Polyhedron Vol. 6, No. 1, p. 1, 1987
Printed in Great Britain

0277-5387/87 $3.00+.00
Pergamon Journals Ltd

HARRY IRVING: A TRIBUTE

R. J. P. WILLIAMS and R. D. GILLARD

Harry Irving was born on 19 November 1905, and has recently, close to his eightieth birthday, retired from the Chair of Analytical Science (which he founded in 1979) at the University of Cape Town. He spent much of the earlier part of his career in Oxford, until he moved to Leeds in 1961 as Professor of Inorganic and Structural Chemistry.

He was initially an organic chemist, becoming later active in analytical and coordination chemistry, but his interests have always remained unusually wide, ranging over the whole field of solution and structural chemistry. It is intriguing that the second and the penultimate paper (separated by 55 years!) in his remarkably varied list of work both deal with a chloral hydrate.

Irving's seminal contributions are chiefly in the area of the relations between the stability of metal complexes of ligands and their structures (both of the ligands and of the complexes). A few of these classes of ligands (such as dithizones, amino-alcohols and complexones: he was of course the translator of Schwarzenbach's book in 1957) are represented in this collection of papers in his honour.

Professor Irving was remarkably percipient in introducing new ideas: quite apart from the Irving–Williams series, he commented very early on steric hindrance influencing stability constants, on kinetic properties of metal ions, on conformations of chelate rings, on solvent extraction in inorganic analysis, and on synergic effects in equilibria. It is salutary to realize that his first doctoral student was R. J. P. Williams (from 1948 when Professor Irving was already aged 43).

Involvement under his tutelage with ideas of stability, reactivity and structure has led Professor Irving's students and collaborators in many new directions. Several are represented in this volume (bio-inorganic chemistry, optical resolutions and stereochemical isomerism, vibrational spectra as a means of studying speciation in solution, and X-ray crystallography for the establishment and confirmation of isomeric structure).

Harry Irving has been, in three universities, a moving spirit for many chemists. While he was one of those who helped to revitalize inorganic chemistry, he also gave to his colleagues and students a wider perspective of a cultured life based on music and dance. He is truly a balanced man. This tribute is dedicated to a many-faceted man of great culture as a mark of affection and respect by his students and associates.

Polyhedron Vol. 6, No. 1, pp. 3–11, 1987
Printed in Great Britain

0277–5387/87 $3.00+.00
Pergamon Journals Ltd

PROFESSOR H. M. N. H. IRVING: LIST OF PUBLISHED WORKS

1929

The action of potassium cyanide on chloroaldehydes. F. D. Chattaway and H. Irving, *J. Chem. Soc.* 1929, 1038.

1930

The interaction of butyl chloral hydrate and 2:4-dihalogen-substituted phenylhydrazines. F. D. Chattaway and H. Irving, *J. Chem. Soc.* 1930, 87.

1931

The condensation of butyl chloral hydrate with aryl hydrazines. F. D. Chattaway and H. Irving, *J. Chem. Soc.* 1931, 751.

The 4-hydroxy-1-aryl-5-methylpyrazoles. F. D. Chattaway and H. Irving, *J. Chem. Soc.* 1931, 786.

2:4:6-Trichlorophenylhydrazine. F. D. Chattaway and H. Irving, *J. Chem. Soc.* 1931, 1740.

1:3-Benzdioxin. F. D. Chattaway and H. Irving, *J. Chem. Soc.* 1931, 2492.

1932

The condensation of butyl chloral hydrate with aryl hydrazines. F. D. Chattaway and H. Irving, *J. Am. Chem. Soc.* 1932, **54**, 263.

1933

2:4:6-Trichloroaniline. F. D. Chattaway and H. Irving, *J. Chem. Soc.* 1933, 142.

The $\alpha\alpha\beta$-trihalogenated butaldehydes. F. D. Chattaway, H. Irving and G. H. Outhwaite, *J. Chem. Soc.* 1933, 993.

1934

The action of alkalis on substituted benzdioxins. F. D. Chattaway and H. Irving, *J. Chem. Soc.* 1934, 325.

1935

An historical account of Pharaoh's serpents. H. Irving, *Sci. Prog. (London)* 1935, **30**, 62.

The action of halogens upon the arylhydrazones of unsaturated aldehydes. F. D. Chattaway and H. Irving, *J. Chem. Soc.* 1935, 90.

1936

The action of amines upon esters. Part I. H. Irving, *J. Chem. Soc.* 1936, 797.

1937

The applications of floating equilibrium to the determination of density. H. Irving, *Sci. Prog. (London)* 1937, **31**, 654.

1940

The interaction of arylhydrazines and halogenated aldehydes. H. Irving, *J. Chem. Soc.* 1940, 813.

The alleged reduction of the phenylurethane of trichlorolactic ester and nitrile by dilute aqueous alkali. H. Irving and H. Marston, *J. Chem. Soc.* 1940, 1512.

1941

Bunsen's salt. H. Irving and G. W. Cherry, *J. Chem. Soc.* 1941, 25.

1943

The action of alkalis on substituted benzdioxins. H. Irving and (in part) E. G. Curtis, *J. Chem. Soc.* 1943, 319.

1948

The action of amines on esters, Part II. H. Irving and H. I. Fuller, *J. Chem. Soc.* 1948, 1989.

The order of stability of metal complexes. H. Irving and R. J. P. Williams, *Nature (London)* 1948, **162**, 746.

Reversion: a new procedure in absorptiometry. H. Irving, G. Andrew and E. J. Risdon, *Nature (London)* 1948, **161**, 805.

Analytical chemistry. H. Irving, *Annu. Rep. Prog. Chem.* 1948, **45**, 316.

1949

The absorptiometric determination of traces of metals. Reversion: a new procedure. H. Irving, E. J. Risdon and G. Andrew, *J. Chem. Soc.* 1949, 537.

Studies with dithizone. Part I. The determination of traces of mercury. H. Irving, G. Andrew and E. J. Risdon, *J. Chem. Soc.* 1949, 541.

Steric hindrance in analytical chemistry. Part I. H. Irving, E. J. Butler and M. F. Ring, *J. Chem. Soc.* 1949, 1489.

Metal complexes and partition equilibria. H. Irving and R. J. P. Williams, *J. Chem. Soc.* 1949, 1841.

Studies with dithizone. Part II. Dithizone as a monobasic acid. H. Irving, S. J. H. Cooke, S. C. Woodger and R. J. P. Williams, *J. Chem. Soc.* 1949, 1847.

The dissociation constant of 8-hydroxyquinoline. H. Irving, J. A. D. Ewart and J. T. Wilson, *J. Chem. Soc.* 1949, 2672.

Analytical chemistry. H. Irving, *Annu. Rep. Prog. Chem.* 1949, **46**, 268.

1950

The effect of time and temperature on potentials measured with the glass electrode. H. Irving and R. J. P. Williams, *J. Chem. Soc.* 1950, 2890.

1951

The centenary of Penny's process: A landmark in the history of analytical chemistry. H. Irving, *Sci. Prog. (London)* 1951, **39**, 63.

The stability of co-ordination compounds in aqueous solution. H. Irving, In *Proceedings of the First Conference on Coordination Chemistry*, I.C.I. Report No. BRL/146 (1951).

Solvent extraction and its applications to inorganic analysis. H. M. Irving, *Q. Rev.* 1951, **5**, 200.

The valencies of the transition elements in the metallic

state. W. Hume-Rothery, H. M. Irving and R. J. P. Williams, *Proc. R. Soc.* (*London*) 1951, **208A**, 431.

1952

Studies with dithizone. Part III. The extraction constant of zinc dithizonate. H. Irving, C. F. Bell and R. J. P. Williams, *J. Chem. Soc.* 1952, 357.

Studies with dithizone. Part IV. The dissociation constant of dithizone. H. Irving and C. F. Bell, *J. Chem. Soc.* 1952, 1261.

Cinnolines, Part XXIX. E. J. Alford, H. Irving, (Miss) H. S. Marsh and K. Schofield, *J. Chem. Soc.* 1952, 3009.

Some factors controlling the selectivity of organic reagents. H. Irving and R. J. P. Williams, *Analyst* (*London*) 1952, **77**, 813.

The solvent extraction of Group IIIB metal halides. H. Irving and F. J. C. Rossotti, *Analyst* (*London*) 1952, **77**, 801.

The solvent extraction of indium. H. Irving, F. J. C. Rossotti and J. G. Drysdale, *Nature* (*London*) 1952, **162**, 619.

S-methyl dithizone and the structure of the metal dithizonates. H. Irving and C. F. Bell, *Nature* (*London*) 1952, **169**, 756.

1953

Partition chromatography. H. Irving and R. J. P. Williams, *Sci. Prog.* (*London*) 1953, **163**, 418.

The stability of transition metal complexes. H. Irving and R. J. P. Williams, *J. Chem. Soc.* 1953, 3192.

Methods for computing successive stability constants from experimental formation curves. H. Irving and (Mrs) H. S. Rossotti, *J. Chem. Soc.* 1953, 3397.

Steric hindrance in analytical chemistry, Part II. The interaction of ferrous salts with 2-substituted 1:10-phenanthrolines. H. Irving, M. J. Cabel and D. Mellor, *J. Chem. Soc.* 1953, 3417.

Studies with dithizone. Part V. A comparison of routes for the synthesis of [^{35}S]dithizones. H. Irving and C. F. Bell, *J. Chem. Soc.* 1953, 3538.

A reversion method for the absorptiometric determination of traces of lead with dithizone. H. Irving and E. J. Butler, *Analyst* (*London*) 1953, **78**, 571.

1954

The stabilities of complexes formed by some bivalent metals with *N*-alkylated substituted ethylenediamines. H. Irving and J. M. M. Griffiths, *J. Chem. Soc.* 1954, 213.

Inorganic chemical kinetics and reactions. H. Irving, *Nature* (*London*) 1954, **173**, 670.

The calculation of formation curves of metal complexes from pH-titration curves in mixed solvents. H. Irving and (Mrs) H. S. Rossotti, *J. Chem. Soc.* 1954, 2904.

The stabilities of some metal complexes of 8-hydroxyquiniline and related substances. H. Irving and (Mrs) H. S. Rossotti, *J. Chem. Soc.* 1954, 2910.

The influence of ring-size on the stability of metal chelates. H. Irving, R. J. P. Williams, D. J. Ferrett and A. E. Williams, *J. Chem. Soc.* 1954, 3494.

8-Hydroxyquinaldinic acid. H. Irving and A. R. Pinnington, *J. Chem. Soc.* 1954, 3782.

The stability constants of the indium halides. H. Irving and B. G. F. Carleson, *J. Chem. Soc.* 1954, 4390

Studies with dithizone. Part VI. *S*-alkyl dithizone. H. Irving and C. F. Bell, *J. Chem. Soc.* 1954, 4253.

The kinetics and mechanism of inorganic reactions in solution. Introductory survey. H. Irving, *Chem. Soc., Spec. Publ.* 1954, **1**, 1.

1955

Steric hindrance in analytical chemistry. Part III. 1,2′-Pyridylisoquinoline and the ferroin reaction. H. Irving and A. Hampton, *J. Chem. Soc.* 1955, 430.

The determination of the dissociation constants of dibasic acids. H. Irving, (Mrs) H. S. Rossotti and G. Harris, *Analyst* (*London*) 1955, **80**, 83.

The theoretical basis of "sensitivity tests" and their application to some potential organic reagents for metals. H. Irving and (Mrs) H. S. Rossotti, *Analyst* (*London*) 1955, **80**, 245.

An investigation of 5-nitroso-oxine as an analytical reagent. H. Irving, R. G. W. Hollingshead and G. Harris, *Analyst* (*London*) 1955, **80**, 260.

A general treatment of the solvent extraction of inorganic compounds. H. Irving, F. J. C. Rossotti and R. J. P. Williams, *J. Chem. Soc.* 1955, 1906.

The extraction of indium at tracer concentrations from acid bromide solutions into methylisobutyl ketone. H. Irving and F. J. C. Rossotti, *J. Chem. Soc.* 1955, 1927.

The extraction of indium at macro concentrations from hydrobromic acid into methylisobutyl ketone and diethyl ether. H. Irving and F. J. C. Rossotti, *J. Chem. Soc.* 1955, 1938.

The extraction of indium halides into organic solvents. H. Irving and F. J. C. Rossotti, *J. Chem. Soc.* 1955, 1946.

A new application of the theory of corresponding solutions to measurements of the stabilities of some metal complexes. H. Irving and D. H. Mellor, *J. Chem. Soc.* 1955, 3457.

1956

The extraction of indium from hydrobromic acid into mixed organic solvents. H. Irving and F. J. C. Rossotti, *J. Chem. Soc.* 1956, 2475.

Some relationships among the stabilities of metal complexes. H. Irving and H. Rossotti, *Acta Chem. Scand.* 1956, **10**, 72.

1957

The bromination of 8-hydroxyquinaldine. H. Irving and A. R. Pinnington, *J. Chem. Soc.* 1957, 285.

Some bromine-substituted derivatives of 8-hydroxyquinoline. H. Irving and A. R. Pinnington, *J. Chem. Soc.* 1957, 290.

The determination of indium in rocks and minerals by radioactivation. A. A. Smales, J. van R. Smit and H. Irving, *Analyst* (*London*) 1957, **82**, 539.

The determination of indium in cylindrite by neutron-activation analysis and by other methods. H. Irving, J. van R. Smit and (in part) L. Salmon, *Analyst* (*London*) 1957, **82**, 549.

G. Schwarzenbach, *Complexometric Titrations* (Translated by H. Irving). Methuen, London (1957).

1958

The indium content of rocks and minerals from the Skaergaard intrusion. L. R. Wager, J. van R. Smit and H. Irving, *Geochim. Cosmochim. Acta* 1958, **13**, 81.

Diamagnetism in a quasi-tetrahedral nickel(II) complex. H. Irving and J. B. Gill, *Proc. Chem. Soc., London* 1958, 168.

Steric hindrance in analytical chemistry. Part IV. Some sterically hindered complexones. H. Irving, R. Shelton and (in part) R. Evans, *J. Chem. Soc.* 1958, 3540.

The preparation of metal-free acids, alkalis, and buffer solutions of high purity. H. Irving and J. J. Cox, *Analyst (London)* 1958, **83**, 526.

Opredelenie indiya radioaktivatsionym metodom. H. Irving, *Tr. Kom. Anal. Khim., Akad. Nauk SSSR* 1958, **9**, 249.

A versatile electronic device for counting drops of eluant in chromatography or operating ancillary apparatus after pre-set counts or pre-set times. G. L. Reed and H. Irving, *Analyst (London)* 1958, **84**, 317.

1959

Steric hindrance in analytical chemistry. Part V. A new 2-substituted 8-hydroxyquinoline (oxine). H. Irving and D. J. Clifton, *J. Chem. Soc.* 1959, 288.

Some potential chelating agents derived from benziminazole. H. Irving and O. Weber, *J. Chem. Soc.* 1959, 2296.

Some observations on Job's method of continuous variations and its extension to two-phase systems. H. Irving and T. B. Pierce, *J. Chem. Soc.* 1959, 2565.

Metal complexes of 2-aminomethylbenzimidazole. H. Irving and O. Weber, *J. Chem. Soc.* 1959, 2560.

An automatic titrimeter for plotting true-scale titration curves. H. Irving and L. D. Pettit, *Analyst (London)* 1959, **84**, 641.

The stability of metal complexes, Plenary Lecture to the Fourth International Congress on Co-ordination Chemistry. H. Irving, *Chem. Soc., Spec. Publ.* 1959, **13**, 13.

A novel relationship between the stability of certain metal halides and the absorption spectra of their complexes with dithizone. H. Irving and J. J. Cox, *Proc. Chem. Soc., London* 1959, 324.

Synergic effects in the solvent extraction of uranium. H. Irving and D. N. Edgington, *Proc. Chem. Soc., London* 1959, 360.

1960

The structure of some di-(3-methyl-1,5-diarylformazyl)-nickel(II) complexes. H. Irving, J. B. Gill and (in part) W. R. Cross, *J. Chem. Soc.* 1960, 2087.

The photochemical decomposition of diphenyliodonium iodide. H. Irving and R. W. Reid, *J. Chem. Soc.* 1960, 2078.

The electronic absorption spectra of some diaryliodonium salts. H. Irving, G. P. A. Turner and R. W. Reid, *J. Chem. Soc.* 1960, 2082.

(Methyl isocyanide)copper(I) iodide. H. Irving and M. Jonason, *J. Chem. Soc.* 1960, 2095.

Synergic effects in the solvent extraction of the actinides. Part I. Uranium(VI). H. Irving and D. N. Edgington, *J. Inorg. Nucl. Chem.* 1960, **15**, 158.

The determination of trace quantities of silver in trade effluents. T. B. Pierce and H. Irving, *Analyst (London)* 1960, **85**, 166.

Solubilities of metal chelates of α-amino acids. H. Irving and L. D. Pettit, *Chem. Ind. (London)* 1960, 1268.

The solvent extraction of solvated ion-pairs: a theoretical approach. H. Irving and D. C. Lewis, *Proc. Chem. Soc., London* 1960, 222.

A procedure for determining the molar extinction coefficients of metal dithizonates. H. Irving and R. S. Ramakrishna, *Analyst (London)* 1960, **85**, 860.

The resolution of (±)-propylenediamine by a stereospecific reaction. H. Irving and R. D. Gillard, *J. Chem. Soc.* 1960, 5266.

Stability of metal complexes and their measurement polarographically, Plenary Lecture to the 2nd International Congress on Polarography, Cambridge, 1959. H. Irving, In *Advances in Polarography, Proceedings of the 2nd International Conference, Cambridge, England,* 1959, Vol. 1, p. 42. Pergamon Press, Oxford (1960).

1961

Synergic effects in solvent extraction. H. Irving and D. N. Edgington, *Chem. Ind. (London)* 1961, 77.

Studies with dithizone. Part VII. The action of halogens on dithizone and its analogues. H. Irving and R. S. Ramakrishna, *J. Chem. Soc.* 1961, 1272.

Studies with dithizone. Part VIII. Reactions with organometallic compounds. H. Irving and J. J. Cox, *J. Chem. Soc.* 1961, 1470.

Metal complexes of bis-[3-di(carboxymethyl)aminopropyl] ether. The computation of stability constants with the aid of a high-speed digital computer. H. Irving and M. H. Stacey, *J. Chem. Soc.* 1961, 2019.

Studies with dithizone. Part IX. The absorption spectra of mono- and di-*p*-bromosubstituted dithizones and of their metal complexes. H. Irving and R. S. Ramakrishna, *J. Chem. Soc.* 1961, 2118.

A new stereospecific reaction. H. Irving and R. D. Gillard, *J. Chem. Soc.* 1961, 2249.

A comparison of the stabilities of metal chelates containing N, P, and As as donor atoms. H. Irving and L. D. Pettit, In *Advances in the Chemistry of the Coordination Compounds* (Edited by S. Kirschner), p. 412. Macmillan, New York (1961).

Liquid–liquid extraction. H. Irving, In *Treatise on Analytical Chemistry* (Edited by I. M. Kolthoff and P. J. Elving), Chap. 31, p. 1309. Interscience, New York (1961).

Synergic effects in the solvent extraction of the actinides. Part II. Plutonium(VI) and neptunium(V). H. Irving and D. N. Edgington, *J. Inorg. Nucl. Chem.* 1961, **20**, 314.

Synergic effects in the solvent extraction of the actinides. Part III. Tetravalent actinides. H. Irving and D. N. Edgington, *J. Inorg. Nucl. Chem.* 1961, **20**, 321.

Synergic effects in the solvent extraction of the actinides. Part IV. Trivalent plutonium, americium and europium. H. Irving and D. N. Edgington, *J. Inorg. Nucl. Chem.* 1961, **21**, 169.

1962

The contributions of π-bonding to the stabilities of metal complexes in solution, and a correlation with Hammett's σ-factor. H. Irving and J. J. R. F. da Silva, *Proc. Chem. Soc., London* 1962, 250.

Observations on the computation of stability constants by Olerup's graphical procedure. H. Irving, *J. Chem. Soc.* 1962, 4056.

Steric hindrance in analytical chemistry. Part VI. 1-Methyl- and 1,6-dimethyl-3,4,5-triazaphenanthrene as reagents for iron and copper. E. A. Hobday, M. Tomlinson and H. Irving, *J. Chem. Soc.* 1962, 4914.

The stability of metal complexes of 1,10-phenanthroline and its analogues. Part I. 1,10-Phenanthroline and 2,2′-bipyridyl. H. Irving and D. H. Mellor, *J. Chem. Soc.* 1962, 5222.

The stability of metal complexes of 1,10-phenanthroline and its analogues. Part II. 2-Methyl- and 2,9-dimethylphenanthroline. H. Irving and D. H. Mellor, *J. Chem. Soc.* 1962, 5237.

The stability of metal complexes of 1,10-phenanthroline and its analogues. Part III. 5-Methyl-1,10-phenanthroline. W. A. E. McBryde, (Mrs) D. A. Brisbin and H. Irving, *J. Chem. Soc.* 1962, 5245.

The complexes formed by thallium(I), the alkali metals, and other monovalent ions. H. Irving and J. J. R. F. da Silva, In *Proceedings of the 7th International Congress on Coordination Chemistry, Stockholm* 1962, p. 108.

1963

The stabilities of complexes of thallium(I) and the alkali metals with uramildiacetic acid. H. Irving and J. J. R. F. da Silva, *J. Chem. Soc.* 1963, 448.

The stabilities of complexes of uramildiacetic acid and its homologues. H. Irving and J. J. R. F. da Silva, *J. Chem. Soc.* 1963, 458.

Studies with dithizone. Part X. Reactions with organomercury(II) compounds. H. Irving and J. J. Cox, *J. Chem. Soc.* 1963, 466.

The adsorption of some anionic complexes on a cation-exchange resin. H. Irving and G. T. Woods, *J. Chem. Soc.* 1963, 939.

Metal complexes of *N*-(2-pyridylmethyl)iminodiacetic acid. H. Irving and J. J. R. F. da Silva, *J. Chem. Soc.* 1963, 945.

Complexones containing heterocyclic donor oxygen atoms. H. Irving and J. J. R. F. da Silva, *J. Chem. Soc.* 1963, 1144.

The stabilities of metal complexes of some *C*-substituted derivatives of glycine. H. Irving and L. D. Pettit, *J. Chem. Soc.* 1963, 1546.

The stabilities of metal complexes of 1,4-piperazinediacetic acid. H. Irving and L. D. Pettit, *J. Chem. Soc.* 1963, 3051.

Steric hindrance in analytical chemistry with special reference to the reactions of analogs of 8-hydroxyquinoline. H. Irving and L. D. Pettit, In *Analytical Chemistry, Proceedings of the International Symposium, Birmingham University, England,* 1962, p. 122 (1963).

The stabilities of metal complexes of some derivatives of iminodiacetic acid. H. Irving and J. J. R. F. da Silva, *J. Chem. Soc.* 1963, 3308.

Studies with dithizone. Part XI. Reactions with *p*-fluorophenyl- and *p*-iodophenyl-mercury(II) compounds. H. Irving and A. M. Kiwan, *J. Chem. Soc.* 1963, 4288.

The Three Cultures, Inaugural Lecture. H. Irving, Leeds University Press, Leeds (1963).

1964

Infra-red absorption spectra of complexes of thiourea. K. Swaminathan and H. M. N. H. Irving, *J. Inorg. Nucl. Chem.* 1964, **26**, 1291.

The purification of hydrobromic and hydriodic acids by ion-exchange. H. Irving and P. D. Wilson, *Chem. Ind. (London)* 1964, 653.

An absorptiometric determination of perchlorate by means of a novel coloured liquid anion exchanger. W. E. Clifford and H. Irving, *Anal. Chim. Acta* 1964, **31**, 1.

The stability of the chloride complexes of europium. H. M. N. H. Irving and P. K. Khopkar, *J. Inorg. Nucl. Chem.* 1964, **26**, 1561.

The stabilities of complexes of the rare earths with propylenediaminetetraacetic acid. H. M. N. H. Irving and J. P. Conesa, *J. Inorg. Nucl. Chem.* 1964, **26**, 1945.

The absorption of polybromide ions on an anion exchange resin. H. M. N. H. Irving and P. D. Wilson, *J. Inorg. Nucl. Chem.* 1964, **26**, 2235.

Studies of ligands containing elements of Group V. Part I. L. D. Pettit and H. M. N. H. Irving, *J. Chem. Soc.* 1964, 5336.

H. Irving and R. J. P. Williams, *Separation Methods in Analytical Chemistry. Liquid–Liquid Extraction*, p. 1309. Wiley Interscience, New York (1964).

1965

A simple preparation of meso-stilbenediamine. H. M. N. H. Irving and (Miss) R. M. Parkins, *J. Inorg. Nucl. Chem.* 1965, **27**, 270.

1,1′-Diaminobicyclohexyl and the stability of its metal complexes. M. L. Tomlinson, M. L. H. Sharp and H. M. N. H. Irving, *J. Chem. Soc.* 1965, 603.

The extraction of copper(II) from acetate buffers by solutions of acetylacetone in benzene. H. M. N. H. Irving and N. S. Al-Niaimi, *J. Inorg. Nucl. Chem.* 1965, **27**, 419.

Synergic effects in solvent extraction. Part VI. The solvent extraction of copper(II) from acetate buffers by mixtures of acetylacetone and 4-methylpyridine. H. M. N. H. Irving and N. S. Al-Niaimi, *J. Inorg. Nucl. Chem.* 1965, **27**, 717.

The stabilities of the metal complexes of optically active amino-acids. R. D. Gillard, H. M. Irving, R. Parkins, N. C. Payne and L. D. Pettit, *Proc. Chem. Soc., London* 1965, 81.

Determination of small amounts of long-chain alkylamines in aqueous solution. H. M. N. H. Irving and A. D. Damodaran, *Analyst (London)* 1965, **90**, 180.

Synergistische Wirkingen bei der flüssig–flüssig Extraktion (Synergic effects in liquid–liquid extraction). H. M. N. H. Irving, *Angew. Chem.* 1965, **77**, 57; *Angew. Chem., Int. Ed. Engl.* 1965, **4**, 95.

Synergic effects in solvent extraction. Part VII. Divalent transition metals. H. M. N. H. Irving and D. N. Edgington, *J. Inorg. Nucl. Chem.* 1965, **27**, 1359.

Synergic effects in solvent extraction. Part VIII. The solvent extraction of copper(II) from acetate buffers by mixtures of acetylacetone with quinoline or isoquinoline. H. M. N. H. Irving and N. S. Al-Niaimi, *J. Inorg. Nucl. Chem.* 1965, **27**, 1671.

A new method for the determination of perchlorate by means of a coloured anion exchanger. H. M. N. H. Irving and A. D. Damodaran, *Analyst* (*London*) 1965, **90**, 443.

Synergic effects in solvent extraction. Part IX. The effect of isoquinoline and 4-methylpyridine on the distribution of diacetylbisbenzoylhydrazone nickel(II) between benzene and aqueous buffers. H. M. N. H. Irving and N. S. Al-Niaimi, *J. Inorg. Nucl. Chem.* 1965, **27**, 2231.

The synthesis of some new complexones and a discussion of the problems that arose in the determination of their acid dissociation constants. H. M. N. H. Irving, L. D. Pettit and M. G. Miles, *Proc. Soc. Anal. Chem.* 1965, **2**, 139.

Conformational aspects of chelate rings. R. D. Gillard and H. M. N. H. Irving, *Chem. Rev.* 1965, **65**, 603.

The solvent extraction of mixed complexes. H. Irving, In *Proceedings of the Symposium on Coordination Chemistry, Tihany, Hungary*, 1964, p. 219. Akademiai Kiado, Budapest (1965).

1966

Stability constants of complexes of thiourea with nickel, cobalt, and bismuth. K. Swaminathan and H. M. N. H. Irving, *J. Inorg. Nucl. Chem.* 1966, **28**, 171.

Electron exchange catalysis in the formation of the EDTA complex of chromium(III) and its photometric determination. H. M. N. H. Irving and W. R. Tomlinson, *Chemist–Analyst* 1966, **55**, 14.

Aryl derivatives of nitrilotriacetic acid, and the stability of their proton and metal complexes. H. M. N. H. Irving and M. G. Miles, *J. Chem. Soc. A* 1966, 727.

Meso- and *dl*-2,3-diaminobutane-*NNN'N'*-tetraacetic acid and their metal complexes. H. M. N. H. Irving and (Miss) R. Parkins, *J. Inorg. Nucl. Chem.* 1966, **28**, 1629.

The isomers of complexes of L-aminoacids with copper(II). R. D. Gillard, H. M. Irving, R. M. Parkins, N. C. Payne and L. D. Pettit, *J. Chem. Soc. A* 1966, 1159.

Analogues of nitrilotriacetic acid and the stabilities of their proton and metal complexes. H. M. N. H. Irving and M. G. Miles, *J. Chem. Soc. A* 1966, 1268.

A new method for determining the activity of concentrated solutions of hydrobromic acid. H. M. N. H. Irving and P. D. Wilson, *J. Inorg. Nucl. Chem.* 1966, **28**, 2033.

1967

The interaction of dithizone with allegedly "purified" dioxan. H. M. N. H. Irving and U. S. Mahnot, *Chem. Ind.* (*London*) 1967, 193.

A study of some problems in determining the stoicheiometric proton dissociation constants of complexes by potentiometric titrations using a glass electrode. H. M. N. H. Irving, M. G. Miles and L. D. Pettit, *Anal. Chim. Acta* 1967, **38**, 475.

The determination of small amounts of long-chain tertiary alkylamines and quaternary ammonium salts. H. M. N. H. Irving and J. J. Markham, *Anal. Chim. Acta* 1967, **39**, 7.

Synergism in the solvent extraction of metal chelates. H. M. N. H. Irving, In *Solvent Extraction Chemistry* (Edited by D. Dyrssen, J. O. Liljenzin and J. Rydberg), p. 91. North-Holland, Amsterdam (1967).

William Skey (1835–1900); a centenary in the history of solvent extraction. H. M. N. H. Irving, *Chem. Ind.* (*London*) 1967, 1780.

The extraction of indium halides into organic solvents. Part VII. The distribution of indium between hydrochloric acid and binary solvent mixtures containing isobutyl methyl ketone. H. M. N. H. Irving and D. Lewis, *Ark. Kemi* 1967, **28**, 131.

1968

Stability constants of copper(II) complexes of optically active α-aminoacids. R. D. Gillard, H. M. N. H. Irving and L. D. Pettit, *J. Chem. Soc. A* 1968, 673.

A general graphical method for evaluating experimental results which should fit a linear equation. H. M. N. H. Irving, *Analyst* (*London*) 1968, **93**, 273.

Complexes of hydroxyacids containing two different metals. H. M. N. H. Irving and W. R. Tomlinson, *Chem. Commun.* 1968, 497.

The extraction of copper(I), lead(II) and tin(IV) from hydrochloric acid by solutions of tetra-*n*-hexylammonium chloride in ethylene dichloride. H. M. N. H. Irving and A. H. Nabilsi, *Anal. Chim. Acta* 1968, **41**, 505.

The extraction of copper(II) from hydrochloric acid by solutions of tetra-*n*-hexylammonium chloride in ethylene dichloride. H. M. N. H. Irving and A. H. Nabilsi, *Anal. Chim. Acta* 1968, **42**, 79.

pH-Meter corrections for titrations in mixtures of water and dioxan. H. M. N. H. Irving and U. S. Mahnot, *J. Inorg. Nucl. Chem.* 1968, **30**, 1215.

The effect of chromium(III) and other ions on the absorptiometric determination of copper using 2,2'-biquinolyl. H. M. N. H. Irving and W. R. Tomlinson, *Talanta* 1968, **15**, 1267.

Studies with dithizone. Part XII. Formation of thiadiazolines by condensation with aldehydes and ketones. H. M. N. H. Irving and U. S. Mahnot, *Talanta* 1968, **15**, 811.

The theory of regular solutions applied to the viscosity of dilute solutions of chromium(III) acetylacetonate in organic solvents. H. M. N. H. Irving and J. S. Smith, *J. Inorg. Nucl. Chem.* 1968, **30**, 1873.

1969

Selenium analogue of dithizone. R. S. Ramakrishna and H. M. N. H. Irving, *Chem. Ind.* (*London*) 1969, 325.

A novel viscometric method for determining the stability constants of a compound of two uncharged species. H. M. N. H. Irving and J. S. Smith, *J. Inorg. Nucl. Chem.* 1969, **31**, 159.

A viscometric study of possible adduct formation between solutions of chromium(III) acetylacetonate and thiourea in methanol. H. M. N. H. Irving and J. S. Smith, *J. Inorg. Nucl. Chem.* 1969, **31**, 169.

Addendum to paper entitled "The theory of regular solutions applied to the viscosity of dilute solutions of chromium(III) acetylacetonate in organic solvents. H. M. N. H. Irving and J. S. Smith, *J. Inorg. Nucl. Chem.* 1969, **31**, 1212.

Studies with dithizone. Part XIII. The extraction of methyl-, benzyl- and *p*-bromophenyl-mercury(II) dithizonates. H. M. N. H. Irving and A. M. Kiwan, *Anal. Chim. Acta* 1969, **45**, 243.

Studies with dithizone. Part XIV. A new oxidation product of dithizone. H. M. N. H. Irving, D. C. Rupainwar and S. S. Sahota, *Anal. Chim. Acta* 1969, **45**, 249.

Studies with dithizone. Part XV. Further reactions with organomercury compounds. H. M. N. H. Irving and A. M. Kiwan, *Anal. Chim. Acta* 1969, **45**, 255.

Studies with dithizone. Part XVI. Water-soluble arylmercury(II) dithizonates and secondary arylmercury(II) dithizonates. H. M. N. H. Irving and A. M. Kiwan, *Anal. Chim. Acta* 1969, **45**, 271.

Studies with dithizone. Part XVII. The extraction constants of organomercury(II) dithizonates. H. M. N. H. Irving and A. M. Kiwan, *Anal. Chim. Acta* 1969, **45**, 447.

A viscometric study of interactions in solutions of bis-(*N*-methylsalicylaldimine)nickel(II). H. M. N. H. Irving and J. S. Smith, *J. Inorg. Nucl. Chem.* 1969, **31**, 2895.

An unusual bicyclic oxidation product of dithizone. W. S. McDonald, H. M. N. H. Irving, G. Raper and D. C. Rupainwar, *Chem. Commun.* 1969, 392.

The non-existence of selenium dithizonate. R. S. Ramakrishna and H. M. N. H. Irving, *Chem. Commun.* 1969, 1356.

Vibrational spectra and force-constant computations of *cis*- and *trans*-dicyanotetrakis(methylisocyanide)-iron(II). R. R. Berrett, B. W. Fitzsimmons, P. Gans, H. M. N. H. Irving and P. Stratton, *J. Chem. Soc. A* 1969, 904.

A viscometric study of iodine–solvent interactions. H. M. N. H. Irving and J. S. Smith, *J. Inorg. Nucl. Chem.* 1969, **31**, 3163.

Studies with dithizone. Part XIX. A photochemical oxidation product of dithizone. H. M. N. H. Irving and D. C. Rupainwar, *Anal. Chim. Acta* 1969, **48**, 187.

Selenazone: the selenium analogue of dithizone. R. S. Ramakrishna and H. M. N. H. Irving, *Anal. Chim. Acta* 1969, **48**, 251.

G. Schwarzenbach and H. Flaschka, *Complexometric Titrations* (2nd English Edition translated and revised by H. M. N. H. Irving). Methuen, London (1969).

The extraction of silver(I) from hydrochloric acid by solutions of tri-*N*-hexylammonium and tetra-*N*-hexylammonium chloride in organic solvents. H. M. N. H. Irving and A. D. Damodaran, *Anal. Chim. Acta* 1969, **48**, 267.

Liquid–liquid extraction. H. M. N. H. Irving, *Minerals Science and Engineering* 1969, **1**, 15.

1970

Selenium dithizonate. H. M. N. H. Irving, *Chem. Commun.* 1970, 519.

The viscosities of dilute solutions of naphthalene in organic solvents and their interpretation in terms of the theory of regular solutions. H. M. N. H. Irving and J. S. Smith, *J. Inorg. Nucl. Chem.* 1970, **32**, 901.

An examination by viscometry of possible stereospecific interaction between chromium(III) acetylacetonate and an optically active ester in benzene solution. H. M. N. H. Irving, R. B. Simpson and J. S. Smith, *J. Inorg. Nucl. Chem.* 1970, **32**, 2275.

Studies with dithizone. Part XX. On the non-existence of selenium dithizonate. R. S. Ramakrishna and H. M. N. H. Irving, *Anal. Chim. Acta* 1970, **49**, 9.

Studies with dithizone. Part XXI. A novel bicyclic oxidation product of dithizone. H. M. N. H. Irving, U. S. Mahnot and D. C. Rupainwar, *Anal. Chim. Acta* 1970, **49**, 261.

Formation constants of europium(III) salicylate complexes and their extraction into isoamyl alcohol. H. M. N. H. Irving and S. P. Sinha, *Anal. Chim. Acta* 1970, **49**, 449.

The extraction of indium from aqueous halide and thiocyanate media by solutions of liquid anion exchangers in organic solvents. H. M. N. H. Irving and A. D. Damodaran, *Anal. Chim. Acta* 1970, **50**, 277.

The synergic extraction of ternary complexes of europium(III). H. M. N. H. Irving and S. P. Sinha, *Anal. Chim. Acta* 1970, **51**, 39.

A novel unimolecular heterolytic fission of the sulphur–sulphur bond in a symmetrical disulphide. A. M. Kiwan and H. M. N. H. Irving, *Chem. Commun.* 1970, 928.

An automatic capillary viscometer. J. S. Smith, H. M. N. H. Irving and R. B. Simpson, *Analyst (London)* 1970, **95**, 743.

The extraction of indium halides into organic solvents. Part VIII. A theoretical approach to the partition of solvated ion-pairs. H. M. N. H. Irving and D. Lewis, *Ark. Kemi* 1970, **32**, 121.

The extraction of indium halides into organic solvents. Part IX. The relative efficiencies of different organic solvents. H. M. N. H. Irving and D. Lewis, *Ark. Kemi* 1970, **32**, 131.

The synergic extraction of the europium(III)–bis-phenanthroline–tris-salicylate complex and the preparation and properties of analogous ternary rare earth complexes. S. P. Sinha and H. M. N. H. Irving, *Anal. Chim. Acta* 1970, **52**, 193.

Formation constants of bis- and tris-complexes of optically active bidentate ligands. A. T. Advani, H. M. N. H. Irving and L. D. Pettit, *J. Chem. Soc. A* 1970, 2649.

Recommended nomenclature for liquid–liquid distribution. H. M. N. H. Irving, *Pure Appl. Chem.* 1970, **21**, 109.

The determination of microgram quantities of mercury(II) and silver(I) by thermometric titration. K. C. Burton and H. M. N. H. Irving, *Anal. Chim. Acta* 1970, **52**, 441.

1971

Divalent metal complexes of *meso*- and *dl*-2,3-diaminobutane-*NNN'N'*-tetraacetic acid. H. M. N. H. Irving and K. Sharpe, *J. Inorg. Nucl. Chem.* 1971, **33**, 203.

Complexes of *meso*- and *dl*-2,3-diaminobutane-*NNN'N'*-tetraacetic acid with rare-earth cations. H. M. N. H. Irving and K. Sharpe, *J. Inorg. Nucl. Chem.* 1971, **33**, 217.

Stabilities of complexes formed by *dl*- and *meso*-2,3-diaminobutane-*NNN'N'*-tetraacetic acid with iron(II) and iron(III). H. M. N. H. Irving and K. Sharpe, *J. Inorg. Nucl. Chem.* 1971, **33**, 233.

The effect of solvent on the electronic absorption spectra of the mesoionic compounds 2,3-diphenyl-2*H*-tetrazolium-5-thiolate and 4-phenyl-1,3,4-thiadiazolium-2-thiolate. A. M. Kiwan and H. M. N. H. Irving, *J. Chem. Soc. B* 1971, 898.

Kinetics of the decomposition of bis-1,5-diphenylformazan-3-yl disulphide and bis-4-phenyl-Δ^2-1,3,4-thiadiazolin-2-yl disulphide in organic solvents. A. M. Kiwan and H. M. N. H. Irving, *J. Chem. Soc. B* 1971, 901.

The extraction of complex cyanides by liquid ion-exchangers. H. M. N. H. Irving and A. D. Damodaran, *Anal. Chim. Acta* 1971, **53**, 267.

The extraction of mercury(II) as cyanide complexes by solutions of long-chain quaternary amines. H. M. N. H. Irving and A. D. Damodaran, *Anal. Chim. Acta* 1971, **53**, 277.

A secondary dithizone complex containing both silver and mercury. H. M. N. H. Irving and T. Nowicka-Jankowska, *Anal. Chim. Acta* 1971, **54**, 55.

Mixed secondary complexes of silver(I) and phenylmercury(II) cations with dithizone. A. M. Kiwan and H. M. N. H. Irving, *Anal. Chim. Acta* 1971, **54**, 351.

Studies with dithizone. Part XXIII. Some observations on secondary mercury(II) dithizonate. T. Nowicka-Jankowska and H. M. N. H. Irving, *Anal. Chim. Acta* 1971, **54**, 489.

Stereoselectivity in the reactions of cobalt(III) complexes of *meso*- and *dl*-2,3-diaminobutanetetraacetic acid with aliphatic diamines. H. M. N. H. Irving and R. Countryman, *J. Inorg. Nucl. Chem.* 1971, **33**, 1819.

The extraction of chromium(III) from aqueous EDTA by solutions of tetrahexylammonium chloride in dichloroethane. H. M. N. H. Irving and R. H. Al-Jarrah, *Anal. Chim. Acta* 1971, **55**, 135.

An automatic capillary viscometer. Part II. Apparatus for viscometric titrations. R. B. Simpson, J. S. Smith and H. M. N. H. Irving, *Analyst* (*London*) 1971, **96**, 550.

Viscometric titrations. A new technique applied to acidimetry and alkalimetry. R. B. Simpson, H. M. N. H. Irving and J. S. Smith, *Anal. Chim. Acta* 1971, **55**, 169.

Studies with dithizone. Part XXV. The deterioration of stock solutions and the identification of two oxidation products. H. M. N. H. Irving, A. M. Kiwan, D. C. Rupainwar and S. S. Sahota, *Anal. Chim. Acta* 1971, **56**, 205.

Steric hindrance to the formation of metal complexes of 2-chloro-1,10-phenanthroline. H. M. N. H. Irving and P. J. Gee, *Anal. Chim. Acta* 1971, **55**, 315.

The crystal structure of primary zinc(II) dithizonate and its relevance to the structures of its *ortho*- and *para*-methyl derivatives. A. Mawby and H. M. N. H. Irving, *Anal. Chim. Acta* 1971, **55**, 269.

Studies with dithizone. Part XXVI. Secondary copper(II) dithizonate. H. M. N. H. Irving and A. M. Kiwan, *Anal. Chim. Acta* 1971, **56**, 435.

Studies with dithizone. Part XXVII. Primary copper(I) dithizonate. A. M. Kiwan and H. M. N. H. Irving, *Anal. Chim. Acta* 1971, **57**, 59.

1972

The crystal structure of primary zinc(II) dithizonate. A. Mawby and H. M. N. H. Irving, *J. Inorg. Nucl. Chem.* 1972, **34**, 109.

The calculation of stability constants of weak complexes from spectrophotometric data. P. Gans and H. M. N. H. Irving, *J. Inorg. Nucl. Chem.* 1972, **34**, 1885.

The viscosity of mixtures of benzene and methanol. H. M. N. H. Irving and R. B. Simpson, *J. Inorg. Nucl. Chem.* 1972, **34**, 2241.

Complexes of chromium(III) with nitrilotriacetic acid and their extraction by solutions of Aliquat-336 in dichloroethane. H. M. N. H. Irving and R. H. Al-Jarrah, *Anal. Chim. Acta* 1972, **60**, 345.

Useful effects of steric hindrance in analytical chemistry. H. M. N. H. Irving, *Proc. Soc. Anal. Chem.* 1972, **9**, 242.

The complexometric determination of cobalt, chromium, and mixtures of bismuth and lead using extractive end-points. H. M. N. H. Irving and R. H. Al-Jarrah, *Chem. Anal.* (*Warsaw*) 1972, **17**, 779.

Observations on the determination of metal–ligand stability constants when the salt background includes potentially complexing anions. H. M. N. H. Irving and M. H. Stacey, *K. Tek. Högskolans Handl.* 1972, **263**, 209.

1973

The extraction of the chromium(III)–EDTA complex by solutions of Aliquat-336 in various organic solvents. H. M. N. H. Irving and R. H. Al-Jarrah, *Anal. Chim. Acta* 1973, **63**, 79.

The extraction of EDTA by solutions of Aliquat-336 in 1,2-dichloroethane. H. M. N. H. Irving and R. H. Al-Jarrah, *Anal. Chim. Acta* 1973, **65**, 77.

The mass spectra of dithizone and some related compounds. P. A. Alsop and H. M. N. H. Irving, *Anal. Chim. Acta* 1973, **65**, 202.

Studies with dithizone. Part XXX. Complexes of metals with *S*-methyldithizone and the methylation of metal dithizonates. H. M. N. H. Irving, A. H. Nabilsi and S. S. Sahota, *Anal. Chim. Acta* 1973, **67**, 135.

The crystal structure of diphenylthiocarbazide. M. Harding, M. J. Adams, P. A. Alsop and H. M. N. H. Irving, *Anal. Chim. Acta* 1973, **67**, 204.

Separation and preconcentration. H. Irving, *Fresenius' Z. Anal. Chem.* 1973, **263**, 264.

1974

A new procedure for determining the metal content of colourless complexonates. H. M. N. H. Irving and R. H. Al-Jarrah, *Anal. Chim. Acta* 1974, **68**, 473.

The extraction of indium halides into organic solvents. X. Synergic effects with solvent mixtures containing alcohols. H. M. N. H. Irving and D. Lewis, *Chem. Scr.* 1974, **5**, 202.

The extraction of indium halides into organic solvents. XI. Synergic effects with solvents containing diethyl ether. H. M. N. H. Irving and D. Lewis, *Chem. Scr.* 1974, **5**, 208.

Application of the solubility parameter concept in liquid–liquid extraction. H. M. N. H. Irving, In *Ion Exchange and Solvent Extraction* (Edited by J. A. Marinsky and Y. Marcus), Vol. 6, Chap. 3, p. 139. Marcel Dekker, New York (1974).

Current uses of liquid–liquid extraction in analytical chemistry. H. Irving, *Chem. Ind. (London)* 1974, **16**, 639.

H. M. N. H. Irving, *The Techniques of Analytical Chemistry, a Short Historical Survey*. H.M. Stationery Office, London (1974).

One hundred years of development in analytical chemistry. Centenary lecture of the Society for Analytical Chemistry. H. M. N. H. Irving, *Analyst (London)* 1974, **99**, 787.

Recommendations on the usage of the terms "equivalent" and "normal". H. M. N. H. Irving, *IUPAC Inf. Bull.* 1974, **26**, 1.

XVth Procter memorial lecture, Fact or fiction? How much do we really know about the chemistry of chromium today? H. M. N. H. Irving, *J. Soc. Leather Technol. Chem.* 1974, **58**, 51.

1975

Fakta, nebo fikce? Co dnes skutečne vime o chemii chromitých sloučenin? H. M. N. H. Irving, *Kožarštvi* 1975, **25**, 59 and 83.

List of trivial names and synonyms (for substances used in analytical chemistry). H. Irving, *IUPAC Inf. Bull.* 1975, **45**, 1.

Preconcentration and separation. H. Irving, *Cron. Chim.* 1975, **46**, 1.

The extraction of various metals as their anionic complexes with EDTA by solutions of Aliquat-336 chloride in 1,2-dichloroethane. H. M. N. H. Irving and R. H. Al-Jarrah, *Anal. Chim. Acta* 1975, **74**, 321.

1976

Separation techniques used in radiochemical procedures. H. M. N. H. Irving, *J. Radioanal. Chem.* 1976, **33**, 287.

1977

Classical methods of analysis. H. M. N. H. Irving, *Pure Appl. Chem.* 1977, **49**, 1575.

The development of analytical techniques. H. M. N. H. Irving, In *Essays on Analytical Chemistry: In Memory of Professor Anders Ringbom* (Edited by E. Wanninen), p. 591. Pergamon Press, Oxford (1977).

Acid strengths of various substituted formazans in ethanolic solution. J. B. Gill, H. M. N. H. Irving and A. Prescott, *J. Chem. Soc., Perkin Trans.* 2 1977, 1683.

H. M. N. H. Irving, *Dithizone*. Analytical Sciences Monographs No. 5, The Chemical Society, London (1977).

1978

The viscosities of isomorphous salts. H. M. N. H. Irving and S. A. Karmali, *J. Inorg. Nucl. Chem.* 1978, **40**, 1401.

Studies with dithizone. Part XXXI. The relationship between $pH_{1/2}$ and molar solubility. H. M. N. H. Irving, N. F. Naqvi and C. G. Tilley, *Anal. Chim. Acta* 1978, **100**, 597.

Recommendations on the usage of the terms "equivalent" and "normal". H. M. N. H. Irving, T. S. West and D. H. Whiffen, *Pure Appl. Chem.* 1978, **50**, 325.

Guide to trivial names, trade names and synonyms for substances used in analytical nomenclature. H. M. N. H. Irving, *Pure Appl. Chem.* 1978, **50**, 339.

Coordination compounds in analytical chemistry. Plenary Lecture, 18th International Conference on Coordination Chemistry, Sao Paulo, Brazil, 1977. H. M. N. H. Irving, *Pure Appl. Chem.* 1978, **50**, 1129.

H. M. N. H. Irving, H. Freiser and T. S. West, *Compendium of Analytical Nomenclature*. Pergamon Press, Oxford (1978).

1979

Crystal structure of bis(2-methyl-8-hydroxyquinolinato)beryllium(II) dihydrate. J. C. van Niekerk, H. M. N. H. Irving and L. R. Nassimbeni, *S. Afr. J. Chem.* 1979, **32**, 85.

Novel intramolecular hydrogen bond to a quasi-aromatic formazan ring: solution conformation and X-ray crystal structure of 3-carboxymethylthio-1,5-diphenylformazan. A. T. Hutton, H. M. N. H. Irving, K. R. Koch, L. R. Nassimbeni and G. Gafner, *J. Chem. Soc., Chem. Commun.* 1979, 57.

Three-coordinate mercury complex: photochromism and molecular structure of phenylmercury(II) dithizonate. A. T. Hutton and H. M. N. H. Irving, *J. Chem. Soc., Chem. Commun.* 1979, 1113.

The crystal and molecular structure of 3-carboxymethylthio-1,5-diphenylformazan. A. T. Hutton, H. M. N. H. Irving, L. R. Nassimbeni and G. Gafner, *Acta Cryst.* 1979, **B35**, 1354.

1980

3-Carboxymethylthio-1,5-diphenylformazan: a potential terdentate ligand with unusual properties. A. T. Hutton and H. M. N. H. Irving, *J. Chem. Soc., Perkin Trans.* 2 1980, 139.

X-Ray crystallographic and spectroscopic study of the configurations of isomeric 3-methylthio-1,5-diarylformazans and their interconversion in solution. A. T. Hutton and H. M. N. H. Irving, *J. Chem. Soc., Chem. Commun.* 1980, 763.

The structures of two condensation products of dithizone. 2-Methyl-3-phenyl-5-phenylazo-1,3,4-thiadiazoline and 5,6-dihydro-4-phenyl-2-phenylazo-4*H*-1,3,4-thiadiazine. P. A. McCallum, H. M. N. H. Irving, A. T. Hutton and L. R. Nassimbeni, *Acta Cryst.* 1980, **B36**, 1626.

Irregular three-coordination in mercury: structures of phenyl- and methylmercury(II) dithizonate. A. T. Hutton, H. M. N. H. Irving, L. R. Nassimbeni and G. Gafner, *Acta Cryst.* 1980, **B36**, 2064.

Isomerism in formazans: structure of the yellow isomer of 3-methylthio-1,5-di(*o*-tolyl)formazan. A. T. Hutton, H. M. N. H. Irving and L. R. Nassimbeni, *Acta Cryst.* 1980, **B36**, 2071.

Spectrophotometric determination of trace amounts of thallium(III) and gold(III) by quantitative oxidation of 3-carboxymethylthio-1,5-diphenylformazan. A. T. Hutton and H. M. N. H. Irving, *Anal. Chim. Acta* 1980, **113**, 113.

Coloured liquid anion-exchangers. H. M. N. H. Irving and J. Hapgood, *Anal. Chim. Acta* 1980, **119**, 207.

The analytical applications of dithizone. H. M. N. H. Irving, *CRC Crit. Rev. Anal. Chem.* 1980, **8**, 321.

1981

The solubility parameters of metal acetylacetonates. H. M. N. H. Irving, J. S. Smith and S. A. Karmali, *J. Inorg. Nucl. Chem.* 1981, **43**, 1139.

Studies with dithizone. Part XXXIII. Effect of temperature on the spectrum in chloroform. H. M. N. H. Irving and A. T. Hutton, *Anal. Chim. Acta* 1981, **128**, 261.

New evidence for the structure of dithizone in solution from ^{1}H and ^{13}C n.m.r. spectra and ^{15}N-labelling. A. T. Hutton and H. M. N. H. Irving, *J. Chem. Soc., Chem. Commun.* 1981, 735.

On the structure of nitroformazans. E. Dijkstra, A. T. Hutton, H. M. N. H. Irving and L. R. Nassimbeni, *Tetrahedron Lett.* 1981, **22**, 4037.

1982

The structure of 1,5-bis(2,6-dimethylphenyl)-3-nitroformazan. E. Dijkstra, A. T. Hutton, H. M. N. H. Irving and L. R. Nassimbeni, *Acta Cryst.* 1982, **B38**, 535.

A tris-complex of 3-mercapto-1,5-diphenylformazan: structure of bismuth dithizonate. M. L. Niven, H. M. N. H. Irving, L. R. Nassimbeni and A. T. Hutton, *Acta Cryst.* 1982, **B38**, 2140.

Studies with dithizone. Part XXXV. A new look at the structure of dithizone in solution. H. M. N. H. Irving and A. T. Hutton, *Anal. Chim. Acta* 1982, **141**, 311.

Isomers of 3-methylthio-1,5-diarylformazans and their interconversion in solution. A. T. Hutton and H. M. N. H. Irving, *J. Chem. Soc., Perkin Trans.* 2 1982, 1117.

Photochromism in organomercury(II) dithizonates. A. T. Hutton and H. M. N. H. Irving, *J. Chem. Soc., Dalton Trans.* 1982, 2299.

Separation techniques: liquid–liquid extraction. H. M. N. H. Irving, In *Treatise on Analytical Chemistry* (Edited by P. J. Elving), 2nd Edn, Vol. 1, Part 5, p. 505. Wiley, New York (1982).

1984

Preparation of chloralide from chloral hydrate: a mechanistic study. S. J. Archer, K. R. Koch and H. M. N. H. Irving, *S. Afr. J. Chem.* 1984, **37**, 62.

1985

Isomerism in parabutylchloral: X-ray crystallographic determinations of 2,4,6-tris(1′,1′,2′-trichloropropyl)-1,3,5-trioxanes. S. J. Archer, H. M. N. H. Irving, K. R. Koch and L. R. Nassimbeni, *J. Cryst. Spectrosc. Res.* 1985, **15**, 333.

A reinvestigation of the "determination" of uranium(VI) and thorium(IV) with dithizone. H. M. N. H. Irving and C. J. Foot, *Anal. Chim. Acta* 1985, **172**, 289.

1986

Studies with dithizone. Part XXXVI. The interaction of thallium(III) with solutions of dithizone in organic solvents. H. M. N. H. Irving, A. H. Nabilsi, A. Mawley, D. C. Rupainwar and C. Sacht, *Anal. Chim. Acta* 1986, **181**, 125.

The boat conformation of α-parachloral. Notes on the revised structures of α- and β-parachloral. S. J. Archer, A. Irving and H. M. N. H. Irving, *J. Cryst. Spectrosc. Res.* 1986, **16**, 283.

Structure and conformation of 6-nitro-2-trichloromethyl-4-dichloromethylene-1,3-benzdioxin: X-ray crystallographic determination. A. Irving and H. M. N. H. Irving, *J. Cryst. Spectrosc. Res.* 1986, **16**, 429.

NOTE ADDED IN PROOF

Since this list was first compiled the following publications have appeared:

Structure of ethanoldiphenylthallium(III) dithizonate. A. Irving and H. M. N. H. Irving, *J. Cryst. Spectrosc. Res.* 1986, **16**, 495.

Structure and conformation of 6-nitro-2-trichloromethyl-1,3-benzdioxin-4-one: X-ray crystallographic determination. A. Irving and H. M. N. H. Irving, *J. Cryst. Spectrosc. Res.* 1986, **16**, 607.

Polyhedron Vol. 6, No. 1, pp. 13–23, 1987
Printed in Great Britain

0277–5387/87 $3.00+.00

STUDIES ON THE EXISTENCE OF A TAUTOMERIC EQUILIBRIUM IN SOLUTIONS OF THE ANALYTICAL REAGENT DITHIZONE

ALAN T. HUTTON*

Department of Analytical Science, University of Cape Town, Rondebosch 7700, South Africa

(*Received* 3 *July* 1986)

Abstract—The traditional view that solutions of dithizone in organic solvents comprise equilibrium mixtures of thiol and thione forms which are individually responsible for the characteristic strong visible absorption bands around 440 and 620 nm is examined critically. Fourier transform ^{1}H and ^{13}C NMR spectroscopic measurements on dithizone, seven of its alkyl-substituted homologues, and on its ^{13}C- and ^{15}N-labelled analogues point to the existence of only a single molecular species in chloroform, benzene or acetone. The marked solvatochromism, however, has yet to be explained. Modifications to established synthetic routes are reported which are especially suitable for the small-scale preparation of isotopically-labelled dithizone analogues.

The analytical reagent dithizone (also known as 1,5-diphenylthiocarbazone or 3-thio-1,5-diphenylformazan and abbreviated here as H_2Dz) was first synthetized just over a century ago in 1878 by Emil Fischer from carbon disulphide and phenylhydrazine,[1] and its structure as the thione (**1**) was established by Corwin and Jackson.[2] The same substance was prepared nearly 50 years after Fischer by the reduction of 3-nitro-1,5-diphenylformazan with ammonium hydrosulphide, and Bamberger *et al.*[3] formulated it as the thiol (**2**). The thiol formulation (**2**) is supported by its ease of oxidation to a disulphide,[4] its acidity ($pK_1 \sim 4.5$) and ready solubility in aqueous alkali, and the formation of the strongly coloured, water-insoluble metal *N,S*-chelate complexes $M(HDz)_n$ which have been used so extensively in absorptiometric trace-metal analysis following liquid–liquid extraction procedures.[5,6] Preparations of dithizone by different synthetic routes [i.e. Fischer's[1] or Bamberger's[3] methods (see Scheme 1)] do not distinguish between the alternative structures **1** and **2**: the thione and thiol forms are clearly tautomers. Since the visible spectra of dithizone in solutions of organic solvents always show two strong absorption bands (cf. Table 1) it has long been assumed that these could be attributed to the individual tautomers, and that dithizone in solution thus exhibited the tautomeric equilibrium **1** ⇋ **2**.[7] It should be noted that each of these tautomers could exist in a considerable number of conformations (viz. 16 stereochemical modifications with a further 48 if charge-separated species are included),[8] though many of these possibilities can be excluded on steric or other grounds.[7]

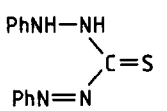

(1)

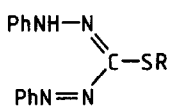

(2) R = H

(3) R = CH_3

Formazans of general formula ArN=N—C(R)=N—NHAr (R = Cl or alkyl) have their main visible absorption band at *ca* 420 nm, and the dithizonate anion, presumably PhN=N—C(S^-)=N—NHPh, absorbs at 470 nm. Since there is commonly a bathochromic shift when chelating agents such as acetylacetone, thenoyltrifluoracetone, 8-quinol-

* M.Sc. and Ph.D. student of Professor H. M. N. H. Irving at the University of Cape Town, 1977–1980; presently "new blood" lecturer in inorganic chemistry at the Department of Pure and Applied Chemistry, The Queen's University, Belfast BT9 5AG, U.K.

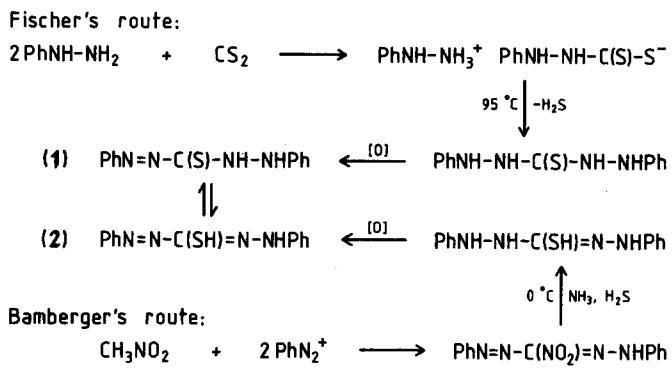

Scheme 1.

inol and 8-mercaptoquinoline form their metal complexes, and since metal complexes of dithizone show a single strong absorption band in the region 450–550 nm, it seems reasonable to assume that the band in dithizone at the lower wavelength (*ca* 440 nm) is due to the thiol form (**2**) and that the change in spectrum when a metal complex is formed is due to the disappearance of the thione band at *ca* 620 nm and a bathochromic shift of the thiol band. The assignment of the band at *ca* 620 nm to the thione form is supported by the data for thiobenzophenone and other thioketones (which absorb near 600 nm) and from studies on the spectra of 2-mercaptobenzothiazoles and thioquinolines and their *S*- and *N*-methyl derivatives.[7]

The classical method of assigning structures to potentially tautomeric systems such as dithizone is to compare the spectra of the parent substance with that of derivatives in which the structure has been locked unambiguously in the thiol or thione form by *S*- or *N*-methylation.[9] This fails in the case

Table 1. The visible absorption spectrum of dithizone in different solvents[a]

Solvent	λ_{max} (nm)		$10^{-3}\,\varepsilon_{max}$ ($m^2\,mol^{-1}$)		R^b
	1	2	1	2	
n-Hexane	617	447	2.76	2.54	1.09
Cyclohexane	623	452	2.70	2.38	1.13
Diethylether	615	440	2.62	2.07	1.27
Carbon disulphide	640	462	2.93	1.91	1.53
Ethanol	596	440	2.73	1.66	1.64
Toluene	622	450	3.31	1.98	1.67
Acetone	610	445	3.26	1.93	1.69
Carbon tetrachloride	620	450	3.46	2.03	1.70
Dioxan	617	446	3.29	1.91	1.72
Benzene	622	453	3.43	1.90	1.81
Chlorobenzene	622	452	3.48	1.83	1.90
Nitrobenzene	627	454	3.19	1.67	1.91
Dioxan–water [1 : 1 (v/v)]	602	446	3.24	1.64	1.98
Nitromethane	607	440	3.77	1.76	2.14
Chloroform	605	440	4.14	1.59	2.60
Tetrachloroethane	607	445	4.24	1.56	2.72

[a] Data from C. F. Bell [D.Phil. thesis, University of Oxford (1952)], W. R. Cross [Part II thesis, University of Oxford (1957)], and similar sources.

[b] R = (absorbance at longer wavelength maximum)/(absorbance at shorter wavelength maximum) ($A_{max,1}/A_{max,2}$).

of dithizone: for while authentic *S*-methyldithizone (**3**) has been synthetized by Irving and Bell,[10] its initially permanganate pink solution in chloroform (λ_{max} 270 and 550 nm, ε_{550} 1225 m^2 mol^{-1}) isomerizes rapidly by first-order kinetics to a yellow isomer (λ_{max} 280, 420 and 540 nm; ε_{420} 1775 m^2 mol^{-1}), the band at 550 nm becoming less intense as that at 420 nm increases. The configurational changes in this system, which are strikingly catalysed by both acids and bases, have recently been elucidated by NMR, IR and visible absorption spectroscopy on **3** and its methyl-substituted homologues and ^{13}C- and ^{15}N-labelled analogues,[11] as well as by X-ray crystallography.[12]

Many of the doubts concerning the existence and structures of thiol and thione forms of dithizone would be resolved if *N*-methylated derivatives such as ArNH—N(Me)—C(S)—N=NAr′, ArN(Me)—NH—C(S)—N=NAr′ and ArN(Me)—N(Me)—C(S)—N=NAr′ could be obtained. Many authors have attempted such syntheses but without success;[2,13,14] in Carlin's Ph.D. dissertation[8] it is stated that these important compounds had been prepared by Barak and Corwin (Ar = Ph, Ar′ = *p*-BrC_6H_4) and various spectra are reported and discussed. No details of these syntheses have ever been published or could be obtained by correspondence. Incidentally, the experimentally verified fact[13] that solutions of dithizone conform strictly with Beer's law enables us to reject Carlin's suggestion[8] that a dimeric form of dithizone (two intermolecularly hydrogen-bonded molecules in the thione form) is one of the species in equilibrium in solution.

The visible absorption spectrum of dithizone is very sensitive to the organic solvent in which it is dissolved. Although changes in the maxima of the two absorption bands are comparatively small [generally ±4% (cf. Table 1)] the magnitudes of the extinction coefficients may vary by as much as 60% and increases in $\varepsilon_{max,1}$ are commonly associated with decreases in $\varepsilon_{max,2}$ so that the "peak ratio" R ($A_{max,1}/A_{max,2}$) can vary from 1.09 in *n*-hexane to 2.72 in tetrachloroethane. (The subscripts 1 and 2 are used to distinguish the longer and shorter wavelengths, respectively.) There appears to be no simple relationship between shifts in λ_1, λ_2, ε_1 or ε_2, or R values with any of the empirical solvent polarity scales Z, E_T or S (which are linearly related),[15] or with Taft's π^* scale,[16] although there is a tendency for R to increase with solvent polarity. There is, however, quite a striking correlation between the R for dithizone and the values (measured in the same solvent) of the concentration ratio [keto]/[enol] for ethylacetoacetate, or the R for 1-(4-methoxy-3,5-dimethyl)phenylazo-2-naphthol, where an equilibrium between azo and hydrazo tautomers has been postulated.[17] This would seem to favour the hypothesis that solutions of dithizone comprise an equilibrium mixture of thione and thiol tautomers.

It must not be overlooked that the value of R is not a simple measure of the relative amounts of the two postulated tautomers in solution and thence of the equilibrium constant of the reaction **1** ⇌ **2**. Specifically, $R = A_{thione}/A_{thiol} = \varepsilon_{thione}[thione]_o l/\varepsilon_{thiol}[thiol]_o l = K_{T,o}(\varepsilon_{thione}/\varepsilon_{thiol})$, where $K_{T,o} = [thione]_o/[thiol]_o$ is the equilibrium constant for the two tautomers present in the organic solvent. There will only be a linear relationship between R and $K_{T,o}$ if $\varepsilon_{thione} = \varepsilon_{thiol}$ or if the ratio $\varepsilon_{thione}/\varepsilon_{thiol}$ is a constant for all solvents. Admittedly Pel'kis and Dubenko[18] deduced that $\varepsilon_{thione} = \varepsilon_{thiol} = 5745$ m^2 mol^{-1} for chloroform, 5768 m^2 mol^{-1} for benzene, and 5745 m^2 mol^{-1} for carbon tetrachloride solutions, but the basis of their argument is unsound.[19]

The application of ^1H NMR spectroscopy to dithizone chemistry has hitherto been indecisive owing to the low solubility of dithizone, although in 1970 Coleman *et al.*,[20] using the more soluble homologue 1,5-di(*o*-ethylphenyl)thiocarbazone in $CDCl_3$, observed δ 1.4 (6H, triplet, CH_3), 3.0 (4H, quartet, CH_2), 7.3, 8.1 (8H, multiplet, Ar*H*), and 12.0 ppm (1.6H, singlet, N*H*). The latter resonance, which disappeared on addition of MeOD, showed no signs of splitting over the range +50 to −45°C, and the authors ruled out the hypothesis of tautomeric equilibrium in favour of a single symmetrical species (as **4**), essentially that subsequently established for the solid-state structure by X-ray crystallography,[21] which shows a nearly planar molecule with extensive delocalization of π-electrons, the C—S distance [1.71(1) Å] corresponding to a thioketone rather than a thiol structure. The same extended *anti,s-trans* structure has recently been reported for the dithizone moiety in the crystal structures of the neutral charge-transfer molecular compounds (H_2Dz)–I_2 and $2(H_2Dz)$–$7I_2$, though the location of the hydrogen atoms was not established.[22]

Although Coleman *et al.*[20] noted the effects on the visible spectrum of changes in solvent they suggest that these "appear to be complicated by acid–base equilibria, trace metal effects and even oxidative decomposition of the dithizone".[20] In our experience none of these factors is involved in the solvatochromism. It is noteworthy that Coleman *et al.*[20] observed only 1.6 protons (instead of 2.0), and when Nabilsi examined the ^1H NMR spectrum of dithizone itself[23] he found signals at δ 0.97 as well as at δ 12.61 ppm of integrated intensity 1:3 and

fully accounting for 2.0 protons. The signal at δ 0.97 ppm was attributed to a non-hydrogen-bonded SH group and Nabilsi suggested that dithizone in $CDCl_3$ solution exhibited a tautomeric equilibrium comprising 25% of the thiol form which might be formulated as **5** or the mesomeric form **6**, together with 75% of a thione form formulated as **4** or **7**.[23]

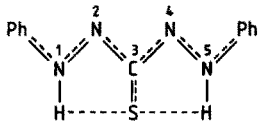

(4)

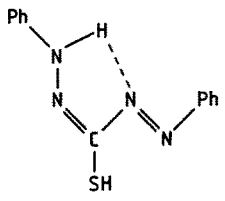

(5)

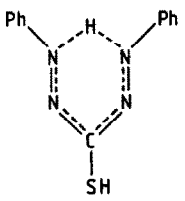

(6)

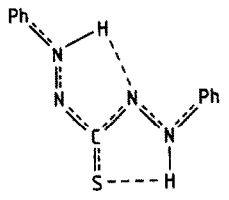

(7)

In view of these and many other discrepancies[7] it was decided to re-examine the solution spectra (particularly by NMR) of dithizone, its alkyl-substituted homologues, and its ^{13}C- and ^{15}N-labelled analogues in search of fresh and possibly decisive data.[24]

RESULTS AND DISCUSSION

Although the use of Fourier transform NMR spectroscopy facilitates measurements on sparingly soluble solutes, to the extent that for the first time good ^1H NMR spectra of dithizone itself were obtained here, it must not be overlooked that residual protons in deuteriated solvents can give rise to spurious signals; a residual line from adventitious $CHCl_3$ enhances the integrated value for aromatic protons so that the intensity of other lines relative to this will be underestimated. In the present work dithizones substituted in their phenyl rings with alkyl groups were used to provide well-defined lines for integration reference and to examine the equivalence or otherwise of the two aryl groups. Using highly purified dithizone Nabilsi's alleged[23] S*H* peak at δ 0.97 ppm could not be reproduced, and this must have originated from solvent or solute impurity or even as a spinning side-band of an intense Me_4Si resonance. Seven alkyl-substituted homologues of dithizone (Table 2) were prepared by Bamberger's method[3] from the corresponding nitroformazans. There were no differences between

Table 2. ^1H NMR spectroscopic data for the 1,5-diarylthiocarbazones in $CDCl_3$, $(CD_3)_2CO$ and C_6D_6[a]

Aryl group	δ(N*H*)[b]	δ(C*H*, CH_2 or CH_3)	δ(Ar*H*)
Phenyl	12.60 12.63 12.84		7.56 7.65 6.93 (m, 10H)
p-Tolyl	12.65 12.63 12.87	2.42 2.39 1.86 (s, 6H)	7.27 7.37 6.60 (d, J = 8.0, 4H) 7.58 7.75 7.05 (d, J = 8.0, 4H)
m-Tolyl	12.54 12.63 12.85	2.43 2.42 1.86 (s, 6H)	7.34 7.43 6.76 (m, 8H)
o-Tolyl	12.80 12.86 13.13	2.63 2.58 2.01 (s, 6H)	7.62 7.62 7.24 (m, 8H)
3,5-Dimethylphenyl	12.49 12.60 12.86	2.36 2.37 1.91 (s, 12H)	6.97 7.04 6.44 (s, 2H) 7.33 7.46 6.86 (s, 4H)
p-Ethylphenyl	12.50 12.60 12.91	1.24 1.24 0.90 (t, J = 7.6, 6H) 2.68 2.70 2.20 (q, J = 7.6, 4H)	7.27 7.38 6.66 (d, J = 8.2, 4H) 7.59 7.77 [c] (d, J = 8.2, 4H)
p-Isopropylphenyl	12.52 12.62 12.96	1.27 1.26 0.96 (d, J = 6.6, 12H) 2.95 2.97 2.48 (h, J = 6.6, 2H)	7.31 7.42 6.74 (d, J = 8.2, 4H) 7.62 7.78 [c] (d, J = 8.2, 4H)
p-*n*-Butylphenyl	12.52 12.50 12.92	0.93 0.93 0.81 (t, J = 6.6, 6H) 1.47 1.47 1.23 (m, 8H) 2.65 2.66 2.23 (t, J = 7.2, 4H)	7.27 7.36 6.69 (d, J = 8.2, 4H) 7.59 7.75 [c] (d, J = 8.2, 4H)

[a] 90-MHz spectra at ambient temperature. Chemical shifts [δ (ppm)] are given for $CDCl_3$, $(CD_3)_2CO$ and C_6D_6 solutions, in that order, relative to $(CH_3)_4Si$. Coupling constants in Hz. Abbreviations used: s, singlet; d, doublet; t, triplet; q, quartet; h, heptet; m, multiplet.

[b] All singlets: all integrate for 2H except in $(CD_3)_2CO$ solutions where the integrals vary from 0.7 to 1.5H due to trace D_2O in the deuterioacetone (see text). All disappear on addition of D_2O.

[c] Obscured by solvent resonance.

the visible absorption spectra of individual compounds measured in $CHCl_3$ or $CDCl_3$; all the compounds show two peaks, one close to 445 nm and one at 620 nm. Their ^1H NMR spectra were measured in each of three solvents, viz. $CDCl_3$, $(CD_3)_2CO$ and C_6D_6, with the results shown in Table 2. In every case the substituent alkyl groups (and hence the two aromatic rings) are found to be exactly equivalent on the NMR time-scale, and spectra at $-50°C$ differed from those at $+60°C$ only by the expected slight narrowing of peaks. The same equivalence follows from examination of the aromatic resonances themselves, and it must be concluded that on the NMR time-scale there is only one (symmetrical) molecule in solution. Furthermore, the singlet due to N*H* at *ca* δ 12.5 ppm always integrates for *exactly* two protons in $CDCl_3$ and C_6D_6, and disappears immediately and completely upon washing with D_2O. In $(CD_3)_2CO$ and N*H* singlets integrate for something less than 2.0 protons but no new peaks arise to account for the missing fractions of protons, and we believe that traces of D_2O in the incompletely dry solvent have exchanged with the imino hydrogens to reduce the intensity of the signals. The effect of traces of D_2O in the NMR solvent is accentuated by the dilute solutions afforded by even the substituted thiocarbazones.

That the two non-aromatic protons in dithizone must be bound to equivalent nitrogen sites, viz. N-1 and N-5 (as **4**), was confirmed by preparing dithizone labelled with ^{15}N at N-1 and N-5 from a sample of 3-nitro-1,5-diphenylformazan, itself prepared by coupling nitromethane in alkaline solution with a diazonium solution prepared from 96 atom-% ^{15}N-enriched aniline, following a modification[24] of Bamberger's general procedure[3] (see Experimental). In the ^1H NMR spectrum of this compound in $CDCl_3$ the N*H* signal at δ 12.60 ppm is split into a doublet with a normal[25] coupling constant value of 90.8 Hz (unchanged at $-50°C$). This value excludes the possibility of a rapid thiol–thione tautomeric equilibrium. In such a tautomeric system the observed spin coupling, J(obs), would be given by a weighted average of the various coupling constants involved,[26] in that case ^1J(S–H) and $^1J(^{15}N–H)$. If P(S) and P(N) represent the mole fractions of the two tautomeric species, then $J(\text{obs}) = {}^1J(\text{S–H})P(\text{S}) + {}^1J(^{15}\text{N–H})P(\text{N})$, and if $^1J(^{15}N–H)$ for an unperturbed N—H bond is assumed to be *ca* 90 Hz,[25] then, since ^1J(S–H) is zero, we find that P(N) = 1 and the protons must be bonded to the N-1 and N-5 atoms of a single species. Thus we have previously found a value for $^1J(^{15}N–H)$ of 92.2 Hz in the yellow *anti,s-trans* form of *S*-methyldithizone (**8**), where tautomerism is impossible, while in the pink *syn,s-cis* form **9a** ⇌ **9b**, where a rapid tautomeric equilibrium does exist, $^1J(^{15}N–H)$ is approximately halved (47.6 Hz).[11]

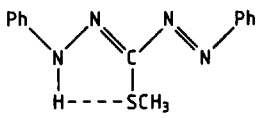

(8)

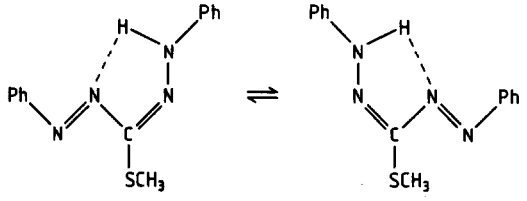

(9a) (9b)

The diphenylthiocarbazide, which is known to have structure **10** (Ar = Ph) in the solid state,[27] is obtained in the course of the synthesis of dithizone. Its ^1H NMR spectrum in $CDCl_3$ shows two N*H* resonances (at δ 6.18 and 8.08 ppm), each integrating for two protons and both disappearing on washing with D_2O. The spectrum of the compound labelled with ^{15}N at N-1 and N-5 shows the signal at δ 6.18 ppm to be split into a doublet with $^1J(^{15}N–H) = 85.2$ Hz. Clearly the N-1 and N-5 protons are not involved in intramolecular exchange, whereas nothing can be said about the protons attached to N-2 and N-4 until the appropriate labelling studies have been carried out. No success attended efforts to obtain ^{15}N NMR signals from the above ^{15}N-labelled compounds whether using broad-band or inverse-gated ^1H-decoupling.[24]

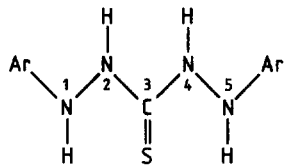

(10)

Further evidence was obtained when dithizone labelled at C-3 with ^{13}C was synthetized from phenylhydrazine and 91 atom-% ^{13}C-enriched carbon disulphide using modifications[24] of Fischer's original synthesis[1,28] suitable for very small scale working (see Experimental). Had $CDCl_3$ solutions of this compound contained thiol and thione forms in slow-enough dynamic equilibrium, the ^{13}C-3

NMR signal from each form might have been individually observable. In fact there is a single peak in the ^{1}H-decoupled spectrum at δ 171.4 ppm downfield from Me_4Si which does not shift or split at $-50°C$. For comparison, the thiocarbonyl resonances in EtNH—C(S)—NHEt and H_2N—C(S)—NH_2 are at 182.8 and 176.7 ppm, respectively.[29] More conclusive, however, is the ^{1}H-coupled spectrum in which the ^{13}C-3 signal splits into a perfectly symmetrical 1:2:1 triplet with $^3J(^{13}C–N–N–H) = 6.0$ Hz (unchanged at $-50°C$) and which collapses to a singlet on washing with D_2O. The same coupling $^3J(H–N–N–^{13}C) = 6.0$ Hz is also found in the ^{1}H NMR spectrum of the ^{13}C-labelled dithizone, where the N*H* peak is split into a doublet, unchanged at $-50°C$ apart from a slight narrowing of the lines. An earlier ^{13}C NMR study of dithizone was inconclusive.[30]

These data, along with the demonstrated magnetic equivalence of the two imino protons and the two aromatic residues, point to the symmetrical structure **4**, as already established by X-ray crystallography for dithizone in the solid state.[21,22] The view that only a single species (as **4**) is present in solution is consistent with the fact that the visible absorption spectrum of dithizone in chloroform does not vary over the temperature range -50 to $+60°C$: in particular, *R* does not change as it would if there were two species in equilibrium. Thus either the two absorption peaks cannot be ascribed to two discrete species (thiol and thione tautomers), or it becomes necessary to accept the surprising conclusion that their interconversion proceeds with no change in enthalpy.[31] Bag and Freiser[32] recently observed that the molar absorptivity of dithizone in cyclohexane is dramatically enhanced by the addition of small quantities of chloroform, and they attributed this to the formation of a 1:2 dithizone–chloroform complex (formation constant $10^{4.0}$). However, the ratio of the two peak heights did not change significantly, indicating that the observed enhancement was not the result of shifting a thiol–thione equilibrium.

The conclusions drawn from these new NMR data, which extend the early measurements of Coleman *et al.*,[20] agree with those drawn from IR measurements.[33] These show a broad band in the region 3100–2800 cm^{-1} with several absorption maxima. On deuteriation this band disappears and is replaced by one at *ca* 2200 cm^{-1} assigned to ν(N—D), while in the region 3100–3000 cm^{-1} only maxima corresponding to aromatic ν(C—H) remain. There are no traces of ν(S—H) bands (expected at *ca* 2600 cm^{-1}). The close similarity between the IR spectrum of dithizone in solution and in the solid state appears to deny the possibility of tautomerism, and it is perhaps significant that the diffuse-reflectance spectrum of solid dithizone shows a clearly defined band at 450 nm (situated similarly to $\lambda_{max,2}$ in organic solutions) with a broad shoulder covering the region 580–610 nm, which roughly corresponds with the location of $\lambda_{max,1}$ in the solution spectra. A recent and thorough Raman vibrational spectroscopic investigation[34] of the acid–base forms of dithizone has indicated that significant structural changes occur when a proton is added to or lost from neutral dithizone (H_2Dz) to form the corresponding conjugate acid of dithizone (H_3Dz^+) or dithizonate anion (HDz^-). Exploitation of resonance intensity enhancement in these systems allowed the Raman spectra of necessarily dilute solutions of the acid–base forms of dithizone to be acquired: the vibrational data[34] obtained from CS_2 solutions of H_2Dz are clearly consistent with the dithizone molecules existing in the single form shown as structure **4**.

There is no reason why a single species in solution, such as **4**, should not give rise to a visible spectrum with two intense visible absorption bands. Indeed, theoretical calculations of the energy and intensity of the electronic transitions in different forms of dithizone have been made (using LCAO MO SCF LCI methods),[35] with some success for the protonated species H_3Dz^+ and the anion HDz^-. For dithizone itself a spectrum with two prominent bands is predicted, the model used being basically the same as **4** (save that one hydrogen atom is bound to sulphur as a thiol). One of these bands is predicted at *ca* 430 nm corresponding to the $\lambda_{max,2}$ found experimentally; the other is located at *ca* 800 nm, which is well away from the experimental values of $\lambda_{max,1}$ (600–640 nm). Moreover, the intensity of this longer-wavelength band is predicted to be less than that at the shorter wavelength, which is never the case [*R* is always > 1 (see Table 1)]. However, it is clear that the simultaneous presence of thione and thiol forms in solutions of dithizone cannot be inferred from the existence of these two visible bands alone.

Of course, such calculations do not take into account the effect of solvent on the spectra and the pronounced solvatochromism remains to be explained, along with the curious relationships which have been noted between the experimental *R* and the equilibrium constant [keto]/[enol] for ethylacetoacetate in the same solvent, or between values of *R* for a series of structurally modified dithizones and the Hammett factors of the substituents.[7] Nevertheless, the new evidence reported here lends overwhelming support to the hypothesis that solutions of dithizone in organic solvents comprise only a single, highly symmetrical, and planar

species, as **4**. A very recent argument[36] in favour of a thiol–thione equilibrium, in which, *inter alia*, the visible absorption spectra of individual thiol and thione forms were calculated by mathematical analysis of the spectra of dithizone in four organic solvents (the assignment of a single band to each tautomer being rejected), fails to explain away the experimental evidence for a single structure provided by the present work. It has been shown in earlier papers that experimental values of $pH_{1/2}$, pK and R can legitimately be used in calculations, although they are compounded of parameters (partition coefficients, acid dissociation constants, molar solubilities etc.) relating to each of the alleged tautomeric forms, and to the equilibrium constant (K_T) governing the interconversion.[37] Thus none of these solvent effects nor, indeed, the existence of a single species (**4**) rather than the equilibrium **1** ⇋ **2**, has any influence on the reliability of the many applications of dithizone in the selective and quantitative spectrophotometric determination of microgram amounts of various metals using the numerous monocolour, mixed-colour or reversion procedures that have been developed over the years.[5,6] A preliminary communication on the work reported here has been published.[38]

EXPERIMENTAL

General and spectroscopic

Special care was taken in cleaning the optical cells, the NMR tubes, and the glassware in which solutions of the thiocarbazones were handled. The cleaning was done by soaking the apparatus in a chromic acid bath, washing with hot water, and then soaking in a strong ammoniacal solution of the disodium salt of ethylenediaminetetraacetic acid. Finally the apparatus was thoroughly rinsed with glass-distilled water and dried in an oven at 130°C. This provided metal-free glassware as tested by a very dilute solution of dithizone in chloroform, which remained pale green when used to rinse the apparatus.

Visible absorption spectra were recorded on a Varian Superscan 3 instrument using 1.00-cm matched quartz cells. Diffuse-reflectance spectra were taken as Nujol mulls on filter paper using a Beckman DK-2A ratio-recording spectrophotometer in the reflectance mode. ^{1}H NMR spectra were measured at 90 MHz on a Bruker WH-90DS Fourier transform spectrometer at ambient temperature (*ca* 32°C) and at −50°C. Chemical shifts are quoted relative to Me_4Si and are accurate to ±0.04 ppm, while coupling constants are estimated to ±0.02 Hz. ^{13}C NMR spectra with broad-band ^{1}H decoupling were measured at ambient temperature and at −50°C on the same spectrometer operating at 22.63 MHz. The ^{1}H-coupled spectra were obtained in the gated proton irradiation mode.[39] Chemical shifts were recorded relative to the $CDCl_3$ signal and related to the standard Me_4Si using the conversion $\delta(Me_4Si) = \delta(CDCl_3) + 76.9$ ppm;[40] they are accurate to an estimated 0.1 ppm. Shiftless relaxation agents were not used. All solvents used for spectroscopic work were of spectroscopic grade, and were purified and dried. Care was taken to ensure no traces of acid were present and to run the $(CD_3)_2CO$ spectra immediately after making up the samples so as to avoid the reported[41] condensation of acetone with dithizones in acid conditions to form the corresponding thiadiazolines.

A comparison of the visible spectrum of dithizone in $CHCl_3$ and $CDCl_3$ was made by purifying a small quantity of dithizone by paper chromatography and extracting the pure dithizone spot into $CHCl_3$ in an optical cell (1.00-cm) and filling with $CHCl_3$ to a mark. After recording this spectrum the solvent was carefully evaporated from the optical cell under reduced pressure and the cell was refilled to the mark with $CDCl_3$. The resulting spectrum was identical to the first.

Preparative work

Glass-distilled water and purified solvents were used throughout the preparative work.

3-*Nitro*-1,5-*diarylformazans*. Sodium hydroxide pellets (4.0 g, 0.10 mol) were dissolved in water (15 cm^3) and cooled in an ice–salt bath to 0°C. A solution of nitromethane (6.4 g, 0.10 mol) in ethanol (35 cm^3) was added slowly with constant mechanical stirring and keeping the temperature below 0°C. Ice water and crushed ice (*ca* 500 g) were added to dissolve the white precipitate and the solution was kept at 0°C until used. The arylamine (0.20 mol), freshly distilled over zinc dust, was added to a mixture of concentrated hydrochloric acid (60 cm^3) and distilled water (100 cm^3) in a 2-l beaker. The resultant clear solution was cooled to 0°C in an ice–salt bath and diazotized by adding dropwise and with mechanical stirring a solution of sodium nitrite (16.6 g, 0.24 mol) in distilled water (30 cm^3). Filtration of the clear yellow solution was not usually necessary and sodium acetate (41 g, 0.5 mol) dissolved in distilled water (120 cm^3) was added dropwise, keeping the temperature at 0°C, to buffer the solution at pH *ca* 4.5. The alkaline nitromethane solution was placed in a separating funnel containing crushed ice and dropped slowly, with vigorous mechanical stirring, into the diazotized

solution. The required 3-nitro-1,5-diarylformazan separated at once as a bright red precipitate, oil or tar. The solution was stirred for a further 1–6 h after which time any tars had turned solid. The solids were collected on a large Buchner funnel by suction and washed with copious quantities of water, while oils were extracted into chloroform, washed with water, dried with $MgSO_4$, and evaporated to dryness. After drying overnight *in vacuo* over silica gel all of these solids recrystallized easily from ethanol to give well-formed maroon or dark-red needles or plates with the characteristics listed in Table 3.

Any tendency to form a tar was minimized by keeping the temperature well below 0°C, by waiting long enough for the nitrogen oxides to escape after diazotization, and by employing pure nitromethane and freshly-distilled arylamines.

A small-scale adaptation of the above procedure[24] was used to synthetize the 3-nitro-1,5-diphenylformazan labelled at N-1 and N-5 with ^{15}N, starting from 0.63 g of 96 atom-% ^{15}N-aniline supplied by BOC Prochem.

1,5-*Diarylthiocarbazones.* 3-Nitro-1,5-diarylformazan (8.0 g) was suspended in absolute ethanol (60 cm^3) in a 100-cm^3 round-bottomed flask and cooled to 0°C in an ice–salt bath. Dry ammonia gas was bubbled through the mixture until it was saturated (10 min) and then hydrogen sulphide gas was passed into the solution until the thiocarbazide (**10**) separated. When reduction was complete as indicated by a change of colour from maroon to yellow, and by the disappearance of unreduced particles of the nitroformazan, the suspension was added in a thin stream to distilled water (200 cm^3) with mechanical stirring, and immediately filtered off by suction. The thiocarbazides were washed with water and dried over silica gel *in vacuo* to give yields of 86–93%. The surface of the dry powders slowly turned from cream to grey-green as oxidation took place. The unstable thiocarbazide compounds (**10**) were oxidized at once to the thiocarbazones by treating with a 5% methanolic potassium hydroxide solution (30 cm^3) at room temperature. After mixing well and breaking up lumps with a stirring rod, a clear dark-red solution was obtained which was immediately neutralized by pouring slowly into ice-cold dilute 0.5 M sulphuric acid (1 l) with vigorous mechanical stirring. After stirring for 1 h the crude 1,5-diarylthiocarbazone was filtered off, washed with water, and dried over silica gel *in vacuo*.

Purification of this product is necessary as oxidation of the thiocarbazone results in small quantities of the corresponding 2,3-diaryl-2*H*-tetrazolium-5-thiolate contaminating the product. Spectroscopically pure dithizonates are usually prepared[42] by an extensive series of extractions from chloroform into a dilute aqueous base, washing the aqueous layer with more chloroform, and re-extraction into chloroform or precipitation from the aqueous phase by acidification. In this work it was found that column chromatography provided a cleaner, quicker method of purification with a greatly enhanced yield.

The crude material (1.0 g) was dissolved in the minimum amount of benzene and added to a chromatographic column (30 × 2.5 cm) of neutral alumina slurried in benzene. Elution with benzene produced a red fore-run. Once this was visibly separated from the dark band at the origin, elution was continued with solutions of acetone in benzene, increasing the acetone concentration rapidly so that pure acetone was used to wash off the last of the red fore-run. The thiocarbazone fraction was collected by adding a 1% solution of sodium bicar-

Table 3. Yield, melting point and microanalytical data[a] for the 3-nitro-1,5-diarylformazans

Aryl group	Yield (%)	M.p. (°C)	% C	% H	% N
Phenyl	57	159–161	58.05 (58.0)	4.1 (4.1)	25.65 (26.0)
Phenyl[b]	68	159–161	58.0 (57.6)	4.0 (4.1)	26.2 (26.55)
p-Tolyl	31	159–162	60.55 (60.6)	5.15 (5.05)	23.2 (23.6)
m-Tolyl	15	155–157	60.65 (60.6)	5.2 (5.05)	23.4 (23.6)
o-Tolyl	13	151–154	60.65 (60.6)	5.1 (5.05)	23.6 (23.6)
3,5-Dimethylphenyl	41	143–145	62.3 (62.8)	5.95 (5.85)	21.3 (21.5)
p-Isopropylphenyl	16	130–133	64.7 (64.6)	6.7 (6.6)	19.35 (19.8)
p-*n*-Butylphenyl	28	126–127	66.2 (66.1)	7.3 (7.1)	18.35 (18.4)

[a] Calculated values are in parentheses.
[b] Labelled at N-1 and N-5 with 96 atom-% ^{15}N.

bonate in water to the column, and the resulting orange eluent was then slowly poured with stirring into dilute aqueous sulphuric acid (0.1 M). After stirring for a further 1 h the fine blue-black precipitate of pure thiocarbazone was collected by filtration, washed with water, and dried over silica gel *in vacuo*. The analyses, melting points, and yields of the thiocarbazones synthetized are given in Table 4.

Smooth oxidation procedure. In the above synthesis the final oxidation of the thiocarbazide to the corresponding thiocarbazone was carried out with methanolic potassium hydroxide: this is actually a disproportionation reaction and the maximum yield of thiocarbazone can be only 50%. It was found[24] that yields of 80–95% of the thiocarbazone could be obtained by smooth oxidation of the thiocarbazide. The thiocarbazide is dissolved or suspended in an organic solvent (*vide infra*) and air is slowly bubbled through the solution until the production of a very deep green colour indicates complete oxidation. Recalcitrant thiocarbazides may require reflux temperatures for acceptably rapid oxidation. Purification is necessary as oxidation of the thiocarbazone again results in small amounts of the corresponding 2,3-diaryl-2*H*-tetrazolium-5-thiolate in the product. This smooth oxidation procedure was applied to the synthesis of dithizone labelled at N-1 and N-5 with ^{15}N.

^{15}N-*labelled dithizone.* 3-Nitro-1,5-diphenylformazan labelled at N-1 and N-5 with 96 atom-% ^{15}N obtained as above (0.60 g) was suspended in ethanol (15 cm^3) and treated with ammonia gas and hydrogen sulphide as described before. Isolation as above gave the ^{15}N-labelled 1,5-diphenylthiocarbazide (0.52 g, 91%). After setting some product aside for NMR spectroscopy, the remainder (0.46 g) was suspended in carbon tetrachloride (300 cm^3) in a 2-l, two-necked round-bottomed flask placed on a heating mantle. A stream of air was bubbled through the solution which was brought to boiling temperature. A long condenser fitted to the flask reduced evaporation of the solvent, but it was necessary to add further portions of solvent periodically. The colour of the solution changed to an intense dark green over *ca* 2 h. Additional solvent (100 cm^3) was then added to dissolve some unoxidized thiocarbazide and after a total of $2\frac{1}{2}$ h of bubbling the carbon tetrachloride was removed on a rotary evaporator. The residue was taken up in the minimum amount of benzene and purified by column chromatography as described above to yield the ^{15}N-labelled dithizone [0.39 g (85% based on thiocarbazide)].

The use of carbon tetrachloride as solvent in this smooth oxidation of the thiocarbazide was found in trial experiments with unlabelled compounds to give a better yield than diethyl ether (72%) or benzene (76%), presumably because of the greater solubility of dithizone in CCl_4.

Reaction of NaHS *with* 3-*chloro*-1,5-*diphenylformazan.* A second route to obtain the ^{15}N-

Table 4. Yield, melting point and microanalytical data[a] for the 1,5-diarylthiocarbazones

Aryl group	Yield[b] (%)	M.p.[c] (°C)	% C	% H	% N
Phenyl[d]	85	166–169	60.15 (60.4)	4.7 (4.7)	22.4 (22.5)
Phenyl[e]	26	167–170	60.9 (61.05)	4.6 (4.7)	21.6 (21.8)
p-Tolyl	28	161–163	63.15 (63.6)	5.55 (5.3)	19.75 (19.8)
m-Tolyl	17	154–158	63.3 (63.6)	5.4 (5.3)	19.75 (19.8)
o-Tolyl	22	135–138	63.2 (63.6)	5.45 (5.3)	19.7 (19.8)
3,5-Dimethylphenyl	28	137–140	65.2 (65.6)	6.1 (6.15)	18.2 (18.0)
p-Isopropylphenyl	14	142–145	67.0 (67.2)	6.5 (6.8)	16.7 (16.5)
p-*n*-Butylphenyl	28	118–120	68.2 (68.6)	7.3 (7.4)	14.95 (15.2)
p-Ethylphenyl	[f]	155–158	65.3 (65.6)	5.9 (6.15)	18.2 (18.0)

[a] Calculated values are in parentheses.

[b] Based on 1,5-diarylthiocarbazide; synthetized using a methanolic KOH oxidation procedure.

[c] All with decomposition.

[d] Labelled at N-1 and N-5 with 96 atom-% ^{15}N; synthetized using a smooth oxidation procedure.

[e] Labelled at C-3 with 91 atom-% ^{13}C; synthetized in one-pot reaction from phenylhydrazine and carbon disulphide.

[f] Sample provided by Prof. H. M. N. H. Irving.

labelled dithizone was investigated which avoids the reduction and low-yield oxidation steps of Bamberger's synthesis.[3] In this route[43] the reactivity of the halogen atom in 3-chloro-1,5-diphenylformazan, PhN=N—C(Cl)=N—NHPh, was exploited in the reaction with sodium hydrogen sulphide to obtain the dithizone directly, either by mechanical shaking at room temperature or by heating under reflux with NaHS. The 3-chloro-1,5-diphenylformazan was obtained by coupling a benzenediazonium solution with dipotassium chloromalonate, itself prepared by the following reaction sequence:

$$CH_2(CO_2Et)_2 \xrightarrow{SO_2Cl_2} ClCH(CO_2Et)_2$$

$$\xrightarrow[EtOH,\,0°C]{KOH} ClCH(CO_2K)_2.$$

This method, however, gave an overall poorer yield in trial runs (*ca* 15% based on aniline) than the route from the nitroformazan, especially if the smooth oxidation procedure was used in the latter route (>50% based on aniline), and so was discarded as a suitable route to the isotopically-labelled dithizone. Further experimental details will be found in Ref. 24.

^{13}C-*labelled dithizone*. This was prepared by a modification of Fischer's original synthesis,[1,28] so adapted that the entire reaction sequence could be carried out in a single vessel with a view to conserving valuable labelled material.[24] Phenylhydrazine (1.42 g, 13.2 mmol) was dissolved in benzene (20 cm^3) in a 50-cm^3 two-necked flask equipped with a magnetic stirrer and a condenser. Carbon disulphide (91 atom-% ^{13}C from BOC Prochem, 0.50 g, 6.6 mmol) was dropped into the solution with constant stirring when the phenylhydrazine salt of the acid PhNH—NH—^{13}C(S)—SH separated as a light-yellow, practically solid sludge. The temperature was gradually raised to 65°C (water bath) when the precipitate gradually dissolved and H_2S was evolved. After *ca* 20 min evolution of H_2S ceased and the thiocarbazide which remained was oxidized by drawing air through the solution while the temperature was increased to 75°C. Additional benzene (20 cm^3) was added, and after 1 h of bubbling the deep green solution was evaporated to dryness and the crude product was purified by column chromatography as described above to give pure ^{13}C-labelled dithizone (0.44 g, 26%).

Acknowledgement—I would like to thank Professor H. M. N. H. Irving for all his help, guidance and friendship over the years, and for passing on and sharing his enthusiasm for the dithizone saga.

REFERENCES

1. E. Fischer, *Annalen* 1878, **190**, 67; E. Fischer and E. Besthorn, *ibid.* 1882, **212**, 316.
2. A. H. Corwin and G. R. Jackson, *J. Am. Chem. Soc.* 1949, **71**, 3698.
3. E. Bamberger, R. Padova and E. Ormerod, *Annalen* 1926, **446**, 260.
4. H. M. N. H. Irving, A. M. Kiwan, D. C. Rupainwar and S. S. Sahota, *Anal. Chim. Acta* 1971, **56**, 205.
5. H. M. N. H. Irving, *Dithizone*. Analytical Sciences Monographs No. 5, The Chemical Society, London (1977).
6. G. Iwantscheff, *Das Dithizon und seine Anwendung in der Mikro- und Spurenanalyse*, 2nd Edn. Verlag Chemie, Weinheim (1972). H. M. N. H. Irving, *CRC Crit. Rev. Anal. Chem.* 1980, **8**, 321.
7. See Ref. 5, pp. 4 and 82, for comprehensive background and references.
8. C. H. Carlin, Ph.D. thesis, The Johns Hopkins University, Baltimore (1966).
9. A. E. Gillam and E. S. Stern, *Introduction to Electronic Absorption Spectroscopy in Organic Chemistry*, p. 229. Edward Arnold, London (1954).
10. H. Irving and C. F. Bell, *Nature (London)* 1952, **169**, 756; *J. Chem. Soc.* 1954, 4253.
11. A. T. Hutton and H. M. N. H. Irving, *J. Chem. Soc., Perkin Trans.* 2 1982, 1117.
12. A. T. Hutton, H. M. N. H. Irving and L. R. Nassimbeni, *Acta Cryst.* 1980, **B36**, 2071.
13. H. M. N. H. Irving, personal communication.
14. D. S. Tarbell, C. W. Todd, M. C. Paulson, E. G. Lindstrom and V. P. Wystrach, *J. Am. Chem. Soc.* 1948, **70**, 1381.
15. C. Reichardt, *Angew. Chem., Int. Ed. Engl.* 1965, **4**, 29.
16. M. J. Kamlet, J. L. M. Abboud and R. W. Taft, *J. Am. Chem. Soc.* 1977, **99**, 6027; *Prog. Phys. Org. Chem.* 1981, **13**, 485.
17. H. Irving, C. F. Bell and W. Ferguson, *Proceedings of the 15th IUPAC Congress, Lisbon*, 1956, p. 181. W. Ferguson, B.Sc. thesis, University of Oxford (1957).
18. P. S. Pel'kis and R. G. Dubenko, *Ukr. Khim. Zh.* 1957, **23**, 748 and 754 (*Chem. Abstr.* 1958, **52**, 14551e and h).
19. See Ref. 5, p. 87.
20. R. A. Coleman, W. H. Foster, J. Kazan and M. Mason, *J. Org. Chem.* 1970, **35**, 2039.
21. P. A. Alsop, Ph.D. thesis, University of London (1971); M. Laing, *J. Chem. Soc., Perkin Trans.* 2 1977, 1248.
22. F. H. Herbstein and W. Schwotzer, *J. Am. Chem. Soc.* 1984, **106**, 2367.
23. A. H. Nabilsi, Ph.D. thesis, University of Leeds (1972).
24. A. T. Hutton, Ph.D. thesis, University of Cape Town (1980).
25. T. Axenrod, In *Nuclear Magnetic Resonance Spectroscopy of Nuclei other than Protons* (Edited by T. Axenrod and G. A. Webb), p. 81. Wiley, New York

(1974). J. W. Lown and S. M. S. Chauhan, *J. Org. Chem.* 1983, **48**, 513.
26. D. Graham and J. S. Waugh, *J. Chem. Phys.* 1957, **27**, 968; G. O. Dudek and E. P. Dudek, *J. Am. Chem. Soc.* 1964, **86**, 4283; L. Mester, A. Stephen and J. Parello, *Tetrahedron Lett.* 1968, 4119; P. B. Fischer, B. L. Kaul and H. Zollinger, *Helv. Chim. Acta* 1968, **51**, 1449.
27. M. Harding, M. J. Adams, P. A. Alsop and H. M. N. H. Irving, *Anal. Chim. Acta* 1973, **67**, 204.
28. J. H. Billman and E. S. Cleland, In *Organic Syntheses* (Edited by E. C. Horning), Collective Vol. 3, p. 360. Wiley, New York (1955).
29. G. C. Levy, R. L. Lichter and G. L. Nelson, *Carbon-13 Nuclear Magnetic Resonance Spectroscopy*, 2nd Edn, p. 165. Wiley Interscience, New York (1980).
30. P. Rashidi-Ranjbar and I. Yavari, *Org. Magn. Reson.* 1981, **16**, 168.
31. H. M. N. H. Irving and A. T. Hutton, *Anal. Chim. Acta* 1981, **128**, 261.
32. S. P. Bag and H. Freiser, *Anal. Chim. Acta* 1982, **136**, 439.
33. A. Janowski and T. Gańko, *Bull. Acad. Pol. Sci., Ser. Sci., Chim.* 1968, **16**, 223; W. Kemula, T. Gańko and A. Janowski, *ibid.* 1971, **19**, 325.
34. J. E. Pemberton and R. P. Buck, *J. Raman Spectrosc.* 1982, **12**, 76.
35. V. Spěváček and V. Spěváčková, *J. Inorg. Nucl. Chem.* 1976, **38**, 1299.
36. H. Wagler and H. Koch, *Talanta* 1984, **31**, 1101.
37. H. M. N. H. Irving and A. T. Hutton, *Anal. Chim. Acta* 1982, **141**, 311; H. M. N. H. Irving, N. F. Naqvi and C. G. Tilley, *ibid.* 1978, **100**, 597.
38. A. T. Hutton and H. M. N. H. Irving, *J. Chem. Soc., Chem. Commun.* 1981, 735.
39. K. Müllen and P. S. Pregosin, *Fourier Transform NMR Techniques: A Practical Approach*, p. 37. Academic Press, London (1976).
40. See Ref. 29, p. 30.
41. H. M. N. H. Irving and U. S. Mahnot, *Talanta* 1968, **15**, 811; P. A. McCallum, H. M. N. H. Irving, A. T. Hutton and L. R. Nassimbeni, *Acta Cryst.* 1980, **B36**, 1626.
42. N. F. Naqvi, Ph.D. thesis, University of Leeds (1966); Ref. 5, p. 67.
43. H. Irving and C. F. Bell, *J. Chem. Soc.* 1953, 3538.

Polyhedron Vol. 6, No. 1, pp. 25–27, 1987
Printed in Great Britain

0277–5387/87 $3.00+.00

CRYSTAL AND MOLECULAR STRUCTURE OF ISOPRENALINE

JOHN F. MALONE* and MASOOD PARVEZ

Department of Chemistry, The Queen's University of Belfast, Belfast BT9 5AG, U.K.

(*Received* 3 *July* 1986)

Abstract—Unlike the related sympathomimetic catecholamines adrenaline and noradrenaline, which exist as zwitterions in the solid state, the β-adrenoreceptor stimulant isoprenaline is shown by crystal structure analysis to contain only neutral atoms. Crystals are monoclinic, space group $P2_1/c$, with $a = 9.93(2)$ Å, $b = 13.56(3)$ Å, $c = 8.13(1)$ Å, and $\beta = 101.6°$. The structure was determined by direct methods and refined to $R = 0.087$ for 1154 independent data. The side chain has the fully extended *anti* conformation.

Inorganic acids form chelates with di- and polyphenols, and with the related catecholamines. For a range of protonated catecholamines in aqueous solution, including isoprenaline (**1**), it has been shown that the first phenolic group is more acidic than the protonated amino group.[1] This has been supported by crystal structure analyses of the catecholamines adrenaline[2] (**2a**) and noradrenaline[3] (**2b**), which possess α- and β-adrenergic activity, and of the structurally-related α-adrenoreceptor stimulant phenylephrine[4] (**3**), which show these compounds to exist as zwitterions in the solid state. In each case it is the *meta*-OH group which donates a proton to the nitrogen atom.

Isoprenaline {isoproterenol [1-(3′,4′-dihydroxyphenyl-2-isopropylaminoethanol]} is the most active of those sympathomimetic amines which act almost exclusively on β-receptors, stimulating the heart muscle as well as dilating the bronchioles. The (−)-isomer (**1**) is 50 times as powerful as the (+)-isomer in circulatory activity in man. On the basis of acid ionization constants in solution an analogous zwitterionic structure would be expected for the solid-state free amine. An earlier crystallographic examination of (±)-isoprenaline in the form of its dihydrated sulphate has been performed,[5] but does not, of course, give any information concerning the ionic state of the free base. The

*On graduating from University College, Dublin (1966) J. F. Malone was appointed by Professor Harry Irving as Demonstrator (1966–1969) in the Department of Inorganic and Structural Chemistry, University of Leeds, and subsequently as Postdoctoral Fellow (1969–1970) and Brotherton Research Lecturer (1970–1973) in the same department. Author to whom correspondence should be addressed.

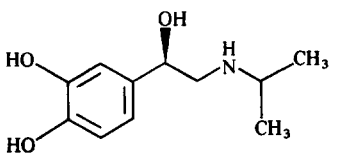

1

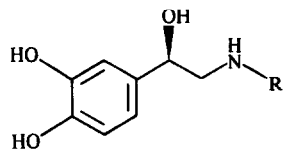

2a R = CH_3
2b R = H

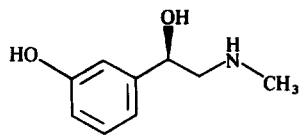

3

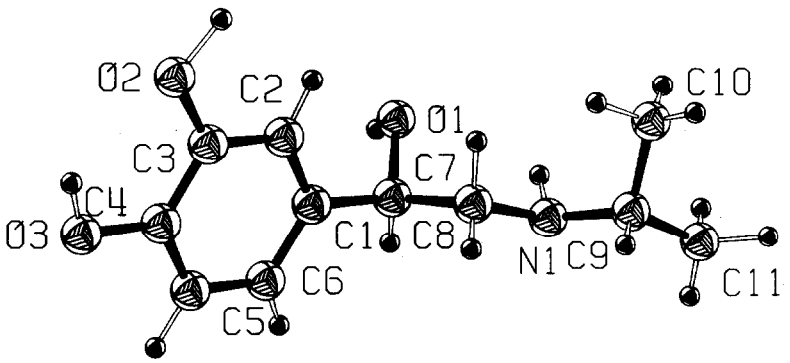

Fig. 1. Isoprenaline: a view of the (−)-isomer. Arbitrary isotropic thermal parameters have been assigned to the atoms.

present study was undertaken in order to establish the molecular characteristics of the free base (±)-isoprenaline and to compare the conformation of this drug with other catecholamines.

EXPERIMENTAL

Crystal data

$C_{11}H_{17}NO_3$, $M = 211.2$, space group $P2_1/c$ (No. 14), $a = 9.93(2)$ Å, $b = 13.56(3)$ Å, $c = 8.13(1)$ Å, $\beta = 101.6°$, $U = 1072.5$ Å^3, $Z = 4$, $D_x = 1.32$ g cm^{-3}, $D_m = 1.32$ g cm^{-3} (by flotation in $CHCl_3$–petroleum ether), λ(Cu-K_α) = 1.5418 Å, $\mu = 7.95$ cm^{-1}, $F(000) = 456$.

Crystals of the free base were obtained from its sulphate by treating with aqueous ammonia under nitrogen. The crystals of (±)-isoprenaline were thin colourless plates. Data were recorded on multiple-film equi-inclination Weissenberg photographs (layers *hk*0–*hk*7) and intensities were measured by a densitometer.* Correction for Lorentz and polarization factors yielded 1154 independent structure factors. The non-hydrogen atoms were located in the E-map with the highest absolute figure of merit obtained via the direct phasing methods of MULTAN.[6] After initial least-squares refinement all 17 hydrogen atoms were located in a difference Fourier synthesis, and were included in the refinement with individual isotropic temperature factors. Non-hydrogen atoms were refined anisotropically. At convergence, R was 0.087. The final weighting scheme was $W = (10 + |F_o| + 0.01|F_o|^3)^{-1}$. A final-difference Fourier showed no significant features.

RESULTS AND DISCUSSION

A projection of the molecule is shown in Fig. 1 and the unit-cell contents in Fig. 2. Table 1 lists the principal bond lengths and angles. A full list of results comprising atomic coordinates, anisotropic temperature factors for non-hydrogen atoms, and bond lengths and angles involving hydrogens has been deposited with the Cambridge Crystallographic Data Centre.†

Although a zwitterionic structure was to be expected on the basis of the solution acid ionization constants this analysis shows the isoprenaline molecule to exist in a non-ionized form in the solid state. All hydrogen atoms were located and successfully refined. As the critical hydrogen atom, namely the *m*-hydroxy atom H(O2), is not hydrogen-bonded to the nitrogen of any adjacent molecule the molecule is clearly present in the neutral form. To confirm this phenolic C—O distances, 1.375(6) and 1.380(5) Å, are normal for phenols, unlike the C—O^- distances of 1.346(5) Å in adrenaline,[2] 1.338(3) Å in noradrenaline[3] and 1.341(3) Å in phenylephrine.[4] The molecular dimensions are normal. The catechol is planar, the maximum deviation of any atom from the benzene ring being 0.009 Å. The deviations of the two H atoms on the phenolic groups from the mean plane of the catechol group are 0.002 and 0.018 Å. The side chain, comprising C(1), C(7), C(8) and N(1), is fully extended (*anti* conformation) as found in (±)-isoprenaline sulphate dihydrate.[5] The side chain is approximately perpendicular (77.4°) to the plane of

* Science Research Council Microdensitometer Service, Rutherford Laboratory.

† Deposited data may be obtained from The Director, Cambridge Crystallographic Data Centre, Lensfield Road, Cambridge.

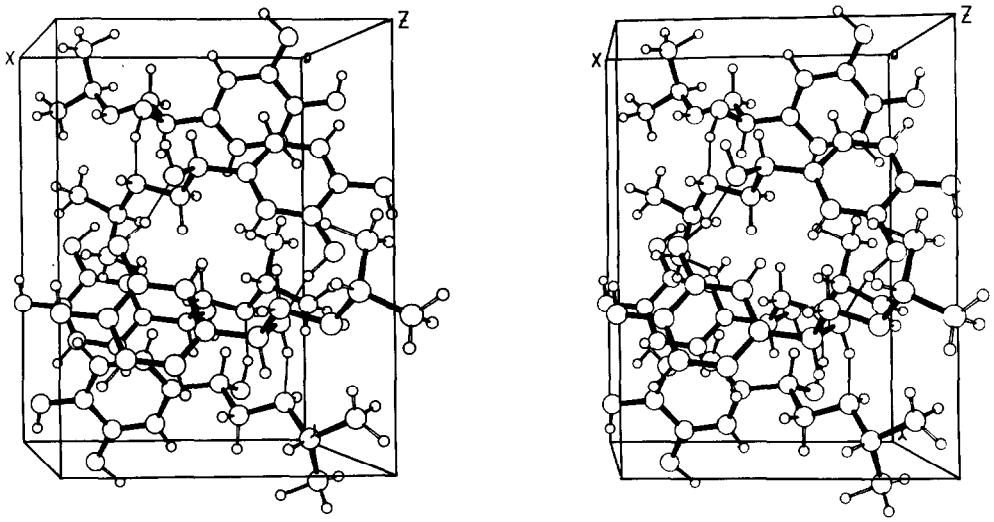

Fig. 2. Stereoview of the crystal structure of (±)-isoprenaline.

Table 1. Interatomic distances (Å) and angles (°)

Distance		Angle	
C(1)—C(2)	1.396(7)	C(1)—C(2)—C(3)	121.0(4)
C(2)—C(3)	1.380(6)	C(2)—C(3)—C(4)	119.7(4)
C(3)—C(4)	1.395(6)	C(3)—C(4)—C(5)	119.9(4)
C(4)—C(5)	1.366(7)	C(4)—C(5)—C(6)	120.1(4)
C(5)—C(6)	1.390(7)	C(5)—C(6)—C(1)	121.1(4)
C(6)—C(1)	1.384(7)	C(2)—C(1)—C(6)	118.1(4)
C(1)—C(7)	1.516(6)	C(2)—C(1)—C(7)	121.6(4)
C(7)—C(8)	1.521(7)	C(6)—C(1)—C(7)	120.2(4)
C(8)—N(1)	1.476(6)	C(1)—C(7)—C(8)	111.3(4)
C(9)—N(1)	1.482(6)	C(1)—C(7)—O(1)	112.2(3)
C(9)—C(10)	1.520(7)	C(8)—C(7)—O(1)	107.5(3)
C(9)—C(11)	1.531(7)	C(7)—C(8)—N(1)	111.2(3)
C(7)—O(1)	1.456(6)	C(8)—N(1)—C(9)	113.0(3)
C(3)—O2)	1.375(6)	C(10)—C(9)—N(1)	113.4(4)
C(4)—O(3)	1.380(5)	C(10)—C(9)—C(11)	110.1(4)
O(1)···O(2)′[a]	2.737(5)	C(11)—C(9)—N(1)	108.5(4)
O(1)···N(1)″[a]	2.796(5)	C(2)—C(3)—O(2)	123.5(4)
O(2)···O(3)‴[a]	2.767(5)	C(4)—C(3)—O(2)	116.7(4)
		C(3)—C(4)—O(3)	121.3(4)
		C(5)—C(4)—O(3)	118.8(4)

[a] Primed, double primed and triple primed atoms are related to unprimed atoms by the transformations $1-x, -y, -z$; $x, \frac{1}{2}-y, \frac{1}{2}-z$; and $-x, -y, -z$, respectively.

the ring system. The C(9) atom of the isopropyl group is in full extension on the side chain. The bond angle C(8)—N(1)—C(9), at 113.0(3)°, is slightly larger than the tetrahedral angle as has been observed in all the previous structures in the phenylethylamine series. The mean C—N bond length [1.479(6) Å] is normal. There is extensive intermolecular hydrogen bonding involving all three oxygens and the nitrogen of each molecule, leading to the compact structure depicted in Fig. 2.

REFERENCES

1. P. J. Antikainen and U. Witikainen, *Acta Chem. Scand.* 1973, **B27**, 2075 (and references therein).
2. A. M. Andersen, *Acta Chem. Scand.* 1975, **B29**, 239.
3. A. M. Andersen, *Acta Chem. Scand.* 1975, **B29**, 871.
4. A. M. Andersen, *Acta Chem. Scand.* 1976, **B30**, 193.
5. M. Mathew and G. J. Palenik, *J. Am. Chem. Soc.* 1971, **93**, 497.
6. G. Germain, P. Main and M. M. Woolfson, *Acta Cryst.* 1971, **A27**, 368.

Polyhedron Vol. 6, No. 1, pp. 29–38, 1987
Printed in Great Britain

0277–5387/87 $3.00+.00

METAL COMPLEXES OF 1,4,10-TRIOXA-7,13-DIAZACYCLOPENTADECANE-*N*,*N*′-DIACETIC ACID

RITA DELGADO, J. J. R. FRAÚSTO DA SILVA*† and M. CÂNDIDA T. A. VAZ

Centro de Química Estrutural, Instituto Superior Técnico, Lisbon, Portugal

(*Received* 3 *July* 1986)

Abstract—The cyclic diaza-crown ether complexone cTOPDA (1,4,10-trioxa-7,13-diazacyclopentadecane-*N*,*N*′-diacetic acid) has been synthesized and characterized by elemental analysis, titration and NMR spectroscopy. Its ionization constants and the stability constants of its ML and M_2L complexes formed with alkali, alkaline-earth and some transition and representative metals were determined at 25.0±0.1°C and ionic strength 0.10 M (Me_4NNO_3). This ligand forms considerably more stable complexes with the transition metals than the analogous tetraoxa-diaza crown ether complexone cTOODA (1,4,10,13-tetraoxa-7,16-diazacyclooctadecane-*N*,*N*′-diacetic acid), but this last ligand favours ions with larger size, particularly K^+. The cobalt(II) complex of cTOPDA is more stable than the nickel(II) complex, hence the Irving–Williams' order of stability is not obeyed for its transition-metal complexes. These effects are discussed in terms of the size of the cavity of the ligand and of the stereochemical constraints that it may impose.

Macrocyclic polyethers ("crown ethers") are well known for their complexation properties towards alkali and alkaline-earth metal ions: a quite remarkable selection can be achieved by changing the number of oxygen donors and the size of the internal cavity of the ligands.[1]

The inclusion in the ring of other types of donor atoms was a logical further step, since it may introduce a range of different effects by changing the affinity towards some metal ions while maintaining the selectivity associated with the relative dimensions of the ions and the cavity of the ligands.

Nitrogen and sulphur, naturally, are particularly interesting heterodonor atoms to investigate, and various studies were indeed carried out with a series of oligo-oxa–oligoaza or oligosulphur macrocycles in the last decade.[2–4]

The properties of such macrocycles as ionophores, models for catalytical centres, solubilizing agents etc. have been extensively discussed, but their analytical applications are limited by their sometimes reduced solubility in water, and by the fact that the stability of their metal complexes in aqueous solution is only moderate. These difficulties may be overcome by synthesizing macrocycles with hydrophylic pendant arms containing extra potential donors, e.g. —NH_2 or —COOH groups. Again, the stereochemical constraints imposed by these new donors may cause variations in the metal-complexing ability of the resulting ligand, which may or may not be of interest for the objectives envisaged.

The polyaza rings, with or without other donor atoms, afford some practical advantages for the introduction of pendant arms since the hydrogen atoms bonded to nitrogen in these ligands can easily be substituted by convenient groups using appropriate reactions; for example, the introduction of —CH_2COOH groups is normally achieved by reaction with chloroacetate or bromoacetate in a basic medium.

These *N*-acetate derivatives of oligoaza macrocycles are, of course, a cyclic version of the well-known polyamino carboxylic acids ("complexones"), widely used in analytical chemistry, adding now the versatility of these complexing agents to the selective character derived from the constraints imposed by the ring that contains several potential donor atoms.

We have previously studied a series of cyclic tetraaza complexones which have indeed some remarkable properties useful for analytical applications,[5]

* Author to whom correspondence should be addressed.
† D.Phil. student of Professor Irving, St. Edmund Hall, Oxford, 1960–1962: now Full Professor in the Chemistry Department, IST, Technical University of Lisbon, Lisbon, Portugal.

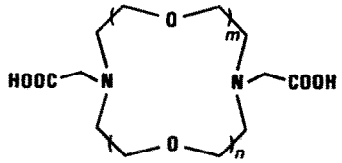

I

Fig. 1. *N*-acetate derivatives of a group of oligo-oxa–oligoaza macrocycles. (a) $m = 2$, $n = 1$: 1,4,10-trioxa-7,13-diazacyclopentadecane-*N*,*N*′-diacetic acid (cTOPDA); (b) $m = 2$, $n = 2$: 1,4,10,13-tetraoxa-7,16-diazacyclooctadecane-*N*,*N*′-diacetic acid (cTOODA); and (c) $m = 1$, $n = 1$: 1,7-dioxa-4,10-diazacyclodecane-*N*,*N*′-diacetic acid (cDODDA).

and in the present work we report the results obtained for a member of a group of *N*-acetate derivatives of oligo-oxa–oligoaza macrocycles—like **Ia** (Fig. 1)—that are expected to display some unusual features due to the combined effects of cavity size, type of donor atoms and stereochemical constraints on the preferred coordination symmetry of some metals.

Compound **Ib** has been studied by other authors,[4,6] and results for **Ic** will be presented in a future paper.

EXPERIMENTAL

Synthesis and characterization of the ligand

cTOPDA dihydrochloride (cTOPDA·2HCl) was prepared by reaction of the corresponding amine [Kryptofix® 21 (Merck–Schuchardt)] with potassium chloroacetate, in aqueous solution at 70°C.

Potassium hydroxide was added at such a rate that the pH was always kept below 10. The reaction was complete after 8 h. The product was precipitated after acidifying the ice-cold solution to pH 0.5, and was recrystallized from a water–ethanol mixture.

cTOPDA·2HCl: m.p. = 205±1°C; *M* (titration) 407. Found: C, 41.0; H, 6.7; N, 6.84%. Required ($C_{14}H_{26}N_2O_7 \cdot 2HCl$): C, 41.3; H, 6.5; N, 6.88%. ^{1}H NMR spectrum [solvent D_2O, reference 2,2,3,3-tetradeutero-3-(trimethylsilyl) propionic acid (DTSS), pD ≅ 2.8]: δ 4.05 (singlet, 4H, acetate groups), 3.84 (triplet, 8H, ring protons), 3.76 (singlet, 4H, ring protons), and 3.68 (triplet, 8H, ring protons).

Reagents

Metal salts. Metal nitrates of analytical-reagent grade were used and solutions were prepared in demineralized water, and standardized by EDTA titrations.

The ionic strength was adjusted with a solution of Me_4NNO_3 (prepared from Me_4NOH and HNO_3 and recrystallized from 80% ethanol).

Carbonate-free Me_4NOH. Carbonate-free solutions of this titrant were prepared directly by dilution of the concentrated product (Merck, 10% aqueous solution) under purified nitrogen. The solutions (*ca* 0.05 M) were standardized by titration with 0.010 M hydrochloric acid. The absence of carbonate was tested regularly, and the solutions were discarded when its concentration reached 0.5% of the concentration of the hydroxide.

Potentiometric titrations

The experimental set-up has been described previously;[5] a Crison Digilab 517 measuring instrument was used together with an Ingold U 1330 glass electrode and a U 1335 saturated calomel reference. The temperature was controlled at 25.0±0.1°C by circulating water through the jacketed titration cell. The ionic strength was kept to 0.10 M by use of tetramethylammonium nitrate as background salt; the ionic product of water in these media was taken as 1.68×10^{-14}.

The glass electrode was calibrated in terms of $[H^+]$ by titrating solutions of hydrochloric acid and potassium hydroxide of known concentrations, and correlating the mV readings with calculated values of $[H^+]$. The $[H^+]$-dependent junction potentials were found to be negligible (from Gran plots), and the correlation between measured e.m.f. and calculated $[H^+]$ was strictly represented by $E = E^{o\prime} + Q \log [H^+]$ for both the acid and alkaline zones, with slightly different values of $E^{o\prime}$. In each zone the relevant value of $E^{o\prime}$, was used; in intermediate pH ranges (4.5–8.5) an average $E^{o\prime}$ value was adopted. With this procedure, experimental and calculated titration curves were completely superimposable. The adequacy of the procedure was tested with ligands for which accurate stability constants of proton and metal complexes are known, e.g. NTA and EDTA.

Other measurements

NMR spectra were recorded with a 100-MHz JEOL JNM 100 PTF spectrometer coupled to a JEOL 980 A computer. Deuterium oxide was the solvent and the reference compound was the sodium salt of DTSS.

Melting points were determined with a Reichert–Thermovar instrument provided with a microscope, and are uncorrected.

Elemental analyses were done with a Perkin–Elmer 240 elemental analyzer.

Calculation of the stability constants

The stability constants of the various species formed were obtained from the experimental data with the aid of the program MINIQUAD[7] and a Data General Eclipse S/140 computer.

Suitable approximate values for the constants were obtained by use of a simpler program, and the values were improved by comparison of the experimental titration curves of the complexones in the presence of the various metal ions with calculated titration curves for values of stability constants close to the estimated values, until a satisfactory superimposition of the curves was achieved. This was done on a 2200 Wang computer coupled to a 2212 plotter. The values for the best superimposition were then refined by the MINIQUAD program. In the present work, the values selected were those for which the calculated relative standard deviation was less than 10%, the "fitting index" was less than 0.003 and the acceptable value of χ^2 at the 95% confidence level for 6 d.f. was less than the value (12.6) obtained following the procedure of other authors.[8,9] The results obtained correspond to a minimum of two experiments for which the ratio C_M/C_L was generally about 1 or 2, except for alkaline-metal ions for which the ratio was 10 or 100.

RESULTS AND DISCUSSION

Titration curves for the ligand studied, alone and in the presence of several metal ions, are shown in Fig. 2.

As it can be seen, the ligand is dibasic with p*k* values of the order of 8–9, corresponding to the ionization from protonated nitrogens. In its di-

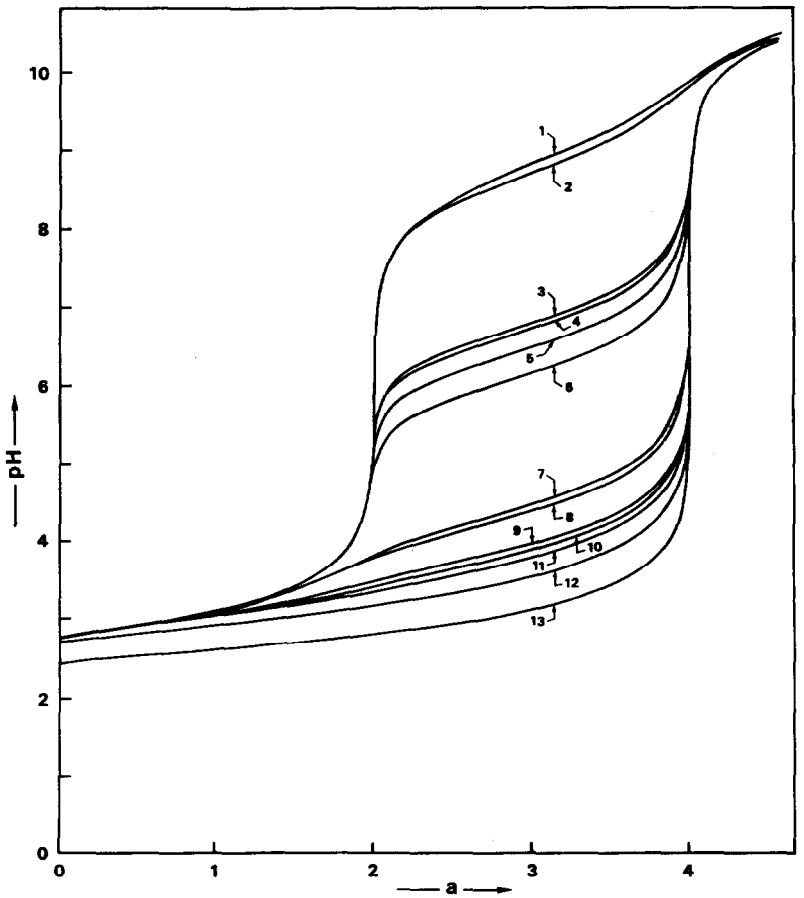

Fig. 2. Titration curves for cTOPDA alone and in the presence of metal ions in 1:1 ratio. $T = 25.0 \pm 0.1$°C, $\mu = 0.1$ M (Me_4NNO_3). (1) cTOPDA alone (10^{-3} M) and with: (2) Na^+ or Li^+, (3) Ba^{2+}, (4) Mg^{2+}, (5) Sr^{2+}, (6) Ca^{2+}, (7) Mn^{2+}, (8) Ni^{2+}, (9) Pb^{2+}, (10) Cd^{2+}, (11) Co^{2+}, (12) Zn^{2+}, and (13) Cu^{2+}.

hydrochloride form, the acetate groups are also protonated and ionize in aqueous solution at low pH; the corresponding pk values are of the order of 2 or lower.

The values of the ionization constants, refined by MINIQUAD, are presented in Table 1, together with those determined by Tazaki *et al.*[6] at 25°C and $\mu = 0.1$ M (KNO_3). Our values were determined at the same temperature and $\mu = 0.10$ M (Me_4NNO_3) both sets of results are presented to allow comparisons. In Table 1 we also include the values of the ionization constants of cTOODA,[4] and of the protonated diaza crown ethers from which cTOODA and cTOPDA were derived, i.e. Kryptofix® 22 and Kryptofix® 21.[10]

The discrepancy between our values and those of Tazaki *et al.*[6] for cTOPDA can be explained easily: the former authors did not taken into account the possibility of formation of K^+ complexes with this ligand and since this does indeed occur ($\log K_{KL} = 1.69$), their pk values are necessarily lower. Compared with the corresponding ionization constants of cTOODA it is seen that cTOPDA is more basic, as expected, since it has less electronegative oxygen atoms in the ring. The pk values for the ionization of these ligands are consistent with those of the corresponding diaza crown ethers from which the ligands were derived.

Concerning the formation of metal complexes, two observations immediately arise from Fig. 1. First, the stability of the complexes of the alkaline-earth metals decreases normally with the increase in the ionic radius of the metal; second, that of the complexes of the transition metals does not follow the "natural" Irving–Williams' order since the cobalt complex is more stable than that of nickel. The zinc complex is also more stable than that of cadmium, but there is no invariant pattern for this pair of metals.

The stability constants of all these complexes were calculated as described in Experimental and are summarized in Table 2, together with the corresponding values for cTOODA, as well as those for EGTA [ethylene bis(oxyethylenenitrilo)tetraacetic acid] and EEDTA [oxy bis(ethylenenitrilo)-tetraacetic acid)],[11] whose linear chains between the substituted nitrogen atoms are similar to the two halves of the structure of cTOPDA. The values of the stability constants of some complexes of cTOPDA obtained by Tazaki *et al.*[6] are also included for comparison, although they are generally incorrect, since they were determined in a complexing medium (KNO_3); furthermore, in the case of the transition metals, only rough approximations were given, due to the slowness of the reactions. In our determinations enough time was given in every case to allow equilibrium to be reached; in the case of iron, manganese, cobalt and nickel this took several hours for each titration, and even in the cases of copper and zinc stable readings were only done several minutes after each addition of titrant. For cadmium and lead, equilibrium was quickly established. Good results were obtained in every case except for iron, probably due to slight oxidation of the metal, even if titrations were carried out under nitrogen.

The correctness of the determinations was checked by carrying out duplicated batch titrations in which several test-tubes containing 1 : 1 and 2 : 1 mixtures of metal and ligand plus variable amounts of titrant Me_4NOH were left for several days in a thermostat, and pH readings were made at regular 1-day intervals. The results obtained in these determinations were very close or identical to those obtained by the normal titrations, but the errors were naturally larger (although less than 0.1 log units).

The excellent results obtained with the demanding MINIQUAD program are also a good indication of the care with which the measurements were made. Two titrations at different metal : ligand ratios (1 : 1 and 2 : 1) were used in each run of the

Table 1. Ionization constants (pk) of some cyclic complexones and the corresponding amines

	cTOPDA · 2HCl	cTOODA · 2HCl	Kryptofix® 21 · 2HCl	Kryptofix® 22 · 2HCl
pk_1	< 1,[a] < 2[b]	—	—	—
pk_2	1.75 ± 0.04,[a] 2.3[b]	2.90 ± 0.10[c]	—	—
pk_3	8.544 ± 0.009,[a] 8.35[b]	7.80 ± 0.02[c]	8.12 ± 0.03[d]	8.15 ± 0.04[d]
pk_4	9.067 ± 0.005,[a] 8.63[b]	8.45 ± 0.02[c]	9.26 ± 0.03[d]	9.30 ± 0.04[d]

[a] Present work: $T = 25.0 \pm 0.1$°C, $\mu = 0.10$ M (Me_4NNO_3).
[b] Tazaki *et al.*:[6] $T = 25.0$°C, $\mu = 0.1$ M (KNO_3).
[c] Chang and Rowland:[4] $T = 25.0$°C, $\mu = 0.1$ M (Me_4NNO_3).
[d] Luboch *et al.*:[10] $T = 25.0$°C, $\mu = 0.1$ M (Et_4NClO_4).

Table 2. Stability constants (log β) of metal complexes of cTOPDA, cTOODA, EGTA and EEDTA

Metal ion	Species	cTOPDA [a]	cTOPDA [b]	cTOODA[c]	EGTA[d]	EEDTA[d]
Li^+	ML	2.139±0.007	—	—		
Na^+	ML	2.72±0.01	2.85	1.95[b]		
K^+	ML	1.69±0.03	—	3.9±0.3		
Mg^{2+}	ML	7.534±0.004	(6.7)	<2[b]	5.28	8.36
Ca^{2+}	ML	8.680±0.003	8.06	8.39±0.06	10.86	9.96
	M_2L	9.9±0.2				
Sr^{2+}	ML	8.023±0.004	7.20	8.29±0.07	8.43	9.24
	M_2L	9.99±0.08				
Ba^{2+}	ML	7.412±0.003	6.74	7.63±0.02	8.30	8.07
Mn^{2+}	ML	12.111±0.006	—	—	12.18	13.7
Fe^{2+}	ML	(13.0)	—	—	11.8	14.2
Co^{2+}	ML	13.72±0.01	(12)	7.00[b]	12.35	(15.2)
	M_2L	16.37±0.05				
Ni^{2+}	ML	12.374±0.008	—	7.39±0.03	13.50	(15.0)
	M_2L	14.3±0.1				
Cu^{2+}	ML	17.79±0.02	>14	14.49±0.03	17.57	18.1
	M_2L	22.79±0.01				
Zn^{2+}	ML	14.442±0.007	(12)	8.42±0.09	12.6	15.2
	M_2L	17.35±0.02				
Cd^{2+}	ML	13.432±0.005	—	11.07±0.03	16.1	16.2
	M_2L	15.62±0.05				
Pb^{2+}	ML	13.255±0.005	—	13.55±0.06	14.71	15.03
	M_2L	15.69±0.03				

[a] Present work: $T = 25.0 \pm 0.1$°C, $\mu = 0.10$ M (Me_4NNO_3).
[b] Tazaki *et al.*:[6] $T = 25.0$°C, $\mu = 0.1$ (KNO_3).
[c] Chang and Rowland:[5] $T = 25.0$°C, $\mu = 0.1$ M (Me_4NNO_3).
[d] Ref. 11.

program and different sets of titrations give results coincident to ±0.05 log units. The values presented in Table 2 correspond to the best outputs of the MINIQUAD program for one set of titrations of each metal–ligand system.

For the other ligands we have used the values available in the literature, and in the cases when more than one set of values are available we have adopted those considered as more reliable (EGTA and EEDTA),[11] or which we considered sufficiently consistent (Kryptofix® 21 and 22).[10]

For the ligand that we have studied we obtained stability constants for the ML and M_2L complexes, and in the cases of Li^+ and Na^+ also for the MHL complexes which are very weak: $\log K_{MHL} = 1.15$ and 0.85, respectively.*

The values quoted for the M_2L complexes are overall constants, i.e. $\log \beta_{ML_2}$; the comparison with the values of $\log K_{ML}$ show that, although the 1 : 1 complexes have a residual affinity to bind a second atom of the metal, this affinity is relatively weak, except in the case of copper, for which the difference $\log \beta_{M_2L} - \log \beta_{ML}$ is 5 log units; for the other metal ions it hardly exceeds 2 log units.

The comparison of our results with those obtained by Chang and Rowland for cTOODA affords interesting results which may also be appreciated in Fig. 3. Hence, whereas the stability constants of the alkaline-earth and Pb^{2+} complexes of cTOODA are approximately equal to those of the corresponding complexes of cTOPDA, but remarkably higher in the case of K^+, the complexes of the first-series transition metals, zinc and cadmium with the first ligand are much less stable than those of the last one, and their stability constants are surprisingly low even in absolute terms, compared with the values for the corresponding complexes of EGTA and EEDTA (Table 2).

This behaviour finds some justification in the degree of fitting of the metal ions to each of the ligands; note that cTOPDA is asymmetric relative

* $K_{MHL} = [MHL]/[M][HL]$.

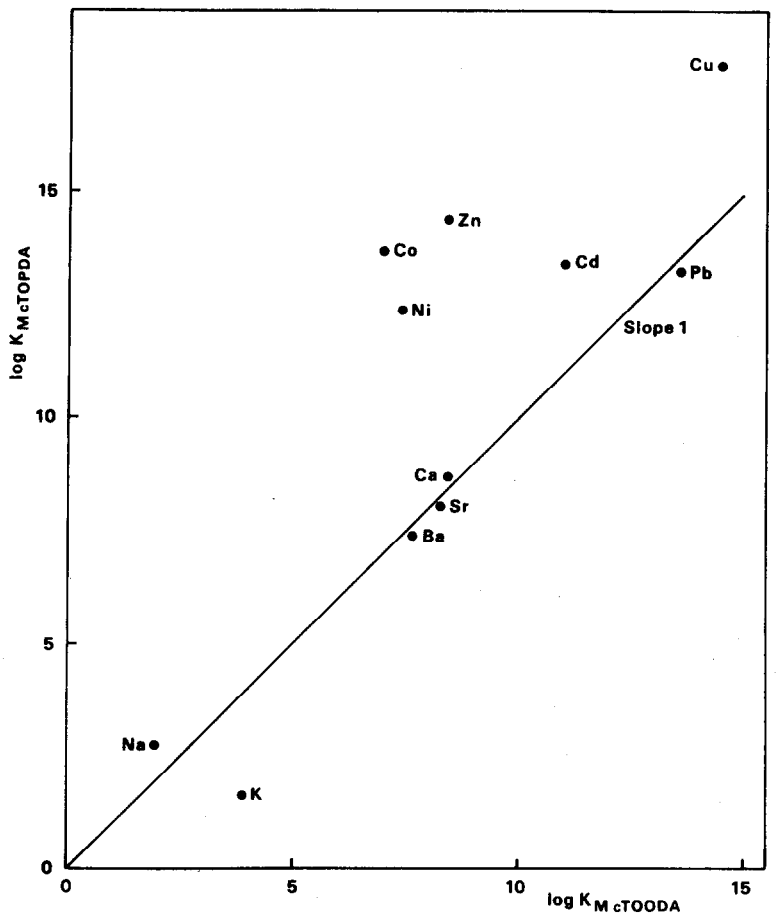

Fig. 3. Correlation of the stability constants ($\log K_{ML}$) of the metal complexes of cTOPDA and cTOODA. A slope 1 straight line would correspond to equal stabilities for the complexes of the two ligands.

to the coordinating nitrogens, hence the metal may be shifted to either side or interact with all atoms, depending on its radius. On this basis we predict that cDODDA will complex the smaller ions even more strongly, and enhance selectivity based on size fitting. This effect becomes clearer when one compares the stability constants of the complexes of cTOPDA on one side and those of the corresponding complexes of EGTA and EEDTA on the other (Fig. 4).

Figure 3 shows that cTOPDA favours the complexation of Cu^{2+}, Zn^{2+}, Co^{2+}, Fe^{2+}, Mn^{2+} and Mg^{2+} relative to EGTA, but when EEDTA is considered instead of EGTA a much better correlation is obtained; the variations in the values of the stability constants on going from EGTA to EEDTA are not substantial for the larger alkaline-earth ions copper and cadmium, but quite considerable for the other transition-metal ions, zinc and magnesium. In both cases, Cd^{2+} is favoured by the non-cyclic ligands.

The behaviour of copper must be considered separately; the structure of its complex with cTOODA has been determined in the solid state by X-ray diffraction[12] and it was found that the metal is tetragonally coordinated with the two nitrogens and the two carboxylate groups in the equatorial plane with two of the ether oxygens of the ligands on opposite sides of the molecule, interacting weakly at longer distances in the axial position. The stability constant of the complex is even smaller than that of the closely similar copper complex of DACODA (1,5-diazacyclooctane-*N*,*N'*-diacetic acid),[13] a ligand that, despite its more basic nitrogen atoms, has no ether oxygen atoms in the ring and, consequently, no other binding interactions besides those of the aminoacetate groups in the equatorial plane. The case of cTOPDA is probably similar, but the axial interaction with the oxygen of the diethyl ether chain seems to be more effective, giving a higher constant than that of Cu(II)cTOODA; this being the case no particular meaning should be attributed

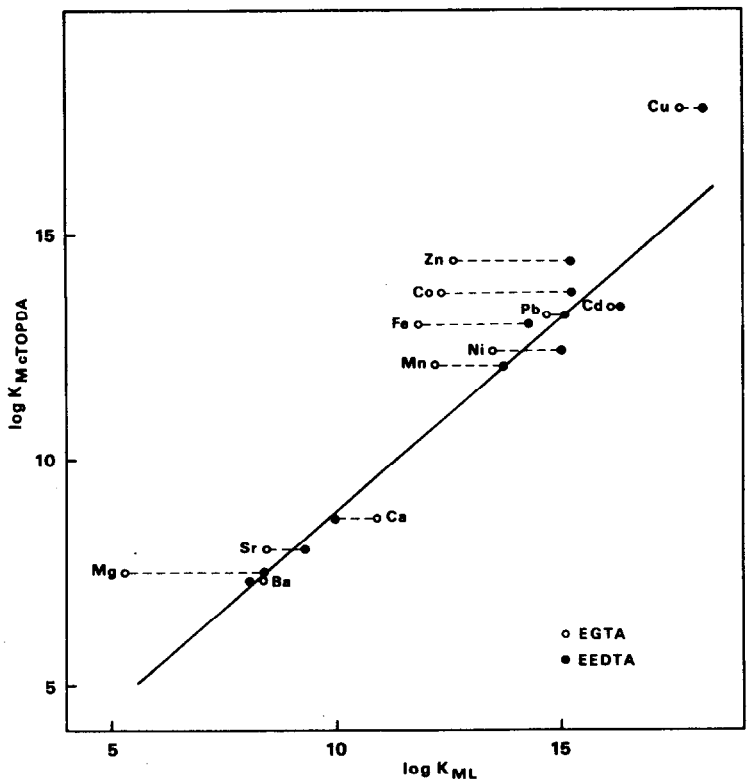

Fig. 4. Correlation of the stability constants ($\log K_{ML}$) of the complexes of cTOPDA and EEDTA (●), showing the shifts when EGTA (○) is considered instead of the latter ligand.

to the location of copper in Fig. 2; it is the type of coordination favoured and not only the size of the ion that is the critical factor in this case.

The conclusions that we derive from these results are that the smaller transition-metal ions tend to bind preferentially to the diaminodiethyl ether *N*,*N'*-diacetate moiety of cTOPDA, similar to EEDTA, whereas the larger alkaline-earth ions, cadmium and lead seem to prefer the other moiety, similar to EGTA.

The larger ligand, cTOODA, naturally prefers the larger ions, and the most favoured is the largest, i.e. K^+. Accordingly, complexes of the smaller metals are destabilized.

These differences of behaviour between cTOPDA and cTOODA must be reflected in the thermodynamic functions for the complexation reactions of each ligand. We expect more favourable enthalpies and entropies of formation of the first-series transition metal, zinc and cadmium complexes of the first ligand (compare thermodynamic data for EEDTA and EGTA complexes), but this idea cannot be confirmed until the relevant data are available (work in progress).

Our final remarks concern the inversion in the normal order of stability of the cobalt and nickel complexes of cTOPDA which is unusual but not specific of this ligand. The effect was already observed in the corresponding amines, i.e. 1,4,10-trioxa-4,13-diazacyclopentadecane or Kryptofix® 21 (denoted by [21]), but not in 1,7-dioxa-4,10-diazacyclododecane (denoted by [11]), neither in 1,4,10,13-tetraoxa-7,16-diazacyclooctadecane nor Kryptofix® 22 (denoted by [22]) (see Table 3).

It therefore seems that the inversion is not directly related to the dimensions of the internal cavity of the ligand—not only cobalt and nickel have similar radii but the inversion is found for a ligand of intermediate cavity size—so we must look into other reasons that may cause this breaking of the normal trend.[14]

Since nickel has a more definite preference for octahedral coordination symmetry than cobalt, it is possible that the inversion is due to a stereochemical constraint of the 15-membered macrocyclic ring, which is asymmetric relative to the two donor-nitrogen atoms, to adopt that favoured configuration. Indeed, the decrease in stability of the complexes of cobalt, nickel and zinc with the increase in the size of the cavity of the ligand from [11] to [21] follows the order Ni > Co, Zn, which is what one would expect from crystal field stabilization energy con-

Table 3. Stability constants of transition-metal complexes of oligo-oxa–oligoaza cyclic amines[a]

Amine	Co^{2+}	Ni^{2+}	Cu^{2+}	Zn^{2+}	Radius of cavity of ligand (Å)
[11]	5.76±0.1	5.91±0.4	8.16±0.11	6.22±0.07	0.8
[21]	5.22±0.08	4.05±0.16	8.15±0.16	5.34±0.08	1.0
[22]	3.25±0.2	3.43±0.32	7.59±0.18	4.31±0.18	1.40

[a] According to Luboch *et al.*:[10] $T = 25.0°C$, $\mu = 0.1$ M (Et_4NClO_4).

siderations if a tetrahedral coordination geometry was favoured.[14,15] Curiously, with the ligand 1-oxa-7,10-dithia-4,13-diaza cyclopentadecane, the normal order of stability Ni > Co is reestablished,[16] which may be due to the combined effects of the higher polarizability of the sulphur atoms and their larger size, compensating for the less adequate geometry of coordination. Nickel and copper will be preferentially favoured in this case and it was found that $\log K_{NiL} = 7.98$ and $\log K_{CuL} = 11.55$, whereas $\log K_{CoL} = 5.42$ and $\log K_{ZnL} = 5.09$.[16]

When one now considers the *N,N'*-diacetate derivatives of Kryptofix® 21 and 22, it is found that the order of stability observed in their respective complexes is maintained, although the stability constants ($\log K_{ML}$) increase by up to 8–9 log units (a rather remarkable effect, compared to the cases of ethylenediamine and ethylenediamine-*N,N'*-diacetic acid, when the increase is only 5–6 log units; the enhancement certainly is of entropic origin).

This seems to imply that the original coordination symmetry in the complexes of the amines is maintained to a large extent, even if the two carboxylate groups are certainly coordinated (or else the stability constants would not increase by such large values). Since the affinity of carboxylate groups for the transition-metal ions (and zinc) does not vary much (note that $\log K_{ML}$ values for the acetate complexes of these metal ions are all similar, close to $\log K_{ML} \sim 1.5$) one would expect, if our hypothesis is valid, just the "normal" effect of increased stability essentially derived from much more favourable entropy changes. Indeed, water and the carboxylate group have similar ligand fields—they are neighbours in the spectrochemical series—hence substitution of coordinated water molecules by carboxylate groups is insufficient to reverse the observed order of the stability $Co^{2+} > Ni^{2+}$ found for the complexes of Kryptofix® 21.

* $Me_6tren \equiv N[CH_2CH_2N(CH_3)_2]_3$.

It is perhaps worth remembering that the Irving–Williams' stability series is a reflexion of the fact that, in octahedral complexes, nitrogen and sulphur favour Fe^{2+}, Ni^{2+} and Cu^{2+} over the other first-series transition metals and zinc, essentially due to larger CFSE, to which one has to add the effect of tetragonal Jahn–Teller distortion in the case of Cu^{2+}. Carboxylate, sulphate or phosphate donors alone are much less effective and differences in stability are smaller since the ligand field strengths of the corresponding ligands are not much different from that of water.

When, however, the symmetry of the complexes changes from the octahedral aqueous ions to tetrahedral or trigonal bipyramidal, due to constrained ligand structures or steric crowding, the situation is different since the Fe^{2+} (d^6) and particularly Co^{2+} (d^7) will then be more favoured in terms of the crystal field stabilization energy, and the "normal" increase in stability expected from the increase in atomic number may not compensate the loss of CFSE for other ions, namely Ni^{2+}, and one may therefore obtain inversions in the Irving–Williams' order of stabilities. Other inversions can, of course, occur due to different effects, such as a spin-pairing in the Fe^{2+} complexes, and are thoroughly discussed in their original paper,[14] but they are not generally verified with the type of ligands used in the present study.

Current examples of inversions resulting from symmetry changes are those of the tetrachloro and tetrabromo complexes of the first-series transition metals and zinc,[17,18] and of the complexes of hexamethylated amino-triethylamine* of type [M(Me_6tren)X],[18] besides that of Kryptofix® 21 and now of cTOPDA, the first complexone type ligand to clearly exhibit this behaviour (note, however, that in the case of EEDTA the $\log K_{ML}$ values of cobalt and nickel complexes are close, and some authors obtained $\log K_{CoL}$ slightly higher than $\log K_{NiL}$). Other examples may be found in the complexes of some biological ligands with distorted

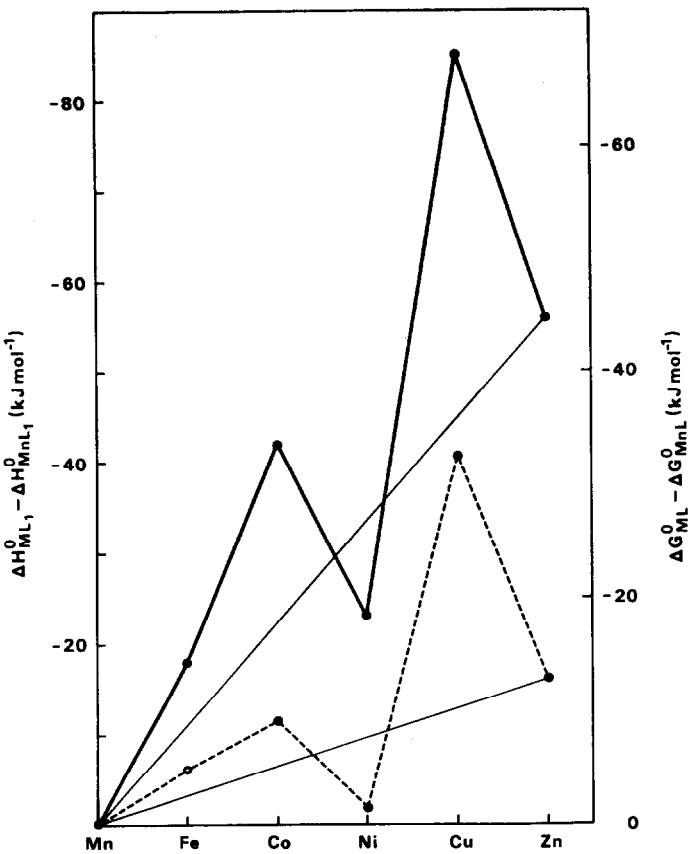

Fig. 5. Relative values of the free-energy and enthalpy changes for the formation of complex compounds from aquo ions. (——) $[M(Me_6tren)Br]^+$: enthalpy changes[18] on the left-hand ordinate; and (– – – –) [McTOPDA]: free-energy changes on the right-hand ordinate.

coordination geometries, which are also a device to increase selectivity. The obvious examples are those of the zinc enzymes with distorted tetrahedral sites in which zinc can be replaced by transition-metal ions, but cobalt is complexed preferentially to nickel.[19]

In the case of the complexes of cTOPDA, the object of the present study, the coordination geometries are not obvious, and electronic spectra do not provide conclusive information because they are not very well-defined. The trend in the free-energy charges on complex formation is similar to that of the enthalpy charges for the complexes $[M(Me_6tren)X]$ (see Fig. 5), and from this one may suggest a trigonal bipyramidal symmetry as a possibility for the transition-metal complexes of cTOPDA, but this will have to be confirmed by other direct experimental evidence and supported by X-ray structure determinations in the solid state.

This paper was submitted in November 1985. Later, a paper by Chang and Ochaya partially on the same subject was published (*Inorg. Chem.* 1986, **25**, 355). The agreement between our values and those obtained by these authors is excellent, with the exception of $\log K_{CuL}$.

REFERENCES

1. J.-M. Lehn, *Struct. Bonding* (*Berlin*) 1973, **16**, 1; A. I. Popov and J.-M. Lehn, In *Coordination Chemistry of Macrocyclic Compounds* (Edited by G. A. Melson), p. 537. Plenum Press, New York (1979).
2. S. Kulstad and L. Å. Malmsten, *J. Inorg. Nucl. Chem.* 1981, **43**, 1299 (and references therein).
3. F. Arnaud-Neu, B. Spiess and M. Schwing-Weill, *Helv. Chim. Acta* 1977, **60**, 2633.
4. C. A. Chang and M. E. Rowland, *Inorg. Chem.* 1983, **22**, 3866.
5. R. Delgado and J. J. R. Fraústo da Silva, *Talanta* 1982, **29**, 815.
6. M. Tazaki, K. Nita, M. Takagi and K. Ueno, *Chem. Lett.* (*Jpn*) 1982, 571.
7. P. Gans, A. Vacca and A. Sabatini, *Talanta* 1974, **21**, 53; *Inorg. Chim. Acta* 1976, **18**, 237.
8. A. Sabatini and A. Vacca, *Coord. Chem. Rev.* 1975, **16**, 161.
9. R. N. Sylva and M. R. Davidson, *J. Chem. Soc., Dalton Trans.* 1979, 465.
10. E. Luboch, A. Cygan and J. F. Biernat, *Inorg. Chim. Acta* 1983, **68**, 201.

11. A. Martell and R. Smith, *Critical Stability Constants*, Vol. 1. Plenum Press, New York (1974).
12. T. Uechi, I. Ueda, M. Tazaki, M. Tagaki and K. Ueno, *Acta Cryst.* 1982, **B38**, 433.
13. E. J. Billo, *Inorg. Nucl. Chem. Lett.* 1975, **11**, 491.
14. H. Irving and R. J. P. Williams, *J. Chem. Soc.* 1953, 3192.
15. F. A. Cotton and G. Wilkinson, *Advanced Inorganic Chemistry*, 4th edn, pp. 686, 768. John Wiley, New York (1980).
16. R. Louis, I. Arnaud-Neu, R. Weiss and M. J. Schwing-Weill, *Inorg. Nucl. Chem. Lett.* 1977, **13**, 31.
17. A. B. Blake and F. A. Cotton, *Inorg. Chem.* 1964, **3**, 5.
18. P. Paoletti and M. Ciampolini, *Inorg. Chem.* 1967, **6**, 64.
19. R. J. P. Williams, *J. Mol. Catal.* 1985, **30**, 1.

Polyhedron Vol. 6, No. 1, pp. 39–44, 1987
Printed in Great Britain

0277–5387/87 $3.00+.00
Pergamon Journals Ltd

COPPER COMPLEXES OF PYRIDINE 2-ALDEHYDE AND 2-ACETYLPYRIDINE THIOSEMICARBAZONES

C. F. BELL,* K. A. K. LOTT and N. HEARN

Department of Chemistry, Brunel University, Middlesex UB8 3PH, U.K.

(*Received* 3 *July* 1986)

Abstract—Copper complexes of two heterocyclic thiosemicarbazones were synthesized and characterized by magnetic-moment measurement, and ESR and IR spectroscopy. Implications of the magnetic and spectral data in relation to the structures of the complexes are discussed.

The applications of thiosemicarbazones in the analysis of metals have been well-known for many years. Recent reviews have summarized developments in analytical aspects[1] and structural information on transition-metal complexes of thiosemicarbazones.[2,3] Dithizone (1,5-diphenyldithiocarbazone) is one of the most versatile of all analytical reagents for metals, and our knowledge of its chelating properties and those of the thiosemicarbazone moiety in related ligands owes much to the pioneering work of Professor Harry Irving and co-workers.[4]

Biological activity associated with thiosemicarbazones was first reported[5] in 1946. Their action as antimicrobial and antiviral agents has been reviewed recently by Levinson,[6] and Perrin and Stünzl.[7] In some cases, it is clear that the highest *in vivo* activity is associated with a metal complex rather than the thiosemicarbazone itself.[6] Thus, although the thiosemicarbazone of pyridine 2-carbaldehyde (also known as 2-formylpyridine thiosemicarbazone and abbreviated below as HPATS) has marked anti-tumour activity,[8] its copper complex, $Cu(PATS)^+$, is much more potent, as determined by single-cell survival of Chinese hamster ovary cells.[9] Again, the anti-tumour activity *in vivo* and the cytotoxicity *in vitro* of the agent 3-ethoxy-2-oxobutyraldehyde bisthiosemicarbazone (KTS) is believed to depend on specific and unique properties of its copper(II) chelate, such as its basicity and its interaction with other ligands, rather than on the sequestering action of the ligand itself.[10] There is little information on the structures of transition-metal complexes of HPATS and related ligands in the literature which can be related to their biological properties. We have now studied in some detail the reaction products between copper compounds and HPATS [and of 2-acetylpyridine thiosemicarbazone (MePATS)], and now report on some of their magnetic and spectroscopic properties. Both ligands act as tridentate chelators, via N(1), N(2) and S donors (**I**).

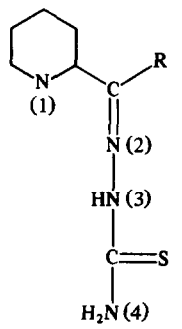

I R = H, HPATS: R = CH_3, MeHPATS

EXPERIMENTAL

Syntheses

HPATS was prepared and purified by the procedure of Hemmerich *et al.*[11] M.p. (after recrystallization from methanol) = 209°C (lit. = 210°C).

* BA (Part II) Oxford (1949–1950) and D.Phil. (1950–1952), both supervised by Professor Irving, and subsequently at Brunel University, Uxbridge. Author to whom correspondence should be addressed.

MePATS was prepared similarly using 2-acetylpyridine. M.p. = 158°C [after recrystallization from 1 : 1 (v/v) ethanol–water] (lit. = 160°C).

(Pyridine-2-carbaldehyde thiosemicarbazone) copper(II) nitrate, $Cu(HPATS)(NO_3)_2$, was made by using the method of Ablov *et al.*[12] for the analogous complex of 8-quinoline aldehyde thiosemicarbazone. It was isolated as a blue-green crystalline solid and purified by solution in water containing a little nitric acid, filtration and then the addition of KNO_3 solution to the filtrate to precipitate the complex. Analysis: Cu, 16.9% [$Cu(HPATS)(NO_3)_2$ requires 17.3%].

(Pyridine 2-carbaldehyde thiosemicarbazone) copper(II) dichloride, $Cu(HPATS)Cl_2$, was prepared by the addition of a hot ethanolic solution of copper(II) chloride (0.0166 mol dm^{-3}) to an equimolar amount of HPATS in solution in *n*-butyl acetate under reflux. An olive-green precipitate formed immediately, which was filtered off after cooling the mixture, and then washed successively with small portions of ethanol and diethylether. M.p. = 220°C. Analysis: C, 26.9; H, 2.8; N, 17.7; Cl, 22.8; Cu, 19.1%. $Cu(HPATS)Cl_2$ requires: C, 26.7; H, 2.5; N, 17.8; Cl, 22.5; Cu, 20.2%.

(Pyridine 2-carbaldehyde thiosemicarbazonato) copper(II) acetate, $Cu(PATS)OCOCH_3$, was prepared by the methods of Hemmerich *et al.*[11] and Antholine *et al.*[13] The first procedure gave the purer product, a dark-green solid with black reflex. M.p. *ca* 228°C (decomp.). It was recrystallized from DMF. Analysis: C, 35.8; H, 3.4; N, 19.2; S, 10.6%. $Cu(PATS)OCOCH_3$ requires: C, 35.8; H, 3.3; N, 18.6; S, 10.6%.

(Pyridine 2-carbaldehyde thiosemicarbazonato) copper(II) chloride, Cu(PATS)Cl, was prepared according to Bhoon[14] by refluxing equimolar solutions in DMF of copper(II) chloride and HPATS. Over a period of 1 h under reflux, a green precipitate formed initially, but slowly dissolved to give a deep-green solution. Excess solvent was distilled off under reduced pressure and water added to the concentrate to precipitate the complex as a dark-brown solid. It was filtered, washed well with water and acetone, and finally dried *in vacuo* over P_2O_5. Although appreciably soluble in DMF and DMSO, it did not prove possible to recover the complex without some decomposition. M.p. = 220–222°C (decomp.). Analysis: C, 30.8; H, 2.5; N, 20.0; Cl, 12.8; Cu, 20.9%. Cu(PATS)Cl requires: C, 30.22; H, 2.52; N, 20.18; Cl, 12.54; Cu, 20.20%.

(Pyridine 2-carbaldehyde thiosemicarbazonato) copper(II) thiocyanate, Cu(PATS)SCN, was precipitated by the addition of an equimolar amount of NH_4SCN in aqueous solution to $Cu(HPATS)(NO_3)_2$ in water. It was isolated as a yellowish-green, paramagnetic solid. Analysis: C, 31.7; H, 2.6; N, 23.9; S, 21.8%. Cu(PATS)SCN requires: C, 31.9; H, 2.3; N, 23.3; S, 21.3%.

(Pyridine 2-carbaldehyde thiosemicarbazone) copper(I) chloride, Cu(PATS)Cl, was prepared by Bhoon's method using copper(I) chloride freshly prepared by the reduction of an aqueous solution of copper sulphate with SO_2 in the presence of dissolved sodium chloride. The complex was isolated as a diamagnetic black solid decomposing at *ca* 240°C. It was not purified further. Analysis: C, 28.5; H, 2.4; N, 18.7; Cu, 22.8%. Cu(HPATS)Cl requires: C, 30.1; H, 2.9; N, 20.1; Cu, 22.5%.

(2-Acetylpyridine thiosemicarbazonato) copper(II) acetate, $Cu(MePATS)OCOCH_3$, and (2-acetylpyridine thiosemicarbazone) copper(II) dichloride, $Cu(MePATS)Cl_2$, were prepared in a similar manner to the HPATS complexes in small quantity for ESR measurements.

ESR spectra of powdered samples and solutions in DMSO at room temperature, and of frozen solutions in DMSO at 77 K, were measured using a Varian E3 ESR spectrometer with DPPH as the reference material. Magnetic-susceptibility measurements were performed by the Gouy method at room temperature. IR spectra were recorded as KBr discs using a Unicam SP2000 IR spectrophotometer. C, H, N, Cl and S analyses were performed by Butterworth Laboratories Ltd, Teddington, Middx. Cu analyses were carried out on aqueous solutions, prepared by dissolving the complexes in dilute nitric acid, using a Perkin–Elmer 2380 atomic absorption spectrometer.

RESULTS AND DISCUSSION

The stoichiometry of the complexes prepared appears to indicate that copper is coordinated by the neutral ligand in $Cu(HPATS)(NO_3)_2$, $Cu(HPATS)Cl_2$ and Cu(I)(HPATS)Cl, and by the singly-charged anion formed by loss of a proton from the thiol form of the ligand in $Cu(PATS)OCOCH_3$, Cu(PATS)Cl and Cu(PATS)(SCN). However, the complex $Cu(PATS)^+$ is known to be very stable ($\log K = 16.90$), and shows[15] no tendency to dissociate at pH values as low as 1.4. Some changes in the electronic spectrum of CuL^+ in aqueous solution from pH 4 to 2[15,16] are associated with protonation of the ligand and indicate that $Cu(HPATS)^{2+}$ is a reasonably strong acid. Complexes containing the neutral ligand therefore only result from reactions in weakly acidic aqueous media or non-aqueous solvents of low polarity.

Magnetic and ESR parameters are given in Table 1. The magneton numbers of $Cu(PATS)OCOCH_3$,

Table 1. Magneton number (X) for Cu complexes (293 K) and ESR data (on solutions in DMSO at 77 K)

Compound	$X_{293\,K}$	$g_\parallel$	$A_\parallel^{Cu}$ (G)	$A_{iso}^{Cu\,a}$ (G)
$Cu(HPATS)Cl_2$	1.51	2.18	155	72
$Cu(PATS)OCOCH_3$	1.83	2.18	175	75
Cu(PATS)Cl	1.89	2.17	163	75
Cu(PATS)SCN		2.18	165	
$Cu(MeHPATS)Cl_2$		2.18	155	75
$Cu(MePATS)OCOCH_3$	1.89	2.16	180	
	$g_\perp$ estimated as ~ 2.03			

[a] Estimated from solution spectra at room temperature.

Cu(PATS)Cl and $Cu(MePATS)OCOCH_3$ all lie close to the spin-only value (1.73) for a d^9-ion, and are consistent with planar or nearly-planar coordination around copper. The ligand is known[2] to coordinate Ni(II) with two sets of coplanar NNS donor atoms to form two chelate rings in $Ni(PATS)_2$, so it is likely that Cu(II) shows four-coordination in these complexes with the last position occupied by an O or Cl donor. There is no magnetic evidence here for any Cu–Cu interaction.

The magneton number of 1.51 recorded for $Cu(HPATS)Cl_2$ is significantly below the spin-only value, perhaps because of metal–metal interaction. The organic ligand should be a tridentate chelator, so it is probable that the Cu(II) ion is in some kind of distorted five-coordinate geometry in this complex.

The ESR spectra (Figs 1 and 2) show similar features to those reported by Antholine *et al.*[15] for solutions containing $Cu(PATS)^+$ ions in 0.1 M KCl and 30% DMSO at 77 K. These workers reported $g_\parallel = 2.204$ and $A_\parallel^{Cu} = 186$ G for this species. For a related complex, CuKTS, doped in Ni, ESR parameters are:[17] $g_\parallel = 2.13$, $g_\perp = 2.035$, and $A_\parallel^{Cu} = 184$ G at 77 K; the value of A_{iso}^{Cu} was estimated to be 87 G. Our values for $g_\parallel$ lie in the range 2.16–2.18, i.e. smaller than reported for $Cu(PATS)^+$. In the case of the four-coordinate complexes, $A_\parallel^{Cu}$ values lie between 163 and 180 G, and the differences probably reflect the different nature of the ligand atom in the fourth coordination position in DMSO solutions. With $Cu(PATS)OCOCH_3$ and $Cu(MePATS)OCOCH_3$, $A_\parallel^{Cu}$ values are close to those reported by Antholine *et al.*[15] for KCl–DMSO solutions of the complex $Cu(PATS)OCOCH_3$. The replacement of acetate by the chloride or thiocyanate ligands produces lower values of $A_\parallel^{Cu}$ because of the greater electronegativity of these ligands. In DMSO solution, it is very likely that solvent molecules coordinate the metal above and below the plane to give a tetragonally-distorted six-

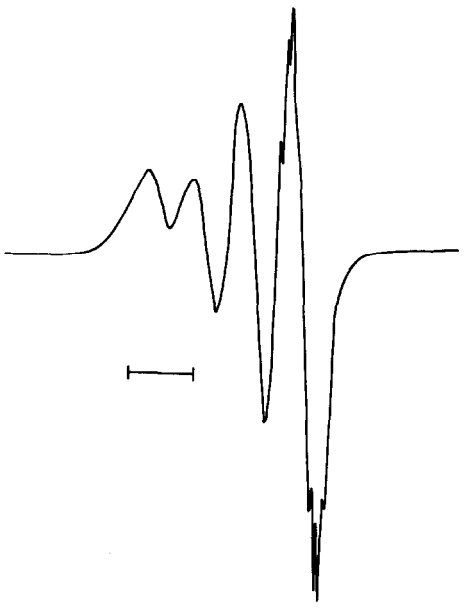

Fig. 1. X-band ESR spectrum of $Cu(MePATS)Cl_2$ dissolved in DMSO ($T = 293$ K). Bar represents 100 G.

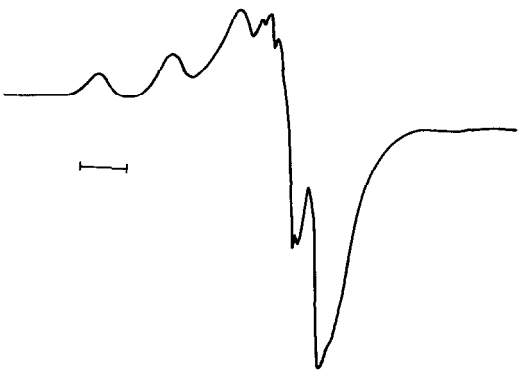

Fig. 2. X-band ESR spectrum of $Cu(MePATS)Cl_2$ dissolved in DMSO ($T = 77$ K). Bar represents 100 G.

Table 2. IR spectral bands (cm^{-1}) involving donor atoms (excluding heterocyclic N)

HPATS	$Cu(HPATS)(NO_3)_2$	$Cu(HPATS)Cl_2$	$Cu(PATS)OCOCH_3$	Cu(PATS)Cl	Cu(PATS)SCN	Cu(I)(HPATS)Cl	Assignment[a]
3440s	3380s	3350m	3410m	3460m	3400s	3280m	
3270s	3290m		3295w	3280m	3295w		$\nu(NH)+\nu(NH_2)$
3163s	3150s	3100m	3165m	3130m	3100m	3100m	
	3030s	3030w					
1530s	—	1520w	—	1535m	—	—	$\delta(NH)+\nu(CN)$
1470s	1480s	1475m	1485vw	1485s	1480m	1480m	$\nu(CS)+\nu(CN)+\delta(NH_2)$
		1455m					
1300s	1310m	1300m	1300w	1290m	1290m	1290w	$\nu(CS)+\nu(CN)+\delta(NH_2)$
1150s	1160s	1195s	1170s	1170s	1170s	1170m	
1120s	1102s	1130w	1155w	1155m	1150s	1160sh	$\delta(NH_2)$ or ν(N—C—S)
		1102s	1115w				
825s	825m	835w	815vw	—	815w	—	ν(CS)
780s	795s	775s	790s	780s	775s	780w	

[a] Assignments according to Refs 2, and 19–21.

coordination. It is noteworthy that, for Cu(HPATS)Cl_2 and Cu(MeHPATS)Cl_2, $A_{\parallel}^{Cu}$ is lower still (155 G). This may be due to the different coordination number, but Hathaway[18] has cautioned against the use of ESR spectral data to try to develop a firm criterion of the stereochemistry of Cu(II) complexes because of the variety of regular and distorted geometries the metal can show on coordination. In general, our spectra do not show the hyperfine splitting from the two nitrogen donors. In Cu(MeHPATS)Cl_2, the spectrum shows clear evidence for at least a seven-line hyperfine splitting pattern in accordance with the presence of two non-equivalent nitrogens bonded to Cu. If they were equivalent, only a five-line hyperfine structure would be expected.

IR spectral data are summarized in Table 2. In HPATS itself vibrational stretches of the —NH and —NH_2 groups give rise to a multiple absorption band between 3160 and 3440 cm^{-1}. For most complexes studied, these move to lower frequencies as a result of coordination. The ligand shows strong multiple absorption centred at 1530 cm^{-1}, probably a major contributor being a combination of a CN stretch coupled with an N—H deformation mode. This disappears in most complexes, evidence of the loss of the N—H proton upon complexation. The band noted at 1535 cm^{-1} in Cu(PATS)Cl does not have the multiple structure that characterizes the ligand spectrum in this frequency region and its appearance does not necessarily conflict with the belief that the proton must have been lost on complex formation.

Following Campbell and Greszkowiak,[20] we have identified ligand bands at 1470 and 1300 cm^{-1} with a combination of CS and CN stretching and NH_2 deformation modes. The 1470-cm^{-1} band moves to slightly higher frequencies in the complexes.

Thiosemicarbazones typically show a strong absorption around 825 cm^{-1}. With the exception of Cu$(NO_3)_2$(HPATS), other complexes show virtually no band in this region. Other authors have noted the shift of this band to lower frequencies by about 100 cm^{-1} in the ligand complexes, and accordingly have assigned it to a CS stretching mode. This would certainly be strongly affected by S-bonding to a metal atom. If this assignment is correct, then CuS bonding is present in all the complexes reported except Cu(HPATS)$(NO_3)_2$. The nitrate does have atypical properties, being freely water-soluble, and thus possesses salt-like characteristics. At most, it would appear that the ligand is bound only by N(1) and N(3). Possibly, even N(1) is not involved, for it is this heterocyclic N that is protonated in acid solution,[22] i.e. the sort of solvent medium from which this complex is precipitated. Absorption bands arising from pyridine ring vibrations are not tabulated. Those found at 1590 and 1570 cm^{-1} in the ligand HPATS (usually identified as pyI and pyII bands) uniformly move to higher frequencies in all complexes. On this evidence, it appears that the heterocyclic N is bonded to the copper in every case. The IR spectrum of Cu(I)(HPATS)Cl shows very little difference from those of Cu(PATS)Cl and Cu(PATS)SCN with regard to the absorption bands of the organic ligand, indicating that a change in the oxidation state of the metal has little effect on the bonding within the chelate rings. A possible mechanism[9] for the anti-tumour activity of $Cu(PATS)^+$ is reduction to Cu(I) complex by thiols, followed by release of HPATS, and then the binding of this to inhibit ribonucleoside diphosphate reductase action. Alternatively, the complex itself may function by binding donor groups *in vivo* in the fourth coordination position round copper. Further study of copper(I)–HPATS complexes with other ligands would be helpful in the elucidation of the mechanism of biological action.

REFERENCES

1. R. B. Singh, B. S. Garg and R. P. Singh, *Talanta* 1978, **25**, 619.
2. M. J. M. Campbell, *Coord. Chem. Rev.* 1975, **15**, 279.
3. S. Padhyé and G. B. Kauffman, *Coord. Chem. Rev.* 1985, **63**, 127.
4. H. M. N. H. Irving, *Dithizone*. Analytical Science Monograph No. 5, The Chemical Society, London (1977).
5. G. Domagk, R. Behnich, F. Mietzsch and H. Schmidt, *Naturwissenschaften* 1946, **33**, 315.
6. W. E. Levinson, *Antibiot. Chemother.* 1980, **27**, 288.
7. D. D. Perrin and H. Stünzl, In *Metal Ions in Biological Systems* (Edited by H. Sigel), Vol. 14, p. 207. Marcel Dekker, New York.
8. R. W. Brockman, J. R. Thompson, M. J. Bell and H. E. Skipper, *Cancer Res.* 1956, **16**, 167.
9. W. E. Antholine, P. Gunn and L. E. Hopwood, *Int. J. Radiat. Oncology, Biol. Phys.* 1981, **7**, 491.
10. H. G. Petering and G. J. Van Giessen, In *Biochemistry of Copper* (Edited by P. Peisach, P. Aisen and W. E. Blumberg), p. 197. Academic Press, New York (1966).
11. P. Hemmerich, B. Prys and H. Erlenmeyer, *Helv. Chim. Acta* 1958, **41**, 2058.
12. A. V. Ablov, N. V. Gerbeleu and B. T. Oloi, *Russ. J. Inorg. Chem.* 1971, **16**, 99.
13. W. E. Antholine, J. M. Knight and D. H. Petering, *J. Med. Chem.* 1976, **19**, 339.
14. N. K. Bhoon, *Polyhedron* 1983, **2**, 365.
15. W. E. Antholine, J. M. Knight and D. H. Petering, *Inorg. Chem.* 1977, **16**, 569.

16. J. M. Cano Pavon and P. Bendito, *Inf. Quim. Anal.* 1972, **26**, 20.
17. W. E. Antholine, R. Basosi, J. S. Hyde, S. Lyman and D. H. Petering, *Inorg. Chem.* 1984, **23**, 3543.
18. B. J. Hathaway, *Coord. Chem. Rev.* 1983, **52**, 87.
19. M. Mashima, *Bull. Chem. Soc. Jpn* 1964, **37**, 976.
20. M. J. M. Campbell and R. Greszkowiak, *J. Chem. Soc. A* 1967, 396.
21. P. D. Mooney, *Diss. Abstr. Int. B* 1972, **33**, 640.
22. D. J. Leggett and W. A. E. McBryde, *Talanta* 1974, **21**, 1005.

Polyhedron Vol. 6, No. 1, pp. 45–52, 1987
Printed in Great Britain

0277–5387/87 $3.00+.00

INFLUENCE OF THE PROLINE RESIDUE ON THE CO-ORDINATION OF Cu(II) TO PEPTIDES CONTAINING -PRO- AND -PRO-PRO- SUBUNITS

LESLIE D. PETTIT,*† CYNARA LIVERA and IAN STEEL

Department of Inorganic Chemistry, The University, Leeds LS2 9JT, U.K.

MICHEL BATAILLE* and CLAUDE CARDON

Laboratoire de Chimie Biologique, U.A. du CNRS No. 217, Université des Sciences et Techniques de Lille, 59655 Villeneuve d'Ascq, France

and

GRAZYNA FORMICKA-KOZLOWSKA

Institute of Chemistry, University of Wroclaw, 50383 Wroclaw, Poland

(*Received* 3 *July* 1986)

Abstract—The synthesis of the series of peptides identified in the neuropeptide Nereidine, $(Pro\text{-}Pro\text{-}Gly)_n$ where $n = 1$, 2 or 3, is reported together with a potentiometric and spectroscopic study of their complexes with Cu(II) at 25°C and $I = 0.10$ mol dm^{-3} (KNO_3). All three peptides behave similarly, forming [CuL] species at low pH followed by $[CuL_2]$ and, at higher pH, $[CuH_{-1}L]$. This complex involves co-ordination through the amide nitrogen of the first glycine residue forming an eight-membered chelate ring. Increase in the length of the peptide chain (i.e. increasing n from 1 to 2 or 3) does not affect the complexed species formed. The results of a potentiometric study of the Cu(II) complexes of the series of tetrapeptides Pro-Ala-Ala-Ala, Ala-Pro-Ala-Ala, Ala-Ala-Pro-Ala and Ala-Ala-Ala-Pro are also reported. The behave similarly to complexes of the analogous ligands based on glycine, showing an even clearer "break-point" effect in Cu(II) co-ordination.

Cu(II) forms very stable complexes with simple oligopeptides such as tetraglycine. Below pH 5 it co-ordinates through the terminal amino group and neighbouring carbonyl oxygen to give a [CuL] complex with one nitrogen co-ordinated (charges omitted for clarity). Above this pH it is able to deprotonate the amide nitrogens of peptide linkages successively to form N^-—Cu bonds, and give the planar species $[CuH_{-1}L]$ (an NN complex) up to $[CuH_{-3}L]$ (an NNNN complex).[1] The peptide is now locked into a tightly bent conformation. Inclusion of a proline (Pro) residue into the peptide sequence prevents this mode of co-ordination since Pro does not possess an ionizable amide proton; hence it acts as a "break-point" to the co-ordination of Cu(II). This encourages the formation of large chelate rings of up to 17 atoms with the peptides locked in a bent or folded conformation.[2,3] In proteins β-turns (regions where the peptide chain folds back on itself) give the globular structure necessary for biological activity, and it has been shown that Pro is the amino acid residue most frequently responsible for these β-turns.[4] Recent ^{13}C NMR studies of tetrapeptides containing three alanine (Ala) residues with one Pro have confirmed the importance of Pro in the second position of the sequence in the formation of bent or folded conformations.[5] Potentiometric and spectroscopic studies of Cu(II) complexes of the corresponding

* Authors to whom correspondence should be addressed.

† L. D. Pettit was a student at Keble College, Oxford, 1954–1960, where Professor Irving was his tutor in inorganic chemistry, and supervisor for his Part II and D.Phil. Since 1961 he has been at Leeds University, where he is now a Reader and where Professor Irving was his Head of Department from 1961 to 1971.

tetrapeptides containing glycine (Gly) in place of Ala have shown quantitatively how the Cu(II) ion can lock the peptide in this folded conformation.[2,3] Peptides which can act as neurotransmitters frequently contain one or more Pro residues,[6] and it has been suggested that Cu(II) ions could activate these molecules by locking them in biologically active conformations.[7]

To pursue these suggestions we have extended the study of tetrapeptides containing Pro with three Gly residues to cover peptides containing paired Pro residues. The series of peptides of general formula (Pro-Pro-Gly)$_n$ where $n = 1$, 2 or 3, has been synthesized and their Cu(II) complexes studied potentiometrically and spectroscopically. A number of biologically active peptides contain the subunit -Pro-Pro-Gly, e.g. bradykinin, a smooth muscle stimulant, starts with the sequence Arg-Pro-Pro-Gly-···, and the head activator neuropeptide of hydra starts with *p*-Glu-Pro-Pro-Gly-···.[8] One of the simplest sequences containing this subunit is found in the neuropeptide Nereidine which has been isolated from the cerebral ganglion of the polychaete annelid (marine worm) *Nereis*.[9] This peptide shows specific physiological activity in the inhibition of sexual differentiation, and in the somatic changes associated with the epitoky of the worm, and tests are available to examine the activity of model peptide fragments *in vitro* for hormonal activity.[10] The study of the peptide Nereidine gave a fraction which showed a high hormonal activity, and which contained the hexapeptide Pro-Pro-Gly-Pro-Pro-Gly, and the sequence -Gly-Pro-Pro-Gly- appeared to be the active portion.[11] Hence, the peptides selected should be good model compounds.

In addition we have studied the analogues of the tetrapeptides based on Pro-Gly-Gly-Gly but which contain Ala residues instead of the Gly residues.[2] These were chosen because the tetrapeptides are based on optically active amino acids (i.e. L-Ala) rather than the inactive Gly, and so should show a more organized conformation. In addition they have been studied by ^{13}C NMR.[5] Complexes formed between Cu(II) and the tetrapeptides with Pro in positions 1, 3 and 4 (but not in position 2) have previously been studied spectroscopically.[12]

EXPERIMENTAL

Organic syntheses

The peptides based on Pro-Pro-Gly were synthesized by standard liquid-phase methods using Bu^t-OCO-L-Pro (*t*-Boc-Pro), L-Pro-CH_2-Ph·HCl (Pro-Bzl·HCl) and Gly-CH_2-Ph·HCl (Gly-Bzl·HCl) as starting materials. The syntheses are outlined below:

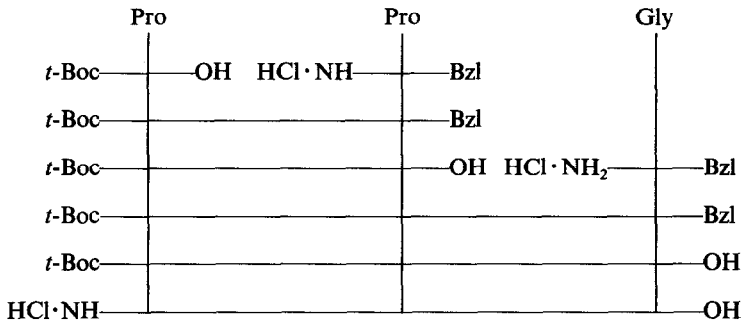

C-protected derivatives (in chloroform solution) were neutralized with triethylamine before coupling. Coupling reagents were dicyclohexylcarbodiimide (Merck) and 1-hydroxybenzotriazole (Aldrich). Benzyl groups were removed by hydrogenolysis using 10% Pd on charcoal as catalyst and *t*-Boc was cleaved using HCl (4 mol dm^{-3}) in dioxan. The tripeptide was purified by gel filtration (Sephadex G 15, eluant, water) and lyophylized. Percentages of amino acid residues (Pro : Gly = 2 : 1) were confirmed by amino acid analysis.

Oligomers of this tripeptide, (Pro-Pro-Gly)$_2$ and (Pro-Pro-Gly)$_3$, were obtained by the same procedure.

The tetrapeptides Pro-Ala-Ala-Ala, Ala-Pro-Ala-Ala, Ala-Ala-Pro-Ala and Ala-Ala-Ala-Pro were prepared as described previously.[5]

Potentiometric studies

Stability constants for H^+ and Cu^{2+} complexes were calculated from titration curves carried out at 25°C using total volumes of 1.5–2 cm^3. Alkali was added from a 0.1- or a 0.25-cm^3 micrometer syringe which had been calibrated by both weight titration and the titration of standardized materials. Changes in pH were followed using a glass electrode calibrated in H^+ concentrations with $HClO_4$.[13] All solutions were of ionic strength 0.10 mol dm^{-3} (KNO_3) and peptide concentrations of 0.003 mol dm^{-3}. Cal-

culations were made with the aid of the SUPERQUAD computer program.[14] This allows for the refinement of total ligand concentrations, and was able to confirm the agreement between calculated values and those found from Gran plots.[15] A further advantage of this technique is that the concentration of free acetate, a frequent impurity in peptide samples, could be measured and allowance made for this in the calculations.[3] The only peptide containing a significant concentration of acetate ions was Pro-Pro-Gly. The validity of the technique is confirmed by the observation that the stability constants calculated for this ligand are entirely compatible with those found for the comparable ligands. In all cases duplicate or triplicate titrations were carried out at Cu : L ratios of 1 : 1 and 1 : 2. The standard deviations quoted were computed by SUPERQUAD and refer to random errors only. They give, however, a good indication of the importance of the particular species in the equilibrium.

Spectroscopic studies

Solutions were of the same concentrations as those used in the potentiometric studies. Absorption spectra were recorded on a Beckman UV5240 spectrophotometer and circular dichroism (CD) spectra were measured on an automatic recording spectropolarimeter, JASCO-J-20. All CD spectra are expressed in terms of $\Delta\varepsilon$ ($\varepsilon_l - \varepsilon_r$). Electron paramagnetic resonance spectra were obtained on a JEOL JES-ME-3X spectrometer at liquid-nitrogen temperature and 9.13 GHz.

RESULTS AND DISCUSSION

Peptides with two Pro residues: the Pro-Pro-Gly series

The series of three peptides Pro-Pro-Gly, (Pro-Pro-Gly)$_2$ and (Pro-Pro-Gly)$_3$ was studied since these are the fragments studied in work on Nereidine.[11]

Protonation constants are given in Table 1. Values for the protonation of the amino group are almost independent of chain length, and only a little above that for Pro-Gly, as would be expected. Protonation of the carboxylate is favoured in the longer chains, possibly as a result of conformational differences, but the small differences found cannot influence the stabilities of the copper complexes.

Cu(II) complex stability constants are also given in Table 1, together with those for Pro-Gly,[16] while the species distribution curves for 1 : 1 and 3 : 1 peptide : metal mixtures are given in Fig. 1. Spectroscopic data for 3 : 1 peptide : Cu(II) mixtures are given in Table 2.

With Pro-Pro-Gly at low pH the first complex to form is the [CuL] species. This will be co-ordinated through the terminal amino nitrogen and the oxygen of the neighbouring peptide carbonyl group to give a 1N complex, comparable in structure to that found with, for example, Gly-Gly. However with these ligands containing the Pro-Pro fragment the [CuL] species has a much larger pH range of existence than with Gly-Gly, as demonstrated in Fig. 1. This is a result of the "break-point" effect of the Pro residue in position 2. Since this residue does not possess an ionizable peptide amide proton it cannot form a [CuH$_{-1}$L] complex comparable to that formed by Gly-Gly. Rather the only way to form a chelated complex through a peptide amide nitrogen is to bond to the peptide link of the Gly residue, the third residue in the chain. The species so formed will then be an NN complex spanning the first and third residues to form an eight-membered chelate ring as shown in Fig. 2. Co-ordination through the carbonyl oxygen of the first peptide linkage (as in [CuL]) is impossible on steric ground when both Pro residues are of the same chirality. The species so formed would be expected to be less stable than the [CuH$_{-1}$L] species with Gly-Gly but, as with Ala-Pro-Ala-Ala studied below, the conformation of the Pro residue would bring the co-ordinating centres sufficiently close together to allow easy bonding to the Cu(II). This chelation is represented quantitatively by $\log K_1'$ in Table 1, and is comparable to that with Ala-Pro-Ala-Ala.

Since the [CuH$_{-1}$L] species does not possess any further ionizable peptide protons, the [CuH$_{-2}$L] species which forms above pH 10 must be the result of hydrolysis of a co-ordinated water molecule, and is therefore still an NN complex. This is supported by the value for the protonation constant ($\log K_2' = 9.96$), which is very close to that found for the comparable reaction with Ala-Ala-Ala-Pro (9.83) (see Table 1). As an alternative to the formation of a [CuH$_{-1}$L] species, [CuL] could co-ordinate a second peptide molecule to give the bis complex [CuL$_2$]. This species would be an NN complex but would not contain any Cu—N$^-$ covalent bonds. Such a species formed between pH 6 and 8 in 1 : 1 peptide : Cu(II) mixtures where it was only a minor species in the absence of excess peptide (see Fig. 1), and was similar in importance to the comparable species formed by Ala-Pro-Ala-Ala (see Fig. 3). In the presence of excess peptide (e.g. 3 : 1 mixtures) this bis complex becomes the major species over the pH range 7–9.5, and the [CuH$_{-1}$L] complex is never predominant (see Fig. 1). As a result the spectroscopic data in Table 2 show charge-transfer

Table 1. Proton and Cu(II) complex stability constants at 25°C and $I = 0.10$ mol dm^{-3} (KNO_3), with estimated standard deviations in parentheses

Peptide	H^+ complexes		
	$\log K_{HL}$	$\log \beta_{H_2L}$	$\log K_{H_2L}$
Pro-Pro-Gly	9.15(1)	12.32(1)	3.17
(Pro-Pro-Gly)$_2$	9.13(1)	12.57(2)	3.44
(Pro-Pro-Gly)$_3$	9.11(1)	12.48(3)	3.37
Pro-Gly[a]	9.06	12.16	3.10
Pro-Ala-Ala-Ala	8.37(1)	11.5(1)	3.1[b]
Ala-Pro-Ala-Ala	8.283(3)	11.594(7)	3.311
Ala-Ala-Pro-Ala	8.202(4)	11.542(8)	3.340
Ala-Ala-Ala-Pro	8.200(3)	11.361(6)	3.161
Ala-Ala-Ala[c]	8.08	11.44	3.36
Ala-Ala-Ala-Ala[d]	8.13	11.65	3.52

	Cu^{2+} complexes, Log β values				
	[CuL]	[CuH$_{-1}$L]	[CuH$_{-2}$L]	[CuH$_{-3}$L]	[CuL$_2$]
Pro-Pro-Gly	6.05(2)	−1.75(5)	−11.71(3)		11.00(3)
(Pro-Pro-Gly)$_2$	6.27(1)	−1.38(3)	−11.49(1)		11.19(2)
(Pro-Pro-Gly)$_3$	5.83(4)	−1.92(6)	−11.86(4)		10.63(10)
Pro-Gly[a]	6.64	2.63	−6.85		
Pro-Ala-Ala-Ala	5.59(1)	−0.21(3)	−7.47(4)	−16.1(1)	
Ala-Pro-Ala-Ala	5.01(1)	−2.64(4)	−11.69(3)	−21.35(3)	9.04(1)
Ala-Ala-Pro-Ala	5.33(3)	−0.20(1)	−10.18(4)	−19.70(2)	
Ala-Ala-Ala-Pro	5.27(4)	−0.36(2)	−7.56(2)	−17.39(3)	
Ala-Ala-Ala[c]	4.64	0.18	−6.45	−18.75	
Ala-Ala-Ala-Ala[d]	4.77	−0.45	−8.09	−17.33	

	Stepwise protonation constants of complexes[e]		
	$\log K'_1$	$\log K'_2$	$\log K'_3$
Pro-Pro-Gly	7.81	9.96	
(Pro-Pro-Gly)$_2$	7.65	10.11	
(Pro-Pro-Gly)$_3$	7.75	9.94	
Pro-Gly	4.01	9.48	
Pro-Ala-Ala-Ala	5.80	7.26	8.6
Ala-Pro-Ala-Ala	7.65	9.05	9.66
Ala-Ala-Pro-Ala	5.53	9.98	9.52
Ala-Ala-Ala-Pro	5.63	7.92	9.83
Ala-Ala-Ala-Ala[d]	5.22	7.64	9.24

[a] Reference 16.
[b] Unreliable since standard deviation large.
[c] Reference 17.
[d] Reference 18.
[e] $K'_1 = [CuL]/[CuH_{-1}L][H]$, $K'_2 = [CuH_{-1}L]/[CuH_{-2}L][H]$, and $K'_3 = [CuH_{-2}L]/[CuH_{-3}L][H]$.

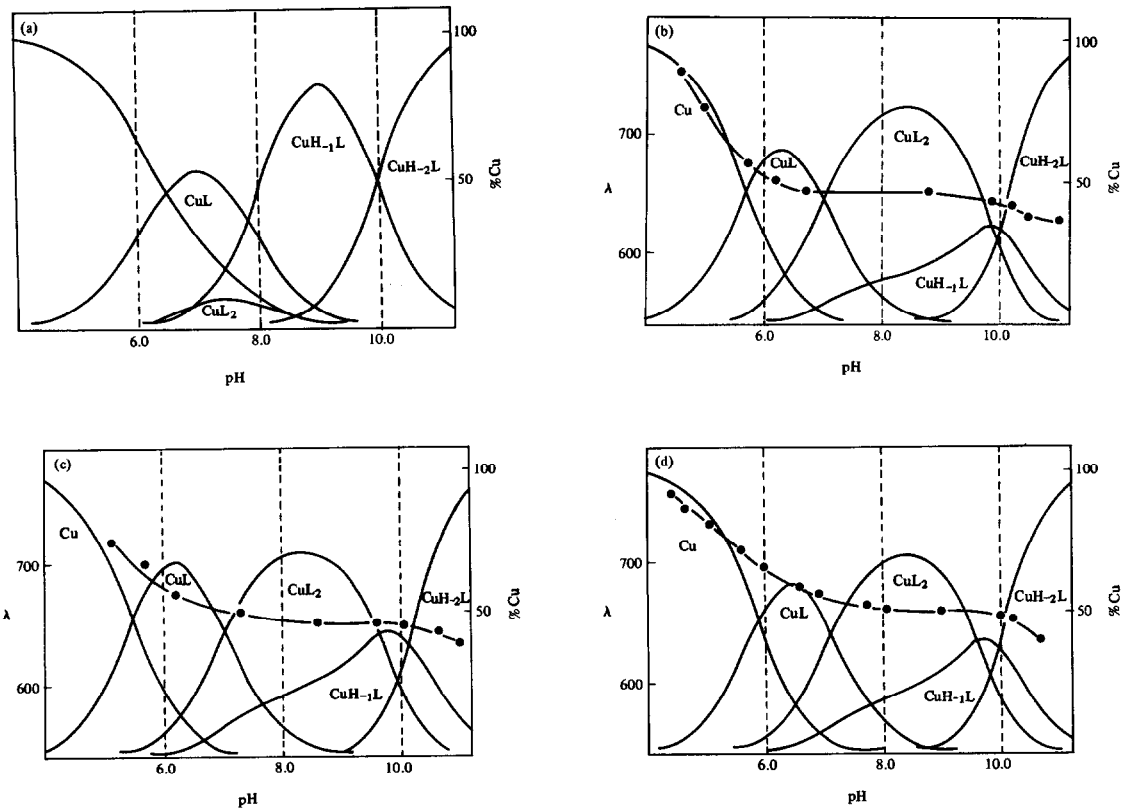

Fig. 1. Species distribution curves for Cu(II) complexes [0.001 mol dm^{-3} Cu(II)]: (a) Pro-Pro-Gly : Cu = 1 : 1, (b) Pro-Pro-Gly : Cu = 3 : 1 with *d–d* band maxima, (c) $(Pro\text{-}Pro\text{-}Gly)_2$: Cu = 3 : 1 with *d–d* band maxima, and (d) $(Pro\text{-}Pro\text{-}Gly)_3$: Cu = 3 : 1 with *d–d* band maxima.

bands characteristic of Cu ← NH= co-ordination only (280–290 nm), although the band in the visible region (630–650 nm) is characteristic of NN co-ordination to Cu(II). It was difficult to gather reliable spectroscopic data above pH 9.5 as a result of solubility problems. The same problem arose at pH 10 in the potentiometric titrations, suggesting that the species $[CuH_{-2}L]$ has a low solubility in water.

The spectroscopic studies therefore confirm the potentiometric results. This is demonstrated for the *d–d* transition energy in Fig. 1, where it is seen that the flat portion of the curve of absorption maximum against pH coincides closely with the range of existence of the NN complexes. This is also supported by the ESR spectra reported in Table 2.

Results for the Cu(II) complexes of the peptides $(Pro\text{-}Pro\text{-}Gly)_2$ and $(Pro\text{-}Pro\text{-}Gly)_3$ are surprisingly similar to those with Pro-Pro-Gly. The spectra are almost completely superimposible, and the stability constants are remarkably similar, giving very similar species distribution curves (see Fig. 1). There are small differences in the magnitudes of the constants, probably as a result of differing chain formations as the peptide chain length increases, but these have only a minor effect on the species actually found. These results suggest that the mode of co-ordination is independent of chain length and that the only co-ordinating centres are the amino-terminal nitrogen atom and the peptide nitrogen of the first Gly residue. At first sight this is surprising since co-ordination through the carboxylate oxygen would

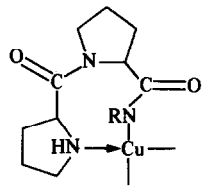

R = $CH_2CO_2^-$

Fig. 2. Donor centres in the $[CuH_{-1}L]$ complex of Pro-Pro-Gly. Co-ordination around the Cu(II) ion may be either *cis* or *trans*, although *trans* co-ordination introduces considerable strain. For conformational reasons co-ordination of the carboxylate oxygen also introduces strain.

Table 2. Spectroscopic data for Cu(II) complexes of peptides containing the Pro-Pro- subunit: peptide : Cu(II) = 3 : 1

Peptide	pH	Major species	Visible λ (nm) (ε)	CD λ (nm) [$\Delta\varepsilon$ ($\varepsilon_l - \varepsilon_r$)]	ESR $A_\parallel$ (G)	ESR $g_\parallel$
Pro-Pro-Gly	4.7–6.0	[CuL]		654 (−0.003) 270 (−0.03)	146	2.328
	6.5–9.5	[CuL_2]	650 (105)	680 (+0.004) 535 (−0.001) 280 (−0.02)	160	2.271
	> 10	[$CuH_{-2}L$]	630 (60)	670 (−0.005) 290 (−0.007)	170	2.265
$(Pro\text{-}Pro\text{-}Gly)_2$	5.0–6.0	[CuL]		685 (−0.01) 280 (−0.01)	150	2.321
	6.5–9.5	[CuL_2]	650 (95)	670 (+0.003) 560sh (+) 280 (−0.05)	160	2.269
	> 10	[$CuH_{-2}L$]	630 (70)	690 (−0.006) 280 (−0.02)	172	2.262
$(Pro\text{-}Pro\text{-}Gly)_3$	5.0–6.5	[CuL]		665 (−0.005) 272 (−0.03)	152	2.318
	6.5–9.0	[CuL_2]	660 (105)	680 (+0.002) 580 (−0.001) 280 (−0.04)	158	2.270
	> 10	[$CuH_{-2}L$]	625 (70)	675 (−0.005) 280 (−0.02)	170	2.260

be expected in the [$CuH_{-1}L$] complex of Pro-Pro-Gly, but not in those of the hexa- and nonapeptides. However, a study of scale models shows that this carboxylate can co-ordinate only by introducing considerable strain into the chelate ring as a result of the conformation of the two Pro rings which force the Gly terminal away from potential planar co-ordination sites on the copper (see Fig. 2). Hence, the thermodynamic contribution of carboxylate co-ordination would be small. In all cases the proton ionization to give the [$CuH_{-2}L$] species is a result of water hydrolysis, hence the values for this ionization (e.g. K'_2) are very similar.

Peptides with one Pro residue: the Pro-Ala-Ala-Ala series

Protonation constants are presented in Table 1 in addition to those of Ala-Ala-Ala[17] and Ala-Ala-Ala-Ala.[18] The value of $\log K_{HL}$ (i.e. imino or amine protonation) is greatest with the Pro residue in position 1 of the tetrapeptide chain, and gradually falls to a "base" value of $\log K_{HL} = 8.20$ as the Pro residue is moved along the chain. This value is close to that for Ala-Ala-Ala-Ala (8.13).[18] It has been shown by ^{1}H NMR[19] and IR[20] techniques that, in organic solvents, the folded conformation of alanine oligopeptides predominates, and that di- and tripeptides containing alanine in their zwitterionic forms adopt intramolecularly hydrogen bonded folded conformations even in aqueous solution.[21] More recently a combined CD and ^{13}C NMR investigation has shown that the presence of a Pro residue in positions 2 and 4 of a tetrapeptide favours the formation of folded conformations, while Pro in position 3 favours unfolding. Ionization was accompanied by a distinct increase in the amount of folded conformation independently of the position of the Pro residue within the tetrapeptide chain.[5] This could be the source of variations in carboxylate protonation constants, although the value for Pro-Ala-Ala-Ala does seem to be abnormally low. However, with this tetrapeptide the statistics of the computer fit were poor below pH 4, although they were good above this value. Errors in the value for K_{H_2L} would have no influence on stability constants of the copper complexes.

Cu(II) complex stability constants are also given

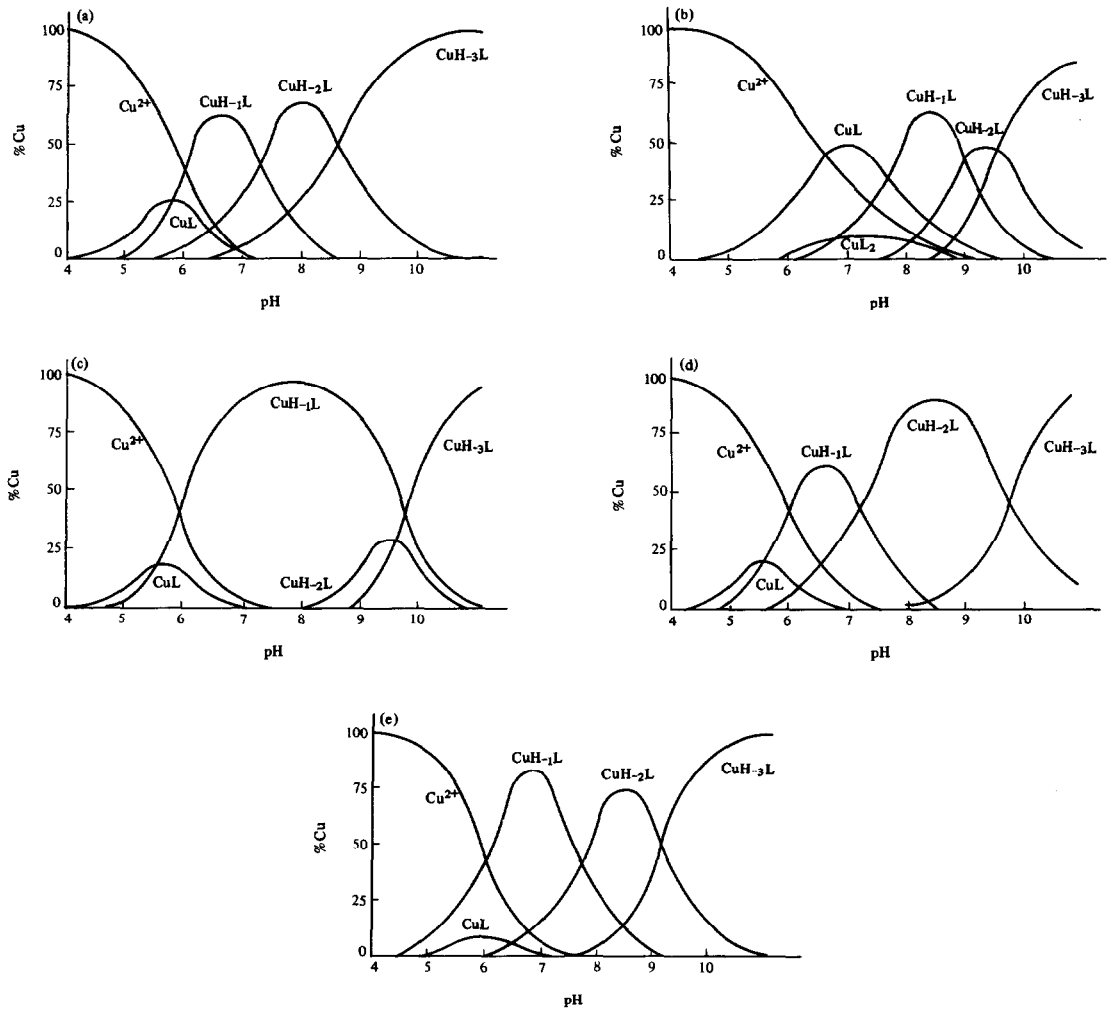

Fig. 3. Species distribution curves for Cu(II) complexes (peptide:Cu = 1:1, 0.001 mol dm^{-3}): (a) Pro-Ala-Ala-Ala, (b) Ala-Pro-Ala-Ala, (c) Ala-Ala-Pro-Ala, (d) Ala-Ala-Ala-Pro, and (e) Ala-Ala-Ala-Ala.[18]

in Table 1, together with stepwise protonation constants. Species distribution curves for 1:1 peptide:copper mixtures are given in Fig. 3, together with those calculated for tetraalanine. In all cases four complexed species were characterized in the pH range 4–10, namely [CuL] (a 1N complex), $[CuH_{-1}L]$ (NN), $[CuH_{-2}L]$ (NNN) and $[CuH_{-3}L]$ (NNNN). In addition a $[CuL_2]$ complex was present with Ala-Pro-Ala-Ala. These species are the same as found with the analogous ligands based on Gly.[2]

The species distribution curves confirm the essentially similar behaviour between peptides based on Gly and those based on Ala. Pro-Ala-Ala-Ala, as expected, behaves similarly to Ala-Ala-Ala-Ala, since it has three secondary peptide nitrogens and, hence, can form an NNNN complex, while Ala-Ala-Ala-Pro resembles Ala-Ala-Ala, having only two successive secondary nitrogens. The most important resemblance is when -Pro- is in the second position, when formation of the $[CuH_{-1}L]$ species is delayed until above pH 7. On the other hand, when it is in the third position this species becomes the predominant complex over the pH range 6–10. Hence, the tetrapeptides containing Ala residues confirm the "break-point" effect identified clearly in the Gly analogues.[2] In fact, comparison of the species distribution curves with those for the Gly analogues shows the effect to be even more marked with the Ala peptides. For example, with Ala-Ala-Pro-Ala the $[CuH_{-1}L]$ complex is more significant than with the Gly analogue, while the $[CuH_{-2}L]$ species is less significant.

The species distribution curves for Cu(II) complexes with Pro-Ala-Ala-Ala and Ala-Ala-Ala-Pro anticipated in the spectroscopic study[12] are shown to be reasonably accurate, but there are significant

differences with Ala-Ala-Pro-Ala. This is probably a result of difficulties in interpreting the spectroscopic data which suggested two different NN co-ordinated species over the pH range of 5–10, and failed to identify an NNN species at high pH. The $[CuH_{-2}L]$ complex (NNN) is never a major species [see Fig. 3(c)], and would be difficult to detect spectroscopically unless the optimum pH (9.5) was selected. This $[CuH_{-2}L]$ complex was detected spectroscopically with Gly-Gly-Pro-Gly,[2] which behaves very similarly to its Ala analogue.

Acknowledgement—We wish to thank Dr K. Sobczyk for providing the samples of Pro-Ala-Ala-Ala, Ala-Pro-Ala-Ala, Ala-Ala-Pro-Ala and Ala-Ala-Ala-Pro.

REFERENCES

1. H. Sigel and R. B. Martin, *Chem. Rev.* 1982, **82**, 385 (and references therein).
2. L. D. Pettit, I. Steel, G. Formicka-Kozlowska, H. Koslowski, T. Tatarowski and M. Bataille, *J. Chem. Soc., Dalton Trans.* 1985, 535.
3. L. D. Pettit, I. Steel, T. Kowalik, H. Kozlowski and M. Bataille, *J. Chem. Soc., Dalton Trans.* 1985, 1201.
4. P. Y. Chou and G. D. Fasman, *J. Mol. Biol.* 1977, **115**, 135.
5. I. Z. Siemion, K. Sobczyk and E. Nawrocka, *Int. J. Pept. Protein Res.* 1982, **19**, 439.
6. F. E. Bloom, *Annu. Rev. Pharmacol. Toxicol.* 1983, **23**, 151.
7. L. D. Pettit and G. Formicka-Kozlowska, *Neurosci. Lett.* 1984, **50**, 53.
8. H. C. Schaller, S. Hoffmeister and H. Bodenmuller, In *Biosynthesis, Metabolism and Mode of Action in Invertebrate Hormones* (Edited by J. Hoffman and M. Porchet), p.5. Springer, Berlin (1984).
9. M. Durchon, *Ann. Sci. Nat., Zool. Biol. Anim.* 1956, **18**, 269.
10. M. Durchon, In *Biosynthesis, Metabolism and Mode of Action of Invertebrate Hormones* (Edited by J. Hoffmann and M. Porchet), p. 10. Springer, Berlin (1984).
11. M. Porchet, N. Dhainaut-Courtois, C. Cardon and M. Bataille, In *Neurosecretion and the Biology of Neuropeptides* (Edited by H. Kobayshi), p. 377. Springer, Berlin (1985).
12. G. Formicka-Kozlowska, H. Kozlowski, I. Z. Siemion, K. Sobczyk and E. Nawrocka, *J. Inorg. Biochem.* 1981, **15**, 201.
13. H. M. Irving, M. G. Miles and L. D. Pettit, *Anal. Chim. Acta* 1967, **38**, 475.
14. P. Gans, A Sabatini and A. Vacca, *J. Chem. Soc., Dalton Trans.* 1985, 1196.
15. G. Gran, *Acta Chem. Scand.* 1950, **4**, 559; *Analyst* 1952, **77**, 661.
16. H. Sigel, *Inorg. Chem.* 1975, **14**, 1535.
17. G. F. Bryce and F. R. N. Gurd, *J. Biol. Chem.* 1966, **241**, 1439.
18. B. Decock-Le Reverend, L. Andrianarijaona, C. Livera, L. D. Pettit, I. Steel and H. Kozlowski, *J. Chem. Soc., Dalton Trans.* 1986, 2221.
19. M. Goodman, N. Ueyama and F. Naider, *Biopolymers* 1975, **14**, 901.
20. J. E. Shields, S. T. McDowell, J. Pavlos and G. R. Gray, *J. Am. Chem. Soc.* 1968, **90**, 3549.
21. S. Blanchard, *J. Mol. Struct.* 1977, **38**, 51.

Polyhedron Vol. 6, No. 1, pp. 53–60, 1987
Printed in Great Britain

0277-5387/87 $3.00+.00

POTENTIOMETRIC INVESTIGATIONS OF THE EQUILIBRIA BETWEEN CAFFEIC ACID AND COPPER(II), ZINC(II), IRON(II) AND HYDROGEN IONS IN AQUEOUS SOLUTION

PETER WILLIAM LINDER* and ALEXANDER VOYÉ†

Department of Physical Chemistry, University of Cape Town, Rondebosch 7700, South Africa

(*Received* 3 *July* 1986)

Abstract—Interactions in aqueous solution of caffeate with copper(II), zinc(II), iron(II) and iron(III) have been investigated. Virtually instantaneous and complete reduction of iron(III) was observed. Glass electrode potentiometry was used to determine the speciation and corresponding formation constants of caffeate with each of the other three metal ions named. Conditions were: temperature, 25°C; ionic strength, 0.100 mol dm^{-3} with respect to chloride. Values obtained for the logarithms of the stepwise protonation constants of the singly protonated dianion of caffeate (L^{2-}) are 8.72 and 4.41. The titration data carried out in the presence of the three metal(II) ions can be explained by postulating the major complexes: LCu, $\log\beta_{110} = 6.02$; $LCuH^{-}_{-1}$, $\log\beta_{11-1} = 0.25$; $L_3Cu_2H^{5-}_{-3}$, $\log\beta_{32-3} = 0.97$; $LZnH^{-}_{-1}$, $\log\beta_{11-1} = -3.03$; $L_3ZnH^{6-}_{-2}$, $\log\beta_{31-2} = -5.51$; LFe, $\log\beta_{110} = 3.86$; $LFeH^{-}_{-1}$, $\log\beta_{11-1} = -3.83$; $L_3FeH^{6-}_{-2}$, $\log\beta_{31-2} = -6.14$, together with a variety of minor species. Complexation in the major species involves, predominantly, chelation by the catecholic site of caffeate whereas coordination to the carboxylate group together with catechol-type chelation featured amongst the minor species. The tendency of copper(II) to form oligonuclear complexes is evident. A single dinuclear iron(II) complex was also found amongst the minor species.

The bioavailability to plants of metal ions is greatly influenced by coordinating ligands which may be present in the soil or in the synthetic nutrient solutions in which the plants grow.[1] To contribute to the understanding of the role of complexation in the uptake of metals by plants, we are undertaking chemical speciation studies by means of computer simulation of soil and nutrient solutions.[2,3]

Of special interest are phenolic compounds that tend to be exuded by the roots of certain plants when subjected to conditions under which the availability of iron is adversely affected.[4–6] The most important of these phenolic compounds is *trans*-3-(3,4-dihydroxy phenyl)-propenoic acid.[7] Caffeic acid is believed to participate not only in the transport of iron from the surrounding soil solution to the roots but also in the reduction of iron(III) to iron(II).[5] In this regard it has been established that the bioavailable form of iron is the iron(II) aquo ion.[8] Apart from this, caffeic acid can also potentially form complexes with various other metal ions that occur in nutrient and soil solutions. Thus, it forms an essential component for inclusion in our computer-based speciation models. There is however a paucity of data in the literature for caffeate–metal–proton complexes. For this reason we have undertaken the investigation described in this paper.

EXPERIMENTAL

Chemicals

Caffeic acid (Aldrich) was purified by double recrystallization from water. (Found: C, 60.3; H, 4.5%. Calc. for $C_9H_8O_4$: C, 60.0; H, 4.5%.) 0.1 mol dm^{-3} hydrochloric acid was prepared from

* Colleague of Professor Harry Irving in the School of Chemical Sciences, University of Cape Town, since 1976. Author to whom correspondence should be addressed.

† Undergraduate and honours student in the School of Chemical Sciences, University of Cape Town (1979–1982).

Merck Titrisol ampoules and standardized against borax (Merck, G.R.) which had been recrystallized and stored as described by Vogel.[9] Sodium hydroxide solutions were freshly prepared at frequent intervals by dilution of the contents of Merck Titrisol ampoules under nitrogen. These solutions were standardized against potassium hydrogen phthalate (Merck, G.R.) as well as with the standardized hydrochloric acid. Zinc(II) chloride solution was made up by dissolving accurately weighed amounts of granulated zinc metal (Merck, G.R.) in concentrated hydrochloric acid (BDH, "Aristar"). The dissolution process was facilitated by adding a piece of platinum foil to the solution. Copper(II) chloride solution was made up from the dihydrated cupric chloride salt (Merck, G.R.). Iron(III) chloride solution was made up by dilution of a 60% (w/v) ferric chloride solution (BDH, Analar). Both the copper(II) and iron(III) chloride solutions were standardized against EDTA (B. Owen Jones) according to the procedure described by Schwarzenbach.[10] The EDTA was standardized against the aforementioned zinc(II) solution. Iron(II) chloride solutions, free from iron(III) as indicated by the spot test with potassium thiocyanate,[11] were obtained by dissolving accurately weighed quantities of iron powder (Merck, G.R.) which had just previously been reduced at 500°C under hydrogen in freshly degassed, refluxed concentrated hydrochloric acid (BDH, "Aristar"). All of the solutions were prepared using carbonate-free boiled out, glass-distilled water, and were made up to a total chloride concentration of 0.100 mol dm^{-3} using solid sodium chloride (BDH, "Aristar"). The acid content of the metal chloride solutions was determined by titration with standardized sodium hydroxide using the method of Gran.[12] The acid content of the iron(III) chloride solution was determined by difference after passing through a cation exchange column [BDH, Amberlite IR-120(H)].

Potentiometric measurements

Protonation constants for caffeic acid and formation constants for the ligand–metal complexes were determined by potentiometric titrations carried out in Metrohm EA876-20/-50 titration vessels maintained at 25 ± 0.1°C. The electrodes were two Metrohm EA109 glass electrodes used alternately, and a Metrohm EA404 calomel reference electrode containing a saturated sodium chloride solution (BDH, "Aristar") as electrolyte. A nitrogen atmosphere, purified as already described,[13] was maintained in the titration vessel during the titrations. In the protonation constant determinations, solutions containing caffeic acid, sodium hydroxide and chloride were titrated with hydrochloric acid–chloride solution, followed by the reverse titration with sodium hydroxide–chloride solution. This particular sequence was followed owing to the greater ease of dissolving caffeic acid in alkaline compared with acid solutions. The titrants were added from a Metrohm Dosimat E635-20 piston burette controlled by a Metrohm Titroprocessor E636, which also measured and recorded the emf of the cell, together with the corresponding volume of titrant added. The data obtained were used to calibrate the electrodes and determine the protonation constants simultaneously.[14]

For the complexation titrations, caffeic acid in sodium chloride–sodium hydroxide solutions was first titrated with hydrochloric acid–chloride solution as described in the previous paragraph. Immediately following this, accurately measured quantities of metal chloride solutions were added from a Metrohm EA274-50 manual piston burette. The solutions were then titrated "back" towards the basic region with sodium hydroxide–chloride solution. This two stage procedure had the advantage of providing protonation data which were used for calibrating the electrodes *in situ*, specifically for each individual titration.

Computations

The caffeate protonation constants and the electrode calibration parameters were determined by applying the programs MAGEC[14] and MINIQUAD[15] alternately to the relevant titration data, according to the procedure already described.[14]

The complexation data were initially processed by the program ZPLOT[16] in order to obtain experimental formation curves of $\bar{Z}_{obs}$ vs $-\log$ [free ligand], and subsequently by MINIQUAD in order to obtain "best"-fitting chemical models and refined formation constants (β_{pqr}).* To facilitate hypothesis testing, the formation constants corresponding to the finally chosen chemical models were used to generate theoretical formation curves of $\bar{Z}_{calc}$ vs $-\log$ [free ligand] by means of the program PSEUDOPLOT.[17] The degree of matching between the experimental and the theoretical formation curves gave a measure of the validity and the accuracy of the proposed chemical models. Lastly the constants corresponding to the finally proposed

* β_{pqr} refer to the general complex $L_pM_qH_r$, where L = ligand, M = metal ion and H = proton. When $r = -1$, this refers to proton removal from the complex or to hydroxyl ion addition.

chemical models were processed by the program HALTAFALL[18] to give profiles of the distribution of each complex species as a function of pH.

RESULTS AND DISCUSSION

Protonations

Several forward and reverse titrations of caffeic acid were carried out over a pH range of about 2–12, with total initial concentrations of the ligand ranging from 0.0038 to 0.0187 mol dm^{-3}. No attempt was made to determine the first protonation constant of the trianion of caffeic acid [which probably has a pK_1 of *ca* 13 (cf. catechol[19])] because of uncertainties arising from deviations of the glass electrodes from Nernstian behaviour together with a non-constant ionic strength of the solution for pH > 12. Therefore in this paper the ligand species L^{2-} is taken as the dianion (**1**).

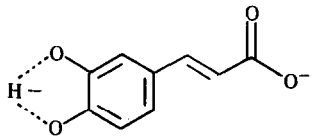

1

The very strong basicity of the third dissociable proton has been attributed mainly to electrostatic attraction of the nearby negative charge and, to a smaller extent, to hydrogen bonding between the hydroxyl and phenoxide groups.[20] All the titrations gave superimposable curves of $\bar{Z}_{obs}$ vs $-\log[H^+]$, indicating the formation of solely the monomeric protonated species HL^- and H_2L (i.e. no evidence for any oligomeric species could be found).

Satisfactory statistical fits of the parameters to the data were indicated by reasonable values of the MAGEC objective function (0.012 cm^6), the MINIQUAD *R*-factor (0.0043) and χ^2 (23.9). Values found for the two protonation constants are presented in Table 1 together with literature values for the same and various related ligands. Allowing for variation in ionic strength and background medium the agreement between our protonation constants and those determined by Timberlake[21] is quite acceptable. The sites of protonation were ascertained by comparison of our constants with those for the other ligands included in Table 1. In this respect catechol was an obvious choice for the catecholate site, and acetate was selected as a suitable model of the carboxylate group of caffeate. The values in Table 1 indicate that K_2^H corresponds to protonation of either one of the catecholate oxygen atoms and K_3^H refers to protonation of the carboxylate group. It should also be noted that the catecholic proton of caffeic acid is somewhat more acidic than that of catechol itself, which might suggest some electron-withdrawing effect of the carboxylate moiety being operative across the double bond of the side chain. This does not seem to be the case with 3,4-dihydroxy hydrocinnamic acid, which has a fully saturated side chain, the value for $\log K_2^H$ being close to that for catechol.[22]

Complexations

Meaningful titrations of the iron(III)–caffeate system could not be carried out successfully owing to rapid reduction to iron(II), as indicated by 1,10-phenanthroline spot tests.[11] Even in the initial, very acidic solutions, reduction of the iron(III) was found to be appreciable. On the other hand,

Table 1. Logarithms of the stepwise protonation constants (K_n^H)[a] for caffeate[b]

Ligand	Log K_1^H	Log K_2^H	*d*	Log K_3^H	*d*	Medium (mol dm^{-3})	*T* (°C)	Reference
Caffeate	—	8.72	0.002	4.41	0.002	0.1 Na[Cl]	25	This study
(dianion)	—	8.76		4.49		0.05 KNO_3	25	21
Catecholate	13.05	9.229		—		1.0 KNO_3	25	19
	12.08	9.37		—		0.1 KCl	25	28
3,4-Dihydroxy hydrocinnamate	11.6	9.36		4.56		0.1 $NaClO_4$	30	22
Acetate	4.499	—		—		0.1 Na[Cl]	25	24

[a] K_n^H is defined here as the associative constant, i.e. for the reaction:

$$LH_n + H \rightleftharpoons LH_{n+1},$$

with $n = 0$, 1 or 2.

[b] Literature constants for related ligands are included for comparison. *d* = standard deviation of $\log K_n^H$.

titrations with iron(II), copper(II) and zinc(II) presented no problems. A series of replicated titrations of caffeate with the latter three metal ion species were carried out using initial total ligand and total metal concentrations covering the ranges 0.0034–0.0275 and 0.0021–0.0038 mol dm^{-3}, respectively. This resulted in ligand : metal ratios ranging from 1 : 1 to 5 : 1 for iron(II), 7 : 1 for copper(II), and 10 : 1 for zinc(II). In the cases of iron(II) and zinc(II), precipitation occurred early in the 1 : 1 ratio titrations and these data were thus discarded. The pH values ranged from 3.3 to *ca* 7 for copper(II), 6–9 for zinc(II), and 5–8.5 for iron(II). The purpose of using such varying initial concentrations was to facilitate the search for not only binary complexes but also protonated, hydroxo and oligonuclear species. Indeed, although titrations with identical starting conditions gave superimposable formation curves indicating good experimental reproducibility, titrations with different ligand : metal ratios gave non-overlapping formation curves in fact as exemplified by copper(II) in Fig. 1 a large degree of back-fanning was observed for all three systems studied. This feature indicates the presence of not only mononuclear binary complexes but also of hydroxo species. Much of the back-fanning is, however, probably attributable to the loss of the very basic third dissociable proton of the ligand on complexation. This is, of course, indistinguishable from the formation of hydroxo species. Further, because of the existence of two potential coordinating sites on the ligand, the formation of oligonuclear hydroxo complexes was considered to be plausible. Hence, numerous combinations of the stoichiometric coefficients *p*, *q* and *r* were tried for the three metal–caffeate systems in applying MINIQUAD to the potentiometric data. Metal hydrolysis reactions of the sort described by Baes and Mesmer[23] were incorporated into every chemical model tried. The most consistent sets of complexes found for the three metal–caffeate systems, together with their respective formation constants, standard deviations, MINIQUAD *R*-factors and χ^2 values are presented in Table 2. Also given, for the purposes of comparison, are formation constants taken from the literature for the catechol–metal ion and 3,4-dihydroxy hydrocinnamate–metal ion systems. No caffeate–metal ion formation constants have been reported in the literature except for the 21 – 2 complex with copper(II),[21] which was, however, not found, although it was searched for in the present study.

The validity of the three chemical models was illustrated by excellent matching of the experimental $\bar{Z}_{obs}$ vs $-\log[L^{2-}]$ points with the corresponding theoretical formation curves as generated PSEUDOPLOT using the refined formation constants given in Table 2. This can be clearly seen for example in the case of the caffeic acid–copper(II) system presented in Fig. 1. Figures 2–4 show typical species distributions for the

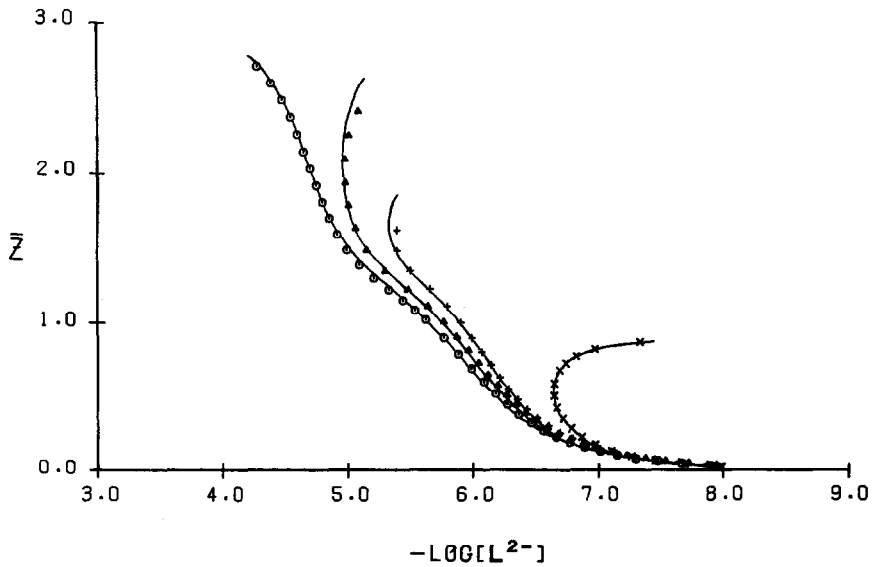

Fig. 1. PSEUDOPLOT formation curves calculated from the caffeate–proton and caffeate–copper(II) formation constants in Tables 1 and 2, plotted together with experimental ZPLOT points. Initial concentrations (10^{-3} mol dm^{-3}) of caffeic acid and copper(II), respectively, are: 3.38 and 3.75 (×), 6.57 and 3.08 (+), 7.81 and 2.75 (▲), and 15.05 and 2.08 (⊙).

Table 2. Logarithms of the stability constants (β_{pqr}) for the complexes of caffeic acid at 25°C and $I = 0.1$ mol dm^{-3} Na[Cl][a]

Metal	Complex No.	p	q	r	Log β_{pqr}	d	n	R	χ^2	Literature data [ligand, T (°C), I (mol dm^{-3}), log β]	Reference
Cu^{2+}	**1**	1	1	1	10.46	0.020	473	0.00254	73.6		
	2	1	1	0	6.02	0.012					
	3	1	1	−1	0.25	0.008				$Hcat^-$,[b] 25, 0.1 KCl, $\log\beta_{11-1} = 0.96$	28
	5	2	1	−2	—					$Hcat^-$, 25, 0.15 $NaClO_4$, $\log\beta_{21-2} = -0.94$	13
	7	1	2	−1	3.54	0.038					
	9	3	2	−3	0.97	0.016					
	10	2	3	−2	7.41	0.024					
Zn^{2+}	**2**	1	1	0	2.99	0.056	458	0.00249	175.4		
	3	1	1	−1	−3.03	0.005				$Hcat^-$, 25, 0.1 KNO_3, $\log\beta_{11-1} = -3.30$	29
	4	2	1	−1	−0.39	0.034				$Hhyd^{2-}$,[b] 30, 0.1 $NaClO_4$ $\log\beta_{11-1} = -2.96$	22
	5	2	1	−2	−8.21	0.022				$Hcat^-$, 25, 0.1 KNO_3, $\log\beta_{21-2} = -8.9$	29
	6	3	1	−2	−5.51	0.017				$Hhyd^{2-}$, 30, 0.1 $NaClO_4$, $\log\beta_{21-2} = -8.4$	22
Fe^{2+}	**2**	1	1	0	3.86	0.034	262	0.00765	111.8	$Hcat^-$, 25, 1.0 KNO_3, $\log\beta_{110} = 3.52$	19
	3	1	1	−1	−3.83	0.054				$Hcat^-$, 25, 1.0 KNO_3, $\log\beta_{11-1} = -5.10$	19
	4	2	1	−1	−0.36	0.025					
	6	3	1	−2	−6.14	0.023					
	8	1	2	0	6.69	0.093					

[a] d = standard deviation in log β, n = number of observations, R = Hamilton R-factor calculated by MINIQUAD, and χ^2 indicates the deviation from normal distribution of the residuals in total concentrations from MINIQUAD output.

[b] Formation constants for the alternatively defined ligands $Hcat^-$ and $Hhyd^{2-}$ calculated from values reported for catecholate^{2-} (cat^{2-}) and 3,4-dihydroxy hydrocinnamate^{3-} (hyd^{3-}) in the references stated.

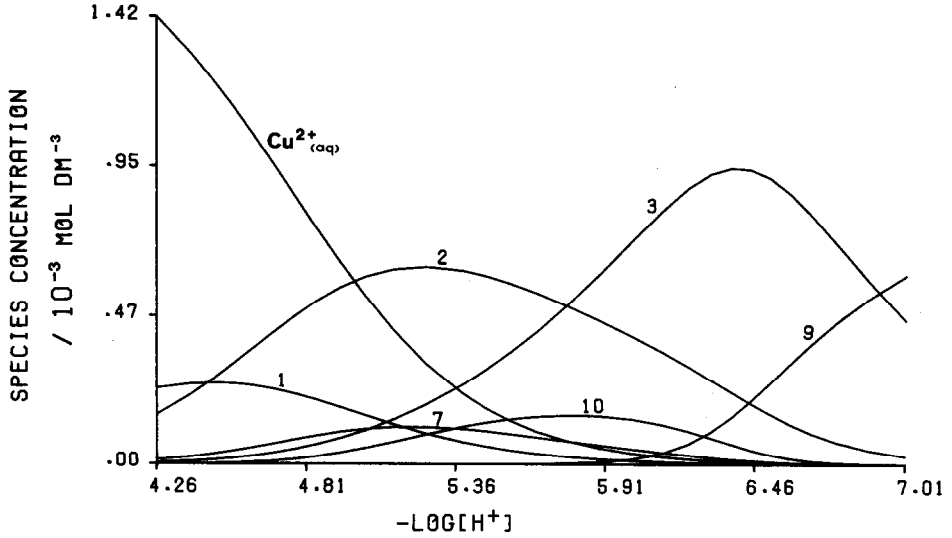

Fig. 2. Distribution of species in the copper(II)–caffeic acid system. Total concentrations (10^{-3} mol dm^{-3}) are: copper(II), 2.03; and caffeic acid, 8.62. Species: (1) LMH, (2) LM, (3) LMH_{-1}, (7) LM_2H_{-1}, (9) $L_3M_2H_{-3}$, and (10) $L_2M_3H_{-2}$.

copper(II)–, zinc(II)– and iron(II)–caffeate systems as functions of pH.

The complexes suggested in Table 2 are all chemically plausible and may, through reference to Figs 2–4, be roughly divided into major and minor species. As a broad generalization, it is to be expected that major species would tend to involve, predominantly, chelation of the metal ions by the more strongly coordinating catecholate site on the caffeate ligands, whereas coordination to the carboxylate moieties would tend to appear more commmonly and, in some cases, concomitantly with catecholate chelation, amongst the minor species. In the range of lower pH values,the major species formed by all three metals are mono complexes, being 11−1 in the case of zinc(II), 110 in the case of iron(II), and both 110 and 11−1 in the case of copper(II). The iron(II) 11−1 species occurs towards higher pH values and the zinc(II) 110 complex appears as a minor species. Our 11−1 constants for copper(II)–caffeate and zinc(II)–caffeate compare favourably with those reported in the literature for complexation of these metal ions by catechol, indicating chelation of the metal ions by

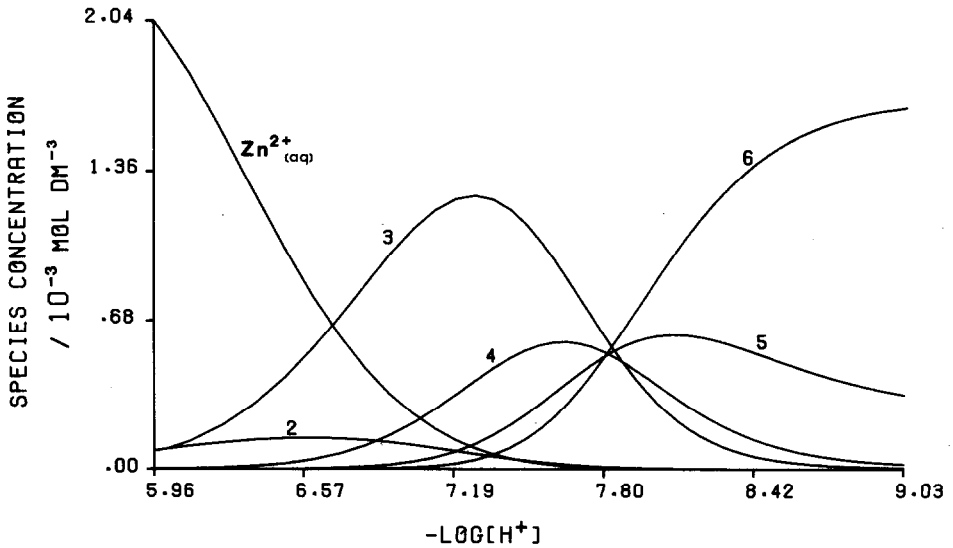

Fig. 3. Distribution of species in the zinc(II)–caffeic acid system. Total concentrations (10^{-3} mol dm^{-3}) are: zinc(II), 2.60; and caffeic acid, 26.1. Species: (2) LM, (3) LMH_{-1}, (4) L_2MH_{-1}, (5) L_2MH_{-2}, and (6) L_3MH_{-2}.

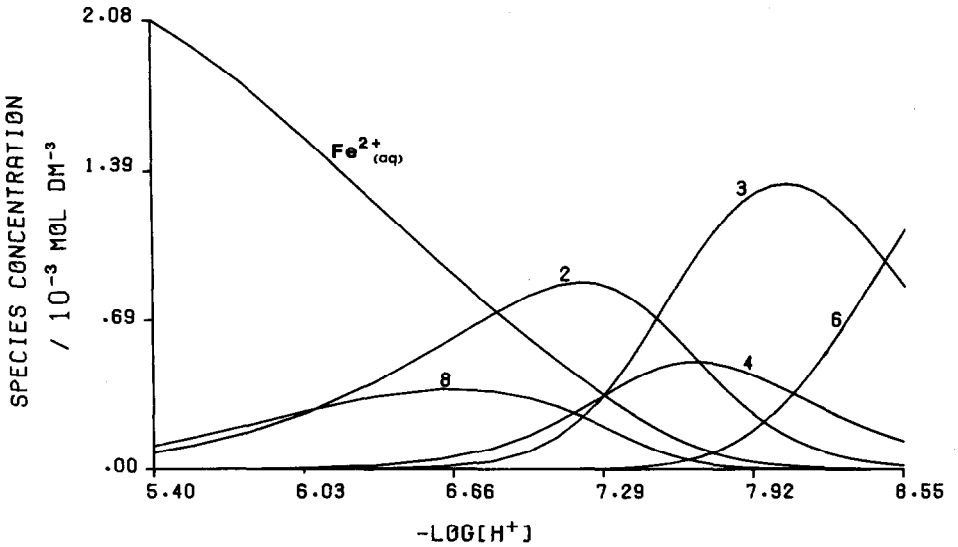

Fig. 4. Distribution of species in the iron(II)–caffeic acid system. Total concentrations (10^{-3} mol dm^{-3}) are: iron(II), 2.98; and caffeic acid, 14.9. Species: (2) LM, (3) LMH_{-1}, (4) L_2MH_{-1}, (6) L_3MH_{-2}, and (8) LM_2.

the fully deprotonated catecholate moiety of caffeate. The alternative of complexation at the carboxylate group of caffeate with a completely deprotonated catecholic site is very unlikely, considering the pH regions ($\ll 12$) in which the complexes occur. Although our constants for the iron(II)–caffeate 11 – 1 complex does not agree closely with the literature value for the corresponding iron(II)–catecholate complex (see Table 2), it is felt that the range of existence of the former complex, namely pH 6–9, approximately, tends to favour catecholate-type chelation over carboxylate complexation, in conformity with the 11 – 1 copper(II)– and zinc(II)–caffeate complexes. As far as the 110 caffeate complexes are concerned, the most likely structure seems to be with chelation at the singly protonated catecholate site and the carboxylate group deprotonated. Although this mode of complexation has not been reported for the copper(II)–catechol system,[13,19] it has been found for the copper(II)–3,5-di-*t*-butylpyrocatechol and iron(II)–catechol systems.[19] Furthermore, our formation constant for the iron(II)–caffeate 110 complex compares quite favourably with that reported in the literature for the corresponding iron(II)–catecholate complex,[19] taking into account the differences in ionic strength and background medium between the two respective investigations. Complexation by the carboxylate group of caffeate, with the catecholate site singly protonated, seems unlikely in view of the significant differences between our 110 metal–caffeate constants and corresponding metal–acetate constants reported in the literature.[24,25] Structures for the 110 metal–caffeate complexes with chelation at the completely deprotonated catecholate site and protonation of the carboxylate group are thought to be unlikely, at least towards higher pH values, for the following reasons. Figures 2–4 indicate the 110 complexes to be present in significant concentrations up to pH values of 7, 7.8 and 8.5 for the copper(II), zinc(II) and iron(II) systems, respectively. In contrast, a protonated carboxylate group is expected to be essentially non-existent at pH values greater than 6.5. At lower pH values a microspecies with protonated carboxylate could contribute towards the 110 macro-stoichiometry, however. The minor species (111), which is unique to copper(II) amongst the caffeate complexes listed in Table 2, could have one of three possible structures. The first, with metal–ion complexation at the fully protonated catecholate site is intuitively unlikely as the corresponding species in the catecholate–copper(II) system was searched for but not found.[13] Furthermore, the carboxylate moiety of caffeate is likely to be protonated in the pH region in which the 111 complex exists. The logarithmic equilibrium constant for the reaction:

$$Cu^{2+} + HL^{-} \rightleftharpoons LCuH^{+},$$

namely, 1.75, is virtually identical to the logarithm of the formation constant of copper(II) with acetate.[24] This agreement lends support to a structure in which complexation occurs at the carboxylate group with a fully protonated catecholate site. A third possible structure with complexation at the singly protonated catecholate site and with the carboxylate group protonated is, however, also

quite likely, because the 111 complex is seen from Fig. 2 to exist over the same pH region in which the 102 protonated ligand species, LH_2, is found. Furthermore, the logarithmic equilibrium constant for the reaction:

$$LCu + H^+ \rightleftharpoons LCuH^+,$$

namely, 4.44, is virtually identical to the $\log K_3^H$, corresponding to protonation of the carboxylate group of caffeate. This lends support to the third alternative because the foregoing considerations of various possible structures for the 110 caffeate complexes of copper(II), zinc(II) and iron(II) tend to favour those with chelation at the singly protonated catecholate site and a deprotonated carboxylate group.

Mononuclear bis(caffeate) complexes appear only as relatively minor species, and of zinc(II) and iron(II) only, not of copper(II). Mononuclear tris-(caffeate) complexes appear in our chemical models as major zinc(II) and iron(II) species. In the light of the foregoing arguments regarding the mono(caffeate) complexes, it is thought that the predominant complexation mode in the bis and tris complexes is metal chelation at the catecholate site, resulting in coordination numbers ranging from 4 to 6.

Towards higher pH values, the only major copper(II) complex of caffeate that we have found, is the dinuclear species (32−3). This, together with the minor copper(II) complexes (23−2 and 12−1), occurring in the lower-pH range, illustrate the tendency of copper(II) to form oligonuclear complexes with ligands possessing two coordination sites.[13,26,27] In these complexes, the copper(II) plays the role of a link between adjoining ligands. Since the caffeic acid molecules in the copper(II) complexes (32−3 and 23−2) are completely deprotonated, it seems likely that all the catecholic sites are involved in the complexation. With regard to the copper(II) complex (12−1) and the analogous minor iron(II) species (120) it seems self-evident that a metal ion is coordinated at each end of the ligand molecule.

Acknowledgements—Grateful acknowledgement is expressed to the University of Cape Town and the South African Council for Scientific and Industrial Research for generous grants. We also thank the University of Cape Town Computer Service for the smooth running of our programs on the Univac 1100/81.

REFERENCES

1. W. L. Lindsay, In *The Plant Root and its Environment* (Edited by E. W. Carson), p. 507. University Press of Virginia, Charlottesville (1974).
2. K. Murray and P. W. Linder, *J. Soil Sci.* 1983, **34**, 511.
3. K. Murray and P. W. Linder, *J. Soil Sci.* 1984, **35**, 217.
4. C. L. Tipton and J. Thowsen, *Iowa State J. Res.* 1983, **57**, 409.
5. R. A. Olsen, J. C. Brown, J. H. Bennet and D. Blume, *J. Plant Nutr.* 1982, **5**, 433.
6. V. Römheld and H. Marschner, *J. Plant Nutr.* 1981, **3**, 551.
7. V. Römheld and H. Marschner, *Plant Physiol.* 1983, **71**, 949.
8. R. L. Chaney, J. C. Brown and L. O. Tiffen, *Plant Physiol.* 1972, **50**, 208.
9. A. Vogel, *Textbook of Quantitative Inorganic Analysis*, 4th Edn. Longmans, New York (1981).
10. G. Schwarzenbach, *Complexometric Titrations.* Methuen, London (1957).
11. F. Feigl and V. Anger, *Spot Tests in Inorganic Analysis.* Elsevier, Amsterdam (1972).
12. F. J. C. Rossotti and H. Rossotti, *J. Chem. Educ.* 1965, **42**, 375.
13. G. V. Fazakerley, P. W. Linder, R. G. Torrington and M. R. W. Wright, *J. Chem. Soc., Dalton Trans.* 1979, 1872.
14. P. M. May, D. R. Williams, P. W. Linder and R. G. Torrington, *Talanta* 1982, **29**, 249.
15 A. Sabatini, A. Vacca and P. Gans, *Talanta* 1974, **21**, 53 ; P. Gans, A. Sabatini and A. Vacca, *Inorg. Chim. Acta* 1976, **18**, 237.
16. D. R. Williams, *J. Chem. Soc., Dalton Trans.* 1973, 1064.
17. A. M. Corrie, G. K. R. Makar, M. L. D. Touche and D. R. Williams, *J. Chem. Soc., Dalton Trans.* 1975, 105.
18. N. Ingri, W. Kakalowicz, L. G. Sillén and B. Warnquist, *Talanta* 1967, **14**, 1261 ; B. Elquist, *ibid.* 1969, **16**, 1502.
19. C. A. Tyson and A. E. Martel, *J. Am. Chem. Soc.* 1968, **90**, 3379.
20. R. K. Boggess and R. B. Martin, *J. Am. Chem. Soc.* 1975, **97**, 3076.
21. C. F. Timberlake, *J. Chem. Soc.* 1959, 2795.
22. V. T. Athavale, L. H. Prabhu and D. G. Vartak, *J. Inorg. Nucl. Chem.* 1966, **28**, 1237.
23. C. F. Baes, Jr and R. E. Mesmer, *The Hydrolysis of Cations.* John Wiley, New York (1976).
24. P. W. Linder, R. G. Torrington and U. A. Seemann, *Talanta* 1983, **30**, 295.
25. A. E. Martell and R. M. Smith, *Critical Stability Constants*, Vol. 3, *Other Organic Ligands.* Plenum Press, New York (1976).
26. J. E. Gorton and R. F. Jameson, *J. Chem. Soc. A* 1968, 2615; *J. Chem. Soc., Dalton Trans.* 1972, 304.
27. A. Gergely and T. Kiss, *Inorg. Chim. Acta* 1976, **16**, 51.
28. R. F. Jameson and W. F. S. Neillie, *J. Inorg. Nucl. Chem.* 1965, **27**, 2623.
29. R. F. Jameson and W. F. S. Neillie, *J. Inorg. Nucl. Chem.* 1966, **28**, 2667.

Polyhedron Vol. 6, No. 1, pp. 61–69, 1987
Printed in Great Britain

0277–5387/87 $3.00+.00

THE BIOCHEMISTRY OF ZINC

R. J. P. WILLIAMS*

University of Oxford, Inorganic Chemistry Laboratory, South Parks Road, Oxford OX1 3QR, U.K.

(*Received* 3 *July* 1986)

Abstract—The biochemistry of zinc is now beginning to be understood. The background to this understanding is a deep knowledge of the chemistry of the element. In this article I shall show some of the ways in which evolution has searched for and found the outstanding potential of zinc in catalysts. As a background an analogy is drawn with man's efforts to evolve analytical methods of high selectivity for the estimation of zinc. The article also illustrates some of my own interests in zinc which started in Professor Irving's laboratory.

The biochemistry of zinc must start from a firm basis in the chemistry of zinc. My first detailed knowledge of that chemistry was during my earliest days as a research student and pupil of Professor Harry Irving. I came to him in 1947 with a determined interest in trace elements and he set me a problem in analysis and the understanding of analytical method. (He had previously been my tutor in inorganic chemistry.) The problem was to be the understanding of the estimation of zinc by the extraction method, followed by colorimetry, using the organic reagent dithizone. The close relationship between analytical chemistry and the selective principles behind trace-element function in biology was soon obvious, and I have never forgotten that lesson. Even if we look at the coordination sphere of the complex between zinc and dithizone

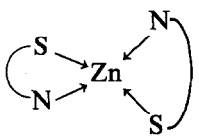

we see two interesting features: (1) the sulphur–nitrogen coordination, and (2) the tetrahedral geometry. We shall refer to both again and again.

There was little known of the structural chemistry of zinc in 1947, nor indeed of its thermodynamics and kinetics. However, earlier work on extraction and analytical methods had demonstrated that zinc was not the element which reacted at the lowest pH with almost any reagent. This distinction belonged to other metals such as mercury, lead, perhaps silver, and, if oxidation could be avoided, copper. Thus, zinc was not a very powerful binding reagent. Curiously (to us at the time) this power of binding was exactly the pattern of the Qualitative Analysis Tables which I had learnt at school and which Dr Irving had taught for some time in undergraduate chemistry. All chemists should know these Tables. Mercury, lead, silver and copper are precipitated before zinc by almost any reagent, e.g. sulphide.

Inspection of the literature showed that, in fact, of all the known analytical organic reagents for metal ions none reacted more readily with zinc than with copper. However, none reacted more readily with manganese than with zinc. With this hint of the appearance of a metal ion series of reactivities we had to stop and think, since there could have been two reasons why metal ions might combine in a preferred order. The first is a matter of affinity (thermodynamics) and the second a matter of speed (kinetics). In 1947 it was not apparent that any of the analytical methods depended on the establishment of equilibrium. In fact it fell to me under Irving's guidance to demonstrate by experiment that the observed series was due to equilibrium not kinetic controls. Dr Irving and I showed this by using a shaking machine working over many hours to produce equilibrium in the extractions of metal ions by dithizone. We showed then that the affinity

* R. J. P. Williams was an undergraduate at Merton College, Oxford (1944–1948), taught inorganic chemistry by Dr Irving, and did his Part II and D.Phil. with Irving. He was a tutor and lecturer at Wadham College, Oxford (1955–1972), before becoming the Napier Royal Society Research Professor at Oxford.

for dithizone at equilibrium with metal ions was in the order of divalent ions:

$$Zn < Cu > Ni > Co > (Fe) > Mn \geqslant Mg = Ca = \text{zero}. \quad (1)$$

Now it was just at this time that Jannick Bjerrum's fine thesis became available to us. In it he demonstrated that equilibrium binding constants could be determined in a single phase, water, for the interaction of metal ions with *neutral* ligands. The order for ethylenediamine was the same as that given above. Thus, we knew that the order did not depend on a phase change (extraction or precipitation) but that there was a fundamental thermodynamic order of interaction energies which was also not dependent on the donor atom, oxygen, nitrogen or sulphur (each shown separately); was not dependent on the anionic character of the ligand; and was not dependent on solvent. Others, especially Mellor and his group in Australia, and Calvin and his group in U.S.A., were approaching the same conclusion. The problem lay in the fact that, although the above order was (almost) universal, any persistent regularity disappeared if data for mercury, lead, cadmium or other ions were included in the series.

Dr Irving and I discovered the reason for the simplicity of the order (1). The metal ions in the order are of very similar size, but their electron affinities change smoothly along the series to a maximum at copper(II) and fall back at zinc. Inclusion of ions of different sizes confuses the description since now readius and ionization energy changes are randomly scattered. In Fig. 1 is plotted the function z/r against the ionization energy from metal ions to the divalent state. The "a"/"b" classification, sometimes unwisely called the hard/soft classification, falls out immediately and so does the Irving–Williams series. Following the evidence of analytical extraction procedures we had uncovered a very simple rule of great general use, i.e. series (1). The rule is almost independent of ligand type, the number of ligands bound, of ligand geometry, and of stereochemistry. The fact that there was a correlation with two central-field parameters, ionization energy and z/r, meant that it was independent of crystal (ligand) field angular polarization, though this adds a term which in octahedral geometry follows the series:

$$Mn < Fe < Co < Ni > Cu > Zn. \quad (2)$$

Just as it is a mistake to use soft and hard as a classification of "a" and "b" metal ions so is it a mistake to overstress the contribution of angular polarization energies to the energy of complex ion formation. It is a fact, as we showed in our very early papers, that series (1) not (2) dominates spectroscopic perturbations of ligand spectra in complexes, i.e. their IR and UV spectra, and the effect

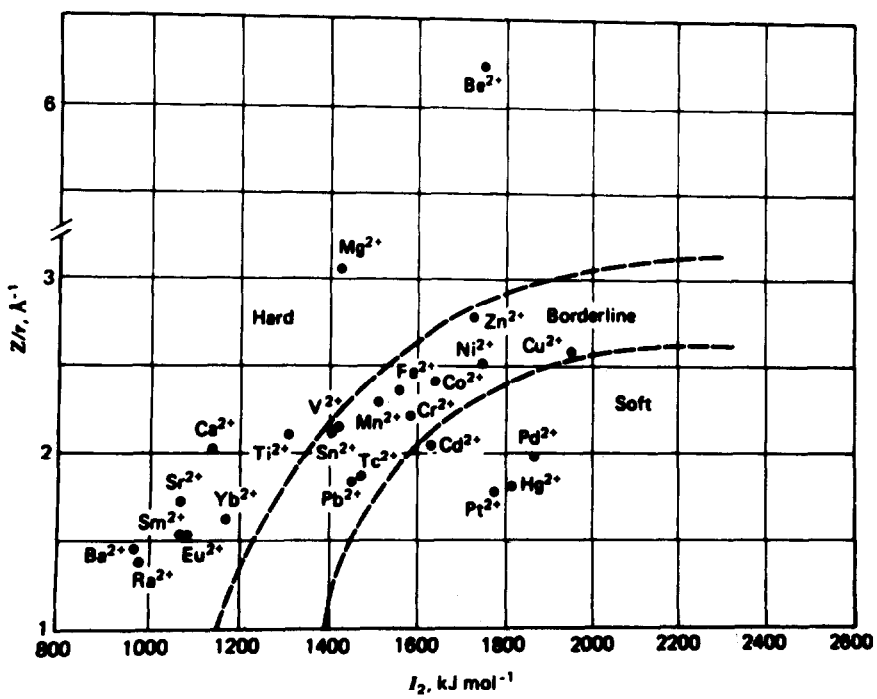

Fig. 1. Plot of z/r against ionization potential for divalent ions showing the classification of metal ions and the Irving–Williams series.

of metal ions as Lewis acids in catalysis. Therefore, the polarization of the ligand by the metal follows order (1). I return to these points later since they must be appreciated if the subtle nature of the use of zinc in biology is to be understood.

Now the background to metal ion–ligand affinity has been given it should also be noticed that the differences in the Irving–Williams order increases as the polarizability of the donor atom increases in the series:

$$O < N < S.$$

This means that there is an increase in selectivity of organic reagents such as dithizone (N,S) over 8-hydroxyquinoline (N,O). Again, this is a lesson of immediate applicability to biological systems. It means that combinations of N- and S-donors can be used to select out powerfully transition metals and B-subgroup metals from A-subgroup metals and that they can also be used to select one transition-metal ion from another. Again, curiously this follows from the way in which the Qualitative Analysis Tables instruct one to proceed. [The classifications in those Tables are in fact of necessity the classifications of elements in biology (Table 1).] The basic idea is the removal of one element, e.g. copper, by one reagent, sulphide, by a phase transfer precipitation before the determination of a second metal, e.g. zinc, in the residual phase. Further metal ions are precipitated as carbonates, an O-ligand. An example is the precipitation of copper as a sulphide at pH < 2 in Group IIA of the Qualitative Analysis Tables followed by filtration. The precipitation of zinc sulphide is at pH = 10 in Group IVA of the same Tables. This shows the large difference between zinc and copper sulphide chemistry. Calcium and magnesium are analysed later by oxygen atom donors. The implication as far as this article is concerned is that biological systems must be able to use a variety of organic ligands to complex metal ions, to control pH in different compartments, and to transfer ions from compartment to compartment in order to keep elements away from one another. In turn, this implies that biological systems have *local* equilibria and use boundaries, membranes, to keep different reaction possibilities under kinetic separation. Biological systems pump ions and compounds across membranes which permits isolation of reactions just as a separation procedure in analyses, e.g. precipitation, uses the removal of one phase, an organic solvent or a precipitate, to carry one set of compounds into a separate set of reaction possibilities. However all these possibilities are preconditioned by binding affinities as revealed in the Irving–Williams series.

Before passing on we note that pumps can be devised and are so devised in biology that they recognize *shape*. The use of the energy of transfer through a membrane depends on a triggering kinetic step. It does not then matter if two compounds bind equally in a thermodynamic sense so long as, for example, the one which is tetrahedral can trigger but the one which is octahedral can not. A tetrahedral zinc complex may traverse the membrane because it is pumped unidirectionally after triggering, but an octahedral nickel complex is unable to pass the membrane at all since it fails to trigger the energy source. In biology the *shape* of complex ions, of ions themselves, of small molecules, of proteins and so on decides the compartment into which they are pumped. We shall see that zinc is readily separated and put in its place by the use of binding energies and the curiosities of its stereochemistry (Fig. 2).

Table 1. Classification of cations in biological systems[a–c]

Na^+, K^+	Mg^{2+}, Ca^{2+}	Zn^{2+}	Fe, Cu, Co, Mo
Charge-carriers	Structure formers and triggers	Super-acid catalysts	Redox catalysts
Mobile	Semi-mobile	Static	Static
Oxygen-anion binding	Oxygen-anion binding	Nitrogen/sulphur ligands	Nitrogen/sulphur ligands
Weak complexes	Moderately strong complexes	Strong complexes	Strong complexes
Very fast exchange	Moderately fast exchange	No exchange	No exchange

[a] R. J. P. Williams, In *Current Topics in Bioenergetics* (Edited by A. Sanadi), Vol. 3, p. 80. Academic Press, New York (1969).

[b] R. J. P. Williams, *R. Inst. Chem. Rev.* 1968, **1**, 13.

[c] B. L. Vallee and R. J. P. Williams, *Chem. Br.* 1968, **4**, 397; R. J. P. Williams, In *The Enzymes* (Edited by P. D. Boyer, H. Lardy and K. Myrback), Vol. 1, p. 391. Academic Press, New York (1959).

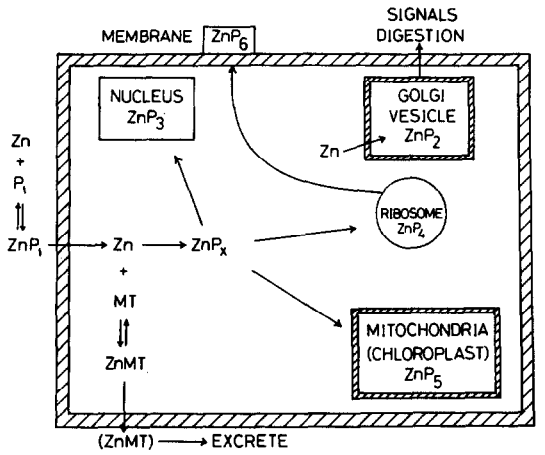

Fig. 2. Transport of zinc complexes in and out of cells. P is any protein carrier or enzyme, MT is metallothionine.

THE DISPOSITION OF ZINC IN BIOLOGICAL SPACE

General inspection of the biological systems shows that, whereas copper is rejected by cells from internal compartments especially the cytoplasm, zinc is not. In general zinc is pumped into vesicles in the cytoplasm or is held in the cytoplasm. In general copper is pushed into totally extracellular spaces. Copper becomes the catalyst (in enzymes) for extracellular oxidations while zinc becomes associated with control and triggering reactions in vesicles, e.g. hormonal release, as well as directly with some special enzymes for digestion (see Table 1 and Fig. 2). The observed distribution of high zinc gives a very good clue to its utilization, especially against the background of its chemistry.

KINETIC CONSIDERATIONS

The work Dr Irving and I carried out did not only reveal the thermodynamic order, the Irving–Williams series, and the basis of a wider appreciation of stability constant data in solution such as the introduction of high-spin–low-spin changes within the series, e.g. that of the complexes of the dipyridyls, and the importance of stereochemistry but it nearly gave us a crystal field theory too. We clearly observed that the involvement of the empty orbitals of the *d*-shell at nickel affected the number of ligands taken up equally. It fell to Dr L. E. Orgel to show us the proper theoretical framework for these observations. We did observe another feature of the reactions of complex ions—some were faster than others. It was the work of Eigen and Taube which gave the underlying explanations once again in terms of *d*-shell filling. This gave a quite new order, that of the rates of substitution of ligands around a metal ion:

$$Zn, Mn > Cu > Fe > Co > Ni > \text{low-spin systems.}$$

Notice that zinc is placed in the very fast reacting groups.

Now in any reaction system we can reduce the rate expression to a dependence on several steps: (1) the formation of the appropriate units in a complex, (2) the formation of the correct stereochemistry in that complex, (3) the readiness of the system to pass along a set of reaction intermediates, and (4) the ease of disruption of the final products. We should also add two other considerations: (5) the absence of alternative unwanted paths, and (6) the spatial separation of the reaction system from other such systems could be desirable so that only one set of transformations is carried out in one part of space. Without much mental effort an overview of the value of zinc in a reaction system begins to appear. (1) It binds well though not as well as copper. (2) It has very selective stereochemical possibilities which can be altered easily since it has no strong preferences for a field of given symmetry—no ligand field terms. (3) It exchanges ligands rapidly. (4) It can release rapidly ligands which are chemically changed, i.e. the products. (5) It does not take part in redox reactions. (6) It is readily transferred into special compartments using (1) and (2) together with pumps. Add to this background the fact that zinc is quite soluble in water at pH = 7, and is therefore available to biology, and we have an ion, zinc, which is preferable to almost any other cation to be the favourite choice as an acid–base catalyst in water on grounds of availability, power and absence of redox properties. Biology uses zinc for just these three reasons. Before looking further at the catalytic potential of zinc we must observe that its binding potential and lack of redox properties are extremely valuable in other respects. Because it binds strongly to, say, thiolate groups and does not catalyse their oxidation, it protects them. This is common in the cross-linking of rubbers. Biology will be seen to use this protection of thiolate groups in a number of ways. We discuss catalysis first.

ZINC ENZYMES

Figure 3 shows the pattern of reaction rates for zinc enzymes when the zinc is substituted by other metal ions. The Irving–Williams order of Lewis acid strength has disappeared but not the binding strength to the isolated enzyme. Clearly stereochemical requirements dominate thermodynamics in this enzymic rate series and there is a clear

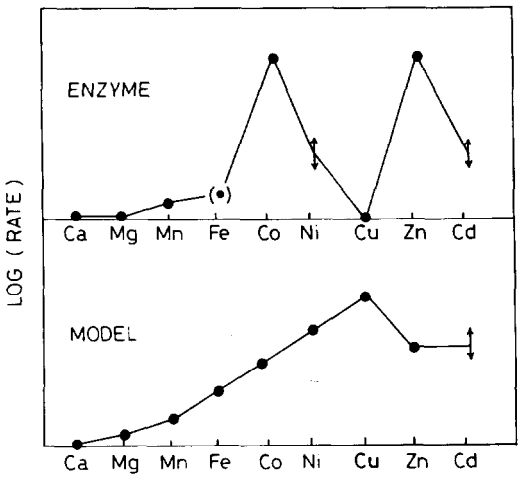

Fig. 3. Plot (below) of the rates of Lewis acid catalysis by free metal ions of model substrates. Shown above is the rate of catalysis by metallo-enzymes in which the native zinc has been replaced by a series of other metal ions.

demand for cations which do not prefer octahedral geometry, i.e. zinc and cobalt. We can draw somewhat convincing reaction pathways, e.g. for carbonic anhydrase (Fig. 4) which show how nicely zinc can aid any catalysis by its fast switches in stereochemistry and by its polarizing power, e.g. in hydroxide generation. I think however that if it had been discovered that copper(II) was at the heart of carbonic anhydrase we could have drawn equally convincing diagrams of its reaction patterns since it has a greater polarizing power and reacts rapidly. After all, it is at the heart of superoxide dismutase. Intrinsically, copper(II) is a better Lewis acid catalyst. The use of zinc to the exclusion of copper in most hydrolytic enzymes has led to the perfecting in a *zinc* enzyme of a pathway peculiar to *zinc* chemistry but zinc was not chosen for its catalytic potential alone. It was selected for the absence of redox reactions. In fact there are no acid–base reactions in biology which are catalysed by copper enzymes. There are a few apparent acid–base transformations where the metal ion in the enzyme is not zinc, but there is the suggestion here that some of these at least go by free-radical paths which zinc can not assist, e.g. diol rearrangements (cobalt in B_{12}), decarboxylations (iron–sulphur), and hydroxy acid rearrangements, aconitase (iron–sulphur). Zinc dominates in all the simple reactions such as ester, amide, ether hydrolyses of biology, and it is here where oxidation must be avoided.

The organic chemist may well ask "but why use zinc at all?" when most hydrolytic enzymes are good catalysts without any metal ion. Here the organic chemist is not observing his own chemical systems closely. The catalysis of reactions in organic chemistry can use extremes of pH so that H^+ and OH^-, even RO^-, are useful free attacking groups. However it is not infrequent for the organic chemist to switch to the use of $AlCl_3$, $ZnCl_2$ etc. as Lewis acid catalysts when he can not control pH, e.g. in organic solvents. Why did he not choose to add organic acids and bases as catalysts? The simple answer is that there are no organic compounds of simple construction which show the high and highly exposed electron affinity of tri- (aluminium) and divalent (zinc) metal ions even in organic solvents. Putting it bluntly, organic chemistry does not supply good attacking groups for either acid or redox reactions at neutral pH. This is the function of metal

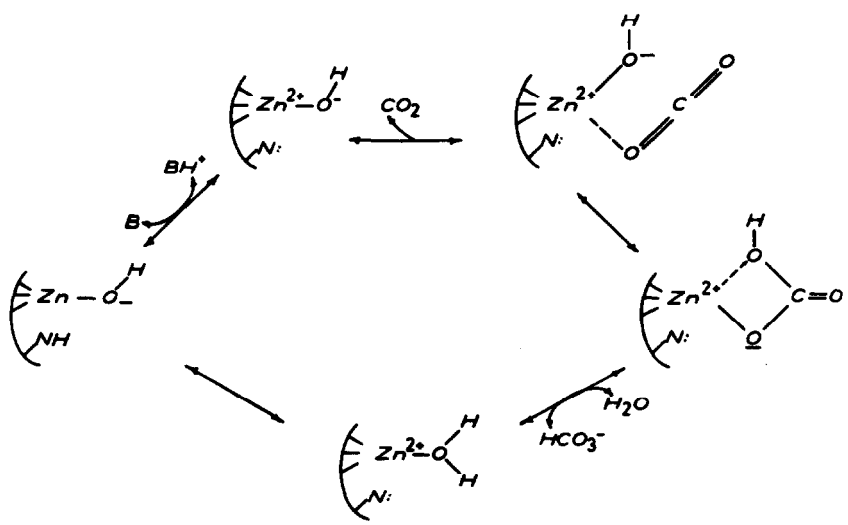

Fig. 4. Proposed outline scheme for the catalysis of the CO_2+H_2O reaction by the zinc enzyme carbonic anhydrase.

Table 2. Comparison between zinc and non-zinc enzymes[a]

Reaction	Zinc-dependent enzyme substrate	Metal-independent enzyme substrate
Hydration	CO_2, levalinic acid	None
Protein hydrolysis	Carboxy-terminal, amino-terminal and dipeptides	Endopeptide None(?)
Phosphate ester hydrolysis	Terminal phosphate	Phosphate transfer
RNA/DNA hydrolysis	Non-specified nucleotides	Ribonucleotides
RNA/DNA polymerase	No specific base	None
β-Lactamase	Penicillins	Penicillins
Aldolase	Several aldols	Several aldols
Phospholipase	(C) Lipid esters	(A) Lipid esters

[a] Generally zinc is employed when the substrate is small, e.g. CO_2, or when the reaction is non-specific, e.g. alkaline phosphatase, RNA polymerase and terminal proteases.

ions or bare H^+ and OH^-. Let us look at acid–base catalysis more closely.

Molecules can be broken rapidly in catalysed steps only by readjusting the bond energies along a pathway. There are two ways of doing this: (1) the bonds can be twisted and stretched, or (2) neighbouring attacking groups can be introduced. Both modes are catalytic. Metal ions are helpful as are any binding modes in (1) but they are unique in (2). Enzymes formed from organic units can only supply very many binding centres for purpose (2) and poorish attacking groups. It follows that if a substrate has many points of attachment to an enzyme it can be twisted and torn apart by an organic template which recognizes the shape of the intermediate better than that of the substrate and, with a little help from friendly disposed but weak organic acids and bases, e.g. in chymotrypsin, which breaks large peptides. However, if the reaction involves a small molecule then the binding must be through very simple attachment, distortion of the substrate is difficult, and catalysis now requires good attacking groups, e.g. zinc. Zinc can activate the smallest of molecules, H_2O, the participant in all hydrolyses. Thus we observe that it is in the hydrolytic reactions of small substrates that zinc is most used (Table 2). (These points are general to the functional use of all metal ions in biological catalyses.)

I do not want to press on with a detailed discussion of the catalytic chemistry of zinc in enzymes. I believe this to be but one area of interest and there are possibly two other areas of zinc action in biology which merit further analysis: (1) protection of thiolates, and (2) triggering. Before passing to these points, however, I would not like three features of the binding of zinc in enzymes and other proteins to be missed (Fig. 5). The zinc is invariably bound to more than one nitrogen or thiolate, and is bound by at least three groups in total to give it *chelate* stability and closely adjusted stereochemistry in the site. If zinc were bound to a smaller number of groups it would not be bound with sufficient strength for permanent (irreversible) attachment. The binding in enzymes is linked to the fold energy of the protein so that the zinc is cooperatively fixed to its site—it does not exchange readily from the enzymes. Note that the zinc enzymes have tight β-sheet folds (Fig. 6). The stereochemistry in the enzymes is carefully tuned to make function optimal—the entatic state tuning of Vallee and Williams, but minor adjustments are permitted to allow flow along a reaction pathway. I shall not elaborate further but I would remind the

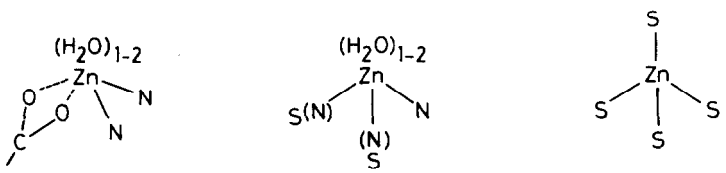

Fig. 5. Different, entatic, geometries of zinc in enzymes. Left: carboxypeptidase, and middle: carbonic anhydrase (N) and alcohol dehydrogenase (S). The right-hand structure shows zinc as a cross-linking agent.

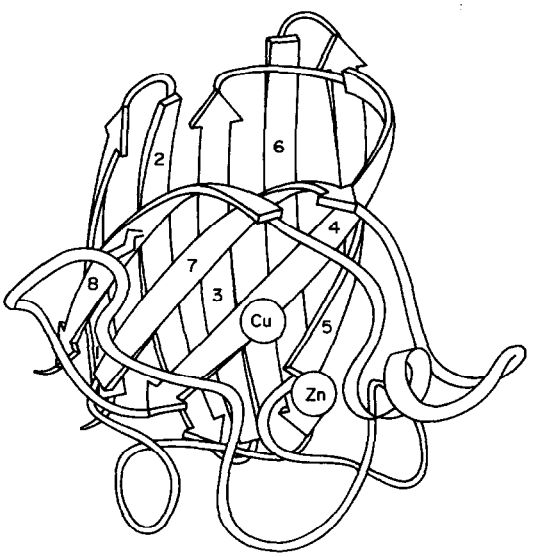

Fig. 6. Outline structure of Cu/Zn superoxide dismutase showing the β-barrel.

reader of the tricks used in analytical chemistry. Dr Irving's favourite, using organic reagents and phase transfer to generate selective determinations of metal ions, is very closely akin to biology's use of organic binding groups not only to control metal ion functions but where they are used and their usefulness.

CROSS-LINKING BY ZINC

Zinc cross-linking is not too unusual in intracellular enzymes. In fact the use of zinc to stabilize a structure is useful in that it can replace the conventional biological cross-links formed from oxidized dithiols, —S—S— bridges, in the extracellular medium. Zinc then provides a centre free from one-electron reactions, which other metals and disulphide could not do, and inside the cell, which is a reducing medium. The cross-links are often now in fact from one RS^- to another through zinc, and the zinc site is frequently in the middle of four such RS^- groups, e.g. in alcohol dehydrogenase and aspartate transcarbamylase (Fig. 5). An alternative cross-link known in one enzyme, the Cu/Zn superoxide dismutase, uses a number of imidazoles, here four again in an approximate tetrahedron. In this last case the zinc is close to the copper at the active site and directly generates the ligand geometry around the copper (Fig. 6). Copper is in a truly entatic condition brought about in part by the zinc. A recent example of unknown importance as yet is the finding of zinc in cytochrome oxidase.

The use of cross-links in enzymes is to be contrasted with the use in other kinds of protein. The best known is the keratin filaments of the tails (flagellae) of such cells as sperm. Here zinc helps to generate a stable yet flexible structure for the motor of this cell. Note that the male reproductive tract is full of zinc—is this to help to keep sperm healthy and moving?

Recently Klug and coworkers have described an impressive example of zinc cross-links in a transcriptase factor. Some 9 or 10 zinc atoms are bound in a repeated domain of a protein which in turn binds to DNA. The on and off reactions of zinc may well be related to the conformations of the protein and its interaction energies with the DNA. Thus zinc could control transcription. We are reminded of two series of experiments. The first showed that zinc is essential for growth of humans and zinc deficiency causes developmental retardation. The second showed that if zinc is replaced by other elements such as cobalt or manganese in *Euglena gracilis* growth media then the genetic machinery suffers some peculiar irregularities.

Finally there are the uses of zinc in some quite peculiar structures such as the tapetum of the eyes of animals with night-vision. Here the zinc is in crystals of zinc cysteinate, it is said. Another use is in the stabilization of the "teeth" of the larvae of insects such as locusts where it is thought the zinc acts as cross-link of phenolate polymers in a form of sclerotin.

ZINC CHEMICAL TRIGGERS

A way of triggering a biological system is to remove an inhibitor. The simplest examples are the breaking of chemical bonds in proenzymes to give enzymes. Thus an inhibitory peptide is broken away from prochymotrypsin, i.e. chymotrypsinogen, to give chymotrypsin. This process is quite sluggish, involving the breakdown of covalent bonds. An alternative mode of triggering of this kind is by the breaking of ionic bonds, and naturally this involves metal ions. Although the following case is not known to be true it looks extremely plausible.

It is now known that many enzymes which breakdown storage proteins to release peptide hormones are thiolate- and zinc-dependent. Such enzymes must be stored ready for use but this has its risks since the thiolates can be readily oxidized. A solution to this problem is to store them with the protein which contains the hormonal peptide in the presence of zinc which both protects the reactive site and inhibits oxidation. The zinc binding must be weak, say two bonds only so that dissociation is fast. In other words a container is needed and a compartment (vesicle) in which there is a somewhat concentrated zinc solution. The zinc is protective

but to be so and readily released it has to be in only moderately strongly held and therefore in fairly high concentration, say 10^{-7} M free zinc ions, in order to function. The situation is unlike that in the above zinc enzymes when the zinc is a catalytic component and is bound almost irreversibly with a constant of 10^{-10} M, although the two modes of action are not mutually exclusive. Now this hypothesis explains immediately the high concentration of zinc in many peptide hormone containing vesicles, e.g. in the brain (endorphins) and the pancreas (insulin). It also explains the presence of high zinc in parts of the sperm and pollen which require proteases to trigger many events—e.g. fertilization. However, the use of zinc in this way needs a mode of concentrating the zinc in the vesicles—a zinc pump.

THE ZINC PUMPS

The way in which zinc is removed from cells to vesicles is unknown. Metallothionine (see Fig. 2) may well be used to export zinc completely from the cell. The same protein is used to expel both copper and to trap cadmium. Thus, metallothionine is one substrate for the pumps. However, zinc goes into compartments where there is no copper. We must suppose that there are special transport pumps for the zinc since we know that zinc is in high concentration in very local biological volumes—vesicles. We have not yet found this pump.

The control of zinc levels in a cell may also be through the protein metallothionine. It is known that this protein has a four metal atom and a three metal atom cluster in two separate domains. All the metal ions are tetrahedrally coordinated to four thiolate groups so that the metals generate a fold. Without the metal ions the protein is in a random coil. The general picture of the function of metallothionine is given in Fig. 3. The zinc-free protein can pass information to DNA. If the zinc concentration rises, or the copper or cadmium concentrations rise, the protein is removed from the DNA and the RNA for production of protein is transcribed. The excess metal is bound. If it is copper or cadmium it is exported probably via lysozymal vesicles. If it is zinc it is pumped into other vesicles for use with proteases for example.

ZINC MECHANICAL TRIGGERS: REMOTE TRIGGERS

The way in which calcium triggers the calmodulin proteins has been outlined in essential detail. It is a very similar mechanism to that for the triggering of hemoglobin allosteric conformations by the iron high-spin–low-spin switch. We have proposed that the triggering of the pumps for ion transfer is similar. In each case the selective binding of, respectively, calcium, oxygen, protons, sodium or calcium, or indeed any channel-opening or pump-regulating molecule, depends upon the rearrangement of helical rods (Fig. 7). These proteins are not built from extended β-sheets as are most enzymes (Fig. 6). The essential difference between an extended sheet and a set of helices is that a sheet provides the more stable long-range two-dimensional order while the rod gives only a one-dimensional long-range order. (Note that a two-stranded sheet is a useful flexible device.) It is easier to rotate rods than sheets and, since the sheets are often closed round in enzymes by loops, it is easier to slide rods. Rods not sheets are the essence of mechanical devices in man's machines, and for very good reason. The mechanical not the catalytic devices of biology are based therefore on helical rods probably

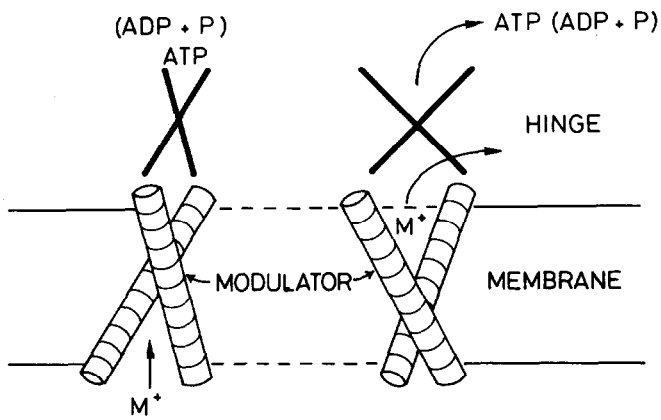

Fig. 7. Proposed scheme for the trigger action of a helical protein. A metal ion such as calcium binds, and by so doing twists and displaces the helices. The displacement drives an enzyme to a new state. The device can be used in reverse to transport ions using the energy of the enzyme reaction.

of necessity. Enzymes can not be so simply based on helices alone since the rods in proteins are weakly cross-linked for the most part by hydrophilic forces of poor directional quality and do not give a framework for selectivity. We shall turn attention away from the enzyme structures which are relatively rigid to the more loosely constructed proteins.

METAL ANTAGONISMS AND REPLACEMENTS

The elements most similar to zinc are cobalt(II) and cadmium. There is no problem from cobalt in living systems since it is rare, but it is an extremely valuable probe atom since its spectroscopic properties and its general chemical similarity with zinc allow it to be functional and observable. This type of isomorphic replacement is very similar to that observed in spinels, being dependent on size and stereochemistry. The easy introduction of the larger cadmium ion into zinc sites is somewhat adjustable. Unfortunately this substitution can lead to major problems *in vivo*. Cadmium poisoning is one of several man-made diseases grouped together under pollution. Metallothionine offers considerable protection, as one would expect from the simple analysis tables, since CdS is precipitated in Group II but not ZnS. Cadmium can be readily determined using dithizone, which brings us back to the beginning of this article and my research work started under Dr H. Irving.

CONCLUSION

I hope, Harry, that you enjoy this article. It has some (probably too much) of the personal provocative approach which you typify. I hope that it contains some of the disciplined constraints which you taught. I think it is thoughtful, reflective and cheeky. The study of chemistry or biochemistry is not dull but full of surprise, and there is the need for flexibility of thought. If my article is to be a compliment to you then I truly hope that it contains these elements. The supervisor is the father of the pupil and inheritable characteristics are inevitably transferred. Apart from my research, I have also tried to see to it through my pupils—your grandchildren—that the inheritance does not die out. They are responsible for much of the work in which I have been involved. As far as the family tree of the chemistry rather than the people is concerned, zinc dithizone was the father of this article.

Acknowledgements—I have not provided references for this article since they can all be obtained from reviews of zinc biochemistry in many review series on bio-inorganic chemistry. I am grateful to the editors of *Endeavour* for permission to reproduce several figures from my article in *Endeavour, New Series*, 1984, **8**, 65, which also has the necessary references.

Polyhedron Vol. 6, No. 1, pp. 71–78, 1987
Printed in Great Britain

0277–5387/87 $3.00+.00

TIN(II) CHLORIDE IN THE ANALYTICAL CHEMISTRY OF THE PLATINUM METALS: FROM THE "PURPLE OF CASSIUS" TO POLYURETHANE FOAMS

KARIM F. G. BRACKENBURY, LYNN JONES, IRIS NEL, KLAUS R. KOCH* and JEAN M. WYRLEY-BIRCH

Department of Analytical Science, University of Cape Town, P. Bag, Rondesbosch 7700, South Africa

(*Received* 3 *July* 1986)

Abstract—Tin(II) chloride has played a central role in the non-instrumental analytical chemistry of the platinum group metals, the characteristic reaction between tin(II) chloride and platinum(II/IV) chloride having been documented for more than 180 years. The intense colour of hydrochloric acid solutions containing small amounts of Pt(II/IV) and tin(II) chloride constituted one of the first trace colorimetric methods for the determination of Pt in the sub parts per million range. Similar spectrophotometric methods of trace analysis for Rh have been known for more than half a century. Remarkably the detailed nature of the interaction of tin(II) chloride with the platinum group metals has only been elucidated relatively recently, and there is evidence of recent renewed interest in platinum group metal complexes involving the $SnCl_3^-$ moiety as ligand. We wish here to give a brief history of the use of tin(II) chloride in the analytical chemistry of the platinum group metals, highlighted by some of our recent work involving the selective immobilization of chloro(trichlorostannato)platinum/rhodium complex anions by polyurethane foams as a means of separation and pre-concentration of small amounts of Rh and Pt.

HISTORICAL PERSPECTIVE

The characteristic reaction between tin(II) chloride and gold(III) chloride in dilute aqueous solution certainly ranks alongside one of the earliest qualitative colorimetric methods for the detection of small quantities of Au. The discovery of the "purple of Cassius" is attributed to one Dr A. Cassius,[1] at Leyden, in the year 1663.[2] Although the analytical potential of the "purple of Cassius" was probably not initially recognized, nor indeed of interest,[1] the purple-red colouration produced when a solution containing gold(III) chloride is treated with tin(II) chloride had already become well-established as a sensitive method for the detection of traces of Au in mid-nineteenth-century textbooks of qualitative chemical analysis.[3,4] The nature of the precipitated "purple of Cassius" remained poorly understood long after its discovery, although evidence that the purple colour was essentially due to a form of colloidal metallic Au dates to 1780.[1] Nevertheless it was to be more than a century before Schneider[5] and Zsigmondy[6] clearly established the true colloidal nature of the "purple of Cassius" as well as the conditions for its formation. Presently it is generally accepted that the "purple of Cassius" consists mainly of finely dispersed metallic Au, adsorbed onto an insoluble form of hydrous stannic oxide.[1,6] Essentially then, the formation of the "purple of Cassius" by reaction between tin(II) chloride and gold(III) chloride may be described as redox in nature, although this view is probably an oversimplification in the light of recent evidence of the formation of complexes of gold involving Au—Sn bonds,[7] in which the $SnCl_3^-$ moiety behaves as a Lewis acid.

Although we have not been able to establish a definite link between the "purple of Cassius" and the discovery of a similarly characteristic reaction

* KRK was appointed lecturer in the newly established Department of Analytical Science at UCT under the Headship of Professor H. M. N. H. Irving (1979–1984). Author to whom correspondence should be addressed.

between tin(II) chloride and platinum(II/IV) chloride, it seems reasonable to postulate that such a link exists. W. H. Wollaston, one of the early pioneers in the chemistry of Pt,[8] first reported the characteristic red-brown colour produced when an acid solution of platinum(II/IV) chloride is treated with excess tin(II) chloride in 1804.[9] Evidently the intense blood-red colour so produced was rapidly adopted as a sensitive qualitative spot test for the presence of Pt, alongside the "purple of Cassius".[3,4] Indeed, the tin(II) chloride spot test for traces of Pt still enjoys prominence in present-day texts,[10,11] as one of the more sensitive tests available, 25×10^{-9} g Pt being easily detectable.

Early attempts to elucidate the nature of the reaction between Pt salts and tin(II) chloride were undoubtedly influenced by comparison with studies of the "purple of Cassius". Nevertheless, Wöhler and Spengel[12] recognized that the red reaction product was extractable into ether, thus ruling out a possible coloidal suspension of finely divided metallic Pt. On the other hand, the idea of reduction of platinum(II/IV) to a metallic state by tin(II) chloride seems so firmly lodged, that recently revised text-books,[10,11] still regard Pt as being reduced to "colloidal Pt" or "to the elementary state". The extractable nature of the intensely red Pt–Sn compound(s) was later exploited by Wölbing who, in 1934, not only demonstrated a quantitative colorimetric method for the determination of small amounts of Pt, but also utilized an ethylacetate extraction procedure to separate Pt from other noble metals.[13]

Nearly two decades later, Ayres and Meyer undertook a series of detailed spectrophotometric investigations of the reaction between tin(II) chloride and Pt,[14–17] Pd[15] and Rh[15] in HCl. Attempts to understand the nature of these chromogenic reactions[14,15] went in hand with a critical evaluation of these colorimetric methods for the determination of some of the platinum metals.[18,19] Such studies convincingly established the utility of tin(II) chloride as a colorimetric reagent for the microdetermination of Pt(II/IV) by measuring the absorption maximum at $\lambda_{max} = 310$ nm (molar absorptivity 3.95×10^4). The reductive power of tin(II) chloride undoubtedly influenced these early attempts to characterize the red Pt–Sn reaction product(s). Thus, Ayres and Meyer postulated the formation of a tetrapositive $[PtSn_4Cl_4]^{4+}$ cation, in which Pt was thought to be reduced to a zerovalent state.[17] This confusion is understandable, since it has only recently been shown conclusively that some platinum group metals in their highest common oxidation states, viz. Pt(IV), Rh(III) and Ru(IV), are certainly reduced to lower formal oxidation states, Pt(II),[20] Rh(I)[21] and Ru(III/II)[22] by tin(II) chloride in aqueous HCl solution. Although complete reduction of Pt (and Rh) by tin(II) chloride is possible under more forcing conditions in HCl, the circumstances under which this occurs have yet to be clearly demonstrated. On the contrary tin(II) chloride is thought to stabilize Pt(II) to further reduction by molecular hydrogen (see below).[23,24]

The true nature of the highly coloured species formed by reaction of Pt(II) and Rh(III) with tin(II) chloride was first revealed by two independent groups. In the same year, Stolberg and coworkers,[25] as well as Davies *et al.*,[26] showed that complex Pt(II) and Rh(III) *anions* containing $SnCl_3^-$ moieties could be precipitated with bulky cations. Thus Cramer *et al.*[25] isolated compounds such as red $[(C_6H_5)_3PCH_3]_3[Pt(SnCl_3)_5]$ and yellow $[(C_6H_3)_3PCH_3]_2[PtCl_2(SnCl_3)_2]$, along with neutral $[Pt(P(C_6H_5)_3)_2(SnCl_3)Cl]$, while Davies *et al.*[26] reported isolation of $[(CH_3)_4N]_4[Rh_2Sn_4Cl_{14}]$. These preliminary reports were soon followed by a detailed investigation by Young *et al.*,[27] in which the syntheses and properties of a considerable number of neutral and anionic complexes of Pt, Rh, Ir and Ru with tin(II) chloride, were reported. In each of these compounds a direct M—Sn bond was postulated, involving the $SnCl_3^-$ moiety as ligand. An X-ray diffraction study of the unusual $[(C_6H_5)_3PCH_3]_3[Pt(SnCl_3)_5]$ complex confirmed directly the trigonal bipyramidal structure of the pentakis(trichlorostannato)platinum(II) anion, showing discrete Pt—Sn bonds (mean length 2.54 Å).[28] This report was followed shortly by the X-ray crystal structure of a highly unusual trigonal bipyramidal Pt–Sn cluster $(C_8H_{12})_3Pt(SnCl_3)_2$ in which the Pt atoms form a triangle, capped by two Sn atoms (Pt—Sn distances 2.80 Å).[29] The latter structure clearly illustrates the uncertainty in the formal oxidation state of the Pt atoms; a simplistic view yields an oxidation state of +2/3 per Pt atom, assuming Sn(II).

Tin(II) *chloride as reducing agent*

At this point it may be appropriate to emphasize the dual role of tin(II) chloride both as reducing agent as well as ligand in the form of the $SnCl_3^-$ moiety. Although to our knowledge relatively little work has been undertaken concerning redox reactions with the platinum group metals in general, it has been established that Pt(IV) in HCl is certainly rapidly reduced by tin(II) chloride according to an overall rate law: $-d[Pt]/dt = k_{obs}[Pt(IV)][Sn(II)]$, where $k_{obs} = 473 \pm 22$ dm^3 mol^{-1} s^{-1} at 297 K.[20] This reduction is followed by a slower complex formation in which the Pt(II) state appears to be

stabilized to further reduction (see below). In the case of Rh(III), Ir(IV) and Ru(III/IV) reduction to Rh(I),[21] Ir(III)[30] [or Ir(I)][27] and Ru(III/II)[31-33] is also known to occur, but no detailed kinetic studies have appeared. The circumstances under which reduction does occur are in any event not fully understood as it appears for example that Rh(III) is only reduced to Rh(I) in the presence of sufficient excess tin(II) chloride,[21] in order to stabilize the Rh(I) by complex formation with $SnCl_3^-$. The behaviour of Pd(II) on the other hand resembles that of Au(III) most closely, in that the reaction of $PdCl_4^{2-}$ with tin(II) chloride in HCl leads to the formation of transient red-brown and yellow complexes of probable formulation $[PdCl_{4-n}(SnCl_3)_n]^{2-}$ ($n = 1$–4),[34] followed by the formation of an unstable dark green hydrosol, from which ultimately metallic Pd may be recovered. This hydrosol of Pd is not extractable into organic solvents such as 4-methylpentan-2-one (MIBK). Since the chloro(trichlorostannato)platinum(II) complex anions may be readily extracted into MIBK, this difference between Pd(II) and Pt(II) may be conveniently exploited for the quantitative separation of these two metals by extraction with MIBK in the presence of a reasonable excess of tin(II) chloride. Figure 1 shows the distribution of equimolar amounts of Pt(II) and Pd(II) (3×10^{-2} mmol) between 2.4 mol dm^{-3} HCl containing an excess (3×10^{-1} mmol) $SnCl_2$ and various mixtures of MIBK and *n*-hexane [% (v/v)]. Extractions were performed 20 min after mixing of solutions, during which time the Pd hydrosol is fully developed. By controlling the HCl concentration, the amount of tin(II) chloride present, the contact time and the organic-phase composition, quantitative separation of Pt(II) from a 10-fold molar excess of Pd(II) is readily possible.

Trichlorostannato anion as ligand

Interest in Pt(II) complexes involving the trichlorostannato ligands was probably encouraged by the discovery reported in 1963 that solutions containing chloro(trichlorostannato)platinum(II) complex anions readily catalyse homogeneous hydrogenation of ethylene and acetylene at room temperature and low H_2 pressures.[25] Following this early report of the catalytic properties of Pt–Sn complexes, the highly selective hydrogenation of oils such as methyl linolenate to unconjugated dienes has been studied in detail,[23] while homogeneous olefin hydroformylation catalysis by platinum(II) group IVB metal halide complexes has been examined.[24,35] Recently Saito *et al.* proposed a rhodium–tin(II) chloride catalytic system for photo-enhanced dehydrogenation of propan-2-ol.[36,37] The latter system shows promise in the quest to convert solar energy into useful chemical energy, in the form of hydrogen. The role of tin(II) chloride in these catalytic systems is not completely understood, although actively under investigation.[38] It is, however, generally agreed that the $SnCl_3^-$ ligand:

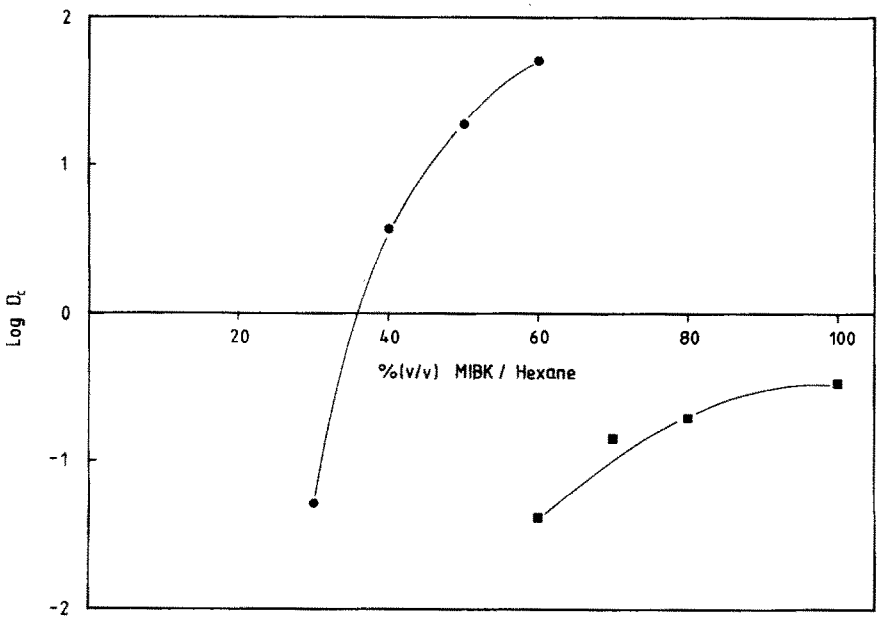

Fig. 1. Distribution coefficients (log D_c) of Pt(II) and Pd(II) between 2.4 mol dm^{-3} HCl and various mixtures of MIBK in *n*-hexane [% (v/v)], in the presence of excess tin(II) chloride at 295 K [Sn(II): $M = 10$ (M = mol Pt+Pd)].

(a) stabilizes Pt(II) to reduction by H_2 to the metallic state with the formation of complex hydride species,[23,24] and (b) the strongly "π-acid" nature of the $SnCl_3^-$ ligand[39] labilizes the often kinetically inert complexes of the platinum group metals to ligand substitution.

A consequence of (a) above is the facile formation of a variety of platinum group metal complex hydrides[40] such as $[Pt(SnCl_3)_4H]^{3-}$ and $H_2Ir(SnCl_3)(PPh_3)_3$. In this context, we have recently observed the formation of a transient complex hydride species of Rh, on simply extracting rhodium(III) chloride from dilute HCl containing excess tin(II) chloride into 4-methylpentan-2-one.[41] This species is best formulated to be $[RhH(SnCl_3)_4Cl]^{3-}$ on the basis of ^{119}Sn NMR evidence. Incidentally, the advent of routine multinuclear Fourier transform (FT) NMR has resulted in great advances in the chemistry of the platinum group metals involving the trichlorostannato ligand, since two naturally occurring isotopes, ^{117}Sn and ^{119}Sn, both have spin $I = \frac{1}{2}$ and, at 7.61 and 8.58% natural abundance, respectively, are easily observed by modern FT NMR spectroscopy.[42] Consequently many authors have used ^{119}Sn–$\{^1H\}$, ^{31}P–$\{^1H\}$ and ^{195}Pt–$\{^1H\}$ NMR spectroscopy to elucidate the fundamental solution chemistry of Pt(II) complexes involving the $SnCl_3^-$ ligand.[38,43–46] Similar studies involving Rh[36,37,41] and Ru[30,47] have been reported.

In the realm of analytical chemistry, the strong *trans* effect of the $SnCl_3^-$ moiety as ligand (comparable to CN^- and CO),[39] has been usefully exploited as a catalyst of ligand substitutions in the usually kinetically inert platinum group metals. Thus a number of solvent extraction schemes for the platinum group metals by a variety of organic extractants have utilized tin(II) chloride as a reducing as well as a "labilizing" agent.[48] The extractive separation of Rh from Ir by diphenylthiourea is catalysed by tin(II) chloride for example, and appears to be quantitative only in the presence of the latter reagent.[49] Similar use of tin(II) chloride was reported by Mojski:[50] the extraction efficiency of Pt, Rh, Ru and Ir by triphenylphosphine from HCl into 1,2-dichloroethane is considerably increased in the presence of tin(II) chloride. Although the role of tin(II) chloride in promoting rapid ligand substitutions of the inert platinum group metals is undisputed, the mechanism of the "labilizing" effect of tin(II) chloride sometimes involves the extraction of complexes containing the $SnCl_3^-$ ligands. In this context we have shown that the extraction of $PtCl_4^{2-}$ by triphenylphosphine in the presence of tin(II) chloride involves the transient formation and extraction of $[Pt(SnCl_3)Cl(PPh_3)_2]$ and $[Pt(SnCl_3)_2(PPh_3)_2]$ into the organic phase, followed by eventual disproportionation of such species, with back extraction of tin(II/IV) chloride into the aqueous phase.[51]

POLYURETHANE FOAM EXTRACTIONS OF THE PLATINUM GROUP METALS

Flexible polyurethane foams are ubiquitous in everyday life, the remarkable versatility of this polymer having prompted the manufacture of a myriad of products for a wide variety of applications. In 1980, about 3×10^6 tons of urethane polymer was consumed worldwide.[52] The versatility of this polymer has recently been extended into the realm of analytical chemistry by the discovery of Bowen[53] that flexible polyurethane foams have the capacity to absorb a large variety of organic and inorganic substances. Amongst the various types of metal complexes that are sorbed by the polyurethane polymer is a group of highly polarizable complex anions such as $AuCl_4^-$ and $FeCl_4^-$, and a host of other transition-metal thiocyanate complexes including those of Rh, Pt and Pd.[54] The continuing interest in the use of polyurethane foams in the separation and pre-concentration of a large range of substances is underscored by the publication of a monograph[55] and a CRC handbook[56] devoted entirely to this subject.

We have recently reported an efficient method for the semi-selective sorption of Pt(II) from dilute hydrochloric acid in the presence of sufficient tin(II) chloride.[57] Detailed studies have been carried out involving the sorption of Pt(II) and Rh(III) from HCl by polyurethane foams in the presence of tin(II) chloride, and it is some of these results we wish to report briefly here.

Chloro(trichlorostannato)platinum(II) complex anions are rapidly and efficiently sorbed by polyurethane foams from 0.5–5.0 mol dm^{-3} HCl solution. The maximum sorptive capacity of the foam with respect to platinum [C(Pt)] depends on the temperature, HCl concentration, the Sn(II):Pt(II) ratio, as well as the presence of alkali earth metal cations, notably K^+. The presence of K^+ ions has a marked depressive effect on the value of C(Pt). Table 1 shows some typical C(Pt) values at 25 and 40°C for a variety of solution conditions. Evidently even at relatively low Sn(II):Pt(II) mole ratios (R_a) in solution, considerable quantities of Pt are sorbed by the foam. Furthermore, we have found that, at 1.0 mol dm^{-3} HCl, the amount of Pt sorbed per unit mass of foam reaches a peak at a value of R_a = 4–5, only to decrease slightly and level off at $R_a > 10$ (Fig. 2). By simultaneous monitoring of the quan-

Table 1. Maximum sorptive capacity of polyurethane foam (cf. Fig. 2) for Pt(II) in 1.0 mol dm^{-3} HCl containing tin(II) chloride, measured for various initial Pt(II) concentrations

[Pt] ($\mu g\ cm^{-3}$)	Sn(II)/Pt	Maximum capacity (mol kg^{-1})			
		$T = 25°C$		$T = 40°C$	
		2	5	2	5
50		0.39	0.50	0.26	0.44
100		0.51	0.59	0.39	0.60
150		0.57	0.58	0.48	0.65
200		0.68	0.66	0.52	0.61

tity of Sn that is coextracted with the Pt, we have determined the average mole Sn : Pt ratio of species sorbed by the foam (R_f). As may be seen from Fig. 2 the value of R_f tends to 5 in the presence of sufficient Sn(II) in solution.

These data suggest that the species preferentially sorbed by the polyurethane foam is the $[Pt(SnCl_3)_5]^{3-}$ complex anion. Nelson and Alcock[58] have recently re-examined the crystal and solution structure of $[(C_6H_5)_3PCH_3]_3[Pt(SnCl_3)_5]$, and found that the $[Pt(SnCl_3)_5]^{3-}$ anion retains its trigonal bipyramidal structure in solution. Furthermore, these authors found no ^{119}Sn and ^{195}Pt NMR evidence of $[Pt(SnCl_3)_5]^{3-}$ dissociating into products such as $[Pt(SnCl_3)_4]^{2-}$ or $[Pt(SnCl_3)_2Cl_2]^{2-}$ in acetone solutions. We have previously examined the solvent extraction of $PtCl_4^{2-}$ in the presence of $SnCl_2$ from HCl into MIBK.[59] Examination of an MIBK extract [obtained from 2 M HCl with Sn(II) : Pt(II) = 10] by means of 186.5-MHz ^{119}Sn NMR showed evidence of only a single set of resonances at 303 K; [$\delta(^{119}Sn) = -127.9$ ppm relative to $(CH_4)_4Sn$, $^1J(^{195}Pt–^{119}Sn) = 16{,}028$ Hz, $^2J(^{117}Sn–^{119}Sn) = 6252$ Hz]. This resonance may be assigned to the $[Pt(SnCl_3)_5]^{3-}$ complex anion on the basis of very similar spin–spin coupling data from the work of Nelson [$^1J(^{195}Pt–^{119}Sn) = 16{,}030$ Hz, $^2J(^{117}Sn–^{119}Sn) = 6230$ Hz].[58]

It is thus reasonable to postulate that, in the case of polyurethane foam extractions, a similar species

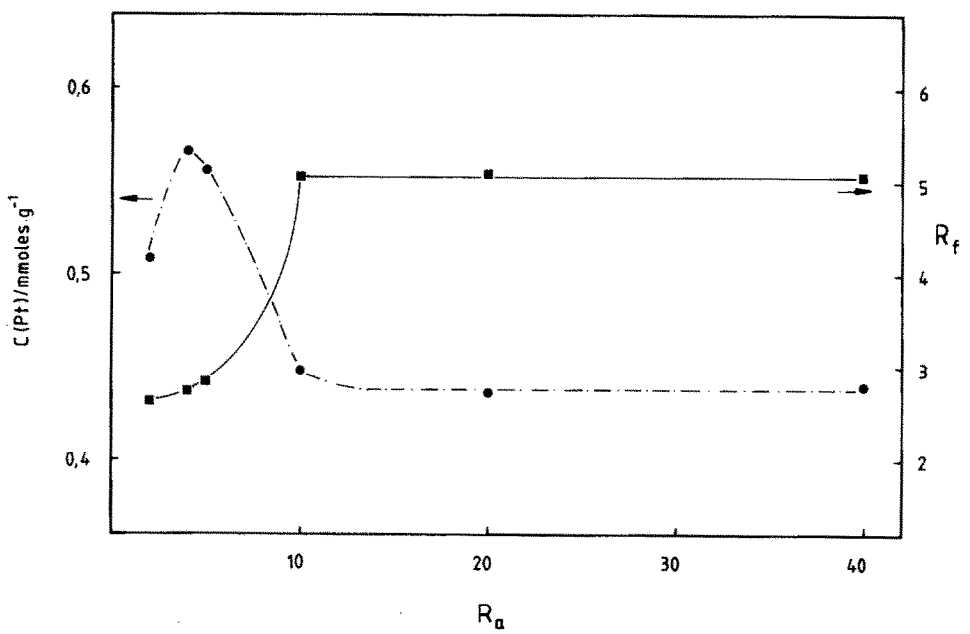

Fig. 2. Variation of the maximum sorptive capacity [C(Pt)] of polyurethane foam [prepared from polypropylene oxide (MW 3400) and an 80 : 20 (v/v) mixture of 2,4- and 2,6-toluene diisocyanate] toward Pt(II) in 1.0 mol dm^{-3} HCl at 298 K as a function of the Sn(II) : Pt mole ratio (R_a). Also shown is the Sn : Pt mole ratio, as observed on the foam (R_f).

Table 2. Recovery and separation of Pt(II) and Ir(IV) by polyurethane foam from 2.0 mol dm^{-3} HCl at room temperature, in the presence of sufficient tin(II) chloride

Platinum[a]		Iridium[b]		Conditions
Taken (mg)	Found (mg)	Taken (mg)	Found (mg)	Sn(II)/M ratio[c]
0.25 ($n = 10$)	0.23±0.01	—	—	30
0.50 ($n = 10$)	0.51±0.03	—	—	30
1.00 ($n = 10$)	1.03±0.06	—	—	30
2.50 ($n = 7$)	2.52±0.06	2.46	2.41±0.08	30
1.00 ($n = 5$)	1.00±0.01	9.85	9.55±0.4	30
0.10 ($n = 6$)	0.095±0.006	9.85	9.82±0.3	30

[a] Platinum found sorbed by 400-mg block of foam.
[b] Iridium left in solution.
[c] Sn(II) : M mole ratio, M = Pt + Ir.

may be involved, especially in view of the observed Sn : Pt ratios found on the foam.

On a more practical level, we have found that small amounts of Pt can be quantitatively sorbed by polyurethane foams as a means of pre-concentration of this metal. The Pt-loaded foam may then be readily dissolved in hot HNO_3–HCl for subsequent analysis. In this way 250 μg Pt may readily be recovered from a 250-cm^3 solution by a 100-mg block of foam, representing a concentration factor of *ca* 2.5×10^3. Table 2 shows some of the results of Pt separation and recovery experiments. It is clear that, in the presence of sufficient Sn(II), satisfactory recoveries of up to 100 μg Pt per 200 cm^3 solution are achieved even in the presence of a 10^2-fold molar excess of Ir(IV) in 2 mol dm^{-3} HCl.

Rhodium(III) chloride reacts fairly rapidly with tin(II) chloride, and in a similar fashion to Pt(II) in dilute HCl, a variety of Rh(III) and Rh(I) chloro(trichlorostannato)rhodium(III/I) complex anions are formed.[21,26,27] We have examined the extraction of rhodium(III) chloride from dilute HCl containing sufficient tin(II) chloride into MIBK.[60] In this manner, Rh may be readily separated from Ru and Ir, since the formation of correspondingly extractable chloro(trichlorostannato)ruthenium and chloro(trichlorostannato)iridium does not occur at room temperature. On this basis, it might be expected that polyurethane foams should sorb chloro(trichlorostannato)rhodium complex anions. This expectation is amply confirmed by results shown in Fig. 3.

In contrast to the sorption of Pt, it appears that a greater excess of tin(II) chloride results in increasing amount of Rh being sorbed by (cf. Fig. 2). Furthermore, analysis of the of samples loaded foam yields Sn : Rh ratios in the range 3.6–4.5, suggesting that a variety of chloro-(trichlorostannato)rhodium(III/I) species may be simultaneously sorbed by the foam. Such an idea is supported by an ^{119}Sn NMR study of an MIBK extract of an HCl solution containing $RhCl_3 \cdot 3H_2O$ and excess $SnCl_2$. We have found that at least seven sets of ^{119}Sn resonances are observable in MIBK extracts obtained under various conditions:[60] of these, $[Rh(SnCl_3)_5Cl]^{3-}$ [$\delta(^{119}Sn) = -117.5$ ppm, $^1J(^{103}Rh–^{119}Sn) = 558$ Hz, $^2J(^{117}Sn–^{119}Sn) = 1943$ Hz], $[Rh(SnCl_3)_4Cl_2]^{3-}$ [$\delta(^{119}Sn) = -209.6$ ppm; $^1J(^{103}Rh–^{119}Sn) = 587$ Hz, $^2J(^{117}Sn–^{119}Sn) = 2216$ Hz], and $[Rh(SnCl_3)_3Cl_3]^{3-}$ [$\delta(^{119}Sn) = -369.3$ ppm, $^1J(^{103}Rh–^{119}Sn) = 731$ Hz, $^2J(^{117}Sn–^{119}Sn) = 3034$ Hz] have been positively assigned in good agreement with the work of Saito.[21] In addition, as already referred to above, we have also identified a hydrido species $[RhH(SnCl_3)_4Cl]^{3-}$, in the MIBK phase.[41] It is thus reasonable to propose that a qualitatively similar distribution of species may be sorbed by the polyurethane foam, as suggested by the observed trends (Fig. 3). We have carried out a detailed study of the optimum conditions of sorption of chloro(trichlorostannato)-rhodium(I/III) complexes by polyurethane foams, and found that rhodium may quantitatively be separated from iridium and ruthenium by this means. Details of this work are, however, to be published elsewhere.[61]

In conclusion, we have found that small amounts of Pt(II/IV) and Rh(III) are remarkably efficiently removed from dilute HCl containing a reasonable excess of tin(II) chloride by means of polyurethane foams. Neither Ir(IV) nor Ru(III/IV) is appreciably retained by the polyurethane polymer under similar

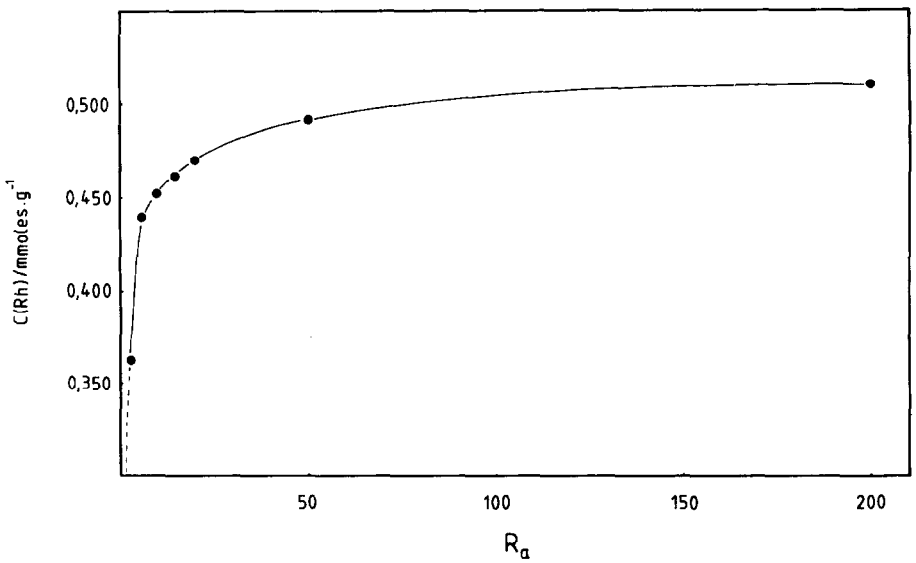

Fig. 3. Sorptive capacity of polyurethane foam toward Rh(III)[C(Rh)] as a function of the Sn(II): Rh(III) mole ratio (R_a) from 2.0 mol dm^{-3} HCl at 313 K.

conditions, hence a clean separation of Pt and Rh from Ir and Ru is possible. Preliminary work indicates that the immobilized Pt and Rh may be conveniently stripped from the polyurethane foam by hot (60°C) 2.5–5.0% (v/v) conc. HCl in ethanol, leading to essentially quantitative recovery of the noble metal. The presence of relatively large amounts of base metals such as Cu, Zn, Ni, Co, Mn and Fe does not significantly affect the immobilization of Pt and Rh in the presence of tin(II) chloride by polyurethane foam. Finally the Sn may be removed from either Pt or Rh by distillation of the volatile $SnBr_4$ at relatively low temperatures.

Acknowledgements—We would like to pay tribute to Professor H. M. N. H. Irving on the occasion of his 81st birthday. We hope that this will be a fitting contribution to mark this occasion. We gratefully acknowledge generous financial assistance from the University of Cape Town, the CSIR (IN and LJ), and MINTEK (KFGB and JMWB), as well as AECI (IN).

REFERENCES

1. Gmelin, *Handbuch der Anorganischen Chemie*: *Gold*, Vol. 62(1), pp. 79 and 92. Verlag Chemie, Weinheim (1950).
2. R. von Wagner, *Manual of Chemical Technology*, p. 452. J. and A. Churchill, London (1904).
3. C. R. Fresenius (Translated by C. E. Groves), *Qualitative Chemical Analysis*, 10th Edn, p. 158. J. and A. Churchill, London (1887).
4. A. H. Sexton, *Outlines of Qualitative Analysis*, 3rd Edn, p. 45. C. Griffin, London (1892).
5. E. A. Schneider, *Z. Anorg. Chem.* 1894, **5**, 80.
6. R. Zsigmondy, *Justus Liebigs Ann. Chem.* 1898, **301** 361.
7. R. J. Puddephatt, *The Chemistry of Gold*, Monograph 16, Topics in Inorganic and General Chemistry, p. 169. Elsevier, Amsterdam (1978).
8. L. B. Hunt, *Platinum Met. Rev.* 1985, **29**, 30.
9. W. H. Wollaston, *Philos. Trans.* 1804, 427.
10. F. Feigl and V. Anger, *Spot Tests in Inorganic Analysis*, 6th English Edn, p. 394. Elsevier, Amsterdam (1972).
11. G. Svehla, *Vogel's Textbook of Macro and Semimicro Quantitative Inorganic Analysis*, 5th Edn, p. 517. Longmans, London (1979).
12. L. Wöhler and A. Spengel, *Z. Chem. Ind. Kolloide* 1910, **7**, 243.
13. H. Wölbing, *Ber.* 1934, **67B**, 773.
14. G. H. Ayres and A. S. Meyer, *Anal. Chem.* 1951, **23**, 299.
15. G. H. Ayres, *Anal. Chem.* 1953, **25**, 1623.
16. O. I. Milner and G. F. Shipman, *Anal. Chem.* 1955, **27**, 1476.
17. G. H. Ayres and A. S. Meyer, *J. Am. Chem. Soc.* 1955, **77**, 2671.
18. F. E. Beamish and W. A. E. McBryde, *Anal. Chim. Acta* 1958, **18**, 551.
19. S. S. Berman and E. C. Goodhue, *Can. J. Chem.* 1959, **37**, 370.
20. K. G. Moodley and M. J. Nicol, *J. Chem. Soc., Dalton Trans.* 1977, 239.
21. H. Moriyama, T. Aoki, S. Shinoda and Y. Saito, *J. Chem. Soc., Dalton Trans.* 1981, 639.
22. H. Remy and A. Lührs, *Ber.* 1929, **62**, 200.
23. E. N. Frankel, E. A. Emben, H. Itatani and J. C. Bailar, *J. Org. Chem.* 1967, **32**, 1447.
24. I. Schwager and J. F. Knifton, *J. Catal.* 1976, **45**, 256.

25. R. D. Cramer, E. L. Jenner, R. V. Linday, Jr and U. G. Stolberg, *J. Am. Chem. Soc.* 1963, **85**, 1691.
26. A. G. Davies, . Wilkinson and J. F. Young, *J. Am. Chem. Soc.* 1963, **85**, 1692.
27. J. F. Young, R. D. Gillard and G. Wilkinson, *J. Chem. Soc.* 1964, 5176.
28. R. D. Cramer, R. V. Lindsey, C. T. Prewitt and U. G. Stolberg, *J. Am. Chem. Soc.* 1965, **87**, 658.
29. L. J. Guggenberger, *J. Chem. Soc., Chem. Commun.* 1968, 512.
30. R. C. Taylor, J. F. Young and G. Wilkinson, *Inorg. Chem.* 1966, **5**, 20.
31. H. Okuno, T. Ishimori, K. Mizumachi and H. Ihochi, *Bull. Chem. Soc. Jpn* 1971, **44**, 415.
32. L. J. Farrugia, B. R. James, C. R. Lassigne and E. J. Wells, *Can. J. Chem.* 1982, **60**, 1304.
33. M. Mukaida, *Bull. Chem. Soc. Jpn* 1970, **43**, 3805.
34. V. I. Shlenskaya, A. A. Biryukov and L. N. Moryakova, *Russ. J. Inorg. Chem. (Engl. Transl.)* 1969, **14**, 256.
35. Y. Kawabata, T. Hayashi and I. Ogata, *J. Chem. Soc., Chem. Commun.* 1979, 462.
36. S. Shinoda, H. Moriyama, Y. Kise and Y. Saito, *J. Chem. Soc., Chem. Commun.* 1978, 348.
37. H. Moriyama, T. Aoki, S. Shinoda and Y. Saito, *J. Chem. Soc., Perkin Trans.* 2 1982, 369.
38. G. K. Anderson, H. C. Clark and J. A. Davies, *Inorg. Chem.* 1983, **22**, 427.
39. D. R. Coulson, *J. Am. Chem. Soc.* 1976, **98**, 3111.
40. H. D. Kaesz and R. B. Saillant, *Chem. Rev.* 1972, **72**, 231.
41. K. R. Koch and J. M. Wyrley-Birch, *Inorg. Chim. Acta* 1985, **102**, L5.
42. C. Brevard and P. Granger, *Handbook of High Resolution Multinuclear NMR*, p. 168. John Wiley, New York (1981).
43. P. S. Pregosin and S. Ning Sze, *Helv. Chim. Acta* 1978, **61**, 1848.
44. K. A. Ostoja Starzewski and P. S. Pregosin, *Angew. Chem.* 1980, **92**, 323.
45. J. H. Nelson, V. Cooper and R. W. Rudolph, *Inorg. Nucl. Chem. Lett.* 1980, **16**, 263.
46. A. Albatini, P. S. Pregosin and H. Ruegger, *Inorg. Chem.* 1984, **23**, 3223.
47. H. Moriyama, T. Aoki, S. Shinoda and Y. Saito, *J. Chem. Soc., Chem. Commun.* 1982, 500.
48. F. B. Beamish, *The Analytical Chemistry of Noble Metals*. Pergamon Press, Oxford (1966).
49. A. Diamontatos and A. A. Verbeek, *Anal. Chim. Acta* 1977, **91**, 287.
50. M. Mojski, *Talanta* 1980, **27**, 7.
51. K. R. Koch and J. E. Yates, *Anal. Chim. Acta* 1983, **147**, 235.
52. *Kirk–Othmer Encyclopedia of Chemical Technology*, 3rd Edn., Vol. 23, p. 576. John Wiley, New York (1983).
53. H. J. M. Bowen, *J. Chem. Soc.* 1970, 1082.
54. S. J. Al-Bazi and A. Chow, *Talanta* 1984, **31**, 815.
55. G. J. Moody and J. D. R. Thomas, *Chromatographic Separation and Extraction with Foamed Plastics and Rubbers*. Marcel Dekker, New York (1982).
56. T. Braun, J. D. Navratil and A. B. Farag, *Polyurethane Foam Sorbents in Separation Science*. CRC Press, Boca Raton, FL (1985).
57. K. R. Koch and I. Nel, *Analyst* 1985, 217.
58. J. H. Nelson and N. W. Alcock, *Inorg. Chem.* 1982, **21**, 1196.
59. N. Ahmed and K. R. Koch, *Anal. Chim. Acta* 1984, **162**, 347.
60. K. R. Koch and J. M. Wyrley-Birch, unpublished results and M.Sc. thesis (JMWB) (1984).
61. L. Jones, I. Nel and K. R. Koch, *Anal. Chim. Acta* 1986, **182**, 61.

Polyhedron Vol. 6, No. 1, pp. 79–84, 1987
Printed in Great Britain

0277–5387/87 $3.00+.00

SPECTROCHEMISTRY OF SOLUTIONS—XVII.* VIBRATIONAL SPECTRA OF CYANO-PALLADIUM(II) COMPLEXES IN LIQUID-AMMONIA SOLUTIONS

PETER GANS,† J. BERNARD GILL†‡ and DOUGLAS MacINTOSH

Department of Inorganic and Structural Chemistry, The University, Leeds LS2 9JT, U.K.

(*Received* 3 *July* 1986)

Abstract—Complexation of Pd^{2+} by CN^- in liquid ammonia has been studied by means of IR and Raman spectra of the solutions. Stepwise complexation occurs up to the square-planar 4:1 species. In the 2:1 step *trans*-$Pd(CN)_2$ is initially formed at subambient temperatures but slowly equilibrates ($t_{1/2}$ = 6 h) at 293 K into a mixture containing both the *cis* and the *trans* isomers. The 2:1 and 4:1 complexes appear to be thermodynamically very stable. All the 11 C—N stretching modes of vibration of $[(NH_3)_3Pd(CN)]^+$, *cis*- and *trans*-$[(NH_3)_2Pd(CN)_2]$, $[(NH_3)Pd(CN)_3]^-$ and $[Pd(CN)_4]^-$ have been observed and assigned. There is no spectroscopic evidence for multinuclear complexation involving bridging CN^- groups.

We report on the complexation of palladium(II) by cyanide ligands in liquid ammonia. This work forms part of a much wider area of our investigations which encompasses a vibrational spectroscopic, as well as an electrochemical, attack on the problem of identifying the various species which occur when cations and anions or ligands interact in liquid-ammonia solutions.

In most protonic solvents, such as water and the lower alcohols, the cyanide salts of heavy metals are insoluble. In previous papers we have shown how liquid ammonia is particularly useful as a medium for the study of water-insoluble metal cyanides in solution. For instance, the stepwise complexation by CN^- of silver(I)[2] and mercury(II)[1] can be followed in the Raman, usually between 200 and 300 K, by collecting the spectra of a range of solutions at different ligand : metal ratios.

The complexation scheme of silver by cyanide is complicated because it involves both geometry changes on the silver(I) centre and equilibria between linkage isomers. Ligation of mercury(II) by cyanide in ammonia contrasts with that on silver(I) because complexation occurs by the simple stepwise replacement of ammonia molecules in the tetrahedral inner coordination sphere of the Ag^+ ion. Like AgCN and $Hg(CN)_2$, $Pd(CN)_2$ is also soluble in liquid ammonia. A high solubility of these cyanides is favoured because the metal cations possess high energies of solvation in liquid ammonia, much greater than the corresponding values for the aqueous system. All three compounds have high lattice energies, and a consideration of these together with their solvation energies indicates that ammoniation of Ag^+, Hg^{2+} and Pd^{2+} cations is a highly enthalpically favoured process. Thus, ligation of the three metal cations, even by powerful and strong donor ligands, might be expected to be competitively at a disadvantage compared with the solvation process. This is not the case for the ligation of Ag^+ and Hg^{2+} by the CN^- anion in ammonia:[3] in Ag^+–CN^- mixtures, $\log K_1 \sim 7$, $\log K_2 \sim 9$, and $\log K_3 \sim 1.5$. However, it is the case for phosphines, and for thiocyanate, for which further ligation is not detectable either spectroscopically[4] or poten-

* For Part XVI see Ref. 1.

† As an undergraduate at Keble College, Oxford (1954–1958), J. B. Gill was tutored in inorganic chemistry, and was supervised for Part II of his B.A. degree, by Dr Irving. After a period in industry and Edinburgh University, he joined Professor Irving again at Leeds University in 1965 as a Lecturer in the Department of Inorganic and Structural Chemistry. P. Gans was appointed in 1964 by Professor Irving as Teaching Fellow in the Department of Inorganic and Structural Chemistry and became a Lecturer in 1966.

‡ Author to whom correspondence should be addressed.

tiometrically[3] after the first step: for SCN^-–Pd^{2+} mixtures, $\log K_1 \sim 0.7$.

Our earlier papers have described some of the methods used to identify ion-associated[5] and complexed species[1,2,4] in ammonia solutions from their Raman spectra. To facilitate analysis of the spectra we established our own methods of computer-assisted curve resolution (VIPER),[6,7] and smoothing and derivative convolution processes.[8] These assist in: (i) the identification of the species present, and (ii) a much improved estimation of the positions of the bands which underly the spectral profiles. In the work presented here we have obtained Raman spectra from solutions of cyano-palladium(II) complexes at various $[CN^-]/[Pd^{2+}]$ ratios (S). It should also be noted that for the first time we have been able to bring into use the new techniques which we have been developing to facilitate measurement of IR spectra of liquid-ammonia solutions at ambient temperatures.[9] Principally, it is through the use of IR spectroscopy that we have been able to observe and monitor the kinetically slow process of ligand exchange which occurs in the cyano-palladium(II) system in liquid ammonia.

EXPERIMENTAL

The techniques for examining the Raman spectra of solutions in liquid ammonia have been described previously.[1,2,4] Ammonia solutions of $Pd(NH_3)_4(NO_3)_2$, at concentrations of *ca* $300 = R = (\text{mol } NH_3)/(\text{atoms of Pd})$, and KCN were sealed in round glass tubes at various S. The Raman spectra were recorded within 24 h of the preparation of the mixtures, and thereafter at intervals of time up to about 4 months. All the techniques we normally apply to obtain good spectra with maximm signal: noise ratio and minimum band distortion were used. The spectra, recorded on our modified Coderg RS100 Raman spectrometer, were calibrated against a Hg line at 2187.7 cm^{-1}.

IR spectra were obtained in our new pressure cell. This contains CaF_2 windows in a piston–cylinder assembly constructed within a block of the thermoplastic Kel-F. This material is resistant to attack by ionic solutions in liquid ammonia, though it should be noted that it is destroyed by solutions of alkali metals in ammonia. A full report on the construction and the use of the cell for analytically quantitative IR determinations is presented elsewhere.[9] This includes a description of the method of solvent spectrum subtraction.

Spectra were recorded on a Pye–Unicam ratio-recording SP3-300 IR spectrometer using a cell pathlength of 50 μm. Each spectrum was collected as nine coadded scans on a Hewlett–Packard 9845A computer. The solute spectra were studied in absorbance units after subtraction of the background (solvent spectrum) from the spectra of the solutions. Spectra were recorded at intervals of approximately 0, 1, 2, 4, 8, 12, 24, 36, 48 and 72 h after the preparation of the solutions.

The salts were recrystallized from liquid ammonia.

RESULTS AND DISCUSSION

Following reports in the literature[10] on the coordination of ligands around the Pd^{2+} ion in both the solid state and in aqeuous solutions[11] there is no reason to assume that any coordination arrangement other than a square-planar array of CN^- groups exists around Pd^{2+} in liquid ammonia. All our spectroscopic evidence supports this. The IR and Raman spectra of the CN^-–Pd^{2+} set of complexes in ammonia consists of bands which all lie between 2125 and 2152 cm^{-1}. In those solutions in which the ratio of $S \leqslant 4$ no band due to free cyanide ligand is observed in the region around 2056 cm^{-1}, but immediately the solution composition exceeds $S = 4$ a band appears at this frequency. From this we can conclude that the formation of $[Pd(CN)_4]^{2-}$ is thermodynamically a very favourable process in liquid ammonia, and that no further complexation occurs beyond the 4:1 stage.

Both the Raman and the IR spectra were scanned to 2350 cm^{-1}. The absence of features due to C—N stretching vibrations, in regions other than those indicated above, provides good spectroscopic evidence that no multinuclear species containing bridging CN^- groups form in the system.

The observed spectra are compatible with a stepwise process of addition of CN^- ligands to the Pd^{2+} metal ion. However, this is complicated by a slow exchange reaction which manifests itself in changes observed in the spectra in the course of 2–3 days. We have monitored these changes in the IR spectra, but we have used the Raman data to identify band positions because of the better resolution which can be achieved with the latter. It was impractical to follow spectrum changes with time in the Raman.

All the nine bands listed in Table 1 have been identified in the Raman spectra, but only five bands can be positively identified in the IR spectra. Attempts were made to identify underlying features in the IR spectra by computer-assisted curve fitting, but extensive overlapping of bands, their relatively low absorbances ($\varepsilon \sim 2$ mol^{-1} m^2), and the low resultant signal: noise ratios in the solvent-subtracted spectra led to a high correlation between band parameters.[12] None the less,it was clear from

Table 1. Frequencies of bands observed in the Raman spectra of solutions of various mixtures of CN^- and Pd^{2+} in liquid ammonia[a]

		Band								
		A	B	C	D	E	F	G	H	I
Frequency (cm^{-1})		2150	2148	2145	2142	2141	2138	2136	2134	2134
Assignment	Time	$[Pd(CN)_4]^{2-}$	$[Pd(CN)_3]^-$	*cis*-$Pd(CN)_2$	*trans*-$Pd(CN)_2$	*cis*-$Pd(CN)_2$	$[Pd(CN)_4]^{2-}$	$[Pd(CN)_3]^-$	$[Pd(CN)_3]^-$	$[Pd(CN)]^+$
Symmetry	(days)	A_{1g}	A_1	A_1	A_g	B_1	B_{1g}	B_1	A_1	A_1
$S = 0.5$						1 (p)				2 ($\alpha = 0.1$)
$S = 1.0$	0					4				5 ($\alpha = 0.1$)
	7					4				5
$S = 1.12$[b]	0			2		5				5
	7				1					1
$S = 1.5$	0			2		3				2
	14				2					1
$S = 2.0$	0			3	←	4 (p)	→			2 ($\alpha = 0.2$)
	14			2	←	4	→			1
$S = 2.1$[b]	0			2	←	2	→			1
	7			2	←	4	→			1
$S = 2.5$			2 (p)	6 (p)	←	4	→	1 (dp)?[c]	2 ($p = 0.5$)	
$S = 3.0$	0		7	4				2 (dp)	1	
	1		5	5				2 (dp)	2	
$S = 3.5$		5 (p)					1 (dp)			
$S = 4.0$	0	6 (p)					1 (dp)			
	7	6 (p)					1 (dp)			
$S = 6.4$		6(p)					1 (dp)			

[a] The numbers indicate approximate relative intensities of component bands.

[b] These samples were made up and stored at −40°C until the first spectrum was recorded. Thereafter they were allowed to stand at ambient temperature.

[c] This band is found only in the one polarized spectrum. It is a weak feature and is lost between bands D and I of the 11 polarized spectra.

these attempts at curve resolution that more than five bands should be used to describe the IR spectra.

Assuming that linkage isomerism may be excluded, it is only at the 2 : 1 stage of complexation that isomerism is possible, i.e. *cis-* and *trans-*$[(NH_3)_2Pd(CN)_2]$. The species formed in the stepwise addition of CN^- to Pd^{2+} should give rise to a possible total of eight Raman and seven IR bands if the system just passes through the *cis* isomer, and seven Raman and six IR bands if complexation involves only the *trans* species. Because nine Raman bands and at least five IR bands can be identified we conclude that both *cis-* and *trans-*$[(NH_3)_2Pd(CN)_2]$ can be found in the solutions with compositions $S \leqslant 2$. To describe this pattern of complexes in the equilibria up to the 4 : 1 stage a total of nine Raman and eight IR bands, representing a total of 11 C—N stretching vibrations, are required. These must include six coincidences, and four mutual exclusions.

Description of the Raman spectra

S = 0.5. Two bands are observed at 2141 cm^{-1} (D/E) and 2134 cm^{-1} (H): both are polarized [E ($\rho = 0.02$), and H ($\rho = 0.1$)]. Because band H, at the lower frequency, is twice as intense as band E we identify it with the A_1 C—N stretching vibration of $[(NH_3)_3Pd(CN)]^+$.

S = 1.0. The same two bands, D/E and H, are observed but the intensity of band D/E is substantially increased relative to band H, and the assignment of band E to a 2 : 1 species is consistent with the attribution of band H to $[(NH_3)_3Pd(CN)]^+$. No significant change is found in this spectrum with the passage of time.

S = 1.12 *and* 1.5. The relative intensity trends observed in the spectra of the solutions at $S = 0.5$ and 1.0 continue in those spectra taken within 24 h of the preparation of the solutions, but a third band at 2145 cm^{-1} (C) appears at a somewhat lower relative intensity. Band C increases in relative intensity as S increases. Spectra taken 7–14 days after the preparation of these solutions change completely to become simple two-band spectra. Although the lower-frequency band H remains a substantive part of these spectra the peak of the feature at 2142 cm^{-1} (D) is shifted slightly with respect to the band at 2141 cm^{-1} (E), and therefore can be identified as a separate feature.

S = 2.0 *and* 2.1. Three peaks, all of which change their relative intensities with time, appear in the spectra. The band of maximum intensity coincides in frequency with band D (observed in the spectrum of a solution at $S = 1.5$ left to stand for several days). The highest-frequency band at 2145 cm^{-1} is in the same position as band C observed soon after an $S = 1.5$ solution has been mixed. After several days band C is reduced in intensity relative to the feature at 2141/2142 cm^{-1}. Band H which is still seen in these spectra is markedly lower in relative intensity that it is in the spectra of the solutions at lower S. It is important to note that the polarization ratio of band H is appreciably higher ($\rho = 0.2$) for these solutions. After a period of 14 days no further changes are observed in the spectra. Four Raman bands are required to be attributed to the vibrations of $[(NH_3)_3Pd(CN)]^+$, and *cis-* and *trans-*$[(NH_3)_2Pd(CN)_2]$. We have already assigned band H to the A_1-vibration of the first of these. On the basis of its polarization ($\rho = 0.02$), and that we might expect the *trans* effect to determine the preferred species, we assign band D (clearly identified in the spectrum of a solution at $S = 1.5$ after several days) to the A_g-vibration of *trans-*$[(NH_3)_2Pd(CN)_2]$, leaving the two bands at 2145 cm^{-1} (C) and 2141 cm^{-1} (E) to be assigned to the *cis-*$[(NH_3)_2Pd(CN)_2]$ isomer. Here assignment poses a problem because the bands at 2142 cm^{-1} and 2141 cm^{-1} severely overlap each other and polarizibility measurements cannot assist. However, we believe that there is some degree of depolarization in this region. Also the band at 2142 cm^{-1} (D) is fairly symmetrical in the spectra taken after several days. Thus it is not unreasonable to infer that band E at 2141 cm^{-1} is a relatively weak feature of the spectra severely masked by band D. Because the band at 2145 cm^{-1} is highly polarized ($\rho = 0.04$) we are inclined to make a tentative assignment of band C to the polarized A_1-vibration of *cis-*$[(NH_3)_2Pd(CN)_2]$ leaving the depolarized (?) band E at 2141 cm^{-1} assigned to its B_1-mode.

S = 2.5 *and* 3.0. The spectrum at $S = 2.5$ exhibits four distinct features at 2148 cm^{-1} (B), 2145 cm^{-1} (C), 2142 cm^{-1} (D and/or E), and 2134 cm^{-1} (H or I). In the perpendicular polarized spectrum bands B, C and D disappear leaving a broad flat-topped region between 2140 and 2132 cm^{-1}. This signifies the existence of two further bands, one at 2136 cm^{-1} (G), the other coincident in frequency with band H at 2134 cm^{-1} (I). Band G does not contribute sufficiently to the parallel polarized spectrum to make itself apparent through the spectral envelope, but its presence in the perpendicularly polarized spectrum indicates that it is a comparatively weak feature with a non-zero polarization ratio. We are fortunate in being able to identify an additional band I at 2134 cm^{-1} by means of the increase in polarization ratio (from $\rho = 0.2$ to $\rho = 0.5$) at this frequency with increase in S from 2.0 to 3.0. At $S = 3$ bands B, C, G and I are observed; these change in relative intensities in the manner which

might be expected as a 2:1 gives is promoted to a 3:1 species. Using the polarization properties we assign band I to the depolarized B_1-vibration of $[(NH_3)Pd(CN)_3]^-$, leaving the bands at 2148 cm^{-1} (B) and 2136 cm^{-1} (G) to be attributed to its two A_1-vibrations.

S = 3.5 *and* 4.0. Two bands, not observed in the spectra described above, appear at 2150 cm^{-1} (A) and 2138 cm^{-1} (F), in an intensity ratio of 6:1. Band A is a highly polarized intense feature ($\rho = 0.01$), whilst band F is depolarized. They are obviously attributable to the symmetrical A_{1g} and the B_{1g} stretching vibrations respectively, of square-planar $[Pd(CN)_4]^{2-}$. The absence of any feature, other than bands A and F, leads us to conclude that complexation to $[Pd(CN)_4]^{2-}$ is complete at $S = 4.0$ and that this complex is thermodynamically very stable.

S = 6.3. No further change occurs in the spectrum when S is increased above 4, but it is to be noted that a band due to free CN^- appears at 2056 cm^{-1} as early as $S = 4.1$, indicating that stepwise complexation is complete at the 4:1 stage.

Description of the IR spectra

IR measurements have enabled us to assign the two Raman-inactive bands. They have also enabled us to monitor the changes in solution composition at ambient temperature during the first 2 days after preparation. At $S \leqslant 2$ the spectra change significantly up to about 50 h; at $S = 3$ changes are complete within 3 h. Five different bands can be clearly discerned and the directions in which they change with time are shown in Table 2.

S = 1 *and* 2. Three features are identifiable at 2141 cm^{-1} (E), 2134 cm^{-1} (H) and 2127 cm^{-1} (K). Relative to the band at 2134 cm^{-1}, which we associate with the C—N stretching frequency of $[(NH_3)_3Pd(CN)]^+$ because of its coincidence with band H of the Raman spectra, the intensities of both the other bands change with time; the band at 2141 cm^{-1} increases and that at 2127 cm^{-1} decreases. No band is observed in the Raman at as low a frequency as 2127 cm^{-1}, and accordingly we can unambiguously assign band K to the Raman-inactive B_{1u} vibration of *trans*-$[(NH_3)_2Pd(CN)_2]$. The highest-frequency band at 2141 cm^{-1} could (on the basis of coincidences with Raman frequencies) be associated with band E (the B_1-vibration of *cis*-$[(NH_3)_2Pd(CN)_2]$. After considering the direction of the changes in the relative intensities of bands E and K we conclude that *trans*-$[(NH_3)_2Pd(CN)_2]$, which forms after the solutions are mixed, reduces in concentration with time giving way to some *cis*-$[(NH_3)_2Pd(CN)_2]$. The overall increase in intensity of the band at *ca* 2141 cm^{-1} (in the Raman) is consistent with an increase in the concentration of the *cis* isomer. Concurrently the band at 2142 cm^{-1} due to the *trans* isomer, in parallel with band K, decreases in relative intensity. The increase in intensity of the feature E compared with the cor-

Table 2. Bands observed in the IR spectra of solutions containing CN^- ligands mixed with Pd^{2+} cations in liquid ammonia at 293 K[a]

Band	B	E	H
Frequency (cm^{-1})	2146	2141	2134
Assignment	$[(NH_3)Pd(CN)_3]^-$	*cis*-$[(NH_3)_2Pd(CN)_2]$	$[(NH_3)_3Pd(CN)]^+$
Symmetry	A_1	B_1	A_1
$S = 1$		↑	|
$S = 2$		↑	|
$S = 3$	|		
$S = 4$			

Band	I	J	K
Frequency (cm^{-1})	2134	2128	2127
Assignment	$[(NH_3)Pd(CN)_3]^-$	$[Pd(CN)_4]^{2-}$	*trans*-$[(NH_3)_2Pd(CN)_2]$
Symmetry	A_1	E_u	B_{1u}
$S = 1$			↓
$S = 2$			↓
$S = 3$	|		↓
$S = 4$		|	

[a] Arrows indicate the direction of intensity changes of the component bands with time. With solutions at $S = 1$ and 2 there is no detectable change after 50 h; for $S = 3$, it is 4 h.

responding loss of intensity under the K feature is good evidence for slow replacement of the *trans* by the *cis* isomer. Assessments of the changes in the band areas suggests an approximate half-life for the *cis–trans* interconversion of about 6 h. After about 50 h all three bands (E, H and K) are present in the spectra, and we conclude that the system contains an equilibrium which includes $[(NH_3)_3Pd(CN)]^+$ and both *cis*- and *trans*-$[(NH_3)_2Pd(CN)_2]$, and perhaps some $[(NH_3)Pd(CN)_3]^-$.

S = 3. At this composition changes in the spectra are complete within 3 h. A small feature is suggested on some of the profiles at *ca* 2136 cm^{-1} to support the assignment of band G (found in the Raman) to $[(NH_3)Pd(CN)_3]^-$. The most distinctive new feature is the relatively small band at 2146 cm^{-1}. This should be associated with band B seen in the Raman at 2148 cm^{-1} and assigned to the A_1-vibration of $[(NH_3)Pd(CN)_3]^-$. As this band is of relatively low intensity it is tempting to suggest that the proportion of $[(NH_3)Pd(CN)_3]^-$ in a solution of $S = 3$ is relatively low, and, because the principal components of the mixture are the 2 : 1 isomers and $[(NH_3)Pd(CN)_3]^-$, that the third stepwise stability constant K_3 is comparatively low.

S = 4. This spectrum consists of a single symmetrical band at 2128 cm^{-1} (J). Because this is absent from the Raman spectra we can unambiguously assign it to the doubly-degenerate E_u-mode of square-planar $[Pd(CN)_4]^{2-}$.

CONCLUSIONS

(1) The Raman and IR spectra of mixtures of Pd^{2+} and CN^- in liquid-ammonia solutions have enabled frequencies to be assigned to all the 11 C—N stretching vibrations of the five square-planar complexes as follows:

2150 cm^{-1}, A_{1g}, $[Pd(CN)_4]^{2-}$;
2148 cm^{-1}, A_1, $[(NH_3)Pd(CN)_3]^-$;
2145 cm^{-1}, A_1, *cis*-$[(NH_3)_2Pd(CN)_2]$;
2142 cm^{-1}, A_g, *trans*-$[(NH_3)_2Pd(CN)_2]$;
2141 cm^{-1}, B_1, *cis*-$[(NH_3)_2Pd(CN)_2]$;
2138 cm^{-1}, B_{1g}, $[Pd(CN_4)]^{2-}$;
2136 cm^{-1}, B_1, $[(NH_3)Pd(CN)_3]^-$;
2134 cm^{-1}, A_1, $[(NH_3)_3Pd(CN)]^+$;
2134 cm^{-1}, A_1, $[(NH_3)Pd(CN)_3]^-$;
2128 cm^{-1}, E_u, $[Pd(CN)_4]^{2-}$;
2127 cm^{-1}, B_{1u}, *trans*-$[(NH_3)_2Pd(CN)_2]$.

(2) A slow interconversion of *trans*-$[(NH_3)_2Pd(CN)_2]$ and *cis*-$[(NH_3)_2Pd(CN)_2]$ ($t_{1/2} \sim 6$ h) can be followed in the IR spectra. This results in a solution at equilibrium containing $[(NH_3)_3Pd(CN)]^+$ and both the *cis* and *trans* isomers.

(3) Complexation of Pd^{2+} by CN^- in liquid ammonia does not proceed beyond the 4 : 1 stage.

(4) The relative intensities of component bands in the spectra suggest that the formation steps to the 2 : 1 and 4 : 1 species are thermodynamically favoured processes.

(5) There is no spectroscopic evidence for the existence of multinuclear complexes with bridging cyano groups.

Acknowledgements—We are grateful to the Science and Engineering Research Council for a Research Grant (GR/B/00817) towards the cost of the IR spectroscopic and computer equipment, for the provision of a Postgraduate Studentship to DM, and to Goodfellow Metals who gave support as the Cooperating Body.

REFERENCES

1. P. Gans, J. B. Gill and G. J. Earl, *J. Chem. Soc., Dalton Trans.* 1985, 663.
2. P. Gans, J. B. Gill, M. Griffin and P. Cahill, *J. Chem. Soc., Dalton Trans.* 1981, 968.
3. Y. M. Cheek, P. Gans and J. B. Gill, *J. Chem. Soc., Chem. Commun.* 1985, 628.
4. P. Gans, J. B. Gill and M. Griffin, *J. Chem. Soc., Faraday Trans.* 1 1978, 432.
5. J. B. Gill, *Pure Appl. Chem.* 1981, **53**, 1365.
6. P. Gans and J. B. Gill, *Appl. Spectrosc.* 1977, **31**, 451.
7. P. Gans, *Comput. Chem.* 1977, **1**, 291.
8. P. Gans and J. B. Gill, *Appl. Spectrosc.* 1983, **37**, 515.
9. P. Gans, J. B. Gill, Y. M. Cheek and C. Reyner, *Spectrochim. Acta* 1986, **42**, 1349.
10. A. G. Sharpe, *The Chemistry of Cyano Complexes of the Transition Metals*, p. 244. Academic Press, London (1976).
11. G. J. Kubas and L. H. Jones, *Inorg. Chem.* 1974, **13**, 2816.
12. P. Gans and J. B. Gill, *Anal. Chem.* 1980, **52**, 351.

Polyhedron Vol. 6, No. 1, pp. 85–94, 1987
Printed in Great Britain

0277–5387/87 $3.00+.00

APPLICATION OF SPECTROSCOPIC TECHNIQUES TO THE COMPLEXES FORMED BY REACTION OF ZEISE'S SALT DERIVATIVES WITH CARBON MONOXIDE

PHILIP S. HALL and DAVID A. THORNTON*

Department of Inorganic Chemistry, University of Cape Town, Rondebosch 7700, South Africa

and

GARY A. FOULDS

Department of Chemical Engineering, University of Cape Town, Rondebosch 7700, South Africa

(*Received* 3 *July* 1986)

Abstract—IR, ^{1}H NMR and electronic spectra are reported for the complexes *trans*-[$PtX_2(CO)(L)$] (X = Cl or Br; L = NH_3, pyridine, pyridine-*N*-oxide, aniline or imidazole) and *trans*-[$Pt_2X_4(CO)_2$(pyrazine)] (X = Cl or Br). Assignments for the internal ligand modes and metal–ligand vibrations are deduced from the band shifts caused by deuteration of the ligands (L). The simplicity of the IR spectra, particularly in the $\nu(C{\equiv}O)$ region, is consistent with a *trans*-configuration. The ^{1}H NMR data show ^{195}Pt–H coupling at ambient temperature, suggesting a slow exchange, unlike the corresponding ethylene complexes which are highly fluxional at ambient temperatures. Assignments are provided for the UV spectra and the previously reported red shift is observed in the $5d(Pt) \rightarrow \pi^*$ transition which results from the replacement of Cl by Br in the complexes.

Recently, we reported a vibrational study of the complexes *trans*-[$PtX_2(C_2H_4)(L)$], where L represents various oxygen and nitrogen donor ligands.[1] The facile displacement of the ethylene from these complexes[2,3] has enabled us to prepare a large number of platinum carbonyl complexes of the type *trans*-[$PtX_2(CO)(L)$] and *trans*-[$Pt_2X_4(CO)_2$(pyrazine)]. In this paper, IR, ^{1}H NMR, UV and MS have been used to examine the nature of these complexes which differ considerably from their ethylene-containing precursors.

EXPERIMENTAL

The complexes *trans*-[$PtX_2(C_2H_4)(L)$] [X = Cl or Br; L = aniline (an), pyridine *N*-oxide (pyO), pyridine (py), NH_3, imidazole (Him) or pyrazine (pz)] and *trans*-[$Pt_2X_4(C_2H_4)_2$(pz)] were prepared using methods described in the literature.[1,4] Prior to the formation of the new carbonyl analogues of the above complexes, the chloroform and *n*-hexane solvents required were dried and distilled over P_2O_5 and Na, respectively. This is essential to prevent the rapid decomposition of the moisture-sensitive carbonyl complexes and the precipitation of elemental platinum.[5]

(*a*) *Preparation of* trans-[$PtX_2(CO)(L)$] (X = Cl *or* Br; L = an *or* Him)

trans-[$PtX_2(C_2H_4)(L)$] (X = Cl or Br; L = an or Him) (1 mmol) was dissolved in dry chloroform (30 cm^3), and carbon monoxide was bubbled through the solution with stirring, during which time the temperature of the solution was maintained at about 30°C. After several minutes (3–60 min, depending on L) the colour of the solution changed from bright yellow to pale greenish-yellow. At this point the solution was concentrated by evaporation

*In 1976, David Thornton invited Professor Harry Irving to the University of Cape Town as visiting Professor in Inorganic Chemistry. He stayed on to become the University's first Professor of Analytical Science until his retirement in 1984 at the age of 79. Author to whom correspondence should be addressed.

of chloroform using a stream of warm dry air. On addition of dry *n*-hexane (20 cm^3) to the point of cloudiness, the product was precipitated. The products, *trans*-[$PtX_2(CO)(L)$] (X = Cl or Br; L = an or Him) were isolated by vacuum filtration, washed with *n*-hexane and stored over silica gel in a vacuum desiccator (<0.1 mmHg) at −5°C.

(*b*) *Preparation of* trans-[$PtX_2(CO)(py)$] (X = Cl *or* Br)

trans-[$PtX_2(CO)(py)$] (X = Cl or Br) was prepared from *trans*-[$PtX_2(C_2H_4)(py)$] (X = Cl or Br) as described in (a), except that *n*-hexane (10 cm^3) was added before the cloudiness occurred, and the resulting solution was placed over silica gel in a large partly evacuated desiccator and stored at −5°C overnight, during which time the solvent evaporated resulting in the formation of needle-like crystals of *trans*-[$PtX_2(CO)(py)$] (X = Cl or Br) which were collected and stored as described in (a).

(*c*) *Attempted preparation of* trans-[$PtX_2(CO)(pz)$] (X = Cl *or* Br)

(1) Attempts to prepare *trans*-[$PtX_2(CO)(pz)$] (X = Cl or Br) from *trans*-[$PtX_2(C_2H_4)(pz)$] using the method described in (a) resulted in the formation of the bridged complex *trans*-[$Pt_2X_4(CO)_2(pz)$] in quantitative yield.

(2) H[$Pt(CO)X_3$] (X = Cl or Br) (1 mmol), prepared as described by Gribov *et al.*,[6] was dissolved in chloroform. Reaction of this solution with pyrazine in various molar ratios always resulted in the formation of *trans*-[$Pt_2X_4(CO)_2(pz)$], while the addition of a large excess of pyrazine (>10 mmol) resulted in the formation of *trans*-[$PtX_2(pz)_2$].[7]

(3) Crystals of $[PtCl_2(CO)_2]_2$, prepared as described in the literature[8,9] were dissolved in chloroform and allowed to react with pyrazine, in various molar ratios. All attempts resulted either in no reaction or in the formation of either *trans*-[$Pt_2Cl_4(CO)_2(pz)$] or *trans*-[$PtCl_2(pz)_2$].

(4) The salts [NR_4][$PtX_3(CO)$] (X = Cl or Br, R = Pr^n_4 or Bu^n_4) were prepared as described by Browning *et al.*[10] Reaction of these salts with pyrazine, in various molar ratios, resulted either in no reaction or in the formation of *trans*-[$PtX_2(pz)_2$].

(*d*) *Preparation of* trans-[$Pt_2X_4(CO)_2(pz)$] (X = Cl *or* Br)

[$Pt_2X_4(CO)_2(pz)$] was prepared from [$Pt_2X_4(C_2H_4)_2(pz)$] as described in (a), except for the fact that larger volumes of chloroform (~ 70 cm^3) are required to dissolve the ethylene complexes.

The purity and composition of all the compounds were determined by microanalysis (C, H and N) (Table 1). The deuterated complexes were similarly prepared using the following labelled compounds supplied by Merck, Sharp & Dohme (Canada) Ltd (isotopic purity in parentheses): ammonia-d_3 (99%), aniline-d_5 (98%), and imidazole-d_4 (98%); and the following compounds supplied by BOC Prochem Ltd: pyridine-d_5 (99%) and pyridine-d_5 *N*-oxide (98%). The deuteroimine groups of 1,2,4,5-tetradeuteroimidazole (Him-d_4) undergo rapid exchange

Table 1. Analytical data

Compound	Calculated			Found			Molecular weight (mass spectrum)[a]
	% C	% H	% N	% C	% H	% N	
trans-[$PtCl_2(CO)(an)$]	21.7	1.8	3.6	21.8	1.9	3.7	386
trans-[$PtCl_2(CO)(pyO)$]	18.5	1.3	3.6	18.6	1.3	3.5	[b]
trans-[$PtCl_2(CO)(py)$]	19.3	1.4	3.8	19.2	1.4	3.8	372
trans-[$PtCl_2(CO)(NH_3)$]	3.9	1.0	4.5	4.0	1.0	4.5	310
trans-[$PtCl_2(CO)(Him)$]	13.3	1.1	7.7	13.3	1.1	7.7	361
trans-[$PtBr_2(CO)(an)$]	17.7	1.5	2.9	17.6	1.5	2.9	474
trans-[$PtBr_2(CO)(pyO)$]	15.1	1.1	2.9	15.1	1.1	2.9	[b]
trans-[$PtBr_2(CO)(py)$]	15.6	1.1	3.0	15.7	1.1	3.1	460
trans-[$PtBr_2(CO)(NH_3)$]	3.0	0.8	3.5	3.0	0.8	3.5	398
trans-[$PtBr_2(CO)(Him)$]	10.7	0.9	6.2	10.7	0.9	6.2	449
trans-[$Pt_2Cl_4(CO)_2(pz)$]	10.8	0.6	4.2	10.9	0.6	4.2	666
trans-[$Pt_2Br_4(CO)_2(pz)$]	8.5	0.5	3.3	8.7	0.6	3.3	842

[a] Based on ^{195}Pt, ^{35}Cl and ^{79}Br.

[b] Greater *m/z* observed.

in aqueous or ethanolic solution to yield complexes containing 2,4,5-trideuteroimidazole (Him-d_3).

The ^{1}H NMR spectra were run at ambient temperature on a Bruker WH-90 spectrometer using CD_3COCD_3 as the solvent and TMS as reference. The IR spectra were determined as Nujol mulls (4000–1500 and 1300–300 cm^{-1}) or hexachlorobutadiene mulls (4000–1700 and 1500–1300 cm^{-1}) between CsBr plates on a Perkin–Elmer 983 spectrophotometer, and as Nujol mulls between polyethylene plates (500–80 cm^{-1}) on a Digilab FTS-16 B/D interferometer. The UV spectra were determined on a Varian Superscan 3 spectrophotometer using CH_3OH as solvent. Mass spectra were measured on a VG Micromass 16/F instrument operating in the electron impact mode, with electron beam energy = 70 eV, ion-accelerating voltage = 3 kV, and with ion source temperatures in the range 100–195°C. Microanalyses were performed by Mr W. R. T. Hemsted of the University of Cape Town.

RESULTS AND DISCUSSION

IR spectra

The spectrum of each compound was determined twice, firstly in the unlabelled form and secondly with the ligand (L) in the deuterated form. The frequency data and assignments for the internal ligand modes of the complexes are listed in Table 2, while the far-IR frequencies are given in Table 3.

The internal vibrations of the ligands, L, are assigned to those bands which shift significantly on deuteration of L, with more specific assignments made from their ν^D/ν^H ratios.[11] Assignments are made in relation to the analogous ethylene compounds[1] and earlier use of the ν^D/ν^H ratio in complexes of aniline,[11] pyridine[11] and imidazole,[12] while the assignments for the pyridine *N*-oxide complexes follow those reported from a normal coordinate analysis of the free ligand.[13–15]

The ν(C≡O) frequencies were determined in chloroform, as well as in Nujol mulls. The former resulted in a single sharp band, while the latter sometimes resulted in splittings which may arise from rotational fine structure in the solid state.[6] The simplicity of the IR spectrum in the ν(C≡O) region is consistent with *trans* coordination.

The far-IR assignments are in good accord with previous work[10,16,17] on related complexes and the δ(Pt—C≡O) band is at higher frequency than that of ν(Pt—C) as expected in metal carbonyls.[18,19] Only one previous IR study of complexes of this type has been reported,[6] in which Gribov and co-workers reported the IR spectrum of *trans*-$[PtCl_2(CO)(NH_3)]$. Two bands were observed in the skeletal region, at 532 and 477 cm^{-1}, both of which were attributed to δ(Pt—C≡O) deformations. We now attribute these to the deformation δ(Pt—C≡O) and stretching ν(Pt—C), respectively. As expected, the ν(Pt—N) frequency is substantially lower in the complexes *trans*-$[Pt_2X_4(CO)(pz)]$ (where the pyrazine is bridging) than in the complexes where similar ligands are terminal, e.g. *trans*-$[PtX_2(CO)(py)]$.

^{1}H NMR *spectra*

The ^{1}H NMR data for the complexes are given in Table 4. Examination of the data reveals that some of the complexes show ^{195}Pt–H coupling. The complexes *trans*-$[PtX_2(CO)(Him)]$ (X = Cl or Br) and *trans*-$[PtBr_2(CO)(py)]$ exhibit coupling at ambient temperature while *trans*-$[PtCl_2(CO)(py)]$ exhibits coupling at reduced temperatures. This suggests that ligand exchange is relatively slow in the former three complexes, with pyridine being more labile in the latter. The above is in direct contrast to the analogous ethylene complexes,[1,20] *trans*-$[PtX_2(C_2H_4)(L)]$, where exchange is rapid at ambient temperature as indicated by an absence of ^{195}Pt–H coupling. This emphasizes the weaker "*trans* effect" of carbon monoxide relative to C_2H_4.

^{195}Pt–H coupling was not observed in the complexes *trans*-$[PtX_2(CO)(L)]$ (X = Cl or Br, L = pyO or an), probably because the protons are separated by at least four bonds from the platinum atom. The absence of coupling in the complexes *trans*-$[Pt_2X_4(CO)_2(pz)]$ may indicate rapid exchange but this is not easy to verify since all four protons are equivalent when the pyrazine plays a bridging role.

Electronic spectra

The electronic spectral data are listed in Tables 5 and 6. By analogy with similar complexes previously studied[21–23] we expect to observe the $\pi \rightarrow \pi^*$(CO) transition as well as the $5d$Pt $\rightarrow \pi^*$(CO) inverse-charge-transfer and the $X^- \rightarrow Pt^{2+}$ charge-transfer bands. In addition, in complexes where L is a ligand which has π-electrons present, there is the possibility of a $5d$Pt $-\pi^*$(ligand) inverse-charge-transfer transition. Since some of the transitions overlap, giving rise to broad bands, some of the assignments are tentative. We observe the previously reported[23] red shift in the $5d$(Pt) $\rightarrow \pi^*$ transition which results from the replacement of Cl by Br in the complexes.

Table 2. Internal ligand frequencies (cm^{-1}) and assignments for the complexes *trans*-[$PtX_2(CO)(L)$] and *trans*-[$Pt_2X_4(CO)_2(pz)$]

	X = Cl		X = Br			
L	Unlabelled	L-deuterated	Unlabelled	L-deuterated	Assignment[a]	
NH_3	3292	2459	3280	2420		
	3200	2427	3201	2369	ν(N—H)	
		2377		2331		
	2145	2145	2128	2126		
	2139	2138			ν(C≡O)	
	(2129)[b]	(2130)	(2126)	(2125)		
	1636	1296	1626	1287	NH_2 scissor	
	1535	1210	1529	1202		
	1294	1073	1289	1067	NH_2 twist	
	784	505	782	772	NH_2 wag	
py	3122	2603	3098	2599		
	3110	2479	3075	2476	ν(C—H)	
	3059	2359	3048	2359		
			3041	2331		
	2123	2121	2126	2126		
			2111	2111	ν(C≡O)	
	(2133)	(2133)	(2128)	(2128)		
	1612	1571	1609	1568		(8a)
		1536	1599	1534	ν(ring)	(8b)
	1483	1327	1483	1325		(19a)
	1451	1238	1451	1238		(19b)
	1354	894	1352	789		(14)
	1242	845	1243	739		(3)
	1218	839	1213	641	δ(C—H)	(9a)
	1213	835				
	1157	830	1160	678		(15)
			1092	1042		(18b)
	1072	983	1076	982	δ(ring)	
	1022	1030	1020	1033		(12)
	941	804	870		γ(C—H)	(10b)
	760	778	762	739	δ(ring)	(11)
			758	733		
	688	638	692	532	γ(C—H)	
	685		689	529		(4)
	660	631	660	559	δ(ring)	(6a)
	507	503	507	504		
	503	498			γ(ring)	
	433	397	440	403		(16b)
			437			
pyO	3134	2335	3113	2395		
	3109	2315	3078	2331	ν(C—H)	
	3083	2308	3063	2307		
	3055	2284	3036	2284		
	2108	2108	2097	2101		
			2052	2049	ν(C≡O)	
	(2117)	(2117)	(2113)	(2113)		
	1615	1571	1612	1569	ν(ring)+ν(N—O)	
		1549		1547		(4)
	1473	1353	1473	1351	ν(ring)	(5)
	1259	1141	1262	1145	ν(N—O)	(6)
	1245	1248			ν(ring)	
	1197	1196	1194	1195		

Table 2. (*Cont.*)

	X = Cl		X = Br			
L	Unlabelled	L-deuterated	Unlabelled	L-deuterated	Assignment[a]	
pyO	1186	875	1171	875		(7)
	1173	859	1159	858		(18)
	1156	844	1156	843	δ(C—H)	
	1153	830	1095	829		(19)
	1094	817	1070	787		(8)
	1068	782	1056	1040		
	1053	1040	1033	1017	δ(ring)	(9)
	1027	1009	1026	994		
	1004	989	1004	988		
			967	778		
	935	765	933	764		
	831	567	830	573	γ(C—H)	
			814	564		
			804	545		
	776	531	773	531		(27)
	669	657	673	655		(28)
			637	636	γ(ring)	
	598	567	591	573		
an	3229	3229	3262	3263		
	3182	3184	3213	3214	ν(N—H)	
	3123	3118	3108	3102		
	3051	2390	3045	2359		
	3025	2366	3007	2331	ν(C—H)	
		2331				
	2121	2144	2119	2122		
		2120			ν(C≡O)	
	(2130)	(2130)	(2125)	(2125)		
	1599	1581	1599	1579	ν(ring)	
		1573	1595			
	1575	1563	1569	1559	NH_2 scissor	
			1561			
	1493	1424	1493	1377		
	1471	1380	1466	1299	ν(ring)	
	1216	1206	1198	1166		
	1191	1137	1180	1135		
	1178	1173	1162	1158	NH_2 twist	
			1145	1022		
	1073	842	1069	842		
	1028	822	1029	822	δ(C—H)	
			973	790		
			909	765		
			798	749	ν(ring)	
	767	769	760	764	NH_2 wag	
	756	757	742	738		
	691	657	691	534	ν(C—H)	
	643	617	578	529	δ(ring)	
	580	574	554		NH_2 rock	
	530	531	483	465	γ(ring)	
Him	3550	3348	3345	3343	ν(N—H)	
	3179	2597	3173	2597		
	3157	2369	3153	2366		
	3136	2338	3131	2336	ν(C—H)	
	2965	2883	2964			
	2847	2597	2849			

Table 2. (*Cont.*)

L	X = Cl		X = Br		Assignment[a]
	Unlabelled	L-deuterated	Unlabelled	L-deuterated	
Him	2129	2129	2123	2122	
	2116	2116	2109	2109	ν(C≡O)
	(2127)	(2127)	(2121)	(2121)	
	1545	1493	1545	1491	
	1516	1471	1515	1473	
	1510	1452	1510		
			1495	1417	ν(ring)
	1483	1429	1479	1404	
	1428	1400	1429	1373	
	1328	1193	1328	1291	
	1272	1283	1271	1278	δ(N—H)
	1261	945	1265	945	
	1225	978	1221	977	
	1183	896	1191	894	
	1131	876	1131	875	δ(C—H)
	1096	867	1102	867	
	1073	828	1072	828	
	1067	820	1068	821	
	853	772	852	774	
	837	739	835	738	
	753	729	751	727	δ(ring)
	744		742		
	708	707	695	695	
	653	589	653	587	
	646	582	645	581	γ(ring)
	613	521	611	564	
	504	497	504	502	
trans-[$Pt_2X_4(CO)_2$(pz)]					
	3120	2331	3146	2359	
	3094	2312	3115	2341	
	3045	2299	3101	2323	ν(C—H)
	3023	2287	3068	2297	
	2993	2273	3051	2277	
	2131	2131	2136	2135	
	2082	2082	2089	2089	ν(C≡O)
	(2134)	(2136)	(2138)	(2139)	
	1490	1291	1493	1297	
	1437	1172	1433	1189	ν(ring)
	1422	1160	1426	1180	
	1166	1136	1172	1174	
	1131	884	1126	886	δ(C—H)
	1122	850	1120	860	
	1103	1095	1104		
	1090	1060	1091	1061	ν(ring)
	1013	1011			
	977	976	973	987	
	823	662	824	687	
			816	657	
	742	724	761	723	γ(ring)
	552	536	552	531	
	472	452	472	441	
	460				

[a] Band numbers refer to those given in Ref. 1.

[b] Values in parentheses are those obtained in chloroform solution.

Table 3. Metal–ligand frequencies and ligand isotopically-induced shifts (cm^{-1}) in the IR spectra of the complexes *trans*-$[PtX_2(CO)(L)]$ and *trans*-$[Pt_2X_4(CO)_2(pz)]$[a]

L, X	δ(Pt—C≡O)	ν(Pt—C)	ν(Pt—N) or ν(Pt—O)	ν(Pt—Cl)	Other
NH_3, Cl	531(0)	465(6)	479(7)	349(1)	208(3) 168(3) 152(1) 123(0)
py, Cl	541(3)	479(0)	226(13)	353(0)	215(2) 159(1) 124(1)
pyO, Cl	580(5)	508(1)	440(23) 413(20)	352(1)	216(2) 158(1) 129(1)
an, Cl	557(0)	484(4)	477(17) 369(11)	345(0)	215(−) 172(5) 132(0) 104(−)
Him, Cl	543(3) 485(2)	538(2)	252(13)	350(0)	162(0) 128(0) 99(1) 84(1)
trans-$[Pt_2Cl_4(CO)_2(pz)]$	510(7)	486(2)	186(1)	357(1)	151(4) 126(2)
NH_3, Br	528(0)	481(3)	466(8)	254(0)	205(4) 174(2) 99(1) 90(1)
py, Br	544(4) 507(3)	488(0)	230(19)	261(1)	185(10) 102(0) 80(2)
pyO, Br	576(6) 490(8)	511(1)	436(19) 402(14)	258(1)	222(6) 180(−) 134(3)
an, Br	530(3)	493(2)	434(20)	254(0)	219(−) 207(6) 165(−) 149(5)
Him, Br	538(0)	479(0)	229(8)	271(6)	196(6) 97(2) 85(−)
trans-$[Pt_2Br_4(CO)_2(pz)]$	510(6)	493(1)	174(6)	259(1)	144(2) 100(0) 88(0)

[a] Numbers in parentheses are the shifts (cm^{-1}) induced by ligand deuteration.

Table 4. ^{1}H NMR data

Complex	X	Chemical shift (ppm)			J_{Pt-H}		
		H_a	H_b	H_c	J_{Pt-H_a}	J_{Pt-H_b}	J_{Pt-H_c}
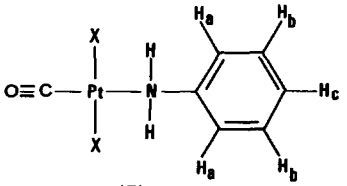 (I)	Cl	Multiplet at 7.36			[a]	[a]	[a]
	Br	Multiplet at 7.42			[a]	[a]	[a]
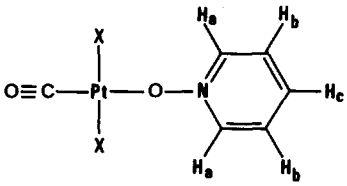 (II)	Cl	8.73	7.97	8.23	[a]	[a]	[a]
	Br	8.71	7.98	8.23	[a]	[a]	[a]
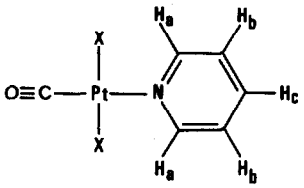 (III)	Cl	8.78	7.76	8.22	30[b]	[a]	[a]
	Br	8.78	7.72	8.18	29	[a]	[a]
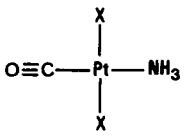 (IV)	Cl	4.46 broad					
	Br	4.47 broad					
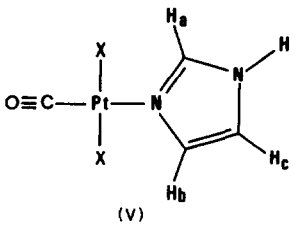 (V)	Cl	8.48	7.52	7.40	17	18	[a]
	Br	8.51	7.53	7.40	18	18	[a]
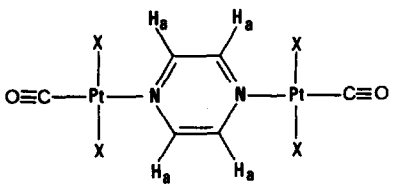 (VI)	Cl	9.26			[a]		
	Br	9.17			[a]		

[a] Not observed.
[b] Coupling observed at 270 K.

Table 5. UV data for the complexes *trans*-$[PtX_2(CO)(L)]$ and *trans*-$[Pt_2X_4(CO)_2(pz)]$ (X = Cl)[a]

L	λ_{max} (nm)	ε	Assignment
NH_3	200	16,605	$Cl^- \rightarrow Pt^{2+}$
	240	5766	$\pi \rightarrow \pi^*(CO)$
	278	3228	$5d(Pt) \rightarrow \pi^*(CO)$
py	201	14,942	$Cl^- \rightarrow Pt^{2+}$
	239	3704	$\pi \rightarrow \pi^*(CO)$
	254	4342	$\pi \rightarrow \pi^*(py)$
	284	894	$5d(Pt) \rightarrow \pi^*(CO)$, $5d(Pt) \rightarrow \pi^*(py)$
pyO	204	23,322	$Cl^- \rightarrow Pt^{2+}$
	263[b]	14,730	$\pi \rightarrow \pi^*(CO)$, $\pi \rightarrow \pi^*(pyO)$, $5d(Pt) \rightarrow \pi^*(CO)$
an	201	19,233	$Cl^- \rightarrow Pt^{2+}$
	234	7659	$\pi \rightarrow \pi^*(CO)$, $\pi \rightarrow \pi^*(an)$
	278	2042	$5d(Pt) \rightarrow \pi^*(CO)$
Him	201	15,748	$Cl^- \rightarrow Pt^{2+}$
	236	4209	$\pi \rightarrow \pi^*(CO)$
	247	4480	$\pi \rightarrow \pi^*(Him)$
	278	2444	$5d(Pt) \rightarrow \pi^*(CO)$, $5d(Pt) \rightarrow \pi^*(Him)$
			trans-$[Pt_2Cl_4(CO)_2(pz)]$
	209	28,012	$Cl^- \rightarrow Pt^{2+}$
	265	17,336	$\pi \rightarrow \pi^*(pz)$, $\pi \rightarrow \pi^*(CO)$
	320[b]	2930	$5d(Pt) \rightarrow \pi^*(CO)$, $5d(Pt) \rightarrow \pi^*(pz)$

[a] CH_3OH used as the solvent.
[b] Broad band.

Table 6. UV data for the complexes *trans*-$[PtX_2(CO)(L)]$ and *trans*-$[Pt_2X_4(CO)_2(pz)]$ (X = Br)[a]

L	λ_{max} (nm)	ε	Assignment
NH_3	205	34,551	$Br^- \rightarrow Pt^{2+}$
	240	2675	$\pi \rightarrow \pi^*(CO)$
	290	1115	$5d(Pt) \rightarrow \pi^*(CO)$
py	203	29,571	$Br^- \rightarrow Pt^{2+}$
	249	4743	$\pi \rightarrow \pi^*(CO)$
	255	4902	$\pi \rightarrow \pi^*(py)$
	295	1107	$5d(Pt) \rightarrow \pi^*(CO)$, $5d(Pt) \rightarrow \pi^*(py)$
pyO	206	38,350	$Br^- \rightarrow Pt^{2+}$
	263[b]	14,792	$\pi \rightarrow \pi^*(CO)$, $\pi \rightarrow \pi^*(pyO)$, $5d(Pt) \rightarrow \pi^*(CO)$
an	202	34,273	$Br^- \rightarrow Pt^{2+}$
	238	8047	$\pi \rightarrow \pi^*(CO)$, $\pi \rightarrow \pi^*(CO)$
	282	2077	$5d(Pt) \rightarrow \pi^*(CO)$
Him	206	31,187	$Br^- \rightarrow Pt^{2+}$
	242	2859	$\pi \rightarrow \pi^*(CO)$
	255	2079	$\pi \rightarrow \pi^*(Him)$
	290	780	$5d(Pt) \rightarrow \pi^*(CO)$, $5d(Pt) \rightarrow \pi^*(Him)$
			trans-$[Pt_2Br_4(CO)_2(pz)]$
	213	33,005	$Br^- \rightarrow Pt^{2+}$
	263	18,803	$\pi \rightarrow \pi^*(pz)$, $\pi \rightarrow \pi^*(CO)$
	318[b]	2725	$5d(Pt) \rightarrow \pi^*(CO)$, $5d(Pt) \rightarrow \pi^*(pz)$

[a] CH_3OH used as the solvent.
[b] Broad band.

Acknowledgement—We thank the Foundation for Research Development of the CSIR for financial assistance.

REFERENCES

1. T. P. Auf der Heyde, G. A. Foulds and D. A. Thornton, *J. Mol. Struct.* 1983, **98**, 11.
2. W. H. Clement and M. Orchin, *J. Organomet. Chem.* 1965, **3**, 98.
3. F. Basolo and R. G. Pearson, *Mechanisms of Inorganic Reactions*, 2nd Edn, p. 376. Wiley, New York (1967).
4. G. A. Foulds, D. A. Thornton and J. Yates, *J. Mol. Struct.* 1983, **98**, 315.
5. M. Orchin and P. J. Schmidt, *Inorg. Chim. Acta, Rev.* 1968, **1**, 123.
6. L. A. Gribov, A. D. Gel'man, F. A. Zakhavova and M. M. Orlova, *Russ. J. Inorg. Chem.* 1960, **5**, 473.
7. G. A. Foulds and D. A. Thornton, *Spectrochim. Acta* 1981, **37A**, 917.
8. R. J. Irving and E. A. Magnusson, *J. Chem. Soc.* 1956, 1860.
9. F. Mylius and F. Foerster, *Chem. Ber.* 1891, **24**, 2424.
10. J. Browning, P. L. Goggin, R. J. Goodfellow, M. G. Norton, A. J. M. Rattray, B. F. Taylor and J. Mink, *J. Chem. Soc., Dalton Trans.* 1977, 2061.
11. G. A. Foulds, J. B. Hodgson, A. T. Hutton, G. C. Percy, P. E. Rutherford and D. A. Thornton, *Spectrosc. Lett.* 1979, **12**, 25.
12. J. B. Hodgson, G. C. Percy and D. A. Thornton, *J. Mol. Struct.* 1980, **66**, 75.
13. A. Gambi and S. Ghersetti, *Spectrosc. Lett.* 1977, **8**, 627.
14. V. Tabaick, V. Pellegrin and M. Gonthard, *Spectrochim. Acta* 1979, **35A**, 1055.
15. M. Cordes and J. L. Walter, *Spectrochim. Acta* 1968, **24A**, 237.
16. M. J. Cleare and W. P. Griffith, *J. Chem. Soc.* 1969, 37.
17. P. L. Goggin and R. J. Goodfellow, *J. Chem. Soc., Dalton Trans.* 1973, 2355.
18. K. Nakamoto, *Infrared Spectra of Inorganic and Coordination Compounds*, 2nd Edn, p. 197. Plenum Press, New York.
19. F. Carderazzo, R. Ercoli and G. Natta, *Organic Syntheses via Metal Carbonyls*, p. 1. Wiley Interscience, New York (1968).
20. G. A. Foulds, G. E. Jackson and D. A. Thornton, *J. Mol. Struct.* 1983, **98**, 232.
21. D. Sutton, *Electronic Spectra of Transition Metal Complexes*. McGraw-Hill, London (1968).
22. G. A. Foulds and D. A. Thornton, *J. Mol. Struct.* 1983, **98**, 309.
23. M. A. M. Meesters, D. J. Stufkens and K. Vriese, *Inorg. Chim. Acta* 1975, **14**, 25.

Polyhedron Vol. 6, No. 1, pp. 95–99, 1987
Printed in Great Britain

0277–5387/87 $3.00+.00

REDOX REACTION ON TREATING *fac*- OR *mer*-[Mo(CO)$_3$(dppm-*PP'*)(dppm-*P*)] (dppm = $Ph_2PCH_2PPh_2$) WITH Hg(SCN)$_2$ AND CRYSTAL STRUCTURE OF THE SEVEN-COORDINATE PRODUCT [Mo(CO)$_2$(NCS)$_2$(dppm-*PP'*)(dppm-*P*)]

ADRIAN BLAGG, ALAN T. HUTTON* and BERNARD L. SHAW

School of Chemistry, University of Leeds, Leeds LS2 9JT, U.K.

(*Received* 3 *July* 1986)

Abstract—[Mo(CO)$_2$(NCS)$_2$(dppm-*PP'*)(dppm-*P*)] (dppm = $Ph_2PCH_2PPh_2$) is formed in a rapid and clean redox reaction when *fac*- or *mer*-[Mo(CO)$_3$(dppm-*PP'*)(dppm-*P*)] is treated with Hg(SCN)$_2$: dppm-chelate ring-opening with formation of a heterobimetallic species is not observed. The X-ray crystal structure of the product shows the molecule to contain seven-coordinate Mo(II) with "*cis*" CO groups, both monodentate and chelating dppm ligands, and with *N*-bonded NCS groups. The coordination geometry is intermediate between a capped trigonal prism and a capped octahedron. Crystals of [Mo(CO)$_2$(NCS)$_2$(dppm-*PP'*)(dppm-*P*)] are orthorhombic, space group $Pna2_1$, with $a = 21.583(7)$ Å, $b = 12.775(4)$ Å, $c = 18.484(5)$ Å, and $Z = 4$; the final R factor was 0.046 for 3181 observed reflections.

We have described the reactions of Group VI metal carbonyl bis(diphenylphosphino)methane (dppm) derivatives of types *fac*-[M^1(CO)$_3$(dppm-*PP'*)(dppm-*P*)] (M^1 = Mo or W) or *mer*-[M^1(CO)$_3$(dppm-*PP'*)(dppm-*P*)] (M^1 = Cr, Mo or W) with labile Rh(I) or Ir(I) carbonyls to give high yields of heterobimetallic complexes containing the *trans,trans*-[M^1(μ-dppm)$_2$M^2] (M^2 = Rh or Ir) skeleton.[1] Similar dppm-chelate ring-opening reactions are induced by the treatment of [M^1(CO)$_3$(dppm-*PP'*)(dppm-*P*)] with copper(I) chloride or iodide, or with (Ph_3P)AgCN, resulting in stable heterobimetallics of type [M^1(CO)$_3$(μ-dppm)$_2$M^{2}X] (M^1 = Cr, Mo or W; M^2 = Cu, X = Cl or I; M^2 = Ag, X = CN), and preliminary results show that treatment with (Ph_3P)AuCl gives similar heterobimetallic complexes containing a [M^1(μ-dppm)$_2$Au] (M^1 = Mo or W) frame.[2] Mixed Group VI metal–platinum complexes of type [M^1(CO)$_3$(μ-dppm)$_2$PtH(X)] (M^1 = Cr, Mo or W; X = Cl or Br) have also been prepared by treating *mer*-[M^1(CO)$_3$(dppm-*PP'*)(dppm-*P*)] with *trans*-[PtH(X)(PPh_3)$_2$].[3]

RESULTS AND DISCUSSION

We report here on a different and contrasting behaviour when mercury(II) salts are used: these generally oxidize [Mo(CO)$_3$(dppm-*PP'*)(dppm-*P*)] to a mononuclear Mo(II) complex rather than induce ring-opening and formation of a heterobimetallic species. Thus treatment of *fac*- or *mer*-[Mo(CO)$_3$(dppm-*PP'*)(dppm-*P*)] with $HgCl_2$ in dichloromethane at 20°C gives [Mo(CO)$_2$(dppm-*PP'*)$_2$Cl]Cl in good (> 60%) yield, together with metallic mercury. We have also prepared this complex by treating *cis*-[Mo(CO)$_2$(dppm-*PP'*)$_2$] with chlorine; the corresponding bromo and iodo complexes [Mo(CO)$_2$(dppm-*PP'*)$_2$X]X (X = Br or I) have been prepared previously by treating *cis*-[Mo(CO)$_2$(dppm-*PP'*)$_2$] with X_2.[4]

Similarly, treatment of either *fac*- or *mer*-[Mo(CO)$_3$(dppm-*PP'*)(dppm-*P*)] with Hg(SCN)$_2$ in dichloromethane gives mercury metal and golden yellow crystals of the seven-coordinate Mo(II) complex [Mo(CO)$_2$(NCS)$_2$(dppm-*PP'*)(dppm-*P*)] in a

* M.Sc. and Ph.D. student with Professor H. M. N. H. Irving at the University of Cape Town (1977–1980); presently "new blood" lecturer in inorganic chemistry at the Department of Pure and Applied Chemistry, The Queen's University, Belfast BT9 5AG, U.K. Author to whom all correspondence should be addressed.

very rapid and clean reaction. This complex has previously been prepared by treating $[MoCl_2(CO)_4]$ with ammonium thiocyanate followed by dppm, and our IR data (Nujol mull: ν_{CN} 2095 and 2070 cm^{-1}, ν_{CO} 1960 and 1890 cm^{-1}) are very similar to those reported before.[5] The $^{31}P-\{^1H\}$ NMR spectrum of $[Mo(CO)_2(NCS)_2$(dppm-*PP'*)(dppm-*P*)] in CD_2Cl_2 (not previously recorded) showed: a doublet at δ −25.3 ppm, assigned to the non-coordinating phosphorus atom; a multiplet at 34.6 ppm due to the coordinated phosphorus atom of the monodentate dppm ligand; and a broad hump at 5.3 ppm, assigned to the chelating dppm phosphorus atoms. At −50°C this broad resonance was resolved into two 1 : 1 : 1 : 1 quartets at −17.2 and 28.2 ppm, the temperature dependence of the spectrum presumably a result of ligand scrambling about the seven-coordinate molybdenum(II) centre.

It seems likely that the Mo(II) complexes described above are formed *via* Mo–Hg bonded intermediates. Treatment of $[M(CO)_4$(bipy)] (M = Mo or W, bipy = 2,2′-bipyridine) with HgX_2 (X = Cl, Br, I or SCN) has been shown to give complexes of type $[M(CO)_3$(bipy)$(HgX)X]$.[6,7] These M–Hg species were found to be unstable in polar solvents, decomposing to give metallic mercury.[7] Thus we tentatively propose that *fac*- or *mer*-$[Mo(CO)_3$(dppm-*PP'*)(dppm-*P*)] initially reacts with HgX_2 to give $[Mo(CO)_2$(dppm-*PP'*)(dppm-*P*)(HgX)X], which subsequently decomposes to give the observed product and mercury metal.

Single crystals of $[Mo(CO)_2(NCS)_2$(dppm-*PP'*)(dppm-*P*)] suitable for an X-ray diffraction study were obtained as golden yellow prisms from acetone–methanol. The structure (Fig. 1) confirms the seven-coordination around Mo(II) with "*cis*" CO groups, both bi- and monodentate dppm ligands, and with *N*-bonded NCS ligands; all these features were predicted from the IR and ^1H NMR data.[5] The choice of an idealized coordination geometry in a seven-coordinate complex is often not simple and has been the subject of several recent articles.[8–11] One simple procedure is to compare the interbond angles at the metal centre (Table 1) with the values computed for various idealized polyhedra.[8,10–12] This procedure reveals the coordination geometry about the Mo(II) centre to be intermediate between a capped trigonal prism [with N(1) in the unique capping position, P(1), N(2), P(3) and C(4) in the capped quadrilateral face, and P(2) and C(3) in the unique edge] and a capped octahedron [with C(3) in the capping position, P(2), P(3) and C(4) in the capped face, and P(1), N(1) and N(2) in the uncapped face]. This geometry is similar to several other M(II) complexes (M = Cr, Mo or W) containing CO and PR_3 ligands,[8] e.g. $[MoCl_2(CO)_2(PMe_2Ph)_3]$,[13] and in particular the interbond angles at Mo in the present structure are very

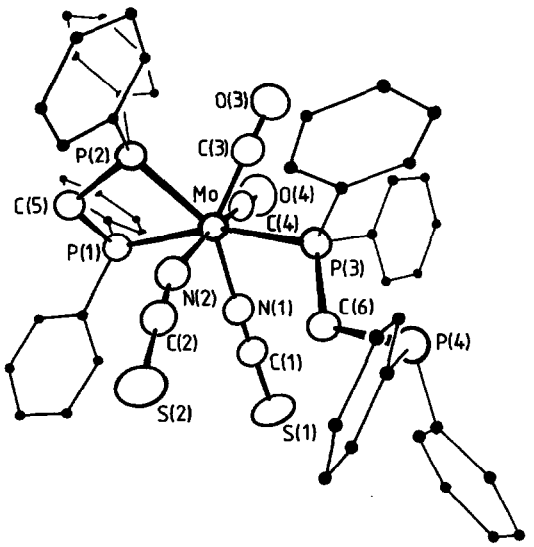

Fig. 1. Molecular structure of $[Mo(CO)_2(NCS)_2$(dppm-*PP'*)(dppm-*P*)], showing the principal atomic numbering.

Table 1. Bond lengths (Å) and angles (°) for $[Mo(CO)_2(NCS)_2$(dppm-*PP'*)(dppm-*P*)], with estimated standard deviations in parentheses

(a) Coordination sphere	
Mo—N(1)	2.159(7)
Mo—N(2)	2.195(8)
Mo—C(3)	1.96(1)
Mo—C(4)	1.98(1)
Mo—P(1)	2.597(3)
Mo—P(2)	2.514(2)
Mo—P(3)	2.554(2)
N(2)—Mo—C(4)	169.2(3)
P(1)—Mo—P(3)	160.0(1)
N(1)—Mo—P(2)	148.5(2)
N(1)—Mo—C(3)	140.4(4)
P(1)—Mo—C(3)	126.3(3)
P(2)—Mo—P(3)	126.2(1)
N(2)—Mo—C(3)	115.7(3)
P(2)—Mo—C(4)	107.8(3)
P(3)—Mo—C(4)	99.9(3)
P(1)—Mo—C(4)	90.9(3)
P(1)—Mo—N(1)	86.7(2)
N(1)—Mo—N(2)	85.1(3)
P(1)—Mo—N(2)	84.9(2)
N(1)—Mo—C(4)	84.8(3)
N(2)—Mo—P(3)	81.5(2)
N(2)—Mo—P(2)	79.4(2)
N(1)—Mo—P(3)	77.6(2)
C(3)—Mo—C(4)	74.8(4)
P(3)—Mo—C(3)	73.2(3)
P(2)—Mo—C(3)	71.0(3)
P(1)—Mo—P(2)	64.8(1)

(*continued*)

Table 1 (*continued*)

(b) Ligand geometry (selected parameters)	
N(1)—C(1)	1.15(1)
N(2)—C(2)	1.15(1)
C(1)—S(1)	1.65(1)
C(2)—S(2)	1.63(1)
C(3)—O(3)	1.16(1)
C(4)—O(4)	1.15(1)
P(1)—C(5)	1.86(1)
P(2)—C(5)	1.82(1)
P(3)—C(6)	1.84(1)
P(4)—C(6)	1.90(1)
P(1)—C(11)	1.834(5)
P(1)—C(21)	1.818(5)
P(2)—C(31)	1.841(5)
P(2)—C(41)	1.812(5)
P(3)—C(51)	1.840(5)
P(3)—C(61)	1.833(5)
P(4)—C(71)	1.868(5)
P(4)—C(81)	1.850(6)
Mo—N(1)—C(1)	175.8(7)
Mo—N(2)—C(2)	159.7(7)
N(1)—C(1)—S(1)	178.7(8)
N(2)—C(2)—S(2)	177.4(8)
Mo—C(3)—O(3)	176.8(9)
Mo—C(4)—O(4)	178.4(8)
Mo—P(1)—C(5)	92.5(3)
Mo—P(2)—C(5)	96.3(3)
P(1)—C(5)—P(2)	96.0(4)
Mo—P(3)—C(6)	112.3(3)
P(3)—C(6)—P(4)	113.8(5)

close to those reported for the complex [$MoCl_2(CO)_2$(dppm-*PP'*)(dppm-*P*)],[14] in which the introduction of a chelate ring accentuates the distortion more towards the capped trigonal prismatic than the capped octahedral geometry.

The Mo—N bond lengths (see Table 1) differ by *ca* 0.04 Å with the shorter bond [Mo—N(1)] being in the unique capping position of the capped trigonal prismatic structure, and similar differences are found in the corresponding Mo—Cl bond lengths of the two dichloro complexes mentioned above,[13,14] the shorter bond again being in this site. The Mo—P bond lengths (see Table 1) are all different, in the sequence Mo—P(1) > Mo—P(3) > Mo—P(2), and the same pattern is found in several related complexes, e.g. [$MoCl_2(CO)_2$(dppm-*PP'*)(dppm-*P*)].[14] Competition for the metal $d\pi$ electrons presumably lengthens the Mo—P(1) and Mo—P(3) bonds, which are mutually *trans*, whereas the Mo—P(2) bond is the shortest since it is nearly *trans* to an NCS group which does not compete as strongly for metal $d\pi$ electrons. The Mo—P(1) bond may be the longest of the Mo—P bonds because it is additionally somewhat *trans* to the carbonyl group C(3)—O(3) (see Table 1 for angles). The chelate ring angle P(1)—C(5)—P(2) of 96.0(4)° is significantly larger in the present complex than in [$MoCl_2(CO)_2$(dppm-*PP'*)(dppm-*P*)], where it is 90(1)°,[14] though the present value is in the middle of the range reported in a compilation of data for structures containing chelating dppm.[15] As in the homologous dichloro complex,[14] the four-membered chelate ring is puckered with the methylene C(5) displaced towards N(2) and away from the two carbonyl groups, allowing the bulky phenyl rings to avoid unfavourable intramolecular contacts. This puckering can be considered to be quite strong as measured by the relatively small P(1)—Mo—P(2) bite angle of 64.8(1)° and relatively large distance of the methylene C(5) atom from the P(1)—Mo—P(2) plane (0.67 Å) (see Ref. 15 for an analysis of chelating dppm stereochemistry).

It is noticeable that one of the isothiocyanate groups is bonded to the metal centre in a markedly non-linear fashion [Mo—N(2)—C(2) = 159.7(7)°], but the angle falls well within the range defined by other structural determinations of complexes containing *N*-bonded thiocyanate ligands.[16–18] The smaller Mo—N(2)—C(2) angle [159.7(7)° compared to Mo—N(1)—C(1) of 175.8(7)°] within the present structure is probably the result of having a CO ligand virtually *trans* [N(2)—Mo—C(4) = 169.2(3)°] to the isothiocyanate group, the resultant decrease in electron density available for bonding being reflected in predominance of the resonance form $S{=}C{=}N\overset{M}{\diagup}$ rather than $\bar{S}{-}C{\equiv}\overset{+}{N}{-}M$, though the correlation of N–C and C–S distances with the M–N–C angles in this structure is not as distinct as in others.[17,18] Steric or packing effects within the crystal have also been invoked to explain bent M–N–CS angles,[18] but there are no intermolecular contacts significantly less than the sum of van der Waals' radii in the present structure, and the low crystal density (D_c = 1.35 g cm^{-3}) is indicative of the somewhat loose packing of the molecules within the crystal.

EXPERIMENTAL

Reactions were carried out in an atmosphere of dry dinitrogen in deaerated, dried solvents. IR spectra were recorded on a Perkin–Elmer 457 grating spectrometer and ^{31}P–{^1H} NMR spectra were recorded on a JEOL FX100 instrument operating at 40.25 MHz and with positive chemical shifts to high frequency relative to 85% H_3PO_4.

Preparation of [$Mo(CO)_2(NCS)_2$(dppm-*PP'*)(dppm-*P*)]

A stirred solution of *fac*-[$Mo(CO)_3$(dppm-*PP'*)(dppm-*P*)] (0.200 g, 0.21 mmol) in dichloromethane (8 cm^3) was treated with $Hg(SCN)_2$ (0.067 g, 0.21 mmol). The solution turned red almost immediately and carbon monoxide was evolved. After 30 min of stirring a small volume of methanol (*ca* 3 cm^3) was added to aid deposition of metallic mercury. The reaction mixture was filtered and methanol added to precipitate out golden yellow crystals of [$Mo(CO)_2(NCS)_2$(dppm-*PP'*)(dppm-*P*)]. Yield 0.096 g (44%). Analysis found (required): C, 62.4 (62.6); H, 4.2 (4.3); N, 2.6 (2.7)%. A similar yield was obtained when *mer*-[$Mo(CO)_3$(dppm-*PP'*)(dppm-*P*)] was used as the starting material.

Crystal data

$C_{54}H_{44}MoN_2O_2P_4S_2$, $M = 1036.91$, orthorhombic, $a = 21.583(7)$ Å, $b = 12.775(4)$ Å, $c = 18.484(5)$ Å, $U = 5096(2)$ $Å^3$, space group $Pna2_1$ (No. 33), $Z = 4$, $D_c = 1.35$ g cm^{-3}, $F(000) = 2128$, graphite-monochromated Mo-K_α radiation, $\lambda = 0.71069$ Å, μ(Mo-K_α) = 4.93 cm^{-1}. Golden yellow prisms from acetone–methanol. Crystal dimensions (distance to faces from centre): 0.155 (100, $\bar{1}00$), 0.148 (011, $0\bar{1}\bar{1}$), 0.165 ($0\bar{1}1$, $01\bar{1}$) mm.

Structure determination

Cell dimensions and their standard deviations were obtained by least-squares refinement of diffractometer setting angles for 15 automatically-centred reflections having $34° < 2\theta < 39°$. Intensities of 3405 independent reflections (h, k, l; $4° < 2\theta < 45°$) were measured on a Syntex $P2_1$ diffractometer in the ω–2θ scan mode using scan speeds, according to a prescan intensity, between 2 and 29° min^{-1}, and with the scans running from 1° below $K_{\alpha1}$ to 1° above $K_{\alpha2}$. The structure analysis used the 3181 reflections with $I > 2\sigma(I)$ after correction for Lorentz and polarization factors; absorption effects were corrected numerically (maximum and minimum transmission factors for full data set = 0.89 and 0.83).[19]

Solution by Patterson and difference syntheses was followed by full-matrix least-squares refinement with anisotropic thermal parameters for all atoms except H and the phenyl ring C atoms, using the SHELX program system.[19] The phenyl rings were refined as rigid groups with idealized D_{6h}-geometry, the C atoms having individual isotropic thermal parameters and C—C distances of 1.395 Å. All H atoms, many of which were found in difference maps, were included in the calculation at idealized positions with C—H fixed at 1.08 Å; their isotropic temperature factors were treated as two single parameters (for aromatic or methylene H). The refinement for 251 parameters converged to $R = 0.046$ and $R_w = \Sigma w^{1/2}\Delta/\Sigma w^{1/2}|F_o| = 0.048$, employing the weighting scheme $w = 1/(\sigma^2 F_o + 0.0004F_o^2)$ to give a flat analysis of variance with increasing $\sin\theta$ and $(F_o/F_{max})^{1/2}$. Refinement of the alternative enantiomorphic specification gave larger R-factors (though not significantly so) and the original structure was retained.* A final difference map was featureless. Complex neutral-atom scattering factors were calculated from the analytical approximation and coefficients given in Ref. 20.

Acknowledgements—We thank the SERC for support and the University of Leeds for a Fellowship (to A.T.H.).

*Atomic coordinates, thermal parameters, full bond length and angle data, and structure factor values have been deposited as supplementary material with the Editor from whom copies are available on request. Atomic coordinates have also been deposited with the Cambridge Crystallographic Data Centre.

REFERENCES

1. A. Blagg, G. R. Cooper, P. G. Pringle, R. Robson and B. L. Shaw, *J. Chem. Soc., Chem. Commun.* 1984, 933.
2. A. Blagg, A. T. Hutton, B. L. Shaw and M. Thornton-Pett, *Inorg. Chim. Acta* 1985, **100**, L33.
3. A. Blagg and B. L. Shaw, unpublished work.
4. A. M. Bond, R. Colton and J. J. Jackowski, *Inorg. Chem.* 1975, **14**, 2526.
5. R. Colton and G. R. Scollary, *Aust. J. Chem.* 1968, **21**, 1435.
6. K. Edgar, B. F. G. Johnson, J. Lewis and S. B. Wild, *J. Chem. Soc. A* 1968, 2851; P. D. Brotherton, J. M. Epstein, A. H. White and S. B. Wild, *Aust. J. Chem.* 1974, **27**, 2667.
7. M. P. Pardo and M. Cano, *J. Organomet. Chem.* 1984, **260**, 81.
8. M. G. B. Drew, *Prog. Inorg. Chem.* 1977, **23**, 67.
9. S. J. Lippard, *Prog. Inorg. Chem.* 1976, **21**, 91; E. L. Muetterties and L. J. Guggenberger, *J. Am. Chem. Soc.* 1974, **96**, 1748; 1977, **99**, 3893; J. K. Kouba and S. S. Wreford, *Inorg. Chem.* 1976, **15**, 1463; 1978, **17**, 1696; E. B. Dreyer, C. T. Lam and S. J. Lippard, *Inorg. Chem.* 1979, **18**, 1904; P. Brant, F. A.

Cotton, J. C. Sekutowski, T. E. Wood and R. A. Walton, *J. Am. Chem. Soc.* 1979, **101**, 6588.
10. D. J. Szalda, J. C. Dewan and S. J. Lippard, *Inorg. Chem.* 1981, **20**, 3851.
11. C. M. Giandomenico, J. C. Dewan and S. J. Lippard, *J. Am. Chem. Soc.* 1981, **103**, 1407.
12. R. Hoffmann, B. F. Beier, E. L. Muetterties and A. R. Rossi, *Inorg. Chem.* 1977, **16**, 511.
13. A. Mawby and G. E. Pringle, *J. Inorg. Nucl. Chem.* 1972, **34**, 517.
14. M. G. B. Drew, A. P. Wolters and I. B. Tomkins, *J. Chem. Soc., Dalton Trans.* 1977, 974.
15. P. W. R. Corfield, J. C. Dewan and S. J. Lippard, *Inorg. Chem.* 1983, **22**, 3424.
16. A. Ferrari, A. Braibanti, G. Bigliardi and A. M. Lanfredi, *Acta Cryst.* 1965, **18**, 367.
17. A. C. Hazell, *J. Chem. Soc.* 1963, 5745.
18. J. R. Knox and K. Eriks, *Inorg. Chem.* 1968, 7, 84.
19. G. M. Sheldrick, *SHELX-76 Program System.* University of Cambridge (1976).
20. J. A. Ibers and W. C. Hamilton (Eds), *International Tables for X-Ray Crystallography*, Vol. 4. Kynoch Press, Birmingham (1974).

Polyhedron Vol. 6, No. 1, pp. 101–103, 1987
Printed in Great Britain

0277–5387/87 $3.00+.00

SUBSTITUTION INERTNESS OF $[Ir(H_2O)_6]^{3+}$

SILVIA E. CASTILLO-BLUM and A. GEOFFREY SYKES*

Department of Inorganic Chemistry, The University,
Newcastle upon Tyne NE1 7RU, U.K.

and

HEINZ GAMSJÄGER

Institut für Physikalische Chemie, Montanuniversität, A-8700 Leoben, Austria

(*Received* 3 *July* 1986)

Abstract—Ligand substitution properties of the recently characterized pale-yellow $[Ir(H_2O)_6]^{3+}$ ion in perchlorate solutions, have been investigated. At 120°C in sealed tubes observations on the exchange with $H_2{}^{18}O$ are impaired by a spurious oxidation to purple Ir(IV). Over extended periods at 40°C the ion has been shown to be extremely inert, and the rate constants for substitution of Cl^- into $[Ir(H_2O)_6]^{3+}$ is estimated to be $< 2 \times 10^{-9}$ $M^{-1}\,s^{-1}$.

The aqua ion of Ir(III), first reported in 1976, is now well characterized as $[Ir(H_2O)_6]^{3+}$.[1–3] Studies on hexa-aqua ions remain of fundamental importance in considering the properties of different oxidation states. Of particular interest are the trends in substitution kinetic behaviour of metals in the same group of the Periodic Table. Present findings are discussed in the context of the substitution behaviour of other metal ions, including $[Al(H_2O)_6]^{3+}$ and $[Ga(H_2O)_6]^{3+}$.[4]

EXPERIMENTAL

Materials

Stock solutions of $[Ir(H_2O)_6]^{3+}$ (0.02 M) in 2 M $HClO_4$ were prepared by treatment of $[IrCl_6]^{3-}$ or $[IrCl_6]^{2-}$ (Johnson Matthey) with OH^-, precipitation of $[Ir(OH)_3(H_2O)_3]$, and dissolving this in 0.1 M $HClO_4$ as previously described.[1,2] Final purification was from a Dowex ion-exchange column. The ion was characterized by its UV–visible peaks, λ (nm) [ε ($M^{-1}\,cm^{-1}$)] at 310 (32.5) and 265 (41). Sodium perchlorate, $NaClO_4 \cdot H_2O$, and sodium chloride (both BDH, Analar) were used without further purification. Sodium thiocyanate (BDH, Laboratory Reagent) was recrystallized 3 times from ethanol.

Kinetic studies

Solutions of $[Ir(H_2O)_6]^{3+}$ ($\sim 4 \times 10^{-3}$ M) in 1.0 M $HClO_4$ containing added ^{18}O-enriched H_2O were sealed in glass ampoules and placed in an oven at 120°C (CARE!). Other studies were at 40°C with Cl^- and NCS^- as substituents. The pH of the latter solutions was adjusted to values in the range 1–2 by addition of saturated $NaHCO_3$ (BDH, Analar). The acid dissociation (pK_a) for $[Ir(H_2O)_6]^{3+}$ is 4.37.[3] The spectrum remained unchanged, and it was assumed that no significant amounts of carbonate remained. No information is available on the spectrum of $[Ir(H_2O)_5Cl]^{2+}$, but from the trends observed[5] for the formation of $[Rh(H_2O)_5Cl]^{2+}$ from $[Rh(H_2O)_6]^{3+}$ significant changes are expected. Formation of thiocyanato complexes generally give rise to large absorbance changes in the near UV.

*A.G.S. was lecturer/colleague of Professor Irving, University of Leeds (1961–1971), and moved to the University of Newcastle in 1980. Author to whom correspondence should be addressed.

RESULTS

Over intervals of ~ 3 h at 120°C pale-yellow solutions of $[Ir(H_2O)_6]^{3+}$ became purple. The colour obtained is the same as that of the Ir(IV) product, at present of uncertain molecularity (not monomer), obtained in electrochemical studies on $[Ir(H_2O)_6]^{3+}$, peak at 541 nm.[6] The same behaviour was observed when solutions were sealed under N_2, and in a test with Ag^+ no Cl^- was detected. This does not rule out formation of other oxidation states of chlorine. It was concluded that high temperatures are not appropriate for studies over long time intervals of the H_2O exchange on $[Ir(H_2O)_6]^{3+}$.

At 40°C the following experiments were carried out with $[Ir(H_2O)_6]^{3+}$ at 2.3×10^{-3} M. First with [NaCl] = 2.3 M, $[H^+] = 0.010$ M, $I = 3.0$ M ($NaClO_4$), and then with [NaCl] = 3.7 M, $[H^+] = 0.10$ M, $I = 3.9$ M, no absorbance changes in the 250–350-nm range were observed over 10 and 15 days, respectively. With [NaNCS] = 1.0 M, $[H^+] = 0.010$ M, $I = 2.0$ M ($NaClO_4$), absorbance changes matched those for a solution with no $[Ir(H_2O)_6]^{3+}$ added, and can be attributed to side reactions of NCS^-.[7] Even with the generous allowance that the time the Cl^- runs were monitored for is equal to the half-life of the reaction, a rate constant of 1.4×10^{-8} M^{-1} s^{-1}, comparable to that for $[Rh(H_2O)_6]^{3+}$, is obtained. More realistically assuming that < 10% reaction occurs in this time we fix the rate constant limit for the reaction of $[Ir(H_2O)_6]^{3+}$ with Cl^- at $< 2 \times 10^{-9}$ M^{-1} s^{-1}. In arriving at this estimate an allowance has been made for the conjugate-base $[H^+]^{-1}$ pathway, which it is assumed contributes to the same extent as in the reaction with $[Rh(H_2O)_6]^{3+}$.[8] In the latter $[Rh(H_2O)_5OH]^{2+}$ has been shown to be ~ 6000 times more reactive than $[Rh(H_2O)_6]^{3+}$.

DISCUSSION

It is concluded from these studies that $[Ir(H_2O)_6]^{3+}$ is extremely inert, probably more inert than $[Rh(H_2O)_6]^{3+}$, and therefore the most inert of hexa-aqua ions at present known. Substitution studies on the d^6-ions $[Co(H_2O)_6]^{3+}$ and $[Rh(H_2O)_6]^{3+}$ have previously indicated significant rate law contributions from $[H^+]^{-1}$-dependent terms.[8,9] Experiments on $[Ir(H_2O)_6]^{3+}$ were at pH 1–2 to gain maximum benefit from such $[H^+]^{-1}$ terms in the rate law. The increase in inertness in going from $[Co(H_2O)_6]^{3+}$ to $[Rh(H_2O)_6]^{3+}$, and then to $[Ir(H_2O)_6]^{3+}$ (see Table 1), is in keeping with the effect of increasing ligand-field stabilization.[10] A similar overall trend has been observed for H_2O exchange of the aquapentaammine complexes, $[Co(NH_3)_5(H_2O)]^{3+}$, $[Rh(NH_3)_5(H_2O)]^{3+}$ and $[Ir(NH_3)_5(H_2O)]^{3+}$, although here it is interesting that the volumes of activation 1.2, −4.1 and −3.2 cm^3 mol^{-1}, respectively, indicate a possible change in mechanism from I_d (for Co) towards I_a (for Rh and Ir).[11–13] Participation of some high-spin $[Co(H_2O)_6]^{3+}$ cannot be ruled out as a contributing factor to the faster rate constants observed for this ion.

In sharp contrast the rate constant (25°C) for 1 : 1 Cl^- anation of $[Mo(H_2O)_6]^{3+}$ (4.6×10^{-3} M^{-1} s^{-1}) is some 10^5 times bigger than for $[Cr(H_2O)_6]^{3+}$ (2.9×10^{-8} M^{-1} s^{-1}), and with NCS^- a similar ratio is obtained.[14,15] The low d-electron population, and increase in associative character with increasing size ($4d > 3d$) of the d-orbitals, provides a likely explanation. The associative character of $[Mo(H_2O)_6]^{3+}$ is comparable to that of the more labile $[V(H_2O)_6]^{3+}$ (d^2) and $[Ti(H_2O)_6]^{3+}$ (d^1) ions, which have H_2O exchange rate constants (25°C) of 495 and 1.81×10^5 s^{-1}, respectively.[4]

Table 1. Comparisons of rate constants for substitution[a]

Reaction	Temperature (°C)	k	Reference
$[Co(H_2O)_6]^{3+} + Cl^-$	25	$\leqslant 2$ M^{-1} s^{-1}	8
$[Rh(H_2O)_6]^{3+} + Cl^-$	40	~ 10^{-8} M^{-1} s^{-1}	9
$[Ir(H_2O)_6]^{3+} + Cl^-$	40	$< 2 \times 10^{-9}$ M^{-1} s^{-1}[b]	This work
$[Co(NH_3)_5(H_2O)]^{3+} + H_2O$	25	5.7×10^{-6} s^{-1}	11
$[Rh(NH_3)_5(H_2O)]^{3+} + H_2O$	25	8.4×10^{-6} s^{-1}	12
$[Ir(NH_3)_5(H_2O)]^{3+} + H_2O$	25	6.1×10^{-8} s^{-1}	13

[a] Contributions from $[H^+]^{-1}$-dependent terms are not included in the first three entries.

[b] An $[H^+]^{-1}$ contribution of similar proportion to that observed for $[Rh(H_2O)_6]^{3+}$ has been allowed for in this estimate.

While it is possible that other hexa-aqua ions of early transition metals may be identified, the availability of an associative route for ligand exchange means that these are unlikely to be very inert. Indeed it is unlikely that there will be a more inert II or III state hexa-aqua ion than $[Ir(H_2O)_6]^{3+}$ in the Periodic Table, and only if $[Pt(H_2O)_6]^{4+}$ is at some time prepared is a more inert ion of this kind likely to be obtained.

A further comparison of interest is that for H_2O exchange (25°C) on $[Al(H_2O)_6]^{3+}$ (1.29 s^{-1}) and $[Ga(H_2O)_6]^{3+}$ (403 s^{-1}), where the size of the metal ion and electrostatics determine the pattern of behaviour observed.[4] Both reactions are assigned an I_d-mechanism from the magnitude of volumes of activation (+5.7 and +5.0 $cm^3\ mol^{-1}$, respectively). This trend also parallels that of characteristic rate constants for water exchange on $[Zn(H_2O)_6]^{2+}$ (3×10^7 s^{-1}), $[Cd(H_2O)_6]^{2+}$ (2×10^8 s^{-1}) and $[Hg(H_2O)_6]^{2+}$ (2×10^9 s^{-1}).[16]

Acknowledgements—S.E.C.-B thanks the National Autonomous University of Mexico (U.N.A.M.) for postgraduate support. We are most grateful to Johnson Matthey for the loan of Ir samples.

REFERENCES

1. P. Beutler and H. Gamsjäger, *J. Chem. Soc., Chem. Commun.* 1976, 554.
2. P. Beutler, H. Gamsjäger and P. Naertschi, *Chimia (Switz)* 1978, **32**, 163.
3. H. Gamsjäger and P. Beutler, *J. Chem. Soc., Dalton Trans.* 1979, 1415.
4. A. Hugi, D. Hugi, L. Helm and A. E. Merbach, Abstracts of the XXIII International Coordination Chemistry Conference, Boulder, Colorado, August 1984, and personal communication.
5. W. Plumb and G. M. Harris, *Inorg. Chem.* 1964, **3**, 542.
6. S. E. Castillo-Blum, D. T. Richens and A. G. Sykes, *J. Chem. Soc., Chem. Commun.* 1986, 1120.
7. A. A. Newman, *Chemistry and Biochemistry of Thiocyanic Acid and its Derivatives*. Academic Press, New York (1975).
8. K. Swaminathan and G. M. Harris, *J. Am. Chem. Soc.* 1966, **88**, 4411.
9. T. G. Conocchioli, G. H. Nancollas and N. Sutin, *Inorg. Chem.* 1965, **5**, 1.
10. F. Basolo and R. G. Pearson, *Mechanisms of Inorganic Reactions*, 2nd Edn, p. 145. Wiley, New York (1967).
11. H. R. Hunt and H. Taube, *J. Am. Chem. Soc.* 1958, **80**, 2642.
12. T. W. Swaddle and D. R. Stranks, *J. Am. Chem. Soc.* 1972, **94**, 8357.
13. S. B. Tong and T. W. Swaddle, *Inorg. Chem.* 1974, **13**, 1538.
14. Y. Sasaki and A. G. Sykes, *J. Chem. Soc., Dalton Trans.* 1975, 1048.
15. (a) J. H. Espenson, *Inorg. Chem.* 1969, **8**, 1554; D. Thusius, *Inorg. Chem.* 1971, **10**, 1106 (and references therein); (b) J. P. Hunt and R. A. Plane, *J. Am. Chem. Soc.* 1954, **76**, 5960.
16. E.g. M. Eigen, *Coordination Chemistry*, p. 102 and Ref. 10, p. 154. Butterworths, London (1963).

Polyhedron Vol. 6, No. 1, pp. 105–110, 1987
Printed in Great Britain

0277–5387/87 $3.00+.00

OPTICALLY ACTIVE COORDINATION COMPOUNDS—XLVI.* RESOLUTION OF TRIS-DI-IMINE COMPOUNDS OF CHROMIUM(III) USING *fac*-(+)TRIS[L-CYSTEINESULPHINATO (2−)-*S,N*]COBALTATE(III)

P. S. CARTWRIGHT, R. D. GILLARD† and E. R. J. SILLANPÄÄ‡

Department of Chemistry, University College, Cardiff CF1 1XL, U.K.

(*Received* 3 *July* 1986)

Abstract—The resolving agent $K_3[Co(L\text{-cysu})_3]\cdot nH_2O$ [cysu = cysteinesulphinato(2−)-*S,N*] is further characterized: $n = 3$ or 6 are distinct compounds. A new solid acid of composition $\{H_3(H_2O)_3[Co(L\text{-cysu})_3]\}$ is described. The new cation tris-5,5′-dimethyl-2,2′-bipyridylchromium(III) is described and its resolution [with those of tris-1,10-phenanthrolinechromium(III) and tris-2,2′-bipyridylchromium(III)].

Schubert[2] studied the reaction between cobalt(III) and L-cysteine in basic aqueous solution, and the reaction of the product with hydrogen peroxide. Neville and Gorin[3] further investigated linkage isomerism in the system, showing that bidentate cysteine coordinates to cobalt(III) via the nitrogen and sulphur atoms. Gorin *et al.*[4] confirmed the mode of coordination, rectified some errors in Neville's earlier paper, and suggested the potential stereoselectivity of the reaction, without further investigating it.

Gillard and Maskill,[5] from chiroptical properties, found stereospecific formation of only one isomer of the tris-cysteinatocobalt(III) complex. Conversion by hydrogen peroxide of thiolate to sulphinate ligand was taken as a chemical correlation of optical configuration. They followed up Schubert's observation[2] that the potassium(+)-tris(L-cysu)cobaltate(III) [cysu = cysteinesulphinato(2−)-*S,N*] forms a precipitate with $[Coen_3]Br_3$ (en = ethylenediamine) by showing that this was a diastereomeric salt, containing the resolved cation, $(+)[Coen_3]^{3+}$. Dollimore and Gillard[6] then used this type of reaction to resolve, for the first time, a series of bis- and tris-chelate bpy and phen derivatives (bpy = 2,2′-bipyridyl, phen = 1,10-phenanthroline), together with the complete series $[Co(en)_x(phen)_{3-x}]^{3+}$ ($x = 0$–3).[7]

More recently, Kane-Maguire and Hallock[8] have used this versatile resolving agent, which lately became available commercially, to resolve the $[Crbpy_3]^{3+}$ cation, previously partially resolved by Mason and Peart,[9] who employed (−)barium tris(catechyl)arsenate(V).

We now report in detail on the synthesis and properties of hydrates of potassium(+)tris(L-cysu)-cobaltate(III) and some derivatives, the resolution of $[Crbpy_3]^{3+}$ (which had already been described[8]), a resolution of $[Crphen_3]^{3+}$ with this resolving agent for the first time,[10] and the preparation and resolution of a new cation, $[Crdmbpy_3]^{3+}$ (dmbpy = 5,5′-dimethyl-2,2′-bipyridyl).

EXPERIMENTAL

Physical measurements

Electronic spectra were measured with Cary 17 and Unicam SP8000 spectrophotometers, calibrated for wavelength and absorbance with holmium oxide and acidified potassium dichromate, respectively.[11] Circular dichroism (CD) spectra were measured using a Jobin Yvon CNRS–Rousel–Jouan Dichrographe III spectrophotometer. IR

* For Part XLIII see Ref. 1.

† R.D.G. was tutored by Professor Irving at St. Edmund Hall, Oxford (1956–1960), when an undergraduate, and did Part II of the Oxford B.A. and the B.Sc. under his supervision. Author to whom correspondence should be addressed.

‡ Permanent address: Department of Chemistry, University of Turku, SF-20500 Turku, Finland.

spectra were recorded, as Nujol mulls, on a Perkin–Elmer 783. NMR spectra were run on a Bruker WM360 spectrometer. Thermogravimetric analyses were obtained with a Stanton Redcroft thermogravimetric TG 750 balance in a dynamic nitrogen atmosphere at a heating rate of 10°C min^{-1}. Microanalyses (C, H and N) were performed by the microanalytical laboratory, Department of Chemistry, University College, Cardiff.

General

All preparations and reactions involving potassium(+)tris(L-cysu)cobaltate(III) were carried out in vessels shielded from direct light. Solvents were of reagent grade purity.

Preparations

Potassium(+)tris(L-cysu)cobaltate(III). A solution of $[Co(NH_3)_6]Cl_3$ (5.34 g, 0.02 mol) in water (150 cm^3) was deoxygenated (N_2 bubbler, 15–20 min) and L-cysteine (12.12 g, 0.10 mol) and KOH (16.84 g, 0.30 mol) were added. The mixture was heated in the dark at 70°C until ammonia could no longer be detected ($\simeq$ 8 h), then ethanol (150 cm^3) was added. A green precipitate of potassium(+)tris[L-cysteinato-*S,N*]cobaltate(III) formed immediately: the mixture was cooled to 0°C, filtered very rapidly, and the collected solid washed with ethanol (2×50 cm^3). This still-moist precipitate was added slowly ($\simeq$ 1 h) to hydrogen peroxide (100 cm^3, 100 vol), keeping the temperature below 10°C. The resulting mixture was allowed to warm slowly to room temperature during 4 h (to ensure complete oxidation). Ethanol (300 cm^3) was added, and the yellow precipitate of potassium(+)tris(L-cysu)cobaltate(III)·$6H_2O$ filtered off and washed with ethanol (2×50 cm^3). Recrystallization was done in two ways. (a) If ethanol was allowed to diffuse slowly into a concentrated aqueous solution of potassium(+)tris(L-cysu)-cobaltate(III), then long, hair-like yellow crystals of the hexahydrate were obtained (Table 1). (b) If recrystallization was done quickly from water–ethanol (2:1.5 by volume), a more compact material was obtained, analysing again as the hexahydrate. The products were dried for several days *in vacuo* over P_2O_5. The yield typically was 3.1 g (21.0% based on $[Co(NH_3)_6]Cl_3$). The trihydrate was obtained by extended desiccation of the hexahydrate (28 days) *in vacuo* over P_2O_5, the material being fluffier and lighter in colour than the hexahydrate (Table 1).

The yellow, hair-like material is very soluble in water, but insoluble in organic solvents. Attempts to modify the morphology of the crystals, i.e. recrystallizing in the presence of LiBr and urea, failed to give anything but hair-like products.

The complex is formed stereoselectively, the ^{13}C NMR spectrum (Table 2) showing only three lines of equal intensity, indicating formation of the facial isomer, as reported by Dollimore and Gillard.[6,7] Separation of isomers of potassium(+)tris(L-cysu)-

Table 1. Microanalytical and thermogravimetric results

Complex	Calculated				Found				Residue[a]
	C	H	N	H_2O	C	H	N	H_2O[a]	
$K_3(+)[Co(L\text{-cysu})_3]\cdot 6H_2O$	14.7	3.7	5.7	14.6	14.9	3.5	5.5	14.5	47% black powder
$K_3(+)[Co(L\text{-cysu})_3]\cdot 3H_2O$	15.8	3.1	6.1	7.9	15.8	3.8	6.1	8.2	37% black powder
"$H_3(+)[Co(L\text{-cysu})_3]\cdot 3H_2O$"	19.0	4.2	7.5	9.5	19.8	4.5	6.9	9.8	17%
$Ba_3(+)[Co(L\text{-cysu})_3]_2\cdot 8H_2O$	13.7	2.9	5.3	9.1	13.6	3.0	4.5	9.0	57% grey ash
$[Crbipy_3](ClO_4)_3\cdot \frac{1}{2}H_2O$[b]	43.5	3.0	10.2	1.1	43.5	3.3	10.3	1.1	Yellow powder (150°C)
$[Crbipy_3](ClO_4)_3\cdot 2H_2O$[b]	42.1	3.3	9.8	4.2	42.2	2.7	10.1	4.5	Yellow powder (150°C)
$[Crphen_3](ClO_4)_3\cdot 2H_2O$[b]	46.6	3.0	9.1	3.9	46.6	2.9	9.0	4.0	Golden powder (150°C)
$[Crdmbpy_3](ClO_4)_3\cdot 6H_2O$[b]	42.8	4.7	8.3	10.6	4.1	4.1	8.0	10.1	Opaque yellow flakes (150°C)
$[Crdmbpy_3](ClO_4)_3\cdot 5H_2O\cdot \frac{1}{2}MeCN$[b]	43.8	4.7	9.0	11.0[c]	4.5	4.5	8.9	11.5[c]	Opaque yellow cubes (150°C)

[a] Thermogravimetric result.

[b] Heated only to 150°C owing to explosive nature of perchlorate.

[c] This value includes $\frac{1}{2}$MeCN of crystallization.

Table 2. ^{13}C NMR results (in D_2O at 35°C)

	δ	Assignment
$K_3(+)[Co(L\text{-cysu})_3]\cdot 6H_2O$	56.3s	Asymmetric carbon
	68.7s	Methylene carbon
	176.5s	Carboxyl carbon
Photoreduced $K_3(+)[Co(L\text{-cysu})_3]$	56.4w	Unphotolysed complex
	57.4s	
	58.0s	
	61.4s	
	67.8s	
	68.2s	
	68.8w	Unphotolysed complex
	176.8w	Unphotolysed complex
	177.2s	Carboxyl carbons
	177.7s	
	179.0s	

cobaltate(III) was attempted by ion exchange chromatography using QAE Sephadex A-25, but only one band was obtained, the chiroptical properties of samples withdrawn from leading and trailing edges of this band being identical. The CD and UV–visible spectra of potassium(+)tris(L-cysu)-cobaltate(III) compared well with the literature[5,6] (Table 3). The hexahydrate showed IR bands at (cm^{-1}): 3500s, 3250s, 3215s, 1600s, 1305m, 1285w, 1268m, 1208s, 1188s, 1168s, 1110s, 1100s, 1063s, 1050s, 992w, 980w, 936s, 930s, 878m, 871m, 807s, 756m, 730m, 690vw, 555m, 540m, 505w, 470s, 387m, 340m and 290m. The complex is photosensitive, the surface of the solid and a solution becoming dark orange in sunlight over 72 h. The changes in electronic and CD spectra are as those reported by Dollimore and Gillard.[6] The ^{13}C NMR spectrum is much more complex for this photoreduced complex (Table 2), indicating the possible formation of the meridional isomer. However, on standing in bright sunlight for 10 days or more, the resultant pink solution shows a broad, less intense absorption maximum *ca* 525 nm with a much less intense shoulder at 310 nm. The CD spectrum shows a small negative peak at 570 nm, together with positive and negative peaks at 523 and 464 nm, respectively, all with $\Delta\varepsilon$ values much reduced from those of the parent potassium tris(L-cysu)-cobaltate(III) (see Table 3).

Tris-fac-[L-*cysteinesulfinato*(−)-S,N]*cobalt*(III). Typically, sulphuric acid (0.5 M, 2cm^3) was added to potassium(+)tris(L-cysu)cobaltate(III) (100 mg in 5 cm^3 H_2O) to give a yellow solid which was collected and washed with ethanol and ether. This compound is very insoluble in most solvents and analyses as the acid salt (see Table 1) of the (+)tris(L-cysu)cobaltate(III) anion, $\{H_3(H_2O)_3\{Co(L\text{-cysu})_2\}\}$. This acid salt shows IR bands (Nujol mulls) at (cm^{-1}): 3490m, 3280m, 3240s, 3210m, 1730m, 1710s, 1410s, 1378s, 1295w, 1245w, 1222s, 1198s, 1185m, 1168m, 1110s, 1070m, 1060s, 1038m, 980w and 932w. On pH titration of potassium(+)tris(L-cysu)cobaltate(III) vs acid, precipitation began after only 1 mole equivalent of acid was added. The identical CD spectrum of the acid salt redissolved in base to that of the potassium(+)tris(L-cysu)cobaltate(III) showed there was no change in optical configuration on acidification.

Preparation of a Ba^{2+} salt is easy, by simple metathesis, adding an aqueous solution of barium chloride to a concentrated solution of potassium(+)tris(L-cysu)cobaltate(III). However, crystal shape remains very similar. The hair-like, yellow material analyses as the octahydrate, $Ba_3(+)[Co(L\text{-cysu})_3]_2\cdot 8H_2O$ (Table 1).

Tris-di-iminechromium(III)*perchlorate*. These compounds were made by prior isolation of chromium(II) acetate. $HClO_4$ (70 cm^3, 1 M) was allowed to drip onto chromium(II) acetate (3 g) in a nitrogen atmosphere, and the resulting blue solution of Cr(II) filtered through glass wool into a suspension of di-imine (5 g) in water (150 cm^3). The dark precipitate which formed was collected, washed with ethanol, ether and was added to $HClO_4$ (100 cm^3, 1 M), with oxygen bubbled through for several hours. The yellow precipitate of $[Cr(\text{di-imine})_3](ClO_4)_3\cdot nH_2O$ was then collected by filtration and washed with ethanol and ether. The method of recrystallization depended on the di-imine present. For $[Crbpy_3](ClO_4)_3\cdot nH_2O$, recrystallization was

Table 3. Absorption and CD results

Complex	Absorption		CD		
	λ (nm)	ε (l mol^{-1} cm^{-1})		λ (nm)	$\Delta\varepsilon$ (l mol^{-1} cm^{-1})
$K_3(+)[Co(L\text{-cysu})_3]\cdot 6H_2O$[a]	406	830		435	−3.71
	308	33,470		390	+3.70
				316	+13.30
				279	−15.70
Final pink photoreduced solution	525	295		570	−0.20
	310	7820		523	+0.75
				464	−1.40
$[Crbpy_3](ClO_4)_3\cdot 2H_2O$[b]	456	261	D(+)	459	−0.94
	428	675		347	−14.46
	405	937		313	−60.30
	357	6754		263	+6.63
	344	9150	L(−)	459	+1.11
	312	26,580		347	+16.47
	275	17,650		313	+75.90
	267	17,865		263	−12.66
$[Crphen_3](ClO_4)_3\cdot 2H_2O$[c]	430	681	D(+)	454	+2.42
	405	846		437	+1.95
	355	3524		326	+35.43
	318	11,630		284	+174.18
	267	55,200		274	+183.00
				259	−118.00
			L(−)	454	−2.20
				437	−1.89
				326	−48.80
				284	−185.71
				274	−195.16
				259	+132.20
$[Crdmbpy_3](ClO_4)_3\cdot 6H_2O$	480	363	D(+)	477	+0.61
	446	895		367	+11.90
	423	1065		327	+38.25
	410	989		299	+5.77
	368	7690		279	−11.55
	356	9890	L(−)	477	−0.66
	322	27,231		367	−16.60
				327	−50.53
	287	21,580		299	−7.04
				279	+13.67
$[Crdmbpy_3](ClO_4)_3\cdot 5H_2O\cdot \frac{1}{2}MeCN$	480	361			
	446	901			
	423	1059			
	410	991			
	368	8160			
	356	10,560			
	322	28,430			
	287	19,430			
	238	48,990			

[a] Literature[6] gives λ (ε): 406 (824), and 308 (29,000); λ ($\Delta\varepsilon$): 438 (−3.83), and 274 (−11.9).

[b] Literature[12] gives λ (ε): 455 (260), 398 (900), and 312 (23,000). Literature[8] gives λ ($\Delta\varepsilon$): 460 (+1.1) and 315 (70 ± 10%) read from very small digram of spectrum.

[c] Literature[10] gives λ (ε): 426 (384).

carried out from 0.01 M $HClO_4$, yielding two crystal types. The first-formed crystals were yellow needles, analysing as $n = 2$; orange crystals began to form thereafter, with $n = \frac{1}{2}$ (see Table 1). The electronic spectra of both forms compared with the literature[12] (Table 3).

$[Crphen_3](ClO_4)_3 \cdot 2H_2O$ was quite insoluble in 0.01 M $HClO_4$, and was therefore recrystallized from water, giving small, golden yellow crystals. Only the dihydrate was formed (Table 1). The electronic spectrum (Table 3) compared well with the literature,[10] but the molar extinction coefficients measured here were considerably higher.

The new compound $[Crdmbpy_3](ClO_4)_3 \cdot nH_2O$ was first recrystallized from 0.01 M $HClO_4$ to give flaky yellow plates, analysing as the hexahydrate (Table 1). Cubic yellow crystals of composition $[Crdmbpy_3](ClO_4)_3 \cdot 5H_2O \cdot \frac{1}{2}MeCN$ were obtained by dissolving in the minimum amount of water–acetonitrile (50 : 50 by volume) and allowing slow evaporation of solvents. The complex compound is soluble in acetonitrile, nitromethane, acetone, DMF and DMSO, quite soluble in water and insoluble in ethanol, THF, dichloromethane and ether. $[Crdmbpy_3](ClO_4)_3 \cdot 5H_2O \cdot \frac{1}{2}MeCN$ shows IR bands at (cm^{-1}): 3500mbr, 2250mw, 1606m, 1580m, 1508m, 1320m, 1280w, 1235m, 1148w, 1160m, 1190sbr, 930mw, 835m, 700w, 665m, 654w, 621s, 538w, 508w, 440wsh, 422m, 390w and 366m. The electronic spectrum is shown in Table 3 and Fig. 1.

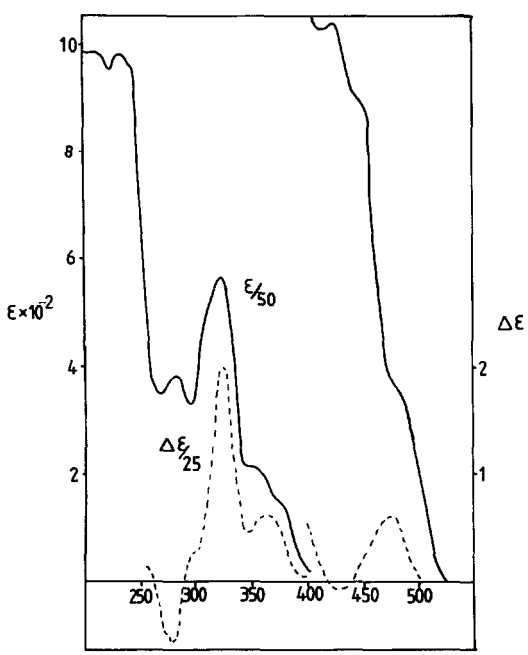

Fig. 1. Electronic absorption (——) and CD (– – – –) spectra of $[Crdmbpy_3]^{3+}$ in water.

Resolution of Δ–Λ$[Cr(di\text{-}imine)_3](ClO_4)_3$. The resolutions were performed in two ways with similar results—the compound was either converted to the chloride salt (Dowex FFIP ion exchange resin, Cl^- form) (cf. Kane-Maguire and Hallock[8]) or a solution of the perchlorate salt was used.

$[Cr(di\text{-}imine)_3]X_3$ (1 mmol) was dissolved in warm water (100 cm^3) and a solution of potassium(+)tris(L-cysu)cobaltate(III)$\cdot 6H_2O$ (0.367 g, 0.5 mmol) in 10 cm^3 water added. For $[Crphen_3]X_3$ and $[Crbpy_3]X_3$, the diastereoisomer (+)$[Cr(di\text{-}imine)_3]$(+)$[Co(L\text{-}cysu)_3]$ was precipitated on cooling in ice for 10 min, and was filtered off, washed with ethanol (25 cm^3) and ether (25 cm^3), and dissolved in 750 cm^3 warm (35°C) water, and ion exchanged for Cl^-. The volume of solution was then reduced to 75 cm^3 and excess $NaClO_4$ added. The (+)$[Cr(di\text{-}imine)_3](ClO_4)_3 \cdot nH_2O$, which separated, was then filtered off, washed with ethanol and ether, and a large excess of $NaClO_4$ added to the filtrate, yielding a more optically active product. The $[Crdmbpy_3]X_3$ gave no diastereomeric precipitate in water. In this case, ethanol was added slowly until precipitation was complete. The same procedure was then adopted, but the more soluble diastereoisomer was dissolved in only 100 cm^3 water.

An excess of $NaClO_4$ was added to the original filtrate, containing (−)$[Cr(di\text{-}imine)_3]^{3+}$, and the resulting precipitate collected and washed with ethanol and ether. An excess of $NaClO_4$ was again added to the filtrate to give a more optically active product. In all cases, the second crop of product, i.e. the more soluble portion, was always the optically pure compound. [$NaClO_4$ could be replaced by $NH_4(PF_6)$ throughout.]

All CD spectral profiles (see Table 3) are consistent with the (+)$[Cr(di\text{-}imine)_3]^{3+}$ cation having the M(C_3) or Λ(C_3) configuration,[13] supported by the fact[6,14] that each (+)$[Cr(di\text{-}imine)_3]^{3+}$ cation forms the less soluble diastereoisomer with the (+)$[Co(L\text{-}cysu)_3]^{3-}$ anion.

It appears also from the CD spectra[6] that (+)$[Mbpy_3]^{3+}$ (M = Cr, Rh or Co) all have related configurations as do (+)$[Mphen_3]^{3+}$.

DISCUSSION

The usefulness of potassium(+)tris(L-cysu)-cobaltate(III) as a means of resolving triply charged cations has been further extended, providing a comparison of configuration within the resolved $[Mbpy_3]^{3+}$ series (M = Cr, Co or Rh), together with a similar comparison within the analogous $[Mphen_3]^{3+}$ series.

Schubert[2] in his original paper, isolated the tri-

hydrate of potassium(+)tris(L-cysu)cobaltate(III) whereas Dollimore and Gillard[6] obtained the hexahydrate. We have obtained both compositions, the trihydrate made from the initially formed hexahydrate by prolonged desiccation *in vacuo*. The structure of potassium(+)tris(L-cysu)colbatate(III) and its photoreduction product have been probed by ^{13}C NMR spectroscopy, and there seems to be a change from facial to meridional geometry on photolysis. The solid trihydrated tribasic acid containing (+)tris(L-cysu)cobaltate(III) has been characterized, the IR spectrum showing a shift of the carboxyl stretching frequency from 1600 to 1700 cm^{-1} on protonation, a process which was found to be reversible, with no loss of optical activity.

A new cation, $[Crdmbpy_3]^{3+}$, has been prepared and resolved, the $(+)[Crdmbpy_3]^{3+}$ having a CD profile consistent with its having the $\Lambda(C_3)$ configuration, as well as forming the less soluble diastereoisomer with potassium(+)tris(L-cysu)-cobaltate(III).

Acknowledgements—We wish to thank the University of Turku for study leave to one of us (E.R.J.S.), during which this work was done, and the Academy of Finland (E.R.J.S.) for financial support.

REFERENCES

1. R. D. Gillard, F. L. Wimmer and J. P. G. Richards, *J. Chem. Soc., Dalton Trans.* 1985, 253.
2. M. P. Schubert, *J. Am. Chem. Soc.* 1933, **55**, 3336.
3. R. G. Neville and G. Gorin, *J. Am. Chem. Soc.* 1956, **78**, 4893.
4. G. Gorin, J. F. Spessard, G. A. Webber and J. P. Oliver, *J. Am. Chem. Soc.* 1959, **81**, 3191.
5. R. D. Gillard and R. Maskill, *Chem. Commun.* 1968, 160.
6. L. S. Dollimore and R. D. Gillard, *J. Chem. Soc., Dalton Trans.* 1973, 933.
7. L. S. Dollimore and R. D. Gillard, *J. Chem. Soc., Dalton Trans.* 1975, 369.
8. N. A. P. Kane-Maguire and J. S. Hallock, *Inorg. Chim. Acta* 1979, **35**, L309.
9. S. F. Mason and B. J. Peart, *J. Chem. Soc., Dalton Trans.* 1973, 949.
10. C. S. Lee, E. M. Gorton, H. M. Neumann and H. R. Hunt, Jr, *Inorg. Chem.* 1966, **5**, 1397.
11. C. Burgess and A. Knowles, *Standards in Absorption Spectrometry*. Chapman & Hall, London (1981).
12. E. Konig and S. Herzog, *J. Inorg. Nucl. Chem.* 1970, **32**, 585.
13. A. J. McCaffery, S. F. Mason and R. E. Ballard, *J. Chem. Soc.* 1965, 2883.
14. K. Garbett and R. D. Gillard, *J. Chem. Soc. A* 1966, 802.

Polyhedron Vol. 6, No. 1, pp. 111–117, 1987
Printed in Great Britain

0277–5387/87 $3.00+.00

RHODIUM- AND IRIDIUM–MANGANESE CARBONYL COMPLEXES CONTAINING BRIDGING $Ph_2PCH_2PPh_2$ LIGANDS

STUART W. CARR and BERNARD L. SHAW*

School of Chemistry, The University, Leeds LS2 9JT, U.K.

(*Received* 3 *July* 1986)

Abstract—Treatment of *mer,cis*-[$MnCl(CO)_2$(dppm-*PP'*)(dppm-*P*)] with [$Rh_2Cl_2(CO)_4$] in the presence of CO and PF_6^- gives [$Cl(OC)_2Mn(\mu$-dppm$)_2Rh(CO)_2]PF_6$ which might have a bridging chloride ligand. Similar treatment of *mer,cis*-[$MnBr(CO)_2$(dppm-*PP'*)(dppm-*P*)] gave [$Br(OC)_2Mn(\mu$-dppm$)_2Rh(CO)_2]PF_6$ which ^{31}P–{^1H} NMR spectroscopy showed to be a mixture of two closely related species. Treatment of *mer,cis*-[$MnCl(CO)_2$(dppm-*PP'*)(dppm-*P*)] with [$Rh_2Cl_2(CO)_4$] at −30°C probably gave [$Cl(OC)_2Mn(\mu$-dppm$)_2$ $Rh(CO)_2]Cl$ but this decomposes above 0°C: the corresponding dibromide was made similarly and is somewhat more stable than the dichloride. Treatment of *mer,cis*-[$MnX(CO)_2$(dppm-*PP'*)(dppm-*P*)] (X = Cl or Br) with [$IrCl(CO)_2$(*p*-toluidine)] and CO–PF_6^- gave [$X(OC)_2Mn(\mu$-dppm$)_2Ir(CO)_2]PF_6$. Neutral complexes of type [$X(OC)_2Mn(\mu$-dppm$)_2Ir(CO)X'$] (X and X′ = Cl or Br) are very labile and rapidly decompose to give $[Ir(CO)$(dppm-*PP'*$)_2]^+$ and other (unidentified) products. Treatment of *mer,cis*-[$MnX(CO)_2$(dppm-*PP'*)(dppm-*P*)] with [$RhH(CO)(PPh_3)_3$] gave [$X(OC)Mn(\mu$-dppm$)_2(\mu$-H)(μ-CO)Rh(CO)] (X = Cl or Br). These heterobimetallic compounds generally showed broad ^{31}P–{^1H} resonances for the *P* nuclei bonded to Mn at *ca* 20°C due to some coupling with the ^{55}Mn nucleus ($I = \frac{5}{2}$, 100% abundant), but at −30°C these resonances sharpened up due to more rapid quadrupolar relaxation at the lower temperature. NMR and IR data are given.

RESULTS AND DISCUSSION

In a previous paper[1] we showed that manganese(I) complexes of type [$MnX(CO)_2$(dppm-*PP'*)(dppm-*P*)] (dppm ≡ $Ph_2PCH_2PPh_2$) of configurations **1a** (X = Cl) or **1b** (X = Br) underwent ring-opening reactions with platinum complexes, e.g. [$Pt(PPh_3)_4$] or *trans*-[$PtHCl(PPh_3)_2$], to give mixed manganese–platinum complexes containing the moiety $Mn(\mu$-dppm$)_2Pt$. In the present paper we describe similar attempts to effect ring-opening reactions with rhodium(I) or iridium(I) carbonyl derivatives.

In preliminary (NMR) studies we found that treatment of complexes of types **1a** or **b** with [$Rh_2Cl_2(CO)_4$] or [$IrCl(CO)_2$(*p*-toluidine)] gave cationic heterobimetallics but these were labile (see below), and more stable products could be obtained by mixing these reactants in the presence of CO and a large anion, such as PF_6^-. These salts with PF_6^- will be discussed first.

Treatment of a solution of the chloro complex (**1a**) with the equivalent amount of [$Rh_2Cl_2(CO)_4$] in the presence of CO and NH_4PF_6 gave a salt, formulated as [$Cl(OC)_2Mn(\mu$-dppm$)_2Rh(CO)_2$] PF_6. The formulation follows from the elemental analysis (Table 1) and the spectroscopic data. In particular the ^{31}P–{^1H} NMR spectrum, at −30°C, showed a pattern typical of an AA′XX′M spin system (M = ^{103}Rh) with deceptively simple triplets and $|^2J(P_AP_X)+{}^4J(P_AP_{X'})| = 54$ Hz (data in Table 2). There was also a resonance due to PF_6^-. At higher temperatures the resonance pattern of the *P* nuclei bonded to manganese broaden due to a slowing down of the quadrupolar relaxation of the ^{55}Mn nucleus ($I = \frac{5}{2}$, 100% abundant). The ^1H–{^{31}P} NMR spectrum of [$Cl(OC)_2Mn$

* Lecturer (1962), Reader (1966) and Professor (1971) in the Department of Inorganic and Structural Chemistry, University of Leeds. Author to whom correspondence should be addressed.

Table 1. IR and analytical data

	IR data for carbonyl region [ν(C≡O) (cm^{-1})]		Analyses (%)[d]			Λ[e] (Ω^{-1} cm^2 mol^{-1})
	Solid[ab]	Solution[bc]	C	H	X	
$[Cl(CO)_2Mn(\mu\text{-dppm})_2Rh(CO)_2]PF_6$	1858w, 1885w, 1942s, 1999s	1865w, 1930m,br, 2001s	53.6 (53.2)	3.5 (3.6)	2.8 (2.9)	22
$[Br(CO)_2Mn(\mu\text{-dppm})_2Rh(CO)_2]PF_6$	1815w, 1860m, 1888w, 1932s, 1950sh, 1998s	1855w,br, 1930m,br, 2002s	51.4 (51.3)	3.4 (3.5)	6.5 (6.3)	21
$[Br(CO)_2Mn(\mu\text{-dppm})_2Rh(CO)_2]Br$	1804m, 1830m, 1920s, 1985s	1805w, 1932m, 2008s	53.7 (54.1)	3.9 (3.7)	13.2 (13.3)	19
$[Br(CO)_2Mn(\mu\text{-dppm})_2Rh(CO)_2]Cl$	1820m, 1850w, 1910s, 1920s, 1983s, 1990sh	1847w, 1916s, 1984s	55.4 (56.2)	4.0 (3.8)	1.37 (1.30)[f]	17
$[Cl(CO)_2Mn(\mu\text{-dppm})_2Ir(CO)_2]PF_6$	1805m, 1859m, 1931s, 1980s	1805m, 1863w, 1927m, 1990s	49.4 (49.6)	3.6 (3.4)	2.9 (2.7)	19
$[Br(CO)_2Mn(\mu\text{-dppm})_2Ir(CO)_2]PF_6$	1782m, 1812s, 1823sh, 1980s, 1990sh	1799m,br, 1923m,br, 1990s,br	47.7 (47.9)	3.3 (3.3)	5.8 (5.9)	20
$[Br(CO)_2Mn(\mu\text{-dppm})_2Ir(CO)Cl]$	1842m, 1920s, 1980s	1845m, 1921s, 1982s	54.2 (52.4)	4.2 (3.7)		2
$[Cl(CO)Mn(\mu\text{-dppm})_2(\mu\text{-H})(\mu\text{-CO})Rh(CO)]$	1760m, 1849s, 1870s	1770m, 1870s, 1940s	60.8 (60.4)	4.3 (4.2)	3.4 (3.6)	2
$[Br(CO)Mn(\mu\text{-dppm})_2(\mu\text{-H})(\mu\text{-CO})Rh(CO)]$	1760m, 1852s, 1940s, 1948s	1772m, 1871s, 1945s	58.3 (58.0)	4.1 (3.8)	7.3 (7.0)	2

[a] As Nujol mulls.

[b] s, strong; m, medium; w, weak; sh, shoulder; br, broad.

[c] Recorded in dichloromethane solution.

[d] Calculated values in parentheses.

[e] As a *ca* 10^{-3} M solution in nitrobenzene at 20°C.

[f] Total halogen determination: titre of $Hg(No_3)_2$ solution (cm^3) [the calculated titre (cm^3) is given in parentheses].

Table 2. $^{31}P-\{^1H\}^{ab}$ and $^1H-\{^{31}P\}^{bc}$ NMR data

					Methylene PCH_2P			
					21°C		Low-temperature	
	$\delta(P_A)^d$	$\delta(P_X)^d$	^1J(RhP)	N^e	$\delta(CH_2)$	^2J(HH)	$\delta(CH_2)$	^2J(HH)
$[Cl(CO)_2Mn(\mu\text{-dppm})_2Rh(CO)_2]PF_6$	49.6	22.4	110	54	3.91 3.44	13.9		
$[Br(CO)_2Mn(\mu\text{-dppm})_2Rh(CO)_2]PF_6$	51.9[f]	23.1	103	64	3.95 3.49	7	3.96,[f] 3.47 4.01,[g] 3.53	13.3 (−20°C) 13.7 (−20°C)
	50.1[g]	22.8	110	53				
$[Cl(CO)_2Mn(\mu\text{-dppm})_2Rh(CO)_2]Cl$	49.8	22.5	110	52				
$[Br(CO)_2Mn(\mu\text{-dppm})_2Rh(CO)_2]Br$	50.3	22.8	103	64	3.70		3.95, 3.57	12.7 (−50°C)
$[Br(CO)_2Mn(\mu\text{-dppm})_2Rh(CO)_2]Cl$	49.7	22.5	110	54	3.61		3.80, 3.37	12.7 (−50°C)
$[Cl(CO)_2Mn(\mu\text{-dppm})_2Ir(CO)_2]PF_6$	50.9	5.2		60	3.52		3.77, 3.27	13.7 (−50°C)
$[Br(CO)_2Mn(\mu\text{-dppm})_2Ir(CO)_2]PF_6$	51.9	2.8		69	3.60		3.84, 3.41	≈14 (−40°C)
	51.4	5.7		58				
$[Br(CO)_2Mn(\mu\text{-dppm})_2Ir(CO)Cl]$	63.2	−6.2		68	4.31		4.39, 4.23	≈11 (−50°C)
	56.7	−11.8		68				
							Hydride resonance at 21°C	
$[Cl(CO)Mn(\mu\text{-dppm})_2(\mu\text{-H})(\mu\text{-CO})Rh(CO)]$	69.7	24.7	120	120	3.43 2.91	13.7	δH(Rh) −17.2, ^1J(RhH) = 28.3	
$[Br(CO)Mn(\mu\text{-dppm})_2(\mu\text{-H})(\mu\text{-CO})Rh(CO)]$	69.2	25.2	117	120	3.32 2.96	13.6	δH(Rh) −16.5, ^1J(RhH) = 28.9	

[a] Chemical shifts (δ) in ppm (±0.1 ppm) relative to 85% H_3PO_4 (positive shift to higher frequency); coupling constants (J) in Hz (±2 Hz). Spectra were recorded at −30°C.
[b] In CD_2Cl_2solution.
[c] Chemical shifts (δ) in ppm (±0.01 ppm) relative to tetramethylsilane; coupling constants (J) in Hz (±0.3 ppm).
[d] P_A and P_X refer to the phosphorus atoms coordinated to manganese and rhodium or iridium, respectivcly.
[e] $N = {}^2J(P_AP_X) + {}^4J(P_AP_{X'})$.
[f] Major isomer.
[g] Minor isomer.

(μ-dppm)$_2$Rh(CO)$_2$]PF$_6$ showed an AB pattern due to the CH_2 protons (data in Table 2). The IR spectrum (Nujol mull) of this complex showed bands at 1858w, 1885w, 1942s and 1999s cm^{-1}, indicative of terminal C≡O, with the possibility of a weak bridging interaction associated with the lowest-frequency band. Bridging carbonyls are common in bimetallic-μ-dppm chemistry.[2-6] Sometimes the bridging is strong and of the "ketonic" type as in [ClPd(μ-CO)(μ-dppm)$_2$PdCl],[2] sometimes it is strong and sideways on (σ, π) as in [(OC)$_2$Mn(μ-CO)(μ-dppm)$_2$Mn(CO)$_2$],[3-5] but frequently it is weak, such as in [(OC)$_2$Mn(μ-CO)(μ-dppm)$_2$PdBr][6] and many other complexes. A band at 225 cm^{-1}, absent from the spectrum of the corresponding bromide (see below), is tentatively assigned to a bridging chlorine, i.e. the cation is formulated as [(OC)$_2$Mn(μ-Cl)(μ-dppm)$_2$Rh(CO)$_2$]$^+$. Treatment of the bromo complex (**1b**) with CO–NH$_4$PF$_6$ and [Rh$_2$Cl$_2$(CO)$_4$] or [Rh$_2$Br$_2$(CO)$_4$] gave a corresponding product, [Br(OC)$_2$Mn(μ-dppm)$_2$Rh(CO)$_2$]PF$_6$.

Elemental analytical data for this complex are given in Table 1 together with IR data [ν(CO)]. The ^{31}P–{^{1}H} NMR spectrum of this product, at −30°C showed it to be a mixture of two closely related complexes (data in Table 2): possibly one isomer has bridging Br and the other bridging (semi-bridging) CO. At higher temperatures the resonance pattern of the phosphorus atoms bonded to manganese broadened due to a slowing down of the quadrupolar relaxation of the manganese nucleus. The spectra at −30 and +21°C are shown in Fig. 1. The ^{1}H–{^{31}P} NMR spectrum of [Br(OC)$_2$Mn(μ-dppm)$_2$Rh(CO)$_2$]PF$_6$ at +20°C showed a broad AB pattern, which separated into two well-defined AB patterns at −20°C [see Fig. 2 (data in Table 2)]. We find that these products of type [X(OC)$_2$Mn(μ-dppm)$_2$Rh(CO)$_2$]PF$_6$ (X = Cl or Br) are stable in CH_2Cl_2 solutions at 20°C over a period of a week (^{31}P–{^{1}H} NMR evidence). Also, from NMR evidence, they did not react with NaOPr^i, NaOMe, H$^+$ or Et$_3$BH$^-$ at 20°C. When treated with TlBF$_4$ (1 equivalent) and CNMe or CNBu^t they reacted to give a mixture of products, which we did not separate.

In a ^{31}P–{^{1}H} NMR study we found that [MnCl(CO)$_2$(dppm-*PP'*)(dppm-*P*)] (**1a**), when treated with an equivalent amount of [Rh$_2$Cl$_2$(CO)$_4$] in CD_2Cl_2 at −30°C, gave a heterobimetallic containing an Mn(μ-dppm)$_2$Rh moiety in high yield (data in Table 2). However, when allowed to warm up, e.g. to above 0°C, this product decomposed to give a mixture, and no bimetallic complex was isolated. The corresponding dibromide [Br(OC)$_2$Mn(μ-dppm)$_2$Rh(CO)$_2$]Br was much more stable and was made by treating [MnBr(CO)$_2$(dppm-*PP'*)(dppm-*P*)] with [Rh$_2$Br$_2$(CO)$_4$] at *ca* 20°C. The product was obtained analytically pure (see Table 1), and was characterized by NMR and IR spectroscopy (Tables 1 and 2). It was stable in dichloromethane solution for about 2 h at 20°C, but then started to decompose. Treatment of **1b** with [Rh$_2$Cl$_2$(CO)$_4$] gave a product, formulated as [Br(OC)$_2$Mn(μ-dppm)$_2$Rh(CO)$_2$]Cl (characterizing data in Tables 1 and 2). Details of the preparation of both these complexes are given in Experimental. We also converted [Br(OC)$_2$Mn(μ-dppm)$_2$Rh(CO)$_2$]PF$_6$ into [Br(OC)$_2$Mn(μ-dppm)$_2$Rh(CO)$_2$]Br by treating it with an excess of Me$_4$NBr in a dichloromethane–methanol mixture at 21°C. Details are in Experimental.

We also prepared the manganese-iridium cationic complexes [X(OC)$_2$Mn(μ-dppm)$_2$Ir(CO)$_2$] (X = Cl or Br) as the PF$_6$ salts, by treating [MnX(CO)$_2$(dppm-*PP'*)(dppm-*P*)] with [IrCl(CO)$_2$(*p*-toluidine)] in an atmosphere of CO and in the presence of NH$_4$PF$_6$. Preparative details are in Experimental and characterizing data in Tables 1 and 2. As with the corresponding rhodium complexes, discussed above, the bromide showed the presence of two complexes (isomers), whereas the chloride showed only one.

Neutral species of type [X(OC)$_2$Mn(μ-dppm)$_2$Ir(CO)X'] are very labile, more labile than the rhodium analogues. Treatment of [MnBr(CO)$_2$(dppm-*PP'*)(dppm-*P*)] with [IrCl(CO)$_2$(*p*-toluidine)] gave a solid product, formulated as [Br(OC)$_2$Mn(μ-dppm)$_2$IrCl(CO)], which was not obtained pure, and in CD_2Cl_2 solution decomposed to give [Ir(CO)(dppm-*PP'*)$_2$]$^+$[7], and other (unidentified) products. Considerable amounts of [Ir(CO)(dppm-*PP'*)$_2$]$^+$ were detected by ^{31}P–{^{1}H} NMR spectroscopy *ca* 10 min after dissolution of [Br(OC)$_2$Mn(μ-dppm)$_2$IrCl(CO)] in CD_2Cl_2 at 20°C. Treatment of [X(OC)$_2$Mn(μ-dppm)$_2$Ir(CO)$_2$]$^+$ with LiX or Me$_4$NX (X = Cl or Br), did not give any detectable quantity of [X(OC)$_2$Mn(μ-dppm)$_2$IrX(CO)]: instead [Ir(CO)(dppm-*PP'*)$_2$]$^+$[7] was formed.

We have also treated [RhH(CO)(PPh$_3$)$_3$] with [MnX(CO)$_2$(dppm-*PP'*)(dppm-*P*)] (X = Cl or Br) in hot benzene. This gave heterobimetallics of the expected composition [X(OC)$_2$Mn(μ-dppm)$_2$RhH(CO)] (preparative details are in Experimental and characterizing data in Tables 1 and 2). In particular the ^{31}P–{^{1}H} NMR spectra showed AA'XX'M patterns (Table 2). The ^{1}H–{^{31}P} NMR spectra at 21°C showed AB CH_2 patterns and a hydride resonance at δ *ca* −17, with couplings to ^{103}Rh of 28–29 Hz. Selective decoupling, ^{1}H–{^{31}P},

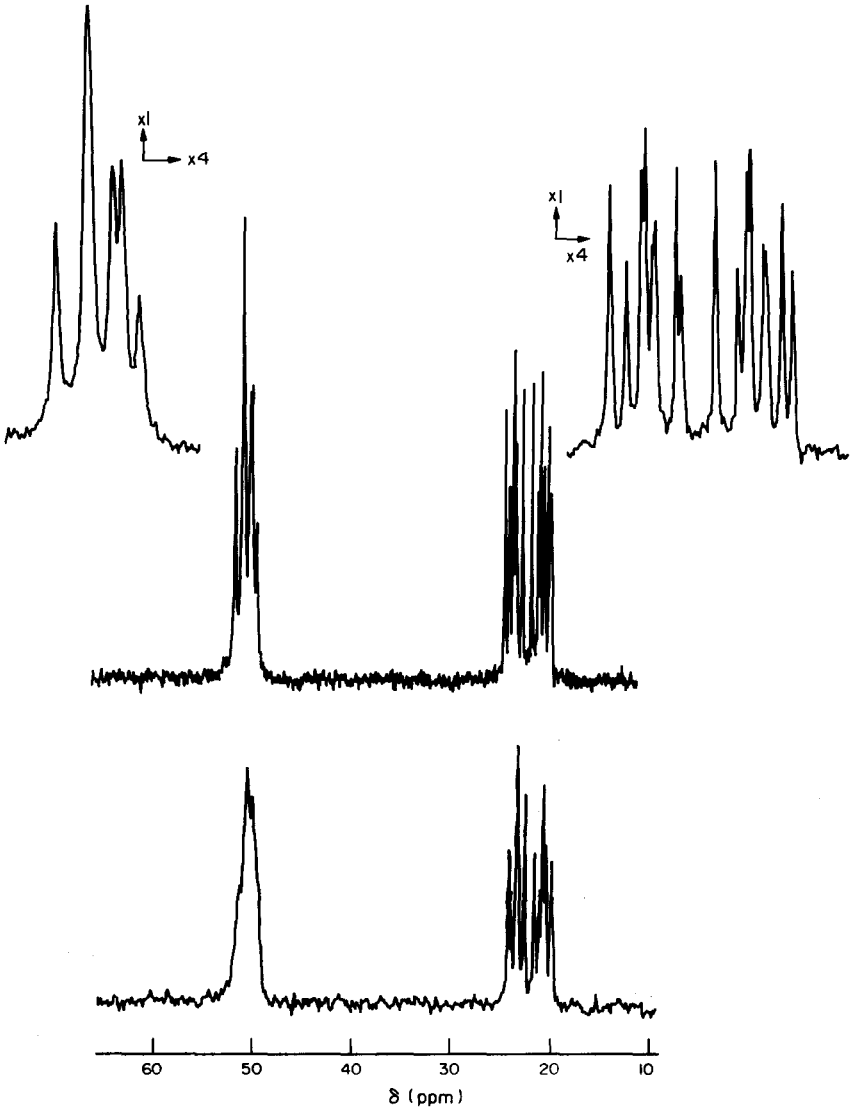

Fig. 1. $^{31}P-\{^1H\}$ NMR spectrum of $[Br(CO)_2Mn(\mu\text{-dppm})_2Rh(CO)_2]PF_6$ (mixture of two isomers) in CD_2Cl_2 at: (a) 21°C, and (b) −30°C.

of each P in turn gave ^1H patterns of the AA′MP and XX′MP types, i.e. the hydride is coupled to all four P nuclei. This result suggests that the hydride is bridging. We tentatively formulate these compounds as $[X(OC)Mn(\mu\text{-H})(\mu\text{-dppm})_2(\mu\text{-CO})Rh(CO)]$: one of the bands due to ν(CO) is at the very low value of 1760 cm^{-1} (Table 2), indicative of bridging CO.

EXPERIMENTAL

All reactions were performed in an atmosphere of dry dinitrogen in degassed solvents. Dichloromethane was dried over molecular sieves (type 4A) and benzene over sodium wire. IR spectra were recorded in either Nujol mulls between KBr plates or in dichloromethane solution on a Perkin–Elmer 257 grating IR spectrometer. Unless otherwise stated, NMR spectra were recorded on a JEOL FX100 instrument at 99.55 MHz (^1H) or 40.25 MHz (^{31}P) using solvent references as internal standards and referenced to TMS or 85% H_3PO_4 as appropriate.

$[Cl(CO)_2Mn(\mu\text{-dppm})_2Rh(CO)_2]PF_6$

A solution of $[Rh_2(CO)_4Cl_2]$ (0.020 g, 0.055 mmol) in dichloromethane (1 cm^3) was added dropwise to a stirred mixture of *mer,cis*-$[Mn(CO)_2$(dppm-*PP′*)(dppm-*P*)Cl]^1 (0.100 g, 0.11 mmol) dissolved in dichloromethane (10 cm^3) and ammonium hexafluorophosphate (0.18 g, 1.1 mmol) in methanol

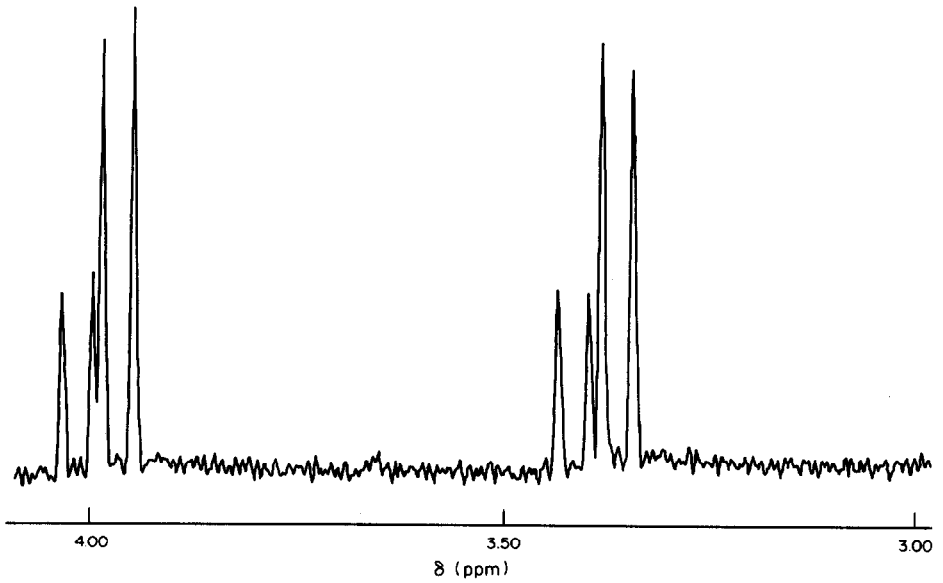

Fig. 2. ^1H–$\{^{31}P\}$ NMR spectrum of the PCH_2P region of $[Br(CO)_2Mn(\mu\text{-dppm})_2Rh(CO)_2]PF_6$ (mixture of two isomers) in CD_2Cl_2 at −30°C.

(10 cm^3) with CO bubbling into the solution. Upon addition of the $[Rh_2(CO)_4Cl_2]$ a bright yellow solution resulted which was stirred under CO for an hour. The resulting mixture was evaporated to dryness under reduced pressure. The required product was extracted into dichloromethane, the solution filtered, and *n*-hexane added until the solution became turbid. This mixture was set aside at −20°C for several hours to give a yellow microcrystalline solid. Yield 0.091 g (68%). The bromo analogue $[Br(CO)_2Mn(\mu\text{-dppm})_2Rh(CO)_2]PF_6$ was prepared by a similar procedure from *mer,cis*-$[Mn(CO)_2$(dppm-*PP'*)(dppm-*P*)Br] and $[Rh_2(CO)_4Cl_2]$ or $[Rh_2(CO)_4Br_2]$ in 78 and 79% yield, respectively.

$[Br(CO)_2Mn(\mu\text{-dppm})_2Rh(CO)_2]Br$

Using $[Rh_2(CO)_4Br_2]$. A solution of $[Rh_2(CO)_4Br_2]$ (0.023 g, 0.047 mmol) in dichloromethane (1 cm^3) was added dropwise to a solution of *mer,cis*-$[Mn(CO)_2$(dppm-*PP'*)(dppm-*P*)Br] (0.100 g, 0.095 mmol) in dichloromethane (5 cm^3) to give a clear yellow solution. *n*-Hexane was then added to precipitate the product which was collected and washed with diethyl ether to give a yellow microcrystalline solid. Yield 0.091 g (81%). The analogous bromide–chloride complex $[Br(CO)_2Mn(\mu\text{-dppm})_2Rh(CO)_2]Cl$ was prepared similarly in 83% yield.

From $[Br(CO)_2Mn(\mu\text{-dppm})_2Rh(CO)_2]PF_6$. A solution of $[Br(CO)_2Mn(\mu\text{-dppm})_2Rh(CO)_2]PF_6$ (0.120 g, 0.095 mmol) in dichloromethane (20 cm^3) was added to a degassed solution of tetramethylammonium bromide (0.240 g, 1.56 mmol) in methanol (20 cm^3). The volume of the mixture was reduced slowly to *ca* 20 cm^3 under reduced pressure. The yellow microcrystalline product was collected and washed with water, methanol and diethyl ether. Yield 0.077 g (69%).

$[Cl(CO)_2Mn(\mu\text{-dppm})_2Ir(CO)_2]PF_6$

A solution of $[Ir(CO)_2Cl$(*p*-toluidine)] (0.043 g, 0.11 mmol) in dichloromethane (2 cm^3) was added dropwise to a stirred mixture of *mer,cis*-$[Mn(CO)_2$(dppm-*PP'*)(dppm-*P*)Cl] (0.100 g, 0.11 mmol) dissolved in dichloromethane (15 cm^3), and ammonium hexafluorophosphate (0.087 g, 0.55 mmol) in methanol (10 cm^3), with CO bubbling into the mixture. The resulting yellow solution was stirred under CO for 1 h. The resulting mixture was evaporated to dryness under reduced pressure. The required product was extracted into dichloromethane, the solution filtered, and *n*-hexane added until the solution became turbid. The mixture was then set aside at −20°C for several hours to give a yellow microcrystalline solid. Yield 0.097 g (71%). The bromo analogue $[Br(CO)_2Mn(\mu\text{-dppm})_2Ir(CO)_2]PF_6$ was prepared analogously in 85% yield.

$[Br(CO)_2Mn(\mu\text{-dppm})_2Ir(CO)Cl]$

A solution of $[Ir(CO)_2Cl$(*p*-toluidine)] (0.037 g, 0.095 mmol) in dichloromethane (1 cm^3) was added

to a solution of [Mn(CO)$_2$(dppm-*PP'*)(dppm-*P*)Br] (0.100 g, 0.095 mmol) in dichloromethane (5 cm^3). The resultant orange solution was stirred for 2 min and evaporated to dryness under reduced pressure. The resultant solid was triturated with diethyl ether to give an orange microcrystalline solid. Yield 0.097 g.

[Cl(CO)Mn(μ-dppm)$_2$(μ-H)(μ-CO)Rh(CO)]

A mixture of [MnCl(CO)$_2$(dppm-*PP'*)(dppm-*P*)] (0.100 g, 0.11 mmol) and [RhH(CO)(PPh$_3$)$_3$] (0.100 g, 0.11 mmol) was refluxed in benzene (5 cm^3) for 2 h. The resulting brown solution was cooled to ambient temperature. Light petroleum (b.p. 30–40°C) (10 cm^3) was then added and the mixture set aside at 5°C for *ca* 3 h. A brown microcrystalline solid product was collected. Yield 0.088 g (73%). The bromo analogue [Br(CO)Mn(μ-dppm)$_2$(μ-H)(μ-CO)Rh(CO)] was prepared similarly in 77% yield.

Acknowledgements—We thank the S.E.R.C. for support and Johnson Matthey Ltd for the generous loan of rare metal salts.

REFERENCES

1. S. W. Carr, B. L. Shaw and M. Thornton-Pett, *J. Chem. Soc., Dalton Trans.* 1985, 2131.
2. L. S. Benner and A. L. Balch, *J. Am. Chem. Soc.* 1978, **100**, 6099.
3. R. Colton and C. J. Commons, *Aust. J. Chem.* 1975, **28**, 1673.
4. H. C. Aspinall and A. J. Deeming, *J. Chem. Soc., Chem. Commun.* 1981, 724.
5. J. A. Marsella and K. G. Caulton, *Organometallics* 1982, **1**, 274.
6. B. F. Hoskins, R. J. Steen and T. W. Turney, *J. Chem. Soc., Dalton Trans.* 1984, 1831.
7. J. S. Miller and K. G. Caulton, *J. Am. Chem. Soc.* 1975, **97**, 1067.

Polyhedron Vol. 6, No. 2, pp. 119–157, 1987
Printed in Great Britain

0277–5387/87 $3.00+.00
Pergamon Journals Ltd

POLYHEDRON REPORT NUMBER 18

THE ORGANOMETALLIC CHEMISTRY OF PHOSPHAZENES

HARRY R. ALLCOCK,* JAMES L. DESORCIE and GEOFFREY H. RIDING
Department of Chemistry, The Pennsylvania State University, University Park, PA 16802, U.S.A.

CONTENTS

I. BACKGROUND

Phosphazene chemistry† is a well-established field that lies at the interface between inorganic and organic chemistry. Its origins can be traced back to the early 1800s when several investigators[1–5]

* Author to whom correspondence should be addressed.

† This field was known as phosphonitrilic chemistry in the early literature.

isolated and studied two unusual heterocyclic compounds with formulae $(NPCl_2)_3$ and $(NPCl_2)_4$ from the reaction of phosphorus pentachloride with ammonia or ammonium chloride.

Since that time, a diverse class of ring systems and linear species has been developed,[6] all the members of which are characterized by a cyclic or linear skeleton of alternating phosphorus and nitrogen atoms, with two side groups attached to each phosphorus. Some typical general structures are shown in **1–4** (Scheme 1). In addition, a subclass exists, comprised of short-chain linear phosphazenes (**5–7**) (Scheme 1) with terminal phosphorus atoms that bear three end groups. The side groups in **1–7** can be halogens or a wide variety of organic or organometallic units.

Perhaps the most striking characteristic of phosphazenes is the existence of extensive polymeric series of rings (**1–3**) and linear chains (**5–7**) that culminate in very high molecular weight polymers (**4**).[6,7] Some of these polymers are known to be linear, but the possibility exists that others are giant macrocyclic species. Ring systems that contain up to 40 repeating units have been detected[8] and larger rings are undoubtedly accessible. Short-chain linear species of type **5–7** are known that contain up to six phosphorus atoms, but this class almost certainly extends as a continuous series that culminates in linear high polymers. A resemblance to the organosiloxane polymeric series will be evident.

Of these three classes of phosphazenes (rings, short chains and high polymers), the least is known about the short-chain species. They are generally difficult to synthesize, isolate and study,[6] and only a few of them have been characterized in detail.[9] However, they are valuable because of their role as small-molecule reaction and structural models for the high polymers.[9]

The structural chemistry and organic-reaction chemistry of cyclic phosphazenes comprises by far the most established branch of this area. The organometallic chemistry is still in the developmental stage. An important facet of cyclophosphazene chemistry is its relationship to the high-polymer chemistry, since small-molecule rings are excellent models for exploratory reactions that can be applied subsequently at the high-polymer level.[10]

The linear or macrocyclic high polymers (**4**) have been known for only a few years,[11–14] but already they form the basis of an extensive chemistry and a growing industrial technology.[15] In a

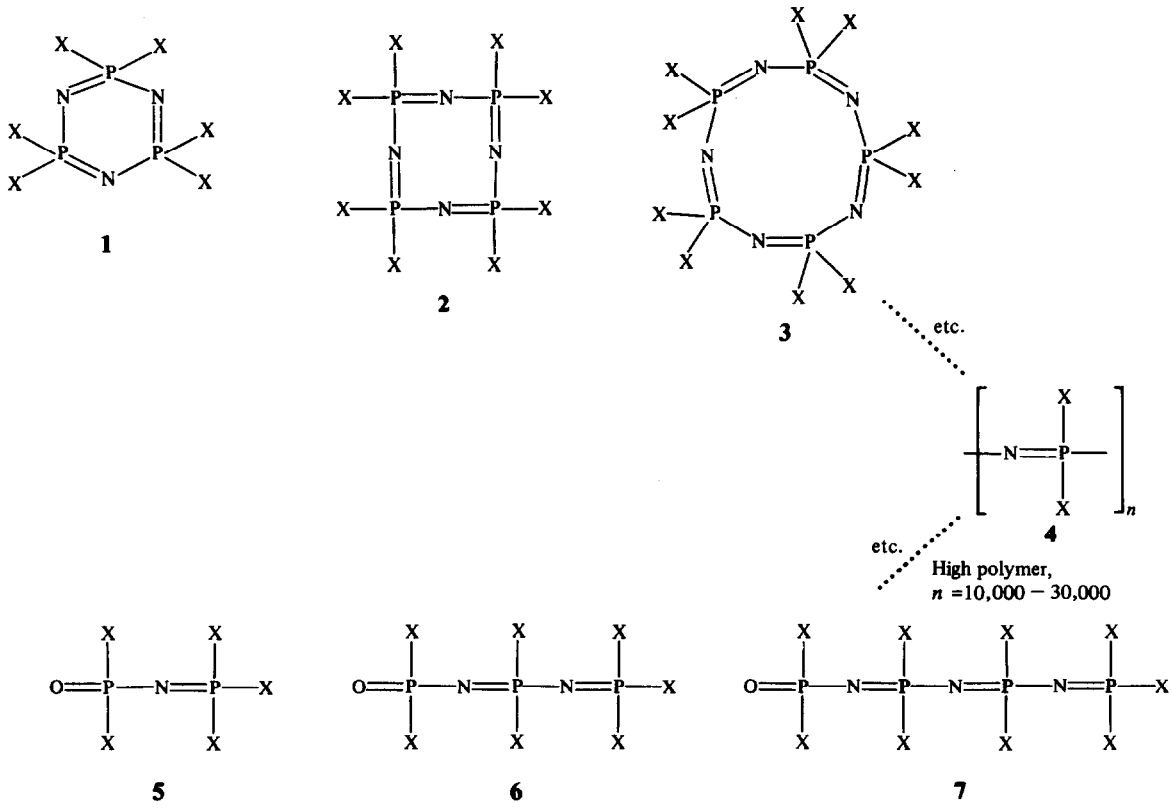

Scheme 1.

practical sense, the high-polymer chemistry provides the driving force for nearly all modern research on phosphazenes.

Historically, the development of phosphazene chemistry can be divided into three phases. Initially, from the 1800s to the 1940s, an emphasis on the Main-Group inorganic chemistry of these compounds was evident.[6] During this period, the synthesis and hydrolysis reactions of halogenophosphazenes [structures **1** and **2** (X = Cl)] were developed.[16]

Beginning in the 1950s and extending into the early 1970s, the second phase involved the development of the organic chemistry of cyclophosphazenes.[17–24] Most of this work revolved around the nucleophilic substitution reactions of chlorocyclophosphazenes such as $(NPCl_2)_3$ (**8**) or $(NPCl_2)_4$ with reagents such as simple alkoxides, aryloxides, or primary or secondary amines. Examples of these transformations are shown in the formation of **9** and **10** (Scheme 2). Much of this chemistry involved studies of the substitution mechanisms (S_N1 or S_N2), and the patterns of halogen replacement (*gem* or non*gem*, and *cis* or *trans*), often aided by NMR analysis and, in a few cases, by X-ray diffraction studies.[6,17–24]

The most recent phase, which began in the late 1960s and early 1970s, has been characterized by three main research thrusts: (a) investigation of the detailed structure of phosphazenes, especially by NMR spectroscopy and X-ray diffraction; (b) development of the high-polymer chemistry in both its fundamental and use-oriented aspects; and (c) the emergence of a diverse organometallic chemistry of phosphazenes. This latter topic is the subject of this review.

II. ORGANOMETALLIC CHEMISTRY—OVERVIEW

To understand the present significance of the organometallic chemistry of phosphazenes, it is necessary to consider some of the reasons for the widespread interest in the macromolecular chemistry of these compounds.

High polymers, in general, are the focus of much research because: (a) in the solid state they form fibers, films, glasses and elastomers that are widely used in modern technology; and (b) because, increasingly, macromolecules are being employed as biomedical materials; immobilization carriers for chemotherapeutic agents, enzymes or transition-metal catalysts; as solid electrolytes; and as electronic conductors. Phosphazene high polymers are being developed or considered for use in all these areas.[15,25–34]

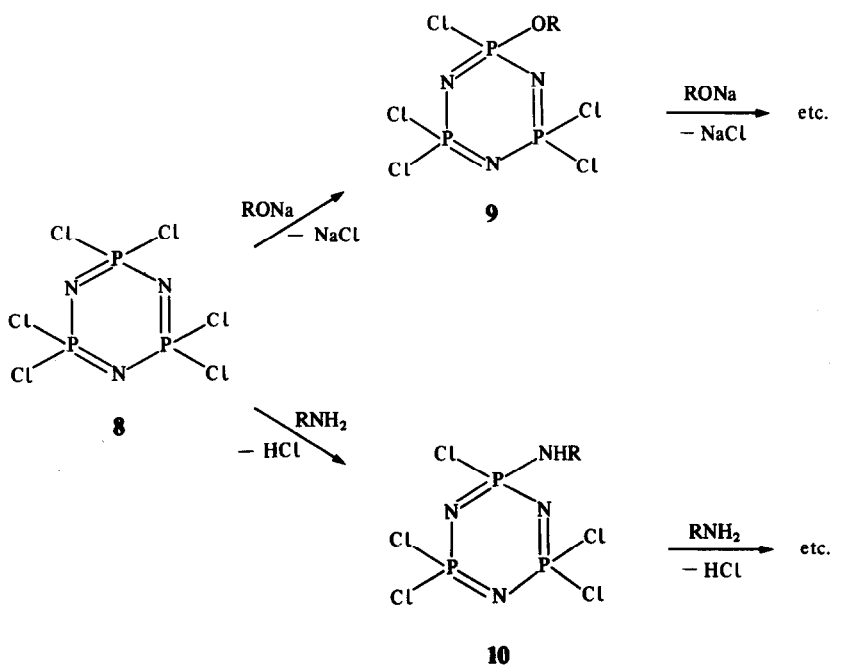

8 **9** **10**

Scheme 2.

Phosphazene high-polymer chemistry began with its organic-derivative chemistry. The main synthesis pathways leading to these macromolecules were discovered in our laboratories and are summarized in Scheme 3. Hexachlorocyclotriphosphazene (**8**), prepared from phosphorus pentachloride and ammonium chloride, is polymerized thermally in the molten state to the transparent, rubbery high polymer, poly(dichlorophosphazene) (**11**).[11] Replacement of the chlorine atoms in **11** by organic nucleophiles yields a wide variety of single- and mixed-substituent derivatives of general formulae **12**–**14**.[11–15] Given the wide variety of organic nucleophiles available to chemists, it is clear that an almost infinite variety of different polymer structures and properties are accessible via these reactions. By the beginning of 1986, roughly 300 different organophosphazene polymers had been synthesized and studied.

Interest in the organometallic chemistry of phosphazenes has expanded mainly because it was perceived (at least in our research group) that the use of organometallic reagents instead of organic nucleophiles as substitution reagents might allow the synthesis of two new classes of cyclo- and polyphosphazenes—those with alkyl or aryl groups linked directly to the inorganic skeleton through carbon–phosphorus bonds, and those with transition-metal organometallic units in the side-group structure.

High-polymeric phosphazenes with alkyl or aryl side groups should be chemically unreactive and stable at high temperatures [they would be structural analogues of poly(organosiloxanes)]. The alkyl or aryl groups could be introduced at the cyclic trimer or tetramer level, in which case the resultant organosphophazenes would be candidates for ring-opening polymerization to high polymers. Alternatively, the alkyl or aryl groups could be introduced directly at the macromolecular level by reactions analogous to those shown in Scheme 3. These possibilities are illustrated in Scheme 4. Polyphosphazenes with transition metals in the side-group structure would be valuable molecules for a wide variety of studies related to catalysts, electrode mediators, electronic conductors etc.

In this review, we discuss both types of chemistry, beginning with the reactions of phosphazenes with Main-Group organometallic reagents followed by the transition-metal chemistry. We will mention work from a number of sources, but, in the second half of the review, we will focus mainly on recent work from our own laboratory.

III. REACTIONS WITH MAIN-GROUP ORGANOMETALLIC REAGENTS

1. *General factors*

The reactions between halogenophosphazenes and Main-Group organometallic reagents have been studied in detail during the past 20 years. These reactions can be complex, and some of the

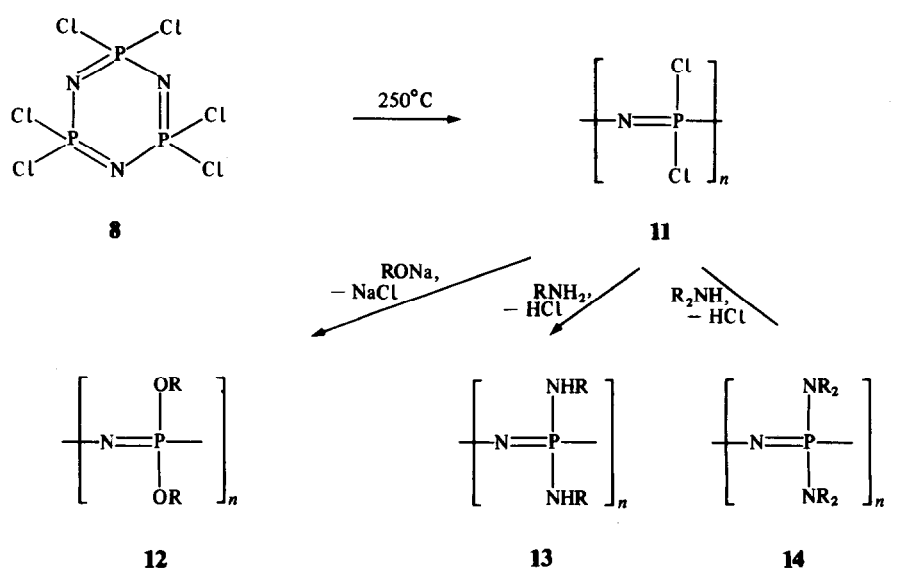

8 **11** **12** **13** **14**

Scheme 3.

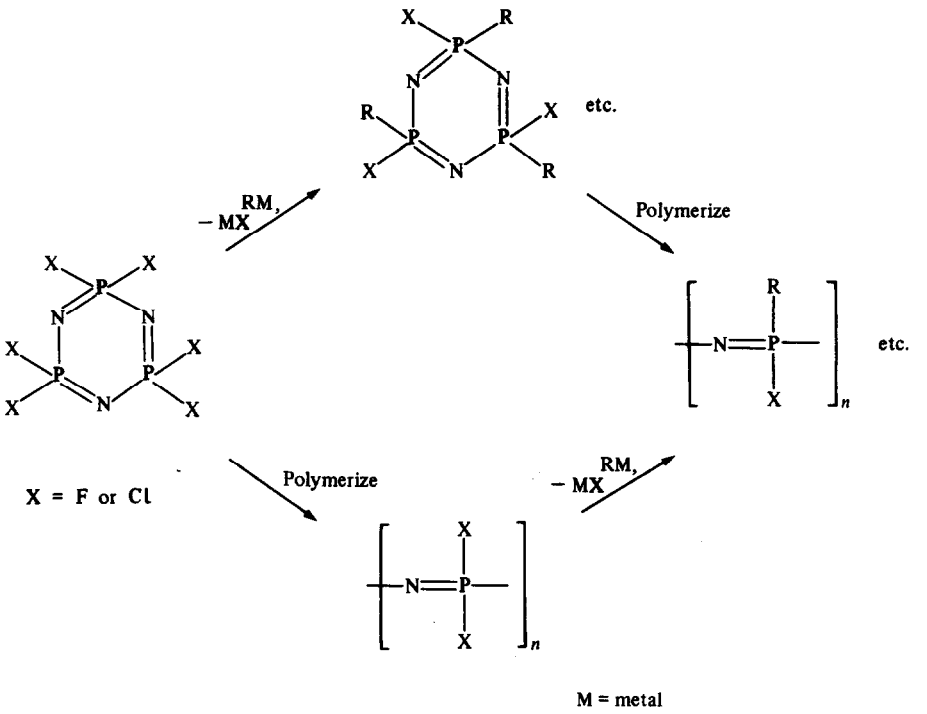

Scheme 4.

earlier work in this area has had to be reinterpreted as the degree of complexity has been recognized.

By analogy with the organic substitution chemistry of phosphazenes, it was originally assumed that organometallic compounds, such as Grignard or organolithium reagents, would participate in simple substitution reactions with halogenophosphazenes to yield alkyl or aryl derivatives of general formulae **15** or **16** [eqn (1)]. However, it is now known that nucleophilic substitution is only one of several reactions that can take place; the others include metal–halogen exchange, proton abstraction from organic side groups, and skeletal cleavage reactions.

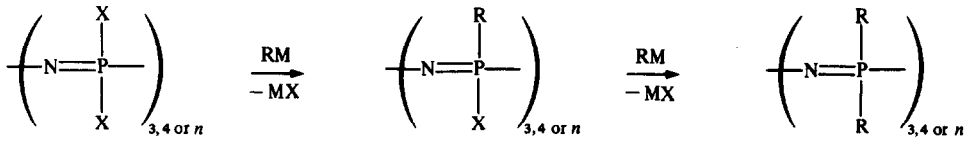

(1)

15 **16**

The exact course of the reaction depends on the type of organometallic reagent used. However, a more critical influence is exerted by the type of phosphazene. Chlorophosphazenes often generate quite different reaction patterns from fluorophosphazenes. Moreover, the degree of polymerization plays a significant role. Cyclic trimers react in a different manner from cyclic tetramers, and linear high polymers may show striking differences from the cyclic oligomers. For this reason, our discussion of the Main-Group organometallic chemistry is divided into four categories, based on the type of phosphazene substrate that is involved. These categories are: (1) organometallic reactions with cyclic fluorophosphazenes; (2) reactions with cyclic chlorophosphazenes; (3) reactions of high-polymeric, linear fluoro- and chlorophosphazenes; and (4) interactions between organometallic reagents and organophosphazenes, i.e. species that bear organic side groups that are capable of reactions with organometallic compounds.

2. *Reactions of cyclic fluorophosphazenes*

(a) *Aryllithium reagents.* The simplest reactions between halogenophosphazenes and Main-Group organometallic compounds are those between small-molecule cyclic *fluoro*phosphazenes

and aryllithium reagents. The key experiments with this system were performed by Moeller and coworkers,[35–38] starting in 1962, and the topic was subsequently developed by Allen, Paddock and Chivers.[38–44] The overall transformations at the cyclic-trimer level are summarized in eqn (2).

$$\underset{\textbf{17}}{(NPF_2)_3} \xrightarrow[-LiF]{ArLi} \underset{\textbf{18}}{N_3P_3F_{6-n}Ar_n} \qquad (2)$$

Arylphosphazene derivatives have been isolated in which the aryl side group is C_6H_5, $C_6H_3D_2$, C_6D_5, C_6F_5, *p*-C_6H_4F, *m*-C_6H_4F, *p*-C_6H_4Cl, *p*-$C_6H_4OCH_3$, *o*-$C_6H_4CH_3$, *p*-$C_6H_4CH_3$ and *p*-$C_6H_4N(CH_3)_2$.

The main products are the mono- and disubstituted species, but replacement of the remaining four fluorine atoms is difficult to accomplish by this method. A maximum of four fluorine atoms can be replaced by a combination of aryllithium and Friedel–Crafts reactions,[37–39,42,43] but the reactivity to fluorine replacement clearly declines as additional aryl groups are attached to the phosphazene ring. Species of type **18** have been used to probe the nature of the electronic interactions between the organic and inorganic pi systems.[39,41,44] They are also valuable molecules for polymerization to alkylfluorophosphazene high polymers (**20**) [eqn (3)].[45]

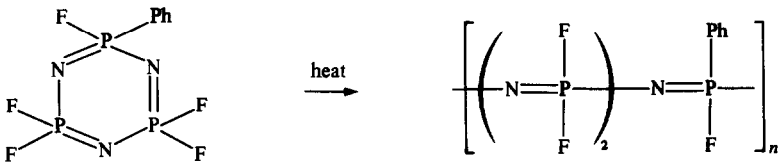

19 **20** $n \approx 1000$ (3)

The fluorine replacement pattern that occurs in the conversion of **17** to **18** has been studied in some detail.[46] At the disubstitution stage, three geometrical isomers (excluding enantiomers) are possible (**21–23**). Aryllithium reagents react predominantly via a 1,3-replacement pathway. For example, $(NPF_2)_3$ interacts with two equivalents of phenyllithium to give **21**, **22** and **23** in a 3 : 1 : 0.25 ratio.[36] The more sterically sensitive *o*-$CH_3C_6H_4Li$ reagent gives the 1,3-product only.

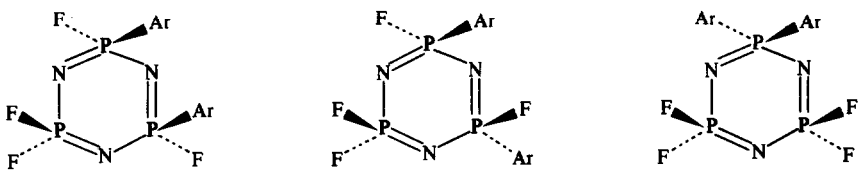

21 1,3 - *cis* (non*gem*) **22** 1,3 - *trans* (non*gem*) **23** 1,1- (*gem*)

These reactions of $(NPF_2)_3$ with aryllithium reagents are striking in their simplicity when compared to the systems to be discussed. For example, aryl Grignard reagents react with $(NPF_2)_3$ by a more complex pathway,[43,47] since products such as the bi(cyclophosphazene) (**24**)[43] are formed. Species of this structure are normally formed by a metal–halogen exchange process.

(b) *Alkyllithium reagents.* The cyclic trimer $(NPF_2)_3$ reacts with methyl- *n*-butyl-, *t*-butyl or cyclohexyllithium reagents to give mainly monosubstituted products of formula $N_3P_3F_5Alk$.[35,48–52] Small amounts of geminal disubstituted products, $N_3P_3F_4Alk_2$, are also formed when methyl- or *n*-butylithium are used.[48,50,51] *t*-Butyllithium gives the non*gem*–*trans* derivative. Presumably geminal substitution is difficult because of steric hindrance effects. It is believed that methyl- and *n*-butyllithium reagents can not only participate in fluorine substitution processes, but many also induce proton abstraction from the alpha position of alkyl groups already attached to the ring. This reaction can lead to decomposition reactions.

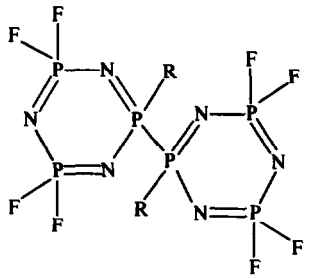

24

Paddock and coworkers[48,53] have made a detailed study of the reactions of methyllithium with octafluorocyclotetraphosphazene, $(NPF_2)_4$. The reaction proceeds predominantly via a 1,1- and 1,1,5,5-fluorine replacement pathway to give species **25** and **26**. Electronic effects within the inorganic ring have been proposed to explain this pattern. However, further fluorine replacement can occur to give the permethyl derivative, $[NP(CH_3)_2]_4$.[48,54] Higher cyclic analogues, such as $(NPF_2)_{6-10}$, react with methylmagnesium bromide to yield $[NP(CH_3)_2]_{6-10}$.[55] *t*-Butyllithium replaces up to two fluorine atoms in $(NPF_2)_4$.[50]

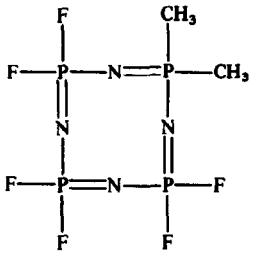

25

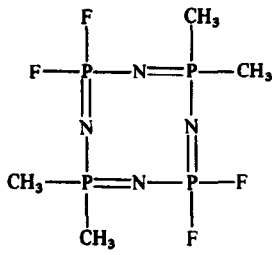

26

An appreciable amount of research has been carried out recently by Allen and others on the reactions of unsaturated alkyllithium reagents with $(NPF_2)_3$ and $(NPF_2)_4$.[49,56–60] A motivation for some of this work has been the synthesis of cyclophosphazenes that undergo vinyl- or acetylenic polymerization through the pendent organic reactive site.[46,61,62] Thus, compounds of formula $N_3P_3F_5R$ have been prepared where R is $CH_2{=}CH{-}$, $CH_3CH{=}CH{-}$, $CH_2{=}C(CH_3){-}$, $CH_2{=}C(OC_2H_5){-}$, $CH_2{=}C(OCH_3){-}$, $C_6H_5C{\equiv}C{-}$ or $(CH_3)_3SiC{\equiv}C{-}$. In general, further reaction yields 1,1-disubstituted products.[56–59] Electron donation from the α-CH_3O or α-C_2H_5O substituents favors substitution.[56,57] This electron supply renders the olefinic center less susceptible to anionic attack and subsequent degradation.

2-Lithio-1-methylpyrrole reacts with $(NPF_2)_{3-6}$ to replace one fluorine atom per ring.[60]

3. *Reactions of cyclic chlorophosphazenes*

(a) *Grignard reagents.* Cyclic *chloro*phosphazenes participate in the widest variety of organometallic reactions. Substitution reactions, skeletal cleavage, metal–halogen exchange, ether cleavage, and ring-contraction processes have all been detected. The preponderance of one reaction over another depends on the type of organometallic reagent, the size of the phosphazene ring, and the solvent used for the reaction. With all these variables, it is perhaps not surprising that different opinions have arisen over the products and mechanisms of particular reactions. Fortunately, enough is now known to allow general principles to be recognized.

Early workers in this field reported that $(NPCl_2)_3$ reacts with phenyl magnesium bromide to give the hexaphenyl derivative, $(NPPh_2)_3$.[63,64] A reinvestigation of this reaction by Biddlestone and Shaw[65–67] yielded the information that, when diethyl ether was used as a solvent, only traces (1–5%) of $(NPPh_2)_3$ were formed, and that this was generated indirectly. The mechanism proposed by these workers involved an initial cleavage of the phosphazene ring, replacement of chlorine atoms in the linear product by phenyl groups, followed by a small amount of recyclization. When diphenyl-

magnesium in dioxane was used in place of phenylmagnesium bromide in ether, a complex mixture was formed which contained linear phosphazenes, a trace of $(NPPh_2)_3$, and a bi(cyclophosphazene). It was proposed that most of these products were formed via phosphazenylmagnesium intermediates.

In our laboratory, Allcock, Desorcie, Harris and Brennan have examined similar reactions in some detail, but with the use of tetrahydrofuran as a reaction solvent.[68–70] Under these conditions, $(NPCl_2)_3$ reacts with a variety of alkyl and aryl Grignard reagents to yield *cyclic* substitution products. No ring-cleavage products were detected. The principal products are the monosubstituted trimer (**27**) and the ring-linked bi(cyclophosphazene) (**28**).

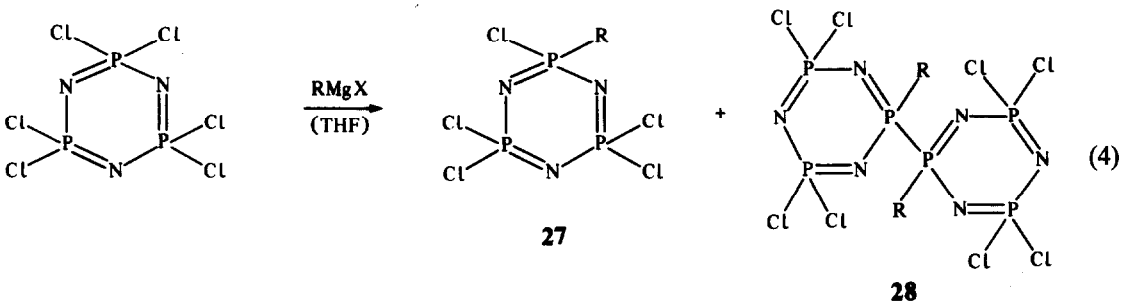

27 **28** (4)

The relative proportions of **27** and **28** are critically dependent on the steric size of the organic group in RMgX. As shown in Table 1, the relative percentage of the monoalkyl product (**27**) in the mixture increases as the size of the alkyl group increases. Phenylmagnesium chloride reacts to give **28** exclusively.

It might be supposed that species **27** would be formed by direct nucleophilic replacement of chlorine by the group R. However, the experimental evidence is in favor of an alternative mechanism in which a metal–halogen exchange pathway is responsible for the fomation of both **27** and **28**.

The initial metal–halogen interaction between $(NPCl_2)_3$ and the Grignard reagent generates a metallophosphazene intermediate (**29**) (Scheme 5). Species **29** contains a trivalent, tricoordinate phosphorus atom which readily participates in chlorine replacement with a molecule of Grignard reagent to yield **30**. At this stage, two possibilities exist. Metal–halogen exchange between **30** and $(NPCl_2)_3$ could generate product **27** and another molecule of **29**. Alternatively, a ring-coupling reaction between **30** and **27** could occur to yield the bi(cyclo) product (**28**). Steric hindrance by bulky alkyl groups inhibits the ring-coupling process. Indirect evidence for the participation of **30** has been obtained by the isolation of **31** from the reaction of $(NPCl_2)_3$ with CH_3MgX or C_6H_5MgX in the presence of iodomethane.

The further reaction of species **27** with Grignard reagents leads to replacement of the geminal chlorine atom by what appears to be a straightforward nucleophilic substitution process to give

Table 1. Reactions of alkyl and aryl Grignard reagents with $(NPCl_2)_3$ in tetrahydrofuran at 66°C[a]

Grignard reagent	% **27**	% **28**
CH_3MgCl	15	85
C_2H_5MgCl	62	38
n-C_3H_7MgCl	64	36
n-C_4H_9MgCl	69	31
i-C_3H_7MgCl	100	0
t-C_4H_9MgCl	50[b]	0
$(CH_3)_3SiCH_2MgCl$	100	0
C_6H_5MgCl	0	100

[a] Percentages represent relative yields of cyclic products isolated.

[b] Remainder of phosphazene components of unreacted $(NPCl_2)_3$.

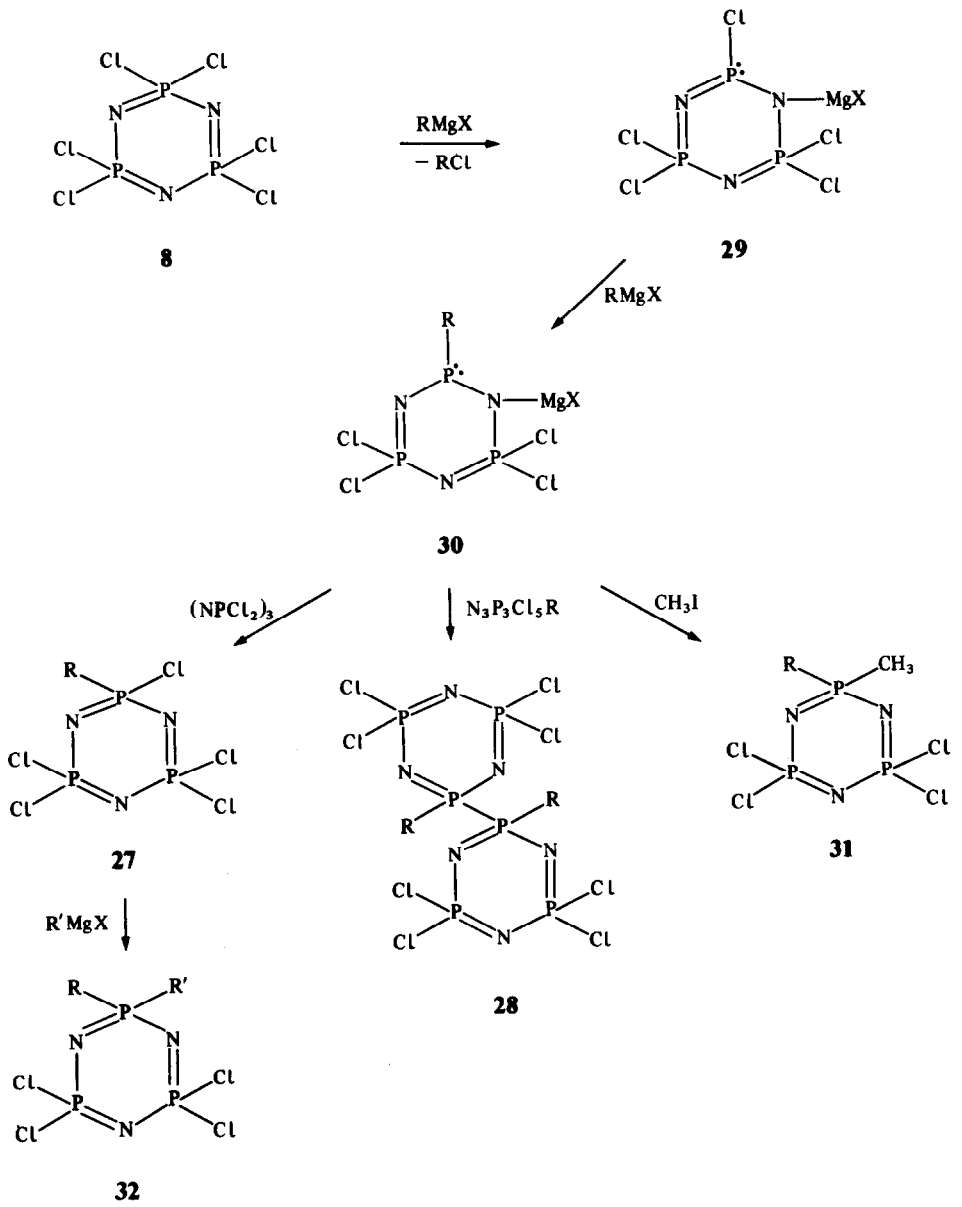

Scheme 5.

species of structure **32**.[69,70] Use of this method has allowed the synthesis of a number of *gem*-alkyl–aryl derivatives by Harris and coworkers.[71]

The reactions of the cyclic tetramer $(NPCl_2)_4$ with Grignard reagents are characterized by both substitution and ring cleavage.[72–74] Thus, the reaction products include cyclic tetrameric species of types **33–35**, and cyclic trimers of type **36–38** formed by skeletal cleavage and ring contraction. The data in Table 2 illustrate how the products vary with changes in group R in RMgX.[72–74]

The mechanism of this ring contraction, first proposed by Shaw,[72,73] is shown in Scheme 6. The initial interaction of $(NPCl_2)_4$ with RMgX results in ring cleavage to form species **39**, which undergoes 1,6-intramolecular nucleophilic displacement to form **40**. Replacement of the chlorine atoms of the pendent unit by reaction with Grignard reagent then yields **36**. This last step seems plausible since the octachloro analogue of **40** has been shown to react with phenylmagnesium bromide to give **36**, with the side-group chlorine atoms reacting first.[75] Species **38** has been isolated from the reaction of $(NPCl_2)_4$ with butylmagnesium halide. (The isopropoxy group is a product of the reaction of a remaining chlorine atom with isopropanol used in the purification process.[74]) A further complication in this type of reaction arises because the ring-contraction process in the

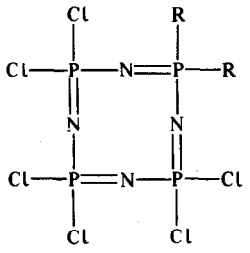

33

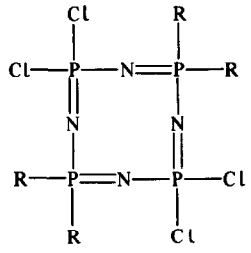

34

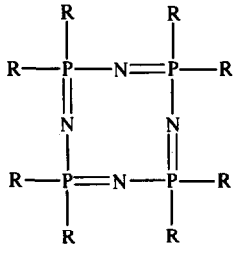

35

For **33**, R = CH_3 ;[75] for **34** and **35**, R = C_6H_5[73,74]

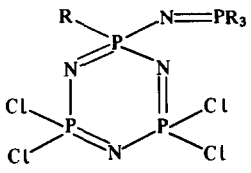

36

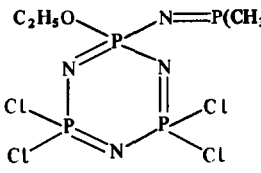

37[75]

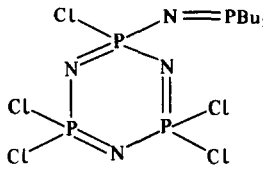

38[75]

R = CH_3, n-C_4H_9 or C_6H_5[73–75]

presence of Grignard reagents can also involve cleavage of the ethers used as solvent. Thus, species **37** is formed by reaction with diethyl ether in the presence of methylmagnesium bromide.[74]

This propensity for alkoxyphosphazene formation during Grignard-mediated reactions is especially noticeable when aminophosphazenes react with Grignard reagents.[76,77] A reaction studied recently in our laboratory is shown in eqn (5). Compound **41** reacts with alkylmagnesium halides

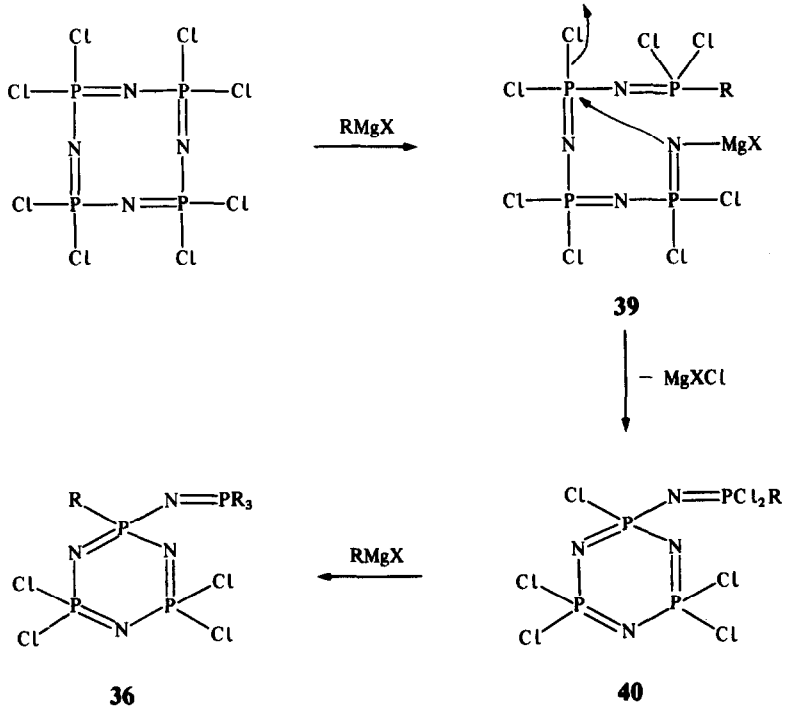

Scheme 6.

Table 2. Cyclic phosphazene products obtained from the reactions of alkyl and aryl Grignard reagents with $(NPCl_2)_4$ in diethyl ether

Grignard reagent	% $(NPCl_2)_4$[a]	% 33	% 34	% 35	% 36	% 37	% 38
CH_3MgBr	40	2	0	0	19	12	0
n-C_4H_9MgCl	35	0	0	0	15	0	7
C_6H_5MgBr	0	0	10	2	70	0	0

[a] Unreacted $(NPCl_2)_4$ recovered.

to generate two types of products, depicted as **42** and **43**. Species **43** with an ethoxy side group, is formed by cleavage of the diethyl ether solvent. The mechanism of this ether cleavage is believed to involve a magnesium halide induced removal of chloride ion from phosphorus, followed by an attack by the resultant phosphazenium ion on the oxygen of an ether molecule.[77]

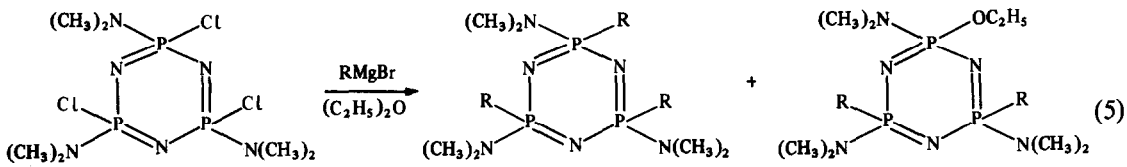

(5)

41 **42** **43**

However, it is possible to maximize the conversion to **42** and discriminate against formation of **43** by the use of a large excess of Grignard reagent in a minimum amount of diethyl ether solvent. Removal of the dimethylamino groups by treatment with hydrogen chloride yields species such as **44** and **45**. These compounds are valuable starting points for further organometallic or organic substitution reactions, because they provide routes to compounds that are not accessible via the direct reaction of $(NPCl_2)_3$ with Grignard reagents. Moreover, compounds such as **44** and **45** can be polymerized to linear macromolecules that contain alkyl groups bonded directly to the skeleton.

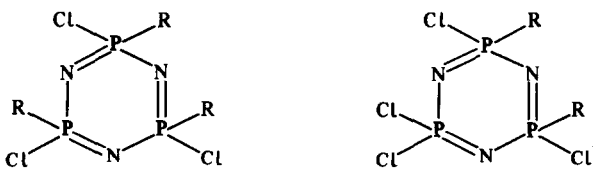

44 **45**

(b) *Organocopper reagents.* In our laboratory, it has been shown that many of the complications inherent in the reaction of chlorophosphazenes with Grignard reagents can be avoided by the use of organocopper reagents.[78–84] Thus, reactions between $(NPCl_2)_3$ and alkyl Grignard reagents in the presence of $[n\text{-}Bu_3PCuI]_4$ lead first to the formation of copper–phosphazene complexes (**46**) (Scheme 7). Reaction of **46** with alkyl halides yields *gem*-dialkyl derivatives (**47**). Treatment of **46** with 2-propanol generates a series of hydridophosphazenes (**48**), which are valuable intermediates for replacement of the hydrogen by chlorine, bromine or iodine to give **49**.

The reactions outlined in Scheme 7 have been explored for systems where R = CH_3, C_2H_5, n-C_3H_7, n-C_4H_9, i-C_3H_7, i-C_4H_9, t-C_4H_9 or $CH_2{=}CH{-}CH_2{-}$. Arylcopper reagents do not function in the same way. They react with $(NPCl_2)_3$ to give *gem*-diarylcyclotriphosphazenes and ring-cleavage products. The group R′, introduced by treatment of **46** with an alkyl halide, can vary over a very wide range from methyl to allyl, 2-methoxyallyl or propynyl.[81–84] However, the introduction of bulky R′ groups is limited by steric effects.

The key intermediate in all these transformations induced by organocopper reagents is the copper–phosphazene species **46**. It has not been isolated, but it has been studied by ^{31}P NMR spectroscopy and by reaction stoichiometry.[79] It has proved to be one of the most valuable organo-

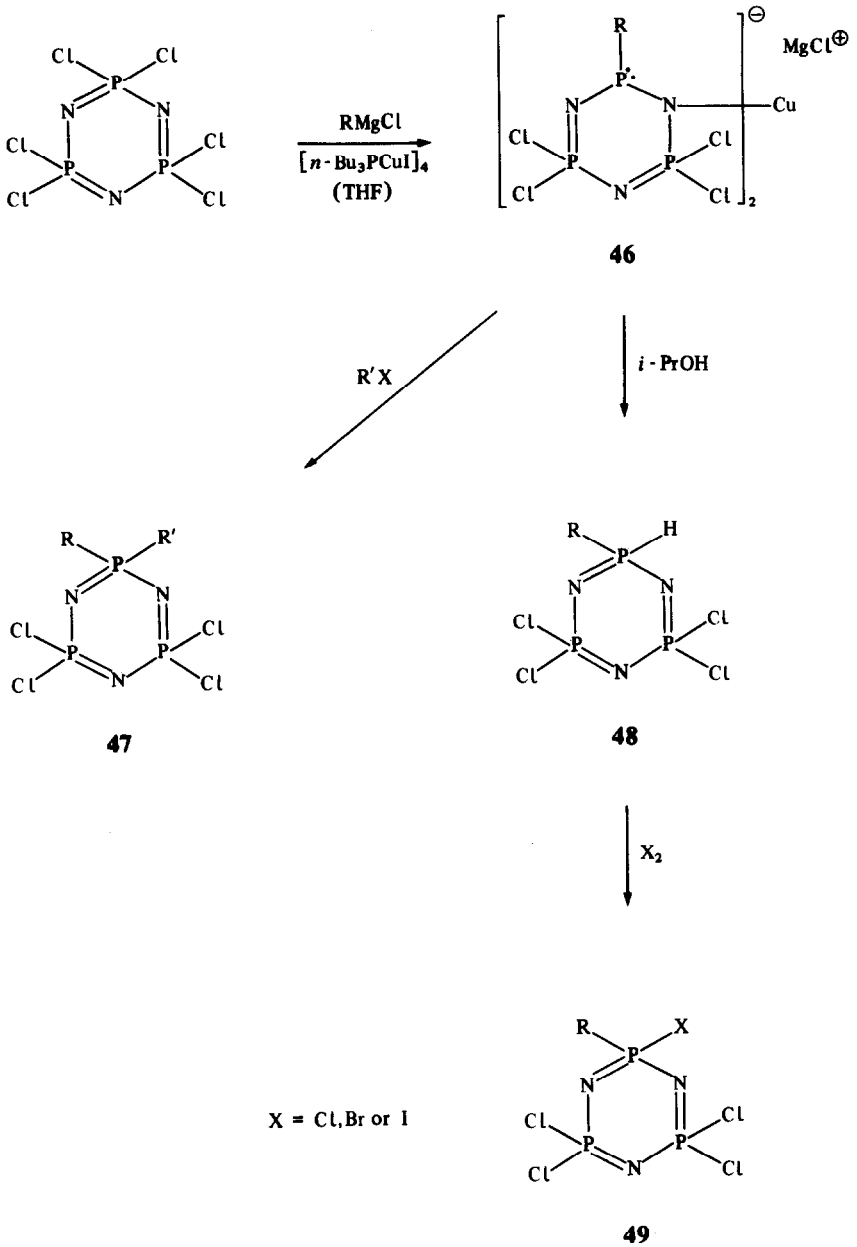

Scheme 7.

metallic species yet discovered in phosphazene chemistry, since it provides access to a diverse range of products of types **47** and **49**, many of which can be converted readily to linear high polymers.[85–87]

(c) *Lithiophosphazenes.* The hydridophosphazene (**48**) provides an entrée into phosphazene anion chemistry. Treatment of **48** with methyllithium at low temperatures yields the phosphazene anion (**50**) (Scheme 8). Interaction of this with prop-2-ynyl bromide[84] gives the propynyl phosphazene (**51**). In the presence of excess methyllithium, species **52** and **53** are also isolated. Compounds **51** and **53** form pi complexes with cobalt carbonyls, and these will be discussed later.

Phenyl derivatives of the copper–phosphazene intermediate (**46**) have not yet been isolated. Thus, for some time, phenyl analogues of **48** and **49** could not be synthesized. This limitation was removed by the discovery by Connolly in our laboratory that the phenylbi(cyclotriphosphazene) (**54**) undergoes P—P bond cleavage in the presence of lithium triethylborohydride to give the stabilized anion shown as **55**. Species **55** behaves in a similar manner to the copper–phosphazene intermediate[88] when treated with proton sources or alkyl halides. This allows the syntheses of *gem-*

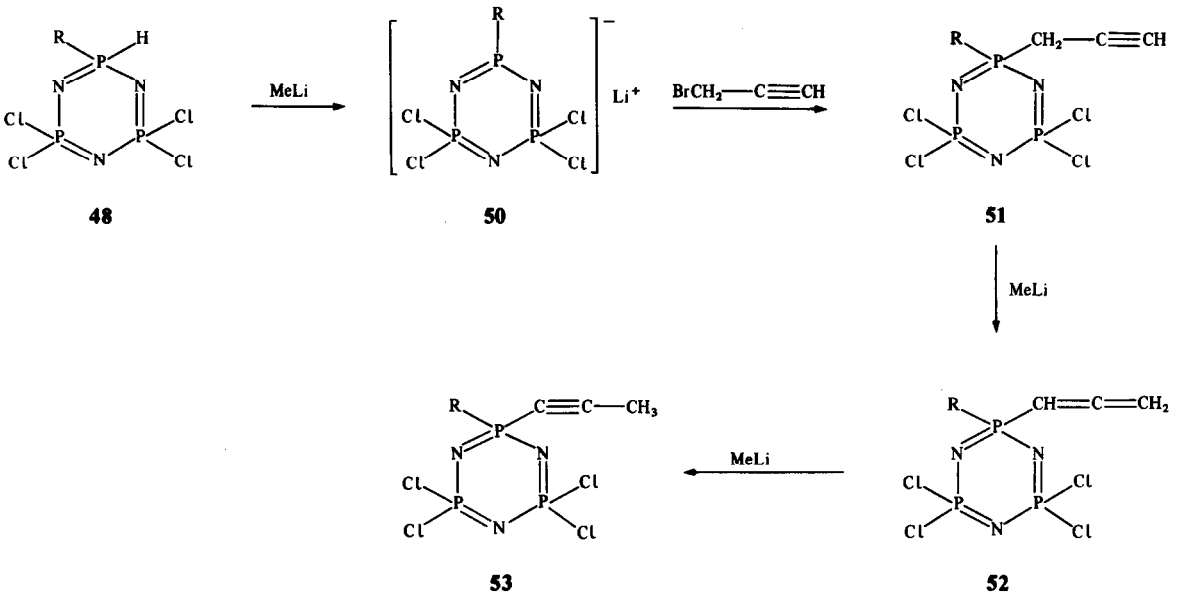

48 50 51 52 53

Scheme 8.

diorganophosphazenes in which one organic unit is an aromatic group. These, too, are valuable precursors to phosphazene high polymers.

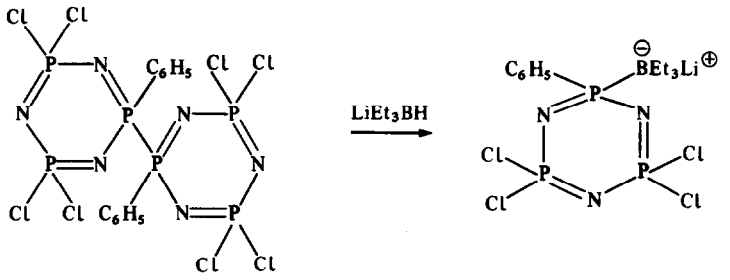

54 55 (6)

(d) *Organolithium reagents.* Simple organolithium compounds appear to be unsuitable reagents for the replacement of chlorine atoms in $(NPCl_2)_3$ by organic groups. Ring-cleavage reactions predominate when $(NPCl_2)_3$ reacts with methyl- or phenyllithium,[89,90] although traces of methylcyclophosphazene products have been isolated.[90] However, van de Grampel and Winter[91] recently reported that the principal product from the reaction of $(NPCl_2)_3$ with methyllithium in tetrahydrofuran at $-20°C$ is a hydridophosphazene. The formation of this compound suggests a metal–halogen exchange process. The same authors[92] also found that the tetramer $(NPCl_2)_4$ reacts with methyllithium to give ring-linked bi(cyclo) tetramers as well as hydridophosphazenes. These products reinforce the view that metal–halogen exchange reactions can occur with organolithium reagents.

On the other hand, Allcock, Scopelianos and O'Brien have shown[93,94] that lithiocarboranes react with $(NPCl_2)_3$ to give monosubstituted products such as **56**. Similar compounds (**57**) are formed by

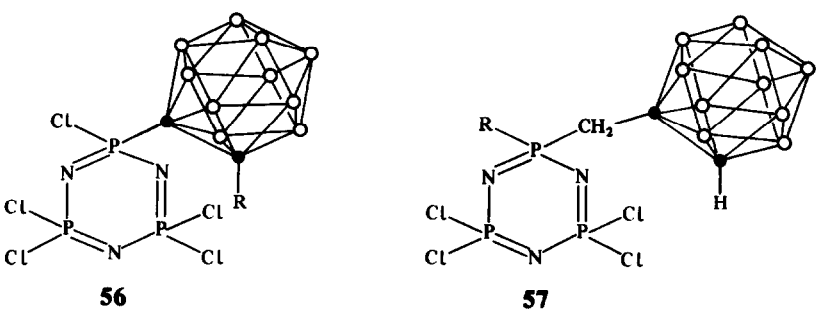

56 57

○ = BH, ● = C

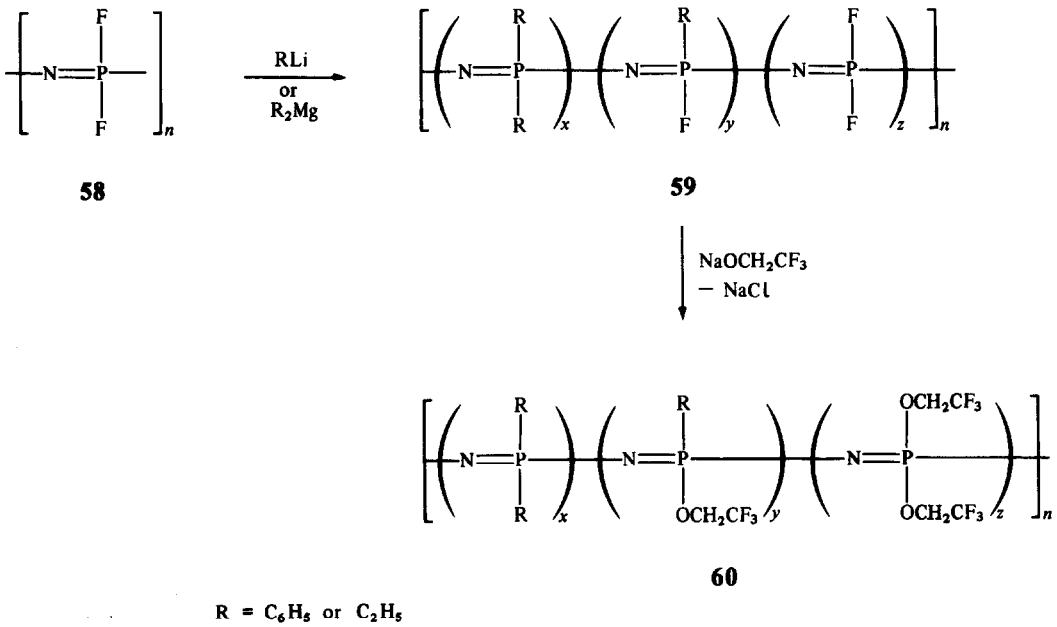

Scheme 9.

the reactions of acetylenic phosphazenes (**51**) with decaborane. Such species polymerize to linear macromolecules when heated, and can be converted to *nido*-carboranes and employed as carrier species for transition metals (see later).

(e) *Organoaluminum and organosodium reagents.* Harris and Jackson[95] have shown that trimethylaluminum reacts with $(NPCl_2)_3$ to yield $N_3P_3Cl_2(CH_3)_4$ in good yield. The substitution follows mainly a geminal substitution pathway.

Burg and Caron[96] found many years ago that sodium acetylide reacts with $(NPCl_2)_3$, but the reaction has not been explored in detail.

4. *Reactions of high-polymeric halogenophosphazenes*

As discussed in an earlier section, two alternative organometallic routes exist for the synthesis of phosphazene high polymers that bear alkyl or aryl side groups linked to the chain via C—P bonds.* In the first route, the organic groups are introduced at the cyclic trimer level and the trimer is then polymerized. In the second method, an attempt is made to introduce the organic groups at the high-polymer level by organometallic substitution processes. We have explored this second possibility in some detail, making use of the results from the "model" reactions with cyclic trimers or tetramers.[10]

First, it must be emphasized that the problems involved in carrying out such reactions with high polymers are highly challenging. The complexity of the reaction at the cyclic-oligomer level, as just described, provides a hint of the difficulties to be expected. Moreover, it can be anticipated that skeletal cleavage reactions would be severely detrimental for high polymers, because shortening of the chains would lower the usefulness of the polymers. Nevertheless, some progress has been made.

It can be anticipated from the results described up to this point that *fluoro*phosphazenes are more appealing substrates for most organometallic reactions than are chlorophosphazenes. The fluoro derivatives are less prone to metal–halogen exchange processes and are perhaps less susceptible to skeletal cleavage. Thus, the reactions of poly(difluorophosphazene) (**58**) have been examined as well as those of poly(dichlorophosphazene) (**62**).

Evans and Patterson in our laboratory showed that poly(difluorophosphazene) reacts cleanly with phenyllithium or diethylmagnesium to yield partly substituted macromolecular products (**59**)[97(a)] (Scheme 9). The remaining fluorine atoms can be replaced by treatment with sodium tri-

* An alternative direct-synthesis route also exists, as reported by P. Wisian-Neilson and R. H. Neilson.[97(b)]

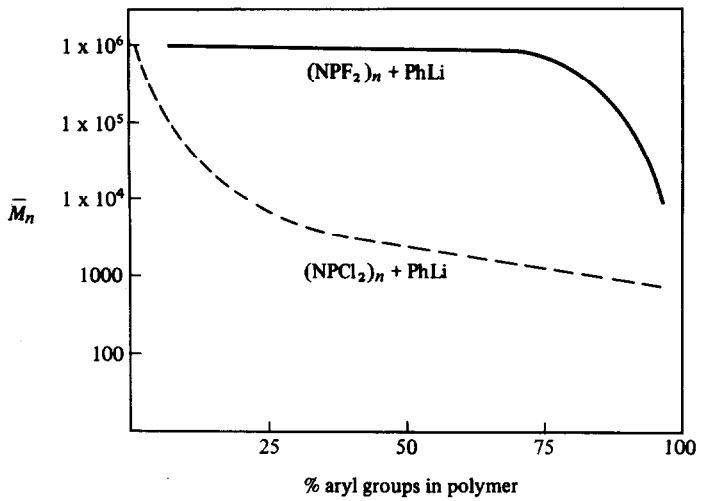

Fig. 1. Comparison of the variation in average molecular weight for $[NP(C_6H_5)_x(OCH_2CF_3)_y]_n$ vs the percentage of phenyl groups attached to the backbone. The broken curve represents the behavior of the system when $(NPCl_2)_n$ is used as a reaction substrate. The solid line illustrates the behavior with $(NPF_2)_n$. From Allcock *et al.*[98]

fluoroethoxide to give a hydrolytically stable high polymer (**60**). The phenyltrifluoroethoxy polymers are film-forming materials with molecular weights above 1×10^6.[98] The substitution reaction with phenyllithium appears to be mainly geminal.[98] It proceeds with no evidence of chain cleavage until roughly 70% of the fluorine atoms have been replaced. Beyond this point, the chain length decreases rapidly (Fig. 1). It is speculated that strong electron withdrawal by the fluorine atoms shields the system against chain cleavage by reducing the basicity of the skeletal nitrogen atoms. However, once 70% of the fluorine atoms have been replaced by phenyl, this protection is reduced, and chain cleavage becomes a major contributor to the reaction.[98]

Methyllithium reacts with $(NPF_2)_n$ to replace fluorine atoms by methyl groups and, at the same time, crosslinks the chains.[99] The cross-linking process appears to involve proton abstraction from pendent methyl groups by methyllithium, followed by attack of the resultant anionic site on a P—F bond in another chain. Evidence for this mechanism was provided by a small-molecule simulation in which octamethylcyclotetraphosphazene was treated with methyllithium to generate the carbanion. This species then reacted with $(NPF_2)_3$ to yield compounds **61**.

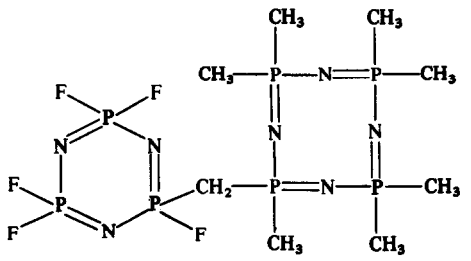

61

Poly(dichlorophosphazene) (**62**) reacts with a deficiency of phenyllithium[100,101] by a geminal substitution process to yield **63**, and the remaining chlorine atoms can be replaced by treatment with alkoxide or amino nucleophiles to give species such as **64** or **65** (Scheme 10).[100] However, chain shortening occurs almost from the beginning of the organometallic reaction (Fig. 1). A similar molecular-weight decline occurs when $(NPCl_2)_n$ reacts with lithiocarboranes.[94] Organomagnesium, organosodium and organozinc reagents also react with $(NPCl_2)_n$ by a complex mechanism.[102] In this sense, the ring-contraction reactions of $(NPCl_2)_4$ provide a good model for what occurs in the high polymer.

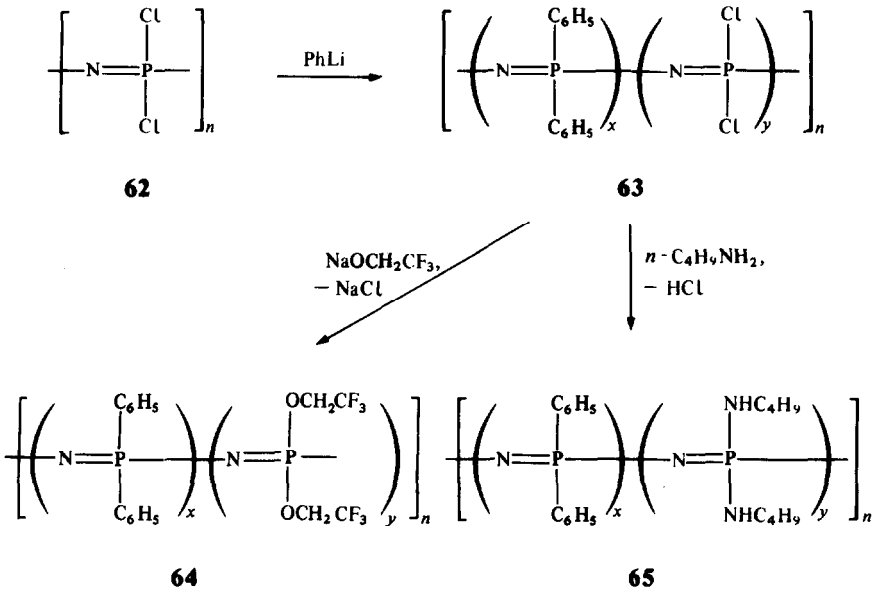

62 **63** **64** **65**

Scheme 10.

5. *Reactions of organophosphazenes*

In principle, the wide array of reactions between Main-Group organometallic reagents and organic compounds can be applied to organic groups that are linked to a phosphazene ring or chain. If conditions are favorable, these side-group reactions may occur without phosphazene skeletal cleavage.[103] Such organic-type reactions offer the prospect of greatly increasing the structures available in phosphazene chemistry. As will be seen later in the section on transition-metal derivatives, this route is of special importance for the synthesis of polymer-bound catalysts.

The possibilities for organometallic transformations at the side groups are so broad that only three examples will be given here. First, Paddock and coworkers have investigated the alkyllithium-induced metal–hydrogen exchange reactions on methyl groups attached to phosphazene rings.[104,105] Compounds such as **66** are formed and can be used as substrates for reactions with electrophiles such as CH_3I, $(CH_3)_3SiCl$, $(CH_3)_3GeCl$, $(CH_3)_3SnCl$, $C_6H_5C(O)C_2H_5$, CO_2, $(CH_3)_2SiCl_2$ and $(CH_3)_2AsI$.[105]

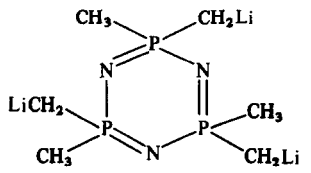

66

Second, we have shown[106] that trifluoroethoxyphosphazenes such as **67** (Scheme 11) react with organolithium reagents to undergo metal–hydrogen exchange at the α-carbon atoms (**68**). Treatment of **68** with a variety of electrophiles allows access to products such as **69–72**.

Finally, as shown in Scheme 12, metal–halogen exchange reactions can be carried out at aryloxy groups attached to a phosphazene ring or chain.[107–109] Allcock, Evans and Fuller used reactions of this type to prepare a wide range of functionalized aryloxyphosphazenes, some of which (**78**) are good carrier molecules for transition-metal organometallic species.

IV. TRANSITION-METAL CHEMISTRY

1. *General features*

The transition-metal chemistry of phosphazenes is of recent origin but has developed rapidly, particularly during the past 5 years. In the preceding sections, an emphasis was placed on the striking

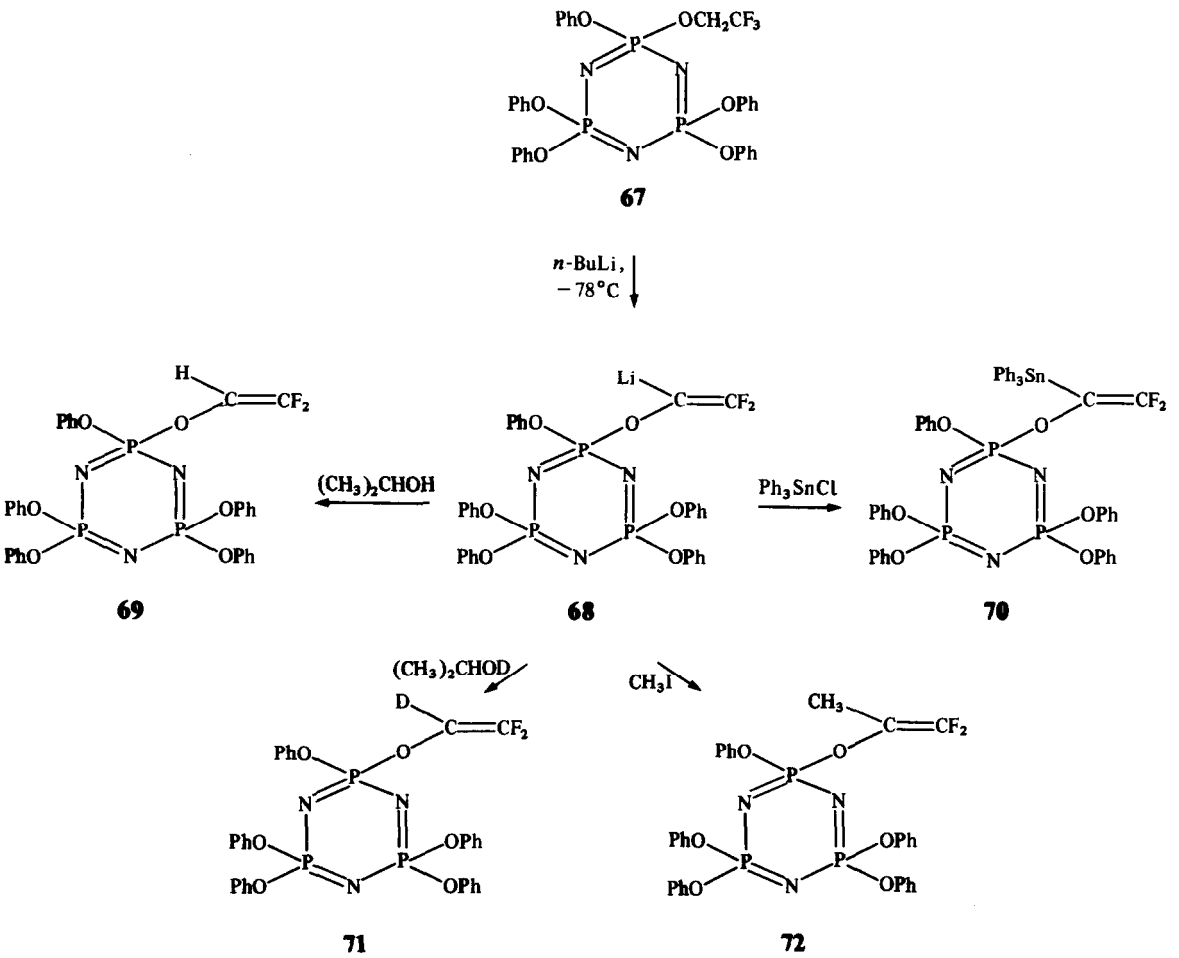

Scheme 11.

differences between the reactions of fluoro-, chloro- and organophosphazenes, and on the role played by skeletal ring or chain size. In transition-metal organometallic chemistry, these differences are still evident, but the most important feature is the nature of the organometallic reagent and the mode of linkage of the transition metal to the phosphazene. The Main-Group organometallic chemistry is valuable in so far as it provides a means for the attachment of organic groups to phosphazenes. The transition-metal organometallic chemistry is important as a method for the linkage of transition metals to phosphazenes.

The mode of attachment of transition metals to cyclic or high-polymeric phosphazenes can be divided into four general categories: (1) use of the electron-donor coordination properties of the skeletal nitrogen atoms of phosphazenes; (2) attachment of the transition metal through ionic, "salt-type" linkages; (3) direct covalent binding between a transition metal and a skeletal phosphorus atom; and (4) attachment of the metal to an organic ligand that is itself connected as a side group to a skeletal phosphorus atom. The first two of these do not fall strictly into the category of organometallic systems, but they are discussed here briefly to provide perspective.

2. *Complexes between metals and skeletal nitrogen atoms*

Each skeletal nitrogen atom of a phosphazene bears a lone pair of electrons (**79**). The remaining nonsigma bonding electrons, one from phosphorus and one from nitrogen, are believed to participate in a d_{π}–p_{π} bond that makes use of a nitrogen $2p_z$ orbital and one of several phosphazene $3d$ orbitals.[110] Delocalization of these pi electrons occurs over three skeletal atoms only[111] in a way that permits

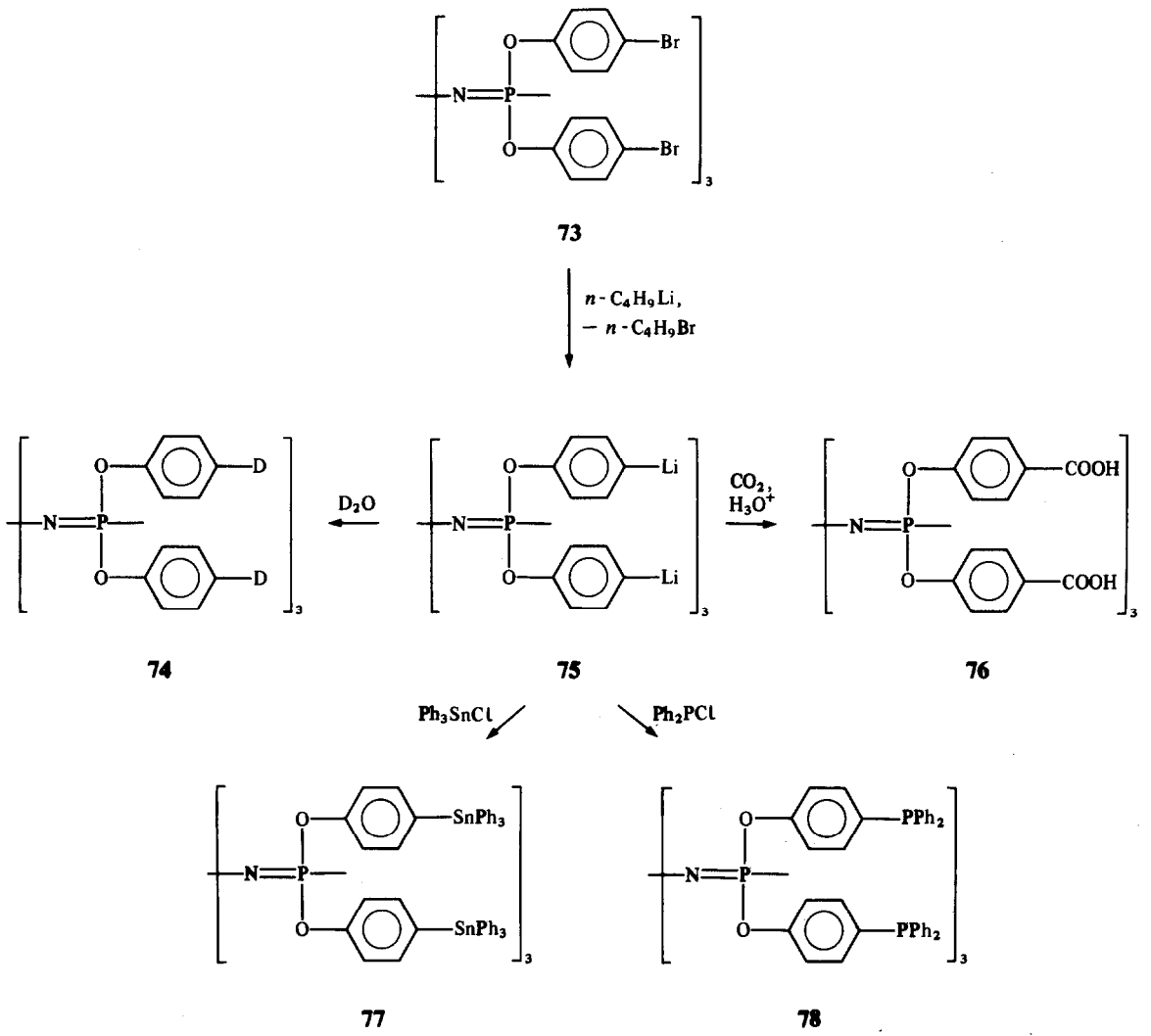

Scheme 12.

an equalization of bond lengths around a ring or along a chain, and gives the superficial appearance of aromaticity without the existence of long-range delocalization effects.[14,15,112]

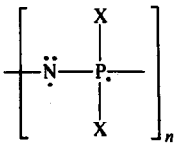

79

The availability of each lone pair of electrons for coordination to metals depends on the side group X. Electron-withdrawing side groups, such as fluorine or trifluoroethoxy, reduce the basicity of skeletal nitrogen but, at the same time, strengthen the skeletal bonds, probably by causing a contraction of the phosphorus *d*-orbitals and improving their overlap efficiency. Conversely, when the side group is an electron-supplying unit, such as methyl, alkylamino etc., the basicity of the skeletal nitrogen atoms is enhanced and they can now bind protons, alkyl cations, or transition metals.

(a) *Metal halide complexes.* One of the earliest complexes of this type was reported by Dyson[113] who allowed $[NP(CH_3)_2]_4$ to react with anhydrous copper(II) chloride in methyl ethyl ketone as a

solvent. A subsequent X-ray diffraction study of this complex by Trotter and Whitlow[114] showed that the molecule had the structure shown in **80**.

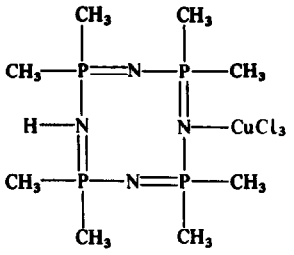

80

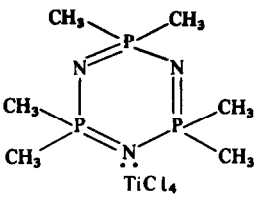

81

Lappert and Srivastava[115] found that $[NP(CH_3)_2]_3$ interacts with titanium tetrachloride in dichloromethane solution to yield the stable crystalline compound shown in **81**. Later, Schmidpeter *et al.*[116] allowed compound **82** to react with nickel, palladium and platinum dichlorides to yield the bis(thionato) metal(II) complexes shown in **83**. An X-ray structure determination by Ahmed[117] of the nickel derivative, where R = CH_3, showed a square planar bischelating geometry that involved a skeletal nitrogen atom and an exocyclic sulfur atom from two phosphazene rings.

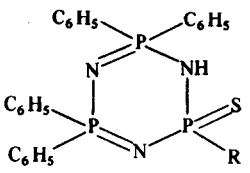

82

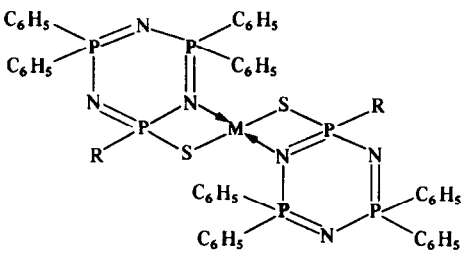

83

R = CH_3, *p*-$C_6H_4OCH_3$ or OC_6H_5
M = Ni, Pd or Pt

Among the aminophosphazenes reported to form metal halide complexes are species such as $[NP(NHPr^n)_2]_3$ (with Co^{2+}, Ni^{2+} or Cu^{2+} halides) and $[NPNHBu^n)_2]_3$ (with Co^{2+}) in acetonitrile.[118] However, these structures have not yet been studied crystallographically.

More is known about the bidentate platinum complexes formed by $[NP(NHCH_3)_2]_4$ and $[NP(NHCH_3)_2]_n$. Allcock *et al.*[119] found that, in the presence of 18-crown-6-ether, K_2PtCl_4 reacts with these phosphazenes to form the square planar complexes shown in **84** and **85**. In the cyclic tetrameric system, it was shown by X-ray diffraction analysis that the metal is coordinated in a transannular fashion to the 2,6-*skeletal* nitrogen atoms.[120] A similar situation is found when the substrate is $[NP(CH_3)_2]_4$ and the reagent is $PtCl_2$ in benzene.[119] The high-polymeric aminophosphazene similarly forms a $PtCl_2$ complex by means of the skeletal nitrogen atoms.[119] The composition of this complex was $[NP(NHCH_3)_2]_n[PtCl_2]_x$ ($x:n \simeq 1:17$). These platinum complexes are of interest as

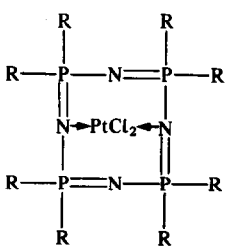

84

R = $NHCH_3$ or CH_3

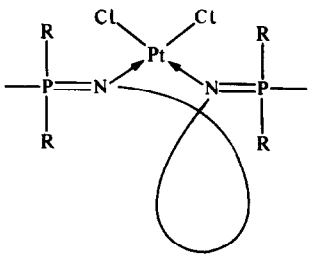

85

R = $NHCH_3$

antitumor drugs. The high polymeric derivative (**85**) has been shown to function as a water-soluble anticancer agent with restricted transmission through semipermeable membranes.

This pattern of transannular linkage with aminophosphazenes extends in higher cyclic species to the formation of macrocyclic chelation systems. For example, Paddock, Trotter and coworkers[121] showed that the cyclic hexamer, $[NP(NMe_2)_2]_6$, reacts with the chlorides of Mn^{2+}, Fe^{2+}, Co^{2+} and Zn^{2+} in methyl ethyl ketone to give macrocyclic chelates of the type shown in **86**.

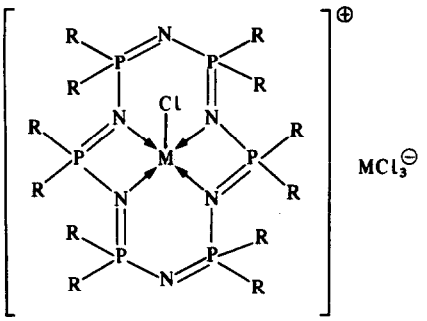

86

R = $N(CH_3)_2$

The cobalt complex was examined by X-ray diffraction techniques[122] and was found to possess a structure in which four of the six skeletal nitrogen atoms occupy the basal site of a distorted square pyramid, with a chlorine atom at the apical position. The analogous copper(II) chloride complex, $[(NP(NMe_2)_2)_6CuCl]^+[CuCl_2]^-$, has a similar structure, but with the counterion reduced to the Cu(I) state.[123,124]

(b) *Metal carbonyl complexes.* In principle, aminophosphazenes have three different types of sites for the binding of transition metals—skeletal nitrogen atoms, side-group nitrogen atoms, and ring or chain pi electrons. Which linkage system wins in the competition for the metal atom is a matter of some interest.

The aminocyclotetraphosphazene, $[NP(NMe_2)_2]_4$, reacts with tungsten carbonyl to give a pale yellow crystalline material that was shown by Paddock, Trotter and their coworkers to have the molecular structure shown in **87**.[125,126]

As indicated in **87**, the phosphazene functions as a bidentate *cis-σ* ligand, with the metal being coordinate by one ring nitrogen and one side-group nitrogen.[126]

A different situation exists when coordination to the side group is impossible. The cyclic tetramer $[NP(CH_3)_2]_4$ reacts with molybdenum or tungsten hexacarbonyl in the melt at 160°C to yield a yellow compound (**88**).[127,128]

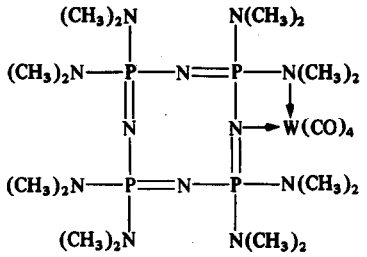

87

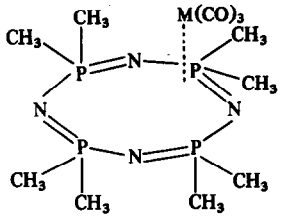

88

The molybdenum analogue of **88** has also been studied by Cotton *et al.*,[129] but no firm conclusions could be drawn about the mode of metal binding. Related compounds have also been prepared from $[NP(CH_3)_2]_5$ and molybdenum or tungsten carbonyl.[127] It has been reported that $(NPCl_2)_3$ reacts with $Cr(CO)_3(CH_3CN)_3$ to yield a species of formula $(NPCl_2)_3 \cdot Cr(CO)_3$,[130] but the structure of the product has not been determined.

3. *Ionic, salt-type species*

The skeletal nitrogen atoms in aminophosphazenes and alkylphosphazenes can acquire a proton or alkyl cation to generate onium-type sites that function as counterions for metallo anions.

Thus, $[NP(NMe_2)_2]_3$ with $CoCl_2$ gives the salt-type species $[(NP(NMe_2)_2)_3H]_2^+[CoCl_4]^{2-}$; $(NPMe_2)_4$ with the same reagent yields $[(NPMe_2)_4H]_2^+[CoCl_4]^{2-}$;[113,131-133] $[NP(NHMe)_2]_4$ with K_2PtCl_4 in acid gave $[(NP(NHMe_2)_2]_4]^{2+}[PtCl_4]^{2-}$, and $[NPMe_2]_4$ gave $[(NPMe_2)_4H_2]^{2+}[PtCl_4]^{2-}$.[119] A hexamolybdate salt of formula $[(NP(NMe_2))_3H]_2^+$ was also formed when $[NP(NMe_2)_2]_3$ reacted with MoO_3 in water.[134] Similarly, the methyl iodide quaternary salt of $[NPMe_2]_4$, $[N_4P_4Me_9]^+I^-$, reacts with chromium or molybdenum hexacarbonyl to displace one carbon monoxide ligand and generate the species $[N_4P_4Me_9]^+[M(CO)_5I]^-$.[127]

4. *Species with metal–phosphorus covalent bonds*

Compounds that contain phosphazene rings or chains linked directly to transition metals through phosphorus–metal covalent bonds were discovered only recently by Greigger, Wagner, Suszko and Riding[135-142] in our laboratories. These constitute an unusual class of compounds that are true hybrids of Main-Group ring systems with transition-metal carbonyl species. Nearly all the developments in this area have been at the cyclic trimeric or tetrameric level, but very recently, the first high polymeric analogues have been isolated. These are prototypes for yet unsynthesized species of type **89**, which would be hybrids of polymers and metals. It is possible that this chemistry might eventually lead to the synthesis of "outrigger" metallo polymers of type **90**.

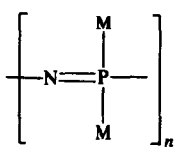

89

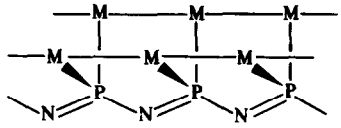

90

Three basic synthetic techniques have been applied to the preparation of small-molecule metallophosphazenes of this type. These are: (a) reaction of transition-metal anions with halogenophosphazenes by a nucleophilic-type substitution process; (b) metal–metal exchange processes to replace one metal already attached to the phosphazene ring by another metal; and (c) the reactions of phosphazene anions with organometallic metal halides which function as electrophiles.

(a) *Reactions of transition-metal nucleophiles with halogenophosphazenes.* These reactions can be viewed as counterparts of the organic and Main-Group organometallic substitution reactions discussed earlier. The first examples of this type of reaction involved the interactions of the most nucleophilic transition-metal carbonyl anions, $[Fe(CO)_2(\eta\text{-}C_5H_5)]^-$ and $[Ru(CO)_2(\eta\text{-}C_5H_5)]^-$, with $(NPF_2)_3$.[135-137] The potassium salts of these anions react with $(NPF_2)_3$ first to give the monosubstituted derivatives (**92** and **95**) in moderate yield (Scheme 13). Further reaction of the iron derivative (**92**) with an excess of $K^+[Fe(CO)_2(\eta\text{-}C_5H_5)]^-$ results in the replacement of the geminal fluorine atom to yield **93** as pale yellow crystals.[136] Exposure of this compound to light results in the loss of one carbon monoxide ligand and the formation of a spirocyclic phosphazene with a metal–metal bond (**94**).[135,136]

The analogous reaction between excess $K^+[Ru(CO)_2(\eta\text{-}C_5H_5)]^-$ and **95** yielded only the spirocyclic compound **96**.[137] The noncyclized, dimetallo intermediate is apparently too prone to decarbonylation to permit its isolation and identification. A mixed-metal derivative (**97**) was prepared by the reaction of $K^+[Fe(CO)_2(\eta\text{-}C_5H_5)]^-$ with the monoruthenium phosphazene (**95**) and this product undergoes facile photolytic decarbonylation to yield the mixed-metal spirocyclic species **98**. However, the converse reaction, that involves treatment of the monoiron phosphazene (**80**) with $K^+[Ru(CO)_2(\eta\text{-}C_5H_5)]^-$, failed to give the same mixed-metal species. Instead, compound **99** was formed,[137] presumably by an attack by the incoming organometallic anion on the phosphorus–metal bond.

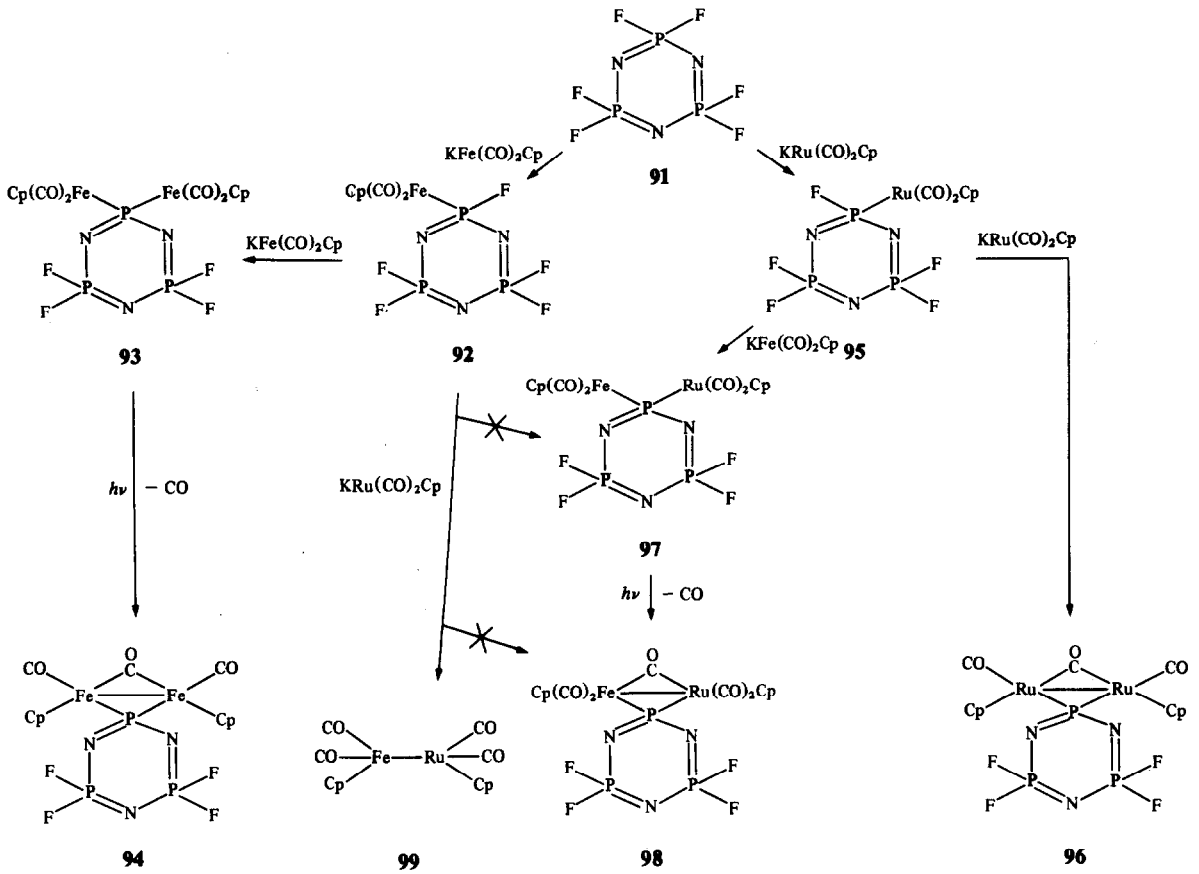

Scheme 13.

No products have yet been isolated in which any of the four remaining fluorine atoms have been replaced by the metallo units. In fact, there appears to be a severe deactivating influence on the nongeminal sites that suggests a strong electron supply from the organometallic moiety into the phosphazene ring.

The structures of **93**, **94** and **98** have been confirmed by X-ray crystallographic studies.[135–137] The influence of the metallo units on the phosphazene ring can be seen in the distortion of ring bond angles and bond lengths.[135–137]

As might be expected from the comparisons between fluoro- and chlorophosphazenes discussed earlier, the reactions between transition-metal anions and $(NPCl_2)_3$ or $(NPCl_2)_4$ are more complex than with $(NPF_2)_3$. Both substitution and cation–halogen exchange are possible with the chlorophosphazenes.

The tetra-*n*-butylammonium salts of the chromium, molybdenum and tungsten anions, $[M(CO)_3(\eta\text{-}C_5H_5)]^-$, react with $(NPCl_2)_3$ in methylene chloride to yield the monometallophosphazenes (**100** and **101**).[138] The structures of **100** and **101** (M = Mo) have been confirmed by

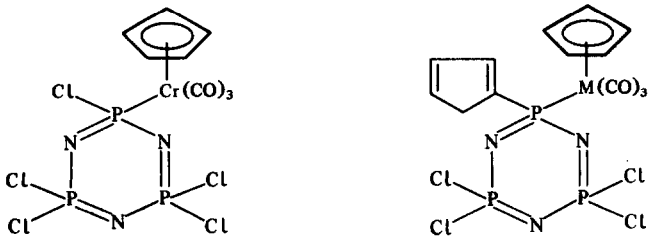

100 **101**

M = Mo or W

X-ray crystal structure analysis.[138] Thus, the chromium derivative (**100**) appears to be the product of a straightforward substitution reaction.

However, the reactions with the molybdenum and tungsten anions are more complex, since a cyclopentadiene unit appears as a substituent at the geminal position. The identification of $MCl(CO)_3(\eta\text{-}C_5H_5)$ from these reactions strongly suggests contributions from a cation–halogen exchange reaction. Further evidence in favor of this interpretation is the isolation of species **102** from reactions in which $(NPCl_2)_3$ reacts with $[W(CO)_3(\eta\text{-}C_5H_5)]^-$ in the presence of methyl iodide.[138]

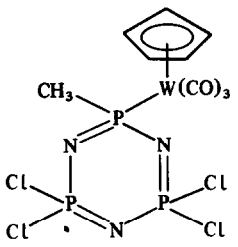

102

Organometallic dianions also react with chlorophosphazenes.[139,140] Disodium octacarbonyl diferrate, $Na_2Fe_2(CO)_8$, interacts with $(NPCl_2)_3$ in tetrahydrofuran to give the spirocyclic diiron phosphazene shown as **103** in Scheme 14, together with smaller amounts of the triiron cluster phosphazenes (**104**). The source of this latter species is of some interest. It appears to be formed by the reaction of **103** with neutral iron carbonyl species, such as $Fe_2(CO)_9$, which are present in the reaction mixture. Treatment of pure **103** with $Fe_2(CO)_9$ under the same reaction conditions yields **104**. Moreover, treatment of **103** with $Ru_3(CO)_{12}$ gave the diiron–monoruthenium cluster phosphazenes depicted as **105**. X-ray crystal structures have been obtained for compounds **103–105**.[139,140] These confirm that the third metal of the cluster is coordinatively bound to the adjacent ring nitrogen atom. The structures also demonstrate that appreciable phosphazene ring distortion accompanies this interaction.

Similar reactions occur with the chlorophosphazene cyclic tetramer, $(NPCl_2)_4$.[140] The reaction of $Na_2Fe_2(CO)_8$ with $(NPCl_2)_4$ led to the isolation of species **106** and **107**.

As mentioned earlier, these substitution reactions are of interest not only for their exploratory

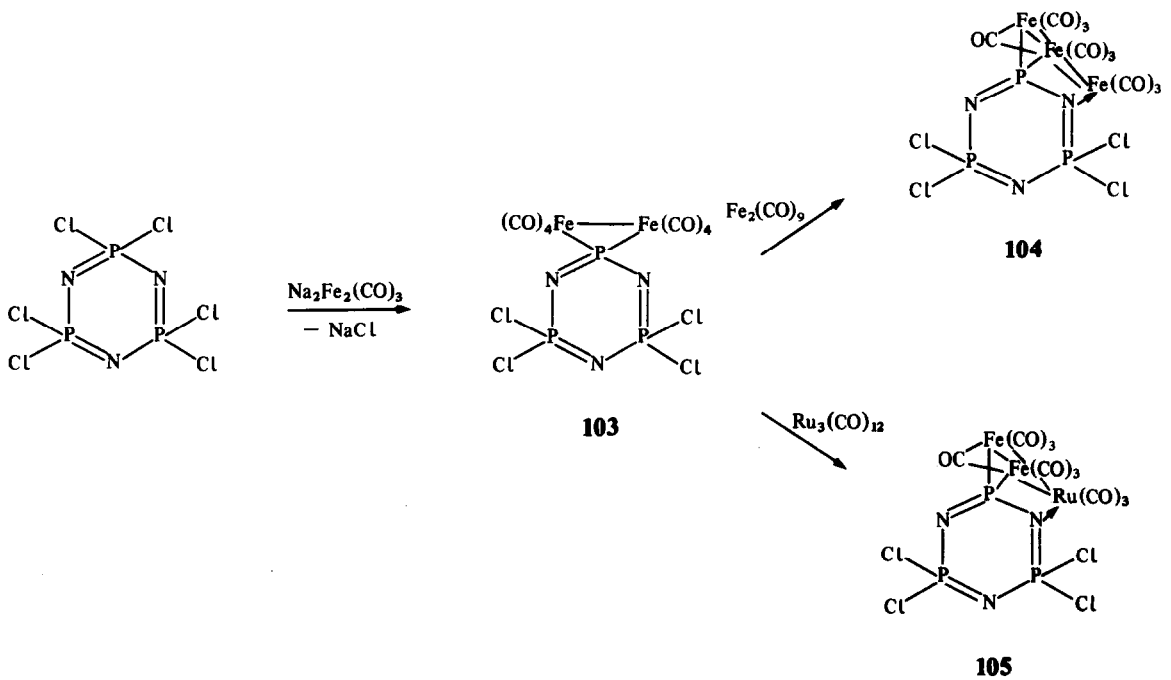

Scheme 14.

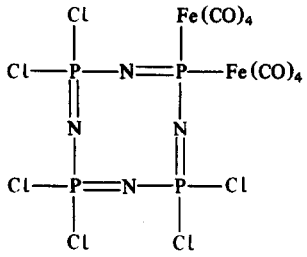

106

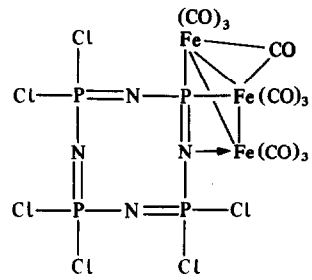

107

and fundamental value, but also because they offer a means for the incorporation of metals and metallo clusters into phosphazene high polymers. Thus, the long-range significance of these structures may lie eventually in their relationship to electroactive, magnetically-active, or catalytically-active macromolecules.

(b) *Metal–metal exchange reactions.* Species **103** not only adds additional metal atoms to generate trimetallo species, but it can also function as a substrate for replacement of one metal by another. Thus, **103** reacts with $Co_2(CO)_8$ to give the dicobalt–monoiron derivative shown as **108**, in which two $Co(CO)_3$ units are now covalently bound to phosphorus, and the one remaining iron atom is displaced into a peripheral position, and is coordinatively bound to a ring nitrogen atom.[141]

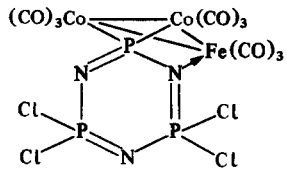

108

Reaction of **103** with the cyclopentadienyl cobalt carbonyl, $Co(CO)_2(\eta\text{-}C_5H_5)$, results first in the replacement of one iron unit to give **109**, while further reaction results in replacement of the second iron to generate **110**[141] (Scheme 15). However, **103** reacts with $Rh(CO)_2(\eta\text{-}C_5H_5)$ to give **111** directly. The structures of **108–110** were confirmed by X-ray diffraction.[141] Species **108** was also examined by Mössbauer spectroscopy.[141]

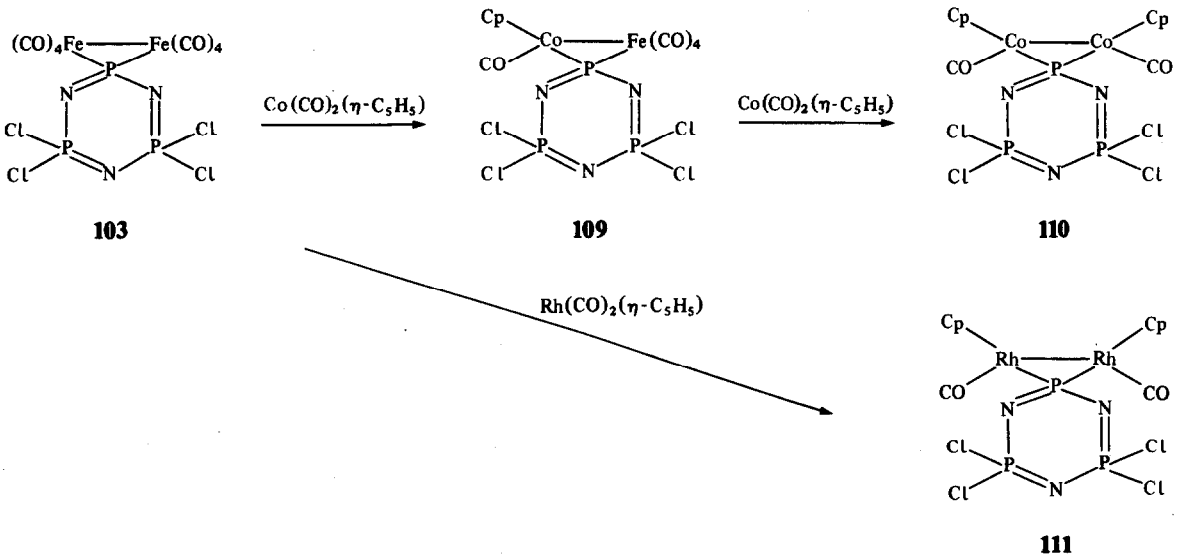

Scheme 15.

(c) *Reactions of phosphazene anions with organometallic electrophiles.* The reactions outlined in the preceding sections yield new compounds that are important from a structural viewpoint. However, when chlorophosphazenes are employed as the reaction substrates, metal–halogen exchange processes are always possible. At the small-molecule level this is not a problem because the products can always be isolated, albeit occasionally, in very low yields.

On the other hand, if such syntheses are to be used at the macromolecular level, the side reactions would impose severe penalties. Thus, two choices remain—either the use of fluorophosphazene high polymers as substrates (and these are soluble only in fluorocarbon solvents) or the development of an alternative method for the formation of phosphorus–metal bonds in these compounds.

As discussed earlier, phosphazene anions are accessible, and these react with organic electrophiles. We have recently shown that they also react with halogeno-transition-metal carbonyl compounds.[122] Thus, the phosphazene anion (**112**) prepared from the hydridophosphazene and methyllithium at −78°C in tetrahydrofuran reacts with $FeI(CO)_2(\eta\text{-}C_5H_5)$ to yield the iron-bound phosphazene (**113**).

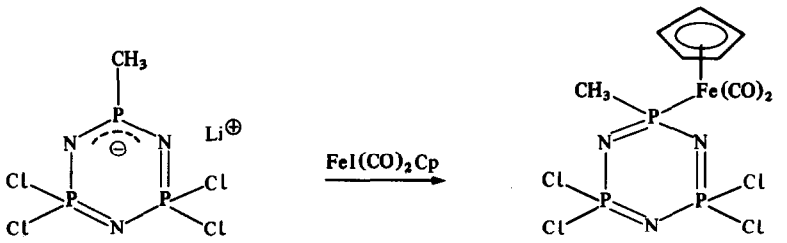

(7)

112 **113**

A similar reaction has been carried out with a phenylphosphazene anion analogous to **112**, but with the anion prepared by P—P bond cleavage of a phenyl bi(cyclophosphazene) with lithium triethylborohydride in the manner discussed earlier. The structure of **113** was confirmed by X-ray diffraction techniques. Ruthenium, chromium, molybdenum and tungsten *gem*-phenyl counterparts of **113** have also been prepared by similar techniques.

5. *Transition metals linked to pendent spacer groups*

A wide variety of methods can be envisaged for the binding of transition-metal organometallic units to organic or inorganic side groups, themselves attached to a phosphazene ring or chain (**114**). In our laboratory, we have examined a number of these possibilities, often making use of the following protocol. First, a phosphazene is synthesized that bears side groups with terminal binding sites for transition metals. Second, a complex is made by interaction of the side group with the metal. Third, the properties of the complex (catalysis, polymerization etc.) are studied. The advantage of this procedure is that it is possible to make use of well-established transition-metal coordination reactions. This has allowed much of the work in this area to be tested first at the small-molecule level, and then extended to the high polymers.

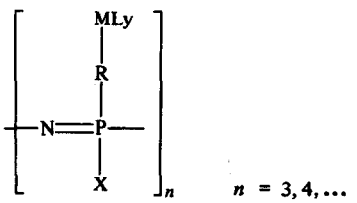

114

Six areas of chemistry have been developed by the use of this approach: (a) binding of iron porphyrins to phosphazenes either through pendent imidazole units or by covalent binding to the skeleton, (b) linkage of copper phthalocyanines to phosphazenes via organic spacer groups, (c) attachment of phosphine units to aryloxy substituent groups followed by coordination to transition-

metal complexes, (d) conversion of *closo*-carboranylphosphazenes to *nido*-carboranyl derivatives and subsequent reaction with metal complexes, (e) attachment of metallocene units to phosphazenes through P—C bonds, and (f) addition of metal carbonyls to phosphazenes that bear pendent acetylenic side groups. The first two approaches will be mentioned only briefly, because organometallic species are not involved.

(a) *Polyphosphazenes as carrier molecules for iron porphyrins.* Several different systems have been studied,[143,144] and these are depicted schematically as **115–117**. In each case, the Fe(III) porphyrin system was prepared first, and this was reduced to the Fe(II) form by treatment with dithionite.

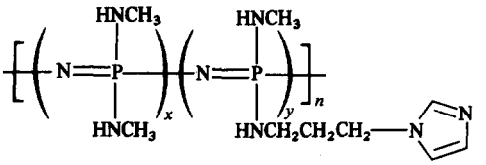

115

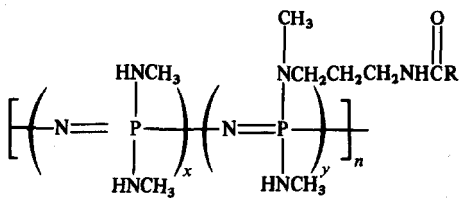

116

$x = 10y, \quad n \approx 15{,}000$

R = CH_2—CH_2—C(=O)—N(H)—C_6H_4—porphyrin (from **117a**)

R = CH_2—CH_2—porphyrin (from **117b**)

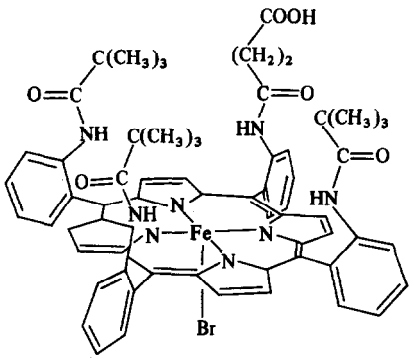

117a

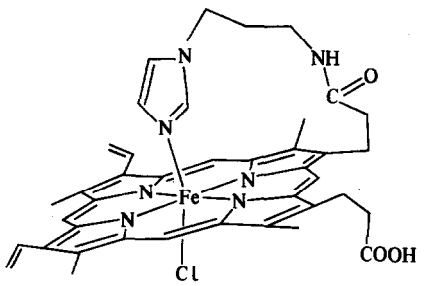

117b

When heme or hemin interacts with the basic, water-soluble control polymer $[NP(NHMe)_2]_n$ in aqueous media, weak (probably acid–base type) adducts are formed that involve pendent carboxylic acid units of the porphyrin ring.[143] The products are bis-aquo-heme or hematin–hemin hydroxide derivatives. By contrast, the polyphosphazene with a pendent imidazole unit (**115**) binds strongly to both heme and hemin via coordination of the imidazole function to the iron atoms to give six-coordinate metal systems. In aqueous media, the heme complex of **115** is irreversibly oxidized to the Fe(III) form in the presence of oxygen. However, the same polymeric complex in the form of thin solid films undergoes cycling between the Fe(II) and Fe(III) forms in the presence or absence of oxygen, with the *polymer* apparently functioning as an internal reducing agent. This is an interesting phenomenon from the viewpoint of potential electrode mediator catalysis.

Covalent binding of Collman-type picket fence and Traylor-type iron porphyrins to a carrier polyphosphazene has also been accomplished (**116** and **117**), and the oxygen-binding behavior and electrochemical characteristics have been studied.[144]

Although not strictly part of the organometallic chemistry of phosphazenes, it should be noted that copper phthalocyanines have been linked to cyclic and high-polymer phosphazenes via organic spacer groups.[145] These generate electrically semiconducting solids when doped with iodine.

(b) *Phosphine-linked phosphazenes.* As mentioned earlier, Main-Group organometallic chemistry

has been used to prepare several cyclic and high-polymeric phosphazenes that bear pendent triarylphosphine groups. Typical compounds of this type are shown as **118–120**.[146]

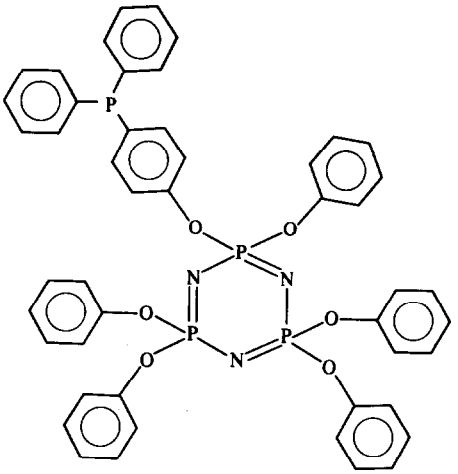

118

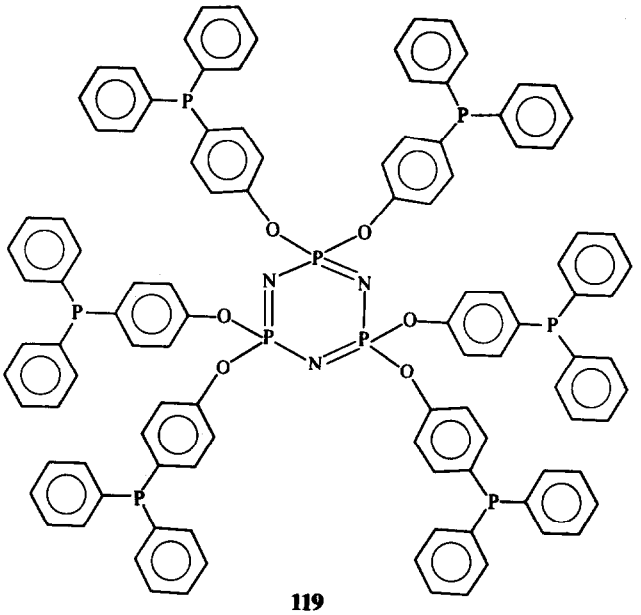

119

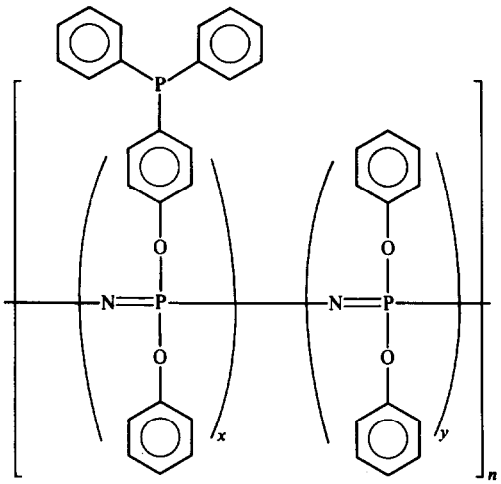

120

These compounds are of interest from three points of view. First, the question exists of whether coordination to a metal would take place through the pendent phosphine unit or through the skeletal nitrogen atoms. In fact, for all the cases studied so far {in which the metallo species was AuCl, $H_2Os_3(CO)_{10}$, $Mn(CO)_2THF(\eta\text{-}C_5H_5)$, $Fe(CO)_3(PhCH{=}CHCOCH_3)$ or $[RhCl(CO)_2]_2$}, the coordination has involved the pendent phosphine groups only.[146] This can be attributed to the relatively low basicity of the skeletal nitrogen atoms when weakly electron-withdrawing side groups, such as phenoxy, are present, and to steric shielding of the nitrogen atoms by the aryloxy groups.

The second question bears on the behavior of all species in which a transition metal is linked to a carrier molecule. If the transition metal can form a diphosphine complex, does this lead to the formation of *inter*molecular crosslinks as phosphine units from different carrier molecules bond to the same metal atom or, in the case of species **119** and **120**, is *intra*molecular linkage preferred, to generate a transannular or intrachain coupled system?

Monophosphine complexes were obtained with the gold, osmium and manganese complexes.[146] However, the iron and rhodium organometallic species formed diphosphine complexes, with both intra- and intermolecular coupling to the phosphines in species **119**. The high polymer **120** underwent

insolubilization through cross-linking in the presence of the same organometallic reagents.[146] A similar cross-linking process was detected when **120** reacted with cobalt carbonyl.[147]

The third question concerns the catalytic activity of transition-metal organometallic species linked to **118–120**. The osmium complexes of **118–120** were catalysts for the isomerization of 1-hexene to 2-hexene.[146] Moreover, the cobalt carbonyl adducts of **118** and **120** were active as hydroformylation catalysts.[147] The main disadvantage of the high-polymer cobalt hydroformylation system is the slow decline in catalytic activity in successive catalytic cycles, which is due to a cobalt-mediated cleavage of the bond that links the pendent phosphorus atom to the supporting aryloxy group. Thus, the phosphino function is lost, and the cobalt escapes with it.[147]

(c) *Metallo-carboranyl-linked phosphazenes.* As discussed in an earlier section, *closo*-carboranyl phosphazenes can be prepared either by the reactions of lithiocarboranes with chlorophosphazenes or by the interaction of propynylphosphazenes with decaborane.[94,148] Such *closo*-carboranyl phosphazenes can be converted to the *nido*-carboranyl anion derivatives by treatment with a base.[148]

When a methylene spacer group separates the carboranyl unit from the phosphazene ring (**121**) or chain (**123**), the *nido*-carboranyl anion units can be induced to form complexes with transition-metal species.[148] For example, compounds **121** and **123** react with $RhCl(PPh_3)_3$ to yield neutral complexes (**122** and **124**) with the transition metal associated with the open face of the carboranyl unit. Similarly, the dianionic derivatives (**125** and **127**) react with $Mo(CO)_6$ or $W(CO)_6$ to form the dianionic complexes depicted as **126** and **128**, in which the metal carbonyl units are bound to the open face of the carborane *and* the phosphazene skeleton.

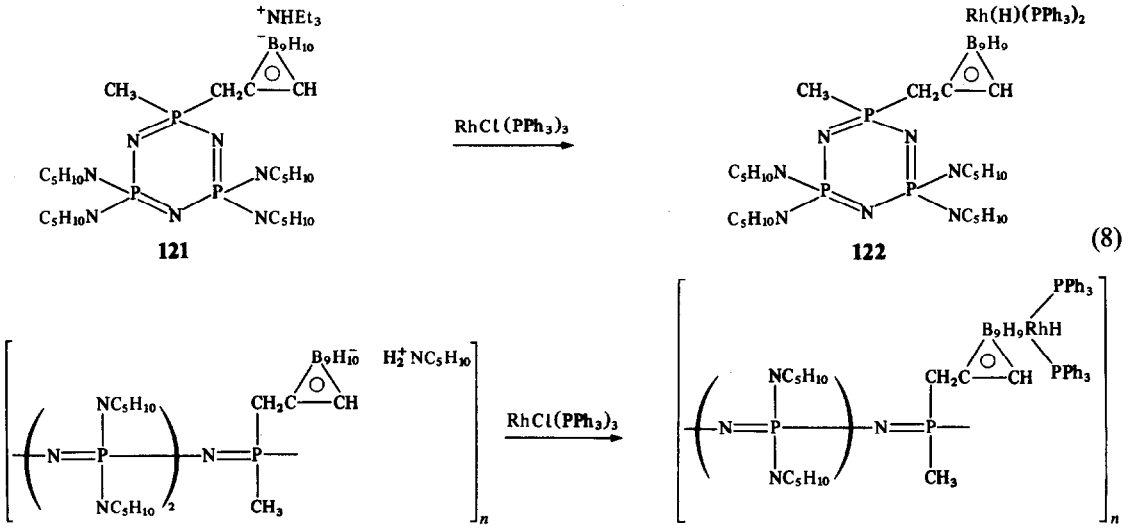

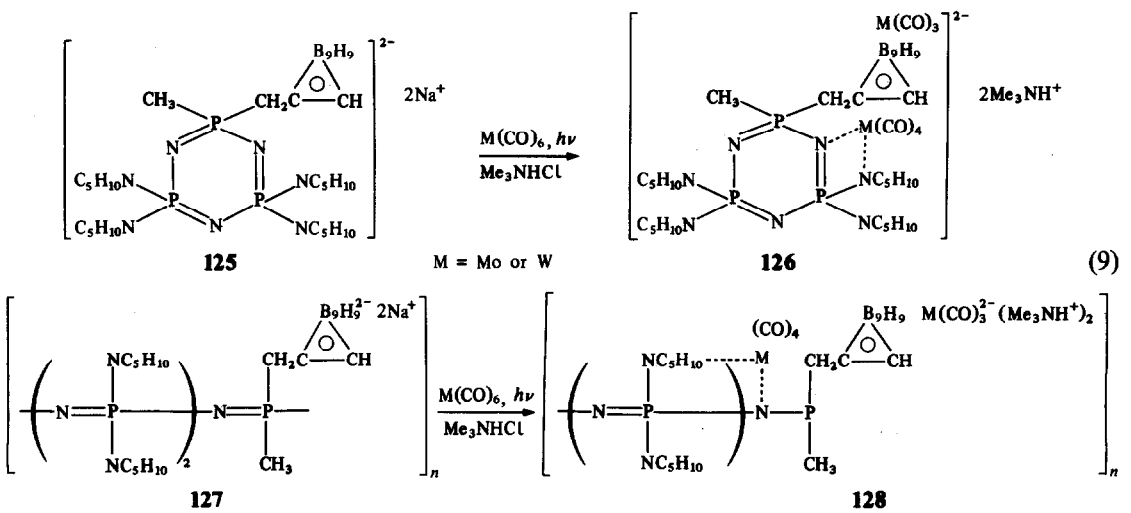

If the methylene spacer group between the carboranyl function and the phosphazene skeleton is not present as, for example, in species **56** discussed earlier, then although *nido*-carborane anion formation is possible, no transition-metal derivatives could be formed. We presume that steric shielding of the open face of the carborane by the phosphazene ring is responsible for this behavior.[148]

(d) *Metallocene-linked phosphazenes.* The reactions between lithiometallocenes and halogenophosphazenes have been studied intensively in our laboratories by Lavin, Riding and Suszko.[149–153] These reactions have led to the isolation of the first hybrid phosphazene–metallocene compounds, species that have proved to be of considerable interest from a structural point of view[149–151] and as starting materials for the preparation of metallocenylphosphazene high polymers.[152]

The reactions of lithiometallocenes with chloro- and fluorophosphazenes can be understood in terms of the mechanisms discussed earlier for the reactions of organolithium reagents with the same substrates. Specifically, the reactions of lithioferrocene or lithioruthenocene with *fluoro*phosphazenes are cleaner than the corresponding reactions with chlorophosphazenes. With fluorophosphazenes, the main reaction is substitution, i.e. replacement of fluorine atoms by metallocene units. With chlorophosphazenes, the reactions are complex, with substitution being accompanied by metal–halogen exchange and associated side reactions, such as ring coupling, metal–hydrogen exchange, skeletal cleavage and so on. The simpler reactions with fluorophosphazenes will be discussed first.

(i) Reactions of mono- and dilithiometallocenes with $(NPF_2)_3$ or $(NPF_2)_4$. These interactions are summarized in Scheme 16.[149,150] Thus, $(NPF_2)_3$ and $(NPF_2)_4$ react with lithioferrocene or lithioruthenocene first to yield the monosubstituted products (**129** and **131**). Further substitution then takes place at a nongeminal site to give the disubstituted products (**130** and **132**).

Dilithioferrocene or dilithioruthenocene react with the trimer, $(NPF_2)_3$, to give predominantly the transannular-linked (ansa) product (**133**). This reaction also yields a small quantity of an intermolecular-coupled product (**134**) with the ruthenium system. The dilithiometallocenes also react with the cyclic tetramer, $(NPF_2)_4$, in a similar manner to give the isomeric transannular products (**135** and **136**). Most of these structures have been confirmed by X-ray crystallography,[149–151] and all the structures have been verified by NMR analysis.

Of special interest from a structural point of view is the fact that the transannular tetramer **135** (where M = Ru) reacts further with dilithioruthenocene to generate the "double transannular" tetramer shown as **137**.[153] An X-ray study of this compound has shown that, as in the case of all the other transannular metallocenyl phosphazenes, the ring strain is accommodated almost entirely by the phosphazene ring through puckering. Thus, in **137**, the cyclic tetrameric phosphazene ring assumes a highly puckered boat conformation in order to allow two cyclopentadienyl units in each metallocene unit to retain their coplanarity. Moreover, the shape of the molecule **137** is such that the remaining fluorine atoms cannot be replaced by conventional organic nucleophiles such as sodium trifluoroethoxide. Presumably, a S_N2-type backside attack on the phosphorus atom is inhibited by steric shielding.

It should also be noted that dilithio-bis-benzenechromium reacts with $(NPF_2)_3$ to form a transannular derivative.[154]

(ii) Reactions between mono- and dilithiometallocenes and $(NPCl_2)_3$ or $(NPCl_2)_4$. In Scheme 17 we summarize some of the products that are formed when $(NPCl_2)_3$ reacts with the mono- or dilithiometallocenes.[109] Monolithioferrocene or monolithioruthenocene reacts to give the monosubstituted derivative (**138**) together with the asymmetrical bi(cyclophosphazene) (**139**). Product **139** is reminiscent of the species formed when Grignard reagents react with $(NPCl_2)_3$, and is a clear indication that metal–halogen exchange reactions are involved with lithiometallocene reactions also.

Further evidence for the involvement of metal–halogen exchange processes is provided by the reactions of the dilithiometallocenes with $(NPCl_2)_3$. As shown in Scheme 17, the products from these reactions include **140** and **141**, in which a chlorine atom has replaced one of the lithium atoms and, in the case of dilithioferrocene in the presence of TMEDA, species **142**, in which a ferrocenyl unit bridges the P—P bond of a bi(cyclophosphazene) compound.[150] These structures have been confirmed by X-ray crystallography and NMR analysis.[150]

A reaction mechanism has been proposed that explains the formation of all these products (**138–142**).[150] The mechanism most compatible with the data is based on the assumption that the *first* step is probably metal–halogen exchange to give species **143** (Scheme 18). By substitution, this then yields species **144** which, by reaction with $(NPCl_2)_3$, gives **139**. Species **138** could be formed by

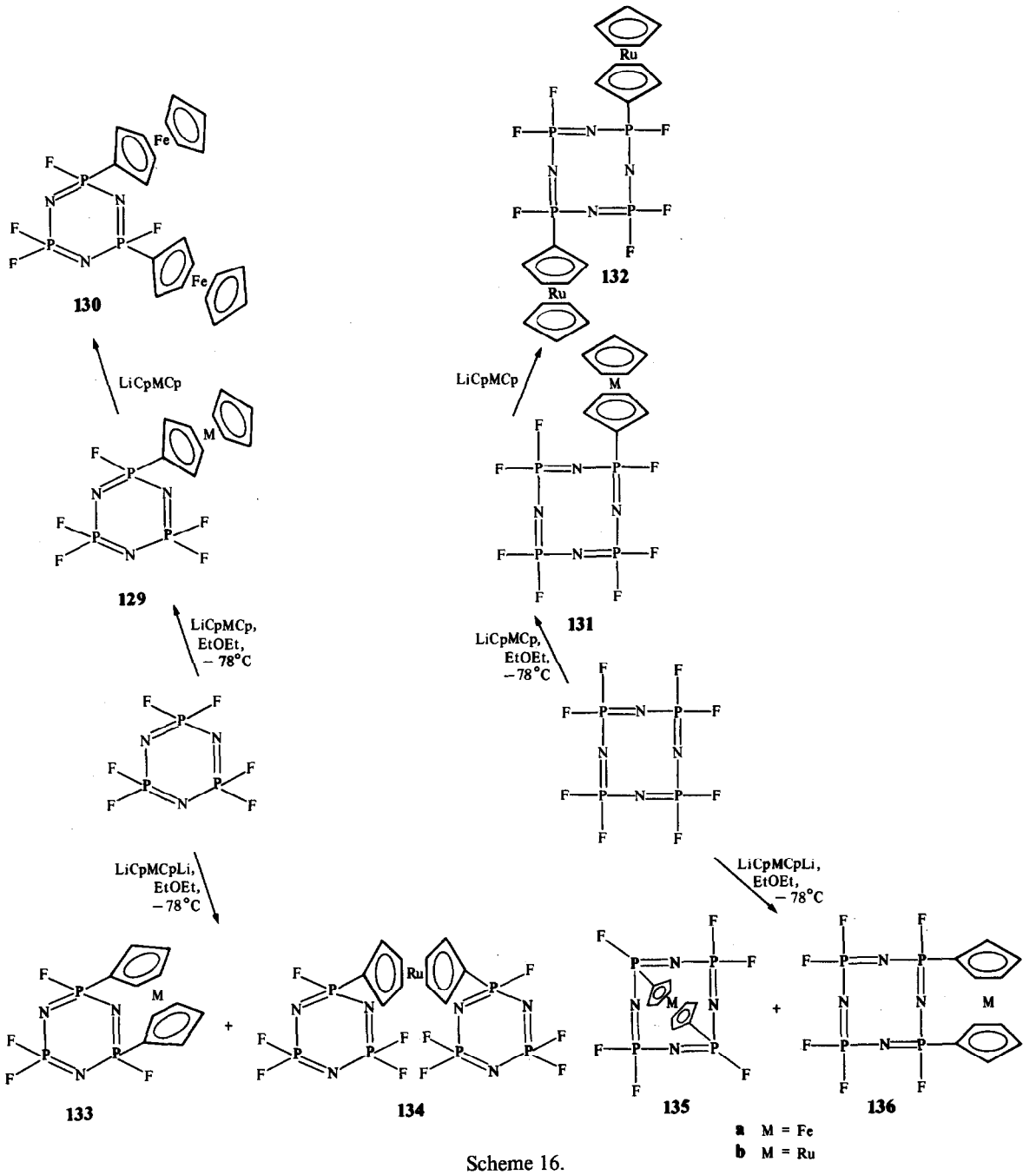
Ru
132
LiCpMCp
M
131
LiCpMCp,
EtOEt,
−78°C
Fe
130
LiCpMCp
M
129
LiCpMCp,
EtOEt,
−78°C
LiCpMCpLi,
EtOEt,
−78°C
LiCpMCpLi,
EtOEt,
−78°C
M
Ru
133
134
135
136
a M = Fe
b M = Ru

Scheme 16.

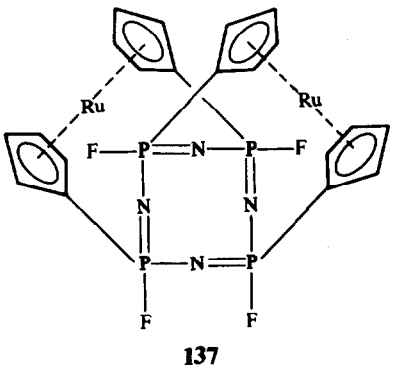
Ru
Ru
137

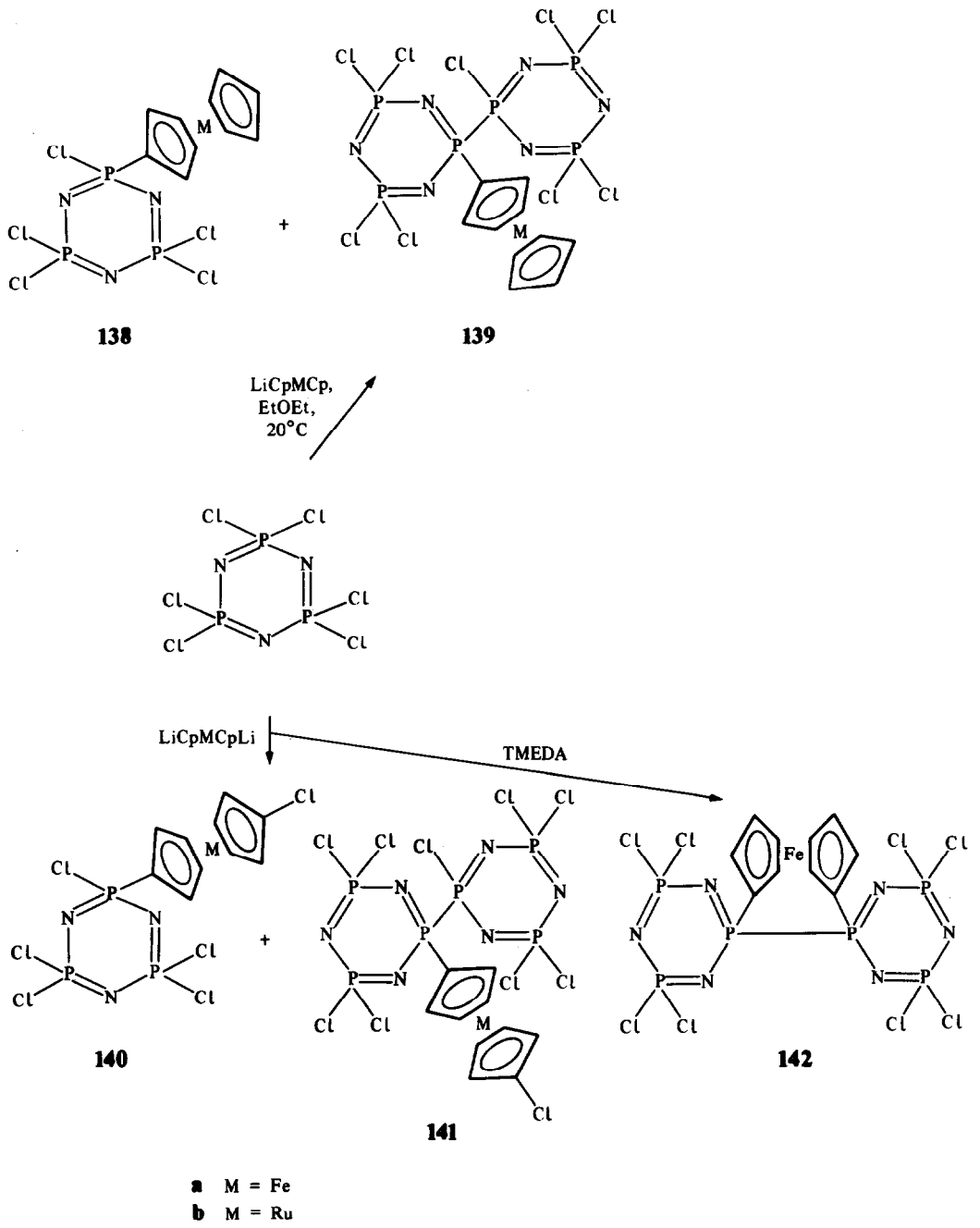

Scheme 17.

abstraction of a chlorine atom from $(NPCl_2)_3$ by **144**. This mechanism appears to be an unnecessarily complex one for the formation of **138**, which could, in principle, be formed directly by a substitution reaction between $(NPCl_2)_3$ and the lithiometallocene. Indeed, the experimental data from the reaction with monolithiometallocenes do not distinguish between these two mechanisms for formation of **138**. However, the data from the reaction with the *di*lithiometallocenes favor a pathway to **138** that proceeds via reactions (c)–(e) (Scheme 18).

In terms of this mechanism, the appearance of a chlorine atom in **140** and **141** in the place previously occupied by lithium, can be explained by metal–halogen exchange. In this context, the overall influence of metal–halogen exchange can be summarized in one reaction, between a mixture of $(NPCl_2)_3$ and $(NPCl_2)_4$ and either mono- or dilithioferrocene.[151] The product (**145**) has both a

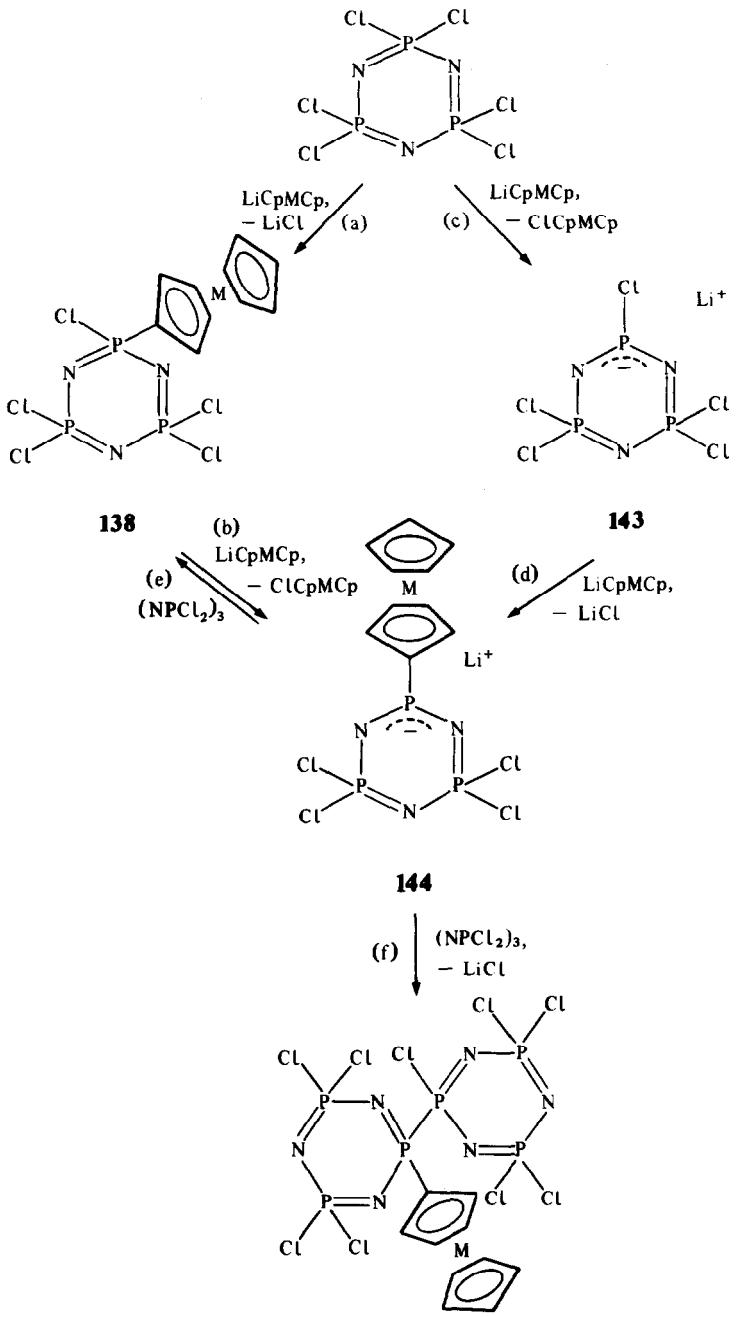
LiCpMCp,
– LiCl
(a)
(c)
LiCpMCp,
– ClCpMCp
M
Li+
138
143
(b)
LiCpMCp,
– ClCpMCp
(e)
(NPCl2)3
(d)
LiCpMCp,
– LiCl
144
(f)
(NPCl2)3,
– LiCl
139

Scheme 18.

ring-linking P—P bond and (in the case of dilithioferrocene) a chlorine atom in place of a lithium atom. The structure of **145** (where X = H) has been confirmed by X-ray crystallography.[151]

$$(NPCl_2)_3 + (NPCl_2)_4 \xrightarrow[\text{LiCpFeCpLi, X = Cl}]{\text{LiCpFeCp, X = H}}$$

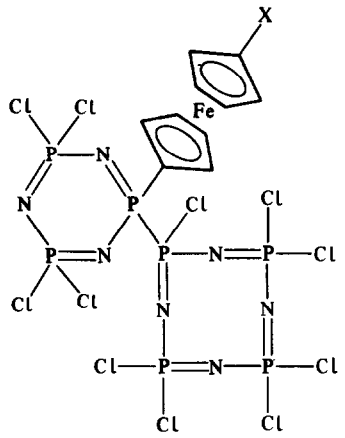

(10)

145

a X = H
b X = Cl

In the absence of the trimer, the tetramer $(NPCl_2)_4$ reacts with monolithioferrocene to yield the ring-contracted species (**146**).[151] The formation of this product can be understood by the mechanism shown in Scheme 19.[151]

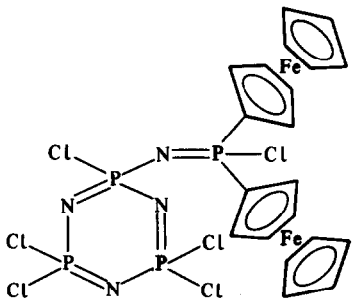

146

(iii) High-polymeric metallocenylphosphazenes. Cyclotriphosphazenes, such as **129** or **138** are of interest not only from a synthetic and structural point of view but also because they can be induced to undergo thermal phosphazene ring-opening polymerization to give linear higher polymers with metallocenyl side groups. Release of phosphazene ring strain in **138** induces a more facile polymerization reaction than in the case of **129**. The fluorine atoms can then be replaced by treatment with organic nucleophiles, such as sodium trifluoroethoxide, to yield water- and heat-stable polymers (**148**, **150** and **152**). The molecular weights of these polymers are in the range of 2×10^6, which corresponds to an average of roughly 5000 repeating units per chain. These reactions are summarized in Schemes 20–22.[152]

The copolymerization reaction shown in Scheme 22 provides a method for the incorporation of two different types of metal centers into the same macromolecule. This is of prospective interest for catalyst, electrode mediator, or electronically-active applications. Polymers of types **148** and **150** are weak semiconductors when doped with iodine.

(e) *Metallo complexes formed by acetylenic phosphazenes.* Finally it is possible through the use of organolithium- or organocopper-mediated reactions to synthesize cyclophosphazenes with phenylacetylenic or propynyl side groups attached to the phosphazene ring.[60,85] It is well-known that acetylenic units form pi complexes with transition metals, especially dicobalt carbonyl species, and that such complexes can serve as catalysts for the cyclotrimerization of acetylenes to benzene derivatives. Chivers[60] first reported a cobalt–phosphazene compound of this type (**153**).

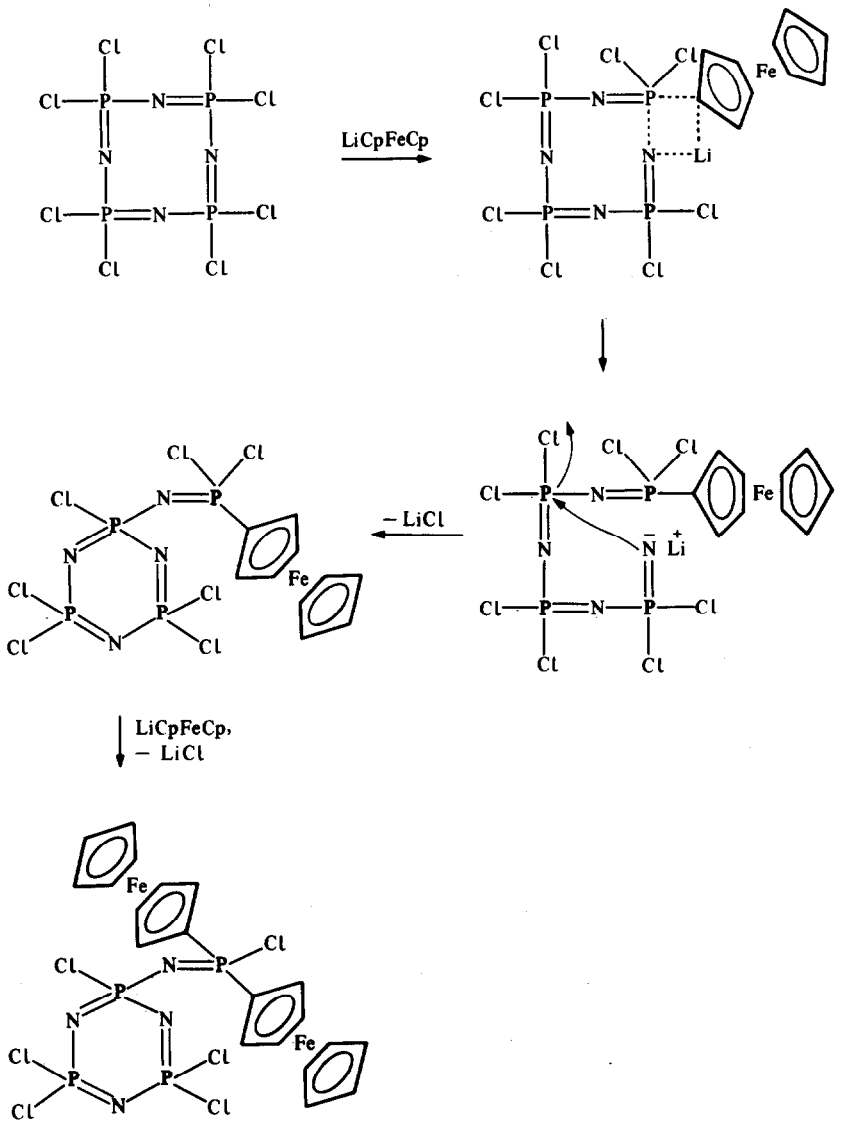

Scheme 19.

We have explored the application of these principles to a broad series of propynyl phosphazenes synthesized in our laboratory.[85] In particular, a number of propynylphosphazenes have been treated with cobalt octacarbonyl to yield the complexes shown as **154** and **155**.[155] Species **154** and **155** induce the cyclotrimerization of diphenylacetylene or phenylacetylene. They also induce the co-oligomerization of propynylphosphazenes with phenylacetylenes to yield benzenoid products with pendent phosphazene rings. Evidence was also obtained that prop-2-ynyl derivatives (but not prop-1-ynyl derivatives) themselves cyclotrimerize to yield benzene rings with three pendent cyclophosphazene rings.

V. CONCLUSIONS

It will be clear that the organometallic chemistry of phosphazenes is a rich and diverse field of study, and one that will form the basis of more extensive explorations in the future.

At the fundamental level, the challenge for the future will be to understand the sometimes complex reaction mechanisms, to expand the chemistry into new areas of transition-metal reactions, to study the novel forms of binding between transition metals and phosphazenes, and to probe the

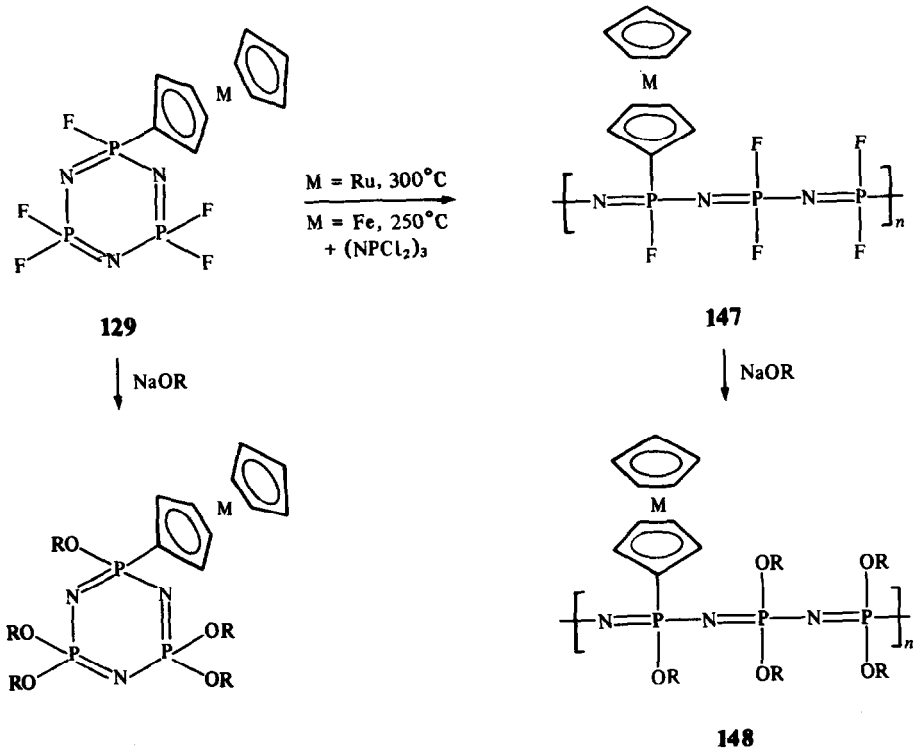

129 **147** **148**

Scheme 20.

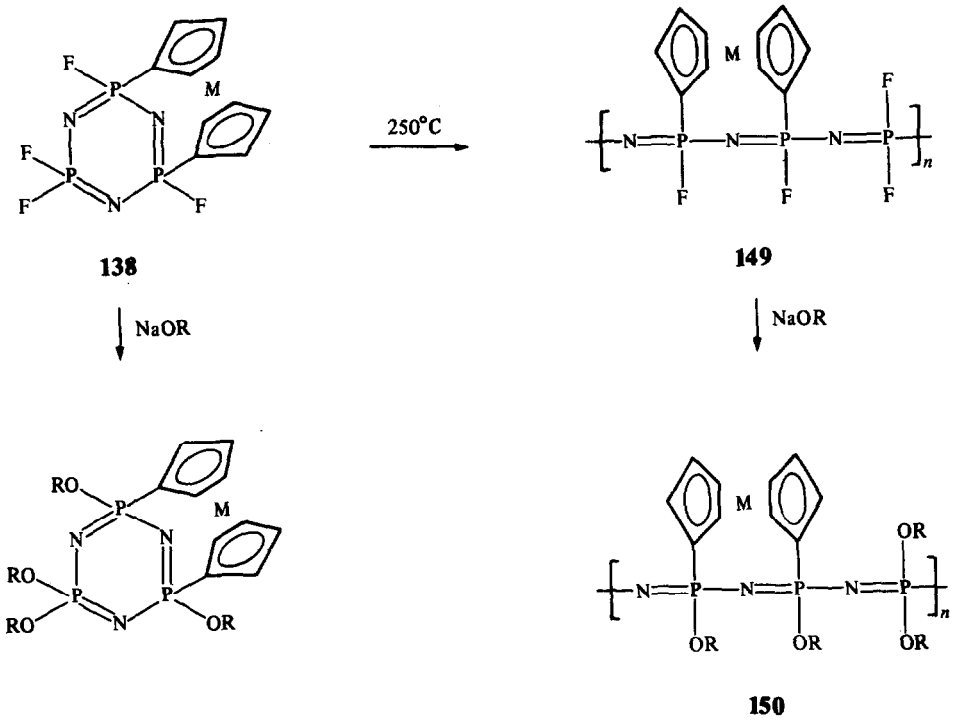

138 **149** **150**

OR = OCH_2CF_3

Scheme 21.

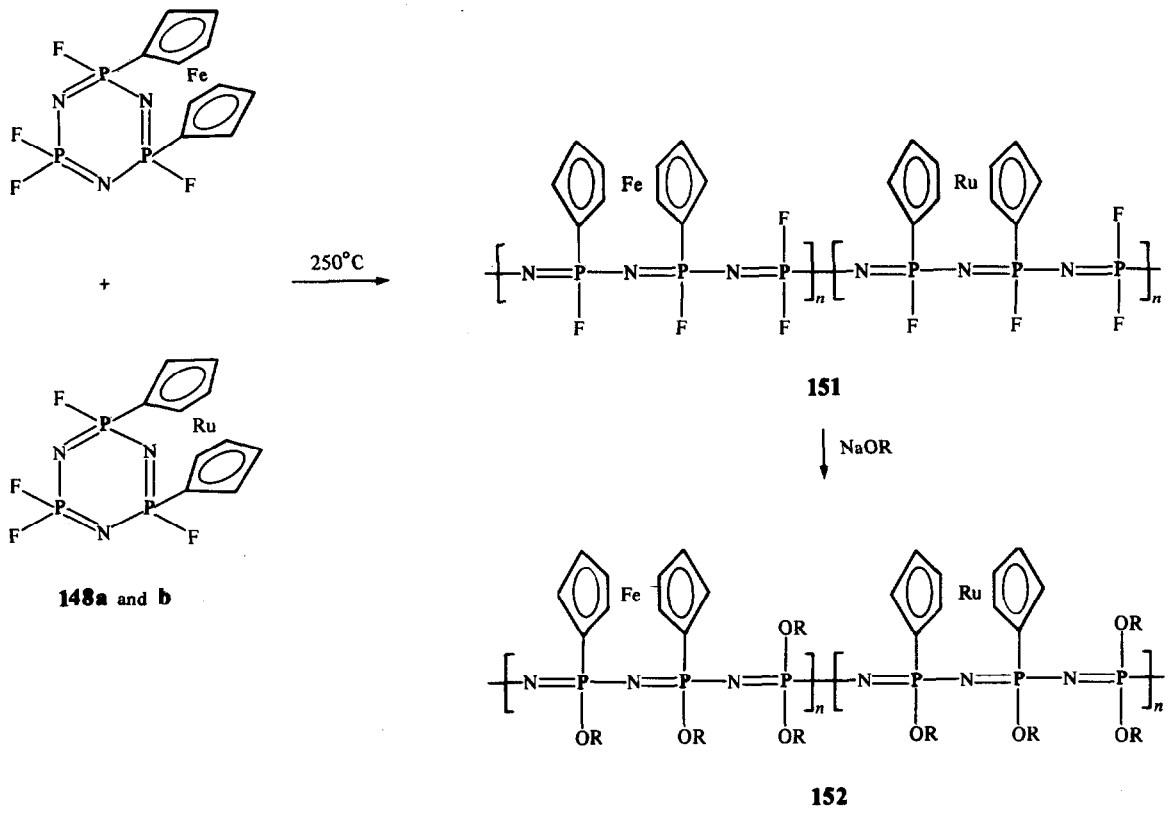

Scheme 22.

possibility that metallocene-type sandwich complexes can be prepared with a metal bound to the pi electrons of a phosphazene ring.

The use-oriented prospects for this area of chemistry are also promising. Examples have been given of polymer-bound catalysts that utilize the polyphosphazene chain, and of organometallic

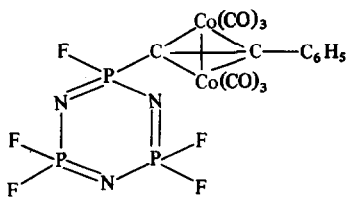

153

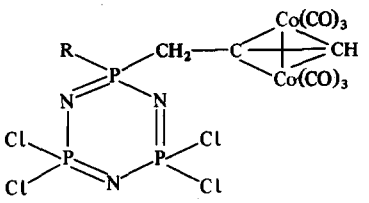

154

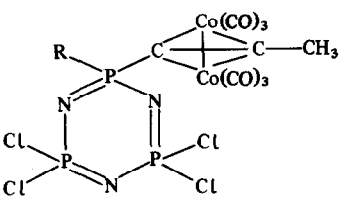

155

R = CH_3, C_2H_5, n-C_3H_7, n-C_4H_9, i-C_3H_7, t-C_4H_9 or C_3H_5

phosphazene high polymers that are actual or prospective semiconductors, electrode mediator catalysts, magnetic disk or tape precursors, or metal-containing preceramic meterials. The organic-type chemistry of phosphazenes has dominated the development of this field until recently. The time now seems ripe for a much increased emphasis on the organometallic aspects.

Acknowledgements—Our work on the organometallic chemistry of phosphazenes has been generously supported by the U.S. Army Research Office, the Office of Naval Research, Air Force Office of Scientific Research, and NASA.

REFERENCES

1. H. Rose, *Ann. Chem.* 1834, **11**, 131.
2. J. Liebig, *Ann. Chem.* 1834, **11**, 139.
3. C. Gerhardt, *C. R. Acad. Sci.* 1846, **22**, 858.
4. J. H. Gladstone and J. D. Holmes, *J. Chem. Soc.* 1864, **17**, 225.
5. W. Couldridge, *J. Chem. Soc.* 1888, **53**, 398.
6. H. R. Allcock, *Phosphorus–Nitrogen Compounds*. Academic Press, New York (1972).
7. H. R. Allcock, *Polymer* 1980, **21**, 673.
8. R. T. Oakley, S. J. Rettig, N. L. Paddock and J. Trotter, *J. Am. Chem. Soc.* 1985, **107**, 6923 (footnote 16b).
9. See, for instance, H. R. Allcock, N. M. Tollefson, R. A. Arcus and R. R. Whittle, *J. Am. Chem. Soc.* 1985, **107**, 5166.
10. H. R. Allcock, *Acc. Chem. Res.* 1979, **12**, 351.
11. H. R. Allcock and R. L. Kugel, *J. Am. Chem. Soc.* 1965, **87**, 4216.
12. H. R. Allcock, R. L. Kugel and K. J. Valan, *Inorg. Chem.* 1966, **5**, 1709.
13. H. R. Allcock and R. L. Kugel, *Inorg. Chem.* 1966, **5**, 1716.
14. H. R. Allcock, *Sci. Prog.* 1980, **66**, 355; *Rings, Clusters, and Polymers of the Main Groups Elements. ACS Symp. Ser.* (Edited by A. H. Cowley) 1983, **232**, 40.
15. H. R. Allcock, *Chem. Eng. News* 1985, **63**, 22.
16. L. F. Audrieth, R. Steinman and A. D. F. Toy, *Chem. Rev.* 1943, **32**, 109.
17. H. Bode, K. Butow and G. Lienau, *Chem. Ber.* 1948, **81**, 547.
18. E. T. McBee, H. R. Allcock, R. Caputo, A. Kalmus and C. W. Roberts, *U.S. Gov. Astia Rep.* 1959, AD 209, 669.
19. R. Ratz, H. Schroeder, H. Ulrich, E. Kober aand C. Grundmann, *J. Am. Chem. Soc.* 1982, **84**, 551.
20. B. W. Fitzsimmons and R. A. Shaw, *J. Chem. Soc.* 1964, 1735.
21. M. Becke-Goehring, K. John and E. Fluck, *Z. Anorg. Allg. Chem.* 1959, **302**, 103.
22. K. John, T. Moeller and L. F. Audrieth, *J. Am. Chem. Soc.* 1960, **82**, 5616.
23. T. Moeller and S. Lanoux, *Inorg. Chem.* 1963, **2**, 1061.
24. S. K. Ray and R. A. Shaw, *J. Chem. Soc.* 1961, 872.
25. D. P. Tate, *J. Polym. Sci., Polym. Symp.* 1974, **48**, 33.
26. (a) R. E. Singler, N. S. Schneider and G. L. Hagnauer, *Polym. Eng. Sci.* 1975, **15**, 322; (b) R. E. Singler, G. L. Hagnauer and R. W. Sicka, *ACS Symp. Ser.* (Edited by J. C. Arthur) 1984, **260**, 143.
27. P. M. Blonsky, D. F. Shriver, P. E. Austin and H. R. Allcock, *J. Am. Chem. Soc.* 1984, **106**, 6854.
28. H. R. Allcock and T. J. Fuller, *Macromolecules* 1980, **13**, 1338.
29. H. R. Allcock, P. E. Austin and T. X. Neenan, *Macromolecules* 1982, **15**, 689.
30. T. X. Neenan and H. R. Allcock, *Biomaterials* 1982, **3**, 78.
31. H. R. Allcock, T. X. Neenan and W. C. Kossa, *Macromolecules* 1982, **15**, 693.
32. H. R. Allcock, P. P. Greigger, J. E. Gardner and J. L. Schmutz, *J. Am. Chem. Soc.* 1979, **101**, 606.
33. H. R. Allcock, W. C. Hymer and P. E. Austin, *Macromolecules* 1983, **16**, 1401.
34. H. R. Allcock and S. Kwon, *Macromolecules* 1986, **19**, 1502.
35. T. Moeller and F. Tsang, *Chem. Ind. (London)* 1962, 361.
36. C. W. Allen and T. Moeller, *Inorg. Chem.* 1968, **7**, 2177.
37. C. W. Allen, F. Y. Tsang and T. Moeller, *Inorg. Chem.* 1968, **7**, 2183.
38. C. W. Allen and T. Moeller, *Inorg. Synth.* 1970, **12**, 293.
39. C. W. Allen and A. J. White, *Inorg. Chem.* 1974, **13**, 1220.
40. C. W. Allen and P. L. Toch, *J. Chem. Soc., Dalton Trans.* 1974, 1685.
41. T. Chivers and N. L. Paddock, *Inorg. Chem.* 1972, **11**, 848.
42. C. W. Allen, G. E. Brunst and M. E. Perlman, *Inorg. Chim. Acta* 1980, **41**, 265.
43. C. W. Allen and P. L. Toch, *Inorg. Chem.* 1981, **20**, 8.

44. C. W. Allen and J. C. Green, *Inorg. Chem.* 1980, **19**, 1719.
45. H. R. Allcock and G. Y. Moore, *Macromolecules* 1975, **8**, 377.
46. C. W. Allen, *Ind. Eng. Chem. Prod. Res. Dev.* 1981, **20**, 77.
47. C. W. Allen, *J. Chem. Soc., Chem. Commun.* 1970, 152.
48. N. L. Paddock, T. N. Ranganathan and S. M. Todd, *Can. J. Chem.* 1971, **49**, 164.
49. E. Niecke, H. Thamm and O. Glemser, *Z. Naturforsch.* 1971, **26B**, 366.
50. T. Moeller, F. Amedeo and F. Y. Tsang, *Inorg. Nucl. Chem. Lett.* 1965, **1**, 49.
51. K. Ramachandran and C. W. Allen, *J. Am. Chem. Soc.* 1982, **104**, 2396.
52. J. Blumentritt and T. Moeller, *Inorg. Nucl. Chem. Lett.* 1978, **14**, 263.
53. T. N. Ranganathan, S. M. Todd and N. L. Paddock, *Inorg. Chem.* 1973, **12**, 316.
54. H. T. Searle, J. Dyson, T. N. Ranganathan and N. L. Paddock, *J. Chem. Soc., Dalton Trans.* 1975, 203.
55. K. D. Gallicano, R. T. Oakley, N. L. Paddock, S. J. Rettig and J. Trotter, *Can. J. Chem.* 1977, **55**, 304.
56. J. G. DuPont and C. W. Allen, *Inorg. Chem.* 1978, **17**, 3093.
57. C. W. Allen and R. P. Bright, *Inorg. Chem.* 1983, **22**, 1291.
58. C. W. Allen, J. L. Desorcie and K. Ramachandran, *J. Chem. Soc., Dalton Trans.* 1984, 2843.
59. T. Chivers, *Inorg. Nucl. Chem. Lett.* 1971, **7**, 827.
60. R. D. Sharma, S. J. Rettig, N. L. Paddock and J. Trotter, *Can. J. Chem.* 1982, **60**, 535.
61. J. G. DuPont and C. W. Allen, *Macromolecules* 1979, **12**, 169.
62. C. W. Allen and J. G. DuPont, *Ind. Eng. Chem. Prod. Res. Dev.* 1979, **18**, 80.
63. G. Rosset, *C. R. Acad. Sci.* 1925, **180**, 750.
64. H. Bode and H. Bach, *Chem. Ber.* 1942, **75B**, 215.
65. M. Biddlestone and R. A. Shaw, *J. Chem. Soc. A* 1969, 178.
66. M. Biddlestone and R. A. Shaw, *J. Chem. Soc., Chem. Commun.* 1968, 407.
67. M. Biddlestone and R. A. Shaw, *J. Chem. Soc. A* 1971, 2715.
68. P. J. Harris, J. L. Desorcie and H. R. Allcock, *J. Chem. Soc., Chem. Commun.* 1981, 852.
69. H. R. Allcock, J. L. Desorcie and P. J. Harris, *J. Am. Chem. Soc.* 1983, **105**, 2814.
70. H. R. Allcock, D. J. Brennan and J. G. Graaskamp, unpublished work.
71. P. J. Harris, K. B. Williams and B. L. Fisher, *J. Org. Chem.* 1984, **49**, 406.
72. M. Biddlestone and R. A. Shaw, *J. Chem. Soc., Chem. Commun.* 1965, 205.
73. M. Biddlestone and R. A. Shaw, *J. Chem. Soc. A* 1970, 1750.
74. K. D. Lavin, Ph.D. thesis, The Pennsylvania State University, University Park (1985).
75. M. K. Feldt and T. Moeller, *J. Inorg. Nucl. Chem.* 1968, **30**, 2351.
76. G. Tesi and P. J. Slota, *Proc. Chem. Soc., London* 1960, 404.
77. H. R. Allcock, J. L. Desorcie and L. J. Wagner, *Inorg. Chem.* 1985, **24**, 333.
78. P. J. Harris and H. R. Allcock, *J. Am. Chem. Soc.* 1978, **100**, 6512.
79. H. R. Allcock and P. J. Harris, *J. Am. Chem. Soc.* 1979, **101**, 6221.
80. H. R. Allcock and P. J. Harris, *Inorg. Chem.* 1981, **20**, 2844.
81. P. J. Harris and H. R. Allcock, *J. Chem. Soc., Chem. Commun.* 1979, 714.
82. H. R. Allcock, P. J. Harris and M. S. Connolly, *Inorg. Chem.* 1981, **20**, 11.
83. P. J. Harris, M. A. Schwalke, V. Liu and B. L. Fisher, *Inorg. Chem.* 1983, **22**, 1812.
84. H. R. Allcock, P. J. Harris and R. A. Nissan, *J. Am. Chem. Soc.* 1981, **103**, 2256.
85. R. J. Ritchie, P. J. Harris and H. R. Allcock, *Macromolecules* 1979, **12**, 1014.
86. H. R. Allcock, R. J. Ritchie and P. J. Harris, *Macromolecules* 1980, **13**, 1332.
87. H. R. Allcock and M. S. Connolly, *Macromolecules* 1985, **18**, 1330.
88. H. R. Allcock, M. S. Connolly and R. R. Whittle, *Organometallics* 1983, **2**, 1514.
89. M. Biddlestone and R. A. Shaw, *Phosphorus Relat. Group V Elem.* 1973, **3**, 95.
90. P. J. Harris and C. L. Fadeley, *Inorg. Chem.* 1983, **22**, 561.
91. H. Winter and J. C. van de Grampel, *J. Chem. Soc., Chem. Commun.* 1984, 489.
92. H. Winter and J. C. van de Grampel, *Recl. Trav. Chim. Pays-Bas* 1984, **103**, 241.
93. A. G. Scopelianos, J. P. O'Brien and H. R. Allcock, *J. Chem. Soc., Chem. Commun.* 1980, 198.
94. H. R. Allcock, A. G. Scopelianos, J. P. O'Brien and M. Y. Bernheim, *J. Am. Chem. Soc.* 1981, **103**, 350.
95. P. J. Harris and L. A. Jackson, *Organometallics* 1983, **2**, 1477.
96. A. B. Burg and A. P. Caron, *J. Am. Chem. Soc.* 1959, **81**, 836.
97. (a) H. R. Allcock, D. B. Patterson and T. L. Evans, *J. Am. Chem. Soc.* 1977, **99**, 6095; (b) R. H. Neilson and P. Wisian-Neilson, *J. Am. Chem. Soc.* 1980, **102**, 2848.
98. H. R. Allcock, T. L. Evans and D. B. Patterson, *Macromolecules* 1980, **13**, 201.
99. T. L. Evans, D. B. Patterson, P. R. Suszko and H. R. Allcock, *Macromolecules* 1981, **14**, 218.
100. H. R. Allcock and C. T.-W. Chu, *Macromolecules* 1979, **12**, 551.
101. J. R. MacCallum and J. Tanner, *J. Polym. Sci., Part A* 1968, **6**, 3163.
102. C. F. Liu and R. L. Evans, U.S. Patent 3,169,933 (1965); *C.A.* 1965, **63**, 704e.
103. H. R. Allcock, R. L. Kugel and E. J. Walsh, *J. Chem. Soc., Chem. Commun.* 1970, 1283.

104. H. P. Calhoun, R. H. Lindstrom, R. T. Oakley, N. L. Paddock and S. M. Todd, *J. Chem. Soc., Chem. Commun.* 1975, 343.
105. K. D. Gallicano, R. T. Oakley, N. L. Paddock and R. D. Sharma, *Can. J. Chem.* 1981, **59**, 2654.
106. H. R. Allcock, P. R. Suszko and T. L. Evans, *Organometallics* 1982, **1**, 1443.
107. T. L. Evans, T. J. Fuller and H. R. Allcock, *J. Am. Chem. Soc.* 1979, **101**, 242.
108. H. R. Allcock, T. L. Evans and T. J. Fuller, *Inorg. Chem.* 1980, **19**, 1026.
109. H. R. Allcock, T. J. Fuller and T. L. Evans, *Macromolecules* 1980, **13**, 1325.
110. N. L. Paddock, *Q. Rev. Chem. Soc.* (*London*) 1964, **18**, 168.
111. M. J. S. Dewar, E. A. C. Lucken and M. A. Whitehead, *J. Chem. Soc.* 1960, 2423.
112. H. R. Allcock, *Chem. Rev.* 1972, **72**, 315.
113. J. Dyson, Ph.D. thesis, University of Manchester, Manchester (1964).
114. J. Trotter and S. H. Whitlow, *J. Chem. Soc. A* 1970, 455.
115. M. F. Lappert and G. Srivastava, *J. Chem. Soc. A* 1966, 210.
116. A. Schmidpeter, K. Blanck and F. R. Ahmed, *Angew. Chem., Int. Ed. Engl.* 1976, **15**, 488.
117. F. R. Ahmed, *Acta Cryst.* 1976, **B32**, 3078.
118. T. Moeller and S. G. Kokalis, *J. Inorg. Nucl. Chem.* 1963, **25**, 875.
119. H. R. Allcock, R. W. Allen and J. P. O'Brien, *J. Am. Chem. Soc.* 1977, **99**, 3984.
120. R. W. Allen, J. P. O'Brien and H. R. Allcock, *J. Am. Chem. Soc.* 1977, **99**, 3987.
121. W. Harrison, N. L. Paddock, J. Trotter and J. N. Wingfield, *J. Chem. Soc., Chem. Commun.* 1972, 23.
122. W. Harrison and J. Trotter, *J. Chem. Soc., Dalton Trans.* 1973, 61.
123. W. C. Marsh, N. L. Paddock, C. J. Stewart and J. Trotter, *J. Chem. Soc., Chem. Commun.* 1970, 1190.
124. W. C. Marsh and J. Trotter, *J. Chem. Soc. A* 1971, 1482.
125. H. P. Calhoun, N. L. Paddock, J. Trotter and J. N. Wingfield, *J. Chem. Soc., Chem. Commun.* 1972, 875.
126. H. P. Calhoun, N. L. Paddock and J. Trotter, *J. Chem. Soc., Dalton Trans.* 1973, 2708.
127. N. L. Paddock, T. N. Ranganathan and J. N. Wingfield, *J. Chem. Soc., Dalton Trans.* 1973, 1578.
128. J. Dyson and N. L. Paddock, *J. Chem. Soc., Chem. Commun.* 1966, 191.
129. F. A. Cotton, G. A. Rusholme and A. Shaver, *J. Coord. Chem.* 1973, **3**, 99.
130. N. K. Hata and R. O. Harris, *J. Chem. Soc., Chem. Commun.* 1972, 407.
131. Al. L. Macdonald and J. Trotter, *Can. J. Chem.* 1974, **52**, 734.
132. J. Trotter, S. H. Whitlaw and N. L. Paddock, *J. Chem. Soc., Chem. Commun.* 1969, 695.
133. J. Trotter and S. H. Whitlaw, *J. Chem. Soc. A* 1970, 460.
134. H. R. Allcock, E. C. Bissell and E. T. Shawl, *J. Am. Chem. Soc.* 1972, **94**, 8603.
135. P. P. Greigger and H. R. Allcock, *J. Am. Chem. Soc.* 1979, **101**, 2492.
136. H. R. Allcock, P. P. Greigger, L. J. Wagner and M. Y. Bernheim, *Inorg. Chem.* 1981, **20**, 716.
137. H. R. Allcock, L. J. Wagner and M. L. Levin, *J. Am. Chem. Soc.* 1983, **105**, 1321.
138. H. R. Allcock, G. H. Riding and R. R. Whittle, *J. Am. Chem. Soc.* 1984, **106**, 5561.
139. P. R. Suszko, R. R. Whittle and H. R. Allcock, *J. Chem. Soc., Chem. Commun.* 1982, 649.
140. H. R. Allcock, P. R. Suszko, L. J. Wagner, R. R. Whittle and B. Boso, *J. Am. Chem. Soc.* 1984, **106**, 4966.
141. H. R. Allcock, P. R. Suszko, L. J. Wagner, R. R. Whittle and B. Boso, *Organometallics* 1985, **4**, 446.
142. R. A. Nissan, M. S. Connolly, M. G. L. Mirabelli, R. R. Whittle and H. R. Allcock, *J. Chem. Soc., Chem. Commun.* 1983, 822; H. R. Allcock, M. N. Mang, G. H. Riding and R. R. Whittle, *Organometallics* (in press).
143. H. R. Allcock, P. P. Greigger, J. E. Gardner and J. L. Schmutz, *J. Am. Chem. Soc.* 1979, **101**, 606.
144. H. R. Allcock, T. X. Neenan and B. Boso, *Inorg. Chem.* 1985, **24**, 2656.
145. H. R. Allcock and T. X. Neenan, *Macromolecules* 1986, **19**, 1495.
146. H. R. Allcock, K. D. Lavin, N. M. Tollefson and T. L. Evans, *Organometallics* 1983, **2**, 267.
147. R. A. Dubois, P. E. Garrou, K. D. Lavin and H. R. Allcock, *Organometallics* 1984, **3**, 649.
148. H. R. Allcock, A. G. Scopelianos, R. R. Whittle and N. M. Tollefson, *J. Am. Chem. Soc.* 1983, **105**, 1316.
149. P. R. Suszko, R. R. Whittle and H. R. Allcock, *J. Chem. Soc., Chem. Commun.* 1982, 960.
150. H. R. Allcock, K. D. Lavin, G. H. Riding, P. R. Suszko and R. R. Whittle, *J. Am. Chem. Soc.* 1984, **106**, 2337.
151. H. R. Allcock, K. D. Lavin, G. H. Riding and R. R. Whittle, *Organometallics* 1984, **3**, 663.
152. H. R. Allcock, K. D. Lavin and G. H. Riding, *Macromolecules* 1985, **18**, 1340.
153. K. D. Lavin, G. H. Riding, M. Parvez and H. R. Allcock, *J. Chem. Soc., Chem. Commun.* 1986, 117.
154. G. H. Riding and H. R. Allcock, *Organometallics* (in press).
155. H. R. Allcock, R. A. Nissan, P. J. Harris and R. R. Whittle, *Organometallics* 1984, **3**, 432.

Polyhedron Vol. 6, No. 2, pp. 159–162, 1987
Printed in Great Britain

0277–5387/87 $3.00+.00
Pergamon Journals Ltd

PREPARATION AND STRUCTURAL PROPERTIES OF A NEW MIXED-METAL BINUCLEAR COMPLEX WITH 4-CYANOPYRIDINE BRIDGING THE PENTAAMMINERUTHENIUM(II) AND THE PENTACYANOFERRATE(II) MOIETIES*

EDGARDO H. CUTIN and NÉSTOR E. KATZ†

Instituto de Química Física, Facultad de Bioquímica, Química y Farmacia, Universidad Nacional de Tucumán, Ayacucho 491, 4000 San Miguel de Tucumán, Argentina

(*Received* 18 *September* 1985; *accepted* 6 *November* 1985)

Abstract—A new binuclear complex, of formula $Na[(NH_3)_5Ru(4\text{-cypy})Fe(CN)_5]\cdot 6H_2O$, with 4-cypy = 4-cyanopyridine, is described. It can be prepared by reaction in aqueous solution, of stoichiometric amounts of $[Ru(NH_3)_5(4\text{-cypy})]Br_2$ and $Na_3[Fe(CN)_5(NH_3)]\cdot 3H_2O$ and is insoluble in water and stable in the solid state. Spectral data point to the structure

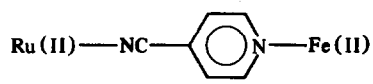

and the observed hypsochromic shifts of the MLCT bands in the UV–Vis spectrum and the diminished shift to lower frequencies observed in the IR spectrum for the nitrile stretching frequency, when compared to the parent complexes, indicate a reduxed π-backbonding interaction between the metals and the bridging ligand. It is concluded that the asymmetry of 4-cypy causes weak π-resonance interaction between both metallic centers.

Bridged polynuclear complexes are systems of interest in various fields, such as the study of mechanisms of biological redox reactions[1] and the generation of chemical potential energy from solar light absorption.[2] Therefore, important efforts have been made in the synthesis and characterization, by spectroscopic or electrochemical techniques, of new mixed-metal complexes.[3–6] In a recent work,[7] a new complex formed by association of $[Fe(CN)_5(NH_3)]^{3-}$ and 4-cypy (4-cypy = 4-cyanopyridine) at a molar ratio of 2:1 has been described. It was found that the cyanide group gives rise to a bridge between both pentacyanoferrate(II) moieties which is much more stable than that derived from the ambidentate ligand 4-cypy.

In this work, we report the preparation and spectral properties of a new mixed-metal dimer with 4-cypy bridging the pentaammineruthenium(II) and the pentacyanoferrate(II) moieties; both of which are able to interact through strong π-backbonding with aromatic nitrogen heterocycles.[8] This new binuclear species has spectroscopic characteristics that differ from similar dimers bridged by symmetric ligands.[9] By analyzing its UV–Vis and IR spectra, the influence of the asymmetric nature of 4-cypy on the structure of the mixed-metal complex can be assessed.

EXPERIMENTAL

Analytical reagent compounds were used for all preparations described in this work. Doubly distilled water was redistilled from alkaline permanganate in an all-glass apparatus.

* Presented at the "IV Congreso Argentino de Fisicoquimica", Rio Cuarto, Argentina, September 1985.

† Member of the "Carrera del Investigador Cientifico", CONICET, Argentina. Author to whom correspondence should be addressed.

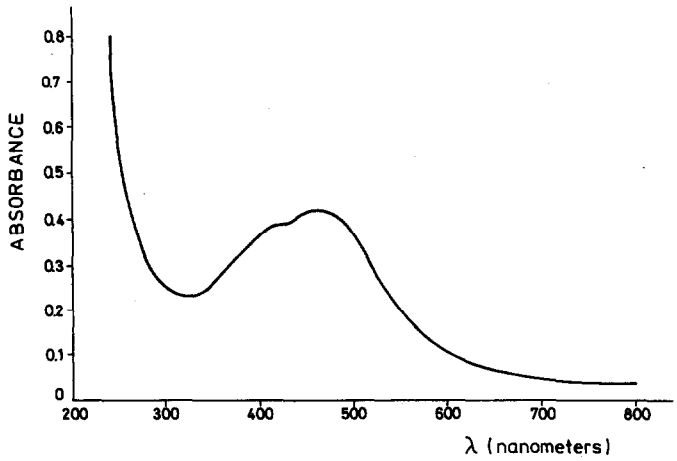

Fig. 1. UV–Vis spectrum of the complex $Na[(NH_3)_5Ru(4\text{-cypy})Fe(CN)_5]\cdot 6H_2O$, as KBr pellet.

4-Cyanopyridinepentaammineruthenium(II) was obtained by a published method.[10] $[Ru(NH_3)_5Cl]Cl_2$ necessary for the previous preparation was synthesized by the method of Allen *et al.*[11] The complexes $Na_5[Fe(CN)_5(SO_3)]\cdot 2H_2O$ and $Na_3[Fe(CN)_5(NH_3)]\cdot 3H_2O$ were obtained according to previous works.[12,13]

Forty-three mg of $Na_3[Fe(CN)_5(NH_3)]\cdot 3H_2O$ were added to 3 cm^3 of a solution in triply distilled water (at room temperature) containing an equimolar amount (60 mg) of $[Ru(NH_3)_5(4\text{-cypy})]Br_2$. The first complex aquates rapidly,[14] while the latter is substitution inert and insensitive to air oxidation.[10] The dark-red product formed precipitated immediately; after 15 min the solid was collected in a sintered glass filter, washed twice with water, ethanol and ether, and dried under vacuum in a desiccator over KOH. In an alternative preparation, 40 mg of $[Ru(NH_3)_5(4\text{-cypy})]Br_2$ were dissolved in 5 cm^3 of triply distilled water and then an equimolar amount of $Na_5[Fe(CN)_5(SO_3)]\cdot 2H_2O$ was added. The precipitate was treated in the same way as above. Both products gave identical IR spectra.

Carbon, hydrogen and nitrogen analyses were performed at UMYMFOR Laboratories, Buenos Aires, Argentina. Iron analysis was done by atomic absorption spectroscopy on a Varian Techtron AA spectrometer; sodium nitroprusside being the selected standard. Ruthenium analysis was carried out by boiling in peroxydisulfate (in KOH), filtering and recording the absorbance at 415 nm[15] on a Metrolab RC325 spectrophotometer.

Electronic spectra were recorded on a Shimadzu UV-300 spectrophotometer. IR spectra were obtained by using a Perkin–Elmer 580B spectrophotometer. All measurements were carried out with KBr pellets. Different samples gave reproducible results, indicating stability in the solid phase.

RESULTS AND DISCUSSION

Chemical analyses gave the following results. Found: Fe, 10.1; Ru, 16.4; C, 21.1; H, 4.4; N, 25.1%. Calc. for $Na[(NH_3)_5Ru(4\text{-cypy})Fe(CN)_5]\cdot 6H_2O$: Fe, 9.2; Ru, 16.6; C, 21.7; H, 5.1; N, 27.7%. The error observed for nitrogen analysis can be attributed to the exchange of NH_3 by H_2O.[1] Insolubility in water can be related to the hydrophobic periphery of the ion; this fact has already been observed in $[(CN)_5Fe(4\text{-cypy})Rh(NH_3)_5]\cdot 6H_2O$.[3]

Figure 1 shows the UV–Vis spectrum of the complex under study. Formation of a 4-cypy bridge between Fe(II) and Ru(II) is evidenced by the two peaks protruding from the broad asymmetric band, at 418 and 470 nm. The $[Ru(NH_3)_5(4\text{-cypy})]^{2+}$ complex presents a metal-to-ligand charge-transfer (MLCT) absorption at 425 nm, corresponding to coordination of Ru(II) to the nitrile end of 4-cypy.[10] On the other hand, the $[Fe(CN)_5(4\text{-cypy})]^{3-}$ complex has a MLCT band at 476 nm, indicating coordination of Fe(II) to the pyridine N of 4-cypy.[16–18] The bands observed for the dimeric complex at 418 and 470 nm are then shifted to higher frequencies with respect to the monomeric complexes and can be surely assigned, by analogy, to electron transfers $d_\pi(Ru) \rightarrow \pi^*$ (nitrile end of 4-cypy) and $d_\pi(Fe) \rightarrow \pi^*$ (pyridine ring of 4-cypy), respectively. The hypsochromic displacements are similar to those found for the $[(Ru(NH_3)_5)_2(4\text{-cypy})]^{4+}$ complex,[1] and are considered "anomalous" when compared with other structurally related systems.[9] This effect can be explained on the basis of the asymmetrical nature of the bridging ligand. π-Backbonding from Fe(II)

Table 1. IR spectra of 4-cyanopyridine (4-cypy) complexes, as KBr pellets: wavenumbers in cm^{-1}

$[R(4\text{-cypy})]Br_2$[a]	$Na_3[F(4\text{-cypy})]\cdot 10H_2O$[b]	$Na[RF(4\text{-cypy})]\cdot 6H_2O$[c]	Description of modes
	3440 br, s	3430 3320 br, s 3270	$\nu(H_2O)$, $\nu(NH)$
		3190 sh 2850 w	$\nu(CH)$
2179 s	2242 m	2183 w	$\nu(CN)$ (nitrile)
	2050 vs	2062 vs	$\nu(CN)$ (cyanide)
	1618 br, m	1620 br, m	$\delta(H_2O)$
1602 s		1595 m	
	1560 vw	1541 w	
		1501 w	ν_{ring}
1485 m	1484 m	1489 w	
1421 m		1430 m	
	1402 m	1410 sh	
		1288 br, w	$\delta(NH_3)$
	1260 m	1225 sh	$\delta(CH)$
	1210 w	1142 vw	
	1080 vw	1062 vw	
	1015 w	852 vw	
	822 m	828 w	$\delta_{ring}+\nu_{ring}+$ other ligand vibrations
		795 w	
		768 w	
		700 w	
	564 m	575 w	
		557 sh	
		511 w	
	478 vw	485 w	ν(FeN), ν(RuN), δ(FeC) etc.
	432 vw	430 sh	
		410 sh	
		398 vw	
		393 vw	
		374 vw	

Abbreviations: F = $Fe(CN)_5$; R = $Ru(NH_3)_5$; vs, very strong; s, strong; m, medium; w, weak; vw, very weak; ν, stretching; δ, in-plane deformation.

[a] Reference 10.

[b] Reference 18.

[c] This work.

to the pyridine ring must raise the energy of the π^*-orbital of the nitrile end of 4-cypy, while π-backbonding from Ru(II) to NC must increase the energy of the π^*-orbital of the aromatic heterocycle.[19] These charge transfers usually surpass electrostatic effects. Therefore, and because the energy of the MLCT is related to the energy of the ligand LUMO,[1] the energies of both electron transfers increase, resulting in higher absorption frequencies respect to the parent complexes. A weak π-resonance interaction thus seems to be present in the binuclear ion.

Table 1 shows data from IR spectra of the studied complex and the corresponding monomers. The proposed assignments are tentative. The stretching frequency of the nitrile group of 4-cypy is shifted 60 cm^{-1} below the value for the free ligand (2243 cm^{-1}). This lowering, already observed for the $[Ru(NH_3)_5(4\text{-cypy})]^{2+}$ complex,[10] can be attributed to the strong π-backbonding capacity of the $Ru(NH_3)_5^{2+}$ moiety and is another evidence of bonding of Ru(II) to the nitrile end of the bridging ligand. For the monomer complex $[Ru(NH_3)_5(4\text{-cypy})]Br_2$, the decrease is $\Delta\nu(CN) = -64$ cm^{-1},[10] while for the dimer $[(Ru(NH_3)_5)_2(4\text{-cypy})](ClO_4)_4$, $\Delta\nu(CN) = -53$ cm^{-1}.[1] The value observed here is thus intermediate between these species, a fact which can be accounted for—as already stated when discussing the electronic spectrum—by the reduction of π-backbonding from Ru(II) to the NC

group of 4-cypy due to coordination of $Fe(CN)_5^{3-}$ to the pyridine N of 4-cypy, and also by the lower π-backbonding capacity of this latter moiety compared to the $Ru(NH_3)_5^{2+}$ group.[8]

As illustrated in Table 1, the IR band assigned to cyanide stretching frequencies at 2062 cm^{-1} falls in the range expected for cyanoferrate(II) complexes.[9] On the other hand, the band corresponding to the symmetric deformation of NH_3 (1288 cm^{-1}) is characteristic of ammine complexes of Ru(II).[9] Finally, the shifts observed for the pyridine ring vibrations with respect to the monomers confirm bonding of a metal center to pyridine N.[18]

Results from IR studies agree with those from UV–Vis, so that we conclude that the new species, of structure

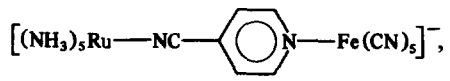

is stable in the solid state, with localized (II) oxidation states for Fe and Ru. The spectral properties indicate weak π-resonance interaction in the unsymmetrical bridge.

Acknowledgements—We thank CONICET and UNT for financial support, Dr C. O. Della Védova and Lic. D. B. Soria for running spectra and Dr G. Bossi for help in AA measurements.

REFERENCES

1. D. E. Richardson and H. Taube, *J. Am. Chem. Soc.* 1983, **105**, 40.
2. J. A. Gelroth, J. E. Figard and J. D. Petersen, *J. Am. Chem. Soc.* 1979, **101**, 3649.
3. K. J. Pfenning, L. Lee, H. D. Wohlers and J. D. Petersen, *Inorg. Chem.* 1982, **21**, 2477.
4. K. J. Moore, L. Lee, G. A. M. Abott and J. D. Petersen, *Inorg. Chem.* 1983, **22**, 1108.
5. K. J. Moore, L. Lee and J. D. Petersen, *Inorg. Chem.* 1983, **22**, 1244.
6. K. J. Moore, L. Lee, J. E. Figard, J. A. Gelroth, A. J. Stinson, H. D. Wohlers and J. D. Petersen, *J. Am. Chem. Soc.* 1983, **105**, 2274.
7. A. Ben Altabef, S. A. Brandán and N. E. Katz, *Polyhedron* 1985, **4**, 227.
8. H. E. Toma and J. M. Malin, *Inorg. Chem.* 1973, **12**, 1039.
9. A. Yeh, A. Haim, M. Tanner and A. Ludi, *Inorg. Chim. Acta* 1979, **33**, 51.
10. R. E. Clarke and P. C. Ford, *Inorg. Chem.* 1970, **9**, 495.
11. A. D. Allen, F. Bottomley, R. O. Harris, V. P. Reinsalu and C. V. Senoff, *J. Am. Chem. Soc.* 1967, **89**, 5595.
12. E. J. Baran and A. Müller, *Z. Anorg. Allg. Chem.* 1969, **368**, 144.
13. D. J. Kenney, T. P. Flynn and J. B. Gallini, *J. Inorg. Nucl. Chem.* 1961, **20**, 75.
14. H. E. Toma and J. M. Malin, *Inorg. Chem.* 1974, **13**, 1772.
15. J. L. Woodhead and J. M. Fletcher, *J. Chem. Soc.* 1961, 5039.
16. A. P. Szecsy, S. S. Miller and A. Haim, *Inorg. Chim. Acta* 1978, **28**, 189.
17. J. E. Figard, J. V. Paukstelis, E. F. Byrne and J. D. Petersen, *J. Am. Chem. Soc.*, 1977, **99**, 8417.
18. N. G. del V. Moreno, N. E. Katz, J. A. Olabe and P. J. Aymonino, *Inorg. Chim. Acta* 1979, **35**, 183.
19. P. T. T. Wong, *J. Chem. Phys.* 1983, **78**, 4840.

Polyhedron Vol. 6, No. 2, pp. 163–173, 1987
Printed in Great Britain

0277–5387/87 $3.00+.00
Pergamon Journals Ltd

PHENYLIMIDO ETHOXO COMPLEXES OF TUNGSTEN(VI): CRYSTAL AND MOLECULAR STRUCTURE OF DICHLORO-DI-μ-ETHOXOTETRAETHOXOBIS(PHENYLIMIDO)DITUNGSTEN(VI)

PAUL A. BATES, ALASTAIR J. NIELSON* and JOYCE M. WATERS†

Department of Chemistry, University of Auckland, Private Bag, Auckland, New Zealand

(*Received* 28 *October* 1985; *accepted* 11 *March* 1986)

Abstract—Reaction of $[W(NPh)Cl_4]_2$ with various quantities of ethanol and *t*-butylamine leads to $[W(NPh)(\mu\text{-}OEt)(OEt)_3]_2$, $[W(NPh)(\mu\text{-}OEt)(OEt)_2Cl]$ and $[W(NPh)(OEt)Cl_3(NH_2CMe_3)]$. A 1:1 proportionation reaction of $[W(NPh)Cl_4]_2$ and $[W(NPh)(\mu\text{-}OEt)(OEt)_3]$ gives $[W(NPh)(\mu\text{-}OEt)(OEt)Cl_2]_2$, whereas a 3:1 proportionation gives $[W(NPh)(\mu\text{-}OEt)Cl_3]_2$. Bridge-splitting reactions of $[W(NPh)(\mu\text{-}OEt)Cl_3]_2$, with PMe_3 or Et_4NCl give $[W(NPh)(OEt)Cl_3(PMe_3)]$ and $[W(NPh)(OEt)Cl_4][Et_4N]$. $[W(NPh)(\mu\text{-}OEt)Cl_3]_2$ reacts with Ph_3CCl to give $[W(NPh)(OEt)Cl_4][Ph_3C]$ and $[W(NPh)Cl_4]_2$ reacts with Ph_3COEt to give $[W(NPh)Cl_4(OEt)][Ph_3C]$. The trityl complexes do not react further to give amido complexes (W—$NCPh_3Ph$). The products were characterized by analytical data, IR, ^1H and ^{13}C NMR spectroscopy. The crystal and molecular structure of $[W(NPh)(\mu\text{-}OEt)(OEt)_2Cl]_2$ was determined from single-crystal X-ray diffractometer data. The crystals are triclinic with $a = 9.637(2)$ Å, $b = 11.135(1)$ Å, $c = 8.016(1)$ Å, $\alpha = 108.47(1)°$, $\beta = 105.51(1)°$, $\gamma = 91.51(1)°$, and space group $P\bar{1}$. The structure was solved by Patterson and Fourier methods and refined to $R = 0.039$ for the 1450 observed data. The molecule is a dimer with the two halves centrosymmetrically related. Both W atoms adopt a distorted octahedral coordination geometry and are linked by two ethoxo bridges. *Trans* to the bridging donors is a linear phenylimido group with a W—N bond length of 1.759(9) Å and a W—N—C bond angle of 172.4(9)°. The remaining octahedral sites are filled by a chloro ligand and two *cis*-orientated alkoxide ligands where the W—O bond distances of 1.835(9) and 1.865(7) Å indicate both ligands participate in π-bonding to the metal.

Many examples of Group VI transition-metal organoimido complexes (M≡NR) are known[1] but few also contain the alkoxide ligand. Those reported to date are the dialkoxides $[(Me_3SiO)_2M(N\text{-}t\text{-}Bu)_2]$[2] (M = Cr or Mo), $[(t\text{-}BuO)_2W(N\text{-}t\text{-}Bu)_2]$[3] and $[WO(NR)(OEt)_2]_n$.[4] Alkoxide ligands are of interest in organoimido chemistry since competitive π-donation from a suitably orientated alkoxide ligand can weaken the very stable, four-electron metal–nitrogen bond, increasing the potential for further reaction at the nitrogen atom.[5–7] In addition, structural features exhibited by the complexes can be affected by the size of the alkoxide R group.[8] We report here the preparation and characterization of mixed chloride–ethoxide phenylimido complexes of tungsten(VI) which complete the series $[W(NPh)(OEt)_xCl_{4-x}]_2$ and demonstrate further relationships between W—OR bonding and structure–reactivity considerations.

RESULTS AND DISCUSSION

In benzene solution phenylimido tungsten tetrachloride $[W(NPh)Cl_4]_2$ reacts with 8 equivalents of EtOH in the presence of excess anhydrous ammonia to give a yellow air- and moisture-sensitive crystalline solid analysing as $[W(NPh)(OEt)_4]_n$, for which the dimeric structure $[W(NPh)(\mu\text{-}OEt)(OEt)_3]_2$ (**1**) is proposed, based on the crystallographically determined methoxo analogue $[W(NPh)(\mu\text{-}OMe)(OMe)_3]_2$.[8] Using ammonia the

* Author to whom correspondence should be addressed.
† Present address: Department of Chemistry, Massey University, Palmerston North, New Zealand.

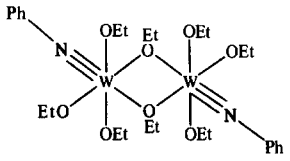

1

yield of **1** is low but with *t*-butylamine and petroleum ether as solvent the yield is increased to over 70%. The reaction produces 8 equivalents of *t*-butylamine hydrochloride after approximately 4 h. If more than 8 equivalents of alcohol and amine are used or the reaction period is shortened, the product reacts with the excess when the solution is concentrated, producing a red gummy contamination product which NMR analysis indicates is a mixture.

Reaction of 6 equivalents of EtOH and Me_3CNH_2 with phenylimido tungsten tetrachloride failed to give a petroleum ether soluble product, but extraction of the yellow amine hydrochloride residue with toluene gave, after crystallization, a yellow complex which analysed as $[W(NPh)(OEt)_3Cl]_n$. An X-ray crystal structure determination (see later) showed the dimeric ethoxo-bridged structure (**2**). The complex was also obtained in varying

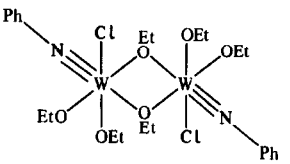

2

yield by toluene extraction of the amine hydrochloride residues produced during formation of the tetraethoxide (**1**) and this complex is the product of further reaction of **2** with 2 equivalents of EtOH and *t*-butylamine.

Four equivalents of EtOH and Me_3CNH_2 reacted with phenylimido tungsten tetrachloride in benzene to give 4 equivalents of amine hydrochloride but the yellow oily product obtained from solution was shown by IR and NMR spectroscopy to be a mixture. However a proportionation reaction between 1 equivalent each of **1** and phenylimido tungsten tetrachloride in benzene gave a yellow crystalline material analysing as $[W(NPh)(OEt)_2Cl_2]_n$ for which an ethoxy-bridged structure (either **3** or **4**) is preferred based on the crystallographically determined ethoxide bridge in **2**.

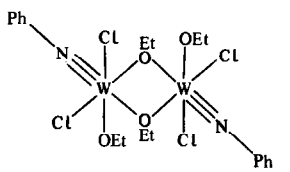

3

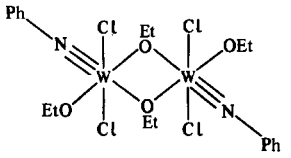

4

Phenylimido tungsten tetrachloride reacted with 2 equivalents of EtOH and Me_3CNH_2, giving a red solution from which the monomeric complex $[W(NPh)(OEt)Cl_3(NH_2CMe_3)]$ (**5**) was obtained.

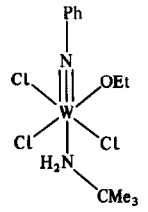

5

The amino ligand lying *trans* to the imido group is preferred for this complex, based on the X-ray structure of $[W(NPh)(OCMe_3)_3Cl(NH_2CMe_3)]$ where the amine ligates *trans* to the imido function.[8] Proportionation of 1 equivalent of **1** with 3 equivalents of phenylimido tungsten tetrachloride in benzene led to a purple-brown solid analysing as $[W(NPh)(OEt)Cl_3]_n$ for which the dimeric ethoxy-bridged structure (**6**) is assigned on the basis of its

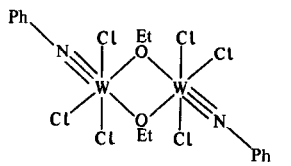

6

IR spectrum. The complex was also obtained by reacting 1 equivalent of $[W(NPh)(OEt)_2Cl_2]_2$ with one of phenylimido tungsten tetrachloride.

Studies carried out on complexes **1–6** to determine the stabilizing effects of the alkoxo ligands and imido ligand reactivity showed the complexes to be surprisingly inert. For example, the ethoxo bridge in complexes **1–3** could not be split with strong σ-donor ligands such as PMe_3, nor was there any tendency to form anionic species by the addition of Ph_4PCl or Et_4NCl. This contrasts with the chemistry of $[W(NPh)Cl_4]_2$ where $[W(NPh)Cl_4(PMe_3)]$[9] and the $[W(NPh)Cl_5]^-$[10] anion are easily formed, and demonstrates the stability of the alkoxo bridge. However, reaction of stoichiometric amounts of PMe_3, Me_3CNH_2 or Et_4NCl with $[W(NPh)(\mu\text{-}OEt)Cl_3]_2$ (**6**) gave the monomeric complexes $[W(NPh)(OEt)Cl_3(PMe_3)]$ (**7**), **5** and $[W(NPh)(OEt)Cl_4][Et_4N]$ (**8**), respec-

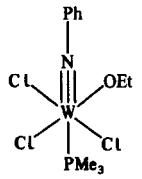

7

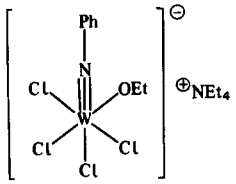

8

tively, suggesting that the bridge in the monoethoxo complex is more easily broken. Further, the room-temperature reaction of excess PMe_3 with **6** in THF did not reduce the complex to tungsten(V) as is the case with $[W(NPh)Cl_4]_2$ which readily reduces to $[W(NPh)Cl_3(PMe_3)_2]$.[9] This complex was, however, obtained after prolonged heating of **6** with the phosphine but no reduced ethoxy complexes could be isolated. Reduction of $[W(NPh)Cl_4]_2$ with sodium–mercury amalgam in the presence of a σ-donor ligand (L) gives rise to the tungsten(IV) complexes $[W(NPh)Cl_2L_3]$[11] but similarly based experiments with the mono- and diethoxo complexes, which are apparently reduced, have so far given intractable products. The tetraethoxide species (**1**) fails to react at all.

For the Group V metals, the imido nitrogen is expected to function as a nucleophile but examples are extremely rare.[12] We have shown that protonation of the W≡NPh bond gives rise to amido complexes (W—NHPh),[6] and bis-imido complexes of molybdenum are known to react with MeBr to produce $PhNMe_2$.[13] We were interested to test the effects of alkyl halide addition to the bridged dimers in the hope of generating amido complexes by the following reaction:

$$[W(NPh)(OEt)_xCl_y]_n + nRX \rightarrow n[W(NPh)(OEt)_xCl_yX^{\ominus}][R^{\oplus}] \rightarrow n[W(NRPh)(OEt)_xCl_yX].$$

All complexes tested failed to react at room temperature with alkyl halides (RX = MeI, MeBr or EtBr) in a variety of solvents and most were resistant to heat. For example, the tetraethoxo complex (**1**) remained unchanged in benzene after heating with MeI to 150°C in a pressure bottle (pressure developed = 700 kPa). However, with Ph_3CCl, $[W(NPh)(\mu\text{-}OEt)Cl_3]_2$ was found to react at room temperature to give $[W(NPh)(OEt)Cl_4][Ph_3C]$ (**9**).

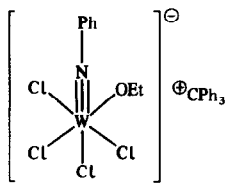

9

This complex, which persisted as a non-crystalline material, analysed as a dichloromethane solvate and was a 1 : 1 conductor in acetonitrile. Reaction of phenylimido tungsten tetrachloride with Ph_3COEt gave a similar anionic complex consistent with the formulation $[W(NPh)Cl_4(OEt)][Ph_3C]$ (**10**),

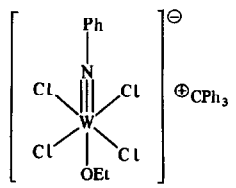

10

whereas $[W(NPh)(OEt)_2Cl_2]_2$ was obtained from the reaction between $[W(NPh)(\mu\text{-}OEt)Cl_3]_2$ and Ph_3COEt. The anionic complexes **9** and **10** are apparently stable in solution and we have so far been unable to obtain evidence for any rearrangement to an amido complex.

IR spectra

Organoimido complexes generally show strong absorptions characteristic of the metal–imide vibration between 1100 and 1300 cm^{-1} [11] but in the present complexes this region is obscured by bands arising from the alkoxide ligand. All the compounds do, however, show strong absorptions at approximately 1350 cm^{-1} in KEL-F or as a shoulder of Nujol. For phenylimido rhenium complexes this absorption shifts to a lower wavenumber on ^{15}N-substitution making it a good candidate for $\nu(W{\equiv}NR)$[5] although $\nu(C{-}N)$ bands for aromatic amines also fall in this region but these are usually weak. Raman spectra of **1** and **2**[14] show the 1350-cm^{-1} band to be intense and polarizable, indicating that it arises from multiple bonding where a sufficient electron density is present to give an induced dipole in the Raman effect. In Table 1 the 1350-cm^{-1} bands found in the IR spectrum of the complexes are shown as ν(WNC).

Assignment of C—O and M—O stretching vibrations is straightforward for the complexes since problems of structural complexity and low

Table 1. IR spectral data (cm^{-1}) for tungsten(VI) phenylimido ethoxide complexes[a]

Complex	ν(WNC)	ν(C—O_t)	ν(C—O_b)	ν(W—O_t)	ν(W—O_b)	ν(W—Cl)
[W(NPh)(μ-OEt)(OEt)$_3$]$_2$ (**1**)	1345	1050	1025	590	510	—
[W(NPh)(μ-OEt)(OEt)$_2$Cl]$_2$(**2**)	1350	1040	1020	640	525	285
[W(NPh)(μ-OEt)(OEt)Cl$_2$]$_2$ (**3** and **4**)	1338	1038	985	622, 618	538	332, 308, 278
[W(NPh)(μ-OEt)Cl$_3$]$_2$ (**6**)	1340	—	975	—	540	348, 322, 295
[W(NPh)(OEt)Cl$_3$(NH$_2$CMe$_3$)] (**5**)	1343	1020	—	630	—	335, 318, 280
[W(NPh)(OEt)Cl$_3$(PMe$_3$)] (**7**)	1350	1005	—	600	—	338, 310, 280
[W(NPh)(OEt)Cl$_4$][Et$_4$N] (**8**)	1350	1020	—	618	—	330, 305, 265
[W(NPh)(OEt)Cl$_4$][Ph$_3$C] (**9**)	1350	1020	—	618	—	320, 280
[W(NPh)Cl$_4$(OEt)][Ph$_3$C] (**10**)	1350	1020	—	622	—	320, 280

[a] t = terminal, b = bridging.

molecular symmetry normally associated with alkoxides are absent. Although the complexes show a series of ν(C—O) bands between 1150 and 850 cm^{-1}, which are characteristic of metal alkoxides in general,[15] only the strongest are shown in Table 1. The monomeric complexes [W(NPh)(OEt)Cl$_3$(L)] (L = NH_2CMe_3 or PMe_3) and [W(NPh)(OEt)Cl$_4$][Et_4N] show a single strong absorption in the ν(C—O) region (1000–960 cm^{-1}) which are from necessity assigned to a terminal mode as also must the M—O band in the region of 600 cm^{-1}.[16] For the parent complex (**6**) both ν(C—O) and ν(M—O) lie at a lower wavelength, which is a characteristic feature of bridging modes in metal alkoxides.[15] The diethoxo complex (**3**) shows absorptions at 1038 and 985 cm^{-1}, suggesting both terminal and bridging modes where the *tri-* and *tetra*ethoxo complexes (**2** and **1**) are similar but show an increasing intensity of the terminal mode with increasing number of terminal ethoxides.

In the far IR **6** shows three W—Cl stretching bands as expected for a *mer* arrangement of three metal chlorides[17] and this is repeated for the monomeric derivatives (**5** and **7**). Comparison of the absorption intensities at 330 and 280 cm^{-1} shows that for the *tri*chloro complex (**6**) the 348-cm^{-1} band dominates, for the dichloro complex, (**3**), the intensities are equal whereas for the monochloro complex (**2**) only one band at 285 cm^{-1} is present. This suggests that the latter absorption may be indicative of a chloro group *trans* to an ethoxide ligand.

NMR spectra

The proton NMR spectra of the complexes (Table 2) show the alkoxide ligand CH_2 resonance in the vicinity of 5 ppm. **6** shows a well-defined quartet as do the other complexes containing only one ethoxide ligand. **2** and **3** exhibit complicated sets of quartets arising from intramolecular exchange of alkoxide ligands but no attempt has been made to obtain frozen-out spectra as it is well established that α-protons of bridging alkoxides absorb upfield of terminal alkoxides.[15] Interestingly, the CH_2 resonances of **1** are less complicated, involving only two sets of quartets in an approximate 2 : 1 ratio, which suggests less intramolecular exchange or a greater magnetic equivalence of the ethoxides in the absence of chloro ligands. For the trityl complexes **9** and **10** the appearance of the CH_2 quartet in the vicinity of 5 ppm confirms the ethoxo group exists as a tungsten alkoxide and not as $EtOCPh_3$. The spectra do not, however, distinguish between a chloro or an ethoxo function lying *trans* to the imido function.

Several of the complexes show well-resolved aromatic resonances which appear to approach first-order spectra. However, as with $[W(NPh)Cl_4(NCEt)]$,[9] the coupling constants are identical indicating deceptive simplicity.[18] In general, anisotropy effects associated with the imido function result in a downfield shift for the *ortho* protons whereas the *para* proton lies upfield.

In the ^{13}C NMR spectra (Table 2) the terminal ethoxide CH_2 resonance of the monoethoxide monomers is observed near 82 ppm as is the case for the trityl complexes (**9** and **10**). $[W(NPh)(\mu\text{-}OEt)Cl_3]_2$ is sparingly soluble but what does dissolve shows the CH_2 resonance also at 82 ppm, suggesting that in solution the complex may well exist as a monomer (cf. IR evidence for a bridging ethoxide in the solid). $[W(NPh)(OEt)_2Cl_2]_2$ shows two resonances in this region and a further two near 77 ppm, suggesting two isomeric forms (**3** and **4**). However, the sets of resonances may be a consequence of intramolecular exchange since several resonances appear for both **1** and **2**. With the greater substitution by ethoxide ligands in these complexes the resonances shift upfield until, in the case of the tetraethoxide, all resonances appear in the vicinity of 72 ppm with no strictly terminal CH_2 resonances (82 ppm) apparent at all.

The complexes show strong deshielding of the aromatic ring *ipso* carbons similar to nitrobenzene where electron withdrawal from the ring occurs.[19] Little change occurs for the *meta* carbons, whereas *ortho* and *para* carbons are affected to differing extents. Downfield shifts of α-carbon resonances in *t*-butylimido complexes of Group V metals are associated with a greater electron density in the W≡N bond,[12] hence, assuming that the analogy holds for *ipso* carbons in the phenylimido complexes, comparative W≡N bond strengths should be demonstrable. The $L_xW{\equiv}N$ substituent effects on the ring carbons compared with benzene are shown in Table 2, and show increasingly greater positive *ipso* carbons and more negative *ortho* and *para* carbons as the number of ethoxide ligands increases. Although the shifts are small it would appear that the tetraethoxo complex (**1**) contains the strongest W≡N bond.

Description and discussion of the X-ray crystal structure of **2**

An X-ray crystal structure determination of **2** showed the molecule to be dimeric with the two halves centrosymmetrically related (Fig. 1). Each tungsten atom adopts a distorted octahedral coordination geometry with the oxygen atoms of two ethoxy groups forming bridges between them. The phenylimido ligand lies *trans* to one of these bridges with a terminal ethoxo group lying *trans* to the other. The remaining octahedral sites are filled by a terminal ethoxide and a chloro ligand lying mutu-

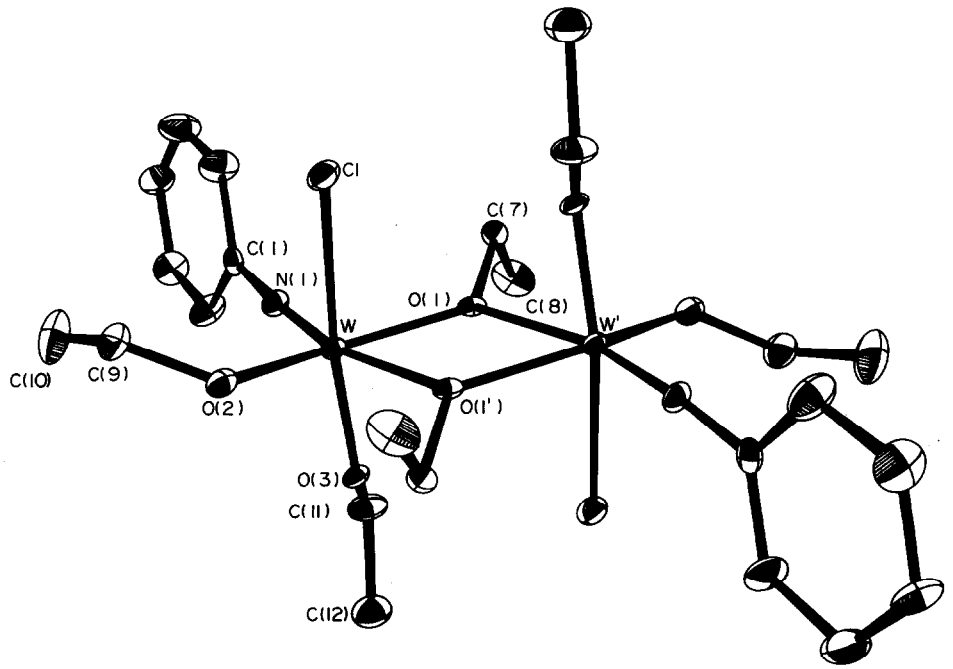

Fig. 1. $[W(NPh)(\mu\text{-}OEt)(OEt)_2Cl]_2$ molecule. Thermal ellipsoids have been drawn at the 50% probability level. Hydrogen atoms have been omitted for clarity.

Table 2. NMR spectral data (ppm) for tungsten(VI) phenylimido ethoxide complexes[a]

Complex	^{1}H NMR[b]		
	CH_2	CH_3	Aromatics
$[W(NPh)(\mu\text{-}OEt)(OEt)_3]_2$ (1)	4.45–4.05	1.00–1.45	6.50–7.50
$[W(NPh)(\mu\text{-}OEt)(OEt)_2Cl]_2$ (2)	4.68–4.70	1.10–1.58	6.82–7.60
$[W(NPh)(\mu\text{-}OEt)(OEt)Cl_2]_2$ (3 and 4)	4.90–5.85	1.10–1.70(t)	6.98–7.80
$[W(NPh)(\mu\text{-}OEt)Cl_3]_2$ (6)	5.10–5.80	1.20–1.42(t)	6.90–7.75
$[W(NPh)(OEt)Cl_3(NH_2CMe_3)]$ (5)[c]	5.55–5.96(q)	1.35–1.58(t, obscured)	6.80–7.70
$[W(NPh)(OEt)Cl_3(PMe_3)]$ (7)[f]	5.21–5.75(q)	1.20–1.6(2t, obscured)	6.82–7.60
$[W(NPh)(OEt)Cl_4][Et_4N]$ (8)[g]	5.45–5.90(q)	1.30–1.60(t, obscured)	6.80–7.80
$[W(NPh)(OEt)Cl_4][Ph_3C]$ (9)[h]	5.20–5.60(q)	1.08–1.40(t)	6.85–7.40
$[W(NPh)Cl_4(OEt)][Ph_3C]$ (10)[h]	5.38–5.80(q)	1.25–1.58(t)	7.04–7.58

[a] Spectra obtained in $CDCl_3$ solution.

[b] t = triplet, q = quartet.

[c] *Ortho* and *meta* tentative assignments (*meta* carbon based on 128.5), *para* assignment made from relative peak height.

[d] Data relative to benzene (128.5 ppm) in parentheses. Positive values indicate deshielding, negative values indicate shielding.

[e] *t*-Butylamino resonances at $\delta = 1.52$ (^{1}H NMR); and $\delta = 28.0$ and 55.3 (^{13}C NMR).

[f] PMe_3 resonances at $\delta = 1.57$, 1.66, 1.75 and 1.85 (^{1}H NMR); and $\delta = 12.9$, 13.5, 15.2 and 15.6 (^{13}C NMR).

[g] Et_4N resonances at $\delta = 1.3$–1.6 (CH_3) and 3.0–3.5 (CH_2) (^{1}H NMR); and $\delta = 7.6$ (CH_3) and 52.4 (CH_2) (^{13}C NMR).

[h] CH_2Cl_2 resonance at $\delta = 5.5$ (^{1}H NMR), and 56.6 (^{13}C NMR).

ally *trans*. (Bond distances and angles are given in Tables 3 and 4.) There are no unusual intermolecular contacts.

The phenylimido ligand is essentially linear with a W—N(1)—C(1) angle of 172.4(9)°. The distance of 1.759(9) Å for the W—N bond indicates considerable multiple-bond character, the separation lying within the range of values (1.61–1.77 Å)[8,9,11,20] found in other tungsten organoimido complexes. A

Table 3. Bond distances (Å) for $[W(NPh)(\mu\text{-}OEt)(OEt)_2Cl]_2$ (standard deviations in parentheses)

W—Cl	2.454(3)
W—O(1)	2.003(8)
W—O(1′)	2.213(8)
W—O(2)	1.835(9)
W—O(3)	1.865(7)
W—N	1.759(9)
O(1)—C(7)	1.44(1)
O(2)—C(9)	1.47(2)
O(3)—C(11)	1.44(2)
N(1)—C(1)	1.36(1)
C(7)—C(8)	1.50(2)
C(9)—C(10)	1.43(2)
C(11)—C(12)	1.49(2)

Table 4. Bond angles (°) for $[W(NPh)(\mu\text{-}OEt)(OEt)_2Cl]_2$ (standard deviations in parentheses)

Cl—W—O(1)	84.1(2)
Cl—W—O(1′)	86.1(2)
Cl—W—O(2)	85.6(3)
Cl—W—O(3)	169.3(2)
Cl—W—N	90.1(3)
O(1)—W—O(1′)	69.7(3)
O(1)—W—O(2)	156.8(3)
O(1)—W—O(3)	92.0(3)
O(1)—W—N	96.6(4)
O(1′)—W—O(2)	89.0(3)
O(1′)—W—O(3)	83.2(3)
O(1′)—W—N	166.1(4)
O(2)—W—O(3)	94.4(4)
O(2)—W—N	104.1(4)
O(3)—W—N	100.3(4)
W—O(1)—W′	110.3(3)
W—O(1)—C(7)	126.8(7)
W′—O(1)—C(7)	118.6(7)
W—O(2)—C(9)	139(1)
W—O(3)—C(11)	129.7(8)
W—N—C(1)	172.4(9)
N(1)—C(1)—C(2)	121.0(6)
N(1)—C(1)—C(6)	119.0(6)
O(1)—C(7)—C(8)	111(1)
O(2)—C(9)—C(10)	110(2)
O(3)—C(11)—C(12)	109(1)

Table 2 (*cont.*)

^{13}C NMR[cd]					
CH_2	CH_3	*Ipso*	*Ortho*	*Meta*	*Para*
72.2, 71.1, 70.6	19.7, 19.2, 18.0	152.3 (+23.8)	127.4 (−1.1)	127.9 (−0.6)	125.8 (−2.7)
78.6, 74.5, 72.5	18.5, 18.3, 17.9	151.1 (+22.6)	128.0 (−0.5)	127.8 (−0.7)	128.4 (−0.1)
81.0, 80.6, 78.1, 76.5	17.8, 17.4, 16.9	150.4 (+21.9)	129.1 (+0.6)	127.7 (−0.8)	131.3, 130.7 (+2.8)
82.8	17.1	149.7 (+21.2)	129.8 (+1.3)	127.8 (−0.7)	131.7 (+3.2)
83.1	17.1	148.9 (+20.2)	130.2 (+1.7)	127.6 (−0.9)	131.4 (+2.9)
81.7	17.4	149.1 (+20.6)	130.4 (+1.9)	128.1 (−0.4)	131.9 (+3.4)
81.8	17.1	148.5 (+20.0)	130.0 (+1.5)	127.6 (−0.9)	130.5 (+2.0)
82.6	17.0	149.4 (+20.9)	129.5 (+1.0)	127.6 (−0.9)	131.3 (+2.8)
82.7	17.1	150.0 (+21.5)	129.7 (+1.2)	127.6 (−0.9)	131.6 (+3.1)

value of 1.71 Å is predicted for a W–N triple bond acting as a four-electron donor.[1]

The W—O(1′) bond [2.213(8) Å] is longer than the W—O(1) bond length [2.003(8) Å], resulting in the asymmetric bridging arrangement whereby lone-pair donation from oxygen occurs *trans* to the imido function. The W—O—W′ bond angle of 110.3(3)° is comparable with that found in $[W(NPh)(\mu\text{-}OMe)(OMe)_3]_2$.[8] The W—O bond lengths of the terminal akoxides at 1.835(9) and 1.865(7) Å are shorter than those forming the bridging structure whereas the W—Cl bond length at 2.454(3) Å lies within the range of values (2.24–2.48 Å) found in other complexes of tungsten.[9,11,21]

The octahedral coordination geometry is distorted away from the ideal with the tungsten atom displaced 0.28 Å above the coordination plane made by the four atoms [O(1), O(2), O(3) and Cl(1)] which lie *cis* to the imido function. This feature is common in other imido complexes and also in those containing the related nitrido ligand.[22] Formation of the ethoxide bridge also contributes to the distortion with the O(1)—W—O(1′) angle being reduced to 69.7(3)°. There are no significant intramolecular contact distances below 3.5 Å in the molecule. Minimal interaction between the phenyl ring and the terminal ethoxide ligands is attained by rotation of the phenyl ring about the N—C(1) bond to a point between the two *cis*-ethoxide groups. As a result the torsion angle, W—N—C(1)—C(2) is 11.0°.

Several implications result from these structural details. Alkoxide ligands formally act as one-electron donors for the purpose of the EAN rule but π-donation involving the oxygen lone pairs allows the ligand to act as a three-electron donor [forming a double bond (M=OR)] or in rare cases as a five-electron donor (M≡OR).[5] The W—O(1) bond length of 2.003(8) Å suggests that this ligand acts as a one-electron donor to W(1).[23] Applying the 18-electron rule with all the alkoxides acting as one-electron donors, the molecule becomes a 16-electron species. Chlorine is a poor π-donor in comparison with an alkoxide and this is reflected by the W—Cl bond length [2.454(3) Å], lying towards the upper limit (2.48 Å) of W—Cl bond lengths.[21] However, the two terminal alkoxide W—O bond lengths [1.835(9) and 1.865(7) Å] are short, lying within the range found for W=OR bonds,[23] so that a measure of π-bonding exists in both. Thus, while an 18-electron configuration may be attained by either **a** or **b**, the structure shows an average of two canonical forms. However, the alkoxide better able to π-bond (shorter bond length and wider W—O—C angle) lies *trans* to the bridging alkoxide. The *cis*-

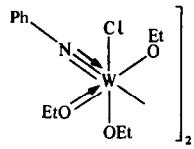

a

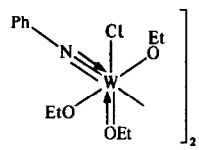

b

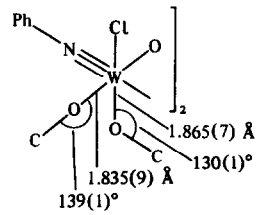

alkoxide arrangement allows the two electrons to be more effectively spread than would *trans*-terminal alkoxides as in the former case the *trans* ligands do not compete for π-bonding orbitals.

In $[W(NPh)(\mu\text{-}OMe)(OMe)_3]$ and [W(NPh)(OC-

$Me_3)_3Cl(NH_2CMe_3)]$ where *trans*-alkoxides do exist,[8] the two electrons can be spread over two sets of *cis*-alkoxides, the situation being reflected by similar W—O bond lengths within each molecule. For $[W(NPh)(OEt)_2Cl_2]_2$ either chlorine or alkoxide ligands may orientate *trans* to an alkoxo bridge giving *cis* or *trans* isomers (**3** and **4**) of comparable energy. In the absence of ethoxide acting as a five-electron donor, an ethoxy bridge in $[W(NPh)(\mu\text{-}OEt)Cl_3]_2$ leaves the complex as a 16-electron species which may account for the bridge-splitting reactions giving complexes capable of attaining an 18-electron configuration.

EXPERIMENTAL

$[WOCl_4]_2$ was prepared by reaction of WO_3 with thionyl chloride[24] and $[W(NPh)Cl_4]_2$ by reaction of $[WOCl_4]_2$ with phenyl isocyanate.[11] Trimethylphosphine was prepared by a literature method.[25] Trityl ethoxide was prepared by refluxing trityl chloride with ethanol and triethylamine in benzene and recrystallizing the product from petroleum ether at −20°C. Tetraethyl ammonium chloride was dried at 100°C *in vacuo* for 24 h and stored in a Schlenk tube. Ethanol was dried and fractionally distilled over magnesium ethoxide. *t*-Butylamine was distilled from calcium hydride and stored in a Schlenk flask. Petroleum ether (b.p. range 40–60°C), toluene and benzene were distilled over sodium wire and dichloromethane over calcium hydride. All distillations were carried out under N_2 treated to remove oxygen and water,[26] as were manipulations using bench-top air-sensitive techniques.[26] Infrared spectra were recorded on a Perkin–Elmer 597 spectrometer, ^1H NMR on a Varian T60 Model spectrometer and ^{13}C NMR spectra on a JEOL FX60 spectrometer. Analytical data were obtained by Professor A. D. Campbell and associates, University of Otago, New Zealand. Melting points were determined in sealed tubes under nitrogen on an electro-thermal melting-point apparatus and are uncorrected.

Di - μ - ethoxohexaethoxobis(phenylimido)ditungsten(VI) (**1**)

t-Butylamine (2.7 cm^3, 25.6 mmol) and ethanol (1.5 cm^3, 25.7 mmol) in petroleum ether (50 cm^3) were added to phenylimido tungsten tetrachloride (2.7 g, 3.2 mmol) suspended in petroleum ether (100 cm^3) and the mixture stirred for 6 h. The yellow solution was filtered from the precipitate of *t*-butylamine hydrochloride which was extracted several times with petroleum ether (30 cm^3). The combined filtrates were reduced to *ca* 5 cm^3 and the solution allowed to stand giving the complex as yellow microcrystals. The product was filtered, washed with petroleum ether (2 cm^3 cooled to 0°C), and dried *in vacuo* (1.63 g, 55%) (m.p. 106–110°C). (Found: C, 36.8; H, 5.8; N, 3.0%. $C_{28}H_{50}N_2O_8W_2$ requires: C, 36.9; H, 5.5; N, 3.1%.)

IR (Nujol) bands at 1565w, 1342s, 1275w, 1142m, 1090s, 1050s, 1022s, 986w, 908s, 982m, 760m, 720w, 690m, 620m, 586s, 542m, 508s, 460m, 395w and 325w cm^{-1}.

The product, sufficiently pure for further reaction, was obtained by stripping the solvent completely from the combined filtrates and washing the product with a small quantity of cold petroleum ether (2 cm^3) to remove an orange gummy material also present. Using this method the yield of complex increases to 2.13 g (72%).

Dichloro - di - μ - ethoxotetraethoxobis(phenylimido)ditungsten(VI) (**2**)

t-Butylamine (1.1 cm^3, 15 mmol) and ethanol (0.7 cm^3, 12 mmol) in petroleum ether (50 cm^3) were added to phenylimido tungsten tetrachloride (1.2 g, 1.5 mmol) suspended in petroleum ether (60 cm^3), and the mixture was stirred for 4 h, after which the solution was filtered and the solvent discarded. The pale yellow residue was extracted with warm toluene (2 × 30 cm^3) and the combined extracts filtered. Reduction of the volume to *ca* 5 cm^3 and standing the solution at −20°C gave the complex as yellow crystals (0.82 g, 64%) [m.p. 148–152°C (dec.)]. (Found: C, 32.5; H, 4.6; N, 3.1%. $C_{24}H_{40}Cl_2N_2O_6W_2$ requires: C, 32.3; H, 4.5; N, 3.1%.)

IR (Nujol) bands at 1580w, 1430s, 1355s, 1272m, 1090s, 1030s, 920s, 882s, 805w, 760s, 688s, 640s, 600m, 555s, 528s, 480s, 382m, 326m, 320m and 284 cm^{-1}.

Bulk quantities of the complex may be obtained by extracting the reaction residue with benzene (50 cm^3), filtering the solution, removing the solvent and washing the crystalline solid with petroleum ether (30 cm^3). Analytical data are similar to the recrystallized product. (Found: C, 32.1; H, 4.7; N, 3.1%.)

Tetrachloro - di - μ - ethoxodiethoxobis(phenylimido)ditungsten(VI) (**3**)

1 (0.6 g, 0.66 mmol) in benzene (25 cm^3) was added to phenylimido tungsten tetrachloride (0.55 g, 0.66 mmol) in benzene (30 cm^3) and the mixture stirred for 6 h. The orange-yellow solution was filtered and the solvent removed, to give a yellow crystalline solid which was dissolved in hot toluene (25

cm^3). The solution was filtered, the volume reduced to *ca* 5 cm^3 and the solution allowed to stand at −20°C, giving the complex as yellow crystals which were filtered, washed with petroleum ether (20 cm^3) and dried *in vacuo* (0.38 g, 66%) [m.p. 168–170°C (melts with decomposition)]. (Found: C, 27.9; H, 3.7; N, 3.2%. $C_{20}H_{30}Cl_4N_2O_4W_2$ requires: C, 27.5; H, 3.7; N, 3.2%.)

IR (Nujol) bands at 1440s, 1400w, 1350w, 1080m, 1040s, 1020s, 986s, 920s, 862s, 825m, 755s, 718m, 680m, 624s, 615s, 550s, 535s, 575s, 390w, 330s, 305m and 280 cm^{-1}.

The complex may be obtained sufficiently pure for further reaction by filtering the reaction mixture, stripping the solvent, washing the crystalline residue with petroleum ether (30 cm^3), and drying the product *in vacuo*.

(b) Trityl ethoxide (0.35 g, 1.2 mmol) in dichloromethane (30 cm^3) was added to a suspension of hexachloro - di - μ - ethoxobis(phenylimido)ditungsten(VI) (**6**) (0.52 g, 0.6 mmol) in dichloromethane (40 cm^3) and the mixture stirred for 4 h. The orange-yellow solution was filtered and the solvent removed *in vacuo* to give an orange gum which was washed with petroleum ether (2 × 25 cm^3) followed by acetonitrile (1 cm^3). The yellow residue was filtered, washed further with acetonitrile (0.5 cm^3), filtered again and dried *in vacuo* (0.3 g, 57%). Physical and spectroscopic properties were identical to the product prepared under (a).

t - *Butylaminetrichloroethoxo(phenylimido)tungsten*(VI) (**5**)

(a) *t*-Butylamine (0.628 cm^3, 6 mmol) was added to phenylimido tungsten tetrachloride (1.25 g, 1.5 mmol) in benzene (30 cm^3) and the mixture was stirred for 4 h. The orange-red solution was filtered and the solvent removed to give an orange-yellow crystalline solid. The product was dissolved in toluene (30 cm^3), the volume reduced to *ca* 15 cm^3 and the solution allowed to stand at −5°C, giving the complex as red-brown crystals which were filtered off and dried *in vacuo* (1.1 g, 73%) (m.p. 62–65°C). {Found: C, 30.1; H, 4.9; N, 4.8%. $C_{12}H_{22}Cl_3N_2OW$ [i.e. $W(NPh)Cl_3(OEt)(NH_2CMe_3)\cdot\frac{1}{2}PhMe$] requires: C, 30.4; H, 4.4; N, 5.4%.}

IR (Nujol) bands at 3125m, 3100m, 1558m, 1505w, 1390w, 1343m, 1295m, 1202m, 1150m, 1020s, 990m, 912s, 885m, 823w, 760s, 738m, 678m, 650m, 630s, 620m, 544m, 445m, 418m, 392w, 335s, 318s and 280s cm^{-1}

(b) *t*-Butylamine (0.6 cm^3, 5.7 mmol) in petroleum ether (40 cm^3) was added to **6** (1.2 g, 1.4 mmol) in petroleum ether (50 cm^3) and the mixture was stirred for 15 h. The orange solid was filtered off, extracted with benzene (30 cm^3), and the solvent removed to give the complex as a red-brown crystalline solid which was washed with petroleum ether (30 cm^3), filtered and dried *in vacuo* (0.8 g, 87%). Physical and spectroscopic properties were identical to the product prepared under (a).

Hexachloro - di - μ - ethoxobis(phenylimido)ditungsten(VI) (**6**)

(a) **1** (1.2 g, 1.3 mmol) in benzene (40 cm^3) was added to a suspension of phenylimido tungsten tetrachloride (3.31 g, 3.9 mmol) in benzene (40 cm^3) and the mixture stirred for 4 h to give a purple-brown precipitate. The solution volume was reduced to *ca* 20 cm^3, whereupon further solid was deposited. The product was filtered, washed twice with benzene (2 cm^3) and dried *in vacuo* giving the complex as purple-brown microcrystals (4.05 g, 90%) (slow decomposition above 100°C). (Found: C, 22.9; H, 2.6; N, 2.9%. $C_{16}H_{20}Cl_6N_2O_2W_2$ requires: C, 22.5; H, 2.4; N, 3.3%.)

IR (Nujol) bands at 1280w, 1150w, 1080w, 1058w, 1020w, 975s, 915w, 840s, 755, 618m, 574m, 618m, 550s, 544s, 470m, 384w, 350s, 324m and 292w cm^{-1}.

(b) Tetrachloro - di - μ - ethoxodiethoxobis(phenylimido)ditungsten(VI) (**3**) (0.1 g, 0.1 mmol) in benzene (10 cm^3) was added to a suspension of phenylimido tungsten tetrachloride (0.1 g, 0.1 mmol) in benzene (5 cm^3) and the mixture stirred for 3 h. The volume of the red-brown solution was reduced to *ca* 5 cm^3, whereupon purple-brown microcrystals of the complex were deposited. These were filtered off, washed with petroleum ether and dried *in vacuo*. Physical and spectroscopic properties were identical to the product prepared under (a).

Trichloroethoxo(phenylimido)trimethylphosphinetungsten(VI) (**7**)

Trimethylphosphine (0.13 cm^3, 1.2 mmol) in petroleum ether (30 cm^3) was added to **6** (0.5 g, 0.6 mmol) suspended in petroleum ether (50 cm^3), and the mixture was stirred for 15 h. The solid was filtered, washed with petroleum ether, and dried *in vacuo* leaving the complex as yellow microcrystals (0.54 g, 93%) [m.p. > 140°C (dec.)]. (Found: C, 25.6; H, 4.1; N, 2.6%. $C_{11}H_{19}Cl_3NOPW$ requires: C, 26.3; H, 3.8; N, 2.8%.)

IR (Nujol) bands at 1240m, 1305w, 1285m, 1280w, 1235w, 1278m, 1005s, 990s, 950s, 908s, 850w, 775s, 750m, 720w, 686s, 590m, 555m, 430w, 400w, 338s, 310m, 280s and 250 cm^{-1}.

Tetraethylammonium tetrachloroethoxophenylimidotungstate(VI) (**8**)

Tetraethylammonium chloride (0.175 g, 1.05 mmol) in dichloromethane (30 cm^3) was added to **6** (0.45 g, 0.5 mmol) suspended in dichloromethane (30 cm^3), and the mixture stirred for 2 h. The orange-red solution was filtered and the solvent removed giving a red oil from which crystalline material slowly formed on standing. The product was continually washed, with petroleum ether, filtered, and ground up until the complex was obtained as an orange powder after drying *in vacuo* (0.6 g, 96%). (Found: C, 32.9; H, 5.4; N, 4.6%. $C_{16}H_{30}Cl_4N_2OW$ requires: C, 32.5; H, 5.1; N, 4.7%.) Λ_m(MeCN) = 100.5 Ω^{-1} cm^2 mol^{-1}.

IR (Nujol) bands at 1345s, 1297m, 1250w, 1170m, 1080m, 1020s, 985m, 904s, 984m, 762s, 718w, 684m, 618m, 558m, 474w, 440w, 395w, 330s, 302s and 268s cm^{-1}.

Triphenylcarbonium tetrachloroethoxo(phenylimido)tungstate(VI) (**9** *and* **10**)

(a) Trityl chloride (0.67 g, 2.4 mmol) in dichloromethane (30 cm^3) was added to **6** (1.0 g, 1.2 mmol) in dichloromethane (40 cm^3), and the mixture was stirred for 3 h. The yellow-brown solution was filtered and the solvent removed to give a gummy material which slowly solidified after continual washing with petroleum ether and drying *in vacuo* (1.6 g, 96%). (Found: C, 41.5; H, 3.7; N, 1.5%. $C_{57}H_{56}Cl_{14}N_2O_2W_2$ {i.e. $([W(NPh)Cl_4(O\text{-}Et)][CPh_3]\cdot 1.5CH_2Cl_2$} requires: C, 41.1; H, 3.4; N, 1.7%.) Λ_m(MeCN) = 76.8 Ω^{-1} cm^2 mol^{-1}.

IR (smear) 3100m, 3025m, 2958s, 2925m, 1625m, 1575s, 1560m, 1475s, 1445s, 1370w, 1350s, 1290m, 1260m, 1180m, 1160w, 1080m, 1060m, 1020s, 990s, 910m, 860m, 795s, 758s, 735s, 695s, 680m, 618m, 600m, 550w, 520w, 465m, 400m, 318s, 280s and 250m cm^{-1}.

(b) Trityl ethoxide (0.62 g, 2.2 mmol) in dichloromethane (30 cm^3) was added to phenylimido tungsten tetrachloride dimer (0.9 g, 1.1 mmol) in dichloromethane (40 cm^3), and the mixture was stirred for 4 h. The yellow-brown solution was filtered and the solvent removed to give a gummy material which produced a non-crystalline brown solid after extensive washing with petroleum ether and drying *in vacuo*. (Found: C, 42.6; H, 3.7; N, 1.4%. $C_{28}H_{27}Cl_6NOW$ {i.e. $[W(NPh)Cl_4(O\text{-}Et)][CPh_3]\cdot CH_2Cl_2$} requires: C, 42.6; H, 3.5; N, 1.8%.) Λ_m(MeCN) = 81.7 Ω^{-1} cm^2 mol^{-1}.

IR (smear) identical to that prepared under (a).

X-ray data collection and structure solution

A single crystal of **2** was sealed under nitrogen in a glass capillary and mounted on an Enraf–Nonius CAD4 diffractometer. Cell constants were determined from a least-squares refinement of the setting angles of 25 reflections.

Crystal data. $C_{24}H_{40}Cl_2N_2O_6W_2$, $M = 891.2$, triclinic, space group $P\bar{1}$, $a = 9.637(2)$ Å, $b = 11.135(1)$ Å, $c = 8.016(1)$ Å, $\alpha = 108.47(1)°$, $\beta = 105.51(1)°$, $\gamma = 91.51(1)°$, $U = 780.4(4)$ Å^3, $Z = 1$, $d_c = 1.90$ g cm^{-3}, μ(Mo-K_α) = 80.1 cm^{-1}. A total of 1915 independent data was collected ($\theta_{max} = 22°$) with Mo-K_α radiation using the ω–2θ scan mode. A variable ω-scan width of $(0.8+0.347\tan\theta)°$ was calculated for each reflection as well as a variable horizontal aperture width of $(1.80+1.20\tan\theta)$ mm. A maximum scan time of 50 s was set for each reflection where $\theta \leqslant 18°$ but this was decreased to 40 s for the remainder of the data to speed up the collection. A marked drop in intensity of the three standards monitored was noted during data collection (final intensities had fallen to 65% of their starting value) and the data were scaled to take account of this. An empirical absorption correction was applied[27] with maximum and minimum transmission factors of 0.999 and 0.783, respectively.

The structure was solved by the heavy-atom method and refined by a full-matrix least-squares technique with anisotropic thermal parameters assumed for all non-hydrogen atoms. Final R and R_w values of 0.039 and 0.038, respectively, were calculated for the 167 variables and 1450 data for which $F^2 > 3\sigma(F^2)$. In the refinement the atoms of the phenyl ring were treated as a rigid group (C—C = 1.395 Å and C—H = 1.08 Å). Hydrogen atoms were included in the calculations riding on the carbon atoms to which they were attached (C—H = 1.08 Å) and with group temperature factors determined for each of their various types. Atomic scattering factors were taken from the tabulations of Cromer and Mann,[28] and anomalous dispersion corrections from Cromer and Liberman.[29] The function minimized was $\Sigma W(|F_o|-|F_c|)^2$ with the weight, W, being defined as $0.9316/[\sigma^2(F)+0.001898F^2]$. Final atomic co-ordinates with anisotropic thermal parameters, tables of calculated hydrogen sites and lists of F_o/F_c values have been deposited with the Editor as supplementary material.*

* Atomic co-ordinates for the structure have also been deposited with the Cambridge Crystallographic Data Centre for inclusion in their Data Base. Copies are also available on request from the Editor.

REFERENCES

1. W. A. Nugent and B. L. Haymore, *Coord. Chem. Rev.* 1980, **31**, 123.
2. W. A. Nugent and R. L. Harlow, *J. Chem. Soc., Chem. Commun.* 1979, 342.
3. W. A. Nugent, *Inorg. Chem.* 1983, **22**, 965.
4. A. A. Kuznetsova, Yu. G. Podzolko and Yu. A. Buslaev, *Russ. J. Inorg. Chem.* 1969, **14**, 393.
5. G. V. Goeden and B. L. Haymore, *Inorg. Chem.* 1983, **22**, 157.
6. P. A. Bates, A. J. Nielson and J. M. Waters, *Polyhedron* 1985, **4**, 999.
7. D. M. T. Chan, W. C. Fultz, W. A. Nugent, D. R. Roe and T. H. Tulip, *J. Am. Chem. Soc.* 1985, **107**, 251; D. M. T. Chan and W. A. Nugent, *Inorg. Chem.* 1985, **24**, 1422.
8. A. J. Nielson, J. M. Waters and D. C. Bradley, *Polyhedron* 1985, **4**, 285.
9. A. J. Nielson and J. M. Waters, *Aust. J. Chem.* 1983, **36**, 243.
10. S. F. Pederson and R. R. Schrock, *J. Am. Chem. Soc.* 1982, **104**, 7483.
11. D. C. Bradley, M. B. Hursthouse, K. M. A. Malik, A. J. Nielson and R. L. Short, *J. Chem. Soc., Dalton Trans.* 1983, 2651.
12. W. A. Nugent, R. J. McKinney, R. V. Kasowski and F. A. Van-Catledge, *Inorg. Chim. Acta* 1982, **65**, L91.
13. W. A. Nugent and R. L. Harlow, *Abstracts, National Meeting of the American Chemical Society* 1980, 179, No. PETR-26.
14. W. P. Griffith, A. J. Nielson and M. J. Taylor, unpublished data.
15. D. C. Bradley, R. C. Mehrotra and D. P. Gaur, *Metal Alkoxides.* Academic Press, New York (1978).
16. C. G. Barraclough, D. C. Bradley, J. Lewis and I. M. Thomas, *J. Chem. Soc.* 1961, 2601; C. T. Lynch, K. S. Mazdiyasni, J. S. Smith and W. J. Crawford, *Anal. Chem.* 1964, **36**, 2332.
17. J. Chatt, C. J. Leigh and J. L. Frost, *J. Chem Soc. (A)* 1969, 1674.
18. L. M. Jackman and S. Sternhell, *Applications of Nuclear Magnetic Resonance in Organic Chemistry*, 2nd Edn, p. 150. Pergamon Press, New York (1978).
19. G. C. Levey, R. L. Lichter and G. L. Nelson, *Carbon-13 Nuclear Magnetic Resonance Spectroscopy*, 2nd Edn, p. 111. Wiley, New York (1980).
20. D. C. Bradley, M. B. Hursthouse, K. M. A. Malik and A. J. Nielson, *J. Chem. Soc., Chem. Commun.* 1981, 103; M. G. B. Drew, K. C. Moss and N. Rolfe, *Inorg. Nucl. Chem. Lett.* 1971, 7, 1219; M. G. B. Drew, G. W. A. Fowles, D. A. Rice annd N. Rolfe, *J. Chem. Soc., Chem. Commun.* 1971, 231.
21. V. W. Eichler and H. J. Seifert, *Z. Anorg. Allg. Chem.* 1977, **431**, 123.
22. D. Bright and J. A. Ibers, *Inorg. Chem.* 1969, **16**, 703; 709.
23. M. H. Chisholm, *Polyhedron* 1981, **2**, 681.
24. R. Colton and I. B. Tonkins, *Aust. J. Chem.* 1965, **18**, 447.
25. W. Wolfsberger and H. Schmidbaur, *Synth. React. Inorg. Met.-Org. Chem.* 1974, **4**, 149.
26. A. J. Nielson, *Chem. N.Z.* 1985, **49**, 11.
27. A. C. T. North, D. C. Philips and F. S. Mathews, *Acta Cryst.* 1968, **A24**, 351.
28. D. T. Cromer and J. Mann, *Acta Cryst.* 1968, **A24**, 321.
29. D. T. Cromer and D. Liberman, *J. Chem. Phys.* 1970, **53**, 1891.

Polyhedron Vol. 6, No. 2, pp. 175–179, 1987
Printed in Great Britain

0277–5387/87 $3.00+.00
Pergamon Journals Ltd

COMPLEXES OF 2,2′-BIPYRIMIDINE WITH SOME LANTHANIDES

QASSEM JARADAT and TALAL AKASHEH*

Chemistry Department, Yarmouk University, Irbid, Jordan

(*Received* 20 *August* 1985; *accepted after revision* 13 *May* 1986)

Abstract—Complexes of the lanthanide ions, La^{3+}, Eu^{3+}, Ce^{3+}, Yb^{3+} and Ho^{3+} as well as that of Y^{3+} with the ligand 2,2′-bipyrimidine have been prepared and their physico-chemical properties studied.

Complexes of lanthanides with nitrogen-donor ligands of weak basicity have been known for some time.[1–3] However, 2,2′-bipyridine,[4,5] 1,10-phenanthroline,[6–8] terpyridine[9] and 1,3,5-tri(2-pyridil)-2,4,6-triazine[10] yield complexes whose thermal stability is high, but were found to be unstable in aqueous solution.[8] Water often displaces the ligands to an extent that conventional physical methods in solution often fail to give information about the complexes. Nevertheless, phenanthroline has been shown to change the UV–vis spectra in water. Furthermore, the idea that oxygen donor ligands are more competitive towards the lanthanides has been shown to be erroneous provided the right solvent is chosen.[12,13]

Lanthanide complexes show exceptionally high coordination numbers and this was best established by X-ray crystallography.[4,5]

2,2′-Bipyrimidine (bpm) has recently become a popular substitute for 2,2′-bipyridine in many metal complexes.[14,15] Bpm also acts as a bridging ligand forming bimetallic complexes.[14,15] In this work we report the preparation and characterization of bpm complexes with Y^{3+} and the lanthanides La^{3+}, Ho^{3+}, Ce^{3+}, Eu^{3+} and Yb^{3+}

EXPERIMENTAL

2,2′-Bipyrimidine (Lancaster Synthesis) was recrystallised from benzene. All metal salts were purchased from Laborat and used without further purification. All solvents were AR grade.

UV–vis and IR spectra were recorded using Pye–Unicam SP8-100 and SP-300 spectrophotometers, respectively. NMR spectra were recorded on a Bruker WP80SY instrument. A Harris meter was used for conductivity measurements. Elemental analysis was done by Butterworths Laboratories, England.

The ligand 2,2′-bipyrimidine was reacted with the lanthanide salts listed in Table 1 under the given conditions. The pale yellow Ce^{3+} complex melts and resolidifies at 330°C, while all other complexes do not melt or decompose below 350°C.

$LaCl_3 \cdot 6H_2O$

To a stirred solution of $LaCl_3 \cdot 6H_2O$ (0.23 g, 0.6 mmole) in 20 cm^3 of hot ethanol, was added a hot solution of bipyrimidine (0.19 g, 1.2 mmole) in ethanol (15 cm^3). A white precipitate appeared almost immediately. After 2 min of stirring, the mixture was cooled and filtered. The solid was washed with hot ethanol (twice), ether, and dried by suction. The yield was 0.25 g (66%). The complex does not melt or decompose up to 350°C.

RESULTS AND DISCUSSION

The elemental analysis for the complexes is shown in Table 2. Although the exact coordination number and structure cannot be determined from any of the physical measurements done in this work, it can be safely assumed that Y^{3+} and Eu^{3+} complexes have a bridging bipyrimidine with two metal centres. These were the only bimetallic species we

* Author to whom correspondence should be addressed.

Table 1. Synthesis of the complexes in ethanol

Lanthanide salt	Ligand to metal mole ratio	Reaction time and condition	Purification	Yield
$HoCl_3 \cdot 6H_2O$	1 : 1	hot stirring; 10 min	wash with ethanol	52%
$YbCl_3 \cdot 6H_2O$	1 : 1	reflux; 1 h	crystallize from ethanol	35%
$EuCl_3 \cdot 6H_2O$	2 : 3	hot; 2 min	wash: hot ethanol and ether	47%
$Ce(NO_3)_3 \cdot 6H_2O$	1 : 1	reflux; 30 min	wash: acetone, ether	82%
$YCl_3 \cdot 6H_2O$	1 : 1	hot stirring; 90 min	wash: ethanol	73%

Table 2. Elemental analyses of the metal complexes

Compound	%C Found (Calc.)	%H Found (Calc.)	%N Found (Calc.)
$La(bpm)_2Cl_3 \cdot 3H_2O$	31.2 (31.0)	3.3 (3.0)	18.3 (18.2)
$Ho(bpm)_2Cl_3 \cdot 6H_2O$	27.6 (27.5)	3.4 (3.4)	16.2 (16.2)
$Yb(bpm)_2Cl_3 \cdot 7H_2O$	26.2 (26.6)	3.4 (3.6)	15.6 (15.5)
$Eu_2(bpm)_3Cl_6 \cdot 8H_2O$	25.0 (25.4)	3.0 (3.0)	14.8 (14.8)
$Ce(bpm)_3(NO_3)_3 \cdot 2H_2O$	29.4 (28.9)	2.7 (2.4)	22.1 (22.7)
$Y_2(bpm)_3Cl_6 \cdot 7H_2O$	28.8 (29.1)	3.4 (3.3)	17.4 (17.0)

Table 3. UV–vis spectra and conductivities of the complexes in DMF

Compound	λ_{max} (nm)	$\varepsilon \times 10^{-3}$ ($l.mole^{-1}\ cm^{-1}$)	Λ_m ($ohm^{-1}\ cm^2\ mol^{-1}$)
2,2′-bipyrimidine	288 (sh)	0.99	—
	266	2.38	—
$La(bpm)_2Cl_3 \cdot 3H_2O$	290	1.50	94
	266	2.90	—
$Ho(bpm)_2Cl_3 \cdot 6H_2O$	291	1.62	84
	266	3.19	—
$Y_2(bpm)_3Cl_6 \cdot 7H_2O$	290	1.72	153
	266	3.33	—
$Eu_2(bpm)_3Cl_6 \cdot 8H_2O$	288	2.05	168
	266	4.18	—
$Yb(bpm)_2Cl_3 \cdot 7H_2O$	292	1.17	63
	266	2.55	—
$Ce(bpm)_3(NO_3)_3 \cdot 2H_2O$	289	2.82	130
	266	3.76	—

Table 4. Proton NMR spectra of complexes[a]

2,2′-bipyrimidine[32]	d : 9.21 ; t : 7.78
$La(bpm)_2Cl_3 \cdot 3H_2O$	d : 9.24 ; t : 7.77
$Eu_2(bpm)_3Cl_6 \cdot 8H_2O$	d : 9.20 ; t : 7.95
$Y_2(bpm)_3Cl_6 \cdot 7H_2O$	d : 9.10 ; t : 7.72
$Ce(bpm)_3(NO_3)_3 \cdot 2H_2O$	d : 9.00 ; t : 7.66
$Yb(bpm)_2Cl_3 \cdot 7H_2O$	d : 9.13 ; t : 7.76
$Ho(bpm)_2Cl_3 \cdot 6H_2O$	d : 8.42 ; t : 7.32

d = doublet, t = triplet.
[a] Chemical shifts are in ppm, solvent is deuterated DMF.

could obtain. Attempts to prepare pure bimetallic species from the other five salts failed. The tendency to form bimetallic species could be explained by weak σ-bonding and favourable π-bonding. When a metal atom is attached on one side of the ligand, strong σ-bonding withdraws the charge density from the ligands thus making the non-bonding electrons on the other side less available for complexation. π-back donation would have the opposite effect. Thus weak σ-bonding and/or stronger π-bonding (and favourable mole ratios) seem to favour the bimetallic Eu^{3+} species over the other lanthanides studied. Y^{3+} has a noble gas configuration with no *f* or *d* orbitals capable of exhibiting ligand field stabilisation. Hence an overall weak bonding tends to retain the charge density on the ligand allowing formation of a bridge between the two Y^{3+} centres.

Table 3 shows UV bands for the complexes. Since the complexes show the free (bpm) spectrum in water, DMF was used as the solvent. The bands in bpm are assigned as π,π^* (266 nm) and n,π^* (288 nm) based on experimental[14,15] and theoretical results.[16] The intensity of the bands increases and only small shifts in the n,π^* transition are observed. This indicates that the metal–ligand bonds, though existent in DMF, are probably weak (and of course non-existent in water). This result is also consistent with the NMR chemical shifts (Table 4) which differ only slightly from bpm except for the fact that Yb^{3+} and Ho^{3+} give broader and less-resolved spectra.

The best evidence for the existence of the complex species in DMF comes from conductivity (Table 3). La^{3+}, Ho^{3+} and Yb^{3+} yield results indicating a 1 : 1 electrolyte ratio, with two chlorines within the coordination sphere. Europium, cerium and yttrium give results consistent with a 2 : 1 electrolyte ratio, thus confirming the complexed species and the number of coordinated anions (four for Cl^- in Eu and Y; one NO_3^- for Ce). By contrast the conductivity in water is much higher due to free salts (for example, the europium complex yields a molar conductivity of 897 $ohm^{-1}\ cm^2\ mol^{-1}$ indicating the dissociation into two Eu^{3+} (hydrated) and six Cl^- ions).

The high thermal stability of the solids and the lability of the complexes in water is consistent with bpy and phen results.[1–6,12,13]

The IR results are shown in Table 5 for the solids in KBr discs. By comparison with bpm the ν(C=N) band in the ring increases in frequency except for Ce (decreases by 1 cm^{-1}). The effect varies from a shift of 2 cm^{-1} in La and Ho to a maximum of 12 cm^{-1} in Yb. The rise in this frequency is due to complexation.[17–19] Sigma bonding (as in protonation) causes a rise in the frequency while π-bonding causes a decrease.[17] The small effect in the present complexes compared to those of Pt, Pd, Os and Rh[15,20,21] is ascribed to weaker bonding. The CN band is broadened in the complexes and therefore masks the C=C band (1547 cm^{-1} in bpm). Other bands in the table show varying degrees of shifts, the biggest being in the ring breathing mode (1029 cm^{-1} in bpm). Bands in the regions 3300–3500 cm^{-1} and 1625–1640 cm^{-1} are due to lattice and coordinated water. A band in the range 500–750 cm^{-1} is usually assigned to coordinated water.[22] In our case such a band might very well be the band around 685 cm^{-1} (of varying strength) which appears in all complexes except that of yttrium. The cerium complex shows an γ(N—O—N) at 1320 cm^{-1} indicating uncoordinated NO_3^- and γ(N—O—N) at 1546 cm^{-1}(s) indicating a mono-coordinated NO_3^-.[14]

In conclusion, we have been able to extend the behaviour of 2,2′-bipyridine towards lanthanides to the ligand 2,2′-bipyrimidine. The latter's bridging properties have also been made use of in the case of two complexes. X-ray analysis of the solid complexes should determine the high coordination number expected by comparison to those of 2,2′-bipyridine.[4,5,12,13]

Table 5. IR spectra of 2,2′-bipyrimidine and its complexes[a]

	ν(O—H)	ν(C=N)	ν(C=C)	Ring stretching	β(C—H)	Ring breathing	γ(C—H)	Ring bending	γ(H—O—H)	Unassigned
bpm		1558(s)	1547(s)	1403(s)	1140(m)	1029(m)	823(m) 765(w)	637(w)		3012(w) 3038(w) 3072(s) 1115(w) 1107(m) 788(w) 683(w)
$La(bpm)_2Cl_3 \cdot 3H_2O$	3300(m.b)	1560(s)	—	1409(s)	1138(m)	1007(m)	822(m) 758(s)	650(s)	1640(m)	689(m)
$Ho(bpm)_2Cl_3 \cdot 6H_2O$	3400(m.b)	1560(s)	1540(sh)	1404(s)	1142(w)	1000(m)	815(m) 758(s)	647(m)	1625(w.b)	1260(w)
$Yb(bpm)_2Cl_3 \cdot 7H_2O$	3500(s.b)	1570(s)	—	1403(s)	1150(m)	1000(m)	820(m) 765(s)	650(s)	—	1150(m) 690(m)
$Ce(bpm)_3(NO)_3 \cdot 2H_2O$[b]	3360(m.b)	1557(s)	—	1398(s)	1132(m)	1005(s)	818(s) 751(s)	643(s)	1630(sh)	3090(w) 2970(sh) 1450(b) 1240(sh) 1198(m) 1162(w) 1105(w) 1087(sh) 1078(m) 1061(sh) 1036(s) 1005(sh) 1000(m) 989(m) 879(w) 850(m) 818(s) 810(s) 770(w) 720(s) 677(s)
$Eu_2(bpm)_3Cl_6 \cdot 8H_2O$	3400(s.b)	1565(s)	—	1408(s)	1140(w)	1005(w)	752(s)	650(m)	1625(m)	682(w)
$Y_2(bpm)_3Cl_6 \cdot 7H_2O$	3500(s.b)	1565(s)	—	1403(s)	1145(w)	1002(w)	838(w) 765(s)	645(m)	1638(m)	1083(w)

[a] Assignments based on ref. 17.
[b] (N—O—N) free = 1320 (b); (N—O—N mono-coordinated) = 1546 (s).

REFERENCES

1. F. A. Hart and F. P. Laming, *Proc. Chem. Soc., London* 1963, 107.
2. N. I. Lobanov and V. A. Smirnova, *Zh. Neorg. Khim.* 1963, **8**, 2208.
3. N. I. Lobanov and V. A. Smirnova, *Zh. Neorg. Khim.* 1963, **8**, 2206.
4. A. R. Al-Karaghouli and J. S. Wood, *J. Am. Chem. Soc.* 1968, **90**, 6548.
5. A. R. Al-Karaghouli and J. S. Wood, *Inorg. Chem.* 1972, **11**, 2293.
6. S. P. Sinha and H. M. N. H. Irving, *Anal. Chem. Acta* 1970, **52**, 193.
7. K. K. Rohargi and S. K. Sen Gupta, *J. Inorg. Nucl. Chem.* 1970, **32**, 2247.
8. F. A. Hart and F. P. Laming, *J. Inorg. Nucl. Chem.* 1964, **26**, 579.
9. D. A. Durham, G. H. Frost and F. A. Hart, *J. Inorg. Nucl. Chem.* 1969, **31**, 833.
10. D. A. Durham, G. H. Frost and F. A. Hart, *J. Inorg. Nucl. Chem.* 1969, **31**, 571.
11. L. I. Kononenko and N. S. Poluektov, *Rus. J. Inorg. Chem.* 1962, **7**, 965.
12. T. Moeller, In *Complexes of the Lanthanides in MTP International Review of Science* (Edited by K. G. Bagnall), Series 1, Vol. 7, p. 275. Butterworths, London (1972).
13. J. H. Forsberg, *Coord. Chem. Rev.* 1973, **10**, 195.
14. P. A. Westcott, Ph.D. Thesis, Colorado State University (1971).
15. Q. Jaradat, K. Barqawi and T. S. Akasheh, *Inorg. Chim. Acta* 1986, **116**, 63.
16. V. Barone, C. Cauletti, F. Lelji, M. N. Piancastelli and N. Ruso, *J. Am. Chem. Soc.* 1982, **104**, 4571.
17. A. R. Katritzky and P. J. Taylor, In *Methods in Heterocyclic Chemistry* (Edited by A. R. Katritzky), Vol. 4, p. 325. Academic Press, New York (1971).
18. P. T. T. Wong and D. G. Brewer, *Can. J. Chem.* 1968, **46**, 131.
19. D. Cook, *Can. J. Chem.* 1964, **42**, 1964.
20. M. P. Kiernar and A. Ludi, *J. Chem. Soc., Dalton Trans.* 1978, **9**, 1127.
21. V. F. Sutcliffe and G. B. Young, *Polyhedron* 1984, **3**, 87.
22. K. Nakomoto, *Infrared and Raman Spectra of Inorganic and Coordination Compounds*, p. 227, 3rd edn. Wiley, New York (1978).

Polyhedron Vol. 6, No. 2, pp. 181–187, 1987
Printed in Great Britain

0277–5387/87 $3.00+.00

THE STRUCTURE OF AQUA-HYDROXO DOUBLE SALTS

MICHAEL ARDON* and AVI BINO

Department of Inorganic and Analytical Chemistry, The Hebrew University of Jersualem, 91904 Jerusalem, Israel

and

W. GREGORY JACKSON

Department of Chemistry, The University of New South Wales, Duntroon, A.C.T. 2600, Australia

(*Received* 3 *March* 1986; *accepted* 19 *May* 1986)

Abstract—The preparation and structure of two so-called aqua-hydroxo double salts of cobalt(III) are reported. X-ray structural analysis showed the compounds not to be double salts of two distinct mononuclear cations but to contain one binuclear cation in which the two equivalent cobalt atoms are bridged by a hydrogen oxide ligand (μ-H_3O_2).

Compound **1**, *trans*-$\{[Co(en)_2NO_2]_2(H_3O_2)\}(ClO_4)_3 \cdot 2H_2O$ forms monoclinic crystals, space group $P2_1/n$, with $a = 12.098(2)$ Å, $b = 8.981(1)$ Å, $c = 14.415(2)$ Å, $\beta = 93.39(2)°$, $V = 1563(1)$ Å^3 and $Z = 2$. Compound **2**, *trans*-$\{[Co(en)_2NCS]_2(H_3O_2)\}(CF_3SO_3)_3 \cdot H_2O$ forms triclinic crystals, space group $P\bar{1}$ with $a = 12.864(2)$ Å, $b = 14.429(2)$ Å, $c = 11.177(1)$ Å, $\alpha = 105.21(3)°$, $\beta = 100.33(2)°$, $\gamma = 65.96(2)°$, $V = 1822(1)$ Å^3 and $Z = 2$.

The two structures were refined by least-squares methods to residuals of $R = 0.077$, $R_w = 0.087$ and $R = 0.063$, $R_w = 0.069$, respectively. In **1**, the dimer resides on a crystallographic inversion center and the O···O separation in the H_3O_2 bridge is 2.412(9) Å. In **2** there is no crystallographic symmetry imposed upon the dimer but the two Co—O(H_3O_2) distances are identical within the experimental error. The O···O length in the H_3O_2 unit is 2.415(6) Å.

The structural features of classical hydroxoaqua ions $[ML_4(H_2O)OH]^{(n-1)+}$ were reported recently.[1] These ions, which may be obtained by neutralization of the diaqua ion $[ML_4(H_2O)_2]^{n+}$ with one equivalent of OH^- ions, are not mononuclear in the crystalline state, but binuclear or polynuclear. Each metal atom in these species is bridged by two *hydrogen oxide* ligands (H_3O_2) to neighboring metal atoms: *cis*-hydroxoaqua ions are doubly bridged dimers, $[L_4M(H_3O_2)_2ML_4]^{2(n-1)+}$, while *trans*-hydroxoaqua ions form chains of metal atoms linked by single H_3O_2 bridges $\cdots M(L_4)(H_3O_2)M(L_4)(H_3O_2)\cdots$.[1] The centered hydrogen bond between the two oxygen atoms of the H_3O_2 ligand is short[1,2] and very strong.[3] Hydrogen oxide bridging between the metal atoms persists in concentrated aqueous solutions.[4]

Neutralization of a *monoaqua* ion such as $[ML_5(H_2O)]^{n+}$ by one equivalent of OH^- produces the classical, mononuclear hydroxo ion $[ML_5(OH)]^{(n-1)+}$. If less than one equivalent of OH^- is added, a mixture of monoaqua and monohydroxo ions is obtained, and at pH = pK_a the ratio of these two species is, of course, 1:1. When such a 1:1 solution is concentrated, either the salt of the aqua ion or that of the hydroxo ion will crystallize, depending on their relative solubilities. However, in some cases neither the aqua salt nor the hydroxo salt but an 'aqua hydroxo double salt' such as $[Co(en)_2(OH_2)N_3][Co(en)_2(OH)N_3](ClO_4)_3$ will precipitate.[5] The results of our earlier work[1] raised the

* Author to whom correspondence should be addressed.

possibility that these so called double salts were symmetric binuclear ions bridged by a single H_3O_2 ligand. The present investigation was undertaken to test this assumption. Herein, the preparation and structure of two typical 'double salts' *trans*-$\{[Co(en)_2(NO_2)]_2(H_3O_2)\}(ClO_4)_3 \cdot 2H_2O$, **1** and *trans*-$\{[Co(en)_2(NCS)]_2(H_3O_2)\}(CF_3SO_3)_3 \cdot H_2O$, **2** are reported.

EXPERIMENTAL

Preparations

trans-$\{[Co(en)_2NO_2]_2(H_3O_2)\}(ClO_4)_3 \cdot 2H_2O$, **1**. To *trans*-$[Co(en)_2(NO_2)(NO_3)]NO_3$[6] (5.9 g) in H_2O (30 cm^3) were added NaOH (1.35 g) and $NaClO_4$ (10 g). After 10 min, 2.13 cm^3 of $HClO_4$ 70.0% were added. The golden crystalline precipitate, which began to form immediately, was filtered after 1 h and washed with ethanol and ether. Suitable crystals for the X-ray study were obtained from the filtrate at 0°C after 24 h.

trans-$\{[Co(en)_2NCS]_2(H_3O_2)\}(CF_3SO_3)_3 \cdot H_2O$, **2**. A solution of *trans*-$[Co(en)_2(NCS)OH]NCS \cdot H_2O$[7] (5.0 g) in $HClO_4$ (4 M, 15 cm^3) was neutralized to pH $\approx$ 7 with NaOH (4 M, 17 cm^3), whereupon *trans*-$\{[Co(en)_2(NCS)]_2(H_3O_2)\}(ClO_3)_3 \cdot H_2O$ (5.3 g, 85%) crystallized. The product was washed with ethanol and ether, and air-dried. Recrystallization from a saturated aqueous solution using $NaClO_4$ (5 M) precipitant and cooling yielded red prisms. Found: C, 14.5; H, 4.4; N, 16.8; S, 7.8; Cl, 13.0%. Calc. for $Co_2C_{10}H_{37}N_{10}Cl_3O_{15}S_2$: C, 15.54; H, 4.52; N, 16.97; S, 7.77; Cl, 12.88%. Its visible absorption spectrum in water (self-buffered) was exactly intermediate between those in 0.01 M $HClO_4$ [$\varepsilon_{max}(538) = 184.6$] and 0.01 M NaOH [$\varepsilon_{max}(508) = 99.0$] indicating that the solution consisted of a 1:1 mixture of the hydroxo and the aqua ions with no evident interaction between them (see discussion section). Crystals of the ClO_4^- salt were found to be unsuitable for an X-ray study. A small sample (0.05 g) was dissolved in 10 cm^3 of $NaCF_3SO_3$ (2.5 M) and the solution was kept at 4°C. Red prisms of **2** were obtained after 24 h.

Two other complexes of the same group $[Co(en)_2A]_2(H_3O_2)(ClO_4)_3$ were prepared, A = N_3^-,[5a] CN^-,[5b] but suitable crystals for X-ray studies could not be obtained.

X-ray crystallography

Crystallographic data and other pertinent information are given in Table 1. Data were measured by using a ω–2θ motion. The scan width, $\Delta\omega$, for each reflection was 1° with a scan time of 20 s. Background measurements were made for another 20 s at both limits of each scan. Three standard reflections were monitored every 60 min. No systematic variations in intensities were found for either compound. For each crystal, Lorentz and polarization corrections were applied. For **1** and **2**, ψ-scans of several reflections indicated that no absorption corrections were necessary. The heavy atom positions in **1** and **2** were obtained from a three-dimensional Patterson function.[8]

In **1**, anisotropic thermal parameters were used for all non-hydrogen atoms of the complex and for the perchlorate chlorine atoms. All the perchlorate oxygens were refined isotropically. There are two kinds of perchlorate ions in the asymmetric unit, both exhibit twofold disorder. The first, Cl(1), is disordered about the crystallographic inversion center at 0, $\frac{1}{2}$, 0. The two disordered tetrahedra share one edge [O(11)—O(11′)]. The chlorine and two of the oxygen atoms, O(12) and O(13) were refined with a half occupancy factor and O(11) with a full one. The difference Fourier map showed that the central chlorine atom, Cl(2), of the second perchlorate ion was surrounding by eight peaks, indicating a twofold disorder of the oxygen atoms. Each of the two disordered ClO_4^- units at this location was treated as a rigid body with a fixed Cl—O distance of 1.50 Å. The eight oxygen atoms [O(14) through O(21)] were refined with a half occupancy factor and Cl(2) with a full one.

Hydrogen atoms of the en ligands were introduced at calculated positions as fixed contributions to F. The two hydrogen atoms of the H_3O_2 ligand, H(1) and H(2) were located from the difference Fourier map. H(1) was found to reside on a crystallographic inversion center at 0, $\frac{1}{2}$, $\frac{1}{2}$. H(1) and H(2) were introduced in fixed positions and their thermal parameters were included in the least-squares refinement [$U = 0.05(3)$ and 0.09(5), respectively].

In **2**, anisotropic thermal parameters were used for cobalt, sulfur, fluorine and oxygen atoms and isotropic ones for all carbon atoms and for the oxygen atom of the lattice water molecule, OL. The two terminal hydrogen atoms of the $H_3O_2^-$ unit, H(1) and H(2) and all the amine hydrogen atoms of the en ligands were located from the difference Fourier map and their positional parameters were included in the final cycles using the riding model. The positions of the methylene hydrogen atoms in the en ligands were calculated and were included in the final cycles as fixed contribution to F. The thermal parameter for all the hydrogen atoms was $U = 0.05$. The structure was refined using two blocks, the first included all the atoms of the dimeric

Table 1. Crystallographic data[a]

	Compound 1	Compound 2
Formula	$C_8Cl_3Co_2H_{39}N_{10}O_{20}$	$C_{13}Co_2F_9H_{37}N_{10}O_{12}S_5$
FW	819.67	974.66
Space group	$P2_1/n$	$P\bar{1}$
a (Å)[b]	12.098(2)	12.864(2)
b (Å)	8.981(1)	14.429(2)
c (Å)	14.415(2)	11.177(1)
α (deg)	—	105.21(3)
β (deg)	93.39(2)	100.33(2)
γ (deg)	—	65.96(2)
V (Å^3)	1563(1)	1822(1)
Z	2	2
d (calc.) (g cm^{-3})	1.741	1.776
μ (cm^{-1})	13.26	12.23
Crystal color and habit	orange prisms	red prisms
Crystal size (mm)	$0.33\times0.50\times0.65$	$0.36\times0.30\times0.25$
Range of 2θ (deg)	3–50	3–45
Observations	$\pm h, k, l$	$\pm h, \pm k, l$
Systematic reflection absences	$h0l$, $h+l=2n+1$	—
	$0k0$, $k=2n+1$	—
No. of data collected	3068	4663
No. of unique data	2724	4663
Data with $F_o^2 > 3\sigma(F_o^2)$	2202	3126
R	0.077	0.063
R_w	0.087	0.069

[a] Data were collected at 20 ± 2°C on a PW 1100 Philips four-circle diffractometer using Mo-K_α ($\lambda = 0.71069$ Å) radiation monochromatized by a graphite crystal.

[b] Unit cell dimensions were obtained by a least-squares fit of 25 reflections in the range $12° < \theta < 16°$.

cation and the crystal water oxygen OL and the second included all the atoms of the three $CF_3SO_3^-$ ions. Values of the atomic scattering factors and the anomalous terms were taken from the conventional sources.[9]

The discrepancy indices $R_1 = \sum||F_o|-|F_c||/\sum|F_o|$ and $R_w = [\sum w(|F_o|-|F_c|)^2/\sum w|F_o|^2]^{1/2}(w = 1/\sigma^2|F|)$ are listed in Table 1. Lists of atomic positional and thermal parameters and observed and calculated structure factors have been deposited as supplementary material with the Editor, from whom copies are available on request. Atomic co-ordinates have also been deposited with the Cambridge Crystallographic Data Centre.

RESULTS

Compound **1**: trans-$[Co(en)_2(NO_2)]_2(H_3O_2)(ClO_4)_3\cdot 2H_2O$

The bond distances and angles are presented in Table 2. Figure 1 shows the numbering scheme of **1**. With $Z = 2$ in space group $P2_1/n$ there is only half a $\{[Co(en)_2(NO_2)]_2(H_3O_2)\}^{3+}$ ion in the asymmetric unit, with the other half related to it by a crystallographic inversion center at 0, $\frac{1}{2}$, $\frac{1}{2}$. This inversion center is located midway between the two oxygen atoms of the hydrogen oxide unit (O1 and O1′). There are six perchlorate ions in the cell. Four occupy general positions and two reside on twofold crystallographic inversion centers. All these perchlorate units are subjected to a twofold disorder as described in the Experimental section.

The O···O separation and other relevant distances and angles concerning the $H_3O_2^-$ units are listed in Table 4.

Compound **2**: trans-$[Co(en)_2(NCS)]_2(H_3O_2)(CF_3SO_3)_3\cdot H_2O$

Table 3 gives the important bond lengths and angles. Figure 2 shows the numbering scheme in the dimer. With $Z = 2$ in the cell of space group $P\bar{1}$ there is no crystallographic symmetry imposed upon the

Table 2. Important bond lengths (Å) and bond angles (°) for **1**

Bond lengths			
Co—O(1)	1.906(6)	N(2)—C(1)	1.46(1)
Co—N(1)	1.900(7)	N(3)—C(2)	1.47(1)
Co—N(2)	1.947(7)	N(4)—C(3)	1.48(1)
Co—N(3)	1.954(7)	N(5)—C(4)	1.48(1)
Co—N(4)	1.952(6)	C(1)—C(2)	1.46(1)
Co—N(5)	1.950(7)	C(3)—C(4)	1.51(1)
O(1)—O(1)′	2.412(9)	Cl(1)—O(11)	1.50(1)
O(1)—H(1)	1.206(6)	Cl(1)—O(11)′	1.55(1)
O(1)—H(2)	0.817(6)	Cl(1)—O(12)	1.51(1)
O(2)—N(1)	1.21(1)	Cl(1)—O(13)	1.44(2)
O(3)—N(1)	1.224(9)		
Bond angles			
O(1)—Co—N(1)	178.7(3)	Co—N(1)—O(2)	120.3(6)
O(1)—Co—N(2)	90.5(3)	Co—N(1)—O(3)	121.4(6)
O(1)—Co—N(3)	87.7(3)	O(2)—N(1)—O(3)	118.3(7)
O(1)—Co—N(4)	91.1(3)	Co—N(2)—C(1)	110.1(6)
O(1)—Co—N(5)	89.7(3)	Co—N(3)—C(2)	109.2(7)
N(1)—Co—N(2)	88.7(3)	Co—N(4)—C(3)	108.4(6)
N(1)—Co—N(3)	91.2(3)	Co—N(5)—C(4)	110.4(6)
N(1)—Co—N(4)	90.0(3)	N(2)—C(1)—C(2)	110.5(9)
N(1)—Co—N(5)	91.1(3)	N(3)—C(2)—C(1)	109.2(1)
N(2)—Co—N(3)	85.9(3)	N(4)—C(3)—C(4)	109.2(8)
N(2)—Co—N(4)	93.2(3)	N(5)—C(4)—C(3)	105.9(8)
N(2)—Co—N(5)	179.4(3)	O(11)—Cl(1)—O(11)′	95.8(7)
N(3)—Co—N(4)	178.4(3)	O(11)—Cl(1)—O(12)	114.4(9)
N(3)—Co—N(5)	94.7(3)	O(11)—Cl(1)—O(13)	115.7(1)
N(4)—Co—N(5)	86.2(3)	O(11)′—Cl(1)—O(12)	114.2(8)
Co—O(1)—H(2)	127.3(6)	O(11)′—Cl(1)—O(13)	115(1)
Co—O(1)—O(1)′	129.8(3)	O(12)—Cl(1)—O(13)	102(1)
H(2)—O(1)—O(1)′	97.9(5)		

complex. Structural features concerning the $H_3O_2^-$ bridge are summarized in Table 4. The $CF_3SO_3^-$ ions are hydrogen bonded through the oxygen atoms to en nitrogen atoms with O···N distances in the normal range of 2.90–3.00 Å. The two terminal hydrogen atoms of the $H_3O_2^-$ unit form two hydrogen bonds: O(1)—O(8) (O_3SCF_3) and O(2)—O(3) (O_3SCF_3) with distances of 2.86(1) Å and 2.89(1) Å, respectively.

DISCUSSION

A double salt formulation for compound **1**, $[Co(en)_2(NO_2)(H_2O)][Co(en)_2(NO_2)(OH)](ClO_4)_3 \cdot$

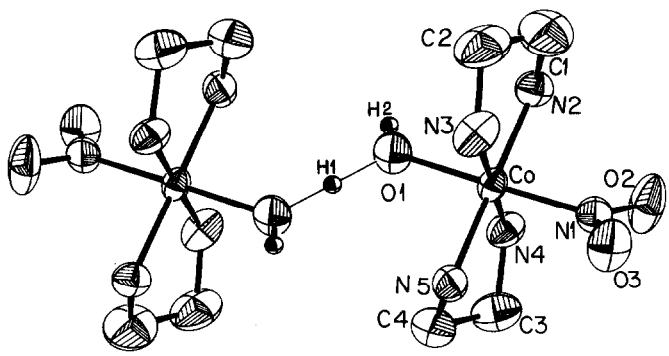

Fig. 1. The structure of *trans*-$[NO_2(en)_2Co(H_3O_2)Co(en)_2NO_2]^{3+}$ as found in **1**. The thermal ellipsoids are of 50% probability. The hydrogen atoms were given an arbitrary thermal parameter.

Table 3. Important bond lengths (Å) and bond angles (°) for **2**

Bond lengths			
Co(1)—O(1)	1.911(5)	Co(2)—N(9)	1.960(8)
Co(1)—N(1)	1.887(7)	Co(2)—N(10)	1.952(7)
Co(1)—N(2)	1.948(9)	S(1)—C(1)	1.62(1)
Co(1)—N(3)	1.952(7)	S(2)—C(6)	1.62(1)
Co(1)—N(4)	1.961(9)	O(1)—H(1)	1.067(9)
Co(1)—N(5)	1.944(6)	O(2)—H(2)	0.959(8)
Co(2)—O(2)	1.916(5)	O(1)—O(2)	2.415(6)
Co(2)—N(6)	1.882(7)	N(1)—C(1)	1.14(1)
Co(2)—N(7)	1.949(8)	N(6)—C(6)	1.17(1)
Co(2)—N(8)	1.940(7)		
Bond angles			
O(1)—Co(1)—N(1)	178.7(4)	N(6)—Co(2)—N(7)	89.4(4)
O(1)—Co(1)—N(2)	90.9(3)	N(6)—Co(2)—N(8)	91.4(4)
O(1)—Co(1)—N(3)	91.4(4)	N(6)—Co(2)—N(9)	89.7(4)
O(1)—Co(1)—N(4)	89.1(3)	N(6)—Co(2)—N(10)	89.2(4)
O(1)—Co(1)—N(5)	89.0(3)	N(7)—Co(2)—N(8)	86.8(4)
N(1)—Co(1)—N(2)	88.8(4)	N(7)—Co(2)—N(9)	178.8(4)
N(1)—Co(1)—N(3)	89.8(4)	N(7)—Co(2)—N(10)	93.8(4)
N(1)—Co(1)—N(4)	91.2(4)	N(8)—Co(2)—N(9)	94.0(4)
N(1)—Co(1)—N(5)	89.7(4)	N(8)—Co(2)—N(10)	179.2(4)
N(2)—Co(1)—N(3)	86.0(4)	N(9)—Co(2)—N(10)	85.5(4)
N(2)—Co(1)—N(4)	179.5(4)	Co(1)—O(1)—H(1)	103.1(7)
N(2)—Co(1)—N(5)	93.7(4)	Co(2)—O(2)—H(2)	106.1(7)
N(3)—Co(1)—N(4)	93.5(4)	H(1)—O(1)—O(2)	117.9(6)
N(3)—Co(1)—N(5)	179.5(3)	O(1)—O(2)—H(2)	107.7(7)
N(4)—Co(1)—N(5)	86.8(4)	Co(1)—O(1)—O(2)	135.9(3)
O(2)—Co(2)—N(6)	179.0(3)	Co(2)—O(2)—O(1)	132.3(3)
O(2)—Co(2)—N(7)	89.9(3)	Co(1)—N(1)—C(1)	171.0(9)
O(2)—Co(2)—N(8)	87.9(3)	Co(2)—N(6)—C(6)	166.5(8)
O(2)—Co(2)—N(9)	91.0(3)	S(1)—C(1)—N(1)	178(1)
O(2)—Co(2)—N(10)	91.5(3)	S(2)—C(6)—N(6)	178.8(1)

$2H_2O$, implies the existence of *two* distinct cationic species in the crystal, an aqua ion and a hydroxo ion, having two different Co—O distances. Structures **1** and **2** are not of this kind. They are definitely not double salts, but salts of a single unique, binuclear cation $[(en)_2XCo(H_3O_2)CoX(en)_2]^{3+}$ (X = NO_2, NCS). The two cobalt atoms in this cation have identical coordination spheres. They have the features of neither a hydroxo nor an aqua ion. The Co—$O(H_3O_2)$ distance, is intermediate between those found in hydroxo and aqua ions. In **1** the two M—$O(H_3O_2)$ distances of 1.906(6) Å are symmetry

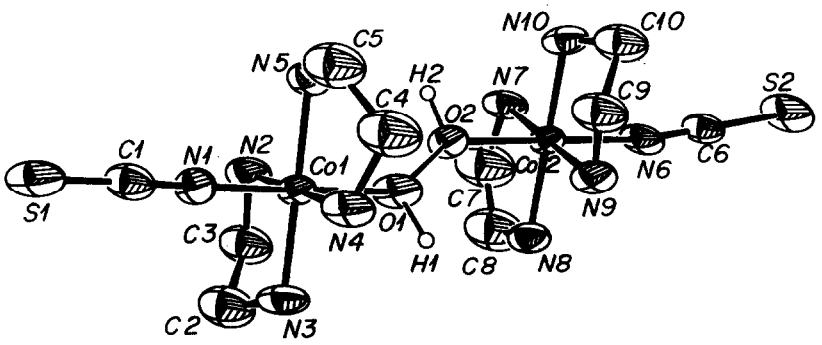

Fig. 2. The structure of *trans*-$[SCN(en)_2Co(H_3O_2)Co(en)_2NCS]^{3+}$ as found in **2**. The thermal ellipsoids are of 50% probability. The hydrogen atoms were given an arbitrary thermal parameter.

Table 4. Structural data for **1**, **2** and other compounds containing H_3O_2 bridges

Compound	Distance (Å)			M—O···O—M torsional angle (deg)
	O—O(H_3O_2)	M—O(H_3O_2)	M—M	
1, *trans*-{[Co(en)$_2$(NO_2)]$_2$(H_3O_2)}(ClO_4)$_3$·2H_2O	2.412(9)	1.906(6)	5.67	180
2, *trans*-{[Co(en)$_2$(NCS)]$_2$(H_3O_2)}(CF_3SO_3)$_3$·H_2O	2.415(6)	1.911(5) 1.916(5)	5.77	174.3(4)
trans-[Co(en)$_2$(H_3O_2)](ClO_4)$_2$[1]	2.441(2)	1.916(1)	5.72	180
{[Mo_3O_2(pr)$_6$(H_2O)$_2$]$_2$(H_3O_2)}Br_3·6H_2O[12]	2.52(1)	2.009(7)	5.63	180

related whereas in **2** they are identical within the experimental error—1.911(5) Å and 1.916(5) Å (Table 4). These distances are shorter than the average distance reported for the Co—O(H_2O) bond (1.94 Å)[10] but slightly longer than the Co—O(OH) distance (1.89 Å).[11] Due to the limitation of the X-ray technique, the exact position of the central hydrogen atom in the $H_3O_2^-$ bridge cannot be located. However, the fact that the two M—O(H_3O_2) distances in both structures are identical supports the assumption that the O···H···O bond is symmetrical.

The O···O distances in the $H_3O_2^-$ bridges of **1** and **2**, 2.412(9) Å and 2.415(6) Å, respectively, are significantly shorter than those found in other compounds with $H_3O_2^-$ bridges (2.44–2.54 Å).[1,12] The decrease in the O···O separation is possibly the result of an inductive effect of the electron withdrawing NO_2^- and NCS^- ligands in the *trans* position. From Table 4 it can be seen that the torsional angle of the M—O···O—M system in **1** and **2** is 180° and 174.3(4)°, respectively. This arrangement yields the longest M—M distances and the smallest interactions between the two positively charged metal centers. The same angle was found in other $H_3O_2^-$ bridged complexes of mono- and polynuclear species.[1,12]

Structures **1** and **2** are, as far as we know, the first reported structures of classical aqua-hydroxo 'double salts'. The binuclear $H_3O_2^-$ bridged structure found in these compounds may be expected in other so-called double salts, because the strong H-bond of the $H_3O_2^-$ bridge (~ 100 kJ mol^{-1})[1] makes this structure more stable than a hypothetical species with distinct mononuclear hydroxo and aqua ions. However, before the general role of H_3O_2 bridging in coordination chemistry was outlined,[1] a double salt formulation such as [Co(en)$_2$(NO_2)OH]·[Co(en)$_2$(NO_2)H_2O](ClO_4)$_3$ seemed to be more justified than a symmetric formulation such as [Co(en)$_2$(OH)(NO_2)]$_2$(ClO_4)$_2$·$HClO_4$ which would imply the existence of an acid salt of a hydroxo-complex. The authors were therefore pleasantly surprised to find, while preparing this manuscript, a paper by Alfred Werner (1907)[13] which proposed an essentially correct formulation for this class of compounds, later mistaken for double salts. This paper, bearing the title "Uber anomale anorganische Oxonium Salze, eine neue Klasse basischer Salze" (on anomalous oxonium salts, a new class of basic salts) reports the composition of basic salts of *trans*-[Co(NH_3)$_4$(NO_2)H_2O]$^{2+}$. The structure proposed by Werner for the chloride salt was:

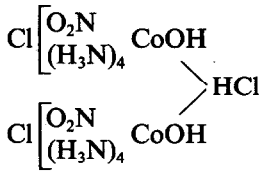

Werner's idea that a hydrogen atom may be bonded to two (or more) oxygen atoms was proposed in an even earlier paper (1902), where the idea of a symmetric hydrogen bond was first used although not explicitly.[14] It is remarkable that Werner applied the idea of hydrogen bonding to structural problems as early as 1902, long before it was first put forward by Latimer and Rodebush as an explanation of the physical properties of water and related liquids.[15]

It was recently shown[4] by Three-Phase Vapor Tensiometry (TPVT) that in moderately concentrated aqueous solutions (~0.1 M) the ion [Cr(bpy)$_2$(H_2O)(OH)]$^{2+}$ is in equilibrium with a significant proportion of the binuclear ion [(bpy)$_2$Cr(H_3O_2)$_2$Cr(bpy)$_2$]$^{4+}$. This doubly bridged dimer is dissociated completely at lower concentrations.[16] Solutions of two other *cis*-hydroxoaqua ions were shown to have the same property.[17] In view of these results, it was of interest to consider the existence of *singly* bridged binuclear ions such as {Co(en)$_2$(NO_2)]$_2$(H_3O_2)}$^{3+}$ in solution. Preliminary results of TPVT measurements of the perchlorate

salt of this ion suggested that at comparable concentration (~0.1 M) such binuclear ions do not exist.[17] This result is supported by the spectrum of the double salt in solution which failed to indicate any interaction between the aqua-ion and the hydroxo-ion (see Experimental section). The higher thermodynamic stability of a doubly bridged dimer in solution, compared to a singly bridged dimer, is the result of two factors: the higher bond energy of the former, which possesses *two* very strong H-bonds (compared to *one* in the latter), and the chelate effect.

Acknowledgements—The authors are grateful to the Fund for Basic Research administered by The Israel Academy of Sciences and Humanities for financial support. One of us (WGJ) acknowledges financial support from the Australian Research Grants Scheme.

REFERENCES

1. M. Ardon and A. Bino, *Inorg. Chem.* 1985, **24**, 1343.
2. The O—O separation is 2.4–2.5 Å in 10 compounds investigated by us. A notable exception is the structure of *cis*-aquahydroxobis(2-pyridylmethylamine)chromium(III) dithionate, determined by S. Larsen, K. B. Nielsen and I. Trabjerg, *Acta Chem. Scand.* 1983, **A37**, 833. In this structure the formation of two $H_3O_2^-$ bridges between two chromium atoms is blocked by the dithionate ion. The chromium atoms in this salt form chains linked by longer hydrogen bonds between the oxygen ligands [2.586(6) Å].
3. 'Very strong hydrogen bonds' have been defined as H bonds with an O—O separation of less than 2.5 Å: J. Emsley, D. J. Jones and J. Lucas, *Rev. Inorg. Chem.* 1981, **3**, 105.
4. M. Ardon and B. Magyar, *J. Am. Chem. Soc.* 1984, **106**, 3359.
5. (a) W. G. Jackson and A. M. Sargeson, *Inorg. Chem.* 1978, **17**, 1348. (b) W. G. Jackson, Unpublished results.
6. A. Werner, *Liebig Ann.* 1912, **386**, 1.
7. C. K. Ingold, R. S. Nyholm and M. L. Tobe, *J. Chem. Soc.* 1956, 1691.
8. All crystallographic computing was done on a CYBER 74 Computer at the Hebrew University of Jerusalem, using the SHELX 1977 structure determination package.
9. (a) D. J. Cromer and J. T. Waber, *International Tables for X-ray Crystallography*, Vol. IV. Kynoch Press, Birmingham, England (1974). (b) R. F. Stewart, E. R. Davidson and W. T. Simpson, *J. Chem. Phys.* 1965, **42**, 3175.
10. Y. Kanazawa and T. Matsumoto, *Acta Cryst.* 1976, **B32**, 282.
11. E. S. Kucharski, B. W. Skelton and A. H. White, *Aust. J. Chem.* 1978, **31**, 47.
12. (a) A. Bino and D. Gibson, *J. Am. Chem. Soc.* 1982, **104**, 4383. (b) A. Bino and D. Gibson, *Inorg. Chem.* 1984, **23**, 109.
13. A. Werner, *Ber.* 1907, **40**, 4122.
14. A. Werner, *Liebig Ann.* 1902, **322**, 296.
15. W. M. Latimer and W. H. Rodebush, *J. Am. Chem. Soc.* 1920, **42**, 1419.
16. M. Ardon, Unpublished results.
17. M. Ardon and B. Magyar, Unpublished results.

Polyhedron Vol. 6, No. 2, pp. 189–195, 1987
Printed in Great Britain

0277–5387/87 $3.00+.00

INSERTION OF TRIVALENT URANIUM IN MACROCYCLIC CROWN-ETHERS: EXAFS AND X-RAY STRUCTURAL ANALYSES

A. DEJEAN, P. CHARPIN,* G. FOLCHER and P. RIGNY

IRDI/DESICP/DPC/SCM CEA-CEN/SACLAY, 91191 Gif sur Yvette Cedex, France

and

A. NAVAZA and G. TSOUCARIS

Laboratoire de Physique, Centre Pharmaceutique, 92290 Chatenay-Malabry, France

(*Received* 3 *March* 1986; *accepted* 19 *May* 1986)

Abstract—The structure of the first U(III) macrocyclic coordinated complex, $[U(III)(BH_4)_2$ dicyclohexyl-(18-crown-6)$]_2U(IV)Cl_5(BH_4)$ (complex **I**), has been determined from three-dimensional X-ray diffraction data. The metal atom in trivalent state is inserted in the crown cavity as a monovalent cation $[U(BH_4)_2]^+$. This compound resulted from a partial oxidation in a dichloromethane solution of $U_3(III)(BH_4)_9$[dicyclohexyl-(18-crown-6)$]_2$ (complex **II**).

EXAFS analysis performed on powdered sample of the homologue of complex **II**, $U_3(BH_4)_9$[18-crown-6$]_2$ (complex **III**) has shown the presence of carbon atoms in the vicinity of the uranium atom and hence has proved that all the oxygen atoms of the crown-ether are directly coordinated to the metal.

In parallel, an EXAFS study on the uranyl complex UO_2(18-crown-6)$(ClO_4)_2$ (complex **IV**) has verified the insertion of the uranyl ion in the solid state, and given evidence for its partial de-insertion in an acetonitrile solution.

Insertion of uranium in macrocyclic crown-ethers has been proved in solution for the valencies VI,[1] V,[2] IV[3] and III.[4] However, insertion in the solid phase has been shown only for VI[5] and IV[3,6] valencies by X-ray crystal structures. A variety of crown-ether complexes of uranium(III) have been studied in the powder state,[4,7–10] but little evidence exists to support the idea that direct coordination of uranium to the oxygen atoms of the crown cavity has been achieved, due to the great difficulty in obtaining and keeping crystals of these very unstable compounds.

From a dichloromethane solution of $U_3(BH_4)_9(dcc)_2$[4] [dcc = dicyclohexyl-(18-crown-6)] (complex **II**), a partially oxidized product, $[U(III)(BH_4)_2dcc]_2[U(IV)Cl_5BH_4]$ has been crystallized (complex **I**). The formula has been established from the single crystal diffraction analysis presented in this paper: two oxidation states, (III) and (IV), coexist in the compound. Coexistence of (IV) and (VI) oxidation states have been observed previously in the oxidized product $[U(IV)Cl_3$(18-crown-6)$]_2$ $[U(VI)O_2Cl_3(OH)(H_2O)]\cdot CH_3NO_2$;[6] in both cases the uranium inserted in the crown-ether has kept its initial oxidation state.

Since no suitable crystal of either of the compounds $U_3(BH_4)_9dcc_2$ or $U_3(BH_4)_9$(18-crown-6$)_2$ could be obtained, we have studied the latter in the powder state with extended X-ray absorption fine structure (EXAFS) analysis at the uranium *L*(III) absorption edge. This technique leads to determination of the radial environment of the uranium atom;[11] consequently it may show the presence of a carbon shell around the absorbing metal[12–14] which would support the idea of the insertion of the uranium(III) into the crown-ether. We have chosen to analyse the compound $U_3(BH_4)_9$(18-crown-6$)_2$ with the unsubstituted crown since it was expected to give a simpler EXAFS spectrum.

To determine the number of neighbours and their

* Author to whom correspondence should be addressed.

distances to the uranium atom, we needed standard compounds with known structures close to those of studied compounds. $U(BH_4)_4$[15] and UO_2(18-crown-6)$(ClO_4)_2$[1] (complex **IV**) were chosen for this purpose, though the latter does not have X-ray determined distances (the direct complexation of uranyl by the 18-crown-6 is known, but twinned crystals have rendered a structure solution to determine the U—O and U—C distances impossible). U—O distances for this complex have been obtained from EXAFS using $UO_2(CH_2COO)_3Na$[11] as a standard compound. We have considered U—C distances as being the same as those found in the insertion complex [UO_2(18-crown-6)(dcc)].[5] The similar configuration of macrocycles (18-crown-6)[6] and dcc,[7] when they are complexed with the cation UCl_3^+, provides a justification for this extrapolation. All EXAFS results refer to the parameters attributed to the solid [UO_2(18-crown-6)$(ClO_4)_2$] (complex **IV**). EXAFS spectra of this complex in the solid phase and in an acetonitrile solution have been compared to test the power of this technique to prove the metal insertion in a macrocyclic ligand in our experimental conditions [in solution UO_2(18-crown-6)$(ClO_4)_2$ is known to be an insertion complex[1]].

EXPERIMENTAL

Complexes **II**, **III** and **IV** were prepared as previously described.[1,4] The solutions studied either in acetonitrile (complex **IV**) or dichloromethane (complex **II**) were saturated. Numerous attempts at recrystallization were performed to obtain suitable single crystals of complex **I**.

Structural X-ray analysis

X-ray data for complex **I**. $U_3(BH_4)Cl_5(O_6C_{20}H_{36})_2$: $M = 1710$, tetragonal $P\bar{4}$, $a = 18.227$ (7), $c = 9.757(2)$ Å, $V = 3241$ Å^3, $Z = 2$; $\rho_{calc} = 1.75$ Mg m^{-3}, μ(Mo-K_α) = 7.34 mm^{-1}; brown single crystal of approximate dimensions $400 \times 250 \times 250$ μm mounted in a capillary in an argon atmosphere. 3250 intensity data were recorded ($1.5° < \theta < 25°$) on a CAD4 diffractometer using graphite-monochromated Mo-K_α radiation with $\omega/2\theta$ scans. Intensities were monitored by three standard reflections every hour and orientation checked every 50 reflections. The large width and weak intensity of most of the reflections showed the crystal imperfection, though the crystal was the best diffracting one. The data were corrected for intensity decay (−23% in 20 h), for absorption (empirical correction ranged from 0.362 to 1.686), and for Lorentz-polarization effects. Direct methods (Multan[16]) and Patterson function led to the choice of space group and location of the two independent uranium atoms. The other atoms were positioned by difference Fourier maps. The structure was refined to $R = 0.097$ for 899 independent reflections with $I > 2.5\sigma(I)$. Only thermal parameters of uranium and chlorine atoms were refined anisotropically. The final difference Fourier map showed residual peaks (height $2e$/Å^3) in the vicinity of the U(III) inserted in the crown-ether. All the parameters were determined with high standard deviations; the poor quality of data did not permit better accuracy. All the calculations were performed with the Enraf–Nonius/SDP program chain.[17]

EXAFS analysis. EXAFS oscillations of complexes **III** and **IV** were recorded at the uranium L(III) absorption edge (room temperature). The data were collected at the EXAFS-I station of LURE (the French synchrotron radiation facility) under the standard operating conditions of the storage-ring DCI.[18] The data reduction was performed as described elsewhere.[11,19] The powder samples were enclosed between several sheets of adhesive tape. The solutions were contained in a cell with mylar windows.

DISCUSSION

X-ray structure of complex **I**

The packing, given in Fig. 1, is built from alternatively negative and positive charged planes along the [001] direction; two new ionic species are present in this structure.

$[U(IV)Cl_5BH_4]^{2-}$ *anion.* The uranium(IV) has a pseudo-octahedral environment (Table 1, Fig. 1). A crystallographic two-fold axis lies along the Cl(22)—U(2)—B(21) line. The U(2)—B(21) distance [2.70(9) Å] corresponds to a bidentate terminal borohydride BH_4^- as in $U(BH_4)_4[OP(C_6H_5)_3]_2 \cdot 2C_6H_6$.[20] The C_2 symmetry is maintained in this type of coordination.

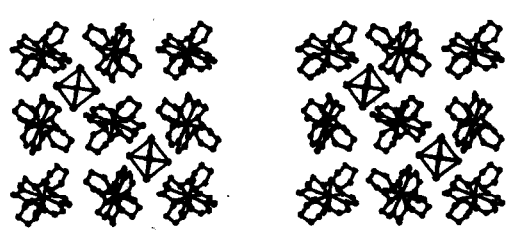

Fig. 1. Stereoscopic ORTEP packing of complex **I**.

Table 1. Bond distances (Å) around the uranium atoms in complex I

U(1)—B(11)	2.44(12)	U(1)—C(2)	3.61(15)
U(1)—B(12)	2.69(16)	U(1)—C(3)	3.97(15)
U(1)—O(1)	2.83(7)	U(1)—C(5)	3.39(15)
U(1)—O(4)	2.82(8)	U(1)—C(6)	3.50(15)
U(1)—O(7)	2.48(8)	U(1)—C(8)	3.49(15)
U(1)—O(10)	2.48(7)	U(1)—C(9)	3.56(14)
U(1)—O(13)	2.56(8)	U(1)—C(11)	3.26(15)
U(1)—O(16)	3.05(9)	U(1)—C(12)	3.19(15)
		U(1)—C(14)	3.88(15)
		U(1)—C(15)	4.07(15)
U(2)—B(21)	2.70(9)	U(1)—C(17)	3.68(15)
U(2)—Cl(22)	2.66(3)	U(1)—C(18)	3.72(13)
U(2)—Cl(23)	2.61(3)		
U(2)—Cl(24)	2.58(4)		

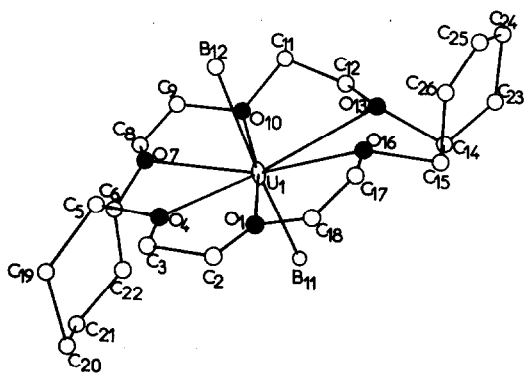

Fig. 2. Atomic numbering in $[U(BH_4)_2dcc]^+$.

$[U(III)(BH_4)_2(dcc)]$ *cation* (Table 1, Figs 1 and 2). The uranium(III) ion is inserted in the crown-ether, and is coordinated to two BH_4^- lying in axial positions on each side of the crown [B(12)—U(1)—B(11) = 173(5)°]. U—B distances have been reported for many U(IV) compounds with BH_4^- or $BH_3CH_3^-$ ligand;[21,22] for U(III) compounds only coordination with $BH_3CH_3^-$ has been published.[23] The distances U(1)—B in the cation (average, 2.57 Å) correspond to tridentate terminal borohydrides. The distances and angles of dcc are severely affected by the weak diffracting power of the crystal; high standard deviations have been usually observed in all described uranium crown-ether compounds.[3,5,6] The mean aliphatic C—C distances are 1.50(17) Å either in the cyclic ether ring or in the cyclohexyl rings; the mean C—O bond length is 1.49(17) Å. The configuration of the dcc is *cis–anti–cis* (isomer B) in the conformation $|^{ax\ eq}_{eq\ ax}|$. This conformation corresponds to a pseudo-symmetry centre located on the centre of gravity of the crown. This pseudo-centre is supported by the cyclic ether ring (Table 3) and by the anions in the packing (Fig. 1) but the U(1) atom does not lie on it: it is located closer to O(7), O(10) and O(13) than to O(4), O(1) and O(16) atoms significantly out of the well-fitted least-square equatorial plane of the ether oxygens (Table 2). This planar configuration may be due to the steric hindrance of the BH_4^- hydrogens. In the $UO_2(dcc)(ClO_4)_2$[5] compound, in which no steric hindrance with UO_2^{2+} oxygen atoms exists, the ether oxygens are more dispersed on both sides of the least-squares equatorial plane. These two structural determinations support the tendency for an inserted linear ion with $D_{\infty h}$ local symmetry to crystallize rather with the B isomer of dcc from a mixture of its A (*cis–syn–cis*) and B isomers. The UCl_3^+ [3,6] ion and $La(III)(NO_3)_3$[23] molecule, having C_2 symmetry, crystallize rather with the A isomer of the dcc.

EXAFS analysis

Complex IV (*solid*). Figure 3(a) shows the Fourier Transform (FT) of EXAFS oscillations of the standard compound $UO_2(CH_3COO)_3Na$. The first peak corresponds to the U—O_2 axial, the second to

Table 2. Deviations (Å) from the least-squares plane through the polyether-oxygen atoms in complex I

O(1)	−0.04(7)	U(1)	−0.212(6)
O(4)	0.07(7)	B(11)	−2.61(12)
O(7)	0.00(8)	B(12)	2.48(16)
O(10)	−0.11(7)		
O(13)	0.15(8)		
O(16)	−0.08(8)		

Table 3. Torsion angles (degrees) of the polyether in complex I

(a) in the cyclic ether ring			
$O_1C_2C_3C_4$	+69	$O_{10}C_{11}C_{12}O_{13}$	−23
$C_2C_3O_4C_5$	−173	$C_{11}C_{12}O_{13}C_{14}$	−125
$C_3O_4C_5C_6$	−153	$C_{12}O_{13}C_{14}C_{15}$	+172
$O_4C_5C_6O_7$	−73	$O_{13}C_{14}C_{15}O_{16}$	+13
$C_5C_6O_7C_8$	−148	$C_{14}C_{15}O_{16}C_{17}$	−169
$C_6O_7C_8C_9$	−177	$C_{15}O_{16}C_{17}C_{18}$	+171
$O_7C_8C_9O_{10}$	+6	$O_{16}C_{17}C_{18}O_1$	−70
$C_8C_9O_{10}C_{11}$	+169	$C_{17}C_{18}O_1C_2$	−171
$C_9O_{10}C_{11}C_{12}$	−164	$C_{18}O_1C_2C_3$	+160
(b) in the cyclohexyl rings			
$C_5C_{19}C_{20}C_{21}$	−12	$C_{14}C_{23}C_{24}C_{25}$	+41
$C_{19}C_{20}C_{21}C_{22}$	+52	$C_{23}C_{24}C_{25}C_{26}$	−21
$C_{20}C_{21}C_{22}C_6$	−48	$C_{24}C_{25}C_{26}C_{15}$	+43
$C_{21}C_{22}C_6C_5$	+37	$C_{25}C_{26}C_{15}C_{14}$	−68
$C_{22}C_6C_5C_{19}$	−37	$C_{26}C_{15}C_{14}C_{23}$	+48
$C_6C_5C_{19}C_{20}$	+67	$C_{15}C_{14}C_{23}C_{24}$	−53

the U—O_6 equatorial distances; no U—C_3 equatorial peak is detected.

Figure 3(b) gives the FT of complex **IV**. In addition to the two axial and equatorial U–O peaks, a third peak corresponding to U–C is observed. The fit of parameters[19] for this compound is presented in Table 4. An error of about 25% on the atom number of the UO axial shell (uranyl) is obtained when fitting is performed with the standard (method a). The atom number of the equatorial shell is then affected by error. To improve the result we have fitted the equatorial shell with the amplitude and phase parameters of the axial shell of the compound itself[11] (method b). We thus verified the presence of the six oxygen atoms of the crown-ether around the uranyl. Average distances of 1.73 and 2.54 Å have been deduced for U–O axial and U–O equatorial, respectively.

Complex **IV** (*acetonitrile solution*). Figure 3(c) shows the FT of this solution. The presence of the three peaks corresponding to U–O axial, U–O equatorial and U–C, is the proof of the insertion of the uranyl in the crown-ether. The fit with parameters of the solid compound as standard (Table 5) gives too small equatorial oxygen and carbon numbers, although the axial oxygen number is correct. This fact and the short U—O equatorial distance led us to suspect a partial de-insertion of the uranyl. If non-inserted, uranyl, in acetonitrile solution would be coordinated only to five CH_3CN molecules. $UO_2(N_3)_3N(C_2H_5)_4$[11] has been chosen as standard to fit the U–N parameters. We have then fitted the first equatorial shell of the uranyl with oxygen and nitrogen atoms (Table 5). The atom numbers and the U—O and U—N distances obtained confirm a partial de-insertion: 2/3 UO_2 (18-crown-6)$^{2+}$ and 1/3 $UO_2(CH_3CN)_5^{2+}$ (error

Table 4. Fitted parameters of UO_2(18-crown-6)$(ClO_4)_2$ in the solid phase, with amplitude and phase parameters[19] from: (a) the standard $UO_2(CH_3COO)_3Na$ (UO_2: $R = 1.755$ Å, UO_6: $R = 2.459$ Å);[11] (b) the first shell of UO_2(18-crown-6)$(ClO_4)_2$: ($\gamma = 0.4$, UO_2: $R = 1.73$ Å)[11]

Pairs	N	R (Å)	$\Delta\sigma^2$ (10^3 Å^2)	ΔE_0 (eV)
UO_2 axial (a)	1.5	1.73	0.01	1.2
UO_6 equatorial (a)	5.2	2.54	3.39	1.7
UO_6 equatorial (b)	6.7	2.54	2.80	5.6

Table 5. Fitted parameters of UO_2(18-crown-6)$(ClO_4)_2$ in CH_2CN saturated solution, with amplitude and phase parameters[19] from the same solid compound (UO_2: $R = 1.73$ Å, UO_6: $R = 2.54$ Å, UC_{12}: $R = 3.44$ Å) and from the compound $UO_2(N_3)_3N(C_2H_5)_4$ (UO_2: $R = 1.74$ Å, UN_5: $R = 2.46$ Å)[11]

Pairs	N	R (Å)	$\Delta\sigma^2$ (10^3 Å^2)	ΔE_0 (eV)
UO_2 axial	2.2	1.73	0.00	−1.0
UO_6 equatorial	4.8	2.51	0.70	0.2
UC_{12} equatorial	8.1	3.44	0.00	0.1
UOx	3.5	2.53	0.02	0
UNy	1.7	2.45	0.00	

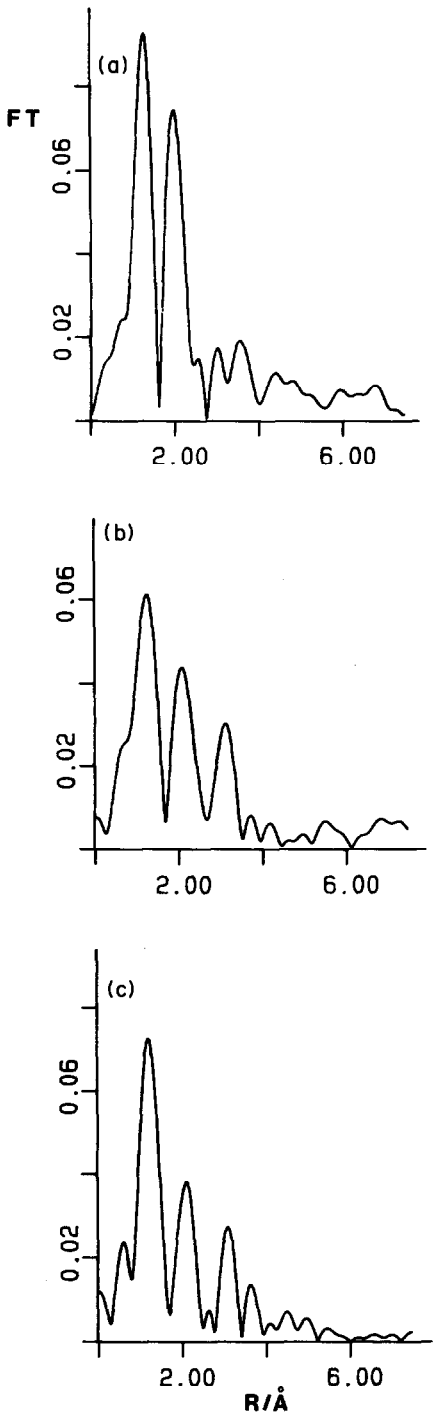

Fig. 3. Fourier transforms of EXAFS oscillations for: (a) $UO_2(CH_3COO)_3Na$, (b) UO_2(18-crown-6)$(ClO_4)_2$ (solid), and (c) UO_2(18-crown-6)$(ClO_4)_2$ (solution in CH_3CN).

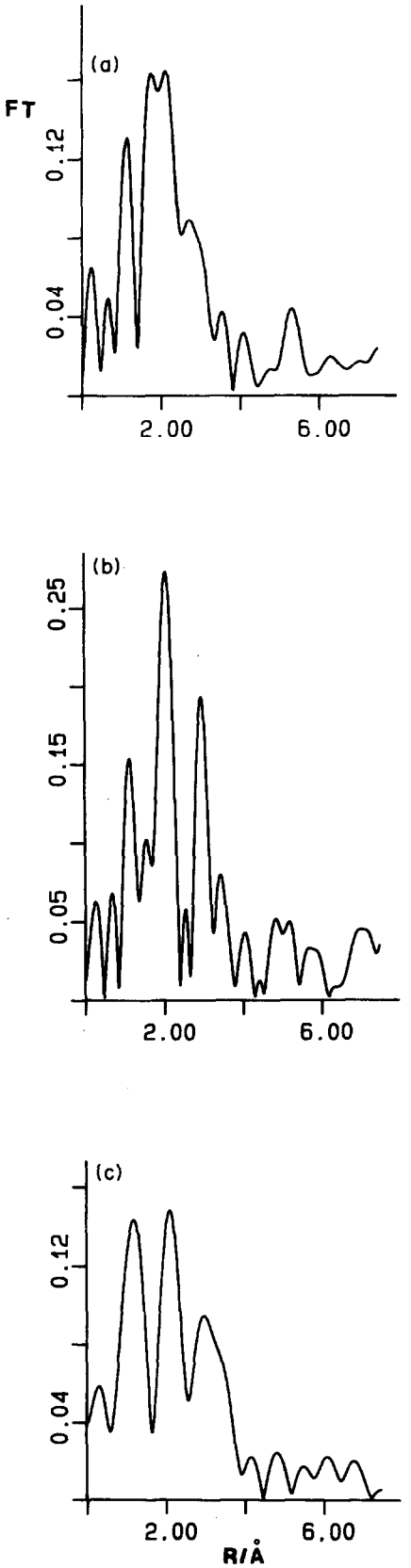

Fig. 4. Fourier transforms of EXAFS oscillations for: (a) $U(BH_4)_4$, (b) $U_3(BH_4)_9$(18-crown-6)$_2$, and (c) $U_3(BH_4)_9(dbc)_2$.

about 10%). The radial environment of the inserted uranium is the same in solid and solution states.

Complex III (*solid*). Figure 4(a) gives the FT of $U(BH_4)_4$ standard compound. The presence of the first peak at 1.7 Å indicates a weak oxidation of the

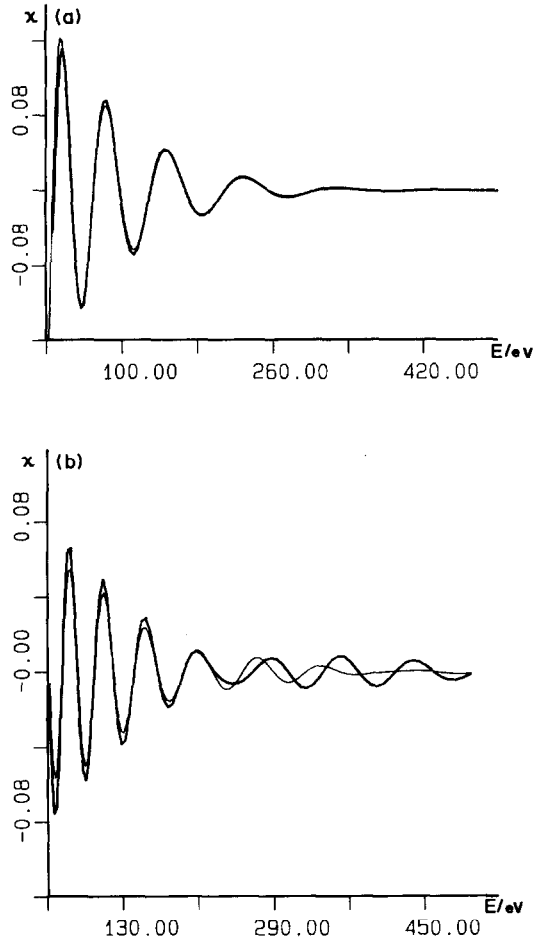

Fig. 5. EXAFS oscillations of $U_3(BH_4)_9$(18-crown-6)$_2$: (a) UOB shell, and (b) UC shell. (—) Fourier filtered experimental EXAFS spectra, (—) theoretical fit.

sample, the second peak corresponds to the U–B pairs.

Figure 4(b) shows the FT of complex **III**. Three peaks are present: the first one as above is due to a weak oxidation (10%) of the sample, the second and the third peak (U–O, U–B and U–C, respectively) are attributed to the complexation of the uranium(III) with the crown-ether. Table 6 and Fig. 5 give the results of the fit for the second and third shells using the following model: all the crown-ethers contain an axial $U(BH_4)_2^+$ ion like the complex **I** and the non-inserted uranium atoms are surrounded by five BH_4^- ions.[4] This model implies fitting of the U–B_3 and U–O_4 pairs to the second peak and U–C_8 pairs to the third peak, which has been split to improve the fit. The result is excellent for the second shell, but not so good for the third one on account of the high background of experimental filtered spectra. The large distance U—B (2.95 Å) implies the presence of some bidentate

Table 6. Fitted parameters of $U_3(BH_4)_9$(18-crown-6)$_2$ in solid phase with amplitude and phase parameters[19] from the solid compound UO_2(18-crown-6)$(ClO_4)_2$ (UO_6: R = 2.54 Å, UC_{12}: R = 3.44(7) Å) and $U(BH_4)_4$: (UB_6: R = 2.75 Å).[15]

Pairs	N	R (Å)	$\Delta\sigma^2$ (10^3 Å^2)	ΔE_0 (eV)
OU	4.0±0.6	2.51±0.01	4.7±0.4	−8±1
UB	3.0±0.4	2.95±0.04	3.4±0.4	
UC	6.0±0.7	3.47±0.03	0.11±0.03	−6±2
	2.0±0.2	4.14±0.03	0.00	

BH_4^- in the structure. The split of the carbon shell corresponds to an important dispersion around the uranium. This fact and the high σ value of the U–O shell shows that the uranium(III) would not be located on the symmetry center of the crown-ether as in complex **I**.

The FT of the [U_3(III)$(BH_4)_9$(dibenzo 18-crown-6)$_2$] is given on Fig. 4(c). The peak corresponding to U–C pairs is present and proves the insertion of U(III) in the crown, but the strong oxidation (first peak) does not allow quantitative results to be given.

CONCLUSION

The EXAFS technique, which is well-known as a useful tool to obtain structural features which cannot be drawn from X-ray crystal structure analysis, has been shown to be useful in the particular case of uranium, either in powdered solid samples or solutions. The interpretation based on the knowledge of structural information on related compounds of uranyl has given evidence of the partial de-insertion of uranyl in solution and of the insertion of uranium(III) in a series of crown-ethers.

Acknowledgements—The authors thank D. Vigner and M. Lance for technical assistance in the X-ray part of this work.

REFERENCES

1. G. Folcher, P. Charpin, R. M. Costes, N. Keller and G. C. de Villardi, *Inorg. Chim. Acta* 1979, **34**, 87.
2. G. Folcher, J. Lambard and G. C. de Villardi, *Inorg. Chim. Acta* 1980, **45**, L59.
3. G. C. de Villardi, P. Charpin, R. M. Costes, G. Folcher, P. Plurien, P. Rigny and C. de Rango, *J. Chem. Soc., Chem. Commun.* 1978, 90.
4. A. Dejean-Meyer, G. Folcher and H. Marquet-Ellis, *J. Chim. Phys.* 1983, **80**, 579.
5. A. Navaza, F. Villain and P. Charpin, *Polyhedron* 1984, **3**, 143.

6. G. Bombieri, G. de Paoli and A. Immirzi, *J. Inorg. Nucl. Chem.* 1978, **40**, 1889.
7. D. C. Moody, R. A. Penneman and K. V. Salazar, *Inorg. Chem.* 1979, **18**, 208.
8. J. I. Bullock and A. E. Storey, *Inorg. Chim. Acta* 1979, **36**, L399.
9. D. C. Moody, A. J. Zozulin and K. V. Salazar, *Inorg. Chem.* 1982, **21**, 3856.
10. F. A. Hart and M. Tajik, *Inorg. Chim. Acta* 1983, **71**, 169.
11. P. Charpin, A. Dejean, G. Folcher, P. Rigny and A. Navaza, *J. Chim. Phys.* 1985, **82**, 925.
12. J. Goulon, Ch. Goulon, F. Niedercorn, C. Selve and B. Castro, *Tetrahedron* 1981, **37**, 3707.
13. P. Richard, J. L. Poncet, J. M. Barbe, R. Guilard, J. Goulon, D. Rinaldi, A. Cartier and P. Tola, *J. Chem. Soc., Dalton Trans.* 1982, 1451.
14. J. Goulon and C. Goulon-Ginet, *Pure Appl. Chem.* 1982, **12**, 2307.
15. E. R. Bernstein, W. C. Hamilton, T. A. Kiederling, S. J. La Placa, S. J. Lippard and J. J. Mayerle, *Inorg. Chem.* 1972, **11**, 3009.
16. P. Main, S. J. Fiske, S. E. Hull, L. Lessinger, G. Germain, J. P. Declercq and M. M. Woolfson, *A System of Computer Programs for the Automatic Solution of Crystal Structures from X-ray Diffraction Data*. Universities of York, U.K. and Louvain, Belgium (1982).
17. B. A. Frenz and associates, *Structure Determination Package*, College Station, TX 77840, U.S.A. and Enraf–Nonius, Delft, Holland (1983).
18. D. Raoux, J. Petiau, P. Bondot, G. Calas, A. Fontaine, P. Lagarde, P. Levi, G. Loupias and A. Sadoc, *Rev. Phys. Appl.* 1980, **15**, 1079.
19. The EXAFS oscillation $\chi(k)$ is described by the approximate formula: D. E. Sayers, E. A. Stern and F. W. Lytle, *Phys. Rev. Lett.* 1971, **27**, 1204 (see also ref. 18)

$$\chi(k) = \frac{1}{k}\sum_i \frac{N_i}{R_i^2}\exp(-2\sigma_i^2 k^2) \times \exp\left(-\frac{\gamma R_i}{k}\right) f_i(r,k)\cdot\sin[2kR_i+\Phi_i(k)]$$

k is the photoelectron wave vector: $k = [(2me/h^2)(E-Eo)]^{1/2}$. The fitted parameters are: N_i the atom number of the ith shell, R_i the average distance which separates the absorbing atom from these N_i scattering atoms, σ_i the deviation from this distance R_i and Eo the origin of the energy above which the photoelectron is free, the amplitudes and phases, f_i and Φ_i, being obtained from standard compounds.
20. P. Charpin, M. Lance, E. Soulie, D. Vigner and H. Marquet-Ellis, *Acta Cryst.* 1985, **C41**, 1723.
21. N. Edelstein, *Inorg. Chem.* 1981, **20**, 297.
22. R. Shinomoto, E. Gamp, N. Edelstein and D. H. Templeton, *Inorg. Chem.* 1983, **22**, 2351.
23. J. Brennan, R. Shinomoto, A. Zalkin and N. Edelstein, *Inorg. Chem.* 1984, **23**, 4143.
24. M. E. Harman, F. A. Hart, M. B. Hursthouse, G. P. Moss and P. R. Raithby, *J. Chem. Soc., Chem. Commun.* 1976, 396.

Polyhedron Vol. 6, No. 2, pp. 197–203, 1987
Printed in Great Britain

0277–5387/87 $3.00+.00
Pergamon Journals Ltd

INFLUENCE OF THE STRUCTURE OF ALKYL DERIVATIVES OF SALICYLALDEHYDE OXIME UPON THE EXTRACTION RATE OF COPPER FROM DILUTED ACIDIC SOLUTIONS

D. STEPNIAK-BINIAKIEWICZ and J. SZYMANOWSKI*

Technical University of Poznan, Pl. Sklodowskiej-Curie Poznan, Poland

and

V. V. TARASOV

Mendeleew Institute of Chemical Technology, Moscow, U.S.S.R.

(*Received* 17 *January* 1985; *accepted after revision* 28 *May* 1986)

Abstract—Individual pure alkyl derivatives of salicylaldehyde oxime were used for copper extraction using the short-time phase contacting method. The influence of the oxime structure upon the extraction rate and the surface activity was discussed. It was found that the reaction can proceed at the interface and in the bulk of the aqueous phase. The bulk-phase process is dominant for oximes having less than four carbon atoms in the alkyl group, while the interfacial process is dominant for oximes having more than six carbon atoms.

The use of hydroxyoximes as copper extractants has created new possibilities for hydrometallurgy because this extraction technique has been applied to the production of such relatively cheap and large tonnage metals as copper.

However, the slow rate of metal extraction by means of chelating agents is one of the basic drawbacks of this technique. Many papers[1–15] have been published on this subject dealing with physicochemical and mechanistic problems, as well as with its technological aspects. In most of these cases commercial products manufactured by Henkel, Acorga or Shell were used. These products, although carefully purified, contain many components such as different isomers and homologues of the particular active extracting agents and alkylphenol. Some other impurities of the starting materials, especially present in commercial nonylphenol, or formed as by products during the manufacture of the hydroxyoximes, may also be present. All these components can influence the rate of copper extraction, especially if one takes into account the possibility of the surface reaction or the parallel mechanism of the interface and bulk aqueous reactions, which are dependent not only upon the rate of the chemical step but also upon the rates of the diffusion steps and the adsorption of the extracting agent and impurities at the interface. The relative ratio of the interfacial to the bulk reaction may be changed by different extraction conditions, e.g. the method used, and the composition of the aqueous phase, as well as by the structure of the extracting agent, and the type and amount of impurities present in the extractant.

The aim of this work was to determine the extraction rates for different homologues of the alkyl derivatives of salicylaldehyde oxime having from 1 to 12 carbon atoms in the normal or branched alkyl chain, and to discuss the influence of the oxime structure upon the extraction rate and the place of the chemical step.

EXPERIMENTAL

Materials

Ten different pure individual hydroxyoximes (Table 1) of the following structure:

* Author to whom correspondence should be addressed.

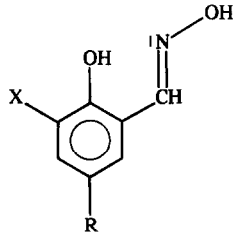

were used as copper extractants. Their analytical data have been given in previous papers.[16,17]

Copper solutions were prepared from copper sulphate (AR grade, POCh Gliwice, Poland), Sulphuric acid (AR grade) was used to adjust the pH. Octane and *p*-xylene were used as diluents.

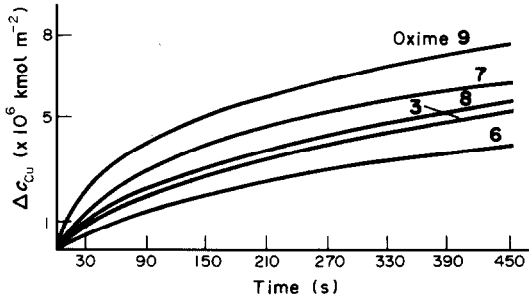

Fig. 1. Influence of the structure of oxime upon the amount of copper transferred into xylene phase (pH = 3.0, $c_{Cu^{2+}} = 0.015$ mol dm^{-3}, $c_{oxime} = 0.025$ mol dm^{-3}).

Kinetic measurements

The short-time phase contacting method described by Yagodin *et al.*[18,19] was used. The conditions for the kinetic measurements were as follows: temperature = 293 K, oxime concentration = 0.003–0.05 mol dm^{-3} copper concentration = 0.015 mol dm^{-3}, pH of the aqueous phase = 3, volume of the aqueous phase = 15.0×10^{-9} m^3, and interface surface = 6.43×10^{-6} m^2.

Additional measurements

Interfacial tensions were determined at 293 K by the drop volume method[20,21] using mutually presaturated organic and aqueous phases. Twice redistilled water was used. The aqueous phase was adjusted by sulphuric acid to pH = 2. The time for the drop to grow was not less than 5 min, and usually 10–15 min.

Distribution coefficients of the oximes at 293 K were determined between 0.05 mol dm^{-3} solutions in xylene and the aqueous phase as adjusted by sulphuric acid to pH 3. The content of the oxime in the aqueous phase was determined spectrophotometrically.[22]

RESULTS

Sample curves showing the amount of copper transferred through the interface during extraction by different hydroxyoximes under the same experimental conditions are presented in Fig. 1. One can observe significant differences for the investigated hydroxyoximes. The extraction rate increases with decrease in the length of the alkyl radical in the 5-position. Oximes having a branched alkyl show a higher extraction rate than their analogues containing a normal alkyl. The introduction of a bulky

Table 1. Structure, molecular weights, distribution coefficients and aggregation numbers of hydroxyoximes

Oxime	R	X	Molecular weights	Log_{10} distribution coefficient[a]	Aggregation number[b]
1	CH_3	H	151	1.22	—
2	C_2H_5	H	165	1.77	1.04
3	*n*-C_4H_9	H	193	2.65	—
4	*n*-C_6H_{13}	H	221	2.95	—
5	*n*-C_8H_{17}	H	259	3.21	1.07
6	*n*-$C_{12}H_{25}$	H	305	3.75	—
7	*t*-C_4H_9	H	193	2.32	1.08
8	*t*-C_8H_{17}	H	259	3.09	1.10
9	*t*-C_8H_{17}	NO_2	304	—	—
10	*t*-C_4H_9	*t*-C_4H_9	259	—	—

[a] In xylene–aqueous system (293 K).
[b] Measured in benzene at 293 K for $c = 0.10$ mol dm^{-3}.

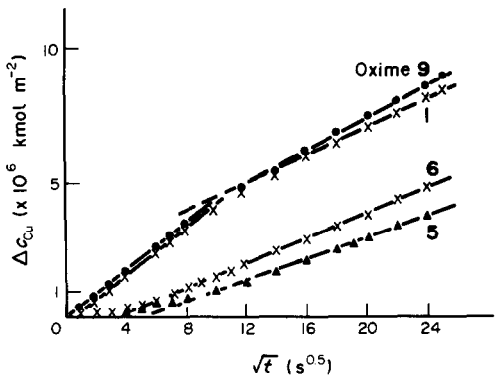

Fig. 2. Relationship between the copper transferred and the square root of the extraction time (xylene, pH = 3.0, $c_{Cu^{2+}} = 0.015$ mol dm^{-3}, $c_{oxime} = 0.025$, 0.05, 0.025 and 0.009 mol dm^{-3}).

t-butyl group in the neighbourhood of the phenolic group (oxime **10**) diminishes the extraction rate so much (about 15 times compared to oxime **7**) that, under the same experimental conditions, the measurement of the extraction rate becomes impossible. However, the electronegative NO_2 group at the 3-position sharply increases the extraction rate. Analogous conclusions can be derived when the results obtained under other experimental conditions, i.e. for different oxime concentrations and octane used as a diluent, are considered.

Figure 2 shows the relationships between the amount of copper transferred to the organic phase and the square root of the extraction time. In most cases the shape of the obtained curves is typical for an interfacial process.[18] At the beginning of the process ($t = 0$) the rate of diffusion is infinitely high or at least very high, and the process rate is determined by the rate of the reaction step. However, after a very short period, usually not exceeding a few tens of seconds, the rates of the diffusion step decrease so significantly that diffusion begins to control the process rate. In this case the considered relationship can be described by the following equations:

$$\Delta c_{Cu} = A + B\sqrt{t},$$

where B is related to the appropriate diffusivities. The extrapolation of the above relation to $\Delta c_{Cu} = 0$ gives the value of the square root of the transient time, which is necessary to convert the process from the kinetic to the diffusion regime.

The value of the transient time (Table 2) increases with the length of the alkyl group of the considered oximes and with the decreasing concentration of the oximes in the organic phase. The direction of the change is similar to the change in the oxime concentration in the aqueous phase, and suggests an increasing role for the interfacial process with the increase in the oxime hydrophobicity and the decrease in the oxime concentration in the organic phase.

Some kinetic curves obtained for an oxime concentration of 0.5 mol dm^{-3}, with the exception of compound **6** (having a long alkyl group), show an atypical shape (Fig. 2). In these cases extraction periods are observed with two different characteristic straight-line slopes and different transient time values. Moreover, for oximes with a lower hydrophobicity, e.g. a shorter-length alkyl or nitro group, this atypical shape of the kinetic curves is also observed in the case of lower oxime concentrations in the organic phase. This suggests a more complex character for the process. Although extraction begins at the interface, the reaction in the bulk of the aqueous phase is also important. The contribution of the bulk reaction increases with the oxime concentration and with the decrease in the alkyl length. For compounds **1** and **9** the first

Table 2. Values of transient time (diluent = xylene, $c_{Cu} = 0.015$ mol dm^{-3})

	Oxime concentration (mol dm^{-3})							
Oxime	0.05	0.025	0.015	0.012	0.009	0.006	0.0045	0.003
1	0.0[a]	0.1	1.5	2.8	3.5	5.3	7.4	9.0
3	1.9[a]	2.0	3.2	3.7	3.9	—	—	—
5	2.5[a]	3.0	3.9	4.3	4.9	5.2	—	—
6	3.0	3.4	4.0	4.3	5.0	5.9	—	—
7	1.7[a]	1.8	1.7	2.1	4.1	4.6	6.3	—
8	1.6[a]	2.0	3.0	5.0[b]	—	—	—	—

[a] For the first extraction period.
[b] $c_{oxime} = 0.01$ mol dm^{-3}.

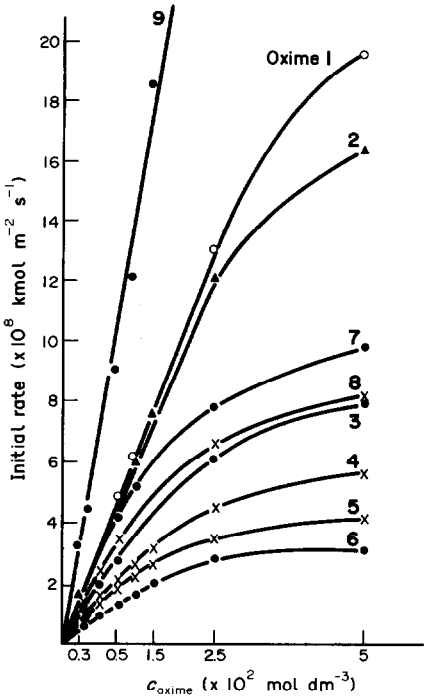

Fig. 3. Influence of the structure of the oxime upon the initial extraction rate (xylene).

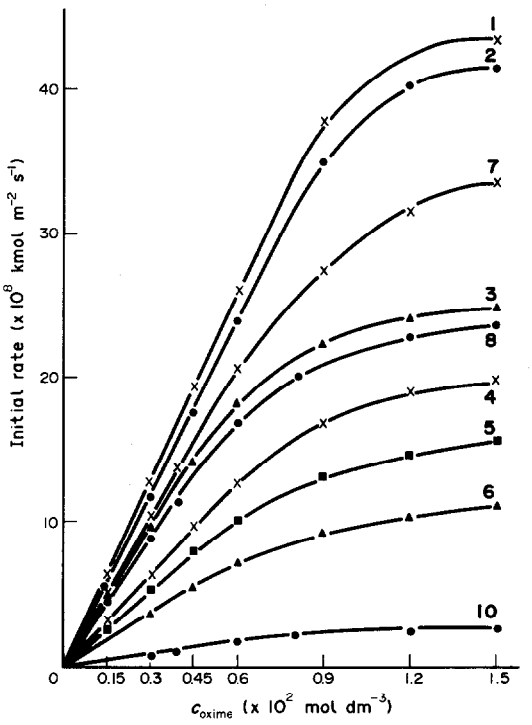

Fig. 4. Influence of the structure of the oxime upon the initial extraction rate (octane).

transient time is equal to zero, which suggests that, even in the first few seconds, the reaction proceeds in the bulk of the aqueous phase and is controlled by diffusional processes. This is in agreement with the independent results of Tarasov *et al.*[13,14] who investigated copper extraction by 2-hydroxy-5-octylbenzophenone oximes using the short-time phase contacting method, and with those of Szymanowski *et al.*,[15,23] who have discussed the influence of the oxime structure upon the extraction rate of copper determined in a Lewis cell, and by the AKUFVE and drop methods.

Figures 3 and 4 show the initial extraction rates obtained by graphical differentiation for $t = 0$ for the oximes considered at different concentrations in the organic phase. Only for compounds **1** and **9** were straight lines obtained for almost the entire range of concentrations considered, which is typical for the bulk reaction. For the other homologues the relationships are not linear and the influence of the oxime concentration decreases as both the concentration and the length of the alkyl increase. For homologues having a higher molecular mass (containing 8–12 carbon atoms in the alkyl group) and higher oxime concentrations (0.025–0.05 mol dm^{-3} for xylene and 0.009–0.015 mol dm^{-3} for octane) the extraction rate is almost constant and independent of oxime concentration. Thus, for oximes with an appropriately long alkyl (more than 12 carbon atoms) the initial extraction rate does not depend upon the length and structure of the alkyl (Fig. 5). This demonstrates the interfacial reaction for oximes having a long alkyl.

The interception points of the asymptotes correspond to four or five carbon atoms in the alkyl. Thus, for the oximes having a normal alkyl the interfacial and bulk reactions dominate for those oximes containing not less than six or not more than three carbon atoms in the alkyl, respectively. This is in agreement with the oxime distribution coefficients (Fig. 6). For oximes containing less than six carbon atoms in the alkyl the extraction rate increases sharply with the decrease in the distribution coefficient (below $\log_{10} P_{RH} = 3$), while for the oximes having more carbon atoms in the alkyl the influence of the distribution coefficient upon the extraction rate is small or almost negligible.

The character of the relationships shown in Fig. 5 is similar to that described in previous work[23] when the results obtained by the Lewis cell method were discussed. In both the methods compared the interface was not renewed and kept constant, which is especially important when the interfacial mechanism is considered.

The influence of the oxime concentration upon interfacial tension is shown in Fig. 7. Relationships typical for surfactants were obtained, i.e. with the increase in the length of the alkyl the interfacial

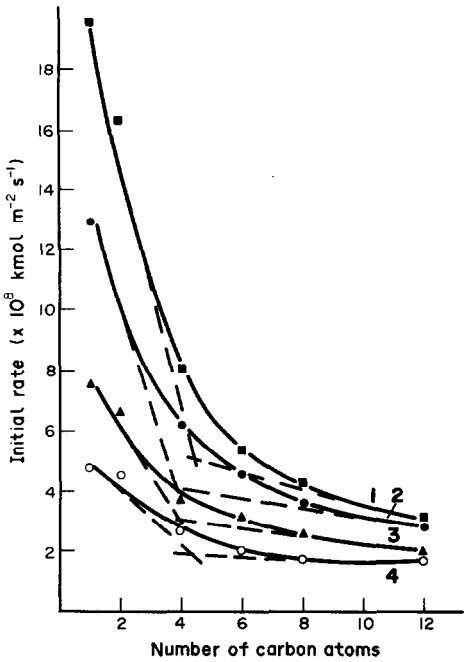

Fig. 5. Influence of the number of carbon atoms in the alkyl upon the initial extraction rate (xylene, curves 1, 2, 3 and 4 = c_{oxime} = 0.05, 0.025, 0.015 and 0.009 mol dm^{-3}, respectively).

tension decreases more efficiently. However, due to the low solubilities the region of critical micelle concentration was not obtained. Only in the case of the oximes having a branched alkyl was the opposite dependence observed. In octane–aqueous systems lower interfacial tensions are observed than in the xylene–aqueous interphase. The values of the excess surface calculated from the Gibbs isotherm:

$$\Gamma = \frac{0.43}{RT}\,\frac{d\gamma}{d(\log c_{oxime})},$$

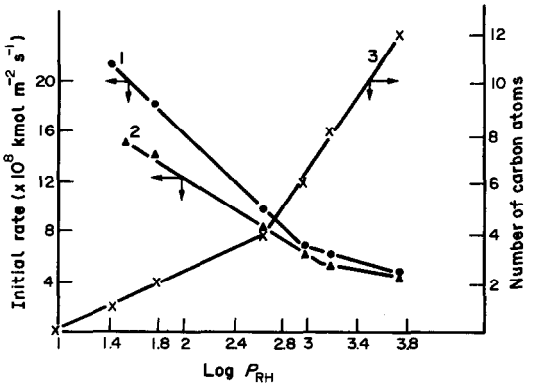

Fig. 6. Relationship between copper extraction rate and the distribution coefficient of the oximes (xylene, curves 1 and 2 = c_{oxime} = 0.05 and 0.025 mol dm^{-3}, respectively; curve 3 = relationship between the distribution coefficient and the number of carbon atoms in the alkyl).

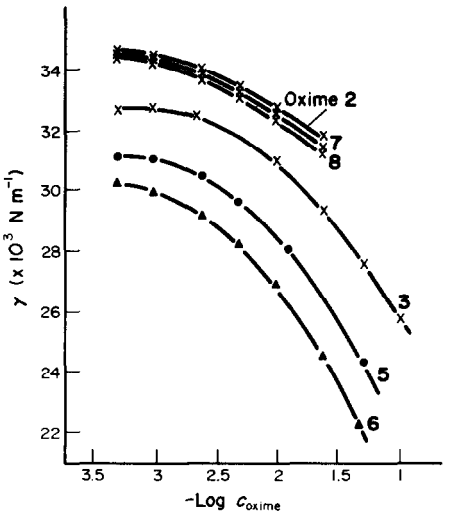

Fig. 7. Interfacial tension isotherms (xylene, 293 K).

are similar for all the oximes considered and vary in the ranges 5–7 × 10^{13} and 16–20 × 10^{13} molecules cm^{-2} for xylene and octane, respectively. This is connected with the similar slopes of the discussed interfacial tension isotherms. Thus the calculated values of the surface excess do not explain the observed differences in the extraction rates. This can be explained by the fact that, in the drop volume method, the equilibrium values of the interfacial tensions are observed after a characteristic time, which depends upon the structure of the considered compounds and the type of system considered. For typical surfactants usually only a few or a few tens of seconds are necessary to achieve equilibrium at the surface of the growing drop. However, in the present case the time for achieving equilibrium is much greater,[8,24] and, therefore, for our oximes dissolved in octane and xylene we estimated it as being equal to about 5 and 10 min, respectively. This means that, although the phases were presaturated, the adsorption or rather the orientation at the interface proceeds so slowly that the extraction rate in such systems should not be correlated with the equilibrium surface activity of the extractant. For extraction systems dynamic methods of measuring the interfacial tension should be elaborated and used. This explains another shape of the kinetic curves obtained by means of AKUFVE method.[23]

For a selected hydroxyoxime the extraction rate and surface activity, measured as a decrease in the interfacial tension, increase as the oxime concentration increases. Thus, in such a case the extraction rate can be proportional to the surface activity.[11,25] However, when different hydroxyoximes are considered quite opposite relationships between the extraction rate and the surface activity

are observed. For constant oxime concentrations the surface activity of the homologous series of oximes considered increases as the length of the alkyl increases, but the extraction rate significantly decreases. This means that under the same conditions the extraction rate does not depend upon the excess surface, but upon the depth of oxime penetration into the aqueous layers near the interface. This further supports our previous conclusions correlating the extraction rate with the hydrophilic–lipophilic balance.[15]

CONCLUSIONS

Our investigations carried out by means of the short-time phase contacting method in which pure individual hydroxyoximes were used showed that copper extraction may proceed both at the interface and in the bulk of the aqueous phase. For oximes having a long alkyl, typical kinetic curves ($\Delta c_{Cu} = A + B\sqrt{t}$) characterized by a relatively short transient time (usually a few or a few tens of seconds) and a constant slope were obtained, which demonstrate that the extraction process occurs at the interface. For hydroxyoximes having a short alkyl or the additional electronegative nitro group atypical curves characterized by two different slope constants were obtained, which suggests a more complex character for the process and the importance of the bulk reaction. The mutual ratios of the interfacial and bulk processes depend not only upon the hydrophobicity of the oximes but also upon the extraction conditions, such as oxime concentration and diluent type. The bulk-phase process dominates for alkyl derivatives of salicylaldehyde oximes having no more than three carbon atoms in the alkyl group, while the surface process dominates for homologues containing not less than six carbon atoms in the alkyl. For compounds containing the electronegative nitro group at the 3-position the bulk-phase process is favoured.

The initial extraction rate depends upon the oxime structure and the length of the alkyl. Higher extraction rates are observed in octane than in xylene. The extraction rate decreases with the increase in the alkyl length in the 5-position. Oximes having a branched alkyl show higher extraction rates than their analogues having a normal alkyl. The nitro group in the 3-position sharply increases the extraction rate while the bulky *t*-butyl group in the 3-position so sharply decreases the extraction rate that it can not even be measured. The oxime structure and extraction conditions also influence the values for the time needed to convert extraction from the kinetic to the diffusion regime. This transient time increases as the oxime concentration decreases and as the length of the alkyl group increases.

The surface activity of the homologous series of oximes increases as the length of the alkyl increases. This suggests that the extraction rate does not depend upon the surface excess under the same extraction conditions but upon the depth of the oxime penetration into the aqueous layers near the interface. This supports the idea correlating the extraction rate with the hydrophile–lipophile balance.

Acknowledgement—We wish to thank Prof. G. A. Yagodin for his generous help and all his advice.

REFERENCES

1. A. W. Ashbrook, *Coord. Chem. Rev.* 1975, **16**, 285.
2. D. S. Flett, *Acc. Chem. Res.* 1977, **10**, 99.
3. C. A. Fleming, M. J. Nicol, R. D. Hancock and N. P. Finkelstein, *J. Appl. Chem. Biotechnol.* 1978, **28**, 443.
4. C. Hanson, M. A. Hughes and R. J. Whewell, *J. Appl. Chem. Biotechnol.* 1978, **28**, 426.
5. A. J. van der Zeeuw and R. Kok, *Proc. ISEC'77, Montreal* 1977, CIM Special Volume, Vol. 21, p. 86 (1979).
6. L. Hummelstedt, E. Paatero, T. Nyberg and L. Rosenback, *Proc. ISEC'80, Liège* 1980, Vol. 2 (19A), paper 80-73 (1980).
7. G. A. Yagodin, S. Yu. Ivakhno and V. V. Tarasov, *Proc. ISEC'80, Liège* 1980, Vol. 3 (15B), paper 80-140 (1980).
8. I. Komasawa, T. Otake and T. Muraoka, *J. Chem. Eng. Jpn* 1980, **13**, 204.
9. M. Cox, C. G. Hirons and D. S. Flett, *Proc. ISEC'80, Liège* 1980, Vol. 1 (2A), paper 80-118 (1980).
10. H. Freiser, *Proc. ISEC'80, Liège* 1980, Vol. 1, paper 80-II (1980).
11. J. S. Preston and Z. B. Luklinska, *J. Inorg. Nucl. Chem.* 1980, **42**, 431.
12. E. Uhlig, *Coord. Chem. Rev.* 1982, **43**, 299.
13. V. V. Tarasov, G. Yagodin, A. Pichugin and S. Ivakhno, *Proc. ISED'83, Denver* 1983, p. 299 (1983).
14. G. Yagodin, V. V. Tarasov and A. Pichugin, *Proc. ISED'83, Denver* 1983, p. 20 (1983).
15. J. Szymanowski, *Polyhedron* 1985, **4**, 269.
16. D. Stepniak-Biniakiewicz and J. Szymanowski, *Hydrometallurgy* 1981, **7**, 299.
17. D. Stepniak-Biniekiewicz, *Pol. J. Chem.* 1979, **7/8**, 1567.
18. V. V. Tarasov, Avtoreferat dissertatsii doktora khimicheskikh nauk Mezhfaznye yavlenija i kinetika ekhstrakcii neorganicheskikh vechehestv., Moskwa, MKhTI im. Mendeleeva (1980).
19. V. V. Tarasov, G. Yagodin and A. B. Ivanow, *Izv. Vuzov Khim. Khim. Tekhnol.* 1977, **204**, 530.
20. W. D. Harkins and F. E. Brown, *J. Am. Chem. Soc.* 1919, **41**, 499.

21. T. A. B. Al-Diwan, M. A. Hughes and R. J. Whewell, *J. Inorg. Nucl. Chem.* 1977, **39**, 1419.
22. A. W. Ashbrook, *Anal. Chim. Acta* 1972, **58**, 115.
23. J. Szymanowski, M. Cox and C. Hirons, *J. Chem. Technol. Biotechnol.* 1984, **34A**, 218.
24. J. M. R. de Carvalho and M. J. Slater, *Proc. ISEC'83, Denver* 1983, p. 297 (1983).
25. R. J. Whewell, M. H. Hughes and C. Hanson, *Advances in Extractive Metallurgy*, p. 21. IMN, London (1977).

Polyhedron Vol. 6, No. 2, pp. 205–211, 1987
Printed in Great Britain

0277–5387/87 $3.00+.00
Pergamon Journals Ltd

DIAGNOSTIC FEATURES FOR THE LINKAGE ISOMERISM OF THE OXIMATO GROUP: CHARACTERIZATION OF SOME Cu(II), Co(II) AND U(VI) COMPLEXES OF A DIOXIME SCHIFF-BASE LIGAND*

A. O. BAGHLAF, M. M. ALY† and N. S. GANJI

Chemistry Department, Faulty of Science, King Abdulaziz University, Jeddah, Saudi Arabia

(*Received* 18 *April* 1985; *accepted after revision* 28 *May* 1986)

Abstract—The reactions of the dioxime ligand *N,N'*-ethylenebis(isonitrosoacetylacetoneimine) with Cu(II), Co(II) and U(VI) ions produced metal complexes with the oximato groups coordinated through both oxygens, both nitrogens or one oxygen and one nitrogen. Some interconversion of isomers was observed. The U(VI) complexes reacted with Ni(II) acetate to produce the Ni(II) analogue of the Cu(II) complex with the oxygen coordination isomer. The observed linkage isomerism of the oximato group and the suggested formulations of the metal complexes are based on analytical, electronic and vibrational spectra, and magnetic-moment evidence.

Structural studies on the transition-metal complexes of either α-dioxime[1–5] or vicinal oxime–imine ligands[1,6–9] have revealed several interesting aspects. The most interesting one is related to the ability of the oximato group to coordinate to the metal ion through either the oximino oxygen or the oximino nitrogen.[1] However, the possible interconversion of the linkage isomers was not dealt with in most of these reports, although this is considered a deciding factor in the characterization of the coordination mode. We wish to report an investigation on the Cu(II), Co(II) and U(VI) complexes of the Schiff-base *N,N'*-ethylenebis(isonitrosoacetylacetoneimine) (H_2L). This ligand comprises features of both a dioxime and vicinal oxime–imine ligand.[10,11] This study is also related to that of the nitrosation products[12] of the metal complexes of *N,N'*-ethylenebis(acetylacetoneimine).

EXPERIMENTAL

Reagent grade chemicals were used. The ligand (H_2L) was prepared by a published method.[10] The IR spectra of the metal complexes were measured as KBr pellets using a Perkin–Elmer 683 spectrophotometer. The electronic spectra were carried out with a Pye–Unicam S.P. 8000 spectrophotometer. Magnetic susceptibilities were measured at 25°C by the Gouy method where mercuric tetrathiocyanatocobaltate(II) was the magnetic-susceptibility standard. Diamagnetic corrections were effected by employing Pascal's constants.[13] The magnetic moments were calculated from the equation $\mu_{eff} = 2.84\sqrt{\chi_M^{corr}T}$. Carbon, hydrogen and nitrogen analyses were determined at the analytical unit of King Abdulaziz University. Standard methods were used for the determination of the metal ions. All metal complexes were dried *in vacuo* over phosphorus pentoxide.

Preparation of the metal complexes and their reactions

(1) *Reactions of* H_2L *with* Cu(II) *acetate monohydrate in aqueous solution.* (a) Complex **I**: A filtered aqueous solution (100 cm^3) of $(CH_3CO_2)Cu \cdot H_2O$ (1.42 g, 0.0071 mol) was added to a warmed aqueous suspension (100 cm^3) of the equimolar concentration of the ligand (2.0 g). The reaction solution was boiled for 2 h and left for 12 h to precipitate the yellowish-brown complex **I**. This was filtered off, washed with water and dried [2.1 g, 86%

* This paper is part of the M.Sc. thesis of N. S. Ganji.

† Author to whom correspondence should be addressed. Present address: Chemistry Department, Faculty of Science, Shebin El-Kom, El-Menoufia University, Egypt.

yield)]. This complex was recovered unchanged from either boiling chloroform (2 h) or after digestion in pyridine (4 h) and decomposed when refluxed with piperidine (1 h).

(b) Complex **II**: This complex was prepared as described in (a) by boiling the reaction solution for 1 h and cooling to precipitate the reddish-violet complex which was filtered off, washed with water and dried [1.7 g (70% yield)]. It was found to be stable after refluxing for 1 h in chloroform, piperidine or pyridine.

(2) *Reaction of* H_2L *with* Cu(II) *acetate monohydrate in absolute ethanol.* This reaction was carried out in ethanol, using the procedure described in 1(a) with a 14-h reaction time, to produce complex **I** [1.6 g (66% yield)].

(3) *Conversion of complex* **I** *to complex* **III.** The powdered complex **I** (3.44 g, 0.01 mol) was added to pyridine (15 cm^3). The reaction solution was refluxed for 2 h and diluted with benzene (200 cm^3) to precipitate complex **III.** This was filtered off, washed with benzene and dried [3.0 g (87% yield)].

(4) *Template reaction of isonitrosoacetylacetone with* Cu(II) *acetate monohydrate and ethylenediamine* (2 : 1 : 1 *molar ratio*) *in ethanol.* An ethylenediamine (0.42 g, 0.007 mol) solution in ethanol (50 cm^3) was added to that (200 cm^3) of $(CH_3CO_2)_2Cu \cdot H_2O$ (1.4 g, 0.007 mol). The resulting solution was added to a solution (50 cm^3) of isonitrosoacetylacetone (1.81 g, 0.014 mol). The resulting reaction solution was warmed for 1 h and left for 14 h to precipitate complex **I** which was filtered off, washed with ethanol and dried [1.9 g (79% yield)].

(5) *Complex* **IV.** This complex was prepared in water, as described in 1(a), from the 5 : 1 molar ratio reaction of $CoCl_2 \cdot 6H_2O$ (6.0 g, 0.025 mol) with H_2L (1.42 g, 0.005 mol). The precipitated red complex was filtered off, washed with water and dried [1.5 g (88% yield)].

(6) *Complexes* **V** *and* **VI.** The ethanolic solution (100 cm^3) of the $UO_2X_2 \cdot nH_2O$ [X = acetate, $n = 2$ (4.24 g, 0.01 mol); X = nitrate, $n = 6$ (5.02 g, 0.01 mol)] was added to an equimolar-concentration suspension of the ligand (2.82 g) in ethanol (200 cm^3). The stirred reaction solution was warmed for 4 h. The precipitated complex was filtered off, washed with boiling ethanol and dried [complex **V** = 2.2 g (33% yield); complex **VI** = 1.9 g (28% yield)].

(7) *Reaction of complex* **V** *or* **VI** *with* Ni(II) *acetate tetrahydrate.* An ethanolic solution (100 cm^3) of $(CH_3CO_2)_2Ni \cdot 4H_2O$ (1.0 g, 0.004 mol) was added to a powdered equimolar-concentration suspension of the U(VI) complex (2.69 g of complex **V** or **VI**) in ethanol (50 cm^3). The reaction solution was warmed while stirring for 4 h and left for 14 h. The precipitated complex was filtered off and extracted with chloroform (30 cm^3). The chloroform extract was concentrated to precipitate the yellow Ni(II) complex analogue of complex **I** [0.32 g (24% yield)]. This Ni(II) complex was characterized by elemental analyses, and electronic and vibrational spectra, as well as by comparing with an authentic sample prepared as described earlier.[11]

RESULTS AND DISCUSSION

The analytical (Table 1) and spectral data (Tables 2 and 3) are compatible with regarding the structure of the complexes formed from the 1 : 1 molar ratio

Table 1

Complex	Suggested formulation	Elemental analyses (%)[a] C	H	N	Metal	Colour
I	LCu ($C_{12}H_{16}N_4O_4Cu$)	41.7 (41.9)	4.8 (4.7)	16.2 (16.3)	18.8 (18.5)	Yellowish-brown
II	LCu ($C_{12}H_{16}N_4O_4Cu$)	42.1 (41.9)	4.7 (4.7)	16.7 (16.3)	18.1 (18.5)	Reddish-violet
III	LCu ($C_{12}H_{16}N_4O_4Cu$)	41.4 (41.9)	4.6 (4.7)	16.5 (16.3)	18.5 (18.5)	Brown
IV	LCo ($C_{12}H_{16}N_4O_4Co$)	42.8 (42.5)	4.8 (4.7)	16.8 (16.5)	17.1 (17.4)	Red
V	$HLUO_2 \cdot en \cdot Ac$ ($C_{16}H_{28}N_6O_8U$)	28.0 (28.7)	4.2 (4.2)	12.0 (12.5)	36.2 (35.5)	Brownish-yellow
VI	$HLUO_2 \cdot en \cdot NO_3$ ($C_{14}H_{25}N_7O_9U$)	24.5 (25.0)	3.8 (3.7)	14.7 (14.6)	34.9 (35.3)	Brownish-yellow

[a] Calculated values in parentheses.

Table 2. Assignments of the vibrational bands (cm^{-1}) of the metal complexes[a]

	Assignment						
	ν(C=O)			ν(N—O)			
Complex	*N*-coordination	*O*-coordination	ν(C=N)	*N*-coordination	*O*-coordination	δ(N—O)	ν(metal–ligand)
		1688(s)			1141(s)	832(w)	592(m)
I	—	1680(s)	1585(m)	—	1135(s)	772(w)	480(m)
						832(w)	592(m)
II	1660(s)	—	1604(m)	1160(s)	—	775(w)	465(m)
							592(m)
		1688(s)	1603(m)			832(w)	480(m)
III	1660(s)	1680(s)	1585(m)	1160(s)	1142(s)	772(w)	465(m)
						835(w)	597(m)
IV	—	1688(s)	1610(m)	—	1146(s)	778(w)	505(m)
		1693(s)[b]	1630(m)[b]		1102(s)	830(w)	592(m)
V	—	1680(s)	1604(m)	—	1073(s)[b]	790(w)	580(m)
		1693(s)[b]	1630(m)[b]		1102(s)	832(w)	593(m)
VI	—	1680(s)	1603(m)	—	1073(s)[b]	794(w)	582(m)

[a] s = strong, m = medium, w = weak.
[b] Bands associated with the non-ionized part of the ligand.

reaction of $(CH_3CO_2)_2Cu \cdot H_2O$ with H_2L to be dependent on the solvent used (water or ethanol) and the time of reaction. These reactions are schematically represented in Fig. 1. Thus, the reaction of the ligand with the metal acetate in either water or ethanol led, after a 14-h reaction time, to the formation of the yellowish-brown complex **I** (Fig. 2). However, in the case of a 1-h reaction time the reddish-violet complex **II** was formed in water. The IR spectrum of complex **I** revealed ν(C=O) vibrations at 1688 and 1680 cm^{-1} [compared to ν(C=O) of the dimeric ligand[10] at 1700, 1690, 1678 and 1662 cm^{-1}]. These bands are located in the 1690–1670-cm^{-1} region which was tentatively associated with six-membered chelate ring in the vicinal oxime–imine Ni(II) complexes.[8,9] Furthermore, the ν(C=O) vibrations could be compared in position and intensity with the reported[12] spectrum of the mononitrosation product [ν(C=O) at 1679 cm^{-1})] of *N,N'*-ethylenebis(acetylacetoneimine)copper(II) whose structure (see complex **A** in Fig. 2) was shown,[14] from X-ray structural data, to comprise the six-membered chelate ring with the oximino oxygen coordination to Cu(II). The ν(N—O) vibrations of complex **I**, are located at identical frequencies (1141 and 1135 cm^{-1}) to those of the reported spectrum of the mononitrosation product which is additional evidence for the structure of this complex [ν(N—O) of the ligand[10] appeared at 1062 and 1025 cm^{-1}]. The splitting of ν(N—O) into two bands (separated by 6 cm^{-1}) is attributed to the non-equivalence of the two six-membered chelate rings in the planar structure of the complex rather than to any side coordination by the oximino oxygen. This is because the magnetic moment of complex **I** was found to be 1.81 BM, which is near the spin-only value for one unpaired electron of the d^9 Cu(II) ion, and, therefore, molecular association is unlikely since it would lead to spin–spin interactions and lower the magnetic moment below the spin-only value.

It is noteworthy in this connection that the reported IR spectrum of the complex prepared by Masuda *et al.*[12] from the complete nitrosation of

Table 3. Electronic spectra of the metal complexes in chloroform or as a Nujol mull

Complex	Solvent	λ_{max} (nm) [values in parentheses are molar absorptivities (l mol cm^{-1})]
I	Nujol	520, 390
	$CHCl_3$	503 (1350), 365 (6670), 282 (13,500)
II	Nujol	554, 510, 388
	$CHCl_3$	503 (1360), 366 (6150), 282 (12,600)
III	Nujol	355
	$CHCl_3$[a]	505, 365, 282
IV	Nujol	546, 516, 466, 386, 346
V	$CHCl_3$[a]	355
VI	$CHCl_3$[a]	340

[a] Saturated solution of the sparingly soluble complex.

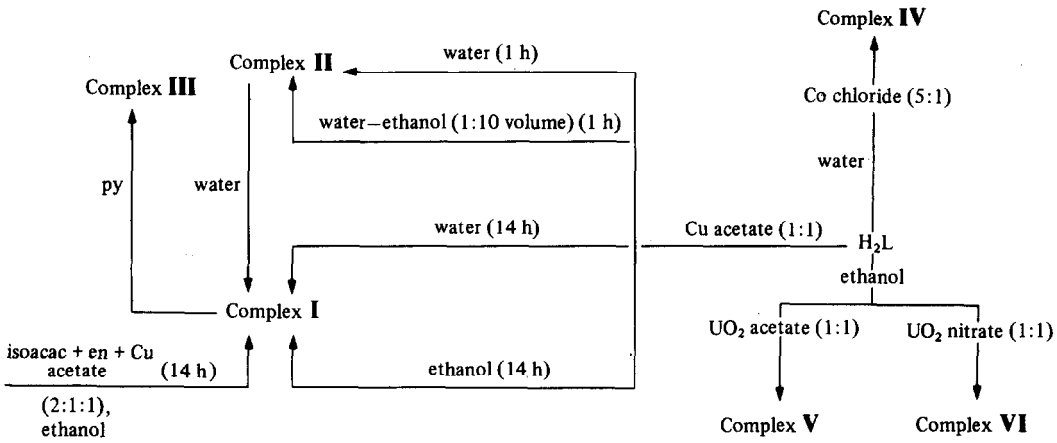

Fig. 1. Schematic representation for the reactions of the ligand with the metal ions and the reactivity of some of the Cu(II) complexes (isoacac, en, py and pip refer to isonitrosoacetylacetone, ethylenediamine, pyridine and piperidine, respectively).

N,N'-ethylenebis(acetylacetoneimine)copper(II) is identical to that of complex **I**. Accordingly, it is believed that its structure is identical to that of our complex **I** and not the reported[12] structure, which suggests coordination of the oximato group through the oximino nitrogen. This conclusion is also applicable to the dark-brown complex reported by Bose and Patel[15] who used the same preparative method of Masuda *et al.*,[12] and proposed a structure based on the *N*-coordination. Moreover, it is in agreement with the structure of the mononitrosation product (*O*-coordination) and, therefore, it should be expected that the nitrosation of the second chelate ring would proceed similarly. This argument is substantiated by the characterization of the red-violet complex **II** (Fig. 2). This complex was prepared from the 1-h reaction of the ligand with $(CH_3CO_2)_2Cu \cdot H_2O$ (1 : 1 molar ratio) in water

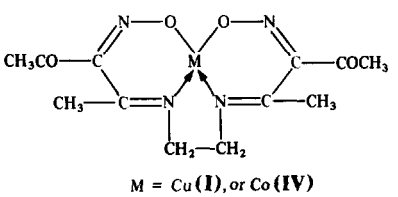

M = Cu(**I**), or Co(**IV**)

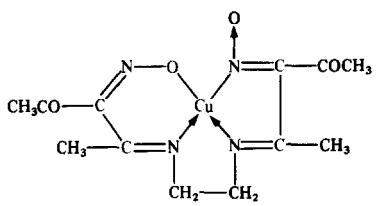

III

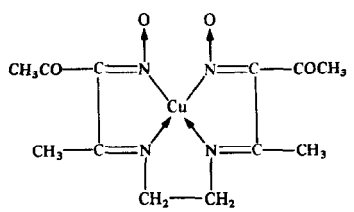

II

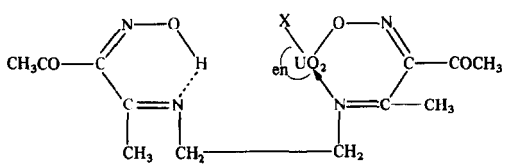

X = acetate(**V**), or nitrate(**VI**)

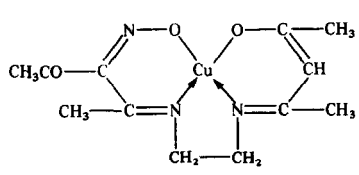

A

Fig. 2. Suggested formulations of the metal complexes **I–VI** and their relation to the mononitrosation product complex (**A**).

or water–ethanol (1 : 10) (see Fig. 1). The ν(C=O) of complex **II** was located at a lower frequency (1660 cm^{-1}) than that of complex **I** (Table 2). This vibration is located in the 1660–1630-cm^{-1} region of the carbonyl group[8,9] attached to a five-membered chelate ring in the vicinal oxime–imino complexes of Ni(II). Furthermore, it occurs at a lower frequency than that of complex **I** as well as that of the mononitrosation product (Fig. 2) of *N,N'*-ethylenebis(acetylacetoneimine)copper(II). It is suggested, therefore, that the chelate rings in complex **II** are of the five-membered type which requires the oximato group to be coordinated to the metal ion through the oximino nitrogen. The observed ν(N—O) in complex **II** is located at a higher frequency (1160 cm^{-1}) than that of complex **I** (1142 and 1135 cm^{-1}) (Table 2). This accords with the suggested structures of complexes **I** and **II** since coordination by the oximino nitrogen will produce an N—O bond with a greater double-bond character and consequently a higher ν(N—O) than is the case with oximino-oxygen coordination of less double-bond character for the N—O bond and a lower ν(N—O). The magnetic moment of complex **II** was found to be 1.78 BM, which is comparable with the spin-only value of the unpaired electron of Cu(II). The suggested structures of complexes **I** and **II** represented a new example for the isomeric linkage for the oximato group whereby both the oximato groups are coordinated through the oximino oxygen and the oximino nitrogen, respectively. Complex **II** (*N*-coordination) was converted to complex **I** (*O*-coordination) by allowing the aqueous reaction solution of **II** to stand at room temperature for 14 h. This conversion implied the stability of the *O*-coordination mode of the six-membered chelate ring over the *N*-coordination mode of the five-membered chelate ring.

Complex **I** decomposed in boiling piperidine and was recovered unchanged from boiling chloroform or after stirring in pyridine for 14 h. However, on refluxing its solution in pyridine for 1 h complex **III** was formed, which is formulated as shown in Fig. 2. The vibrational features of this complex regarding the stretching vibrations of the carbonyl and oximato groups are diagnostic for the presence of the isomeric linkage behaviour of the oximato group within the same complex, whereby it exhibits *O*- and N-coordination to produce six- and five-membered chelate rings, respectively. Thus, the IR spectrum of the complex revealed the presence of two distinct ν(C=O) vibrations for the carbonyl groups. The higher-frequency vibrations (1688 and 1680 cm^{-1}) are located in the 1690–1670-cm^{-1} region of the carbonyl group attached to a six-membered chelate ring [in the oxime–imino complexes[8] of Cu(II) and Ni(II)] whereas the lower-frequency band is located in the 1660–1630-cm^{-1} region of the five-membered chelate ring. Similarly, the ν(N—O) vibrations are separated by two distinct and well-resolved bands where the higher frequency (1160 cm^{-1}) is ascribed to the oximino-nitrogen coordination (greater double-bond character for the N—O bond) whereas the lower frequency (1142 cm^{-1}) is associated with the oximino-oxygen coordination (less double-bond character for the N—O bond).

The action of pyridine in the conversion of complex **I** to complex **III** should proceed through dissociation of the metal–oxygen bond of the oximato group. This step could result from the axial ligation of pyridine to the metal atom. Charge redistribution on the oximato group will lead to its coordination through the oximino nitrogen. The magnetic moment of complex **III** (1.82 BM) indicated that molecular association is unlikely as was the case with complexes **I** and **II**. The Ni(II) analogue to complex **III** was prepared from the reaction of H_2L with $(CH_3CO_2)_2Ni \cdot 4H_2O$ in ethanol.[11] The location of the vibrational bands of the carbonyl in the Ni(II) and Cu(II) complexes are identical. However, this similarity does not extend to the ν(N—O) since it is related to the stability of the chelate ring itself which comprises the metal ion.

It is of interest to compare ν(C=N) and the Cu–ligand stretching vibrations of complex **III** (which showed an isomeric linkage of the oximato group in the same complex) with those of complexes **I** (*O*-coordination) and **II** (*N*-coordination) where the oximato groups exhibited one mode of the coordination in the same complex. Thus the ν(C=N) of complex **I** is located[16] at a lower frequency (1585 cm^{-1}) than complex **II** (1604 cm^{-1}). This implied a higher contribution from the imino nitrogen to the strength of the chelate ring in the case of the six-membered chelate ring. Both these vibrations were detected from complex **III** where both five- and six-membered chelate rings are present. The ν(Cu—N) (imino nitrogen) appeared at 592 cm^{-1} in complexes **I–III**, where the ligand had no vibrational bands.[17] In complex **I** with *O*-coordination of the oximato group, a band appeared at 480 cm^{-1}, whereas in complex **II** with *N*-coordination this band was shifted to 465 cm^{-1}. It is therefore safe to assign the 480-cm^{-1} band to ν(Cu—O) (oximino oxygen) and the 465-cm^{-1} band to ν(Cu—N) (oximino nitrogen). These assignments are supported by the presence of those two bands in the case of complex **III** with isomeric coordination.

The electronic spectra of the metal complexes **I–III** are summarized in Table 3. The Nujol mull spectra of complexes **I–III** are indicative of a planar

structure.[18] The chloroform solutions of complexes **I–III** are red, although they have different colours in the solid state (Table 1). The positions of the absorption peaks observed from the Nujol mull spectra are not identical with those of the solution spectra. Moreover, the intensities of these maxima are higher than the usually encountered[18] values. The absorption peak of the ligand at 315 nm is shifted to 282 nm in complexes **I–III**. In view of these observations it is best to consider all these bands as charge-transfer transitions generated from intramolecular electronic interactions.

The reaction of $CoCl_2 \cdot 6H_2O$ with the ligand (5 : 1 molar ratio) led to the formation of the red complex **IV**. The IR spectrum of this complex was identical with that of the Cu(II) complex **I** with regard to ν(C=O), ν(N—O) and ν(metal–ligand) vibrations. It is suggested therefore that the structure of complex **IV** comprises *O*-coordination of the oximato group in a similar manner to that described for complex **I** (Fig. 2). The magnetic moment of complex **IV** (1.71 BM) indicates a low-spin Co(II) complex and its visible spectrum (Table 3) is typical of a square-planer Co(II) complex.[19] The ν(C=N) band in complex **IV** is shifted to a higher frequency (15 cm^{-1}) than the corresponding vibration of the Cu(II) complex **I** of the same structure. This is ascribed to the weaker contribution of the imino nitrogen to the strength of the chelate ring in the case of the Co(II) complex compared to the Cu(II) complex.

The reaction of H_2L with either $(CH_3CO_2)_2UO_2 \cdot 2H_2O$ or $UO_2(NO_3)_2 \cdot 6H_2O$ (1 : 1 molar ratio) led to the formation of the yellowish-brown uranyl complexes **V** and **VI**, respectively. The formulations of these complexes (Fig. 2) are compatible with analytical (Table 1), spectral (Tables 2 and 3) and chemical-reactivity evidence. The formation of complexes **V** and **VI** is explained by the following reactions:

H_2L = (isoacac)$_2$enimine

$$\xrightleftharpoons{C_2H_5OH} 2\text{Hisoacac} + \text{en}, \quad (1)$$

$$H_2L + UO_2X_2 + \text{en} \longrightarrow HLUO_2X \cdot \text{en} + HX, \quad (2)$$

where Hisoacac = isonitrosoacetylacetone, X = acetate (complex **V**) or nitrate (complex **VI**), and en = ethylenediamine. The IR spectra of the complexes **V** and **VI** are almost identical with regard to ν(C=O), ν(C=N) and ν(N—O) vibrations. The presence of two well-resolved ν(C=O) (1693 and 1680 cm^{-1}) is indicative of two non-equivalent carbonyl groups. The higher-frequency band is identical with that observed from the ligand[10] itself whereas the lower-frequency band is located at a comparable frequency to that observed from the carbonyl group attached to the six-membered chelate ring of the vicinal oxime–imine complexes of Ni(II)[8] and Cu(II)[14] as well as from complexes **I** and **IV** [*O*-coordination (see Fig. 2)]. The associated ν(N—O) bands are located at 1073 cm^{-1} for the non-ionized part (shifted from 1062 cm^{-1} in the case of H_2L) and at 1102 cm^{-1} for the six-membered chelate ring. The latter band is located at a lower frequency (30 cm^{-1}) than the comparable ν(N—O) of complexes **I** and **IV** with an identical chelate ring. This observation could be explained by the weaker U—O bond (oxygen of the oximato group in complexes **V** and **VI** compared to the M—O bond in complexes **I** and **IV**. The ν(C=N) vibrations of the chelate ring and the non-ionized part of the ligand were located at 1604 and 1630 cm^{-1}, respectively (shifted from 1635 cm^{-1} in the case of H_2L). The acetato group in complex **V** showed a ν_{as} centred at 1545 cm^{-1}, and the splitting of this band (1555, 1550 and 1540 cm^{-1}) is indicative of coordinate crowding in the equatorial plane of the uranyl ion. Bidentate coordination is suggested for the acetato group by comparing the ν_{as} in this case with other acetato complexes of the metal ion.[20] The $\nu(NH_2)$ of the bidentate ethylenediamine is broad (centred around 3250 cm^{-1}) and mixed with the broad ν(OH) (centred at 3400 cm^{-1}) of the non-ionized part of the ligand. The IR spectrum of complex **VI** did not show any strong band in the 1350–1400-cm^{-1} region of the free nitrate ion but revealed instead a vibrational band at 1485 cm^{-1} which is assigned to ν(N—O) of the coordinated nitrato broup. Other stretching vibrations for nitrato group were observed at 2580, 2495, 1720 and 745 cm^{-1}. These bands are located at comparable locations to those of the known bidentate nitrate[21,22] of the uranyl ion. Accordingly, it is suggested that the U(VI) ion in complexes **V** and **VI** had achieved 6-coordination in the equatorial plane [two from the chelate ring, two from ethylenediamine and two from either the acetato or the nitrato group (see Fig. 2)]. The ν(U—N) (imino nitrogen) is located near 600 cm^{-1} as in complexes **I–IV**. The strong ν(O—U—O) stretching vibration is located at 910 cm^{-1} as in other cases of uranyl complexes of Schiff bases.[21]

The electronic spectra of the sparingly soluble complex **V** (a single peak at 355 nm) and complex **VI** (a single peak at 340 nm) is typical of the uranyl complexes which usually show absorption peaks in the 340–500-nm region related to the UO_2^{2+} entity.[23] The suggested half-ionization of the ligand in complexes **VI** and **VII** is consistent with a similar behaviour of the trivalent lanthanides complexes of Schiff-bases.[24] Moreover, the reaction of

uranyl nitrate with the related H_2L produced the adduct $UO_2(H_2L)(NO_3)_2$ in which the ligand behaved[21] as a neutral bidentate molecule.

Chemical evidence for the suggested formulations of complexes **V** and **VI** is derived from their reaction with $(CH_3CO_2)_2Ni \cdot 4H_2O$ (1 : 1 molar ratio in ethanol). This reaction led to the formation of a Ni(II) complexes which has been characterized, by analytical and spectral evidence, as the previously reported[11] Ni(II) analogue of complex **I**. The formation of the latter complex is explained by the following metal exchange reaction:

$$HLUO_2 \cdot en \cdot X + (CH_3CO_2)_2Ni \xrightarrow{C_2H_5OH} LNi + (CH_3CO_2)_2UO_2 + en + HX. \quad (3)$$

The freed diamine in reaction (3) reacted with the initially formed Ni(II) complex **III** analogue to form that of complex **I**, which is in accordance with our earlier[11] observation regarding the reactivity of the former complex with the diamine.

REFERENCES

1. A. Chakravorty, *Coord. Chem. Rev.* 1974, **13**, 1.
2. R. H. Holm and M. J. O'Connor, *Prog. Inorg. Chem.* 1971, **14**, 277.
3. J. S. Miller and A. J. Epstein, *Prog. Inorg. Chem.* 1976, **20**, 100.
4. T. W. Thomas and A. E. Underhill, *Chem. Soc. Rev.* 1972, **1**, 99.
5. M. S. Ma and R. J. Angelici, *Inorg. Chem.* 1980, **19**, 363.
6. M. J. Lacey, C. G. Macdonald, J. S. Shannon and P. J. Collin, *Aust. J. Chem.* 1970, **23**, 2279.
7. M. J. Lacey, C. G. Macdonald, J. F. McConnell and J. S. Shannon, *J. Chem. Soc., Chem. Commun.* 1971, 1206.
8. M. J. Lacey, J. S. Shannon and C. G. Macdonald, *J. Chem. Soc., Dalton Trans.* 1974, 1215.
9. K. S. Bose, B. C. Sharma and C. C. Patel, *Inorg. Chem.* 1973, **12**, 120.
10. M. M. Aly and F. A. El-Said, *J. Inorg. Nucl. Chem.* 1981, **43**, 287.
11. M. M. Aly, A. O. Baghlaf and N. S. Ganji, *Polyhedron* 1985, **4**, 1301.
12. I. Masuda, M. Tamaki and K. Shinra, *Bull. Chem. Soc. Jpn* 1969, **42**, 157.
13. J. Lewis and R. G. Wilkins, *Modern Coordination Chemistry*, p. 403. Interscience, New York (1960).
14. M. B. Cingi, A. C. Villa, A. G. Manfredotti, C. Guastini and M. Nardelli, *Acta Cryst.* 1972, **B28**, 1075.
15. K. S. Bose and C. C. Patel, *J. Inorg. Nucl. Chem.* 1971, **33**, 2947.
16. J. E. Kovacic, *Spectrochim. Acta* 1967, **23A**, 183.
17. D. B. Powell and N. Sheppard, *J. Chem. Soc.* 1956, 3108.
18. A. B. P. Lever, *Inorganic Electronic Spectroscopy*, p. 355. Elsevier, Amsterdam (1968).
19. A. B. P. Lever, *Inorganic Electronic Spectroscopy*, p. 328. Elsevier, Amsterdam (1968).
20. M. Casellato and P. A. Vigato, *Coord. Chem. Rev.* 1978, **25**, 85.
21. B. Kim, C. Miyake and S. Iomoto, *J. Inorg. Nucl. Chem.* 1975, **37**, 963.
22. N. F. Curtis and Y. M. Curtis, *Inorg. Chem.* 1965, **4**, 804.
23. A. Pasini, M. Gullotti and E. Cesarotti, *J. Inorg. Nucl. Chem.* 1972, **34**, 3821.
24. H. A. Tayim, M. Absi, A. Darwish and S. K. Thabet, *Inorg. Nucl. Chem. Lett.* 1975, **11**, 395.

Polyhedron Vol. 6, No. 2, pp. 213–218, 1987
Printed in Great Britain

0277–5387/87 $3.00+.00

ANDERSON-TYPE HETEROPOLYANIONS OF MOLYBDENUM(VI) AND TUNGSTEN(VI)

KENJI NOMIYA, TAKEO TAKAHASHI, TAKAHIRO SHIRAI and MAKOTO MIWA*

Department of Industrial Chemistry, Faculty of Engineering, Seikei University, Musashino, Tokyo 180, Japan

(*Received* 7 *April* 1986; *accepted* 28 *May* 1986)

Abstract—The previously reported preparation of some Anderson-type molybdopolyanions containing divalent metal ions (Zn, Cu, Co or Mn) as a heteroatom has been reinvestigated. The molybdopolyanions of Zn(II) and Cu(II) were confirmed, although the Cu(II) polyanion was not stable and could not be recrystallized. On the other hand, the polyanions of Co(II) and Mn(II) could not be reproduced. Another type of heteropoly compound, $[X(H_2O)_{6-x}(Mo_7O_{24})]^{4-}$ [X = Cu(II), Co(II) or Mn(II)], was isolated as solids, which are not stable thermally. The mixed-type Anderson polyanions, $[Ni(II)Mo_{6-x}W_xO_{24}H_6]^{4-}$, which have been questioned as mixtures of species with different x values, were also reinvestigated using IR, UV absorption and MCD spectra. They are single species, but not mixtures, although some positional isomers may be present for the compounds where $x = 2$–4. The possibility of oxidation of the heteroatom with the Anderson structure maintained was examined. The oxidation of $[Ni(II)Mo_6O_{24}H_6]^{4-}$ by the $S_2O_8^{2-}$ ion in aqueous solution gave the Waugh-type $[Ni(IV)Mo_9O_{32}]^{6-}$ polyanion, whereas the oxidation of $[Ni(II)W_6O_{24}H_6]^{4-}$ gave no heteropoly compound.

Anderson-type heteropolyanions, represented by the general formula $[XM_6O_{24}H_x]^{n-}$, possess a heteroatom (X) in a central octahedral cavity of the crown by edge-sharing six octahedral MO_6 (M = Mo or W).[1] These polyanions become a family for a number of 2+, 3+, 4+, 6+ and 7+ metal ions as the heteroatom. They have been classified into A ($x = 0$) and B ($x = 6$) types by the number of attached protons, although some polyanions with x other than 0 or 6 have been recently reported.[2,3] Most of them have been tabulated in books.[1,4] However, some questionable compounds are also involved there. In this work, we have done three experimental studies. The first is related to members of the family of B-type molybdopolyanions, especially the polyanions containing some divalent metal ions [Zn(II), Cu(II), Co(II) or Mn(II)] other than Ni(II), which have been first reported by LaGinestra *et al.*,[5] and later questioned by Malik *et al.*[6] The second is a reinvestigation by spectroscopic (IR, UV absorption and MCD) methods of the mixed-type Ni(II) molybdotungstopolyanions previously reported by Matijevic *et al.*[7] The last concerns the possibility of the oxidation of Ni(II) molybdo- and tungstopolyanions leading to the corresponding Ni(IV) ones with the polyanion structure maintained.

EXPERIMENTAL

Electronic absorption spectra were measured by a Hitachi 340 spectrophotometer with an attached computer-key board. MCD spectra were recorded by a JASCO J-40AS spectropolarimeter mounted with a 10.0-kG electromagnet. IR spectra were recorded with a JASCO IR-G spectrophotometer. Measurements were made at room temperature.

Preparations

$(NH_4)_3[X(III)Mo_6O_{24}H_6]\cdot 7H_2O$ *and* $(NH_4)_4[X(II)Mo_6O_{24}H_6]\cdot 5H_2O$. B-type molybdopolyanions

* Author to whom correspondence should be addressed.

containing tervalent metal ions (Cr, Al or Fe) and Ni(II) ion were obtained as crystals by the traditional method:[8] adding an aqueous solution of metal sulphates or alums (3.1×10^{-3} mol) in 20 cm^3 water into a boiling aqueous solution of $(NH_4)_6Mo_7O_{24} \cdot 4H_2O$ (5 g, 4.2×10^{-3} mol) dissolved in 80 cm^3 water, further evaporating on a steam-bath, filtering the hot solution and cooling. In the preparation of the Co(III) polyanion, a mixed aqueous solution (30 cm^3) of $CoSO_4 \cdot 7H_2O$ (4.2 g, 0.015 mol) and 30% aqueous H_2O_2 (2 g) was added into the boiling solution of aqueous heptamolybdate (30.9 g, 2.5×10^{-2} mol in 260 cm^3 water). These compounds were recrystallized twice from water. The colour and analytical data are listed in Table 1. Visible absorption spectra of the Co(III), Cr(III) and Ni(II) compounds are in good agreement with the previous data.[9] When the colourless Fe(III) polyanion was dissolved in water, the solution was a wine-red colour due to the dissociation and/or the hydrolysis.

The preparation of B-type Anderson molybdopolyanions containing divalent metal ions (Ni, Zn, Co or Mn) has been reported by LaGinestra *et al.*[5] However, some questionable points were seen. They stated that such polyanions must be prepared without boiling: however, the Ni(II) and Zn(II) compounds were actually obtained from boiling solutions. The Zn(II) compound was obtained as colourless crystals by adding an aqueous solution of $ZnSO_4 \cdot 7H_2O$ (1 g, 3×10^{-3} mol in 20 cm^3 water) into a boiled solution of heptamolybdate (5 g, 4.2×10^{-3} mol in 80 cm^3 water). It was recrystallized twice from water. Analytical data are listed in Table 1. This compound was very soluble in water. Further, the Cu(II) compound was obtained by adding Cu(II) sulphate solution (0.75 g, 3×10^{-3} mol in 20 cm^3 water) into the boiled solution of heptamolybdate (5 g, 4.2×10^{-3} mol in 80 cm^3 water), filtering the yellow insoluble precipitate produced, cooling the filtrate, and adding excess amounts of acetonitrile. The light blue solid obtained was insoluble in water and not stable thermally. The Co(II) and Mn(II) compounds were not obtained from boiling solutions. Any changes in the pH of the initial heptamolybdate solution and in the reaction time gave mixtures of the initial materials and the bluish violet [for Co(II)] or yellow [for Mn(II)] insoluble solids. On the other hand, from the experiments without boiling, the Cu(II), Co(II) and Mn(II) compounds could be obtained, which were insoluble in water and not stable thermally. They were prepared by concentrating the mixed aqueous solutions of the metal sulphates and heptamolybdate without heating and/or adding excess amounts of acetonitrile. However, their spectra were not identical with the characteristic IR spectra of the Anderson molybdopolyanions.

Table 1. Colour and analytical data for $(NH_3)_3[X(III)Mo_6O_{24}H_6] \cdot 7H_2O$ and $(NH_4)_4[X(II)Mo_6O_{24}H_6] \cdot 5H_2O$

X	Colour	Found (%)		Calculated (%)	
		N	H	N	H
Co(III)	Blue-green	2.4	3.6	2.7	3.5
Cr(III)	Reddish-violet	2.4	3.6	2.7	3.5
Fe(III)	Colourless	2.4	3.6	2.7	3.5
Al(III)	Colourless	2.4	3.7	2.7	3.6
Ni(II)	Sky-blue	2.7	4.6	2.7	4.7
Zn(II)	Colourless	2.3	4.5	2.7	4.7

$(NH_4)_4[Ni(II)Mo_{6-x}W_xO_{24}H_6] \cdot 5H_2O$. B-type Ni(II) molybdotungstopolyanions ($x = 1, 3, 5$ or 6) were prepared according to two methods of Matijevic *et al.*[7] Method 1 is based on the dropwise addition of an aqueous solution of Ni(II) sulphate into boiling solutions containing appropriate molar ratios of Mo and W, where the source of Mo is $(NH_4)_6Mo_7O_{24} \cdot 4H_2O$ for $x = 0$, $Na_2MoO_4 \cdot 2H_2O$ for $x = 1$, and MoO_3 for $x = 2$–5; and the source of W is $Na_2WO_4 \cdot 2H_2O$ for all x. Method 2 is based on heating above 80°C aqueous solutions containing appropriate molar mixtures of already isolated $x = 0$ or 6 compounds, and cooling spontaneously to room temperature. All compounds, recrystallized twice from water, were obtained as sky-blue crystals. Analytical results for all the compounds were in good agreement within the experimental error. However, they do not lead to direct evidence for these mixed species, because they cannot be discriminated from those of mixtures of species with different compositions.

(Na, K)$_8[Ni(IV)W_6O_{24}] \cdot nH_2O$. An A-type Ni(IV) tungstopolyanion was obtained by the modification of the preparation of the isostructural Mn(IV) tungstopolyanion.[12] A solution of $Na_2WO_4 \cdot 2H_2O$ (20 g, 0.06 mol) in 100 cm^3 water was boiled, into which $NiSO_4 \cdot 6H_2O$ (2.6 g, 0.01 mol) in 10 cm^3 water was slowly added. Further, a fine powder of $K_2S_2O_8$ (5.4 g, 0.02 mol) was added. The boiling was continued for about 15 min, with occasional additions of water. The reaction mixture was poured into an equal amount of hot water and the solution kept at 80°C for about 30 min on the steam-bath. The black crystals formed were filtered, washed with water, and dried (yield 2.5 g). This compound was slightly soluble in water and insoluble in most other solvents.

Oxidation of Ni(II) *molybdo- and tungstopolyanions*

When an aqueous solution of $(NH_4)_4[Ni(II)Mo_6O_{24}H_6]\cdot 5H_2O$ containing $(NH_4)_2S_2O_8$ was heated, a colour change was seen; from sky-blue it turned gradually to black. After the homogeneous black solution was left standing at room temperature, the colourless precipitates produced were filtered off. The black crystals obtained from the filtrate showed IR spectra identical with that of the Waugh-type heteropoly compound $(NH_4)_6[Ni(IV)Mo_9O_{32}]$, which was prepared separately.[13] On the other hand, in the analogous experiments using $(NH_4)_4[Ni(II)W_6O_{24}H_6]\cdot 5H_2O$, no heteropoly compound could be obtained. In this reaction, the solution became blackish via yellowish-brown, but then it turned to green. Further addition of $(NH_4)_2S_2O_8$ showed no more colour change. Only the mixture of decomposed materials was given.

RESULTS AND DISCUSSION

B-type molybdopolyanions with divalent metal ions as a heteroatom

In the Anderson heteropolyanion, each heteroatom forms an octahedral complex of six oxygens for A-type and of six OH groups for B-type. Thus, the visible absorption spectra of B-type polyanions of Co(III), Cr(III) and Ni(II) are comparable with that of the corresponding hexaaqua complexes,[9] although the peak intensities of the polyanions are smaller as shown in Table 2. IR spectra of Anderson-type $[X(III)Mo_6O_{24}H_6]^{3-}$ [X(III) = Co(III), Cr(III), Fe(III) or Al(III)] are presented in Fig. 1. The bands due to the heteroatom are seen only in the region less than 450 cm^{-1}. Since the IR spectra in the 950–900- and 650–550-cm^{-1} regions become independent of the sort of heteroatom, they can be said to be in the pattern common to the B-type Anderson molybdopolyanions. In fact, the Ni(II), Zn(II) and Cu(II) molybdopolyanions show the characteristic IR spectra (Fig. 2). The IR spectrum previously shown for the Mn(II) compound by LaGinestra *et al.*[5] is evidently different from these patterns.

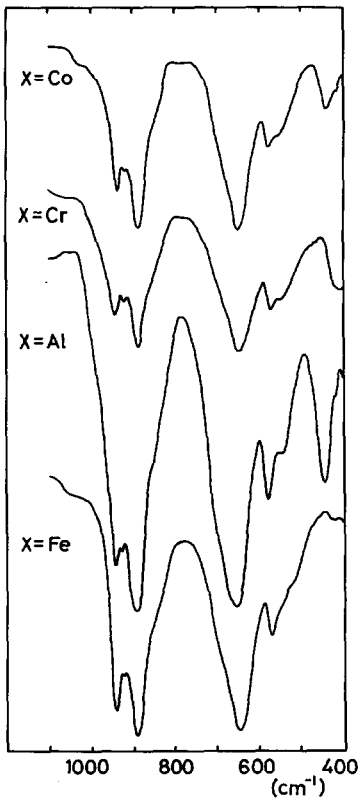

Fig. 1. Solid IR spectra of Anderson-type $[X(III)Mo_6O_{24}H_6]^{3-}$ polyanions.

Table 2. Spectral data of visible and near-IR absorption of Anderson-type molybdopolyanions of Co(III), Cr(III) and Ni(II)

	λ ($\times 10^{-3}$ cm^{-1}) (ε)		
$[Co(III)Mo_6O_{24}H_6]^{3-}$	16.5 (18.6)	24.2 (18.4)	
$[Co(H_2O)_6]^{3+}$ [a]	16.5 (40)	25.0 (50)	
$[Cr(III)Mo_6O_{24}H_6]^{3-}$	18.5 (7.8)	25.3 (9.5)	
$[Cr(H_2O)_6]^{3+}$ [a]	17.4 (13.3)	24.6 (15.3)	
$[Ni(II)Mo_6O_{24}H_6]^{4-}$	9.3 (1.6)	13.7 (1.2)	15.6 (1.8)
$[Ni(H_2O)_6]^{2+}$ [a]	8.5 (2.0)	13.8 (2.1)	15.2 (1.9)
$[SiNiMo_{11}O_{40}H_2]^{6-}$ [b]	8.6 (5.3)	14.5 (6)	

[a] Ref. 10.
[b] Ref. 11.

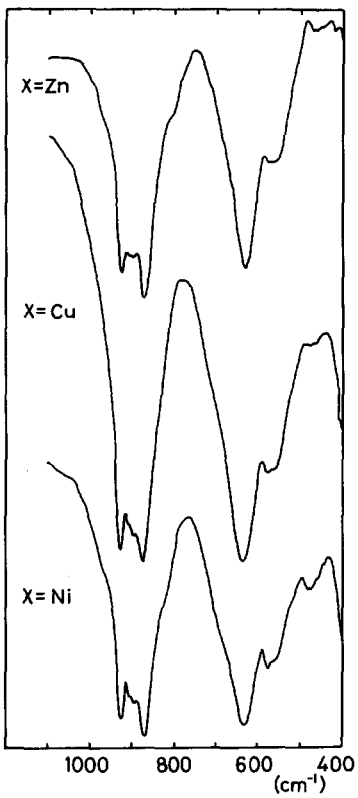

Fig. 2. Solid IR spectra of Anderson-type $[X(II)Mo_6O_{24}H_6]^{4-}$ polyanions.

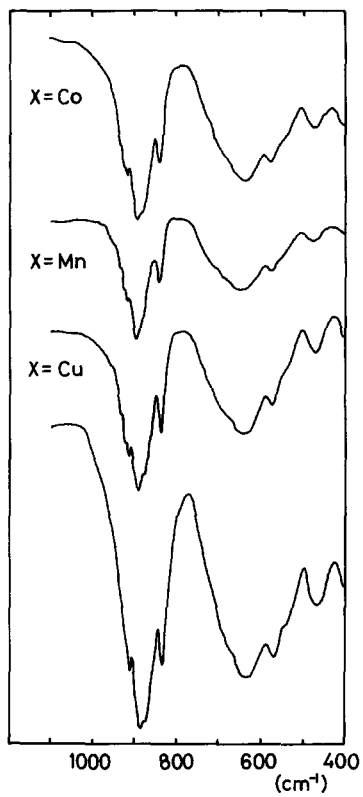

Fig. 3. Solid IR spectra of the 1:1 metal ion (X): $Mo_7O_{24}^{6-}$ complexes and $Mo_7O_{24}^{6-}$ alone (on the bottom).

Although they have attributed the disagreement to the different formulae due to the number of hydrates, it presumably accounted for the compound itself. On the other hand, the IR spectrum presented by them as that of the Co(II) compound is apparently similar to the characteristic patterns. We have occasionally obtained the compound showing such an IR spectrum from the reaction involving boiling with a Co(II) sulphate solution and an aqueous heptamolybdate solution adjusted to pH 4.46. However, such a compound was a minor product.

The Cu(II), Co(II) and Mn(II) compounds obtained from the experiments without boiling were not of the Anderson type, but like the Mo_7O_{24} polyanion. These compounds showed IR spectra very similar to that of the $[Mo_7O_{24}]^{6-}$ polyanion, except for the slightly broad bands in the 650–550-cm^{-1} region and the *ca* 10 cm^{-1} shift to the high-frequency region of the bands at *ca* 900 cm^{-1} (Fig. 3). They were insoluble in water and could not be recrystallized. Heating the aqueous suspension led to decomposition. These compounds are probably the $[X(H_2O)_{6-x}(Mo_7O_{24})]^{4-}$-type 1:1 complex, which was first proposed by Malik *et al.*,[6] from the Job method of continuous variation in an aqueous solution of metal sulphate and heptamolybdate. As a related complex, we have previously isolated the 1:2 Ce(III):Mo_7O_{24} complex as orange-red crystals from an aqueous solution containing ammonium Ce(III) nitrate and ammonium heptamolybdate.[14,15] The preparation was done only at room temperature, and the Ce(III) complex obtained was also insoluble in water, and not stable thermally.

The Anderson heteropolyanion is one of the most well-known polyanions and it constitutes a family with a number of heteroatoms.[1,4] We propose that the Co(II) and Mn(II) ions should be excluded from the Anderson family and entered into another category of polyanion.

Mixed-type $[Ni(II)Mo_{6-x}W_xO_{24}H_6]^{4-}$ *polyanions*

For these mixed polyanions, the possibility has been pointed that they are mixtures of polyanions with different x values.[1] However, it was easily confirmed from the IR spectra that the $x = 3$ compound obtained by method 1 differed from an equimolar mixture of the $x = 0$ and $x = 6$ compounds.

Further, the IR spectra of the $x = 3$ compounds obtained by methods 1 and 2 were identical, as shown in Fig. 4. The IR spectra of each mixed polyanion were subtly different, and all of them resembled that of the $x = 6$ rather than the $x = 0$ compound as a whole.

In aqueous solution, these mixed polyanions showed the behaviour of a single species. Figure 5 shows the UV and MCD spectra of the $x = 0$, 1, 3, 5 and 6 compounds obtained by method 1. MCD spectra evidently indicate that they are single species, but not a mixture of species with different compositions, because the peak positions are quite different.

We can see some implications for the formation of the mixed Anderson cage in the experiments by method 2, and also in the recrystallization process for the $x = 0$ and $x = 6$ compounds. When an aqueous solution containing the Ni(II) Anderson polyanion is heated above 80°C, a colour change of the solution is observed from sky-blue to green. During the cooling process to room temperature, it returns to the original sky-blue. The green solution will be due to the Ni(II) aqua ion produced by dissociation of the polyanion. Therefore, it seems that, during the cooling process, the Anderson cage is formed around the Ni(II) ion as a core. The mixed Anderson cage will be formed on the basis of the reorientation of randomly distributed Mo and W oxo ions at the high temperature. Thus, the experiments by two methods do not exclude the possibility that the $x = 3$ compound, and also the $x = 2$ and $x = 4$ compounds, contain some positional isomers.

Oxidation of Ni(II) *molybdo- and tungstopolyanions*

The oxidation of the $[Ni(II)Mo_6O_{24}H_6]^{4-}$ polyanion by the $S_2O_8^{2-}$ ion in aqueous solution led to the formation of a Waugh-type $[Ni(IV)Mo_9O_{32}]^{6-}$ polyanion, which was isolated separately.[13] The valency of the heteroatom can be changed and the polyanion cage is simultaneously transformed. On the other hand, the oxidation of $[Ni(II)W_6O_{24}H_6]^{4-}$ gave the decomposition mixture, but no heteropoly compound. The same initial materials have been used in the preparations of $[Ni(IV)W_6O_{24}]^{8-}$ and $[Ni(II)W_6O_{24}H_6]^{4-}$ polyanions, except for the

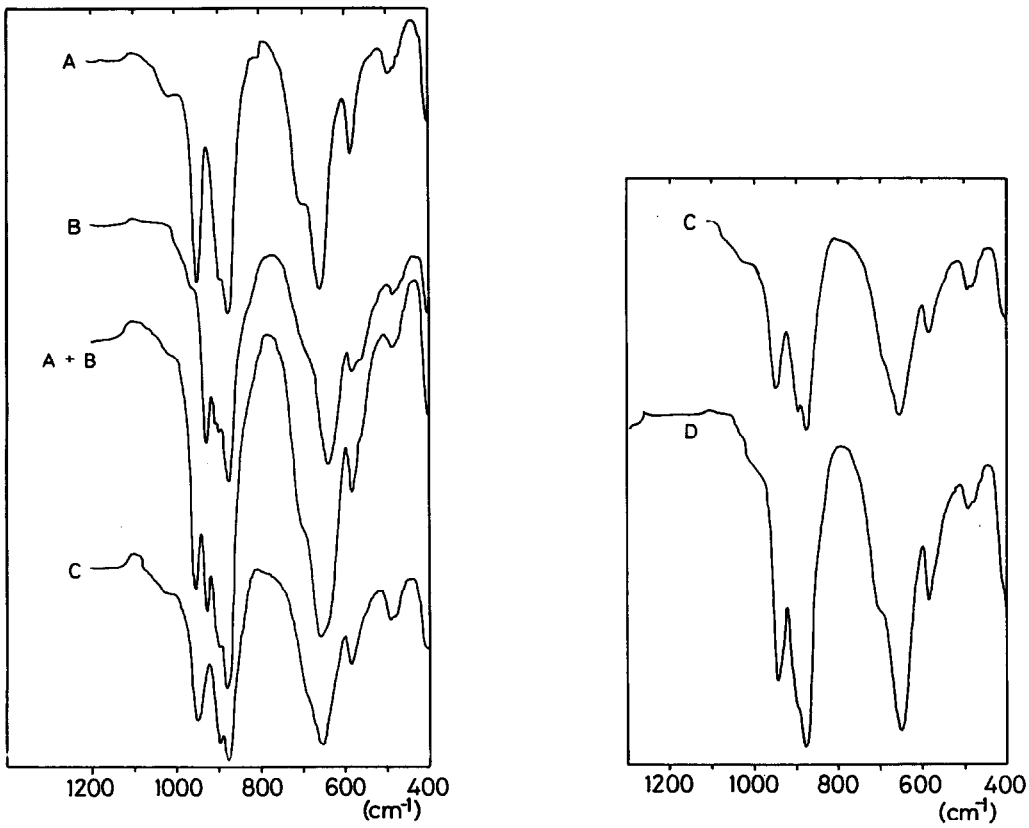

Fig. 4. Solid IR spectra of $[Ni(II)Mo_{6-x}W_xO_{24}H_6]^{4-}$ polyanions; $x = 6$ (A) and 0 (B) compounds, equimolar mixture (A + B) of them, and $x = 3$ compounds obtained by methods 1 (C) and 2 (D).

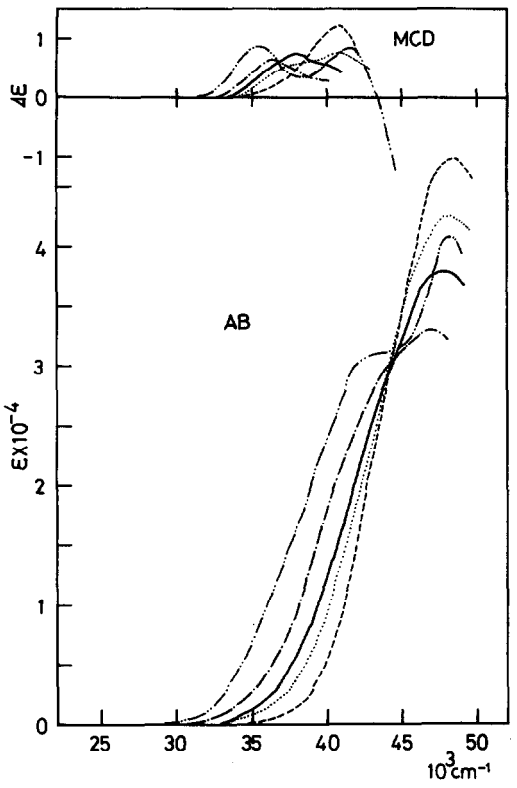

Fig. 5. UV absorption and MCD spectra of $[Ni(II)Mo_{6-x}W_xO_{24}H_6]^{4-}$ polyanions: $x = 0$ (——), $x = 1$ (—·——), $x = 3$ (———), $x = 5$ (·····), and $x = 6$ (– – –).

addition of the $S_2O_8^{2-}$ ion in the former. Thus, this oxidation experiment suggests that the formation of the $[Ni(IV)W_6O_{24}]^{8-}$ polyanion does not proceed through the oxidation of the already formed $[Ni(II)W_6O_{24}H_6]^{4-}$ polyanion. In a Keggin-type polyanion, the valency of the central heteroatom can be changed sometimes by chemical oxidation, with the polyanion structure maintained, such as $[Co(II)W_{12}O_{40}]^{6-} \rightarrow [Co(III)W_{12}O_{40}]^{5-}$ [16,17] and $[Cu(I)W_{12}O_{40}]^{7-} \rightarrow [Cu(II)W_{12}O_{40}]^{6-}$,[18] reactions which proceed by the outer-sphere mechanism of an electron transfer.[18,19] In this case, the Anderson structure may be thermally less stable than the Keggin structure.

REFERENCES

1. M. T. Pope, *Heteropoly and Isopoly Oxometalates*. p. 21. Springer, New York (1983).
2. U. Lee, A. Kobayashi and Y. Sasaki, *Acta Cryst.* 1983, **C39**, 817.
3. U. Lee and Y. Sasaki, *Chem. Lett.* 1984, 1297.
4. F. A. Cotton and G. Wilkinson, *Advanced Inorganic Chemistry*, 4th Edn, p. 852. John Wiley, New York (1980).
5. A. LaGinestra, F. Giannetta and P. Fiorucci, *Gazz. Chim. Ital.* 1968, **98**, 1197.
6. A. Malik, S. A. Zubaili and S. Khan, *J. Chem. Soc., Dalton Trans.* 1977, 1049.
7. E. Matijevic, M. Kerker, H. Bayer and F. Theubert, *Inorg. Chem.* 1963, **2**, 581.
8. R. D. Hall, *J. Am. Chem. Soc.* 1907, **29**, 692.
9. Y. Shimura, H. Ito and R. Tsuchida, *Nippon Kagaku Zasshi* 1954, **75**, 560.
10. D. Sutton, *Electronic Spectra of Transition Metal Complexes*. McGraw-Hill, New York (1968).
11. S. A. Malik, *J. Inorg. Nucl. Chem.* 1970, **32**, 2425.
12. V. S. Sergienko, V. N. Molchanov, M. A. Porai-Koshits and E. A. Torchenkova, *Koord. Khim.* 1979, **5**, 936; *Sov. J. Coord. Chem. (Engl. Trans.)* 1979, **5**, 740.
13. K. Nomiya, R. Kobayashi and M. Miwa, *Polyhedron* 1985, **4**, 149.
14. M.-J. Schwing-Weill, *Bull. Soc. Chim. Fr.* 1972, 1754.
15. K. Nomiya, H. Murasaki and M. Miwa, unpublished results.
16. L. C. W. Baker and T. P. McCutcheon, *J. Am. Chem. Soc.* 1956, **78**, 4503.
17. K. Nomiya, R. Kobayashi and M. Miwa, *Bull. Chem. Soc. Jpn* 1983, **56**, 2272.
18. A. G. Lappin and R. D. Peacock, *Inorg. Chim. Acta* 1980, **46**, L71.
19. P. G. Rasmussen and C. H. Brubaker, *Inorg. Chem.* 1964, **3**, 977.

Polyhedron Vol. 6, No. 2, pp. 219–223, 1987
Printed in Great Britain

0277–5387/87 $3.00+.00

PENTACOORDINATED COMPLEXES OF ORGANOTELLURIUM(IV) HALIDES WITH TERTIARY PHOSPHINE SELENIDES

T. N. SRIVASTAVA,* JAI DEO SINGH and SANJAY KUMAR SRIVASTAVA

Chemistry Department, University of Lucknow, Lucknow 226007, India

(*Received* 17 *April* 1986; *accepted* 28 *May* 1986)

Abstract—The pentacoordinated tellurium(IV) complexes [$R_2TeCl_2 \cdot L$] [R = C_6H_5 or *p*-$CH_3OC_6H_4$; L = Ph_3PSe, (*p*-$MeC_6H_4)_3PSe$, Bu_3PSe or $Ph_2P(Se)(CH_2)_2(Se)PPh_2$] were obtained by the reaction of R_2TeCl_2 with L under anhydrous conditions. The complexes have been characterized by spectral (IR, ^1H NMR and ^{31}P NMR) studies. The reaction of $RTeCl_3$ and L, however, yields tellurium/selenium metal. $^1J(^{31}P–^{77}Se)$ coupling constant data suggest complexation. In case of bidentate donor bases only one donor site is used in coordination. The complexes possess distorted octahedral geometry around a central tellurium atom which is surrounded by five groups and one vacant site occupied by a lone pair.

The coordination chemistry of phosphine selenides is little known compared to that of phosphine, phosphine oxides and sulfides.[1] There are only a few reports on the complexes of P=Se bases with some soft acceptors[2–6] such as Pt(II), Pd(II), Ag(I), Zn(II), Cd(II) and Hg(II). A few coordination compounds of the main-group metals Pb(II), Sn(II) and Sn(IV) have also been reported,[7,8] but the corresponding reactions with organometals have not been studied. There is a single paper describing the coordination behaviour of P=Se with (PhTeBr).[9] In continuation of our interest in the synthesis and reactivity of organotellurium(IV) compounds,[10] we report herein the synthesis of such complexes with organotellurium(IV).

EXPERIMENTAL

All manipulations were carried out under dry nitrogen. $TeCl_4$ (BDH) was used as such. Ph_2TeCl_2,[11] (*p*-$MeOC_6H_4)_2TeCl_2$,[12] Me_2TeI_2,[13] (*p*-$MeOC_6H_4)TeCl_3$,[14] and $Ph_2Te(OCOCF_3)_2$ and $Me_2Te(OCOCF_3)_2$[15] were prepared by literature methods. Tertiary phosphine selenides were prepared from the phosphine and KSeCN in CH_3CN[16] or by direct reaction of elemental selenium (red) with phosphines in refluxing toluene.[17] ^1H NMR spectra of the compounds were recorded in $CDCl_3$, using TMS as the internal standard on a Varian 90-D spectrometer. ^{31}P NMR spectra were obtained using a JEOL-PFT 400 Fourier transform spectrometer operating at 40.5 MHz. Samples were contained in spinning 10-mm tubes with $CDCl_3$ as the solvent system with a 1-mm capillary tube containing 85% H_3PO_4 as a reference. The molecular complexes were obtained by the direct interaction of the Lewis acids and bases in dichloromethane.

Reaction of R_2TeCl_2 (R = Ph *or* *p*-$MeOC_6H_4$) *with bases*

In a typical experiment a mixture of Ph_2TeCl_2 (3.52 g, 10 mmol) and Ph_3PSe (3.41 g, 10 mmol) in dichloromethane (~30 cm^3) was refluxed for 4 h, and the excess solvent distilled off. The solution was concentrated to crystallization, yielding [$Ph_2TeCl_2 \cdot SePPh_3$]. Similar products were obtained using $Ph_2P(Se)(CH_2)_2(Se)PPh_2$ as a base and $Me_2Te(OCOCF_3)_2$ as an acceptor.

Reaction of (*p*-$MeOC_6H_4)TeCl_3$ *with bases*

In a representative experiment, a mixture of (*p*-$MeOC_6H_4)TeCl_3$ and Ph_3PSe in a 1:1 molar ratio was stirred in dichloromethane at room temperature. The reaction mixture after a few minutes deposited selenium and tellurium metals. Similarly, Me_2TeI_2 and Me_2TeCl_2 with Ph_3PSe

* Author to whom correspondence should be addressed.

Table 1. Analytical data for $R_2TeCl_2 \cdot L$

	Complex	Yield (%)	M.p. (°C)	Elemental analysis: found (calc.) (%)					IR absorptions of P═Se (cm^{-1})[a]		
				C	H	Cl	Se	Te	ν_1	ν_2	$\Delta(\nu^1-\nu^2)$
1	$[Ph_2TeCl_2 \cdot SePPh_3]$	82	119	51.6 (51.9)	3.4 (3.6)	10.2 (10.2)	11.2 (11.4)	18.1 (18.4)	562	553	−9
2	$[Ph_2TeCl_2 \cdot SePBu_3]$	85	109	45.0 (45.5)	5.6 (5.8)	11.1 (11.2)	12.1 (12.5)	20.0 (20.1)	511	503	−8
3	$[Ph_2TeCl_2 \cdot Ph_2P(Se)(CH_2)_2(Se)PPh_2]$	80	149	50.1 (50.2)	3.4 (3.7)	7.5 (7.8)	17.2 (17.4)	13.7 (14.0)	537	528	−9
4	$[Ph_2TeCl_2 \cdot SeP(p\text{-}CH_3OC_6H_4)_3]$	75	134	53.6 (53.8)	4.0 (4.2)	9.3 (9.6)	10.1 (10.7)	17.2 (17.3)	544	534	−10
5	$[(p\text{-}MeOC_6H_4)_2TeCl_2 \cdot SePPh_3]$	80	131	50.7 (50.9)	3.6 (3.8)	9.0 (9.4)	10.3 (10.5)	16.8 (16.9)	562	551	−11
6	$[(p\text{-}MeOC_6H_4)_2TeCl_2 \cdot SePBu_3]$	79	114	44.7 (45.0)	5.6 (5.9)	10.1 (10.2)	11.3 (11.4)	18.2 (18.4)	511	501	−10
7	$[(p\text{-}MeOC_6H_4)_2TeCl_2 \cdot SeP(p\text{-}CH_3OC_6H_4)_3]$	83	152	52.4 (52.9)	4.1 (4.4)	8.5 (8.9)	9.8 (9.9)	15.6 (16.0)	544	535	−9
8	$[(p\text{-}MeOC_6H_4)_2TeCl_2 \cdot Ph_2P(Se)(CH_2)_2(Se)PPh_2]$	85	158	49.3 (49.5)	3.6 (3.9)	7.1 (7.3)	16.1 (16.3)	13.1 (13.2)	537	527	−10
9	$[2(p\text{-}MeOC_6H_4)_2TeCl_2 \cdot Ph_2P(Se)(CH_2)_2(Se)PPh_2]$	87	117	46.8 (46.9)	3.7 (3.8)	10.1 (10.3)	11.2 (11.4)	18.4 (18.5)	537	525	−12
10	$[Me_2Te(OCOCF_3)_2 \cdot Ph_2P(Se)(CH_2)_2(Se)PPh_2]$	80	135	40.6 (40.9)	3.1 (3.2)	—	16.3 (16.8)	13.3 (13.6)	537	526	−11
11	$[Ph_2Te(OCOCF_3)_2 \cdot Ph_2P(Se)(CH_2)_2(Se)PPh_2]$	85	118	42.5 (42.9)	3.1 (3.2)	—	14.4 (14.8)	11.6 (12.0)	537	523	−14

[a] ν_1 in ligand and ν_2 in complex.

and $Ph_2P(Se)(CH_2)_2(Se)PPh_2$ deposited free metals and failed to yield stable adducts.

RESULTS AND DISCUSSION

The analytical data for the adducts (Table 1) correspond to a 1 : 1 (M : L) stoichiometry except for $[2(p\text{-}MeOC_6H_4)_2TeCl_2 \cdot Ph_2P(Se)(CH_2)_2(Se)PPh_2]$ which has a 2 : 1 (M : L) mole ratio and possesses a bridging ligand. All complexes are white crystalline solids having sharp melting points. They are normally stable but deposit selenium metal on standing for a long time. The complexes possess very offensive odours. They are soluble in common organic solvents such as MeOH, EtOH, CH_2Cl_2, MeCN, Me_2SO, Me_2NCHO and $PhNO_2$. The molar conductances of 10^{-3} M solutions of the complexes in MeOH and MeCN at room temperature indicate their non-electrolytic nature.

All known organoselenophosphorus compounds belong to the P(IV)–Se(II) class. Thus, selenium can be bonded to a phosphorus atom by a single (σ) bond or by a double bond of p_π–d_π (Se $4p_\pi \rightarrow$ P $3d_\pi$) type. P═Se can be considered as essentially a double bond because 3*d* orbitals of phosphorus are available for π-bonding. The p_π–d_π bonding arises from donation of non-bonding $4p_\pi$ electrons of the selenium atom into vacant 3*d* orbitals of phosphorus. This double-bond character in these ligands and the presence of valence *s*-electron density at the nucleus of the selenium atom is more than twice that for phosphorus, which would normally lead to a larger coordinating centre. Depending upon the relative importance of the two resonating hybrid structures the selenium atom will effectively retain from one to two electron lone pairs which have most of the selenium *s*-character, and thus may coordinate to a metal atom in one of the following ways:

$$R_3P{=}Se: \rightarrow M \leftrightarrow R_3P^+\dot{S}e\dot{:}^- \rightarrow M.$$

IR spectra

The IR spectra of the complexes were recorded in the range 4000–400 cm^{-1}. The diagnostic absorptions are discussed below.

Complexes with phosphine selenides

The ν(P═Se) reported in various phosphine selenides lies in the range 511–562 cm^{-1}, and undergoes a negative shift of 8–14 cm^{-1} on coordination. A shift of 10–20 cm^{-1} in ν(P═Se) has been reported for zinc, cadmium, mercury and nickel complexes.[3,18]

The shift is attributed to a weakening of the secondary p_π–d_π bonds between the selenium and the phosphorus atom in the complexes. It is observed that only a small change in the P═Se stretching frequency occurs compared to the corresponding ν(P═O) and ν(P═S) absorptions[18] in the corresponding complexes. This is reasonable since the vibrations involving the relatively heavy selenium atom would be less sensitive to coordination than those with the lighter phosphorus, oxygen or sulphur atoms.

^{1}H *NMR spectral studies*

The ^{1}H NMR values are given in Table 2. The salient features of the spectra are discussed below.

In the ^{1}H NMR spectra of $[(p\text{-}MeOC_6H_4)_2TeCl_2 \cdot Ph_2P(Se)(CH_2)_2(Se)PPh_2]$ (1 : 1 M : L) and $[2(p\text{-}MeOC_6H_4)_2TeCl_2 \cdot Ph_2P(Se)(CH_2)_2(Se)PPh_2]$ (2 : 1 M : L), the —CH_2 protons are doubled due to coupling with the ^{31}P nucleus. The methyl protons of the p-$MeOC_6H_4$ group show a doublet in the 1 : 1 complex. In the 2 : 1 complex the two methyl singlets are separated and are centred at 3.75 and 3.68. However, the two complexes show a single spot in TLC, ruling out the presence of a mixture of the 2 : 1 and 1 : 1 adducts. The structural change may be due to participation of both selenium atoms of the bidentate ligand in coordination, giving rise to a bridging ligand between the two tellurium atoms. The structure of bis(diphenylphosphinoselenide)-ethane favours more a bite and an orientation of the lone pairs for bridging two metals atoms

Table 2. ^{1}H NMR spectral data

Complex[a]	Chemical shift (ppm)
5	3.72, s, 6H (p-CH_3O); 6.88, d, 4H (*meta*-protons); 7.94, d, 4H [*ortho* protons of (p-$CH_3OC_6H_4$)]; 7.2–7.85, m, 15H (C_6H_5)$_3$P
7	2.3, s, 9H (C_6H_4—CH_3); 3.73, s, 6H (p-CH_3O); 6.8–8.0, m, 20H (phenyl protons)
8	2.84, d, 4H (—CH_2CH_2—); 3.76, d, 6H (p-CH_3O); 6.92, d, 4H (*meta* protons) 7.95, d, 4H [*ortho* protons of (p-$CH_3OC_6H_4$)—]; 6.5–8.0, m, 20H [phenyl protons of Ph_2P(Se)]
9	2.82, d, 4H (—CH_2CH_2); 3.75, 3.68, s, 12H (p-CH_3O) 6.90, d, 8H [*ortho* protons of (p-$CH_3OC_6H_4$)—]; 6.6–8.0, m, 20H [phenyl protons of Ph_2P(Se)—]

[a] See Table 1.

Table 3. ^{31}P NMR data for $[R_2TeCl_2 \cdot L]$

L in the complex $(p\text{-}MeOC_6H_4)_2TeCl_2 \cdot L$	$\delta(P)$ (ppm)	$\delta(P)$ (ppm)	$^1J(^{31}P\text{–}^{77}Se)$ (Hz)	$\Delta(^{31}P\text{–}^{77}Se)$ (Hz)
Ph_3PSe	35.3	2.4	700.4	−35.6
	(32.9)[a]		(736)	
$Ph_2P(Se)(CH_2)_2(Se)PPh_2$	35.98	2.38	635.1	−100.9
	(33.6)[a]		832.2 (736)	+96.2

[a] Free-ligand values.[24]

rather than forming a chelate ring around a single metal.[19] It is concluded that diphosphine selenide acts as a bridging ligand between two tellurium atoms, as reported for diphosphine complexes with other metals.[20–22]

^{31}P *NMR spectra*

^{31}P NMR spectra of a few complexes were obtained at room temperature and the data are listed in Table 3.

From the ^{31}P NMR data the following facts are deduced:

(i) $J_{P\text{–}Se}(^{31}P\text{–}^{77}Se)$ is sensitive toward coordination and possesses a lower value compared to that for the free ligand. Such a change is attributed to coordination of P=Se to the metal atom through selenium.[23,24]

(ii) In the complex $[(p\text{-}MeOC_6H_4)_2TeCl_2 \cdot SePPh_3]$ the $\delta(P)$ and $^1J(^{31}P\text{–}^{77}Se)$ decrease on coordination, indicating Se → Te bonding.[17,23]

(iii) In the complex $[(p\text{-}MeOC_6H_4)_2TeCl_2 \cdot Ph_2P(Se)(CH_2)_2(Se)PPh_2]$ two sets of ^{77}Se satellites of equal intensity, with $^1J(^{31}P\text{–}^{77}Se) = 635.1$ and 832.2 Hz, are observed. The former coupling constant $[\Delta^1J(^{31}P\text{–}^{77}Se = -100.9$ Hz] is due to coordination from the selenium atom, while the other, being higher ($\Delta^1J = +96.2$ Hz) than that in the free ligand, may be due to an uncoordinated selenium atom.[25] Thus, from spectral data it may be concluded that the complexes possess an octahedral geometry around a tellurium atom with one site being occupied by a lone pair of electrons. The structures of the complexes may be as shown below.

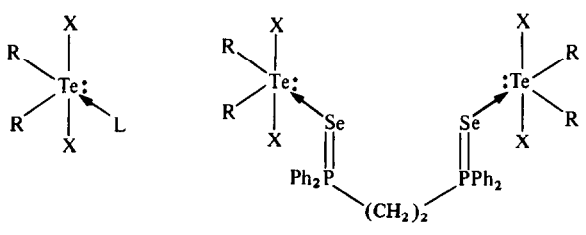

R = CH_3, C_6H_5 or p-$MeOC_6H_4$; X = Cl or $OCOCF_3$

Acknowledgements—Financial assistance from the Council of Scientific and Industrial Research, New Delhi, and the University Grant Commission, New Delhi, in support of the present work is gratefully acknowledged.

REFERENCES

1. N. M. Karayannis, C. M. Mikulski and L. L. Pyrlewski, *Inorg. Chim. Acta, Rev.* 1977, **5**, 69.
2. T. Allman and R. G. Geol. *Can. J. Chem.* 1984, **60**, 615, 621.
3. A. J. Blake and G. P. McQuillan, *J. Chem. Soc., Dalton Trans.* 1984, 1849.
4. D. J. Williams and K. J. Wynne, *Inorg. Chem.* 1976, **15**, 1449.
5. E. W. Abel, S. K. Bhargwa, K. G. Orell and V. Sik, *Inorg. Chim. Acta* 1981, **49**, 25.
6. I. J. Colquhoun and W. McFarlane, *J. Chem. Soc., Dalton Trans.* 1981, 658.
7. M. J. Fernandezcid, M. P. Pazos Perez, J. Sordo, J. S. Casas, M. R. Bermego and M. Gayoso, *An. Quim., Ser. B* 1982, **78**, 190.
8. P. A. W. Dean, *Can. J. Chem.* 1982, **60**, 2921.
9. S. Hauge and O. Vikane, *Acta Chem. Scand.* 1973, **27**, 3596.
10. T. N. Srivastava, Jai Deo Singh and Shashi Mehrotra, *Indian J. Chem.* 1985, **24A**, 849.
11. R. C. Paul, K. K. Bhasin and R. K. Chadha, *J. Inorg. Nucl. Chem.* 1975, **37**, 2337.
12. J. Bergman, *Tetrahedron* 1972, **28**, 3323.
13. R. H. Vernon, *J. Chem. Soc.* 1920, **117**, 86.
14. G. T. Morgan and R. E. Kellett, *J. Chem. Soc.* 1926, 1089.
15. T. N. Srivastava and Jai Deo Singh, *Indian J. Chem.* (communicated).
16. P. Nicpon and D. W. Meek, *Inorg. Chem.* 1966, **5**, 1297.
17. S. O. Grim, E. D. Walton and L. C. Satek, *Can. J. Chem.* 1980, **58**, 1476.
18. M. G. King and G. P. McQuillan, *J. Chem. Soc. A* 1967, 898.
19. C. H. Lindsay, L. S. Benner and A. L. Balch, *Inorg. Chem.* 1980, **19**, 3503.

20. M. M. Olmstead, C. H. Lindsay, L. S. Benner and A. L. Balch, *J. Organomet. Chem.* 1979, **179**, 289.
21. V. G. Kumar Das, *J. Inorg. Nucl. Chem.* 1976, **38**, 1241.
22. F. A. Cotton, G. G. Stanley and R. A. Walton, *Inorg. Chem.* 1978, **17**, 2099.
23. P. A. W. Dean, *Can. J. Chem.* 1979, **57**, 754.
24. S. O. Grim, E. D. Walton and L. C. Satck, *Inorg. Chim. Acta* 1978, **27**, L115.
25. P. A. W. Dean and M. K. Hughes, *Can. J. Chem.* 1980, **58**, 180.

Polyhedron Vol. 6, No. 2, pp. 225–254, 1987
Printed in Great Britain

0277-5387/87 $3.00+.00
Pergamon Journals Ltd

SINGLE-CRYSTAL OPTICAL ABSORPTION SPECTRA FOR MAGNUS-TYPE SALTS OF PALLADIUM AND PLATINUM

MICHAEL L. RODGERS[1] and DON S. MARTIN†

Chemistry Department and Energy and Mineral Resources Research Institute, Iowa State University, Ames, IA 50011, U.S.A.

(*Received* 5 *December* 1985; *accepted after revision* 4 *June* 1986)

Abstract—Polarized single-crystal absorption spectra in the region 800–250 nm were recorded at 300 and 6 K for the 20 possible Magnus-type crystals containing the $PtCl_4^{2-}$, $PtBr_4^{2-}$, $PdCl_4^{2-}$ and $PdBr_4^{2-}$ anions, and the $[Pt(NH_3)_4]^{2+}$, $[Pt(CH_3NH_2)_4]^{2+}$, $[Pt(en)_2]^{2+}$, $[Pd(NH_3)_4]^{2+}$ and $[Pd(en)]^{2+}$ cations. Metal–metal distances were obtained from X-ray diffraction determination of crystal axes. A complete set of X-ray diffraction intensities was collected for 2659 reflections over four octants for crystals of $Pt(en)_2PdCl_4$. Triclinic cell parameters were: $a:b:c = 11.711(7):8.480(6):6.801(2)$ Å; $\alpha:\beta:\gamma = 96.10(4):91.08(4):106.74(8)°$; $V = 642.3(2)$ Å^3; $Z = 2$. However, only 20 very weak reflections occurred that would conflict with a body-centered space group. Refinement in $I\bar{1}$ yielded Pt, Pd, Cl and N positions satisfactory for spectra interpretation. C positions could not be satisfactorily established and refinement in $P1$, $I1$ or $P\bar{1}$ did not converge. The spectra at 6 K provided resolution into components not available at room temperature. The temperature dependence of intensities and in some cases resolution of vibrational structure in the bands was helpful in making transition assignments. For $Pt(NH_3)_4PtCl_4$ a very sharp electric dipole allowed band, not previously observed, was found just above the d–d transitions with x,y polarization (normal to the stacking direction). Similar bands occurred in the $PtCl_4^{2-}$ salts with other Pt cations. The evidence is summarized for assignment of these bands as interionic electron transfers (anion-$d_{xz,yz}$ → cation-p_z). This evidence implies that the very intense absorption at *ca* 35,000 cm^{-1}, z-polarized (along the stacking axis), is also an interionic electron transfer (anion-d_{z^2} → cation-p_z). These results together with shifts of the intraionic $d \rightarrow d$ transitions suggest that the d_{z^2}-orbital in the free MX_4^{2-} ions lies close in energy to the $d_{xz,yz}$-orbitals. Spectra of $PdCl_4^{2-}$ salts with the Pt cations reveal broad dipole-allowed transitions above the intramolecular $d \rightarrow d$ transitions. It appears likely that they are interionic electron transfers. However, their characteristics indicate they cannot be anion-$d \rightarrow$ cation-d nor anion-$d \rightarrow$ cation-p_z transitions. Hence they are most likely anion-$L\pi \rightarrow$ cation-$d\sigma^*$ transitions. The results indicated that Pt was more effective than Pd in shifting d–d transitions in the region of 3.25–3.55 Å. These shifts, except for the $^1A_{1g} \rightarrow {}^1A_{2g}$ transitions, were strongly dependent on the metal–metal distance with cations of the same metal.

The green compound $Pt(NH_3)_4PtCl_4$ first described by Magnus[2] in 1828 is commonly known as Magnus' Green Salt (MGS). Since the compound is formed from the normally colorless $[Pt(NH_3)_4]^{2+}$ cation and the normally red $PtCl_4^{2-}$ anion, it has been the subject of numerous speculations throughout the years. The anomalous color is apparently the result of close face-to-face stacking of alternating cations and anions in one-dimensional arrays with Pt–Pt spacings of 3.24 Å.[3,4] Indeed, a polymorph, Magnus' Pink Salt, without the one-dimensional stacks, has the normally expected color.

The Magnus-type salts consist of similar one-dimensional stacks of MA_4^{2+} cations and $M'X_4^{2-}$

† Author to whom correspondence should be addressed.

anions. In the present work single-crystal polarized absorption spectra have been recorded at room temperature and 6K for the 20 possible Magnus-type salts with M and M′ = Pt or Pd, X = Cl or Br, and A = NH_3, CH_3NH_2 or half the chelating group ethylenediamine (en).

Previously, single-crystal spectra for MGS of very limited quality were reported by Yamada.[5] Day *et al.*[6,7] published single-crystal spectra for MGS, $Pt(CH_3NH_2)_4PtCl_4$ and $Pt(C_2H_5NH_2)_4PtCl_4$ at room temperature while Martin *et al.*[8] presented 300- and 15-K spectra for MGS. The various Magnus-type salts occur with a variety of colors. Miller[9] as well as Day *et al.*[6] have tabulated wave numbers for peaks and some shoulders observed in the diffuse reflectance for a number of the Magnus-type salts. Anex and coworkers[10,11] have used single-crystal polarized specular reflectance spectra to characterize the high-intensity, high-energy transition in a number of Magnus-type salts. Such specular reflection spectra nicely complement the transmission-absorption spectra since they provide polarization information about intense bands that are beyond the capability of absorption measurements. Yamada[5] and Miller[9,12] considered the anomalous color to originate in a band-to-band type of transitions in Magnus-type salts. However, Day[13] has argued that the visible-region spectra were essentially anion spectra in which a number of transitions had been red-shifted. The red shifts for *d–d* transition were attributed to the repulsion interactions between anion electrons and electrons of the adjacent cations. A red shift of an intense *z*-polarized transition was suggested to be the result of transition dipole–dipole interactions. On the other hand Anex and coworkers[10,11] have argued that the intense absorption band for ammonia–chloride Magnus-type salts of Pt and Pd involves a "delocalized" transition without further specification.

The low-temperature spectra in the present study provide resolution into a greater number of bands than can be discerned at room temperature, and also a vibrational structure has appeared in some bands. The temperature dependence of the band intensities is useful since permanent electric dipole allowed transitions will have little temperature dependence, whereas vibronically-enabled transitions (Herzburg–Teller type) decrease significantly in intensity as the temperature falls from room temperature to liquid-helium temperatures. The use of different amines provides some variation in the M–M′ stacking distances which in turn causes a number of band shifts and intensity changes. With the large number of compounds involved, the rather severe testing of any theory or rationalization of orbital and transition energies is now possible.

EXPERIMENTAL

Preparation of crystals

The preparation of the complex anion salts K_2PtCl_4, K_2PtBr_4, K_2PdCl_4 and K_2PdBr_4 has been described previously.[14–16] To prepare the cation complexes, *ca* 50 mg of the potassium salt of the chloride or bromide complex was dissolved in a minimum of water. A concentrated aqueous solution of NH_3 or the indicated amine was added until the Magnus-type salt formed. The reaction mixture was heated until the Magnus-type salt had redissolved and most of the liquid had evaporated. The remaining solution was added to 500 cm^3 of a solution formed from 45% diethyl ether, 45% acetone and 10% ethanol. The white precipitate was stored over a concentrated aqueous solution of the amine to minimize ligand replacement reactions.

Attempts to prepare the compounds $Pd(CH_3NH_2)_4Cl_2$ and $Pd(CH_3NH_2)_4Br_2$ by this technique produced very poor yields of impure products that were unsuitable for use in the Magnus-type salt synthesis. Hence, only 20 Magnus-type salts were prepared of the 24 possible with two metals, two halides and three amines.

Thin crystals were mostly grown in the film of solutions between glass plates by the technique utilized in the earlier study of MGS in our laboratory.[8] Larger crystals were prepared in a crystal grower which consisted of a 25-mm horizontal cyclindrical vessel divided into three compartments by fine sintered-glass discs. The anion salt solution was placed in one end compartment, the cation salt in the other end compartment, and a potassium halide solution in the center compartment. Crystals normally formed on the surfaces of the sintered-disc dividers.

Crystallographic methods

Atoji *et al.*[4] showed that the MGS crystals possess a tetragonal unit cell with the ions stacked face-to-face along the *c*-axis so that the metal atoms are spaced apart by a distance of *c*/2. Miller[12] reported from powder film data that the Magnus-type salts containing methylamine ligands in the cations also formed tetragonal crystals. From the *c*-axis lengths and the optical properties, he concluded that the ions stacked along the tetragonal axis similar to MGS for all the compounds for which he had data. However, the Magnus-type salt with ethylenediamine-complexed cations crystallized as needles with triclinic lattices. Optical examinations of all our ethylenediamine crystals showed that optical extinctions were not appreciably wavelength-dependent, and one extinction was aligned with the

needle axis. The strong dichromism of the crystals indicated that the needle axis, which we have always designated as the *c*-axis, provided essentially the *z*-polarized spectra for the complex. For 16 of the 19 compounds other than MGS itself, we were able to mount suitable crystals on the goniometer head of a four-circle X-ray diffractometer, constructed in the Ames Laboratory of the U.S.D.O.E. This instrument was interfaced with a PDP 15 computer. Automatic indexing was accomplished by an interactive program ALICE of Jacobson.[17] These indexing experiments also provided the indices of the well-developed faces which served for the crystal spectroscopy and the volumes of the unit cells needed for evaluating spectroscopic intensities. These crystallographic axes and angles, determined without any symmetry constraints, are shown in Table 1. The results are in good agreement with tetragonal assignments for the ammine and methylamine salts. Variations in a and b, and between α, β and γ, indicate uncertainties in the axes of about ± 0.02 Å, and in the angles of about 0.1°, in agreement with our experience. Three of the sets of lattice parameters in Table 1 are those of Miller, who collected X-ray powder data for eight of the compounds since we did not index these crystals. For four of the five compounds for which both Miller and we collected data, agreement of axes were within the 0.02-Å uncertainty. However, for $Pt(CH_3NH_2)_4PtBr_4$ our $a:b:c$ axes were 0.16, 0.15 and 0.13 Å larger than Miller's. It should be noted that Miller's values would place $Pt(CH_3NH_2)_4PtBr_4$ unexpectedly in a smaller cell than $Pt(CH_3NH_2)_4PdBr_4$ and would give $Pt(CH_3NH_2)_4PtBr_4$ an unexpectedly smaller *c*-axis than $Pt(NH_3)_4PtBr_4$.

Since no information was available for the triclinic structure of any ethylenediamine compound, a full X-ray diffraction structure determination was attempted for $Pt(en)_2PdCl_4$. Intensity data were collected for 2659 reflections in the four octants hkl, $\bar{h}k\bar{l}$, $\bar{h}kl$ and $h\bar{k}l$. Mo-K_α radiation with a wavelength of 0.70964 Å was utilized. A scintillation counter scanned the peaks in a series of 0.01° steps in ω. The intensities of a set of three standard reflections were measured after each accumulation of intensities for 75 reflections.

From 20 independent reflections with $24° < 2\theta < 40°$ the lattice parameters were determined by the program LATT.[18] The final cell parameters were: $a:b:c = 11.711(7):8.480(6):6.801(2)$ Å, $\alpha:\beta:\gamma = 96.10(4):91.08(4):106.74(8)°$; $V = 642.3(2)$ Å^3. A total of 1244 independent reflections were observed with intensities greater than the limit for statistical significance, viz. $|F_o| > 3\sigma(F_o)$. Data were corrected for both absorption and Lorentz polarization. For all but 20 very weak reflec-

Table 1. Cell constants and metal–metal distances for the Magnus-type salts

Salt	a (Å)	b (Å)	c (Å)	α (°)	β (°)	γ (°)	d(M–M) (Å)
$Pt(NH_3)_4PtCl_4$[a]	9.03	9.03	6.49	90.0	90.0	90.0	3.24
$Pt(NH_3)_4PdCl_4$	8.967	8.927	6.465	90.0	89.9	90.0	3.23
$Pt(NH_3)_4PtBr_4$	9.279	9.279	6.626	90.0	90.0	90.0	3.31
$Pt(NH_3)_4PdBr_4$	9.317	9.317	6.645	90.1	90.1	89.8	3.32
$Pt(CH_3NH_2)_4PtCl_4$	10.373	10.351	6.486	90.1	89.9	90.0	3.24
$Pt(CH_3NH_2)_4PdCl_4$	10.358	10.358	6.491	90.0	90.0	90.0	3.25
$Pt(CH_3NH_2)_4PtBr_4$	10.711	10.695	6.743	90.0	90.1	90.0	3.37
$Pt(CH_3NH_2)_4PdBr_4$	10.651	10.664	6.695	90.2	90.1	90.0	3.35
$Pt(en)_2PtCl_4$	12.341	8.167	6.826	92.0	94.5	108.9	3.41
$Pt(en)_2PdCl_4$	11.711	8.480	6.801	96.10	91.08	106.74	3.40
$Pt(en)_2PtBr_4$	12.177	8.551	7.015	99.0	89.4	106.2	3.51
$Pt(en)_2PdBr_4$	12.201	8.538	7.051	98.9	89.8	106.1	3.53
$Pd(NH_3)_4PtCl_4$[b]	9.00	9.00	6.50	90.0	90.0	90.0	3.25
$Pd(NH_3)_4PdCl_4$[b]	8.96	8.96	6.49	90.0	90.0	90.0	3.25
$Pd(NH_3)_4PtBr_4$	9.355	9.352	6.664	89.8	90.0	90.2	3.33
$Pd(NH_3)_4PdBr_4$[b]	9.32	9.32	6.66	90.0	90.0	90.0	3.33
$Pd(en)_2PtCl_4$	12.292	8.175	6.819	92.9	95.8	109.4	3.41
$Pd(en)_2PdCl_4$	12.294	8.754	6.870	110.6	82.9	109.9	3.44
$Pd(en)_2PtBr_4$	12.588	8.426	7.096	95.2	96.3	106.1	3.55
$Pd(en)_2PdBr_4$	12.445	8.800	7.104	108.5	83.9	108.0	3.55

[a] Reference 4.
[b] Reference 12.

tions $h+k+l$ were even. Thus, although the data indicated a P lattice ($Z = 2$) apparently the heavy atoms, Pt and Pd, were very close to body-centered, I, positions. With the heavy atoms, which dominate the X-ray scattering, in I positions, it appeared expedient to conduct the preliminary refinements in $I\bar{1}$. An initial Patterson map in $I\bar{1}$ clearly indicated the Cl positions. These positions, introduced into the program FOUR,[19] generated an electron density map by a least-squares fitting of the observed and calculated structure factors. The structure refinement was developed stepwise with the Pt and Pd in the fixed positions, initially by block diagonals and finally with full-matrix anisotropic temperature factors for the Pt, Pd, Cl and N atoms in the structure. However, convergence could not be attained with anisotropic temperature factors for the C atoms and isotropic factors were utilized to give R and R_w values of 0.126 and 0.147, respectively.

The positions of the Pt, Pd, Cl and N atoms at this point are included in Table 2, and important interatomic distances and angles are in Table 3. It is to be noted that the Pd—Cl bonds of 2.316(8) and 2.319(8) Å, the Pt—N bonds of 2.04(2) and 2.08(3) Å, and the Cl—Pd—Cl angle of 89.5(3)° meet very reasonable expectations. However, the indicated C—C distance at this stage was 1.43 Å, unreasonably low for a single-bond distance.

A number of refinement procedures to improve the structure were attempted. The introduction of disorder represented by a partial exchange of Pt and Pd atoms did not improve the refinement, and changes in the occupancy factors were toward the nondisordered occupancy. The partial occupancy of two sites for the C atoms, individually as well as together, were tested. The value of R could be reduced only to 0.125 and reasonable C—C bond lengths were still not attained. When the space group $P\bar{1}$ was tried, convergence in the refinement of the metal atom positions was not attained. In addition, improvement by refinement in $P1$, $I1$ starting with the $I\bar{1}$ positions could not be achieved.

Table 2. Indicated atom positions from the partial X-ray diffraction structure of $Pt(en)_2PdCl_4$ refined under $I\bar{1}$

Atom	x	y	z
Pt	0	0	0
Pd	0.5000	0.5000	0
Cl1	0.5238(8)	0.783(1)	0.024(1)
Cl2	0.7054(7)	0.554(1)	0.002(1)
N1	0.007(3)	0.245(3)	0.015(5)
N2	0.818(3)	−0.028(3)	−0.007(5)

Table 3. Some distances and angles in $Pt(en)_2PdCl_4$

Atoms	Distance (Å)	Atoms	Angle (°)
Pt—Pd	3.400(5)	Cl1—Pd—Cl2	89.5(3)
Pd—Cl1	2.319(8)	N1—Pt—N2	81.5(11)
Pd—Cl2	2.316(8)	Cl1—Pd—Pt	87.6(2)
Pt—N1	2.04(2)	Cl2—Pd—Pt	87.9(2)
Pt—N2	2.08(3)	N1—Pt—Pd	86.6(10)
		N2—Pt—Pd	89.4(9)

With these unsatisfactory results the structure determination was abandoned.

It is believed that the positions of Pt, Pd, Cl and N atoms in the crystal are rather accurately established. Apparently, there is disorder in the C positions that is not characterized by X-ray diffraction because of the dominant scattering by the much heavier metal atoms. However, the orientations established for the Pt—N and the Pd—Cl bond are important in identifying some of the electronic transitions in the crystal spectra (see below).

Spectroscopic methods

The procedures we have used for recording polarized crystal spectra at temperatures down to 6 K have been described previously.[20,21]

The crystals were mounted over small holes in a Pt foil. The dimensions of the hole were such that the crystal completely covered the hole so no light which did not pass through the crystal was transmitted. The holes were made by denting the sheet and then abrading the surface with fine emery paper. A sheet might be dented 20 times in order to make a single hole. A fine-point sewing needle was used to make indentations for round holes which could be made as small as 20 μm. However, since many of the crystals were long needles, it was frequently advantageous to use the edge of a new razor blade to make the indentations which would form slits. These slits covered by the crystal could be aligned with the image of the slit in the spectrophotometer sample compartment to provide much greater transmitted light than a round hole.

Generally, from 6 to 10 crystal spectra were measured for each Magnus-type salt; and all of the tabulated bands in the spectra were observed in at least two crystals. It was important to use crystals of widely different thicknesses since weak features would be masked by variations in the base lines for very thin crystals, and more intense bands would not provide sufficient transmitted light in thick crys-

tals. The thickness of at least one crystal for each salt was measured by observing a crystal edge under a microscope equipped with a calibrated reticle. Variations in crystal thickness as well as difficulties in focus limited the uncertainty of such measurements to not less than 20%. For MGS itself, several crystals were found which possessed sufficiently good optical faces that well developed interference waves were developed in the absorbance vs wavelength recording because of multiple internal reflections of the light beam. The thickness of crystals in our previous study[8] of MGS utilized these waves to estimate crystal thickness and indices of refraction. In a subsequent paper[16] it was shown that neglect of dispersion will introduce considerable error into the calculations of crystal thickness and index of refraction. The technique of this latter paper was utilized to calculate the crystal thickness of an MGS crystal which was 4.16(8) μm thick. The indicated index of refraction for a-polarized light was $n_{a\text{-Na-D}} = 1.85$ and $1/n_a(\mathrm{d}n_a/\mathrm{d}\bar{\nu}) = 2.6 \times 10^{-6}$ cm. This compares with the value 1.90 reported earlier and was consistent with the observation that n_a was substantially less than the index of 1.93 for a calibration liquid.

The low-temperature spectra provided better resolution of electronic bands than the room-temperature ones. Even so, it was sometimes found useful to resolve Gaussian components by the damped least-squares procedure of Paponsek and Pliva.[22]

RESULTS AND DISCUSSION

A review of the spectra and excited states of the Pt(II) and Pd(II) square-planar tetrahalide complexes is appropriate since the spectra of the Magnus-type salts have frequently been considered to be just those of the anions perturbed by the close cation neighbors in the solid state. For this discussion we are utilizing the molecular-orbital energy scheme illustrated in Fig. 1. For the "strong-field" d^8-complexes in D_{4h}-symmetry, the lowest unoccupied molecular orbital (LUMO) is the antibonding b_{1g}^*-orbital derived essentially from the $d_{x^2-y^2}$- and the ligand σ-orbitals. All electrons are paired so a ground state of $^1A_{1g}$ is indicated. Our present assignments for the transitions of the four anions are given in the first columns of Tables 4–7. They have been inferred from solution spectra as well as single-crystal spectra of the potassium salts where the distance between the metal atoms along a tetragonal axis is greater than 4.1 Å.[15,23,24]

According to the orbital-energy diagram, the low-energy transitions should be the relatively low-intensity, electric dipole forbidden $d \rightarrow d$ tran-

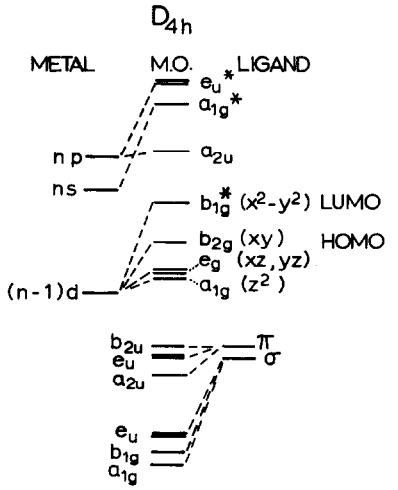

Fig. 1. Ordering of molecular-orbital energies for d^8-ions in D_{4h}-symmetry. The gerade ligand π-orbitals have been omitted for clarity.

sitions, which "borrow" intensity from higher allowed transitions by vibronic perturbations. The lowest electronic transition in this case would be a spin-forbidden singlet–triplet transition which attains intensity as a consequence of spin–orbit coupling in addition to the vibronic perturbations. At higher energies a series of electric dipole allowed transitions can occur due to excited $^1A_{2u}$-states, which will yield z-polarized transitions, and ^1E_u-states, which will give the x,y polarized transitions. Allowed $^1A_{2u}$- and ^1E_u-states can arise from the halide ligand to metal charge transfer (LMCT) $L\pi \rightarrow d^*_{x^2-y^2}$ transitions. At a somewhat higher energy will be another degenerate pair of LMCT $L\sigma \rightarrow d^*_{x^2-y^2}$ transitions to ^1E_u-states. In addition, possible electric dipole allowed $d \rightarrow p$ transitions may be spectroscopically accessible, viz. states $^1A_{2u}$, $nd_{z^2} \rightarrow (n+1)p_z$ and ^1E_u, $nd_{xz,yz} \rightarrow (n+1)p_z$.

There is a striking difference between the intense dipole-allowed transitions of the Pt and Pd complexes. In aqueous solution $PdCl_4^{2-}$ shows two intense bands at 37,400 cm^{-1} (ε = 9300 cm^{-1} M^{-1}) and 45,000 cm^{-1} (ε = 25,800 cm^{-1} M^{-1}).[16] Polarized crystal spectra of K_2PdCl_4 show that both of these bands must be largely x,y-polarized. There is a much weaker peak at 37,400 cm^{-1} in z-polarization. The temperature dependence of the intensity for this weaker peak indicates that it is electric dipole allowed despite its lower intensity. The z-polarized absorption could be followed to 44,000 cm^{-1}, and there was no indication of a peak in the vicinity of 45,000–46,000 cm^{-1} for it. These results justify the assignment of absorption at *ca* 37,500 cm^{-1} to the L-πMCT transitions and the 45,000-cm^{-1} absorption to L-σMCT. Jorgensen[25] indicated that mixing

Table 4. Transition assignments for $PtCl_4^{2-}$ in Magnus-type salts

Localized excited state: transition	$\bar{\nu}$ (cm^{-1})					
	K_2PtCl_4	$Pd(en)_2PtCl_4$	$Pd(NH_3)_4PtCl_4$	$Pt(en)_2PtCl_4$	$Pt(CH_3NH_2)_4PtCl_4$	$Pt(NH_3)_4PtCl_4$
$^1E_u : L\sigma \rightarrow d^*_{x^2-y^2}$						
$^1A_{2u} : d_{z^2} \rightarrow p_z$	44,100					
$^1E_u : d_{xz,yz} \rightarrow p_z$	46,000					
$^1A_{2u} : L\pi \rightarrow d^*_{x^2-y^2}$	(43,000)					
$^1E_u : L\pi \rightarrow d^*_{x^2-y^2}$	42,400					
$^1B_{1g} : d_{z^2} \rightarrow d^*_{x^2-y^2}$	30,000	26,500	25,000	25,000	—	23,500
$^1E_g : d_{xz,yz} \rightarrow d^*_{x^2-y^2}$	30,000	27,500	26,000	28,000	25,500	25,300
$^1A_{2g} : d_{xy} \rightarrow d^*_{x^2-y^2}$	26,400	26,800	25,300	24,800	24,800	24,900
Triplet states						
$E'_1 : {}^3A_{2g}, {}^3E_g, {}^3B_{1g}$	24,200			(19,500)	(18,000)	
$A'_2 : {}^3E_g$ $E'_1 : {}^3A_{2g}, {}^3E_g, {}^3B_{1g}$	21,000	19,600	18,900	17,000	16,600	16,000
$B'_1 : {}^3E_g$ $E'_1 : {}^3A_{2g}, {}^3E_g, {}^3B_{1g}$	18,500					

Table 5. Transition assignments for $PtBr_4^{2-}$ in Magnus-type salts

Localized excited state : transition	$\bar{\nu}$ (cm^{-1})					
	K_2PtBr_4	$Pd(en)_2PtBr_4$	$Pd(NH_3)_4PtBr_4$	$Pt(en)_2PtBr_4$	$Pt(CH_3NH_2)_4PtBr_4$	$Pt(NH_3)_4PtBr_4$
$^1E_u : L\sigma \rightarrow d^*_{x^2-y^2}$	48,000					
$^1A_{2u} : d_{z^2} \rightarrow p_z$						
$^1E_u : d_{xz,yz} \rightarrow p_z$	48,000					
$^1A_{2u} : L\pi \rightarrow d^*_{x^2-y^2}$	37,000					
$^1E_u : L\pi \rightarrow d^*_{x^2-y^2}$	37,000					
$^1B_{1g} : d_{z^2} \rightarrow d^*_{x^2-y^2}$	27,000	25,800	(24,000)	23,700	22,200	21,400
$^1E_g : d_{xz,yz} \rightarrow d^*_{x^2-y^2}$	27,000	25,800	(25,000)	26,900	24,000	23,700
$^1A_{2g} : d_{xy} \rightarrow d^*_{x^2-y^2}$	24,400	23,800	23,800	23,700	24,000	23,700
Triplet states						
$E'_1 : {}^3A_{2g}, {}^3E_g, {}^3B_{1g}$	22,700					
$A'_2 : {}^3E_g$ $E'_1 : {}^3A_{2g}, {}^3E_g, {}^3B_{1g}$	19,000	18,500	18,000	17,500	16,600	16,500
$B'_1 : {}^3E_g$ $E'_1 : {}^3A_{2g}, {}^3E_g, {}^3B_{1g}$	17,500					

Table 6. Localized transition assignments for $PdCl_4^{2-}$ in Magnus-type salts

Localized excited state: transition	$\bar{\nu}$ (cm^{-1})					
	K_2PdCl_4	$Pd(en)_2PdCl_4$	$Pd(NH_3)_4PdCl_4$	$Pt(en)_2PdCl_4$	$Pt(CH_3NH_2)_4PdCl_4$	$Pt(NH_3)_4PdCl_4$
$^1E_u : L\sigma \rightarrow d^*_{x^2-y^2}$	45,000					
$^1A_{2u} : d_{z^2} \rightarrow p_z$						
$^1E_u : d_{xz,yz} \rightarrow p_z$						
$^1A_{2u} : L\pi \rightarrow d^*_{x^2-y^2}$	36,900		34,200			
$^1E_u : L\pi \rightarrow d^*_{x^2-y^2}$	36,500					
$^1B_{1g} : d_{z^2} \rightarrow d^*_{x^2-y^2}$	21,700	20,700	20,700	17,800	16,800	16,200
$^1E_g : d_{xz,yz} \rightarrow d^*_{x^2-y^2}$	22,100	20,700	20,700	(20,300)	(20,100)	(20,100)
$^1A_{2g} : d_{xy} \rightarrow d^*_{x^2-y^2}$	20,200	19,800	19,200	19,500	19,500	19,300
Triplet states						
$E'_1 : {}^3A_{2g}, {}^3E_g, {}^3B_{1g}$						
$A'_2 : {}^3E_g$ $E'_1 : {}^3A_{2g}, {}^3E_g, {}^3B_{1g}$	17,400	16,000	—	(15,000)	14,500	13,800
$B'_1 : {}^3E_g$ $E'_1 : {}^3A_{2g}, {}^3E_g, {}^3B_{1g}$	16,000					

Table 7. Localized transition assignments for $PdBr_4^{2-}$ in Magnus-type salts

Localized excited states : transition	$\bar{\nu}$ (cm^{-1})					
	K_2PdBr_4	$Pd(en)_2PdBr_4$	$Pd(NH_3)_4PdBr_4$	$Pt(en)_2PdBr_4$	$Pt(CH_3NH_2)_4PdBr_4$	$Pt(NH_3)_4PdBr_4$
$^1E_u : L\sigma \rightarrow d^*_{x^2-y^2}$	40,000					
$^1A_{2u} : d_{z^2} \rightarrow p_z$						
$^1E_u : d_{xz,yz} \rightarrow p_z$						
$^1A_{2u} : L\pi \rightarrow d^*_{x^2-y^2}$	30,900	29,700	30,400	29,800	29,500	
$^1E_u : L\pi \rightarrow d^*_{x^2-y^2}$	30,200				28,000	
$^1B_{1g} : d_{z^2} \rightarrow d^*_{x^2-y^2}$	22,100	20,000	18,700	18,300	16,500	16,000
$^1E_g : d_{xz,yz} \rightarrow d^*_{x^2-y^2}$	22,100	20,000	(19,100)	(19,100)	19,500	(19,300)
$^1A_{2g} : d_{xy} \rightarrow d^*_{x^2-y^2}$	20,200	19,200	19,200	19,100	19,200	18,700
Triplet states						
$E'_1 : {}^3A_{2g}, {}^3E_g, {}^3B_{1g}$						
$A'_2 : {}^3E_g$ $E'_1 : {}^3A_{2g}, {}^3E_g, {}^3B_{1g}$	17,400			14,500		
$B'_1 : {}^3E_g$ $E'_1 : {}^3A_{2g}, {}^3E_g, {}^3B_{1g}$	15,700					

of the σ- and π-orbital states would greatly enhance the ^1E_u, x,y absorption at 37,500 cm^{-1}. For the $^1A_{2u}$ transition with the electron-orbital designation of $b_{2u} \rightarrow b_{1g}^*$ there is no mixing possible for the σ- and π-orbitals; and, in z-polarization, the transition must be pure L-πMCT.

The spectra for the $PdBr_4^{2-}$ ion support this assignment as well. The LMCT transitions are expected to occur at a lower energy than for the corresponding chloride complexes. Thus an intense x,y-polarized band at 30,700 cm^{-1} corresponds to the L-πMCT, ^1E_u transition; and a still stronger band at 40,400 cm^{-1} corresponds to the L-σMCT, ^1E_u transition. A much weaker electric dipole allowed band in z-polarization at 30,900 cm^{-1} is the L-πMCT, $^1A_{2u}$ transition. There is no z-polarized band near 40,000 cm^{-1}.

In contrast to the Pd complexes there is a very intense peak at 46,000 cm^{-1} in $PtCl_4^{2-}$ with a weaker shoulder at 43,000 cm^{-1}. Polarized-reflectance spectra by Anex and Takeuchi[26] showed that in this region the z-polarized band was more intense than the x,y-polarized absorption. This difference between the Pt and Pd complexes has been attributed to $d \rightarrow p_z$ transitions in this region for the platinum. Recently Isci and Mason[27] have observed A-terms in the magnetic circular dichroism (MCD) spectra of $PtCl_4^{2-}$ in this region, which indicate the presence of two ^1E_u-transitions so that they believe that the L-πMCT as well as the $d \rightarrow p_z$ transitions are in the vicinity of 43,000–46,000 cm^{-1}. The presence of the L-πMCT transition is also supported by the spectra of $PtBr_4^{2-}$ where an intense x,y-polarized band is seen at the lower energy of 37,000 cm^{-1}, where there is only a weak absorption in z-polarization.

Three of the four spin-allowed d–d transitions can be assigned unambiguously for all four of the anions. The transition to the $^1A_{2g}$-state $d_{xy} \rightarrow \sigma^*(d_{x^2-y^2})$ is predicted from consideration of all the molecular vibrations of the square-planar MX_4^{2-} ion to be forbidden in z-polarization. This selection rule is apparently exact since a pure x,y band is observed in each complex (it is at 26,400 cm^{-1} for $PtCl_4^{2-}$).[20] In addition, the ^1E_g [$d_{xz,yz} \rightarrow \sigma^*(d_{x^2-y^2})$] states have been identified in aqueous solution by an A-term in the MCD spectra.[28,29] In $PtCl_4^{2-}$ this ^1E_g-states can be associated with the peak at 30,300 cm^{-1} (aqueous), 29,200-z, 29,800-xy (15-K crystal).

Although there is a consensus in the assignment of these $^1A_{2g}$ and ^1E_g d–d states, the situation is much less clear with respect to the third spin-allowed $d \rightarrow d$ state, the $^1B_{1g}$, $d_{z^2} \rightarrow \sigma^*(d_{x^2-y^2})$. For some time it was assigned to a weak shoulder at 38,000 cm^{-1} in $PtCl_4^{2-}$ solution and at 36,500 cm^{-1} in K_2PtCl_4. Such an assignment was proposed by Chatt *et al.*,[30] Jørgensen[31] and supported by semiempirical MO calculations of Basch and Gray[32] and Cotton and Harris.[33] There is a band at about 21,000 cm^{-1} seen in both c- and x,y polarizations, which although weaker than the $^1A_{2g}$- and ^1E_g-bands does have 20–30% of the intensity of these. There are much weaker features still at 17,000 and 23,000 cm^{-1} which can be logically assigned as spin-forbidden transitions; but the intensity of the 21,000-cm^{-1} band is anomalous. Martin and Lenhardt[34] suggested that the $^1B_{1g}$-state might be associated with the 21,000-cm^{-1} band. However, a ligand field calculation,[35] which included spin–orbit coupling and the electron–electron repulsion Slater–Condon parameters F_2 and F_4, which were considered reasonable at the time, indicated the $^3B_{1g}$-states would fall in the region of 14,000 cm^{-1} where there was no detectable absorption. However, two sets of seemingly satisfactory parameters were obtained which placed calculated $d \rightarrow d$ transitions at observed band energies in the spectra. One set placed the $^1B_{1g}$-state of 35,300 cm^{-1} whereas the alternative placed it at 29,700 cm^{-1}, in close proximity to the ^1E_g-band and impossible to resolve from it. Elding and Olsson[36] indicated that the shift in the 35,500-cm^{-1} band, as Cl^- ligands were replaced by H_2O, was different from $d \rightarrow d$ transitions and favored placing the $^1B_{1g}$-band at about 29,700 cm^{-1}. Tuszynski and Gliemann,[37] on the other hand, have performed ligand field calculations which placed the $^1B_{1g}$ back at the 21,000-cm^{-1} anomalous-intensity peak of $PtCl_4^{2-}$. For this computation they used considerably smaller electron–electron repulsion parameters than have usually been applied to transition-metal complexes. Hence, the spin-forbidden $^3B_{1g}$-transitions were placed no lower than 17,000 cm^{-1}.

A very similar situation occurs for the d–d transitions of $PtBr_4^{2-}$. The $^1A_{2g}$- and ^1E_g-transitions are indicated unambiguously, and there is an anomalous-intensity band at lower energies.[15] For the $PdCl_4^{2-}$ and $PdBr_4^{2-}$ ions again the $^1A_{2g}$- and ^1E_g-transitions are identifiable.[16,38] These states have a much smaller separation than in the Pt anions so the peaks are not separable in x,y-polarization. Spin-forbidden transitions are much weaker with the lighter Pd atom. Such very weak transitions were observed below the $^1A_{2g}$- and ^1E_g-transitions. There is no third, anomalous-intensity band so the $^1B_{1g}$-band must either lie too close to the $^1A_{2g}$- and ^1E_g-bands to be resolved from them or else must be at a considerably higher energy. In the latter case for K_2PdCl_4 the $^1B_{1g}$-band would have to lie at least 8000 cm^{-1} above the $^1A_{2g}$-band and would fall under the tail of the L-πMCT band.

The spectrum of the colorless $[Pt(NH_3)_4]^{2+}$ ion in aqueous solution is available from the work of Isci and Mason.[39] They assigned a broad maximum at 35,000 cm^{-1} ($\varepsilon = 40$ cm^{-1} M^{-1}) to the $^3A_{2g}$- and ^3E_g-states; and an intense peak ($\varepsilon = 10{,}000$ cm^{-1} M^{-1} at 50,950 cm^{-1}) was assigned as the $d \rightarrow p$ transitions. Very weakly defined shoulders on this intense band at 41,000 and 45,000 cm^{-1} were then assigned as $^1A_{1g} \rightarrow {}^1A_{2g}$ ($d_{xy} \rightarrow d^*_{x^2-y^2}$), ^1E_g ($d_{xz,yz} \rightarrow d^*_{x^2-y^2}$) and $^1A_{1g} \rightarrow {}^1B_{1g}$ ($d_{z^2} \rightarrow d^*_{x^2-y^2}$), respectively. Thus, the transitions all have much higher energies then the corresponding ones in the anions. As a consequence simple halide salts of this cation are colorless.

The single-crystal absorption spectra for all the Magnus salts studied are shown in Figs 2–24. Some comments about the site symmetries are relevant before a consideration of the spectra. The anions for the tetraamine and the tetra(methylamine) salts are in tetragonal sites, and the spectra are measured for a $h,k,0$ face. The c-polarization for such faces gives an explicit molecular z-polarization and the polarization normal to c gives an accurate molecular x,y polarization for a degenerate pair of transitions that have been labelled in the figures.

The partially determined structure determination for the $Pt(en)_2PdCl_4$ can serve to assign polarizations for the group of salts with ethylenediamine complexes. From the atom positions and bond angles of $Pt(en)_2PdCl_4$ in Tables 2 and 3 the following inferences may be drawn. The $PdCl_4^{2-}$ ion is very nearly square-planar ion with D_{4h}-symmetry. In $[Pt(en)_2]^{2+}$, the PtN_4 grouping of atoms must be nearly planar, exactly so if there is a $\bar{1}$-symmetry. The angles between the Pt—N bonds in the chelate ring however are only 81.5° so the PtN_4 grouping must be considered to have approximately D_{2h}-symmetry. The ions stack along the c-axis, and it is apparent from the Pt—Pd—Cl and the Pd—Pt—N angles that the normals to the planar groups are within about 3° of the c-axis. The crystals were needles with the c-axis as the needle axis. The needle axes for all the ethylenediamine salts were invariably observed as a polarization (extinction) direction for one of the two waves transmitted by the indicated $h,k,0$ face, although this is not required by crystallographic symmetry for triclinic systems. The two polarizations directions have been labeled as molecular z-polarization for the c-polarization and $\perp z$ polarization for the normal-to-c polarization. We have used this designation rather than x,y polarization since a nearly D_{4h} $PtBr_4^{2-}$ in $K_2PtBr_4 \cdot 2H_2O$ exhibited absorptions differing by a factor of 2 normal to its z-axis in an orthorhombic crystal.[40]

The arrangement of the bonds in the counter cations also need to be considered because of their influence on some possible interionic electron transfer transitions. For MGS itself which is the one tetragonal salt with a complete crystal structure[4] the Pt—N and Pt—Cl bonds can be considered as partially staggered since the $[Pt(NH_3)]^{2+}$ is rotated by 28° about the c-axis from an eclipsed configuration with the $PtCl_4^{2-}$. Both ions occupy a $4/m$ site. From our partial determination of $Pt(en)_2PdCl_4$ the bisector of the N—Pt—N angle in the cation is within 1.7° of being parallel to the bisector of the Cl—Pd—Cl bond angle in the anion. Hence, the ions can be considered as eclipsed as is possible with very approximately mmm (D_{2h}) symmetry.

MGS

Day[13] has maintained that the color and transitions in the visible region of MGS can be explained by the shift of $d \rightarrow d$ transitions of the anions due to the close proximity of the neighboring cations. The d_{xy} and the $d_{x^2-y^2}$ metal orbitals which are concentrated in the plane of the ion are presumably influenced least by the presence of neighbors, and the transition to an $^1A_{2g}$-state, d_{xy} (b_{2g}) $\rightarrow d^*_{x^2-y^2}$ (b_{1g}), is expected to be shifted very little. However, the $d_{xz,yz}$ (e_g) orbitals which place more electron density out of the plane are expected to be influenced more. Repulsions between the $d_{xz,yz}$-electrons and the electrons of the cation are expected to raise the energy of $d_{xz,yz}$-electrons and result in a red shift of the ^1E_g-transition. The transition to the $^1B_{1g}$-state ($d_{z^2} \rightarrow d^*_{x^2-y^2}$) should be red-shifted an even greater amount because of the high electron density placed along the z-axis.

The $^1A_{2g}$-band, which is forbidden in z-polarization, is clearly evident in the potassium salts of the four anions, which also possess a vibrational structure, exhibiting a long Franck–Condon progression. This transition can usually be identified in the Magnus-type salts from its polarization, and in a number of cases a vibrational structure is resolvable as well.

Crystal spectra for $Pt(NH_3)_4PtCl_4$. considerably superior to any recorded previously, are shown in Fig. 2. For x,y polarization there is only a single broad $d \rightarrow d$ band at *ca* 24,800 cm^{-1}, whereas K_2PtCl_4 has two bands at 26,400 and 30,300 cm^{-1}. The very narrow peak at 31,800 cm^{-1} is unlike any d–d transition observed previously for Pt(II) salts and will be discussed later. Hence, it is concluded that the ^1E_g-band, placed by consensus at *ca* 30,000 cm^{-1} in K_2PtCl_4, has been red-shifted by about 5500 cm^{-1} to about 25,300 cm^{-1} in MGS. A faint vibrational structure with maximum amplitude at

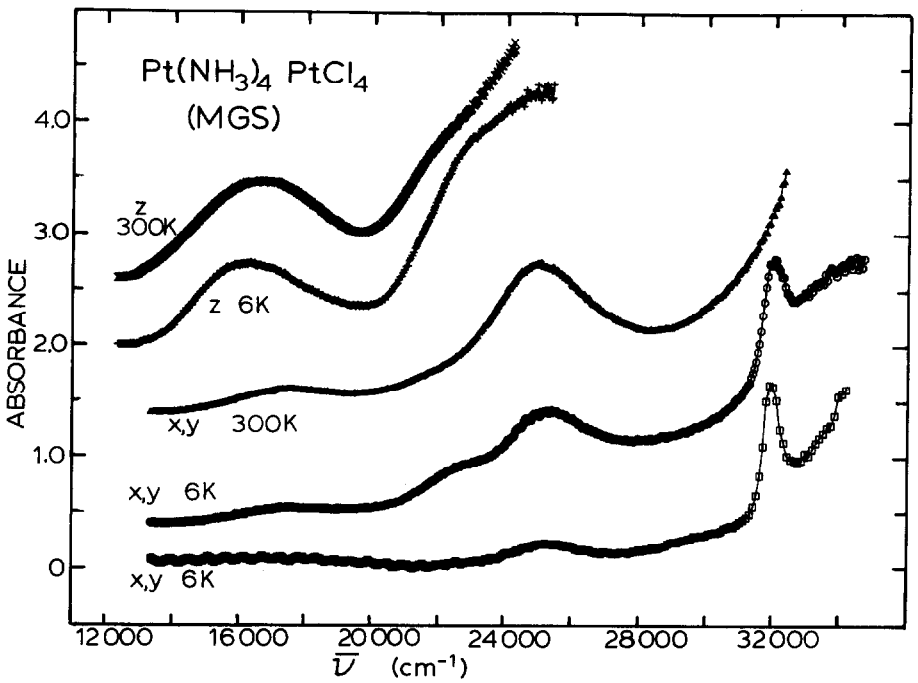

Fig. 2. Polarized single-crystal spectra for $Pt(NH_3)_4PtCl_4$ (MGS). The upper four spectra are for a 12.3-μm-thick crystal. The lowest curve is for a 4-μm-thick crystal.

24,900 cm^{-1} is evident in the 6 K–x,y spectrum of the 12.3-μm crystal in Fig. 2, indicating the presence of the $^1A_{2g}$-band which has been shifted by only 1500 cm^{-1} from K_2PtCl_4. In x,y polarization MGS appears yellow in color. The green color results from the z- or c-polarization of the crystals where there is a low-absorption "window" in the spectrum in the vicinity of 20,000 cm^{-1}. The specular-reflectance spectra[10,11] indicate an intense absorption peak at 35,000 cm^{-1}, some 10,000 cm^{-1} below the highest peak in $PtCl_4^{2-}$ solutions. Although a peak in the vicinity of 25,000 cm^{-1} in z-polarization was at one time reported,[6,7] it has been shown[8] that this was a consequence of either a finite elipticity of the polarizer or depolarization at the surface of the crystal; and the absorption rises rapidly in the vicinity of 25,000 cm^{-1}. However, the low-energy transitions apparently "borrow" z-intensity from the intense band at 35,000 cm^{-1}, and absorption in the vicinity of a maximum at 16,000 cm^{-1} is at least an order of magnitude greater than in the x,y polarization. The peak at 16,000 cm^{-1} is presumably the peak at 21,000 cm^{-1} in K_2PtCl_4 which has been red-shifted by the proximity of the neighboring ions. Since this red shift is only 5000 cm^{-1} and no greater than the shift of the ^1E_g-band, we have concluded that the 21,000-cm^{-1} anomalous-intensity band in K_2PtCl_4 is not the $^1B_{1g}$ ($d_{z^2} \rightarrow d^*_{x^2-y^2}$) band, and must therefore be assigned to spin-forbidden transitions. Such bands become allowed by virtue of spin–orbit coupling, which mix in spin-allowed transitions; their symmetry must be treated by the double rotational group D_4'. Probably, most intensity will be in transition to A_2'-, B_2'- and E_1'-states since the $^1A_{2g}$, $^1B_{1g}$ and ^1E_g wave functions, respectively, are basis functions for these double-group irreducible representations. The assignment of the three resolvable spin-forbidden bands of K_2PtCl_4 to the double groups, based on the ligand field parameter B in ref. 35 are included in Table 4. It is noted that all of the bands contain contributions for transitions from all four orbitals, d_{xy}, d_{xz}, d_{yz} and d_{z^2} so a red shift no greater than that of the ^1E_g-band is reasonable. We are therefore placing the $^1B_{1g}$-transition in the 30,000-cm^{-1} band at $PtCl_4^{2-}$ where it is not resolvable from the ^1E_g-transition. In MGS we assign it to the fairly weak feature, a shoulder at 23,500 cm^{-1}. In this case its red shift is 6500 cm^{-1}, significantly greater than for the $^1B_{1g}$-band. Moncuit[41] has reported a theoretical treatment of the intensities of vibronically allowed d–d transitions of $PtCl_4^{2-}$. His calculations predict that, although the $^1B_{1g}$-band is vibronically allowed in both polarizations, the $z:x,y$ oscillator strength ratio at 0 K is nearly 40 and the x,y oscillator strength of the $^1B_{1g}$-transition is 0.12 times that for the $^1A_{2g}$-transition and 0.08 times that for the x,y-component of the ^1E_g-transition. Hence, this assignment of the relatively weak 23,500-cm^{-1} component appears to be quite consistent with these computations.

A new feature in the MGS spectra of the present

work is the remarkably sharp, narrow band seen at 31,800 cm^{-1} in the 6K–x,y-spectra of Fig. 2. The improved crystal specimens and techniques permitted the observation of this band. In previous reports of this spectrum for MGS the scans were terminated on the rapidly rising portion of this band. The narrow width of this band, not over 200 cm^{-1} at half-height, is unlike any of the other d–d bands in which an electron is excited into the $d^*_{x^2-y^2}$-orbital, and which have half-widths of the order of 2000 cm^{-1}. Even so, the measurements are unquestionably subject to instrumental limitations. For example, this peak for the 4-μm-thick crystal in Fig. 2 with the better resolution appears as high or higher than that for the 12.3-μm crystal. (The waves in the low-absorption region of the 4-μm crystal are due to interference from the multiple reflections in the optical faces of the crystal.) In Fig. 3, scans of this peak at a series of temperatures show that the peak height increases as the peak narrows with lower temperatures and the integrated intensity is relatively temperature independent. This is in contrast to the vibronically allowed bands and indicates that the transition is effectively electric dipole allowed, although it has a relatively low transition moment. An unusual feature is the shift of the peak to longer wavelengths as the crystal is cooled. This is in contrast to most sharp electronic bands in crystal spectra where the shift is to shorter wavelengths as thermal excitation of phonon states are reduced at lower temperature. Since there appears to be no logical molecular transition for this band, we are proposing an anion → cation (A → C) electron transfer. Since all the indicated transitions to the $d^*_{x^2-y^2}$ (σ-antibonding) orbitals are broad, we suggest that this transition must be to an orbital not involved in the σ-bonding. The most reasonable orbital would seem to be the $(p_z)_C$ orbital. A $(d_{xz,yz})_A \rightarrow (p_z)_C$ electron transfer would be dipole-allowed for x,y polarization. The intensity would depend upon the overlap of the cation and anion orbitals which, of course, is not high. It is not possible to predict the energy of such a transition since it would depend upon the ionization energy of the anion, the electron affinity of the cation and the lattice energy changes induced by replacing doubly charged ions by a pair of singly charged ions. The $(p_z)_C$ orbital has a suitable σ-symmetry for forming a bond to adjacent $(d_{z^2})_A$ orbitals and in solid-state parlance would be considered to form a pair of one-dimensional bands. The observed transition would then be a band-to-band transition. However, the energy separation of the bands, indicated by the transition wave numbers together with the narrowness of the optical bands preclude any significant bonding between the ions.

An examination of the spectra of other $PtCl_4^{2-}$ salts shows that similar sharp peaks are clearly evident in the salts with Pt cations. In $Pt(CH_3NH_2)_4PtCl_4$ with nearly the same Pt—Pt distance as MGS the peak is at 31,800 cm^{-1} as well, whereas for $Pt(en)_2PtCl_4$ with significantly higher

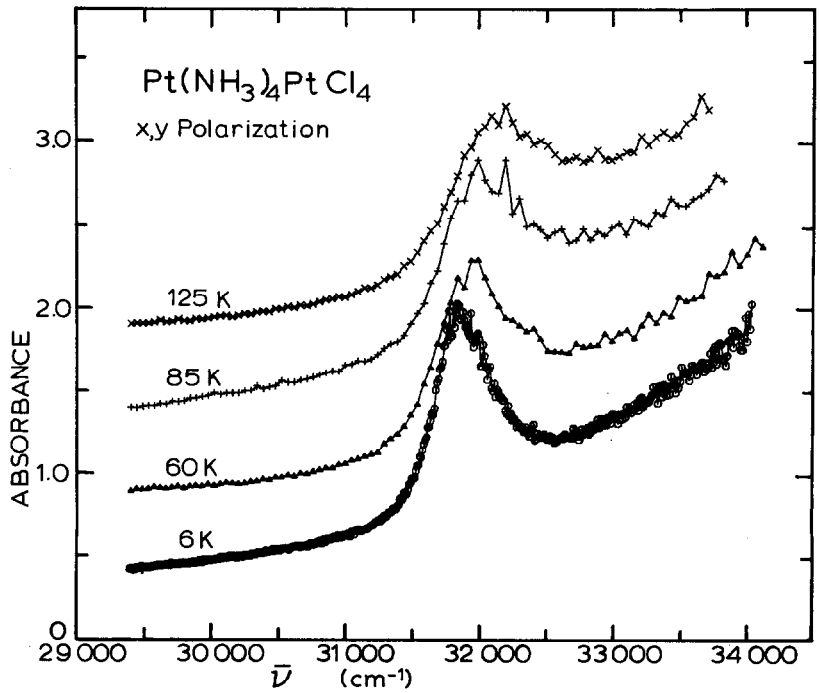

Fig. 3. Temperature dependence of the narrow high-energy band in the 4-μm MGS crystal of Fig. 2 for x,y polarization.

Pt—Pt distances the band is at higher energy (33,600 cm^{-1}). There was no evidence for such a narrow band in the $PtCl_4^{2-}$ with Pd cations. However, the 6-K scans could only be extended to 31,700 cm^{-1} for the $[Pd(en)_2]^{2+}$ compound and to 32,500 cm^{-1} for the $[Pd(NH_3)_4]^{2+}$ compound.

The foregoing information now provides some insights into the assignment of the intense absorption maximum at 35,000 cm^{-1} in z-polarization in MGS. Day[13] attributed this to the $d_{z^2} \rightarrow p_z$ transition in $PtCl_4^{2-}$ which had been shifted to a lower energy by 10,000 cm^{-1}. In the treatment of absorption in crystals as Frenkel excitons, energy shifts are predicted as a consequence of the interactions of transition dipoles which will therefore by intensity-dependent.[42] As Day showed with rather widely separated one-dimensional chains extending in the z-direction, a z-polarized transition is shifted to lower energies and x,y-polarized bands are shifted to high energies by one half as much. The shifts are proportional to the transition moments squared and to a first approximation inversely proportional to the cube of the separation of the moments. According to the theory, the shift for a z-directed 1.0 e Å transition moment with 6.48 Å separation of the moments in a one-dimensional chain is less than 2000 cm^{-1}, much less than the required 10,000 cm^{-1}. In addition, in our spectra for $Pt(CH_3NH_2)_4PdBr_4$ (Fig. 20) a truncated very intense band is seen that must have a maximum at about 28,000 cm^{-1}. This is assigned as the intense L-$\pi \rightarrow$ M charge-transfer band that occurs at about the same energy (30,200 cm^{-1}) in $PdBr_4^{2-}$ solutions. Hence, no significant blue shift of this intense band has occurred in this Magnus-type salt with 3.35-Å spacing between the oppositely charged ions. Therefore, we believe that the 35,000-cm^{-1} band of MGS cannot be the simple molecular $d_{z^2} \rightarrow p_z$ transition.

If the $n-d_{z^2}$ orbital on the anion metal atom is destabilized by the repulsions with the cation electrons, then the $(n+1)p_z$ orbital must be destabilized to an even greater extent. It is our contention that such orbital destabilizations take the transitions involving the anion p_z-orbitals out of the spectroscopic region and to such a high energy that it cannot participate in significant interionic bonding. We therefore prefer to assign this 35,000-cm^{-1} transition to the $(d_{z^2})_A \rightarrow (p_z)_C$ interionic electron transition. If one considers only a linear system of two cation metal atoms about an anion metal there will be a $\Sigma_g^+ \rightarrow \Sigma_u^+$ transition which will be polarized in the z-direction. This is an equivalent interionic transition, except that it involves a d_{z^2}-electron rather than a $d_{xz,yz}$-electron, to the one we assigned to the 31,800-cm^{-1} band in x,y polarization, consistent with our conclusion that the d_{z^2}-orbital lies close in energy to the d_{xz}- and d_{yz}-orbitals. The major problem then is the explanation for the striking difference in intensities in these similar types of transition since the one with polarization in the stacking direction is so much stronger.

For treating the intensities, a one-dimensional array of alternating anion and cation metal atoms will be considered along the z-axis. There are a total of N cells, each contain one anion at $z = \frac{1}{4}$ and one cation at $z = \frac{3}{4}$ in the array. With the usual neglect of end effects, orthogonal and normalized wave functions for the one-dimensional bands will have the form:

$$\psi_{1,n} = (1/\sqrt{N}) \sum_j e^{2\pi inj/N} d_{z^2,A,j}, \quad (1)$$

$$\psi_{2,m} = (1/\sqrt{N}) \sum_j e^{2\pi imj/N} p_{z,C,j}, \quad (2)$$

$$\psi_{3,l} = (1/\sqrt{N}) \sum_j e^{2\pi ilj/N} d_{xz,A,j}, \quad (3)$$

where $1 \leqslant j \leqslant N$ is the index of the cell in the chain, and l, m, n are the quantum numbers 0, 1, ... $N-1$ for the states in the band. Since the d_{z^2}- and p_z-orbitals each have σ-symmetry with respect to the z-axis there may be some interaction between the $\psi_{1,n}$ and $\psi_{2,m}$ wave functions. Only an overlap between adjacent anions and cations will be significant. For a one-electron treatment the matrix elements will be:

$$H_{1,n;1,n} = \langle d_{z^2,A,j}|H|d_{z^2,A,j}\rangle, \quad (4)$$

$$H_{2,m;2,m} = \langle p_{z,C,j}|H|p_{z,C,j}\rangle, \quad (5)$$

$$H_{1,n;2,m} = \frac{1}{N}\sum_j \{e^{2\pi i(m-n)j/N}\langle d_{z^2,A,j}|H|p_{z,C,j}\rangle + e^{-2\pi nj/N} e^{2\pi im(j-1)/N}\langle d_{z^2,A,j}|H|p_{z,C,j-1}\rangle\}. \quad (6)$$

Equation (6) can be rewritten as:

$$H_{1,n;2,m} = \frac{1}{N}\sum e^{2\pi i(m-n)j/N}\{d_{z^2,A,j}|H|p_{z,C,j}\rangle + e^{-2\pi im/N}\langle d_{z^2,A,j}|H|p_{z,C,j-1}\rangle\}. \quad (7)$$

The sum is zero unless $m = n$, and the problem therefore reduces to a set of $N2 \times 2$ secular equations. In addition, since:

$$\langle d_{z^2,A,j}|H|p_{z,C,j}\rangle = -\langle d_{z^2,A,j}|H|p_{z,C,j-1}\rangle, \quad (8)$$

the matrix elements can be reduced to:

$$H_{1,n;2,n} = \langle d_{z^2,A,j}|H|p_{z,C,j}\rangle(1-e^{-2\pi in/N}). \quad (9)$$

The roots of these secular equations will give a band of states, filled with electron pairs below $\langle d_{z^2,A,j}|H|d_{z^2,A,j}\rangle$, and an empty band above $\langle p_{z,C,j}|H|p_{z,C,j}\rangle$. If the interaction integral in equation (9) is small, the bands will be narrow; and a

wave function with neglect of overlap can be written for the filled- and empty-band orbitals, respectively:

$$\Psi_{\mathrm{I},n} = (1-\alpha_n^2)^{1/2}\psi_{1,n} - \alpha_n\psi_{2,n} \tag{10}$$

and

$$\Psi_{\mathrm{II},n} = \alpha_n\psi_{1,n} + (1-\alpha_n^2)^{1/2}\psi_{2,n}.$$

In the present case $|\alpha_n| \ll 1$.

The z-component for a transition moment of a $\psi_{\mathrm{I},m} \rightarrow \psi_{\mathrm{II},n}$ excitation is:

$$\mu_z(m \rightarrow n) = \frac{1}{N}\Big\langle \sum_j e^{2\pi ijm/N} \times [(1-\alpha_m^2)^{1/2} d_{z^2,A,j} - \alpha_m p_{z,C,j}]|ez| \times \sum_j e^{2\pi in/N}[\alpha_n d_{z^2,A,j} + (1-\alpha_n^2)^{1/2} p_{z,C,j}]\Big\rangle. \tag{11}$$

This expression can be rewritten with the assumption of zero overlap between nonadjacent anions and/or cations:

$$\begin{aligned}\mu_z(m \rightarrow n) = \frac{e}{N}\sum_j e^{2\pi i(n-m)j/N} &\times \{(1-\alpha_m^2)^{1/2}\alpha_n\langle d_{z^2,A,j}|z|d_{z^2,A,j}\rangle \\ &- \alpha_m(1-\alpha_n^2)^{1/2}\langle p_{z,C,j}|z|p_{z,C,j}\rangle \\ &+ (1-\alpha_m^2)^{1/2}(1-\alpha_n^2)^{1/2}[\langle d_{z^2,A,j}|z|p_{z,C,j}\rangle \\ &+ e^{-2\pi in/N}\langle d_{z^2,A,j}|z|p_{z,C,j-1}\rangle] \\ &- \alpha_m\alpha_n[\langle p_{z,C,j}|z|d_{z^2,A,j}\rangle \\ &+ e^{2\pi in/N}\langle p_{z,C,j}|z|d_{z^2,A,j+1}\rangle]\}. \end{aligned} \tag{12}$$

If the z-axis origin is placed at the center of the one-dimensional stack of ions then the $|z|$ operator in equation (12) can be replaced by $|Z_j + z_j|$, where Z_j is the z-coordinate of the center of the j cell and z_j is the coordinate measured from Z_j. With this substitution in equation (12) the summation provides nonzero values only for the transitions where $n = m$. Since

$$d_{z^2,A,j}|Z_j + z_j|d_{z^2,A,j} = Z_j - c/4,$$

$$p_{z,C,j}|Z_z + z_j|p_{z,C,j} = Z_j + c/4,$$

and

$$\sum_j Z_j = 0,$$

the final expression for μ_z becomes:

$$\begin{aligned}\mu_z(n \rightarrow n) = e\{&\alpha_n(1-\alpha_n^2)^{1/2}(-c/2) \\ &+ (1-\alpha_n^2)[\langle d_{z^2,A,j}|z_j|p_{z,C,j}\rangle \\ &+ e^{-2\pi in/N}\langle d_{z^2,A,j}|z_j|p_{z,C,j-1}\rangle] \\ &- \alpha^2[\langle p_{z,C,j}|z_j|d_{z^2,A,j}\rangle \\ &+ e^{2\pi in/N}\langle p_{z,C,j}|z_j|d_{z^2,A,j+1}\rangle]\}. \end{aligned} \tag{13}$$

On the other hand the x-component of $\psi_{3,m} \rightarrow \Psi_{\mathrm{II},n}$ is:

$$\mu_x(m \rightarrow n) = \frac{1}{N}\Big\langle \sum_j e^{2\pi ijm/N} d_{xz,A,j}|e\,x| \times \sum e^{2\pi ijn/N}[\alpha_n d_{z^2} - (1-\alpha_n^2)^{1/2} p_{z,C,j}]\Big\rangle. \tag{14}$$

Again, only transitions between states with $m = n$ are allowed. This equation leads to the final expression:

$$\mu_x(n \rightarrow n) = -e\langle d_{xz,A,j}|x|p_{z,C,j}\rangle \times (1-\alpha_n^2)^{1/2}[1 + e^{-2\pi in/N}]. \tag{15}$$

This expression contains a factor dependent on overlap of the d_A- and p_C-orbitals, and a factor in square brackets which describes the variation in intensity across the band. They are expected to be of the same order of magnitude as the overlap terms for $\mu_z(n \rightarrow n)$ in equation (13). The high intensity of the z-polarized intensity then resides in the first term of expression (13) where, although α_n is small, $\alpha_n(c/2)$ is orders of magnitude greater than the integrals involving overlap. This is in essence the same argument utilized by Robin and Day,[43] who used a localized rather than a band description to account for the high intensity of transitions polarized in the stacking (z) direction for mixed-valence compounds, [Pt(II)A_2X_2][Pt(IV)A_2X_4]. In those cases square-planar Pt(II)A_2X_2 complexes stack alternately with octahedral Pt(IV)A_2X_4 complexes. Very intense z-polarized absorption occurs because of mixing of the $d_{z^2,\mathrm{II}}$, $d_{z^2,\mathrm{IV}}$ orbitals whereas dipole-allowed x,y polarization transitions have orders of magnitude lower intensity. This treatment requires that anion $p_{z,A}$-orbitals not be mixed significantly with the $(d_{z^2})_A$–$(p_z)_C$ bands since their presence would enhance the x,y-polarized transitions equally with the z-polarized transition.

One disturbing question is the sharpness of the x,y A → C transfer transition and the high absorption over a wide region in z-polarization in MGS. It is apparent that z-polarized transition "borrow" intensity from the 35,000-cm^{-1} peak and the intensity of the borrowing increases as the distance between transitions decreases. The spin-forbidden $d \rightarrow d$ transitions in the $[Pt(NH_3)_4]^{2+}$ are placed at 35,000 cm^{-1} and with some red shift as occurs in the anion may well be in the vicinity of 30,000 → 32,000 cm^{-1}. Their contribution may broaden the absorption somewhat. It may also be that the reflectance techniques are subject to saturation effects which appear to a broaden a peak so that an accurate picture of the width of the z-polarized absorption is not available.

Spectra of $PtCl_4^{2-}$ *salts*

The shifts of the $d \rightarrow d$ transitions of the other $PtCl_4^{2-}$ salts can be compared with MGS. Although the crystal in Fig. 4 for $Pt(CH_3NH_2)_4PtCl_4$ was too thin for identification of the $^1B_{1g}$-band, the $^1A_{2g}$, ^1E_g and the spin-forbidden band all lie very close to the values in MGS. However, for $Pt(en)_2PtCl_4$ in Fig. 5, the $^1A_{2g}$-band can be assigned from the well-developed vibrational structure which is a maximum on the shoulder at 24,800 cm^{-1}. The peak at 28,00 cm^{-1} is due to the ^1E_g-band that has been shifted only about 2000 cm^{-1} from K_2PtCl_4. Enhancement of intensity in z-polarization is not as great as in MGS, and a peak can be identified at 24,500 cm^{-1} which is assigned to the $^1B_{1g}$-band. Also the spin-forbidden band at 17,000 cm^{-1} has not been shifted as far as with the other two Pt cations. For the Pd salts there is much less intensity enhancement in the z-polarization. For $Pd(NH_3)_4PtCl_4$ in Fig. 6 the x,y peak at 26,000 cm^{-1} is assigned to the ^1E_g-band, and the feeble vibrational structure indicates the $^1A_{2g}$-band is at 25,300 cm^{-1}. The maximum in z-polarization occurs below that in x,y polarization so that the $^1B_{1g}$-band is placed at 25,000 cm^{-1}. For $Pd(en)_2PtCl_4$ in Fig. 7 the $^1A_{2g}$- and ^1E_g-transitions are well resolved in x,y-polarization and the $^1B_{1g}$-transition would be placed at about 26,500 cm^{-1} from the z-polarized absorption of a crystal that was only 15 μm thick. Thus the shift of the spin-allowed d–d bands are perhaps surprisingly similar with the Pt and Pd cations. Although the corresponding Pt and Pd salts give separations that are surprisingly similar, the extension of the d-orbitals in Pd are usually considered considerably less than in Pt. In contrast to the spin-allowed transitions, the shift of the band at 21,000 cm^{-1} in K_2PtCl_4 which we are assigning as spin-forbidden is shifted much less with the Pd cations and appears at 19,600 cm^{-1}.

Spectra for the $PtBr_4^{2-}$ *salts*

The metal–metal separations range from 0.07–0.14 Å higher for the $PtBr_4^{2-}$ salts than with $PtCl_4^{2-}$. For the d–d transitions there is generally a similar but small red shift of the transition energies from K_2PtBr_4 through the salt series. $Pt(NH_3)_4PdBr_4$ in Fig. 8 shows a merged $^1A_{2g}$, ^1E_g peak which requires only a 3300-cm^{-1} shift of the ^1E_g-band from K_2PtBr_4 compared to 4700 cm^{-1} for the Pt–Cl system. The $^1B_{1g}$-band is evident from the z-polarized band. The $Pt(CH_3NH_2)_4PtBr_4$ spectra in Fig. 9 are for a very small thin crystal, and distinct base-line problems are evident. For $Pt(en)_2PtBr_4$ in Fig. 10 there is very little shift of the ^1E_g-band but the z-polarization indicates a distinct shift of 3300 cm^{-1} for the $^1B_{1g}$-band. The spin-forbidden peaks of the $PtBr_4^{2-}$ salts with Pt cations are at very nearly the same wavenumber as for $PtCl_4^{2-}$ which implies

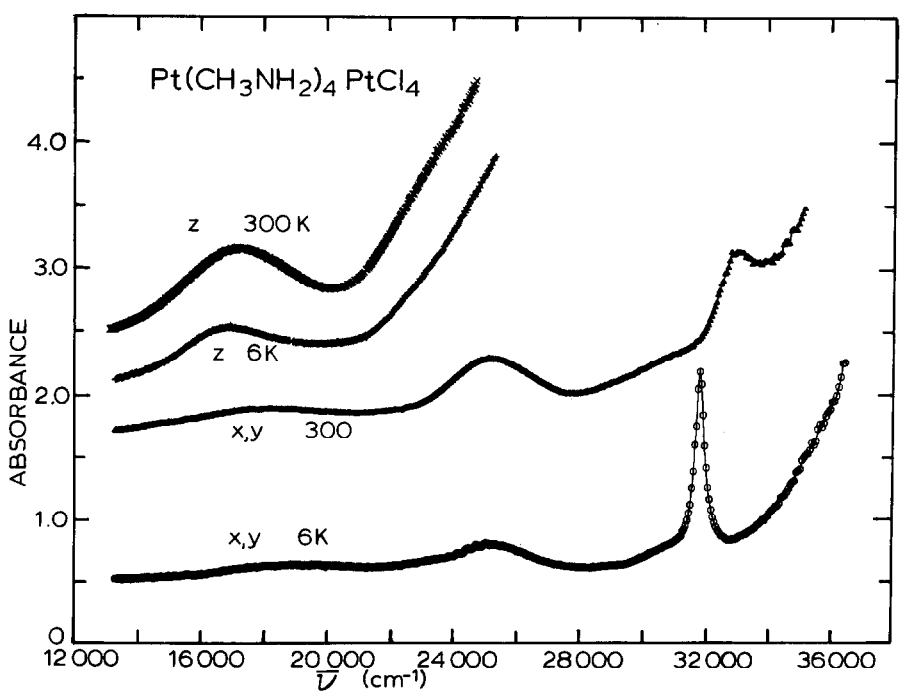

Fig. 4. Polarized spectra for $Pt(CH_3NH_2)_4PtCl_4$ crystal, 6 μm thick.

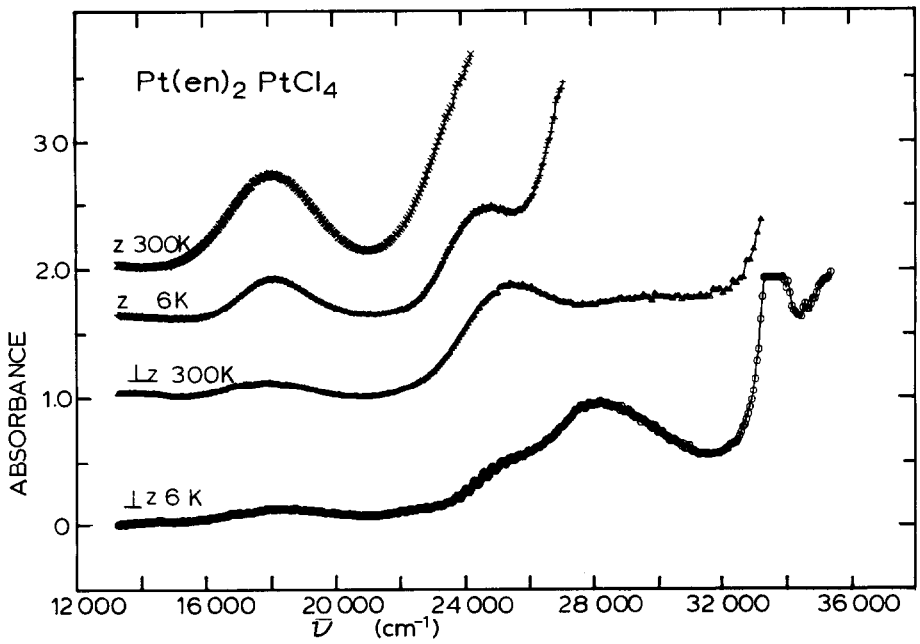

Fig. 5. Polarized single-crystal spectra for $Pt(en)_2PtCl_4$ crystal, 16 μm thick.

that the shifts for the $PtBr_4^{2-}$ transitions are about 2000 cm^{-1} smaller. For $[Pd(NH_3)_4PtBr_4]^{2-}$ (Fig. 11) there appears to be a merged broad peak that contains the $^1A_{2g}$- and ^1E_g-bands. The z-polarized spectrum indicates that the $^1B_{1g}$-transition is very close to the others. For $Pd(en)_2PtBr_4$ in Fig. 12 the appearance of two peaks indicates that the $^1E_{1g}$-band has shifted by no more than 1200 cm^{-1} from K_2PtBr_4 and the z-polarized spectra suggest that the $^1B_{1g}$-band is contained in this band as well. In the Pd salts the one identifiable spin-forbidden band is shifted very little from K_2PtBr_4.

The intense ^1E_u charge-transfer band, at 37,000 cm^{-1} in K_2PtBr_4, conceals any A → C electron-

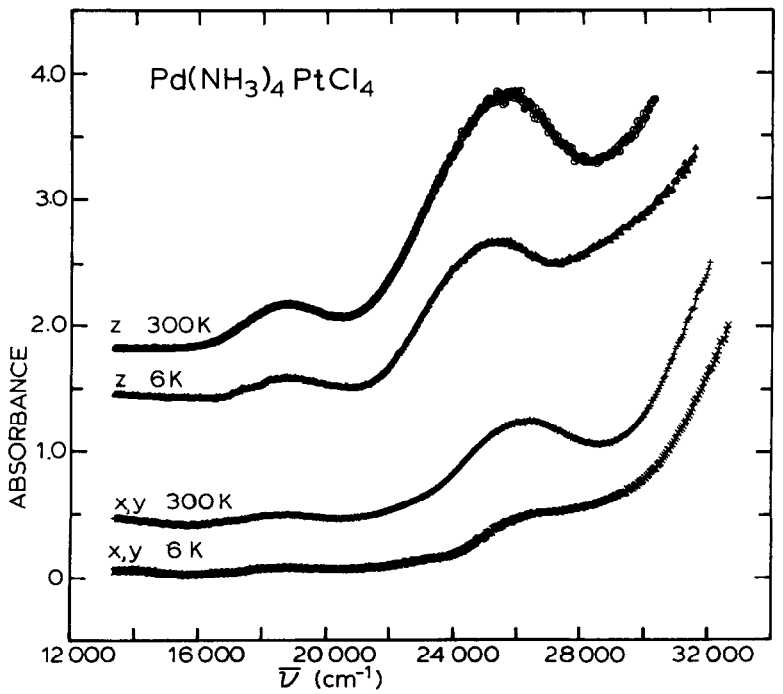

Fig. 6. Polarized spectra for $Pd(NH_3)_4PtCl_4$ crystal, 13 μm thick.

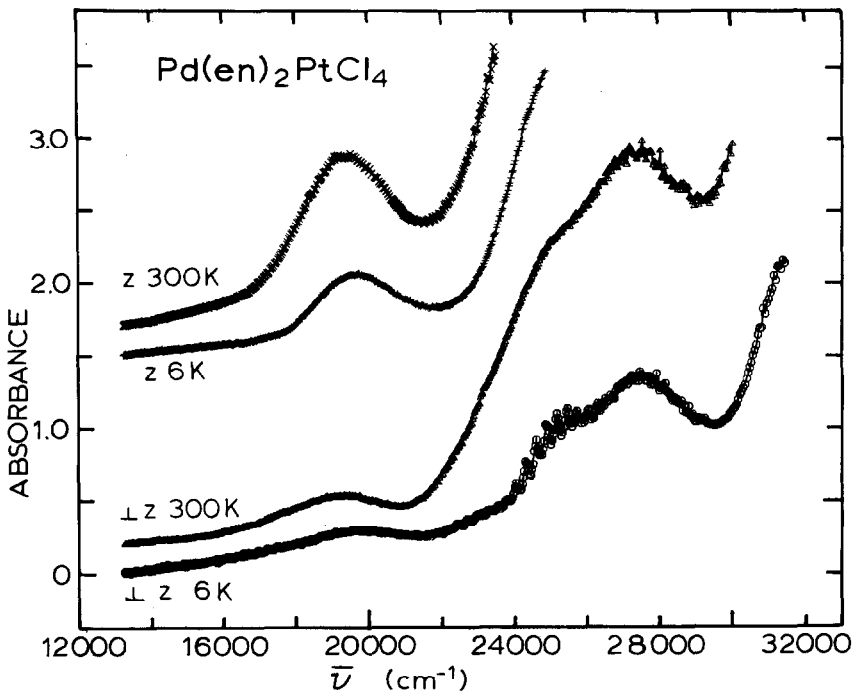

Fig. 7. Polarized spectra for $Pd(en)_2PtCl_4$ crystal, 26 μm thick.

transfer transitions in x,y polarization which might be expected at somewhat higher energies than in $PtCl_4^{2-}$ salts. The z-polarized intensity of the $PtBr_4^{2-}$ salts does not appear to be enhanced as strongly as in the $PtCl_4^{2-}$ salts. In addition, no vibrational structure for the $^1A_{2g}$-band was evident.

Spectra of $PdCl_4^{2-}$ *salts*

For K_2PdCl_4 the $^1A_{2g}$-band exhibits a vibrational structure which is centered at 20,800 cm^{-1}. In the $d \rightarrow d$ transition region the x,y-absorption intensity is significantly greater than the z-absorption inten-

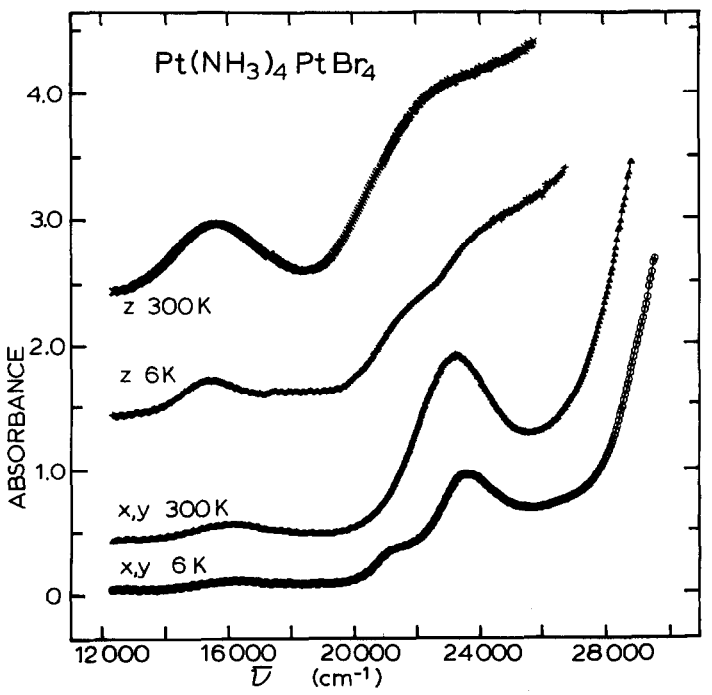

Fig. 8. Polarized spectra for $Pt(NH_3)_4PtBr_4$ crystal, 8 μm thick.

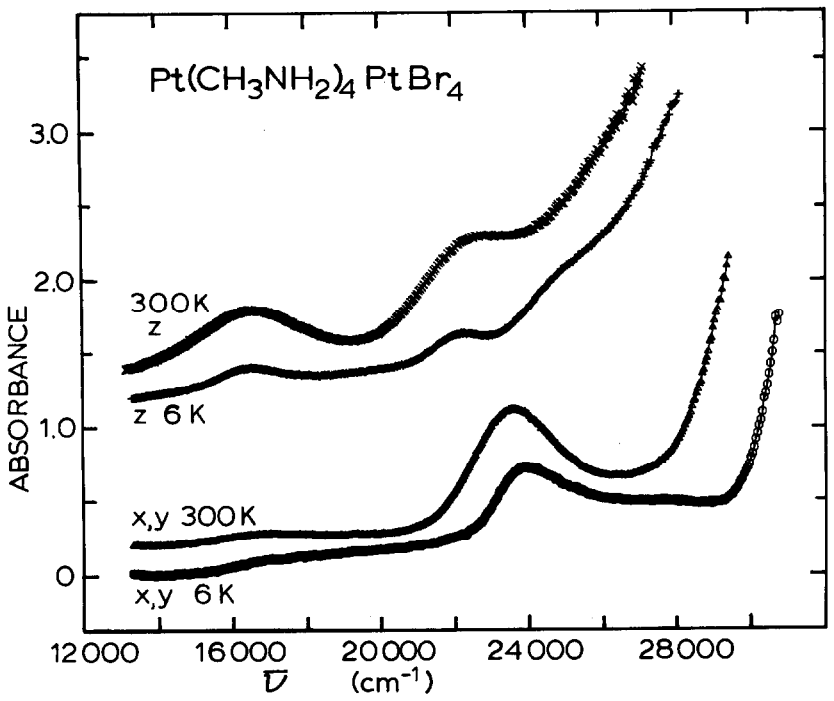

Fig. 9. Polarized spectra for $Pt(CH_3NH_2)_4PtBr_4$ crystal, 4.0 μm thick.

sity. There is only a very low absorption from 24,000 to 30,000 cm^{-1}; consequently the ^1E_g- and $^1B_{1g}$-transitions are assigned at *ca* 22,000 cm^{-1} and are not well resolved from the $^1A_{2g}$-band. All the $PdCl_4^{2-}$ Magnus-type salts show vibrational structure in the x,y or $\perp z$ polarization. The center of this structure is taken as the $^1A_{2g}$-transition energy which ranges only 300–900 cm^{-1} below the K_2PdCl_4 assignment. For $Pt(NH_3)_4PdCl_4$ in Fig. 13 there is some absorption in x,y polarization with no resolvable single peak in the region of 22,000–26,500 cm^{-1}. However, in z-polarization there is a broad-

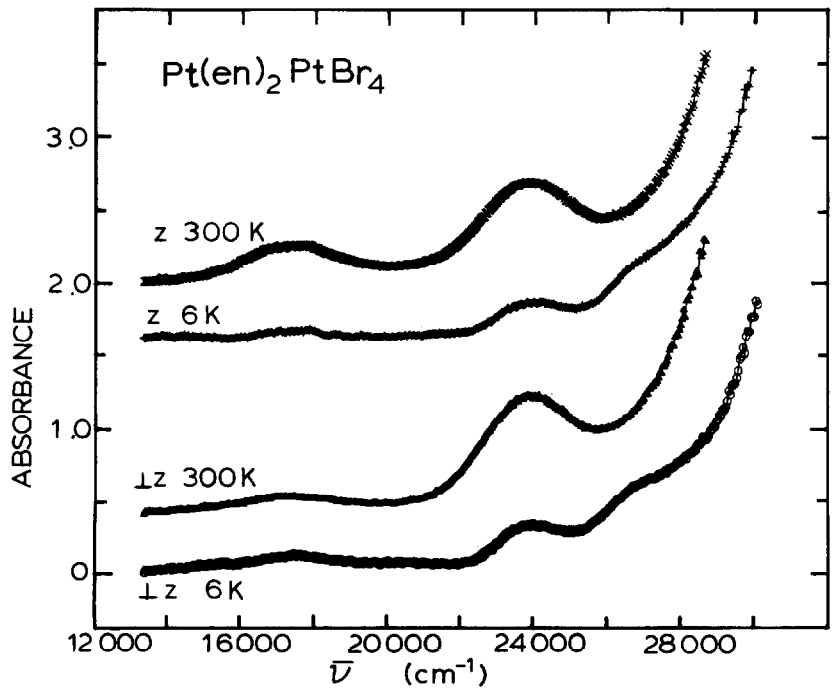

Fig. 10. Polarized spectra for $Pt(en)_2PtBr_4$ crystal, 7 μm thick.

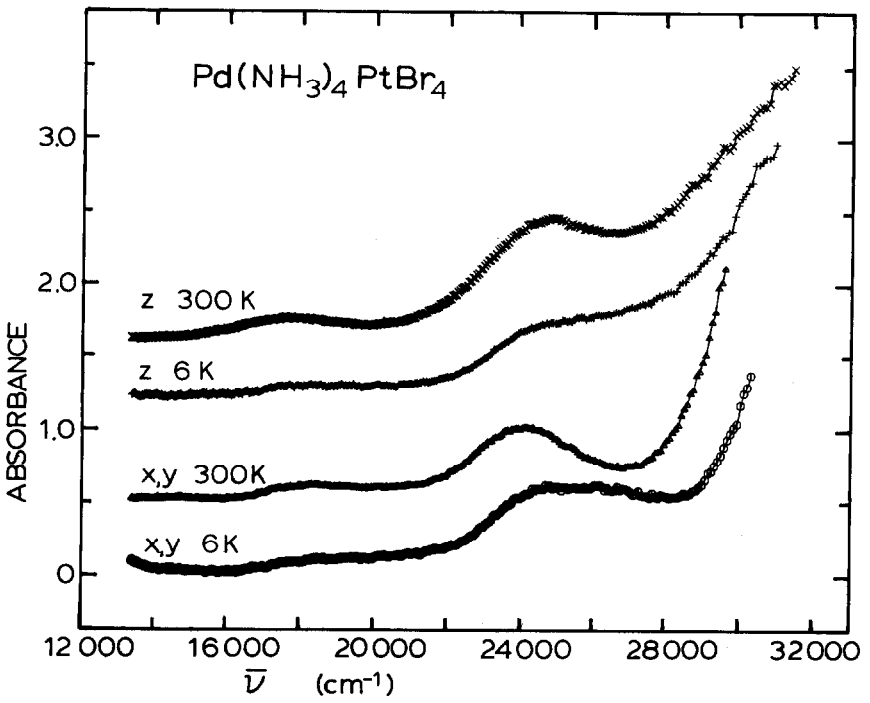

Fig. 11. Polarized spectra for $Pd(NH_3)_4PtBr_4$ crystal, 6 μm thick.

peak maximum at 22,400 cm^{-1} which is more intense than the $^1A_{2g}$-band in x,y polarization. Furthermore, this 22,400-cm^{-1} peak does not decrease in intensity at low temperatures as do the $d \rightarrow d$ transitions. $Pt(CH_3NH_2)_4PdCl_4$ in Fig. 14 shows a similar absorption in this region with the z-polarized peak at 23,000 cm^{-1}. In $Pt(en)_2PdCl_4$ (Fig. 16) the z-polarized peak has moved to still higher energy (25,400 cm^{-1}). In addition, for this salt there is also a well-resolved band in x,y polarization at this energy. There is little absorption from 22,000–25,000 cm^{-1} for the two $PdCl_4^{2-}$ Magnus-type salts

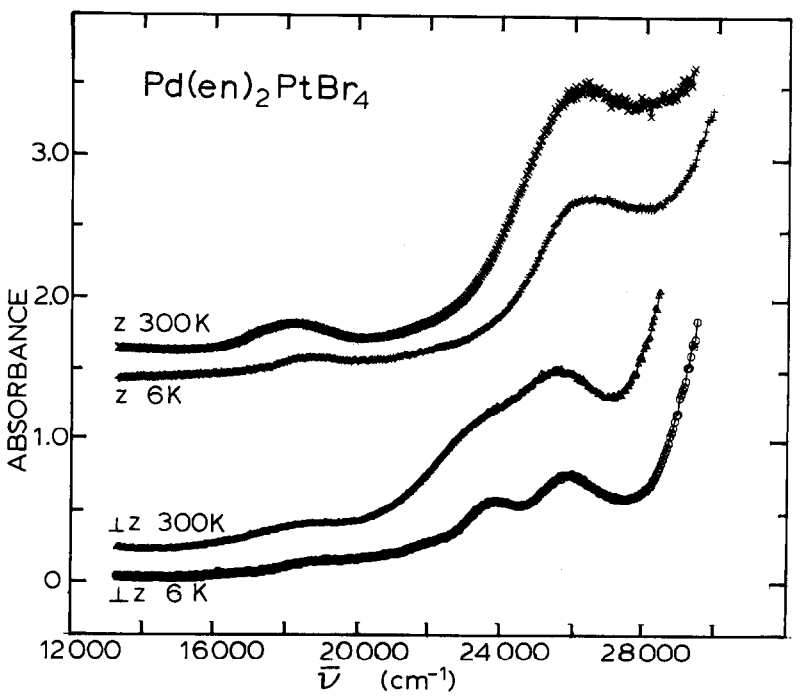

Fig. 12. Polarized spectra for $Pd(en)_2PtBr_4$ crystal, 8 μm thick.

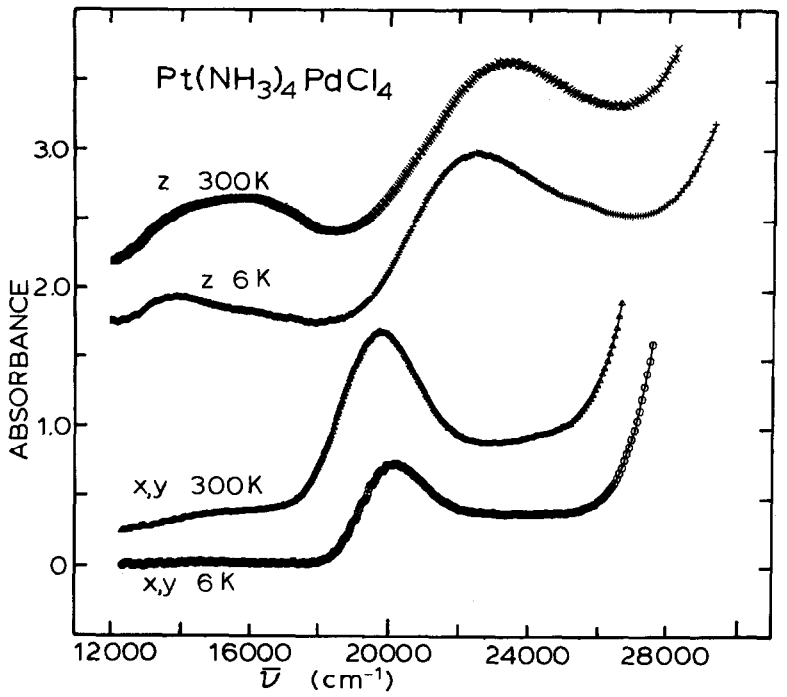

Fig. 13. Polarized spectra for $Pt(NH_3)_4PdCl_4$ crystal, 9 μm thick.

with Pd cations (Figs 17 and 18). We have concluded that the absorption in this region is not due to intraionic $d \rightarrow d$ transitions, but that it must be attributed to some solid-state effects which will be discussed later. In $Pt(NH_3)_4PdCl_4$ there are two components clearly apparent in z-polarizations at energies below the $^1A_{2g}$-transition, viz. at 13,800 and 16,200 cm^{-1}. The peak at 16,200 cm^{-1} is more intense at room temperature than the other but becomes much less intense at 6 K. We assign this

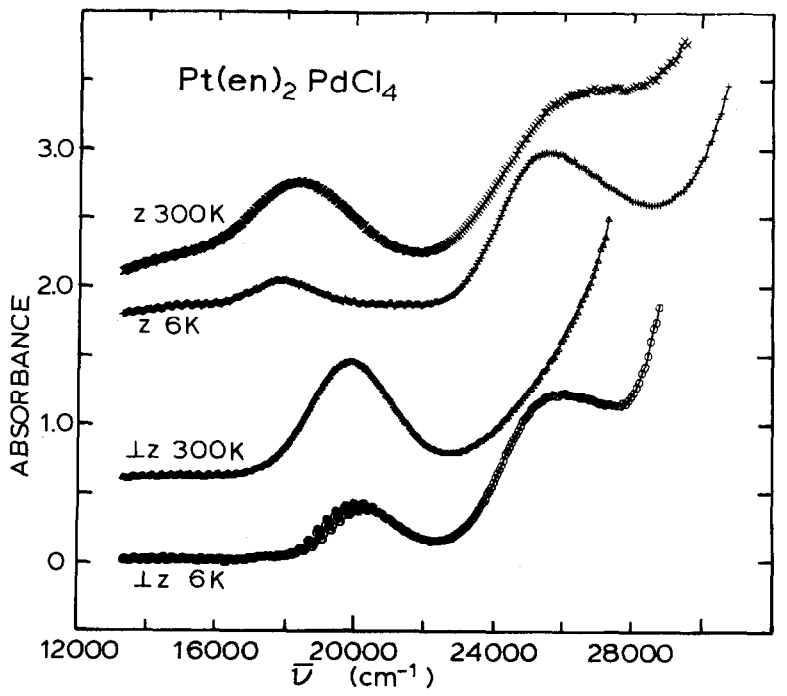

Fig. 14. Polarized spectra for $Pt(en)_2PdCl_4$ crystal, 8 μm thick.

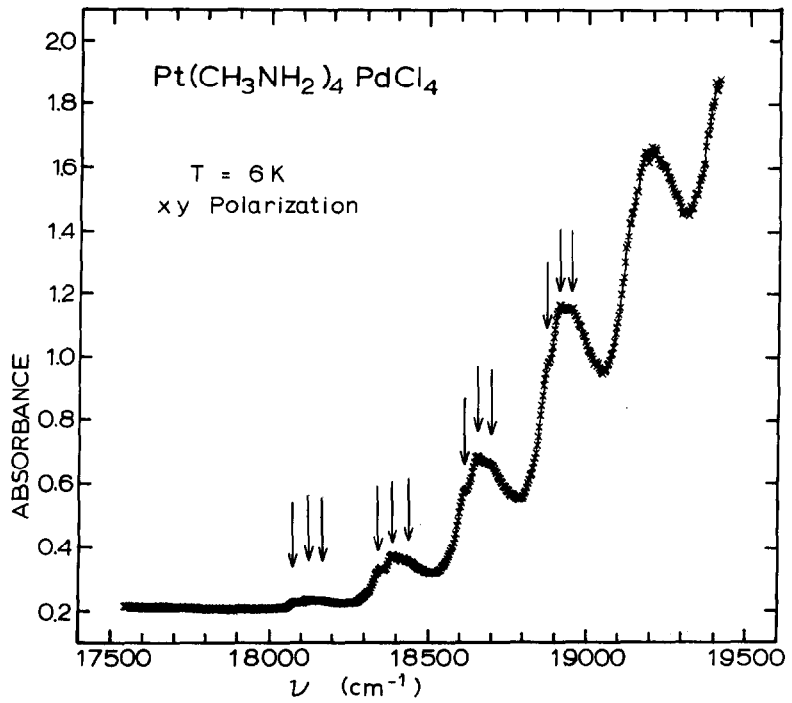

Fig. 15. Spectrum in x,y polarization at 6 K for $Pt(CH_3NH_2)_4PdCl_4$ crystal, 70 μm thick.

16,500-cm^{-1}-transition as $^1B_{1g}$. The z-polarized component of this becomes vibronically allowed by virtue of only a B_{2u} molecular vibration. This vibrational frequency is not accessible in either IR or Raman spectroscopy. However, it is a pure bending mode and is expected to have a lower frequency than a stretching vibration. The temperature dependence of a vibronically enabled transition is expected to increase as the vibrational frequency decreases. Hence, our assignment is based primarily

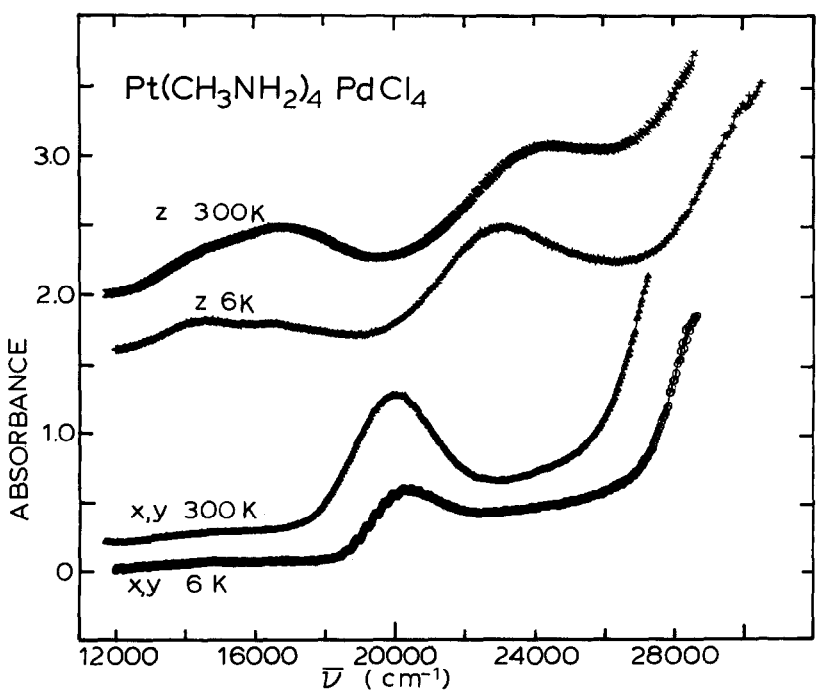

Fig. 16. Polarized spectra for $Pt(CH_3NH_2)_4PdCl_4$ crystal, 11 μm thick.

on this temperature dependence. The 13,800-cm^{-1} component would then be a spin-forbidden band. The assignment of the 16,200-cm^{-1} band as the $^1B_{1g}$-transition appears to be consistent with the theoretical treatment of vibronic intensities of $PdCl_4^{2-}$ by Enry and Moncuit.[44] They predict an oscillator strength ratio $f(z)/f(x, y)$ of 20 for the $^1B_{1g}$-transition of $PdCl_4^{2-}$ with the $^1A_{2g}$-transition in x,y-polarization about 4 times as intense as the z-component of $^1B_{1g}$. However, they placed the $^1B_{1g}$-transition at 30,000 cm^{-1} which would enhance its intensity since at that energy it would be much closer to the allowed transition from which it borrowed intensity.

With $Pt(CH_3NH_2)_4PdCl_4$ the low-energy absorption is very similar to $Pt(NH_3)_4PdCl_4$, and for it the $^1B_{1g}$-band can be placed at 16,800 cm^{-1} and the spin-forbidden band at 14,300 cm^{-1}. With $Pt(en)_2PdCl_4$ in Fig. 16 the $^1B_{1g}$ has not been so strongly red-shifted and a z-polarized band is evident at *ca* 17,800 cm^{-1}. For all of the $PdCl_4^{2-}$ Magnus-type salts with Pt cations the ^1E_g must be placed in the vicinity of the $^1A_{2g}$-band. For the two $PdCl_4^{2-}$ salts with Pd cations, all of the $d \rightarrow d$ transitions must fall under a single band, the transitions appearing somewhat closer together than in K_2PdCl_4.

A number of possibilities were considered for the dipole-allowed bands appearing at 22,000–26,000 cm^{-1} in the $PdCl_4^{2-}$ salts with Pt cations. Could they be spin-forbidden L-πMCT bands that were red-shifted by the proximity of cation neighbors? The $Pd(NH_3)_4PdCl_4$ crystal, whose spectra are shown in Fig. 17, was very thin so the spin-allowed L-πMCT ($b_{2g} \rightarrow b_{1g}^*$) transition can be identified at 34,000 cm^{-1}. This is a red shift of 2900 cm^{-1} from K_2PdCl_4. In this transition the chloride MO is a linear combination of p_z-orbitals with a node in the molecular plane. Electron repulsions with cation electrons might account for the red shift. However, the only spin-forbidden transition which becomes electric dipole allowed by spin–orbit coupling involves transfers from chloride p_x, p_y orbitals which concentrate electron density in the molecular plane so a lower electron repulsion should occur. In the $PdBr_4^{2-}$ salts the repulsion of electrons in the π-orbitals with the neighbors might be expected to be greater, such repulsions together with the lower energy of the LMCT would serve to obscure the $d \rightarrow d$ transitions which clearly does not occur.

It seems necessary therefore to assign these transitions to $A \rightarrow C$ electron transfers and logical assignments must be sought. An assignment of $d_A \rightarrow (p_z)_C$ does not seem likely. First, there is not the high intensity in z-polarization nor the narrow peak in x,y polarization seen for Pt–Pt $A \rightarrow C$ transitions. Besides, Anex[11] and coworkers have seen a high z-intensity at 40,400 cm^{-1} in specular reflectance spectra for $Pt(NH_3)_4PdCl_4$ which they correlated with the $Pt(NH_3)_4PtCl_4$ band at 35,000 cm^{-1}. The possibility of $d_A \rightarrow (d_{x^2-y^2}^*)_C$ was also considered. For a staggered arrangement of metal–ligand bonds, the $(d_{xy})_A$ transition will provide an electric dipole allowed transition. However, in an eclipsed arrangement this transition is forbidden. For $Pt(en)_2PdCl_4$ with very close to anion D_{2h} local symmetry, this transition is forbidden and there seems no way to account for such a strong z-component

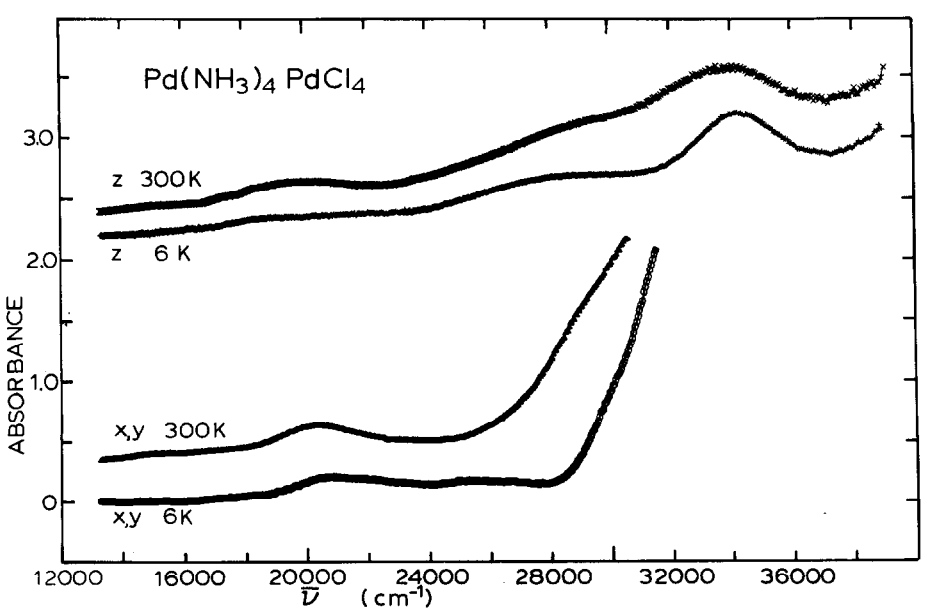

Fig. 17. Polarized spectra for $Pd(NH_3)_4PdCl_4$ crystal, 3.1 μm thick.

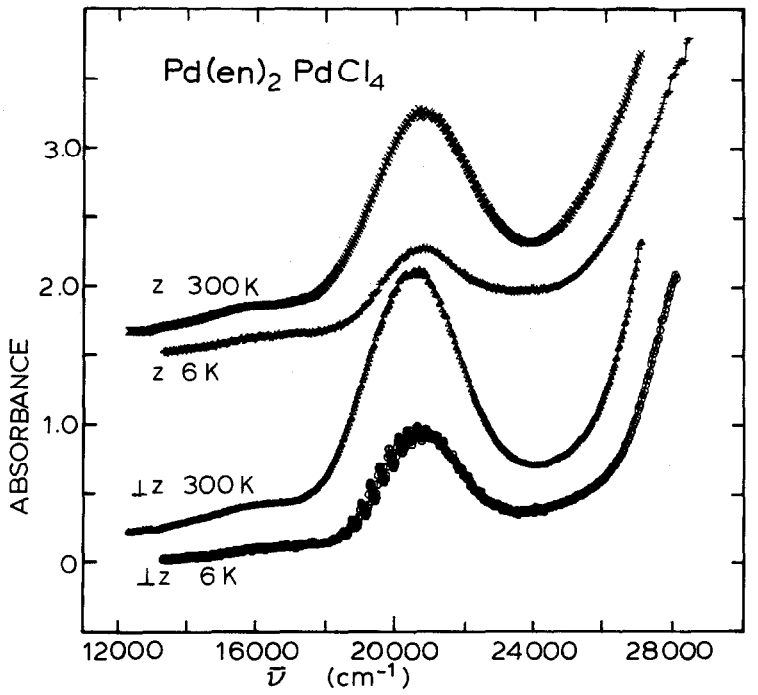

Fig. 18. Polarized spectra for $Pd(en)_2PdCl_4$ crystal, 40 μm thick.

at 25,400 cm^{-1} as an $d_A \rightarrow d_C$ transition. We believe the best assignment to be an $(L\pi)_A \rightarrow [\sigma^*(d_{x^2-y^2})]_C$ transition. There are such transitions with orbital symmetries for an electric dipole allowed character in both polarizations. However, orbital overlap for such transitions would be expected to be very low.

Spectra of $PdBr_4^{2-}$ *salts*

Most $PdBr_4^{2-}$ spectra shown in Figs 19–24 were for such thin crystals that the $^1A_{2u}$ L-πMCT band was evident. It occurred at about the same energy at which it occurs in K_2PdBr_4. As mentioned pre-

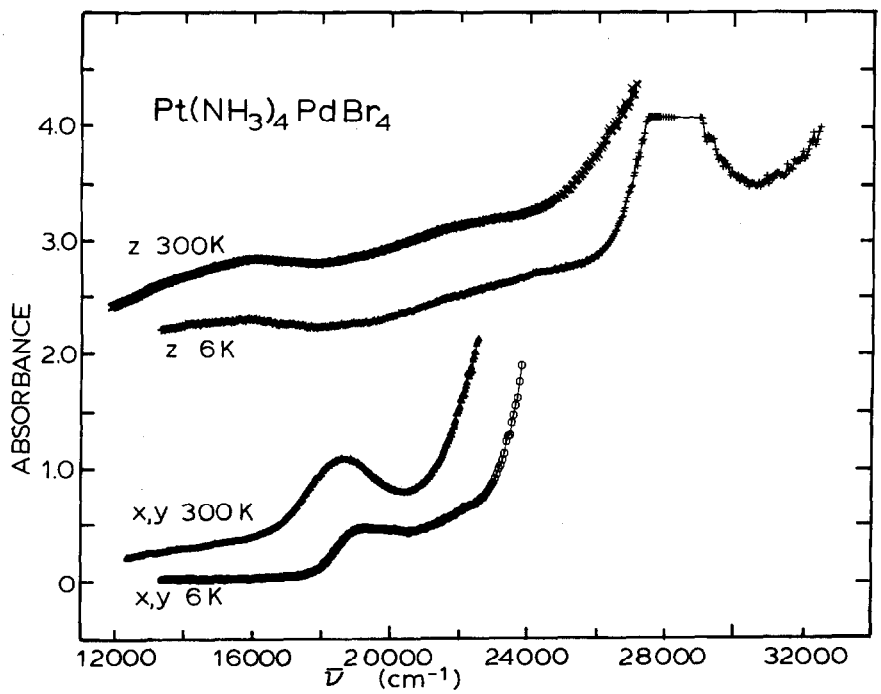

Fig. 19. Polarized spectra for $Pt(NH_3)_4PdBr_4$ crystal, 10 μm thick.

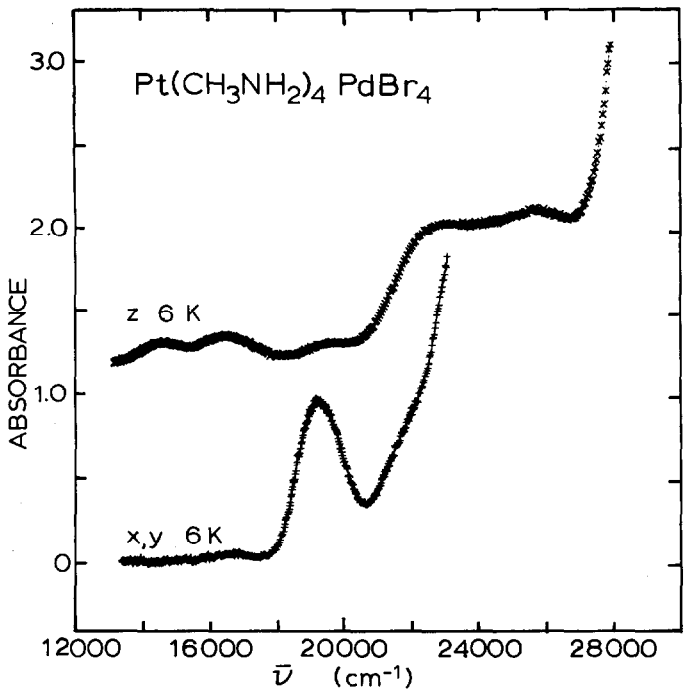

Fig. 20. Polarized spectra for $Pt(CH_3NH_2)_4PdBr_4$ crystal, 13 μm thick.

viously, the truncated ^1E_u L-πMCT band could be observed for the 3-μm crystal to place this transition at *ca* 28,000 cm^{-1}. The proximity of this intense transition enhances x,y intensities among the $d \rightarrow d$ transitions. Each of the $PdBr_4^{2-}$ salts had a moderately strong band with a strong temperature dependence for the intensity in x,y polarization that ranged from 18,700 to 19,200 cm^{-1} which could be associated with the $^1A_{2g}$-transition which is at 20,200 cm^{-1} in K_2PdBr_4. Vibrational structure was not as strongly developed as for the $PdCl_4^{2-}$ salts and indeed was barely evident only in the 13-μm $Pt(CH_3NH_2)_4PdBr_4$. The $^1B_{1g}$-band is generally placed with the z-polarized absorption below the $^1A_{2g}$-region. In the 13-μm $Pt(CH_3NH_2)_4PdBr_4$ crystal (Fig. 20) there are clearly two weak peaks in this region. The $^1B_{1g}$-transition can be associated with the 16,500-cm^{-1} peak which had a higher tem-

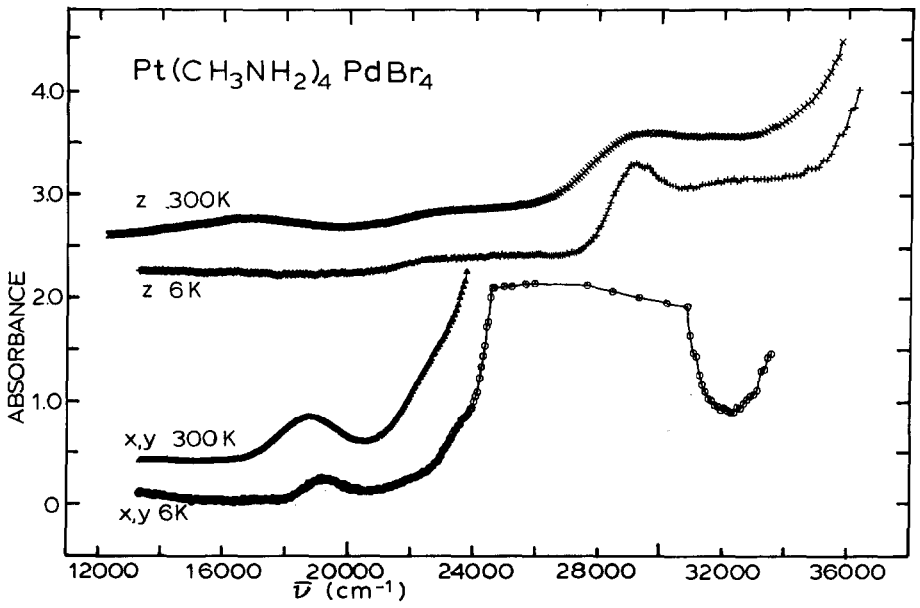

Fig. 21. Polarized spectra for $Pt(CH_3NH_2)_4PdBr_4$ crystal, 3 μm thick.

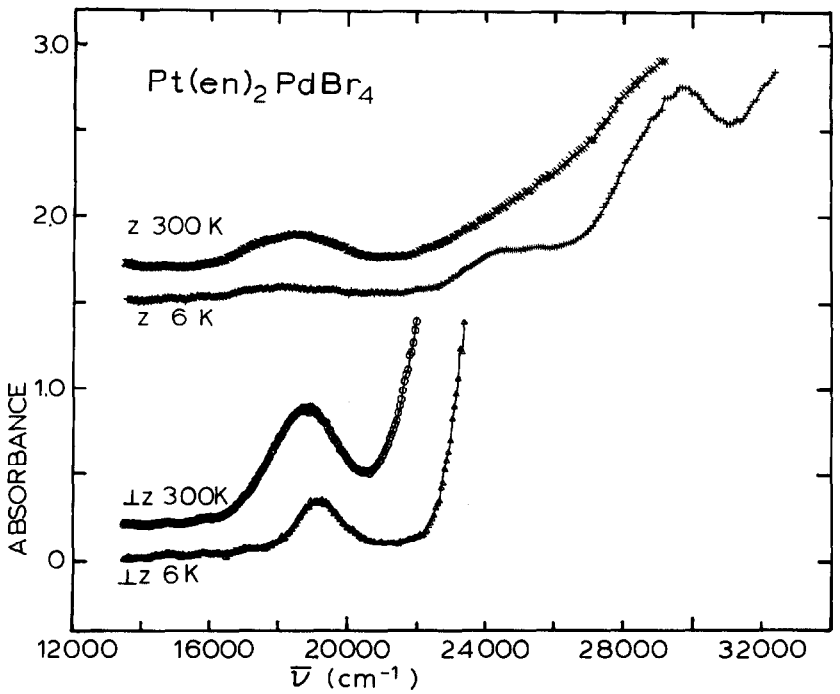

Fig. 22. Polarized spectra for $Pt(en)_2PdBr_4$ crystal, 5 μm thick.

perature dependence, and the 14,500-cm^{-1} band is then a spin-forbidden band. Again, the ^1E_g-transition must be placed close to the $^1A_{2g}$-band. Unfortunately, the relatively low z-polarized absorption does not clearly indicate this transition because of strong x,y enhancement. Absorption above 22,000 cm^{-1} can logically be attributed to molecular L-$\pi \rightarrow$ M charge transfer.

There is no absorption apparent that can be correlated to the $(L\pi)_A \rightarrow [\sigma^*(d_{x^2-y^2})]_C$ bands assigned the $PdCl_4^{2-}$ salts with Pt cations. Since they do involve electron transfers from halides a lower energy might be expected for bromide. However, the increase in interionic spacing will produce a counteracting energy shift and also should serve to reduce the intensity appreciably.

Vibrational structure in the spectra

As was commented earlier, vibrational structure was present in the $^1A_{2g}$-band of the potassium as well as many of the Magnus-type salts of the anions.

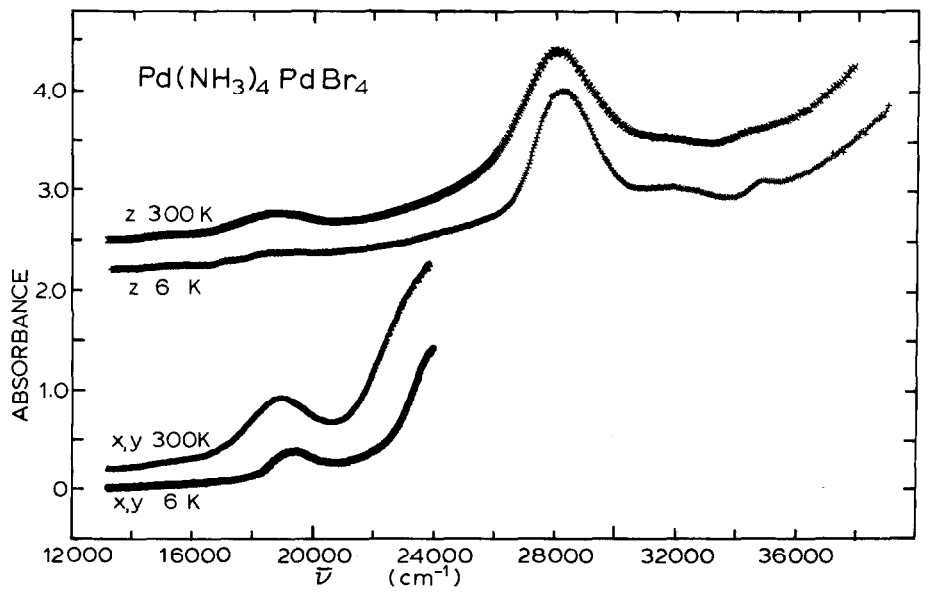

Fig. 23. Polarized spectra for $Pd(NH_3)_4PdBr_4$ crystal, 3.1 μm thick.

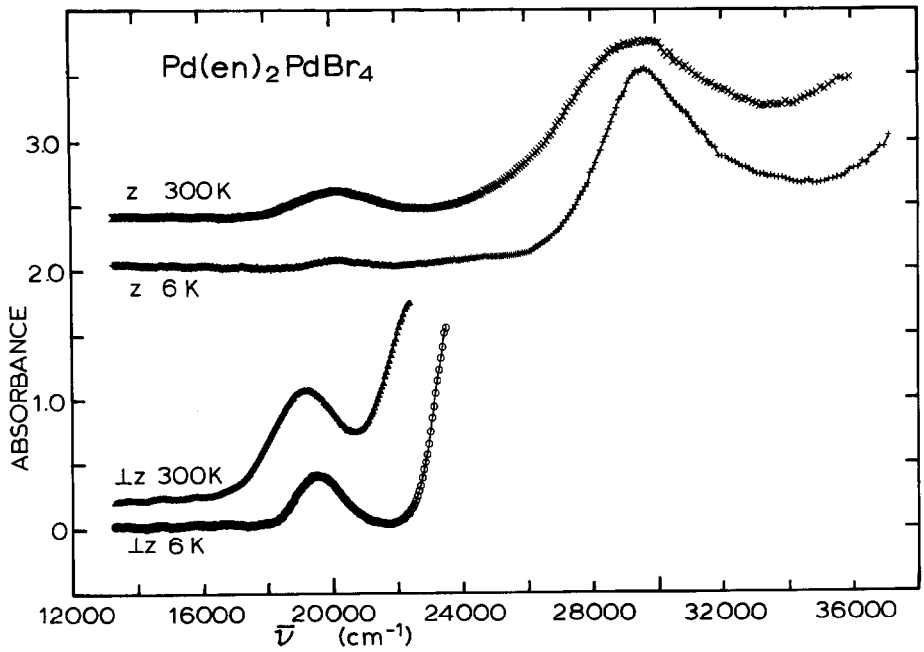

Fig. 24. Polarized spectra for $Pd(en)_2PdBr_4$ crystal, 5 μm thick.

This structure indicated the presence of long Franck–Condon progressions in a totally symmetric vibration of the excited state, which would be the ν_1 stretching vibration for the MX bonds. It is consistent with a relaxation of the bonds in the excited state that would be expected for excitation of an electron into a σ-antibonding orbital. An examination of the spectra in the figures shows that the vibrational structure is generally most highly developed in the ethylenediamine and least developed in the ammonia complex salts. Now vibrational detail will be lost when there are a distribution of sites persisting even at helium temperatures which have transition energies which differ in energy by the order of ν_1. These shifts in transition energies may result from interactions of electrons in the orbitals involved in the transition with neighboring atoms. For the $^1A_{2g}$-transition the two orbitals involved are mostly the d_{xy} and $d_{x^2-y^2}$, concentrated in the plane of the atoms in the ion. Since these two orbitals would be subject less to external influences, it is logical that this transition would have the most highly developed vibrational structure. Rotation of NH_3 groups about the M—N bond can result in site differences being frozen in at low temperatures which compromise the vibrational detail. With the more limited motion imposed by the methyl group in methylamine and especially by the chelate ring with ethylenediamine ligands, the vibrational structure is enhanced. Also the salts with chloride complexes with higher values of ν_1 generally had better developed vibrational structure than those of the bromide complexes.

For cases where five or more vibrational components could be read from the spectra, their wavenumbers were fitted to the component number by linear least squares. The indicated values of $\bar{\nu}_1$ for the $^1A_{2g}$-transition are included in Table 8 together with the indicated standard deviations. Ground state values for $\bar{\nu}_1$, available from the Raman spectra of the potassium salts, are listed in Table 8. The values of $\bar{\nu}_1$ for the excited $^1A_{2g}$-state are quite comparable to those observed in the potassium salts. They are quite generally 12–15% lower than the $\bar{\nu}_1$ for the ground state in the potassium salts. The value for $\bar{\nu}_1$ for the salts with ammonia complexes appear 5–10 cm^{-1} lower than those for salts with methylamine or ethylenediamine complexes. The one exception to this rule may be $Pd(NH_3)_4PdCl_4$; however, the value for this compound does have a large 6-cm^{-1} standard deviation.

For a thick crystal of $Pt(CH_3NH_2)_4PdCl_4$ sufficiently high resolution was attained, as shown in Fig. 15, that clearly each vibrational peak was comprised of three components. This result suggests that three separate vibrations provide vibronic perturbation which induce the necessary transition dipole moment. An E_u vibration symmetry is required for the $^1A_{2g}$-transition and the square-planar ions possess only two E_u-vibrations, ν_6 (an asymmetric stretch) and ν_7 (an in-plane bending mode). From IR spectra these vibrations are set

Table 8. Vibrational structure in Franck–Condon progressions for Magnus-type salts

Compound	$\bar{\nu}^a$ for potassium salts: Ground state Raman spectrum	Excited state
K_2PtCl_4	332[b]	290[c]
K_2PtBr_4	205[b]	170[d]
K_2PdCl_4	307[b]	264[e]
K_2PdBr_4	192[b]	164[e]
	ν_1'[a] for $^1A_{1g} \rightarrow A_{2g}$ transition (x,y or $\perp z$-polarization)	
$Pt(NH_3)_4PtCl_4$	277 (±5)	(6)[f]
$Pt(CH_3NH_2)_4PtCl_4$	283 (±3)	(7)
$Pt(en)_2PtCl_4$	281 (±1)	(9)
$Pd(en)_2PtCl_4$	278 (±2)	(11)
$Pt(en)_2PtBr_4$	176 (±3)	(7)
$Pd(en)_2PtBr_4$	172 (±3)	(9)
$Pt(NH_3)PdCl_4$	255 (±2)	(11)
$Pt(CH_3NH_2)_4PdCl_4$	265 (±2)	(13)
$Pt(en)_2PdCl_4$	260 (±1)	(14)
$Pd(NH_3)_4PdCl_4$	262 (±6)	(6)
$Pd(en)_2PdCl_4$	262 (±2)	(15)
$Pt(CH_3NH_2)_4PdBr_4$	170 (±6)	(5)
$Pt(en)_2PdBr_4$	172 (±2)	(5)
$Pd(NH_3)_4PdBr_4$	160 (±2)	(7)
$Pd(en)_2PdBr_4$	172 (±3)	(8)
Triplet bands		
$Pd(en)_2PdCl_4$ (z-polarization 14,793–17,391)	260 (±1)	(11)
(x,y polarization 14,174–15,798)	268 (±4)	(7)
$Pt(en)_2PtCl_4$ ($\perp z$ polarization 21,940–23,370)	286 (±2)	(6)

[a] $\bar{\nu}_1$ in cm^{-1}.
[b] Reference 45.
[c] Reference 46.
[d] Reference 15.
[e] Reference 16.
[f] Values in parentheses indicate the number of components in least-squares analysis.

at 335 and 195 cm^{-1}, respectively.[47] It is logical to assign the largest, central component of each peak to the ν_6 stretching vibration $+n\bar{\nu}_1$ vibrations in the Franck–Condon progressions. The second strongest component in each peak is the lowest member that occurs only *ca* 40 cm^{-1} below the ν_6-peak. We would assign this to the ν_7 bending vibration. The weakest feature is quite broad and seems likely due to a lattice or phonon band. Thus in a peak the component would be assigned $\nu_L+(n+1)\nu_1$. This means there would be such a component too weak to be observed below the first peak. The indicated separation of the bending and stretching component of only 40 cm^{-1} is very low in view of the difference of 140 cm^{-1} for ν_6–ν_7 in the ground state from IR spectra. Harrison *et al.*[48] observed a similar arrangement of components in the $^1A_{2g}$-absorption for $PdCl_4^{2-}$ in a Cs_2HfCl_6 host crystal with somewhat greater resolution. In that case the bending, ν_7, components was 70 cm^{-1} below the stretching, ν_6, components. Since the A_{1g} stretching vibration for the $^1A_{2g}$-state is only 44 cm^{-1} lower than in the ground state, it probably indicates that some feature in the ion packing of $Pt(CH_3NH_2)_4PdCl_4$, perhaps hydrogen bonding between Cl and N atoms, serves to raise the bending vibration frequency for ν_7.

For a very thick crystal of $Pd(en)_2PdCl_4$ (105 μm), vibrational structure was resolved for separate low-energy triplet bands in z- as well as x,y polarization. The indicated A_{1g} vibrational frequencies, given in Table 8, were not within the statistical uncertainty different from those for the $^1A_{2g}$ band.

Finally, vibrational structure appears in x,y polarization on a weak component which is below the $^1A_{2g}$-band and the assigned $^1B_{1g}$-peak seen in z-polarization of $Pt(en)_2PtCl_4$, which must be for one of the triplet bands, largely ^3E_u. The indicated A_{1g}-frequency, given in Table 8 is about 5 cm^{-1} higher than for the $^1A_{2g}$-band.

SUMMARY

The collection of single-crystal absorption spectra that are now available permit some important conclusions about this interesting class of compounds. First of all, the planar nature of the ions provides a close contact of the metal atoms as these alternating cations and anions stack in one-dimensional arrays. There is some orbital overlap between the metal atoms in the cations and anions. However, there appears to be negligible covalent bonding or delocalization as occurs in the mixed-valence chains with the planar $Pt(CN)_4$ groups, which have much smaller Pt—Pt distances and metallic conductivity. There is, however, sufficient overlap with the 3.25–3.5-Å metal spacing to permit interionic electron-transfer transitions and these account for a higher absorption of polarized light with the electric vector oriented in stacking direction that has been recognized as a characteristic of a number of these compounds. It is especially important to this assignment that the expected interionic electron transfer with polarization normal to the stacking direction can now be identified in some of the cases.

The energies of a number of *d–d* transitions for the anions are highly sensitive to differences in the metal–metal spacings in the region of 3.25–3.6 Å. These differences in the band frequencies account for the anomalous colors which have drawn attention to these compounds. Controversy over where to place the d_{z^2}-orbital with respect to the other *d*-orbitals has simmered for the past 25 years. Our results provide, we believe, good but perhaps not overwhelming evidence for placing the d_{z^2} and the $d_{xz,yz}$ pair close together in the free MX_4^{2-} ion so the $^1B_{1g}$- and ^1E_g-bands are not resolved in aqueous solution or in the potassium salts. One general conclusion is that the valence shell orbitals of Pd are more compact than the corresponding orbitals of Pt. Thus the Pt cations gave greater shifts of aborption bands and higher interionic electron transfer probabilities for a given anion. The results were also consistent with a much lower $d \rightarrow p$ excitation energy for Pt compared to Pd.

Finally, we believe that the earlier assignment of intermolecular electron-transfer transitions for the molecular compounds of $Pt(en)Cl_2$ and $Pt(en)Br_2$ should be reconsidered.[49,50] These nearly planar molecules stack face to face in one-dimensional arrays in orthorhombic crystals. Metal–metal spacings are 3.39 and 3.50 Å, respectively. Both have an intense absorption band polarized in the stacking direction. Polarized reflectance spectroscopy by Anex and Peltier[51] places the peak at 35,100 cm^{-1}. Diffuse-reflectance spectra on the other hand showed maxima at 37,500 and 36,700 cm^{-1}, respectively, for the chloride and bromide compounds. Thus they each have a strong band similar to those in the $PtCl_4^{2-}$ and $PtBr_4^{2-}$ Magnus-type salts. In view of the present work, it appears logical now to assign this transition as an intermolecular $d_{z^2} \rightarrow p_z$ electron transfer rather than as the red-shifted intramolecular $d_{z^2} \rightarrow p_z$ originally proposed. Although the neutral molecules would be expected to have greater ionization energy and electron affinity than the anion and cation, the formation of an ion-pair would greatly increase the lattice energy. The narrow band, indicated to arise from a dipole-allowed transition, polarized normal to the stacking direction at 33,100 and 33,500 cm^{-1} for the chloride and bromide would then correspond to intermolecular $d_{yz} \rightarrow p_z$ electron transfer rather than the intermolecular $d_{yz} \rightarrow d^*_{xy}$ transition proposed. (In this case the axes were selected so that the d_{xy} was the *d*-orbital involved in the σ-bonds to the ligands[50].) This transition occurred among the normal intramolecular $d \rightarrow d$ transitions. Although for these crystals the metal–metal distances permitted the intermolecular electron transfer transitions, they were sufficiently large that no significant red shift of the spin-forbidden *d–d* bands occurred as in the case of many of the Magnus-type salts with ethylenediamine cations.

Acknowledgements—We acknowledge the assistance of Professor R. A. Jacobson who made available the X-ray diffraction equipment in the crystal structure determination. The authors are grateful for the support of this work under the NSF grants CHE 76-83665 and CHE 80-007442.

REFERENCES

1. From the dissertation submitted in partial fulfillment of the requirements for the Ph.D. degree, Iowa State University (1984).
2. G. Magnus, *Ann. Phys. Chem. J. C. Poggendorf* 1828, **14**, 242.
3. E. G. Cox, *J. Chem. Soc.* 1932, 1912.
4. M. Atoji, J. W. Richardson and R. E. Rundle, *J. Am. Chem. Soc.* 1957, **79**, 3017.
5. S. Yamada, *J. Am. Chem. Soc.* 1951, **73**, 1579.
6. P. Day, A. F. Orchard, A. J. Thomson and R. J. P. Williams, *J. Chem. Phys.* 1965, **42**, 1973.
7. P. Day, A. F. Orchard, A. V. Thomson and R. J. P. Williams, *J. Chem. Phys.* 1965, **42**, 3763.
8. D. S. Martin, Jr, R. M. Rush, R. J. Kroening and P. E. Fanwick, *Inorg. Chem.* 1972, **12**, 301.
9. J. R. Miller, *J. Chem. Soc.* 1965, 715.
10. B. G. Anex, M. E. Ross and M. W. Hedgcock, *J. Chem. Phys.* 1967, **46**, 1090.
11. B. G. Anex, S. I. Foster and F. Fucaloro, *Chem. Phys. Lett.* 1973, **18**, 126.
12. J. R. Miller, *J. Chem. Soc.* 1961, 4452.
13. P. Day, *Inorg. Chim. Acta, Rev.* 1969, **3**, 81.
14. C. I. Sanders and D. S. Martin, Jr, *J. Am. Chem. Soc.* 1961, **83**, 807.
15. R. F. Kroening, R. M. Rush, D. S. Martin, Jr and J. C. Clardy, *Inorg. Chem.* 1974, **13**, 1366.
16. R. M. Rush, D. S. Martin, Jr and R. G. LeGrand, *Inorg. Chem.* 1975, **14**, 2543.
17. R. A. Jacobson. *An Algorithm for Automatic Indexing on Bravais Lattice Selection. Programs BLIND and ALICE.* Report IS-3469, Ames Laboratory, USAEC, Iowa State University, Ames, IA (1974).
18. F. Takusagawa, unpublished results from Ames Laboratory of the U.S.D.O.E., Iowa State University, Ames, IA.
19. R. L. Lapp and R. A. Jacobson, *FOUR: A Generallized Crystallographic Fourier Program.* Ames Laboratory, U.S.D.O.E., Report IS-4737, Iowa State University, Ames, IA (1980).
20. D. S. Martin, *Inorg. Chim. Acta, Rev.* 1971, **5**, 107.
21. P. E. Fanwick, D. S. Martin, T. R. Webb, G. A. Robbins and R. A. Newman, *Inorg. Chem.* 1978, **17**, 2723.
22. D. Paponsek and J. Pliva, *Collect. Czech. Chem. Commun.* 1965, **30**, 3007.
23. R. H. Mais, P. G. Owston and A. M. Wood, *Acta Cryst.* 1972, **B28**, 393.

24. D. S. Martin, Jr, J. L. Bonte, R. M. Rush and R. A. Jacobson, *Acta Cryst.* 1975, **B31**, 2538.
25. C. K. Jørgensen, *Prog. Inorg. Chem.* 1970, **12**, 130.
26. B. G. Anex and N. Takeuchi, *J. Am. Chem. Soc.* 1974, **96**, 4411.
27. H. Isci and W. R. Mason, *Inorg. Chem.* 1984, **23**, 1565.
28. D. S. Martin, Jr, J. G. Foss, M. E. McCarville, M. A. Tucker and A. J. Kassman, *Inorg. Chem.* 1966, **5**, 491.
29. A. J. McCaffery, P. N. Schatz and P. J. Stephens, *J. Am. Chem. Soc.* 1968, **90**, 5730.
30. J. Chatt, G. A. Gamlen and L. E. Orgel, *J. Chem. Soc.* 1958, 486.
31. C. K. Jørgensen, *Adv. Chem. Phys.* 1963, **5**, 33.
32. H. Basch and H. B. Gray, *Inorg. Chem.* 1967, **6**, 365.
33. F. A. Cotton and C. B. Harris, *Inorg. Chem.* 1967, **6**, 369.
34. D. S. Martin and C. A. Lenhardt, *Inorg. Chem.* 1964, **3**, 1368.
35. D. S. Martin, Jr, M. A. Tucker and A. J. Kassman, *Inorg. Chem.* 1966, **5**, 1298.
36. L. I. Elding and L. F. Olsson, *J. Phys. Chem.* 1978, **82**, 69.
37. W. Tuszynski and G. Gliemann, *Z. Naturforsch.* 1979, **34A**, 211.
38. E. Franke and C. Moncuit, *C. R. Acad. Sci., Ser. B* 1970, **271**, 741.
39. H. Isci and W. R. Mason, *Inorg. Nucl. Chem. Lett.* 1972, **8**, 885.
40. T. J. Peters, R. F. Kroening and D. S. Martin, *Inorg. Chem.* 1978, **17**, 2302.
41. C. Moncuit, *Theor. Chim. Acta* 1975, **39**, 255.
42. D. P. Craig and S. H. Walmsley, *Excitons in Molecular Crystals*, Chap. 3. W. A. Benjamin, New York (1968).
43. M. B. Robin and P. Day, *Adv. Inorg. Chem. Radiochem.* 1967, **10**, 247.
44. M. Erny and C. Moncuit, *Theor. Chim. Acta* 1982, **61**, 29.
45. P. J. Hendra, *J. Chem. Soc. A* 1967, 1298.
46. D. S. Martin, M. A. Tucker and A. J. Kassman, *Inorg. Chem.* 1965, **4**, 1682.
47. D. M. Adams and R. W. Berg, *J. Chem. Soc., Dalton Trans.* 1976, 52.
48. T. G. Harrison, H. H. Patterson and J. J. Godfrey, *Inorg. Chem.* 1976, **15**, 1291.
49. D. S. Martin, L. D. Hunter, R. Kroening and R. F. Coley, *J. Am. Chem. Soc.* 1971, **93**, 5433.
50. R. F. Kroening, L. D. Hunter, R. M. Rush, J. C. Clardy and D. S. Martin, *J. Phys. Chem.* 1973, **77**, 3077.
51. B. G. Anex and W. P. Peltier, *Inorg. Chem.* 1983, **22**, 643.

Polyhedron Vol. 6, No. 2, pp. 255–259, 1987
Printed in Great Britain

0277–5387/87 $3.00+.00

^{95}Mo AND ^{183}W NMR STUDIES OF TRIPLY BONDED DINUCLEAR M(III) AND RELATED M≡C (M = Mo OR W) COMPLEXES

CHARLES G. YOUNG, EDWARD M. KOBER and JOHN H. ENEMARK*

Department of Chemistry, University of Arizona, Tucson, AZ 85721, U.S.A.

(*Received* 27 *May* 1986; *accepted* 4 *June* 1986)

Abstract—^{95}Mo and ^{183}W NMR data are reported for a series of dinuclear triply bonded M(III) (M = Mo or W unless specified) and related $[M{\equiv}CR]^{3+}$ complexes. Complexes of general formulae M_2L_6 (L = $[OCMe_3]^-$ or $[NMe_2]^-$; M = Mo, L = $[CH_2CMe_3]^-$, $[CH_2SiMe_3]^-$, $[OCH_2CMe_3]^-$ or $[OCHMe_2]^-$) and $M_2(OCHMe_2)_6L_2$ (L = C_5H_5N, $\frac{1}{2}Me_2PCH_2CH_2PMe_2$ or $\frac{1}{2}MeNHCH_2CH_2NHMe$) exhibit very deshielded resonances in the δ-2430–3695 (M = Mo) and δ-4196–4736 (M = W) regions. The novel $M_2(O_2CMe)_4(CH_2CMe_3)_2$ complexes exhibit resonances which are shielded relative to the above complexes and related $M_2(O_2CR)_4$ complexes. The $M(CXMe_3)(CH_2XMe_3)_3$ (X = C or Si) complexes, which contain formal M≡C triple bonds, exhibit resonances at δ 1400 and 1845 (M = Mo), and δ 2867 and 3613 (M = W), respectively. The tungsten alkylidyne complexes exhibit septet ^{183}W resonances due to coupling of ^{183}W and $CH_2XMe_3^-$ protons ($^2J_{W-H}$ = 10.5 Hz). The magnitude of the nuclear shielding in these related species increases in the order: $[M{\equiv}M]^{4+}$ $(\sigma^2\pi^4\delta^2)$ < $[M{\equiv}M]^{6+}$ $(\sigma^2\pi^4)$ < $[M{\equiv}M]^{6+}$ $(\pi^4\delta^2)$ ~ $[M{\equiv}C]^{3+}$ < $[M{\equiv}N]^{3+}$. The nuclear deshielding appears to be related to the extreme covalency of the multiple bond in which the metals are involved.

Metal NMR has developed into a powerful probe of the solution structure, reactivity and dynamics of coordination and organometallic compounds. In particular, ^{95}Mo and ^{183}W NMR spectroscopies have experienced sustained development since the first solution studies were reported 10 years ago.[1] Molybdenum complexes of oxidation states 0–VI have now been characterized by ^{95}Mo NMR, and ^{183}W NMR has been applied to tungsten complexes of oxidation states 0, II and VI.[2] While mononuclear complexes of M(0), M(II), M(IV) and M(VI) (M = Mo or W hereafter) generally possess the diamagnetism necessary for NMR observation, the study of M(V), M(III) and M(I) complexes by NMR is restricted to dinuclear or otherwise spin-paired complexes. Interestingly, dinuclear complexes possessing direct metal–metal bonds exhibit unique ^{95}Mo and ^{183}W NMR properties. Quadruply bonded $[M{\equiv}M]^{4+}$ complexes, for example, exhibit the most deshielded resonances known (δ 3225–4150 for Mo,[3,4] and δ 6760 for W[5]). In contrast, mononuclear M(II) complexes exhibit resonances at the other extreme of the chemical-shift range (δ 50 to −2075 for Mo, and δ −2400 to −4037 for W[2]).

The origin of the extreme deshielding in the $[M{\equiv}M]^{4+}$ complexes is unclear. In order to better understand such phenomena we have investigated the metal NMR properties of other complexes containing metal–metal bonds. Here, we report ^{95}Mo and ^{183}W NMR data for a series of dinuclear triply bonded Mo(III) complexes (**A** and **B**), several of their *N*- and *P*-donor ligand adducts (**C**), and related complexes containing triply bonded M≡C fragments (**D** and **E**). This work represents the first study of such complexes by ^{95}Mo and ^{183}W NMR spectroscopies, and provides a basis for the routine characterization of such species by these NMR techniques. A preliminary account of the ^{95}Mo NMR spectra of the $[M{\equiv}Mo]^{6+}$ complexes has appeared.[6]

* Author to whom correspondence should be addressed.

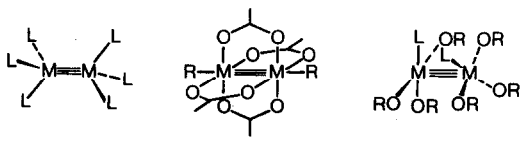

A B C

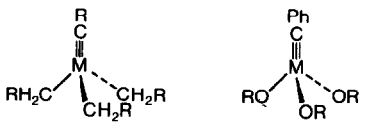

D E

EXPERIMENTAL

The compounds M_2L_6 (L = alkyl,[7,8] alkoxide[9,10] or amide[11,12]), $M_2(O_2CMe)_4(CH_2CMe_3)_2$,[13] $M(CXMe_3)_3(CH_2XMe_3)_3$ (X = C or Si[14–16]), and $W(CPh)(OCMe_3)_3$,[17] were prepared according to published procedures or adaptions thereof. The $M_2(OCHMe_2)_6L_2$ (L = py, ½dmpe or ½Me_2en[10,18]) were prepared *in situ* from $M_2(NMe_2)_6$, $HOCHMe_2$ and L.* The NMR samples were prepared under anaerobic conditions using dried and deoxygenated solvents.

The NMR spectra were recorded on a Bruker WM250 NMR spectrometer. The ^{95}Mo NMR spectra were measured with a 10-mm molybdenum probe (16.3-MHz). To reduce the effects of probe ringing a Doty Scientific duplexer and preamplifier with a 16-MHz center was inserted between the probe and the Bruker broadband preamplifier. The duplexer was gated off during the pulse and 5 μs after the pulse. With this arrangement the preacquisition delay was reduced to 100 μs. The transmitter output was amplified with a Heathkit SB-201 (1-kW) linear amplifier. The input was attenuated to give a 26-μs 90° pulse. A 2 M $Na_2[MoO_4]$ solution in D_2O, effective pH 11, was used as the external standard. Spectra were run unlocked; no drift of the spectrometer was detected when the external standard was measured between samples. Typically 10^4–10^5 transients were accumulated.

The ^{183}W NMR spectra were measured at 10.28 MHz using a 10-mm broadband (7.6–31.2-MHz) probe. The duplexer and preamplifier described above was inserted between the probe and the broadband preamplifier to reduce the effects of probe ringing. A preacquisition delay of 320 μs was employed. The transmitter output was amplified as described above and the input was attenuated to give a 90-μs 90° pulse. A 40-μs pulse was employed in data acquisition and the spectrometer was locked on the deuterium signal of C_6D_6. The ^{183}W chemical shifts were referenced to an external standard of 2 M $Na_2[WO_4]$ in D_2O, effective pH 11.

RESULTS AND DISCUSSION

Dinuclear triply metal–metal-bonded complexes of type Mo_2L_6 (L = $[CH_2CMe_3]^-$, $[CH_2SiM_3]^-$, $[OCMe_3]^-$, $[OCH_2CMe_3]^-$, $[OCHMe_2]^-$ or $[NMe_2]^-$) exhibit ^{95}Mo NMR resonances over the chemical-shift range δ 2430–3695, a deshielded portion of the known chemical-shift range.[2] The shielding of the ^{95}Mo nuclei in these complexes increases in the order: alkyl < 3° alkoxide < 2° and 1° alkoxide < dialkylamide. The resonances are not as deshielded as those of quadruply bonded Mo(II) complexes,[3,4] but their chemical shifts are almost certainly a consequence of the metal–metal bond. The relatively narrow linewidths of the Mo(III) complexes (120–1320 Hz) contrast with the broad resonances of the Mo(II) dimers (up to 1960 Hz at elevated temperatures).[3] The broader resonance of $Mo_2(NMe_2)_6$ could result from enhanced quadrupolar relaxation of ^{95}Mo bonded to ^{14}N.

The tungsten complexes W_2L_6 (L = $[OCMe_3]^-$ or $[NMe_2]^-$) also exhibit very deshielded resonances (δ 4196 and 4489, respectively) and exhibit the same ligand-dependent order as that found for the molybdenum complexes. The W_2L_6 (L = $[OCHMe_2]^-$ or $[OCH_2CMe_3]^-$) complexes have not been isolated due to their decomposition to the tetrameric hydrido W(IV) complexes, $W_4(OR)_{14}H_2$.[19] We could not detect signals from dilute solutions of the $W_2(CH_2CMe_3)_6$ and $W_2(CH_2SiMe_3)_6$ complexes.

The $M_2(OCHMe_2)_6$ complexes readily react with amine and phosphine ligands to form triply bonded adduct complexes, $M_2(OCHMe_2)_6L_2$ (L = py, ½dmpe or ½Me_2en[10,18]). These adducts exhibit chemical shifts which are slightly deshielded compared to the precursors, $M_2(OCHMe_2)_6$. For the molybdenum complexes the magnitude of the deshielding ranges from 435 ppm for the dmpe adduct to *ca* 280 ppm for the *N*-donor ligand adducts. Similar deshielding is observed in the tungsten complexes which exhibit resonances between δ 4380 and 4736. ^{183}W–^{31}P spin–spin coupling is observed in the phosphine complex $W_2(OCHMe_2)_6$(dmpe). The values of the one- and two-bond ^{183}W–^{31}P couplings, 228 and 19 Hz, respectively, are in good agreement with those derived from the ^{31}P NMR spectrum of the related complex, $W_2(OCH_2CMe_3)_6(PMe_3)_2$ (^1J = 240 Hz, ^2J = 20 Hz).[18] The shielding trend of

*Abbreviations used: Me = methyl, py = pyridine, dmpe = 1,2-bis(dimethylphosphino)ethane, and Me_2en = 1,4-dimethylethylenediamine.

Table 1. ^{95}Mo and ^{183}W NMR data[a]

Compound	M = Mo		M = W[b]	
	δ	$W_{1/2}$ (Hz)	δ	J (Hz)
M(III) complexes				
$M_2(CH_2CMe_3)_6$	3695	530	[c]	
$M_2(CH_2SiMe_3)_6$	3625	530	[c]	
$M_2(OCMe_3)_6$	2645	120	4489	
$M_2(OCH_2CMe_3)_6$	2445	600	[d]	
$M_2(OCHMe_2)_6$	2445	350	[d]	
$M_2(NMe_2)_6$	2430	1320	4196	
$M_2(OCHMe_2)_6$(dmpe)	2880	850	4736	$^2J_{W-P} = 228$ $^2J_{W-P} = 19$
$M_2(OCHMe_2)_6(py)_2$	2725	1000	[c]	
$M_2(OCHMe_2)_6(Me_2en)$	2720	950	4380	
$M_2(O_2CMe)_4(CH_2CMe_3)_2$	2040	1460	2653	
M≡C complexes				
$M(CSiMe_3)(CH_2SiMe_3)_3$	1845	16	3613	$^2J_{W-H} = 10.5$
$M(CCMe_3)(CH_2CMe_3)_3$	1400	16	2867	$^2J_{W-H} = 10.5$
$M(CPh)(OCMe_3)_3$	[c]		2526	

[a] ^{95}Mo and ^{183}W NMR spectra recorded in toluene and d^6-benzene, respectively.
[b] For ^{183}W spectra $W_{1/2} = 10$ Hz.
[c] Not observed.
[d] These complexes are not known.

the *N*- and *P*-donor ligands observed here is the opposite to that observed in a variety of mononuclear $M(S_2CNEt_2)_2(CO)_2L$ adducts.[20] The above triply bonded dinuclear Mo(III) complexes possess a $\sigma^2\pi^4$ triple-bond electron configuration. The deshielded nature of their resonances is clearly reminiscent of the deshielded resonances of the Mo(II) complexes $Mo_2(O_2CR)_4$,[3,4] which possess a $\sigma^2\pi^4\delta^2$ electron configuration.

The novel dinuclear complexes $M_2(O_2CMe)_4(CH_2CMe_3)_2$ are extraordinary in that they possess a formal metal–metal triple bond of $\pi^4\delta^2$ configuration, i.e. there is no σ-bond. Their metal resonances are substantially more shielded than the quadruply bonded $M_2(O_2CR_2)_4$ precursors. For example, $Mo_2(O_2CMe)_4(CH_2CMe_3)_2$ has δ 2040, whereas $Mo_2(O_2CMe)_4$ has δ 3700–3770, depending upon the experimental conditions.[3] The structures and bond lengths of both types of compounds are similar: the $M_2(O_2CMe)_4(CH_2CMe_3)_2$ species have neopentyl ligands in the axial positions, aligned with the metal–metal vector (**B**). The ^{95}Mo NMR data for the related pair of complexes, $Mo_2(O_2CCF_3)_4$ and $Mo_2(O_2CCF_3)_4(py)_2$, also show shielding of the metal resonances (*ca* 200 ppm) upon axial ligation by the pyridine ligands.[4]

As a compliment to the above studies we have also examined the NMR properties of the alkylidyne complexes $L_3M{\equiv}CR$ (L = alkoxide or alkyl). Although these species formally contain a Mo(VI) center, homolytic cleavage of the rather covalent M≡C triple bond would generate half of the $[M{\equiv}M]^{6+}$ ($\sigma^2\pi^4$) core. The alkylidyne–Mo(VI) complexes $Mo(CXMe_3)(CH_2XMe_3)_3$ exhibit resonances at δ 1845 (X = Si) and δ 1400 (X = C), which are toward the deshielded end of the known chemical-shift range of monomeric Mo(VI) complexes.[2] The tungsten analogues also exhibit deshielded ^{183}W resonances (X = Si, δ 3613; X = C, δ 2867) as does the related $W(CPh)(OCMe_3)_3$ complex (δ 2526). Although more shielded than the resonances of the M_2L_6 species, the $L_3M{\equiv}CR$ resonances are significantly deshielded relative to the resonances of complexes containing metal–nitrogen triple bonds, e.g. $MoN(OCMe_3)_3$ (δ 55).[21] The photoelectron spectra of the metal–alkylidyne and metal–nitride complexes reveal that the metal–alkylidyne triple bond is much more covalent than the metal–nitride triple bond.[22] The greater covalency of the M≡C multiple bond may contribute to the deshielding of the metal nuclei. Interestingly, the alkylidyne carbon nuclei are also extremely de-

shielded [$\delta(^{13}C)$ *ca* 330].[15] The metal resonances for the Si-containing complexes are considerably more deshielded than the neopentyl derivatives consistent with a general deshielding influence for β-Si in substituted alkylidyne complexes. In contrast, the metal chemical shifts of the $M_2(CH_2XMe_3)_6$ (X = C or Si) complexes are quite similar. These observations suggest that the deshielding effect of the β-Si atom is mediated through the electronic structure of the metal–alkylidyne fragment, in support of a covalent M≡C bond being associated with the deshielding of the metal nuclei.

Both tungsten–alkylidyne complexes exhibit septet resonances (see Fig. 1) produced by the coupling of ^{183}W to six equivalent $C\underline{H}_2XMe_3$ protons: the magnitude of this two-bond coupling is 10.5 Hz. This is the first reported two-bond ^{183}W–^1H coupling to be derived from a ^{183}W spectrum, and the potential of such a coupling to characterize complexes with mixtures of alkyl, alkylidene and alkylidyne ligands is obvious. The value of the coupling is in close agreement with that derived from the ^1H spectrum of $W(CSiMe_3)(CH_2SiMe_3)_3$.[14] A similar coupling has not been previously reported for $W(CCMe_3)(CH_2CMe_3)_3$.[15,16]

The ^{95}Mo and ^{183}W chemical shifts of analogous pairs of complexes are often related by linear expressions which yield shielding sensitivities[2] [defined as $\Delta\delta(^{183}W)/\Delta\delta(^{95}Mo)$]. Several diverse classes of Mo and W compounds exhibit shielding sensitivities of 1.3–1.7.[20,23–26] For the complexes under discussion a broad correlation with a shielding sensitivity of *ca* 1.5 is observed when all data, except those for the $M_2(O_2CMe)_4(CH_2CMe_3)_2$ complexes, are considered. This correlation may be indicative of a common electronic origin for the deshielding in the $[M{\equiv}M]^{4+}$ ($\sigma^2\pi^4\delta^2$), $[M{\equiv}M]^{6+}$ ($\sigma^2\pi^4$) and $[M{\equiv}CR]^{3+}$ ($\sigma^2\pi^4$) species.

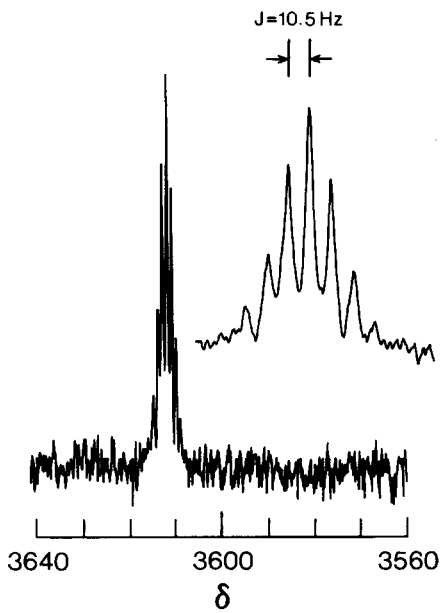

Fig. 1. ^{183}W NMR spectrum of $W(CSiMe_3)(CH_2SiMe_3)_3$ in d^6-benzene. The insert shows an expansion of the septet resonance. Acquisition parameters were: spectral width, 5 kHz; acquisition time, 1.638 s; digital resolution, 0.61 Hz (point)$^{-1}$; number of scans, 17,400.

Detailed theoretical calculations of the nuclear shielding are not yet feasible for large polyelectron atoms such as Mo and W. However, it is generally recognized that the paramagnetic term in the Ramsey equation for nuclear shielding dominates the chemical-shift differences among transition-metal compounds by mixing the angular momentum of appropriate metal excited states into the ground state.[27] For some series of complexes the metal chemical shift is inversely correlated with the energy of the lowest electronic transition of the molecule.[28–30] In other instances there is no correlation between the energy of the first excited state and the metal chemical shift.[2,31] The latter situation applies to the present study. The lowest-energy excited states of the $M_2(O_2CR)_4$ and $M_2(O_2CR)_4(R')_2$ species occur at similar energies,[32] yet their chemical shifts are quite disparate. On the other hand, the lowest-energy excited states of the $M_2(NR_2)_6$, $M_2(OR)_6$ and $M_2(OR)_6L_2$ complexes are rather different,[22,33] yet their chemical shifts span a relatively narrow range. These observations are consistent with the assignments for the lowest-energy electronic transitions in these complexes. For example, the lowest-energy transitions in the $[M{\equiv}M]^{4+}$ ($\sigma^2\pi^4\delta^2$) and $[M{\equiv}M]^{6+}$ ($\pi^4\delta^2$) complexes are $\delta \rightarrow \delta^*$ and $\delta \rightarrow \pi^*$ (O_2CR) (MLCT) in origin. Neither of these transitions should be an important contributor to the nuclear shielding. The $\delta \rightarrow \delta^*$ transition leaves the angular momentum unchanged, and the $\delta \rightarrow \pi^*$ (O_2CR) (MLCT) excitation removes the electron from the metal center. On the other hand, the metal-centered transitions of the $[M{\equiv}M]^{6+}$ unit which occur at higher energies ($\delta \rightarrow \pi^*$, $\delta \rightarrow \sigma^*$, $\pi \rightarrow \delta^*$ and $\pi \rightarrow \sigma^*$) could be very important contributors to the nuclear shielding.[4]

In conclusion, deshielding of the metal nuclei in multiply bonded dinuclear species appears to be related to the strongly covalent nature of the bonding present in such complexes. For the complexes studied herein the magnitude of the nuclear shielding increases in the order: $[M{\equiv}M]^{4+}$ ($\sigma^2\pi^4\delta^2$) < $[M{\equiv}M]^{6+}$ ($\sigma^2\pi^4$) < $[M{\equiv}M]^{6+}$ ($\pi^4\delta^2$) ~ $[M{\equiv}C]^{3+}$ < $[M{\equiv}N]^{3+}$. There is no clear correlation of the chemical shift with the HOMO–LUMO energy gap, which underscores the import-

ance of the entire excited state manifold to the paramagnetic term of the chemical shift.

Acknowledgements—We thank the U.S. Department of Agriculture for supporting this work with grant No. 84-CRCR-1-1416, Dr K. A. Christensen for his technical assistance with the NMR spectrometer, Dr M. Minelli for some preliminary experiments, and Mr Bill Van der Sluys for providing samples of the $M_2(O_2CMe)_4$ $(CH_2CMe_3)_2$ complexes.

REFERENCES

1. R. R. Vold and R. L. Vold, *J. Mag. Reson.* 1975, **19**, 365; J. Banck and A. Schwenk, *Ann. Physik.* 1975, **B20**, 75.
2. M. Minelli, J. H. Enemark, R. T. C. Brownlee, M. J. O'Connor and A. G. Wedd, *Coord. Chem. Rev.* 1985, **68**, 169.
3. (a) S. F. Gheller, T. W. Hambley, R. T. C. Brownlee, M. J. O'Connor, M. R. Snow and A. G. Wedd, *J. Am. Chem. Soc.* 1983, **105**, 1527; (b) B. P. Shehan, M. Kony, R. T. C. Brownlee, M. J. O'Connor and A. G. Wedd, *J. Magn. Reson.* 1985, **63**, 343.
4. R. A. Grieves and J. Mason, *Polyhedron* 1986, **5**, 415.
5. D. J. Santure, K. W. McLaughlan, J. C. Huffman and A. P. Sattelberger, *Inorg. Chem.* 1983, **22**, 1877.
6. C. G. Young, M. Minelli, J. H. Enemark, G. Miessler, N. Janietz, H. Kauermann and J. Wachter, *Polyhedron* 1986, **5**, 407.
7. W. Mowat, A. Shortland, G. Yagupsky, N. J. Hill, M. Yagupsky and G. Wilkinson, *J. Chem. Soc., Dalton Trans.* 1972, 533.
8. M. H. Chisholm, F. A. Cotton, M. W. Extine and B. R. Stults, *Inorg. Chem.* 1976, **15**, 2252.
9. M. H. Chisholm, F. A. Cotton, C. A. Murillo and W. W. Reichert, *Inorg. Chem.* 1977, **16**, 1801.
10. M. Akiyama, M. H. Chisholm, F. A. Cotton, M. W. Extine, D. A. Haitko, D. Little and P. E. Fanwick, *Inorg. Chem.* 1979, **18**, 2266.
11. M. H. Chisholm, F. A. Cotton, B. A. Frenz, W. W. Reichert, L. W. Shive and B. R. Stults, *J. Am. Chem. Soc.* 1976, **98**, 4469.
12. M. H. Chisholm, F. A. Cotton, M. W. Extine and B. R. Stults, *J. Am. Chem. Soc.* 1976, **98**, 4477.
13. M. H. Chisholm, D. M. Hoffman, J. C. Huffman, W. G. Van Der Sluys and S. Russo, *J. Am. Chem. Soc.* 1984, **106**, 5386.
14. R. A. Andersen, M. H. Chisholm, J. F. Gibson, W. W. Reichert, I. P. Rothwell and G. Wilkinson, *Inorg. Chem.* 1981, **20**, 3934.
15. D. N. Clark and R. R. Schrock, *J. Am. Chem. Soc.* 1978, **100**, 6774.
16. R. R. Schrock, D. N. Clark, J. Sancho, J. H. Wengrovius, S. M. Rocklage and S. F. Pederson, *Organometallics* 1982, **1**, 1645.
17. R. R. Schrock, M. L. Listemann and L. G. Sturgeoff, *J. Am. Chem. Soc.* 1982, **104**, 4291.
18. M. J. Chetcuti, M. H. Chisholm, J. C. Huffman and J. Leonelli, *J. Am. Chem. Soc.* 1983, **105**, 292.
19. N. Akiyama, D. Little, M. H. Chisholm, D. A. Haitko, F. A. Cotton and M. W. Extine, *J. Am. Chem. Soc.* 1979, **101**, 2504.
20. C. G. Young and J. H. Enemark, *Aust. J. Chem.* 1986, **39**, 997.
21. M. Minelli, C. G. Young and J. H. Enemark, *Inorg. Chem.* 1985, **24**, 1111.
22. E. M. Kober and D. L. Lichtenberger, unpublished results.
23. S. F. Gheller, T. W. Hambley, J. R. Rodgers, R. T. C. Brownlee, M. J. O'Connor, M. R. Snow and A. G. Wedd, *Inorg. Chem.* 1984, **23**, 2519.
24. J. Y. LeGall, M. M. Kubicki and F. Y. Petillon, *J. Organomet. Chem.* 1981, **221**, 287.
25. H. C. E. McFarlane, W. McFarlane and D. S. Rycroft, *J. Chem. Soc., Dalton Trans.* 1976, 1616.
26. G. T. Andrews, I. J. Colquhoun, W. McFarlane and S. O. Grim, *J. Chem. Soc., Dalton Trans.* 1982, 2353.
27. A. G. Wedd, In *NMR of Newly Accessible Nuclei* (Edited by P. Laszlo), Vol. 1, p. 79. Academic Press, New York (1983).
28. S. F. Gheller, P. A. Ganzzana, A. F. Masters, R. T. C. Brownlee, M. J. O'Connor, A. G. Wedd, J. R. Rodgers and M. R. Snow, *Inorg. Chim. Acta* 1981, **54**, L131.
29. S. F. Gheller, T. W. Hambley, R. T. C. Brownlee, M. J. O'Connor, M. R. Snow and A. G. Wedd, *Aust. J. Chem.* 1982, **35**, 2183.
30. M. Minelli, J. H. Enemark, K. Wieghardt and M. Hahn, *Inorg. Chem.* 1983, **22**, 3952.
31. M. Minelli, J. L. Hubbard and J. H. Enemark, *Inorg. Chem.* 1984, **23**, 970.
32. M. H. Chisholm, D. L. Clark, J. C. Huffman, W. G. Van Der Sluys, E. M. Kober, D. L. Lichtenberger and B. E. Bursten, manuscript in preparation.
33. M. H. Chisholm and E. M. Kober, manuscript in preparation.

Polyhedron Vol. 6, No. 2, pp. 261–267, 1987
Printed in Great Britain

0277–5387/87 $3.00+.00
Pergamon Journals Ltd

SYNTHESIS, MOLECULAR STRUCTURE AND SPECTROSCOPIC CHARACTERIZATION OF $Mo(CO)_2I_2(\eta^2\text{-dppm})(\eta^1\text{-dppm})$

F. ALBERT COTTON* and MAREK MATUSZ

Department of Chemistry and Laboratory for Molecular Structure and Bonding, Texas A&M University, College Station, TX 77843, U.S.A.

(*Received* 4 *February* 1986; *accepted* 18 *June* 1986)

Abstract—A new, high-yield method has been developed for the preparation of $Mo(CO)_2I_2(\eta^2\text{-dppm})(\eta^1\text{-dppm})$. The title compound was prepared by the reaction of $[Et_4N][Mo(CO)_4I_3]$ with dppm in benzene in 95% yield. It has been characterized by a single-crystal X-ray study. The crystallographic data are as follows: monoclinic, space group $P2_1/n$, $a = 19.023(4)$ Å, $b = 14.439(3)$ Å, $c = 20.141(5)$ Å, $\beta = 100.45(2)°$, $V = 5440(2)$ Å^3, $Z = 4$. The geometry around the central metal atom could be considered as either a distortion from a capped octahedron with a carbonyl in a capping position or from a trigonal prism with the iodine capping a rectangular face. The solution behavior of $Mo(CO)_2I_2(dppm)_2$ was examined with ^{31}P NMR, which showed it to be fluxional.

Recently we have been investigating the possibility of forming multiply bonded heteroatomic dimers. One of the designed approaches would be to have a bidentate, dangling ligand on one metal atom. The dangling ligand might then coordinate to a second metal atom, bringing it close enough for an M—M′ bond to be formed, with the dangling ligand(s) becoming a bridge spanning the dimetallic core. For such a purpose the starting material would have to meet at least the following criteria:

(1) contain a metal that easily forms multiple bonds, or

(2) have the metal already in a suitable oxidation state.

Of the possible bidentate ligands, phosphines are of the greatest practical interest, with bis(diphenylphosphino)methane (dppm) being one of the best choices.

There are only a few examples in the chemical literature of complexes with dangling diphosphines.[1–7] At first we focused our attention on Mo(II) and Mo(III) compounds, since they fulfill the above requirements. A search of the chemical literature then revealed that a promising candidate for our experiments already existed and has been structurally characterized. $Mo(CO)_2Cl_2(dppm)_2$ was first prepared[3] by Colton *et al.*, and then later structurally characterized[7] as possessing a seven-coordinate molybdenum atom with two carbonyl groups, two chlorine atoms, one chelating diphosphine ligand and one dangling dppm ligand.

The reported synthesis of $Mo(CO)_2Cl_2(dppm)_2$ utilized the following reactions:

$$Mo(CO)_6 + Cl_2 \rightarrow Mo(CO)_4Cl_2,$$

$$Mo(CO)_4Cl_2 + 2dppm \rightarrow Mo(CO)_2Cl_2(dppm)_2.$$

In our hands the first step, i.e. the oxidative halogenation of molybdenum hexacarbonyl, has proved to be unreliable. In view of recent structural characterization of other $M_2(CO)_8X_4$ type dimers[8,9] it is possible that dimeric $Mo_2(CO)_8Cl_4$ instead of monomeric $Mo(CO)_4Cl_2$ is the product of chlorination of $Mo(CO)_6$, and that this may lead to poor yields of $Mo(CO)_2Cl_2(dppm)_2$.

We turned our attention to the corresponding bromo and iodo compounds. We found that $Mo(CO)_2I_2(dppm)_2$ (**1**) had been prepared by the following procedure:[10]

$$Mo(CO)_6 + dppm \rightarrow Mo(CO)_4dppm$$

$$\xrightarrow{I_2} \alpha,\beta Mo(CO)_3I_2dppm$$

$$\xrightarrow{dppm} Mo(CO)_2I_2(dppm)_2.$$

*Author to whom correspondence should be addressed.

This method gives not only the molecular compound $Mo(CO)_2I_2(dppm)_2$, but also the *cis* and *trans* isomers of $[Mo(CO)_2I(dppm)_2]I$, which have to be separated. We therefore searched for an alternative method of preparation of **1**.

After trying several reactions we found that the desired product could be synthesized in 95% yield by the following procedure:

$$[R_4N][Mo(CO)_4I_3] + 2dppm \rightarrow Mo(CO)_2I_2(dppm)_2 + R_4NI.$$

The starting material, $[R_4N][Mo(CO)_4I_3]$, can be easily prepared in a high-yield, one-pot synthesis from $Mo(CO)_6$. Compound **1** had not been structurally characterized, and some unusual stereochemistry might be found in a relatively crowded, presumably seven-coordinate molecule. The molecular structure was therefore determined by single-crystal X-ray studies.

During the routine spectroscopic characterization we discovered that the ^{31}P NMR spectrum was temperature-dependent, indicating fluxional behavior of $Mo(CO)_2I_2(dppm)_2$ in solution. The low-temperature ^{31}P spectrum is in accord with the observed solid-state structure.

EXPERIMENTAL

General

Standard Schlenk tube techniques were employed throughout. All solvents were dried and freshly distilled prior to use. Tetraethylammonium iodide was purchased from Aldrich Chemical Co. and used as received.

Formation of $[Et_4N][Mo(CO)_4I_3]$[11]

Molybdenum hexacarbonyl (9.08 g, 0.0344 mol) and Et_4NI (9.19 g, 0.0359 mol) were charged into a 500-cm^3, round-bottom flask. 100 cm^3 of THF was added and the reaction mixture was refluxed for 1.5 h. After that time the color of the reaction mixture was bright yellow, indicating the formation of $[Et_4N][Mo(CO)_5I]$, which can be isolated by adding ether and refrigerating. If any unreacted $Mo(CO)_6$ is still present, the reaction mixture should be filtered while still hot. The bright yellow solution was cooled and 8.7 g (0.0344 mol) of elemental iodine was added from an addition finger during a period of 5 min. The reaction mixture was stirred vigorously during that time. Addition of each portion of iodine was accompanied by evolution of carbon monoxide. After all the iodine was added, the reaction mixture was stirred for an additional 15 min. It was dark orange at this time. 100 cm^3 of diethyl ether was added to initiate precipitation and the reaction mixture was refrigerated overnight. The crystalline product was filtered, washed with ether and vacuum dried. The yield was 18.1 g (73%) of dark yellow crystals. An additional 2.4 g of the product could be recovered from the mother liquor, bringing the yield to 83%.

$Mo(CO)_2I_2(dppm)_2$ (**1**)

$[Et_4N][Mo(CO)_4I_3]$ (1.0 g, 1.40 mmol), 1.6 g (6.1 mmol) of dppm and 40 cm^3 of benzene were stirred at room temperature. The reaction proceeded with CO evolution and an orange precipitate was deposited. After 6 h of stirring the reaction mixture was brought to a boil and filtered hot. Remaining solids were treated with an additional 40 cm^3 of hot benzene and filtered. A white solid (Et_4NI) remained on the filter stick. The combined filtrates were treated with 100 cm^3 of hexane and refrigerated. The product was filtered, washed with hexane and vacuum dried, to give a yield of 1.55 g (95%) of orange-red crystalline material. The complex is air-stable in the solid state, but it is light-sensitive both in the solid state and in solution. Found: C, 55.5; H, 4.1%. Calc. for $Mo(CO)_2I_2(dppm)_2 \cdot C_6H_6$: C, 55.6; H, 4.0%. IR spectrum (Nujol mull): $\nu(CO) = 1930(s)$ and $1850(s)$ cm^{-1}. Solution spectra (chloroform and toluene) were essentially identical. Electronic spectrum (chloroform solution): $\lambda_{max} = 450$ nm (sh), and 350 nm (sh).

Measurements

Elemental analyses were performed by Galbraith Laboratories Inc. IR spectra were recorded on a Perkin–Elmer 785 spectrophotometer. The electronic spectra were recorded on a chloroform solution using a Cary 17D spectrophotometer. $^{31}P-\{^1H\}$ NMR spectra were recorded on a Varian XL 200 spectrometer at an operating frequency of 80.98 MHz in $CDCl_3$ solutions. 85% H_3PO_4 was used as an external standard. For the variable-temperature measurements the sample was referenced to H_3PO_4 at room temperature.

X-ray crystallographic procedures

Single crystals of **1** were grown by layering hexane on top of a benzene solution of the complex. The diffraction data were collected on a P3 autodiffractometer. Lorentz, polarization and absorption corrections were applied to the data. Standard

Table 1. Crystal data for $Mo(CO)_2I_2(dppm)_2 \cdot C_6H_6$

Formula	$MoI_2P_4O_2C_{58}H_{50}$
Formula weight	1252.69
Space group	$P2_1/n$
Systematic absences	$h0l: h+l \neq 2n$; $0k0: k \neq 2n$
a (Å)	19.023(4)
b (Å)	14.439(3)
c (Å)	20.141(5)
α (°)	90.0
β (°)	100.45(2)
γ (°)	90.0
V (Å^3)	5440(2)
Z	4
d_{calc} (g cm^{-3})	1.529
Crystal size (mm)	$0.2 \times 0.3 \times 0.6$
μ(Mo-K_α) (cm^{-1})	15.128
Data collection instrument	P3
Radiation (monochromated in incident beam)	Mo-K_α ($\lambda_\alpha^- = 0.71073$ Å)
Orientation reflections [number, range (2θ) (°)]	25, $16 < 2\theta < 25$
Temperature (°C)	27
Scan method	2θ–ω
Data collection range (2θ) (°)	4–45
Number of unique data, total with $F_o^2 > 3\sigma(F_o^2)$	5469, 4354
Number of parameters refined	569
Transmission factors (max, min)	0.9987, 0.8640
R^a	0.0416
$R_w{}^b$	0.0555
Quality-of-fit indicator^c	1.17
Largest shift/esd (final cycle)	0.84
Largest peak (e Å^{-3})	0.60

$^a R = \Sigma \, ||F_o| - |F_c|| / \Sigma \, |F_o|$.
$^b R_w = [\Sigma \, w(|F_o| - |F_c|)^2 / \Sigma \, w|F_o|^2]^{1/2}$; $w = 1/\sigma^2(|F_o|)$.
^{c} Quality of fit $= [\Sigma \, w(|F_o| - |F_c|)^2 / (N_{obs} - N_{parameters})]^{1/2}$.

procedures were used to process the data.[12]* The solution of the structure was initiated by placing the Mo atom at a position obtained from the $Mo(CO)_2Cl_2(dppm)_2 \cdot C_6H_6$ structure[7] (x- and z-coordinates were reversed). Additional atoms were located from the alternating least-squares cycles and difference Fourier maps. All the nonhydrogen atoms with the exception of the benzene molecule present as solvent of crystallization and C(44) were refined anisotropically. The structure converged to a value of $R = 0.0416$. The final difference Fourier map was featureless with a highest peak of 0.60 e Å^{-3}. All the relevant crystallographic data are presented in Table 1.

* Calculations were done on the VAX 11/780 computer at the Department of Chemistry, Texas A&M University, College Station, Texas, with a VAX-SDP software package.

RESULTS AND DISCUSSION

Synthesis

Preparation of **1** proceeds through the following synthetic steps:

$$Mo(CO)_6 + R_4NI \rightarrow [R_4N][Mo(CO)_5I] + CO$$

$$\xrightarrow{I_2} [R_4N][Mo(CO)_4I_3]$$

$$\xrightarrow{dppm} Mo(CO)_2I_2(dppm)_2 + 2CO + R_4NI.$$

The first stage entails thermal CO substitution of $Mo(CO)_6$ by tetraalkylammonium iodide. The reaction is of a general type, and has been widely used with other alkylammonium salts. The product, $[R_4N][Mo(CO_5)I]$, was not routinely isolated, but oxidized *in situ* with elemental iodine. The iodine has the advantage of being a mild oxidiz-

ing agent and it is easy to handle. The oxidation proceeds rapidly, with high yields. Despite the earlier reports of the extreme instability of $[R_4N][Mo(CO)_3I_3]$, we found that it can be isolated and conveniently handled. In the absence of light and air the complex could be stored for several days. The last step in the preparative procedure, the ligand substitution with dppm, gives the desired compound (**1**) with yields over 95%. A variety of tetralkylammonium salts have been tried (ethyl, propyl and butyl), with tetraethylammonium being the most convenient.

The preparation of **1**, by the method of Colton[10] has several disadvantages, namely, lower yields, and, in addition to the desired molecular complex $Mo(CO)_2I_2(dppm)_2$, *cis*- and *trans*-$[Mo(CO)_2I(dppm)_2]I$ are also formed.

Colton and coworkers also investigated reactions of $[Mo(CO)_4X_3]^-$ with dppm,[13] but under their conditions only the ionic complex $[Mo(CO)_2I_2dppm)_2]I$ was formed.

The preparation of **1** via the route employed for the synthesis of $Mo(CO)_2Cl_2(dppm)_2$ is not feasible because diiodotetracarbonyl molybdenum is inaccessible.

Our method of preparation of **1** gives only the molecular complex, uncontaminated by the ionic isomers. $Mo(CO)_2I_2(dppm)_2$ can be recrystallized from dichloromethane–hexane, but refluxing of dichloromethane solutions of **1** or even their prolonged storage leads to the formation of ionic species.

Spectroscopy

The IR spectrum shows two strong C≡O absorptions at 1947 and 1869 cm^{-1} in toluene (1940 and 1865 cm^{-1} in $CHCl_3$).

Figure 1 represents a series of variable-temperature ^{31}P studies of **1** in $CDCl_3$ solution.

At −40°C (Fig. 1a) the spectrum consists of four groups of peaks (integration 1 : 1 : 1 : 1), indicating that all four phosphorus atoms are nonequivalent, which is in accord with the solid-state structure. The assignment of all the lines in the spectrum is given in Fig. 1a. There are four chemical shifts (ppm) (12.64, 7.78, −25.40 and −43.04) and four coupling constants (Hz) (30.50, 84.7, 168 and 22.3). A large coupling constant (J_{AD} = 168 Hz) is probably between P(3) and P(2), since these are the most *trans* phosphorus atoms. The second largest coupling is observed for P(1) and P(2) in the chelating dppm (J_{DB} = 84.7 Hz). Small coupling constants are observed for the two phosphorus atoms in the dangling dppm (J_{AC} = 30.5 Hz) and between P(3) and P(1) (J_{AB} = 22.3 Hz). The doublet at −25.40 ppm is assigned to uncoordinated phosphorus. This value is consistent with that of free dppm. The coupling to the second phosphorus atom in this dppm molecule splits the signal into a doublet. One of the chelating phosphorus atoms is shifted upfield to −43.04 ppm, an unusual chemical shift, since phosphorus atoms in a five-membered ring are usually shifted downfield from the corresponding uncoordinated phosphines.

Upon warming, the resonances due to P(1) and P(2) start broadening. Also the J_{AB} coupling is "lost" in the P(3) resonance. At room temperature (Fig. 1d) the resonances of P(1) and P(2) are broad, and the fine structure of (P3) is very poorly resolved, except for the AC coupling. The dangling phosphorus P(4) is still present as a sharp doublet, suggesting that fluxionality does not involve opening of the chelating ring, and closing with an uncoordinated phosphorus P(4). There are at least two possible exchange mechanisms for **1**. One is a dissociative mechanism, involving dissociation of iodide from the capping position in the trigonal prism. The trigonal prism can then rearrange to an octahedron, rendering the phosphorus atoms equivalent. Another possibility is a simple rearrangement between capped trigonal prisms[14] which can be achieved easily by compressing and elongating bonds (see Fig. 2). As the temperature increases the sharp doublet assigned to the uncoordinated phosphorus atom begins to broaden as well, but it has been observed that **1** is decomposed in boiling dichloromethane or even at room temperature over a period of days.

Molecular structure

Selected bond distances and angles for **1** are listed in Table 2. Figure 3 presents a labelled ORTEP diagram of **1** along with a labelling scheme.* The molecule is seven-coordinate with the molybdenum atom bonded to two carbonyl groups, three phosphorus atoms and two iodine atoms. One of the dppm ligands is bidentate, but the second one is only monodentate. This type of structure has been postulated and observed before. The structure is distorted from a capped octahedron with CO(2) capping the P(1)–P(3)–1C(1) face and a trigonal prism with the I(1) capping the C(1)–P(2)–I(2)–

* *Supplementary material available.* Atomic positional parameters, full listing of bond angles, bond distances, isotropic-equivalent displacement parameters, and observed and calculated structure factors (28 pp.). Copies are available from the Editor. Atomic coordinates have also been deposited with the Cambridge Crystallographic Data Centre.

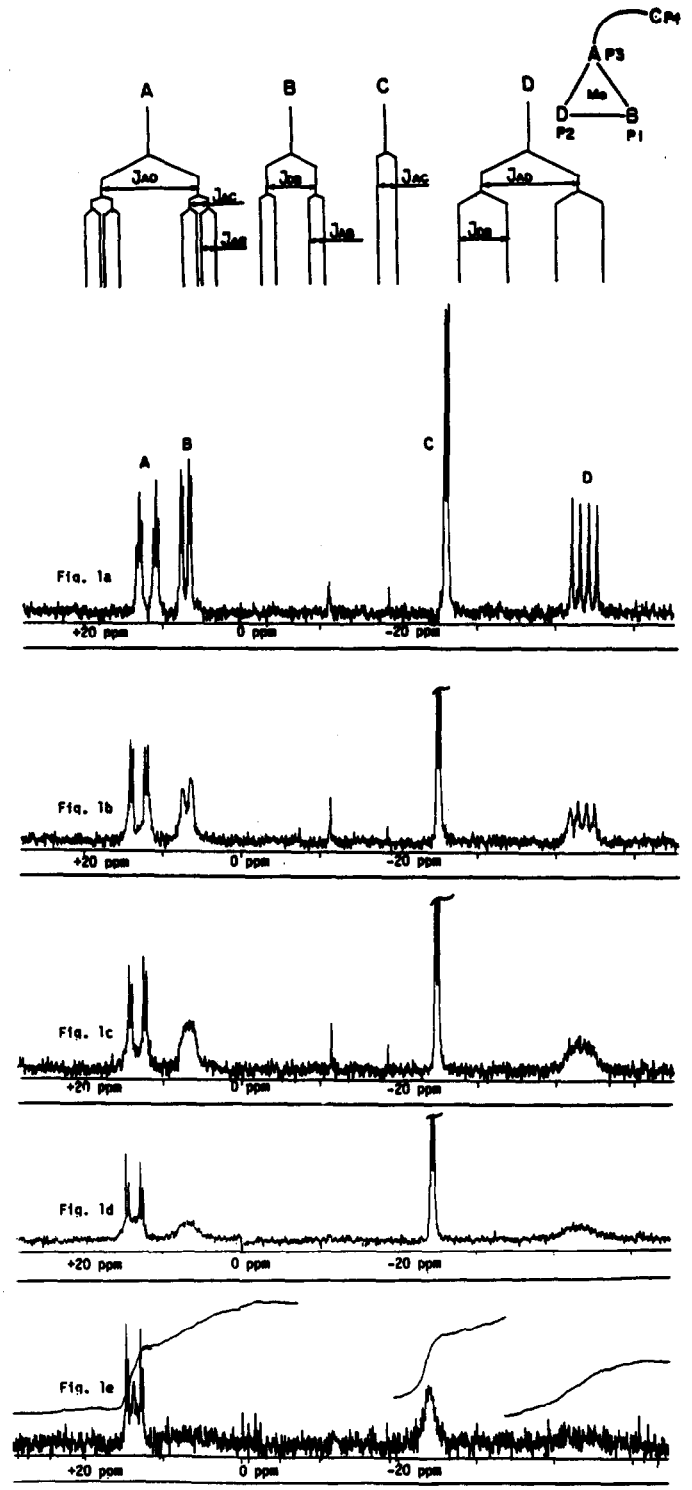

Fig. 1. Variable-temperature $^{31}P-\{^1H\}$ NMR studies. Referenced to H_3PO_4 as an external standard at room temperature. (a) −40°C, (b) 0°C, (c) 10°C, (d) 25°C, and (e) 40°C. Peak assignment on top of Fig. 1a.

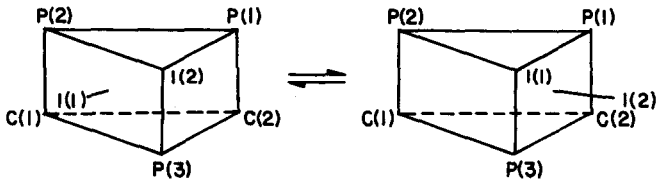

Fig. 2. Idealized capped trigonal prism geometry showing one of the possible exchange mechanisms.

Table 2. Selected bond distances (Å) and angles (°) for $Mo(CO)_2I_2(dppm)_2 \cdot C_6H_6$[a]

Atom 1	Atom 2	Distance
Mo(1)	I(1)	2.846(1)
Mo(1)	I(2)	2.904(1)
Mo(1)	P(1)	2.491(2)
Mo(1)	P(2)	2.589(2)
Mo(1)	P(3)	2.574(2)
Mo(1)	C(1)	1.957(10)
Mo(1)	C(2)	1.945(9)
P(1)	C(3)	1.827(8)
P(2)	C(3)	1.839(8)
P(3)	C(4)	1.850(8)
P(4)	C(4)	1.866(9)
O(1)	C(1)	1.136(10)
O(2)	C(2)	1.160(10)

Atom 1	Atom 2	Atom 3	Angle
I(1)	Mo(1)	I(2)	86.77(3)
I(1)	Mo(1)	P(1)	145.35(6)
I(1)	Mo(1)	P(2)	82.98(5)
I(1)	Mo(1)	P(3)	83.64(6)
I(1)	Mo(1)	C(1)	80.9(3)
I(1)	Mo(1)	C(2)	142.5(3)
I(2)	Mo(1)	P(1)	82.86(5)
I(2)	Mo(1)	P(2)	86.64(5)
I(2)	Mo(1)	P(3)	83.21(5)
I(2)	Mo(1)	C(1)	167.6(3)
I(2)	Mo(1)	C(2)	116.4(3)
P(1)	Mo(1)	P(2)	63.53(7)
P(1)	Mo(1)	P(3)	127.40(8)
P(1)	Mo(1)	C(1)	106.3(3)
P(1)	Mo(1)	C(2)	70.4(3)
P(2)	Mo(1)	P(3)	163.62(7)
P(2)	Mo(1)	C(1)	89.9(3)
P(2)	Mo(1)	C(2)	124.9(3)
P(3)	Mo(1)	C(1)	97.2(3)
P(3)	Mo(1)	C(2)	71.4(3)
C(1)	Mo(1)	C(2)	75.2(4)
Mo(1)	P(1)	C(3)	97.8(3)
Mo(1)	P(2)	C(3)	94.2(3)
Mo(1)	P(3)	C(4)	116.6(3)
Mo(1)	C(1)	O(1)	174.8(8)
Mo(1)	C(2)	O(2)	174.6(8)
P(1)	C(3)	P(2)	93.7(4)
P(3)	C(4)	P(4)	115.2(4)

[a] Numbers in parentheses are estimated standard deviations in the least significant digits.

Table 3. Comparison of selected bond angles (°) for $Mo(CO)_2X_2(dppm)_2$

Angle	X = Cl	X = I
P(1)—Mo—P(2)	63.5(2)	63.53(7)
P(1)—Mo—P(3)	126.4(2)	127.40(8)
P(2)—Mo—P(3)	163.1(2)	163.62(7)
X(1)—Mo—X(2)	86.7(2)	86.77(3)
C(1)—Mo—C(2)	73.5(1)	75.2(4)
X(1)—Mo—C(1)	115.5(7)	80.9(3)
X(1)—Mo—C(2)	141.5(7)	142.5(3)
X(2)—Mo—C(1)	170.4(7)	167.6(3)
X(2)—Mo—C(2)	83.9(8)	116.4(3)
X(1)—Mo—P(1)	147.8(2)	145.35(6)
X(1)—Mo—P(2)	80.0(2)	82.98(5)
X(1)—Mo—P(3)	81.2(2)	83.64(6)

P(3) rectangular face (see Fig. 2). The principal distances (in Å) in the molecule are: Mo(1)—I(1) = 2.846(1), Mo(1)—I(2) = 2.904(2), Mo(1)—P(1) = 2.491(2), Mo(1)—P(2) = 2.589(2), Mo(1)—P(3) = 2.574(2), Mo(1)—C(1) = 1.957(10), and Mo(1)—C(2) = 1.945(9). All the distances are with the normal range and require no further comment. All the angles are almost identical to those observed in the chloro analogue, Table 3, demonstrating that substitution of chlorides by iodides had almost no effect on the molecular structure.

Concluding remarks

We have developed a new synthetic method for the preparation of $Mo(CO)_2I_2(\eta_2\text{-dppm})(\eta_1\text{-dppm})$. The title complex has been characterized by a single-crystal X-ray diffraction. The central molybdenum atom is seven-coordinate with two iodine atoms, two carbonyl groups and three phosphorus atoms forming the immediate coordination sphere. One of the dppm ligands is chelating, the other one has one dangling phosphorus atom. The geometry around the central molybdenum atom is distorted from a capped octahedron or a capped trigonal prism. Variable-temperature ^{31}P NMR studies revealed that the molecule is fluxional in solution. The reac-

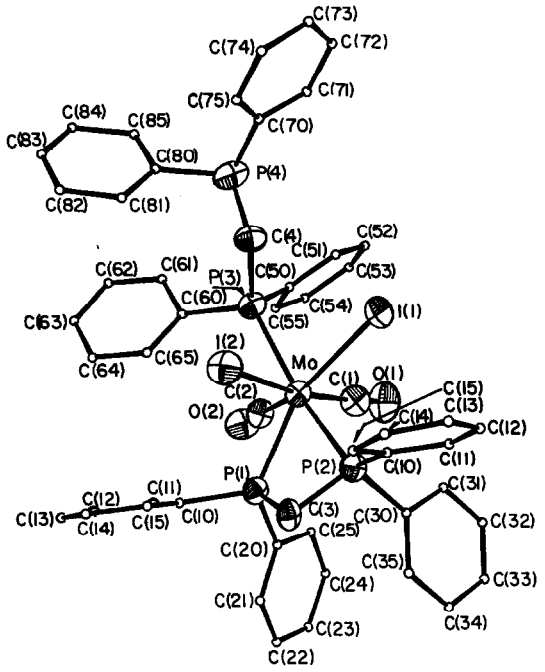

Fig. 3. ORTEP drawing of $Mo(CO)_2I_2(dppm)_2$.

tivity of **1** in the formation of heterobimetallic dimers, as well as its photochemical behavior are currently under investigation.

Acknowledgement—We thank the National Science Foundation for support.

REFERENCES

1. R. J. Puddephatt, *Chemistry of Bis(diphenylphosphino)methane*, p. 103. Chemical Society Reviews, London (1983).
2. E. E. Isaacs and W. A. G. Graham, *Inorg. Chem.* 1975, **14**, 2560.
3. M. W. Anker, R. Colton and I. B. Tomkins, *Aust. J. Chem.* 1968, **21**, 1143.
4. M. W. Anker, R. Colton and I. B. Tomkins, *Aust. J. Chem.* 1968, **21**, 1159.
5. R. L. Keiter, A. L. Rheingold, J. J. Hamerski and C. K. Castle, *Organometallics* 1983, **2**, 1635.
6. R. L. Keiter, Y. Y. Sun, J. W. Brodack and L. W. Cary, *J. Am. Chem. Soc.* 1979, **101**, 2638.
7. M. G. B. Drew, A. P. Walters and I. B. Tomkins, *J. Chem. Soc., Dalton Trans.* 1977, 974.
8. F. A. Cotton, L. R. Falvello and J. H. Meadows, *Inorg. Chem.* 1985, **24**, 514.
9. F. Calderazzo, R. Poli and P. F. Zanazzi, manuscript in preparation.
10. R. Colton and J. J. Howard, *Aust. J. Chem.* 1970, **23**, 223.
11. S. N. J. Burgmayer and J. L. Templeton, *Inorg. Chem.* 1985, **24**, 2224.
12. (a) A. Bino, F. A. Cotton and P. E. Fanwick, *Inorg. Chem.* 1979, **18**, 3558; (b) F. A. Cotton, B. A. Frenz, G. Deganello and A. J. Shaver, *J. Organomet. Chem.* 1973, **50**, 227; (c) A. C. T. North, D. C. Phillips and F. S. Matthews, *Acta Cryst.* 1968, **A39**, 158.
13. R. Colton and J. J. Howard, *Aust. J. Chem.* 1969, **22**, 2543.
14. For a review of seven-coordinate complexes and isomerization see: M. G. B. Drew, *Prog. Inorg. Chem.* 1977, **23**, 67.

Polyhedron Vol. 6, No. 2, pp. 269–273, 1987
Printed in Great Britain

0277–5387/87 $3.00 + .00

KINETICS OF THE REVERSIBLE PHOTOAQUATION OF THE OCTACYANOMOLYBDATE(IV) ION*

VILMOS GÁSPÁR and MIHÁLY T. BECK†

Department of Physical Chemistry, Institute of Chemistry, Kossuth Lajos University, Debrecen, P.O. Box 7, H-4010, Hungary

(*Received* 4 *June* 1986; *accepted* 23 *June* 1986)

Abstract—The kinetics of the photoaquation of the octacyanomolybdate(IV) ion in aqueous solution were studied by potentiometric and spectrophotometric methods. In an alkaline medium a simple scheme analogous to the photoaquation of the hexacyanoferrate(II) ion describes the process. The values of the constants of the kinetic equation are: $\Phi = 1.0$, $k_8 = (6.55 \pm 0.8) \times 10^{-9}\ s^{-1}$, and $k_{-8} = (7.88 \pm 0.5) \times 10^{-2}\ mol^{-1}\ dm^3\ s^{-1}$ (pH = 10.5). The reversibility of the photoaquation is also explained by the scheme. A simultaneous measurement of free cyanide ion concentration and the absorbance at 512 nm shows that the red coloured transition product is a heptacyano complex.

The kinetics and mechanism of the photoaquation of different cyano complexes have been intensively studied for a long time.[1] Nevertheless, the reversible photoaquation of hexacyanoferrate(II) and octacyanomolybdate(IV) ions remained unsolved. In an earlier paper we dealt with the kinetics of the photoaquation of the hexacyanoferrate(II) ion.[2] It was shown that a simple scheme (see Fig. 3 in Ref. 2) explains all the experimental observations. The success of those experiments is due to the application of a cyanide-selective electrode. This sensor can sensitively monitor both the thermal reactions and the photoreactions without perturbing the system, even if the conversions are very small. Since there are many similarities in the photochemistry of the two cyano complexes, we have tried to investigate the photoaquation of the octacyanomolybdate(IV) ion in an alkaline medium by applying the same experimental and computational methods as in the case of the hexacyanoferrate(II) ion.[2]

The aqueous solution of the complex ion is stable in the dark. The rate constant of its thermal aquation reaction was determined by Wilson *et al.*[3] Its value is $8.5 \times 10^{-8}\ s^{-1}$. It is well known[1] that on illumination by sunlight or 365-nm monochromatic light the yellow coloured aqueous solution of the complex turns to red and hydrogen cyanide is formed simultaneously. By interrupting the illumination, the solution turns back to its original yellow. The photoreaction is reversible. If, however, the irradiation time is longer, the transient red colour disappears and the solution turns irreversibly green and finally blue. Formation of a blue precipitate can also be observed at a high concentration of the complex.

Mitra and Mohan[4] isolated a yellow complex as a potassium salt by addition of a calculated amount of KOH to the red solution. The composition of this yellow complex was $K_4MO(CN)_7(OH)$. Their experiments suggest that the blue product is formed by *photolysis* of *this* complex ion, rather than, as previously supposed, by a series of thermal reactions. A careful investigation of this blue product showed that it should be a mixture of different

*Dedicated to Professor Viktor Gutmann on the occasion of his 65th birthday.

†Author to whom correspondence should be addressed.

species. Their results can be summarized by the following scheme:

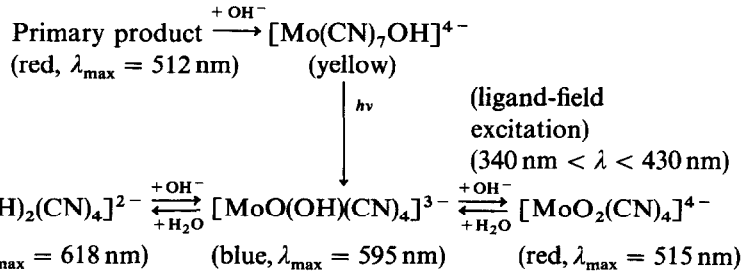

Surprisingly, the composition of the primary product is still a subject of controversy in the literature. A number of investigations[5-8] support the following simple reaction (A) as the primary process:

$$[Mo(CN)_8]^{4-} \overset{h\nu(LF),\,+H_2O}{\rightleftharpoons} [Mo(CN)_7(H_2O)]^{3-} + CN^-. \quad \text{(A)}$$
(yellow) (red)

Jakob *et al.*[9] proposed reaction (B) that results in an increase in the coordination number:

$$[Mo(CN)_8]^{4-} \overset{h\nu(LF),\,+2H_2O}{\rightleftharpoons} [Mo(CN)_8(H_2O)_2]^{4-}. \quad \text{(B)}$$

Reaction (C) was suggested by different authors[10,11] according to spectrophotometric investigations:

$$[Mo(CN)_8]^{4-} \overset{h\nu(LF),\,+OH^-}{\rightleftharpoons} [Mo(CN)_7(OH)]^{3-} + CN^-. \quad \text{(C)}$$

The conductometric and pH titration curves[12] of the photolysed solutions of octacyanomolybdic acid corresponding to the stage of maximum optical density at 512 nm showed a sharp minimum and an inflexion, respectively, at 4 equivalents of KOH per mole of the complex. First the three strong H^+ ions were neutralized and then in a slow reaction 1 equivalent of the base was consumed. This latest process was attributed to a ligand exchange reaction, in which the coordinated water molecule of the product of reaction (A) was replaced by an OH^- ion. According to these observations, reactions (B) and (C) cannot be taken into account as the main photoreactions.

Our esperimental set-up allows us to determine simultaneously the free cyanide ion concentration and the optical density at the characteristic wavelength of the red species. Therefore we can perform a *direct* experimental investigation of the primary process. Only such an experiment can finally resolve the controversy.

We hoped that an exact kinetic investigation of the photoaquation by our method[2] would result in an accurate value of the quantum yield, since rather different values were determined earlier by different methods (Table 1.)

EXPERIMENTAL

Potassium octacyanomolybdate(IV) dihydrate was obtained by the method of Van de Poel and Neumann.[14] The yellow crystals were recrystallized 4 or 5 times from ethanol solutions. Purity was controlled by a spectrophotometric method (ε = 15,540 mol^{-1} dm^3 cm^{-1} at 240 nm).

(A) Investigation of the stoichiometry of the primary photoreaction

120 cm^3 of 2.5 × 10^{-3} mol dm^{-3} potassium octacyanomolybdate(IV) solution was put into a 150 cm^3 beaker. The pH of the solution was adjusted to 10.3 by adding a few drops of 1.0 M

Table 1. Quantum yield (Φ) of the photoaquation of the octacyanomolybdate(IV) ion on the exposure to 365-nm light

Method	Φ	Reference
Determination of OH^- production, initial pH = 6–7	0.8–0.9	6
Determination of the initial rate of the decrease in $[Mo(CN)_8]^{4-}$ concentration by spectrophotometric method in 0.1 M KOH solution	~1	11
Determination of cyanide ion production by spectrophotometric method, pH = 8–12 in borate buffer	0.15	13

carbonate-free sodium hydroxide solution. The solution was kept in the dark and under an argon atmosphere for at least 30 min. The free cyanide concentration was monitored potentiometrically by using an OP-711-D-I ion-selective electrode and a Radiometer Type K401 saturated calomel electrode with an OP-205 Radelkis mV-meter. The pH of the solution was measured by a combined glass electrode (GK 301 B Radiometer) and a PHM-51 Radiometer mV-meter. A Hitachi–Perkin–Elmer 139 single-beam spectrophotometer was used for determination of the absorbance of the red product at 512 nm. The optical length of the flow-cell was 0.51 cm. The solution was stirred with a magnetic stirrer.

After reaching an equilibrium state in the dark, the solution was irradiated by sunlight. (Although sunlight is not monochromatic, its intensity is much more higher than that of the lamp used in our standard photochemical experiments. Therefore, on illumination by sunlight the red state was reached within a few minutes.)

The side of the beaker opposite to the direction of the irradiation was covered with an aluminium foil to maintain nearly the same intensity of irradiation in the whole volume of the solution.

(B) Kinetics of the photoaquation in an alkaline medium

A detailed description of the photochemical device is given in our earlier paper.[2] In these experiments, however, the light source was a TUNGSRAM PRK-2 medium-pressure mercury lamp. The constant intensity of irradiation was measured by the ferrioxalate method.[15] It amounts to $2.1 \pm 0.1 \times 10^{-10}$ mol of photons (365 nm) cm^{-2} s. For monitoring the reaction, the same electrodes and mV-meters were used as described in part (A) of this section.

RESULTS AND DISCUSSION

Figure 1 shows the simultaneous changes in the absorbance at 512 nm and the free cyanide concentration on exposure to sunlight. The cyanide ion concentration increases monotonically to a final value that corresponds to 1.8 mol of free cyanide

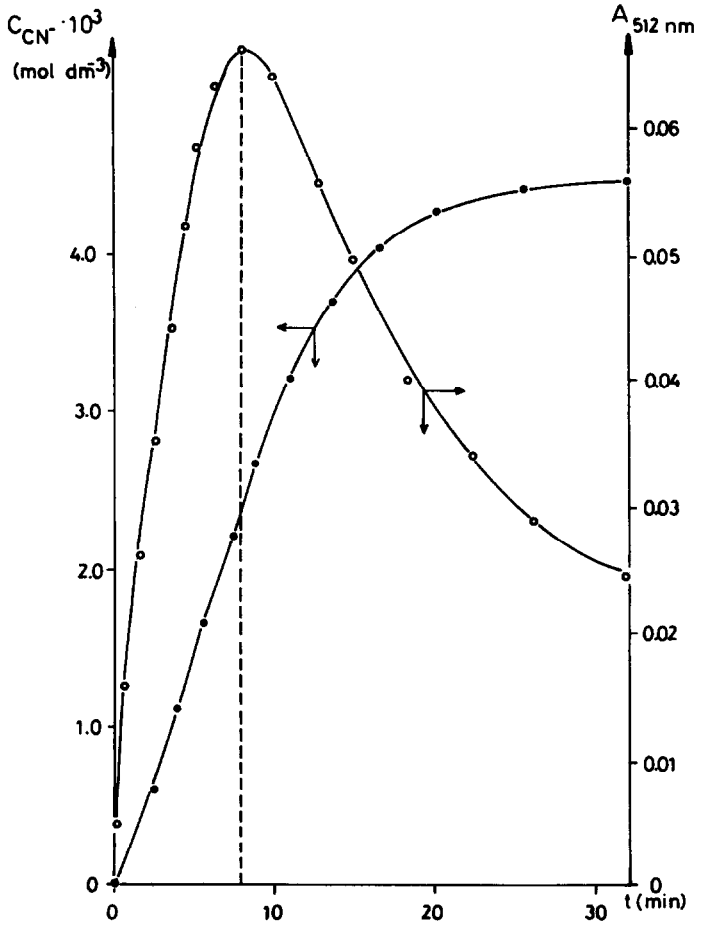

Fig. 1. Simultaneous change in the free cyanide ion concentration (●) and absorbance (○) at 512 nm on exposure to sunlight. $[Mo(CN)]_o^{4-} = 2.5 \times 10^{-3}$ mol dm^{-3}.

ion released by 1 mol of the initial complex ion. The absorbance changes according to a maximum curve. At the maximum value the free cyanide ion concentration is 2.35×10^{-3} mol dm^{-3}. Since in a strongly alkaline solution the amount of hydrogen cyanide formed can be neglected, the kinetic mean coordination number ($\bar{n}_t$) can be calculated by the following equation:

$$\bar{n}_t = \frac{T_{CN} - [CN^-]_t}{T_{Mo}}$$

where T_{CN} and T_{Mo} are the analytical concentrations, and $[CN^-]_t$ is the actual concentration of the free cyanide ion. At the maximum value of the absorbance $\bar{n}_{max} = 7.06$. *This value is in good agreement with the stoichiometry proposed by reaction (A).*

The roughly estimated molar absorbance of the red species is about 50 mol^{-1} dm^3 cm^{-1}. Its magnitude is consistent with the fact that the ligand-field transitions are symmetry-forbidden.

The small decrease (0.1–0.2 pH units) in pH during the irradiation confirms the reaction scheme of Mitra and Mohan.[4]

When the intensity of the irradiating light is small as in our kinetic experiments and the time of illumination is not too long, the reaction system remains in the so-called reversible stage. Figure 2 shows a few periods of the alternating increase and decrease in the free cyanide concentration in the subsequent periods of illumination and darkness.

This behaviour of the system can be qualitatively described by scheme (D), neglecting the decomposition and the ligand exchange reaction of the red species:

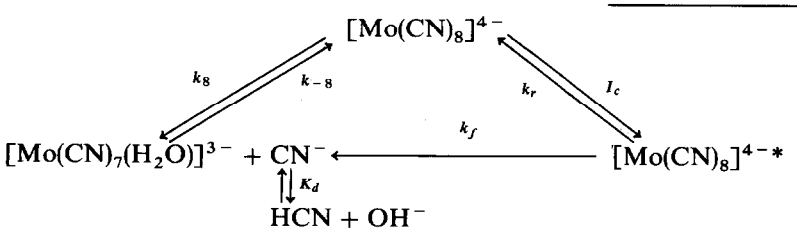

(D)

This scheme is completely analogous to the scheme applied for the description of the kinetics of the photoaquation of the hexacyanoferrate(II) ion in alkaline solution. (The water molecules are systematically omitted from the scheme.) I_c is the average number of moles of photons (365 nm) absorbed by the complex ion per unit volume and unit time. In our experiments it amounts to 6.3×10^{-8} mol of photons dm^{-3} s^{-1}. $[Mo(CN)_8]^{4-*}$ is the excited state of the complex ion. k_r and k_f are the first-order rate constants of the recombination and decomposition of the excited complex ion, respectively. k_8 and k_{-8} are the rate constants of the thermal reactions. K_d is the dissociation constant of hydrogen cyanide.

Introducing the quantum yield Φ $[= k_f/(k_f + k_r)]$ and applying the steady-state approximation for the concentration of the excited complex ion, the following rate equation can be derived:

$$-\frac{d[Mo(CN)_8]^{4-}}{dt} = \frac{d[Mo(CN)_7(H_2O)]^{3-}}{dt} = \Phi I_c + k_8[Mo(CN)_8]^{4-} - k_{-8}[Mo(CN)_7(H_2O)^{3-}][CN^-].$$

Taking into account that the total amount of cyanide released by the complex ion always equals the concentration of the heptacyano complex ion, the concentration of hydrogen cyanide, cyanide and hydroxide ions can be calculated as the components of an acid–base equilibrium system. The exact values of the constants of the kinetic equation were calculated by a least-squares method from the linear algebraic system of the equations given for the parameters. The calculation of the kinetic curves (full lines in Fig. 2) was based on the required combination of the fourth-order Runge–Kutta and Newton–Raphson numerical methods. The values of the constants are: $\Phi = 1.0$, $k_8 = (6.55 \pm 0.8) \times 10^{-9}$ s^{-1}, and $k_{-8} = (7.88 \pm 0.5) \times 10^{-2}$ mol^{-1} dm^3 s^{-1}. According to these data the photostationary (A^*) and thermal-equilibrium (A) values of free cyanide ion concentration can be calculated. As is shown by Fig. 2, the difference between these values is nearly one order of magnitude only. The reversibility of the photoaquation can be interpreted in the light of the two stable solutions, depending on the conditions.

Applying the definition of the $\bar{n}_t$, its change during the reaction can be easily calculated (see dashed line in Fig. 2). The conversions in both photoreactions and thermal reactions are small (1.98 and 0.11%, respectively). Nevertheless, these very small changes could be exactly determined because of the high sensitivity of the cyanide ion selective electrode.

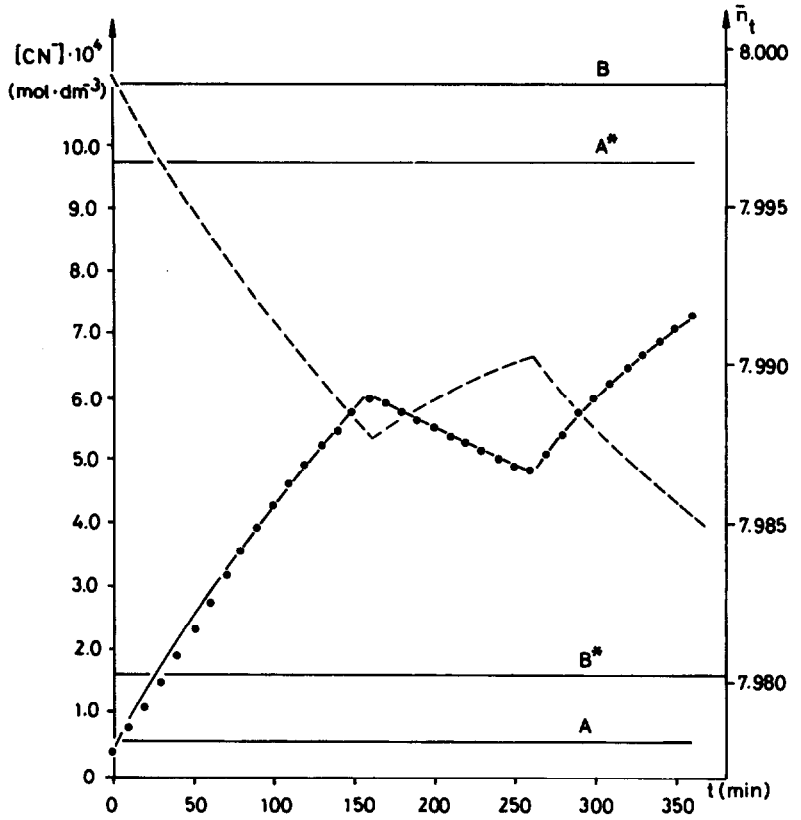

Fig. 2. Experimental (●) and calculated (full line) changes in the free cyanide ion concentration in 5.0×10^{-2} mol dm^{-3} octacyanomolybdate(IV) solution at pH = 10.5. The order of periods is: illumination, darkness, illumination. Dashed line: calculated change in the kinetic mean coordination number ($\bar{n}_t$). *A* and *A** are the thermal and photostationary values of the free cyanide ion concentration, respectively. *B* and *B** are the analogous values of the coordination number.

It follows from the kinetic data that the stability constant of the eighth complex (K_8) ($=k_{-8}/k_8$) is $(1.2 \pm 0.1) \times 10^7$ mol^{-1} dm^3. Unfortunately, no reference *data* are available in the literature on the stability of the complex ion or on the stepwise complex formation reactions. Our result is consistent with the fact that the hexacyanoferrate(II) ion is more stable in alkaline solution and its K_6 value[2] is higher by a factor of 5.

One should take into consideration that scheme (D) is correct only in the case of small conversions. For describing the complete photochemical decomposition of the octacyanomolybdate(IV) ion, scheme (D) should be simply extended by the reaction scheme of Mitra and Mohan.[4]

REFERENCES

1. V. Balzani and V. Carassiti, *Photochemistry of Coordination Compounds*. Academic Press, New York (1970).
2. V. Gáspár and M. T. Beck, *Polyhedron* 1983, **2**, 378.
3. R. D. Wilson, V. S. Sastri and C. H. Langford, *Can. J. Chem.* 1971, **49**, 679.
4. R. P. Mitra and H. Mohan, *J. Inorg. Nucl. Chem.* 1974, **36**, 3739.
5. V. Carassiti and V. Balzani, *Ann. Chim. (Rome)* 1960, **50**, 630.
6. V. Balzani, M. Monfrin and L. Moggi, *Inorg. Chem.* 1969, **8**, 47.
7. A. W. Adamson, J. P. Welker and M. Volpe, *J. Am. Chem. Soc.* 1950, **72**, 4030.
8. A. W. Adamson and J. J. Perummareddi, *Inorg. Chem.* 1965, **4**, 247.
9. W. Jakob, A. Samotus and Z. Stasicka, *Rocz. Chem.* 1962, **36**, 611; *ibid.* 1966, **40**, 967; *ibid.* 1966, **40**, 1383; *Z. Naturforsch.* 1966, **21B**, 819.
10. V. Carassiti, A. M. Mavirangeli and V. Balzani, *Ann. Chim. (Rome)* 1960, **50**, 790.
11. A. Samotus, Z. Stasicka, A. Dudek and L. Nadzeija, *Rocz. Chem.* 1971, **45**, 299.
12. R. P. Mitra, B. K. Sharma and H. Mohan, *Can. J. Chem.* 1969, **47**, 2317.
13. E. J. Bowen, *J. Chem. Soc.* 1935, 76.
14. J. Van de Poel and H. M. Neumann, *Inorg. Synth.* 1968, **11**, 53.
15. C. G. Hatchard and C. A. Parker, *Proc. R. Soc. London* 1956, **A235**, 518.

Polyhedron Vol. 6, No. 2, pp. 275–279, 1987
Printed in Great Britain

0277–5387/87 $3.00 + .00

SOME ORGANOPEROXO COMPLEXES OF MOLYBDENUM AND TUNGSTEN

M. T. H. TARAFDER* and A. R. KHAN

Department of Chemistry, University of Rajshahi, Rajshahi, Bangladesh

(*Received* 17 *April* 1986; *accepted* 23 *June* 1986)

Abstract—Several new peroxo complexes of molybdenum and tungsten containing different organic ligands have been prepared. The complexes have the compositions $[Mo(O)(O_2)L_2]$, $[Mo(O)_2(O_2)L(H_3O)]^+$, $[Mo(O)(O_2)L']$ and $[W(O)(O_2)L_2]$ [L = oxoquinolino, aniline-2-carboxylate, 2-aminophenoxide, picolinato or 2-carboxylatoquinolino ligand; L′ = *N*-(2-oxophenyl)salicylidenimino ligand], respectively. The complexes were found to oxidize allyl alcohol, and also PPh_3 and $AsPh_3$, to their oxides. The IR spectra of the complexes indicate that the frequency of the ν_1-mode of the $M(O_2)$ grouping, which is essentially an O—O stretch, decreases with the increase in atomic number of metals in a particular group.

In recent years, there has been considerable interest in the dioxygen complexes of transition metals because of their coordination chemistry as well as their role in synthetic organic chemistry.[1–10] Dioxygen itself is a reactive entity but, since it has a triplet ground state, its direct combination with organic molecules is a spin-forbidden process.[2] Transition metals having multiple spin and oxidation states can readily interact with dioxygen, and, in some cases, they form isolable oxygen adducts.

Investigations into the fixation and activation of molecular oxygen by transition metals were largely initiated to understand the bondings and structures of such compounds, but later these were found to be both stoichiometric and catalytic reagents for epoxidation of olefins, allyl alcohols etc. We have been interested to extend such a study with new hetero ligand peroxo complexes of molybdenum and tungsten. We report here the synthesis of these complexes and their possible oxygen transfer reactions.

EXPERIMENTAL

Physical measurements

IR spectra (as KBr discs) were recorded with a Pye–Unicam SP3-300 IR spectrophotometer. Conductivities of solutions in nitrobenzene or *N*, *N*′-dimethylformamide (DMF) were measured at 298 K with a conductivity bridge type M.C.3 (Electronic Switchgear Ltd, London). 10^{-3} M solutions of the complexes were used for this purpose.

Reagents

All chemicals used were of reagent grade and were used as supplied by Merck.

Analyses

Molybdenum and tungsten were determined gravimetrically.[11] Methanolic solutions of the peroxo complexes were titrated with Ce(IV) to determine the number of active oxygen atoms present.[11] Carbon and hydrogen analyses were done by Mikroanalytisches Labor Pascher, Germany.

Preparation of the Schiff base (L′)

This was prepared from 2-aminophenol and salicylaldehyde following the published procedure.[6]

Preparation of complexes

General method for the preparation of complexes (**1**, **3**, **4**, **6** *and* **7**): $M(O)(O_2)L_2$ [M = Mo(VI) *or* W(VI), L = *picolinato or 2-carboxylatoquinolino ligands*]. A suspension of MO_3 (0.013 mol) in 30%

*Author to whom correspondence should be addressed.

H_2O_2 (50 cm^3) was stirred overnight at 45–50°C to get a clear solution. This was cooled to 0°C when a solution of organic ligand L (0.026 mol) in acetone (20 cm^3) was added to it. The mixture was stirred while cooling at the same time in an ice–salt bath. A bright yellow precipitate appeared, which was washed successively with water and *n*-hexane, and dried *in vacuo* over P_4O_{10}.

Preparation of $H^+[Mo(O)_2(O_2)(C_6H_4NH_2COO)(H_2O)]$. The same procedure was applied to 2.2 g (0.0153 mol) of molybdic acid and 2.1 g (0.0153 mol) of 2-aminobenzoic acid. Yield 3.0 g (62%) of the complex.

Preparation of $[Mo(O)(O_2)C_{13}H_9NO_2]$. This was prepared from 1.5 g (0.01 mol) of molybdic acid and 2.4 g (0.01 mol) of *N*-(2-hydroxyphenyl)salicylidenimine. Yield 2.5 g (67%) of the complex.

Reaction of **1** *with allyl alcohol (reaction A)*

Compound **1** (6.5 g, 0.015 mol) was suspended in 20 cm^3 of tetrahydrofuran (THF), and a stoichiometric amount of allyl alcohol was added. The mixture was refluxed at 60°C for 24 h. Microdistillation under *ca* 19 mmHg yielded glycidol [0.5 g (57%)] at 145–150°C. The glycidol was identified from its boiling point.

Catalytic reaction of **1** *and* H_2O_2 *with allyl alcohol (reaction B)*

A 25-cm^3 quantity of allyl alcohol (21.3 g, 0.367 mol) was dissolved in 20 cm^3 of dioxane and 1.1 g of **1** was added followed by 25 cm^3 of 30% H_2O_2. The mixture was kept under reflux at 90°C for 24 h. The reaction mixture was filtered and the filtrate distilled at 19 mmHg pressure. The fraction collected at 175–180°C was identified as glycerol [18 g (53% yield)].

Reaction of **3** *with triphenylphosphine (reaction C)*

A solution of triphenylphosphine (0.7 g, 0.0026 mol) in THF (20 cm^3) was added to a solution of **3** (0.94 g, 0.0026 mol) in the same solvent (60 cm^3). The mixture was refluxed for 48 h. TLC indicated that the reaction was complete. The solution was filtered and the residue collected. A yellowish white powder was recovered from the filtrate which was identified as $OPPh_3$ [m.p. 155–157°C (lit. 157°C)].

Reaction of **4** *with triphenylarsine (reaction D)*

A solution of triphenylarsine (0.68 g, 0.0022 mol) in THF (30 cm^3) was added to a solution of **4** (0.86 g, 0.0022 mol) in the same solvent (70 cm^3). The mixture was refluxed for 72 h. TLC indicated that arsine was converted entirely into arsine oxide. The solution was filtered and the residue collected. Evaporation of the filtrate yielded the product [m.p. 187–189°C (lit. 189°C)].

Complexes **6** and **7** were also found to be effective stoichiometric reagents for the oxidation of PPh_3 and $AsPh_3$ to their oxides.

RESULTS AND DISCUSSION

The analytical and molar-conductance data (Table 1) are consistent with a seven-fold coordination of the metal atom. Titrations of methanolic solutions of the peroxo complexes with Ce(IV) indicated that **1**–**7** were monoperoxo complexes. The molar-conductance values indicated that all of the complexes were non-electrolytes in solution except for **2** which exhibited a value characteristic of a 1:1 electrolyte in DMF (Table 1). Literature values[12] for 1:1 electrolytes are comparable to ours. Alkalimetric titration of **2** indicated an inflection point at pH 6.3 which corresponds to the neutralization of the outer-sphere proton.

IR spectral data are shown in Table 2. The ν(O—H) band at 3405 cm^{-1}, observed in the free 8-hydroxyquinoline disappears upon coordination, which indicates deprotonation and coordination at the oxygen site. Further, in compounds **1** and **7**, the decrease in ν(C=N), by 50 and 30 cm^{-1}, respectively, relative to the free-ligand value (1610 cm^{-1}) indicates coordination by the heterocyclic nitrogen.[4,9,13] The shifting of ν(C=N) modes thus suggest that Mo(VI) acts as a stronger acceptor than W(VI). Complexes **2** and **3** show two ν(N—H_2) bands (Table 2) significantly lower than the values for 2-aminobenzoic acid and 2-aminophenol (3390, 3300 and 3414, 3342 cm^{-1}).[6] Complexes **2**, **4** and **6** show a decrease in ν(C=O) by 48, 85 and 77 cm^{-1}, respectively, from the free-ligand values, indicating carboxylate binding in the complexes.[4,6,13] In **4** and **6**, the appearance of ν(C=N) at 1595 and 1590 cm^{-1}, respectively, suggest that the heterocyclic nitrogen is coordinated to the metal atom. The Schiff-base *N*-(2-hydroxyphenyl)-salicylidenimine in complex **5** behaves as a tridentate–dinegative ligand coordinating at the imino nitrogen and two oxygen atoms.[6] In complex **5**, the decrease in ν(C=N) by 25 cm^{-1} relative to the free-ligand value[6] indicates coordination through the imino nitrogen atom.[14,15] The ν(O—H) band

Table 1. Analytical data and other physical properties of Mo(VI) and W(VI) peroxo complexes[a]

No.	Compound	% metal		% carbon		% hydrogen		% peroxide		Molar conductance
		Calc.	Found	Calc.	Found	Calc.	Found	Calc.	Found	(Ω^{-1} cm^2 mol^{-1})
1	$[Mo(O)(O_2)(C_9H_6NO)_2]$	22.2	22.0	50.0	50.0	2.8	2.7	7.4	7.4	0
2	$H^+[Mo(O)_2(O_2)(C_6H_4NH_2COO)(H_2O)]$	30.5	30.3	26.6	26.5	2.8	2.8	10.2	10.2	65.5
3	$[Mo(O)(O_2)(C_6H_4NH_2O)_2]$	26.6	26.6	40.0	39.8	3.3	3.3	8.9	8.9	0.2
4	$[Mo(O)(O_2)(C_5H_4NCOO)_2]$	24.6	24.4	36.9	36.8	2.0	2.0	8.2	8.2	0.2
5	$[Mo(O)(O_2)C_{13}H_9NO_2]$	25.8	25.6	42.0	41.8	2.4	2.4	8.6	8.6	0.5
6	$[Mo(O)(O_2)(C_9H_6NCOO)_2]$	19.6	19.6	49.2	49.1	2.5	2.4	6.5	6.5	0
7	$[W(O)(O_2)(C_9H_6NO)_2]$	35.4	35.3	41.5	41.3	2.3	2.3	6.1	6.1	0

[a]The organic moieties for the compounds indicated are:

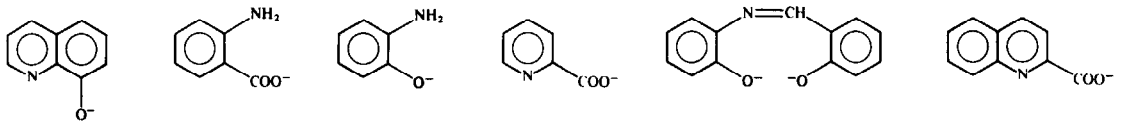

1 and 7 2 3 4 5 6

Table 2. IR spectral data for the Mo(VI) and W(VI) complexes[a] [band maxima (cm^{-1})]

Compound	ν(O—H)	$\nu(NH_2)$	ν(C=O)	ν(C=N)	ν(M=O)	ν_1(O—O)	ν_3(M<O,O>)	ν_2(M<O,O>)	ν(M—O′)	ν(M—N)
1				1560s	950s	848vs	637vs	538s	400w	312s
2	3400br	3270m 3175m	1632vs		945s	860vs	660s	550vs	375m	290sh
3		3315m 3260m			947s	850vs	640s	590m	400w	280w
4			1640vs	1595m	955s	870s	650vs	600w	400vs	300m
5				1615m	950s	900s	680m	600m	385s	295m
6			1628vs	1590s	960s	865s	670s	612m	405m	285m
7				1580s	940vs	825vs	645s	575m	400w	270m

[a]Relative band intensities are denoted by vs, s, m, w, sh and br, meaning very strong, strong, medium, weak, shoulder and broad, respectively.

observed in the free Schiff-base at 3290 cm^{-1} disappears upon coordination, which indicates deprotonation and coordination at the oxygen site. Further support for M—O′ (O′ = oxygen in organic ligand, M = Mo or W) and M—N bondings in **1–7** are evident from the appearance of ν(M—O′) and ν(M—N) modes at 375–405 and 280–312 cm^{-1}, respectively. All of the complexes display ν(M=O modes.[5]

The metal–peroxo grouping gives rise to three IR-active vibrational modes. These are predominantly O—O stretching (ν_1), the symmetric M—O stretch (ν_2), and the antisymmetric M—O stretch (ν_3). The characteristic ν_1(O—O) modes of **1–6** appear at 848–900 cm^{-1}. There is a decrease in ν_1 upon passing from molybdenum complexes to the tungsten complex **7**. The ν_1-mode was found to decrease further in the peroxo complex of uranium.[6] The ν_3 and ν_2-modes in **1–7** appear at 637–680 and 538–612 cm^{-1}, respectively. The assignments shown in Table 2 are based on comparisons with other peroxo complexes of molybdenum and tungsten.[4,5,16,17]

Reactivity

Peroxo complexes of melybdenum and tungsten were not explosive. These were found to liberate iodine on treatment with aqueous iodide. So that the possible reactivity of the present peroxo complexes toward olefinic compounds could be explored, compound **1** was allowed to react stoichiometrically with allyl alcohol (reaction A) which produced glycidol as indicated by an IR band at 1055 cm^{-1} assigned to a C—O—C stretching mode.[7,18] With H_2O_2 and only a catalytic amount of **1** (reaction B), the product isolated was glycerol as indicated by its boiling point. The IR spectrum was identical with that of an authentic sample. A possible reaction path is shown in Scheme 1.

Reactions C and D produced $OPPh_3$ and $OAsPh_3$, respectively. The products showed IR bands at 1190 and 880 cm^{-1}, assigned to ν(P=O) and ν(As=O) modes, respectively.[19,20] IR spectra of the metal residues of reactions C and D showed the disappearance of ν_1(O—O) bands, thereby indicating the transfer of peroxo oxygens to the substrates.

REFERENCES

1. H. Mimoun, I. S. de Roch and L. Sajus, *Tetrahedron* 1979, **26**, 37.
2. H. Mimoun, *J. Mol. Catal.* 1980, **7**, 1.
3. D. A. Muccigrosse, S. E. Jacobson, P. A. Apgar and F. Mares, *J. Am. Chem. Soc.* 1978, **100**, 7063.
4. S. E. Jacobson, R. Tang and F. Mares, *Inorg. Chem.* 1978, **17**, 3055.
5. A. D. Westland, F. Haque and J. M. Bouchard, *Inorg. Chem.* 1980, **19**, 225.
6. A. D. Westland and M. T. H. Tarafder, *Inorg. Chem.* 1981, **20**, 3992.
7. A. D. Westland and M. T. H. Tarafder, *Inorg. Chem.* 1982, **21**, 3228.
8. O. Bertolini, V. Conte, F. DiFuria and G. Modena, *Nouv. J. Chim.* 1985, **9**, 157.
9. M. T. H. Tarafder and M. A. Latif Miah, *Inorg. Chem.* 1986, **25**, 2265.
10. M. T. H. Tarafder and Alauddin Ahmed, *Indian J. Chem.* (in press).
11. A. I. Vogel, *A Text Book of Quantitative Inorganic Analysis*, 3rd Edn. Longmans, Green, London (1961).
12. W. J. Geary, *Coord. Chem. Rev.* 1971, **7**, 113.
13. H. Minoun, M. Postel, F. Casabianca, J. Fischer and A. Mitschler, *Inorg. Chem.* 1982, **21**, 1303.
14. J. E. Kovacic, *Spectrochim. Acta* 1967, **23A**, 183.
15. M. Akbar Ali, *Can. J. Chem.* 1980, **58**, 727.
16. E. Wendling, *Bull. Soc. Chim. Fr.* 1967, 16.
17. W. P. Griffith, *J. Chem. Soc.* 1964, 5428.
18. G. A. Olah and J. Weleh, *J. Org. Chem.* 1978, **43**, 2830.
19. D. Brown, J. Hill and C. E. F. Rickard, *J. Chem. Soc. A* 1970, 499.
20. J. Burnstein, M. Halman, S. Pinchas and D. Samuel, *J. Chem. Soc.* 1964, 821.

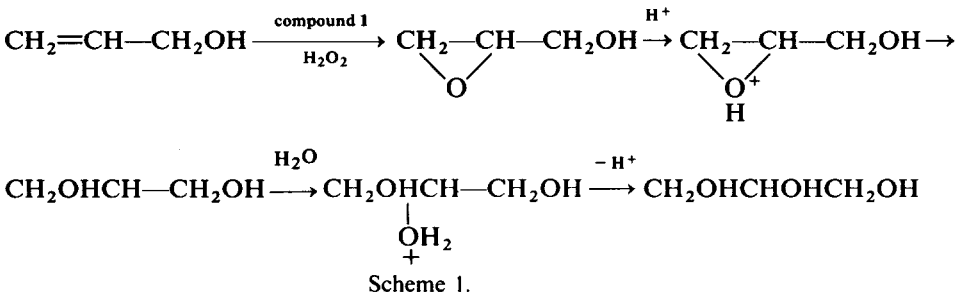

Scheme 1.

Polyhedron Vol. 6, No. 2, pp. 281–283, 1987
Printed in Great Britain

0277–5387/87 $3.00+.00

HAVE $Cp^*_2MoOCl_2$ AND $Cp^*_2WOCl_2$ EVER BEEN ISOLATED? ON THE REPRODUCIBILITY OF THE REPORTED SYNTHESES

PIETRO DIVERSI, GIOVANNI INGROSSO, ANTONIO LUCHERINI* and MARCO LANDUCCI

Dipartimento di Chimica e Chimica Industriale, Università di Pisa, Via Risorgimento 35, 56100 Pisa, Italy

(*Received* 15 *May* 1986; *accepted* 23 *June* 1986)

Abstract—The literature reports on the syntheses of $Cp^*_2MOCl_2$ (M = Mo or W, Cp* = cyclopentadienyl or indenyl) could not be confirmed, and attempts to prepare $(C_5H_5)_2MoOI_2$ by oxidative addition of I_2 to $(\eta^5\text{-}C_5H_5)_2MoO$ failed.

We were interested in studying the reactivity of the complexes $Cp^*_2MOCl_2$ (M = Mo or W; Cp* = C_5H_5, C_5Me_5 or indenyl) as suitable starting materials in organometallic chemistry and catalysis.

The preparation of the cyclopentadienyl and indenyl complexes, according to the following equation:

$$MOCl_4 + 2Cp^*H\,(\text{or } Cp^*Na) \xrightarrow{THF,\Delta} Cp^*_2MOCl_2 + 2HCl\,(\text{or NaCl})$$

has been reported by Multani *et al.*[1–6] since 1968 without mentioning possible problems in the isolation and crystallization of the products. These syntheses appeared very simple, and suitable to be extended to the preparation of $(C_5Me_5)_2MOCl_2$.

Surprisingly all the attempts to prepare these compounds were unsuccessful. This fact, in addition to the recent reports[7,8] on the failure to confirm the synthesis of $(C_5H_5)_2WOCl_2$ and other preparations by Multani *et al.*, stimulated us to relate our results.

RESULTS AND DISCUSSION

Molybdenum and tungsten oxide tetrachlorides

It has been repeatedly asserted by Multani *et al.*[2,3,5,9] that the $MOCl_4$ oxychlorides, necessary for the synthesis of the title complexes, were prepared from MO_3 in refluxing $SOCl_2$, following the preparation described by Colton and Tomkins.[10]

We have found that only $MoOCl_4$ could be easily obtained by this way, since WO_3 did not react in refluxing $SOCl_2$ even when a long reaction time (48 h) was employed. We succeeded in preparing $WOCl_4$ either by reacting WO_3 with an excess of S_2Cl_2 at 180°C,[11] or from tungstic acid (Fluka) in refluxing $SOCl_2$ for 3 h (yield 75% of sublimed product). This last route, which is analogous to that reported by Colton and Tomkins[10] who prepared $MoOCl_4$ from sodium molybdate and $SOCl_2$, has been independently discovered by Crabtree and Hlatky.[7]

Reaction of molybdenum and tungsten oxychlorides with Cp*H

According to the literature method,[1–6] the $MOCl_4$ oxychlorides were reacted with an excess of Cp*H ($[Cp^*H]/[MOCl_4]$ = 3–4) in refluxing THF for 6–8 h, giving dark-blue or black products insoluble in pentane and diethyl ether, hardly soluble in benzene, chloroform and methylene chloride, and partly soluble in THF. These solubilities were very much different from those reported for the expected complexes, and all attempts to obtain pure crystalline compounds failed. Moreover the raction products were found not to be inert to water, in contrast to the literature report.[4] Although the IR spectra were not well resolved, bands at 950–980 cm^{-1}, attributable to the stretching of M=O, were observed. The ^1H NMR spectra of

*Author to whom correspondence should be addressed.

the $CDCl_3$ or C_6D_6 extracts showed enlarged signals in the region of the Cp* resonances that might be indicative of a mixture of products and/or the presence of paramagnetic impurities. The results of elemental analyses changed from run to run, and in general the carbon and chlorine percentages were markedly lower than those calculated for the expected products.

In the case of the reaction of $WOCl_4$ with indene, the elemental analysis of the residue to the extraction (THF) of the crude reaction product gave a chlorine percentage close to that expected for $(C_9H_7)_2WOCl_2$, but a carbon percentage clearly lower; the elemental analysis of the product recovered from the THF extracts gave results that were consistent with the formulations $(C_9H_7)_3WOCl$ or $(C_9H_7)_3WOCl \cdot THF$ (see Experimental).

On the basis of these results, and of some reports[6,12] on the preparation of complexes of type Cp^*_4MoO on reaction of $Cp^*_2MoOCl_2$ or $MoOCl_4$ with Cp*Na, we repeated the reactions using a [Cp*H]/[$MOCl_4$] molar ratio of 2: we obtained again insoluble dark-blue or black crude products.

The same results were obtained by adding the Cp*H reagent at low temperature (−20°C), or varying the reaction time, or the solvent (benzene, diethyl ether or *n*-hexane), or carrying out the reaction in the presence of diethylamine as HCl trapper.

Since several alkyl complexes of type $(C_5H_5)_2WOR_2$ (R = Me, Et, Ph or CH_2Ph) were prepared[3] by alkylation of $(C_5H_5)_2WOCl_2$, we tried to obtain the methyl derivatives by the treatment of the crude residues with MeMgI in diethyl ether: we could not obtain any pentane-soluble product nor isolate other organometallic compounds.

Reactions of the molybdenum and tungsten oxychlorides with Cp*Na

In spite of many attempts carried out according to the described procedure,[1-6] we failed to obtain $(C_5H_5)_2MOCl_2$ by reacting $MOCl_4$ oxychlorides with two equivalents of C_5H_5Na in refluxing THF for 3–4 h. Instead brown-black precipitates were obtained, which were extracted with THF. Addition of *n*-hexane to these solutions caused the precipitation of blue-black compounds, whose IR analyses were indicative of the presence of C_5H_5 and M=O groups; however elemental analyses gave carbon and chlorine percentages lower by far than those calculated for the desired products (M = Mo, Found: C, 30.4; H, 3.7; Cl, 16.6%. Calc. for $C_{10}H_{10}Cl_2MoO$: C, 38.4; H, 3.2; Cl, 22.7%. M = W, Found: C, 21.6; H, 2.9; Cl, 12.5%. Calc. for $C_{10}H_{10}Cl_2OW$: C, 30.0; H, 2.5; Cl, 17.7%.)

In the case of the reactions of the $MOCl_4$ oxychlorides with C_9H_7Na in refluxing THF no precipitate formed: evaporation of the solvent led to residues insoluble in benzene and diethyl ether. Attempts to eliminate NaCl by washing with H_2O gave insoluble blue-black residues whose elemental analyses were very different (chlorine percentages always lower than 6%) from those calculated for the expected complexes.

Variations in some reaction parameters such as temperature (−20 to +20°C) or medium (*n*-hexane, diethyl ether or benzene) did not cause any improvement.

Since we were interested in the synthesis of Group VI transition metal metallacycles,[13] we treated the crude mixture obtained from the reaction of $MoOCl_4$ and C_5H_5Na with an excess of 1,4-dilithiobutane in diethyl ether. Chromatographic purification of the pentane-soluble materials on a column of neutral alumina yielded a small quantity of orange-red crystals identified as bis(η^5-cyclopentadienyl)molybdenacyclopentane by elemental analysis and by comparison of its ^1H NMR spectrum with that of an authentic sample.[13] We do not know whether $(\eta^5\text{-}C_5H_5)_2Mo(CH_2CH_2CH_2CH_2)$ is derived from the alkylation of the $(\eta^5\text{-}C_5H_5)_2MoCl_2$ compound, or from $(C_5H_5)_2MoOCl_2$, 1,4-dilithiobutane behaving both as a reducing and an alkylating agent.

Alkylation of the other crude mixtures obtained from $MOCl_4$ and Cp*Na with 1,4-dilithiobutane failed to give identifiable organometallic compounds.

Reaction of bis(cyclopentadienyl)molybdenum oxide with I_2

In the attempt to obtain $(C_5H_5)_2MoOI_2$ by an alternative route, we reacted the $(\eta^5\text{-}C_5H_5)_2MoO$ complex[14] with I_2 in THF at room temperature, but the desired oxidative addition of I_2 did not occur, and we recovered a precipitate (59% yield) identified as $(\eta^5\text{-}C_5H_5)_2MoI_2$ by comparison of its IR and ^1H NMR spectra with those of an authentic sample.[15] No organometallic compound was isolated from the THF solution.

In contrast to the literature reports[1-6] the reactions described here failed to give the desired compounds, leading always to mixtures of insoluble, intractable compounds.

We cannot, of course, exclude the possibility that our failure to repeat the described syntheses of the title compounds is due to some unpublished but important experimental detail. However, on the basis of these and other[7] efforts to repeat this

chemistry, we would suggest that one must be careful before choosing $Cp^*_2MOCl_2$ complexes as starting materials.

EXPERIMENTAL

All operations were carried out under dinitrogen or argon by Schlenk techniques. Diethylether and THF were first refluxed and distilled from sodium, and then from lithium aluminum hydride. Pentane and benzene were washed free of olefins or thiophene with concentrated sulphuric acid, dried on calcium chloride, and then distilled from lithium aluminum hydride. Unless otherwise stated, other solvents were reagent grade, and were degassed under reduced pressure and dried on molecular sieves before use.

IR spectra were run on a Perkin–Elmer 283-B instrument. ^1H NMR spectra were run at 60 MHz on a Varian T60 instrument using $SiMe_4$ as the internal standard. Microanalyses were performed by the Laboratorio di Microanalisi of the Istituto di Chimica Organica, Facoltà di Farmacia, Università di Pisa.

$MoOCl_4$,[10] $WOCl_4$,[7] C_5H_5Na,[16] C_9H_7Na,[17] $Li(CH_2)_4Li$[18] and $(\eta^5\text{-}C_5H_5)_2MoO$[14] were prepared as described.

The reactions of $MOCl_4$ with Cp*H (or Cp*Na) were performed as described,[1–6] or with the variations described in Results and Discussion; the resulting solid products were washed with diethyl ether and pentane, and then dried *in vacuo* (0.1 mmHg). The reactions of 1,4-dilithiobutane with the crude products obtained by reacting $MOCl_4$ oxychlorides with Cp*Na were carried out according to the described procedures.[13]

Reaction of $WOCl_4$ *with indene*

$WOCl_4$ (1.20 g, 3.52 mmol) dissolved in benzene (50 cm^3) was treated with freshly distilled indene (1.8 cm^3, 15.4 mmol). The resulting mixture was refluxed for 14 h and then the brown solid formed was separated, washed with diethyl ether (3 × 30 cm^3) and extracted with THF (2 × 50 cm^3). The insoluble black residue was recovered and dried *in vacuo*. (Found: C, 35.3; H, 2.7; Cl, 15.4%. Calc. for $C_{18}H_{14}Cl_2OW$: C, 43.2; H, 2.8; Cl, 14.2%.) Evaporation to dryness of the THF extracts gave a brown solid which was washed with pentane and dried *in vacuo*. (Found: C, 58.3; H, 4.6; Cl, 6.5%. Calc. for $C_{27}H_{21}ClOW$: C, 55.8; H, 3.6; Cl, 6.1%. Calc. for $C_{31}H_{29}ClO_2W$: C, 57.0; H, 4.5; Cl, 5.5%.)

Reaction of $(\eta^5\text{-}C_5H_5)_2MoO$ *with* I_2

$(\eta^5\text{-}C_5H_5)_2MoO$ (0.241 g, 1.0 mmol) dissolved in THF (50 cm^3) was treated with I_2 (1.0 mmol, 4 cm^3 of a 0.25 mol dm^{-3} THF solution). The resulting mixture was stirred at room temperature for 4 h and then the black solid formed was separated, washed with diethyl ether (3 × 10 cm^3), and dried *in vacuo*. $(\eta^5\text{-}C_5H_5)_2MoI_2$ (0.284 g, 59% yield) was obtained. (Found: C, 25.6; H, 2.6; I, 53.1%. Calc. for $C_{10}H_{10}I_2Mo$: C, 25.0; H, 2.4; I, 52.7%.)

Acknowledgement—This work was supported by a grant from the Ministero della Pubblica Istruzione, Rome.

REFERENCES

1. S. P. Anand, R. K. Multani and B. D. Jain, *Curr. Sci.* 1968, **37**, 487.
2. S. P. Anand, R. K. Multani and B. D. Jain, *J. Organomet. Chem.* 1969, **17**, 423.
3. S. P. Anand, R. K. Multani and B. D. Jain, *J. Organomet. Chem.* 1969, **19**, 387.
4. S. P. Anand, R. K. Multani and B. D. Jain, *J. Organomet. Chem.* 1970, **24**, 427.
5. S. P. Anand, R. K. Multani and B. D. Jain, *J. Organomet. Chem.* 1971, **28**, 265.
6. K. M. Sharma and S. P. Anand, *J. Prakt. Chem.* 1973, **315**, 258.
7. R. H. Crabtree and G. G. Hlatky, *Polyhedron* 1985, **4**, 521.
8. G. B. Deacon, T. D. Tuong and D. G. Vince, *Polyhedron* 1983, **2**, 969.
9. S. P. Anand, R. K. Multani and B. D. Jain, *Bull. Chem. Soc. Jpn* 1969, **42**, 3459.
10. R. Colton and I. B. Tomkins, *Aust. J. Chem.* 1965, **18**, 447.
11. H. Funk, W. Weiss and G. Mohaupt, *Z. Anorg. Allg. Chem.* 1960, **304**, 238.
12. K. C. Goyal and B. D. Khosla, *Curr. Sci.* 1980, **49**, 469.
13. P. Diversi, G. Ingrosso, A. Lucherini, W. Porzio and M. Zocchi, *J. Chem. Soc., Dalton Trans.* 1983, 967.
14. M. L. H. Green, A. H. Lynch and M. G. Swanwick, *J. Chem. Soc., Dalton Trans.* 1972, 1445.
15. R. L. Cooper and M. L. H. Green, *J. Chem. Soc. A* 1967, 1155.
16. R. B. King and F. G. A. Stone, *Inorg. Syn.* 1963, **7**, 99.
17. R. B. King and A. Efraty, *J. Organomet. Chem.* 1970, **23**, 527.
18. J. X. McDermott, M. E. Wilson and G. M. Whitesides, *J. Am. Chem. Soc.* 1976, **98**, 6529.

Polyhedron Vol. 6, No. 2, pp. 285–288, 1987
Printed in Great Britain

0277–5387/87 $3.00+.00

COMPLEXES OF 1-(2′-HYDROXYBENZYL)-2-(2′-HYDROXYPHENYL)-BENZIMIDAZOLE WITH U(VI) AND Ce(IV)

K. M. M. S. PRAKASH, L. D. PRABHAKAR* and M. C. CHOWDARY

Department of Chemistry, Sri Krishnadevaraya University, Anantapur 515003, India

(*Received* 9 *December* 1985; *accepted after revision* 27 *June* 1986)

Abstract—Some new U(VI) and Ce(IV) complexes of 1-(2′-hydroxybenzyl)-2-(2′-hydroxyphenyl)-benzimidazole have been prepared and characterized by spectral, magnetic and conductance studies. IR spectral data suggests that the ligand in all the complexes is monodenate through the tertiary nitrogen and that the phenolic oxygen is free from coordination. Conductivity measurements indicate that the nitrate and acetate complexes of U(VI) are non-electrolytes, whereas the nitrate complex of Ce(IV) is a 1:1 electrolyte.

Uranyl complexes with various nitrogen and oxygen donars have been extensively reviewed.[1–7] Recently the Schiff's base compounds have aroused new interest because of their high stability, and they can be used for selective chemical separations.[8,9] Herein we report the synthesis and characterization of the uranyl and cerium complexes.

EXPERIMENTAL

Physico-chemical measurements

Elemental (C, H and N) analyses of the complexes were recorded in the Analytical Division, Regional Research Laboratory, Hyderabad, India. IR spectra were recorded in both Nujol mulls and KBr pellets on a Perkin–Elmer 983 G IR spectrophotometer. Magnetic susceptibilities for the solid compounds were determined by the Guoy method using $Hg[Co(NCS)_4]$ as standard. The molar conductances of the complexes were determined by using Systronics direct reading Conductivity Meter 303.

Synthesis and characteristics of the ligand

1-(2′-Hydroxybenzyl)-2-(2′-hydroxyphenyl)-benzimidazole was prepared according to Subbarao and Ratnam[10] by refluxing 1,2-phenylenediamine with salicylaldehyde (1:3) in glacial acetic acid. The white product that separated was recrystallized from MeOH.

The IR spectra measured in KBr pellets showed a peak at 1480 cm^{-1} which can be assigned to $\nu(C{=}N)$ stretching. A peak at 3500–3700 cm^{-1} corresponding to the free phenolic —OH is not observed; instead a peak at 3300 cm^{-1} confirms the intramolecular hydrogen bonding of the two —OH groups.[11–13] Based on the above observations the structure of the ligand can be represented as

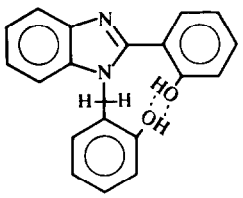

	C	H	N
Calculated	75.9	5.6	8.9
Experimental	75.8	5.8	8.7

Preparation of the compound

The complexes were prepared by refluxing methanolic solutions of ligand and corresponding metal salts at 70–80°C. The solution containing the complex was evaporated *in vacuo* until the solid crystallizes. The precipitates were filtered off and washed with aqueous MeOH. The product was dried *in vacuo* for 24 h.

Physical properties

Uranyl(VI) nitrate, uranyl(VI) acetate and Ce(IV) nitrate complexes are soluble in MeOH, DMSO

*Author to whom correspondence should be addressed.

Table 1. Elemental and conductance data

% metal		% C		% H		% N			Molar	
Exp.	Calc.	Exp.	Calc.	Exp.	Calc.	Exp.	Calc.	Solvent	conductance	Complex
33.9	32.3	39.8	39.2	2.8	3.0	3.8	3.8	MeOH	31.25	$[UO_2L(OAc)_2]_2 \cdot 4H_2O$
								DMF	12.04	
								DMSO	48.18	
21.2	22.0	44.6	44.5	2.9	3.0	7.7	7.8	MeOH	—	$[UO_2L_2(NO_3)_2] \cdot 3H_2O$
								DMF	27.02	
								DMSO	54.05	
22.6	23.2	47.0	47.8	3.2	3.2	5.3	5.6	MeOH	—	$[UO_2L_2SO_4]_2 \cdot 3H_2O$
								DMF		
								DMSO	—	
22.1	22.7	46.2	46.0	3.1	3.1	5.3	5.4	MeOH	—	$[UO_2L_2Cl_2] \cdot 4H_2O$
								DMF	—	
								DMSO	—	
11.8	12.8	47.2	47.1	3.1	3.1	11.3	11.0	MeOH	125.00	$[Ce(NO_3)_3L_2]NO_3 \cdot 4H_2O$
								DMF	151.00	
								DMSO	145.83	
12.9	13.5	49.4	49.8	3.2	3.1	5.8	5.8	MeOH	—	$[CeL_2(SO_4)_2] \cdot 4H_2O$
								DMF	—	
								DMSO	—	

and DMF. All the complexes are crystalline powders, decomposed only by strong hot perchloric acid.

Chemical analysis

Uranium was determined by the oxine method as U_3O_8 and cerium was estimated by the Ce(IV) iodate method and subsequent ignition to CeO_2.[14]

RESULTS AND DISCUSSION

Analytical data of the complexes and ligand are shown in Table 1. The ligand has two potential sites for co-ordination, the pyridine nitrogen and the phenolic oxygen atom. Since no change was observed in the pH of the free-ligand solution and its solution after complexation, it can be inferred that the ligand has not been deprotonated. This fact is also supported by the IR spectra where the shift corresponding to the —OH stretching vibration is not observed.

IR spectra

IR spectra of the ligand and its metal chelates* shows a strong IR absorption around 3300 cm^{-1} which is due to —OH stretching vibrations associated with intramolecular hydrogen bonding.[12,13] The hydrated complexes also show a strong absorption in the same region. There is no absorption at 1605 and 900 cm^{-1} corresponding to stretching, and scissoring and rocking modes of vibration of co-ordinated water. Beyond 1600 cm^{-1} the first absorption band in the ligand appears between 1590 and 1450 cm^{-1}, which can be attributed to the C=C of the phenyl ring and the C=N stretching frequency. The ν(C=N) band in the ligand observed at 1480 cm^{-1} is shifted to 1470 cm^{-1} in its complexes. Hence it can be concluded that co-ordination takes place through the pyridine nitrogen and the ligand acts as a neutral one.

The unco-ordinated nitrate (D_{3h}) is expected to exhibit three IR-active fundamentals: $\nu_2(A_2)$, 831 cm^{-1}; $\nu_3(E)$, 1390 cm^{-1}; and $\nu_4(E')$, 790 cm^{-1}; whereas a co-ordinated nitrate (C_{2v}) exhibits six such fundamentals:[15] $\nu_4(B_1)$, 1530–1480 cm^{-1}; $\nu_1(A_1)$, 1290 cm^{-1}; $\nu_2(A_1)$, 1030 cm^{-1}; $\nu_5(B_2)$, 810 cm^{-1}; $\nu_3(A_1)$, 740 cm^{-1}; and $\nu_6(B_1)$, 731 cm^{-1}. In the nitrate complexes of Ce(IV) and U(VI) the $\nu_4(B_1)$ mode falls in the range 1435–1460 cm^{-1} and $\nu_1(A_1)$ in the range 1250–1320 cm^{-1}. The magnitude of $\nu_4 - \nu_1 \neq (140–185\ cm^{-1})$ in these complexes might be considered to be in favour of the bidentate character of the C_{2v} nitrate,[16] though this has not been considered as a good criterion to distinguish between a bidentate and a monodentate nitrate by Kowano and Osokio.[17] A very weak band at 1010–1035 cm^{-1} is assigned to the $\nu_2(A_1)$ mode and those in the region 790–815 cm^{-1} to the $\nu_5(B_2)$ mode of the C_{2v} nitrate. The $\nu_6(B_1)$ mode is

*A table of IR spectral data has been deposited with the Editor as supplementary material.

not observed in both of the nitrate-containing complexes, similar to results of Mishra *et al.*[18] In the sulphate complexes the peaks at 1050, 1160 and 1230 cm^{-1} can be attributed to the bidentate bridging sulphate groups.[16,19] The sharp peak at 1550 cm^{-1} which is absent in the ligand and other complexes is attributed to the ν_{assy}-mode of the monodentate acetate group.[15] The metal–chloride stretching frequency of the uranyl chloride is observed in the range 250–350 cm^{-1} as a weak band, which is absent in the ligand.[20,21]

The uranyl ion exhibits[22,23] three vibrational frequencies: a symmetric (ν_1), asymmetric (ν_3), and stretching and bending (ν_2) frequency. With the linear uranyl ion, only the asymmetric stretching is easily observed in the normal IR spectrum, since the bending frequency is predicted to be around 200 cm^{-1} and the symmetric stretching is IR-inactive. The observed frequencies (890–920 cm^{-1}) lie below that found for an aqueous solution of UO_2^{2+}.

Conductance measurements

The molar conductance of the complexes are shown in Table 1. All the complexes except the Ce(IV) nitrate complex, show a low conductance in DMSO, DMF and MeOH which shows that they behave as non-electrolytes[24] in these solvents. The Ce(IV) nitrate complex shows a conductance attributable to a uni-univalent electrolyte, $[Ce(NO_3)_3L_2]^+NO_3^-$, in all solvents, which indicates that three of the four nitrate groups are in a co-ordination sphere whereas the fourth one is out of the sphere. Thus it can be concluded that only in the Ce(IV) nitrate complex is the nitrate group acting as ionic, monodentate and bidentate. The ability of the nitrate group to function as both a monodentate and a bidentate ligand has been recognized earlier.

Magnetic susceptibilities

All complexes are diamagnetic, as generally expected for $5f^0$U(VI) and $4f^0$Ce(IV) compounds, and it can be concluded that reduction of the metal does not take place under the influence of the ligand.

Acknowledgements—Professor G. Aravamudan of the Indian Institute of Technology, Madras, and Professors V. Krishnan and M. Munichandraiah of the Indian Institute of Science, Bangalore, are thanked for their interest in this work. We wish to thank Professors S. Hussain and P. Raviprasad of the Regional Research Laboratories, Hyderabad, for their help in C, H and N analyses. Thanks are due to the Council of Scientific and Industrial Research, New Delhi, for awarding Senior Research Fellowships to two of the authors (KMMSP and LDP).

REFERENCES

1. K. W. Bagnall, *Chemistry of Actinide Elements*, p. 188. Elsevier, Amsterdam (1972).
2. A. F. Trotman-Dickenson, *Comprehensive Inorganic Chemistry*, Vol. 5, p. 462. Pergamon Press, Oxford (1973).
3. K. W. Bagnall, In *Halogen Chemistry* (Edited by V. Trutamann), Vol. 3, p. 363. Academic Press, London (1967).
4. D. Brown, *Halides of Lanthanides and Actinides*, p. 121. Wiley, London (1968).
5. A. E. Comyns, *Chem. Rev.* 1960, **60,** 115.
6. K. W. Bagnall, *Chemistry of Actinide Elements*, p. 154. Elsevier, Amsterdam (1972).
7. A. F. Trotman-Dickenson, *Comprehensive Inorganic Chemistry*, Vol. 5, p. 301. Pergamon Press, Oxford (1973).
8. G. Bandoli, D. A. Clemente and U. Croatte, IV *Conv. Naz. Chim. Inorg. Venezia*, 1971, Comm. F_7; G. Bandoli, D. A. Clementee, M. Croatte and P. A. Vigato, *J. Chem. Soc., Chem. Commun.* 1971, 1330.
9. P. A. Vigato, S. Degetto, M. Vidali and L. Cattalini, IV *Conv. Naz. Chem. Inorg. Venezia*, 1971, Comm. F_3.
10. N. S. Subbarao and C. V. Ratnam, *Curr. Sci.* 1955, **24,** 299.
11. A. Palm and H. Werbin, *Can. J. Chem.* 1953, **31,** 1004.
12. R. Blinc and D. Hadzi, *J. Chem. Soc.* 1958, **45,** 36.
13. L. E. Khoo and F. E. Smith, *Polyhedron*, 1982, **1,** 213.
14. A. I. Vogel, *Text Book of Quantitative Inorganic Analysis Including Elementary Instrumental Analysis*, pp. 458 and 487. English Language Book Society, Longman (1978).
15. S. Satpathy and B. Sahoo, *J. Inorg. Nucl. Chem.* 1971, **33,** 1971.
16. K. Nakamoto, *Infrared Spectra of Inorganic and Co-ordination Compounds*, p. 161. Wiley, New York (1963).
17. Y. Kawano and M. K. L. Osokio, *J. Inorg. Nucl. Chem.* 1977, **39,** 701.
18. A. Mishra, M. P. Singh and J. P. Singh, *J. Indian Chem. Soc.* 1980, **57,** 249.
19. P. R. Hall, C. H. C. Keinnard and R. A. Plowman, *J. Inorg. Nucl. Chem.* 1966, **28,** 467.
20. S. P. Gosh, P. Hathaachavjee and L. K. Mishra, *J. Indian Chem. Soc.* 1974, **51,** 308.
21. Mangal Singh and Manmohan Singh, *Indian J. Chem.* 1983, **22A,** 522.
22. H. R. Hoekstra, *Inorg. Chem.* 1963, **2,** 492.
23. L. H. Zones, *Spectrochim. Acta* 1958, **10,** 395.
24. V. V. Savant and C. C. Patel, *J. Inorg. Nucl. Chem.*

1972, **34,** 1462.
25. S. Satpathy and B. Sahoo, *J. Inorg. Nucl. Chem.* 1970, **32,** 2223.
26. Buddha Dev Sen and B. V. M. D. Mahone, *J. Inorg. Nucl. Chem.* 1972, **34,** 3509.
27. T. J. Lane, I. Nakagawa, J. L. Walter and A. J. Kandathil, *Inorg. Chem.* 1962, **1,** 267.
28. N. Logan and B. B. Simpson, *Spectrochim. Acta* 1965, **21,** 857.
29. J. I. Bullock, *J. Inorg. Nucl. Chem.* 1967, **29,** 2257.
30. B. S. Manhas, Trikhak and M. Singh, *Indian J. Chem.* 1978, **16A,** 431.
31. A. Kleimslein and I. Gabe, *Anst-Mni I.S. XIV*, 1968, 139.
32. K. Nakamoto, *Infrared Spectra of Inorganic and Coordination Compounds.* Wiley, London (1963).
33. A. D. Allen and T. Theophanides, *Can. J. Chem.* 1964, **42,** 1551.
34. J. R. Durig, Rolyton, D. Link and B. Mitchel, *Spectrochim. Acta* 1965, **21,** 1367.
35. J. R. Durig and D. W. Wertz, *Appl. Spectrosc.* 1968, **22,** 63.
36. N. S. Biradar and V. H. Kulkarni, *J. Inorg. Nucl. Chem.* 1971, **33,** 3867.

Polyhedron Vol. 6, No. 2, pp. 289–293, 1987
Printed in Great Britain

0277–5387/87 $3.00+.00

PREPARATION OF NOVEL PENTAAZA MACROCYCLIC SCHIFF BASE LIGANDS AND APPLICATION OF ONE AS A HIGHLY SELECTIVE EXTRACTANT FOR COPPER(II)

TAKAYUKI MATSUSHITA,* KAZUHIKO TAKAISHI, MANABU FUJIWARA and TOSHIYUKI SHONO

Department of Applied Chemistry, Faculty of Engineering, Osaka University, Yamadaoka, Suita, Osaka 565, Japan

(*Received* 17 *December* 1985; *accepted after revision* 27 *June* 1986)

Abstract—The novel macrocyclic Schiff base ligands L^1, L^2 and L^3 were prepared by the condensation of *N,N'*-bis(2-formyl-4-nitrophenyl)ethylenediamine with ethylenediamine, bis(3-aminopropyl)amine and *N,N*-bis(3-aminopropyl)methylamine, respectively, under high-dilution conditions. Their complexing abilities and extractabilities for transition-metal ions have been investigated and L^2 has been found to be an excellent extractant for copper(II).

Many macrocyclic ligands, such as crown ethers and polyaza compounds, have been extensively synthesized and their complexation with metal ions investigated. However, the complexation and extractability of unsaturated polyaza macrocycles for transition-metal ions have been little studied so far. Zolotov *et al.* reported several tetraaza macrocyclic Schiff base ligands which can selectively extract copper(II).[1–3]

Recently, we have reported that the dinitro-substituted ligand of 5,7,12,14-tetramethyl-1,4,8,11-tetraazacyclotetradeca-1,5,7,12-tetraene has a much more efficient extraction rate and selectivity for copper(II) than the parent macrocycle.[4] Moreover, we have reported that the polymeric ligands containing a tetraaza macrocyclic Schiff base in the polymer backbone can be applied as effective extractants[5,6] and adsorbents[7] selective for copper(II).

In this paper, we will describe the preparation of novel pentaaza macrocycle Schiff base ligands (Fig. 1) and their extractabilities for transition-metal ions such as copper(II), nickel(II) and cobalt(II).

*Author to whom correspondence should be addressed.

EXPERIMENTAL

Preparation of macrocyclic Schiff base ligands

N,N'-bis(2-formyl-4-nitrophenyl)ethylenediamine was prepared as yellow crystals, according to the methods described in the literature.[8,9]

L^1, L^2 and L^3 stand for 7,8,15,16,17,18-hexahydro-3,12-dinitrobenzo [*e, m*] [1,4,8,11] tetraazacyclotetradecane, 7,8,9,10,11,12,13,20,21,22,23-undecahydro-3,17-dinitrodibenzo[*e,r*] [1,4,8,12,16] pentaazacyclononadecane and 7,8,9,11,12,13,20,21,22,23-decahydro-*N*(10)-methyl-3,17-dinitro dibenzo[*e,r*][1,4,8,12,16]pentaazacyclononadecane, respectively.

These ligands were obtained as yellow crystals as follows: A solution of the required diamine or triamine in 50 cm^3 of *N,N*-dimethylformamide (DMF) was added slowly with stirring to a solution of 0.358 g (1 mmol) of *N,N'*-bis(2-formyl-4-nitrophenyl)ethylenediamine in 500 cm^3 of DMF which had been warmed at about 65°C. The yellow solution was stirred for 24 h at 65°C, and then the solvent was removed under reduced pressure. The resulting yellow powder was collected on a glass filter, washed with ethanol, and dried *in vacuo*. The yields of the ligands were 70–80%.

L^1: m.p. 299–300°C (decomp.). Found: C, 56.5; H, 4.7; N, 21.9%. Calc. for $C_{18}H_{18}N_6O_4$: C, 56.5; H, 4.7; N, 22.0%. IR (in KBr disc): 1635, 1605,

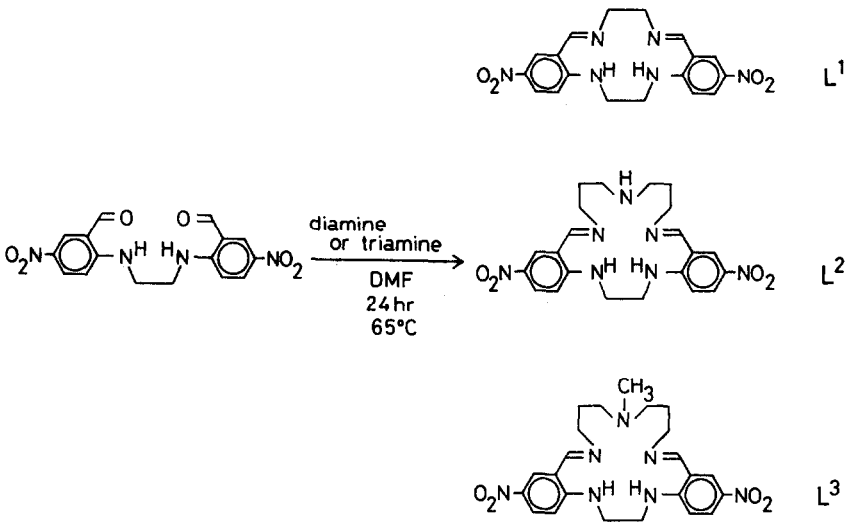

Fig. 1. Synthesis of macrocyclic Schiff base ligands.

1580, 1540, 1495, 1435, 1330, 1300, 1235, 1195, 1150, 1105 and 750 cm^{-1}. MS: m/z = 382 (M^+ = 382).

L^2: m.p. 213–214°C (decomp.). Found: C, 57.9; H, 6.0; N, 21.1%. Calc. for $C_{22}N_{27}N_7O_4$: C, 58.3; H, 6.0; N, 21.6%. IR (in KBr disc): 3300, 2920, 2825, 1635, 1605, 1580, 1535, 1495, 1455, 1430, 1320, 1295, 1185, 1155, 1105, 940, 905, 820 and 750 cm^{-1}. MS: m/z = 453 (M^+ = 453). ^1H NMR (in $CDCl_3$): δ (ppm) = 1.54–2.00 (m, 6H, CH_2—$C\underline{H}_2$—CH_2 and C_6H_3—N$\underline{H}$—CH_2); 2.76–2.98 (t, 4H, $C\underline{H}_2$—NH—$C\underline{H}_2$); 3.58–3.88 (m, 8H, C_6H_3—NH—$C\underline{H}_2$ and CH=N—$C\underline{H}_2$); 3.98 (s, H, CH_2—N$\underline{H}$—CH_2); 6.60–8.26 (m, 6H, $C_6\underline{H}_3$); and 8.41 (s, H, C$\underline{H}$=N).

L^3: m.p.: 252–253°C (decomp.). Found: C, 58.8; H, 6.2; N, 21.0%. Calc. for $C_{23}H_{29}N_7O_4$: C, 59.1; H, 6.2; N, 21.0%. IR (in KBr disc): 3300, 2925, 2835, 2775, 1635, 1605, 1580, 1535, 1495, 1450, 1325, 1300, 1195, 1155, 1105, 820 and 750 cm^{-1}. MS: m/z = 467 (M^+ = 467). ^1H NMR (in $CDCl_3$): δ (ppm) = 1.62–1.90 (m, 6H, CH_2—$C\underline{H}_2$—CH_2 and C_6H_3—N$\underline{H}$); 2.15 (s, 3H, N—$C\underline{H}_3$); 2.42–2.62 (t, 4H, $C\underline{H}_2$—N—CH_3); 3.60–3.78 (m, 8H, CH=N—$C\underline{H}_2$ and C_6H_3—NH—$C\underline{H}_2$); 6.58–8.26 (m, 6H, $C_6\underline{H}_3$); and 8.35 (s, 2H, C$\underline{H}$=N). These assignments were made according to those for the analogous compounds described in the literature.[10,11]

Preparation of copper(II) and nickel(II) complexes with L^1

The copper(II) and nickel(II) complexes with L^1 were prepared according to the literature,[9,12] and confirmed by the elemental analyses.

Preparation of copper(II) and nickel(II) complexes with L^2

To a DMF solution (100 cm^3) of copper(II) acetate monohydrate (0.2 g, 1 mmol) was added L^2 (0.45 g, 1 mmol), the solution was stirred for 2 h at 50°C, and then the solvent was removed to dryness under reduced pressure. The resulting brown powder was collected on a glass filter, washed with ethanol, and recrystallized from DMF. The yield was 79%. Found: C, 50.4; H, 4.9; N, 18.2%. Calc. for $Cu(C_{22}H_{25}N_7O_4)$: C, 51.3; H, 4.9; N, 19.0%. IR (in KBr disc): 1610, 1590, 1535, 1490, 1430, 1275, 1245, 1180, 1150, 1105, 820, 750 and 690 cm^{-1}.

A nickel(II) complex of L^2 was obtained in a similar manner to that described for the copper(II) complex, using nickel(II) acetate tetrahydrate in place of the copper salt. It was recrystallized from DMF. The yield was 76%. Found: C, 50.9; H, 4.9; N, 18.8%. Calc. for $Ni(C_{22}H_{25}N_7O_4)$: C, 51.8; H, 4.9; N, 19.2%. IR (in KBr disc): 1610, 1590, 1535, 1485, 1430, 1285, 1250, 1185, 1155, 1100, 800, 750 and 690 cm^{-1}.

Preparation of copper(II) and nickel(II) complexes with L^3

Both copper(II) and nickel(II) complexes with L^3 were obtained in a similar manner to those described for L^2. These were recrystallized from DMF. The yield of the copper(II) complex was 83%. Found: C, 52.0; H, 5.1; N, 18.5%. Calc. for $Cu(C_{23}H_{27}N_7O_4)$: C, 52.2; H, 5.1; N, 18.5%. IR (in KBr disc): 1605, 1590, 1535, 1490, 1435, 1400, 1285, 1245, 1160, 1105, 805, 750 and 700 cm^{-1}.

The yield of the nickel(II) complex was 78%. Found: C, 52.3; H, 5.2; N, 18.8%. Calc. for $Ni(C_{23}H_{27}N_7O_4)$: C, 52.7; H, 5.2; N, 18.7%. IR (in KBr disc): 1605, 1585, 1535, 1485, 1430, 1395, 1285, 1250, 1200, 1155, 1100, 795, 750 and 700 cm^{-1}.

Procedure for solvent extractions

Solvent extractions were carried out as described previously.[6]

Measurements

All measurements were carried out as described previously.[6]

Materials

All reagents were of reagent grade. DMF was distilled over CaH_2 under reduced pressure prior to use. Other solvents were purified by the usual manner. Water was deionized. Acetate buffer solutions (0.2 M) were used for adjusting pH from pH 3.5 to 5.8. The pH values below 3.5 or above 5.8 were adjusted by the addition of adequate amounts of 1 M hydrochloric acid or sodium hydroxide.

RESULTS AND DISCUSSION

The novel pentaaza macrocyclic Schiff base ligands were obtained in good yields by a high-dilution method. Their copper(II) and nickel(II) complexes were prepared by the reaction of the free ligands with metal ions and characterized by electronic spectroscopy. Moreover, these ligands were applied as extractants for transition-metal ions, and L^2 was found to be a highly selective extractant for copper(II).

Electronic spectra

Figure 2 shows the electronic spectra of the free ligands L^2 [Fig. 2(A)] and L^3 [Fig. 2(B)] and their copper(II) and nickel(II) complexes in DMF. L^2 and L^3 have an intense absorption band at 25.3 and 25.6 $\times 10^3$ cm^{-1}, respectively, which can be assigned to the $\pi \rightarrow \pi^*$ transitions. The spectra of the complexes show the absorption band shifted to lower energies: 21.9 $\times 10^3$ cm^{-1} for $Cu(L^2\text{-}2H)$, 20.4 $\times 10^3$ cm^{-1} for $Ni(L^2\text{-}2H)$, 21.8 $\times 10^3$ cm^{-1} for $Cu(L^3\text{-}2H)$ and 20.2 $\times 10^3$ cm^{-1} for $Ni(L^3\text{-}2H)$. These absorption bands can be assigned to the transitions from the same origin as the ligands. Moreover, in the visible region, the spectra of $Cu(L^2\text{-}2H)$ and $Cu(L^3\text{-}2H)$ exhibit an absorption band at 16.7 and 16.1 $\times 10^3$ cm^{-1}, respectively, which can be assigned to ligand field transitions. As for the nickel(II) complexes, the shoulder band was observed around 16.7 and 16.1 $\times 10^3$ cm^{-1} for $Ni(L^2\text{-}2H)$ and $Ni(L^3\text{-}2H)$, respectively. These bands can also be assigned to ligand field transitions.

The magnetic susceptibilities of $Ni(L^2\text{-}2H)$ and $Ni(L^3\text{-}2H)$ are diamagnetic, suggesting that the nickel(II) ion of these complexes may adopt a four-coordinate planar configuration. On the other hand, for $Cu(L^2\text{-}2H)$ and $Cu(L^3\text{-}2H)$ a coordinate environment about the copper(II) ion, four- or five-coordinate, could not be determined from the available data.

Solvent extractions by L^1, L^2 and L^3

Extractabilities of L^1–L^3 toward transition-metal ions such as copper(II), nickel(II) and cobalt(II) have been studied under various conditions.

Effect of shaking time on extraction

Figure 3 shows plots of percentage of copper(II) extracted by L^1–L^3 against shaking time. The concentrations of the extractants in chloroform and of the metal ion in the aqueous phase were 1 $\times 10^{-3}$ and 1 $\times 10^{-4}$ M, respectively, and the pH of the aqueous phase was adjusted to nearly 6.7 using a 0.2 M acetate buffer solution plus appropriate amounts of an aqueous solution of sodium hydroxide. The extraction rate by L^2 was found to be much faster than those by L^1 and L^2. Moreover, the percentage of copper(II) extracted by L^2 reached nearly 100% within 30 min, whereas with L^1 and L^3 only 20 and 40% of copper(II), respectively, were transferred into the organic phase after shaking for 4 h. The large difference in the extraction rates between L^2 and L^3 may arise from the difference in their hydrophilicity: the former possesses a secondary amino group (—CH_2NHCH_2—) which is more hydrophilic than the tertiary amino group [—$CH_2N(CH_3)CH_2$—] of the latter.

On the other hand, no nickel(II) and cobalt(II) were extracted by these extractants under the same conditions as the copper(II) case after shaking for 8 h.

Effect of pH on extraction by L^2

Figure 4 shows the effect of the pH of the aqueous phase on extractions of copper(II), nickel(II) and cobalt(II) by L^2. The extractions were made under the following conditions. The concentrations of L^2 in chloroform and of the metal ions in the aqueous

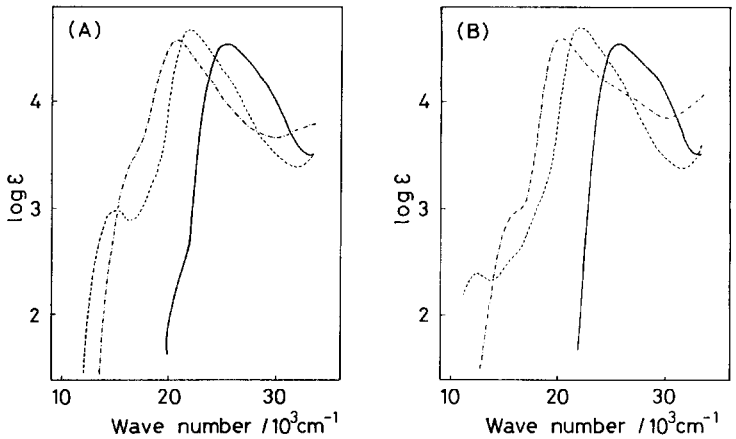

Fig. 2. Electronic spectra in DMF. (A)(——) L^2, (– – –)Cu(L^2-2H), and (–·–·–): Ni(L^2-2H). (B)(——) L^3, (– – –)Cu(L^3-2H), and (–·–·–): Ni(L^3-2H).

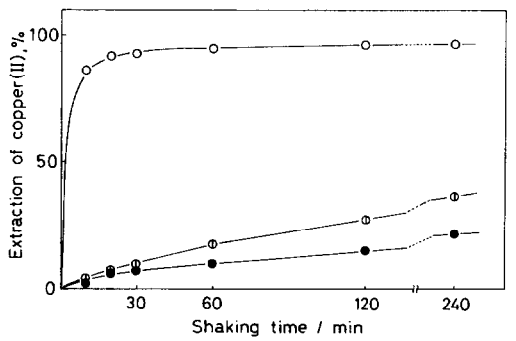

Fig. 3. Effect of shaking time on extraction of copper(II) (1×10^{-4} M) by L^1, L^2 and L^3 (1×10^{-3} M) at pH 6.7. (●)L^1, (○)L^2, and (Φ)L^3.

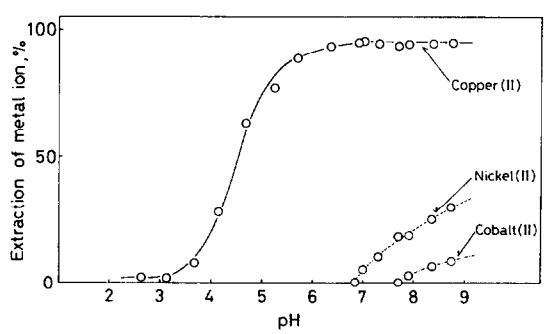

Fig. 4. pH dependence of extraction of metal ions (1×10^{-4} M) by L^2 (1×10^{-3} M). Shaking time 2 h.

phase were 1×10^{-3} and 1×10^{-4} M, respectively. The shaking time was 2 h for all systems. No copper(II) was extracted in the pH region below 3.0. The extraction began to occur at pH 3.5 and its percentage increased with increasing pH of the aqueous phase and reached nearly 100% in the pH region above 6.5. No nickel(II) or cobalt(II) as extracted at a pH lower than 7.0 or 7.8, respectively. Moreover, the percentage extractions of these metal ions were much less than that of copper(II). These results indicate that the selective extraction of copper(II) by L^2 can be achieved by adjusting the pH of the aqueous phase to about 6.7.

From these results L^2 is considered to be a better extractant than the tetraaza macrocyclic Schiff base ligands which were reported previously by us[4,5] in its extraction rate, efficiency and selectivity for copper(II).

Relationship between distribution factor and pH or extractant concentration

In order to identify the species of copper(II) extracted by L^2, the relationship between the distribution factors of copper(II) and the pH or extractant concentration was investigated. The slope of the plot of the logarithm of the copper(II) distribution factor ($\log D$) vs the pH of the aqueous phase is about 2, which indicates that two hydrogen ions of L^2 should be substituted through complexation with copper(II). Moreover, the plot of $\log D$ vs $\log [L^2]$ is linear over the range of L^2 concentration of 1×10^{-3}–1×10^{-4} M, and its slope is nearly unity. This suggests that the ratio of copper(II) to L^2 in the extracted species is 1:1. These results indicate that the copper(II) is extracted by L^2 as the neutral complex Cu(L^2-2H).

Recovery of copper(II) extracted by L^2

The copper(II) extracted by L^2 was recovered by treatment with aqueous solutions of hydrochloric acid as follows. The copper(II) in the aqueous phase was completely extracted into the organic phase of L^2 by shaking for 2 h at pH 6.7 and then the aqueous phase was separated and removed. A dilute hydrochloric acid solution was added to the

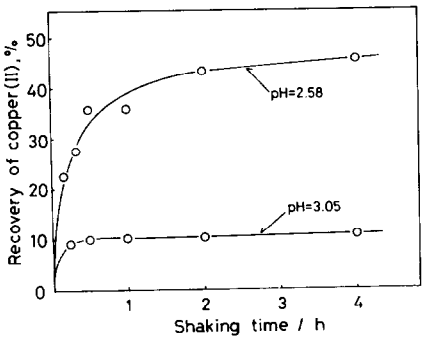

Fig. 5. Back-extraction of copper(II) (1×10^{-4} M) with acidic solutions after complete extraction by L^2 (1×10^{-3} M).

remaining organic phase and it was shaken for an appropriate time. The copper(II) back-extracted into the hydrochloric acid solution was determined by atomic absorption spectrometry. The results are shown in Fig. 5. When an aqueous solution of pH 3.05 was used, the percentage of recovered copper(II) was very low (*ca* 10%) after shaking for 4 h. With an aqueous solution of pH 2.58, it reached *ca* 45% after shaking for 4 h. However, in this case, nearly 20% of the extractant in the organic phase was found to decompose, which was determined spectrophotometrically. Moreover, with an aqueous solution with a pH lower than 1.0, nearly 100% of copper(II) was recovered, but almost all the extractant in the organic phase was found to decompose.

REFERENCES

1. Yu. A. Zolotov, V. P. Bodnja, G. A. Larikova, N. V. Niz'eva, G. A. Vlasava and E. V. Rybakova, *Zh. Anal. Khim.* 1982, **32,** 1543.
2. Yu. A. Zolotov, N. V. Niz'eva, V. P. Ionov, D. M. Kumina and O. V. Ivanov, *Mikrochim. Acta* 1983, **1,** 381.
3. Yu. A. Zolotov, V. P. Ionov, N. V. Niz'eva and A. A. Formanovski, *Dokl. Akad. Nauk SSSR,* 1984, **277,** 1145.
4. M. Fujiwara, T. Matsushita and T. Shono, *Polyhedron* 1984, **3,** 1357.
5. T. Matsushita, N. Kubota, M. Fujiwara and T. Shono, *Chem. Lett.* 1984, 657.
6. N. Kubota, M. Fujiwara, T. Matsushita and T. Shono, *Polyhedron* 1985, **4,** 1051.
7. M. Fujiwara, Y. Nakajima, T. Matsushita and T. Shono, *Polyhedron* 1985, **4,** 1859.
8. H. H. Hodgson and H. G. Beard, *J. Chem. Soc.* 1926, 147.
9. D. St. C. Black and M. J. Lane, *Aust. J. Chem.* 1970, **23,** 2039.
10. E. Kwiatkowski, T. Ossowski and A. Jankowska, *Polyhedron* 1985, **4,** 1191.
11. K. Sakata, M. Hashimoto, N. Tagami and Y. Murakami, *Bull. Chem. Soc. Jpn* 1980, **53,** 2262.
12. D. St. C. Black and P. W. Kortt, *Aust. J. Chem.* 1972, **25,** 281.

Polyhedron Vol. 6, No. 2, pp. 295–302, 1987
Printed in Great Britain

0277–5387/87 $3.00+.00

SYNTHESIS OF [*N,N'*-PHENYLENEBIS(SALICYLIDENIMINATO)] MONONITROSYLIRON AND ITS CHARACTERIZATION IN THE SOLID STATE (IR, EPR, MÖSSBAUER, X-RAY ANALYSIS AND MAGNETIC SUSCEPTIBILITY)

O. R. LEEUWENKAMP and C. M. PLUG

Department of Pharmaceutical Analysis and Analytical Chemistry, Subfaculty of Pharmacy, Gorlaeus Laboratories, State University Leiden, P.O. Box 9502, 2300 RA Leiden, The Netherlands

and

A. BULT*

Department of Analytical Pharmacy, Subfaculty of Pharmacy, State University Utrecht, Catharijnesingel 60, 3511 GH Utrecht, The Netherlands

(*Received* 17 *December* 1985; *accepted after revision* 27 *June* 1986)

Abstract—Appreciable changes in effective magnetic moment, isomer shift (I_s) and quadrupole splitting (ΔE_q) (Mössbauer spectra) as well as in the EPR spectra occur upon cooling a sample of the title compound [Fe(salophen)NO] at a temperature of about 180 K. The observed changes are consistent with a $S = 3/2 \rightleftarrows S = 1/2$ spin crossover. At 300 K $I_s = 0.29$ and $\Delta E_q = 0.198\,\text{mm s}^{-1}$, while for a sample temperature of 100 K values are observed of 0.15 and $1.738\,\text{mm s}^{-1}$, respectively. In the EPR spectrum of polycrystalline samples a broad signal is observed. At 100 K two sharp lines corresponding to $g_\perp = 2.108$ and $g_\parallel = 2.211$ are present. The EPR spectrum for 12 K is nearly identical to the spectrum obtained at 100 K. The physicochemical properties of the complex resemble strongly those of the analogue [Fe(salen)NO] and consequently rationalization of the results in terms of the MO diagram for the latter complex can be given. From the magnetic susceptibility and Mössbauer data a separation of the orbitals—involved in the spin-crossover process—of about $300\,\text{cm}^{-1}$ was calculated. Analysis of the magnetic-susceptibility data further reveals, via the large values found for $\Delta S^\ominus$ ($286.2\,\text{J mol}^{-1}\,\text{K}^{-1}$) and $\Delta H^\ominus$ ($28.9\,\text{kJ mol}^{-1}$), that the spin crossover is accompanied by a relative large change in the bonding distances and/or angles. In oxygen- and/or water-containing solutions the complex is rapidly transformed into the μ-oxo-dimer $[\text{Fe(salophen)}]_2\text{O}$.

The pentacyanonitrosylferrate or nitroprusside dianion is very interesting from several points of view. The properties of this anion have been recently reviewed.[1] Nitroprusside is frequently used as a reagent for detection and/or determination of a wide variety of nucleophillic species—generated in (strongly) alkaline medium from compounds such as thiols, ketones, aldehydes, phenols, pyrrols, indols and thioureas—and sulphite. Moreover, nitroprusside is a potent hypotensive drug. Unfortunately, a number of drawbacks limits its therapeutic use. Nitroprusside is administered by (intravenous) infusion (in the clinic), because the drug is not absorbed after oral administration. Secondly, nitroprusside is especially light-sensitive in (infusion) solutions. On the other hand, the drug is toxic due to the *in vivo* loss of the cyanide ligands. Reactivity, and most probably the biological activity as well, are related to the Fe(II)–NO^+ moiety.

Therefore, our ultimate aim was the synthesis of

*Author to whom correspondence should be addressed.

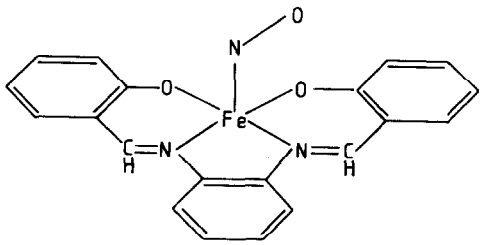

Fig. 1. Structure of [Fe(salophen)NO].

stable and less toxic (mono)nitrosyl analogues of nitroprusside with at least a comparable hypotensive action. In general the separations of the orbitals involved in the ligand coordination in iron nitrosyl complexes are small.[2] As a consequence both the stability of iron mononitrosyl complexes and the character of the nitrosyl group (NO^+, NO^0 or NO^-) are sensitive to subtle changes in the properties of the coordinated ligands. A survey of the literature on mononitrosyl iron complexes reveals that only a minority of these compounds are to a certain extent stable in the solid state and in solution. On the basis of the anionic multidentate ligands present in the relatively stable complexes porphinato,[3] phthalocyanato,[4] dithiolato,[5] dithiocarbamato[6] and Schiff base[7-9] mononitrosyl coordination compounds can be distinguished. Apparently, π-extended systems possess stabilizing properties towards iron nitrosyl complexes. This is not surprising, since cyanide present in the comparatively stable nitroprusside ion is a strong field ligand with an exceptional $d\pi$-accepting ability.

An alternative approach to the preparation of nitroprusside analogues is the replacement of the central metal ion by Ru(II). In this ion the fully occupied t_{2g}^6-orbitals extend far more into space and consequently strong back-bonding interactions with common π-acceptor ligands such as NO^+ occur.[10-13] For this reason Ru(II) nitrosyl complexes can be formally regarded as Ru–NO^+ and are in general relatively stable. Unfortunately, Ru(II) complexes are both mutagenic and carcinogenic.[14]

In order to obtain more insight into the role of conjugation in stabilizing mononitrosyl iron complexes, the phenylene analogue of [*N*,*N*′-ethylenebis(salicylideniminato)]nitrosylferrate, [Fe(salophen)NO] (Fig. 1), was prepared and its physicochemical features were compared to those of [Fe(salen)NO] which was recently characterized by Wells *et al.*[8]

Finally, the stability of [Fe(salophen)NO] was investigated in the solid state and in solution, employing the intensity of the characteristic nitrosyl stretching frequency in the IR spectrum as criterion.

EXPERIMENTAL

Reagents and ligands

Sodium acetate, sodium nitrite, *o*-phenylenediamine and sulfuric acid (Merck analytical grade), ferrous perchlorate hexahydrate (Ventron), salicylaldehyde (Baker reagent grade), methanol and ethanol (Baker analytical grade) were used in the synthetic procedures. The ligands *o*-ethylene- and *o*-phenylenebissalicylideniminato were obtained by condensation of the respective diamines with salicylaldehyde (1:2) in refluxing ethanol. The crop of yellow and orange crystals was subsequently thoroughly washed with ethanol and recrystallized from ethanol.

Preparation of [Fe(salophen)NO]

Earnshaw *et al.*[7] prepared [Fe(salen)NO] via the extremely air-sensitive [Fe(salen)] complex. In our method the desired nitrosyl complex is produced in one step, circumventing the unstable intermediate. 0.32 g powdered ligand was added to 30 cm^3 methanol, which was deoxygenated by purging with nitrogen purified via a BTS tower. Thereafter, a 0.16 g sodium acetate (0.02 M) and 0.36 g ferrous perchlorate (0.01 M) were added. Immediately NO gas, generated from sodium nitrite by dropwise addition of 2 M sulfuric acid and purified by passage through a 30% KOH solution and a column of KOH pellets,[15] was bubbled through the well-stirred reaction medium. The solution turned black and a black product precipitated. After 1.5 h the excess NO gas was removed by purging with nitrogen and the black microcrystalline material was filtered, washed with 30 cm^3 deoxygenated methanol under a stream of nitrogen and finally dried *in vacuo* for 1.5 h.

Found: Fe; 13.7%. Calc. for [Fe(salophen)NO] ($FeC_{20}H_{14}N_3O_3$): Fe, 14.0%. ν_{NO} = 1720 cm^{-1} (KBr, Nujol mull).

Preparation of [Fe(salen)NO] *and* [Co(salophen)NO]

The complex [Fe(salen)NO] was prepared in an analogous way. In the synthesis of [Co(salophen)NO] Co(II) acetate tetrahydrate was used, while sodium acetate was omitted.

[Fe(salen)NO]: ν_{NO} = 1710 cm^{-1} (KBr); [Co(salophen)NO]: ν_{NO} = 1640 cm^{-1} (KBr).

Physical measurements

Powder X-ray diffractograms were recorded by means of a Philips diffractometer, type PW 1025/25 using Cu-K_α radiation (λ = 1.5418 Å).

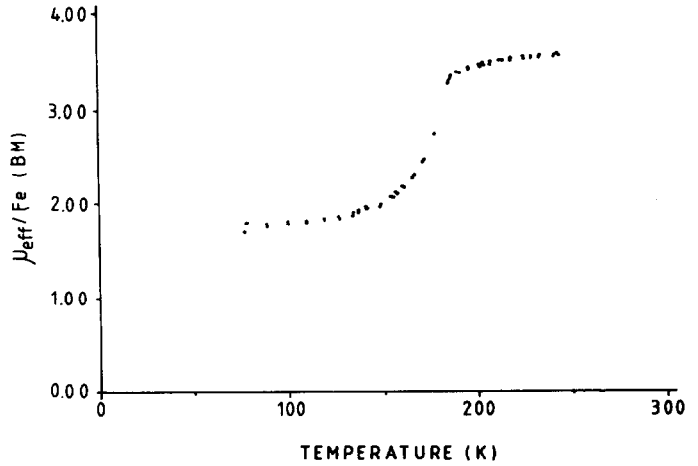

Fig. 2. Effective magnetic moment (μ_{eff}) for [Fe(salophen)NO] in the temperature range 80–300 K.

The magnetic properties of [Fe(salophen)NO] were determined in the temperature range 2–300 K. The high-temperature susceptibility ($T > 77$ K) was measured using a Faraday balance. In the low-temperature range susceptibility and magnetization measurements were performed using a PAR vibrating sample magnetometer. Field-dependent magnetization curves were recorded at liquid-He temperature applying fields up to 5.6 T. All susceptibility data were corrected for diamagnetism of the samples[16] and the sample holder.

The IR spectra were recorded for both the KBr pellet and the Nujol mull by means of a Beckman IR-10 spectrometer in the frequency range 4000–200 cm^{-1}. For the Mössbauer experiments a conventional constant-acceleration type spectrometer was applied. The source was ^{57}Co diffused in rhodium. All isomer shifts (I_s) are relative to sodium nitroprusside.

The EPR spectra for a polycrystalline sample of [Fe(salophen)NO] were recorded at room temperature, and 100 and 12 K on a Varian E 3 at X-band frequencies, employing a 9.22-GHz field modulation.

RESULTS

Magnetic susceptibility

The data for polycrystalline [Fe(salophen)NO] are represented in Fig. 2.

These results closely resemble those for [Fe(salen)NO]. At about 180 K a spin crossover occurs. Above the crossover temperature (T_c) the effective magnetic moment (μ_{eff}) is approximately 3.9, while at temperatures below T_c the effective magnetic moment is about 1.9. These values are very close to the spin-only values for $S = \frac{3}{2}$ (3.88) and $S = \frac{1}{2}$ (1.73), respectively. In addition a magnetic phase transition due to antiferromagnetic coupling of the Fe centres is observed at $T = 6$ K (Fig. 3).

The magnetic-susceptibility data can be treated according to eqn (1):

$$\mu_{eff}^2 = \alpha \cdot \mu_{S=3/2}^2 + (1 - \alpha)\mu_{S=1/2}^2, \qquad (1)$$

in which $\mu_{S=3/2}$ and $\mu_{S=1/2}$ are the theoretical spin-only values of 3.88 and 1.73. The equilibrium constant at various temperatures for the spin crossover (K_{eq}^T) can be calculated by eqn (2):

$$K_{eq}^T = \alpha/(1 - \alpha), \qquad (2)$$

where α denotes the fraction in the high-spin state. Subsequently, eqn (3):

$$\ln K_{eq}^T = \Delta S^{\ominus}/R - \Delta H^{\ominus}/RT \qquad (3)$$

offers the possibility of calculating both enthalpic and entropic changes accompanying the spin transition. In Fig. 4 the plot of $\ln K_{eq}^T$ vs T^{-1} is given. From this plot values of 286.2 J mol^{-1} K^{-1} and 28.9 kJ mol^{-1} were calculated for $\Delta S^{\ominus}$ and $\Delta H^{\ominus}$. The $\Delta S^{\ominus}$ value comprises an electronic entropy change related to a difference in spin multiplicity and state degeneracy for the high- and low-spin states. In theory the electronic entropy change for the present case equals $R \ln(\frac{4}{2}) = 5.8$ J mol^{-1} K^{-1}. Thus the calculated value for $\Delta S^{\ominus}$ may almost entirely be ascribed to changes in bond distances and/or bond angle occurring concomitantly with the spin-crossover process. The value of 286.2 J mol^{-1} K^{-1} is very high. Petty *et al.*[17] found

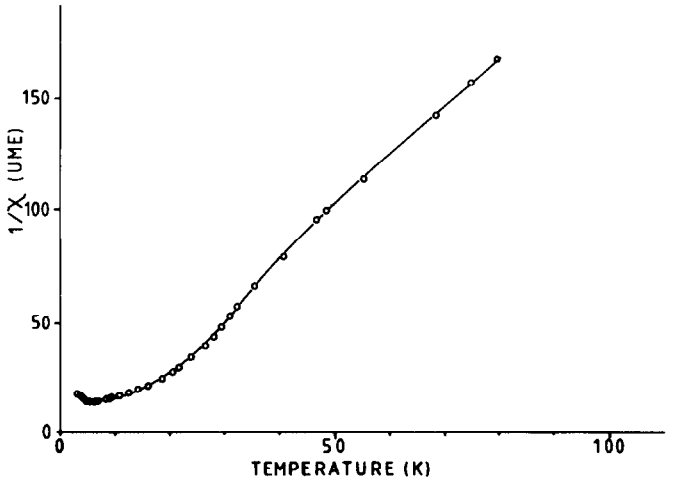

Fig. 3. Reciprocal magnetic susceptibility ($1/\chi$) for [Fe(salophen)NO] in the temperature range 2–80 K.

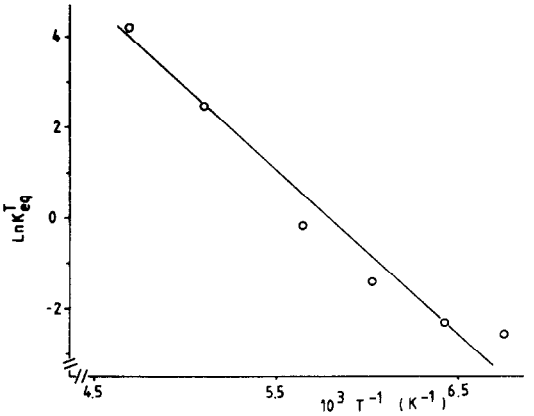

Fig. 4. Plot of $\ln K_{eq}^{T}$ vs T^{-1}.

Table 1. Mössbauer spectroscopy data for [Fe(salophen)NO]

T (K)	ΔE_q (mm s^{-1})	I_s (mm s^{-1})[a]
300	0.198	−0.29
220	0.292	−0.30
200	0.364	−0.29
180	1.231	−0.19
160	1.576	−0.15
130	1.705	−0.15
100	1.738	−0.15

[a]Relative to sodium nitroprusside.

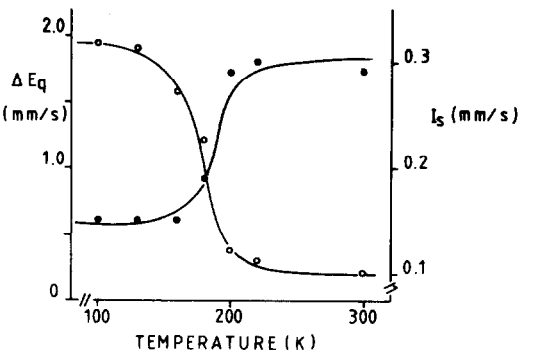

Fig. 5. Variation of quadrupole splitting (ΔE_q) (open circles) and isomer shift (I_s) (closed circles) with temperature in the range 100–300 K.

a value of 112.2 J mol^{-1} K^{-1} for an iron(II) complex. Apparently, large changes in bonding distances and/or angles occur during the spin crossover. A change in bonding distance of 0.1–0.2 Å is reasonable.[16] Assuming a change equal to 0.2 Å, the expected inner coordination sphere reorganization energy is 25.1 kJ mol^{-1}.[18] As a consequence, the estimated electronic contribution to the observed enthalpic change amounts to 28.9 − 25.1 = 3.8 kJ mol^{-1}. This value reflects the separation of the electronic levels involved in the spin transition and is estimated as 300 cm^{-1}.

Mössbauer spectroscopy

In the Mössbauer experiments performed at various temperatures the spin transition is also observed at $T_c = 180$ K. The Mössbauer data are summarized in Table 1. In Fig. 5 the variation in the quadrupole splitting (ΔE_q) and I_s with temperature is depicted. Representative Mössbauer spectra for $T = 293$, 200, 160 and 100 K are given in Fig. 6. The magnetic-susceptibility and Mössbauer data are thus in good agreement. The quadrupole-splitting values at each temperature [$\Delta E_q(T)$] are related to the quadrupole splitting at $T = 0$ K [$\Delta E_q(0)$] via eqn (4):[19]

$$\Delta E_q(T) = \Delta E_q(0) \tanh(\Delta \tfrac{1}{2} kT). \quad (4)$$

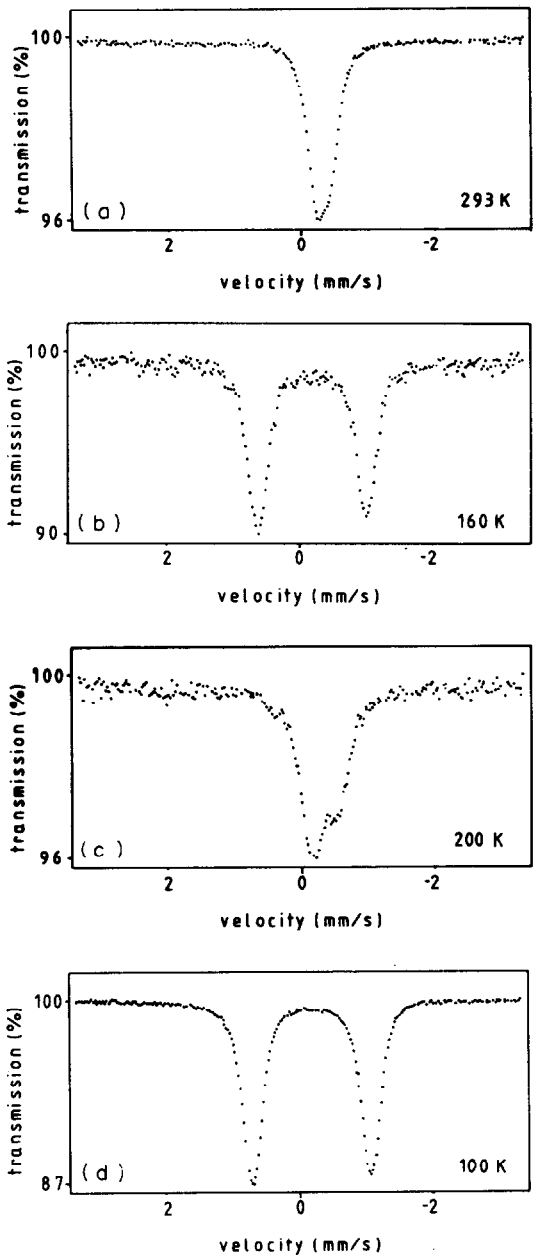

Fig. 6. Mössbauer spectra for [Fe(salophen)NO] at the indicated temperatures.

In eqn (4) Δ represents the separation of the levels playing a role in the spin crossover. Using for $\Delta E_q(0)$ the extrapolated value of $1.83\,\mathrm{mm\,s^{-1}}$ a reasonable fit between experimental and calculated values is obtained for $\Delta = 280\,\mathrm{cm^{-1}}$. This value is relatively close to the value of $300\,\mathrm{cm^{-1}}$ derived from the susceptibility data.

X-ray analysis

The X-ray powder diffraction pattern of [Fe(salophen)NO] can be indexed in an orthorhombic space group. The cell parameters are $a = 16.74$ Å, $b = 17.32$ Å and $c = 10.65$ Å. Systematic absences indicate *P*222 to be the most likely space group. Data for the observed reflections with 2θ between 10 and 25° are presented in Table 2. The results agree qualitatively with the reported structure for one of the modifications of the related Co complex [Co(salophen)].[20] The cell parameters are about the same for both complexes, but in the case of the iron compound the *c*-parameter is doubled with respect to the value for the Co compound. This is probably due to the presence of the NO moiety in the Fe complex and to the larger size of the central Fe ion. Both conditions may give rise to a shift

Table 2. X-ray powder diffraction data for [Fe(salophen)NO]

2θ (°)	*hkl*
10.22	020
13.20	021
13.45	201
14.18	121
14.52	211
16.07	130
17.35	012
17.47	102, 031
17.97	301
19.51	022
20.23	122
20.48	040, 212, 231
21.06	400
23.54	420
24.48	241

DISCUSSION

Comparison of the magnetic behaviour, EPR, IR and Mössbauer parameters of [Fe(salen)NO] and [Fe(salophen)NO] leads to the conclusion that only minor changes occur upon extension of the conjugation in the equatorial Schiff base ligand. This is consistent with the observation that μ_{eff} for the $S = \frac{1}{2}$ and $\frac{3}{2}$ spin states approximates the theoretical spin-only values, suggesting a limited admixture of the salophen orbitals and the metal *d*-orbitals. Lack of suitable orbitals on the phenolic oxygen may account for a slight degree of delocalization involving the equatorial ligand. Because of the similarities in the properties of [Fe(salen)NO] and [Fe(salophen)NO] the MO description proposed by Wells *et al.*[8] (Fig. 8) might be used for the explanation of the observed features of [Fe(salophen)NO]. The relatively low nitrosyl stretching frequency of 1720 cm^{-1} is, according to Gaughan *et al.*,[21] indicative either of an Fe(II)–NO^0 or an

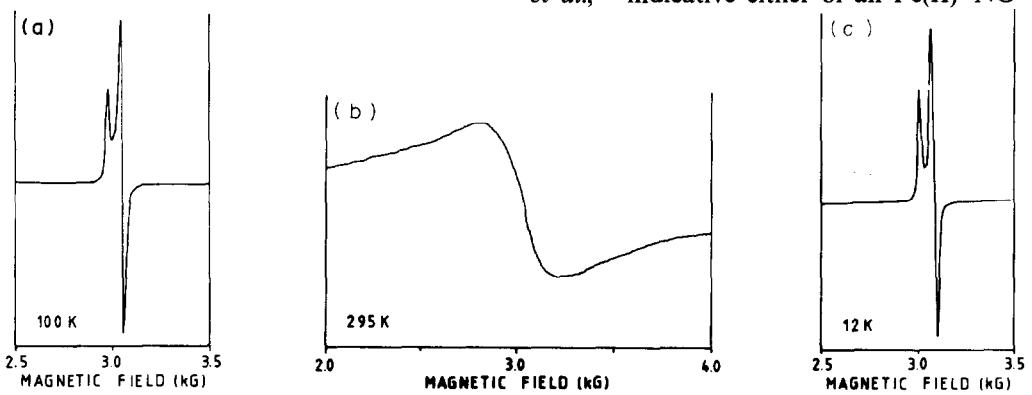

Fig. 7. Polycrystalline EPR spectra for [Fe(salophen)]NO]. The sample temperatures are indicated.

coordination. In the structure of the orthorhombic modification of the Co complex the *c*-axis is perpendicular to the almost planar ligand. Alternation of the assumed out-of-plane shift of the Fe atom in the positive and negative direction will result in a doubling of the translation symmetry along the *c*-axis with respect to the original structure.

EPR spectroscopy

Figure 7 shows the EPR spectra for polycrystalline [Fe(salophen)NO]. At $T = 295$ K a broad polycrystalline EPR signal is observed. Upon lowering the sample temperature the EPR spectrum changes markedly at about 180 K. At $T = 100$ K two sharp lines are observed which correspond to $g_\perp = 2.108$ and $g_\parallel = 2.211$. The EPR spectrum for $T = 12$ K is practically the same with $g_\perp = 2.090$ and $g_\parallel = 2.195$.

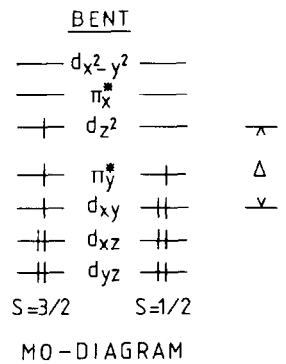

Fig. 8. MO diagram for an $\{FeNO\}^7$ complex with a bent geometry.

Fe(III)–NO^- moiety. In the given MO diagram six *d*-electrons are placed in orbitals with a predominant *d*-character, while one electron resides mainly in the antibonding π_y^*-orbital. Thus, the high-temperature state can be formally regarded as

temperature state can be formally regarded as Fe(II)–NO. Furthermore, the NO stretching frequency for [Co(salophen)NO] is 1640 cm^{-1}. The decline in the NO stretching frequency, going from d^6 [Fe(salophen)NO] to d^8 [CO(salophen)NO] is in agreement with the orbital leveling as given by Wells *et al.*[8] In the Co analogue a second *d*-electron is placed in the π_y^*-orbital leading to substantial weakening of the bond between the *N* and the O atom in the nitrosyl group.

As suggested by the large values found for ΔH^0 and ΔS^0, the spin-crossover process is accompanied by structural changes, i.e. changes in bond distances and/or angles. X-ray analysis of [Fe(salophen)NO] at 293 K suggests that in the high-spin state the Fe ion is displaced out of the plane of the Schiff base ligand. Wells *et al.*[8] derive from their Mössbauer experiments that on going from the $S = \frac{3}{2}$ state to the $S = \frac{1}{2}$ state the recoil-free fraction increases. These authors attribute this phenomenon to the movement of the iron atom from an out-of-plane position to an in-plane position. It is clear that this implies a change in bond distances and angles. Therefore, changes in the bond distances and angles must be taken into account in the interpretation of the Mössbauer parameters. Wells *et al.*,[8] however, neglect these changes in their explanation given for the variation of Mössbauer parameters with temperature. According to the MO diagram, the spin crossover consists in the transfer of electron density from the d_{xy}-orbital to the d_{z^2}-orbital. The d_{z^2}-orbital possesses less *d*-character because of overlap between the d_{z^2}- and the σ^*-orbital. As a consequence the electric field gradient (EFG) and thus the quadrupole splitting is larger for the $S = \frac{1}{2}$ state. At the same time the Fe atom moves into the plane of the equatorial salophen ligand and consequently the bond distances (*r*) become shorter. This effect will also lead to an increase in the EFG, since the EFG is proportional to r^{-3}. As a result of these two cooperative effects the quadrupole splitting will greatly change in the neighbourhood of the spin conversion temperature (180 K). On the other hand a relatively small decrease in I_s is observed. This indicates the effective *s*-electron density as experienced by the iron nucleus in the $S = \frac{1}{2}$ state to be smaller. The spin crossover is apparently associated with an increase in shielding of the *s*-type iron electrons due to transfer of electron density from the σ^*-type d_{z^2}-orbital to the d_{xy}-orbital.

The complex [Fe(salophen)NO] is relatively stable in the solid state. No decrease in the intensity of the nitrosyl stretching frequency (1720 cm^{-1}) was observed over a period of 2 months. By contrast, in oxygen- and/or water-containing solutions a red precipitate is rapidly formed. The observed peak at 820 cm^{-1} in the IR spectrum of the red material points to the formation of the μ-oxo-dimer [Fe(salophen)]$_2$O.[22,23] Gulotti *et al.*[24] have reported that the μ-oxo-dimer [Fe(salen)]$_2$O is cleaved in the presence of excess cyanide, while [Fe(salen)(CN)$_2$] is slowly converted into the oxygen-bridged species. Most probably this type of dimirization can be prevented by a (strong) ligand at the sixth position. Placing a sixth ligand along the *z*-axis will lift the d_{xz}-, d_{yz}- and especially the d_{z^2}-orbital. This may result in an orbital leveling very similar to the orbital configuration in the nitroprusside ion.[25]

In conclusion [Fe(salophen)NO] is not a suitable nitroprusside analogue. Most probably replacement of the four equatorial cyanide ligands in nitroprusside by an anionic multidentate with exceptional $d\pi$-accepting ability may result in a stable Fe(II)–NO^+ complex.

REFERENCES

1. O. R. Leeuwenkamp, W. P. van Bennekom, E. J. van der Mark and A. Bult, *Pharm. Weekblad Sci. Ed.* 1984, **6**, 129.
2. J. H. Enemark and R. D. Feltham, *Coord. Chem. Rev.* 1974, **13**, 339.
3. W. R. Scheidt and M. E. Frisse, *J. Am. Chem. Soc.* 1975, **97**, 17.
4. C. Ercolani and C. Neri, *J. Chem. Soc.* 1967, 1715.
5. J. A. McCleverty, N. M. Atherton, J. Locke, E. J. Whinton and C. J. Winscom, *J. Am. Chem. Soc.* 1967, **89**, 6082.
6. W. Silverthorn and R. D. Feltham, *Inorg. Chem.* 1967, **6**, 1662.
7. A. Earnshaw, E. A. King and L. F. Larkworthy, *J. Chem. Soc.* A 1969, 2459.
8. F. V. Wells, S. W. McCann, H. H. Hendrickson and R. D. Feltham, *Inorg. Chem.* 1982, **21**, 2306.
9. Y. Numata, K. Kubokara, Y. Nonaka, M. Okawa and S. Kida, *Inorg. Chim. Acta* 1980, **43**, 193.
10. J. Gibson, *Nature (London)* 1962, **196**, 64.
11. B. A. Goodman, J. B. Raynor and M. C. R. Symons, *J. Chem. Soc. A* 1969, 2572.
12. F. Bottomley, *Coord. Chem. Rev.* 1978, **26**, 7.
13. S. D. Pell and J. N. Armor, *Inorg. Chem.* 1973, **12**, 873.
14. M. J. Clarke, In *Metal Complexes in Biological Systems* (Edited by H. Sigel), Vol. 11, p. 231. Marcel Dekker, New York (1980).
15. O. Bostrup, *Inorg. Synth.* 1966, **8**, 191.
16. B. N. Figgis and J. Lewis, *Modern Coordination Chemistry*, Interscience, New York (1960).
17. R. H. Petty, E. V. Dose, M. F. Tweedle and L. J. Wilson, *Inorg. Chem.* 1978, **17**, 1064, 1071.
18. H. C. Stynes and J. A. Ibers, *Inorg. Chem.* 1971, **10**, 2304.
19. T. C. Gibbs, *Principles of Mössbauer Spectroscopy*, p. 108. Chapman & Hall, London (1976).
20. N. B. Panor, M. Calligaris, P. Delise, G. Dodic, G.

Nardin and L. Randaccio, *J. Chem. Soc., Dalton Trans.* 1976, 2478.
21. A. P. Gaughan, B. L. Haymore, J. A. Ibers, W. H. Myers, T. F. Myers and D. W. Meek, *J. Am. Chem. Soc.* 1973, **95**, 6859.
22. R. H. Niswander and A. E. Martell, *Inorg. Chem.* 1978, **17**, 2341.
23. T. Mashusita, H. Kono, M. Nishino and T. Shono, *Bull. Chem. Soc. Jpn* 1982, **55**, 2581.
24. M. Gulotti, L. Casella, A. Pasini, and R. Ugo, *J. Chem. Soc., Dalton Trans.* 1977, 339.
25. P. T. Manoharan and H. B. Gray, *J. Am. Chem. Soc.* 1966, **87**, 823.

Polyhedron Vol. 6, No. 2, pp. 303–308, 1987
Printed in Great Britain

0277–5387/87 $3.00+.00

EQUILIBRIA IN AQUEOUS SOLUTION BETWEEN Be(II) AND IMINODIACETIC, *N*-METHYLIMINODIACETIC, *N*-ETHYLIMINODIACETIC AND *N*-PROPYLIMINODIACETIC ACIDS

A. MEDEROS,* S. DOMINGUEZ and M. J. MORALES

Departamento de Química Inorgánica, Facultad de Quimica, Universidad de La Laguna, Tenerife, Canary Islands, Spain

and

F. BRITO and E. CHINEA

Laboratorio de Equilibrios en Solución, Escuela de Quimica, Facultad de Ciencias, Universidad Central de Venezuela, Caracas, Venezuela

(*Received* 19 *December* 1985; *accepted after revision* 27 *June* 1986)

Abstract—The complex species formed in aqueous solution between Be(II) and iminodiacetic, *N*-methyliminodiacetic, *N*-ethyliminodiacetic and *N*-propyliminodiacetic acids were studied at 25°C and ionic strength 0.5 M in Na ClO_4. The application of the least-squares computer program LETAGROP to the experimental potentiometric data, taking into account hydrolysis of the Be(II) ion, indicates that, upon varying the ligand–metal relationship, only the monohydroxide complex $[Be(OH)C]^-$ (H_2C ligand) is formed in significant amounts for the four systems studied. The formation constants β_{pr} (11, −11 and −21) of the protonated species of the ligands, β_{pq} (−12 and −33) of the hydrolytic species of Be(II), and β_{pqr} (−311) of the complex $[Be(OH)C]^-$ were determined.

The coordinating properties of Be(II) in aqueous solution with polyaminocarboxylic acids have, in general, been very little studied,[1–3] probably because of the strong tendency to hydrolyse displayed by the small Be(II) cation.[4] In some cases where such a study has been carried out, as with iminodiacetic acid (IDA), the results have been contradictory: Dyatlova *et al.*[5–7] found that IDA *did not form complexes with* Be(II). No references to the same are to be found in the tables of stability constants.[1–3] However, more recently, Jain *et al.*[9] and Dubey *et al.*[8] have determined from potentiometric measurements the stability constant of the neutral complex BeC (ligand H_2C). But these authors have not taken into consideration the hydrolysis of Be(II) in their calculations.

In our studies in aqueous solution of the systems Be(II)-EDTA[10,11] (EDTA = ethylenediaminetetraacetic acid) and Be(II)–NTA[12] (NTA = nitrilotriacetic acid) we have found upon analysing the experimental potentionmetric data by means of the NERNST/LETA/GRAFICA[13] version of the LETAGROP[14] program that the species resulting from hydrolysis of Be(II) must be taken into consideration in the calculations in order to determine the complex species really present in the solution and to obtain correct values of the stability constants. Otherwise, the values obtained are higher than the true ones, since the acidity due to hydrolysis of the non-complexed Be(II) is included in the value of the stability constant obtained.

For these reasons we decided to reinvestigate in this work the Be(II)–IDA system in aqueous solution. The analogous Be(II)–MIDA (MIDA = *N*-methyliminodiacetic acid), Be(II)–EIDA (EIDA = *N*-ethyliminodiacetic acid) and Be(II)–PIDA (PIDA = *N*-propyliminodiacetic acid) systems have also been studied, no references to these having been found in the literature.

*Author to whom correspondence should be addressed.

EXPERIMENTAL

Reagents

IDA was prepared by recrystallization of IDA (Merck, analytical grade). MIDA, EIDA and PIDA were synthesized by reacting methylamine, ethylamine and *n*-propylamine (Merck, products for synthesis), respectively, with previously neutralized chloroactic acid, following the procedure described by Souchay *et al.*[15] The previously obtained barium salts gave the corresponding acid on adding conc. H_2SO_4. The acids were purified by recrystallization in water–isopropanol mixtures, and were identified by their potentiometric equivalents, and NMR and mass spectra.

The solution of $Be(ClO_4)_2$ was prepared by reacting metallic Be (Spex Industries Inc.) with an excess of $HClO_4$ (Merck, analytical grade), its free acidity[16] being determined, as well as the concentration of Be(II) in aqueous solution which was evaluated gravimetrically.[17,18] The carbonate-free sodium hydroxide solution was prepared according to the school of Sillén[19] and standardized against potassium hydrogen phthalate. $NaClO_4$ was prepared by recrystallization of $NaClO_4$ (Merck, analytical grade).

Apparatus and titration procedures

The potentiometric titrations were carried out in an inert argon atmosphere, at 25 ± 0.0.5°C, ionic strength 0.5 M in $NaClO_4$, using a Radiometer Type PHM-64 potentiometer, a Radiometer G 202 B glass electrode and a K 401 calomel electrode. The cell constants were determined according to the method of Biedermann and Sillén,[20] the liquid junction potentials being found to be negligible within the margins of $[H^+]$ studied. It was found that $pK_w = 13.72$, in excellent agreement with reported data.[21]

Measurements were taken of the ligands alone at the following concentrations: IDA, MIDA and EIDA (C_L = 10 and 20 mM); PIDA (C_L = 10 and 5.7 mM). Be(II) was measured alone (C_M = 10 and 20 mM) in order to study hydrolysis, and the ligands in the presence of Be(II) at the following concentrations and ligand: metal ratios: C_M = 10, 20 and 40 mM and 1:1, 2:1, 4:1 and 6:1 ratios for IDA and EIDA; C_M = 10 mM, and 1:1, 2:1 and 4:1 ratios for MIDA; and C_M = 10, 20 and 40 mM, and 1:1 ratio for PIDA.

Data treatment

The experimental potentiometric data were analysed by means of the NERNST/LETA/GRAFICA version[13] of the LEGATROP program,[14] based on a generalized form of the least-squares method that establishes the best model and best values of the β_{pqr} constants, minimizing the function $U = \sum(Z_{exp} - Z_{calc})^2$, Z being the average number of disassociated protons for the total concentration of ligand (Z_C) or for the total concentration of metal (Z_B). The LETAGROP calculations also give the standard deviations $\sigma(Z)$ and $\sigma(\log \beta_{pqr})$.[22] The computations were performed on a Burroughs 6700 computer (Facultad de Ciencias, Universidad Central de Venezuela, Caracas).

RESULTS AND DISCUSSION

Hydrolysis of Be(II)

The aquo cation $Be(H_2(O)_4^{2+}$ only exists in a strongly acid medium.[4] Since the work of Kakihana and Sillén,[23] later confirmed by other authors,[24–29] it has been established that the main product of the hydrolysis of Be^{2+}, in solutions more concentrated than 1 mM, is the trinuclear species $[Be_3(OH)_3]^{3+}$. In a more acidic medium, the dinuclear species $[Be_2(OH)]^{3+}$ has been identified, the percentage of formation of which increases with the concentration of beryllium.[26] The species $Be(OH)_2$ has been proposed before precipitation of the hydroxide[22,25,26,29] in a small proportion because of the very little solubility of $Be(OH)_2$ in water.[4] Mesmer and Baes[4,27] question of the existence of this species at concentrations above 1 mM, and from the studies of Bertin *et al.*[26] it is deduced that neither is it present at concentrations of 10 mM or over.

Prior to our study of the coordinating capacity in aqueous solution of Be(II) with different iminodiacetic ligands, we investigated the hydrolysis of Be(II) under the same conditions of temperature (25°C) and ionic strength (0.5 M in $NaC1O_4$). We also used concentrations of Be(II) of 10 and 20 mM, similar to those employed in the study of the coordinating capacity.

The constants β_{-pq} are defined by means of equilibrium (1):

$$qBe^{2+} + pH_2O \rightleftharpoons [Be_q(OH)_p]^{(2q-p)+} + pH^+. \quad (1)$$

The model that best fits the experimental results is that which considers the presence of the hydroxylated species $Be_2(OH)^{3+}$ and $Be_3(OH)_3^{3+}$ in the range of concentrations and pH values (2.5–5.3) studied. Forty-eight experimental points of the two potentiometric titrations carried out were used for

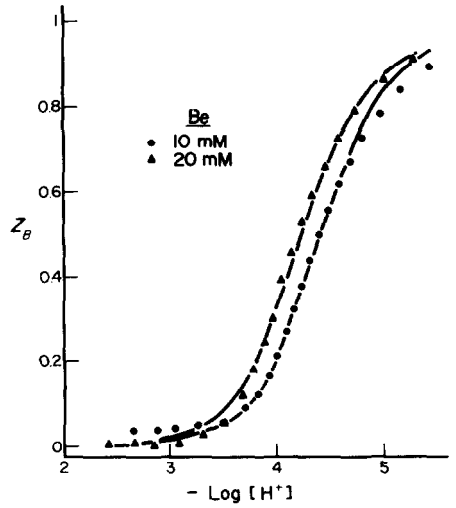

Fig. 1. Z_B vs log[H^+] curves of the hydrolysis of Be(II). Full curves have been calculated using the constants β_{pq} found.

the calculations. It was found that:

$-\text{Log}\,\beta_{-12}$	$\text{Log}\,\beta_{-33}$	Standard deviation [$\sigma(Z)$]	Reference
3.20	8.92 ± 0.08	0.018	Present work
3.20	8.81		26

in good agreement with other authors[4,23-27,29] and especially with Bertin *et al.*[26] who worked at the same ionic strength and temperature. Figure 1 shows the excellent agreement between the experimental curves Z vs $-\log[H^+]$ and those calculated from the values found for β_{-12} and β_{-33}. It should be noted that $Z \to 1$ in accordance with the major formation of the species $(Be_3(OH)_3]^{3+}$.

Ionization constants of the acids

From the values obtained for the constants β_{pr} corresponding to equilibrium (2):

$$pH^+ + rH_2C \rightleftharpoons [H_p(H_2C)_r]^{p+} \qquad (2)$$

the ionization constants of the acids (K_i) given in Table 1 could readily be determined.

The values of pK_i are in good agreement with those found at 25°C and ionic strength 0.1 M in KCl,[30] and with those found for IDA[1,2,31-34] and MIDA[2,35] at 25°C and ionic strength 0.5 M in $NaClO_4$. It is observed that the order of basicity of the N atom[36] (equilibrium HC^-/C^{2-}) is IDA < MIDA < EIDA ≤ PIDA, which order corresponds to the electron donor effect to the corresponding alkyl radical.

Formation constants of the complexes formed

The formation constants β_{pqr} are defined by means of equilibrium (3):

$$pH^+ + qBe^{2+} + rH_2C \rightleftharpoons [H_pBe_q(H_2C)_r]^{(p+2q)+}. \qquad (3)$$

Since, according to Dyatlova *et al.*[5-7] IDA does not form complex with Be(II), we first applied the model FONDO (species $[Be_2(OH)]^{3+}$, $[Be_3(OH)_3]^{3+}$, H_3C^+, HC^- and C^{2-}) to the potentiometric curves of the four systems studied, implying the non-formation of complexes. The Z_c vs $-\text{Log}[H^+]$ experimental curves for the ligand-metal ratios of 1:1 and 2:1 shift slightly to the left with regard to the calculated curves, this effect being most visible at pH ≃ 5 or over. This seems to indicate the presence of a supplementary acidity due to the formation of complex species. Since Jain *et al.*[8] and Dubey *et al.*[9] have affirmed the formation of the complex BeC for IDA acid, and considering the possible formation of the complex $BeHC^+$, the possible presence of these complexes is now analysed, by using the models FONDO + $BeHC^+$, FONDO + BeC and FONDO + $BeHC^+$ + BeC. A shift to the left in the experimental curves Z_C vs $-\log[H^+]$ continues to exist with respect to the calculated curves; therefore the supplementary acidity does not seem to be due to these complexes. A summary of the calculations for the IDA–Be(II) and MIDA–Be(II) systems is given in Table 2 and shows that the constants β_{pqr} are very badly defined for these complexes, so if the complex species $BeHC^+$ and BeC exist in these systems they would be present in a practically negligible amount. The calculation for the PIDA–Be(II) system shows that the species BeC is practically non-existent.

If the complex BeC is only formed in the curves for the ligand: metal ratio of 1:1, $Z \to 2$, but it can be observed from the experimental data in Fig. 2 (the other three systems behave analogously) that at the ratio 1:1 the curves inflect at a value of $Z > 2$. These values are attained shortly before turbidity is reached for all the R–IDA–Be(II) systems. This result is a qualitative proof of the presence of a complex with $p/r > 2$, which could be $[Be(OH)C]^-$.

From Fig. 2 it can also be deduced that the complex species will be formed at $Z > 1$ (pH > 3.5). At these pH values and at the concentration of Be(II) studied, in accordance with Bertin *et al.*[26]

Table 1. Formation constants (β_{pr}) and ionization constants (K_i) of IDA, MIDA, EIDA and PIDA (25°C, I = 0.5 M in $NaClO_4$)

	$-\text{Log}\ \beta_{pr}$			
pr	IDA	MIDA	EIDA	PIDA
+11	−1.79 ± 0.02	−1.60 ± 0.08	−1.59 ± 0.09	−1.45 ± 0.01
−11	2.56 ± 0.01	2.28 ± 0.02	2.32 ± 0.03	2.23 ± 0.03
−21	11.83 ± 0.01	11.79 ± 0.01	12.21 ± 0.04	12.18 ± 0.04
[a/b]	2/63	2/63	2/47	1/34
[c]	0.003	0.012	0.007	0.004
[d]	2.4–5.6	2.2–4.7	2.2–11.3	2.3–11.2
[a/b]	2/38	2/55		
[c]	0.005	0.007		
[d]	6.3–9.6	5.9–10.6		

	Equilibrium (pK_i)			
	H_3C^+/H_2C	H_2C/HC^-	HC^-/C^{2-}	[e]
IDA	1.79 ± 0.02	2.56 ± 0.01	9.27 ± 0.01	9.32
MIDA	1.60 ± 0.08	2.28 ± 0.02	9.50 ± 0.03	9.61
EIDA	1.51 ± 0.09	2.32 ± 0.03	9.89 ± 0.07	9.95
PIDA	1.45 ± 0.01	2.23 ± 0.03	9.95 ± 0.07	10.02

[a] Number of titrations.
[b] Number of experimental points.
[c] Standard deviations [$\sigma(Z)$].
[d] $-\text{Log}[H^+]$ range. For IDA and MIDA, the values of β_{11} and β_{-11} on the one hand and that of β_{-21} on the other were calculated separately.
[e] At 25°C and I = 0.1 M in KCl.[30]

Table 2. LETAGROP calculations for the IDA-Be(II), MIDA-Be(II), EIDA-Be(II) and PIDA Be(II) systems

System	[a/b]	[c]	C_M(mM)	Z	Species	$-\text{Log}\ \beta_{pqr}$	$\sigma(Z)$[d]
IDA	4/94	1,2,4,6	10		BeC	5.98(> 5.73)	0.020
	4/94	1,2,4,6	10		$[BeHC]^+$	1.90(> 1.68)	0.019
	12/299	1,2,4,6	10,20,40	> 0.8	$[Be_3(OH)_3C_3]^{3-}$	30.40(> 30.0)	0.025
	4/97	1,2,4,6	10	> 0.8	$[Be(OH)C]^-$	11.60 ± 0.06	0.014
	12/299	1,2,4,6	10,20,40	> 0.8	$[Be(OH)C]^-$	11.58 ± 0.13	0.022
MIDA	3/73	1,2,4	10		BeC	5.28(> 5.05)	0.052
	3/73	1,2,4	10		$[BeHC]^+$	1.68(> 1.15)	0.054
	3/90	1,2,4	10	> 1	$[Be(OH)C]^-$	11.31 ± 0.04	0.034
	3/73	1,2,4	10	0.15–2.07	[Be(OH)C]	11.31 ± 0.19	0.039
EIDA	6/108	1,2	10,20,40	> 1	$[Be(OH)C]^-$	11.40 ± 0.10	0.030
	12/183	1,2,4,6	10,20,40	0.00–1.60	[Be(OH)C]	11.43 ± 0.19	0.056
	12/201	1,2,4,6	10,20,40	> 1	[Be(OH)C]	11.47 ± 0.15	0.041
PIDA	3/73	1	10,20,40	> 1	BeC	0	
	3/73	1	10,20,40	> 1	$[Be_2(OH)C_2]$	14.5(> 14.2)	0.035
	3/73	1	10,20,40	> 1	[Be(OH)C]	11.54 ± 0.21	0.031

[a] Number of titrations.
[b] Number of experimental points.
[c] Ligand/metal.
[d] Standard deviation.

and our results (Fig. 1), the hydrolytic species of Be(II) are mainly present, $[Be_2(OH)]^{3+}$ and especially $[Be_3(OH)_3]^{3+}$. On the other hand, Thomas *et al.*[37–39] have shown that the trimer species $[Be_3(OH)_3(H_2O)_6]^{3+}$ is not destroyed if the ligands are mono- or didentate, since the tetra-coordination of the Be(II) is then maintained, displacing one or two molecules of water for each

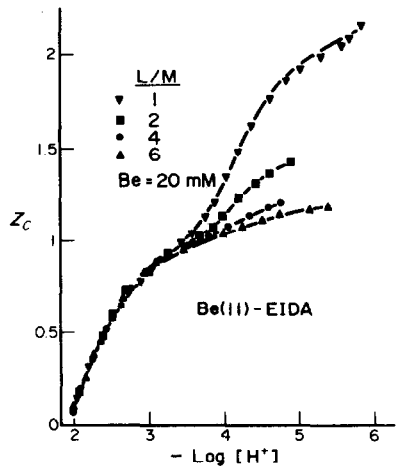

Fig. 2. Z_C vs $-\log[H^+]$ curves of the EIDA–Be(II) system. Full curves = calculated curves (Model "FONDO + $[Be(OH)C]^-$", using β_{-311} in Table 3).

atom of Be(II). Considering the possibility that the R–IDA ligands display a behaviour similar to that of bidentate ligands, we tried the models FONDO + $[Be_2(OH)C_2]^-$, and FONDO + $[Be_3(OH)_3C_3]^{3-}$. The data presented in Table 2 for IDA and PIDA show that good limits of tolerance are not obtained for the constants β_{pqr}, therefore permitting us to discount the presence in significant amounts of the binuclear species $[Be_2(OH)C_2]^-$ and the trinuclear species $[Be_3(OH)_3C_3]^{3-}$.

The presence was then confirmed of the mononuclear species $[Be(OH)C]^-$, by applying the model FONDO + $[Be(OH)C]^-$. The constant β_{-311} is well defined for the four R–IDA–Be(II) systems studied, as manifested in the summary of LETAGROP calculations given in Table 2. The values fit better if the calculations are carried out at $Z > 1$. The best values found are given in Table 3. Figure 2 shows a good fit between the experimental $Z_C$vs $-\log[H^+]$ curves and those calculated from the values of β_{-311} given in Table 3. Analogous curves are obtained for the other three systems. The curves calculated for the model FONDO + $[Be(OH)C]^-$ practically coincides with the curve calculated for the model FONDO up to pH $\simeq$ 5. It is deduced that the complex $[Be(OH)C]^-$ is mainly formed at pH > 5. This result is best observed in the diagram of species distribution presented in Fig. 3 for the IDA–Be(II) system. Analogous distribution diagrams are obtained for the other three systems. The species $[Be(OH)C]^-$ begins to form in small amounts at pH > 4, but mainly at pH > 5. The limited margin of existence of the species $[Be(OH)C]^-$ is conditioned by the great stability of the hydrolytic species $[Be_3(OH)_3]^{3+}$. In Fig. 3 it is

Table 3. Formation constants (B_{pqr}) and stability constants (K) of the complex $[Be(OH)C]^-$ of IDA, MIDA, EIDA and PIDA (25°C, I = 0.5 M in $NaClO_4$)

Acid	$-\text{Log}\,\beta_{-311}$	Log K	Log K	Log K	Log K
IDA	11.60 ± 0.06	13.95	16.83[a]		
MIDA	11.31 ± 0.04	14.20	16.15[b]	13.53[c]	
EIDA	11.40 ± 0.10	14.53		13.80[c]	
PIDA	11.54 ± 0.21	14.36		13.48[c]	11.28[d]

[a] Cu(II), 25°C, I = 0.1 M in KCl[1]
[b] Cu(II), 20°C, I = 0.1 M in KCl.[1]
[c] Pb(II),25°C, I = 0.1 M in $NaNO_3$.[41]
[d] Fe(II), 25°C, I = 0.1 M in KCl.[30]

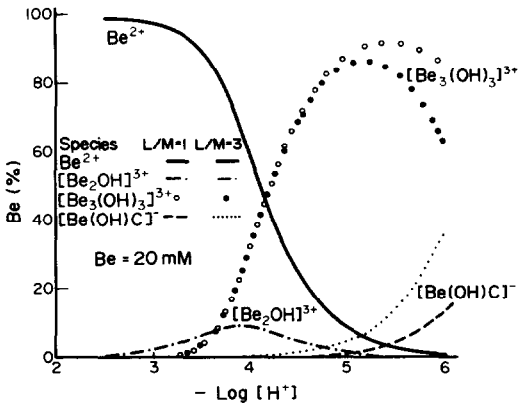

Fig. 3. Species distribution as a function of $-\log[H^+]$ for the IDA–Be(II) system.

observed that as the concentration of the ligand increases, the proportion of the complex $[Be(OH)C]^-$ increases and that of the species $[Be_3(OH)_3]^{3+}$ decreases. That is, the complex $[Be(OH)C]^-$ is fundamentally formed by means of equilibrium (4):

$$\frac{1}{3}[Be_3(OH)_3]^{3+} + HC^- \rightleftharpoons [Be(OH)C]^- + H^+ \quad (4)$$

which accounts for the supplementary acidity observed in Fig. 3 upon formation of the complex $[Be(OH)C]^-$.

The R–IDA ligands act, therefore, as tridentate ligands, destroying the trinuclear species $[Be_3(OH)_3]^{3+}$. The OH^- will occupy fourth place in the tetrahedron of coordination[40] of the Be(II), leading us to propose the structure in Fig. 4 for the complex $[Be(OH)C]^-$. The species $BeC(H_2O)$ is unstable, since if it were formed it would undergo rapid hydrolysis, stabilizing the species $[Be(OH)C]^-$. But the experimental data are more

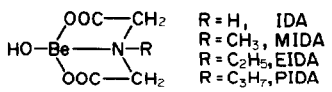

Fig. 4. Structure proposed for the complex $[Be(OH)C]^-$.

in accordance with its formation from the trimer species $[Be_3[OH_3]^{3+}$ (Fig. 3). NTA and such stabilize the neutral complex BeC^- (H_3C ligands),[12] because the ligand is tetradentate and satisfies the coordination necessities of the Be(II).[40]

The values of the constant β_{-311} are practically identical for the four ligands studied (Table 3). The values of the stability constant K of the complex $[Be(OH)C]^-$ are also given in Table 3, according to equilibrium (5):

$$Be^{2+} + C^{2-} + OH^- \rightleftharpoons [Be(OH)C]^-, \quad (5)$$

readily calculated from β_{-311} (Table 3), β_{-21} (Table 1) and K_w, the ionic product of the water. Upon comparison with other values of $\log K$ for $[M(OH)C]^-$ complexes (Table 3), it is found that the complexes of Be(II) are more stable than those of Fe(II), somewhat more stable than those of Pb(II) and less stable than those of Cu(II).

REFERENCES

1. A. E. Martell and R. M. Smith, *Critical Stability Constants*, Vol. 1, *Amino Acids*. Plenum Press, New York (1974).
2. A. E. Martell and R. M. Smith, *Critical Stability Constants*,. Vol. 5, *First Supplement*. Plenum Press, New York (1982).
3. D. D. Perrin, *Stability Constants of Metal–Ion Complexes. Part B: Organic Ligands*. Pergamon Press, Oxford (1979).
4. C. F. Baes, Jr and R. E. Mesmer, *The Hydrolysis of Cations*, John Wiley, New York (1976).
5. N. M. Dyatlova, M. I. Kabachnik, T. Y Medved, M. V. Rudomino and Y. F. Belugin, *Dokl. Akad. Nauk SSSR* 1965, **161**, 607.
6. N. M. Dyatlova, V. V. Medyntsev and B. V. Zhadanov. *Chem. Abstr.* 1968, **69**, 6572j.
7 N. M. Dyatlova, V. V. Medyntsev and B. V. Zhadanov, *Chem. Abstr.* 1968, **68**, 16594m.
8. U. Jain, V. Kumari, R. C. Sharma and G. K. Chaturvedi, *J. Chim. Phys.* 1977, **74**, 1038.
9. S. N. Dubey, A. Singh and D. M. Puri, *J. Inorg. Nucl. Chem.* 1981, **43**, 407.
10. A. Mederos, S. Dominguez, M. Hernández-Padilla, F. Brito and E. Chinea, *Bol. Soc. Quim. Perú* 1984, **50**, 277.
11. A. Mederos, J. M. Felipe, M. Hernández-Padilla, F. Brito, E. Chinea and K. Bazdikian, *J. Coord. Chem.* 1986, **14**, 277.
12. A. Mederos, S. Dominguez, A. M. Medina, F. Brito, E. Chinea and K. Bazdikian, to be published.
13. F. Brito and J. M. Gonçalves, Project No. 51.78.31-51-1228, CONICIT, Caracas, Venezuela (1981).
14. R. Arneck, L. G. Sillén and O. Wahlberg, *Ark. Kemi* 1959, **31**, 353.
15. P. Souchay, N. Israily and P. Gouzerh, *Bull. Soc. Chim. Fr.* 1966, 3917.
16. G. Gran, *Analyst* 1952, **77**, 661.
17. J. Huré, M. Kremer and F. Bequer, *Anal. Chim, Acta* 1952, **7**, 37.
18. R. Pribil, *Analytical Applications of EDTA and Related Compounds*. Pergamon Press, Braunschweig (1972).
19. F. Brito and N. Ingri, *An. Quim* 1960, **56B**, 165.
20. G. Biedermann and L. G. Sillén, *Ark. Kemi* 1953, **5**, 425.
21. G. Lagerström, *Acta Chem. Scand.* 1959, **13**, 722.
22. L. G. Sillén, *Acta Chem. Scand.* 1962, **16**, 159; L. G. Sillén and B. Warnqvist, *Ark. Kemi* 1969, **31**, 341.
23. H. Kakihana and L. G. Sillén, *Acta Chem. Scand.* 1956, **10**, 985.
24. B. Carrell and A. Olin, *Acta Chem. Scand.* 1961, **15**, 1875.
25. S. Hietanen and L. G. Sillén, *Acta Chem. Scand.* 1964. **18**, 1015.
26. F. Bertin, G. Thomas and J. C. Merlin, *Bull. Soc. Chim. Fr.* 1967, 2393.
27. R. E. Mesmer and C. F. Baes, *Inorg. Chem.* 1967, **6**, 1951.
28. M. K. Cooper, D. E. J. Garman and D. W. Yaniuk, *J. Chem. Soc., Dalton Trans.* 1974. 1281.
29. A. Vanni, M. C. Gennaro and G. Ostacoli, *J. Inorg. Nucl. Chem.* 1975, **37**, 1443.
30. A. Mederos, S. Dominguez, A. M. Medina, F. Brito and E. Chinea, *Polyhedron* 1986, **5**, 1247.
31. A. Napoli, *Gazz. Chim. Ital.* 1972, **102**, 724.
32. A. Liberti and A. Napoli, *J. Inorg, Nucl. Chem.* 1971, **33**, 89.
33. E. Collange and G. Thomas, *Anal. Chim. Acta* 1973, **65**, 87.
34. G. M. Sergeev and I. A. Korshunov, *Radiokhimiya* 1973. **15**, 618.
35. A. Napoli, *J. Inorg. Nucl. Chem.* 1977, **39**, 463.
36. G. Schwarzenbach, H. Ackerman and P. Ruckstuhl, *Helv, Chim. Acta* 1949, **32**, 1175.
37. F. Bertin and G. Thomas, *Bull. Soc. Chim. Fr.* 1968, 1225.
38. G. Duc, F. Bertin and G. Thomas, *Bull. Soc. Chim. Fr.* 1974, 793; 1975, 495; 1976, 414; 1977, 196 and 645.
39. G. Duc, and G. Thomas, *Bull. Soc. Chim. Fr.* 1979, 163; 1980, I–169.
40. J. Burgess, *Metal Ions in Solution*. Ellis Horwood, Chichester (1978).
41. A. Mederos, S. Dominguez and A. M. Medina, *An. Quim.* (in press).

Polyhedron Vol. 6, No. 2, pp. 309–314, 1987
Printed in Great Britain

0277–5387/87 $3.00 + .00

TOPOLOGY AND CHEMISTRY OF POLYOXOMETALATES: INORGANIC POLYMERS FORMED BY CONNECTING OCTAHEDRAL UNITS, HETERO- AND ISOPOLYANIONS, AND THEIR STRUCTURAL STABILITY

KENJI NOMIYA

Department of Industrial Chemistry, Faculty of Engineering, Seikei University, Musashino, Tokyo 180, Japan

(*Received* 24 *February* 1986; *accepted after revision* 27 *June* 1986)

Abstract—The structure of inorganic polymers such as hetero- and isopolyanions formed by connecting some MO_6 octahedra is topologically discussed on the basis of the mode of connectivity of the octahedral components. The path in the inorganic polymer and the closed loop in the polyanion, which are contours continuously linked by *trans*-located bridging vertices (oxygens) in each constituent octahedron, are discussed. The previously reported three rationalizations of the polyanion structure are standardized; the first is Lipscomb's proposal on the number of terminal vertices within each octahedral unit of actual polyanions, the second is Pope's classification of all polyanions according to Lipscomb's proposal, and the third is our presentation of the structural stability based on the number of closed loops. A topological definition of a polyanion is provided by the Lipscomb–Pope condition; the polyanion is a condensation compound of some octahedral units where each octahedron has one or two mutually *cis*-located terminal oxygens. The structure of the polyanion skeleton is determined by the combination of the structural parameters *A*, *B* and *C*, where *A* is the number of MO_6 octahedral components constituting the polyanion skeleton, *B* the number of MO_6 units constituting the closed loop, and *C* the number of closed loops. The closed loop is directly related to the mode of connectivity of the octahedral units and significantly contributes to the structural stability. The combination of the structural parameters *A*, *B* and *C* represents the topological character of the polyanion. The topological isomer with an identical combination is distinguished from the chemical isomer with an identical composition.

Hetero- and isopolyanions in chemistry are included in an inorganic polymer formed by connecting some MO_6 octahedral units, that is, by repeating their corner and/or edge sharings. They have also been considered as assemblages of metal–oxygen octahedra, or as fragments of metal-oxide lattices and close-packed arrays.[1] Topology has provided us with some tools for classifying geometrical figures as a bounded and closed set, or a compact set, an arcwise connectivity, Euler's characteristics and so on.[2] As shown in elementary topology, these items have a mathematically common property, the topological invariant, which all homeomorphic figures necessarily possess.* However, they are not always a powerful tool for the topology of the polyanion structure as a geometrical aggregate of octahedral units. In this paper, we have discussed the polyanion structure and its stability by using a new idea concerning the connec-

*The theorem for the topological invariant is well-known. Theorem. If two figures (*A* and *B*) are homeomorphic, the following three propositions are presented. (1) If *A* is the compact set, *B* is also the compact set, (2) if *A* is arcwise-connected, *B* is also arcwise-connected, and (3) their Euler's characteristics are equal.

The contraposition of the theorem has been practically used for classification of the figures. For two figures (*A* and *B*): (1) if *A* is the compact set and *B* is not, *A* is not homoemorphic with *B*, (2) if *A* is arcwise-connected and *B* is not, *A* is not homeomorphic with *B*; and (3) if their Euler's characteristics are different from each other, they are not homeomorphic.

tivity of octahedral components, the path and the closed loop, which are contours continuously linked by *trans*-located bridging vertices in each octahedron. The polyanion is topologically defined by the Lipscomb–Pope condition.[3,4]

RESULTS AND DISCUSSION

The path

For instance, in a hypothetical inorganic polymer (I), M_nO_{4n+2}, formed only by edge sharing, and a polymer (II), M_nO_{5n+1}, formed only by corner sharing of n MO_6 octahedral units [Fig. 1(a)], both are arcwise-connected, because they have a continuous linkage of octahedral components. Further, they have an identical Euler's characteristic; $\chi = V$ (vertex) $- E$ (edge) $+ F$ (face) $= n + 1$, because $V = 4n + 2$, $E = 11n + 1$, and $F = 8n$ for polymer **I**; and $V = 5n + 1$, $E = 12n$, and $F = 8n$ for polymer **II**. The topological invariant is a necessary but not a sufficient condition for homeomorphic figures.* Therefore, these two polymers cannot be discriminated in a simple way. In these polymers, six vertices of an octahedron and a connecting mode are essential points. Each octahedron could not be substituted by a spherical ball, although they are homeomorphic with each other. Here we intend to propose that a path becomes a tool classifying the structure of such polymers. The path is defined as the contour continuously linked by *trans*-located bridging vertices (oxygens) in each MO_6 octahedron, O—M—O—·····—M—O. The path starts from a vertex in the terminal octahedron. It should pass through all the octahedral units. In the above example, there exist two paths in polymer **I**, but only one path in **II** [Fig. 1(b)]. The analogous polymer formed only by face sharings, M_nO_{3n+3} ($V = 3n + 3$, $E = 9n + 3$, and $F = 6n + 2$), has three paths. However, this polymer is homeomorphic with a monomeric polyhedron and a spherical ball, because none of the linking octahedra have terminal vertices. In fact, it has an Euler's characteristic of 2, independent of n. It follows, therefore, that this polymer is distinct from polymers **I** and **II**. The path is a stricter condition than the arcwise connectivity. In polymer **I**, if each edge sharing is transformed into corner sharing by "scissoring" the shared edges, many corner-sharing polymers are produced. All of them, of course, have equal Euler's characteristics. Only one of them, polymer **II**, has one path and the others have no path despite the continuous linkage of all the octahedral components. If some edge sharings are transformed into corner sharings by "scissoring", a number of polymers containing both corner and edge sharings are produced. Only limited polymers have one path. Some examples are depicted in Fig. 2.

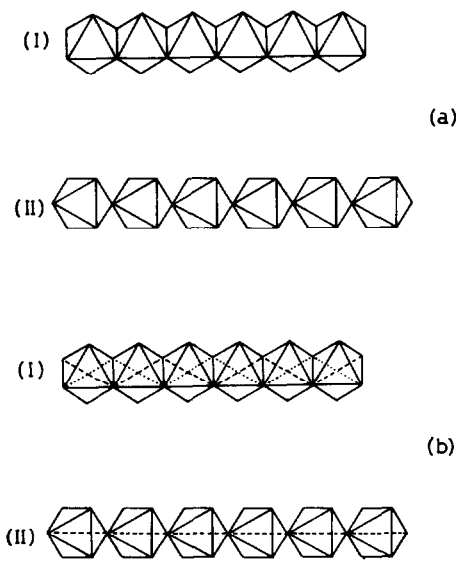

Fig. 1. (a) Hypothetical inorganic polymers formed by edge and corner sharings of n octahedral MO_6 units: **I** with general formula of M_nO_{4n+2}, and **II** with that of M_nO_{5n+1}, respectively. They are drawn as $n = 6$ for convenience. Both have an identical Euler's characteristic: $\chi = V$ (vertex) $- E$ (edge) $+ F$ (face) $= n + 1$. (b) Classification of **I** and **II** by path. There are two paths represented by broken and dotted lines in **I** and one path by a broken line in **II**.

The next examples are the polymers M_3O_{14} (**III**), M_3O_{14} (**IV**) and M_3O_{13} (**V**) formed by the edge sharing of three octahedra (Fig. 3). They are fundamental fragments which frequently appear in many polyanion structures.[1] The difference between polymers **III** and **IV** is an edge-sharing site of a terminal octahedron. Three octahedra in polymer **V** share an edge with each other. These polymers also have an equal Euler's characteristic ($\chi = 4$), as readily confirmed. Polymer **V** can be certainly discriminated from **IV** and **III** by the arcwise connectivity resulting from a removal of one octahedron. However, the path provides a more evident difference; there exist two paths in **III**, one in **IV** and none in **V** (Fig. 3). Since the path is related to the mode of connectivity of each octahedron, it is meaningful in the topology of an inorganic polymer.

In polymers **I** and **II**, a condensation by edge, corner or face sharing between two terminal octahedra leads to cyclization, although it needs an appropriate number of linking octahedra. The

*See footnote on p. 309.

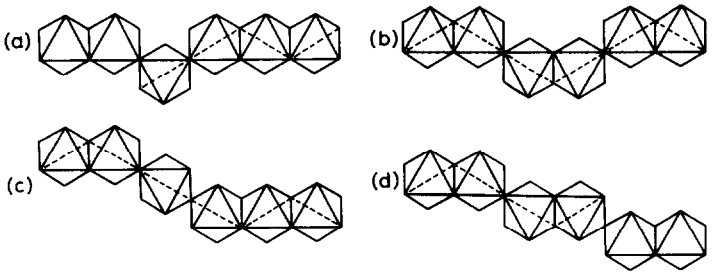

Fig. 2. Inorganic polymers containing both edge and corner sharings produced by "scissoring" of I. There is one path in (b) and (c), but no path in (a) and (d).

propagation of an inorganic polymer by the condensation of some octahedral units ceases on cyclization, because a linear-type condensation is endless. This not only applies to the main chain but also to the side chain or the branch. Evidently, the number of terminal vertices (oxygens) of condensating octahedra decreases on cyclization. The cyclic polymer (I'), M_nO_{4n} ($V = 4n$, $E = 11n$ and $F = 8n$; $\chi = n$), derived from polymer **I**, and the cyclic polymer (II'), M_nO_{5n} ($V = 5n$, $E = 12n$ and $F = 8n$; $\chi = n$), derived from polymer **II**, have two and one path, respectively [Fig. 4(a)]. In these cases, the path forms a closed linkage. Incidentally, polymers **I** and **II** are not homeomorphic with the cyclic polymers **I'** and **II'**, because the Euler's characteristics are different.* The cyclic polymers **I'** and **II'** have two and four terminal vertices in each octahedron, respectively. This implies that polymer **I'** has a higher degree of condensation than **II'**. Here it is noteworthy that the cyclization is independent of the connecting positions between the two condensating octahedra. In the cyclic polymers, closed linkages sometimes exist, but more frequently they do not. This is exemplified in polymer **II'**, where the probability of having a closed linkage is 1/5 [Fig. 4(b)].

The Lipscomb–Pope condition and the polyanions

Although the polyanion is an inorganic polymer, we should discuss them separately. The reason is that the inorganic polymer which is a condensation compound of octahedral units includes the polyanion, but the condensation compound is not always a polyanion. Thus, the definition of the polyanion is required.

Lipscomb[3] has previously proposed that MO_6 octahedra polymerize in aqueous solution to give stable polyanions in which no octahedron terminates in three or more terminal oxygens. In fact, in the actual polyanions hitherto known, the number of terminal oxygens in each octahedral component is less than or equal to two. According to this proposal, Pope[4] has classified the known polyanions into three types; type I comprising each octahedron with a single terminal oxygen, type II comprising each octahedron with two mutually *cis*-located terminal oxygens, and type III containing both sorts of octahedron. Lipscomb's proposal requires that multiple condensations of octahedral units are absolutely necessary for the formation of

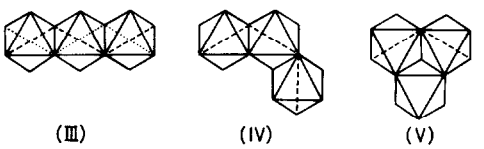

Fig. 3. Polymers formed by edge sharing of three octahedra and classification by path. There are two, one and no path in **III**, **IV** and **V**, respectively.

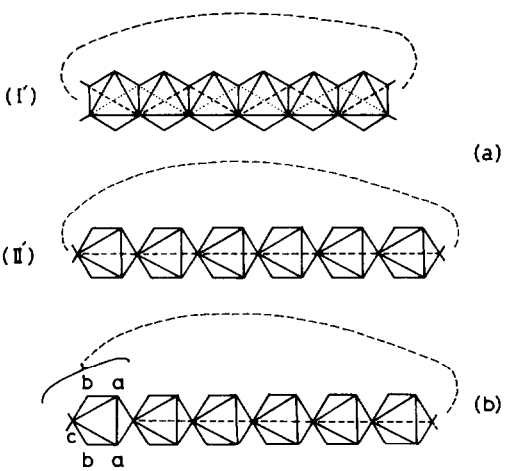

Fig. 4. (a) Cyclic polymers derived from **I** and **II** and path; **I'** with general formula of M_nO_{4n} and **II'** with that of M_nO_{5n}. They have an identical Euler's characteristic; $\chi = n$. (b) Connectivity and path in cyclic polymer **II'**. Only when the cyclization is completed at point *c* does one closed linkage exist.

*See footnote on p. 309.

the polyanion, because the number of nonbridging oxygens in the monomeric octahedron, six, should decrease to less than or equal to two. The formation of the polyanion is certainly well described by the proposal. Further this can be considered to be the necessary and sufficient condition for the condensation compound being the polyanion. Thus, the topological definition of the polyanion is given by the Lipscomb–Pope condition; the polyanion is the condensation compound of octahedral units where each octahedron has one or two mutually *cis*-located terminal oxygens.

Here it should be noted that the Lipscomb–Pope condition concerns the number of terminal oxygens in each octahedral unit derived from the already formed polyanions. Coordination by a heteroatom and modification by attaching water, hydroxy and some organic groups can sometimes convert the terminal oxygens into nonterminal ones. Accordingly, it is possible that the Lipscomb–Pope condition can be satisfied by such modifications, even though it is not satisfied by the original skeleton. Furthermore, it is silent about whether the polyanion is stable or not.

As referred to in the definition, none of the examples of inorganic polymers (**I**–**V**) and the cyclic polymer **II**′ are polyanions. The cyclic polymer **I**′ has two terminal oxygens in each octahedron; however, it is also ruled out, because of their *trans* location.

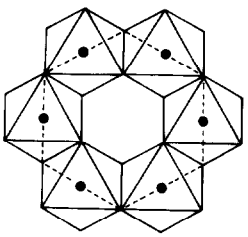

(VI)

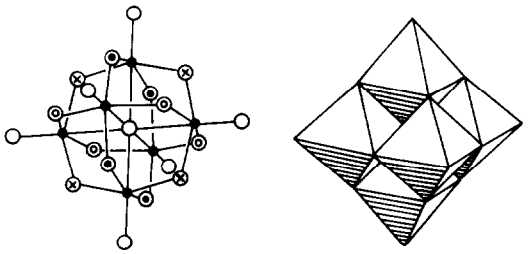

(VII)

Fig. 5. Path and closed loop for polyanions formed by edge sharings of six octahedra; one path in **VI** constitutes one closed loop. In **VII**, there is no path through all the octahedra, but three closed loops through four octahedra. In **VI** and **VII**, the filled small circles are metal (M) atoms and in the framework bond model of **VII** the uniformly marked circles (oxygens) identify one closed loop. The polyhedral skeletons of **VI** and **VII** are actually seen in the Anderson polyanion and the $[M_6O_{19}]^{n-}$ isopolyanion, respectively.

The closed loop and structural stability

The path is a convenient tool for distinguishing some inorganic polymers consisting of the same number of octahedral units. This can also be applied to a polyanion. We frequently find that the route along the path forms the closed linkage passing through only bridging vertices. Generally, when the starting vertex of the contour is the same as the end vertex, we have called it a closed loop.[5(a)] The closed loop does not necessarily pass through all octahedral units in the polyanion. There sometimes exist some local closed loops passing through partial octahedral units. This point may be different from the path in the polymer. However, the closed loop also becomes a topological tool for distinguishing some polyanions. When the path is a closed linkage, it is essentially a closed loop. These are shown in Fig. 5.

The formation of a closed loop is directly related to the mode of connectivity of the octahedral components. Further, the combination of the structural parameters *A*, *B* and *C*, where *A* is the number of MO_6 octahedral components constituting the polyanion skeleton, *B* the number of MO_6 units constituting the closed loop, and *C* the number of closed loops, represents a one-to-one correspondence with many actual polyanion structures.[5(a)–(d)] Thus, this combination is representative of the topological character of the polyanion. As a matter of fact, a number of polyanions are more conveniently classified by *A*, *B* and *C* than by the Euler's characteristic. Here it should be noted that in the heteropolyanions the number of heteroatoms themselves, and some elements and groups regarded as the heteroatom, do not contribute to the structural parameters, especially to parameter *A*, and the closed loop is only applied to the polyanion skeleton as an aggregate of octahedra.

If polyanions with different structures have an identical combination of *A*, *B* and *C*, they should be topologically isomeric. Since the topological isomer is not related to a chemical formula or composition, it is not always chemically isomeric. Some mechanisms for the interconversions between α- (**VIII**) and β-$[Mo_8O_{26}]^{4-}$ (**IX**) isopolyanions,

and between Anderson-type $[XMo_6O_{24}H_6]^{n-}$ (X) and Lindqvist-type $[Mo_7O_{24}]^{6-}$ (XI) polyanions, have been previously proposed by some workers (Fig. 6).[6,7] However, α- and β-$[Mo_8O_{26}]^{4-}$ polyanions are chemical isomers, but not topological isomers, because the structural parameters are $A = 6$, $(B, C) = (6, 1)$ in the former, and $A = 8$, $(B, C) = (4, 2)$ in the latter.[5(a)] On the other hand, the Anderson-type $[XMo_6O_{24}H_6]^{n-}$ heteropolyanion, the Lindqvist-type $[Mo_7O_{24}]^{6-}$ and the α-$[Mo_8O_{26}]^{4-}$ isopolyanions are topological isomers, but not chemical isomers, because these polyanions have identical parameters $[A = 6, (B, C) = (6, 1)]$[5(a)] in spite of different chemical compositions. Recently Pope and coworkers[8] have prepared new heteropolytungstoarsonates, $[RAsW_7O_{27}H]^{7-}$ (R = CH_3, C_6H_5 or p-NH_2—C_6H_4) (XII), and discussed the mechanism for the interconversion with the "topologically" related compound, the Lindqvist-type $[W_7O_{24}]^{6-}$ polyanion. The former parameters are $A = 7$, $(B, C) = (6, 1)$, but the latter ones are $A = 6$, $(B, C) = (6, 1)$, because the central nonoxo WO_6 octahedron in the Lindqvist structure has been treated as a heteroatom.[5(a)] Thus, these polyanions are neither chemically nor topologically isomeric. However, the $[(RAs)_2W_6O_{25}H]^{5-}$(XIII) polyanion $[A = 6, (B, C) = (6, 1)]$, which is rapidly induced from XII in aqueous solution, is topologically isomeric with the $[W_7O_{24}]^{6-}$ isopolyanion (Fig. 7).

Apart from the above points, the closed loop is chemically meaningful and it significantly contributes to the stability of the polyanion, since the cyclic π-bonding system along the loop can be considered. The π-bonding character of bridging oxygens has been experimentally confirmed.[6(a)] We[5(a)] have previously proposed the structural stability of the polyanion skeleton on the basis of the number of closed loops and defined the stability index (η) as the number of closed loops per MO_6 octahedral unit. It has been estimated from the

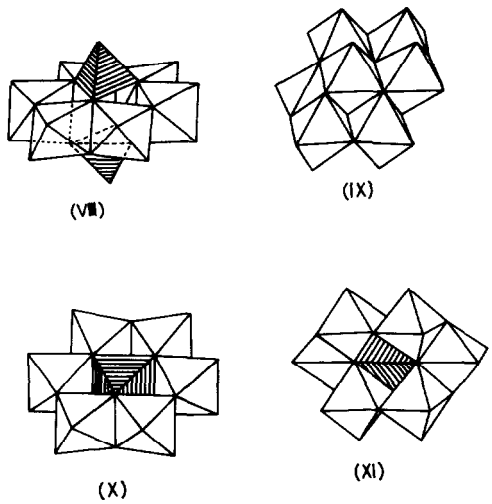

Fig. 6. Polyhedral models of some polyanions; α-$[Mo_8O_{26}]^{4-}$ (VIII), β-$[Mo_8O_{26}]^{4-}$ (IX), Anderson-type $[XM_6O_{24}H_6]^{n-}$ (X) and Lindqvist-type $[M_7O_{24}]^{6-}$ (XI) structures. Shaded polyhedra are the heteroatom or the groups regarded as it.

structural parameters A, B and C as $\eta = (\Sigma BC)/A$. This, in turn, represents the proportion of octahedral components constituting the closed loop to the total number of octahedral units of the polyanion. The product BC shows the number of bridging oxygens on the closed loops. The summation is more than, equal to, or less than the number of actual bridging oxygens according to the multiplicity of the loop passing through the same vertex (bridging oxygen). η has been estimated for a number of actual polyanions[5(a)–(d)] and its properties have been summarized as general rules: (1) polyanions with a larger index are more stabilized; (2) polyanions with an identical index within the same series of constituting elements (M ion and heteroatom) can be interconverted, or converted from one polyanion to another; (3) the index reveals the degree of condensation; (4) when a heteropolyanion decomposes, or degrades, into

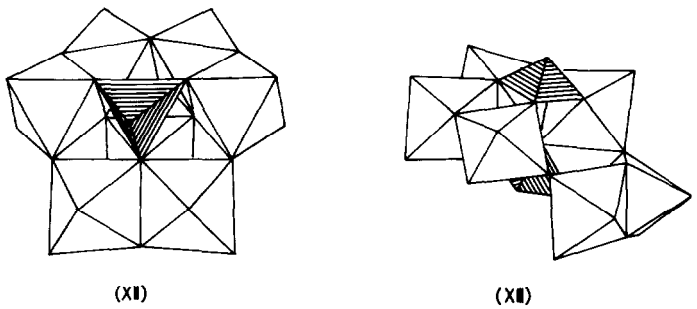

Fig. 7. Polyhedral models of $[RAsW_7O_{27}H]^{7-}$ (XII)[8] and $[(RAs)_2W_6O_{25}H]^{5-}$ (XIII)[1] polyanions. The tetrahedral part of the $RAsO_3$ group is shaded.

some isopolyanions under an appropriate condition, the isopolyanion possessing the largest index is predominantly produced; and (5) the real heteropoly and isopoly compounds with a smaller index are stabilized by some supporting factors other than the structural one.

Acknowledgment—I thank Professor M. Miwa of Seikei University for his helpful advice.

REFERENCES

1. M. T. Pope, *Heteropoly and Isopoly Oxometalates*, Chap. 2. Springer, New York (1983).
2. (a) A. H. Wallace, *An Introduction to Algebraic Topology*. Pergamon Press, New York (1957). (b) B. H. Arnold, *Intuitive Concepts in Elementary Topology*. Prentice-Hall, Englewood Cliffs, NJ (1962). (c) A. Brown, *Elements of Modern Topology*. McGraw-Hill, Maidenhead (1968). (d) I. Tamura, *Topology* (Japanese). Iwanami Shoten, Tokyo (1974).
3. W. N. Lipscomb, *Inorg. Chem.* 1965, **4**, 132.
4. M. T. Pope, *Inorg. Chem.* 1972, **11**, 1973.
5. (a) K. Nomiya and M. Miwa, *Polyhedron* 1984, **3**, 341, 1171; (b) K. Nomiya and M. Miwa, *ibid.* 1985, **4**, 89; (c) K. Nomiya and M. Miwa, *ibid.* 1985, **4**, 675; (d) K. Nomiya and M. Miwa, *ibid.* 1985, **4**, 1407.
6. W. G. Klemperer and W. Shum, *J. Am. Chem. Soc.* 1976, **98**, 8291.
7. A. F. Masters, S. F. Gheller, R. T. C. Brownlee, M. J. O'Connor and A. G. Wedd, *Inorg. Chem.* 1980, **19**, 3866.
8. G. B. Jameson, M. T. Pope and S. H. Wasfi, *J. Am. Chem. Soc.* 1985, **107**, 4911.

Polyhedron Vol. 6, No. 2, pp. 315–317, 1987
Printed in Great Britain.

0277–5387/87 $3.00 + .00

SYNTHESIS AND MOLECULAR STRUCTURES OF COMPLEXES OF $TlBrI_2$ WITH PYRIDINE *N*-OXIDE AND SOME SUBSTITUTED PYRIDINE *N*-OXIDES

M. R. BERMEJO,* E. SOLLEIRO and A. RODRÍGUEZ

Departamento de Química Inorgánica, Facultade de Química, Universidade de Santiago de Compostela, Galiza, Spain

and

A. CASTIÑEIRAS

Departamento de Química Inorgánica, Facultade de Farmacia, Universidade de Santiago de Compostela, Galiza, Spain

(*Received* 25 *February* 1986; *accepted after revision* 27 *June* 1986)

Abstract—The following compounds, $TlBrI_2(PyO)_2$, $TlBrI_2(2\text{-}PicO)_2$, $TlBrI_2(3\text{-}PicO)_2$, $TlBrI_2(4\text{-}PicO)_2$, $TlBrI_2(4\text{-}Cl\text{-}PyO)_2$, $TlBrI_2(4\text{-}CN\text{-}PyO)_2$, $TlBrI_2(4\text{-}NO_2\text{-}PyO)_2$ and $TlBrI_2(4\text{-}CH_3O\text{-}PyO)_2$, have been prepared and characterized by elemental analysis. The solids behave as non-electrolytes in acetonitrile solution and are monomers in benzene. Vibrational (IR and Raman) spectra suggest that the most probable structure is that of a trigonal bipyramid with the halogen atoms in equatorial positions and the two ligands in axial positions.

Our previous work reported the detailed characterization of $TlI_3 \cdot L_2$[1] and $TlClI_2 \cdot L_2$[2] complexes, following a new and simple synthesis procedure which is an improvement on the one published by Cotton.[3]

We now report the synthesis and structural characterization of interhalogen derivatives of thallium(III) of type $TlBrI_2 \cdot L_2$. The selected ligands are: pyridine *N*-oxide (PyO), 2-, 3- and 4-methylpyridine *N*-oxide (2-PicO, 3-PicO and 4-PicO), 4-chloropyridine *N*-oxide (4-Cl-PyO), 4-cyanopyridine *N*-oxide (4-CN-PyO), 4-nitropyridine *N*-oxide ($4\text{-}NO_2\text{-}PyO$) and 4-methoxypyridine *N*-oxide ($4\text{-}CH_3O\text{-}PyO$). $TlBrI_2 \cdot 2PyO$ has been prepared previously[4] but it is prepared now for comparison.

EXPERIMENTAL

Measurements and material

IR spectra were recorded on a Perkin–Elmer 180 spectrophotometer with a far-IR accessory and the Raman spectra with a Jarrel–Ash spectrophotometer (Ar^+ laser, 5145 Å). The conductivity measurements were carried out with a WTW LF-3 type conductivity bridge and an LTA type electrode using 10^{-3} M solutions in acetonitrile, and the molecular weights of those complexes that were sufficiently soluble were determined in benzene in a Knauer vapour pressure osmometer. Standard procedures were used for determining the elements. All products were of reagent grade and the solvents were dried by standard procedures.

Synthesis of the complexes

They were prepared by the addition of a solution of iodine in acetonitrile, drop by drop, with magnetic stirring, to a TlBr suspension and the donor in the same solvent. As the addition proceeds the TlI can be observed dissolving as a consequence of the formation of the new $TlBrI_2 \cdot 2L$ compounds which are often soluble in the selected solvent. The transparent solution formed is stirred for a few hours and concentrated in the vacuum line. Some solids were recrystallized in acetonitrile.

*Author to whom correspondence should be addressed.

RESULTS AND DISCUSSION

All the compounds were prepared in a 1:2 molar ratio as coloured solids (some of them crystalline). The compounds are photo- and air-stable, with the exception of $TlBrI_2(4\text{-}NO_2\text{-}PyO)_2$ which is hydrolyzed slowly by air (in acid medium the hydrolysis is very fast). They are soluble in solvents with lower dielectric constants. The molecular weights show that the compounds exist as monomers, at least in benzene, in agreement with data obtained for similar compounds.[1,3-5] The milimolar conductivities in acetonitrile (see Table 1) are lower than the values reported for 1:1 electrolytes,[6] and show their non-electrolytic behaviour in this solvent.

The most significative bands of the IR spectra of the ligands and adducts are shown in Table 2. The ligand bands have been assigned according to Shindo[7] and Karayannis.[8]

The position of the ν(N—O) vibration mode in the compounds is shifted toward lower wavenumbers ($\Delta\nu \simeq 20\text{–}49\,cm^{-1}$), showing that the coordination takes place through the oxygen atom of the N—O group. The strong band, close to $850\,cm^{-1}$ and assigned to δ(N—O), undergoes small shifts which have been ascribed to two competitive effects[9] and have also been detected in other complexes with these aromatic amine oxides.[2,4,8,10]

The ν(Tl—Br), ν(Tl—I), ν(T1—O) and δ(Tl—X) bands that appear between 500 and $50\,cm^{-1}$ contain information concerning the structure of the complexes. The assignments of the ν(Tl—Br) and ν(Tl—I) vibrations has been accomplished by comparing the spectra of our complexes with the assignments made in other thallium halide complexes[1,2,4,5] prepared by us, and taking into account that, according to Carty,[11] the ν(Tl—Br)/ν(Tl—Cl) and ν(Tl—I)/ν(Tl—Cl) ratios must be 0.7 and 0.6, respectively. The bands appearing at 130 and $150\,cm^{-1}$ have been taken as δ(Tl—Br) and δ(Tl—I) modes, respectively, as has been suggested by Walton[12] and McWhinnie.[13] The position of the ν(Tl—O) band has been placed at $300\,cm^{-1}$ according to the assignments of other papers.[1,5] These assignments are listed in Table 2.

X-ray diffraction studies of the complexes $TlCl_3(4\text{-}CN\text{-}PyO)_2$,[14] $TlI_3(2\text{-}PicO)_2$,[15] $TlBr_3(TPPO)_2$,[16] $TlBr_3(PyO)_2$,[17] $TlBr_2I(TPPO)_2$[18] and $TlClBrI(TPPO)_2$,[19] have confirmed the presence in these crystals of slightly distorted trigonal bipyramidal molecules. Recently $TlBrI_2(TPPO)_2$[20] and $TlBrI_2(4\text{-}PicO)_2$[21] have been studied. The unit cell of $TlBrI_2(4\text{-}PicO)_2$ is orthorhombic, space group *Pnna*, and the structure consists of discrete molecules which have distorted trigonal bipyramidal geometry. The thallium atom is coordinated to two iodine atoms and a bromine atom in equatorial positions, and by two ligands in the axial positions.

The small number of bands present in the vibrational spectra of the complexes and their position may exclude the presence of covalent dimeric or polymeric structures and ionic forms.[1,22,23]

For our $TlBrI_2$ compounds the presence of monomer trigonal bipyramidal species must be expected. For this kind of systems there are three different spatial arrangements with thallium C_{2v}, C_s or C_1 local symmetries. All of them originate one ν(Tl—Br), two ν(Tl—I) and two ν(Tl—O), all IR- and Raman-active. The number of bands present in the IR spectra of these compounds is compatible with a *bpt* structure, in spite of us being able to find only a band which can be assigned to a Tl—O stretching mode. However, the Raman spectra show a band at *ca* $270\,cm^{-1}$, which can be assigned to the symmetrical Tl—O stretching mode, which should be stronger in Raman than in IR spectra.

Table 1. Analytical data and some physical properties of the compounds

Compounds	Colour	% C[a]	% H[a]	% N[a]	% Tl[a]	M.p. (°C)	Λ_M[b]	M_m[c]
$TlBrI_2(PyO)_2$	Orange	16.7 (16.5)	1.2 (1.4)	4.0 (3.9)	27.4 (28.1)	138	38.37	691 (728)
$TlBrI_2(4\text{-}Cl\text{-}PyO)_2$	Orange	15.4 (15.1)	1.0 (1.0)	3.4 (3.5)	25.7 (25.6)	126	45.56	792 (797)
$TlBrI_2(4\text{-}NO_2\text{-}PyO)_2$	Orange	14.7 (14.7)	0.8 (1.0)	6.7 (6.9)	25.4 (25.0)	88 (d)[d]	41.57	—
$TlBrI_2(4\text{-}CN\text{-}PyO)_2$	Red	18.3 (18.5)	1.0 (1.0)	6.9 (7.2)	25.7 (26.3)	139 (d)	49.14	—
$TlBrI_2(4\text{-}CH_3O\text{-}PyO)_2$	Yellow	18.4 (18.3)	1.7 (1.8)	3.5 (3.6)	25.5 (25.9)	86	23.55	808 (788)
$TlBrI_2(2\text{-}PicO)_2$	Orange	19.2 (19.1)	1.7 (1.9)	3.4 (3.7)	25.9 (27.0)	127	35.47	750 (756)
$TlBrI_2(3\text{-}PicO)_2$	Orange	19.0 (19.1)	1.8 (1.9)	3.6 (3.7)	26.8 (27.0)	135–136	39.16	758 (756)
$TlBrI_2(4\text{-}PicO)_2$	Red	19.1 (19.1)	1.8 (1.9)	3.5 (3.7)	27.4 (27.0)	140	40.45	753 (756)

[a]The theoretical values are given in parentheses.
[b]Concentration in 10^{-3} M acetonitrile.
[c]Molecular weight measured in benzene.
[d]Decomposition.

Table 2. Most significant bands of the ligands and the complexes[a] in the IR spectra

Compound	ν(N—O)	δ(N—O)	ν(Tl—O)	ν(Tl—Br)	ν(Tl—I)	Other bands
PyO	1.243vs	842s	—	—	—	515m, 460s
$TlBrI_2(PyO)_2$	1.210vs	833s	293vs	189s	165s, 150sh	518vs, 460s, 410s, 130m[b]
4-Cl-PyO	1.248vs	848s	—	—	—	480m, 334m, 280m
$TlBrI_2$(4-Cl-PyO)$_2$	1.205s	837s	—	210s	169s, 154m	465m, 368s, 279m, 192m
4-NO_2-PyO	1.273vs	861m	—	—	—	455m, 360m, 220s
$TlBrI_2$(4-NO_2-PyO)$_2$	1.224vs	850s	330m	192s	170s, br	455m, 370m, 232m, 118m[b]
4-CN-PyO	1.275vs	845s	—	—	—	455m, 410m, 220m
$TlBrI_2$(4-CN-PyO)$_2$	1.239vs	850s	290m	200s	169vs, br	455m, 425m, 128[b]w, 105[b]w
4CH_3O-PyO	1.213vs	850s	—	—	—	455s, 400s, 310w, 250s
$TlBrI_2$(4CH_3O-PyO)$_2$	1.192vs	839s	292m	197s	161, 155sh	462s, 403s, 252s, 107[b]m
2-PicO	1.242vs	855s	—	—	—	470s, 454s, 342m, 270w, 255w, 230m
$TlBrI_2$(2-PicO)$_2$	1.205vs	841s	313s	200s	170s, 160m	468s, 455s, 345m, 232m, 129w,[b] 107w[b]
3-PicO	1.278vs	—	—	—	—	492s, 438m, 308m
$TlBrI_2$(3-PicO)$_2$	1.258s	—	292m	188s	168s, 154m	485s, 438m, 308m, 203w, 122w,[b] 107w[b]
4-PicO	1.228vs	852s	—	—	—	473s, 465m, 336s, 317d
$TlBrI_2$(4-PicO)$_2$	1.192s	827s	—	217s	180s, 170s	479s, 470s, 378s, 327w, 122m[b]

[a]Abbreviations: m, medium; s, strong; w, weak; sh, shoulder; br, broad; v, very.
[b]Band assigned to δ(Tl—X).

Finally, the most probable structure for $TlBrI_2 \cdot L_2$ compounds is a trigonal bipyramid with the halogen atoms in equatorial positions and the two ligands in axial positions.

Acknowledgement—We thank the Xunta de Galicia (Galiza, Spain) for financial support of this work.

REFERENCES

1. M. R. Bermejo and M. Gayoso, *Synth. React. Inorg. Met-Org. Chem.* 1985, **15**, 951.
2. M. R. Bermejo, M. Isabel Fernández, J. García Taboada and M. Gayoso, *Synth. React. Inorg. Met-Org. Chem.* 1986, **16**, 327.
3. F. A. Cotton, B. F. G. Johnson and R. M. Wing, *Inorg. Chem.* 1965, **4**, 502.
4. M. R. Bermejo, J. Irisarri and M. Gayoso, *Synth. React. Inorg. Met-Org. Chem.* 1985, **15**, 197.
5. M. V. Castaño, A. Sánchez, M. R. Bermejo and M. Gayoso, *An. Quim.* 1983, **79B**, 357.
6. W. J. Geary, *Coord. Chem. Rev.* 1971, **7**, 81.
7. H. Shindo, *Chem. Pharm. Bull.* 1956, **4**, 460; 1958, **6**, 117; 1959, **7**, 791.
8. N. M. Karayannis, L. L. Pytlewski and C. M. Mikulski, *Coord. Chem. Rev.* 1973, **11**, 93.
9. I. S. Ahuja and P. Rastogi, *J. Inorg. Nucl. Chem.* 1970, **32**, 1381.
10. J. R. Masaguer, J. S. Casas, J. Sordo, M. R. Bermejo and M. V. Castaño, *Inorg. Chim. Acta* 1977, **24**, 227.
11. A. J. Carty, *Coord. Chem. Rev.* 1969, **4**, 29.
12. R. A. Walton, *Inorg. Chem.* 1968, **7**, 640, 1927.
13. J. R. Hudman, M. Patel and W. R. McWhinnie, *Inorg. Chim. Acta* 1970, **4**, 161.
14. E. Gutiérrez-Puebla, A. Vegas and S. García-Blanco, *Acta Cryst.* 1980, **B36**, 145.
15. M. R. Bermejo, A. Castiñeiras, M. Gayoso, W. Hiller, U. Englert and J. Strähle, *Z. Naturforsch.* 1984, **39B**, 1159.
16. S. E. Jeffs, R. W. H. Small and I. J. Worrall, *Acta Cryst.* 1984, **C40**, 381.
17. C. Ruiz-Valero, E. Gutierrez-Puebla and A. Monge, *An. Quím.* 1984, **80B**, 474; W. Hiller, M. E. García-Fernández, M. R. Bermejo and M. V. Castaño, *Acta Cryst.* 1986, **C42**, 60.
18. A. Castiñeiras, W. Hiller, M. R. Bermejo and M. Gayoso, *Acta Cryst.* (in press).
19. M. R. Bermejo, A. Fernández, A. Castiñeiras and W. Hiller, *Inorg. Chem.* (submitted).
20. A. Castiñeiras, W. Hiller, J. Strähle, M. R. Bermejo and M. Gayoso, *An. Quim.* (in press).
21. W. Hiller, A. Castiñeiras, M. E. García Fernández, M. R. Bermejo, J. Bravo and A. Sánchez, *Z. Naturforsch.* (in press).
22. R. A. Walton, *J. Inorg. Nucl. Chem.* 1970, **32**, 2875.
23. K. Arai, T. Chiba and K. Aida, *J. Inorg. Nucl. Chem.* 1981, **43**, 1986.

Polyhedron Vol. 6, No. 2, pp. 319–327, 1987
Printed in Great Britain

0277-5387/87 $3.00+.00

COMPLEXES OF TRIMETHYLPLATINUM(IV) HALIDES WITH OPTICALLY ACTIVE SCHIFF BASE LIGANDS

EDWARD W. ABEL, KENNETH KITE* and PHILLIP S. PERKINS

Department of Chemistry, University of Exeter, Exeter EX4 4QD, U.K.

(*Received* 3 *June* 1986; *accepted* 27 *June* 1986)

Abstract—The complexes $[(PtMe_3X)C_6H_4NC(R):NCH(Ph)Me]$ (X = Cl, Br or I; R = H or Me) of the Schiff bases derived from (*S*)-(−)-α-methylbenzylamine and 2-pyridinecarboxaldehyde and 2-acetylpyridine, respectively, have been prepared and characterized by 400-MHz ^1H NMR spectroscopy. The diastereoisomeric mixtures have been separated, but rapid isomerization is observed in solution.

The *fac*-methyl groups in trimethylplatinum(IV) compounds[1] make the octahedrally coordinated metal a chiral centre whenever there are three different *trans* substituents, or multidentate ligands which remove the planes of symmetry. No optically active $PtMe_3^+$ complexes have been reported to date, though in the closely related complex $(\eta^5\text{-}C_5H_5)Pt(CH_3)(C_2H_5)(COCH_3)$ the pseudo-tetrahedral or "piano stool" disposition of ligands confers optical isomerism. The ^{13}C and ^1H NMR signals from all four ligands in this complex are split in the presence of a chiral shift reagent[2,3] but it was not possible to resolve the isomers.

The addition of an optically active ligand of defined chirality (*S*) to a prochiral metal centre will necessarily generate two diastereoisomers during synthesis, with optical configurations (*S*)(*R*) and (*S*)(*S*) at the (ligand)(metal) atoms, respectively. This has been elegantly exploited by Brunner and co-workers,[4] who found that "piano stool" complexes of type $[(\eta^5\text{-}C_5H_5)Mn(NO)(CO)_2]^+$ could be resolved by replacing one of the CO groups with an optically active *t*-phosphine,[5] and the octahedral complexes *fac*-$[(CO)_3M(PPh_3)(L\text{–}L)]$ (M = Cr, Mo or W) by using a chiral Schiff base (L–L).[6] The direct parallels with *fac*-trimethylplatinum(IV) led us to prepare the complexes $[PtMe_3X(L\text{–}L)]$, where X = Cl, Br or I, and (L–L) = the Schiff bases **I** and **II** made from the condensation of 2-pyridinecarboxaldehyde and 2-acetylpyridine, respectively, with the optically active primary amine (*S*)-(−)-α-methylbenzylamine, and to study their optical stability by ^1H NMR spectroscopy. Another feature of interest in these complexes is their similarity to the thioether compounds $[(PtMe_3X)MeS(CH_2)_2SMe]$, which undergo an intramolecular fluxion at high temperatures that causes a coalescence of the ^1H NMR signals from the Pt—Me groups. The most plausible mechanism for this process is a "pancake flip" rotation of the thioether.[7] Such a mechanism applied to the Schiff base complexes would interconvert the two diastereoisomers, and a ligand flip process has been suggested by Brunner to explain the isomerization of diastereoisomers of some square pyramidal Mo(I) complexes of I.[8]

EXPERIMENTAL

Literature methods were used to prepare trimethylplatinum iodide[9] and sulphate,[10] from which the bromide and chloride were obtained by reaction with the appropriate potassium halide.[11] 2-Pyridinecarboxaldehyde, 2-acetylpyridine and (*S*)-(−)-α-methylbenzylamine were commercial samples (Aldrich) whose purity was checked by NMR spectroscopy before use.

The Schiff base ligands $C_6H_4NC(R):NCH(Ph)Me$ (**I**, R = H; **II**, R = Me) were made by the method of Brunner and Herrmann[12] in 82 and 76% yield for **I** and **II**, respectively. They were purified by low-temperature recrystallization from diethyl ether, and characterized by mass spectroscopy, optical rotation and NMR spectroscopy in $CDCl_3$ solution [**I**, *m/z* 210 (210); $[\alpha]^{589\,nm}$ = +7.36°; δ 1.60 d (3H) (*J* = 6.7 Hz); 4.63 q (1H) (*J* = 6.6 Hz); 7.36 m (5H); and 8.46 s (1H): **II**, *m/z* 223–225 (224); $[\alpha]^{589\,nm}$ = +90.4°; δ 1.53 d (3H)

*Author to whom correspondence should be addressed.

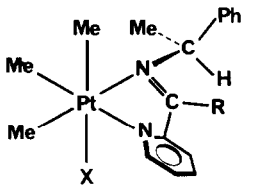

Fig. 1. Structure of the Schiff base complexes [**IA**, R = H, X = Cl; **IB**, R = H, X = Br; **IC**, R = H, X = I; **IIA**, R = Me, X = Cl; **IIB**, R = Me, X = Br; **IIC**, R = Me, X = I].

(J = 6.7 Hz), 2.40 s (3H), 4.89 q (1H) (J = 6.5 Hz), and 7.2–7.4 m (5H)]. Reported NMR data[8] for **I** and **II** are in agreement, allowing for the different solvent system. Optical rotation data are reported for **II** alone, and show that the specific rotation is very wavelength-sensitive, the most comparable value being +101° at 579 nm.

The trimethylplatinum(IV) complexes **IA–C** and **IIA–C** (Fig. 1) were made by the same general method, the following for **IIC** being typical. A mixture of trimethylplatinum(IV) iodide (0.25 g, 0.68 mmol*) and **II** (0.155 g, 0.69 mmol) in chloroform (15 cm^3) was refluxed overnight. The solution was evaporated to dryness, and the solid recrystallized twice from dichloromethane–light petroleum as fine yellow crystals (0.24 g, 59.7%).

^{1}H NMR spectra were recorded at 400 MHz on a Bruker WH-400 spectrometer and at 100 MHz on a JEOL PS/PFT-100 equipped with standard accessories for variable-temperature work. The ^{13}C NMR spectra were recorded on a JEOL GX-270 spectrometer. Band shape analyses were carried out with a version of the DNMR programme of Kleier and Binsch[13] modified to calculate spectral changes based on six initial chemical configurations. Far-IR spectra were run in polythene discs on a Grubb–Parsons/NPL Cube interferometer linked to an Apple II microcomputer. Molecular weights were determined by vapour pressure osmometry, and mass spectra were obtained on a single focussing VG-Micromass MM-30 spectrometer using electron ionization at a potential of 70 eV and probe temperatures of 145 and 200°C.

RESULTS AND DISCUSSION

Complexes **IA–C** and **IIA–C** were prepared from the appropriate trimethylplatinum(IV) halide and an equimolar quantity of the ligand as yellow or orange solids. Analytical and far-IR data (Table 1) are consistent with the mononuclear structure in Fig. 1.

The bromides and iodides crystallized as rhombic or needle-like crystals from CH_2Cl_2–MeOH (1:1 by volume). The chlorides separated as oils, which turned solid on prolonged pumping. The melting ranges indicate isomeric mixtures, the bromides and iodides showing signs of change up to 20°C before the onset of melting. Lower values for the chlorides and their reluctance to crystallize shows a marked change in ease of crystal packing with increase in halide size. Monomeric molecular ions were seen in the mass spectra of all of the complexes. The mononuclear structure in solution was confirmed by vapour pressure osmometry on the iodides in chloroform and the similarity of the NMR data for all three halides. The presence of coordinated X^- was confirmed by the observation of terminal Pt—X stretches in the far IR, these modes being uniformly lower in the complexes of ligand **II**.

^{1}H *NMR spectra*

The 400-MHz ^{1}H NMR spectra of both series of complexes confirm the structures in Fig. 1 and show clear evidence of the presence of two diastereoisomers in every case. For reasons that will be apparent later, it is convenient to discuss the spectra of the two series separately. The spectroscopic data for complexes **IA–C** are recorded in Table 2, aromatic protons (non-first-order multiplets) being omitted as they give no extra structural information.

In the spectra of **IA–C** each diastereoisomer (**a** and **b**) shows six sets of signals (including the aromatic protons) almost all of which are clearly resolved at 400 MHz. The isomers are present in different proportions as expected, and the relative amounts of each are reflected in all six regions of the spectrum, making assignments unambiguous. Relative proportions of one isomer (averaged from all the signals) are 1.34, 1.04 and 0.88 for **IA**, **IB** and **IC**, respectively. Of the three Pt—Me signals for each isomer (Fig. 2), two show $^2J(^{195}Pt–^1H)$ values expected[14] for methyls *trans* to N (68.9–71.7 Hz) and one shows ^2J values for methyls *trans* to halide, with the latter invariably at higher field as is usual in this type of complex.[15] These highest-field signals clearly show that for **IA** and **IB** (X = Cl or Br) the most abundant isomer has its methyl *trans* to X signal at higher field while for **IC** (X = I) the situation is reversed. The more abundant isomer usually has a slightly higher ^2J value for methyls *trans* to N, and in one of the pair of isomers the

*Based on the molar unit $PtMe_3I$.

Table 1. Colour, melting-point, analytical, molar-mass and far-IR data for the $PtMe_3$(IV) complexes

Complex[a]	Halide	Colour	M.p. (°C)	Analytical data[b] % C	% H	% N	Molecular[b] ion *m/z*	(Pt—X) (cm^{-1})
IA	Cl	Pale yellow	77.5–80.5	43.5	5.2	5.6	481–487	234
				(42.0)	(4.8)	(5.8)	(485.9)	
IB	Br	Yellow	205.4–206.7	38.6	4.3	5.3	527–533	135
				(38.5)	(4.4)	(5.3)	(530.4)	
IC	I	Yellow	207.6–208.2	35.1	3.8	5.0	576–578[c]	122
				(35.4)	(4.0)	(4.8)	(577.4)	
IIA	Cl	Pale yellow	83.6–87.4	41.1	4.9	5.4	497–503	230
				(43.2)	(5.0)	(5.6)	(499.9)	
IIB	Br	Orange	184.2–187.1	39.7	4.7	5.0	544–546	130
				(39.7)	(4.6)	(5.1)	(544.4)	
IIC	I	Yellow	193.5–195.8	36.7	4.2	4.8	591–593[d]	105
				(36.6)	(4.3)	(4.7)	(591.4)	

[a]Numbering as in Fig. 1.
[b]Calculated values in parentheses.
[c]Osmometrically in $CHCl_3$ = 576 ± 5.
[d]Osmometrically in $CHCl_3$ = 594 ± 16.

Table 2. 400-MHz ^1H NMR data for complexes IA–C

Complex No.	X	Isomer	Population (%)	N=C—H δ (ppm)	^3J (Hz)	^4J (Hz)	C*—H δ (ppm)[a]	C*—Me δ (ppm)	^3J (Hz)	N—Pt—Me δ (ppm)	^2J (Hz)	X—Pt—Me δ (ppm)	^2J (Hz)
IC	I	**a**	46.3	8.249	28.9	1.3	5.929	1.764	7.0	1.615	71.7	0.758	72.8
										1.527	70.0		
		b	40.9	8.513	29.2	1.3	5.641	1.978	7.0	1.517	71.3	0.587	72.8
										1.500	71.3		
		a'	7.4	8.452	27.6	1.3	5.592	1.908	6.9	1.338	71.2	0.440	74.8
										1.318	69.2		
		b'	5.4	8.312	27.3	1.3	5.778	1.764	7.0	1.390	70.0	0.577	74.8
										1.328	69.2		
IB	Br	**a**	47.3	8.564	28.6	1.4	5.568	1.905	6.9	1.458	70.4	0.482	74.6
										1.378	70.5		
		b	45.4	8.314	28.3	1.3	5.773	1.755	7.0	1.396	69.2	0.650	74.7
										1.367	69.3		
		a'	4.1	n/s[b]	—	—	n/s	1.881	7.1	1.313	70.0	0.422	74.6
										n/s	—		
		b'	3.2	n/s	—	—	n/s	1.612	6.7	1.311	70.0	0.570	74.1
										n/s	—		
IA	Cl	**a**	57.3	8.515	28.1	1.3	5.544	1.844	6.7	1.315	70.4	0.426	74.8
										1.295	68.9		
		b	42.7	8.345	27.5	1.3	5.719	1.756	7.0	1.371	69.9	0.580	75.1
										1.312	68.9		

[a]Average for non-first-order multiplets.
[b]Not seen.

two Pt—Me signals for methyls *trans* to N have a much narrower chemical-shift separation.

Each isomer shows the same pattern of signals assignable to the PhC*H(Me) group, viz. a doublet (^3J = 6.7–7.0 Hz, 3H) (Fig. 2), a non-first-order multiplet (1H) with ^3J couplings to both ^{195}Pt and the C—Me protons (Fig. 3), and a low-field multiplet (5H) for the aromatic protons. For *one* of the isomers (the one resonating at lower field in each case) the C*—H(Me) signals show a marked depen-

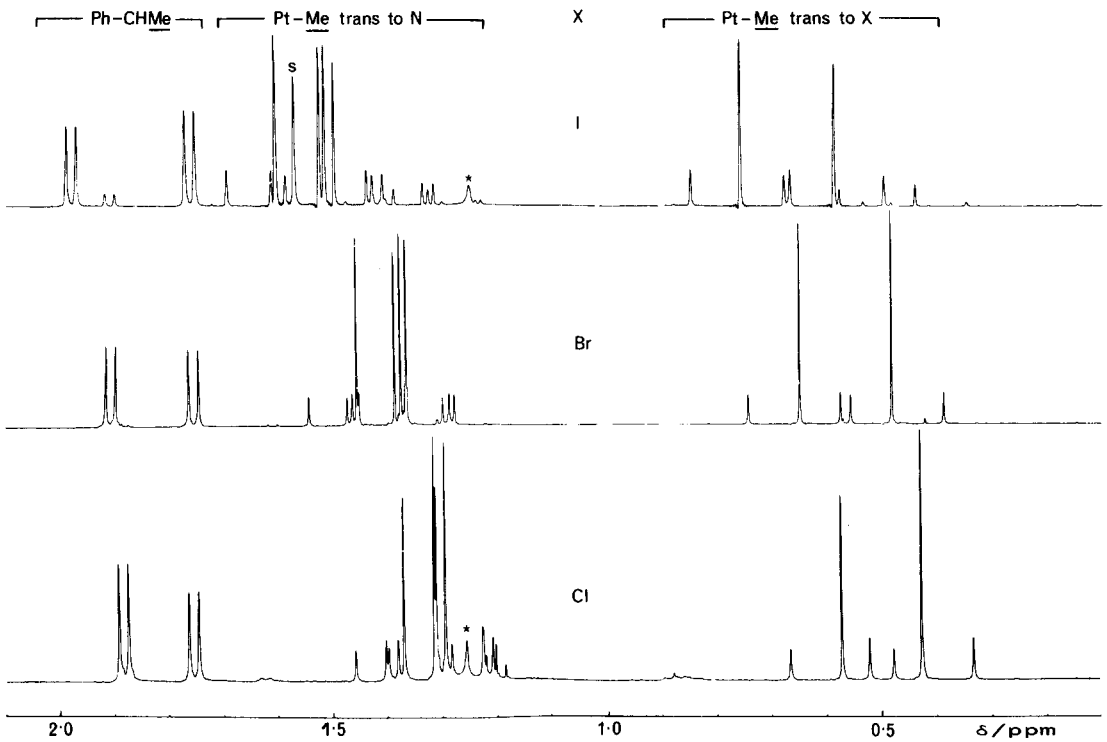

Fig. 2. 400-MHz ^{1}H NMR spectra of complexes IA–C in the region 0–2.0 ppm showing the Pt—Me (right) and Ph—CMe signals and the isomer populations (S = solvent, * = impurity).

dence on halide, moving downfield from chloride to iodide. The proton of the CH=N group appears further downfield, and the signals, split by coupling to ^{195}Pt (^3J = *ca* 28 Hz), also show long-range coupling (J = *ca* 1.3 Hz) to one of the pyridine protons, which implies that the coupled protons are in a planar configuration.

Close examination of the spectra of **IB** and **IC** reveals a second set of low-intensity signals which in relative intensity reflect the proportions of the major pair of isomers. The peak-for-peak correspondence throughout the spectra (where peaks are not overlapped), and the J values for the coupled signals show that each major isomer (**a** and **b**) has a very similar "ghost" (labelled **a′** and **b′**), though the chemical shifts show considerable differences. The variation in abundance of these additional signals with halide ($I^- > Br^- > Cl^-$) leads us to conclude that they may be attributed to *rotamers* arising from restricted rotation about the benzyl–nitrogen bond caused by a steric clash between the phenyl ring and the halide. Molecular models show that this is reasonable, but do not reveal any specially favoured configuration. Assignments of **a′** and **b′** are based on relative signal intensities alone, and do not necessarily imply that they are the rotamers of major isomers **a** and **b**, respectively.

For complexes **IIA–C** very similar spectra resulted, the most prominent difference being the expected replacement of the triplet of doublets at low field by a 1:4:1 triplet at *ca* 2.1 ppm (^4J = ~ 3.6–3.8 Hz) from the N=C(Me) protons coupled to platinum. Spectral data in Table 3 show that two isomers (**a** and **b**) are present, but for this series the relative isomer ratio is barely altered by a change in halide, and there are no additional "ghost" signals. The methyl group probably inhibits the N—C* bond rotation and locks the structure in one rotameric conformation. The ^2J values for Pt—Me groups *trans* to N indicate that for all complexes both Pt—N bonds are stronger[14,15] than in **IA–C**. In a series of $PtMe_3^+$ complexes containing a substituted salicylaldimine and 3,5-lutidine[16] the two Pt—Me signals could be readily distinguished by their ^2J values (65.7–68.1 Hz *trans* to imine N and 71.3–72.3 Hz *trans* to lutidine N), with the former invariably at lower field. In both **IA–C** and **IIA–C** the distinction is more difficult to make as the ^2J values are much closer together, though in **IIA–C** the Pt–Me signal at lowest field (except for **IIBb**) has the smaller ^2J value, so it is likely that this is a methyl *trans* to imine N.

^{13}C *NMR study*

Further characterization of one of the complexes (**IB**) was done by recording a 270-MHz proton-decoupled ^{13}C NMR spectrum. Data are given in

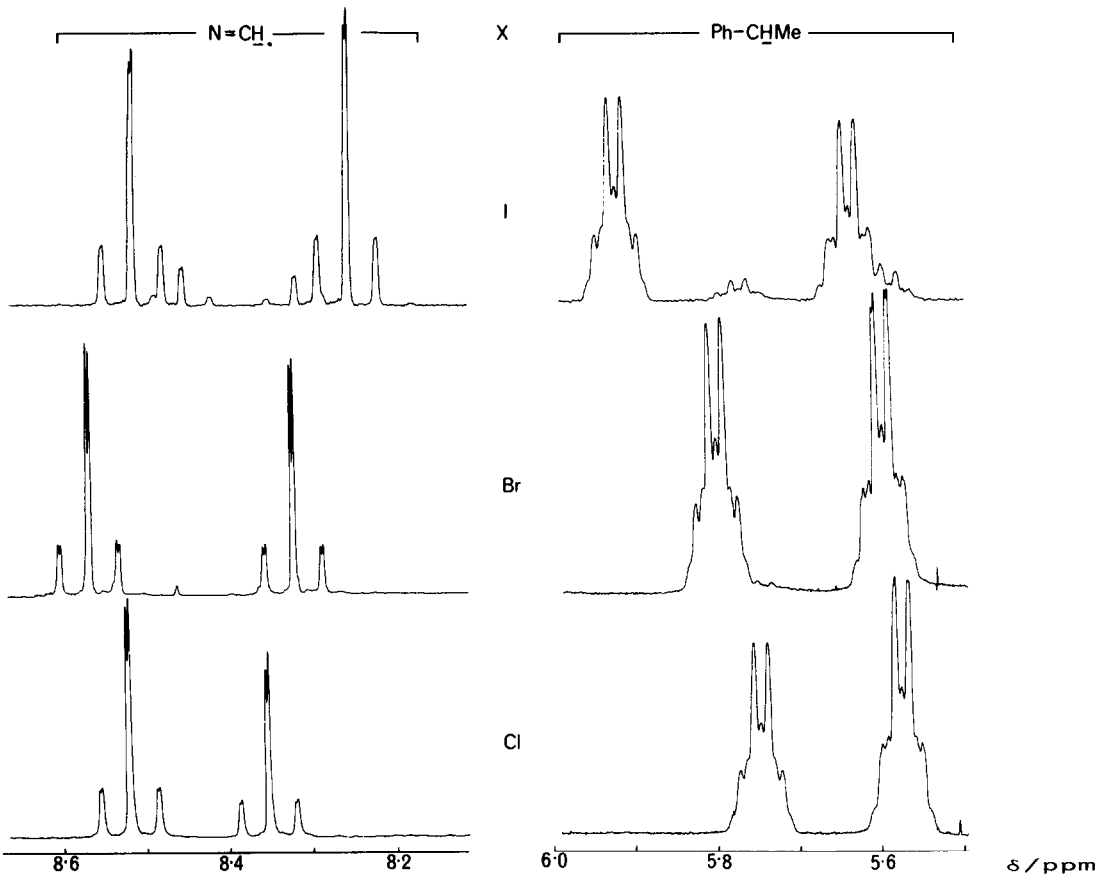

Fig. 3. 400-MHz ^{1}H NMR spectra of complexes IA–C showing the N=CH (left) and Ph—CH (right) proton signals.

Table 3. 400-MHz ^{1}H NMR data for complexes 11A–C

Complex				N=C—me		C*—H	C*—Me		N—Pt—Me		X—Pt—Me	
No.	X	Isomer	Population (%)	δ (ppm)	^4J (Hz)	δ (ppm)[a]	δ (ppm)	^3J (Hz)	δ (ppm)	^2J (Hz)	δ (ppm)	^2J (Hz)
									1.517	69.1		
IIC	I	a	55.5	2.215	3.82	6.172	1.827	7.17	1.428	69.7	0.685	72.5
									1.535	69.0		
		b	44.5	2.147	3.78	6.040	2.096	7.15	1.412	69.4	0.838	73.0
IIB	Br	a	54.7	2.124	3.8	6.144	1.809	7.18	1.374	68.4	0.564	74.5
									1.299	69.1		
									1.395	68.4		
		b	45.3	2.120	3.6	6.023	2.031	7.14	1.296	67.9	0.720	74.8
									1.243	67.8		
IIA	Cl	a	55.4	2.108	—	6.060	1.767	7.10	1.170	68.4	0.457	75.1
									1.264	68.3		
		b	44.6	2.071	—	5.958	1.942	7.10	1.161	68.4	0.618	75.3

[a]Average value of non-first-order multiplets.

Table 4 with assignments shown in Fig. 4. Signal assignments are based on $^1J(^{195}Pt)$ couplings, chemical-shift values, and the fact that signal intensities decrease in the order $CH_3 > CH_2 > CH > C$ due to relaxation effects.[17] Coupling to ^{195}Pt through two or more bonds was also evident, making possible the complete assignment of the pyridine ring carbons. The spectrum was too noisy for

Table 4. Proton-decoupled 270-MHz ^{13}C NMR data[a] for complex **IB** with assignments shown in Fig. 4

	Diastereoisomer 1 (48.1%)		Diastereoisomer 2 (51.9%)	
Assignment	δ (ppm)	J (Hz)	δ (ppm)	J (Hz)
a	−6.005	678.8	−6.066	675.7
b	−4.691	670.0	−4.912	667.4
c	−0.359	701.7	−0.390	698.6
d	21.360	—	19.229	—
e	63.745	16.61	63.936	16.09
f	163.708	—	163.426	—
g	154.533	7.28	154.410	8.30
h	127.627	12.98	127.736	12.98
i	138.987	—	138.987	—
j	128.436	6.23[b]	128.711	6.23[b]
k	146.947	17.64	147.085	17.64
l	138.796	5.71	138.238	7.78
mm′	129.109	—	129.109	—
nn′ [c]	129.032	—	129.032	—
o	128.635	—	128.635	—
	128.192	—	128.192	—

[a]In $CDCl_3$ solution.
[b]Approximate value due to overlap with aromatic signals.
[c]Aromatic region, assignment uncertain owing to coincidental overlap.

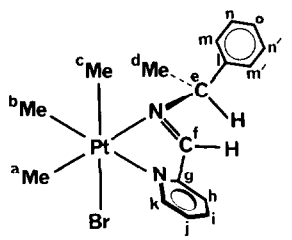

Fig. 4. Structure of **IB** with environmental assignments for the ^{13}C NMR spectrum (Table 4).

rotamers to be detected, but the relative populations of the two major isomers agree with values from the 400-MHz ^1H spectra. Pt—Me groups *trans* to X^- showed higher ^1J values than those *trans* to N, paralleling the ^2J values from the proton spectra.

Separation of the isomers

Initial attempts were made to separate the isomers of **IB** and **C** and **IIB** and **C** by fractional crystallization from a range of single- and mixed-solvent systems, and by thin-layer chromatography (tlc) on Kieselgel 60F. In every case an ^1H NMR spectrum of the product showed no isomeric enrichment. A sample of **IIC** showed some broadening on the tlc plates, but column chromatography on Kieselgel 60F with CCl_4 followed by CH_2Cl_2 gave head and tail fractions with the same isomer abundance. The reason for this behaviour became apparent when samples of the solids **IIA–C** were washed with small aliquots of CCl_4. The *remaining* solid in each case was enriched with one isomer, the percentage enrichment (determined by 100-MHz NMR spectra) being dependent on the halide (I^- = 90.4%, Br^- = 86.4%, Cl^- = 60.0%). However, on standing in $CDCl_3$ the relative proportions of the isomers gradually changed to the quilibrium populations shown in Table 3, the half-life for the iodide complex **IIC** being 13.6 min at 19°C. Clearly this propensity for the isomers to interconvert in solution at room temperature frustrated attempts to separate them, but enabled the isomerization to be followed kinetically.

Interconversion of the isomers

A time-dependent set of ^1H NMR spectra for complexes **IIA–C** in $CDCl_3$ was obtained at 100 MHz, and the spectral changes in the Pt–Me region for the iodide complex are shown in Fig. 5. Changes in the population of the isomers **a** and **b** are clearly seen in the two highest intensity high-field signals. The first-order rate constant for the intramolecular process **a** = **b** was calculated by plotting $\ln x$ against time, where x is the percentage by which the more abundant isomer exceeds its equilibrium value. For first-order kinetics this prod-

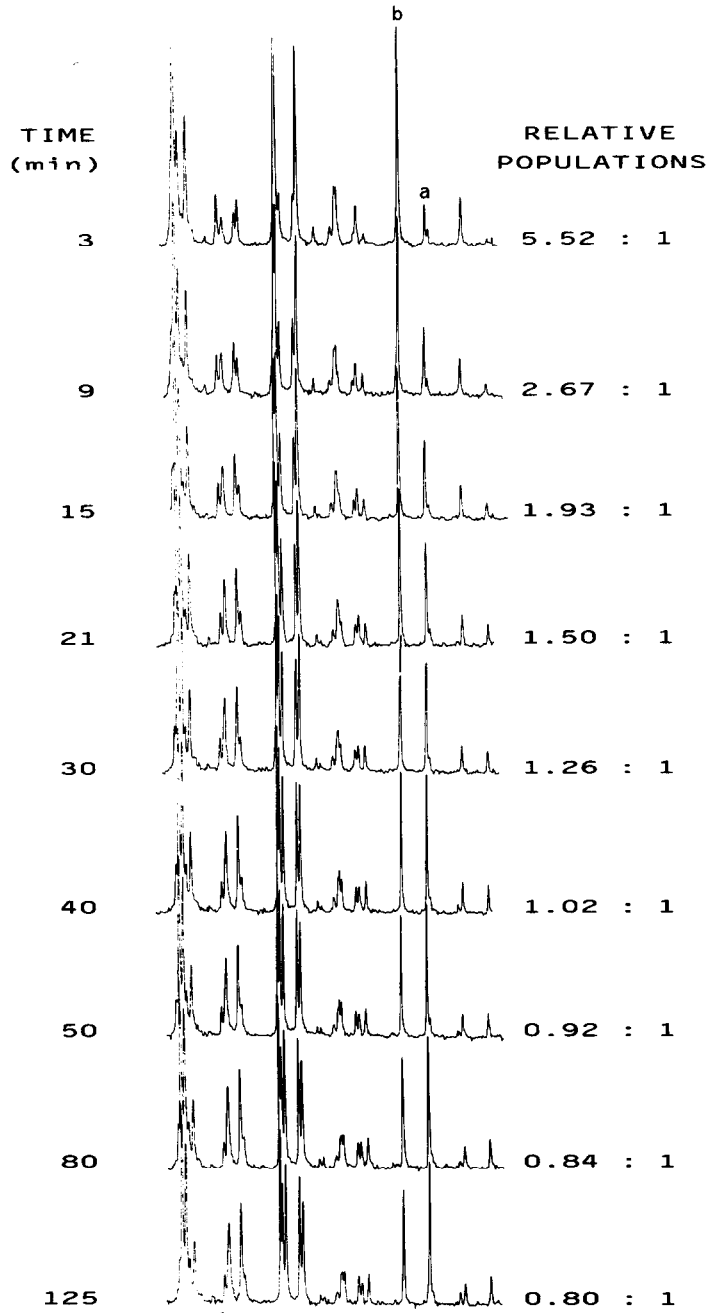

Fig. 5. Time-dependent 100-MHz ^{1}H NMR spectra of **IIC** in $CDCl_3$ at ambient temperature, showing relative populations (**b**:**a**) of isomers **b** and **a**.

uces a straight line with gradient $-k$. Values of x were obtained from the relationship:

$$x = a_t^N - a_\infty^N,$$

where a_t^N is the normalized amount of **a** at time t given by:

$$a_t^N = \frac{a_t}{a_\infty + b_\infty}$$

Data are recorded in Table 5. Owing to the low initial enrichment obtainable for the chloride **IIA**, it was not possible to get accurate rate data, though the interconversion was clearly slower than for the bromide. An additional run on the bromide complex **IIB** using a more dilute solution gave an almost identical rate for the interconversion (Fig. 6), implying that the process is not solvent-dependent. The more than doubling of the rate on raising the temperature by 11°C is as expected for the first-

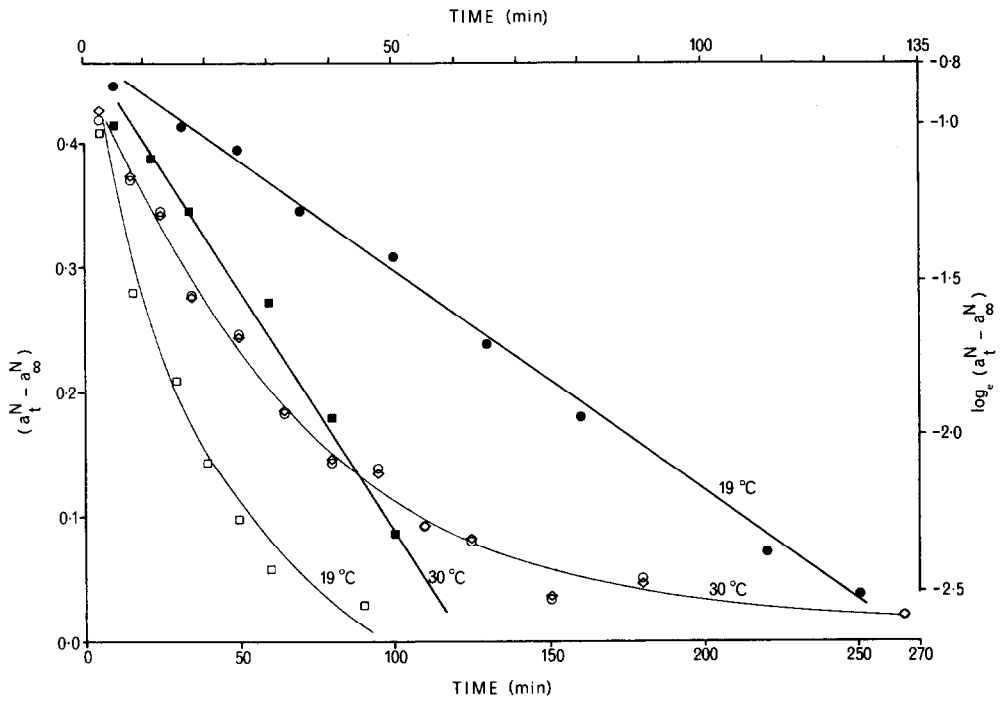

Fig. 6. Isomerization of **IIB** and $CDCl_3$ showing exponential (□ and ○) and $\log_e$ (■ and ●) plots. Curves ○ and ◇ refer to isothermal runs at different concentrations.

Table 5. First-order rate constants for the isomerization of **IIB** and **IIC**

Complex	Halide	Temperature (°C)	$t_{\frac{1}{2}}$ (min)	k $(min)^{-1}$
IIB	Br	19	48.3	0.014
IIB	Br	30	22.0	0.032
IIC	I	19	13.6	0.05

order kinetics, and the process causing the isomerization is therefore intramolecular.

High-temperature NMR spectra

A DNMR study of the thioether complexes mentioned earlier revealed a high-temperature intramolecular fluxion[6] which causes the ^1H NMR signals from the Pt–Me groups to coalesce. As the isomers of the iodide complex **IIC** show the fastest rate of interconversion, the 100-MHz NMR spectra of the iodides were examined at high temperatures to see whether a Pt—Me scrambling process would occur. Complex **IC** showed no spectral changes up to 115°C ($CDCl_3$, sealed tube) so it seems likely that this series does not show high-temperature fluxionality. When complex **IIC** was studied in the same solvent, spectral collapse was seen to begin at 100°C, but as the broadening was not complete at the highest temperature accessible in this solvent (115°C) a different solvent system (CD_3NO_2–$C_6D_5NO_2$, 2:3 by volume, sealed tube) was used. Here spectral collapse began at a much lower temperature (65°C), implying that the process was solvent-dependent. This was confirmed by the failure of attempts to simulate the spectra using a program structured for purely intramolecular mechanisms.[13]

Evidence for a high-temperature fluxional process was seen in the spectral changes of the N=C—Me proton signals of **IIC**. The pair of triplets at room temperature broaden and coalesce to a single sharp triplet at 150°C. However, on raising the temperature by a further 10–20°C this triplet disappeared and was replaced by a low-intensity multiplet. On cooling to room temperature, the final spectrum was identical to the initial one, minus the pair of triplets from the N=C—Me group. A substantial increase in the signal from residual CH_3NO_2 in the solvent region strongly suggests a CD_3 for CH_3 group exchange on the ligand. A repetition of this experiment using free ligand in the same solvent system showed no exchange. We are uncertain whether it is just atom (H–D) or group (CH_3–CD_3) exchange.

General discussion

The $PtMe_3$(IV) complexes are the first reported which contain neutral bidentate Schiff base ligands,

which compared to the ionic salicylaldiminates[16] are poorer donors via the imine N. A parallel was found with the formerly analogous complexes *fac*-$[(CO)_3M(PPh_3)(L\text{–}L)]$ (M = Cr, Mo or W; L–L = **I**)[6] and *fac*-$[(CO)_3MnBr(L\text{–}L)]$ (L–L = **I**)[18] which contain a d^6-metal, in that each compound exists in solution as a mixture of two diastereoisomeric forms (**a** and **b**) having either the (*R*)(*S*) or the (*S*)(*S*) configuration at the metal and benzyl carbon atoms, respectively. The apparent rapid interconversion of **a** and **b** in solution was surprising, in view of the success of the $PtMe_3^+$ ion as a probe to identify the *meso* and racemic forms of some chelating diarsines.[19,20] In particular, the reaction of $[PtMe_3I(diarsine)]$ with $AgPF_6$ in the presence of pyridine to give $[PtMe_3(py)(diarsine)]^+$ with *meso*-$[C_6H_4(AsMePh)_2]$ proceeded stereospecifically for both isomers of the iodide (arsine methyls pointing towards or away from the halide),[19] indicating that the $PtMe_3$ group and the arsine retain the same stereochemical relationship during the reaction. The stronger Pt—As bond (^2J = *ca* 65 Hz) may be responsible. The mechanism by which isomers **a** and **b** interconvert is apparently first-order, and a "ligand flip" of the Schiff base is one possibility.

It is not possible to say which isomer has which configuration, but the ^1H NMR parameters for all the C*(Me)H ligand signals are considerably halide-sensitive, suggesting a difference in conformation with respect to the axial Pt—X bond. It is possible to ascribe the additional isomers of **IA** and **IB** to rotamers, on the basis of the variation in abundance with halide size (greatest in the more sterically crowded iodide), and also the failure to detect them in **IIA–C**, where the additional ligand methyl group presumably favours one rotameric form.

REFERENCES

1. T. G. Appleton, J. R. Hall and L. Lambert, *Inorg. Chim. Acta* 1978, **29**, 89.
2. A. Shaver, *Can. J. Chem.* 1978, **56**, 2281.
3. G. Hamer and A. Shaver, *Can. J. Chem.* 1980, **58**, 211.
4. H. Brunner, *Top. Curr. Chem.* 1975, **56**, 67; *Adv. Organomet. Chem.* 1980, **18**, 151.
5. H. Brunner and J. Doppelberger, *Chem. Ber.* 1978, **111**, 673.
6. H. Brunner and W. A. Herrmann, *J. Organomet. Chem.* 1973, **57**, 183.
7. E. W. Abel, S. K. Bhargava and K. G. Orrell, *Prog. Inorg. Chem.* 1984, **32**, 95.
8. H. Brunner and W. A. Herrmann, *J. Organomet. Chem.* 1974, **74**, 423.
9. J. C. Baldwin and W. C. Kaska, *Inorg. Chem.* 1975, **14**, 2020.
10. D. E. Clegg and J. R. Hall, *Spectrochim. Acta* 1965, **21**, 357.
11. D. E. Clegg and J. R. Hall, *J. Organomet. Chem.* 1970, **22**, 491.
12. H. Brunner and W. Herrmann, *Chem. Ber.* 1972, **105**, 770.
13. D. A. Kleier and G. Binsch, *DNMR3 Program* 165, *Quantum Chemistry Program Exchange.* Indiana University, **10**, 165 (1970).
14. T. G. Appleton, H. C. Clark and L. E. Manzer, *Coord. Chem. Rev.* 1973, **10**, 335.
15. D. E. Clegg, J. R. Hall and G. A. Swile, *J. Organomet. Chem.* 1972, **38**, 403.
16. J. R. Hall and G. A. Swile, *Aust. J. Chem.* 1975, **28**, 1507.
17. G. C. Levy, R. L. Lichter and G. L. Nelson, *Carbon-13 Nuclear Magnetic Resonance*, 2nd Edn. Wiley Interscience, New York (1980).
18. H. Brunner and M. Lappus, *Z. Naturforsch.* 1974, **29B**, 363.
19. A. J. Cheney and B. L. Shaw, *J. Chem. Soc. A* 1971, 3545, 3549.
20. K. Henrick and S. B. Wild, *J. Chem. Soc., Dalton Trans.* 1975, 1506.

Polyhedron Vol. 6, No. 2, pp. 329–335, 1987
Printed in Great Britain.

0277–5387/87 $3.00 + .00

PALLADIUM COMPLEXES WITH BIOLOGICAL LIGANDS—II.* KINETICS AND MECHANISM OF PYRIDOXAL-5′-PHOSPHATE AND PYRIDOXAMINE-5′-PHOSPHATE REACTIONS WITH PD(II)

MOHAMED S. EL-EZABY,† HAYAT M. MARAFIE and HUSAM M. ABU-SOÛD‡

Chemistry Department, Faculty of Science, University of Kuwait, Kuwait

(*Received* 9 *December* 1985; *accepted* 30 *June* 1986)

Abstract—The kinetics of the interaction of either pyridoxal-5′-phosphate (PLP) or pyridoxamine phosphate (PMP) with Pd(II) have been studied in acidic aqueous solution at 37°C and ionic strength 0.15 M (NaCl). The observed dependence of the rate constant k_{obs} on the total ligand concentration (T_L) at a given pH is as follows for each system: $k_{obs}(PLP) = A + BT_{PLP}$ and $k_{obs}(PMP) = C + DT_{PMP}$. The parameters A–D are pH-dependent. It has been suggested that, in the case of the Pd(II)–PLP and Pd(II)–PMP systems, the prior fast formation of a $Pd(H \cdot VB_6P)Cl_3$ (VB_6 = vitamin B_6) complex species has been assumed.

Pd(II) complexes with non-phosphorylated vitamin B_6 (VB_6) compounds have been shown to have inhibitory effects on some cell divisions.[2] The stopped-flow method has been used to study the kinetics of their formation in aqueous solution.[2] It has been concluded that the 1:1 complexes were formed relatively faster than the 2:1 species, specially in the case of the pyridoxal (PL)– and pyridoxamine (PM)–Pd(II) systems. It has been also concluded that possibly $PdCl_4^{2-}$ as well as $[PdCl_3(OH)]^{2-}$ are the Pd(II) reactive species in their complex formation with VB_6. In the present work the interaction of the phosphorylated VB_6 compounds with Pd(II) has been studied under identical conditions to the previous investigation[3] in order to examine the effect of the phosphate group on the complex formation kinetics.

EXPERIMENTAL

A stock solution of Pd(II) chloride (0.1 M) was prepared in 1.0 M HCl. The Pd(II) concentration was checked by a gravimetric method as Pd(dimethylglyoxime)$_2$.[4] Pyridoxal-5′-phosphate (PLP) and pyridoxamine phosphate (PMP) were analytically pure chemicals and were used without purification. Stock solutions (0.1 M) of the ligands were prepared by dissolving the right amount in deionized double distilled water and kept in the dark at 4°C. In all measurements, the ionic strength was kept constant at 0.15 M (NaCl).

Measurements

Kinetic measurements were done using a Durrum stopped-flow apparatus. The optical path length was 20.0 mm. The mixing syringes and cuvette were thermostated at 37°C. The observed pseudo-first-order rate constants were calculated from data for up to 85% completion of the reaction. Measurements of pH were carried out using a Radiometer pH-meter type 62 equipped with a combined glass electrode (GK 2301C). The pH meter was calibrated before use with radiometer buffer solutions (pH 4.00 and 7.00). Spectrophotometric measurements were carried out on a Pye–Unicam SP8-100 spectrophotometer. The concentration range of the ligands used was $(0.25–1.75) \times 10^{-2}$ M. The Pd(II) concentration was kept constant at 2.5×10^{-4} M.

*For Part I see Ref. 1.

†Author to whom correspondence should be addressed.

‡Present address: Chemistry Department, University of Essex, Essex, U.K.

RESULTS AND DISCUSSION

Pd(II)–*PLP system*

The spectral band of Pd(II) in the visible region was lost when a 10 times concentration of PLP was added at pH = 2.00 (Fig. 1). This was taken as an indication of the complex formation between Pd(II) and PLP. In order to determine if the phosphate group was involved in the complex formation or not, a solution of NaH_2PO_4 was added to a Pd(II) solution under identical experimental conditions to the above. The Pd(II) spectra in the visible region and in the pH range 2–6 were the same in the absence and in the presence of the phosphate solution A wavelength (λ) of 470 nm has been selected to carry out the kinetic study in the pH range 2.25–4.50 where PLP has a practically minimum absorption. Figure 2 shows the dependence of the observed rate constant (k_{obs}) (under pseudo-first-order conditions) as a function of the pH. On the other hand, Fig. 3 shows the linear dependence of k_{obs} on the total concentration of PLP (T_{PLP}) at interpolated values of pH. At any particular pH these linear relations can be represented by the following equation:

$$k_{obs}(PLP) = A + BT_{PLP}, \quad (1)$$

where A and B are the intercept and slope values at various pH values. Table 1 depicts the values of A and B at interpolated pH values. In analogy to the PL–Pd(II) system[3] it may be reasonable to assume that the 1:1 complex is formed relatively faster than the 2:1 complex. A mechanism similar to what has been proposed (Scheme 1) for PL–Pd(II) systems may be applied to the PLP–Pd(II) system. In this case, however, we have several species of PLP existing under the experimental

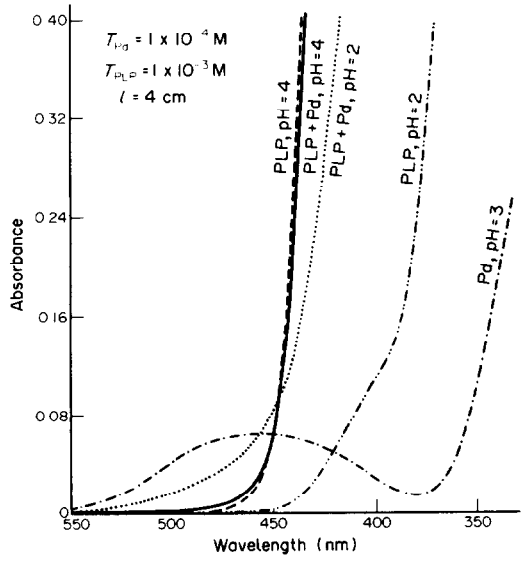

Fig. 1. Absorption spectra of Pd(II)–PLP system at various pH values.

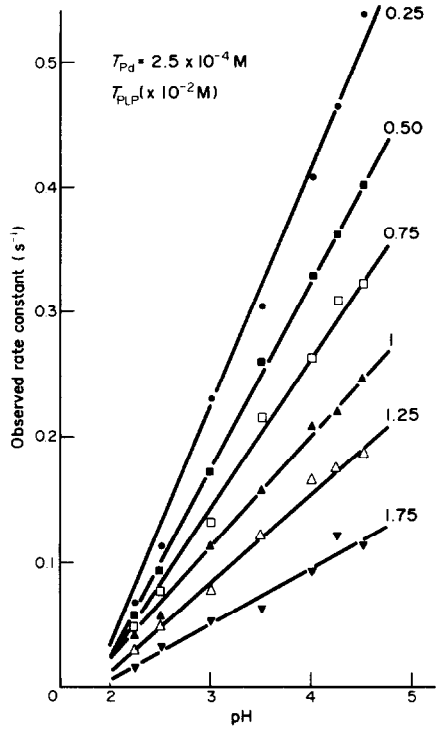

Fig. 2. Dependence of k_{obs}(PLP) of Pd(II)–PLP system on pH at various T_{PLP} values.

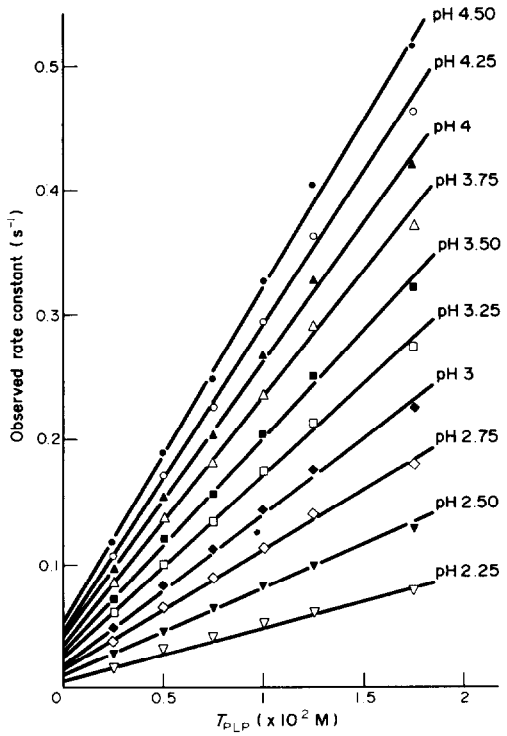

Fig. 3. k_{obs}(PLP) as function of T_{PLP} at interpolated pH values.

conditions used, namely H_4PLP^+, H_3PLP, H_2PLP^- and $HPLP^{2-}$ (Table 2). There is also the possibility that two species of Pd(II) may exist, $PdCl_4^{2-}$ and $[PdCl_3OH)]^{2-}$. Other chloro and/or hydroxy species of Pd(II) may be ignored since the solutions have a relatively high chloride ion concentration ($\simeq 0.15$ M) and are acidic (pH $\leqslant 4.5$).

$$\begin{array}{l} H_4PLP^+ \\ \downarrow\uparrow \\ H_3PLP \\ \downarrow\uparrow \\ PdCl_4^{2-} + H_2PLP^- \overset{K'_{1C}}{\rightleftarrows} [Pd(H_2PLP)Cl_3]^{2-} + Cl^- \qquad \text{(i)} \\ \downarrow\uparrow K_{OH} \qquad\qquad \downarrow\uparrow K'_{OH} \\ [PdCl_3(OH)]^{2-} + H_2PLP^- \rightleftarrows [Pd(H_2PLP)Cl_2OH]^{2-} + Cl^- \qquad \text{(ii)} \end{array}$$

$$[Pd(H_2PLP)Cl_3]^{2-} + H_3PLP \rightleftarrows [Pd(H_2PLP)_2Cl_2]^{2-} + Cl^- + H^+; k'_1, k'_{-1} \qquad \text{(a)}$$

$$\begin{array}{l} \qquad\qquad\qquad\qquad\qquad\qquad\qquad\qquad \downarrow\uparrow K_{2PLP} \\ [Pd(H_2PLP)Cl_3]^{2-} + H_2PLP^- \rightleftarrows [Pd(H_2PLP)_2Cl_2]^{2-} + Cl^-; k'_2, k'_{-2} \qquad \text{(b)} \\ \quad K'_{OH} \downarrow\uparrow +OH^- \\ [Pd(H_2PLP)Cl_2OH]^{2-} + H_3PLP \rightleftarrows [Pd(H_2PLP)_2Cl_2]^{2-} + H_2O; k'_3, k'_{-3} \qquad \text{(c)} \end{array}$$

$$[Pd(H_2PLP)Cl_2OH]^{2-} + H_2PLP^- \rightleftarrows [Pd(H_2PLP)_2Cl_2]^{2-} + OH^-; k'_4, k'_{-4} \qquad \text{(d)}$$

Scheme 1.

Table 1. Values of A and B at various interpolated pH values

pH[a]	$A \times 10^3$	B	R^b	$A[H^+]^{-1} \times 10^{-2}$	$B([H^+] + K_{2PLP})[H^+]^{-1} \times 10^{-2}$
2.25	8.4 ± 1.9	4.20 ± 0.2	0.996	0.02	0.04
2.50	13.8 ± 2.0	6.8 ± 0.2	0.998	0.04	0.08
2.75	17.7 ± 2.8	9.5 ± 0.3	0.998	0.10	0.11
3.00	23.7 ± 3.2	11.8 ± 0.3	0.999	0.24	0.15
3.25	27.2 ± 4.2	14.4 ± 0.4	0.999	0.48	0.21
3.50	33.5 ± 4.5	16.8 ± 0.4	0.999	1.06	0.31
3.75	38.7 ± 5.8	19.3 ± 0.6	0.998	2.18	0.48
4.00	42.2 ± 6.4	22.0 ± 0.6	0.998	4.22	0.74
4.10	45.5 ± 6.0	22.9 ± 0.0	0.999	5.73	0.98
4.15	47.0 ± 6.8	23.4 ± 0.6	0.998	6.64	1.00
4.20	48.0 ± 7.0	23.9 ± 0.7	0.998	7.60	1.21
4.25	49.3 ± 7.1	24.2 ± 0.7	0.998	8.77	1.34
4.30	48.9 ± 6.7	24.9 ± 0.6	0.998	9.76	1.49
4.35	50.8 ± 6.7	25.4 ± 0.6	0.999	11.38	1.71
4.40	52.5 ± 7.4	25.8 ± 0.7	0.999	13.18	1.95
4.45	53.6 ± 7.5	26.2 ± 0.7	0.998	15.10	2.22
4.50	53.5 ± 8.0	26.9 ± 0.8	0.998	16.92	2.48

[a]Interpolated values.
[b]Correlation coefficient.

Table 2. Pertinent values of log K mentioned in this work

	Log K		
Equilibrium reaction	L = PLP[a]	L = PMP[b]	Others
$H_5L \rightleftarrows H_4L + H^+$	—	~1.20(—PO_3OH_2)	
$H_4L \rightleftarrows H_3L + H^+$	−1.60	−3.05(—PO_3OH)	
$H_3L \rightleftarrows H_2L + H^+$	−3.58	−5.38(—PO_3OH)	
$H_2L \rightleftarrows HL + H^+$	−6.41	−8.62	
$HL \rightleftarrows L + H^+$	−9.24	−11.77	
$H_2O \rightleftarrows H^+ + OH^-$	—	—	13.38[a]
$PdCl_4^{2-} \rightleftarrows Pd^{2+} + 4Cl^-$	—	—	11.11[c]
$[PdCl_3(OH)]^{2-} + Cl^- \rightleftarrows PdCl_4 + OH^-$	—	—	−5.70[d]

[a]N. Al-Awadi, M. S. El-Ezaby and H. M. Abu-Soûd, *Inorg. Chim. Acta* 1982, **67**, 131.
[b]M. S. El-Ezaby and S. Fareed, unpublished work.
[c]L. G. Sillén and A. E. Martell, *Stability Constants of the Metal–Ion Complexes.* Special Publication No. 17 (1964).
[d]A. I. Kazakova and B. V. Ptitsym *Zh. Inorg. Khim.* 1967, **12**, 620.

The integrated rate equation describing the above mechanism is as previously reported:[3]

$$\ln \frac{(C_{\text{IIPLP}})_{eq}}{(C_{\text{IIPLP}})_{eq} - (C_{\text{IIPLP}})_t} = \{Q_8 + Q_7 T_{\text{PLP}}/Q_2([\text{H}^+] + K_{2\text{PLP}})\}t, \quad (2)$$

where:

$$Q_8 = k'_{-1}[\text{H}^+][\text{Cl}^-] + k'_{-2}[\text{Cl}^-] + k'_{-3} + k'_{-4}[\text{OH}^-],$$

$$Q_7 = k'_1[\text{H}^+] + k'_2 K_{2\text{PLP}} + k'_3 K'_{\text{OH}} K_w[\text{Cl}^-]^{-1} + k'_4 K_{2\text{PLP}} K'_{\text{OH}}[\text{OH}^-][\text{Cl}^-]^{-1},$$

$$Q'_2 = 1 + K'_{\text{OH}}[\text{OH}^-][\text{Cl}^-]^{-1} \simeq 1,$$

and

$$k_{\text{obs}} = Q_8 + Q_7 T_{\text{PLP}}/Q'_2([\text{H}^+] + K_{2\text{PLP}}) \quad (3)$$

and

$$A = Q_8,$$

$$B = Q_7/([\text{H}^+] + K_{2\text{PLP}}) \text{ if } Q'_2 = 1.$$

If $A[\text{H}^+]^{-1}$ is plotted vs $[\text{H}^+]^{-1}$ a quadratic curve is produced [Fig. 4(a)] which is represented by the following equation:

$$A[\text{H}^+]^{-1} = a_0 + a_1[\text{H}^+]^{-1} + a_2[\text{H}^+]^{-2}, \quad (4)$$

where $a_0 \simeq 0$, $a_1 = (4.3 \pm 0.1) \times 10^{-2}$ and $a_2 = (3.9 \pm 0.4) \times 10^{-7}$. These coefficients correspond to k'_1, $(k'_{-2}[\text{Cl}^-] + k'_{-3})$ and $k'_{-4}K_w$ (K_w = ionic product of H_2O), respectively. The probable values of the k's are listed in Table 3. On the other hand, the plot of $B([\text{H}^+] + K_{2\text{PLP}})[\text{H}^+]^{-1}$ vs $[\text{H}^+]^{-1}$ is also quadratic [Fig. 4(b)]. The relationship follows the equation:

$$B([\text{H}^+] + K_{2\text{PLP}})[\text{H}^+]^{-1} = b_0 + b_1[\text{H}^+]^{-1} + b_2[\text{H}^+]^{-2}, \quad (5)$$

where b_0, b_1 and b_2 have the values 7.4 ± 1, $(6.6 \pm 0.2) \times 10^{-3}$ and $(3.1 \pm 0.6) \times 10^{-9}$, respectively. These parameters correspond to k'_1, $k'_2 K_{2\text{PLP}} + k'_3 K'_{\text{OH}}$ $K_w[\text{Cl}^-]^{-1}$ and $k'_4 K_{2\text{PLP}} K'_{\text{OH}} K_w[\text{Cl}^-]^{-1}$, respectively. The values of micro-rate constants are listed in Table 3 after the adoption of reasonable assumptions shown in the footnotes to the table.

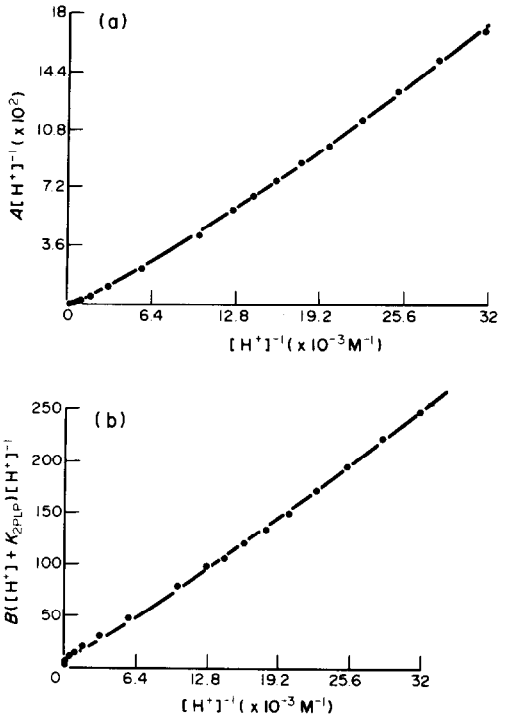

Fig. 4. (a) Dependence of $A[\text{H}^+]^{-1}$ on $[\text{H}^+]^{-1}$. (b) Dependence of $B([\text{H}^+] + K_{2\text{PLP}})[\text{H}^+]^{-1}$ on $[\text{H}^+]^{-1}$.

Pd(II)–*PMP system*

The addition of a solution of PMP to that of Pd(II) in the pH range 2.0–5.0 caused considerable spectral changes in the latter in the visible region as shown in Fig. 5. Similar to the Pd(II)–PLP system no precipitation was observed in the pH range used. The kinetic runs were done at $\lambda = 470$ nm in the pH range 2.5–5.0. Figure 6 shows the dependence of pseudo-first-order rate constants [k_{obs}(PMP)] on the pH and the total PMP concentration (T_{PMP}). Figure 7 shows the dependence of k_{obs}(PMP) on T_{PMP} at interpolated pH values obtained from Fig. 6. The dependence is linear and is expressed by the following equation:

$$k_{\text{obs}}(\text{PMP}) = C + DT_{\text{PMP}}, \quad (6)$$

where C and D are pH-dependent parameters. The values of these parameters are listed in Table 4.

The reaction mechanism describing the data expressed by eqn (6) is similar to that shown in Scheme 1 except that the PMP species are different. In this case we have possibly four species in the pH range 2.5–5.0, namely H_5PMP^{2+}, H_4PMP^+, H_3PMP and H_2PMP^- (Table 2), and the reactive ones are likely H_4PMP^+ and/or H_3PMP, since the phosphate group has been excluded from possible ligation with Pd(II). Now, if H_4PMP^+ is the

Table 3. Summary of the micro-rate constants mentioned in this work

System	k	Magnitude of k	Equilibrium constant (K)
PLP–Pd(II)	k'_1, k'_{-1}	7.4, ~0	$\gg 7.4$
	k'_2, k'_{-2}[a]	25, 0.3	$\geqslant 86$
	k'_3, k'_{-3}[a]	2.4×10^{10}, 4.3×10^{-2}	5.6×10^{11}
	k'_4, k'_{-4}[b]	4×10^7, 9.4×10^6	0.42
PMP–Pd(II)	k''_1, k''_{-1}	~0, 10.9	~0
	k''_2, k''_2[c]	19.4, 0.14	1.4×10^2
	k''_3, k''_{-3}[c]	8.3×10^5, 2.2×10^{-2}	3.8×10^7
	k''_4, k''_{-4}[b]	8.1×10^4, 1.45×10^6	$\geqslant 5.6 \times 10^{-2}$

[a]The assumption was $k_{-2}[Cl^-] \gg k_{-3}$ such that $k_{-2}k_{-3} = a_1$ and vice versa: similarly $k'_2K_{2PLP} \gg k'_3K'_{OH}K_w[Cl^-]^{-1}$ such that $k'_2K_{2PLP} = b_1$ and vice versa.

[b]K'_{OH} was assumed to be equal to $10^{5.7}$.

[c]Similar to the above: either $k''_2K_{2PMP} \gg k''_3K_{OH}K_w[Cl^-]^{-1}$ or vice versa, and either $k''_{-2}[Cl^-]^{-1} > k''_{-3}$ or vice versa.

ligating species PMP may be monodentate and if H_3PMP is the ligating species it will be bidentate. In both cases the metaoxy group is one of the ligation sites and in H_2PMP^- the amino group may act as the second ligating site: in that case a switch in the pK values may occur. If we assume that the formation of a 1:1 species is too fast to be detected by a stopped-flow technique and the kinetics of the reaction are describing the formation of a 2:1 species with H_2PMP^-, then the mechanism may be treated similarly to Scheme 1. The plot of $C[H^+]^{-1}$ vs $[H^+]^{-1}$ is quadratic [Fig. 8(a)] and can be represented by the equation:

$$C[H^+]^{-1} = c_0 + c_1[H^+]^{-1} + c_2[H^+]^{-2}, \quad (7)$$

where $c_0 = k''_{-1} = 10.87 \pm 11.02$, $c_1 = k''_{-2}[Cl^-] + k''_{-3} = (2.18 \pm 0.07) \times 10^{-2}$, and $c_2 = k''_{-4}K_w = (6.04 \pm 0.75) \times 10^{-8}$. The probable values of the k''s are listed in Table 3. The plot of $D([H^+] + K_{2PMP})[H^+]^{-1}$ vs $[H^+]^{-1}$ is quadratic [Fig. 8(b)], i.e.:

$$D([H^+] + K_{2PMP})[H^+]^{-1} = d_0 + d_1[H^+]^{-1} + d_2[H^+]^{-2}. \quad (8)$$

d_0, d_1 and d_2 have the values ~0, $(1.73 \pm 0.06) \times 10^{-2}$ and $(1.01 \pm 0.06) \times 10^{-7}$, respectively. These values stand for k''_1, $k''_2K_{2PMP} + k''_3K'_{OH}K_w[Cl^-]^{-1}$ and $k''_4K_{2PMP}K'_{OH}$

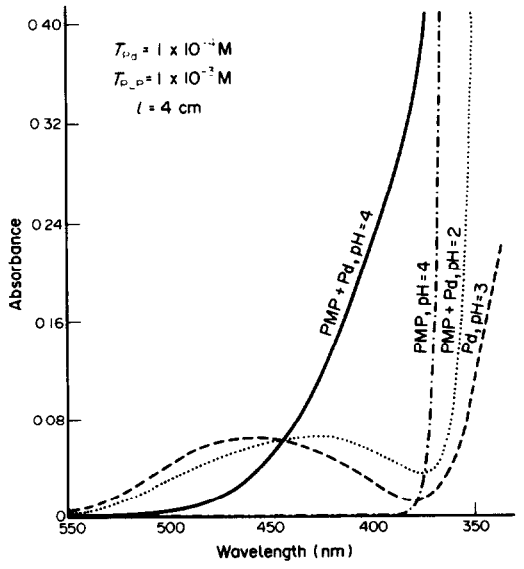

Fig. 5. Absorption spectra of Pd(II)–PMP system at various pH values.

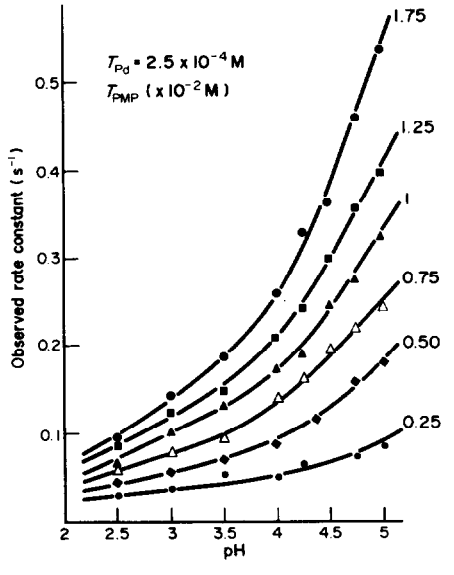

Fig. 6. Dependence of k_{obs}(PMP) on pH at various T_{PMP} values.

Table 4. Values of parameters C and D at interpolated pH values for the PMP–Pd(II) system and other pertinent functions

pH[a]	$C \times 10^{3}$[b]	D[b]	$C[H^+]^{-1} \times 10^{-2}$	$D([H^+] + K_{2PMP})[H^+]^{-1} \times 10^{-2}$
2.5	20.6 ± 4.1	4.9 ± 0.4	0.06	0.06
2.75	22.4 ± 5.1	5.9 ± 0.5	0.13	0.09
3.00	24.0 ± 5.7	7.1 ± 0.6	0.24	0.13
3.25	26.1 ± 6.2	8.1 ± 0.6	0.46	0.21
3.50	25.0 ± 6.2	9.8 ± 0.6	0.79	0.37
3.75	26.2 ± 8.4	11.5 ± 0.8	1.47	0.68
4.00	26.3 ± 8.2	14.0 ± 0.8	2.63	1.38
4.10	24.9 ± 8.6	15.2 ± 0.8	3.14	1.87
4.20	24.6 ± 9.1	16.6 ± 0.9	3.90	2.51
4.25	24.9 ± 8.1	17.3 ± 0.7	4.43	2.92
4.35	23.2 ± 8.2	19.0 ± 0.8	5.19	3.94
4.45	23.5 ± 7.6	20.4 ± 0.7	6.64	5.24
4.50	21.4 ± 6.5	21.5 ± 0.6	6.77	6.20
4.60	24.1 ± 8.1	22.8 ± 0.8	9.59	8.33
4.70	25.1 ± 7.8	24.5 ± 0.8	12.56	11.15
4.75	26.0 ± 7.6	25.3 ± 0.7	14.63	12.78
4.85	26.6 ± 7.7	27.0 ± 0.7	18.81	17.45
4.95	27.1 ± 7.5	28.9 ± 0.7	24.15	23.24
5.00	27.9 ± 8.2	29.8 ± 0.8	27.89	26.81

[a]Interpolated pH values.
[b]Correlated coefficient = 0.999.

$K_w[Cl^-]^{-1}$. Table 3 lists the values of micro-rate constants after reasonable assumptions have been made (see the footnote to the table).

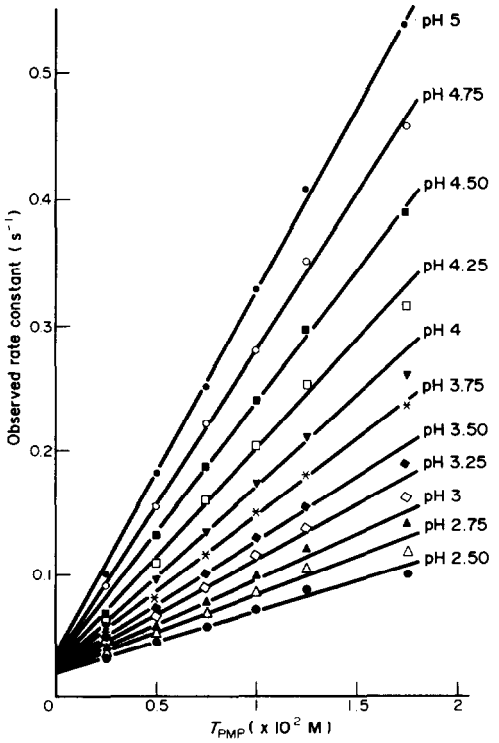

Fig. 7. k_{obs}(PMP) as function of T_{PMP} at interpolated pH values.

Conclusion

The complexes of Pd(II) with PLP and PMP are different from those with PL and PM in that they are more soluble. Although the phosphate group did not take part in complex formation yet they enhance kinetically the complexation with the other

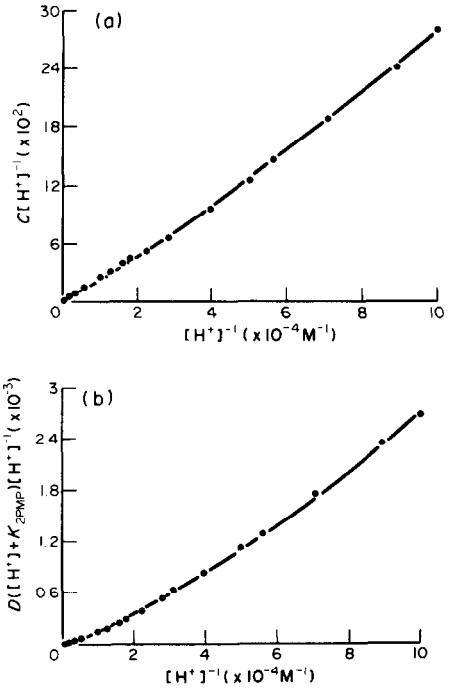

Fig. 8. (a) Dependence of $C[H^+]^{-1}$ on $[H^+]^{-1}$. (b) Dependence of $D([H^+] + K_{2PMP})[H^+]^{-1}$ on $[H^+]^{-1}$.

ligating sites (Table 3). The most interesting feature of the Pd(II) complexes with PLP and PMP is that reaction (c) in Scheme 1 is highly significant in the formation of the products and reaction (d) is the least significant. One should expect that the converse is true since the ligand is less protonated with the free ligating sites available for metal ion complexation. However, this may reflect the fact that OH^- substitution with ligands is favorable with highly protonated species. This conclusion indicates that hydrolyzed species are more reactive than non-hydrolyzed species. The presence of two chloride ions in the product complex formula does not necessarily indicate that they are inner-sphere ligands. If PLP or PMP act as a monodentate ligand the two chloride ions are likely to be of an inner-sphere type. Conversely, if they are bidentate ligands it is likely that the chloride species are not inner-sphere species.

Acknowledgements—We would like to thank Kuwait University for supporting the research project SC021 and sled money SDC 120 and SDC 121.

REFERENCES

1. N. A. Al-Salem, M. S. El-Ezaby, H. M. Marafie and H. M. Abu-Soûd, *Polyhedron* 1986, **5**, 633.
2. N. M. Moussa, A. Laham, M. S. El-Ezaby, N. A. Al-Salem, M. Abu Zeid, G. S. Mahmoud, A. Kabarity and S. Mazrooei, *J. Inorg. Biochem.* 1982, **17**, 185.
3. M. S. El-Ezaby and H. M. Abu-Soûd, *Inorg. Chim. Acta* 1982, **67**, 121.
4. A. I. Vogel, *Quantitative Inorganic Analysis*, 3rd Edn. Longmans, London (1966).

Polyhedron Vol. 6, No. 2, pp. 337–339, 1987
Printed in Great Britain

0277–5387/87 $3.00+.00

COMMUNICATION

A KINETICS METHOD FOR THE IDENTIFICATION OF COORDINATIVELY-UNSATURATED SUBSTITUTED METAL CARBONYL TRANSIENTS: *CIS*-[(TRIPHENYLPHOSPHINE)TETRACARBONYLTUNGSTEN(0)]*

GERARD R. DOBSON,† KHALIL J. ASALI, STEPHEN S. BASSON and CHARLES B. DOBSON

Center for Organometallic Research and Department of Chemistry, North Texas State University, Denton, TX 76203-5068, U.S.A.

(*Received* 4 *June* 1986; *accepted after revision* 28 *July* 1986)

Abstract—The specifically solvated, five-coordinate intermediate [(triphenylphosphine)-tetracarbonyltungsten(0)] was produced via pulsed laser flash photolysis from *cis*-(piperidine)(triphenylphosphine)tetracarbonyltungsten(0) in chlorobenzene. This five-coordinate species was identified through comparison of the "competition ratio", k_2/k_{-1}, for its interaction with piperidine (governed by k_{-1}) and tri(isopropyl) phosphite (governed by k_2) as determined through parallel flash photometric and thermal studies. This method offers a broadly applicable means of identification of transients generated upon flash photolysis and of obtaining values of all rate constants for ligand-displacement reactions of substituted octahedral metal carbonyls by Lewis bases.

Flash photolysis of metal carbonyls in solution ultimately generates specifically solvated, coordinatively unsaturated transients in their electronic ground-states which are implicated as key intermediates in metal carbonyl substitution reactions or which participate in a variety of homogeneous catalytic pathways;[1,2] UV and/or visible light are most commonly employed in transient detection. For the mononuclear parent carbonyls, identification of the photogenerated transients poses little difficulty since the number of possible primary photoproducts is very limited; thus, for $M(CO)_6$ (M = Cr, Mo or W), $[M(CO)_5]$ is the only reasonable candidate. For *substituted* metal carbonyls, however, e.g. for $LM(CO)_5$ (L = phosphines, phosphites) several possible photogenerated species resulting from M—CO or M—L bond-breaking or isomerization can be envisioned. While UV–vis detection conveniently monitors rates of reaction of the photogenerated species, their spectra are relatively featureless and generally similar.[3] Under usual circumstances the various postulated transients are also expected to exhibit similar (bimolecular) rate behavior; thus it is difficult to distinguish among them.

We report parallel photochemical and thermal rate studies of such species which afford complementary kinetics data of sufficient complexity and congruence to provide unequivocal identification of the photogenerated intermediate. This method, which is broadly applicable, has been employed in the identification of *cis*-$[Ph_3PW(CO)_4]$ (**1**) and the determination of the rate data for the ligand displacement

$$cis\text{-(piperidine)}(Ph_3P)W(CO)_4 + L \rightarrow cis\text{-(L)}(Ph_3P)W(CO)_4{}^4 + \text{piperidine} \quad (1)$$

for which **1** has been found to be both a photochemically and thermally generated intermediate.

It has been observed that complexes containing chelating rings coordinating through both N and

*Part 59 of the series, Octahedral metal carbonyls. For Part 58, see Ref. 10.

†Author to whom correspondence should be addressed.

P, e.g. $(NP)Mo(CO)_4$ (NP = 1-diethylamino-2-diphenylphosphinoethane) react both thermally[5,6] and photolytically[7] via metal–nitrogen bond fission to afford largely specifically solvated[8] $[(\eta^1\text{-}NP)Mo(CO)_4]$ intermediates in which the solvated coordination site is *cis* to L. This being the case, *cis*-(pip)$(Ph_3P)W(CO)_4$ [pip = piperidine (**2**)] was selected as a species likely to afford **1** upon photolysis and thermolysis. The relatively inert W complex was selected to avoid competitive thermal reactions during photolysis. The complex was synthesized from $W(CO)_6$ via *cis*-$(pip)_2W(CO)_4$ employing the method of Darensbourg and Kump.[9] Analytical, flash photolysis and thermal kinetics data are consistent with stoichiometry (1) and with mechanism (2).

Pulsed laser flash photolysis reactions of **2** (355 nm photolyzing and 430 nm analyzing wavelengths) were carried out in chlorobenzene over ~20–35°C in the presence of varying flooding concentrations of L (= triethyl phosphite, tri(*iso*-propyl) phosphite and triphenylphosphine) and, separately, of pip, employing equipment and

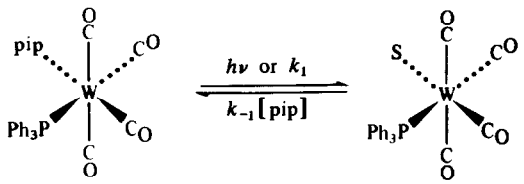

S = solvent (chlorobenzene)

$$-S \downarrow k_2[L] \quad (2)$$

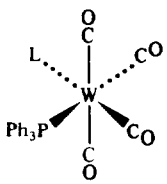

methods described previously.[7] Plots of absorbance vs time for disappearance of the photogenerated transient exhibited logarithmic decay; from these plots were extracted pseudo-first-order rate constants, k_{obsd}. Plots of k_{obsd} vs [L] obeyed the rate law

$$k_{obsd} = k[L] \quad (3)$$

consistent with loss of pip and bimolecular interaction of (**1**) with L (the step governed by k_2) or with pip (the step governed by k_{-1}) as outlined in eqn (2).

Thermal reactions of **2** in the presence of large excesses of *both* pip and L, also proceeding via the stoichiometry given in eqn (1) were also studied over long periods of time in sealed cells[10] monitoring 425 nm in chlorobenzene at 33.3°C, a temperature at which the flash photolysis studies were also carried out. In terms of the pseudo-first-order rate constants, k'_{obsd}, rate data were consistent with the rate law

$$k'_{obsd} = k'[L]/([pip] + k''[L]). \quad (4)$$

This rate law is consistent with mechanism (2), where $k' = k_1k_2/k_{-1}$ and $k'' = k_2/k_{-1}$, the 'competition ratio' for bimolecular rate constants of interaction of **1** with L and pip, respectively. The rate constant for unimolecular dissociation of pip from **2** [k_1, scheme (2)] may be calculated as k''/k'; all rate constants for both the photochemical and thermal pathways at ~20–35°C are exhibited in Table 1.

It is to be noted that the 'competition ratio', $k'' = k_2/k_{-1}$, determined from the tnermal data may be compared to this same ratio obtained from the *photochemical* data; the values (Table 1) are the same, within experimental error. The adherence of both the thermal and photochemical reactions to both a common stoichiometric expression and rate law, and the agreement between rate constants (the 'competition ratios') obtained through independent thermal and photochemical rate studies carried out under identical reaction conditions provide compelling evidence in support of this mechanism and show that **1** is the thermally and photochemically generated transient. There is no evidence for stereochemical rearrangement in **1** on the timescale of processes governed by k_{-1} or k_2.[11]

Activation parameters for interaction of both $P(OiPr)_3$ and pip with **1** are also given in Table 1. They agree within experimental error, as might be expected given the relatively non-discriminating nature of the intermediate, and exhibit entropies of activation near zero, reasonable for a solvent–L exchange process. Rates of bimolecular interaction of pip and L with solvated **1** vary in the order pip > $P(OEt)_3$ > PPh_3 > $P(OiPr)_3$, which suggests a dominant (but not exclusive) steric influence on reaction rate. A similar conclusion has been drawn through ligand-competition studies of the closely-related *cis*-(amine)(L)$Mo(CO)_4$ complexes.[12]

Acknowledgments—The support of this research by the Robert A. Welch Foundation (Grant no. B-434), the National Science Foundation (Grant CHE 84-15153) and the North Texas State University Faculty Research Fund is gratefully acknowledged. We thank Dr Paul H. Wermer

Table 1. Rate constants for displacement of piperidine (pip) from *cis*-(pip)$(PPh_3)W(CO)_4$ complexes by L (= phosphine, phosphite) in chlorobenzene

T (°C)	L	10^6k_1 (s^{-1})	$10^{-4}k_{-1}$[a] ($M^{-1}s^{-1}$)	$10^{-4}k_2$ ($M^{-1}s^{-1}$)	k_2/k_{-1} (M^{-1})
21.1[b,c]	$P(OiPr)_3$[d]	—	2.04(9)	1.13(6)	0.55(6)
23.3[c]		—	2.42(11)	—	—
33.3[c,f]		—	5.57(1)	2.4(3)	0.43(6)
33.3[e,f]		1.12(3)	—	—	0.53(2)
34.3[c]		—	5.3(8)	3.2(3)	0.61(15)
21.1[c]	$P(OEt)_3$	—	—	1.79(4)	0.88(6)
21.1[c]	PPh_3	—	—	1.45(5)	0.71(6)

[a] $\Delta H‡ = 13.2(13)$ kcal mol^{-1}, $\Delta S‡ = 6.2(42)$ cal $°C^{-1}$ mol^{-1}.
[b] Values extrapolated from data at 23.3–34.3°C.
[c] Photochemical data.
[d] $\Delta H‡ = 12.4(20)$ kcal mol^{-1}, $\Delta S‡ = 2.8(36)$ cal $°C^{-1}$ mol^{-1}.
[e] Thermal data.
[f] $K_{eq} = [1]/[2]$ [eqn (3)] $= 2.01(5) \times 10^{-11}$, $\Delta G = 14.98(1)$ kcal mol^{-1}.

and Dr Saber E. Mansour for experimental assistance. The pulsed laser flash photolysis studies and analyses of the data were performed at the Center for Fast Kinetics Research (CFKR) at the University of Texas at Austin. The CFKR is supported jointly by the Biotechnology Branch of the Division of Research Resources of the National Institutes of Health (Grant RR00886) and by the University of Texas at Austin. The experimental help and technical expertise of the staff at CFKR, in particular that of Dr Stephen J. Atherton, are greatly appreciated. K.J.A. thanks King Saud University, Abha Branch, Abha, Saudi Arabia for sabbatical leave.

REFERENCES

1. J. J. Turner and M. Poliakoff, *ACS Symp. Ser.* 1983, **211,** 35.
2. M. Wrighton, J. S. Graff, R. J. Kaslauskas, J. C. Mitchener and C. J. Reichel, *Pure Appl. Chem.* 1982, **54,** 161.
3. D. J. Darensbourg and M. A. Murphy, *J. Am. Chem. Soc.* 1978, **100,** 463.
4. W. A. Schenk, *J. Organomet. Chem.* 1980, **184,** 195.
5. W. J. Knebel and R. J. Angelici, *Inorg. Chem.* 1974, **13,** 627.
6. S. E. Mansour, Dissertation, North Texas State University (1985).
7. G. R. Dobson, I. Bernal, M. G. Reisner, C. B. Dobson and S. E. Mansour, *J. Am. Chem. Soc.* 1985, **107,** 525.
8. J. Simon and K. S. Peters, *Chem. Phys. Lett.* 1983, **98,** 53.
9. D. J. Darensbourg and R. J. Kump, *Inorg. Chem.* 1978, **17,** 2680.
10. G. R. Dobson, S. S. Basson and C. B. Dobson, *Inorg. Chim. Acta* 1985, **105,** L17.
11. G. R. Dobson, H. H. Awad and S. S. Basson, *Inorg. Chim. Acta* 1986, **118,** L5; cf. D. J. Darensbourg, G. R. Dobson and A. Moradi-Araghi, *J. Organomet. Chem.* 1976, **116,** C17.
12. C. L. Hyde and D. J. Darensbourg, *Inorg. Chem.* 1973, **12,** 1286.

Polyhedron Vol. 6, No. 2, pp. 341–343, 1987
Printed in Great Britain

0277–5387/87 $3.00+.00

COMMUNICATION

SYNTHESIS AND X-RAY CRYSTAL STRUCTURE OF A DINUCLEAR PLATINUM HYDRIDE COMPLEX OF TETRACYANOBIIMIDAZOLE

J. CARLOS BAYÓN

Departament de Química, Universitat Autònoma de Barcelona, Bellaterra, Barcelona, Spain

and

J. BRUCE KOLOWICH and PAUL G. RASMUSSEN*

Department of Chemistry, University of Michigan, Ann Arbor, MI 48109, U.S.A.

(*Received* 19 *June* 1986; *accepted* 15 *August* 1986)

Abstract—Reaction of the diacid form of tetracyanobiimidazole via oxidative addition with two equivalents of $Pt(PPh_3)_4$ produces a dinuclear complex whose structure is solved by X-ray analysis. The presence of dihydride is confirmed by observation of IR shift of a deuterium-labelled compound.

The reaction of protic acids with platinum(0)tetrakisphosphines via oxidative addition to form platinic hydrides has been well documented in the literature. Earlier works have described numerous examples of reaction of Pt(0) with mineral acids[1] and imides[2] to produce such hydride compounds, but reactions with oxyacids do not produce compounds of similar stability.[3] Hydride-containing dinuclear complexes of platinum without bridging hydrides are rare,[4–7] and are not the product of reaction of a diacid with two equivalents of a Pt(0) species.

We now report the synthesis of a symmetrical platinum(II)hydrido dinuclear compound formed by the oxidative addition of a non-oxygen diacid, 4,4′,5,5′-tetracyano-2,2′-biimidazole ($C_{10}N_8H_2$), to two equivalents of tetrakistriphenylphosphineplatinum(0). The white, air-stable reaction product, $HPt(PPh_3)_2(C_{10}N_8)(PPh_3)_2PtH$, precipitates quantitatively on stirring for 1 h in tetrahydrofuran, regardless of the stoichiometric ratios added to the reaction mixture. Crystals of this compound suitable for X-ray analysis were prepared by allowing a mixture of the reactants to stand overnight in a new flask. Once the compound was prepared, it showed no solubility in common laboratory solvents except those which react with the hydride.

Chemical characterization of the dinuclear compound included elemental analysis and IR spectra. Principle characterization of the structure was the result of X-ray analysis (Fig. 1).† From this we find the geometry about the platinum to be a slightly distorted square-planar, with angles P1—Pt—N1 99.8° and P2—Pt—N1 95.0°. The atoms P1, P2, Pt and N1 are coplanar, and this plane is almost exactly perpendicular to that of the central ligand. The bonded distance of 2.125 Å for Pt—N1 compares to the non-bonded distance of 3.027 Å for Pt—N3′. Examination of packing plots from all axes revealed no strong intermolecular association.

*Author to whom correspondence should be addressed

†Crystal data: $C_{82}H_{62}N_8P_2Pt_2$, $M = 1611.58$, triclinic, space group $P\bar{1}$, $a = 13.397$ Å, $b = 14.734$ Å, $c = 12.379$ Å, $\alpha = 100.82°$, $\beta = 115.90°$, $\gamma = 64.65°$, $U = 1986$ Å^3, $Z = 1$, $D_{calc} = 1.408$ g cm^{-3}, μ(Mo-K_α) = 36.81 cm^{-1}, λ(Mo-K_α) = 0.71069 Å, $N = 4614$, $NP = 479$, $R = 0.0283$, non-hydrogen atoms anisotropic, hydrogens fixed but not refined. Tables of atomic positional and thermal parameters, bond lengths and angles and F_o/F_c values have been deposited as supplementary material with the Editor from whom copies are available on request. Atomic coordinates have also been deposited with the Cambridge Crystallographic Data Centre.

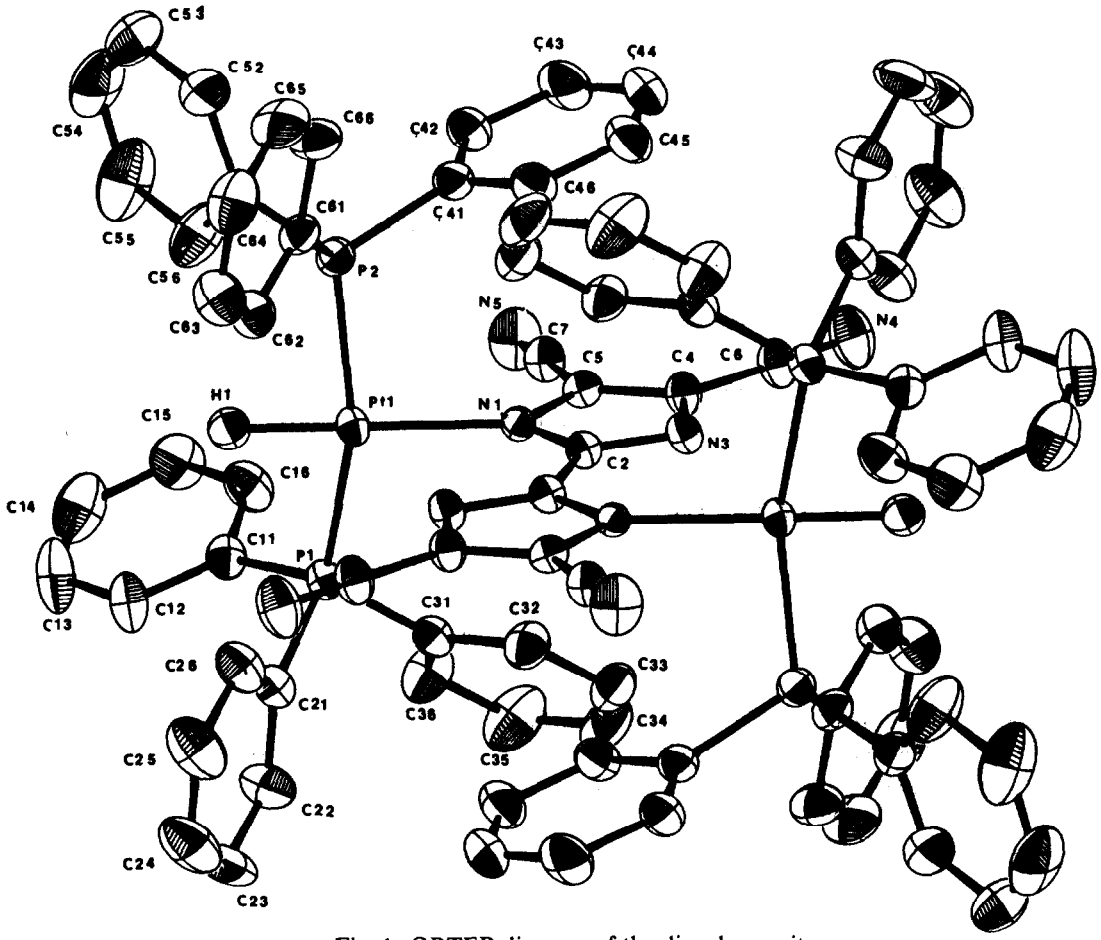

Fig. 1. ORTEP diagram of the dinuclear unit.

Stereoplots of these packings indicated that interaction was mainly confined to the phenyl ring periphery of the molecule. This is the first example of coordination of this type for tetracyanobiimidazole. More commonly expected are dinuclear species with quadridentate binding to the ring nitrogens,[8] or mononuclear bidentate species with the metal atom bound to one side of the ligand.[9]

The hydride was verified via isotopic labeling and observance of the shift in frequency for the IR Pt—H resonance. Labeling was accomplished by stirring the acid form of the ligand in D_2O at 5°C for several hours. This deuterated form of the ligand ($D_2C_{10}N_8$) was then allowed to react with two equivalents of tetrakistriphenylphosphine-platinum(0). The resulting product was identical in appearance and solubility to the protic analog. IR spectra of the two compounds were virtually identical, except for the hydride–deuteride bands. The hydride band at 2196 cm^{-1} was absent in the deuteride spectrum, and as expected, a new resonance had appeared at 1621 cm^{-1}.

Investigations of this unusual molecule are continuing with synthetic attempts to probe the hydride reactivity.

Acknowledgements—P.G.R. acknowledges support from the donors of the Petroleum Research Fund administered by the American Chemical Society. J.C.B. acknowledges support from CIRIT (Catalonia). J.B.K. acknowledges support from the H. Judson Osterhof fellowship of the Rackham Graduate School.

REFERENCES

1. F. Cariati, R. Ugo and F. Bonati, *Inorg. Chem.* 1966, **5**, 1128.
2. D. M. Roundhill, *Inorg. Chem.* 1970, **9**, 254.
3. D. Carmona, R. Thouvenot, L. M. Venanzi, F. Bachechi and L. Zambonelli, *J. Organomet. Chem.* 1983, **250**, 589.
4. R. S. Paonessa, A. L. Prignano and W. C. Trogler, *Organometallics* 1985, **4**, 647.
5. R. S. Paonessa and W. C. Trogler, *Inorg. Chem.* 1983, **22**, 1038.
6. M. Auburn, M. Ciriano, J. A. K. Howard, M. Murray, N. J. Pugh, J. L. Spencer, F. G. A. Stone and P.

Woodward, *J. Chem. Soc., Dalton Trans.* 1980, 659.
7. T. H. Tulip, T. Yamagata, T. Yoshida, R. D. Wilson, J. A. Ibers and S. Otsuka, *Inorg. Chem.* 1979, **18,** 2239.
8. P. G. Rasmussen, J. E. Anderson and J. C. Bayón, *Inorg. Chim. Acta* 1984, **87,** 159.
9. P. G. Rasmussen, J. E. Anderson, O. H. Bailey and J. C. Bayón, *J. Am. Chem. Soc.* 1985, **107,** 279.

Woodward, *J. Chem. Soc., Dalton Trans.* 1980, 659.
7. T. H. Tulip, T. Yamagata, T. Yoshida, R. D. Wilson, J. A. Ibers and S. Otsuka, *Inorg. Chem.* 1979, **18,** 2239.
8. P. G. Rasmussen, J. E. Anderson and J. C. Bayón, *Inorg. Chim. Acta* 1984, **87,** 159.
9. P. G. Rasmussen, J. E. Anderson, O. H. Bailey and J. C. Bayón, *J. Am. Chem. Soc.* 1985, **107,** 279.

Polyhedron Vol. 6, No. 2, pp. 345–346, 1987
Printed in Great Britain

0277–5387/87 $3.00+.00

COMMUNICATION

ON THE NATURE OF ACTIVATION OF ANCHORED RHODIUM CATALYSTS BY BOROHYDRIDE

B. VISWANATHAN* and D. RAMESH

Department of Chemistry, Indian Institute of Technology, Madras, India

(*Received* 15 *July* 1986; *accepted* 4 *September* 1986)

Abstract—The nature of the active polymer anchored rhodium catalysts used for hydrogenation has been deduced to be a mono- or dihydridorhodium(III) species.

Rhodium complexes anchored on polymers containing ligands like phosphine[1] and anthranilic acid derivatives[2] have been employed as hydrogenation catalysts. The systems containing polymers with anthranilic acid derivatives were synthesized from $RhCl_3$ and were subsequently treated with $NaBH_4$.[2] In this process,[2] it is considered that Rh(III) is reduced to Rh(I) as evidenced from the colour change observed as well as from XPS results. The purpose of this communication is to examine the nature of activation caused in the catalyst as a result of borohydride treatment.†

Normally, rhodium (III) chloride complexes containing nitrogen ligands on treatment with borohydride yield either mono- or dihydrido species by nucleophilic displacement of chloride or undergoes reduction to Rh(I) or Rh(O).[4] It is also known that a dihydrorhodium(III) complex can be obtained by oxidative addition of molecular hydrogen to Rh(I) species.[5] It is therefore deduced that treatment of Rh(III) complexes with borohydride (which can also act as a source for hydrogen[6]) can result in a di- or monohydridorhodium(III) complex depending upon the nature of the ligands. However, hydrido species could not be formed from Rh(III) complexes by treatment with other reducing agents like sodium amalgam, hypophosphorus acid or molecular hydrogen.[4] It is likely, therefore, that the active hydrogenating polymer-anchored catalysts can contain Rh(III) hydrido species. The reports available in the literature[2] have unfortunately identified this species as Rh(I) on the basis of a low value (~308 eV) of the binding energy of the Rh $3d_{5/2}$ emission. Furlani *et al.*[7] have analysed the XPS data of a number of rhodium compounds and have shown that: (i) the binding energy as well as the FWHM of Rh 3*d* line is strongly dependent on the nature and the number of co-ordinating species, and (ii) the rhodium species on the polymer surfaces are predominantly in the higher oxidation state. The lower binding energy values for Rh $3d_{5/2}$ (~308 eV) observed for these species could arise from: (i) the initial-state chemical shifts resulting from the nature of the ligands, and (ii) the final-state relaxation shifts whose contribution could be significant especially in view of the extended nature of the polymer backbone used.

Borane generated during borohydride treatment[6] could also bind to the polymer (the presence of highly charged boron species is also reported in polymer-bound nickel catalysts[8]) and can activate the olefin. This could also account, at least partially, for the hydrogenation activity observed.

The hypotheses proposed in this letter, however, await further support from IR data of the active catalyst for ν_{B-H} (2300–2500 cm^{-1}), ν_{Rh-H} (1700–2200 cm^{-1}) and $\nu_{Rh-H-Rh(bridged)}$ (1150 cm^{-1}).[9]

*Author to whom correspondence should be addressed.

†Even though metallic rhodium is effective for the hydrogenation of olefins,[3] its role on polymer-anchored systems without elution is doubtful. In addition, the existence of Rh(0) was never identified by XPS.[2]

REFERENCES

1. (a) C. U. Pittman, Jr, In *Comprehensive Organometallic Chemistry* (Edited by G. Wilkinson), Vol. 8, p. 553. Pergamon Press, Oxford (1982); (b) R. A. W. Johnstone and A. H. Wilby, *Chem. Rev.* 1985, **85**, 129.
2. (a) N. L. Holy, *Tetrahedron Lett.* 1977, 3703; (b) N. L.

2. (a) N. L. Holy, *Tetrahedron Lett.* 1977, 3703; (b) N. L. Holy, *J. Org. Chem.* 1979, **44**, 239.
3. C. A. Brown and H. C. Brown, *J. Am. Chem. Soc.* 1962, **84**, 1495.
4. R. D. Gillard and G. Wilkinson, *J. Chem. Soc.* 1963, 3594.
5. (a) J. F. Young, J. A. Osborn, F. H. Jardine and G. Wilkinson, *J. Chem. Soc., Chem. Commun.* 1965, 131; (b) for a general discussion on activation and addition of hydrogen see B. R. James, In *Comprehensive Organometallic Chemistry* (Edited by G. Wilkinson), Vol. 8, p. 285. Pergamon Press, Oxford (1982).
6. A. Hajos, *Complex Hydrides—Studies in Organic Chemistry—1*, p. 43, Elsevier, Amsterdam (1979).
7. C. Furlani, G. Mattogno, G. Polenzetti, G. Sbarana and G. Valentini, *J. Catal.* 1985, **94**, 335 (and references cited therein).
8. N. L. Holy and R. Shalvoy, *J. Org. Chem.* 1980, **45**, 1418.
9. C. White, D. S. Gill, J. W. Kang, H. B. Lee and P. M. Maitilis, *J. Chem. Soc., Chem. Commun.* 1971, 734 (and references cited therein).

Polyhedron Vol. 6, No. 2, p. 347, 1977
Pergamon Journals Ltd. Printed in Great Britain

BOOK REVIEW

Structure and Bonding, Vol. 62, Clusters.
Springer, Berlin, 1985. ISBN 3-540-15731-X, 116 pp., DM 980

The latest volume of this popular series of reviews contains three surveys of aspects of polynuclear metal compounds. Each review is valuable and each shows a different way in which a review can help us master chemical information: by surveying a field for the first time, by updating our knowledge of a busy area previously well covered, or by writing an essay which is itself a contribution to science.

Günther Gliemann and Hartmut Yersin from Regensburg provide a well organized article on one-dimensional $[Pt(CN)_4]^{2-}$ species. They emphasize electronic spectra, both absorption and emission, and include effects of pressure and magnetic fields, but they do not deal with the one-dimensional electric conductance which is already well known. General inorganic chemists may find the level of theory rather tough, but they will be pleased by the many excellent diagrams of polarized single crystal spectra.

Albert Cotton and Richard Walton have updated their book on multiply bonded cluster complexes by reviewing recent work, mostly their own, on dinuclear compounds of this type. The metals covered are Cr, Mo, W, Tc, Re, Ru, Os and Pt, but not in any special order, nor at equal length. There are also short sections on spectroscopy and a note on M_2 molecules. I was sorry not to see anything about Nb=Nb bonds, so this is not quite a comprehensive study. For that matter there are plenty of interesting dinuclear complexes which are not metal–metal bonded, as in Mo and Cu chemistry, and we must take care not to forget these while we get excited about quadruple bonds. Despite these criticisms I enjoyed reading how the field is now developing from structural and bonding studies to include redox and ligand reactions. Those familiar with Dr Cotton's work will enjoy or be bored by the usual pointed refutations of the results of other workers, especially theoreticians and Russians.

The most valuable review of the three is Günter Schmid's essay about large cluster molecules. Using purely geometric arguments he explains why such a molecule as $[Au_{55}(PPh_3)_{12}Cl_6]$ is found. No molecular orbitals, no electron counting, just a simple analysis of a cubic close-packed cubo-octahedron of 55 metal atoms, the size of phosphines (at the 12 remaining vertices) and the spaces left for chlorines (over the six square faces). Dr Schmid goes on to show where these structures are found, how they are non-rigid, and how electron counting rules which apply to smaller clusters are weak here. There is a short note on magnetochemistry and this splendid essay concludes with some striking electron micrographs of Au_{55} clusters.

PETER THORNTON

Department of Chemistry
Queen Mary College
London E1 4NS, U.K.

Polyhedron Vol. 6, No. 2, p. 349, 1987
Pergamon Journals Ltd. Printed in Great Britain

ANNOUNCEMENT

POLYHEDRON PUBLICATION AWARD

Pergamon Journals Ltd is pleased to announce the award annually of a cash prize of $1000 for the best paper published in *Polyhedron*.

The award will be made to the authors of the original research paper (not including *Polyhedron* Reports) judged to be the best on the basis of scientific originality, significance, clarity and style of presentation. The first award will be made for a paper published in Volume 6, 1987. Members of the Editorial Board will each be invited to nominate two papers for the award and the final selection will be made by an anonymous committee appointed by the Editors who themselves will not be eligible for the award.

The recipient of the first award will be notified early in 1988.

Polyhedron Vol. 6, No. 3, pp. 351–382, 1987
Printed in Great Britain

0277–5387/87 $3.00+.00

POLYHEDRON REPORT NUMBER 19

NAKED PHOSPHORUS ATOMS AND UNITS IN TRANSITION-METAL COMPOUNDS*

MASSIMO DI VAIRA and PIERO STOPPIONI†

Dipartimento di Chimica, Università di Firenze, Via Maragliano, 77, 50144 Firenze, Italia

and

MAURIZIO PERUZZINI

Istituto I.S.S.E.C.C., C.N.R., Via J. Nardi, 39, 50132 Firenze, Italia

CONTENTS

I. INTRODUCTION

Transition metals give rise to a large number of clusters which vary in nature from the simple aggregates of metal atoms to complex systems formed by transition-metal atoms and ligands of various sorts, such as carbonyls, hydrides, olefins and phosphines, as well as by interstitial atoms.[1] Metal and non-metal main-group elements, on the other hand, form a numerous class of "naked clusters". neutral or ionic, having no peripheral ligands, such as P_4, P_4S_3, Bi_5^{3+}, Bi_9^{5+}, Sn_5^{2+}, Ge_9^{2-} etc.[2] One of the most viable and stimulating fields in the chemistry of the transition metals and main-group elements is the one related to the synthesis and characterization of new cluster compounds in which main-group elements and transition-metal ligand units form linkages to each other. Among such compounds those containing naked P atoms are quickly growing in number, being at the centre of the interest of many chemists.

This report deals with compounds which contain unsubstituted P atoms or small units of such atoms bound to transition-metal–ligand moieties, and covers the literature up to the end of 1985. It focuses on three topics: (a) the survey of metal compounds containing from one to six naked P atoms, with particular emphasis on their structures and the synthetic routes leading to these

*Dedicated to Professor Luigi Sacconi on the occasion of his 75th birthday.

†Author to whom correspondence should be addressed.

compounds; (b) the examination of the reactivity of such naked P atoms or units towards additional metal–ligand moieties; and (c) the collection of ^{31}P NMR data for the compounds. Up to now no exhaustive review of this field has been published. Only cyclotriphosphorus compounds have been reviewed by Di Vaira and Sacconi,[3] while Riess, considering the coordination chemistry of polycyclic tetraphosphorus compounds,[4] has reported on the transition-metal complexes obtained by using such cage molecules as parent compounds. Finally, a recent review by Scherer on the coordinating ability of multiply bonded systems of the Group V elements has included some compounds containing the P_2 unit.[5]

II. SYNTHESES AND STRUCTURES OF COMPOUNDS WITH NAKED PHOSPHORUS ATOMS

The number of naked P atoms contained in the compounds described until now, where such P atoms are bound to metal–ligand moieties, ranges from one to six, excluding five. It was considered convenient for the discussion to group the complexes according to the number of their unsubstituted P atoms. Whenever two or more naked P atoms are present in a compound they are also bound *inter se* so that it is possible to refer to P_2, P_3, P_4 or P_6 fragments interacting with metal–ligand moieties. Moreover, numerous species having three, two or one P atom may be considered to originate from the tetrahedral P_4 molecule by progressive replacement of its atoms by appropriate metal–ligand systems. Scheme 1 summarizes the bonding modes of the mono- or polyphosphorus units of the latter type to transition-metal moieties, schematically denoted by M. On the other hand, in Scheme 1 no reference is made either to the species with P atoms in interstitial or semi-interstitial positions, which occur among the transition-metal carbonyl clusters, or to the compounds containing P units that cannot be considered as fragments of the P_4 molecule. The latter compounds have either more than four P atoms or contain chains of such atoms. All of the compounds which do not match the structural features and bonding modes summarized in Scheme 1 are included in the section devoted to miscellaneous derivatives.

II.1. *Intact* P_4 *molecule as ligand*

The first compounds which were claimed to contain the *tetrahedro*-tetraphosphorus molecule linked to a metal atom were described in 1971 by Ginsberg and Lindsell.[6,7] They were isolated by reacting Rh(I) or Ir(I) tertiary phosphine or arsine complexes with white phosphorus at low temperatures; the list of the compounds is reported in Table 1. The complexes are stable under an inert atmosphere in the solid state, whereas they slowly decompose in solution even under nitrogen. Scheme 2 shows the synthesis of $[RhCl(\eta^2\text{-}P_4)(PPh_3)_2]$ (**1**). Several pieces of evidence suggested the presence of the intact P_4 molecule in all of these compounds although it was not possible to establish how the molecule was linked to the metal atom. More recently strong evidence for the coordination mode of the P_4 species in **1** was obtained by means of $^{31}P\text{-}\{^1H\}$ NMR spectroscopy,[8] whereas the definitive proof by X-ray diffraction analysis[9] could be achieved only later due to the high reactivity of the compound at room temperature. The NMR data showed the equivalence of the two phosphines and were consistent with an A_2B_2 spin system due to the P_4 ligand, each line being doubled by ^{103}Rh (Table 4); such a pattern suggests that the P_4 molecule acts as an η^2-ligand toward the metal atom. The crystallographic analysis has shown that the metal-bonded P–P edge is essentially perpendicular to the best plane through the metal atom and the other donor atoms (Fig. 1). The most important deformation of the P_4 moiety from the tetrahedral shape with 2.21 Å edge, possessed by the free molecule,[10] is due to lengthening (by *ca* 0.25 Å) of the metal-bonded edge upon coordination. EHMO calculations suggest strong similarities between η^2-coordinated P_4 and η^2-alkene ligands.[9]

Six years after the communication by Ginsberg and Lindsell[6] Schmid and Kempny reported[11] the synthesis of an iron carbonyl derivative containing the P_4 molecule (Scheme 3), having the formula $[\{Fe(CO)_4\}_3(P_4)]$ (**2**). The complex was characterized by elemental analysis, and by Mössbauer and IR spectra.[11] Its extreme instability in solution prevented a better characterization.

The first transition-metal compounds containing the P_4 ligand and endowed with a sufficiently high stability to allow X-ray structural investigations were obtained by Sacconi and coworkers in

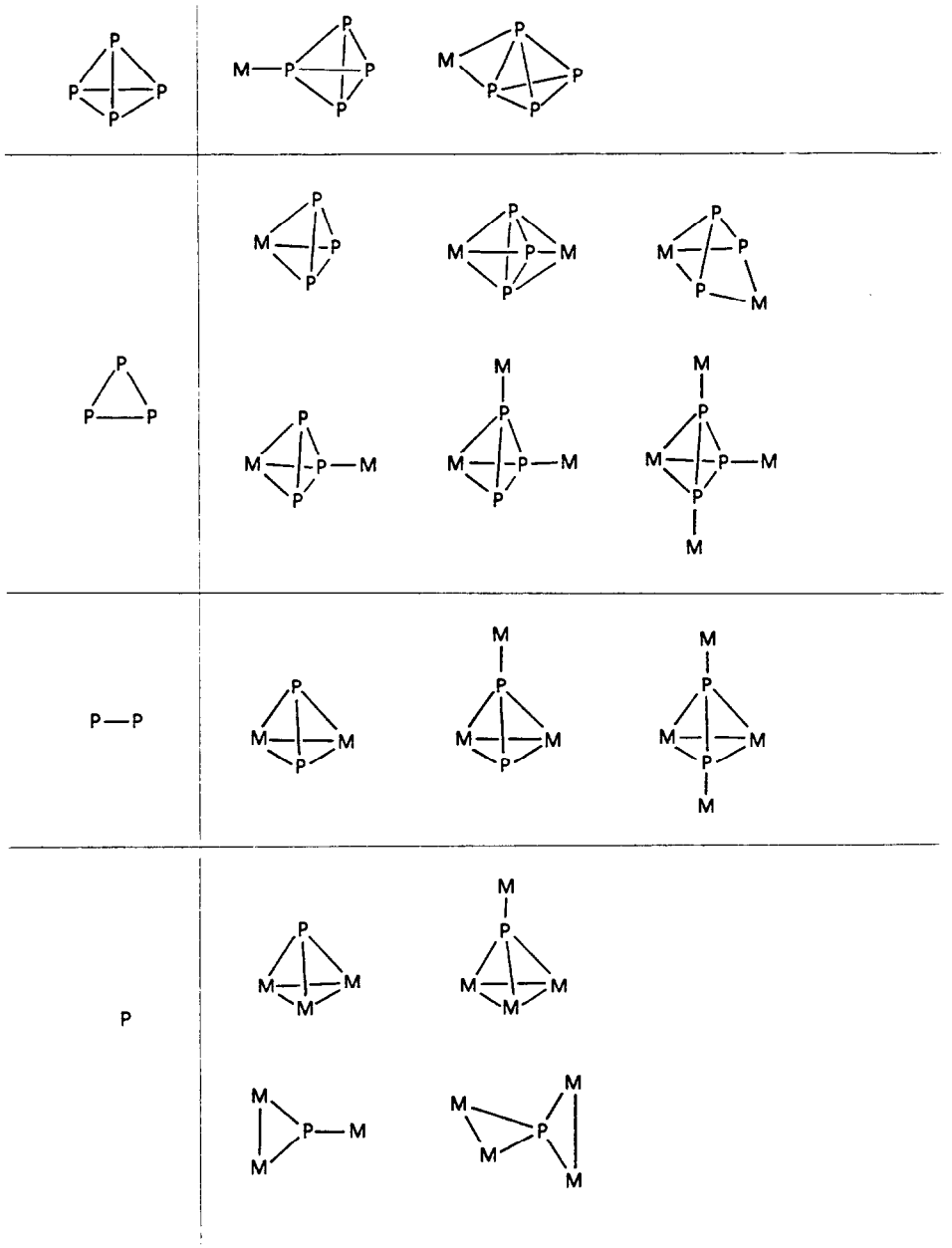

Scheme 1.

Table 1. Rhodium and iridium complexes containing the intact P_4 molecule as a ligand[a]

Compound	Color	M.p. (°C)
$[RhCl(\eta^2\text{-}P_4)(PPh_3)_2]$	Yellow	171–173 d
$[RhBr(\eta^2\text{-}P_4)(PPh_3)_2]$	Yellow	166–167 d
$[RhI(\eta^2\text{-}P_4)(PPh_3)_2]$	Yellow	153–156 d
$[RhCl(\eta^2\text{-}P_4)(AsPh_3)_2]$	Yellow	104–106 d
$[RhCl(\eta^2\text{-}P_4)(Pm\text{-}tol_3)_2]$	Yellow	132–134 d
$[RhCl(\eta^2\text{-}P_4)(Pp\text{-}tol_3)_2]$	Yellow	110–115 d
$[IrCl(\eta^2\text{-}P_4)(PPh_3)_2]$	Orange	158–161 d

[a]References 6 and 7.

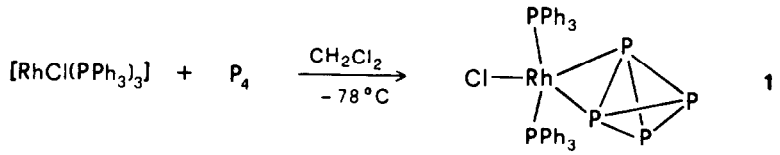

Scheme 2.

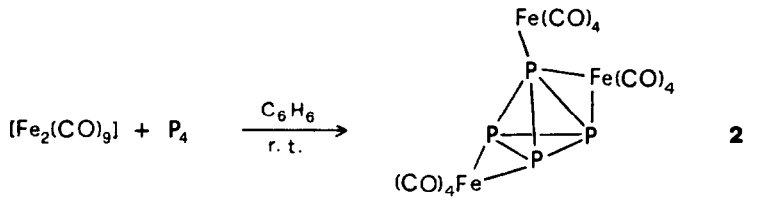

Scheme 3.

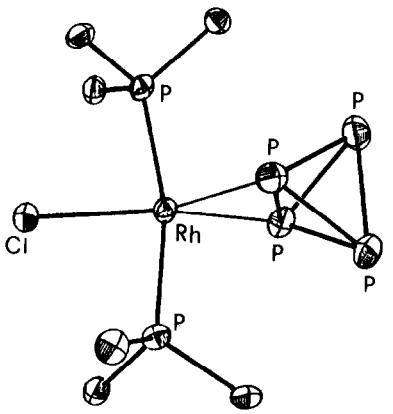

Fig. 1. Central part of $[RhCl(\eta^2\text{-}P_4)(PPh_3)_2]$.

1979.[12] Reaction of the trigonal pyramidal Ni(0) complex $[(np_3)Ni]$ [np_3 = tris(2-diphenylphosphinoethyl)amine] with white phosphorus in THF at *ca* 0°C leads to the diamagnetic compound $[(np_3)Ni(\eta^1\text{-}P_4)]$ (3), which readily precipitates (Scheme 4). It is slightly air-sensitive in the solid state and is insoluble in all common organic solvents. On substitution of $[(np_3)Pd]$ for $[(np_3)Ni]$, the $[(np_3)Pd(\eta^1\text{-}P_4)]$ (4) complex is obtained by the above procedure.[13] This is isomorphous with the nickel analogue, whose structure has been determined (Fig. 2).[12] The metal atom in $[(np_3)Ni(\eta^1\text{-}P_4)]$ is bound to the three P atoms of the np_3 ligand and to one P atom of the P_4 unit in a nearly

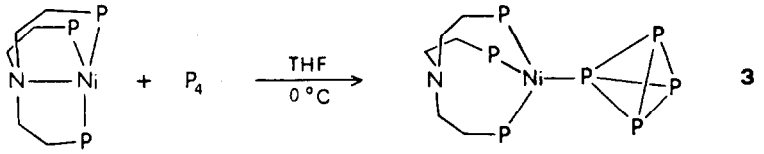

Scheme 4.

regular tetrahedral arrangement. The N atom of the np_3 ligand is uncoordinated whereas in the educt compound it is linked to the metal atom. Upon coordination the P_4 unit undergoes a small distortion from the regular tetrahedral geometry toward that of a slightly elongated trigonal pyramid whose apex points toward the metal atom. The P_{basal}—P_{apical} distance [2.20(3) Å] is indeed significantly longer than the P_{basal}—P_{basal} one [2.09(3) Å]. Such deformation of the tetrahedral P_4 unit and the short Ni—P bond [1.99(1) Å] are indicative of appreciable interaction between the

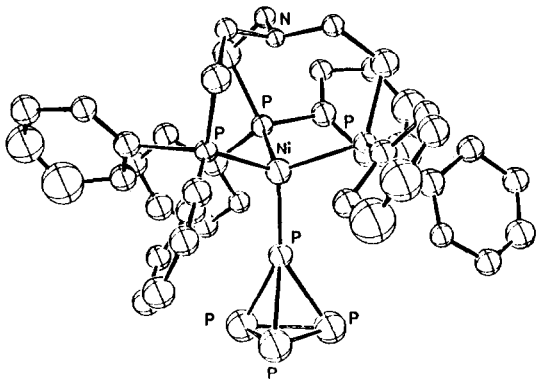

Fig. 2. Structure of the $[(np_3)(\eta^1\text{-}P_4)]$ molecule.

$[(np_3)Ni]$ moiety and the P_4 ligand. The formation and stability of these P_4 adducts are probably due to properties of the np_3 ligand, such as its flexibility, the nature of its donor set, its ability to impose a proper symmetry on the metal environment and the shielding effects due to its phenyl groups.[3]

The compounds reported until now show that the P_4 molecule may be bound as an η^1- or η^2-ligand to transition-metal moieties. Extended Hückel calculations have been carried out on models of η^1-, η^2- and η^3-complexes of P_4 with ML_3 fragments.[14] The η^1-square-planar and the η^2-arrangement with C_{2v}-symmetry should be preferred by a d^8-ML_3 fragment whereas the η^1-tetrahedral geometry is expected to be the most stable one for d^{10}-ML_3. The η^3-coordination should be possible with appropriate metal–ligand moieties, although no complex of this type has been described so far.

II.2. *Compounds containing the cyclotriphosphorus unit*

II.2(i) *Mononuclear metal complexes.* The first transition-metal compound containing the cyclotriphosphorus unit was reported in 1976 by Vizi-Orosz while investigating the reaction of white phosphorus with $[Co_2(CO)_8]$ under various conditions.[15] Such a reaction leads to a mixture of the carbonyl derivatives **5–8** (Scheme 5) which were separated by means of silica gel column chromatography with hexane as eluant. The relative amounts of compounds **5–8** in the mixture are controlled by the reaction conditions; in particular, the cyclotriphosphorus derivative (**5**) was obtained in the highest yield (*ca* 40%) by carrying out the reaction in an autoclave at 50°C under a 120 atm CO pressure. The yellow crystals of **5** ignite spontaneously in the air. IR data suggest that **5** has the same geometry as $[Co(CO)_3(\eta^3\text{-}As_3)]$,[16] which consists of a $Co(CO)_3$ group coordinated to a triangular As_3 fragment. Therefore **5** should contain a $Co(CO)_3$ group bound to a triangular P_3 unit. The same mixture of compounds **5–8** was also obtained by reacting $[Co_2(CO)_8]$ or $[Co(CO_4]^-$ in THF and hexane with phosphorus trihalides[15] under CO (1 atm); by this reaction **5** is obtained in a very low yield. Compound **6**, which contains the P_2 unit, will be described in some detail in Section II.3 whereas compounds **7** and **8**, having single P atoms, are postponed until Section II.4. It is worth noting at this point, however, that **5–8** form a group of related compounds, containing a tetrahedral array of Co and naked P atoms, which may be considered to originate from that of the P_4 molecule through stepwise replacement of its P atoms by the isolobal $Co(CO)_3$ units (Scheme 5).[17] Compounds **5–7**, with the general formula $[\{Co(CO)_3\}_nP_{4-n}]$ (n = 1, 2 or 3), may undergo rearrangements to each other in the presence of suitable reagents.[18]

Up to now the largest class of mononuclear metal compounds containing the cyclotriphosphorus unit corresponds to the formula $[(triphos)M(\eta^3\text{-}P_3)]^{n+}$ [M = Co,[19] Rh[20] or Ir;[20] n = 0: M = Ni,[21,22] Pd[13] or Pt;[13] n = 1: triphos = 1,1,1-tris(diphenylphosphinomethyl)ethane]. The first derivative of this series, $[(triphos)Co(\eta^3\text{-}P_3)]$ (**9**), was obtained by reacting hydrated Co(II) salts of poorly coordinating anions with white phosphorus in the presence of triphos at *ca* 40°C (Scheme 6).[19] Orange crystals of the product separate after the addition of ethanol. An excess of white phosphorus with respect to cobalt is a crucial factor for obtaining **9**; by reacting the cobalt salts and triphos with a lower amount of phosphorus ($Co:P_4$ = 2:1) the dinuclear triple decker sandwich complex

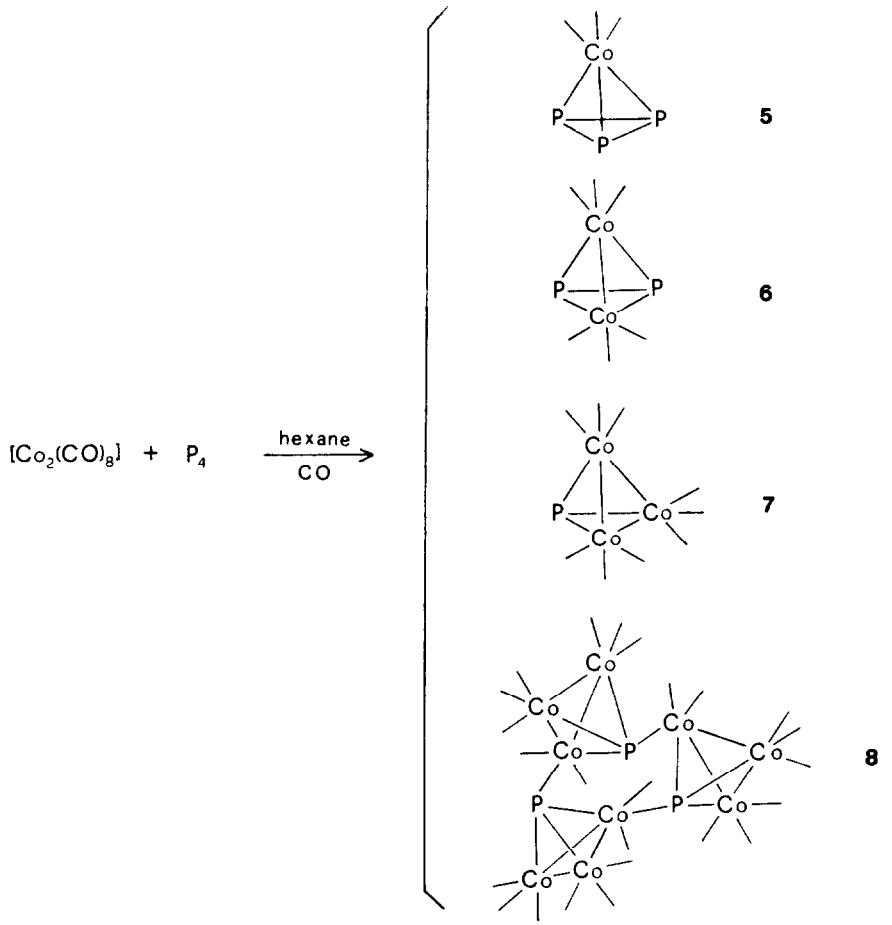

Scheme 5.

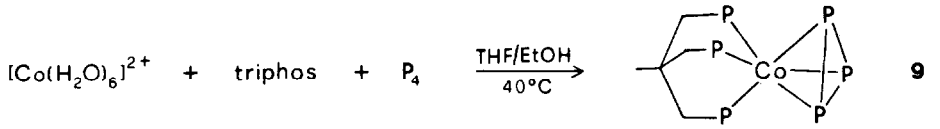

Scheme 6.

[(triphos)Co(μ,η^3-P_3)Co(triphos)](BF_4)$_2$ is obtained [see Section II.2(ii)].[23] The structure of **9**, which is typical of the complexes of this class, is shown in Fig. 3. The metal atom is coordinated by the three P atoms of the triphos ligand and by those of the *cyclo*-P_3 group, the two sets of donor atoms being nearly staggered. A strictly similar coordination geometry exists in [(np_3)Co(η^3-P_3)] (**10**) where the nitrogen atom of the tripod ligand is uncoordinated.[24] Simple electron counting shows that removal of the nitrogen lone pair from the coordination sphere of the metal atom allows this to achieve the 18-electron configuration.

The rhodium (**11**), and iridium (**12**), analogues of [(triphos)Co(η^3-P_3)] were obtained by allowing the complexes [RhCl(C_2H_4)$_2$]$_2$ and [IrCl(CO)(PPh_3)$_2$], respectively, to react with P_4 in the presence of triphos.[20] These compounds are isomorphous with each other as well as with the cobalt complex **9**.[19] The [$MCl_2(PBu_3)$]$_2$ complexes (M = Pd or Pt) in the presence of triphos and P_4 yield the cationic complexes of *cyclo*-P_3, [(triphos)Pd(η^3-P_3)]$^+$ (**13**) and [(triphos)Pt(η^3-P_3)]$^+$ (**14**), which were isolated as the BF_4^- salts.[13] The corresponding nickel derivative [(triphos)Ni(η^3-P_3)]BF_4 (**15**) was synthesized by a different procedure,[21] i.e. cleavage of the P_4S_3 cage molecule by the Ni(II) ion in the presence of triphos (Scheme 7). The structures of both the BF_4^- and the I_3^- salts of the

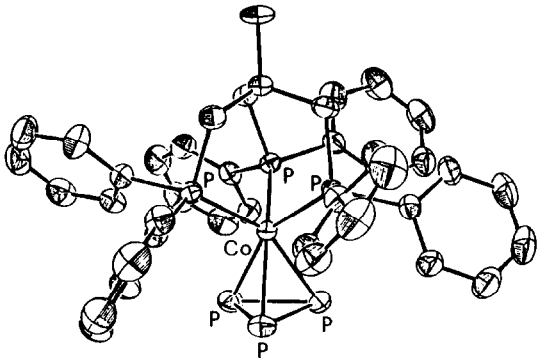

Fig. 3. View of the complex molecule [(triphos)Co(η^3-P_3)].

$$[Ni(H_2O)_6]^{2+} + \text{triphos} + P_4S_3 \xrightarrow[\text{reflux}]{THF/C_6H_6} \quad \mathbf{15}$$

Scheme 7.

nickel complex, which are mutually isomorphous, have been determined.[21,22] Although the coordination geometry of the cationic complexes is closely similar to that of the neutral compounds of the cobalt group there are significant differences between their M—P and P—P bond distances. In particular, the M—P(triphos) distances are consistently longer in the cationic complexes than in the neutral ones.[21] It should be noted in passing that formation of the mononuclear *cyclo*-P_3 derivatives with phosphine ligands by the procedures exploited up to now has invariably involved reduction of the metal atom relative to its oxidation state in the parent compound. The mononuclear cyclotriphosphorus derivatives may be considered, on the other hand, to originate from the tetrahedral P_4 molecule by replacement of one of its P atoms by an LM (M = Co, Rh or Ir; L = triphos or np_3) or LM^+ (M = Ni, Pd or Pt; L = triphos) moiety. Such substituent groups, as well as the $Co(CO)_3$ unit of Scheme 5, are three-electron donors according to Wade's rules:[25] in this sense they are equivalent to the P atom they are considered to replace in the P_4 cage. Such considerations provide the simplest bonding approach to the mononuclear *cyclo*-P_3 derivatives. Substantial interaction occurs between the orbitals of the LM fragment and properly oriented orbitals of the η^3-P_3 ligand.[3]

Taking into account the isolobal relationship between organometallic fragments[26] it is not surprising that the $CpMo(CO)_2$ (Cp = η^5-cyclopentadienyl) and $Cp^*Mo(CO)_2$ (Cp^* = η^5-pentamethylcyclopentadienyl) fragments, that have similar frontier orbitals to those of CoL_3, stabilize compounds containing the *cyclo*-P_3 unit. Scherer *et al.*[27] have reported that the P_4 molecule undergoes cleavage in the presence of the reactive molybdenum dimer complex $[CpMo(CO)_2]_2$ in boiling toluene, yielding different compounds (Scheme 8) which have been separated by column chromatography on florisil with a toluene–pentane mixture as eluant. The presence of the cyclotriphosphorus unit η^3-bound to the $CpMo(CO)_2$ fragment, compound **16**, has been ascertained on the basis of NMR data[27] and by an X-ray diffraction study.[28] The structure has shown that the Mo atom and those of the *cyclo*-P_3 unit form a trigonal pyramid. The P_3 ligand has the shape of a nearly equilateral triangle with mean P—P bond lengths in good agreement with those existing in the compounds [(triphos)M(η^3-P_3)] (M = Co, Rh or Ir)[19,20] and [(np_3)Co(η^3-P_3)].[24] Compound **17**, containing the bridging P_2 unit, is considered in Section II.3. The pentamethylcyclopentadienyl dicarbonyl molybdenum dimer, $[Cp^*Mo(CO)_2]_2$, reacts with P_4 in high boiling solvents[29] yielding a mixture of compounds (Scheme 9) which have been separated by chromatography on florisil. **18** contains the cyclotriphosphorus unit η^3-bound to one $Cp^*Mo(CO)_2$ fragment as indicated by NMR data. As in the case of the Cp analogue[27,28] no restriction to rotation of the P_3 unit has been observed even at *ca* −80 °C. Compound **18** can also be prepared from $[Cp^*Mo(CO)_2]_2$ and

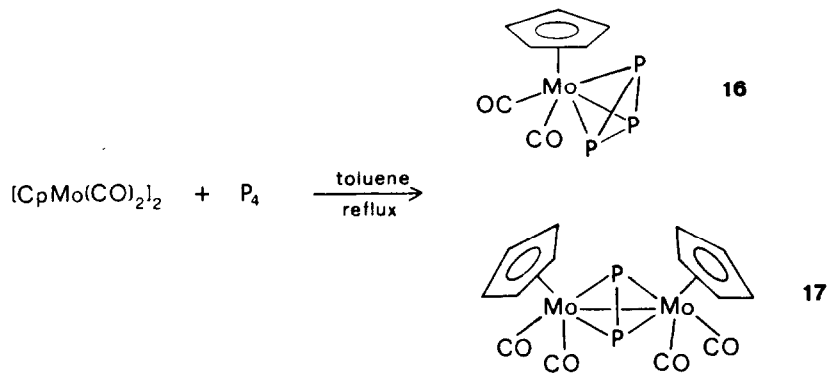

Scheme 8.

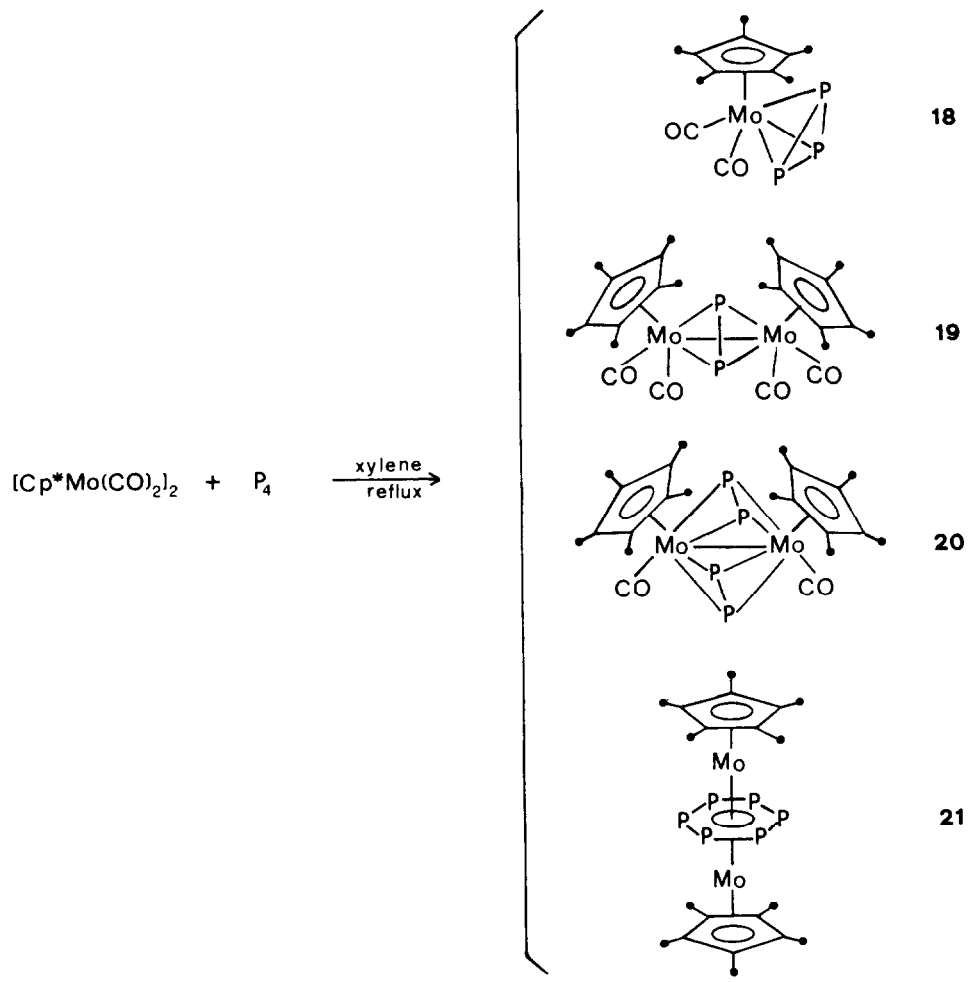

Scheme 9.

P_4S_3.[30] Compounds **19–21**, which contain P_2 or P_6 ligands, will be described in Sections II.3 and II.5, respectively. Compounds **16–19** present tetrahedral cores of molybdenum–ligand units and of naked P atoms corresponding to two members of the mixed tetrahedrane cluster family with the general formula $[(MoL)_nP_{4-n}]$ [$n = 1$, 2 or 3; MoL = $CpMo(CO)_2$ or $Cp^*Mo(CO)_2$] which parallels that already described for the cobalt derivatives (Scheme 5) of formula $[\{Co(CO)_3\}_nP_{4-n}]$ ($n = 1, 2$ or 3).

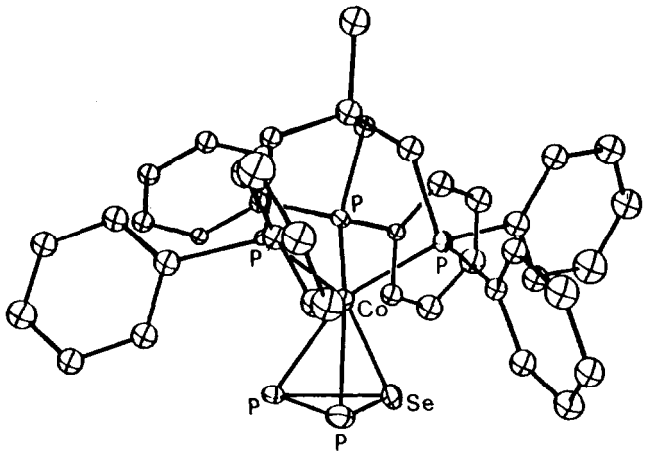

Fig. 4. View of the $[(triphos)Co(\eta^3\text{-}P_2Se)]^+$ cation.

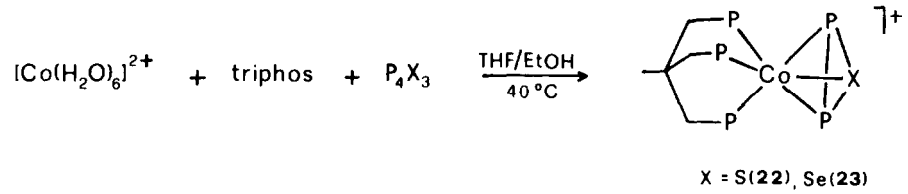

Scheme 10.

The inorganic heterocycles thiadiphosphirene, P_2S, and selenadiphosphirene, P_2Se, are closely related to the cyclotriphosphorus unit from which they may be considered to originate by replacing one P atom with a chalcogen (S or Se) atom. Such fragments are stabilized by the cobalt–triphos moiety. The reaction of Co(II) tetrafluoroborate in the presence of the tripod ligand triphos with the appropriate tetraphosphorus trichalcogenide, P_4S_3 or P_4Se_3, affords the compounds $[(triphos)Co(\eta^3\text{-}P_2S)]BF_4$ (**22**) and $[(triphos)Co(\eta^3\text{-}P_2Se)]BF_4$ (**23**), which are air-stable in the solid state (Scheme 10).[31,32] The reaction leading to compounds **22** and **23** provides an interesting example of cleavage of the tetraphosphorus trichalcogenide molecules P_4X_3 (X = S or Se) by the cobalt–triphos system. A different cleavage of the same cage molecules, yielding cyclotriphosphorus derivatives, Scheme 7, occurs with the nickel–triphos system.[21] Such reactions provide examples of selective activation of cage molecules controlled by transition-metal–ligand systems.

The crystal structures of the isomorphous compounds **22** and **23** consist of $[(triphos)Co(\eta^3\text{-}P_2X)]^+$ cations (X = S or Se) and BF_4^- anions, as well as of interposed benzene solvate molecules. A perspective view of the $[(triphos)Co(\eta^3\text{-}P_2Se)]^+$ cation is shown in Fig. 4.[32] The metal atom is in a six-coordinate environment formed by the triphos P atoms and by the atoms of the heterocyclic P_2X unit in a staggered arrangement similar to that found for the simple-sandwich complexes formed by the cyclotriphosphorus homocyclic ring.[3] The P_2S and P_2Se triangular units in the two compounds are disordered about the pseudo-three-fold axis of each cation so that the chalcogen atom (S or Se) is distributed over the three vertexes of the triangle.[32] The mean of the interatomic distances in the P_2S ring is slightly shorter than the value found for the *cyclo*-P_3 unit in the neutral $[(triphos)Co(\eta^3\text{-}P_3)]$[19] compound and is close to that existing in the $[(triphos)Ni(\eta^3\text{-}P_3)]^+$ cation.[21,22] Both the distances within the P_2Se group and those from this group to the metal atom are considerably affected by the presence of the large Se atom in the heterocyclic ring.

The above compounds containing the P_3 and P_2X (X = S or Se) triatomic units form a large series of isostructural and isoelectronic compounds whose ^{31}P NMR data have been considered.[21,32] This has allowed the detecting of some trends in the NMR parameters (chemical shifts and coupling constants) of the P atoms belonging both to the polyphosphine ligand and to the triatomic unit. The P(triphos) chemical shifts for the compounds $[(triphos)M(\eta^3\text{-}P_3)]$ (M = Co, Rh or Ir) and

[(triphos)M(η^3-P_3)]BF_4 (M = Ni, Pd or Pt) decrease rather smoothly and with similar trends on descending each metal atom group.[21] Such trends are consistent with that reported for phosphine complexes formed by metal atoms of different transition rows, having the same coordination number, molecular geometry, phosphine ligand and oxidation state of the metal atom. The P(triphos) chemical shift is essentially unchanged on replacing the P_3 with the heteroatomic P_2X (X = S or Se) units in the cobalt derivatives [(triphos)Co(η^3-P_2X)]BF_4.[32] The P(η^3-P_3) chemical-shift values, on the other hand, do not vary smoothly on changing the metal atom within each group of compounds although they exhibit similar trends for the neutral compounds [(triphos)M(η^3-P_3)] (M = Co, Rh or Ir) and the cationic complexes [(triphos)M(η^3-P_3)]BF_4(M = Ni, Pd or Pt). Remarkably, the ^1J[M–P(η^3-P_3)] coupling constants for M = Rh or Pt{^1J[Rh – P(η^3-P_3)] = 13 Hz and ^1J[Pt–P(η^3-P_3)] = 171 Hz} are smaller, by more than one order of magnitude, than the ^{1}J[M–P(triphos)] ones, which in turn are in the usual range for the phosphine complexes of such metals. The relative positions of the P_2X (X = S or Se) ^{31}P signals in the [(triphos)Co(η^3-P_2X)]BF_4 compounds, the P_2Se signal occurring at lower field than the P_2S one, exhibit decreasing $\delta(^{31}P)$ values with increasing size of the heteroatom.

II.2(ii) *Triple decker sandwich complexes.* The cyclotriphosphorus and the isoelectronic thiadiphosphirene and selenadiphosphirene units may also act as bridging units between two metal atoms, yielding a large class of triple-decker complexes[3] that have been well characterized by Sacconi and coworkers. Dinuclear-sandwich complexes having the cyclotriphosphorus unit as the internal slice have been obtained up to now by the following procedures:[33–37]

(a) By allowing stoichiometric amounts of white phosphorus, hydrated metal salt and phosphane ligand to react in solution. THF solutions of P_4 and of the ligand have generally been used, whereas the hydrated metal salt was dissolved in ethanol. Scheme 11 summarizes the synthesis of [(triphos)Co(μ,η^3-P_3)Co(triphos)]$(BF_4)_2$.[23] By this procedure only symmetric-sandwich compounds are obtained.

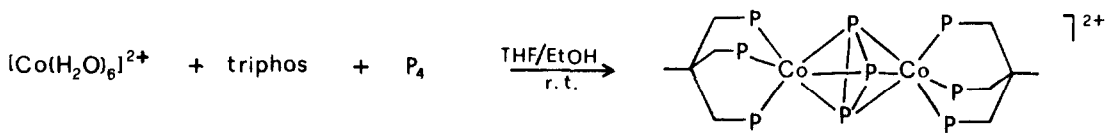

Scheme 11.

(b) By allowing a mononuclear complex [(triphos)M(η^3-P_3)]$^{n+}$ (M = Co, Rh or Ir; n = 0: M = Ni, Pd or Pt; n = 1) or [(triphos)Co(η^3-P_2X)]$^+$ (X = S or Se), to react with a hydrated metal salt or a metal complex in solution, in the presence of the appropriate tripod ligand. The synthesis of [(triphos)Co(μ, η^3-P_2S)Co(triphos)]$(BF_4)_2$ by this procedure[36] is reported in Scheme 12. All reactants were generally dissolved in CH_2Cl_2 or Me_2CO, except for the hydrated metal salts, which were dissolved in ethanol. In this way both symmetric and asymmetric complexes are obtained. In the latter, the metal atoms and/or the external ligands may be different.

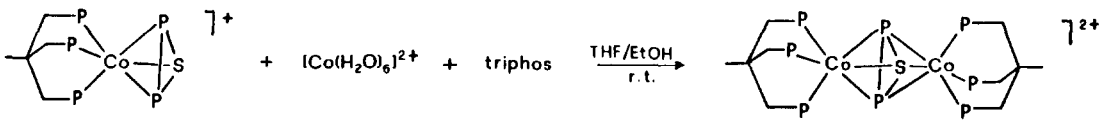

Scheme 12.

(c) By reducing the dinuclear *cyclo*-P_3 complexes obtained by the procedures described in (a) or (b) with $NaBH_4$ in acetone–ethanol. The [(triphos)Co(μ, η^3-P_3)Co(triphos)]$^+$ monocation has been obtained in this way (Scheme 13).[23] It has been recently reported that the *cyclo*-P_3 unit may be also generated by cleavage of the cage silylphosphane $P_7(SiMe_3)_3$ and trapped in the [(triphos)M(μ,η^3-P_3)M(triphos)]$^{2+}$ cations (M = Co or Ni).[38]

All triple-decker complexes of this type, which are listed in Table 2, are stable in the solid state. They are also rather stable in solution, except for the unsymmetrical compounds formed by two metal atoms of different transition-metal series, which decompose rather quickly. In all of these

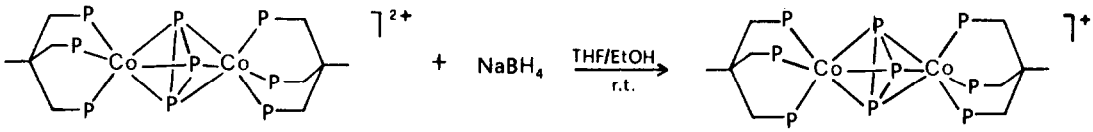

Scheme 13.

Table 2. Triple decker sandwich complexes containing the triphosphirene and thiadiphosphirene cyclic units as internal ligands

Compound	Synthesis[a]	VEN[b]	μ_{eff}[c]	Reference
[(triphos)Co(μ, η^3-P_3)Fe(etriphos)][PF_6]$_2$	a	30	Diam.	33
[(triphos)Co(μ, η^3-P_3)Co(triphos)][Y]$_2$[d]	a, b	31	2.20	23
[(triphos)Co(μ, η^3-P_3)Rh(triphos)][Y]$_2$[d]	b	31	2.20	34, 35
[(triphos)Co(μ, η^3-P_3)Ir(triphos)][BF_4]$_2$	b	31	1.95	34, 35
[(triphos)Co(μ, η^3-P_3)Co(etriphos)][BPh_4]$_2$	b	31	2.29	33
[(triphos)Co(μ, η^3-P_3)Co(triphos)]BPh_4	c	32	3.13	23
[(triphos)Co(μ, η^3-P_3)Ni(triphos)][BPh_4]$_2$	b	32	3.14	23
[(triphos)Rh(μ, η^3-P_3)Rh(triphos)][BPh_4]$_2$	b	32	Diam.	34, 35
[(triphos)Ni(μ, η^3-P_3)Rh(triphos)][Y]$_2$[d]	b	32	1.64	34, 35
[(triphos)Co(μ, η^3-P_3)Ni(etriphos)][BPh_4]$_2$	b	32	3.12	33
[(triphos)Co(μ, η^3-P_2S)Co(triphos)][BF_4]$_2$	b	32	1.35	36
[(triphos)Co(μ, η^3-P_2S)Rh(triphos)][BF_4]$_2$	b	32	1.50	36
[(triphos)Rh(μ, η^3-P_2S)Rh(triphos)][BPh_4]$_2$	b	32	1.42	36
[(triphos)Ni(μ, η^3-P_3)Ni(triphos)][Y]$_2$[d]	a, b	33	2.09	23
[(triphos)Ni(μ, η^3-P_3)Ni(triphos)]BPh_4	c	34	Diam.	23
[(triphos)Ni(μ, η^3-P_3)Pd(triphos)]BF_4	b	34	Diam.	37
[(triphos)Pd(μ, η^3-P_3)Pd(triphos)BPh_4	a	34	Diam.	13
[(np_3)Pd(μ, η^3-P_3)Pd(np_3)]BF_4	a	34	Diam.	13

[a]The key for a, b and c is reported in the text.
[b]VEN = valence electron number.
[c]Room temperature.
[d]Y = BPh_4 or BF_4.

triple-decker derivatives the external layers are formed by the triphos, etriphos [etriphos = 1, 1, 1-tris(diethylphosphinomethyl)ethane] or np_3 ligands, whereas the internal slice is formed by the *cyclo*-P_3 or *cyclo*-P_2X (X = S or Se) group. Each metal atom is bonded to the three P atoms of one external ligand and to the three atoms of the bridging η^3-P_3 or η^3-P_2X ring in a six-coordinate arrangement. A typical example is provided by the structure of the dication in the compound [(triphos)Pd(μ, η^3-P_3)Pd(triphos)]BPh_4, shown in Fig. 5.[13] A simplified approach to the bonding, magnetic properties, and redox behaviour of the complexes here described has already been reported.[3] The triple-decker dications [(triphos)M(μ, η^3-P_2S)M′(triphos)]$^{2+}$ (M = M′ = Co, or Rh; M = Co, M′ = Rh) recently reported,[36] which contain the heteroatomic P_2S ring, undergo autoreduction and exhibit transferability of the triatomic unit between metal–ligand moieties. Such features, which have never been observed for cyclotriphosphorus derivatives, suggest that cleavage of bonds between the metal and ring atoms is easier when the ring is heteroatomic.

II.3. *Compounds containing the diphosphorus unit*

The compounds containing the unsubstituted diphosphorus unit so far reported are relatively few compared with the *cyclo*-P_3 derivatives. The first compound containing the diphosphorus ligand, having the formula [{$Co(CO)_3$}$_2$(μ, η^2-P_2)] (**6**) was isolated by Markò and coworkers in 1973 as a red oil.[39] It was obtained by reacting Na[$Co(CO)_4$] with PCl_3 or PBr_3 in THF solution at room temperature (Scheme 14). The compound was assigned a structure with a tetrahedral Co_2P_2 core in which two vertexes are occupied by the P_2 unit and the other two by the $Co(CO)_3$ fragments. Such a Co_2P_2 core was proposed by comparing the IR spectrum of the compound with

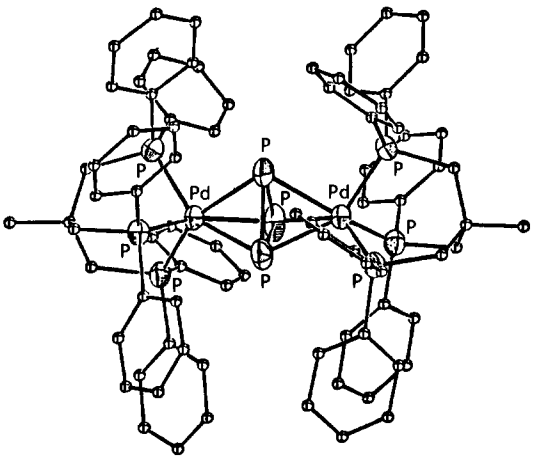

Fig. 5. View of the [(triphos)Pd(μ, η^3-P_3)Pd(triphos)]$^+$ cation.

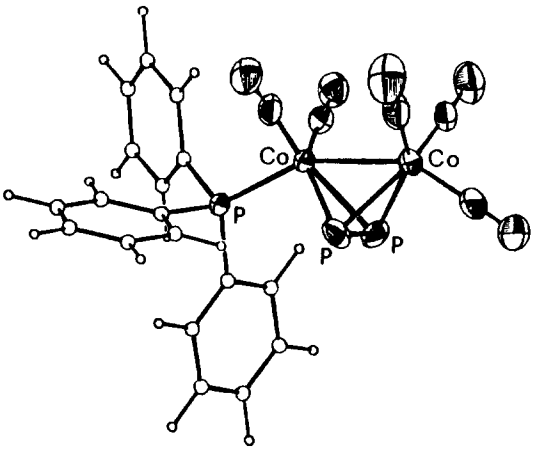

Fig. 6. View of the [{$Co_2(CO)_5PPh_3$}(μ,η^2-P_2)] molecule.

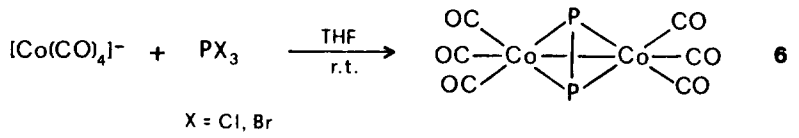

Scheme 14.

those of the related arsenic, [{$Co(CO)_3$}$_2$(μ,η^2-As_2)],[40] and alkyne, [{$Co(CO)_3$}$_2${μ,η^2-$(CR)_2$}],[41] derivatives. The geometry of the former was in turn suggested by consideration of the structure of the compound [{$Co(CO)_2(PPh_3)$}$_2$(μ,η^2-As_2)] which had been isolated from the carbonyl derivative in the presence of a large excess of triphenylphosphine.[42] The substitution of a CO by a PPh_3 group on each cobalt atom in [{$Co(CO)_3$}$_2$(μ,η^2-As_2)] actually yields a compound retaining the Co_2As_2 tetrahedral core. By carrying out a similar substitution reaction on **6** a crystalline compound of formula [{$Co_2(CO)_5(PPh_3)$}(μ,η^2-P_2)] (**24**) was obtained.[43] The X-ray analysis of **24** (Fig. 6) has shown that the skeleton of the molecule is a completely bonded Co_2P_2 fragment. The six coordination about each Co atom can be viewed as octahedral-like with a bent Co—Co bond. The Co_2P_2 tetrahedral fragment is slightly distorted due to translation of the P_2 unit toward the triphenylphosphine-substituted Co atom.

Scherer and coworkers have recently isolated from the reaction of white phosphorus with [$CpMo(CO)_2$]$_2$[27] and [$Cp^*Mo(CO)_2$]$_2$[29] three compounds, containing diphosphorus units, with

the formulae $[\{CpMo(CO)_2\}_2(\mu,\eta^2\text{-}P_2)]$ (**17**), $[\{Cp^*Mo(CO)_2\}_2(\mu,\eta^2\text{-}P_2)]$ (**19**) and $[Cp^*Mo(CO)(\mu,\eta^2\text{-}P_2)]_2$ (**20**). The reactions leading to these derivatives are reported in Schemes 8 and 9. Compound **19** has also been obtained by cleavage of the P_4S_3 cage molecule in the presence of $[Cp^*Mo(CO)_2]_2$.[30] On the other hand **17** has also been synthesized by reacting $[CpMoX(CO)_3]$ (X = Cl or Br) with the silylphosphines $P(SiMe_3)_3$, $PH(SiMe_3)_2$ and $PH_2(SiMe_3)$.[44] The crystal structure of **17** has been determined.[27] The molecule contains a pseudotetrahedral Mo_2P_2 core and each metal atom bears a cyclopentadienyl group and two CO groups as coligands; the $CpMo(CO)_2$ moieties are in a *trans* arrangement with respect to the metal–metal edge. The pentamethyl derivative (**19**) has been assigned the same structure as **17** on the basis of NMR and IR measurements.[29] As shown in Scheme 9, from the reaction of $[Cp^*Mo(CO)_2]_2$ and P_4 a second derivative containing the P_2 ligand is also obtained, i.e. $[Cp^*Mo(CO)(\mu,\eta^2\text{-}P_2)]_2$ (**20**). Mass and NMR data suggest a structure consisting of two Mo_2P_2 tetrahedra with a common Mo–Mo edge and a *cis* arrangement of the Cp* and CO ligands.[29]

Two more reports on compounds containing the diphosphorus unit have recently appeared. The first one is from Chisholm and coworkers.[45] The reaction of Markò's compound (**6**) with $[W_2(OPr^i)_6(py)_2]$ yields the compound $[W_2(OPr^i)_6(py)(\mu,\eta^2\text{-}P_2)]$ (**25**) (Scheme 15). Its crystal structure shows a pseudo-tetrahedral W_2P_2 unit with an alkoxide group bridging the two

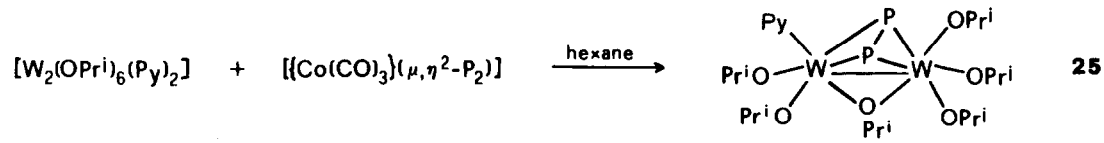

25

Scheme 15.

metals.[45] The substitution of the $Co(CO)_3$ fragment in the parent compound with the d^3 isolobal $W(OR)_3$ and $W(OR)_3(py)$ fragments[45] allows one to state, from a different point of view, that the diphosphorus unit may be transferred between metal moieties. It should also be mentioned at this point that the homometallic triple-decker compound $[(triphos)Rh(\mu,\eta^3\text{-}P_2S)Rh(triphos)][BPh_4]_2$ (**26**)[36] has been obtained by reacting the simple-sandwich complex (**22**) with a large excess of $[(triphos)Rh]^+$ generated *in situ* in the presence of $NaBPh_4$ (Scheme 16). Also this reaction proves that "naked" pnicogen units may be transferred between isolobal transition-metal fragments. Such interesting behaviour could open new routes to the synthesis of organometallic compounds containing small units of pnicogen atoms.

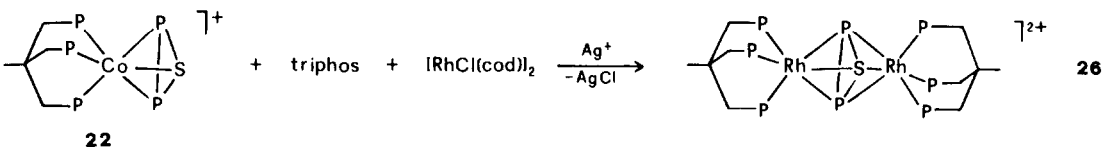

26

Scheme 16.

The second report, by Schäfer *et al.*, deals with the reaction of silylphosphines with Ni(II) complexes containing a bidentate phosphine ligand (Scheme 17).[46] Such reactions surprisingly yield diphosphorus derivatives of formula $[\{NiL\}_2(\mu,\eta^2\text{-}P_2)]$ [where L = bis(diethylphosphino)ethane (**27**), bis(dicyclohexylphosphino)ethane (**28**) or bis(diphenylphosphino)ethane (**29**)]. The crystal structure of **27** (Fig. 7) shows that each Ni atom is surrounded by four P atoms in a nearly planar arrangement, with two P atoms provided by a diphosphine ligand and the other two by the bridging diphosphorus unit. The two coordination planes are nearly perpendicular. The P_2 unit in all of the compounds described so far acts as a four-electron donor. On the other hand Huttner and coworkers have obtained compounds in which such a ligand acts as an eight-electron donor.[47] The tetracarbonyl anion $[Co(CO)_4]^-$ reacts with organometallic compounds, which have halophosphines as coligands (Scheme 18), to yield compounds where P_2 is side-on bridging two $Co(CO)_3$ units and each phosphorus of the P_2 ligand is furthermore terminally bonded to one metal–ligand ML fragment [ML = $Cr(CO)_5$ (**30**), $W(CO)_5$ (**31**) or $CpMn(CO)_2$ (**32**)]. The crystal structure of the

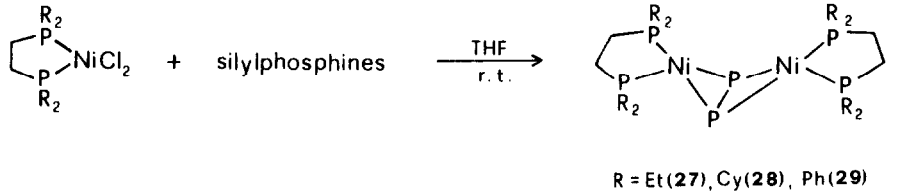

Scheme 17.

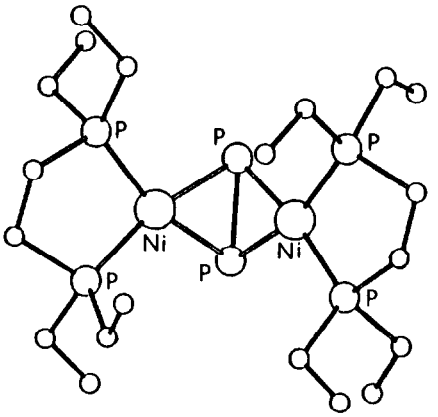

Fig. 7. Structure of $[\{(Et_2PCH_2CH_2PEt_2)Ni\}_2(\mu,\eta^2\text{-}P_2)]$.

compound $[\{[Co(CO)_3]_2(\mu, \eta^2\text{-}P_2)\}\{Cr(CO)_5\}_2]$ is reported in Fig. 8.[47] Selected structural data for compounds with the P_2 ligand and a tetrahedrane M_2P_2 core are listed in Table 3.

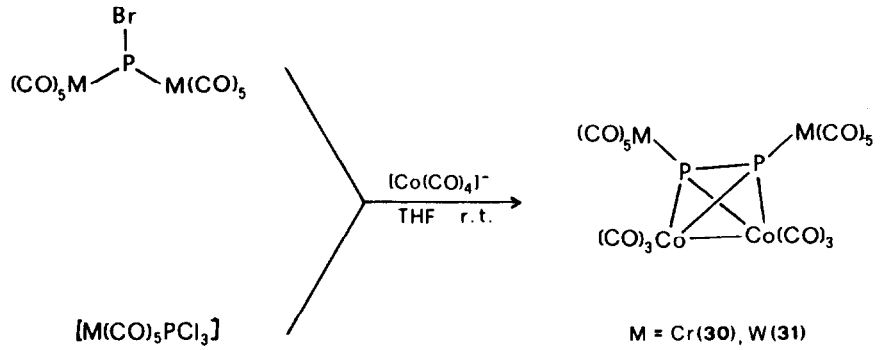

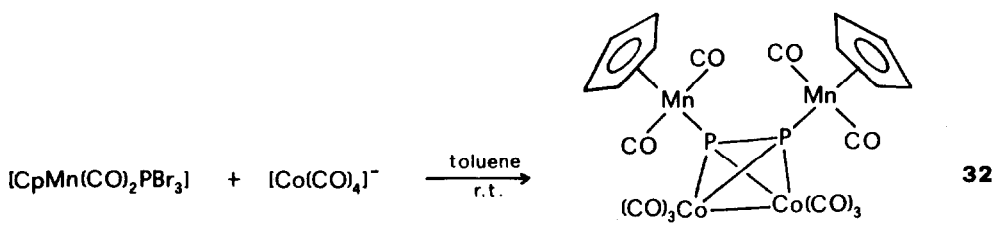

Scheme 18.

Compound **33**, which has been isolated from the reaction mixture of $[Cp^*Mo(CO)_2]_2$ with P_4S_3,[48] contains an S_2 ligand side-on bonded to two Cp*Mo fragments and a bent PSP group whose P atoms are linked to the molybdenum centres (Scheme 19). Compound **33** is transformed in the presence of $[Co_2(CO)_8]$, yielding **34** which contains the unprecedented PS ligand. The geometry of **34**, proposed on the basis of spectral data and the crystal structure of the analogous

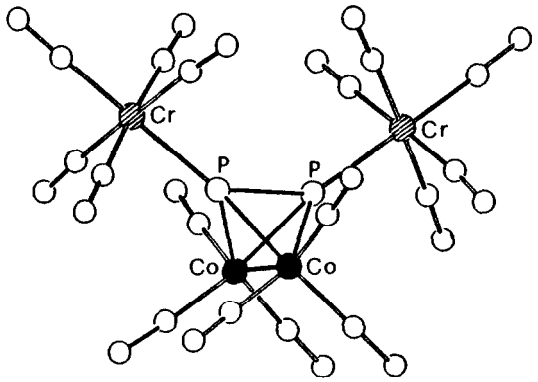

Fig. 8. Structure of the tetranuclear complex $[\{[Co(CO)_3]_2(\mu,\eta^2\text{-}P_2)\}\{Cr(CO)_5\}_2]$.

Table 3. Bond distances in the tetrahedrane clusters containing the P_2 unit[a]

Compound	P—P	P—M	M—M	Reference
24 $[\{Co_2(CO)_5(PPh_3)\}(\mu,\eta^2\text{-}P_2)]$	2.019(9)	2.264(5)	2.574(3)	43
30 $[\{[Co(CO)_3]_2(\mu,\eta^2\text{-}P_2)\}\{Cr(CO)_5\}_2]$[b]	2.060(5)	2.247(4)	2.565(3)	47
54 $[\{[Co(CO)_3]_2(\mu,\eta^2\text{-}P_2)\}\{Cr(CO)_5\}\{W(CO)_5\}]$[c]	2.061(3)	2.250(2)	2.573(1)	67
25 $[W_2(OPr^i)_6(py)(\mu,\eta^2\text{-}P_2)]$	2.154(4)	2.453(3)	2.695(1)	45
27 $[\{(Et_2PCH_2CH_2PEt_2)Ni\}_2(\mu,\eta^2\text{-}P_2)]$	2.121(6)	2.234(4)	2.908(3)	46
17 $[\{CpMo(CO)_2\}_2(\mu,\eta^2\text{-}P_2)]$	2.079(2)	2.507(1)	3.022(1)	27
52 $[\{[CpMo(CO)_2]_2(\mu,\eta^2\text{-}P_2)\}\{Re_2(CO)_6(\mu\text{-}Br)_2\}]$[d]	2.093(8)	2.467(4)	3.077(2)	66
53 $[\{[CpMo(CO)_2]_2(\mu,\eta^2\text{-}P_2)\}_2\{Re_2(CO)_6Br_2\}]$[e]	2.071(9)	2.487(7)	3.034(2)	66
55 $[\{Cp^*Mo(CO)(\mu,\eta^2\text{-}P_2)\}_2\{Cr(CO)_5\}_2]$[f]	2.067(5)	[g]	2.905(1)	5

[a]Averages over chemically equivalent bond distances (Å) are reported.
[b]P—Cr_{mean} = 2.278(4) Å.
[c]The mean P—M distance (M = Cr or W) is 2.361(2) Å. The Cr and W atoms were disordered, each with 50% occupancy of the metal sites.
[d]P—Re_{mean} = 2.490(4) Å.
[e]P—Re_{mean} = 2.483(7) Å.
[f]P—Cr distances not reported.
[g]Not reported.

arsenic derivative, presents a Mo_2Co triangle bridged by two μ_3-S atoms, with a PS ligand acting as a bridge between two Mo atoms.[48]

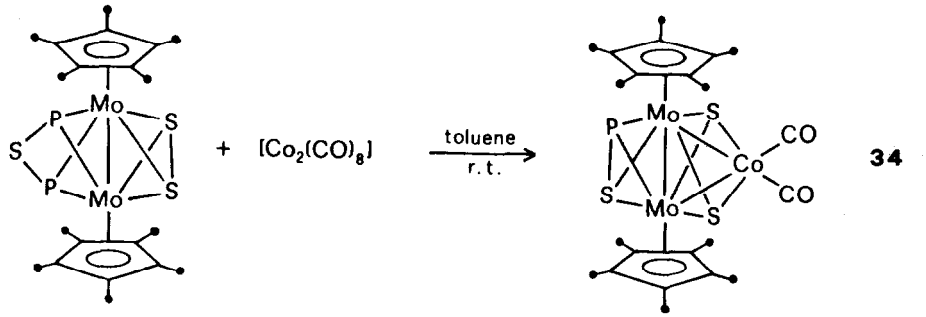

33 **34**

Scheme 19.

P_2 and PS ligands act as side-on bridging units in all of the complexes reported up to now, spanning two vertexes of tetrahedrane clusters in which the other two vertexes bear metal–ligand moieties. Such a core is opened toward a butterfly geometry only in the case of the nickel derivatives

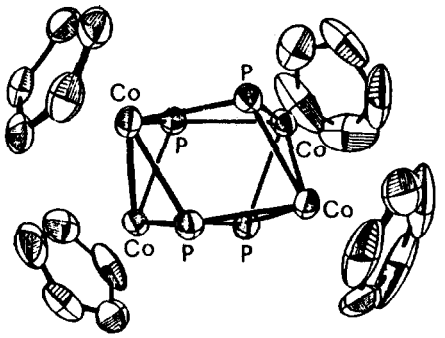

Fig. 9. View of the $[(CpCoP)_4]$ molecule.

27–29.[46] The synthesis of compounds of this type may be achieved by using an excess of the organometallic complex as the source of a metal fragment and various phosphorus derivatives as the parent compounds of the P_2 unit. Despite the apparent unpredictability in the synthesis of the present compounds two general routes may be singled out: (a) reaction of dimetallic derivatives, that easily originate mononuclear metal–ligand fragments isoelectronic to phosphorus, with labile small cluster molecules such as P_4 and P_4S_3; and (b) reaction of metal–ligand or phosphido anions, such as $[Co(CO)_4]^-$ or $[P(SiMe_3)_2]^-$, with halophosphine or phosphine halide complexes such as $[Cr(CO)_5PCl_3]$, $[NiCl_2(dppe)]$ [dppe = bis(diphenylphosphino)ethane] and so on. Procedures of type (b) yield diphosphorus derivatives from compounds containing single phosphorus atoms.

II.4. *Compounds containing single phosphorus atoms*

Transition-metal compounds which contain single P atoms are relatively few. In such derivatives the P atom acts as a bridging ligand between three or more metal–ligand fragments. It may be involved in a pseudo-tetrahedral, planar or spirane-like arrangement.

$$[CpCo(CO)_2] + P_4 \xrightarrow[\text{reflux}]{\text{toluene}} [(CpCoP)_4] \quad \mathbf{35}$$

Scheme 20.

The first compound that was reported to contain single naked P atoms belongs to the class of compounds having the pnicogen atom in a tetrahedral array as a μ_3-ligand. $[(CpCoP)_4]$ (**35**) was obtained in low yield by Simon and Dahl[49] by reacting $[CpCo(CO)_2]$ with the stoichiometric amount of white phosphorus in toluene under an inert atmosphere (Scheme 20). Compound **35** has been characterized by IR and mass spectrometry, and by X-ray diffraction analysis. The molecule has a cubane-like architecture (Fig. 9). Each cobalt atom is surrounded by one cyclopentadienyl ligand, three P atoms, and one Co atom, so that it achieves the closed-shell electronic configuration. The Co_4P_4 core is significantly deformed from the idealized cubic geometry that occurs in other cubane-like structures such as those of compounds with the M_4S_4 core.

The monophosphido compound $[\{Co(CO)_3\}_3(\mu_3\text{-P})]$ (**7**) is one of the products isolated from the reaction of cobalt carbonyl and white phosphorus (Scheme 5);[15] it has also been obtained from phosphorus trihalides and $[Co(CO)_4]^-$ salts.[15] Compound **7** is the most reactive of all the members of the mixed-cluster family $[\{Co(CO)_3\}_nP_{4-n}]$ ($n = 1, 2$ or 3). It has been characterized by comparing its IR spectrum with that of the analogous arsenic derivative $[\{Co(CO)_3\}_3(\mu_3\text{-As})]$.[50] Compound **7** has a great tendency to undergo cyclotrimerization with the loss of carbon monoxide to yield **8** (Scheme 21).[15] IR studies in hexane solution have shown that the lifetime of **7** is restricted to a few minutes.[15] The monomeric compound **7** has been stabilized by adding to its solutions suitable metal–ligand units like $Fe(CO)_4$ generated *in situ* from $[Fe_2(CO)_9]$ in THF that act as scavengers for **7**, to give **36**, before it undergoes cyclotrimerization (Scheme 22).[15,50]

Compounds of formula $[\{[Co(CO)_3]_3\}(\mu_4\text{-P})\{M(CO)_5\}]$ [M = Cr (**37**), Mo (**38**) or W (**39**)] have been unexpectedly obtained[18] by reacting **6** and **5**, which contain P_2 and P_3 units, respectively, with Group VI hexacarbonyls under UV radiation. Compounds **37–39** have the same structure as

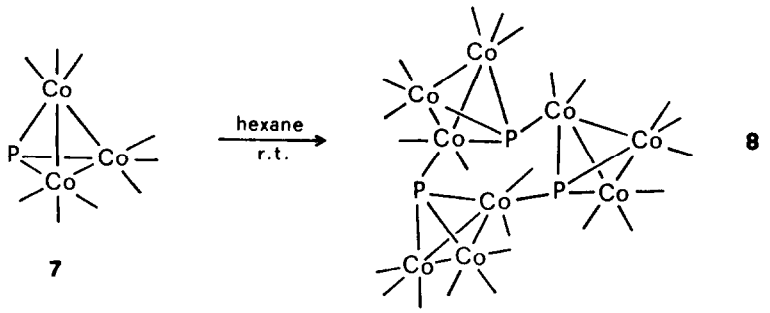

CO ligands omitted for clarity

Scheme 21.

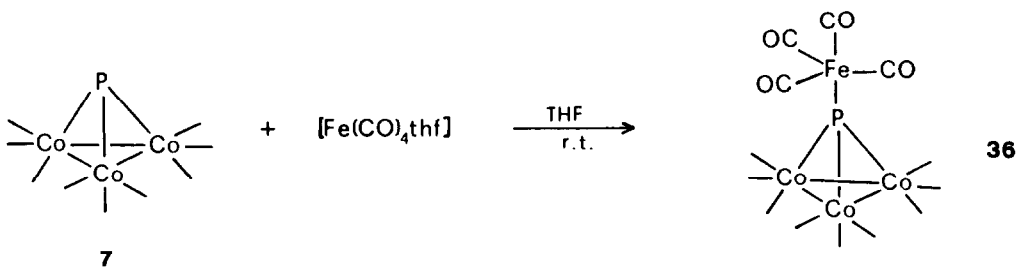

CO ligands omitted for clarity

Scheme 22.

the iron derivative **36** in Scheme 22, with the $M(CO)_5$ fragments replacing the $Fe(CO)_4$ unit. In the present synthesis the educt compounds **5** and **6**, which have pseudotetrahedral P_3M and P_2M_2 [$M = Co(CO)_3$] cores, undergo rearrangement, yielding products with a PM_3 core. A monophosphorus derivative having a PCo_3 core has been also obtained by reacting an oxidized P atom of PSX_3 (X = Cl or Br)[39] with $Na[Co(CO)_4]$ (Scheme 23). Such a reaction yields a

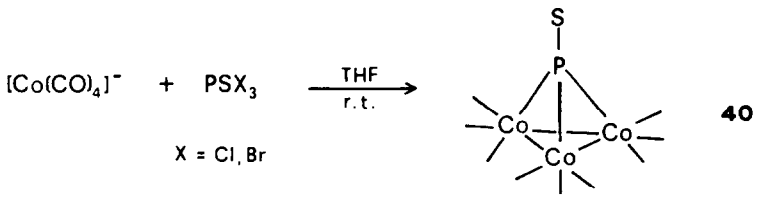

CO ligands omitted for clarity

Scheme 23.

thiophosphoryl complex (**40**) having a pseudotetrahedral core where each Co atom bears three carbonyl ligands and the P atom is also bound to an S atom. In terms of structure and bonding **7** is closely related to the phosphalkyne complexes $[\{Co_2(CO)_3\}_2(\mu,\eta^2\text{-PCR})]$ in which a CR unit (R = Me, Ph or $SiMe_3$) may be assumed to replace one of the isolobal $Co(CO)_3$ fragments in **7**. Such compounds have been recently considered by several workers[51–54] and have been prepared for example by reacting cobalt carbonyl with (ω,ω'-dihaloalkyl)-dihalophosphines (Scheme 24).[51]

Iridium trichloride reacts at 80°C with PF_3 at pressures of 80–200 atm to give orange crystals of the compound with formula $[\{Ir(PF_3)_3\}_3(\mu_3\text{-P})]$ (**41**) in very poor yield (Scheme 25).[55] Mass spectra suggest for **41** a tetrahedrane geometry with a PIr_3 core where each Ir atom is linked to

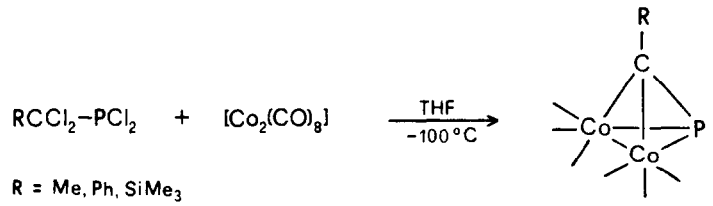

Scheme 24.

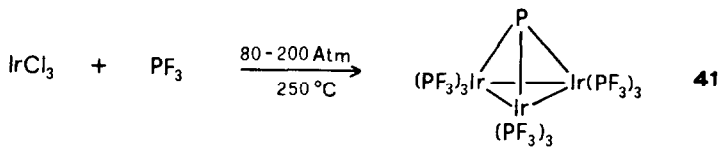

Scheme 25.

three trifluorophosphine ligands. In all complexes described above each isolated P atom always occupies a vertex of a tetrahedron and invariably acts as a μ_3- or μ_4-ligand. On the other hand, different coordination geometries are also possible for naked P atoms in transition-metal complexes and some of them have been recently achieved by Huttner and coworkers.

Compound **42** was isolated through reductive dehalogenation of $[CpMn(CO)_2PBr_3]$ with $[Fe_2(CO)_9]$ (Scheme 26).[56] The nature of **42** has been confirmed by chemical–physical measurements; the structure of the compound is shown in Fig. 10. It presents two trigonally coordinated P atoms, each linked to two iron tricarbonyl fragments and one $CpMn(CO)_2$ moiety. The short Mn—P bond distance is considered to be indicative of significant P(π)–metal $d(\pi)$ interaction.[56] The P atoms in **42** exhibit an unusual downfield shift in the ^{31}P NMR spectrum (see Section IV).

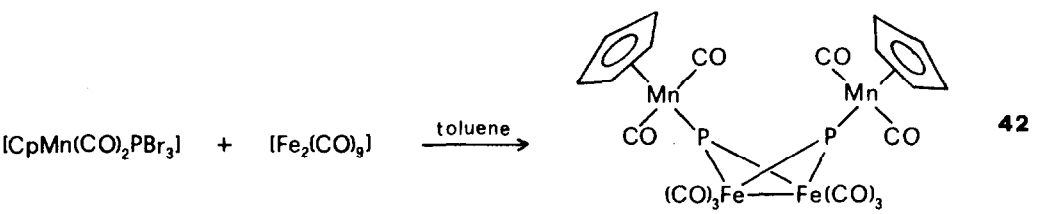

Scheme 26.

More recently a second example of a P atom bridging three metal atoms in a trigonal planar array has been reported.[57] Compound **43** was obtained by reacting the bromophosphinidene complex $[\{Cr(CO)_5\}_2PBr]$ with the strong nucleophile anion $[CpW(CO)_3]^-$ in dry THF (Scheme 27). The P atom forms a three-membered ring with the W and one Cr atom, while the second $Cr(CO)_5$ group is exocyclic. The short bond distance between the exocyclic Cr and the P atom suggests a P–Cr interaction analogous to that which is considered to exist in **42**. The P atom is in an approximately trigonal planar geometry.

The reaction of $[Fe_2(CO)_9]$ with PCl_3 leads to the crystalline compound **44** (Scheme 28).[58] Determination of its crystal structure (Fig. 11) has shown that a $Fe_2(CO)_8$ group is joined to a $Fe_2(CO)_6(\mu\text{-Cl})$ one by a P atom that is linked to all four transition-metal atoms, acting as a spiro centre. Compound **44** is the first, and up to now unique, compound in which a P atom acts as the joining centre between two cyclic fragments.

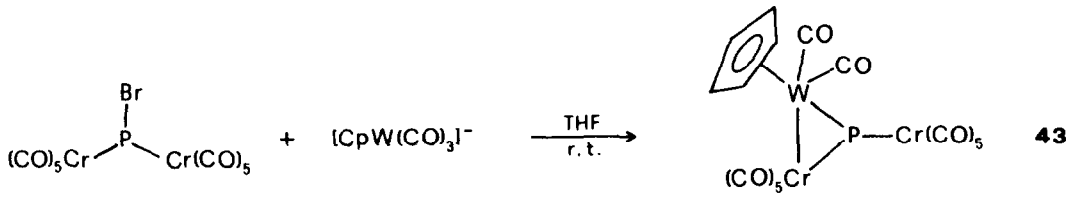

Scheme 27.

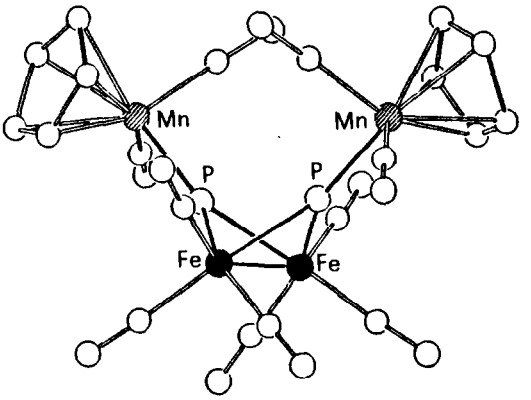

Fig. 10. Molecular structure of $[\{Fe_2(CO)_6\}(\mu_3\text{-}P)_2\{CpMn(CO)_2\}_2]$.

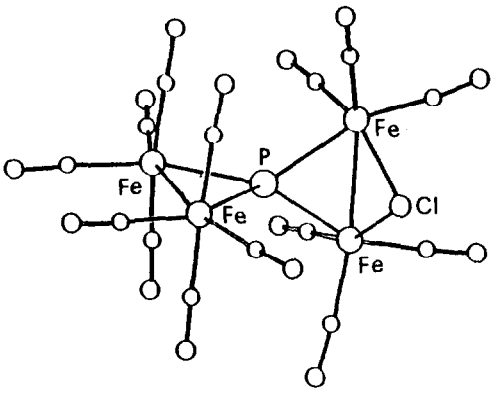

Fig. 11. View of the spirane-like molecule $[\{Fe_2(CO)_8\}\{Fe_2(CO)_6(\mu\text{-}Cl)\}(\mu_4\text{-}P)]$.

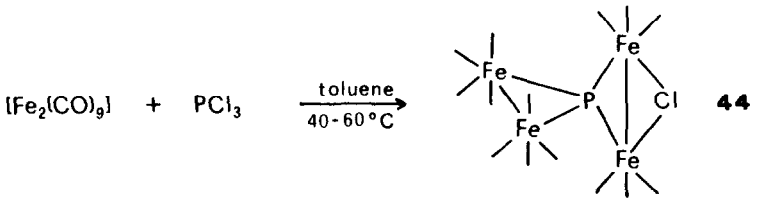

CO ligands omitted for clarity

Scheme 28.

In most of the compounds considered up to this point, containing the P_4, P_3 or P_2 units, or single naked P atoms, the pnicogen atoms occupy some of the vertexes of a polyhedron, the other vertexes being occupied by metal–ligand fragments. A few examples of different P atom environments

are provided by the compounds containing the intact P_4 molecule η^1-bound to the metal atom,[12,13] by the iron carbonyl derivative **44**[58] described above, and by complexes **42** and **43**, which contain a P atom in a trigonal planar environment.[56,57]

On the other hand, compounds have been reported in which one naked P atom is encapsulated in a interstitial or semi-interstitial position inside metal carbonyl clusters with which it shares all of its valence electrons. Vidal *et al.* have isolated compound **45**, with the formula $[NEt_3Bz]_2[Rh_9(CO)_{21}P]$,[59] by reacting $[Rh(acac)(CO)_2]$ with triphenylphosphine in a high boiling solvent under high pressures of H_2 and CO (Scheme 29). By carrying out the same reaction in the

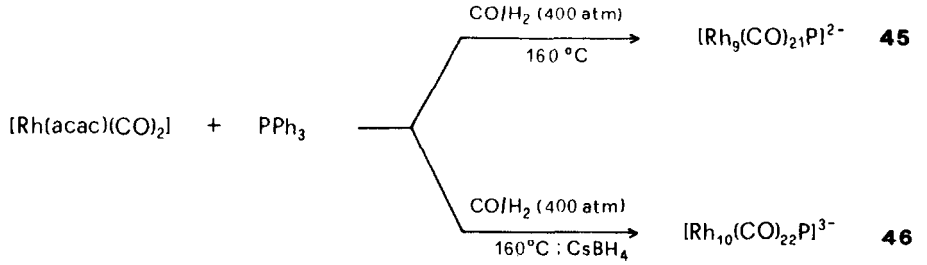

Scheme 29.

presence of a reducing agent such as $CsBH_4$, compound **46**, containing the cluster anion $[Rh_{10}(CO)_{22}P]^{3-}$, has been isolated.[60] The two compounds have been characterized by X-ray analyses and their structures are closely related. The $[Rh_9(CO)_{21}P]^{2-}$ anion (Fig. 12) consists of eight Rh atoms arranged at the corners of a cubic antiprism, with the ninth Rh atom capping one of the two square faces. The P atom is located inside the cavity of the cluster anion while the carbonyl ligands are bonded both terminally and in a bridging position. The carbonyl ligands show fluxionality in solution; the same behaviour is suggested for the rhodium skeleton according to the 10 line multiplet [δ = 283.2 ppm, J(Rh–P) = 38.5 Hz] exhibited by the ^{31}P NMR spectrum of the compound.[59] The structure of the cluster anion in **46** consists of a square antiprism capped by two Rh atoms sitting on the square faces, with a bare P atom located at the geometrical centre of the polyhedron. This anion also presents scrambling of both the carbonyl ligands and the rhodium skeleton, the latter process being evidenced by an odd-line pattern of 11 lines at 369.3 ppm.[60] The constancy of this pattern even at −45°C is indicative of the persistence of skeletal scrambling at low temperatures. Variable-temperature multinuclear NMR studies[61,62] on the above rhodium carbonyl cluster derivatives, **45** and **46**, have been carried out, and it has been found that the skeleton is static at the lowest temperatures attained. In both compounds the time-averaged value of J(Rh–P) is close to the weighted mean of the low-temperature Rh–P couplings. It seems probable

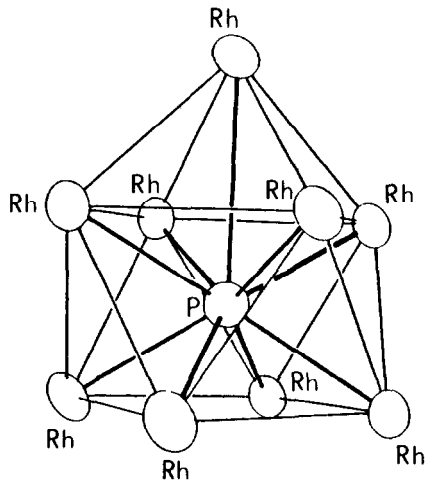

Fig. 12. Structure of the $[Rh_9(CO)_{21}P]^{2-}$ anion without the CO ligands.

that the migratory pathways of the metallic skeletons are similar to the rearrangements found for the boron polyhedra in boron hydrides.

The cobalt carbonyl salt $Na[Co(CO)_4]$ reacts with PCl_3 in THF, yielding the anion $[Co_6(CO)_{16}P]^-$ (**47**), which has been isolated as the potassium salt (Scheme 30).[63] Different salts of **47** have been obtained by metathesis in aqueous methanol; the tetraphenylphosphonium derivative has been investigated by X-ray diffraction analysis.[64] The anion **47** (Fig. 13) contains a six-metal atom array consisting of a chain of four edge-sharing triangles surrounding a semi-interstitial P atom. This phosphide ligand is probably in an intermediate condition between that of an external bridging P atom (sharing three electrons) and that of an interstitial atom (sharing five electrons). Such an array is rather uncommon and may be rationalized considering the dimensions of the Co and P atoms. The radius ratio r_P/r_{Co} is such that a P atom cannot occupy the cavity of an octahedron or of a regular trigonal prism formed by six Co atoms. The above Co_6 open array may be considered as a part of the surface of a larger polyhedron, namely an icosahedron.[64]

$$[Co(CO)_4]^- + PCl_3 \xrightarrow[KBr]{THF} K[Co_6(CO)_{16}P] \quad \mathbf{47}$$

Scheme 30.

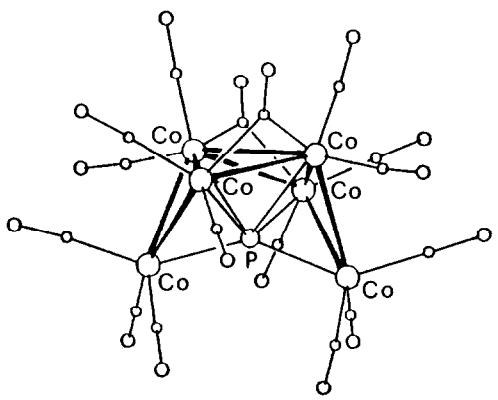

Fig. 13. View of the $[Co_6(CO)_{16}P]^-$ anion.

II.5. *Miscellaneous compounds*

In the previous sections the compounds have been grouped according to the number of bare P atoms that they contain, and considering the P_3 and P_2 units, or the isolated P atoms, as derived from the P_4 molecule by replacement of one, two or three of its atoms. In this section compounds are grouped which contain either units formed by more than four naked P atoms or chains of P atoms that cannot be considered to ideally originate from the P_4 molecule by processes in which its atoms are replaced, preserving the tetrahedral arrangement.

$[Cp^*Mo(CO)_2]_2$ reacts with white phosphorus yielding compounds **18–20** that contain P_3 or P_2 units (Scheme 9).[29] From the same reaction also compound **21** has been isolated, which is a triple-decker sandwich complex containing hexaphosphabenzene as the central bridging ligand. The crystal structure of $[\{Cp^*Mo\}_2(\mu,\eta^6\text{-}P_6)]$ (Fig. 14) shows the triple-decker arrangement with the P_6 ring forming the internal slice between two Mo atoms, each bonded in addition to a pentamethylcyclopentadienyl group which acts as an external ligand. Both Cp* rings and the P_6 ring are planar and parallel to each other. The average P—P distance (2.170 Å) lies in the range expected for such a moiety.[29] The ^1H and $^{31}P\text{-}\{^1H\}$ NMR spectra (Table 4) provide evidence for the equivalence of the methyl groups of Cp* as well as for that of the P atoms of the hexaphosphabenzene ring. The latter unit, stabilized by complexation, may be considered to derive from benzene by the isoelectronic replacement of one P atom for each CH group. This triple decker sandwich complex has 28 valence electrons.

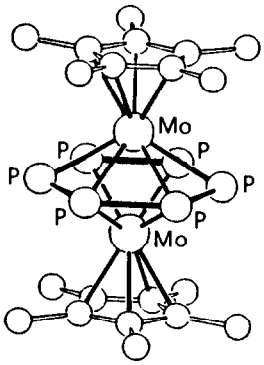

Fig. 14. Molecular structure of $[(CpMo)_2(\mu,\eta^6\text{-}P_6)]$.

Another compound to be reported in this section is that with the formula $[Co(Ph_2PCH_2PPh_2PPPPPPh_2CH_2PPh_2)]BF_4$ (**48**).[65] It has been isolated by reacting under an inert atmosphere white phosphorus, cobalt tetrafluoroborate hydrate and the ligand bis(diphenylphosphino)methane (dppm) (Scheme 31). This complex contains an unusual zigzag type tetraphosphorus fragment 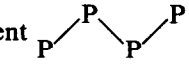 and apparently arises from a P_4 molecule which has been forced to

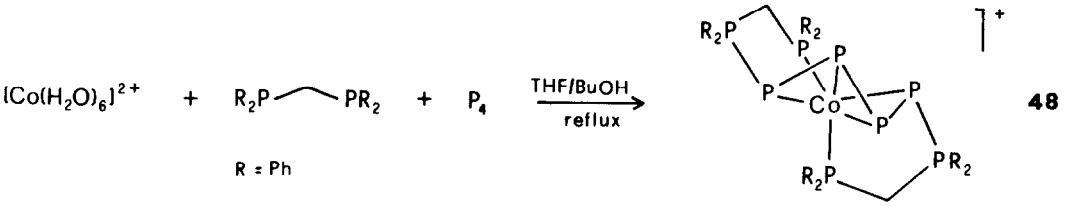

Scheme 31.

rearrange to a linear P_4 chain. The crystal structure reveals (Fig. 15) that a novel ligand, $Ph_2PCH_2PPh_2PPPPPPh_2CH_2PPh_2$, resulting from opening of the P_4 molecule in the presence of two dppm ligands, has been formed. The metal atom has a very distorted octahedral coordination geometry in which the new ligand coordinates through all of the P atoms of the P_4 chain and two of the four P atoms belonging to the dppm moieties; the dppm P atoms linked to the P_4 chain are uncoordinated. Among the P—P bonds within the 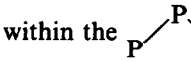 chain, the central one, 2.197 Å, is somewhat longer than the external bonds, 2.171 and 2.173 Å. The latter values are intermediate between those expected for double and single P–P bonds.[65] The above reaction involves oxidation of the P_4 molecule which is then nucleophilically attacked by the dppm P atoms. This compound can be used instead of white phosphorus to obtain the *cyclo*-P_3 derivative $[(triphos)Co(\eta^3\text{-}P_3)]$.[19]

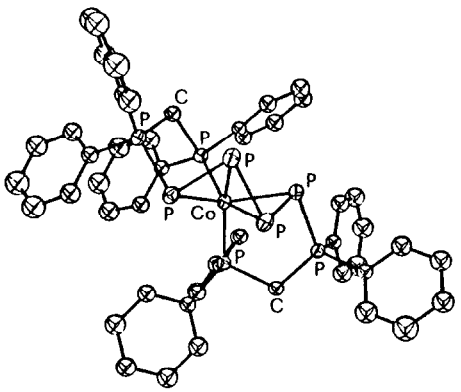

Fig. 15. View of the complex cation $[Co(Ph_2PCH_2PPh_2PPPPPPh_2CH_2PPh_2)]^+$.

III. REACTIVITY OF COORDINATED PHOSPHORUS ATOMS AND UNITS

Most of the unsubstituted P atoms which are contained in the derivatives that have been described in Section II present non-bonding electrons which should be available for further, terminal or bridging, interactions with transition-metal–ligand units or with electrophilic organic reagents. Furthermore, the complexes present additional potentially reactive sites at the P—P and P—M bonds. The compounds containing naked P atoms or units may therefore provide the starting material for numerous derivatives. Up to now the reactivity of the above compounds toward metal–ligand fragments, but not toward organic reagents, has been investigated. The following possibilities have been detected: (a) bonding by a single P atom to one metal centre, (b) interaction between three P atoms and one metal–ligand fragment, (c) interaction of one P atom with more than one metal centre, and (d) cleavage of a P—P bond by appropriate metal–ligand moieties.

The naked P atoms of the compounds reported in Section II may act as predominantly σ- or π-donors, depending on the conditions, and the compounds themselves may function as the building blocks for cluster compounds or may provide the substrate for the insertion of new metal–ligand moieties.

III.1. *σ- and π-donor abilities*

Naked P atoms, whether bound individually to metal centres or included in polyatomic units like P_2, P_3 and so on, have been found to be capable of acting as electron donors. If the chemical properties of the compounds containing single P atoms are compared with those of compounds containing P_2 or P_3 units it appears that the former derivatives are more basic than the latter. Thus **7**, described in Section II, is stable only for a short time in solution, where it forms the trimeric compound **8** (Scheme 21).[15] The monotetrahedrane species has been stabilized by allowing the single pnicogen atom to coordinate to an additional metal centre, as that in $Fe(CO)_4$ (**36**)[15,50] or $M(CO)_5$ [M = Cr (**37**), Mo (**38**) or W (**39**)].[18] Such a strong donor ability of single P atoms in tetrahedrane-type compounds is also confirmed by the chemical behaviour of the pnicogen atom in phosphalkyne complexes.[51–54] For example, the compounds $[\{Co(CO)_3\}_2(\mu, \eta^2\text{-PCR})]$ (R = Me, Ph or $SiMe_3$)[51] undergo cyclotrimerization in a few days (Scheme 32) but readily form adducts with chromium group carbonyls (Scheme 33). Such adducts contain the $M(CO)_5$ fragment bonded to the P atom of the phosphalkyne ligand as evidenced by NMR and IR spectra.[51]

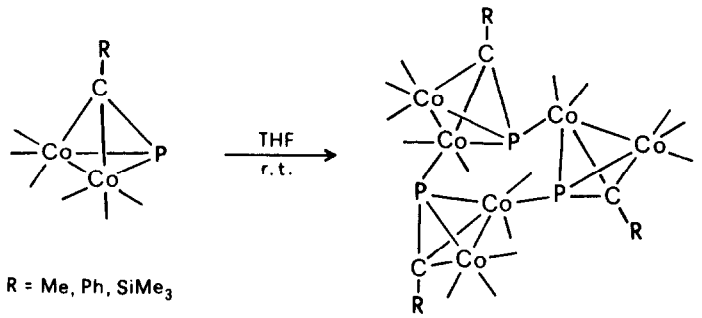

Scheme 32.

The molybdenum derivative **17** reacts with $[M(CO)_5thf]$[5,66] (Scheme 34), yielding the compounds $[\{CpMo(CO)_2\}_2(\mu,\eta^2\text{-}P_2)\{M(CO)_5\}_2]$ [M = Cr (**49**), Mo (**50**) or W (**51**)] which have the same Mo_2P_2 core as the parent compound and have in addition an $M(CO)_5$ fragment bound to each P atom of the P_2 unit. A similar donation of electron pairs by the P_2 bridge occurs also in the reaction with the compound $[Re_2Br_2(CO)_6(thf)_2]$, where two $Re(CO)_3thf$ units are bridged by the

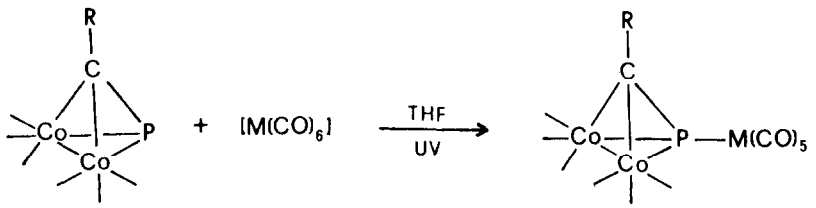

R = Me, Ph, $SiMe_3$

M = Cr, Mo, W

CO ligands omitted for clarity

Scheme 33.

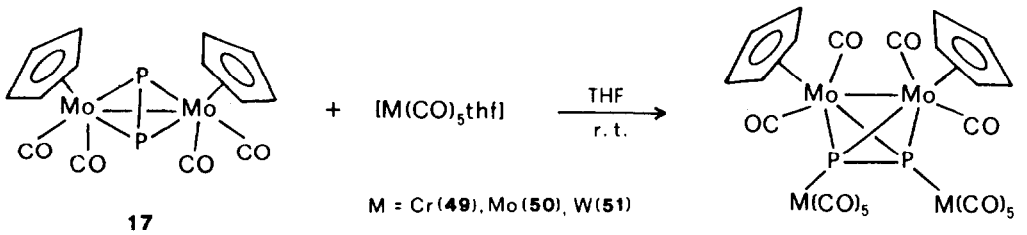

Scheme 34.

Br atoms, which yields **52** (Scheme 35).[66] In the latter the Re_2Br_2 four-membered ring is bridged by the Mo_2P_2 cluster. A THF solution of complex **52** is transformed to **53**[66] where the two Re atoms and the P_2 units of two complex ligands form a planar six-membered ring. Each Re atom is in a six-coordinate environment formed by two P atoms of different $[\{CpMo(CO)_2\}_2(\mu,\eta^2\text{-}P_2)]$ fragments, by three carbonyl groups and by one Br atom. The crystal structures of the two rhenium derivatives **52** and **53**[66] show that the bond lengths and angles of the coordinated Mo_2P_2 tetrahedra in both compounds differ very little from those of the uncoordinated molecule.[27] The donor ability of the P_2 unit in the $[\{Co(CO)_3\}_2(\mu,\eta^2\text{-}P_2)]$ cluster[39] as well as in its phosphine-substituted derivatives[42] has been proved recently.[67] Such compounds react with the metal carbonyl fragments $M(CO)_5$ (M = Cr, Mo or W) and $Fe(CO)_4$, yielding mono- or bimetallated derivatives depending on the ratio of the reagents (Scheme 36). The bimetallated derivatives could be also prepared starting from the monometallated compounds by addition of a further portion of the adduct (Scheme 36). This route allowed to prepare compounds in which two different transition-metal–ligand moieties are linked to the coordinated P_2 unit. The crystal structures of a homo-bimetallated compound, $[\{[Co(CO)_3]_2(\mu,\eta^2\text{-}P_2)\}\{Cr(CO)_5\}_2]$[47] (**30**), and of a hetero-bimetallated compound, $[\{[Co(CO)_3]_2(\mu,\eta^2\text{-}P_2)\}\{Cr(CO)_5\}\{W(CO)_5\}]$[67] (**54**), have been reported. Each $M(CO)_5$ (M = Cr or W) group in these compounds is bound to one P of the P_2 unit. The geometry of the Co_2P_2 core is substantially unchanged from that existing in the parent compound, the most significant difference being due to lengthening of the P—P bond (Table 3).

The double tetrahedrane complex **20**, containing two P_2 units,[39] reacts with $[Cr(CO)_5thf]$ to give (Scheme 37) the bimetallated derivative **55** in which each $Cr(CO)_5$ fragment is coordinated to one P atom of a P_2 ligand, which then functions as a six-electron donor.[5] Also the mononuclear neutral *cyclo*-P_3 complexes $[(triphos)M(\eta^3\text{-}P_3)]$ exhibit affinity for electron-acceptor groups like metal carbonyl fragments and related compounds. The cobalt derivative **9** reacts with $[Cr(CO)_6]$ under UV irradiation,[19,68] to afford (Scheme 38) complex **56** or **57**, depending on the amounts of reagents. No compound with more than two $Cr(CO)_5$ groups attached to the *cyclo*-P_3 unit of the parent complex **9** could be isolated. The adduct **58**, in which each P atom of the cyclotriphosphorus ligand of **9** is linked to an additional metal centre, has been synthesized (Scheme 38) by using the

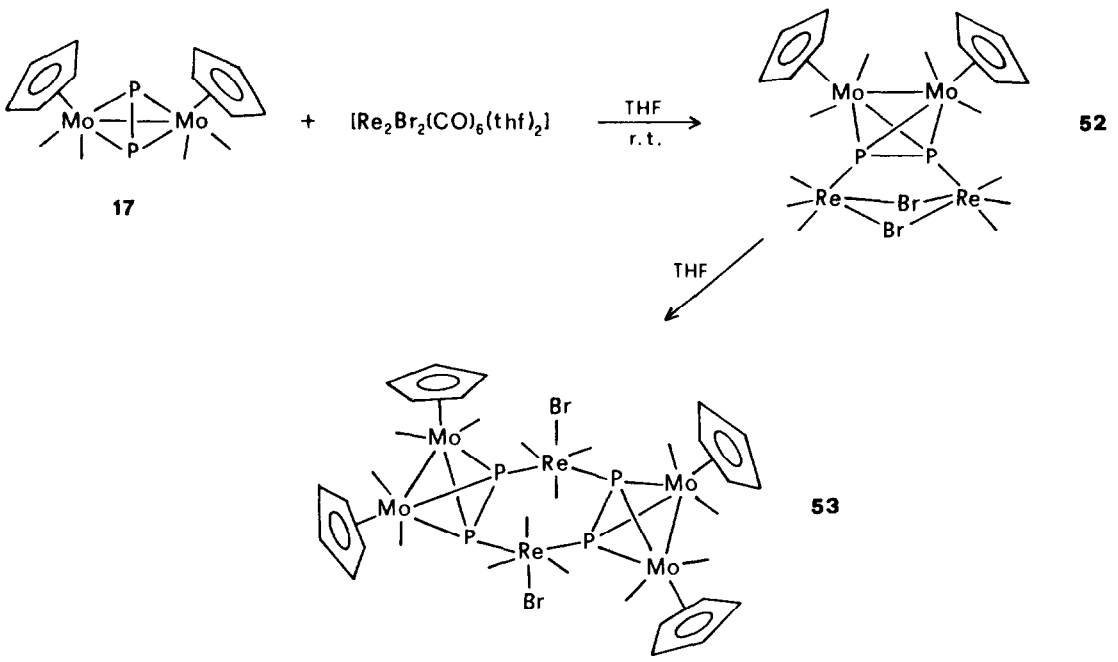

CO ligands omitted for clarity

Scheme 35.

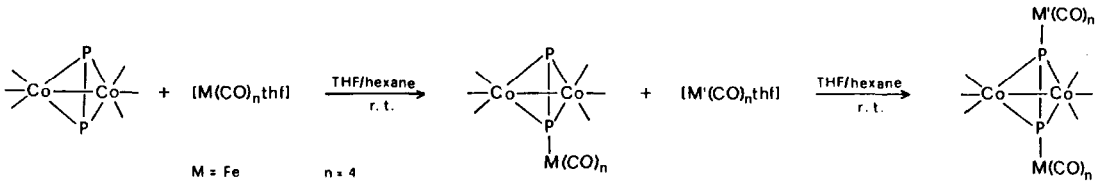

Scheme 36.

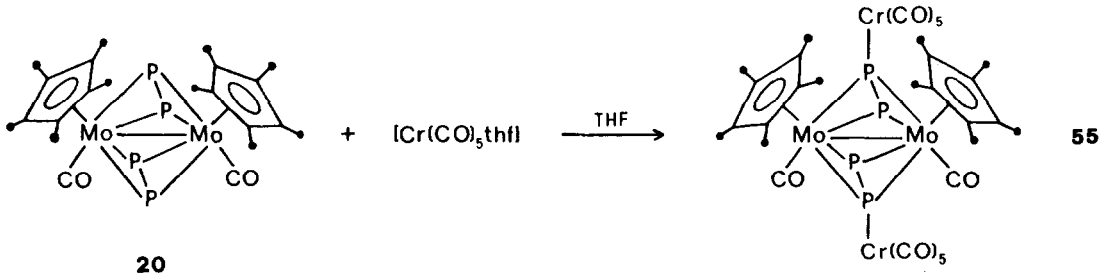

Scheme 37.

$CpMn(CO)_2$ fragment with similar electronic properties but lower steric requirements than $Cr(CO)_5$.[69] The structures of **57** and **58** show that the Cr or Mn atoms are displaced from the plane of the *cyclo*-P_3 unit on the opposite side to that of the Co atom. Bond distances within the cyclotriphosphorus group are essentially unchanged relative to those in **9**. The zigzag tetraphosphorus fragment of compound **48** reacts with $[W(CO)_6]$ in THF solution under UV radiation to form the $[Co(Ph_2PCH_2PPh_2PPPPPPh_2CH_2PPh_2)\{W(CO)_5\}]BPh_4$ derivative (**59**).[70] The

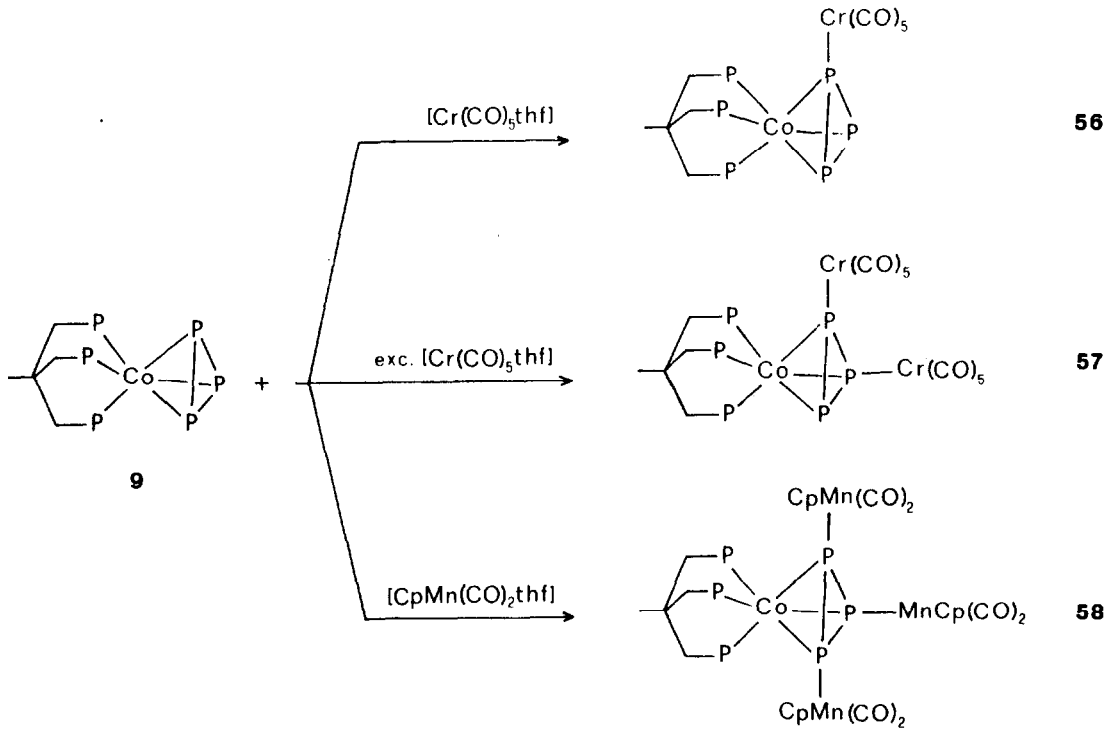

Scheme 38.

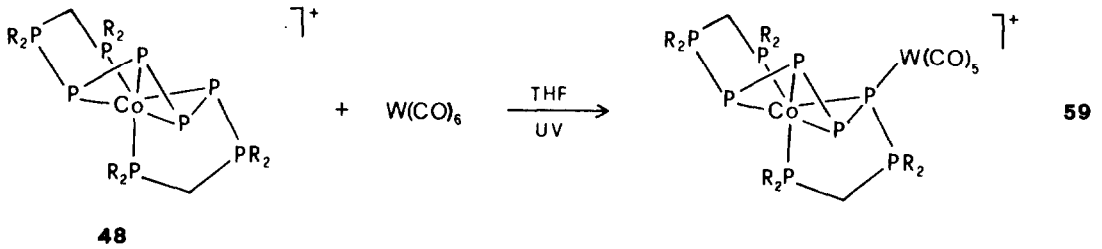

Scheme 39.

structure of the compound shows that one of the inner P atoms of the 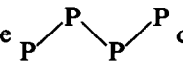 chain is linked to the W atom of the $W(CO)_5$ fragment. The coordination geometry around the Co atom is essentially unchanged with respect to that of the mononuclear donor complex.

The mononuclear $[(triphos)M(\eta^3\text{-}P_3)]^{n+}$ (M = Co, Rh or Ir; $n = 0$: M = Ni, Pd or Pt; $n = 1$) complexes moreover react with appropriate metal–ligand fragments to yield the previously described triple-decker sandwich complexes [see Section II.2(ii)] in which the triangular P_3 unit acts as the internal layer between two metal–ligand moieties. The same reactivity is exhibited also by the mononuclear compounds **22** and **23** which contain P_2X (X = S or Se) units. Such reactions reveal the π-bonding ability of the coordinated cyclotriphosphorus ligand. None of the other P units, i.e. the P_2 one and the tetrahedral or zigzag P_4, have been found up to now to be able to bind to one metal centre through two or more P atoms acting as π-donors.

III.2. *Phosphorus complexes as building blocks in clusters*

The Lewis base character of coordinating P atoms or units that has been considered in the previous section is at the origin of the tendency of the compounds containing such units to yield polymetallic derivatives in which either single P atoms or the three P atoms of the *cyclo*-P_3 unit

are bound to a metal centre. Recently two cluster compounds have been described in which the P_3 fragment of the [(triphos)M(η^3-P_3)] (M = Co or Ir) molecule acts as a capping ligand for unusual units containing Cu and Br atoms.[71,72] The cobalt derivative **9** dissolved in CH_2Cl_2 reacts with a suspension of CuBr, affording **60** (Scheme 40).[71] The molecule of this compound consists of two [(triphos)Co(η^3-P_3)] units held together by a hexagonal Cu_6 fragment (Fig. 16) whose edges are all symmetrically bridged by bromine atoms lying approximately in the Cu_6 plane. The P atoms of the two cyclotriphosphorus units and the Cu atoms are at the vertexes of a cuboctahedron. The presence of one lone pair on each P atom of the P_3 fragments as well as the arrangement of the P_3 and Cu_6 rings suggest that bonding should be considered to be essentially delocalized.

When the iridium derivative **12** is allowed to react with CuBr in a molar ratio of 1:2 the novel ionic compound **61** is obtained (Scheme 40).[72] In the cluster cation (Fig. 17) three molecules of [(triphos)Ir(η^3-P_3)] are held together via the P_3 ligands by the central Cu_5Br_4 framework. The five Cu atoms are at the vertexes of a distorted trigonal bipyramid whose lower edges are bridged by Br atoms, while each upper triangular face is unsymmetrically capped by the P_3 group of one [(triphos)Ir(η^3-P_3)] moiety. The fourth Br atom is terminally bonded to the Cu atom in the upper apical position. The Cu atoms display three different coordination geometries. The Cu atom at the lower vertex is trigonally coordinated by three Br atoms. Each equatorial Cu atom is in an approximately tetrahedral environment formed by one bridging Br atom and three P atoms belonging to two *cyclo*-P_3 groups. Finally, the fifth Cu atom is tetrahedrally coordinated by the terminal Br atom and three P atoms, each provided by a different cyclotriphosphorus group.

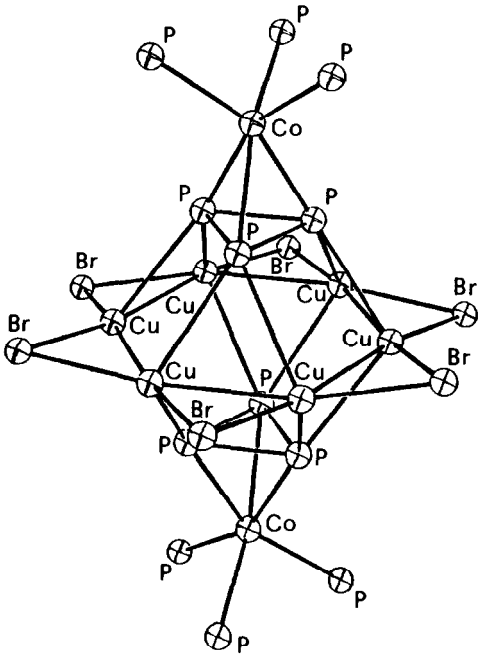

Fig. 16. Skeleton of the [{(triphos)Co(η^3-P_3)}$_2$($CuBr)_6$] molecule.

$$[(\text{triphos})\text{Co}(\eta^3\text{-}P_3)] + \text{CuBr} \xrightarrow[\text{r.t.}]{CH_2Cl_2} [\{(\text{triphos})\text{Co}(\eta^3\text{-}P_3)\}_2(CuBr)_6] \quad \mathbf{60}$$

$$[(\text{triphos})\text{Ir}(\eta^3\text{-}P_3)] + \text{CuBr} \xrightarrow[\text{r.t.}]{CH_2Cl_2} [\{(\text{triphos})\text{Ir}(\eta^3\text{-}P_3)\}_3Cu_5Br_4][CuBr_2] \quad \mathbf{61}$$

Scheme 40.

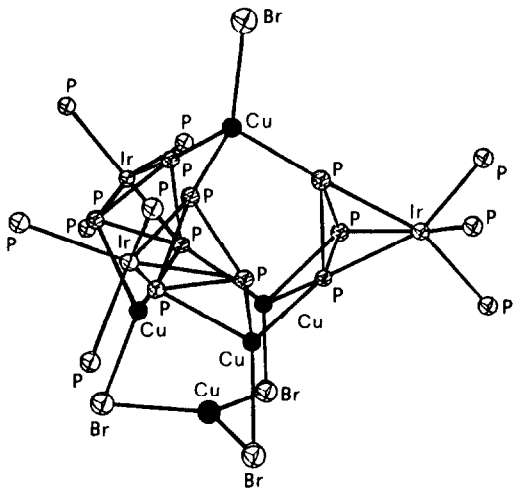

Fig. 17. Framework of the cluster cation $[\{(triphos)Ir(\eta^3\text{-}P_3)\}_3Cu_5Br_4]^+$.

III.3. P—P *bond activation*

A further type of reaction exhibited by compounds containing bare P atoms or units is the cleavage of a P—P bond. The activation of such bonds without complete disruption of the molecule is difficult for small molecules containing few unsubstituted P atoms. The only reports on this subject deal with the opening of a P—P bond in the P_4[73–77] and P_4S_3[78,79] cages.

The activation of P—P bonds in the unsubstituted P units bound to transition-metal moieties has been considered even less: the only report presently available deals with the insertion of the $Pt(PPh_3)_2$ group into a P—P bond of the cyclotriphosphorus ligand in $[(triphos)Ni(\eta^3\text{-}P_3)]BF_4$ (**15**).[80] Insertion reactions of diphenylcarbene CPh_2[81] and the carbene-like fragments $M(PPh_3)_2$ (M = Pd or Pt)[82] occur also into a bond of the thiadiphosphirene and thiadiarsirene units in the compounds $[(triphos)Co(\eta^3\text{-}E_2S)]BF_4$ (E = P[31,32] or As[83]) which are isoelectronic to **15**. The cationic compound **15** reacts with $[(\eta^2\text{-}C_2H_4)Pt(PPh_3)_2]$ to give the cation $[(triphos)Ni\{P_3Pt(PPh_3)_2\}]^+$ (**62**) that has been isolated as the tetraphenylborate salt (Scheme 41).[80] The structure of **62** shows that the $Pt(PPh_3)_2$ fragment inserts into a P—P bond of the cyclotriphosphorus ring. The Ni atom is coordinated by the three P atoms of the triphos ligand and by the atoms of the P_3 unit. The latter is considerably distorted from the regular triangular shape that it has in the parent compound **15**, since the bond into which insertion of the $Pt(PPh_3)_2$ moiety occurs lengthens to 2.53 Å, whereas the other two bond distances average 2.17 Å. The Pt atom is in a nearly planar arrangement formed by the two PPh_3 P atoms and by the two atoms defining the long side of the distorted P_3 group. The dihedral angle between the plane of the triatomic unit and the best plane through the four atoms surrounding the Pt atom is *ca* 128°.

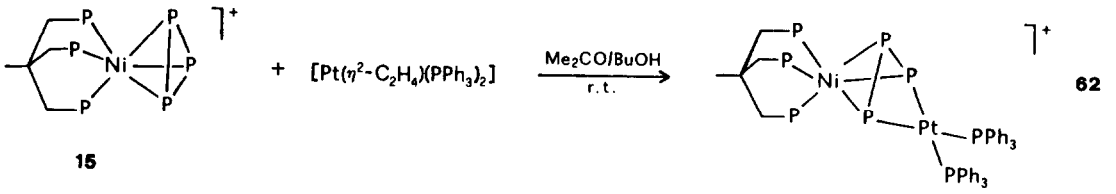

15 **62**

Scheme 41.

The ^{31}P NMR spectra of compound **62** at room temperature (Table 4) exhibit a single broad signal for the P atoms of the triphos ligand, the opened P_3 unit and the two PPh_3 groups. The resonances due to the two triphenylphosphines, which are bound to Pt, are accompanied by satellites. Such a pattern suggests a dynamic behaviour for the compound. Some broadening of the

signals occurs only at −95°C, showing a low activation energy for the process that goes on in solution.[80] Further studies are in progress in order to obtain limiting low-temperature spectra.

The [(triphos)Co(η^3-E_2S)]BF_4 (E = P or As)[31,32,83] compounds which are isoelectronic and isostructural to **15** react with [(η^2-C_2H_4)M(PPh_3)$_2$] (M = Pd or Pt),[81] yielding a series of compounds with the formula [(triphos)Co{$E_2SM(PPh_3)_2$}]BPh_4 (E = P or As, M = Pd or Pt) which have essentially the same geometry and exhibit the same behaviour in solution as **62**

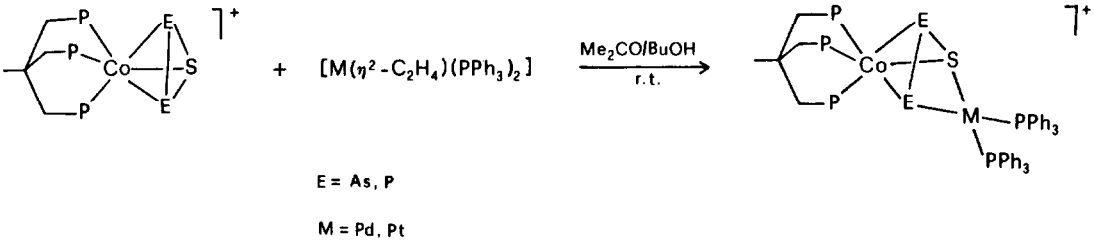

E = As, P

M = Pd, Pt

Scheme 42.

(Scheme 42). The insertion is considered to occur into one of the heteroatomic P—S or As—S bonds rather than into the P—P or As—As bond; such reactions are nevertheless reported here due to their close similarity with the process leading to **62**. Moreover the [(triphos)Co(η^3-As_2S)]BF_4 derivative[83] in the presence of CPh_2 generated *in situ* from CPh_2N_2 yields the compound [(triphos)Co{$SAsC(Ph_2)As$}]BF_4 (**63**), whose cation contains the four-membered 3,3-diphenyl-1,2,4-thiadiarsete unit 1,2,4-η^3-bound to the (triphos)Co moiety (Scheme 43).[82] Such a ring, containing three main group naked atoms and the diphenylcarbene C atom, is obtained through insertion of the CPh_2 moiety into the homoatomic bond of the As_2S unit. The generation of 3,3-diphenyl-1,2,4-thiadiarsete on the one hand, and of the platina- and pallada-triphosphete, -thiadiarsete and -thiadiphosphete units on the other hand, points to the similarities in the reactivity of all the triatomic units on the parent compounds which have been used. These results also substantiate the expected similarities in behaviour between the isolobal fragments $M(PR_3)_2$ and CR_2, even though the latter contain such atoms, as Pd or Pt on the one hand, and C on the other hand, which are considerably different from each other in most respects.

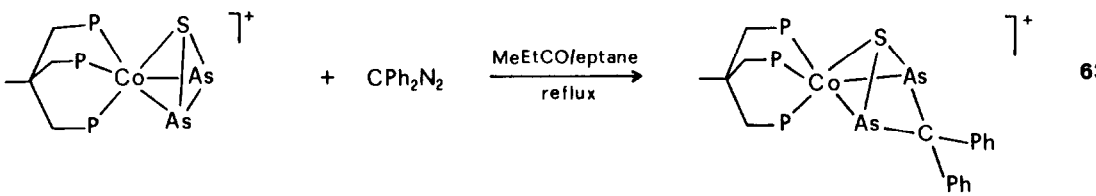

63

Scheme 43.

IV. NMR DATA FOR THE COMPLEXES

The ^{31}P NMR chemical shifts which have been reported for "naked" P atoms in transition-metal compounds are gathered in Table 4. Inspection of the data reveals a very broad range for the chemical shifts of the unsubstituted P atoms, the lowest shift occurring at +977 ppm for [{[$Fe(CO)_3$]$_2$(μ, η^2-P_2)}{$CpMn(CO)_2$}$_2$] (**42**) and the highest one at −351.5 ppm for [$CpMo(CO)_2$(η^3-P_3)] (**16**). The [(triphos)M(η^3-P_3)] (M = Co, Rh or Ir), [(triphos)M(η^3-P_3)]BF_4 (M = Ni, Pd or Pt) and [(triphos)Co(η^3-P_2X)]BF_4 (X = S or Se) compounds form an isostructural and isoelectronic series for which definite trends in the values of chemical shifts upon substitution of the metal atom or of one atom in the triangular unit have been observed, as already mentioned in Section II.2(i). The other compounds included in this survey, however, differ from each other in one or more important features, such as the nature of the metal atom and the overall electron count, the nature and number of ligands, or the molecular geometry, even though they may contain the same group of naked P atoms. For these reasons as well as for the rather small number of

compounds known, belonging to each of the classes considered here, it seems impossible to detect any definite trends in most of the ^{31}P NMR data pertaining to the unsubstituted P atoms in transition-metal compounds, except for the following general tendencies: (a) the ^{31}P chemical shifts move to higher field as the number of naked P atoms forming the units increases; (b) unsubstituted P atoms bound to magnetically active metal atoms exhibit very small coupling constants (Table 5) compared to those reported for phosphines; and (c) the P_6 and P_3 units exhibit a fluxional behavior at room temperature that persists at low temperatures consistently with the expected low energy barriers to the rotation of such units.

Table 4. ^{31}P chemical shifts[a] for naked phosphorus compounds[b]

Compound	Solvent	$\delta(^{31}P)$	Reference
Compound containing the P_6 unit			
21 $[\{Cp^*Mo\}_2(\mu,\eta^6\text{-}P_6)]$	CD_2Cl_2	−315.6(s)	29
Compounds containing the P_4 ligand			
1 $[RhCl(\eta^2\text{-}P_4)(PPh_3)_2]$[c]	CD_2Cl_2	−279.4(m) −284.0(m)	8
2 $[\{Fe(CO)_4\}_3(P_4)]$	C_6D_6	21(s)	11
Compounds containing the P_3 unit			
16 $[CpMo(CO)_2(\eta^3\text{-}P_3)]$	C_6D_6	−351.5(s)	27
18 $[Cp^*Mo(CO)_2(\eta^3\text{-}P_3)]$	C_6D_6	−336.5(s)	29
9 $[(triphos)Co(\eta^3\text{-}P_3)]$	CD_2Cl_2	−276.2(b)	21
11 $[(triphos)Rh(\eta^3\text{-}P_3)]$	CD_2Cl_2	−270.8(q)	8, 21
12 $[(triphos)Ir(\eta^3\text{-}P_3)]$	CD_2Cl_2	−312.9(q)	21
15 $[(triphos)Ni(\eta^3\text{-}P_3)]BF_4$	CD_2Cl_2	−155.7(q)	21
13 $[(triphos)Pd(\eta^3\text{-}P_3)BF_4$	CD_2Cl_2	−132.9(q)	21
14 $[(triphos)Pt(\eta^3\text{-}P_3)]BF_4$	CD_2Cl_2	−217.4(q)	21
22 $[(triphos)Co(\eta^3\text{-}P_2S)]BF_4$	CD_2Cl_2	−210.9(b)	32
23 $[(triphos)Co(\eta^3\text{-}P_2Se)]BF_4$	CD_2Cl_2	−145.5(q)	32
62 $[(triphos)Ni\{P_3Pt(PPh_3)_2\}]BPh_4$	CD_2Cl_2	−103.5(m)	80
Compounds containing the P_2 unit			
17 $[\{CpMo(CO)_2\}_2(\mu,\eta^2\text{-}P_2)]$	C_7D_8	−42.9(s)	27
19 $[\{Cp^*Mo(CO)_2\}_2(\mu,\eta^2\text{-}P_2)]$	C_6D_6	−48.4(s)	29
20 $[Cp^*Mo(CO)(\mu,\eta^2\text{-}P_2)]_2$	C_6D_6	−101.9 −131.4	29
27 $[\{(Et_2PCH_2CH_2PEt_2)Ni\}_2(\mu,\eta^2\text{-}P_2)]$	C_7D_8	133(q)	46
28 $[\{(Cy_2PCH_2CH_2PCy_2)Ni\}_2(\mu,\eta^2\text{-}P_2)]$	C_7D_8	135(q)	46
29 $[\{(Ph_2PCH_2CH_2PPh_2)Ni\}_2(\mu,\eta^2\text{-}P_2)]$	C_7D_8	161(q)	46
30 $[\{(Co(CO)_3]_2(\mu,\eta^2\text{-}P_2)\}\{Cr(CO)_5\}_2]$	C_7D_8	146(s)	47
31 $[\{(Co(CO)_3]_2(\mu,\eta^2\text{-}P_2)\}\{W(CO)_5\}_2]$	CD_2Cl_2	44(s)	47
32 $[\{(Co(CO)_3]_2(\mu,\eta^2\text{-}P_2)\}\{CpMn(CO)_2\}_2]$	C_7D_8	197(s)	47
49 $[\{(CpMo(CO)_2]_2(\mu,\eta^2\text{-}P_2)\}\{Cr(CO)_5\}_2]$	C_4D_8O	−36.7(s)	66
52 $[\{(CpMo(CO)_2]_2(\mu,\eta^2\text{-}P_2)\}\{Re_2Br_2(CO)_6\}]$	CD_2Cl_2	−78.5(s)	66
Compounds containing single P atoms			
42 $[\{[Fe_2(CO)_6](\mu\text{-}P)_2\}\{CpMn(CO)_2\}_2]$[d]	C_7D_8	977(s)	56
43 $[\{CpW(CO)_2\}\{Cr(CO)_5\}_2(\mu_3\text{-}P)]$[e]	CD_2Cl_2	945(s)	57
44 $[\{Fe_2(CO)_8\}\{Fe_2(CO)_6(\mu\text{-}Cl)\}(\mu_4\text{-}P)]$		433(s)	58
45 $[NEt_3Bz]_2[Rh_9(CO)_{21}P]$	$(CD_3)_2CO$	282.3(m)	59, 62
46 $[NEt_3Bz]_3[Rh_{10}(CO)_{22}P]$[f]	$(CD_3)_2CO$	369.3(m)	60, 62
47 $[PPh_4][Co_6(CO)_{16}P]$[g]	C_4D_8O	486.2(b)	63

[a] Positive chemical shifts are to low field of external H_3PO_4 (85%); s = singlet, q = quartet, m = multiplet, b = broad signal.

[b] Only the resonances due to naked P atoms are listed.

[c] 251 K.

[d] 293 K.

[e] 252 K.

[f] 182 K.

[g] 189 K.

Table 5. Direct coupling constants between naked phosphorus and metal atoms

Compound		^1J(Hz)	Reference
1 $[RhCl(\eta^2\text{-}P_4)(PPh_3)_2]$	$^1J(Rh\text{-}\eta^2\text{-}P_4)$	33.9	8
11 $[(triphos)Rh(\eta^3\text{-}P_3)]$	$^1J(Rh\text{-}\eta^3\text{-}P_3)$	28.0	21
14 $[(triphos)Pt(\eta^3\text{-}P_3)]BF_4$	$^1J(Pt\text{-}\eta^3\text{-}P_3)$	171	21
45 $[NEt_3Bz]_2[Rh_9(CO)_{11}P]$	$^1J(Rh\text{-}P)^a$	38.5	62
46 $[NEt_3Bz]_3[Rh_{10}(CO)_{22}P]$	$^1J(Rh\text{-}P)^a$	31.7	62

[a]Time-averaged value.

REFERENCES

1. B. F. G. Johnson (Ed.), *Transition Metal Clusters*. Wiley Interscience, Chichester (1980).
2. J. D. Corbett, *Chem. Rev.* 1985, **85**, 383 (and references therein).
3. M. Di Vaira and L. Sacconi, *Angew. Chem., Int. Ed. Engl.* 1982, **21**, 330.
4. J. G. Riess, In *Rings, Clusters, and Polymers of Main Group Elements* (Edited by A. H. Cowley), p. 17. ACS Symposium Series 232, Washington, DC (1983).
5. O. J. Scherer, *Angew. Chem., Int. Ed. Engl.* 1985, **24**, 924.
6. A. P. Ginsberg and W. E. Lindsell, *J. Am. Chem. Soc.* 1971, **93**, 2082.
7. A. P. Ginsberg, W. E. Lindsell and W. E. Silverthorn, *Trans. N. Y. Acad. Sci.* 1971, **33**, 303.
8. W. E. Lindsell, *J. Chem. Soc., Chem. Commun.* 1982, 1422.
9. W. E. Lindsell, K. J. McCullogh and A. J. Welch, *J. Am. Chem. Soc.* 1983, **105**, 4487.
10. L. E. Sutton (Ed.), Chemical Society, Special Publication No. 11 (1958).
11. G. Schmid and H. P. Kempny, *Z. Anorg. Allg. Chem.* 1977, **432**, 160.
12. P. Dapporto, S. Midollini and L. Sacconi, *Angew. Chem., Int. Ed. Engl.* 1979, **18**, 469.
13. P. Dapporto, L. Sacconi, P. Stoppioni and F. Zanobini, *Inorg. Chem.* 1981, **20**, 3834.
14. S. Kang, T. A. Albright and J. Silvestre, *Croat. Chem. Acta* 1984, **57**, 1355.
15. A. Vizi-Orosz, *J. Organomet. Chem.* 1976, **111**, 61.
16. A. S. Foust, M. S. Foster and L. F. Dahl, *J. Am. Chem. Soc.* 1969, **91**, 5631.
17. L. Markò, *Gazz. Chim. Ital.* 1979, **109**, 247.
18. A. Vizi-Orosz, V. Galamb, G. Pàlyi and L. Markò, *J. Organomet. Chem.* 1981, **216**, 105.
19. C. A. Ghilardi, S. Midollini, A. Orlandini and L. Sacconi, *Inorg. Chem.* 1980, **19**, 301.
20. C. Bianchini, C. Mealli, A. Meli and L. Sacconi, *Inorg. Chim. Acta* 1979, **37**, L543.
21. M. Di Vaira, L. Sacconi and P. Stoppioni, *J. Organomet. Chem.* 1983, **250**, 183.
22. M. Di Vaira, M. Peruzzini and P. Stoppioni, *Acta Cryst.* 1983, **C39**, 1210.
23. M. Di Vaira, S. Midollini and L. Sacconi, *J. Am. Chem. Soc.* 1979, **101**, 1757.
24. F. Cecconi, P. Dapporto, S. Midollini and L. Sacconi, *Inorg. Chem.* 1978, **17**, 3292.
25. K. Wade, *Inorg. Nucl. Chem. Lett.* 1972, **8**, 559.
26. R. Hoffmann, *Angew. Chem., Int. Ed. Engl.* 1982, **21**, 711; F. G. A. Stone, *Acc. Chem. Res.* 1981, **14**, 318 (and references therein).
27. O. J. Scherer, H. Sitzmann and G. Wolmershäuser, *J. Organomet. Chem.* 1984, **268**, C9.
28. O. J. Scherer, H. Sitzmann and G. Wolmershäuser, *Acta Cryst.* 1985, **C41**, 1761.
29. O. J. Scherer, H. Sitzmann and G. Wolmershäuser, *Angew. Chem., Int. Ed. Engl.* 1985, **24**, 351.
30. I. Bernal, H. Brunner, W. Meier, H. Pfisterer, J. Wachter and M. L. Ziegler, *Angew. Chem., Int. Ed. Engl.* 1984, **23**, 438.
31. M. Di Vaira, M. Peruzzini and P. Stoppioni, *J. Chem. Soc., Chem. Commun.* 1982, 894.
32. M. Di Vaira, M. Peruzzini and P. Stoppioni, *J. Chem. Soc., Dalton Trans.* 1984, 359.
33. C. Bianchini, M. Di Vaira, A. Meli and L. Sacconi, *Inorg. Chem.* 1981, **20**, 1169.
34. C. Bianchini, M. Di Vaira, A. Meli and L. Sacconi, *J. Am. Chem. Soc.* 1981, **103**, 1448.
35. C. Bianchini, M. Di Vaira, A. Meli and L. Sacconi, *Angew. Chem., Int. Ed. Engl.* 1980, **19**, 405.
36. M. Di Vaira, F. Mani, S. Moneti, M. Peruzzini, L. Sacconi and P. Stoppioni, *Inorg. Chem.* 1985, **24**, 2230.
37. M. Di Vaira, M. Peruzzini and P. Stoppioni, unpublished results.
38. M. Peruzzini and P. Stoppioni, *J. Organomet. Chem.* 1985, **288**, C44.
39. A. Vizi-Orosz, G. Pàlyi and L. Markò, *J. Organomet. Chem.* 1973, **60**, C25.
40. A. S. Foust, M. S. Foster and L. F. Dahl, *J. Am. Chem. Soc.* 1969, **91**, 5633; A. S. Foust, C. F. Campana, J. D. Sinclair and L. F. Dahl, *Inorg. Chem.* 1979, **18**, 3047.
41. G. Bor, *Chem. Ber.* 1963, **96**, 2644.
42. G. Varadi, A. Vizi-Orosz, S. Vastag and G. Pàlyi, *J. Organomet. Chem.* 1976, **108**, 225.
43. C. F. Campana, A. Vizi-Orosz, G. Pàlyi, L. Markò and L. F. Dahl, *Inorg. Chem.* 1979, **18**, 3054.

44. See footnote 3 in Ref. 66.
45. M. H. Chisholm, K. Folting, J. C. Huffman and J. J. Koh, *Polyhedron* 1985, **4**, 893.
46. H. Schäfer, D. Binder and D. Fenske, *Angew. Chem., Int. Ed. Engl.* 1985, **24**, 522.
47. H. Lang, L. Zsolnai and G. Huttner, *Angew. Chem., Int. Ed. Engl.* 1983, **22**, 976; *Angew. Chem. Suppl.* 1983, 1463.
48. H. Brunner, H. Kauermann, U. Klement, J. Wachter, T. Zahn and M. L. Ziegler, *Angew. Chem., Int. Ed. Engl.* 1985, **24**, 132.
49. G. L. Simon and L. F. Dahl, *J. Am. Chem. Soc.* 1973, **95**, 2175.
50. A. Vizi-Orosz, V. Galamb, G. Pàlyi, L. Markò, G. Bor and G. Natile, *J. Organomet. Chem.* 1976, **107**, 235.
51. D. Seyferth, J. S. Merola and R. S. Henderson, *Organometallics* 1982, **1**, 859.
52. G. Becker, W. A. Herrmann, W. Kalcher, G. W. Kriechbaum, C. Pahl, C. T. Wagner and L. M. Ziegler, *Angew. Chem., Int. Ed. Engl.* 1983, **22**, 413.
53. A. H. Cowley, *Polyhedron* 1984, **3**, 389 (and references therein).
54. M. F. Meidine, C. J. Meir, S. Morton and J. F. Nixon, *J. Organomet. Chem.* 1985, **297**, 255 (and references therein).
55. T. Kruck, G. Sylvester and I. P. Kunau, *Z. Naturforsch.* 1973, **28B**, 38.
56. H. Lang, L. Zsolnai and G. Huttner, *Angew. Chem., Int. Ed. Engl.* 1983, **22**, 976; *Angew. Chem. Suppl.* 1983, 1451.
57. G. Huttner, U. Weber, B. Sigwarth, O. Scheidsteger, H. Lang and L. Zsolnai, *J. Organomet. Chem.* 1985, **282**, 331.
58. G. Huttner, G. Mohr, B. Pritzlaff, J. von Seyerl and L. Zsolnai, *Chem. Ber.* 1982, **115**, 2044.
59. J. L. Vidal, W. E. Walker, R. L. Pruett and R. C. Schoening, *Inorg. Chem.* 1979, **18**, 129.
60. J. L. Vidal, W. E. Walker and R. C. Schoening, *Inorg. Chem.* 1981, **20**, 238.
61. O. A. Gansow, D. S. Gill, F. J. Bennis, J. R. Hutchinson, J. L. Vidal and R. C. Schoening, *J. Am. Chem. Soc.* 1981, **102**, 2449.
62. B. T. Heaton, L. Strona, R. Della Pergola, J. L. Vidal and R. C. Schoening, *J. Chem. Soc., Dalton Trans.* 1983, 1941.
63. P. Chini, G. Ciani, S. Martinengo, A. Sironi, L. Longhetti and B. T. Heaton, *J. Chem. Soc., Chem. Commun.* 1979, 188.
64. G. Ciani and L. Sironi, *J. Organomet. Chem.* 1983, **241**, 385.
65. F. Cecconi, C. A. Ghilardi, S. Midollini and A. Orlandini, *J. Am. Chem. Soc.* 1984, **106**, 3667.
66. O. J. Scherer, H. Sitzmann and G. Wolmershäuser, *Angew. Chem., Int. Ed. Engl.* 1984, **23**, 968.
67. A. Vizi-Orosz, G. Pàlyi, L. Markò, R. Boese and G. Schmid, *J. Organomet. Chem.* 1985, **288**, 179.
68. S. Midollini, A. Orlandini and L. Sacconi, *Angew. Chem., Int. Ed. Engl.* 1979, **18**, 81.
69. C. Mealli, S. Midollini, S. Moneti and L. Sacconi, *Cryst. Struct. Commun.* 1980, **9**, 1017.
70. F. Cecconi, C. A. Ghilardi, S. Midollini and A. Orlandini, *XVII Congresso Nazionale Chimica Inorganica*, p. 275. Cefalù (1984).
71. F. Cecconi, C. A. Ghilardi, S. Midollini and A. Orlandini, *J. Chem. Soc., Chem. Commun.* 1982, 229.
72. F. Cecconi, C. A. Ghilardi, S. Midollini and A. Orlandini, *Angew. Chem., Int. Ed. Engl.* 1983, **22**, 554.
73. M. Baudler, H. Suchomel, G. Fürstenberg and U. Schings, *Angew. Chem., Int. Ed. Engl.* 1981, **20**, 1044.
74. E. Niecke, R. Rüger and B. Krebs, *Angew. Chem., Int. Ed. Engl.* 1982, **21**, 544.
75. W. W. Schoeller and C. Lerch, *Inorg. Chem.* 1983, **22**, 2992.
76. A. Schmidpeter, G. Burget, H. G. von Schnering and D. Weber, *Angew. Chem., Int. Ed. Engl.* 1984, **23**, 816.
77. R. Riedel, H. D. Hausen and E. Fluck, *Angew. Chem., Int. Ed. Engl.* 1985, **24**, 1056.
78. C. A. Ghilardi, S. Midollini and A. Orlandini, *Angew. Chem., Int. Ed. Engl.* 1983, **22**, 790.
79. M. Di Vaira, M. Peruzzini and P. Stoppioni, *J. Chem. Soc., Dalton Trans.* 1985, 291.
80. G. Baldi, M. Di Vaira, L. Niccolai, M. Peruzzini and P. Stoppioni, *IX European Crystallographic Meeting*, p. 164. Torino (1985). M. Di Vaira, B. Mann, M. Peruzzini and P. Stoppioni, unpublished results.
81. M. Di Vaira, S. Moneti, M. Peruzzini and P. Stoppioni, *J. Organomet. Chem.* 1984, **266**, C8; M. Di Vaira, M. Peruzzini and P. Stoppioni, unpublished results.
82. M. Di Vaira, L. Niccolai, M. Peruzzini and P. Stoppioni, *Organometallics* 1985, **4**, 1888.
83. M. Di Vaira, P. Innocenti, S. Moneti, M. Peruzzini and P. Stoppioni, *Inorg. Chim. Acta* 1984, **83**, 161.

Polyhedron Vol. 6, No. 3, pp. 383–386, 1987
Printed in Great Britain

0277–5387/87 $3.00+.00

THERMAL BEHAVIOUR, ^{119}Sn MÖSSBAUER AND IR SPECTROSCOPIC STUDIES OF SOME DIORGANOTIN(IV)CARBOHYDRATES

JOHN D. DONALDSON and SUSAN M. GRIMES

Department of Chemistry, The City University, Northampton Square, London EC1V 0HB, U.K.

LORENZO PELLERITO* and M. ASSUNTA GIRASOLO

Istituto di Chimica Generale, Via Archirafi 26, 90123 Palermo, Italy

PETER J. SMITH

International Tin Research Institute, Frazer Road, Perivale, Greenford, Middlesex, U.K.

and

ANTONIO CAMBRIA and MARIA FAMÀ

Istituto di Chimica Biologica, Viale Andrea Doria 6, 95125 Catania, Italy

(*Received* 18 *April* 1986; *accepted after revision* 27 *June* 1986)

Abstract—The synthesis of diorganotincarbohydrates {R_2SnL [R = Me, Bu or Oct; L = aldotetrose (erythrose), aldopentoses (arabinose or ribose), ketohexoses (fructose or sorbose), aldohexoses (galactose or glucose) or 6-deoxyaldohexose (rhamnose)]} is reported. IR and ^{119}Sn Mössbauer spectra are consistent with the presence of tin–carbohydrate oxygen bonds in the compounds and with a trigonal bipyramidal arrangement of two alkyl and three O-containing groups about the tin atoms. The thermal decomposition of the compounds is shown to fall into one of three categories, viz: (1) aldose derivatives that decompose without melting to give SnO as the final tin-containing product, (2) ketose derivatives that decompose without melting to give SnO_2 as the final tin-containing product, and (3) aldose derivatives that melt and then decompose to give either SnO or SnO_2.

Studies on the interaction between carbohydrates and inorganic compounds have been reported for both solid and solution phases,[1–9] and an extensive review on this subject has been published.[8] There is, however, very little information on organometallic derivatives of the carbohydrates.[10–13] As part of a research program developed in our laboratories to investigate the bonding of diorganotin oxide moieties to nucleoside,[14] we now report the synthesis of some diorganotin compounds with several monosaccharides and their characterization by IR and Mössbauer spectroscopic data. Since there are no reports in the literature dealing with the modes of decomposition of the type of compounds prepared in this work, we have also studied the fate of the tin atom on thermal decomposition of the compounds.

EXPERIMENTAL

The compounds were obtained by refluxing equimolar quantities of the carbohydrate (J. T. Backer Chemicals B.V., Deventer, Holland) and the diorganotin oxide (gift from Schering AG, Bergkamen) in anhydrous methanol. Some products precipitated

*Author to whom correspondence should be addressed.

immediately from the mixture while others were obtained after removal of the solvent by rotary evaporation. The products were washed with the minimum of methanol, and dried *in vacuo*.

C and H analyses were performed at the Laboratorio di Chimica Organica, Milano. Analytical data for the compounds prepared are given in Table 1.

IR spectra were obtained as mulls of Nujol and hexaclorobutadiene in the region 4000–200 cm^{-1} using a Perkin–Elmer model 983G IR spectrometer. ^{119}Sn Mössbauer spectra were measured at liquid-nitrogen temperature with a constant acceleration and a triangular waveform, using a Laben 8001 multichannel analyzer, a Mössbauer closed refrigerator system [model 21SC Cryodyne Cryocooler (CTI-Cryogenics, U.S.A.)] and a digital temperature controller (model DRC-80C, Lake Shore Cryotronics Inc., U.S.A.).

The thermal behaviour of the complexes was studied on a Stanton Redcroft STA 780 simultaneous thermal analyser.

RESULTS AND DISCUSSION

IR vibrational data

The analytical data in Table 1 and the IR data (Table 2) are consistent with the formation of compounds of type R_2SnL (L = carbohydrato moiety) by replacement of the oxygen atom in R_2SnO (R = Me, Bu or Oct) with carbohydrate groups.

Changes occurred in the 1200–1000- and 600–400-cm^{-1} regions of the spectra for the new compounds in comparison with the carbohydrates.

These changes are typical of: (1) the replacements of C—O vibrations of the COH groups of the carbohydrate with C—O vibrations of COSn groups[16–20] in the complex, and (2) the appearance of vibrational frequencies arising from Sn—C[16,21] and Sn—O bonds.[21,22]

Table 1. Analytical data (calculated % values in parentheses) and ^{119}Sn Mössbauer parameters of some diorganotin(IV)carbohydrates[ab]

Compound	C (%)	H (%)	δ^c	$\Delta E_{exp}{}^d$
Bu_2Snerythrose	41.9	6.6	1.16	2.78
($Bu_2SnC_4H_6O_4$)	(41.1)	(6.9)		
Oct_2Snerythrose	52.4	9.0	1.18	2.84
($Oct_2SnC_4H_6O_4$)	(51.8)	(8.7)		
Bu_2Snarabinose	40.7	7.0	1.25	3.07
($Bu_2SnC_5H_8O_5$)	(41.0)	(6.9)		
Bu_2Snribose	40.9	6.7	1.22	2.95
($Bu_2SnC_5H_8O_5$)	(41.0)	(6.9)		
Bu_2Snfructose	39.9	6.9	1.21	2.94
($Bu_2SnC_6H_{10}O_6$)	(40.9)	(6.9)		
Me_2Sngalactose	29.5	5.6	1.20	2.95
($Me_2SnC_6H_{10}O_6$)	(29.4)	(4.9)		
Bu_2Sngalactose	40.5	6.9	1.22	2.95
($Bu_2SnC_6H_{10}O_6$)	(40.9)	(6.9)		
Oct_2Sngalactose	51.2	8.9	1.04	2.87
($Oct_2SnC_6H_{10}O_6$)	(50.5)	(8.5)		
Me_2Snglucose	28.5	5.2	1.16	3.05
($Me_2SnC_6H_{10}O_6$)	(29.4)	(4.9)		
Bu_2Snglucose	40.4	7.1	1.23	3.03
($Bu_2SnC_6H_{10}O_6$)	(40.9)	(6.9)		
Bu_2Snrhamnose	42.3	7.3	1.17	2.78
($Bu_2SnC_6H_{10}O_5$)	(42.6)	(7.1)		
Bu_2Snsorbose	40.6	7.0	1.21	2.95
($Bu_2SnC_6H_{10}O_6$)	(40.9)	(6.9)		

[a]Arabinose = β-D(−)arabinopyranose, erythrose = β-D(−)erythrofuranose, fructose = β-D(−)fructopyranose, galactose = α-D(+)galactopyranose, glucose = α-D(+)glucopyranose, rhamnose = α-L(+)-rhamnopyranose, ribose = β-D(−)ribopyranose and sorbose = β-L(−) sorbopyranose.[15]

[b]Absorber thickness (mg ^{119}Sn cm^{-2}) was ≈0.5. Mössbauer parameters were determined at 77.3 K; $\delta \pm 0.03$ mm s^{-1}, $\Delta E \pm 0.02$ mm s^{-1}.

[c]Isomer shift with respect to room-temperature $CaSnO_3$.

[d]Experimental nuclear quadrupole splitting. The calculated nuclear quadrupole splitting was 2.673 mm s^{-1}; the partial quadrupole splittings used in the point charge model formalism were according to Refs 25–27.

Mössbauer data

The ^{119}Sn Mössbauer isomer shifts (Table 1) are characteristic of dialkyltin(IV) derivatives.[23] Both the shifts and quadrupole splittings increased from the values for R_2SnO compounds (for R = Me, $\delta = 0.92$, $\Delta E = 1.82$ mm s^{-1}; for R = Bu, $\delta = 1.08$, $\Delta E = 2.06$ mm s^{-1}; for R = Oct, $\delta = 0.97$, $\Delta E = 2.00$ mm s^{-1}).

The increase in the shifts show that the bonds between tin and the carbohydrate oxygen atoms are more covalent in character than the Sn—O bonds in R_2SnO.

The increases in the splittings must result from increases in the asymmetry of the tin *p*- or *d*-electron density on formation of the carbohydrate derivatives from the oxides. The Mössbauer spectra showed for all the investigated complexes only one doublet, which strongly supported the occurrence of only one tin environment, excluding in such a way the possible coexistence of both five- and six-coordinated tin atoms in the complexes as was found by Holzapfel *et al.*[13] in methyl-4,6-*O*-benzylidene-2,3-*O*-dibutylstannilene-α-D-mannopyrano-

Table 2. More relevant IR absorption bands for some diorganotin (IV)carbohydrates[a]

Compound	ν(CO) in COSn	ν(SnC)	ν(SnO)
Bu_2Snerythrose	1105m, 1080w	570m,bd, 515w	455w, 415w
Oct_2Snerythrose	1105m, 1075m	599s, 559s	435s
Bu_2Snarabinose	1110w, 1075m	596m, 520w	475m, 420w
Bu_2Snribose	1110w, 1078m	598m, 522w	453w, 425m
Bu_2Snfructose	1105sh, 1080s	590w, 520w	450m, 420m
Me_2Sngalactose	1110w, 1090w	572m, 545m	428w
Bu_2Sngalactose	1105sh, 1082vs	560w, 520w	458s
Oct_2Sngalactose	1105m, 1080s	564s, 535w	470w, 430sh
Me_2Snglucose	1110s, 1078m	578s, 552m	430s
Bu_2Snglucose	1115m, 1076s, bd	598s, 520w	460w, 415m
Bu_2Snrhamnose	1113w, 1080s, bd	595w, 512w	462m, 420w
Bu_2Snsorbose	1105w, 1090sh	578w, 550w	450m, 415w

[a]Measured in the range 4000–180 cm^{-1} as Nujol and hexachlorobutadiene mulls: s = strong, m = medium, w = weak, sh = shoulder, bd = broad and v = very.

side by X-ray investigation.

The quadrupole-splitting data for the dialkyltin oxides have been interpreted in terms of a polymeric network with five-coordinate tin atoms[23] and the values of the splittings for the carbohydrate derivatives are also consistent with trigonal bipyramidal C_2SnO_3 coordination with equatorial Sn—C bonds.[14] The dibutylstannylene derivative of methyl-4-6-di-*O*-benzylidene-α-D-glucopyranoside, which is likely to have a tin environment similar to those in the carbohydrates prepared in this work, is known to have a trigonal bipyramidal five-coordinated structure.[24]

Assuming the tin coordination in Fig. 1, the nuclear quadrupole splittings can be rationalized in terms of the point charge model formalism using literature values for the partial quadrupole splitting of alkyl and oxygen-bonding groups (Table 1).[25–27]

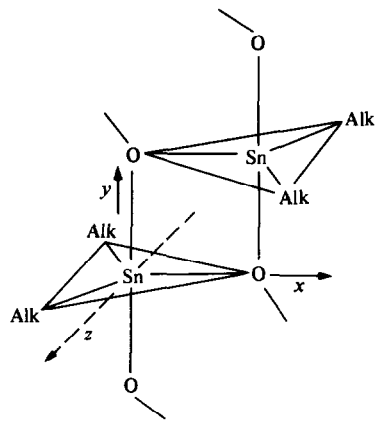

Fig. 1.

Thermal decomposition

The results show that the thermal decomposition of the complexes fall into one of three main types: viz. (1) those sugar derivatives which break down in two stages, leaving a residue of stannous oxide; (2) those which pyrolyse in a two-step process to give either SnO_2 or SnO_2 and carbon as products of decomposition, and finally (3) those compounds which melt before decomposition and give either SnO or SnO_2 as residues.

Table 3 list the dialkyltin(IV)carbohydrates under these categories.

It appears that the fate of tin during decomposition to give either a tin(II) or tin(IV) species as a product is dependent on the nature of the sugar. Monosaccharides are divided principally into two categories, those which are polyhydroxyaldehydes (aldoses) and those which are polyhydroxyketones (ketoses). Of the sugars studied here most are aldoses but fructose and sorbose are examples of ketoses. The dialkyltin(IV) derivatives of the aldoses (compounds **1–6**) are shown to decompose without melting to give SnO, whilst the derivatives of the ketoses (compounds **7** and **8**) give SnO_2, again without melting.

These results are consistent with the reducing properties of aldoses resulting in the reduction of tin(IV) to tin(II), and the oxidation of the aldehyde group of the aldoses to aldonic acids.

No such reducing reactions occur with ketoses.

The reactions in these two categories deal with the decomposition of the tin species in the solid state but different criteria apply to the third group of compounds in which melting procedes the decomposition.

Table 3. Thermal behaviour of some diorganotin(IV)carbohydrates

1	2	3
1 Bu_2Snerythrose	**7** Bu_2Snfructose	**9** Oct_2Snerythrose (m.p. 101°C)
2 Bu_2Snarabinose	**8** Bu_2Snsorbose	**10** Me_2Sngalactose (m.p. 163°C)
3 Bu_2Snribose		**11** Oct_2Sngalactose (m.p. 97°C)
4 Bu_2Sngalactose		**12** Me_2Snglucose (m.p. 155°C)
5 Bu_2Snglucose		
6 Bu_2Snrhamnose		

In a molten system, the final tin product depends not only on the nature of the sugar but also on the nature of the molten tin species. One of the aldose derivatives (compound **12**) decomposes to give the expected tin product, SnO, but this is not always the case. It is found that the aldose derivatives (compounds **9–11**) decompose from melts to give SnO_2 and not the reduced tin species, SnO, as the final tin product.

Acknowledgements—Financial support from NATO (grant No. 1762), from the Consiglio Nazionale delle Ricerche (Roma), from the Ministero della Pubblica Istruzione (Roma) and from S.E.R.C. and the International Tin Research Institute (for a studentship to S.M.G.) is gratefully acknowledged.

REFERENCES

1. S. J. Angyal and K. P. Davies, *J. Chem. Soc. Chem. Commun.* 1971, 500.
2. S. J. Angyal, *Aust. J. Chem.* 1972, **25**, 1957.
3. D. G. Craig, N. C. Stephenson and J. D. Stevens, *Carbohydr. Res.* 1972, **22**, 496.
4. W. J. Cook and C. E. Bugg, *Carbohydr. Res.* 1973, **131**, 265 (and references therein).
5. S. J. Angyal, *Pure Appl. Chem.* 1973, **35**, 131.
6. S. J. Angyal, D. Greeves and V. A. Pickles, *Carbohydr. Res.* 1974, **35**, 165.
7. J. Ollis, V. J. James, S. J. Angyal and P. M. Pojer, *Carbohydr. Res.* 1978, **60**, 219 (and references therein).
8. S. J. Angyal, *Chem. Soc. Rev.* 1980, **9**, 415 (and references therein).
9. M. Tonkovic, O. Hadzija and Nagy-Czako, *Inorg. Chim. Acta* 1983, **80**, 251.
10. A. J. Crowe and P. J. Smith, *J. Organomet. Chem.* 1976, **110**, C59 (and references therein).
11. A. F. Husain and R. C. Poller, *J. Organomet. Chem.* 1976, **118**, C11 (and references therein).
12. D. Wagner, J. P. H. Verheyden and J. G. Moffatt, *J. Org. Chem.* 1974, **39**, 24.
13. C. W. Holzapfel, J. M. Koekemoer, C. F. Marais, G. J. Kruger and J. A. Pretorius, *S. Afr. J. Chem.* 1982, **80**, 35.
14. G. Ruisi, M. T. Lo Giudice and L. Pellerito, *Inorg. Chim. Acta* 1984, **93**, 161 (and references therein).
15. W. Pigman and D. Horton, In *The Carbohydrates: Chemistry and Biochemistry* (Edited by W. Pigman and D. Horton), Vol. 1A, p. 1. Academic Press, New York (1972).
16. L. Pellerito, G. Ruisi, R. Barbieri and M. T. Lo Giudice, *Inorg. Chim. Acta* 1977, **21**, L33 (and references therein).
17. C. L. Angell, *J. Chem. Soc.* 1961, 504.
18. L. P. Khun, *Anal. Chem.* 1950, **22**, 276.
19. T. Shimanouchi, M. Tsuboi and Y. Kyokogu, *Infrared Spectra of Nucleic Acids and Related Compounds, Adv. Chem. Phys.* 1964, **7**, 435.
20. D. M. Adams, *Metal–Ligand and Related Vibrations.* E. Arnold, London (1967).
21. F. K. Butcher, W. Gerrard, E. F. Money, R. G. Rees and H. A. Willis, *Spectrochim. Acta* 1964, **20**, 51.
22. J. Mendelsohn, A. Marchand and J. Valadè, *J. Organomet. Chem.* 1966, **6**, 25.
23. V. I. Goldanskii, E. F. Makarov, R. A. Stukan, V. A. Trukhtanov and V. V. Khrapov, *Dokl. Akad. Nauk SSSR* 1963, **151**, 357.
24. J. D. David, C. Pascard and M. Cesario, *Nouv. J. Chem.* 1979, **3**, 63 (and references therein).
25. G. M. Bancroft, V. G. Kumar Das, T. K. Sham and M. G. Clark, *J. Chem. Soc., Dalton Trans.* 1976, 643.
26. G. M. Bancroft and R. H. Platt, *Adv. Inorg. Chem. Radiochem.* 1972, **15**, 59 (and references therein).
27. C. D. Hager, F. Huber, A. Silvestri and R. Barbieri, *Inorg. Chim. Acta* 1981, **49**, 31 (and references therein).

Polyhedron Vol. 6, No. 3, pp. 387–391, 1987
Printed in Great Britain

0277–5387/87 $3.00+.00

RUTHENIUM(III) PERCHLORATE COMPLEXES WITH PURINES, PYRIMIDINES AND NUCLEOSIDES

BADAR TAQUI KHAN,* AHMED GAFFURI, P. NAGESWARA RAO and S. M. ZAKEERUDDIN

Department of Chemistry, Osmania University, Hyderabad-7, India

(*Received* 14 *February* 1986; *accepted* 30 *June* 1986)

Abstract—Ru(III) perchlorate complexes of purine and pyrimidine bases and their nucleosides, viz. adenine, adenosine, guanine, guanosine, hypoxanthine, inosine, cytosine, cytidine, uracil, uridine, thymine and thymidine, were synthesized. The compounds were characterized by elemental analysis, IR, electronic and ^{1}H NMR spectroscopy, and conductivity measurements. In the complexes of purine bases and nucleosides the ligand binding site is found to be N_7, whereas in the case of complexes of pyrimidine bases and their nucleosides N_3 is the binding site.

Recently there has been an upsurge of interest in the complexes of purines, pyrimidines and nucleosides with metal ions.[1–6] This is mainly because of their role in biochemical processes involving nucleic acids.[7] The platinum group metal complexes of purines, pyrimidines and their derivatives were found to possess antitumor and antibacterial activity.[8–11] Interest has been mostly focussed on the complexes of Pt(II) and Pd(II),[1–6] and the ruthenium complexes of purines, pyrimidines and the nucleosides have been little studied.[12,13] Earlier we reported on the complexes of Ru(II) and Ru(III)[6,14,15] with purines, pyrimidines and nucleosides. Since the perchlorate anion as a ligand or as a counter ion can give rise to an interesting series of complexes, we report in the present paper the synthesis of Ru(III) perchlorate complexes of the purines adenine, guanine and hypoxanthine, and the pyrimidines uracil, cytosine and thymine, and their nucleosides. Except for hypoxanthine and inosine the purines, pyrimidines and their nucleosides studied are the natural constituents of DNA and RNA molecules. The complexes reported are binary Ru(III) purine, pyrimidine or nucleoside complexes with perchlorate present either at the outer coordination sphere or in the inner coordination sphere of the metal ion. The complexes are soluble in water which makes them useful candidates for biological studies.

*Author to whom correspondence should be addressed.

EXPERIMENTAL

Ruthenium perchlorate was prepared by a metathesis reaction of ruthenium trichloride trihydrate obtained from Alfa Ventron (U.S.A.) and silver perchlorate obtained from BDH (London, U.K.). Purines, pyrimidines and nucleosides were purchased from Sigma Chemicals (U.S.A.). All solvents used were of high purity and distilled in the laboratory before use. Elemental analyses were obtained from CSIRO (Australia). Conductivity data were measured on a digital conductivity meter No. DI 909. The IR spectra were recorded in KBr pellets on a Perkin–Elmer 577 spectrophotometer. The electronic spectra were recorded on Beckman model 26 and Varian 635 M spectrophotometers. NMR was recorded on Varian A-60 and JEOL HA-100 spectrophotometers.

Preparation of Ru(III) *perchlorate*

Ruthenium trichloride trihydrate (0.5 mmol, 0.13 g) was dissolved in alcohol (15 cm^3), and to this an alcoholic solution of silver perchlorate (0.5 mmol, 0.31 g) was added. The precipitated silver chloride was separated by repeated centrifugation, and the filtrate was taken as Ru(III) perchloroate.

Preparation of complexes

Triperchloratobis(adenine)methanolruthenium-(III)methanolate $\{(Ru(ade)_2(CH_3OH)(ClO_4)_3b]\cdot CH_3OH\}$ (1),diaquo-tetra(adenosine)ruthen-

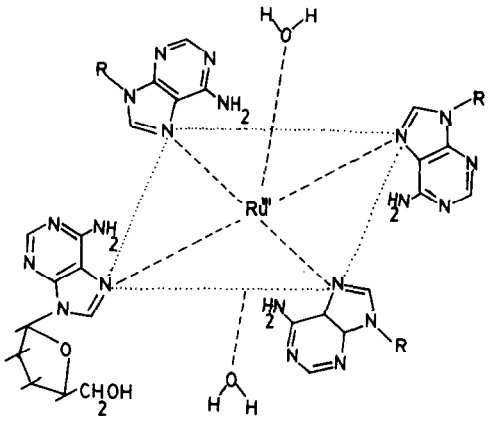

R = RIBOSE

Fig. 1.

ium(III) perchlorate $\{[Ru\text{-}(adenos)_4\text{-}(H_2O)_2]\text{-}(ClO_4)_3\}$ (**2**), pentaaquo(guanine)-ruthenium-(III)perchlorate $\{[Ru(gua)(H_2O)_5](ClO_4)_3\}$(**3**), aquopenta-(guanosine)ruthenium(III) perchlorate-$\{[Ru(guanos)_5\text{-}(H_2O)](ClO_4)_3\}$ (**4**), tris(cytosine)-trimeth-anolruthenium(III) perchlorate methanolate $\{[Ru(cyt)_3\text{-}(CH_3OH\}_3](ClO_4)_3\cdot CH_3OH\}$(**5**), aquopenta(cytidine)-ruthenium(III) perchlorate dihydrate $\{[Ru(cyd)_5\text{-}(H_2O)](ClO_4)_3\cdot 2H_2O\}$ (**6**), hexa(uracil)ruthenium(III)perchlorate hydrate $\{[Ru(ura)_6](ClO_4)_3\cdot H_2O\}$ (**7**), bis-perchlorato-triaquo(uridine)ruthenium(III) perchloratehydrate $\{[Ru(urd)(H_2O)_3(ClO_4)_2](ClO_4)\cdot H_2O\}$ (**8**), perchloratodiaquotris (thymine) ruthenium (III) perchlorate$\{[Ru(thy)_3(H_2O)_2(ClO_4)](ClO_4)_2\}$ (**9**), tetraaquobis(thymidine)ruthenium(III) perchlorate $\{[Ru(thd)_2(H_2O)_4]\text{-}(ClO_4)_3\}$ (**10**), diaquotetra(hypoxanthine)ruthenium(III)perchlorate $\{[Ru(hyp)_4(H_2O)_2](ClO_4)_3\}$ (**11**), aquopenta-(inosine)ruthenium(III) perchlorate $\{[Ru(ino)_5(H_2O)]\text{-}(ClO_4)_3\}$ (**12**).

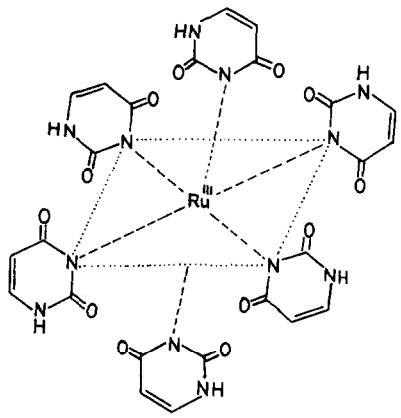

Fig. 3.

In a general method for the preparation of complexes **1–12** an appropriate quantity of ruthenium perchlorate in water is added to the required concentration of an aqueous solution of purine, pyrimidine or nucleoside. The resulting solution was refluxed on a water bath for 6–8 h and then left at room temperature overnight when complexes **1–12** separated out. The complexes were filtered, washed with acetone or ether, recrystallized from water–methanol, dried *in vacuo* and kept in a desiccator. Yield 60–70%,

The recrystallized complexes were characterized by elemental analyses, conductivity measurements, IR, electronic and NMR spectra. The analytical and conductivity data of the complexes are presented in Table 1.

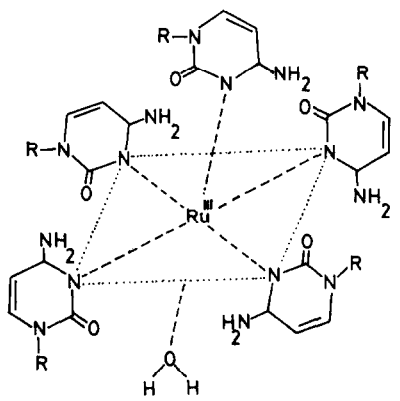

R = RIBOSE

Fig. 2.

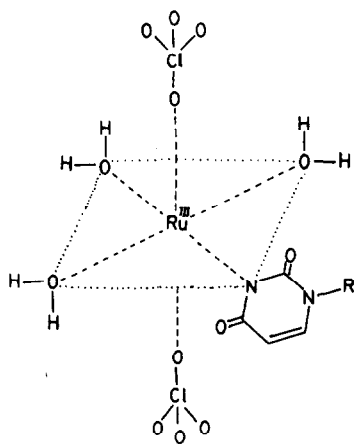

R = RIBOSE

Fig. 4.

Table 1. Characterization and conductivity data of Ru(III) perchlorate complexes

No.	Complex	Colour	Analysis [% found (calc.)] Carbon	Hydrogen	Nitrogen	Conductivity (mho cm^2 mol^{-1})
1	$[Ru(ade)_2(CH_3OH)(ClO_4)_3]\cdot CH_3OH$	Brown	19.6 (19.5)	2.4 (2.4)	19.7 (19.0)	14.6[a]
2	$[Ru(adenos)_4(H_2O)_2](ClO_4)_3$	Dark brown	31.8 (31.9)	3.8 (3.7)	18.6 (18.6)	280
3	$[Ru(gua)(H_2O)_5](ClO_4)_3$	Dark brown	9.3 (9.4)	2.3 (2.3)	10.6 (10.9)	308
4	$[Ru(guanos)_5(H_2O)](ClO_4)_3$	Chocolate brown	33.7 (32.7)	3.5 (3.6)	18.9 (19.1)	280
5	$[Ru(cyt)_3(CH_3OH)_3](ClO_4)_3\cdot CH_3OH$	Red brown	22.3 (22.6)	3.6 (3.7)	14.6 (14.8)	200
6	$[Ru(cyd)_5(H_2O)](ClO_4)_3\cdot 2H_2O$	Brown	32.9 (32.9)	4.2 (4.3)	12.6 (12.6)	225
7	$[Ru(ura)_6](ClO_4)_3\cdot H_2O$	Dark brown	26.4 (26.5)	2.4 (2.4)	15.5 (15.4)	280
8	$[Ru(urd)(H_2O)_3(ClO_4)_2](ClO_4)\cdot H_2O$	Dark brown	14.4 (14.6)	2.4 (2.9)	3.9 (3.9)	88.6
9	$[Ru(thy)_3(H_2O)_2(ClO_4)](ClO_4)_2$	Dark brown	22.1 (22.4)	2.7 (2.4)	10.3 (10.6)	123[b]
10	$[Ru(thd)_2(H_2O)_4](ClO_4)_3$	Brown	25.5 (25.0)	3.7 (3.7)	5.8 (5.8)	300
11	$[Ru(hyp)_4(H_2O)_2](ClO_4)_3$	Violet	24.9 (24.6)	2.4 (2.6)	22.8 (23.0)	360
12	$[Ru(ino)_5(H_2O)](ClO_4)_3$	Dark brown	31.1 (30.7)	3.5 (3.5)	15.4 (15.9)	250

[a]In DMSO.
[b]In alcohol.

RESULTS AND DISCUSSION

The ligational frequencies of importance in the complexes of purines, pyrimidines and nucleosides studied in this investigation are the ν(C=C), ν(C=N) and ν(C=O) modes. The ν(C=C) and ν(C=N) of the purines, pyrimidines and nucleosides are observed around 1450–1600 cm^{-1} and undergo a significant shift ($\sim$50 cm^{-1}) on complexation compared to the frequencies in the free ligand, indicating the involvement of ring nitrogens in coordination to the metal ion. The ligational ν(C=O) and $\delta(NH_2)$ modes observed around 1700 and 1680 cm^{-1}, respectively, are very slightly shifted on complexation, excluding the coordination of the C=O or NH_2 group of the ligands to the metal ion. The ν(OH) mode of coordinated water or methanol appears as a medium band around 3300–3400 cm^{-1}. The presence of a coordinated perchlorate in complexes **1**, **8** and **9** is observed as doubly split[16–20] ν_3- and ν_4-modes of perchlorate around 1080 and 620 cm^{-1}. The ν_1-mode of perchlorate becomes IR-active on coordination and is observed around 910 cm^{-1} as a medium peak. The presence of exclusively ionic perchlorate in complexes **2–7** and **10–12** is observed as single peaks around 1080 and 620 cm^{-1}, corresponding to the ν_3- and ν_4-modes of perchlorate which are fundamental vibrations of this group.[16–20] The presence of both ionic and coordinated perchlorate in complexes **8** and **9** is observed as triply split ν_3- and ν_4-peaks around 1080 and 620 cm^{-1}. The ν_1-mode is observed around 920 cm^{-1}. The IR spectra of the complexes exhibit a ν(M—N) around 520 cm^{-1}.[21]

The electronic spectra of the complexes and their assignments[22] are given in Table 2 and some structures are depicted in Figs 1–4.

In order to determine the binding sites of the ligands used, the NMR spectra of the complexes were of great help. The NMR spectra were recorded in D_2O. The solubility of complex **1** precludes the NMR investigation. The NMR spectrum of complex **2** exhibits peaks at δ 8.20 and 8.64 ppm corresponding to C_2H and C_8H protons, respectively, of adenosine. The peak corresponding to the C_8H protons is shifted downfield by 0.28 ppm in the complex compared to that of the ligand, whereas C_2H protons remain unaffected on complexation. This indicates that adenosine is bound to the metal ion through N_7. On the basis of the NMR spectrum of the rhodium complex of adenine[23] in which the C_8H protons alone are shifted and on the earlier

Table 2. Electronic spectra of Ru(III) perchlorate complexes

No.	Complex	λ_{max} (nm)	ε_{max} ($mol^{-1}\,cm^{-1}$)	Point group	Probable transition
1	$[Ru(ade)_2(CH_3OH)(ClO_4)_3]\cdot CH_3OH$	270[a]	13.25×10^3	C_{2v}	$\pi-\pi^*$
		368	41.6×10^2		$^2A_2 \rightarrow {}^2B_1$
		556	12.5×10^2		$^2A_2 \rightarrow {}^2B_2$
2	$[Ru(adenos)_4(H_2O)_2](ClO_4)_3$[b]	258	49.46×10^3	D_{4h}	$\pi-\pi^*$
		354	4.86×10^3		$d-d$
		546	8.50×10^2		$^2B_2 \rightarrow {}^2B_1$
		714	566		$^2B_2 \rightarrow {}^2A_1$
3	$[Ru(gua)(H_2O)_5](ClO_4)_3$	248	8.22×10^3	C_{4v}	$\pi-\pi^*$
		354	1.2×10^3		$^2A_1 \rightarrow {}^2B_1$
		542	434		$^2A_1 \rightarrow {}^2B_2$
4	$[Ru(guanos)_5(H_2O)](ClO_4)_3$	252	42.25×10^3	C_{4v}	$\pi-\pi^*$
		356	8.16×10^3		$^2A_1 \rightarrow {}^2B_1$
5	$[Ru(cyt)_3(CH_3OH)_3](ClO_4)_3\cdot CH_3OH$	270	15.69×10^3	C_{2v}	$\pi-\pi^*$
		360	234		$^2A_2 \rightarrow {}^2B_1$
		560	65		$^2A_2 \rightarrow {}^2B_2$
		690	56		$^2A_2 \rightarrow {}^2A_1$
6	$[Ru(cyd)_5(H_2O)](ClO_4)_3\cdot 2H_2O$[c]	270	56.92×10^3	C_{4v}	$\pi-\pi^*$
		362	5.99×10^3		$^2A_1 \rightarrow {}^2B_1$
		538	942		$^2A_1 \rightarrow {}^2B_2$
7	$[Ru(ura)_6](ClO_4)_3\cdot H_2O$[d]	260	14.10×10^3	O_h	$\pi-\pi^*$
		355	322		$^2T_{2g} \rightarrow {}^2E_g$
		560	30		$^2T_{2g} \rightarrow {}^4T_{2g}$
		755	14		$^2T_{2g} \rightarrow {}^4T_{1g}$
8	$[Ru(urd)(H_2O)_3(ClO_4)_2](ClO_4)\cdot H_2O$[e]	264	257×10^3	C_{2v}	$\pi-\pi^*$
		336	415		$^2A_2 \rightarrow {}^2B_1$
		527	48		$^2A_2 \rightarrow {}^2B_2$
		722	25		$^2A_2 \rightarrow {}^2A_1$
9	$[Ru(thy)_3(H_2O)_2(ClO_4)](ClO_4)_2$	278[f]	12.13×10^3	C_s	$\pi-\pi^*$
		372	14.9×10^2		$d-d$
		552	368		$d-d$
10	$[Ru(thd)_2(H_2O)_4](ClO_4)_3$	264	85.71×10^3	D_{4h}	$\pi-\pi^*$
		344	2.79×10^3		$d-d$
		560	1540		$^2B_2 \rightarrow {}^2B_1$
11	$[Ru(hyp)_4(H_2O)_2](ClO_4)_3$	260	5.8×10^3	D_{4h}	$\pi-\pi^*$
		365	248		$d-d$
		560	95		$^2B_2 \rightarrow {}^2B_1$
12	$[Ru(ino)_5(H_2O)](ClO_4)_3$	250	24.7×10^4	C_{4v}	$\pi-\pi^*$
		362	40.65×10^2		$^2A_1 \rightarrow {}^2B_1$
		542	12.33×10^2		$^2A_1 \rightarrow {}^2B_2$

[a]In DMSO.
[b]Figure 1.
[c]Figure 2.
[d]Figure 3.
[e]Figure 4.
[f]In alcohol.

work on adenine complexes,[24] it can also be proposed that the adenine in complex **1** is coordinated through N_7. In the NMR spectrum of complex **3** the peak at 7.88 ppm for the C_8H protons shows a downfield shift of about 0.2 ppm, indicating that N_7 is the binding site in guanine. In complex **4** the NMR peak for C_8H protons at 8.80 ppm shows a shift of about 1.0 ppm, which is evidence for the coordination of the N_7 of guanosine to the metal ion. On the basis of the above discussion, hypoxanthine, which is also a purine base, and its nucleoside inosine can be assumed to be coordinated through N_7 in complexes **11** and **12**. Earlier literature also supports this assumption.[13] In the NMR spectrum of complex **5** the peaks at 5.26 and 7.20 ppm correspond to the C_5H and C_6H resonance, respectively, of cytosine. The peak at 5.26 ppm shows a greater upfield shift than the one at

7.20 ppm, indicating the coordination of cytosine to the metal ion through N_3. The peak at 1.8 ppm in complex **5** shows the presence of coordinated methanol. In complex **6**, the NMR spectrum shows peaks at 5.48 and 7.64 ppm. The peak at 5.48 ppm corresponding to C_5H protons shows a greater shift than the C_6H protons, indicating that the binding site in cytidine is N_3. The NMR spectrum of complex **7** exhibits two peaks for the C_5H and C_6H protons at 5.60 and 7.56 ppm, respectively. The C_5H peak shows a greater upfield shift than the C_6H peak, indicating that uracil is coordinated to the metal ion through N_3. On the basis of earlier work on uridine[1] and the NMR of the complex of uracil, uridine in complex **8** may also be proposed to be coordinated to the metal ion through N_3. The NMR spectrum of complex **10** exhibits two peaks at 1.76 and 7.5 ppm, corresponding to methyl and C_6H protons, respectively. The peak at 7.5 ppm shows a shift of about 0.20 ppm, indicating that N_3 is the binding site in thymidine. On this basis and by comparison with the complexes of other pyrimidine bases in this paper and the earlier work on Pt(II) thymine complexes,[25] the thymine in complex **9** is assumed to be bound to the metal ion through N_3.

To summarize, in the present investigation the purine bases and nucleosides studied are coordinated to the metal ion through N_7 whereas in the case of pyrimidine bases and nucleosides N_3 is the binding site.

Acknowledgement—P. N. R. (Pool officer) and S. M. Z. (Senior Research Fellow) thank the CSIR, New Delhi, India, for financial assistance.

REFERENCES

1. S. Mansey, B. Rosenberg and A. J. Thompson, *J. Am. Chem. Soc.* 1973, **95**, 1633.
2. P. C. Kong and T. Theophanides, *Inorg. Chem.* 1974, **13**, 1981.
3. K. P. Beaumont, C. A. McAulife and M. E. Friedman, *Inorg. Chim. Acta* 1977, **25**, 241.
4. C. M. Mikuluski, D. Delacato and D. Braccia, *Inorg. Chim. Acta* 1984, **93**, L19.
5. Badar Taqui Khan, S. Vijaya Kumari, K. Murali Mohan and G. Narsa Goud, *Polyhedron* 1985, **4**, 1617.
6. Badar Taqui Khan, Ahmed Gaffuri and M. R. Somayajulu, *Indian J. Chem.* 1981, **13**, 199.
7. G. L. Eichorn, *Adv. Chem. Ser.* 1967, **62**, 378.
8. S. Kirschner, Y. K. Wei, D. Fransis and J. G. Bergman, *J. Med. Chem.* 1966, **9**, 369.
9. B. Rosenberg, *Platinum Met. Rev.* 1971, **15**, 42.
10. M. J. Cleare and J. D. Hoeshele, *Platinum Met. Rev.* 1973, **15**, 42.
11. B. Rosenberg, In *Nucleic Acid Metal Ion Interactions* (Edited by T. G. Spiro), Vol. 1, p. 127. Marcel Dekker, New York (1979).
12. E. Symn, C. M. Flynn and R. B. Martin, *Theor. Chim. Acta* 1976, **42**, 23.
13. M. J. Clarke, *Inorg. Chem.* 1977, **16**, 738.
14. Badar Taqui Khan, Aneesa Mehmood and M. M. Taqui Khan, *J. Inorg. Nucl. Chem.* 1979, **40**, 1934.
15. Badar Taqui Khan, M. R. Somayajulu and M. M. Taqui Khan, *J. Inorg. Nucl. Chem.* 1978, **40**, 1251.
16. B. J. Hathaway and A. E. Underhill, *J. Chem. Soc.* 1961, 3091.
17. B. J. Hathaway, D. G. Holali and M. Hudson, *J. Chem. Soc.* 1963, 4586.
18. A. E. Wickenden and R. A. Krause, *Inorg. Chem.* 1965, **4**, 404.
19. S. F. Parkvic and D. W. Meek, *Inorg. Chem.* 1965, **4**, 1091.
20. M. E. Farago, J. M. James and V. C. G. Trew, *J. Chem. Soc. A* 1967, 820.
21. K. Nakamoto, *Infrared Spectra of Inorganic and Coordination Compounds*. Wiley, New York (1970).
22. A. B. P. Lever, *Inorganic Electronic Spectroscopy*. Elsevier, Amsterdam (1968).
23. Ahmed Gaffuri, Ph.D. thesis submitted to Osmania University, Hyderabad, India (1982).
24. Badar Taqui Khan and S. Vijaya Kumari, *Indian J. Chem.* 1980, **19A**, 452.
25. B. Lippert and U. Schubert, *Inorg. Chim. Acta* 1981, **56**, 15.

Polyhedron Vol. 6, No. 3, pp. 393–396, 1987
Printed in Great Britain

0277–5387/87 $3.00+.00
Pergamon Journals Ltd

THE INTERACTION OF 2-ACYLPYRIDINES WITH METHYLTIN, PHENYLTIN AND STANNIC CHLORIDES

H. T. BOZIMO and J. J. BONIRE*

Department of Chemistry, Ahmadu Bello University, Zaria, Nigeria

(*Received* 20 *December* 1985; *accepted after revision* 7 *July* 1986)

Abstract—1:1 Lewis acid: Lewis base adducts are obtained from the reaction of 2-benzoylpyridine with $MeSnCl_3$, $SnCl_4$ and $PhSnCl_3$, and of 2-pyridine carboxaldehyde with $PhSnCl_3$. The Lewis bases bind to the organotin Lewis acids through both N and O atoms of the acylpyridines. But 2-acetylpyridine reacts in a different manner with the organotin chlorides, giving what appear to be 1:2 adducts with $MeSnCl_3$, $SnCl_4$, $PhSnCl_3$ and Ph_2SnCl_2; and a product with Me_2SnCl_2 that has yet to be characterized. This suggests that, with organotin Lewis acids, 2-acylpyridines with an α-hydrogen atom on the side-chain reacts differently from 2-acylpyridines without side-chain α-hydrogen atoms.

With an acyl substituent at the 2-position on the pyridine ring (**I**) (Fig. 1) several possibilities arise in the mode of association of the Lewis base with a suitable Lewis acid: the carbonyl oxygen could coordinate along with the nitrogen on the Lewis acid, or the nitrogen could coordinate alone, being less electronegative than oxygen. Or the Lewis base might fail to bind at all because of steric repulsion if the acyl group is bulky. Also, for certain acyl groups, tautomerization in the side-chain could influence the mode of interaction between the acylpyridine and the organotin Lewis acid.

Studies of the interaction of a few 2-acylpyridines with some transition metals have been previously reported.[1–4] 2-Acetylpyridine and 2-benzoylpyridine were found to bind with both N and O on the Lewis acids studied. Jain,[5] in his study of the interaction of 2-acetylpyridine with stannic chloride, obtained what he identified as a 1:1 adduct.

According to the principle of hard and soft acids and bases, the presence of inductively positive organic groups on tetravalent tin would confer softness on the latter.[6,7] The mode of interaction of acylpyridines with transition metal Lewis acids might therefore differ from that with organotin chlorides.

No report appears to have been made so far of the interaction of organotin halides with 2-acylpyridines. We report herein a study of the mode of reaction

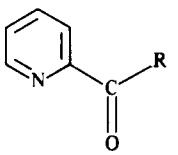

R = H, CH_3 or C_6H_5

Fig. 1.

of 2-acetylpyridine (2-AcPy), 2-benzoylpyridine (2-BzPy), and 2-pyridine carboxaldehyde (2-PyCHO) with methyltin chlorides, phenyltin chlorides and stannic chloride.

EXPERIMENTAL

All the reagents were ANALAR grade. The organotin chlorides and stannic chloride, and the Lewis bases were obtained from Aldrich Chemical Co.

Dichloromethane was purified by washing successively with 5% sodium carbonate solution and water, and drying over anhydrous $CaCl_2$ before distillation.

Melting points are uncorrected.

IR spectra (KBr and CsI discs) were obtained using Perkin–Elmer PE-700 and PE-710-B spectrometers.

^1H NMR spectra (in DMSO-d_6 with internal TMS reference) were obtained using a Varian T-60 spectrometer operating at a probe temperature of 38°C.

Elemental analyses (C, H, N and Cl) were carried

*Author to whom correspondence should be addressed.

out by Scandinavian Analytical Laboratories. Tin content was determined locally according to the method of Farnsworth *et al.*[8]

Preparations

Solutions (containing about 1 mmol solute in 6 cm^3 solvent) of the Lewis acid and Lewis base were mixed in a solute molar ratio of 1:2. The resulting clear mixtures were left overnight at a temperature of about 5°C to give crystalline products. The crystals were washed four times with solvent or recrystallized and dried *in vacuo*.

RESULTS AND DISCUSSION

Table 1 summarizes the methods of preparation, physical properties and elemental analytical results of the various complexes. The analytical results suggest 1:1 complex formation between benzoyl pyridine and $MeSnCl_3$, $SnCl_4$ and $PhSnCl_3$. The last two complexes decomposed on heating.

The reaction of 2-pyridine carboxaldehyde with $MeSnCl_3$, $PhSnCl_3$ and $SnCl_4$ gave a stable isolable product only with $PhSnCl_3$, Elemental analysis of this product suggested a 1:1 adduct.

Reaction of 2-acetylpyridine with $MeSnCl_3$, $PhSnCl_3$, diphenyltin dichloride (Ph_2SnCl_2) and $SnCl_4$ yielded products that were clearly different from the corresponding products with 2-benzoylpyridine. Elemental analysis of the 2-acetylpyridine products suggested 1:2 adduct formation. On the other hand, the analytical results of the reaction product with Me_2SnCl_2 conformed neither with 1:1 nor with 1:2 adduct formation. With the exception of the adduct with Ph_2SnCl_2, these adducts all decomposed at a lower temperature than the corresponding 2-BzPy complexes.

IR spectra

With 2-benzoylpyridine, complex formation resulted in a ligand carbonyl band shift from 1660 cm^{-1} to about 1610 cm^{-1}. From the work of Plytzanopoulos *et al.*[2-4] it can be inferred that this shift is an indication of binding through the carbonyl oxygen atom. For all the complexes an aromatic C=C band shift from 1580 to 1595 cm^{-1} was observed. This is an indication of binding through the nitrogen atom of the pyridine ring. Thus, taken with the inference from the elemental analyses, it can be concluded that benzoylpyridine behaves as a bidentate ligand with the tin Lewis acids. Similar evidence shows that 2-pyridine carboxaldehyde also behaves as a bidentate ligand.

The adducts with 2-acetylpyridine all lack the 1700 cm^{-1} band which is observed in the free base. All except the adduct with Me_2SnCl_2 show a band at about 3450 cm^{-1} which is assignable to —OH. The usual parent ring band shift from 1580 cm^{-1} to about 1600 cm^{-1} was observed in all the complexes. The evidence suggests, first, adduct formation through the nitrogen rather than the oxygen atom and, second, the tautomerization (enolization) of the side-chain. But because the band at 1640 cm^{-1} was broad and extended to about 1650 cm^{-1} it was not possible to confirm the presence of a band for the vinyllic C=C which would have been expected at about 1645 cm^{-1}.

The IR spectrum of the 2-acetylpyridine adduct of Me_2SnCl_2 showed no band above 3100 cm^{-1}, suggesting that no enolization occurred, and that the band at 1640 cm^{-1} was probably due to a coordinated carbonyl (Table 2).

^1H NMR spectra

The ^1H NMR spectra of the 2-benzoylpyridine adducts were simple and, except for slight downfield shifts of the ligand signals, directly derivable from those of the uncomplexed starting materials. The spectrum of the 2-pyridine carboxaldehyde complex with $PhSnCl_3$ was also simple.

The 2-acetylpyridine complexes were more complicated. The stannic chloride adduct showed singlets at 1.95, 2.40, 3.00, 5.80 and 7.00 ppm, in addition to the 2.70 ppm singlet for the $COCH_3$ side-chain. The aromatic ring of the ligand showed a complex multiplet between 9.50 and 7.00 ppm.

The spectra of the $PhSnCl_3$ complexes were relatively simple and supported the molecular formulae suggested by the elemental analyses.

The spectrum of the $MeSnCl_3$ complex showed a new singlet at 2.15 ppm in addition to those expected for $MeSnCl_3$ · bis-2-AcPy. But the most complex spectrum, which we have still not been able to interpret, is that of the reaction product of 2-acetylpyridine with Me_2SnCl_2. The spectrum lacks the singlet at 2.70 ppm for the —$COCH_3$ of the starting Lewis base but shows a signal at 2.30 ppm. The signal for the aromatic rings shows a complex pattern between 7.20 and 8.15 ppm. The mass spectrum of the product gave no indication of a simple 1:1 or 1:2 adduct. It showed a base peak at 207, an apparent molecular ion at 394, and other major peaks at 135, 155, 170, 185 and 224.

The results show a variety of reaction patterns between acylpyridines and organotin Lewis acids. 2-Benzoylpyridine acts as a bidentate ligand to give 1:1 adducts with the tin derivatives. Also, 2-pyridine carboxaldehyde reacts, at least with $PhSnCl_3$, to give a 1:1 adduct. 2-Acetlypyridine reacts with $PhSnCl_3$ and Ph_2SnCl_2 to give 1:2 adducts in which the ligand is coordinated through the nitrogen atom. Adduct

Table 1. Preparation and physical proeprties of the complexes

Complex	Medium of prep.	Special precautions	Appearance of crystals	Mode of purification	Melting point (°C)	Elemental analysis (%)					
							C	H	Cl	N	Sn
$CH_3SnCl_3 \cdot$ 2-BzPy	CH_2Cl_2		Greenish yellow	Washing	182–183	Found	36.9	2.9		3.3	28.4
						Calc.	36.9	2.8		3.3	28.0
$SnCl_4 \cdot$ 2-zPy	CH_2Cl_2	Reactants mixed with cooling	Greenish yellow	Washing	271–273 (d)	Found	32.6	2.1	32.3	3.1	26.8
						Calc.	32.5	2.0	32.0	3.2	26.8
$PhSnCl_3 \cdot$ 2-BzPy	CH_2Cl_2		Light yellow	Washing	209–211 (d)	Found	44.3	2.8		2.8	24.8
						Calc.	44.5	2.9		2.9	24.5
$CH_3SnCl_3 \cdot$ bis-2-AcPy	CH_2Cl_2		Dirty white	Washing	195 (d)	Found	36.7	3.2		5.6	24.9
						Calc.	37.3	3.5		5.8	24.6
$SnCl_4 \cdot$ bis-2-AcPy	Ch_2Cl_2		Light yellow	Washing	253–255 (d)	Found	32.9	2.9	28.4	5.4	23.8
						Calc.	33.4	2.8	28.3	5.6	23.6
$PhSnCl_3 \cdot$ bis-2-AcPy	CH_2Cl_2		Dirty white	Washing	189–191 (d)	Found	43.7	3.6		5.1	22.1
						Calc.	44.1	3.5		5.2	21.8
$Ph_2SnCl_2 \cdot$ bis-2-AcPy	CCl_4		Yellow	Recrystallized from 1:1 toluene-diisopropyl ether	125–127	Found	53.1	4.0		4.4	20.5
						Calc.	53.3	4.1		4.8	20.3
$PhSnCl_3 \cdot$ 2-PyCHO	CH_2Cl_2	Warm solvent: product filtered after 2 h	Brown	Washing	112–115	Found	34.9	2.6	26.8	3.5	29.4
						Calc.	35.2	2.4	26.0	3.4	29.0
Product of Me_2SnCl_2 + 2-AcPy	CH_2Cl_2	Mixture left standing for 2 days	Colourless	Recrystallized from acetonitrile	185 (d)	Found	27.3	3.5		3.2	39.8
						Calc.	41.6	2.4		6.1	25.8

Table 2. IR spectral (cm^{-1}) data of complexes of $MeSnCl_3$, Ph_2SnCl_2, $PhSnCl_3$ and $SnCl_4$ with 2-BzPy, 2-AcPy and 2-PyCHO

Complex	O—H	C—H(arom)	C=O	C=C(Py)	Sn—Ph	Sn—Me	Sn—Cl
$MeSnCl_3 \cdot$ 2-BzPy		3060w	1620s	1595s		795m	
$SnCl_4 \cdot$ 2BzPy		3060w	1610s	1600s			325s
$PhSnCl_3 \cdot$ 2-BzPy		3100w	1610s	1595s	1065w		320s
$PhSnCl_3 \cdot$ 2PyCHO		3100w	1630s	1595s	1065w		320s
$MeSnCl_3 \cdot$ bis-2-AcPy	3500w	3050w	16302	1600s		795m	280s
$SnCl_4 \cdot$ bis-2-AcPy	3450m	3100w	1620s	1600s			325s
$PhSnCl_3 \cdot$ bis-2-AcPy	3450m	3100w	1610s	1600s	1060w		
$PhSnCl_2 \cdot$ bis-2-AcPy	3500w	3050w	1630s	1600s	1060w		
Product of Me_2SnCl_2 + 2-AcPy		3070m	1640s	1600		795s	

formation in this instance also seems to lead to extensive enolization in the ligand side-chain. With $SnCl_4$ and $MeSnCl_3$, 2-acetylpyridine gives reaction products which, from the elemental analyses, appear to be 1:2 adducts but for which spectroscopic data suggest structures that are more complex than the other simple adducts. It has not yet been possible to deduce meaningful structures from the spectroscopic data for these products.

REFERENCES

1. J. D. Ortego, D. D. Waters and S. C. Steele, *J. Inorg. Nucl. Chem.* 1974, **36**, 751.
2. M. Plytzanopoulos, G. Pneumatikakis, N. Hadjiliades and D. Katakis, *J. Inorg. Nucl. Chem.* 1977, **39**, 965.
3. M. Plytzanopoulos and G. Pneumaticakis, *Chim. Chron.* 1979, **8**, 281.
4. M. Plytzanopoulos, G. Pneumatikakis, N. Hadjiliadis, D. Katakis and V. Papadopoulos, *Chim. Chron.* 1979, **8**, 109.
5. S. C. Jain, *Labdev, Part A* 1970, **8**(4), 169.
6. R. C. Poller, *The Chemistry of Organotin Compounds*, p. 186. Logos Press, New York (1970).
7. Tse-Lok Ho, *Chem. Rev.* 1975, **75**, 1.
8. N. Farnworth and J. Pekola, *Analyt. Chem.* 1959, **31**, /410.
9. N. S. Gill, R. H. Nuttal, D. E. Scaife and D. W. A. Sharp, *J. Inorg. Nucl. Chem.* 1961, **18**, 79.
10. P. C. H. Mitchell, *J. Inorg. Nucl. Chem.* 1961, **21**, 382.
11. A. I. Popov, J. C. Marshall, F. B. Stute and W. B. Person, *J. Am. Chem. Soc.* 1961, **83**, 3586.

Polyhedron Vol. 6, No. 3, pp. 397–400, 1987
Printed in Great Britain

0277-5387/87 $3.00+.00

REACTION OF PHENYLTIN CHLORIDES WITH SILVER TRIFLUOROACETATE

J. J. BONIRE

Department of Chemistry, Ahmadu Bello University, Zaria, Nigeria

(*Received* 5 *July* 1985; *accepted after revision* 7 *July* 1986)

Abstract—Ph_3SnCl and $PhSnCl_3$ reacted with $AgOCOCF_3$ to give $Ph_3SnOCOCF_3$ and $PhSn(OCOCF_3)_3$ respectively, but Ph_2SnCl_2 gave an oil which breaks down and rearranges by a radical mechanism to give the ditin compound $Ph_2Sn_2(OCOCF_3)_4$.

In a previous paper,[1] I reported the synthesis of some pyridine complexes of tri- and dimethyltin trifluoroacetates resulting from a study of the substitution reactions of organotin chloride pyridine adducts.

In continuation of this study, it was discovered that the pyridine adducts of diphenyltin dichloride react with silver trifluoroacetate to produce, not the expected pyridine adducts of diphenyltin bistrifluoroacetate, but salts of the pyridine Lewis bases.

Although there is a great deal of literature on the synthesis of organotin carboxylates,[2,3] there has been no report on any reaction of phenyltin chlorides with silver trifluoroacetate.

In trying to understand why diphenyltin dichloride pyridine adducts do not react with silver trifluoroacetate to give pyridine adducts of diphenyltin bistrifluoroacetate, a study of the reaction of silver trifluoroacetate with phenyltin chlorides has been undertaken, and this paper reports the results.

EXPERIMENTAL

All reagents were obtained from BDH, Aldrich, or Alfa; elemental analyses were done by the Scandinavian Microanalytical Laboratories; Sn analysis was done locally using the method of Farnsworth.[4]

IR spectra (CsI disc) were obtained using Perkin–Elmer SP 700 and 800 spectrometers; Raman and mass spectra were determined by the Butterworth Analytical Laboratories.

Dry acetone was prepared by refluxing an AnalaR grade of acetone with *p*-toluenesulphonyl chloride (1 g/l of acetone) for 45 min, and distilling.

Reaction of Ph_3SnCl *with* $AgOCOCF_3$

Triphenyltin chloride (3.85 g, 0.01 M) and silver trifluoroacetate (2.21 g, 0.01 g), each in dry acetone (50 cm^3) were mixed. The precipitated silver chloride was coagulated by boiling the mixture for 10 min in the dark, and filtered off. The clear filtrate was evaporated to dryness giving a white powder. The product (3.60 g, dry) was recrystallized 3 times from 40–60 petroleum spirit; analyses (below) show that it is triphenyltin trifluoroacetate.

Reaction of $PhSnCl_3$ *with* $AgOCOCF_3$

Phenyltin trichloride (1.51 g, 0.005 M) and silver trifluoroacetate (9.95 g, 0.015 M), each in 100 cm^3 of dry acetone, were mixed. The precipitated silver chloride was removed as above, and the clear light yellow filtrate concentrated by evaporation into a thick oil. The oil, on standing, hardened into an unpurifiable brown solid.

Extraction of the oil into 40–60 petroleum spirit, followed by boiling under reflux for 30 min, yielded a fine, white powder which was shown by analysis to be phenyltin tristrifluoroacetate.

Reaction of Ph_2SnCl_2 *with* $AgOCOCF_3$

Diphenyltin dichloride (3.44 g, 0.01 M) and silver trifluoroacetate (5.53 g, 0.025 M), each in 50 cm^3 of dry acetone, were mixed. After removal of the precipitated silver chloride the clear filtrate was concentrated into a colourless viscous oil.

The 'oil' was extracted into cold, aromatic hydrocarbon-free 40–60 petroleum spirit. Warming of the solution started the production of a white

Table 1. Elemental analysis results and IR spectra (CsI disc) of the products

Compound	Yield (%)	Melting point (°C) (uncorrected)	Elemental analysis Found C	H	Sn	Calculated C	H	Sn	IR spectra (cm^{-1}) O—C—O (assym)	O—C—O (sym)	Sn—O—C
$(C_6H_5)_3SnOCOCF_3$	77.80	120–122	51.8	3.4	25.6	51.9	3.2	25.6	1640vs	1440m	990m
$C_6H_5Sn(OCOCF_3)_3$	54.60	>360	27.0	1.1	22.6	26.9	0.9	22.2	1640vs	1440m	1085m
$(C_6H_5)_2Sn_2(OCOCF_3)_4$	36.50	>360	28.1	1.6	28.6	28.4	1.2	28.1	1610s	1430m	995m

paste, and the reaction continued in an exponential manner for several days as the solution was boiled under reflux. After four days, the fine granular precipitate was filtered off, washed four times with aromatic hydrocarbon-free petrol (40–60), and dried (2.5 g). Analyses showed the powder to be $Ph_2Sn_2(OCOCF_3)_4$.

RESULTS AND DISCUSSION

Table 1 shows the elemental analytical results for the products. Ph_3SnCl, $PhSnCl_3$ and Ph_2SnCl_2 reacted with $AgOCOCF_3$ to give products which the elemental analysis results have suggested to be $Ph_3SnOCOCF_3$, $PhSn(OCOCF_3)_3$, $PhSn(OCOCF_3)_2$, respectively.

The ^1H NMR spectra of the products obtained for Ph_3SnCl and Ph_2SnCl_2, in deuterodimethyl sulphoxide (*d*-DMSO), were simple and similar, giving multiplets assignable to the phenyl ring protons at δ 7.40 and 7.75 ppm. The product obtained from $PhSnCl_3$, however, dissolved in *d*-DMSO only with much heating, and gave just a singlet at δ 7.30 ppm (assignable to benzene protons) thereby raising the suggestion of the breakdown of the product in hot *d*-DMSO instead of a simple dissolution.

The IR (CsI discs) spectral data of the products are also shown in Table 1. The spectra of the three products were similar, showing intense bands for a bridge type of O—C—O bond among others.

A mass spectrum of the solid product obtained from Ph_2SnCl_2 gave the highest mass unit of 423, assignable to $C_6H_5Sn(OCOCF_3)_2$ but its Raman spectrum showed bands at Raman shifts of 139, 147, 183, 565, 852, 1000 and 1026 cm^{-1}. Taking into account the works of Brown *et al.*[5] and Bulliner *et al.*,[6] the Raman shift at 147 cm^{-1} has been assigned to an Sn—Sn bond in the compound. A UV spectrum of the compound in DMSO gave a band with a λ_{max} at 273 nm, assignable to an Sn—Sn bond, according to the reports of Drenth *et al.*[7] and Poller.[8] Further, the decolouration of a CCl_4 bromine solution by the compound makes it safe to conclude that the molecule of the compound contains an Sn—Sn bond, since the Sn—Sn bond is known to be broken by the halogens.

From the elemental analysis results and the above deductions the molecular formula of the solid product obtained from Ph_2SnCl_2 is $Ph_2Sn_2(OCOCF_3)_4$ or $[PhSn(OCOCF_3)_2]_2$, with an Sn—Sn linkage.

The elemental and spectral analyses have shown that Ph_3SnCl, $PhSnCl_3$ and Ph_2SnCl_2 react with $AgOCOCF_3$ to yield $Ph_3SnOCOCF_3$, $PhSn(OCOCF_3)_3$ and $Ph_2Sn_2(OCOCF_3)_4$, respectively. The synthesis of $Ph_3SnOCOCF_3$ is not new,[2] but its preparation using $AgOCOCF_3$ appears to be.

The $Ph_2Sn_2(OCOCF_3)_4$, dirty white and powdery, did not melt below 360°C. It dissolved only in highly nucleophilic solvents like dimethylsulphoxide and dimethylformamide.

Benzene was produced along with $Ph_2Sn_2(OCOCF_3)_4$ when the "oil" obtained from the reaction of Ph_2SnCl_2 with $AgOCOCF_3$ was heated in aromatic, hydrocarbon-free 40–60 petroleum spirit. The production of benzene, first indicated by ^1H NMR spectroscopy, was confirmed by subjecting a distillate of the reaction mixture to nitration with 1:1 c. H_2SO_4/c. HNO_3; crystals of *m*-dinitrobenzene were obtained. It was also found that $Ph_2Sn_2(OCOCF_3)_4$ was produced from the oil in petrol under UV and sun light. Prolonged heating of a CCl_4 extract of the oil yielded a powder that had identical spectral properties with $Ph_2Sn(OCOCF_3)_4$, and biphenyl. Heating of a benzene extract of the oil also yielded biphenyl, confirmed by spectroscopy and TLC, along with $Ph_2Sn_2(OCOCF_3)_4$. It was also found that addition of benzoquinone, a radical scavenger, to a petrol extract of the "oil" inhibited the production of $Ph_2Sn_2(OCOCF_3)_4$ when the mixture was heated.

A tin elemental analysis of the "oil" in its driest form gave an Sn content of 20.92%; further drying made the oil solidify to an amorphous light yellow powder with an Sn content of 26.75%. The IR and ^1H NMR spectra of the "oil" did not appear much different from those of $Ph_2Sn_2(OCOCF_3)_4$. There was no indication that benzene was produced along with the "oil" from Ph_2SnCl_2. Also, a Lassaigne test did not show the presence of Cl in the oil. It does appear then that the 'oil' was $Ph_2Sn(OCOCF_3)_2$.

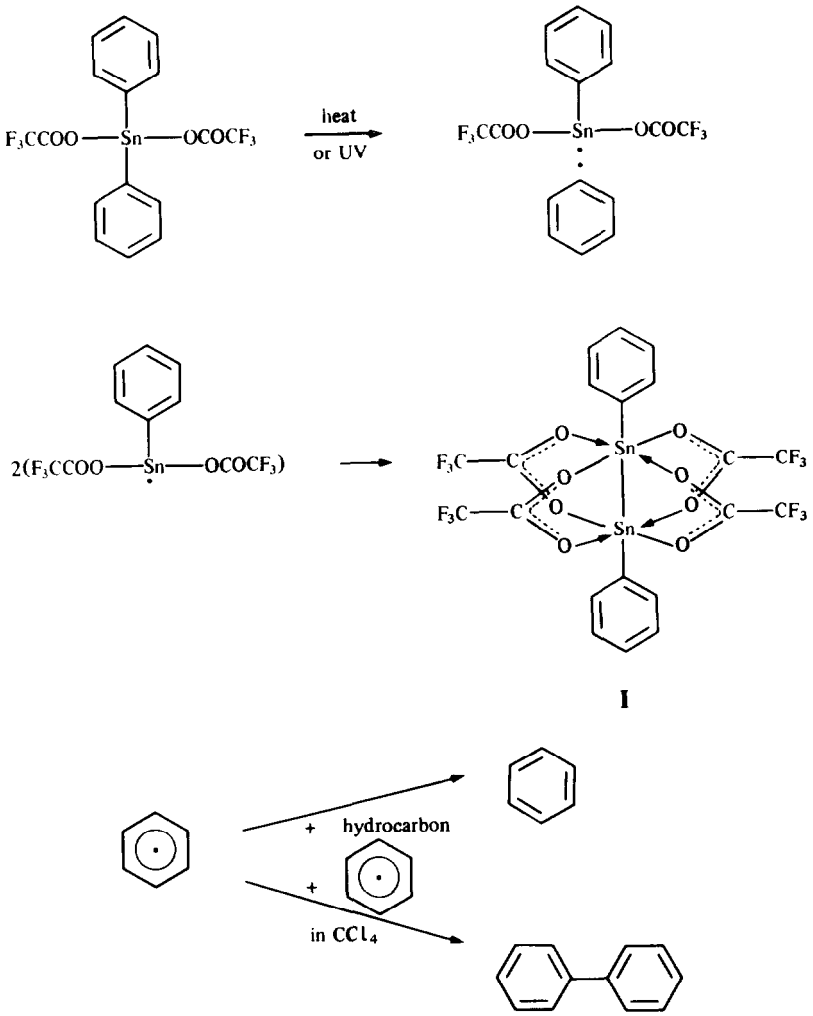

I

Fig. 1. Behaviour of $Ph_2Sn(OCOCF_3)_2$ when heated in non-polar media and UV light.

The production of the $Ph_2Sn_2(OCOCF_3)_4$ from the 'oil' in petroleum spirit is exponential, a mode typical of radical reactions. This suggestion has further being strengthened by the ability of UV and sun light, in addition to heat, to initiate the production of the compound in non-polar media only; and by the ability of benzoquinone, a radical scavenger, to stop or inhibit its production. Benzene was produced along with $Ph_2Sn_2(OCOCF_3)_4$ in petrol, and biphenyl in CCl_4 and benzene solvents. These suggest an initial radical break of the Sn—phenyl bond, a union of two $Ph\dot{S}n(OCOCF_3)_2$ radicals, and the union of two phenyl radicals or the abstraction of a hydrogen radical from petroleum spirit by a phenyl radical, as shown in Fig. 1.

Benzene is obtained in petrol and biphenyl in CCl_4 probably because it is easier to homolytically break a C—H bond than a C—Cl bond.

The symmetrical nature of the structure (I) suggested above would explain the high melting point of the compound; its internal coordination would explain why pyridine adducts of Ph_2SnCl_2 do not react with $AgOCOCF_3$ to give pyridine adducts of $Ph_2Sn(OCOCF_3)_2$, as well as the poor solubility of $Ph_2Sn_2(OCOCF_3)_4$ in many solvents.

It cannot be said at this stage that all diphenyltin dicarboxylates would react as above in non-polar media. It is possible that the electron-withdrawing ability of the phenyl ring of $Ph_2Sn(OCOCF_3)_2$ happened to compare with that of the $Sn(OCOCF_3)_2$ moiety, thereby making possible a homolytic fission of the Sn—phenyl bond. $Ph_2Sn(OCOCH_3)_2$, reportedly first synthesized by Graddon and Rana, [10] remained stable when heated in non-polar media.

REFERENCES

1. J. J. Bonire, *Polyhedron* 1985, **4**, 1707.
2. B. F. E. Ford and J. R. Sams, *J. Organomet. Chem.* 1971, **31**, 47.

3. A. Roy and A. K. Ghosh, *Inorg. Chim. Acta* 1977, **24,** L89.
4. M. Farnsworth and J. Pekola, *Analyt. Chem.* 1959, **31,** 410.
5. M. P. Brown, E. Cartmel and G. W. A. Fowles, *J. Chem. Soc.* 1960, 506.
6. P. A. Bulliner, C. P. Quicksall and T. G. Spiro, *Inorg. Chem.* 1971, **10,** 13.
7. W. Drenth, M. J. Janssen and G. J. M. Van Der Kerk, *J. Organomet. Chem.* 1964, **2,** 265.
8. R. C. Poller, *The Chemistry of Organotin Compounds*, p. 259. Logos Press, New York (1970).
9. R. C. Poller, *The Chemistry of Organotin Compounds*, p. 145. Logos Press, New York (1970).
10. D. P. Graddon and B. A. Rana, *J. Organomet. Chem.* 1977, **136,** 19.

Polyhedron Vol. 6, No. 3, pp. 401–402, 1987
Printed in Great Britain

0277–5387/87 $3.00 + .00

POLAROGRAPHIC STUDY OF THE COMPOSITION AND STABILITY CONSTANTS OF THALLIUM(I) CYCLOHEXYLTHIOGLYCOLATE COMPLEXES

USHA GUPTA and A. L. J. RAO*

Department of Chemistry, Punjabi University, Patiala 147002, India

(*Received* 20 *March* 1986; *accepted after revision* 7 *July* 1986)

Abstract—The complexation of thallium(I) by cyclohexylthioglycolate (CyHTG) has been studied polarographically. The reduction of Tl^+ in cyclohexylthioglycolate solution has been found to be reversible and diffusion controlled involving a one-electron transfer process. Potential vs concentration data at 0.5 M ionic strength are interpreted on the basis of the formation of two complex species, TlA and TlA_2^-. The logarithms of the stability constants of these complexes are 1.73, 3.176 at 20°C, 1.77, 3.342 at 30°C and 1.87, 3.398 at 40°C, respectively. The values of $\Delta G^\ominus$, $\Delta H^\ominus$ and $\Delta S^\ominus$ have been calculated at 30°C.

Mercapto compounds containing active SH and COOH groups have a wide variety of applications. The polarographic behaviour of Tl^+ has been studied in various media with different complexing reagents such as ethylene bis-(3-mercaptopropionate),[1] ethylthioglycolate,[2] ethane-1,2-dithiol,[1] butylthioglycolate,[3] furfuryl mercaptan,[4] 2-mercapto ethanol[5] and β-mercaptopropionic acid.[6] In the present investigations the complexation of cyclohexylthioglycolate with thallium(I) has been studied polarographically to determine the composition and stability constants of the complex ions formed. The values of $\Delta G^\ominus$, $\Delta H^\ominus$ and $\Delta S^\ominus$ have also been calculated and are reported in this paper.

EXPERIMENTAL

Cyclohexylthioglycolate (CyHTG) was used as metal binding agent. It was synthesized by the method given by Gambarov,[7] and was standardized. A stock solution of the reagent was prepared in pure ethanol. A 2 M solution of KNO_3 was used as the supporting electrolyte and 0.1% Triton X-100 as the maximum suppressor. All solutions used in the polarographic measurements had in addition to CyHTG, a Tl^+ concentration of 1.0 mM, 0.5 M KNO_3 and 0.002% Triton X-100 in 50% ethanolic media at pH 6.0. The CyHTG concentration was varied from 0.005 to 0.03 M. A manual Toshniwal polarograph (CLO_2 type) and saturated calomel electrode were used. The necessary correction for the iR drop and residual current were applied in determining the half-wave potential and diffusion current data, respectively.

The plot of i_d vs $\sqrt{h}$ and i_d vs C (C = concentration of thallium) is linear, indicating the diffusion-controlled nature of the reduction wave. The values of slopes from log plots (i.e. plot of log $i/i_d - i$ vs $E \cdot d \cdot e$) agreed with the theoretical values for one-electron transfer. The half-wave potential shifted toward more negative values with increasing CyHTG concentration indicating complex formation. The diffusion current and half-wave potential values are recorded in Table 1. A plot of $E_{1/2}$ as a function of log (CyHTG) showed the curvature indicating the formation of more than one complex. The method of Deford and Hume[8] was applied to the calculation of stability constants for the two complexes TlA and TlA_2^-. Thermodynamic parameters $\Delta G^\ominus$, $\Delta H^\ominus$ and $\Delta S^\ominus$ were also evaluated at 30°C for the two complexes and the results are summarized in Table 2. The percentage distribution of thallium present in different forms as a function of log (CyHTG) has been calculated and the results are presented in Fig. 1.

*Author to whom correspondence should be addressed.

Table 1. Half-wave potentials, diffusion current and values of the various functions at 20°C

Concentration of ligand (M)	i_d (μA)	$-E_{1/2}$ *vs* SCE (V)	$F_0(X)$	$F_1(X)$	$F_2(X)$
0.000	0.554	0.460	—	—	—
0.005	4.048	0.480	1.288	57.6	720
0.010	3.774	0.490	1.640	64.9	1090
0.015	3.542	0.502	2.135	65.7	1440
0.020	3.238	0.510	2.673	83.7	1484
0.025	3.036	0.520	3.377	95.0	1640
0.030	2.834	0.530	4.285	109.5	1850

Table 2. Stability constants and their thermodynamic functions at 30°C

Composition	Stability constants 20°C	Stability constants 30°C	$\Delta G^{\ominus}$ (kJ mol^{-1})	$\Delta H^{\ominus}$ (kJ mol^{-1})	$\Delta S^{\ominus}$ (J K^{-1} mol^{-1})
1:1	54	60	−10.5	6.8	57
1:2	1.5×10^3	2.2×10^3	−19.2	29.3	159

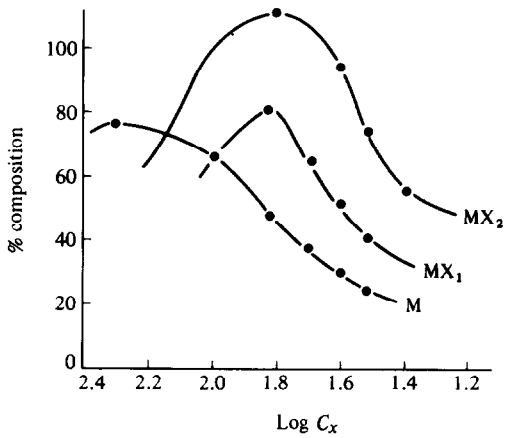

Fig. 1. Distribution diagrams for thallium–cyclohexylthioglycolate system.

Acknowledgement—Financial assistance of CSIR to one of the authors (U.G.) is gratefully acknowledged.

REFERENCES

1. R. S. Saxena and U. S. Chaturvedi, *J. Inorg. Nucl. Chem.* 1972, **34**, 2964.
2. R. S. Saxena and U. S. Chaturvedi, *J. Inorg. Nucl. Chem.* 1972, **34**, 913.
3. R. S. Saxena and M. C. Saxena, *Indian J. Chem.* 1976, **14A**, 628.
4. R. S. Saxena and S. S. Sheelwant, *Labdev.* 1974, **12**, 124.
5. R. S. Saxena and G. L. Khandelwal, *J. Indian Chem. Soc.* 1976, **53**, 970.
6. R. S. Saxena, K. C. Gupta and M. L. Mittal, *Indian J. Chem.* 1969, **7**, 374.
7. D. G. Gambarov, K. Z. Guseinov and R. Fati-Zade, *Org. Reagentry Anal. Khim. Tezisy. Dokl. Vses. 4th Knof.* 1976, **1**, 111; *Chem. Abatr.* 1977, **87**, 193132X.
8. D. D. DeFord and D. N. Hume, *J. Am. Chem. Soc.* 1951, **73**, 5321.

Polyhedron Vol. 6, No. 3, pp. 403–409, 1987
Printed in Great Britain

0277–5387/87 $3.00+.00

THE KINETICS AND MECHANISMS OF THE CATALYSED DECOMPOSITION OF HYDROGEN PEROXIDE BY ETHYLENEDIAMINETETRA(METHYLENEPHOSPHONATO) COMPLEX OF MANGANESE(II)

E. N. RIZKALLA,* S. S. ANIS and L. H. KHALIL

Faculty of Science, Ain Shams University, Abbassia, Cairo, Egypt

(*Received* 8 *April* 1986; *accepted after revision* 7 *July* 1986)

Abstract—The decomposition of H_2O_2 in the presence of ethylenediaminetetra(methylenephosphonato)manganate(II) complex, [Mn(II)Y] (Y represents the $(CH_2–N(CH_2PO_3H_2)_2)_2$ anion), was studied at various temperatures. The rate law:

$$\frac{-d[H_2O_2]}{dt} = \frac{K_a[H^+](k_2 + k_1K_1[H^+])}{(1 + K_a[H^+])(1 + K_1[H^+])}[MnY]_{aq}[H_2O_2]_T$$

holds over the pH range 9.0–10.30. A mechanism involving Mn(IV) and peroxy intermediates is suggested. In strongly alkaline solutions, Mn(IV) species hydrolyse to give colloidal MnO_2. At 30°C, the specific rate constants for the reactions:

$$[Mn(III)Y(OH)]^{6-} + H_2O_2 \xrightarrow{k_1} [Mn(III)Y(OOH)]^{6-} + H_2O$$

and

$$[Mn(III)Y]^{5-} + H_2O_2 \xrightarrow{k_2} [Mn(III)Y(H_2O_2)]^{5-}$$

were determined to be $k_1 = 33\,M^{-1}s^{-1}$ and $k_2 = 2.2\,M^{-1}s^{-1}$. The corresponding activation parameters are, $\Delta H_1^{\ominus} = 17 \pm 4\,kJ\,mol^{-1}$; $\Delta S_1^{\ominus} = -165 \pm 15\,J\,K^{-1}\,mol^{-1}$; $\Delta H_2^{\ominus} = 83 \pm kJ\,mol^{-1}$ and $\Delta S_2^{\ominus} = 37 \pm 55\,J\,K^{-1}\,mol^{-1}$.

The kinetics of oxidation of hydrogen peroxide by potentially oxidizing aquo metal ions in acidic media has been thoroughly investigated.[1–3] In the case of aquo manganese(III) species, two different mechanisms were postulated to cope with the observed rate data. In one set of experiments,[4] the data were analysed using a bimolecular rate equation and the apparent second-order rate constants were found to vary with varying the initial [Mn(III)], [Mn(II)], $[H_2O_2]$ and $[H^+]$ concentrations. The results indicated a first-order dependency on both [Mn(III)] and $[H_2O_2]$ and an inverse dependence on [Mn(II)]. Wells and Mays,[5] on the other hand, investigated the same system under comparable experimental conditions and found that the rate of reaction is first order in [Mn(III)] and independent of both [Mn(II)] and $[H_2O_2]$ concentrations. The enhancement in optical density at 470 nm after mixing with peroxide was attributed to the formation of a new [Mn(III)-OOH] peroxo species which decomposes slowly to the products. The discrepancy in both experiments was attributed to the inappropriate use of the bimolecular rate equation.[6] Analysis of the optical densities available for an individual run in Ref. 4 gave a reasonable first-order plot with k_{obs} approximately half of that estimated from the measurements of Wells *et al.*[5]

Disproportionation of H_2O_2 in the presence of

*Author to whom correspondence should be addressed. Current address: Chemistry Department, Florida State University, Tallahassee, FL 32306-3006, U.S.A.

manganese-polyaminocarboxylates is limited to the report of Jones and Hamm.[7] The reaction of Mn(III)-CyDTA with H_2O_2 was studied in the pH range of 2–4 and found to be first-order in $[H_2O_2]$, second-order in [Mn(III)-CyDTA] and inversely dependent on both $[H^+]$ and [Mn(II)-CyDTA] concentrations. The mechanism suggested involves a fast formation of a ternary peroxo intermediate followed by the slow decomposition of these species. Such ternary complexes were also proposed for the reaction of Fe(III)-EDTA[8] and Cr(III)-EDTA[9] with hydrogen peroxide at higher pH (~6–10). In these systems, the rate was found to be first-order in both H_2O_2 and the complex species. The disagreement in the rate equation for Mn-CyDTA compared to the closely resembling Fe(III) and Cr(III) systems arises from the differences in the reactions considered in both cases. Although iron and chromium chelates were shown to act as catalyst centres for the disproportionation of H_2O_2, Mn(III)-CyDTA was shown to react with H_2O_2 to give Mn(II)-CyDTA and oxygen with an overall stoichiometry of $[Mn(III)\text{-}CyDTA]/[H_2O_2] = 2.06$. Contrary to the peroxidatic systems, the rate-determining step in the catalytic studies is that involving peroxide substitution in the inner sphere of the metal ion.

In the present investigation, we extend these studies to the Mn-ENTMP–H_2O_2 system [ENTMP = ethylenediaminetetra(methylenephosphonic) acid, $\{CH_2\text{-}N(CH_2PO_3H_2)_2\}_2$]. A slight excess of ENTMP was always present to ensure that manganese was present only in the complexed form.

EXPERIMENTAL

Materials

Ethylenediaminetetra(methylenephosphonic) acid, H_8ENTMP, was kindly donated by Monsanto Chemical Co., St. Louis, MO and was recrystallized by precipitating the ligand as the tetra lead salt, filtered, washed and allowed to react with H_2S for 2 h. The black residue of lead sulphide was removed by filtration and the mother liquor containing the ligand in the acid form was freeze dried. The purity of the ligand was checked by potentiometric titration of a suitable sample with a standard CO_2-free sodium hydroxide. Also, the ^1H NMR spectrum showed the presence of only a doublet and a singlet assigned to the α-methylene and the β-backbone protons respectively.[10] Manganese(II) chloride hexahydrate, sodium nitrate, sodium hydroxide and hydrogen peroxide were B.D.H. AnalaR grade.

The Mn(II)-ENTMP complex was prepared by adding 0.001 mol of the manganese salt solution to an equimolar amount of the ligand aqueous solution slowly with a constant stirring. The mixture was warmed and the pH was raised to 7–8 with Na_2CO_3. Twice the stoichiometric amount of magnesium nitrate was then added and the mixture was left to stand overnight. The pale pinkish crystals formed were filtered, dried and analysed for the constituent elements and found to agree well with the empirical formula $Na_2Mg_2[MnY]\cdot 18H_2O$; here and elsewhere Y represents the anion of ethylenediaminetetra(methylenephosphonate).

Spectral and cyclic voltametry measurements

Visible spectral measurements were obtained with a Tracor Northern Optical Multichannel Analyzer. The system composed of a Tracor Northern 6050 spectrometer containing a Czerny–Turner spectrograph connected to a Tracor Northern 1710 Multichannel Analyzer and a Houston Omnigraphic 2000 X-Y recorder. Wavelength calibration was achieved with a holmium oxide filter and the measurements were obtained using a 1.00-cm path length quartz cuvette.

Cyclic voltammograms were obtained using an EG&G Princeton Applied Research model 174A polarographic analyser. A conventional three-electrode system was used with a glassy carbon working electrode, a Pt wire counter electrode and a saturated sodium chloride–calomel electrode as a reference. The electrochemical solutions were isolated from the reference electrode via asbestos fritte. The voltammograms were recorded on a Houston Omnigraphic 2000 X-Y recorder and the scan rate used was $50\,mV\,s^{-1}$.

Kinetic procedure

In all kinetic measurements, fresh solutions of the manganese complex were prepared by dissolving the appropriate weight in the minimum amount of hydrochloric acid. The pH was then adjusted to the desired value by the addition of either glycine buffer[11] or ammonia buffer. Sodium nitrate was added to maintain the ionic strength at 0.10 M unless otherwise specified. The mixture was thermostated in a controlled temperature bath and the kinetic run was started by injecting the peroxide into the solution. Samples of the reaction mixture were removed at set time intervals and the reaction was quenched by KI/H_2SO_4 mixture. The liberated iodine equivalent to the residual peroxide contents was then determined iodometrically.[11]

All calculations were carried out using an IBM PC.

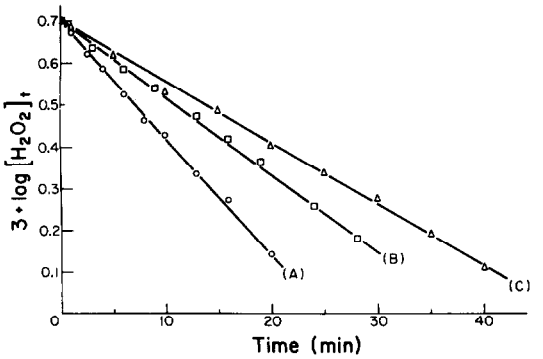

Fig. 1. Variation of residual peroxide concentration with time for the decomposition of hydrogen peroxide in the presence of $[MnY]_{aq}$: $[H_2O_2] = 5.0\,mM$, $[MnY]_{aq} = 0.0555\,mM$, $I = 0.10\,M$ (KNO_3). (A) pH = 9.88 (40°C); (B) pH = 9.80 (35°C); (C) pH = 9.79 (30°C).

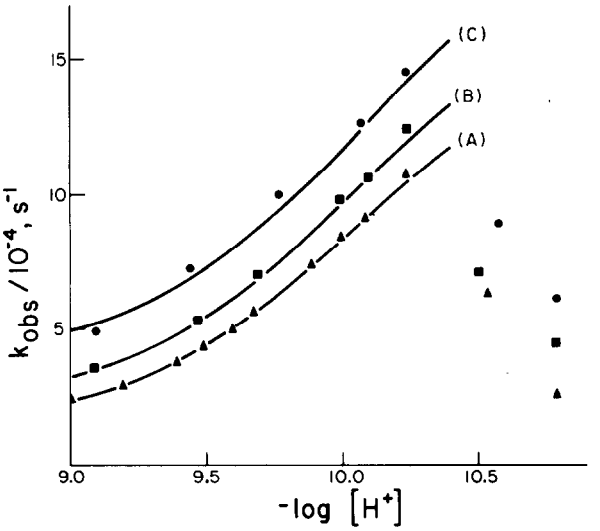

Fig. 2. Dependency of the rate constants on the pH of the medium. Solid lines represent the calculated values from eqn (5) at different pH values; the solid symbols are those obtained experimentally. (A) 30°C; (B) 35°C; (C) 40°C.

RESULTS AND DISCUSSION

The dependence of the reaction rate of the catalytic process

$$2H_2O_2 \rightarrow O_2 + 2H_2O \qquad (1)$$

on the initial conditions of the reaction mixture (namely pH, catalyst concentration, temperature and ionic strength) was investigated. Pseudo-first-order conditions were maintained in all runs by the use of a large excess of H_2O_2 over that of the manganese complex. Semi-logarithmic plots of the residual peroxide contents as a function of time were found to be linear up to a degree of completion of two half-lives or more. Representative sample plots obtained at $-\log[H^+] = 9.7$ and at various temperatures, are shown in Fig. 1. In most cases, the limiting ratio of $[H_2O_2]/[MnY]$ at 75% reaction completion is greater than 22. Only in a few cases, where the dependence of the reaction rate on the catalyst concentration is studied, did this ratio approach 6–7. The influence of the concentration of the catalyst on the disproportionation reaction was determined at several pHs and temperatures. In all cases, the rate is linearly proportional to the catalyst concentration. The slopes of these lines are a function of the medium pH and the temperature of the reaction mixture.

The rate constants determined for mixtures of fixed initial H_2O_2 and complex concentrations at variable pHs are illustrated in Fig. 2. At the three temperatures studied, the values of k_{obs} are an increasing function of pH in the range of 9.0–10.3. At higher alkalinity, the catalytic sensitivity is markedly retarded and approaches zero at pH > 11. A summary of all the results obtained at various reaction conditions is listed in Table 1.

Earlier equilibrium studies on the reaction of manganese salts with ENTMP is limited to the reports of Kabachnik *et al.*[12] and Kurochkina *et al.*[13] Manganese(II) reacts with the phosphonate ligand to form MnH_4Y^{2-} at pH ≃ 5. With increasing the pH of the medium, the complex deprotonates successively, leading to the formation of the normal complex $[MnY]^{6-}$ and the following equilibria hold

$$MnH_{n-1}Y^{-(7-n)} + H^+ \rightleftharpoons MnH_nY^{-(6-n)}$$

$$K_n = [MnH_nY^{-(6-n)}]/[MnH_{n-1}Y^{-(7-n)}][H^+] \qquad (2)$$

$$Mn^{2+} + Y^{8-} \rightleftharpoons MnY^{6-}$$

$$\beta_{101} = [MnY^{6-}]/[Mn^{2+}][Y^{8-}] \qquad (3)$$

where $pK_n = 9.06$, 7.51, 6.22 and 5.32 for $n = 1$, 2, 3 and 4, respectively, and $\log\beta_{101} = 12.70$.

The study is not as complete for manganic species and only the constant for the reaction

$$Mn^{3+} + H_2Y^{6-} \rightleftharpoons MnH_2Y^{3-} \qquad (4)$$

was evaluated to be $\log\beta_{121} = 11.20$[13] compared with $\log\beta_{121} = 7.00$ for the corresponding equilibria with Mn^{2+}. The authors showed also that the auto-reduction of manganese(III) reaches a minimum at pH ⩾ 9.[13]

According to these data in the pH range of 9.0–10.3 the ratio of [Mn(II)HY]/[Mn(II)Y] decreases from 0.72 to 0.06. Since pK_1 for trivalent ENTMP

Table 1. Observed rate constants for the decomposition of hydrogen peroxide in the presence of Mn-ENTMP complex: $[H_2O_2] = 5.0\,mM$, $I = 0.10\,M\,(KNO_3)$

$-\log[H^+]$	Temperature (°C)	$[MnY]^a_{aq}/10^{-5}$ (M)	$k_{obs}/10^{-4}$ (s^{-1})
9.01	30	5.549	2.40 ± 0.15
9.09	35	5.549	3.61 ± 0.23
9.09	40	5.549	4.90 ± 0.32
9.19	30	5.549	2.95 ± 0.18
9.39	30	5.549	3.83 ± 0.24
9.47	35	5.549	5.32 ± 0.35
9.44	40	5.549	7.30 ± 0.50
9.49	30	5.549	4.42 ± 0.28
9.60	30	5.549	5.00 ± 0.32
9.68	30	5.549	5.68 ± 0.37
9.68	30	11.098	10.90 ± 0.80
9.69	30	16.647	16.10 ± 1.30
9.68	30	19.422	19.00 ± 1.62
9.69[b]	30	5.549	6.50 ± 0.44
9.68[c]	30	5.549	6.72 ± 0.45
9.68[d]	30	5.549	6.90 ± 0.47
9.69	35	5.549	7.03 ± 0.48
9.69	35	11.098	13.81 ± 1.07
9.71	35	16.647	20.09 ± 1.74
9.77	35	5.549	7.60 ± 0.52
9.77	40	5.549	10.00 ± 0.72
9.89	30	5.549	7.40 ± 0.51
9.99	35	5.549	9.83 ± 0.71
10.01	30	5.549	8.45 ± 0.59
10.09	30	5.549	9.15 ± 0.65
10.09	35	5.549	10.70 ± 0.78
10.07	40	5.549	12.65 ± 0.96
10.24	30	5.549	10.76 ± 0.79
10.24	35	5.549	12.40 ± 0.94
10.24	40	5.549	14.50 ± 1.14
10.54	30	5.549	6.27 ± 0.42
10.51	35	5.549	7.05 ± 0.48
10.57	40	5.549	8.90 ± 0.63
10.79	30	5.549	2.60 ± 0.16
10.69	30	11.098	6.40 ± 0.43
10.69	30	15.260	8.80 ± 0.62
10.79	35	5.549	4.44 ± 0.28
10.79	35	15.260	12.17 ± 0.92
10.79	40	5.549	6.10 ± 0.41
10.84	40	15.260	16.39 ± 1.33
10.77	45	5.549	8.08 ± 0.56

[a]Manganese concentration in all forms.
[b]$I = 0.30\,M\,(KNO_3)$.
[c]$I = 0.50\,M\,(KNO_3)$.
[d]$I = 0.75\,M\,(KNO_3)$.

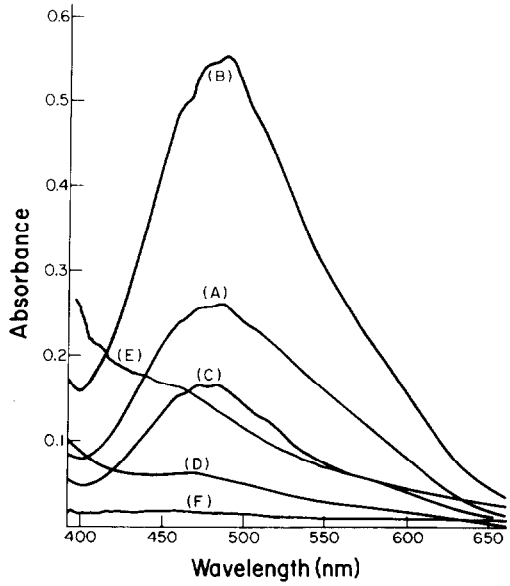

Fig. 3. Absorption spectra recorded after 15 min of mixing $[MnY]_{aq}$ with hydrogen peroxide. (A) $[MnY]_{aq} = 10$ mM (pH = 6.31); (B) $[MnY]_{aq} = 6$ mM (pH = 7.12); (C) $[MnY]_{aq} = 4$ mM (pH = 7.88); (D) $[MnY]_{aq} = 2$ mM (pH = 10.03); (E) $[MnY]_{aq} = 2.5$ mM (pH = 10.67); and (F) $[MnY]_{aq} = 2.5$ mM (no peroxide).

complexes is ~7.0,[14] only [Mn(III)Y] species are dominant at pH > 9.0.

The spectral characteristics of Mn-ENTMP complexes were investigated over the pH range 5–12. In the absence of H_2O_2, Mn(II)-ENTMP has a very weak absorption over the entire pH range ($\varepsilon_{max} = 4.0\,M^{-1}\,cm^{-1}$). Addition of H_2O_2 to the mixture is accompanied by subsequent changes in colour depending on the pH of the medium. The course of the colour changes is pale pink → intense purple → yellowish pink → yellow at pH 6.3, 7.1, 7.9 and 10.0, respectively. The colour intensity reaches a maximum after 15 min of peroxide addition except at pH 10 where the yellow colour is developed instantaneously. Increasing the pH to 10.7 intensifies the yellow colour which turns to brown upon standing for 3 h followed by the deposition of MnO_2 and the pH drifts to 12.5. Figure 3 illustrates the spectral envelopes observed. The presence of a strong band at 485–495 nm in the pH range 6.3–7.9 can be assigned to the spin-allowed $^5E_g \leftarrow {}^5B_{1g}$ transition for Mn(III) in a distorted O_h symmetry.[15] These spectra resemble closely those obtained by mixing Mn(III)-pyrophosphate with ENTMP.[13] At all pHs, the colour is reversible and disappears upon the depletion of the peroxide. Hamm and Suwyn[16] attributed the change in colour from pink to yellow in the case of Mn(III)-CyDTA to the formation of the monohydroxo complex ($pK = 8.11$). At higher pHs, the formation of the unstable intense yellow-brown solutions was attributed to the formation of an oxo-Mn(IV) complex.[15] The very few reports on the spectra of Mn(IV) complexes suggests the presence of two spin-allowed transitions in the regions 355–520 and 460–628 nm assigned to $^4T_{1g} \leftarrow {}^4A_{2g}$ and $^4T_{2g} \leftarrow {}^4A_{2g}$ transitions, respectively.[17] The

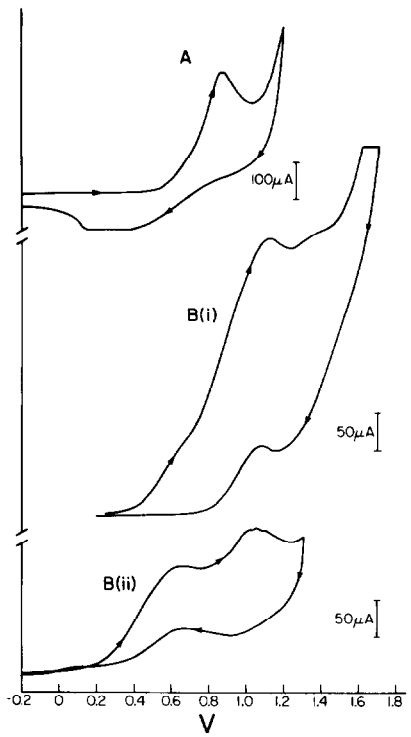

Fig. 4. Cyclic voltammograms obtained during the electro-oxidation of $[MnY]_{aq}$. (A) No peroxide (pH = 7.96); (B) in the presence of excess peroxide: (i) pH = 6.93; (ii) pH = 11.61.

spectra of Mn-ENTMP–H_2O_2 at pH 10 shows the presence of two new bands at 468 and 587 nm and the latter was masked by the intense absorption at 460 nm when the solution pH was raised to 10.7 and higher.

The cyclic voltammograms obtained for Mn(II)-ENTMP in the absence of peroxide and at pH 8.0 displayed a reversible peak with an $E^{\circ\prime}_{MnY}$ of 0.81 V vs NHE (Fig. 4A). The small cathodic current observed relative to the anodic current is presumably due to the adsorbability of the phosphonate complex on the electrode surface.[18] The voltammogram obtained for the Mn-ENTMP–H_2O_2 mixture (pH $\simeq$ 7), shows the presence of an anodic peak at E_{pa} 1.13 V and a small hump at 1.42 V and the reversed scan gave rise to a cathodic peak at E_{pc} of 1.14 V. In strongly alkaline solutions (pH = 11.6), the intensity of the anodic peak at higher potential increased at the expense of the first one. Also, the potentials of all the peaks were negatively shifted by $\sim$0.40 V. The low potential anodic peak is probably associated with the oxidation of the residual Mn(II) to Mn(III). The observed negative shift in the potential with increasing the pH of the medium is attributed to the changes in Mn(II) speciation. At pH 7, the dominant species are MnH_2Y^{4-} and MnH_3Y^{3-}; in strongly alkaline media, the electron-rich MnY^{6-} [and/or $Mn(OH)Y^{7-}$] species are dominant. The pair of peaks observed at higher potential involves a two-electron transfer reaction as indicated by the difference in ($E_{pa} - E_{pc}$). This is tentatively assigned to the oxidation of the $[Mn(III)YX]^{6-}$ complex to $[Mn(IV)YX]^{4-}$, where X is a coordinated OH^- or OOH^- group.

The kinetic data obtained in the pH region 9.0–10.3 were processed using the program KINETIC based on the SIMPLEX algorithm and written by W. Cacheris. The program allows simultaneous calculation of the rate constants associated with two reactants and their conjugate bases. Different models were considered for the reaction of H_2O_2 (and/or HOO^-) with MnY^{5-} and/or $MnY(OH)^{6-}$ complexes. Among all probabilities, only that which consider the reaction of neutral H_2O_2 with both complex species gave the best fit. The absence of ionic strength dependency of the rate constants is in support of this assumption. These results are consistent with the rate law

$$\frac{-d[H_2O_2]}{dt} = k_{obs}[MnY]_{aq}[H_2O_2]_T$$

$$= \frac{K_a[H^+](k_2 + k_1K_1[H^+])}{(1 + K_a[H^+])(1 + K_1[H^+])} [MnY]_{aq}[H_2O_2]_T \quad (5)$$

where $[MnY]_{aq}$ is the manganese concentration in all forms, K_a is the protonation constant of H_2O_2 ($pK_a = 11.75$),[19] k_1 and k_2 are the rate constants observed in the presence of $MnY(OH)^{6-}$ and MnY^{5-} species respectively, and K_1 is the protonation constant for the reaction

$$MnY(OH)^{6-} + H^+ \rightleftharpoons MnY^{5-}. \quad (6)$$

A summary of all the constants calculated together with the activation parameters are listed in Table 2. The error limits of the activation parameters were obtained at 90% confidence following standard procedures.[20] As a further check, the rate constants obtained were used to calculate the values of k_{obs} at different pHs. The solid lines shown in Fig. 2 represent these theoretical calculations; the solid symbols are the experimental values.

In the very early stages of the reaction and at the specified conditions for the kinetic runs ($[H_2O_2] \gg [MnY]_{aq}$; pH $\geqslant$ 9), most of the manganese species will resume oxidation state III. Therefore, the catalytic process is initiated by the reaction of these complexes with the peroxide. The spectral data shown in Fig. 3 are not conclusive about

Table 2. The rate constants and the activation parameters for the catalytic decomposition of hydrogen peroxide in the presence of Mn-ENTMP complex

Temperature (°C)	k_1 ($M^{-1}s^{-1}$)	k_2 ($M^{-1}s^{-1}$)	pK_1
30	33 ± 2.4	2.2 ± 0.03	10.1 ± 0.06
35	36 ± 3.3	3.7 ± 0.18	10.1 ± 0.10
40	42 ± 2.5	6.7 ± 0.31	10.1 ± 0.08
$\Delta H_1^{\ominus} = 17 \pm 4\,kJ\,mol^{-1}$,		$\Delta H_2^{\ominus} = 83 \pm 16\,kJ\,mol^{-1}$	
$\Delta S_1^{\ominus} = -165 \pm 15\,JK^{-1}\,mol^{-1}$,		$\Delta S_2^{\ominus} = 37 \pm 55\,JK^{-1}\,mol^{-1}$	

the involvement of peroxy intermediates in the mechanism. The band position is slightly blue-shifted by ~15 nm compared to that reported in Ref. 13. This shift could be due to the formation of such intermediates or perhaps an anticipated shift due to the presence of the auxiliary pyrophosphate ligand.

The negative entropy associated with the $[Mn(III)Y(OH)]^{6-}$ route suggests that substitution of H_2O_2 for the coordinated OH^- group is the rate-limiting step as in other polyaminocarboxylate systems.[8(a),9] The positive entropy observed for the [Mn(III)Y] pathway, can also be attributed to the solvent reorganization accompanying the intramolecular charge-transfer RDS.[21] However, changes in complex ion hydration can arise from H_2O_2 substitution for one of the coordinated dinegative phosphonate groups. The marked change in the energy barrier for both pathways argues for the involvement of different leaving groups. A possible mechanism consistent with these observations is

$$[Mn(III)Y(OH)]^{6-} + H_2O_2 \xrightarrow{k_1} [Mn(III)Y(OOH)]^{6-} + H_2O \quad (7)$$

$$[Mn(III)Y]^{5-} + H_2O_2 \xrightarrow{k_2} [Mn(III)Y(H_2O_2)]^{5-}. \quad (8)$$

The reaction may propagate via one-electron oxidation steps with the liberation of $OH^{\cdot}$ radicals. Accordingly

$$[Mn(III)Y(OOH)]^{6-} \rightarrow [Mn(IV)Y(O)]^{6-} + OH^{\cdot} \quad (9)$$

$$[Mn(III)Y(H_2O_2)]^{5-} \rightarrow [Mn(IV)Y(OH)]^{5-} + OH^{\cdot} \quad (10)$$

$$H_2O_2 + OH^{\cdot} \rightarrow H_2O + H^+ + O_2^{\cdot -} \quad (11)$$

$$[Mn(IV)Y(O)]^{6-} + H_2O + O_2^{\cdot -} \rightarrow [Mn(III)Y(OH)]^{6-} + O_2 + OH^- \quad (12)$$

$$[Mn(IV)Y(OH)]^{5-} + O_2^{\cdot -} \rightarrow [Mn(III)Y(OH)]^{6-} + O_2. \quad (13)$$

In strongly alkaline media, the oxo-Mn(IV) species undergo further hydrolysis leading to the formation of colloidal MnO_2 which, in turn, reduces the catalytic activity as evidenced by the kinetic observations.

Acknowledgements—The authors wish to thank Mrs S. Clark and Mr G. Peppin for their assistance with the spectral and CV measurements.

REFERENCES

1. (a) C. F. Wells and M. Husain, *Trans. Faraday Soc.* 1971, **67**, 760; (b) J. H. Baxendale and C. F. Wells, *Trans. Faraday Soc.* 1957, **53**, 800.
2. (a) W. G. Barb, J. H. Baxendale, P. George and K. R. Hargrave, *Trans. Faraday Soc.* 1951, **47**, 591; (b) M. L. Kremer and G. Stein, *Trans. Faraday Soc.* 1962, **58**, 702; 1963, **59**, 2535; (c) C. Walling and A. Goosen, *J. Am. Chem. Soc.* 1973, **95**, 2987.
3. (a) C. F. Wells and M. Husain, *J. Chem. Soc. A* 1970, 1013; (b) G. Czapski, B. H. J. Bielski and N. Sutin, *J. Phys. Chem.* 1963, **67**, 201; (c) G. Czapski and A. Samuni, *Israel J. Chem.* 1969, **7**, 361; (d) A. Samuni and G. Czapski, *J. Chem. Soc. A* 1973, 487; (e) H. A. Mahlman, R. W. Mathews and T. J. Sworski, *J. Phys. Chem.* 1971, **75**, 250.
4. G. Davies, L. J. Kirschenbaum and K. Kustin, *Inorg. Chem.* 1968, **7**, 146.
5. C. F. Wells and D. Mays, *J. Chem. Soc. A* 1968, 665.
6. C. F. Wells and D. Fox, *J. Inorg. Nucl. Chem.* 1976, **38**, 107.
7. T. E. Jones and R. E. Hamm, *Inorg. Chem.* 1974, **13**, 1940.
8. (a) E. N. Rizkalla, O. H. El-Shafey and N. M. Guindy, *Inorg. Chim. Acta* 1982, **57**, 199; (b) K. C. Francis, D. Cummins and J. Oakes, *J. Chem. Soc., Dalton Trans.* 1985, 493.

9. E. N. Rizkalla, S. S. Anis and M. S. Antonious, *Inorg. Chim. Acta* 1985, **97**, 165.
10. E. N. Rizkalla and G. R. Choppin, *Inorg. Chem.* 1983, **22**, 1487.
11. A. I. Vogel, *A Text Book of Quantitative Inorganic Analysis Including Elementary Instrumental Analysis*, 2nd edn. Longmans, London (1966).
12. M. I. Kabachnik, I. M. Dyatlova, T. Ya. Medved, Ya. F. Belugin and V. V. Sidorenko, *Dokl. Akad. Nauk SSSR* 1967, **175**, 351.
13. L. V. Kurochkina, N. I. Pechurova, N. I. Snezhko and V. I. Spitsyn, *Russ. J. Inorg. Chem.* 1978, **23**, 2676.
14. E. N. Rizkalla, *Rev. Inorg. Chem.* 1983, **5**, 223.
15. J. Stein, J. P. Fackler, Jr., G. J. McClune, J. A. Fee and L. T. Chan, *Inorg. Chem.* 1979, **18**, 3511.
16. R. E. Hamm and M. A. Suwyn, *Inorg. Chem.* 1967, **6**, 139.
17. A. B. P. Lever, *Inorganic Electronic Spectroscopy*. Elsevier, Amsterdam (1968).
18. H. R. Rawls, T. Bartels and J. Arends, *J. Colloid Interface Sci.* 1982, **87**, 339.
19. V. A. Kargin, *Z. Anorg. Allg. Chem.* 1929, **183**, 77.
20. E. S. Swinbourne, *Analysis of Kinetic Data*. Nelson, London (1971).
21. (a) A. J. Miralles, R. E. Armstrong and A. Haim, *J. Am. Chem. Soc.* 1977, **99**, 1416; (b) A. Szecsy and A. Haim, *J. Am. Chem. Soc.* 1981, **103**, 1679; (c) *J. Am. Chem. Soc.* 1982, **104**, 3063.

Polyhedron Vol. 6, No. 3, pp. 411–416, 1987
Printed in Great Britain

0277-5387/87 $3.00+.00

FACILE SYNTHESIS OF ANTIMONY DITHIOCARBAMATE COMPLEXES

RYOKI NOMURA,* AKIHISA TAKABE and HARUO MATSUDA

Department of Applied Chemistry, Faculty of Engineering, Osaka University, Yamada-Oka, Suita, Osaka 565, Japan

(*Received* 7 *May* 1986; *accepted* 7 *July* 1986)

Abstract—Antimony(III) oxide could react readily with dithiocarbamic acids ($R^1R^2NCS_2$-H, where R^1, $R^2 = C_1$–C_8 alkyls, alkylenes and $C_2H_4OC_2H_4$) and gave the corresponding antimony(III) dithiocarbamates in good yields (45–94%) at 15°C. Novel β-hydroxy or β-cyanoethyl dithiocarbamates were prepared via the condensation in 88–98% yields (R^1, $R^2 = CH_2CH_2OH$, $R^1 = Me$, and $R^2 = CH_2CH_2OH$; $R^1 = Bu^n$, and $R^2 = CH_2CH_2CN$). The larger anisobidenticity among the antimony dithiocarbamate complexes was introduced in the Sb-S_2CN moieties by hydrogen bonding from β-hydroxyl groups which was confirmed by IR, and ^1H and ^{13}C NMR spectroscopy. The quinquevalent inorganic Sb_2O_5 and Sb_2S_5, and organometallic $PhSbO_3H_2$ and Ph_3SbO, gave tervalent products. In the reactions with diethylamine and CS_2 the former three compounds afforded the corresponding dithiocarbamates and the last gave triphenylstibine, but Ph_4SbOH gave the quinquevalent $Ph_4SbS_2CNEt_2$.

Only two methods for the preparation of antimony dithiocarbamate complexes, of both Sb(III) or Sb(V), and also of inorganic or organometallic, have been available to date:[1] (i) metathesis reaction between antimony chloride and sodium or ammonium dithiocarbamate salts;[2–5] (ii) insertion of CS_2 into Sb–amide bonds[6–8]

$$Sb_2O_3 + 6R_2NCS_2H \rightarrow 2Sb(S_2CNR_2)_3 + 3H_2O. \quad (1)$$

In this paper we wish to report a facile and more operative procedure for the preparation of the antimony dithiocarbamates. We found that antimony(III) oxide could be condensed with dithiocarbamic acids, formed from dialkylamines and carbon disulphide *in situ*, to give the corresponding antimony(III) dithiocarbamates in good yields even at room temperature.[9] The reaction was not sensitive to moisture, air and temperature, and was a clean process because of the very small contamination by sodium and/or chlorine. We have extended the reaction to β-substituted amines, e.g. bis(hydroxyethyl)amine, and also succeeded in obtaining organoantimony dithiocarbamates such as tetraphenylstibonium dithiocarbamates. We have also investigated the effect of β-substituents on the dithiocarbamate bonding by means of IR, ^1H and ^{13}C NMR.

EXPERIMENTAL

General

Melting points were measured with a Yanaco micro-melting point apparatus and were uncorrected. IR spectra were recorded on a Hitachi 260-30 spectrophotometer using a KBr disk or KRS-5 windows. ^1H and ^{13}C NMR spectra were performed with a Hitachi R90H FT spectrometer (2.1138T). Cryoscopical molecular weights were measured in benzene or DMSO using a Beckmann thermometer (accuracy ±0.001°C) and indicated that the obtained dithiocarbamate complexes were monomeric in the solution. X-Ray fluorescence analysis was executed using a Rigaku 0600 type analyser (30 kV–5 mA, secondary target Ti), and showed no detectable peaks due to chlorine or sodium atoms, although the samples prepared from the metathesis

*Author to whom correspondence should be addressed.

process contained these contaminators even after some recrystallizations with respect to the peak observation.

Materials

Antimony trioxide (Sb_2O_3, Kanto Chemical Co., Inc., Tokyo) was used without purification. Tetraphenylstibonium hydroxide was prepared by basic hydrolysis of tetraphenylstibonium bromide.[10] Phenylstibonic acid ($PhSbO_3H_2$) was synthesized as reported by Doak and Steinman.[11] Triphenylstibine oxide was obtained by hydrogen peroxide oxidation of triphenylstibine.[12] These organoantimony oxides gave satisfactory analyses. Other reagents and solvents were used after purification.

Reactions

Typical procedures are described below. $Sb(S_2CNEt_2)_3$: into a suspension of Sb_2O_3 (5 mmol) in 20 cm^3 of acetonitrile and 30 mmol diethylamine, CS_2 (30 mmol) was added dropwise at 15°C. The precipitates of Sb_2O_3 disappeared with the reaction and then a yellow solution was obtained. After 1 h of stirring, the volatiles were evaporated *in vacuo*. The resulting yellow mass was then dissolved into hot $CHCl_3$ and filtered. Recrystallization was performed by addition of cold methanol to the chloroform solution. Antimony tris(diethyldithiocarbamate), was obtained as yellow needles, m.p. 133–135°C (lit. 136–137°C[7]), 88%.

$Sb(S_2CN(Me)CH_2CH_2OH)_3$: the reaction of Sb_2O_3 (5 mmol), *N*-methylethanolamine (36 mmol) and CS_2 (30 mmol) in 20 cm^3 of methanol gave a dark yellow gum after stirring for 2 h at 15°C. The gum was filtered off and washed with cold methanol in order to remove unreacted ethanolamine. The dithiocarbamate was recrystallized from MeOH–$CHCl_3$, m.p. 156–159°C, in 98% yield. Yields and analytical and spectral data of the synthesized dithiocarbamates are presented in Tables 1 and 2, respectively.

RESULTS AND DISCUSSION

The direct condensation of antimony(III) oxide (Sb_2O_3) and dithiocarbamic acids proceeded smoothly at 15°C and gave the corresponding antimony(III) dithiocarbamates ($Sbdtc_3$) in good yields. The results of the reaction are summarized in Table 1. Dialkylamines, cyclic amines and β-substituted amines could be converted into the $Sbdtc_3$ in 1–4 h. Reactions using Sb_2S_3, Sb_2O_5 and Sb_2S_5 also occurred, but the yields of the dithiocarbamate were somewhat lower compared to Sb_2O_3.

In the case of diethylamine, a solvent effect was investigated. Aprotic solvents such as acetonitrile, benzene and chloroform, irrespective of their own polarity, promoted the reaction, however, protic ones—such as methanol and water—resulted in lower yields of $Sbdtc_3$. The basicity of the starting amines (based on their pK_a values[15]) seems not to affect the reaction at all. Instead, steric hindrance largely decreases the formation of $Sbdtc_3$: for example, di(isopropyl)amine gave $Sb(S_2CNPr^i_2)$ in only 45% yield, while dipropylamine afforded $Sb(S_2CNPr^n_2)_3$ in 77% yield. Based on the above-mentioned results, we believed that the formation of $Sbdtc_3$ proceeded via stepwise condensation of Sb_2O_3 and the dithiocarbamic acids as shown below. A similar process has been reported for the case of arsenic(III) oxide and dithiocarbamic acids by Sugiyama *et al.*[14] The first step in the scheme may be rate-limiting because unreacted antimony oxide and the dithiocarbamic acids were recovered.

The most characteristic merit of this procedure is the fact that amines which have labile substituents against basic or acidic conditions could be converted to corresponding substituted $Sbdtc_3$. Thus, reactions involving the β-hydroxy or β-cyano derivatives, such as diethanolamine, *N*-methylethanolamine and butyl cyanoethylamine, gave the novel substituted dithiocarbamates in good yields with minor modification to the reaction conditions; namely, methanol was rather favourable in these reactions in place of acetonitrile.

On the other hand, some efforts on the reaction of organoantimony oxides and dithiocarbamic acids have been reported.[2,3,7] Most of the authors in the literature have used organic antimony(III) oxides in oxygen–sulphur exchange reactions. We have found that two phenylantimony(V) oxides were reduced to antimony(III) species during the condensation. Thus, phenylstibonic acid ($PhSbO_3H_2$) gave phenylantimony(III) bis(diethyldithiocarbamate) in good yield, while triphenylstibine oxide did not give any dithiocarbamate complexes, but gave the corresponding thiuram disulphide $[(Et_2NCS_2)_2]$ and triphenylstibine quantitatively. On the other hand, tetraphenylstibonium hydroxide could be converted into quinquevalent tetraphenylstibonium dithiocarbamate but in low yield.

IR spectra

It has been reported that ν(C···N) and ν(C···S) modes of the Sbdtc species appeared in the regions of 1450–1550 and 950–1050 cm^{-1}, respectively.[4,7,16–18] These bands reflect both the π character of the C—N bonds and denticity of the CS_2 moiety, respectively.

Table 1. Preparation of antimony dithiocarbamates from the reaction of antimony oxides, amines and CS_2 at 15°C[a]

Amines (R^1R^2NH)				Time	Yield
R^1	R^2	pK_a[b]	Solvent	(h)	(%)
(1) Sb_2O_3					
Et	Et	10.93	MeCN	1	88
			H_2O	1	52
			EtOH	1	41
			$CHCl_3$	1	85
			C_6H_6	1	79
Pr^n	Pr^n	11.00	MeCN	1	77
Pr^i	Pr^i	11.05	MeCN	1	45
Bu^n	Bu^n	11.31	MeCN	1	86
Bu^i	Bu^i	10.82	MeCN	1	69
Bn[c]	Bn		EtOH	1	94
Oc[d]	Oc		MeCN	4	54
$(CH_2)_4$		11.11	MeCN	4	80
$(CH_2)_5$		11.12	MeCN	1	79
$C_2H_4OC_2H_4$		8.36[e]	C_6H_6[f]	2	89
C_2H_4OH	C_2H_4OH	8.80	MeOH	2	88
Me	C_2H_4OH	(9.72)[g]	MeOH	2	98
Bu	C_2H_4CN		MeCN	o.n.[h]	90
(2) $PhSbO_3H_2$					
Et	Et		MeCN	4	80
(3) Ph_4SbOH					
Et	Et		MeCN	1.5	30

[a]Reaction conditions: antimony oxides, 5 mmol; amines, 30 mmol; CS_2, 30 mmol; solvents, 20 cm^3 and the isolated yields were presented here.

[b]Taken from Ref. 15.

[c]Bn denotes benzyl.

[d]Oc denotes 2-ethylhexyl.

[e]Ref. 20.

[f]Reflux.

[g]pK_a value for *N*-methyl-2-propanolamine.

[h]Overnight.

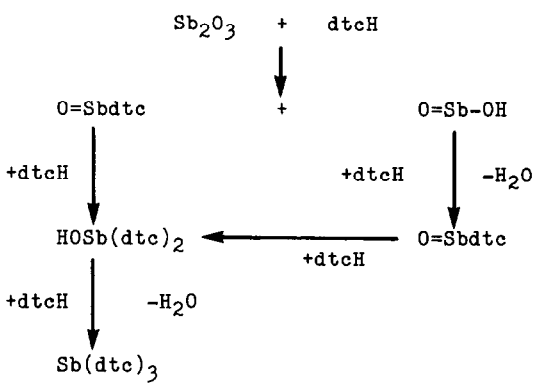

Scheme 1.

The ν(C···N) band of $Sb(S_2CNPr^i_2)_3$ appeared as a doublet at 1475 and 1440 cm^{-1}, and the ν(C···S) band shifted to 1030 cm^{-1} in comparison with those of other $Sbdtc_3$. The splitting and the higher wave number shift indicated larger π bond character in C—N bonds and monodenticity of the CS_2 moiety in $Sb(S_2CNPr^i_2)_3$, compared with other dialkyl derivatives. The larger monodenticity may be attributable to its large steric hindrance.

The existence of β-hydroxy group greatly affected the ν(C···N) and ν(C···S) bands in the two hydroxyethyl derivatives, $Sb[S_2CN(CH_2CH_2OH)_2]_3$ and $Sb[S_2CN(Me)CH_2CH_2OH]_3$. Both ν(C···N) and ν(C···S) bands in the former were split into doublets with low wave number shifts and in the latter 10 cm^{-1} splitting could be observed in the ν(C···S) band. These results indicated the possibility that the anisobidenticity of CS_2 moiety was increased or that monodentate and bidentate CS_2 moieties co-existed. These were caused by intramolecular hydrogen bonding between O—H and C—S bonds.[18]

Table 2. Analytical and spectral data for synthesized antimony dithiocarbamates

R^1	R^2	m.p. (lit.)[a] (°C)	Formula	Found (calc.) (%) C	H	N	IR[b] ν(C···N)	ν(C···S)	^{1}H NMR[c,d] δ(α)	δ(β)	δ(γ)	δ(δ)
Et	Et	133–135 (136–137)[e]	$C_{15}H_{30}N_3S_6Sb$	31.8 (31.8	5.4 5.3	7.4 7.4)	1492s	995m	3.86q	1.28t		
Pr^n	Pr^n	149.5–151	$C_{21}H_{42}N_3S_6Sb$	38.8 (38.8	6.6 6.5	6.4 6.5)	1480s	980m	3.74q	1.76sx	0.92t	
Pr^i	Pr^i	146–147	$C_{21}H_{42}N_3S_6Sb$	38.6 (38.8	6.6 6.5	6.4 6.5)	1475m 1440m	1030bd	n.d.	1.44bd		
Bu^n	Bu^n	73–75 (78–79)[f]	$C_{27}H_{54}N_3S_6Sb$	44.8 (44.1	7.7 7.4	5.8 5.7)	1483s	980m	3.76t	1.28m	1.70m	0.92t
Bu^i	Bu^i	105–107 (96–97)[g]	$C_{27}H_{54}N_3S_6Sb$	44.2 (44.1	7.4 7.4	5.8 5.7)	1478s	985m	3.66d	2.36m	0.92d	
Bn^h	Bn	132–134.5 (137–138)[g]	$C_{45}H_{42}N_3S_6Sb$	58.7 (57.6	4.7 4.5	4.2 4.5)	1495ms	1000m	5.08s	7.48m[q]		
Oc^i	Oc	oil (oil at 0°C)[f]	$C_{51}H_{102}N_3S_6Sb$	57.6 (57.1	9.9 9.6	3.8 3.9)	1480s	980m	3.78d	1.84–2.28m 1.10–1.70m, 0.90t[j]		
$(CH_2)_4$		238–240 (224–225)[g]	$C_{15}H_{24}N_3S_6Sb$	31.7 (32.1	4.3 4.3	7.5 7.5)	1460ms	1002m	3.80bdm	2.00bdm		
$(CH_2)_5$		236–238 (236–238)[g]	$C_{18}H_{30}N_3S_6Sb$	36.1 (35.9	5.2 5.0	6.5 7.0)	1480s	1000m	3.9–4.1m	1.5–1.8m		
$C_2H_4OC_2H_4$		265–268	$C_{15}H_{24}N_3O_3S_6Sb$	29.6 (29.6	4.1 4.0	6.9 6.9)	1480s	1000m	4.12t	3.74t		
C_2H_4OH	C_2H_4OH	143–144[k]	$C_{15}H_{30}N_3O_6S_6Sb$	27.1 (27.2	4.5 4.6	6.2 6.3)	1493s 1468s	982sh 978m	4.06t	3.91q	4.98t[l,m]	
Me	C_2H_4OH	156–159[k]	$C_{12}H_{24}N_3O_3S_6Sb$	24.8 (25.2	4.3 4.2	7.2 7.3)	1492s	982m 972m	3.36t 3.88t	3.68q	4.94t[l,m]	
Bu^n	C_2H_4CN	106–107	$C_{24}H_{39}N_6S_6Sb$	39.6 (39.7	5.3 5.4	11.4 11.6)	1492s	975m	4.14t 3.94t	1.78qn 2.95t	1.40sx	0.98t
Et^n	Et	149–151 (150.3)[q]	$C_{16}H_{25}N_2S_4Sb$	38.7 (39.0	5.2 5.1	5.7 5.7)[o]		985m	3.84q	1.27t	7.30, 8.10[p]	
Et^r	Et	163.5–166	$C_{29}H_{30}NS_2Sb$	59.8 (60.2	5.2 5.2	2.5 2.4)	1470s	1015m	3.65q	1.12t	7.18, 7.53[p]	

[a]Generally recrystallized from $CHCl_3$–MeOH.

[b]KBr disk or KRS-5 windows (neat): s, strong; ms, medium strong; m, medium; bd, broad peak.

[c]In $CDCl_3$ unless otherwise noted.

[d]s, singlet; d, doublet; t, triplet; q, quartet; qn, quintet; sx, sextet; bd, broad signals; m, multiplet; n.d., not detected.

[e]Ref. 8. [f]Ref. 21. [g]Ref. 9. [h]Bn denotes benzyl. [i]Oc denotes 2-ethylhexyl. [j]Signals of two kinds of end methyl were coalesced. [k]Recrystallized from methanol. [l]δ(O*H*). [m]In Me_2SO-d_6. [n]$PhSb(S_2CNEt_2)_2$. [o]Could not be resolved. [p]δ(*Ph*-Sb). [q]Ref. 7. [r]$Ph_4Sb(S_2CNEt_2)$.

Table 3. ^{13}C NMR spectral data for the antimony dithiocarbamates[a]

Dithiocarbamates	Solvent	$\delta(N^{13}CS_2)$	δ(*N*-alkyl) α	β	γ	δ	Others[b]
$Sb(S_2CNEt_2)_3$	$CDCl_3$	199.2	48.3	12.3			
	Me_2SO-d_6	196.9	48.0	12.0			
$Sb(S_2CNPr^i_2)_3$	$CDCl_3$	199.3	54.0[c]	20.0			
$Sb[S_2CN(CH_2CH_2OH)_2]_3$	Me_2SO-d_6	198.7	57.8	57.1			
$Sb[S_2CN(Me)CH_2CH_2OH]_3$	Me_2SO-d_6	198.2	43.0				
			57.9	57.1			
$Sb[S_2CN(Bu)CH_2CH_2CN]_3$	$CDCl_3$	202.5	55.5	29.3	20.2	13.9	117.4[d]
			49.4	15.8			
$PhSb(S_2CNEt_2)_2$	$CDCl_3$	197.6	48.3	12.2			128.1(*m*), 128.2(*p*), 134.9(*o*), 148.9(*ipso*)
$Ph_4Sb(S_2CNEt_2)$	$CDCl_3$	200.7	50.0	12.1			127.6(*m*), 128.3(*p*), 134.9(*o*), 151.2(*ipso*)

[a]Conditions: 5–15 wt% solution, pulse interval 1.5 s, pulse width 45°, number of pulses 500–4000, resolution 0.12 Hz.

[b]Signals of ring carbons were assignable by using the reported data of several phenylantimony compounds (Refs 23 and 24).

[c]$\Delta(\nu_{2/1})$: 27.7 Hz.

[d]$\delta(^{13}C{\equiv}N)$.

The $\nu(C{\cdots}S)$ band of $Ph_4SbS_2CNEt_2$ appeared in the higher wave-number region (1015 cm^{-1}) from which a larger ionicity of Sb—S_2C bonding was expected. Recently, Stevens and Trooster[19] have reported that the analogous $Me_4SbS_2CNEt_2$ showed an ionic structure by means of Mössbauer spectroscopy.

NMR spectra

Results of ^1H NMR measurements are also presented in Table 2. No remarkable change was observed other than some broadening in the signals of *N*-alkyl protons as reported by Sharma *et al.*[18] In particular, we could not detect the methine proton signal of $Sb(S_2CNPr^i_2)_3$. This may be derived from slow rotation around the C—N bonds. Such a significant line broadening in the isopropyl derivative was also observed in ^{13}C NMR signals. The $\Delta(\nu_{1/2})$ of methine carbon was 27.7 Hz.

^{13}C NMR investigation of the obtained Sbdtc was also carried out and the results are shown in Table 3. $\delta(N^{13}CS_2)$ of $Sb(S_2CNEt_2)_3$ in $CDCl_3$ appeared at 199.2 ppm which was between the reported chemical shifts, 198.7[17] and 199.5.[20] Dipolar solvent, Me_2SO-d_6 shifted $\delta(N^{13}CS_2)$ of $Sb(S_2CNEt_2)_3$ to higher field by about 2.3 ppm. The up-field shift of $\delta(N^{13}CS_2)$ in $PhSb(S_2CNEt_2)_2$ could be explained by its higher fraction of oxidation number (oxidation number/coordination number)[17] and supported the penta-coordinated structure reported by Meinema and Noltes.[7] Apparently, in the ionic $Ph_4SbS_2CNEt_2$ $\delta(N^{13}CS_2)$ shifted to lower field by about 1.5 ppm compared with $Sb(S_2CNEt_2)_3$.

In the β-hydroxy substituted dithiocarbamates, single and higher $\delta(N^{13}CS_2)$ shifts were detected, although the anisobidenticity was enhanced as suggested by the IR spectra. In general, an increase of the anisobidenticity has been considered to decrease the δ values. In this case, such lower field shifts were mainly attributable to an increase of total π character in whole NCS_2 moieties. As shown in **2**, the hydrogen bonding pulls the *p*-electrons in N atoms introducing an increase in total π character. Thus, it is reasonable that the increasing of double bond character in C—N bonds compensated for the decrease in C—S bonds.

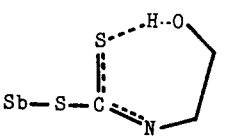

2

Scheme 2.

The most awkward feature was faced on the higher $\delta(N^{13}CS_2)$ in β-cyanoethyl derivative because there was no notable change in vibrational mode. We tentatively deduced that the large lower field shift of ~3.3 ppm was brought about by the coordination of the end cyano group which cancelled the formal positive charge at a central antimony atom, and then decreased the fraction of oxidation number.

Thus, an introduction of polar substituents in

the end of *N*-alkyl group was found to cause a significant alternation on the bonding between the central antimony atoms and the ligands. It was found that the $\delta(N^{13}CS_2)$ of β-substituted antimony dithiocarbamates appeared in the most low field among these simple alkyl dithiocarbamates (193–200 ppm).[17]

Acknowledgement—One of the authors (RN) is grateful for financial support from the Ministry of Education, Japanese Government, Grant-in-Aid for Scientific Research No. 59750674.

REFERENCES

1. G. D. Thorn and R. A. Ludwig, *The Dithiocarbamates and Related Compounds*, pp. 7–37. Elsevier, Amsterdam (1962).
2. E. J. Kupchik and P. J. Calabretta, *Inorg. Chem.* 1965, **4**, 973.
3. E. J. Kupchik and C. T. Teisen, *J. Organomet. Chem.* 1968, **11**, 627.
4. A. Ouchi, M. Shiomi, F. Ebina, T. Uehiro and Y. Yoshino, *Bull. Chem. Soc. Japan* 1978, **51**, 3511.
5. M. Meula-Zigon, J. R. Dias and S. Gomiscek, *Vestn. Slov. Khem. Drus.* 1982, **29**, 23; *Chem. Abstr.* 1982, **96**, 209818z.
6. G. Otertel, H. Molz and H. Holtzschmidt, *Ger. Pat.* 1,170,393 (1964).
7. H. A. Meinema and J. G. Noltes, *J. Organomet. Chem.* 1970, **25**, 139.
8. G. E. Manoussakis and P. Karayamidis, *Inorg. Nucl. Chem. Lett.* 1970, **6**, 71.
9. G. E. Manoussakis and C. A. Tsipis, *J. Inorg. Nucl. Chem.* 1973, **35**, 743.
10. R. Nomura, M. Kori and H. Matsuda, *Chem. Lett.* 1985, 579.
11. H. E. Affsprung and H. E. May, *Analyt. Chem.* 1960, **32**, 1164; K. D. Moffett, J. R. Simula and H. A. Potraz, *Analyt. Chem.* 1956, **28**, 1356.
12. G. O. Doak and H. G. Steinman, *J. Am. Chem. Soc.* 1946, **68**, 1987.
13. H. Matsuda, A. Baba, R. Nomura, M. Kori and S. Ogawa, *Ind. Engng Chem., Prod. Res. Dev.* 1985, **24**, 239.
14. T. Yamashita, I. Okuda and H. Sugiyama, *J. Synth. Org. Chem. Japan* 1978, **36**, 12.
15. G. G. Grau, Konstanten der elektrolytischen Dissoziation. In *Landolt-Boernstein, Band II, Teil 7*, pp. 898–917. Springer, Berlin (1960).
16. M. Lalia-Kantouri, A. George and G. E. Manoussakis, *J. Inorg. Nucl. Chem.* 1977, **39**, 1741.
17. H. L. M. van Gaal, J. W. Diesveld, F. W. Pijpers and J. G. M. van der Linden, *Inorg. Chem.* 1979, **18**, 3251.
18. C. P. Sharma, N. Kumar, M. C. Khandpal, S. Sharma and V. G. Bhide, *J. Inorg. Nucl. Chem.* 1981, **43**, 923.
19. J. G. Stevens and J. M. Trooster, *J. Chem. Soc., Dalton Trans.* 1979, 740.
20. M. Yamazaki, M. Teranishi, R. Igarashi and J. Niwa, *J. Chem. Soc. Japan, Chem. Ind. Chem.* 1980, 1723.
21. H. K. Hall, Jr, *J. Am. Chem. Soc.* 1956, **78**, 2570.
22. H. H. Farmer, B. W. Malone and H. F. Tompkins, *Lubr. Engng* 1967, **23**, 57.
23. J. Havranek and A. Lycka, *Sb. Ved. Pr. Vys. Sk. Chem. Technol., Pardubice* 1980, **43**, 123.
24. A. Ouchi, M. Nakatani, Y. Takahashi, S. Kitazima, T. Sugihara, M. Matsumoto, T. Uehiro, K. Kitano, K. Kawashima and H. Honda *Sci. Pap. Coll. Gen. Educ., Univ. Tokyo* 1975, **25**, 73.

Polyhedron Vol. 6, No. 3, pp. 417–421, 1987
Printed in Great Britain

0277-5387/87 $3.00+.00

COMPLEXATION OF SOME MACROCYCLIC POLYETHERS CONTAINING CONVERGENT METHOXYARYL OR PHENOLIC GROUPS WITH ALKALI CATIONS IN METHANOL

P. L. ZANONATO, P. DI BERNARDO and A. CASSOL*

Dipartimento di Chimica Inorganica, Metallorganica ed Analitica dell'Università, Via Loredan 4, 35131 Padua, Italy

and

G. TOMAT

Istituto di Chimica e Tecnologia dei Radioelementi del C.N.R., C.so Stati Uniti, 35100 Padua, Italy

(*Received* 12 *May* 1986; *accepted* 7 *July* 1986)

Abstract—Log K, ΔH and ΔS values for the 1:1 reactions at 25°C in methanol solution of Na^+, K^+ and Cs^+ with 2-methoxy-1,3-xylyl-15-crown-4 (**I**), 2-methoxy-1,3-xylyl-18-crown-5 (**II**), 2-hydroxy-1,3-xylyl-15-crown-4 (**III**), and 2-hydroxy-1,3-xylyl-18-crown-5 (**IV**) were determined by a calorimetric titration procedure. Log K values for the systems with Na^+ and K^+ were also determined by potentiometry with ion-selective electrodes. For a given cation the stability constants for the complexes with the 18-membered cycles **II** and **IV** are higher than those for the complexes with the 15-membered cycles **I** and **III**. For the ligand having the same ring size the methoxy-crown complex is always more stable than the hydroxy-crown one. The macrocyclic effect shown by the two 18-membered cycles is the result of favourable entropic factors.

A wide variety of thermodynamic parameters are now available for the complexation of cations with crown ethers.[1] The process of the ion–polyether association depends on several factors related to the characteristic properties of ligand, reacting ion and solvent.

Various modifications have been made to the basic crown ether structure in an attempt to influence the ion-binding characteristics of the ligands. Among these modifications a number of macrocyclic polyethers containing convergent methoxyaryl or phenolic groups have been reported.[2–5]

The complexing properties of macrocyclic systems bearing convergent methoxyaryl groups have been investigated by determining the free energies of their association with alkali metal and ammonium and alkylammonium picrates in chloroform.[2,4]

The host–guest complexation of a series of crown ethers bearing an intra-annular phenolic group with alkali metal cations, ammonia and primary amines has been well characterized mainly on the basis of structural studies.[5]

Recently we have examined how the ability of a crown ether to bond lanthanide ions is influenced by a convergent methoxyaryl group.[6,7]

Since no thermodynamic parameters for the reactions of these crown ether derivatives with metal ions are available in the literature, we planned to perform a calorimetric study of the interactions of two crown ether methoxyaryls (**I** and **II**) and two crown ether phenols (**III** and **IV**) with Na^+, K^+ and Cs^+ cations in anhydrous methanol solution.

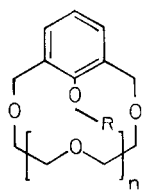

	n	R
I	2	CH_3
II	3	CH_3
III	2	H
IV	3	H

*Author to whom correspondence should be addressed.

From the experimental data, log K, ΔH and $T\Delta S$ values for the reactions examined were calculated. Log K values for the complexes with Na^+ and K^+ were also determined by potentiometry with ion-selective electrodes.

EXPERIMENTAL

Materials

The macrocyclic ligands I–IV were synthesized by condensation of 2,6-bis(bromomethyl)anisole with the appropriate polyethylene glycol, following the procedures described by McKervey *et al.*[3,5] The NaCl, KCl and CsCl salts (Baker) were dried at 120°C for 24 h and stored in a desiccator over P_2O_5. The absolute methanol (Baker Analyzed Reagent) was found by Karl Fischer titration to contain less than 0.01% H_2O. The concentration of NaCl, KCl and CsCl solutions were determined gravimetrically. The macrocycle solutions were prepared by dissolving known weights of each compound in methanol and by dilution. All solutions and reagents were handled and stored in a glove box filled with an inert recirculating atmosphere.

Calorimetric measurements

The calorimetric measurements were made at 25°C using a LKB 8721-2 Precision Calorimeter. The heats of reaction were determined by titrating the metal ion solution in the reaction vessel with successive additions of the ligand solution from a piston burette. Heat of dilution was measured by adding the solution of the cyclic polyether to the pure solvent.

Log K and ΔH values were calculated from calorimetric data using the least-squares program LETAGROP KALLE.[8]

Potentiometric measurements

The concentration of the uncomplexed metal cation was measured with ion-selective electrodes. A Philips G15 Na electrode was used for Na^+ and a Philips G15 K electrode for K^+. The electrodes were stepwise conditioned in aqueous solutions of increasing methanol content up to pure methanol. A calomel reference electrode was used. The electrode was connected to the measuring solution via a bridge containing 0.01 M $N(C_2H_5)_4Br$ in methanol.

A closed glass cell equipped with inlets for the electrodes and the titrant and a magnetic stirrer was used for the measurements. The temperature of the system was maintained at 25.0 ± 0.1°C with a bath of circulating water. The e.m.f. was measured with a Radiometer PHM64 pH meter. The cation selective glass electrodes were calibrated by using standard solutions of the corresponding alkali metal ion in the concentration range 10^{-5}–30×10^{-3} M.

Three runs of measurements were carried out for each cation/polyether system. Each run was started by measuring the e.m.f. of the salt solution (concentration range 10^{-3}–20×10^{-3} M). The polyether solution was added from a piston burette and the new e.m.f. value was measured after each increment.

The stability constant of the 1:1 complex, K, was computed from the relationship

$$K = \frac{C_M - [M^+]}{(C_L - C_M + [M^+]) \cdot [M^+]}$$

where $[M^+]$ is the measured equilibrium concentration of the free metal ion, and C_L and C_M are the total polyether and metal ion concentrations, respectively. Refined values of K were obtained using the least-squares program MINIQUAD.[9]

In the treatment of both potentiometric and calorimetric data we assumed that the alkali metal chlorides are completely dissociated in methanol. This assumption was proved to be justifiable by other authors[10,11] and has been applied in a number of investigations on the interaction of alkali metal cations with macrocycles in methanol.[1]

RESULTS AND DISCUSSION

Log K, ΔH and $T\Delta S$ values for the reactions of Na^+, K^+ and Cs^+ with the macrocyclic ligands studied in methanol are given in Table 1. Also included in this table, for comparison, are the corresponding values for the reactions with two simple crown ethers and their linear counterparts.

For all the systems investigated the heat generated was sufficient to allow log K, ΔH and $T\Delta S$ to be calculated, except for the Na^+/hydroxy-15-crown-4 system. In this case only a rough value of log K calculated from potentiometric data is reported. For the other systems the reliability of the log K values computed from calorimetric data is indicated by the excellent agreement with the corresponding values obtained from independent potentiometric measurements.

In all cases where the heat generated was sufficient, the log K and ΔH values computed on the assumption of 1:1 complexing were found to describe adequately the reaction occurring in the calorimeter. Reactions of stoichiometry 1:1 were also indicated by the potentiometric data treatment. Only for the reactions of methoxy-18-crown-5 with

Table 1. Log K (M^{-1}), ΔH ($kJ\,M^{-1}$) and $T\Delta S$ ($kJ\,M^{-1}$) for reactions of Na^+, K^+ and Cs^+ with polyethers in methanol at 25°C (estimated standard deviations in parentheses)

Ligand	Na^+			K^+			Cs^+		
	log K	ΔH	$T\Delta S$	log K	ΔH	$T\Delta S$	log K	ΔH	$T\Delta S$
Methoxy-15-crown-4 (I)	1.14(3)	− 8.4(4)	−2.0	1.97(4)	−19.9(2)	−8.7	1.81(3)	−20.0(4)	−9.7
	1.11(3)[a]			2.00(3)[a]					
Methoxy-18-crown-5 (II)	2.30(1)	−15.9(3)	−2.8	3.52(4)	−24.7(1)	−4.6	2.76(2)	−22.8(4)	−7.0
	2.28(2)[a]			3.48(2)[a]					
Hydroxy-15-crown-4 (III)	—	—	—	1.26(3)	−12.5(6)	−5.3	1.30(4)	−11.7(8)	−4.3
	~0.8[a]			1.24(4)[a]					
Hydroxy-18-crown-5 (IV)	2.25(2)	−22.2(3)	−9.5	3.18(2)	−33.5(2)	−15.3	2.62(2)	−33.5(8)	−18.5
	2.23(2)[a]			3.15(3)[a]					
15-Crown-5[b]	3.30	−22.6	−3.8	3.35	−32.6	−13.4	2.62	−31.9	−17.0
18-Crown-6[c]	4.36	−35.5	−10.3	6.06	−56.1	−21.6	4.79	−47.2	−19.9
H_3C—O⌒O⌒O⌒O⌒O—CH_3 (TeG)[d]	1.44	−15.1	−6.8	1.59	−28.5	−19.4	1.43	−21.9	−13.7
H_3C—O⌒O⌒O⌒O⌒O⌒O—CH_3 (PG)[d]	1.54	−19.7	−11.0	2.07	−44.7	−32.8	1.76	−38.6	−28.6

[a] Values calculated by potentiometry.
[b] From Ref. 15.
[c] From Ref. 14.
[d] From Ref. 16(e).

K^+ and Cs^+ were the experimental data consistent with a small amount of 1:2 (metal:ligand) complexing.

The data in Table 1 show that all the complexes formed are enthalpy stabilized, whereas the entropy change opposes their formation. The stability sequence for the three alkali metal ions with all the four ligands is $K^+ > Cs^+ > Na^+$, except for the relative positions of K^+ and Cs^+ with the ligand hydroxy-15-crown-4.

For each of the three cations the stability constants for the complexes with the 18-membered cycles **II** and **IV** are at least one order of magnitude higher than those for the complexes with the 15-membered cycles **I** and **III**. This difference in stability is mainly due to the enthalpic contribution, which is more favourable with the larger macrocycles, as would be expected if the magnitude of ΔH is related to the number of oxygen donor atoms in the ring.[12,13]

Comparison of $\log K$ values for the complexes with methoxy and hydroxy derivatives having the same ring size shows that for each cation the methoxy-crown complex is always more stable than the hydroxy-crown one. Taking into account steric hindrance factors, a reversed trend should be expected. A similar behaviour was found by Cram *et al.*[2] in their investigations on the ion binding properties of binaphthyl-crown ethers bearing two methoxyaryl or, alternatively, two phenolic groups with alkali metal picrates in chloroform. The reason for the observed difference was attributed to the existence of strong intramolecular hydrogen bonds of the phenolic groups with the crown ether *O*-atoms in the uncomplexed macrocyclic polyethers. Complex formation requires the cleavage of these hydrogen bonds.

The well-established intramolecular O—H···O hydrogen bonding in the pure hydroxy-18-crown-5 (**IV**)[5] further supports this hypothesis for the system examined here.

It is also of interest to compare the complexing behaviour of the methoxy and hydroxy derivatives with that of the simple crown ethers which have a corresponding ring framework and the same number of oxygen donor atoms, i.e. 18-crown-6 and 15-crown-5. As can be seen in Table 1, both the simple crown ethers form more stable adducts than the corresponding methoxy- and hydroxy-crown with all the three cations. A similar behaviour was noted in the case of methoxy-18-crown-5 compared with the dicyclohexyl-18-crown-6 in chloroform.[4] The poorer complexing ability of the methoxy and hydroxy derivatives can be accounted for by structural factors. Indeed, a functional group attached to the 2-position of the 1,3-xylyl subunit can easily adopt an intra-annular orientation toward the centre of the cavity defined by the macro-ring. This conformation has to change upon complexation in order to allow a more favourable interaction between the cation and the ligand donor atoms. The energy required for this change is expected to have a destabilizing effect on the resulting metal complex.[13]

A consideration of the thermodynamic values reported in Table 1 shows that the lower stability of the methoxy- and hydroxy-crown complexes compared with that of the corresponding simple crown complexes is the result of less favourable enthalpic factors, which seems in accord with the notion that unfavourable conformational energetics are primarily responsible for the observed difference.

An additional minor contribution to this difference in stability could be ascribed to the fact that the methoxy- or hydroxy-oxygen is probably a poorer ligand for cations than purely aliphatic oxygens because of the electron-withdrawing effect of the attached aryl group.

Is this lowering of stability so great to remove the macrocyclic effect? Useful information to answer this question can be obtained by comparing $\log K$, ΔH and $T\Delta S$ values for the systems here examined with the corresponding values for the complexes of their open-chain counterparts. Among a number of available data referring to reaction of alkali metal ions with open-chain polyethers,[16] we have chosen and reported in Table 1 a complete set of stability constants and thermodynamic values for the complexes of Na^+, K^+ and Cs^+ with tetraethylene glycol dimethyl ether (TeG) and pentaethylene glycol dimethyl ether (PG), in methanol at 25°C, recently reported.[16e] To our knowledge no study has been carried out on the complexing properties of open-chain polyethers based on the 1,3-xylyl subunit, and so TeG and PG appear to be the best counterparts available for a comparison with the methoxy- and hydroxy-crowns having five and six oxygens, respectively.

The data listed in Table 1 show that all the complexes formed by a given alkali metal ion with pentaoxa-ligands **I**, **III** and TeG have stability constants of the same order of magnitude. It is difficult to admit any significant macrocyclic effect for the two 15-membered crown derivatives. Instead, a comparison of exaoxa-cycles **II** and **IV** with PG clearly indicates a greater stability for the crown derivatives complexes (maximum $\Delta \log K = 1.5$), which can be attributed to the macrocyclic effect. This is particularly true for the methoxy-18-crown-5 ligand where no interference of transannular hydrogen bonding is present. A consider-

ation of thermodynamic values shows that this macrocyclic effect is caused entirely by favourable entropic factors.

From a comparison of the data for the reaction of Na^+ and K^+ with 18-crown-6, PG and PeG (pentaaethylene glycol), Izatt *et al.* concluded that the macrocyclic effect is primarily the result of favourable enthalpic factors, not entropic factors.[16(d)] At least two effects, depending on structural peculiarities of **II** and **IV**, can be invoked to account for these different conclusions concerning the thermodynamic origin of the macrocyclic effect. (i) Owing to unfavourable conformation of methoxy- and hydroxy-crown a greater energy is required to place the donor atoms in their proper bonding locations, lowering in this way the stabilizing enthalpy change, as mentioned above. (ii) The more rigid structure imposed by the 1,3-xylyl subunit decreases the unfavourable internal entropy change upon complexation.

REFERENCES

1. R. M. Izatt, J. S. Bradshaw, S. A. Nielsen, J. D. Lamb and J. J. Christensen, *Chem. Rev.* 1985, **85,** 271.
2. K. E. Koenig, R. C. Helegson and D. J. Cram, *J. Am. Chem. Soc.* 1976, **98,** 4018.
3. M. A. McKervey and D. L. Mulholland, *J. Chem. Soc., Chem. Commun.* 1977, 438.
4. K. E. Koenig, G. M. Lein, P. Stuckler, T. Kaneda and D. J. Cram, *J. Am. Chem. Soc.* 1979, **101,** 3553.
5. C. M. Browne, G. Ferguson, M. A. McKervey, D. L. Mulholland, Th. O'Connor and M. Parvez, *J. Am. Chem. Soc.* 1985, **107,** 2703.
6. G. Tomat, G. Valle, A. Cassol and P. Di Bernardo, *Inorg. Chim. Acta* 1983, **76,** L13.
7. G. Tomat, G. Valle, P. Di Barnardo and P. L. Zanonato, *Inorg. Chim. Acta* 1985, **110,** 113.
8. R. Arnek, *Ark. Kemi* 1970, **32,** 81.
9. P. Gans, A. Sabatini and A. Vacca, *Inorg. Chim. Acta* 1976, **18,** 237.
10. H. K. Frensdorff, *J. Am. Chem. Soc.* 1971, **93,** 600.
11. G. Michaux and J. Reisse, *J. Am. Chem. Soc.* 1982, **104,** 6895.
12. R. M. Izatt, R. E. Terry, D. P. Nelson, Y. Chan, D. J. Eatough, J. S. Bradshaw, L. D. Hansen and J. J. Christensen, *J. Am. Chem. Soc.* 1976, **98,** 7626.
13. M. L. Campbell, N. K. Dalley, R. M. Izatt and J. D. Lamb, *Acta Cryst.* 1981, **B37,** 1664.
14. J. D. Lamb, R. M. Izatt, C. S. Swain and J. J. Christensen, *J. Am. Chem. Soc.* 1980, **102,** 475.
15. R. B. Davidson, R. M. Izatt, J. J. Christensen, R. A. Schultz, D. M. Dishong and G. W. Gokel, *J. Org. Chem.* 1984, **49,** 5080.
16. (a) C. J. Pedersen and H. K. Frendorff, *Angew. Chem., Int. Ed. Engl* 1972, **11,** 16; (b) L. Favretto, *Ann. Chim.* 1976, **66,** 621; (c) L. Favretto, *Ann. Chim.* 1981, **71,** 163; (d) B. L. Haymore, J. D. Lamb, R. M. Izatt and J. J. Christensen, *Inorg. Chem.* 1982, **21,** 1958; (e) H. J. Buschmann, *Z. Phys. Chem.* 1984, **139,** 113; (f) H. J. Buschmann, *Polyhedron* 1985, **4,** 2039.

Polyhedron Vol. 6, No. 3, pp. 423–425, 1987
Printed in Great Britain

0277–5387/87 $3.00+.00

NEW γ,γ′-DISUBSTITUTED DERIVATIVES OF MACROCYCLIC JÄGER-TYPE Ni(II) COMPLEXES

JULITA EILMES

Institute of Chemistry, Jagiellonian University, Karasia 3, 30-060 Cracow, Poland

(*Received* 28 *May* 1986; *accepted* 7 *July* 1986)

Abstract—The reaction of [Bzo_2Me_4[14]hexaenato(2−)N_4]Ni(II) and [$Bzo_2Me_2Ph_2$ [14]hexaenato(2−)N_4]Ni(II) with glutaryl chloride leads to new γ,γ′-disubstituted derivatives having γ,δ-unsaturated-δ-lactonic rings as substituents. The demetalation of the new complexes by means of gaseous HCl is described. The new compounds were characterized by elemental analysis, IR, ^{1}H NMR and MS data.

The γ-position of six-membered diiminato chelate rings has been found to be a reactive nucleophilic centre. In an earlier report the reactivity of Jäger-type macrocyclic Ni(II) complexes towards benzoyl chloride was described.[1] Since there is continuing interest in the preparation of peripherally substituted macrocyclic complexes, it seemed interesting to use the dichlorides of dicarboxylic aliphatic acids as acylating agents.

It is believed that the reaction with such difunctional electrophilic reagents will give rise to a variety of derivatives. First of all, γ,γ′-disubstituted complexes are expected to be formed. It is also possible that, depending on the length of the aliphatic chains, more complicated compounds can be produced. Bi- and polynuclear systems linked by the difunctional acyl groups, and lacunar-type complexes seem to be also accessible in this way.

This paper summarizes the results of the reaction of Jäger-type Ni(II) complexes with glutaryl chloride.

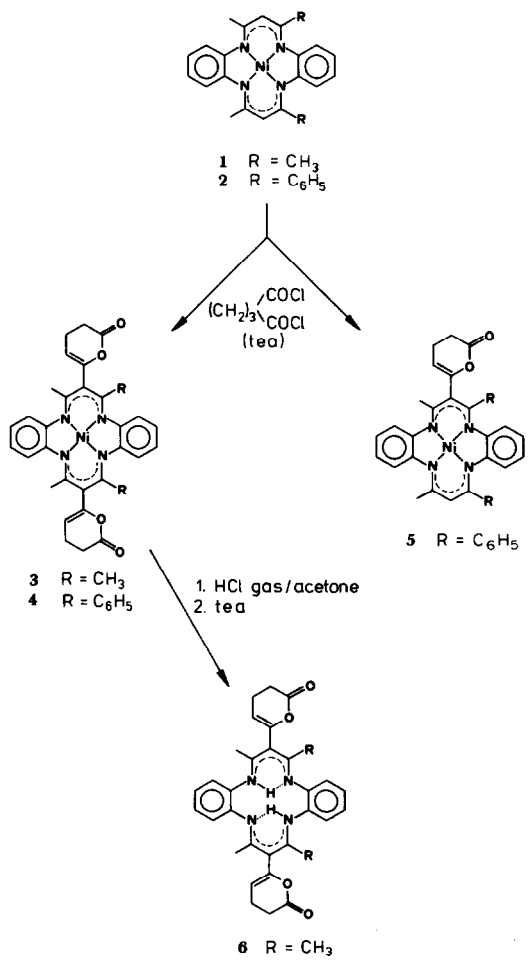

RESULTS

The reaction of the complex **1** and glutaryl chloride in the 1:2 molar ratio in the presence of triethylamine was performed in refluxing benzene. In this manner γ,γ′-disubstituted compound **3**, with two γ,δ-unsaturated-δ-lactonic rings as substituents, was obtained in good yield.

The sterically more crowded complex **2** had to be acylated with an excess of the acylating agent, otherwise about equal quantities of unreacted complex **2**, monosubstituted product **5** and disubstituted complex **4** were isolated from the reaction mixture.

Demetalation of these disubstituted complexes

was conducted in the manner similar to that earlier described.[1] This procedure, however, appeared to be inefficient for complex **4** which underwent a partial decomposition with the loss of substituents.

DISCUSSION

The formation of γ,δ-unsaturated-δ-lactonic rings connected with the macro cyclic ring at δ-carbon atoms, can be explained in terms of intramolecular *O*-acylation within the glutaryl groups. Examples of this type of lactonization and discussions of the mechanism are described in the literature.[2-4] The reaction is considered to involve enolization of the ketomethylene group or alternatively formation of a saturated chlorolactonic intermediate. Further elimination of hydrogen chloride gives rise to the final unsaturated product.

Evidence for the proposed structure of the products **3–6** is given by spectral ^{1}H FT NMR and IR data. ^{1}H NMR spectra show a signal corresponding to the protons of vinyl groups in the region typical for unsaturated δ-lactones.[5] This signal appears as a triplet at δ 5.35, 5.0, 5.0, 5.5 ppm ($J \sim 4$ Hz), for the compounds **3–6**, respectively. Protons of the —CH_2—CH_2— groups which are an A_2B_2 part of the A_2B_2X pattern give rise to a complicated multiplet in the region of aliphatic protons. When the vinyl signals are decoupled, this multiplet collapses to an A_2B_2 multiplet. Conversely, irradiation with the frequency of the adjacent methylene protons causes the vinyl signal to appear as a sharp singlet. The other lines in the ^{1}H NMR spectra are fully consistent with the structure of the macrocyclic framework.

The IR spectra show an intense absorption of a carbonyl group in the region which is characteristic for γ,δ-unsaturated-δ-lactons[5,6] at 1750 cm^{-1}. A band of middle intensity at 1680 cm^{-1} corresponds to the C=C stretching vibration and is typical for an endocyclic double bond of γ,δ-unsaturated-δ-lactons.[4,6]

The presence of signals of parent molecular ions in the mass spectra is supporting evidence for the proposed structure of the products.

EXPERIMENTAL

Melting points are uncorrected. IR spectra were recorded in Nujol and hexachlorobutadiene on a Zeiss UR-10 spectrometer. ^{1}H NMR spectra were taken on a Tesla BS 567A, 100 MHz instrument in $CDCl_3$ using TMS as internal standard. Mass spectra were taken on an LKB 900 instrument.

Parent complexes **1** and **2** were prepared by a procedure described earlier.[7,8]

Reaction of [Bzo_2Me_4[14]hexaenato(2−)N_4] Ni(II) (**1**) *with glutaryl chloride*

3.75 g (0.02 mol) of glutaryl chloride, diluted with 5 cm^3 of benzene was added dropwise to a slurry of complex **1** (4 g, 0.01 mol) and triethylamine (5 cm^3) in dry benzene (80 cm^3). The reaction mixture, protected from moisture, was heated under gentle reflux for 2 h with stirring and then left overnight at room temperature. A grey-green precipitate was filtered off, dried and washed carefully with hot water to separate the product from triethylamine hydrochloride. The crude, green product was dried and recrystallized from dimethylformamide–water. Yield 5.5 g (93%). M.p. 320°C.

Found (**3**): C, 64.7; H, 5.0; N, 9.3; Ni, 10.0%. Calc. for $C_{32}H_{30}N_4O_4Ni$: C, 64.8; H, 5.1; N, 9.4; Ni, 9.9%. MS: 592 (P^{+58}Ni). IR (cm^{-1}): 1680(s) (νC=C), 1750(s) (νC=O). ^{1}H NMR (δ (ppm)]: 2.2 (s, 12H) —CH_3, 2.5 (m, 8H)—CH_2—CH_2—, 5.35 (b.t, 2H) =CH—, 6.7 (b.s, 8H)—*o*-C_6H_4.

Reaction of [$Bzo_2Me_2Ph_2$[14]hexaenato(2−)N_4] Ni(II) (**2**) *with glutaryl chloride*

The reaction of the complex **2** (5.24 g, 0.01 mol) with glutaryl chloride (6.8 g, 0.04 mol) and triethylamine (13 cm^3) in dry benzene (150 cm^3) was carried out for 3.5 h in the same way as described above. After standing for 24 h a colourless precipitate of triethylamine hydrochloride was filtered off and benzene was removed from the filtrate on a rotatory evaporator. Green, resinous product was dissolved in acetone and diluted with cold water. A green solid product which appeared in the solution was filtered off. The crude complex **4** was purified by dissolving in a small amount of dimethylformamide and re-precipitating with cold water. Yield 6.6 g (92%). M.p. 280°C.

A 1:2 molar ratio of reagents produces a mixture of approximately equal quantities of the parent complex **2**, monosubstituted product **5** and disubstituted complex **4** (TLC). The separation of these complexes was performed chromatographically on silica gel (0.05–0.2 mm, Merck) using benzene, chloroform–benzene (1:1), and chloroform as eluents.

Found (**4**): C, 69.9; H, 4.7; N, 7.7; Ni, 8.3%. Calc. for $C_{42}H_{34}N_4O_4Ni$: C, 70.3; H, 4.8; N, 7.8; Ni, 8.2%. MS: 716 (P^{+58}Ni). IR (cm^{-1}): 1680 (m) (νC=C), 1760 (s) (νC=O). ^{1}H NMR [δ (ppm)]: 2.0 (m, 8H)—H_2—CH_2—, 2.3 (s, 6H)—CH_3, 5.0 (b.t, 2H)=CH—, 5.7 (m, 4H) AA′BB′—*o*-C_6H_4, 6.8 (m, 4H)—*o*-C_6H_4, 7.3 (m, 10H)—C_6H_5.

Found (**5**): C, 71.8; H, 4.5; N, 9.1; Ni, 9.8%. Calc. for $C_{37}H_{30}N_4O_2Ni$: C, 71.5; H, 4.9; N, 9.0; Ni, 9.4%.

MS: 620 (P^{+58}Ni). IR (cm^{-1}): 1680(m) (νC=C), 1750(s) (νC=O). ^1H NMR [δ(ppm)]: 2.0 (m, 4H)[—CH_2—CH_2—, 2.2 (s, 3H)—CH_3, 2.3 (s, 3H)—H_3, 4.9 (s, 1H)=CH—, 5.0 (b.t, 1H)=CH—(lact.), 5.7 (m, 4H) AA'BB'—o-C_6H_4, 6.7 (m, 4H)—o-C_6H_4, 7.4 (m, 10H)—C_6H_5.

Demetalation of the complex **3**

A stream of anhydrous hydrogen chloride was passed through a magnetically stirred suspension of complex **3** (3 g) in 150 cm^3 of acetone. The colour of the reaction mixture changed slowly from dark green to orange-yellow and a yellow precipitate began to appear. After about 15 min, the passage of hydrogen chloride was stopped and the tightly closed reaction flask was left overnight under magnetic stirring. Crystalline solid material which accumulated was filtered off, washed with acetone and dried. It was then treated with dilute (1:10) hydrochloric acid to dissolve the nickel chloride. Orange, undissolved solid was filtered off, washed carefully with dilute hydrochloric acid and then immediately with acetone, while still wet. The deprotonation of this hydrochloride of the disubstituted ligand was achieved with the use of triethylamine by the previously described procedure.[1] Recrystallization of the crude product from dimethylformamide–water afforded the ligand **6** as yellow crystals. Yield 1.6 g (59%). M.p. 280°C.

Found (**6**): C, 71.2; H, 5.9; N, 10.2%. Calc. for $C_{32}H_{32}N_4O_4$: C, 71.6; H, 6.0; N, 10.4%. MS: 536 (P^+), IR (cm^{-1}): 1680 (m) (νC=C), 1750 (s) (νC=O), 2700–2900 (v.w) (νN—H), ^1H NMR: 2.2 (s, 12H)—CH_3, 2.6 (m, 8H)—CH_2—CH_2—, 5.5 (t, 2H, J = 4 Hz)=CH—, 7.1 (s, 8H)—o-C_6H_4, 14.5 (broad, 2H) N—H (in py-D_5).

Acknowledgement—This research was supported financially by the Polish Academy of Sciences.

REFERENCES

1. J. Eilmes, *Polyhedron* 1985, **4**, 943.
2. R. B. Turner, *J. Am. Chem. Soc.* 1950, **72**, 579.
3. R. B. Woodward, F. Sondheimer, D. Taub, K. Heusler and W. M. McLamore, *J. Am. Chem. Soc.* 1952, **74**, 4223.
4. J. A. Hartman, A. J. Tomasewski and A. S. Dreiding, *J. Am. Chem. Soc.* 1956, **78**, 5662.
5. D. Rosenthal, P. Grabowich, E. F. Sabo and J. Fried, *J. Am. Chem. Soc.* 1963, **85**, 3971.
6. H. Rosenkrantz and M. Gut, *Helv. Chim. Acta* 1953, **36**, 1000.
7. F. A. L'Eplattenier and A. Pugin, *Helv. Chim. Acta* 1975, **58**, 917.
8. J. Eilmes, D. Pelan and E. Sledziewska, *Bull. Acad. Pol. Sci.* 1980, **28**, 371.

Polyhedron Vol. 6, No. 3, pp. 427–433, 1987
Printed in Great Britain

0277-5387/87 $3.00+.00

SYNTHESIS AND CHARACTERIZATION OF COPPER(II) BIS(DIZIRCONIUM-*ENNEA*-ALKOXIDES)

R. K. DUBEY, A. SINGH and R. C. MEHROTRA*

Department of Chemistry, University of Rajasthan, Jaipur 302004, India

(*Received* 18 *February* 1986; *accepted* 17 *July* 1986)

Abstract—Copper(II) bis(dizirconium-*ennea*-isopropoxide), $[Cu\{Zr_2(OPr^i)_9\}_2]$, has been synthesized by the interaction of $CuCl_2$ with $K\{Zr_2(OPr^i)_9\}$ in a 1:2 molar ratio. The compound undergoes exchange reactions with alcohols of varying steric bulk to yield products of the composition, $[Cu\{Zr_2(OR)_9\}_2]$ (where R = Me, Et, Pr^n, Bu^n, Bu^i and Bu^s); $[Cu\{Zr_2(OPr^i)_6(OEt)_3\}_2]$; $[Cu\{Zr_2(OPr^i)_6(OBu^s)_3\}_2]$; $[Cu\{Zr_2OPr^i)_3(OBu^s)_6\}_2]$; $[Cu\{Zr_2(OPr^i)_7(OBu^t)_2\}_2]$; $[Cu\{Zr_2(OPr^i)_3(OBu^t)_6\}_2]$; and $[Cu\{Zr_2(OPr^i)_4(OAm^t)_5\}_2]$. These derivatives have been characterized by IR, electronic and ESR studies as well as by magnetic susceptibility and molecular weight determinations.

For many years, the alkoxide chemistry of transition metals has centred mainly on the earlier members of the series.[1] During the past few years we have made a detailed study of simple as well as some bimetallic alkoxides of later transition metals.[2–6] The synthesis and alcoholysis reactions of simple copper alkoxides,[1–3] $\{Cu(OR)_2\}_n$ as well as of bis-tetraisopropoxyaluminates $[Cu\{Al(OPr^i)_4\}_2]$ have been described over the past few years by our laboratory.[4]

In view of an unprecedented interest in the bimetallic alkoxides as a source of ceramic and other materials,[7] we report in this paper the synthesis, reactivity and structural characteristics (with the help of IR, electronic, ESR and magnetic studies) of some novel copper bis(dizirconium-*ennea*-alkoxides), $[Cu\{Zr_2(OR)_9\}_2]$.

EXPERIMENTAL

Glass apparatus with standard joints were used throughout the experimental work and stringent precautions were taken to exclude moisture.

Anhydrous $CuCl_2$ was prepared by heating the hydrated $CuCl_2 \cdot 2H_2O$ (B.D.H.) in a current of dry HCl gas. (Found: Cu, 47.3; Cl, 52.7%. Calc. for $CuCl_2$: Cu, 47.2; Cl, 52.8%.) $K\{Zr_2(OPr^i)_9\}$ was synthesized[8] by the (1:2 molar) reaction of $KOPr^i$ with $Zr(OPr^i)_4 \cdot Pr^iOH$ in Pr^iOH. Found: Zr, 24.6; OPr^i, 70.4%. Calc. for $K\{Zr_2(OPr^i)_9\}$: Zr, 24.2; OPr^i, 70.6%.)

Copper in bimetallic alkoxides was estimated iodometrically[9] and zirconium was estimated as oxide after precipitation as mandelate. Alcohols were determined by an oxidimetric method[10] after using a correction for copper(II) content of the sample.

The magnetic susceptibility measurements were made on a Gouy balance using $Hg[Co(CNS)_4]$ as standard. The magnetic moments, μ_{eff}, were calculated by the expression: $\mu_{eff} = 2.84\sqrt{\chi_M^{corr} \cdot T}$ (where χ_M^{corr} is the observed molar susceptibility after correction for the diamagnetism of the constituent atoms).

Preparation of $[Cu\{Zr_2(OPr^i)_9\}_2]$

To a suspension of $CuCl_2$ (0.34 g, 2.52 mmol) in Pr^iOH (*ca* 5 cm^3) was added a benzene solution (*ca* 35 cm^3) of $K\{Zr_2(OPr^i)_9\}$ (3.7 g, 5.03 mmol) and the reaction mixture was refluxed for *ca* 5 h, during which the colour of the reaction mixture changed from light green to bluish green. The precipitated KCl was filtered, and the filtrate concentrated (*ca* 15 cm^3) and left at room temperature for a few hours to afford a bluish green crystalline product (3.10 g, 83.8%). The product was further recrystallized unchanged from *n*-hexane. Analysis and physical characteristics of $[Cu\{Zr_2(OPr^i)_9\}_2]$ are given in Table 1.

*Author to whom correspondence should be addressed.

Table 1. Synthesis and alcohol interchange reactions of $[Cu\{Zr_2(OPr^i)_9\}_2]$

Sl. No.	Reactants (g)	Product (g) and reaction conditions[a,b,c]	Physical state of product	Analysis (%) found (calc.) Cu	Zr	OPr^i	Pr^iOH liberated (g)
1.	$CuCl_2$ + 2K$\{Zr_2(OPr^i)_9\}$ 0.34 3.79	$[Cu\{Zr_2(OPr^i)_9\}_2]$ 3.10 (3.70)	Bluish green crystalline solid	4.1 (4.3)	24.6 (24.4)	70.4 (71.3)	
2.	$[Cu\{Zr_2(OPr^i)_9\}_2]$ + MeOH 2.00 ~40 cm^3	$[Cu\{Zr_2(OMe)_9\}_2]^a$ 1.30 (1.32)	Turqoise colour powdery solid	6.0 (6.4)	35.5 (37.0)		
3.	$[Cu\{Zr_2(OPr^i)_9\}_2]$ + MeOH 1.43 0.19	$[Cu\{Zr_2(OPr^i)_6(OMe)_3\}_2]^a$ 1.24 (1.26)	Green colour solid	4.7 (4.8)	28.4 (27.6)		
4.	$[Cu\{Zr_2(OPr^i)_9\}_2]$ + MeOH 1.25 0.33	$[Cu\{Zr_2(OPr^i)_3(OMe)_6\}_2]^a$ 0.94 (0.96)	Green colour solid	5.4 (5.5)	32.1 (31.6)		
5.	$[Cu\{Zr_2(OPr^i)_9\}_2]$ + MeOH 1.82 0.55	$[Cu\{Zr_2(OPr^i)_2(OMe)_7\}_2]^a$ 1.32 (1.32)	Turquoise solid	5.6 (5.8)	33.9 (33.2)		
6.	$[Cu\{Zr_2(OPr^i)_9\}_2]$ + EtOH 1.27 ~35 cm^3	$[Cu\{Zr_2(OEt)_9\}_2]^b$ 0.89 (1.05)	Turquoise colour solid	5.0 (5.1)	30.3 (29.4)	63.0[d] (65.5)[d]	
7.	$[Cu\{Zr_2(OPr^i)_9\}_2]$ + EtOH 1.00 ~25 cm^3	$[Cu\{Zr_2(OPr^i)_6(OEt)_3\}_2]^b$ 0.93 (0.94)	Green solid	4.4 (4.5)	26.4 (25.9)		
8.	$[Cu\{Zr_2(OPr^i)_9\}_2]$ + Pr^nOH 1.23 ~30 cm^3	$[Cu\{Zr_2(OPr^n)_9\}_2]^b$ 1.22 (1.23)	Turquoise colour solid	4.0 (4.3)	24.8 (24.4)		
9.	$[Cu\{Zr_2(OPr^i)_9\}_2]$ + Bu^nOH 0.73 ~40 cm^3	$[Cu\{Zr_2(OBu^n)_9\}_2]^b$ 0.79 (0.85)	Sea green foamy solid	3.6 (3.6)	21.6 (20.9)		
10.	$[Cu\{Zr_2(OPr^i)_9\}_2]$ + Bu^iOH 2.10 ~40 cm^3	$[Cu\{Zr_2(OBu^i)_9\}_2]^b$ 2.35 (2.44)	Green colour crystalline solid	3.6 (3.6)	21.4 (20.9)		
11.	$[Cu\{Zr_2(OPr^i)_9\}_2]$ + Bu^sOH 1.32 ~20 cm^3	$[Cu\{Zr_2(OPr^i)_6(OBu^s)_3\}_2]^a$ 1.37 (1.39)	Green colour solid	4.0 (4.0)	23.7 (23.1)	44.6 (45.0)	
12.	$[Cu\{Zr_2(OPr^i)_9\}_2]$ + Bu^sOH 1.20 ~20 cm^3	$[Cu\{Zr_2(OPr^i)_3(OBu^s)_6\}_2]$ 1.24 (1.33)	Green colour solid	4.0 (3.8)	24.4 (22.0)	22.5 (21.3)	
13.	$[Cu\{Zr_2(OPr^i)_9\}_2]$ + Bu^sOH 2.10 ~35 cm^3	$[Cu\{Zr_2(OBu^s)_9\}_2]^c$ 2.28 (2.45)	Green colour solid	3.6 (3.6)	21.5 (20.9)		1.5 (1.5)
14.	$[Cu\{Zr_2(OPr^i)_9\}_2]$ + Bu^tOH 1.24 ~25 cm^3	$[Cu\{Zr_2(OPr^i)_7(OBu^t)_2\}_2]^b$ 1.26 (1.28)	Green solid	5.0 (4.1)	24.2 (23.6)	53.0 (53.4)	
15.	$[Cu\{Zr_2(OPr^i)_9\}_2]$ + Bu^tOH 1.94 ~40 cm^3	$[Cu\{Zr_2(OPr^i)_3(OBu^t)_6\}_2]^c$ 2.10 (2.15)	Sea green solid	3.8 (3.8)	22.6 (22.0)	21.0 (21.3)	0.9 (0.9)
16.	$[Cu\{Zr_2(OPr^i)_9\}_2]$ + Am^tOH 1.84 ~40 cm^3	$[Cu\{Zr_2(OPr^i)_4(OAm^t)_5\}_2]^c$ 2.05 (2.18)	Green solid	3.5 (3.6)	21.3 (20.6)	26.1 (26.7)	0.7 (0.7)

[a]Reaction at room temperature.
[b]Reaction in refluxing benzene, without azeotropic removal of Pr^iOH.
[c]Reaction in refluxing benzene with azeotropic removal of liberated Pr^iOH.
[d]Observed as well as calculated values in this case refer to "ethoxy" content.

Alcoholysis reactions of $[Cu\{Zr_2(OPr^i)_9\}_2]$

(*a*) *With* MeOH *in different molar ratios*

(i) *With excess of* MeOH. A slight heat was evolved on addition of an excess of methanol (*ca* 40 cm^3) to a benzene solution (*ca* 30 cm^3) of $[Cu\{Zr_2(OPr^i)_9\}_2]$ (2.00 g). The reaction mixture was stirred for *ca* 6 h, during which its colour changed from bluish green to turquoise and an insoluble product separated out. The solid with the composition $[Cu\{Zr_2(OMe)_9\}_2]$ was isolated (1.24 g, 94%) by decantation and dried under reduced pressure.

(ii) *With* MeOH *in* 1:6 *molar ratio.* The above reaction was repeated in 1:6 molar ratio $[Cu\{Zr_2(OPr^i)_9\}_2]$ (1.43 g, 0.95 mmol) with MeOH (0.19 g, 5.93 mmol) in benzene (*ca* 15 cm^3). Although the colour of the solution became lighter, it remained clear even after 6 h of stirring, after which the volatile components were removed under reduced pressure yielding a green solid (1.24 g, 98%), which was purified by volatilization at 180°C/0.2 mm to afford a green coloured solid of composition $[Cu\{Zr_2(OPr^i)_6(OMe)_3\}_2]$.

(iii) *With* MeOH *in* 1:12 *molar ratio.* From the reaction of $[Cu\{Zr_2(OPr^i)_9\}_2]$ (1.25 g, 0.83 mmol) with MeOH (0.33 g, 10.30 mmol) in benzene, under conditions similar to those in the previous experiment, a green coloured solid product (0.94 g, 98%) of formula $[Cu\{Zr_2(OPr^i)_3(OMe)_6\}_2]$ could be isolated.

(iv) *With* MeOH *in* 1:14 *molar ratio.* Interaction of $[Cu\{Zr_2(OPr^i)_9\}_2]$ (1.82 g, 1.21 mmol) with methanol (0.55 g, 17.18 mmol) in benzene resulted in the appearance of turbidity after *ca* 4 h. The reaction mixture was allowed to stand at room temperature overnight. After filtration of the insoluble material and drying it under reduced pressure a turquoise

coloured solid compound (1.32 g, 100%) of composition $[Cu\{Zr_2(OPr^i)_2(OMe)_7\}_2]$ was isolated.

(*b*) *With excess of* EtOH (*at room temperature*). To a benzene solution (*ca* 10 cm^3) of $[Cu\{Zr_2(OPr^i)_9\}_2]$ (1.00 g) was added an excess of ethanol (*ca* 25 cm^3) and the mixture was stirred for *ca* 6 h at room temperature. The solvent was removed from the clear solution under reduced pressure, affording a green solid (0.93, 98%) product which corresponded in analysis to $[Cu\{Zr_2(OPr^i)_6(OEt)_3\}_2]$.

(*c*) *With excess of* EtOH (*under refluxing conditions*). $[Cu\{Zr_2(OPr^i)_9\}_2]$ (1.27 g) was dissolved in benzene (*ca* 20 cm^3) and treated with an excess of EtOH (*ca* 35 cm^3) and the mixture was refluxed for *ca* 6 h during which the colour changed from bluish green to turquoise. After stripping off the solvent, a turquoise coloured solid (0.89 g, 85%) product of composition $[Cu\{Zr_2(OEt)_9\}_2]$ was isolated. In a similar manner derivatives of *n*-propanol, *n*-butanol and *i*-butanol were prepared.

(*d*) *With excess of* Bu^sOH *at room temperature.* To a benzene solution (*ca* 20 cm^3) of $[Cu\{Zr_2(OPr^i)_9\}_2]$ (1.32 g) was added an excess of *s*-butanol (*ca* 20 cm^3). The reaction mixture was stirred for *ca* 6 h, after which the solvent was stripped off under reduced pressure to afford a green solid, (1.37 g, 98%) which corresponded in analysis to $[Cu\{Zr_2(OPr^i)_6(OBu^s)_3\}_2]$.

(*e*) *With excess of* Bu^sOH *in refluxing benzene* (*without azeotropic fractionation of* Pr^iOH). To a benzene (*ca* 15 cm^3) solution of $[Cu\{Zr_2(OPr^i)_9\}_2]$ (1.20 g) was added *s*-butanol (*ca* 20 cm^3). The reaction mixture was refluxed for *ca* 5 h, after which the solvent was removed under reduced pressure, yielding a green solid product (1.24 g, 93%) with composition $[Cu\{Zr_2(OPr^i)_3(OBu^s)_6\}_2]$.

(*f*) *With excess of* Bu^tOH *in refluxing benzene* (*without azeotropic fractionation of* Pr^iOH). Bu^tOH (*ca* 25 cm^3) was added to the benzene solution (*ca* 10 cm^3) of $[Cu\{Zr_2(OPr^i)_9\}_2]$ (1.24 g). After refluxing the mixture for *ca* 4 h, the solvent was removed under reduced pressure and finally a green coloured solid (1.26 g, 98%) product of composition $[Cu\{Zr_2(OPr^i)_7(OBu^t)_2\}_2]$ was obtained.

(*g*) *Alcoholysis reaction with excess of* Bu^sOH (*with continuous azeotropic removal of* Pr^iOH). To a benzene solution (*ca* 15 cm^3) of $[Cu\{Zr_2(OPr^i)_9\}_2]$ (2.10 g) was added *s*-butanol (*ca* 35 cm^3). The reaction mixture was refluxed for *ca* 7 h, during which the liberated isopropanol was continuously fractionated out azeotropically. After complete removal of the isopropanol, the solvent was removed under reduced pressure to yield a green coloured solid compound (2.28 g, 93%) of the composition corresponding to $[Cu\{Zr_2(OBu^s)_9\}_2]$.

(*h*) *With excess of* Bu^tOH *and* Am^tOH (*with continuous azeotropic fractionation of* Pr^iOH). To a benzene solution (*ca* 15 cm^3) of $[Cu\{Zr_2(OPr^i)_9\}_2]$ (1.94 g) was added *t*-butanol (*ca* 40 cm^3). The reaction mixture was refluxed for *ca* 25 h with continuous azeotropic removal of the liberated isopropanol, which was collected and estimated. The reaction was stopped when isopropanol could no longer be detected in the azeotrope; the solvent was removed from the final reaction mixture under reduced pressure to yield a green solid product (2.10 g, 97%) of composition $[Cu\{Zr_2(OPr^i)_3(OBu^t)_6\}_2]$.

The reaction with excess of *t*-amyl alcohol was carried out in a similar manner.

Analyses as well as physical characteristics for all the products isolated from the above reactions are compiled in Table 1.

RESULTS AND DISCUSSION

The reaction of copper(II) chloride (anhydrous) with $K\{Zr_2(PPr^i)_9\}$ in 1:2 molar ratio in benzene containing a few drops of isopropanol (which probably facilitates the dissolution of $CuCl_2$ in the solvent) affords quantitatively the bimetallic isopropoxide of copper(II), $[Cu\{Zr_2(OPr^i)_9\}_2]$:

$$CuCl_2 + 2K\{Zr_2(OPr^i)_9\} \xrightarrow[\text{reflux}]{\text{PhH}} [Cu\{Zr_2(OPr^i)_9\}_2] + 2KCl\downarrow.$$

The bluish green solid product can be purified unchanged by volatilisation (230°C/0.2 mm) or recrystallization (from Pr^iOH/C_6H_6 or *n*-hexane); it shows monomeric behaviour in freezing benzene.

The alcoholysis reactions of the isopropoxide derivative $[Cu\{Zr_2(OPr^i)_9\}_2]$ with different alcohols have shown interesting results in the following order of reactivity:

$$\underbrace{\text{MeOH} \gg \text{EtOH, } n\text{-PrOH, } n\text{-BuOH, } i\text{-BuOH}}_{\text{(a)}} \gg \text{s-BuOH} \gg \underbrace{t\text{-BuOH, } t\text{-AmOH}}_{\text{(c)}}$$
(b)

For example, with methanol the replacement of the isopropoxy group is quantitative even at room temperature:

$$[Cu\{Zr_2(OPr^i)_9\}_2] + 18\underset{\text{(excess)}}{MeOH} \rightarrow [Cu\{Zr_2(OMe)_9\}_2] + 18Pr^iOH\uparrow.$$

On the other hand, with EtOH, *n*-PrOH, *n*-

BuOH, *i*-BuOH and *s*-BuOH at room temperature only six isopropoxy groups out of 18 could be replaced:

$$[Cu\{Zr_2(OPr^i)_9\}_2] + \underset{(excess)}{6ROH} \rightarrow [Cu\{Zr_2(OPr^i)_6(OR)_3\}_2] + 6Pr^iOH\uparrow$$

The primary alcohols out of the above could effect complete replacement of isopropanol in $[Cu\{Zr_2(OPr^i)_9\}_2]$ when the reaction was carried out under refluxing conditions:

$$[Cu\{Zr_2(OPr^i)_9\}_2] + \underset{(excess)}{18ROH} \xrightarrow[reflux]{PhH} [Cu\{Zr_2(OR)_9\}_2] + 18Pr^iOH\uparrow$$

(where R = Et, Pr^n, Bu^n and Bu^i).

However, even in refluxing benzene, the reaction with an excess of *s*-butanol yielded a product corresponding in analysis to $[Cu\{Zr_2(OPr^i)_3(OBu^s)_6\}_2]$:

$$[Cu\{Zr_2OPr^i)_9\}_2] + \underset{(excess)}{12Bu^sOH} \xrightarrow[reflux]{PhH} [Cu\{Zr_2(OPr^i)_3(OBu^s)_6\}_2] + 12Pr^iOH\uparrow.$$

The complete replacement of isopropoxy groups with *s*-butanol was possible when the liberated isopropanol was continuously fractionated out from the refluxing reaction mixture.

$$[Cu\{Zr_2(OPr^i)_9\}_2] + \underset{(excess)}{18Bu^sOH} \rightarrow [Cu\{Zr_2(OBu^s)_9\}_2] + 18Pr^iOH\uparrow.$$

At room temperature, no reaction appeared to take place between $[Cu\{Zr_2(OPr^i)_9\}_2]$ and *t*-butanol. In refluxing benzene, however, four isopropoxy groups could be replaced:

$$[Cu\{Zr_2(OPr^i)_9\}_2] + \underset{(excess)}{4Bu^tOH} \rightarrow [Cu\{Zr_2(OPr^i)_7(OBu^t)_2\}_2] + 4Pr^iOH\uparrow.$$

The above reaction under the condition of azeotropic removal (for *ca* 25 h) of Pr^iOH finally gave a solid product which corresponded in analysis to $[Cu\{Zr_2(OPr^i)_3(OBu^t)_6\}_2]$:

$$[Cu\{Zr_2(OPr^i)_9\}_2] + \underset{(excess)}{12Bu^tOH} \rightarrow [Cu\{Zr_2(OPr^i)_3(OBu^t)_6\}_2] + 12Pr^iOH\uparrow.$$

The product obtained as a result of the reaction with Am^tOH (with azeotropic fractionation) corresponded in analysis to $[Cu\{Zr_2(OPr^i)_4(OAm^t)_5\}_2]$.

In a number of publications from these laboratories it has been shown that in alcoholysis reactions of alkoxides of earlier transition metals (e.g. Zr),[11] the terminal isopropoxy groups are replaced with greater facility than the alkoxy groups bridging the metal atoms. In the case of mixed methoxide isopropoxide, although the interchange occurs initially at the terminal positions, the methoxy groups tend to change the bridging positions, so that the molecule finally tends to show properties ascribable to the greater steric bulk of the terminal isopropoxy groups.[11] Further, the alcoholysis reactions of such (zirconium) isopropoxides with more ramified tertiary alcohols do not tend to go to completion. More recently, it has been shown that, as far as bimetallic alkoxides of later transition metals (like copper)[4] are concerned, the alkoxy groups bridging copper with main group metals like aluminium tend to show no difference in the facility with which these are replaced in alcoholysis reactions.

In order to understand the results of the alcoholysis reactions of $[Cu\{Zr_2(OPr^i)_9\}_2]$ with different alcohols, it becomes necessary to postulate a plausible structure for the same. In an earlier publication[11] from these laboratories, a plausible structure was suggested for $K\{Zr_2(OPr^i)_9\}$, which appears to have received some corroboration in the structure determined recently[12] for $K\{U_2(OCMe_3)_9\}$. As it would be rather speculative to suggest a structure for the derivatives $[Cu\{Zr_2(OR)_9\}_2]$ described in these investigations, the structure may be considered similar to that of $K\{U_2(OCHe_3)_9\}$ which is reproduced in Fig. 1, with the copper atom in place of potassium; the 6-coordinated copper ion is held by two bridging and one terminal oxygen atom from each $\{Zr_2(OPr^i)_9\}^-$ moiety:

In the structure suggested above, ignoring the alkoxy bridge between Zr and Cu, there are three bridging alkoxy groups between each pair of zirconium atoms and every zirconium atom has three terminal groups. The results of alcoholysis reactions can, therefore, be explained easily on the following lines: (i) only 12 groups are replaced by alcohols of group (a) and *s*-butanol at room temperature; (ii) both types of alkoxy groups are replaced by alcohols (a) under refluxing and by methanol at room temperature; (iii) only partial replacement of terminal groups with *t*-butanol occurs under refluxing conditions, and all the terminal groups 12 are replaced by *t*-butanol under refluxing and continuous removal of the liberated isopropanol azeotropically; it may be further concluded that the

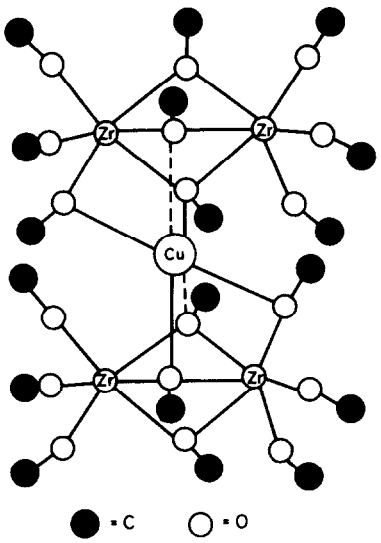

Fig. 1.

last stages of this final reaction become too slow with *t*-amyl alcohol. The alcoholysis of $[Cu\{Zr_2(OPr^i)_9\}_2]$ with methanol is quite facile at room temperature; by carrying out the methanolysis reactions in different molar ratios it has been shown that the derivatives $[Cu\{Zr_2(OPr^i)_6(OMe)_3\}_2]$ and $[Cu\{Zr_2(OPr^i)_3(OMe)_6\}_2]$ are soluble but further replacement tends to make the product insoluble. As mentioned above, it may be that the replacement of isopropoxy by methoxy groups occurs initially at the terminal positions, but in view of their (OMe) tendency to form stronger bridging bonds, these tend to shift to the latter positions. The volatility of the derivative $[Cu\{Zr_2(OPr^i)_6(OMe)_3\}_2]$ can be explained on the basis of all the methoxy groups occupying the bridging positions. Further, the presence of three isopropoxy and three methoxy groups on the terminal positions on zirconium atoms tends to hinder further association and hence the product remains soluble and becomes insoluble only when more than three OPr^i groups per zirconium atom are replaced by OMe groups.

All these bimetallic alkoxides of copper(II) are highly soluble (except the homoleptic methoxide derivative, which is insoluble) in common organic solvents (such as benzene, carbon tetrachloride and *n*-hexane), but these depict lower solubility in parent alcohols.

The analytical data and physical characteristics of these derivatives are compiled in Table 1.

IR studies

The IR spectra (in the range 4000–400 cm^{-1}) of these compounds exhibited structurally significant bands[13,14] (Table 2) at 950–1160 cm^{-1} for ν(C—O)M, and 510–580 cm^{-1} for the ν(Zr—O) and at 440–470 cm^{-1} ν(Cu—O).

Electronic spectral studies

The electronic spectra of a large number of copper(II) complexes are reported in the literature and it is believed that the absorption connected with the $^2E_g \rightarrow {}^2T_{2g}$ transition is characteristic of octahedral geometry.[15] However, in a tetragonal ligand field it may split into two bands, $^2A_{1g} \rightarrow {}^2B_{1g}(\nu_1)$ and $^2E_g \rightarrow {}^2B_{1g}(\nu_2)$, in the visible

Table 2. IR and room temperature magnetic moments of bimetallic alkoxides of copper(II)

Sl. No.	Compound	ν(C—O)M	ν(Zr—O)	ν(Cu—O)	μ_{eff} (BM)
1.	$[Cu\{Zr_2(OMe)_9\}_2]$	1150, br, 1020m, 950m	580w, 540w	470m	1.59
2.	$[Cu\{Zr_2(OEt)_9\}_2]$	1130, 950s, 1000s	570s	460m	1.74
3.	$[Cu\{Zr_2(OPr^n)_9\}_2]$	1150s, 1080m, 1015m	560m, 530m	460m	1.82
4.	$[Cu\{Zr_2(OBu^n)_9\}_2]$	1160m, 1120m, 1000s, 950m	570w	460w	—
5.	$[Cu\{Zr_2(OBu^i)_9\}_2]$	1140s, 1070s, 1010m	560m	460m	1.81
6.	$[Cu\{Zr_2(OPr^i)_9\}_2]$	1160m, 1130m, 1015m, 945m	560mbr	470mbr	1.69
7.	$[Cu\{Zr_2(OBu^s)_9\}_2]$	1160m, 1130w, 1015w, 960w	570wbr	470wbr	1.79
8.	$[Cu\{Zr_2(OPr^i)_3(OBu^t)_6\}_2]$	1160m, 1090m, 995m	510mbr	440m	1.81
9.	$[Cu\{Zr_2(OPr^i)_4(OAm^t)_5\}_2]$	1140m, 1100w, 1055m, 1025m	550m	450wbr	1.80

Table 3. Electronic spectral parameters of bimetallic alkoxides of copper(II) with Zr(IV)

Sl. No.	Compound	Medium	Observed transitions (kK)[a] ν_2	ν_1
1.	$[Cu\{Zr_2(OPr^i)_9\}_2]$	(i) Benzene	15.4	17.8(sh)
		(ii) THF	15.2	—
		(iii) Pyridine	14.8	—
2.	$[Cu\{Zr_2(OEt)_9\}_2]$	Benzene	15.5	17.5(sh)
3.	$[Cu\{Zr_2(OBu^n)_9\}_2]$	THF	14.9	—
4.	$[Cu\{Zr_2(OBu^i)_9\}_2]$	Benzene	15.1	17.8(sh)
5.	$[Cu\{Zr_2(OBu^s)_9\}_2]$	Benzene	15.4	17.9(sh)
6.	$[Cu\{Zr_2(OPr^i)_3(OBu^t)_6\}_2]$	Benzene	15.1	17.2(sh)

[a] $1\,kK = 1000\,cm^{-1}$.

region, possibly due to distortion.[15,16] The electronic spectra of the bimetallic alkoxides of copper(II) studied here showed broad asymmetric bands at 15.3 and 17.5 kK (Table 3), are characteristic of distorted octahedral geometry[17] in tetragonal ligand field. The visible spectral studies of $[Cu\{Zr_2(OPr^i)_9\}_2]$ in different solvents (non-coordinating and coordinating) reveal: (i) disappearance of the higher frequency bands (ν_1); and (ii) shifting of ν_2 bands towards lower frequency side with increasing coordinating tendency of the solvent.

In view of the above findings a sandwich-type structure (Fig. 1) can be suggested for the derivatives $[Cu\{Zr_2(OR)_9\}_2]$ in which $\{Zr_2(OR)_9\}^-$ units behave as tridentate ligands conferring a distorted octahedral geometry on copper(II). It is of interest that for the compound $K(U_2(OCMe_3)_9\}$ the crystal structure[12] is similar to that suggested above.

Magnetic studies

For the Cu^{2+} ion (d^9) having only one unpaired electron, the spin-only magnetic moment should be 1.73 BM. However, the observed values are generally higher due to some orbital contribution.

The observed magnetic moments (at room temperature) for these new bimetallic copper(II) alkoxides are in the 1.69–1.81 BM range and are in agreement with reported values (1.8–2.4 BM) for Cu(II)d^9 systems. The slightly lower value (1.59 BM) observed only in the case of the methoxide derivative, possibly due to its polymeric nature, is given in Table 2.

The low temperature (77.8–295 K) magnetic susceptibilities have been made on $[Cu\{Zr_2(OBu^n)_9\}_2]$ and indicated a decrease in magnetic moment with lowering of temperature. The plot of T vs $1/\chi_M^{corr}$ is a straight line showing Curie–Weiss behaviour with $\theta = -17$ K suggestive of antiferromagnetic exchange. The variable temperature magnetic susceptibility data are given in Table 4.

ESR studies

The ESR spectra of polycrystalline Cu^{2+} derivatives exhibits two types of g values, $g_\parallel$ and $g_\perp$, and these have been used to distinguish[18] unambiguously between $d_{x^2-y^2}$ (or d_{xy}) ground state on one hand and $d_{x^2-y^2}$ ground state on the other hand. For example, in $d_{x^2-y^2}$ (or d_{xy}) ground state ESR spectrum indicate $g_\parallel > g_\perp > 2.02$ in most cases whilst a d_{z^2} ground term usually gives a spectrum with $g_\perp > g_\parallel \sim 2.00$. The bimetallic alkoxides of copper(II), studied here, show a pronounced peak (for which $g_\perp \sim 2.10$) and a broad shallow quadruplet peak (for which $g_\parallel \sim 2.40$). These observations are characteristic[19,20] of axially distorted octahedral copper(II) complexes in which the unpaired electron is present in the $d_{x^2-y^2}$.

In an axial symmetry the g values are related by the expression $G = (g_\parallel - 2)/(g_\perp - 2)$, which measures the exchange interaction between copper centres in the polycrystalline solid,[21] if $G > 4$ exchange interaction is negligible, values of $G < 4$ indicate considerable exchange interaction in the

Table 4. Magnetic susceptibility of $[Cu\{Zr_2(OBu^n)_9\}_2]$ at different temperatures

Temperature (K)	$\chi_g \times 10^6$ (c.g.s.)	$\chi_M \times 10^6$ (c.g.s.)	$\chi_M^{corr} \times 10^6$ (c.g.s.)	μ_{eff} (BM)
77.8	1.732	3017.46	4126.12	1.60
86.6	1.542	2687.30	3795.96	1.62
110.0	1.118	1949.22	3057.88	1.64
131.0	0.8607	1499.74	2608.40	1.65
140.2	0.8121	1414.98	2523.64	1.68
174.2	0.5302	923.90	2032.56	1.68
190.0	0.4579	797.88	1906.54	1.70
220.0	0.3289	573.15	1681.81	1.72
295.5	0.1013	176.47	1285.13	1.74

Table 5. g values of copper(II) bimetallic alkoxides from ESR spectra

Sl. No.	Compound	$H_{\parallel}$ field (Gauss)	$g_{\parallel}$	$H_{\perp}$ field (Gauss)	$g_{\perp}$	g_{av}[a]	G[a]
1.	$[Cu\{Zr_2(OMe)_9\}_2]$	2900	2.342	3300	2.087	2.172	3.93
2.	$[Cu\{Zr_2(OPr^i)_9\}_2]$	3150	2.352	3550	2.094	2.182	3.74
3.	$[Cu\{Zr_2(OBu^n)_9\}_2]$	3050	2.324	3480	2.101	2.175	3.20
4.	$[Cu\{Zr_2(OEt)_9\}_2]$[b]	2660	2.435	3040	2.130	2.231	3.34
5.	$[Cu\{Zr_2(OPr^n)_9\}_2]$[b]	2680	2.416	3100	2.089	2.198	4.67
6.	$[Cu\{Zr_2(OPr^i)_9\}_2]$[b]	2660	2.435	3060	2.116	2.22	3.75
7.	$[Cu\{Zr_2(OBu^n)_9\}_2]$[b]	2660	2.434	3040	2.130	2.231	3.34
8.	$[Cu\{Zr_2(OPr^i)_9\}_2]$[a]	—	—	3265	2.103	—	—
9.	$[Cu\{Zr_2(OPr^i)_3(OBu^t)_6\}_2]$[c]	—	—	3340	2.105	—	—

[a] $g_{av} = 1/3(g_{\parallel} + 2g_{\perp})$; $G = (g_{\parallel} - 2)/(g_{\perp} - 2)$.

[b] Spectra have been recorded in polycrystalline solid state at L.N.T. ($\sim$77 K).

[c] Spectra have been recorded in carbon tetrachloride solution at room temperature ($\sim$25°C).

solid complexes. The calculated G values are given in Table 5. The g_{av} values were calculated according to the relation $g_{av} = 1/3(g_{\parallel} + g_{\perp})$ and gave values in the range 2.23 ± 0.07 which are in agreement with an orbitally non-degenerate ground state.[22]

Acknowledgements—The authors wish to thank Professor S. Mitra, T.I.F.R. Bombay (India) and R.S.I.C. Bombay for providing facilities for ESR and magnetic susceptibility measurement. One of the authors (R.K.D.) is grateful to D.S.T. for providing a senior research fellowship.

REFERENCES

1. R. C. Mehrotra, *Adv. Inorg. Radiochem.* 1983, **26**, 269.
2. J. V. Singh, B. P. Barnwal and R. C. Mehrotra, *Z. Anorg. Allgem. Chem.* 1981, **477**, 235.
3. J. V. Singh, Ph.D. thesis, University of Delhi, India (1980).
4. R. C. Mehrotra, J. V. Singh, *Z. Anorg. Chem.* 1984, **512**, 221.
5. R. C. Mehrotra and J. V. Singh, *J. Coord. Chem.* 1984, **13**, 273.
6. R. C. Mehrotra and J. V. Singh, *Inorg. Chem.* 1984, **23**, 1046.
7. J. D. Mackenzie, *J. Non-cryst. Solids* 1982, **48**, 1.
8. R. C. Mehrotra and M. M. Agrawal, *J. Chem. Soc. A* 1967, 1026.
9. A. I. Vogel, *A Text Book of Quantitative Inorganic Analysis*. Longman, London (1978).
10. R. C. Mehrotra, *J. Ind. Chem. Soc.* 1953, **30**, 585.
11. D. C. Bradley, R. C. Mehrotra and D. P. Gaur, *Metal Alkoxides*. Academic Press, London (1978).
12. F. A. Cotton, O. Marler and W. Schwotzer, *Inorg. Chem.* 1984, **23**, 4211.
13. K. Nakamoto, *Infrared Spectra of Inorganic and Coordination Compounds*. Wiley Interscience, London (1970).
14. L. J. Bellamy, *The Infrared Spectra of Complex Molecules*. Chapman & Hall, London (1975).
15. A. B. P. Lever, *Inorganic Electronic Spectroscopy*, 2nd edn. Elsevier, Amsterdam (1984).
16. C. K. Jorgensen, *Acta Chem. Scand.* 1954, **8**, 1495.
17. H. J. Stoklosa, J. R. Wasson, E. V. Brown, H. W. Richardson and E. Hatfield, *Inorg. Chem.* 1975, **14**, 2378.
18. M. C. Jain, A. K. Srivastava and P. C. Jain, *Inorg. Chim. Acta* 1977, **23**, 199.
19. H. G. K. Sundar and K. J. Rao, *J. Non-cryst. Solids* 1982, **50**, 137; *Chem. Abstr.* 1982, **97**, 83898.
20. B. J. Hathaway and D. E. Billing, *Coord. Chem. Rev.* 1970, **5**, 143.
21. I. M. Procter, B. J. Hathaway and P. Nicholls, *J. Chem. Soc. A* 1968, 1678.
22. B. N. Figgis, *Introduction to Ligand Field*, p. 296. Interscience, New York (1966).

Polyhedron Vol. 6, No. 3, pp. 435–440, 1987
Printed in Great Britain.

0277-5387/87 $3.00 + .00

DISILOXANE-CONTAINING DIFUNCTIONAL COMPOUNDS: SYNTHESIS AND REACTIVITY OF 1,3-BIS-(*p*-ISOCYANATOPHENYL) DISILOXANES*

N. D. GHATGE† and S. S. MOHITE

Division of Polymer Chemistry, National Chemical Laboratory, Pune 411008, India

(*Received* 11 *November* 1985; *accepted after revision* 17 *July* 1986)

Abstract—Disiloxane-containing diisocyanates having the following general structure:

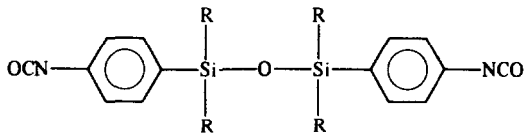

where R = CH_3 and C_6H_5, have been synthesized by the Curtius rearrangement of acid diazides. Both the diazides and one diisocyanate (R = C_6H_5) are new. The other diisocyanate (R = CH_3) was prepared by following a new synthetic route. All the compounds were characterized by IR and ^1H NMR spectroscopy. The reactivity of the diisocyanates with 2-ethyl-1-hexanol was studied using the IR spectroscopic technique.

The uniqueness of the isocyanates lies in their high reactivity towards compounds containing active hydrogen atoms, leading to wide-ranging applications in organic as well as polymer chemistry. Isocyanates can serve as the backbone for a wide variety of polymers other than the conventional polyurethanes and polyureas.[1]

During our research on the syntheses of silicon-containing diisocyanates[2,3] we have synthesized and characterized the following disiloxane-containing diisocyanates which were obtained from the corresponding diacids via the Curtius rearrangement of acid diazides:

(i) 1,3-bis-(*p*-isocyanatophenyl)-1,1,3,3-tetramethyldisiloxane (DMIS);
(ii) 1,3-bis-(*p*-isocyanatophenyl)-1,1,3,3-tetraphenyldisiloxane (DPIS).

DPIS is a new compound. DMIS was previously prepared by Bonnet and Marechal by the phosgenation of the corresponding diamine,[4,5] however, in the present study DMIS was prepared by following a different synthetic route. Both the diazides were synthesized for the first time.

*NCL Communication No. 3935

†Author to whom correspondence should be addressed. Present address: R & D Division (Polymer), Bharati Vidyapeeth, Erandawane, Pune 411038, India.

EXPERIMENTAL

Synthesis

p-Tolyldimethylchlorosilane (DMSCL). To a solution of dimethyldichlorosilane (105 g, 0.81 mol) in dry ether (100 cm^3), an ethereal solution of *p*-tolylmagnesium bromide [prepared from magnesium (12.15 g, 0.5 g atoms) and *p*-bromotoluene (85.5 g, 0.5 mol) in dry ether (200 cm^3)] was added dropwise with stirring. The reaction mixture was stirred for an additional 12 h after the addition had been completed. The supernatant liquid was then poured from the salts which had formed, and the latter were washed with 150 cm^3 of dry ether. After distillation of solvent and unreacted dimethyldichlorosilane, vacuum was applied and 59.96 g (65%) of the product boiling at 95°C (11 mmHg) were obtained.

p-Tolyldiphenylchlorosilane (DPSCL). An ethereal solution of *p*-tolylmagnesium bromide [prepared from magnesium (12.15 g, 0.5 g atoms) and *p*-bromotoluene (85.5 g, 0.5 mol) in dry ether (200 cm^3)] was added dropwise with stirring to a solution of diphenyldichlorosilane (253 g, 1 mol) in dry ether (100 cm^3). The reaction mixture was refluxed for 2 h. The ether was distilled out, at the same time dry toluene (300 cm^3) was added dropwise and the reaction mixture was refluxed for 4 h. After the magnesium salts were filtered off,

toluene was removed under reduced pressure. The fractional distillation gave 114.14 g (74%) of DPSCL.

p-*Tolyldiphenylsilanol* (*DPOH*). A drop of phenolphthalein indicator was added to a solution of DPSCL (61.7 g, 0.2 mol) in ether (300 cm^3). Sodium hydroxide solution (1 N) was added with vigorous stirring till a light pink colour was obtained. The ether layer was separated, washed with water and dried over sodium sulphate. After removal of ether, the solid obtained was recrystallized from hexane to afford 52.20 g (90%) of DPOH.

1,3-*Bis*-(p-*tolyl*)-1,1,3,3-*tetramethyldisiloxane* (*DMDM*). A solution of DMSCL (40 g, 0.217 mol) in ether (250 cm^3) was shaken with successive portions of cold water until the water was no longer acidic. The ether layer was then dried and after removal of the ether, the liquid residue was distilled under reduced pressure to obtain 26.9 g (79%) of DMDM.

1,3-*Bis*-(p-*tolyl*)-1,1,3,3-*tetraphenyldisiloxane* (*DPDM*). A mixture of DPOH (72 g, 0.248 mol) and sodium hydroxide solution (4 cm^3, 0.1 N) was heated at 218°C for 1.5 h, during which time water was eliminated. The temperature was then raised to 260°C for 1 h and the melt was allowed to cool. The product was purified by recrystallization from heptane. Yield: 65 g (95%).

1,3-*Bis*-(p-*carboxyphenyl*)-1,1,3,3-*tetramethyldisiloxane* (*DMAC*). The temperature of the solution of DMDM (30 g, 0.095 mol) in water (100 cm^3) and pyridine (200 cm^3) was raised to 95°C, and potassium permanganate was added portionwise to maintain a slow reflux. The mixture was then refluxed for 3 h. The excess permanganate was destroyed by adding methanol. The MnO_2 was removed by filtration and washed with a large volume of boiling water, and the washings were combined with the filtrate. The filtrate, after removal of excess pyridine was treated with activated charcoal and acidified with dilute HCl. The precipitated acid was collected by filtration, washed with water, then dissolved in sodium carbonate solution, again treated with activated charcoal and finally acidified with HCl to get 25 g (70%) of DMAC after recrystallization from alcohol.

1,3-*Bis*-(p-*carboxyphenyl*)-1,1,3,3-*tetraphenyldisiloxane* (*DPAC*). A mixture of glacial acetic acid (620 cm^3) and acetic anhydride (200 cm^3) was cooled to −5°C and concentrated sulphuric acid (50 cm^3) was added dropwise with stirring. The mixture was allowed to warm to 10°C and DPDM (43 g, 0.0765 mol; in 11 g portion) and chromium trioxide (76.8 g, in 19 g portions) were added with rapid stirring. The portions of the chromium trioxide were added at 0.5 h intervals, followed 10 min later by a portion of DPDM with the temperature maintained at 10–14°C during the additions. After the additions were complete, stirring was continued for 3 h at 12–17°C and the mixture was poured over crushed ice. The precipitated acid was filtered, washed thoroughly with water and dried. It was further washed with methylene chloride (150 cm^3) by stirring for 30 min. Treatment with charcoal and recrystallization from ethanol afforded 32.4 g (68%) of DPAC.

1,3-*Bis*-(p-*chlorocarbonylphenyl*)-1,1,3,3-*tetraphenyldisiloxane* (*DPACL*). DPAC (20 g, 0.032 mol) and thionyl chloride (150 cm^3) were refluxed for 8 h. Excess of thionyl chloride was removed under reduced pressure and the residue was recrystallized from dry toluene. Yield: 14 g (66%).

1,3-*Bis*-(p-*chlorocarbonylphenyl*)-1,1,3,3-*tetramethyldisiloxane* (*DMACL*). This compound was synthesized by following a similar procedure as that described for DPACL.

1,3-*Bis*-(p-*azidocarbonylphenyl*)-1,1,3,3-*tetraphenyldisiloxane* (*DPAZ*). (a) To a cooled (5°C) solution of sodium azide (2.60 g, 0.04 mol) in water (15 cm^3) was added a solution of DPACL (6.59 g, 0.01 mol) in methylene chloride (15 cm^3) with efficient stirring. After stirring for 20 min, the water layer was separated and the methylene chloride layer was washed with water and dried over sodium sulphate. The methylene chloride was removed under reduced pressure to obtain 4.64 g (69%) of DPAZ.

(b) The suspension of DPAC (6.22 g, 0.01 mol) in acetone (40 cm^3) was cooled to 0°C and triethylamine (2.02 g, 0.02 mol) in acetone (15 cm^3) was added over a period of 10 min. The reaction mixture was stirred for further 10 min and then a solution of ethyl chloroformate (2.17 g, 0.02 mol) in acetone (15 cm^3) was added at 0°C over a period of 10 min. The resulting reaction mixture was stirred for 1 h at the same temperature and then a solution of sodium azide (2.60 g, 0.04 mol) in water (60 cm^3) was added dropwise. Finally, the reaction mixture was stirred for 4 h at 0°C and then poured into 200 cm^3 of ice-cold water. The solid was collected by filtration. It was dissolved in methylene chloride and dried over sodium sulphate. After filtration, methylene chloride was removed under reduced pressure to get 5.71 g (85% of DPAZ).

1,3-*Bis*-(p-*azidocarbonylphenyl*)-1,1,3,3-*tetramethyldisiloxane* (*DMAZ*). The reaction conditions described for the synthesis of DPAZ were followed to obtain DMAZ—by both routes (a) and (b).

1,3-*Bis*-(p-*isocyanatophenyl*)-1,1,3,3-*tetraphenyldisiloxane* (*DPIS*). A solution of DPAZ (3.36 g, 0.005 mol) in dry benzene (35 cm^3) was refluxed for 12 h. The benzene was removed by distillation under

reduced pressure and the residue was recrystallized from dry hexane. Yield: 2.84 g (92%).

1,3-*Bis*-(p-*isocyanatophenyl*)-1,1,3,3-*tetramethyldisiloxane* (*DMIS*). The procedure described for the preparation of DPIS was used to obtain DMIS.

Reactivity measurements

The intense absorption of IR caused by the isocynate group was used for plotting the course of the reaction. The IR spectra were recorded on a PYE UNICAM SP-3 300 IR spectrophotometer equipped with sodium chloride cells. The instrument was previously calibrated with standard polystyrene film. All measurements were done at 24 ± 1°C with the same pair of cells (path length 0.5 mm).

Reaction of DMIS with 2-ethyl-1-hexanol. In a 10 cm^3 volumetric flask, a 0.02 M solution of DMIS was prepared by dissolving 73.6 mg of it in dry benzene up to the mark. It was used as standard solution. In another 10 cm^3 volumetric flask, 73.6 mg of DMIS and 520 mg of 2-ethyl-1-hexanol were dissolved in dry benzene and the solution was standardized to 10 cm^3. This was the reaction mixture, 0.02 M with respect to diisocyanate and 0.4 M with respect to 2-ethyl-1-hexanol. Absorption (A_s) was recorded by scanning the IR spectrum of the standard solution which filled the cell. The reaction mixture was also run for IR spectrum in the cell, and absorbance (A_t) at different time, t, was recorded. The percentage of unreacted isocyanate was calculated with the help of A_s and A_t values.

Reaction of DPIS with 2-ethyl-1-hexanol. The procedure described for DMIS–2-ethyl-1-hexanol reaction was used for this reaction also.

RESULTS AND DISCUSSION

The scheme for the synthesis of diisocyanates is outlined in Fig. 1.

The physical characteristics and spectral data (IR and ^1H NMR) of the compounds prepared are given in Table 1.

The compounds DMSCL[6] and DPSCL[7] were prepared from the Grignard reagent of *p*-bromotoluene and excess of the appropriate dichlorosilane. All the reactions were carried out under a dry and inert atmosphere.

The hydrolysis and concurrent dehydration of DMSCL gave DMDM.[8]

An ethereal solution of DPSCL with a drop of phenolphthalein indicator was hydrolysed by sodium hydroxide solution at room temperature. A light pink colour ensured the completion of hydrolysis. In this case the free silanol, DPOH, rather than disiloxane, results. It was identified as silanol by the fact that the benzene (dry) solution reacted with sodium. Also a band at 3300 cm^{-1} in the IR spectrum and D_2O exchange in the NMR spectrum confirmed the presence of an OH group.

The dehydration of DPOH in the presence of sodium hydroxide at elevated temperature[8] afforded DPDM.

The oxidation of DMDM was carried out with potassium permanganate in pyridine/water mixture as described by Speck.[8] The complete oxidation of the aryl CH_3 groups was confirmed by the ^1H NMR spectrum of the resulting compound in pyridine which showed the absence of singlet peak of aryl CH_3 at δ 2.20 ppm.

DPAC was prepared following chromic acid oxidation of DPDM as reported by Breed and Wiley[9] but with a different purification procedure. Before washing the DPAC by methylene chloride, the ^1H NMR spectrum showed a peak at δ 2.27 ppm due to aryl CH_3. After washing with methylene chloride the spectrum showed the absence of the peak at 2.27 clearly indicating the removal of DPDM.

The diacid chlorides, DMACL[10] and DPACL,[9] were prepared by reacting the corresponding diacids with excess of thionyl chloride at reflux temperature.

The synthesis of the two new acyl azides was accomplished by two reaction pathways. Method (a) consists of treating DMACL/DPACL in methylene chloride with sodium azide in water. The other method (b) involved the conversion of carboxylic groups of diacids (DMAC and DPAC) into the azido carbonyl groups by an adaptation of the elegant Weinstock modification of the Curtius reaction.[11] The diacids were treated successively with 2 moles each of triethylamine, ethyl chloroformate and sodium azide. This is a "one-flask" reaction which does not involve the isolation of intermediate compounds and gives the product in pure form with good yields. A strong absorption band at 2130 cm^{-1} is observed which is due to the asymmetric stretching vibration of the N_3 group. A slight splitting of this absorption band is observed which may be explained as due to Fermi interaction with a combination tone involving the N_3 symmetric or C—N stretching vibration and other low-lying frequencies.[12]

The desired disiloxane-containing diisocyanates were obtained by the thermal decomposition of the corresponding acid diazides. The Curtius rearrangement was carried out in dry benzene at reflux temperature. The rearrangement took place

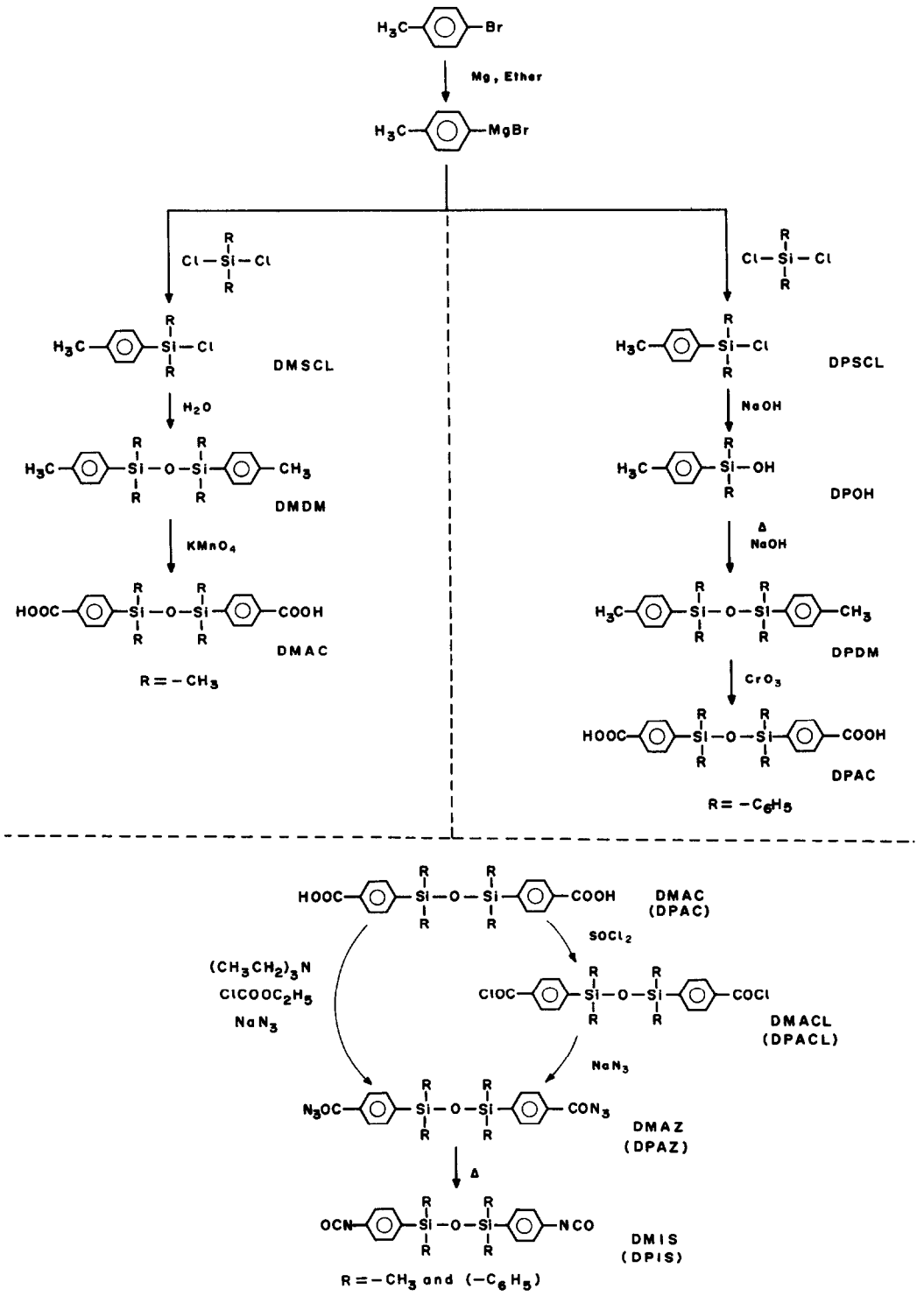

Fig. 1. Synthesis of disiloxane-containing diisocyanates.

Table 1. Physical characteristics and spectral data of the compounds

Compound	Yield (%)	m.p./b.p. [°C/(mm)]	^{1}H NMR[a] [δ (ppm)]	IR (cm^{-1})
DMSCL	65	95/(11)	0.33 (s, Si—CH_3, 6H), 2.0 (s, Ar—CH_3, 3H) 6.73 (d, Ar—H *ortho* to Si, 2H), 7.13 (d, Ar—H *ortho* to CH_3, 2H)[b]	550 (Si—Cl), 800, 840, 1260 (Si—CH_3)[g]
DPSCL	74	180–185/(0.2)	2.33 (s, Ar—CH_3, 3H), 6.86–7.60 (m, Ar—H, 14H)[b]	550 (Si—Cl) 705, 1120, 1430 (Si—C_6H_5)[h]
DPOH	90	94–95	2.27 (s, Ar—CH_3, 3H) 4.0 (s, Si—OH, 1H; exchangeable with D_2O), 7.53–6.77 (m, Ar—H, 14H)[b]	705, 1120, 1430 (Si—C_6—H_5), 3300 (OH)[h]
DMDM	79	140–142/(0.2)	0.27 (s, Si—CH_3, 12H), 2.20 (s, Ar—CH_3, 6H), 6.78 (d, Ar—H *ortho* to Si, 4H), 7.10 (d, Ar—H *ortho* to CH_3, 4H)[b]	800, 840, 1260 (Si—CH_3), 1060 (Si—O—Si)[g]
DPDM	93	157–159	2.27 (s, Ar—CH_3, 6H), 6.70–7.30 (m, Ar—H, 28H)[b]	710, 1120, 1435 (Si—C_6H_5), 1100 (Si—O—Si)[h]
DMAC	70	244–246	0.33 (s, Si—CH_3, 12H) 7.42 (d, Ar—H *ortho* to Si, 4H), 7.73 (d, Ar—H *ortho* to COOH, 4H)[c]	800, 840, 1260 (Si—CH_3), 1070 (Si—O—Si), 2300–3300 (COOH), 1680 (C=O)[h]
DPAC	68	248–250	7.22–7.53 (m, Ar—H *ortho* to Si and Si—C_6H_5, 24H), 7.68 (d, Ar—H *ortho* to —COOH, 4H)[c]	705, 1120, 1430 (Si—C_6H_5), 1100 (Si—O—Si), 2300–3300 (COOH), 1690 (C=O)[h]
DMACL	72	55	0.39 (s, Si—CH_3, 12H), 7.50 (d, Ar—H *ortho* to Si, 4H), 7.90 (d, Ar—H *ortho* to COCl, 4H)[d]	800, 840, 1260 (Si—CH_3), 1090 (Si—O—Si) 1750, 1780 (—COCl)[h]
DPACL	66	194–195	7.05–7.65 (m, Ar—H *ortho* to Si and Si—C_6H_5, 24H),	710, 1120, 1435 (Si—C_6H_5), 1100 (Si—O—Si), 1745, 1780 (—COCl)[h]
DMAZ	72[e] 87[f]	Liquid	0.33 (s, Si—CH_3, 12H), 7.33 (d, Ar—H *ortho* to Si, 4H), 7.73 (d, Ar—H *ortho* to CON_3, 4H)[d]	800, 840, 1260 (Si—CH_3), 1070 (Si—O—Si), 2130 (N_3 asymmetric), 1700 (>C=O)[g]
DPAZ	69[e] 85[f]	95	7.0–7.60 (m, Ar—H *ortho* to Si and Si—C_6H_5, 24H), 7.83 (d, Ar—H *ortho* to CON_3, 4H)[b]	705, 1120, 1430 (Si—C_6H_5), 1090 (Si—O—Si), 2130 (N_3 asymmetric), 1700 (C=O)[h]
DMIS	90	155/(0.1)	0.33 (s, Si—CH_3, 12H) 6.78 (d, Ar—H *ortho* to Si, 4H), 7.23 (d, Ar—H *ortho* to NCO, 4H)[d]	800, 840, 1260 (Si—CH_3), 1070 (Si—O—Si), 2280 (NCO)[g]
DPIS	92	55	6.87 (d, Ar—H *ortho* to NCO, 4H), 7.0–7.47 (m, Ar—H *ortho* to Si and Si—C_6H_5, 24H)[b]	705, 1120, 1430 (Si—C_6H_5), 1100 (Si—O—Si), 2280 (NCO)[h]

[a]Assignment given in parentheses: s = singlet, d = doublet, m = multiplet.
[b]CCl_4.
[c]DMSO-d_6.
[d]$CDCl_3$.
[e]Acid chloride–sodium azide method.
[f]Mixed anhydride–sodium azide method.
[g]Smear.
[h]Nujol.

smoothly and required 12 h for completion (confirmed by IR spectra taken after every 2 h). During the rearrangement, CON_3 rearranges to NCO with evolution of nitrogen. Hence, the aryl protons which were *ortho* to CON_3 in azidocarbonyl compounds became *ortho* to NCO in isocyanate, thereby producing an upfield chemical shift.

The method of Ghatge and Dandge[13] was followed for plotting the course of the reaction between the diisocyanates and 2-ethyl-1-hexanol. Although the alcohol isocyanate reactions have been shown to follow second-order kinetics, approximately first-order kinetics can be assumed to be due to the large excess of the alcohol used. The pseudo-first-order reaction rate constants for diisocyanates at various degrees of reaction along with the time required for completion of reaction at these degrees are given in Table 2. Bailey *et al.*[14] have shown that the electron-withdrawing substituent groups increase the reactivity of the isocyanate group by increasing the partial positive charge on the isocyanate carbon. In contrast, the electron-donating substituent groups decrease the reactivity of the isocyanate group by increasing the electronegativity of the carbon atom of the isocyanate group. However, in the present investigation CH_3 and C_6H_5 groups may not be expected to influence the reactivities of the isocyanate groups in the neighbouring aromatic rings because of the presence of saturated silicon atoms in between the aromatic nuclei.

Acknowledgement—One of the authors (S.S.M.) is thankful to the Council of Scientific and Industrial Research, New Delhi (India) for the award of a Junior Research Fellowship during the tenure of this work.

REFERENCES

1. H. Ulrich, *J. Polym. Sci., Makromol. Rev.* 1976, **11,** 93.
2. N. D. Ghatge and J. Y. Jadhav, *Synth. React. Inorg. Met.–Org. Chem.* 1984, **14,** 83.
3. N. D. Ghatge and P. P. Wadgaonkar, *J. Polym. Mat.* 1984, **1,** 161.
4. (a) Union Carbide Corp., Neth. Pat. 6,410,323 (1965); (b) E. J. Pepe, Union Carbide Corp., Ger. Offen. 1,906,259 (1969).
5. J.-C. Bonnet and E. Marechal, *Bull. Soc. Chim. Fr.* 1972, 3561.
6. D. W. Lewis and G. C. Gainer, *J. Am. Chem. Soc.* 1952 **74,** 2931.
7. A. K. Shubber and R. L. Dannley, *J. Org. Chem.* 1971, **36,** 3784.
8. S. B. Speck, *J. Org. Chem.* 1953, **18,** 1689.
9. L. W. Breed and J. C. Wiley, Jr, *J. Organomet. Chem.* 1975, **102,** 29.
10. E. P. Micheev and G. N. Malnova, *J. Prakt. Chem.* 1964, **23,** 206.
11. J. Weinstock, *J. Org. Chem.* 1961, **26,** 3511.
12. E. Lieber, C. N. R. Rao, A. E. Thomas, E. Oftedahl, R. Minnis and C. V. Nambury, *Spectrochim. Acta* 1963, **19,** 1135.
13. N. D. Ghatge and D. K. Dandge, *Angew. Markromol. Chem.* 1976, **49,** 129.
14. M. E. Bailey, V. Kriss and R. G. Spaunburgh, *Ind. Engng Chem.* 1956, **48,** 794.

Polyhedron Vol. 6, No. 3, pp. 441–446, 1987
Printed in Great Britain

0277–5387/87 $3.00+.00

γ-RADIOLYSIS OF MONOGERMANE AND THE FORMATION OF SOLID GERMANIUM HYDRIDE POLYMERS

R. BELLUATI, M. CASTIGLIONI and P. VOLPE*

Istituto di Chimica Generale ed Inorganica, Università di Torino, Corso M. d'Azeglio 48, 10125 Torino, Italy

and

M. C. GENNARO

Dipartimento di Chimica Analitica, Università di Torino, Via P. Giuria 5, 10125 Torino, Italy

(*Received* 15 *November* 1985; *accepted after revision* 17 *July* 1986)

Abstract—H_2, Ge_2H_6 and a solid material $(GeH_x)_n$ ($x = 0.55$–1.81) are produced by γ-radiolysis of GeH_4. The relative amount of all the products and the composition of the solid are reported vs the pressure of GeH_4 in the sample and the radiation dose. The composition of the solid approaches the formula Ge_nH_{2n} as the pressure increases while the production of H_2 and Ge_2H_6 decreases.

Until some years ago research on the IVth group semi-conductors was directed to the preparation of crystalline materials of very high purity.[1] Only recently has attention been focused, at least for silicon, on the amorphous form in an effort to obtain cheaper and more efficient material for solar photovoltaic cells. It has been demonstrated that amorphous silicon cells (containing a small percentage of bonded hydrogen) can collect the energy of the solar spectrum with higher efficiency than monocrystal cells.[1]

Germanium has not yet been considered for solar cell technology, but because its energy gap is lower than that of silicon, it might be added to silicon to build solar cells of higher efficiency utilizing the sun's spectrum in the lower energy region.[1]

The decomposition of monogermane has been studied by thermal methods and by mercury photosensitization. Thermal decomposition in a static system has been interpreted as caused by both a zero-order reaction occurring on the surface of the reaction vessel and a first-order reaction occurring in the gas phase, the former being predominant at low pressures and the latter at higher pressures.[2]

To our knowledge no radiolysis studies have been reported for GeH_4. Radiolytical decomposition is a suitable method to get useful information on mechanisms which can be easily transferable to other decomposition methods, such as glow-discharge—which is one of the most popular techniques used for the commercial production of amorphous semiconductors.

In this study we report the first results of the $\gamma + GeH_4$ experiments. T-labelled GeH_4 was used the better to trace the hydrogen content of the products.

EXPERIMENTAL

GeH_4 was prepared by reduction of GeO_2 with KBH_4.[3] After purification from CO_2, it was mixed with ^3He, sealed in quartz ampoules, and neutron bombarded for T-labelling with the nuclear recoil method.[4] The irradiated mixture was purified by gas chromatography using a 1 m × 1 cm i.d. column filled with Chromosorb 102, 60/80 mesh (J. Manville) at 310 K, He carrier 300 cm^3 min^{-1}. The T-labelled GeH_4 was then diluted with pure unlabelled GeH_4 to a specific activity of 5.62×10^3 Bq cm^{-3} at STP as measured by a static ion chamber (Nuclear Chicago).

*Author to whom correspondence should be addressed.

Germane, or mixtures of germane with oxygen or neon, sealed in Pyrex cylindrical ampoules (10 cm^3 vol.) were radiolysed with ^{60}Co γ-rays in a Gamma cell 200 (Atomic Energy of Canada Ltd.) at a dose rate of 150 Gy min^{-1} for total doses of 1.0×10^5, 8.0×10^5 and 1.2×10^6 Gy.

Several samples were prepared for each radiation dose, filling pressure and composition of the mixture, in order to carry out, for all experimental conditions, the gas-phase analysis and that of the solid product, both for Ge and H content.

The gas phase was analysed on a Cary-Loenco radio gas chromatograph[4] using 2 m × 0.6 cm i.d. columns in the 280–353 K temperature range; Chromosorb 102 (60/80 mesh) was used to get a good separation of HT and GeH_3T; G.C. Durapack *n*-octane porasil C, 80/100 mesh (Waters Associates) was used to separate HT + GeH_3T, Ge_2H_5T and higher germanes.

After the analysis of the gas phase one half of the samples were washed with concentrated nitric acid to dissolve the solid product. The acidic solution was analysed for Ge content by plasma emission spectroscopy. A DC Spectraspan IV (SMI Andover) spectrometer was employed. A two-point calibration method was used. The remaining samples were analysed for the H (T) content by combustion at 980 K in a wet oxygen stream.[5] The stream at the exit of the combustion tube was collected in a 10 cm^3 of cooled distilled water. The collected water was mixed with 10 cm^3 of Instagel (United Technologies Packard) scintillation cocktail and counted in a Tri-Carb (Packard) liquid scintillator counter (9.1% efficiency).

RESULTS

Gas-phase products

At the temperature of the irradiation (300–315 K depending on the irradiation time) the gaseous products of the radiolysis of GeH_4 are H_2, Ge_2H_6 and traces of Ge_3H_8 (the last easily detectable only in the higher dose and pressure runs). Figure 1 shows the trends of the labelled products yields as a function of the dose at 6.7 and 1.6×10^2 kPa. The products' yields increase with the dose, reaching, at 1.2×10^6 Gy, the total values of 9 and 5% in samples at 6.7 and 1.6×10^2 kPa, respectively—indicating that H_2 and Ge_2H_6 are primary products. Figure 2 shows the trend of the GeH_4 decomposition as a function of the pressure at the dose of 8×10^5 Gy. No strong dependence of the radiolytic products upon the reactant pressure can be observed, especially in the case of the Ge_2H_5T production, indicating that the experiments have been performed in the 'high-pressure region'.[6] Due to experimental difficulties the 'low-pressure region' has not been studied.

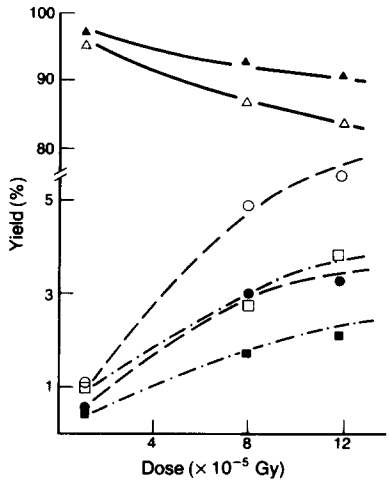

Fig. 1. Yields of GeH_3T, HT and Ge_2H_5T at 6.7 kPa (light points) and at 1.6×10^2 kPa (black points) as function of the absorbed dose: (——) GeH_3T, (-----) HT, and (-·-·-) Ge_2H_5T.

Figure 2 also shows the effect of added inert gas (Ne). When Ne is added the decomposition increases and the yields of the products are higher than those obtained not only at the same total pressure but even at the same reactant pressure.

Table 1 shows that the addition of O_2 as a radical scavenger has no effects on the Ge_2H_5T yield and only minor effects on the HT yield.

It should be pointed out that the results reported in Figs 1 and 2 refer only to the observed labelled products. Actually GeH_3T^* decomposes via a route leading to HT or H_2, and hence to GeH_2 or GeHT, respectively, with the same probability (see Discussion). By radio GC only the products containing the label will be detected, consequently the observed yields of both HT and Ge_2H_5T are only half of the actual hydrogen and digermane yields from GeH_3T^*.

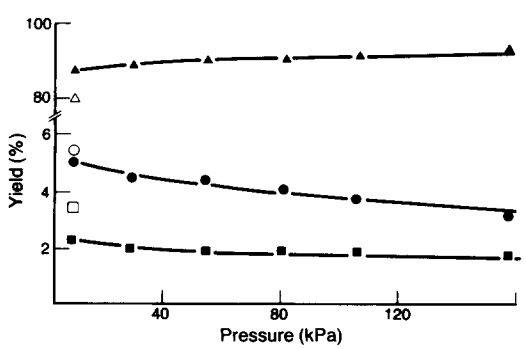

Fig. 2. Yield (%) in the system γ + GeH_4 as a function of the reactant pressure: (▲) GeH_4, (●) HT, and (■) Ge_2H_5T. △, ○ and □ = the same products in the presence of Ne (2:1). Dose = 8×10^5 Gy.

Table 1. Effect of oxygen on yield of products

Oxygen (kPa)	Products: Ge in solid total Ge (wt%)	T (solid)	HT (% of total activity)	Ge_2H_5T
2.7	3.79	1.8	2.40	1.8
6.6	3.98	1.35	2.61	1.8
13.3	4.18	1.65	2.82	1.5
20.0	3.87	2.01	2.77	1.3

The solid product

The solid product appears as a dark brown waxy material which covers the lower wall of the ampoule. In the oxygen-containing samples, the solid product is pale yellow, indicating the possible presence of hydrated oxides.

The compound is quite stable, in fact combustion of identical samples performed after prolonged exposures to the atmosphere gave the same results. The compound is remarkably different from the so-called "polymeric GeH_x"[3] which indeed contains oxygen.

Table 2 shows the composition of the solid as a function of the sample composition, pressure and the total dose. As expected the solid contains a lower fraction of the total Ge as the pressure increases and also its composition is pressure dependent: the H/Ge ratio is higher when obtained at higher pressures. The samples containing Ne show fairly enhanced yields.

Experiments carried out with ampoules filled with glass wool showed no surface effect, the observed deposition of the solid over the bottom of the ampoule also confirms the absence of any appreciable wall effect.

Table 2. Composition of the solid vs pressure and dose

Pressure GeH_4 (kPa)	Ne (kPa)	Dose (Gy)	Total T in solid (%)	Wt of Ge in solid (mg)	H/Ge ratio in solid
6.7		1×10^5	0.52	0.080	0.55
53.3		1×10^5	0.25	0.196	0.86
80.0		1×10^5	0.29	0.228	1.29
160.0		1×10^5	0.28	0.392	1.47
6.7		8×10^5	1.93	0.224	0.73
26.7		8×10^5	1.86	0.735	0.86
53.3		8×10^5	1.79	1.093	1.11
80.0		8×10^5	1.81	1.680	1.10
106.6		8×10^5	1.84	2.056	1.81
6.7		12×10^5	3.01	0.323	0.78
53.3		12×10^5	2.76	1.756	1.06
80.0		12×10^5	2.61	1.867	1.42
160.0		12×10^5	2.43	3.017	1.61
6.7	13.4	8×10^5	3.47	0.372	0.77

Table 3. *G* values of reactant and products at various pressures at the dose of 8×10^5 Gy

Pressure (kPa)	*G*: $-GeH_4$	H_2	Ge_2H_6	Ge (solid)
6.7	19.5 ± 2.1	17.1 ± 1.3	6.9 ± 1.5	16.5 ± 0.7
53.3	15.7 ± 1.8	15.1 ± 2.5	5.4 ± 0.6	10.1 ± 1.2
106.6	12.6 ± 0.4	11.9 ± 1.9	5.1 ± 1.0	8.2 ± 0.9
160	9.4 ± 1.1	9.2 ± 0.7	4.8 ± 0.8	6.3 ± 1.1

The *G* values for all the components of the system at 8×10^5 Gy and various pressures are reported in Table 3. The values at 1.0×10^5 Gy are about 1.5 times higher and those at 12×10^5 Gy do not differ substantially from those reported in the table, showing a stabilization at the per 100 eV yields over 8×10^5 Gy; a similar trend has been observed for SiH_4.[7]

DISCUSSION

In gas-phase radiolysis both radicals and ions are responsible for the final products. Apart from the mechanistic point of view, it is interesting to consider evidence for ionic reaction paths, to determine whether their contribution is significant, and whether their final products are expected to be different from those of the radical path.

The average energy absorbed for the formation of an ion pair (W) in the gas phase is about 5.3×10^{-18} J (34 eV) which is appreciably greater than the first ionization potential (I) of any gas.[8] The excess energy ($W - I$) is then available to form excited molecules. The ionization potential of GeH_4 has been found to be about 1.7×10^{-18} J (10.7 eV),[9] therefore in the upper limiting conditions, three molecules could be excited at about 1.2×10^{-18} J (7.7 eV) per each ion pair formed.

Moreover from the relation $G = 3M/N$, where M = number of molecules transformed, N = number of ions formed, it can be calculated that in our high-pressure conditions (where G has the lower value) $N = M/3$, i.e. the ions could account for ~25% of the reactive species. On the other hand, at least for H_2 production, the per 100 eV yield obtained in absence of ions, as in mercury-photosensitized decomposition of GeH_4 with 7.7×10^{-19} J (4.8 eV) photons, is the same as in our experiments at 6.3 kPa.[10] Besides, if an ionic mechanism similar to that of silane is supposed, the first step will give $GeH_3^+ + H$ and/or $GeH_2^+ + H_2$.[14] In the first instance scavengable hydrogen is produced, which has been observed to be a minor product. In the second instance molecu-

lar hydrogen is produced and the reactions of GeH_2^+ will produce detectable amounts of higher germanes (see below). It can then be inferred that for GeH_4 radiolysis the behaviour of the ions will not sensibly differ from that of radicals.

The following discussion will then deal with radicals, though some considerations could also apply to GeH_2^* species. Previous decomposition studies of GeH_4 suggest that excited GeH_4^* molecules could react as follows[10]

$$GeH_4^* + M \rightarrow GeH_4 + M \quad (1)$$

$$GeH_4^* \rightarrow GeH_3 + H \quad (2)$$

$$GeH_4^* \rightarrow GeH_2 + H_2 \quad (3)$$

$$GeH_4^* \rightarrow GeH + H_2 + H. \quad (4)$$

Reaction (2) involves the rupture of H_3G—H bond and hence requires at least 346 kJ mol^{-1}, while reaction (3) requires an activation energy of about 200 kJ mol^{-1} [12] and is then much more probable even in radiation and nuclear chemistry where the available excitation energies may be very high.[4]

As hypothesized above, if only three molecules could be excited for each ion formed, their excitation energy should be 1.2×10^{-18} J. In such conditions the unimolecular rate constants for reactions (2) and (3), calculated from equation (5):[13]

$$K_a = \alpha\nu\left(\frac{E + E_z - E_0}{E + E_z}\right)^{s-1} \quad (5)$$

are $1.4 \times 10^{10}\,s^{-1}$ and $1.9 \times 10^{12}\,s^{-1}$, respectively.

However in our mean experimental conditions (80.0 kPa and 8.0×10^5 Gy) the calculated mean energy absorbed per molecule is only about 9.8×10^{-20} J, so that the effective excitation energy of the GeH_4 molecule should be in the 1.2×10^{-18}–9.8×10^{-20} J range, with a higher probability for intermediate values. In such an energy range reaction (2) could then be easily suppressed by collision deactivation.

Furthermore experiments performed at 160 kPa and 1.2×10^6 Gy with variable amounts of O_2 (Table 1) show that the HT yield is scarcely affected by the scavenger; this finding makes it possible to exclude significant contributions of reactions (2) and (4) to the decomposition.

To sum up, it appears that the primary decomposition of excited GeH_4 species occurs mainly according to reaction (3), leading to H_2 and germylene (GeH_2).

The decomposition reaction (3) is, however, in competition with the stabilization reaction (1), which is of increasing importance as the collision frequency increases.

The poor pressure dependence of $-(GeH_3T)$ indicates that K_{dec} is greater than the collision frequency ω (ranging from 1.3×10^8 to 1.6×10^9) at least by one order of magnitude, i.e. $\sim 10^{10}$.

The calculation based on eqn (5) indicates that such a reaction rate requires an excitation energy of at least about 4.5×10^{-19} J, which is a reasonable value between the mean energy absorbed per molecule (9.8×10^{-20} J) at 8×10^5 Gy and the maximum energy of 1.2×10^{-18} J assuming only three excited molecules per ion pair.

The finding that GeH_2 is the main reactive species produced by decomposition of GeH_4^* suggests that germylene is the precursor of Ge_2H_6 through the insertion reaction (6), as it has been observed also in recoil Ge chemistry,[9] and of the solid product.

$$GeH_2 + GeH_4 \rightarrow Ge_2H_6. \quad (6)$$

The small pressure dependence of digermane yield could suggest that GeH_2 is very reactive by reaction (6), also at low energy content.

Actually the amount of germylene in the system decreases by about 6% (i.e. as $-GeH_4$) as the pressure increases from 6.3 to 160 kPa. If Ge_2H_6 is assumed to be produced by reaction of GeH_2, its yield reported in Fig. 2, is apparently only scarcely affected by the pressure; in fact the yield of reaction (6) is sharply dependent upon the collisional survival of GeH_2, and competes with the decomposition reactions (7) and (8)

$$GeH_2 + M \rightarrow Ge + H_2 + M \quad (7)$$

$$GeH_2 + M \rightarrow GeH + H + M \quad (8)$$

both of which are thermochemically feasible. It is suggested that they compete in the ratio 9:1.[12]

The solid product formation could be attributed to two different reaction sequences: (a) excited germylene insertion into the Ge—H bond of GeH_4, followed by hydrogen elimination and chain propagation as it has been suggested for the ionic mechanism in SiH_4[14,15] and for the radical mechanism in methylgermane.[16] Such a sequence will lead to a solid with a composition very close to Ge_nH_{2n} at any pressure condition and to the formation of detectable amounts of higher germanes. (b) Aggregation of Ge, GeH species [from reactions (7) and (8)] and perhaps GeH_2, leading to a hydrogen-poor solid. The composition of the solid reported in Table 2 and the absence of any substan-

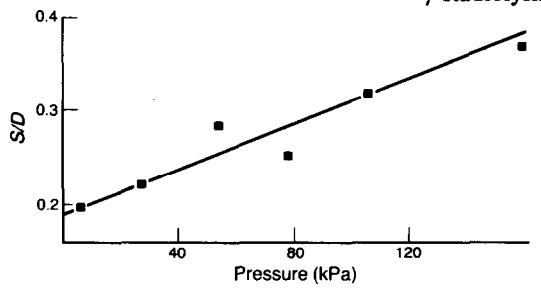

Fig. 3. Stabilization/decomposition for germilene radicals, vs total pressure. Intercept = 0.194; slope = 0.00118.

tial amount of higher germanes strongly supports this second reaction sequence.

The energetics of the reactivity of GeH_2 can be studied considering the competition between reactions (6), and (7) + (8). Using the symbology of decomposition–stabilization studies, we can call S (stabilized in gas phase) the fraction of GeH_2 species which reacts to Ge_2H_6 and D the fraction which through decompositions (7) + (8) is found in the solid.

Then the apparent rate constant for the unimolecular decomposition of germylene can be obtained by eqn (9) at the pressure where $D/S = 1$.

$$K_a = P\left(\frac{S}{D}\right)^{-1} Z \qquad (9)$$

Z is the collision number and P the pressure in torr. Z has been obtained using $\sigma_{GeH_4} = 5.1 \times 10^{-8}$ cm; D is the ratio (Ge in solid GeH_4) and S is (Ge_2H_6/−GeH_4). The plot of S/D vs pressure (Fig. 3) is linear enough to support the hypothesis that both Ge_2H_6 and the solid are formed in direct competition from the same precursor.[17] Linear least-square interpolation in Fig. 3 indicates that $D/S = 1$ at 7.2×10^5 kPa pressure, where the apparent unimolecular decomposition rate constant K_a for reaction (7) is: $ZP = K_a = 7.2 \times 10^9\,s^{-1}$.

The excitation energy for reaction (7), calculated by eqn (5) using the above rate constant, overcomes the activation energy used (1.18×10^{-19} J molecule^{-1})[12] by less than 1.6×10^{-22} J (0.001 eV). Because the energy used as activation energy is the lowest possible value for E_a, other values (2–3 times larger) have been tested. Nevertheless the decomposition rate does not change substantially, because the high decomposition rate is due to the very small number of degree of freedom of the GeH_2. Using the simplified RRK formula (i.e. neglecting te zero point energy E_z), K_a becomes one order of magnitude higher than ZP at an excitation energy 6.4×10^{-21} J higher than E_a. However, it should be noted that by neglecting the zero point energy, at low excitation energy, uncorrected values for K_a are obtained.[18]

It therefore appears quite strange that so much GeH_2 can be found in so narrow energy a range ($E - E_a$) to give the observed 'stabilization' yield (i.e. digermane).

The above findings can be explained taking into account that GeH_4^* molecules can undergo decomposition before or after any collision with the surroundings. GeH_2 species obtained by decomposition before collisions may carry higher excitation energy and be easily decomposed [reactions (7) + (8)], whereas the species obtained after collisions may be in a very low excitation state and be quite stable also. As the pressure increases the fraction of GeH_2 in low energy states increases and the ratio (Ge_2H_6/Ge in solid), i.e. S/D, is enhanced. As a consequence, the amount of undecomposed GeH_2 increases; this then takes part in the formation of the solid, which thus becomes richer in hydrogen.

Although the results at lower radiation doses and pressure (Table 2) are probably affected by larger errors, the composition of the solid does not appear to change in the 1.0×10^5–1.2×10^6 Gy range. This indicates that the solid is not sensibly affected by radiation damage up to 1.2×10^6 Gy, at least as far as the loss of hydrogen is concerned.

We also tested the influence of inert gas bath (Ne) at the lowest pressure. The sharp increase of volatile products, mainly HT, at the same partial pressures of GeH_4 indicates that the added Ne not only is unable to quench the excited GeH_4^* molecules but also favours some collisional decomposition [reaction (3b)] and consequently the insertion reaction (6)

$$GeH_4^* + Ne \rightarrow GeH_2 + H_2 + Ne. \qquad (3b)$$

The added Ne also affects the amount of the solid, the composition of which is apparently the same as that obtained from pure GeH_4.

Oxygen added as scavenger leads to a solid which appears different from that obtained from pure GeH_4. The analytical procedure used in this work, for the study of the solid has been devoted to the sole determination of the H/Ge ratio. Oxygen is known to react with radicals GeH_x, though its reactivity with such species is not known.[9] Nevertheless it can be inferred that the solid contains germanoxane chains, in fact the presence of oxygen does not affect the H/Ge ratio, indicating that oxygen does not substitute hydrogen atoms but

rather is inserted between two Ge atoms. The nature of the oxygen-containing solid will be the subject of a further report.

CONCLUSION

Though the bond dissociation energy for Si—H is higher than for Ge—H (378 vs 346 kJ mol^{-1}),[11] GeH_4 appears to be somewhat more stable than SiH_4 towards radiolysis, e.g. at 6.7 kPa: $G(-SiH_4) = 22$,[14] $G(-GeH_4) = 19$. Also for the formation of the solid the G values for silane[19] are higher than for germane, moreover the hydrogen content of the former is lower than for the latter. On the other hand some other contradictory properties of silicon and germanium compounds have been already pointed out. Possibly the nature of germanium d orbitals is relevant to this behaviour.[20]

The ionic contribution to the radiolysis of GeH_4 has been considered as similar to the radical contribution. However, the specific contribution of the ionic mechanism to the overall process should be tested, even if at very low pressures, by means of instrumental techniques such as MS and ICR spectrometry.

The deposition rate of the solid film, which is a determining parameter for practical application, has been estimated (for the 150 Gy min^{-1} dose rate), to range from 0.05–0.10 μm h^{-1} at the lowest pressure to 2–4 μm h^{-1} at the highest pressure. The above values are comparable with those usually observed for glow discharge deposition of amorphous silicon.

Acknowledgement—The authors wish to acknowledge the co-operation of the staff of the FRAE Institute of the CNR for sample irradiations and absorbed dose measurements.

REFERENCES

1. W. Fuhs, *Endeavour* 1984, **8**, 145.
2. K. Tamaru, M. Boudart and H. Taylor, *J. Phys. Chem.* 1955, **59**, 801.
3. W. L. Jolly and J. E. Drake, *Inorg. Synth.* 1963, **7**, 36.
4. M. Castiglioni and P. Volpe, *Polyhedron* 1983, **2**, 225.
5. D. E. Vance, M. E. Smith and G. R. Waterbury, Los Alamos Scientific Laboratory Report, L.A. 7716, UCLA (April 1979).
6. R. Weston Jr and H. A. Schwarz, *Chemical Kinetics*, p. 119. Prentice-Hall, Englewood Cliffs, NJ (1972).
7. W. Ando and S. Oae, *Bull. Chem. Soc. Jpn* 1962, **35**, 7540.
8. J. W. T. Spinks and R. J. Woods, *An Introduction to Radiation Chemistry*, pp. 5–7. J. Wiley, New York (1964).
9. P. P. Gaspar and J. J. Frost, *J. Am. Chem. Soc.* 1973, **95**, 6567.
10. Y. Rousseau and G. J. Mains, *J. Phys. Chem.* 1966, **70**, 3158.
11. M. J. Almond, A. M. Doncaster, P. N. Noble and R. Walsh, *J. Am. Chem. Soc.* 1982, **104**, 4717.
12. C. G. Newman, J. Dzarnoski, M. A. Ring and H. E. O'Neal, *Int. J. Chem. Kinet.* 1980, **12**, 661.
13. W. Frost, *Theory of Unimolecular Reactions*, p. 82 ff. Academic Press, New York (1973).
14. J. F. Schmidt and F. W. Lampe, *J. Phys. Chem.* 1969, **73**, 2706.
15. G. W. Steward, J. M. S. Henis and P. P. Gaspar, *J. Chem. Phys.* 1973, **58**, 890.
16. J. Dzarnoski, H. E. O'Neal and M. A. Ring, *J. Am. Chem. Soc.* 1981, **103**, 5740.
17. D. C. Fee and S. S. Markowitz, *J. Phys. Chem.* 1974, **78**, 347.
18. P. C. Jordan, *J. Chem. Phys.* 1966, **44**, 3400.
19. M. Castiglioni, M. Tuninetti and P. Volpe, *Gazz. Chim. Ital.* 1983, **113**, 457.
20. E. A. V. Ebsworth, *Volatile Silicon Compounds*, p. 4 ff. Pergamon Press, Oxford (1963).

Polyhedron Vol. 6, No. 3, pp. 447–453, 1987
Printed in Great Britain

0277–5387/87 $3.00+.00
Pergamon Journals Ltd

STABILITY CONSTANTS OF THE TERNARY COMPLEXES OF PALLADIUM(II) WITH THIODIPROPANOIC ACID AND CHLORIDE ION

S. HERNÁNDEZ CASSOU* and H. ITURRIAGA MARTÍNEZ†

Departamento de Química Analítica, Facultad de Ciencias, Universidad Autónoma de Barcelona, Bellaterra, Barcelona, Spain

(*Received* 6 *June* 1986; *accepted* 24 *July* 1986)

Abstract—The formation of the ternary complexes between palladium(II) ions and 3,3′-thiodipropanoic acid (TDPA) and chloride ion as ligands has been studied using spectrophotometric methods in acidic aqueous media with a constant ionic strength 0.5 M ($Na^+, H^+)(Cl_4^-, Cl^-$). The stoichiometries of the detected ternary complexes are: $[Pd(TDPA)Cl_3]^-$, $[Pd(TDPA)_2Cl_2]$ and $[Pd(TDPA)_2Cl]^+$. The spectrophotometric characteristics and the equilibrium constants for the different ternary species have been calculated with the LETAGROP-SPEFO computer program.

The ability of $Pd^{2+}(aq)$ to form different complexes with chloride ions is well known and the equilibrium constants corresponding to this binary system have been already summarized in the literature.[1] In a previous communication[2] the direct complexation between $Pd^{2+}(aq)$ and thiodipropanoic acid (TDPA) without chloride ions being present in the medium was studied and the values of the equilibrium constants of the resulting complexes $[Pd(TDPA)]^{2+}$ and $[Pd(TDPA)_2]^{2+}$ were reported.[2] Likewise, ternary systems containing palladium(II), chloride ions and thioethers[3–5] or sulphur-related compounds[6,7] have also been described and some of these results indicate that TDPA would be able to form this kind of mixed complex in a similar way. On this basis, and following our previous research with thio- and dithiodiacids,[2] a fundamental spectrophotometric study was carried out to elucidate the displacement reactions which could be produced when these two ligands (TDPA and chloride) compete for the same central atom (palladium) in acidic media.

EXPERIMENTAL

Apparatus and reagents

The apparatus has been previously described.[2]

Sodium chloride (Merck analytical reagent grade) was dried at 110°C and used without further treatment.

Hydrochloric acid (Probus analytical reagent grade) was standardized with HgO, KI.

All other reagents and solutions have been already indicated.[2]

Preliminary studies

Spectral characteristics. In the range of palladium concentration studied (10^{-5}–10^{-4} M), the species tetrachloropalladate(II), in aqueous media, shows two absorption bands: a broad one around 280 nm and a sharper one at 222 nm.

In the experimental conditions of this work, the predominant binary species from the system Pd–TDPA that has to be considered is the complex $Pd(TDPA)_2$, which denotes an absorption maxima at 272 nm.[2]

Initial assays evidenced the formation of ternary complexes $[Pd–TDPA–Cl]^-$ which presented a shoulder at 234 nm, and new absorption bands at the 280–300 nm zone shifted to higher wavelengths with respect to that of the binary systems.

*Present address: Departamento de Química Analítica, Facultad de Ciencias, Universidad de Barcelona, Barcelona, Spain.

†Author to whom correspondence should be addressed.

Variation of absorbance with pH. No changes in the absorbance value of solutions with $C_{Pd} = 10^{-5}$ M, $C_{TDPA} = 10^{-2}$ M and $C_{Cl} = 1.0$ M were observed when the pH was varied in the range 0.7–2.1. Therefore a $pC_H = 1.3$ was chosen to avoid problems with hydroxocomplexes of palladium in a way similar to that of a previous work.[2]

Variation of absorbance with time. The absorbance values of 10 solutions containing $C_{Pd} = 2.7 \times 10^{-5}$ M, $C_{TDPA} = 4 \times 10^{-4}$ M and chloride concentration in the range 1.7×10^{-4}–6.1×10^{-2} M were followed during two days, and indicated that during this period of time the solutions were stable.

Ionic strength. Some preliminary attempts were made with solutions containing different concentrations of chloride (3, 1 or 0.5 M depending on the series), a palladium concentration of 10^{-5} M and TDPA:Pd ratios of 1, 5, 50, 100 and 1000. These studies showed that, as could be predicted, TDPA molecules more easily replaced the chloride ions from the ternary complexes at lower concentrations of chloride. In consequence, and to work in experimental conditions analogous to those of a previous paper,[2] a total ionic strength of 0.5 M was chosen for the following studies.

RESULTS AND DISCUSSION

Because the species in solution, corresponding to the different binary and ternary systems, could be numerous it was necessary to establish the experimental conditions in such a way that only $[Pd(TDPA)_2]^{2+}$, $[PdCl_4]^{2-}$ and mixed complexes predominate. Two series of solutions were outlined: (i) a series with constant concentrations of metal and TDPA, 5.3×10^{-5} and 8.0×10^{-4} M, respectively, varying the concentration of chloride in the range 1.0×10^{-4}–10^{-1} M; and (ii) a series with constant concentrations of metal and chloride, 5.3×10^{-5} and 0.4 M, respectively, varying the concentration in the range of TDPA 2×10^{-5}–1.8×10^{-3} M.

The analytical concentration of hydrogen in all solutions was $pC_H = 1.3$ and the total ionic strength was always kept constant at 0.5 M (Na^+, H^+) (ClO_4^-, Cl^-). Some spectra corresponding to each series can be seen in Figs 1 and 2, respectively. Thirty minutes after each solution had been prepared, its absorbance values were read at different wavelengths in the range 320–235 nm in order to get enough experimental data to study quantitatively all species absorbing in the wavelength zone. The TRIANG[8] numerical program was simultaneously applied to both series of solutions. It was possible to conclude that at least two ternary species were present in solution if an error matrix from 0.004–0.009 was tolerated, and a third one, probably present in low proportion appeared for an error matrix <0.004.

Treatment of the experimental data

The spectra of Figs 1 and 2 show that mixed species are gradually formed. It can be observed that the band of $[Pd(TDPA)_2]^{2+}$ (Fig. 1) decreases and shifts to higher wavelengths, and finally a well-defined band around 300 nm appears. In Figure 2, the 280 nm band corresponding to $[PdCl_4]^{2-}$ also shifts, and it is possible to appreciate two new zones, one at 290 nm and other at 300 nm. It seems that the final species at 300 nm is the same in both series. On this basis, and taking into account that at $pC_H = 1.3$ TDPA acts as a monodentate ligand,[2] the ternary complexes could be: (i) $[Pd(TDPA)Cl_3]^-$ and $[Pd(TDPA)_2Cl_2]$ resulting from the displacement of chloride ions in $[PdCl_4]^{2-}$ by TDPA molecules; and (ii) $[Pd(TDPA)_2Cl]^+$ and $[Pd(TDPA)_2Cl_2]$ formed when chloride ions are added to the $[Pd(TDPA)_2]$ complex, trying to satisfy the four coordination positions of palladium(II).

The system can be represented by the following equations:

$$[PdCl_4]^{2-} + TDPA \rightleftharpoons [Pd(TDPA)Cl_3]^- + Cl^-;$$

$$K_1 = \frac{[[Pd(TDPA)Cl_3]^-][Cl^-]}{[[PdCl_4]^{2-}][TDPA]} \quad (1)$$

$$[Pd(TDPA)Cl_3]^- + TDPA \rightleftharpoons [Pd(TDPA)_2Cl_2] + Cl^-;$$

$$K_2 = \frac{[Pd(TDPA)_2Cl_2][Cl^-]}{[[Pd(TDPA)Cl_3]^-][TDPA]} \quad (2)$$

$$[Pd(TDPA)_2]^{2+} + Cl^- \rightleftharpoons [Pd(TDPA)_2Cl]^+;$$

$$K_3 = \frac{[[Pd(TDPA)_2Cl]^+]}{[[Pd(TDPA)_2]^{2+}[Cl^-]} \quad (3)$$

where TDPA represents the totally protonated form of the ligand. In the following, the charges of the species will be omitted.

Graphical methods. Newman and Hume's method[9] was used to corroborate this initial hypothesis. This graphical method has already been applied to displacement reactions between palladium chloride and some thioethers similar to thiodipropanoic acid.[3] The method must be followed in conditions where the coordination of the central atom is completely fulfilled and, in this

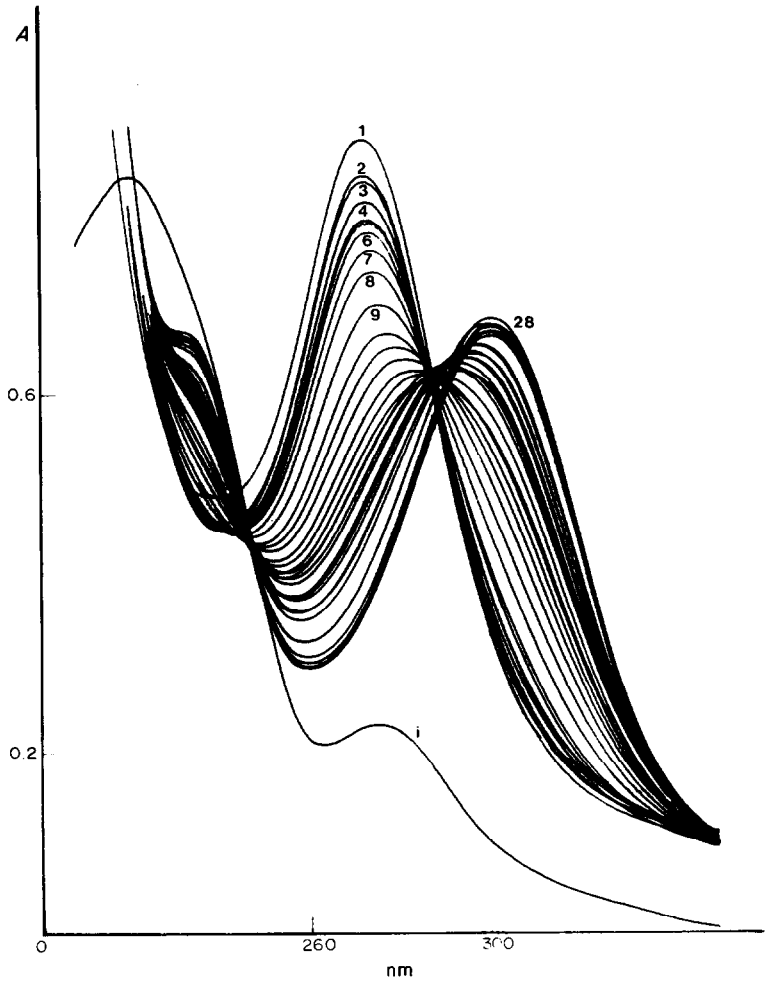

Fig. 1. Absorption spectra of Pd–TDPA–Cl system. Displacement of Pd–TDPA complexes. All solutions contained a concentration of palladium and TDPA equal to 5.3×10^{-5} and 8×10^{-4} M, respectively, and the chloride concentration was: (1) none, (2) 1.01×10^{-4} M, (3) 2.02×10^{-4} M, (4) 3.03×10^{-4} M, (5) 4.04×10^{-4} M, (6) 5.05×10^{-4} M, (7) 6.06×10^{-4} M, (8) 8.08×10^{-4} M, (9) 1.01×10^{-3} M, (10) 1.51×10^{-3} M,...,(28) 4.00×10^{-2} M. Solution (i) contained 5.3×10^{-5} Pd^{2+}, 3×10^{-2} M Cl^- and no TDPA was present.

work, only eqns (1) and (2) satisfy them. Two equations analogous to those of Newman and Hume were derived:

—two species, $PdCl_4$ and $Pd(TDPA)Cl_3$, exist and both absorb

$$|(\varepsilon_{PdCl_4} \cdot C_{Pd}) - A| \frac{C_{Cl}}{C_{TDPA}} = A \cdot K_1 - C_{Pd} \cdot \varepsilon_{Pd(TDPA)Cl_3} \cdot K_1 \quad (4)$$

—two species, $Pd(TDPA)Cl_3$ and $Pd(TDPA)_2Cl_2$, exist and only one, $Pd(TDPA)_2Cl_2$, absorbs.

$$A = \frac{1}{K_2}(-A)\frac{C_{Cl}}{C_{TDPA}} + \varepsilon_{Pd(TDPA)_2Cl_2} \cdot C_{Pd} \quad (5)$$

where C_{Pd}, C_{Cl} and C_{TDPA} are the analytical concentrations of palladium, chloride and thiodipropanoic acid, respectively and A is the experimental absorbance. The molar absorptivities of $[PdCl_4]^{2-}$ at different wavelengths, ε_{PdCl_4}, were obtained from a separate experiment, which is indicated in the next section on numerical methods. When ε_{PdCl_4} is known then K_1 and $\varepsilon_{Pd(TDPA)Cl_3}$ at 280 and 290 nm, from eqn (4), and K_2 and $\varepsilon_{Pd(TDPA)_2Cl_2}$ at 310 and 320 nm, from eqn (5), can be calculated and these results are given in the table 1.

Numerical methods. Newman and Hume's method needs the molar absorptivities of the tetrachloropalladate complex. So a series of solutions with high chloride concentration (3 M) and palladium varying between 3.2×10^{-5} and 6.4×10^{-5} M was prepared. The molar absorptivities obtained are shown in Table 2 at some wavelengths and agree with those of Pitombo *et al.*[3] At a chloride

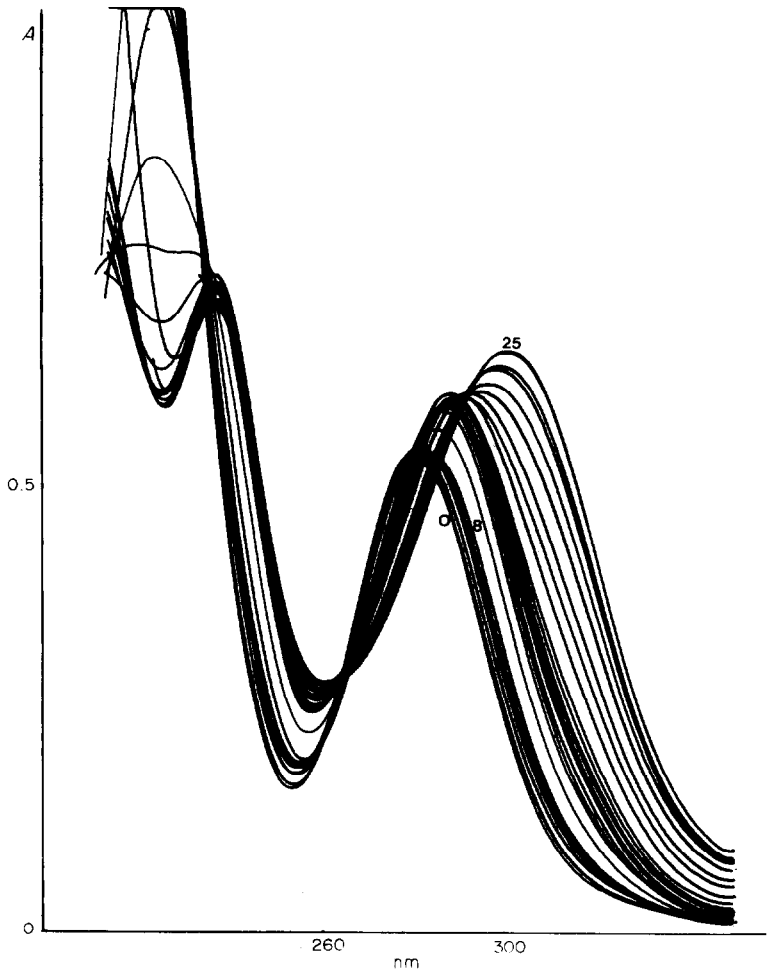

Fig. 2. Absorption spectra of Pd–TDPA–Cl system. Displacement of palladium chlorocomplexes. All solutions contained a concentration of palladium and chloride equal to 5.3×10^{-5} M and 0.4 M, respectively, and the TDPA concentration was: (1) 1×10^{-5} M, (2) 1.2×10^{-5} M, (3) 1.4×10^{-5} M, (4) 1.6×10^{-5} M, (5) 1.8×10^{-5} M, (6) 2.2×10^{-5} M, (7) 2.6×10^{-5} M, (8) 4.0×10^{-5} M, (9) 5.0×10^{-5} M, (10) 6.0×10^{-5} M,..., (25) 1.8×10^{-3} M.

Table 1. Results obtained by means of Newman and Hume's method[9]

Wavelength (nm)	$\varepsilon_{Pd(TDPA)Cl_3}$ ($l\,mol^{-1}\,cm^{-1}$)	Log K_1	$\varepsilon_{Pd(TDPA)_2Cl_2}$ ($l\,mol^{-1}\,cm^{-1}$)	Log K_2
280	9475	4.03		
290	11,981	4.10		
310			12,290	3.30
320			8571	3.26

concentration of 0.4 M, the species $[PdCl_3]^-$ must also be considered (it can be present up to 5%); then a series in these conditions and with palladium concentrations in the range 3.2×10^{-5}–6.4×10^{-5} M was prepared. Table 2 also gives the molar absorptivities of $[PdCl_3]^-$, and the overall stability constants of the palladium binary species with chloride ion, β_4 and β_3, calculated by means of the LETAGROP-SPEFO program[10] were $\log\beta_4 = 11.39$ and $\log\beta_3 = 10.27$ which are in concordance with the results of Ref. 1. The LETAGROP-SPEFO computer program was used to treat simultaneously the experimental data from eight wavelengths. Because of the difficulty of the whole system, the binary systems (molar absorptivities and equilibrium constants) were fixed and only those of the ternary species were left to refine. The initial refinement cycle was done with the values found by graphical methods. The final computer results are listed in Table 3 where overall formation constants for the system

$$pPd^{2+} + q\text{TDPA} + rCl^- \rightleftharpoons [Pd_p(\text{TDPA})_qCl_r]^{(2p-r)+}$$

are expressed as $\log\beta_{pqr} \pm 3\sigma_{(\beta)}$, where σ is the

Table 2. Molar absorptivities of chlorocomplexes of palladium(II) and their global equilibrium constants calculated with the LETAGROP-SPEFO program

	Wavelength (nm)							
	260	270	280	285	290	295	300	310
$\varepsilon_{PdCl_4^{2-}}$ ($l\,mol^{-1}\,cm^{-1}$)	3623 ± 15	8851 ± 37	11,503 ± 53	10,569 ± 46	8578 ± 35	6225 ± 23	4137 ± 17	1562 ± 15
$\varepsilon_{PdCl_3^-}$ ($l\,mol^{-1}\,cm^{-1}$)	2156 ± 139	136 ± 117	227 ± 186	841 ± 173	1183 ± 176	1287 ± 126	1300 ± 103	1047 ± 102

$\log\beta_4$	$\log\beta_3$	$\sigma(Y)$	U_{min}
11.39 ± 0.01	10.27 ± 0.03	0.0024	0.30×10^{-3}

Table 3. Final values of overall equilibrium constants and molar absorptivities obtained with the LETAGROP-SPEFO program: $I = 0.5\,M\ (Na^+, H^+)\ (ClO_4^-, Cl^-)$

$$pPd^{2+} + q\text{TDPA} + rCl^- \rightleftharpoons [Pd_p(\text{TDPA})_qCl_r]^{(2p-r)+};\ \beta_{pqr} = \frac{[[Pd_p(\text{TDPA})_qCl_r]^{(2p-r)+}]}{[Pd^{2+}]^p[\text{TDPA}]^q[Cl^-]^r}$$

$\log\beta_{113}$	$\log\beta_{122}$	$\log\beta_{121}$	$\sigma(Y)$	U_{min}
16.92 ± 0.09	19.79 ± 0.13	17.28 ± 0.12	0.011	4.26×10^{-2}

	260	270	280	285	290	295	300	310
$\varepsilon_{Pd(TDPA)Cl_3}$ ($l\,mol^{-1}\,cm^{-1}$)	5170 ± 38	6799 ± 46	9830 ± 70	11,029 ± 104	11,307 ± 115	10,449 ± 90	8848 ± 50	5431 ± 81
$\varepsilon_{Pd(TDPA)_2Cl_2}$ ($l\,mol^{-1}\,cm^{-1}$)	5018 ± 36	5519 ± 44	8158 ± 67	9942 ± 99	11,684 ± 110	13,052 ± 86	13,775 ± 48	12,694 ± 77
$\varepsilon_{Pd(TDPA)_2Cl}$ ($l\,mol^{-1}\,cm^{-1}$)	12,222 ± 43	15,533 ± 52	14,945 ± 79	13,090 ± 118	10,737 + 130	8360 ± 102	6306 ± 57	3520 ± 91

Table 4. Comparison between different binary and ternary equilibrium systems of Pd–TDPA–Cl. The constants of equilibria (I)–(IV) have been derived from β_{pqr} values of the Table 3 and K_i'' and K_i'' values from this table

	Equilibrium constant	Reference
(I) $[PdCl_4]^{2-}(aq) + TDPA \rightleftharpoons [Pd(TDPA)Cl_3]^- + Cl^-$	$\log K_1 = 5.42$	This work
(II) $[Pd(TDPA)Cl_3]^- + TDPA \rightleftharpoons [Pd(TDPA)_2Cl_2] + Cl^-$	$\log K_2 = 2.87$	This work
(III) $[Pd(TDPA)_2(H_2O)_2]^{2+} + Cl^- \rightleftharpoons [Pd(TDPA)_2Cl(H_2O)]^+ + H_2O$	$\log K_3 = 4.30$	This work
(IV) $[Pd(TDPA)_2Cl(H_2O)]^+ + Cl^- \rightleftharpoons [Pd(TDPA)_2Cl_2] + H_2O$	$\log K_4 = 2.51$	This work
(V) $[Pd(H_2O)_4]^{2+} + TDPA \rightleftharpoons [Pd(TDPA)(H_2O)_3]^{2+} + H_2O$	$\log K_1' = 7.40$	2
(VI) $[Pd(TDPA)(H_2O)_3]^{2+} + TDPA \rightleftharpoons Pd(TDPA)_2(H_2O)_2]^{2+} + H_2O$	$\log K_2' = 5.58$	2
(VII) $[Pd(H_2O)_4]^{2+} + Cl^- \rightleftharpoons [PdCl(H_2O)_3]^+ + H_2O$	$\log K_1'' = 4.47$	1
(VIII) $[PdCl(H_2O)_3]^+ + Cl^- \rightleftharpoons [PdCl_2(H_2O)_2] + H_2O$	$\log K_2'' = 3.27$	1
(IX) $[PdCl_2(H_2O)_2] + Cl^- \rightleftharpoons [PdCl_3(H_2O)]^- + H_2O$	$\log K_3'' = 2.46$	1
(X) $[PdCl_3(H_2O)]^- + Cl^- \rightleftharpoons [PdCl_4]^{2-}(aq) + H_2O$	$\log K_4'' = 1.30$	1

standard deviation. As can be seen, the molar absorptivities calculated by numerical and graphical methods are in agreement (the differences oscillate between 3 and 6%), more so if the complexity of the solution system is taken into account.

The particular stoichiometries and types of the ternary complexes found in this study reinforce our previous work[2] about the monodentate character of 3,3′-thiodipropanoic acid when it reacts with palladium(II) in highly acidic solutions (where the TDPA will be totally protonated) supposing that the coordination number of this cation is four. Table 4 shows all the equilibria of the binary and ternary systems of Pd–TDPA–Cl which can be compared in this way. If the Pd^{2+} ion, in the absence of chloride, is considered surrounded by water, $[Pd(H_2O)_4]^{2+}$, then the displacement by TDPA of one molecule of water is approximately 100 units easier than the analogous case with chloride in $[PdCl_4]^{2-}$ species. The ratios K_1/K_2 and K_1'/K_2' (2.55 and 1.82 in logarithmic units, respectively) would indicate that there is an extra effect in the steric hindrance of chloride, with respect to the water, when a second bulky molecule of TDPA approximates in both cases. Obviously, the lower values of second stepwise constants compared to the first ones are due to this hindrance.

The $-I$ effect of the COOH group, which is mentioned in some works,[3] would be very much diminished in the mixed complexes with TDPA because in this system the carboxylic group is in the γ-position with regard to the sulphur atom, and in consequence the values of these equilibrium constants would be greater, although for TDPA only one chloride is displaced and two chlorides were substituted in the COOH case.

The comparison between equilibria III and VII of Table 4 shows that the constants in these two

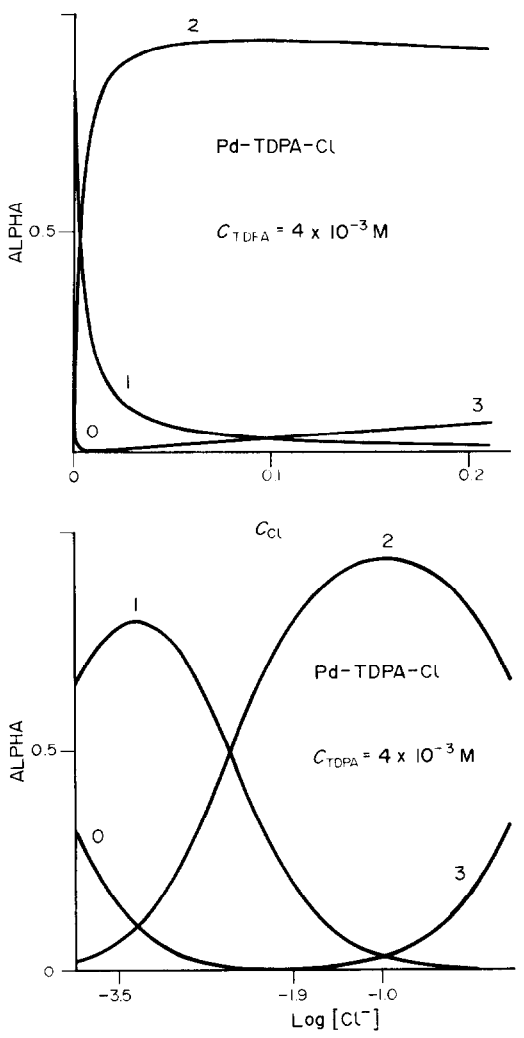

Fig. 3. Species distribution diagrams of Pd–TDPA–Cl system calculated by the Haltafall program: (0) $[Pd(TDPA)_2]$, (1) $Pd(TDPA)_2Cl]$, (2) $[Pd(TDPA)_2Cl_2]$, (3) $[Pd(TDPA)Cl_3]$.

systems are nearly equal, $\log K_3 = 4.30$ and $\log K_1'' = 4.47$, and it is possible to conclude, in consequence, that the behavior of TDPA in $[Pd(TDPA)_2]^{2+}$ is like a monodentate ligand because the tendency of chloride ion to coordinate with $[Pd(TDPA)_2(H_2O)_2]^{2+}$ or $[Pd(H_2O)_4]^{2+}$ is exactly the same. Moreover, in both cases, there is a mononegative anion (Cl^-) that approximates to a dispositive cation, $[Pd(H_2O)_4]^{2+}$ or $[Pd(TDPA)_2(H_2O)]^{2+}$, indicating that the electrostatic effect of the attraction predominates over the hindrance of TDPA with respect to chloride and, of course, this would only be possible if the TDPA is totally protonated and is coordinated only by the sulphur atom.

Recently Kragten *et al.*[11] have studied the palladium(II)–EDTA–chloride system and they have found a value of $\log K = 5.3 \pm 0.1$ for the equilibrium

$$PdH_2Y + Cl^- \rightleftharpoons PdH_2YCl^-$$

in agreement with the result calculated in this paper for the formation constant of equilibrium III, which is similar.

Figure 3 shows the species distribution diagrams, calculated from the final equilibrium constants by means of the computer program Haltfall,[12] and indicates that the species $[Pd(TDPA)_2Cl_2]$ is predominant (>90%) over a wide range of the chloride concentration. Then, on the basis of this complex, it would be possible to develop a method for the determination of palladium(II) by TDPA in the presence of chloride ion.

REFERENCES

1. R. M. Smith and A. E. Martell, *Critical Stability Constants*, Vol. 4. Plenum Press, New York (1976).
2. J. Coello, S. Hernández Cassou and H. Iturriaga Martínez, *Polyhedron* 1986, **5**, 1777.
3. L. R. M. Pitombo and E. De Oliveira, *Anal. Chim. Acta* 1978, **101**, 177.
4. E. Casassas, J. J. Arias and F. García, *J. Chim. Phys.* 1977, **74**, 424.
5. S. E. Livingstone, *Q. Rev. Chem. Soc.* 1965, **19**, 386.
6. B. Morelli, *Analyst* 1984, **109**, 47.
7. L. Canovese, L. Cattalini, G. Marangoni and G. Michelon, *J. Coord. Chem.* 1982, **12**, 63.
8. F. R. Hartley, C. Burgess and R. M. Alcock, *Solution Equilibria*, 1st Edn, p. 313. Ellis Horwood, England (1980).
9. L. Newman and D. Hume, *J. Am. Chem. Soc.* 1957, **79**, 4571.
10. L. G. Sillén and B. Warnqvist, *Arkiv Kemi* 1969, **31**, 315.
11. J. Kragten and L. G. Decnop-Weever, *Talanta* 1983, **30**, 449.
12. N. Ingri, W. Kakolowicz, L. G. Sillén and B. Warnqvist, *Talanta* 1967, **14**, 1261.

Polyhedron Vol. 6, No. 3, pp. 455–459, 1987
Printed in Great Britain

0277-5387/87 $3.00+.00

OXOVANADIUM(IV) COMPLEXES WITH 2-(2′-PYRIDYL)BENZIMIDAZOLE

P. K. NATH, N. C. MISRA,* V. CHAKRAVORTTY and K. C. DASH†

Departments of Chemistry and *Physics, Utkal University, Bhubaneswar 751004, India

(*Received* 11 *June* 1986; *accepted* 24 *July* 1986)

Abstract—The bidentate ligand, 2-(2′-pyridyl)benzimidazole (PBH), forms both five- and six-coordinated complexes with oxovanadium(IV), (VO^{2+}). The complexes $[VO(PBH)_2](NCS)_2$, $[VO(PBH)SO_4]$ and $[VO(PBH)_2]SO_4$ are five-coordinated while $[VO(PBH)_2X]X$ (X = Cl, Br or NO_3) are six-coordinated. Elemental analyses, electrical conductivity in non-aqueous media, electronic and IR spectra, mass and EPR spectra, magnetic susceptibility measurements and thermal analysis (TGA, DTG or DTA) studies adequately characterize the complexes.

The chemistry of oxovanadium(IV) has received considerable attention[1] as the VO^{2+} unit can readily coordinate four and five donor atoms to form VOL_4 and VOL_5 complexes, respectively. Additional interest has been generated due to the increasing discoveries of the biological importance of vanadium.[2] Several types of invertebrates accumulate vanadium in their blood. Thus, the ascidian seaworm *Phallusia mammilata* has a blood concentration of vanadium up to 1900 p.p.m., which represents more than a 10^6-fold concentration with respect to the sea-water in which it lives.[3] In this instance, vanadium was believed to play a role in the oxygen transport cycle.[4] Vanadium is also known to be an essential nutrient in higher life forms,[2,5] where it is involved in phospholipid oxidation, sulphur metabolism and cholesterol biosynthesis[6] and also plays a role in other biochemical processes. Oxovanadium(IV) complexes find use in chemical-reactivity studies either as models for V—O bond reactivity[7] or as potential free-radical like activators of organic and inorganic molecules. Oxovanadium(IV) porphyrins are commonly found in petroleum,[8] although their origin is not clear. Furthermore, the chemistry of vanadium is also of interest due to its close similarity to molybdenum, which is an essential co-factor in a number of oxidation–reduction enzymes.[9,10]

The ligand, 2-(2′-pyridyl)benzimidazole (PBH, see Scheme 1) is of interest in view of its similarity with 2,2′-bipyridyl and 1,10-phenanthroline in containing the —N=C—C=N— grouping and as it contains the imidazole group, which is present in many important biological systems. It also has potential use as a biochemical, anticancer and analytical reagent. The complexes formed due to the interaction of this ligand with dioxouranium(VI) and thorium(IV) have already been reported by us.[11] In continuation of our earlier work on imidazoles[12–14] and on the complexes of vanadium,[15,16] we report here the complexes formed by the interaction of several oxovanadium(IV) compounds with the ligand 2-(2′-pyridyl)benzimidazole. All of these complexes were adequately characterized on the basis of a number of spectral techniques in addition to the data based on analyses, electrical conductivity, magnetic susceptibility and thermogravimetric analyses.

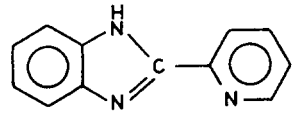

(PBH)

Scheme 1.

†Author to whom correspondence should be addressed.

EXPERIMENTAL

Materials

The ligand 2(2′-pyridyl)benzimidazole was synthesized as reported earlier.[11] V_2O_5 and $VOSO_4 \cdot 5H_2O$ were BDH reagent grade chemicals and were used as such. Syrupy $VOCl_2$ and $VOBr_2$ were prepared by a literature method.[17] $VO(NO_3)_2$ was obtained in solution by treating $VOSO_4$ with NaOH and treating the precipitated $VO(OH)_2$ with 50% HNO_3 followed by concentration of this solution.

Analyses

Vanadium was estimated either as V_2O_5 or as $AgVO_3$[18]; Cl and Br were estimated as silver halides and S as $BaSO_4$ after fusion of the sample with NaOH and Na_2O_2 and extraction of the melt with H_2O followed by acidification and addition of either $AgNO_3$ or $BaCl_2$, respectively. C, H and N microanalyses were made using a Carlo Erba instrument in CDRI, Lucknow. All melting points were determined in sealed capillaries and are uncorrected.

Physical measurements

The room temperature magnetic moments were determined in a Gouy balance using $HgCo(CNS)_4$ as calibrant. The electrical conductivity was measured in DMF solution ($\sim 10^{-3}$ M) using a Systronics 304 digital conductivity bridge and a dip type Pt cell with a cell constant of 1.0. The electronic spectra were recorded in a Varian 634 spectrophotometer and IR spectra were recorded as KBr pellets or polyethylene discs in the range 4000–200 cm^{-1} in a Perkin–Elmer 983 spectrophotometer. The EPR spectra were recorded as polycrystalline solids in a Varian E-4 spectrometer operating at X-band frequency. The mass spectra were recorded in a Varian CH-7 MAT spectrometer operating at an electron energy of 70 eV. The ion source was maintained at 473 K and the emission current was 300 μA. The thermogravimetric measurements were made using a Shimadzu DT-30 thermalanalyser which records T, TG, DTG and DTA simultaneously.*

Synthesis of complexes

Chloro bis-2-(2′-pyridyl)benzimidazole oxovanadium(IV) chloride, $[VO(PBH)_2Cl]Cl$ (**1**). Syrupy $VOCl_2$ (1 mmol) in acetone (5 cm^3) was added dropwise to the ligand PBH (2 mmol, 0.49 g) in the same solvent (5 cm^3) with stirring when a light green-yellow precipitate formed. The mixture was stirred further for 30 min under reflux, cooled and the solid filtered, washed with small aliquots of acetone, followed by ether and dried *in vacuo*.

Bromo bis-2-(2′-pyridyl)benzimidazole oxovanadium(IV) bromide, $[VO(PBH)_2Br]Br$ (**2**). Addition of aq. $VOBr_2$ (1 mmol) in acetone (5 cm^3) to PBH (2 mmol, 0.4 g) with stirring yields a viscous green liquid which was dissolved in 1:1 acetone–ethanol mixture and stored in a refrigerator for 12 h when green solid deposited. This was collected on a frit, washed with acetone–ethanol mixture and dried *in vacuo*.

Nitrato bis-2-(2′-pyridyl)benzimidazole oxovanadium(IV) nitrate, $[VO(PBH)_2(NO_3)]NO_3$ (**3**). Syrupy $VO(NO_3)_2$ (1 mmol) in acetone (5 cm^3) and PBH (2 mmol, 0.4 g) in acetone (5 cm^3) on stirring for 30 min yields a green compound, which was collected and dried as above.

Bis-2-(2′pyridyl)benzimidazole oxovanadium(IV) thiocyanate, $[VO(PBH)_2](CNS)_2$ (**4**). $VO(CNS)_2$, prepared by metathesis of aq. $VOCl_2$ and NH_4CNS in EtOH, was added dropwise to a stoichiometric amount of PBH in EtOH, and stirred for 1 h. The volume was reduced and the resultant concentrate was stored in a refrigerator for 12 h. A brown-yellow solid deposited, which was collected, washed with Et_2O and dried *in vacuo*.

Bis-2-(2′-pyridyl)benzimidazole oxovanadium(IV) sulphate, $[VO(PBH)_2]SO_4$ (**5**). $VOSO_4$ (1 mmol, 0.26 g) dissolved in 1:1 ethanol–water mixture was added to PBH (2 mmol, 0.4 g) in EtOH with stirring. A bulky yellow precipitate formed immediately and the mixture stirred for 30 min for completion of reaction. The compound was collected on a frit washed with small volumes of acetone, followed by ether and dried *in vacuo*.

Sulphato 2-(2′-pyridyl)benzimidazole oxovanadium(IV), $[VO(PBH)SO_4]$ (**6**). $VOSO_4$ (1 mmol, 0.26 g) dissolved in DMF was added to a solution of PBH (1 mmol, 0.2 g) in DMF and stirred. Initially the solution turned green from which on further stirring a grey powder separated out. This was collected, washed with EtOH and then ether and dried *in vacuo*.

RESULTS AND DISCUSSION

The compounds reported in this work are presented in Table 1 along with their analytical data, conductance, magnetic moments and the EPR $\langle g \rangle$ parameters. The conductance measurements were made in dilute solutions ($\sim 10^{-3}$ M) of DMF, $MeNO_2$ and MeOH. On the basis of observed

*The TGA and DTA data have been deposited with the Editor as supplementary data available on request.

Table 1. Colour, analyses, conductivity data, magnetic moment and EPR parameters $\langle g \rangle$ of oxovanadium complexes with PBH ligand

Compound	Colour	Analytical data; found (calc.) % V	C	H	N	Λ_M (in DMF)	μ_{eff} (BM)	$\langle g \rangle$
$[VO(PBH)_2Cl]Cl$	Green yellow	10.2 (9.7)	54.4 (54.5)	3.5 (3.4)	15.8 (15.9)	63.1	1.86	1.993
$[VO(PBH)_2Br]Br$	Green	9.0 (8.3)	46.5 (46.7)	2.8 (2.9)	3.4 (3.6)	89.8	1.70	2.002
$[VO(PBH)_2NO_3]NO_3$	Brown yellow	8.5 (8.8)	49.5 (49.6)	3.2 (3.1)	19.1 (19.3)	58.0	1.82	1.997
$[VO(PBH)_2](CNS)_2$	Green yellow	10.9 (10.7)	54.4 (54.4)	3.1 (3.1)	19.6 (19.5)	170.0	1.87	1.99
$[VO(PBH)_2]SO_4$	Yellow	9.5 (9.2)	52.0 (52.0)	3.2 (3.2)	15.0 (15.2)	57.4	1.78	1.989
$[VO(PBH)SO_4]$	Grey	13.8 (14.2)	40.0 (40.2)	2.2 (2.5)	11.5 (11.7)	25.0	1.79	1.9835

Table 2. Prominent IR absorption bands of VO^{2+} complexes with PBH ligand (in cm^{-1})[a]

Complex	ν(V=O)	Anion vibrational modes				Remarks
$[VO(PBH)_2Cl]Cl$	980					
$[VO(PBH)_2Br]Br$	980					
$[VO(PBH)_2(NO_3)]NO_3$	985	1400				Ionic NO_3^-
		1255	1060	750		Unidentate NO_3^-
$[VO(PBH)_2](CNS)_2$	980	2074				Ionic CNS^-
$[VO(PBH)_2](SO_4)$	982	1100	1000	620	450	Ionic SO_4^{2-}
$[VO(PBH)SO_4]$	985	1060	985	605		Bidentate SO_4^{2-}

[a]In all cases the following important ligand vibrations were observed: ν(N—H), 3400–3500; ν(C=N), 1590–1610; pyridine ring vibration, 1560–1580; N—H out of plane deformation 790–800 cm^{-1}.

conductivity values in these solvents,[19–21] the $[VO(PBH)_2X]X$ (X = Cl, Br or NO_3) and $[VO(PBH)_2]SO_4$ are formulated as 1:1 electrolytes, the $[VO(PBH)_2](NCS)_2$ as a 1:2 electrolyte and $[VO(PBH)SO_4]$ as a non-electrolyte. The electronic spectra of the complexes in solution exhibit ligand-field bands in the 17–19 and 12–13 kK regions corresponding to the $b_2 \rightarrow b_1$ and $b_2 \rightarrow c$ transitions.[22–24]

The IR spectra were recorded in the 4000–200 cm^{-1} region and in all cases the spectra due to the ligand, the polyatomic anions and the ν(V=O) were observed. The prominent ligand bands are either split or shifted due to coordination.[25] The IR spectra show that the ligand is coordinated in a bidentate manner through the unsaturated N atom and the N atom of the pyridine ring.[26] The $[VO(PBH)_2(NO_3)](NO_3)$ complex has a strong band at 1400 cm^{-1} due to the ionic nitrate group and bands at 1255, 1060 and 750 cm^{-1} corresponding to the ν_1, ν_2 and ν_3 vibrations for the nitrate group coordinated in a unidentate manner.[27,28] The thiocyanate complex has a strong absorption band at 2074 cm^{-1} due to the ionic thiocyanate group[29,30] in $[VO(PBH)_2](CNS)_2$ which is in agreement with the conductivity data. The sulphato complex $[VO(PBH)SO_4]$ has IR bands at 1060, 605 and 985 cm^{-1} corresponding to the bidentate coordination[31] of SO_4^{2-} group and the sulphate complex $[VO(PBH)_2]SO_4$ exhibits bands at 1000, 450, 1100 and 620 due to the ν_1, ν_2, ν_3, ν_4 vibrations, respectively of the uncoordinated ionic sulphate group.[32] The ν(V=O) stretching frequency is observed in all complexes at 980–985 cm^{-1} region except for the $[VO(PBH)_2NO_3]NO_3$ complex where it occurs at 998 cm^{-1}. These values indicate that V=O bond in VO^{2+} consists of a combination of σ-bond and p_π–d_π donation of electrons from the vanadyl oxygen to the vanadium atom.[24]

The observed magnetic moments of these complexes are approximately in agreement with the spin-only value of a d^1 system,[33,34] where the orbital contribution to the magnetic moment is quenched[35] due to the strong axial ligand field in oxovanadium(IV) complexes. Antiferromagnetic couplings of spin are also not observed at room

temperature[36] and the complexes do not exhibit any dependence on the magnetic field strength indicating the absence of ferromagnetic interactions. The results of magnetic moment studies are supported by the measurement of EPR spectra of polycrystalline compounds at X-band frequencies at room temperature. In all cases the g_{av} values lie in the range 1.983–2.002 close to the free-electron spin-only value of 2.0023. Both this result and the fact that the anisotropy of the g values is small in comparison with that for the magnetically similar d^9 complexes indicate that the axial component to the ligand field is high and the unpaired electron lies in an orbital of b_2 symmetry. In all cases the EPR signal appears as unresolved broad line except for the $[VO(PBH)_2(NO_3)](NO_3)$ complex, which shows[37] fairly well resolved hyperfine lines due to ^{51}V ($I = 7/2$). The anisotropic g values for this complex are $g_{\|}$ 1.957 and $g_{\perp}$ 2.017 with a g_{av} of 1.997; $A_{\|}$ is 175 G and $A_{\perp}$ is 60 G. The g_{av} values for $[VO(PBH)_2](CNS)_2$ and $[VO(PBH)_2]SO_4$ are 1.99 and 1.89, respectively, which are very close, indicating that the extent of delocalization in both cases are almost similar due to identical structural and electronic environment around vanadium. In both cases the five-coordinate $[VO(PBH)_2]^{2+}$ species is present as is clear from both conductance and IR results. The other five-coordinate species containing the bidentate PBH ligand and the bidentate sulphate group, $[VO(PBH)SO_4]$, also has a similar g_{av} value of 1.984. Incorporating a weak donor, e.g. Cl, Br or NO_3, in the vacant sixth position results in an increase of the g_{av} value towards the free-electron value for $[VO(PBH)_2X]X$ (X = Cl, Br or NO_3) complexes.

The mass spectra of the ligand and the complexes were investigated and in no case was the complex molecular ion nor any fragment of the ligand involving the metal ion obtained. In all cases peaks corresponding to the ligand molecule and its fragmentation products were obtained. The ligand molecular peak is obtained at m/z 195, from which two successive losses of HCN give peaks at m/z 168 and 141. Two prominent fragmentation peaks are obtained at m/z 90 and 91 corresponding to loss of $C_6H_5N_2$ or $C_6H_4N_2$. Thermal studies of simple ligand and the complexes were carried out. The PBH ligand gives a sharp endothermic peak at 221°C where it melts and around 450°C the entire ligand is volatilized leaving no residue. For the oxovanadium(IV) complexes with this ligand, the decomposition takes place in several stages corresponding to the loss of ligand in varying proportions, ultimately giving V_2O_5 as the end product. However, in some cases around 800–900°C there is considerable volatilization of the residue leaving only 3–4% residue, a fact which was substantiated by heating the compounds at the same temperature in a furnace and estimating the loss on heating. Such thermal behaviour was observed earlier for copper(II) complexes with imidazoles.[38]

Acknowledgements—The authors thank Dr J. Subramanian of North Eastern Hill University, Shillong and Dr G. Krishnamoorthy of TIFR, Bombay for EPR spectra and Mr C. R. Panda of this Department for thermal analysis. One of the authors (K.C.D.) thanks the UGC for a National Fellowship and P.K.N. thanks the Government of Orissa for leave of absence.

REFERENCES

1. J. Selbin, *Coord. Chem. Rev.* 1966, **1**, 293.
2. T. G. F. Hudson, *Vanadium–Toxicology and Biological Significance*. Elsevier, New York (1964).
3. J. H. Swineheart, W. R. Biggs, D. J. Halko and N. C. Schroeder, *Biol. Bull.* 1974, **146**, 302.
4. D. B. Carlisle, *Proc. R. Soc.* 1968, **171B**, 31.
5. L. L. Hopkins, Jr and H. E. Mohr, In *Newer Trace Elements in Nutrition* (Edited by W. Mertz and W. E. Cornatzer). Marcel Dekker, New York (1971).
6. G. L. Curran and R. E. Burch, *Proc. University of Missouri Annual Conf. Trace Subst. Envir. Health*, Ist, 1967, 96.
7. M. Pasqualli, A. Torres-Filho and C. Floriani, *J. Chem. Soc. Chem. Commun.* 1975, 534.
8. G. W. Hodgson, B. L. Baker and E. Peake, In *Fundamental Aspects of Petroleum Geochemistry* (Edited by B. Nagy and U. Colombo). Elsevier, New York (1967).
9. L. W. Amos and D. T. Sawyer, *Inorg. Chem.* 1974, **13**, 78.
10. H. R. Mahler and E. H. Cordes, *Biological Chemistry*, 2nd Edn. Harper & Row, New York (1971).
11. K. C. Dash and H. N. Mohanta, *J. Inorg. Nucl. Chem.* 1978, **40**, 499.
12. K. C. Dash and P. Pujari, *J. Inorg. Nucl. Chem.* 1975, **37**, 2061.
13. K. C. Dash and G. Roy Chaudhury, *J. Mol. Struct.* 1981, **72**, 269.
14. J. K. Das and K. C. Dash, *Polyhedron* 1985, **4**, 1109.
15. P. K. Nath and K. C. Dash, *Indian J. Chem. A* (in press).
16. P. K. Nath, N. C. Mishra, V. Chakravortty and K. C. Dash, *Z. Naturforsch.* 1986, **41B**, 111.
17. J. Selbin and L. H. Holmes, *J. Inorg. Nucl. Chem.* 1962, **24**, 1111.
18. A. I. Vogel, *A Text Book of Quantitative Inorganic Analysis*, 3rd edn. Longmans, London (1962).
19. N. S. Gill and R. S. Nyholm, *J. Chem. Soc.* 1959, 3997.
20. J. V. Quagliano, J. Fujita, G. Franz, D. J. Philips and S. Y. Tyree, *J. Am. Chem. Soc.* 1961, **83**, 3770.
21. W. J. Geary, *Coord. Chem. Rev.* 1971, **7**, 81.
22. L. G. Vanquickenborne and S. P. McGlynn, *Theor.*

Chim. Acta 1968, **9**, 390.
23. C. J. Ballhausen and H. B. Gray, *Inorg. Chem.* 1962, **1**, 111.
24. C. E. Mannix and A. P. Zipp, *J. Inorg. Nucl. Chem.* 1979, **41**, 59.
25. M. Goldstein, E. F. Mooney, A. Anderson and H. A. Gebbie, *Spectrochim. Acta* 1965, **21**, 105.
26. T. J. Lane, I. Nakagawa, J. L. Walter and A. J. Kandathill, *Inorg. Chem.* 1962, **1**, 267.
27. C. C. Addison and W. B. Simpson, *J. Chem. Soc.* 1965, 598.
28. R. W. Hester and E. L. Grossman, *Inorg. Chem.* 1966, **5**, 1308.
29. J. L. Burmeister, *Coord. Chem. Rev.* 1968, **3**, 225.
30. R. A. Bailey, S. L. Kozak, T. W. Michelsen and W. N. Mills, *Coord. Chem. Rev.* 1971, **6**, 407.
31. E. P. Hertzenberg and J. C. Bailar, Jr, *Inorg. Chem.* 1971, **10**, 2371.
32. K. Nakamoto, *Infrared Spectra of Inorganic and Coordination Compounds.* John Wiley, New York (1963).
33. R. L. Dutta and G. P. Sengupta, *J. Ind. Chem. Soc.* 1972, **49**, 919.
34. A. Pasini and M. Gullotti, *J. Coord. Chem.* 1974, **3**, 319.
35. R. J. H. Clark, *The Chemistry of Titanium and Vanadium.* Elsevier, Amsterdam (1968).
36. B. N. Figgis and J. Lewis, In *Modern Coordination Chemistry* (Edited by J. Lewis and R. G. Wilkins), p. 400. Interscience, New York (1960).
37. B. A. Goodman and J. B. Raynor, In *Advances in Inorganic Chemistry and Radiochemistry* (Edited by H. J. Emeléus and A. G. Sharpe), Vol. 13, p. 135. Academic Press, New York (1970).
38. Ch. K. C. Mohapatra and K. C. Dash, *J. Inorg. Nucl. Chem.* 1977, **39**, 1253.

Polyhedron Vol. 6, No. 3, pp. 461–463, 1987
Printed in Great Britain

0277-5387/87 $3.00+.00

THE INTERACTION OF NITROGEN AND SULPHUR DONOR MACROCYCLIC LIGANDS WITH DIRHODIUM(II) TETRACARBOXYLATES

ALAN J. HOLDER, MARTIN SCHRÖDER* and T. ANTHONY STEPHENSON*

Department of Chemistry, West Mains Road, University of Edinburgh, Edinburgh EH9 3JJ, U.K.

(*Received* 11 *March* 1986; *accepted* 24 *July* 1986)

Abstract—Reaction of dirhodium(II) tetracarboxylates $[Rh_2(O_2CR)_4]$ with 1,4,8,11-tetraazacyclotetradecane (cyclam, L_1) under ambient conditions leads to the formation of the stable adducts $[Rh_2(O_2CR)_4(cyclam)]_n$. Under similar conditions reaction of dirhodium(II) tetracarboxylates with the tridentate macrocycles 1,4,7-triazacyclononane (L_3), *N,N',N''*-trimethyl-1,4,7-triazacyclononane (L_4) and 1,4,7-trithiacyclononane (L_5) gives adducts of 3:2 stoichiometry $[\{Rh_2(O_2CR)_4\}_3(L)_2]_n$. The stoichiometries of these polymeric adducts illustrate the *exo* manner in which the macrocyclic ligands bind to the binuclear metal substrates.

Extensive work on dirhodium(II) tetracarboxylates $[Rh_2(O_2CR)_4X_n]$ ($n = 1, 2$) has been carried out chiefly to study the variations in Rh—Rh and Rh—X bond lengths as a function of substituent X (X = C, N, O, P or S donor ligands) and carboxylate moiety.[1] The dirhodium(II) tetracarboxylates can react therefore either via carboxylate exchange with another carboxylate or bridging ligand (e.g. CO_3^{2-}, SO_4^{2-}), or via adduct formation by replacement of X. The exchange reaction with the unsaturated tetradentate macrocycle L (L = 5,7,12,14-tetramethyldibenzo[b, i] [1,4,8,11]-tetraazacyclotetra-2,4,6,9,11,13-hexaene) yields the binuclear complex $[Rh_2L_2]$ containing an unsupported metal–metal bond;[2] the related binuclear species $[Rh_2(OEP)_2]$[3] and $[Rh_2(dmg)_2(PPh_3)_2]$[4] have also been synthesized but via monomeric precursors, while bi- and polydentate ligands have been shown to form adducts linking dirhodium(II) tetracarboxylate units in a polymeric chain, e.g. $[Rh_2(O_2CEt)_4(DDA)]$ (DDA = durenediamine).[5]

We report here a study on the interactions of dirhodium(II) tetracarboxylates with saturated tetra- and tridentate macrocycles L_1–L_5. These ligands incorporate suitable donor arrays for adduct formation with the $[Rh_2(O_2CR)_4]$ moiety, and also for potential carboxylate exchange to generate new cationic macrocyclic complexes.

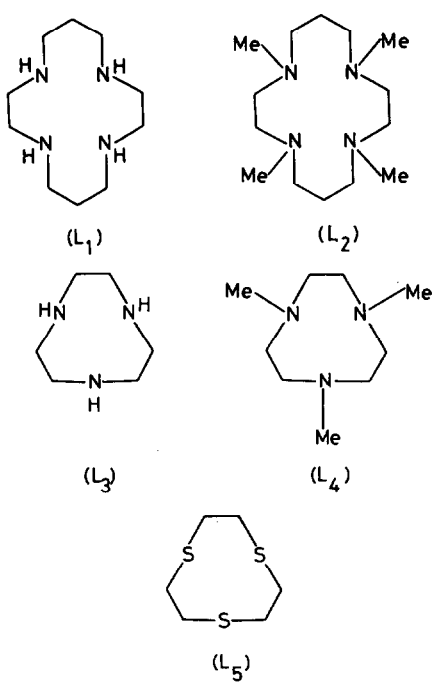

RESULTS AND DISCUSSION

Dirhodium(II) tetraacetate, -propionate, -butyrate, -pivalate and 4-^{t}butylbenzoate react as solutions or slurries in methanol with one equivalent

*Author to whom correspondence should be addressed.
*Deceased.

Table 1. Analytical data for adducts of rhodium(II) tetracarboxylates[a]

(a) $Rh_2(O_2CR)_4(L_1)$	% C	% H	% N
R = Me	33.1 (33.7)	5.6 (5.6)	8.5 (8.7)
Et	38.0 (37.8)	6.3 (6.4)	8.2 (8.0)
"Pr	41.3 (41.4)	7.1 (6.9)	7.6 (7.4)
CMe_3	44.7 (44.5)	7.4 (7.5)	6.7 (6.9)
$C_6H_4CMe_3$	57.9 (58.2)	6.9 (6.9)	4.8 (5.0)

(b) $[Rh_2(O_2CR)_4]_3(L_3)_2$	% C	% H	% N
R = Me	27.2 (27.3)	4.4 (4.2)	5.3 (5.3)
Et	32.8 (32.9)	5.1 (5.2)	4.8 (4.8)
"Pr	38.1 (37.5)	6.2 (6.0)	4.3 (4.4)

(c) $[Rh_2(O_2CR)_4]_3(L_4)_2$	% C	% H	% N
R = Me	29.3 (30.2)	4.9 (4.7)	5.0 (5.0)
Et	36.0 (35.3)	5.9 (5.6)	4.4 (4.6)

(d) $[Rh_2(O_2CR)_4]_3(L_5)_2$	% C	% H	% S
R = Me	26.2 (25.6)	3.8 (3.6)	
Et	30.8 (31.1)	4.5 (4.6)	9.5 (10.4)
"Pr	35.5 (35.6)	5.4 (5.4)	9.7 (9.5)

[a]Expected values in parentheses.

of cyclam (L_1) at room temperature to give pink products. These compounds were obtained in virtually quantitative yield and analysed for $[Rh_2(O_2CR)_4(L_1)]_n$ (Table 1). The nature of the products isolated was independent of the molar ratio of $[Rh_2(O_2CR)_4]$:cyclam used (1:1 to 1:10). IR spectra showed absorptions due to N—H stretching vibrations near 3300–3200 cm^{-1}, these bands being sharper than for the free ligand L_1. As well as bands due to L_1, bands characteristic of the parent carboxylate were retained with $\nu_{asym}(CO_2)$ near 1600 cm^{-1} and $\nu_{sym}(CO_2)$ near 1420 cm^{-1}. ^1H NMR spectra of the more soluble adducts confirm the ratio of L_1 to carboxylate as 1:4. Confirmatory evidence for the retention of the $[Rh_2(O_2CR)_4]$ unit was obtained from the ready conversion of these 1:1 adducts to the known 1:2 pyridine adducts $[Rh_2(O_2CR)_4py_2]$ on reaction with an excess of pyridine.

The 1:1 stoichiometry is indicative of a chain polymeric structure in which L_1 is bound via two of its four nitrogen donors to separate $[Rh_2(O_2CR)_4]$ units, with the other two nitrogen donor atoms remaining unbound. A polymeric structure would account for the general insolubility of these compounds.

Reaction of dirhodium(II) tetracarboxylates with L_2(1,4,8,11-tetramethyl-1,4,8,11-tetraazacyclotetradecane) and 1,4,8,11-tetrathiacyclotetradecane gave pink polymeric products of stoichiometry $[\{Rh_2(O_2CR)_4\}_2(L)]_n$.

The tridentate macrocyclic ligands L_3–L_5 react with the dirhodium(II) tetracarboxylates to yield pink polymeric adducts; in these cases however a stoichiometry of $[\{Rh_2(O_2CR)_4\}_3(L)_2]_n$ gave best agreement with the analytical data (Table 1). This stoichiometry is consistent with that expected for a network structure in which each nitrogen or sulphur donor atom of the macrocycle is coordinated to separate rhodium centres. Again, IR spectral evidence confirmed the presence of the macrocyclic ligand and retention of the $[Rh_2(O_2CR)_4]$ moiety.

The pink colour (λ_{max} = 535 nm for $[Rh_2(O_2CPr)_4(L_1)]_n$ in benzene) of all the products is consistent with adduct formation via nitrogen or sulphur coordination to $[Rh_2(O_2CR)_4]$.[6] Heating $[Rh_2(O_2CR)_4L]_n$ or $[\{Rh_2(O_2CR)_4\}_3(L)_2]_n$ in $CHCl_3$ in the presence of excess of L yields red solutions presumably containing the species $[Rh_2(O_2CR)_4(L)_2]$; these compounds however could not be obtained in the solid state, the less soluble polymeric adducts being isolated in each case.

In contrast to the above reactions in which the carboxylate bridged framework is retained, preliminary studies indicate that treatment of $[Os_2(O_2CR)_4Cl_2]$ (R = Me, "Pr) with L_1 in CH_2Cl_2 at room temperature gives air-sensitive, diamagnetic purple cations of probable formula $[Os(O_2CR)(L_1)]_n^{n+}$ (n = 1 or 2). With $[Ru_2(O_2CR)_4Cl]$ and L_1 in THF under reflux, air-sensitive yellow solids of similar stoichiometry can be isolated. Oxidative dehydrogenation reactions of the cyclam ligand in these systems likely;[7] further studies on these and related osmium and ruthenium compounds are now in progress.

EXPERIMENTAL

Except where otherwise stated all reactions were performed under a nitrogen atmosphere using Schlenk tube techniques and distilled solvents. Methanol and ethanol were distilled from magnesium; benzene and THF were dried over sodium, and for the latter benzophenone was added. Dichloromethane was dried over calcium hydride and distilled. IR spectra were recorded on a Perkin–Elmer 548 spectrometer as Nujol and hexachlorobutadiene mulls. ^1H NMR spectra were recorded on

a Bruker WP80 (80 MHz) spectrometer. Electronic spectra were obtained on a SP8 400 spectrophotometer while elemental analyses were carried out at the Chemistry Departments of the University of Edinburgh and University of St Andrews. L_1 and L_2 were purchased from Aldrich Chemical Co.; L_3 L_5 were prepared by the literature procedures.[8-10]

Preparation of $[Rh_2(O_2CR)_4]$

$[Rh_2(O_2CMe)_4(MeOH)_2]$ was prepared via the literature method.[11] The corresponding propionate, butyrate and pivalate complexes were prepared by exchange reaction of the acetate in neat carboxylic acid. The solution was refluxed for 1 h and the excess acid evaporated *in vacuo*. The 4-^{t}butylbenzoate derivative was obtained by heating the acetate in a melt of 4-^{t}butylbenzoic acid for 4 h. The exchanged complex was recovered by dissolving the cooled residue in ethanol and collecting the product by filtration. The purity of the acetate and 4-^{t}butylbenzoate was checked by preparation of their pyridine adducts.

Preparation of cyclam (L_1) *adducts of* $[Rh_2(O_2CR)_4]$

The dirhodium(II) tetracarboxylates were reacted with a slight molar excess of cyclam (L_1) at room temperature as slurries (acetate, 4-^{t}butylbenzoate) or solutions (propionate, butyrate and pivalate) in methanol. For the solutions, reaction was fast to give pink precipitates of $[Rh_2(O_2CR)_4(L_1)]_n$. Similar products were obtained for the acetate and 4-^{t}butylbenzoate but a reaction time of 24 h was required for completion. The adducts of L_2 were obtained in a similar manner.

Preparation of adducts of L_3–L_5 *with* $[Rh_2(O_2CR)_4]$

Dirhodium(II) tetraacetate was reacted with L_3 or L_4 in aqueous solution, and in acetone–methanol for L_5. The dirhodium(II) tetrapropionate and tetrabutyrate analogues were reacted with L_3 or L_4 in acetone–water, and in acetone alone for L_5. In each case, the adduct precipitates out in almost quantitative yield.

Acknowledgements—We thank the SERC for financial support (to A.J.H.), Johnson Matthey PLC for very generous loans of platinum metals, and Mr M. N. Bell for preparation of L_5.

REFERENCES

1. T. R. Felthouse, *Prog. Inorg. Chem.* 1982, **29**, 73.
2. L. F. Warren and V. L. Goedken, *J. Chem. Soc., Chem. Commun.* 1978, 909.
3. J. P. Collman, C. E. Barnes, P. N. Swepston and J. A. Ibers, *J. Am. Chem. Soc.* 1984, **106**, 3500.
4. K. G. Caulton and F. A. Cotton, *J. Am. Chem. Soc.*, 1971, **93**, 1914.
5. F. A. Cotton and T. R. Felthouse, *Inorg. Chem.* 1981, **20**, 600.
6. S. A. Johnson, H. R. Hunt and H. M. Neumann, *Inorg. Chem.* 1963, **2**, 900.
7. C.-K. Poon and C.-M. Che, *Inorg. Chem.* 1981, **20**, 1640.
8. J. E. Richman and T. J. Atkins, *J. Am. Chem. Soc.*, 1974, **96**, 2268; A. McAuley, P. R. Norman and O. Olubuyide, *Inorg. Chem.* 1984, **23**, 1938.
9. K. Wieghardt, P. Chaudhuri, B. Nuber and J. Weiss, *Inorg. Chem.* 1982, **21**, 3086.
10. W. N. Setzer, C. A. Ogle, G. S. Wilson and R. S. Glass, *Inorg. Chem.* 1983, **22**, 266; D. Sellman and L. Zapf, *Angew. Chem., Int. Ed. Engl.* 1984, **23**, 807.
11. P. Legzdins, R. W. Mitchell, G. L. Rempel, J. D. Ruddick and G. Wilkinson, *J. Chem. Soc. A* 1970, 3322.

Polyhedron Vol. 6, No. 3, pp. 465–471, 1987
Printed in Great Britain

0277–5387/87 $3.00+.00

MOLYBDENUM(IV) DIMERIC COMPLEXES WITH *N*-ALKYLPHENOTHIAZINES AND THEIR INTERACTIONS WITH L-CYSTEINE, L-HISTIDINE, 1,10-PHENANTHROLINE AND 2,2′-BIPYRIDYL

B. KESHAVAN* and J. SEETHARAMAPPA

Department of Post-graduate Studies and Research in Chemistry, University of Mysore, Mysore 570006, India

(*Received* 12 *February* 1986; *accepted after revision* 24 *July* 1986)

Abstract—The synthesis and structure elucidation of the dimeric form of molybdenum(IV) oxo-complexes with *N*-alkylphenothiazines as ligands have been studied. These complexes were identified by IR and electronic spectra, magnetic susceptibility, DTA, TGA, conductometric and analytical data. These results permit us to assign the formula $Mo_2O_4(L)_2(H_2O)_2$ (where L = *N*-alkylphenothiazine). Some interactions of these complexes with biologically important compounds like L-cysteine and histidine and potential ligands such as 1,10-phenanthroline and 2,2′-bipyridyl have been reported.

It is well known that molybdenum as a trace element plays an important role in metabolic processes.[1] Complexes of molybdenum(V) and (VI) with cysteine[2,3] histidine,[4] other amino acids[5] and organic sulphur compounds[6] are of interest as models for molybdenum-containing enzymes. These enzymes are known to catalyse a number of important biological oxo-transfer reactions where valence of molybdenum cycles between molybdenum(VI) and molybdenum(IV) states in their reaction with substrates and subsequent reactivation.[7]

N-Alkylphenothiazines (NAP) are versatile anticholinergic and antihistamine compounds.[8] Formation of complex or cation radical between platinum metals and phenothiazines in aqueous media has provided a basis for the spectrophotometric determination of platinum metals[9–12] and complexometric determination of palladium.[13] Recently the possible use of metal–phenothiazine complexes as fungicides and a considerable increase in the fungicidal activity by complexation of phenothiazines with copper(II) and dioxygenyl uranium(II) have been reported.[14] In view of the importance of phenothiazines as analytical reagents, metal–phenothiazine complexes as fungicides and molybdenum(V)–cysteine or histidine complexes as possible models for molybdoenzymes, it was considered worthwhile to study the molybdenum(IV)–NAP complexes and their interactions.

In this paper, we report the synthesis and characterization of molybdenum(IV)–NAP complexes and their interactions with biologically important compounds such as L-cysteine and histidine and potential ligands like 1,10-phenanthroline and 2,2′-bipyridyl (Fig. 1).

EXPERIMENTAL

Materials

$(NH_4)_6Mo_7O_{24}\cdot 4H_2O$, L-cysteine, L-histidine hydrochloride monohydrate, 1,10-phenanthroline and 2,2′-bipyridyl were BDH Analar grade.

NAP: CPH, PMH, BPD, PPP, PPC and MTM from Bayer A.G., Leverkusen, F.R.G.: MH and PDM from Byk Gulden Pharmazeutika, Konstanz, F.R.G. were used as received. Dimethyl formamide (DMF) and dimethyl sulphoxide (DMSO) were BDH Analar products.

Analytical procedures

Elemental analysis were performed at Bioorganic chemistry division, Bhaba Atomic Research Centre, Bombay, India. Molybdenum was deter-

*Author to whom correspondence should be addressed.

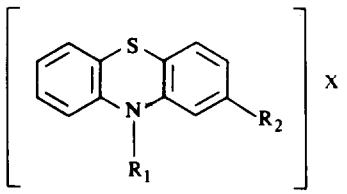

Chlorpromazine hydrochloride: $R_1 = (CH_2)_3NMe_2$, R_2= Cl, and X = HCl
Promethazine hydrochloride: $R_1 = CH_2CHMeNMe_2$, R_2= H, and X = HCl
Butaperazine dimaleinate: $R_1 = (CH_2)_3N(CH_2)_4NMe$, $R_2 = CO(CH_2)_3Me$, and X = dimaleinate
Propionylpromazine phosphate: $R_1 = (CH_2)_3NMe_2$, $R_2 = COCH_2Me$, and X = phosphate
Propericiazine: $R_1 = (CH_2)_3NC_5H_9OH$, R_2= CN, and X = –
Methotrimeprazine: $R_1 = CH_2CHMeCH_2NMe$, R_2OMe, and X = –
Mepazine hydrochloride: $R_1 = CH_2CH(CH_2)_4NMe$, R_2= H, and X = HCl
Perazine dimaleinate: $R_1 = (CH_2)_3N(CH_2)_4NMe$, R_2= H, and X = dimalonate

Fig. 1. Structure of *N*-alkylphenothiazines.

mined by atomic absorption (AA/AE spectrophotometer model 751) after decomposing the complexes with a 1:1 mixture of concentrated sulphuric and nitric acids. The analytical data are given in Table 1.

Methods

The magnetic susceptibilities were determined by the Gouy method at *room temperature* using $Hg[Co(SCN)_4]$ as calibrant ($\chi_g = 16.4$ c.g.s.u.). Molar susceptibilities were corrected for the diamagnetism for the constituent molecules and magnetic moments calculated according to the formula $\mu = 2.84\ (\chi'_M \cdot T)^{0.5}$ BM where χ'_M is the corrected molar susceptibility.[15]

The IR spectra were recorded on a Perkin–Elmer spectrophotometer model 781. The samples were pressed in KBr pellets. Far IR spectra were obtained using a Polytech far-IR spectrophotometer model 30. The samples were examined as polythene pellets. The important IR absorption bands for these complexes are listed in Table 2.

The UV–VIS spectra of the complexes in DMF were measured in the range 200–800 nm on a Beckman spectrophotometer model DB. The results obtained are given in Table 3. The electrical conductances of the complexes were measured in DMF using Philips PR 9500 conductivity bridge. Thermal analysis was carried out on a Stanton Redcraft TG 750/770 electrobalance with a heating rate of 6°C min^{-1} in air. The X-ray diffraction data was obtained using JEOL X-ray diffractometer model JDX-8P with a monochromatic Fe K_α ($\lambda = 1.934$ Å) as the source.

Preparation of the complexes

$(NH_4)_6Mo_7O_{24} \cdot 4H_2O$ (2.1 g) dissolved in 2 M hydrochloric acid (30 cm^3) was added to a solution of CPH (3.0 g) in water (50 cm^3) with vigorous stirring. There was an immediate formation of the solid complex. The suspension was set aside for 2 h, filtered, washed several times with water, then with ethanol and dried *in vacuo* over fused $CaCl_2$. Yield 76%.

The above procedure was repeated for the preparation of the complexes with other phenothiazines. The yield varied from 67–79%.

Interaction of molybdenum(IV)*–NAP complexes with* L-*cysteine*, L-*histidine*, 1,10-*phenanthroline and* 2,2′-*bipyridyl*

Molybdenum(IV)–NAP complex (1.8 g) dissolved in DMF (60 cm^3) was treated with L-cysteine (2.6 g) in 2 M hydrochloric acid (80 cm^3) or with an aqueous solution of histidine (2.75 g). The solid complexes separated immediately, were filtered, washed with ethanol and dried *in vacuo* over fused $CaCl_2$.

Molybdenum(IV)–NAP complex (1.4 g) dissolved in DMF (50 cm^3) was added to the DMF solution of 1,10-phenanthroline (2.45 g in 90 cm^3) or with 2,2′-bipyridyl (23.2 g in 80 cm^3). The suspension was set aside for 1 h, filtered, washed with ethanol and dried *in vacuo* over $CaCl_2$.

DISCUSSION

The interaction of $(NH_4)_6Mo_7O_{24} \cdot 4H_2O$ with NAP results in the formation of molybdenum(IV) complex. The reduction of molybdenum(VI) to molybdenum(IV) may be attributed to the behaviour of phenothiazines which are excellent electron donors.[16] The analytical data presented in Table 1

Table 1. Colour, analytical data and molar conductance of molybdenum(IV)–NAP complexes

Complex	Colour	Found (calc.) (%)				Λ_m (ohm^{-1} cm^{-1} mol^{-1})
		C	H	N	Mo	
$Mo_2O_4(CP)_2(H_2O)_2$	Pale yellow	43.7 (43.9)	4.3 (4.5)	6.2 (6.0)	20.8 (20.7)	19.7
$Mo_2O_4(PM)_2(H_2O)_2$	Pale yellow	47.6 (47.4)	4.8 (5.1)	6.4 (6.5)	22.5 (22.3)	20.3
$Mo_2O_4(BP)_2(H_2O)_2$	Pale yellow	51.8 (51.9)	5.7 (6.0)	7.8 (7.6)	17.4 (17.3)	18.9
$Mo_2O_4(PP)_2(H_2O)_2$	Yellowish-brown	50.7 (50.6)	4.8 (5.2)	5.0 (5.6)	19.8 (19.3)	19.5
$Mo_2O_4(PPC)_2(H_2O)_2$	Pale yellow	49.8 (49.3)	4.6 (4.9)	8.5 (8.2)	19.0 (18.8)	21.4
$Mo_2O_4(MTM)_2(H_2O)_2$	Bluish grey	46.8 (46.7)	4.7 (5.2)	6.1 (6.1)	20.4 (20.9)	20.6
$Mo_2O_4(M)_2(H_2O)_2$	Pale yellow	50.5 (50.0)	5.1 (5.3)	6.4 (6.1)	21.2 (21.0)	23.8
$Mo_2O_4(P)_2(H_2O)_2$	Yellowish-brown	50.2 (49.5)	6.0 (5.6)	8.3 (8.7)	19.6 (19.8)	22.7

correspond with the formula $Mo_2O_4(L)_2(H_2O)_2$, where L = CP, PM, BP, PP, PPC, MTM, M or P (hydrochloride, maleinate, phosphate and malonate remain in solution and do not take part in coordination).

The complexes are coloured, non-hygroscopic and are stable at room temperature for long periods. They do not possess sharp melting points. The complexes are insoluble in common organic solvents but soluble in DMF and DMSO. The molar conductance of the complexes in DMF given in Table 1 indicate the non-electrolytic nature of the complexes and the ion-exchange studies show that the complexes are neutral. These are in consistent with the stoichiometry assumed for the complexes on the basis of analytical data.

Magnetic properties

The magnetic susceptibility measurements for the dioxo-bridge molybdenum(IV) complexes suggest the spin–spin interactions through the oxygen bridges in the dimeric complexes or by direct metal–metal bond comparable to that found in other complexes of molybdenum(IV) which have been reported.[17]

IR spectra

The selected IR frequencies of the dimeric molybdenum(IV)–NAP complexes are given in Table 2. The IR spectra of $Mo_2O_4(L)_2(H_2O)_2$ complexes contain five bands assignable to the

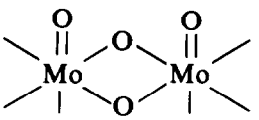

moiety. The strong bands observed at 965–945 cm^{-1} are due to terminal Mo=O vibrations. The antisymmetric stretching mode is not found. However the presence of the symmetric stretching mode is quite sufficient to designate a *cis* disposition of the two terminal Mo=O in the dimeric complexes.[18] The antisymmetric and symmetric vibrations due to the Mo—O bridge are found at 680–658 and 452–425 cm^{-1}, respectively. These values are in good agreement with those found in complexes suggested to have an MoO_2Mo bridge.[17,19,20] All these complexes exhibit strong and broad bands at 3500–3110 cm^{-1} which are assigned to coordinated water. The Mo—N bond is confirmed by the presence of the medium intensive band at 356–334 cm^{-1}.

Bands observed in the 2860–2825 cm^{-1} region

Table 2. IR absorption maxima (cm^{-1}) of molybdenum(IV)–NAP complexes

Complex	ν_s(Mo=O)	ν_a(Mo—O_b)	ν_s(Mo—O_b)	ν(Mo—N)	$\nu(H_2O)$
$Mo_2O_4(CP)_2(H_2O)_2$	952	670	445	340	3120
					3500
$Mo_2O_4(PM)_2(H_2O)_2$	956	672	448	354	3115
					3450
$Mo_2O_4(BP)_2(H_2O)_2$	950	658	452	356	3110
					3445
$Mo_2O_4(PP)_2(H_2O)_2$	945	674	428	342	3140
					3452
$Mo_2O_4(PPC)_2(H_2O)_2$	965	680	450	334	3118
					3464
$Mo_2O_4(MTM)_2(H_2O)_2$	962	672	436	340	3225
					3455
$Mo_2O_4(M)_2(H_2O)_2$	964	678	446	352	3232
					3468
$Mo_2O_4(P)_2(H_2O)_2$	948	666	425	348	3230
					3442

of the NAP IR spectra may be assigned to the heterocyclic nitrogen atom attached to an alkyl group.[21] In the IR spectra of the corresponding complexes, this band is either disappeared or has been shifted to higher frequency ($\Delta\nu = 30$–$40\,cm^{-1}$) suggesting the coordination of heterocyclic nitrogen atom.

In NAP, R_3NH^+ interaction with Cl^- gives rise to a broad band in the 2500–2300 cm^{-1} region.[22] A broad band observed at 2600–2350 cm^{-1} region in the IR spectra of the ligands corresponds to the $CH_2NR_2H^+$ (R = Me, Et or Bu) together with X^- (X = Cl, PO_4, malonate and maleinate). In the IR spectra of the corresponding complexes of molybdenum(IV), this band has totally disappeared indicating that the tertiary nitrogen atom of the side chain is the another site of coordination.

Visible and UV spectra

All the complexes studied here show a peak or shoulder at 652–742 and 530–598 nm, which are assigned to $^2B_2 \rightarrow {}^2E(I)$ and $^2B_2 \rightarrow {}^2B_1$ transitions,[17,19] respectively. The three bands observed at 306–320, 272–300 and 250–262 nm are attributed to intraligand transitions. The electronic spectra of the NAP also consist of three bands at the same wavelength and differences are not significant.

TGA and DTA

TG studies indicate that the decomposition pattern consists of two steps (Table 4). The first step consists of the loss of water molecules at 118–184°C. The second step involves the decomposition of the organic moiety and oxidation until the formation of MoO_3. In the above two cases, the intermediate was revealed by elemental analysis and IR data and the end product was identified by X-ray diffraction method (Table 5). The DTA studies show that the loss of water molecules is accompanied by an endothermic process at ~140°C and the formation of MoO_3 at 590–698°C by an exothermic process.

Interactions of molybdenum(IV)–NAP complexes with some biologically important and potential ligands

The interactions of molybdenum(IV)–NAP complexes with biologically important ligands such as L-cysteine, L-histidine and potential ligands like 1,10-phenanthroline and 2,2′-bipyridyl were carried out to find the ease of substitution of the coordinated ligands. These interactions result in the immediate formation of solid complexes by displacement of the phenothiazine ligands. The molybdenum(IV) complexes thus obtained are quite stable for long periods. They exhibit low magnetic moments in accordance with the dimeric molybdenum(IV)–NAP complexes due either to spin–spin interaction or to direct metal–metal bond.

The analytical and magnetic data are given in Table 6, show that there is no significant change in the composition or structure of the substituted products.

The IR spectra of all these complexes possess a strong band at 970–930 cm^{-1} assigned to the stretching vibration of the Mo=O group. The bridged vibrations of the Mo=O group are

Table 3. Electronic spectra of molybdenum(IV)–NAP complexes

Complex	λ (nm)	$\bar{\nu}$ (kK)	ε	Transition
$Mo_2O_4(CP)_2(H_2O)_2$	720	13.8	44	$^2B_2 \rightarrow {}^2E(I)$
	530	18.5	710	$^2B_2 \rightarrow {}^2B_1$
	310	32.5	16,260	Intraligand
	292	33.8	30,826	Intraligand
	254	40.1	64,815	Intraligand
$Mo_2O_4(PM)_2(H_2O)_2$	742	13.3	56	$^2B_2 \rightarrow {}^2E(I)$
	560	19.5	828	$^2B_2 \rightarrow {}^2B_1$
	312	34.2	6280	Intraligand
	284	33.4	28,452	Intraligand
	262	38.4	38,625	Intraligand
$Mo_2O_4(BP)_2(H_2O)_2$	730	14.2	65	$^2B_2 \rightarrow {}^2E(I)$
	546	18.3	728	$^2B_2 \rightarrow {}^2B_1$
	308	32.8	15,780	Intraligand
	288	34.9	27,695	Intraligand
	255	38.8	36,585	Intraligand
$Mo_2O_4(PP)_2(H_2O)_2$	690	15.8	286	$^2B_2 \rightarrow {}^2E(I)$
	594	16.7	325	$^2B_2 \rightarrow {}^2B_1$
	312	32.2	25,258	Intraligand
	278	32.9	17.354	Intraligand
	255	38.8	60,765	Intraligand
$Mo_2O_4(PPC)_2(H_2O)_2$	735	13.5	48	$^2B_2 \rightarrow {}^2E(I)$
	552	18.8	764	$^2B_2 \rightarrow {}^2B_1$
	320	31.6	15,064	Intraligand
	285	33.6	32,125	Intraligand
	260	38.1	37,845	Intraligand
$Mo_2O_4(MTM)_2(H_2O)_2$	652	15.5	41	$^2B_2 \rightarrow {}^2E(I)$
	598	16.6	356	$^2B_2 \rightarrow {}^2B_1$
	310	32.5	16,426	Intraligand
	300	33.2	25,068	Intraligand
	252	39.8	61,144	Intraligand
$Mo_2O_4(M)_2(H_2O)_2$	728	13.9	58	$^2B_2 \rightarrow {}^2E(I)$
	555	21.5	926	$^2B_2 \rightarrow {}^2B_1$
	315	32.5	15,658	Intraligand
	286	33.9	29,152	Intraligand
	256	39.2	52,675	Intraligand
$Mo_2O_4(P)_2(H_2O)_2$	702	14.4	270	$^2B_2 \rightarrow {}^2E(I)$
	598	16.6	425	$^2B_2 \rightarrow {}^2B_1$
	306	32.6	16,356	Intraligand
	272	35.5	29,654	Intraligand
	250	39.7	36,547	Intraligand

observed at 752–740 and 462–434 cm^{-1}. The medium intensive bands at 3224 and 3218 cm^{-1} in the molybdenum(IV)–cysteine complex and at 3240 and 3232 cm^{-1} bands in the molybdenum(IV)–histidine complex are assigned to NH_2 stretching modes. In these complexes, the COO group exhibits bands at 1654–1588 cm^{-1}. For complexes with 1,10-phenanthroline and 2,2′-bipyridyl, the assignments of bands to metal–oxygen bridge vibrations[23–25] are become uncertain because of the ligand vibrations in the same region (800–700 cm^{-1}). The presence of 1,10-phenanthroline is shown by the characteristic bands at 1632, 1420, 1308, 846 and 732 cm^{-1}. The weak band at 788 cm^{-1} and the strong band at 772 cm^{-1} indicate the coordination of 2,2′-bipyridyl in the complex. The medium band at 345 cm^{-1} in all complexes is attributed to the Mo—N bond. The strong and broad bands at 3465–3218 cm^{-1} are assigned to coordinated water. These assignments are consist-

Table 4. Thermogravimetric data for molybdenum(IV)–NAP complexes

Complex	Temperature range (°C)	Weight loss (%) Found (Calc.)	Probable phase
$Mo_2O_4(CP)_2(H_2O)_2$	124–182	3.7 (3.9)	$Mo_2O_4(CP)_2$
	605–693	84.3 (84.5)	MoO_3
$Mo_2O_4(PM)_2(H_2O)_2$	125–184	4.3 (4.2)	$Mo_2O_4(PM)_2$
	624–693	83.7 (83.3)	MoO_3
$Mo_2O_4(BP)_2(H_2O)_2$	120–182	3.4 (3.2)	$Mo_2O_4(BP)_2$
	612–689	86.8 (87.0)	MoO_3
$Mo_2O_4(PP)_2(H_2O)_2$	118–179	3.9 (3.6)	$Mo_2O_4(PP)_2$
	618–692	85.7 (85.5)	MoO_3
$Mo_2O_4(PPC)_2(H_2O)_2$	122–181	3.4 (3.5)	$Mo_2O_4(PPC)_2$
	621–690	85.7 (85.9)	MoO_3
$Mo_2O_4(MTM)_2(H_2O)_2$	121–183	3.6 (3.9)	$Mo_2O_4(MTM)_2$
	590–694	84.5 (84.3)	MoO_3
$Mo_2O_4(M)_2(H_2O)_2$	122–178	3.6 (3.9)	$Mo_2O_4(M)_2$
	598–688	84.3 (84.2)	MoO_3
$Mo_2O_4(P)_2(H_2O)_2$	123–182	3.8 (3.7)	$Mo_2O_4(P)_2$
	608–698	85.4 (85.2)	MoO_3

Table 5. Powdered X-ray diffraction data of MoO_3

d (Å)	I/I_1 (%)
3.26	100
3.80	82.1
3.46	60.9
6.94	34.2
2.65	35.1
2.31	31.0
1.85	21.3
2.70	18.9
2.27	17.8
1.74	17.0

ent with the molybdenum(V) complexes of L-cysteine,[2] histidine,[4] 1,10-phenanthroline[23,24] and 2,2′-bipyridyl[23,25] reported earlier.

In the light of the above discussions, we propose the structure given in Fig. 2 for the molybdenum(IV)–NAP complexes.

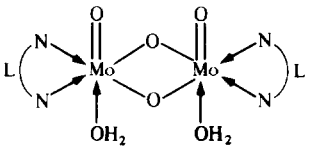

Fig. 2. Structure of molybdenum(IV)–*N*-alkylphenothiazine complex.

Acknowledgements—We thank M/s Bayer A.G., Leverkusen and Byk Gulden Pharmazeutika, Konstanz, F.R.G. for supplying pure NAP. One of us (J.S.) thanks the University of Mysore for financial support. We also thank one of the referees for pointing out an error in the original manuscript.

REFERENCES

1. E. J. Hewitt, *Biol. Rev.* 1959, **34**, 333.
2. L. R. Melby, *Inorg. Chem.* 1969, **8**, 349.
3. A. Kay and P. C. H. Mitchell, *J. Chem. Soc. A* 1970, 2421.
4. L. Russell Melby, *Inorg. Chem.* 1969, **8**, 1539.

Table 6. Analytical and magnetic data of the molybdenum(IV)–substituted complexes

Complex	Found (Calc.) % C	H	N	Mo	μ_{eff} (BM)
$[Mo_2O_4(Cyst)_2(H_2O)_2]^{2-}$	13.6(13.5)	3.0(3.4)	5.4(5.2)	36.2(35.9)	0.23
$[Mo_2O_4(Hist)_2(H_2O)_2]^{2-}$	23.7(23.9)	3.8(3.6)	13.7(13.9)	32.1(31.9)	0.34
$Mo_2O_4(Phen)_2(H_2O)_2$	44.3(44.2)	3.0(3.1)	8.3(8.6)	29.7(29.4)	0.28
$Mo_2O_4(Bipy)_2(H_2O)_2$	40.0(39.7)	3.2(3.3)	9.4(9.3)	31.6(31.7)	0.25

5. H. Eguchi, T. Takeuchi, A. Ouchi and A. Furuhashi, *Bull. Chem. Soc. Jpn* 1969, **42,** 3585.
6. L. S. Meriwether, W. F. Marzluff and W. G. Hodgson, *Nature* 1966, **212,** 465.
7. R. H. Holm and J. M. Berg, *Pure Appl. Chem.* 1984, **56,** 1645.
8. S. H. Snyder, *Am. J. Psychiatry* 1976, **133,** 197.
9. B. Keshavan and P. Nagaraja, *Indian J. Chem.* 1983, **22A,** 725.
10. H. S. Gowda and B. Keshavan, *Mikrochim. Acta* 1975, 437.
11. H. S. Gowda and B. Keshavan, *Z. Anal. Chem.* 1975, **273,** 31.
12. H. S. Gowda and B. Keshavan, *Indian J. Chem.* 1976, **14A,** 293.
13. B. Keshavan, *Analyst* 1981, **106,** 461.
14. A. K. Jain, K. D. Jain and A. K. Katiar, *J. Indian Chem. Soc.* 1976, **43,** 938.
15. P. W. Selwood, *Magnetochemistry*. Interscience, New York (1956).
16. P. C. Dwivedi, K. G. Rao, S. N. Bhat and C. N. R. Rao, *Spectrochim. Acta* 1975, **31A,** 129.
17. J. Hyde and J. Zubieta, *J. Inorg. Chem.* 1977, **39,** 289.
18. F. A. Cotton, D. L. Hunter, L. Ricard and R. Weiss, *J. Coord. Chem.* 1974, **3,** 259.
19. R. Lozano, A. Doadrio and A. L. Doadrio, *Polyhedron* 1982, **1,** 163.
20. W. E. Newton, L. Corbin, C. Bravard, J. E. Searles and J. W. McDonald, *Inorg. Chem.* 1974, **13,** 1100.
21. S. P. Garg, N. M. Srivasta and V. N. Sharma, *J. Indian Chem. Soc.* 1975, **52,** 1160.
22. Katritzky and A. J. Boulton (Editors), *Advances in Heterocyclic Chemistry*, Vol. 9, p. 336. Academic Press, New York (1968).
23. A. Komura, Y. Ikeda and H. Imanaga, *Bull. Chem. Soc. Jpn* 1976, **49,** 131.
24. A. K. Saha and M. C. Halder, *J. Inorg. Nucl. Chem.* 1972, **34,** 3097.
25. A. K. Saha and A. K. Banerjee, *J. Inorg. Nucl. Chem.* 1972, **34,** 697.

5. H. Eguchi, T. Takeuchi, A. Ouchi and A. Furuhashi, *Bull. Chem. Soc. Jpn* 1969, **42,** 3585.
6. L. S. Meriwether, W. F. Marzluff and W. G. Hodgson, *Nature* 1966, **212,** 465.
7. R. H. Holm and J. M. Berg, *Pure Appl. Chem.* 1984, **56,** 1645.
8. S. H. Snyder, *Am. J. Psychiatry* 1976, **133,** 197.
9. B. Keshavan and P. Nagaraja, *Indian J. Chem.* 1983, **22A,** 725.
10. H. S. Gowda and B. Keshavan, *Mikrochim. Acta* 1975, 437.
11. H. S. Gowda and B. Keshavan, *Z. Anal. Chem.* 1975, **273,** 31.
12. H. S. Gowda and B. Keshavan, *Indian J. Chem.* 1976, **14A,** 293.
13. B. Keshavan, *Analyst* 1981, **106,** 461.
14. A. K. Jain, K. D. Jain and A. K. Katiar, *J. Indian Chem. Soc.* 1976, **43,** 938.
15. P. W. Selwood, *Magnetochemistry*. Interscience, New York (1956).
16. P. C. Dwivedi, K. G. Rao, S. N. Bhat and C. N. R. Rao, *Spectrochim. Acta* 1975, **31A,** 129.
17. J. Hyde and J. Zubieta, *J. Inorg. Chem.* 1977, **39,** 289.
18. F. A. Cotton, D. L. Hunter, L. Ricard and R. Weiss, *J. Coord. Chem.* 1974, **3,** 259.
19. R. Lozano, A. Doadrio and A. L. Doadrio, *Polyhedron* 1982, **1,** 163.
20. W. E. Newton, L. Corbin, C. Bravard, J. E. Searles and J. W. McDonald, *Inorg. Chem.* 1974, **13,** 1100.
21. S. P. Garg, N. M. Srivasta and V. N. Sharma, *J. Indian Chem. Soc.* 1975, **52,** 1160.
22. Katritzky and A. J. Boulton (Editors), *Advances in Heterocyclic Chemistry*, Vol. 9, p. 336. Academic Press, New York (1968).
23. A. Komura, Y. Ikeda and H. Imanaga, *Bull. Chem. Soc. Jpn* 1976, **49,** 131.
24. A. K. Saha and M. C. Halder, *J. Inorg. Nucl. Chem.* 1972, **34,** 3097.
25. A. K. Saha and A. K. Banerjee, *J. Inorg. Nucl. Chem.* 1972, **34,** 697.

Polyhedron Vol. 6, No. 3, pp. 473–478, 1987
Printed in Great Britain

0277–5387/87 $3.00+.00

ELECTROCHEMICAL STUDY OF DINUCLEAR RUTHENIUM(II)–ARENE COMPOUNDS: ELECTROGENERATION OF Ru(II)–Ru(I) SPECIES

F. ESTEVAN, P. LAHUERTA* and J. LATORRE

Departamento de Química Inorgánica, Facultad de Químicas, Universidad de Valencia, Burjassot, Valencia, Spain

and

A. SANCHEZ and C. SIEIRO

Departamento de Química Física, Universidad Autonoma de Madrid, Madrid, Spain

(*Received* 7 *March* 1986; *accepted after revision* 24 *July* 1986)

Abstract—The preparation and characterization of Ru(II)–arene compounds $[\{RuCl_2(p\text{-cym})\}_2(\mu\text{-L-L})]$ where *p*-cym = *p*-$MeC_6H_4CHMe_2$; and L-L = diphenylphosphinomethane (**I**), 1,1′-bisdiphenylphosphinoferrocene (**II**), pyrazine (**III**) and 4,4′-bipyridine (**IV**), are described. Electrochemical data for these compounds obtained by cyclic voltammetry and coulometry are reported. The electrochemical reduction of compounds **I** or **II** yields ruthenium(0) species. However, compounds **III** or **IV** containing ligands with delocalized π orbitals undergo one-electron reduction. The ESR signal detected during the electrolysis of compounds **III** or **IV** is consistent with one delocalized electron through the whole dinuclear unit.

The electrochemical oxidation of dinuclear Ru(II)–Ru(II) compounds has been extensively studied.[1–3] In some cases two single-electron transfer processes are observed and the mixed valence compound Ru(II)–Ru(III) can be isolated.[1] The electrochemical reduction which would generate *a priori* Ru(II)–Ru(I) or Ru(I)–Ru(I) species has been studied much less.

We have recently described how the electrochemical reduction of compounds of the type $\{RuCl_2(arene)\}_2$ generates Ru(I) compounds of only limited stability in solution at room temperature.[4] The number of Ru(I) compounds described in the literature is very limited and in all the cases where a metal–metal bond is present.[5]

The electrochemical generation of Ru(I) species seems to be possible only if a metal–metal bond can be formed. We assumed that by using adequate bridging ligands we could stabilize binuclear Ru(I)–Ru(I) compounds. So we have prepared and studied the electrochemical properties of several new dinuclear ruthenium compounds containing phosphorus bridging ligands. Other compounds containing nitrogen ligands with delocalized π orbitals are also studied.

EXPERIMENTAL

All solvents were reagent grade and were degassed and dried prior to use by standard procedures. All the reactions were carried out under argon using the Schlenk technique, although the isolated compounds were air-stable.

Preparation of the compounds

$\{RuCl_2(p\text{-cym})\}_2$, $\{RuCl_2(p\text{-cym})\}_2$dppe and $[\{Ru_2Cl_3(p\text{-cym})_2\}BPh_4]$ were prepared by literature methods.[6–8]

(*a*) $[\{RuCl_2(p\text{-cym})\}_2(\mu\text{-dppm})]$ (**I**). A solution of dppm (77 mg, 0.2 mmol) in CH_2Cl_2 (5 cm^3) was added to a solution of $\{RuCl_2(p\text{-cym})\}_2$ (122 mg,

*Author to whom correspondence should be addressed.

0.2 mmol) in CH_2Cl_2 (10 cm^3). The solvent was evaporated under reduced pressure and upon addition of hexane a red precipitate was formed. The precipitate was filtered, washed with hexane and dried *in vacuo*. Yield 72%. Found: C, 50.3; H, 4.9%. Calc. for $C_{45}H_{50}Cl_4P_2Ru_2 \cdot CH_2Cl_2$: C, 51.0; H, 4.7%.

(*b*) $[\{RuCl_2(p\text{-cym})\}_2\{\mu\text{-}Fe(C_5H_4PPh_2)_2\}]$ **(II)**. A solution of $Fe(C_5H_4PPh_2)_2$ (73 mg, 0.13 mmol) in CH_2Cl_2 (3 cm^3) was added to a solution of $\{RuCl_2(p\text{-cym})\}_2$ (80 mg, 0.13 mmol) in CH_2Cl_2 (6 cm^3). Hexane was added and the solvent evaporated under reduced pressure. The red precipitate was filtered, washed with hexane and dried *in vacuo*. Yield 87%. Found: C, 56.1; H, 5.1%. Calc. for $C_{54}H_{56}Cl_4FeP_2Ru_2$: C, 55.6; H, 4.8%.

(*c*) $[\{RuCl_2(p\text{-cym})\}_2(\mu\text{-pyz})]$ **(III)**. A solution of pyrazine (16 mg, 0.2 mmol) in CH_2Cl_2 (3 cm^3) was added to a solution of $\{RuCl_2(p\text{-cym})\}_2$ (122 mg, 0.2 mmol) in CH_2Cl_2 (10 cm^3). At 10 min the solution was cloudy and in 1 h the precipitation of an orange-yellow compound was completed. The precipitate was filtered, washed with CH_2Cl_2 and dried *in vacuo*. Yield 70%. Found: C, 39.8; H, 4.6; N, 3.7%. Calc. for $C_{24}H_{32}Cl_4N_2Ru_2$: C, 41.0; H, 4.5; N, 4.0%.

(*d*) $[\{RuCl_2(p\text{-cym})\}_2(\mu\text{-4,4'-bipy})]$. **(IV)**. A solution of 4,4'-bipyridine (39 mg, 0.25 mmol) in CH_2Cl_2 (5 cm^3) was added to a solution of $\{RuCl_2(p\text{-cym})\}_2$ (153 mg, 0.25 mmol) in CH_2Cl_2 (15 cm^3). The solution was stirred for 2 h at room temperature, during which a yellow precipitate was formed. The precipitate was filtered, washed with CH_2Cl_2 and dried *in vacuo*. Yield 76%. Found: C, 46.3; H, 4.6; N, 3.3%. Calc. for $C_{30}H_{36}Cl_4N_2Ru_2$: C, 46.8; H, 4.6; N, 3.6%.

Instrumental

IR spectra were recorded on a Pye–Unicam SP-2000 spectrometer. NMR spectra were recorded on a Brucker AC-200 spectrometer. ESR spectra were recorded on a Varian E-12 spectrometer provided with a 100 kHz field modulation. The g factor was obtained by means of relation $g = 0.714484\nu$ (MHz)/H(G) where the magnetic field H (in Gauss) at the sample was measured using a Gaussmeter and the microwave frequency (ν) (in MHz) was measured with a high precision frequency meter.

For complicated spectra the hyperfine coupling constants were obtained by comparing experimental and computer-simulated spectra, assuming a Lorentzian line-shape.

The electrochemical experiments were carried out in a three-electrode cell. The working and auxiliary electrodes were platinum, the reference was a saturated calomel electrode, electrically connected to the non-aqueous solution by a "salt-bridge" containing the non-aqueous solvent and the supporting electrolyte.

Cyclic voltammograms were obtained with a programming function generator 305 H.Q. Instruments which was connected to a 552 Amel potentiostat and recorded with a Riken-Denshi F 35 x–y recorder.

The solvents were THF, freshly distilled over Na–benzophenone and DMSO dried by elution through a column of activated alumina and distilled under reduced pressure. The supporting electrolyte was Bu_4NPF_6 recrystallized from ethanol and dried at 80°C *in vacuo* for 48 h.

In order to prove the presence of paramagnetic binuclear Ru(II)–Ru(I) species, we carried out simultaneous ESR and electrochemical experiments. The electrolysis is performed by placing a special flat cell inside the microwave cavity of the X-band spectrometer. We used the Willmad and Glass Co. Electrolytic Cell Assembly for ESR studies.

To obtain ESR spectra with high resolution, we prepared dilute solution of the studied compounds (1 mM) and used very low microwave power (2–5 mW). The solutions were degassed for 30 min to avoid the scavenging effect of dissolved oxygen. All the electrochemical experiments were carried out under an inert atmosphere.

RESULTS AND DISCUSSION

Compounds I–IV are prepared by reacting $\{RuCl_2(p\text{-cym})\}_2$ with a stoichiometric amount of the ligand L-L in CH_2Cl_2 at room temperature. Compounds **III** and **IV** are of limited solubility in CH_2Cl_2 or THF and all the spectroscopic and electrochemical measurements have been performed in DMSO. The compounds are non-electrolytes in solution. (The measurements of conductivity were carried out in CH_2Cl_2 for compounds **I** or **II** and in DMSO for compounds **III** or **IV**.)

^1H and ^{31}P NMR spectra support the dinuclear stoichiometry $[(p\text{-cym})RuCl_2(\mu\text{-L-L})RuCl_2(p\text{-cym})]$ proposed for these compounds (Table 1). Compounds **I** and **II** show singlet signals in the ^{31}P NMR spectra at 21.1 and 18.3 ppm, respectively, indicating that both phosphorus nuclei are coordinated.

The four protons of the pyrazine ligand in compound **III** are equivalent and they appear as a sharp resonance at $\delta = 9.03$ ppm. Both C_5H_4N moieties of the bipy ligand in compound **IV** give two doublets in the ^1H NMR spectrum at 9.1 and 7.4 ppm ($J = 7$ Hz). All the proton resonances corresponding to the *p*-cymene ligand are also observed for compounds **I–IV**.

Table 1. Spectroscopic data for the compounds[a,b]

Compound	^{1}H NMR[c,d,g] Co-ordinated arene protons	^{1}H NMR[c,d,g] Others	^{31}P NMR[e]	ν_{Ru-Cl} (cm^{-1})
$[\{RuCl_2(p\text{-cym})\}_2(\mu\text{-dppm})]$	5.15, 4.90 (H_A, H_B, *J* 6); 2.47 (sp, $CHCH_3$)	7.6(m), 7.2(m)	21.1(s)	292
	1.90(s, CH_3); 0.93 (d, $CHCH_3$, *J* 7)	4.5(t)		281
$[\{RuCl_2(p\text{-cym})\}_2\{\mu\text{-Fe}(C_5H_4PPh_2)_2\}]$	4.16, 3.87 (H_A, H_B, *J* 6); 2.52 (sp, $CHCH_3$)	7.37, 7.73	18.3(s)	296
	1.70(s, CH_3); 0.95 (d, $CHCH_3$, *J* 7)	5.06		280
$[\{RuCl_2(p\text{-cym})\}_2(\mu\text{-pyz})]$[f]	5.43, 5.27 (H_A, H_B, *J* 6); 3.02 (sp, $CHCH_3$)	9.03(s)		288
	1.58 (s, CH_3); 1.28 (d, $CHCH_3$, *J* 8)			284
$[\{RuCl_2(p\text{-cym})\}_2(\mu\text{-4,4'-bipy})]$[f]	5.49, 5.29 (H_A, H_B, *J* 6); 3.07 (sp, $CHCH_3$)	9.16 (d, *J* 7)		291
	1.58 (s, CH_3); 1.25 (d, $CHCH_3$, J 8)	7.45 (d, *J* 7)		281

[a] Measured in $CDCl_3$ at room temperature.

[b] Abbreviations: s, singlet; d, doublet; t, triplet; sp, septet; m, multiplet.

[c] Chemical shifts relative to Me_4Si.

[d] *J* in Hz.

[e] Chemical shifts relative to H_3PO_4.

[f] Measured in (d_6)DMSO.

[g] Labelling of *p*-cymene protons:

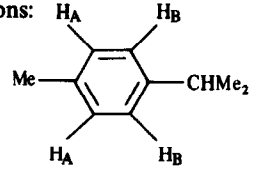

Assignment of resonances to H_A and H_B is arbitrary.

Table 2. Electrochemical parameters for the compounds

Compound	E_p^{red}		E_p^{ox}
	A_1	A_2	A_3'
$[\{RuCl_2(p\text{-cym})\}_2(\mu\text{-dppm})]^a$	-1.64^c		1.40^d
$[\{RuCl_2(p\text{-cym})\}_2(\mu\text{-dppe})]^a$	-1.58^c	-1.70^c	1.14^d
$[\{RuCl_2(p\text{-cym})\}_2\{\mu\text{-Fe}(C_5H_4PPh_2)_2\}]^a$	-1.92^c		0.64^d
$[\{RuCl_2(p\text{-cym})\}_2(\mu\text{-pyz})]^b$	-1.30^c	-2.12^c	
$[\{RuCl_2(p\text{-cym})\}_2(\mu\text{-4,4'-bipy})]^b$	-1.28^c	-1.86^c	
$[\{Ru_2Cl_3(p\text{-cym})_2\}BPh_4]^a$	-0.74		

[a]Conditions: 0.1 M Bu_4NPF_6 in THF; scan rate 100 mV s^{-1}.
[b]Conditions: 0.1 M Bu_4NPF_6 in DMSO; scan rate 100 mV s^{-1}.
[c]Irreversible cathodic peak.
[d]Reversible anodic peak.

A compound of stoichiometry $[RuCl_2(p\text{-cym})(dppm)]$ has been previously described,[9] suggesting that the phosphine coordinates to the ruthenium atom only through one phosphorus atom. We have repeated the reported preparative method, obtaining the same spectroscopic and analytical results as for compound **I**. The bidentate coordination of dppm ligand is evident from the analytical data and from the integration of the ^1H NMR signals which fit better a bimetallic stoichiometry.

Electrochemical data

Table 2 summarizes the electrochemical data for compounds **I–IV** as well as for $[\{RuCl_2(p\text{-cym})\}_2(\mu\text{-dppe})]$ (**V**) and $[\{Ru_2(Cl_3(p\text{-cym})_2\}BPh_4]$ (**VI**). Compounds containing phosphorus ligands reduce at higher potential values. $Fe(C_5H_4PPh_2)_2$ behaves as a stronger electron donor ligand than dppm or dppe and consequently compound **II** reduces with more difficulty than compounds **I** or **V**. Only one reduction peak is observed for compounds **I–IV**, while compound **V** shows some splitting in the first process.

Potential-controlled electrolysis on the plateau of peak A_1 gives a consumption of 4 F mol^{-1} for compounds **I**, **II** and **V**. This indicates that in A_1 a complicated process yielding Ru(0) species takes place.

According to this, these three compounds do not show any clear tendency to stabilize the oxidation state (I) as observed for $\{RuCl_2(p\text{-cym})\}_2$. They behave like other mononuclear compounds such as $RuCl_2(p\text{-cym})PPh_3$. This compound shows two close reduction peaks, A_1 (−1.54 V) and A_2 (−1.64 V) each corresponding to one-electron transfer processes.

Compounds **I**, **II** and **V** oxidize reversibly with **II** showing the lowest oxidation potential.

Another aspect related to the electrochemical behaviour of $\{RuCl_2(p\text{-cym})\}_2$ is the fact that the first reduction peak A_1 at −0.98 V corresponds to the simultaneous reduction of both Ru atoms. No evidence of an intermediate Ru(II)–Ru(I) species has been observed.

We considered the cationic species $\{Ru_2Cl_3(p\text{-cym})_2\}^+$ an interesting compound to generate Ru(II)–Ru(I) species. As cationic compounds usually reduce at lower potentials than neutral ones with the same oxidation state, we should expect $\{Ru_2Cl_3(p\text{-cym})_2\}^+$ to show a separate reduction peak corresponding to Ru(II)–Ru(II) → Ru(II)–Ru(I) process. This compound reduces at −0.74 V. The exhaustive electrolysis at this potential value gives a consumption of 1 F mol^{-1}. From the resulting solution, $\{RuCl_2(p\text{-cym})\}_2$ can be isolated in a low yield. This indicates that the product of the reduction is not stable and shows a chemical evolution, probably such as Ru(II)–Ru(I) → Ru(II)–Ru(II) + Ru(I)–Ru(I). EPR measurements on the reduced solution of $\{Ru_2Cl_3(p\text{-cym})\}^+$ fail to show any evidence of a paramagnetic species in solution.

Another possible way to stabilize mixed valence species might be the use of bridging ligands capable of delocalizing electron density as pyrazine or 4,4'-bipyridine.

The complexes $[\{RuCl_2(p\text{-cym})\}_2(\mu\text{-pyz})]$ and $[\{RuCl_2(p\text{-cym})\}_2(\mu\text{-4,4'-bipy})]$ show a monoelectronic reduction peak at −1.28 V assignable to the Ru(II)–Ru(II) → Ru(II)–Ru(I) process. This reduction peak is in both cases irreversible. A second reduction peak is also observed for each compound. The potential values for the second peak are very similar to the reduction potential values of the corresponding ligands pyz and 4,4'-bipy.

The reduced species are fairly stable in solution and have been detected by ESR spectroscopy. The

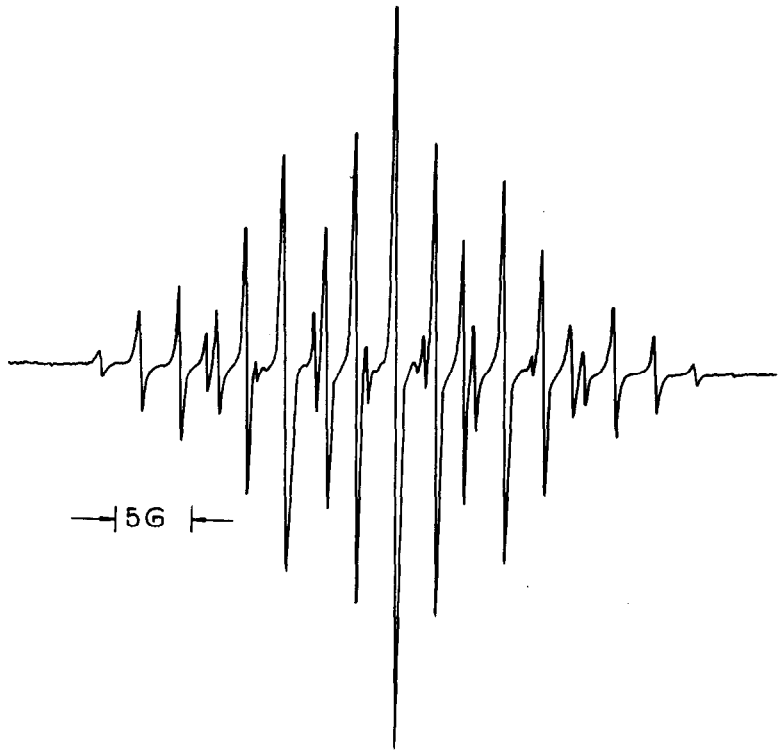

Fig. 1. EPR spectrum of reduced [{$RuCl_2$(*p*-cym)}$_2$(μ-pyz)].

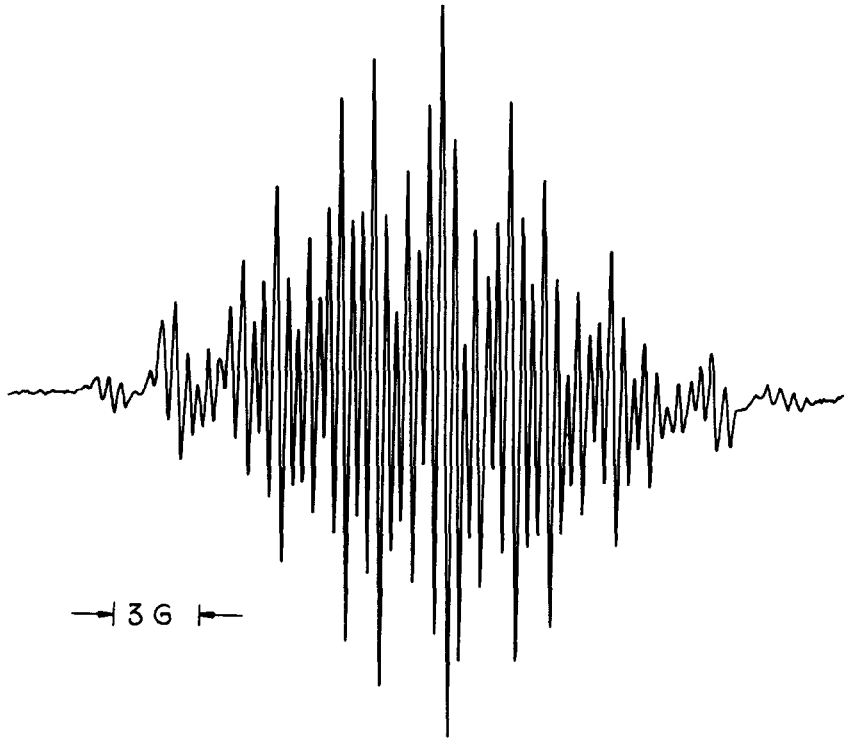

Fig. 2. EPR spectrum of reduced [{$RuCl_2$(*p*-cym)}$_2$(μ-4,4′-bipy)].

ESR spectra obtained are shown in Figs 1 and 2. These spectra are very well resolved and show a metal–ligand isotropic superhyperfine interaction. The spectrum of the reduced complex $[\{RuCl_2(p\text{-cym})\}_2(\mu\text{-pyz})]$ is composed of two quintets with the following hyperfine splittings: $a_N = 7.20$ G and $a_H = 2.65$ G (pyrazine ring protons). Its g factor is 2.0036.

The spectrum of the reduced complex $[\{RuCl_2(p\text{-cym})\}_2(\mu\text{-4,4'-bipy})]$ is complicated and from its analysis by simulation assuming Lorentzian line-shape, three hyperfine coupling constants were obtained, whose values (in G) are: 3.50 (Q, 1:2:3:2:1), 2.35 (Q, 1:4:6:4:1) and 0.45 (Q, 1:4:6:4:1). The first quintet corresponds to the nitrogen splittings and we assign the quintets with 2.35 and 0.45 G to the *ortho* and *meta* protons of the bipyridine rings, respectively. This assignment is based on the analysis of the canonical structure of this compound. Its g factor is 2.0030. Further studies of these and other related ruthenium arene complexes containing ligands with delocalized π orbitals are in progress.

Acknowledgement—We thank Comisión Asesora de Investigación Científica y Técnica (CAICYT) for financial support under grant no. 3275/83.

REFERENCES

1. J. C. Curtis, J. S. Berntein and T. J. Meyer, *Inorg. Chem.* 1985, **24**, 385.
2. R. W. Callahan, G. M. Brown and T. J. Meyer, *Inorg. Chem.* 1975, **14**, 1443.
3. T. Easton, G. A. Heath, T. A. Stephenson and M. Bochman, *J. Chem. Soc., Chem. Commun.* 1985, 514.
4. P. Lahuerta and J. Latorre, Submitted to *J. Chem. Research.*
5. G. Wilkinson *et al.* (Editors), *Comprehensive Organometallic Organometallic Chemistry.* Pergamon Press, Oxford (1982).
6. M. A. Bennett, T. N. Huang, T. W. Matheson and A. K. Smith, *Inorg. Synth.* 1982, **21**, 75.
7. F. Faraone, G. A. Loprete and G. Tresoldi, *Inorg. Chim. Acta* 1979, **34**, L251.
8. R. O. Gould, C. L. Jones, T. A. Stephenson and D. A. Tocher, *J. Organomet. Chem.* 1984, **264**, 365.
9. R. A. Zelonka and M. C. Baird, *Can. J. Chem.* 1972, **50**, 3063.

Polyhedron Vol. 6, No. 3, pp. 479–482, 1987
Printed in Great Britain

0277-5387/87 $3.00+.00

COMMENTS ON THE CLAIMED NOVEL COMPOUND CYCLOHEPTATRIENYL THALLIUM(III) DICHLORIDE

M. B. MILLIKAN and B. D. JAMES*

Department of Chemistry, La Trobe University, Bundoora, Victoria 3083, Australia

(*Received* 1 *July* 1986; *accepted* 24 *July* 1986)

Abstract—Reaction of pyridinium pentachlorothallate(III) with cycloheptatriene and triethylamine in dichloromethane yielded the pyridine adduct $(C_5H_6N)TlCl_4 \cdot C_5H_5N$ and not the novel complex originally claimed. Cycloheptatriene does not interact at all with the metal under the experimental conditions.

Cycloheptriene forms well-known complexes of the $C_7H_7^+$ ligand when a hydride has been abstracted from the parent hydrocarbon. The ligand formally is a six-electron donor akin to $C_5H_5^-$ and C_6H_6. Similarly, a formal seven-electron donor function is obtained if a hydrogen atom is abstracted (e.g. by using Pt).[1,2] A third ligating function has been claimed for cycloheptatriene: namely that of acting as $C_7H_7^-$ after proton abstraction from the parent. This was proposed on the basis of a number of reactions reported with various transition metal chlorides such as $TaCl_5$ and $WOCl_4$ in refluxing benzene, when hydrogen chloride was evolved.[3,4]

An extension of this function to Main Group compounds of Sn(IV), Pb(IV) and Tl(III) was also claimed, although only the thallium reaction has apparently been published.[5] The reaction involved the interaction of pyridinium pentachlorothallate(III) with the hydrocarbon in dichloromethane, using triethylamine as a proton abstractor:

$$(C_5H_6N)TlCl_5 + C_7H_8 + (C_2H_5)_3N \rightarrow C_7H_7TlCl_2 + 2C_5H_6NCl + (C_2H_5)_3NHCl.$$

On the basis of the reported IR spectral frequencies, a π-bonding function for the C_7 ligand was suggested. This seemed unusual because cyclic hydrocarbon derivatives of Group III metals do not generally form well-defined π-bonded complexes in the same manner as transition metals. For example, the species $C_5H_5MR_2$ (M = Al, Ga or In; R = CH_3, C_2H_5) appear to form a series in which the C_5 ring is not bonded in a η^5 manner.[6] Likewise none of the rings in tris(cyclopentadienyl) indium can be classified as π-bonded in the 'sandwich' manner.[7] While the large Tl(III) cation probably could accommodate a π-bonded planar ring, it seemed more likely that the marked stability of di-organothallium(III) compounds would tend to force a product to that stoichiometry or, alternatively, sufficient electron density would be donated to the metal to cause its facile reduction to the +I state.[8]

Of further interest to us was the reactivity of the chlorothallate reagent. Leaving aside for the moment the confusion over whether the authors' description of the use of the pentachlorothallate really meant that reagent,[9] it appeared to be a possibility that one mole equivalent of the amine added to $(C_5H_6N)_2TlCl_5$ could form a donor–acceptor complex as was found with dimethylsulfoxide.[10] In addition, unless the product was exceptionally stable, it seemed unlikely that cycloheptatriene ($pK_a \sim 30$[11]) would be deprotonated by the amine under the mild reaction conditions reported. In view of the novel nature of the reported compound, we have reinvestigated the stated synthetic procedure, using both $(C_5H_6N)_2TlCl_5$ and $(C_5H_6N)TlCl_4$ as starting materials.

EXPERIMENTAL

Pyridinium salts of $TlCl_5^{2-}$ and $TlCl_4^-$ were prepared from Tl_2O_3 as described previously[9,12] and triethylamine and cycloheptatriene of good commercial quality were purified according to the directions given by Perrin *et al.*[13] Reactions were

*Author to whom correspondence should be addressed.

Table 1. Microanalytical results[a]

Sample	% C	% H	% N	% Cl	Product
A	23.5 (23.8)	2.3 (2.2)	5.6 (5.5)	27.9 (28.1)	$(C_5H_6N)TlCl_4 \cdot C_5H_5N$
B	28.3 (29.0)	2.8 (2.8)	6.7 (6.8)	29.1 (28.5)	$(C_5H_6N)_2TlCl_5 \cdot C_5H_5N$
C	18.5 (18.6)	1.9 (1.9)		32.6 (33.0)	$(C_5H_6N)_3Tl_2Cl_9$
D	12.5 (14.1)	1.3 (1.4)		33.9 (33.3)	$(C_5H_6N)TlCl_4$

[a]Microanalyses were performed by AMDEL, Melbourne or by Malissa and Reuter, Engelskirchen, F.R.G. Values in parentheses are those calculated for the product suggested.

performed in a N_2-filled glovebox and manipulations were performed using appropriate vacuum line procedures when necessary.

The reaction described by Kumar and Sharma[5] was performed with both possible chlorothallate starting materials as described below.

(i) *Using* $(C_5H_6N)_2TlCl_5$. Equimolar quantities (10 mmol) of pyridinium pentachlorothallate (5.4 g), cycloheptatriene (0.92 g) and triethylamine (1.0 g) were mixed in CH_2Cl_2 (350 cm^3) and left to stand for ½ h at 18°C in a glovebox. A slight turbidity was observed and was removed by filtration through a G4 frit. This operation caused some white crystals, m.p. 151°C, to precipitate in the filtrate. Once these had been removed, the remainder of the filtrate was concentrated on a vacuum line and yielded two more crops of the same material, m.p. 151°C. Microanalysis: sample A (Table 1).

(ii) *Using* $(C_5H_6N)TlCl_4$. The above procedure was repeated with equimolar quantities (2 mmol) of $(C_5H_6N)TlCl_4$ (1.0 g), triethylamine and cycloheptatriene. After 1 h, a slightly cloudy orange solution was obtained which was filtered to remove the very fine suspension. Part of the resulting solution was concentrated on a rotary evaporator (under a N_2 bleed), while the remainder was concentrated on a hot-water bath in the air. Both methods yielded a brown-orange oil, but operations in air result in the oil decomposing faster as evidenced by its progressive darkening.

The oil obtained from the rotary evaporator was examined by ^{13}C NMR spectroscopy (JEOL JNM-PS-100 PFT instrument operating at 25 MHz; ~600 pulses, 2.5 s repetition time; $CDCl_3$ solution) (Table 2).

The potential for triethylamine and cycloheptatriene to react separately with each of the chlorothallate reagents was examined as described below.

Reactions with triethylamine

(i) *Pyridinium pentachlorothallate*(III). To a solution of $(C_5H_6N)_2TlCl_5$ (2 g, 4 mmol) in 200 cm^3 CH_2Cl_2 was added an equimolar amount of triethylamine (0.51 cm^3). The mixture was allowed to stand for 1 h after which the cloudiness was removed using filter aid and the resulting clear solution was concentrated on a vacuum line. The white solid which separated on concentrating the solution had a m.p. 144–145°C. Microanalysis: sample B (Table 1).

(ii) *Pyridinium tetrachlorothallate*(III). A similar reaction was performed using $(C_5H_6N)TlCl_4$ (1.0 g, 2.3 mmol) and triethylamine (0.35 cm^3). The slightly cloudy orange solution obtained after ~1½ h was filtered and separated into two portions. One of these was evaporated quickly on a vacuum line and the oil so obtained was redissolved in $CDCl_3$ for a ^{13}C NMR spectrum. The remainder was concentrated on a hot water bath and also yielded an oil from which thallium(I) chloride precipitated over some hours.

Reactions with cycloheptatriene

(i) *Pyridinium pentachlorothallate*(III). To a solution of $(C_5H_6N)_2TlCl_5$ (1.92 g, 3.5 mmol) in 300 cm^3, was added cycloheptatriene (0.37 cm^3) and the mixture allowed to stand for ~1 h after which it was concentrated on a vacuum line to yield a white solid, m.p. 130°C. Microanalysis: sample C (Table 1).

(ii) *Pyridinium tetrachlorothallate*(III). In a similar reaction, $(C_5H_6N)TlCl_4$ (1.0 g, 2.3 mmol) was mixed with cycloheptatriene (0.25 cm^3) in CH_2Cl_2 (300 cm^3). The very fine white solid which developed over ~4 h was removed by filtration and the filtrate was concentrated on a vacuum line to yield a crystalline material. Microanalysis: sample D (Table 1).

RESULTS

Microanalytical data obtained on the precipitated products are given in Table 1, while the ^{13}C NMR spectra obtained on the oily products are presented in Table 2. Samples A and B appear to be chlorothallate–pyridine adducts and their IR spectral data are given in Table 3.

Table 2. ^{13}C NMR spectra in $CDCl_3$

Sample	Chemical shift (ppm)	Peak height (%)	Assignment
$(C_5H_6N)TlCl_4 + (C_2H_5)_3N + C_7H_8$ (orange-brown oil—fresh sample)	29.67	13.24	C7
	120.74	14.42	C1
	126.50	11.75	C2
	130.87	17.05	C3
			C_7h_8
	124.13	19.19	
	136.93	19.72	pyH^+
	144.13	30.54	
	9.10	42.94	
	46.78	85.86	$(C_2H_5)_3N$
$(C_5H_6N)TlCl_4 + (C_2H_5)_3N$ (orange-brown oil—fresh sample)	124.07	11.75	
	136.67	17.36	pyH^+
	149.25	29.07	
	9.28	37.48	
	46.66	109.50 O/F	$(C_2H_5)_3N$
Triethylamine (distilled)	11.71	41.54	
	46.35	100.82 O/F	
Cycloheptatriene (distilled)	27.97 (28.8)[a]	181.16	C7
	120.74 (123.3)	46.24	C1
	126.50 (129.8)	53.90	C2
	130.92 (134.1)	57.03	C3
Reference compounds			
$(C_5H_5)M(C_7H_7)$(M = Cr, Mo, Ti or Zr)[b]	80–90		One peak, seven equiv. C atoms
η^6-C_7H_8 in $Cr(CO)_3(\eta^6$-$C_7H_8)$[b]	23.48		C7
	24.17		C7
	57.61		C1
	58.15		C6
	99.47		C3
	100.22		C4
	101.73		C2
	102.27		C5

[a]Values in parentheses are taken from Ref. 17.
[b]Values obtained from Ref. 18.

DISCUSSION

It is quite clear from the results obtained here that an 85% yield of a red-brown compound with formula $C_7H_7TlCl_2$ was not obtained under the conditions described by Kumar and Sharma.[5] From the pentachlorothallate(III) starting material, the colorless product obtained analyzed well for the adduct $(C_5H_6N)TlCl_4 \cdot C_5H_5N$ and this formulation was supported by the IR spectrum which displayed vibrations characteristic of coordinated pyridine[14] in addition to those of the pyridinium ion (Table 3). Evidence for interaction of the metal with cycloheptatriene was not forthcoming. Using the tetrachlorothallate(III) instead, an orange oil could be isolated, but this was unstable at room temperature and decomposed within 5 h. The ^{13}C NMR spectrum obtained while the sample was still fresh showed that those peaks which were due to cycloheptatriene were virtually unchanged from those of the pure hydrocarbon (Table 2). Certainly, they bore no resemblance to those spectra which have been reported for authentic η^7-C_7H_7 or even for η^6-C_7H_8 complexes, in which considerable shifts are observed for the various C resonances.

In the absence of the amine, cycloheptatriene also did not interact with the thallium center. Its addition to a solution of $(C_5H_6N)_2TlCl_5$ caused $(C_5H_6N)_3Tl_2Cl_9$ to separate. It appears that the hydrocarbon merely changes the properties of the solvent, so as to shift the chlorothallate equilibrium in favor of the rather stable enneachloride. With $(C_5H_6N)TlCl_4$, somewhat impure starting material was the only solid product obtained.

Any orange colors which were observed appeared to arise from oxidation of the amine by $(C_5H_6N)TlCl_4$. Highly colored materials have been

Table 3. IR spectra of chlorothallate–pyridine adducts (KBr pellets)

Compound	Assignments		
	$C_5H_6N^+$ Ion	Coordinated C_5H_5N	ν(Tl—Cl)
$(C_5H_6N)_2TlCl_5 \cdot C_5H_5N$	3340–2600 w, br; 1635 m; 1607 m; 1595 m; 1532 s; 1488 s; 1385 w; 1365 sh; 1325 w; 1260 sh; 1241 w; 1198 m; 1164 m; 1050 sh; 1040 sh; 740 s; 610 s; 610 s; 674 s; 389 w	1446 s; 1350 w; 1208 m; 1152 w; 1060 m; 1032 m; 1010 m; 865 w, br; 755 m; 698 s; 631 m; 417 m	295 s, 235 s
$(C_5H_6N)TlCl_4 \cdot C_5H_5N$	1040 m; 1607 not well resolved; 560 w,br		260 (sh), 230 s
$Mn(C_5H_5N)_2Cl_2$[a]		1442, 1362, 1223, 1152, 1076, 1005, 691, 625, 417	

[a]From Ref. 4.

recognized from such reactions for many years, but these have not been investigated further.[8] There was a small (~2.5 ppm) downfield shift for the C_1 atom of the amine when the reaction occurred. This change in the NMR spectrum was, however, very much larger than was observed for any of the carbon atoms of the cycloheptatriene.

It is evident, then, that the major role of the amine in the reaction mixture is to remove a proton from the pyridinium cation rather than from the cycloheptatriene, which thus remains unreacted. Free pyridine is thereby released and is able to form an adduct with one of the chlorothallate species in solution. Such proton transfer behavior is quite consistent with the relative acidities of the species involved: cycloheptatriene, being an exceptionally weak acid, while triethylamine ($K_b = 5.6 \times 10^{-4}$) is a stronger base than pyridine ($K_b = 2.3 \times 10^{-9}$).[15]

Consequently, we remain unconvinced of the π-cycloheptatrienyl thallium(III) dichloride reported by Kumar and Sharma and are left querying whether some essential experimental details were omitted from their paper. We have had cause to complain before about what appeared to be unreliable analytical procedures employed by this group[9,16] but in this instance in which there appears to be no resemblance at all to the product claimed, the standard of the work appears to be very disappointing.

REFERENCES

1. G. E. Coates, M. L. H. Green and K. Wade, *Organometallic Compounds*, Vol. 2, Chap. 6. Methuen, London (1968).
2. M. A. Bennett, *Adv. Organomet. Chem.* 1966, **4**, 353.
3. K. M. Sharma, S. K. Anand, R. K. Multani and B. D. Jain, *J. Organomet. Chem.* 1970, **21**, 389.
4. K. M. Sharma, S. K. Anand, R. K. Multani and B. D. Jain, *J. Organomet. Chem.* 1970, **23**, 173.
5. K. Numar and R. K. Sharma, *Chem. Ind.* 1974, 773.
6. D. G. Tuck, In *Comprehensive Organometallic Chemistry* (Edited by G. Wilkinson), Vol. 1, Chap. 7. Pergamon Press, Oxford (1982).
7. F. W. B. Einstein, M. M. Gilbert and D. G. Tuck, *Inorg. Chem.* 1972, **11**, 2832.
8. A. G. Lee, *The Chemistry of Thallium*. Elsevier, Amsterdam (1971).
9. M. B. Millikan and B. D. James, *Inorg. Chim. Acta* 1980, **44**, L93.
10. B. D. James, M. B. Millikan and M. F. Mackay, *Inorg. Chim. Acta* 1983, **77**, L251.
11. A. Streitwieser, Jr, *Molecular Orbital Theory for Organic Chemists*, Chap. 14. Wiley, New York (1961).
12. M. B. Millikan and B. D. James, *Inorg. Chim. Acta* 1984, **81**, 109.
13. D. D. Perrin, W. L. F. Armarego and D. R. Perrin, *Purification of Laboratory Chemicals*, 2nd edn. Pergamon Press, Oxford (1980).
14. N. S. Gill, R. H. Nuttall, D. E. Scaife and D. W. A. Sharp, *J. Inorg. Nucl. Chem.* 1961, **18**, 79.
15. R. T. Morrison and R. N. Boyd, *Organic Chemistry*, 3rd edn. Allyn & Bacon, Boston (1973).
16. M. B. Millikan and B. D. James, *J. Inorg. Nucl. Chem.* 1981, **43**, 1175.
17. G. C. Levy and G. L. Nelson, *Carbon-13 Nuclear Magnetic Resonance for Organic Chemists*. Wiley–Interscience, New York (1972).
18. B. E. Mann and B. F. Taylor, ^{13}C *NMR Data for Organometallic Compounds*. Academic Press, London (1981).

Polyhedron Vol. 6, No. 3, pp. 483–488, 1987
Printed in Great Britain

0277–5387/87 $3.00+.00

THE SOLUBILIZATION OF METALLIC GOLD AND SILVER: EXPLANATION OF TWO SIXTH-CENTURY CHINESE PROTOCHEMICAL RECIPES

ANTHONY R. BUTLER, CHRISTOPHER GLIDEWELL,*
SHEILA M. GLIDEWELL and SHAREE E. PRITCHARD

Chemistry Department, University of St Andrews, St Andrews, Fife KY16 9ST, U.K.

and

JOSEPH NEEDHAM

The Needham Research Institute, East Asian History of Science Library, Cambridge CB2 2BB, U.K.

(*Received* 28 *April* 1986; *accepted* 24 *July* 1986)

Abstract—According to two early Chinese protochemical procedures, metallic gold and silver can be brought into solution by a mixture of nitre and vinegar, together with iron(II) sulphate and various organic additives, respectively. We conclude that for the solubilization of gold, iodide formed by reduction of iodate, a common impurity in crude nitrate deposits, is required, but that the nitrate has no role other than to introduce the iodate: for the solubilization of silver, nitrite formed by reduction of nitrate by organic matter is essential. The role of iron(II) sulphate in the solubilization of gold appears to be the reduction of iodate.

The properties of gold have exerted a unique fascination from the earliest times[1,2] to the present day.[2,3]

Because of its ability to resist corrosion, medieval Chinese protochemists considered gold as one of the keys to immortality. By its consumption it was hoped a man would be able so to refine his body so that he would never grow old or die. Moreover, Ko Hung, in the *Bao-pu zi*, a text of *ca.* AD 300 indicates that artificial 'Alchemical Gold' was regarded as superior to natural gold as an ingredient of the elixirs of immortality. The challenge was to render gold in a form suitable for use as a drug.

Consequently the two techniques of aurifaction (the conversion of other materials into gold; cf. aurifiction, involving wilful deceit[2]) and of solubilization to form potable gold were of the utmost importance, and upon them much effort was expended. To understand the practical, as well as the philosophical, background of the protochemists of early medieval China it is important that these techniques be subjected to experimental scrutiny.

One published method for the production of potable gold is that described in the protochemical manual, the *San-shi-liu Shui Fa*[4] (*Thirty-six Methods for the Bringing of Solids into Aqueous Solutions*). Needham *et al.*[5] have published a full translation of this text, and have dated it as of about the sixth century AD. However, some of the procedures described in the *San-shi-liu Shui Fa* probably date from as early as the second century BC:[5] some are described in the *Bao-pu zi* of Ko-Hung, and others come from the *San-shi-liu Shui Ching* (*Manual of the Thirty-six Aqueous Solutions*) which predates Ko Hung. As printing was in use in China during the eighth century AD, it is probable that the copy of the *San-shi-liu Shui Fa* which survives is an accurate reproduction of the sixth-century original. While the *San-shi-liu Shui Fa* is tersely written with precise and unambiguous instructions for bringing various minerals into solution, many of the procedures appear at first sight to be rather startling, for example the solubilization

*Author to whom correspondence should be addressed.

of mercury sulphide or of elemental lead using only very dilute acetic acid (vinegar), and potassium nitrate (nitre), together with copper sulphate in the case of mercury sulphide.

However, experimental study of the solubilization of mercury sulphide showed[6] that in the presence of chloride, a common impurity in naturally occurring nitre, dissolution of HgS proceeds readily with formation of $HgCl_2$ and sulphate: similarly, the solubilization of elemental lead was shown[7] to be dependent upon the presence of traces of nitrite, again a common impurity in nitre exposed to organic materials such as the hollow bamboo tubes prescribed[5] as the reaction vessels. Given the presence of only chloride or nitrite, respectively, the otherwise wholly insoluble mercury(II) sulphide and metallic lead readily dissolve in dilute acetic acid/nitre mixtures, confirming the accuracy at least for these two procedures of the observations recorded in the *San-shi-liu Shui Fa.*

The procedure for the production of tin(IV) sulphide (mosaic gold) described in the *Bao-pu zi* of Ko Hung, provides a further example of the accuracy of observation and description displayed by the early Chinese protochemists: according to the essentials of this recipe, mosaic gold (SnS_2) is produced by heating elemental tin with potassium alum, $KAl(SO_4)_2$. This would require the sulphate ion to act as a powerful oxidant, itself being reduced to sulphide. Experimental study of Ko Hung's procedure confirms the formation of SnS_2 from alum or, more simply, from aluminium sulphate:[8]

$$\rightarrow \tfrac{2}{3}\,Al_2(SO_4)_3 + 4Sn \rightarrow \tfrac{2}{3}\,Al_2O_3 + 3SnO_2 + SnS_2.$$

Thermochemical calculations on this, and similar processes, indicate[8] that the principal driving force for the reaction is the formation of tin(IV) oxide, but that most metal sulphates should be capable of oxidising elemental tin to ($3SnO_2 + SnS_2$). Similarly aluminium sulphate should be capable, thermodynamically, of oxidising elemental hydrogen to ($3H_2O + H_2S$):[9] experimental verification of this point predates its thermochemical prediction by *ca.* 150 years.[10]

The experimental verification[6–8] of the essential correctness of three apparently remarkable recipes from the *San-shi-liu Shui Fa* and the *Bao-pu zi* indicates most strongly that chemical procedures given in early Chinese sources, no matter how unlikely they may at first appear in the content of modern chemical knowledge, ought not to be dismissed without experimental investigation.[11]

The solubilization of gold

The *San-shi-lui Shui Fa* procedure is as follows:[4,5]

(29) *Huang-jin shui*—an aqueous solution of gold. 1 lb of gold and 2 lb of green vitriol (*lü fan*), sealed in a bamboo tube with lacquer and placed in vinegar for 50 days will form an aqueous solution.

Green vitriol is the mineral copperas or melanterite, iron(II) sulphate heptahydrate, $FeSO_4 \cdot 7H_2O$ (but see below). Unlike most of the *San-shi-lui Shui Fa* recipes, this procedure does not explicitly mention the addition of nitre, just as one of the recipes for dissolution of mercury sulphide does not include the addition of any liquid phase, although vinegar is clearly required.[5,6] However the commentary in the *Huang-Di Jiu Ding Shen Dan Jing Jue* (*Explanation of the Yellow Emperor's Manual of the Nine-vessel Magical Elixir*)[12] states that 'all the methods depend upon the use of nitre'.[5] Needham *et al.* regard the occasional omission of similar vinegar or nitre from the directions given in the *San-Shi-liu Shui Fa* as no more than inadvertence, or considered unnecessary by the author.

The recipe as it stands immediately poses problems: Needham comments[5] that 'one cannot feel that the gold recipe gave the alchemists much satisfaction'. Uniquely amongst the metallic elements, gold forms no aqua ions which are stable in aqueous media, and hence in the absence of coordinating ligands gold cannot be oxidized from the elemental state at any pH in aqueous solution.[13] To dissolve metallic gold in aqueous media, both an oxidizing agent and a good coordinating ligand for a class b (soft) metal ion are required: neither alone is sufficient. Both acetate and nitrate are extremely poor ligands towards soft cations, and hence it seemed probable that any dissolution of metallic gold in acetic acid/potassium nitrate mixtures would be dependent upon the presence of specific impurities, as found for the dissolution in such media of mercury(II) sulphide[6] and of metallic lead.[7]

We first confirmed that acetic acid/potassium nitrate mixtures do not dissolve metallic gold. Under our normal experimental conditions (see Experimental section) we estimate that dissolution of as little as 0.5% of the original charge of metallic gold would be accurately and reproducibly measurable. In fact in these experiments, no gold was detected in solution even after a reaction time of 70 days, thus confirming the requirement of an impurity if any gold is to be brought into solution by such a solution.

We then surveyed the effects not only of iron(II)

salts and potassium alum, a common ingredient in the recipes of the *San-shi-liu Shui Fa*, but also of likely impurities in the potassium nitrate. The production of potassium nitrate, by extraction from soil, remained as a primitive technique from ancient times until well into the present century,[14] and the composition of the end-product varied widely depending upon the area of production. While samples containing up to 97% KNO_3 were found[14] in some areas, other samples contained as little as 50% ($NaNO_3 + KNO_3$): with nitrate contents averaging ~70–75%, the scope for various active impurities to be present is wide.

Potassium alum, a common ingredient in *San-shi-liu Shui Fa* procedures, was without effect, as were the iron(II) salts, iron(II) chloride, sulphate, and gluconate. The impurities found earlier to be important in the solubilization of mercury (II) sulphide[6] and metallic lead,[7] namely chloride and nitrite, respectively, were also wholly ineffective, as was iodate(V), $[IO_3]^-$. Of the plausible impurities, only iodide is really effective in promoting the solubilization of gold, although bromide has a very modest effect. Further investigation showed that not only was nitrite wholly ineffective alone, and in combinations with iron(II) salts, with chloride, or with potassium alum, but that it completely suppressed the solubilizing action of iodide, by oxidizing it all to elemental iodine. Iodine was shown independently to be entirely ineffective as an additive, although a mixture of iodide and iodine, i.e. tri-iodide $[I_3]^-$, was extremely active. These observations all support the view that the primary role of the iodide is to act as a complexation agent towards gold and that any further additive in combination with iodide which destroys this capability will suppress the solubilizing action of iodide.

For standard 10-mg charges of gold wire in acetic acid/potassium nitrate mixture in the presence of added potassium iodide, the extent of dissolution increases with time for any non-zero level of iodide added, and the rate of dissolution increases with KI level, attaining a constant rate around 5% added KI. When the potassium nitrate was omitted entirely, dissolution still occurred for all non-zero levels of added KI, and the general pattern of the dependence of the reaction upon KI level was unchanged: however, there was a modest, but wholly reproducible *increase* in the rate of dissolution at any level of added KI. Hence potassium nitrate is not an essential requirement for the production of the aqueous gold solutions described in the *San-shi-liu Shui Fa*, save only as a possible means for the introduction of the crucial impurity, iodide.

Examination of the standard reduction e.m.f.s[15] for the half reactions:

$$Au + 2I^- \rightarrow [AuI_2]^- + e^-$$

$$e^- + H^+ + \tfrac{1}{4}O_2 \rightarrow \tfrac{1}{2}H_2O$$

shows that the oxidation of gold, by atmospheric oxygen in the presence of iodide as ligand, is thermodynamically feasible at any pH below 8: hence in dilute acetic acid media, the sole requirements for the solubilization of gold as the iodocomplex $[AuI_2]^-$ are air and iodide ions, and the possible sources of iodide in the *San-shi-liu Shui Fa* recipe must now be considered.

Although iodide is absent from nitrate deposits, iodate $[IO_3]^-$ is a common impurity.[16–18] Iodate is very readily reduced by iron(II), in dilute acetic acid, to yield iodine, although iodide is absent. The standard reduction e.m.f.s[15] show that, in isolation, iron(II) cannot reduce iodine to iodide, but that such reduction is possible in strongly acid media ($pH < 1$) when coupled to the oxidative complexation of gold to yield $[AuI_2]^-$. Such strongly acidic solutions are probably not relevant to the *San-shi-liu Shui Fa* procedure, but organic matter (cf. the use of bamboo tubes sealed with lacquer which are prescribed[5] as reaction vessels in the *San-shi-liu Shui Fa* recipe for the preparation of an aqueous solution of gold) will readily reduce iodine to iodide, as required for the complexation of gold in soluble $[AuI_2]^-$.

Hence the primary role of the potassium nitrate in this recipe is to introduce the common impurity, iodate, as the primary source of the crucial iodide; the role of the iron(II) sulphate is to effect the reduction of iodate to iodine; and the role of the lacquer-sealed bamboo tubes is to act not only as a reaction vessel (for which purpose alone any container would suffice) but, most importantly, as the final reductant of iodine to iodide.

In the published procedure the ingredient *lü fan* was translated[5] as green vitriol, $FeSO_4 \cdot 7H_2O$. However, there is the possibility[19] of confusion of the terms for iron sulphate and copper sulphate, with the possibility therefore that the recipe in the *San-shi-liu Shui Fa* actually calls for blue vitriol instead of green vitriol, i.e. for copper(II) sulphate. The possible involvement of copper is interesting in view of reports[20,21] that metallic gold is somewhat soluble in hot HCl solutions of copper(II) chloride, although much less soluble at normal temperature. However, under similar reaction conditions,[20,21] none of copper(II) sulphate, iron(II) sulphate or iron(III) sulphate in sulphuric acid effected solution unless chloride was added.

Substitution of copper sulphate for iron(II) sulphate has no effect alone on the solubilization of gold, but diminishes the effectiveness of iodide: although, unlike iron(II), copper(II) cannot (cf. Ref. 15) reduce iodate to iodine, it will however readily oxidize iodide to iodine:

$$Cu^{2+} + 2I^- \rightarrow CuI(s) + \tfrac{1}{2}I_2.$$

If *lü fan* were interpreted[5,19] to mean copper(II) sulphate instead of iron(II) sulphate, the quantity prescribed by the recipe[5] would be sufficient to prevent any reduction of iodine-containing precursors to iodide: all would be converted to elemental iodine and the wholly insoluble copper(I) iodide, and solubilization of gold would be prevented. Hence, experiment discounts the possibility that *lü fan* here means copper(II) sulphate and confirms the rendering[5] of this term as iron(II) sulphate.

The solubilisation of silver

We have also investigated briefly the solubilization of metallic silver, for which the *San-shi-liu Shui Fa* procedure[4,5] is as follows:

(30) *Bai-yin shui*—an aqueous solution of silver. 1 lb of silver, 2 pints of clear wheat sauce, 2 pints of vinegar, and 1 pint of wine made from glutinous millet and the fruits of the *mu jing* shrub; sealed in a bamboo tube with lacquer put in vinegar for 30 days will form an aqueous solution.

Glutinous millet (*Qi Shu*) is *Panicum miliaceum*, and *mu jing* is *Vitex negundo*, both medicinal plants.[5,22] As in the gold recipe, no explicit mention is made of nitre: as before its omission is inadvertent. For the sake of simplicity, we have investigated the solubilization of silver only in the context of those components of the *San-shi-liu Shui Fa* procedure which are reproducibly accessible: thus we have omitted all of the organic components, apart from the acetic acid, just as in our previous investigation of the solubilization of cinnabar.[6]

Although silver metal readily dissolves in nitric acid, Mellor records[23] a number of reports in the older literature that it does so only in the presence of nitrite. Preliminary experiments with mixtures of 60% acetic acid with various concentrations of potassium nitrate showed that no dissolution occurred in the absence of added nitrite. For standard 100-mg charges of silver wire in acetic acid–nitre mixtures (see Experimental section) the initial rate of silver dissolution, as measured by the extent of reaction, after 24 h varied linearly with concentration of added nitrite, for nitrite levels between zero and 0.4%.

In weakly acidic aqueous media, as here, the nitrite anion is protonated to yield either the nitrosonium cation, NO^+, or its mono-solvate, the nitrous acidium ion $H_2NO_2^+$:[24,25] the nitrosonium cation has an electron affinity 9.27 eV[26] rather greater than that first ionization energy of silver, 7.57 eV,[27] and hence, even when solvation energies and the sublimation energy of silver are taken into account, the nitrosonium ion is expected to oxidize silver metal, with an overall $\Delta H^{\ominus}$ in aqueous solution of $\sim 80\,kJ\,mol^{-1}$. Consistent with this, we observed that solutions of nitrosonium tetrafluoroborate in either acetonitrile or sulpholane (tetramethylene sulphone) readily oxidized and solubilized metallic silver: the nitronium ion also readily oxidized metallic silver under these conditions although at a higher rate. Thus a 100-mg charge of solver was 49% dissolved after 30 min exposure to $10\,cm^3$ of $0.5\,mol\,cm^{-3}$ $NOBF_4$, but 81% dissolved after 30 min exposure to $10\,cm^3$ of $0.5\,mol\,dm^{-3}$ NO_2BF_4: when the solution was $0.5\,mol\,dm^{-3}$ in each salt, the silver charge was wholly dissolved in 30 min.

These observations confirm that, as in the solubilization of metallic lead,[7] the crucial impurity is nitrite, without which the standard nitre/acetic acid mixture will not effect dissolution. Nitrite is of course readily formed from nitrate in the presence of organic matter acting as a reducing agent, such as the organic components prescribed in the *San-shi-liu Shui Fa* procedure.[5]

The mechanistic role of nitrite has not been investigated in this work, but it is possible that its efficacy depends upon the possibility of a simple one-electron redox reaction with silver, to producing silver(I) and the volatile by-product nitrogen(II) oxide:

$$Ag + NO_2^- + 2H^+ \rightarrow Ag^+ + H_2O + NO.$$

DISCUSSION

Each of the four procedures from the *San-shi-liu Shui Fa* which has been investigated by contemporary chemical techniques, namely the solubilization of mercury(II) sulphide (cinnabar),[6] and metallic lead,[7] gold and silver depends for its effectiveness upon the presence of a highly specific impurity: nitrite for metallic lead or silver, chloride for mercury(II) sulphide, and iodide for gold. We have shown above a plausible source of the iodide in the

original[5] reaction mixture, while chloride is also[28] a common impurity in crude nitre: nitrite is readily formed from nitrate by the reducing agents, such as the organic matter frequently found in *San-shi-liu Shui Fa* procedures.

While in a number of procedures the additives other than nitre and vinegar may appear somewhat capricious, for those examples which we have investigated, these additives appear to have a chemical purpose. Thus in the solubilization of cinnabar,[6] copper sulphate is prescribed[5] as an additive, whose purpose is to catalyse the oxidation by nitrate of the chloride impurity to give elemental chlorine, which in turn acts as the primary oxidant of mercury(II) sulphide, yielding mercury(II) chloride, and sulphite. For the solubilization of metallic silver, which depends upon the formation of nitrite by reduction of nitrate, the original recipe[5] prescribes (see above) the addition of several organic components other than bamboo and lacquer, while the recipe for gold, whose solubilisation has no such requirement for nitrite, prescribes none of these. It is therefore interesting that the recipe[5] for the solubilization of elemental sulphur, which has not yet been reinvestigated in modern times, requires mulberry dew, presumably as a crucial additive.

Potassium alum was found above to exhibit no effect on the solubilization of gold by nitre–vinegar mixtures. Use was made of this lack of action of alum solutions upon gold in early medieval Colombian metallurgy[29,30] in the process of gilding of copper objects, and of enriching in gold the surface of copper–gold alloys (*tumbaga*). Upon heating the alloy or mixture in air, the gold is unaffected but the copper is oxidized to copper(I) oxide, Cu_2O. Experiment shows that aqueous potassium alum solutions are sufficiently acidic to dissolve the copper(I) oxide, while leaving the metallic gold unchanged: repeated application of heat, followed by treatment with the acidic alum solution therefore leads to a surface layer composed almost entirely of metallic gold, even when the original alloy is copper-rich. The process relies first on the ability of air to oxidize copper but r t gold to the metal oxide, and secondly on the solubility of copper(I) oxide, but not gold, in aqueous potassium alum solution.

EXPERIMENTAL

Gold and silver wire, of 0.5 mm diameter, and 99.9% minimum purity were obtained from Alfa, and were used as received. Iodine, of Analar quality, was exhaustively washed with distilled water, dried, and then sublimed. All other chemicals were of the best quality commercially available, and were used as received.

Gold and silver concentrations were measured in solution using a Perkin–Elmer model 360 atomic absorption spectrophotometer, interfaced to a BBC microcomputer for curve analysis and interpolation: multiple sampling (between 5 and 10 aliquots per solution) was routinely employed. All measurements were made on experiments conducted in triplicate.

In a typical experiment, 10 mg of gold wire was placed in 10 cm^3 of aqueous acetic acid (either 30 or 60% w/v) together with appropriate additives. Potassium nitrate, potassium iodide and iron(II) sulphate were at one of the concentrations 0, 0.2, 0.5, 1, 2, 5%; potassium chloride or bromide were at one of 0, 1, 2 or 5%; sodium or potassium nitrite was at 0, 0.5 or 2%; other additives were generally at 0 or 2%. Reaction mixtures were shaken, in air, continuously at 21°C, and the metal concentrations monitored over periods ranging up to 70 days. Under these conditions $[AuI_2]^-$ only is formed: $[AuI_4]^-$ requires[31] large concentrations of free iodine for stability.

Acknowledgement—We thank the Leverhulme Trust for their support of this work.

REFERENCES

1. *Genesis*, 2:11–12.
2. J. Needham, *Science and Civilisation in China*, Vol. 5, Part 2, *Spagyrical Discovery and Invention: Magisteries of Gold and Immortality*. Cambridge University Press, Cambridge (1974).
3. Y. Jiang, S. Alvarez, and R. Hoffmann, *Inorg. Chem.* 1985, **24**, 749.
4. 三十六水法 (*pīnyīn* Romanization).
5. Ts'ao T'ien-Ch'in, Ho Ping-Yu, and J. Needham, *Ambix* 1959 **7**, 122.
6. A. R. Butler, C. Glidewell, and J. Needham, *J. Chem. Res.* 1980, 47, (M) 0817.
7. S. E. MacKerron, M.Sc. thesis, University of St Andrews (1983).
8. A. R. Butler, C. Glidewell, J. Needham and S. Pritchard, *Chem. Br.* 1983, **19**, 132.
9. A. R. Butler, C. Glidewell and S. M. Glidewell, *Thermochim. Acta* 1986, **106**, 355.
10. F. Wöhler, *Annalen* 1845, **53**, 422.
11. A. R. Butler, C. Glidewell and S. E. Pritchard, *Interdiscip. Sci. Rev.* 1986, **11**, 88.
12. *Dao Zang* (*Daoist Patrology*), first printed in the *Northern Sung* (AD 1111–1117); see also, L. Wieger, *Taoisme*, Vol. 1 Bibliographie Générale, No. 878. Mission Press, Hsien-hsien (1911).
13. R. J. Puddephatt, *The Chemistry of Gold*. Elsevier, Amsterdam (1978).
14. *Chinese Economic Monthly* 1925, **2**, 8.

15. A. J. Bard, R. Parsons and J. Jordan, *Standard Potentials in Aqueous Solution.* Marcel Dekker (IUPAC), New York (1985).
16. E. S. Dana, *Textbook of Mineralogy.* John Wiley, London (1922).
17. J. W. Mellor, *Comprehensive Treatise on Inorganic and Theoretical Chemistry*, Suppl. II, Part 1. Longmans, London (1956).
18. V. M. Goldschmidt, *Geochemistry.* Oxford University Press, London (1954).
19. B. E. Read and C. Pak, *Compendium of Minerals and Stones used in Chinese Medicine from the Pên Tshao Kang Mu.* French Bookstore, Peking (1936).
20. H. N. Stokes, *Ecol. Geol.* 1908, **1**, 644.
21. W. J. McCaughey, *J. Am. Chem. Soc.* 1909, **31**, 1261.
22. B. E. Read, *Chinese Medicinal Plants from the Pên Tshao Kang Mu.* French Bookstore, Peking (1936).
23. J. W. Mellor, *Comprehensive Treatise on Inorganic and Theoretical Chemistry*, Vol. 3, p. 351. Longmans, London (1923).
24. J. H. Ridd, *Adv. Phys. Org. Chem.* 1978, **16**, 1.
25. D. L. H. Williams, *Adv. Phys. Org. Chem.* 1983, **19**, 381.
26. C. Jungen and E. Miescher, *Can. J. Phys.* 1969, **47**, 1769.
27. B. Lakatos, J. Bohus and G. Medgyesi, *Acta Chim. Hung.* 1959, **20**, 1.
28. K. H. Wedepohl, *Handbook of Geochemistry.* Springer, Berlin (1969).
29. W. C. Root, *J. Chem. Educ.* 1951, **28**, 76.
30. W. C. Root, In *Essays in Pre-Columbian Art and Archaeology* (Edited by S. K. Lothrop), p. 251. Harvard University Press, Cambridge, MA (1961).
31. Å. Håkansson and L. Johansson, *Chem. Scr.* 1975, **7**, 201.

Polyhedron Vol. 6, No. 2, pp. 489–495, 1987
Printed in Great Britain

0277–5387/87 $3.00+.00

^{13}C and ^{14}N ISOTROPIC NMR SHIFTS IN ANIONIC NITRATOLANTHANATE(III) COMPLEXES WITH QUATERNARY CATIONS

NAILIN CHEN, PHIL J. WITTON, CLIVE E. HOLLOWAY and IAN M. WALKER*

Department of Chemistry, York University, Downsview, Ontario, Canada M3J 1P3

(*Received* 21 *April* 1986; *accepted after revision* 28 *July* 1986)

Abstract—The ^{14}N NMR of nitrate ion coordinated to paramagnetic lanthanide cations in a series of penta- and hexanitratolanthanate(III) anions has been recorded in nitrobenzene–dichloromethane mixtures for all naturally occuring members of the lanthanide series except gadolinium. The nitrate ^{14}N signals show large shifts from their normal values in diamagnetic environments. These isotropic shifts are analysed in terms of a mixture of Fermi contact and through-space dipolar effects. The nitrogen and carbon isotropic shifts from the ammonium cation were shown to be exclusively dipolar in nature. Estimation of the approximate relative amounts of contact and dipolar shift in the nitrate isotropic shifts was attempted. Mixtures of diamagnetic and paramagnetic complexes show separate nitrate ^{14}N resonance signals under our operating conditions. A brief discussion of the kinetics of exchange of nitrate ion between different lanthanide environments is presented.

NMR spectra of salts of the type $[R_4N]_a(MX_n)$ containing paramagnetic metal ions M in moderate dielectric solvents are unusual in that the signals of probe nuclei on the R_4N^+ cation are shifted from their normal frequencies.[1] This is a consequence of the formation of ion-pairs or higher aggregates in solution. These cation isotropic NMR shifts have often been shown, at least for protons, to be due to a predominantly axial dipolar shift mechanism. It is therefore possible to obtain some measure of the structure of the cation in the ion-pair complex. In so doing, use is made of the well-known dependence of the dipolar shift on distances and angles (see below).

Paramagnetic anions of formula $Ln(NO_3)_5^{2-}$ have been shown to be effective shift reagents for R_4N^+ cations, and we have already presented proton NMR isotropic shifts and structural information on several ion-paired systems containing these anions.[2] This choice of anion has several advantages over those derived from the common beta-diketonate shift reagents, including low cost and insensitivity to moderate amounts of hydroxylic solvents.

X-ray studies on salts containing this type of anion show that nitrate acts as a bidentate chelating ligand.[3] It is often convenient for many purposes, in view of the short bite distance of nitrate, to view the 10-coordinate $Ln(NO_3)_5^{2-}$ ion as a trigonal bipyramid. Twelve-coordinate $Ln(NO_3)_6^{3-}$ ions also exist, but are less common.[4,5]

There are several small details concerning the proton isotropic shift patterns in $Ln(NO_3)_5^{2-}$ salts which have puzzled us for some time. It is well known that in a normally behaved, isostructural series of lanthanide complexes of axial symmetry, the Tb, Dy and Ho homologues give shifts in the same direction, while the Er, Tm and Yb homologues give NMR shifts in the opposite direction.[6] In our system, $Er(NO_3)_5^{2-}$ is distinctly anomalous, causing cation isotropic shifts in the same direction as does $Ho(NO_3)_5^{2-}$.

In view of this interesting anomaly, we decided to learn more about the magnetic properties of the $Ln(NO_3)_5^{2-}$ anions in solution, by means of NMR spectroscopy. The most convenient probe nucleus is the almost 100% abundant ^{14}N of the nitrate ion. A great deal of useful information would also be available from studies of the rarer and considerably less sensitive ^{17}O nucleus.[7]

In general, the isotropic shift, $\Delta_T^M(i)$, at the ith

*Author to whom correspondence should be addressed.

nucleus in a metal complex M consists of three terms, the through-space axial and rhombic dipolar shifts $\Delta^M_{ax}(i)$ and $\Delta^M_{rh}(i)$, and the through-bond Fermi contact shift $\Delta^M_c(i)$.

$$\Delta^M_T(i) = \Delta^M_{ax}(i) + \Delta^M_{rh}(i) + \Delta^M_c(i). \quad (1)$$

Since the nitrate nitrogen is separated from the paramagnetic centre by only two bonds, large Fermi contact contributions to the isotropic shift are expected. Fortunately, recent theoretical developments due to Golding and Halton,[8] Bleaney *et al.*[9,10] and Reilley *et al.*[11] now make it possible to partition the observed isotropic shift of a nucleus into its contact and dipolar parts. In this article, we apply these approaches in order to elucidate the origins of the isotropic shift in both the cationic and anionic parts of the homologous series $(R_4N)_{x-3}Ln(NO_3)_x$, where R is *n*-butyl or *n*-propyl, and $x = 5$ or 6. A complete set of ^{13}C isotropic shifts for the cations has also been recorded, and is used to effect a separation of the nitrate isotropic shift into contact and dipolar parts.

In addition, we report preliminary results on the kinetics of nitrate exchange between paramagnetic environments.

EXPERIMENTAL

The preparation of all complexes has been previously described.[5] All solvents used were reagent grade, and were dried over molecular sieves before use. NMR spectra for solutions of 0.15–0.20 mol l^{-1} concentration were obtained at 5.74 MHz (^{14}N) and 20.0 MHz (^{13}C) on a Varian FT-80 NMR spectrometer, using 10-mm sample tubes and the external D_2O lock. ^{13}C spectra were obtained in the proton-decoupled mode, using pulse parameters appropriate for best sensitivity. ^{14}N spectra were obtained using a near 90° pulse with minimum acquisition time (~0.2 s) such that line-shape distortions were avoided, while the advantages of a short T_1 were retained.

The internal reference for the carbon spectra was TMS, while the chosen internal reference for the nitrogen spectra was nitrobenzene. In order to provide a solvent suitable for both ^{14}N and ^{13}C measurements, so that all reported shifts would be measured under identical conditions, a mixture of 10% (v/v) TMS, and 10% (v/v) nitrobenzene in dichloromethane was adopted as the standard solvent for isotropic shift work. Kinetic measurements were made in acetone, which had been dried for at least 48 h over molecular sieves.

RESULTS

^{13}C *Chemical shifts*

Spin-decoupled ^{13}C spectra of quaternary cations are markedly superior to proton spectra in paramagnetic salts, since broadening and signal overlap are nearly always absent. The data reported in Table 1 therefore represent a major improvement in quality over the proton data which we reported earlier.[5] The carbon isotropic shifts are reported in ppm with respect to the corresponding signal of the $Lu(NO_3)_5^{2-}$ salt. A positive shift represents a shift to high field (low frequency).

As with proton spectra, only one signal for a given carbon is observed, even in mixtures of paramagnetic and diamagnetic lanthanide salts. This is a consequence of fast exchange of cations between different ion-pairs.

^{14}N *Chemical shifts*

The spectra of the diamagnetic standards $(Bu_4N)_2Lu(NO_3)_5$ and $(Bu_4N)_3La(NO_3)_6$ in acetone consist of a sharp resonance at high field due to the cation, and a broader resonance due to nitrate at low field. The data are reported in Table 1. Careful measurements have shown that under our experimental conditions, the chemical shift of nitrobenzene is coincident with that of nitrate in diamagnetic environments. Isotropic shifts of the nitrate resonance are therefore referred to the internal standard, nitrobenzene, a positive shift being to high field, as in the carbon spectra. The width of the nitrobenzene signal introduces a small error into our isotropic shifts; we estimate this to be at most 2 ppm.

Studies of the pentanitrato complexes in low dielectric solvents such as acetone, dichloromethane and nitrobenzene show that the nitrate isotropic shift is not sensitive to either solvent or concentration.

^{14}N *Linewidth studies*

The width of the nitrate resonance in free tetrapropylammonium nitrate is broader in organic solvents such as acetone than it is in water (width at half height = 6 Hz in water). Changes in viscosity cannot account for this effect. Increased ion association in the organic solvents is a more likely explanation. The nitrate resonance also broadens considerably on formation of the diamagnetic $Lu(NO_3)_5^{2-}$ complex (width at half height = 40 Hz in acetone). This effect can be due to both an increase in the correlation time associated with a

Table 1. Isotropic shift data for nitratolanthanate salts: $[R_4N]_{x-3}Ln(NO_3)_x$

Ln	x	Nitrate $\Delta_T^M(NO_3)^{a,b}$ (ppm)	Cation $\Delta_T^M(^{14}N)^{a,c}$ (ppm)	Cation $\Delta_T^M(\alpha\text{-}C)^{a,d}$ (ppm)	Cation SR_β^e	Cation SR_γ^e
Ce	6	23	−0.9	−0.3	0.7	0.3
Ce[f]	5	30				
Pr	6	75	−2.3	−0.2	0.7	0.5
Pr[f]	5	90				
Nd	6	95	−1.9	−0.4	0.7	0.5
Nd[f]	5	116				
Sm	5	15	+1.4	−0.1	1	1
Eu	5	−172	−0.4	+0.7	0.7	0.5
Tb	5	−388	−6.0	−4.3	0.6	0.23
Dy	5	−277	−7.0	−6.6	0.65	0.35
Ho	5	−140	−8.4	−7.6	0.66	0.39
Er	5	−60	−5.5	−3.8	0.66	0.39
Tm	5	−56	2.3	3.7	0.65	0.35
Yb	5	−12	1.5	1.7	0.65	0.35

[a]Isotropic shifts in ppm with respect to the corresponding resonances in the diamagnetic Lu complex. Upfield shifts are indicated by a positive sign. The solvent is 10% (v/v) TMS and 10% nitrobenzene in dichloromethane. Unless otherwise indicated, the cation is tetra-*n*-butylammonium.

[b]The ^{14}N isotropic NMR shift of coordinated nitrate ion. The uncertainty is ±2 ppm.

[c]The ^{14}N isotropic shift of the central tetrabutylammonium nitrogen. The cation signal occurs 306.8 ppm to high field of nitrobenzene in the Lu complex. The uncertainty is ±2 ppm.

[d]The $^{\beta}C$ isotropic shift of the α-carbon of the tetrabutylammonium ion. The α-signal occurs at 58.9 ppm with respect to TMS in the Lu derivative.

[e]SR_i is defined as the ratio of the isotropic shift on the *i*th carbon with respect to the α-carbon, i.e. $\Delta_T^M(i\text{-}C)/\Delta_T^M(\alpha\text{-}C)$. The β- and γ-carbon signals are at 24.1 and 19.9 ppm with respect to TMS in the Lu derivative, respectively.

[f]Data recorded on tetra-*n*-propylammonium salts in acetone.

larger anion, as well as the induction of a field-gradient at the quadrupolar nitrogen nucleus.

The quadrupolar broadening increases markedly on cooling for all salts, a factor which may be primarily due to an increase in viscosity. The paramagnetic lanthanide ions exert about the same broadening effect on the nitrate signal (width at half height = 100 ± 20 Hz) in this solvent mixture. The sole exception is the Gd complex, in which the resonance signals of all nuclei are unobservably broad.

DISCUSSION

Isotropic shifts

We now provide a short synopsis of the modern theory used in the analysis of isotropic NMR shifts.[11,12] It is customary to write the dipolar shift expression as the product of metal dependent factors D_{1M} and D_{2M}, appropriate to axial and rhombic symmetry, respectively, and axial and rhombic geometric factors $G_1(i)$ and $G_2(i)$, which depend only on the metal–nucleus distance, R_i, and on angles θ_i, ϕ_i:

$$\Delta_{ax}^M(i) + \Delta_{rh}^M(i) = G_1(i)D_{1M} + G_2(i)D_{2M} \qquad (2)$$

where

$$G_1(i) = R_i^{-3}(3\cos^2\theta_i - 1)$$

and

$$G_2(i) = R_i^{-3}(\sin^2\theta_i \cos 2\phi_i).$$

The angles are as defined in Ref. 12. The Fermi contact shift is written as the product of the metal-dependent effective spin magnetization, $\langle S_z\rangle_M$, and

the hyperfine coupling constant, A_i:

$$\Delta_c^M(i) = A_i\langle S_z\rangle_M. \quad (3)$$

It can be shown[12] that on combining and rearranging these equations:

$$\Delta_T^M(i)/\langle S_z\rangle_M = A_i + K[D_{1M}/\langle S_z\rangle_M] \quad (4a)$$

Thus, a plot of $\Delta_T^M(i)/\langle S_z\rangle_M$ vs $D_{1M}/\langle S_z\rangle_M$ should result in a straight line of intercept A_i, and slope K, where

$$K = G_1(i) + D_{2M}G_2(i)/D_{1M}. \quad (4b)$$

Straight line behaviour will result in our case only if the following conditions are met:

(a) The ion pair complexes must all have the same structure on a time average. In addition, the coordination polyhedron about the lanthanide ion must not vary significantly across the lanthanide series;
(b) rhombic terms are unimportant, or:
(c) there is a proportionality between D_{1M} and D_{2M} which extends across the lanthanide series:
(d) the hyperfine coupling constant, A_i, is constant across the lanthanide series.

Values of D_{1M} have been given by Bleaney *et al.*,[9,10] while values of $\langle S_z\rangle_M$ are available from Golding and Halton.[8]

Cation isotropic shifts

Since the cation nuclei are many bonds removed from the paramagnetic centre, Fermi contact terms would be expected to be very small. This can be seen by comparing the α-carbon isotropic shifts in Table 1 with the proton data previously reported for these systems.[5] The isotropic shifts for proton and carbon are nearly the same in sign and magnitude, as would be expected for nuclei which occupy nearly the same average positions in space. The cation nitrogen data show considerable scatter due in part to the larger uncertainty; nonetheless, they are essentially in agreement with the carbon shifts. Thus the predominant mechanism is dipolar for $Ln(NO_3)_5^{2-}$ complexes. This is in strong contrast to the behaviour of tetrahalocobaltate(II) ion pairs, in which cation proton and carbon isotropic shifts are in opposite directions[13] due to the presence of sizeable contact contributions in the ^{13}C spectra.

For systems in which the contact term is absent, a plot of $\Delta_T^M(i)$ vs D_{1M} should give a straight line, provided the rhombic terms are well-behaved [see (c) above], and that the ion-pair complexes are isostructural.

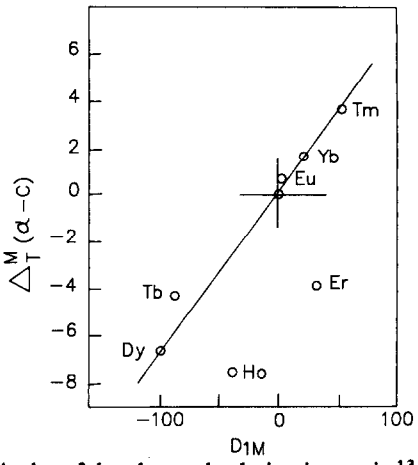

Fig. 1. A plot of the observed solution isotropic ^{13}C NMR shifts at the α-carbon of the cation, $\Delta_T^M(\alpha\text{-C})$, vs Bleaney factors D_{1M} for $[(C_4H_9)_4N]_2Ln(NO_3)_5$ complexes. The data are taken from Table 1.

In Fig. 1, we show such a plot for the α-carbon isotropic shift data for the $[(n\text{-}C_4H_9)_4N]_2Ln(NO_3)_5$ series, for which a straight line may be drawn through nearly all of the lathanide data. We note that Tb gives a small positive deviation, while Ho and Er give significant negative deviations.

Recently, single crystal ESR data have been obtained on $[(C_6H_5)_4As]_2Yb(NO_3)_5$ in a diluent host lattice. Three unequal g factors were observed,[14] showing that in a magnetic sense, the trigonal bipyramid model, with its implicit axial symmetry, is not an accurate description for this type of ion in the solid state. It now appears from consideration of Fig. 1 that rhombic terms must also be considered to make a significant contribution to the cation isotropic shifts in solution. The reason why most lanthanides lie on the line is probably that D_{1M} and D_{2M} are in the same ratio for these complexes; this proportionality breaks down significantly for Ho and Er, however.

We have been aware for some time that the ratios of shifts of cation nuclei, SR_i, are independent of the metal ion. This is apparent in all of the proton studies,[2,5] and can also be seen from Table 1. This behaviour is due to the fact that the cationic part of this system shows effective axial symmetry. The reader may consult Refs 15 and 16 for a further discussion of this problem. In short, the ratios of the shifts of the ith and jth NMR signal will be independent of the metal ion, and will appear to be axial-dipolar, even though the magnetic properties of the anion are rhombic.

Nitrate isotropic shifts

In separating the contact and dipolar parts of the isotropic shift, we make use of eqn (4). The relevant quantities have been collected in Table 2,

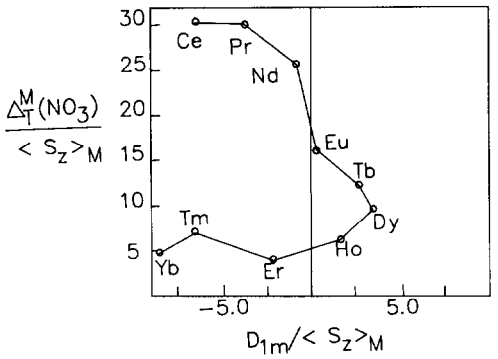

Fig. 2. A plot of $\Delta_T^M(NO_3)/\langle S_z\rangle_M$ vs $D_{1M}/\langle S_z\rangle_M$ for the $Ln(NO_3)_5^{2-}$ complexes. Here, $\Delta_T^M(NO_3)$ is the observed solution ^{14}N isotropic shift at the nitrate ion coordinated to lanthanide ion M, D_{1M} is the corresponding Bleaney factor, and $\langle S_z\rangle_M$ is the effective spin magnetization. The data are taken from Table 2.

Table 2. Analysis of istropic shift data[a]

Ln	$\Delta_T^M(NO_3)/\langle S_z\rangle_M$	$D_{1M}/\langle S_z\rangle_M$	$\Delta_T^M(\alpha\text{-C})/\langle S_z\rangle_M$
Ce[b]	30.6	−6.44	—
Pr	30.3	−3.70	—
Nd	25.8	−0.94	—
Sm	243	11.1	—
Eu	16.1	−0.37	−0.07
Tb	12.2	2.70	0.14
Dy	9.7	3.50	0.23
Ho	6.2	1.72	0.34
Er	3.9	−2.15	0.25
Tm	6.9	−6.46	−0.45
Yb	4.7	−8.50	−0.66

[a]Nitrate isotropic shifts taken from Table 1 for penta-nitrato-complexes. Values of $\langle S_z\rangle_M$ were taken from Ref. 8, while values of D_{1M} were taken from Refs 9, 10.

[b]Data for Ce, Pr and Nd are from $[(C_3H_7)_4N]_2Ln(NO_3)_5$ salts in acetone. All other data are from $[(C_4H_9)_4N]_2Ln(NO_3)_5$ salts in dichloro-methane–nitrobenzene–TMS mixture.

and a plot of $\Delta_T^M(NO_3)/\langle S_z\rangle_M$ vs $D_{1M}/\langle S_z\rangle_M$ is shown in Fig. 2.

We note the total lack of linearity; the plot suggests that all three mechanisms are significant contributors to the overall isotropic shift. The $Sm(NO_3)_5^{2-}$ ion has a considerably larger nitrate shift than expected from the $\langle S_z\rangle_M$ value quoted for this ion by Golding and Halton.[8] Although the sign of the shift is consistent with theory, the ratio $\Delta_T^{Sm}(NO_3)/\langle S_z\rangle_{Sm} = 243$ is grossly out of line (Table 2). Interestingly, $Eu(NO_3)_5^{2-}$ seems well-behaved, although it should exhibit similar problems.[8] The derivation of accurate values for $\langle S_z\rangle_M$ for Eu and Sm complexes has been the subject of a recent article.[17]

Recently, a modification of eqn (4) has been

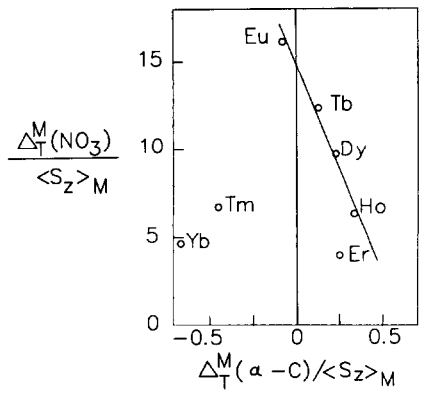

Fig. 3. A plot of $\Delta_T^M(NO_3)/\langle S_z\rangle_M$ vs $\Delta_T^M(\alpha\text{-C})/\langle S_z\rangle_M$ for the $Ln(NO_3)_5^{2-}$ complexes. $\Delta_T^M(NO_3)$ is the observed solution isotropic ^{14}N NMR shift at coordinated nitrate, $\Delta_T^M(\alpha\text{-C})$ is the solution ^{13}C isotropic shift at the cation α-carbon, and $\langle S_z\rangle_M$ is the effective spin magnetisation. The data are taken from Table 2.

suggested by Pinkerton and co-workers.[18–20] The shift of a nucleus which has both contact and dipolar terms may be written:*

$$\Delta_T^M(i)/\langle S_z\rangle_M = A_i + C[\Delta_T^M(j)/\langle S_z\rangle_M] \quad (5)$$

where $\Delta_T^M(j)$ is the shift at a nucleus which is predominantly dipolar in nature. Thus a plot of $\Delta_T^M(i)/\langle S_z\rangle_M$ vs $\Delta_T^M(j)/\langle S_z\rangle_M$ will give a straight line of intercept A_i, assuming the system obeys the conditions for good behaviour (see above). The slope of this plot, C, is a complicated function of D_{1M}, D_{2M} and the geometric factors, and contains no readily useful information.

The value of this method has been amply demonstrated for the series of complexes $[(C_6H_5)_4As]Ln(S_2PR_2)_4$, where R represents a series of alkyl and alkoxy substituents.[18–20] This treatment has the advantage that it compensates for deficiencies in the theoretical values of D_{1M}. In addition, the method appears to be very well adapted to showing up subtle changes in solution geometry.

Choosing the α-carbon shifts as our contact-free shifts, we show such a plot in Fig. 3. Data for the early lanthanides have been omitted, due to variations in stoichiometry; also, the small size of the carbon shifts for these systems renders any conclusions not very meaningful. Several points emerge from this plot: much better linearity is obvious for the four ions Eu–Ho than was found in Fig. 2. The erbium value now lies closer to the Eu–Ho line than before, although the deviation is still significant. The Pinkerton method thus at least

*Our notation is a modification of that used by Pinkerton and co-workers, in order to make it compatible with that of Shelling *et al.*[12]

Table 3. Separation of the ^{14}N isotropic shift in nitrate ion[a]

Ln	$\Delta^M_T(NO_3)$	$\Delta^M_c(NO_3)$	$\Delta^M_{dip}(NO_3)$
Eu	−172	−160	−12
Tb	−388	−477	89
Dy	−277	−428	151
Ho	−140	−339	199

[a]Data in ppm.

partially compensates for the presence of rhombic shift effects in the $Ln(NO_3)_5^{2-}$ system.

We may use these four points in an attempt to estimate the size of the contact shift. Taking the intercept $A_i = 16$ from the plot, and multiplying by the appropriate $\langle S_z \rangle_M$ value, we obtain the contact terms shown in Table 3; application of eqn (1) then yields the dipolar term. The reader is cautioned that these numbers are order-of-magnitude estimates only. It appears safe to conclude, however, that the contact and dipolar contributions are opposite in sign for the ions Tb, Dy and Ho.

Figures 2 and 3 reveal distinctly anomalous behaviour for Tm and Yb data. It has likewise been found[18–20] that data for the $Ln(S_2PR_2)_4^-$ cannot be fitted to one straight line; rather the early lanthanides Ce–Dy fall on one line, while the heavy lanthanides Ho–Yb fall on a line of opposite slope. There appears to be a different A_i value associated with each group of lanthanides. It has been postulated that a structural change in the coordination polyhedron can account for this behaviour, but with the retention of axial symmetry.

It is entirely possible that some of the anomalies which we have noted in the $Ln(NO_3)_5^{2-}$ ion-pairs are due to structural changes. We suspect that breakdown of any of the conditions (a)–(d) could also lead to anomalies in our system, but there does not appear to be any definitive way to pinpoint the precise cause of the breakdown at present.

Kinetics of nitrate exchange

There are relatively few kinetic studies which use ^{14}N as the probe nucleus, probably because the range is somewhat limited by the quadrupolar broadening referred to earlier. In the present case, we have carried out two kinds of experiments:

(1) Exchange of nitrate ion between diamagnetic $Ln(NO_3)_5^{2-}$ or $LuLn(NO_3)_5^{2-}$ and a paramagnetic $Ln(NO_3)_5^{2-}$ complex in acetone.
(2) Exchange of non-coordinated nitrate, as the tetrapropylammonium salt, with paramagnetic $Ln(NO_3)_5^{2-}$ complexes in acetone.

The total concentrations of salts were varied, but in order to simplify the analysis, and to maximize the sensitivity for both peaks, the systems were always studied under conditions of equal site populations. Thus, in the experiments of type 2, the ratio of NO_3^- to paramagnetic $LnNO_3)_5^{2-}$ was always kept as 5:1. The approximate standard equations for two-site line-shape kinetics were used.[21] Despite the broadness of the resonances, the very large shifts permit the same approximations to be used as for non-quadrupolar nuclei. Spectral data were observed from both the fast and slow exchange sides of the coalescence condition, but only the fast exchange data were used for kinetic analysis, in order to minimize quadrupolar broadening problems.

Our results are as follows:

(a) Rates of exchange between small diamagnetic and paramagnetic centres such as Y and Ho, or Lu and Ho do not depend significantly on the metal ion. Thus, small differences in ionic radii do not show up in the kinetics. The $\Delta G\dagger$ values range from +14 to +15 kcal mol^{-1}, while the coalescence temperature varies from 35 to 60°C.

(b) Changing the total concentration of such a mixture has no effect on the rate of reaction. The reaction is thus pseudo-first order in both complex species.

(c) Comparison of data for $Y(NO_3)_5^{2-}$–$Ho(NO_3)_5^{2-}$ exchange with data for $Ho(NO_3)_5^{2-}$–NO_3^- exchange at the same conditions shows that the coalescence temperatures are essentially the same within experimental error (+2°C). We conclude from this that the reactions involving heavy lanthanides are not catalysed by nitrate; this implies a dissociative mechanism. The following scheme is therefore suggested:

$$Ho(NO_3)_5^{2-} \xrightarrow{slow} Ho(NO_3)_4^- + NO_3^-$$

$$Y(NO_3)_5^{2-} \xrightarrow{slow} Y(NO_3)_4^- + NO_3^-*$$

$$NO_3^-* + Ho(NO_3)_4^- \xrightarrow{fast} [Ho(NO_3)_4(NO_3)^*]^{2-}.$$

The large metal ions Ce, Pr, Nd behave differently. Examination of $[(C_3H_7)_4N]_2Ln(NO_3)_5$ and $[(C_3H_7)_4N]_2Ln(NO_3)_5$ were carried out in acetone, as before. Addition of $(C_3H_7)_4NNO_3$ to solutions of either series gives only one line at temperatures where the heavy lanthanides gave two lines; this indicates fast exchange between free and coordinated nitrate. Further, it can be seen from Table 1 that the solution isotropic shifts in the $Ln(NO_3)_5^{2-}$ are very nearly 5/6 as large as those in the $Ln(NO_3)_5^{2-}$ series (Ln = Ce, Pr, Nd). This

observation can be explained by the dissociation reaction:

$$Ln(NO_3)_6^{3-} \underset{slow}{\overset{fast}{\rightleftharpoons}} Ln(NO_3)_5^{2-} + NO_3^-$$

permitting fast exchange of free and coordinated nitrate.

Conclusions

The axial symmetry observed in the organic ligands in the $Ln(S_2PR_2)_4$ complexes[18-20] is not observed in the $Ln(NO_3)_5^{2-}$ complexes. This may seem surprising, since the ligands are both bidentate chelating, and the approximate structural analogy between a tetrahedron in the former case and a trigonal bipyramid in the latter is not without some foundation. The reasons for this difference in behaviour are unclear; however, we have shown that it is inaccurate to describe these pentanitrato-anions as trigonal bipyramids in solution.
solution.

Lanthanide coordination polyhedra are fluctional. It is safe to say therefore that each nitrate ion in these anionic complexes can experience several different magnetic environments over the life of the NMR experiment. This averaging takes place in such a way that both rhombic and axial dipolar terms are generally present in the dipolar shift for both the organic cation and the nitrate anion. In addition, we have detected a large Fermi contact term in the nitrate spectrum.

We have undertaken a preliminary investigation of the kinetics of nitrate exchange in these systems. The exchange reaction appears to take place by a dissociative mechanism for the heavier lanthanides. The exchange rates in the earlier lanthanides are generally faster, and there is evidence that $Ln(NO_3)_6^{3-}$ species undergo dissociation in acetone solution.

Acknowledgement—The authors would like to thank the National Science and Engineering Research Council of Canada for their financial support.

REFERENCES

1. G. N. LaMar, *J. Chem. Phys.* 1964, **41**, 2992.
2. (a) M. S. Quereshi, L. Rosenthal and I. M. Walker, *J. Coord. Chem.* 1976, **5**, 77; (b) M. S. Quereshi and I. M. Walker, *Inorg. Chem.* 1975, **14**, 2187; (c) M. S. Quereshi and I. M. Walker, *Inorg. Chem.* 1974, **13**, 2896.
3. J. G. Bunzli, B. Klein, G. O. Pradervand and P. Porcher, *Inorg. Chem.* 1983, **22**, 3763, and references contained therein.
4. (a) T. A. Beineke and J. Delgaudio, *Inorg. Chem.* 1968, **7**, 715; (b) A. Zalkin, J. D. Forrester and D. H. Templeton, *J. Chem. Phys.* 1963, **39**, 2881.
5. I. M. Walker and D. H. Weeden, *Inorg. Chem.* 1973, **12**, 772.
6. W. D. Horrocks, Jr, and J. P. Sipe, III, *J. Am. Chem. Soc.* 1971, **93**, 6800.
7. J. Reuben and D. Fiat, *J. Chem. Phys.* 1969, **51**, 4909.
8. R. M. Golding and M. P. Halton, *Aust. J. Chem.* 1972, **25**, 2577.
9. B. Bleaney, *J. Magn. Reson.* 1972, **8**, 91.
10. B. Bleaney, C. M. Dobson, B. A. Levine, R. B. Martin, R. J. P. Williams and A. V. Xavier, *J. Chem. Soc. Chem. Commun.* 1972, 791.
11. C. N. Reilley, B. W. Good and R. D. Allendorfer, *Analyt. Chem.* 1976, **48**, 1446.
12. J. G. Shelling, M. E. Bjornson, R. S. Hodges, A. K. Taneja and B. D. Sykes, *J. Magn. Reson.* 1984, **57**, 99.
13. I. Bertini, C. Luchinat and E. Borghi, *Inorg. Chem.* 1981, **20**, 303.
14. W. Urland and R. Kremer, *Inorg. Chem.* 1984, **23**, 1550.
15. J. M. Briggs, G. P. Moss, E. W. Randall and K. D. Sales, *J. Chem. Soc. Chem. Commun.* 1972, 1180.
16. I. M. Walker, L. Rosenthal and M. S. Quereshi, *Inorg. Chem.* 1971, **10**, 2463.
17. A. A. Pinkerton, M. Rossier and S. Spiliadis, *J. Magn. Reson.* 1985, **64**, 420.
18. S. Spiliadis and A. A. Pinkerton, *Inorg. Chim. Acta* 1983, **75**, 125.
19. A. A. Pinkerton and W. L. Earl, *J. Chem. Soc. Dalton Trans.* 1978, 267.
20. S. Spiliadis and A. A. Pinkerton, *J. Chem. Soc. Dalton Trans.* 1982, 1815.
21. J. Sandström, *Dynamic NMR Spectroscopy*, Chap. 6. Academic Press, New York (1982).

Polyhedron Vol. 6, No. 3, pp. 497–502, 1987
Printed in Great Britain

0277–5387/87 $3.00+.00

SOLVENT EFFECT ON THE LIQUID–LIQUID PARTITION COEFFICIENTS OF BIS(DIMETHYLDITHIOCARBAMATO)NICKEL(II) AND BIS(THENOYLTRIFLUOROACETONATO)NICKEL(II)

NOBUO SUZUKI,* SATORU MATSUMORA and HISANORI IMURA

Department of Chemistry, Faculty of Science, Tohoku University, Sendai 980, Japan

(*Received* 18 *February* 1986; *accepted* 8 *May* 1986)

Abstract—Partition coefficients of nickel(II) chelates with thenoyltrifluoroacetone (Htta) and dimethyldithiocarbamic acid (Hdmdtc) into various organic solvents were measured at 25°C. The effect of solvent on the partitition coefficients was evaluated with the aid of a modified equation of the regular solution theory. A great difference in the partition coefficients between $Ni(tta)_2$ and $Ni(dmdtc)_2$ can be interpreted by a preferential solute–solvent interaction for the former chelate. The ability of the divalent metal chelates to accept additional solvation is an important factor governing the partition coefficient.

Recently the liquid–liquid partition coefficient (P) of organic chemicals has been used as a simple measure for the prediction of permeation of these compounds into the environment.[1] Fundamentally the partition coefficient is the key process governing the separation efficiency of the compounds of interest including metal species in chemical separation methods such as solvent extraction and liquid chromatography. It is a surprising fact that only a few systematic studies on the partition coefficient of different kinds of nonelectrolytes, including metal complex compounds, have been made.[2]

In some pioneering work done in 1964, the partition coefficients of β-diketones and their scandium tris-chelates were measured in different organic solvent systems and discussed with the aid of the regular solution theory,[3–5] and one of the important conclusions was expressed as $\log P_{MA_n} = (V_{MA_n}/V_{HA}) \log P_{HA} + C$ where V denotes molar volume, and subscripts MA_n and HA are metal chelate and acidic chelating ligand, respectively. This relation was confirmed experimentally for several types of metal chelates.[6–10] In this original equation, the second term of the right-hand side expressed as C is a correction factor depending on experimental conditions, and ideally this constant term can be neglected. If so this equation simply shows that the partition coefficient of the metal chelate combined with n moles of chelating ligands into an organic solvent is always simply the nth power of the partition coefficient of the chelating ligand into the same organic solvent under the assumption that $V_{MA_n}/V_{HA} \simeq n$.[2,4] In other words, the partition coefficients of the same type of metal chelates MA_n into an organic solvent are equal to each other and not influenced by the central metal ion itself. More detailed studies on the partition coefficient of metal chelates with different central metal ions have been done previously,[7] where the partition coefficients of seven acetylacetonate chelates with Pt(II), Pd(II), Be(II), VO(IV), Cr(III), Al(III) and Co(III) were studied, and an apparent discrepancy from the original equation was discussed in relation to the hydration to chelates. The solute–solvent interaction including hydration may differ in different combinations of central metal ions and acidic chelating ligands.

In this study, the partition coefficients of nickel(II) chelates with thenoyltrifluoroacetone (which is one of β-diketones having oxygen donor atoms) and with dimethyldithiocarbamic acid (which is one of dithiocarbamate family having sulfur donor atoms) are determined in the liquid–liquid system of different organic solvents and an aqueous perchlorate solution. These β-diketones and dithiocarbamates are quite popular chelating agents and extensively exploited in the solvent extraction of

* Author to whom correspondence should be addressed.

metal ions. The partition coefficients are also compared with those for the copper(II) chelates.[9,10]

EXPERIMENTAL

Reagents and apparatus

Thenoyltrifluoroacetone (Htta) was obtained from Dojindo Laboratories and purified by vacuum sublimation. Sodium dimethyldithiocarbamate (Nadmdtc·$2H_2O$) was obtained from Tokyo Kasei Co., Ltd. and purified by recrystallization from acetone–absolute ether. Nickel(II) thenoyltrifluoroacetonate chelate was synthesized in the usual way and recrystallized from 75–99% ethanol. Nickel(II) dimethyldithiocarbamate chelate was obtained from Tokyo Kasei Co., Ltd. and purified by vacuum sublimation. The results of the elemental analysis of each chelate were as follows: $Ni(tta)_2 \cdot 2H_2O$ (Found: C, 35.9; H, 2.2; S, 11.7%; Calc.: C, 35.8; H, 2.2; S, 11.9%); $Ni(dmdtc)_2$ (Found: C, 24.2; H, 3.9; N, 9.4; Calc.: C, 24.1; H, 4.0; N, 9.4%). Based on the experimental results obtained by thermogravimetry, in which the dehydration of $Ni(tta)_2 \cdot 2H_2O$ and its thermal decomposition were observed at 123–156°C and 230°C, respectively, anhydrous $Ni(tta)_2$ was prepared by heating the hydrated chelate at 135–140°C for 2 h.

Carrier-free ^{57}Ni was produced by 24 MeV α-bombardment of iron foil (99.99% purity) with a cyclotron of Tohoku University and isolated by means of anion exchange chromatography (column): Dowex 1X8, 8 mm × 150 mm) with 10 M hydrochloric acid. The effluent was evaporated to dryness and dissolved in 0.01 M perchloric acid. Then carrier-free ^{57}Ni solution was added to an aliquot of a standard solution of nickel(II) perchlorate prepared from the high purity metal (99.99% purity), evaporated to dryness and dissolved in 0.01 M perchloric acid. Other reagents and apparatus were the same as those used previously.[8]

Procedures

An aqueous sodium perchlorate solution (ionic strength 0.10) prepared from 0.01 M perchloric acid and 0.01 M sodium hydroxide was shaken with 0.01–0.10 M Htta in an organic solvent to attain a preliminary equilibrium. A 10-μl portion of 5×10^{-5}–5×10^{-2} M nickel(II) solution labeled with ^{57}Ni was added to the contents and shaken for 2–12 h at 25±0.5°C. In the case of dimethyldithiocarbamate, the aqueous perchlorate solution (ionic strength 0.10) of pH 7–8 containing 1×10^{-4}–1×10^{-2} M Nadmdtc and 2×10^{-7}–1×10^{-4} M radioactive nickel(II) was shaken with an organic solvent for 15–60 min at 25±0.5°C. After centrifuging, an aliquot (0.1–3 ml) was very carefully taken from each phase. The γ-activities of both phases were measured with a well-type NaI(Tl) scintillation counter and the distribution ratio (D) of nickel(II) was calculated. The equilibrium pH value was measured with a glass electrode. Attainment of the partition equilibrium was always checked by forward extraction and backward extraction. Additionally, the partition coefficients of copper(II) thenoyltrifluoroacetonate chelate into isobutylmethyl ketone and diisobutyl ketone were measured in the same way as described previously.[9]

RESULTS AND DISCUSSION

Figure 1 shows typical extraction curves of nickel(II) thenoyltrifluoroacetonate into benzene, isobutylmethyl ketone, and diisobutyl ketone as well as nickel(II) dimethyldithiocarbamate into heptane. The concentration of each chelating anion in the aqueous phase [A^-] was calculated by using the acid dissociation constant and the partition coefficient of Htta[9] and Hdmdtc.[10] In principle the partition coefficient of metal chelate can be directly determined as the limiting value of the distribution ratio in the plateau region. However, since the partition coefficient of $Ni(tta)_2$ in ketone solvents was too high to be accurately measured by this technique, it was determined from the linear section with the slope of two of the distribution curves as shown in

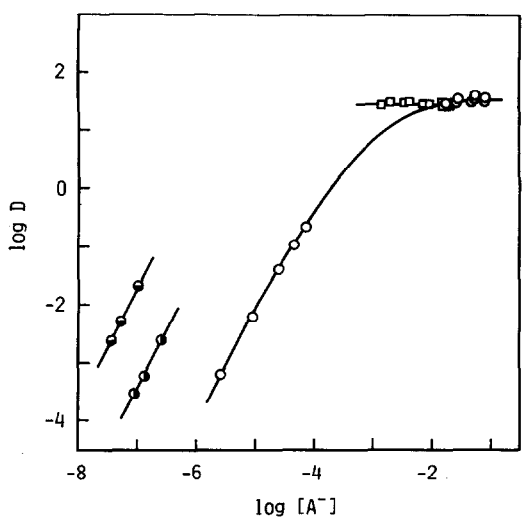

Fig. 1. Distribution ratio of nickel(II) *vs* concentration of chelating anion in the aqueous phase. Initial concentration of Htta: 0.08–0.11 M; pH 2.0–8.2. Initial concentration of Nadmdtc: 0.002–0.020 M; pH 6.0–8.5. ○ Htta–benzene; ◒ Htta–isobutylmethyl ketone; ◑ Htta–diisobutyl ketone; □ Nadmdtc–heptane.

Table 1. Partition coefficients of $Ni(tta)_2$ into benzene

[Ni(II)]/M	[Htta]/M	pH	log P_M
8.3×10^{-8}	0.10	8.12	1.591
3.5×10^{-7}	0.11	7.92	1.594
3.5×10^{-7}	0.11	8.21	1.550
8.7×10^{-7}	0.11	7.44	1.439
8.7×10^{-7}	0.11	7.77	1.522
8.7×10^{-7}	0.11	7.92	1.530
8.7×10^{-7}	0.11	8.21	1.512
1.6×10^{-6}	0.11	7.94	1.436

Fig. 1. The linear section is expressed by $D = P_M\beta_2[A^-]^2$[9] and the overall chelate formation constant β_2 does not depend on the organic solvent itself, hence we can use β_2 determined by analyzing the extraction curve in an appropriate solvent system where P_M is obtained directly from the plateau region. Here from the distribution curve in benzene, β_2 for $Ni(tta)_2$ is obtained as $10^{6.54}$. The β_2 for $Ni(tta)_2$ has not been reported yet, but this value may be comparable with those for Ni(II) chelates with other β-diketones; β_2 for trifluoroacetylacetonate and benzoyltrifluoroacetonate are $10^{6.68}$ and $10^{6.68}$, respectively.[11]

It has been said that nickel(II) chelates, especially with β-diketone, show a strong tendency to form a polymerized species such as $[Ni(\beta\text{-diketonate})_2]_3$ in organic solvent.[12] The partition coefficients of nickel(II) chelates into nonpolar solvents were measured at different initial concentrations of chelates. The results for nickel(II) chelate with thenoyltrifluoroacetonate are listed in Table 1. A constant P_M value for each chelate is obtained within experimental uncertainty. The same was true for nickel(II) chelates with dimethyldithiocarbamate in carbon tetrachloride solvent. These results show that both nickel(II) chelates in the concentration range as low as 10^{-8}–10^{-6} M are present as a monomeric species in both organic and aqueous phases.

The P_M values of $Ni(tta)_2$ and $Ni(dmdtc)_2$ between various organic solvents and 0.10 M perchlorate solution are summarized in Table 2 together with those of the corresponding copper (II) chelates.[9,10] A large solvent effect on the partition coefficients of these chelates is clearly observed. In the thenoyltrifluoroacetonate system, a greater difference in the partition coefficients between nickel(II) and copper(II) chelates is observed, that is, the partition coefficients of copper(II) chelate are larger than those of nickel(II) chelate by a factor of 10^4 in most of the solvents. In the dimethyldithiocarbamate system, the partition coefficient of copper(II) chelate is roughly the same or a little larger than that of nickel(II) chelate.

Following the regular solution concept the partition coefficient of a nonelectrolyte, expressed in a molar fraction scale, can be formulated as[8]

$$\ln P_s^\circ = \frac{V_s}{RT}[C_{ww} - C_{oo} + 2(C_{so} - C'_{sw})] \qquad (1)$$

where V and C are the molar volume and the cohesive energy density, respectively, and the subscripts s, w and o denote solute, water and organic solvent, respectively. In this formulation, the parameter C'_{sw} involves overall interaction between solute and water. If the geometric mean approximation is valid for C_{so}, eqn (1) can be rewritten by the solubility parameters δ as

$$\frac{RT}{V_s}\ln P_s^\circ + C_{oo} = 2\delta_s\delta_o + C_{ww} - 2C'_{sw}. \qquad (2)$$

Table 2. Partition coefficients ($\log P_M$) of nickel(II) and copper(II) chelates with thenoyltrifluoroacetonate and dimethyldithiocarbamate at 25°C

No.	Organic solvent	$Ni(tta)_2$	$Cu(tta)_2$[c]	$Ni(dmdtc)_2$	$Cu(dmdtc)_2$[d]
1	Hexane	-1.05 ± 0.10	3.094	1.38 ± 0.02	2.23
2	Heptane	-1.23 ± 0.14	3.047	1.45 ± 0.03	2.21
3	Carbon tetrachloride	0.02 ± 0.15	4.570	3.11 ± 0.05	3.71
4	Isopropylbenzene	0.51 ± 0.02	4.959	3.69 ± 0.03	4.31
5	Benzene	1.52 ± 0.06	5.489	4.05 ± 0.08	4.57
6	Dibutyl ether	2.18 ± 0.17	5.222	2.74 ± 0.03	3.42
7	Diisobutyl ketone	4.12 ± 0.05[a]	6.08[ab]		
8	Isobutylmethyl ketone	5.84 ± 0.02[a]	6.67[ab]		

[a] Calculated from $P_M = D/(\beta_2[A^-]^2)$ by knowing β_2, see the text.
[b] Average of two measurements.
[c] Ref. 9.
[d] Ref. 10.

A linear relationship between the left-hand side of eqn (2) and δ_o can be expected, and the apparent solubility parameter of the solute δ_s, can be obtained from the slope. Figure 2 shows the plots for $Ni(dmdtc)_2$ together with those for Hdmdtc and $Cu(dmdtc)_2$ reported previously.[10] The molar volume of $Ni(dmdtc)_2$ was assumed to be the same as that of $Cu(dmdtc)_2$, i.e. 190 cm^3 mol^{-1}.[10] The plots for each solute give a good linear relationship apart from the plots in dibutyl ether solvent. The apparent solubility parameter of $Ni(dmdtc)_2$ obtained was 13.3 $cal^{1/2}$ $cm^{-3/2}$, slightly larger than that for Hdmdtc (δ: 12.2) and $Cu(dmdtc)_2$ (δ: 12.7).

Figure 3 shows the same type of plots for $Ni(tta)_2$, $Cu(tta)_2$ and Htta, but Htta is a tautomeric mixture of keto and enol isomers hence the partition coefficient of the enol type of Htta is plotted in Fig. 3.[3,13] Here the molar volume of the nickel(II) chelate was assumed to be the same as that of the copper(II) chelate, 304 cm^3 mol^{-1}.[9] For each solute, a good linear relationship holds for nonpolar solvents, but a positive deviation is clearly observed in polar solvents such as ether and ketone. The apparent solubility parameter of $Ni(tta)_2$ is obtained to be 11.0 $cal^{1/2}$ $cm^{-3/2}$ from the slope of the straight line drawn for nonpolar solvents. This value is the same as that of $Cu(tta)_2$.[9] A similarity between the solubility parameter of $Ni(tta)_2$ and that of $Cu(tta)_2$ suggests a similarity in the chemical state of these extractable chelates in nonpolar solvents. If $Ni(tta)_2$ is extracted as a dihydrate (or monohydrate) species into nonpolar solvents, its apparent solubility parameter can

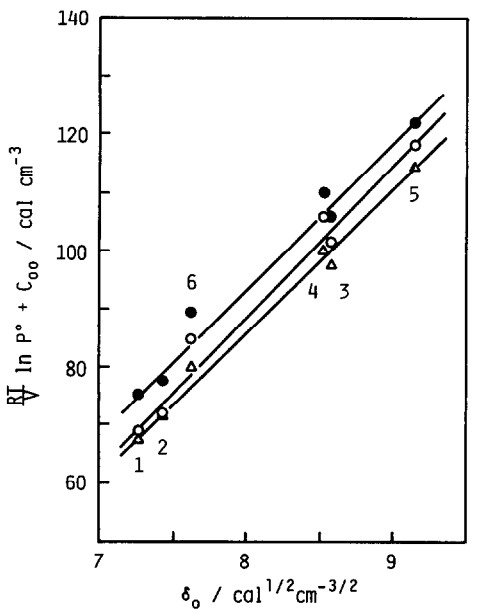

Fig. 2. Evaluation of partition coefficients with eqn (2). The numbers correspond to those in Table 2. ○ $Ni(dmdtc)_2$; ● $Cu(dmdtc)_2$;[10] △ Hdmdtc.[10]

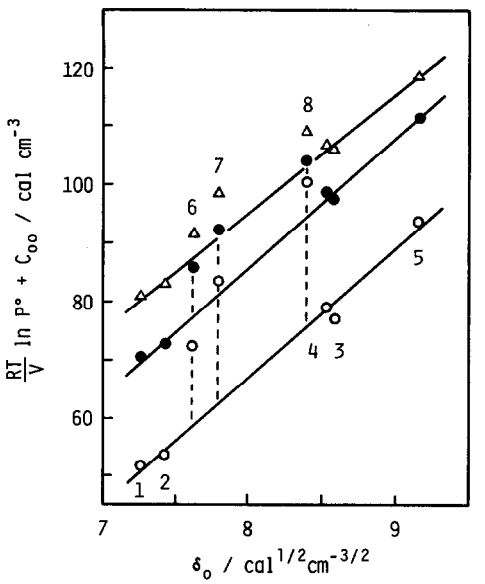

Fig. 3. Evaluation of partition coefficients with eqn (2). The numbers correspond to those in Table 2. ○ $Ni(tta)_2$; ● $Cu(tta)_2$;[9] △ Htta(enol).[9]

be expected to be larger than that of $Cu(tta)_2$, which is extracted without appreciable hydration in nonpolar solvents, due to a contribution of the coordinated water having a high solubility parameter (δ: 23.4). Accordingly, it may be speculated that $Ni(tta)_2$ is not extracted as a rigid hydrated state in the nonpolar solvents. The plots for polar solvents always deviate from the straight line and the extent of deviation is greatly different in different solutes. The observed deviation may be ascribed to additional interaction between the solute and these polar solvents.

Under the assumption that eqn (2) holds for the partition coefficients of acidic chelating ligand P_A°, and also for that of its metal chelate, P_M°, the following relation is readily derived

$$\log P_M^\circ = \frac{V_M}{V_A}\log P_A^\circ + \frac{2V_M}{2.303RT}(\delta_M - \delta_A)\delta_o + \frac{2V_M}{2.303RT}(C'_{wA} - C'_{wM}). \quad (3)$$

The plots of $\log P_M^\circ$ *vs* $\log P_A^\circ$ in thenoyltrifluoroacetonate and dimethyldithiocarbamate systems are shown in Fig. 4. The plots for both $Ni(dmdtc)_2$ and $Cu(dmdtc)_2$ are close to the *ideal* straight line with the slope of two passing through the origin. This *ideal* straight line can be expected when the second and third terms on the right-hand side of eqn (3) are negligible, and this is fulfilled at $\delta_M \simeq \delta_A$ and $C'_{wA} \simeq C'_{wM}$. On the other hand, the plots for $Ni(tta)_2$ and $Cu(tta)_2$, particularly for the

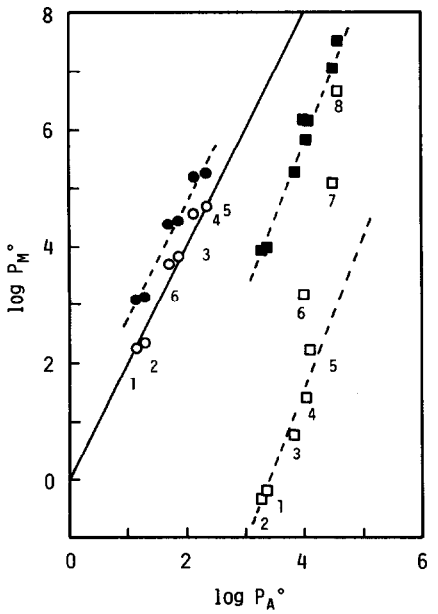

Fig. 4. Linear free energy relationship between the partition coefficients of acidic chelating ligand and its divalent metal chelate. The numbers correspond to those in Table 2. ○ $Ni(dmdtc)_2$; ● $Cu(dmdtc)_2$;[10] □ $Ni(tta)_2$; ■ $Cu(tta)_2$.[9]

former chelate, are in a region remarkably lower than those of the dimethyldithiocarbamate system. By knowing a similarity between the solubility parameters of the solutes $Ni(tta)_2$, $Cu(tta)_2$ (δ: 11.0)[9] and Htta(enol) (δ: 10.2),[9] it is considered that such a lower straight line observed for $Ni(tta)_2$ is caused by a large negative contribution of the third term in eqn (3), i.e. $C'_{wM} > C'_{wA}$. Additionally, the plots for $Ni(tta)_2$ in ether and ketone solvents deviate remarkably from the straight line drawn for the nonpolar solvents. These results suggest that an interaction with water in the aqueous phase is the dominant factor governing the partition coefficient of $Ni(tta)_2$ and also that an interaction of this chelate with polar organic solvents also plays an important role. A preferential solvation of water to $Ni(tta)_2$ over $Ni(dmdtc)_2$, $Cu(dmdtc)_2$ and $Cu(tta)_2$ is demonstrated by the next experiment. A known amount of the anhydrous chelates was left under a constant vapor pressure of water, 9.76 mmHg, which is maintained by an equilibrium atmosphere over 10 mol kg^{-1} lithium chloride solution at 25°C. The result is shown in Fig. 5 where the amount of water absorbed into the chelates was determined by weight variation. Only the $Ni(tta)_2$ chelate gradually takes up water until an equilibrium weight corresponding to $Ni(tta)_2 \cdot 2H_2O$.

A characteristic trend of $Ni(tta)_2$ in the liquid–liquid partition is demonstrated also by a linear free energy relationship between the partition coefficient

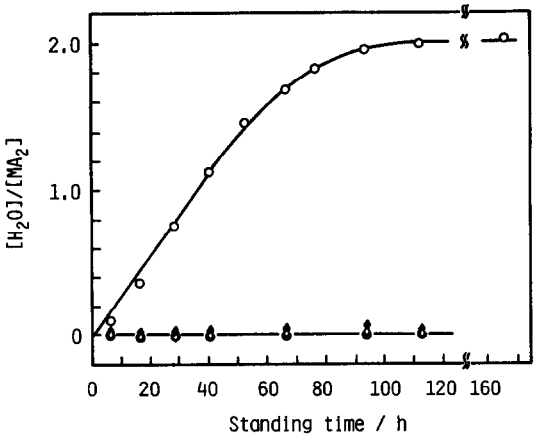

Fig. 5. Hydration of the divalent metal chelates under a constant vapor pressure of water (9.76 mmHg) at 25°C. ○ $Ni(tta)_2$; ● $Cu(tta)_2$; ◇ $Ni(dmdtc)_2$; ◆ $Cu(dmdtc)_2$.

of nickel(II) chelate, P_{Ni}, and that of copper(II) chelate, P_{Cu}, with a given chelating ligand. The relationship is simply derived from eqn (2) as

$$\log P°_{Ni} = \frac{V_{Ni}}{V_{Cu}} \log P°_{Cu} + \frac{2V_{Ni}}{2.303RT}(\delta_{Ni} - \delta_{Cu})\delta_o + \frac{2V_{Ni}}{2.303RT}(C'_{wCu} - C'_{wNi}). \quad (4)$$

The plots of $\log P_{Ni}°$ *vs* $\log P_{Cu}°$ are shown in Fig. 6.

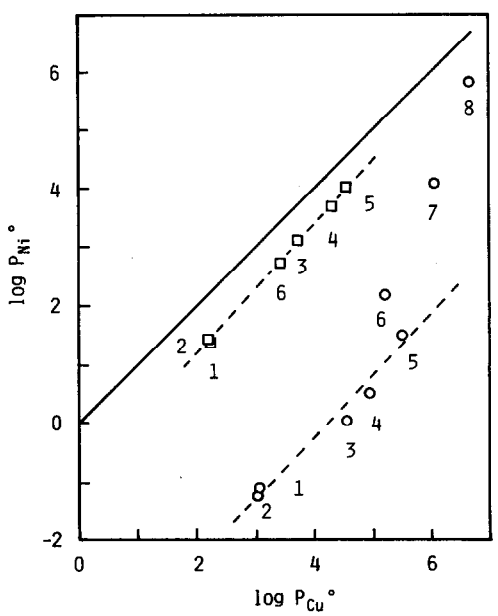

Fig. 6. Linear free energy relationship between the partition coefficients of nickel(II) chelate and copper(II) chelate. The numbers correspond to those in Table 2. □ dimethyldithiocarbamate; ○ thenoyltrifluoroacetonate.

The plots of two metal chelates with dimethyldithiocarbamate are close to the straight line with the unit slope passing through the origin, and this is reasonably understood by considering that the second and third terms in eqn (4) are almost negligible as discussed above. On the other hand, the plots of two metal chelates with thenoyltrifluoroacetonate show a linear correlation with the unit slope of nonpolar solvents, but have a large negative intercept due to much larger solvation of water to $Ni(tta)_2$ compared to $Cu(tta)_2$, and it is again clear that the plots for polar organic solvents deviate remarkably from the straight line due to an appreciable interaction of these polar organic solvents with $Ni(tta)_2$. A noticeable difference in the solute–water and the solute–polar organic solvent interaction observed in two nickel(II) chelates with thenoyltrifluoroacetonate and dimethyldithiocarbamate may be ascribed to the chemical nature of these chelates. Nickel(II) chelate with thenoyltrifluoroacetonate has a strong tendency to form a high-spin complex, by readily forming an adduct compound with donor molecules, such as polar solvents including water, and takes an octahedral structure. On the other hand, dimethyldithiocarbamate chelate involving sulfur donor atoms is a diamagnetic complex with a square planar structure, and shows very little tendency towards coordination of additional donor molecules.[14] In this connection, the partition coefficient of $Ni(dmdtc)_2$ into heptane was measured in the presence of tributylphosphate (tbp), this having a higher coordination ability. The addition of tbp in as high a concentration as 0.10 M has little influence on the P_M ($\log P_M$: 1.66 ± 0.12). This result shows the great difficulty of further coordination of such a strong Lewis base as tbp to $Ni(dmdtc)_2$.

In conclusion, the partition coefficient of nickel(II) chelate with dimethyldithiocarbamate can be quantitatively evaluated by the simple equation based on the regular solution concept, but the partition coefficient of nickel(II) chelate with thenoyltrifluoroacetonate is highly susceptible to water and polar organic solvents. A large difference in the partition coefficients of two nickel(II) chelates with different chelating ligands but of a similar stoichiometry MA_2 is clearly demonstrated.

REFERENCES

1. Test guideline for the determination of the partition coefficient in the system *n*-octanol/water, OECD Chemicals Testing Programme, Berlin (1979).
2. H. M. N. H. Irving, Application of the solubility concept in liquid–liquid extraction, In *Ion Exchange and Solvent Extraction* (Edited by J. A. Marinsky and Y. Marcus), Vol. 6, p. 139. Marcel Dekker, New York (1974).
3. T. Wakahayashi, S. Oki, T. Omori and N. Suzuki, *J. Inorg. Nucl. Chem.* 1964, **26**, 2255.
4. T. Omori, T. Wakahayashi, S. Oki and N. Suzuki, *J. Inorg. Nucl. Chem.* 1964, **26**, 2265.
5. S. Oki, T. Omori, T. Wakahayashi and N. Suzuki, *J. Inorg. Nucl. Chem.* 1965, **27**, 1141.
6. N. Suzuki, M. Itoh and H. Watarai, *Polyhedron* 1982, **1**, 383.
7. H. Watarai, H. Oshima and N. Suzuki, *Quant. Struct. Act. Relat.* 1984, **3**, 17.
8. H. Imura and N. Suzuki, *J. Radioanal. Nucl. Chem.* 1985, **88**, 63.
9. H. Imura and N. Suzuki, *Talanta* 1985, **32**, 785.
10. H. Imura, S. Matsumora and N. Suzuki, *Bull. Chem. Soc. Jpn* 1986, **59**, 621.
11. T. Sekine, S. Iwahori and R. Murai, *J. Inorg. Nucl. Chem.* 1977, **38**, 363.
12. F. A. Cotton and J. P. Fackler, Jr., *J. Am. Chem. Soc.* 1961, **83**, 2818.
13. N. Suzuki and K. Akiba, *J. Inorg. Nucl. Chem.* 1971, **33**, 1169.
14. L. Pauling, *The Nature of the Chemical Bond.* Cornell University Press (1960).

Polyhedron Vol. 6, No. 3, pp. 503–506, 1987
Printed in Great Britain

0277–5387/87 $3.00+.00

THE $^1A_1 \rightarrow {}^1E$ TRANSITION AS A MEASURE OF THE π-ACCEPTOR ABILITY IN $M(CO)_5L$ COMPLEXES

C. DÍAZ* and N. YUTRONIC

Universidad de Chile, Facultad de Ciencias, Casilla 653, Santiago, Chile

(*Received* 28 *August* 1985; *accepted after revision* 13 *May* 1986)

Abstract—It has been found that the position of the λ_{max} for d–d $^1A_1 \rightarrow {}^1E$ transition for $M(CO)_5L$ (M = Cr, Mo and W) complexes is determined by the π-acceptor ability of the L ligand estimated by the Graham π-parameter. The utility of electronic spectra data in the determination of the π-acceptor property of ligands is discussed.

In general, the transfer of electrons from the metal to the ligand (π-back-bonding) in metal carbonyl compounds depends on the properties of the metal and the ligand. For a constant metal this π-back-bonding depends solely of the nature of the ligand and several techniques have been used for the investigation of this matter: IR,[1–4] photoelectron[5] and ^{13}C NMR spectroscopy.[6] Theoretical studies[7] also have been made for a major understanding of this problem.

Although carbonyl frequencies ν(C—O) and force constants k_1 and k_2 have been largely employed in the estimation of the π-acceptor capacity of the ligand L in the $M(CO)_5L$ system,[1,4,8] the M—C bond distances obtained from X-ray crystallographic studies are actually most used.[9,10] Nevertheless, this technique can be employed only for those compounds for which suitable crystals can be obtained. As a more simple method of determining this property the estimation of the π-acceptor ability of L ligand in complexes $M(CO)_5L$ (M = Cr, Mo and W) from their UV–vis spectra is proposed in this paper and its validity and reliability discussed.

RESULTS AND DISCUSSION

As a measure of the π-acceptor ability of ligand we have used the Graham π-parameter[11] because it appears as the best method to estimate this property; in fact this parameter correlates well with the M—C *trans* bond distance in $Cr(CO)_5L$ complexes.[12] Thus the decrease of Cr—CO (*trans*) length bond has been usually discussed on the basis of the π-acceptor capacity of the L ligand.[10]

The π-acceptor ability expressed by the Graham π-parameter was calculated for the $M(CO)_5L$ complexes through the k_1 (axial) and k_2 (equatorial) Cotton–Kraihanzel force constants obtained from the carbonyl ν(C—O) stretching frequencies, previously reported in the literature.[2,3,13,14] For the complexes $[M(CO)_5(THF)]$ (M = Cr, W) no carbonyl stretching and UV–vis data have been reported. Hence they were obtained through irradiation of a solution of $M(CO)_6$ and the ligand in THF as solvent.[14] Because they are highly unstable they cannot be isolated and the IR and visible spectra were recorded from freshly prepared solutions of the complexes. The complex $[Cr(CO)_5(C_6H_5SH)]$ was synthesized from the reaction of $[Cr(CO)_5(THF)]$ photochemically generated with C_6H_5SH and subsequent purification.[14] The yellow solid obtained is highly unstable and the IR and UV–vis spectra were rapidly recorded.

The lowest energy absorption in the complexes $M(CO)_5L$ have been assigned to the ligand field $^1A(e^4b_2^2) \rightarrow {}^{1,3}E(e^3b_2^2a_1^1)$ transition[15,17] (see Fig. 1). Variations of λ for this transition as a function of the acceptor ability of L expressed by the Graham π-parameter are illustrated in Fig. 2 in which λ_{max} is plotted *vs* π for 16 complexes $Cr(CO)_5L$. For $Mo(CO)_5L$ and $W(CO)_5L$ complexes (Figs 3, 4) similar relationships are obtained. Sources for the λ_{max} (nm) and ν_{CO} or k_{CO} data are: 1, $[Cr(CO)_5$ THF] (this work); 2, $[Cr(CO)_5SPMe_3]$;[25] 3, $[Cr(CO)_5HNC_5H_{10}]$;[25] 4, $[Cr(CO)_5(OMe\ C_6H_4SCH_2)_2]$;[26] 5, $[Cr(CO)_5S(N\langle\rangle O)_2]$;[14] 6,

* Author to whom correspondence should be addressed.

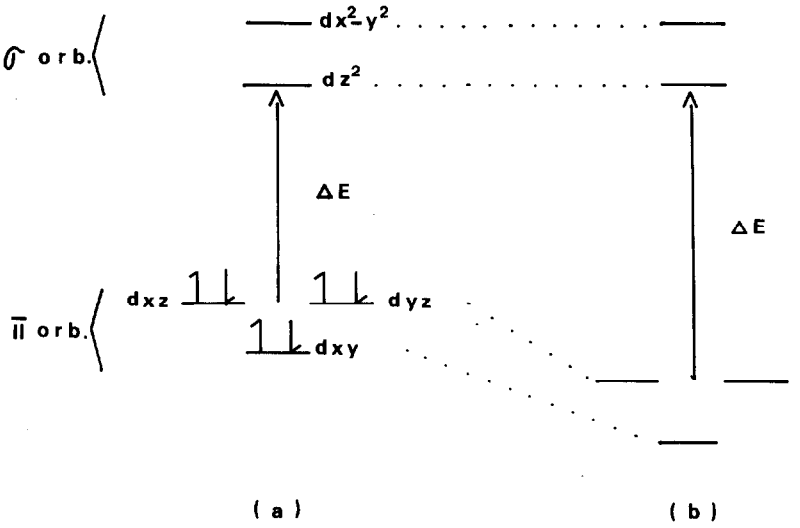

Fig. 1. One-electron energy ordering for $C_{4v}d^6$ $M(CO)_5L$ complexes (a) and effect on π-level at increase of π-back-bonding (b).

$[Cr(CO)_5S(N(CH_2\text{-}C_6H_5)_2)_2]$;[14] 7, $[Cr(CO)_5SPh_2]$;[13] 8, $[Cr(CO)_5(bte)]$;[26] 9, $[Cr(CO)_5S(CH_2Ph)_2]$;[13] 10, $[Cr(CO)_5PhSH]$ (this work); 11, $[Cr(CO)_5EtS(CH_2)_2SEt]$;[26] 12, $[Cr(CO)_5S(CH_2)_3SCH_2]$;[13] 13, $[Cr(CO)_5PPh_3]$;[2,25] 14, $[Cr(CO)_5i\text{-}PrNC]$;[6] 15, $[Cr(CO)_5SCMe_2]$;[27] 16, $[Cr(CO)_5P(C_6H_{11})_3]$;[25,2] 17, $[Cr(CO)_5PEt_3]$;[6] 18, $[Cr(CO)_5P(OPh)_3]$;[25,2] 19, $[Cr(CO)_6]$;[2] 20, $[Mo(CO)_5HNC_5H_{10}]$;[25,2] 21, $[Mo(CO)_5NEt_3]$;[28,2] 22, $[Mo(CO)_5H_2NC_6H_{11}]$;[28,2] 23, $[Mo(CO)_5(bte)]$;[26] 24, $[Mo(CO)_5SEt_2]$;[28,2] 25, $[Mo(CO)_5SCMe_2]$;[27] 26, $[Mo(CO)_5PPh_3]$;[2] 27, $[Mo(CO)_6]$;[28] 28, $[W(CO)_5Et_2O]$;[28] 29, $[W(CO)_5THF]$ (this work); 30, $[W(CO)_5Py]$;[28,2] 31, $[W(CO)_5H_2NC_6H_{11}]$;[28,2] 32, $[W(CO)_5S(N\langle\rangle O)_2]$;[14] 33, $[W(CO)_5PhSH]$ (this work); 34, $[(W(CO)_5)_2(tmdto)]$;[25] 35, $[(W(CO)_5)_2(2,9\ dtd)]$;[25] 36, $[W(CO)_5SCPh_2]$;[27] 37, $[W(CO)_5SCMe_2]$;[27] 38, $[W(CO)_5PPh_3]$;[25,2] 39, $[W(CO)_6]$;[28,2] (bte = $CMe_3SCH_2CH_2SCMe_3$; 2,9 dtd = $MeS(CH_2)_6SMe$; tmdto = $BuS(CH_2)_2SBu$.

The points lie within straight lines:

1. $\lambda_{max}Cr(CO)_5L = -137.7\pi + 407.2$ (1)

2. $\lambda_{max}Mo(CO)_5L = -136.0\pi + 387.84$ (2)

3. $\lambda_{max}W(CO)_5L = -141.74\pi + 391.75.$ (3)

From Figs 3–4 it is immediately evident that, from an increase of π-acceptor capacity of L, a decrease of λ_{max} for the transitions is observed and vice versa.

This trend can be qualitatively understood if we consider the one-electron energy ordering for $C_{4v}d^6$ $M(CO)_5L$ complexes[18] which is shown in the scheme of Fig. 1.

A better π-acceptor ligand causes a decrease in interelectron repulsion by π-back-bonding M → L interaction and therefore a stabilization of the π levels. Consequently a Δ increase and a diminution of λ_{max} is obtained. On the contrary, poor π-acceptor (or π-donor, π with negative values) produces an increase of the energy of π level, and hence a decrease of Δ.

Accordingly a relationship of the type $1/\lambda = a\pi$ could be expected rather than equations (1)–(3) but better correlations were obtained in these latter expressions. When λ^{-1} is plotted against parameter π a smooth curve is obtained, due to the deviation of extremes points. This effect is less notorious when the data are fitted by linear correlation of λ with π. Further straightforward expressions are practically most useful.

From Figs 2–4, however, it is observed that somewhat different values of π give similar values of λ_{max}: hence for these cases λ_{max} could be used only roughly as a measure of the π-acceptor capacity of ligands. From this can be concluded that λ_{max} is not able to distinguish ligands with only slightly different acceptor ability.

Table 1. π values calculated from IR and UV–vis data for $M(CO)_5L$, L = 4-vinyl pyridine, and for $W(CO)_5(Te{=}CPh_2)$

	π(IR)	π(UV–vis)
$Cr(CO)_5$(4-VP)	−0.07	−0.05
$Mo(CO)_5$(4-VP)	−0.01	−0.06
$W(CO)_5$(4-VP)	−0.09	−0.086
$W(CO)_5(Te{=}CPh_2)$	0.11	0.22

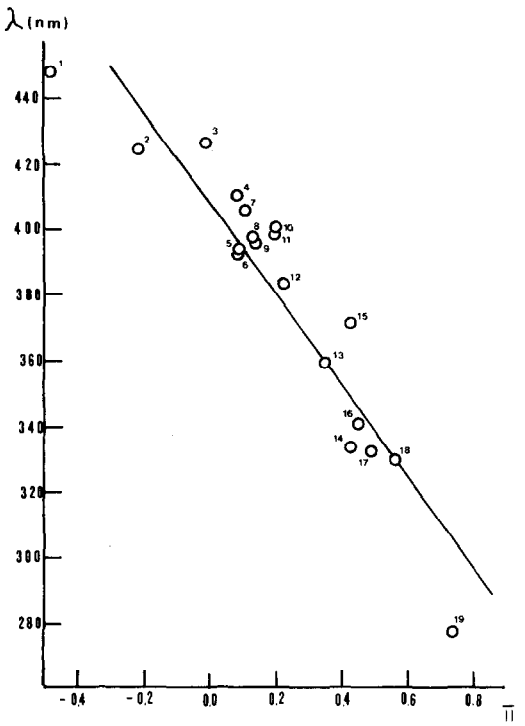

Fig. 2. Dependence from the π-acceptor capacity of λ_{max} for $Cr(CO)_5L$.

Data for $M(CO)_5L$, L = carbenes[19] and thioureas,[20,21] fall out of the relationships (1)–(3).

It is noteworthy that the slopes of the straight lines shown in Figs 2–4 are equal. From this it can be concluded that the π-acceptor ability measured by the relationships 1, 2 and 3 is a property that

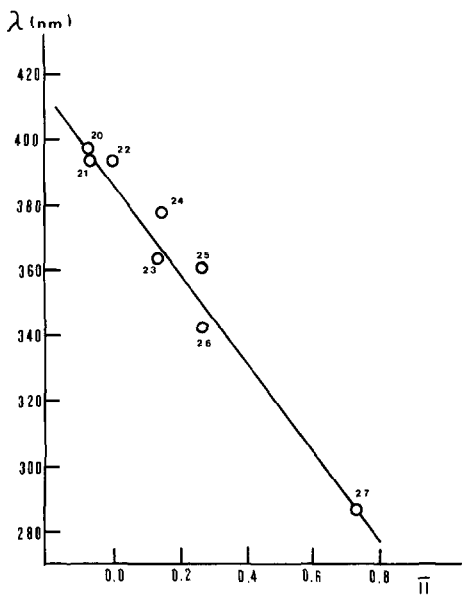

Fig. 3. Dependence from the π acceptor capacity on λ_{max} for $Mo(CO)_5L$.

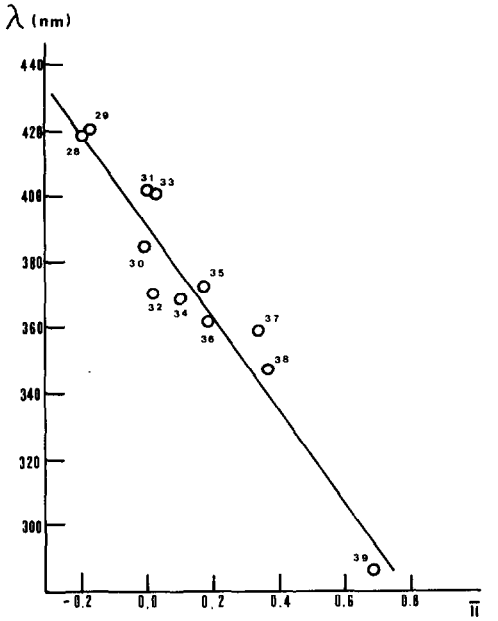

Fig. 4. Dependence from the π-acceptor capacity on λ_{max} for $W(CO)_5L$.

does not depend on the metal (Cr, Mo or W) and hence λ_{max} can be viewed as a sort of 'spectrochemical series' for π-bonding neutral ligands.

As an example of the validity of equations (1)–(3) we have estimated the π parameter from UV–vis data for $M(CO)_5$(4-VP) (4-VP = 4-vinyl pyridine; M = Cr, Mo and W) reported recently.[22] This is shown in Table 1 where the values are close that those calculated from IR data. For the complex $[W(CO)_5(Te{=}CPh_2)]$[23] a satisfactory agreement was also found.

These results suggest that in spite of the fact that UV–vis spectral data are rarely included in the characterization of $M(CO)_5L$ derivatives,[24] electronic spectra can afford valuable information about the π-acceptor ability of the ligand similar to that obtained by IR spectroscopy and other methods. The estimation of this property using UV–vis data is particularly useful when the $M(CO)_5L$ is not soluble in apolar and inert solvents, in such a case it is not possible to record the IR spectra in the C—O stretching region which precludes the estimation of the π-parameter. Then, a diffuse reflectance spectra should be utilized for estimation of the π-acceptor capacity.

REFERENCES

1. W. A. Horrocks and R. C. Taylor, *Inorg. Chem.* 1963, **2**, 723.
2. D. M. Adams, *Metal–Ligand Vibrations*. Arlond, London (1967).

3. G. Dobson, I. N. Stolz and R. K. Sheline, *Adv. Inorg. Chem. Radiochem.* 1965, **8**, 1.
4. F. A. Cotton and C. S. Kraihanzel, *J. Am. Chem. Soc.* 1962, **83**, 4432.
5. H. Daamen, A. Oskam and D. J. Stufkens, *Inorg. Chim. Acta* 1980, **38**, 71 and references cited therein.
6. G. M. Bodner, *Inorg. Chem.* 1975, **14**, 2694.
7. J. B. Johnson and W. G. Klemperer, *J. Am. Chem. Soc.* 1977, **99**, 7132.
8. R. A. Brown and G. R. Dobson, *Inorg. Chim. Acta* 1972, **6**, 65.
9. A. Carty, N. J. Taylor, A. W. Coleman and M. F. Lappert, *J. Chem. Soc., Chem. Commun.* 1979, 639.
10. C. M. Burschka, F. F. Baumman and W. A. Schenk, *Z. Anorg. Allg. Chem.* 1983, **502**, 191.
11. W. A. Graham, *Inorg. Chem.* 1968, **7**, 315.
12. We have found a satisfactory relationship between the π-parameter and the Cr—C length. For 15 compounds $Cr(CO)_5L$ the points lie on a straight line: $d(Cr—C) = 0.104\pi + 1.81$.
13. H. G. Raubenheimer, S. Lotz, H. W. Vilgeon and A. A. Chalmers, *J. Organomet. Chem.* 1978, **152**, 73.
14. C. Díaz and G. González, *Inorg. Chim. Acta* 1984, **85**, 61.
15. M. J. Wrighton, D. L. Morse, M. B. Gray and D. K. Ottensen, *J. Am. Chem. Soc.* 1976, **98**, 1111.
16. D. A. Wensky and K. Wensky, *Spectrochim. Acta* 1975, **31A**, 23.
17. C. C. Frazier and H. Kisch, *Inorg. Chem.* 1978, **17**, 2736.
18. M. Wrighton, *Chem. Rev.* 1974, **74**, 401.
19. M. Y. Darensbourg and D. J. Darensbourg, *Inorg. Chem.* 1970, **9**, 32.
20. J. Granifo, J. Costamagna, A. Garrao and M. Pieber, *J. Inorg. Nucl. Chem.* 1980, **42**, 1587.
21. A. O. Baghlaf, M. Ishaq and A. S. Deifuliah, *Polyhedron* 1984, **3**, 235.
22. J. M. Kelly and C. Long, *J. Organomet. Chem.* 1982, **235**, 315.
23. H. Fisher and S. Zeugner, *J. Organomet. Chem.* 1983, **252C**, 63.
24. Numerous articles with the synthesis and characterization of $M(CO)_5L$ complexes have been recently reported but they do not contain spectral UV–vis data. See for example: G. J. Kruger, L. Linford and H. G. Raubenheimer, *J. Chem. Soc., Dalton Trans.* 1984, 2377 and J. Grobe, M. Köhne-Wachter and D. Le Van, *J. Organomet. Chem.* 1985, **280**, 331.
25. E. W. Ainscough, E. J. Birch and A. M. Brodie, *Inorg. Chim. Acta* 1976, **20**, 187.
26. J. A. Connor and G. Hudson, *J. Chem. Soc., Dalton Trans.* 1975, 1025.
27. R. G. Gingerich and R. J. Angelici, *J. Organomet. Chem.* 1977, **132**, 377.
28. M. Wrighton, G. S. Hammond and H. B. Gray, *J. Am. Chem. Soc.* 1971, **93**, 4336.

Polyhedron Vol. 6, No. 3, pp. 507–512, 1987
Printed in Great Britain

0277–5387/87 $3.00+.00

THERMAL DECOMPOSITION OF ORGANOINDIUM COMPOUNDS AND PREPARATION OF INDIUM–TIN-OXIDE FILMS

RYOKI NOMURA,* SHIN'JI INAZAWA and HARUO MATSUDA

Department of Applied Chemistry, Faculty of Engineering, Osaka University, Yamada-Oka, Suita, Osaka 565, Japan

and

SHUJI SAEKI

Institute of Research and Development, Daiichi-Kogyo-Seiyaku Co. Ltd, Shimogyo-ku, Kyoto 600, Japan

(*Received* 11 *February* 1986; *accepted* 29 *July* 1986)

Abstract—Organoindium compounds of general formula Bu_2InX [where X is OBu^t, OPh, O_2CEt, O_2CPh, $O_2CCH(Et)(CH_2)_3CH_3$ or $C_5H_7O_2$ (acetylacetonate)] were synthesized, and their thermal decomposition was investigated by means of thermogravimetry. The main pyrolysis of the dibutylindium compounds was exothermic and their thermal weight loss occurred below *ca* 400°C. In contrast, metallo-organics such as $In(acac)_3$ and $In[O_2CCH(Et)(CH_2)_3CH_3]_3$ decomposed endothermically in the temperature range between 190 and 480°C. Chemical liquid pyrolysis of dibutylindium octanoate and propionate in *p*-xylene below 450°C, along with dibutyltin oxide as a dopant, gave highly conductive (*ca* 10^{-3} Ω cm) and transparent indium–tin-oxide films.

The chemistry of organoindium compounds has been one of the less studied areas of organometallic chemistry, and synthetically and industrially they have been almost ignored.[1] Recently, studies on the organoindiums have increased since MOCVD (metal organic chemical vapour deposition, alternatively termed OMCVD) techniques for the production of III/V semiconductor thin films have been remarkably developed.[2] However, MOCVD has usually been carried out with indium trialkyls, and the use of organoindium compounds other than the trialkyls has been limited.

On the other hand, some recent reports have shown that indium–tin-oxide (ITO) films as one example of III/VI semiconductors, which are most useful as conducting and transparent oxide films for displays or solar cell windows,[3] could be prepared by chemical pyrolysis of metallo-organics of indium such as chelates,[4,5] acylates[6] and alkoxides.[7–9] However, the chemical pyrolytic preparation of ITO films by using such metallo-organics must usually be carried out with substrate temperatures greater than about 500°C to obtain highly conductive films.

We expected that the chemical liquid pyrolysis of organoindium compounds, because of the lability of their In—C bonds[10] compared with metallo-organics, could give highly conductive ITO films even at moderate temperatures. However, the thermal behaviour of the organoindium derivatives is not known in detail. Hence, we investigated the thermal decomposition of organoindium compounds (Bu_2InX) [where X is OBu^t, OPh, O_2CEt, O_2CPh, $O_2CCH(Et)(CH_2)_3CH_3$ or $C_5H_7O_2$ [acetylacetonate (acac)], aiming at establishment of suitable organometallics for the preparation of ITO films by means of chemical liquid pyrolysis.

* Author to whom correspondence should be addressed.

EXPERIMENTAL

General

IR and ^{1}H NMR spectra were recorded on a Hitachi 260-30 spectrophotometer and a JEOL JMX-100 spectrometer, respectively. Thermogravimetric analyses were performed with a Rigaku DG-C1H type thermogravimeter. Film thickness was measured by a multiple reflection interferometer, using nitric acid etched samples as reported by Ogihara and Kinugawa.[4] Surface resistivity of the films was measured with a Tycoon 841 type four-probe apparatus, a Takasago CCP10-1MR Dc constant-current power supply and Sanwa 9000EA digital multimeter. Indium chloride ($InCl_3 \cdot 3.5H_2O$), indium tris(2-ethylhexanoate) and dibutyltin oxide as a dopant were from commercial sources.

Preparation of organoindium compounds

Tributylindium was synthesized by the Grignard method reported by Runge *et al.*[11] by using $InCl_3$ which was prepared by dehydration of commercial $InCl_3 \cdot 3.5H_2O$ *in vacuo* (10^{-4} torr) at 160°C for 1 h. The crude tributylindium was purified by distillation twice *in vacuo* [yield 60%, b.p. 117°C/3 torr (lit.[12] 86–7°C/0.4 torr)]. Dibutylindium derivatives were then prepared by the direct reaction of the corresponding oxygen acids with tributylindium in ether as reported by Clark and Pickard,[13] and were recrystallized from ether or distilled *in vacuo*. The results of the analyses and the properties of the dibutylindium derivatives are summarized in Table 1. In addition, it is very interesting that tributylindium was converted into pure indium tris(acetylacetonate) quantitatively in acetylacetone solution: m.p. 188–190°C (lit.[15] 186°C); IR (KBr): 440 cm^{-1} (ν_{In-O}); ^{1}H NMR ($CDCl_3$): δ 2.00s (6H, CH_3), 5.41s (1H, CH). Found: C, 44.2; H, 5.3. Calc. for $C_{15}H_{21}InO_6$; C, 43.7; H, 5.1%.

Film preparation

ITO films were prepared as follows. To 10 cm^3 of absolute *p*-xylene, prescribed amounts of organoindium compounds and dibutyltin oxide were dissolved (boiled if necessary). About 100 μl of the resulting solution was dropped upon a glass sub-

Table 1. Properties of prepared dibutylindium derivatives

Bu_2InX X	B.p. or m.p. (°C) (torr)	Yield (%)	Found (%) [calc. (%)] C	H	Formula	Chemical shifts[a] (δ)
OBu^t[b]	125 (0.01)	75	48.1 (47.6	9.4 9.0)	$C_{12}H_{27}InO$	0.70 (J = 8.4 Hz), 0.90t (J = 6.0 Hz), 1.17 and 1.26s, 1.26sx, 1.62m ($A_2B_2B'_2$ type)
OPh[c]	167 (0.01)	76	51.7 (52.0	7.5 7.2)	$C_{14}H_{23}InO$	0.83t (J = 6.6 Hz), 1.07t (J = 7.5 Hz), 1.30 sx, 1.62m ($A_2B_2B'_2$ type), 6.61d, 6.80d, 7.15t (J = 7.2 Hz)
acac[d]	89–90	88	47.8 (47.6	7.9 7.7)	$C_{13}H_{25}InO_2$	0.88t (J = 6.6 Hz), 0.9–1.8m, 1.88s, 5.24s
OCOEt[e]	140 (0.01)	83	43.0 (43.7	8.1 7.7)	$C_{11}H_{23}InO_2$	0.89t (J = 7.3 Hz), 1.06t (J = 7.0 Hz) 1.0–2.0m, 2.22q (J = 7.0 Hz)
OCOPh[f]	140 (0.01)	73	50.7 (51.4	7.0 6.6)	$C_{15}H_{23}InO_2$	0.88t (J = 6.3 Hz), 0.90t (J = 8.1 Hz), 1.30sx, 1.65m ($A_2B_2B'_2$ type), 7.42dd (*meta*, J_{om} = 7.5 Hz, J_{mp} = 2.4 Hz), 7.45m (*para*), 7.99dd (*ortho*)
OCOC$_7$[g,h]	220	80	50.6 (51.6	8.8 8.9)	$C_{16}H_{33}InO_2$	0.8–1.9m, 3.5–3.8bd m

[a] Bu_3In (Et_2O): δ 0.57t (In—CH_2, J = 8.1 Hz), 0.87t (CH_3, J = 7.5 Hz), 1.32sx (CH_3CH_2), 1.62m (CH_2CH_2In).
[b] ν_{In-O} 480 cm^{-1}.
[c] ν_{In-O} 510 cm^{-1}.
[d] ν_{In-O} 420 cm^{-1}.
[e] ν_{CO} 1550 cm^{-1}.
[f] ν_{CO} 1550 cm^{-1}.
[g] 2-Ethylhexanoate.
[h] ν_{CO} 1555 cm^{-1}.

strate (Matsunami slide glass No. S-111, 76 × 26 mm) and spread over the surface by tipping. The substrate was then heated in air at 100°C for 40 min, resulting in the formation of a transparent film. However, films thus obtained were not conductive. The films on the substrate were then baked in a quartz tube at 350–500°C for 1 h in air.

RESULTS AND DISCUSSION

The results of the thermogravimetric analyses of the dibutylindium derivatives along with two metallo-organics of indium are summarized in Table 2 and typical thermograms are presented in Fig. 1. The thermal weight loss of indium tris(acetylacetonate) and indium tris(2-ethylhexanoate), which are the most popular metallo-organics for the preparation of ITO films,[4–6] occurred sharply at *ca* 300 and 380°C, respectively, along with large endothermic DTA peaks. The weight loss, however, continued beyond 400°C. The sharp and endothermic decomposition indicates that bond dissociation between the indium atom and ligands is the initial process, and degradation of ligands follows later.

The behaviour of dibutylindium derivatives in thermal decomposition seems apparently opposite to that of the metallo-organics. The dibutylindiums were found to decompose *via* complex multi-steps as can be seen from TG and DTA curves. The main thermal decomposition process is exothermic, and occurred below 300°C. Thus, it can be said that these dibutylindium compounds are superior to the metallo-organics for the preparation of ITO films at lower temperatures. Travkin *et al.*[15] and Aleksandrov *et al.*[16] have reported that trialkylindiums, including tributylindium, decomposed exothermically at temperatures between 200 and 300°C.

$Bu_2In(acac)$

Three peaks appeared in the DTA curve. A sharp endothermic peak at 83°C means that $Bu_2In(acac)$ melts at this temperature. The exothermic and broad DTA peak centered at 260°C seems to characterize the thermal decomposition of $Bu_2In(acac)$, in contrast to the other metallo-organics. The main thermal weight loss occurred exothermically and the presence of one inflection point was observed at 260°C, based on DTG. At the point of inflexion, the weight loss reached 35.5%, which corresponds to the loss of two Bu groups.

The main decomposition process ceased at 310°C, after a weight loss of 56.4%. Thus, $Bu_2In(acac)$ was pyrolysed into In_2O_3 up to 310°C. The

Table 2. Results of thermogravimetric analyses of dibutylindium derivatives[a]

	TG				DTA	
X	Start and end of weight loss (°C)		Total weight loss (%) Obsd	Calc.[b]	Endothermic (°C)	Exothermic (°C)
			(1) Bu_2InX			
OBu[t]	60	350[c]	*ca* 100	55.1	330	280
OPh	96	431	58.1	56.9		301, 383
acac	101	381	67.9	57.6	83[d]	261, 372
OCOEt	45	353	53.9	54.1		200, 320
$OCOC_7$[e]	115	400	63.1	62.7	231[d]	366
			(2) InX_3			
acac	188	476	70.2	66.3	190[d], 306	419
$OCOC_7$[e]	189	431	74.5	74.5	242[d], 382	

[a] Conditions of thermal analyses as follows: temperature range rt–650°C, heating rate 5°C min^{-1}, reference α-alumina, range TG, ±50 mg, DTA 100 mV, under N_2.

[b] Calculation was done with the hypothesis that the organoindium compounds was perfectly converted into In_2O_3.

[c] Volatilized.

[d] Melting point.

[e] 2-Ethylhexanoate.

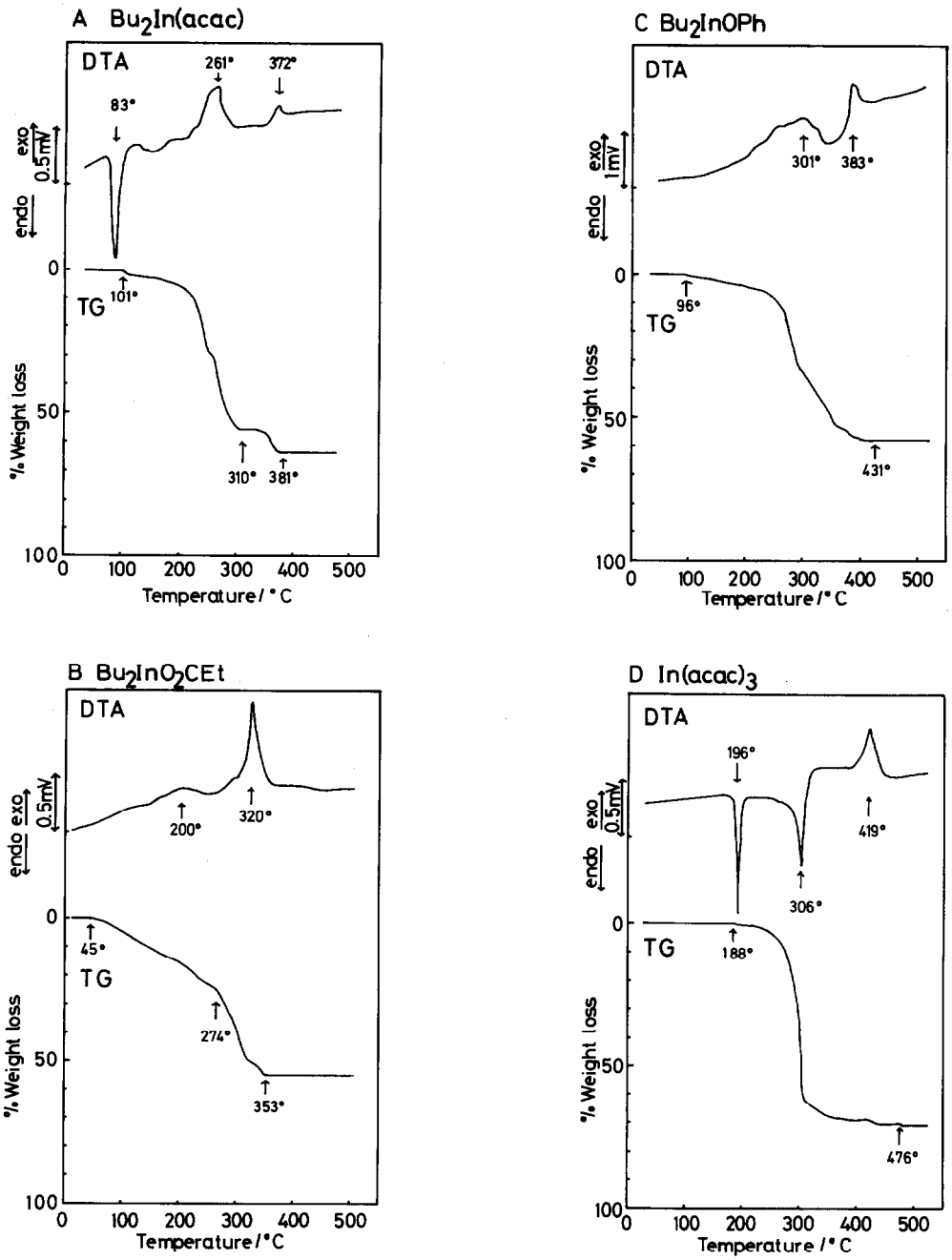

Fig. 1. Thermograms of organoindium compounds: (A) $Bu_2In(acac)$, (B) $Bu_2In(O_2CEt)$, (C) $Bu_2In(OPh)$, and (D) $In(acac)_3$.

weight loss again started exothermically at 350°C and finally ended at 381°C, followed by indium metal deposition. In general, because of the insufficiency of oxygen, organoindium derivatives employed here often gave an oxygen-deficient indium oxide or indium metal via pyrolysis under an inert atmosphere. In the decomposition of $Bu_2In(acac)$, a trace of carbon contamination derived from butyl substituents might catalyse the reduction of the resulting indium oxide. However, it is important that the temperature for decomposition into In_2O_3 was about 100°C lower than that of $In(acac)_3$.

$Bu_2In(O_2CEt)$ *and* $Bu_2In[O_2CCH(Et)(CH_2)_3CH_3]$

These acylates did not give indium metal on thermal decomposition. The main decomposition processes are also exothermic, but the exothermic DTA peaks shifted to a higher temperature compared to

$Bu_2In(acac)$. Especially for $Bu_2In(O_2CEt)$, a significant weight loss was observed over a wide range of temperature, 45–353°C. Although a clear inflection point was present at 274°C in the TG curve, where the total weight loss could be read as 23.3%, the weight loss could not be correlated with the simple liberation of any individual substituent. In addition, the controlled degradation experiment of $Bu_2In(O_2CEt)$ at 250°C for 1 h under N_2 gave *ca* 30% of butyl propionate.

Hence, the thermal decomposition of $Bu_2In(O_2CEt)$ evidently proceeded via a complex process, such as the combination of free-radical elimination of the butyl group bonded to central indium atoms to give alkanes, hydride transfer to afford alkenes as in the thermal decomposition of indium trialkyls,[15,16] and reductive-elimination to form butyl propionate. As shown in TG and DTA, dibutylindium 2-ethylhexanoate, possessing a long carbon chain, behaved rather similarly to $Bu_2In(acac)$ and no weight loss far below the m.p. was detected.

$Bu_2In(OR)$ (R = Bu^t *and* Ph)

The thermal behaviour of $Bu_2In(OBu^t)$ could not be investigated in detail because it vaporized above 330°C. An exothermic peak at 280°C was observed, which indicated that the dibutylindium *tert*-butoxide was partially decomposed. In the case of the phenoxide, two exothermic peaks at 301 and 383°C were observed. Thus, the decomposition process could be divided into two steps. In the former step, $Bu_2In(OPh)$ lost two butyl groups and, in the latter, the Ph group was formally liberated, based on % weight loss observation. Thus, $Bu_2In(OPh)$ can be said to be thermally the most stable of the organoindium compounds employed here.

Preparation of ITO films and their resistivities

In this study, we selected Bu_2SnO as a source of tin dopant, because of its high reactivities to active hydrogen compounds[17] and towards other organometallics to give Sn—O—metal bonds on heating.[18] Thus, we expected that if indium alkoxide or indium hydroxide were formed in the primary pyrolysis of organoindium compounds,[19] an In—O—Sn linkage or even network could be easily afforded by disproportionation with dibutyltin oxide. The formation of an In—O—Sn linkage disperses Sn moieties uniformly over the indium oxide layers. Results of the preparation of ITO films when the ITO solution in *p*-xylene was heated at 120°C for 40 min and baked at 450°C for 1 h are summarized in Table 3.

Clear and transparent ITO films were obtained by using dibutylindium acylates or acetylacetonate. Volatile $Bu_2In(OBu^t)$ gave no film and relatively stable $Bu_2In(OPh)$ afford opaque and highly resistive films. in contrast, dibutylindium acylates yielded highly conductive films: in the lower end of the order of 10^{-3} Ω cm. The temperature dependency of the ITO film resistivities was further investigated using the octanoate, which afforded the most conductive ITO films. The resistivity reached

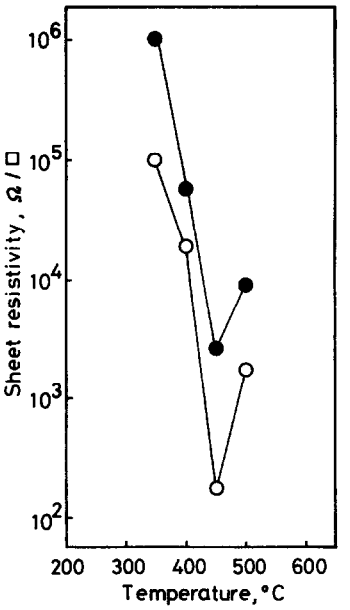

Fig. 2. Relation between sheet resistivities of ITO films prepared from $Bu_2In(O_2CCH(Et)(CH_2)_3CH_3)$ with or without Bu_2SnO and baking temperature; solvent was *p*-xylene and the dibutylindium octanoate concentration was kept at 5 wt %. The Bu_2SnO content varied between 0 (●) and 2 wt % (○), with respect to the indium compounds.

Table 3. Resistivity of ITO films prepared from dibutylindium compounds and dibutyltin oxide[ab]

Bu_2InX X	Film thickness (Å)	Resistivity (Ω cm)	Appearance
OBu^t	—	$> 10^2$	—
OPh	2000	$> 10^2$	Opaque
acac	3100	7.1×10^{-1}	Clear
O_2CEt	860	3.5×10^{-3}	Clear
O_2CC_7[c]	1400	1.9×10^{-3}	Clear

[a] ITO solution composition: solvent, *p*-xylene; organoindium compounds, 5 wt %; Bu_2SnO as dopant, 0.25 wt %.

[b] Conditions of ITO film preparation: 100°C, 40 min; 450°C, 1 h.

[c] 2-Ethylhexanoate.

a minimum at 450°C and then increased with rise in temperature. In chemical pyrolysis, the resistivity has been reported generally to decrease with temperature till 600°C.[6] An increase in resistivity with rising temperature above 450°C resulted from the partial reduction of deposited In_2O_3 derived from the organoindium compounds into indium metal or oxygen-deficient indium oxides.

In conclusion, the organoindium compounds containing at least one In—O bond are thermally unstable relative to the corresponding metallo-organics. Thus, the chemical pyrolysis of the organoindium compounds could give highly conductive ITO films even at 400–450°C.

Acknowledgement—Financial support from the Ministry of Education, Japanese Government, is gratefully acknowledged.

REFERENCES

1. D. G. Tuck, In *Comprehensive Organometallic Chemistry* (Edited by G. Wilkinson), Vol. 1, Chap. 7. Pergamon Press, Oxford (1982).
2. R. J. M. Griffiths, *Chem. Ind. (London)* 1985, 247.
3. K. L. Chopra, S. Major and D. K. Pandya, *Thin Solid Films* 1983, **102**, 1.
4. S. Ogihara and K. Kinugawa, *Yogyo-Kyokai-Shi* 1982, **90**, 157 (*CA* 1982, **96**, 227205b).
5. L. A. Ryabova, *Thin Solid Films* 1982, **92**, 327; *Izv. Akad. Nauk SSSR, Neorg. Mater.* 1980, **16**, 1120.
6. A. Tsunashima, T. Asai, K. Kodaira and T. Matsushita, *Chem. Lett.* 1978, 855.
7. K. Miyazawa, *Jpn Kokai* 79 164284 (*CA* 1980, **92**, 207767a).
8. H. Dislich, *Glastech. Ber.* 1984, **57**, 229.
9. Mitsubishi Metal Corp. *Jpn. Kokai* 84 198606 (*CA* 1984, **102**, 158989p).
10. P. J. Barker and J. N. Winter, In *The Chemistry of Metal–Carbon Bonds* (Edited by F. R. Hartley and S. Patai), Vol. 2, Chap. 3. John Wiley, New York (1985); M. E. O'Neil and K. Wade, In *Comprehensive Organometallic Chemistry* (Edited by G. Wilkinson), Vol. 1, pp. 5–8. Pergamon Press, Oxford (1982).
11. F. Runge, W. Zimmermann, H. Pfeiffer and I. Pfeiffer, *Z. Anorg. Allg. Chem.* 1951, **267**, 39.
12. H. Raymond and J.-P. Laurent, *Bull. Soc. Chim. Fr.* 1966, 3454.
13. H. C. Clark and A. L. Pickard, *J. Organomet. Chem.* 1967, **8**, 427.
14. J. J. Habeeb and D. G. Pickard, *Inorg. Synth.* 1979, **19**, 261.
15. N. N. Travkin, B. K. Shachkov, I. G. Tonoyan and B. I. Kozyrkin, *Zh. Obshch. Khim.* 1978, **48**, 2678; *J. Gen. Chem. U.S.S.R.* 1979, **48**, 2428.
16. Yu. A. Aleksandrov, O. N. Druzhkov, Yu. Yu. Baryshnikov, T. K. Postnikova, G. I. Makin and B. I. Kozyrkin, *Zh. Obshch. Khim.* 1980, **50**, 2642; *J. Gen. Chem. U.S.S.R.* 1981, **50**, 2129.
17. B. J. Aylett, *Organometallic Compounds*, 4th Edn, p. 221. Chapman & Hall, London (1979); A. G. Davies and P. J. Smith, In *Comprehensive Organometallic Chemistry* (Edited by G. Wilkinson), Vol. 2, pp. 551, 564 and 578–581. Pergamon Press, Oxford (1982).
18. A. G. Davies and P. G. Harrison, *J. Organomet. Chem.* 1967, **10**, 31; A. G. Davies, P. G. Harrison and P. R. Polan, *ibid.* 1967, **10**, 33; H. Matsuda, F. Mori, A. Kashiwa and S. Matsuda, *ibid.* 1972, **34**, 341.
19. C. F. Cullis, A. Fish and R. T. Pollard, *Trans. Faraday Soc.* 1964, **60**, 2224.

Polyhedron Vol. 6, No. 3, pp. 513–517, 1987
Printed in Great Britain

0277–5387/87 $3.00+.00

SYNTHESES AND PROPERTIES OF *STRATI-BIS* COPPER(II) COMPLEXES WITH $[N_2O_2]_2$ TYPE SCHIFF BASES

MASAAKI NAKAMURA,* TAKESHI MASUMOTO and FUMIAKI KAI

Department of Chemistry, Faculty of Science, Kumamoto University, Kumamoto 860, Japan

(*Received* 1 *May* 1986; *accepted* 29 *July* 1986)

Abstract—The new *"strati-bis"* Schiff base ligands, H_4(R,R′-sabzta), and their binuclear copper(II) complexes, Cu_2(R,R′-sabzta), were prepared and characterized, where H_4(R,R′-sabzta) denotes 1,2,3,4-tetrakis(R′-salicylideneamino)-2,3-bis(R-phenyl)butane (R = H or *p*-Cl; R′ = H, 5-Me or 5-Bu^t). No substantial differences in the electronic and ESR spectra were observed between these binuclear and the corresponding mononuclear copper(II) complexes. In each of those binuclear complexes, only one redox wave was observed at nearly the same potential as their corresponding mononuclear complexes. The redox wave was tentatively assigned to a total two-electron transfer process, Cu(II)–Cu(II) → Cu(I)–Cu(I), involving two one-electron reduction waves. These spectral and electrochemical properties of the binuclear complexes could be attributed to the two copper(II) ions not interacting through the intramolecular π–π stacking of the two metal coordination planes.

"*Strati-bis*" binuclear complexes in which the two metal coordination planes are held in a face-to-face manner by flexible or non-flexible linkages have been investigated as model systems for the active sites of some biological bimetal systems.[1–3] It has been mainly focused on bis(porphyrin) metal complexes, whereas studies on the metal complexes with Schiff bases are few in number.

Previously, Ōkawa *et al.*[4–8] reported the syntheses and characterization of *strati-bis* Schiff base ligands, 1,2,3,4-tetrakis(R′-salicylideneamino)-2,3-dimethylbutane [H_4(R′-sata)] and 1,2-bis(R′-salicylideneamino)-1,2-bis(R′-salicylideneaminomethyl)-cyclohexane [H_4(R′-sacta)] (R′ are the substituents on salicylaldehyde), and their binuclear metal complexes. The metal ions in these complexes are held in the "salen-like" donation site [H_2(salen) = 1,2-bis(salicylideneamino)ethane] and their two [MN_2O_2] coordination planes can be stacked in a face-to-face manner in solution. The stacked species of these complexes showed the unique properties in contrast with the corresponding mononuclear complexes. The most striking characteristics of the species are the facile reduction to the mixed valence [M(II)–M(I) or M(III)–M(II)] complexes and considerable stabilization of these reduced species. This can be rationalized in terms of the electron delocalization over the whole molecule by the π–π stacking of the two metal coordination planes.

In this study, the new *strati-bis* Schiff base ligands which contain the aromatic rings as the substituents on the tetraamine moiety, 1,2,3,4-tetrakis(R′-salicylideneamino)-2,3-diphenylbutane [H_4(R′-sabzta)] and 1,2,3,4-tetrakis(R′-salicylideneamino-2,3-bis-(4-chlorophenyl)butane [H_4(*p*-Cl,R′-sabzta)] (R′ are the substituents on the salicylaldehyde), and their binuclear copper(II) complexes were prepared and characterized. The structures of these ligands are given in Fig. 1. Each ligand has also two "salen-like" donating sites which are linked to each other making a bond between carbon atoms of the ethylenediamine moieties. It is expected in the present complexes that the two metal coordination planes would be stacked in a face-to-face manner and the two aromatic rings at the tetraamine moiety stacked to each other by molecular model considerations. The spectroscopic and redox properties of those complexes were investigated in connection with the effects of the introduced aromatic rings on the π–π stacking between the two metal coordination planes.

* Author to whom correspondence should be addressed.

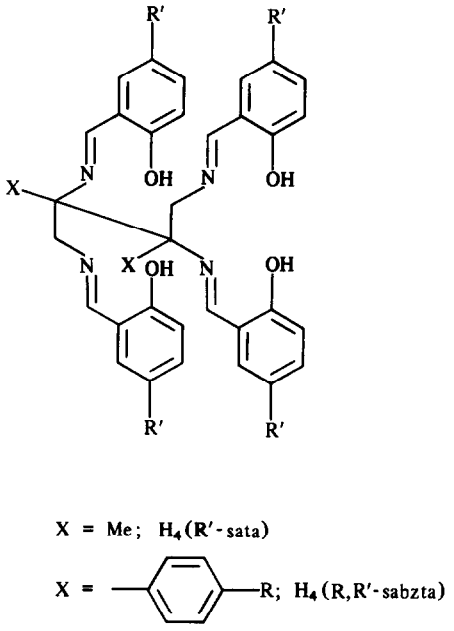

Fig. 1. Chemical structures of H_4(R'-sata) and H_4(R,R'-sabzta).

EXPERIMENTAL

Synthesis

1,2-Bis(4-chlorophenyl)ethanedione was prepared by the method described in the literature.[9] 1,2,3,4-Tetraamino-2,3-diphenylbutane and 1,2,3,4-tetraamino-2,3-bis(4-chlorophenyl)butane were synthesized in nearly the same way as 1,2,3,4-tetraamino-2,3-dimethylbutane[4] from 1,2-diphenylethanedione and 1,2-bis(4-chlorophenyl)ethanedione, respectively. 5-Methyl- and 5-*t*-butylsalicylaldehyde were prepared by the formylation (Duff's reaction)[10] of 4-methyl- and 4-*t*-butylphenol, respectively. The binucleating ligands, H_4(R,R'-sabzta) (R = H or *p*-Cl; R' = H, 5-Me or 5-Bu^t), were prepared by the condensation of the tetraamine and salicylaldehyde or its derivatives in ethanol in a 1 : 4 mole ratio.

Cu_2(sabzta). Copper(II) acetate monohydrate (1.44 mmol) and H_4(sabzta) (0.72 mmol) were suspended in absolute ethanol (20 cm^3) and the mixture was refluxed for 4 h. A purple crystalline powder formed was collected. The product was recrystallized from a chloroform–ethanol mixture. Found: C, 63.1; H, 4.3; N, 6.6%. Calc. for $C_{44}H_{34}N_4O_4Cu_2 \cdot \frac{3}{2}H_2O$: C, 63.2; H, 4.5; N, 6.7%.

Cu_2(5-Me-sabzta). Copper(II) acetate monohydrate (1.92 mmol) and H_4(5-Me-sabzta) (0.96 mmol) were suspended in absolute ethanol (20 cm^3) and the mixture was refluxed for 4 h. The green crystalline powder precipitated was collected and washed with a small amount of ethanol, the product was dissolved in chloroform and the solution was passed through a silica gel column (3 × 15 cm). The eluant was concentrated to *ca* 5 cm^3 and allowed to stand overnight at room temperature to give Cu_2(5-Me-sabzta) as a purple crystalline powder. Found: C, 65.0; H, 5.0; N, 6.1%. Calc. for $C_{48}H_{42}N_4O_4Cu_2 \cdot H_2O$: C, 65.2; H, 5.0; N, 6.3%.

Cu_2(5-Bu^t-sabzta). A mixture of copper(II) acetate monohydrate (1.92 mmol), H_4(5-Bu^t-sabzta) (0.96 mmol), and triethylamine (3.84 mmol) in absolute ethanol (20 cm^3) was refluxed for 3 h. The purple powder precipitated was collected. The purple crystal was obtained by recrystallization of the crude product from ethanol–chloroform. Found: C, 68.4; H, 7.0; N, 5.0%. Calc. for $C_{60}H_{60}N_4O_4Cu_2 \cdot 2C_2H_5OH$: C, 68.2; H, 7.0; N, 5.0%.

Cu_2(*p*-Cl-sabzta). This complex was obtained as a purple crystalline powder by reacting copper(II) acetate monohydrate (2.06 mmol) and H_4(*p*-Cl-sabzta) (1.03 mmol) in absolute ethanol (20 cm^3) in a way similar to that for Cu_2(5-Me-sabzta). Found: C, 53.6; H, 3.6; N, 5.4%. Calc. for $C_{44}H_{32}N_4O_4Cl_2Cu_2 \cdot CHCl_3 \cdot \frac{1}{2}H_2O$: C, 53.7; H, 3.4; N, 5.6%.

Cu_2(*p*-Cl,5-Me-sabzta). This complex was also obtained as a purple crystalline powder by reacting copper(II) acetate monohydrate (2.06 mmol) and H_4(*p*-Cl,5-Me-sabzta) (1.03 mmol) in absolute ethanol (20 cm^3) in a way similar to that for Cu_2(5-Me-sabzta). Found: C, 61.5; H, 4.5; N, 5.8%. Calc. for $C_{48}H_{40}N_4O_4Cl_2Cu_2$: C, 61.7; H, 4.3; N, 6.0%.

The mononuclear copper(II) complexes, Cu(R,R'-sabzen) (R = H or *p*-Cl, R' = H or 5-Me), were synthesized by the method described in the literature.[11]

Measurements

IR spectra were recorded on a JASCO IRA-1 grating spectrometer on a KBr disk. ^{1}H NMR spectra were recorded on a Hitachi–Perkin–Elmer R-24 spectrometer with tetramethylsilane as the internal reference. Electronic spectra were recorded on a Hitachi 220 A recording spectrophotometer in dichloromethane. Polarograms were recorded on a Yanagimoto voltammetric analyzer Model P-1000 in dichloromethane containing 0.1 mol dm^{-3} tetrabutylammonium perchlorate (TBAP) as the supporting electrolyte. A three-electrode cell was used for measurements, in which the working electrode is a dropping mercury electrode or a glassy carbon, and the auxiliary electrode a platinum coil. A saturated calomel electrode (SCE) was used as the reference electrode. In practice, instead of the reference

electrode an internal standard, the ferrocene–ferricinium(1+) couple, was utilized.[12] ESR spectra were measured with a JES-FE3X ESR instrument in frozen chloroform solutions near liquid-nitrogen temperature and at room temperature.

RESULTS AND DISCUSSION

The synthesis of new tetraamines, 1,2,3,4-tetraamino-2,3-diphenylbutane and 1,2,3,4-tetraamino-2,3-bis(4-chlorophenyl)butane, were carried out in the way similar to that for 1,2,3,4-tetraamino-2,3-dimethylbutane.[4,5] In these processes, each diaminodinitrile, 1,2-dicyano-1,2-diphenyl-1,2-ethanediamine and 1,2-dicyano-1,2-bis(4-chlorophenyl)-1,2-ethanediamine, gave two isomers which can be attributed to two geometrical isomers (*meso*- and *dl*-); one is liquid and the other is solid. The presence of two products of diaminodinitrile is similar to the case of 2,3-dicyano-2,3-butanediamine.[4,5] In this study, the solid product can be attributed to the *dl*-isomer by comparing with the case of the previous reports[4,5] which used $LiAlH_4$ reduction. In Fig. 1, the structures of the binucleating ligands H_4(R′-sata) and H_4(R,R′-sabzta) of the *dl*-tetraamines are shown.

The IR spectra of these complexes showed strong absorption bands at 1625–1628 and 1530–1535 cm^{-1} which could be assigned to a stretching vibration of the azomethine moiety and a skeletal vibration of the aromatic ring of the ligands, respectively. The frequencies of these characteristic bands are similar to those of the corresponding mononuclear copper(II) complexes, Cu(R,R′-sabzen) [R = H or *p*-Cl, R′ = H or 5-Me, H_2(R,R′-sabzen) = 1-(R-phenyl)-1,2-bis(R′-salicylidene amino)ethane], and other copper(II) complexes with "salen" type ligands.

Electronic spectra of the complexes obtained were measured in dichloromethane. The results are given in Table 1 and the spectrum of Cu_2(sabzta) is shown as an example in Fig. 2, together with the spectrum of Cu(sabzen). The absorption bands which can be assigned to a *d–d* transition of the central copper(II) ion are observed near 17,000 cm^{-1} with no substantial change in the frequency and the intensity between the binuclear and mononuclear complexes. This implies that the copper(II) ions of the binuclear complexes, as well as the mononuclear complexes, have a square planar configuration involving a $[CuN_2O_2]$ chromophore as already demonstrated for Cu(salen).[13] The bands near 27,000 cm^{-1} can be assigned to the π–π^* trans-

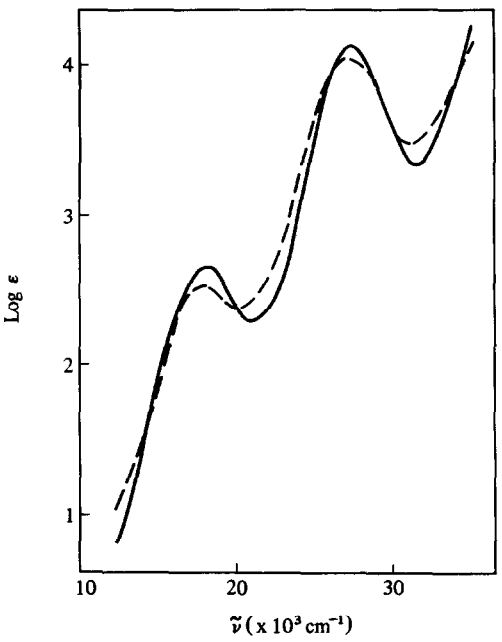

Fig. 2. Electronic spectra of: (——) Cu_2(sabzta), and (– – –) Cu(sabzen) in dichloromethane.

Table 1. Electronic spectral data for the complexes

Complex	$\tilde{\nu}_{max}$ ($\times 10^3$ cm^{-1}) (ε)	
	d–d	π–π^*
Cu_2(sabzta)	17.6 (422)	27.2 (13,000)
Cu(sabzen)	17.6 (325)	27.1 (11,400)
Cu_2(5-Me-sabzta)	18.0 (322)	26.3 (12,200)
Cu(5-Me-sabzen)	17.7 (338)	26.3 (10,800)
Cu_2(5-Bu′-sabzta)	17.7 (457)	26.5 (12,200)
Cu_2(*p*-Cl-sabzta)	17.6 (391)	27.0 (12,000)
Cu(*p*-Cl-sabzen)	17.6 (416)	27.0 (12,600)
Cu_2(*p*-Cl,5-Me-sabzta)	17.6 (431)	26.2 (12,400)
Cu(*p*-Cl,5-Me-sabzen)	17.6 (423)	26.5 (11,800)

Table 2. ESR parameters of the complexes

Complex	g_{av}	A_{av} (G)	$g_{\parallel}$	$A_{\parallel}$ (G)
Cu_2(sabzta)	2.11	91.1	2.18	203
Cu(sabzen)	2.11	84.4	2.17	206
Cu_2(5-Me-sabzta)	2.08	91.1	2.17	206
Cu(5-Me-sabzen)	2.11	83.9	2.18	200
Cu_2(5-Bu′-sabzta)	2.11	78.8	2.20	199
Cu_2(*p*-Cl-sabzta)	2.11	88.3	2.17	201
Cu(*p*-Cl-sabzen)	2.11	87.8	2.18	200
Cu_2(*p*-Cl,5-Me-sabzta)	2.12	89.4	2.17	204
Cu(*p*-Cl,5-Me-sabzen)	2.10	90.0	2.17	204

Table 3. Polarographic data of the complexes

Complex	$E_{1/2}$ (DME) (V vs E_{Fc-Fc^+})[a]	Slope (mV)	$E_{1/2}$ (GCE) (V vs E_{Fc-Fc^+})
Cu_2(sabzta)	−1.72	43	−1.73
Cu(sabzen)	−1.71	44	−1.69
Cu_2(5-Me-sabzta)	−1.79	42	−1.81
Cu(5-Me-sabzen)	−1.82	48	−1.78
Cu_2(*p*-Cl-sabzta)	−1.74	39	−1.73
Cu(*p*-Cl-sabzen)	−1.72	44	−1.71
Cu_2(*p*-Cl,5-Me-sabzta)	−1.78	46	−1.79
Cu(*p*-Cl,5-Me-sabzen)	−1.77	46	−1.75

[a] E_{Fc-Fc^+} is the oxidation potential of the ferrocene–ferricinium couple.

ition involving the azomethine π-character.[14] It is observed that there is no appreciable difference in the frequency between the bands of Cu(salpn) [H_2(salpn) = 1,2-bis(salicylideneamino)propane] (27,250 cm^{-1})[4] and Cu(R-sabzen) (27,000–27,100 cm^{-1}). This suggests that the substitution of a methyl group for aromatic rings at the ethylenediamine moiety of the ligands does not affect the electronic states of the azomethine moiety. Furthermore, the binuclear copper(II) complexes also showed the π–π^* transition band at essentially the same frequency as the mononuclear complexes, which implies the absence of appreciable π–π interaction between the two [CuN_2O_2] coordination planes of these complexes.

ESR spectra of the complexes obtained were measured at room and liquid-nitrogen temperature in chloroform solution, and the results are given in Table 2. All the spectra have the four-line hyperfine structure at both temperatures and a typical axial pattern ($g_\parallel > g_\perp$) at liquid-nitrogen temperature. These results suggest that the geometry around the copper(II) ions of the present binuclear complexes is almost the same as that of the mononuclear complexes and the intra- and intermolecular magnetic interaction between the copper(II) ions of the binuclear complexes are negligible.

Redox properties of the complexes obtained were examined by DC and differential-pulse polarography in dichloromethane containing 0.1 mol dm^{-3} TBAP as a supporting electrolyte. The differential-pulse polarograms were recorded by a dropping mercury electrode (DME) and a glassy carbon electrode (GCE). In Table 3, the half-wave potential and the slope of the potential vs log $(i/i_d - i)$ plot are given. The wave observed around −1.7 vs E_{Fc-Fc^+} in the mononuclear complexes is assigned to a quasi-reversible one-electron transfer process, Cu(II) → Cu(I), on the basis of their potentials and slopes (44–48 mV). On the other hand, only one redox wave was observed in the binuclear complexes at essentially the same potential as their corresponding mononuclear complexes. These redox waves can be also attributed to an apparent quasi-reversible one-electron transfer process, judging from the results of the standard polarographic plot of potential vs log $(i/i_d - i)$. The electrochemical properties of the present binuclear complexes resembled closely those of Cu_2(5-Me-sata) and Cu_2(5-Bu^t-sata),[4,5] in which the Cu(II)–Cu(II) species are reduced to Cu(I)–Cu(I) species by two simultaneous monoelectronic steps at nearly the same potential as those of the corresponding mononuclear complexes. From the resemblance of the electrochemical properties between Cu_2(R,R′-sabzta) and Cu_2(R′-sata), it is concluded that the apparent one-electron reduction wave for the former complexes can be assigned to a total two-electron transfer involving two one-electron reduction waves at the same potential. The results indicated that the two [CuN_2O_2] chromophores of the present binuclear complexes do not interact each other. This can be attributed to the steric hindrance of aromatic rings as substituents on the tetraamine moiety.

Acknowledgements—We wish to express our thanks to Professor Sigeo Kida and Associate Professor Hisashi Ōkawa of Kyushu University for help in obtaining the ESR and electrochemical data.

REFERENCES

1. N. E. Kagan, D. Mauzerall and R. B. Merrifield, *J. Am. Chem. Soc.* 1977, **99**, 5484.
2. M. R. Wasielewski, W. A. Svec and B. T. Cope, *J. Am. Chem. Soc.* 1978, **100**, 1961.

3. H. Ogoshi, H. Sugimoto and Z. Yoshida, *Tetrahedron Lett.* 1977, 169.
4. T. Izumitani, M. Nakamura, H. Ōkawa and S. Kida, *Bull. Chem. Soc. Jpn* 1982, **55**, 2122.
5. H. Ōkawa, M. Kakimoto, T. Izumitani, M. Nakamura and S. Kida, *Bull. Chem. Soc. Jpn* 1983, **56**, 149.
6. M. Nakamura, H. Ōkawa and S. Kida, *Inorg. Chim. Acta* 1983, **75**, 9.
7. M. Nakamura, *Bull. Chem. Soc. Jpn* 1983, **56**, 2529.
8. H. Ōkawa, A. Honda, M. Nakamura and S. Kida, *J. Chem. Soc., Dalton Trans.* 1985, 59.
9. H. T. Clarke and E. E. Dreger, *Organic Synthesis Colloquium*, 2nd Edn, Vol. 1, p. 87. Wiley, New York (1956).
10. J. C. Duff, *J. Chem. Soc.* 1941, 547.
11. S. Maeda, M. Nakamura, T. Shinmyouzu, H. Ōkawa and S. Kida, *Mem. Fac. Sci., Kyushu Univ., Ser. C* 1985, **15**, 71.
12. R. R. Gagné, C. A. Koval and G. C. Lisensky, *Inorg. Chem.* 1980, **19**, 2885.
13. E. N. Baker, D. Hall and T. N. Waters, *J. Chem. Soc. A* 1970, 406.
14. R. S. Dowing and F. L. Urback, *J. Am. Chem. Soc.* 1969, **91**, 5977.

Polyhedron Vol. 6, No. 3, pp. 519–524, 1987
Printed in Great Britain

0277–5387/87 $3.00+.00

CHARGE-TRANSFER ABSORPTION SPECTRA OF SOME TUNGSTEN(VI) AND MOLYBDENUM(VI) POLYOXOANIONS

KENJI NOMIYA, YOSHINOBU SUGIE, KOICHI AMIMOTO and MAKOTO MIWA*

Department of Industrial Chemistry, Faculty of Engineering, Seikei University, Musashino, Tokyo 180, Japan

(*Received* 7 *April* 1986; *accepted* 29 *July* 1986)

Abstract—The charge-transfer (CT) absorption spectra in the UV region (30,000–50,000 cm^{-1}) of most W(VI) and Mo(VI) polyoxoanions, attributed to the oxygen-to-metal transitions, are interpreted on the basis of structural considerations through edge- and/or corner-sharings of some octahedral units. Polyoxoanions studied here are classified into two groups according to a common fragment constituting their structures; one group contains an 'M_5O_{18}' fragment [M = W(VI) and Mo(VI)] such as Weakley-type $[Ce(IV)(W_5O_{18})_2]^{8-}$ anion, $[W_{10}O_{32}]^{4-}$ and $[M'W_5O_{19}]^{n-}$ [M′ = V(V), Nb(V), W(VI)] polyanions and the other contains an A-α-'XM_9O_{34}' fragment (X = heteroatom) such as Keggin-type $[\alpha\text{-}XM_{12}O_{40}]^{n-}$ and Dawson-type $[\alpha\text{-}P_2M_{18}O_{62}]^{6-}$ heteropolyanions. The first- and second-lowest energy CT (LECT) bands of the respective group are qualitatively discussed from the CT interactions among some fragments.

UV absorption spectra of most polyoxometalates (hetero- and isopolyanions of W and Mo) have been attributed to the charge-transfer (CT) transitions of oxygens to W(VI) and Mo(VI). In the polyoxometalates, there exists two or three chromophores due to the bonding with metal ion of unshared (terminal) oxygens, edge- and/or corner-shared oxygens. The bonding between terminal oxygen and metal ion possesses greater double-bond character and its CT transition appears usually in the highest energy region (> 40,000 cm^{-1}). The absorptions due to the other chromophores are seen in the lower energy region. This is assumed from the facts that new absorption bands due to the formation of M—O—M bridges are observed in the 30,000–40,000 cm^{-1} region as well as the absorption maximum in the higher energy region by acidifying the aqueous solution of molybdate and tungstate.[1] Although such spectra should be significantly related to the structural feature through edge- and/or corner-sharings of octahedral units, a rational interpretation involving origins of the first- and second-lowest energy charge-transfer (LECT) bands has not yet been given.[2] The purpose of this work is to provide an interpretation of the CT absorption spectral data of some polyoxometalates on the basis of structural considerations. We here assume that the formation of polyanion from some fragments and some octahedral units results from a stabilization by edge- and/or corner-sharing interaction between building blocks 'A' (HOMO) and 'B' (LUMO), where the HOMO level of 'A' has an oxygen character and the LUMO one of 'B' has a metal character. In this approach, the LECT bands are qualitatively understood from a CT interaction between the HOMO and the LUMO levels. Using a similar model, Madic *et al.*[3] have recently explained the origin of the red colour of the vanadium(V) dimer. Applying the model to our absorption spectral data of some W(VI) and Mo(VI) polyoxometalates, it is convenient to abstract a building block 'A' as a common fragment constituting their structures. From the structural considerations as shown in Figs 1 and 2,[4] two fragments are selected as such for 'A'; one is 'M_5O_{18}' (M = W, Mo) for Weakley-type $[Ce(IV)(W_5O_{18})_2]^{8-}$, $[W_{10}O_{32}]^{4-}$ and $[M'W_5O_{19}]^{n-}$ (M′ = V, Nb, W) polyoxoanions and the other A-α-'XM_9O_{34}' (X = heteroatom) for Keggin and Dawson α-heteropolyanions.

* Author to whom correspondence should be addressed.

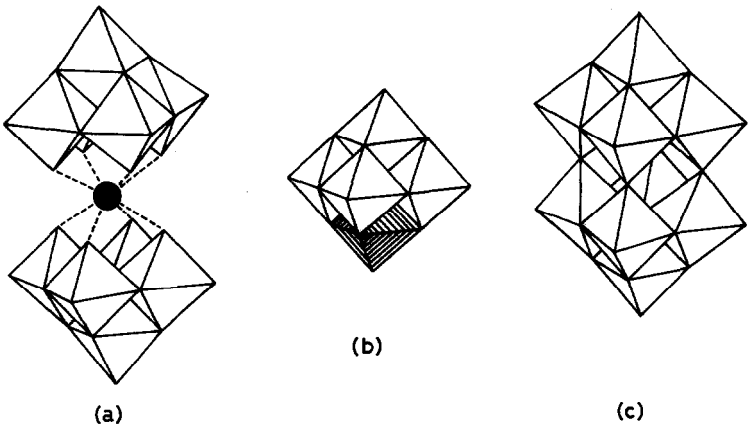

Fig. 1. Polyhedral models of polyanion-group containing 'M_5O_{18}' fragment; Weakley-type $[X(W_5O_{18})_2]^{n-}$ polyanion (a), $[M'M_5O_{19}]^{n-}$ polyanion (b) and $[W_{10}O_{32}]^{4-}$ isopolyanion (c). In (a), central filled circle shows the X (rare-earth) atom and the geometry around it is square antiprismatic. Each of two 'W_5O_{18}' fragments coordinates to X atom as a quadridentate ligand. In (b), a shaded octahedron represents a substituting M′ atom (V, Mo, W, Nb and so on) and the residual part corresponds to the 'W_5O_{18}' fragment (M = W and Mo). In (c), two 'W_5O_{18}' fragments are linked by corner-sharings to D_{4h} symmetry.

EXPERIMENTAL

Measurements

UV absorption spectra were measured by a Hitachi 340-spectrophotometer with a computer keyboard attached. Solvents were acetonitrile distilled before use for tetrabutylammonium (TBA) salt and redistilled water for some lacunary species. IR spectra were recorded with a JASCO IR-G spectrophotometer. All measurements were made at room temperature.

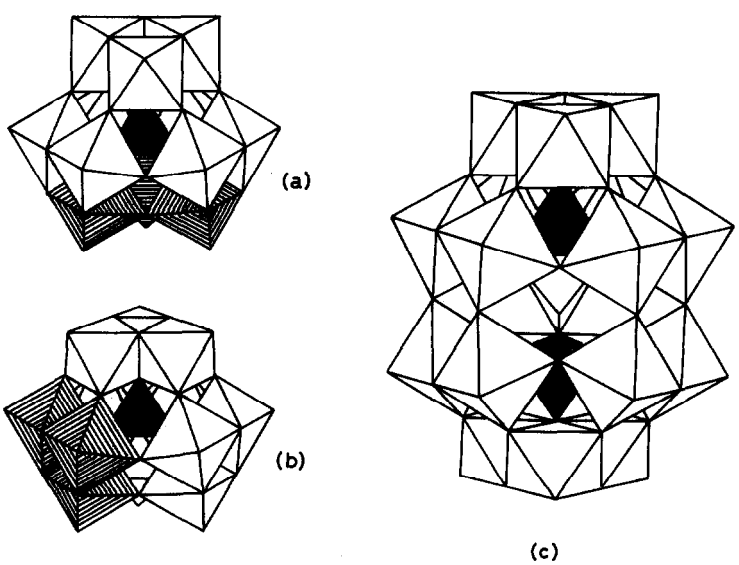

Fig. 2. Polyhedral models of polyanion-group containing 'XM_9O_{34}' fragment; Keggin $[\alpha\text{-}XM_{12}O_{40}]^{n-}$ (a), Keggin $[\beta\text{-}XM_{12}O_{40}]^{n-}$ (b) and Dawson $[\alpha\text{-}X_2M_{18}O_{62}]^{6-}$ (c) heteropolyanions. Central filled tetrahedra show the heteroatom X. In (a), the residual part other than three shaded octahedra corresponds to A-α-'XM_9O_{34}' fragment. In (b), upper M_3O_{13} unit rotates 60° with respect to the Keggin α-structure. The residual part other than shaded M_3O_{13} unit corresponds to B-β-'XM_9O_{34}' fragment. The notation of α and β of the 'XM_9O_{34}' is based on the parent Keggin structure and that of A and B is based on the positions of three octahedra removed. In (c), two A-α-'XM_9O_{34}' fragments are linked by corner-sharings to D_{3h} symmetry.

Table 1. Analytical results

Formula	Found (%)			Calc. (%)		
	C	H	N	C	H	N
$[(C_4H_9)_4N]_4[W_{10}O_{32}]$	23.0	4.5	1.8	23.2	4.4	1.7
$[(C_4H_9)_4N]_2[W_6O_{19}]$	20.3	3.9	1.5	20.3	3.8	1.5
$[(C_4H_9)_4N]_2[Mo_6O_{19}]$	28.2	5.4	2.1	28.2	5.3	2.1
$[(C_4H_9)_4N]_6[\alpha\text{-}P_2W_{18}O_{62}]$	19.8	3.9	1.5	19.8	3.7	1.4
$[(C_4H_9)_4N]_5H[\alpha\text{-}P_2Mo_{18}O_{62}]$	23.8	4.8	1.8	24.1	4.6	1.8
$[(C_4H_9)_4N]_3[\alpha\text{-}PW_{12}O_{40}]$	15.9	3.0	1.1	16.0	3.0	1.2
$[(C_4H_9)_4N]_3[\alpha\text{-}PMo_{12}O_{40}]$	22.7	4.3	1.6	22.6	4.3	1.7
$[(C_4H_9)_4N]_4[\alpha\text{-}SiW_{12}O_{40}]$	20.0	3.6	1.4	20.0	3.8	1.5
$[(C_4H_9)_4N]_4[\beta\text{-}SiW_{12}O_{40}]$	20.1	3.6	1.4			
$[(C_4H_9)_4N]_4[\alpha\text{-}SiMo_{12}O_{40}]$	27.5	5.1	1.9	27.6	5.2	2.0
$[(C_4H_9)_4N]_3Na[\beta\text{-}SiMo_{12}O_{40}]$	22.7	4.2	1.6	22.4	4.2	1.6
$[(C_4H_9)_4N]_4[\alpha\text{-}GeW_{12}O_{40}]$	19.7	3.7	1.4	19.8	3.7	1.4
$[(C_4H_9)_4N]_4[\beta\text{-}GeW_{12}O_{40}]$	19.9	3.9	1.5			
$[(C_4H_9)_4N]_4[\alpha\text{-}GeMo_{12}O_{40}]$	27.1	5.0	2.0	27.1	5.1	2.0
$[(C_4H_9)_4N]_4[\beta\text{-}GeMo_{12}O_{40}]$	27.1	5.0	1.9			
$[(C_4H_9)_4N]_4K[\alpha\text{-}BW_{12}O_{40}]$	20.1	3.9	1.6	19.9	3.8	1.5

Preparations

The TBA salts of polyanions were prepared according to procedures previously described; $(TBA)_4[W_{10}O_{32}]$,[5] $(TBA)_2[M_6O_{19}]$ (M = W, Mo),[6] $(TBA)_6[\alpha\text{-}P_2W_{18}O_{62}]$,[6] $(TBA)_5H[\alpha\text{-}P_2Mo_{18}O_{62}]$,[6] $(TBA)_3[\alpha\text{-}PW_{12}O_{40}]$ (M = W, Mo),[7] $(TBA)_4[\alpha\text{-}SiM_{12}O_{40}]$ (M = W, Mo),[7] $(TBA)_4[\beta\text{-}SiW_{12}O_{40}]$,[7] $(TBA)_3Na[\beta\text{-}SiMo_{12}O_{40}]$,[7] $(TBA)_4[\alpha\text{-}GeM_{12}O_{40}]$ (M = W, Mo),[7] $(TBA)_4[\beta\text{-}GeM_{12}O_{40}]$ (M = W, Mo)[7] and $(TBA)_4K[\alpha\text{-}BW_{12}O_{40}]$.[7] They were isolated without any solvation. These compounds were identified by elemental analysis of the counterion part, shown in Table 1, and by comparison of the spectra (Table 2) with the already established IR spectra of the polyanion moiety.[5,8–11] Some lacunary species were also prepared according to the literature: $K_7[\alpha\text{-}PW_{11}O_{39}]\cdot 28H_2O$,[12] Na_3H_6

Table 2. Absorption spectral data in acetonitrile solution

Compound	Absorption maximum (cm^{-1}) (ε: $mol^{-1}\,dm^3\,cm^{-1}$)
$[W_{10}O_{32}]^{4-}$	30,800 (14,000), 38,000 (16,500), 45,700 (50,000)
$[W_6O_{19}]^{2-}$	31,300 (3400)sh, 36,200 (14,900), 47,600 (30,000)
$[Mo_6O_{19}]^{2-}$	30,800 (6600), 39,100 (13,100), 45,100 (22,000)
$[\alpha\text{-}P_2W_{18}O_{62}]^{6-}$	33,200 (32,500), 40,000 (52,000)
$[\alpha\text{-}P_2Mo_{18}O_{62}]^{6-}$	31,400 (21,700), 41,700 (109,000)sh
$[\alpha\text{-}PW_{12}O_{40}]^{3-}$	37,700 (45,700)
$[\alpha\text{-}PMo_{12}O_{40}]^{3-}$	32,300 (22,300)
$[\alpha\text{-}SiW_{12}O_{40}]^{4-}$	37,900 (50,900)
$[\beta\text{-}SiW_{12}O_{40}]^{4-}$	37,700 (35,200)
$[\alpha\text{-}SiMo_{12}O_{40}]^{4-}$	32,900 (19,500), 39,700 (49,300)sh
$[\beta\text{-}SiMo_{12}O_{40}]^{4-}$	32,900 (16,900)
$[\alpha\text{-}GeW_{12}O_{40}]^{4-}$	37,600 (46,900)
$[\beta\text{-}GeW_{12}O_{40}]^{4-}$	37,200 (29,600)
$[\alpha\text{-}GeMo_{12}O_{40}]^{4-}$	33,300 (19,200), 41,000 (61,200)sh
$[\beta\text{-}GeMo_{12}O_{40}]^{4-}$	33,000 (18,500)
$[\alpha\text{-}BW_{12}O_{40}]^{5-}$	39,100 (45,200)
$[PW_{11}O_{39}]^{7-}$	40,700 (46,200)[a]
$[A\text{-}\alpha\text{-}PMo_9O_{34}]^{9-}$	43,100 (52,600),[a] 48,000 (92,900)[a]
$[\beta\text{-}PW_9O_{34}]^{9-}$	40,000 (32,400)[a]

[a] In water.

$[A\text{-}\alpha\text{-}PMo_9O_{34}]\cdot 13H_2O$[13] and $Na_8H[B\text{-}\beta\text{-}PW_9O_{34}]\cdot 24H_2O$.[13]

RESULTS AND DISCUSSION

1. *Group containing* 'M_5O_{18}' *fragment*

The position and intensity of absorption maxima of this polyanion group are depicted as a bar graph in Fig. 3. The fragment 'M_5O_{18}' itself has not been found because of its instability. However, derivatives are seen as in the ligand of the Weakley-type polyanion $[X(W_5O_{18})_2]^{n-}$ (X = rare-earth metal ion), the $[W_{10}O_{32}]^{4-}$ isopolyanion resulting from corner-sharing between two 'W_5O_{18}' fragments and also the $[M'W_5O_{19}]$-type isopolyanion (M' = V, Mo, W, Nb and so on) from edge-sharing between 'W_5O_{18}' and '$M'O_6$' units.

For the UV spectrum in the aqueous media of the $[Ce(IV)(W_5O_{18})_2]^{8-}$ polyanion, we have previously assigned two CT bands of the ligand-to-Ce(IV) and the intra-ligand by MCD measurement.[14] The absorption maxima and intensities are 30,000 cm^{-1} (ε 5600) and 38,000 cm^{-1} (ε 19,000), respectively. In this polyanion, the geometry around the central Ce(IV) ion is square antiprismatic and two 'W_5O_{18}' ligands contribute independently to the intensity of the intra-ligand CT. On the other hand, the UV spectrum of $[W_{10}O_{32}]^{4-}$ polyanion, formed by the corner-sharings between two 'W_5O_{18}' units, shows three CT bands; 30,800 cm^{-1} (ε 14,000), 38,000 cm^{-1} (ε 16,500) and 45,700 cm^{-1} (ε 50,000). It should be noted that the position and intensity of the second LECT are very close to those of the intra-ligand CT of the Weakley polyanion. This indicates that the two half-units of the $[W_{10}O_{32}]^{4-}$ polyanion contribute independently to the second LECT. The first LECT band is a new absorption, which could not be seen in the 'W_5O_{18}' unit alone, and probably stems from an interaction between two identical fragments. When two 'W_5O_{18}' units approach in the manner that four oxygen-legs of each unit face each other and finally two sets of four legs coalesce into one, a large delocalization of charge through the corner-shared oxygens linking two units can be expected. This leads to the formation of stable $[W_{10}O_{32}]^{4-}$ polyanion and a new lower-energy CT becomes possible. Thus, the first LECT is considered to be a transition through such oxygens.

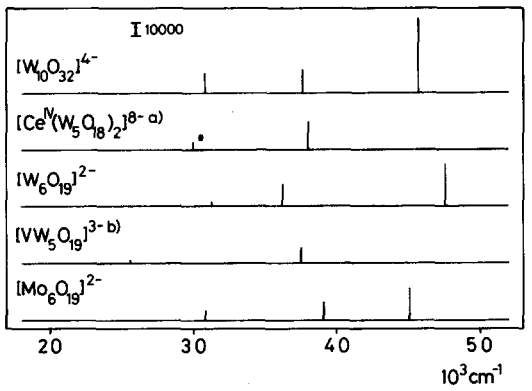

Fig. 3. Bar graphs of absorption maxima of a polyanion-group containing 'M_5O_{18}' (M = W and Mo) fragment. Height shows relative intensity and abscissa shows wavenumber. The data of (a) and (b) are reported in Refs 14 and 15, respectively. Asterisked peak indicates a CT band of ligand-to-Ce(IV).

Another way of stabilizing a 'W_5O_{18}' fragment is found in the formation of a $[M'W_5O_{19}]^{n-}$-type polyanion by edge-sharings between '$M'O_6$' and 'W_5O_{18}' units. In this polyanion-series, an intra-'W_5O_{18}' CT and new inter-CT transitions are expected. The absorption band of the former CT should appear near 38,000 cm^{-1} as observed in the intra-CT of Weakley polyanion and in the second LECT of $[W_{10}O_{32}]^{4-}$ isopolyanion. On the other hand, the band of the latter CT presumably depends strongly upon the electronegativity of M' atom, if it is assumed that the group overlap of edge-sharing interaction is unchanged by M' atom. The optical electronegativity χ of some M' atoms has been previously estimated by So and Pope;[2] χ = 2.7 for V(V), 2.5 for Mo(VI), 2.3 for W(VI) and 2.0 for Nb(V). In the Figs 4a–c, the HOMO–LUMO interaction models leading to the formation of $[M'W_5O_{19}]^{n-}$ polyanion are depicted. In Fig. 4a at least two inter-CT bands are possible in the lower energy region than the intra-CT band, while in Figs 4b and c at least one inter-CT band is expected. In the model of Fig. 4b, the inter-CT will shift to the higher energy region against the more electronegative M' atom, because the HOMO level of '$M'O_6$' becomes energetically lower.

The $[W_6O_{19}]^{2-}$ polyanion shows the first LECT as a weak and broad shoulder band at ~ 31,300 cm^{-1} (ε 3400) and the second LECT as a prominent band at 36,200 cm^{-1} (ε 14,900). Moreover, the first and second LECT measured in methanol solution of $[VW_5O_{19}]^{3-}$ polyanion, which contains the most electronegative V(V) atom substituted, are reported at 25,600 cm^{-1} (ε 2580) and 37,500 cm^{-1} (ε 11,000), respectively.[15] If the second LECT bands can be attributed to the intra-'W_5O_{18}' CT transitions, the first LECT bands are assigned to the inter-CT ones. This feature rules out the transitions based on the model of Fig. 4a and is consistent with the transitions by the model of Fig. 4c, where the LUMO level of '$M'O_6$' is lying between HOMO and LUMO levels of 'W_5O_{18}'. Dabbabi and Boyer[16] have pre-

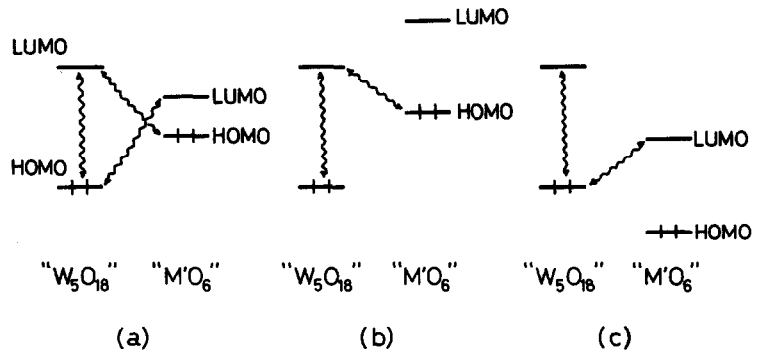

Fig. 4. Formation of $[M'W_5O_{19}]^{n-}$-type polyanion and the models of HOMO–LUMO interaction between 'W_5O_{18}' and '$M'O_6$' fragments. HOMO and LUMO levels of '$M'O_6$' fragment in (a), only the HOMO level in (b) and only the LUMO level in (c) are situated between HOMO and LUMO levels of 'W_5O_{18}' fragment. Wave-like lines represents the HOMO–LUMO interaction leading to the formation of polyanion. Degeneracy of HOMO and LUMO levels is out of consideration.

viously reported an absorption maximum of the $[NbW_5O_{19}]^{3-}$ polyanion, substituted with the less electronegative Nb(V) atom, at 36,600 cm^{-1} (ε 11,300). However, they have not referred to other low energy bands.

On the other hand, the UV spectrum of the $[Mo_6O_{19}]^{2-}$ polyanion shows the first LECT at 30,800 cm^{-1} (ε 6600) and the second one at 39,100 cm^{-1} (ε 13,100). They are clearly separated in contrast to those of an isostructural tungsto-analogue. Using the model of Fig. 4c, these bands are also assigned to the inter- and intra-CT transitions, respectively. The clear separation implies that (i) the LUMO–LUMO gap between 'Mo_5O_{18}' and 'MoO_6' fragments is larger than that between 'W_5O_{18}' and 'WO_6' and (ii) the HOMO–LUMO gap of 'Mo_5O_{18}' itself is larger than that of 'W_5O_{18}'.

2. *Group containing* A-α-'XM_9O_{34}' *fragment*

Analogous approaches are also applied to the interpretation of the CT spectra of Keggin $[\alpha\text{-}XM_{12}O_{40}]^{n-}$ and Dawson $[\alpha\text{-}P_2M_{18}O_{62}]^{6-}$ (M = Mo or W) polyanions (abbreviated to α-XM_{12} and α-P_2M_{18}, respectively, hereafter) in solution. Their absorption maxima and intensities are shown as bar graphs in Figs 5 and 6. When the A-α-'PM_9' fragment is considered as a common unit in these polyanions, the Keggin anion comprises edge- and corner-sharings of A-α-'PM_9' with three 'MO_6' units and the Dawson anion corner-shares two A-α-'PM_9' fragments. In the Keggin anion it should be noted that three 'MO_6' units inserted into the A-α-'XM_9' fragment by edge(corner)-sharings result in mutual corner(edge)-sharings.

The A-α-'PM_9' fragment actually exists as some protonated forms of $[PM_9O_{34}]^{9-}$ polyanion. As shown in Fig. 5, the second LECT position (41,700 cm^{-1}) of Dawson α-P_2Mo_{18} polyanion is situated near the first LECT (43,100 cm^{-1}) of A-α-PMo_9 polyanion which corresponds to the half-unit structure of the Dawson anion, and further the intensity (ε 109,000) of the former LECT is about twice that of the latter (ε 52,600). Thus, just like the $[W_{10}O_{32}]^{4-}$ polyanion, the LECT of α-P_2Mo_{18} (31,400 cm^{-1}; ε 21,700) can be assigned to the CT transition containing corner-sharing oxygens which link two A-

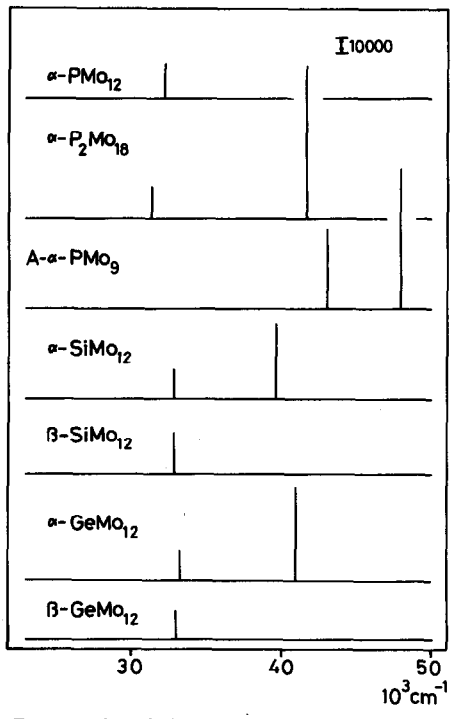

Fig. 5. Bar graphs of absorption maxima of a polyanion-group containing 'XMo_9O_{34}' (X = P, Si, Ge) fragment. Height shows relative intensity and abscissa shows wavenumber.

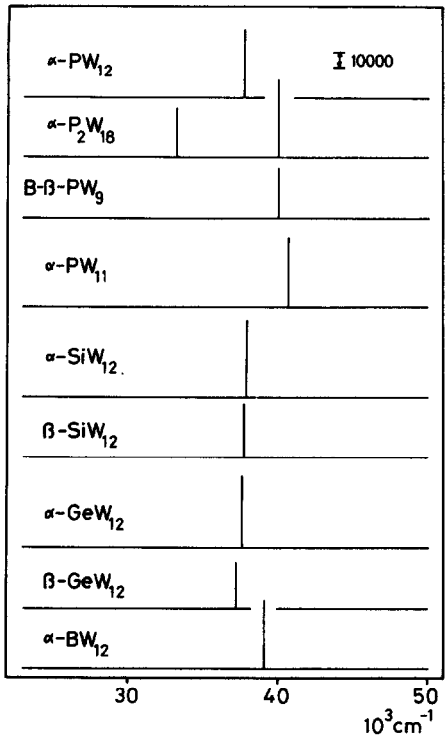

Fig. 6. Bar graphs of absorption maxima of a polyanion-group containing 'XW_9O_{34}' (X = P, Si, Ge, B) fragment. Height shows relative intensity and abscissa shows wavenumber.

α-'PMo_9' fragments and the second LECT to the intra-CT of the fragment.

The Keggin α- and β-molybdopolyanions show the first LECT bands, independent of heteroatoms, at energetically close positions ($\sim$ 33,000 cm^{-1}) to that of Dawson α-molybdopolyanion. Furthermore, some Keggin polyanions such as α-$SiMo_{12}$ and α-$GeMo_{12}$ show explicitly the second LECT bands as broad shoulders near the second LECT position in the Dawson polyanion. These facts suggest that the A-α-'XMo_9' unit becomes a discrete chromophore-group and all the first LECT bands of four geometrical isomers (A-α, B-α, A-β and B-β) of the 'XMo_9' fragment are also energetically comparable. An equivalent energy appearance of the first LECT bands of Keggin and Dawson molybdopolyanions indicates that the stabilization of the Dawson anion by corner-sharing interaction becomes nearly equal to that of the Keggin ones by the interactions between 'XMo_9' and three 'MoO_6' fragments. Moreover, a large LUMO–LUMO gap between A-α-'XMo_9' and 'MoO_6' units can be proposed.

On the other hand, the first LECT at 33,200 cm^{-1} (ε 32,500) and the second LECT at 40,000 cm^{-1} (ε 52,000) of the Dawson α-P_2W_{18} polyanion are assigned to the CT transition due to the corner-sharing oxygens which link two identical fragments and the intra-CT transition of the fragment, respectively. Although a reference band, i.e. the first LECT of the A-α-type tungsto-fragment is not provided, it is assumed not to deviate significantly from the second LECT of the Dawson tungstopolyanion and further to be close to the LECT position of the B-β isomer of the PW_9 polyanion as shown in Fig. 6. In contrast to the molybdopolyanions, all Keggin tungstopolyanions except the α-BW_{12} anion show the first LECT located at $\sim$ 38,000 cm^{-1}, which is lower by $\sim$ 2000 cm^{-1} than the assumed position of the A-α-'XW_9' fragment, and no second LECT. This probably accounts for the averaging of the inter- and intra-CT due to small LUMO–LUMO gap between 'XW_9' and 'WO_6' fragments.

REFERENCES

1. R. I. Buckley and R. J. H. Clark, *Coord. Chem. Rev.* 1985, **65**, 167 and references cited therein.
2. H. So and M. T. Pope, *Inorg. Chem.* 1972, **11**, 1441.
3. C. Madic, G. M. Begun, R. L. Hahn, J. P. Launay and W. E. Thiessen, *Inorg. Chem.* 1984, **23**, 469.
4. M. T. Pope, *Heteropoly and Isopoly Oxometalates.* Springer-Verlag, New York (1983).
5. A. Chemseddine, C. Sanchez, J. Livage, J. P. Launay and M. Fournier, *Inorg. Chem.* 1984, **23**, 2609.
6. M. Filowitz, R. K. C. Ho, W. G. Klemperer and W. Shum, *Inorg. Chem.* 1979, **18**, 93.
7. C. Rocchiccioli-Deltcheff, M, Fournier, R. Franck and R. Thouvenot, *Inorg. Chem.* 1983, **22**, 207.
8. R. Thouvenot, M. Fournier, R. Franck and C. Rocchiccioli-Deltcheff, *Inorg. Chem.* 1984, **23**, 598.
9. K. F. Jahr, J. Fuchs and R. Oberhauser, *Chem. Ber.* 1968, **101**, 477.
10. C. Rocchiccioli-Deltcheff, R. Thouvenot and M. Fouassier, *Inorg. Chem.* 1982, **21**, 30.
11. J. F. Garvey and M. T. Pope, *Inorg. Chem.* 1978, **17**, 1115.
12. A. Komura, M. Hayashi and H. Imanaga, *Bull. Chem. Soc. Jpn* 1976, **49**, 87.
13. R. Massart, R. Contant, J-M. Fruchart, J-P. Ciabrini and M. Fournier, *Inorg. Chem.* 1977, **16**, 2916.
14. K. Nomiya, H. Murasaki and M. Miwa, *Polyhedron* 1985, **4**, 1793.
15. C. M. Flynn, Jr. and M. T. Pope, *Inorg. Chem.* 1971, **10**, 2524.
16. M. Dabbabi and M. Boyer, *J. Inorg. Nucl. Chem.* 1976, **38**, 1011.

Polyhedron Vol. 6, No. 3, pp. 525–529, 1987
Printed in Great Britain

0277–5387/87 $3.00+.00

THE SYNTHESIS AND STRUCTURE OF BIS(ACETYLACETONATO)(2-HYDROXYPHENOLATO)-ALUMINIUM: A STABLE DIMER

E. W. MEIJER

Philips Research Laboratories, P.O. Box 80.000, 5600 JA Eindhoven, The Netherlands

(*Received* 12 *November* 1985; *accepted after revision* 29 *July* 1986)

Abstract—The dimeric structure of bis(acetylacetonato)(2-hydroxyphenolato)aluminium (I) has been elucidated using NMR spectroscopy and vapour phase osmometry. It has been shown that in solution the three geometrical isomers of the dimer are in equilibrium with monomeric species. At high concentrations even trimeric and/or polymeric species have to be considered in the equilibrium.

The homopolymerization of epoxides is catalysed by the combination of tris(acetylacetonato)aluminium (II) and phenols.[1,2] Catechol (III) has proved to be the most effective phenol. We have observed by NMR and HPLC the formation of a reactive intermediate in the homopolymerization of cyclohexene oxide.[3] This intermediate proves to be the actual catalytic species and is the reaction product of II and III.[3]

Although a long history exists on the structure, properties, and chemistry of aluminium alkoxides[4] and β-diketonates,[5] knowledge of the reactions of II with phenols is limited to monodentate ligands.[6] Bidentate ligands are only studied in reactions with aluminium alkoxides[4] and aluminium salts.[7] Most studies are dealing with the complexation of aluminium alkoxides or mixed alkoxide-β-diketonates. In a recent paper Wengrovius *et al.* described the synthesis of several dimeric complexes of Al(OR)(β-diketonate)$_2$.[8] These dimers are thermally unstable in solution and decompose via ligand disproportionation. No monomer–dimer equilibrium is observed, probably due to the unfavourable five-coordinated aluminium in the monomer. We have synthesized bis(acetylacetonato)(2-hydroxyphenolato)aluminium (I) from II and III as an example of Al(OR)(β-diketonate)$_2$, in which the OR group is provided with a hydroxy functionality. We have studied in detail the dimeric structure of this effective catalyst for ring-opening polymerization by NMR spectroscopy.

EXPERIMENTAL

Preparation of bis(acetylacetonato)(2-hydroxyphenolato)aluminium (I)

Catechol (5.0 g, 45 mmol) was added to a solution of 9.6 g (29 mmol) tris(acetylacetonato)aluminium in 500 cm^3 of diethylether and the mixture was refluxed for 48 h. The product precipitated during the reaction and was collected by filtration, thoroughly washed with diethylether and dried at reduced pressure, affording 2.4 g (10.2 mmol, 35%) spectroscopically pure bis(acetylacetonato)(2-hydroxyphenolato)aluminium, m.p. 192–194°C (dec.). An analytically pure sample was obtained upon crystallization from benzene, m.p. 195°C. Found: C, 56.9; H, 5.5; Al, 8.0. Calc. for ($C_{32}H_{38}O_{12}Al_2$): C, 57.5; H, 5.7; Al, 8.1%. HPLC analysis of the raw reaction mixture showed the presence of II, III, acetylacetone, and a product with the same retention time as I.

Measurements

The ^{1}H- and ^{13}C-NMR spectra were recorded at 80 and 20 MHz respectively with a Bruker WP-80-SY spectrometer. ^{27}Al-NMR spectra were recorded at 52 MHz with a Nicolet NT200. Solid state ^{13}C-NMR spectra were recorded at 100 MHz with a Bruker MSL 400 using CP/MASS and TOSS for side band reduction. The two-dimensional NOE

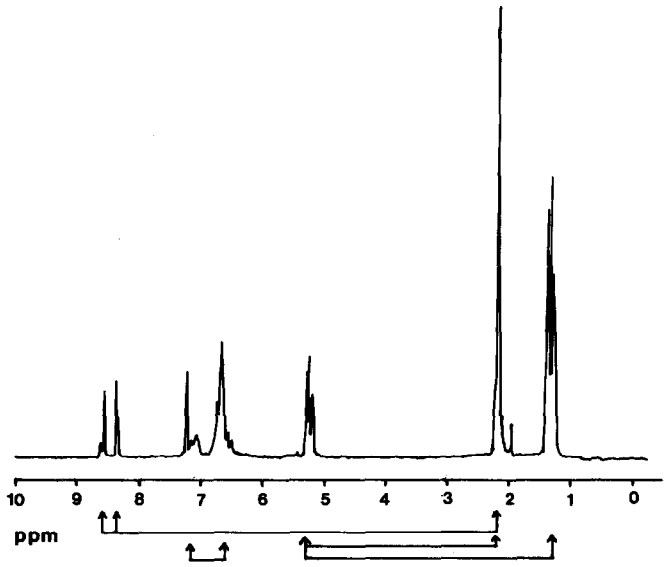

Fig. 1. ^{1}H-NMR spectrum of a freshly prepared sample of **I** in $CDCl_3$; the connectivities indicated at the bottom are NOE interactions as measured with a mixing time of 1.4 s.

(NOESY) and COSY spectra were recorded at 250 MHz with a Bruker AM 250, using mixing times of 0.9, 1.4, and 1.9 s, respectively. The chemical shifts are reported in δ units (parts per million) relative to $CHCl_3$ and converted to δ TMS values using δ $CHCl_3$ = 7.25 ppm. The vapour phase osmometric measurements were performed at the analytical department of the university of Groningen using 0.5% solutions in $CHCl_3$ at a temperature of 37°C.

RESULTS AND DISCUSSION

The reaction of **II** and **III** in ether at reflux temperature for 48 h yields **I** as a white precipitate in 35% yield. The substitution of a second acetylacetonate ligand is not observed despite a high ratio **III** over **II**. The ^{1}H-NMR spectrum of a freshly prepared sample of **I** in $CDCl_3$ is depicted in Fig. 1. The difference in chemical shift for the methyl groups of the acetylacetonate moiety (δ = 2.2–2.0 vs δ = 1.3–1.1 ppm) is remarkable. The three resonances at δ = 8.3, 8.5 and 8.55 ppm indicate the presence of three isomers. This is supported by the observation that the relative intensities of the three isomers are dependent on the history of the sample (twice vs not recrystallized). The proximity of protons within **I** is assessed in a two-dimensional nuclear Overhauser enhancement (NOE) exper-

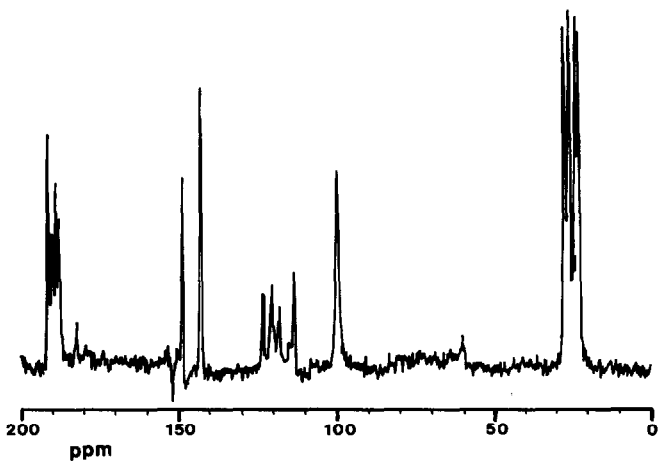

Fig. 2. ^{13}C-NMR spectrum of **I** in the solid state using CP/MASS.

iment. The NOE connectivities are indicated in Fig. 1. Besides the expected connectivities on the basis of adjacent hydrogens in the molecule, the experiment indicates a remarkable short distance between the acidic phenol hydrogens and the downfield CH_3 group of the acetylacetonate ligand. A solid state ^{13}C-NMR spectrum of **I** shows four resonances for both the carbonyl carbons and the methyl carbons of the acetylacetonate moiety (Fig. 2).

The NMR data cannot be explained by a simple monomeric structure of bis(acetylacetonato)(2-hydroxyphenolato)aluminium. However, the data are in complete accordance with a dimeric structure of **I**, in which the catechol ligands are responsible for the bridging (see Scheme 1). A CPK model of the dimer shows that the two benzene rings are located perpendicular to each other and that three geometrical isomers are possible, in which the four acetylacetonate ligands are all orientated longitudinally, all transversally, or in a combination of two longitudinal and two transverse dentations with respect to the Al–Al axis, respectively. Furthermore and most striking, the two phenolic hydroxyl groups are forced to close proximity at the same site of the dimer molecule offering a very acid proton by hydrogen bonding of these two hydroxyl groups. The model also clearly demonstrates that one CH_3 group of each acetylacetonate moiety is located in the shielding zone of the benzene ring, while the other is situated in the deshielding zone. Models of monomer and trimer do not show these (de)shielding effects.

We propose that the first step in the reaction of

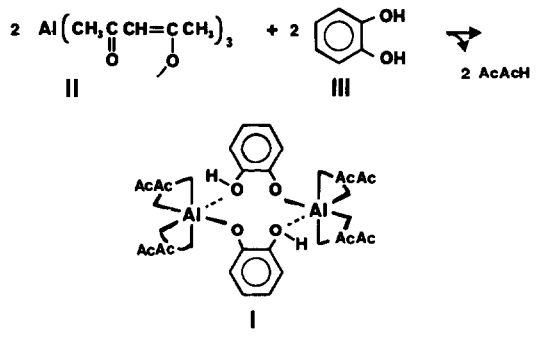

Scheme 1.

II and **III** consists of a ligand exchange equilibrium between catechol and acetylacetone. This equilibrium has been confirmed by HPLC analysis.[3] The primary monomeric product bis(acetylacetonato)(2-hydroxyphenolato)aluminium is in equilibrium with its dimer **I**, which separates from the reaction mixture. The ratio **II** over **III** and their concentrations determine the yield of **I**. Dimer **I** is an amorphous mixture of three isomers and is stable in air.

Dynamic NMR spectroscopy

When a sample of **I** in $CDCl_3$ was stored for several hours at room temperature the ^1H-NMR spectrum (see Fig. 3) deviated from that of a freshly prepared sample (Fig. 1). Apparently the dimer partially dissociates into monomeric species, to which the resonances at $\delta = 1.94$ and $\delta = 5.42$ ppm can

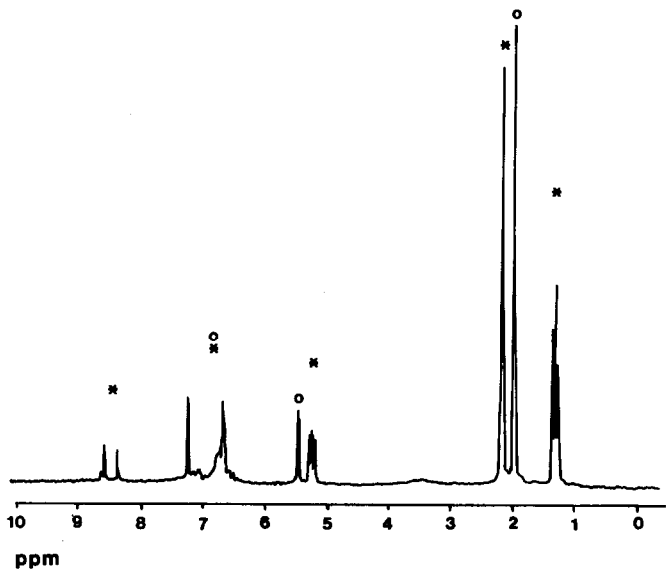

Fig. 3. ^1H-NMR spectrum of a sample of **I** in $CDCl_3$ after 2 h storing at room temperature; the resonances indicated with * correspond to dimer and with ○ to monomer.

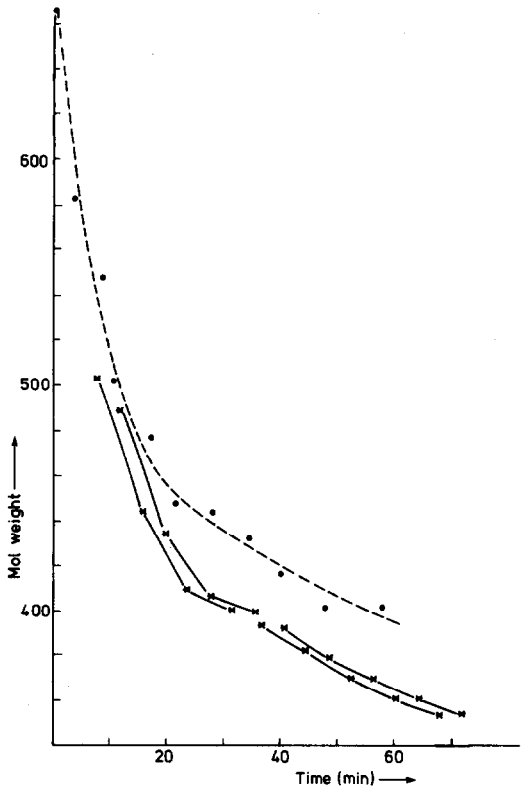

Fig. 4. The change in molecular weight in time of a solution of I in $CHCl_3$ using VPO (*) and in $CDCl_3$ using ^{1}H-NMR (●).

be assigned. The spin-lattice relaxation times for all hydrogens of the dimer are shorter than the T_1 values of the corresponding atoms in the monomer. The information obtained from ^{27}Al-NMR spectroscopy is scarce. The singlet for dimer and monomer of I are indistinguishable, while the resonance is shifted 2 ppm upfield and broadened by a factor of 1.5 with respect to the tris(acetylacetonato)-aluminium resonance.

The dissociation of I is confirmed by vapour phase osmometry. The changes in molecular weight during the dissociation of the dimer I were measured using a dilute solution of $CHCl_3$ at 37°C (Fig. 4). At these low concentrations a simple dimer–monomer equilibrium was observed in which the equilibrium constant is high. The observed decrease in molecular weight in time is in full agreement with the NMR kinetic measurements in $CDCl_3$ under the same conditions (Fig. 4).

The equilibrium constant of the dimer–monomer interchange proved to be dependent on concentration, solvent and temperature. Lowering the concentration of I furnishes a higher degree of dissociation. Variable temperature ^{1}H-NMR spectroscopy of I in ODCB-d_4 were performed to study the dynamics of the geometrical isomerization in the dimer and of the dimer–monomer equilibrium. The results are presented in Fig. 5. As the temperature was raised the resonances due to the acidic phenol hydrogens of the three isomers of the dimer were shifted upfield and coalesced at 138°C. This coalescence corresponds to an isomerization of the acetylacetonate ligands. The $\Delta G^{\neq}$ of isomerization of the three isomers is established at 21.7 ± 0.7 kcal/mol. This free energy of activation is similar to those found for the isomerization of the octahedral tris(β-diketonato) complexes,[9] but significantly higher than found for the Al(OR)(β-diketonate)$_2$ dimers.[8] This observation is consistent with a normal β-diketonate octahedral isomerization, without going through a transition state in which one of the catecholate–aluminium bonds is broken. Furthermore, no coalescence was observed for the intermolecular dimer–monomer interchange.

At the high concentrations of I, used in this experiment, no linear correlation was found for the logarithm of the equilibrium constant (K) and the reciprocal temperature when K was calculated on the basis of a dissociation of the dimer alone (Fig. 5). Satisfactory fits could only be obtained when it was assumed that at high dimer concentrations trimeric or even polymeric species were involved.

The results presented above force us to propose that the reaction of II and III furnishes the dimer of bis(acetylacetonato)(2-hydroxyphenolato)aluminium (I). The dimer is present in three geometrical isomers and in solution these isomers are

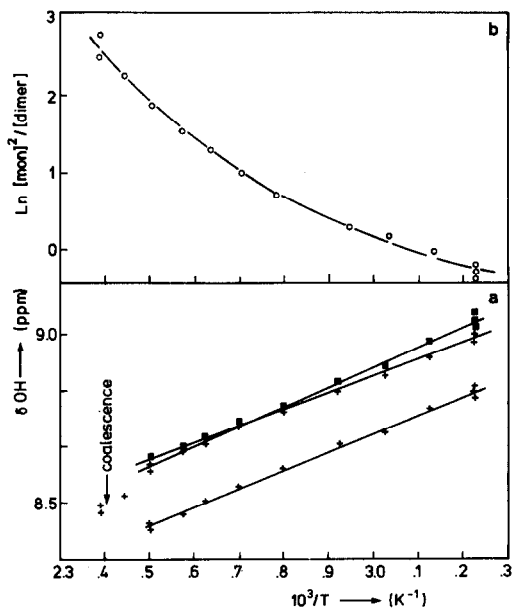

Fig. 5. (a) The chemical shift of the acid phenolic hydrogens of the dimer as a function of temperature. (b) The calculated equilibrium constant as a function of temperature.

in equilibrium with monomeric and polymeric species. The unique structure of the dimer, with the close proximity of the acidic phenol hydrogens and both catechol ligands attached to two aluminium atoms, makes **I** an active catalytic species. Investigations concerning the catalytic role of **I** in the ring-opening of epoxides is in progress.[3]

Acknowledgements—We thank the Bruker company for obtaining the solid state ^{13}C-NMR spectra and gratefully acknowledge J. P. H. Heynen and Dr F. W. van der Wey for stimulating discussions.

REFERENCES

1. M. Markovits, U.S. Patent 3,812,214 (1973).
2. M. Markovits, In *Chemistry and Properties of Crosslinked Polymers* (Edited by S. S. Labana), p. 49. Academic Press, New York (1977).
3. E. W. Meijer, J. P. H. Heynen and F. W. van der Wey, to be published.
4. D. C. Bradley, R. C. Mehrotra, and D. P. Gaur, *Metal Alkoxides*. Academic Press, London (1978).
5. R. C. Mehrotra, R. Bohra and D. P. Gaur, *Metal β-Diketonates and Allied Derivatives*. Academic Press, London (1978).
6. M. M. Aly, *J. Inorg. Nucl. Chem.* 1973, **35**, 537.
7. R. A. Hancock and S. T. Orszulik, *Polyhedron* 1982, **1**, 313.
8. J. H. Wengrovius, M. F. Garbauskas, E. A. Williams, R. C. Going, P. E. Donahne and J. F. Smits, *J. Am. Chem. Soc.* 1986, **108**, 982.
9. N. Serpone and D. G. Bickley, In *Progress in Inorganic Chemistry* (Edited by J. O. Edwards), Vol. 17, p. 391. Wiley, New York (1972).

Polyhedron Vol. 6, No. 3, pp. 531–533, 1987
Printed in Great Britain

0277–5387/87 $3.00+.00

HYDROLYSIS REACTION OF INORGANIC CYCLOPHOSPHATES AT VARIOUS ACID STRENGTHS

GENICHIRO KURA

Department of Chemistry, Fukuoka University of Education, Akama, Munakata, Fukuoka 811-41, Japan

(*Received* 14 *July* 1986; *accepted* 29 *July* 1986)

Abstract—Hydrolysis rate constants of six-, eight-, twelve- and sixteen-membered inorganic cyclophosphates at various acid strengths at 40°C were determined. Six-membered cyclotriphosphate was the most rapidly hydrolyzed at almost all acid concentrations, as a result of its interaction with hydrogen ion, and strain in the six-membered ring structure. The hydrolysis rate of the cyclophosphate which has a stronger affinity with hydrogen ions was faster than that of others. Binding of hydrogen ions renders the phosphorus atoms more susceptible to nucleophilic attack by water molecules.

Of the cyclophosphates ($M(I)_nP_nO_{3n}$) classified as a condensed phosphate which are produced by the condensation reaction of oxoacids of phosphorus of oxidation number five, cyclo-tri- and cyclo-tetraphosphate have been well known and studied by a number of investigators.[1]

The existence of cyclophosphates with degrees of polymerization greater than four in the aqueous solution of Graham's salt was first reported by Van Wazer and Karl-Kroupa in 1956.[2] In 1965, cyclopenta- and cyclo-hexaphosphate were prepared by Thilo and Schülke from the fractional precipitation of Graham's salt.[3] The synthesis of cyclo-hexa- and cyclo-octaphosphate from the source material other than Graham's salt were reported by Griffith and Buxton,[4] and by Schülke,[5] respectively. Cyclo-heptaphosphate was first isolated by the use of an anion-exchange dextran gel column by the author and Ohashi.[6]

Various properties of these higher-membered cyclophosphates have been investigated from various viewpoints.[7] These cyclophosphates are very interesting electrolytes because of their high negative charge on relatively compact molecular structures. When using these anions in the aqueous state for various purposes, their hydrolysis properties must be known clearly.

The hydrolysis reaction of cyclo-tri-, cyclo-tetra-, cyclo-hexa- and cyclo-octaphosphate have been investigated using automatic anion-exchange chromatography.[8–10] The half-life period of the hydrolysis reaction of cyclo-triphosphate in 0.1. M HCl solution at 40°C is 1.87 h and this phosphate is the most unstable. Those of cyclo-tetra- and cyclo-hexaphosphate are 16.1 and 11.4 h, respectively, and these are relatively stable compared with the cyclo-octaphosphate, with the highest degree of polymerization in the cyclophosphate series, for which the half-life is 4.53 h. The stability of the P—O—P bonds in the ring structure decreases from tetramer to octamer. This decrease is ascribed to the increase of the affinity between cyclophosphate and hydrogen ion due to the increase of the flexibility of ring structure. In acidic solutions, the degree of interactions with hydrogen ions has been considered[10] as the major factor affecting the hydrolysis rate of cyclophosphates.

This paper reports the hydrolysis rate of cyclophosphates at various hydrogen ion concentrations.

Cyclophosphate is abbreviated to P_{nm} where n is the degree of polymerization.

EXPERIMENTAL

Materials

As an anion-exchanger, Hitachi Custom Ion No. 2630 and TSK Gel SAX were used. Inorganic cyclophosphates were prepared by the methods described in our earlier paper.[7]

Chromatographic system

The separation and detection system was as described earlier.[10]

Hydrolysis procedure

The initial concentration of cyclo-octaphosphate to be hydrolyzed was varied from 9×10^{-3} to 5×10^{-5} M to study the effect of the initial concentration on the hydrolysis rate at 40°C in 0.1 M HCl. Then the initial concentration of the cyclophosphate to be hydrolyzed was adjusted to 1.25×10^{-3} M. Hydrochloric acid was added to each solution to control acid strength. The hydrolysis reaction was then performed in a water bath, the temperature of which was maintained within ±0.1°C. At measured time intervals, the hydrolysis reaction of sample solutions withdrawn was stopped by a rapid neutralization and cooling. The sample solutions were stored in a refrigerator until taken out for analysis.

RESULTS AND DISCUSSION

When cyclophosphate is hydrolyzed, the corresponding linear phosphate with the same degree of polymerization is first observed. Subsequently the linear phosphate degrades to the lower linear phosphates. To determine the hydrolysis rate of the parent phosphate, it is necessary to separate the phosphate from the hydrolysis products. We have successfully applied the automatic anion-exchange chromatographic system to the analysis of the hydrolysis samples. As mentioned previously,[8] the initial concentration of cyclophosphates affects the hydrolysis rate constant. We measured the half-life period of the hydrolysis rate of cyclo-octaphosphate of various initial concentrations in 0.1 M HCl at 40°C. As shown in Fig. 1, a constant value of half-life period was obtained when the initial concentration of cyclo-octaphosphate was lower than 1.25×10^{-3} M. Then, the initial concentration was fixed at 1.25×10^{-3} M and the hydrolysis rate in HCl solution of various concentrations was measured at 40°C.

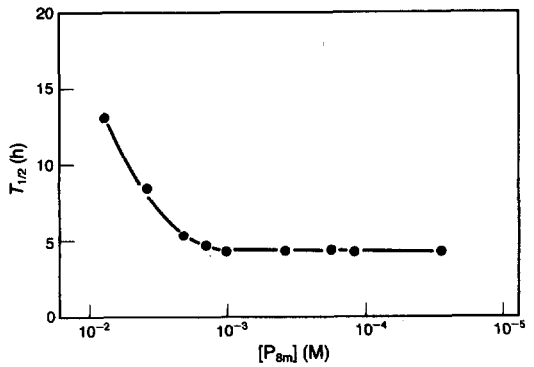

Fig. 1. Concentration dependence of half-life period of cyclo-octaphosphate hydrolysis in 0.1 M HCl at 40°C.

The rate of the hydrolysis reaction of cyclophosphates in 0.1 M HCl solution was first order. The basicity of cyclophosphate anion for hydrogen ion is relatively weak compared with linear phosphates, however, the interaction with hydrogen ion was observed and some dissociation constants of cyclophosphoric acids were determined.[7] The first-order rate equation can be presented as follows,

$$-\frac{dc}{dt} = k_0[P_nO_{3n}^{n-}] + k_1[HP_nO_{3n}^{1-n}] + \cdots + k_n[H_nP_nO_{3n}] \quad (1)$$

where k_i and c are the rate constant of the individual protonated species and the total concentration of the phosphate, respectively. When the molar fraction of the protonated species, $H_iP_nO_{3n}^{i-n}$ is defined as X_i for the total concentration, the rate equation is represented as

$$-\frac{dc}{dt} = (k_0X_0 + k_1X_1 + \cdots + k_nX_n)c. \quad (2)$$

Equation (2) is rearranged to

$$-\frac{dc}{dt} = k_{obsd}c \quad (3)$$

where k_{obsd} is a function of X_i, and varies with hydrogen ion concentration. A relation of k_{obsd} and $-\log[H^+]$ is shown in Fig. 2. The apparent rate constant k_{obsd} increases with the increase of hydrogen ion concentration. If the value of X_i is known accurately, k_i can be calculated from the combination of k_{obsd} and X_i at various hydrogen ion concentrations. Because of lack of enough data on the acid dissociation constants of $H_nP_nO_{3n}$ accurate values of X_i and k_i could not be obtained.

However, the author has tried to predict an

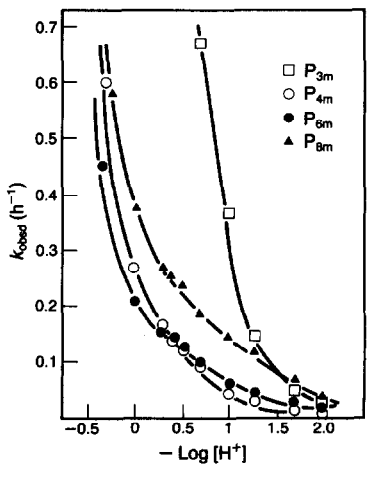

Fig. 2. Hydrolysis rate constants for cyclophosphates at various acid strengths at 40°C.

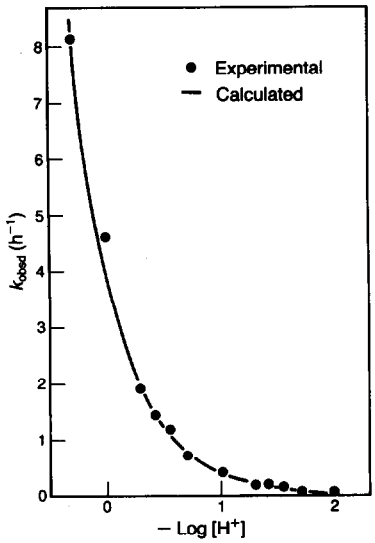

Fig. 3. Hydrolysis rate constants of cyclo-triphosphate at various acid strengths at 40°C.

approximate value of k_i for cyclo-triphosphate system from the very rough estimation of the acid dissociation constants of $H_3P_3O_9$. We have already obtained the linear relation between pK_{an} of $HP_nO_{3n}^{1-n}$ acid and the anion charge, n.[7] Using this linear relation and taking into account the statistical factor, K_{a1}, K_{a2} and K_{a3} of $H_3P_3O_9$ acid were estimated as 18.9, 1.6 and 0.1, respectively, at ionic strength 0.1. By neglecting the difference in the ionic strength, the molar fraction of the individual protonated species, X_i at each hydrogen ion concentration was calculated by using these K_{ai} values. From the set of k_{obsd} and X_i values and by the use of successive approximations, a rough value of the rate constant of the individual protonated species was determined as $k_0 = 4 \times 10^{-4}$, $k_1 = 0.5$, $k_2 = 5$ and $k_3 = 100\ h^{-1}$. The solid line in Fig. 3 presents the k_{obsd} value calculated from these constants. Coincidence of the calculated and experimental value is satisfactory.

The large difference between k_0 and k_1 values suggest that the hydrolysis rate of cyclophosphates are greatly accelerated by the bonding with hydrogen ion. The cyclo-triphosphate of the smallest six-membered ring in the cyclophosphate series is very readily hydrolyzed. This instability is ascribed not only to the interaction with hydrogen ion but to the strain in the six-membered ring structure. The strain has been supposed to be the reason of the non-existence of cyclo-diphosphate anion containing two PO_4 tetrahedra.[1] The next-most unstable species is the sixteen-membered cyclo-octaphosphate, which has the largest ring structure. The phosphate has so much flexibility in its ring structure that the affinity with the hydrogen ion increases. This is suggested as the reason of the increase in k_{obsd}. Cyclo-tetra- and cyclo-hexaphosphate have similar stability, however, at lower hydrogen ion concentration cyclo-hexaphosphate is much more rapidly hydrolyzed as a result of the increase of proton affinity. In neutral aqueous solution, hydrolysis rates of these four cyclophosphates are very slow even in boiling water.

REFERENCES

1. J. R. Van Wazer, *Phosphorus and Its Compounds.* Interscience, New York (1958).
2. J. R. Van Wazer and E. Karl-Kroupa, *J. Am. Chem. Soc.* 1956, **78**, 1772.
3. E. Thilo and U. Schülke, *Z. Anorg. Allgem. Chem.* 1965, **341**, 293.
4. E. J. Griffith and R. L. Buxton, *Inorg. Chem.* 1965, **4**, 549.
5. U. Schülke, *Z. Anorg. Allgem. Chem.* 1968, **360**, 231.
6. G. Kura and S. Ohashi, *J. Chromat.* 1971, **56**, 111.
7. G. Kura and S. Ohashi, *J. Inorg. Nucl. Chem.* 1976, **38**, 1151.
8. G. Kura, T. Nakashima and F. Oshima, *J. Chromat.* 1981, **219**, 385.
9. G. Kura, *J. Chromat.* 1982, **246**, 73.
10. G. Kura, *Bull. Chem. Soc. Jpn* 1983, **56**, 3769.

Polyhedron Vol. 6, No. 3, pp. 535–538, 1987
Printed in Great Britain

0277–5387/87 $3.00+.00

SPECTROPHOTOMETRIC STUDY OF SOME ALKALINE-EARTH AND OF SILVER COMPLEXES WITH DIBENZO-30-CROWN-10 IN METHANOL, DIMETHYLFORMAMIDE AND DIMETHYLSULFOXIDE SOLUTIONS

MOHAMMAD BAGHER GHOLIVAND, SOHEILA KASHANIAN and MOJTABA SHAMSIPUR*

Department of Chemistry, Razi University, Bakhtaran, Iran

(*Received* 21 *May* 1986; *accepted after revision* 31 *July* 1986)

Abstract—The interaction between Ag^+, Ca^{2+}, Sr^{2+} and Ba^{2+} ions and the cyclic polyether dibenzo-30-crown-10 (DB30C10) in methanol, dimethylformamide and dimethylsulfoxide solutions has been studied by a visible spectroscopic technique, using murexide as a metal ion indicator. The stabilities of the resulting complexes were determined. Strontium ion was found to form the most stable complex with the ligand in all three solvents used. There is an inverse relationship between the stabilities of the complexes and the Gutmann donicity of the solvents. The effect of the solvent on the stability of the alkaline-earth complexes is most notable with DB30C10–Ca^{2+} and the least with DB30C10–Ba^{2+}. The data obtained in this study support the existence of a 'wrap around' structure for the above complexes in solutions.

Among the macrocyclic crown ethers first synthesized by Pedersen,[1] large ligands, such as dibenzo-13-crown-10 (DB30C10), have some interesting properties. These are very flexible molecules, with enough oxygen atoms in the ring to enable them to twist around a metal ion of suitable size to envelope it completely and form a three-dimensional 'wrap around' complex.[2–5]

Some alkali complexes of large crown ethers (i.e. larger than 18-crown-6) have been studied in different solvents.[3–6,14] Negative enthalpies and entropies of complexation of cesium ion complexes of large crowns in different non-aqueous solvents, which are definitely solvent dependent, have been reported.[4,5] It is assumed that the decrease in the conformational entropy of the large crown ethers, from a rather flexible free molecule to a rigid 'wrap around' complex, would be the main reason for the large negative values of entropy changes.

Despite the interesting properties of large crowns, not much attention has been focused on the study of metal ion complexes of these ligands, so that the information for understanding their behavior in solution is quite sparse.

It was of interest to us to study the interactions of alkaline earth and of silver ions with a large crown ether, capable of forming three-dimensional complexes with these cations. In this paper, we report the study of Ag^+, Ca^{2+}, Sr^{2+} and Ba^{2+} complexes with DB30C10 in methanol, dimethylformamide and dimethylsulfoxide solutions, by a previously described visible spectroscopic technique, using murexide as a metal ion indicator.[7,8]

EXPERIMENTAL

DB10C10 was synthesized by a slight modification of Pedersen's method.[1] The product was recrystallized from reagent grade acetone and vacuum dried. Methanol (Baker, MeOH), dimethylformamide (Fisher, DMF) and dimethylsulfoxide (Fisher, DMSO) were purified and dried by the previously described method.[9] Reagent grade murexide (Merck), calcium chloride (Merck), strontium nitrate (Merck), barium chloride (Fluka), and silver nitrate (Merck), were dried over P_2O_5 under vacuum for 72 h. All spectra were obtained with a model 34 Beckman UV-Vis spectrometer at $25 \pm 1°C$.

The formation constants for the metal ion–

*Author to whom correspondence should be addressed.

murexide complexes were determined from the spectra of a series of solutions in which varying amounts of the metal ions were added to a fixed concentration of murexide in different solvents. The formation constants of various DB30C10 complexes were determined by recording the spectra of a series of solutions containing varying amounts of the crown ether and fixed concentrations of metal ion and murexide. Attainment of equilibrium was checked by the observation of no further change in the spectra after several hours. Errors associated with the various formation constants were reported as ± standard deviations.

RESULTS AND DISCUSSION

In order to determine the stabilities of metal ion–murexide and metal ion–DB30C10 complexes, the spectra of a series of solutions of fixed murexide concentration and varying concentrations of the metal ions and ligand were recorded. In all cases, maximum absorption of free and complexed murexide molecules were separated by 20–55 nm. All spectra presented satisfactory isobestic points. The deviations of the spectra from the isobestic points were at most ± 5%. The spectra of mixtures of murexide, strontium ion and DB30C10 in DMSO are shown in Fig. 1. All the calculated formation constants for metal ion–murexide and metal ion–DB30C10 complexes are presented in Table 1. The relationships between the stabilities of the DB30Cl0 complexes of alkaline-earth ions and their crystal radii[10] in different solvents are shown in Fig. 2.

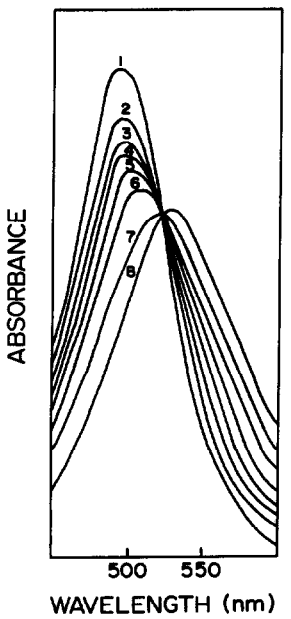

Fig. 1. Visible spectra of mixtures of murexide (m, 2.0×10^{-5} M), Sr^{2+} ion, and DB30C10 in DMSO at 25°C. 1, m+Sr^{2+} (8.0×10^{-5} M); 2, m+Sr^{2+} (6.0×10^{-5} M); 3, m+Sr^{2+} (4.0×10^{-5} M); 4, m+Sr^{2+} (4.0×10^{-5} M)+DB30C10 (8.0×10^{-5} M); 5, m+Sr^{2+} (4.0×10^{-5} M)+DB30C10 (1.2×10^{-4} M); 6, m+Sr^{2+} (2.0×10^{-5} M); 7, m+Sr^{2+} (1.0×10^{-5} M); 8, m alone.

Table 1. Log K_f of different Ag^+ and alkaline-earth cation complexes with murexide and DB30C10 in various solvents at 25°C

Solvent	Cation	Murexide	DB30C10
MeOH (DN = 25.7)[a]	Ag^+	3.87±0.07	4.31±0.19
	Ca^{2+}	6.09±0.09	4.25±0.14
	Sr^+	5.68±0.10	4.74±0.12
	Ba^{2+}	5.40±0.11	4.37±0.13
DMF (DN = 26.6)	Ag^+	4.33±0.11	3.42±0.14
	Ca^{2+}	3.98±0.08	3.28±0.13
	Sr^{2+}	4.52±0.09	3.86±0.11
	Ba^{2+}	4.43±0.07	3.51±0.09
DMSO (DN = 29.8)	Ca^{2+}	4.64±0.06	2.92±0.09
	Sr^{2+}	4.35±0.09	3.61±0.15
	Ba^{2+}	4.05±0.07	3.40±0.2

[a] DN = donor number, Ref. 11.

All of our solvents have relatively high dielectric constants and at the very low salt concentration we used, (10^{-4}–10^{-5} M), the amount of ion pairing with the free cation, and especially with the large complex ion, is negligible. Therefore, the nature of the anion should not influence the complexation reaction.

As it can be seen, the solvent plays a very fundamental role in the complexation reactions. There is an inverse relationship between log K_f of the metal ion–DB30C10 complexes and the donor (or sol-

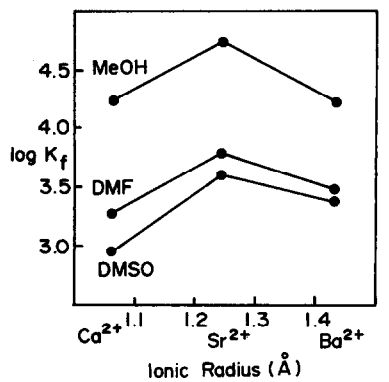

Fig. 2. Stability constants of the alkaline-earth–DB30C10 complexes vs ionic radii of the cations in various solvents at 25°C.

vating) ability of the solvents, as expressed by the Gutmann donor number.[11] In fact, the complexation takes place by replacement of the inner solvation shell of the cation by crown ether oxygen atoms. Thus, there is a competition between macrocycle and solvent molecules for cations in solution. As a result, in solvents with higher solvating power there is a drastic decrease in the stabilities of the crown complexes. The same solvent effect has already been reported for different alkali ion–crown ether complexes in various solvents.[5,12,13]

It is interesting to note that the solvent effect on the stability constants of the alkaline-earth complexes is most notable with DB30C10–Ca^{2+} and the least with DB30C10–Ba^{2+} complex. Since the Ba^{2+} ion is rather weakly solvated because of the low charge density of the cation, it is not surprising that the stability of its complex is less affected by the nature of the solvent molecules. On the other hand, the charge density of the calcium ion is much greater than that of the larger sized strontium and barium ions, which results in a much stronger solvent–cation interaction for this ion. Thus, the solvent effect on the stability of the DB30C10–Ca^{2+} complex is more evident.

Figure 2 shows that the variation of the stability of the three alkaline-earth–DB30C10 complexes with the size of the cations in all solvents used follows the same trend. Strontium ion forms the most stable complex with the ligand in all three solvents used. The stabilities of the other alkaline-earth complexes are about the same within experimental error. In the study of the complexes of large flexible crown ethers that are capable of forming of a three-dimensional 'wrap around' complex, we would expect to see the maximum binding energy when fit conditions are optimized. Metal ions with smaller or larger radii would fail to achieve the maximum stability because of the repulsive forces resulting from the effects of oxygen atoms of the ring on each ether, and/or steric hindrance inhibiting the ligand from achieving the 'best fit' configuration. Among the alkali ions, potassium has been shown to have the best size to fit inside the cavity of the twisted DB30C10 ligand, resulting in a complete 'wrap around' structure both in solid state[2] and in solution.[3,4]

Results obtained in this study for Ca^{2+}, Sr^{2+} and Ba^{2+} complexes with DB30C10 make it clear that the barium ion is too large to form a complete 'wrap around' complex. Thus just some, but not all, of the oxygen atoms of the ring can bond the cation; consequently a weaker complex results. On the other hand, the calcium ion is too small for the cavity of the twisted ligand. In this case, the ligand can still form the 'wrap around' structure, but here the oxygen atoms of the ligand have to be in close proximity, and the resulting repulsive forces weaken the complex. The strontium ion, with ionic size very close to that of the potassium ion,[10] seems to have the most suitable size for this ligand and, therefore, its resulting 'wrap around' complexes are the most stable ones in all three solvents.

The stability of the DB30C10–K^+ complex in methanol solution has been reported by Chock,[14] and is $\log K_f = 4.57 \pm 0.11$ which is somewhat less stable than DB30C10–Sr^{2+} ($\log K_f = 4.74 \pm 0.12$) probably because of the higher charge of Sr^{2+} ion. In contrast, monovalent silver ion, with about the same ionic radius as bivalent calcium ion,[10] despite its lower charge, forms a more stable complex with DB30C10 in MeOH and DMF solutions (Table 1). This is because in the case of small cations, such as Ag^+ and Ca^{2+} ions, the hydration energy of the cations becomes predominant in the complexation reactions. Thus, considering the competition between the solvent and the ligand for the cations, the much larger solvation effect of the bivalent cation over the monovalent cation results in a more univalent complex. Similar results have been reported for dicyclohexyl-18-crown-6 complexes with sodium and calcium ions.[15,16]

Acknowledgement—The authors gratefully acknowledge the support of this work by a research grant from the Ministry of Culture and Higher Education of the Islamic Republic of Iran.

REFERENCES

1. C. J. Pedersen, *J. Am. Chem. Soc.* 1967, **89**, 7017.
2. M. A. Bush and M. R. Truter, *J. Chem. Soc., Perkin Trans.* 1972, **2**, 345.
3. D. Live and S. I. Chan, *J. Am. Chem. Soc.* 1976, **48**, 3769.
4. M. Shamsipur and A. I. Popov, *J. Am. Chem. Soc.* 1979, **101**, 4051.
5. M. Shamsipur, G. Rounaghi and A. I. Popov, *J. Solution Chem.* 1980, **9**, 701.
6. R. M. Izatt, J. J. Christensen and D. J. Eatough, In *Coordination Chemistry of Macrocyclic Compounds* (Edited by G. A. Melson), Chapter 1. Plenum Press, New York (1979).
7. V. M. Loyola, R. Pizer and R. G. Wilkins, *J. Am. Chem. Soc.* 1977, **99**, 7185.
8. R. Pizer and R. Selzer, *Inorg. Chem.* 1983, **22**, 1359.
9. M. S. Greenberg and A. I. Popov, *Spectrochim. Acta* 1975, **31A**, 697.
10. J. M. Lehn, *Struct. Bonding* 1973, **16**, 1.
11. V. Gutmann and E. Wychera, *Inorg. Nucl. Chem. Lett.* 1966, **2**, 257.
12. A. J. Smetana and A. I. Popov, *J. Solution Chem.* 1980, **9**, 183.

13. J. D. Lin and A. I. Popov, *J. Am. Chem. Soc.* 1981, **103**, 3773.
14. P. B. Chock, *Proc. Natl. Acad. Sci., USA* 1972, **69**, 1939.
15. R. M. Izatt, D. P. Nelson, J. H. Rytting, B. L. Haymore and J. J. Christensen, *J. Am. Chem. Soc.* 1971, **93**, 1619.
16. J. J. Christensen, J. D. Hill and R. M. Izatt, *Science* 1971, **174**, 459.

Polyhedron Vol. 6, No. 3, pp. 539–542, 1987
Printed in Great Britain

0277–5387/87 $3.00+.00

OXIDATIVE ADDITION REACTION BETWEEN LAWESSON'S REAGENT AND $Pt(C_2H_4)(PPh_3)_2$: THE PREPARATION AND X-RAY STRUCTURE OF $[Pt\{(S_2P(S)(C_6H_4OMe)\}(PPh_3)_2]$

RAY JONES, DAVID J. WILLIAMS, PAUL T. WOOD and J. DEREK WOOLLINS*

Department of Chemistry, Imperial College of Science and Technology, South Kensington, London SW7 2AY, U.K.

(*Received* 9 *June* 1986; *accepted* 4 *August* 1986)

Abstract—Reaction of Lawesson's reagent (**1**) with $Pt(C_2H_4)(PPh_3)_2$ in benzene gives *cis*-$Pt\{S_2P(S)(C_6H_4OMe)\}(PPh_3)_2$ (**2**), in 63% yield. (**2**) was characterised by IR, ^{31}P NMR and X-ray crystallography: monoclinic, space group $P2_1/c$ with $a = 10.489(3)$, $b = 18.373(7)$ and $c = 22.591(9)$ Å, $\beta = 91.34(3)°$. The molecule has square planar platinum co-ordination with non-equivalent Pt—S bond lengths [2.369(2), 2.351(2) Å] and a folded (19.4° dihedral angle) PtS_2P ring. The P—S bond lengths are equal.

The preparation of transition metal complexes containing alkoxythiophosphate ligands is an important area of research since the zinc compounds in particular are useful lubricant additives.[1,2] Surprisingly, although a great deal of work has been reported[3,4] on RPS_2^- complexes there has been only one report on the preparation of thiophosphoryl compounds.[5] Organoperthiophosphinic acid anhydride dimers $P_2R_2S_4$ are readily prepared, synthetically useful sulphurating agents both in organic synthesis[6] and, more recently, in the preparation of a molybdenum sulphur compound.[7] However, their potential as source reagents in the preparation of new metal complexes has not been established. We wish to report the results of our investigations into the cleavage reaction of Lawesson's reagent (**1**) (R = *p*-$MeOC_6H_4$) with $Pt(C_2H_4)(PPh_3)_2$. The product of this reaction, *cis*-$Pt\{S_2P(S)(C_6H_4OMe)\}(PPh_3)_2$ (**2**) was characterized by IR/Raman, ^{31}P NMR and X-ray crystallography.

EXPERIMENTAL

All chemicals were of reagent grade. K_2PtCl_4 and Lawesson's reagent were purchased from Johnson Matthey and Aldrich Chem. Co. respectively and were used without further purification. $Pt(C_2H_4)(PPh_3)_2$ was prepared as described in the literature.[8] All manipulations were carried out under argon. Solvents were dried before use: thf, diethyl-ether and benzene were distilled from Na/benzophenone; dichloromethane was distilled from calcium hydride. ^{31}P–[^1H] NMR spectra were recorded on a JEOL FX90Q spectrometer and are referred to external 85% H_3PO_4. IR spectra were obtained as KBr discs using a Perkin–Elmer 683 spectrometer. Raman spectra were obtained using a SPEX Ramalog system (647.1 nm excitation Innova 90 laser). Elemental analyses were performed by the microanalytical department of Imperial College and by Pascher, FRG.

Preparation of $Pt\{S_2P(S)(C_6H_4OMe)\}(PPh_3)_2$ (2)

Degassed thf (10 cm^3) was added to $Pt(C_2H_4)(PPh_3)_2$ (50 mg, 0.07 mmol) and Lawesson's reagent (30 mg, 0.07 mmol) and the resulting yellow solution was stirred for 1 h during which time it darkened to orange. The solution was evaporated to dryness *in vacuo*. The resulting solid was extracted with dichloromethane (5 cm^3) and to this solution was added benzene (2 cm^3) and diethyl ether (30 cm^3). Cooling to −20°C gave the product as pale yellow crystals (40 mg, 63%). ^{31}P–[^1H] NMR (thf/$CDCl_3$) $\delta = 18.62$ $^1J[^{31}P–^{195}Pt]$ 3254 Hz, $\delta = 87.75$ $^2J[^{31}P–^{195}Pt]$ 225 Hz. ^{13}C $\delta = 55.9$ (singlet, 1) OMe group, $\delta = 112–136$ (multiplet, 42) phenyl rings. Analysis: Found, C, 51.2; H, 3.9. Required for the dichloromethane solvate. $C_{44}H_{39}Cl_2OP_3PtS_3$: C, 50.9; H, 3.8%.

* Author to whom correspondence should be addressed.

Crystals suitable for X-ray analysis were obtained by addition of chloroform to a thf solution of (2).

Crystal data

$C_{43}H_{37}OP_3S_3Pt \cdot 0.2(X_3)$,* $M = 961.14$,† monoclinic, $a = 10.489(3)$, $b = 18.373(7)$, $c = 22.591(9)$ Å, $\beta = 91.34(3)°$, $U = 4352(3)$ Å^3, space group $P2_1/c$, $Z = 4$, $D_c = 1.47$ g cm^{-3}.† Yellow, air stable prisms, dimensions $0.10 \times 0.15 \times 0.40$ mm, μ(Cu-K_α) = 87 cm^{-1},† $\bar{\lambda} = 1.54178$ Å, $F(000) = 1910$.†

Data collection and processing

Nicolet R3m diffractometer, ω-scan method, ($\theta \leqslant 50°$), graphite monochromated Cu-K_α radiation; 4342 independent measured reflections, 3945 observed [$|F_o| > 3\sigma(|F_o|)$], corrected for Lorentz and polarisation factors; numerical absorption correction (face indexed crystal).

Structure analysis and refinement

The structure was solved by the heavy atom method and all the non-hydrogen atoms refined anisotropically. The hydrogen atoms were idealised (C—H = 0.96 Å), assigned isotropic thermal parameters $U(H) = 1.2U\text{eq}(C)$ and allowed to ride on their parent carbons. An unidentified solvent fragment was located from a ΔF map and refined isotropically as three 20% occupancy carbon atoms. Refinement was by block-cascade full-matrix least squares to $R = 0.031$ ($R = \Sigma[|F_o| - |F_c|]/\Sigma|F_o|$), $R_w = 0.034$ ($w^{-1} = \sigma^2(F) + 0.00042F^2$).‡ The maximum residual electron density in the final ΔF map was 0.6 e Å^{-3} and the mean and maximum shifts/error in the final refinement cycle were 0.004 and 0.029 respectively. Computations were carried out on an Eclipse S140 computer using the SHELXTL program system[9] and published scattering factors.[10]

* X represents unidentified solvent fragment assigned atomic mass of carbon.

† Includes contribution from unidentified solvent fragment.

‡ Final values of atomic positional and thermal coefficients and lists of F_o/F_c values have been deposited as supplementary data with the Editor, from whom copies are available on request. Atomic coordinates have also been deposited with the Cambridge Crystallographic Data Centre.

RESULTS AND DISCUSSION

Reaction of Lawesson's reagent (1) with (η^2-ethene)bis(triphenylphosphine) platinum(0) in thf proceeds smoothly at room temperature to give (2) in good yield [equation (1)]. It is somewhat surprising that heterolytic cleavage of the P_2S_2 ring has taken place. The absence of any metal complex containing P(III) is good evidence that (1) is not readily dissociated in solution. A speculative mechanism for the formation of (2) would involve initial coordination of (1) via sulphur followed by elimination of an RPS fragment. We do not consider it likely that a four-membered P_2S_2Pt ring is an intermediate (although some workers have proposed this type of species for a titanium complex[5]) since this type of system would not readily rearrange to (2). The ^{31}P NMR of the crude reaction mixture contains several bands between 70 and 100 ppm and these are tentatively assigned to cyclic $(RPS)_n$ species

$$Pt(C_2H_4)(PPh_3)_2 + P_2S_4(C_6H_4OMe)_2 \rightarrow Pt\{S_2P(S)(C_6H_4OMe)\}(PPh_3)_2 + \frac{1}{n}(MeOC_6H_4PS)_n. \quad (1)$$

Characterisation of (2) was accomplished by IR, NMR, microanalysis and X-ray crystallography. The vibrational spectra of (2) contain the expected bands due to triphenylphosphine and the C_6H_4OMe group. (1) has a band at 694 cm^{-1}, due to ν(P═S), in its Raman spectrum and this band is observed at 692 cm^{-1} in (2), consistent with the P(V) oxidation state. In the low frequency region the ν(M—S) vibration in (2) is seen at 369 and 357 cm^{-1} in the IR and Raman respectively. The ^{31}P NMR of (2) (Fig. 1) consists of two singlets with platinum satellites. The band due to the PPh_3 groups is seen at $\delta = 18.62$ with $^1J[^{195}Pt-^{31}P] = 3254$ Hz appropriate to a Pt(II) complex with phosphorus *trans* to sulphur. The thiophosphoryl group gives rise to a resonance at $\delta = 87.75$ with $^2J[^{195}Pt-^{31}P] = 225$ Hz. For comparison, in (1) $\delta = 77.9$ ppm (thf/$CDCl_3$). The ^{2}J in (2) is intermediate in magnitude between those observed for $Pt(S_2P(OEt)_2)_2$ (3) (445 Hz) and $Pt(S_2P(OEt)_2)_2(PPh_3)$ (4) (120, monodentate ligand and 336 Hz, bidentate ligands).[11] These values suggest that there is less π-delocalisation in the PtS_2P ring of (2) than in (3) or (4) which is reasonable since (2) is dianionic whilst the chelate ligands in (3) and (4) are monoanionic and, formally, contain P═S groups.

The crystal structure of (2) reveals (Fig. 2, Table

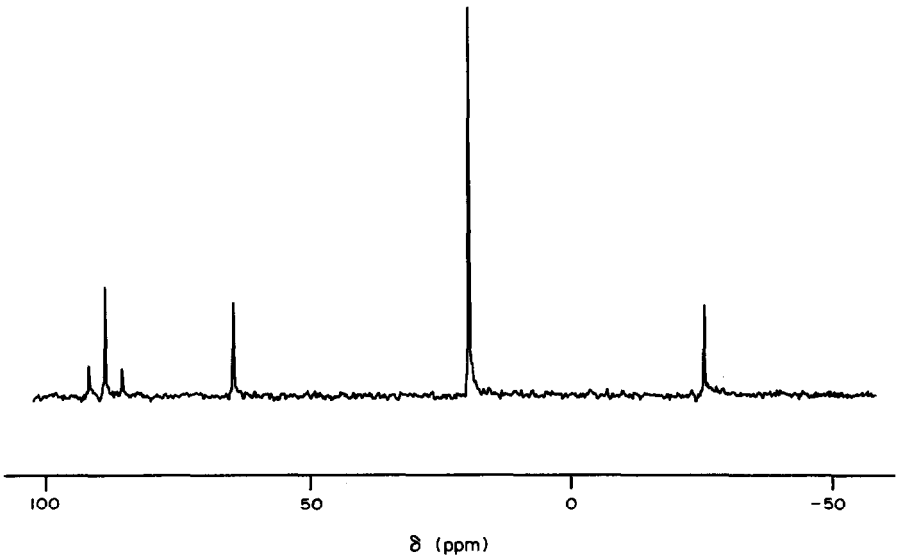

Fig. 1. ^{31}P–[^1H] NMR of **2**.

1) square planar co-ordination of the platinum by two *cis*-triphenylphosphine groups and a bidentate $(MeOC_6H_4)(S)PS_2^{2-}$ ligand. The ligand shell of the platinum, Pt, S(1), S(2), P(1), P(2), has a maximum deviation from planarity of 0.056 Å for S(2). As is commonly observed, steric effects force apart the phosphine ligands with a P(1)—Pt—P(2) angle of 101.2(1)° whilst S(1)—Pt—S(2) is contracted to 81.7(1)°. The Pt—P distances [2.291(2) and 2.293(2) Å] are normal for a Pt(II) complex. The X-ray structure of Lawesson's reagent has not been reported, though the structures of $PhSPS_2PSPh$ (**5**), $MeSPS_2PSMe$ (**6**) and the related titanium complex (**7**) have been established.[5,12,13] Comparison of the geometry in the four-membered rings in (**2**), (**4**)–(**7**) reveals some interesting features. In both (**5**) and (**6**) the structures contain a crystallographic centre of symmetry at the centre of the rings and are therefore planar. However, in the metal complexes (**2**) (**4**) and (**7**) there are varying degrees of distortion of the four-membered rings, the rings being folded with dihedral angles between the MS_2 and PS_2 planes of 19.4°, 10.2° and 12.9° respectively. In (**2**) a consequence of this significant dihedral angle is a displacement of P(3) of 0.48 Å from the ML_4 plane; this results in pseudo-axial/equatorial dispositions of the exocyclic sulphur atom and the $MeOC_6H_4$ group relative to the ML_4 plane. In all cases except (**5**) the two ring P—S distances are equivalent. In (**5**) there is a small, but statistically significant, difference in the bond lengths [2.108(2) and 2.133(2) Å]. The P—S bond lengths do vary between the different compounds. The shortest values are in (**4**), 1.97(2) and 2.00(1) Å, whilst (**2**) and (**7**) are intermediate, 2.063(2), 2.065(2) and 2.062(1), 2.060(1) Å respectively, and the longest distances are in (**5**) and (**6**), 2.108(2), 2.133(2) and 2.141(6) Å respectively. The M—S bonds differ in length within (**2**), (**4**) and (**7**) though the differences in (**4**) are probably not statistically significant. In (**2**) the Pt—S distances are 2.369(2) and 2.351(2) Å and in (**7**) Ti—S are 2.490(1) and 2.464(1) Å respectively. In (**2**) there is an accompanying non-equivalence of the P(1)—Pt—S(1) and P(2)—Pt—S(2) angles, 87.4(1) and 89.8(1)° respectively. There is no ready explanation for this effect and we note that the ^{31}P NMR spectrum of (**2**) shows only one type of PPh_3 environment in solution. The exocyclic P(3)=S(3), 1.945(3) Å, is intermediate in length between the values for the equivalent bonds in (**5**) and (**7**), 1.920(2) and 1.970(1) Å respectively. There appears to be an inverse correlation between the *exo* and *endo* P—S bond lengths. The differences in the ring

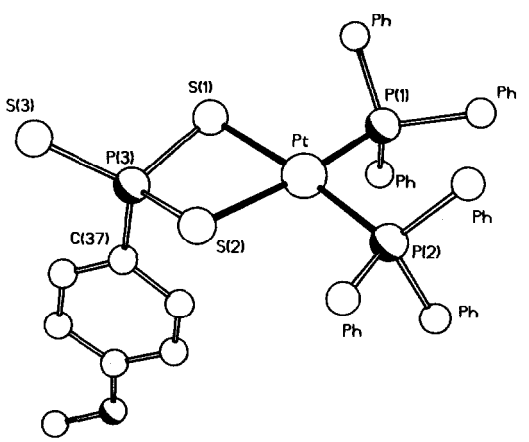

Fig. 2. Crystal structure of $Pt\{S_2P(S)C_6H_4OMe)\}(PPh_3)_2$ (**2**); phenyl rings omitted for clarity.

Table 1. Selected bond distances (Å) and angles (deg) for $Pt\{S_2P(S)(C_6H_4OMe)\}(PPh_3)_2$ (**2**)

Pt—S(1)	2.369(2)	Pt—S(2)	2.351(2)
Pt—P(1)	2.291(2)	Pt—P(2)	2.293(2)
S(1)—P(3)	2.063(2)	S(2)—P(3)	2.065(2)
S(3)—P(3)	1.945(3)	P(1)—C(1)	1.829(7)
P(1)—C(7)	1.828(6)	P(1)—C(13)	1.829(7)
P(2)—C(19)	1.827(7)	P(2)—C(25)	1.809(7)
P(2)—C(31)	1.835(7)	P(3)—C(37)	1.828(7)
S(1)—Pt—S(2)	81.7(1)	S(1)—Pt—P(1)	87.4(1)
S(2)—Pt—P(1)	168.3(1)	S(1)—Pt—P(2)	171.4(1)
S(2)—Pt—P(2)	89.8(1)	P(1)—Pt—P(2)	101.2(1)
S(1)—P(3)—S(2)	96.8(1)	S(1)—P(3)—S(3)	115.4(1)
S(2)—P(3)—S(3)	117.9(1)	Pt—S(1)—P(3)	88.9(1)
Pt—S(2)—P(3)	89.3(1)	Pt—P(1)—C(1)	112.2(2)
Pt—P(1)—C(7)	110.6(2)	Pt—P(1)—C(13)	121.2(2)
Pt—P(2)—C(19)	114.4(2)	Pt—P(2)—C(25)	115.8(2)
Pt—P(2)—C(31)	112.0(2)	S(2)—P(3)—C(37)	106.5(3)
S(3)—P(3)—C(37)	111.2(3)	S(1)—P(3)—C(37)	107.6(2)

P—S bond lengths between (**2**), (**4**) and (**5**) may be indicative of differences in the extent of π-delocalisation in the various compounds and the effect on the phosphorus NMR of the metal complexes was mentioned above.

Acknowledgements—P.T.W. is grateful to the SERC and Esso Chemicals for a CASE studentship.

REFERENCES

1. D. Klaman (Ed.), *Lubricants and Related Products.* Verlag Chemie, Weinheim, F.R.G. (1984).
2. P. G. Harrison, M. J. Begley, T. Kikabhai and F. Killer, *J. Chem. Soc., Dalton Trans.* 1986, 925 and references therein.
3. J. R. Wasson, G. M. Waltermann and A. J. Stoklosa, *Topics Current Chem.* 1973, **35**, 65.
4. W. Kuchen and H. Hertel, *Angew. Chem. Int. Ed. Engl.* 1969, **8**, 89.
5. G. A. Zank and T. B. Rauchfuss, *Organometallics* 1984, **3**, 1191.
6. R. A. Cherkasov, G. A. Kutrev and N. Pudovik, *Tetrahedron* 1985, **14**, 2567.
7. H. Keck, W. Kuchen and J. Mathow, *Inorg. Synth.* 1986, **XXIII**, 118.
8. C. D. Cook and C. S. Jauhal, *J. Am. Chem. Soc.* 1968, **90**, 1464.
9. G. M. Sheldrick, *SHELXTL, An Integrated System for Solving, Refining, and Displaying Crystal Structures from Diffraction Data.* University of Gottingen, Gottingen, F.R.G. (1978), Revision 4.1 (August 1983).
10. *International Tables for X-ray Crystallography*, Vol. 4. Kynoch Press, Birmingham (1974).
11. J. P. Fackler, Jr, L. D. Thompson, I. J. B. Lin, T. A. Stephenson, R. O. Gould, J. M. C. Alison and A. J. F. Fraser, *Inorg. Chem.* 1982, **21**, 2397.
12. C. Lensch, W. Clegg and G. M. Sheldrick, *J. Chem. Soc., Dalton Trans.* 1984, 723.
13. R. E. Banks, R. N. Haszeldine and H. Sutcliffe, *J. Chem. Soc.* 1964, 4066.

Polyhedron Vol. 6, No. 3, pp. 543–547, 1987
Printed in Great Britain

0277–5387/87 $3.00+.00

CRYSTAL STRUCTURES OF $[Co\{P(OPh)_3\}_4(HgX)]$, X = Cl, Br; NON-LINEARITY OF Co—Hg—X ARISING FROM INTRAMOLECULAR PHOSPHORUS–MERCURY INTERACTIONS

DAVID M. L. GOODGAME,* ALEXANDRA M. Z. SLAWIN and DAVID J. WILLIAMS*

Chemistry Department, Imperial College of Science and Technology, London SW7 2AY, U.K.

(*Received* 10 *June* 1986; *accepted* 4 *August* 1986)

Abstract—Single crystal X-ray diffraction studies have been carried out on the compounds $[Co\{P(OPh)_3\}_4(HgX)]$, X = Cl, Br. Crystals of the bromide, (**1**), are monoclinic, $C2$, $a = 22.391(4)$, $b = 13.643(3)$, $c = 22.851(6)$ Å, $\beta = 101.37(2)°$, $Z = 4$. The structure was refined on 4388 reflections to $R = 0.059$. Crystals of the chloride (**2**), are monoclinic, $C2$, $a = 22.300(5)$, $b = 13.632(3)$, $c = 22.743(4)$ Å, $\beta = 100.98(2)°$, $Z = 4$. The structure was refined on 4124 reflections to $R = 0.061$. In each case the molecule adopts a distorted trigonal bipyramidal geometry with a non-linear P(1)—Co—Hg axis, with corresponding short intramolecular Hg—P contacts. The Co—Hg—X (X = Cl, Br) chain is also significantly bent. Raman spectral data for the compounds, and for the iodide analogue, are also reported.

Many compounds are known which contain a mercury atom bonded to a transition metal atom. X-Ray structural studies on complexes of the type L_nMHgX, where X is a halogen atom, have shown that when the mercury is bonded to only one transition metal, M, the M—Hg—X unit is essentially linear, though deviations of up to ~ 20° from this linearity have been reported.[1–6]

These distortions of the M—Hg—X group have arisen because of intermolecular interactions between the Hg atom in one molecule and one or more halogen atoms from neighbouring molecules. In $(\eta^5\text{-}C_5H_5)Mo(CO)_3HgCl$, for example, each Hg atom interacts with the chlorine atoms of two neighbouring molecules at distances Hg···Cl of 3.079(3) and 3.078(4) Å resulting in a 160° bond angle for Mo—Hg—Cl.[6] We report here the structures of the compounds $[Co\{P(OPh)_3\}_4(HgX)]$, X = Cl, Br, described by Anderson and co-workers,[7] and some Raman spectral data for the complexes and for their iodo-analogue.

* Authors to whom correspondence should be addressed.

EXPERIMENTAL

Samples of $[Co\{P(OPh)_3\}_4(HgX)]$, X = Cl, Br, I, were prepared by the method of Anderson *et al.*[7] and crystallized from acetone/water.

The Raman spectra were obtained on the solid samples using a Spex Ramalog V instrument with a Coherent model 52 Krypton ion laser. The exciting lines used were 568.2 nm for the chloride complex and 647.1 nm for the bromide and iodide. Data were collected using a Spex Datamate computer controller.

X-Ray studies

Crystal data. (**1**) $C_{72}H_{60}O_{12}P_4BrCoHg$, monoclinic, $a = 22.391(4)$, $b = 13.643(3)$, $c = 22.851(6)$ Å, $\beta = 101.37(2)°$, $U = 6844$ Å^3, space group $C2$, $Z = 4$, $M = 1580.6$, $D_c = 1.53$ g cm^{-3}, μCu-$K_a = 84$ cm^{-1}.

(**2**) $C_{72}H_{60}O_{12}P_4ClCoHg \cdot C_{1.5}$, monoclinic, $a = 22.300(5)$, $b = 13.632(3)$, $c = 22.743(4)$ Å, $\beta = 100.98(2)°$, $U = 6787$ Å^3, space group $C2$, $Z = 4$, $M = 1554.2$, $D_c = 1.52$ g cm^{-3}, μCu-$K_\alpha = 81$ cm^{-1}.

Measurements. Refined unit cell parameters were obtained by centring in (**1**) 11, and in (**2**) 18 reflections on a Nicolet R3m diffractometer. Using the omega scan measuring routine, in (**1**) 4817, and in (**2**) 4813 independent reflections ($\theta \leqslant 58°$) were measured with Cu-K_α radiation (graphite monochromator). Of these in (**1**) 4388 and in (**2**) 4124 had $|F_o| > 3\sigma(|F_o|)$ and were considered observed. Lorentz and polarisation corrections were applied. In (**1**) a numerical absorption correction (face indexed crystal) was applied. In (**2**) an empirical absorption correction based on 324 azimuthal measurements was applied.

Structure analysis. The structure of (**1**) was solved by the heavy atom method, which gave the position of the mercury atom. All other non-hydrogen atoms were located from subsequent ΔF maps. Because of the large number of atoms in the structure, the geometries of the phenyl rings were idealised, C—C = 1.395, C—H = 0.96 Å, and the groups refined as rigid bodies. The ring carbon atoms were assigned individual isotropic thermal parameters which were allowed to refine. The hydrogen atoms were given constrained isotropic thermal parameters $U(\mathrm{H}) = 1.2U(\mathrm{C})$. The remaining atoms were refined anisotropically.*

Structure (**2**), being isostructural with (**1**), was solved by refining the coordinates of (**1**), omitting the bromine atom, using the data for (**2**) and allowing the halogen to come up in a ΔF map. This also revealed the presence of three partial atoms of an unidentified solvent fragment. These were refined isotropically, as carbons each with a site occupancy of 0.5. The remaining refinement procedure was as for (**1**).

The polarities of the structures were in both cases determined by *R*-factor tests. Refinement in both cases was by block-cascade full-matrix least-squares to for (**1**) $R = 0.059$, $R_w = 0.064$ $[w^{-1} = \sigma^2(F) + 0.00266F^2]$, and (**2**) $R = 0.061$, $R_w = 0.062$ $[w^{-1} = \sigma^2(F) + 0.00154F^2]$. Computations were carried out on an Eclipse S140 computer using the SHELXTL program system.[8] Scattering factors were taken from the *International Tables for X-Ray Crystallography*.[9]

Final atomic coordinates, thermal parameters and structure factors have been deposited with the Editor as supplementary data. Atomic coordinates have also been deposited with the Cambridge Crystallographic Data Centre.

* Allowing anisotropic thermal values for the ring carbon atoms increased significantly the number of variable parameters but did not produce any improvement in the *R* values. Final refinement was therefore carried out using isotropic values.

RESULTS AND DISCUSSION

Tables 1 and 2 give selected bond lengths and angles for (**1**) and (**2**). Figure 1 shows a perspective view of (**1**).

In view of the very close correspondence between the geometries of the two structures we shall quote average numerical values in the following discussion. The cobalt has distorted trigonal bipyramidal geometry (Fig. 2) with all four Co—P bonds the same length, within statistical significance. The cobalt atom is displaced 0.21 Å (in both structures) towards P(1) relative to the P(4)—P(7)—P(10) plane. The P(1)—Co—Hg axis is bent with a P(1)—Co—Hg angle of 172.8(1)°. This bending of the Co—Hg bond relative to the axis of the bipyramid takes place in the direction of the Co—P(4)—P(10) plane, with resulting short contacts between the mercury atom and P(4) [3.035(5) Å] and P(10) [2.949(7) Å]. The Hg—Co bond is inclined by 68° to the Co—P(4)—P(10) plane. The Hg—P(7) distance is significantly longer (3.36 Å). There are notable departures from trigonal geometry for the three equatorial phosphorus atoms, the angles at cobalt being: P(4)P(7) 109.4(3)°, P(7)P(10) 118.4(3)°, and P(4)P(10) 129.2(3)°.

The Co—Hg bond [2.484(3) Å] is towards the lower end of the range (2.43–2.71 Å) found for the nine reported structures containing Co—Hg bonds, and consistent for essentially two-coordinate mercury.[10–18] The Co—Hg—X (X = Cl, Br) unit is significantly bent [172.8(2)°].

There are no major differences in the P—O bond distances in these structures and they are all in accord with expected values.

The coordination geometry about the cobalt atom can be thought of either in terms of a distortion from an idealised trigonal bipyramidal geometry, as observed[16] in $Hg\{Co[P(OCH_3)_3]_4\}_2$,

Table 1. Selected comparative bond lengths (Å) for (**1**) and (**2**)

Atoms	(**1**) X = Br	(**2**) X = Cl
Co—Hg	2.485(2)	2.481(2)
Co—P(1)	2.116(4)	2.107(4)
Co—P(4)	2.131(5)	2.130(6)
Co—P(7)	2.122(5)	2.129(5)
Co—P(10)	2.098(5)	2.109(6)
Hg—X	2.505(2)	2.385(6)
Hg—P(4)	3.029(3)	3.040(3)
Hg—P(10)	2.947(5)	2.950(5)

Table 2. Selected comparative bond angles (deg) for (1) and (2)

Atoms	(1) X = Br	(2) X = Cl
P(1)—Co—P(4)	98.3(2)	98.3(2)
P(1)—Co—P(7)	93.7(2)	93.3(2)
P(1)—Co—P(10)	95.0(2)	95.0(2)
P(4)—Co—P(7)	109.5(2)	109.3(2)
P(4)—Co—P(10)	129.4(2)	128.9(2)
P(7)—Co—P(10)	118.0(2)	118.8(2)
P(1)—Co—Hg	172.6(1)	173.0(1)
P(4)—Co—Hg	81.6(1)	82.1(1)
P(7)—Co—Hg	93.2(1)	93.1(1)
P(10)—Co—Hg	79.5(1)	79.5(1)
Co—Hg—X	163.1(1)	163.8(1)

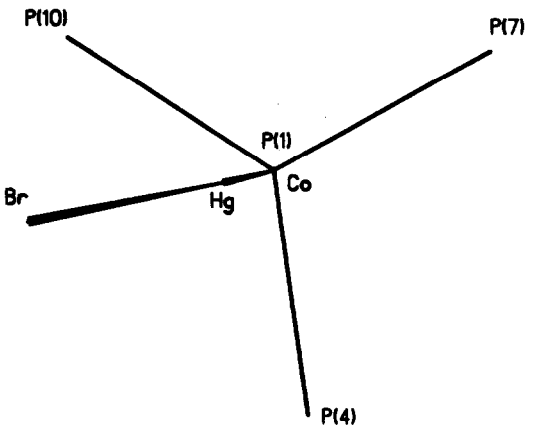

Fig. 2. Perspective view normal to the P(4)—P(7)—P(10) plane of the nucleus of the structure of (1).

or a distortion from tetrahedral geometry resulting from the insertion of the Hg—Br unit. In the latter case this insertion could take place either along the three-fold direction of the CoP_4 tetrahedron or along one of the two-fold axes. On balance, we favour the distorted tetrahedral geometry because of the observed equivalence in the lengths of the four Co—P bonds. Also the preferred geometry for a CoL_4 complex of Co(−I) is tetrahedral.[19] In trigonal pyramidal geometry one would expect the Co—P(1) bond to be longer than the other three, though this could be influenced by the *trans*-disposition of the mercury atom.

Neither of these arguments, however, resolves the

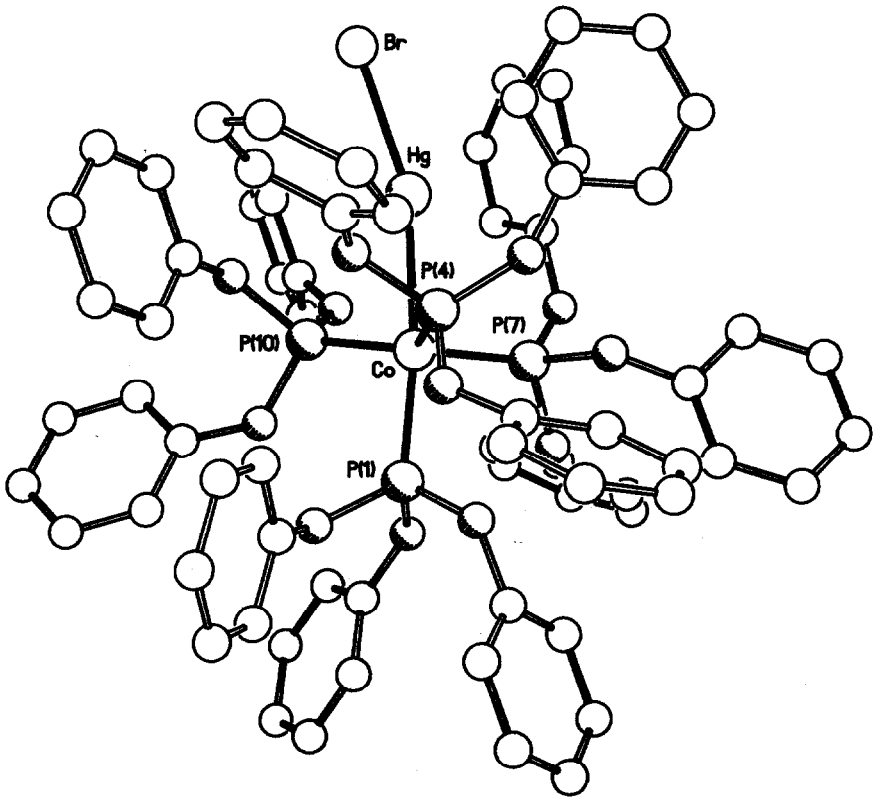

Fig. 1. Molecular structure of $[Co\{P(OPh)_3\}_4HgBr]$.

question as to whether the interactions between the mercury atom and P(4) and P(10) are repulsive or attractive. Both of these Hg—P distances are significantly shorter than the sum of the van der Waals' radii of the component atoms, and both P(4) and P(10) have larger angles at the cobalt atom, with respect to P(1), than does P(7). On the other hand, the angle formed by P(4) and P(10) at cobalt [129.2(3)°] is significantly larger than the other two equatorial angles. Further evidence for interactions between P(4), P(10) and the mercury is provided by the significant bending of the Co—Hg—X chain. Steric factors due to the phenyl rings appear to play no significant part in causing this bending, as the effect is the same regardless of the size of the halogen atom (Fig. 3).

Raman spectra

The bands observed in the Raman spectra of $[Co\{P(OPh)_3\}_4(HgX)]$ below 400 cm^{-1} are listed in Table 3. In each case, the dominant feature is a strong, halogen dependent band at 278 cm^{-1} (X = Cl), 198 cm^{-1} (X = Br) and 160 cm^{-1} (X = I) which is readily assigned as ν(Hg—X). [In using this designation we recognize that the actual mode concerned is not pure ν(Hg—X) but will have at least some ν(Co—Hg) character, particularly in the case of the iodide.] The values for ν(Hg—Br) and ν(Hg—I) are close to those reported[20] for Ph—Hg—Br (199 cm^{-1} IR; 193 cm^{-1} Raman) and Ph—Hg—I (160 cm^{-1} IR; 156 cm^{-1} Raman), but ν(Hg—Cl) is higher in Ph—Hg—Cl (330 cm^{-1} IR; 316 cm^{-1} Raman). Values of ν(Hg—Cl) in the range 252–219 cm^{-1} are, however, commonly found for other M—Hg—Cl species.[21]

Table 3. Low frequency (< 400 cm^{-1}) Raman bands (cm^{-1}) for the complexes $Co[P(OPh)_3]_4(HgX)$, X = Cl, Br, I

X = Cl	Br	I	Assignment[a]
278s	—	—	ν(Hg—Cl)
210br m	215br m	201br m	ν(Co—P)
—	198s	160s	ν(Hg—X)
129m	128m	109m	ν(Co—Hg)

[a] Designations represent likely major contribution as there will be significant mixing, particularly when X = Br and I.

Bearing in mind the masses of the phosphite ligands bonded to cobalt, the ν(Co—Hg) bands in $[Co\{P(OPh)_3\}_4(HgX)]$ would be expected to be at quite low frequencies. Even when Hg is bonded to first row transition metal ions linked to relatively light ligands, such as CO, the modes approximating to ν(Hg—M) are below 200 cm^{-1}.[21] The large mass of the $Co[P(OPh)_3]_4$ unit would be expected to lower ν(Co—Hg) even further. It seems probable that the medium intensity bands at 129 cm^{-1} (X = Cl), 128 cm^{-1} (X = Br) and 109 cm^{-1} (X = I) in the Raman spectra of $[Co\{P(OPh)_3\}_4(HgX)]$ are due to modes with significant ν(Co—Hg) character. On the basis of literature assignments of ν(M—P) for other phosphite complexes of low-valent M atoms,[22] the broad, medium intensity bands in the 200–215 cm^{-1} region are assigned to ν(Co—P).

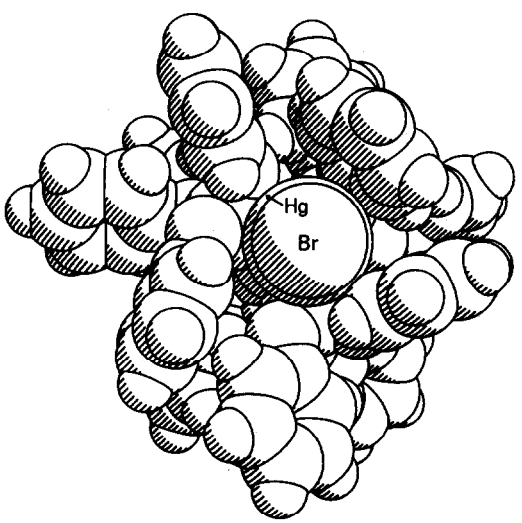

Fig. 3. Space filling representation of (1) viewed along the Br–Hg axis.

Acknowledgements-We thank the SERC for the diffractometer and for a Research Studentship (to A.M.Z.S.), Mr M. Mulinder, Miss A. M. Pedley, and Mr M. J. Tozer for samples of the complexes, and Dr N. J. Campbell for running the Raman spectra under the ULIRS scheme.

REFERENCES

1. H. W. Baird and L. F. Dahl, *J. Organomet. Chem.* 1967, **7**, 503.
2. C. L. Raston, A. H. White and S. B. Wild, *Aust. J. Chem.* 1976, **29**, 1905.
3. P. D. Brotherton, C. L. Raston, A. H. White and S. B. Wild, *J. Chem. Soc., Dalton Trans.* 1976, 1799.
4. M. M. Mickiewicz, C. L. Raston, A. H. White and S. B. Wild, *Aust. J. Chem.* 1977, **30**, 1685.
5. M. J. Albright, M. D. Glick and J. P. Oliver, *J. Organomet. Chem.* 1978, **161**, 221.
6. C. Bueno and M. R. Churchill, *Inorg. Chem.* 1981, **20**, 2197.
7. L. B. Anderson, H. L. Conder, R. A. Kudaroski, C.

Kriley, K. J. Holibaugh and J. Winland, *Inorg. Chem.* 1982, **21**, 2095.
8. G. M. Sheldrick, *SHELXTL, An Integrated System for Solving, Refining, and Displaying Crystal Structures from Diffraction Data*, Revision 4.1. University of Gottingen, F.R.G. (1983).
9. *International Tables for X-Ray Crystallography*, Vol. IV, pp. 99–149. Kynoch Press, Birmingham, England (1974).
10. R. F. Bryan and A. R. Manning, *J. Chem. Soc., Chem. Commun.* 1968, 1316.
11. I. W. Nowell and D. R. Russell, *J. Chem. Soc., Dalton Trans.* 1972, 2393.
12. I. W. Nowell and D. R. Russell, *J. Chem. Soc., Dalton Trans.* 1972, 2396.
13. R. F. Bryan and H. P. Weber, *Acta Cryst.* 1966, **21**, A138.
14. D. N. Duffy, K. M. Mackay, B. K. Nicholson and W. T. Robinson, *J. Chem. Soc., Dalton Trans.* 1981, 381.
15. C. A. Ghilardi, S. Midollini and S. Moneti, *J. Chem. Soc., Chem. Commun.* 1981, 865.
16. E. L. Muetterties, J. R. Bleeke, Z.-Y. Yang and V. W. Day, *J. Am. Chem. Soc.* 1982, **104**, 2940.
17. F. Cecconi, C. A. Ghilardi, S. Midollini and S. Moneti, *J. Chem. Soc., Dalton Trans.* 1983, 349.
18. J. M. Burlitch, J. M. Ragosta and M. C. Vanderveer, *Acta Cryst.* 1984, **C40**, 1549.
19. F. A. Cotton and G. Wilkinson, *Advanced Inorganic Chemistry*, 4th edn. p. 767. Wiley Interscience, New York (1980).
20. P. L. Goggin and D. M. McEwan, *J. Chem. Res. (S)* 1978, 171.
21. T. G. Spiro, *Progr. Inorg. Chem.* 1970, **11**, 1.
22. J. G. Verkade, *Coord. Chem. Rev.* 1972/73, **9**, 1.

Polyhedron Vol. 6, No. 3, pp. 549–562, 1987
Printed in Great Britain

0277–5387/87 $3.00+.00

CATIONIC COMPLEXES OF TRIMETHYLPLATINUM(IV) WITH TRIDENTATE LIGANDS—II. FLUXIONAL BEHAVIOUR

EDWARD W. ABEL, KENNETH KITE* and PHILLIP S. PERKINS

Department of Chemistry, University of Exeter, Exeter EX4 4QD, U.K.

(*Received* 22 *July* 1986; *accepted* 8 *August* 1986)

Abstract—Variable temperature ^{1}H NMR studies on the ionic compounds $[PtMe_3\{MeE(CH_2)_nE'(CH_2)_nEMe\}]^+X^-$ ($n = 3$, E = E′ = S: $n = 2$, E = Se or S; E′ = O, S, Se: $n = 2$, E = S, E′ = SS: X = I, BPh_4 or BF_4) have shown that pyramidal inversion takes place only at the terminal chalcogen atoms. High-temperature studies on these complexes and $[PtMe_3\{(H_2NCH_2CH_2)_2E'\}]^+BF_4^-$ (E′ = O or SS) show that only those with E′ = O undergo ligand scrambling processes. Computer simulation of the static and dynamic spectra gives accurate energy barriers for both fluxional processes.

Earlier studies[1] on the fluxional behaviour of uncharged complexes of trimethylplatinum(IV) halides with bidentate thioethers and selenoethers $[(PtMe_3X)MeE(CH_2)_nE'Me]$ ($n = 2$ and 3, E = E′ = S and Se: $n = 2$, E = S, E′ = Se; X = Cl^-, Br^-, I^-) have shown that pyramidal inversion at E and E′ takes place in an uncorrelated manner, and that the inversion energy barriers are higher at Se than at S, and higher in the five- compared to the six-membered rings. We now consider the effect of introducing a third potential inverting centre into the system using tridentate ligands of the general type $MeE(CH_2)_nE'(CH_2)_nEMe$, which should form charged complexes. The effect of ring size has been examined with the ligands having $n = 2$ and 3, and E = E′ = S. Ligands having E = S or Se allow us to test the relative rates of inversion of these atoms, and whether the expected inversion at the terminal chalcogens is uncorrelated here also. Molecular models indicate that inversion at the central atom E′ is likely to be disfavoured on steric grounds, but this possibility has been explored using ligands with E′ = O, S and Se. Additionally, ligands with E′ = O and SS may be used to test respectively the effect of a significantly weaker donor to Pt(IV) than N, S or Se,[2] and the possibility of a 1,2-metallotropic shift between the SS atoms. Two ligands with no possibility of inversion at the terminal donor atoms $[(H_2NCH_2CH_2)_2E']$ (E′ = O or SS) are included for comparison. The tridentate ligands allow us to explore the effect of a third donor atom on any high temperature ligand scrambling processes comparable to those reported for complexes of the bidentate ligands. Characterisation of these complexes is reported in an earlier paper.[3]

EXPERIMENTAL

The compounds were prepared and characterised as described.[3] The ^{1}H NMR spectra were recorded at 100 MHz on a JEOL PS/PFT-100 equipped with standard accessories for variable temperature work. Temperature measurements were made using a copper–constantan thermocouple. The 400 MHz spectra were run on a Bruker WH-400 spectrometer.

Band shape analyses were carried out using a modified version of the DNMR programme of Kleier and Binsch.[4] Computer simulated spectra were fitted visually, and energy parameters derived from standard Arrhenius and Eyring plots are based on least-square fitting. The errors quoted for the free energies of activation $\Delta G^{\ddagger}$ are based on the numerical difference between the standard deviations of $\Delta H^{\ddagger}$ and $T\Delta S^{\ddagger}$ (where $T = 298.15$ K) following the practice of Binsch and Kessler.[5]

RESULTS AND DISCUSSION

In considering the ^{1}H DNMR behaviour of the compounds shown in Fig. 1, it is convenient to distinguish the low temperature pyramidal inversion processes from the ligand scrambling which is a feature of the spectra at higher temperatures.

* Author to whom correspondence should be addressed.

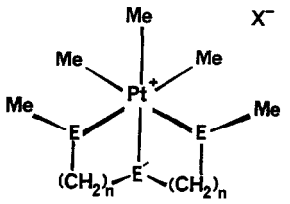

Complex	n	E	E'	X^-
I	3	S	S	BF_4^-
II	2	S	O	BF_4^-
III	2	S	S	BPh_4^-
IIIa	2	S	S	I^-
IV	2	S	Se	I^-
V	2	Se	O	BF_4^-
VI	2	Se	S	BF_4^-
VII	2	Se	Se	BF_4^-
VIII	2	S	-SS-	BF_4^-

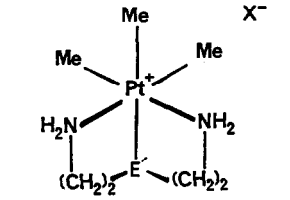

Complex	E'	X^-
IX	O	BF_4^-
X	-SS-	BF_4^-

Fig. 1. Structures of the cationic complexes $[PtMe_3\{MeE(CH_2)_nE'(CH_2)_nEMe\}]^+$ ($n = 3$; E = E′ = S: $n = 2$; E = S or Se, E′ = O, S, Se: $n = 2$; E = S, E′ = SS) and $[PtMe_3(NH_2CH_2CH_2)_2E]^+$ (E = O or SS).

Low-temperature studies

In the majority of the compounds the tridentate ligand is symmetrical with three potential inverting centres (compounds **I–VII**). For compound **VIII** (E′ = SS) which lacks a plane of symmetry more complicated behaviour is found, while compounds **IX** and **X** with chalcogen atoms present only in the middle of the ligand show no spectral changes in this temperature range. ^1H NMR data at the fast and slow inversion limits are recorded in Table 1, with assignments as indicated in Fig. 2. The coupling constants are in the expected ranges found for complexes with the analogous bidentate ligands,[1] and will not be discussed further.

The temperature variations observed in the spectrum of $[PtMe_3\{(MeSCH_2CH_2)_2S\}]^+$ (**III**) are typical of complexes (**I–VII**). The S atoms are centres of chirality, so that in the absence of sulphur inversion four diastereoisomers are possible, a degenerate pair of *dl*-isomers and two distinct *meso*-isomers (Fig. 3). Inversion at the central S atom would give another set of four diastereoisomers. There is, however, no experimental evidence for the presence of more than one set of diastereoisomers, and molecular models show that such a central S atom

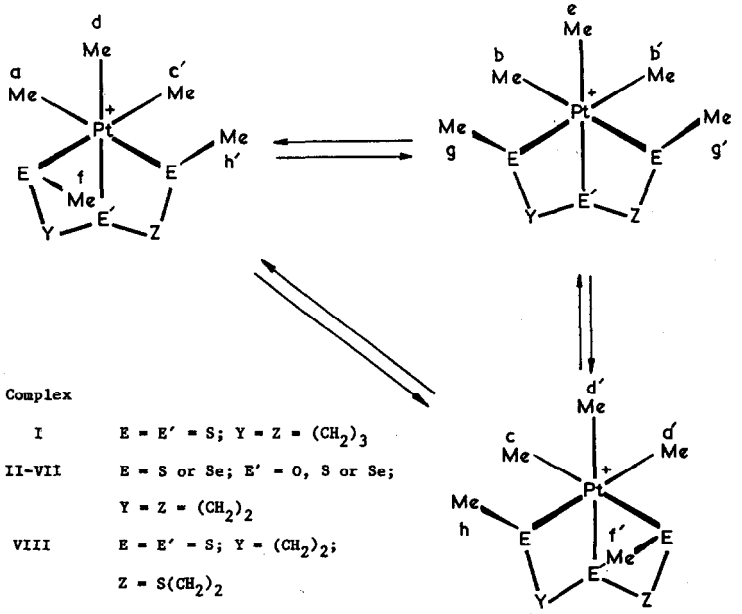

Complex	
I	E = E′ = S; Y = Z = $(CH_2)_3$
II-VII	E = S or Se; E′ = O, S or Se; Y = Z = $(CH_2)_2$
VIII	E = E′ = S; Y = $(CH_2)_2$; Z = $S(CH_2)_2$

Fig. 2. Environmental assignment of isomers for complexes **I–VIII**.

Table 1. ^{1}H NMR data for the thio- and selenoether complexes at the fast and slow inversion limits

Complex	Temperature (°C)	Pt—Me(*trans* to E)[a] δ/ppm (*J*/Hz)			Pt—Me(*trans* to E′)[a] δ/ppm (*J*/Hz)		E—Me[a] δ/ppm (*J*/Hz)		
		a a′[b]	b b′	c c′	d d′	e	f f′	g g′	h h′
I	−77.3	1.13(65.6)	1.02(65.7)	0.92(65.8)	0.78(66.9)	0.78(66.9)		2.29(16.5)	
	+26.0		1.05(65.9)		0.82(66.4)			2.30(15.3)	
II	−45.0	1.02(66.0)	0.98(66.3)	0.95(66.3)	1.09(81.9)	1.12(81.7)	2.49(13.3)	2.35(16.9)	2.36(16.9)
	+1.3		1.08(66.2)		1.21(81.6)			2.49(15.1)	
IIIa	−61.4	0.95(66.8)	0.91(66.8)	0.88(66.8)	1.00(67.1)	1.04(67.4)	2.63(13.7)	2.33(16.0)	2.34(16.0)
	+16.8		0.94(67.0)		1.03(67.0)			2.44(14.8)	
IV	−54.1	0.97(67.4)	0.92(66.9)	0.89(66.7)	1.03(67.1)	1.10(66.9)	2.60(14.2)	2.32(16.1)	2.37(15.6)
	+29.0		0.95(67.1)		1.08(66.9)			2.43(14.7)	
VI	−56.5	0.81(67.4)	0.89(66.7)	0.89(66.2)	1.02(67.4)	1.02(67.4)	2.28(10.5)	2.12(13.2)	2.13(12.9)
	+78.4		1.02(67.1)		1.16(67.4)			2.30(11.0)	
VII	−0.4	0.63(66.3)	0.58(67.4)	0.62(67.3)	0.79(67.1)	0.80(67.5)	2.02(11.0)	1.85(13.2)	1.86(12.8)
	+83.2		1.01(67.3)		1.18(67.3)			2.30(12.0)	
VIII	−67.1	1.24(66.0)	1.27(65.8)	1.20(65.8)	1.07(69.0)	1.07(69.0)	2.65(12.8)	2.32(16.2)	2.32(16.4)
		0.80(65.9)	0.88(65.9)	0.88(65.9)	1.03(68.9)		2.55(12.2)	2.37(16.6)	2.33(16.7)
	+33.0	1.27(66.0)		0.89(66.2)	1.07(68.8)		2.45(15.3)		2.40(15.4)

[a] Assignments as in Fig. 2.

[b] Primed letters apply only to complex **VIII**.

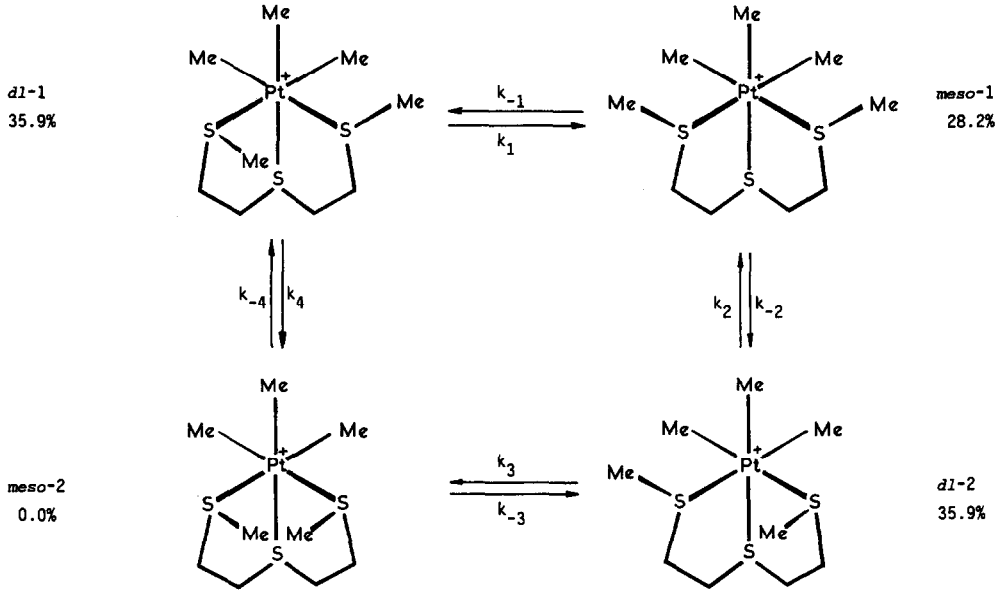

Fig. 3. Diastereoisomers of $[PtMe_3(MeSCH_2CH_2)_2S]^+$ showing isomer abundance.

inversion would lead to a highly strained conformation. With the supporting evidence that there are also no changes attributable to central chalcogen atom inversion in the spectra of compounds **IX** and **X**, it is reasonable to conclude that this process is energetically inaccessible, and the problem is simplified to one involving four interconvertible diastereoisomers.

At low temperatures (−54.6°C), the S—Me region of the spectrum of **III** contains only three signals (plus ^{195}Pt satellites) (Fig. 4), assignable to the two *dl*-isomers and one of the *meso* isomers. This assignment is confirmed by the presence of five signals in the Pt—Me region, a set of three in the rate 1 : 1 : 1 from the asymmetric *dl*-isomers, and two signals ratio 2 : 1 from the one *meso*-isomer (Fig. 5). No signals from the second *meso*-isomer could be detected, possibly due to coincidental over-

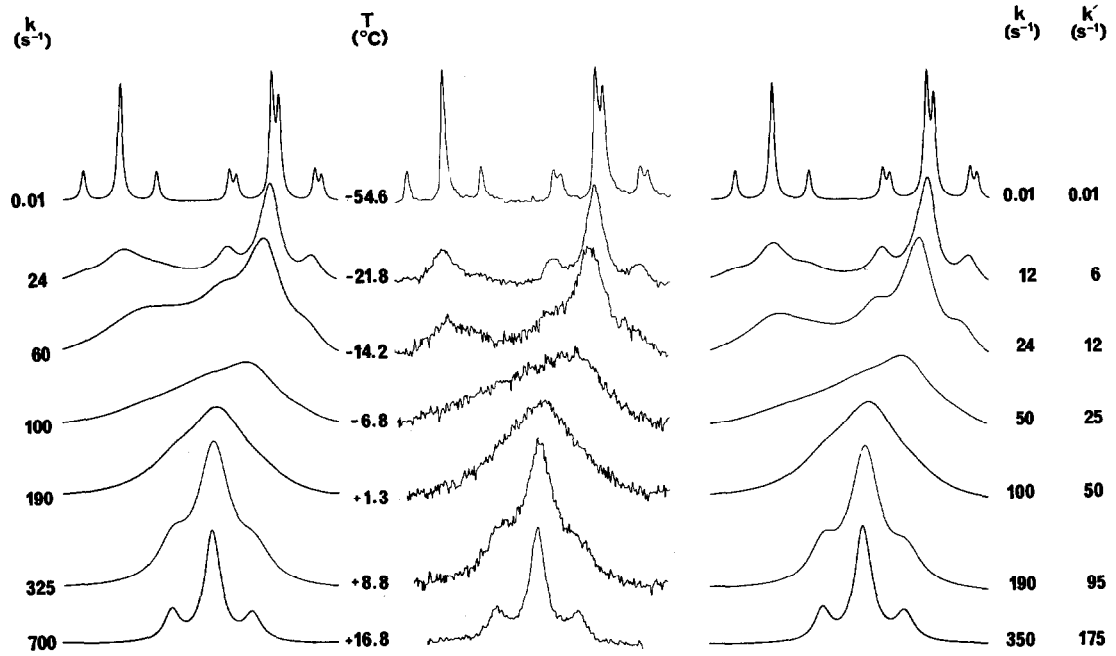

Fig. 4. Experimental and computer synthesised variable temperature ^1H NMR spectra of $[PtMe_3(MeSCH_2CH_2)_2S]^+I^-$ in the S—Me region.

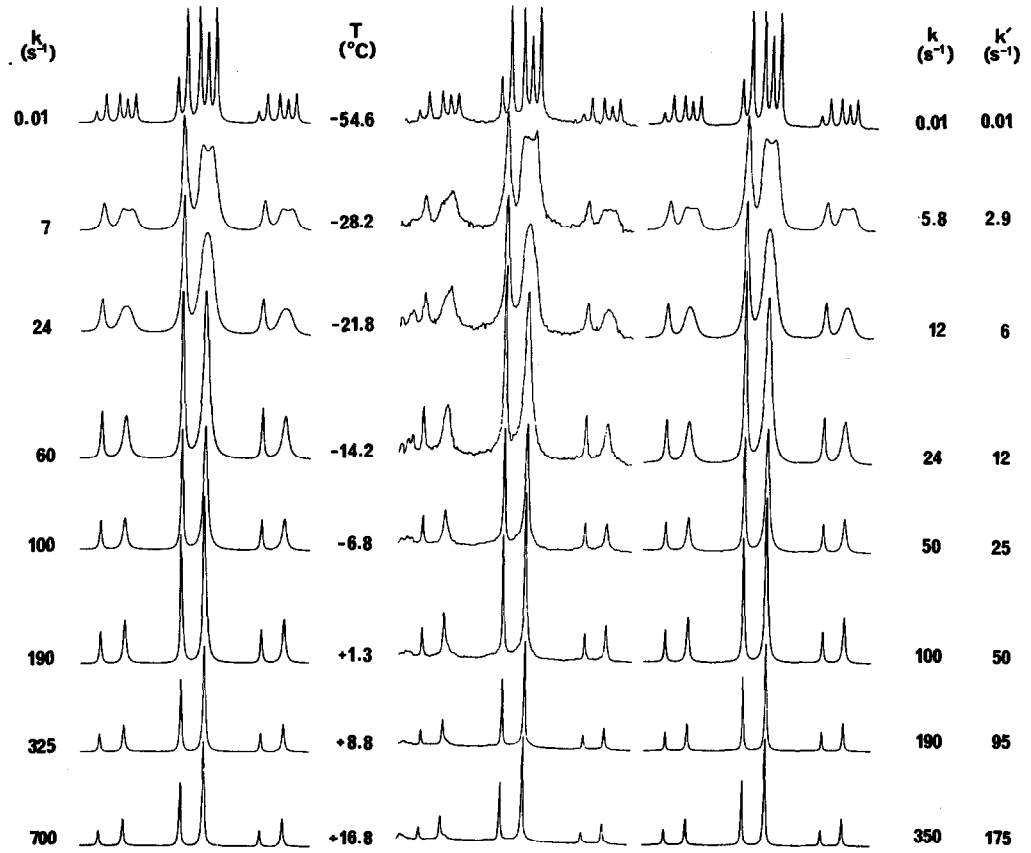

Fig. 5. Experimental and computer synthesised variable temperature ^1H NMR spectra of $[PtMe_3(MeSCH_2CH_2)_2S]^+I^-$ in the Pt—Me region.

lap of the signals, but much more probably to a very low abundance for this isomer. Molecular models of *meso*-2 show severe steric interaction between the two S—Me groups, and our analysis below assumes an assignment of the signals to the *meso*-1 form and the *dl*-pair (see below). Signal area determinations gave the relative isomer populations shown in Fig. 3.

On warming the sample, the three SMe signals coalesced as a result of S-inversion, until at 16.8°C a single averaged peak (with ^{195}Pt satellites) was observed (Fig. 4). At the same time the PtMe signals coalesced to two, with intensity ratio 2:1 (Fig. 5). Both regions showed complete retention of coupling to ^{195}Pt at all temperatures, proving that a non-dissociative fluxional process was responsible for the changes. Computer simulation of the spectra was performed assuming that the isomers were interconverted by pyramidal inversion at the sulphur atoms (Fig. 3). Since the two *dl*-isomers are identical, it necessarily follows that $k_1 = k_2$ $(= k)$, and $k_3 = k_4$ $(= k'')$. As no *meso*-2 isomer was evident, the initial assumption was made that $k_3 = k_4 = 0$, thus reducing the spin problem to one involving three isomers (Fig. 6, spin system 1). However, while it was possible to obtain good agreement between simulated and experimental spectra in both the S—Me and Pt—Me regions, the k values necessary for the former were 5–10% higher than for the latter. Compromise values could be found which gave reasonable agreement in both regions, but the need to consider an alternative spin system was clear. Since the signal to noise ratio and peak width at the low temperature limit would allow for up to 4% of the *meso*-2 isomer, the initial assumption was revised, and allowance made for the presence of very small amounts of *meso*-2, so that rate constant k_3 and k_4 now have equal but non-zero values, and spin-system 2 (Fig. 6) applies. A simplification of this system is possible by combining the effects of k_3 and k_4 in the form of one rate constant k' which represents the overall rate of interconversion of the two *dl*-isomers via a short-lived *meso*-2 intermediate (spin system 3). This implies a practically simultaneous inversion at both sulphur atoms. Simulations based on spin system 3 gave excellent agreement with the observed spectra in both S—Me and Pt—Me regions throughout the temperature range studied. The simulated spectra using spin system 1 (left of figures) and spin system

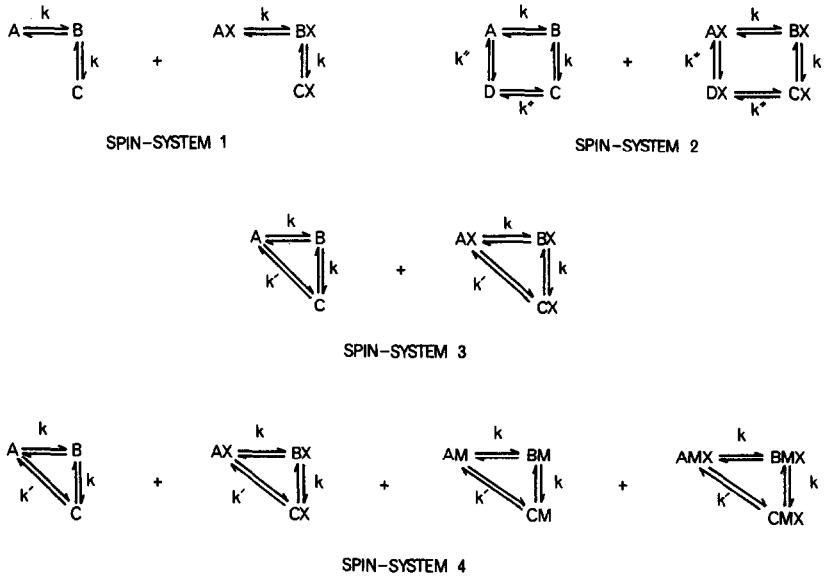

Fig. 6. Spin systems on which the computer synthesised spectra are based. A, B, C and D refer to the proton environments in the *dl*-1, *meso*-1, *dl*-2 and *meso*-2 isomers in Fig. 2 respectively. X denotes the ^{195}Pt nucleus and M the ^{77}Se nucleus.

3 are compared with the experimental spectra in Figs 4 and 5 (note the incompatibility of the spectra at −14.2°C using the former system). Spin-system 3 was also used for compounds **I**, **II** and **IV–VII**, since inclusion of the spin-active selenium nuclei in the computations (spin system 4) had negligible effect on the overall line shape.

For the symmetrical compound **I** $[PtMe_3\{(MeSCH_2CH_2CH_2)_2S\}]^+$ good agreement was obtained only when k' was put equal to zero. In this complex the two six-membered rings undergo rapid ring reversal even at −56.5°C, and molecular models show that this process increases the steric interaction in the *meso*-2 isomer such that it is inaccessible as an intermediate for the *dl–dl* interconversion. This is supported by the observation that the *dl*-isomers are only 12.3% abundant compared to *c.* 35% for the corresponding five-membered ring systems (Table 2). The low-temperature spectrum of **I** in the S—Me region could not be assigned owing to signal overlap and the relatively low abundance of the *dl*-invertomers, and energy barriers were obtained from the Pt—Me region only. The spectra of **V** proved impossible to simulate, as selenium inversion takes place in the same temperature range as Pt—Me scrambling (*vide infra*).

The spectral changes shown by the unsymmetrical ion **VIII** are more complex, as four pairs of *dl*-isomers are possible (Fig. 7), each of which has a non-superimposable mirror image (though as the respective mirror images give identical NMR spectra, only one set of conformers needs to be considered). At −67.1°C (the slow inversion limit), the S—Me region of the 400 MHz spectrum shows six signals assignable to *dl*-1, *dl*-2 and *dl*-3. The remaining undetected isomer is analogous to the *meso*-2 isomer in **I–VII**, and its absence may be explained by the same reasoning. The assignment is confirmed by the presence of either signals in the Pt—Me region (the ninth methyl signal overlaps). The spectra at 100 MHz were not so clearly resolved, but it was possible to use the data from 400 MHz spectra to simulate them. Figure 7 illustrates how the conformers are related by the rate constants k_1–k_5, but similar reasoning to that used for **I–VII** shows that only k_1, k_2 and k_3 are needed

Table 2. Relative isomer abundance for the thio- and selenoether complexes at the slow inversion limits

Complex	Relative percentage abundance[a] *dl*-1	*meso*-1	*dl*-2
I	12.3	75.4	12.3
II	39.0	22.0	39.0
III	35.9	28.2	35.9
IV	33.5	33.0	33.5
VI	36.5	27.0	36.5
VII	36.0	28.0	36.0
VIII	48.8	33.5[b]	17.7[c]

[a] Isomers refer to Fig. 3 (for **I–VII**) and to Fig. 7 (for **VIII**): the *meso*-2 isomers (*dl*-4 for **VIII**) were not detected.

[b] *dl*-2 for **VIII**.

[c] *dl*-3 for **VIII**.

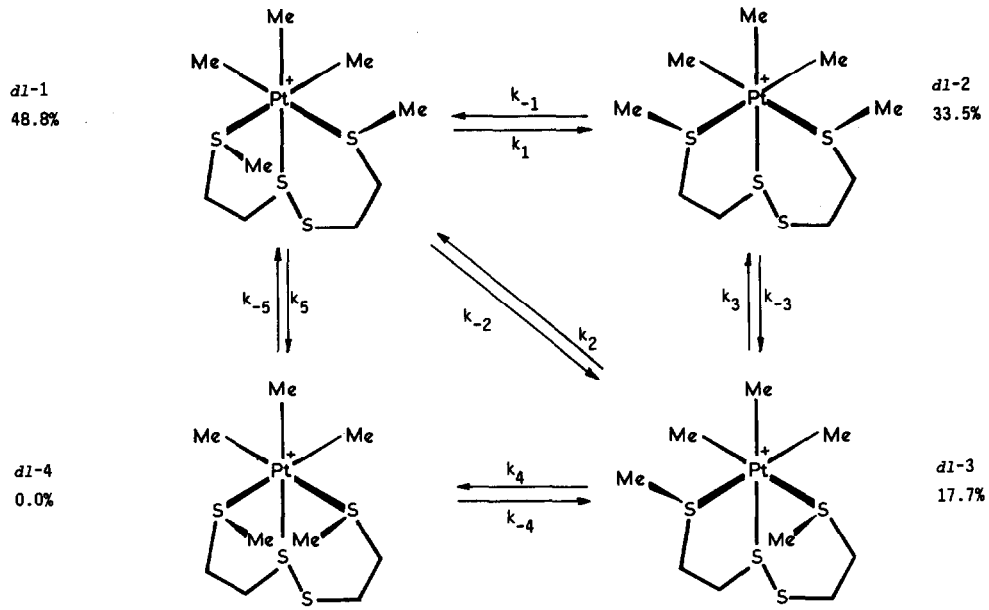

Fig. 7. Diastereoisomers of $[PtMe_3(MeSCH_2CH_2S)_2]^+$ showing isomer abundance.

for successful simulation. Comparison of data obtained with compounds **I** and **III** (containing six- and five-membered rings respectively) shows it is reasonable to assume that $k_3 > k_1 > k_2$ at all temperatures.

On warming compound **VIII**, spectral changes occur in two distinct stages (Figs 8 and 9). From −67 to −27°C signals (spectra a–g) from *dl*-1 stay sharp, so simulations were done assuming $k_1 = k_2 = 0.01\ s^{-1}$. By the onset of the second stage collapse (−27 to +33°C) (spectra g–m), a linear correlation between $\log_{10} k_3$ and $1/T$ had already been established, thus enabling values of k_3 to be estimated by extrapolation. Manipulation of the three rate constants gave excellent agreement between experimental and simulated spectra throughout the two ranges. The k values determined are given in Table 3, and the energy barriers to inversion in Table 4.

As found for the bidentate analogues,[1] the inversion rates for this series of compounds are extremely fast compared to those found for sulphoxides,[6] selenoxides,[7] thiosulphinates[8] and sulphonium ions.[9] As expected, the free energies of activation at the selenium atoms are *c.* 15 kJ mol^{-1} higher than those for sulphur inversion, presumably due to increased *s*-character of the lone pair on the chalcogen atom. The energy barriers to inversion at E (Fig. 1) were found to depend on the central chalcogen E′ in the order Se ~ S > 0, which is related to the length of the Pt—E bond reflected in the ^2J(Pt—Me) coupling constants. The markedly weaker Pt—O bond clearly makes the transition state more accessible,[10] and predominates over the competing effect of decreasing the chalcogen—carbon bond length and decreasing electron density at platinum.

Comparison of complexes **I**, **III** and **VIII** reveals a decrease of *c.* 9 kJ mol^{-1} in inversion energy barriers as the heterocyclic ring changes from five to six members, consistent with results obtained elsewhere.[1,10–12] In complex **VIII** the inversion energy barriers for the five- and the six-membered

Table 3. Rate constants and temperatures for the variable temperature ^1H NMR spectra of complex **VIII** in Figs 8 and 9

Spectrum	Temperature (°C)	Rate constants[a] k (s^{-1})		
		k_1	k_2	k_3
a	−67.1	0.01	0.01	0.7
b	−57.1	0.01	0.01	2.8
c	−52.7	0.01	0.01	5.2
d	−47.3	0.01	0.01	11.2
e	−42.1	0.4	0.2	20.0
f	−31.9	1.2	0.7	60.0
g	−27.3	2.4	1.2	102.0
h	−20.6	5.6	2.4	202.0
i	−7.0	24.0	8.0	732.0
j	−0.7	40.0	15.0	1270.0
k	+12.9	145.0	45.0	3840.0
l	+22.5	370.0	160.0	7889.0
m	+33.0	800.0	250.0	8000.0

[a] For assignments of the rate processes see Fig. 7.

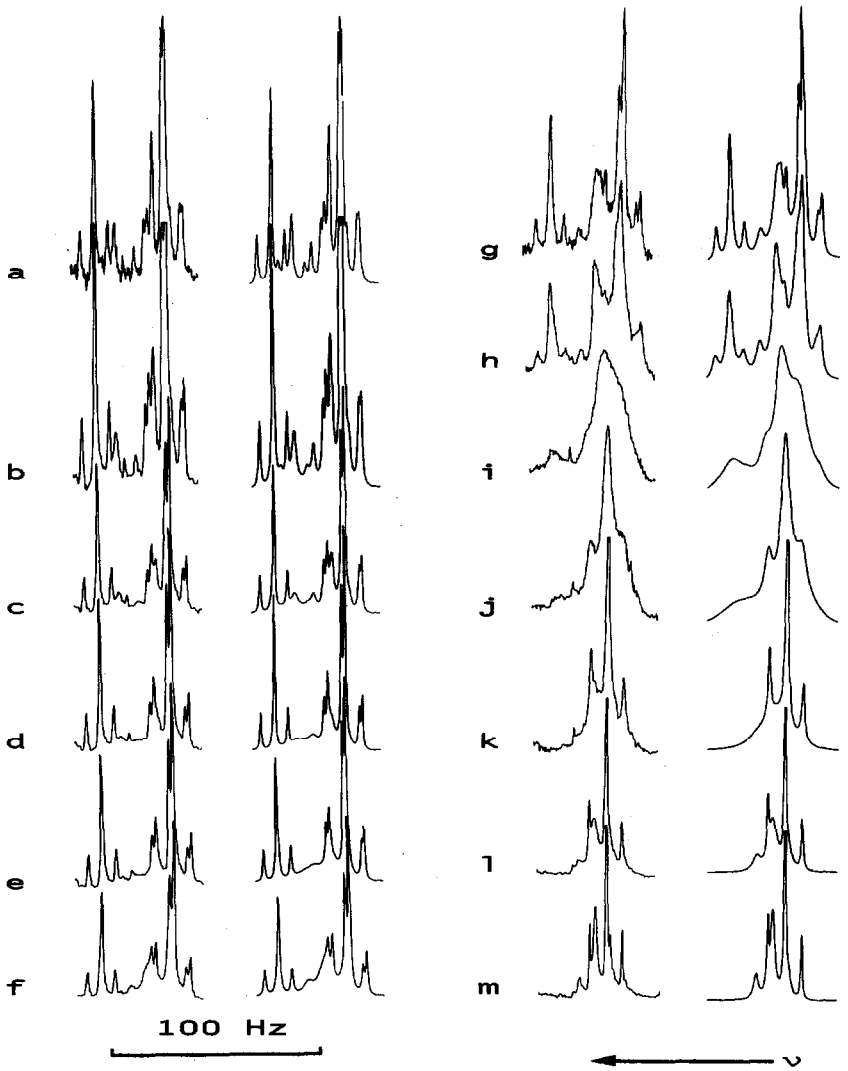

Fig. 8. Experimental and computer synthesised variable temperature ^1H NMR spectra of $[PtMe_3(MeSCH_2CH_2S)_2]^+BF_4^-$ showing the effects of sulphur inversion on the S—Me signals.

Table 4. Energy parameters for the pyramidal inversion processes

Complex[a]	Mechanism[b]	E_a (kJ mol^{-1})	$\log_{10} A$	ΔH^* (kJ mol^{-1})	ΔG^* (kJ mol^{-1})	ΔS^* (J mol^{-1} K^{-1})
I	*k*	49.0±0.44	12.35±0.10	44.0±0.44	48.4±0.13	−15±1.94
	k'	—	—	—	—	—
II	*k*	61.0±1.18	13.94±0.24	59.0±1.19	54.7±0.19	15±4.6
	k'	64.0±1.52	14.20±0.30	62.0±1.52	55.9±0.24	20±5.9
IIIa	*k*	53.7±0.35	12.22±0.07	51.4±0.36	56.9±0.04	−18±1.30
	k'	53.5±0.30	11.90±0.06	51.3±0.32	58.7±0.04	−24±1.20
IV	*k*	61.1±1.70	13.70±0.34	59.0±1.70	56.0±0.23	10±6.50
	k'	59.0±1.57	13.04±0.31	57.0±1.57	58.0±0.22	−2±6.01
VI	*k*	66.0±1.15	12.00±0.20	63.0±1.17	71.0±0.1	−25±3.6
	k'	66.0±1.15	11.70±0.20	63.0±1.17	72.7±0.1	−31±3.6
VII	*k*	70.0±0.67	12.57±0.10	67.0±0.69	71.2±0.07	−13±2.07
	k'	74.0±1.84	12.92±0.29	71.0±1.86	73.4±0.19	−7±5.60
VIII	k_1	60.0±0.66	13.15±0.13	58.0±0.65	58.0±0.09	0±2.47
	k_2	56.0±1.30	11.91±0.26	54.0±1.29	60.8±0.17	−24±4.90
	k_3	52.6±0.17	13.19±0.04	50.6±0.17	50.3±0.04	1±0.69

[a] Complexes assigned as in Fig. 2.

[b] *k* and *k'* as shown in Fig. 6 (spin system 3). k_1, k_2 and k_3 as shown in Fig. 7.

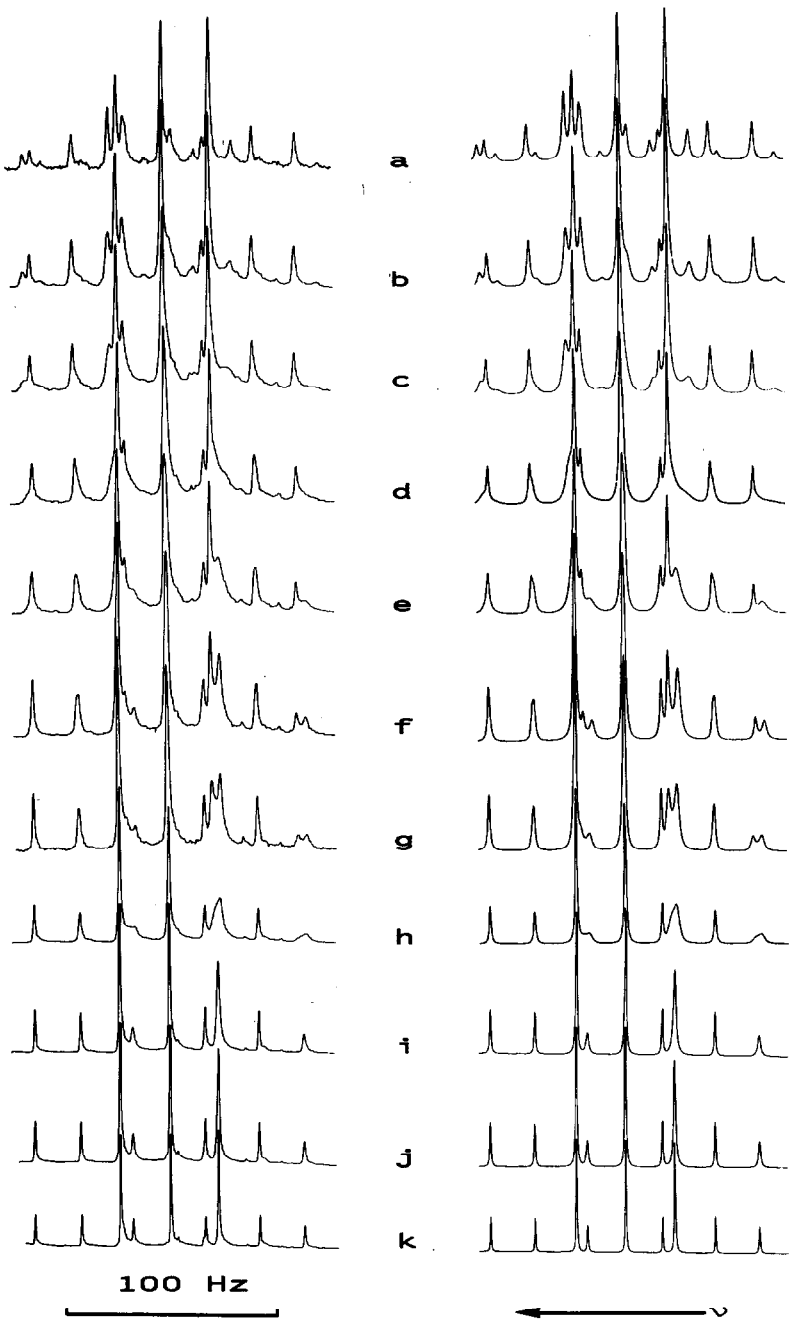

Fig. 9. Experimental and computer synthesised variable temperature ^{1}H NMR spectra of $[PtMe_3(MeSCH_2CH_2S)_2]^+BF_4^-$ showing the effects of sulphur inversion of the Pt—Me signals.

rings are both higher than those found for the five-membered rings in **II–IV** and the six-membered rings in **I**. These observations are not unexpected on steric grounds, and reflect trends that have been observed for the incorporation of different numbers of sulphur atoms into six-membered rings.[13]

High-temperature studies

The behaviour of the compounds at high temperatures falls into one of three categories depending on the Pt–ligand bonding modes. For complexes **I, III, IV, VI** and **VII** the spectral changes associated with **III** are typical. With iodide as counter ion (**IIIa**), at *c.* 75°C (Fig. 10A), an additional set of lines (plus ^{195}Pt satellites) appears in the Pt—Me region and a new singlet at *c.* δ 2.2 (Table 5). A Pt—Me signal with ^2J = 69.3 Hz shows that a neutral iodide-coordinated complex[1] has been formed by displacement of a terminally coordinated sulphur atom. The ligand clearly prefers to form a five-membered ring rather than the eight-membered

ring that would result if the central sulphur atom were displaced. Furthermore ^2J values for Pt—Me groups *trans* to sulphur increase by *c.* 4 Hz when the uncharged complex is formed, showing a decreased Pt—S bond strength. The analogous complex with BPh_4^- as counter ion (**III**) was non-fluxional when heated in DMSO-d_6 up to 135°C (Fig. 10C). The other members of this group were also non-fluxional at high temperatures, though there was slight evidence of peak broadening and changes in the coupling constants that showed the onset of ligand dissociation.

Complexes **VIII** and **X** have the metal coordinated to the central disulphide group. Similar systems are known to undergo 1,2 shifts at high temperatures,[14] and the same process here would give a highly fluxional pseudo-seven-coordinated system. The spectrum of a solution of **VIII** in DMSO-d_6 showed three Pt—Me signals (plus ^{195}Pt satellites) at room temperature. On warming, spectral collapse

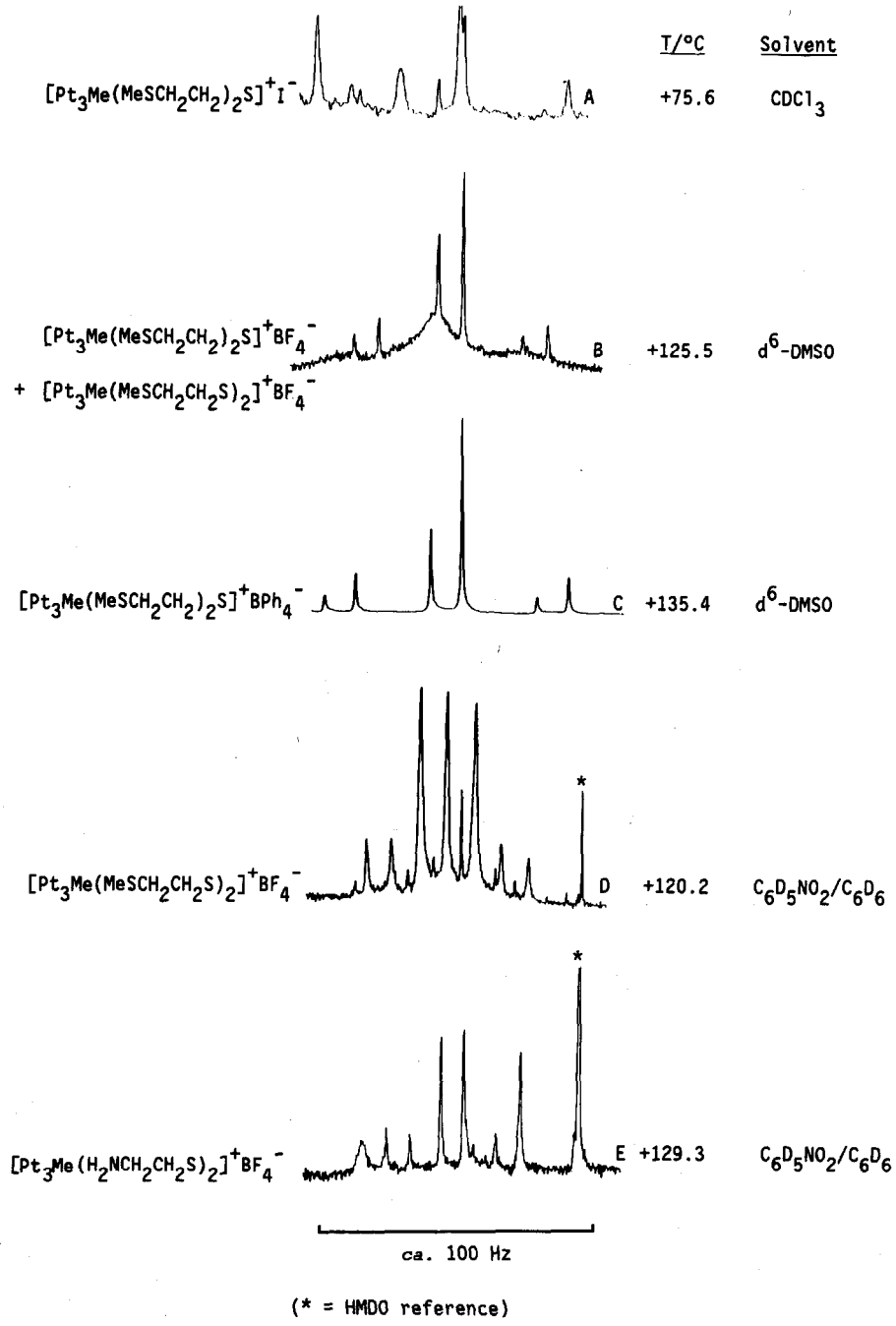

Fig. 10. High temperature ^{1}H NMR spectra (Pt—Me region) for representative complexes.

Table 5. ^{1}H NMR data for the thio- and selenoether complexes at high temperatures

Complex		Temperature (°C)	Pt—Me(*trans* to EMe or NH_2) δ/ppm (J/Hz)	Pt—Me(*trans* to central E′) δ/ppm (J/Hz)	EMe or NH_2 δ/ppm (J/Hz)	Solvent (reference)
$[PtMe_3[(MeSCH_2CH_2)_2S]^+I^-$	**IIIa**	25.0	0.94 (66.9)	1.02 (67.1)	2.47 (14.4)	$CDCl_3$
		75.6	0.96 (66.9)	1.04 (66.9)	2.46 (13.7)	(TMS)
			1.52 (71.3)	1.52 (71.3)	2.18[b]	
			0.97 (69.6)[a]			
$[PtMe_3(MeSCH_2CH_2)_2S]^+BPh_4^-$	**III**	25.0	0.93 (67.4)	0.94 (67.1)	2.29 (15.5)	DMSO-d_6
		122.3	0.89 (67.6)	0.99 (67.4)	2.32 (14.9)	(TMS)
$[PtMe_3(MeSCH_2CH_2CH_2)_2S]^+BF_4^-$	**I**	27.0	0.89 (64.2)	0.69 (63.8)	2.28 (15.0)	DMSO-d_6
		175.0	0.99[c] (74.3)	0.81 (66.2)	2.24 [d]	(TMS)
$[PtMe_3(MeSeCH_2CH_2)_2Se]^+BF_4^-$	**VII**	82.0	0.98 (66.6)	1.15 (66.8)	2.33 (13.9)	DMSO-d_6
		147.0	1.07 (67.5)	1.23 (67.5)	2.42 (13.1)	(HMDO)
$[PtMe_3(MeSCH_2CH_2S)_2]^+BF_4^-$	**VIII**	25.0	1.23 (66.2)	1.10 (69.1)	[e]	DMSO-d_6
			0.87 (66.7)			
		126.0	0.99 (67.6)		[e]	(HMDO)
$[PtMe_3(MeSCH_2CH_2S)_2]^+BF_4^-$	**VIII**	66.8	1.11 (66.0)	0.95 (69.0)	2.33 (14.9)	$C_6D_6NO_2/C_6D_6$
			0.77 (66.4)			
		141.0	1.11 (69.1)[f]	0.95 (69.1)[f]	2.23 (15.3)	(HMDO)
			0.77 (69.1)[f]			
$[PtMe_3(H_2NCH_2CH_2)_2S]^+BF_4^-$	**X**	27.5	0.86 (67.9)	0.42 (67.9)	1.99 —	$C_6D_6NO_2/C_6D_6$
			1.06 (68.6)			(HMDO)
		150.0	0.86 (67.9)	0.40 (68.4)	[g] —	
			0.98 (68.6)			
$[PtMe_3(MeSCH_2CH_2)_2O]^+BF_4^-$	**II**	9.8	0.98 (65.9)	1.09 (81.5)	2.40 (15.6)	$C_6D_6NO_2/C_6D_6$
		101.0	1.10 (71.6)		2.45 (14.9)	(HMDO)
$[PtMe_3(MeSeCH_2CH_2)_2O]^+BF_4^-$	**V**	−27.5[h]	1.03 (66.7)		2.19 (12.2)	$CDCl_3$
			1.09 (63.0)			
					2.48 (10.7)	(TMS)
		93.0	1.17 (71.3)		2.29 [d]	
$[PtMe_3(H_2NCH_2CH_2)_2O]^+BF_4^-$	**IX**	11.5	0.77 (68.4)	1.27 (83.4)	2.08 —	$C_6D_6NO_2/C_6D_6$
		110.0	0.89 (73.2)		1.64 —	(HMDO)

[a] Pt—Me *trans* to coordinated iodide.
[b] Uncoordinated S—Me group.
[c] Broad signal, $\Delta\nu_{1/2} = 2.8$ Hz.
[d] Broad signal, $\Delta\nu_{1/2} = 16$ Hz.
[e] S—Me region not recorded.
[f] Approximate values, $\Delta\nu_{1/2} = 7.8$ Hz.
[g] NH_2 protons not seen.
[h] Very complex non-first order spectrum, major peaks shown.

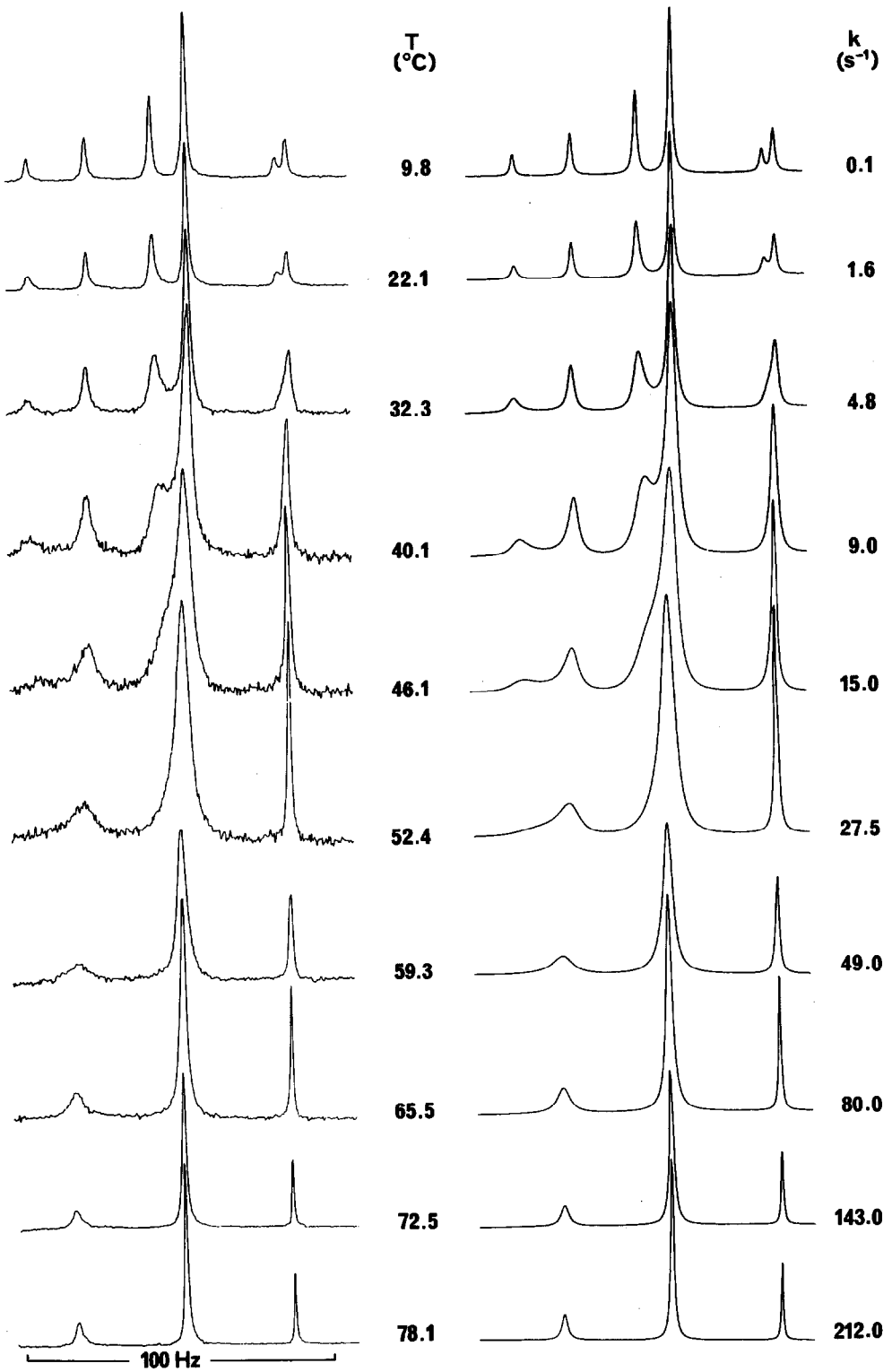

Fig. 11. Experimental and computer synthesised ^1H NMR spectra of $[PtMe_3(MeSCH_2CH_2)_2O]^+$ BF_4^- showing the effects of scrambling of the Pt—Me signals.

occurred until at 155°C only one broad Pt—Me signal (plus satellites) was apparent. This effect is illustrated with a mixture of **III** and **VIII** at 125°C (Fig. 10B) which clearly shows that while the disulphide complex undergoes methyl scrambling (one broad peak), the sulphide complex remains rigid and exhibits two sharp signals. A second high temperature run on **VIII** using a different solvent ($C_6D_5NO_2/C_6D_6$; 2:1 by volume) showed that the fluxional behaviour of **VIII** was solvent dependent. In this solvent three broadened lines are present at 120°C (Fig. 10D) whereas in DMSO the signals had coalesced at this temperature (Fig. 10B). Further heating showed spectral changes comparable to those observed in DMSO, but at 150°C decomposition of the complex occurred. By comparison the ^{1}H NMR spectrum of **X** in DMSO shows three signals (plus ^{195}Pt satellites) at room temperature which stay sharp on warming to 130°C with very little change in chemical shifts or coupling constants (Fig. 10E). Evidently **X** is non-fluxional in the temperature range studied.

Finally, complexes **II**, **V** and **IX** undergo fluxional changes resulting from the centrally coordinated oxygen atom. The inherent weakness of the Pt—O bond[15–18] favours dissociation leading to a stereochemically non-rigid five-coordinate intermediate. Coalescence of the Pt—Me signals was observed for each of these complexes with complete retention of coupling to ^{195}Pt. The spectral changes observed for **II** are reproduced in Fig. 11. Similar changes were recorded for **IX**, but for **V** inversion at Se occurs over the same temperature range as methyl scrambling. For **II** and **IX**, computer simulation gave excellent agreement between experimental and simulated spectra when a single rate constant was used ($A \rightleftarrows B + AX \rightleftarrows BX$; A = PtMe *trans* to N, S or Se, B = PtMe *trans* to O, X = ^{195}Pt). Simulated spectra for **II** are reproduced alongside the experimental spectra in Fig. 11 and the rate constants measured for **II** and **IX** are given in Table 6.

This study shows that ligand scrambling via a 120° pseudo-rotation of the tridentate ligand does not occur for this type of complex, in contrast to the bidentate analogues, for which a 'pancake flip' movement of the bidentate ligands has been well established elsewhere.[19] One explanation may be that the tridentate ligands are more strongly bound, the increase in Pt—ligand bond strength shown by the decrease in Pt—Me coupling of *c.* 4 Hz being enough to inhibit ligand scrambling processes. Spectral changes associated with the disulphide complexes show that here the fluxional process is solvent dependent, which points to a dissociative mechanism. However, this work does show that the rate of dissociation is also dependent on the

Table 6. Energy parameters for the high-temperature scrambling processes in complexes **II** and **IX**

	Complex	E_a (kJ mol^{-1})	$\log_{10} A$	ΔH^+ (kJ mol^{-1})	ΔG^+ (kJ mol^{-1})	ΔS^+ (kJ mol^{-1})
(II)	$[PtMe_3(MeSCH_2CH_2)_2O]^+BF_4^-$	75±0.6	13.5±0.1	71.1±0.1	72±0.6	4±1.9
(IX)	$[PtMe_3(H_2NCH_2CH_2)_2O]^+BF_4^-$	79±0.8	13.2±0.1	76±0.8	76.6±0.1	−1±2.3

presence of both terminal chalcogen and disulphide coordination. Complexes with a coordinated oxygen atom undergo high-temperature ligand scrambling that is fully reversible and purely intramolecular. The energy parameters are slightly affected by the nature of the terminal bonding and therefore a value for $\Delta G^{\ddagger}$ of around 75 kJ mol^{-1} can be expected for ligand scrambling and selenium inversion in complex **V**.

REFERENCES

1. E. W. Abel, S. K. Bhargava, K. Kite, K. G. Orrell, V. Sik and B. L. Williams, *J. Chem. Soc., Dalton Trans.* 1982, 583, and references therein.
2. T. G. Appleton, H. C. Clark and L. E. Manzer, *Coord. Chem. Rev.* 1973, **10**, 335.
3. E. W. Abel, K. Kite and P. S. Perkins, *Polyhedron* 1986, **5**, 1459.
4. D. A. Kleier and G. Binsch, *'D.NMR. 3', Quantum Chemistry Program Exchange* 1970, 1, 165.
5. G. Binsch and H. Kessler, *Angew. Chem. Int. Edn.* 1980, **19**, 411.
6. D. R. Rayner, A. J. Gordon and K. Mislow, *J. Am. Chem. Soc.* 1968, **90**, 4845.
7. M. Oki and H. Iwamura, *Tetrahedron* 1966, 217.
8. P. Koch and R. L. Tomilson, *J. Am. Chem. Soc.* 1968, **90**, 5938.
9. R. J. Cross, T. H. Green and R. Keat, *J. Chem. Soc., Dalton Trans.* 1976, 1150.
10. E. W. Abel, M. Booth and K. G. Orrell, *J. Chem. Soc., Dalton Trans.* 1980, 1582.
11. A. R. Rauk, L. C. Allen and K. Mislow, *Angew. Chem. Int. Edn.* 1970, **9**, 400.
12. E. W. Abel, S. K. Bhargava and K. G. Orrell, *Prog. Inorg. Chem.* 1984, **32**, 1.
13. N. L. Allinger, M. J. Hickey and J. Kao, *J. Am. Chem. Soc.* 1976, **98**, 2741.
14. E. W. Abel, S. K. Bhargava, T. E. Mackenzie, P. K. Mittal, K. G. Orrell and V. Sik, *J. Chem. Soc., Chem. Commun.* 1982, 535.
15. F. P. Dwyer, N. S. Gill, E. C. Gyarfas and F. Lions, *J. Am. Chem. Soc.* 1953, **75**, 1526.
16. J. R. Lotz, B. P. Block and W. C. Fernelius, *J. Phys. Chem.* 1959, **63**, 541.
17. M. Ciampolini and N. Nardi, *Inorg. Chem.* 1967, **6**, 445.
18. R. Barbucci and A. Vacca, *J. Chem. Soc., Dalton Trans.* 1974, 2363.
19. E. W. Abel, S. K. Bhargava and K. G. Orrell, *Prog. Inorg. Chem.* 1984, **2**, 94.

Polyhedron Vol. 6, No. 3, pp. 563–569, 1987
Printed in Great Britain

0277–5387/87 $3.00+.00

ON THE EXTRACTION WITH LONG-CHAIN AMINES—XXXVII. THE EXTRACTION OF LEAD(II) BY TRILAURYLAMINE AND TRILAURYLAMMONIUM, TRI-*n*-OCTYLAMMONIUM AND TRI-*n*-HEXYLAMMONIUM CHLORIDES DISSOLVED IN BENZENE

M. P. ELIZALDE,* J. M. CASTRESANA, L. A. FERNANDEZ and M. E. ASTIGARRAGA

Departamento de Quimica, Universidad del Pais Vasco, Apartado 644, 48080 Bilbao, Spain

(*Received* 27 *May* 1986; *accepted* 12 *August* 1986)

Abstract—The extraction of Pb(II) from 1.0 mol dm^{-3} NaCl with trilaurylamine (TLA) and trilaurylammonium, tri-*n*-octylammonium and tri-*n*-hexylammonium chlorides (TLAHCl, TOAHCl and THAHCl) dissolved in benzene has been studied at 298 K. The extraction of Pb(II) by TLA and TLAHCl can be explained by the formation of the species (TLAHCl)($PbCl_2$) and $(TLAHCl)_3(PbCl_2)$ in the organic phase. The use of TOAHCl and THAHCl as extractants leads to the formation of the same kind of species in the organic phase indicating that the length of the alkylic chain of the amine does not influence the metal extraction. Conditional equilibrium constants for the extracted species are given.

The extraction of lead from chloride solutions by long-chain tertiary amines has been scarcely studied.[1–4] Furthermore, information about lead extraction by other amine and quaternary ammonium salts is also rather scarce[5–10] if compared with the larger number of studies performed with inner and outer transition metal ions.

The lack of information about the extraction behaviour of Pb(II) in these systems together with its great environmental importance made us initiate a study on the extraction of this metal from aqueous 1.0 mol dm^{-3} NaCl solutions by trilaurylamine (TLA) dissolved in benzene.

This work is part of a systematic study on the extraction of metal chlorides by long-chain tertiary alkylamines and presents a detailed description of the factors affecting the extraction such as the aqueous pH (in the extraction by TLA alone), the ammonium salt concentration [extraction by trilaurylammonium chloride (TLAHCl)] and the length of the amine chain [extraction by tri-*n*-octylammonium and tri-*n*-hexylammonium chlorides (TOAHCl and THAHCl)]. The effect of the ionic strength in the extraction of Pb(II) by TLAHCl will be discussed in a subsequent publication. The data in the present study have been treated by graphical and numerical methods in order to ascertain the composition of the species extracted as well as the extraction constants.

EXPERIMENTAL

Reagents

Lead chloride, $PbCl_2 \cdot H_2O$ (Merck, p.a.), was purified by recrystallization before use and analysed trimetrically according to standard methods.[11] Sodium chloride (Merck, p.a.) was recrystallized as described elsewhere.[12] TLA, benzene and mercaptosuccinic acid (Merck, p.a.) were used as supplied. TLAHCl, TOAHCl and THAHCl were prepared from TLA (Merck, p.a.), TOA (Eastman Kodak, p.a.), and THA (Eastman Kodak, p.a.), as described in Ref. 13. Distilled deionised water was used throughout the work. All other chemicals were of analytical-grade quality.

Experimental procedure

Equal volumes (10 cm^3) of organic solutions containing TLA or the ammonium salts in benzene

* Author to whom correspondence should be addressed.

ranging from 0.005 to 0.100 mol dm^{-3} were shaken with aqueous solutions of Pb(II) in 1.0 mol dm^{-3} NaCl using special stoppered tubes on a continuous rotating rack. The total concentration of Pb(II) was varied from 0.2 to 0.8 mmol dm^{-3}. The free hydrogen ion concentration was varied from 10^{-5} to 10^{-1} mol dm^{-3} when using TLA, and kept around 10^{-2} mol dm^{-3} when the ammonium salts were used as extractants. Preliminary experiments showed that extraction equilibrium was attained within 2 min although a shaking time of 15 min was always used.

After centrifugation, aliquots of the aqueous phases were taken for analysis. The metal concentration was measured spectrophotometrically using mercaptosuccinic acid in $Na_2B_4O_7$–NaOH buffer at pH = 10.5.[14] By measuring the concentration of Pb(II) in the organic phase after its stripping with NaOH, the mass balance for lead could be checked.

RESULTS AND GRAPHICAL DATA TREATMENT

Extraction by the amine

The extraction of Pb(II) by TLA dissolved in benzene can be described by:

$$j\mathrm{Pb}^{2+} + n\mathrm{Cl}^- + q\mathrm{H}^+ + p\mathrm{TLA}_{\mathrm{org}} \rightleftharpoons \mathrm{TLA}_p\mathrm{H}_q\mathrm{Pb}_j\mathrm{Cl}_{n\,\mathrm{org}}, \quad (1)$$

for which the stroichiometric equilibrium constant is given by:

$$\beta_{pqjn} = \frac{[\mathrm{TLA}_p\mathrm{H}_q\mathrm{Pb}_j\mathrm{Cl}_n]_{\mathrm{org}}}{[\mathrm{Pb}^{2+}]^j[\mathrm{Cl}^-]^n[\mathrm{H}^+]^q[\mathrm{TLA}]^p}. \quad (2)$$

The stoichiometric distribution coefficient of Pb(II) is given by:

$$D = C_{\mathrm{Pb,org}}/C_{\mathrm{Pb,aq}} = \sum_p\sum_q\sum_j\sum_n j\beta'_{pqjn}[\mathrm{Cl}^-]^n[\mathrm{Pb}^{2+}]^{j-1}[\mathrm{H}^+]^q[\mathrm{TLA}]^p \quad (3)$$

β'_{pqjn} being a conditional formation constant defined by:

$$\beta'_{pqjn} = \beta_{pqjn}\alpha_{\mathrm{Pb}}^{-1}. \quad (4)$$

The side-reaction coefficient α_{Pb} remained constant since the chloride concentration was kept constant and the contribution of metal hydroxo-complexes can be considered negligible in the pH range studied.

The experimental results, $\log D = f(\mathrm{pH})$ at several total concentrations of TLA are given in Fig. 1. Additional experiments carried out at several total Pb(II) concentrations indicated absence of polynuclear lead species in the organic phase.

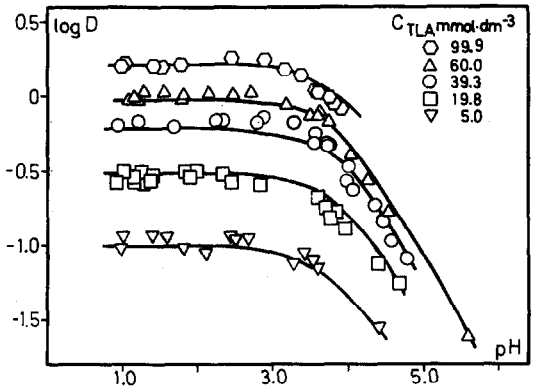

Fig. 1. Plot of $\log D$ vs pH data for the different total concentration of TLA. The solid lines have been drawn using the proposed extraction constants.

On the other hand, a preliminary analysis of the data in Fig. 1 made by plotting $\log D = F(\log [\mathrm{TLA}]_{\mathrm{org}})$ at selected fixed pH values gave rise to curves of increasing slope indicating the extraction of more than one lead species. Hence, assuming as simplest hypothesis the formation of two species with stoichiometries $\mathrm{TLA}_p\mathrm{H}_q\mathrm{PbCl}_n$ and $\mathrm{TLA}_r\mathrm{H}_s\mathrm{PbCl}_m$, the distribution coefficient can be expressed, according to eqn (3), by:

$$D = \beta'_{pqn}[\mathrm{Cl}^-]^n[\mathrm{TLA}]^p[\mathrm{H}^+]^q + \beta'_{rsm}[\mathrm{Cl}^-]^m[\mathrm{TLA}]^r[\mathrm{H}^+]^s \quad (5)$$

where β'_{pqn} and β'_{rsm} are the respective conditional extraction constants.

Equation (5) can be rearranged to:

$$\frac{D}{\beta'_{rsm}[\mathrm{Cl}^-]^m[\mathrm{TLA}]^r[\mathrm{H}^+]^s} = 1 + \frac{\beta'_{pqn}}{\beta'_{rsm}}[\mathrm{Cl}^-]^{n-m}[\mathrm{TLA}]^{p-r}[\mathrm{H}^+]^{q-s}. \quad (6)$$

The experimental functions $(\log D - \log [\mathrm{TLA}]_{\mathrm{org}}) = f(\log [\mathrm{TLA}]_{\mathrm{org}})$ obtained for different integer values of r, at constant selected pH values, were compared with:

$$\log Y = \log(1 + X^i) = f(\log X), \quad (7)$$

where Y and X are normalized variables defined by:

$$Y = \frac{D}{\beta'_{rsm}[\mathrm{Cl}^-]^m[\mathrm{TLA}]^r[\mathrm{H}^+]^s}, \quad (8)$$

$$X = \left(\frac{\beta'_{pqn}}{\beta'_{rsm}}[\mathrm{Cl}^-]^{n-m}[\mathrm{H}^+]^{q-s}\right)^{1/(p-r)}[\mathrm{TLA}]_{\mathrm{org}}, \quad (9)$$

and $i = p - r$.

Free TLA concentrations were calculated from the mass balance for the reagent by neglecting the contribution from the lead species due to the high

C_{TLA}/C_{Pb} ratio used in the experiments:

$$C_{TLA} = [TLA]_{org} + \beta_{11}[TLA]_{org}[Cl^-][H^+] + 2\beta_{22}[TLA]^2_{org}[Cl^-]^2[H^+]^2, \quad (10)$$

where β_{11} and β_{22} were taken from Ref. 13.

The best agreement between experimental and theoretical functions, for which the position of best fit is shown in Fig. 2, was found for $i = 2$ and $r = 1$. Therefore, the value of the stoichiometric coefficient p equals 3.

In order to determine the stoichiometric coefficients s and q, as well as the extraction constants, the differences between experimental and theoretical functions defined by:

$$\Delta Y = (\log D - \log[TLA]_{org}) - \log Y = \log \beta'_{rsm}[Cl^-]^m - s\,pH, \quad (11)$$

$$\Delta X = \log[TLA]_{org} - \log X = -\frac{1}{p-r}\log\frac{\beta'_{pqn}}{\beta'_{rsm}}[Cl^-]^{n-m} + \frac{q-s}{p-r}pH \quad (12)$$

were plotted as a function of pH as shown in Fig. 3. Straight lines of slope values -1 and 1, respectively, were observed from which the values $s = 1$ and $q = 3$ can be deduced from eqns (11) and (12).

From the intercepts on both axes in Fig. 3, values of the extraction constants for the species $(TLAHCl)(PbCl_2)$ and $(TLAHCl)_3(PbCl_2)$ were obtained. The number of chloride ions in the extracted species has been deduced from the electroneutrality condition in the organic phase. Values of the constants are collected in Table 1.

Extraction with the ammonium salts

The extraction of Pb(II) from chloride medium with TLAHCl, TOAHCl and THAHCl, generically

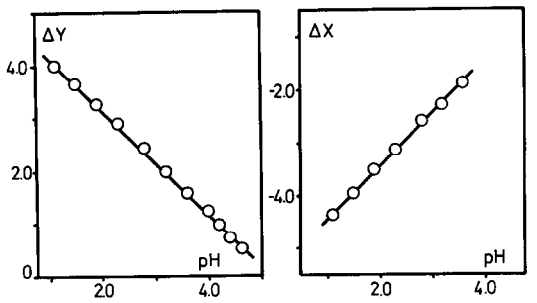

Fig. 3. Differences on both axes in Fig. 2 as a function of pH.

represented by R_3NHCl, can be described by:

$$jPb^{2+} + 2jCl^- + zR_3NHCl_{org} \rightleftharpoons (R_3NHCl)_zPb_jCl_{2j\,org}. \quad (13)$$

Since Pb(II) is only present in tracer amounts, polynuclear complexes of lead in the organic phase need not to be considered. This assumption is supported by the fact that the curves $\log D$ vs $\log C_{R_3NHCl}$ coincide for different Pb(II) concentrations (cf. Fig. 4).

Taking into account the mass balance equation for the metal, with k'_{z2} being the conditional extraction constant for reaction (13), the distribution coefficient of Pb(II) can be expressed by:

$$D = \sum_z k'_{z2}[Cl^-]^2[R_3NHCl]^z_{org}. \quad (14)$$

In order to deduce values of the stoichiometric coefficient z, the functions $\log D = f(\log [R_3NHCl]_{org})$ have been obtained using the aggregation constants for TLAHCl, TOAHCl and THAHCl given in Refs 13, 15 and 16, respectively. The contribution of the lead species to the mass balance equations for the ammonium salts has been

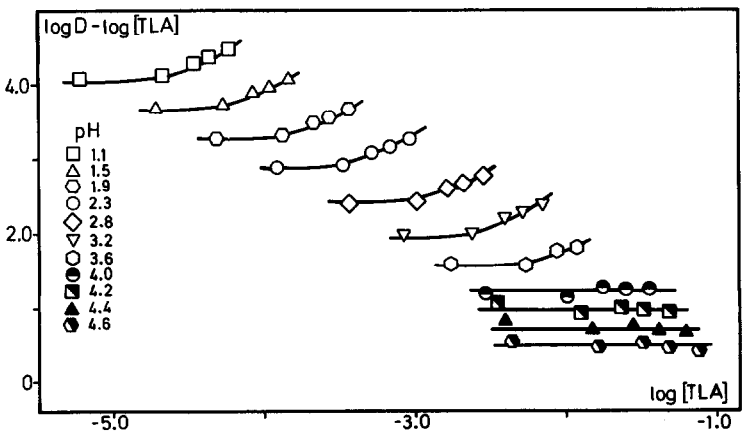

Fig. 2. Comparison between the experimental functions $\log D - \log[TLA] = f(\log [TLA])$ and the theoretical $\log Y = \log(1 + X^2) = f(\log X)$ in the best-fit position.

Table 1. Values of the conditional extraction constants obtained by the graphical and numerical data treatments

	TLA		TLAHCl	
	Log β'_{113}	Log β'_{335}	Log k'_{12}	Log k'_{32}
Graphical	5.15	16.15	1.49	4.91
LETAGROP	5.19±0.03	16.11±0.07	1.54±0.03	4.82±0.10
	TOAHCl		THAHCl	
	Log k'_{12}	Log k'_{32}	Log k'_{12}	Log k'_{32}
Graphical	1.55	5.23	1.50	5.36
LETAGROP	1.54±0.05	5.29±0.10	1.52±0.06	5.48±0.07

considered as negligible since lead is present in tracer amounts. The plots are presented in Fig. 5. It can be appreciated that similar curves, with a lower limiting slope value close to 1.0 and higher ones when increasing the concentration of the extractants, are obtained for the three systems studied. Therefore, assuming the formation in the organic phase of two metallic species with $z = 1$ and $z = z$, eqn (14) can be transformed into:

$$Dk'_{12}[Cl^-]^2[R_3NHCl]_{org}^{-1} = 1 + k'_{z2}(k'_{12})^{-1}[R_3NHCl]_{org}^{z-1}. \quad (15)$$

In a similar way to the treatment carried out with the results of the Pb(II)–TLA system, the experimental functions $(\log D - \log [R_3NHCl]_{org}) =$

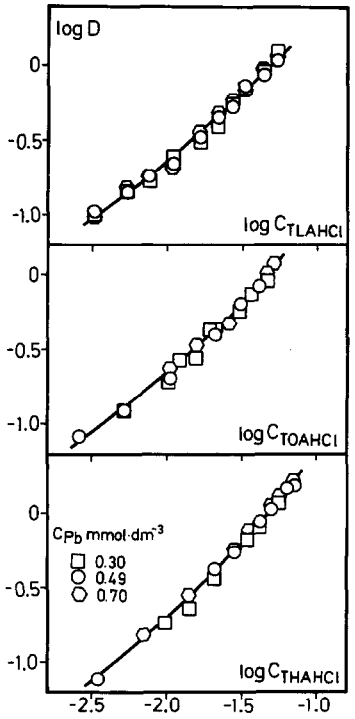

Fig. 4. Plot of log D vs log C_{R_3NHCl} data at different total Pb(II) concentrations. Continuous lines have been drawn using the proposed extraction constants.

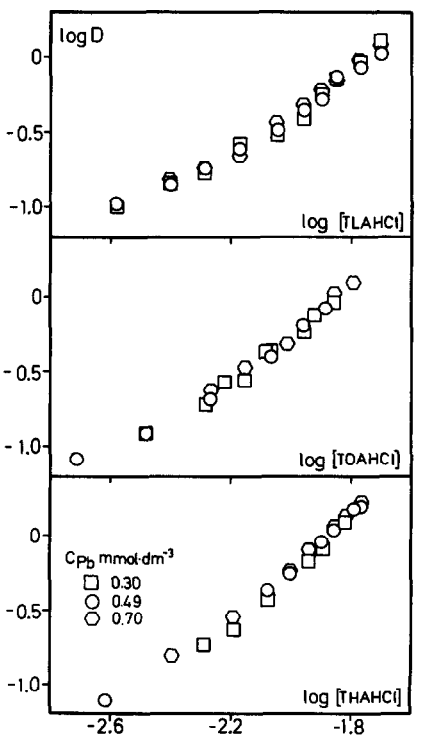

Fig. 5. Log D as a function of the free ammonium salts concentrations at the different Pb(II) concentrations.

$f(\log[R_3NHCl]_{org})$ were compared with the theoretical curves defined by eqn (7), with:

$$Y = Dk'_{12}[Cl^-]^2[R_3NHCl]_{org}^{-1}, \quad (16)$$

$$X = (k'_{z2}/k'_{12})^{1/(z-1)}[R_3NHCl]_{org}, \quad (17)$$

$$i = z^{-1}. \quad (18)$$

The best fit in the three systems was obtained from $i = 2$, as shown in Fig. 6 where the theoretical curves have been drawn with $i = 2$, indicating $z = 3$. From the differences on both axes, values of the conditional constants for the extraction of the species $(R_3NHCl)(PbCl_2)$ and $(R_3NHCl)_3(PbCl_2)$ collected in Table 1 were deduced.

Numerical treatment

The version DISTR[17] of the general minimizing program LETAGROP for the treatment of distribution data was used for the refinement of the graphically obtained equilibrium constants. The function to be minimized is the error squares sum, U, defined by:

$$U = \sum_{N_p} (\log D_{calc} - \log D_{exp})^2, \quad (19)$$

with D_{exp} being the experimentally measured distribution coefficient, D_{calc} the corresponding quantity calculated by the program and N_p the number

Table 2. Values of U_{min} and $\sigma(\log D)$ for the different combination of complexes tried in the extraction of Pb(II) by TLA, TLAHCl, TOAHCl and THAHCl

	Species (n,p,q)	U_{min}	$\sigma(\log D)$	Rejected
TLA	(3,1,1), (4,2,2)	0.475	0.072	
	(3,1,1), (5,3,3)	0.384	0.065	
	(3,1,1), (6,4,4)	0.439	0.070	
	(3,1,1), (4,2,2), (5,3,3)	0.384	0.067	
	(3,1,1), (5,3,3), (6,4,4)	0.384	0.065	
	Species $(1,z)$			
TLAHCl	(1,2)	1.439	0.223	
	(1,1), (1,2)	0.037	0.040	
	(1,1), (1,3)	0.022	0.029	
	(1,1), (1,4)	0.023	0.030	
	(1,1), (1,5)	0.031	0.036	
	(1,1), (1,2), (1,3)	0.022	0.029	(1,2)
	(1,1), (1,2), (1,4)	0.022	0.031	
	(1,1), (1,3), (1,4)	0.021	0.030	
	(1,1), (1,3), (1,5)	0.022	0.030	
TOAHCl	(1,2)	0.520	0.166	
	(1,3)	2.931	0.393	
	(1,1), (1,2)	0.021	0.037	
	(1,1), (1,3)	0.014	0.030	
	(1,1), (1,4)	0.017	0.033	
	(1,1), (1,5)	0.024	0.040	
	(1,1), (1,2), (1,3)	0.014	0.030	(1,2)
	(1,1), (1,2), (1,4)	0.013	0.031	
	(1,1), (1,3), (1,4)	0.014	0.031	
	(1,1), (1,3), (1,5)	0.014	0.031	
THAHCl	(1,2)	0.165	0.093	
	(1,3)	0.172	0.301	
	(1,1), (1,2)	0.028	0.042	
	(1,1), (1,3)	0.016	0.032	
	(1,1), (1,4)	0.024	0.039	
	(1,1), (1,5)	0.042	0.051	
	(1,1), (1,2), (1,3)	0.017	0.033	
	(1,1), (1,2), (1,4)	0.017	0.034	
	(1,1), (1,3), (1,4)	0.016	0.032	(1,4)
	(1,1), (1,3), (1,5)	0.016	0.032	(1,5)

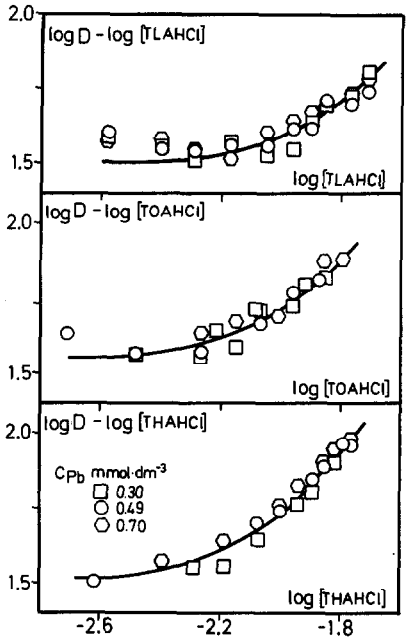

Fig. 6. Comparison between the experimental functions $\log D - \log[R_3NHCl] = f(\log[R_3NHCl])$ and the theoretical $\log Y = \log(1+X^2) = f(\log X)$ in the best-fit positions.

of experimental points. Together with the U_{min} values, the standard deviation $\sigma(\log D)$ is also given for each set of complexes.

From Table 2 it can seen that the graphically obtained model gives the lowest values for U_{min} and $\sigma(\log D)$ for the three systems studied. Models containing more than two metallic extracted species did not improve the fit to the experimental data. The conditional equilibrium constants obtained by numerical treatment are given in Table 1. With the proposed extraction constant values the theoretical $\log D = f(\mathrm{pH})_{C_{TLA}}$ and $\log D = f(\log C_{R_3NHCl})_{C_{pB}}$ functions have been plotted together with the experimental points in Figs 1 and 4, respectively.

Conclusions

The extraction of Pb(II) from chloride medium by TLA and TLAHCl dissolved in benzene can be explained by the formation of $(TLAHCl)(PbCl_2)$ and $(TLAHCl)_3(PbCl_2)$. Taking into account the values of the conditional extraction constants collected in Table 1 for the extraction of Pb(II) by TLA and TLAHCl, the value of the equilibrium extraction constant β_{11} for the reaction:

$$TLA_{org} + H^+ + Cl^- \overset{\beta_{11}}{\rightleftharpoons} TLAHCl_{org} \quad (20)$$

can be obtained combining the reactions:

$$Pb^{2+} + 3Cl^- + TLA_{org} + H^+ \rightleftharpoons (TLAHCl)(PbCl_2)_{org}, \quad (21)$$

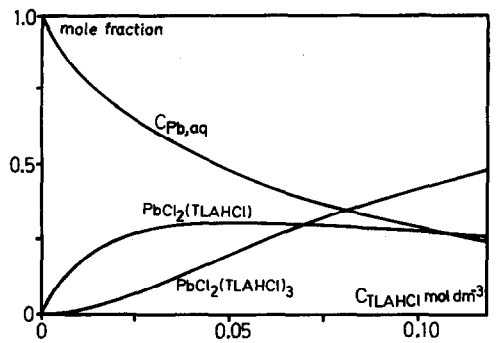

Fig. 7. Distribution diagram of Pb(II) species in the system Pb(II)–Cl^-/TLAHCl–benzene at pH = 2.00.

$$Pb^{2+} + 2Cl^- + TLAHCl_{org} \rightleftharpoons (TLAHCl)(PbCl_2)_{org}, \quad (22)$$

and

$$Pb^{2+} + 5Cl^- + 3TLA_{org} + H^+ \rightleftharpoons (TLAHCl)_3(PbCl_2)_{org}, \quad (23)$$

$$Pb^{2+} + 2Cl^- + 3TLAHCl_{org} \rightleftharpoons (TLAHCl)_3(PbCl_2)_{org}. \quad (24)$$

The values of $\log\beta_{11} = 3.65$ and $\log\beta_{11} = 3.76$ obtained in this way agree acceptably with that obtained by two phase titrations, $\log\beta_{11} = 3.78 \pm 0.06$.[13] This supports the validity of the model proposed.

The same model applies to TOAHCl and THAHCl. This supports the hypothesis that the length of the alkyl chain does not influence the composition of the metal species formed. Similar conclusions were drawn by Aguilar[18] in the extraction of Zn(II) by the three amines.

As an example of the predominance of the metallic species in the systems studied, Fig. 7 shows the distribution diagram of Pb(II) as a function of C_{TLAHCl}. It can be appreciated that $(TLAHCl)(PbCl_2)$ is predominant at low values of the reagent concentration whereas when increasing this concentration the metallic ion is mainly extracted as $(TLAHCl)_3(PbCl_2)$.

Acknowledgements—The interest of Professor Erik Högfeldt in this work is greatefully acknowledged. The authors wish to acknowledge also Professor M. Aguilar for his scientific guidance and personal help. L.A.F. is indebted to the Basque Government for the scholarship received.

REFERENCES

1. J. C. Sheppard and R. Warnock, *J. Inorg. Nucl. Chem.* 1964, **26**, 1421.

2. T. Suzuki and T. Sotobayashi, *J. Chem. Soc. Jpn* 1966, **87**, 587.
3. A. R. Selmer-Olsen, *Acta Chem. Scand.* 1966, **20**, 16.
4. M. Y. Mirza, M. Ejaz, A. R. Sani, S. Ullah, M. Rashid and G. Samdani, *Anal. Chim. Acta* 1967, **37**, 402.
5. H. G. Petrov, *U.S. At. Energy Comm. Rept.* TID-5772 (1960).
6. G. Nakagawa, *Nippon Kakagu Zasshi* 1960, **81**, 1255.
7. T. Suzuki and T. Sotobayashi, *Jpn. Anal.* 1965, **14**, 414.
8. T. Ishimori and E. Nakamura, *Data of Inorganic Solvent Extraction, Res. Rept. Japan At. Energy Res. Inst.*, JAERI, 1963, 1047; 1964, 1062; 1966, 1106.
9. V. F. Borbat, A. V. Burgaeva and P. I. Bobikov, *Tsvetn. Met.* 1966, **7**, 43.
10. H. Irving and H. Nabilsi, *Anal. Chim. Acta* 1968, **41**, 505.
11. A. Vogel, *Textbook of Quantitative Inorganic Analysis*, 4th Edn. Longman, London (1964).
12. *Some Laboratory Methods.* Mimeograph from the Department of Inorganic Chemistry. The Royal Institute of Technology, Stockholm (1959).
13. M. Muhammed, J. Szabon and E. Högfeldt, *Chem. Scr.* 1974, **6**, 61.
14. F. D. Snell, *Photometric and Fluorometric Methods of Analysis*, Part I. Wiley Interscience, New York (1978).
15. M. Aguilar and E. Högfeldt, *Chem. Scr.* 1972, **2**, 149.
16. M. Aguilar and E. Högfeldt, *Chem. Scr.* 1973, **3**, 107.
17. D. H. Liem, *Acta Chem. Scand.* 1971, **25**, 1521.
18. M. Aguilar, *Chem. Scr.* 1974, **5**, 213.

Polyhedron Vol. 6, No. 3, pp. 571–576, 1987
Printed in Great Britain

0277–5387/87 $3.00+.00

^1H AND ^{13}C NMR SPECTRA OF Pd(II) AND Pt(II) AMINOPOLYCARBOXYLATES

M. G. BASALLOTE, R. VILAPLANA and F. GONZÁLEZ-VÍLCHEZ*

Departamento de Química Inorgánica, Facultad de Ciencias de Cádiz, Apartado 40, Puerto Real (Cádiz), Spain

(*Received* 5 *February* 1986; *accepted after revision* 12 *August* 1986)

Abstract—^1H and ^{13}C NMR spectra of palladium and platinum aminopolycarboxylate complexes have been studied. The spectra of $[M(Y\text{-}H_4)Cl_2]$, $[M(Y\text{-}H_2)]$ and $(Y\text{-}H_6)[MCl_4]$ compounds (M = Pd or Pt; Y = EDTA, PDTA or CDTA) dissolved in DMSO-d_6 are discussed. Proton spectra are less complicated than those recorded in D_2O solution because of faster nitrogen inversion. Carbon spectra clearly demonstrate bidentate and tetradentate behaviour of these ligands.

Palladium and platinum complexes of aminopolycarboxylates have been extensively studied in recent years.[1–6] Most of these complexes can be classified into two types: dichlorocomplexes with bidentate aminopolycarboxylate and complexes where the ligand acts as tetradentate (Fig. 1). IR spectroscopy is very useful for distinguishing both types of compounds. Thus, dichlorocomplexes show a single band at *ca* 1700 cm^{-1}, which corresponds to $\nu_{C=O}$(COOH), whereas complexes with tetradentate aminopolycarboxylates show two bands at *ca* 1700 and 1600 cm^{-1}, the first one corresponding to the stretching of carbonyls in COOH groups and the second one to those in carboxylate groups.[7]

Although IR spectra of D_2O solutions of these compounds can be obtained,[8–10] they are very complicated and a complete assignment is not possible because of many overlapping bands. For this reason, it is impossible in many cases to determine if the spectrum corresponds to a single compound or to a mixture. In this sense, NMR spectroscopy provides an easily available technique that can be advantageously used for studying the nature of complexes in solution. Proton spectra have been used so far for this purpose.[11–14] D_2O has been commonly used as solvent, with AB patterns being frequently observed for CH_2(ac) protons (Fig. 1). The actual pattern of these signals for an octahedral complex depends on the rates of inversion of the nitrogen atoms and on the labilities of metal–nitrogen and metal–oxygen bonds. Intramolecular scrambling processes also affect the pattern of CH_2(ac) signals.[11,12,15,16] This results in extremely complicated spectra, specially for complexes of asymmetric aminopolycarboxylates.[12,17,18] Moreover, new complications appear due to acid- and base-catalyzed deuteration processes, that occur with different rates for the several types of CH_2(ac) protons.[17–20] In square-planar complexes, intramolecular scrambling processes are less complicated, but inversion of nitrogen atoms may be slow on the NMR time scale, giving rise to AB patterns. Other authors[21,22] have observed complicated spectra with overlapping quartets for Pd–EDTA and Pt–EDTA complexes in D_2O because of the existence of more than one complex in solution.

^{13}C NMR spectra have been less used for studying the nature of aminopolycarboxylate complexes.[23–25] However, when they are recorded with proton decoupling, they are less complicated than proton spectra and may be used for obtaining complementary information.

In this paper, we report ^1H and ^{13}C NMR spectra of DMSO-d_6 solutions of Pd(II) and Pt(I) complexes with EDTA, PDTA and CDTA. These compounds illustrate both bidentate and tetradentate behaviour of aminopolycarboxylates. $(Y\text{-}H_6)[MCl_4]$ salts have been also obtained and included in the study.

* Author to whom correspondence should be addressed.

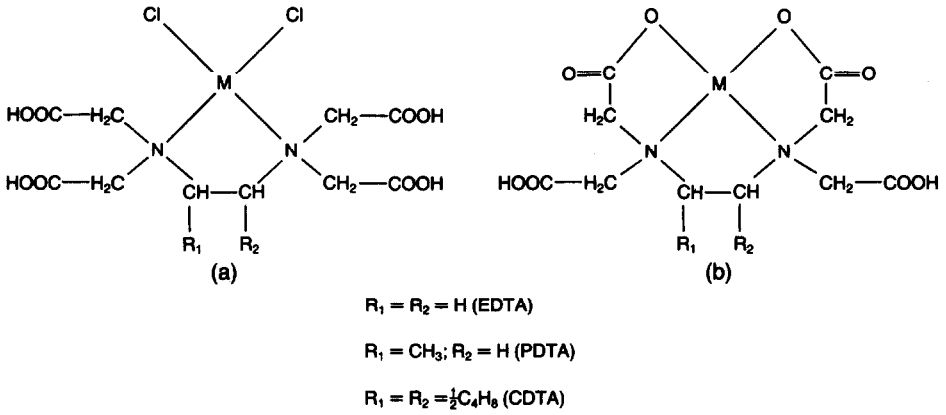

Fig. 1. Aminopolycarboxylate complexes of Pd(II) and Pt(II): (a) dichloro complexes, and (b) complexes with tetradentate aminopolycarboxylate.

EXPERIMENTAL

All compounds were synthesized as described in another paper.[26] Samples for obtaining NMR spectra were prepared by dissolving 50–100 mg of compound in 0.5 cm^3 of DMSO-d_6. Solutions were placed in 5-mm tubes and TMS was added as internal reference.

NMR spectra were recorded at the probe temperature (40°C) with a Varian FT-80A spectrometer.

RESULTS AND DISCUSSION

EDTA complexes

The shifts of the signals in the ^1H and ^{13}C spectra of EDTA complexes are shown in Table 1. Proton spectra of (EDTA-H_6)[$PtCl_4$] and [Pd(EDTA-H_4)Cl_2]·$5H_2O$ are similar to that of free EDTA except for the displacement to lower field of both signals. However, in the spectrum of [Pt(EDTA-H_4)Cl_2]·$5H_2O$ a quartet appears for CH_2(ac) pro-

Table 1. NMR spectra of EDTA complexes (all chemical shifts are reported in ppm and referenced to TMS)[ab]

Compound	(a) ^1H spectra CH_2(ac)	CH_2(en)	
EDTA-H_4	3.45	2.78	
[Pd(EDTA-H_4)Cl_2]·$5H_2O$	3.79	3.14	
(EDTA-H_6)[$PtCl_4$]	3.90	3.25	
[Pt(EDTA-H_4)Cl_2]·$5H_2O$	4.24[b]	3.41	
[Pd(EDTA-H_2)]·$5H_2O$	3.74, 3.93	3.23, 3.08	
Compound	(b) ^{13}C spectra CH_2(ac)	CH_2(en)	COOH
EDTA-H_4	54.62	51.38	172.15
[Pd(EDTA-H_4)Cl_2]·$5H_2O$	54.38	50.94	170.50
(EDTA-H_6)[$PtCl_4$]	54.33	50.81	169.78
[Pt(EDTA-H_4)Cl_2]·$5H_2O$	57.77	55.00	168.95
[Pd(EDTA-H_2)]·$5H_2O$	54.38, 56.70	52.97	170.21, 169.06

[a] Abbreviations used: ac = acetate arm, en = ethylenediamine backbone.
[b] AB quartet with $\delta_A - \delta_B = 0.49$ ppm and $J_{AB} = 17.7$ Hz.

tons, in a similar way to that observed for palladium complexes in D_2O solution.[21] Thus, interchange of metal–nitrogen bonds is slower for the platinum complex than for its palladium analogue. The absence of AB splitting in the spectrum of (EDTA-H_6)[$PtCl_4$] shows that protonation of nitrogen atoms does not cause inversion of these atoms to be slow on the NMR time scale.

Carbon spectra of these compounds also show two signals for CH_2(ac) groups, with one more for the carbons of free carboxylic groups. All of these signals are little displaced from their positions in free EDTA. There is a single exception, which corresponds to both types of CH_2 in the spectrum of [Pt(EDTA-H_4)Cl_2]·$5H_2O$. These signals are displaced more than 3 ppm to lower field with respect to the other compounds. This behaviour also resembles that of analogous complexes in D_2O solution.[23–25]

Tetradentate coordination of EDTA results in more complicated spectra. From symmetry considerations, two AB quartets and one A_2B_2 multiplet must appear for CH_2(ac) and CH_2(en) protons, respectively. However, the proton spectrum of [Pd(EDTA-H_2)]·$5H_2O$ shows two singlets for every type of CH_2 groups. In the case of CH_2(en), both signals appear near their positions in the spectra of dichlorocomplexes, and they must correspond to a degenerate A_2B_2 pattern. In the case of CH_2(ac), both singlets result from collapse of AB quartets, and one of them is displaced to lower field because of palladium–carboxylate coordination. This collapse of AB patterns has been previously observed by many workers for several aminopolycarboxylate complexes.[19–21,27,28] The carbon spectrum shows two signals for both carbonyl and methylene carbons of acetate groups, and one more for CH_2(en). This spectrum is also consistent with tetradentate coordination of EDTA and it suggests that there is not interconversion between coordinated and free acetate arms.

PDTA complexes

Proton spectrum of PDTA in D_2O shows two AB quartets for CH_2(ac) [Fig. 2(a)]. This pattern is due to the asymmetry caused by the methyl group and to the slow inversion of nitrogen atoms.[11–14] However, when the spectrum is recorded in DMSO-d_6 solution, two singlets at 3.50 and 3.43 ppm are observed for these protons [Fig. 2(b)]. So, it is concluded that inversion is faster in DMSO-d_6 than in D_2O, what results in simpler spectra. In palladium and platinum complexes (Table 2), these signals are displaced to lower field, as in the case of the EDTA analogue complexes. A displacement is also observed for the doublets of CH_2(en) and CH_3, although no significant changes of the coupling constants are detected. The spectra of [Pt(PDTA-H_4)Cl_2]·$2H_2O$ is similar to that of the analogous EDTA complex with AB quartets appearing for CH_2(ac) protons.

The methyl group appears at 12.93 ppm in the carbon spectrum of free PDTA and it causes the splitting of the CH_2(ac) and COOH signals (Table 2). It is interesting to note that [Pt(PDTA-H_4)Cl_2]·$2H_2O$ does not show a behaviour similar to the EDTA dichlorocomplex, i.e. the signals of

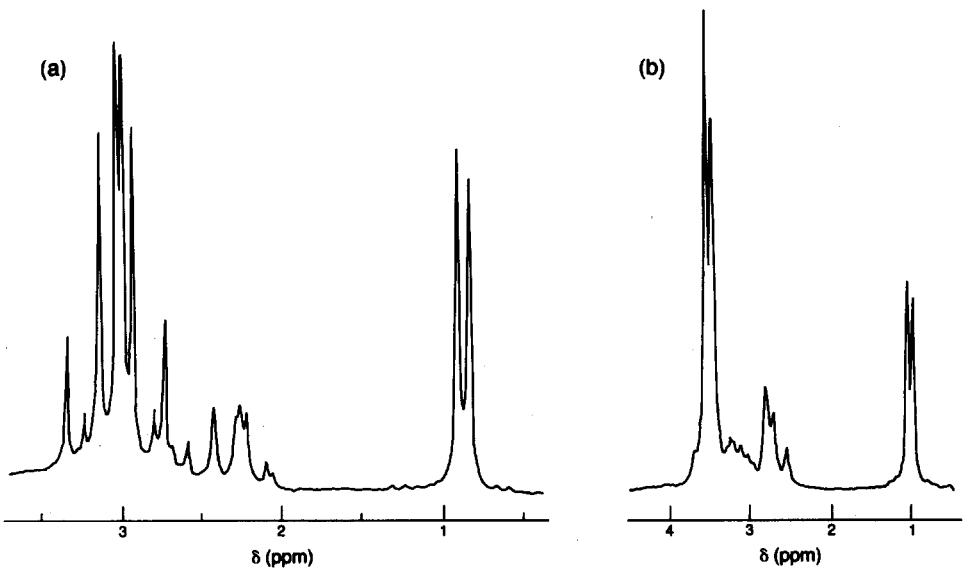

Fig. 2. ^1H NMR spectrum of PDTA: (a) D_2O solution, and (b) DMSO-d_6 solution.

Table 2. NMR spectra of PDTA complexes (all chemical shifts are reported in ppm and referenced to TMS)

Compound	(a) ^{1}H spectra[ab] CH_2(ac)	CH_2(en)	CH_3
PDTA-H_4	3.50, 3.43	2.70 (6.7)	0.93 (5.8)
[Pd(PDTA-H_4)Cl_2]	3.91, 3.74	3.03 (6.4)	1.11 (5.7)
(PDTA-H_6)[$PtCl_4$]	3.91, 3.76	3.04 (6.4)	1.11 (5.9)
[Pt(PDTA-H_4)Cl_2]·$2H_2O$	3.99[c]		1.10 (6.0)

Compound	(b) ^{13}C spectra CH_2(ac)	CH_2(en)	CH_3	CH	COOH
PDTA-H_4	54.35, 52.43	59.11	12.93	57.93	172.30, 171.86
[Pd(PDTA-H_4)Cl_2]	54.11, 51.78	57.78	10.67	54.37	170.83, 169.24
(PDTA-H_6)[$PtCl_4$]	54.13, 51.81	57.80	10.68	54.39	170.85, 169.27
[Pt(PDTA-H_4)Cl_2]·$2H_2O$	54.38, 52.39	56.39	12.69	55.53	171.94, 171.69

[a] CH proton gives a multiplet superimposed to other signals.
[b] Coupling constants values (Hz) included in parentheses.
[c] Corresponds to the most intense of signals appearing between 3.50 and 4.76 ppm.

CH_2(ac) are only slightly displaced. The spectra of complexes with tetradentate PDTA are even more complicated and difficult to interpret. In the case of [Pd(PDTA-H_2)]·$4H_2O$, a mixture of complexes seems to be formed in DMSO-d_6 solution. Moreover, the spectra of [Pt(PDTA-H_2)]·$3H_2O$ change with time and they are practically coincident with those of free PDTA when the equilibrium state is attached (2 days after preparation of the sample). These results can be interpreted in terms of partial or total substitution of PDTA by DMSO, and it indicates that caution must be taken when interpreting spectra of similar compounds. It is, however, surprising that this reaction only occurs for complexes with tetradentate PDTA and not for dichlorocomplexes.

CDTA complexes

Dichlorocomplexes of Pd(II) and Pt(II) with CDTA could not be isolated in the solid state, although they are formed in aqueous solution.[26]

Table 3. NMR spectra of CDTA complexes (all chemical shifts are reported in ppm and referenced to TMS)

Compound	(a) ^{1}H spectra CH_2(ac)	CH(en)	$CH_2(\beta)_{ec}$	$CH_2(\gamma)_{ec}$	$CH_2(\beta, \gamma)_{ax}$
CDTA-H_4	3.53	2.95	2.00	1.66	1.17
(CDTA-H_6)[$PdCl_4$]·$2H_2O$	3.75	3.16	2.07	1.67	1.24
(CDTA-H_6)[$PtCl_4$]·$2H_2O$	3.80	3.20	2.07	1.72	1.29

Compound	(b) ^{13}C spectra CH_2(ac)	CH(en)	$CH_2(\beta)$	$CH_2(\gamma)$	COOH
CDTA-H_4	52.12	62.01	25.25	24.31	171.21
(CDTA-H_6)[$PdCl_4$]·$2H_2O$	51.69	62.22	24.06	23.68	170.18
(CDTA-H_6)[$PtCl_4$]·$2H_2O$	52.00	62.37	24.03	23.61	169.99
[Pd(CDTA-H_2)]·H_2O	64.81, 59.19	78.47	26.59	24.01	178.83, 176.35
	58.83, 55.92	70.38	25.74	23.65	168.31, 167.84

$(CDTA\text{-}H_6)[MCl_4]$ salts (M = Pd or Pt) give NMR spectra similar to free CDTA (Table 3). It is important to note that AB patterns are not observed in the proton spectra because of fast inversion of nitrogen atoms. The singlet of CH_2(ac) protons is displaced from 3.53 ppm in CDTA to 3.75 and 3.80 ppm in the salts.

The signals of protons in the cyclohexane ring are very broad because of multiple couplings between many types of symmetrically different atoms. The assignment included in Table 3 has been performed by integration of the signals and comparing their positions with literature data.[29,30] This part of the spectrum is similar to that of CDTA in D_2O except for the appearance of a single signal for $CH_2(\beta)_{ax}$ and $CH_2(\gamma)_{ax}$.

Carbon spectra of CDTA and $(CDTA\text{-}H_6)[MCl_4]$ salts are also very similar, with a single signal for COOH, CH_2(ac) and CH(en). The CH(en) signal appears at lower field than in EDTA and PDTA, showing that substitution in the ethylenediamine backbone leads to a displacement of the signal to higher δ values. The signals of carbon atoms in β- and γ-positions of cyclohexane ring are easily recognized in the spectra.

The spectra of $[Pd(CDTA\text{-}H_2)]\cdot H_2O$ are much more complicated. Coordination of carboxylate groups results again in the nonequivalence of atoms. The assignment of signals in the proton spectrum is difficult because it consists of a mountain of broad resonances. Despite its complexity, the carbon spectrum reveals clearly the tetradentate character of the ligand, with a signal appearing for every carbon atom. Coordinated carboxylate carbons appear at 178.83 and 176.35 ppm, and free carboxylic carbons at 168.31 and 167.84 ppm. The assignment of CH_2(ac) and CH(en) resonances has been performed with the aid of the APT spectrum.

The use of DMSO-d_6 as solvent for obtaining NMR spectra of aminopolycarboxylates results in higher rates of nitrogen inversion, what causes CH_2(ac) protons to appear as singlets in proton spectra. This is clearly seen in the spectra of free PDTA and CDTA, where singlets appear for those protons, in contrast to the spectra recorded in D_2O solutions, where AB patterns are observed. Protonation of nitrogen atoms does not cause important differences in the rate of nitrogen inversion, as shown by the maintenance of the singlets in the spectra of $(PDTA\text{-}H_6)[PtCl_4]$ and $(CDTA\text{-}H_6)[MCl_4]$ salts. When aminopolycarboxylates coordinate to Pd(II) ion, fast exchange of Pd—N bonds also results in the appearance of singlets for acetate protons. However, the spectra of platinum dichlorocomplexes show AB quartets for these protons because of slow interchange of Pt—N bonds. In any case, proton spectra recorded in DMSO-d_6 solutions are easier to interpret than those obtained in D_2O.

An interesting observation is that either protonation of nitrogen atoms or coordination to a metal ion in a bidentate way results in similar displacements to lower field of the signals of CH_2(ac) and CH_2(en), as shown in Table 4. This result may be important for characterization of analogous complexes.

When carboxylate groups are also coordinated, a further displacement of the signal of coordinated acetate CH_2 is observed, although those of CH_2(en) and uncoordinated acetate CH_2 are still equally displaced. However, carboxylate coordination causes complicated proton spectra due to the nonequivalence of different types of CH_2(ac) and CH_2(en) groups. In this sense, ^{13}C NMR spectroscopy can be more useful for studying coordination of aminopolycarboxylates to d^8 ions. The spectra of free ligands are very simple, with one signal for every type of different carbon atoms. Substitution results in a displacement to higher δ values of the resonances of carbon atoms in the ethylenediamine backbone of the molecule.

When these ligands are protonated or coordinated to a metal ion in a bidentate way, the appearance of the spectra is maintained, with small displacements of the signals. However, for those complexes where exchange of metal–nitrogen bonds is slow, an important displacement of CH_2(ac) signal to higher δ values is observed. The same effect is observed when the ligand is linked in a tetradentate way. In this latter case, more resonances appear in the spectra because of the nonequivalence of coordinated and uncoordinated acetate arms.

Another interesting observation is the absence of ^{195}Pt–^1H or ^{195}Pt–^{13}C coupling (^{195}Pt: $I = 1/2$, 34% abundance) in the spectra of the platinum chlorocomplexes. In these cases, the rate of Pt–N

Table 4. $\Delta_{CH_2} = \delta_{CH_2}(\text{complex}) - \delta_{CH_2}(\text{ligand})$

Compound	Δ_{CH_2}(ac)	Δ_{CH_2}(en)
$[Pd(EDTA\text{-}H_4)Cl_2]\cdot 5H_2O$	+0.34	+0.36
$(EDTA\text{-}H_6)[PtCl_4]$	+0.45	+0.47
$[Pt(EDTA\text{-}H_4)Cl_2]\cdot 5H_2O$	+0.79[a]	+0.63
$[Pd(PDTA\text{-}H_4)Cl_2]$	+0.36[b]	+0.33
$(PDTA\text{-}H_6)[PtCl_4]$	+0.37[b]	+0.34
$(CDTA\text{-}H_6)[PdCl_4]\cdot 2H_2O$	+0.22	+0.21
$(CDTA\text{-}H_6)[PtCl_4]\cdot 2H_2O$	+0.27	+0.25

[a] Considering the center of the quartet.
[b] Considering the media of both signals.

interchange is slow and so, the absence of ^{195}Pt side bands can not be explained in terms of a rapid interchange causing the ^{195}Pt nucleus to loose its magnetic character. There are some previous reports of platinum complexes where the absence of ^{195}Pt side bands can not be related to ligand exchange, and the results have been interpreted as a consequence of a dominant chemical shift anisotropy relaxation mechanism.[31,32] The absence of ^{195}Pt side bands can not be used as an evidence of lack of metal coordination because of the AB patterns and of the magnitude of the displacements observed for those complexes where Pt–N interchange is slow.

Although the species studied in this paper have been previously characterized in solid state,[1–6,26,33] some doubt can appear about their nature in solution because of the simplicity of the spectra. This result differs greatly from those previously reported for Pd–EDTA and Pt–EDTA systems in D_2O solution.[21,22] In both cases complicated spectra reveal the existence of several species in solution and so spectra obtained in D_2O can not be used for characterization purposes. In the case of DMSO-d_6 solutions, spectra are more simple with a number of signals equivalent to the expected for the proposed structures from symmetry considerations. Reaction of platinum complexes with DMSO must be ruled out except in the case of $[Pt(PDTA\text{-}H_2)]\cdot 3H_2O$, where the equilibrium spectra are identical to those of free PDTA. In the other cases there is a displacement of the signals from their positions in the spectra of free ligand. These displacements are consequence of protonation or metal coordination, as revealed by the spectra of complexes with tetradentate aminopolycarboxylates, where the displacements of the signals of uncoordinated acetate arms are similar to those observed for bidentate complexes.

REFERENCES

1. D. H. Busch and J. C. Bailar, *J. Am. Chem. Soc.* 1956, **78**, 716.
2. N. A. Ezerskaya and V. N. Filimonova, *Russ. J. Inorg. Chem.* 1965, **10**, 1444.
3. D. J. Robinson and C. H. L. Kennard, *J. Chem. Soc. A* 1970, 1008.
4. S. González-García and F. González-Vílchez, *An. Quim.* 1970, **66**, 875.
5. N. A. Ezerskaya, T. P. Solovykh and L. K. Schubochkin, *Koord. Khim.* 1980, **6**, 1064.
6. F. González-Vílchez, J. M. López-Alcalá and M. García Basallote, *An. Quim.* 1983, **79**, 51.
7. D. H. Busch and J. C. Bailar, *J. Am. Chem. Soc.* 1953, **75**, 4574.
8. D. T. Sawyer and J. E. Tackett, *J. Am. Chem. Soc.* 1963, **85**, 314.
9. K. Nakamoto, Y. Morimoti and A. E. Martell, *J. Am. Chem. Soc.* 1963, **85**, 308.
10. N. A. Ezerskaya, I. N. Kiseleva and B. V. Zhadanov, *Russ. J. Inorg. Chem.* 1970, **15**, 533.
11. R. J. Day and C. N. Reilley, *Anal. Chem.* 1964, **36**, 1073.
12. R. J. Day and C. N. Reilley, *Anal. Chem.* 1965, **37**, 1326.
13. R. J. Kula, D. T. Sawyer, S. I. Chan and C. M. Finley, *J. Am. Chem. Soc.* 1963, **85**, 2930.
14. J. L. Sudmeier and C. N. Reilley, *Anal. Chem.* 1964, **36**, 1707.
15. P. A. Baisden, G. R. Choppin and B. B. Garrett, *Inorg. Chem.* 1977, **16**, 1367.
16. M. C. Gennaro and P. Mirti, *Nouv. J. Chim.* 1981, **5**, 495.
17. J. B. Terrill and C. N. Reilley, *Inorg. Chem.* 1966, **5**, 1988.
18. J. L. Sudmeier, A. J. Senzel and G. L. Blackmer, *Inorg. Chem.* 1971, **10**, 90.
19. P. F. Coleman, J. I. Legg and J. Steele, *Inorg. Chem.* 1970, **9**, 937.
20. G. L. Blackmer and J. L. Sudmeier, *Inorg. Chem.* 1971, **10**, 2019.
21. Y. O. Aochi and D. T. Sawyer, *Inorg. Chem.* 1966, **5**, 2085.
22. L. E. Erickson, J. W. McDonald, J. K. Howie and R. P. Clow, *J. Am. Chem. Soc.* 1968, **90**, 6371.
23. G. R. Choppin, P. A. Baisden and S. A. Khan, *Inorg. Chem.* 1979, **18**, 1330.
24. G. R. Choppin, S. A. Khan and G. C. Levy, *Spectrosc. Lett.* 1980, **13**, 205.
25. M. A. Freeman, F. A. Schultz and C. N. Reilley, *Inorg. Chem.* 1982, **21**, 567.
26. M. G. Basallote, R. Vilaplana and F. González-Vílchez, submitted for publication.
27. B. J. Fuhr and D. L. Rabenstein, *Inorg. Chem.* 1973, **12**, 1868.
28. P. Balgavy, P. Novomesky and J. Majer, *Inorg. Chim. Acta* 1980, **38**, 233.
29. N. Muller and W. C. Tosch, *J. Chem. Phys.* 1962, **37**, 1167.
30. K. Okamoto, M. Noji and Y. Kidani, *Bull. Chem. Soc. Jpn* 1981, **54**, 713.
31. J. Y. Lallemand, J. Soulié and J. C. Chottard, *J. Chem. Soc., Chem. Commun.* 1980, 436.
32. I. M. Ismail, S. J. S. Kerrison and P. J. Sadler, *Polyhedron* 1982, **1**, 57.
33. E. N. Duesler, R. E. Tapscott, M. G. Basallote and F. González-Vílchez, *Acta Cryst.* 1985, **C41**, 678.

Polyhedron Vol. 6, No. 3, pp. 577–581, 1987
Printed in Great Britain

0277–5387/87 $3.00+.00

POTASSIUM-39 NUCLEAR MAGNETIC RESONANCE STUDY OF THE COMPLEXATION OF POTASSIUM THIOCYANATE BY DIBENZO-30-CROWN-10 IN NITROMETHANE

HARALD D. H. STÖVER, MARC ROBILLARD and CHRISTIAN DETELLIER*

Ottawa-Carleton Chemistry Institute, University of Ottawa Campus, Ottawa(Ont.) K1N 9B4, Canada

(*Received* 25 *April* 1986; *accepted* 15 *August* 1986)

Abstract—A 2:1 potassium:dibenzo-30-crown-10 complex is formed in nitromethane solution. Taking into account the ion-pairing equilibrium of KSCN in that solvent, an equilibrium constant for the 2:1 complex formation ($K_{2c} = 52 \pm 5$) has been calculated. The characteristic K-39 relaxation rate and chemical shift of the 2:1 complex are compatible with an open structure of the crown, in which the two potassium cations are exposed to the solvent molecules and the thiocyanate counteranion.

Large crown ethers are known to wrap around alkali metal cations in both solid state and solution. The wrapping of dibenzo-30-crown-10 (DB30C10) around the potassium cation has been shown by the X-ray crystal structures of the potassium iodide DB30C10[1] and of the potassium thiocyanate DB30C10 complexes.[2] The main difference between the X-ray structures of the uncomplexed and the potassium complexed DB30C10 consists in the conversion of four anti C–O conformations of the uncomplexed crown into four gauche C–O conformations in the complex.[1]

In solution, evidence has been given by H-1 and C-13 NMR that the K^+–DB30C10 complex has the same configuration as in the crystal, with complete desolvation of the cation upon complexation.[3,4] The Na^+–DB30Cl0 complex displays a different configuration[3] and complexes with other stoichiometries (2:1 and 3:2) are formed as well.[4,5] Dibenzo-24-crown-8 (DB24C8) wraps around the sodium cation, expelling the solvent molecules from the first solvation shell.[6] With tetraphenylborate as the counteranion, $(n+1)$: n Na^+: DB24C8 aggregates are formed to a small extent.[7,8] Wrapping of ligands around the alkali metal cations is also observed in the case of acyclic polyethers.[9,10]

K-39 is a quadrupolar nucleus ($I = 3/2$) whose receptivity is only 2.69 compared to C-13. This explains why potassium has been much less used than sodium for direct metal cation NMR studies.[11] Shih and Popov have published a K-39 NMR study of potassium salts in non-aqueous solvents.[12] Kinetics studies of the complexation of the potassium cation with dibenzo-18-crown-6[13] and 18-crown-6[14] have been carried out in various solvents. Neurohr *et al.*[15] studied the complexation of K^+ with several ionophores using K-39 NMR and the K^- anion has been observed both in solution and in crystalline potassides.[16,17]

We report here a K-39 NMR study of the complexation of K^+ by DB30C10 in nitromethane. We show that a 2:1 K^+:DB30C10 complex coexists with the 1:1 complex in nitromethane solutions. Taking into account the ion-pairing equilibrium of KSCN in that solvent, we calculate an equilibrium constant for the 2:1 complex formation and the characteristic values of the relaxation rate and chemical shift of the 2:1 complex.

EXPERIMENTAL

After recrystallization from ethylacetate, dibenzo-30-crown-10 (Parish Chem.) was vacuum-dried at 60°C for several hours. Potassium thiocyanate (Aldrich, 98%+) was dried under vacuum at 60°C for at least three hours prior to use. Nitromethane

* Author to whom correspondence should be addressed.

(Baker) was dried under reflux over calcium hydride, fractionally distilled, and stored over 4 Å molecular sieves, under argon.

Measurements of K-39 chemical shifts and bandwidths at half-height were made at 21°C on a Varian XL-300 NMR spectrometer operating at 13.997 MHz. The K-39 chemical shifts are expressed relative to 0.1 M KCl in H_2O (10% D_2O v/v). Bandwidths at half-height were measured graphically. We checked that all the bands obtained had a Lorentzian shape. A line broadening of up to 5 Hz was used. The 90° pulse length was 90 μs. The transverse relaxation rates were derived from the linewidths. The longitudinal relaxation times were measured using a 180°–τ–90° pulse sequence, and T_1 was calculated using a three-parameters non-linear regression.

Procedures for the non-linear regression analysis of the chemical shifts and of the linewidths data were described previously.[5,7]

RESULTS

Figure 1 shows the K-39 NMR chemical shifts of KSCN solution in nitromethane as a function of ρ, the ratio [DB30C10]/[KSCN]. Contrary to what we have observed in other non-aqueous solvents (pyridine, acetone, acetonitrile),[18] the chemical shift variation in the range $0 < \rho < 1$ is not linear, which indicates either the step-wise formation of two or more complexes[5,7] or ionic association, or a combination of both. The observed curvature depends upon the total concentration of potassium thiocyanate, being more pronounced at higher concentrations. For $\rho \geqslant 1.0$, the chemical shift values are constant ($\delta = 13.0$ ppm), regardless of the total KSCN concentration. This is indicative of the formation of a stable 1:1 K^+:DB30C10 complex ($\log K_c > 5$).[4] The "wrapped around" structure is confirmed by the similarity of the observed K-39 chemical shifts of the 1:1 complex in various non-aqueous solvents.[18]

In order to test for the influence of ion pairing phenomena upon the observed chemical shift variation, we have carried out a concentration study. Figure 2 shows the K-39 chemical shift dependence upon the KSCN concentration (10^{-3} M to 7×10^{-2} M) in nitromethane. The observed curvature can be accounted for by a simple ion-pairing model [eqn (1)],

$$(K^+)_s + (SCN^-)_s \overset{K_p}{\rightleftharpoons} (K, SCN)_s \qquad (1)$$

where $(K^+)_s$ and $(SCN^-)_s$ stand for the solvated potassium cation and the solvated thiocyanate anion respectively. $(K, SCN)_s$ refers to an ion pair. Equation (1) leads to eqns 2 and 3 describing the observed

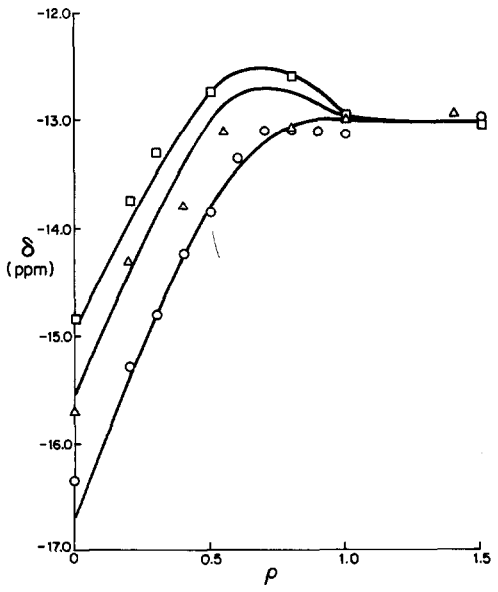

Fig. 1. K-39 chemical shifts as a function of the ratio [DB30C10]/[KSCN] for different total KSCN concentrations. ○: [KSCN] = 0.025 M; △: [KSCN] = 0.050 M; □: [KSCN] = 0.070 M. The data points are experimental and the curves were calculated following the results of the regression analysis displayed in Table 1.

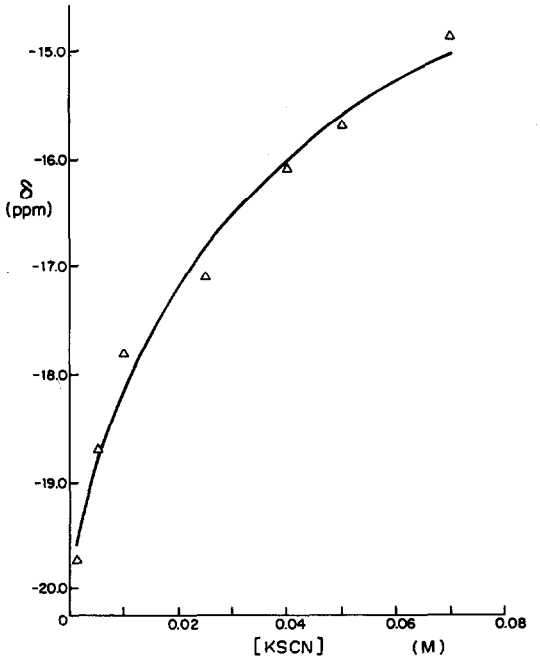

Fig. 2. K-39 chemical shifts as a function of the total KSCN concentration in nitromethane. The data points are experimental and the curve was calculated from the results of the non-linear regression analysis on eqns (2) and (3). $K_p = 24$; $\delta_P = -9.7$ ppm and $\delta_F = -19.8$ ppm; RMS of the fit is equal to 0.3 ppm.

chemical shift as a function of the KSCN concentration,

$$\frac{\delta_{obs}-\delta_P}{\delta_F-\delta_P}=\frac{[(K^+)_s]}{[KSCN]_T} \qquad (2)$$

where δ_{obs}, δ_F and δ_P are, respectively, the observed K-39 chemical shift and the characteristic chemical shifts for the solvated and ion-paired potassium cation. $[(K^+)_s]$ is a function of the ion-pairing equilibrium constant K_p and of the total KSCN concentration, $[KSCN]_T$. This is shown in eqn (3).

$$K_P=\frac{[KSCN]_T-[(K^+)_s]}{[(K^+)_s]^2}. \qquad (3)$$

In Fig. 2, the data points are experimental and the curve is calculated following the results obtained from a non-linear regression analysis on the three parameters, δ_P, δ_F and K_P from eqns (2) and (3).

Figure 3 shows the K-39 linewidths dependence upon the KSCN concentration. The data points are experimental and the curve is calculated following a two-parameters $[(\nu_{1/2})_F$ and $(\nu_{1/2})_P]$ non-linear regression analysis. The agreement between the two sets of independent measurements is good, and this militates in favour of the simple model of ion-pairing [eqn (1)]. In Fig. 1, the data points are experimental and the curves have been calculated following the eqns (1), (4) and (5) and the results given in Table 1.

$$(K^+)_s+(C)_s \overset{K_c}{\rightleftharpoons} (K^+,C)_s \qquad (4)$$

$$(K^+)_s+(K^+,C)_s \overset{K_{2c}}{\rightleftharpoons} (K^+,C,K^+)_s. \qquad (5)$$

$(C)_s$, $(K^+,C)_s$ and $(K^+,C,K^+)_s$ stand for the solvated crown, the solvated 1 : 1 K^+ : DB30C10 complex and the solvated 2 : 1 K^+ : DB30C10 complex, respectively. A two-parameters non-linear regression has been carried out simultaneously on the three curves of Fig. 1, corresponding to different

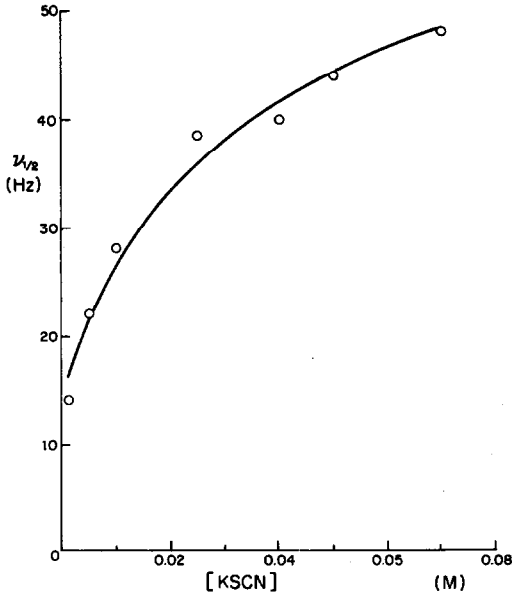

Fig. 3. K-39 linewidths of half-height as a function of the total KSCN concentration in nitromethane. The data points are experimental and the curve was calculated from the results of the non-linear regression analysis on eqns (2) and (3) applied to the linewidths. $(\nu_{1/2})_F = 14$ Hz; $(\nu_{1/2})_P = 87$ Hz. The RMS on the regression was 2.5 Hz.

total potassium concentrations. The two parameters were K_{2c} [eqn (5)] and δ_{2c}, the chemical shift of the 2 : 1 complex. The value of K_c [eqn (4)] in the regression analysis was taken as 10^6, since the equilibrium constant formation of the 1 : 1 complex has been shown to be greater than 10^5 in nitromethane.[4] Moreover, we have checked that values of K_c taken greater than 10^4 do not modify the results of the regression analysis.[5] The observed curvature could not be accounted for by consideration of eqns (1) and (4) only, that is to say that if the complexation of the potassium cation by

Table 1. Values of the parameters involved in eqns (1)–(5)

log K_c[a]	K_p[b]	K_{2c}[d,e]	δ_P[b] (ppm)	δ_F[b] (ppm)	δ_{2c}[d] (ppm)	δ_c[f] (ppm)	$T_{2,P}^{-1}$[c] (Hz)	$T_{2,F}^{-1}$[c] (Hz)	$T_{2,2c}^{-1}$[d] (Hz)	$T_{2,c}^{-1}$[f] (Hz)
> 5	24±3	52±5	−9.7±0.2	−19.8±0.1	−10.5±0.3	−13.0±0.1	270±20	45±3	380±40	220±10

[a] Taken as equal to 6 in the regression procedure.[4]

[b] Obtained from a three-parameters non-linear regression analysis on the experimental data of Fig. 2 and eqns (1)–(3).

[c] From a two-parameters regression on the experimental data of Fig. 3 and eqns (1)–(3). K_p was carried over from [b].

[d] From a two-parameters regression on experimental data of Fig. 1 or 4 and eqns (1), (4) and (5)

[e] Mean value from the two independent determinations of Figs 1 and 4.

[f] Experimental value.

the crown leads to an increase in the ion pairing of the uncomplexed potassium cation [eqn (1)] this effect does not account for the observed curvature. Typically, it accounts for half of it. We had to envisage another hypothesis: namely the 2:1 K^+:DB30C10 complex formation [eqn (5)]. There are precedents in the literature for such stoechiometries in the cases of large crown ethers complexing sodium or potassium cations in non-aqueous solutions.[4,5,7] The non-linear regression analysis gave the results of Table 1. K_P, δ_F and δ_P [eqn (1)] were carried over from the concentration study (Figs 2 and 3).

Figure 4 shows a similar trend in the K-39 linewidth variation as a function of ρ. The characteristic linewidth for the 1:1 complex is 71 Hz when the curve displays a maximum at 77 Hz for a ratio $\rho = 0.7$. The curve of Fig. 4 is calculated from the results of the regression which are given in Table 1. The agreement between the chemical shifts data and the relaxation rates data is again very good, specially if one considers that the regressions of Figs 1 and 4 did not involve more than two fitting parameters: δ_{2c} and K_{2c} in the case of the chemical shifts data, $T_{2,2c}^{-1}$ and K_{2c} in the case of the linewidths data. The agreement between the two independent determinations of K_{2c} is indeed excellent: 54 ± 3 from the linewidths data and 50 ± 5 from the chemical shifts data.

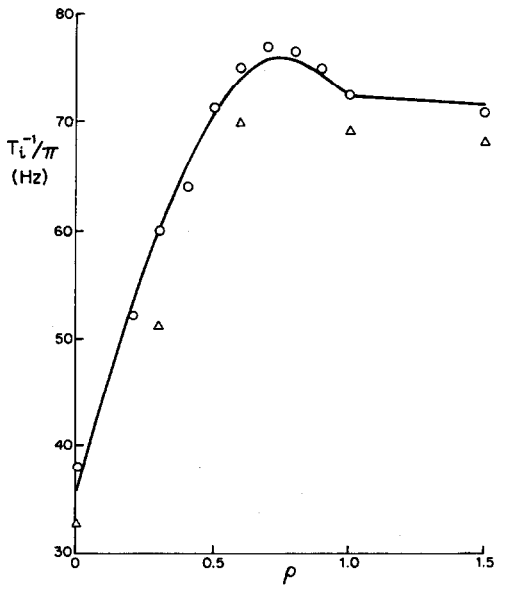

Fig. 4. K-39 transverse and longitudinal relaxation rates as a function of the ratio [DB30C10]/[KSCN] for [KSCN] = 0.025 M. ○: transverse relaxation data ($i = 2$); △: longitudinal relaxation data ($i = 1$). The data points are experimental and the curve was calculated following the values from Table 1.

We have checked that there was no exchange broadening contribution to the linewidth. The variation of the longitudinal relaxation rate as a function of ρ parallels the transverse relaxation rate (Fig. 4). The difference between the two relaxation rates was in the order of magnitude of the expected inhomogeneity contribution to the linewidth.

DISCUSSION

We can account for the KSCN concentration dependence of the chemical shifts and linewidths on the basis of a simple model involving only two thermodynamically stable species: the solvated cation and a solvated ion pair. The observation that the chemical shifts and the linewidths are linearly related is a strong support for this model (combining data of Figs 2 and 3 affords the equation: $\delta = 0.14\nu_{1/2} - 21.7$, with a correlation coefficient of 0.981 on seven data points). The same type of linear relationship was found for ^{23}NaSCN and ^{23}NaI in nitromethane.[19] Maynard *et al.*[20] have mentioned the formation of (K, SCN) ion pairs in dimethylformamide in the course of their kinetic study of the complexation of potassium with 18-crown-6, and KSCN has been shown to associate and dimerize in dioxolane.[21] A similar downfield shift of the K-39 resonance of KSCN in an other poorly coordinating solvent, acetonitrile, has been reported.[12]

The chemical shift of the 1:1 complex, −13.0 ppm, is independent of the nature of the solvent,[18] and is characteristic of an oxygen environment of the potassium cation. The chemical shift of K^+ is −10.5 ppm in acetone and −10 ppm in methanol.[12] The chemical shift of the sandwiched K^+(15-crown-5)$_2$ in dimethylether with K^- as the associated counteranion falls in the same range (−9.9 ppm).[16] Similarly to what we have found previously for the Na-23 chemical shift of the 2:1 Na^+:DB24C8 complex,[5] the K-39 chemical shift of the potassium cation in the 2:1 K^+:DB30C10 complex is not comprised between the two values of the solvated K^+ (−19.8 ppm) and of the 1:1 complexed K^+ (−13.0 ppm). Neurohr *et al.* have reported K-39 chemical shift data for K^+-39 complexed by ionophores.[15] Referencing their values to the commonly accepted standard, K^+ in water, one obtains −24 ppm for the K^+–valinomycin complex where K^+ is embedded into a symmetrical cavity made of six carbonyl oxygens, a situation comparable to the symmetrical environment of the potassium cation in the K^+–DB30C10 complex.[18] The K^+–18C6 complex resonates at −3 ppm in methanol[14,15] or acetone.[14] This value, for a complexed K^+ exposed to the solvent, is in agreement with the one that we determine in the

case of the 2:1 K^+:DB30C10 (−10.5 ppm), since the value at higher field for the latter case is expected on the basis of the lower donicity number of nitromethane, compared to methanol or acetone. However, this chemical shift value does not rule out the possibility of a structure consisting of two ion pairs linked by the large crown ether, since the chemical shift of $(K, SCN)_s$ is −9.7 ppm in nitromethane (Table 1). We should probably envisage the characteristic data of the 2:1 complex given in Table 1 as the weighted average of the two limiting values resulting from the equilibria of eqn (6).

$$(K^+, C, K^+)_s \rightleftharpoons (SCN, K, C, K^+)_s \rightleftharpoons (SCN, K, C, K, SCN)_s. \quad (6)$$

The transverse relaxation rate of the 1:1 complex was found to be twice as large as the one of the 1:1 complex, reflecting the higher dissymetry of the potassium environment in the 2:1 complex. The quadrupolar coupling constant of K^+-39 in the 1:1 complex will be reported and discussed elsewhere.[18]

All our data are consistent with the presence of potassium thiocyanate ion pairs in nitromethane solutions, as well as with the formation of a 2:1 K^+:DB30C10 complex, in addition to the strongly favoured "wrapped around" 1:1 complex.

Acknowledgement—This research has been supported by a grant from Natural Sciences and Engineering Research Council of Canada (NSERCC).

REFERENCES

1. M. A. Bush and M. R. Truter, *J. Chem. Soc., Perkin Trans. II* 1972, 345.
2. J. Hasek, D. Hlavata and K. Huml, *Acta Cryst. B* 1980, **36**, 1782.
3. D. Live and S. I. Chan, *J. Am. Chem. Soc.* 1976, **98**, 3769.
4. M. Shamsipur and A. I. Popov, *J. Am. Chem. Soc.* 1979, **101**, 4051.
5. H. D. H. Stöver, L. J. Maurice, A. Delville and C. Detellier, *Polyhedron* 1985, **4**, 1091.
6. M. Bisnaire, C. Detellier and D. Nadon, *Can. J. Chem.* 1982, **60**, 3071.
7. H. D. H. Stöver, A. Delville and C. Detellier, *J. Am. Chem. Soc.* 1985, **107**, 4167.
8. A. Delville, H. D. H. Stöver and C. Detellier, *J. Am. Chem. Soc.* 1985, **107**, 4172.
9. J. Grandjean, P. Laszlo, F. Vogtle and H. Sieger, *Angew. Chem.* 1978, **17**, 856.
10. J. Grandjean, P. Laszlo, W. Offermann and P. L. Rinaldi, *J. Am. Chem. Soc.* 1981, **103**, 1380.
11. C. Detellier, In *NMR of Newly Accessible Nuclei* (Edited by P. Laszlo), Vol. 2, Chapter 5. Wiley, New York (1983).
12. J. S. Shih and A. I. Popov, *Inorg. Nucl. Chem. Lett.* 1977, **13**, 105.
13. M. Shporer and Z. Luz, *J. Am. Chem. Soc.* 1975, **97**, 665.
14. E. Schmidt and A. I. Popov, *J. Am. Chem. Soc.* 1983, **105**, 1873.
15. K. J. Neurohr, T. Drakenberg, S. Forsen and H. Lilja, *J. Magn. Res.* 1983, **51**, 460.
16. M. L. Tinkham and J. L. Dye, *J. Am. Chem. Soc.* 1985, **107**, 6129.
17. P. P. Edwards, A. S. Ellaboudy and D. M. Holton, *Nature* 1985, **317**, 242.
18. C. Detellier and M. Robillard, *Can. J. Chem.*, submitted.
19. H. D. H. Stöver and C. Detellier, to be published.
20. K. J. Maynard, D. E. Irish, E. M. Eyring and S. Petrucci, *J. Phys. Chem.* 1984, **88**, 729.
21. M. Chabanel and Z. Wang, *J. Phys. Chem.* 1984, **88**, 1441.

Polyhedron Vol. 6, No. 3, pp. 583–586, 1987
Printed in Great Britain

0277–5387/87 $3.00+.00

NONCOVALENT INTERACTIONS IN METAL COMPLEXES—XI.* SYNTHESIS AND STEREOSELECTIVITY OF 1:3 COBALT(III) COMPLEXES OF 1-*l*-MENTHYLOXY-3-ACYLACETONES

S. MAEDA, M. NAKAMURA, H. ŌKAWA† and S. KIDA

Department of Chemistry, Faculty of Science, Kyushu University, Hakozaki, Higashiku, Fukuoka 812, Japan

(*Received* 17 *December* 1985; *accepted after revision* 15 *August* 1986)

Abstract—1 : 3 Cobalt(III) complexes of 1-*l*-menthyloxy-3-acylacetones [*l*-menthyl–O–CH_2–CO–CH_2–CO–R: R = C_2H_5(Et), *n*-C_3H_7 (*n*Pr), *i*-C_3H_7 (*i*Pr), *n*-C_4H_9 (*n*Bu), *i*-C_4H_9 (*i*Bu), *n*-C_5H_{11} (*n*Am), *i*-C_5H_{11} (*i*Am)] have been synthesized, and their stereochemistries were examined. CD and NMR spectra revealed that the complexes of R = Et and *i*Bu preferred the *fac*-Δ configuration while the complexes of R = *i*Pr and *i*Am the *fac*-Λ configuration. The complexes of R = *n*Pr, *n*Bu and *n*Am showed no significant CD at the first *d–d* band. The stereoselectivities of the complexes were discussed in comparison with those of tris(1-*l*-menthyloxy-3-benzoylacetonato)cobalt(III) and its homologs previously reported.

Stereoselectivities of tris(1,3-diketonato)M(III) complexes have been investigated using (+)-hydroxymethylenecamphor (+hmc)[2–4] and (+)-3-acetylcamphor (+atc).[4–6] Resolution of the diastereomers (*fac*-Δ, *fac*-Λ, *mer*-Δ, *mer*-Λ) was achieved for [Cr(+atc)$_3$][5] and [Co(+atc)$_3$],[5,6] and the isomer predominantly formed was shown to be *mer*-Λ. The ratio of the *mer*-Λ, however, is only 45–48% for [Co(+atc)$_3$] and 38% for [Cr(+atc)$_3$], indicating that the stereoselectivities of the complexes are relatively low. Single-crystal X-ray analysis for *mer*-Λ-[Cr(+atc)$_3$][7] suggests no appreciable interligand interaction within a molecule, and the factors governing stereoselectivity in [M(+atc)$_3$] and [M(+hmc)$_3$] are still obscure.

Recently, we have shown that tris(1-*l*-menthyloxy-3-benzoylacetonato)M(III), [M(*l*-moba)$_3$] (M = Co, Cr, Mn, lanthanoid),[8,9] show a high stereoselectivity giving rise to the *fac*-Δ isomer. The stereoselectivity of these complexes can be attributed to intramolecular CH/π interaction[10] (bonding interaction) operating between the phenyl and *l*-menthyl groups (see Fig. 1), because the stereoselectivity is enhanced when (1) the size of the π system becomes larger[1] or (2) the π electron density of the ring is increased.[11] Based on 400 MHz ^{1}H-NMR spectra, tris{1-*l*-menthyloxy-3-(4-methylbenzoyl)acetonato}cobalt(III) [Co(*l*-moba-Me)$_3$] is revealed to be pure *fac*-Δ isomer.[12]

These facts prompted us to examine if intramolecular, interligand "hydrophobic" interaction between alkyl or alicyclic groups can also give rise to a stereoselectivity of tris(1,3-diketonato)M(III) complexes. For this purpose a series of 1-*l*-menthyloxy-3-acylacetones (*l*-menthyl–O–CH_2–CO–CH_2–CO–R) were prepared, whose abbreviations are given in Table 1. The 1 : 3 cobalt(III) complexes of these ligands were obtained, and their configurations were examined by means of CD and ^{1}H-NMR spectra and discussed in terms of intramolecular, interligand *l*-menthyl/alkyl interaction.

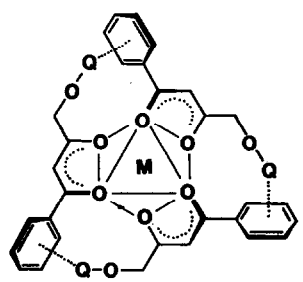

Fig. 1. Schematical representation of CH/π interaction in [M(*l*-moba)$_3$] (Q = *l*-menthyl).

* For Part X see Ref. 1.

† Author to whom correspondence should be addressed.

Table 1. Abbreviations of 1-*l*-menthyloxy-3-acylacetones (*l*-menthyl–O–CH_2–CO–CH_2–CO–R) and elemental analyses of their copper(II) and cobalt(III) complexes

R	Ligands Abbreviation	Found % (Calc. %) Copper(II) complexes C	H	Cobalt(III) complexes C	H
C_2H_5	H(*l*-mo-Et)	64.7 (64.2)	9.5 (9.1)	66.9 (66.9)	9.4 (9.5)
n-C_3H_7	H(*l*-mo-*n*Pr)	65.4 (65.2)	9.5 (9.3)	67.9 (67.8)	9.5 (9.7)
i-C_3H_7	H(*l*-mo-*i*Pr)	65.3 (65.2)	9.5 (9.3)	68.0 (67.8)	9.6 (9.7)
n-C_4H_9	H(*l*-mo-*n*Bu)	66.4 (66.1)	9.6 (9.5)	67.5 (67.6)[a]	9.7 (10.0)[a]
i-C_4H_9	H(*l*-mo-*i*Bu)	66.1 (66.1)	9.6 (9.5)	70.1 (70.4)[b]	10.0 (9.7)[b]
n-C_5H_{11}	H(*l*-mo-*n*Am)	67.3 (66.9)	9.9 (9.7)	69.3 (69.3)	10.1 (10.1)
i-C_5H_{11}	H(*i*-mo-*i*Am)	66.8 (66.9)	9.7 (9.7)	70.9 (71.0)[b]	10.5 (9.9)[b]

[a] Calculated value for mono-methanol adduct.
[b] Calculated value for mono-benzene adduct.

Our preliminary investigation on the complexes of 1-*l*-menthyloxy-3-acetylacetone[13] has suggested that the interligand *l*-menthyl/methyl interaction leads to a stereoselectivity distinctly differing from that in [M(*l*-moba)$_3$] and its homologs.

EXPERIMENTAL

Syntheses

H(*l*-mo-R). To a mixture of ethyl *l*-menthyloxyacetate (2×10^{-2} mole) and NaH (2×10^{-2} mole) in dry ether (50 cm^3) was added dropwise a solution of ketone (1×10^{-2} mole) in dry ether (20 cm^3) at 45°C in 30 min. The mixture was stirred for additional 2 h at this temperature. Unreacted NaH was decomposed by adding ethanol (30 cm^3), and the mixture was poured onto ice-water (100 cm^3) containing hydrochloric acid (5 cm^3). The upper ethereal layer was separated, and the aqueous layer was extracted with two 50 cm^3 portions of ether. The combined ethereal solution was shaken with saturated sodium bicarbonate solution and then with water. To this solution was added a solution of copper(II) acetate monohydrate (3 g) in aqueous ammonia (15%, 50 cm^3), and the mixture was vigorously stirred to give blue mass of the copper(II) complex. It was collected and recrystallized from a chloroform–methanol mixture. The yield was 40–50%.

The copper complex was dissolved in ether (100 cm^3), and the solution was vigorously shaken with 20% sulfuric acid (100 cm^3). The ether layer was separated, washed with a saturated sodium bicarbonate solution and then with water, and dried over anhydrous sodium sulfate. Evaporation of the solvent left H(*l*-mo-R) as a pale yellow, oily substance. The yield based on the copper complex was *ca* 90%.

[Co(*l*-mo-R)$_3$]. To a mixture of cobalt(II) hydroxycarbonate (1.5×10^{-4} mole) and a ligand (1.5×10^{-3} mole) was added dropwise hydrogen peroxide (30%, 10 cm^3) at 90°C. The reaction mixture assumed an intense green color. After being cooled to room temperature, the complex was extracted with ether and the extract was shaken with 3% KOH solution and then with water. The crude product obtained on evaporating the solvent was dissolved in a benzene–methanol (1 : 1) mixture and passed through an alumina column (ϕ 15 mm × 100 mm). Evaporation of the solvent left [Co(*l*-mo-R)$_3$] as a green oily substance. It was dried over P_2O_5 in a vacuum desiccator.

Elemental analyses of the copper(II) and cobalt(III) complexes are given in Table 1.

Physical measurements

The ^{1}H-NMR spectra were recorded on a JEOL Fourier Transform NMR Spectrometer Model FX90Q in $CDCl_3$. Tetramethylsilane was used as an internal standard. The electronic and CD spectra were obtained in CCl_4 on a Shimadzu UV–Visible Recording Spectrometer UV-240 and a JASCO J-500C Spectropolarimeter, respectively. The elemental analyses were obtained at the Elemental Analysis Service Center, Kyushu University.

RESULTS AND DISCUSSION

The ligands H(*l*-mo-R) were identified by elemental analyses of their copper(II) complexes (Table 1) and ^{1}H-NMR spectra (Table 2). Each NMR spectrum of H(*l*-mo-R) shows a broad signal at 14–15 ppm attributable to the enolic proton.[14] The signal for the methine proton on the chelate ring appears at 5.8–5.9 ppm. The signal for the meth-

Table 2. ^{1}H–NMR spectral data for H(*l*-mo-R) and [Co(*l*-mo-R)$_3$]

R	H(*l*-mo-R) Enolic OH	Methine	Methylene	[Co(*l*-mo-R)$_3$] Methine	Methylene
Et	14.0	5.87	4.07(AB)	5.93(b)	3.90–4.44(m)
*n*Pr	14.5	5.84	4.04(AB)	5.90(b)	3.83–4.42(m)
*i*Pr	14.5	5.88	4.06(AB)	5.91–5.93	3.84–4.44(m)
*n*Bu	15.0	5.86	4.07(AB)	5.92(b)	3.90–4.44(m)
*i*Bu	14.5	5.83	4.07(AB)	5.86(b)	3.70–4.42(m)
*n*Am	15.0	5.86	4.07(AB)	5.90(b)	3.90–4.44(m)
*i*Am	14.5	5.85	4.06(AB)	5.92(b)	3.84–4.40(m)

Abbreviations: AB = AB quartet, b = broad, m = multiplet.

ylene protons adjacent to the *l*-menthyloxy group appears at 4.0–4.1 ppm. The AB quartet pattern of this signal is presumably due to the chirality of the neighbouring *l*-menthyl group.[12]

The methine proton signal of [Co(*l*-mo-R)$_3$] is broad and in the case of [Co(*l*-mo-*i*Pr)$_3$] the splitting of the signal is clearly seen. This fact suggests that the stereoselectivity of [Co(*l*-mo-R)$_3$] is not so high as found for [Co(*l*-moba)$_3$] and its homologs, and the *mer* isomer is more or less formed together with the *fac* isomer as the main species. The signal for the methylene protons adjacent to the *l*-menthyloxy group (near 4.2 ppm) is no more AB quartet pattern but essentially multiplet. This suggests that the free rotation about the methylene group is restricted because of the interligand *l*-menthyl/alkyl interaction. A similar NMR pattern is seen for the methylene protons of [Co(*l*-moba-Me)$_3$],[13] which is proved to be of pure *fac*-Δ.

All the complexes show the first *d–d* transition band near 17×10^3, characteristic of tris(1,3-diketonato)cobalt(III) complexes.[15,16] The CD spectra in the first *d–d* band region were measured. A typical CD spectrum is shown in Fig. 2 together with its absorption spectrum, and the numerical data are included in Table 3. As seen in Table 3, [Co(*l*-mo-Et)$_3$], [Co(*l*-mo-*i*Pr)$_3$], [Co(*l*-mo-*i*Bu)$_3$] and [Co(*l*-mo-*i*Am)$_3$] show distinct CD in the first *d–d* band region whereas [Co(*l*-mo-*n*Pr)$_3$], [Co(*l*-mo-*n*Bu)$_3$], and [Co(*l*-mo-*n*Am)$_3$] show practically no CD in this region. The CD for the former complexes probably arises from the dissymmetry about the metal center (configurational effect) but not vicinal effect from the *l*-menthyl group, because no CD is induced for the latter complexes. However, judging from the CD intensities, the stereoselectivity of these complexes is much lower compared with that of [Co(*l*-moba)$_3$] and its homologs. It is also seen from Table 3 that the preferred configuration depends upon the R group; Δ configuration for [Co(*l*-mo-Et)$_3$] and [Co(*l*-mo-*i*Bu)$_3$] whereas Λ configuration for [Co(*l*-mo-*i*Pr)$_3$] and [Co(*l*-mo-*i*Am)$_3$]. For tris(1-*l*-menthyloxy-3-acetylacetonato)cobalt(III) the preferred configuration was Λ.[13]

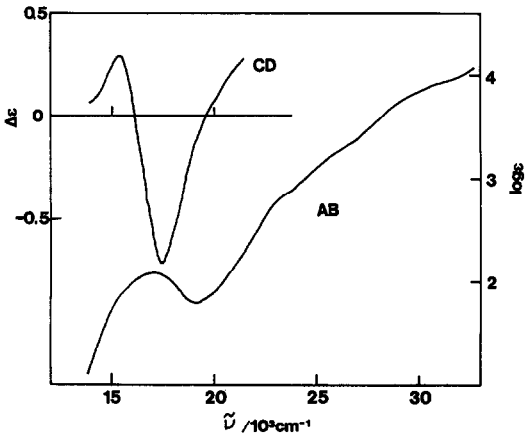

Fig. 2. Absorption (AB) and circular dichroism (CD) spectra of [Co(*l*-mo-Et)$_3$].

Recently we have suggested for [Co(*l*-moba-Me)$_3$][12] that one of the methyl groups of the *l*-menthyl moiety, probably one of the isopropyl group, plays the major role in the CH/π interaction with the aromatic ring. Such a methyl-ring coupling has a directionality, as pointed out by Nishio[10] based on the X-ray analysis for *t*-butyl 1-phenylethyl sulfoxide.[17,18] Because of this directionality, the *l*-menthyl and aryl groups should take a specific orientation to each other when the CH/π interaction operates, and this may lead to a controlled disposition of the diketonate ions about the central metal. The interaction ("association") between alkyl and alicyclic groups seems to have less directionality than CH/π interaction. The CD spectral results for [Co(*l*-mo-R)$_3$] (Table 3) suggest that the *l*-menthyl group can associate with alkyl groups in two different ways: one leads to the predominant formation of the *fac*-Δ isomer (R = Et and *i*Bu) whereas the other to the *fac*-Λ isomer (R = *i*Pr and *i*Am). It is likely that in the complexes

Table 3. Electronic and CD spectral data for the first *d–d* band of [Co(*l*-mo-R)$_3$]

Complex	$\tilde{\nu} \times 10^3$ (cm^{-1}) (log ε)	$\tilde{\nu} \times 10^3$ (cm^{-1}) ($\Delta\varepsilon$)		Preferred configuration
		$^1A_2 \leftarrow {}^1A_1$	$^1E \leftarrow {}^1A_1$	
[Co(*l*-mo-Et)$_3$]	16.8 (2.08)	15.4 (+0.29)	17.4 (−0.72)	Δ
[Co(*l*-mo-*n*Pr)$_3$]	16.8 (2.07)			
[Co(*l*-mo-*i*Pr)$_3$]	16.7 (2.19)	15.2 (−0.19)	17.7 (+0.33)	Λ
[Co(*l*-mo-*n*Bu)$_3$]	16.8 (2.09)			
[Co(*l*-mo-*i*Bu)$_3$]	16.9 (1.95)	15.3 (+0.14)	17.4 (−0.33)	Δ
[Co(*l*-mo-*n*Am)$_3$]	16.8 (2.06)			
[Co(*l*-mo-*i*Am)$_3$]	16.8 (2.01)	15.4 (−0.03)	17.4 (+0.34)	Λ

ε: extinction coefficient in the unit dm^3 mole^{-1} cm^{-1}.

of R = *n*Pr, *n*Bu or *n*Am there is no significant difference in free energy between the two ways of associations and thence no appreciable stereoselectivity is caused in these complexes.

From the present study on [Co(*l*-mo-R)$_3$], together with our previous results for [Co(*l*-moba-R)$_3$] and its homologs, we may conclude that the interligand CH/π interactions are much more effective than the hydrophobic interactions to give rise to stereoselectivities of metal complexes.

REFERENCES

1. M. Nakamura, H. Ōkawa and S. Kida, *Inorg. Chim. Acta* 1984, **96**, 111.
2. I. Lifschitz, *Rec. Trav. Chim.* 1950, **69**, 1495.
3. J. H. Dunlop, R. D. Gillard and R. Ugo, *J. Chem. Soc. A* 1966, 1540.
4. Y. T. Chen and G. W. Everette Jr, *J. Am. Chem. Soc.* 1968, **90**, 6660.
5. R. M. King and G. N. Everette Jr, *Inorg. Chem.* 1971, **10**, 1237.
6. C. S. Springer Jr, R. E. Sievers and B. Feibush, *Inorg. Chem.* 1971, **10**, 1242.
7. W. D. Horrocks Jr, D. L. Johnston and D. MacInnes, *J. Am. Chem. Soc.* 1970, **92**, 7620.
8. H. Ōkawa, K. Ueda and S. Kida, *Inorg. Chem.* 1982, **21**, 1594.
9. M. Nakamura, H. Ōkawa, S. Kida and S. Misumi, *Bull. Chem. Soc. Jpn* 1984, **57**, 3147.
10. M. Nishio, *Kagaku No Ryoiki* 1977, **31**, 998.
11. M. Nakamura, H. Ōkawa and S. Kida, *Bull. Chem. Soc. Jpn* 1985, **58**, 3377.
12. M. Nakamura, M. Kato, H. Ōkawa, T. Ito and S. Kida, presented at the 35th Meeting of Coord. Chem. in Japan, Hiroshima, 11 Oct. 1985.
13. M. Nakamura, H. Ōkawa and S. Kida, *Chem. Lett.* 1981, 547.
14. D. J. Sardella, D. H. Heinert and B. L. Shapiro, *J. Org. Chem.* 1969, **34**, 2817.
15. D. A. Johnson and A. G. Sharpe, *J. Chem. Soc. A* 1966, 798.
16. T. S. Piper, *J. Chem. Phys.* 1961, **35**, 1240.
17. Y. Iitaka, Y. Kodama, K. Nishihata and M. Nishio, *J. Chem. Soc., Chem. Commun.* 1974, 389.
18. Y. Kodama, K. Nishihata, M. Nishio and Y. Iitaka, *J. Chem. Soc., Perkin II* 1976, 1490.

Polyhedron Vol. 6, No. 3, pp. 587–592, 1987
Printed in Great Britain

0277–5387/87 $3.00+.00

TRIORGANOTIN(IV) DERIVATIVES OF FIVE MEMBERED HETEROCYCLIC 2-CARBOXYLIC ACIDS

G. K. SANDHU* and S. P. VERMA

Department of Chemistry, Guru Nanak Dev University, Amritsar 143005, India

(*Received* 6 *March* 1986; *accepted after revision* 15 *August* 1986)

Abstract—A series of 20 complexes of general formula R_3SnL (R = CH_3, n-C_3H_7, n-C_4H_9, C_6H_5, c-C_6H_{11}; L = anion of thiophene 2-, thiophene 2-acetic, furoic 2- and pyrrole 2-carboxylic acids) has been prepared. All of these complexes are monomers except those of triphenyltin(IV) which are polymers and have been characterised by molecular weight determination, IR, ^{1}H-NMR and ^{119m}Sn Mössbauer studies. Tetrahedral and trigonal bipyramidal structures have been assigned and it has been found that none of the ring hetero atoms bond to tin(IV).

Fungicidal and bacteriocidal carboxylates of tributyltin(IV) with furoic and thiophene acids are known through patents.[1,2] Structural information about very few diorganotin(IV)[3] and tributyltin(IV)[4] compounds with furoic and pyrrole acids is available. A possible biological activity is expected from the triorganotin carboxylates reported in this paper since all the hetero atoms of the five membered carboxylic acids are free and are not bonded to tin(IV).

EXPERIMENTAL

Chemicals

Thiophene 2-carboxylic acid (ThioH), thiophene 2-acetic acid (ThioAH), furoic 2-carboxylic acid (FuH) and pyrrole 2-carboxylic acid (PyrH) were obtained from Aldrich Chemicals (England) and are used as such. Trimethyltin(IV) chloride and tributyltin(IV) chloride were procured from Alpha Products (USA) and Fluka Chemicals (Germany), respectively and are used as such while tripropyltin(IV) chloride,[5] triphenyltin(IV) chloride[6] and tricyclohexyltin(IV) chloride[7] were prepared by the reported methods.

Preparation of the sodium salt

Sodium hydroxide (BDH) (4.0 g, 0.1 mole) was added to a solution of ThioH (12.8 g, 0.1 mole) in ethanol (95%, 50 cm^3) and refluxed till a clear solution resulted (pH 7–7.2). After removing the excess alcohol by distillation, dry benzene (20 cm^3) was added to remove water azeotropically using a Dean and Stark trap. Thiophene 2-sodium carboxylate separated out and was filtered, washed several times with acetone and then with dry ether and dried *in vacuo*. Sodium salts of the remaining acids were prepared in a similar way.

Preparation of complexes

To a solution of triorganotin(IV) chloride (0.001 mole) in absolute alcohol (30 cm^3) was added the sodium salt of the acid (0.00104 mole). The reaction mixture was refluxed on a water bath for 3–4 h when a clear solution was produced. From the reaction mixture half of the alcohol was removed by distillation. On cooling some sodium chloride separated which was filtered through a sintered glass funnel (G-4) under reduced pressure. To the clear solution was added thiophene-free dry benzene (20 cm^3) followed by refluxing on a water bath using a Dean and Stark trap for 2 h. Sodium chloride that separates on cooling was filtered. Refluxing followed by cooling and subsequent filtration of the solution was repeated till the removal of sodium chloride was complete. After removing the solvents completely, the residue was dried *in vacuo*. All the compounds are solids except Nos 8, 12 and 18 (Table 1) which are liquids. Compound 12 solidifies on long standing whereas 18 becomes a semi-solid on keeping. Compounds 1–4 and 17–20 have been

* Author to whom correspondence should be addressed.

Table 1. Physical and analytical data of triorganotin(IV) derivatives

Sr No.	Complex	Yield (%)	M.p. (°C)	Analysis (%) Found (Calc.) C	H	S	N	Sn	Mol. wt C[a]	Mol. wt R[b]	Mol. wt Calc.
1.	$(CH_3)_3SnThio$	85	158–9	33.4 (33.0)	3.7 (4.1)	10.9 (11.0)	—	40.6 (40.8)	253.0	270.0	290.7
2.	$(CH_3)_3SnThioA$	82	129–31	34.8 (35.4)	4.0 (4.5)	10.3 (10.5)	—	38.4 (38.9)	—	290.0	304.7
3.	$(CH_3)_3SnFu$	88	196–7	34.5 (34.9)	4.1 (4.3)	—	—	42.8 (43.2)	—	260.0	274.7
4.	$(CH_3)_3SnPyr$	75	139–40	35.2 (35.0)	4.3 (4.7)	—	5.4 (5.1)	43.0 (43.3)	—	259.0	273.7
5.	$(n\text{-}C_3H_7)_3SnThio$	80	89–90	44.5 (44.8)	6.0 (6.4)	8.6 (8.5)	—	31.5 (31.6)	326.1	330.2	374.7
6.	$(n\text{-}C_3H_7)_3SnThioA$	80	74–5	45.9 (46.3)	6.5 (6.6)	8.0 (8.2)	—	30.2 (30.5)	350.4	340.5	388.7
7.	$(n\text{-}C_3H_7)_3SnFu$	84	120–21	46.4 (46.8)	6.7 (6.6)	—	—	32.8 (33.0)	339.3	335.7	358.7
8.	$(n\text{-}C_3H_7)_3SnPyr$[c]	85	—	46.7 (46.9)	6.5 (6.9)	—	3.4 (3.9)	33.0 (33.1)	318.5	320.0	357.7
9.	$(n\text{-}C_4H_9)_3SnThio$	75	63	48.4 (48.9)	6.7 (7.1)	7.8 (7.6)	—	28.3 (28.4)	390.5	380.5	416.7
10.	$(n\text{-}C_4H_9)_3SnThioA$	80	75	49.8 (50.1)	7.1 (7.4)	7.1 (7.4)	—	27.3 (27.5)	399.6	390.8	430.7
11.	$(n\text{-}C_4H_9)_3SnFu$	75	83–85 (86–87)[d]	50.6 (50.9)	7.1 (7.5)	—	—	29.4 (29.6)	388.3	370.2	400.7
12.	$(n\text{-}C_4H_9)_3SnPyr$[e]	75	59–61	50.7 (51.0)	7.4 (7.7)	—	3.15 (3.50)	29.4 (29.7)	379.1	375.6	399.7
13.	$(C_6H_5)_3SnThio$	80	114	57.7 (57.9)	3.7 (3.8)	6.6 (6.7)	—	24.5 (24.9)	459.1	450.8	476.7
14.	$(C_6H_5)_3SnThioA$	70	144–45	58.4 (58.6)	3.8 (4.1)	7.0 (6.5)	—	24.0 (24.2)	—	—	490.7
15.	$(C_6H_5)_3SnFu$[f]	75	190	59.4 (59.9)	4.1 (3.9)	—	—	25.5 (25.8)	—	—	460.7
16.	$(C_6H_5)_3SnPyr$	80	160–62	60.5 (60.0)	3.7 (4.1)	—	3.44 (3.04)	25.5 (25.8)	—	—	459.7
17.	$(c\text{-}C_6H_{11})_3SnThio$	85	119–21	55.4 (55.8)	7.0 (7.3)	6.1 (6.4)	—	23.4 (24.0)	475.5	448.5	494.7
18.	$(c\text{-}C_6H_{11})_3SnThioA$	82	Semi-solid	56.2 (56.6)	7.1 (7.5)	5.9 (6.3)	—	23.1 (23.3)	—	470.0	508.7
19.	$(c\text{-}C_6H_{11})_3SnFu$	80	126–28	57.1 (57.6)	7.1 (7.5)	—	—	24.6 (24.8)	—	427.0	478.7
20.	$(c\text{-}C_6H_{11})_3SnPyr$	75	188–90	57.2 (57.7)	7.5 (7.7)	—	3.2 (2.9)	24.5 (24.8)	—	430.2	477.7

ThioH = thiophene 2-carboxylic acid; ThioAH = thiophene 2-acetic acid; FuH = furan 2-carboxylic acid; PyrH = pyrrole 2-carboxylic acid.

[a] Cryoscopically.

[b] Rast method.

[c] Liquid complex.

[d] Literature value, P. Dunn and T. Norris, *Austral. Defence Sci. Serv. Defence Stand. Labs*, Report 269, Feb. 1964.

[e] Compound solidifies on prolonged standing.

[f] Decomposes.

recrystallized from ethanol while 5–7 and 9–12 from pet-ether (60–80°C). The triphenyltin(IV) derivatives (13–16) could not be recrystallized because of their insolubility in common organic solvents but were washed with pet-ether (40-60°) to remove Ph_3SnCl.

Physical measurements

Melting points were determined in open capillaries and are uncorrected. Elemental analysis was carried out by microanalytical service, Calcutta University, Calcutta. Tin was estimated as SnO_2.[8] Molecular weights were determined both cryoscopically in benzene and by Rast's method (in molten camphor, 175°C). Infrared spectra were recorded on Pye-Unicam $Sp_{3\text{-}300}$ spectrophotometer in KBr and in neat polythene strips in 4000–200 cm^{-1} range. ^{1}H-NMR spectra were recorded on Tesla BS487C (80 MHz) using TMS as internal standard. The ^{119m}Sn Mössbauer spectra were recorded at 77 K on a Ranger Engineering constant acceleration spectrometer equipped with an NaI scintillation counter using $Ca^{119m}SnO_3$ as the source and Ca $^{119m}SnO_3$ was the reference material for zero velocity at room temperature. The velocity calibration was based on β-tin and natural iron foils. The resultant spectra were fitted using standard least squares techniques assuming a Lorentzian shape.

RESULTS AND DISCUSSION

All the complexes except triphenyltin(IV) derivatives are soluble in common organic solvents. The analytical data are given in Table 1. Molecular weight determination of all the complexes except those of triphenyltin(IV) complexes by Rast and cryoscopic methods indicates a monomeric nature of the compounds. Insoluble nature of the triphenyltin(IV) complexes indicates polymeric structures.

The assignments of important infrared bands are shown in Table 2 both for ligands and complexes. A band around 2900–2500 cm^{-1} in the spectra of acids disappears in the spectra of their respective sodium salts and complexes which indicates deprotonation of the carboxylic group. A lower ν(N–H) in the PyrNa as compared to PyrH supports the presence of hydrogen bonding in the PyrH. A higher ν(N–H) value in complexes 4, 8 and 12 or its unchanged value in 16 and 20 show non-participation of nitrogen atom in bonding to tin.

The $\Delta\nu$ value [$\Delta\nu = \nu(COO)_{asym} - \nu(COO)_{sym}$] which is useful in drawing structural inferences in the case of metal carboxylate[9] is used to determine the nature of bonding of the carboxylate to tin(IV). In the seven complexes 8, 12, 13 and 17–20, Table 2, the $\Delta\nu$ value is higher by 90–65 cm^{-1} than in the sodium salts and indicates either asymmetric or a unidentate bonding of the carboxylate group to tin(IV)[10] while in the remaining complexes the carboxylate group behaves in a bidentate manner since $\Delta\nu$ value is comparable to the sodium salt of the acids.[11] However, polymeric triphenyltin(IV) complexes have asymmetrically bonded bridging bidentate carboxylate group since $\nu(COO)_{asym}$ and $\nu(COO)_{sym}$ fall in the range of bridging carboxylates.[12] Observation of both $\nu(Sn–C)_{asym}$ and $\nu(Sn–C)_{sym}$ modes in the infrared spectrum of all the compounds studied rules out the planar arrangement for the SnC skeleton. The assignment of ν(Sn–C) and ν(Sn–O) are consistent with the values reported in literature.[11]

The ^{1}H-NMR spectra of the ligands and soluble complexes are given in Table 3. The carboxylic acid proton signal in the acids disappears in the spectra of all the complexes. However in pyrrole 2-carboxylic acid the two protons of the COOH and the NH groups appear as a broad multiplet which may be due to strong hydrogen bonding. The N–H resonance appears as a broad highfield signal in the spectra of all the pyrrole derivatives which is indicative of the non-participation of the nitrogen atom of the ligand to tin(IV). Integrations tally with the expected ratio. In the derivatives of triphenyltin(IV), the signals for protons of the rings (acid) overlap with those of the aromatic protons and are thus difficult to distinguish. Since a multiplet is observed for CH_3 protons in all the trimethyltin(IV) complexes so a *cis* or a *mer* trigonal bipyramidal structure may be present. However, the possibility of a distorted planar Me_3Sn skeleton cannot be ruled out.

The quadrupole splitting parameter (QS) is very useful for interpreting Mössbauer data.[13] A higher QS value in the range 3.69–3.82 mm s^{-1} for complexes 1, 5 and 9, Table 4, is consistent with five coordination. The ratio ρ = QS/IS also favours a five coordinated structure.[15] $Ph_3SnThio$ which is a monomer has much lower QS value and involves monodentate carboxylate. Both properties are consistent with four coordination for tin as reported for other tri-organotin carboxylates.[16]

CONCLUSIONS

All the four Cy_3Sn, *n*-Pr_3SnPyr, *n*-Bu_3SnPyr and $Ph_3SnThio$ complexes are monomers with a unidentate carboxylate which bonds to tin(IV) tetrahedrally. Mössbauer parameters of $Ph_3SnThio$ further support a four coordinate structure. Me_3Sn-, 1–4, *n*-Pr_3Sn-, 5–7, and *n*-Bu_3Sn-, 9–11,

Table 2. IR spectral data (cm^{-1}, KBr/neat in polythene strips)

Sr No.	Compound	ν(Sn–O)	ν(Sn–C)	$\nu(COO)_{asym}$	$\nu(COO)_{sym}$	$\Delta\nu$	ν(N–H)
	ThioH	—	—	1685s,b	1285s	400	—
	ThioNa	—	—	1550s,b	1340s	210	—
	ThioAH	—	—	1700vs	1225s	475	—
	ThioANa	—	—	1565vs	1350m,sp	215	—
	FuH	—	—	1690vs	1300s	390	—
	FuNa	—	—	1590vs	1370s	220	—
	PyrH	—	—	1670vs	1320s,sp	350	3360s
	PyrNa	—	—	1565vs	1380s	185	3260s
1.	$(CH_3)_3$SnThio	420w,sh	540–500bs	1575vs	1365vs	210	—
2.	$(CH_3)_3$SnThioA	405w, 340m,sp	545s, 475w	1570vs	1355s,sp	215	—
3.	$(CH_3)_3$SnFu	455m,sp	545s,sp, 515sh	1600vs,sp	1365s,sp	235	—
4.	$(CH_3)_3$SnPyr	470s,sp, 400s	550s, 505sh	1575vs,b	1365vs,sp	210	3420s,sp, 3310vs,sp
5.	$(n\text{-}C_3H_7)_3$SnThio	415w,sp	590w, 500m,sp	1575vs	1360vs,sp	215	—
6.	$(n\text{-}C_3H_7)_3$SnThioA	475w,sp, 425w,sp	600m,sp, 505w	1580vs,b	1380sh	200	—
7.	$(n\text{-}C_3H_7)_3$SnFu	450ms,sp, 385w,sp	590m,sp, 500w,sp	1600vs,sp	1365vs,sp	245	—
8.	$(n\text{-}C_3H_7)_3$SnPyr[a]	480m,sp, 385w,sp	595m,sp, 510w,b	1610vs,sp	1350s,sp	260	3490sh, 3290vs,sp
9.	$(n\text{-}C_4H_9)_3$SnThio	425m,sp	600s,sp, 510s,sp	1580vs,b	1355vs,b	225	—
10.	$(n\text{-}C_4H_9)_3$SnThioA	435w,b, 390w	550w,sp, 505w	1595vs,sp	1380s,sp	215	—
11.	$(n\text{-}C_4H_9)_3$SnFu	455m,sp	595w,b, 540m,sp	1600vs,sp	1360s,sp	240	—
12.	$(n\text{-}C_4H_9)_3$SnPyr[a]	490m,sp	605ms,b, 515w,b	1605s,sp	1355s,b	250	3270s,sp
13.	$(C_6H_5)_3$SnThio	340w,b	265w, 245sh	1620vs	1320s,sp	300	—
14.	$(C_6H_5)_3$SnThioA	320w,sp	270w, 230sh	1570vs	1330sh	240	—
15.	$(C_6H_5)_3$SnFu	325w,sp	265m,sp, 250w	1585s,sp	1355ms,sp	230	—
16.	$(C_6H_5)_3$SnPyr	315m,sp	285sh, 275m,sp	1615s,sp	1340s,sp	275	3250vs,b
17.	$(c\text{-}C_6H_{11})_3$SnThio	320m,sp, 280sh	480w,sp, 410m,sp	1620s,sp	1360s,sp	260	—
18.	$(c\text{-}C_6H_{11})_3$SnThioA	280sh	480w, 410m,sp	1645s,sp	1335s,sp	310	—
19.	$(c\text{-}C_6H_{11})_3$SnFu	270sh, 250sh	480w,sp, 410w,sp	1605s,sp	1350s,sp	255	—
20.	$(c\text{-}C_6H_{11})_3$SnPyr	310m,sp, 280w,sp	485m,sp, 415w,sp	1610vs,sp	1350vs,sp	260	3230s,b

$\Delta\nu = \nu(COO)_{asym} - \nu(COO)_{sym}$.

[a] In polythene strips.

s = strong, b = broad, m = medium, w = weak, sp = sharp, sh = shoulder.

Table 3. ^{1}H-NMR data (δ, $CDCl_3/CCl_4$)[a]

Sr No.	Compound	Ring protons H^3	H^5	H^4	R–Sn–R		
	ThioH	7.70 (d, 1H)	7.48 (d, 1H)	6.98 (t, 1H)	—		
	ThioAH	7.05 (bd, 1H)	6.5–6.875 (m, 2H)	—	—		
	FuH	7.60 (d, 1H)	7.43 (t, 1H)	6.55 (t, 1H)	—		
	PyrH	6.85 (t, 1H)	6.63 (t, 1H)	6.05 (q, 1H)	—		
1.	$(CH_3)_3$SnThio	7.75 (d, 1H)	7.53 (d, 1H)	7.32–7.03 (m, 1H)	1.3–0.43 (m, 9H)		
2.	$(CH_3)_3$SnThioA	7.15 (m, 1H)	6.85 (m, 2H)	—	0.58 (s, 9H)		
3.	$(CH_3)_3$SnFu	7.45 (s, 1H)	7.05 (t, 1H)	6.43 (m, 1H)	1.08–0.53 (m, 9H)		
4.	$(CH_3)_3$SnPyr	6.68 (m, 1H)	6.35 (bm, 1H)	6.03 (m, 1H)	1.33–0.28 (m, 9H)		
5.	$(n\text{-}C_3H_7)_3$SnThio	7.75 (d, 1H)	7.50 (d, 1H)	7.10 (t, 1H)	1.73 (m, 6H)	1.38 (m, 6H)	1.04 (t, 9H)
6.	$(n\text{-}C_3H_7)_3$SnThioA	7.08 (m, 1H)	6.80 (m, 2H)	—	1.63 (m, 6H)	1.25 (m, 6H)	0.78 (t, 9H)
7.	$(n\text{-}C_3H_7)_3$SnFu	7.45 (s, 1H)	6.95 (d, 1H)	6.40 (m, 1H)	1.88 (m, 6H)	1.48 (m, 6H)	1.08 (t, 9H)
8.	$(n\text{-}C_3H_7)_3$SnPyr	6.73 (m, 1H)	6.33 (bm, 1H)	6.03 (q, 1H)	1.65 (m, 6H)	1.18 (m, 6H)	1.03 (t, 9H)
9.	$(n\text{-}C_4H_9)_3$SnThio	7.63 (d, 1H)	7.43 (t, 1H)	7.05 (t, 1H)	1.73–1.13 (m, 18H)		0.93 (t, 9H)
10.	$(n\text{-}C_4H_9)_3$SnThioA	7.08 (m, 1H)	6.80 (t, 2H)		2.05–1.08 (m, 18H)		0.73 (t, 9H)
11.	$(n\text{-}C_4H_9)_3$SnFu	7.43 (m, 1H)	6.93 (m, 1H)	6.38 (m, 1H)	1.93–1.23 (m, 18H)		0.88 (t, 9H)
12.	$(n\text{-}C_4H_9)_3$SnPyr	6.73 (s, 1H)	6.30 (bm, 1H)	6.03 (d, 1H)	2.0–1.05 (m, 18H)		0.93 (t, 9H)
13.	$(C_6H_5)_3$SnThio[a]	7.78 (m, 4H)	7.55 (m, 2H)	7.35 (m, 10H) 6.95 (m, 2H)			
14.	$(C_6H_5)_3$SnThioA[b]	—	—	—	—		
15.	$(C_6H_5)_3$SnFu[b]	—	—	—	—		
16.	$(C_6H_5)_3$SnPyr[a]	7.90	7.60	6.78 (bm,5H) 7.30 (m, 7H)	—		
17.	$(c\text{-}C_6H_{11})_3$SnThio	7.83 (m, 1H)	7.55 (d, 1H)	7.13 (m, 1H)	2.43–1.13 (m, 33H)		
18.	$(c\text{-}C_6H_{11})_3$SnThioA	7.25 (bs, 1H)	6.80 (bs, 2h)		2.65–1.00 (m, 33H)		
19.	$(c\text{-}C_6H_{11})_3$SnFu	7.50 (bs, 1H)	7.18 (bs, 1H)	6.45 (bs, 1H)	2.65–1.00 (m, 33H)		
20.	$(c\text{-}C_6H_{11})_3$SnPyr	6.65 (m, 1H)	6.38 (m, 1H)	6.03 (m, 1H)	2.25–1.25 (m, 33H)		

s = singlet; d = doublet; t = triplet; q = quarter; b = broad; m = multiplet.

[a] Soluble in $CDCl_3$ + DMSO(D_6).

[b] Insoluble in $CDCl_3$ and CCl_4.

Table 4. ^{119m}Sn Mössbauer spectral data (80 K, mm s^{-1})

	Complex	IS ± 0.03 (SnO_2)	QS ± 0.06	Line width 1	Line width 2	ρ
1.	$(CH_3)_3SnThio$	1.42	3.69	1.04	1.08	2.598
5.	$(n\text{-}C_3H_7)_3SnThio$	1.54	3.76	1.21	1.14	2.440
9.	$(n\text{-}C_4H_9)_3SnThio$	1.54	3.82	1.36	1.11	2.480
		1.48[a]	3.78	—	—	2.554
13.	$(C_6H_5)_3SnThio$	1.33	2.54	1.21	1.69	1.909

[a] Literature value, D. W. Allen, J. S. Brooks, R. Formstone, A. J. Crowe and P. J. Smith, *J. Organomet. Chem.* 1978, **156**, 359.

derivatives are monomers with a bidentate carboxylate in a five coordinate structure. Mössbauer data of three complexes $Me_3SnThio$, $n\text{-}Pr_3SnThio$ and $n\text{-}Bu_3SnThio$ further support a trigonal bipyramidal structure for these complexes. Three remaining Ph_3Sn-, 14–16, derivatives, which are polymers, have a five coordinate carboxylate bridged structure.

Acknowledgements—One of us (S.P.V.) is grateful to UGC, New Delhi, India for the award of a Teacher Research Fellowship and DAV Managing Committee, Chitergupta Road, New Delhi, India for the grant of study leave.

REFERENCES

1. M. Nakanishi and A. Tsuda, *Yoshitomi Pharmaceutical Industries Ltd.* Japan 15, 690 (1964) 4 August, Applied 30 May 1961 [CA 62: 6513b].
2. *M. and T. International* B.V. Neth. Applied 7312, 329 (Cl CO7f, AOIn) 13 March 1974 [CA 81: 91732b].
3. G. K. Sandhu, N. S. Boparai and S. S. Sandhu Jr, *Synth. React. Inorg. Met.-Org. Chem.* 1980, **10**, 535.
4. D. W. Allen, J. S. Brooks, R. Formstone, A. J. Crowe and P. J. Smith, *J. Organomet. Chem.* 1978, **156**, 359.
5. A. Saitow, E. G. Rochow and D. Seyferth, *J. Org. Chem.* 1958, **23**, 116.
6. D. Seyferth and F. G. A. Stone, *J. Am. Chem. Soc.* 1957, **79**, 515.
7. V. K. Awasthi, S. N. Bhattacharya and M. Verma, *J. Indian Chem. Soc.* 1982, **LIX**, 264.
8. A. I. Vogel, *A Text Book of Quantitative Inorganic Analysis*. English Language Book Society and Longman Group Limited, London (1973).
9. B. Y. K. Ho and J. J. Zuckerman, *Inorg. Chem.* 1973, **12**, 1552.
10. N. W. G. Debye, D. E. Fenton and J. J. Zuckerman, *J. Inorg. Nucl. Chem.* 1972, **34**, 352.
11. G. K. Sandhu, R. Gupta, S. S. Sandhu, R. V. Parish and K. Brown, *J. Organomet. Chem.* 1985, **279**, 373.
12. W. D. Honnick and J. J. Zuckerman, *J. Organomet. Chem.* 1979, **178**, 133.
13. R. V. Parish, In *Mössbauer Spectroscopy Applied to Inorganic Chemistry* (Edited by G. J. Long), Vol. I, p. 52. Plenum Press, New York (1984).
14. G. M. Bancroft, B. W. Davis, N. C. Pyne and T. K. Sham, *J. Chem. Soc., Dalton Trans.* 1975, 973.
15. J. J. Zuckerman, *Adv. Organomet. Chem.* 1970, **9**, 21.
16. B. F. E. Ford and J. R. Sams, *J. Organomet. Chem.* 1969, **19**, 53.

Polyhedron Vol. 6, No. 3, pp. 593–601, 1987
Printed in Great Britain

0277–5387/87 $3.00+.00

EMISSION AND ELECTROCHEMICAL STUDIES OF 2-PYRIDYLCARBONYLMETHYLIDE–RHENIUM(I) COMPLEXES

GEN-ETSU MATSUBAYASHI* and KOSUKE UEYAMA

Department of Applied Chemistry, Faculty of Engineering, Osaka University, Yamada-oka, Suita, Osaka 565, Japan

(*Received* 9 *April* 1986; *accepted* 15 *August* 1986)

Abstract—Re(I)Br(CO)$_3$(2-pyridylcarbonylmethylide) and Re(I)Br(CO)$_3$(2-acetylepyridine) were prepared by reactions of Re(I)Br(CO)$_5$ with 2-pyridylcarbonylmethylides, $C_5H_4NC(O)\bar{C}H\overset{+}{Z}$ [$\overset{+}{Z}$ = $\overset{+}{P}Ph_3$ (Y_P), $\overset{+}{As}Ph_3$ (Y_{As}), $\overset{+}{S}Me_2$ (Y_S) and $\overset{+}{N}C_5H_4R$-4 (Y_{N-R}; R = CN, Ph, H and Me)], and 2-acetylpyridine. These complexes are concluded to assume an octahedral geometry containing the chelation by the carbonyl oxygen and pyridyl nitrogen atoms and the *facial*-coordination of metal carbonyl groups on the basis of IR and ^{1}H-NMR spectra. Although the 2-acetylpyridine complex gave no emission, the Y_P, Y_{As} and Y_S complexes showed an emission due to the metal-to-ligand charge transfer (MLCT) transition at 77 K in MeOH/EtOH (1:4 v/v). On the other hand, the Y_{N-R} complexes showed emissions due to both the MLCT and the intraligand CT transitions. All the present ylide complexes were oxidized at +0.71 to +0.82 V vs Ag/Ag$^+$ in acetonitrile. The Y_P, Y_{As} and Y_S complexes were reduced at −1.91 to −2.00 V, while reduction of the Y_{N-R} complexes occurred on the pyridinium ring of the ylides at less negative potentials (−1.68 to −1.04 V).

Photo-physical properties of charge transfer (CT) transitions between metal ions and ligands have been investigated in order to clarify mechanisms of photo-reactions of organometallic complexes.[1–3] Many rhenium(I) complexes with nitrogen donor ligands were reported to show intensive emissions due to metal-to-ligand CT transitions even at room temperature.[3] Moreover, it is of interest that some of them display multiple emissions due to intraligand and metal-to-ligand CT transitions.[4]

Ylide molecules in which carbanions are directly attached to hetero-atoms, such as phosphorus, arsenic, sulfur and nitrogen, exhibit various unique reactivities that are characteristic of the ylide bonding.[5] Moreover, ylide–metal interactions have attracted much interest.[6,7] However, photo-physical properties of ylides and their metal complexes are little known.[8] Ylide molecules generally exhibit intensive absorption bands due to an intramolecular CT transition[9] and some of them are known to give noticeable emissions caused by this transition.[10] In order to investigate the effect of the ylide structure in the ligand on photo-physical properties of metal complexes, we have chosen rhenium(I)–ylide complexes which have been expected to exhibit intensive emissions.

This paper reports configurations of Re(I)Br(CO)$_3$L (L = several 2-pyridylcarbonylmethylides (**1**) and 2-acetylpyridine) and their emission properties, together with electrochemical behaviors of the complexes.

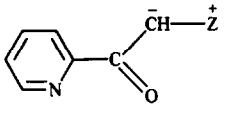

1

$\overset{+}{Z}$ = $\overset{+}{P}Ph_3$ (Y_P)
$\overset{+}{As}Ph_3$ (Y_{As})
$\overset{+}{S}Me_2$ (Y_S)
$\overset{+}{N}C_5H_4R$-4 (Y_{N-R})
R = CN, Ph, H or Me

EXPERIMENTAL

Preparation of 4-substituted pyridinium 2-pyridylcarbonylmethylides

A benzene (25 cm^3) solution of 4-phenylpyridine (1.9 g, 12 mmol) was added to a benzene (25 cm^3)

* Author to whom correspondence should be addressed.

solution of 2-(bromoacetyl)pyridine[11] (2.5 g, 12 mmol) and the mixture was refluxed for 4 h to give white precipitates of 4-phenyl-*N*-(2-pyridylcarbonylmethyl)pyridinium bromide (4.3 g, 98% yield). To its aqueous (150 cm^3) solution was added an aqueous (70 cm^3) solution of K_2CO_3 (3.9 g, 29 mmol) and the precipitates obtained were extracted with dichloromethane (400 cm^3). After the solution was concentrated to one third volume under reduced pressure, it was kept at $-10°C$ overnight to give red crystals of 4-phenylpyridinium 2-pyridylcarbonylmethylide (Y_{N-Ph}) (2.0 g, 61% yield), m.p. 163°C (decomp.). Found: C, 78.5; H, 4.9; N, 10.2. Calc. for $C_{18}H_{14}N_2O$: C, 78.8; H, 5.1; N, 10.2%.

Pyridinium 2-pyridylcarbonylmethylide (Y_{N-H}) was prepared as yellow needles according to the same method described above (43% yield), m.p. 138°C (decomp.). Found: C, 67.9; H, 4.9; N, 12.8. Calc. for $C_{12}H_{10}N_2O \cdot 0.2CH_2Cl_2$: C, 68.1; H, 4.9; N, 13.2%. The presence of solvent molecules was confirmed by the ^{1}H-NMR spectrum.

4-Cyanopyridinium (Y_{N-CN}) and 4-methylpyridinium 2-pyridylcarbonylmethylide (Y_{N-Me}) were prepared according to the literature methods.[12,13]

Preparation of triphenylarsonium (Y_{As}), *triphenylphosphonium* (Y_P) *and dimethylsulfonium* 2-*pyridylcarbonylmethylide* (Y_S)

A methanol (50 cm^3) solution containing triphenylarsine (1.9 g, 6.2 mmol) and 2-(bromoacetyl)pyridine (2.0 g, 9.9 mmol) was stirred overnight at room temperature. After the solvent was evaporated to dryness, the residue was washed with benzene and dried *in vacuo* (1.9 g, 60% yield). To its aqueous (200 cm^3) solution was added an aqueous (60 cm^3) solution of NaOH (5.0 g). White precipitates were filtered off and recrystallized from a mixture of dichloromethane and diethyl ether at $-10°C$ to give white crystals of Y_{As} (1.2 g, 84% yield), m.p. 96°C (decomp.). Found: C, 68.6; H, 5.0; N, 3.2. Calc. for $C_{25}H_{20}NOAs \cdot 0.5H_2O$: C, 69.1; H, 4.9; N, 3.2%. The presence of solvent molecules was confirmed by the IR spectrum.

Y_P and Y_S were prepared according to the literature method.[10]

Preparation of bromotricarbonyl(2-pyridylcarbonylmethylide and 2-acetylpyridine)rhenium(I), ReBr$(CO)_3$L [L = Y_P, Y_{As}, Y_S, Y_{N-R} (R = CN, Ph, H *and* Me) *and* 2-AcPy]

A benzene (60 cm^3) solution of Y_{N-Ph} (56 mg, 0.20 mmol) was added to a benzene (70 cm^3) solution of bromopentacarbonylrhenium(I)[14] (82 mg, 0.20 mmol) and the solution was refluxed for 2 h. Yellow precipitates of $ReBr(CO)_3Y_{N-Ph}$ were filtered off and dried *in vacuo* (86 mg, 83% yield). The other ylide– and 2-acetylpyridine–rhenium(I) complexes were prepared by the similar method.

Melting points, analyses and reaction yields for the rhenium(I) complexes are summarized in Table 1.

n-Butyltrichloro(4-cyanopyridinium 2-pyridylcarbonylmethylide)tin(IV)[15] and 4-substituted (CN, Ph, H and Me)-N-(2-pyridylcarbonylmethyl)pyridinium perchlorates[16] were prepared as described elsewhere.

Physical measurements

IR, ^{1}H-NMR and emission spectra[8] as well as ESR spectra[17] were measured as described previously. For the measurement of emission lifetimes, deaerated methanol/ethanol (1:4 v/v) solutions containing metal complexes were irradiated at 337.1 nm with a pulsed nitrogen-laser (pulse width of ~ 2 ns).[18] Lifetimes were calculated from oscilloscope tracings of the decay of emission intensities.

All cyclic voltammograms were recorded in an acetonitrile solution containing $[NBu^n_4]ClO_4$ (0.05–0.1 mol dm^{-3}) as a supporting electrolyte, as described elsewhere.[16]

Table 1. Melting points, elemental analyses and preparation yields of $ReBr(CO)_3L$

L	M.p. (decomp.) (°C)	Found (calc.) (%) C	H	N	Yield (%)
Y_{N-CN}	210	38.4 (37.1)	2.1 (2.3)	6.7 (7.1)	49
Y_{N-Ph}	267	40.5 (40.4)	2.1 (2.3)	4.5 (4.5)	83
Y_{N-H}	247	33.1 (32.9)	1.9 (1.8)	5.2 (5.1)	74
Y_{N-Me}[a]	180	39.1 (39.1)	2.6 (2.8)	4.6 (4.6)	61
Y_P	300	45.4 (46.0)	2.9 (2.8)	1.9 (1.9)	36
Y_{As}[b]	220	43.4 (44.2)	2.8 (2.7)	1.8 (1.8)	28
Y_S	185	27.3 (27.1)	2.2 (2.1)	2.6 (2.6)	52
2-AcPy	241	25.5 (25.5)	1.5 (1.5)	3.0 (3.0)	54

[a] Contains $0.67C_6H_6$.
[b] Contains $0.17C_6H_6$.

RESULTS AND DISCUSSION

Configuration of the rhenium(I) complexes

The ν(C≡O) bands of $ReBr(CO)_3Y_{N-R}$ and $ReBr(CO)_3$(2-AcPy) are observed at lower frequencies than those of the free ligands, indicating that the ligands coordinate to the rhenium(I) ion through the carbonyl oxygen atom (Table 2).[10] In ^{1}H–NMR spectra of these complexes, the signals of the proton (H_6) bound with the carbon atom adjacent to the pyridyl nitrogen atom are observed at lower fields than those of free ligands, which suggests that Y_{N-R} and 2-AcPy chelate to the rhenium(I) ion through the carbonyl oxygen and pyridyl nitrogen atoms.

In $ReBr(CO)_3Y_S$, the ν(C≡O) bands occurs at a slightly higher frequency than that of the free ylide. This behavior is also the same as $W(CO)_4Y_S$,[10] and the IR spectra due to the coordinating Y_S ligand are almost the same for these two complexes. Since the X-ray crystallographic analysis revealed that $W(CO)_4Y_S$ has the chelate coordination through the carbonyl oxygen and pyridyl nitrogen atoms, the rhenium(I)–Y_S complex seems to assume the same configuration around the metal atom to $W(CO)_4Y_S$. Although the Y_P and Y_{As} complexes also have exhibited the ν(C≡O) bands of the coordinating ylides at slightly higher frequencies than the free ylides, they are reasonably likely to have the chelation by oxygen and nitrogen atoms as well as the Y_S complex. These small higher frequency shifts of the ν(C≡O) bands are in contrast to the large higher frequency shifts (167 and 160 cm^{-1}) of the ν(C≡O) ones which were seen on the chelation by the ylide carbon and pyridyl nitrogen atoms in $PtCl_2Y_S$[19] and $PtCl_2Y_P$.[20]

In the ^{1}H-NMR spectrum of $ReBr(CO)_3Y_P$ in dimethyl sulfoxide-d_6, the spin-spin coupling constant between the ylide proton and ^{31}P nucleus has been measured 18 Hz which is close to 20 Hz of $W(CO)_4Y_P$ having the chelation by the oxygen and nitrogen atoms.[10] Although the magnitude is smaller than 27 Hz of the free Y_P, it is significantly large compared with those (6 and 10 Hz) of $PdCl_2Y_P$ and $PtCl_2Y_P$ having the chelation by the ylide carbon and pyridyl nitrogen atoms.[20] These findings also suggest an sp^2 geometry around the ylide carbon atom of Y_P in the present complex which is caused by the coordination through the carbonyl oxygen atom. In Y_P–, Y_{As}– and Y_S–Re(I) complexes, the H_6 proton signals appear at lower fields than those of free ligands (Table 2). These results support the chelation to the metal through the carbonyl oxygen and pyridyl nitrogen atoms.

All the complexes exhibit the three IR bands in the region of the C≡O stretching frequencies (Table 2), suggesting that the three carbonyl ligands coordinate to the rhenium(I) ion in a *cis*-arrangement (**2**).[21,22] The ^{1}H-NMR spectrum of $ReBr(CO)_3Y_S$ has shown two S–CH_3 signals (2.90 and 2.93 δ in dimethyl sulfoxide-d_6), confirming this configuration.

Table 2. Relevant infrared frequencies (cm^{-1}) and ^{1}H-NMR chemical shifts of $ReBr(CO)_3L$

L	ν(C≡O)[a]			ν(C=O)[b]	δ H_6[c]
Y_{N-CN}	2012	1910	1859	1489 (−42)	8.88 (0.34)
Y_{N-Ph}	2000	1880	1860	1486 (−29)	8.91 (0.36)
Y_{N-H}	2005	1880		1493[d] (−40)	8.88 (0.33)
	(1997	1893	1870)		
Y_{N-Me}	2005	1884	1859	1505 (−24)	8.85 (0.37)
Y_P	2009	1897	1858	1542 (+5)	8.84 (0.38)
Y_{As}	2021	1898	1860	1537 (+34)	8.57 (0.27)
Y_S	2007	1890		1538 (+26)	8.88 (0.36)
	(2006	1897	1872)		
2-AcPy	2019	1929	1891	1618 (−82)	9.18[e] (0.45)

[a] Measured in Nujol mulls and measured in DMF in parentheses.

[b] Measured in Nujol mulls and $\nu(C{=}O)_{complexed} - \nu(C{=}O)_{free}$ in parentheses.

[c] Measured in DMSO-d_6 and $\delta H_{6\,complexed} - \delta H_{6\,free}$ in parentheses.

[d] Measured in a KBr disk.

[e] Measured in CH_2Cl_2.

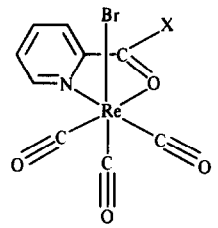

2

$\bar{C}H-\overset{+}{Z}$; Z = $\overset{+}{P}Ph_3$, $\overset{+}{A}sPh_3$, $\overset{+}{S}Me_2$, $\overset{+}{N}C_5H_4R$-4

X = CH_3

R = CN, Ph, H or Me

Electronic absorption spectra

$ReBr(CO)_3$(2-AcPy) exhibits an intensive absorption band at 430 nm in MeOH/EtOH (1 : 4 v/v), while both 2-acetylpyridine and $ReBr(CO)_5$[23] have no band in this region (Fig. 1). This band is reasonably assigned to a metal-to-ligand charge transfer (MLCT) transition, since $ReX(CO)_3L_2$ complexes (L = pyridine and its derivatives,[24] L_2 = di-imines;[22] X = Br and Cl) were reported to exhibit MLCT bands at 290–520 nm. Moreover, this band displays an appreciable blue shift in polar solvents (Table 3), as was seen in MLCT bands of other rhenium(I) complexes,[24,25] which supports this assignment.

Table 3. Solvent dependence on absorption band maxima of $ReBr(CO)_3L$ at 298 K

Solvent	Band (nm) L = 2-AcPy	L = Y_P	L = Y_{N-H}
DMSO	394	378	446
MeCN	423	379	440
MeOH/EtOH (1 : 4 v/v)	430	380	430
CH_2Cl_2	452	388	455
THF	444	391	459
$CHCl_3$	466	391	463

Figure 2 shows the spectrum of $ReBr(CO)_3Y_P$ in MeOH/EtOH (1 : 4 v/v), together with that of free ylide in 2-MeTHF. The band at 380 nm also is attributed to the MLCT transition on the basis of the spectrum of the 2-AcPy–Re(I) complex. Free Y_P exhibits a strong band at 348 nm which can be assigned to an intramolecular CT transition from the negatively charged ylide-carbon to the phosphonium moiety.[5] Assuming the coordination of the carbonyl oxygen-to-rhenium(I) for $ReBr(CO)_3Y_P$, this intraligand CT (ILCT) band of

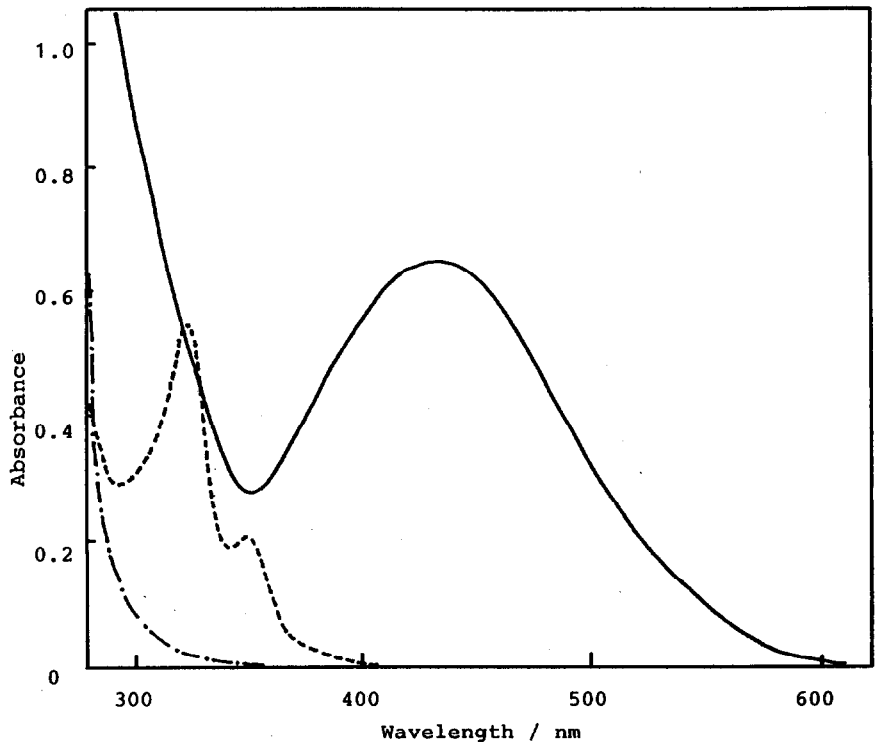

Fig. 1. Electronic absorption spectra of $ReBr(CO)_3$(2-AcPy) (——) in MeOH/EtOH (1 : 4 v/v), $ReBr(CO)_5$ (– – –) and 2-AcPy (– · – · –) in MeCN at 298 K : 3.0×10^{-4} mol dm^{-3}.

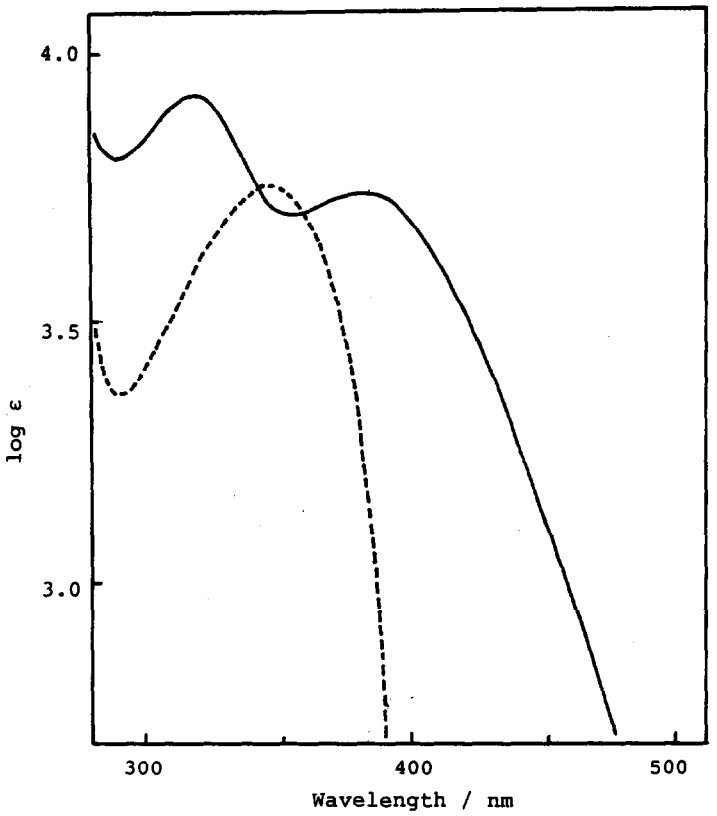

Fig. 2. Electronic absorption spectra of $ReBr(CO)_3Y_P$ (——) in MeOH/EtOH (1 : 4 v/v) and of Y_P (– – –) in 2-MeTHF.

the complex is likely to occur at a higher energy than free Y_P, as was seen in several 4-substituted pyridinium 2-pyridylcarbonylmethylide-$SnBu^nCl_3$ complexes.[15] Hence, the strong band of the Y_P–Re(I) complex observed at 327 nm is possibly due to the ILCT transition. Y_{As}– and Y_S–Re(I) complexes also have exhibited both ILCT and MLCT bands at quite similar wavelengths to the Y_P complex.

The spectra of $ReBr(CO)_3Y_{N-H}$ and free Y_{N-H} in MeOH/EtOH (1 : 4 v/v) are illustrated in Fig. 3. The band at 426 nm observed for free Y_{N-H} is referred to a CT transition from the ylide carbon to the pyridinium ring.[9] On the other hand, the Y_{N-H}–Re(I) complex shows an extremely broad band near 430 nm, where the ILCT band due to the $\bar{C}$–$\overset{+}{N}$ ylide structure and the MLCT one seem to be overlapped. The other Y_{N-R}–Re(I) complexes also exhibit the similar broad absorptions to the Y_{N-H} complex. The absorption maxima of the Y_{N-R} complexes occur at lower energies than the Y_P, Y_{As} and Y_S complexes which are summarized in Table 4. This finding is plausibly indicative of much stabilization of excited states of the Y_{N-R} complexes compared with the Y_P, Y_{As} and Y_S ones, which is

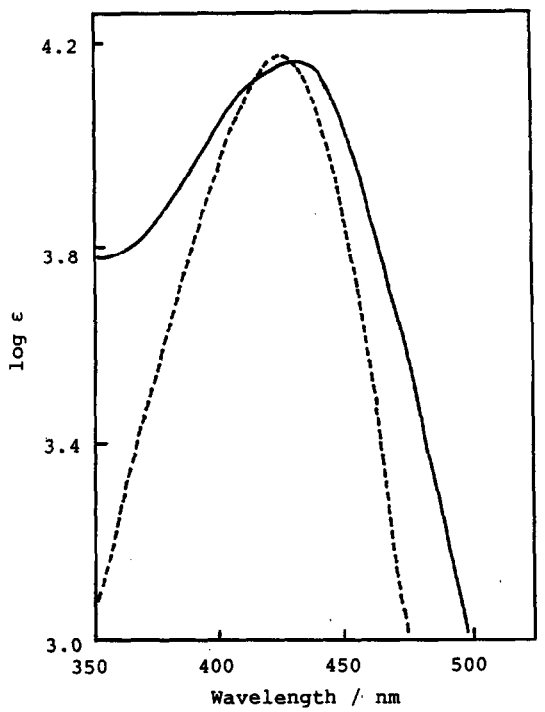

Fig. 3. Electronic absorption spectra of $ReBr(CO)_3Y_{N-H}$ (——) and Y_{N-H} (– – –) in MeOH/EtOH (1 : 4 v/v) at 298 K.

Table 4. Electronic absorption band maxima (nm) of $ReBr(CO)_3L$ complexes and of free ligands in MeOH/EtOH (1 : 4 v/v) at 298 K

L	$ReBr(CO)_3L$ ILCT band (log ε)	$ReBr(CO)_3L$ MLCT band (log ε)	Free L ILCT band (log ε)
Y_{N-CN}	504 (4.03)		473 (4.11)
Y_{N-Ph}	466 (3.58)		459 (4.43)
Y_{N-H}	430 (4.17)		426 (4.17)
Y_{N-Me}	423 (3.96)		423 (4.03)
Y_P	319 (3.94)	380 (3.75)	348 (3.76)[a]
Y_{As}	308 (4.18)	370 (4.01)	329 (3.64)
Y_S	307 (3.93)	369 (3.74)	316 (3.93)
2-AcPy		430 (3.35)	

[a] Measured in 2-MeTHF.

consistent with the electrochemical properties of the complexes as described later.

Emission spectra

Complexes of the type of $ReX(CO)_3L_2$ (L_2 = pyridine and 1,10-phenanthroline derivatives; X = Br and Cl) are known to exhibit intensive emissions due to the MLCT transition even at room temperature.[3,4,23] $ReBr(CO)_3$(2-AcPy), however, has shown no emission even at 77 K, although it contains the coordination of pyridyl nitrogen and shows an intensive absorption band due to the MLCT transition. This is possibly due to any appreciable quenching through the coordinating carbonyl group, considering the fact that $ReBr(CO)_3$(4-acetylpyridine)$_2$ gave a strong emission.[26]

The Y_P, Y_{As} and Y_S complexes have shown appreciable emissions at 77 K. Figure 4 shows the emission spectrum of $ReBr(CO)_3Y_P$ in MeOH/EtOH (1 : 4 v/v) at 77 K, together with its excitation spectrum. The excitation spectrum is almost identical with the absorption spectrum measured at room temperature. Therefore, the emission is attributed to the MLCT transition. The emission lifetime of 10.0 μs also supports the above assignment, since several $ReBr(CO)_3L_2$ (L_2 = pyridine derivatives) had MLCT emission lifetimes of ≈ 40 μs.[3,27]

Although the Y_P complex has the same configuration around the metal as the 2-AcPy complex, the presence of the ylide structure which is adjacent to the coordinating carbonyl group in the former complex seems to play a role in the appearance of the emission. Free Y_P itself has exhibited a noticeable emission due to the intramolecular CT transition based on the ylide structure. Therefore, in the rhenium complex, an effective energy transfer from the ylide CT level to the metal-to-ligand CT one seems to cause the appearance of the emission. The emissive behavior is the same also in the Y_{As}–rhenium(I) complex (Table 4). The Y_S–rhenium(I) complex also has exhibited an MLCT emission,

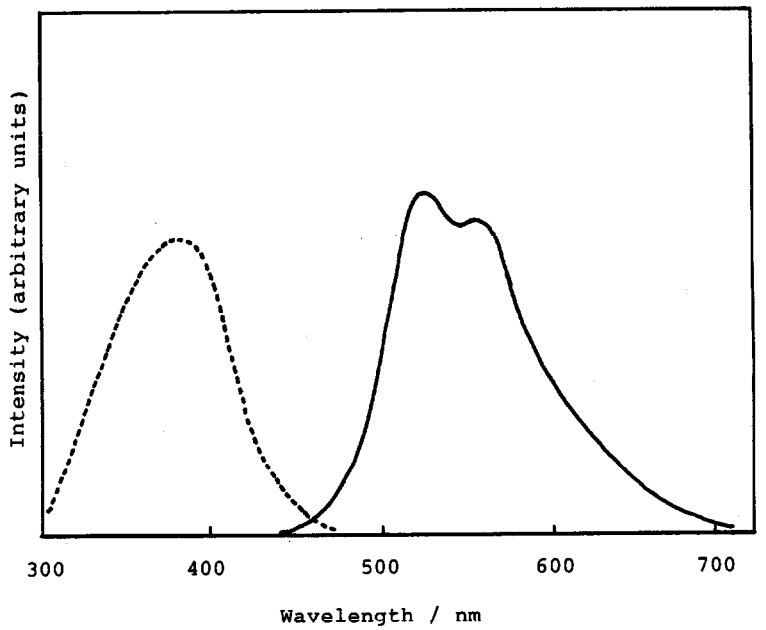

Fig. 4. Emission (——) and excitation (– – –) spectra of $ReBr(CO)_3Y_P$ in MeOH/EtOH (1 : 4 v/v) at 77 K.

although free Y_S has given no emission even at 77 K.

Figure 5 shows the emission and excitation spectra of $ReBr(CO)_3Y_{N-H}$ in MeOH/EtOH (1 : 4 v/v) at 77 K. Since free Y_{N-H} also has exhibited a ylide CT emission at 463 nm, the emission band at 467 nm of the rhenium(I) complex is favorably ascribed to the fluorescence coming from the ILCT transition of the coordinating ylide. The fact that the excitation band essentially agrees with the ILCT absorption band, together with the emission lifetime of < 8 ns, supports this assignment. The complex has another emission band near 632 nm. Although the measurement of the lifetime has been unsuccessful owing to the weak intensity, this emission can be reasonably assigned to the MLCT transition in analogy with the emission bands of the Y_P–, Y_{As}– and Y_S–rhenium(I) complexes. The complex has shown no phosphorescence, while free Y_{N-H} affords a phosphorescence at 460 nm (~ 800 ms) from the carbonyl $^3(n-\pi^*)$ state. This phosphorescence seems to be quenched in the complex owing to the MLCT triplet state which lies at lower energy than the $^3(n-\pi^*)$ state.

As shown in Table 5, in a series of the Y_{N-R} complexes a more electron-withdrawing substituent of the pyridinium ring results in the occurrence of both the ILCT and MLCT emission bands at lower energies.

The observation of the dual emissions in the Y_{N-R} complexes is likely to be related to the energetically closely lying ILCT and MLCT states. As apparent from the absorption spectra of the Y_{N-R} complexes as well as the excitation ones for their emissions, these two excited states have quite similar energies. Hence, both the states can emit simultaneously, although the energy of the MLCT state is relaxed to its lowest level by a radiationless internal conversion, followed by the emission at much lower energy. On the other hand, the Y_P–, Y_{As}– and Y_S–

Table 5. Emission bands (nm) and lifetimes [τ] of $ReBr(CO)_3L$ complexes and of free ligands in MeOH/EtOH (1 : 4 v/v) at 77 K

L	$ReBr(CO)_3L$ ILCT band [τ]	$ReBr(CO)_3L$ MLCT band [τ]	Free L ILCT band
Y_P		521 (556) [10.0 μs]	433[a]
Y_{As}		523 (560) [11.3 μs]	412
Y_S		534 (567) [7.8 μs]	none
Y_{N-Me}	469	626 (680)	460
Y_{N-H}	467 (< 8 ns)	632 (687)	463
Y_{N-Ph}	496	676 (728)	507
2-AcPy		none	

[a] Measured in 2-MeTHF.

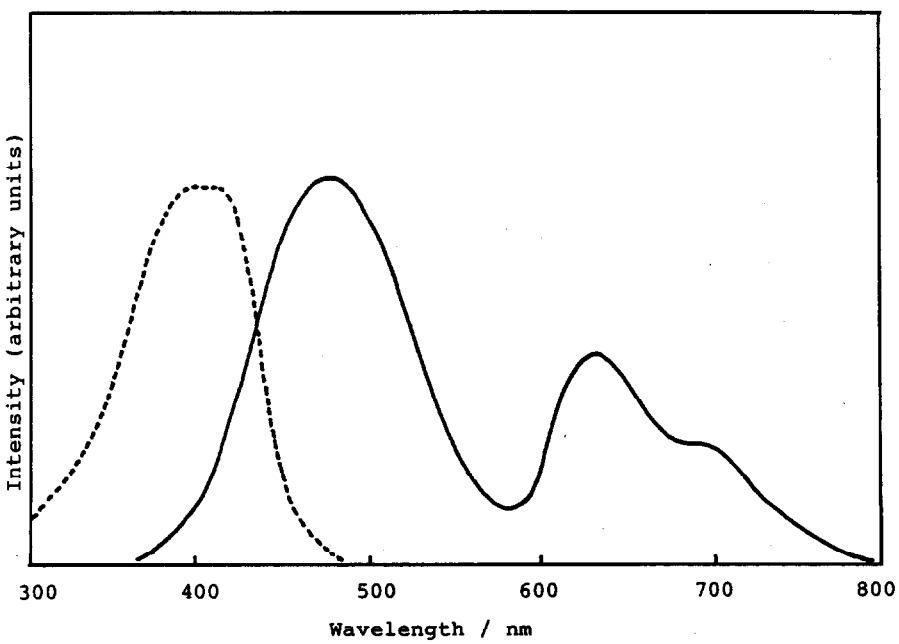

Fig. 5. Emission (——) and excitation (– – –) spectra of $ReBr(CO)_3Y_{N-H}$ in MeOH/EtOH (1 : 4 v/v) at 77 K.

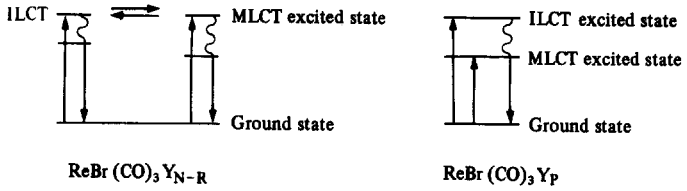

Scheme 1.

rhenium(I) complexes have given only the MLCT emission. In these complexes the ILCT level lies at a considerably higher energy than the MLCT level. Excitation to the ILCT level is followed by an effective radiationless quenching to the MLCT level, resulting in the appearance of only the MLCT emission (Scheme 1).

Electrochemical properties of the rhenium(I) complexes

Electrochemical properties of the $ReBr(CO)_3L$ complexes (L = 2-AcPy and 2-pyridylcarbonylmethylides) have been investigated by cyclic voltammetry. The data are summarized in Table 6. The 2-AcPy complex has revealed an irreversible wave at +1.20 V (vs Ag/Ag^+). This peak seems to correspond to the oxidation from Re(I) to Re(II), since free 2-AcPy has exhibited no anodic peak up to +1.7 V and $ReCl(CO)_3$(2,2′-bipyridine) and $ReCl(CO)_3$(1,10-phenanthroline) were reported to have oxidation peaks at 1.35 and 1.33 V vs SCE, respectively.[27]

The oxidation peaks of the Y_P–, Y_{As}– and Y_S–rhenium(I) complexes have appeared at significantly less positive potentials than that of the 2-AcPy complex. This suggests that these ylide complexes have greater electron densities on the metal compared with the 2-AcPy complex. Increased electron densities on the metal are expected to lead to less favorable reduction. In fact, Y_P–, Y_{As}– and Y_S–rhenium(I) complexes exhibit the cathodic peaks at extremely negative potentials, although the 2-AcPy complex reveals a peak at −1.04 V.

Figure 6 shows the cyclic voltammogram of the Y_{N-CN} complex in acetonitrile. While the irreversible oxidation wave is observed at a similar potential to those of the Y_P, Y_{As} and Y_S complexes, two cathodic peaks appear. The reduction from Re(I) to Re(0) seems to occur at −1.71 V which is close to the reduction potentials of Y_P, Y_{As} and Y_S complexes. The Y_{N-CN} complex has another less negative cathodic peak which accompanies a reversible anodic peak. This peak is reasonably assigned to the reduction process of the pyridinium ring of the ylide ligand on the basis of the following results. (1) At quite a similar potential (−0.94 V) has been observed the reversible cathodic peak also in $Sn(IV)Bu^nCl_3Y_{N-CN}$ in which Y_{N-CN} coordinates to the tin atom through the carbonyl oxygen and pyridyl nitrogen atoms[15] as well as the Y_{N-CN}–rhenium(I) complex. (2) The ESR spectrum measured under the electrochemical reduction of $Sn(IV)Bu^nCl_3Y_{N-CN}$ at −1.2 V has shown the signal at $g = 2.004$ with hyperfine structures, although the signal ($g = 2.003$) of the electrochemically reduced $ReBr(CO)_3Y_{N-CN}$ has not been sufficiently resolved. (3) The cathode peak potentials of the Y_{N-CN}–rhenium(I) complexes are similar to those of the corresponding 4-substituted-(2-pyridylcarbonylmethyl)pyridinium perchlorates ($[Y_{N-R}H]ClO_4$) (see Table 7). Moreover, these peak potentials are very sensitive to the electron-withdrawing property

Table 6. Cathode and anode peak potentials of $ReBr(CO)_3L$[a]

L	E_{pc}	E_{pa}
2-AcPy	−1.05	+1.20
Y_P	−1.91	+0.78
Y_{As}	−1.93	+0.82
Y_S	−2.00	+0.77
Y_{N-Me}	−1.68	+0.71
Y_{N-H}	−1.56	+0.74
Y_{N-Ph}	−1.51	+0.74
Y_{N-CN}	−1.04	+0.81

[a] V vs Ag/Ag^+ in MeCN containing $[NBu^n_4]ClO_4$ (0.05 mol dm^{-3}), measured with a scan rate of 0.1 V s^{-1}.

Table 7. Cathode peak potentials[a] of $[Y_{N-R}H]ClO_4$ and Y_{N-R}

R	$[Y_{N-R}H]ClO_4$	Y_{N-R}
Me	−1.06	−2.02
H	−1.05	−2.08
Ph	−1.43	−1.90
CN	−0.94	−1.50

[a] V vs Ag/Ag^+ in MeCN containing $[NBu^n_4]ClO_4$ (0.05 mol dm^{-3}), measured with a scan rate of 0.1 V s^{-1}.

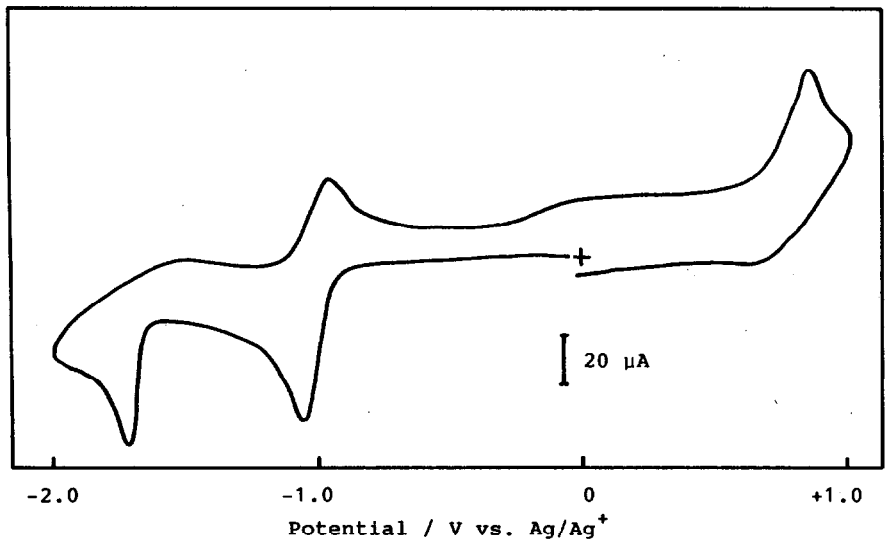

Fig. 6. Cyclic voltammogram of $ReBr(CO)_3Y_{N-CN}$ in MeCN containing $[NBu^n_4]ClO_4$ (0.05 mol dm^{-3}), measured with a scan rate of 0.1 V s^{-1}.

of a substituent on the pyridinium ring; a more electron-withdrawing substituent gives a less negative cathodic peak potential.

Since cathodic peaks of these free pyridinium-ylides have been observed at much more negative potentials (−1.50 V for Y_{N-CN} and −2.02 V for Y_{N-Me}) (Table 7), less negative potentials of the rhenium(I) complexes indicate a significant decrease of the electron density on the pyridinium ring of the ylide caused by coordination through the carbonyl oxygen atom. The fact that the lowest excited states of the Y_{N-R} complexes lie at appreciably low energies compared with those of the Y_P, Y_{As} and Y_S complexes is consistent with the fact that absorption and emission bands of the former complexes occur at much lower energies than those of the latter ones.

Acknowledgements—We wish to express hearty thanks to Professor Toshio Tanaka of Osaka University for his continuous encouragement throughout this study. We thank Dr Masaoki Furue of Osaka University for the measurement of the emission lifetimes.

REFERENCES

1. G. L. Geoffroy and M. S. Wrighton, *Organometallic Photochemistry*. Academic Press, New York (1979).
2. M. Wrighton, *Chem. Rev.* 1974, **74**, 401.
3. M. Wrighton and D. L. Morse, *J. Am. Chem. Soc.* 1974, **96**, 998.
4. P. J. Giordano, S. M. Fredericks, M. S. Wrighton and D. L. Morse, *J. Am. Chem. Soc.* 1978, **100**, 2257.
5. A. W. Johnson, *Ylid Chemistry*. Academic Press, New York (1966).
6. H. Schmidbaur, *Angew. Chem.* 1983, **95**, 980.
7. L. Weber, *Angew. Chem.* 1983, **95**, 539.
8. G. Matsubayashi and S. Akazawa, *Polyhedron* 1985, **4**, 419.
9. I. Zugravescu and M. Petrovanv, N-*Ylid Chemistry*. McGraw-Hill, New York (1974).
10. I. Kawafune and G. Matsubayashi, *Inorg. Chim. Acta* 1983, **70**, 1.
11. G. R. Cremo, W. McG. Morgan and R. Raper, *J. Chem. Soc.* 1937, 965.
12. G. Matsubayashi and Y. Kondo, *J. Organomet. Chem.* 1981, **219**, 269.
13. G. Matsubayashi, *Bull. Chem. Soc. Jpn* 1981, **54**, 915.
14. E. W. Abel and G. Wilkinson, *J. Chem. Soc.* **1959**, 1051.
15. G. Matsubayashi and S. Akazawa, to be published.
16. G. Matsubayashi and K. Ueyama, *Polyhedron* 1985, **4**, 173.
17. K. Ueyama, G. Matsubayashi and T. Tanaka, *Inorg. Chim. Acta* 1984, **87**, 143.
18. M. Furue, K. Sumi and S. Nozakura, *Chem. Lett.* **1981**, 1349.
19. G. Matsubayashi, Y. Kondo, T. Tanaka, S. Nishigaki and K. Nakatsu, *Chem. Lett.* **1979**, 375.
20. G. Matsubayashi, unpublished results.
21. M. S. Wrighton, D. L. Morse and L. Pdungsap, *J. Am. Chem. Soc.* 1975, **97**, 2073.
22. R. W. Balk, D. J. Stufkens and Ad Oskam, *J. Chem. Soc., Dalton Trans.* **1981**, 1124.
23. M. S. Wrighton, D. L. Morse, H. B. Gray and D. K. Ottesen, *J. Am. Chem. Soc.* 1976, **98**, 1111.
24. P. J. Giordano and M. S. Wrighton, *J. Am. Chem. Soc.* 1979, **101**, 2888.
25. M. S. Wrighton and D. L. Morse, *J. Am. Chem. Soc.* 1978, **100**, 5790.
26. S. M. Fredericks and M. S. Wrighton, *J. Am. Chem. Soc.* 1980, **102**, 6166.
27. J. C. Lung, R. A. Faltynek and M. S. Wrighton, *J. Am. Chem. Soc.* 1980, **102**, 7892.

Polyhedron Vol. 6, No. 3, pp. 603–611, 1987
Printed in Great Britain

0277–5387/87 $3.00+.00

KINETICS, ELECTROCHEMISTRY AND RESONANCE RAMAN SPECTRA OF THE (2-MERCAPTOPYRIDINE) (EDTA)RUTHENIUM(III) COMPLEX

HENRIQUE E. TOMA,* and PAULO S. SANTOS

Instituto de Química, Universidade de São Paulo, Caixa Postal 20780, São Paulo, SP, Brazil

and

MARIA P. D. MATTIOLI and LUIZ A. A. OLIVEIRA

Instituto de Química, UNESP, Araraquara, SP, Brazil

(*Received* 15 *April* 1986; *accepted* 29 *July* 1986)

Abstract—The chemistry of the pentadentate edta complexes of ruthenium(III) and (II) with 2-mercaptopyridine (HSpy) has been investigated based on spectroscopic, kinetic and electrochemical techniques. The reaction of $[Ru(III)(edta)H_2O]^-$ with HSpy proceeds with a specific rate of 1.05×10^4 M^{-1} s^{-1} (25°C, I = 0.10 M, acetate buffer), forming a red complex (λ_{max} = 550 nm) which undergoes a relaxation process as a function of pH, with an apparent $pK_a = 4.35$ and $k_{obs} = 0.31$ s^{-1}. The second reaction depends on the concentration of HSpy and leads to a stable green product (λ_{max} = 630 nm). A pronounced enhancement has been observed in the Raman spectra of the complexes, particularly in the region of the metal–ligand vibrations. The electronic and resonance Raman spectra are consistent with the coordination of HSpy via the sulfur atom in the red complex, and with a chelate binding in the green species.

The 2-mercaptopyridine ligand exists (> 99%) in aqueous solution in the tautomeric form (**1B**) with a protonated N-atom,[1] but having available a thione group to bind transition metal ions.[2]

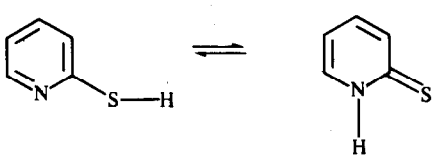

(1)

A **B**

In the course of our studies on linkage isomerism in transition metal complexes[3–5] we observed that the reaction of $[Ru(III)(Hedta)H_2O]$ with 2-mercaptopyridine led to a mixture of red and green species in equilibrium. The complexes have been investigated in detail in the present work, based on resonance Raman spectroscopy, spectroelectrochemistry, cyclic voltammetry and stopped-flow techniques. We concentrated our interest on the dynamics of the equilibrium reactions, stimulated by the extraordinary substitution reactivity of the pentadentate edta complexes of ruthenium(III).[6–8]

EXPERIMENTAL

The $[Ru(III)(Hedta)H_2O]\cdot 4H_2O$ complex was prepared according to the procedures previously described in the literature.[8,10] Found: C, 26.0; N, 5.7; H, 3.7. Calc. for $RuC_{10}N_2H_{23}O_{13}$: C, 25.0; N, 5.83; H, 4.82%. The red [Ru(III)(Hedta) HSpy]·$4H_2O$ complex was prepared by reacting stoichiometric amounts of $[Ru(III)(Hedta)H_2O]$ and 2-mercaptopyridine (Aldrich), and evaporating the solution to dryness, under vacuum, in the presence of concentrated sulfuric acid. Found: C, 31.0; N, 7.1; H, 3.8. Calc. for $RuC_{15}N_3H_{26}O_{12}S$: C, 31.3; N, 7.32; H, 4.40%. The red complex was converted to the green compound by reacting with an excess of ammonium hydroxide and evaporating the sol-

* Author to whom correspondence should be addressed.

ution to dryness, under vacuum. The product was very hygroscopic. The C/N and C/H ratios were consistent with the composition $(NH_4)_2$[Ru(III)(edta)Spy]·nH_2O. The complex anion [Ru(II)(edta)H_2O]$^{2-}$ was prepared *in situ* by the reduction of [Ru(III)(edta)H_2O]$^-$ with zinc amalgam under argon atmosphere. All other reagents were of high purity, and were used as supplied.

The electronic spectra of the complexes were recorded on a Cary 17, or a Hewlett–Packard 8451-A diode array spectrophotometer. Resonance Raman spectra were recorded on a Jarrell-Ash instrument using Spectra Physics argon and krypton ion lasers. Measurements were carried out in aqueous solution, using a spinning cell to avoid local heating and decomposition of the complexes. The relative intensities were measured as peak heights relative to the sulfate Raman band at 994 cm^{-1}. The IR spectra were recorded on a Zeiss Specord 75 instrument, with the samples dispersed in KBr pellets.

Cyclic voltammetry was carried out with a Princeton Applied Research instrument, consisting of a 173 potentiostat and a 175 universal programmer. A gold disc electrode was employed for the measurements, using the conventional Luggin capillary arrangement with the Ag/AgCl (I = 1 M KCl) reference electrode. A platinum wire was used as the auxiliary electrode. The measured potentials were converted to the normal hydrogen scale by adding 0.222 V. For the spectroelectrochemical measurements, the PARC 173 potentiostat was used in parallel with the diode-array spectrophotometer. A three-electrode system was designed for a rectangular quartz cell of 0.03 cm internal path-length. A gold minigrid was used as a transparent working electrode, in the presence of a small Ag/AgCl reference electrode and of a platinum auxiliary electrode. The experiments were carried out at 25°C under semi-infinite diffusion conditions, as described by Kuwana and Winograd.[11]

The determination of the apparent pK_a was carried out spectrophotometrically and by cyclic voltammetry as a function of pH. Cells specially designed for the experiments were used, combining simultaneous pH measurements with absorption spectra and cyclic voltammetry. The substitution kinetics were investigated using a Durrum D-110 stopped-flow instrument equipped with a Kel-F flow system.

RESULTS AND DISCUSSION

The reaction of [Ru(III)(Hedta)H_2O] with 2-mercaptopyridine in neutral or slightly acidic solutions leads to a red complex absorbing at λ_{max} = 550 nm (ε = 2600 M^{-1} cm^{-1}). Above pH 6, the reaction is followed by the conversion of the red species to a green product absorbing at λ_{max} = 630 nm (ε = 1700 M^{-1} cm^{-1}). Within the pH interval from 3 to 6, these species co-exist in equilibrium, with an isosbestic point at 595 nm, as shown in Fig. 1A.

The pK_a measured in this work for the free ligand was 9.72, in agreement with that reported in the literature.[1] In the thione form (**1B**) the N-atom is protonated and the ligand can only bind via the sulfur atom. As a matter of fact, the red color seems to be characteristic of Ru(III)(edta) complexes with sulfur-containing ligands, being consistent with a ligand-to-metal charge-transfer transition.[10] Similar complexes with pyridine ligands display no charge-transfer bands in the visible.

The distribution of the red and green species can be expressed as in a typical acid–base equilibrium (2), with an apparent pK_a of 4.35 ($K_a = k_3/k_{-3}$ = 4.4×10^{-5} M^{-1}) at 25°C and I = 0.10 M lithium *p*-toluenesulfonate (Lipts)

$$\text{red complex} + H_2O \underset{k_{-3}}{\overset{k_3}{\rightleftharpoons}} \text{green complex} + H_3O^+. \quad (2)$$

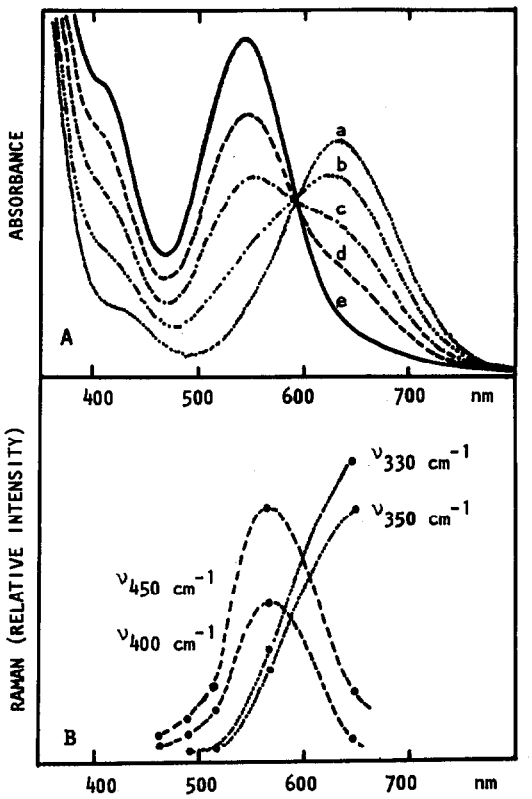

Fig. 1. (A) Electronic spectra of the Ru(III)(edta) complex with 2-mercaptopyridine at pH (a) 6.2; (b) 5.1; (c) 4.4; (d) 4.1; (e) 3.2. (B) Resonance Raman profiles for the most enhanced vibrational bands of the red complex (400, 450 cm^{-1}) and of the green complex (330, 350 cm^{-1}).

Comparative experiments using the 4-mercaptopyridine and 2-mercaptopyridine-N-oxide ligands led exclusively to red products, with no evidence of green species even under strongly alkaline conditions. Presumably, a new chromophore group is present in the green complex, arising from the bidentate properties of the deprotonated 2-mercaptopyridine ligand.

Vibrational spectra

The infrared (IR) and Raman (R) spectra of the 2-mercaptopyridine ligand can be seen in Figs 2A and 3A, respectively. X-ray studies have shown that the ligand molecule exists in the solid state as the thione species (**B**), with a C—S distance of 0.168 nm consistent with 65% double bond character.[12] Based on the examples from the literature, the 'thioamide' I, II, III and IV vibrations[13,14] were tentatively assigned to the observed frequencies at 1360 (w), 1250 (s), 1137 (s) and 740 cm^{-1} (s) in the IR spectra, and at 1375 (w), 1265 (w), 1135 (m) and 737 cm^{-1} (s) in the R spectra, respectively. The ring stretching modes were assigned to the IR peaks at 1610 (w), 1570 (s) 1495 (m), 1440 (m) and to the R peaks at 1613 (w), 1580 (w), 1505 (m), 1450 cm^{-1} (w). The breathing vibrational modes were observed at 980 (m) or 995 cm^{-1} (m) in the IR or R spectra, respectively. The remaining IR bands at 600 (w), 475 (w) and 430 cm^{-1} (w), and R bands at 625 (w), 450 (w) and 395 cm^{-1} (w) are related with the

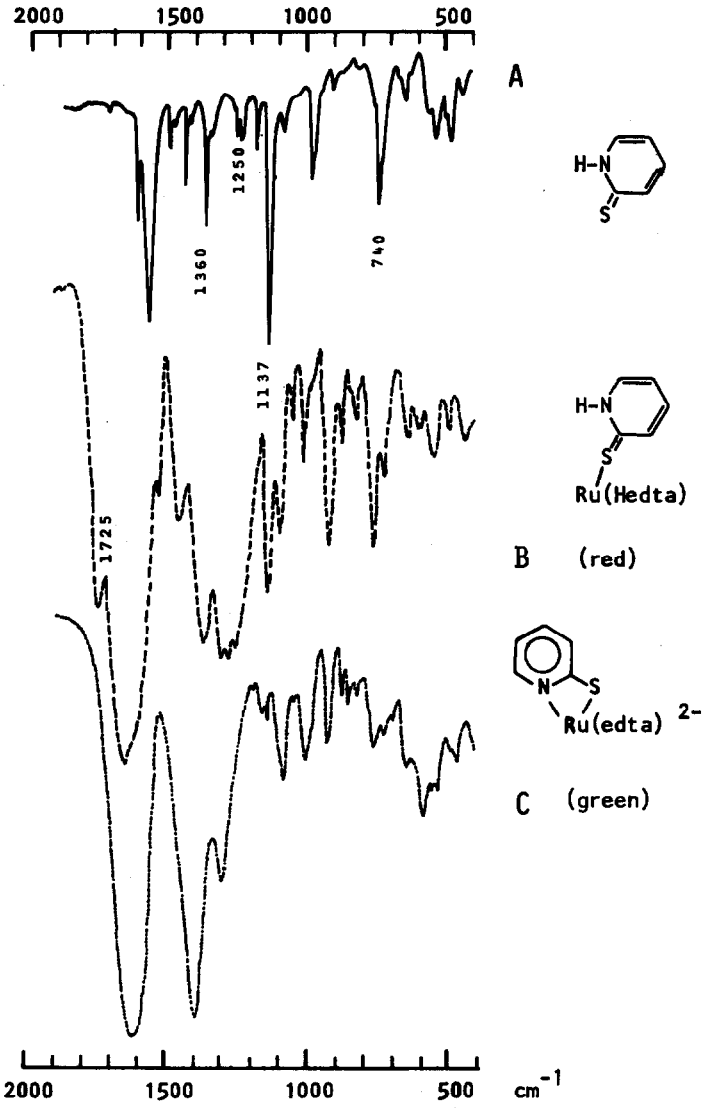

Fig. 2. IR spectra of the 2-mercaptopyridine ligand (A), and of the red (B) and green (C) complexes with Ru(III)(edta) in KBr pellets.

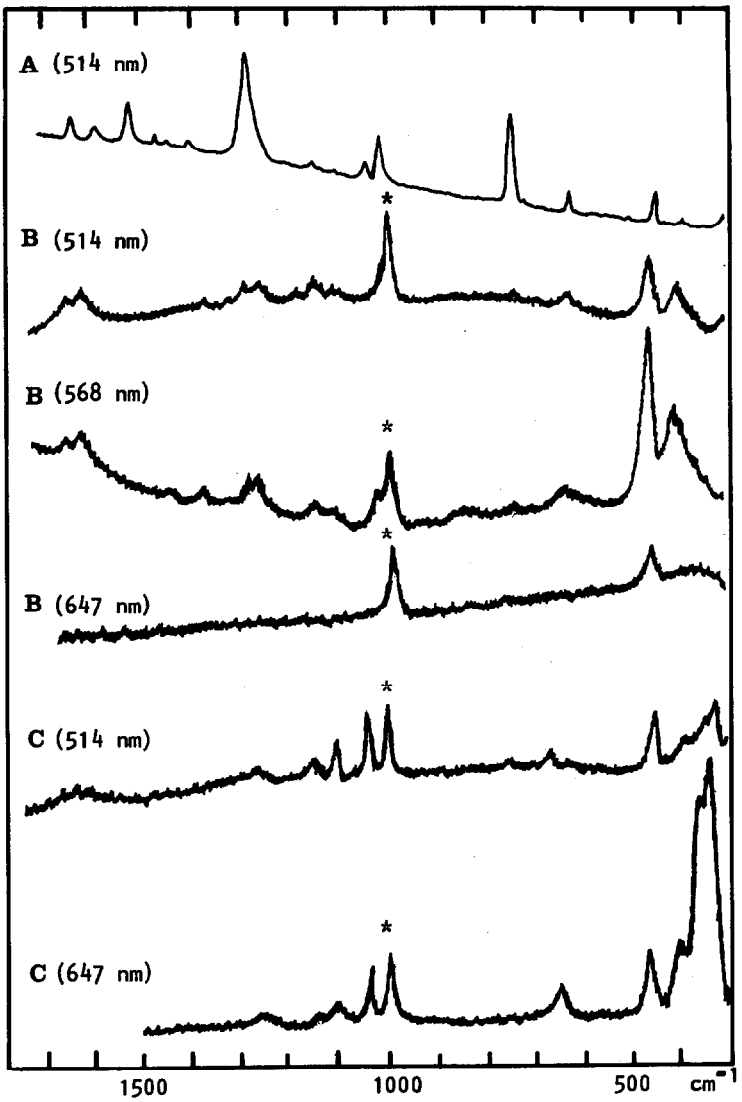

Fig. 3. (A) Raman spectra of the 2-mercaptopyridine ligand in the solid state, and (B) of aqueous solutions of the red (0.5 mM), and green Ru(III) complex (1 mM), at several excitation wavelengths, in the presence of 0.10 M sodium sulfate (* = sulfate band).

several deformation modes involving the C—H and C—C bonds (w = weak, m = medium, s = strong).

The IR spectra of the red [Ru(III)(Hedta) HSpy]·$4H_2O$ and green $(NH_4)_2$[Ru(III)(edta) Spy]·nH_2O complexes (Fig. 2) are complicated by the strong overlap of the vibrational bands of the Ru(Hedta) or Ru(edta)$^-$ moieties with those of the 2-mercaptopyridine ligand. The non-coordinated carboxylic group in the red complex is responsible for the absorption band at 1725 cm^{-1}, in the IR spectra. The ring vibrational bands are masked by the strong absorptions at 1625 cm^{-1} associated with the asymmetric vibrational modes of the carboxylate groups. The thioamide bands are less intense in the red complex, being practically negligible in the green species. This kind of behavior is consistent with the expected decrease of the C=S double bond character due to the coordination to the ruthenium(III) ion. As a matter of fact, for a number of thione ligands coordinated through the sulfur, it has been observed that the C=S stretching band around 1150 cm^{-1} decreases dramatically in intensity and in most cases completely disappears.[15,16]

The R spectra exhibit a resonance effect, leading to an enhancement of the vibrational bands associated with the Ru(III)-HSpy chromophore. In this way, several vibrational bands which are masked in the IR spectra can be detected in the resonance Raman (RR) spectra of the complexes, as shown in Fig. 3. Typical RR excitation profiles for the red and green species are shown in Fig 1B. The maximum

enhancement is observed for the low frequency vibrations at 450 and 400 cm^{-1} for the red species, and at 458, 400, 350 and 330 cm^{-1} for the green one. Because of the specific electronic states involved in the RR effect, the enhanced bands in the region of the metal–ligand vibrations can be particularly useful in the assignment of the chromophore groups. Recent work[17,18] has shown that the metal–sulfur stretching vibrations usually appear in the region of 400–500 cm^{-1}. Therefore, the enhancement observed in this region is consistent with the presence of a Ru(III)—S bond in the complexes. On the other hand, the strongly enhanced vibrational bands at 330 and 350 cm^{-1} are only observed in the spectra of the green species, suggesting the existence of an additional Ru(III)—N bond in a chelate configuration. Although five geometrical isomers are theoretically possible in this case, recent studies[19,20] on tetradentate ruthenium–edta complexes have indicated a *trans* configuration for the carboxylate groups, with the bidentate ligand lying in the plane of the nitrogen atoms. According to these arguments, the following structures can be proposed for the red and green species:

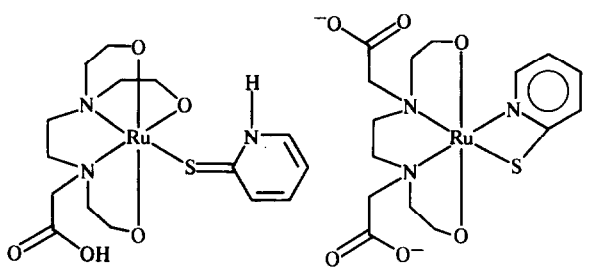

Red complex A **Green complex B** (3)

Kinetic studies

The kinetics of the substitution reactions of $[Ru(III)(Hedta)H_2O]$ with various entering monodentate ligands have been previously investigated by Matsubara and Creutz.[7] The observed rate constants were dependent on the pH, exhibiting a maximum value within the pH range from 2.4 to 7.6, which correspond to the pK_as of the Hedta and H_2O ligands in the complex, respectively.[7,9] In the acetate buffer pH region, the kinetics are associated with the $[Ru(III)(edta)H_2O]^-$ complex. Our preliminary results obtained for the substitution reactions with HSpy were similar to those reported by Matsubara and Creutz.[7] The reactions proceeded according to a pseudo-first-order kinetics for at least two half-lives. The observed rate constants exhibited a maximum, practically constant value in the $4 < pH < 6$ region. However, in contrast with the preceding cases, two successive reactions were detected in this work. The first reaction leading to the red complex was ascribed to the substitution of H_2O by the thione ligand. The second reaction was associated with the partial or total conversion of the red complex to the green one.

Table 1 summarizes the kinetic data for the successive reactions. The observed rate constants for the first reaction are proportional to the concentration of the 2-mercaptopyridine ligand, leading to the specific rates and activation parameters shown in Table 2, along with some related data from the literature, for comparison purposes. The substitution rates for the $[Ru(III)(edta)H_2O]^-$ complex and the corresponding activation parameters depend on the nature of the entering ligands, and are consistent with an associative mechanism, as previously proposed in the literature.

In the presence of acetate buffer, the second reac-

Table 1. Observed rate constants for the substitution reactions in the $[Ru(III)(edta)H_2O]^-$ + 2-mercaptopyridine system

Exp.[a]	T (°C)	[L] (M)	k_{obs} (s^{-1})	$k_{r\rightarrow g}$[b] (s^{-1})
1	20.0	1.00×10^{-3}	9.1	1.9
2	20.0	2.00×10^{-3}	18.1	2.1
3	25.0	1.00×10^{-3}	11.7	3.1
4	25.0	1.50×10^{-3}	14.8	3.1
5	25.0	2.00×10^{-3}	21.4	3.1
6	25.0	2.50×10^{-3}	26.7	3.2
7	30.0	1.00×10^{-3}	13.5	4.6
8	30.0	2.00×10^{-3}	24.8	4.9
9	35.0	2.00×10^{-3}	29.6	7.2
10	40.0	2.00×10^{-3}	38.2	10.0
11	15.5	0.260	0.49×10^{-4}	
12	20.0	0.260	1.78×10^{-4}	
13	25.0	0.208	2.46×10^{-4}	
14	25.0	0.260	2.49×10^{-4}	
15	25.0	0.341	2.49×10^{-4}	
16	30.0	0.260	3.86×10^{-4}	
17	34.5	0.260	6.3×10^{-4}	
18	25.0	4.5×10^{-3}	11.4	
19	25.0	9.0×10^{-3}	21.5	
20	25.0	1.5×10^{-2}	36.3	

[a] $I = 0.10$ M lithium *p*-toluenesulfonate; experiments 1–10 refer to reactions of $[Ru(III)(edta)H_2O]^-$ with L = 2-mercaptopyridine, pH 4.54 (acetate buffer); experiments 11–17 refer to reactions of $[Ru(III)(edta)Spy]^{2-}$ with L = pyridine, pH 5.48 (pyridine buffer); experiments 18–20 refer to reactions of $[Ru(II)(edta)H_2O]^{2-}$ with L = 2-mercaptopyridine, pH 4.54.

[b] Observed rate constants for the conversion of the red complex to the green complex.

Table 2. Kinetic and thermodynamic parameters for some substituted [Ru(III)(edta)L] complexes

Ligand	k_L[a]	$\Delta H^{\neq}$	$\Delta S^{\neq}$	k_{-L}	$K = k_L/k_{-L}$
2-Mercaptopyridine[b]	1.05×10^4	5.8	−20	3.4×10^{-3}	3.1×10^6
Pyridine[c]	6.3×10^3			6.1×10^{-2}	1.0×10^5
Pyrazine[c]	2.0×10^4	5.7	−20	2.0	1.0×10^4
Isonicotinamide[c]	8.3×10^3	6.6	−19	0.7	1.2×10^4
Thiocyanate[c]	2.7×10^2	8.9	−18	0.5	5.4×10^2
	2.5×10^2[d]				
Acetonitrile[c]	3.0×10	8.3	−24	3.2	9

[a] 25°C, acetate buffer.
[b] Monodentate binding, $I = 0.10$ M Lipts.
[c] $I = 0.20$ M potassium trifluoromethanesulfonate, Ref. 7.
[d] $I = 0.10$ M Lipts, this work.

tion proceeds to an equilibrium position [equation (2)], with an apparent $pK_a = 4.35$. The observed rate constants shown in Table 1 do not depend on the concentration of 2-mercopyridine, and are coherent with a relaxation process involving the deprotonation of the coordinated ligand. In this case, the formal equilibrium constant can be expressed by $K = k_3/k_{-3} \cdot [H^+]$, and the observed rate constants are given by $k_{obs} = k_3 + k_{-3} \cdot [H^+]$. The calculated values of k_3 and k_{-3} were 1.9 s^{-1} and 1.2×10^4 M^{-1} s^{-1}, respectively.

It should be noted that the relaxation process observed in this work is relatively slow. Since the proton transfer reactions are diffusion controlled,[21] the measured rate can not be ascribed to a simple acid–base reaction. The changes in the absorption spectra are consistent with an appreciable reorganization of the coordination sphere. Considering that the deprotonated 2-mercaptopyridine ligand is potentially bidentate, the displacement of a coordinated carboxylate group would lead to a chelate chromophore group, as deduced from the RR spectra. This explanation is in harmony with the several examples of chelate complexes of 2-mercaptopyridine, previously reported in the literature.[2,22]

The substitution of the HSpy ligand from the complex was not detected in the presence of a ligand such as thiocyanate, isonicotinamide or pyrazine, because of their unfavorable stability constants (Table 2). However, by using a high excess of pyridine the substitution reaction proceeded to completion, leading to the decay of the characteristic charge-transfer bands in the visible. A pseudo-first-order behavior was observed for at least two half-lives, with a saturation of k_{obs} versus the concentration of the pyridine ligand, as shown in Table 1. A similar behavior has been reported by Matsubara and Creutz[7] for the substitution reactions of [Ru(III)(edta)L] (L = $NCCH_3$ or SCN^-) in the presence of pyrazine, to form [Ru(III)(edta)pz]$^-$. In both cases the observed rate constant was independent of the pyrazine concentration, and practically identical to the dissociation rate constant k_{-L}. No evidence of direct replacement of L by pyrazine has been found, leading to the conclusion that the reaction proceeds through [Ru(III)(edta)H_2O]$^-$ formed by dissociation of [Ru(III)(edta)L].

Based on the considerations from the literature, and on the microscopic reversibility principle, we propose the following mechanism for the substitution reactions in the [Ru(III)(edta)Spy]$^{2-}$ complex:

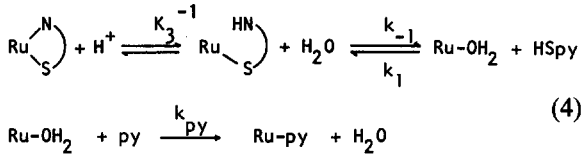

(4)

Assuming a steady-state approximation for the concentration of the [Ru(III)(edta)H_2O]$^-$ complex,

$$-\frac{d[Ru(III)(edta)Spy^{2-}]}{dt} = k_{obs}[Ru(III)(edta)Spy^{2-}] \quad (5)$$

$$k_{obs} = \frac{k_{py}k_{-1}K_3^{-1}[H^+][py]}{k_1[HSpy] + k_{py}[py]}.$$

Under the conditions of this work [py] ≪ [HSpy], and the pyridine term predominates in the denominator of equation (5). Therefore,

$$k_{obs} = k_{-1}K_3^{-1}[H^+] = 2.5 \times 10^{-4}\,s^{-1}.$$

Since $K_3^{-1} = 2.2 \times 10^4$ M^{-1} and $[H^+] = 3.3 \times 10^{-6}$ M, k_{-1} can be calculated as 3.4×10^{-3} s^{-1}. The equilibrium constant for the formation of the red complex is given by $K_1 = k_1/k_{-1} = 3.1 \times 10^6$ M^{-1}.

The substitution reaction of $[Ru(II)(edta)H_2O]^{2-}$ with HSpy was also studied in this work, in order to compare with the Ru(III) reaction. The kinetics was typically of first order for at least two half-lives. The observed rate constants were proportional to the concentration of the HSpy ligand, as shown in Table 1, with $k_2 = 2.45 \pm 0.8 \times 10^3$ M^{-1} s^{-1} at 25°C, $I = 0.10$ M Lipts, pH 4.5 (acetate buffer). This value is two orders of magnitude higher than those reported by Matsubara and Creutz,[7] suggesting an associative mechanism for the substitution reaction in the $[Ru(II)(edta)H_2O]^{2-}$ complex.

Electrochemistry

Cyclic voltammograms of the [Ru(III)(edta) HSpy]$^-$ complex, obtained at several pHs, are shown in Fig. 4. Below pH 3 and above pH 6 only a pair of anodic and cathodic waves can be observed, corresponding to the reversible monoelectronic reduction of the red [Ru(III)(Hedta) HSpy] and green [Ru(III)(edta)Spy]$^{2-}$ species, with $E_{1/2} = 0.134$ V ($D = 4 \times 10^{-6}$ cm^2 s^{-1}) and -0.103 V versus NHE ($D = 4 \times 10^{-6}$ cm^2 s^{-1}), respectively. The spectroelectrochemical behavior of the complexes (Fig. 5) was typically reversible, with a Nernst slope of 0.058 V and $E^\ominus$ values consistent with those obtained from the cyclic voltammograms. The electronic spectra of the ruthenium(II) complexes can also be seen in Fig. 5.

In the pH range from 3 to 6, the equilibrium between the red and green species can be readily detected in the cyclic voltammograms, as shown in Fig. 4A. The apparent pK_a value based on the cathodic peak heights was 4.34 ± 0.05, in agreement with the spectrophotometric results. Three additional points can be explored in the cyclic voltammograms of Fig. 4. The first point is the systematic shift of the anodic and cathodic peaks of the red species as a function of pH. This particular kind of dependence is illustrated in the internal plot of Fig. 4. The Nernst slope of 0.060 V/pH is consistent with a reversible deprotonation of the oxidized complex. The estimated pK_a for the [Ru(III)(Hedta)HSpy] complex was 2.9 ± 0.2. This value is comparable with that previously reported for the $[Ru(III)(Hedta)H_2O]$ complex[9] (p$K_a = 2.36$), involving the deprotonation of the non-coordinated carboxylic group. The corresponding pK_a for the $[Ru(II)(Hedta)H_2O]^-$ complex is 3.20,[9] in comparison with p$K_a \cong 4$ for the [Ru(II)(Hedta)HSpy]$^-$ species, estimated from the second intercept in the internal plot of Fig. 4. The half-wave potential for the reduction of [Ru(III)(edta)HSpy]$^-$, measured at pH 4.5, was 0.082 V versus NHE.

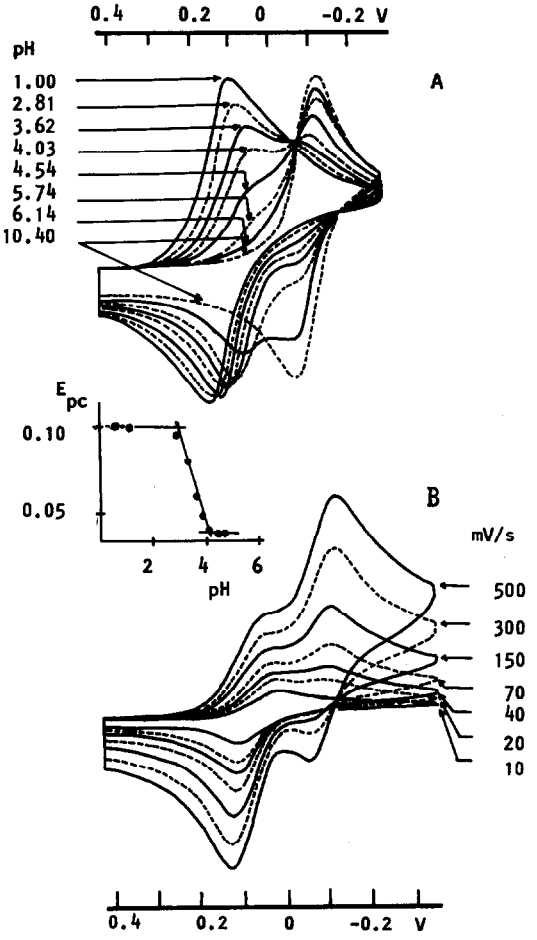

Fig. 4. Cyclic voltammograms of the ruthenium(III)/(II)–(edta) complexes of 2-mercaptopyridine (5 mM, $I = 0.10$ M Lipts, 25°C) at several pHs (scan rate = 0.10 V s^{-1}) and at several potential scan rates (pH = 4.43). The internal plot illustrates a typical dependence of $E_{1/2}$ versus pH for the red species.

Using the redox potentials and equilibrium constants for the Ru(III)(edta) complexes, a complete thermodynamic cycle can be proposed, as shown in Fig. 6, allowing the evaluation of the corresponding parameters for the reduced species.

A second point which has been analyzed in Fig. 4B is the pronounced dependence of the relative heights of the cathodic waves of the red and green species with respect to the potential scan rates. This kind of behavior is consistent with scheme (6) involving an electrochemical process proceeded by

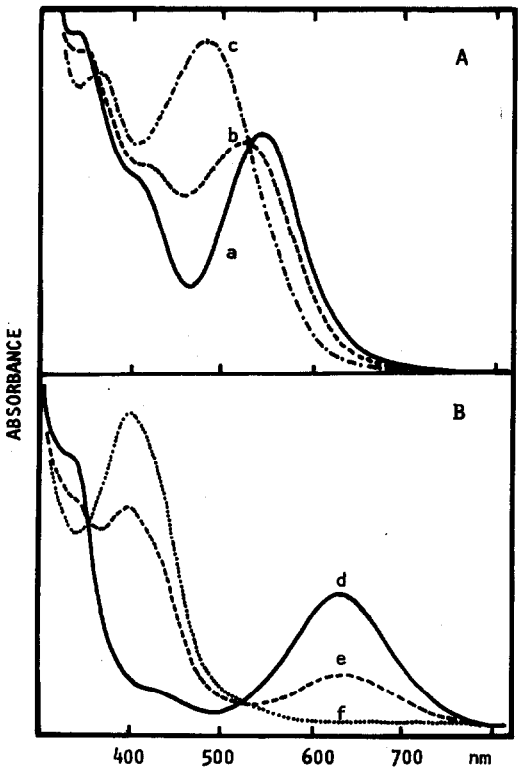

Fig. 5. Spectroelectrochemistry of the ruthenium(III)/(II)–(edta) complexes of 2-mercaptopyridine at (A) pH 2.8, and (B) pH 9.2, $I = 0.10$ M Lipts. Applied potentials. (a) 0.22, (b) 0.32, (c) 0.42, (d) 0.12, (e) −0.13 and (f) −0.28 V versus NHE.

a chemical reaction:

$$[(\text{edta})\text{Ru(III)Spy}]^{2-} + \text{H}^+ \underset{k_3}{\overset{k_{-3}}{\rightleftharpoons}} [(\text{edta})\text{Ru(III)HSpy}]^- \xrightarrow{+e} [(\text{edta})\text{Ru(II)HSpy}]^{2-} \quad (6)$$

At low potential scan rates, the chemical reaction competes with the electrochemical process and the current function becomes dependent on the kinetic constants k_{-3} and k_3, as well as, on the potential scan rates a. In this case, the kinetic constants can be estimated using Nicholson and Shain's[23] equation (7), where i is the observed cathodic current for the red species and i_d is the diffusion-controlled current calculated from the data in the absence of chemical reactions.

$$\frac{i_d}{i} = 1.02 + \frac{0.471}{K}\left(\frac{a}{k_3 + k_{-3}[\text{H}^+]}\right)^{1/2}. \quad (7)$$

Theoretical analysis has shown that the contribution of the green species to the currents measured at the peak potentials of the red species is

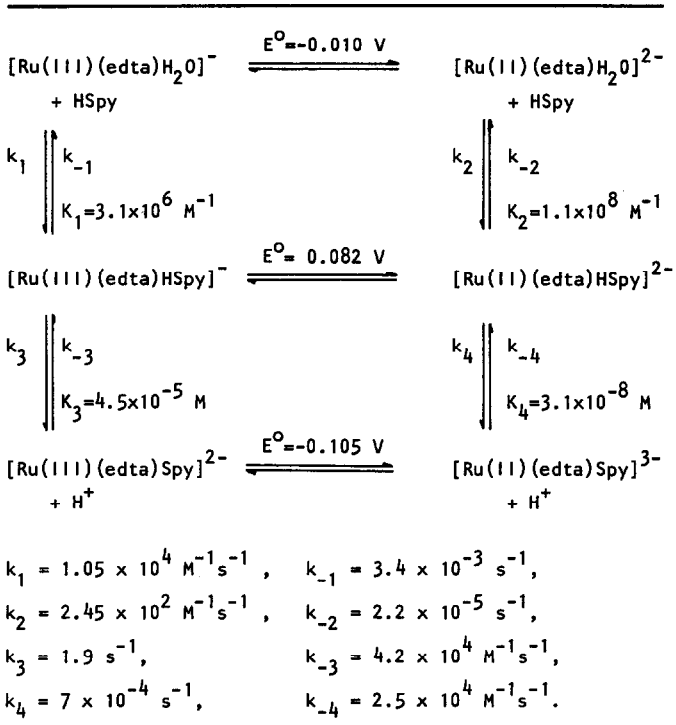

Fig. 6. Thermodynamic cycle for the ruthenium(III)/(II)–(edta) complexes of 2-mercaptopyridine (25°C, $I = 0.10$ M Lipts, pH 4.54 acetate buffer).

practically zero. Typical results for $k_{obs} = k_3 + k_{-3}\cdot[H^+]$ obtained at pH 4.55 and at potential scan rates of 0.200, 0.100, 0.075, 0.050 V s^{-1} were 3.0, 3.3, 3.2 and 3.0 s^{-1}, respectively, with an average of 3.1 ± 0.2 s^{-1}. From the values of K and k_{obs}, the kinetic constants k_3 and k_{-3} were calculated as 1.9 s^{-1} and 4.2×10^4 M^{-1} s^{-1}, respectively, in excellent agreement with the stopped-flow results.

The third interesting aspect is the dependence of the relative heights of the anodic peaks on the potential scan rates, as shown in Fig. 4B. At high rates, the reduced forms of the red and green species are reoxidized rapidly enough during the reverse scan, allowing the evaluation of the interconversion rates from the measurements of the anodic peak heights as a function of time. The observed rate constant, $k_{obs} = k_4 + k_{-4}\cdot[H^+]$, obtained in this way at pH 4.55, was 0.68 ± 0.07 s^{-1}. Based on the equilibrium constant of the ruthenium(II) complex estimated from the thermodynamic cycle in Fig. 6 ($K_4 = k_4/k_{-4}\cdot[H^+]$), we obtained $k_4 = 7 \times 10^{-4}$ s^{-1} and $k_{-4} = 2.5 \times 10^4$ M^{-1} s^{-1}.

A comparison of the thermodynamic and kinetic parameters of the ruthenium(III) and (II) complexes can be seen in Fig. 6. The Ru(II) complexes are relatively more stable and inert than the Ru(III) ones, with $k_{-2} = k_2/K_2 = 5 \times 10^{-5}$ s^{-1}. According to the thermodynamic data, the bidentate ruthenium(II) species is more susceptible to protonation than the corresponding ruthenium(III) analog. The difference, however, is associated with the k_3 and k_4 constants, rather than with the k_{-3} and k_{-4} protonation constants. The higher basicity of the ruthenium(II) mercaptopyridine complex is consistent with the expected backbonding interactions in the system.

Acknowledgements—The support from the FINEP, CAPES and CNPq institutions is gratefully acknowledged.

REFERENCES

1. R. A. Jones and A. R. Katritzky, *J. Chem. Soc.* 1958, 3610.
2. B. P. Kennedy and A. B. P. Lever, *Can. J. Chem.* 1972, **50**, 3488.
3. H. E. Toma, A. A. Batista and H. B. Gray, *J. Am. Chem. Soc.* 1982, **104**, 7509.
4. H. E. Toma, E. Giesbrecht and R. Espinoza, *Can. J. Chem.* 1983, **61**, 2520.
5. H. E. Toma, E. Giesbrecht and R. Espinoza, *J. Chem. Soc., Dalton Trans.* 1985, 2469.
6. N. Oyama and F. C. Anson, *J. Electroanalyt. Chem.* 1978, **8**, 289.
7. T. Matsubara and C. Creutz, *Inorg. Chem.* 1979, **18**, 1956.
8. M. Mukaida, H. Okuno and T. Ishimori, *Nippon Kakagu Zasshi* 1965, **86**, 589.
9. K. Shimizu,T. Matsubara and G. P. Sato, *Bull. Chem. Soc. Jpn* 1974, **47**, 1651.
10. Y. Oshino, T. Uehiro and M. Saito, *Bull. Chem. Soc. Jpn* 1979, **52**, 1060.
11. T. Kuwana and N. Winograd, In *Electroanalytical Chemistry*, ed. A. J. Bard, Vol. 7, pp. 1–78. Marcel Dekker, New York (1974).
12. B. R. Penfold, *Acta Cryst.* 1953, **6**, 707.
13. C. N. N. Rao and R. Venkataraghavan, *Spectrochim. Acta* 1962, **18**, 541.
14. E. Spinner, *J. Chem. Soc.* 1960, 1238.
15. N. Hadjiliadis and T. Theophanides, *Inorg. Chim. Acta* 1975, **15**, 167.
16. N. Kottmair and W. Beck, *Inorg. Chim. Acta* 1979, **34**, 137.
17. A. Grigoratos and N. Katsaros, *Inorg. Chim. Acta* 1985, **108**, 41.
18. P. C. Kong and T. Theophanides, *Bioinorg. Chem.* 1975, **5**, 51.
19. Y. Yoshino, M. Kawahara and M. Saito, *Polyhedron* 1985, **4**, 1019.
20. A. Diamantis and J. V. Dubrawski, *Inorg. Chem.* 1981, **20**, 1142.
21. F. Caldin, *Fast Reactions in Solution*, p. 262. Wiley, New York (1964).
22. S. R. Fletcher and A. C. Skapski, *J. Chem. Soc., Dalton Trans.* 1972, 635.
23. R. S. Nicholson and I. Shain, *Analyt. Chem.* 1964, **36**, 706.

Polyhedron Vol. 6, No. 3, pp. 613–618, 1987
Printed in Great Britain

0277–5387/87 $3.00+.00

A POTENTIOMETRIC STUDY ON COMPLEX FORMATION OF NICKEL(II) AND ZINC(II) IONS WITH 3-(2-NAPHTHYL)-2-MERCAPTOPROPENOIC ACID

ALVARO IZQUIERDO* and JOSE LUIS BELTRAN

Department of Analytical Chemistry, Faculty of Chemistry, University of Barcelona, 08028 Barcelona, Spain

(*Received* 29 *April* 1986; *accepted* 15 *August* 1986)

Abstract—Protonation and complex formation equilibria between zinc and nickel ions with 3-(2-naphthyl)-2-mercaptopropenoic acid (NMPA) have been studied in 50% (v/v) water–ethanol solutions containing 1 M $NaClO_4$ as constant ionic medium at 25°C using glass electrode potentiometry. Initial estimates of complex formation constants were refined with the MINIGLASS program. Protonation constants for the ligand and formation constants for the complexes Ni(NMPA), $Ni(NMPA)_2$, Zn(NMPA)H, Zn(NMPA) and $Zn(NMPA)_2$ are reported.

Studies of several 3-aryl-2-mercaptopropenoic acids as analytical reagents for the spectrophotometric determination of metal ions have been reported because of their selectivity and high sensitivity for certain metal ions as nickel(II),[1] titanium(IV)[2] or molybdenum(VI).[3] Although there are few references about the complexation of metals with these compounds,[4,5] it has been shown that the metal complexes formed with the 3-aryl-2-mercaptopropenoic acids are more stable that the formed with 3-aryl-2-mercaptopropanoic acids;[6] this effect is due to the conjugated double bond between carbonyl and aryl groups.

In biological studies, Foye and Lo[4] reported antibacterial activity for the 3-phenyl-2-mercaptopropenoic acid, and Wagner *et al.*[5] found that the aryl-mercaptopropenoic acids were potent inhibitors of metalloenzymes; it seems that the strong complexation of this type of compounds with metal ions has effect in trace metal metabolism.

In the present work we have studied the complexation of 3-(naphthyl)-2-mercaptopropenoic acid against the nickel(II) and zinc(II) metal ions by glass electrode potentiometry[7] to find the effect of enlarging the 3-aryl group in the stability of complexes with divalent ions. This study has been carried out in water–ethanol medium (50% v/v) because of the low solubility of this ligand in aqueous medium. The ionic strength of medium was 1.00 M in $NaClO_4$, and the temperature was kept constant to 25 ± 0.1°C.

EXPERIMENTAL

Materials

3-(2-Naphthyl)-2-mercaptopropenoic acid (NMPA) was synthesized following the procedure of Campaigne and Cline[8] by condensation of 2-naphthaldehyde with rhodanine, subsequent hydrolysis in alkaline medium, and acidification with mineral acid. By twice recrystallization from benzene under nitrogen the NMPA was obtained as yellow crystals with m.p. 170°C. The purity was determined by potentiometric titration with sodium hydroxide and by iodometric titration with potassium iodate solution.[9] Both sets of titrations were performed in water–ethanol medium because of the low solubility of NMPA in water. Found: C, 64.9; H, 4.32; S, 13.70. Required for $C_{13}H_{10}O_2S$: C, 64.60; H, 4.38; S, 13.90%.

Solutions of NMPA were prepared immediately before use to avoid the oxidation of the mercapto group.

Nickel(II) and zinc(II) perchlorates were pre-

* Author to whom correspondence should be addressed.

pared by dissolving $NiCO_3$ and ZnO, respectively, in a 1 : 1 perchloric acid solution and recrystallized from water. Nickel(II) stock solution was standardized gravimetrically as dimethylglioximate and the zinc(II) solution was determined by complexometric titration with EDTA.[10]

Carbonate-free sodium hydroxide solution in water–ethanol medium (50% v/v) was prepared from sodium hydroxide pellets, and standardized by titration against potassium hydrogen phthalate.

Stock solutions of aqueous perchloric acid were standardized against recrystallized sodium tetraborate.[11]

Solutions were prepared with double distilled water and absolute ethanol, so that all solutions were 50% (v/v) water–ethanol. To maintain ionic strength, the solutions were made up to a perchlorate concentration of 1.00 M by addition of sodium perchlorate stock solution. The ionic medium ($NaClO_4$) was prepared from sodium carbonate and perchloric acid by a literature method.[12]

All solutions were deaerated with nitrogen before use, and all reagents were of analytical grade.

Apparatus

Radiometer PHM 84 pH-meter was used with a Radiometer G 202 B glass electrode and an Ag/AgCl reference electrode[13] in a Wilhelm-type salt bridge.[14] The titrations corresponding to a complex formation with NMPA with Ni(II) and Zn(II) were performed with an automatic titration and data acquisition assembly described in a previous work.[15]

The sodium hydroxide solution was added with a Metrohm E 415 automatic burette. The temperature was controlled by a Selecta mod. Tectron thermostat.

Method

Protonation constants for NMPA and formation constants for their metal complexes were determined by potentiometric titration in a jacketed vessel, thermostatted at 25 ± 0.1°C by circulating water. Acidic solutions (T.S.) containing the reagents (ligand or ligand–metal) were titrated with sodium hydroxide solution, and during the titration pure nitrogen[16] was passed through the solution to remove dissolved oxygen. The variation of free hydrogen ion concentration was measured using the cell:

$$\text{Ag/AgCl(s)} \;\Big|\; \begin{matrix}0.01\text{ M NaCl*}\\ 0.99\text{ M NaClO}_4\end{matrix} \;\Big|\; \begin{matrix}1\text{ M NaClO}_4\text{*}\end{matrix} \;\Big|\; \text{T.S.*} \;\Big|\; \begin{matrix}\text{Glass}\\ \text{electrode}\end{matrix}$$

* 50% (v/v) ethanol–water.

The electrode system was calibrated in terms of hydrogen ion concentration by the Gran method.[17]

Protonation curves of NMPA were obtained at several ligand concentrations, and the complex formation curves were obtained at different metal concentrations and different ligand : metal ratios. The experimental conditions of titrations performed are listed in Table 1. The concentration of ligand is limited by its low solubility, even in the water–ethanol medium.

RESULTS AND DISCUSSION

The protonation curve of NMPA shows two protonation constants, corresponding to carboxylate and thiol groups. By comparing this curve with a set of normalized curves,[18] approximate values

Table 1. Experimental conditions of potentiometric titrations

Titr. number	$[NMPA]_0$ (mM)	$[Ni^{2+}]_0$ (mM)	$[Zn^{2+}]_0$ (mM)	Ligand/metal ratio	Range of $-\log[H]$
1	1.348	—	—	—	3.5–9.5
2	2.250	—	—	—	3.3–9.9
3	2.627	—	—	—	3.3–10.0
4	1.850	0.581	—	3.2	2.3–3.7
5	2.140	0.870	—	2.5	2.2–3.5
6	3.259	1.308	—	2.5	2.3–3.7
7	2.654	2.616	—	1.0	2.4–3.6
8	2.231	—	0.512	4.4	2.0–3.7
9	3.147	—	1.025	3.1	2.0–3.7
10	2.327	—	1.025	2.3	2.0–3.6
11	2.369	—	2.050	1.2	2.0–3.6

found for the constants were $\log(\beta_{101}) = 8.9$ and $\log(\beta_{102}) = 13.05$.

The formation curves for the Ni(II)–NMPA system corresponding to several metal concentrations were all superimposable (Fig. 1); thus indicating that for this system only the mononuclear NiL and NiL_2^{2-} species were present in the concentration range studied. Initial values for stability constants obtained by comparison with normalized curves were $\log(\beta_{110}) = 9.85$ and $\log(\beta_{210}) = 20$.

For the Zn(II)–NMPA system, the formation curves from different titrations were not all superimposables (Fig. 2), as those corresponding to a low ligand : metal ratio show a deviation. Furthermore, the other curves showed no correspondence with the set of normalized curves, showing the presence of another species other than the mononuclear ones.

Numerical calculations of these systems were performed on a HP 9816 S desk computer, by using the MINIGLASS program.[15] The protonation constants were refined using the PKAS procedure; in this case the function minimized (U) is defined by:

$$U = \sum_{i=1}^{n} (-\log[H^+]_{i,\text{exp}} + \log[H^+]_{i,\text{calc}})^2.$$

The complex equilibria between NMPA and Ni(II) and Zn(II) were studied using the COMPLEX procedure of MINIGLASS. For comparison of results, we have used the two possible options, refining by the $-\log[H^+]$ of the solution and by the titrant volume added (V_t). For the Ni(II)–NMPA system, the obtained values of formation constants were consistent with those calculated graphically. In the Zn(II)–NMPA system the best set of species compatible with the experimental data were 1 : 1 : 1, 1 : 1 : 0 and 2 : 1 : 0 (referred to ligand : metal : hydrogen), and the values obtained refining by $-\log[H^+]$ and V_t were virtually the same. With the set of constants obtained for this system, were have constructed the theoretical formation curves for titrations 8–11 (Fig. 3), showing good agreement with the experimental formation curves.

The results of calculations for protonation and complex formation constants, together with the final values, are summarized in Table 2.

By comparing the pK_a values for NMPA calculated from the protonation constants ($pK_{a_1} = 4.16$, $pK_{a_2} = 8.89$) with those of the analogous compound, 3-(1-naphthyl)-2-mercaptopropenoic acid[19] with $pK_{a_1} = 4.07$ and $pK_{a_2} = 9.32$ in the same medium, we have seen that the dissociation constants for the carboxyl groups are very similar, but the acidity of thiol group is higher in 3-(2-naphthyl)-2-mercaptopropenoic acid than in the 1-naphthyl derivative, as might be expected from the different resonant effect in the position 2 of the naphthyl group.

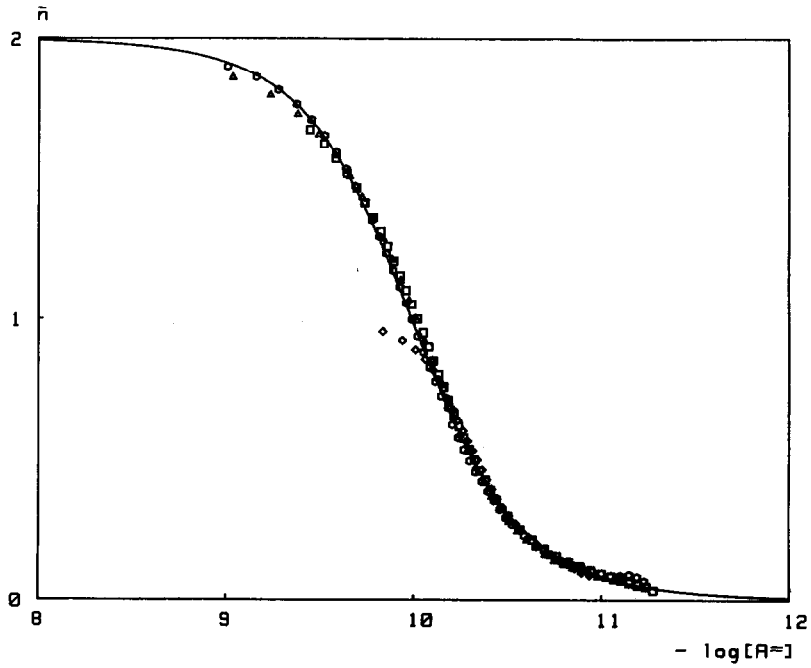

Fig. 1. Experimental formation curves for the Ni(II)–NMPA system. Symbols are: (○) titr. 4, (□) titr. 5, (△) titr. 6 and (◇) titr. 7. Solid line is the theoretical curve after the constants given in Table 2.

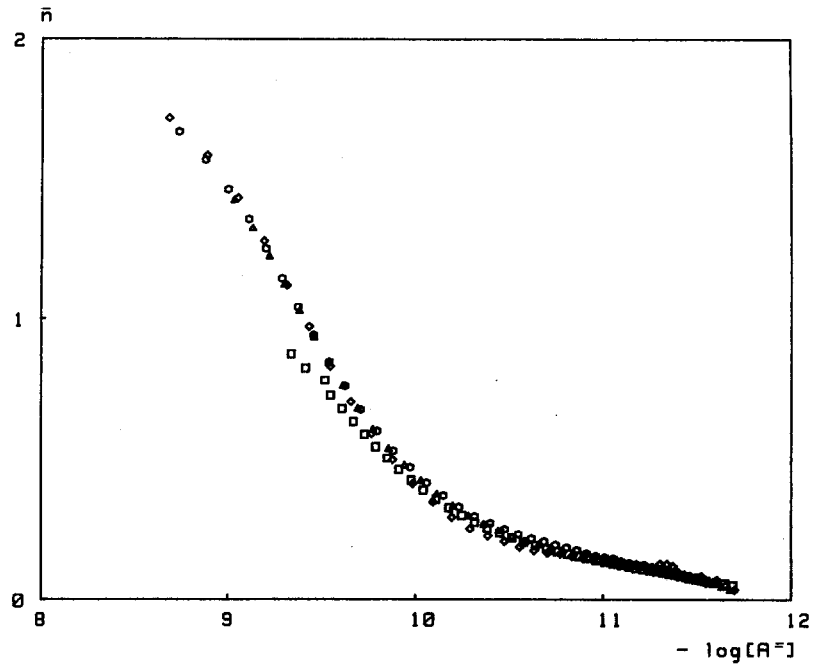

Fig. 2. Experimental formation curves for the Zn(II)–NMPA–H system. Symbols: (◇) titr. 8, (○) titr. 9, (△) titr. 10 and (□) titr. 11.

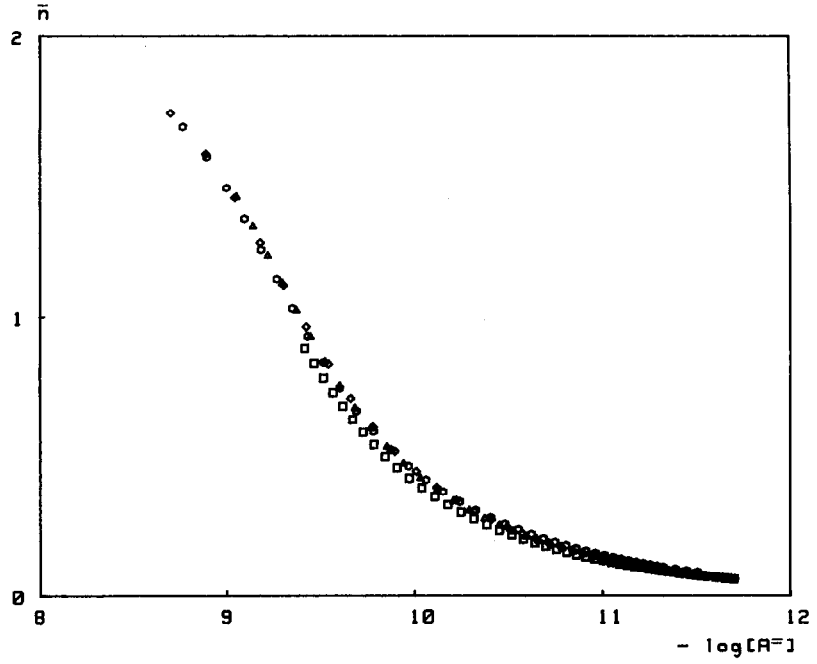

Fig. 3. Calculated formation curves for the Zn(II)–NMPA–H system from the constants of Table 2. Symbols as in Fig. 2.

Table 2. Calculated formation constants (at 25°C, 1 M $NaClO_4$ in water–ethanol 50% medium)

Metal ion	log (β_{lmh})[a] 101	102	111	110	210
H^{+b}	9.890(3)	13.053(5)			
Ni^{2+c}				9.820(8)	19.998(4)
Ni^{2+d}				9.868(11)	19.978(5)
Zn^{2+c}			12.794(7)	9.701(5)	19.047(6)
Zn^{2+d}			12.792(14)	9.695(7)	19.042(7)
Proposed values					
H^+	8.890(3)	13.053(5)			
Ni^{2+}				9.84(4)	19.98(2)
Zn^{2+}			12.79(2)	9.70(2)	19.04(2)

[a] The estimated standard deviation on the final digit is given in parentheses.
[b] Calculated by PKAS procedure.
[c,d] Calculated by COMPLEX procedure (by V_t and $-\log[H]$, respectively).

In reference to complex formation with Ni(II) and Zn(II) ions, the lack of formation of polynuclear species founded in saturated mercaptoacids without arylic substituent with these metal ions, as in mercaptoacetic[20] or 2-mercaptopropanoic[21] acids, can be explained by steric hindrance and the resonance effect between the sulphur atom and the naphthyl group through the conjugated double bond in the 3-aryl-2-mercaptopropenoic acids. Similar evidence was found by Wagner *et al.*[5] in studying the complexation of several 3-aryl-2-mercaptopropenoic acids with these metal ions.

With the final values of constants in Table 2, we have studied the species distribution for the systems Ni(II)–NMPA and Zn(II)–NMPA–H (see Figs 4 and 5) for a metal and ligand concentrations of 1 mM and 3 mM, respectively. The obtained distributions show the high affinity of NMPA for these divalent ions as, at $-\log[H^+] = 4$, less than 1% of metal ion remains uncomplexed. Analytical interest has the reaction of NMPA with the Ni(II) ion, because at this acidity level the complex $Ni(NMPA)^{2-}$ is practically the only Ni(II) species present.

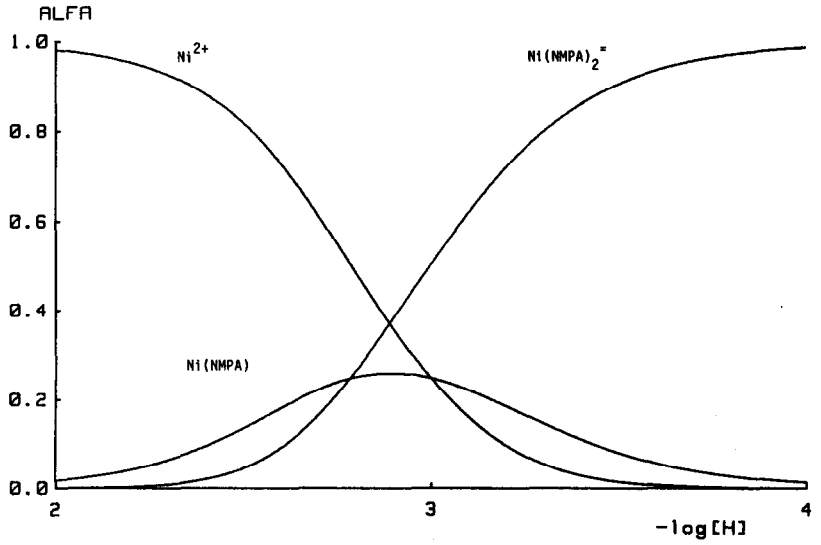

Fig. 4. Species distribution for Ni(II)–NMPA complexes. $[Ni^{2+}] = 1$ mM, [NMPA] = 3 mM.

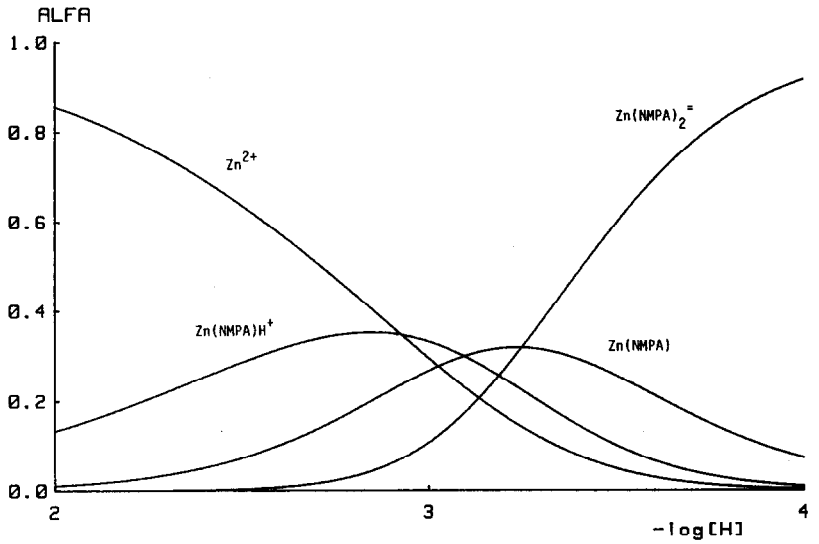

Fig. 5. Species distribution for Zn(II)–NMPA–H complexes. $[Zn^{2+}] = 1$ mM, [NMPA] = 3 mM.

REFERENCES

1. A. Izquierdo and J. Carrasco, *Analyst* 1984, **109**, 605.
2. A. Izquierdo and J. Calmet, *Talanta* 1977, **25**, 56.
3. A. Izquierdo and J. Calmet, *Analusis* 1976, **4**, 200.
4. W. O. Foye and J. R. Lo, *J. Pharma. Sci.* 1972, **61**, 1209.
5. J. Wagner, P. Vitali, J. Schoun and E. Giroux, *Can. J. Chem.* 1977, **55**, 4028.
6. A. Izquierdo, L. García-Puignou and J. Guasch, *Polyhedron* 1986, **5**, 1253.
7. H. S. Rossotti, *Talanta* 1974, **21**, 809.
8. E. Campaigne and R. E. Cline, *J. Org. Chem.* 1956, **21**, 32.
9. Y. Okuda, *Biochem. J. (Jpn)* 1925, **5**, 201.
10. A. I. Vogel, *A Textbook of Quantitative Inorganic Analysis*. Longman, London (1978).
11. D. D. Perrin and B. Dempsey, *Buffers for pH and Metal Ion Control*. Chapman & Hall, London (1974).
12. *Some Laboratory Methods*, The Royal Institute of Technology, Stockholm (1959).
13. A. S. Brown, *J. Am. Chem. Soc.* 1934, **56**, 646.
14. W. Forsling, S. Hietanen and L. G. Sillén, *Acta Chem. Scand.* 1952, **6**, 601.
15. A. Izquierdo and J. L. Beltrán, *Anal. Chim. Acta* 1986, **181**, 87.
16. L. Meites, *Polarographic Techniques*. Wiley, New York (1965).
17. G. Gran, *Analyst* 1952, **77**, 661.
18. L. G. Sillén, *Acta Chem. Scand.* 1956, **10**, 186.
19. A. Izquierdo, E. Bosch and J. L. Beltrán, *Talanta* 1984, **31**, 475.
20. D. D. Perrin and I. G. Sayce, *J. Chem. Soc.* 1967, 82.
21. H. F. De Brabander, A. M. Goeminne and L. C. Van Poucke, *J. Inorg. Nucl. Chem.* 1975, **37**, 799.

Polyhedron Vol. 6, No. 3, pp. 619–626, 1987
Printed in Great Britain

0277–5387/87 $3.00+.00

ELECTRON-RICH BORANES AND RELATED MOLECULES

BRIAN W. CLARE and DAVID L. KEPERT*

School of Chemistry, University of Western Australia, Nedlands, Western Australia, Australia

(*Received* 1 *May* 1986; *accepted* 15 *August* 1986)

Abstract—The mathematical modelling procedure developed previously for predicting the structure of *closo*-$B_nH_n^{2-}$, *nido*-$B_nH_n^{4-}$ and *arachno*-$B_nH_n^{6-}$ has been extended to the next two homologous series, for which the names *eka*-$B_nH_n^{8-}$ and *dva*-$B_nH_n^{10-}$ are proposed. Specific structural predictions are made for each of these molecules, most of which have yet to be synthesised. An atom–electron map is proposed that conveniently shows the relation between the boron hydrides and the hydrocarbons (and related species such as the polyphosphide and polysulfide ions).

The *closo*-boron hydrides, $B_nH_n^{2-}$, consist of polyhedral clusters of boron atoms, the structures of which can be mathematically modelled if it is assumed that each boron atom interacts with every other boron atom in the cluster, the extent of the interaction depending only upon the interatomic distance.[1–3] A useful potential that relates the energy between any pair of boron atoms, u_{B-B}, to the internuclear distance, d_{B-B}, is given by the bi-reciprocal expression (1):

$$u_{B-B} = \frac{1}{d_{B-B}^2} - \frac{1}{d_{B-B}}. \quad (1)$$

In comparison with molecular orbital methods, this technique replaces a small number of very strongly bonding interactions across the interior of the polyhedron by a larger number of weaker cross-polyhedral interactions that have bonding energies comparable to the interactions around the surface of the cluster.

The structures of the *nido*-boron hydrides that are based on the formula $B_nH_n^{4-}$ can be obtained in the same manner if an interaction, u_{B-ep}, between the additional electron pair and each boron atom is incorporated into the model,[4] a suitable expression being:

$$u_{B-ep} = \frac{2.2}{d_{B-ep}^4} - \frac{1.2}{d_{B-ep}}. \quad (2)$$

Increasing the number of electron pairs in the molecule, as in *arachno*-$B_nH_n^{6-}$, requires the addition of an interaction between the electron pairs, u_{ep-ep}, an appropriate expression being:

$$u_{ep-ep} = \frac{0.1}{d_{ep-ep}^4}. \quad (3)$$

In the expressions (1)–(3), energy and distance are both in arbitrary units but nevertheless the stereochemical arrangement of atoms can be accurately predicted.

In this work, these three potentials are used to extrapolate these structural predictions to molecules based on the series $B_nH_n^{8-}$ and $B_nH_n^{10-}$. Some comments are first made on the extent of this area of interest.

THE RELATION BETWEEN THE HOMOLOGOUS SERIES OF BORON HYDRIDES AND THE HOMOLOGOUS SERIES OF HYDROCARBONS

The addition of successive pairs of electrons to the *closo*-boron hydrides, $B_nH_n^{2-}$, forms homologous series based on the formulae *nido*-$B_nH_n^{4-}$ and *arachno*-$B_nH_n^{6-}$, the structural prefixes denoting closed convex polyhedral structures, partially opened out nest-like structures, and more completely opened out and more complex spider web-like structures, respectively. The addition of n electron pairs to the *closo*-compounds would form $B_nH_n^{(2n+2)-}$, isoelectronic with the homologous series of saturated hydrocarbons C_nH_{2n+2}. Progressing in the reverse direction, that is by the removal of an

* Author to whom correspondence should be addressed.

electron pair from the saturated hydrocarbons and the addition of one "bond", forms the cyclic hydrocarbons and the alkenes, C_nH_{2n}. (In this electron counting exercise, a double bond can simply be imagined as a two-membered ring.) Removal of a second electron pair and addition of another bond forms C_nH_{2n-2}, the bicyclic alkanes, monocyclic alkenes, dienes and alkynes. A dominant feature of this area of chemistry is the very large number of structural isomers possible for any chemical composition.

We propose that the relation between the homologous series based on the boron hydrides and the homologous series based on the hydrocarbons is conveniently depicted by the atom–electron map shown in Fig. 1. Each hexagonal cell represents a fixed number of skeletal atoms and a fixed number of electron pairs. The number of skeletal atoms, n, increases on descending the map and the number of electron pairs increase from left to right. The three sloping columns on the left hand side corresponding to the three homologous series of boron hydrides are indicated, as are the three sloping columns on the right hand side corresponding to the first three series of hydrocarbons. It is clear that these two sets of homologous series meet and cross near the top of the map. The top hexagonal cell at $n = 0$ corresponds to H_2, the two cells at $n = 1$ correspond to BH_3 and CH_4, respectively (and isoelectronic species such as BH^{2-} and BH_4^-), the three cells at $n = 2$ correspond to $B_2H_2^{2-}$, B_2H_6 (or C_2H_4) and C_2H_6, respectively, and so on.

The observation that these two sets of homologous series, one based on the boron hydrides and one based on the hydrocarbons, are not parallel with one another leads to a dilemma in chemical

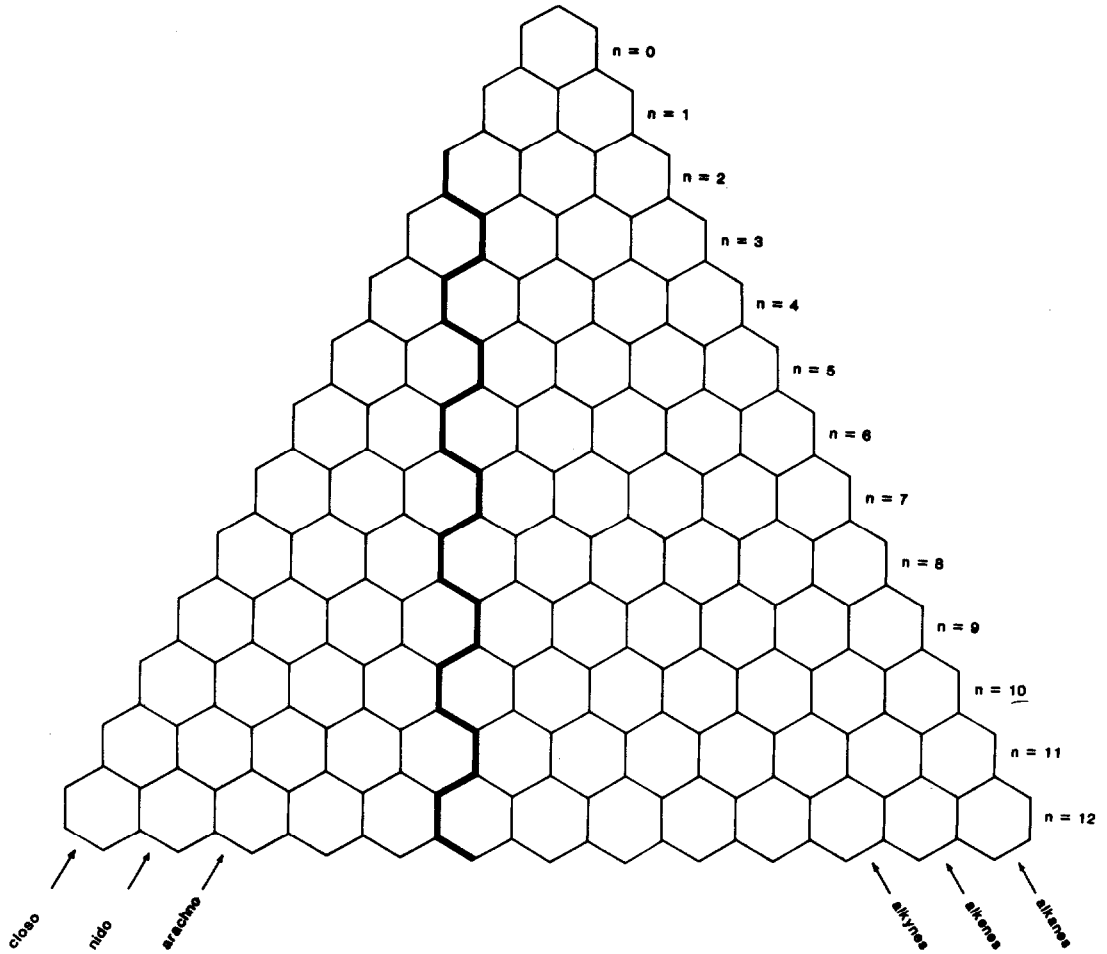

Fig. 1. Atom–electron map. Each hexagonal cell represents a fixed number of atoms and a fixed number of electron pairs, the number of atoms n increasing from top to bottom and the number of electron pairs increasing from left to right. The locations of the first three homologous series of boron hydrides are shown, as are the first three homologous series of hydrocarbons. The heavy zig-zag vertical line represents the left hand limit for which two electron/two atom bonding schemes can be drawn.

nomenclature. Continuation of the structural prefixes, *closo-*, *nido-*, *arachno-* to subsequent series $B_nH_n^{x-}$, where $x = 8$, 10, 12, is not appropriate as the type of structure is expected to depend upon the size of the cluster. Smaller members, for example $B_4H_4^{10-}$ which is isoelectronic with the alkene C_4H_{10}, would be expected to have opened out structures whereas the larger members of the same series, for example $B_{12}H_{12}^{10-}$, would be expected to retain much of the cluster characteristics of the *closo-*, *nido-* and *arachno*-compounds. Prefixes that have been used include *hypho-* and *conjuncto-*. There are very few compounds known of the types $B_nH_n^{8-}$ and $B_nH_n^{10-}$ and until more information is available we propose the use of the following temporary prefixes. The first is *eka-* (Sanskrit: one), which has an illustrious chemical tradition as it was chosen by Mendeleev for unknown elements whose existence was required to fill the spaces in his Periodic Table; it could also be used for the first series beyond the *arachno*-series. The subsequent series would then become *dva-* (Sanskrit: two).

The heavy vertical zig-zag line in Fig. 1 is the left hand limit for which classical two electron/two atom bonding schemes can be drawn for molecules containing skeletal atoms restricted to a valency of four and in which each skeletal atom is bonded to one non-skeletal atom or group, or contains one non-bonding pair of electrons. Examples to the immediate right hand side of this zig-zag line include C_nH_n or P_n (n = even) and $C_n H_{n+1}$ or P_n^- (n = odd). For example, P_7^{3-} [5] and Sb_7^{3-} [6] are adequately represented as analogues of tricycloheptane C_7H_{10}, with P atoms replacing CH groups and P^- ions replacing CH_2 groups.

It is not clear where the right hand limit for compounds based on clusters exists in Fig. 1, although it does appear to overlap the left hand limit of the classical structures.

It is also clear from Fig. 1 that for larger molecules there is an area between the *arachno*-series and the classical structure limit. This area of chemistry is relatively unknown.

These questions are further explored in this paper using the mathematical modelling procedures that have been developed for cluster compounds and summarized above.

RESULTS

As might have been expected, the structural chemistry of the compounds in the area investigated is complicated by the large number of isomers that occur and it did not appear to be feasible to locate all possible minima on the potential energy surfaces. The more stable isomers that have been located so far for each member of the *eka*-$B_nH_n^{8-}$ series are shown in Fig. 2; only those isomers that are within 0.1000 energy units of the most stable structure are shown (Table 1). Similarly Fig. 3 and Table 2 list the more favourable structures found for the *dva*-$B_nH_n^{10-}$ series.

Table 1. Energies (arbitrary units) for those *eka*-$B_nH_n^{8-}$ depicted in Fig. 2 (in the same order)

$B_nH_n^{8-}$	Energies
$B_3H_3^{8-}$	−4.7897
$B_4H_4^{8-}$	−6.8350, −6.7772
$B_5H_5^{8-}$	−9.0768
$B_6H_6^{8-}$	−11.4974, −11.4498, −11.4163
$B_7H_7^{8-}$	−14.1054, −14.1074, −14.1113, −14.1314
$B_8H_8^{8-}$	−16.9436, −17.0434
$B_9H_9^{8-}$	−20.0775, −20.1581, −20.0816
$B_{10}H_{10}^{8-}$	−23.4723, −23.4285, −23.4676, −23.4380
$B_{11}H_{11}^{8-}$	−26.9791, −26.9981, −26.9646
$B_{12}H_{12}^{8-}$	−30.7655, −30.7254

The eka-$B_nH_n^{8-}$ *series*

The calculations show that *eka*-$B_3H_3^{8-}$ is expected to have a bent structure with the three electron pairs in a plane at right angles to the plane of the three skeletal atoms. This structure is in contrast to the equilaterial triangular arrangement predicted[7] for *closo*-$B_3H_3^{2-}$, *nido*-$B_3H_3^{4-}$ and *arachno*-$B_3H_3^{6-}$, an example of the latter structure being Pr_3P_3.[8] Examples of the bent *eka*-$B_3H_3^{8-}$ structure include the isoelectronic propane C_3H_8, and groups of heavier atoms such as P_3^{5-}, S_3^{2-}, Te_3^{2-} and I_3^+.[9-11]

Figure 2 shows the two possible structures for *eka*-$B_4H_4^{8-}$. The first is a four-membered ring as is observed in cyclobutane, C_4H_8, P_4^{4-} and As_4^{4-}.[12,13] The second possible structure is the less stable planar open-chain trapezoidal arrangement. A

Table 2. Energies (arbitrary units) for those *dva*-$B_nH_n^{10-}$ depicted in Fig. 3 (in the same order)

$B_nH_n^{10-}$	Energies
$B_4H_4^{10-}$	−8.5295
$B_5H_5^{10-}$	−11.1750, −11.0988
$B_6H_6^{10-}$	−14.0064, −13.9458
$B_7H_7^{10-}$	−16.9769, −16.9937, −16.9858, −17.0114
$B_8H_8^{10-}$	−20.2880, −20.2926
$B_9H_9^{10-}$	−23.8335, −23.7709
$B_{10}H_{10}^{10-}$	−27.5837, −27.5859
$B_{11}H_{11}^{10-}$	−31.5262, −31.5145
$B_{12}H_{12}^{10-}$	−35.7478

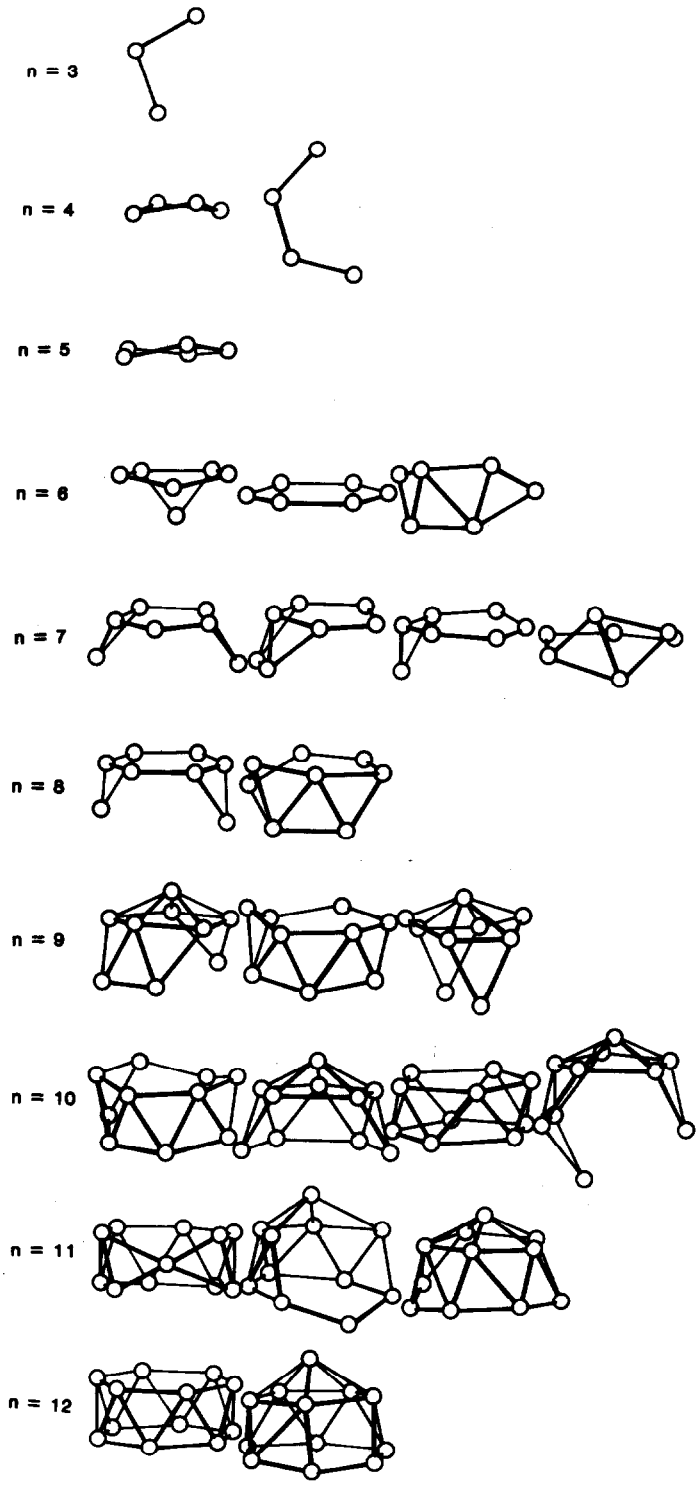

Fig. 2. Structures of *eka*-$B_nH_n^{8-}$.

cyclic structure is also predicted as the most stable arrangement for *eka*-$B_5H_5^{8-}$, or cyclopentene, C_5H_8.

A number of isomers are possible for $B_6H_6^{8-}$. The most stable structure consists of a five-membered ring linked to a three-membered ring while a closely related monocyclic structure is formed by breaking the 1–3 "bond"; both structures can be considered as isomers of C_6H_8. If the three electron pairs are arranged on the same side of the molecule, a structure of four linked triangles is formed, as is observed in $B_6H_{10}(PMe_3)_2$.[14] A fourth isomer, existing as a

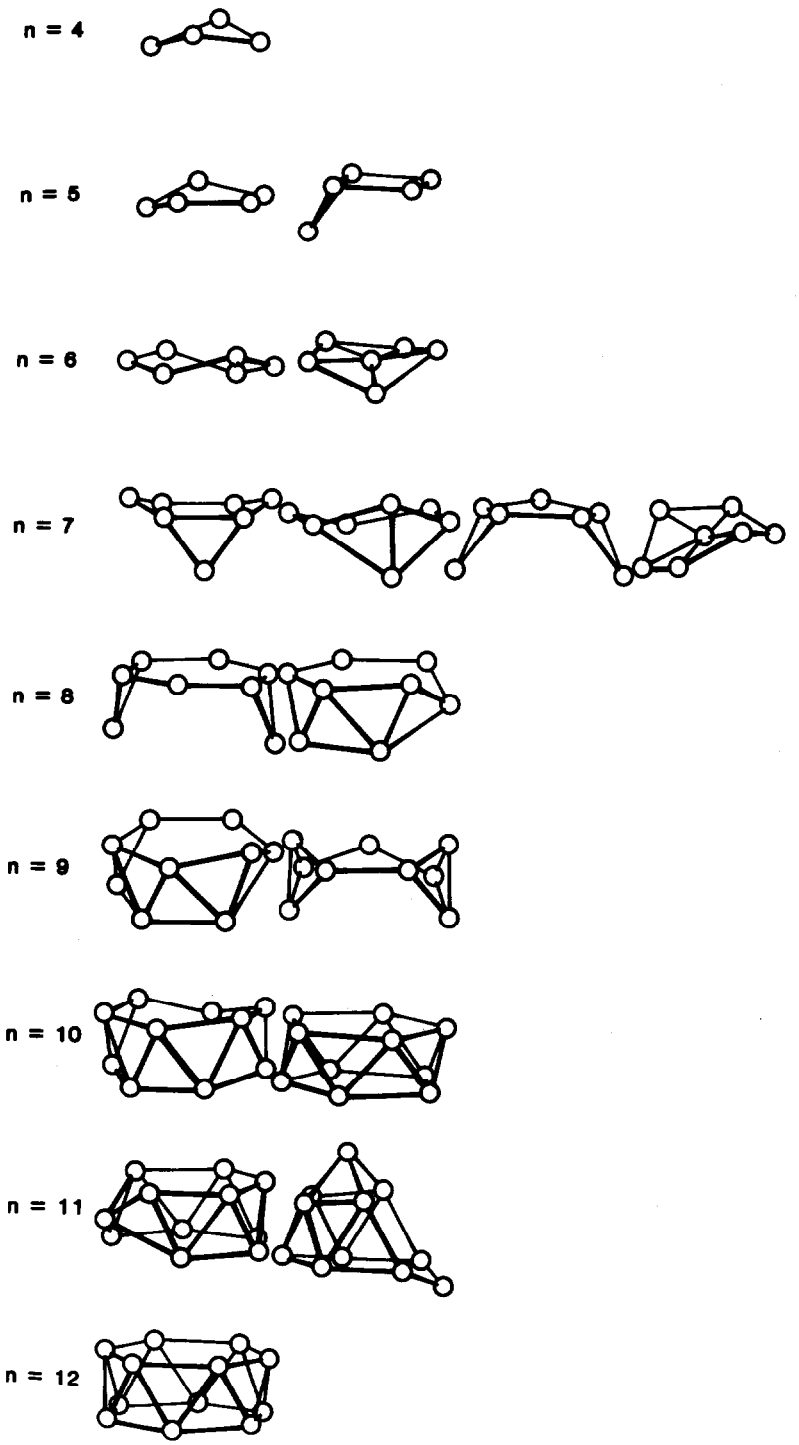

Fig. 3. Structures of *dva*-$B_nH_n^{10-}$.

minimum on the potential energy surface but not shown in Fig. 2 because it is 0.1088 energy units less stable than the bicyclic structure, consists of a trigonal prismatic arrangement of atoms with a pair of electrons outside each of the rectangular faces. This trigonal prismatic structure is experimentally known for Te_6^{4+},[15] although it may be noted that molecular orbital calculations have been used to predict a significant distortion of the prism.[16]

Figure 2 shows that for *eka*-$B_nH_n^{8-}$, where $n = 7$–12, the predicted structures are complex clusters but there appears to be little experimental confirmation for compounds in this area. Some structural relationships are discussed later.

The dva-$B_nH_n^{10-}$ *series*

Ring structures are predicted for $B_4H_4^{10-}$ and $B_5H_5^{10-}$ (Fig. 3) with two pairs of electrons on each side of the ring. In addition, a second isomer is possible for $B_5H_5^{10-}$, with one electron pair on one side of the molecule and three electron pairs on the other side of the molecule. Similarly,the most stable structure for $B_6H_6^{10-}$ is a planar six-membered ring with two electron pairs on each side. This structure is known for the P_6^{4-} anion.[17] It may be noted, however, that the structure of the P_7^{3-} anion[5] (and a number of closely related species[18]), does not have any of the structures shown in Fig. 3 for $B_7H_7^{10-}$, but has a conventional structure based on simple electron pair bonds with octets about each atom.

The larger *dva*-boranes consist of complex clusters of atoms only some of which have high symmetry, for example the pentagonal antiprismatic structure of $B_{10}H_{10}^{10-}$ and the hexagonal antiprismatic structure of $B_{12}H_{12}^{10-}$. Another interesting structure is the second isomer found for $B_{11}'H_{11}^{10-}$ which can be considered as a 156 stack with one atom in the pentagonal plane missing (Fig. 3). This structure has C_{2v} symmetry, the two-fold axis passing through the atom in the bottom right hand corner of the view shown in Fig. 3. Alternatively, this structure can be considered to be based on two linked six-membered rings forming a wedge enclosing the other two atoms, with two pairs of electrons outside each hexagonal ring. Replacement of the two enclosed atoms with electron pairs would form a highly symmetrical D_{3h} structure composed of two three-membered rings and three six-membered rings, with two electron pairs outside each six-membered ring. This structure also occurs as a minimum on the potential energy surface and is predicted for *catur*-$B_9H_9^{14-}$ (*catur*: Sanskrit for *four*) and related molecules including P_9^{5-} and S_9^{4+}.

DISCUSSION

It has been noted previously[4] that one of the isomers for each of the *arachno*-$B_nH_n^{6-}$ compounds has a structure closely related to the single structure for each of the *nido*-$B_nH_n^{4-}$ compounds, in which the single electron pair in the *nido*-compound is replaced by two adjacent electron pairs in the *arachno*-compound. Similarly in this work it is found that many of the *eka*-$B_nH_n^{8-}$ compounds are related to an *arachno*-isomer, and that many of the *dva*-$B_nH_n^{10-}$ isomers are related to an *eka*-isomer. In some instances the same structure is observed across the three series, *arachno*-$B_nH_n^{6-}$, *eka*-$B_nH_n^{8-}$ and *dva*-$B_nH_n^{10-}$. For example, the most stable structure found for $B_5H_5^{6-}$, $B_5H_5^{8-}$ and $B_5H_5^{10-}$ is a pentagonal ring with electron pairs distributed on both sides of the ring. Similarly a hexagonal ring is found for $B_6H_6^{6-}$, $B_6H_6^{8-}$ and $B_6H_6^{10-}$. In $B_7H_7^{x-}$ there are two isomers common across the three series, the first consisting of a hexagon and a triangle sharing an edge, and the second consisting of two edge-shared triangles with three additional atoms completing the ring (Figs 2 and 3). An even more extensive structural series is found for the nonaboranes, where the structure derived from an icosahedron by removal of the three atoms from the same face and replacing them with a region of increasing electron density is found for *nido*-$B_9H_9^{4-}$, *arachno*-$B_9H_9^{6-}$, *eka*-$B_9H_9^{8-}$ (0.1110 energy units less stable than the most stable structure and therefore not shown in Fig. 2) and *dva*-$B_9H_9^{10-}$ (0.2153 energy units higher than the most stable structure and therefore not shown in Fig. 3).

In order to examine the overall structural pattern in these molecules it is instructive to consider the series of twelve atom clusters, $B_{12}H_{12}^{x-}$, where $x = 2$, 4, 6, 8 and 10 (Fig. 4). The *closo*-compound, $B_{12}H_{12}^{2-}$, is a regular icosahedron. The icosahedron is also obtained for *nido*-$B_{12}H_{12}^{4-}$, which contains the additional pair of electrons at the centre of the cluster. The second additional pair of electrons in *arachno*-$B_{12}H_{12}^{6-}$ opens out the polyhedron to form a distorted 156 stack in which one pair of electrons is at the centre of the cluster and the other is outside the hexagonal face. A distorted variant of this structure is found in $C_4Me_4B_8H_8(C_5H_4)Co(C_5H_5)$[19] (the cobalt atom is not part of the cage formed by the four carbon atoms and eight boron atoms). Extension to *eka*-$B_{12}H_{12}^{8-}$ yields two possible isomers as separate potential energy minima. The first is the hexagonal antiprism in which one electron pair is situated in the centre of the cluster with the other two electron pairs situated outside the two hexagonal faces. The second isomer is the 156 stack in which one electron pair is in the interior of the molecule, one near the centre of the hexagonal face and one outside the hexagonal face. Addition of a fourth electron pair to form *dva*-$B_{12}H_{12}^{10-}$ leads only to a distorted hexagonal antiprism with one electron pair near the centre, one outside one hexagonal face and two outside the other.

It is often convenient to consider *nido*-compounds containing less than twelve skeletal atoms to be fragments of icosahedra, the only exception being the small $B_5H_5^{4-}$, which is square pyramidal. Similarly, the *arachno*-compounds can be considered as fragments of an icosahedron or fragments of a 156 stack, or both, the only exception being the square isomer of the small $B_4H_4^{6-}$ anion. These descriptions in terms of fragments of these twelve-vertex polyhedra appear to be more useful

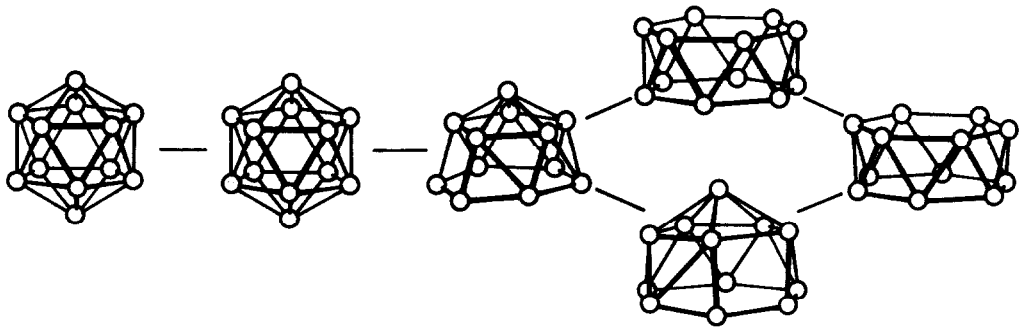

Fig. 4. Structures, from left to right, of *closo*-$B_{12}H_{12}^{2-}$, *nido*-$B_{12}H_{12}^{4-}$, *arachno*-$B_{12}H_{12}^{6-}$, *eka*-$B_{12}H_{12}^{8-}$ (two isomers) and *dva*-$B_{12}H_{12}^{10-}$.

than the description as fragments of the *closo*-compounds.

The structural predictions made in this work in general cannot as yet be verified because boranes corresponding to many of the hexagonal cells in Fig. 1 have not yet been synthesized. A great many carboranes are now known but the vast majority contain only two skeletal carbon atoms as they are usually synthesized by incorporating alkynes into boranes. Care needs to be taken in extrapolating the structural correlations found here to molecules containing other elements. There are two main reasons for this caution:

(1) The atom–atom potential (1) used in this work was derived from the structures of *closo*-$B_8H_8^{2-}$ and *closo*-$B_9H_9^{2-}$.[1] However, mathematical modelling of clusters of the heavier *p*-block elements, for example, Sn_5^{2-}, $TlSn_8^{3-}$ and $TlSn_9^{3-}$, yield significantly "harder" potentials such as:[3]

$$u_{Sn-Sn} = \frac{1}{d_{Sn-Sn}^4} - \frac{1}{d_{Sn-Sn}}.$$

Further extension to transition metal organometallic clusters yields very hard potentials as in, for example, $[Os_5(CO)_{16}]$ and $[Rh_9(CO)_{19}]^{3-}$:[3]

$$u_{Os-Os} = \frac{1}{d_{Os-Os}^{10}} - \frac{1}{d_{Os-Os}^4}.$$

At the present time nearly all the electron-rich compounds beyond the *arachno*-series contain organometallic fragments incorporated into the borane fragment and the resulting distortions make the perception of structural correlations difficult.[20]

Even replacement of a boron atom in the formula of a borane by an isoelectronic carbon cation, C^+, is possible to only a limited extent before substantial structural changes are observed. For example,in *nido*-$C_4Me_4B_8H_8$[21] and *nido*-$C_4Et_4B_8H_8$[20] the C_4B_8 icosahedra are distorted due to the lengthening of the C–C edges so that the coordination number of the carbon atoms is reduced from six to five. In many carbon-rich carboranes the carbon atom is bonded to two terminal groups and the group is displaced out of the cluster of remaining atoms until it approximates to a methylene group bridging two of the remaining cluster atoms.[20] Conversely, it is possible to visualize many carbon-rich carboranes as basic hydrocarbon skeletons in which a CH_2 group is replaced by a BH group, regardless of electron count. Thus $C_4H_4B_6Me_6$ adopts the adamantane structure rather than that expected for *nido*-$B_{10}H_{10}^{4-}$.[22]

(2) The atom–electron pair potential used in this work was derived from *nido*-$B_{10}H_{14}$ and the minimum potential occurs at about the same boron–electron pair distance as the boron–boron distance corresponding to the minimum boron–boron potential.[4] That is, in a borane the electron pair occupies approximately the same space as a boron atom. Thus addition of one electron pair to the tetrahedral *closo*-$B_4H_4^{2-}$ forms *nido*-$B_4H_4^{4-}$ in which the structure is partially opened out and consists of only two triangles sharing an edge.[4] However P_4, As_4 and Sb_4, which have the *nido*-electron count, appear to be regular tetrahedral.[23] This structure can be attributed to the additional electron pair occupying less space than the phosphorus atoms and can be accommodated at the centre of the cluster. The situation can be likened to the contraction of non-bonding pairs of electrons in simple compounds such as $[MX_3(\text{lone pair})]$ as the Periodic Table is descended.[24] Similarly many Zintl phases AX and BX_2 (A = Na, K, Rb, Cs; B = Sr, Ba; X = Si, Ge, Sn, Pb) contain tetrahedral X_4^{4-} ions,[25,26] as do $Na_8(Tl_4)$[27] and $[K(2,2,2\text{-crypt})]_2(Pb_2Sb_2)$.[28] On the other hand, molecules such as P_4 can be simply represented as each phosphorus atom forming simple localized electron pair bonds to the other three phosphorus atoms, with a non-bonding pair of electrons completing a tetrahedral arrangement of electron pairs.

For these heavier elements a second electron pair

is required to form the opened out structure, as in P_4H_2[29] and Si_4^{6-},[30] similar to B_4H_{10} or dicyclobutane, C_4H_6. In these compounds the two electron pairs occupy the *cis*-sites of an octahedron with the four skeletal atoms at the other four vertices. An octahedral structure with electron pairs in *trans*-sites and a square planar arrangement of atoms is compounds such as $[K(crypt)]_2(Sb_4)$,[31] $[K(crypt)]_2(Bi_4)$,[32] $(Se_4)(HS_2O_7)_2$[33] and $(Te_4)(AlCl_4)_2$.[34]

Larger clusters of the *p*-block elements with the *nido*-electron count also have polyhedral structures closely related to the *closo*-compounds and the additional electron pair can again be imagined as being located in the centre of the cavity. Examples include Ge_9^{4-},[35] Sn_9^{4-}[36-38] and Bi_9^{5+}.[39]

In an analogous manner the electron count of the larger transition metal carbonyl clusters can also be interpreted in terms of the 18-electron rule with an additional electron pair being located at the centre of the cluster leading to, for example, the 86 electron octahedral clusters such as $[Rh_6(CO)_{16}]$.

Acknowledgements—These calculations were facilitated by the availability of special rates from the West Australian Regional Computing Centre, for which we are grateful. This work is also sponsored by the Australian Research Grants Scheme.

REFERENCES

1. D. J. Fuller and D. L. Kepert, *Inorg. Chem.* 1982, **21**, 163.
2. D. J. Fuller and D. L. Kepert, *Polyhedron* 1983, **2**, 749.
3. D. J. Fuller and D. L. Kepert, *Inorg. Chem.* 1984, **23**, 3273.
4. B. W. Clare and D. L. Kepert, *Inorg. Chem.* 1984, **23**, 1521.
5. W. Dahlmann and H. G. v. Schnering, *Naturwiss.* 1972, **59**, 420.
6. D. G. Adolphson, J. D. Corbett and D. J. Merryman, *J. Am. Chem. Soc.* 1976, **98**, 7234.
7. B. W. Clare and D. L. Kepert, unpublished.
8. M. Baudler, G. Furstenburg, H. Suchomel and J. Hahn, *Z. anorg. Chem.* 1983, **498**, 57.
9. H. G. v. Schnering, W. Wichelhaus and M. Schulze Nahrup, *Z. anorg. Chem.* 1975, **412**, 193.
10. A. F. Wells, *Structural Inorganic Chemistry*, Fifth Edition, p. 731. Clarendon Press, Oxford (1984).
11. A. Cisar and J. D. Corbett, *Inorg. Chem.* 1977, **16**, 632.
12. S. Rundqvist and N.-O. Ersson, *Arkiv Kemi* 1968, **30**, 103.
13. N. Mandel and J. Donohue, *Acta Cryst.* 1971, **B27**, 2288.
14. M. Mangion, R. K. Hertz, M. L. Denniston, J. R. Long, W. R. Clayton and S. G. Shore, *J. Am. Chem. Soc.* 1976, **98**, 449.
15. R. C. Burns, R. J. Gillespie, W.-C. Luk and D. R. Slim, *Inorg. Chem.* 1979, **18**, 3086.
16. R. C. Burns, R. J. Gillespie, J. A. Barnes and M. J. McGlinchey, *Inorg. Chem.* 1982, **21**, 799.
17. H. P. Abicht, W. Honle and H. G. v. Schnering, *Z. anorg. Chem.* 1984, **519**, 7.
18. H. G. v. Schnering, *Angew. Chem. Int. Ed.* 1981, **20**, 23.
19. R. N. Grimes, J. R. Pipal and E. Sinn, *J. Am. Chem. Soc.* 1979, **101**, 4172.
20. R. N. Grimes, *Adv. Inorg. Chem. and Radiochem.* 1983, **26**, 55.
21. D. P. Freyberg, R. Weiss, E. Sinn and R. N. Grimes, *Inorg. Chem.* 1977, **16**, 1847.
22. I. Rayment and H. M. M. Shearer, *J. Chem. Soc. Dalton Trans.* 1976, 136.
23. J. Donohue, *The Structure of the Elements*. Wiley Interscience, New York (1974).
24. D. L. Kepert, *Inorganic Stereochemistry*. Springer, Heidelberg (1982).
25. H. Schafer, B. Eisenmann and W. Muller, *Angew. Chem. Int. Ed.* 1973, **12**, 694.
26. J. Llanos, R. Nesper and H. G. v. Schnering, *Angew. Chem. Int. Ed.* 1983, **22**, 998.
27. D. A. Hansen and J. F. Smith, *Acta Cryst.* 1967, **22**, 836.
28. S. C. Critchlow and J. D. Corbett, *Inorg. Chem.* 1985, **24**, 979.
29. W. W. Schoeller and C. Lerch, *Inorg. Chem.* 1983, **22**, 2992.
30. B. Eisenmann, K. H. Janzon, H. Schafer and A. Weiss, *Z. Naturforsch.* 1969, **24b**, 457.
31. S. C. Critchlow and J. D. Corbett, *Inorg. Chem.* 1984, **23**, 770.
32. A. Cisar and J. D. Corbett, *Inorg. Chem.* 1977, **16**, 2482.
33. I. D. Brown, D. B. Crump and R. J. Gillespie, *Inorg. Chem.* 1971, **10**, 2319.
34. T. W. Couch, D. A. Lokken and J. D. Corbett, *Inorg. Chem.* 1972, **11**, 357.
35. C. H. E. Belin, J. D. Corbett and A. Cisar, *J. Am. Chem. Soc.* 1977, **99**, 7163.
36. L. Diehl, K. Khodadadeh and J. Strahle, *Ber.* 1976, **109**, 3404.
37. J. D. Corbett and P. A. Edwards, *J. Am. Chem. Soc.* 1977, **99**, 3313.
38. R. C. Burns and J. D. Corbett, *Inorg. Chem.* 1985, **24**, 1489.
39. R. M. Friedman and J. D. Corbett, *Inorg. Chem.* 1973, **12**, 1134.

Polyhedron Vol. 6, No. 3, pp. 627–631, 1987
Printed in Great Britain

0277–5387/87 $3.00+.00

REACTION OF $[Ni(CN)_4]^{2-}$ WITH POLYSULFIDE: SYNTHESIS OF $[Ni(S_4)_2]^{2-}$ AND ITS REACTIONS WITH CARBON DISULFIDE AND ACTIVATED ACETYLENES

K. NAGENDRA UDPA and SABYASACHI SARKAR*

Department of Chemistry, Indian Institute of Technology, Kanpur 208016, India

(*Received* 20 *June* 1986; *accepted* 15 *August* 1986)

Abstract—Bis(tetrasulfido)nickelate(II) is synthesized by the reaction of tetracyanonickelate(II) with polysulfide. The reaction of $[Ni(S_4)_2]^{2-}$ with CS_2 and substituted acetylenes forming the perthiocarbonato and dithiolene complexes is described. The dithiolene complexes are found to be oxidized by one unit. The compounds are characterized by various physicochemical methods. The biorelevance of this work is very briefly outlined.

The dissolution of certain transition metal salts in aqueous ammonium polysulfide solution has long been known and was generally attributed to the formation of soluble metal polysulfides. Although the first example of such a compound came in 1903 when Hofmann and Höchten reported[1] the synthesis of $(NH_4)_2PtS_{15}\cdot 2H_2O$, a systematic approach to a study of these systems started only a few years back. This is mainly due to the advent of the spectroscopic and structural techniques which made it possible to characterize and study these compounds. Since then a host of polysulfido complexes with a variety of metal ions have been synthesized and characterized and a recent review[2] summarizes the results of investigations carried out on these systems so far. The polysulfide ions are capable of coordinating to metal centers in a variety of ways thereby giving complexes with novel structural features. They are purely inorganic chelating ligands and the size of the sulfur chain can be varied by changing the reaction conditions. They can undergo unusual reactions leading to the formation of new novel complexes. They may find applications in catalysis[3] and help in understanding certain biochemical reactions.[4] In this paper we describe the synthesis of $[Ni(S_4)_2]^{2-}$ by the interaction of $[Ni(CN)_4]^{2-}$ with polysulfide and its reactions with carbon disulfide and activated acetylenes forming the perthiocarbonato and dithiolene complexes, respectively.

* Author to whom correspondence should be addressed.

EXPERIMENTAL

Materials and methods

Reagent grade chemicals and solvents were employed. Solvents were distilled before use. $K_2[Ni(CN)_4]\cdot H_2O$,[5] dibenzoylacetylene (DBA),[6] dimethylacetylene dicarboxylate (DMAD)[7] and ammonium polysulfide[8] solution were prepared by literature methods. Potassium polysulfide solution in methanol was prepared by passing a moderately fast stream of hydrogen sulfide gas into a suspension of sulfur (20 g) and potassium hydroxide (4 g) in methanol (100 cm^3) for about 2 h with occasional stirring. The orange–red solution of the polysulfide was filtered to remove the excess sulfur. Only freshly prepared polysulfide solutions were used in the reactions.

C, H and N were analyzed at the Microanalytical Laboratories, I.I.T., Kanpur. Nickel was estimated gravimetrically as the dimethylglyoximate after decomposing the compounds with *aqua regia*. Sulfur in the compounds was oxidized to sulfate by alkaline bromine and estimated as barium sulfate. Electronic spectra were recorded on Cary-17D and Shimadzu UV-190 spectrophotometers. The infrared spectra as CsI pellets were obtained on a Perkin–Elmer Model-580 spectrophotometer. Magnetic susceptibility measurements were carried out on an EG and G Model-150A parallel field vibrating sample magnetometer. Electron spin resonance spectra were obtained on a Varian E-109 EPR system working at X-band frequencies using DPPH as standard.

$(PPh_4)_2[Ni(S_4)_2]$, *Method A*

$K_2[Ni(CN)_4]\cdot H_2O$ (0.5 g, 1.93 mmol) was added with stirring to 25 cm^3 of aqueous ammonium polysulfide solution. After the mixture was stirred for 5 min in a stoppered flask, the dark brown solution was filtered into a solution of PPh_4Cl (1.5 g, 4 mmol) in 25 cm^3 of methanol. Allowing the solution to stand for 30 min gave reddish brown microcrystals, which were filtered, washed with little deoxygenated water, methanol, toluene and finally with diethylether. The product was dried under vacuum; yield 0.77 g (40%).

Method B

PPh_4Cl (1.5 g, 4 mmol) was dissolved in 50 cm^3 of methanolic potassium polysulfide solution. $K_2[Ni(CN)_4]\cdot H_2O$ (0.5 g, 1.93 mmol) dissolved in minimum amount of water (*ca* 1 cm^3) was added with stirring. The resulting solution was boiled on a water bath for 5 min when the color of the solution became very dark brown. It was quickly filtered and the filtrate was allowed to stand in a stoppered flask at room temperature. In about an hour, dark brown crystals precipitated, which were filtered, washed with methanol, toluene and diethylether; yield 0.67 g (35%).

$(Et_4N)_2[Ni(S_4)_2]$

Tetraethylammonium bromide (1.0 g, 4.76 mmol) was dissolved in 50 cm^3 of methanolic potassium polysulfide solution. $K_2[Ni(CN)_4]\cdot H_2O$ (0.5 g, 1.93 mmol) was added in small portions with stirring and the reaction mixture was boiled on a water bath for 10 min. The dark brown solution was filtered and the filtrate was allowed to stand at 5°C for several hours. The precipitated shining black crystals were filtered, washed and dried as described above; yield 0.33 g (30%).

$(PPh_4)_2[Ni(CS_4)_2]$

Carbon disulfide (5 cm^3) was added to a solution of freshly prepared $(PPh_4)_2[Ni(S_4)_2]$ (0.5 g, 0.5 mmol) in dichloromethane (40 cm^3). The solution was stirred for 10 min and filtered. Addition of diethylether to the filtrate gave yellow–brown microcrystals, which were filtered, washed with diethylether and dried; yield 0.36 g (70%).

$(PPh_4)[Ni(S_2C_2(COC_6H_5)_2)_2]$

0.5 g (0.5 mmol) of freshly prepared $(PPh_4)_2[Ni(S_4)_2]$ and DBA (0.25 g, 1.07 mmol) were dissolved in dichloromethane (50 cm^3) and stirred at room temperature for 20 min. The solution was filtered and to the filtrate an excess of petroleum ether (40–60°C) was added. An oily mass separated. The supernatant liquid was decanted off and the oil was repeatedly washed with petroleum ether whereby it solidified. Recrystallization by CH_2Cl_2–petroleum ether gave the product as brown microcrystals; yield 0.2 g (40%).

$(PPh_4)[Ni(S_2C_2(COOCH_3)_2)_2]$

Freshly prepared $(PPh_4)_2[Ni(S_4)_2]$ (0.3 g, 0.3 mmol) and DMAD (0.1 cm^3, 0.81 mmol) were stirred in CH_2Cl_2 at room temperature for 20 min. A work-up similar to the one given above, gave the product as brown microcrystals; yield 0.05 g (20%).

RESULTS AND DISCUSSION

Tetracyanonickelate(II) is one of the most stable complexes of nickel and only very few substitution reactions of this anion are reported in the literature.[9] The ready enhancement of the coordination number of this anion and the synthesis of $[Ni(CN)_3S]^{3-}$ by a curious cyanide elimination reaction by sulfide[10] prompted us to study the elimination of coordinated cyano groups with polysulfide.

The reaction of $[Ni(CN)_4]^{2-}$ and polysulfide is quite facile both in aqueous and methanolic media, $[Ni(S_4)_2]^{2-}$, thus formed was briefly reported by us.[11] Almost simultaneously Müller and coworkers[12] published the X-ray crystal structure of this anion prepared by the reaction of nickel(II) acetate with methanolic ammonium polysulfide. The elemental analysis of this and the other compounds are presented in Table 1. The synthesis of $[Ni(S_4)_2]^{2-}$ probably proceeds by the stepwise replacement of coordinated cyanide ligands. The cyanide is converted into thiocyanate as soon as it gets replaced by reaction with sulfide of the polysulfide. The tentative scheme (Scheme 1) given below for this reaction with the proposal of the formation of the dicyano(tetrasulfido)nickelate(II) as intermediate seems reasonable in the light of the isolation of $[Ni(CN)_2(S_5)]^{2-}$ by the reaction of *in*

$$[Ni(CN)_4]^{2-} \xrightarrow{S_4^{2-}} \{[Ni(CN)_2(S_4)]\}^{2-} + 2CN^-$$

$$\{[Ni(CN)_2(S_4)]\}^{2-} \xrightarrow{S_4^{2-}} [Ni(S_4)_2]^{2-} + 2CN^-$$

$$CN^- + S_x^{2-} \longrightarrow SCN^- + S_{x-1}^{2-}$$

Scheme 1.

Table 1. Analytical data of the complexes

Compound	Analysis: found (calc.) (%) C	H	N	S	Ni
$(PPh_4)_2[Ni(S_4)_2]$	58.4 (58.0)	4.5 (4.0)	—	25.6 (25.8)	5.9 (5.9)
$(Et_4N)_2[Ni(S_4)_2]$	33.4 (33.4)	7.0 (7.0)	5.2 (4.9)	43.8 (44.5)	10.7 (10.3)
$(PPh_4)_2[Ni(CS_4)_2]$	59.4 (59.0)	3.8 (3.9)	—	25.4 (25.2)	5.7 (5.8)
$(PPh_4)[Ni(S_2C_2(COC_6H_5)_2)_2]$	67.1 (67.6)	4.2 (4.0)	—	12.5 (12.9)	6.3 (5.9)
$(PPh_4)[Ni(S_2C_2(COOCH_3)_2)_2]$	53.0 (53.3)	4.3 (3.9)	—	15.5 (15.8)	7.1 (7.3)

situ generated polysulfide using sulfur and KOH in DMF in $[Ni(CN)_4]^{2-}$.[3]

The reaction of $[Ni(S_4)_2]^{2-}$ with CS_2 in dichloromethane readily yields the bis(perthiocarbonato)nickelate(II) anion.[14] Recently, the X-ray crystal structure of this anion has been reported by Coucouvanis and coworkers.[15] The reactivity of $[Ni(S_4)_2]^{2-}$ is further demonstrated by its reactions with substituted acetylenes giving the corresponding dithiolene complexes. The reaction of coordinated polysulfide with activated acetylenes is known for other metal systems also.[2] The interesting feature of our reactions is that the dithiolene complexes formed are found to be oxidized by one unit. The oxidizing agent here could be the sulfur formed as a byproduct in the reaction. The reaction of $[Ni(S_4)_2]^{2-}$ with substituted acetylenes though novel is not without precedence since the synthesis of tetraphenylthiophene by diphenylacetylene using freshly prepared nickel sulfide containing a little excess of sulfur as catalyst led to the isolation of a phenylsubstituted dithiolene complex $[Ni(S_2C_2(C_6H_5)_2)_2]$.[16] Here the formation of the dithiolene complex is proposed to be due to the presence of small amounts of a short-lived nickel tetrasulfide species.

The vibrational spectral data of the complexes are given in Table 2. The IR spectral data of $[Ni(S_4)_2]^{2-}$ agrees well with that reported by Müller and coworkers.[12] The IR spectrum of $[Ni(CS_4)_2]^{2-}$

Table 2. Vibrational spectral data of the complexes

Complex	Important IR frequencies (cm^{-1})	Ref.
$(PPh_4)_2[Ni(S_4)_2]$	480, 430, 370 ν(S–S); 280 ν(Ni–S)	This work
$(PPh_4)_2[Ni(CS_4)_2]$	1030, 965, 910, 850 ν(C=S); 640, 474, 442, 428, 340, 309	This work
$(PPh_4)[Ni(S_2C_2(COC_6H_5)_2)_2]$	1465 ν(C=C); 1660 ν(C=O); 445, 350, 330	This work
$(PPh_4)[Ni(S_2C_2(COOCH_3)_2)_2]$	1522 ν(C=C); 1725 ν(C=O); 600	This work
$(NEt_4)[Ni(S_2C_2H_2)_2]$	1435 ν(C=C); 840 ν(C–S+ring def.); 790 ν(C–S); 705, 694 (ring def.); 311.5, 385 ν(Ni–S)	18
$(NEt_4)[Ni(S_2C_2(CF_3)_2)_2]$	1485 ν(C=C); 918, 847 ν(C–S); 449, 415 ν(Ni–S)	18
$(NEt_4)[Ni(S_2C_2(C_6H_5)_2)_2]$	1475 ν(C=C); 960, 870 ν(C–S); 465, 406 ν(Ni–S+ring def.); 428 ν(Ni–S)	18
$(Et_4N)[Ni(S_2C_2(CN)_2)_2]$	1435 ν(C=C); 2195 ν(C≡N), 1170, 1055 ν(C–S)+ν(C–C), 865 ν(C–S); 457, 365, 357 ν(Ni–S+ring def.)	18

Table 3. Electronic spectral data of the complexes

Complex	Solvent	λ_{max} (ε, l mol^{-1} cm^{-1}) (nm)
$(PPh_4)_2[Ni(S_4)_2]$	KBr	370 480 670
$(PPh_4)_2[Ni(CS_4)_2]$	CH_2Cl_2	318 (1.87×10^4) 360sh (1.26×10^4) 388 (1.57×10^4) 458 (5.80×10^3)
$[Ni(S_2C_2(COC_6H_5)_2)_2]^-$	CH_2Cl_2	322 (1.44×10^3) 350sh (1.29×10^3) 410sh (4.50×10^2) 510 (3.11×10^2)
$[Ni(S_2C_2(COOCH_3)_2)_2]^-$	CH_2Cl_2	315 (1.21×10^4) 370sh (4.96×10^3) 460 (2.58×10^3) 485 (2.63×10^3) 515sh (2.43×10^3) 645 (5.75×10^2)

shows the characteristic absorptions of the coordinated perthiocarbonato group. Recently a band at 905 cm^{-1} in the IR spectrum of $[Ni(CS_4)_2]^{-2}$ has been assigned to the C=S vibration.[15] An earlier report[17] assigns this vibration to a peak at 1035 cm^{-1}. In our IR spectrum we observe three strong bands in the region 1030–900 cm^{-1} and a medium intensity band at 855 cm^{-1}. We tentatively assign these bands to C=S vibrations. The vibrations due to S–S and Ni–S modes appear in the lower region and it is difficult to assign them accurately.

A detailed normal coordinate analysis of nickel dithiolene complexes is reported in the literature.[18] In this series $[Ni(S_2C_2R_2)_2]^n$ ($n = 0, -1, -2$) the perturbed C=C stretching frequency is a rough measure of the C=C bond strength as it couples very little with other modes. In a series of mononegative ions the C=C stretching frequency would be mainly dependent on the substituent group on the acetylenic carbon atoms. When R = COC_6H_5 the C=C stretching frequency is found to be about 60 cm^{-1} less than when R = $COOCH_3$. A lower ν(C=C) in the $-COC_6H_5$ substituted complex indicates a better π-electron delocalization than that in the $-COOCH_3$ substituted dithiolene complex. For comparison some of the data reported for similar complexes are also listed in Table 2.

The electronic spectral data of the complexes are given in Table 3. The solid state electronic spectrum of $[Ni(S_4)_2]^{2-}$ and the solution spectrum of $[Ni(CS_4)_2]^{2-}$ agree well with the reported data of these complexes.[12,17] The characteristic features of the electronic spectra of the monoanionic complexes are the intense absorptions in the visible and near infrared region. These bands are not of *d–d* type but have their origin in some sort of charge transfer. Extensive studies on the electronic spectra of nickel dithiolene complexes have been carried out and the assignments of electronic bands for similar systems are available in the literature.[19]

The monoanionic dithiolene compounds give ESR signals at room temperature in the solid state. The interesting feature of these ESR spectra is the considerable anisotropy of the g-tensor. The observed ESR parameters along with the magnetic moment values are presented in Table 4. Using extended Hückel MO calculations Schlapfer and Nakamoto[18] have calculated the electron density of metal character in the highest occupied molecular orbital for some of the monoanionic nickel dithiolene complexes. The results obtained by them are shown in Table 4. It can be seen that the percent metal character of the HOMO depends markedly on the substituent group present on the dithiolene moiety. A comparison of the percent metal character of the HOMO and the $\langle g \rangle$ values suggests that the percent metal character of the HOMO increases roughly with an increase in the $\langle g \rangle$ value. The complexes isolated in this study have the highest $\langle g \rangle$ values compared to the other compounds listed in Table 3.

Recently, the presence of nickel as Ni(III) (ESR active) has been demonstrated in several hydrogenases.[21] The donor atom in the nickel containing hydrogenases has been found to be sulfur.[22] These enzymes give rhombic ESR signals similar to that

Table 4. Magnetic moments and ESR spectral data for the mononegative dithiolene complexes

Complex	μ_{eff} B.M.	g_1	g_2	g_3	g	% Metal character of the HOMO	Ref.
$[Ni(S_2C_2(COC_6H_5)_2)_2]^-$	1.79	2.143	2.055	2.011	2.0702[a]	—	This work
$[Ni(S_2C_2(COOCH_3)_2)_2]^-$	1.80	2.148	2.064	2.013	2.0725[a]	—	This work
$[Ni(S_2C_2(CN)_2)_2]^-$	1.83	2.160	2.042	1.998	2.0630	38	18, 20
$[Ni(S_2C_2(CF_3)_2)_2]^-$	1.85	2.137	2.044	1.996	2.0618	43	18, 20
$[Ni(S_2C_2(C_6H_5)_2)_2]^-$	1.82	2.122	2.041	1.999	2.0568	23	18, 20
$[Ni(S_2C_2H_2)_2]^-$	—	2.126	2.039	1.996	2.0506	6	18, 20

[a] In CH_2Cl_2 solution.

of the dithiolene complexes described here but the anisotropy is more pronounced and the $\langle g \rangle$ values are quite high.[23] Nonetheless, the formation of ESR active, stable dithiolene complexes of nickel at normal conditions suggests that this could well be the starting point to synthesize model systems of the nickel containing hydrogenase.

REFERENCES

1. K. A. Hofmann and F. Höchtlen, *Chem. Ber.* 1903, **36**, 3090.
2. M. Draganjac and T. B. Rauchfuss, *Angew. Chem. Int. Ed. Engl.* 1985, **24**, 742.
3. A. Müller, *Polyhedron* 1986, **5**, 323.
4. R. H. Holm and J. A. Ibers, *Iron–Sulfur Proteins* (Edited by W. Levenberg), Vol. 3. Academic Press, New York (1977).
5. W. C. Fernelius and J. J. Burbage, *Inorg. Synth.* 1946, **2**, 227.
6. E. R. Lutz and W. R. Smithey Jr, *J. Org. Chem.* 1951, **16**, 51.
7. E. H. Huntress, T. E. Lesslie and J. Bornstein, *Org. Synth. Coll. Vol.* 1963, **4**, 329.
8. G. Brauer, *Handbook of Preparative Inorganic Chemistry*, Vol. I, p. 369. Academic Press, New York (1977).
9. A. G. Sharpe, *The Chemistry of the Cyanocomplexes of the Transition Metals*, p. 235. Academic Press, London (1975).
10. A. N. Sergeeva and K. N. Mikhalevich, *Russ. J. Inorg. Chem.* (*English Transl.*) 1962, **7**, 349.
11. S. Sarkar and K. N. Udupa, *Abstracts of the Third Annual Conference of Indian Council of Chemists.* Dharwad, India (1983).
12. A. Müller, E. Krickemeyer, H. Bögge, W. Clegg and G. M. Sheldrick, *Angew. Chem. Int. Ed. Engl.* 1983, **22**, 1006.
13. K. N. Udupa and S. Sarkar, *J. Organomet. Chem.* 1985, **284**, C36.
14. K. N. Udpa, Ph.D. thesis, I.I.T., Kanpur (1985).
15. D. Coucouvanis, P. R. Patil, M. G. Kanatzidis, B. Detering and N. C. Baenziger, *Inorg. Chem.* 1985, **24**, 24.
16. G. N. Schrauzer and V. Mayweg, *J. Am. Chem. Soc.* 1962, **84**, 3221.
17. D. Coucouvanis and J. P. Fackler Jr, *J. Am. Chem. Soc.* 1967, **89**, 1346.
18. C. W. Schlapfer and K. Nakamoto, *Inorg. Chem.* 1975, **14**, 1338.
19. S. I. Shupack, E. Billig, R. J. H. Clark, R. Williams and H. B. Gray, *J. Am. Chem. Soc.* 1964, **86**, 4594.
20. A. Davison, N. Edelstein, R. H. Holm and A. H. Maki, *Inorg. Chem.* 1963, **2**, 1227.
21. S. P. J. Albracht, K. J. Albrecht-Elimer, D. J. M. Schmedding and E. C. Slater, *Biochim. Biophys. Acta* 1982, **681**, 330.
22. R. A. Scott, M. Czechowski, D. V. Dervartanian, J. LeGall, H. D. Peck Jr. and I. Moura, *Rev. Port. Quim.* 1985, **27**, 67.
23. J. J. G. Moura, M. Teixeira, I. Moura, A. V. Xavier and J. LeGall, *Rev. Port. Quim.* 1985, **27**, 63.

Polyhedron Vol. 6, No. 3, pp. 633–639, 1987
Printed in Great Britain

0277–5387/87 $3.00+.00

STABILITY CONSTANTS OF *N*-ISOBUTYROYL-L-LYSINE AND POLY(*N*-METHACRYLOYL-L-LYSINE) COMPLEXES

A. LEKCHIRI and M. MORCELLET*

Laboratoire de Chimie Macromoleculaire, U.A. 351 du C.N.R.S.,
59655 Villeneuve d'Ascq Cedex, France

and

M. WOZNIAK

Laboratoire d'Hydrométallurgie, Ecole Nationale Supérieure de Chimie de Lille—BP 108,
59652 Villeneuve d'Ascq Cedex, France

(*Received* 9 *July* 1986; *accepted* 15 *August* 1986)

Abstract—The formation constants of the complexes formed between H^+, Cu^{2+}, Ni^{2+}, Co^{2+} and Zn^{2+} and *N*-isobutyroyl-L-lysine (NIBL) [$H_2A^+ = (CH_3)_2CHCONH(CH_2)_4CH(NH_3^+)COOH$] have been determined by potentiometry at 25.0°C and $I = 0.1$ mol dm^{-3} $NaClO_4$. Titration curves of this ligand in the presence of a metal ion did not reveal appreciable complexing in acidic media. At intermediate pH values, after neutralization of the carboxyl group, the presence of the metal ion induces a lowering of the pH value, indicating complex formation. The detection of the species and the determination of the corresponding formation constants has been made with the aid of the MUCOMP refinement program. It has shown that the following species are present in solution: CuA^+, CuA_2, NiA^+, NiA_2, CoA^+, CoA_2, ZnA^+ and ZnA_2. These complexes are likely to be N, O chelates of the glycine type. The cumulative and the stepwise formation constants follow the Irving–Williams series. No evidence was found for the deprotonation of the amide group.

The formation constants of the complexes formed between copper(II) and the polymeric analog of NIBL, poly(*N*-methacryloyl-L-lysine) were determined in the same way. For this purpose, it was necessary to consider as the ligand a hypothetical molecule made up of two repeat units. The results obtained are in good agreement with those of spectroscopic measurements.

We are currently investigating the complex properties of optically active hydrosoluble polymers derived from natural amino acids. These polymers have –C–NH–CH(R)COOH as their side chain where R depends on the nature of the amino acid used for the synthesis. Up to now, polymers derived from alanine ($R = CH_3$), glutamic acid [$R = (CH_2)_2(COOH)$], aspartic acid ($R = CH_2COOH$), asparagine ($R = CH_2CONH_2$) and lysine [$R = (CH_2)_4NH_2$] have been studied.[1–5] As is well known, the ionization and complexing properties of a polymeric ligand are very different from those of a small molecule because the electrostatic interactions between the neighbouring ionizable groups strongly influence all the thermodynamic parameters such as the p*K* values.[6] Thus, to have a best knowledge of the behaviour of these polymers we were led to study low molecular weight compounds considered as models. The present paper reports results obtained with *N*-ε-isobutyroyl-L-lysine $(CH_3)_2CHCONH(CH_2)_4CH(NH_3^+)COOH$ (NIBL), which is the analog of the repeat unit of poly(*N*-ε-methacryloyl-L-lysine) (PNML),[4] using a potentiometric technique. The stability constants of the complexes formed with Cu(II), Ni(II), Co(II) and Zn(II) are compared with those of the lysine (from which NIBL is derived) and glycine complexes.

In a second part of this work, is reported the tentative determination of the formation constants

* Author to whom correspondence should be addressed.

of the complexes of copper(II) with the polymer PNML.

EXPERIMENTAL

Samples

N-ε-isobutyroyl-L-lysine (NIBL) was synthesized by a Schotten Bauman reaction between isobutyroyl chloride and the ε-amino group of L-lysine, the α-amino and carboxyl group being protected by a complex with copper. Details of the experimental procedure will be found elsewhere.[4] NIBL was purified by column chromatography using *n*-butanol as eluant. NIBL was characterized by its rotatory power ($[\alpha]_{546}^{20} = +9.2°$ in water). IR spectroscopy (amide I: 1660 cm^{-1}; amide II: 1525 cm^{-1}; NH: 3300 cm^{-1}; COOH: 1720 cm^{-1}), NMR spectroscopy and elemental analysis. (Found: C, 47.3; H, 8.3; N, 11.0; Cl, 14.2. Calc. for $C_{10}H_{20}N_2O_3$, HCl: C, 47.5; H, 8.3; N, 11.1; Cl, 14.1%.)

Poly(*N*-methacryloyl-L-lysine) (PNML) was prepared by free radical polymerization of *N*-methacryloyl-L-lysine and purified according to a procedure described elsewhere.[4]

Measurements and calculations

The potentiometric data (added volume of sodium hydroxide, pH of the solution) were collected using the automated titration system described elsewhere.[7] Added volumes and pH were measured to a precision of 10^{-4} cm^3 and 10^{-3} pH unit respectively. The studies were carried out at 25.0°C in a 0.10 mol dm^{-3} sodium perchlorate medium and under purified nitrogen. The glass electrode was standardized in the concentration scale with perchloric acid in the presence of 0.10 mol dm^{-3} sodium perchlorate.

Titrations of perchloric acid (2×10^{-3} mol dm^{-3}) with sodium hydroxide (0.25 mol dm^{-3}) were periodically performed in order to check—by using the MUPROT program—the parameters of the measuring cell (zero shift, sensitivity), the ionic product of water as well as the characteristic figures of the titrant (total concentration of the sodium ion and of the carbonate). The carbon dioxide evolution coefficient was fixed at 3×10^{-4}, the liquid junction coefficients remaining always negligible.

Protonation constants for the free ligands were obtained from titrations of the ligands (2×10^{-3} mol dm^{-3}) in the presence of perchloric acid.

The stability constants for the metal complexes were computed from titrations in which the metal: ligand: perchloric acid ratios were 1:1:1, 0.5:1:1, 0.2:1:1, for NIBL and lysine and 0.05:1:1, 0.06:1:1, 0.1:1:1 and 0.2:1:1 for PNML.

The titrations were discontinued when precipitation took place, i.e. when the pH readings became unstable, rejection of such points being also possible during the refinement process on the basis of anomalous residuals. Thus the following maximum pH ranges were used for calculations with Cu(II), Ni(II), Co(II) and Zn(II), respectively: 2.79–10.93; 2.81–10.86; 2.81–9.73; 2.80–11.10. For NIBL and lysine, the data were processed as in earlier studies by use of the MUPROT and MUCOMP multiparametric refinement programs.[7,8] As hydrolysis constants for the metal, the following values were introduced: $Cu_2(OH)_2^{2+}$, $\log \beta_{qj0} = -10.7$; $CoOH^+$: −9.8; $NiOH^+$: −9.3; $ZnOH^+$: −9.8.[9,10]

Besides the stability constants, other parameters such as the total concentration of the ligand, the excess of the strong acid, were simultaneously refined in order to compensate systematic errors. That possibility was evidently used with great care.

RESULTS AND DISCUSSION

The protonation constants of the ligand NIBL are first compared with those of lysine and glycine (Table 1) ($t = 25°C$ and $I = 0.1$ mol dm^{-3} $NaClO_4$).

Table 1. Protonation constants of lysine, NIBL and glycine at 25°C and $I = 0.1$ mol dm^{-3}. Standard deviation (1σ values) are given in parentheses

	Lysine	NIBL	Glycine
$\log K_1$	10.67[a]	9.42(1)[a]	9.56[e]
$(A + H \rightarrow HA)$	10.72[b]		9.68[f]
	10.66[c]		9.45[g]
	10.65(1)[d]		
$\log K_2$	9.14[a]	2.40(1)[d]	2.39[e]
$(HA + H \rightarrow H_2A)$	9.18[b]		2.33[f]
	9.20[c]		2.65[g]
	9.14(1)[d]		
$\log K_3$	2.20[a]		
$(H_2A + H \rightarrow H_3A)$	2.18[b]		
	2.15[c]		
	2.18(1)[d]		

[a] 0.1 mol dm^{-3} KNO_3, Ref. 11.
[b] Ref. 12.
[c] 0.2 mol dm^{-3} KCl, Ref. 13.
[d] 0.1 mol dm^{-3} $NaClO_4$, this work.
[e] 0.1 mol dm^{-3} $NaClO_4$, Ref. 14.
[f] 0.1 mol dm^{-3} $NaClO_4$, Ref. 15.
[g] 0.15 mol dm^{-3} $NaClO_4$, $t = 37°C$, Ref. 16.

Our values for the protonation constants of lysine in 0.1 mol dm^{-3} $NaClO_4$ are in very good agreement with those previously reported by Brookes and Pettit in 0.1 mol dm^{-3} KNO_3.[11] For NIBL, the protonation constants are much closer to those of glycine than those of lysine. This is due to the absence of the ε-amino group which, in lysine, competes with the α-amino group for the uptake of a proton. At 25°C, the pK of the α-amino group in NIBL is significantly lower than in glycine. This may be due to the presence of an amide group in the molecule, which is known to have an acidifying influence.[17]

Titrations in the presence of metal ion were carried out with [ligand]/[metal] molar ratios ranging from $R = 1$–5.

Figure 1 shows typical titration curves of NIBL in the absence of metal and with Cu(II), Ni(II), Zn(II) and Co(II). The lowering of the pH decreases from copper to cobalt indicating decreasing stability constants for the complexes. The stability constants values are reported in Table 2 as overall formation constants $\beta_{qjp} = [M_qH_jA_p]/[M]^q[H]^j[A]^p$, together with values for lysine and glycine. Various models were fitted to the data and the models selected and reported in Table 2 were those giving for each ligand–metal system, the best statistical fit, consistent with chemical logic.

For lysine, our results for copper, nickel and cobalt are in reasonable agreement with those of Refs 11 and 13 taking into account the difference in the nature of the medium.

Nevertheless the $CuHA_2$ complex was found to be about one log unit more stable in 0.1 mol dm^{-3} $NaClO_4$ than in other media.

With nickel, the MH_2A_3 and MA complexes which were assumed by Brookes and Pettit[11] were not found to improve the refinement of the data.

For the lysine–cobalt system, the MH_2A_3 complex which was tentatively assumed in Ref. 11 was rejected in the calculation.

Table 2 also gives values for the lysine–zinc system for which the MHA, MH_2A_2, MHA_2 and MA_2 complexes were found with stability constants intermediate between those of the nickel and cobalt complexes. The ornithine–zinc parent system was recently investigated by Nair *et al.*[20] who found the following set of complexes: MHA, MA and MH_2A_2. Similar differences between the sets of complexes were found for the copper complexes of ornithine and lysine[11] and are related to the lower values of the protonation constants of ornithine compared to lysine.[11]

For NIBL, the titration data were conveniently explained with only two complexes, namely MA and MA_2, for the four metal ions under study. The stability constants decrease from glycine to lysine and NIBL especially for the nickel and cobalt complexes. This is undoubtedly an effect of steric hindrance due to the additional $COCH(CH_3)_2$ group in NIBL compared to lysine.

The stepwise formation constant ($\log K^{A}_{102}$) for the addition of the second ligand:

$$MA + A \rightarrow MA_2 \qquad (1)$$

is given by:

$$\log K^{A}_{102} = \log \beta_{102} - \log \beta_{101}. \qquad (2)$$

The values are 6.80, 4.29, 3.12 and 3.40 for copper, nickel, cobalt and zinc, respectively. They are always lower than the corresponding $\log \beta_{101}$

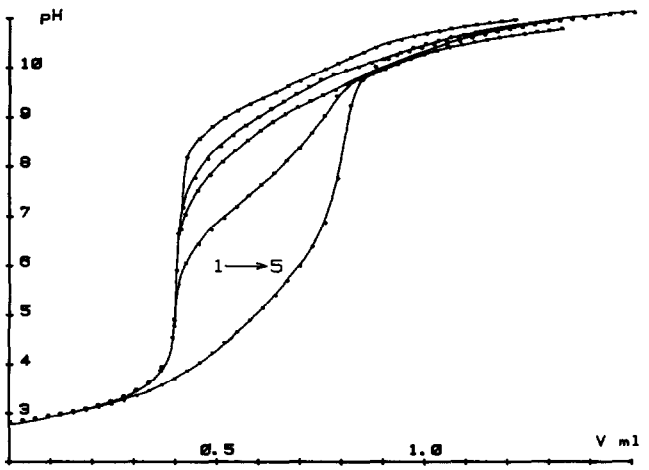

Fig. 1. Titration curves of NIBL and NIBL–metal mixtures in 0.1 mol dm^{-3} $NaClO_4$, 25°C: 1, NIBL; 2, NIBL–Co, $R = 5$; 3, NIBL–Zn, $R = 5$; 4, NIBL–Ni, $R = 2$; 5, NIBL–Cu, $R = 2$.

Table 2. Formation constants for the complexes of lysine, NIBL and glycine at 25°C and $I = 0.1$ mol dm^{-3}. Standard deviations (1σ values) are given in parentheses

		Lysine			NIBL		
		Ref. 11	Ref. 13	This work	This work		
$\log \beta_{qjp}$		in KNO_3	in KCl	in $NaClO_4$	in $NaClO_4$	Glycine	
Cu^{2+}	111	18.29	18.33	18.33(2)			
	122	35.45	35.40	35.58(2)			
	112	25.52	25.32	26.23(2)			
	101	—	—	—	8.00(1)	8.22[a]	8.27[b]
	102	15.05	14.81	14.83(2)	14.80(1)	15.02[a]	15.19[b]
Ni^{2+}	111	15.60		15.60(2)			
	122	30.49		30.47(2)			
	133	44.05		43.95(2)			
	123	34.26		—			
	112	20.43		20.68(5)			
	101	5.75		—	5.21(3)	5.83[c]	5.79[d]
	102	10.34		9.96(2)	9.50(2)	10.74[c]	10.57[d]
	103	—		—	—	~ 14[c]	
Co^{2+}	111	14.50		14.53(2)			
	122	28.41		28.38(2)			
	133	41.45		40.84(5)			
	123	31.6?		—			
	112	18.50		19.08(4)			
	101	—		—	4.26(3)	4.63[c]	
	102	8.46		8.45(5)	7.38(3)	8.50[c]	
	113	—		—	—	—	
Zn^{2+}	111			14.80(2)			
	122			29.29(2)			
	112			20.22(3)			
	101			—	4.89(5)	4.96[c]	
	102			9.02(5)	8.29(5)	9.19[c]	

[a] Ref. 14, 0.1 mol dm^{-3} $NaClO_4$.
[b] Ref. 15, 0.1 mol dm^{-3} $NaClO_4$.
[c] Ref. 18, 0.1 mol dm^{-3} $NaClO_4$.
[d] Ref. 19, 0.1 mol dm^{-3} KNO_3.

values, which means that the coordination of the second ligand to the metal is more difficult than the binding of the first one.

Both the cumulative and stepwise formation constants are in accordance with the Irving–Williams series: Co < Ni < Cu > Zn.[21]

From the comparison between NIBL and glycine, it is clear that the complexes formed by NIBL with metal ions are five-membered ring chelates made up of the amino acid extremity. These glycine-like chelates with N, O donor atoms were confirmed by a spectroscopic study using electronic spectroscopy, circular dichroïsm and electron paramagnetic resonance.[4]

Characteristic ratios may be used to compare the affinity of the ligand A for the metal and the proton:[22] $\log \beta_{101}/\log \beta_{011}$ (Table 3).

Values for NIBL and glycine are very close which confirms that the mode of bonding is similar.

The possible role played by the amide group of NIBL has not yet been discussed. In similar molecules such as dipeptides, which also contain an amino and a peptide group, the CuA complex which first appears is a five-membered chelate involving the terminal NH_2 group and the carbonyl of the amide group. In Gly–gly, for example, the complex has a $\log \beta$ value equal to 5.60.[23–25] In NIBL, a similar complex involving the carbonyl group would be a ten membered chelate ring, much less stable and thus with a $\log \beta$ value much lower than 5.6, which is not the case ($\log \beta = 8.00$). In addition, the second step in the case of Gly–gly, is the deprotonation of the amide group with formation of a $CuH_{-1}A$ complex ($\log \beta = 1.50$[20–22]) which has not

Table 3. Characteristic ratios for complexation and acidity constants

Metal	$\log \beta_{101}/\log \beta_{011}$ NIBL	Glycine[a]	$\log K^{A}_{102}/\log \beta_{101}$ NIBL	Glycine[a]
Cu	0.85	0.86	0.85	0.84
Ni	0.55	0.61	0.82	0.84
Co	0.45	0.48	0.73	0.73
Zn	0.52	—	0.70	—

[a] From Refs 15 and 18.

been evidenced for NIBL. In this case, the five-membered chelate ring between the α-amino and carboxyl groups is largely favoured. Nevertheless, the following relationship:

$$\log \beta_{101} = 2 \log \beta_{010} - 10.7$$

which was established for a number of peptides with a glycine in the N terminal position,[26,27] holds for the CuA complex of NIBL. This indicates that the stability of this complex depends mostly on the basicity of the amino groups as for peptides.

Figure 2 shows the titration curves of the polymeric analog of NIBL, PNML, in the presence of copper.

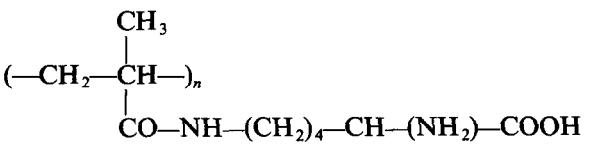

[Ligand]/[metal] ratios ranging from 5 to 20 were used in this case because precipitation of the complexes readily occurred at lower values. With $R = 5$, only the 18 first points of the titration curve were used for calculation. For the same reason, titration curves of PNML in the presence of nickel could not be processed.

Figure 2 shows a large decrease of the pH in the presence of copper, indicating strong complex formation.

In a first step, an attempt was made to calculate the acidity constants of the amino and carboxyl groups of PNML, considered as a simple ligand, and using the concentration C of the repeat unit, whose value was kept constant in the refinement process. In this case the agreement between the calculated curve and the experimental data was rather bad, especially in the high pH range. As said in the introduction, this is due to strong electrostatic interactions between charges of the same sign beared by the polymer chain, with the consequence that pK values are not unique as for the model molecule NIBL.

Thus, in a second step, PNML was considered as a ligand made up of two repeat units, each one being characterized by a different set of two pK values. In that case a fixed concentration $C/2$ was used to take into account the "dimeric" nature of the ligand. Then a satisfactory agreement was found between experimental and calculated data, showing that the polyelectrolyte effect may be well represented, for PNML, by the use of only four acidity constants. The following pK values were found: $pK_1 = 9.47$ and $pK_2 = 10.95$ for the amino groups. For NIBL, $pK = 9.42$ which is very close to pK_1. The somewhat higher value for pK_2 reflects the electrostatic interactions. For the carboxyl groups $pK_3 = 2.88$ ($pK = 2.40$ for NIBL). The pK_4 value is too low to be conveniently refined

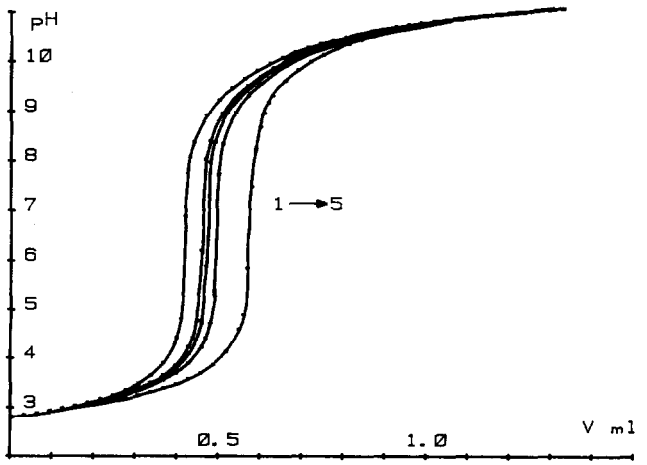

Fig. 2. Titration curves of PNML and PNML–Cu mixtures: 1, PNML; 2, PNML–Cu, $R = 20$; 3, PNML–Cu, $R = 15$; 4, PNML–Cu, $R = 10$; 5, PNML–Cu, $R = 5$.

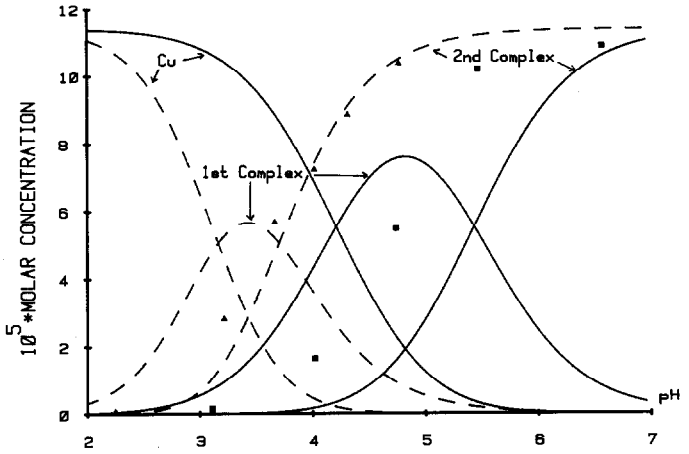

Fig. 3. Species distribution curves for NIBL–Cu and PNML–Cu mixtures, $R = 15$. Full line: NIBL; dotted line PNML. Points are concentration values calculated from circular dichroïsm measurements[4] for the second complex: (■) NIBL; (▲) PNML.

($pK_4 < -\log C/2$). We can consider that this carboxyl group is fully ionized in this concentration range. Thus only three acidity constants are necessary to simulate the titration behaviour of PNML.

This result is not surprising. In fact, this means that, for a given function of repeat unit, the successive elementary deprotonations are controlled only by statistical factors and are equally distributed around the given p*K*s.[28]

In the next step were calculated the formation constants of the PNML–Cu complexes using the MUCOMP program. Two $MA_{0.5}$ and MA complexes (which are the analogs of the MA and MA_2 complexes of NIBL) were found with formation constants equal to 8.68(4) and 16.77(3), respectively.

Using the formation constants of the PNML–Cu and NIBL–Cu complexes, the distribution curves of the species as a function of pH were plotted with the aid of the COMSOL program (Fig. 3). With PNML the first complex is formed at a pH lower than with NIBL and to a lower extent. The second complex forms about 1.5 pH units earlier with PNML than with NIBL. As shown in a previous work[4] this results from the accumulation of the complexing sites along the polymer chain which affects the entropy change of the complexation. The distribution curves obtained from potentiometry (Fig. 3) are in rather good agreement with data obtained from circular dichroïsm measurements[4] (especially for the second complex) if it is considered that the two approaches of the complex formation are very different.

The agreement is fairly good at high pH, i.e. in the domain of formation of the second complex. This suggests that the discrepancy observed at lower pH could result from the contribution of the first complex to the circular dichroïsm.

To our knowledge, this work is the first report on the determination of polyelectrolyte–metal complex formation constants using multiparametric refinement programs. Work is now in progress to extend this approach to other kinds of polyelectrolytes.

Acknowledgement—The authors are greatly indebted to Mrs Anne-Marie Caze for her skilful technical assistance.

REFERENCES

1. C. Methenitis, J. Morcellet-Sauvage and M. Morcellet, *Polym. Bulletin* 1984, **12**, 133.
2. C. Methenitis, J. Morcellet-Sauvage and M. Morcellet, *Polym. Bulletin* 1984, **12**, 141.
3. C. Methenitis, Thesis, Lille (1985).
4. A. Castellano, A. Lekchiri, J. Morcellet and M. Morcellet, submitted to *J. Polym. Sci.*
5. A. Lekchiri, Thesis, Lille (1985).
6. R. Barbucci, M. Casolaro, M. Nocentini, S. Correzi, P. Ferruti and V. Barone, *Macromol.* 1986, **19**, 37.
7. G. Nowogrocki, J. Canonne and M. Wozniak, *Anal. Chim. Acta* 1979, **112**, 185.
8. M. Wozniak and G. Nowogrocki, *J. Chem. Soc., Dalton Trans.* 1981, 2423.
9. K. B. Yatsimirskii and V. P. Vasil'ev, In *Instability Constants of Complex Compounds.* Van Nostrand, Princetown (1960).
10. M. Wozniak, Thesis, Lille (1977).
11. G. Brookes and L. D. Pettit, *J. Chem. Soc., Dalton Trans.* 1976, 42.
12. A. Albert, *Biochem. J.* 1952, **50**, 690.
13. A. Gergely, E. Farkas, I. Nagypal and E. Kas, *J. Inorg. Nucl. Chem.* 1978, **40**, 1709.

14. T. P. I and G. H. Nancollas, *Inorg. Chem.* 1972, **11**, 2414.
15. R. Griesser and H. Sigel, *Inorg. Chem.* 1970, **9**, 1238.
16. M. S. Nair and M. Santappa, *J. Chem. Soc., Dalton Trans.* 1981, 992.
17. J. P. Greenstein and M. Winitz, *Chemistry of the Amino Acids*, Vol. 1, p. 499. Wiley, New York (1961).
18. R. Griesser and H. Sigel, *Inorg. Chem.* 1971, **10**, 2229.
19. M. C. Lim and G. H. Nancollas, *Inorg. Chem.* 1971, **10**, 1957.
20. M. S. Nair, M. S. Pillai and S. K. Ramalingam, *J. Chem. Soc., Dalton Trans.* 1986, 1.
21. H. Irving and R. J. P. Williams, *J. Chem. Soc.* 1953, 3192.
22. H. Irving, R. J. P. Williams, D. J. Ferrett and A. E. Williams, *J. Chem. Soc.* 1954, 3494.
23. A. P. Brunetti, M. C. Lim and G. H. Nancollas, *J. Am. Chem. Soc.* 1968, **90**, 5120.
24. H. Sigel, R. Griesser and B. Prijs, *Z. Naturforsch. B* 1972, **27**, 353.
25. H. Sigel and R. B. Martin, *Chem. Rev.* 1982, **82**, 385.
26. H. Sigel, *Inorg. Chem.* 1971, **10**, 1957.
27. H. Sigel, C. F. Naumann, B. Prijs, D. B. McCormick and M. C. Falk, *Inorg. Chem.* 1977, **16**, 790.
28. J. J. Kankare, *Talanta* 1975, **22**, 1005.

Polyhedron Vol. 6, No. 3, pp. 641–643, 1987
Printed in Great Britain

0277-5387/87 $3.00+.00

COMMUNICATION

A KINETIC STUDY OF THE OXIDATION OF HYDROXYLAMINE BY OCTACYANOTUNGSTATE(V)

ABRAHAM J. VAN WYK,* C. ROBERT DENNIS,† JOHANN G. LEIPOLDT and STEPHEN S. BASSON

Chemistry Department, University of the Orange Free State, Bloemfontein 9300, Republic of South Africa

(*Received* 28 *July* 1986; *accepted* 4 *September* 1986)

Abstract—The kinetics of the oxidation of hydroxylamine by octacyanotungstate(V) ions has been studied over a wide pH range. The reaction is first-order in both oxidant and reductant. The kinetically determined dissociation constants, $K_{a1} = 2.5 \pm 0.5 \times 10^{-6}$ M and $K_{a2} = 3.2 \pm 8.0 \times 10^{-14}$ M, are in agreement with values obtained from the literature.

The reaction of hydroxylamine with a variety of oxidizing agents has been studied.[1] Various oxidation products, i.e. NH_3, $H_2N_2O_2$, N_2 and N_2O, have been reported. These studies were performed in acidic solution (pH 5.6 to 2.5 M H^+) and the reactions were first-order in both oxidant and hydroxylamine.

Autoxidation of hydroxylamine in alkaline solutions was studied by Hughes and co-workers.[2] A deprotonated hydroxylamine species (NH_2O^-) and its acid dissociation constant were reported. Peroxonitrite (ONO_2^-) was formed as an oxidation product, but rapid oxidation with a further hydroxylamine ion yielded nitrite and nitroxyl (NO^-) ions.

The oxidation of hydroxylamine[3] by $Fe(CN)_6^{3-}$ in a weak acidic medium proceeds via an intermediate radical, NH_2O, which is formed by oxidation of NH_2OH. N_2 was detected as the main reaction product. The observed hydrogen ion effect was attributed to acid dissociation of the protonated hydroxylamine species, NH_3OH^+.

The oxidation of hydroxylamine by $W(CN)_8^{3-}$ was performed as part of a research project on the redox properties of the cyano complexes of Mo, W and Fe. Although the oxidation of hydroxylamine in acidic solution is well-studied, very little is known about the reaction in alkaline medium. For this reason the present study was performed over a wide pH range to include results of the alkaline oxidation of hydroxylamine.

EXPERIMENTAL

$Cs_3W(CN)_8 \cdot 2H_2O$ was prepared as described by Leipoldt *et al.*,[4,5] and was used as a primary standard[6] after recrystallization. Hydroxylammonium chloride (Merck *pro analisi*) was used as source of hydroxylamine. The hydroxylammonium chloride solution was neutralized with sodium hydroxide. This solution was renewed daily. All other reagents used were analytical-grade and redistilled water was used throughout.

Kinetic measurements were made in both alkaline and acidic media using Britton–Robinson[7] buffer mixtures or sodium hydroxide solutions at a constant ionic strength. Rate data were obtained by monitoring the decrease in $[W(CN)_8^{3-}]$ on a Durrum D-110 spectrophotometer (faster runs) and a Pye–Unicam SP 1700 spectrophotometer (slower runs) at 357 nm.

Experiments to identify reaction products at pH ~ 6 and $[OH^-] \sim 0.05$ M were carried out by comparing the normal O_2:N_2 ratio of the atmosphere directly above a hydroxylamine solution with the atmosphere resulting from a reaction mixture in a stoppered flask, on a Packard model

*Present address: Research and Process Development, Iscor, Pretoria 0001, Republic of South Africa.

† Author to whom correspondence should be addressed.

Table 1. Observed rate constants for the oxidation of hydroxylamine by $W(CN)_8^{3-}$: $T = 25°C$, $\mu = 0.1$ M

$10^4[W(CN)_8^{3-}]$ (M)	$10^2[NH_2OH]$ (M)	$10^4[W(CN)_8^{3-}]$ (M)	$[OH^-]$ (M)	pH	k_{obsd} (s^{-1})
5.0	0.50			4.73	2.6×10^{-3}
3.0	0.50			4.73	2.6×10^{-3}
2.0	0.50			4.73	2.4×10^{-3}
5.0	0.50	2.0		4.73	2.0×10^{-3}
5.0	0.50	3.0		4.73	1.8×10^{-3}
5.0	0.50	5.0		4.73	1.4×10^{-3}
5.0	1.0			4.73	5.1×10^{-3}
5.0	0.80			4.73	3.9×10^{-3}
5.0	0.50			4.73	2.4×10^{-3}
5.0	0.40			4.73	2.1×10^{-3}
5.0	1.5		0.045		101
3.0	1.5		0.045		99
2.0	1.5		0.045		99
5.0	1.5	2.0	0.045		100
5.0	1.5	3.0	0.045		103
5.0	1.5	5.0	0.045		101
5.0	1.5		0.045		100
5.0	1.2		0.045		82
5.0	0.75		0.045		50
5.0	0.60		0.045		39

472 gas chromatograph. A significant increase in N_2 was detected. Calculations proved that this increase was equal to the stoichiometric amount of N_2 generated by the reaction between $W(CN)_8^{3-}$ and hydroxylamine.

RESULTS AND DISCUSSION

Pseudo-first-order plots of log $[W(CN)_8^{3-}]$ vs time were linear for at least two half-lives. Results in Table 1 show that the reaction is first-order in both oxidant and reductant in a weakly acidic as well as in an alkaline medium. Adding $W(CN)_8^{4-}$ to the reaction mixture caused a decrease in the reaction rate in the acidic medium, but no significant effect was observed in the alkaline medium. This result is indicative of an equilibrium in the reaction pathway in an acidic medium.

Kinetic measurements over a wide pH range (Fig. 1) show the pH dependence of the reaction. These results clearly show two dissociation constants which indicates that three hydroxylamine species are present over the observed pH range. The equilibria [eqns (1) and (2)]

$$NH_3OH^+ \overset{K_{a1}}{\rightleftharpoons} NH_2OH + H^+, \quad (1)$$

$$NH_2OH \overset{K_{a2}}{\rightleftharpoons} NH_2O^- + H^+ \quad (2)$$

are thus operative and the relative reactivities of the

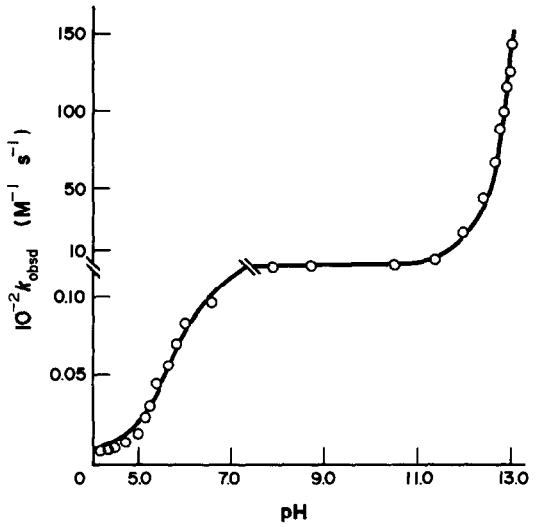

Fig. 1. pH dependence of the oxidation of hydroxylamine by $W(CN)_8^{3-}$: $[W(CN)_8^{3-}] = 5 \times 10^{-4}$ M, $[NH_2OH] = 5 \times 10^{-3}$ M, $\mu = 0.1$ M (NaCl), $T = 25°C$. The solid curve is the computer fit.

species are in the order $NH_3OH^+ < NH_2OH \ll NH_2O^-$.

The product study has shown N_2 to be a reaction product. From this and the observed kinetic results, a reaction mechanism (Scheme 1) is proposed. The oxidation of hydroxylamine in acidic medium proceeds via the $NH_2O^{\cdot}$ radical, which decomposes to N_2 and H_2O. The $NH_2O^{\cdot}$ radical was reported earlier by Gutch and Waters.[8]

$$
\begin{array}{lcl}
NH_3OH^+ + W(CN)_8^{3-} & \underset{k_{-1}}{\overset{k_1}{\rightleftharpoons}} & W(CN)_8^{4-} + NH_2O^{\cdot} + 2H^+ \\
\Big\| K_{a1} & & \\
NH_2OH + W(CN)_8^{3-} & \underset{k_{-2}}{\overset{k_2}{\rightleftharpoons}} & W(CN)_8^{4-} + NH_2O^{\cdot} + H^+ \\
\Big\| K_{a2} & & \\
NH_2O^- + W(CN)_8^{3-} & \xrightarrow{k_3} & W(CN)_8^{4-} + \tfrac{1}{2}N_2 + H_2O
\end{array}
$$

Scheme 1.

From the reaction mechanism, the following rate law is obtained:

$$\frac{-d[W(CN)_8^{3-}]}{dt} = \frac{k_1[H^+]^2 + k_2K_{a1}[H^+] + k_3K_{a1}K_{a2}}{[H^+]^2 + K_{a1}[H^+] + K_{a1}K_{a2}} [W(CN)_8^{3-}][NH_3OH^+]_T. \quad (3)$$

A non-linear least-squares fit of the data in Fig. 1 to the rate law (3) yielded $k_1 = 2 \pm 1 \times 10^{-2}\,M^{-1}s^{-1}$, $k_2 = 12 \pm 4\,M^{-1}s^{-1}$, $k_3 = 8 \pm 2 \times 10^4\,M^{-1}s^{-1}$, $K_{a1} = 2.5 \pm 0.5 \times 10^{-6}$ M ($pK_a = 5.6$), and $K_{a2} = 3.2 \pm 0.8 \times 10^{-14}$ M ($pK_{a2} = 13.5$) under the approximation that $[H^+] = 10^{-pH}$. The obtained pK_a values are in very good agreement with literature values, i.e. $pK_{a1} = 5.82$[9] and $pK_{a2} = 13.7$.[2]

Acknowledgements—We are grateful to the South African C.S.I.R. and the research fund of this university for financial assistance.

REFERENCES

1. W. C. Bray, M. E. Simpson and A. A. Mackenzie, *J. Am. Chem. Soc.* 1919, **41**, 1363; A. Kurtenacker and R. Neusser, *Z. Anorg. Chem.* 1923, **131**, 27; T. H. James, *J. Am. Chem. Soc.* 1939, **61**, 2379; 1940, **62**, 536; 1942, **64**, 731; J. H. Anderson, *Analyst* 1964, **89**, 357; 1966, **91**, 532; W. A. Walters and I. R. Wilson, *J. Chem. Soc. A* 1966, 534; B. J. Thakuria and Y. K. Gupta, *J. Chem. Soc., Dalton Trans.* 1975, 77; G. Bengtsson, *Acta Chem. Scand.* 1973, **27**, 1717, 3053; G. S. Barney, *J. Inorg. Nucl. Chem.* 1976, **38**, 1677; G. J. Bridgart, W. A. Waters and I. R. Wilson, *J. Chem. Soc., Dalton Trans.* 1973, 1582; R. Tomat and A. Rigo, *J. Inorg. Nucl. Chem.* 1974, **36**, 611; N. Rajasekar, R. Subramaniam and E. S. Gould, *Inorg. Chem.* 1983, **22**, 971.
2. M. N. Hughes and H. G. Nicklin, *J. Chem. Soc. A* 1971, 164; M. N. Hughes, H. G. Nicklin and K. Shrimanker, *J. Chem. Soc. A* 1971, 3485.
3. V. K. Jindal, M. C. Agrawal and S. P. Mushran, *J. Chem. Soc. A* 1970, 2060.
4. J. G. Leipoldt, L. D. C. Bok and P. J. Cilliers, *Z. Anorg. Allg. Chem.* 1974, **407**, 350.
5. L. D. C. Bok, J. G. Leipoldt and S. S. Basson, *Z. Anorg. Allg. Chem.* 1975, **415**, 81.
6. S. S. Basson, L. D. C. Bok and S. R. Grobler, *Z. Anal. Chem.* 1974, **268**, 287.
7. D. Dobos, *Electrochemical Data*, Chap. 4, p. 239. Elsevier, New York (1975).
8. C. J. W. Gutch and W. A. Waters, *J. Chem. Soc.* 1965, 751.
9. A. I. Vogel, *A Textbook of Quantitative Inorganic Analysis*, 3rd Edn, p. 1168. Longmans, London (1961).

Polyhedron Vol. 6, No. 3, pp. 645–646, 1987
Printed in Great Britain

0277–5387/87 $3.00+.00

COMMUNICATION

REACTIONS OF M–M BONDED DINUCLEAR ZIRCONIUM(III) COMPLEXES WITH VICINAL DIHALOALKANES AND OLEFINS: A NEW TYPE OF METAL–OLEFIN COMPLEX

F. ALBERT COTTON* and PIOTR A. KIBALA

Department of Chemistry and Laboratory for Molecular Structure and Bonding, Texas A&M University, College Station, TX 77843, U.S.A.

(*Received* 28 *August* 1986; *accepted* 16 *September* 1986)

Abstract—The reaction of $Zr_2X_6(PR_3)_4$ compounds with *vic*-dihalides or with olefins gives $Zr_2X_6(PR_3)_4(C_2R_4)$ compounds in which the mid-point of the olefin lies between the two Zr atoms, providing an unprecedented type of metal–olefin complex.

Dinuclear complexes of types **I** and **II** in which there are usually metal–metal bonds[1] are numerous and have been studied from many points of view. Those of type **I** formed by niobium(III) and tantalum(III), which contain M=M double bonds have proved to be extremely useful starting materials for synthesizing a variety of compounds of these elements.[2] We are conducting studies to extend the applicability of this approach to other elements, especially by oxidative addition reactions. We report here some results with zirconium(III) compounds of type **II** that contain Zr—Zr single bonds wherein they readily undergo clean and unusual reactions with vicinal dihaloalkanes and olefins.

Our first observations were unplanned. When attempting to employ 1,2-$C_2H_4Cl_2$ as a solvent for the bromo analog of $Zr_2Cl_6(PEt_3)_4$,[3] we noted that the solution spontaneously and rapidly changed color from green to orange. A red crystalline product (**1**) was isolated from the reaction mixture. $Zr_2Cl_6(PEt_3)_4$ undergoes a similar reaction with $ClCH_2CH_2Cl$ to produce yellow solutions from which an orange crystalline product (**2**) could be isolated. Both compounds were characterized crystallographically† and were shown to be of the general type $Zr_2X_6(PR_3)_4(CH_2CH_2)$, where X = Cl or Br, and R = Et. The characteristic feature of both molecules is an ethylene bridge perpendicular to the Zr–Zr axis. Figure 1 shows an ORTEP drawing of a $Zr_2X_6P_4(CH_2CH_2)$ fragment and Table 1 lists selected bond distances and angles for $Zr_2Cl_6(PEt_3)_4(CH_2CH_2)$ (**1**) and $Zr_2Br_6(PEt_3)_4(CH_2CH_2)$ (**2**).

With the above results in hand we naturally wondered if $Zr_2X_6(PR_3)_4$ species would react directly with olefins to yield compounds **1** and **2** and similar ones. On reexamining Ref. 3, we found that reactions of ethylene and propene with $Zr_2Cl_6(PEt_3)_4$ had already been reported; however, no crystallographic work had been done and structures with Zr—C σ-bonds were proposed.‡ We have been able to obtain the compound formulated

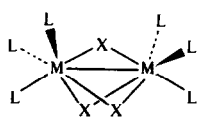

I

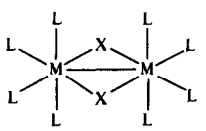

II

*Author to whom correspondence should be addressed.

†Atomic positional and thermal parameters have been deposited with the Editor, from whom copies are available on request. Atomic coordinates have also been sent to the Cambridge Crystallographic Data Centre.

‡This proposal of a σ-bonded structure seemed to be inspired by a previous report concerning $(Cp_2ZrX)_2C_2H_4$ compounds[4] in which a very rough structure determination was used as the basis for suggesting the existence of two Zr—C σ-bonds.

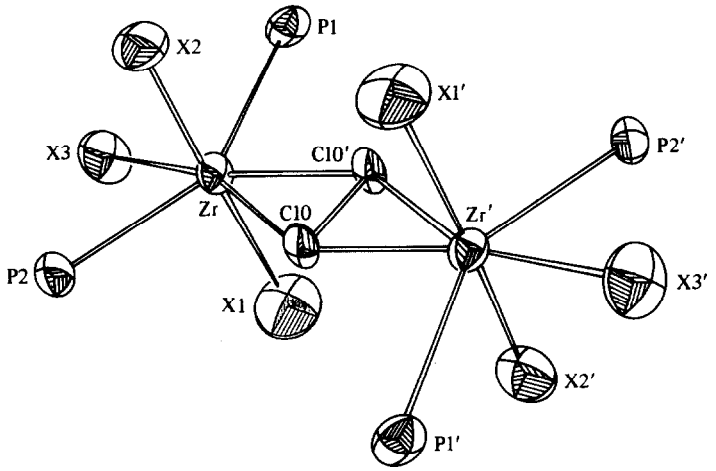

Fig. 1. ORTEP drawing of $[ZrX_3(PR_3)_2]_2(CH_2CH_2)$ molecule with the atom-labelling scheme. The carbon atoms of the PR_3 ligands are removed for clarity. Atoms are represented by their ellipsoids at the 50% probability level.

Table 1. Selected bond distances (Å) and angles (°) for $Zr_2Cl_6(PEt_3)_4(CH_2CH_2)$ and $Zr_2Br_6(PEt_3)_4(CH_2CH_2)$*

	X = Cl	X = Br
Zr—C(10)	2.422(15)	2.41(2)
	2.44(2)	2.40(2)
C(10)—C(10)	1.69(3)	1.56(4)
Zr—X_{axial}	2.472(5)	2.629(3)
Zr—X_{trans}	2.428(5)	2.597(3)
	2.430(5)	2.593(3)
Zr—P_{trans}	2.780(5)	2.798(6)
	2.793(6)	2.785(6)
C(10)—Zr—C(10)'	40.6(7)	37.9(8)
Cl_{trans}—Zr—Cl_{trans}	174.8(2)	172.0(1)
P_{trans}–Zr–P_{trans}	153.0(2)	150.0(2)

*Numbers in parentheses are estimated standard deviations in the least significant digits.

in Ref. 3 as $(Et_3P)_2Cl_3ZrCH_2CH_2Zr(PEt)_2Cl_3$ in crystalline form and we find that it is identical to our compound **2**.

The reaction of $Zr_2X_6(PR_3)_4$ compounds with 1,2-$C_2H_4Cl_2$ (and other vicinal dihalides) is now under detailed study. Evidence now available suggests that two molecules of $Zr_2X_6(PR_3)_4$ react with 1,2-$C_2R_4X'_2$ to produce $[ZrX_3(PR_3)_2]_2$ $C_2R_4 + 2ZrX_3X'(PR_3)_2$.

Molecular-orbital (MO) calculations by the Fenske–Hall method[5] have been carried out to elucidate the bonding in the M_2-(μ_2-η^4-olefin) unit. To our knowledge this type of metal–olefin interaction has not previously been recognized to exist and has not, therefore, been considered from a theoretical point of view. If the molecule is considered to be assembled from two $ZrX_3(PR_3)_2$ units and the $H_2C{=}CH_2$ molecule, we can envision that two major contributions to the bonding will arise. The π-orbital of C_2H_4 and its pair of electrons can interact with a pair of σ-type orbitals on the two Zr atoms. The calculations show that this contribution is spread over a number of b_{1u} MOs rather than being clearly identifiable in any one. Overlap between suitable $d\pi$ orbitals (or $d\pi$–$p\pi$ hybrids) on the metal atoms with the π^*-orbital of C_2H_4, and the population of the resulting b_{2g} bonding orbital by two electrons [nominally the unpaired electrons on the $ZrX_3(PR_3)_2$ fragments] should provide a second important contribution. The calculation shows that this contribution can be clearly identified as the HOMO. Since the calculation shows a very large HOMO to LUMO gap, we are inclined to believe that analogs to these molecules in which there are more electrons may not be obtainable.

Acknowledgements—We thank the Robert A. Welch Foundation (Grant No. A-494) and the National Science Foundation for support.

REFERENCES

1. (a) A. R. Chakravarty, F. A. Cotton, M. P. Diebold, D. B. Lewis and W. J. Roth, *J. Am. Chem. Soc.* 1986, **108**, 971; (b) F. A. Cotton, *Polyhedron* (in press).
2. F. A. Cotton, S. A. Duraj and W. J. Roth, *J. Am. Chem. Soc.* 1984, **106**, 4749.
3. J. H. Wengrovius, R. R. Schrock and C. S. Day, *Inorg. Chem.* 1981, **20**, 1844.
4. (a) H. Sinn and E. Kolk, *J. Organomet. Chem.* 1966, **6**, 373; (b) W. Kaminsky, J. Kopf, H. Sinn and H.-J. Vollmer, *Angew. Chem., Int. Ed. Engl.* 1976, **15**, 629.
5. M. B. Hall and R. F. Fenske, *Inorg. Chem.* 1972, **11**, 768.

Polyhedron Vol. 6, No. 3, pp. 647–649, 1987
Printed in Great Britain

0277–5387/87 $3.00+.00

COMMUNICATION

SYNERGISTIC EFFECTS IN EXTRACTION SUBSTRATES—AN APPLICATION OF THE CONE-PACKING MODEL TO THE SOLVENT EXTRACTION OF URANYL IONS

TANG BER-LIN, YU ZHI-HUI, GUO AO-LING, SUN PENG-NIAN, FENG XI-ZHAN and LI XING-FU*

Application Department, Institute of High Energy Physics, Academia Sinica, P.O. Box 2732, Beijing, China

and

ZHANG DA-CHUAN, ZHU ZHAN-YANG and LIN ZHEN-JIONG

Institute of Biophysics, Adademia Sinica, Beijing, China

(*Received* 25 *November* 1985; *accepted after revision* 22 *September* 1986)

Abstract—Synergistic extraction in mixed substrates has been predicted according to the cone-packing model and confirmed in the uranyl extraction with TBP in mixed solutions of ammonium chloride and sodium acetate. The molecular structure of $UO_2(CH_3COO)Cl(dmf)_2$ (dmf = *N*,*N*-dimethylformamide) confirmed the suggested extraction mechanism.

Although "coordination saturation" is a much used idea in solvent extraction, it is quite a confused concept in that one could understand it as saturation with respect either to coordination number or to coordination space. From our treatment of more than 500 molecular structures of lanthanide and actinide compounds, we have found that the latter offers the best explanation of the observed behaviour in this field.[1–5]

The packing saturation rule summarized in our previous paper[5] was also applied to the solvent extraction of the actinides and lanthanides in order to predict the extracted complexes.[6] In this communication we report the prediction and experimental confirmation of synergistic extraction of the uranyl ion in mixed aqueous substrates by applying the cone-packing model.

So far interest in synergistic extraction has been concentrated in the following ternary system:

$$\text{substrate} + \text{extractant}_1 + \text{extractant}_2.$$

An enhanced extraction efficiency in the mixed extraction substrates has been claimed[7–11] but the mechanism was not reported. We expected that synergism would also be shown in the following system:

$$\text{substrate}_1 + \text{substrate}_2 + \text{extractant},$$

and chose the UO_2^{2+}–NH_4Cl–$Na(CH_3COO)$–CH_3COOH–TBP system to test this assumption. It is clear from Fig. 1 that the complex $UO_2(CH_3COO)Cl(TBP)_2$ (I) has the most favourable packing compared to the other possible complexes, $UO_2Cl_2(TBP)_2$ (II), $UO_2Cl_2(TBP)_3$ (III), $UO_2(CH_3COO)_2TBP$ (IV), and $UO_2(CH_3COO)_2(TBP)_2$ (V). It is therefore expected that a higher extraction efficiency should coincide with the formation of the more stable compound (I).

As shown in Fig. 2, a synergistic effect was found with an acetate:chloride ratio of *ca* 1:3 which shifts

*Author to whom correspondence should be addressed.

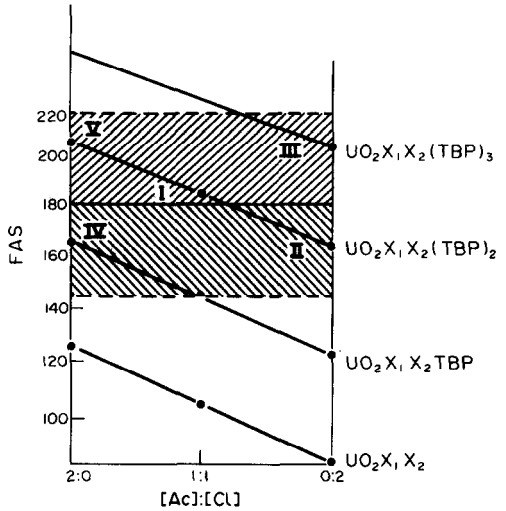

Fig. 1. UO_2^{2+}–Ac-Cl–TBP packing diagram. $X_1 = Ac^-$, $X_2 = Cl^-$.

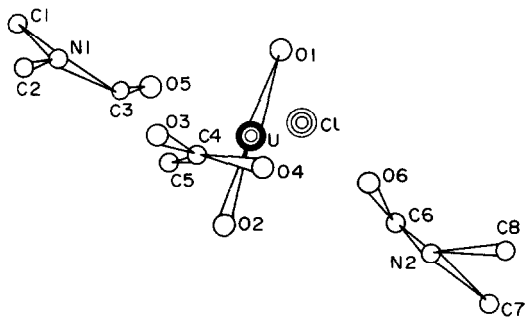

Fig. 3. Structure of $UO_2(CH_3COO)Cl(dmf)_2$:
O1···U = 1.714(18) Å, O2···U = 1.781(21) Å,
O3···U = 2.419(16) Å, O4···U = 2.419(17) Å,
O5···U = 2.353(14) Å, O6···U = 2.363(17) Å,
Cl···U = 2.678(6) Å, Cl···U···O6 = 81.3(5)°,
Cl···U···O5 = 79.6(5)°, O3···U···O5 = 74.3(6)°, and
O4···U···O6 = 87.2(9)°.

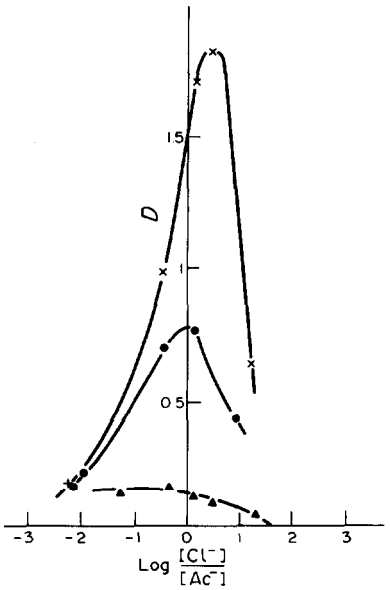

Fig. 2. Uranyl extraction by mixed substrates of different total concentrations: (×) 2.0 N, (●) 1.0 N, and (▲) 0.2 N. $UO_2^{2+} = 9.94 \times 10^{-4}$ mol dm^{-3}.

only slightly on changing the total concentration of the mixed substrates from 2.0 to 0.2 N, but remains constant on varying the uranyl ion concentration. The extracted complex was found to be mainly $UO_2(CH_3COO)Cl(TBP)_2$ by the slope method from which the values of $\log D - \log C$ are 1.91, 1.00 and 1.05, respectively, for TBP, acetate and chloride. By analysing the uranyl ion and chloride concentrations in the organic phase it was found that $[UO_2^{2+}]/[Cl^-]$ fluctuates in the range 0.893–1.23 when the $[Cl^-]:[CH_3COO^-]$ ratio in the aqueous phase was changed from 1:9 to 9:1. The synergistic effect is most marked in the pH range 2.5–3.5 and decreases at lower pH. A similar effect was found with other extractants and other diluents.

A structural study of the mixed-ligand complexes of this type is still in progress.

We have prepared and characterized new compounds $UO_2(CH_3COO)Cl(L)_2$ (L = triphenylphosphine oxide, tributylphosphine oxide, hexamethylphosphoramide or dimethylformamide) and have determined the molecular structure of $UO_2(CH_3COO)Cl(dmf)_2$ (Fig. 3), which confirms our expectation that the extracted complexes are genuine compounds rather than mixtures of uranyl chloride and uranyl acetate complexes.

Acknowledgements—This work was supported by the Science Fund of the Chinese Academy of Science. We thank Prof. K. W. Bagnall for helpful discussion and English revision.

REFERENCES

1. K. W. Bagnall and Li Xing-fu, *J. Chem. Soc., Dalton Trans.* 1982, 1365.
2. Li Xing-fu, Ph.D. thesis, The University of Manchester (1982).
3. Li Xing-fu and R. D. Fischer, *Inorg. Chim. Acta* 1984, **94**, 50.
4. R. D. Fischer and Li Xing-fu, *J. Less-Common Metals*, 1985, **112**, 303.
5. (a) Li Xing-fu, Feng Xi-zhang, Xu Ying-ting, Sun Peng-nian and Shi Jie, *Acta Chim. Sin.* 1985, **43**, 502; (b) Li Xing-fu, Feng Xi-zhang, Xu Ying-ting, Shi Jie, Wang Hai-dung, Liu Li and Sun Peng-nian, *Inorg. Chim. Acta* 1986, **117**, 85.
6. Sun Peng-nian, Shi Jie, Feng Xi-zhang, Xu Ying-

ting, Li Xing-fu, Wang Wen-qing and Yi Min, *Acta Chim. Sin.* 1985, **43**, 597.
7. K. Naito and T. Suzuki, *J. Phys. Chem.* 1962, **66**, 989.
8. A. M. Ross, TID-7508 (1955).
9. W. E. Keder, *J. Inorg. Chem.* 1960, **16**, 138.
10. N. Souka, R. Shabana and F. Hafez, *Microchem. J.* 1976, **21**, 215.
11. N. Souka, R. Shabana and F. Hafez, *Radiochim. Acta* 1975, **22**, 45.

Polyhedron Vol. 6, No. 3, pp. 651–654, 1987
Printed in Great Britain

0277–5387/87 $3.00+.00
Pergamon Journals Ltd

COMMUNICATION

LIGAND SUBSTITUTION REACTIONS OF (BIDENTATO-*O,O* and -*O,N*) BIS(ETHYLENEDIAMINE)COBALT(III) COMPLEXES WITH ETHYLENEDIAMINE CATALYZED BY PHOTOEXCITED TRIS(2,2′-BIPYRIDINE)RUTHENIUM(II) COMPLEX: THE ROLE OF CIRCULARLY POLARIZED LIGHT IN PHOTOIRRADIATION

MASAHIKO ISHIKAWA, KEN-ICHI OKAMOTO and JINSAI HIDAKA

Department of Chemistry, University of Tsukuba, Niihari, Ibaraki 305, Japan

and

HISAHIKO EINAGA†

Institute of Materials Science, University of Tsukuba, Niihari, Ibaraki 305, Japan

(*Received* 4 *July* 1986; *accepted* 27 *October* 1986)

Abstract—The substitution reactions with ethylenediamine of the bidentato-*O,O* ligand of (bidentato-*O,O*)bis(ethylenediamine)cobalt(III) complex have been studied in a weakly alkaline aqueous solution in the presence of tris(2,2′-bipyridine)ruthenium(II) complex under photoirradiation. The reaction was catalyzed by the photoexcited ruthenium(II) complex. Enhanced generation of the photoexcited ruthenium(II) complex and acceleration of the reaction of the bidentato-*O,N* ligand of (bidentato-*O,N*)bis(ethylenediamine)cobalt(III) complex were noticed when the optically active isomer of the ruthenium(II) complex was irradiated by the corresponding circularly polarized light.

It has been reported that the ligand substitution reaction of glycinato ligand in bis(ethylenediamine)glycinatocobalt(III), $[Co(gly)(en)_2]^{2+}$, with ethylenediamine does not proceed at room temperature (25°C) but does proceed at an elevated temperature (60–70°C)[1] or in the presence of triplet state excited tris(2,2′-bipyridine)ruthenium(II), $*[Ru(bpy)_3]^{2+}$, even at room temperature.[2] The $*[Ru(bpy)_3]^{2+}$-catalyzed ligand substitution reaction mechanism has been explained in terms of labilization of $[Co(gly)(en)_2]^{2+}$ by a charge-transfer process between $*[Ru(bpy)_3]^{2+}$ and $[Co(gly)(en)_2]^{2+}$.[2]

Further investigation of the role of $*[Ru(bpy)_3]^{2+}$ on the ligand substitution reaction of carbonatobis(ethylenediamine)cobalt(III), $[Co(CO_3)(en)_2]^{+}$, and bis(ethylenediamine)oxalatocobalt(III), $[Co(ox)(en)_2]^{+}$, with ethylenediamine suggested that the mechanism is general for the (bidentato-*O,O* and -*O,N*) bis (ethylenediamine) cobalt(III) complexes. Furthermore, it was found that the catalytic role of $*[Ru(bpy)_3]^{2+}$ could be enhanced for $[Co(gly)(en)_2]^{2+}$ by using the optically active isomer of $[Ru(bpy)_3]^{2+}$, and by exciting with irradiation by the corresponding circularly polarized light. The present article relates to these investigations.

EXPERIMENTAL

$[Co(CO_3)(en)_2]Cl$ and $[Co(ox)(en)_2]Cl \cdot H_2O$ were prepared and resolved into optically active isomers according to procedures given in the literature.[3,4] All other complexes and reagents used have been described elsewhere.[2]

The $*[Ru(bpy)_3]^{2+}$-catalyzed ligand substitution reaction was followed by procedures given in a

†Author to whom correspondence should be addressed.

previous paper.[2] In addition, excitation of $[Ru(bpy)_3]^{2+}$ at 452 nm by irradiation by left and right circularly polarized light was made by using Polaroid Circular Polarizers, Nos HNCP37L-4 and HNCP37R-4, which were attached in front of the sample holder of the photoirradiation system.[2] Other experimental procedures, including fluorescence quenching of $*[Ru(bpy)_3]^{2+}$, determination of hydroxide ion concentration etc., have been carried out as described elsewhere.[1,2]

RESULTS AND DISCUSSION

Investigation by liquid chromatography [SP-Sephadex C-25 column (Na^+ form); eluant, 0.05 mol dm^{-3} aqueous NaCl] of the photoirradiation reaction solution {initial conditions: 1.00×10^{-2} mol dm^{-3} $[Co(CO_3)(en)_2]^+$, 1.00×10^{-3} mol dm^{-3} $[Ru(bpy)_3]^{2+}$, 2.00 mol dm^{-3} ethylenediamine, pH 12.0 (buffered), room temperature (25°C)}, revealed that $[Co(CO_3)(en)_2]^+$ changed uniquely to $[Co(en)_3]^{3+}$. The amount of $[Co(CO_3)(en)_2]^+$ was decreased linearly with increasing photoirradiation time. Furthermore, no evidence was noticed of the formation of $[Co(en)_3]^{3+}$ in the absence of $[Ru(bpy)_3]^{2+}$. When $[Co(ox)(en)_2]^+$ was used in place of $[Co(CO_3)(en)_2]^+$, a stoichiometric change of $[Co(ox)(en)_2]^+$ to $[Co(en)_3]^{3+}$ by $*[Ru(bpy)_3]^{2+}$ was also found. However, the relation between the decreased amount of $[Co(ox)(en)_2]^+$ and the photoirradiation time [cf. Fig. 1 (for CD data), curves 5 and 6] showed a deviation from linearity. This deviation can be ascribed to the photodecomposition process of $[Co(ox)(en)_2]^+$ (cf. Fig. 1, curve 7).† Hence it is deduced that the ligand substitution reaction of $[Co(bidentato\text{-}O,O)(en)_2]^+$ with ethylenediamine is catalyzed by $*[Ru(bpy)_3]^{2+}$, as in the case of $[Co(gly)(en)_2]^{2+}$.[2]

Stern–Volmer plots were taken at 25°C by monitoring fluorescence intensities at 607 nm of 1.00×10^{-3} mol dm^{-3} $[Ru(bpy)_3]^{2+}$ in relation to concentration (0–2.00×10^{-2} mol dm^{-3}) of $[Co(bidentato\text{-}O,O)(en)_2]^+$. Linear relations with an intercept of unity were obtained for $[Co(CO_3)(en)_2]^+$ and $[Co(ox)(en)_2]^+$ with Stern–Volmer constants of 0.54×10^2 and 0.50×10^2 mol^{-1} dm^3, which can be converted by applying a lifetime of $*[Ru(bpy)_3]^{2+}$ in water at 25°C of 0.6 μs[6,7] to quenching rate constants (k_q) of 0.90×10^8 and 0.83×10^8 mol^{-1} dm^3 s^{-1}, respectively. These data compare well with the rate constant of $[Co(gly)(en)_2]^{2+}$ (1.25×10^8 mol^{-1} dm^3 s^{-1}),[2] corresponding to a diffusion-controlled, outer-sphere charge-transfer between $*[Ru(bpy)_3]^{2+}$ and $[Co(gly)(en)_2]^{2+}$. It should be noted that the Stern–Volmer constant decreases slightly in the following order; $[Co(gly)(en)_2]^{2+} > [Co(CO_3)(en)_2]^+ > [Co(ox)(en)_2]^+$.

The yield for the $*[Ru(bpy)_3]^{2+}$-catalyzed ligand substitution reaction of $[Co(bidentato\text{-}O,O)(en)_2]^+$ with ethylenediamine against $*[Ru(bpy)_3]^{2+}$ generated, Φ^{sub} $\{= (-d[[Co(bidentato\text{-}O,O)(en)_2]^+]/dt)/I_a\Phi^o$, where $I_a\Phi^o$ corresponds to the formation rate of $*[Ru(bpy)_3]^{2+}\}$,[2] was determined on both racemates as well as optically active isomers, and the data are summarized in Table 1. The yield does not depend on the stereochemistries of both the ruthenium(II) and the cobalt(III) complexes; the values are about the same magnitude with, however, a slight decrease in the following order; $[Co(gly)(en)_2]^{2+}$,[2] $> [Co(CO_3)(en)_2]^+ \fallingdotseq [Co(ox)(en)_2]^+$.

From the evidence given above, it is concluded that the mechanism of the $*[Ru(bpy)_3]^{2+}$-catalyzed ligand substitution reaction of $[Co(bidentato\text{-}O,O)(en)_2]^+$ with ethylenediamine is the same as that of $[Co(gly)(en)_2]^{2+}$.[2]

According to the discussion above, there remains an interesting point left unsolved on the role of circularly polarized light on the generation of $*[Ru(bpy)_3]^{2+}$. The $*[Ru(bpy)_3]^{2+}$-catalyzed ligand substitution reaction was followed under irradiation by left or right circularly polarized light at 452 nm of the optically active isomers of both $[Ru(bpy)_3]^{2+}$ and $[Co(bidentato\text{-}O,O)(en)_2]^+$ as well as $[Co(gly)(en)_2]^{2+}$ (cf. Fig. 1). Figure 1 demonstrates that $[Co(gly)(en)_2]^{2+}$ clearly shows the effect of irradiation by circularly polarized light; the rate of the decrease in $[Co(gly)(en)_2]^{2+}$ is enhanced by irradiation by right circularly polarized light on a solution containing $\Delta\text{-}(-)_{589}\text{-}[Ru(bpy)_3]^{2+}$ irrespective of the optical isomerism of $[Co(gly)(en)_2]^{2+}$. This effect can be explained in terms of an enhanced excitation of $\Delta\text{-}(-)_{589}\text{-}[Ru(bpy)_3]^{2+}$ by right circularly polarized light because this isomer shows a negative CD sign at 452 nm. Furthermore, this finding supports our conclusion on the mechanism of the $*[Ru(bpy)_3]^{2+}$-catalyzed ligand substitution reaction of $[Co(gly)(en)_2]^{2+}$,[2] that the overall rate of the reaction is governed by the photoexcitation step of $[Ru(bpy)_3]^{2+}$. We could not obtain any definite indication of the irradiation effect of circularly polarized light on $[Co(bidentato\text{-}O,O)(en)_2]^+$ within our experimental uncertainties. The reason is not clear at present, but we can safely state that the effect may be less pronounced $\{[Co(CO_3)(en)_2]^+\}$ or may be influenced by the

†$[Co(ox)(en)_2]^+$ has been reported not to racemize on photoirradiation.[5]

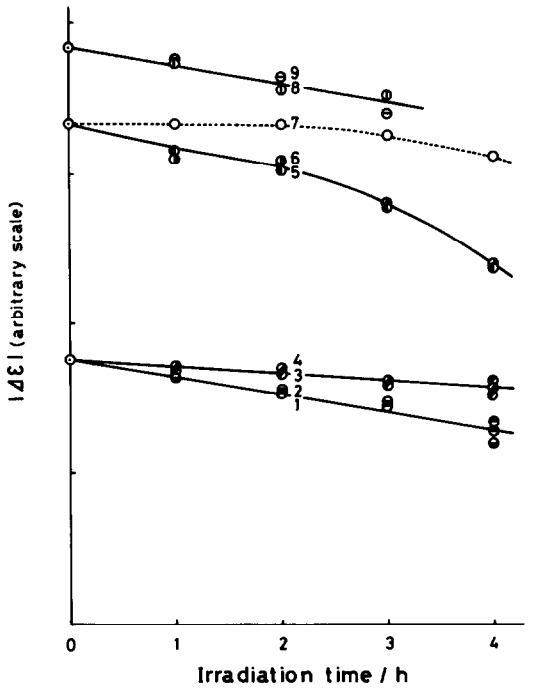

Fig. 1. CD intensity changes of cobalt(III) complexes with irradiation time of circularly polarized light in relation to the coexisting optically active ruthenium(II) complex. [[Co(bidentato-*O,O* or -*O,N*)$(en)_2]^{+ \text{or } 2+}$], 1.00×10^{-2} mol dm^{-3} (initial state); $[[Ru(bpy)_3]^{2+}]$, 1.00×10^{-5} mol dm^{-3}; [en], 2.00 mol dm^{-3}; $[OH^-]$, 1.58×10^{-2} mol dm^{-3} (buffered); and $[Cl^-]$, 1.0 mol dm^{-3}. *T*(°C), 25. Excitation wavelength of circularly polarized light (nm), 452. Wavelength of CD intensity measurement (nm), 509 $\{[Co(gly)(en)_2]^{2+}\}$, 520 $\{[Co(ox)(en)_2]^+\}$, and 530 $\{[Co(CO_3)(en)_2]^+\}$. Notation is as follows:

	$[Co(gly)(en)_2]^{2+}$		$[Co(ox)(en)_2]^+$	$[Co(CO_3)(en)_2]^+$
	Δ-$(-)_{589}$-	Λ-$(+)_{589}$-	Λ-$(+)_{589}$-	Λ-$(+)_{589}$-
Right CPL	1	2	5	9
Left CPL	3	4	6	8

CPL = circularly polarized light. Δ-$(-)_{589}$-$[Ru(bpy)_3]^{2+}$ was used throughout the runs. Curve 7 is a blank run for Λ-$(+)_{589}$-$[Co(ox)(en)_2]^+$ in the absence of Δ-$(-)_{589}$-$[Ru(bpy)_3]^{2+}$.

Table 1. Yield for ligand substitution reaction against $*[Ru(bpy)_3]^{2+}$ generated as determined by the circular dichroism spectral method at 25°C

	$\Phi^{sub\,a}$					
	$[Co(ox)(en)_2]^+$		$[Co(CO_3)(en)_2]^+$		$[Co(gly)(en)_2]^{2+}$	
	Δ-$(-)_{589}$-	Λ-$(+)_{589}$-	Δ-$(-)_{589}$-	Λ-$(+)_{589}$-	Δ-$(-)_{589}$-	Λ-$(+)_{589}$-
$[Ru(bpy)_3]^{2+}$	0.33	0.31	0.34	0.35	0.55[b]	0.55[b]
Δ-$(-)_{589}$-$[Ru(bpy)_3]^{2+}$	0.33	0.31	0.35	0.34	0.52[b]	0.55[b]

[a] $\Phi^{sub} = \{-d[[Co(\text{bidentato-}O,O \text{ or } -O,N)(en)_2]^{+ \text{ or } 2+}]/dt\}/I_a\Phi^o$ (consult the text).

[b] Reference 2. [[Co(bidentato-*O,O* or -*O,N*)$(en)_2]^{+ \text{or } 2+}$], 1.00×10^{-2} mol dm^{-3} (initial state); $[[Ru(bpy)_3]^{2+}]$, 1.00×10^{-5} mol dm^{-3}; [en], 2.00 mol dm^{-3}; $[OH^-]$, 1.58×10^{-2} mol dm^{-3} (buffered); and $[Cl^-]$, 1.0 mol dm^{-3}.

photosensitivity of the cobalt(III) complex $\{[Co(ox)(en)_2]^+\}$.

REFERENCES

1. M. Ishikawa, K. Okamoto, J. Hidaka and H. Einaga, *Polyhedron* 1986, **5**, 1345.
2. M. Ishikawa, K. Okamoto, J. Hidaka and H. Einaga, *Helv. Chim. Acta* 1985, **68**, 2015.
3. H. Fushimi, K. Okamoto, J. Hidaka and H. Einaga, *Inorg. Chim. Acta* 1985, **98**, 47.
4. F. P. Dwyer, I. K. Reid and F. L. Garvan, *J. Am. Chem. Soc.* 1961, **83**, 1285.
5. S. T. Speeds and A. W. Adamson, *Inorg. Chem.* 1962, **1**, 531.
6. J. van Houten and R. J. Watts, *J. Am. Chem. Soc.* 1976, **98**, 4853.

7. M. S. Wrighton (Ed.), *Inorganic and Organometallic Photochemistry*, Chap. 1. American Chemical Society, Washington D.C. (1978).

8. Absolute configurations of the complexes are designated by the IUPAC tentative rule. *Inorg. Chem.* 1970, **9**, 1.

Polyhedron Vol. 6, No. 3, pp. 655–657, 1987
Printed in Great Britain

0277–5387/87 $3.00+.00

COMMUNICATION

UNUSUAL MERCURY–PHOSPHORUS COUPLING CONSTANTS IN THE MERCURY(II) TRIPHOSPHINE COMPLEXES $[Hg(\eta^2\text{-LL})(\eta^1\text{-dppm})]^{2+}$ (LL = dppe OR dppp)*

PAUL PERINGER† and MARIA LUSSER

Institut für Anorganische und Analytische Chemie der Universität Innsbruck, Innrain 52a, A-6020 Innsbruck, Austria

(*Received* 11 *April* 1986; *accepted* 23 *October* 1986)

Abstract—The asymmetric complexes $[Hg(LL)(LL')]^{2+}$ (LL and LL' = dppm, dppe or dppp, LL ≠ LL') are formed in an equilibrium mixture with the corresponding symmetric compounds from $[Hg(Me_2SO)_6](O_3SCF_3)_2$ and the corresponding diphosphines. The bonding mode of dppe and dppp in the mixed complexes is chelating bidentate. The dppm ligands are monodentate and are involved in fast intramolecular exchange of the coordinated phosphorus atoms by the free phosphorus atoms. The mercury triphosphine complexes show unusual Hg–P coupling constants which are explained by the different *s*-character of the ligand–Hg bonds as a result of the fixed geometry of the chelate ligands differing from the ideal geometry of tricoordinate mercury(II).

Anomalous metal–phosphorus coupling constants have been observed when the actual coordination geometry of a metal differs from its ideal geometry.[1]

The platinum tetraphosphine complex [Pt(tripod)PPh_3] [tripod = $CH_3C(CH_2PPh_2)_3$] for example exhibits very different Pt–P coupling constants: 3096 Hz for the tridentate ligand but 5400 Hz for the monodentate phosphine.[1] Approximately the average of these coupling constants has been observed for $[Pt(PPh_3)_4]$.[2] This has been rationalized as follows:[1] the P—Pt—P angles involving the tripod ligand are 93–94°, i.e. essentially smaller than the tetrahedral angle. The Pt–tripod bonds will thus have a smaller *s*-character than tetrahedral Pt—P bonds, consistent with a smaller coupling constant. The Pt—PPh_3 bond will be hybridized to include more *s*-character, corresponding to a larger coupling constant.

Similar observations have been reported for $[Hg(tripod)L]^{2+/+}$, where L stands for a neutral or anionic phosphorus donor ligand.[3] We present here further evidence of this effect in mixed mercury(II) complexes with diphosphine ligands.

RESULTS AND DISCUSSION

In a solution of equimolar quantities of $[Hg(Me_2SO)_6](O_3SCF_3)_2$, dppm and dppe in dichloromethane the new asymmetric complex $[Hg(\eta^2\text{-dppe})(\eta^1\text{-dppm})]^{2+}$ (**1**) is formed in an equilibrium mixture with the symmetric species $[Hg(\eta^2\text{-dppe})_2]^{2+}$ (**2**)[4] and $[Hg(\eta^1\text{-dppm})_2]^{2+}$ (**3**).[4] The coordination sphere of mercury in complexes **1** and **3** is thought to be completed by Me_2SO. Equilibrium (1):

$$2[Hg(\eta^2\text{-dppe})(\eta^1\text{-dppm})] \rightleftharpoons [Hg(\eta^2\text{-dppe})_2]^{2+} + [Hg(\eta^1\text{-dppm})_2]^{2+} \quad (1)$$

occurs rapidly on the preparative time scale, and the equilibrium concentrations are almost statistical as estimated by the integration of the ^{31}P NMR signals.

At ambient temperature, the ^{31}P NMR signals

*dppm = $PPh_2CH_2PPh_2$, dppe = $PPh_2(CH_2)_2PPh_2$, dppp = $PPh_2(CH_2)_3PPh_2$.

†Author to whom correspondence should be addressed.

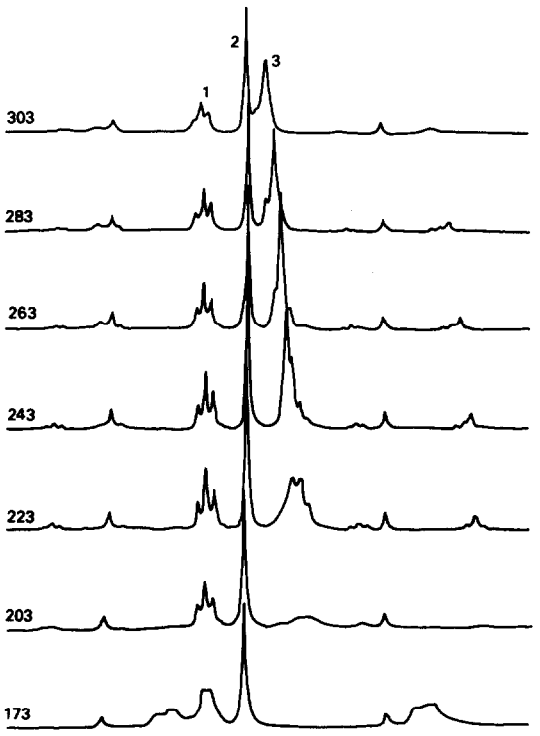

Fig. 1. $^{31}P-\{^1H\}$ NMR spectra of a solution of $[Hg(Me_2SO)_6](O_3SCF_3)_2$, dppm and dppe in a ratio of 1:1:1 in CH_2Cl_2 at different temperatures (in K): (1) dppe part of $[Hg(\eta^1\text{-dppm})(\eta^2\text{-dppe})]^{2+}$, (2) $[Hg(\eta^2\text{-dppe})_2]^{2+}$, and (3) dppm part of $[Hg(\eta^1\text{-dppm})(\eta^2\text{-dppe})]^{2+}$ and $[Hg(\eta^1\text{-dppm})_2]^{2+}$.

are broadened as a result of intermolecular ligand exchange (Fig. 1). At 263 K the ^{31}P NMR spectrum of **1** consists of two triplets attributable to coordinated dppm and dppe together with the corresponding ^{199}Hg satellites originating from the isotopomer containing ^{199}Hg atoms (abundance 16.8%). The ^{199}Hg NMR spectrum at this temperature is a triplet of triplets.

These coupling pattern are not caused by a structure $[Hg(\eta^2\text{-dppe})(\eta^2\text{-dppm})]^{2+}$ but by $[Hg(\eta^2\text{-dppe})(\eta^1\text{-dppm})]^{2+}$ involved in intramolecular exchange of the coordinated phosphorus atoms with the free phosphorus atoms of the η^1-dppm ligands occurring rapidly on the NMR time scale. Upon further cooling the dppm signals broaden, and below 173 K two broadened peaks attributable to the coordinated and the free phosphorus atoms of the η^1-dppm ligands appear, but the slow-exchange limit could not be attained.

Dean and Srivastava[5] reported very recently on the compound $[Hg(\eta^2\text{-dppe})(\eta^2\text{-dppm})]^{2+}$ which is formed from $Hg(SbF_6)_2$, dppe and dppm, but in the absence of Me_2SO. This confirms that the $Hg(\eta^2\text{-dppm})$ ring is readily opened by Me_2SO. This must be caused by the strain of the four-membered HgPCP ring since tertiary phosphines are much stronger ligands for mercury compared to oxygen donor ligands (e.g. Me_2SO). The strain in four-membered metal–dppm rings is a known fact and causes dppm to prefer the bridging bidentate or monodentate bonding mode.[6] An analogous opening of a Hg–dppm chelate ring by Me_2SO has been observed for $[Hg(\eta^2\text{-dppm})_2]^{2+}$ which exists as $[Hg(\eta^1\text{-dppm})_2]^{2+}$ when dissolved in Me_2SO.[4] The NMR parameters of **1** are summarized in Table 1. The ^{199}Hg chemical shift largely corresponds to that of other cationic Hg complexes of type $[Hg(PR_3)_3]^{2+}$.[7] On the other hand the $^{199}Hg-^{31}P$ coupling constants are rather interesting: the one bond coupling constant involving dppe (2456 Hz) is unexpectedly small. The Hg–P coupling constants of cationic mercury phosphine complexes $[Hg(PR_3)_n]^{2+}$ usually decrease with n: they are *ca* 10,000 Hz for $n = 1$,[8] *ca* 5500 Hz for $n = 2$, *ca* 3300 Hz for $n = 3$, and *ca* 2100 Hz for $n = 4$.[7] The Hg–dppe coupling constant of **2** thus more closely resembles that of a mercury tetraphosphine complex than that of a triphosphine complex.

The apparent Hg–dppm coupling at the fast-exchange limit of the end-over-end exchange is actually the mean of the one- and the three-bond mercury–phosphorus couplings. The assumption

Table 1. NMR parameters of $[Hg(LL)(LL')]^{2+}$ [a]

		LL		LL'			T
LL	LL'	δ(P)	J(Hg–P)	δ(P)	J(Hg–P)	δ(Hg)	(K)
dppm	dppe	10.2[b]	2822	32.2	2456	1835	263
dppm	dppp	17.6[c]	2338	36.2	2305	1936	300
dppe	dppp	18.2[d]	1893	16.3	2236	2083	300

[a] Chemical shifts in ppm to high frequency of 85% H_3PO_4 or aqueous $Hg(ClO_4)_2$ [2 mmol HgO (cm^3 60% $HClO_4$)$^{-1}$], coupling constants in Hz.

[b] $^2J\{[P(dppm)–P(dppe)] + {}^4J[P(dppm)–P(dppe)]\}/2 = 63$.

[c] $^2J\{[P(dppm)–P(dppp)] + {}^4J[P(dppm)–P(dppp)]\}/2 = 53$.

[d] $^2J[P(dppe)–P(dppp)] = 49$.

of a ^3J(Hg–P) of ± 70 Hz leads to a ^1J(Hg–P) of *ca* 5600–5700 Hz. This is in the region of Hg–P couplings in complexes of type $[Hg(PR_3)_2]^{2+}$. The average of the coupling constants of Hg to dppm and dppe for **2** on the other hand is in the region typically observed for $[Hg(PR_3)_3]^{2+}$ complexes. The anomalous coupling constants may be explained as those of the Pt(0)[1] or Hg(II)[3] tripod complexes mentioned above. The five-membered rings of M(η^2-dppe) complexes involve P—M—P angles of *ca* 85°. This is essentially smaller than the optimal P—Hg—P angle in **1**, and results in a diminished *s*-character of the Hg—(η^2-dppe) bonds, and therefore in a decreased coupling constant. The Hg—(η^1-dppm) bonds are hybridized to include more *s*-character and have an enlarged Hg–P coupling constant.

The complex $[Hg(\eta^2\text{-dppp})(\eta^1\text{-dppm})]^{2+}$ (**4**) is formed together with the corresponding symmetric compounds from $[Hg(Me_2SO)_6](O_3SCF_3)_2$, dppp and dppm, and behaves similarly to **1**. The NMR data show the same anomalies as **1**, and are included in Table 1.

$[Hg(\eta^2\text{-dppe})(\eta^2\text{-dppp})]^{2+}$ (**5**) is formed from $[Hg(Me_2SO)_6](O_3SCF_3)_2$, dppe and dppp in an equilibrium mixture with $[Hg(\eta^2\text{-dppe})_2]^{2+}$ and $[Hg(\eta^2\text{-dppp})_2]^{2+}$. In contrast to **1** and **4**, **5** contains four-coordinated phosphorus donor atoms. The NMR data of **5** (Table 1) are almost identical to that of $[Hg(\eta^2\text{-dppe})(\eta^2\text{-dppp})](SbF_6)_2$, which has been reported[5] since the acquisition of this data.

EXPERIMENTAL

$[Hg(Me_2SO)_6](O_3SCF_3)_2$ has been prepared as previously described,[9] and all other reagents are commercially available.

The NMR spectra were recorded in the FT mode on a multinuclear Bruker WP-80 spectrometer.

REFERENCES

1. J. Chatt, R. Mason and D. W. Meek, *J. Am. Chem. Soc.* 1975, **97**, 3826.
2. C. A. Tolman, W. C. Seidel and D. H. Gerlach, *J. Am. Chem. Soc.* 1972, **94**, 2669.
3. P. Peringer and M. Lusser, *Inorg. Chim. Acta*, 1986, **117**, L25.
4. P. Peringer and M. Lusser, *Inorg. Chem.* 1985, **24**, 109.
5. P. A. W. Dean and R. S. Srivastava, *Can. J. Chem.* 1985, **63**, 2829.
6. R. J. Puddephatt, *Chem. Soc. Rev.* 1983, 99.
7. R. Colton and D. Dakternieks, *Aust. J. Chem.* 1984, **34**, 323.
8. P. Peringer and M. Lusser, unpublished results.

Polyhedron Vol. 6, No. 3, pp. 659–661, 1987
Pergamon Journals Ltd. Printed in Great Britain

BOOK REVIEWS

Carbosilanes. Synthesis and Reactions. G. Fritz and E. Matern, Springer, Berlin, 1986. ISBN 3-540-15929-0, xii + 258 pp., 40 figs, 74 tables, DM 189.

Carbosilanes are compounds containing a molecular skeleton based on alternating carbon and silicon atoms. The present volume is an authoritative and expert in-depth review of a field which has grown up over the last 40 years.

After a brief scene-setting chapter comparing the chemistries of carbon and silicon, the book proceeds to a consideration of the synthetic routes to carbosilanes. The first route to be discovered was simple gas-phase pyrolysis of methyl silanes. Thus, pyrolysis of $SiMe_4$ yields some 45 different silicon containing products (and a range of hydrocarbons) boiling between 45 and 280°C, plus higher molecular weight silicon compounds. The simplest compounds have linear or one-ring cyclic structures, whilst many (but not all) of the polycyclic derivatives have the "adamantane" type cage, some of these being stable to above 400°C. Chlorinated carbosilanes are similarly obtained from chlorosilanes.

An alternative synthetic route to carbosilanes involves cold plasma; this permits the isolation of compounds decomposed in the thermal routes, notably linear carbosilanes. Another route involves using a copper catalyst to facilitate reaction of silicon with chloromethanes; Lewis acids such as $AlCl_3$ also catalyse rearrangement reactions of carbosilanes. The text discusses the mechanisms believed to occur in these reactions, as well as particular organometallic syntheses.

Chapter 3 treats the reactions of carbosilanes; under appropriate conditions a number of functional groups may be introduced. These include halogenation of Si—H and C—H groups, hydrogenation of Si—Hal, and alkylation with Grignard reagents and organolithium compounds. Generally speaking, it is at the silicon atoms that reaction occurs, but under the right conditions the carbon atoms can be metallated, specific reagents being available for $—CH_2—$ and $\equiv CH$ groups. Metallation with organometallic moieties such as $—Fe(CO)_2(C_5H_5)$ can also be brought about.

The final chapter contains details of all the molecular structures determined for carbosilanes, mainly, of course, by X-ray diffraction methods. Clear diagrams show all bond lengths and angles.

All references (212) are given at the end; a majority of the work cited is by Professor Fritz and his coworkers, a significant amount of it not having been published before.

This reviewer confesses to a total ignorance of carbosilanes before reading this book, but he found the work thoroughly covered, with plenty of illustrations to clarify the often-complicated structures. This is a very neatly produced contribution to keeping us abreast of the substantial area represented by silicon chemistry.

Stanground School **SIMON COTTON**
Peterborough
Cambs, U.K.

The Periodic Table of the Elements, 2nd Edition. R. J. Puddephatt and P. K. Monaghan, Oxford University Press, Oxford, 1986. ISBN 0-19-855515-6 (hbk), ISBN 0-19-855516-4 (pbk), £6.95 (pbk).

The arrangement of the chemical elements in the form known as the Periodic Table is familiar to all except those with a cursory acquaintance with chemistry. Its merits as a way of classifying the elements are illustrated by the way in which it has survived in essentially the same form from a time when many fewer elements were known and when notions of atomic structure were extremely sketchy.

This is the second edition of a book first published 14 years ago, intended for "first year students in universities and technical colleges and for senior secondary school students". Compared with the first edition, it contains about one-fifth as many pages in the text, partly accounted for by a change in typeface but also having significant additions in certain chapters.

After a brief introductory section (which points out that the book is concerned with trends in properties and comparisons between elements, rather than being a catalogue of facts) the second chapter is concerned with a brief summary of quantum theory, which in Chapter 3 is utilized to relate electronic structure to the Periodic Table. Both the traditional (I–VIII) and new IUPAC (1–18) systems of classifying groups are used.

The next three chapters (4–6) treat the main-group elements. The first of these chapters, significantly expanded from the last edition, introduces ideas like ionization energy and electron affinity, showing how these (and atomic and ionic radii) vary within a group. This chapter also outlines some basic principles of chemical bonding. Chapter 5 treats the physical and structural properties of the main-group elements, indicating the relationship between these, both within a group and across a period. Chapter 6 (again significantly expanded) looks at representative compounds (halides, oxides and hydrides) of the elements and shows how the properties of these compounds are related to the properties (i.e. metal/non-metal) of the element itself. The section on the hydrides includes a very brief discussion of the VSEPR model and of hydrogen bonding.

Chapter 7 deals with the transition elements. The chlorides are used to illustrate the property of multiple oxi-

Polyhedron Vol. 6, No. 3, pp. 659–661, 1987
Pergamon Journals Ltd. Printed in Great Britain

BOOK REVIEWS

Carbosilanes. Synthesis and Reactions. G. Fritz and E. Matern, Springer, Berlin, 1986. ISBN 3-540-15929-0, xii + 258 pp., 40 figs, 74 tables, DM 189.

Carbosilanes are compounds containing a molecular skeleton based on alternating carbon and silicon atoms. The present volume is an authoritative and expert in-depth review of a field which has grown up over the last 40 years.

After a brief scene-setting chapter comparing the chemistries of carbon and silicon, the book proceeds to a consideration of the synthetic routes to carbosilanes. The first route to be discovered was simple gas-phase pyrolysis of methyl silanes. Thus, pyrolysis of $SiMe_4$ yields some 45 different silicon containing products (and a range of hydrocarbons) boiling between 45 and 280°C, plus higher molecular weight silicon compounds. The simplest compounds have linear or one-ring cyclic structures, whilst many (but not all) of the polycyclic derivatives have the "adamantane" type cage, some of these being stable to above 400°C. Chlorinated carbosilanes are similarly obtained from chlorosilanes.

An alternative synthetic route to carbosilanes involves cold plasma; this permits the isolation of compounds decomposed in the thermal routes, notably linear carbosilanes. Another route involves using a copper catalyst to facilitate reaction of silicon with chloromethanes; Lewis acids such as $AlCl_3$ also catalyse rearrangement reactions of carbosilanes. The text discusses the mechanisms believed to occur in these reactions, as well as particular organometallic syntheses.

Chapter 3 treats the reactions of carbosilanes; under appropriate conditions a number of functional groups may be introduced. These include halogenation of Si—H and C—H groups, hydrogenation of Si—Hal, and alkylation with Grignard reagents and organolithium compounds. Generally speaking, it is at the silicon atoms that reaction occurs, but under the right conditions the carbon atoms can be metallated, specific reagents being available for $—CH_2—$ and $\equiv CH$ groups. Metallation with organometallic moieties such as $—Fe(CO)_2(C_5H_5)$ can also be brought about.

The final chapter contains details of all the molecular structures determined for carbosilanes, mainly, of course, by X-ray diffraction methods. Clear diagrams show all bond lengths and angles.

All references (212) are given at the end; a majority of the work cited is by Professor Fritz and his coworkers, a significant amount of it not having been published before.

This reviewer confesses to a total ignorance of carbosilanes before reading this book, but he found the work thoroughly covered, with plenty of illustrations to clarify the often-complicated structures. This is a very neatly produced contribution to keeping us abreast of the substantial area represented by silicon chemistry.

Stanground School **SIMON COTTON**
Peterborough
Cambs, U.K.

The Periodic Table of the Elements, 2nd Edition. R. J. Puddephatt and P. K. Monaghan, Oxford University Press, Oxford, 1986. ISBN 0-19-855515-6 (hbk), ISBN 0-19-855516-4 (pbk), £6.95 (pbk).

The arrangement of the chemical elements in the form known as the Periodic Table is familiar to all except those with a cursory acquaintance with chemistry. Its merits as a way of classifying the elements are illustrated by the way in which it has survived in essentially the same form from a time when many fewer elements were known and when notions of atomic structure were extremely sketchy.

This is the second edition of a book first published 14 years ago, intended for "first year students in universities and technical colleges and for senior secondary school students". Compared with the first edition, it contains about one-fifth as many pages in the text, partly accounted for by a change in typeface but also having significant additions in certain chapters.

After a brief introductory section (which points out that the book is concerned with trends in properties and comparisons between elements, rather than being a catalogue of facts) the second chapter is concerned with a brief summary of quantum theory, which in Chapter 3 is utilized to relate electronic structure to the Periodic Table. Both the traditional (I–VIII) and new IUPAC (1–18) systems of classifying groups are used.

The next three chapters (4–6) treat the main-group elements. The first of these chapters, significantly expanded from the last edition, introduces ideas like ionization energy and electron affinity, showing how these (and atomic and ionic radii) vary within a group. This chapter also outlines some basic principles of chemical bonding. Chapter 5 treats the physical and structural properties of the main-group elements, indicating the relationship between these, both within a group and across a period. Chapter 6 (again significantly expanded) looks at representative compounds (halides, oxides and hydrides) of the elements and shows how the properties of these compounds are related to the properties (i.e. metal/non-metal) of the element itself. The section on the hydrides includes a very brief discussion of the VSEPR model and of hydrogen bonding.

Chapter 7 deals with the transition elements. The chlorides are used to illustrate the property of multiple oxi-

dation states, and also how the 4*d* and 5*d* metals tend to utilize higher oxidation states. Trends across the series in ionic and atomic radii, and in properties such as ionization energy, are illustrated, and there is a discussion of hard and soft acids and bases linking with complex formation, and of crystal-field theory. Chapter 8 is a brief (6-page) account of trends in the lanthanide and actinide series.

This book has many solid virtues and is both easy to read and extremely well illustrated. It has no pretence of being a textbook on inorganic chemistry and, indeed, refers the reader to the standard texts in the field. It is also always easy to suggest ways of expanding a short book, but there are some areas that this reviewer would look for. Although it would be covered by cognate texts, a little more account of VSEPR treatment would be welcome, as would some more account of variation in properties across periods. The authors do not state explicitly just which properties are characteristic of transition metals as distinct from other elements, and, finally, it would be nice to see the very old-fashioned table comparing the known properties of germanium with Mendeleev's predictions, if only to illustrate the power of the Periodic system in the hands of a skilled practitioner!

Stanground School **SIMON COTTON**
Peterborough
Cambs, U.K.

Organotitanium Reagents in Organic Synthesis. Manfred T. Reetz, Springer, Berlin, 1986. ISBN 3-540-15784-0, 236 pp., 23 figs, DM 168.

This volume is a timely addition to the Springer series "Reactivity and Structure Concepts in Organic Chemistry". The book is organized in eight concise chapters each with its own comprehensive references. Early chapters cover the preparation and general properties of organotitanium compounds, including a brief treatment of theoretical and spectroscopic aspects. Subsequent chapters describe the major uses of titanium in synthesis. Addition reactions of organotitanium reagents to carbonyl compounds are treated in some detail and with special regard to chemo- and stereoselectivity, and with a separate brief chapter concerning kinetics.

Other areas treated include the use of titanium species as Lewis acid mediators in reactions of enol and allyl silanes, titanium enolate chemistry, and methylenation reactions using titanium-based reagents. The book includes coverage of the literature up to early 1985 along with additional unpublished data from Prof. Reetz's own research group. The excellent organization and layout of this volume make it an enjoyable read as well as a valuable reference book, and it should prove popular and useful to all those involved in organic synthesis.

Department of Chemistry **N. S. SIMPKINS**
Queen Mary College
Mile End Road
London E1 4NS, U.K.

Gmelin Handbook of Inorganic Chemistry, 8th Edition. Sn—Organotin Compounds, Part 13, Other RSn–Oxygen Compounds. Compounds with Two and Three Different Organic Groups Bonded to the Sn Atom. Springer, Berlin, 1986. xii+374 pp., DM 1456.

Organotin chemists will be delighted to see the rapid appearance of this 13th volume on organotin compounds. Like all the previous volumes, it has been compiled by Herbert and Ingeborg Schumann, and it maintains the very high standard of the series.

This volume contains all mononuclear R_3Sn–oxygen compounds with R other than methyl, ethyl, propyl and butyl, and all $R_2R'Sn$– and $RR'R''Sn$–oxygen compounds; the mononuclear restriction means that trialkyltin hydroxides are included, but bis(trialkyltin) oxides are not. The literature is covered up to the end of 1982.

For example, 8 pp. are devoted to the tribenzyltin–oxygen compounds, and cover the hydroxide, alkoxides, phenoxides, ketonates, carboxylates, peroxides, and other miscellaneous derivatives. The section on the corresponding triphenyltin–oxygen compounds is of course much larger (160 pp.). For each compound, details are given of preparations, properties, structure, reactions and applications. Much information is tabulated, and amplified in extensive footnotes. There is an empirical formula index (28 pp.) and a ligand index (59 pp.).

The printing and production are as impeccable as usual.

Doubly welcome is the promise that additional volumes describing other R_3SnO derivatives and tin–oxygen compounds with R_2Sn and RSn groups will follow in the near future.

Department of Chemistry **A. G. DAVIES**
University College London
20 *Gordon Street*
London WC1H 0AJ, U.K.

Gmelin Handbook of Inorganic Chemistry, 8th Edition. Sb—Organoantimony Compounds, Part 4, Compounds of Pentavalent Antimony with Three Sb—C Bonds. Springer, Berlin, 1986. 250 pp., DM 1173.

The first volume of this series covered organoantimony compounds of type R_3Sb, the second covered the compounds R_2SbX and $RSbX_2$, and the third dealt principally with the Sb(V) compounds R_5Sb.

This fourth volume describes pentavalent antimony compounds of types R_3SbX_2 and $R_3Sb{=}X$.

Most readers will be familiar with the Gmelin format. The text is now wholly in English. For each compound, the preparations are first listed, then the physical and spectroscopic properties, with figures of the molecular structure if it has been determined by diffraction

dation states, and also how the 4*d* and 5*d* metals tend to utilize higher oxidation states. Trends across the series in ionic and atomic radii, and in properties such as ionization energy, are illustrated, and there is a discussion of hard and soft acids and bases linking with complex formation, and of crystal-field theory. Chapter 8 is a brief (6-page) account of trends in the lanthanide and actinide series.

This book has many solid virtues and is both easy to read and extremely well illustrated. It has no pretence of being a textbook on inorganic chemistry and, indeed, refers the reader to the standard texts in the field. It is also always easy to suggest ways of expanding a short book, but there are some areas that this reviewer would look for. Although it would be covered by cognate texts, a little more account of VSEPR treatment would be welcome, as would some more account of variation in properties across periods. The authors do not state explicitly just which properties are characteristic of transition metals as distinct from other elements, and, finally, it would be nice to see the very old-fashioned table comparing the known properties of germanium with Mendeleev's predictions, if only to illustrate the power of the Periodic system in the hands of a skilled practitioner!

Stanground School **SIMON COTTON**
Peterborough
Cambs, U.K.

Organotitanium Reagents in Organic Synthesis. Manfred T. Reetz, Springer, Berlin, 1986. ISBN 3-540-15784-0, 236 pp., 23 figs, DM 168.

This volume is a timely addition to the Springer series "Reactivity and Structure Concepts in Organic Chemistry". The book is organized in eight concise chapters each with its own comprehensive references. Early chapters cover the preparation and general properties of organotitanium compounds, including a brief treatment of theoretical and spectroscopic aspects. Subsequent chapters describe the major uses of titanium in synthesis. Addition reactions of organotitanium reagents to carbonyl compounds are treated in some detail and with special regard to chemo- and stereoselectivity, and with a separate brief chapter concerning kinetics.

Other areas treated include the use of titanium species as Lewis acid mediators in reactions of enol and allyl silanes, titanium enolate chemistry, and methylenation reactions using titanium-based reagents. The book includes coverage of the literature up to early 1985 along with additional unpublished data from Prof. Reetz's own research group. The excellent organization and layout of this volume make it an enjoyable read as well as a valuable reference book, and it should prove popular and useful to all those involved in organic synthesis.

Department of Chemistry **N. S. SIMPKINS**
Queen Mary College
Mile End Road
London E1 4NS, U.K.

Gmelin Handbook of Inorganic Chemistry, 8th Edition. Sn—Organotin Compounds, Part 13, Other RSn–Oxygen Compounds. Compounds with Two and Three Different Organic Groups Bonded to the Sn Atom. Springer, Berlin, 1986. xii+374 pp., DM 1456.

Organotin chemists will be delighted to see the rapid appearance of this 13th volume on organotin compounds. Like all the previous volumes, it has been compiled by Herbert and Ingeborg Schumann, and it maintains the very high standard of the series.

This volume contains all mononuclear R_3Sn–oxygen compounds with R other than methyl, ethyl, propyl and butyl, and all $R_2R'Sn$– and $RR'R''Sn$–oxygen compounds; the mononuclear restriction means that trialkyltin hydroxides are included, but bis(trialkyltin) oxides are not. The literature is covered up to the end of 1982.

For example, 8 pp. are devoted to the tribenzyltin–oxygen compounds, and cover the hydroxide, alkoxides, phenoxides, ketonates, carboxylates, peroxides, and other miscellaneous derivatives. The section on the corresponding triphenyltin–oxygen compounds is of course much larger (160 pp.). For each compound, details are given of preparations, properties, structure, reactions and applications. Much information is tabulated, and amplified in extensive footnotes. There is an empirical formula index (28 pp.) and a ligand index (59 pp.).

The printing and production are as impeccable as usual.

Doubly welcome is the promise that additional volumes describing other R_3SnO derivatives and tin–oxygen compounds with R_2Sn and RSn groups will follow in the near future.

Department of Chemistry **A. G. DAVIES**
University College London
20 *Gordon Street*
London WC1H 0AJ, U.K.

Gmelin Handbook of Inorganic Chemistry, 8th Edition. Sb—Organoantimony Compounds, Part 4, Compounds of Pentavalent Antimony with Three Sb—C Bonds. Springer, Berlin, 1986. 250 pp., DM 1173.

The first volume of this series covered organoantimony compounds of type R_3Sb, the second covered the compounds R_2SbX and $RSbX_2$, and the third dealt principally with the Sb(V) compounds R_5Sb.

This fourth volume describes pentavalent antimony compounds of types R_3SbX_2 and $R_3Sb{=}X$.

Most readers will be familiar with the Gmelin format. The text is now wholly in English. For each compound, the preparations are first listed, then the physical and spectroscopic properties, with figures of the molecular structure if it has been determined by diffraction

dation states, and also how the 4*d* and 5*d* metals tend to utilize higher oxidation states. Trends across the series in ionic and atomic radii, and in properties such as ionization energy, are illustrated, and there is a discussion of hard and soft acids and bases linking with complex formation, and of crystal-field theory. Chapter 8 is a brief (6-page) account of trends in the lanthanide and actinide series.

This book has many solid virtues and is both easy to read and extremely well illustrated. It has no pretence of being a textbook on inorganic chemistry and, indeed, refers the reader to the standard texts in the field. It is also always easy to suggest ways of expanding a short book, but there are some areas that this reviewer would look for. Although it would be covered by cognate texts, a little more account of VSEPR treatment would be welcome, as would some more account of variation in properties across periods. The authors do not state explicitly just which properties are characteristic of transition metals as distinct from other elements, and, finally, it would be nice to see the very old-fashioned table comparing the known properties of germanium with Mendeleev's predictions, if only to illustrate the power of the Periodic system in the hands of a skilled practitioner!

Stanground School **SIMON COTTON**
Peterborough
Cambs, U.K.

Organotitanium Reagents in Organic Synthesis. Manfred T. Reetz, Springer, Berlin, 1986. ISBN 3-540-15784-0, 236 pp., 23 figs, DM 168.

This volume is a timely addition to the Springer series "Reactivity and Structure Concepts in Organic Chemistry". The book is organized in eight concise chapters each with its own comprehensive references. Early chapters cover the preparation and general properties of organotitanium compounds, including a brief treatment of theoretical and spectroscopic aspects. Subsequent chapters describe the major uses of titanium in synthesis. Addition reactions of organotitanium reagents to carbonyl compounds are treated in some detail and with special regard to chemo- and stereoselectivity, and with a separate brief chapter concerning kinetics.

Other areas treated include the use of titanium species as Lewis acid mediators in reactions of enol and allyl silanes, titanium enolate chemistry, and methylenation reactions using titanium-based reagents. The book includes coverage of the literature up to early 1985 along with additional unpublished data from Prof. Reetz's own research group. The excellent organization and layout of this volume make it an enjoyable read as well as a valuable reference book, and it should prove popular and useful to all those involved in organic synthesis.

Department of Chemistry **N. S. SIMPKINS**
Queen Mary College
Mile End Road
London E1 4NS, U.K.

Gmelin Handbook of Inorganic Chemistry, 8th Edition. Sn—Organotin Compounds, Part 13, Other RSn–Oxygen Compounds. Compounds with Two and Three Different Organic Groups Bonded to the Sn Atom. Springer, Berlin, 1986. xii+374 pp., DM 1456.

Organotin chemists will be delighted to see the rapid appearance of this 13th volume on organotin compounds. Like all the previous volumes, it has been compiled by Herbert and Ingeborg Schumann, and it maintains the very high standard of the series.

This volume contains all mononuclear R_3Sn–oxygen compounds with R other than methyl, ethyl, propyl and butyl, and all $R_2R'Sn$– and $RR'R''Sn$–oxygen compounds; the mononuclear restriction means that trialkyltin hydroxides are included, but bis(trialkyltin) oxides are not. The literature is covered up to the end of 1982.

For example, 8 pp. are devoted to the tribenzyltin–oxygen compounds, and cover the hydroxide, alkoxides, phenoxides, ketonates, carboxylates, peroxides, and other miscellaneous derivatives. The section on the corresponding triphenyltin–oxygen compounds is of course much larger (160 pp.). For each compound, details are given of preparations, properties, structure, reactions and applications. Much information is tabulated, and amplified in extensive footnotes. There is an empirical formula index (28 pp.) and a ligand index (59 pp.).

The printing and production are as impeccable as usual.

Doubly welcome is the promise that additional volumes describing other R_3SnO derivatives and tin–oxygen compounds with R_2Sn and RSn groups will follow in the near future.

Department of Chemistry **A. G. DAVIES**
University College London
20 *Gordon Street*
London WC1H 0AJ, U.K.

Gmelin Handbook of Inorganic Chemistry, 8th Edition. Sb—Organoantimony Compounds, Part 4, Compounds of Pentavalent Antimony with Three Sb—C Bonds. Springer, Berlin, 1986. 250 pp., DM 1173.

The first volume of this series covered organoantimony compounds of type R_3Sb, the second covered the compounds R_2SbX and $RSbX_2$, and the third dealt principally with the Sb(V) compounds R_5Sb.

This fourth volume describes pentavalent antimony compounds of types R_3SbX_2 and $R_3Sb{=}X$.

Most readers will be familiar with the Gmelin format. The text is now wholly in English. For each compound, the preparations are first listed, then the physical and spectroscopic properties, with figures of the molecular structure if it has been determined by diffraction

dation states, and also how the 4*d* and 5*d* metals tend to utilize higher oxidation states. Trends across the series in ionic and atomic radii, and in properties such as ionization energy, are illustrated, and there is a discussion of hard and soft acids and bases linking with complex formation, and of crystal-field theory. Chapter 8 is a brief (6-page) account of trends in the lanthanide and actinide series.

This book has many solid virtues and is both easy to read and extremely well illustrated. It has no pretence of being a textbook on inorganic chemistry and, indeed, refers the reader to the standard texts in the field. It is also always easy to suggest ways of expanding a short book, but there are some areas that this reviewer would look for. Although it would be covered by cognate texts, a little more account of VSEPR treatment would be welcome, as would some more account of variation in properties across periods. The authors do not state explicitly just which properties are characteristic of transition metals as distinct from other elements, and, finally, it would be nice to see the very old-fashioned table comparing the known properties of germanium with Mendeleev's predictions, if only to illustrate the power of the Periodic system in the hands of a skilled practitioner!

Stanground School **SIMON COTTON**
Peterborough
Cambs, U.K.

Organotitanium Reagents in Organic Synthesis. Manfred T. Reetz, Springer, Berlin, 1986. ISBN 3-540-15784-0, 236 pp., 23 figs, DM 168.

This volume is a timely addition to the Springer series "Reactivity and Structure Concepts in Organic Chemistry". The book is organized in eight concise chapters each with its own comprehensive references. Early chapters cover the preparation and general properties of organotitanium compounds, including a brief treatment of theoretical and spectroscopic aspects. Subsequent chapters describe the major uses of titanium in synthesis. Addition reactions of organotitanium reagents to carbonyl compounds are treated in some detail and with special regard to chemo- and stereoselectivity, and with a separate brief chapter concerning kinetics.

Other areas treated include the use of titanium species as Lewis acid mediators in reactions of enol and allyl silanes, titanium enolate chemistry, and methylenation reactions using titanium-based reagents. The book includes coverage of the literature up to early 1985 along with additional unpublished data from Prof. Reetz's own research group. The excellent organization and layout of this volume make it an enjoyable read as well as a valuable reference book, and it should prove popular and useful to all those involved in organic synthesis.

Department of Chemistry **N. S. SIMPKINS**
Queen Mary College
Mile End Road
London E1 4NS, U.K.

Gmelin Handbook of Inorganic Chemistry, 8th Edition. Sn—Organotin Compounds, Part 13, Other RSn–Oxygen Compounds. Compounds with Two and Three Different Organic Groups Bonded to the Sn Atom. Springer, Berlin, 1986. xii+374 pp., DM 1456.

Organotin chemists will be delighted to see the rapid appearance of this 13th volume on organotin compounds. Like all the previous volumes, it has been compiled by Herbert and Ingeborg Schumann, and it maintains the very high standard of the series.

This volume contains all mononuclear R_3Sn–oxygen compounds with R other than methyl, ethyl, propyl and butyl, and all $R_2R'Sn$– and $RR'R''Sn$–oxygen compounds; the mononuclear restriction means that trialkyltin hydroxides are included, but bis(trialkyltin) oxides are not. The literature is covered up to the end of 1982.

For example, 8 pp. are devoted to the tribenzyltin–oxygen compounds, and cover the hydroxide, alkoxides, phenoxides, ketonates, carboxylates, peroxides, and other miscellaneous derivatives. The section on the corresponding triphenyltin–oxygen compounds is of course much larger (160 pp.). For each compound, details are given of preparations, properties, structure, reactions and applications. Much information is tabulated, and amplified in extensive footnotes. There is an empirical formula index (28 pp.) and a ligand index (59 pp.).

The printing and production are as impeccable as usual.

Doubly welcome is the promise that additional volumes describing other R_3SnO derivatives and tin–oxygen compounds with R_2Sn and RSn groups will follow in the near future.

Department of Chemistry **A. G. DAVIES**
University College London
20 *Gordon Street*
London WC1H 0AJ, U.K.

Gmelin Handbook of Inorganic Chemistry, 8th Edition. Sb—Organoantimony Compounds, Part 4, Compounds of Pentavalent Antimony with Three Sb—C Bonds. Springer, Berlin, 1986. 250 pp., DM 1173.

The first volume of this series covered organoantimony compounds of type R_3Sb, the second covered the compounds R_2SbX and $RSbX_2$, and the third dealt principally with the Sb(V) compounds R_5Sb.

This fourth volume describes pentavalent antimony compounds of types R_3SbX_2 and $R_3Sb{=}X$.

Most readers will be familiar with the Gmelin format. The text is now wholly in English. For each compound, the preparations are first listed, then the physical and spectroscopic properties, with figures of the molecular structure if it has been determined by diffraction

methods. Finally any applications of the compounds are described and references are given at the end of each section. Related compounds {e.g. the triorganoantimony dibenzoates $[R_3Sb(O_2CAr)_2]$}, or related information about a compound (e.g. the preparations of Ph_3SbO) are frequently tabulated.

For example trimethylantimony dichloride is described in 9 pp. This includes tables of the IR and Raman vibration spectra of the solid, of the reactions of Me_2SbCl_3, and of the Raman spectrum of the complex $Me_3SbCl_2 \cdot SbCl_3$, and a figure of the crystal structure of this complex. A list of 84 references completes the section.

Apparently there are now some 1200 publications and 400 patents on organoantimony compounds, more than half of which have been published within the past 10 years, and over 3000 organoantimony compounds have been described. This volume will be invaluable to the growing number of chemists who are interested in this field.

A. G. DAVIES

Department of Chemistry
University College London
20 *Gordon Street*
London WC1H 0AJ, U.K.

Polyhedron Vol. 6, No. 3, p. 663, 1987
Pergamon Journals Ltd. Printed in Great Britain

ANNOUNCEMENT

POLYHEDRON PUBLICATION AWARD

Pergamon Journals Ltd is pleased to announce the award annually of a cash prize of $1000 for the best paper published in *Polyhedron.*

The award will be made to the authors of the original research paper (not including *Polyhedron* Reports) judged to be the best on the basis of scientific originality, significance, clarity and style of presentation. The first award will be made for a paper published in Volume 6, 1987. Members of the Editorial Board will each be invited to nominate two papers for the award and the final selection will be made by an anonymous committee appointed by the Editors who themselves will not be eligible for the award.

The recipient of the first award will be notified early in 1988.

Polyhedron Vol. 6, No. 4, p. 665, 1987
Printed in Great Britain

0277-5387/87 $3.00+.00
Pergamon Journals Ltd

INTRODUCTION

MALCOLM H. CHISHOLM

The discovery by Cotton and coworkers in the mid 1960s that metal atoms could form quadruple bonds with one another heralded a new chapter in inorganic chemistry. Now, after more than 20 years, multiple bonds between metal atoms still provide challenges in terms of theory, spectroscopy and reactivity. In this collection of papers the reader will find articles of topical interest in the field of metal–metal multiple bonds varying from extensive reviews of an area to short contributions dealing with a very specific topic. Clearly the field is maturing. The chemistry is getting richer and more diverse and should prosper well for another two decades or more.

Polyhedron Vol. 6, No. 4, pp. 667–677, 1987
Printed in Great Britain

0277–5387/87 $3.00+.00
Pergamon Journals Ltd

THE STRUCTURES OF METAL–METAL-BONDED EDGE-SHARING BIOCTAHEDRAL COMPLEXES

F. A. COTTON

Department of Chemistry and Laboratory for Molecular Structure and Bonding, Texas A&M University, College Station, TX 77843, U.S.A.

(*Received* 19 *November* 1986)

The edge-sharing bioctahedron presents a broadly applicable and flexible framework within which to examine the interaction between adjacent metal (M) atoms.[1,2] The basic unit is shown in general form in Fig. 1.

The flexibility of this structure motif is due to the following factors:

(1) M may be varied in three ways: (a) atomic number (hence, size); (b) charge; and (c) number of *d*-electrons.

(2) There are at least three non-equivalent types of ligands which may be varied independently:

(a) The terminal ligands X and Z may be the same or different, anionic or neutral, and they may be connected in various ways, viz. Z to Z, X to X or Z to X.

(b) The bridging ligands Y can be varied in size, e.g. O vs S or Se, Cl vs Br or I etc. These size changes by themselves can have a major influence on the strength of the M–M interaction.

(c) The linking of Z to adjacent Z, for example if a ligand such as RCO_2^- or $R_2PCH_2PR_2$ is used, also influences the M–M distance since in this way the repulsive forces between independent Zs are reduced (a point first stressed by Shaik *et al.*[3]).

It should be noted that the highest possible symmetry for compounds of this class is D_{2h}, even if X = Y = Z. The maintenance of this symmetry does not require any special values of the various angles, e.g. X–M–X, Y–M–Y, M–Y–M, Z–M–X or Z–M–Y. It does, however, depend on the existence of two mutually perpendicular planar units, one comprised of the $X_2M(\mu\text{-}Y)_2MX_2$ set and the other of the M_2Z_4 set. There must also be another plane of symmetry perpendicularly bisecting the M ··· M line and containing the Y ligands.

There are a number of cases in which small twists about the M ··· M axis degrade the D_{2h}-symmetry. This is understandable since such a twist can increase the two Z ··· Z distances and the four X ··· Y distances, thus diminishing the repulsive energy in the molecule. An example is shown in Fig. 2. However, the twist angles are generally small (< 10°) and in considering the M–M bonding and other aspects of the electronic structure these twists are generally ignored, and calculations are performed as though D_{2h}-symmetry were fully displayed.

One further prefactory observation concerns the relationship of the various bond angles at the metal atoms to the nature and strength of the M–M interaction. If two regular octahedra are simply joined on a common edge, all angles are 90° (or 2 × 90°), including the M–Y–M angles. This situation is not, however, of any special significance in real cases, and will not be seen except by pure coincidence. In the absence of an M–M bond, numerous repulsive forces, including (and perhaps

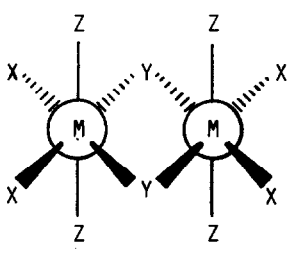

Fig. 1. Generalized, schematic representation of the edge-sharing bioctahedron.

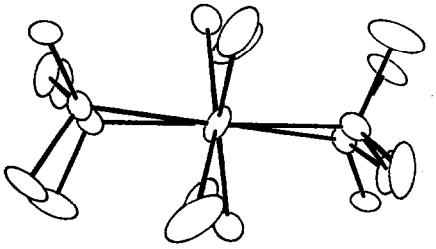

Fig. 2. View of the $Nb_2Cl_6(dmpm)_2$ molecule along the Nb–Nb bond axis. The staggering of the chlorine atoms is clearly shown.

Table 1. M_2Cl_{10} structures

M	M–M (Å)	Mean M—(μ-Cl) (Å)	Mean M—Cl_t (Å)	(μ-Cl)—M—(μ-Cl) (°)	Reference
Nb	3.951(2)	2.55	2.28	78.7	5
Mo	3.84(2)	2.53	2.24	81.4	6
W	3.814(2)	2.52	2.25	81.5	7
Re	3.739(2)	2.47	2.25	81.3	8

especially) the repulsion between the two M atoms themselves, will elongate the structure so as to make the Y–M–Y angles $<90°$ and the M–Y–M angles $>90°$. This will probably indirectly cause the X–M–X angles to become $>90°$.

On the other hand, the drawing together of the metal atoms resulting from a direct M–M bond will have consequences that are the opposite of those just mentioned, i.e. Y–M–Y $> 90°$, M–Y–M $< 90°$, and probably X–M–X $< 90°$.

It is likely that even the formation of an M–M single bond will cause a net contraction of the structure; thus only contracted structures with M–M bonds or extended structures with no M–M bonds are likely to be seen. This is true for all structures presently known. The exact balancing of an attractive (i.e. M–M-bonding) force and the repulsive forces to result in the ideal structure derived from two conjoined octahedra is not to be expected in any real compound. Thus, in general, the existence of an M–M bond will be evident from the structure. Similar considerations were outlined and illustrated many years ago for confacial bioctahedral complexes.[4]

With these considerations in mind, we turn now to a tabulation of the majority of the edge-sharing bioctahedral structures known. We have intentionally excluded from this tabulation compounds with large numbers of strongly π-accepting ligands, e.g. $(OC)_4MnCl_2Mn(CO)_4$, as well as a few other compounds having odd features that place them outside of a mainstream discussion.

METAL PENTAHALIDE DIMERS

We consider these molecules separately because they lack M–M bonds. In general the higher the oxidation state of the M atoms the less likely they are to form M–M bonds, and this is especially true when the bridging atoms are as large as Cl, or larger. The four structurally characterized M_2X_{10} compounds are the chlorides of Nb (d^0), Mo (d^1), W(d^1), and Re (d^2). Their structural parameters are listed in Table 1.

It can be seen that these non-bonded M–M distances are all very long, *ca* 3.8 ± 0.1 Å, and that the stretching out of the central rhombus results in (μ-Cl)—M—(μ-Cl) angles of *ca* 80°. Another consistent characteristic of these structures is the great difference between the M—(μ-Cl) and M—Cl_t bond lengths (*ca* 0.25 Å). In the M–M-bonded structures to be considered later, we shall see very different features.

Before turning to the large group of structures with which this review is mainly concerned, we may note that even for an oxidation number of V, M–M bond formation is possible if other factors are conducive. This point is well illustrated by a condensed structure in which there are $Re_2(V)O_{10}$ units.[9] In $Nd_4Re_2O_{11}$, there are $Re_2(V)O_{10}$ fragments in which the Re–Re distance is 2.421 Å, and the assignment of a Re=Re double bond is straightforward. The presence of small bridging atoms is perhaps the major factor in allowing or even encouraging a close approach of the Re atoms. It is, however, also worth noting that this factor alone does not assure the formation of M–M bonds. In the compound $PbRe_2O_6$, there are connections to the surrounding structure that tend to draw the Re_2O_{10} unit out and the resulting Re–Re distance is 3.102(1) Å (compared to 2.77 Å calculated for idealized edge-sharing ReO_6 octahedra). Presumably no significant Re–Re bonding exists in this case.

GENERAL SURVEY OF STRUCTURES

In Table 2 all of the structural data we wish to examine and discuss here are listed. To facilitate the use of the table, note that it is organized as follows:

(1) d^1–d^1 species: (a) +3, +3; (b) +4, +4; and (c) +5, +5.

(2) d^2–d^2 species: (a) +3, +3; and (b) +4, +4.

(3) d^3–d^3 species: (a) +3, +3; and (b) +4, +4.

(3/4) d^3–d^4 species: (a) +3, +4.

(4) d^4–d^4 species: (a) +3, +3; and (b) +4, +4.

(5) d^5–d^5 species: (a) +3, +3.

In each category, complexes are listed in order of increasing atomic number, e.g. all Mo complexes

Table 2. Listing of edge-sharing bioctahedral structures [formula, M–M bond length (Å), and reference]

1. d^1-d^1 Species

(a) +3, +3

1. 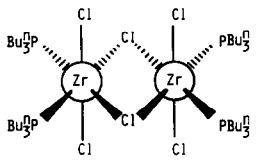 3.182(1) [10]

(b) +4, +4

1. 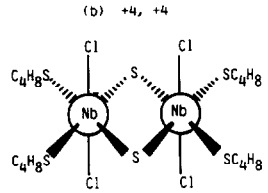 2.868(2) [11]

2. 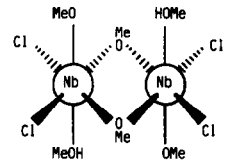 2.781(1) [12]

3. 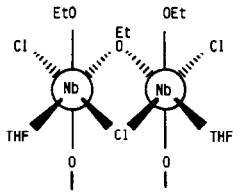 2.891(1) [12]

4. 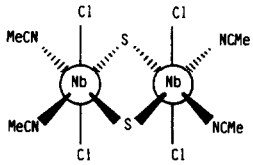 2.862(2), 2.872(2), 2.864(2) (Three independent molecules) [13]

5. 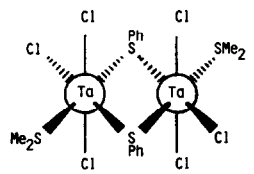 3.165(1) [14]

(c) +5, +5

1. 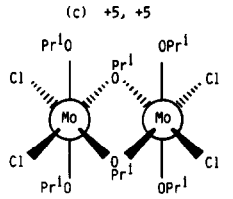 2.731(1) [15]

2. 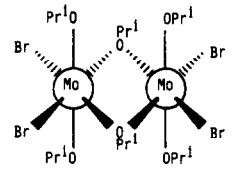 2.739(1) [15]

3. 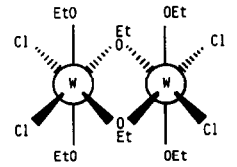 2.715(1) [16]

4. 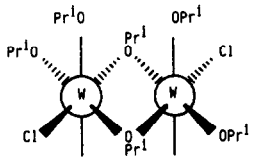 2.784(1) [17]

5. 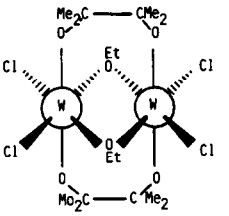 2.701(1) [18]

6. 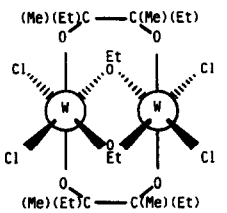 2.691(1) [18]

7. 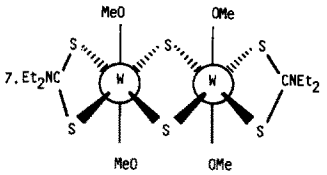

2.791(1) [19]

8. 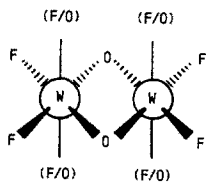

2.620(1) [20]
$[W_2O_4F_6]^{4-}$ with F/O disorder

2. q^2-q^2 Species

(a) +3, +3

1. 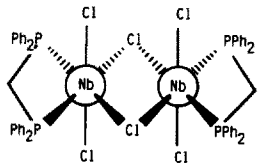

2.696(1) [21]

2. 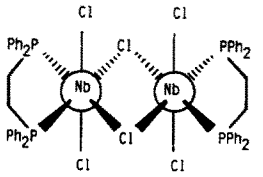

2.729(2) [22]

3. 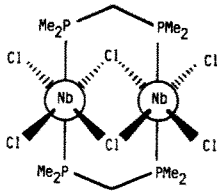

2.711(3) [23]

4. 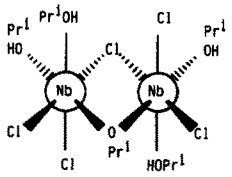

2.611(3) [12]

5. 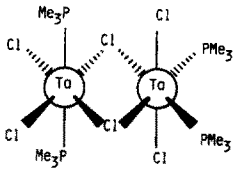

2.721(1) [24]

6. 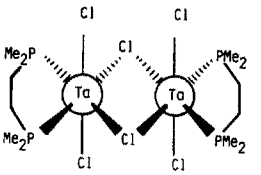

2.710(1) [25]

7. 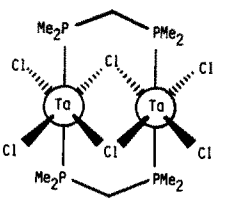

2.692(2) [2]

8. 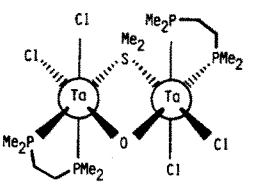

2.726(1) [26]

(b) +4, +4

1. 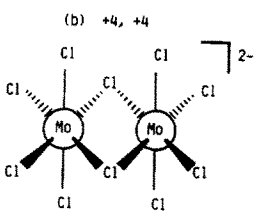

3.80 [27]

2. 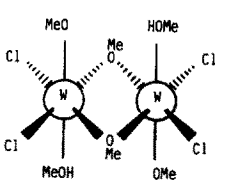

2.481(1) [28]

3. 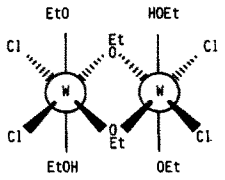

2.483(1) [28]

4. 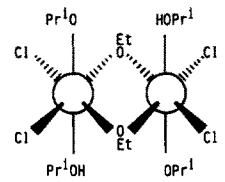

2.488(1)
2.499(1)
(two independent molecules)
[29]

5. 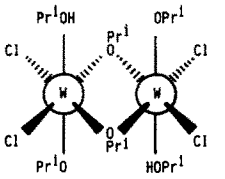

2.514(1)
2.530(1)
(two independent molecules)
[29]

6. 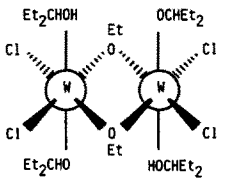

2.489(1)
2.491(1)
two independent molecules
[29]

7. 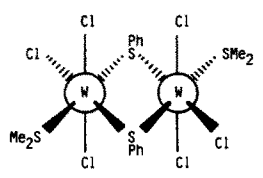

2.759(1) [30]

8. 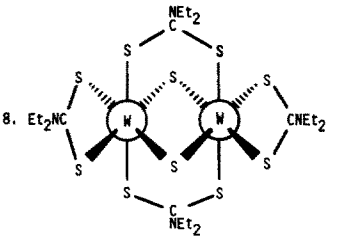

2.530(2) [19]

3. d^3-d^3 Species

(a) +3, +3

1. 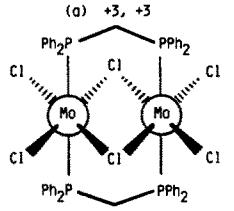

2.789(1) [2]

2. 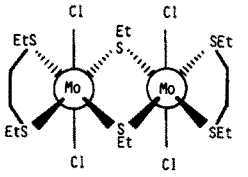

2.682(1) [1]

3. 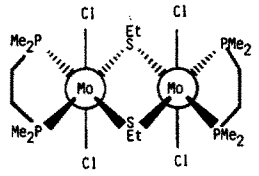

2.712(3) [1]

4. 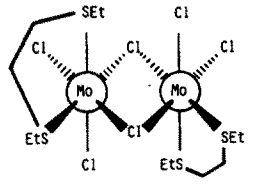

2.735(2) [31]

5. 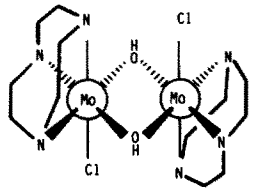

2.501(3) [32]

6. 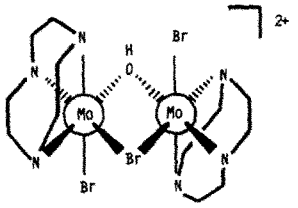 2.558(3) [33]

7. 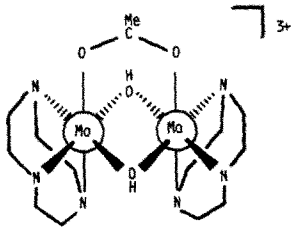 2.471(2) [32]

8. 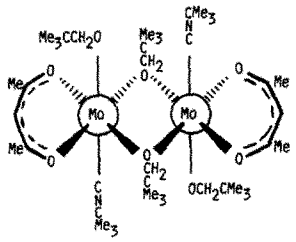 2.508(2) [34]

9. 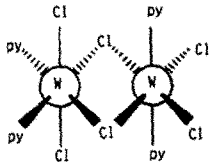 2.737(2) [36]

10. 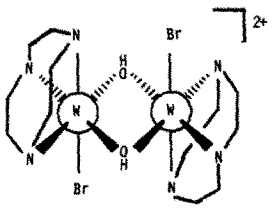 2.477(3) [37]

(b) +4, +4

1. 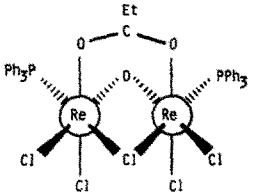 2.522(1) [35]

3/4. d^3-d^4 Species

(a) +3, +4

1. 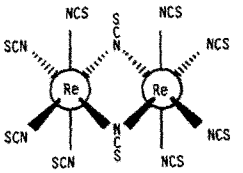 2.613(1) [38,39]

2. 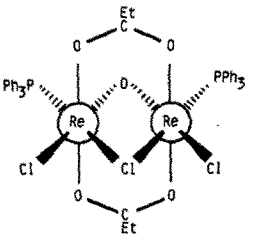 2.514(1) [40]

3. 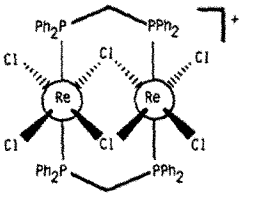 2.682(1) [41]

4. 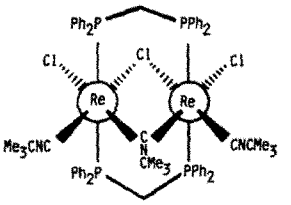 2.704(1) [42]

4. d^4-d^4 Species

(a) +3, +3

1. 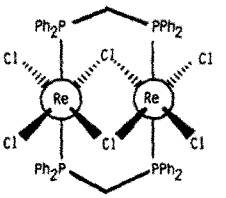 2.616(1) [43]

2. 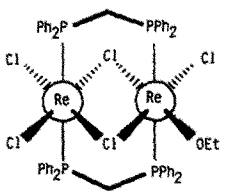 2.667(1) [43]

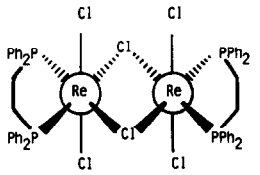

3. 3.809(1) [44]

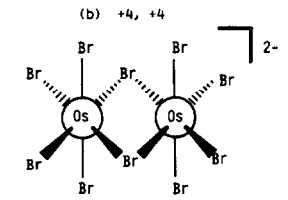

1. 3.788(3) [45]

5. d^5–d^5 Species

(a) +3, +3

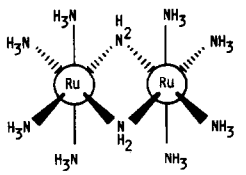

1. 2.625(1) [46]

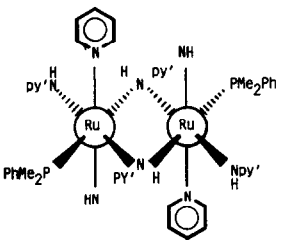

2. 2.573(2) [47]

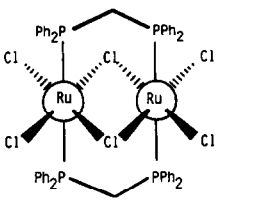

3. 2.933(1) [2]

Note added in proof. The ligand in the above compound 5(a)3 should be $Me_2PCH_2PMe_2$.

before W complexes. Each complex can then be cited by a number, such as 1(b)5, which immediately locates it in the table.

DISCUSSION

The many structures listed in Table 2, 52 in all, afford a very disparate array. No attempt will be made to discuss all of them; instead some important trends will be noted and also a few compounds that present special features will be highlighted. Before doing that, however, we must summarize the electronic structure considerations that are important in determining the M–M bond orders as a function of the number of *d*-electrons on each metal. In doing this we shall be making assertions that arise from the calculations and experiments detailed in Refs 1–3 and 28.

The M–M bonding in an edge-sharing bioctahedron can be formulated in a sort of "zero-ith order" approximation by assuming that the six σ-bonds that each metal atom forms to ligands engage the usual set of orbitals, viz. s, p_x, p_y, p_z, d_{z^2} and $d_{x^2-y^2}$ (where for the moment we use a local, conventional set of Cartesian axes). There are then three *d*-orbitals on each M atom (those conventionally designated as $d\pi$ or t_{2g} orbitals) available to form bonds between the M atoms. They are enabled by symmetry to form σ, σ^*, π, π^*, δ and δ^* combinations. Figure 3(a) shows the three bonding combinations in a schematic way and Fig. 3(b) the relative energies of all the orbitals that would be expected purely on the basis of the differing extents of overlap. From this simple picture we would expect that for complexes of the d^n–d^n type the following bond orders would arise for different values of n: $n = 1$ or 5 single (σ), $n = 2$ or 4 double ($\sigma + \pi$), and $n = 3$ triple ($\sigma + \pi + \delta$).

Even approximate MO calculations (extended Hückel or Fenske–Hall) immediately show that this simple and rigid picture is untrustworthy. Because certain M–ligand interactions can compete in importance with certain M–M interactions, especially at longer M–M distances, the pattern of orbital energies in Fig. 3(b) need not be correct. For our purpose here it will suffice to say that the major ambiguity is in the ordering of the δ- and δ^*-levels. There is reason to believe that both orderings, $\delta < \delta^*$ [as in Fig. 3(b)] and $\delta^* < \delta$, occur in different complexes. In any case, however, the δ-orbital is only weakly bonding and the δ^*-orbital only weakly antibonding, at least in most cases.

With these considerations in mind, we might expect that d^1–d^1 and d^5–d^5 complexes would have the longest M–M bonds, while d^2–d^2 and d^4–d^4 complexes, having net double bonds, would display appreciably shorter M–M distances. The d^3–d^3 systems might be expected to have fairly short bonds, but exactly how they would relate to those in the doubly-bonded systems would depend on

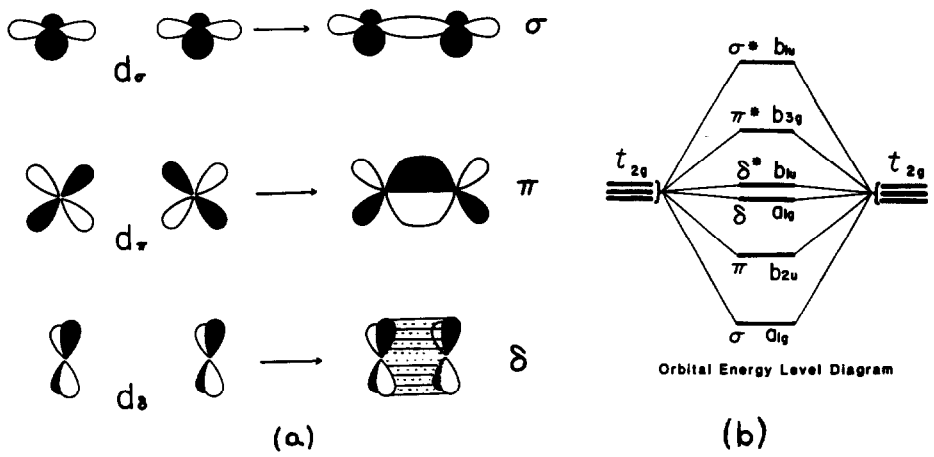

Fig. 3. (a) d–d overlaps giving rise to M–M bonding orbitals of σ, π and δ types. (b) Pattern of energy levels expected purely on the basis of relative orbital overlaps.

the ordering of the δ and δ^* levels.

All of the trends and relationships that are suggested by M–M bonding considerations are subject to major modification when the sizes, and other properties, of the ligands are changed. A particularly prominent and consistent effect is that the smaller bridging ligands promote shorter and stronger M–M bonds, other things (i.e. M charges and d^n-configurations) being equal.

(*a*) *The longest bonds*

The first compound in the table, 1(a)1, has the longest M–M *bonded* distance so far reported, namely a Zr–Zr single bond distance of 3.182(1) Å. This distance probably indicates the approximate upper limit for M–M bonds in this structural context since all other d^1–d^1 singly-bonded systems, compounds 1(b)1–1(b)5 and 1(c)1–1(c)8 have shorter ones. Only 1(b)5 is comparable, with a Ta–Ta distance of 3.165(1) Å. There are a few M–M single bonds formed by d^5–d^5 systems and no doubt more will be discovered, but we might hazard the suggestion that these should not be in any case longer than the longest d^1–d^1 single bonds because of a general contraction in atomic size as we proceed from left to right across the transition series.

(*b*) *The shortest bonds*

There are several that lie in the range 2.471–2.501 Å, namely, those in 2(b)2, 2(b)3, 2(b)4, 2(b)6, 3(a)5, 3(a)7 and 3(a)10. As is evident from their numbers, these are d^2–d^2 and d^3–d^3 systems. These complexes also all contain OR or OH groups as bridging ligands. Thus, with the electron configurations suitable for the formation of double bonds ($\sigma^2\pi^2$) or, considering the weakness of the δ overlaps, approximately double bonds ($\sigma^2\pi^2\delta^2$ or $\sigma^2\pi^2\delta^{*2}$), and with the smallest of bridging ligands, it is entirely understandable that these systems have the shortest M–M distances.

(*c*) *Effect of bridging ligand size*

We have just had occasion to cite the influence of bridging ligands on M–M distance, particularly as a consequence of their size. This is a feature of general importance in this class of compounds as the following examples, chosen from Table 2, will illustrate.

The series of Mo(V) and W(V) complexes, 1(c)1–1(c)6 all have M–M single bonds with M–M distances of about 2.70–2.78 Å. This is in contrast to the Mo_2Cl_{10} and W_2Cl_{10} molecules mentioned earlier in which there are no M—M bonds and the distances are *ca* 3.7 Å. A major factor in this contrasting behavior must be the replacement of μ-Cl groups by μ-OR groups, which are much smaller. It must be noted, however, that all of these bonded complexes also differ from the M_2Cl_{10} species in that there are some terminal OR groups replacing terminal Cl ligands. This too may favor M–M bonding because the π-donating tendency of the OR groups will serve to lessen the effective positive charge on the M atoms, thus making them more able to achieve the necessary d–d overlap for M–M bond formation.

The chloro-bridged complexes of Nb(III), e.g. 2(a)1–2(a)3 have Nb–Nb distances of *ca* 2.71 Å, while in 2(a)4, where one μ-Cl has been replaced by μ-OPr^i, the distance is reduced to 2.61 Å. Admittedly, there are also changes in the set of terminal ligands, so that this comparison is not as unambiguous as one might like. This is but one of the many instances in this field where it would be desirable

to conduct a synthetic program designed to deliver pairs or sets of molecules in which only one feature at a time is changed.

(*d*) *Influences of terminal ligands*

The strength of the M–M bond can be affected by the steric as well as the electronic properties of the terminal ligands, both the X and the Z types (Fig. 1). Shaik *et al.*[3] first called attention to the potential importance of the repulsive force between opposite pairs of Z ligands. Clearly, it is not possible to have M–Z bonds perpendicular to the central molecular plane along with M–M distances in the bonding range (i.e. < 3.2 Å) when the van der Waals' radii of the Z ligands are > 1.6 Å, which is the case for nearly all ligands. To relieve strain the M–Z bonds may bend away from perpendicularity to the central plane, but, in addition, some stretching of the M–M bond may also be caused.

In principle the way to minimize and even eliminate the Z···Z repulsion problem is to have the pairs of Z atoms tied together. There are examples among the known compounds of at least three ways to do this. The use of $R_2PCH_2PR_2$ (R = Ph or Me) is quite common. It is noteworthy, however, that the effectiveness of this approach is open to question. As will be explained under point (e) below, there is one instance in which the use of $Ph_2PCH_2PPh_2$ would appear to be critical to the formation of an M–M bond. However, we can also argue that on comparison of 2(a)1 and 2(a)2, where the diphosphine ligands chelate, with 2(a)3, where the $Me_2PCH_2PMe_2$ ligands span the adjacent axial positions, the "tying-together" does nothing to improve the M–M bonding. Thus, in 2(a)1 and 2(a)2 the Nb=Nb double bonds are 2.70 and 2.73 Å in length, while in 2(a)3 it is 2.71 Å in length. The same relationship is seen for 2(a)6 and 2(a)7 where the Ta=Ta distance in the "tied-together" case is less than 0.02 Å shorter than in the case where all Z-type positions are occupied by Cl atoms. Still another comparison that argues against the effectiveness of the $R_2PCH_2PR_2$ type ligand in enhancing M–M bonding is afforded by 3(a)1 where there are bridging $Ph_2PCH_2PPh_2$ ligands (and Mo–Mo = 2.79 Å) and 3(a)2–3(a)4, where there is no "tying together", and the Mo–Mo distances are in fact appreciably *shorter*, viz. 2.68–2.74 Å. Again, however, the comparison is marred by the fact that other features also differ and it would be safer to prepare and study some more conservatively altered pairs.

The presence of a μ_2-η^2 RCO_2^- ligand across an adjacent pair of Z positions is illustrated by 3(a)7, 3(b)1 and 3/4-2. However, the absence of any appropriate molecules that lack this feature but are otherwise closely similar means that we cannot determine whether such a carboxyl ligand is truly valuable in promoting M—M bond formation.

Finally, we note in 2(b)2–2(b)6 that by having an ROH and an RO ligand on each of the adjacent Z positions a "tying-together" effect arises by intramolecular hydrogen-bond formation. Indeed, in several of these molecules the hydrogen bond may well be a symmetrical one. Curiously, in 1(b)2 which is the Nb homolog of 2(b)2, no such intramolecular hydrogen bonding occurs; instead the two MeOH ligands form hydrogen bonds to neighboring molecules in the crystal.

The nature of the other terminal ligands, the X ligands in Fig. 1, may be less important than that of the Y or Z ligands, but this point remains somewhat moot on the basis of the present data. However, 4(a)1 and 4(a)2 afford evidence that such X-ligand effects can be appreciable. In going from 4(a)1 to 4(a)2 the only change in composition is the replacement of one terminal Cl ligand by an OEt group, but the Re–Re bond length increases from 2.62 to 2.67 Å. The probable reason for this increase is that the alkoxide ligand donates more strongly from its $p\pi$ orbitals to the σ^*- or π^*-orbitals of the Re_2 unit, thus weakening the Re–Re bond.

(*e*) *Comparisons in homologous series*

Because of the marked sensitivity of M–M distances to the identities and properties of the ligands (X, Y and Z), to the formal charges on the M atoms, and to the number of electrons available for M–M bonding, a meaningful search for systematic trends in M–M interaction can be successful only if we examine a series of compounds in which just one of these factors at a time is made to vary. We will summarize here the work on one suitable homologous series; it is actually the only one of sufficient extent to be really informative but no doubt other such series will be studied soon, as synthetic work makes them available.

The series in question here is comprised of complexes 2(a)3, 2(a)7, 3(a)1, 4(a)1 and 5(a)3. They are all of the type shown in the diagram below.

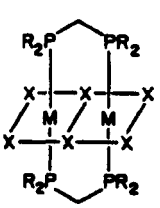

II

R=CH3, C6H5

X=Cl

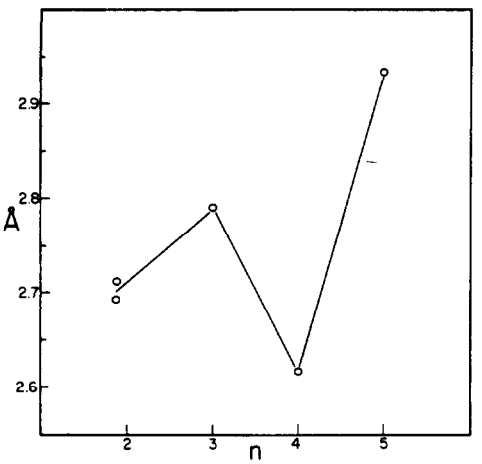

Fig. 4. M–M distances for a series of $M_2Cl_6(\mu\text{-dppm})_2$ or $M_2Cl_6(\mu\text{-dmpm})_2$ compounds covering d^n–d^n interactions form n from 2 to 5. The two points for $n = 2$ are for Nb and Ta compounds.

The details of this work will be found in Ref. 2. The purpose of the study was to employ structural data to infer the ordering of the MOs mainly responsible for M–M bonding. The particular point of uncertainty concerned the relative energies of the δ- and δ^*-levels. As already mentioned, it is not safe to assume that δ must be below δ^*, and it has been shown[2,3] that interaction of filled ligand orbitals with the M d-orbitals that contribute to the δ- and δ^*-levels can reverse this order, placing δ^* below δ.

The way in which M–M bond lengths change through a series of compounds with d^1–d^1, d^2–d^2, d^3–d^3, d^4–d^4 and d^5–d^5 M atom pairs will be different for the two possible relationships of the δ- and δ^*-orbitals. On going from d^1–d^1 to d^2–d^2 we pass from a σ^2 single bond to a $\sigma^2\pi^2$ double bond, and this should cause a marked decrease in M–M distance. Similarly, at the other end of the series, when we pass from the $\sigma^2\pi^2(\delta/\delta^*)^4$ configuration to the $\sigma^2\pi^2(\delta/\delta^*)^4\pi^{*2}$ configuration, there should be a marked increase in the M–M distance. What happens in between these end pairs, that is, between the d^2–d^2 and d^4–d^4 cases will depend on the order of filling the δ- and δ^*-orbitals. If δ is filled first, there should be a "down followed by up" pattern, whereas if δ^* is filled first there should be an "up followed by down" pattern in the M–M distances. These changes in distance should, of course, be smaller than those caused by adding the more strongly bonding or antibonding π- or π^*-electrons.

As shown in Fig. 4, the observed variation in M–M distances through the series from d^1–d^1 to d^5–d^5 is indicative of a σ, π, δ^*, δ, π^*, σ^* sequence of levels.

It should be noted that even in this study, perfect homology was not achieved for several reasons. First, the type of structure required could not be obtained in every case with either $Ph_2PCH_2PPh_2$(dppm) or $Me_2PCH_2PMe_2$(dmpm); instead it was necessary to use one of these in some cases and the other one in the remaining cases. It is not expected that changes in M–M bond length that might be caused by this would be as large as the significant variations observed, but this is a point that ought to be checked, and efforts to do so are underway. Second, the set of complexes used includes some from the second transition (4*d*) series and some from the third (5*d*) series. By examining both the niobium and tantalum compounds it was found (and can be seen in Fig. 4) that the difference is too small to influence the overall pattern of changes.

(*f*) *A puzzling anomaly*

In contradistinction to the type of regular, and understandable, behavior just discussed, there is one particularly puzzling deviation from regularity in a homologous series of complexes. As long ago as 1975 it was reported that in 4(a)3 there is no Re–Re bond, even though a $\sigma^2\pi^2\delta^2\delta^{*2}$ configuration, giving rise to a net double bond, would seem quite possible and even likely. In at least partial explanation of this, Shaik *et al.*[3] suggested that repulsive forces between the axial (Z-type in Fig. 1) Cl atoms might be sufficient to deny the system access to the bonded state. They suggested that in a similar complex where the Z positions were occupied by ligand atoms tied together, the Re=Re double bond would be seen. This prediction was later confirmed when the structures of 4(a)1 and 4(a)2 were determined. Here, the diphosphine ligands are dppms that span the adjacent pairs of Z positions.

However, further work has now shown that this apparently satisfying picture must be too simple; something of importance is omitted from it. We see this by referring to compounds 2(a)1, 2(a)2, 2(a)6, 3(a)2 and 3(a)3, to mention only the most directly pertinent ones. In each of these we have essentially the same type of ligand arrangement as in 4(a)3; indeed in 2(a)2 the composition is identical and in 2(a)6 the only difference is replacement of the chelating dppe ligands by dmpe ligands. In all of these complexes there are M–M bonds with lengths in the range 2.68–2.73 Å, formed by d^2–d^2 or d^3–d^3 M atom pairs. Thus, it appears that simply by adding two more electrons, to reach a d^4–d^4 situation, the formation of an M–M bond is abruptly disfavored.

There is at present no explanation for this discontinuous behavior. Further experimental data that

might serve to define more precisely the properties associated with the discontinuity would certainly be welcome and efforts in that direction are underway in the author's laboratory. Some pertinent synthetic targets are (dmpe)$Cl_4Re(\mu\text{-}Cl)_2ReCl_4$(dmpe), as well as the following pairs (where R = CH_3 or C_6H_5): (dRpe)$Cl_4W(\mu\text{-}Cl)_2WCl_4$(dRpe) and (dRpe)$Cl_4Tc(\mu\text{-}Cl)_2TcCl_4$(dRpe).

Acknowledgements—Support for experimental work in this area as well as for the preparation of this article was provided by the National Science Foundation, and is hereby gratefully acknowledged. I am also happy to thank Dr Kim Dunbar for useful discussions and for reading the manuscript.

REFERENCES

1. F. A. Cotton, M. P. Diebold, C. J. O'Connor and G. L. Powell, *J. Am. Chem. Soc.* 1985, **107**, 7438.
2. A. R. Chakravorty, F. A. Cotton, M. P. Diebold, D. B. Lewis and W. J. Roth, *J. Am. Chem. Soc.* 1986, **108**, 971.
3. S. Shaik, R. Hoffmann, C. R. Fisel and R. H. Summerville, *J. Am. Chem. Soc.* 1980, **102**, 4555.
4. F. A. Cotton and D. A. Ucko, *Inorg. Chim. Acta* 1972, **6**, 161.
5. A. Zalkin and D. E. Sands, *Acta Cryst.* 1958, **11**, 615.
6. D. E. Sands and A. Zalkin, *Acta Cryst.* 1959, **12**, 723.
7. F. A. Cotton and C. E. Rice, *Acta Cryst.* 1978, **B34**, 2833.
8. K. Mucker, G. S. Smith and Q. Johnson, *Acta Cryst.* 1968, **B24**, 874.
9. I. Wentzell, H. Fuess, J. W. Bats and A. K. Cheetham, *Z. Anorg. Allg. Chem.* 1985, **528**, 48.
10. J. H. Wengrovius, R. R. Schrock and C. S. Day, *Inorg. Chem.* 1981, **20**, 1844.
11. M. G. B. Drew, D. A. Rice and D. M. Williams, *J. Chem. Soc., Dalton Trans.* 1985, 417.
12. F. A. Cotton, M. P. Diebold and W. Roth, *Inorg. Chem.* 1985, **24**, 3509.
13. A. J. Benton, M. G. B. Drew, R. J. Hobson and D. A. Rice, *J. Chem. Soc., Dalton Trans.* 1981, 1304.
14. G. C. Campbell, J. M. Canich, F. A. Cotton, S. A. Duraj and J. F. Haw, *Inorg. Chem.* 1986, **25**, 287.
15. M. H. Chisholm, C. C. Kirkpatrick and J. C. Huffman, *Inorg. Chem.* 1981, **20**, 871.
16. F. A. Cotton, D. DeMarco, B. W. S. Kolthammer and R. A. Walton, *Inorg. Chem.* 1981, **20**, 3048.
17. T. J. Barder, F. A. Cotton, D. Lewis, W. Schwotzer, S. M. Tetrick and R. A. Walton, *J. Am. Chem. Soc.* 1984, **106**, 2882.
18. L. B. Anderson, F. A. Cotton, D. DeMarco, L. R. Falvello, S. M. Tetrick and R. A. Walton, *J. Am. Chem. Soc.* 1984, **106**, 4743.
19. A. Bino, F. A. Cotton, Z. Dori and J. C. Sekutowski, *Inorg. Chem.* 1978, **17**, 2946.
20. R. Mattes and K. Mennemann, *Z. Anorg. Allg. Chem.* 1977, **437**, 175.
21. F. A. Cotton and W. R. Roth, *Inorg. Chem.* 1983, **22**, 3654.
22. F. A. Cotton and W. R. Roth, *Inorg. Chim. Acta* 1983, **71**, 175.
23. F. A. Cotton, S. A. Duraj, L. R. Falvello and W. J. Roth, *Inorg. Chem.* 1985, **24**, 4389.
24. A. P. Sattelberger, R. B. Wilson, Jr and J. C. Huffman, *Inorg. Chem.* 1982, **21**, 2392.
25. F. A. Cotton, L. R. Falvello and R. Najjar, *Inorg. Chem.* 1983, **22**, 375.
26. F. A. Cotton and W. J. Roth, *Inorg. Chem.* 1983, **22**, 868.
27. E. Hey, F. Weller and K. Deknicke, *Z. Anorg. Allg. Chem.* 1984, **508**, 86.
28. L. B. Anderson, F. A. Cotton, D. DeMarco, A. Fang, W. H. Ilsley, B. W. S. Kolthammer and R. A. Walton, *J. Am. Chem. Soc.* 1981, **103**, 5078.
29. F. A. Cotton, L. R. Falvello, M. F. Fredrich, D. DeMarco and R. A. Walton, *J. Am. Chem. Soc.* 1983, **105**, 3088.
30. P. M. Boorman, J. M. Ball, K. J. Moynihan, V. D. Patel and J. F. Richardson, *Can. J. Chem.* 1984, **61**, 2809.
31. F. A. Cotton, P. E. Fanwick and J. W. Fitch, *Inorg. Chem.* 1978, **17**, 3254.
32. K. Wieghardt, M. Hahn, W. Swiridoff and J. Weiss, *Inorg. Chem.* 1984, **23**, 94.
33. P. Chanduri, K. Wieghardt, I. Jibril and G. Huttner, *Z. Naturforsch.* 1984, **39B**, 1172.
34. M. H. Chisholm, J. F. Corning, K. Folting, J. C. Huffman, A. L. Ratermann, I. P. Rothwell and W. E. Streib, *Inorg. Chem.* 1984, **23**, 1073.
35 F. A. Cotton and B. M. Foxman, *Inorg. Chem.* 1968, **7**, 1784.
36 R. B. Jackson and W. E. Streib, *Inorg. Chem.* 1971, **10**, 1760.
37 P. Chandhuri, K. Wieghardt, W. Gebert, I. Jibril and G. Huttner, *Z. Anorg. Allg. Chem.* 1985, **521**, 23.
38. F. A. Cotton, A. Davison, W. H. Ilsley and H. S. Trop, *Inorg. Chem.* 1979, **18**, 2719.
39. F. A. Cotton, W. R. Robinson, R. A. Walton and R. Whyman, *Inorg. Chem.* 1967, **6**, 929.
40. F. A. Cotton, R. Eiss and B. M. Foxman, *Inorg. Chem.* 1969, **8**, 950.
41. K. R. Dunbar, D. Powell and R. A. Walton, *Chem. Commun.* 1985, 114.
42. T. J. Barder, D. Powell and R. A. Walton, *Chem. Commun.* 1985, 550.
43. T. J. Barder, F. A. Cotton, D. Lewis, W. Schwotzer, S. M. Tetrick and R. A. Walton, *J. Am. Chem. Soc.* 1984, **106**, 2882.
44. J. A. Jaecker, W. R. Robinson and R. A. Walton, *J. Chem. Soc., Dalton Trans.* 1975, 698.
45. F. A. Cotton, S. A. Duraj, C. C. Hinckley, M. Matusz and W. J. Roth, *Inorg. Chem.* 1984, **23**, 3080.
46. M. T. Flood, R. F. Ziolo, J. E. Earley and H. B. Gray, *Inorg. Chem.*, 1973, **12**, 2153.
47. A. R. Chakravarty, F. A. Cotton and D. A. Tocher, *Inorg. Chem.* 1984, **23**, 4030.

Polyhedron Vol. 6, No. 4, pp. 679–684, 1987
Printed in Great Britain

0277–5387/87 $3.00+.00
Pergamon Journals Ltd

PROBLEMS IN THE THEORETICAL DESCRIPTION OF METAL–METAL MULTIPLE BONDS OR HOW I LEARNED TO HATE THE ELECTRON CORRELATION PROBLEM

MICHAEL B. HALL

Department of Chemistry, Texas A&M University, College Station, TX 77843, U.S.A.

(*Received* 19 *November* 1986)

Abstract—The goal of this article is to present a historical perspective to theoretical calculations of metal–metal multiple bonds, to explain why calculations on these systems are so difficult and to predict the direction of future research in this area.

From the beginning, theory has played an important role in the history of the quadruple bond. The first report[1] of the structure of $K_2Re_2Cl_8 \cdot 2H_2O$ contains an explanation of the short Re–Re bond and the eclipsed Cl ligands in terms of the, now familiar, quadruple bond, $\sigma^2\pi^4\delta^2$. Although some early extended Hückel calculations were performed, 10 years passed before this problem was tackled by more accurate calculations. The first of these was a scattered-wave X-α (SW-Xα) calculation on the $Mo_2Cl_8^{4-}$ ion.[2] This calculation confirmed the $\sigma^2\pi^4\delta^2$ ordering for the orbitals in this ion. Following the initial discovery of the quadruple bond in $Re_2Cl_8^{2-}$, other second- and third-row quadruply bonded systems were prepared. In 1970 the structure of $Cr_2(O_2CCH_3)_4(H_2O)_2$ was determined (Cr–Cr = 2.362 Å) and the molecule was postulated to contain a quadruple Cr–Cr bond.[3] The first *ab initio* calculation was performed on the related $Cr_2(O_2CH)_4$ dimer and published in conjunction with the gas-phase ultraviolet photoelectron (PE) spectrum of $Cr_2(O_2CCH_3)_4$.[4] In this work the authors found that the lowest-energy single-determinant wavefunction was $\sigma^2\pi^2\pi^{*2}\sigma^{*2}$. Thus, they predicted that there was no Cr–Cr bond in this system. They suggested that this was the reason for the somewhat long bond length and they assigned all the metal ionizations to the first band in the PE spectrum.

These conclusions were the beginning of two controversies. The first centered on the nature of the Cr–Cr bonding, i.e. was it or wasn't it a quadruple bond? The second centered on the assignment of the PE spectrum, i.e. were all the Cr ionizations in the first band or was the ionization for the bonding σ-pair at a substantially higher ionization energy (IE)?

In a scientific sense the first controversy was settled rather quickly with the publication of configuration interaction (CI) calculations on $Cr_2(O_2CH)_4$ and related systems.[5,6] However, because the quadruply bonded configuration, $\sigma^2\pi^4\delta^2$, represented such a small part of the wavefunction, a semantic argument, about whether or not these systems have a quadruple bond, continued to be heard.

The second controversy was only settled recently with the publication of the PE spectra of several quadruply bonded tungsten derivatives[7] and local density functional (LDF) calculations on the IE.[8] Previously, the SW-Xα (a scattered-wave LDF approach) results[9(a)] suggested that the σ-ionization was a high IE and that the first band consisted of only the δ- and π-ionizations. Early *ab initio* results[10] suggested that the first band contained all three ionizations. The PE work on tungsten and the improved LDF calculations confirmed the conclusion of the early *ab initio* results.

A similar controversy concerning the assignment of the $Mo_2(O_2CH)_4$ PE spectrum has been resolved and the initial assignment from *ab initio* calculations[10] proved more accurate than that of the Xα-SW calculations.[9(b)] Again, more sophisticated LDF calculations agree with the *ab initio* results.[8]

Before going on with the progress of theoretical developments in this area, we will present a short discussion of the fundamentals of *ab initio* molecular electronic structure calculations as they relate to the problems in calculating the electronic structure of molecules with metal–metal bonds.

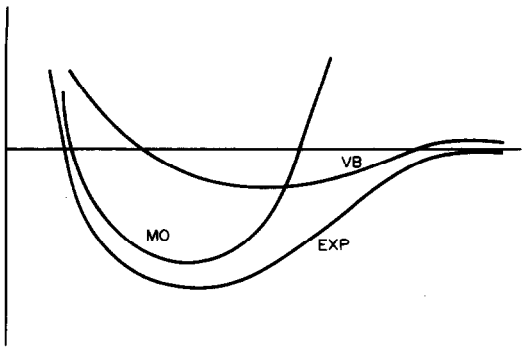

Fig. 1. Schematic potential energy curves are shown for a typical molecular orbital (MO) and valence bond (VB) wavefunction. In comparison with the "experimental" (EXP) curve, the MO wavefunction does not dissociate properly but parallels the EXP curve at short internuclear distances (R), while the VB wavefunction dissociates properly but is too repulsive at shorter R.

THEORETICAL

We will begin with a discussion of the simple diatomic H_2. The two lowest-energy molecular orbitals (MOs) of H_2 are the $1\sigma_g$ and the $1\sigma_u$. The former is the bonding MO, while the latter is the antibonding counterpart. In its ground state H_2 has two electrons in the $1\sigma_g$, i.e. $1\sigma_g^2$. The total wavefunction is the Slater determinant:

$$\Psi_{MO} = |1\sigma_g\alpha 1\sigma_g\beta|, \tag{1}$$

where α and β are the $+\frac{1}{2}$ and the $-\frac{1}{2}$ spin eigenfunction, respectively. The wavefunction must be a Slater determinant in order to obey the Pauli exclusion principle. In the usual linear combination of atomic orbitals (LCAO) approach the $1\sigma_g$ MO is expanded as a linear combination of two atomic-like orbitals, one on each H atom. If we refer to these two functions as a and b, then:

$$1\sigma_g = (a + b)N_+ \tag{2}$$

$$1\sigma_u = (a - b)N_- \tag{3}$$

where $N_\pm$ are the normalization constants.

If one uses a simple MO wavefunction like Ψ_{MO} in eqn (1) to calculate the potential energy curve for H_2, one finds that the energy begins to rise much too rapidly as the internuclear distance increases. This is shown schematically in the curve labelled MO in Fig. 1. The reason for this behavior can be seen, if we expand eqn (1) and substitute the definition of $1\sigma_g$ given in eqn (2). Expansion yields:

$$\Psi_{MO} = [1\sigma_g\alpha(1)1\sigma_g\beta(2) - 1\sigma_g\beta(1)1\sigma_g\alpha(2)]/\sqrt{2}, \tag{4}$$

where (1) and (2) refer to electron labels. We can now factor the space and spin parts

$$\Psi_{MO} = 1\sigma_g(1)1\sigma_g(2)[\alpha(1)\beta(2) - \beta(1)\alpha(2)]/\sqrt{2}, \tag{5}$$

where the latter part $(\alpha\beta - \beta\alpha)/\sqrt{2}$ is the singlet spin function. Expanding the spacial part of the wavefunction by substituting eqn (2) for $1\sigma_g$, we find that:

$$\Psi_{MO} = [a(1) + b(1)]\,[a(2) + b(2)]\,N_+^2(\alpha\beta - \beta\alpha)/\sqrt{2}. \tag{6}$$

We will discontinue writing the singlet spin function with the understanding that it always multiplies the spacial part. Multiplying out the wavefunction, we find that:

$$\Psi_{MO} = [a(1)a(2) + a(1)b(2) + b(1)a(2) + b(1)b(2)]N_+^2. \tag{7}$$

The first term represents a contribution to the wavefunction with both electrons in orbital a, i.e. on one of the H atoms. The second term represents a contribution with one electron in orbital a and the other electron in orbital b, i.e. on different H atoms. The third and fourth terms can be interpreted in a similar manner. Thus, the MO wavefunction suggests that there are equal contributions from both electrons on one H atom and from one electron on one H atom and the other electron on a different H atom. This might be a good approximation when both atoms are close together, but it is clearly incorrect as the molecule dissociates. At a large internuclear distance (R) one should have a wavefunction with one election on each atom, i.e.:

$$\Psi_{VB} = [a(1)b(2) + b(1)a(2)]N. \tag{8}$$

This wavefunction, which is correct at large R, is the simple valence bond (VB) or Heitler–London function. The potential energy curve for this simple VB wavefunction is also shown on Fig. 1. Although it dissociates properly into two neutral atoms, it is too repulsive as R gets shorter because it has no ionic contributions. On the other hand, the MO wavefunction is more accurate at short R, but dissociates improperly into a mixture of neutral and ionic atoms.

What one needs is a wavefunction that looks like an MO function at short R and a VB function at long R. One can achieve this by adding a variable amount of ionic character to the VB wavefunction [eqn (8)]. Alternatively, one can achieve the same wavefunction by doing a CI calculation using the MOs $1\sigma_g$ and $1\sigma_u$. Consider the doubly excited configuration $1\sigma_u^2$; its wavefunction:

$$\Psi'_{MO} = |1\sigma_u\alpha 1\sigma_u\beta|, \tag{9}$$

yields the following after substitution of eqn (3) and neglect of the singlet spin term:

$$\Psi'_{MO} = [a(1)a(2) - a(1)b(2) - b(1)a(2) + b(1)b(2)]N^2_-. \quad (10)$$

Notice that if one subtracts Ψ'_{MO} from Ψ_{MO} one gets Ψ_{VB}. Thus, if we form:

$$\Psi = (1 - \lambda^2)^{1/2}\Psi_{MO} - \lambda\Psi'_{MO} \quad (11)$$

we can use λ as a variational parameter to minimize the total energy at each point in the potential energy curve. As R gets large, λ will approach $1/\sqrt{2}$. Thus, the wavefunction in eqn (11) represents the simplest form for a wavefunction which is qualitatively correct over the entire potential-energy curve.

The process of adding to the simple MO wavefunction configurations which are excited with respect to the simple MO function is called CI. If one also varies the form of the MOs $1\sigma_g$ and $1\sigma_u$ as one varies λ, one has a multiconfiguration self-consistent-field (MCSCF) procedure. For this particular case of two electrons and two orbitals, the MCSCF wavefunction in eqn (11) is the same as the wavefunction obtained from other procedures such as generalized molecular orbital (GMO), generalized valence bond (GVB), and antisymmetric product of strongly-orthogonal geminals (APSG).

Although these procedures will not be equivalent for more complicated cases, their goal is the same: to correct for the deficiencies in the simple MO wavefunction by using more than one configuration to represent the wavefunction. The overall error in the MO wavefunction is usually referred to as the electron correlation error. The electrons in the MO wavefunction are uncorrelated, i.e. one electron does not know about the actual position of the other electrons, only about their average position. Thus, in the simple MO wavefunction, the electrons are equally likely to be found together on the same atom [$a(1)a(2)$ like terms] as on different atoms [$a(1)b(2)$ like terms]. When the motion of the electrons is correlated as in eqn (11) the electrons are less likely to be found together in the same atom or region of space and are more likely to be found in different atoms or regions of space.

The wavefunction in eqn (11) only represents a fraction of the total correlation energy. Because of this the potential-energy curve calculated with this wavefunction is still not exactly parallel to the experimental curve. Generally, the predicted bond distance is now too long and the dissociation energy is still too small because the wavefunction [eqn (11)] is more accurate at a large R than at small R. This discrepancy is related to the relative energy of the resonance:

$$H + H \leftrightarrow H^+ + H^-. \quad (12)$$

The simple MO model suggests both sides are of equal weight (same energy) while the simple MCSCF [eqn (11)] suggests that the left side of eqn (12) is more important. Although the simple MCSCF is basically correct, it underestimates the importance of the right side of eqn (12) because it has not calculated correctly the electron affinity of H. When additional electron correlation is added, the relative energies of the two sides of eqn (12) are calculated correctly and the potential-energy curve now parallels the experimental curve.

A correlated wavefunction like that in eqn (11) presents a problem for the calculation of the bond order (BO). The usual scheme for calculating a BO in MO theory is:

$$BO = \tfrac{1}{2}[(\text{No. of } e^- \text{ in bonding MO}) - (\text{No. of } e^- \text{ in antibonding MO})]. \quad (13)$$

Thus, for the simple MO wavefunction the BO = 1, but for the wavefunction in eqn (11):

$$BO = \tfrac{1}{2}[2(1 - \lambda^2) - 2\lambda^2] = 1 - 2\lambda^2. \quad (14)$$

As the molecule dissociates this BO approaches zero because at large R the $1\sigma_g$ and $1\sigma_u$ have an equal number of electrons. Even at the equilibrium distance the BO < 1.0. A considerably different view is apparent if we remember that, when $\lambda = 1/\sqrt{2}$, its value at $R = \infty$, the wavefunction Ψ in eqn (11) is identical to the Ψ_{VB} in eqn (8). From the valence bond viewpoint the wavefunction in eqn (8) represents a single bond, i.e. BO = 1. Thus, the same wavefunction has a BO(MO) = 0 and a BO(VB) = 1. The MO BO, as calculated by eqn (13) or (14), changes with R and reflects the strength of the bond. On the other hand the VB BO is one over the entire potential-energy curve and, thus, represents a formal BO.

RESULTS AND DISCUSSION

We can now discuss in some detail the "true" nature of the bonding in the chromium dimers. The first column in Table 1 shows the important configurations and occupation numbers from a GMO-CI calculation[11] on $Cr_2(O_2CH)_4$ at a Cr–Cr distance of 2.3 Å. The single most important configuration is the quadruple bond $\sigma^2\pi^4\delta^2$, but it only makes up about 12% of the wavefunction. The remainder of the wavefunction is made of configurations in which electrons from the bonding orbitals occupied in the $\sigma^2\pi^4\delta^2$ configuration are excited

Table 1. Comparison of quadruple-bond strength

	$Cr_2(O_2CH)_4$[a]	$Cr_2((NH)_2CH)_4$[b]
	Orbital occupations	
σ	1.47	1.73
π	2.44	3.33
δ	1.18	1.51
δ^*	0.82	0.49
π^*	1.56	0.67
σ^*	0.53	0.27
	Important configurations[c]	
$\sigma^2\pi^4\delta^2$	0.117	0.482
$\sigma^2\pi^4\delta^{2*2}$	0.054	0.085
$\sigma^2\pi^2\delta^2\pi^{*2}$	0.083	0.094
$\pi^4\delta^2\sigma^{*2}$	0.017	0.019

[a] Values for molecule at 2.3 Å.

[b] Values for molecule at 1.9 Å.

[c] Values represent the sum of the square of the coefficients corresponding to different spin components of the same configuration.

into the antibonding orbitals σ^*, π^* or δ^*. The most important configurations are those in which two electrons from a bonding orbital are excited into the corresponding antibonding one such as $\delta^2 \rightarrow \delta^{*2}$. These doubly excited configurations provide an important part of the left–right near-degenerate correlation that was described in the previous section.

This Cr–Cr quadruple bond is unusual compared to most chemical bonds at their equilibrium distance, because the contribution of the leading configuration is so small and the importance of the other configurations is so large. In "typical" molecules the leading configuration makes up more than 80% of the wavefunction at the equilibrium distance. It is only as the bond length gets longer that the importance of the leading configuration (all bonding MOs occupied) decreases and the others increase. Thus, these chromium dimers appear to be similar to a more typical bond at a long bond distance. And, one would expect the Cr–Cr bond energy to be rather small and the potential energy to be rather shallow. This theoretical result is consistent with the long and variable bond lengths found in the dichromium tetracarboxylates.

Another way of presenting the electronic structure of these dimers is shown also in Table 1 where the orbital occupations are given. These are determined from summations over all configurations in the wavefunction. Although the single most important term in the wavefunction is the quadruple bonding configuration $\sigma^2\pi^4\delta^2$, a calculation of the BO from the occupation numbers in Table 1 yields a BO of 1.1. Thus, this quadruple bond is only expected to be as strong as a "typical" single Cr–Cr bond. Naturally, this difference, between a formal (VB) BO of 4 and a much smaller calculated BO, led to some disagreement over whether these systems should be properly termed as having a quadruple bond.[6,12]

All of the dichromium tetracarboxylates have some type of axial coordination. Thus far, attempts to prevent this axial ligation have failed. The impetus for trying this was the belief that the Cr–Cr distance would shorten when the axial ligands are removed.[13] The first "supershort" Cr–Cr bond (< 1.9 Å) was found in $Cr_2(DMP)_4$ (DMP = 2,6-dimethoxyphenyl anion). In this molecule we have a much more basic bridging ligand, no axial ligands and a Cr–Cr bond length of 1.847 Å. The results of a theoretical calculation on a model for these "supershort" dimers is given in the second column of Table 1. Now, the quadruple bond configuration $\sigma^2\pi^4\delta^2$ makes up nearly 50% of the wavefunction and the calculated BO has risen to 2.6. Clearly, there has been a dramatic change in the bonding. Our theoretical work[14] on $Cr_2(O_2CH)_4$, $Cr_2(O(NH)CH)_4$ and $Cr_2((NH)_2CH)_4$ suggests that a major factor influencing the Cr–Cr bond length was the basicity of the bridging ligand. GMO-CI calculations of the potential-energy curve for $Cr_2(O_2CH)_4$ and $Cr_2((NH)_2CH)_4$ reveal minima at 2.41 and 1.93 Å, respectively. The implication of these results is that one must have ligands more basic than carboxylates to have "supershort" Cr–Cr bonds and that removal of the axial ligands from a tetracarboxylate will not result in a "supershort" Cr–Cr bond. Previous CI calculations[15] of $Cr_2(O_2CH)_4$ with and without two axially coordinated H_2O molecules also suggested that little change in the Cr–Cr bond length would result from removal of the two axial ligands.

The experimental work on the question of the relative importance of the bridging vs axial ligand in determining the Cr–Cr bond length is somewhat ambiguous. Cotton and coworkers have clearly shown that if one adds axial ligands to one of the supershort bonds the bond will lengthen.[16] In this study the parent molecule, $Cr_2[(2\text{-xylyl})NC(CH_3)O]_4$, has a Cr–Cr bond length of 1.937 Å. Adding one THF axial ligand lengthened the bond by 0.086 Å, adding a second THF axial ligand lengthened the previous one by 0.198 Å, and replacing both THF ligands in the last complex by two pyridine ligands lengthened the bond by another 0.133 Å. Clearly, the addition of axial ligands to one of the molecules with short Cr–Cr bonds will cause those bonds to lengthen.

However, will removal of axial ligands from one of the systems with a long bond cause those bonds

to shorten? The answer here is not as clear. Thus far all attempts to prepare a tetracarboxylate dimer of chromium without axial coordination have been unsuccessful. If one replaces two axial pyridine ligands by two H_2O molecules in the tetraformate or tetraacetate derivative one finds a shortening of only 0.041 and 0.007 Å, respectively.[17] This change in bond distance is much smaller than that observed for a similar ligand exchange in $Cr_2[(2\text{-xylyl})NC(CH_3)O]_4L_2$. Cotton and Wang studied the structure of a number of $Cr_2(O_2CR)_4L_2$ molecules and plotted the value of the Cr–Cr bond distance against the pK_a of the acid HO_2CR and the pK_a of L, where L was pyridine or substituted pyridine.[18] The correlation for a give class of compounds was nearly linear and different classes of compounds had parallel lines. The slope of these lines, $\Delta Cr\text{–}Cr/\Delta pK_a$, was -0.04 Å/pK_a for changes in the bridging ligand and $+0.007$ Å/pK_a for changes in the axial ligand. Thus, strengthening the basicity of the bridging ligands was much more effective in shortening the Cr–Cr bond length than weakening basicity of the axial ligands. In other words, the tetracarboxylate dimers seem to be more sensitive to the nature of the bridging ligands than the axial ligands. How much shortening will occur when one removes the axial ligands from $Cr_2(O_2CR)_4L_2$ dimers is not clear.

The ultimate experiments would be, of course, on $Cr_2(O_2CR)_4$ in the gas phase. Two experiments of this type have been performed. The electron diffraction of $Cr_2(O_2CCH_3)_4$ has been reported by Ketkar and Fink.[19] They reported a Cr–Cr bond length of 1.966 Å, but the solution of this problem was complicated because the peaks in the radial distribution for Cr–Cr and Cr–O overlapped strongly. The gas-phase ultraviolet PE spectra of a variety of dichromium species have been reported.[4,20] If one compares the low-energy region of $Cr_2(O_2CCH_3)_4$ with the same region in the PE spectra of "supershort" dimers one finds substantial differences that are best explained by assuming that the Cr–Cr bond of the tetraacetate is substantially longer than that of the "supershort" dimers. Thus, the only two gas-phase experiments appear to lead to different conclusions on the length of dichromium tetraacetate without axial ligands.

In principle one could resolve this discrepancy through more accurate calculations. To date, attempts to improve the theoretical results have been less than satisfactory.[21,22] As more complete MCSCF procedures and CI calculations have been performed, the Cr–Cr bond distance in the tetraformate model systems has gotten longer and longer. These results essentially mean that all of the previous results obtained a minimum in the potential-energy curve because of a cancellation of errors. One may argue that this cancellation is not entirely fortuitous and that those previous results are essentially correct. However, it is not very satisfying when improved calculations yield inferior results. As we mentioned in the theoretical section, calculations on small diatomics that result in bond distances which are too long are a result of the failure to properly account for the difference in the atomic IP and EA. Thus, these improved calculations may be neglecting important atomic-like electron correlation as they improve the molecular correlation (left–right near-degenerate). Goddard and coworkers[23] have suggested that this is the reason that nearly all previous calculations on the simple diatomic Cr_2 have failed to obtain the correct bond distances of 1.73 Å. These workers have empirically adjusted an atomic coulomb repulsion integral to bring theoretical ΔH for the reaction $2Cr^0 = Cr^+ + Cr^-$ into line with experiment. Using this adjusted integral they were successful in calculating the bond distance in Cr_2. Others have emphasized the change in the correlation energy of the other electrons in the system as one forms the metal–metal bond.[24] This is sometimes referred to as the differential correlation energy and played an important role in the calculation of the dissociation energy of the Mo≡Mo triple bond.[25]*

One unusual feature of theoretical work in this area that it is apparently easier to calculate the bond energy and bond distance of the heavier dimolybdenum systems than dichromium. Usually, quantum chemistry is easier on the lighter molecule (fewer electrons). However, the overlap between the 4*d* orbitals is sufficiently larger than the overlap between 3*d* orbitals that the dimolybdenum system can be calculated accurately with a more modest treatment of the electron correlation. This theoretical problem actually manifests itself in the chemistry and structure of these systems. Thus, the Mo≡Mo bond distance is essentially constant regardless of ligands, while the Cr≡Cr bond distance has the largest range of any known bond of a given order.

The chapter on Cr≡Cr bonds is not yet closed. We do not have a complete understanding of how to calculate the bond distance or dissociation energy correctly. Furthermore, we do not understand the relative importance of all the factors which determine the wide variation of Cr≡Cr bond lengths.

* Although early LDF calculations suggested a larger dissociation energy than our *ab initio* results, the most recent and sophisticated LDF calculations[26] now yield dissociation energies similar to our prediction.

Also, there has been little *ab initio* theoretical work on the excited states of systems such as these. One of the few complete studies is that by Hay[27] on $Re_2Cl_8^{2-}$. In this paper I have tried to give the reader an appreciation of the problems encountered in calculating accurate properties of the dichromium species. Future theoretical work in this area will be directed toward these remaining problems.

REFERENCES

1. (a) F. A. Cotton, N. F. Curtis, C. B. Harris, B. F. G. Johnson, S. J. Lippard, J. T. Mague, W. R. Robinson and J. S. Wood, *Science* 1964, **145**, 1305; (b) F. A. Cotton and C. B. Harris, *Inorg. Chem.* 1965, **4**, 330; (c) F. A. Cotton, *Inorg. Chem.* 1965, **4**, 334.
2. J. G. Norman and H. J. Kolari, *J. Chem. Soc., Chem. Commun.* 1974, 303; *J. Am. Chem. Soc.* 1975, **97**, 33.
3. F. A. Cotton, B. G. DeBoer, M. D. La Prade, J. R. Pipal and D. A. Ucko, *J. Am. Chem. Soc.* 1970, **93**, 2926; *Acta Cryst.* 1971, **B27**, 1664.
4. C. D. Garner, I. H. Hillier, M. F. Guest, J. C. Green and A. W. Coleman, *Chem. Phys. Lett.* 1976, **41**, 91.
5. M. Benard and A. Veillard, *Nouv. J. Chim.* 1977, **1**, 97.
6. M. F. Guest, I. H. Hillier and C. D. Garner, *Chem. Phys. Lett.* 1977, **48**, 587.
7. (a) G. M. Bancroft, E. Pellach, A. P. Sattelberger and K. W. McLaughlin, *J. Chem. Soc., Chem. Commun.* 1982, 752; (b) E. M. Kober and D. L. Lichtenberger, *J. Am. Chem. Soc.* 1985, **107**, 7199.
8. T. Ziegler, *J. Am. Chem. Soc.* 1985, **107**, 4453.
9. (a) F. A. Cotton and G. G. Stanley, *Inorg. Chem.* 1977, **16**, 2668; (b) J. G. Norman, H. J. Kolari, H. B. Gray and W. C. Trogler, *Inorg. Chem.* 1977, **16**, 987.
10. (a) I. H. Hillier, C. D. Garner, G. R. Mitcheson and M. F. Guest, *J. Chem. Soc., Chem. Commun.* 1978, 204; (b) M. Benard, *J. Am. Chem. Soc.* 1978, **100**, 2354; (c) M. F. Guest, C. D. Garner, I. H. Hillier and I. B. Walton, *J. Chem. Soc., Faraday* II 1978, **74**, 2092.
11. R. A. Kok and M. B. Hall, *Inorg. Chem.* 1985, **24**, 1542.
12. F. A. Cotton and R. A. Walton, *Multiple Bonds between Metal Atoms*, p. 339. Wiley, Interscience, New York (1982).
13. *Ibid.*, p. 154.
14. (a) R. A. Kok and M. B. Hall, *Inorg. Chem.* 1985, **24**, 1542; (b) R. A. Kok and M. B. Hall, *J. Am. Chem. Soc.* 1983, **105**, 676.
15. R. Wiest and M. Benard, *Chem. Phys. Lett.* 1983, **98**, 102.
16. S. Baral, F. A. Cotton and W. H. Ilsley, *Inorg. Chem.* 1981, **20**, 2696; F. A. Cotton, W. H. Ilsley and W. Kaim, *J. Am. Chem. Soc.* 1980, **102**, 3464.
17. F. A. Cotton and G. W. Rice, *Inorg. Chem.* 1978, **17**, 688; F. A. Cotton, M. W. Extine and G. W. Rice, *Inorg. Chem.* 1978, **17**, 176; F. A. Cotton, B. G. De Boer, M. D. La Prade, J. R. Pipal and D. A. Ucko, *Acta Cryst.* 1971, **B27**, 1664; F. A. Cotton and T. R. Felthouse, *Inorg. Chem.* 1980, **19**, 328.
18. F. A. Cotton and W. Wang, *Nouv. J. Chim.* 1984, **8**, 331.
19. S. N. Ketkar and M. Fink, *J. Am. Chem. Soc.* 1985, **107**, 338.
20. (a) A. W. Coleman, J. C. Green, A. J. Hayes, E. A. Seddon, D. R. Lloyd and Y. Niwa, *J. Chem. Soc., Dalton Trans.* 1979, **75**, 485; (b) C. D. Garner, I. H. Hillier, A. A. MacDowell, I. B. Walton and M. F. Guest, *J. Chem. Soc., Faraday Trans.* 2, 1979, **75**, 485; (c) C. D. Garner, I. H. Hillier, B. J. Knight, A. A. MacDowell, I. B. Walton and M. F. Guest, *J. Chem. Soc., Faraday Trans.* 2 1980, **76**, 885.
21. M. Benard, personal communication.
22. I. H. Hillier, personal communication.
23. M. M. Goodgame and W. A. Goddard III, *Phys. Rev. Lett.* 1985, **54**, 661.
24. M. Benard and R. Wiest, *Chem. Phys. Lett.* 1985, **122**, 447; R. Wiest, A. Strich, J. Demuynck, M. Benard and P. E. M. Siegbahn, *Chem. Phys. Lett.* 1985, **122**, 453.
25. R. A. Kok and M. B. Hall, *Inorg. Chem.* 1983, **22**, 728.
26. T. Ziegler, V. Tschinke and A. Becke, *Polyhedron* 1987, **6**, 685.
27. P. J. Hay, *J. Am. Chem. Soc.* 1982, **104**, 7007.

Polyhedron Vol. 6, No. 4, pp. 685–693, 1987
Printed in Great Britain

0277–5387/87 $3.00+.00

A THEORETICAL STUDY ON THE STRENGTH OF MULTIPLE METAL–METAL BONDS IN BINUCLEAR COMPLEXES AND TRANSITION-METAL DIMERS BY A NON-LOCAL DENSITY FUNCTIONAL METHOD

TOM ZIEGLER,* and VINCENZO TSCHINKE

Department of Chemistry, University of Calgary, Calgary, Alberta, Canada

and

AXEL BECKE

Department of Chemistry, Queens University, Kingston, Ontario, Canada

(*Received* 19 *November* 1986)

Abstract—The strength of multiple metal–metal bonds in the metal dimers M_2 (M = Cr, Mo or W) and binuclear complexes $M_2(OH)_6$ (M = Cr, Mo or W), $M_2Cl_4(PH_3)_4$ (M = V, Cr, Mn, Nb, Mo, Tc, Ta, W or Re) has been studied by a non-local density functional theory. The method employed here provides metal–metal bond energies [D(M–M)] in good accord with experiments for Cr_2 and Mo_2, and predicts that W_2 of the three dimers M_2 (M = Cr, Mo or W) has the strongest metal–metal bond with D(W–W) = 426 kJ mol^{-1} and R(W–W) = 2.03 Å. Among the binuclear complexes studied here we find the 3d elements to form relatively weak metal–metal bonds (40–100 kJ mol^{-1}), compared to the 4d and 5d elements with bonding energies ranging from 250 to 450 kJ mol^{-1}. The metal–metal bond for a homologous series is calculated to be up to 100 kJ mol^{-1} stronger for the 5d complex, than for the 4d complex. An energy decomposition of D(M–M) revealed that the σ-bond is somewhat stronger than each of the π-bonds, and one order of magnitude stronger than the δ-bond. For the same transition metal we find D(M–M) to be larger for $M_2(PH_3)_4Cl_4$ (M = Cr, Mo or W) than for $M_2(OH)_6$ (M = Cr, Mo or W), and attribute this to a stronger π-interaction in the former series. While many of the findings here are in agreement with previous HFS studies, the order of stability $D(3d–3d) \ll D(4d–4d) < D(5d–5d)$ differs from the order $D(3d–3d) \ll D(5d–5d) < D(4d–4d)$ obtained by the HFS method, and the present method provides in general more modest values for D(M–M) than the HFS scheme.

Cotton's description[1] of the metal–metal bond in terms of orbitals with local σ, π and δ axial symmetries has been immensely useful in codifying[2] the increasing number of synthesized binuclear complexes, and account for their chemical and spectroscopic properties. It is thus not surprising that much effort, both experimentally[2–4] and theoretically[5–8] have gone into expanding on Cotton's original scheme by: (a) probing the relative energies of the σ-, π- and δ-type orbitals; (b) assessing variations in the metal–metal bond lengths with changes in the metal–metal bond order; and (c) determining the metal–metal bond strength and the respective contributions from the σ-, π- and δ-bonds.

LOW-ENERGY PHOTOELECTRON SPECTROSCOPIC STUDIES ON BINUCLEAR COMPLEXES, AND THEIR THEORETICAL INTERPRETATION

One of the experimental technics with the strongest bearings on the points raised under (a) is low-energy photoelectron (PE) spectroscopy,[3] which in

* Author to whom correspondence should be addressed.

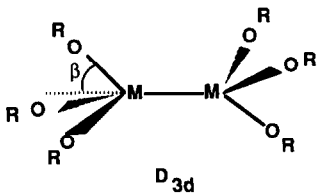

D_{3d}

1a

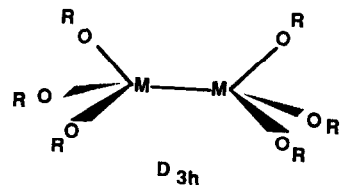

D_{3h}

1b

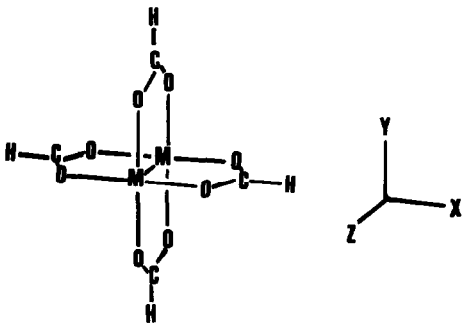

2

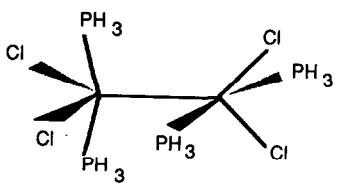

D_{2d}

3

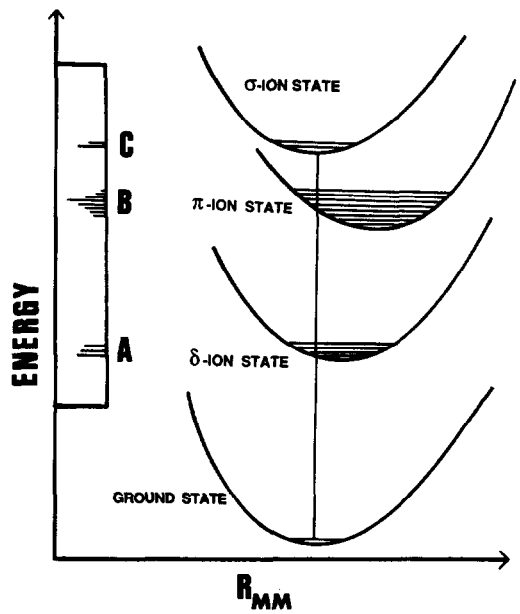

Fig. 1. Schematic representation of the energy for a quadruple bonded binuclear complex M_2L_{2n} in its ground state and first three ion states, corresponding to ionizations out of the σ, π and δ bonding orbitals, as a function of the metal–metal bond distance (R_{MM}). Schematic representation of the three first PE bands with expected shapes are given as A, B and C, respectively.

conjunction with theoretical calculations[5,6] can provide information on the relative energies of the states corresponding to ionizations of electrons out of the σ, π and δ metal–metal bonding orbitals. The triple bonded M_2L_6 (M = Mo or W, L = OR or NR_2)[3(c)] complexes (**1a**) as well as the quadruple bonded complexes $M_2(O_2CR)_4$ (M = Cr, Mo or W)[3(a)] and $M_2Cl_4(PR_3)_4$ (M = Mo or W)[3(b)] (**2** and **3**) have been particularly well studied[3] by PE spectroscopy since their volatility makes them well suited for this experimental technic.

We have previously found[5(c)] in our interpretation of the recorded PE spectra for the quadruple bonded systems, based on HFS calculations, that the first three bands corresponded to ionizations out of the σ, π and δ metal–metal bonding orbitals, respectively, with ionization out of the ligand based orbitals at somewhat higher energies, and a similar assignment has also been reached by *ab initio* calculations[6(a)] for $M_2(O_2CH)_4$ (M = Cr or Mo). It is indicated in Fig. 1, where we schematically present the energies of the three first-ion states of $[M_2(O_2CR)_4]^+$ or $[M_2Cl_4(PR_3)_4]^+$ relative to the ground state of the neutral molecules as a function of the metal–metal bond distance (R_{MM}), that the first ionization for the quadrupole bonded systems, according to our previous calculations takes place from the δ-orbital, whereas the second ionization, which, depending on the system, is 1–2 eV higher in energy, corresponds to the π-orbital. There has been some controversy[2] over the position of the ionization band due to the σ-orbital. We find[5(c)] the σ-ionization to be of higher energy than the π-ionization by 1 eV of less (Fig. 1).

All theoretical calculations to date[3(c),5(c)] indicate that the first two bands in the recorded PE spectra of the triple bonded M_2L_6 (L = OR or NR_2)[3(c)] complexes correspond to ionizations from the π- and σ-orbitals, respectively, with the σ-ionization around 1 eV higher in energy than the π-ionization.

DEPENDENCE OF R_{MM} ON THE FORMAL METAL–METAL BOND ORDER

Photoelectron spectroscopy can also in principle determine the change in R_{MM} on ionization of an

electron out of the metal–metal bonding orbitals, and thus address the point raised under (b) concerning the variation in R_{MM} as a function of the formal bond order. So far only an estimate of the change in R_{MM} from the ionization out of the δ-orbitals has been obtained experimentally.[3(e)] The influence of the δ^*-occupation on R_{MM} has further been studied[9] by X-ray diffraction methods for the series $[Re_2Cl_4(PR_3)_4]^{n+}$ ($n = 2$, 1 or 0).

We have previously calculated[5(c)] the difference in R_{MM} between the ground state and the three first-ion states of some quadruple bonded complexes. We found, perhaps not surprisingly, that an ionization out of the weakly bonding δ-orbital leads to a modest elongation of R_{MM} of around 0.04 Å, whereas the ionization out of the strongly bonding π-orbital results in a substantial elongation (~ -15 Å). What was surprising, however, was the negligible change in R_{MM}, 0.01 Å or less, accompanying the ionization from the strongly metal–metal bonding σ-orbital (Fig. 1). An analyses of this puzzling result revealed that the ionization from the σ-orbital not only reduces the bond order but also the exchange repulsion. The two factors have adverse effects on the metal–metal bond distance which cancels.[5(c)]

The different extent to which R_{MM} is influenced by ionizations out of the σ-, π- and δ-orbitals should have consequences for the shapes of the different ionization bands, with band B (Fig. 1) due to the π-ionization being rather broad, and band C due to the σ-ionization being rather narrow. This is in fact what has been observed by Bancroft *et al.*[3(a)] in the case of $W_2(O_2CCF_3)_4$. For other quadruple bonded systems[2] the width of band B seems to be comparable to the σ–π separation, resulting in overlaps of bands B and C.

STRENGTH OF THE METAL–METAL BOND IN BINUCLEAR COMPLEXES

The strength of the metal–metal bond, let alone the respective σ, π and δ contributions, has been exceedingly difficult to determine experimentally,[4] since calorimetric measurements of the metal–metal bond energy [D(M–M)] in M_2L_n complexes is hampered by an uncertainty in the M–L dissociation energy, an uncertainty that is multiplied by n in the final estimate of D(M–M).

Attempts on the other hand to estimate D(M–M) from *ab initio* calculations are faced with the formidable task of describing the correlated motion of the electrons in the metal–metal bond, and only a few attempts have so far been reported.[7] We have recently calculated D(M–M)[8] with the aid of the HFS method according to Baerends *et al.*[10(a)] for some M_2L_6 and $M_2Cl_4(Ph_3)_4$ systems with quadruple or triple bonds, and decomposed D(M–M) into its σ-, π- and δ-components. We found[8] the σ-bond to be slightly stronger than each of the π-bonds, and one order of magnitude stronger than the δ-bond. In absolute terms triple or quadruple bond strengths of 3*d* elements were calculated by the HFS method to be in the range 150–300 kJ mol^{-1}, whereas the corresponding bond energies for 4*d* and 5*d* elements were in the 400–600 kJ mol^{-1} bracket. Multiple metal–metal bonds, even for the heavier 4*d* and 5*d* elements are thus according to our HFS calculations in strength more comparable to the triple bond in P_2 than the triple bond in N_2.

RECENT ADVANCES IN DENSITY FUNCTION THEORY

Experience with the HFS (or Xα) method, accummulated over the past decade, seems to indicate that calculated bond distances and force constants as well as spectroscopic energy differences, such as ionization potentials and electronic excitation energies, are in good to fair agreement with experimental results, whereas calculated bond energies compare less satisfactorily with experiment.

The HFS method is an approximation to the density functional theory of Kohn and Sham[11(a)] in much the same way as *ab initio* Hartree–Fock theory is an approximation to many body theories including configuration interaction, since both methods completely neglect the correlation between electrons of different spins.[12] Recent advances in density functional theory,[13] which in many ways parallels the development of post-HFS methods, has lead to remedies for the lack of correlation between electrons of different spins and other shortcomings of the HFS method by including two corrections to the HFS energy expression E_{HFS}:

$$E_{BS} = E_{HFS} + E_C + E_X^{NL}. \quad (1)$$

The first correction term E_C in eqn (1) proposed by Stoll *et al.*[11(b)] represents the correlation between electrons of different spins, whereas the second correction term E_X^{NL}, according to Becke,[11(c)] represents a non-local correction to the HFS exchange energy E_X.

We shall now demonstrate that the modified HFS method, based on the energy expression of eqn (1), in the cases of Cr_2 and Mo_2 provides bond energies D(M–M) in good agreement with the accurate experimental values for D(Cr–Cr) and D(Mo–Mo).[14] Following this evaluation of the

method based on eqn (1), calculated D(M–M) and R_{MM} will be presented for the triple bonded compounds $M_2Cl_4(PH_3)_4$ (M = V, Nb, Ta, Mn, Tc or Re) and $M_2(OH)_6$ (M = Cr, Mo or V) as well as the quadruple bonded complexes $M_2Cl_4(PR_3)_4$ (M = Cr, Mo or W).

COMPUTATIONAL DETAILS

All calculations were based on the LCAO–HFS program system according to Baerends *et al.*[10(a)] or its relativistic extension due to Snijders *et al.*[15] with only minor modifications to allow for Becke's non-local exchange correction[16] as well as correlation between electrons of different spins in the formulation by Stoll,[11(b)] based on Vosko's parametrization[16] from electron gas data. Bond energies were evaluated by the generalized transition-state method[17(a)]* or its relativistic extension.[17(b)]

A triple ζ-STO basis[10(b),(c)] was used for 1*s* on H, 3*s*, 3*p* on Cl and P, as well as *ns*, *np*, *nd* and $(n+1)s$, $(n+1)p$ on the transition metals, augmented with a single 3*d* STO on P and three $(n+1)f$ STOs on the metals. Electrons in shells of lower energy were considered as core and treated by the frozen-core approximation according to the procedure Baerends *et al.*[10(a)] The total molecular electron density was fitted in each SCF iteration by an auxiliary basis[10(d)] of *s*, *p*, *d*, *f* and *g* STOs, centered on the different atoms in order to represent the Coulomb and exchange potentials accurately.[10(a)] The SCF part of the calculations, as well as the optimizations of R_{MM}, included, of the correction terms in eqn (1), only E_C, corresponding to the correlation between electrons of different spins. The wave functions generated from this type of SCF calculation were then used to calculate Becke's non-local exchange corrections (E_X^{NL}) at the optimized R_{MM}, in order to evaluate E_{BS} of eqn (1) as well as the D(M–M). Efforts[18] are under way to include D_X^{NL} in the SCF part of the calculations as well as in the geometry optimizations.

THE CALCULATED METAL–METAL BOND STRENGTH OF THE DIMERS Cr_2, Mo_2 AND W_2

The metal dimers Cr_2 and Mo_2 are among the few species with multiple metal–metal bonds for which quite accurate experimental bond energies are available,[14] and our primary aim here has been to compare those values to calculated bond energies based on eqn (1) in order to evaluate the accuracy of E_{BS}. A more extensive account of the bonding in electron-poor metal dimers with multiple metal–metal bonds involving group 4–7 transition metals is in preparation,[18] and we note that several theoretical accounts of the bonding in Cr_2 and Mo_2 have already appeared, based on *ab initio*[14] and density functional theory.[19] No calculation has, however, been reported on W_2, nor are there any experimental data available.

Table 1. Calculated bond energies [D(M–M)] (eV) and metal–metal bond distances (R_{MM}) (Å) for Cr_2, Mo_2 and W_2

	D(M–M)		R_{MM}	
M_2	Calc.	Exp.	Calc.	Exp.
Cr_2	1.75	1.56 ± 0.2	1.65	1.69
Mo_2	4.03	4.18 ± 0.2	1.95	1.93
W_2	4.41(3.54)[a]	—	2.03(2.07)[a]	—

[a]Non-relativistic results.

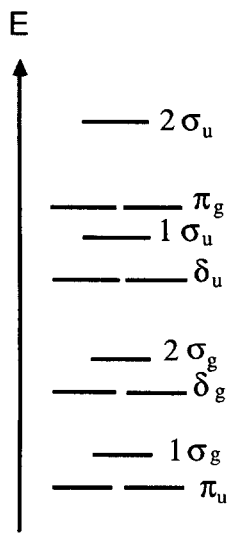

Fig. 2. Orbital-level diagram for M_2, with orbitals classified according to $D_{\infty v}$-symmetry.

The bond energies presented in Table 1 were based on spin-unrestricted calculations using $C_{\infty v}$- rather than $D_{\infty v}$-symmetry constraints, in order to allow for the polarization of electrons with different spins towards opposite metal centers. Thus, whereas the ground-state configuration for M_2 (M = Cr, Mo or W) in a single-determint description under $D_{\infty v}$-symmetry constraints is $1\sigma_g^2 2\sigma_g^2 \pi_u^4 \delta_g^4$ (see Fig. 2), a reduction in symmetry to $C_{\infty v}$ allows for the partial occupation of the anti-bonding orbitals $1\sigma_u$, $2\sigma_u$, π_g and δ_u, where equal occupation of bonding and anti-bonding orbitals (Fig. 2) corresponds to complete polarization of *d*-valence elec-

*The generalized transition state procedure is not only applicable to the HFS method but can be extended to any energy density functional such as E_{BS}, as we have done in the present work.

trons with different spins to the opposite metal centers.

The bond energies in Table 1 were calculated by evaluating the energy difference:

$$\Delta E = 2^*E(^7S) - E(M_2) \qquad (2)$$

between two metal atoms in a ^7S state corresponding to the $nd^5(n+1)s^1$ configuration and M_2. ΔE represents for Cr_2 and Mo_2 the bond energies D(Cr–Cr) and D(Mo–Mo), respectively, since Cr and Mo both have a spherical ^7S ground state. The W atom, however, has a ^{5}D ground state with the configuration $5d^46s^2$, and we have thus for W_2 subtracted the experimental energy difference (0.37 eV)[20] between the ^5D and ^7S states of W twice from ΔE in order to arrive at D(W–W) in Table 1.

The calculated bond energies and R_{MM} for Cr_2 and Mo_2 are in good accord with experimental values, as can be seen from Table 1. We have, in contrast to other calculations based on density functional theory,[19] in the present work employed $(n+1)f$ polarization functions. There contributions on the bond energies are modest, 0.2–0.4 eV, and our results conform, among the other density functional calculations in particular, well to those of Baykara *et al.*,[19] although a slightly different energy functional was used in their work.

We predict that W_2 after the inclusion of relativistic effects (Table 1) should have a stronger metal–metal bond than Mo_2 with an R_{MM} of 2.03 Å. The bonding interaction is, even in the non-relativistic case, stronger in W_2 than in Mo_2 if the two metal atoms are referred to the same ^7S reference state.

The single-determint wave functions for Mo_2 and W_2 converged at the equilibrium distance under $C_{\infty v}$ constraints to nearly $D_{\infty v}$ symmetry with a $1\sigma_g^2 2\sigma_g^2 \pi_u^4 \delta_g^4$ configuration. The two molecules have thus, with a formal bond order of six, a hexuple metal–metal bond. For Cr_2, where bonding d–d overlaps are weaker than in Mo_2 or W_2, the converged single determinantal wave function had, at the equilibrium distance, a broken $C_{\infty v}$-symmetry with the configuration $1\sigma_g^2 2\sigma_g^2 \pi_u^4 \delta_g^{3\cdot 4} \delta_u^{\cdot 6}$, indicating substantial spin polarization in the δ-framework, and a formal bond order of less than six. We refer to Baykara *et al.*[19] for an authoratative analyses of the bonding in Cr_2 and Mo_2 at different R_{MM}.

CALCULATIONS OF D(M–M) FOR $M_2(OH)_6$ (M = Cr, Mo OR W) AND $M_2Cl_4(PH_3)_4$ (M = V, Cr, Mn, Nb, Mo, Tc, Ta, W OR Re)

The $M_2(OH)_6$ (M = Mo or W) systems were taken as models for the known alkoxy complexes $M_2(OR)_6$ (M = Mo or W), and together with $Cr_2(OH)_6$, for which the alkoxy analogues are unknown, given a staggered conformation (**1a**). All geometrical parameters, except for R_{MM} were taken from Ref. 8(a), where we previously have discussed the relative stabilities of $M_2(OH)_6$ in the staggered (**1a**) and eclipsed (**1b**) conformations. The many-electron wave function for $M_2(OH)_6$ of $D_{(3d)}$ symmetry was represented by a single Slater determinant corresponding to the $\pi^4\sigma^2$ electronic configuration.

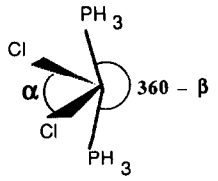

4

The observed structures of $M_2Cl_4(PR_3)_4$ for M = Mo, W or Re are those of two deformed $MCl_2(PR_3)_2$ fragments (**4**) combined into a staggered conformation (2) with the Cl—M—Cl angle (α) close to 130° and the P—M—P angle (β) close to 165°. The structures of the model systems $M_2Cl_4(PH_3)_4$ were taken from Ref. 8(b), except for R_{MM}, which we have reoptimized for each system. The many-electron wave function for the d^3–d^3 complexes $M_2Cl_4(PH_3)_4$ (M = V, Nb or Ta) and the d^5–d^5 complexes $M_2Cl_4(PH_3)_4$ (M = Mn, Tc or Re) were represented by a single Slater determinant under $D_{(2d)}$ symmetry constraints corresponding to the $\sigma^2\pi^4$ and $\sigma^2\pi^4\delta^2\delta^{*2}$ electronic configurations, respectively. The d^4–d^4 systems $M_2Cl_4(PH_3)_4$ (M = Cr, Mo or W) were represented by a two-determint wave function as:

$$\Psi = C_1|\overset{+}{\sigma}\overset{-}{\sigma}\overset{+}{\pi_1}\overset{-}{\pi_1}\overset{+}{\pi_2}\overset{-}{\pi_2}\overset{+}{\delta}\overset{-}{\delta}| + C_2|\overset{+}{\sigma}\overset{-}{\sigma}\overset{+}{\pi_1}\overset{-}{\pi_1}\overset{+}{\pi_2}\overset{-}{\pi_2}\overset{+}{\delta^*}\overset{-}{\delta^*}| \qquad (3)$$

according to the method by Noodleman *et al.*,[21] in order to allow for spin polarization in the δ framework.

The D(M–M) given in Tables 2–5 were calculated as the energy difference between M_2L_{2n} and two ML_n fragments in a high-spin ground-state configuration.

We have in previous studies decomposed D(M–M) according to:

$$D(M\text{–}M) = -\Delta E^o - \Delta E_\sigma - \Delta E_\pi - \Delta E_\delta - \Delta E_T - \Delta E_R. \qquad (4)$$

Table 2. Optimized metal–metal bond distances, and decomposition of calculated bonding energies, for $M_2(OH)_6$ (M = Cr, Mo or W)

	R_{MM}		E (kJ mol^{-1})			
$M_2(OH)_6$	(Å)	D(M–M)	ΔE^o	ΔE_σ	ΔE_π	ΔE_R
$Cr_2(OH)_6$	1.91	31.8	644.4	−335.6	−340.6	—
$Mo_2(OH)_6$	2.22	258.2	545.6	−347.1	−456.7	—
$W_2(OH)_6$	2.30	360.1	473.4	−348.5	−419.7	−65.3[a]

[a]Contributions to bonding energy from relativistic effects are given by $-\Delta E_R$. The bonding energy is given as $D(M–M) = -\Delta E^o - \Delta E_\sigma - \Delta E_\pi - \Delta E_R$.

Table 3. Optimized metal–metal bond distances, and decomposition of calculated bonding energies, for $M_2Cl_4(PH_3)_4$ (M = Cr, Mo or W)

	R_{MM}		E (kJ mol^{-1})				
$M_2Cl_4(PH_3)_4$	(Å)	D(M–M)[a]	ΔE^o	ΔE_σ	ΔE_π	ΔE_δ	ΔE_R
$Cr_2Cl_4(PH_3)_4$	1.89	102	655	−274	−473	−10	—
$Mo_2Cl_4(PH_3)_4$	2.16	371	643	−345	−620	−49	—
$W_2Cl_4(PH_3)_4$	2.29	460	419	−316	−525	−24	−14

[a]The bonding energy is given as $D(M–M) = -\Delta E^o - \Delta E_\sigma - \Delta E_\pi - \Delta E_\delta - \Delta E_R$, where $-\Delta E_R$ is the contribution from relativistic effects to bonding energy.

Table 4. Optimized metal–metal bond distances, and decomposition of calculated bonding energies, for $M_2Cl_4(PH_3)_4$ (M = Mn, Tc or Re)

	R_{MM}		E (kJ mol^{-1})				
$M_2Cl_4(PH_3)_4$	(Å)	D(M–M)[a]	ΔE^o	ΔE_σ	ΔE_π	ΔE_δ	ΔE_R
$Mn_2Cl_4(PH_3)_4$	1.92	99	650	−291	−451	−7	—
$Tc_2Cl_4(PH_3)_4$	2.17	337	614	−355	−591	−5	—
$Re_2Cl_4(PH_3)_4$	2.29	441	427	−328	−520	−9	−11

[a]The bonding energy is given as $D(M–M) = \Delta E^o - \Delta E_\sigma - \Delta E_\pi - \Delta E_\delta - \Delta E_R$, where $-\Delta E_R$ is the contribution from relativistic effects to bonding energy.

Table 5. Optimized metal–metal bond distances, and decomposition of calculated bonding energies, for $M_2Cl_4(PH_3)_4$ (M = V, Nb or Ta)

	R_{MM}		E (kJ mol^{-1})				
$M_2Cl_4(PH_3)_4$	(Å)	D(M–M)	ΔE^o	ΔE_σ	ΔE_π	ΔE_T	ΔE_R
$V_2Cl_4(PH_3)_4$	2.04	67	521	−253	−481	146	—
$Nb_2Cl_4(PH_3)_4$	2.30	259	562	−328	−651	159	—
$Ta_2Cl_4(PH_3)_4$	2.51	297	404	−304	−562	173	−8

[a]The bonding energy is given as $D(M–M) = -\Delta E^o - \Delta E_\sigma - \Delta E_\pi - \Delta E_T - \Delta E_R$, where $-\Delta E_R$ is the contribution from relativistic effects to D(M–M) and ΔE_T twice the energy required to promote $MCl_2(PH_3)_2$ from the $b_2^1a_2^1a_1^1$ ground-state configuration to $b_2^1a_1^1b_1^1$ (see text).

Here ΔE^o is the (steric) interaction energy between two high-spin ML_n fragments of opposite spin polarization at the positions they will take up in the combined M_2L_{2n} complex. The term ΔE^o is positive and destabilizing. The terms ΔE_σ, ΔE_π and ΔE represent the stabilization of the metal–metal bond from the pairing up of electrons with opposite spin polarization on the two fragments in orbitals

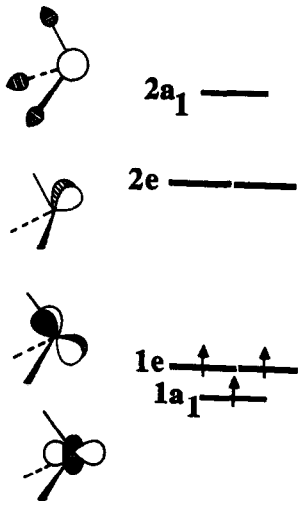

Fig. 3. Orbital-level diagram for $M(OH)_3$ of C_{3v} -symmetry.

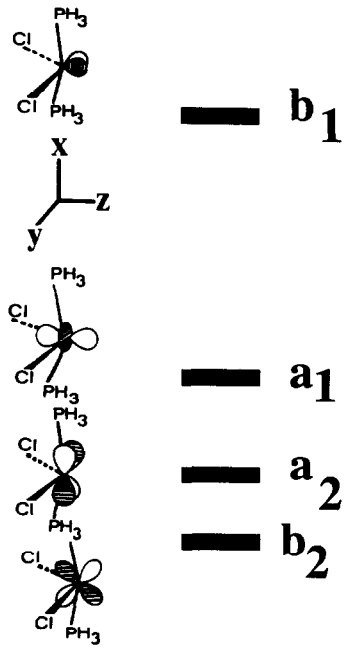

Fig. 4. Orbital-level diagram for $MCl_2(PH_3)_2$ of C_{2v}-symmetry.

with local δ, π and δ axial symmetries, as the electron density is allowed to relax to that of the first M_2L_{2n} complex. Thus, $-\Delta E_\sigma$, $-\Delta E_\pi$ and $-\Delta E_\delta$ represent the respective σ, π and δ components of D(M–M). Two $M(OH)_3$ (M = Cr, Mo or V) fragments with the $1a_1^1 1e_x^1 1e_y^1$ ground-state configurations (see Fig. 3) correlate directly with $^2\pi^4$ configuration of the $M_2(OH)_6$ complexes, and the two $MCl_2(PH_3)_2$ fragments of groups 6 and 7 metals with $1a_1^1 1a_2^1 1b_2^1 1b_1^1$ and $1a_1^1 1a_2^2 1b_2^1 1b_1^1$ configurations, respectively (see Fig. 4) correlates also directly with the respective $\sigma^2\pi^4\delta^2$ and $\delta^2\pi^4\delta^2\delta^{*2}$ ground-state configurations of the combined $M_2Cl_4(PH_3)_4$ complexes. However, two $MCl_2(PH_3)_2$ fragments of group 5 metals with the $1a_1^1 1a_2^1 1b_2^1$ configuration correlates with the excited $\sigma^2\pi^2\delta^2$ configuration of $M_2Cl_4(PH_3)_4$ rather than the ground-state configuration $\sigma^2\pi^4$. We must thus before combining them promote the two $MCl_2(PH_3)_2$ fragments to the $1a_1^1 1b_2^1 1b_1^1$ configuration correlating with the $\sigma^2\pi^4$ configuration. The energy required for this promotion is ΔE_T of eqn (4). The term $-\Delta E_E$, evaluated only[8] for complexes of 5*d* elements, constitutes the contribution to D(M–M) from relativistic effects. The decomposition of D(M–M) in eqn (4), if somewhat arbitrary, should hopefully help to pinpoint the factors responsible for the difference in the strength of the metal–metal bond of the various systems under investigation.

Our calculations here indicate that the metal–metal bond in binuclear complexes between elements of the first transition series is relatively weak (40–100 kJ mol^{-1}) in comparison to metal–metal bonds between the heavier congeners in the second and third transition series (Tables 2–5). This is understandable since 3*d* orbitals are more contracted than their 4*d* and 5*d* counterparts, with smaller *d*–*d* bonding overlaps, and consequently small bonding contributions from $-\Delta E_\sigma$, ΔE_π and $-\Delta E_\delta$ to D(M–M) (see Tables 2–5). The repulsive steric interaction ΔE^o is further relatively large for complexes of 3*d* elements, since the short metal–metal bond distance allows for substantial four-electron destabilizing interactions between the occupied core-like 3*d*, 3*p* orbitals of the two metal centers of almost the same radial extent as 3*d*. Known neutral binuclear complexes of 3*d* elements, such as $Cr_2(O_2CR)_4$, have bidentate ligands with coordination to both metal centers, and we intend to investigate to what extent this arrangement might stabilize the metal–metal bond. The order of stability D(V–V) < D(Cr–Cr) ~ D(Mn–Mn) between $M_2Cl_4(PH_3)_4$ complexes of 3*d* elements is deceiving in the sense that the interaction between two $VCl_2(PH_3)_2$ fragments with the valence configuration $1a_1^1 1b_1^1 1b_2^1$ in $M_2Cl_4(PH_3)_4$ is stronger than the corresponding interactions between two $CrCl_2(PH_3)_2$ or $MnCl_2(PH_3)_2$ complexes in their respective ground-state configurations. Thus, in our analysis it is the required promotion energy ΔE_T which gives rise to the small value for D(V–V).

We find for a pair of homologous binuclear complexes with 4*d* and 5*d* elements from the same triad, such as $Mo_2(OH)_6$ and $W_2(OH)_6$, that the complex of the 5*d* elements invariably has the stronger metal–metal bond (Tables 2–5). In going from a 4*d* complex to the 5*d* homologue one observes (Tables 2–5) a reduction in the σ, π and

δ bonding contributions, in particular from $-\Delta E_\pi$, as well as a reduction in ΔE^o due to the four-electron destabilizing interactions between *ns*, *np* core-like orbitals on the two metal centers. Of the two reductions, both of which can be explained as due to the longer metal–metal bond distance for 5*d* elements in comparison with their lighter 4*d* congeners, the reduction in ΔE^o prevails over the reduction in the σ, π and δ bonding contributions, resulting in a stronger metal–metal bond for the 5*d* complex than its 4*d* homologue. We note again that the stability orders D(Nb–Nb) $\ll$ D(Tc–Tc) $<$ D(Mo–Mo) and D(Ta–Ta) $\ll$ D(Re–Re) $<$ D(W–W) in $M_2Cl_4(PH_3)_4$ are deceiving in that the smaller values for D(Nb–Nb) and D(Ta–Ta) are due to the promotion energies ΔE_T.

It follows from the deliberation given here that the trend in D(M–M) down a triad is set by a competition between attractive ($-\Delta E_\sigma$, $-\Delta E_\pi$ and $-\Delta E_\delta$) and repulsive (ΔE^o) interactions. The attractive interactions can be increased by shortening the metal–metal bond, but *not* without increasing the repulsive interaction ΔE^o as well. For good metal–metal bonding elements we need the *nd* orbitals to be relatively diffuse and the corresponding *ns*, *np* core-like orbitals in comparison as contracted as possible. This criterion is best met by the 5*d* elements. The elements of the first transition series have on the other hand relatively contracted 3*d* orbitals as well as 3*s*, 3*p* core orbitals of nearly the same radial extent as 3*d*. The 3*d* elements are for this reason poor metal–metal bonders. This situation might well change in such cases as Cu_2, Ag_2 and Au_2, where the metal–metal bond distance is long and due primary to the $(n+1)s$–$(n+1)s$ bonding overlaps.

There are two important differences between $M_2(OH)_6$ complexes and the $M_2Cl_4(PH_3)_4$ systems. The first is a greater contribution from relativistic effects ($-\Delta E_R$) to D(M–M) in $W_2(OH)_6$ compared to $M_2Cl_4(PH_3)_4$ (M = Ta, W or Re) as a consequence of a larger participation from $(n+1)s$ in the σ-orbital of $W_2(OH)_6$ compared to the σ-orbital of the $M_2Cl_4(PH_3)_4$ (M = Ta, W or Re) systems.[8] The second difference is a stronger π-bond in $M_2Cl_4(PH_3)_4$ compared to $M_2(OH)_6$ for metals of the same transition-metal series. In $M_2Cl_4(PH_3)_4$ the π-bond is between the two well-directed fragment orbitals $1b_1$ and $1b_2$ (Fig 4 and **6**) where in particular the lobes of the anti-bonding $1b_1$ orbital on one fragment is polarized towards $1b_2$ of the other fragment (**6**). The π-bonding overlaps in $M_2Cl_4(PH_3)_4$ were, for M = Cr, Mo or W, calculated as 0.19, 0.30 and 0.27, respectively.

In $M_2(OH)_6$, with two trigonal $M(OH)_3$ fragments at $\beta = 80°$ (**1a**) one finds on the other hand

the interaction in the π-orbital **7** to be less than optimal[8(a)] due to the tilt of the two 1*e* fragment orbitals involved. The overlaps between the 1*e* orbitals (**7**) are as a consequence relatively small, 0.08, 0.13 and 0.11 for M = Cr, Mo and W, respectively. The weaker π-interaction in $M_2(OH)_6$ is the major factor responsible for the modest strength of the metal–metal bond in $M_2OH)_6$ compared to $M_2Cl_4(Cl)_4$ of the same transition metals.

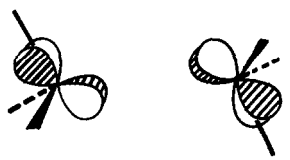

$$S = 2/3\ S_\pi - 1/3\ S_\delta$$

The present set of calculations, based on the energy expression in eqn (1), provides σ, π and δ bonding interactions as well as R_{MM} comparable to those found in previous HFS studies[8] on the same systems. We note that the σ-bond is somewhat stronger than each of the π-bonds, and for the quadruple bonded complexes one order of magnitude stronger than the δ-bond. The steric interaction energy calculated here is, on the other hand, larger than the ΔE^o values evaluated in previous HFS studies,[8] and the D(M–M) based on eqn (1) as a consequence smaller than the D(M–M) values due to the HFS method. It is a general feature of the present method, as demonstrated in recent studies on both diatomics[11(c)] and polyatomic molecules[13(c)] of main-group elements, that the bond energies based on eqn (1) are smaller and more in line with experiment than the bonding energies obtained by the HFS method. The bond energy calculated here for $Cr_2(OH)_6$ is further in reasonable agreement with the value for D(Cr–Cr) obtained in a recent *ab initio* calculation[7(b)] on the related Cr_2H_6 complex.

Acknowledgements—We would like to thank Professor E. J. Baerends and the theoretical chemistry group at the Free University in Amsterdam for providing us with a copy of their HFS program. This investigation was supported by the Natural Sciences and Engineering earch Council of Canada (NSERC).

REFERENCES

1. F. A. Cotton, *Inorg. Chem.* 1965, **4**, 334.
2. F. A. Cotton and R. A. Walton, *Multiple Bonds between Metal Atoms.* Wiley, New York (1982).
3. (a) G. M. Bancroft, E. Pellach, A. P. Sattelberger and K. W. McLaughlin, *J. Chem. Soc., Chem. Commun.* 1982, 752; (b) F. A. Cotton, J. L. Hubbard, D. L. Lichtenberger and I. Shim, *J. Am. Chem. Soc.* 1982, **104**, 679; (c) B. E. Bursten, F. A. Cotton, J. C. Green, E. A. Seddon and G. G. Stanley, *J. Am. Chem. Soc.* 1980, **102**, 4579; (d) A. W. Coleman, J. C. Green, A. J. Hayes, E. A. Seddon, D. R. Lloyd and Y. Niwa, *J. Chem. Soc., Dalton Trans.* 1979, 485; (e) D. L. Lichtenberger and C. H. Blevine II, *J. Am. Chem. Soc.* 1984, **106**, 1936.
4. (a) F. A. Adedeji, K. J. Cavell, S. Cavell, J. A. Connor, G. Pilcher, H. A. Skinner and M. T. Zafarani-Moattar, *J. Chem. Soc., Faraday* I 1979, **75**, 603; (b) K. J. Cavell, C. D. Garner, G. Pilcher and S. Parkes, *J. Chem. Soc., Dalton Trans.* 1979, 1714.
5. (a) J. C. Norman, H. J. Kolari, H. B. Gray and W. C. Trogler, *Inorg. Chem.* 1977, **12**, 987; (b) F. A. Cotton and G. G. Stanley, *Inorg. Chem.* 1977, **16**, 2668; (c) T. Ziegler, *J. Am. Chem. Soc.* 1985, **107**, 4453.
6. (a) P. M. Atha, T. H. Hillier and M. F. Guest, *Mol. Phys.* 1982, **46**, 437; (b) M. Benard, *J. Am. Chem. Soc.* 1978, **100**, 2354.
7. (a) R. A. Kok and M. B. Hall, *Inorg. Chem.* 1983, **22**, 728; (b) R. Wiest, A. Strich, J. Demuynck, M. Benard and P. E. M. Siegbahn, *Chem. Phys. Lett.* 1985, **122**, 453.
8. (a) T. Ziegler, *J. Am. Chem. Soc.* 1983, **105**, 7543; (b) T. Ziegler, *J. Am. Chem. Soc.* 1984, **106**, 5901.
9. F. A. Cotton, K. R. Dunbar, R. L. Falvello, M. Tomas and R. A. Walton, *J. Am. Chem. Soc.* 1983, **105**, 4950.
10. (a) E. J. Baerends, D. E. Ellis and P. Ros, *Chem. Phys.* 1973, **2**, 41; (b) G. J. Snijders, E. J. Baerends and P. Vernooijs, *At. Nucl. Data Tables* 1982, **26**, 483; (c) P. Vernooijs, G. J. Snijders and E. J. Baerends, Slater type basis functions for the whole periodic system. Internal Report, Free University, Amsterdam, The Netherlands (1981); (d) J. Krijn and E. J. Baerends, Fit functions in the HFS-method. Internal Report (in Dutch), Free University, Amsterdam, The Netherlands (1984).
11. (a) W. Kohn and L. J. Sham, *Phys. Rev.* 1965, **140**, A1133; (b) H. Stoll, E. Golka and H. Preuss, *Theor. Chim. Acta* 1980, **55**, 29; (c) A. Becke, *J. Chem. Phys.* (in press).
12. T. Ziegler, A. Rauk and E. J. Baerends, *Theor. Chim. Acta* 1977, **43**, 261.
13. (a) R. M. Dreizler and J. da Providencia (Eds), *Density Functional Methods in Physics.* Plenum, New York (1985); (b) J. Avery and J. P. Dahl (Eds), *Local Density Approximations in Quantum Chemistry and Solid State Physics.* Plenum, New York (1984); (c) R. M. Erdahl and V. H. Smith, Jr (Eds), *Density Matrices and Density Functionals.* D. Reidel, Dordrecht (in press).
14. (a) I. Shim, *K. Dan. Vidensk. Selsk. Mat.-Fys. Medd.* 1985, **41**, 47 (and references therein); (b) W. Weltner and R. J. Van Zee, *Annu. Rev. Phys. Chem.* 1984, **35**, 291.
15. G. J. Snijders, E. J. Baerends and P. Ros, *Mol. Phys.* 1979, **38**, 1909.
16. S. H. Vosko, L. Wilk and M. Nusair, *Can. J. Phys.* 1980, **58**, 1200.
17. (a) T. Ziegler and A. Rauk, *Theor. Chim. Acta* 1977, **46**, 1; (b) T. Ziegler, G. J. Snijders and E. J. Baerends, *J. Chem. Phys.* 1981, **74**, 1271.
18. A. Becke, V. Tschinke and T. Ziegler, work in progress.
19. N. A. Baykara, B. N. McMaster and D. R. Salahub, *Mol. Phys.* 1984, **52**, 891 (and references therein).
20. C. E. Moore, *Atomic Energy Levels*, Vol. 3. National Bureau of Standards.
21. L. Noodleman, *J. Chem. Phys.* 1981, **74**, 5737.

Polyhedron Vol. 6, No. 4, pp. 695–704, 1987
Printed in Great Britain

0277-5387/87 $3.00+.00
Pergamon Journals Ltd

THEORETICAL DESCRIPTION OF METAL–METAL MULTIPLE BONDS IN $M_2(O_2CH)_4$ COMPOUNDS USING THE Xα-SW MO METHOD

BRUCE E. BURSTEN*

Department of Chemistry, The Ohio State University, Columbus, OH 43210, U.S.A.

and

DAVID L. CLARK†

Department of Chemistry, Indiana University, Bloomington, IN 47405, U.S.A.

(*Received* 19 *November* 1986)

Since the discovery of the metal–metal (M–M) quadruple bond in $Re_2Cl_8^{2-}$, the chemical literature has exploded with experimental and theoretical investigations into the nature of M–M multiple bonding.[1] As chemists, we like to think of multiple bonds most simply as derived from the overlap of atomic orbitals of σ-, π- and δ-symmetry, giving rise to multiple bonds corresponding to valence configurations such as $\sigma^2\pi^4$, $\sigma^2\pi^4\delta^2$, $\sigma^2\pi^4\delta^2\delta^{*2}$ or even $\pi^4\delta^2$. A major problem is that such descriptions, although attractive and simple, are oversimplifications when applied to the interpretation of spectroscopic data. Indeed, the quantitative description of M–M multiple bonding has provided an exceptional challenge to theoretical electronic structure methods. More recently, the problems associated with the calculation of the properties of transition-metal dimers containing heavy elements, most notably the necessity of including relativistic effects, have received greater attention. In this regard, density functional methods such as the various Xα molecular-orbital (MO) formalisms[2] hold an important position in inorganic chemistry since they provide a significantly less expensive alternative to *ab initio* methods for complex systems, they preserve an orbital description with which nontheoretical chemists are most comfortable, and they allow for the easy incorporation of relativistic effects. The Xα-SW method, in particular, has had an important role in the development of quantitative descriptions of multiple M–M bond electronic structure, a role in which it continues today, albeit subject to greater criticism than in the past. In the spirit of this Symposium-in-Print, we wish to critically assess some of the successes and failures of the Xα-SW MO method as applied to systems involving multiple bonds between transition-metal atoms. In doing so, we will draw primarily, but not exclusively, on the recent results we and others have obtained for $M_2(O_2CH)_4$ systems.

THE $\delta \rightarrow \delta^*$ TRANSITION ENERGY

For molecules with M–M quadruple bonds with an approximate valence MO configuration $\sigma^2\pi^4\delta^2$, and triple bonds of approximate valence MO configuration $\pi^4\delta^2$, the lowest-energy electronic transition is expected to be from the occupied δ-bonding orbital to the unoccupied δ-antibonding orbital: the so-called $\delta \rightarrow \delta^*$ transition. This transition is perhaps the most studied electronic phenomenon in such multiply bonded systems and a detailed review of the spectroscopy is provided by Hopkins and Gray in this symposium. The theoretical interest in the $\delta \rightarrow \delta^*$ transition energy has grown in tandem with experimental interest, particularly since the factors which influence the transition energy are not well understood from first principles. There have been major difficulties in the calculation of $\delta \rightarrow \delta^*$ transition energies using MO theory, but this is not surprising in view of the weakness of the interaction between the two orbitals of δ-symmetry. The M–M δ-orbital overlap is

*Camille and Henry Dreyfus Teacher-Scholar (1984–1989), and Fellow of the Alfred P. Sloan Foundation (1985–1987). Author to whom correspondence should be addressed.

†Indiana University General Electric Fellow (1985–1986).

small enough that the two paired electrons may substantially localize, one on each metal, rather than delocalizing between the two centers as assumed in MO theory. The resulting situation is thus parallel to the breakdown in MO theory for dihydrogen at the dissociation limit, wherein the presence of low-lying electronic states of the same symmetry as the ground state renders the single configuration description of bonding inadequate. In fact, interaction of the δ-electrons is so weak that it is subject to this same problem even at the equilibrium internuclear distance! Hay has performed a detailed GVB-CI study of the state energetics of $Re_2Cl_8^{2-}$ and convincingly demonstrated that a single-configuration MO wave function is quite inadequate for describing the relative energetics of the states resulting from the δ- and δ^*-orbitals due to the severity of the correlation problem.[3] In fact, the GVB-CI treatment predicts nearly complete localization of the δ-electrons. The inadequacy of the single-configuration descriptions of the ground ("δ^2") and excited ("$\delta^1\delta^{*1}$") states has a profound effect on the calculation of the $\delta \rightarrow \delta^*$ transition energy using *any* MO method. A very simple, two Slater determinant CI description of the ground state, and singlet and triplet excited states of a typical quadruple bond leads to the conclusion that the transition is nearly completely dominated by two-electron repulsions rather than orbital energy (one-electron) terms.[4] Thus, the Xα-SW method, through Slater's transition-state formalism, usually underestimates the $\delta \rightarrow \delta^*$ transition by approximately a factor of two, but adequately calculates transitions between the other, more strongly bonding orbitals in the M–M bonding manifold (see Table 1). It is recognized[5] that the Xα exchange potential does introduce some correlation between electrons of opposite spin, and this observation prompted Noodleman and Norman to cast the Xα-SW method in a valence-bond formalism.[6] Their application of this Xα valence-bond method to the $\delta \rightarrow \delta^*$ transition in $Mo_2Cl_8^{4-}$ has resulted in a tremendous improvement in the $\delta \rightarrow \delta^*$ transition energy from 9.2×10^3 cm^{-1} (Xα-SW)[7] to $15.2 \times 10^3\,cm^{-1}$ (experimental value $18.8 \times 10^3\,cm^{-1}$).

The $\delta \rightarrow \delta^*$ transitions in systems with a bond order of 3.5, corresponding to $\sigma^2\pi^4\delta^1$ or $\sigma^2\pi^4\delta^2\delta^{*1}$ configurations are typically in the near IR region of the spectrum (*ca* $6000\,cm^{-1}$), much lower in energy than the corresponding transition in quadruply bonded complexes. MO methods have been very successful in the calculation of these transition energies,[8] despite the fact that they result from weak δ- and δ^*-interactions (Table 1). The reason for this is very clear; the removal or addition of one electron from or to the quadruply bonded configuration $\delta^2\delta^{*0}$ eliminates the low-lying excited state with the same symmetry as the ground state, and hence mitigates the extent of configuration interaction which will occur.

M–M σ-BONDING

Xα-SW calculations on $M_2(O_2CH)_4$ molecules reveal some interesting differences in M–M σ-bonding between Cr, Mo and W. The Xα-SW calculations in general yield two components to the M–M σ-bond, the $4a_{1g}$ and the $5a_{1g}$ molecular orbitals. One can envision these orbitals as the result of the interaction of a nearly pure d_{z^2} σ_g orbital of an M_2^{4+} fragment with the symmetric combination of four formate lone-pair orbitals. This interaction gives rise to the 4*a*1*g* and 5*a*1*g* orbitals which are M–O bonding and antibonding (respectively) between the torus (or "doughnut") of the σ_g-orbital and formate lone-pair orbitals, as depicted qualitatively in **I**.

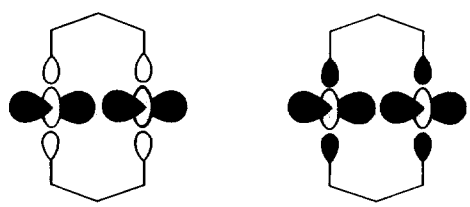

I

As expected from simple perturbation theory, the amount of mixing between the M_2^{4+} σ_g and formate orbitals will depend on the relative energetics and magnitude of overlap between the σ_g and the formate levels. Weak 3*d*–3*d* bonding in Cr_2 systems results in a sizable energetic separation between the Cr–Cr σ and formate orbitals and very little metal–ligand (M–L) mixing is observed as depicted qualitatively in Fig. 1. Conversely, stronger 4*d*–4*d* and 5*d*–5*d* bonding between Mo_2 and W_2 centers (respectively) lowers the M–M σ-orbital in energy, allowing for a better energetic match, and hence greater M–L mixing occurs between metal and formate levels in Mo–Mo and W–W systems (Fig. 1). The extent of M–L mixing can be gauged by the percentage of metal contribution to the $5a_{1g}$ and $4a_{1g}$ orbitals of $M_2(O_2CH)_4$ which are 98 and 20% for M = Cr,[9] 48 and 75% for M = Mo,[7] 59 and 54% for M = W (nonrelativistic),[10] and 69 and 51% for M = W (relativistic).[10] In the case of $Cr_2(O_2CH)_4$, the $5a_{1g}$ orbital is best described as the Cr–Cr σ-bond (98% Cr), and the $4a_{1g}$ is best described as the Cr–O bonding level. However, in $Mo_2(O_2CH)_4$ and $W_2(O_2CH)_4$, stronger M–L mixing results in two orbitals with substantial M–

Table 1. A comparison of experimental and Xα-SW $\delta \rightarrow \delta^*$ transition energies in M–M multiply bonded compounds

Compound	ν_{max} ($\delta \rightarrow \delta^*$) ($\times 10^3\,cm^{-1}$)	Xα-SW ($\times 10^3\,cm^{-1}$)	Valence configuration
$Mo_2Cl_8^{4-}$	18.8	9.2	$\sigma^2\pi^4\delta^2$
$Re_2Cl_8^{2-}$	14.2	7.0	$\sigma^2\pi^4\delta^2$
$Mo_2(O_2CH)_4$	22.9	14.7	$\sigma^2\pi^4\delta^2$
$W_2(O_2CH)_4$	23.0	12.3	$\sigma^2\pi^4\delta^2$
$Tc_2Cl_8^{3-}$	5.9	6.0	$\sigma^2\pi^4\delta^2\delta^{*1}$
$[Re_2Cl_4(PH_3)_4]^+$	6.6	5.6	$\sigma^2\pi^4\delta^2\delta^{*1}$

M σ character, and it becomes difficult to label either the $4a_{1g}$ or $5a_{1g}$ orbital as the "principal" M–M σ-bond. There are clearly two MOs with substantial M–M σ character, and together they are equivalent to one strong metal–metal σ-bond. The simple description of the quadruple bond as $\sigma^2\pi^4\delta^2$ is thus rendered inadequate due to metal–ligand mixing in the orbitals of a_{1g}-symmetry for the 4*d* and 5*d* metals.

Another feature evident in the a_{1g} M–M σ-bonding orbitals is the involvement of virtual $(n + 1)s$ atomic orbitals which contribute further to the stabilization of M–M and M–L bonding. There is essentially no Cr as 4*s* atomic orbital participation to the 3*d*–3*d* σ-bond of $Cr_2(O_2CH)_4$,[9] whereas we find a significant contribution of W 6*s* atomic orbital participation to the 5*d*–5*d* σ-bond of $W_2(O_2CH)_4$.[10] The increased $(n + 1)s$ contribution to M–M σ-bonding is a combined result of decreased *nd* and $(n + 1)s$ atomic orbital energy differences, and the increased importance of relativistic effects for third-row relative to first-row transition metals. These latter effects will be examined more closely in the next section.

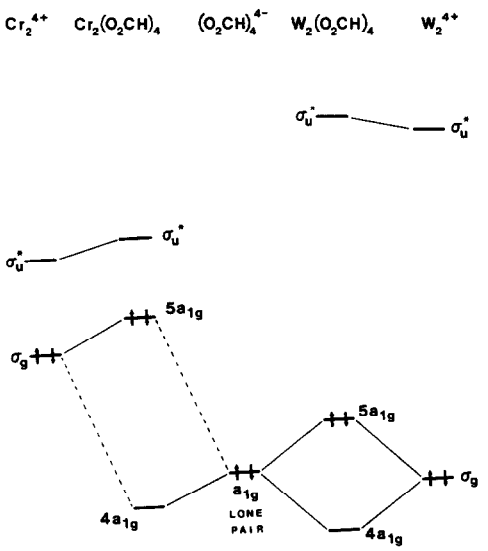

Fig. 1. Qualitative molecular-orbital diagram comparing the interaction of the Cr_2^{4+} and W_2^{4+} σ_g-orbitals with the symmetric a_{1g} carboxylate oxygen lone-pair orbital.

CONSEQUENCES OF RELATIVISTIC CORRECTIONS TO M–M σ-BONDING

One of the great advantages of the Xα-SW method is the ease with which relativistic corrections can be incorporated for heavy elements such as the third-row transition metals or the actinides. We have previously reported the major effects of including the "quasi-relativistic" corrections of Wood and Boring[11] on organouranium complexes,[12] and we are finding nearly as profound an influence of these on the valence electronic structure of metal–metal multiple bonds. Shown in Fig. 2 is a comparison of our relativistic and nonrelativistic calculations on the $W_2(O_2CH)_4$ molecule.[10] The two components of the W–W σ-bond are labeled along with the percent metal character of the predominantly M-based MOs. The relativistic corrections cause large energy shifts in the W core levels and similar shifts in valence orbitals containing significant W character, while, as expected, the primarily O-, C- and H-based MOs are scarcely affected. The changes induced in the bonding picture upon inclusion of relativistic effects are consistent with the expected influence of mass–velocity corrections on the W atomic orbitals.[13] The inner *s*-orbitals, having the highest classical velocities, are the most profoundly affected orbitals. The relativistic mass increase results in a contraction of all the *s*-orbitals with a concomitant decrease in their orbital energies. This effect is mimicked by the *p*-orbitals although the contraction and stabilization is much less pronounced than for the *s*-orbitals. The metal *d*- and *f*-electrons, which have a much smaller probability of attaining a classical velocity close to *c*, are primarily influenced by the contraction of the *s*- and *p*-orbitals. The contraction of these latter orbitals results in an expansion and

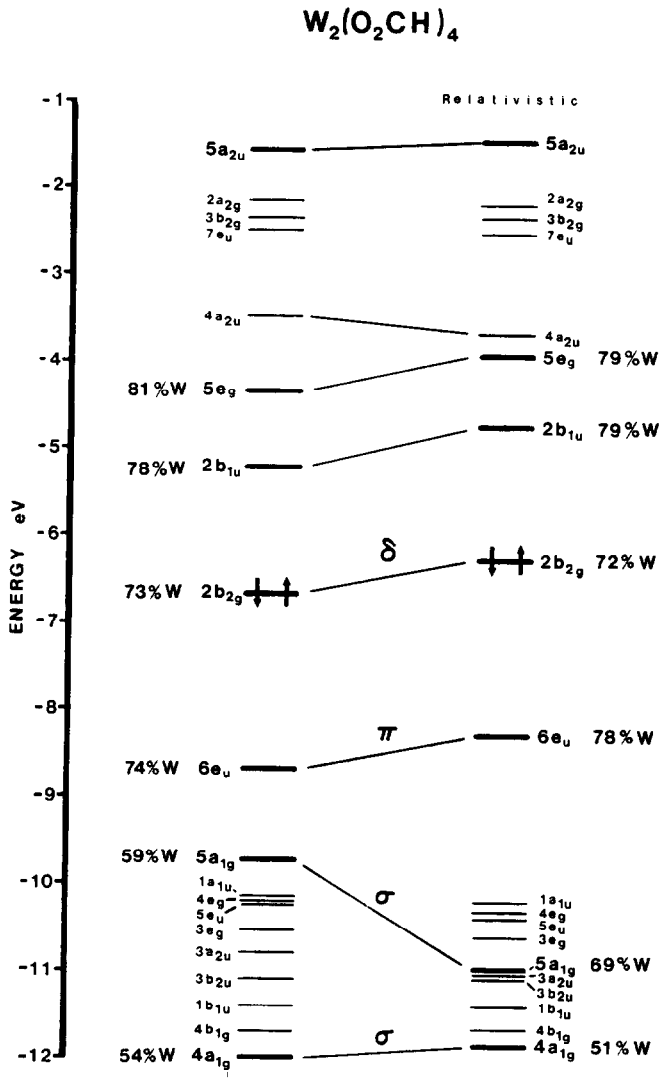

Fig. 2. Nonrelativistic and relativistic converged Xα-SW eigenvalues for $W_2(O_2CH)_4$. Primarily W-based levels are in bold face along with their percentage of W contribution. The HOMO is marked with arrows. Adapted from Ref. 10.

rise in energy of the *d*- and *f*-orbitals.

In Fig. 2 it is seen that the relativistic shifts in the orbital energies are in the expected directions. The valence levels containing significant W 5*d* character rise in energy with the exception of the $5a_{1g}$ σ-orbital; without relativistic corrections, this orbital has 17% W 6*s* and 38% W 5*d* character, and the substantial 6*s* character causes this orbital to drop in energy upon the inclusion of relativistic effects. Upon stabilization, the $5a_{1g}$ σ-orbital acquires significantly more W 6*s* character (26%) and somewhat less W 5*d* character (36%). The W 6*s* orbital contribution to this orbital represents a mixing of the 6*s*–6*s* σ-bonding orbital, normally unoccupied, with the 5*d*–5*d* σ-bonding orbital. Thus the relativistic corrections have their most profound effect on orbitals of σ-symmetry.

The importance of increased *s*-orbital participation to the M–M σ-bond needs some amplification. The *s*–*s* σ-bonding orbital was shown to be important in explaining the extremely short bond distances found for naked-metal diatomics such as Mo_2 which has a singlet ground state with a closed-shell $1\sigma_g^2 1\pi_u^4 1\delta_g^4 2\sigma_g^2$ configuration.[14,15] The $2\sigma_g$ orbital of Mo_2 represents the 5*s*–5*s* σ-bond, while the $1\sigma_g$ represents the 4*d*–4*d* σ-bond. Contour plots of the $1\sigma_g$ and $2\sigma_g$ orbitals[14] of Mo_2 are shown in comparison with the $4a_{1g}$ and $5a_{1g}$ orbitals[10] of $W_2(O_2CH)_4$ in Fig. 3. The $2\sigma_g$ orbital, representing the 5*s*–5*s* σ interaction in Mo_2 shows a striking similarity to the $5a_{1g}$ σ-orbital of $W_2(O_2CH)_4$, further emphasizing the importance of the 6*s*–6*s* contribution to the $5a_{1g}$ orbital in $W_2(O_2CH)_4$. We will show later that *s*-orbital participation is also

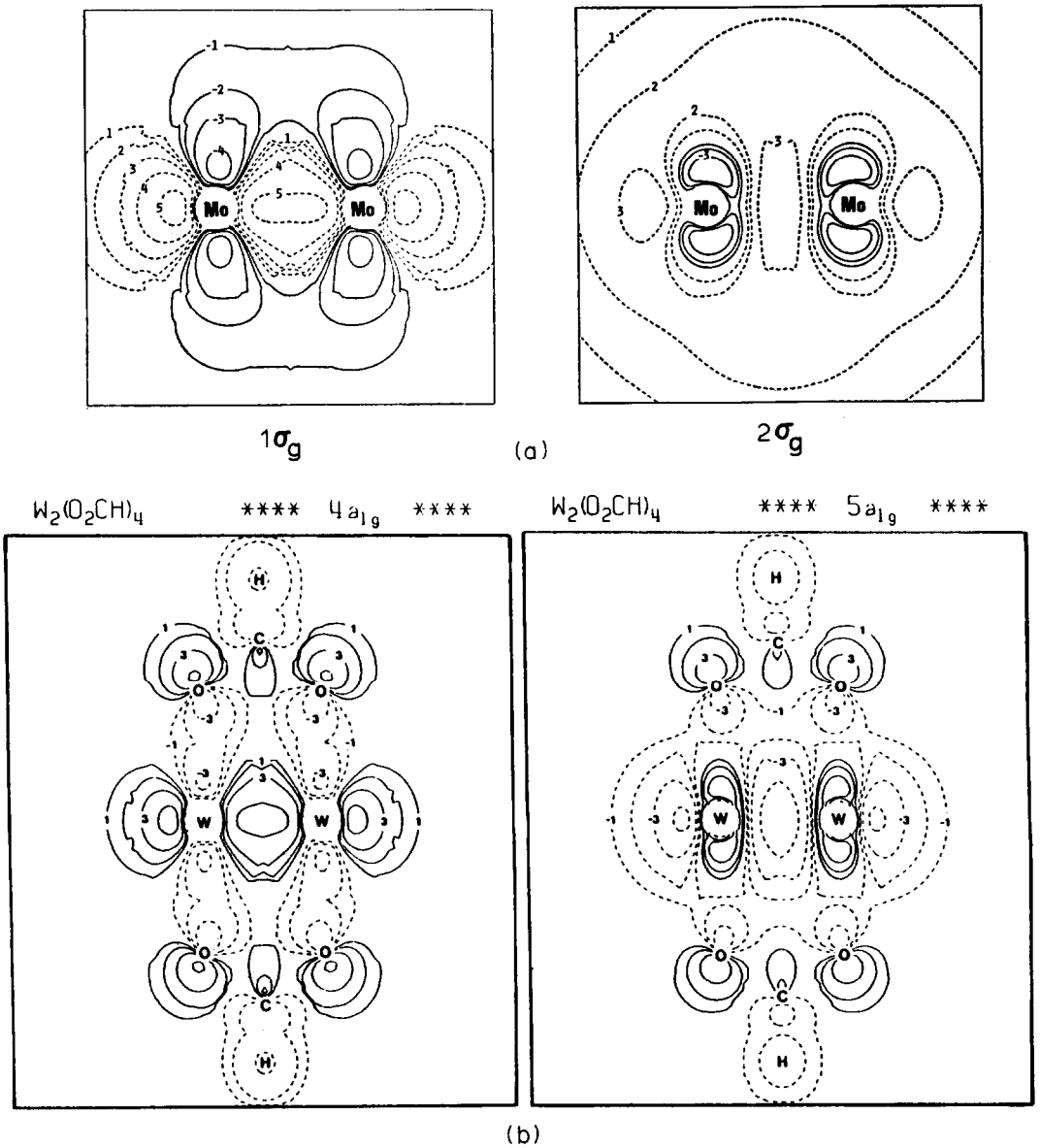

Fig. 3. (a) Contour plots of the $1\sigma_g$ and $2\sigma_g$ orbitals of Mo_2 at 1.929 Å. The contour values are ± 1; ± 2, ± 3, ± 4 and $\pm 5 = \pm 0.015$, ± 0.030, ± 0.060, ± 0.120 and $\pm 0.240\ e\text{Å}^{-3}$, respectively. Adapted from Ref. 14. (b) Contour plots of the $4a_{1g}$ and $5a_{1g}$ molecular orbitals of $W_2(O_2CH)_4$. These plots are in the horizontal mirror plane containing the W atoms and two of the formate ligands. Contour values are ± 1, ± 2, ± 3 and $\pm 4 = \pm 0.02$, ± 0.04, ± 0.08 and $\pm 0.16\ e\text{Å}^{-3}$, respectively. Adapted from Ref. 10.

an important consideration in the electronic effects of axial ligation.

What effect does this valence *s* and *dσ* hybridization have on metal–metal σ-bond strength? We feel that the answer to this question is parallel to that given by Mulliken years ago when considering the effect of *s* and *pσ* hybridization in homonuclear diatomics such as N_2.[16] In the N_2 molecule (ground-state configuration $1\sigma_g^2 1\sigma_u^2 2\sigma_g^2 2\sigma_u^2 1\pi_u^4 3\sigma_g^2$) there is major *s* and *pσ* hybridization in the $2\sigma_g$, $2\sigma_u$ and $3\sigma_g$ MOs. Positive *s*-*pσ* hybridization in $2\sigma_g$ makes the MO strongly bonding, while negative *s*–*pσ* hybridization in $3\sigma_g$ makes it only weakly bonding. This "forced hybridization" is a simple consequence of the requirement of orthogonality among LCAO MOs of the same symmetry. The result of the *s*–*pσ* hybridization is a decrease in the overlap population and a resultant loss of bond strength in the $3\sigma_g$ orbital. This, of course, does not mean that N_2 has a weak σ-bond, for now these three σ MOs of N_2 are equivalent to one strong σ-bond. This situation is not at all unlike that observed for $M_2(O_2CH)_4$ compounds of second- and third-row transition metals.

THE EFFECTS OF AXIAL LIGATION ON THE M–M σ-BOND

Xα-SW calculations on a variety of $M_2(O_2CH)_4$ and $M_2(O_2CH)_4L_2$ compounds have helped to reveal both quantitative and qualitative details of the electronic effects of axial ligation.[10,17–20] We will first consider the qualitative picture of axial ligation and then discuss the effects for first vs third-row metals.

All of the calculations indicate that the interaction of the $M_2(O_2CH)_4$ moiety with an axial ligand is essentially a σ-only interaction. It is found that the M–M π, δ, δ^*, π^* and formate orbitals all have nearly identical energies in $M_2(O_2CH)_4$ and $M_2(O_2CH)_4L_2$ calculations. Even for axial ligands containing π lone-pairs, the π lone-pair orbitals are found to be essentially noninteracting with the $M_2(O_2CH)_4$ moiety. The symmetric combination of the two ligand σ lone-pair orbitals interacts with the M–M σ-bonding orbitals ($4a_{1g}$ and $5a_{1g}$); while the antisymmetric combination interacts with the M–M σ^*-orbitals, which are of a_{2u}-symmetry. The consequences of these interactions depends in part on the strength of the original M–M σ-bond and the energetic placement of the L_2 orbitals.

The important first-order M–M bond weakening upon axial ligand coordination results from axial ligand lone-pair donation into the M–M σ^*-orbital. The magnitude of the donation is reflected by the amount of M–M σ^* character found in occupied MOs and will be related to the strength of the original M–M σ-bond. In the case of $Cr_2(O_2CH)_4$ compounds,[9,17] weak $3d$–$3d$ σ-bonding results in a low-lying Cr–Cr σ^*-orbital, whereas the much stronger $5d$–$5d$ σ-bonding in $W_2(O_2CH)_4$ results in a relatively high lying W–W σ^*-orbital.[10] This criterion would suggest that for the same axial ligand (e.g. THF), the L_2 interaction should be able to introduce qualitatively more M–M σ^* character into the occupied orbitals of the Cr_2L_2 than the W_2L_2 system.

The second important interaction is between the occupied M–M σ-bonding orbital and the symmetric combination of the axial L_2 orbitals. The Xα-SW calculations[17] on $Cr_2(O_2CH)_4(H_2O)_2$ present the result that weak Cr–Cr σ-bonding places the symmetric L_2 combination lower in energy than the Cr–Cr σ-orbital. This interaction destabilizes the Cr–Cr σ-orbital by Cr–L σ-antibonding while the L-localized level is stabilized by Cr–L σ-bonding. In contrast, the much stronger W–W σ-bonding is expected to find the W–W σ-orbitals lower in energy than the symmetric L_2 combination, and interaction will stabilize the W–W σ-bond. This comparison is shown qualitatively in the interaction diagram of Fig. 4, and accounts

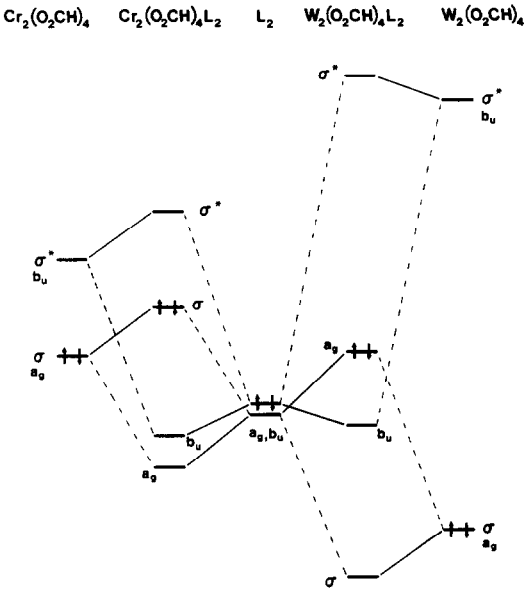

Fig. 4. Qualitative molecular-orbital diagram comparing the interaction of a neutral donor ligand L with $Cr_2(O_2CH)_4$ and $W_2(O_2CH)_4$. Only the σ interactions are depicted for clarity.

qualitatively for the extreme sensitivity and insensitivity of Cr–Cr and W–W bond lengths (respectively) in the presence of neutral axial donors.

In our recent relativistic calculations[10] on the model compound $W_2(O_2CH)_4(CH_3)_2$ we found that the interaction of the symmetric combination of L_2 orbitals with the W–W σ-bonding orbitals resulted in a significant increase in the contribution of the $6s$–$6s$ σ-bonding orbital in both W–W and W–L σ-bonding. The correlation of the MO of $W_2(O_2CH)_4(CH_3)_2$ with those of its component fragments $W_2(O_2CH)_4$ and $(CH_3)_2$ is shown in Fig. 5. One feature emphasized in Fig. 5 is that axial ligand interaction is essentially a σ-only interaction, and as expected, the M–M π, δ, δ^*, π^*, M–L and formate levels in $W_2(O_2CH)_4(CH_3)_2$ are essentially unperturbed by interaction of $W_2(O_2CH)_4$ with the axial ligands.

The symmetric combination of the $(CH_3)_2$ orbital interacts with both the $4a_{1g}$ and $5a_{1g}$ components of the W–W σ-bond. The stronger interaction is with the $5a_{1g}$ component since it is both spatially and energetically favored over the $4a_{1g}$ orbital. This interaction results in formation of the W–C σ-bonding $13a_g$ and σ-antibonding $16a_g$ MO which are occupied and unoccupied, respectively. The filled $13a_g$ orbital has 35% W character of which 63% is W $6s$. As was the case for its $5a_{1g}$ precursor, this represents a contribution of the $6s$–$6s$ σ-bonding orbital in W–CH_3 σ-bonding. The more important observation in the a_g interaction is that

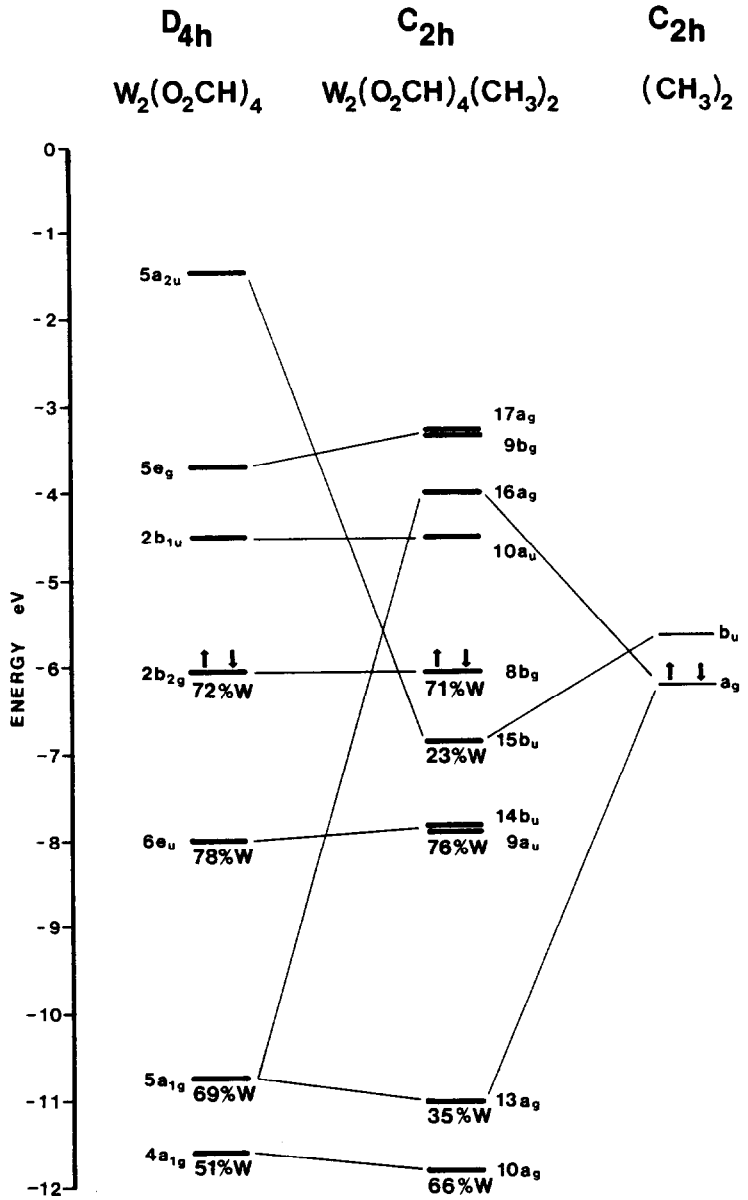

Fig. 5. Results of relativistic SCF-Xα-SW calculations on $W_2(O_2CH)_4(CH_3)_2$. This diagram shows the correlation of the orbitals of $W_2(O_2CH)_4(CH_3)_2$ to those of $W_2(O_2CH)_4$ and $(CH_3)_2$. Only those levels involved in W–W bonding or antibonding are shown. The highest occupied orbitals are depicted with arrows. Adapted from Ref. 10.

the $4a_{1g}$ MO, the principal component of the $5d$–$5d$ σ-bond, is actually stabilized by the interaction and acquires more W $5d$ character. A contour plot of the resulting $10a_g$ orbital of $W_2(O_2CH)_4(CH_3)_2$ is shown in Fig. 6, and can be compared to the $4a_{1g}$ $5d$–$5d$ σ component of $W_2(O_2CH)_4$ shown in Fig. 3.

The antisymmetric combination of the $(CH_3)_2$ orbital interacts with the $5a_{2u}$ W–W σ^*-orbital of $W_2(O_2CH)_4$, generating the W–C σ-bonding and σ-antibonding orbitals which are occupied and unoccupied, respectively (Fig. 6). The filled $15b_u$ orbital is 49% C and 23% W, of which this small amount of W character is allocated between s, p and d angular contributions. For $W_2(O_2CH)_4(CH_3)_2$, we find a rather peculiar result of strong M–M bonding in consort with strong M–L bonding in the axial position as demonstrated by the observation that experimentally both $W_2(O_2CR')_4$ and $W_2(O_2CR')_4R_2$ compounds have identical W–W bond distances.[21] Formally, the $W_2(O_2CH)_4(CH_3)_2$ molecule can be considered as having a W_2^{6+} core, and thus a d^3–d^3 triple bond of *approximate* valence MO configuration $\pi^4\delta^2$. We

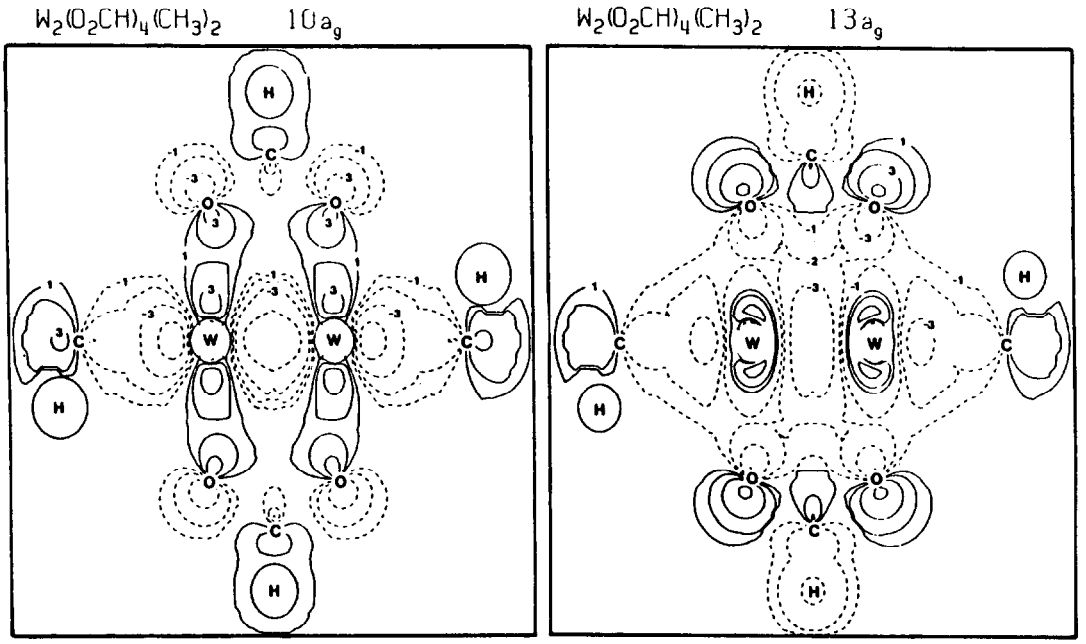

Fig. 6. Contour plots of the $10a_g$ and $13a_g$ molecular orbitals of $W_2(O_2CH)_4(CH_3)_2$. These plots are in the horizontal mirror plane containing the W atoms, two of the formate ligands, the axial C atoms, and two of the C—H bonds. Contour values are the same as those in Fig. 3(b). Adapted from Ref. 10.

emphasize that this is simply an approximation, and an aesthetically simple way to differentiate this type of d^3–d^3 dimer from one with a $\sigma^2\pi^4$ configuration. The $\pi^4\delta^2$ triple bond however suffers from a severe "σ-problem". Extensive mixing between W–W, W–CH_3 and W–O_2CH σ-bonding is so severe that we cannot asign any given orbital to any one symmetry type (i.e. M–M σ or M–L σ). There are clearly occupied MOs with substantial W–W σ character in the $\pi^4\delta^2$ triple bond as emphasized in the contour plots. Using our model of axial ligation we can readily see that the strong W–W and W–C bonding in $W_2(O_2CH)_4(CH_3)_2$ is the result of several factors. (1) Strong W–W bonding results in a very high energy W–W σ^*-orbital and little axial ligand donation into the W–W σ^*-orbital is observed. Due to the small amount of W–W σ^* character found in occupied orbitals, the W–W bond is not significantly weakened by the interaction. (2) The $4a_{1g}$ component of the $5d$–$5d$ σ-bond is scarcely affected by the axial ligation and thus remains a strong, occupied component of W–W σ-bonding in $W_2(O_2CH)_4(CH_3)_2$. (3) The major interaction of the symmetric combination of $(CH_3)_2$ orbitals is with the $5a_{1g}$ component of the W–W σ-bond, resulting in a significant contribution of the $6s$–$6s$ σ-bonding orbital in both W–W and W–C σ-bonding.

It is our belief that the participation of the s–s σ-bonding orbital is largely responsible for the electronic structural differences between first-, second- and third-row multiple M–M-bonded systems. The importance of this point needs some amplification. If the s–s σ-bonding orbital is unimportant, as it most certainly is in Cr–Cr quadruply bonded systems, the interactions of both the symmetric and antisymmetric L_2 orbitals with an M–M quadruple bond must necessarily weaken and lengthen the M–M bond. The antisymmetric combination donates into the M–M σ^*-orbital, an interaction which obviously will weaken the M–M bond. The symmetric combination will interact with the M–M σ-bond, resulting in M–L bonding and antibonding orbitals which are occupied and unoccupied, respectively. Thus, a portion of the M–M σ-bond is found in unoccupied orbitals, again weakening the M–M interaction. The importance of the s–s σ-bonding orbital in W systems, which is due in large part to the relativistic stabilization of the W $6s$ orbitals, is that it provides another mechanism by which the symmetric L_2 orbital can interact with the dimetal core. The participation of s orbitals has been found to be important in the M–M σ- and σ^*-orbitals of second-row dimers as well, although the $5s$ participation in $Mo_2(O_2CH)_4$ is not nearly so pronounced as the $6s$ participation in $W_2(O_2CH)_4$. It is our belief that this $5s$ participation accounts in part to the insensitivity of the Mo–Mo bond length in axial adducts of dimolybdenum tetracarboxylates as compared to the extreme sensi-

tivity of the corresponding Cr dimers. As an illustration we note that the W–W distances in $W_2(O_2CMe)_4$ and $W_2(O_2CMe)_4(CH_2Bu^t)_2$ are both 2.189 Å,[21] whereas a slight lengthening from 2.090 to 2.134 Å is observed for the respective Mo–analogues,[22] presumably due to the smaller degree of 5*s*–5*s* σ-participation in the Mo_2 system.

CALCULATED IONIZATION ENERGIES OF THE M–M σ-BOND

The initial assignment[23] of the low-energy photoelectron (PE) spectrum of $W_2(O_2CCF_3)_4$ has been the focus of considerable attention and, at least initially, considerable controversy.[24] Of particular note was the assignment of a very sharp band at 9.71 eV in the PE spectrum to ionization from the W–W σ-bond, an ionization less than 1 eV above that assigned to ionization from the π-bond. Recent experimental studies of Kober and Lichtenberger[25] have confirmed these assignments, which are somewhat disheartening in view of our expectations based on the relativistic Xα-SW calculations on $W_2(O_2CH)_4$. The δ–π separation of *ca* 1.8 eV is in good quantitative agreement with the predictions (2.0 eV) of the Xα-SW calculations. However, the calculations place the first σ ionization (from the $5a_{1g}$ orbital) 2.3 eV below the π-ionization. This is, in fact, a general observation in that Xα-SW calculations on M–M quadruply bonded systems *always* place the σ-orbitals well below the π-orbitals. By contrast, Ziegler's relativistic Hartree–Fock–Slater (DV-Xα) calculation[26] on $W_2(O_2CH)_4$ yields a σ–π splitting of 0.5 eV, in good agreement with the experimental results. Similarly, Xα–SW calculations[7] on $Mo_2(O_2CH)_4$ give a σ–π splitting on the order of 1.0 eV, whereas recent DV-Xα calculations[27] on the same molecule predicts the σ- and π-ionizations to be almost isoenergetic, a result also obtained using multiconfiguration *ab initio* methods.[28] It thus appears that discrete variational and scattered-wave solutions to the Xα method differ with respect to the placement of the σ-orbital in $M_2(O_2CH)_4$ compounds. We believe that the inability of the Xα-SW method to properly place the σ-orbitals is due to some of the assumptions of the overlapping-sphere formalism which is the accepted practice for such calculations. For these very short M–M bonds, the atomic spheres of the M atoms overlap substantially, and the largest errors in the description of the M–M interaction are expected to occur for those orbitals which have their maximum interatomic interactions in the overlap region. This will not be a serious problem for the δ- and π-orbitals, but could be (and apparently is) for the σ-orbitals. Sattelberger and Scioly[29] have found that the Xα-SW energies of the σ-orbitals of $W_2(O_2CH)_4$ are extremely sensitive to the choice of sphere radii, consistent with the above conjecture. The DV-Xα method, which does not employ the scattered-wave method of solution, is apparently able to more correctly model the M–M σ-interaction. It is our expectation that recognition of this apparent flaw in the Xα-SW method will lead to further examination of its causes and corrections.

CONCLUSIONS

The Xα-SW method occupies a unique role in multiple M–M bond chemistry. Beginning with Norman and Kolari's seminal work on $Mo_2Cl_8^{4-}$ and $Mo_2(O_2CH)_4$,[30] the method has been one of the most widely used quantitative electronic structural tools in this area of chemistry. The application of the method to multiple metal–metal bonds was not unjustified as the results of the calculations more often than not led to new insights about the bonding and energetics of these systems. In fact, in nearly all cases, the Xα-SW method provides results which are in excellent *qualitative* and very often (but not always) excellent *quantitative* agreement with experimental data.

It must be recognized, however, that the Xα-SW method is not a panacea for all aspects of the multiple bonding between M atoms. We have tried to present not only the successes of the method, but also areas in which it fails. Two of these are particularly notable for this Symposium: the calculation of $\delta \rightarrow \delta^*$ transition energies, and the energies of M–M σ-bonding orbitals. The former is, of course, a flaw of MO theory and there is no corrective recourse within a single-configuration description. The latter must be acknowledged as an area in which the Xα-SW method provides poor quantitative agreement with experiment. It is our hope that these discussions provide the impetus for further investigation into the source(s) of these problems.

Acknowledgments—We thank Dr A. P. Sattelberger of the Los Alamos National Laboratory, and Professor D. L. Lichtenberger of the University of Arizona for helpful discussions. D.L.C. gratefully acknowledges M. H. Chisholm of Indiana University for helpful discussions and financial support through a SOHIO fellowship during the period in which this research was undertaken.

REFERENCES

1. F. A. Cotton and R. A. Walton, *Multiple Bonds between Metal Atoms*. Wiley, New York (1982).
2. (a) J. C. Slater, *Quantum Theory of Molecules and*

Solids. The Self-Consistent Field for Molecules and Solids, Vol. 4. McGraw-Hill, New York (1974); (b) K. H. Johnson, *Annu. Rev. Phys. Chem.* 1975, **26**, 39; (c) D. A. Case, *Annu. Rev. Phys. Chem.* 1982, **33**, 151.
3. P. J. Hay, *J. Am. Chem. Soc.* 1978, **100**, 2897.
4. B. E. Bursten and T. W. Clayton, Jr, *Abstracts of Papers*, 191st National Meeting of the American Chemical Society, New York, NY. American Chemical Society, Washington D.C. (1986). PHYS 31.
5. R. P. Messmer and D. R. Salahub, *J. Chem. Phys.* 1976, **65**, 779.
6. L. Noodleman and J. G. Norman, Jr, *J. Chem. Phys.* 1979, **70**, 4903.
7. J. G. Norman, Jr, H. J. Kolari, H. B. Gray and W. C. Trogler, *Inorg. Chem.* 1977, **16**, 987.
8. See, for example: B. E. Bursten, F. A. Cotton, P. E. Fanwick, G. G. Stanley and R. A. Walton, *J. Am. Chem. Soc.* 1983, **105**, 2606.
9. F. A. Cotton and G. G. Stanley, *Inorg. Chem.* 1977, **16**, 2668.
10. M. D. Braydich, B. E. Bursten, M. H. Chisholm and D. L. Clark, *J. Am. Chem. Soc.* 1985, **107**, 4459.
11. J. H. Wood and A. M. Boring, *Phys. Rev. B.* 1978, **18**, 2701.
12. B. E. Bursten and A. Fang, *Inorg. Chim. Acta* 1985, **110**, 153.
13. Many excellent reviews exist, for example: (a) K. S. Pitzer, *Acc. Chem. Res.* 1979, **12**, 271; (b) P. Pyykko and J. Desclaux, *Acc. Chem. Res.* 1979, **12**, 276; (c) J. G. Snijders and P. Pyykko, *Chem. Phys. Lett.* 1980, **75**, 5; (d) T. Ziegler, J. G. Snijders and E. J. Baerends, *Chem. Phys. Lett.* 1980, **75**, 1.
14. B. E. Bursten and F. A. Cotton, *Symp. Faraday Soc.* 1980, **14**, 180.
15. B. E. Bursten, F. A. Cotton and M. B. Hall, *J. Am. Chem. Soc.* 1980, **102**, 6348.
16. R. S. Mulliken, *J. Chem. Phys.* 1951, **19**, 912; **23**, 2338.
17. B. E. Bursten, F. A. Cotton and G. G. Stanley, unpublished results.
18. B. E. Bursten and F. A. Cotton, *Inorg. Chem.* 1981, **20**, 3042.
19. J. G. Norman, Jr, G. E. Renzoni and D. A. Case, *J. Am. Chem. Soc.* 1979, **101**, 5256.
20. J. G. Norman, Jr and H. J. Kolari, *J. Am. Chem. Soc.* 1978, **100**, 791.
21. M. H. Chisholm, D. M. Hoffman, J. C. Huffman, W. G. Van Der Sluys and S. Russo, *J. Am. Chem. Soc.* 1984, **106**, 5386.
22. M. H. Chisholm, D. L. Clark, J. C. Huffman, W. G. Van Der Sluys, E. M. Kober, D. L. Lichtenberger and B. E. Bursten, manuscript in preparation.
23. (a) G. M. Bancroft, E. Pellach, A. P. Sattelberger and K. W. McLaughlin, *J. Chem. Soc., Chem. Comm.* 1982, 752; (b) A. P. Sattelberger, In *Inorganic Chemistry: Towards the 21st Century* (Edited by M. H. Chisholm), p. 291. American Chemical Society, Washington D.C. (1983).
24. (a) D. L. Lichtenberger, *Abstracts of Papers*, 187th National Meeting of the American Chemical Society, St. Louis, MO (1984). INOR 48; (b) D. L. Lichtenberger, In *Inorganic Chemistry: Towards the 21st Century* (Edited by M. H. Chisholm), p. 301. American Chemical Society, Washington D.C. (1983).
25. E. M. Kober and D. L. Lichtenberger, *J. Am. Chem. Soc.* 1985, **107**, 7199.
26. T. Ziegler, *J. Am. Chem. Soc.* 1985, **107**, 4453.
27. M. C. Manning, G. F. Holland, D. E. Ellis and W. C. Trogler, *J. Phys. Chem.* 1983, **87**, 3083.
28. P. M. Atha, I. H. Hillier and M. F. Guest, *Mol. Phys.* 1982, **46**, 437.
29. A. J. Scioly, Ph.D. thesis, University of Michigan (1985).
30. (a) J. G. Norman, Jr and H. J. Kolari, *J. Chem. Soc., Chem. Commun.* 1974, 303; (b) J. G. Norman, Jr and H. J. Kolari, *J. Am. Chem. Soc.* 1975, **97**, 33; (c) J. G. Norman, Jr and H. J. Kolari, *J. Chem. Soc., Chem. Commun.* 1975, 649.

Polyhedron Vol. 6, No. 4, pp. 705–714, 1987
Printed in Great Britain

0277–5387/87 $3.00+.00
Pergamon Journals Ltd

$\delta \rightarrow \delta^*$ REVISITED: WHAT THE ENERGIES AND INTENSITIES MEAN†

MICHAEL D. HOPKINS and HARRY B. GRAY

Arthur Amos Noyes Laboratory, California Institute of Technology, Pasadena, CA 91125, U.S.A.

and

VINCENT M. MISKOWSKI

Applied Sciences and Microgravity Experiments Section, Jet Propulsion Laboratory, California Institute of Technology, Pasadena, CA 91109, U.S.A.

(*Received* 19 *November* 1986)

Abstract—Attempts to extract estimates of the δ-bond strength of quadruply metal–metal-bonded molecules from their $\delta \rightarrow \delta^*$ electronic transitions have been hindered in the past by limited understanding of the origins of the energies and intensities of these transitions. We show that the energies of the $\delta \rightarrow \delta^*$ transitions of a wide variety of these molecules are adequately interpreted in terms of a simple zero-differential-overlap model that yields one-electron δ–δ^* splittings of 5000–10,000 cm^{-1} and two-electron exchange terms $[K(\delta, \delta^*)]$ of 5000–8000 cm^{-1}. Because of the magnitude of K, singlet–triplet $\delta \rightarrow \delta^*$ splittings are very large, and configuration interaction is important for the correct description of the ground state. The intrinsic intensity of $^1(\delta \rightarrow \delta^*)$ is estimated to be quite low. The considerable intensities observed in many cases do not correlate with δ-bond strength, but instead reflect intensity stealing from charge-transfer excited states as a result of δ,δ^*-orbital mixing with ligand orbitals. The intrinsic δ-bond stabilization is estimated to be on the order of 10 kcal mol^{-1}.

In 1964 Cotton proposed[1] the existence of a metal–metal δ-bond for $Re_2Cl_8^{2-}$ in order to account for its diamagnetism and eclipsed (D_{4h}) geometry. The d^4–d^4 electron count yields, within this molecular orbital framework, a $[\sigma^2\pi^4\delta^2]$ electronic configuration and a low-lying empty δ^* antibonding orbital, with the δ-HOMO and δ^*-LUMO being derived from metal d_{xy}-orbitals. The δ-bond completes a metal–metal quadruple bond.

A central question in the years following this discovery has concerned the strength of the δ-bond. A primary experimental probe in this regard has been the determination of the spectroscopic energies of the electronic transitions between the δ- and δ^*-orbitals. The earliest attempts along these lines were adversely affected by the primitive calculation methods that were then available,[2] and extremely inflated estimates of δ-bond strength, as well as incorrect spectroscopic assignments, resulted.

Work on three different fronts ushered in a new era in this field during 1973–75. On the theoretical side, calculations employing the then-novel SCF-Xα-SW method were published by Norman and Kolari,[3] and Mortola *et al.*[4] The postulated molecular-orbital ordering was confirmed, although the splitting of the one-electron δ- and δ^*-levels was much smaller than had previously been envisioned. Meanwhile, Cowman and Gray[5] showed that the lowest-energy visible absorption in the electronic spectrum of $Re_2Cl_8^{2-}$ ($\nu_{max} = 14{,}700\ cm^{-1}$, $\varepsilon \simeq 2500$) and related quadruply bonded compounds could be assigned to the $^1(\delta \rightarrow \delta^*)$ transition on the basis of its molecular z-polarization and pronounced vibronic structure in the metal–metal

† Contribution No. 7482 from the Arthur Amos Noyes Laboratory.

stretching mode ν_1. While the energy and intensity of this transition seemed to indicate a moderate δ interaction, the small decrease in ν_1 in the $^1(\delta\delta^*)$ excited state relative to the ground state suggested that this bond was quite weak. Finally, the method of resonance Raman spectroscopy was applied by Clark and Franks.[6] Excitation into the recently assigned $^1(\delta \rightarrow \delta^*)$ transition of $Mo_2Cl_8^{4-}$ resulted in very strong and selective resonance enhancement of ν_1, which was manifested as long overtone progressions in this mode. This result strongly indicated a metal–metal-localized transition, consistent with the single-crystal assignment.

Numerous subsequent investigations have amply supported the 1973–1975 work, while considerably expanding upon it. Unfortunately, as has been emphasized in two recent papers,[7,8] the desired correlations between $^1(\delta \rightarrow \delta^*)$ transition energies and intensities and the strength of the δ-bond have been elusive. A key example is presented by $Mo_2(O_2CCH_3)_4$ and related molybdenum carboxylates, which have among the shortest metal–metal distances of all second and third transition-series quadruply bonded dimers.[2] Although the $^1(\delta \rightarrow \delta^*)$ transition of this compound appears at relatively high energy (23,000 cm^{-1}), which seems intuitively consistent with its short bond length, it is also weak ($\varepsilon = 150$)—so weak, in fact, that the vibronically induced, x,y-polarized intensity is of comparable magnitude to the orbitally allowed, z-polarized intensity.[9]

Why is this transition simultaneously of so much higher energy and lower intensity for $Mo_2(O_2CCH_3)_4$ than for $Re_2Cl_8^{2-}$, and what, if any, inferences can be made about δ-bond strength? We attempt to answer these questions in this paper.

THE ENERGIES

We adopt a time-tested model, one originally developed for the $\pi \rightarrow \pi^*$ transition of ethylene and subsequently applied to many organic molecules.[10] We initially assume that δ-symmetry orbitals have pure metal character; mixing with ligands is ignored. The δ- and δ^*-orbitals are then derived from symmetric and antisymmetric linear combinations of face-to-face d_{xy}-orbitals on atoms A and B:

$$\phi_1 = [2(1+S)]^{-1/2}[d_{xy}(\mathrm{A}) + d_{xy}(\mathrm{B})] \equiv \delta,$$
$$\phi_2 = [2(1-S)]^{-1/2}[d_{xy}(\mathrm{A}) - d_{xy}(\mathrm{B})] \equiv \delta^*,$$

where S is the orbital overlap.

Four states, consistent with the Pauli principle, can be constructed from the δ- and δ^*-levels:

$$\Phi_1 = |\phi_1\phi_1| \equiv {}^1(\delta^2),$$
$$\Phi_2 = |\phi_2\phi_2| \equiv {}^1(\delta^{*2}),$$
$$\Phi_T = 2^{-1/2}\{|\phi_1\phi_2| - |\phi_2\phi_1|\} \equiv {}^3(\delta\delta^*),$$
$$\Phi_V = 2^{-1/2}\{|\phi_1\phi_2| + |\phi_2\phi_1|\} \equiv {}^1(\delta\delta^*).$$

We now write out the state energies, taking care to include the off-diagonal interaction between Φ_1 and Φ_2:

$$E_V = W_1 + W_2 + J_{12} + K_{12},$$
$$E_T = W_1 + W_2 + J_{12} - K_{12},$$
$$E(\Phi_1,\Phi_2): \begin{vmatrix} 2W_1 + J_{11} - \lambda & K_{12} \\ K_{12} & 2W_2 + J_{22} - \lambda \end{vmatrix} = 0.$$

The W_i are core integrals consisting of one-electron terms, J_{ii} and J_{ij} are one- and two-center coulomb repulsion integrals, and K_{12} is the exchange integral.

Invoking the zero-differential-overlap approximation, as is well established[10] for organic molecules, results in $J_{11} = J_{22} = J_{12}$. If we additionally adopt the average energy of the one-electron δ- and δ^*-levels, $\frac{1}{2}(W_1 + W_2)$, as a reference point, we eliminate the Js from the expressions and arrive at:

$$E_V = K,$$
$$E_T = -K,$$
$$E(\Phi_1,\Phi_2): \begin{vmatrix} -\Delta W - \lambda & K \\ K & \Delta W - \lambda \end{vmatrix} = 0,$$

where we have dropped the subscript on $K = K_{12}$ and set $\Delta W = W_2 - W_1$. We finally note that K is given by:

$$K = \tfrac{1}{2}[(aa\,|\,aa) - (aa\,|\,bb)],$$

where $(aa\,|\,aa)$ is the energy required to transfer a δ-electron from metal center A to metal center B at infinite A–B distance (R). The $(aa\,|\,bb)$ term is an electrostatic correction[10,11] to finite R, which is approximately given by e^2/R in the point-charge limit.

In Fig. 1 we show the internuclear-distance dependence of the δ,δ^*-manifold of states according to this simple theory. The strong dependence of ΔW on $R(\mathrm{M_2})$ (decreasing to larger R) and the weaker but much longer range $1/R$ dependence of K (increasing to larger R) have both been qualitatively indicated. It is well understood for bonding–antibonding transitions in strongly bonded dimers that K is large; using the above analysis, it is estimated to be on the order of 30,000 cm^{-1} for ethylene.[10(b)] The situation for weakly bonding cases is less well appreciated,

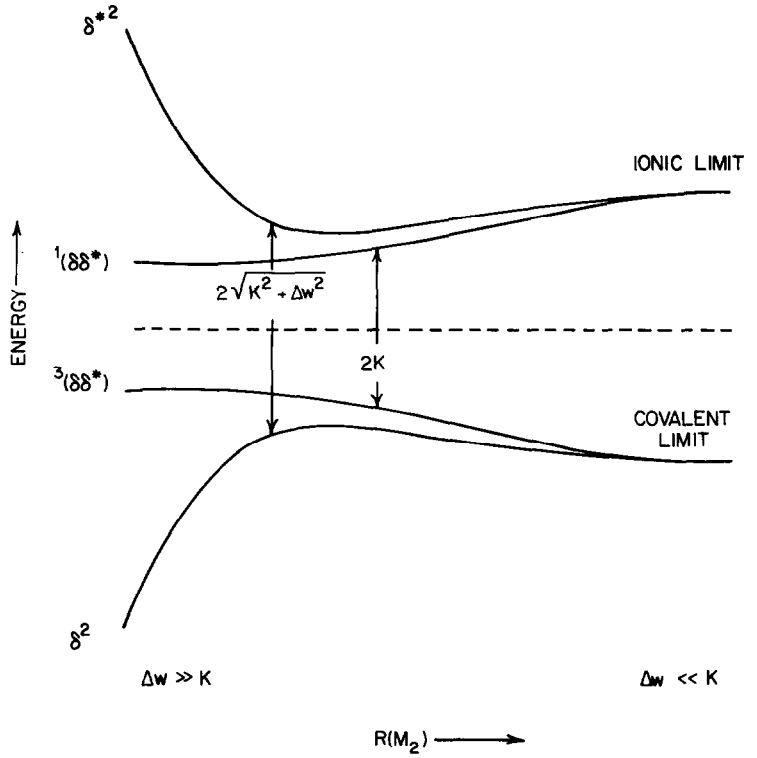

Fig. 1. Dependence of the energies of the δ,δ^*-manifold of electronic states upon metal–metal distance.

however. Even in the absence of bonding between A and B ($\Delta W = 0$), there will be a singlet "bonding–antibonding" (A-to-B charge-transfer) transition of energy $2K$; for the archetypical weakly metal–metal-interacting dimer, namely $Cu_2(O_2CCH_3)_4(OH_2)_2$, K has been estimated (neglecting ligand interactions) to be 50,000 cm^{-1}.[11] The ionic and covalent limits indicated in Fig. 1 are most easily visualized by contrasting the ionic contribution of K to the $^1(\delta\delta^*)$ state with the δ^2 and $^3(\delta\delta^*)$ states:

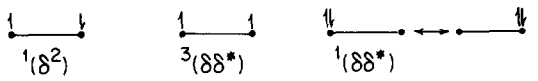

In order to attempt to fit this simple theory to experiment, we need at least two transition energies, but, unfortunately, only $^1(\delta \rightarrow \delta^*)$ is well established experimentally. However, there are now many examples of dimers either one-electron oxidized or reduced relative to the full quadruple bond configuration, i.e. with δ^1 or $\delta^2\delta^{*1}$ ground states. At the same theoretical level as our preceding analysis, the $^2(\delta \rightarrow \delta^*)$ transition of such molecules appears at exactly ΔW, since the contributions of the two-electron terms to the transition energy cancel each other. Numerous structural studies have shown that there is very little effect on metal–metal bond length as a result of such one-electron oxidation or reduction;[2] indeed, even two-electron oxidation or reduction does not produce large changes.[12] Since ΔW can accordingly be expected to be little affected, we propose to perform theoretical fits of the $^1(\delta \rightarrow \delta^*)$ [$^1(\delta^2)$ ground state] energies using values of ΔW derived from the $^2(\delta \rightarrow \delta^*)$ transition energies of their redox congeners.

Table 1 shows our results for the available experimental data. Also included are some comparisons with results from SCF-Xα-SW calculations. It has been observed in the past that calculations of δ–δ^* orbital energy differences for doublet ground-state molecules are in excellent agreement with observed $\delta \rightarrow \delta^*$ transition energies, and this can be traced to the good accounting of valence one-electron terms, but poor accounting of correlation energy, that this theory achieves. We note that such calculations for δ^2 ground-state molecules also give good agreement with the $^2(\delta \rightarrow \delta^*)$ transition energies of one-electron-oxidized or one-electron-reduced species, in agreement with one of our assumptions.

The derived parameters in Table 1 are values of K and predictions of $^3(\delta \rightarrow \delta^*)$ transition energies. As to the former, we observe that, despite a very large range of $^1(\delta \rightarrow \delta^*)$ transition energies, the calculated Ks are all roughly similar: ~6000–

Table 1. $\delta \rightarrow \delta^*$ Electronic transition parameters for selected quadruply bonded complexes[a]

Compound	Observed		ΔW^b (Xα)	Calculated	
	$^1(\delta \rightarrow \delta^*)$	$^2(\delta \rightarrow \delta^*) \equiv \Delta W$		K	$^3(\delta \rightarrow \delta^*)$
$Mo_2(O_2CPr^n)_4^{0/+}$	22,700[c]	13,300[c]	12,200[d]	7450	7790
$Mo_2(SO_4)_4^{4-/3-}$	19,420[e]	7140[e]	—	8400	2630
$Mo_2Cl_4(PMe_3)_4$	17,090[f]	—	8070[gh]	6640	3810
			8390[hi]	6490	4120
$Tc_2Cl_8^{2-/3-}$	14,750[j]	6500[k]	5820[l]	5940	2860
$Re_2(O_2CBu^t)_4Cl_2^{0/-}$	20,200[m]	14,490[n]	—	4900	10,390
$W_2Cl_4(PMe_3)_4^{0/+}$	15,150[f]	7350[o]	7340[gp]	5790	3570
$Re_2Cl_4(PMe_2Ph)_4^{2+/+}$	13,890[q]	7350[q]	5650[r]	5000	3890
$Re_2Cl_6(PEt_3)_2^{0/-}$	13,950[s]	6560[n]	—	5430	3090

[a] All energies (cm^{-1}) refer to vertical transitions, thus to band maxima. Calculated values are based upon the observed $\delta \rightarrow \delta^*$ transition energies except for $Mo_2Cl_4(PMe_3)_4$, where the $X\alpha\Delta W$ values were used together with the $^1(\delta \rightarrow \delta^*)$ energy.

[b] Calculated values of ΔW are for the $[\sigma^2\pi^4\delta^2]$ electronic configuration, except as noted.

[c] Reference 33(a).

[d] References 3(b) and 18. Calculated for $Mo_2(O_2CH)_4$.

[e] F. A. Cotton, D. S. Martin, P. E. Fanwick, T. J. Peters and T. R. Webb, *J. Am. Chem. Soc.* 1976, **98**, 4681; P. E. Fanwick, D. S. Martin, T. R. Webb, G. A. Robbins and R. A. Newman, *Inorg. Chem.* 1978, **17**, 2723; D. K. Erwin, G. L. Geoffory, H. B. Gray, G. S. Hammond, E. I. Solomon, W. C. Trogler and A. A. Zagars, *J. Am. Chem. Soc.* 1977, **99**, 3620.

[f] Reference 8.

[g] Reference 16(a).

[h] Calculated for $Mo_2Cl_4(PH_3)_4$.

[i] Reference 16(b).

[j] F. A. Cotton, L. Daniels, A. Davison and C. Orvig, *Inorg. Chem.* 1981, **20**, 3050.

[k] F. A. Cotton, P. E. Fanwick, L. D. Gage, B. J. Kalbacher and D. S. Martin, *J. Am. Chem. Soc.* 1977, **98**, 5642.

[l] Calculated for the $[\sigma^2\pi^4\delta^2\delta^{*1}]$ electronic configuration: F. A. Cotton and B. J. Kalbacher, *Inorg. Chem.* 1977, **16**, 2386.

[m] D. S. Martin, H.-W. Huang and R. A. Newman, *Inorg. Chem.* 1984, **23**, 699; D. M. Collins, F. A. Cotton and L. D. Gage, *ibid.* 1979, **18**, 1712.

[n] K. R. Dunbar and R. A. Walton, *Inorg. Chem.* 1985, **24**, 5.

[o] M. D. Hopkins, unpublished results.

[p] Calculated for $W_2Cl_4(PH_3)_4$.

[q] Reference 12(b).

[r] Calculated for the $Re_2Cl_4(PH_3)_4^+$ ion: B. E. Bursten, F. A. Cotton, P. E. Fanwick, G. G. Stanley and R. A. Walton, *J. Am. Chem. Soc.* 1983, **105**, 2606.

[s] V. M. Miskowski, unpublished results.

8000 cm^{-1} for second transition-series examples, and ~5000–6000 cm^{-1} for the third row. Inasmuch as these values are of comparable magnitude to the corresponding ΔWs, configuration interaction (CI) is clearly of importance in determining the ground-state energy. Nonetheless, $^1(\delta^2)$ is still a fairly good representation of the ground state. For example, the values of K and ΔW for $Re_2Cl_4(PMe_2Ph)_4^{2+}$ can be used to calculate the CI-mixed ground-state wavefunction as $0.956\Phi_1 + -0.295\Phi_2$, where Φ_1 and Φ_2 are the pure $^1(\delta^2)$ and $^1(\delta^{*2})$ state wavefunctions defined earlier. The occupation numbers (twice the squares of the coefficients) of the δ- and δ^*-orbitals are thus 1.83 and 0.17.

The 3890-cm^{-1} triplet $\delta\delta^*$ energy calculated for $Re_2Cl_4(PMe_2Ph)_4^{2+}$ is in good agreement with an *ab initio* estimate by Hay[13] of 3200 cm^{-1} for $Re_2Cl_8^{2-}$; Hay's estimate of the magnitude of CI mixing is also similar to ours. There is also experimental evidence that bears out the large singlet–triplet $\delta\delta^*$ splitting inferred by these calculations.[14,15] As our present analysis shows, this is *not* a consequence of CI, but of the large magnitude of K, as is illustrated in Fig. 2. While CI leaves the singlet–triplet $\delta\delta^*$ splitting unaffected, the effects on excitation energies are dramatic. If it were not for CI, the triplet

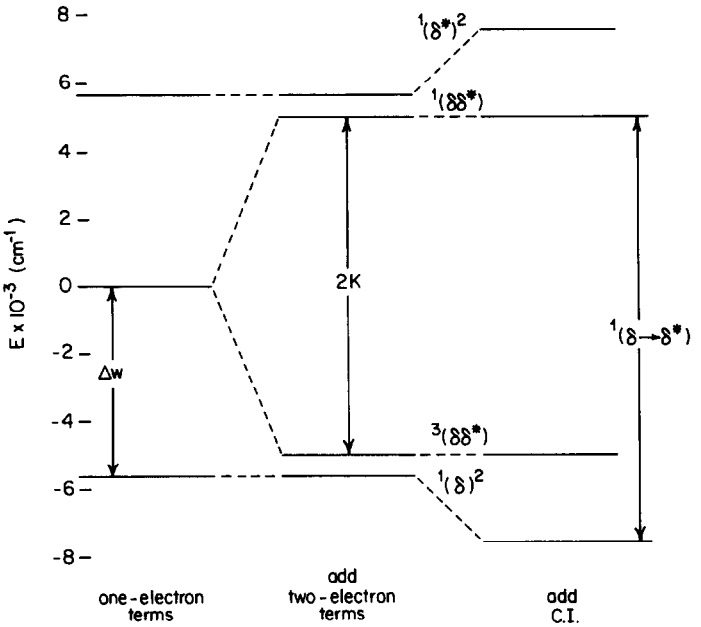

Fig. 2. Relative energies of the δ,δ^*-manifold of electronic states with and without configuration interaction. Parameters used are those for $Re_2Cl_4(PMe_2Ph)_4^{+}$ (Table 1.)

state would be close to being the ground state. But CI will make a singlet the ground state, even in the case of almost no δ interaction,[11] such as for copper acetate, despite small terms[11] neglected in our analysis that would favor a triplet ground state.

A second and completely different experimental approach to these questions can be taken. When diphosphines (e.g. $R_2PCH_2CH_2PR_2$) bridge dimers of the form β-$M_2X_4(P\text{–}P)_2$, where X is a halide, ligand-backbone strain enforces noneclipsed geometries. The torsional angle (χ) is equal to 0° for the eclipsed and 45° for the staggered ($\Delta W = 0$) geometry. A theoretical prediction of the behavior of the δ,δ^* states is very similar to that shown in Fig. 1,[15] but K is independent of rotation angle, according to the approximations defined earlier. The observed singlet "$\delta \rightarrow \delta^*$"* transition energy of the nearly staggered ($\chi = 40°$) compound β-$Mo_2Cl_4(dmpe)_2$ [dmpe = 1,2-bis(dimethylphosphino)ethane] is 12,450 cm^{-1}, which should be very near $2K$; †we thus estimate $K = 6200\,cm^{-1}$. Moreover, the rigorously eclipsed but otherwise very similar compound $Mo_2Cl_4(PMe_3)_4$ displays $^1(\delta \rightarrow \delta^*)$ at 17,090 cm^{-1}.[8] In combination with the above estimate of K, this value yields $\Delta W(\chi = 0°) = 8950\,cm^{-1}$. The agreement of these derived parameters, both with calculated one-electron δ–δ^* splittings of the model complex $Mo_2Cl_4(PH_3)_4$ obtained by the SCF-Xα-SW (8070 cm^{-1})[16(a)] and LCAO-HFS transition-state methods (8390 cm^{-1}),[16(b)] is very good.*

We now return to the anomalous case of the molybdenum carboxylates. Our analysis shows that they, and also the Re(III) carboxylates, are exceptional in having ΔW about twice as large as the other complexes. This has been previously predicted by SCF-Xα-SW calculations.[3(b),18] Of key importance is that these calculations indicate that the effect is due primarily to the interaction of δ and δ^* with carboxylate orbitals, rather than to an exceptionally large metal–metal δ-interaction; we shall return to this point shortly. There is an interesting prediction in Table 1: the large ΔW of the carboxylates results in *all* $\delta \rightarrow \delta^*$ transitions being exceptionally high-energy, including the as yet unobserved $^3(\delta \rightarrow \delta^*)$ transition.

Many attempts have been made in the past to correlate $^1(\delta \rightarrow \delta^*)$ energies with the strength of metal–metal interaction. We conclude that there is

*$^1(\delta \rightarrow \delta^*)$ is, of course, an incorrect designation in this case since the singlet ground state is nearly an equal mixture of $^1(\delta^2)$ and $^1(\delta^{*2})$. The transition actually corresponds to metal-to-metal charge transfer.

† The extinction coefficient is only 210. For rigorous D_{4d}-symmetry the transition is dipole-forbidden.

* The experimental dependence of the $^1(\delta \rightarrow \delta^*)$ energy upon torsional angle[17] is simulated very well by a calculation including the simple CI advocated here.

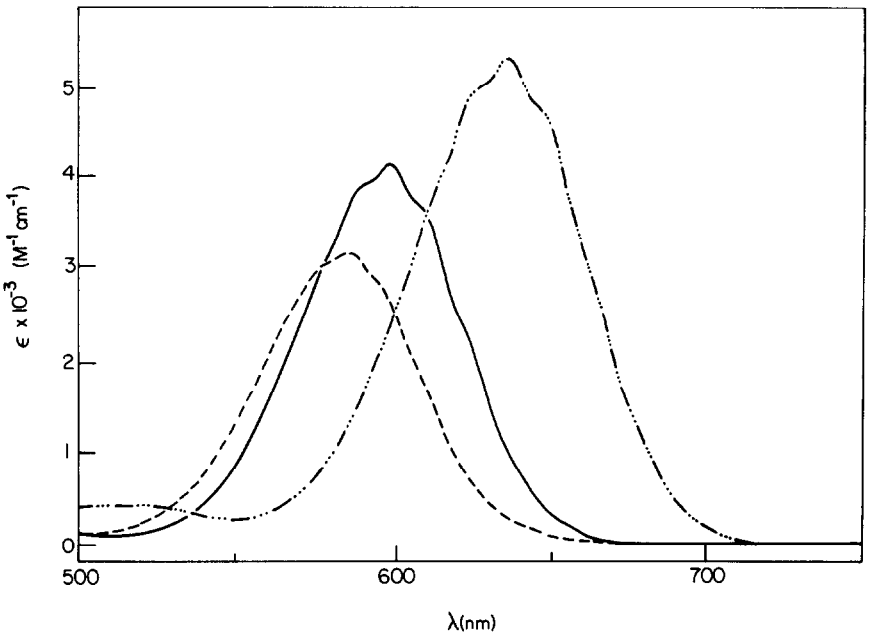

Fig. 3. Electronic absorption spectra of $Mo_2X_4(PMe_3)_4$ in 2-methylpentane solution at 300 K: X = Cl (– – – –), Br (———), or I (—···—).

a correlation of the one-electron δ–δ^* splitting with the $^1(\delta \rightarrow \delta^*)$ energy, but that it is not a simple one because two-electron terms are important. Certainly, small shifts in $^1(\delta$–$\delta^*)$ cannot be casually attributed solely to variation in metal–metal interaction, and comparisons between compounds of metals in different transition series are particularly treacherous, since two-electron integrals such as K typically decrease down a column.[19]

Having achieved some conceptual feeling for the factors involved in determining the relative energies of the δ,δ^*-manifold of states, we now turn to the question of the transition intensities.

THE INTENSITIES

In Table 2 we present selected $^1(\delta \rightarrow \delta^*)$ energy and intensity data. Groups A–C manifest a consistent trend: as the halide ligands become more reducing, the $^1(\delta \rightarrow \delta^*)$ transition both red shifts and increases in intensity.[7] Such metal–metal bond-length data as are available for these halide series fail to show a distinct correlation with the $^1(\delta \rightarrow \delta^*)$ energy or intensity. This is particularly notable for group C,[8] the spectra of which are reproduced in Fig. 3.

We suggest that the observed intensity trends are due to mixing of the "zero-order" $^1(\delta \rightarrow \delta^*)$ transition with X → M charge-transfer (CT) transitions, rather than to changes in metal–metal interactions.[8] Indeed, calculations show considerable (2–25%) halide character in the δ- and δ^*-orbitals. As the LMCT states shift to lower energy, mixing increases. That the effect on intensity should be much more dramatic than that on energy is reasonable if the inherent intensity of $\delta \rightarrow \delta^*$ is small; small amounts of mixing with intense LMCT transitions can then greatly affect intensity.

We should emphasize that a mixing mechanism involving more than nonspecific interactions with nearby LMCT states is required. First, the dominant molecular z-polarization of $\delta \rightarrow \delta^*$ requires that the interacting LMCT states also be z-polarized (LMCT states of x,y-polarization might be involved in the rather strong x,y-polarized vibronic component observed in several cases). Furthermore, effective mixing requires[20] that the two transitions have a common orbital; the LMCT must therefore be a transition of type $b_{2g}(\text{ligand}) \rightarrow b_{1u}(\delta^*)$ (D_{4h}-symmetry). Both the $M_2X_8^{n-}$ and $Mo_2X_4(PMe_3)_4$ compounds have a π(X) orbital of the appropriate symmetry, and the proposed mixing mechanism is therefore viable.

There are precedents for such an intensity-stealing mechanism among mononuclear transition-metal complexes. Well-established examples are the CoX_4^{2-} ions (X = Cl, Br or I), for which *ab initio* calculations[21(a)] strongly support LMCT mixing as the explanation for the exceptionally high[21(b)] (for a d–d transition) oscillator strength of 5.09×10^{-3} for the $^4A_2 \rightarrow {}^4T_1$ transition of $CoCl_4^{2-}$ at 14,700 cm^{-1}. The oscillator strength of this transition for CoI_4^{2-} is 8.12×10^{-3}, the increase relative to $CoCl_4^{2-}$ being consistent with a decreased

Table 2. Energies and intensities of $^1(\delta \rightarrow \delta^*)$ transitions for selected quadruply bonded complexes[a]

Group	Compound	ν_{max} (cm^{-1})	ε_{max} ($M^{-1}cm^{-1}$)	$R(M_2)$ (Å)
A	$Re_2F_8^{2-}$	17,920[b]	810	—
	$Re_2Cl_8^{2-}$	14,700[c]	2340	2.222[d]
	$Re_2Cl_6(PEt_3)_2$	13,950[e]	2610	2.222[f]
	$Re_2Br_8^{2-}$	14,000[e]	2980	2.226–2.228[g]
	$Re_2I_8^{2-}$	12,800[h]	—	—
B	$Mo_2Cl_8^{4-}$	19,610[i]	960	2.129–2.150[j]
	$Mo_2Br_8^{4-}$	19,460[i]	1170	2.135[k]
	$Mo_2(NCS)_8^{4-}$	14,500[l]	2600	2.162–2.177[l]
C	$Mo_2Cl_4(PMe_3)_4$	17,090[m]	3110	2.130[n]
	$Mo_2Br_4(PMe_3)_4$	16,720[m]	4060	2.125[m]
	$Mo_2I_4(PMe_3)_4$	15,720[m]	5250	2.127[m]
D	$Re_2(O_2CBu^t)_4Cl_2$	20,200[o]	180	2.236[o]
	$Mo_2(O_2CH)_4$	22,800[p]	120	2.091[q]
	$Mo_2(SO_4)_4^{4-}$	19,420[r]	170	2.110[s]
	Mo_2^{4+}(aq)	19,800[t]	340	—

[a]Reference for ε_{max} is the same as that for ν_{max} in each case.

[b]G. Peters and W. Preetz, *Z. Naturforsch.* 1979, **34b**, 1767.

[c]F. A. Cotton, N. F. Curtis, B. F. G. Johnson and W. R. Robinson, *Inorg. Chem.* 1965, **4**, 326.

[d]F. A. Cotton, B. A. Frenz, B. R. Stults and T. R. Webb, *J. Am. Chem. Soc.* 1976, **98**, 2768.

[e]V. M. Miskowski, unpublished results.

[f]F. A. Cotton and B. M. Foxman, *Inorg. Chem.* 1968, **7**, 2135.

[g]F. A. Cotton, B. G. DeBoer and M. Jeremic, *Inorg. Chem.* 1970, **9**, 2143; H.-W. Huang and D. S. Martin, *ibid.* 1985, **24**, 96.

[h]W. Preetz and L. Rudzik, *Angew. Chem., Int. Ed. Engl.* 1979, **18**, 150.

[i]W. C. Trogler, D. K. Erwin, G. L. Geoffroy and H. B. Gray, *J. Am. Chem. Soc.* 1978, **100**, 1160.

[j]J. V. Brencic and F. A. Cotton, *Inorg. Chem.* 1969, **8**, 7; J. V. Brencic and F. A. Cotton, *ibid.* 1969, **8**, 2698; J. V. Brencic and F. A. Cotton, *ibid.* 1970, **9**, 346; I. Leben and P. Segedin, *Inorg. Chim. Acta* 1984, **85**, 181.

[k]J. V. Brencic, I. Leben and P. Segedin, *Z. Anorg. Allg. Chem.* 1976, **427**, 85.

[l]A. Bino, F. A. Cotton and P. E. Fanwick, *Inorg. Chem.* 1979, **18**, 3558.

[m]Reference 8.

[n]F. A. Cotton, M. W. Extine, T. R. Felthouse, B. W. S. Kolthammer and D. G. Lay, *J. Am. Chem. Soc.* 1981, **103**, 4040.

[o]D. M. Collins, F. A. Cotton and L. D. Gage, *Inorg. Chem.* 1979, **18**, 1712.

[p]Reference 18.

[q]F. A. Cotton, J. G. Norman, Jr, B. R. Stults and T. R. Webb, *J. Coord. Chem.* 1976, **5**, 217.

[r]D. K. Erwin, G. L. Geoffroy, H. B. Gray, G. S. Hammond, E. I. Solomon, W. C. Trogler and A. A. Zagars, *J. Am. Chem. Soc.* 1977, **99**, 3620.

[s]F. A. Cotton, B. A. Frenz, E. Pedersen and T. R. Webb, *Inorg. Chem.* 1975, **14**, 391.

[t]A. R. Bowen and H. Taube, *Inorg. Chem.* 1974, **13**, 2245.

energy gap between the ligand-field and LMCT transitions; the lowest strong bands of the latter type [assigned[21(c)] to transitions to $^4T_1$ states, so that mixing is possible] occur[21(c)] at 42,600 cm^{-1} for $CoCl_4^{2-}$ and 25,000 cm^{-1} for CoI_4^{2-}.

Just what is the intrinsic or "metal–metal" intensity of $^1(\delta \rightarrow \delta^*)$? We believe that the answer is revealed by group D of Table 2. The one-electron δ–δ^* splitting for the molybdenum carboxylates was earlier indicated to be among the largest

known; this low intensity ($f < 10^{-3}$) represents the intrinsic metal–metal-induced intensity. Group D also includes examples with smaller ΔWs such as $Mo_2(SO_4)_4^{4-}$. That the δ-interaction (the magnitude of which is directly related to this low intrinsic intensity) should be so very weak, is, of course, not surprising.

Accordingly, the vast majority of the $^1(\delta \rightarrow \delta^*)$ intensity for molecules such as $Re_2Cl_8^{2-}$ is stolen from LMCT transitions. This does not mean that $^1(\delta \rightarrow \delta^*)$ is not a predominantly metal–metal-localized transition; excited distortions, as indicated by resonance Raman and low-temperature electronic spectroscopic studies, unequivocally indicate a high degree of metal–metal character. Rather, a small amount of LMCT character mixed into the transition completely dominates the intensity. It is worth considering why there is little LMCT intensity-lending for group D of Table 2. We see two major reasons. First, complexes with oxygen donor ligands should have much higher energy LMCT states than Cl^-, Br^- or I-containing compounds, according to optical electronegativities.[22]† The low $\delta \rightarrow \delta^*$ intensity for $Re_2F_8^{2-}$ (group A, Table 2) has a similar explanation. Second, the Mo_2(carboxylate)$_4$ structure imposes O–Mo–Mo angles very near 90°. As a result, z-polarized CT transitions will accidentally carry very little intensity, and CT mixing with $\delta \rightarrow \delta^*$ would therefore be an ineffective intensity-stealing mechanism, regardless of the amount of ligand character mixed into the δ- and δ^*-orbitals.

THE ENERGIES RECONSIDERED

We will now reconsider our treatment of the energies of the δ,δ^*-manifold of states. We analyzed them with a model that assumed pure d-orbitals, yet, in order to explain intensities, we found it necessary to invoke mixing with LMCT transitions. Are these approaches contradictory?

Treatments such as we have set out are fundamentally empirical, but no more so than the traditional $10Dq$ one-electron parameter, and B and C two-electron parameters of mononuclear d–d spectroscopy. That these single-center parameters are sensitive to the nature of the ligands is well known, and this, of course, is due to the ligand-field orbitals not being pure d-orbitals. While d–d spectra can be empirically analyzed in terms of crystal-field theory, it has been emphasized[24] that the derived parameters have theoretically nebulous meaning because of this mixing with ligand orbitals. It has nonetheless historically proven fruitful to analyze spectra in this way, and to correlate derived parameters with ligand properties.

Some insight into the ligand dependence of K is gained by consideration of the torsionally distorted compound β-$Mo_2Br_4(dmpe)_4$, which has $\chi = 36°$,[17(b)] similar to its chloride analogue (*vide supra*), and a $^1(\delta \rightarrow \delta^*)$ transition energy of 11,800 cm^{-1}. Taking this as the zero-δ-interaction limit, we estimate $K = 5900\,cm^{-1}$, and, from the $^1(\delta \rightarrow \delta^*)$ energy of $Mo_2Br_4(PMe_3)_4$,[8] (ΔW ($\chi = 0°$) = 9070 cm^{-1}. The differences of these parameters from those of the chloride analogues (*vide supra*) are quite small, but seem to be concentrated in a reduction of K. This results in a reduction of the energy of the $^1(\delta \rightarrow \delta^*)$ transition of about the same magnitude for both $Mo_2X_4(PMe_3)_4$ and β-$Mo_2X_4(dmpe)_2$, upon exchange of bromide for chloride, despite the large difference in transition energy for eclipsed and staggered conformers. The correlations of Cotton *et al.*[17(b)] suggest a rather constant $^1(\delta \rightarrow \delta^*)$ energy difference between chloride and bromide complexes as χ is varied, consistent with the chloride–bromide energy difference always being due to K. That two-electron integrals such as K should be smaller for bromide than for chloride complexes has precedent for mononuclear complexes, and is a manifestation of the nephelauxetic effect.[19] K for all of these complexes is undoubtedly greatly reduced from the value for a diatomic reference (M_2^{n+}) because of such ligand interactions.

What about ΔW? We have already mentioned that its anomalously large value for $Mo_2(O_2CR)_4$ reflects ligand interactions. Insight into the extent of this interaction is provided by examination of carboxylate-bridged compounds in which the metal–metal antibonding orbitals are partially occupied. The π^*- and δ^*-levels of such species are energetically close,[25] resulting in high-spin ground states of quartet $[\pi^{*2}\delta^{*1}]$ for[26(a)] $Ru_2(O_2CR)_4Cl$ ($R \simeq 2.28$ Å)[27] and triplet $[\pi^{*1}\delta^{*1}]$ for[26(b)] $Os_2(O_2CR)_4Cl_2$ ($R \simeq 2.31$ Å);[28] the bond lengths are to be compared to 2.19 and 2.24 Å, respectively,

* In our discussion of intensities, we have emphasized mixing of electronic transitions rather than of orbitals because it is likely that excited-state mixing is much larger than ground-state mixing, as a result of closer energetic proximity. Thus, an attempt to analyze these effects based solely upon ground-state wavefunctions would be incomplete.

† There appears to be a fairly low energy metal-to-ligand charge-transfer band for the $M_2(O_2CR)_4$ (M = Mo, W or Re) complexes.[23] However, this intense CT band is attributed to a transition of the wrong polarization ($\perp$ molecular z) to mix with $^1(\delta \rightarrow \delta^*)$, and there are, in fact,[3(b),18] no low-lying carboxylate orbitals of the right symmetry to yield a z-polarized $\delta \rightarrow$ carboxylate CT transition.

for[29] $M_2(O_2CC(CH_3)_3)_4Cl_2$ (M = Tc or Re). The $^2(\delta \rightarrow \delta^*)$ transitions (so termed because of the half-occupancy of δ^*) of the ruthenium and osmium compounds are centered at 9100 cm^{-1} (ε40) and 11,800 cm^{-1} (ε75), respectively.[26] These values of ΔW may additionally be compared with calculated values of 8942 cm^{-1} for $Ru_2(O_2CH)_4Cl_2^{-}$[25] and 8100 cm^{-1} for $Rh_2(O_2CH)_4(OH_2)_2$[30] (R = 2.39 Å); the π^* and δ^*-orbitals of the latter are fully occupied.

The reduction in ΔW for these compounds as antibonding orbitals are populated and R increases seems to reflect decreasing metal–metal δ-bonding interaction. It does not, however, extrapolate to zero as the bond length continues to increase, which supports an important role for metal–carboxylate interactions in maintaining large δ–δ^* separations. It is interesting that the Rh_2(II, II) value is about 6000 cm^{-1} smaller than the values for the carboxylate-bridged quadruple bond entries of Table 1. Since the direct δ interaction must be very weak indeed for the Rh_2(II,II) compound, 6000 cm^{-1} is a rough estimate of the metal–metal bonding contribution to ΔW for the Mo_2(II, II), Tc_2(III, III) and Re_2(III, III) carboxylate compounds, and it is, in fact, very similar to the values of ΔW estimated for the noncarboxylate entries of Table 1.[30]

CONCLUSIONS AND IMPLICATIONS

Our treatment of $\delta \rightarrow \delta^*$ electronic transitions leads to the conclusion that the metal–metal δ-bond is quite weak. Intrinsic metal–metal-bonding-induced one-electron δ–δ^* splittings for quadruply bonded dimers* are only about 6000–9000 cm^{-1} (corresponding to a stabilization of ~10 kcal mol^{-1}) and the intrinsic intensity for the bonding–antibonding $\delta \rightarrow \delta^*$ transition is accordingly very weak.

Interpretation of experimental data for $\delta \rightarrow \delta^*$ electronic transitions has been complicated by two previously poorly understood factors. First, there is a very large contribution of a two-electron (ionic) term to the observed transition energy. Second, mixing with ligand orbitals has profound effects upon both intensities and energies of $\delta \rightarrow \delta^*$ transitions. With regard to this latter point, it is important to note that our emphasis on sensitivity to ligands of the formally metal–metal-localized $^1(\delta \rightarrow \delta^*)$ transition is in accord with a previous discussion.[7] However, we differ with the earlier work in that we do not infer large changes in the extent of δ-bonding interactions as a function of ligand electronegativity.[8]

We finally consider the consequence of our conclusion that the $^1(\delta \rightarrow \delta^*)$ excited state has a great deal of ionic character. Excited states of this type are, in principle, subject to the phenomenon of sudden polarization, in which they can distort to the localized ionic configuration M^+M^-.[32] As we show elsewhere,[33] analyses of the vibronic structure of several examples of $^1(\delta \rightarrow \delta^*)$ transitions support the existence of such excited-state distortions. Of relevance to our present discussion of excited-state energies is that Chakravarty *et al.* recently reported[34] the preparation of $(EtO)_2Cl_2Re$-$ReCl_2(PPh_3)_2$, for which structural data suggest a considerable contribution of the polar Re(II)–Re(IV) form to the ground state of the formally quadruply bonded (eclipsed) molecule. The compound is reported to show a band at 8400 cm^{-1} (ε2800); we suggest that this band be assigned to $^1(\delta \rightarrow \delta^*)$, where electron-repulsion differences between ground and excited state have been greatly reduced, thus lowering the transition energy to near the one-electron value.

* We have emphasized analysis of ΔW based solely on the $\delta \rightarrow \delta^*$ transitions themselves. An alternate approach is to estimate δ–δ^* splittings as the difference in energy between transitions involving δ and δ^* and a third, common orbital, as in many cases the two-electron contributions should roughly cancel out. We have been able to obtain sufficiently reliable spectroscopic assignments with which to attempt this approach for only one class of compounds: the $[\sigma^2\pi^4\delta^0]$-configured $Mo_2(HPO_4)_4^{2-}$ ion and its δ^1 and δ^2 analogues $Mo_2(SO_4)_4^{3-/4-}$.[31] Assignment of the $\pi \rightarrow \delta$ and $\pi \rightarrow \delta^*$ transitions leads to estimates of ΔW of 5100, 7200 and 8500 cm^{-1} for the δ^0, δ^1 and δ^2 compounds, respectively. These estimates of ΔW are quite consistent with those of Table 1. That ΔW varies as δ is depopulated indicates a shortcoming of one of the approximations used in our earlier analysis, but the variation is not so large as to invalidate it.

Acknowledgements—M. D. H. thanks the Sun Co. and Standard Oil Co. (Ohio) for providing graduate fellowships. This work was supported by National Science Foundation Grant CHE84-19828 (H.B.G.). Part of the research included in this paper was carried out at the Jet Propulsion Laboratory, California Institute of Technology, under contract with the National Aeronautics and Space Administration.

REFERENCES

1. F. A. Cotton, N. F. Curtis, C. B. Harris, B. F. G. Johnson, S. J. Lippard, J. T. Mague, W. R. Robinson and J. S. Wood, *Science* 1964, **145**, 1305.
2. F. A. Cotton and R. A. Walton, *Multiple Bonds between Metal Atoms*. Wiley, New York (1982).
3. (a) J. G. Norman, Jr and H. J. Kolari, *J. Chem. Soc.*,

Chem. Commun. 1974, 303; (b) J. G. Norman, Jr and H. J. Kolari, *ibid.* 1975, 649; (c) J. G. Norman, Jr and H. J. Kolari, *J. Am. Chem. Soc.* 1975, **97**, 33.
4. (a) A. P. Mortola, J. W. Moskowitz and N. Rösch, *Int. J. Quantum Chem. Symp.* 1974, **8**, 161; (b) A. P. Mortola, J. W. Moskowitz, N. Rösch, C. D. Cowman and H. B. Gray, *Chem. Phys. Lett.* 1975, **32**, 283.
5. C. D. Cowman and H. B. Gray, *J. Am. Chem. Soc.* 1973, **95**, 8177.
6. (a) R. J. H. Clark and M. L. Franks, *J. Chem. Soc., Chem. Commun.* 1974, 316; (b) R. J. H. Clark and M. L. Franks, *J. Am. Chem. Soc.* 1975, **97**, 2691.
7. M. C. Manning and W. C. Trogler, *J. Am. Chem. Soc.* 1983, **105**, 5311.
8. M. D. Hopkins, W. P. Schaefer, M. J. Bronikowski, W. J. Woodruff, V. M. Miskowski, R. F. Dallinger and H. B. Gray, *J. Am. Chem. Soc.* 1987, **109**, 408.
9. D. S. Martin, R. A. Newman and P. E. Fanwick, *Inorg. Chem.* 1979, **18**, 2511.
10. (a) C. A. Coulson and I. Fischer, *Philos. Mag.* 1949, **40**, 386; (b) R. G. Parr, *The Quantum Theory of Molecular Electronic Structure*. W. A. Benjamin, New York (1964); (c) K. Ohno, *Adv. Quantum Chem.* 1967, **3**, 239.
11. A. E. Hansen and C. J. Ballhausen, *Trans. Faraday Soc.* 1965, **61**, 631.
12. (a) A. Bino and F. A. Cotton, *Inorg. Chem.* 1979, **18**, 3562; (b) F. A. Cotton, K. R. Dunbar, L. R. Falvello, M. Tomas and R. A. Walton, *J. Am. Chem. Soc.* 1983, **105**, 4950.
13. P. J. Hay, *J. Am. Chem. Soc.* 1982, **104**, 7007.
14. (a) T. C. Zietlow, M. D. Hopkins and H. B. Gray, *J. Solid State Chem.* 1985, **57**, 112; (b) V. M. Miskowski, R. A. Goldbeck, D. S. Kliger and H. B. Gray, *Inorg. Chem.* 1979, **18**, 86.
15. M. D. Hopkins, T. C. Zietlow, V. M. Miskowski and H. B. Gray, *J. Am. Chem. Soc.* 1985, **107**, 510.
16. (a) F. A. Cotton, J. L. Hubbard, D. L. Lichtenberger and I. Shim, *J. Am. Chem. Soc.* 1982, **104**, 679; (b) T. Ziegler, personal communication. For further details on this calculation, see: T. Ziegler, *J. Am. Chem. Soc.* 1984, **106**, 5901.
17. (a) M. D. Hopkins and H. B. Gray, to be submitted for publication; (b) F. L. Campbell III, F. A. Cotton and G. L. Powell, *Inorg. Chem.* 1985, **24**, 177.
18. J. G. Norman, Jr, H. J. Kolari, H. B. Gray and W. C. Trogler, *Inorg. Chem.* 1977, **16**, 987.
19. C. K. Jørgensen, *Modern Aspects of Ligand Field Theory*, Chap. 23. North-Holland, Amsterdam (1971).
20. R. F. Fenske, *J. Am. Chem. Soc.* 1967, **89**, 252.
21. (a) I. H. Hillier, J. Kendrick, F. E. Mabbs and C. D. Garner, *J. Am. Chem. Soc.* 1976, **98**, 395; (b) F. A. Cotton, D. M. L. Goodgame and M. Goodgame, *ibid.* 1961, **83**, 4690; (c) B. D. Bird and P. Day, *J. Chem. Phys.* 1968, **49**, 392.
22. C. K. Jørgensen, *Prog. Inorg. Chem.* 1970, **12**, 101.
23. D. J. Santure, J. C. Huffman and A. P. Sattelberger, *Inorg. Chem.* 1985, **24**, 371.
24. C. J. Ballhausen, *Molecular Electronic Structures of Transition Metal Complexes*, Chap. 2. McGraw-Hill, New York (1979).
25. J. G. Norman, Jr, G. E. Renzoni and D. A. Case, *J. Am. Chem. Soc.* 1979, **101**, 5256.
26. (a) V. M. Miskowski, T. M. Loehr and H. B. Gray, *Inorg. Chem.* (submitted for publication); (b) V. M. Miskowski and H. B. Gray, to be submitted for publication.
27. A. Bino, F. A. Cotton and T. R. Felthouse, *Inorg. Chem.* 1979, **18**, 2599.
28. (a) T. Behling, G. Wilkinson, T. A. Stephenson, D. A. Tocher and M. D. Walkinshaw, *J. Chem. Soc., Dalton Trans.* 1983, 2109; (b) F. A. Cotton, A. R. Chakravarty, D. A. Tocher and T. A. Stephenson, *Inorg. Chim. Acta* 1984, **87**, 115.
29. F. A. Cotton and L. D. Gage, *Nouv. J. Chim.* 1977, **1**, 441.
30. J. G. Norman, Jr and H. J. Kolari, *J. Am. Chem. Soc.* 1978, **100**, 791.
31. M. D. Hopkins, V. M. Miskowski and H. B. Gray, *J. Am. Chem. Soc.* 1986, **108**, 959.
32. M. Benard and A. Veillard, *Chem. Phys. Lett.* 1982, **90**, 160.
33. (a) M. D. Hopkins, Ph.D. thesis, California Institute of Technology, Pasadena, California (1986); (b) M. D. Hopkins, V. M. Miskowski and H. B. Gray, to be submitted for publication.
34. A. R. Chakravarty, F. A. Cotton, R. A. Cutler, S. M. Tetrick and R. A. Walton, *J. Am. Chem. Soc.* 1985, **107**, 4795.

Polyhedron Vol. 6, No. 4, pp. 715–721, 1987
Printed in Great Britain

0277–5387/87 $3.00+.00
Pergamon Journals Ltd

OPTICAL ACTIVITY OF QUADRUPLY BONDED DIMOLYBDENUM AND DIRHENIUM COMPLEXES

ROBERT D. PEACOCK

Department of Chemistry, The University, Glasgow G12 8QQ, U.K.

(*Received* 19 *November* 1986)

Abstract—A simple metal-localized model relating the optical activity of configurationally chiral quadruply bonded complexes is presented. The predictions of the model are tested against the available data and some applications to structural and electronic assignments are discussed.

The majority of quadruply bonded dimeric metal complexes have the eclipsed ligand configuration exemplified by the structures[1] of $[Mo_2Cl_8]^{4-}$ and $[Re_2Cl_8]^{2-}$. Indeed the eclipsed geometry was one of the main reasons for the original postulation of quadruple bonds in these complexes. There is, however, an important minority of quadruply bonded complexes where due to ligand constraints or crystal packing the molecules have a staggered or partially staggered geometry about the metal–metal bond. Such molecules are necessarily chiral. Because the chromophore (in this case the Mo_2 or Re_2 unit) is chiral we call such complexes chromophorically chiral or more usually configurationally chiral. Good examples are complexes of the type β-$[Mo_2X_4(PP)_2]$, where X is halide or pseudohalide and PP represents a bidentate phosphine such as dppe or a substituted analogue; the β in the formula indicates that the phosphine is bridging the two molybdenum atoms and so engendering the twist. When the phosphine is achiral, such as dppe itself, the metal complex will be formed as a racemic mixture of the Λ and Δ forms (Fig. 1) and a solution of the complex will not show optical activity. Sometimes such racemic complexes crystallize as enantiomorphic single crystals in which all the molecules in any particular crystal are of the same hand. This happens[2] for example in β-$[Mo_2Cl_4(dmpe)_2]$.* Since the molecules are kinetically labile, however, they racemize rapidly on dissolution of the crystal and the resulting solution is optically inactive. More commonly racemic compounds crystallize as racemic crystals with equal numbers of Λ and Δ forms in the unit cell. An example[3] of this behaviour is β-$[Mo_2Cl_4(dppe)_2]$. There are a few examples of complexes containing bidentate ligands or ligands such as dmpe, which usually result in eclipsed complexes, where presumably because of packing forces the molecule is slightly twisted in the crystal. An example of this phenomenon is $[Mo_2(SCN)_4(dppm)_2]$ which has a twist of 13°.[4]

If a complex contains chiral ligands it is necessarily chiral. This ligand chirality does not always translate itself to the chromophore, however, and so produce a configurationally chiral complex. Complexes with chiral amino acids such as $[Mo_2(L\text{-leucine})_4]^{4+}$ contain[5] planar Mo_2O_2C rings and so have either zero or very small twists. The chelated (α) isomers of the $[Mo_2X_4(PP)_2]$ type complex, in which the ligand forms a five-membered chelate with each molybdenum atom, have an eclipsed geometry[6] and so are not configurationally chiral. A final example is the complex $[Mo_2Cl_4(S\text{-peap})_2]$; although the structure of this complex has not been determined its electronic spectrum is indicative of the eclipsed $Mo_2P_4Cl_4$ chromophore and it shows[7] no measurable circular dichroism (CD) under the $\delta_{xy} \rightarrow \delta^*_{xy}$ transition, indicating again a lack of configurational chirality. When chiral ligands of the type which cause the chromophore to twist are

*Ligand abbreviations: en, 1,2-diaminoethane; *R*-pn, (*R*)-1,2-diaminopropane; dppe, 1,2-bis(diphenylphosphino)ethane; dppp, 1,3-bis(diphenylphosphino)propane; *R*-dppp, (*R*)-1,2-bis(diphenylphosphino)propane; *S,S*-dppb, (*S,S*)-2,3-bis(diphenylphosphino)butane; *S*-chairphos, (*S*)-1,3-bis(diphenylphosphino)butane; *S,S*-skewphos, (*S,S*)-2,4-bis(diphenylphosphino)pentane; *R*-phenphos, (*R*)-1-phenyl-1,2-bis(diphenylphosphino)ethane; *S*-peap, *N,N*-bis(diphenylphosphino)-*S*-α-phenylethylamine.

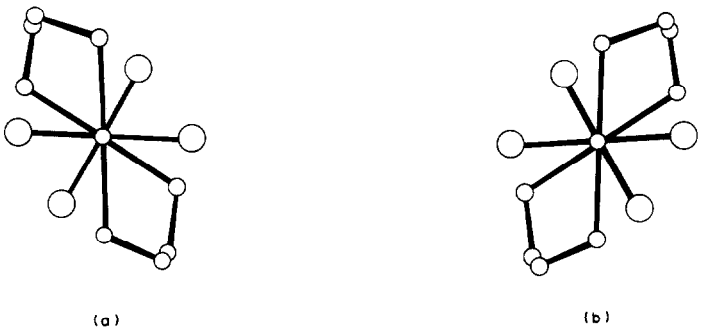

Fig. 1. Λ (a) and Δ (b) forms of a twisted $[Mo_2X_4(PP)_2]$ complex such as $[Mo_2Cl_4(dppe)_2]$.

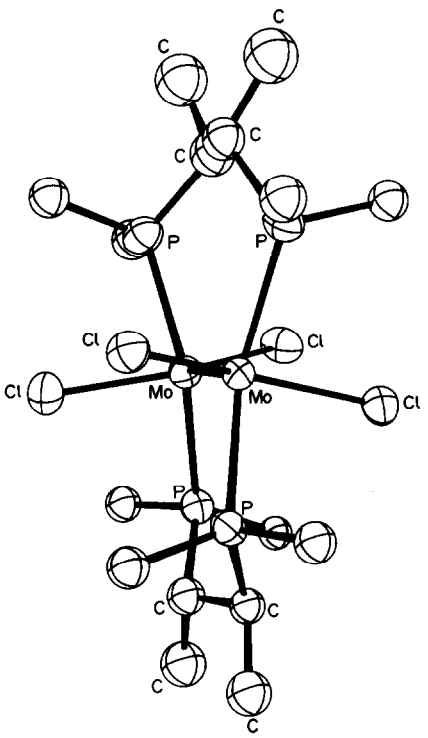

Fig. 2. Molecular structure of Λ-$[Mo_2Cl_4(S,S\text{-dppb})_2]$.

incorporated in a complex, however, we expect the conformational preference of the ligands to effect an asymmetric synthesis and produce only one of the configurational isomers. Thus conformational analysis predicts (and crystallography confirms[8]) that reaction of $[Mo_2Cl_8]^{4-}$ with *S,S*-dppb will produce solely Λ-$[Mo_2Cl_4(S,S\text{-dppb})_2]$. The structure of this molecule is shown in Fig. 2.

In this article we shall concentrate on configurationally chiral complexes for two reasons. Firstly they are expected to show much larger CD spectra under the essentially metal-localized transitions; indeed as indicated above there is usually no detectable CD under the $\delta_{xy} \rightarrow \delta^*_{xy}$ transition in eclipsed chiral complexes. Secondly it is much easier to develop a model which unambiguously relates the CD of the chromophore of a configurationally chiral complex to the geometry of the complex.

THE MODEL

The model we describe is at present a metal-localized model and so applies to those transitions which can be described without explicitly involving ligand orbitals, for example the $\delta_{xy} \rightarrow \delta^*_{xy}$ and $\delta_{xy} \rightarrow \delta_{x^2-y^2}$ transitions. It is worth issuing a caveat at the start: both the energy and intensity of the $\delta_{xy} \rightarrow \delta^*_{xy}$ transition depend quite markedly on the ligator set which implies that the ligand orbitals should not really be ignored in attempting to account for these properties. We expect the metal-localized model to be most applicable when used to compare the spectra of molecules with similar ligands and perhaps also to be better at rationalizing the signs than the magnitudes of the CD spectra. The model has a considerable merit in its simplicity but its validity has to be tested and not assumed.

The $\delta_{xy} \rightarrow \delta^*_{xy}$ transition

The transient charge distribution during the $\delta_{xy} \rightarrow \delta^*_{xy}$ transition of a dimetal complex with eclipsed geometry is shown pictorially in Fig. 3. It can readily be seen that the movement of charge is along the metal–metal bond, i.e. that the transition is *polarized* along the metal–metal bond (*z*-polarized using the conventional co-ordinate system) and so can be excited only by light propagated perpendicular to the metal–metal bond and with electric vector directed parallel to it. This polarization has been experimentally demonstrated in a number of systems,[9] although in some cases, particularly with carboxylic acid or amino acid ligands, there is an additional intensity polarized perpendicular to the metal–metal bond (*xy* polarization) based on false origins.[10] Figure 3 is formally

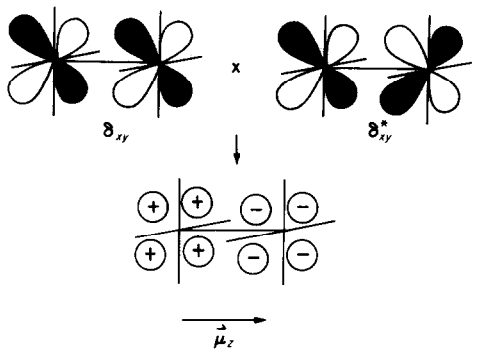

Fig. 3. Transient charge distribution for the $\delta_{xy} \rightarrow \delta^*_{xy}$ transition of an eclipsed chromophore obtained by multiplying the phases of the δ_{xy}- and δ^*_{xy}-orbitals.

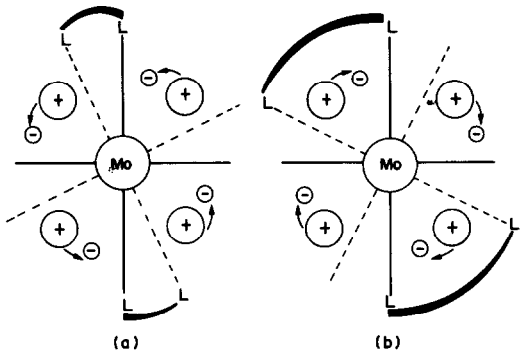

Fig. 4. Transient charge distribution for the $\delta_{xy} \rightarrow \delta^*_{xy}$ transition of a twisted $Mo_2L_4L'_4$ chromophore. (a) On rotating the near set of ligators through an angle of less than 45° in the counterclockwise (Λ) direction the transient charge distribution is that of a left-handed helix. (b) On rotating counterclockwise through an angle of greater than 45° the transition gives rise to a right-handed helical charge displacement.

equivalent to the group-theoretical statement that the produce of the symmetries of the $\delta_{xy}(b_{1g})$ and $\delta^*_{xy}(b_{2u})$ orbitals transform as $z(a_{2u})$ in D_{4h}-symmetry; the corresponding representations in D_{2h} (for the $Mo_2P_4Cl_4$ chromophore) being b_{1g} (δ_{xy}), a_u (δ^*_{xy}) and $b_{1u}(z)$.

When the molecule is configurationally chiral the symmetry of the chromophore drops to D_4 or D_2, and the product of the δ_{xy} and δ^*_{xy} orbital symmetries transform as a_2 or b_1, respectively. The transition thus becomes both electric and magnetic dipole allowed along or around the metal–metal bond and is optically active. In particular it will show the phenomenon of CD, the differential absorption of left and right circularly polarized light. This situation is shown pictorially in Fig. 4 for the Λ absolute configuration. The direction of the transient charge displacement can be obtained by following the signs from +ve to −ve (or vice versa) through the shorter spacial path. There are two situations: in both cases the charge displacement is that of a helix along and around the metal–metal bond but when the twist is between 0 and 45° the helix is left-handed, while for a twist of between 45 and 90° there is a right-handed helical charge displacement. At angles of 0, 45 and 90°, the chromophore is not chiral and the transient charge displacements are a translation, a rotation and a translation along or about the metal–metal bond, respectively.

The absolute sign of the CD associated with the $\delta_{xy} \rightarrow \delta^*_{xy}$ transition may be deduced from the helical charge displacements of Fig. 4. We will establish the sign for the Λ absolute configuration and a twist of less than 45° [Fig. 4(a); left-handed displacement along the metal–metal bond]. The $\delta_{xy} \rightarrow \delta^*_{xy}$ transition must be excited by light propagated perpendicular to the metal–metal bond. Since any helix has the opposite helicity when viewed along or perpendicular to the helix axis, light

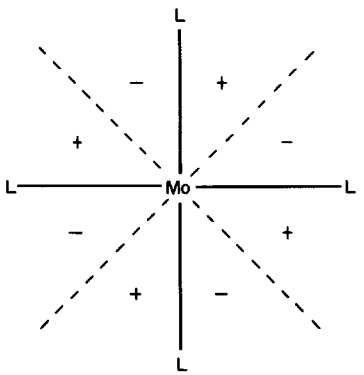

Fig. 5. Sign rule for the CD of the $\delta_{xy} \rightarrow \delta^*_{xy}$ transition. The sign of the CD is that of the sectors containing the rear set of ligating atoms.

propagated perpendicular to the metal–metal bond will see and interact with a right-handed helical charge displacement. Right circularly polarized light interacts more strongly with a right-handed helical charge displacement than does left circularly polarized light. Thus the exctinction coefficient ε_r is larger than ε_l, and the differential extinction coefficient $\Delta\varepsilon$ ($\varepsilon_l - \varepsilon_r$) is negative for the geometry depicted in Fig. 4(a). The sign of the CD changes every 45° and a sign rule can be constructed (Fig. 5) in which the sign of the CD is related to the sense and magnitude of the twist angle.

The variation of the magnitude of the CD with twist angle can be made at least semi-quantitative. The rotational strength of a transition (the area under the CD band) is proportional to the product of the electric and magnetic dipole transition moments:

$$R = \mu \times m.$$

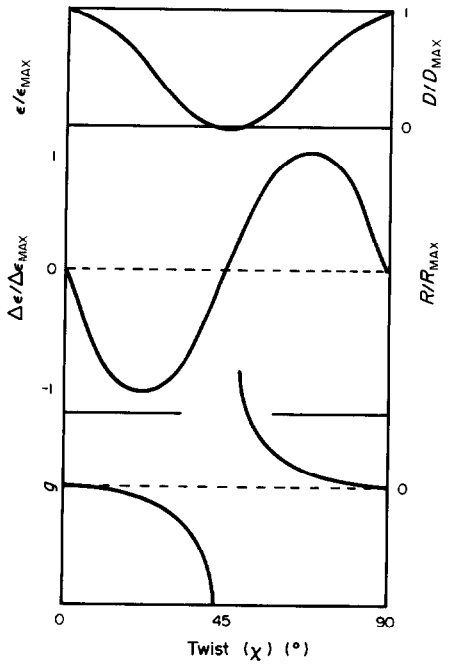

Fig. 6. Variation of dipole strength (D) (and ε), rotational strength (R) (and $\Delta\varepsilon$) and g value with twist angle χ (for the $\delta_{xy} \rightarrow \delta^*_{xy}$ transition of a complex with the Λ absolute configuration).

The electric dipole transition moment is proportional to the angular overlap of the d_{xy} orbitals and is a maximum for the eclipsed configuration; it therefore is proportional to cos 2χ, where χ is the angle of twist about the metal–metal bond. Similarly the magnetic dipole transition moment is proportional to sin 2χ. Thus:

$$R = R_{\mathrm{MAX}} \cos 2\chi \sin 2\chi.$$

The dipole strength (the area under the absorption band) and the g value ($g = 2R/D$ or $\Delta\varepsilon/\varepsilon$) can be written as functions of χ in a similar way:

$$D = D_{\mathrm{MAX}} \cos^2 2\chi,$$

$$g = g_{\mathrm{MAX}} \tan 2\chi.$$

These relations are summarized in Fig. 6.

The $\delta_{xy} \rightarrow \delta_{x^2-y^2}$ transition

In many complexes there is a transition to slightly higher energy of the $\delta_{xy} \rightarrow \delta^*_{xy}$ transition which has a low extinction coefficient but a very large g value. This identifies it as a magnetic dipole transition and the current assignment is to the $\delta_{xy} \rightarrow \delta_{x^2-y^2}$ excitation. The transient charge distribution during this transition is shown in Fig. 7 for the eclipsed

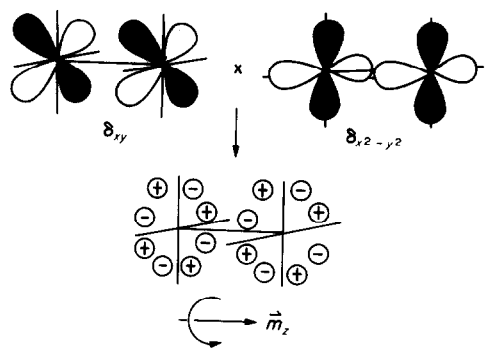

Fig. 7. Transient charge distribution for the $\delta_{xy} \rightarrow \delta_{x^2-y^2}$ transition of an eclipsed chromophore obtained by multiplying the phases of the δ_{xy}- and $\delta_{x^2-y^2}$-orbitals.

geometry and can be seen to involve a rotation of charge around the metal–metal bond ($A_{1g} \rightarrow A_{2g}$ in D_{4h}, $A_{1g} \rightarrow B_{1g}$ in D_{2h}). Twisting the molecule about the metal–metal bond makes the transition electric as well as magnetic dipole allowed. The same analysis as described above for the $\delta_{xy} \rightarrow \delta^*_{xy}$ transition gives[11] a sign rule with the same form but with opposite signs to those of Fig. 6. Thus the CD of the $\delta_{xy} \rightarrow \delta_{x^2-y^2}$ transition is predicted to have opposite sign to that of the $\delta_{xy} \rightarrow \delta^*_{xy}$ transition. The $\delta_{xy} \rightarrow \delta_{x^2-y^2}$ transition is also expected to have a much larger g value than that of the $\delta_{xy} \rightarrow \delta^*_{xy}$ transition because the former is magnetic dipole allowed in the parent achiral symmetry.

How well does the model work?

The main predictions of our model are:

(1) The absolute sign of the CD of the $\delta_{xy} \rightarrow \delta^*_{xy}$ transition is related to the absolute configuration of the molecule and the twist angle as indicated in Fig. 5.

(2) The way in which the magnitudes of the CD and g value of the $\delta_{xy} \rightarrow \delta^*_{xy}$ transition is shown in Fig. 6. As mentioned above we expect the variation of the g value, being the ratio of the magnetic to electric dipole transition moment, to be more accurately described by the metal-localized model than either the absorption intensity or CD. In particular we predict that the g value should be very small for small twists away from 0 or 90°, should vary rather slowly in the 20–30° region but should be large for small deviations from 45°.

(3) The $\delta_{xy} \rightarrow \delta^*_{xy}$ and the $\delta_{xy} \rightarrow \delta_{x^2-y^2}$ transition should have CD of opposite sign.

(4) The g value of the $\delta_{xy} \rightarrow \delta_{x^2-y^2}$ transition should be much larger than that of the $\delta_{xy} \rightarrow \delta^*_{xy}$ transition in the same complex.

So far only two configurationally chiral dimolyb-

denum complexes have had their structures determined[8] by X-ray crystallography: Λ-[Mo_2Cl_4(*S,S*-dppb)$_2$] and Λ-[Mo_2Br_4(*S,S*-dppb)$_2$]. The structure of the former is shown in Fig. 2. It is worth noting that the absolute configuration (Λ) is correctly predicted by conformational analysis of the six-membered $Mo_2P_2C_2$ ring and that a scale model suggests that the twist angle should be in the 20–30° region, agreeing well with the experimental value of 24°. The bromide complex has a similar structure with a very slightly smaller twist angle of 22°. Our model predicts that both complexes should have −ve CD under the $\delta_{xy} \rightarrow \delta^*_{xy}$ transition and +ve CD under the $\delta_{xy} \rightarrow \delta_{x^2-y^2}$ transition. The spectra are illustrated in Fig. 8 and show that this is so. The *g* values for the $\delta_{xy} \rightarrow \delta_{x^2-y^2}$ transition (7.3 and 8.5 × 10^{-2} for the chloride and bromide complexes) are approximately an order of magnitude larger than those for the corresponding $\delta_{xy} \rightarrow \delta^*_{xy}$ transitions and indeed are among the largest *g* values measured for any solution CD spectra. The effect of changing the *S,S*-dppb ligand to *R*-dppp is to produce a complex with Δ absolute configuration, Δ-[Mo_2Cl_4(*R*-dppp)$_2$]. The CD spectra of this complex and of Λ-[Mo_2Cl_4(*S,S*-dppb)$_2$] are shown in Fig. 9, and are seen to be essentially enantiomeric apart from a small wavelength shift due to slightly different twist angles.

The model is equally applicable to quadruply bonded dirhenium complexes. The CD of [Re_2Cl_4(*S,S*-dppb)$_2$]$^{2+}$ produced[12] by *in situ* oxidation of neutral triply bonded [Re_2Cl_4(*S,S*-dppb)$_2$] is shown in Fig. 10. The sign of the CD associated with the $\delta_{xy} \rightarrow \delta^*_{xy}$ transition (at 930 nm, absent in the triply bonded species) is the same as that of Λ-[Mo_2Cl_4(*S,S*-dppb)$_2$] and has a comparable *g* value. This suggests very strongly that the complex (given the Λ configuration dictated by the *S,S*-dppb ligands) has a twist in the region of 20–30°. The fact that the metal-localized model appears to fit rhenium complexes is important because calculations suggest that the δ_{xy} and δ^*_{xy} orbitals in quadruply bonded dirhenium complexes have more ligand character than the analagous dimolybdenum complexes.

Those predictions of our model which it has been possible to test show good agreement with experiment. The one interesting prediction it has not yet been possible to explore is the behaviour of the *g* value when the twist angle is close to 45°. Figure 6 shows that both the dipole and rotational strength tend to zero at 45°. The *g* value for a pure metal-localized transition with only *z*-polarised intensity behaves as a tangent function and tends to infinity as *R* and *D* tend to zero. What happens

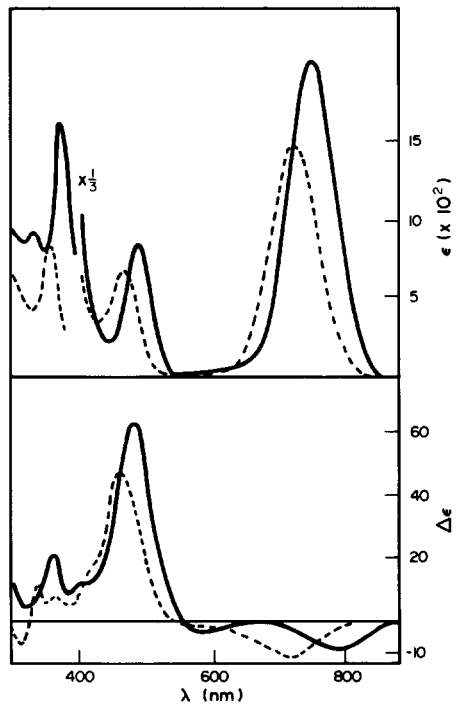

Fig. 8. Absorption and CD spectra of Λ-[Mo_2Br_4(*S,S*-dppb)$_2$] (full line) and Λ-[Mo_2Cl_4(*S,S*-dppb)$_2$] (dashed line), both in dichloromethane solution.

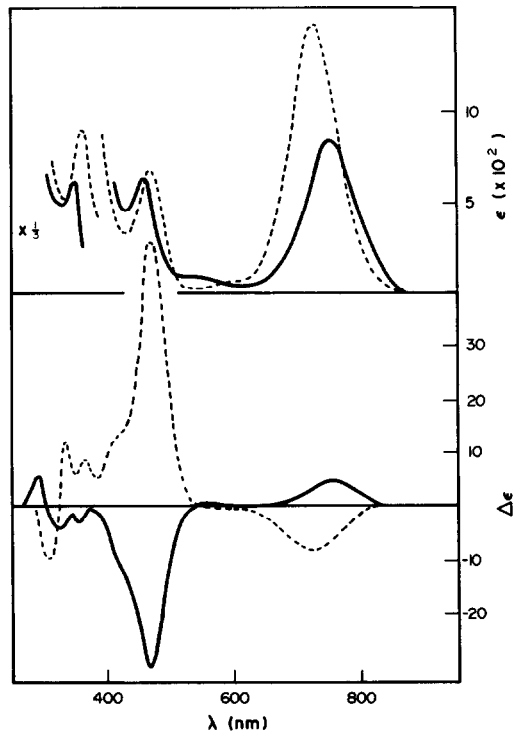

Fig. 9. Absorption and CD spectra of Δ-[Mo_2Cl_4(*R*-dppp)$_2$] (full line) and Λ-[Mo_2Cl_4(*S,S*-dppb)$_2$] (dashed line), both in dichloromethane solution.

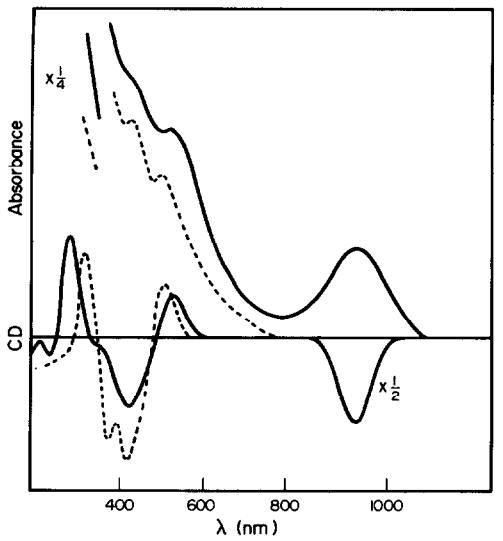

Fig. 10. Absorption and CD spectra of Λ-$[Re_2Cl_4(S,S\text{-dppb})_2]^{2+}$ (full line) and Λ-$[Re_2Cl_4(S,S\text{-dppb})_2]$ (dashed line), both in dichloromethane solution.

to the g value of the $\delta_{xy} \rightarrow \delta^*_{xy}$ transition in a real molecule at angles close to 45° remains to be seen. In the final section we give an indication of the possible uses which CD spectra have in structural assignments and in the detection and assignment of electronic transitions in the spectra of quadruply bonded complexes.

Structural and electronic assignments

The octant nature of the sign rule connecting the CD of the $\delta_{xy} \rightarrow \delta^*_{xy}$ transition to the twist about the metal–metal bond makes the assignment of absolute configuration and/or magnitude of the twist angle from CD spectra ambiguous. Examples of this ambiguity are illustrated by the complexes β-$[Mo_2Cl_4(S\text{-chairphos})_2]$ and β-$[Mo_2Cl_4(S,S\text{-skewphos})_2]$. The ligands have three carbon atoms in the backbone chain and so the complexes contain seven-membered $Mo_2P_2C_3$ rings. Both complexes show negative CD under the $\delta_{xy} \rightarrow \delta^*_{xy}$ transition thus implying either Λ (0–45°) or Δ (45–90°) twists (spectroscopic data for all the complexes discussed in the review are collected in Table 1). Another structural tool available is the experimental correlation between magnitude of the twist angle and energy of the $\delta_{xy} \rightarrow \delta^*_{xy}$ transition due to Campbell *et al.*[13] This too is ambiguous, however, since twists of χ and $(90 - \chi)$ will result in the same energy of the $\delta_{xy} \rightarrow \delta^*_{xy}$ transition. For the two seven-membered ring complexes, therefore, we can predict absolute configurations (twist) of either Λ (18°) or Δ (72°) for β-$[Mo_2Cl_4(S\text{-chairphos})_2]$ and Λ (22°) or Δ (68°) for β-$[Mo_2Cl_4(S,S\text{-skewphos})_2]$. Conformational analysis suggests the larger angle and Δ-configuration in both cases but a recent structural determination[14] on β-$[Mo_2Cl_4(dppp)_2]$, which has an unsubstituted three carbon backbone, shows that this complex has a twist of 22°. Our experience with the six-membered ring complexes shows that backbone substitution drastically alters the twist angle [β-$[Mo_2Cl_4(dppe)_2]$ has a twist of 60° while β-$[Mo_2Cl_4(S,S\text{-dppb})_2]$ has one of 24°] and so we feel that despite the structural results for β-$[Mo_2Cl_4(dppp)_2]$ the twist angles in the methyl-substituted complexes must remain ambiguous at present.

We are on much safer ground if we use CD spectra to decide whether a complex is or is not twisted about the Mo–Mo bond. The chelated complexes α-$[Mo_2Cl_4(S\text{-chairphos})_2]$ and α-$[Mo_2Cl_4(R\text{-dppp})_2]$ show no measurable c.d. under either the $\delta_{xy} \rightarrow \delta^*_{xy}$ or $\delta_{xy} \rightarrow \delta_{x^2-y^2}$ transitions. The amino acid complex $[Mo_2(\text{L-leucine})_4]^{4+}$ has a twist in the crystal of 1.4° and again has no measurable c.d. in the solid-state spectrum under the $\delta_{xy} \rightarrow \delta^*_{xy}$ transition (interestingly it does have a weak but measurable CD in solution perhaps indicating a larger twist). The implication is, therefore, that if the $\delta_{xy} \rightarrow \delta^*_{xy}$ transition has a reasonably large CD the complex must be configurationally chiral. We shall give one example. Until recently $[Mo_2(en)_4]^{4+}$ was the only example[15] of a dimolybdenum complex with saturated amine ligands. The crystal structure has not been determined and it was not known if the 1,2-diaminoethane ligands are chelating or bridging. The analogous complex $[Mo_2(R\text{-pn})_4]^{4+}$ has been synthesized[16] and its absorption and CD spectra are shown in Fig. 11. The CD spectrum shows clearly that we have a configurationally chiral chromophore; the g value for the $\delta_{xy} \rightarrow \delta_{x^2-y^2}$ transition in particular being the largest for any dimolybdenum complex we have measured. There seems no doubt that $[Mo_2(R\text{-pn})_4]^{4+}$, and by extension $[Mo_2(en)_4]^{4+}$, has a twisted chromophore and so most probably contains bridging diamine ligands.

CD spectra are also useful for assigning and identifying electronic transitions. We have already mentioned the assignment of the magnetic dipole $\delta_{xy} \rightarrow \delta_{x^2-y^2}$ transition based on the magnitude of its g value and there seems little doubt that the absorption found around 21,000 cm^{-1} in complexes containing the $Mo_2P_4Cl_4$ chromophore is due to the $\delta_{xy} \rightarrow \delta_{x^2-y^2}$ excitation. As well as this transition and the $\delta_{xy} \rightarrow \delta^*_{xy}$ transition we can clearly identify five more transitions in the c.d. spectrum of Λ-[Mo Cl (*S,S*-dppb)] in the energy region below 350 nm. These are assigned fully in reference 8b. Briefly the very weak feature at 570 nm, which can

Table 1. Energies ($\tilde{\nu}$) and g values for the $\delta_{xy} \rightarrow \delta^*_{xy}$ and $\delta_{xy} \rightarrow \delta_{x^2-y^2}$ transitions of chiral dimolybdenum and dirhenium complexes.

	$\delta_{xy} \rightarrow \delta^*_{xy}$		$\delta_{xy} \rightarrow \delta_{x^2-y^2}$	
	($\times 10^{-3}\,\tilde{\nu}\,\mathrm{cm}^{-1}$)	$g(\Delta\varepsilon/\varepsilon)$ ($\times 10^3$)	($\times 10^{-3}\,\tilde{\nu}\,\mathrm{cm}^{-1}$)	$g(\Delta\varepsilon/\varepsilon)$ ($\times 10^2$)
$[Mo_2Cl_4(S,S\text{-dppb})_2]$	13.70	−5.8	21.05	+7.3
$[Mo_2Cl_4(R\text{-dppb})_2]$	13.33	+7.5	21.74	−6.7
$[Mo_2Cl_4(R\text{-phenphos})_2]$	13.20	+6.0	21.51	−6.2
$[Mo_2Cl_4(S\text{-chairphos})_2]$	14.33	−2.0	21.28	+1.1
$[Mo_2Cl_4(S,S\text{-skewphos})_2]$	13.89	−10.8	20.83	+3.7
$[Mo_2Br_4(S,S\text{-dppb})_2]$	13.24	−3.2	20.70	+8.5
$[Mo_2Br_4(R\text{-dppp})_2]$	12.82	+3.0	20.83	−4.5
$[Mo_2(R\text{-pn})_4]^{4+}$	20.96	−9.1	27.78	+17.0
$[Re_2Cl_4(S,S\text{-dppb})_2]^{2+}$	10.50	−6.0	—	—

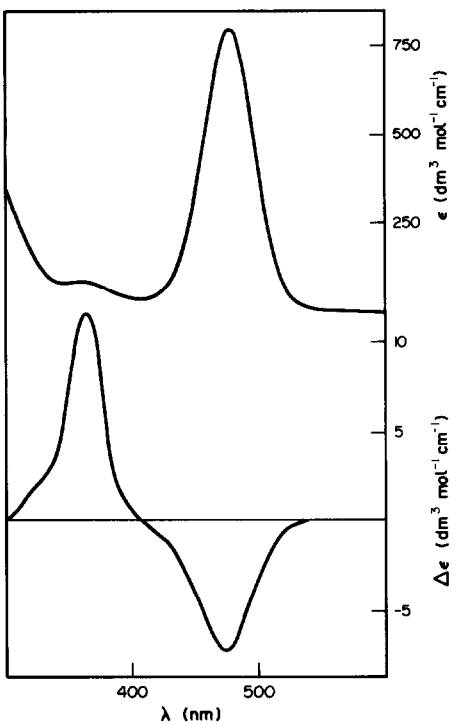

Fig. 11. Absorption and CD spectra of $[Mo_2(R\text{-pn})_4]^{4+}$ as the chloride salt in 10^{-2} mol l^{-1} HCl.

just be discerned in the absorption spectrum and which has the same sign and a similar g value to the $\delta_{xy} \rightarrow \delta^*_{xy}$ transition is assigned as the two-electron $\delta^2_{xy} \rightarrow \delta^{*2}_{xy}$ excitation; the shoulder on the high-energy side of the $\delta_{xy} \rightarrow \delta_{x^2-y^2}$ transition at ~440 nm. is assigned to $\delta_{xy} \rightarrow \delta^*_{x^2-y^2}$ and the final three transitions to the $\pi_{yz} \rightarrow \delta^*_{xy}$, $\pi_{xy} \rightarrow \delta^*_{xy}$ and $\pi_{yz} \rightarrow \delta_{x^2-y^2}$ excitations in increasing energy order.

REFERENCES

1. F. A. Cotton and R. A. Walton, *Multiple Bonds between Metal Atoms*. John Wiley, New York (1982).
2. F. A. Cotton and G. L. Powell, *Inorg. Chem.* 1983, **22**, 1507.
3. P. A. Agaskar and F. A. Cotton, *Inorg. Chem.* 1984, **23**, 3383.
4. E. H. Abbott, K. S. Bose, F. A. Cotton, W. T. Hall and J. C. Sekutowski, *Inorg. Chem.* 1978, **17**, 3240.
5. A. Bino, F. A. Cotton and P. E. Fanwick, *Inorg. Chem.* 1980, **19**, 1215.
6. P. A. Agaskar and F. A. Cotton, *Inorg. Chem.* 1986, **25**, 15.
7. A. McVitie, B.Sc. thesis, University of Glasgow (1983).
8. (a) P. A. Agaskar, F. A. Cotton, I. F. Fraser and R. D. Peacock, *J. Am. Chem. Soc.* 1984, **106**, 1851; (b) P. A. Agaskar, F. A. Cotton, I. F. Fraser, K. Muir, Lj. Manlovich-Muir and R. D. Peacock, *Inorg. Chem.* 1986, **25**, 2511.
9. (a) P. E. Fanwick, D. S. Martin, F. A. Cotton and T. R. Webb, *Inorg. Chem.* 1977, **16**, 2103; (b) F. A. Cotton, D. S. Martin, P. E. Fanwick, T. J. Peters and T. R. Webb, *J. Am. Chem. Soc.* 1976, **98**, 4681.
10. F. A. Cotton, D. S. Martin, T. R. Webb and T. J. Peters, *Inorg. Chem.* 1976, **15**, 1199.
11. I. F. Fraser, A. McVitie and R. D. Peacock, *Polyhedron* 1986, **5**, 39.
12. I. F. Fraser and R. D. Peacock, *J. Chem. Soc. Chem. Commun.* 1985, 1727.
13. F. L. Campbell III, F. A. Cotton and G. L. Powell, *Inorg. Chem.* 1985, **24**, 117.
14. F. A. Cotton, unpublished work quoted in Ref. 8(b).
15. A. R. Bowen and H. Taube, *Inorg. Chem.* 1974, **13**, 2245.
16. I. F. Fraser and R. D. Peacock, *Inorg. Chem.* 1985, **24**, 989.

Polyhedron Vol. 6, No. 4, pp. 723–727, 1987
Printed in Great Britain

0277-5387/87 $3.00+.00

ELECTRONIC ABSORPTION SPECTRA OF M_2L_6 COMPOUNDS CONTAINING METAL–METAL TRIPLE BONDS OF $\sigma^2\pi^4$ CONFIGURATION

M. H. CHISHOLM,* D. L. CLARK, E. M. KOBER† and W. G. VAN DER SLUYS

Department of Chemistry, Indiana University, Bloomington, IN 47401, U.S.A.

(*Received* 19 *November* 1986)

Abstract—The electronic absorption spectra of compounds containing metal–metal triple bonds of $\sigma^2\pi^4$ valence electronic configuration are presented and discussed. The lowest-energy transition of M_2L_6 compounds (M = Mo or W, L = CH_2Bu^t or OBu^t) is expected to be the dipole-allowed $\pi \rightarrow \pi^*$ ($e_u \rightarrow e_g$) transition. This appears to be the case for $M_2(CH_2Bu^t)_6$ and $M_2(OBu^t)_6$ compounds, in which the lowest energy absorption bands occur between 26,000 and 28,000 cm^{-1} ($\varepsilon = 1.1 \times 10^3$–$1.8 \times 10^3\ M^{-1}\,cm^{-1}$). For $M_2(NMe_2)_6$ compounds, the lowest energy absorption is not the $\pi \rightarrow \pi^*$ transition but is assigned instead to a LMCT transition originating from nitrogen lone-pair orbitals, $N_{1p} \rightarrow \pi^*$, observed at 30,800 cm^{-1} ($\varepsilon = 1.4 \times 10^4$–$1.9 \times 10^4\ M^{-1}\,cm^{-1}$). The $\pi \rightarrow \pi^*$ transition is not observed in these compounds, but is presumably masked by the more intense LMCT. These assignments are derived from Xα-SW calculations performed and described by other authors (Bursten *et al.*, *J. Am. Chem. Soc.* 1980, **102**, 4579).

The rapid growth in the synthetic and structural chemistry of dinuclear transition-metal complexes containing strong metal–metal bonds has provided a wealth of information concerning the nature of metal–metal bonding interactions. The study of strong metal–metal bonding interactions initially focused on the family of quadruple bonds of valence configuration $\sigma^2\pi^4\delta^2$ where the combination of sophisticated calculations, electronic absorption, emission, and photoelectron spectroscopic studies have provided a fairly detailed understanding of this class of multiple bond.[1] More recently, active research programs involving the study of metal–metal triple bonds have developed in several major research groups. Again, sophisticated molecular-orbital calculations coupled with photoelectron spectroscopy have demonstrated that triple bonds between metal atoms may contain a variety of valence electronic structures ranging from $\sigma^2\pi^4$ or $\sigma^2\pi^4\delta^2\delta^{*2}$ to the recently discovered $\pi^4\delta^2$ configuration.[2] Although the latter two configurations have been the subject of much recent attention, we note that there has been no study of the electronic absorption spectra of a homologous series of the $\sigma^2\pi^4$ triple bonds. We report here a comparison of the electronic absorption spectra of M_2L_6 compounds (M = Mo or W; L = CH_2Bu^t, NMe_2 or OBu^t) which have the $\sigma^2\pi^4$ valence M–M electronic configuration, and offer a tentative assignment for the lowest-energy transitions.

RESULTS AND DISCUSSIONS

The $\sigma^2\pi^4$ M≡M bond

The simplest of complexes containing the $\sigma^2\pi^4$ M≡M bonding configuration are the unbridged, "ethane-like" d^3–d^3 dinuclear compounds of molybdenum and tungsten of formula M_2L_6 (L = R,[3] NR_2,[3] OR[3] or SAr[4]) depicted in **I**. The qualitative view that the valence electronic structure is composed of one σ- and two π-components has been

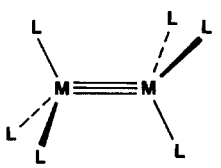

I

* Author to whom correspondence should be addresed.

† Present address: Los Alamos National Laboratory, Los Alamos, NM, U.S.A.

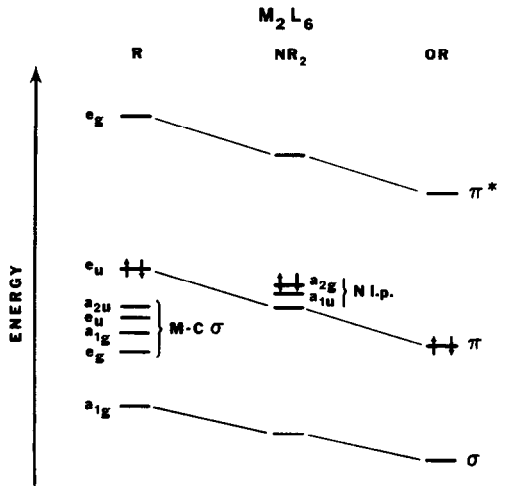

Fig. 1. Qualitative valence energy level diagram for $Mo_2(OR)_6$, $Mo_2(NR)_2)_6$ and $Mo_2(R)_6$ adapted from Reference 2(b).

confirmed by photoelectron spectroscopy[2,5] and a variety of molecular-orbital calculations employing the Xα-SW,[2(a),(b)] Hartree–Fock–Slater,[6] Hartree–Fock,[7] generalized molecular orbital,[8] and extended Hückel[9] methods. The Xα-SW calculations have been performed on $Mo_2(OH)_6$, $Mo_2(NH_2)_6$, $Mo_2(NMe_2)_6$ and $Mo_2(CH_3)_6$, and the projected Xα formalism applied to determine accurate orbital populations and atomic charges for these systems.[2(b)] The latter calculations were shown to be in favorable agreement with the results of photoelectron spectroscopy, and these results are summarized in the form of a qualitative energy level diagram shown in Fig. 1. The lowest unoccupied molecular orbital (LUMO) in each compound was calculated to be a Mo–Mo π*-orbital of e_g-symmetry in the D_{3d} point group.[2(b)] The highest occupied molecular orbital (HOMO) was calculated to be a Mo–Mo π-bonding orbital of e_u-symmetry for L = CH_3 and OH, yet for L = NH_2 and NMe_2 the calculated HOMO was predicted to be a nitrogen lone-pair orbital of either a_{2g}- or a_{1u}-symmetry. These calculations have found support from photoelectron spectroscopic studies.[2(b),5] For L = OR, there is a clear separation in energy between the $\sigma^2\pi^4$ M≡M bonding orbitals and the orbitals of the M–L σ-bonds, and this shows up very nicely in the He(I) and He(II) photoelectron spectra of these compounds. For L = R, extensive mixing is observed between M–M and M–L bonding orbitals which complicates the simple description of the valence electronic structure as $\sigma^2\pi^4$.

Electronic absorption spectra of M_2L_6 compounds

A summary of electronic absorption data and tentative band assignments for a representative series of M_2L_6 compounds (M = Mo or W; L = CH_2Bu^t, NMe_2 or OBu^t) are given in Table 1. A series of electronic absorption spectra comparing homologous Mo and W compounds for L = CH_2Bu^t, NMe_2 and OBu^t are shown in Figs 2–4. For each ligand set, the lowest-energy transition occurs in the UV and tails into the visible region of the spectrum, accounting for the characteristic yellow to red colors of the M_2L_6 compounds.

The ground state of the M_2L_6 systems is $^1A_{1g}$, and symmetry-allowed transitions are to excited states of A_{2u}- and E_u-symmetry in the D_{3d} point group. Thus the M≡M $\pi \rightarrow \pi^*$ ($e_u \rightarrow e_g$) transition is orbitally-allowed and expected to be the lowest-energy transition for compounds where L = CH_2Bu^t or OBu^t. For these compounds, the lowest-energy transitions are observed as relatively weak (ε = 1200–1700 $M^{-1}cm^{-1}$) bands centered between 25,000–27,000 cm^{-1}. These absorptions are tentatively assigned to the dipole-allowed $\pi \rightarrow \pi^*$ ($^1A_{1g} \rightarrow {}^1E_u$) transitions in these molecules. The relatively weak intensity of these transitions presumably arises from a mixing of M–M π and δ character in the π- and π*-orbitals under D_{3d}-symmetry. The PXα results indicate that this δ–π mixing in the occupied π-orbitals is only appreciable in magnitude for L = alkyl.[2(b)] Fenske–Hall calculations performed in our laboratory yield the same result, but, more important, they reveal that the magnitude of δ–π mixing in the π*-orbitals is severe,[10] and we feel that this will have important consequences to the intensity of the $\pi \rightarrow \pi^*$ transition in these compounds. Absorption intensity is expected to increase as the square of the overlap between ground and excited states, and in this regard we note that the intrinsically weak, yet fully-allowed $\delta \rightarrow \delta^*$ transition in quadruply bonded dimers has been rationalized by use of the weak coupling model.[11] A shoulder on the $\pi \rightarrow \pi^*$ transition is observed for $W_2(OBu^t)_6$ but not for $W_2(CH_2Bu^t)_6$ and we propose that this arises from the dipole-allowed, spin-forbidden triplet component $^3(\pi \rightarrow \pi^*)$ of the $\pi \rightarrow \pi^*$ transition. For heavy atoms such as tungsten, the effects of spin–orbit coupling become significant and can contribute to the intensity of forbidden transitions.[12] A slight mixing of triplet character into the ground state, or a mixing of singlet character into the triplet state, will contribute to the intensity of singlet–triplet transitions. The lack of a $^3(\pi \rightarrow \pi^*)$ component for $W_2(CH_2Bu^t)_6$ may be the result of the increased mixing of M–M and M–C bonding orbitals, resulting in a

Table 1. Electronic absorption data for M_2L_6 compounds (M = Mo or W; L = CH_2Bu^t, NMe_2 or OBu^t)[a]

Compound		λ (nm)	λ (cm^{-1})	ε ($M^{-1}cm^{-1}$)	Tentative assignment[b]
$Mo_2(CH_2Bu^t)_6$		368	2.72×10^4	1.7×10^3	$\pi \rightarrow \pi^*$
		303	3.30×10^4	1.2×10^4	$\sigma_{MC} \rightarrow \pi^*$
		263	3.80×10^4	1.9×10^4	NA
		230	4.35×10^4	2.2×10^4	NA
$W_2(CH_2Bu^t)_6$		387	2.58×10^4	1.8×10^3	$\pi \rightarrow \pi^*$
	sh	269	3.72×10^4	6.4×10^3	NA
		232	4.31×10^4	1.9×10^4	NA
$Mo_2(NMe_2)_6$		325	3.08×10^4	1.9×10^4	$N_{1p} \rightarrow \pi^*$
	sh	265	3.77×10^4	2.7×10^4	NA
		240	4.17×10^4	3.7×10^4	NA
$W_2(NMe_2)_6$	sh	360	2.78×10^4	1.0×10^3	$\pi \rightarrow \pi^*$
		282	3.55×10^4	1.7×10^4	$N_{1p} \rightarrow \pi^*$
	sh	235	4.26×10^4	3.0×10^4	NA
$Mo_2(OBu^t)_6$		392	2.55×10^4	1.4×10^3	$\pi \rightarrow \pi^*$
	sh	285	3.50×10^4	6.4×10^3	NA
$W_2(OBu^t)_6$	sh	460	2.17×10^4	6.0×10^2	$^3(\pi \rightarrow \pi^*)$
		378	2.65×10^4	1.6×10^3	$\pi \rightarrow \pi^*$
	sh	250	4.00×10^4	3.9×10^3	NA

[a] Spectra recorded in THF solution using matched 1.0-cm quartz cells.
[b] π and π^* denote the M–M character of predominantly metal-based orbitals. σ_{MC} and N_{1p} denote M–C σ and N lone-pair orbitals, respectively. NA = not assigned.

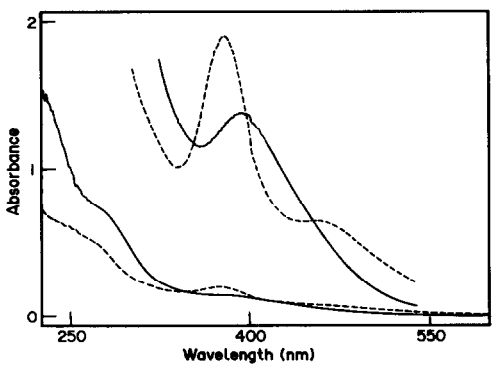

Fig. 2. Comparison of the electronic absorption spectra of $Mo_2(OBu^t)_6$ (solid line) and $W_2(OBu^t)_6$ (dashed line) in THF solutions, at 1.0×10^{-3} and 1.0×10^{-4} M.

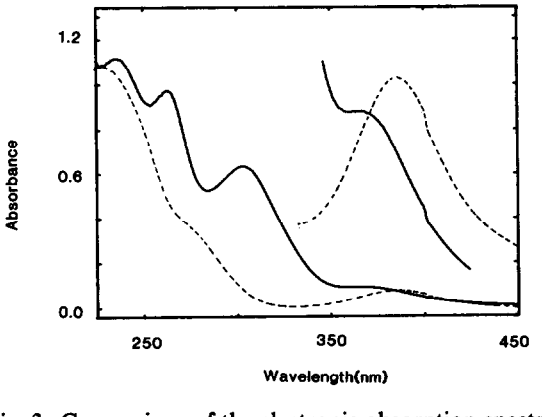

Fig. 3. Comparison of the electronic absorption spectra of $Mo_2(CH_2Bu^t)_6$ (solid line) and $W_2(CH_2Bu^t)_6$ (dashed line) in THF solutions, at 5.7×10^{-4} and 5.7×10^{-5} M.

lower percent metal character in the M–M π-orbitals compared to those of $W_2(OBu^t)_6$.[2(b)]

By contrast, for $M_2(NMe_2)_6$ compounds the lowest-energy transition is expected to be a ligand-to-metal charge transfer transition (LMCT) arising from a nitrogen lone-pair excitation to the M≡M π^*-orbital ($^1A_{1g} \rightarrow {}^1E_u$) ($a_{1u} \rightarrow e_g$) which is in good agreement with the observed absorption energy (30,800 cm^{-1}), and intensity [$\varepsilon = 1.4 \times 10^4$ M^{-1} cm^{-1} (M = Mo) and intensity [$\varepsilon = 1.4 \times 10^4 M^{-1} cm^{-1}$; M = Mo]. Interestingly enough, the LMCT in $W_2(NMe_2)_6$ is found at higher energy ($3.55 \times 10^4 cm^{-1}$) than the corresponding transition in $Mo_2(NMe_2)_6$. This shift uncovers a shoulder at *ca.* 360 nm ($2.78 \times 10^4 cm^{-1}$, $\varepsilon = 1.0 \times 10^3 cm^{-1} M^{-1}$) which is most likely the $\pi \rightarrow \pi^*$ transition. Presumably in $Mo_2(NMe_2)_6$ the $\pi \rightarrow \pi^*$ transition is masked by or hidden beneath the LMCT.

When comparing the spectra of $M_2(CH_2Bu^t)_6$

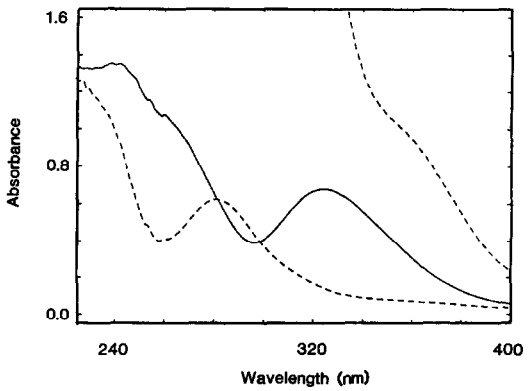

Fig. 4. Comparison of the electronic absorption spectra of $Mo_2(NMe_2)_6$ (solid line) and $W_2(NMe_2)_6$ (dashed line) in THF solutions, at 3.5×10^{-5} M.

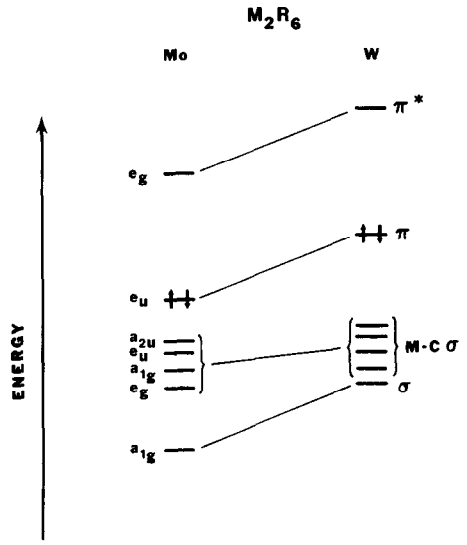

Fig. 5. Qualitative valence energy level diagram describing the differences between $Mo_2(R)_6$ and $W_2(R)_6$.

compounds, transitions are observed for the molybdenum compound which are not observed for the tungsten counterpart. The origin of these absorption features, which occur at higher energy than the $\pi \rightarrow \pi^*$ transitions are admittedly much more speculative. However, the Xα-SW calculations and photoelectron spectroscopic studies indicate that M–C σ-bonding orbitals of a_{2u}- and e_u-symmetry are located energetically just below the M≡M π-bonding orbitals.[2(b)] Transitions from these M–C σ bonding orbitals into the empty M≡M π^*-orbitals are dipole-allowed under D_{3d}-symmetry. Furthermore, from photoelectron spectroscopy it is known that the metal–metal bonding orbitals for tungsten compounds lie higher in energy than those of molybdenum counterparts, yet the metal–carbon orbitals remain at about the same energy.[13] We summarize the effect of changing the metal from molybdenum to tungsten in the form of a qualitative energy level diagram in Fig. 5. Orbitals with large amounts of metal character will be raised in energy for tungsten relative to molybdenum, whereas orbitals with large amounts of carbon character will be relatively unaffected. Thus, while the π to π^* separation remains relatively unchanged, the separation of M–C σ- and M≡M π^*-orbitals is greatly changed. We feel that this diagram qualitatively accounts for the observation of M–C $\sigma \rightarrow$ M≡M π^* transitions at lower energy for molybdenum relative to tungsten.

Concluding remarks

We have presented a summary of the electronic absorption spectra for the prototypical compounds containing metal–metal triple bonds of valence M–M configuration $\sigma^2\pi^4$, namely the M_2L_6 compounds of molybdenum and tungsten. For, M = Mo, W; L = CH_2Bu^t OBu^t and L = NMe_2; M = W the lowest-energy absorptions can reasonably be assigned to the $\pi \rightarrow \pi^*$ transition whereas for M = Mo; L = NMe_2 the lowest-energy absorption is most likely LMCT. The overall understanding of these metal–metal triple bonds from both a theoretical and experimental basis seems quite satisfactory. Calculations using the Xα-SW method have proved useful in the interpretation of both the electronic absorption spectra and the photoelectron spectra. It should be recognized that the valence molecular orbital description of $\sigma^2\pi^4$ is only an approximation, and that this description is dependent on the ligands L, and that the degree of M–M and M–L mixing increases in the order OBu^t to NMe_2 to CH_2Bu^t.

EXPERIMENTAL

Compounds were prepared using standard Schlenk and glove-box techniques as described elsewhere* and were purified by either sublimation

* $Mo_2(CH_2Bu^t)_6$ was prepared from $MoCl_3$ and $LiCH_2Bu^t$: K. J. Ahmed, Ph.D. thesis, Indiana University. $W_2(CH_2Bu^t)_6$ was prepared from $NaW_2Cl_7(THF)_5$ and $LiCH_2Bu^t$: M. H. Chisholm *et al.*, results to be published. $Mo_2(NMe_2)_6$: M. H. Chisholm, F. A. Cotton, B. A. Frenz, W. W. Reichert, L. W. Shrive and B. R. Stults, *J. Am. Chem. Soc.* 1976, **98**, 4469. $W_2(NMe_2)_6$ was prepared from $NaW_2Cl_7(THF)_5$: M. H. Chisholm *et al.*, results to be published. $Mo_2(OBu^t)_6$: M. H. Chisholm, F. A. Cotton, C. A. Murillo and W. W. Reichert, *Inorg. Chem.* 1977, **16**, 1801. $W_2(OBu^t)_6$: M. Akiyama, M. H. Chisholm, F. A. Cotton, M. W. Extine, D. A. Haitko, D. Little and P. E. Fanwick, *Inorg. Chem.* 1978, **18**, 2266.

($L = CH_2Bu^t$ and NMe_2) or recrystallized from hexane ($L = OBu^t$). Prior to examination of the electronic absorption measurements, compound purity was checked by ^1H NMR spectroscopy. Spectral-grade THF was distilled from sodium benzophenone and stored over 3-Å sieves and under nitrogen. Electronic absorption spectra were recorded in THF solution on a Hewlett–Packard 8450A spectrophotometer using matched 1.0-cm quartz cells. As a check on reproducibility, spectra were recorded at various concentrations which allow the estimate of accuracy for ε ($M^{-1}\,cm^{-1}$) listed in Table 1.

Acknowledgements—We thank the National Science Foundation for financial support and Professor B. E. Bursten for helpful discussions. D. L. Clark is the recipient of the 1985–1986 Indiana University General Electric Foundation Fellowship.

REFERENCES

1. F. A. Cotton and R. A. Walton, *Multiple Bonds between Metal Atoms*. Wiley, New York (1982).
2. For triple bonds of $\sigma^2\pi^4$ configuration see: (a) F. A. Cotton, G. G. Stanley, B. J. Kalbacher, J. C. Green, E. A. Seddon and M. H. Chisholm, *Proc. Nat. Acad. Sci. U.S.A.* 1977, **74**, 3109; (b) B. E. Bursten, F. A. Cotton, J. C. Green, E. A. Seddon and G. G. Stanley, *J. Am. Chem. Soc.* 1980, **102**, 4579. For triple bonds of $\sigma^2\pi^4\delta^2\delta^{*2}$ configuration see: (c) D. R. Root, C. H. Blevins, D. L. Lichtenberger, A. P. Sattelberger and R. A. Walton, *J. Am. Chem. Soc.* 1986, **108**, 953; (d) B. E. Bursten, F. A. Cotton, P. E. Fanwick, G. G. Stanley and R. A. Walton, *J. Am. Chem. Soc.* 1983, **105**, 2606. For triple bonds of $\pi^4\delta^2$ configuration see: (e) M. H. Chisholm, D. M. Hoffman, J. C. Huffman, W. G. Van Der Sluys and S. Russo, *J. Am. Chem. Soc.* 1984, **106**, 5386; (f) M. D. Braydich, B. E. Bursten, M. H. Chisholm and D. L. Clark, *J. Am. Chem. Soc.* 1985, **107**, 4459; (g) M. H. Chisholm, D. L. Clark, J. C. Huffman, W. G. Van Der Sluys, E. M. Kober, D. L. Lichtenberger and B. E. Bursten, *J. Am. Chem. Soc.* (submitted for publication).
3. M. H. Chisholm and F. A. Cotton, *Acc. Chem. Res.* 1978, **11**, 356.
4. M. H. Chisholm, J. F. Corning, K. Folting and J. C. Huffman, *Polyhedron* 1985, **4**, 383.
5. E. M. Kober and D. L. Lichtenberger, unpublished results.
6. T. Ziegler, *J. Am. Chem. Soc.* 1983, **105**, 7543.
7. I. H. Hillier, C. D. Garner and G. R. Mitcheson, *J. Chem. Soc., Chem. Commun.* 1978, 204.
8. R. A. Kok and M. B. Hall, *Inorg. Chem.* 1983, **22**, 728.
9. T. A. Albright and R. Hoffmann, *J. Am. Chem. Soc.* 1978, **100**, 7736.
10. M. H. Chisholm and D. L. Clark, unpublished results.
11. W. C. Trogler and H. B. Gray, *Acc. Chem. Res.* 1978, **11**, 232.
12. B. N. Figgis, *Introduction to Ligand Fields*. Wiley, New York (1966).
13. See Ref. 2(g) and also: (a) M. F. Lappert, J. B. Pedley and G. Sharp, *J. Organomet. Chem.* 1974, **66**, 271; (b) S. Evans, J. C. Green, P. J. Joachin, A. F. Orchard, D. W. Turner and J. P. Maier, *J. Chem. Soc., Faraday Trans.* 2 1972, **68**, 905.

Polyhedron Vol. 6, No. 4, pp. 729–740, 1987
Printed in Great Britain

0277–5387/87 $3.00+.00

SOME RECENT DEVELOPMENTS IN THE CHEMISTRY OF MULTIPLY BONDED DIMETAL COMPLEXES THAT CONTAIN THE INTRAMOLECULAR BRIDGING PHOSPHINE LIGANDS $R_2P(CH_2)_nPR_2$

ANDREW C. PRICE and RICHARD A. WALTON*

Department of Chemistry, Purdue University, West Lafayette, IN 47907, U.S.A.

(*Received* 19 *November* 1986)

Abstract—Recent synthetic and structural studies on multiply bonded complexes of stoichiometry $M_2X_4[\mu\text{-}R_2P(CH_2)_nPR_2]_2$ (M = Mo, W or Re; X = Cl, Br or I; R = Me, Et or Ph; $n = 1$ or 2), the ditungsten(III) hydride $W_2(\mu\text{-H})(\mu\text{-Cl})Cl_4(\mu\text{-dppm})_2$ (dppm = $Ph_2PCH_2PPh_2$), $Re_2Cl_4(\mu\text{-dmpm})_3$ (dmpm = $Me_2PCH_2PMe_2$), and $M_2(\mu\text{-Cl})_2Cl_4(\mu\text{-}R_2PCH_2PR_2)_2$ (R = Me or Ph) are surveyed. The first examples of multiply bonded complexes that contain the $Ph_2PCH{=}CHPPh_2$ ligand (abbreviated dppee) are described, viz. the α- and β-isomers of $M_2X_4(dppee)_2$ (M = Mo or Re, X = Cl or Br). The reactions of $Re_2X_4(dppm)_2$ (X = Cl or Br) with RNC, RCN and CO ligands that yield complexes in which a metal–metal multiple bond is preserved are reviewed.

Bidentate phosphine ligands of type $R_2P(CH_2)_nPR_2$ can not only chelate or bind in a monodentate fashion to a single metal center but, in the case of $n = 1$ or 2, they can also bridge dimetal units to give quite stable five- or six-membered rings. Such species can have an important and extensive chemistry, e.g. the $Ph_2PCH_2PPh_2$ (dppm) complexes of the platinum metals.[1] A few years ago it was discovered[2–10] that multiply bonded dimolybdenum(II), ditungsten(II) and dirhenium(II) complexes could be isolated in which such phosphines either chelate to the individual metal centers within the dinuclear unit or form intramolecular bridges between them. In the case of the $Ph_2PCH_2CH_2PPh_2$ ligand (dppe), there are instances where both structural forms have been isolated. These compounds, which are designated α- (for chelating) and β- (for bridging), respectively, have been shown to display a rich chemistry, many aspects of which have been summarized in a text[11] and in two very recent review articles.[12,13] The present article addresses some of the recent developments in this field with a particular emphasis upon the reactions of these systems with the π-acceptor CO and RNC ligands.

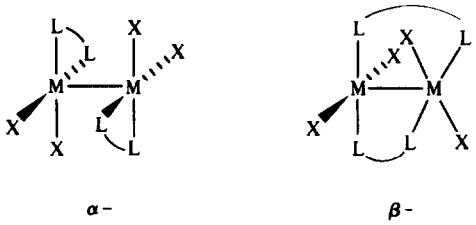

L–L = $Ph_2P(CH_2)_nPPh_2$, X = halide

A. RECENT SYNTHETIC AND STRUCTURAL STUDIES ON MIXED HALIDE–BIDENTATE PHOSPHINE COMPLEXES

Multiply bonded complexes of type $M_2X_4(LL)_2$ [X = halide, LL = $R_2P(CH_2)_nPR_2$] are limited to cases where M = Mo, W or Re. Only work carried out or reported during the last 2 years or so will be summarized here; surveys of earlier studies can be found elsewhere (see Refs 11–13). The quadruply-bonded dimolybdenum(II) complexes $Mo_2X_4(dppm)_2$ (X = Br or I) can be prepared in high yield from $Mo_2Cl_4(dppm)_2$ via simple halide-exchange reactions (using NaX in acetone).[14] Alter-

*Author to whom correspondence should be addressed.

native routes to the iodide complex have recently been devised that involve the decarbonylation of $Mo_2I_4(CO)_8$ in toluene in the presence of dppm, and the reaction of $Mo_2(O_2CCH_3)_4$ with Me_3SiI in toluene with two equivalents of dppm.[15] These synthetic procedures[14,15] have led to two independent crystallographic studies of $Mo_2I_4(dppm)_2$ with a view to comparing its structure with those reported for $Mo_2Cl_4(dppm)_2$[4] and $Mo_2Br_4(dppm)_2$[16] and thereby providing a structural comparison of a homologous series of multiply bonded dinuclear complexes of the type $M_2X_4(LL)_2$ (X = Cl, Br or I). Crystals of $Mo_2I_4(dppm)_2$ grown from toluene were found[15] to contain the molecule in the expected fully eclipsed rotational geometry [the Mo–Mo distance is 2.139(1) Å] with a *trans* bridging arrangement of dppm ligands as is the case for its chloride and bromide analogues.[4,16] However, crystals of this complex which were grown from CH_2Cl_2–CH_3OH are different.[17] There are two independent sets of molecules in the unit cell both of which possess a structure in which the dppm ligands are present in an intramolecular bridging mode with a transoid disposition to one another. One molecule, which resides on a crystallographic inversion center, has the usual eclipsed rotational geometry, while the two symmetry-related molecules in general positions have an Mo–Mo distance of 2.152(2) Å and a twist angle [i.e. average torsional angle (χ)] of 17(2) Å.[17] This is one of the first instances where two quite different rotational geometries are present in the solid state for a molecule of this general type, *a result which indicates that crystal packing forces can play an important role in determining the exact rotational geometry*. While there is crystallographic and chemical evidence that these crystals contain small amounts of chloride and that the true composition may actually be $Mo_2I_{4-x}Cl_x(dppm)_2$, with $x \sim 0.2$, this does not appear to influence the structure in any significant way. Interestingly, the β-form of $Mo_2I_4(dppe)_2$ has recently been prepared and structually characterized and found[18] to possess a structure in which independent molecules in the unit cell have different rotational geometries.

The dimolybdenum(II) complex $Mo_2Cl_4(dmpm)_2$ (dmpm = $Me_2PCH_2PMe_2$) has been prepared by the reactions of dmpm with a mixture of $Mo_2(O_2CCH_3)_4$ and Me_3SiCl in toluene and with a suspension of $K_4Mo_2Cl_8$ in methanol.[19] The latter of these two procedures has also been used to prepare β-$Mo_2Cl_4(depe)_2$ (depe = $Et_2PCH_2CH_2PEt_2$).[20] Crystals of $Mo_2Cl_4(dmpm)_2$ have been shown to possess the usual phosphine-bridge eclipsed structure with an Mo–Mo distance of 2.1253(4) Å. The structure and properties of this complex resemble quite closely those of $Mo_2Cl_4(dppm)_2$.[14] Of special note is the accessibility of several redox processes for $Mo_2Cl_4(dmpm)_2$. Thus, solutions in 0.1 M n-Bu_4NPF_6–CH_2Cl_2 display a reversible process ($i_{p,a}/i_{p,c} \sim 1$) at +0.49 V vs Ag–AgCl, which corresponds to a one-electron oxidation of the bulk complex. An irreversible oxidation is seen at $E_{p,a} = +1.25$ V vs Ag–AgCl, and an irreversible reduction is observed near the solvent limit with $E_{p,c} = -1.75$ V vs Ag–AgCl. The crystal structure determination of β-$Mo_2Cl_4(depe)_2$ has confirmed its staggered rotational geometry [$\chi = 42.7(2)°$].[20] A comparison of this structural data with that for the other quadruply bonded dimolybdenum(II) mixed halide–bidentate phosphine complexes of this type has revealed an inverse linear relationship between the Mo–Mo bond length and cos 2χ (correlation coefficient of 0.9547). From this, the complete loss of the δ-component to the quadruple bond (corresponding to a fully staggered geometry) is seen to lead to an increase of 0.097 Å in the bond length.[20] Further refinements in this correlation can be expected as more structural data are forthcoming.

In the case of ditungsten(II) complexes that contain $R_2P(CH_2)_nPR_2$ ligands, earlier studies have reported $W_2Cl_4(dmpe)_2$ and $W_2Cl_4(dppe)_2$ (dmpe = $Me_2PCH_2CH_2PMe_2$).[5,11,13] These quadruply bonded species are prepared by the reactions of dmpe and dppe with $W_2Cl_4(P\text{-}n\text{-}Bu_3)_4$.[5] When such reactions are carried out between dppm and $W_2Cl_4(P\text{-}n\text{-}Bu_3)_4$ in toluene, the μ-hydrido ditungsten(III) complex $W_2(\mu\text{-}H)(\mu\text{-}Cl)Cl_4(dppm)_2$ (**1**)

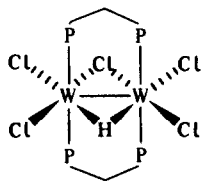

1

is formed.[21] An alternative and more logical synthetic method utilizes the reaction between $W_2(mhp)_4$ (mhp = anion of 2-hydroxy-6-methylpyridine), Me_3SiCl, and dppm in methanol. The W–W distance in **1** is 2.483(1) Å. While the location of the hydride ligand is not apparent from the X-ray crystal structure analysis, its presence has, nonetheless, been confirmed by spectroscopic means. Furthermore, the structural details of this molecule resemble closely those of $W_2(\mu\text{-}H)(\mu\text{-}Cl)Cl_4(4\text{-}Etpy)_4$.[22]

A most useful development in the area of dirhenium(II) chemistry has been the discovery that the

bis-carboxylate complexes $Re_2(O_2CCH_3)_2X_4 \cdot 2L$ (X = Cl, Br or I; L = H_2O or γ-picoline) react with dppm in hot ethanol to give $Re_2X_4(dppm)_2$.[23] When dppe is used in place of dppm, these reactions afford β-$Re_2X_4(dppe)_2$ (X = Cl, Br or I). In the case of X = Cl or Br, the paramagnetic mixed-valent intermediates $Re_2(O_2CCH_3)X_4(dppm)_2$ have been isolated.[23] The reactions of lithium acetate with mixtures of $Re_2(O_2CCH_3)_2X_4 \cdot 2L$ and dppm or with $Re_2(O_2CCH_3)X_4(dppm)_2$ in methanol afford the species $Re_2(O_2CCH_3)_2X_2(dppm)_2$ in good yield.[23] These same complexes can be obtained by a redox reaction in which $Re_2(O_2CCH_3)_4X_2$ is reacted with dppm in refluxing ethanol.[23] The full characterization of these complexes is currently in progress.

The X-ray crystal structure of $Re_2Cl_4(dppm)_2$ has confirmed that this complex has a staggered rotational geometry.[24] The conformation of the two fused metallocyclic rings can be considered to be derived from the twist-boat conformation of the cyclohexane-like ring. For an Re(II)–Re(II) compound in which there is a $\sigma^2\pi^4\delta^2\delta^{*2}$ triple bond that imposes no electronic barrier to rotation, the observed staggered arrangement appears to correspond to an energy minimum. This is easy to visualize in a qualitative sense because a twist about the metal–metal axis relieves repulsive steric interactions. Attempts to prepare $Re_2Cl_4(dmpm)_2$ have led to an unexpected result. The reaction of dmpm with $(n\text{-}Bu_4N)_2Re_2Cl_8$ in methanol or with $Re_2Cl_4(P\text{-}n\text{-}Pr_3)_4$ in ethanol–toluene affords the novel complex $Re_2Cl_4(dmpm)_3$[25] that contains three intramolecular phosphine bridging ligands. The ^1H NMR spectrum of this species displays six broad singlets of approximate equal intensity in accord with six pairs of inequivalent methyl groups. The structure of $Re_2Cl_4(dmpm)_3$ as revealed by X-ray crystallography is shown in Fig. 1.

When the phosphine complexes $Re_2Cl_4(PMe_3)_2(LL)$ [LL = dppm or $Ph_2PNHPPh_2$ (dppa)][26] are reacted with dppe or arphos ($Ph_2PCH_2CH_2AsPh_2$) in hot *n*-butanol, the PMe_3 ligands are displaced to give the mixed-ligand species $Re_2Cl_4(LL)(LL')$ (LL = dppm or dppa, LL' = dppe or arphos).[27] The crystal structure of $Re_2Cl_4(dppm)(dppe)$ has been determined (Fig. 2) and the complex shown[27] to possess a staggered rotational geometry with an Re–Re distance of 2.237(1) Å; this value is intermediate between that of $Re_2Cl_4(dppm)_2$[24] and β-$Re_2Cl_4(dppe)_2$.[9] This structure can also be compared with that of the recently characterized complex β-$Re_2Cl_4(depe)_2$ for which the Re–Re distance is 2.211(1) Å.[20] The reported method for the synthesis of this complex produced it in a 20% yield. In order to utilize this material as a reactant with other ligands, an improved synthetic route has recently been developed.[28] By using $Re_2Cl_4(P\text{-}n\text{-}Pr_3)_4$ in place of $(n\text{-}Bu_4N)_2Re_2Cl_8$ and refluxing this with depe in a mixture of toluene and ethanol, the yield of β-$Re_2Cl_4(depe)_2$ increases to 70%. The bromide derivative has also been synthesized in an analogous manner but proceeds in much lower yield (< 10%) since α-$Re_2Br_4(depe)_2$ is the major product.

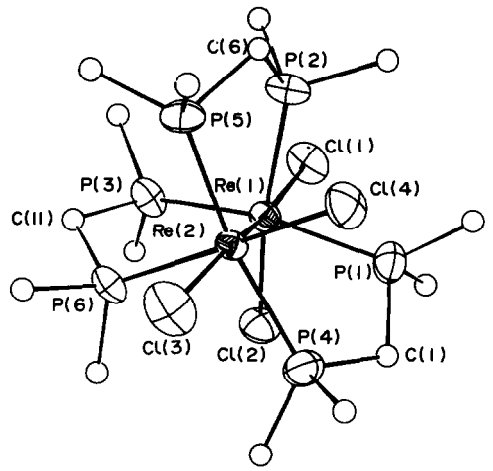

Fig. 1. ORTEP representation of the structure of $Re_2Cl_4(dmpm)_3$.[25] Carbon atoms are represented as circles of arbitrary radius. Other atoms are given as their 35% probability ellipsoids.

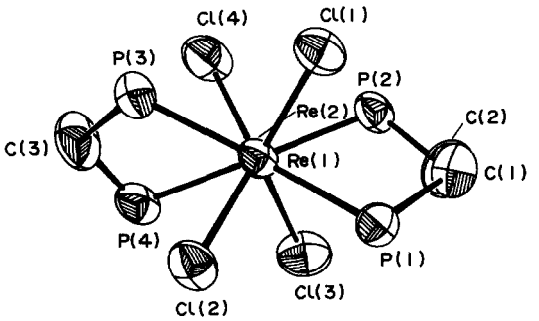

Fig. 2. The ORTEP structure of $Re_2Cl_4(dppm)(dppe)$ as viewed down the Re–Re axis.[27] One rhenium atom has been obscured by the other. Phenyl rings have been omitted for clarity and atoms are given as their 50% probability ellipsoids.

The first studies have now been carried out on multiply bonded dimetal complexes that contain phosphine ligands of the types $R_2PCH{=}CHPR_2$ and $R_2PC{\equiv}CPR_2$. In the case of the ligand *cis*-$Ph_2PCH{=}CHPPh_2$ (abbreviated *cis*-dppee),* it reacts in refluxing alcohol solvents to give α-$Mo_2Cl_4(dppee)_2$ or β-$Mo_2Cl_4(dppee)_2$; the β-

*Sometimes abbreviated ebdp, dppen or Pf=Pf.

isomer is favored by higher reaction temperatures.[29] Solutions of α-$Mo_2Cl_4(dppee)_2$ in CH_2Cl_2 isomerize slowly to the β-isomer at room temperature. Both isomers of the analogous dirhenium(II) complex have also been isolated using reactions (1) and (2):

$$[Re_2X_8]^{2-} + dppee \xrightarrow[\text{reflux}]{\text{MeOH–HCl or EtOH}} \alpha\text{-}Re_2X_4(dppee)_2 \quad (X = Cl \text{ or } Br) \qquad (1)$$

$$Re_2Cl_6(P\text{-}n\text{-}Bu_3)_2 + dppee \xrightarrow[\text{reflux}]{\text{EtOH}} \alpha\text{-}Re_2X_4(dppee)_2$$

$$Re_2X_4(PR_3)_4 + dppee \xrightarrow[\text{reflux}]{\text{benzene}^{\wedge}} \beta\text{-}Re_2X_4(dppee)_2 \quad (X = Cl \text{ or } Br;\ R = Et \text{ or } n\text{-}Pr) \qquad (2)$$

The X-ray crystal structure of β-$Re_2Cl_4(dppee)_2$ has shown that this molecule has a staggered geometry in which the disposition of the pairs of *trans* P–Re–P units is intermediate between that found previously in complexes of type $Re_2Cl_4(PR_3)_4$ and in $Re_2Cl_4(dppe)_2$. This represents the first structure of its kind for a dppee-bridged complex. Although the crystal structure of α-$Re_2X_4(dppee)_2$ has not yet been determined, it is very likely analogous to the structures of α-$Re_2Cl_4(dmpe)_2$[24] and α-$Re_2Cl_4(dppp)_2$ [dppp = $Ph_2P(CH_2)_3PPh_2$][10] both of which possess eclipsed structures with chelating bidentate phosphine ligands. The latter complexes are prepared from the reactions between $(n\text{-}Bu_4N)_2Re_2Cl_8$ and the appropriate phosphine ligand.

Both $Ph_2PC{\equiv}CPPh_2$ and *trans*-$Ph_2PCH{=}CHPPh_2$ (*trans*-dppee) react with $(n\text{-}Bu_4N)_2Re_2Cl_8$ in MeOH–HCl to give "dimer of dimers" species $[(n\text{-}Bu_4N)Re_2Cl_7(LL)_{0.5}]_2$ in which quadruply bonded $[Re_2Cl_7]$ units are linked by intermolecular phosphine bridges. The reaction chemistry of these molecules is currently under investigation.

By using the ligand *S,S*-dppb (*S,S*-$Ph_2PCHMeCHMePPh_2$), the novel chiral complex $Re_2Cl_4(S,S\text{-}dppb)_2$[30] has been synthesized and probably has a similar structure to β-$Re_2Cl_4(dppe)_2$,[9] namely a staggered geometry with a twist between the two $ReCl_2P_2$ units. Oxidation of $Re_2Cl_4(S,S\text{-}dppb)_2$ with $NOPF_6$ in acetonitrile solution yields the mono- and dications $[Re_2Cl_4(S,S\text{-}dppb)_2]^{n+}$ ($n = 1$ or 2).[30] Circular-dichroism experiments indicate that the dication, which contains a Re_2^{6+} core, and therefore a quadruple bond, has a twist angle of less than 45°. This is the first example of a twisted dirhenium complex with a formal quadruple Re–Re bond, and $Re_2Cl_4(S,S\text{-}dppb)_2$ and $[Re_2Cl_4(S,S\text{-}dppb)_2]^{2+}$ are the first configurationally chiral dirhenium complexes reported. They resemble the related dimolybdenum(II) complex $Mo_2Cl_4(S,S\text{-}dppb)_2$ that was studied previously.[31]

Some important studies have been carried out on edge shared bioctahedral complexes of the type $M_2(\mu\text{-}Cl)_2Cl_4(LL)_2$. Following upon the earlier isolation and structural characterization of $Re_2(\mu\text{-}Cl)_2Cl_4(\mu\text{-}dppm)_2$,[32] the redox chemistry of this complex has recently been explored.[33,34] Reduction with cobaltocene yields the monoanion $[(\eta\text{-}C_5H_5)_2Co][Re_2Cl_6(dppm)_2]$ while oxidation using $NOPF_6$ yields the cation $[Re_2Cl_6(dppm)_2]PF_6$. Hydrolysis of the PF_6^- anion in the latter complex gives rise to $[Re_2Cl_6(dppm)_2]\text{-}H_2PO_4 \cdot H_3PO_4 \cdot 4H_2O$ which has been structurally characterized.[33,34] The Re–Re bond length of 2.682 Å (compared with that of 2.616 Å in the neutral precursor) is in accord with a bond order of 1.5 and the $\sigma^2\pi^2\delta^{*2}\delta^1$ electronic configuration. Although $[(\eta\text{-}C_5H_5)_2Co][Re_2Cl_6(dppm)_2]$ has not yet been structurally characterized, its electronic configuration is believed to be $\sigma^2\pi^2\delta^{*2}\delta^2\pi^{*1}$, which is also representative of a metal–metal bond order of 1.5.

Of relevance to the studies on $Re_2Cl_6(dppm)_2$ has been the recent isolation and full structural characterization of the stoichiometrically homologous compounds $Nb_2Cl_6(dmpm)_2$,[35] $Ta_2Cl_6(dmpm)_2$,[36] $Mo_2Cl_6(dppm)_2$,[36] and $Ru_2Cl_6(dmpm)_2$.[36] The structural features for this series of five complexes are very similar and the variations in M–M bond lengths through the d^2–d^2(Nb, Ta), d^3–d^3 (Mo), d^4–d^4(Re) and d^5–d^5(Ru) series of metal atom pairs is consistent with the following electronic configurations: $\sigma^2\pi^2$, $\sigma^2\pi^2\delta^{*2}$, $\sigma^2\pi^2\delta^{*2}\delta^2$ and $\sigma^2\pi^2\delta^{*2}\delta^2\pi^{*2}$.[36] The ditungsten(III) analogue $W_2Cl_6(dppm)_2$ has recently been prepared by the reaction of $W_2Cl_6(THF)_4$ with dppm,[37] but it has not yet been structurally characterized although its monohydrido derivative $W_2(\mu\text{-}H)(\mu\text{-}Cl)Cl_4(\mu\text{-}dppm)_2$ has.[21]

B. PHOSPHINE-BRIDGED DIMETAL COMPLEXES THAT CONTAIN ISOCYANIDE, NITRILE AND CARBONYL LIGANDS

Multiply bonded dimetal complexes that contain monodentate phosphines react with the π-acceptor ligands CO, NO and the alkyl and aryl isocyanides to form mononuclear cleavage products.[38] Recent examples include the carbonylation of $[Re_2Cl_4(PMe_2Ph)_4]^{n+}$ (n = 0, 1 or 2) to give the carbonyl derivatives $ReCl(CO)_3(PMe_2Ph)_2$, $ReCl(CO)_2(PMe_2Ph)_3$ and $ReCl_3(CO)(PMe_2Ph)_3$[39] and the mixed isocyanide–phosphine salts of stoichiometry $[Re(CNR)_4(PR'_3)_2]PF_6$ and $[Re(CNR)_4(PEtPh_2Cl_2]PF_6$ (R = t-Bu or cyclohexyl, R' = Et or n-Pr) from the reactions of $Re_2Cl_4(PR_3)_4$ and $Re_2Cl_6(PEtPh_2)_2$, respectively, with isocyanides.[40] While these cleavage reactions are of considerable synthetic value, relatively little information regarding the mechanisms involved has been gathered since these reactions are quite facile and are difficult to control.

By resorting to the phosphine-bridged complexes $Re_2X_4[R_2P(CH_2)_nPR_2]_2$ (X = halogen, R = alkyl or aryl, n = 1 or 2) we have found that cleavage by carbonyls, isocyanides and nitriles is prevented, presumably due to the very stable Re–Re–P(CH$_2$)$_n$P rings that are formed,* and we have developed the chemistry of these particular class of multiply bonded complexes extensively.

B(i) *Isocyanide derivatives*

$Re_2Cl_4(dppm)_2$ reacts readily with one equivalent of an isocyanide, RNC (R = Me, t-Bu or xylyl), to form the mono-isocyanide adducts $Re_2Cl_4(dppm)_2(CNR)$ in high yield.[41] The ^{1}H NMR spectrum of the t-butyl derivative is in accord with the complex possessing an A-frame type structure (**2**), and an X-ray crystal structure analysis[42] has indeed confirmed this. However, refinement of the structure was frustrated by a disorder problem which involves the Cl and t-BuNC ligands *trans* to the bridging Cl ligand. Nevertheless, an Re–Re distance of 2.30(1) Å is indicative of a multiple bond which is slightly longer than that in the parent complex.[24] A qualitative treatment of the bonding in this complex, a member of a rare class of $M_2(\mu\text{-}L)L_8$ species possessing the A-frame type structure, predicts a slightly weakened triple bond.[42] An especially interesting property of these compounds is the fact that two ν(C≡N) modes at frequencies characteristic of a terminally coordinated RNC ligand are observed in the IR spectra of Nujol mulls, CH_2Cl_2 and benzene solutions. These findings indicate that the complexes exist as a mixture of isomers but only one of which forms suitable crystals for a crystallographic determination. These isomers interconvert rapidly on the NMR time scale.

The bromide derivatives of these isocyanides, viz. $Re_2Br_4(dppm)_2(CNR)$, have also been prepared[42] and show very similar properties to their chloride analogues. Oxidation of these complexes using $NOPF_6$ forms $[Re_2X_4(dppm)_2(CNR)]PF_6$ (X = Cl or Br)[42] which show one ν(C≡N) mode in their IR spectra, indicating that only a single isomer is now present in each case.

The treatment of $Re_2Cl_4(dppm)_2$ with two equivalents of t-BuNC in acetone in the presence of PF_6^- gives yellow and green isomers of stoichiometry $[Re_2Cl_3(dppm)_2(CN\text{-}t\text{-}Bu)_2]PF_6$.[41,43] A comparison of their IR, ^{1}H NMR and ^{31}P–{^{1}H} NMR spectra show that these isomers are structurally very different. Based upon the similarities between the electrochemical redox properties, electronic absorption spectra and NMR spectral properties of these two complexes and related bis-nitrile and mixed isocyanide–nitrile species (*vide infra*) they are suggested to have structures **3a** and **3b**. A novel complex which contains a μ-iminyl ligand

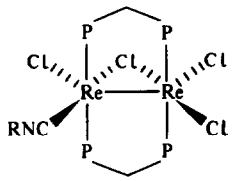

2

R = t-Bu

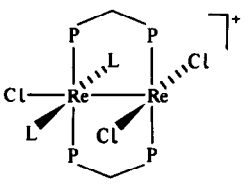

3a

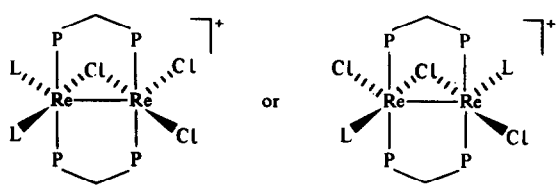

3b

L = t-BuNC

*Both kinetic and thermodynamic factors presumably contribute to the stability of these rings.

$[Re_2Cl_3(dppm)_2(\mu\text{-}C{=}NH\text{-}t\text{-}Bu)(CN\text{-}t\text{-}Bu)_2]PF_6$ has been isolated as a by-product in the synthesis of the green isomer and has been structurally characterized.[43,44] This blue, paramagnetic complex exhibits a well-defined X-band ESR spectrum which may be explained by the fact that the μ-C=NH-*t*-Bu ligand (which symmetrically bridges the two rhenium atoms) is bound as an iminyl moiety with a net -1 charge, giving rise to a Re_2^{5+} core that contains one unpaired electron.

When $Re_2Cl_4(dppm)_2$ is reacted with 3 equivalents of *t*-BuNC in the presence of KPF_6 the green tris-isocyanide complex $[Re_2Cl_3(dppm)_2(CN\text{-}t\text{-}Bu)_3]PF_6$ is produced.[43] This salt and its xylylNC derivative can also be prepared via an alternative route using a mixed isocyanide–nitrile containing species [see Section B(iii)]. While the stoichiometries of these two complexes are identical, their electrochemical redox properties are very different. This suggests that they may be structural isomers. Reduction of the monocation $[Re_2Cl_3(dppm)_2(CNxylyl)_3]PF_6$ with cobaltocene yields the neutral paramagnetic complex $Re_2Cl_3(dppm)_2(CNxylyl)_3$ containing (formally speaking at least) the rare Re_2^{3+} core, while oxidation with $NOPF_6$ gives the paramagnetic dication $[Re_2Cl_3(dppm)_2(CNxylyl)_3](PF_6)_2$ possessing a Re_2^{5+} core. The related *t*-BuNC derivative $[Re_2Cl_3(dppm)_2(CN\text{-}t\text{-}Bu)_3]PF_6$ does not possess any reversible redox chemistry.

A study has recently been carried out which details the reactions of $Mo_2X_4(dppm)_2$ (X = Cl, Br or I) with isocyanide ligands.[14] With one equivalent of RNC (R = *i*-Pr or *t*-Bu) in the presence of $TlPF_6$ (in THF) or KPF_6 (in acetone), the complexes $[Mo_2X_3(dppm)_2(CNR)]PF_6$ are formed. These are the first examples of multiply bonded Mo_2^{4+} complexes that contain coordinated π-acceptor RNC ligands. Reactions with an excess of RNC lead to seven-coordinate mononuclear $[MoX(dppm)(CNR)_4]^+$ and thence to other mononuclear isocyanide-containing species.[14]

B(ii) *Nitrile derivatives*

Nitriles (RCN) also react very readily with $Re_2Cl_4(dppm)_2$ in the presence of KPF_6 to yield the stable, ionic, bis-nitrile complexes $[Re_2Cl_3(dppm)_2(NCR)_2]PF_6$ (R = Me, Et, Ph or 4-PhC_6H_4).[45] These reactions proceed via the intermediacy of rather unstable neutral 1:1 adducts. The 1:2 benzonitrile derivative has been structurally characterized and has both nitrile ligands coordinated to the same rhenium atom (**4**). The Re–Re bond length of 2.270 Å is greater than that generally

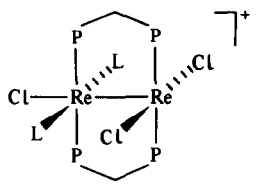

4

L = R'CN

observed in neutral triply bonded dirhenium compounds, and may be explained by the fact that there is a contraction of the Re–Re σ and π bonding orbitals due to the increased positive charge on the molecule, and also the presence of an axially coordinated chloride ligand. The molecule is staggered with a P–Re–Re–P torsion angle of 22°. The bis-nitrile salts react cleanly with $NOPF_6$ to generate the paramagnetic ESR-active dications $[Re_2Cl_3(dppm)_2(NCR)_2](PF_6)_2$[34] which possess the Re_2^{5+} core and a $\sigma^2\pi^4\delta^2\delta^{*1}$ ground-state electronic configuration.

B(iii) *Mixed isocyanide–nitrile derivatives*

Treatment of the monoisocyanides $Re_2Cl_4(dppm)_2(CNR)$ (R = *t*-Bu or xylyl) with an excess of nitrile R'CN (R' = Me, Et or Ph) and KPF_6 affords the mixed isocyanide–nitrile salts $[Re_2Cl_3(dppm)_2(CNR)(NCR')]PF_6$.[43] These have very similar electrochemistry, electronic absorption and NMR spectral properties to those of the bis-nitrile salts discussed in Section B(ii). Even though no structural information is available at the present time, we believe that these complexes have a structure similar to the aforementioned bis-nitrile salts (**4**) and the green isomer $[Re_2Cl_3(dppm)_2(CN\text{-}t\text{-}Bu)_2]PF_6$ (**3a**), i.e. the isocyanide and nitrile ligands are coordinated to the same rhenium atom. These mixed-ligand salts have been oxidized chemically with $NOPF_6$ to yield the paramagnetic dications $[Re_2Cl_3(dppm)_2(CNR)(NCR')](PF_6)_2$ which show[43] complex ESR spectra comparable to those of the bis-nitrile species.[34]

As mentioned in Section B(i), the tris-isocyanide complex $[Re_2Cl_3(dppm)_2(CN\text{-}t\text{-}Bu)_3]PF_6$ is synthesized readily from $Re_2Cl_4(dppm)_2$ and three equivalents of *t*-BuNC. An alternative synthesis is provided through the reaction between $[Re_2Cl_3(dppm)_2(CN\text{-}t\text{-}Bu)(NCEt)]PF_6$ and *t*-BuNC, i.e. substitution of a nitrile by an isocyanide along with the addition of another isocyanide. There is no evidence for the formation of the intermediate $[Re_2Cl_3(dppm)_2(CN\text{-}t\text{-}Bu)_2]PF_6$ which would be expected to occur if a simple

displacement of a nitrile by an isocyanide were the first step in the reaction. Related to this is the reaction between $[Re_2Cl_3(dppm)_2(CNxylyl)(NCPh)]PF_6$ and 2.5 equivalents of xylylNC to give the tris-xylyl isocyanide salt $[Re_2Cl_3(dppm)_2(CNxylyl)_3]PF_6$.[43]

The reactions of $Re_2Cl_4(dppm)_2$ with isocyanide and nitrile ligands which have been discussed in Sections B(i)–(iii) are summarized in Scheme 1.

B(iv) *Carbonyl derivatives*

The isoelectronic nature of CO and isocyanides has prompted a thorough investigation of the reactions between $Re_2X_4(dppm)_2$ (X = Cl or Br) and CO.[46,47] The red monocarbonyls $Re_2X_4(dppm)_2(CO)$ are formed readily when CO is bubbled through a dichloromethane solution of the starting complex for 5 min. Two $\nu(C{\equiv}O)$ modes are observed in the IR spectra (Nujol mull and solution) and these vary in their relative intensities depending on the solvent used. This information, along with NMR spectral data which clearly indicates that a fluxional process is occuring in solution, suggests that isomers are present as is the case for the monoisocyanide species $Re_2X_4(dppm)_2(CNR)$.[41,42] A mechanism which is entirely in accord with the ^1H, ^{13}C and ^{31}P NMR spectral data has been proposed.[46,47] An X-ray crystal structure determination of the chloride derivative on crystals grown from a mixture of CH_2Cl_2 and benzene (5) reveals the characteristic A-frame-like

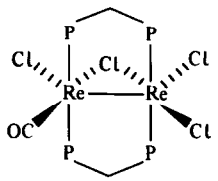

5

structure in which the CO ligand is *trans* to the bridging chloride. The observed Re–Re distance of 2.338 Å is consistent with a triple bond, but an accurate appraisal of the electronic configuration of this species is not yet at hand. However, a qualitative treatment of the bonding[42] in these types of molecules is consistent with the presence of a slightly weakened triple bond.

If CO is bubbled into a CH_2Cl_2 solution of $Re_2Cl_4(dppm)_2$ [or $Re_2Cl_4(dppm)_2(CO)$] for 3 h, the green dicarbonyl $Re_2Cl_4(dppm)_2(CO)_2$ is formed in which one CO ligand bridges the Re–Re bond and the other remains terminal.[46] This dicarbonyl has been characterized by X-ray crystallography, but due to a disorder problem it is impossible to say if the two CO ligands are *cis* or *trans* to each other with respect to the Re–Re axis. However, in light of the reactions of this dicarbonyl with isocyanides and nitriles (*vide infra*), we suggest that the CO ligands are *cis* to one another and reside on the same side of the molecule as in **6**. The Re–Re bond distance of 2.584 Å is far longer than bonds observed in triply bonded complexes with a Re_2^{4+} core. Accordingly, this dicarbonyl can be viewed[46] as containing a Re_2^{6+} core by regarding the bridging CO as divalent, and hence giving rise to a $\sigma^2\pi^2\delta^{*2}\delta^2$ configuration, i.e. a double bond.

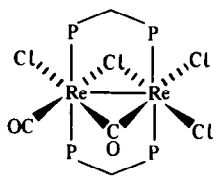

6

B(v) *Mixed carbonyl–isocyanide derivatives*

The monocarbonyl $Re_2Cl_4(dppm)_2(CO)$ reacts with 1 equivalent of an isocyanide to form the neutral complexes of stoichiometry $Re_2Cl_4(dppm)_2(CO)(CNR)$ (R = *i*-Pr, *t*-Bu, xylyl or mesityl).[47] A comparison of their IR spectral properties shows that the alkyl isocyanide derivatives have both π-acceptor ligands terminally bound, but the CO ligand in the aryl isocyanide derivatives bridges the Re–Re bond while the isocyanide remains terminal. Their electrochemical properties and hence their electronic configurations are very different. An X-ray crystal structure of $Re_2Cl_4(dppm)_2(CO)(CNxylyl)$[47] has shown that the CO and xylylNC ligands are *cis* to one another and the Re–Re bond distance of 2.581 Å, which is very close to that of the dicarbonyl $Re_2Cl_4(dppm)_2(CO)_2$,[46] is consistent with an Re–Re double bond. A twinning problem with the crystals of the alkyl isocyanide derivatives have so far prevented us from obtaining any structural data on these unique complexes.

The dicarbonyl reacts with isocyanides in the presence of $TlPF_6$ to give the salts $[Re_2Cl_3(dppm)_2(CO)_2(CNR)]PF_6$ (R = *i*-Pr, *t*-Bu or xylyl).[48,49] No structural information is available on these salts but we suspect that all three chlorides lie on the same side of the molecule, since an X-ray crystal structure on the reduced isopropyl isocyanide complex $Re_2Cl_3(dppm)_2(CO)_2(CN\text{-}i\text{-}Pr)$[49] (*vide infra*) shows this *all-cis* arrangement of ligands. These dicarbonyl–monoisocyanide complexes may be prepared by using two other synthetic procedures, viz. either by stirring the monoisocyanide

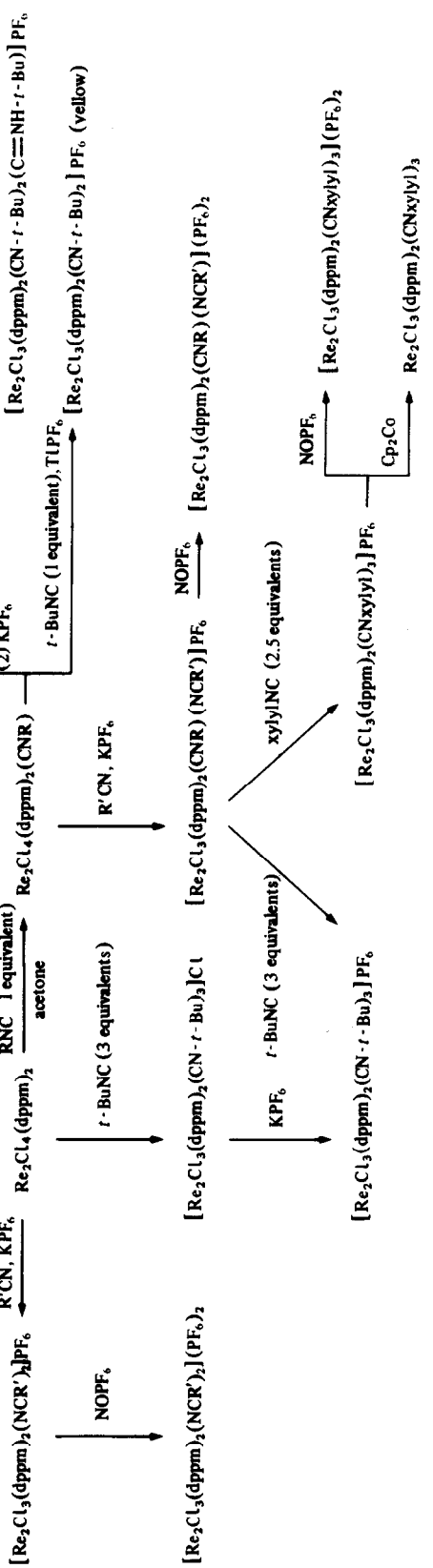

Scheme 1. Reactions of $Re_2Cl_4(dppm)_2$ with isocyanides and nitriles.

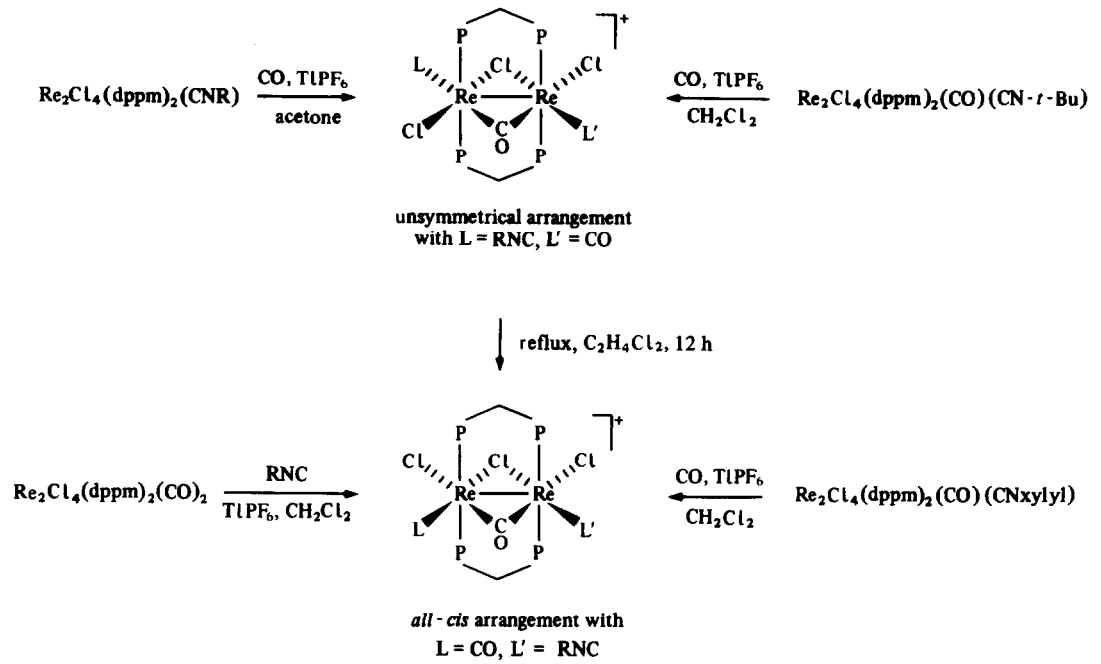

Scheme 2. Synthesis and isomerization of $[Re_2Cl_3(dppm)_2(CO)_2(CNR)]PF_6$ (R = *t*-Bu or xylyl).

$Re_2Cl_4(dppm)_2(CNR)$ or the mixed carbonyl–isocyanide $Re_2Cl_4(dppm)_2(CO)(CNR)$ under an atmosphere of CO in the presence of $TlPF_6$.[49] However, depending on the isocyanide used (*t*-BuNC or xylyl), isomers are formed. The isomer derived from $Re_2Cl_4(dppm)_2(CNR)$ (R = *t*-Bu or xylyl) and $Re_2Cl_4(dppm)_2(CO)(CN\text{-}t\text{-}Bu)$ possesses an unsymmetric arrangement of ligands in the equatorial plane as confirmed by an X-ray crystal structure of $[Re_2Cl_3(dppm)_2(CO)_2(CN\text{-}t\text{-}Bu)]PF_6$ (prepared from the reaction of $Re_2Cl_4(dppm)_2(CN\text{-}t\text{-}Bu)$ with CO–$TlPF_6$). These results are summarized in Scheme 2. However, isomerization to the *all-cis* derivatives occurs upon heating $C_2H_4Cl_2$ solutions of these species over a period of 12 h. This thermal conversion, which leads to some decomposition, must involve bond breaking and reforming. We conclude, therefore, that the *all-cis* configuration is the thermodynamically stable form.

Reduction of these mixed carbonyl–isocyanide salts to the neutral, paramagnetic species $Re_2Cl_3(dppm)_2(CO)_2(CNR)$,[48,49] has been achieved either chemically using cobaltocene, or electrochemically in $n\text{-}Bu_4NPF_6$–CH_2Cl_2 solutions. The X-ray crystal structure of $Re_2Cl_3(dppm)_2(CO)_2(CN\text{-}i\text{-}Pr)$,[49] derived from the dicarbonyl, shows the *all-cis* arrangement of chloride ligands. An Re–Re distance of 2.718 Å is in accord with the complex possessing a $\sigma^2\pi^2\delta^{*2}\delta^2\pi^{*1}$ electronic configuration; this gives rise to a bond order of 1.5 if we regard the bridging CO as divalent, i.e. an Re_2^{5+} core complex.

B(vi) *Mixed carbonyl–nitrile derivatives*

Salts of stoichiometry $[Re_2Cl_3(dppm)_2(CO)(NCR')_2]F_6$[47] and $[Re_2Cl_3(dppm)_2(CO)_2(NCR')]PF_6$[48] (R' = Me, Et or Ph) may be prepared by reacting the mono or dicarbonyls, respectively, with an excess of nitrile in the presence of $TlPF_6$. An X-ray crystal structure of $[Re_2Cl_3(dppm)_2(CO)_2(NCEt)]PF_6$[48] shows the now familiar *all-cis* arrangement of ligands. The Re–Re bond length of 2.586 Å is almost identical with the value of 2.584 Å found in $Re_2Cl_4(dppm)_2(CO)_2$[46] and 2.581 Å in $Re_2Cl_4(dppm)_2(CO)(CNxylyl)$.[47] While the salts $[Re_2Cl_3(dppm)_2(CO)(NCR')_2]PF_6$ have not yet been subject to any crystallographic characterization, their ^1H and $^{31}P\text{-}\{^1H\}$ NMR spectral properties[47] suggest strongly that these complexes must also possess the *all-cis* arrangement of ligands. Although the dicarbonyl complexes can be reduced by cobaltocene to give the fairly air-stable neutral species $Re_2Cl_3(dppm)_2(CO)_2(NCR')$,[48] the bis-nitrile salts are more difficult to reduce and yield the highly air-sensitive $Re_2Cl_3(dppm)_2(CO)(NCR')_2$.[50] This is in accord with the notion that two π-acceptors (in this case CO) are more effective than one at stabilizing low oxidation states.

As discussed in Section B(iii), nitrile ligands have been found to undergo substitution by isocyanides. We have discovered that $[Re_2Cl_3(dppm)_2(CO)_2(NCEt)]PF_6$ reacts with RNC to yield $[Re_2Cl_3(dppm)_2(CO)_2(CNR)]PF_6$[48,50] and free

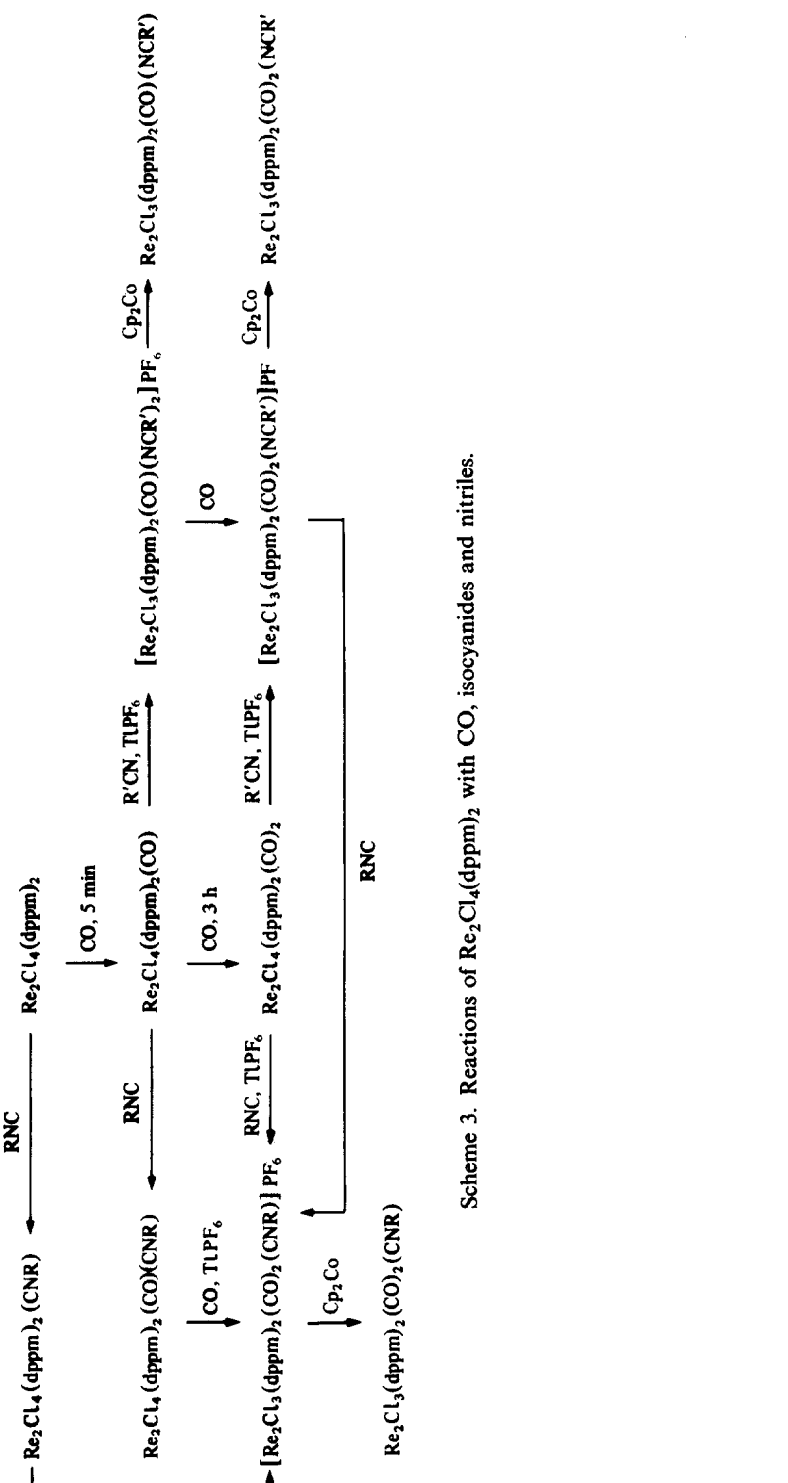

Scheme 3. Reactions of $Re_2Cl_4(dppm)_2$ with CO, isocyanides and nitriles.

nitrile, and $[Re_2Cl_3(dppm)_2(CO)(NCR')_2]PF_6$(R' = Me or Et) reacts with CO to form $[Re_2Cl_3(dppm)_2(CO)_2(NCR')]PF_6$.[50] The latter complex does not react further with CO, although we are still investigating the possibility of synthesizing the tricarbonyl $[Re_2Cl_3(dppm)_2(CO)_3]PF_6$ and a mixed carbonyl–isocyanide–nitrile $[Re_2Cl_3(dppm)_2(CO)(CNR)(NCR')]PF_6$ by this means.

Scheme 3 summarizes the reactions of $Re_2Cl_4(dppm)_2$ with isocyanides, nitriles and CO.

Acknowledgements—Our work in this area has been generously supported by grants from the National Science Foundation. Thanks are due to current members of our research group whose contributions are cited throughout this review. Special acknowledgements are due to Drs T. J. Barder, K. R. Dunbar and L. B. Anderson for their past contributions. Much of the recent structural work described has been carried out by Dr P. E. Fanwick of this department. We also acknowledge a continuing fruitful collaboration with Professor F. A. Cotton of Texas A&M University.

REFERENCES

1. R. J. Puddephatt, *Chem. Soc. Rev.* 1983, 99.
2. S. A. Best, T. J. Smith and R. A. Walton, *Inorg. Chem.* 1978, **17**, 99.
3. F. A. Cotton, P. E. Fanwick, J. W. Fitch, H. D. Glicksman and R. A. Walton, *J. Am. Chem. Soc.* 1979, **101**, 1752.
4. E. H. Abbott, K. S. Bose, F. A. Cotton, W. T. Hall and J. C. Sekutowski, *Inorg. Chem.* 1978, **17**, 3240.
5. R. R. Schrock, L. G. Sturgeoff and P. R. Sharp, *Inorg. Chem.* 1983, **22**, 2801.
6. F. A. Cotton, M. W. Extine, T. R. Felthouse, B. W. Kolthammer and D. G. Lay, *J. Am. Chem. Soc.* 1981, **103**, 4040.
7. F. A. Cotton and T. R. Felthouse, *Inorg. Chem.* 1981, **20**, 3880.
8. J. R. Ebner, D. R. Tyler and R. A. Walton, *Inorg. Chem.* 1976, **15**, 833.
9. F. A. Cotton, G. G. Stanley and R. A. Walton, *Inorg. Chem.* 1978, **17**, 2099.
10. N. F. Cole, F. A. Cotton, G. L. Powell and T. J. Smith, *Inorg. Chem.* 1983, **22**, 2618.
11. F. A. Cotton and R. A. Walton, *Multiple Bonds between Metal Atoms.* J. Wiley, New York (1982) (and references cited therein).
12. R. A. Walton, *Isr. J. Chem.* 1985, **25**, 196.
13. F. A. Cotton and R. A. Walton, *Struct. Bonding (Berlin)* 1985, **62**, 1.
14. W. S. Harwood, J-S. Qi and R. A. Walton, *Polyhedron* 1986, **5**, 15.
15. F. A. Cotton, K. R. Dunbar and R. Poli, *Inorg. Chem.* 1986, **25**, 3700.
16. F. L. Campbell III, F. A. Cotton and G. L. Powell, *Inorg. Chem.* 1984, **23**, 4222.
17. P. E. Fanwick, W. S. Harwood and R. A. Walton, *Inorg. Chim. Acta* 1986, **122**, 7.
18. F. A. Cotton and K. R. Dunbar and M. Matusz, *Inorg. Chem.*, 1986, **25**, 3641.
19. F. A. Cotton, L. R. Falvello, W. S. Harwood, G. L. Powell and R. A. Walton, *Inorg. Chem.* 1986, **25**, 3949.
20. F. L. Campbell III, F. A. Cotton and G. L. Powell, *Inorg. Chem.* 1985, **24**, 4384.
21. P. E. Fanwick, W. S. Harwood and R. A. Walton, *Inorg. Chem.* (accepted).
22. R. T. Carlin and R. E. McCarley, unpublished results.
23. A. R. Cutler, D. R. Derringer and R. A. Walton, unpublished work.
24. T. J. Barder, F. A. Cotton, K. R. Dunbar, G. L. Powell, W. Schwotzer and R. A. Walton, *Inorg. Chem.* 1985, **24**, 2550.
25. L. B. Anderson, F. A. Cotton, L. R. Falvello, W. S. Harwood, D. Lewis and R. A. Walton, *Inorg. Chem.* 1986, **25**, 3637.
26. D. R. Root, C. H. Blevins, D. L. Lichtenberger, A. P. Sattelberger and R. A. Walton, *J. Am. Chem. Soc.* 1986, **108**, 953.
27. P. E. Fanwick, D. R. Root and R. A. Walton, *Inorg. Chem.* 1986, **25**, 4832.
28. L. B. Anderson-Lane, Ph.D. thesis, Purdue University (1985).
29. P. E. Fanwick, M. A. Bakir and R. A. Walton, unpublished work.
30. I. F. Fraser and R. D. Peacock, *J. Chem. Soc., Chem. Commun.* 1985, 1727.
31. P. A. Agaskar, F. A. Cotton, I. F. Fraser and R. D. Peacock, *J. Am. Chem. Soc.* 1984, **106**, 1851.
32. T. J. Barder, F. A. Cotton, D. Lewis, W. Schwotzer, S. M. Tetrick and R. A. Walton, *J. Am. Chem. Soc.* 1984, **106**, 2882.
33. K. R. Dunbar, D. Powell and R. A. Walton, *J. Chem. Soc., Chem. Commun.* 1985, 114.
34. K. R. Dunbar, D. Powell and R. A. Walton, *Inorg. Chem.* 1985, **24**, 2842.
35. F. A. Cotton, S. A. Duraj, L. R. Falvello and W. J. Roth, *Inorg. Chem.* 1985, **24**, 4389.
36. A. R. Chakravarty, F. A. Cotton, M. P. Diebold, D. B. Lewis and W. J. Roth, *J. Am. Chem. Soc.* 1986, **108**, 971.
37. W. S. Harwood and R. A. Walton, unpublished work.
38. R. A. Walton, *ACS Symp. Ser.* 1981, **155**, 207 (and references cited therein).
39. K. R. Dunbar and R. A. Walton, *Inorg. Chim. Acta* 1984, **87**, 185.
40. J. D. Allison, T. E. Wood, R. E. Wild and R. A. Walton, *Inorg. Chem.* 1982, **21**, 3540.
41. L. B. Anderson, T. J. Barder and R. A. Walton, *Inorg. Chem.* 1985, **24**, 1421.
42. L. B. Anderson, T. J. Barder, D. Esjornson, R. A. Walton and B. E. Bursten, *J. Chem. Soc., Dalton Trans.* (accepted for publication).
43. L. B. Anderson, T. J. Barder, F. A. Cotton, K. R. Dunbar, L. R. Falvello and R. A. Walton, *Inorg. Chem.* 1986, **25**, 3629..

44. T. J. Barder, D. Powell and R. A. Walton, *J. Chem. Soc., Chem. Commun.* 1983, 550.
45. T. J. Barder, F. A. Cotton, L. R. Falvello and R. A. Walton, *Inorg. Chem.* 1985, **24**, 1258.
46. F. A. Cotton, L. M. Daniels, K. R. Dunbar, L. R. Falvello, S. M. Tetrick and R. A. Walton, *J. Am. Chem. Soc.* 1985, **107**, 3524.
47. F. A. Cotton, K. R. Dunbar, A. C. Price, W. Schwotzer and R. A. Walton, *J. Am. Chem. Soc.* 1986, **108**, 4843.
48. F. A. Cotton, K. R. Dunbar, L. R. Falvello and R. A. Walton, *Inorg. Chem.* 1985, **24**, 4180.
49. L. B. Anderson, F. A. Cotton, K. R. Dunbar, L. R. Falvello, A. C. Price, A. H. Reid and R. A. Walton, *Inorg. Chem.* (submitted).
50. A. C. Price and R. A. Walton, unpublished work.

Polyhedron Vol. 6, No. 4, pp. 741–757, 1987
Printed in Great Britain

0277–5387/87 $3.00+.00
Pergamon Journals Ltd

SYNTHESIS AND CHARACTERIZATION OF BINUCLEAR TANTALUM HYDRIDE COMPLEXES*

A. J. SCIOLY, M. L. LUETKENS, Jr†, and R. B. WILSON, JR

Department of Chemistry, The University of Michigan, Ann Arbor, MI 48109, U.S.A.

J. C. HUFFMAN

Molecular Structure Center, Indiana University, Bloomington, IN 47405, U.S.A.

and

A. P. SATTELBERGER‡

Inorganic and Structural Chemistry Group (INC-4), Los Alamos National Laboratory, Los Alamos, NM 87545, U.S.A.

(*Received* 19 *November* 1986)

Abstract—Reduction of the quadruply-bridged (2Cl, 2H) tantalum(IV) dimer, $Ta_2Cl_6(PMe_3)_4H_2$ (**2**) with sodium amalgam in glyme or THF at 0°C provides deep green $Ta_2Cl_4(PMe_3)_4H_2$ (**3**) in 70% yield. Dimer **3** has a D_{2d} $Ta_2Cl_4(PMe_3)_4$ substructure which closely resembles that of the quadruply metal–metal-bonded dimer $W_2Cl_4(PMe_3)_4$. The hydride ligands of **3** are located on a diagonal plane, bridging the two tantalum atoms and the Ta–Ta separation is 2.545(1) Å. **3** reacts cleanly with Cl_2, HCl and H_2 in diethyl ether to provide the quadruply-bridged dimers **2**, $Ta_2Cl_5(PMe_3)_4H_3$ (**4**), and $Ta_2Cl_4(PMe_3)_4H_4$ (**5**), respectively, in high yield. Dimer **5** can also be prepared in high yield via thermolysis of the tantalum(IV) hydride $TaCl_2H_2(PMe_3)_4$ (**6**) in refluxing methylcyclohexane. The X-ray structure of **5** shows that the $(\mu\text{-H})_4$ group is staggered by 45° with respect to the eclipsed pyramidal $TaCl_2(PMe_3)_2$ end groups. The molecular symmetry of **5** is D_{2d} and the Ta–Ta separation is 2.511(2)Å. Multiple-scattering Xα calculations on the model compounds $Ta_2Cl_4(PH_3)_4H_2$ and $Ta_2Cl_4(PH_3)_4$ are used to elucidate the ground-state electronic structures of **3** and **5**, and to probe the question of $(\mu\text{-H})_x$ rotation about the metal–metal bonds in these complexes. Crystal data (at 160°C) are as follows: for **3**, monoclinic space group $C2/c$, $a = 18.371(5)$ Å, $b = 9.520(3)$ Å, $c = 18.942(6)$ Å, $\beta = 125.36(2)°$, $V = 2701.8$ Å^3, $Z = 4$, $d_{calc.} = 1.991$ g cm^{-3}; for **5**, tetragonal space group $P4/nbm$, $a = b = 12.579(2)$ Å, $c = 10.205(2)$ Å, $V = 1614.7$ Å^3, $Z = 2$, $d_{calc.} = 1.670$ g cm^{-3}.

The great propensity with which molybdenum and tungsten form metal–metal-bonded dinuclear complexes[2] might lead one to expect the same of their group 5 neighbors, niobium and tantalum. Operating under this assumption, we set out, several years ago, to prepare a number of low-valent ditantalum complexes. Our choice of target molecules was influenced by a report[3] on the syntheses of $W_2Cl_6(PMe_3)_4$ and $W_2Cl_4(PMe_3)_4$. These dimers were obtained by sodium amalgam reduction of polymeric tungsten(IV) chloride in THF, in the presence of trimethylphosphine (PMe_3), and we reasoned that their tantalum(III) and tantalum(II) analogues could be prepared in a similar fashion. This logic held up in the case of $Ta_2Cl_6(PMe_3)_4$ (**1**). Reduction of tantalum(V) chloride with sodium amalgam (2 equivalents) in toluene–PMe_3 provides burgundy red **1** in good yield.[4] The latter adopts

*Metal–metal bonded complexes of the early transition metals—XI. For Part X, see Ref. 1.

†Dow Britton Fellow (1983–1984).

‡Author to whom correspondence should be addressed.

an edge-sharing bioctahedral geometry with axial phosphines on one metal center and equatorial phosphines on the second, and it contains a formal Ta–Ta double bond, represented by a $\sigma^2\pi^2$ ground-state electronic configuration. The synthesis of $Ta_2Cl_4(PMe_3)_4$, a molecule which should contain an unbridged Ta–Ta triple bond ($\sigma^2\pi^4$), has not been achieved. Treatment of **1** with a variety of powerful reducing agents (e.g. NaNp and Na–K) failed to effect its conversion to the desired product. This disappointing result was offset by our observation that the Ta=Ta bond in **1** could be hydrogenated under mild conditions (25°C, 1 atm H_2).[5] The hydrogenation product, viz. $Ta_2Cl_6(PMe_3)_4H_2$ (**2**) is a quadruply-bridged (2Cl, 2H) dimer with pyramidal $TaCl_2(PMe_3)_2$ end groups. Subsequently, we discovered that **2** could be reduced to $Ta_2Cl_4(PMe_3)_4H_2$ (**3**), a doubly hydrogen-bridged tantalum(III) dimer, which may be viewed as the hydrogenation product of the elusive $Ta_2Cl_4(PMe_3)_4$. In this paper, we describe: (1) the synthesis, physicochemical properties and X-ray structure of **3**; (2) the reactions of **3** with Cl_2, HCl and H_2; (3) the X-ray structure of the hydrogenation product, $Ta_2Cl_4(PMe_3)_4H_4$, a molecule with four bridging hydrides; and (4) the electronic structures of **3** and $Ta_2Cl_4(PMe_3)_4H_4$. Preliminary reports of certain aspects of this work have been published.[6,7]

RESULTS

Synthesis and characterization of 3

Reduction of **2** with 2 equivalents of sodium amalgam in ethylene glycol dimethyl ether (glyme) or THF [eqn (1)]:

$$\underset{\mathbf{2}}{Ta_2Cl_6(PMe_3)_4H_2} + 2Na\text{–}Hg \xrightarrow[4\,h,\,0°C]{THF} \underset{\mathbf{3}}{Ta_2Cl_4(PMe_3)_4H_2} + 2NaCl \quad (1)$$

at 0°C provides deep green solutions containing **3**. The latter is isolated as a dark green powder after filtration, solvent removal, extraction of the solid residue with diethyl ether, filtration, and evaporation of the filtrate. These operations provide a spectroscopically pure product in *ca* 70% yield. If only 1 equivalent of sodium amalgam is used, an approximately 1:1 mixture of **2** and **3** is obtained. There is no spectroscopic evidence (NMR or ESR) for the presumed intermediate in the reduction, $Ta_2Cl_5(PMe_3)_4H_2$.

Dimer **3** is very air-sensitive in the solid state, decomposing within seconds after exposure to laboratory air. It is soluble in ethereal and aromatic solvents, and slightly soluble in hexane. **3** decomposes rapidly in chloroform, methylene chloride and acetonitrile. Well-defined products were not obtained from these reactions. The dimeric formulation was established by an osmometric molecular weight measurement in benzene (Calc: 810; Found: 813). Attempts to obtain electron impact or chemical ionization mass spectra were unsuccessful. PMe_3 was the only gas-phase species observed.

The presence, number and location of the hydride ligands were established by NMR and IR techniques. The room-temperature 360-MHz proton NMR spectrum of **3** is shown in Fig. 1. The binomial quintet ($^2J_{PH}$ = 13.4 Hz) at δ 8.52 (area 2) is assigned to a pair of chemically and magnetically equivalent bridging hydride ligands. The resonance at δ 1.52 (area 36) is due to the methyl hydrogens of virtually coupled pseudo-*trans* PMe_3 ligands. The ^{31}P–$\{^1H\}$ NMR spectrum consists of a single resonance at δ + 1.3 which splits into a 1:2:1 triplet ($^2J_{PH}$ = 13.4 Hz) upon selective ^1H-decoupling of the proton NMR resonance at δ 1.52. No significant changes were observed in either the ^1H or ^{31}P NMR spectra on cooling toluene-d_8 solutions of **3** to −90°C.

The location of the hydride ligands in bridging positions is supported by the IR spectra (KBr disc) of $Ta_2Cl_4(PMe_3)_4H_2$ and $Ta_2Cl_4(PMe_3)_4D_2$. The former shows a band of moderate intensity at 1232 cm^{-1} which shifts to 860 cm^{-1} in the spectrum of the deuteride (ν_H/ν_D = 1.43). We assign these bands as the Ta–H(D)–Ta vibrations.

With the preceding data in hand, we initially assumed that **3** was an edge-sharing bioctahedral complex with C_{2h}-symmetry. Such a structure is reminiscent of those found[8,9] for $H_2W_2(CO)_8^{2-}$ and $H_2Re_2(CO)_8$ but it was rejected on steric grounds. In **1**, which has axial phosphines on one metal center and equatorial phosphines on the second, there is clear structural evidence for axial crowding, i.e. the axial ligands are bent back and the $TaCl_2(PMe_3)_2$ end groups twist away from each other.[4] Placing four phosphines in axial positions and (presumably) shortening the metal–metal bond (**1** → **3**) will certainly exacerbate the axial crowding problem. Space-filling molecular models show this quite clearly. The rejection of the C_{2h} structure, the only static model which satisfies the spectroscopic data, raised the obvious question and we turned to X-ray crystallography for the answer.

Solid state structure of 3

In the crystalline state, the compound is composed of discrete molecules of **3**. Final atomic coordinates and isotropic thermal parameters are

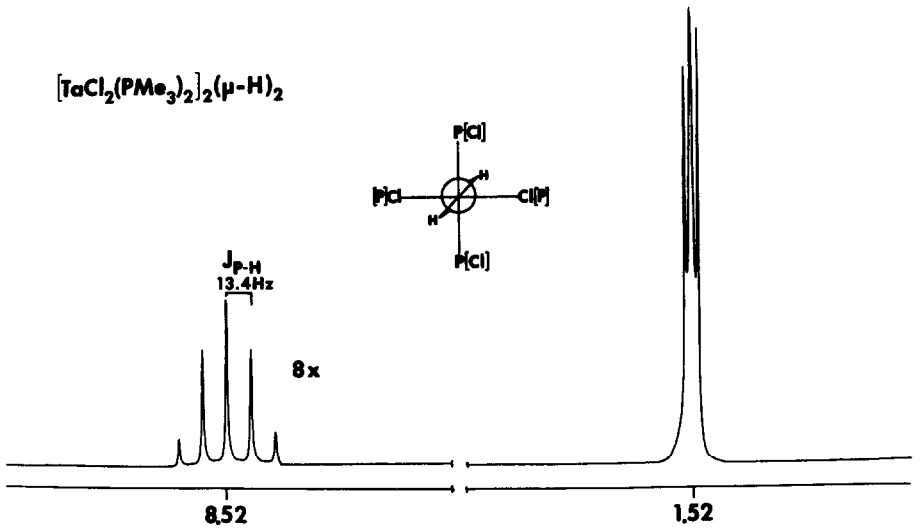

Fig. 1. 360-MHz ^{1}H NMR spectrum of $Ta_2Cl_4(PMe_3)_4H_2$. In this and the following proton NMR spectra, end-on Newman projections are included and the atoms in brackets ([ ]) are associated with the back tantalum.

Table 1. Fractional coordinates and isotropic thermal parameters for $Ta_2Cl_4(PMe_3)_4H_2$[a]

Atom	x	y	z	B_{iso}
Ta(1)	10000*	3890(1)	2500*	10
Ta(2)	10000*	6564(1)	2500*	10
Cl(3)	9743(2)	2778(3)	1227(2)	19
P(4)	8338(2)	3323(3)	1816(2)	18
P(5)	9720(2)	7129(3)	1019(2)	18
Cl(6)	8566(2)	7645(3)	1899(2)	19
C(7)	7551(9)	3978(15)	747(9)	31
C(8)	8122(10)	1453(13)	1708(11)	28
C(9)	7863(10)	3917(17)	2388(11)	33
C(10)	550(9)	6458(15)	879(9)	22
C(11)	9737(16)	9005(15)	836(12)	37
C(12)	8676(11)	6512(18)	72(10)	32

[a]Fractional coordinates are $\times 10^4$ for nonhydrogen atoms and $\times 10^3$ for hydrogen atoms. B_{iso} values are $\times 10$. Isotropic values for those atoms refined anisotropically were calculated using the formula given in: W. C. Hamilton, *Acta Cryst.* 1959, **12**, 609. Parameters marked with an asterisk (*) were not varied.

listed in Table 1. Interatomic distances and angles are provided in Table 2. An ORTEP drawing of **3**, indicating the atom-numbering scheme, is shown in Fig. 2. A two-fold axis, passing through Ta(1) and Ta(2) is required by the space group.

The structure of **3**, excluding the bridging hydrides (*vide infra*), resembles those of the quadruply metal–metal-bonded group 6 dimers $Mo_2Cl_4(PMe_3)_4$ and $W_2Cl_4(PMe_3)_4$.[10] The latter also have eclipsed pyramidal $MCl_2(PMe_3)_2$ end groups and staggered PMe_3 ligands. In **3**, the Ta–Ta–Cl and Ta–Ta–P angles average 115.7[3] and 102.0[1]°, respectively.* Corresponding values in $W_2Cl_4(PMe_3)_4$ are 111.65[9] and 101.14[4]°. The Ta–Cl and Ta–P bond lengths average 2.416[2] and 2.596[4] Å, respectively. These bond distances are comparable to those found for the axial ligands in **1**. The Ta=Ta bond length of 2.545(1) Å is, by a wide margin, the shortest metal–metal double bond yet observed in diniobium or ditantalum chemistry, and it compares favorably with the W=W bond length of 2.530(2) Å found in the isoelectronic tungsten(IV) dimer $W_2S_2(S_2CNEt_2)_4$.[11]

The next feature of **3** to consider is the bridge region. There are two conceivable locations for the hydride ligands, i.e. they are either eclipsed or staggered with respect to the terminal ligands. Our prejudice for the D_2 structure (Fig. 2) is clear but it requires some justification. A careful search of the final difference Fourier map revealed only one peak ($\sim 0.8e$ Å^{-3}) which might reasonably be assigned as H_b. It was located on the diagonal plane 1.97 Å from Ta(1) and 1.86 Å from Ta(2), and the Ta–H_b–Ta angle was 83.1°. The shortest intramolecular contact was H_b–P(5) at 2.54 Å. When the position of H_b was rotated 45° into the eclipsed C_{2v}-conformation, this contact distance shortened to 2.02 Å. These observations favor the D_2 structure but there

*The number in brackets is equal to $[\Sigma_m \Delta_i^2/m(m-1)]^{1/2}$, where Δ_i is the deviation of the ith value in a set of m such values from the arithmetic mean.

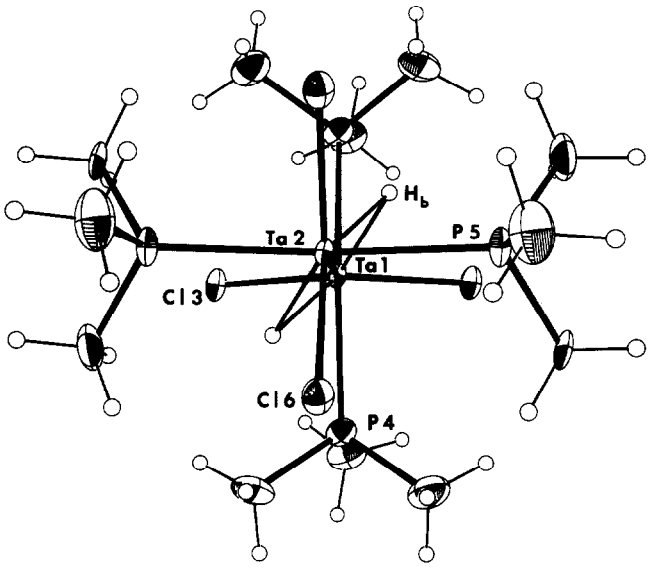

Fig. 2. ORTEP drawing of $Ta_2Cl_4(PMe_3)_4H_2$. Each nonhydrogen atom is represented by a thermal vibration ellipsoid enclosing 50% of its electron density. A crystallographic C_2-axis runs through Ta(1) and Ta(2).

are some complications. These can be summarized as follows. (1) Because of experimental difficulties (see Experimental), the X-ray data were not corrected for absorption [$\mu = 86.32\,cm^{-1}$, (Mo-K_α)]. (2) As a consequence of (1), the final difference map was not as "clean" as one would like. Several peaks of comparable or greater density than H_b were observed near the tantalum (1.5–2.1e Å^{-3}), phosphorus (<0.8e Å^{-3}) and chlorine (<0.8e Å^{-3}) atoms. (3) There are no significant distortions in the $Ta_2Cl_4(PMe_3)_4$ portion of the molecule (Table 2 and supplementary data†) which might be used as corroborating evidence for the location of H_b. In fact, given the number of possible hydride sites, one must accept the possibility that the bridging hydrides are disordered in the solid state. In view of these reservations, H_b was not included in the final stages of refinement.

A static D_2 structure cannot account for the proton NMR spectrum shown in Fig. 1 unless the two P–H coupling constants are accidentally degenerate. An alternative explanation for the apparent magnetic equivalence of $H_b(1)$ and $H_b(2)$, and the one which we favor, is rapid rotation of the bridging ligands about the Ta–Ta axis in solution. We will return to this point later on in the paper.

Reactivity of **3**

3 is very susceptible to binuclear oxidative-addition reactions. Here we describe three representative examples.

(1) Ether solutions of **3** react readily with chlorine at −20°C [eqn (2)]:

$$\underset{\mathbf{3}}{Ta_2Cl_4(PMe_3)_4H_2} + Cl_2 \xrightarrow[1\,h,\,-20°C]{OEt_2} \underset{\mathbf{2}}{Ta_2Cl_6(PMe_3)_4H_2} \quad (2)$$

and deposit a sparingly soluble green powder in 70% yield. The latter has been identified as **2** by comparison of its ^1H NMR spectrum [Fig. 3(a)] with that of an authentic sample[5] prepared by the original route (*vide supra*). As an aside, we note that there are two isomers of **2** (one with C_s-symmetry and one with D_2-symmetry) depending on the disposition of the bridging ligands. In our studies, only the C_s isomer has been detected and it does not rearrange to the D_2 isomer thermally or photochemically.

†Tables of anisotropic thermal parameters and observed and calculated structure factors for **3** and **5**, plus hydrogen atom positions and tortion angles for **3** are available from the Executive Editor, Queen Mary College, London, or the Indiana University Molecular Structure Center, upon request.

Table 2. Selected bond distances (Å) and angles (°) for $Ta_2Cl_4(PMe_3)_4H_2$

A	B	Distance	A	B	C	Angle
Ta(1)	Ta(2)	2.545(1)	Ta(2)	Ta(1)	Cl(3)	116.0(1)
Ta(1)	Cl(3)	2.418(3)	Ta(2)	Ta(1)	P(4)	102.0(1)
Ta(1)	P(4)	2.591(3)	Cl(3)	Ta(1)	Cl(3)′	128.1(1)
Ta(2)	Cl(6)	2.413(3)	Cl(3)	Ta(1)	P(4)	85.2(1)
Ta(2)	P(5)	2.600(3)	P(4)	Ta(1)	P(4)′	155.9(1)
P(4)	C(7)	1.785(14)	Ta(1)	Ta(2)	Cl(6)	115.3(1)
P(4)	C(8)	1.810(12)	Ta(1)	Ta(2)	P(5)	102.0(1)
P(4)	C(9)	1.831(15)	Cl(6)	Ta(2)	Cl(6)′	129.5(1)
P(5)	C(10)	1.807(13)	Cl(6)	Ta(2)	P(5)	85.6(1)
P(5)	C(11)	1.822(14)	P(5)	Ta(2)	P(5)′	156.1(1)
P(5)	C(12)	1.805(16)	Ta(1)	P(4)	C(7)	116.1(5)
			Ta(1)	P(4)	C(8)	112.3(5)
			Ta(1)	P(4)	C(9)	117.8(5)
			C(7)	P(4)	C(8)	103.6(7)
			C(7)	P(4)	C(9)	102.3(7)
			C(8)	P(4)	C(9)	102.9(7)
			Ta(2)	P(5)	C(10)	115.3(5)
			Ta(2)	P(5)	C(11)	113.1(5)
			Ta(2)	P(5)	C(12)	115.9(5)
			C(10)	P(5)	C(11)	102.2(8)
			C(10)	P(5)	C(12)	104.0(7)
			C(11)	P(5)	C(12)	104.8(9)

(2) Ether solutions of **3** also react readily with hydrogen chloride at −20°C [eqn (3)]:

$$\underset{\mathbf{3}}{Ta_2Cl_4(PMe_3)_4H_2} + HCl \xrightarrow[1\,h,\,-20°C]{OEt_2} \underset{\mathbf{4}}{Ta_2Cl_5(PMe_3)_4H_3}. \quad (3)$$

A yellow-green solid (**4**) was isolated by concentration of the suspension and cooling to −40°C (70% yield). Elemental analyses and a molecular-weight measurement suggested that **4** was $Ta_2Cl_5(PMe_3)_4H_3$. If HCl adds to **3** in the same fashion as Cl_2, we expect a dimer with C_2-symmetry. The proton and $^{31}P-\{^1H\}$ NMR spectra are in accord with this expectation. In the former [Fig. 3(b)], we observe two complex hydride multiplets, one at δ 9.68 (area 1) and the other at δ 7.69 (area 2), and two phosphine doublets (each of area 18) at δ 1.60 and 1.29. The chemically equivalent PMe_3 ligands in the C_2 structure are magnetically nonequivalent (an AA′XX′ spin system), and this is consistent with what we observe in the $^{31}P-\{^1H\}$ NMR spectrum (see Experimental).

(3) Ether solutions of **3** react slowly with hydrogen (40 psi) at 25°C [eqn (4)]:

$$\underset{\mathbf{3}}{Ta_2Cl_4(PMe_3)_4H_2} + H_2 \xrightarrow[12\,h,\,25°C]{OEt_2} \underset{\mathbf{5}}{Ta_2Cl_4(PMe_3)_4H_4}. \quad (4)$$

A yellow-green solid (**5**) was isolated from the reaction suspension by concentration and cooling to −40°C (85% yield). Elemental analyses and a molecular-weight measurement indicated that **5** was $Ta_2Cl_4(PMe_3)_4H_4$.* Addition of H_2 across the metal–metal bond of **3** should provide a dimer with D_{2d}-symmetry. The room-temperature ^1H NMR spectrum of **5** [Fig. 3(c)] supports this prediction. A single hydride multiplet is observed at δ 8.79 (area 4) together with one phosphine methyl resonance at δ 1.47 (area 36). Because the hydride resonance is not a simple first-order pattern, we propose that the hydride ligands in **5** are static, i.e. they do not rotate about the Ta–Ta axis. There was no change in the appearance of the hydride resonance up to +100°C in toluene-d_8. Higher temperatures led to decomposition. The $^{31}P-\{^1H\}$ NMR spectrum of **5** (C_6D_6, 25°C) shows a singlet at δ −1.8. Selective ^1H-decoupling of the phosphine methyl resonance broadened this peak, but we were unable to resolve any fine structure. Because the spin system is complex (AA′A″A‴XX′X″X‴), this result is not particularly surprising. Below, we provide definitive proof for the proposed structure of **5**, but first we would like to describe an alternate, and more convenient, synthesis of **5**.

Synthesis of **5** *from* $TaCl_2H_2(PMe_3)_4$

The deep red tantalum(IV) hydride complex, $TaCl_2H_2(PMe_3)_4$ (**6**) can be synthesized, in high yield (≥75%) via reduction of $TaCl_5$ with sodium

*This dimer has been prepared independently by Fellmann[12(b)] and Schrock from monomeric $Ta(CHCMe_3)(H)Cl_2(PMe_3)_3$ and molecular hydrogen.

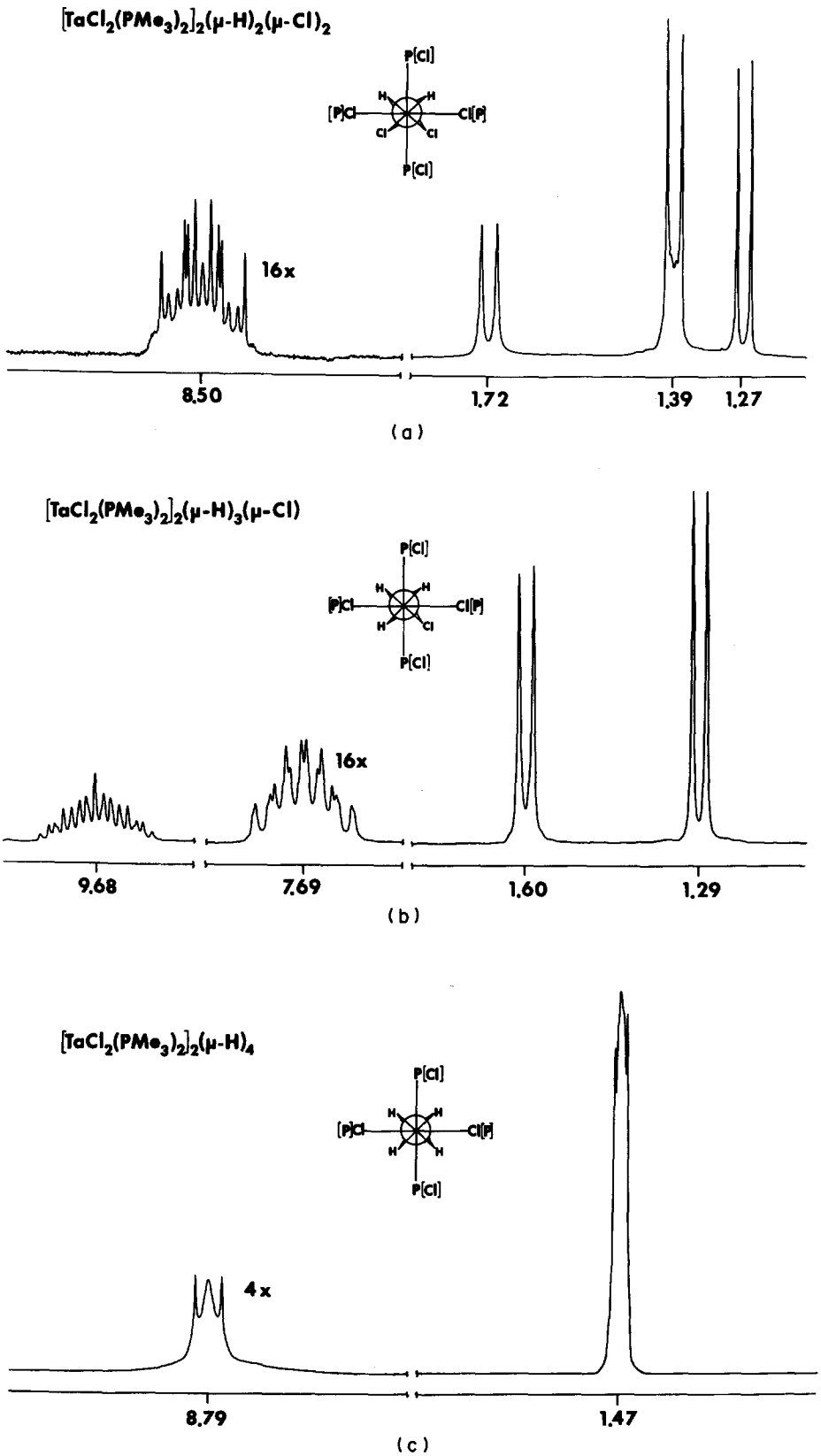

Fig. 3. 360-MHz ^{1}H NMR spectra of: (a) $Ta_2Cl_6(PMe_3)_4H_2$, (b) $Ta_2Cl_5(PMe_3)_4H_3$, and (c) $Ta_2Cl_4(PMe_3)_4H_4$.

amalgam (3 equivalents) in ether and subsequent treatment with molecular hydrogen.[13] The reduc-reduction step generates the tantalum(II) monomer, *trans*-$TaCl_2(PMe_3)_4$, which then oxidatively adds hydrogen to give the paramagnetic dihydride. The latter, as well as its 1,2-bis(dimethylphosphino)-ethane analog, $TaCl_2H_2(dmpe)_2$, have been fully characterized by solution and solid-state ESR, magnetic-susceptibility measurements, and X-ray crystallography.[13,14] As we commented earlier,[13] the isolation of **6** was quite unexpected. We thought that it would decompose to **5** and free phosphine as fast as it was formed. This prejudice was based on a popular misconception that paramagnetic early transition metal hydrides were simply too unstable to permit isolation.[15] **6** does decompose to **5** in solution at 25°C, but the reaction is very slow because the liberated trimethylphosphine inhibits further decomposition of the monomer [eqn (5)]:

$$2\underset{\mathbf{6}}{TaCl_2H_2(PMe_3)_4} \xrightarrow[25°C]{C_6H_6} \underset{\mathbf{5}}{Ta_2Cl_4(PMe_3)_4H_4} + 4PMe_3. \quad (5)$$

In an open system at higher temperatures, however, **6** decomposes readily to **5**. Refluxing methylcyclohexane (b.p. 101°C) is quite suitable for this purpose. This route is a considerable improvement over the original four-step ($TaCl_5 \rightarrow 1 \rightarrow 3 \rightarrow 5$) procedure and provides **5** in *ca* 65% yield based on tantalum pentachloride.

Solid state structure of 5

In the crystalline state, the compound is composed of discrete molecules of **5**. Final atomic coordinates and isotropic thermal parameters are listed in Table 3. Interatomic distances and angles are provided in Table 4. The molecular geometry and atom-numbering scheme are shown in Fig. 4. The pseudo-square planes of chloro and PMe_3 ligands are in the eclipsed conformation, the phosphine ligands are staggered among themselves, and the bridging H_4 group is staggered by 45° with respect to the end groups. The molecular symmetry, D_{2d}, is a *requirement* of the tetragonal space group $P4/nbm$ ($Z = 2$).

The Ta–Ta–Cl and Ta–Ta–P bond angles in **5** are 121.6(1) and 110.3(1)°, respectively. Both are more obtuse than their counterparts in **3** and the increases of 5–8° are almost certainly a reflection of the decrease in the metal–metal separation going from **3** [Ta = Ta, 2.545(1) Å] to **5** [Ta–Ta, 2.511(2) Å]. In the bridge region, the Ta–H_b distance is 1.81(21) Å and the Ta–H_b–Ta angle is 88(4)°. The only other structurally characterized $(\mu\text{-H})_4$ dimer is $Re_2H_8(PEt_2Ph)_4$.[16] Here the metal–metal separation is 2.538(4) Å, the Re–H_b distance is 1.878(7) Å, and the Re–H_b–Re angle is 85.0(3)° (neutron diffraction data).

Table 3. Fractional coordinates and isotropic thermal parameters for $Ta_2Cl_4(PMe_3)_4H_4$[a]

Atom	*x*	*y*	*z*	B_{iso}
Ta(1)	7500*	2500*	3770(1)	18
Cl(2)	8678(3)	1322*	2505(6)	29
P(3)	6127(3)	3873*	−2886(6)	24
C(4)	6012(19)	3988*	−1117(26)	42
C(5)	6380(18)	−215(14)	3470(22)	47
H(1)	669*	82*	73*	53
H(2)	550*	450*	−86*	52
H(3)	581*	−68*	321*	55
H(4)	702*	−48*	308*	55
H(5)	645*	−23*	439*	55
H(6)	750(14)	354(15)	500(13)	21(51)

[a]See footnote to Table 1.

Electronic structure calculations

Why is it that the briding hydrides in **5** do not rotate about the metal–metal bond axis? Why do the bridging hydrides in **3** rotate rapidly about the metal–metal bond axis? In order to answer these questions, we calculated the ground-state electronic structures of the model compounds $Ta_2Cl_4(PH_3)_4H_4$ and $Ta_2Cl_4(PH_3)_4H_2$ using the multiple-scattering Xα method.[17]* For each of these models, the calculation of Xα eigenvalues was first carried out nonrelativistically. Relativistic corrections[18] were then added, and the calculations were reconverged. Additional information on the calculations is provided in Experimental.

$Ta_2Cl_4(PH_3)_4H_4$

The results of the calculations are displayed in Fig. 5, which shows both the nonrelativistic levels and those obtained after approximate relativistic corrections were applied. The energies of the relativistic levels and the atomic contributions to them are presented in Table 5. The levels fall naturally into a number of small groups; these will be discussed in turn.

*The programs we used were written by M. Cook, Harvard University, and B. E. Bursten and G. G. Stanley, Texas A&M University. We are grateful to Professor Bruce Bursten (Ohio State University) for a copy of the programs.

Table 4. Selected bond distances (Å) and angles (°) for $Ta_2Cl_4(PMe_3)_4H_4$

A	B	Distance	A	B	C	Angle
Ta(1)	Ta(1)′	2.511(2)	Ta(1)′	Ta(1)	Cl(2)	121.6(1)
Ta(1)	Cl(2)	2.461(5)	Ta(1)′	Ta(1)	P(3)	110.3(1)
Ta(1)	P(3)	2.604(5)	Cl(2)′	Ta(1)	Cl(2)	116.7(3)
P(3)	C(4)	1.817(22)	Cl(2)	Ta(1)	P(3)	79.5(1)
P(3)	C(5)	1.818(16)	P(3)′	Ta(1)	P(3)	139.5(2)
Ta(1)	H(6)	1.81(21)	Ta(1)	P(3)	C(4)	116.7(9)
			Ta(1)	P(3)	C(5)	112.7(5)
			C(4)	P(3)	C(5)	105.4(8)
			C(5)	P(3)	C(5)′	102.6(12)
			Ta(1)′	Ta(1)	H(6)	46.(3)
			Cl(2)	Ta(1)	H(6)	143.(6)
			P(3)	Ta(1)	H(6)	136.(6)
			Ta(1)′	H(6)	Ta(1)	88.(4)

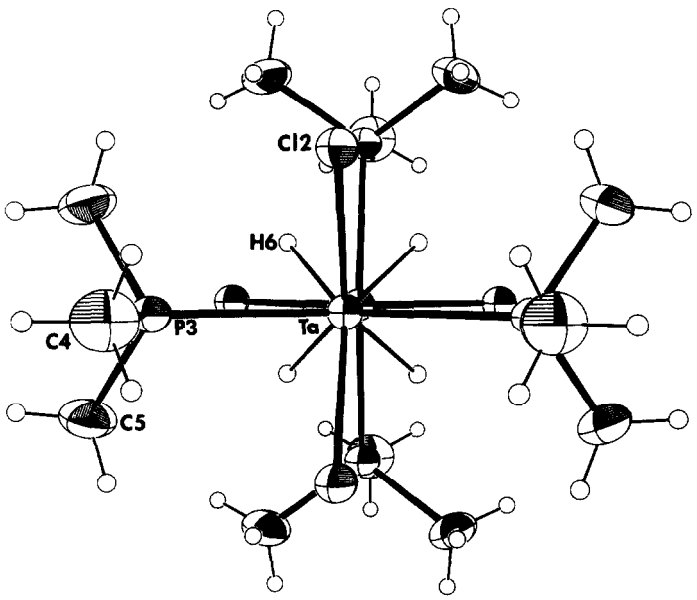

Fig. 4. ORTEP drawing of $Ta_2Cl_4(PMe_3)_4H_4$. Each nonhydrogen atom is represented by a thermal vibration ellipsoid enclosing 50% of its electron density. D_{2d}-symmetry is a space group requirement (see text).

First, we examine the highest occupied molecular orbital (HOMO) and the low-lying virtual orbitals. As seen from the breakdown in Table 5, both the HOMO ($8a_1$) and the lowest unoccupied molecular orbital (LUMO) ($3a_2$) are metal localized with modest contributions from the chloro and phosphorus ligands. A cross-section of the HOMO is shown in Fig. 6. The Ta–Ta interaction is a bonding one, arising from overlap of the $5d_{z^3}$ orbitals. There is also evidence of Ta–P bonding and Ta–Cl antibonding here. The bridging hydrogens make a negligible contribution to this level, which is clearly a Ta–Ta σ-bond. The LUMO (not pictured here) is essentially the δ^*-orbital, i.e. the out-of-phase combination of the $5d_{xy}$ orbitals on the tantalum centers. The HOMO–LUMO gap is 1.26 eV. Other virtual orbitals of note are the $7b_2$ and the $10e$. These are the Ta–Ta σ^*- and π^*-levels, respectively.

Lying below the HOMO are four groups of levels (see Fig. 5): (1) the Ta–P σ-bonding orbitals ($9e$, $7a_1$, $6b_2$; -6.5 to -7.8 eV); (2) the chlorine lone pair orbitals ($3b_1$, $8e$, $2a_2$, $7e$, $5b_2$, $6a_1$; -8.1 to -8.7 eV); (3) the Ta–Cl σ-bonding orbitals ($6e$, $5a_1$, $4b_2$; -9.0 to -9.7 eV); (4) the P–H σ-bonding orbitals ($5e$, $1a_2$, $4e$, $1b_1$, $3b_2$, $4a_1$; -11.8 to -12.0 eV). Both the ordering and the energies of these levels are in accordance with an earlier MS-Xα calculation on $W_2Cl_4(PH_3)_4$.[19]

The four remaining occupied levels in Fig. 5 and Table 5 are those which describe the σ-, π and δ-

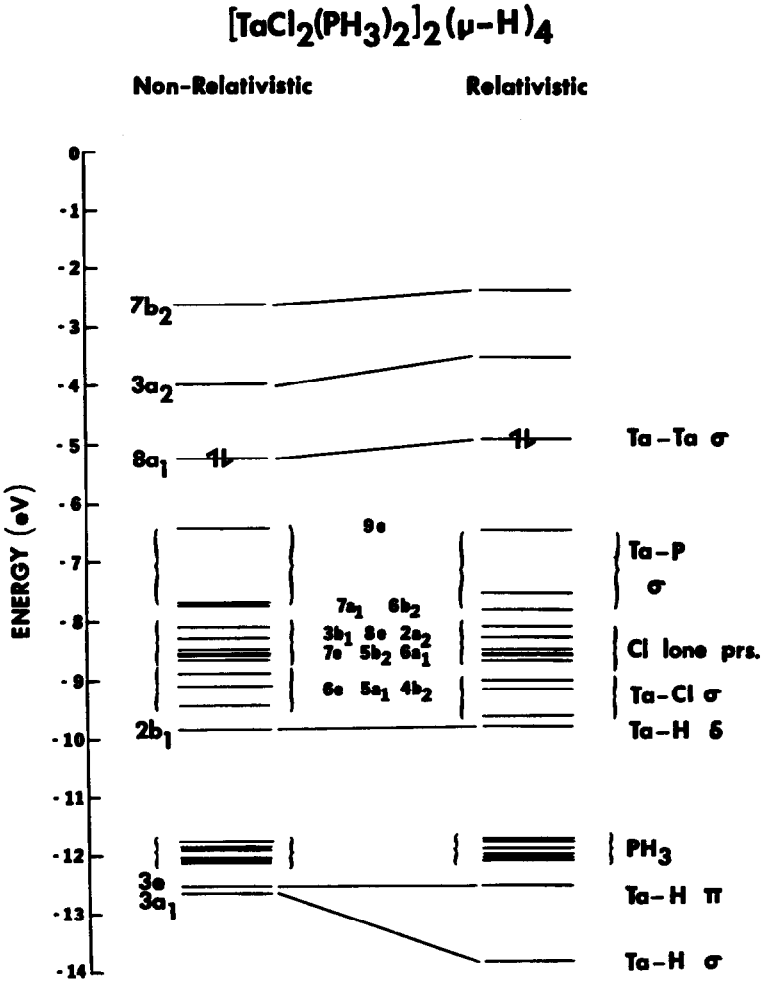

Fig. 5. Summary of the nonrelativistic and relativistic eigenvalues for the model complex $Ta_2Cl_4(PH_3)_4H_4$.

type interactions between the tantalum atoms and the four bridging hydride ligands. The lowest-lying of these is the $\sigma(3a_1, -13.9\,eV)$ and a cross-section of this level is shown in Fig. 7. The interaction here is between the in-phase combination of all four hydrogen 1*s* orbitals, and a pair of tantalum hybrid orbitals (62% 6*s*, 23% $6p_z$ and 14% $5d_{z^2}$). The substantial tantalum 6*s* character in this level is responsible for its marked stabilization. Note also that this is the only level which drops dramatically in energy when relativistic corrections are introduced into the calculations (see Fig. 5). This extra stabilization of the $3a_1$ level is a direct consequence of its high tantalum *s* + *p* character.[20]

At somewhat higher energy are the degenerate π-type levels (3*e*, −12.5 eV), one of which is shown in Fig. 8. Here we have another strong, stabilizing interaction. This one is primarily between the tantalum $5d_{\pm 1}$ orbitals (note the lobular structure about each Ta) and an antisymmetric combination of hydrogen 1*s* orbitals. Finally, at −9.8 eV, we find the $2b_1$ or δ-type level. In-phase overlap of the tantalum $5d_{xy}$ orbitals with the bridging ligand orbitals is the genesis of this level. A cross-section of the $2b_1$ level shows the δ-symmetry quite clearly (Fig. 9).

Now that we have a good picture of the M–M and M–H–M interactions in $Ta_2Cl_4(PH_3)_4H_4$, we are in a position to address the question of $(\mu\text{-H})_4$ rotation in **5**. The σ- and π-interactions are cylindrically symmetric with respect to the Ta–Ta axis and do not engender a conformational preference for the bridging hydride ligands. The same cannot be said for the TaH_4Ta δ-interaction. This bridge bonding component will stabilize the staggered hydride conformation relative to the eclipsed hydride conformation.* Unfortunately, ground-state calculations of the type reported here

*Similar conclusions have been reached in the case of $Re_2H_8(PH_3)_4$, a model for $Re_2H_8(PEt_2Ph)_4$.[16,21]

Table 5. MA-Xα eigenvalues (including relativistic corrections) for $Ta_2Cl_4(PH_3)_4H_4$[a]

Level	Energy (EV)	% Contribution Ta	Cl	P	H1	H2	H3	Int	Out	Ta angular contributions			
$4b_1$	−0.896	15	3	10	1	0	4	60	7	89% D	11% F		
$11e$	−1.004	5	3	5	0	1	0	78	9				
$10a_1$	−1.249	37	9	15	0	0	1	33	5	1% P	98% D	1% F	
$9a_1$	−1.385	16	7	6	0	1	0	62	7	4% S	95% D	1% F	
$8b_2$	−1.614	44	9	16	0	2	0	26	3	4% P	94% D	2% F	
$10e$	−1.637	69	10	7	1	0	0	12	1	99% D	1% F		
$7b_2$	−2.505	65	17	1	0	0	0	16	0	3% S	3% P	93% D	1% F
$3a_2$	−3.671	74	8	2	1	0	0	14	0	100% D			
$8a_1$	−4.932	59	14	7	0	1	4	15	0	1% P	96% D	3% F	
$9e$	−6.514	11	14	49	5	2	0	18	1	38% P	58% D	4% F	
$7a_1$	−7.671	36	0	42	5	1	1	13	1	2% S	6% P	91% D	1% F
$6b_2$	−7.822	26	11	39	6	1	0	16	1	14% S	85% D	1% F	
$3b_1$	−8.166	5	73	0	0	0	10	12	0				
$8e$	−8.376	1	84	0	0	0	1	14	0				
$2a_2$	−8.559	4	79	2	2	0	0	13	0				
$7e$	−8.684	3	71	7	1	1	0	16	0				
$5b_2$	−8.692	5	72	5	0	1	0	16	0				
$6a_1$	−8.728	5	75	1	0	1	1	16	0				
$6e$	−9.059	12	77	1	1	0	2	7	1	43% P	54% D	4% F	
$5a_1$	−9.239	19	73	0	0	0	3	5	1	2% S	22% P	72% D	3% F
$4b_2$	−9.711	16	73	2	0	0	0	8	0	48% S	9% P	40% D	3% F
$2b_1$	−9.814	33	10	4	6	0	39	7	0	91% D	9% F		
$5e$	−11.817	5	1	42	43	5	4	0	0				
$1a_2$	−11.892	0	1	46	52	0	0	0	0				
$4e$	−11.916	4	0	42	24	25	4	0	1				
$1b_1$	−11.999	2	2	45	50	0	2	0	0				
$3b_2$	−12.029	0	0	46	18	35	0	0	1				
$4a_1$	−12.046	1	1	45	18	34	0	0	0				
$3e$	−12.553	35	2	10	4	6	40	3	0	12% P	83% D	5% F	
$3a_1$	−13.908	41	5	3	0	1	46	4	0	62% S	23% P	14% D	

[a]Chlorine 3*s*, phosphorus 3*s*, and core levels have been omitted. The HOMO is $8a_1$. H1 and H2 refer to the out-of-plane and in-plane PH_3 hydrogens, respectively (see text). H3 refers to the bridge hydrogens.

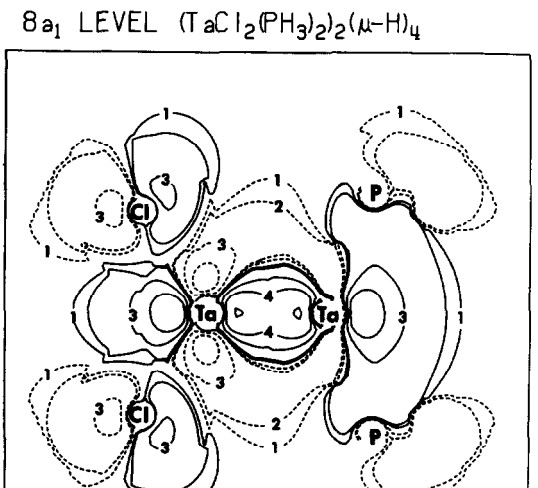

Fig. 6. Cross-section of the $8a_1$ level (HOMO) of $Ta_2Cl_4(PH_3)_4H_4$. For this and all other diagrams, solid lines represent positive wave function values and dashed lines represent negative values. The number 1 represents 0.005 electrons bohr^{-3}, and each succeeding number represents a factor of two increase in electron density, except for 7, which stands for 0.22 electron bohr^{-3}.

do not provide any information on the energetics of $(\mu\text{-H})_4$ rotation about the metal–metal bond. All we can say is that our inability to effect an averaging of spin couplings in **5** from 25 to 100°C is consistent with the presence of a substantial δ-interaction which effectively "locks" the hydride ligands into the staggered conformation. Hoffmann and co-workers[21] have calculated (using extended Hückel methods) a 35 kcal mol^{-1} barrier to $(\mu\text{-H})_4$ rotation in $Re_2H_8(PH_3)_4$, a model for structurally characterized $Re_2H_8(PEt_2Ph)_4$[16] whose $(\mu\text{-H})_4$ group is also staggered by 45° with respect to its eclipsed pyramidal $ReH_2(PEt_2Ph)_2$ end groups. We do not expect a significant difference between $(\mu\text{-H})_4$ rotation barriers in the rhenium(IV) and tantalum(IV) dimers because the orbitals which are depopulated (Re → Ta) are essentially pure M–M σ^*- and δ^*-orbitals and are therefore unaffected by $(\mu\text{-H})_4$ rotation. Note that a barrier greater than *ca* 20 kcal mol^{-1} is all that is required to account for our failure to observe an averaging of spin couplings at +100°C.

$Ta_2Cl_4(PH_3)_4H_2$

The overall electronic structure of this D_2 model compound is quite similar to that of the quadruply

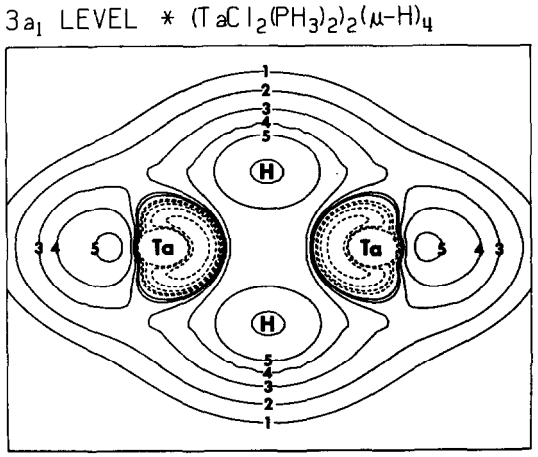

Fig. 7. Cross-section of the $3a_1$ level (Ta–H σ-interaction) of $Ta_2Cl_4(PH_3)_4H_4$.

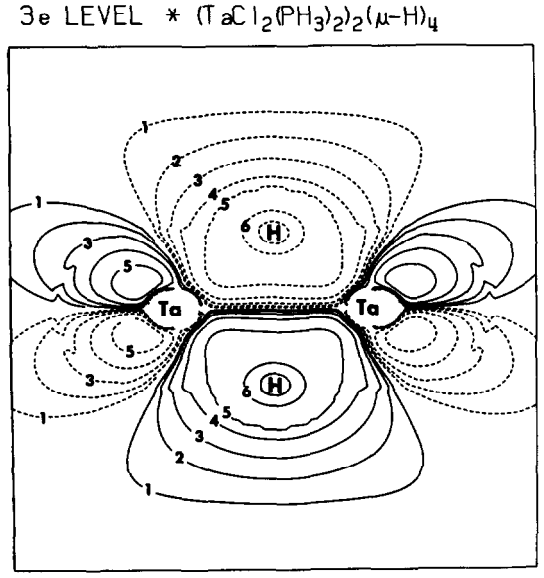

Fig. 8. Cross-section of one component of the $3e$ level (Ta–H π-interaction) of $Ta_2Cl_4(PH_3)_4H_4$.

hydrogen-bridged D_{2d} dimer described above and *we will not discuss it in detail. Rather, the focus* here will be specific changes brought about by removal of two bridging hydrides.

The relativistic energy eigenvalues obtained for $Ta_2Cl_4(PH_3)_4H_2$ are listed in Table 6. Figure 10 is a correlation diagram showing schematically how the Ta–H–Ta interactions change in going from $Ta_2Cl_4(PH_3)_4H_4$ to $Ta_2Cl_4(PH_3)_4H_2$. The σ-interaction remains strong. A cross-section of the $5a$ level of the $(\mu\text{-H})_2$ dimer is very similar to the $3a_1$ level of $Ta_2Cl_4(PH_3)_4H_4$. The most striking change can be seen in the splitting of the π-levels. In the $(\mu\text{-H})_4$ dimer, we have two equivalent TaH_2Ta π-interactions. Removal of a pair of *trans* hydrides

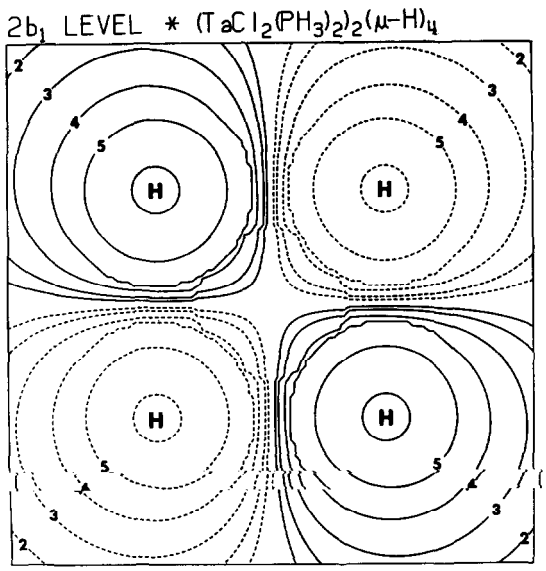

Fig. 9. Cross-section of the $2b_1$ level (Ta–H δ-interaction) of $Ta_2Cl_4(PH_3)_4H_4$, through the four bridging hydride ligands.

from the bridge leaves us with only one and a pair of tantalum $5d_{\pm 1}$ orbitals which overlap to form a weak metal–metal π-bond. The Ta–Ta π-bonding level [$9b_3$ (Fig. 11)] is the HOMO of $Ta_2Cl_4(PH_3)_4H_2$, lying slightly above the Ta–Ta σ-bonding $10a$ level. Finally, we note that the bridge hydrogens of $Ta_2Cl_4(PH_3)_4H_2$ no longer possess a representation of δ-symmetry and, consequently, there is no TaH_2Ta δ-interaction. The δ-level ($2b_1$) of $Ta_2Cl_4(PH_3)_4H_4$ becomes the LUMO ($9b_1$) of $Ta_2Cl_4(PH_3)_4H_2$ and loses all of its hydride character. It is now the (virtual) metal–metal δ-bonding level. The loss of a δ-interaction involving the bridge hydrogens removes the electronic barrier to hydride rotation which was indicated for the $(\mu\text{-H})_4$ dimers (*vide supra*). As a consequence, we expect the barrier for $(\mu\text{-H})_2$ rotation about the Ta–Ta axis of **3** to be lower in energy than the barrier for *$(\mu\text{-H})_4$ rotation about the Ta–Ta axis of* **5**. The proton NMR spectrum of $Ta_2Cl_4(PMe_3)_4H_2$ (Fig. 1) and our inability to effect hydride magnetic nonequivalence in the temperature range -90 to $+25$°C are consistent with this hypothesis and indicate that the barriers differ by at least 10 kcal·mol^{-1}.

DISCUSSION

The preparation of metal–metal-bonded *niobium(III) and tantalum(III) dimers by sodium* amalgam reduction of higher-valent halides or their complexes has ample precedent. The synthesis of

Table 6. MS-Xα Eigenvalues (including relativistic corrections) for $Ta_2Cl_4(PH_3)_4H_2$[a]

Level	Energy (EV)	% Contribution Ta	Cl	P	H1	H2	H3	Int	Out	Ta angular contributions			
$11b_1$	−1.022	36	9	6	5	0	0	38	7	98% D	2% F		
$10b_3$	−1.056	13	2	10	4	2	0	60	9	1% P	98% D	1% F	
$10b_2$	−1.056	14	2	10	4	2	0	59	9	1% P	98% D	1% F	
$10b_1$	−1.397	65	6	0	0	0	0	28	1	7% P	91% D	1% F	
$12a$	−1.635	7	1	11	5	1	1	66	9				
$11a$	−2.410	59	8	3	0	1	2	25	1	2% S	4% P	92% D	1% F
$9b_1$	−2.671	82	4	0	1	0	0	13	0	100% D			
$9b_3$	−4.277	58	4	12	0	1	0	25	1	9% P	90% D	1% F	
$10a$	−4.947	70	8	3	0	0	6	12	0	5% S	91% D	3% F	
$9b_2$	−5.496	11	5	55	0	0	0	26	1	41% P	55% D	5% F	
$8b_3$	−5.620	22	7	46	0	0	0	23	1	12% P	85% D	3% F	
$9a$	−6.697	35	1	43	2	0	0	19	1	4% S	4% P	92% D	1% F
$8b_1$	−6.821	27	2	46	2	0	0	23	1	20% S	1% P	79% D	1% F
$8b_2$	−8.344	2	82	0	0	0	2	14	0				
$8a$	−8.385	4	79	1	2	0	1	13	0				
$7b_3$	−8.447	1	83	0	0	0	0	14	0				
$7b_1$	−8.461	3	79	2	2	0	0	13	0				
$7b_2$	−8.544	2	78	3	0	0	0	16	0				
$6b_3$	−8.552	3	78	3	0	0	0	16	0				
$6b_1$	−8.610	3	79	1	0	0	0	17	0				
$7a$	−8.672	5	75	2	0	1	1	16	0				
$6b_2$	−9.005	12	76	1	1	0	3	6	1	56% P	40% D	4% F	
$5b_3$	−9.271	17	76	0	0	0	0	6	0	18% P	79% D	2% F	
$6a$	−9.330	24	62	1	1	0	8	2	1	19% P	77% D	4% F	
$5b_1$	−9.879	18	75	0	0	0	0	6	1	39% S	5% P	53% D	3% F
$5b_2$	−11.139	29	6	18	9	10	28	0	0	7% P	86% D	7% F	
$5a$	−11.297	27	14	19	13	7	20	0	0	57% S	10% P	29% D	3% F
$4b_3$	−12.191	1	0	47	21	31	0	0	1				
$4b_1$	−12.202	1	0	47	16	35	0	0	1				
$4b_2$	−12.255	1	1	47	36	14	1	0	0				
$3b_1$	−12.393	1	2	47	51	0	0	0	0				
$3b_3$	−12.415	0	1	47	48	4	0	0	0				
$4a$	−12.461	2	1	45	28	21	1	1	1				
$3b_2$	−12.943	13	1	30	22	12	18	4	0	20% P	75% D	5% F	
$3a$	−13.092	13	3	30	25	8	16	5	0	47% S	17% P	33% D	4% F

[a]See footnote to Table 5. The HOMO is $9b_3$.

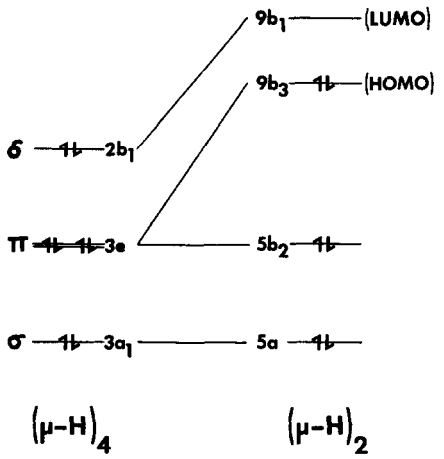

Fig. 10. Schematic correlation diagram uniting the Ta–H interactions in the $(\mu\text{-H})_4$ and $(\mu\text{-H})_2$ dimers.

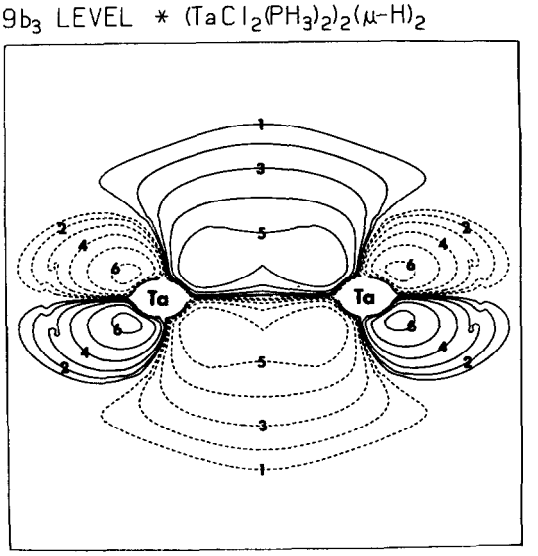

Fig. 11. Cross-section of the $9b_3$ level (HOMO) of $Ta_2Cl_4(PH_3)_4H_2$.

$Ta_2Cl_6(PMe_3)_4$ from $TaCl_5$ was mentioned in the Introduction, but the approach is due to Maas and McCarley.[22] In 1973, these authors prepared a series of $Nb_2X_6(THT)_3$ complexes (X = Cl, Br or I;

THT = tetrahydrothiophene) by Na–Hg reduction of $NbX_4(THT)_2$ in benzene. The synthesis of **3** reported here is novel only in the sense that precursor **2** is a well-defined, metal–metal-bonded tantalum(IV) dimer. The structure of **3**, on the other hand, is unprecedented in niobium(III) or tantalum(III) dimer chemistry. The chloro-bridged species, **1** and $Ta_2Cl_6(dmpe)_2$,[23] adopt edge-sharing bioctahedral geometries while the $M_2X_6(SR_2)_3$ dimers prefer confacial bioctahedral structures.[24]

We can understand the structure of **3** in terms of the following hypothetical transformation. Replacement of the bridging halogens in **1** with smaller hydride ligands must shorten the Ta–Ta separation because effective Ta–H bonding requires that the metals be brought into closer proximity to each other. This, in turn, forces the terminal ligands into pyramidal arrangements to relieve axial–axial interactions. In addition, replacement of the chlorides destroys the δ-interaction shown below, which locks **1** into the edge-sharing geometry. Recall that the hydride ligands in **3** do not possess a representation with δ-symmetry and, therefore, are not constrained to a specific location about the Ta–Ta axis.

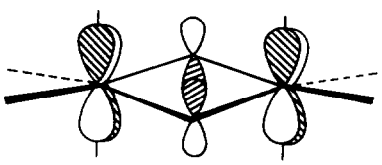

Dimer **3** is the only metal–metal multiply bonded system which reacts readily and cleanly with Cl_2, HCl *and* H_2.* These substrates add across the Ta=Ta bond, decreasing the bond order from two to one, and there are none of the gross structural rearrangements which usually accompany oxidative-addition reactions in metal–metal-bonded complexes.[26] Our observation that only the C_s isomer of **2** is formed in the chlorination reaction also suggests that the addition of X_2 to **3** is a concerted process.

The X-ray structure of dimer **5** confirms that H_2 addition is across the Ta–Ta bond of **3** and also shows the combined effect of four strong Ta–H–Ta interactions on the Ta–Ta separation. The Ta–Ta bond length in **5** is *ca* 0.03 Å shorter than found in **3**, where we have no δ-interaction and only one π-type TaH_2Ta interaction.

The electronic structure calculations on $Ta_2Cl_4(PH_3)_4H_4$ and $Ta_2Cl_4(PH_3)_4H_2$ complement our structural and spectroscopic studies on **3** and **5**. We now have some appreciation of the electronic factors which influence hydride rotation in these systems, and the calculations support the assignments of Ta–Ta bond orders in **3** and **5**. The MS-Xα results can also be used to interpret the optical spectra of **3** and **5**, but this is another story and one which we will relate in a future paper in this series.

The synthesis of **3** and **5** naturally call for a comment on the possible existence of $Ta_2Cl_4(PMe_3)_4$, since the $(\mu\text{-H})_2$ and $(\mu\text{-H})_4$ complexes are the sequential hydrogenation products of this tantalum(II) dimer. *A priori*, we have no reason to believe that $Ta_2Cl_4(PMe_3)_4$ should not exist and efforts to prepare it, or an analogue, continue in our laboratory at Los Alamos. Neither reduction of **1** nor thermolysis of *trans*-$TaCl_2(PMe_3)_4$[27]† have yielded this dimer, but there are other possibilities which merit investigation, e.g. thermally induced reductive elimination of H_2 from **3**, and these are being pursued.

We would be remiss not to mention the recent success of the Cotton group[28] in preparing and structurally characterizing the face-sharing bioctahedral tantalum(II) dimer, $[Ta_2Cl_6(\mu\text{-THT})_3]^2$. The isolation of this material, which contains a formal metal–metal triple bond [Ta–Ta 2.626(1) Å], provides further impetus in the search for molecules containing unbridged Ta–Ta triple bonds.

EXPERIMENTAL

Reagents

Tantalum pentachloride was purchased from Pressure Chemical and sublimed under high vacuum to remove nonvolatile impurities. $Ta_2Cl_6(PMe_3)_4H_2$, $Ta_2Cl_6(PMe_3)_4D_2$ and $TaCl_2H_2(PMe_3)_4$ were prepared and purified by literature procedures.[5,13] Hydrogen (Air products, 99.995%) and deuterium (Linde, 99.5%) were used as received. Chlorine and hydrogen chloride (both from Matheson) were dried by passage through concentrated sulfuric acid.

THF, ether and glyme were dried and freed from dissolved molecular oxygen by distillation under argon from a solution of the solvent, benzophenone, and sodium or potassium. *n*-Hexane was purified

*The Mo–Mo bond of $[CpMo(CO)_2]_2$ will add HI and I_2 thermally but not H_2.[25]

†Thermolysis of *trans*-$TaCl_2(PMe_3)_4$ in refluxing cyclohexane leads to disproportionation and hydride abstraction from the solvent.[27(b)]

by stirring over saturated $KMnO_4$ in 10% sulfuric acid (2 × 6 h). It was then sequentially washed with water, saturated aqueous Na_2CO_3 and water, dried over $MgSO_4$, filtered and distilled under argon from sodium–potassium alloy.

Physical and analytical measurements

Elemental analyses and molecular-weight measurements were performed by Galbraith Laboratories, Knoxville, TN.

IR spectral measurements were made on a Perkin–Elmer Model 1330 spectrometer. Samples were run as KBr discs. NMR spectra were run on Bruker WM-360 and JEOL FX90Q spectrometers. ^{31}P spectra were recorded at 36.20 or 145.80 MHz, and ^1H spectra at 360.1 MHz. Benzene-d_6 was used as a lock solvent for most spectra. Phosphorus chemical shifts (δ) are reported relative to external 85% aqueous H_3PO_4. Negative chemical shifts are assigned to resonances at lower frequency (higher field) than the reference.

General synthetic procedures

Manipulations of air-sensitive reagents and solutions and the workup of reaction products were usually performed within the confines of a helium-filled Vacuum Atmospheres Dri-Lab (HE-43). The latter is equipped with a high capacity Dri-Train (MO-40V), and a Dri-Cold Freezer maintained at −40°C.

$Ta_2Cl_4(PMe_3)_4H_2$ (3)

Inside the drybox, $Ta_2Cl_6(PMe_3)_4H_2$ (3.0 g, 3.41 mmol) was added to 150 cm^3 of THF in a two-neck, 250-cm^3 Morton flask, equipped with a mechanical stirrer and N_2-gas inlet. Sodium amalgam (2.5 cm^3 of 0.5% amalgam, 7.35 mmol of Na) and mercury (8 cm^3) were added and the flask was removed from the drybox. The flask was connected to a source of argon, cooled to 0°C in an ice–salt bath, and the reaction mixture was stirred *vigorously* for 4–5 h. The yellow-green suspension turned dark green during this period. The flask was returned to the drybox, the contents were filtered through *ca* 1 inch of Celite on a 60 cm^3 medium porosity sintered glass frit, and the flask was rinsed with 50 cm^3 of fresh THF. The combined filtrate was stripped to dryness and the solid residue was extracted with diethyl ether (4 × 50 cm^3). After filtration, the combined extracts were stripped to dryness, providing **3** as a dark green powder. Yield 2.01 g (73%).

An analytical sample was obtained by recrystallization from a concentrated ether solution at −40°C.

Calc. for $Ta_2Cl_4(PMe_3)_4H_2$ ($C_{12}H_{38}Cl_4P_4Ta_2$): C, 17.8; H, 4.7; Cl, 17.5%; M_r, 810. Found: C, 17.8; H, 4.7; Cl, 17.8%; M_r, 813.

IR (cm^{-1}): 1232 (m, $\nu_{Ta-H-Ta}$).

^1H NMR (ppm, C_6D_6): 8.52 (quin, 2, J_{PH} = 13.4 Hz, H_b), 1.52 [t, 36, J_{PH} = 3.8 Hz, $P(CH_3)_3$].

^{31}P NMR (ppm, C_6D_6, selective $\{^1H\}$ at 1.52): +1.3 (t, J_{PH} = 13.4 Hz)

The deuteride, $Ta_2Cl_4(PMe_3)_4D_2$, was prepared from $Ta_2Cl_6(PMe_3)_4D_2$ in a similar fashion. IR (cm^{-1}): 860 ($\nu_{Ta-D-Ta}$).

$Ta_2Cl_6(PMe_3)_4H_2$ (2) *from* 3

A 0.25 g (0.31 mmol) sample of **3** was dissolved in 30 cm^2 of ether in a 100-cm^3 Schlenk flask equipped with a N_2-gas inlet, pressure-equalizing dropping funnel and a magnetic stir bar. The solution was cooled to −20°C in a dry ice–acetone bath and 30 cm^3 of a 0.01 M Cl_2–ether solution was added dropwise over the course of 0.5 h. A light green powder precipitated during the addition. The suspension was stirred for an additional 0.5 h at −20°C. Approximately half the ether was removed *in vacuo* and the solid was collected by filtration, washed with hexane (2 × 10 cm^3) and dried. Yield 0.91 g (70%). The spectroscopic properties (NMR and IR) of this material were identical to those reported for **2**.[5] The filtrate was stripped to dryness and checked by NMR. **2** and a trace of unreacted **3** were the only materials detected.

$Ta_2Cl_5(PMe_3)_4H_3$ (4)

A 0.60-g (0.74-mmol) sample of **3** was dissolved in 40 cm of ether in a 100-cm^3 Schlenk flask, equipped as noted above. The solution was cooled to −20°C and 30 cm^3 of a 0.025 M HCl–ether solution was added dropwise over the course of 0.5 h. A light green solid precipitated during the addition. When the latter was complete, the reaction mixture was stirred for an additional 0.5 h at −20°C. Half of the ether was then removed *in vacuo* and the suspension was cooled to −40°C for several hours. The product was filtered, washed with hexane (2 × 10 cm^3) and dried *in vacuo*. Yield 0.45 g (72%). An analytical sample was obtained by recrystallization from ether at −40°C.

Calc. for $Ta_2Cl_5(PMe_3)_4H_3$($C_{12}H_{39}Cl_5P_4Ta_2$): C, 17.0; H, 4.6; Cl, 20.9%; M_r, 846.5. Found: C, 16.9; H, 4.6; Cl, 21.0%; M_r, 853.

IR(cm^{-1}): 1260 (m, $\nu_{Ta-H-Ta}$).

^1H NMR (ppm, C_6D_6): 9.68 (complex m, 1, H_b), 7.69 (complex m, 2, H_b'), 1.60 [d, 18, J_{PH} = 9.3 Hz,

$P(CH_3)_3]$, 1.29 [d, 18, $J_{PH} = 8.8$ Hz, $P'(CH_3)_3]$.

^{31}P NMR (ppm, C_6D_6, $\{^1H\}$): +8.45 [m, 1, $P(CH_3)_3$, $J_{AX} + J_{AX'} = 28.7$ Hz], −13.34 [m, 1, $P'(CH_3)_3$, $J_{AX} + J_{AX'} = 28.7$ Hz].

$Ta_2Cl_4(PMe_3)_4H_4$ (5)

Method A. A 1.00-g sample of **3** was dissolved in 50 cm^3 of ether in a 90-cm^3 Fischer–Porter pressure vessel. The latter was sealed, removed from the drybox, and connected to a source of hydrogen and vacuum. The bomb was evacuated and back-filled with H_2 (40 psi). After 12 h, the bomb was vented, returned to the drybox and half the ether was removed *in vacuo*. The light green suspension was cooled to −40°C for several hours. The product was filtered off, washed with hexane (2 × 10 cm^3) and dried *in vacuo*. Yield 0.85 g (85%). An analytical sample was obtained by recrystallization from ether at −40°C.

Calc. for $Ta_2Cl_4(PMe_3)_4H_4(C_{12}H_{40}Cl_4P_4Ta_2)$: C, 17.8; H, 5.0; Cl, 17.5%; M_r, 812. Found: C, 17.6; H, 5.0; Cl, 17.4%; M_r, 799.

IR (cm^{-1}): 1225 (m, $\nu_{Ta-H-Ta}$).

^1H NMR (ppm, C_6D_6): 8.79 (m, 4, H_b), 1.47 [t, 36, $J_{HP} = 4$ Hz, $P(CH_3)_3]$.

^{31}P NMR (ppm, C_6D_6, $\{^1H\}$): −1.8 (s).

Method B. A freshly recrystallized sample of **6** (2.0 g, 2.6 mmol) was transferred to a 100-cm^3 Schlenk flask containing *ca* 40 cm^3 of methylcyclohexane. The flask was fitted with a reflux condenser and the red suspension was heated at reflux (101°C) for 2 h under a slow argon flush. Over the course of the thermolysis, the color of the suspension turned pale green. The suspension was then cooled to −40°C for several hours, filtered, and the product was washed with hexane (2 × 5 cm^3) and dried *in vacuo*. Yield 1.3 g (89%). The purity of **5** synthesized by this route should be checked by proton NMR. If any **3** is detected, the entire yield is placed in a 90 cm^3 Fischer–Porter pressure vessel together with 20 cm^3 of ether and the vessel is pressurized (40 psi) with H_2 for several hours. The pure product is then isolated by removal of the solvent in vacuo.

X-ray structure determinations

General procedures were the same as those described previously.[29]

$Ta_2Cl_4(PMe_3)_4H_2$. Crystals of **3** were grown by slow cooling of concentrated glyme solutions. The bulk sample consisted of well-formed green-black crystals of various sizes. Attempts to use the smaller crystals for data collection were unsuccessful; omega scans were in excess of 2°. Several of the larger crystals were then fractured and examined. In most cases twinning occurred, yielding cells with equivalent *a*- and *c*-axes, and considerable peak splitting. After numerous attempts, an irregularly-shaped fragment of maximum dimension 0.06 mm was obtained which was not twinned, and data were collected using it. The sample manipulation and mounting were performed in a nitrogen-filled glove bag and the sample was transferred to the goniostat (under N_2) and cooled to −160°C for characterization and data collection (see supplementary data).

The structure was solved by a combination of direct methods, Patterson techniques, and difference Fourier techniques, and refined by full-matrix least squares. All nonhydrogen atoms were located, and their positional and thermal parameters (anisotropic) refined. The molecule lies on a crystallographic two-fold axis and no disorder is apparent in the nonhydrogen positions. Hydrogen atoms, excluding the bridging hydride, were located in a difference Fourier synthesis and refined isotropically. Several of the hydrogen thermal parameters are rather large, and the distances and angles involving the methyl hydrogens indicate they are poorly located.

A final difference Fourier indicated several peaks of density between 0.8 and 2.1e Å^{-3}. While one of these peaks was located in the bridge region, there was sufficient doubt as to preclude its inclusion in the refinement.

$Ta_2Cl_4(PMe_3)_4H_4$. Crystals of **5** were grown by slow cooling of concentrated THF solutions. Inside a nitrogen-filled glove bag, a green block was mounted on a glass fiber, and then transferred to the goniostat where it was cooled to −165°C. The structure was solved by Patterson and Fourier techniques, and refined by full-matrix least squares. The data were corrected for the effects of absorption. All nonhydrogen atoms were located and their positional and anisotropic thermal parameters refined. A difference Fourier synthesis, phased on the nonhydrogen atom parameters, revealed peaks which could be assigned as the hydrogens. When all of these were included in the refinement, two of the methyl group hydrogens failed to converge. For this reason, *all* methyl hydrogens were placed in fixed positions and only the bridging hydrogen was refined. A final difference Fourier map was essentially featureless, the largest peaks being *ca* 0.6e Å^{-3}, located near the tantalum and chlorine atoms. Crystal data are given in Table 7.

Calculations

The multiple-scattering Xα method was applied to the model compounds $Ta_2Cl_4(PH_3)_4H_2$ and $Ta_2Cl_4(PH_3)_4H_4$. Values of α were taken from

Table 7. Crystal data for $Ta_2Cl_4(PMe_3)_4H_2$ and $Ta_2Cl_4(PMe_3)_4H_4$

	3	5
mol formula	$Ta_2Cl_4P_4C_{12}H_{38}$	$Ta_2Cl_4P_4C_{12}H_{38}$
color	green-black	green
crystal dimens, mm	0.06 × 0.06 × 0.05	0.06 × 0.06 × 0.07
space group	C2/c	P4/nbm
temp, °C	− 161	− 165
cell dimens		
a, Å	18.371(5)	12.579(2)
b, Å	9.520(3)	12.579(2)
c, Å	18.942(6)	10.205(2)
β, deg	125.36(2)	90.00
molecules/cell	4	2
d(calcd), g cm^{-3}	1.991	1.670
wavelength, Å	0.71069	0.71069
mol wt	810.04	812.06
linear abs coeff, cm^{-1}	86.32	72.22
max abs	—	0.402
min abs	—	0.499
diffractometer	Picker 4-circle	Picker 4-circle
mode	Θ–2Θ	Θ–2Θ
2Θ range, deg	6–45	6–55
quadrants collected	+ h, + k, ± l	+ h, + k, + l
no. of data with $F_0 \geq 2.33\sigma(F_0)$	2155	656
No. of unique data	2399	897
total data collected	2693	3474
final residuals		
R_F	0.0464	0.0512
R_{wF}	0.0475	0.0402
goodness of fit, last cycle	1.256	1.363
max Δ/σ, last cycle	0.05	0.5

Schwartz,[30] except for hydrogen ($\alpha = 0.77725$)[31] and tantalum, whose α value was extrapolated from Schwartz as 0.69319.[32] For inter- and outer-sphere regions, values of α were calculated as valence-electron weighted averages of the atomic α values.

The starting molecular potentials were a superposition of the Herman–Skillman atomic potentials[33] of the neutral atoms. Atomic spheres were allowed to overlap in accordance with the scheme of Norman.[34] The final radii were chosen as 89% of the atomic number radii. In each calculation, the outer sphere was chosen to be tangent to the outermost atomic sphere.

Coordinates were calculated using the crystallographic data for the individual trimethyl phosphine species. The bond distances and bond angles used for $Ta_2Cl_4(PH_3)_4H_4$ were: Ta–Ta, 2.511 Å; Ta–Cl, 2.461 Å; Ta–P, 2.604 Å; Ta–H, 1.81 Å; Ta–Ta–P, 110.3°; Ta–Ta–Cl, 121.6°; Ta–H–Ta, 88°; P–H, 1.415 Å; Ta–P–H, 110.3°. The geometry was idealized to D_{2d}-symmetry. The corresponding data for the $(\mu\text{-H})_2$ dimer were: Ta–Ta, 2.545 Å; Ta–Cl, 2.416 Å; Ta–P, 2.596 Å; Ta–H, 1.85 Å; Ta–Ta–P, 102°; Ta–Ta–Cl, 116°; Ta–H–Ta, 87°. The PH_3 data were the same as given above and the geometry was idealized to D_2-symmetry.

The molecules were each placed in a coordinate system with its origin at the midpoint of the Ta–Ta bond, the Z-axis colinear with the Ta–Ta bond and the XZ and YZ planes each chosen to include four terminal ligand atoms. Each PH_3 ligand was oriented about the Ta–P bond such that each distal hydrogen atom was in the XZ or YZ plane.

Partial waves up to $l = 0, 2, 2, 3$ and 4 were used for H, P, Cl, Ta and outer sphere, respectively.

For each molecule the calculation of the Xα eigenvalues was first carried out nonrelativistically, until consecutive values of the SCF potential differed by less than 0.001 Ry. Relativistic corrections, viz. Darwin and mass–velocity terms for both core and valence metal orbitals,[21] were then added and the calculation was reconverged.

Acknowledgments—We are grateful to the National Science Foundation for support of this research and to Wrubel Computer Center, Indiana University, for a generous gift of computing time. AJS and APS would like to thank Professor B. E. Bursten (Ohio State) for helpful discussions on the MS-Xα method.

REFERENCES

1. D. J. Santure and A. P. Sattelberger, *Inorg. Chem.* 1985, **24**, 3477.
2. F. A. Cotton and R. A. Walton, *Multiple Bonds between Metal Atoms*. Wiley, New York (1982).
3. P. R. Sharp and R. R. Schrock, *J. Am. Chem. Soc.* 1980, **102**, 1430.
4. A. P. Sattelberger, R. B. Wilson, Jr and J. C. Huffman, *Inorg. Chem.* 1982, **21**, 2392.
5. A. P. Sattelberger, R. B. Wilson, Jr and J. C. Huffman, *Inorg. Chem.* 1982, **21**, 4179.
6. R. B. Wilson, Jr, J. C. Huffman and A. P. Sattelberger, *J. Am. Chem. Soc.* 1982, **104**, 858.
7. A. P. Sattelberger, *Inorganic Chemistry: Toward the 21st Century*, ACS Symposium Series No. 211, p. 291. American Chemical Society, Washington D.C. (1983).
8. M. R. Churchill and S. W-Y. Chang, *Inorg. Chem.* 1974, **13**, 2413.
9. M. J. Bennett, W. A. G. Graham, J. K. Hoyano and W. L. Hutcheon, *J. Am. Chem. Soc.* 1972, **94**, 6232.
10. F. A. Cotton, M. W. Extine, T. R. Felthouse, B. W. S. Kolthammer and D. G. Lay, *J. Am. Chem. Soc.* 1981, **103**, 4040.
11. A. Bino, F. A. Cotton, Z. Dori and J. C. Sekutowski, *Inorg. Chem.* 1978, **17**, 2946.
12. (a) R. R. Schrock and J. D. Fellmann, personal communication; (b) J. D. Fellmann, Ph.D. thesis, Massachusetts Institute of Technology (1980).
13. M. L. Luetkens, Jr, W. L. Elcesser, J. C. Huffman and A. P. Sattelberger, *Inorg. Chem.* 1984, **23**, 1718.
14. J. B. Raynor, A. P. Sattelberger and M. L. Luetkens, Jr, *Inorg. Chim. Acta* 1986, **113**, 51.
15. (a) I. H. Elson, J. K. Kochi, U. Klubunde, G. Parshall and F. N. Tebbe, *J. Am. Chem. Soc.* 1974, **96**, 7374; (b) I. H. Elson and J. K. Kochi, *J. Am. Chem. Soc.*

1975, **97**, 1263.
16. R. Bau, W. E. Carroll, D. W. Hart, R. G. Teller and T. F. Koetzle, *J. Am. Chem. Soc.* 1977, **99**, 3872.
17. (a) J. C. Slater, *Quantum Theory of Molecules and Solids, the Self-Consistent Field of Molecules and Solids*, Vol. 4, McGraw-Hill, New York (1974); (b) K. H. Johnson and F. C. Smith, *Phys. Rev. B* 1972, **5**, 831; (c) K. H. Johnson, *Adv. Quantum Chem.* 1973, **7**, 143; (d) K. H. Johnson, *Annu. Rev. Phys. Chem.* 1975, **25**, 39; (e) D. A. Case, *Annu. Rev. Phys. Chem.* 1982, **33**, 151.
18. J. H. Wood and M. A. Boring, *Phys. Rev. B* 1978, **18**, 2701.
19. F. A. Cotton, J. L. Hubbard, D. L. Lichtenberger and I. Shim, *J. Am. Chem. Soc.* 1982, **104**, 679.
20. P. Pyykko and J.-P. Desclaux, *Acc. Chem. Res.* 1979, **12**, 276.
21. A. Dedieu, T. A. Albright and R. Hoffmann, *J. Am. Chem. Soc.* 1979, **101**, 3141.
22. E. T. Maas and R. E. McCarley, *Inorg. Chem.* 1973, **12**, 1096.
23. F. A. Cotton, L. R. Falvello and R. C. Najjar, *Inorg. Chem.* 1983, **22**, 375.
24. (a) J. L. Templeton, W. C. Dorman, J. C. Clardy and R. E. McCarley, *Inorg. Chem.* 1978, **17**, 1263; (b) F. A. Cotton and R. C. Najjar, *Inorg. Chem.* 1981, **20**, 2716.
25. M. D. Curtis, L. Messerie, N. A. Fotinos and R. F. Gerlach, *Reactivity of Metal–Metal Bonds*, ACS Symposium Series No. 155, Chap. 12. American Chemical Society, Washington D.C. (1981).
26. (a) M. H. Chisholm, *Transition Met. Chem.* 1978, **3**, 321; (b) M. H. Chisholm, C. C. Kirkpatrick and J. C. Huffman, *Inorg. Chem.* 1981, **20**, 871.
27. (a) M. L. Luetkens, Jr, J. C. Huffman and A. P. Sattelberger, *J. Am. Chem. Soc.* 1983, **105**, 4474; (b) M. L. Luetkens, Jr, Ph.D. thesis, The University of Michigan (1984).
28. F. A. Cotton, M. P. Diebold and W. J. Roth, *J. Am. Chem. Soc.* 1986, **108**, 3538.
29. J. C. Huffman, L. N. Lewis and K. G. Caulton, *Inorg. Chem.* 1980, **19**, 2755.
30. K. Schwartz, *Phys. Rev. B* 1972, **5**, 2466.
31. J. C. Slater, *Int. J. Quantum Chem. Symp.* 1973, **7**, 533.
32. K. Schwartz, *Theor. Chim. Acta* 1974, **34**, 225.
33. F. Herman and S. Skillman, *Atomic Structure Calculations*. Prentice-Hall, Englewood Cliffs, NJ (1963).
34. (a) J. G. Norman, Jr, *J. Chem. Phys.* 1974, **61**, 4630; (b) J. G. Norman, Jr, *Mol. Phys.* 1976, **31**, 1191.

Polyhedron Vol. 6, No. 4, pp. 759–782, 1987
Printed in Great Britain

0277–5387/87 $3.00 + .00
Pergamon Journals Ltd

REACTIONS OF THE METAL–METAL TRIPLE BOND IN $Cp_2Mo_2(CO)_4$ AND RELATED COMPLEXES

M. DAVID CURTIS

Department of Chemistry, The University of Michigan, Ann Arbor, MI 48109, U.S.A.

(*Received* 19 *November* 1986)

Abstract—The reactions of the M≡M triple bonds in compounds of type $Cp_2M_2(CO)_4$ (M = Cr, Mo or W) are reviewed. These reactions are grouped under the headings of synthesis and structures of $Cp_2M_2(CO)_4$-type compounds, nucleophilic additions to the M≡M bonds, reactions with 1,3-dipoles, oxidative reactions with nonmetals, and cluster-building reactions. Literature coverage is until the end of 1985 with 102 references.

Our discovery of a simple, high-yield synthesis of the triply-bonded compound $Cp_2Mo_2(CO)_4$ (**1**) and our subsequent demonstration of the diverse chemistry associated with the Mo≡Mo triple bond has stimulated the use of this and related compounds in many new areas. In the 5 years since we first reviewed[1] the chemistry of **1**, the molecule has continued to attract interest and is now a standard, more reactive alternative to $Cp_2Mo_2(CO)_6$ as a starting material in CpMo chemistry.

Most of the new chemistry has been reported for (**1**) or $Cp^*_2Mo_2(CO)_4$ (**2**) ($Cp^* = C_5Me_5$). $Cp_2Cr_2(CO)_4$ shows a disappointing lack of reactivity associated with the Cr≡Cr triple bond, per se, and $Cp_2W_2(CO)_4$ seems to parallel its Mo congener in much of its chemistry. This article reviews work which has been published since the last review[1] as well as unpublished work from the author's laboratory. In order to present a comprehensive picture, some overlap with the previous article occurs here. The literature coverage extends to the end of 1985.

SYNTHESIS AND STRUCTURES OF $Cp_2Mo_2(CO)_4$-TYPE COMPOUNDS

The structure of **1** was shown to have a linear Cp–Mo–Mo–Cp skeleton and four semi-bridging carbonyls.[2] The semi-bridging carbonyls are linear, as opposed to the nonlinear M–CO structure usually associated with semi-bridging carbonyls. It was proposed that these two classes of semi-bridging carbonyls represented donor (linear) and acceptor (nonlinear) interactions.[3,4]

An EHMO calculation for **1** indicated the linear, semi-bridging COs were election acceptors, although no rationale for the bent vs linear classification was proposed.[5] Hall and coworkers[6] have recently reported a PES study of $Cp_2M_2(CO)_4$ (M = Cr, Mo or W) and also have addressed the question of linear vs bent semi-bridging carbonyl groups with Fenske–Hall MO calculations.[6] They find that the geometry of the bridging CO is determined by the nature of the HOMO associated with the metal–metal interaction. If the HOMO is a π^*-orbital (as is usually the case for M–M single bonds between late transition metals), the M–C–O group is bent (**A**), whereas if the HOMO is an M–M π-bond, the M–C–O group is nearly linear (**B**). The calculations show a nest of tightly spaced M–M orbitals of σ-, δ-, δ^*-, π_{xz}- and π_{yz}-symmetry, and are consistent with the observed PES.

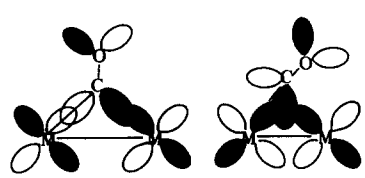

A **B**

The mechanism of the formation of **1** from the thermolysis of a solution of $Cp_2Mo_2(CO)_6$ has been shown[7] to involve loss of CO *without* M–M bond homolysis as originally proposed.[8] The presumed intermediate, $Cp_2Mo_2(CO)_5$, has been observed in a matrix.[9]

The structure of **2** has been determined and shown to have a bent Cp*–Mo–Mo–Cp* axis (ω = 168°).[10] The Mo≡Mo bond length [2.488(3) Å] is somewhat longer than the 2.448(1) Å observed for **1**.[2]

The compound originally reported[11] as (indenyl)$_2$Mo$_2$(CO)$_6$ has been shown by X-ray crystallography to be the triply-bonded tetracarbonyl In$_2$Mo$_2$(CO)$_4$ (**3**).[12] The overall structure closely resembles that of **2** in that only two of the four COs are semi-bridging and the InMoMoIn axis is nonlinear (Fig. 1). The Mo≡Mo distance is 2.500(1) Å. The triply-bonded tetracarbonyl reacts readily with CO at room temperature to give authentic In$_2$Mo$_2$(CO)$_6$.[12] The latter is also obtained from ferricenium ion oxidation of InMo(CO)$_3^-$ [eqn (1)].[12(b),(c)] Thermolysis of the purified hexacarbonyl dimer gives the highest yields of triply-bonded **3** [eqn (2)]:

$$2\mathrm{InMo(CO)_3^-} + 2\mathrm{Cp_2Fe^+} \longrightarrow \mathrm{In_2Mo_2(CO)_6} \qquad (1)$$

In = η^5-indenyl

$$\mathrm{In_2Mo_2(CO)_6} \xrightarrow[-2\mathrm{CO}]{110-140^\circ\mathrm{C}} \mathrm{In_2Mo_2(CO)_4} \qquad (2)$$

(3)

To date, no "indenyl effect" on the reactivity of **3** *vis-à-vis* **1** has been observed, probably because the unsaturation inherent in the Mo≡Mo triple bond overides any such effect.[12(c)]

Oxidation of the TpMo(CO)$_3^-$ anion with Cp$_2$Fe$^+$ gives the *mono*nuclear, 17e radical TpMo(CO)$_3$ (**4**) (Tp = hydridotrispyrazolylborato) [eqn (3)].[13] Refluxing acetonitrile solutions of (**4**) gives the triply-bonded dimer **5** [eqn (4)]:

$$\mathrm{TpMo(CO)_3^-} + \mathrm{Cp_2Fe^+} \longrightarrow \underset{\mathbf{4}}{\mathrm{Cp_2Fe}} + \mathrm{TpMo(CO)_3} \qquad (3)$$

$$2\mathrm{TpMo(CO)_3} \xrightarrow[\Delta]{} \underset{\mathbf{5}}{\mathrm{Tp(CO)_2Mo{\equiv}Mo(CO)_2Tp}} \qquad (4)$$

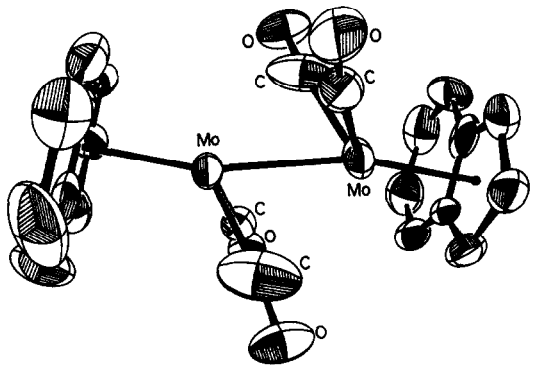

Fig. 1. ORTEP plot of (indenyl)$_2$Mo$_2$(CO)$_4$(Mo≡Mo).

The Tp–Mo–Mo–Tp axis in **5** is also nonlinear and only two of the four carbonyl groups are semi-bridging. The Mo≡Mo distance is 2.507(1) Å. The coordination about each Mo is quasi-octahedral if the metal–metal bond is considered to occupy one coordination site.

The chemistry associated with the Mo≡Mo bond in **5** is rather disappointing. No reaction was observed with acetylenes, Ph_2CN_2, CH_2N_2, S_8, propylene sulfide, P(OMe)$_3$ or H_2. Even CO does not react with **5** at atmospheric pressure. Prolonged reaction of **5** with CO (172 atm, 35°C) gave Mo(CO)$_6$ as the only carbonyl-containing product. In its reactions with Br_2 or I_2, **5** resembles **2** in that CO transfer occurs and RMo(CO)$_3$X (R = Tp or Cp*) are the only carbonyl products isolated.

A mixed Mo≡W triply-bonded compound may be prepared by refluxing a diglyme solution of Cp$_2$Mo$_2$(CO)$_6$ and Cp$_2$W$_2$(CO)$_6$ according to eqn (5).[14] The use of diglyme as solvent also gives an improved synthesis of compound **1**.[14] A mixed Tp–Cp dimer could not be prepared either by heating a solution of TpMo(CO)$_3$ and Cp$_2$Mo$_2$(CO)$_6$ or by mixing TpMo(CO)$_3^-$ with CpMo(CO)$_3$BF$_4$.[13(b)] In the former case, only **1** and unreacted TpMo(CO)$_3$ were recovered, while the latter reaction gave TpMo(CO)$_3$ and Cp$_2$Mo$_2$(CO)$_6$ by an electron-transfer process.

$$\mathrm{Cp_2Mo_2(CO)_6} + \mathrm{Cp_2W_2(CO)_6} \xrightarrow[\Delta]{-\mathrm{CO}} \mathrm{Cp_2M_2(CO)_4} + \mathrm{Cp_2MoW(CO)_4} \qquad (5)$$

M = Mo or W

The $R_2M_2(CO)_4$ compounds described in this section all display the same basic structure. However, the details of their reactivity seem to be influenced enormously by subtle changes in the steric and electronic properties of the groups R. We turn now to a survey of the chemistry associated with the metal–metal multiple bonds. Where warranted, the chemistry of some of the more interesting compounds prepared from **1** and its homologs will also be described.

NUCLEOPHILIC ADDITIONS TO THE M≡M BONDS

Molecular-orbital basis for reactivity

In molecular-orbital parlance, a molecule interacting with a nucleophile must possess a relatively low energy acceptor orbital. Both the Fenske–Hall[6] and EHMO[5,15] calculations on Cp$_2$Mo$_2$(CO)$_4$ show the π^*_{yz} MO to be the LUMO when the Cp rings are centered on the Mo–Mo axis. The π^*_{xz}

orbital lies at slightly higher energy. When the rings are tilted off the Mo–Mo axis as shown in Fig. 2, the energy of the π^*_{xz} orbital drops and it becomes the LUMO.

An inspection of the structures of the products of a variety of nucleophilic additions suggests that the regioselectivity of nucleophilic addition may be controlled by either π^*_{xz} or π^*_{yz}. The energy barrier to bending the CpMoMoCp axis is apparently quite low,[5] so that either path A or path B (Scheme 1) may be followed, depending on subtle electronic and steric requirements of the reactants. Path A seems to be followed by bulkier nucleophiles, e.g. phosphines and phosphites,[8,14] whereas bridging ligands, e.g. cyanide ion,[3] alkynes and diazoalkanes, seem to prefer path B (see below). Isomerization of the products has been noted in some instances (see below), so that the observed geometries of the isolated products may not correspond to those of initial, kinetic products, however.

In any event, simple electron counting suggests that an M=M double bond should result if the *net* result of a reaction is the addition of two electrons to the dimetal unit, an M–M single bond results from adding 4 electrons net, while donation of six electrons disrupts the metal–metal bonding.

Reactions with sulfur-containing reagents

Molybdenum is the chief constituent of many hydrotreating catalysts, especially those used for hydrosulfurization (HDS).[16] The reactions of the Mo≡Mo bond with sulfur-containing molecules has therefore been of interest. Alper and coworkers

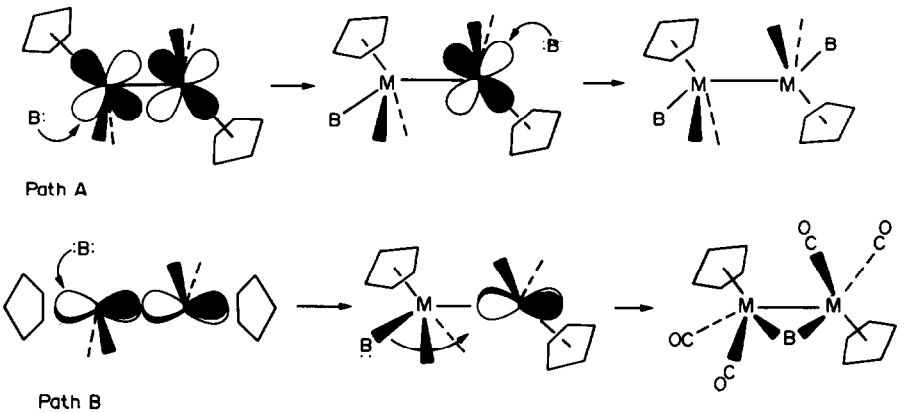

Scheme 1.

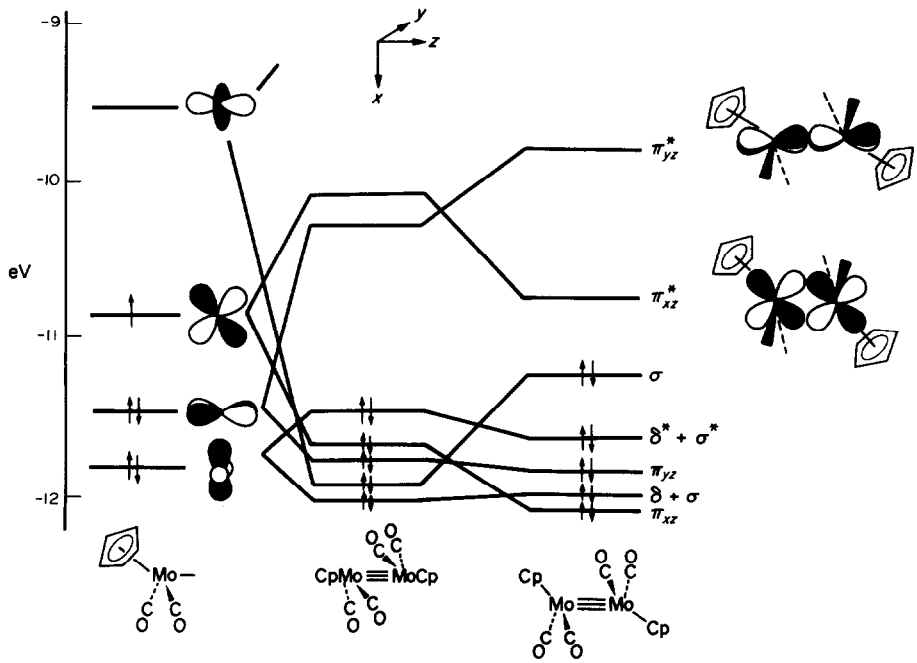

Fig. 2. MO energy levels of $Cp_2Mo_2(CO)_4$ as a function of the Cp–Mo–Mo angle (ω).

have shown that organosulfur compounds bind to the dimetal framework of **1** to give unusual structures [eqns (6)–(8)] [M = $Mo(CO)_2Cp$]:

(6)[17]

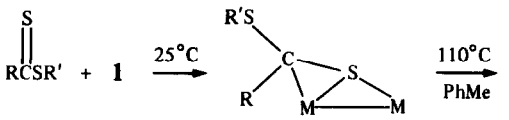

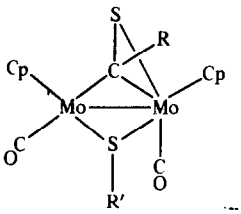

(7)[18]

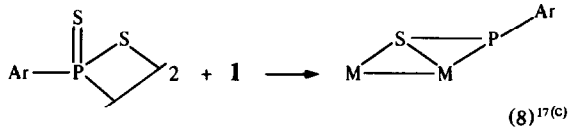

(8)[17(c)]

With Ph_3PS, **1** gives an unusual 1,1-disubstituted product [eqn (9)] rather than the usual 1,2-product shown in path A of Scheme 1.[19]

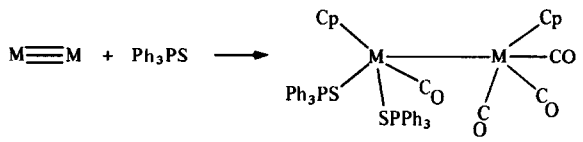

(9)

Isothiocyanates react with $(C_5Me_5)_2Mo_2(CO)_4$ (**2**) according to eqn (10). With a 10-fold excess of RNCS, only the dithiocarbamate was isolated. With a 1:1 ratio of RNCS and **2**, the μ,η^2-isocyanide was produced with a conversion of 6%.[20] Similar isonitrile complexes are produced directly in high yield from the reaction of RNC with **1**.[21]

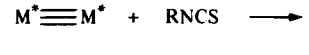

2

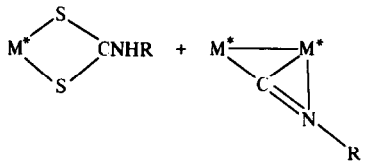

(10)

M* = $Mo(CO)_2Cp^*$

Refluxing a CS_2 solution of **1** gave the CS_2 adduct in *ca* 20% yield [eqn (11)]:[22]

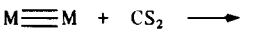

1

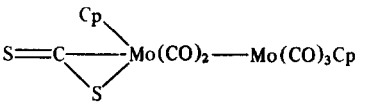

(11)

Reactions with phosphorus-containing nucleophiles

Most simple phosphines or phosphites react with **1** to give the disubstituted dimers corresponding to path A of Scheme 1. The cyclic phosphite (**6**) reacts with **1** with CO *substitution* and retention of the Mo≡Mo triple bond [Mo–Mo distance in **7** = 2.506(1) Å] [eqn (12), L = **6**].[23]

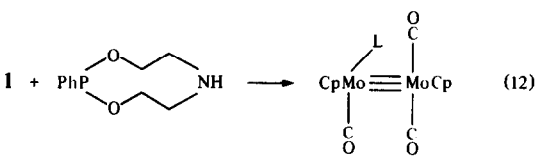

(12)

6 **7**

Compound **7** reacts with CO and isonitriles in the same manner that the parent **1** reacts [eqns (13) and (14)], but with $P(OMe)_3$, the ligand **6** is displaced [eqn (15)].[23] There is no ready explanation for the unusual behavior of phosphite **6**.

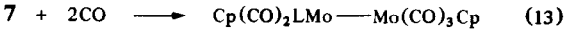

(13)

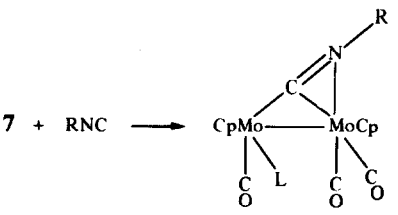

(14)

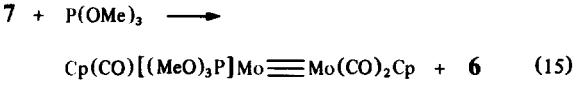

(15)

The reactions of M≡M with ylides are of considerable interest since such reactions could lead to new routes to alkylidene complexes. Unfortunately, these reactions are exceedingly messy and interesting products cannot be obtained in high yield.*

* Reactions of **1** with Me_3PCH_2 or $Me_2P(CH_2)_2^-$ gave very complex mixtures.[24]

The products, **8** and Ph_3P, show that extensive fragmentation of the ligand occurs.[25] The Mo=Mo distance in **8** is 2.885(1) Å.

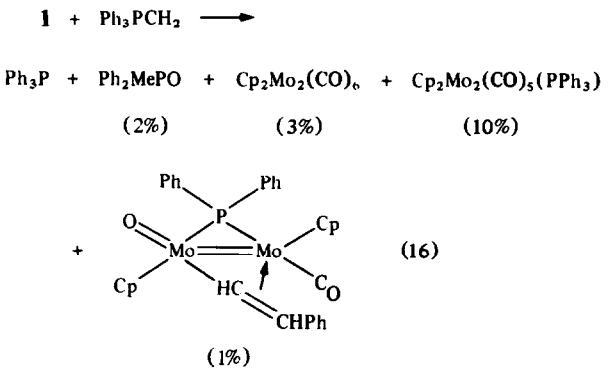

8

The phosphaalkyne $^tBuC{\equiv}P$ reacts with **1** to give an adduct with the same tetrahedrane type structure obtained from **1** and alkynes:[26]

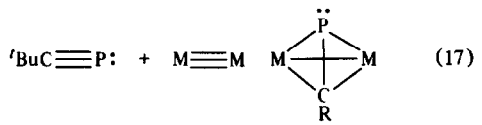

Reactions with alkynes and alkenes

At room temperature, **1** reacts rapidly with all but the most hindered alkynes to give tetrahedrane-type adducts [eqn (18)].[8,27–29] These adducts typically have the following bond lengths (Å): Mo–Mo, 2.98; Mo–C, 2.18; and C–C, 1.33. The ^{13}C chemical shifts of the acetylenic carbons of a variety of adducts of type **9** are collected in Table 1. The values range from δ 29 for a silyl-substituted carbon to *ca* 140 for stannyl substitution. Large differences between two differently substituted carbons in the same coordinated acetylene are evident, viz. 100.7 and 29.3 for $HCCSiMe_3$, and 117 and 40 for $MeCCSiMe_3$. The usual range for C- or H-substitution is 60–90 ppm.

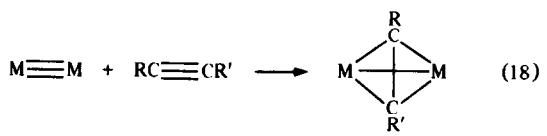

9

These alkyne adducts show interesting reactivity. At higher temperatures (>100°C), they lose CO and react with additional alkynes to form new

Table 1. ^{13}C NMR chemical shifts of acetylene and acetylide dimolybdenum complexes

R[a]	R′	δC	δC′	Reference
H	H[b]	61.9	—	27
Me	Me[b]	82.6	—	27
Co_2Me	Co_2Me	62.0	—	27
H	CH_2CH_2OH	87.2	?	27
H	Et	86.0	60.9	29
Me	$SiMe_3$	117.4	40.4	28
Ph_3Sn	Ph_3Sn	140.4	—	29
H	$SiMe_2Ph$	100.7	29.3	28
—[c]	Ph	185.8	101.8	40

[a] R and R′ are acetylenic substituents in structure **9**.
[b] Free acetylenes resonate at 71.6 and 73.9, respectively.
[c] Acetylide structure **23**.

ligands derived from sequential coupling of two–four alkyne ligands.[28,30–33] The structural types so produced are indicated by **10–13** shown below:

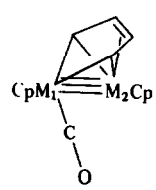

10

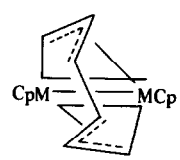

11

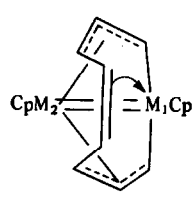

12

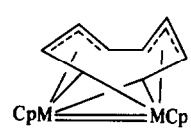

13

When terminal alkynes (RCCH) are employed, the C_4-ring in **10** shows predominate head-to-tail coupling of the two alkynes. The isomers of **11–13** which are formed by the reaction of alkynes with **10** show that the new alkynes which are incorporated may enter at either Mo–C bond in the MoC_4 ring [eqn (19)]. Structures of type **12** are also formed by one electron reduction of the mononuclear, $CpMo(RCCR)_2(NCMe)^+$ complexes.[34]

In addition to the main products shown above, smaller quantities of compounds of type **14** and **15** may be isolated from the reaction mixtures. These compounds are probably formed by the reaction of the triply-bonded precursors **10** and **11** with CO as has been demonstrated in one instance [eqns (20) and (21)]:[32]

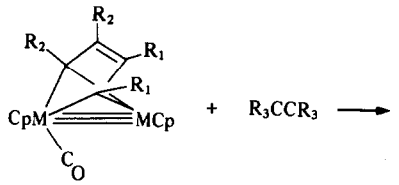

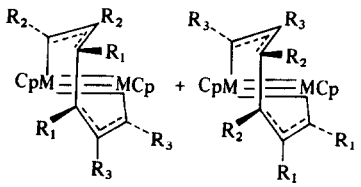

(19)

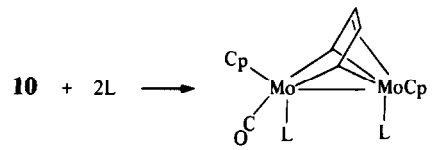

(20)

L = CO or RNC

14

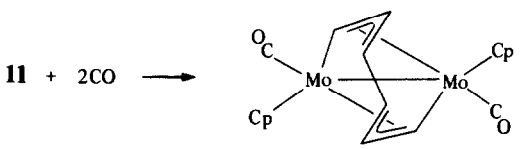

(21)

15

The details of the structures of these alkyne adducts show some interesting features. The terminal carbons of the C_4-fragment in **10** are symmetrically bonded to both metals [*d*-(Cr–C) = 2.025(7) Å avg.] and thus appear to be bridging alkylidene carbons. Their ^{13}C NMR resonance ($\delta \sim 210$ ppm) is consistent with this description.[35] The middle carbons of the M_1C_4 fragment are η^2-bonded to the M_2 metal [$d(M_2–C) = 2.23$ Å]. The M_1C_4 ring system itself appears to be delocalized[36] with equal C–C bond lengths (≈ 1.42 Å avg.).

Structure types **12** and **13** are isomeric. In **12**, both termini (C_t) of the C_8-ligand are very tightly bonded to one metal [$d(M_1–C_t) = 2.08$ Å, $d(M_2–C_t) = 2.23$ Å]. The $M_1–C_t$ distance approaches that expected for Mo=C double bonds,[37] while the $M_2–C_t$ distance is in the range found for Mo—C single bonds. M_2 is η^3-bonded to opposite ends of the C_8-fragment while M_1 is also η^2-bonded to the two central carbons.

In **13**, the two terminal carbons bridge the two metals in a nearly symmetrical manner (the M_2C_2 rhombus has essentially C_2-symmetry with two opposite M–C bonds of length 2.18 Å and another opposite set of two M–C bonds of length 2.14 Å) (cf. structure **10**). The next three carbons from each end of the C_8-chain are η^3-bonded to one metal each and the two halves are joined by a C—C single bond. This description of the bonding differs from that originally proposed.[30,31]

In both isomers, **12** and **13**, the electron count demands a Mo=Mo double bond to achieve an 18-electron count at each Mo.[1] The Mo=Mo distances[31,34] range from 2.595(1) to 2.635(1) Å. This distance compares with *ca* 3.0 Å for bridged M—M single bonds and 2.448(1) Å for the Mo≡Mo bond in **1**.

The mono-alkyne adducts (**9**) are readily protonated by strong acids to produce the μ,η^1,η^2-vinyl complexes **16**.[29,38] The stereochemistry of the protonated product suggested that the proton was delivered to the alkyne moiety via the metal in an intermediate, e.g. **17**. The tungsten analogue of **17** was subsequently observed as a product of the protonation of the carbyne complex $Cp(CO)_2W{\equiv}CR$.[39]

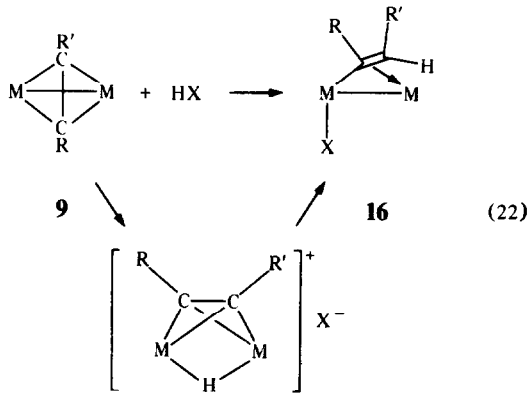

(22)

17

Excess acid protonates the trifluoroacetate group ("X" in **16**) giving coordinatively unsaturated intermediate **18** which is fluxional on the NMR scale. The coordination unsaturation of **18** allows for the oxidative addition of H_2 and subsequent stoichiometric hydrogenation of the alkyne. Under catalytic conditions with a large excess of alkyne, the excess alkyne inhibits the oxidative addition of hydrogen and the alkyne is polymerized instead [eqn (23b)].[29]

Methoxyallene reacts with **1** to give the adduct **19** [eqn (24)]. Fluoroboric acid reacts with **19** to give MeOH and the cation **20**. Cation **20** is also obtained from the reaction of the adduct of methyl propargyl ether (**9**: R = H, R′ = CH_2OMe) with HBF_4 [eqn (25)].[40] Figure 3 is a PLUTO drawing of **20**. This perspective shows that **20** may be regarded as a cationic μ-η^1,η^1,η^3-allenyl complex in which the C_3-fragment is π-bonded to Mo1 and

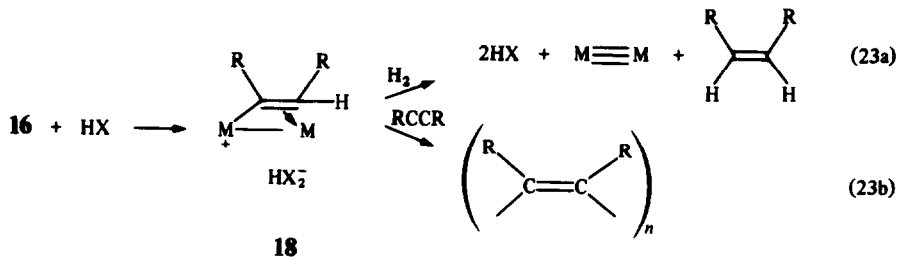

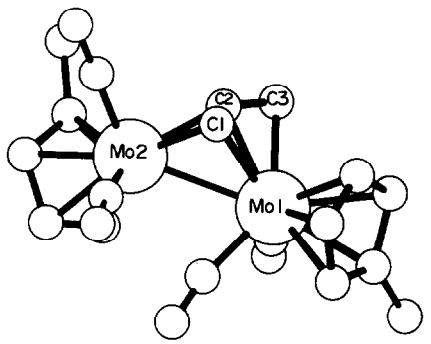

Fig. 3. PLUTO drawing of the cation, $Cp_2Mo_2(CO)_4(\mu\text{-}C_3H_3)^+$ (**20**).

two C—H bonds of the π-allyl group have been replaced with two Mo2–C σ-bonds.

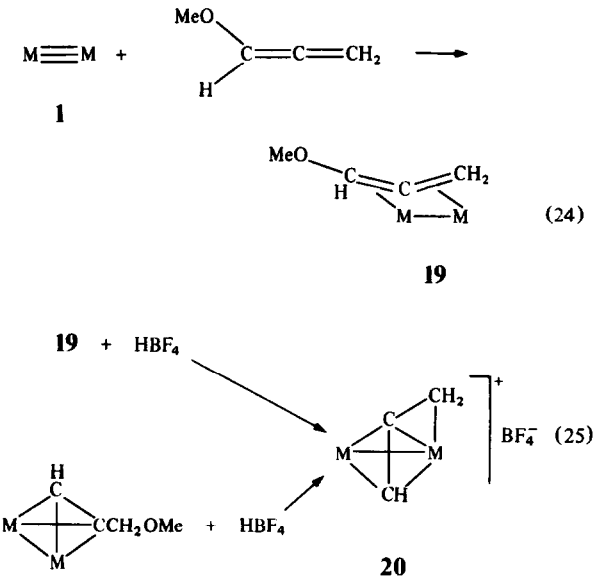

9 (R = H, R′ = CH_2OMe)

Complex **20** is fluxional on the ^1H NMR time scale ($\Delta G^{\pm}$ = 16.9 kcal mol^{-1} at 338 K). At −60°C, the spectrum is consistent with the solid-state structure (two types of Cp groups): δ 6.76 (d, J = 1.7 Hz, =CH), 5.33 (d, J = 1.7, —CH_2), 5.05 (s, —CH_2). At 75°C, the Cp groups are equivalent but the signals due to the C_3H_3 fragment do not vary with temperature. The dynamic process shown in Scheme 2 interconverts enantiomers of **20** via the symmetrically bridged intermediate in which the plane of the C_3H_3 fragment is perpendicular to the Mo–Mo bond. This process resembles the higher energy fluxional processes[27,28] in the acetylene adducts (**9**) and μ-vinyl complexes (**16**).[29,38]

The ^{13}C NMR shifts of the C_3-fragments in **20** and its precursor complexes **19** and **9** (R = H, R′ = CH_2OMe) show interesting trends. We label the MeO-bearing carbon Cα in the precursors. Upon loss of MeO^- to form **20**, Cα of **19** but Cγ of **9** become C1 of **20**. These relationships and the chemical shifts of corresponding carbons are shown below (see Fig. 3 for numbering scheme of **20**):

19	**20**	**9** (R = H, R′ = CH_2OMe)
38 (Cγ) →	76 (C3) ←	76 (Cα)
176 (Cβ) →	118 C2) ←	56 (Cβ)
101 (Cα) →	81 (C1) ←	86 (Cγ)

Insofar as these chemical-shift changes reflect charge redistribution, it is seen that the electronic structure of the C_3-fragment in **20** resembles more closely that of the acetylene adduct **9** than the allene adduct **19**. In particular, the deshielding of Cγ in **19** suggests that positive charge is transferred from Cα to Cγ in the transformation **19** → **20**. This conclusion is borne out by the reactivity of **20** toward nucleophiles [eqn (26)].[40] Even hindered bases, e.g. $^iPr_2NLi$, attack the terminal carbon, C3, to yield alkyne complexes **21**. We have been unsuccessful in attempts to remove a proton from **20**.

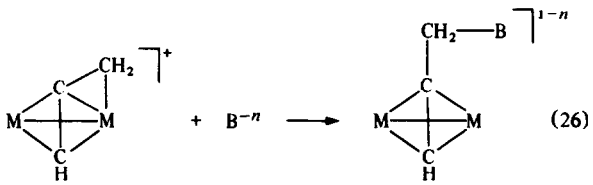

20 **21**

B = Py, $^iPr_2N^-$, MeO^-, CN^- or R_3P

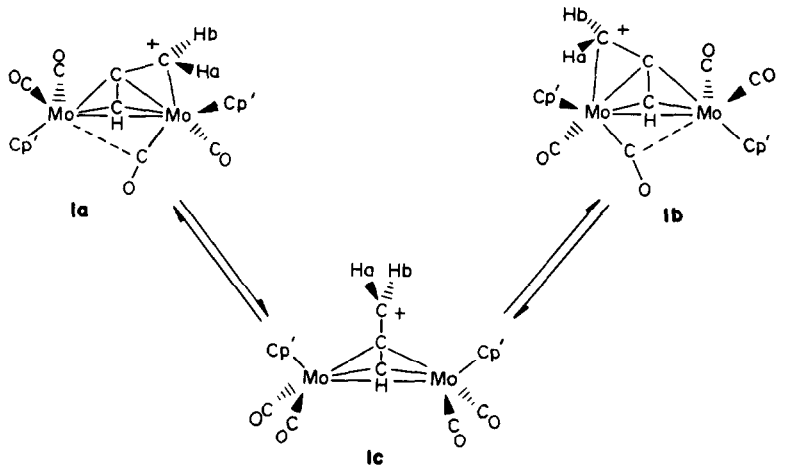

Scheme 2.

Metal carbonyl anions react [eqn(27)] with **20** in a redox manner to give the bis-adduct (**22**)[40] of 1,5-hexadiyne, previously prepared from **1** and the free diyne.[30] The reduction of **20** to give **22** is also accomplished with Na amalgam. Figure 4 is a PLUTO drawing of the structure of **22**.

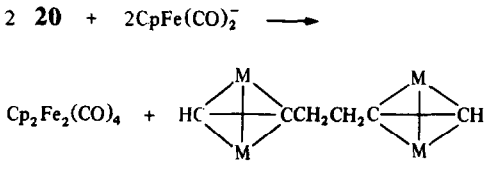

(27)

22

Complexes (**9**) of terminal alkynes react with strong bases, preferably $^{i}Pr_2NLi$ or $NaNH_2$, to produce μ-η^1,η^2-acetylide complexes (**23**) [eqn (28)].[41] The molecular structure of **23** (R = CH_2-OMe) is shown in Fig. 5. The counter ion in this crystal is Na(15-crown-5)$^+$. The Na^+ ion is also chelated by the methoxy oxygen and to one carbonyl oxygen in the solid state. Similar coordination of alkali cations to carbonyl groups has been observed previously.[42] These μ-η^1,η^2-acetylide complexes exhibit the same "windshield wiper" fluxional motion previously established for the

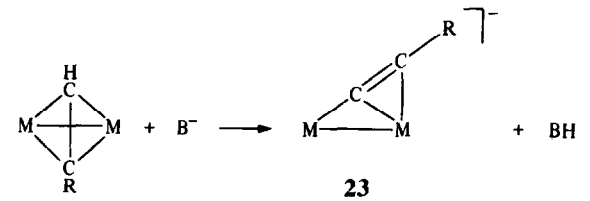

R = Ph or CH_2OMe (28)

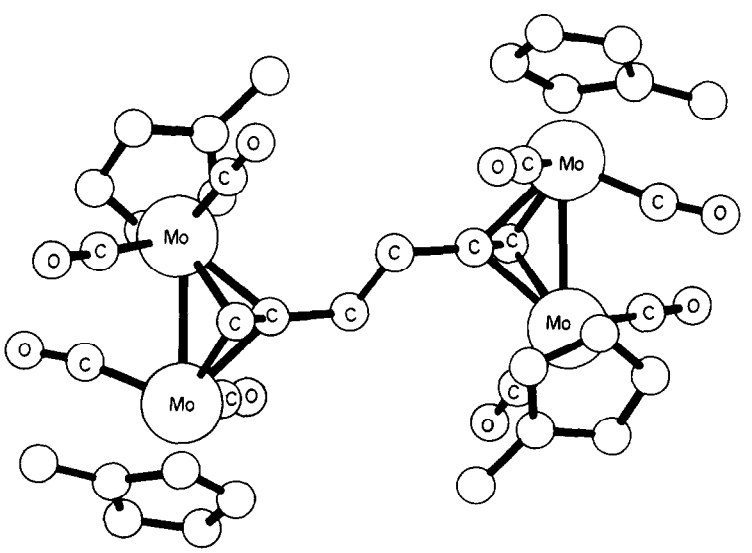

Fig. 4. PLUTO drawing of the 1,5-hexadiyne adduct (**22**) of $Cp_2Mo_2(CO)_4$.

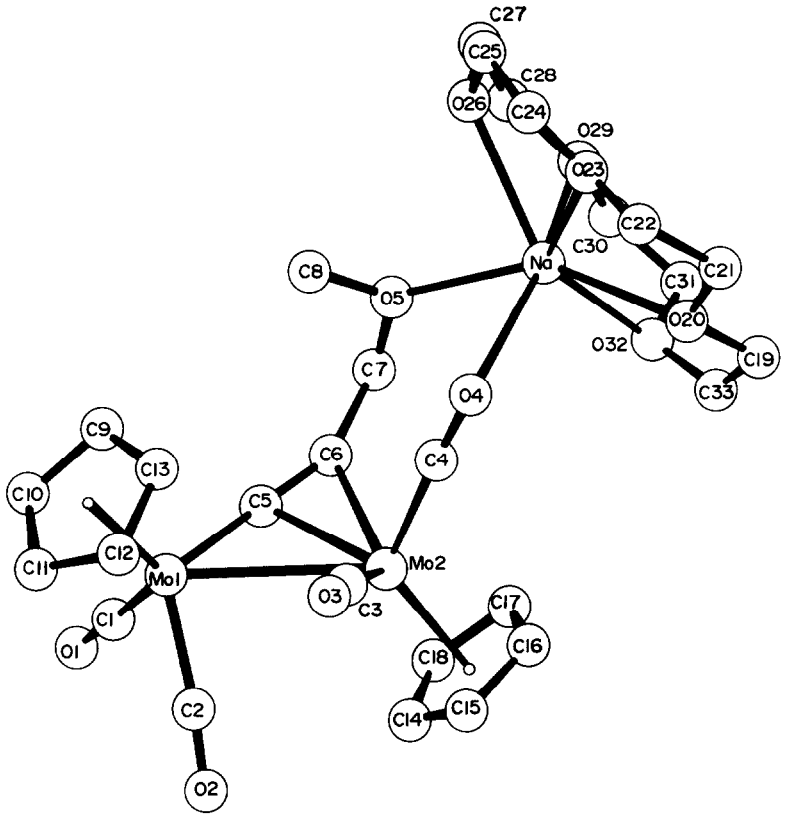

Fig. 5. ORTEP plot of Na(15-crown-5) $Cp_2Mo_2(CO)_4$ (μ-$CCCH_2OMe$) (**23**) showing the coordination of Na^+ to the methoxy and carbonyl oxygens of the anion.

cyanide adduct[3] of **1** and for other μ-η^1,η^2-acetylide adducts.[43,44]

The Mo1–C5 distance in **23** (Fig. 5) is 2.03(1) Å, a distance approaching those observed for Mo=C double bonds.[41] The Mo2–C5 and Mo2–C6 distances [2.285(6) and 2.318(6) Å, respectively] are not unusual for Mo bound to π-systems. The ^{13}C NMR chemical shifts of the acetylide carbons show a remarkable downfield shift in comparison to those in the parent complex **9** (cf. Table 1). The resonances due to C5 and C6 occur at δ 186 and 102, respectively.[41] The former resonance lies toward the downfield side of the range of chemical shifts observed for bridging methylene groups.[35] Thus, both the Mo1–C5 distance and the ^{13}C NMR chemical shift suggest considerable "carbene" character for the terminal carbon of the acetylide bridge in **23**.

The early papers on the reactivity of the Mo≡Mo triple bond reported that **1** does not react with alkenes.[8,27] It was later shown that more severe conditions (1–21 days, 110–130°C) gave complex mixtures from which low yields of structurally interesting compounds could be isolated [eqns (29)–(31)].[45,46]

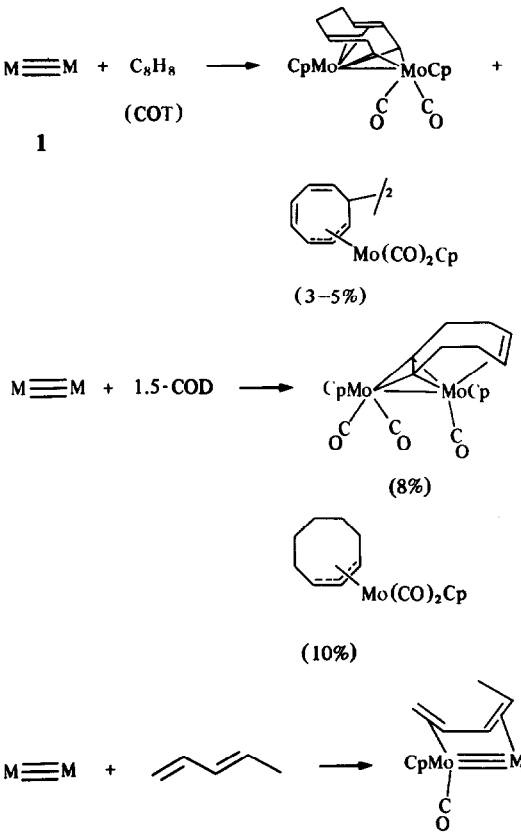

The alkyne adducts (**9**) react with cyclic, conjugated dienes to give products with ligands derived from formal Diels–Adler condensation of the diene with the coordinated alkyne [eqn(32)].[47] The Mo≡Mo bond length in **24** is 2.504(1)Å. All of these rather complex reactions involving alkenes undoubtedly occur with prior loss of CO from **1** or **9**.[32]

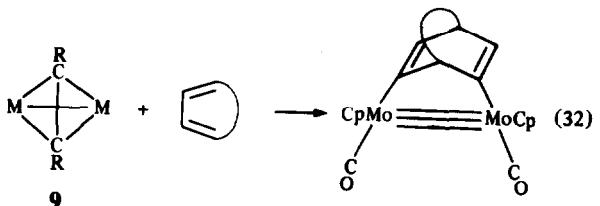

9 **24**

The reactions described in the section amply demonstrate that the easily prepared alkyne adducts of the Mo≡Mo triple bond form the basis for an extensive chemistry of hydrocarbon conversions on a bimetallic center. Even in those reactions which require higher temperatures and proceed with loss of CO, the strength of the Mo≡Mo triple bond serves to maintain the integrity of the dinuclear unit and suppress the formation of mononuclear products.

REACTIONS WITH 1,3-DIPOLES

The reactions of carbon–carbon multiple bonds with 1,3-dipolar reagents have been studied extensively.[48] For example, alkynes normally react with the 1,3-dipole to give the cycloadduct **25**. This adduct may expel the small molecule Y≡Z to give a three-membered ring (**26**) [eqn(33)].

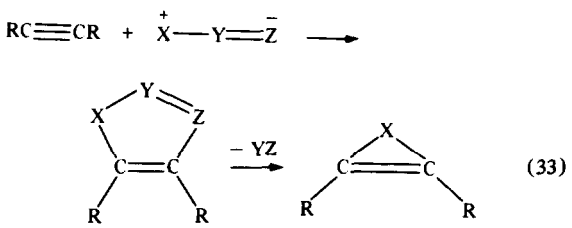

25 **26**

It is therefore of interest to determine how metal–metal multiple bonds interact with 1,3-dipolar reagents. What are the similarities and differences in behavior of metal–metal multiple bonds *vis-à-vis* their well-studied organic counterparts? The answers to such questions lead to increased understanding of factors governing chemical reactivity and, at the same time, provide the synthetic chemist with new routes to molecules of interest in related areas.

Reactions with diazolkanes

Diazoalkanes ($R_2C{=}N_2$) are prototypal 1,3-dipoles. In addition to the interest attached to the bonding of the diazoalkane ligand itself to a dimetal fragment, loss of N_2 from the adduct may give metal alkylidene complexes. The latter compounds are still of interest in connection with CO reduction chemistry.[35]

The coordination chemistry of diazoalkanes with M≡M (**1**) and related complexes has been both rewarding and frustrating in its complexity. No less than *seven* different reaction paths of diazoalkanes with M≡M have been well characterized. These are summarized in Scheme 3. The reaction of **1** with diaryldiazomethanes was the first reaction of this type to be reported and the product was shown to have the unusual bonding mode depicted in **27** (M = $Mo(CO)_2Cp$).[49,50] This structure is isolobal and isoelectronic with the bridging alkylidyne (**28**).[51]

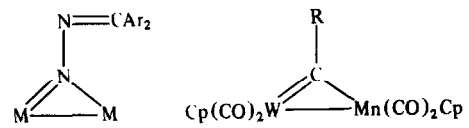

27 **28**

The parent diazomethane ($CH_2{=}N_2$) reacts with **1**, but no stable complex could be isolated—N_2 is evolved and polymethylene is formed.[1] However, CH_2N_2 reacts with the pentamethylcyclopentadienyl analog of **1**, hereinafter denoted by M*≡M* [M* = $Mo(CO)_2(C_5Me_5)$], with loss of N_2 to give an adduct with either structure **29** or **30**.[52,53]

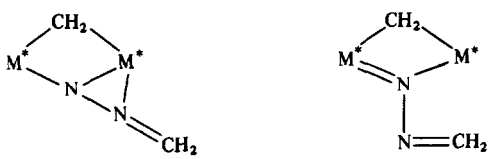

29 **30**

Diazopropane ($Me_2C{=}N_2$) reacts with either M≡M or M*≡M* to give an adduct in which the terminal nitrogen is bonded to both Mo atoms, and the central nitrogen also bonded to one of the Mo atoms.[54,55] In solution, a second isomer of $M_2(N_2CMe_2)$ is present as shown by the NMR spectrum.[50,54]

Ethyl diazoacetate reacts cleanly with M*≡M* to give adduct **31** which has the same coordination mode as the Me_2CN_2 adducts [eqn(34)].[50] An ORTEP plot of the structure of **31** is shown in Fig. 6. The major difference between the structure types **31** and **27** is that in **27** the terminal N donates a

Scheme III, M = Mo(CO)$_2$Cp

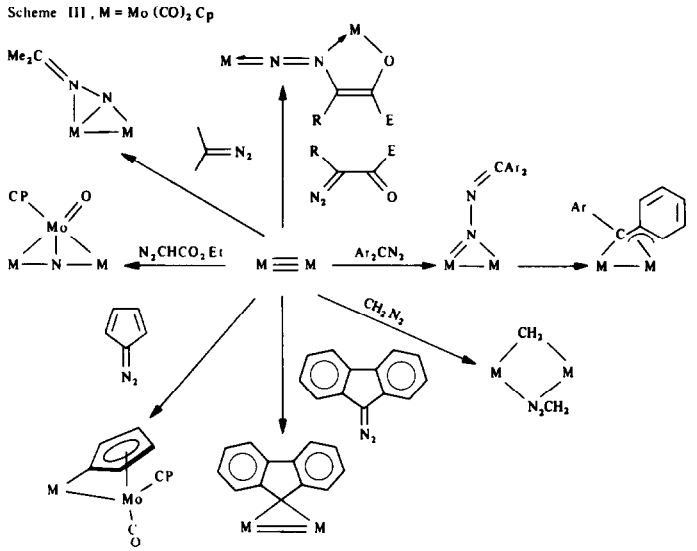

total of four electrons to the dimetal fragment, whereas in **31** the terminal N donates two electrons and the central N donates two also. In spite of their seemingly disparate structures, the bond distances and angles in the N_2C portion of the molecules **27** and **31** are virtually identical.

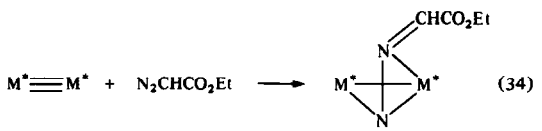

(34)

31

Reaction (34) is surprising because previous work had shown potential donor groups adjacent to the diazo group become coordinated to the metal in these diazoalkane adducts. Thus α-ketodiazoalkanes[56] and diethyl diazomalonate[50,54] react with M≡M or M*≡M* to give products containing a chelate ring which incorporates the keto or carboxyl oxygen [eqn(35)]. In these adducts, the α-keto or α-carboxyl diazoalkane reacts as a six-electron donor so the M≡M bond is completely disrupted.

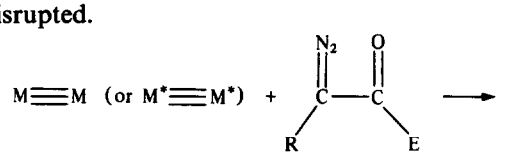

(35)

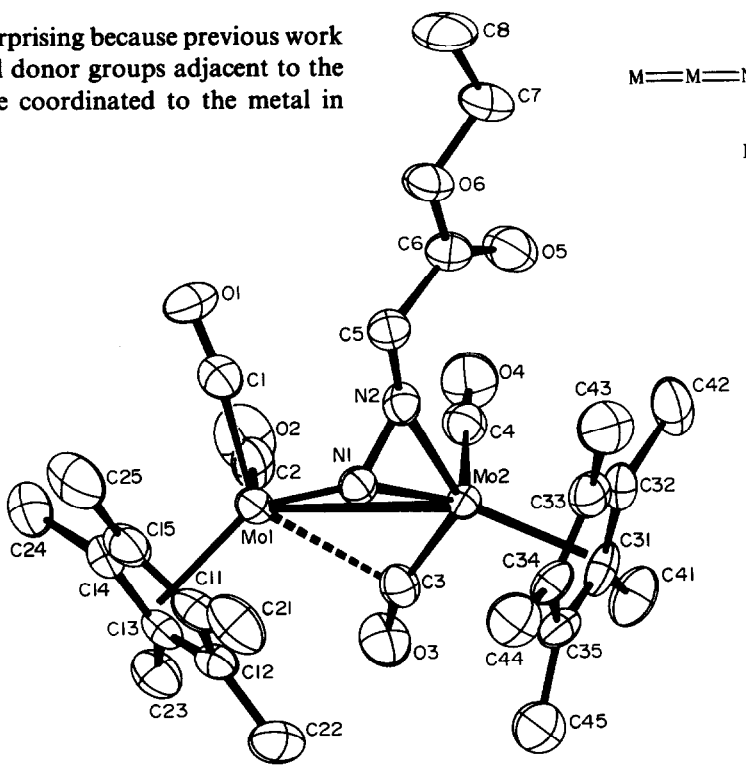

Fig. 6. ORTEP plot of $Cp^*_2Mo_2(CO)_4(N_2CHCO_2Et)$ (**31**).

Ethyl diazoacetate reacts with M≡M (**1**) at temperatures from −78°C to +110°C to give extremely complex mixtures.[54,57] Feasey *et al.* isolated cluster **32** in 5% yield from such a mixture.[57]

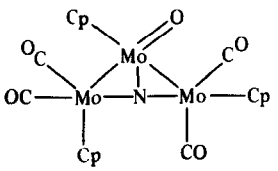

32

The reaction of **1** with the dienophile, diethyl azidodicarboxylate, gives a product (**33**) with a structure related to those depicted in eqn (35).[58] The molecular structure of **33** is shown in Fig. 7.

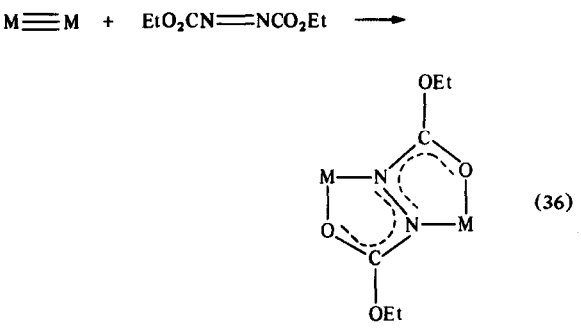

(36)

33

Reactions of diazoalkane adducts

By analogy with the organic chemistry of 1,3-dipolar cycloadducts depicted in eqn (33), it was of interest to investigate the tendency of the diazoalkane adducts of **1** and related compounds to lose N_2 and form dimetallacyclopropenes, i.e. μ-alkylidene complexes.

Herrmann *et al.* found that the adduct of 2-diazopropane and M*≡M* underwent a rearrangement in which the N–N bond was broken, one nitrogen then inserting into an Mo–CO bond to form an isocyanate, and the Me_2CN fragment forming a μ-imido group [eqn (37)].[53]

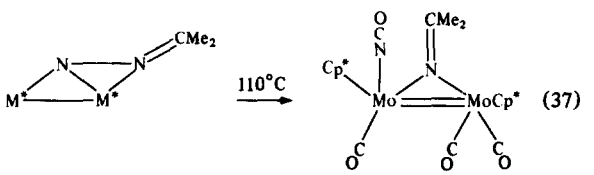

(37)

34

Me_2CN_2 or $C_5H_4N_2$ react with the triply-bonded tungsten complex, $Cp^*_2W_2(CO)_4$, at *ca* −20°C to give the μ-imido isocyanate W complexes analogous to **34**.[59]

The doubly-bonded complex **34**, and its W analog, add one equivalent of CO to form singly-bonded **35**.[53,59] In order for each metal to maintain the 18-electron count during this transformation,

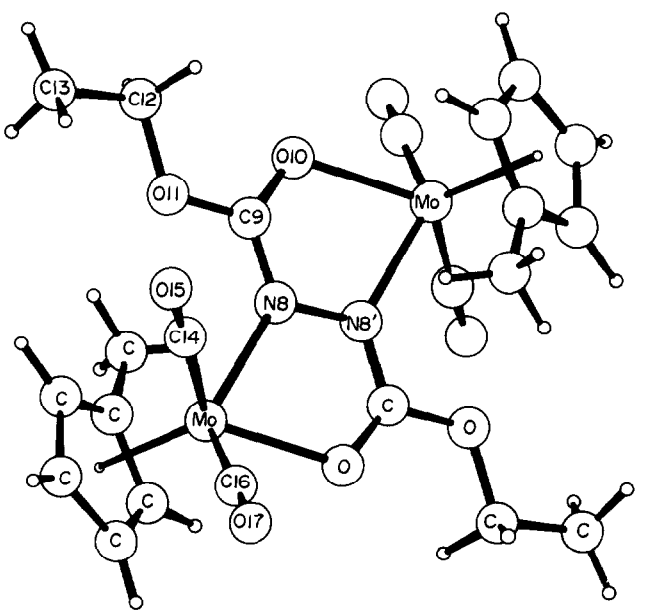

Fig. 7. ORTEP drawing of adduct (**33**) of diethyl azidodicarboxylate and $Cp_2Mo_2(CO)_4$.

an internal redox disproportionation must occur as illustrated in eqn (38).

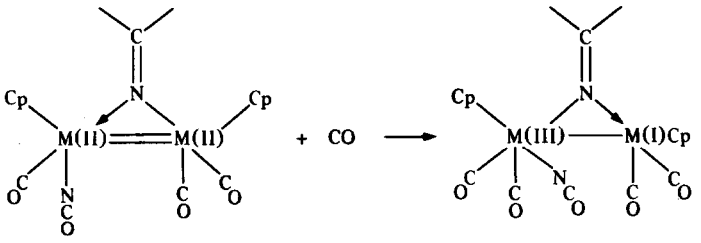

34 35

The adduct with structure **29** or **30** also undergoes an isomerization upon heating, but in this case the nitrogen inserts into the methylene bridge and two methyleneimido ligands are formed [eqn (39)].[53]

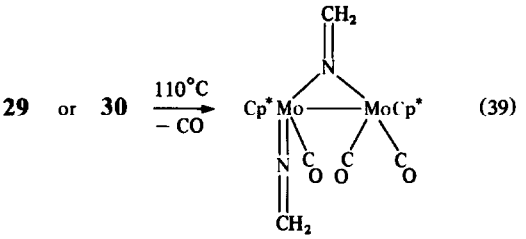

To date, the only diazoalkane adducts which cleanly lose N_2 and form μ-alkylidene complexes were the first to be discovered, viz. the diaryldiazomethane adducts (**27**).[49,50] Heating **27** (Ar = phenyl or *p*-tolyl) to 60°C causes an *intra*molecular loss of dinitrogen. The resulting μ-diarylalkylidenes were shown to have the structure depicted in **36** in which one aryl group has become coordinated to one Mo.[49,50] The intramolecular loss of N_2 from **27** is believed to occur through the 1,3-dipolar cycloadduct (**37**). This view is supported by the fact that the complexes $M_2^*(\mu\text{-}N_2CAr_2)$ do not lose N_2 cleanly, presumably because attainment of the transition state **37** is blocked by steric interactions between the bulky Cp* groups and the aryl groups.[50] Conversely, 9-diazofluorene reacts with **1** with loss of N_2 even below room temperature, presumably because the steric congestion in intermediate **38** is less than that in **37** as shown below. The product is the μ-fluorenylidene complex **39** which now has a Mo=Mo bond [2.798(1) Å] since the aryl groups are tied together and cannot bend over and coordinate to a metal as does the aryl group in **36**. The reactions of the μ-alkylidenes **36** and **39** with small molecules, e.g. CO, H_2, isocyanides and alkynes, are the subject of several reports.[60–62]

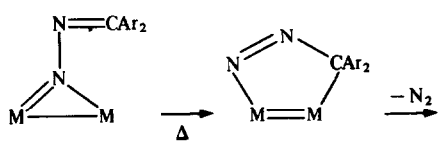

27 37

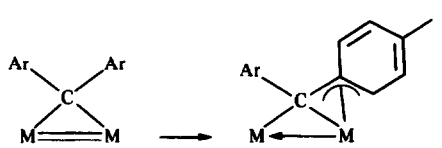

36

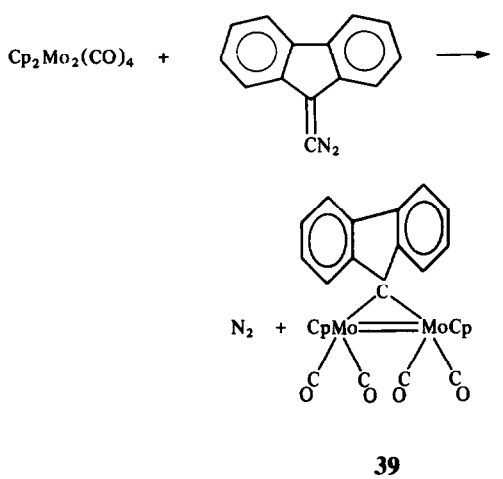

39

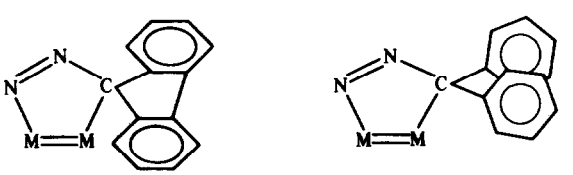

38 37

An uncrowded transition state similar to **38** also explains the facile loss of N_2 and subsequent formation of **40** when diazocyclopentadiene reacts with **1** [eqn (42)].[63]

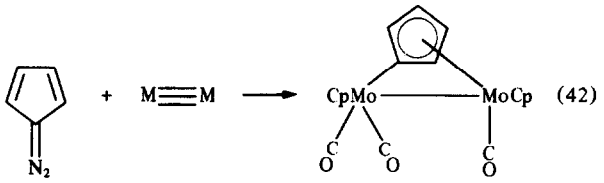

(42)

40

Reactions with other 1,3-*dipoles*

Organoazides are isoelectronic with diazoalkanes. Hence, the interaction of an organoazide with the M≡M triple bond could lead to a dimetallatriazene (the cyclic 1,3-adduct) which would be expected to lose N_2 and form a nitrene complex [eqn (43)].

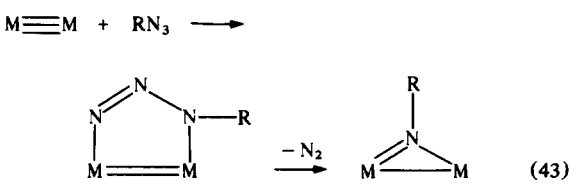

(43)

41

In fact, the reaction of aryl or alkyl azides with **1** follows a different course.[54,64] The *initial* product is probably the nitrene adduct (**41**). However, this initial product reacts with additional azide nearly as fast as it is formed to give the final complex (**42**).

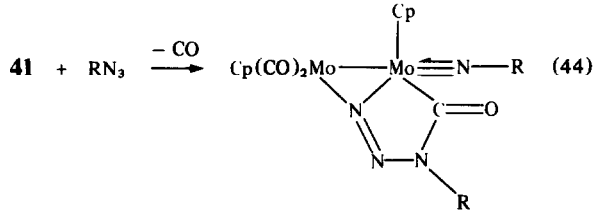

(44)

42

The final product contains a terminal nitrene triply bonded to Mo [Mo≡N = 1.75(1) Å] and a bridging chelate ring formed by attack of the second azide on a coordinated carbonyl. The transformation of a bridging nitrene to a terminal nitrene upon reaction with excess azide has its exact parallel in the transformation of an alkylidene from bridging to terminal upon reaction with excess diazoalkene [eqn (45)].[61] The major difference is that the carbon of the diazoalkane is not sufficiently nucleophilic to attack a coordinated carbonyl as does the N in eqn (44).

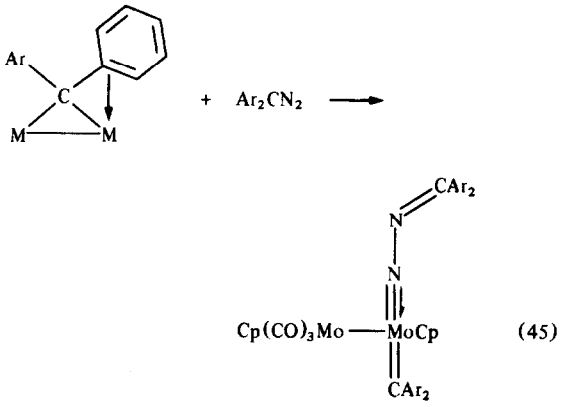

(45)

Cyclopropenes and azirines may be regarded as "masked" 1,3-dipoles.[48] The cyclopropene is a masked vinylcarbene [eqn (46)] and the azirine a masked nitrile ylide [eqn (47a)] or a masked vinyl nitrene [eqn (47b)].

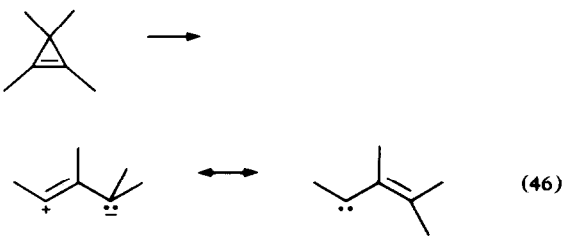

(46)

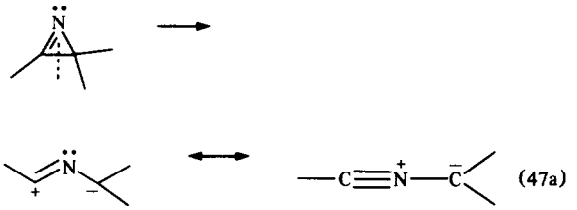

(47a)

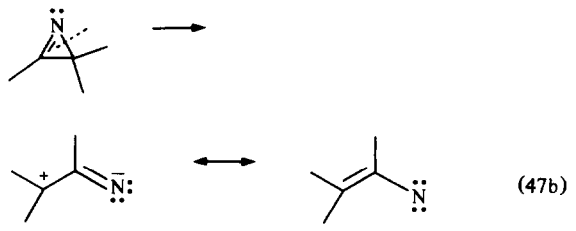

(47b)

In fact, **1** reacts with 1,1-dimethylcyclopropene to give the bridged, vinyl alkylidene (**43**).[65] The pattern of Mo–C (bridge) distances in **43** are very similar to those in **36** as might be expected. Thus, cyclopropene adds to the Mo≡Mo triple bond as if it were a vinyl carbene [cf. eqn (46)].

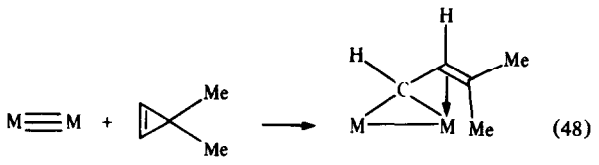

43 (48)

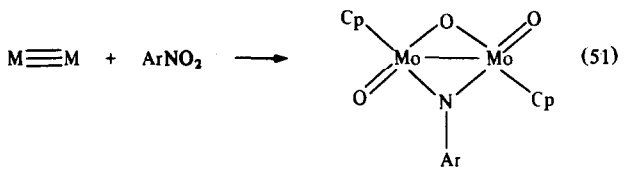

46 (51)

We have found that the Mo≡Mo triple bond is very reactive towards azirines. Compound **1** reacts with 2-phenyl-1-azirine to form a red, thermally labile complex which decomposes above 0°C to a green mixture of products.[66] Green and coworkers have isolated the azaallyl complex **44** by column chromatography from this mixture.[67] The extra proton on the azaallyl ligand presumably comes from the column packing.

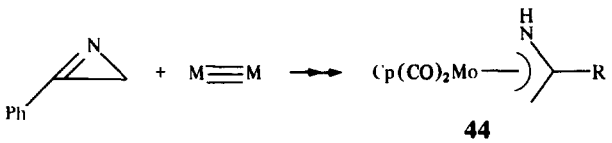

44 (49)

The phenylazirine also reacts with M*≡M* to give a labile adduct. However, 2-phenyl-3,3-dimethyl-1-azirine with M*≡M* gives a thermally stable product believed to have structure **45** on the basis of its NMR spectra (an X-ray structure determination is planned).[66] It thus appears that the azirine ring is behaving as a masked vinyl nitrene in reactions with Mo≡Mo triple bonds.

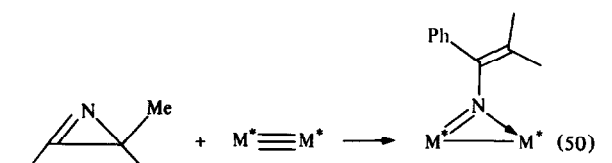

45 (50)

Alper *et al.*[68] have found that nitro arenes ($ArNO_2$) react with **1** or the W-analog to give the complex shown in eqn (51). Although $ArNO_2$ may be classified as a 1,3-dipole,[48] it is doubtful that this property is required for reaction (51) since aryl nitroso compounds (ArNO) react with **1** to give the same products.[68]

The Mo–Mo single bond distance in **46** is only 2.65 Å, a distance which is shorter than the formal Mo=Mo double bonds in compounds **34** and **39** discussed above. In compounds in which the Mo is in a high formal oxidation state, e.g. in **46**, extensive π-bonding with the bridging ligands undoubtedly serves to contract the Mo–Mo bond distance.

Compound **1** reacts slowly with excess carbodiimides in refluxing toluene to give the products shown in eqn (52).[69] The high temperature and slow rate of reaction again suggest that the reaction is proceeding by prior loss of CO from **1** followed by coordination of the carbodiimide. The Mo≡Mo triple bond in **47** reacts with CO to give a saturated derivative $[Cp_2Mo_2(CO)_5(RNCNR)]$.[69]

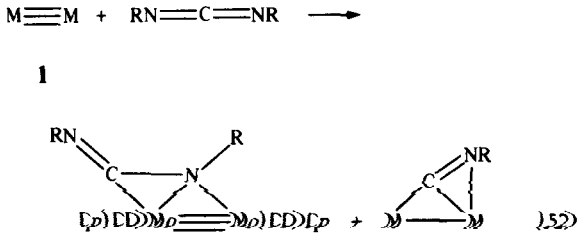

47 (52)

Although many interesting structures are formed by the interaction of 1,3-dipolar reagents with the M≡M triple bonds in **1** and related compounds, only in the decomposition of the adducts of Ar_2CN_2 with **1** [eqn (40)] is there any persuasive evidence that 1,3-dipolar cycloadducts are formed. The lack of cycloadduct formation is in keeping with the different behavior of these M≡M triple bonds *vis-à-vis* C≡C triple bonds. Attack of the nucleophilic end of the 1,3-dipole on a C≡C bond generates a nucleophilic site on the contiguous carbon. Ring closure then occurs when this nucleophilic carbon reacts with the electrophilic end of the dipolar reagent [eqn (53)].

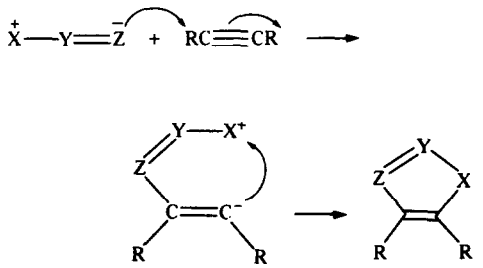

(53)

In contrast, attack by a nucleophile on one end of the M≡M triple bond in **1** generates a 16-electron, *electrophilic* site on the remote metal [eqn(54)] due to collapse of electrons into non-bonding levels which are not available to carbon (see electron-counting arguments in Ref. 1). Thus, there is no charge development which directs ring closure to a 1,3-dipolar cycloadduct. Instead, the preferred reaction path seems to be first coordination of the most nucleophilic portion of the dipolar reagent, followed by rearrangements and/or coordination of other donor functions on the dipolar reagent to eventually "saturate" the M≡M triple bond according to the scheme in eqn (54) (B′ represents any second donor function, i.e. B and B′ may be in the same molecule or on different molecules).

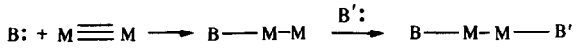

(54)

OXIDATIVE REACTIONS WITH NON-METALS

In our initial explorations of the chemical behavior of compound **1**, we were disappointed in its lack of reactivity toward molecular H_2. However, it was demonstrated recently that photolysis of $CpW(CO)_3H$ gives the μ-dihydride [eqn(55)].[70] Compound **48** is unstable in solution, presumably dissociating to H_2 and $Cp_2W_2(CO)_4$. The C_5Me_5 derivatives are stable, however, and may be prepared by the direct reaction of the M*≡M* bonded compounds with H_2 under UV photolysis.

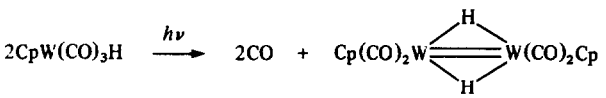

48

(55)

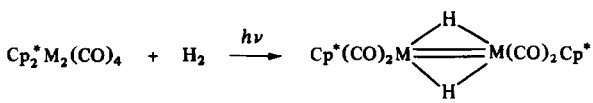

M = Mo or W

(56)

The multiply-bonded Mo dimers show high reactivity toward other non-metals, e.g. P, As, S, Se etc. With white phosphorus, **1** forms tetrahedrane clusters [eqn(57)].[71]

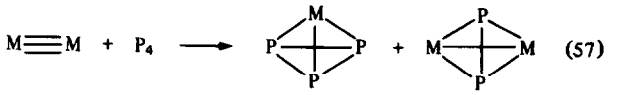

M = $CpMo(CO)_2$

Under more forcing conditions, the derivatives react to give a mixture of structurally novel complexes in low yield [eqn(58)].[72] Included in the products is a triple-decker complex with a P_6-ring sandwiched between two Cp*Mo moieties. The Mo–Mo distance in this complex is 2.647(1) Å and the Mo–P avg. distance is *ca* 2.54 Å. There is some evidence for a ring current associated with the P_6-ring: the Me groups of the Cp* ligands resonate at δ 0.47 instead of their more usual value of *ca* 2.

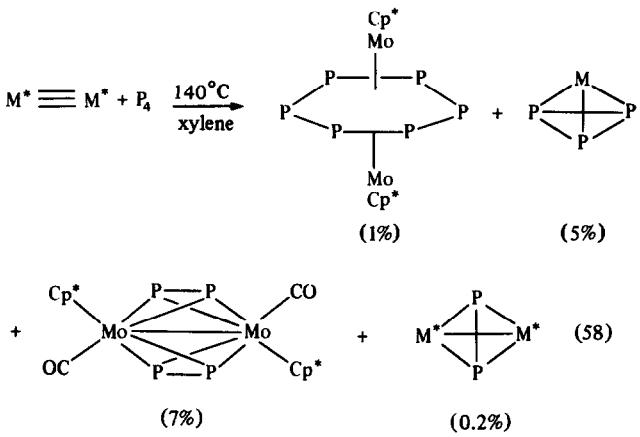

(1%) (5%) (7%) (0.2%)

(58)

Arsenic and its derivatives also react with **1** [or its precursors, $Cp_2Mo_2(CO)_6$ or $CpMo(CO)_3H$] at elevated temperatures to give novel Mo–As clusters [eqns (59),[73] (60),[74] (61),[75] (62)[76] and (63)[77]].

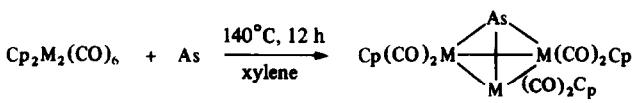

M = Mo, 65%
M = W, 40% **49**

(59)

The structure of **49** is similar to that of the isoelectronic cation, $Cp_3Mo_3(CO)_6S^+$ (see below) except that in **49** the $CpMo(CO)_2$ units are twisted relative to one another in such a way that the cluster has no symmetry, whereas the sulfur cation cluster has approximate C_3-symmetry in the solid state.[78]

Reactions (61)–(63) do not use the triply-bonded dimers as starting material, but the reactions are conducted under conditions where **1** (or **2**) forms rapidly. In any event, the products are so closely

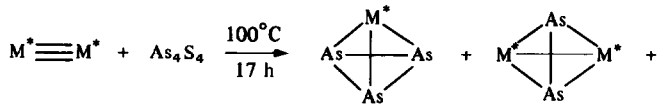

(12%) (4%)

50 **51**

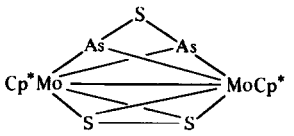

(26%)

52

(60)

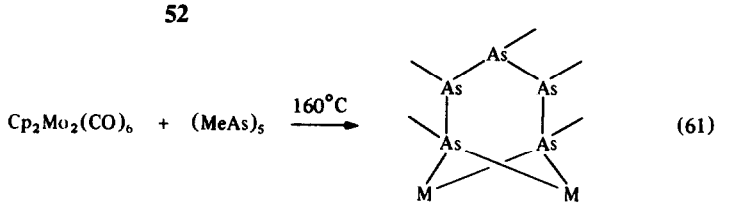

(61)

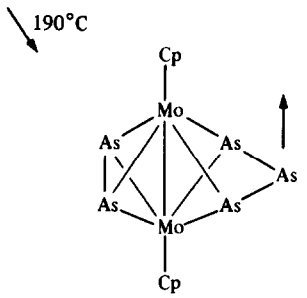

(62)

53

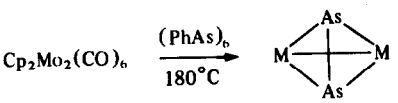

(63)

54

related to those obtained from **1** or **2** that they are included here for completeness.

Compound **53** was described originally by the authors as having a Mo=Mo double bond. However, if the ligands are considered to be μ-As_2^{4-} and μ-As_3^{4-}, then the formal oxidation state of Mo is $+5(d^1)$ so the maximum Mo–Mo bond order is one. The Mo–Mo distance [2.75 Å] is consistent with an Mo–Mo single bond bridged by three or four groups.* Complex **53** is quite unusual nevertheless. The five As atoms are essentially coplanar and the Mo–Mo bond is perpendicular to the As plane. The As atoms are segregated into two groups, As_2 and As_3, and an odd electron is apparently localized on the central As of the μ,η^2-As_3 ligand.[76] Reaction 61 is very similar to the reaction of M≡M with disulfides (RSSR).[8]

The series, M_nAs_{4-n} ($n = 1$–3), is represented by compounds **50**, **51** or **54**, and **49**. The $n = 0$ (As_4) is known in the gas phase, but there is no convincing evidence for the existence of the $n = 4$ member, i.e. M_4.[8,14] The As–As distance in **54** is 2.31 Å, commensurate with an As=As double bond. Complexes **51** and **54** may then be regarded as adducts of

* Mo–Mo distances in a variety of Mo–S dimers and clusters show a strong correlation with the number of sulfide bridges: μ-S, Mo–Mo ≃ 2.9–3.0 Å; 2μ-S, Mo–Mo = 2.75–2.8 Å; 3 or 4μ-S, Mo–Mo = 2.65–2.7 Å.[79]

M≡M with the alkyne analogue As≡As. Synergic bonding reduces the As–As bond order from 3 to 2 in the same manner that the C–C bond order is reduced in the alkyne adducts.

The M≡M triple bond is also quite reactive with the chalcogens. The reaction of **1** with excess sulfur produces red, insoluble polysulfides[78] ($[CpMoS_x]_n$) identical to those obtained from the reaction of $Cp_2Mo_2(CO)_6$ with excess sulfur. However, if the stoichiometry is carefully controlled and $\frac{1}{8}S_8$ (solution in CH_2Cl_2, CS_2 or toluene) is added to the solution of **1** a surprising disproportionation of two dimers into a trimer and a monomer is observed [eqn (64)].

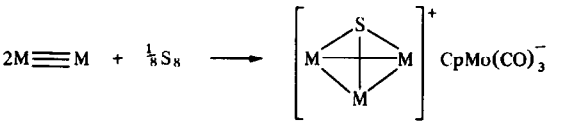

55

(64)

Yields of the cation **55** of 50–70% have been realized. The $CpMo(CO)_3^-$ anion is easily replaced with halide either by adding RX and washing the $CpMo(CO)_3R$ (R = H or Me) away from the salt (**55**·X) with petroleum ether.

The more soluble (and more hindered) Cp* complexes of Cr, Mo and W react with excess sulfur to give discrete tetrasulfide complexes which display an interesting series of isomeric forms.[80] These isomers may have different formal oxidation states due to the formation of S–S bonds in the ligands [eqn (65)]. Prolonged refluxing of the reaction mixture converts **57** into **56**. Under UV photolysis, **58** is converted into **57** which in turn is converted to **56**. Photolysis of **56** regenerates **58** so that a photo-steady-state mixture of all three isomers results.[81]

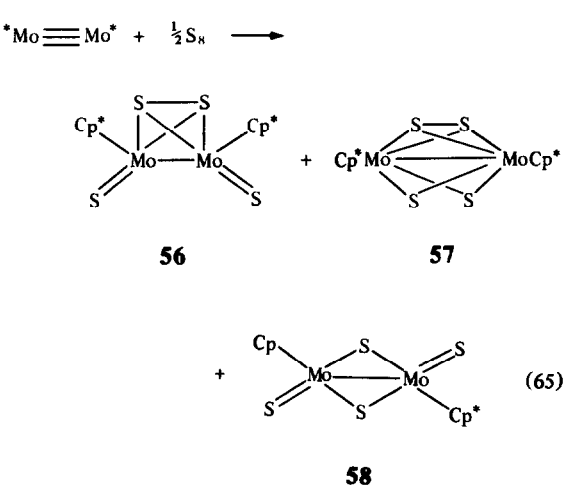

56 **57** **58**

(65)

The reaction of $Cp_2^*W_2(CO)_4$ with sulfur proceeds as in eqn (66). Compound **60** reacts with excess sulfur to form **59**.[80] Similar sulfur compounds to those shown in eqns (65) and (66) may be obtained from either the single-bonded dimers, $Cp_2M_2(CO)_6$, or the hydrides, $CpM(CO)_3H$.[82]

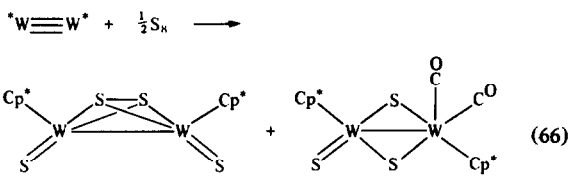

59 **60**

(66)

The Cr≡Cr triple bond in $Cp_2Cr_2(CO)_4$ is reported to react with sulfur as shown in eqns (67) and (68).[83] In our laboratory, we have been unable to obtain the disulfide **62** according to eqn (68); only **61** was isolated.

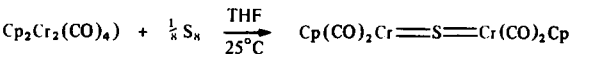

61 (100%)

(67)

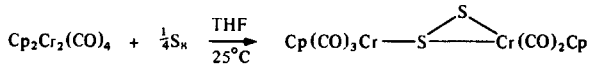

62 (90%)

(68)

The more hindered Cp* complex reacts with excess sulfur to give a 22% yield of the pentasulfide shown in eqn (69).[84(a)] The Cr–Cr distance is 2.489(2) Å, and the Cr–S distances range from 2.24 to 2.35 Å. The S—S and S=S distances are 2.15 and 2.10 Å, respectively.

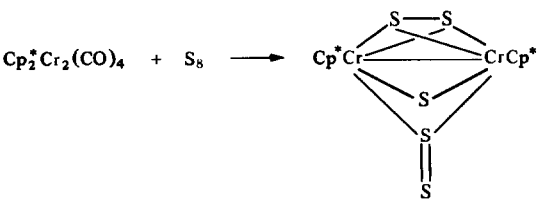

(69)

Compound **1** reacts with SO_2 according to eqn (70).[85]

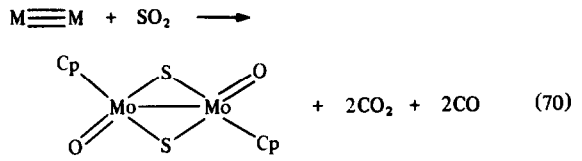

(70)

Results for the heavier chalcogens is limited to the reaction of **2** with Se.[84(b)] A short reaction time gives a 10% conversion to the tetraselenide (**63**); most of the Mo is recovered as unchanged starting material. When a toluene solution of **63** was stirred at 45°C for 3 days, a 45% yield of **64** was obtained following chromatography on silica gel. The source of the oxygen is unknown. The tungsten compound gave the Se analog of **60** [eqn(73)].

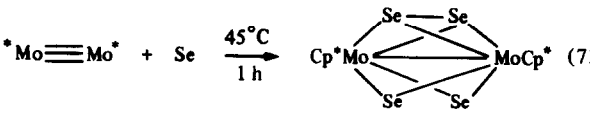

(71)

63

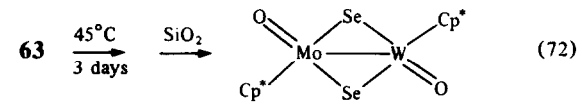

(72)

64

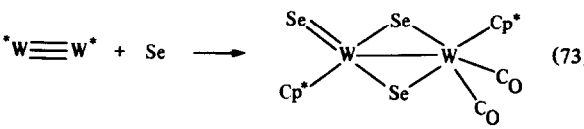

(73)

10%

The M≡M triple bond in **1** reacts readily with halogens to give dinuclear adducts.[86] With I_2, the structure is the μ-diiodide (**65**) but the dichloride is suggested to have the unsymmetrical structure (**66**) on the basis of Cl-XPS and NMR data.

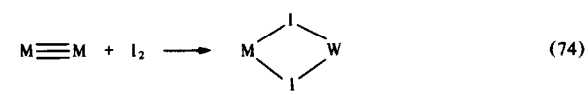

(74)

1 **65**

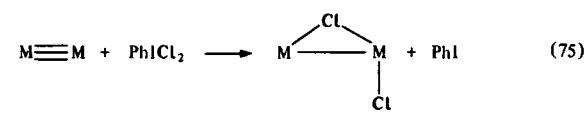

(75)

66

Hydrogen halides, HCl and HI, react with **1** to give the oxidative addition products **67** (X = Cl or I). These hydrohalide adducts react with excess HX to give their respective dihalides (**65** or **66**) and H_2.[86]

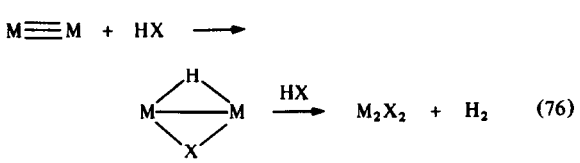

(76)

67

In the oxidative reactions of the type discussed above it makes little difference if the starting complex is saturated $Cp_2M_2(CO)_6$ or $CpM(CO)_3H$, or the unsaturated, multiply-bonded derivatives $Cp_2M_2(CO)_4$, if: (a) elevated temperatures, or (b) a large excess of the non-metal is used in the reaction. The utility of the unsaturation in the M≡M bond is best realized when the reactions are carried out under mild conditions with stoichiometric quantities of reagents. Then the enhanced reactivity of the metal–metal multiple bond is advantageous and allows for the isolation of thermally labile or kinetically controlled products, e.g. **55**, **67** etc.

CLUSTER-BUILDING REACTIONS

One of the most useful properties of carbon–carbon multiple bonds is their ability to polymerize and oligomerize into larger structures which maintain the basic skeleton of the monomers. An analogous oligomerization of metal–metal multiply bonded complexes gives metal clusters. To date, the *simple* olimerization of M≡M bonds as depicted in eqn (77) has not been observed.[14,*] Nevertheless, the M≡M triple bond in **1** has served as a convenient synthon in the construction of trinuclear and tetranuclear clusters containing the M_2 unit.

(77)

In our first paper on the reactivity of **1**, we noted that $(R_3P)_2Pt^{(0)}$ could be added to the M≡M bond to give M_2Pt triangulo clusters.[8] Unfortunately, the instability of these clusters has precluded an X-ray structure determination. Several clusters of types MX_3, M_2X_2 and M_3X are produced in the oxidative reactions of M≡M with non-metals (see above). However, the most useful cluster-building

*Oligomerization of metal–metal multiply bonded species upon loss of ligand[87(a)] or through the formation of ligand bridges[87(b),(c)] has been realized.

reactions of M≡M are those which give ligand-bridged, bimetallic clusters.

Thus, **1** reacts with the disulfide linkage in **68** to give the isomeric clusters **69** and **70**.[88,89] Both **69** and **70** are 62-electron clusters and have five metal–metal bonds in accordance with various electron-counting schemes.[90] They differ primarily in the disposition of the sulfide ligands—in the planar isomer (**69**), the sulfide ligands are on opposite sides of the Mo_2Fe_2 plane (the molecule is centrosymmetric) whereas in **70** the sulfurs are cisoid and the metals are in the more common butterfly geometry. The chromium derivative, $Cp_2Cr_2(CO)_4$, reacts with **68** to give the Cr butterfly analogous to **70**.[91] These $Mo_2Fe_2S_2$ clusters and related $Mo_2Co_2S_3$ clusters[92] are effective catalysts for CO methanation and thiophene HDS when supported on Al_2O_3.[93]

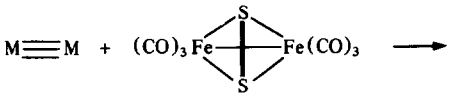

1 **68**

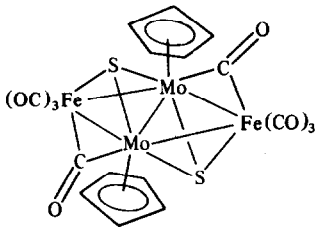

69

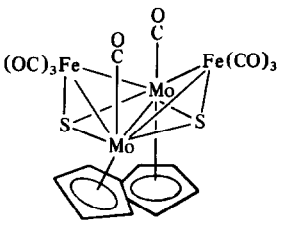

(78)

70

The triple bond in **1** also displaces propene from $Cp_2Mo_2(SCH_2CH(Me)S)_2$ [eqn. (79)] or H_2 from $Cp_2Mo_2(\mu\text{-}SH)_2(\mu\text{-}S)_2$ (**71**) to give the Mo_4S_4 cubane, **72**.[88] This route to these cubanes is the most convenient and allows one to control the substitution on the Cp rings almost at will. The reaction of **71** with $Cp_2W_2(CO)_4$ failed to give the $Cp_4Mo_2W_2S_4$ cubane.[94] The $Cp_4Mo_4S_4$ cubanes are very readily oxidized to mono- or dications, the structures of which have been determined.[95] The PES of the Mo_4S_4 cubanes,[95] their cyclic voltametry, their structural parameters, and an EHMO calculation[94] are all consonant with an electron configuration of $a_1^2e^4t_2^6$ for the six cluster framework electron pairs as originally suggested by Trinh-Toan *et al.*[96]

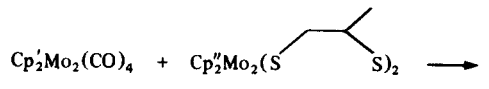

$$Cp'_2Mo_2(CO)_4 + Cp''_2Mo_2(SC_3H_6S)_2 \longrightarrow Cp'_2Cp''_2Mo_4S_4 + 4CO + 2C_3H_8 \quad (79)$$

72

A beautiful illustration of the utility of the isolobal principle is the addition of a metal carbyne to the M≡M bond to give trimetalla-tetrahedrane structures as shown in eqn (80) [cf. eqn (18)].[97]

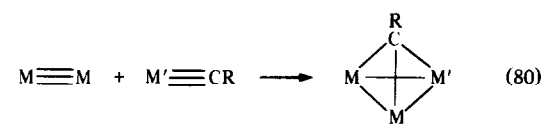

(80)

1 **73**

M = $Cp(CO)_2Mo$, M′ = $Cp(CO)_2W$

Cluster **73** is obtained in quantitative yield when M = Mo and M′ = W. The reaction of the W carbyne with $Cp_2Cr_2(CO)_4$ led to the dimerization of the carbyne [eqn (81)]. It was found that the Cr≡Cr complex *catalyzes* the dimerization of the carbyne.[97]

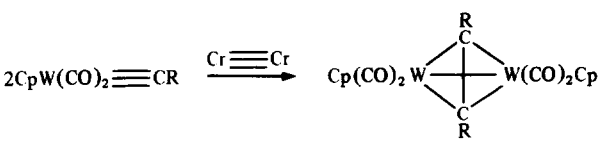

(81)

Green *et al.*[97] found that a complex mixture resulted when **1** was allowed to react with $Br(CO)_4W{\equiv}CR$ in ether. A 22% yield of the trimetallic cluster **73** [M = M′ = $Mo(CO)_2Cp$], was obtained by chromatography of the mixture over Florisil. Cotton and Schwotzer isolated a 20% yield of cluster **74** from the nearly identical reaction (THF solvent, followed by chromatography over silica gel).[98] Either the solvent exerts a strong influence on the course of this reaction, or the reaction mixture reacts further on the chromato-

graphy column to give products which depend on the column packing.

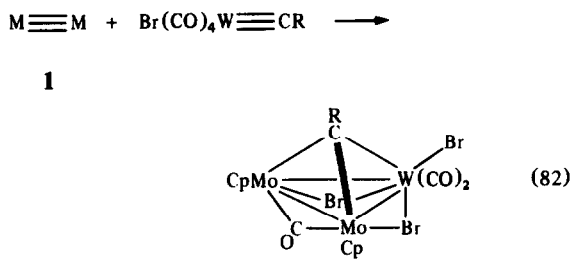

(82)

74

The nitrosyl complexes, $Cp(CO)_2M{\equiv}NO$ (M = Mo or W) react with $Cp_2M'_2(CO)_6$ (M′ = Mo or W) to give trimetallic nitrido clusters (**75**) in a reaction that is superficially related to the reactions of the carbynes above.[99] However, the conditions (200°C, sealed tube, 1 h), low yields, and the demonstrated cleavage of the N–O bond suggest the mechanism of formation of the clusters **75** is not a straightforward addition of the M≡NO bond to the M≡M bond.

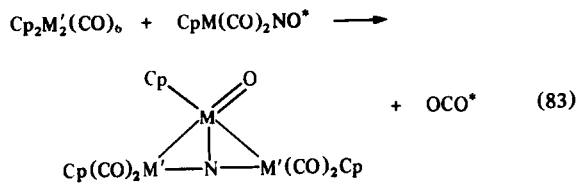

(83)

75

M and M′ = Mo or W

Attempts to insert the M≡M unit into preformed clusters by thermal reactions have been largely unsuccessful.[1] However, **1** does react with Cp*Co $(C_2H_4)_2$ under UV photolysis to give the novel cluster **76** in 20% yield.[100]

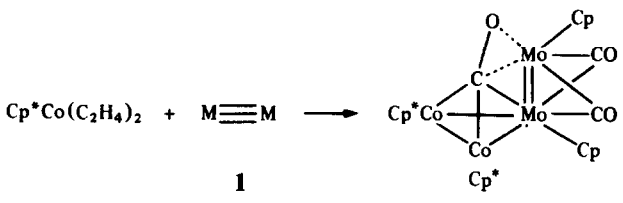

76

(84)

Finally, $Cp_2Ti(CO)_2$ reacts with **1** as shown in eqn (85). The carbonyl groups are transferred from Ti to Mo and the Ti is formally oxidized from Ti(II) to Ti(III). Lewis bases (B) cleave the dimeric structure to give $Cp_2Ti(B)OC(CO)_2MoCp$.[101]

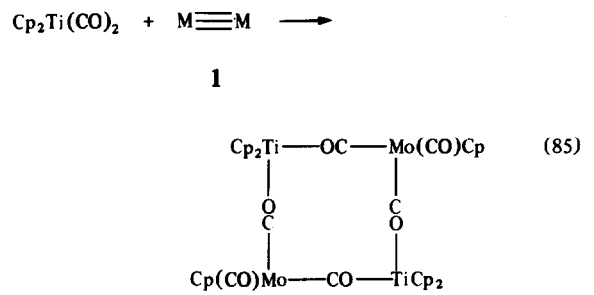

(85)

CONCLUSION

The compounds $Cp_2M_2(CO)_4$ (M = Mo or W) and related substituted-Cp derivatives have proven to be extremely versatile reagents for the elaboration of more complex molecules containing the Cp_2M_2 units. The M≡M units may be thought of as dimetal fragments which have been stripped of two ligands (four electrons) and are thus extremely electrophilic. Consequently, reactions with nucleophiles often occur under very mild conditions so that thermally labile products may be isolated and new bonding modes revealed.

At higher temperatures (>100°C), or under UV photolysis, CO is lost from the M≡M unit and more complex modes of reactivity are often observed. Even here, however, the presence of the metal–metal triple bond may be instrumental in directing the reaction to give dinuclear products. It is well known,[7,8] that the Mo–Mo or W–W *single* bonds in $Cp_2M_2(CO)_6$ complexes are extensively dissociated at elevated temperatures, and these single-bonded dimers often form mononuclear products as a result. In contrast, there is no evidence at all that the triply-bonded dimers dissociate into mononuclear fragments either thermally or under UV photolysis.[102]

The Cr≡Cr triple bond in $Cp_2Cr_2(CO)_4$ and related complexes has hot been as useful a starting material as its Mo and W congeners. Intractable mixtures are often produced.

Finally, a word about the concept of an "inorganic functional group" is appropriate. The term "functional group", as derived from organic chemistry, connotes more than a reactive grouping of atoms in a larger molecule. The term also suggests that a particular grouping of atoms will react in certain specified ways when exposed to certain conditions and/or reagents.

Are the Mo≡Mo and W≡W triple bonds in $Cp_2M_2(CO)_4$ "inorganic functional groups"? They are certainly reactive and some generalizations

concerning their reactivity can be made. However, as the reactions of M≡M with diazoalkanes so amply demonstrate, the course of the reactions of M≡M may be greatly altered by subtle changes in the reagents, the substitution on the Cp ring etc. Under such circumstances, the utility of the functional group *concept* is clearly limited.

The utility of the M≡M *compounds* is not restricted by our limited ability to predict the exact course of the reactions, however. The rational syntheses of the clusters **69–73**, or the metallacyclopropene (**39**) clearly show that the reactivity of the M≡M unit can be extrapolated successfully to new areas. In any event, it is clear that the availability of compounds with metal–metal multiple bonding opens a new dimension to the synthetic chemist, and that the exploration of metal–metal multiple bond reactivity will continue to be an exciting area of research.

Acknowledgements—I thank all my students and coworkers, acknowledged in the references, whose labors have contributed to the work described here. The assistance of the National Science Foundation and Petroleum Research Fund, administered by the American Chemical Society, is gratefully acknowledged.

REFERENCES

1. M. D. Curtis, L. Messerle, N. A. Fotinos and R. F. Gerlach, *ACS Symp. Ser.* 1981, **155**, 221.
2. R. J. Klingler, W. M. Butler and M. D. Curtis, *J. Am. Chem. Soc.* 1978, **100**, 5024.
3. M. D. Curtis, K. R. Han and W. M. Butler, *Inorg. Chem.* 1980, **19**, 2096.
4. C. P. Horowitz and D. F. Shriver, *Adv. Organomet. Chem.* 1984, **23**, 219.
5. E. D. Jemmis, A. R. Pinhas and R. Hoffmann, *J. Am. Chem. Soc.* 1980, **102**, 2576.
6. B. J. Morris-Sherwood, C. B. Powell and M. B. Hall, *J. Am. Chem. Soc.* 1984, **106**, 5079.
7. N. N. Turaki and J. M. Huggins, *Organometallics* 1985, **4**, 1766.
8. M. D. Curtis and R. J. Klingler, *J. Organomet. Chem.* 1978, **17**, 2324.
9. R. H. Hooker, K. A. Mahmoud and A. J. Rest, *J. Organomet. Chem.* 1983, **254**, C25.
10. J.-S. Huang and L. F. Dahl, *J. Organomet. Chem.* 1983, **243**, 57.
11. R. B. King and M. B. Bisnette, *Inorg. Chem.* 1965, **4**, 475.
12. (a) M. A. Greaney, J. S. Merola and T. R. Halbert, *Organometallics* 1985, **4**, 2059; (b) I. Bakkar and M. D. Curtis, Abstracts, 19th ACS National Meeting, Chicago, II 1985, INOR 377; (c) I. Bakkar and M. D. Curtis, to be published.
13. (a) K.-B. Shiu, M. D. Curtis and J. C. Huffman, *Organometallics* 1983, **2**, 936; (b) M. D. Curtis, K.-B. Shiu, W. M. Butler and J. C. Huffman, *J. Am. Chem. Soc.* 1986, **108**, 3335.
14. M. D. Curtis, N. A. Fotinos, L. Messerle and A. P. Sattelberger, *Inorg. Chem.* 1983, **22**, 1559.
15. M. D. Curtis, to be submitted for publication.
16. F. E. Massoth, *Adv. Catal.* 1978, **27**, 265.
17. (a) H. Alper, N. D. Silavwe, G. I. Birnbaum and F. R. Akmed, *J. Am. Chem. Soc.* 1978, **101**, 6582; (b) H. Alper, F. W. B. Einstein, R. Nagai, J.-F. Petrignani and A. C. Willis, *Organometallics* 1983, **2**, 1291; (c) *ibid.* 1983, **2**, 1422.
18. (a) H. Alper, F. W. B. Einstein, F. W. Hartstock and A. C. Willis, *J. Am. Chem. Soc.* 1985, **107**, 173; *Organometallics* 1986, **5**, 9.
19. H. Alper and J. Hartgerink, *J. Organomet. Chem.* 1980, **190**, C25.
20. H. Brunner, H. Buchner, J. Wachter, I. Bernal and W. H. Ries, *J. Organomet. Chem.* 1983, **244**, 247.
21. R. D. Adams, D. A. Katahira and L.-W. Yang, *Organometallics* 1982, **1**, 231.
22. H. Brunner, W. Meier and J. Wachter, *J. Organomet. Chem.* 1981, **210**, C23.
23. J. Wachter, J. G. Riess and A. Mitshler, *Organometallics* 1984, **3**, 714.
24. J. Krause and M. D. Curtis, unpublished results.
25. K. Endrich, R. Korswagen, T. Zahn and M. L. Ziegler, *Angew. Chem., Int. Ed. Engl.* 1982, **21**, 919.
26. (a) J. C. T. R. Burckett-St. Laurent, P. B. Hitchcock. H. W. Kroto and J. F. Nixon, *J. Organomet. Chem.* 1982, **238**, C82; (b) G. Becker, W. A. Herrmann, W. Kalcher, G. W. Kriechbaum, C. Pahl, C. T. Wagner and M. L. Ziegler, *Angew. Chem.* 1983, **95**, 417; *Angew. Chem. Suppl.* 1983, 501.
27. W. I. Bailey, Jr, M. H. Chisholm, F. A. Cotton and L. A. Rankel, *J. Am. Chem. Soc.* 1978, **100**, 5764.
28. J. A. Beck, S. A. R. Knox, R. F. D. Stansfield, F. G. A. Stone, M. J. Winter and P. Woodward, *J. Chem. Soc., Dalton Trans.* 1982, 195.
29. R. F. Gerlach, D. N. Duffy and M. D. Curtis, *Organometallics* 1983, **2**, 1172.
30. S. A. R. Knox, R. F. D. Stansfield, F. G. A. Stone, M. J. Winter and P. Woodward, *J. Chem. Soc., Dalton Trans.* 1982, 173.
31. A. M. Boileau, A. G. Orpen, R. F. D. Stansfield and P. Woodward, *J. Chem. Soc., Dalton Trans.* 1982, 187.
32. S. Slater and E. L. Muetterties, *Inorg. Chem.* 1981, **20**, 946.
33. J. S. Bradley, *J. Organomet. Chem.* 1978, **150**, C1.
34. M. Green, N. C. Norman and A. G. Orpen, *J. Am. Chem. Soc.* 1981, **103**, 1269.
35. W. A. Herrmann, *Adv. Organomet. Chem.* 1982, **20**, 160.
36. D. L. Thorn and R. Hoffmann, *Nouv. J. Chim.* 1979, **3**, 39.
37. M. D. Curtis, K.-B. Shiu and W. M. Butler, *J. Am. Chem. Soc.* 1986, **108**, 1550.
38. J. A. Beck, S. A. R. Knox, G. H. Riding, G. E. Taylor and M. J. Winter, *J. Organomet. Chem.* 1980, **202**, C49.

39. J. C. Jeffery, J. C. V. Laurie, I. Moore and F. G. A. Stone, *J. Organomet. Chem.* 1983, **258**, C37.
40. A. Meyer and M. D. Curtis, submitted to *Organometallics*, 1987.
41. M. D. Curtis and A. Meyer, to be published.
42. D. J. Wink, J. R. Fox and N. J. Cooper, *J. Am. Chem. Soc.* 1985, **107**, 5012.
43. K.-W. Lee and T. L. Brown, *Organometallics* 1985, **4**, 1025.
44. J.-C. Daran, Y. Jeanin and O. Kristianson, *Organometallics* 1985, **4**, 1882.
45. R. Goddard, S. A. R. Knox, R. F. D. Stansfield, F. G. A. Stone, M. J. Winter and P. Woodward, *J. Chem. Soc., Dalton Trans.* 1982, 147.
46. M. Griffiths, S. A. R. Knox, R. F. D. Stansfield, F. G. A. Stone, M. J. Winter and P. Woodward, *J. Chem. Soc., Dalton Trans.* 1982, 159.
47. S. A. R. Knox, R. F. D. Stansfield, R. G. A. Stone, M. J. Winter and P. Woodward, *J. Chem. Soc., Dalton Trans.* 1982, 167.
48. (a) A. Padwa, Ed., 1,3-*Dipolar Cycloaddition Chemistry*, Vols 1 and 2. Wiley Interscience, New York (1984); (b) R. Huisgen, *Angew. Chem., Int. Ed. Engl.* 1963, **2**, 565.
49. L. Messerle and M. D. Curtis, *J. Am. Chem. Soc.* 1980, **102**, 7789.
50. M. D. Curtis, L. Messerle, J. J. D'Errico, W. M. Butler and M. S. Hay, *Organometallics*, 1986, **5**, 2283.
51. J. A. Abad, L. W. Bateman, J. C. Jefferey, K. A. Mead, H. Razay, F. G. A. Stone and P. Woodward, *J. Chem. Soc., Dalton Trans.* 1983, 2075.
52. W. A. Herrmann and L. K. Bell, *J. Organomet. Chem.* 1982, **239**, C4.
53. W. A. Herrmann, L. K. Bell, M. L. Ziegler, K. Pfisterer and C. Dahl, *J. Organomet. Chem.* 1983, **247**, 39.
54. J. J. D'Errico, L. Messerle and M. D. Curtis, *Inorg. Chem.* 1983, **22**, 849 [note: the labelling of isomers 7a and 7b (eqn 2) in this reference are inadvertently interchanged].
55. L. K. Bell, W. A. Herrmann, G. W. Kriechbaum, H. Pfisterer and M. L. Ziegler, *J. Organomet. Chem.* 1982, **240**, 381.
56. (a) L. K. Bell, W. A. Herrmann, M. L. Ziegler and H. Pfisterer, *Organometallics* 1982, **1**, 1673; (b) W. A. Herrmann, G. W. Kriechbaum, M. L. Ziegler and H. Pfisterer, *Angew. Chem., Int. Ed. Engl.* 1982, **21**, 707.
57. N. D. Feasey, S. A. R. Knox and A. G. Orpen, *J. Chem. Soc., Chem. Commun.* 1982, 75.
58. M. D. Curtis and J. J. D'Errico, submitted to *Organometallics*, 1987.
59. W. A. Herrmann and G. Ihl, *J. Organomet. Chem.* 1983, **251**, C1.
60. J. J. D'Errico and M. D. Curtis, *J. Am. Chem. Soc.* 1983, **105**, 4478.
61. L. Messerle and M. D. Curtis, *J. Am. Chem. Soc.* 1982, **104**, 889.
62. M. D. Curtis, L. Messerle, J. J. D'Errico, H. E. Solis and I. D. Barcelo, *J. Can. Chem. Soc.* 1987, **109**, in press.
63. W. A. Herrmann, G. Kriechbaum, C. Bauer, E. Guggolz and M. L. Ziegler, *Angew. Chem., Int. Ed. Engl.* 1981, **20**, 815.
64. W. A. Herrmann, G. W. Kriechbaum, R. Dammel and H. Bock, *J. Organomet. Chem.* 1983, **254**, 219.
65. G. K. Barker, W. E. Carroll, M. Green and A. J. Welch, *J. Chem. Soc., Chem. Commun.* 1980, 1071.
66. M. Hay and M. D. Curtis, to be submitted for publication.
67. M. Green, R. J. Mercer, C. E. Morton and A. G. Orpen, *Angew. Chem., Int. Ed. Engl.* 1985, **24**, 422.
68. (a) H. Alper, J.-F. Petrignani, F. W. B. Einstein and A. C. Willis, *J. Am. Chem. Soc.* 1983, **101**, 1701; (b) J.-F. Petrignani and H. Alper, *Inorg. Chim. Acta* 1983, **77**, 1243.
69. H. Brunner, B. Hoffmann and J. Wachter, *J. Organomet. Chem.* 1983, **252**, C35.
70. H. G. Alt., K. A. Mahmoud and A. J. Rest, *Agnew. Chem., Int. Ed. Eng.* 1983, **22**, 544.
71. O. J. Scherer, H. Sitzmann and G. Wolmershäuser, *J. Organomet. Chem.* 1984, **268**, C9.
72. O. J. Scherer, H. Sitzmann and G. Wolmershäuser, *Angew. Chem., Int. Ed. Engl.* 1985, **24**, 351.
73. K. Blechschmitt, H. Pfisterer, T. Zahn and M. L. Ziegler, *Angew. Chem., Int. Ed. Engl.* 1985, **24**, 66.
74. I. Bernal, H. Brunner, W. Meier, H. Pfisterer, J. Wachter and M. L. Ziegler, *Angew. Chem., Int. Ed. Engl.* 1984, **23**, 438.
75. A. L. Rheingold and M. R. Churchill, *J. Organomet. Chem.* 1983, **243**, 165.
76. A. L. Rheingold, M. J. Foley and P. J. Sullivan, *J. Am. Chem. Soc.* 1982, **104**, 4727.
77. P. J. Sullivan and A. L. Rheingold, *Organometallics* 1982, **1**, 1547.
78. M. D. Curtis and W. M. Butler, *J. Chem. Soc., Chem. Commun.* 1980, 998.
79. P. D. Williams and M. D. Curtis, to be published.
80. H. Brunner, W. Meier, J. Wachter, E. Guggolz, T. Zahn and M. L. Ziegler, *Organometallics* 1982, **1**, 1107.
81. A. E. Bruce and D. R. Tyler, *Inorg. Chem.* 1984, **23**, 3433.
82. (a) O. A. Rajan, M. McKenna, J. Noodlik, R. C. Haltiwanger and M. Rakowski-Dubois, *Organometallics* 1984, **3**, 831; (b) M. Rakowski-Dubois, D. L. Dubois, M. C. Van Derveer and R. C. Haltiwanger, *Inorg. Chem.* 1981, **20**, 3064; (c) D. L. Dubois, W. K. Miller and M. Rakowski-Dubois, *J. Am. Chem. Soc.* 1981, **103**, 3429.
83. L. Y. Goh, T. W. Hambley and G. B. Robertson, *J. Chem. Soc., Chem. Commun.* 1983, 1458.
84. (a) H. Brunner, J. Wachter, E. Guggolz and M. L. Ziegler, *J. Am. Chem. Soc.* 1982, **104**, 1765; (b) H. Brunner, J. Wachter and H. Wintergerst, *J. Organomet. Chem.* 1982, **235**, 77.
85. C. A. Poffenberger, N. H. Tennent and A. Wojcicki,

J. Organomet. Chem. 1980, **191**, 107.
86. M. D. Curtis, N. A. Fotinos, K. R. Han and W. M. Butler, *J. Am. Chem. Soc.* 1983, **105**, 2686.
87. (a) T. R. Ryan and R. E. McCarley, *Inorg. Chem.* 1982, **21**, 2072; (b) M. H. Chisholm, R. J. Errington, K. Folting and J. C. Huffman, *J. Am. Chem. Soc.* 1982, **104**, 2025; (c) M. J. Chetcuti, M. H. Chisholm, J. C. Huffman and J. Lionelli, *ibid.* 1983, **105**, 292.
88. P. D. Williams, M. D. Curtis, D. N. Duffy and W. M. Butler, *Organometallics* 1983, **2**, 165.
89. P. Braunstein, J.-M. Jud, A. Tiripicchio, M. Tiripicchio-Camellini and E. Sappa, *Angew. Chem., Int. Ed. Engl.* 1982, **21**, 307.
90. (a) J. W. Lauher, *J. Am. Chem. Soc.* 1978, **100**, 5305; (b) K. Wade, In *Transition Metal Clusters* (Edited by D. F. G. Johnson) p. 193. Wiley, New York (1980).
91. P. Braunstein, A. Tiripicchio, M. T. Camellini and E. Sappa, *Inorg. Chem.* 1981, **20**, 3586.
92. M. D. Curtis and P. D. Williams, *Inorg. Chem.* 1983, **22**, 2661.
93. M. D. Curtis, J. Schwank, L. Thompson, P. D. Williams, and O. Baralt, Preprint, Fuels Division, American Chemical Society National Meeting, Anaheim CA, September 1986.
94. P. D. Williams and M. D. Curtis, *Inorg. Chem. 1986*, **25**, 4562.
95. J. A. Bandy, C. E. Davies, J. C. Green, M. L. H. Green, K. Prout and D. P. S. Rogers, *J. Chem., Soc. Chem. Commun.* 1983, 1395.
96. Trinh-Toan, B. K. Teo, J. A. Ferguson, T. J. Meyer and L. F. Dahl, *J. Am. Chem. Soc.* 1977, **99**, 408.
97. M. Green, S. J. Porter and F. G. A. Stone, *J. Chem. Soc., Dalton Trans.* 1983, 513.
98. F. A. Cotton and W. Schwotzer, *Angew. Chem., Int. Ed. Engl.* 1982, **31**, 629.
99. N. D. Feasey and S. A. R. Knox, *J. Chem. Soc., Chem. Commun.* 1982, 1062.
100. P. Brun, G. M. Dawkins, M. Green, A. D. Miles, A. G. Orpen and F. G. A. Stone, *J. Chem. Soc., Chem. Commun.* 1982, 926.
101. J. S. Merola, K. S. Campo, R. A. Gentile, M. A. Modrick and S. Zentry, *Organometallics* 1984, **3**, 334.
102. J. L. Robbins and M. S. Wrighton, *Inorg. Chem.* 1981, **20**, 1133.

Polyhedron Vol. 6, No. 4, pp. 783–792, 1987
Printed in Great Britain

0277–5387/87 $3.00+.00

REACTIONS INVOLVING ALKYNES AND TUNGSTEN–TUNGSTEN TRIPLE BONDS SUPPORTED BY ALKOXIDE LIGANDS

MALCOLM H. CHISHOLM,* BRIAN K. CONROY, BRYAN W. EICHHORN, KIRSTEN FOLTING, DAVID M. HOFFMAN, JOHN C. HUFFMAN and NANCY S. MARCHANT

Department of Chemistry and Molecular Structure Center, Indiana University, Bloomington, IN 47405, U.S.A.

(*Received* 19 *November* 1986)

Abstract—$W_2(OR)_6L_n$ compounds [R = Bu^t, $n = 0$; R = Pr^i or Np (Np = neopentyl), L = py (py = pyridine) or $HNMe_2$, $n = 2$] react with alkynes (R′C≡CR′) under mild conditions (hexane solutions, room temperature or below) to yield a variety of products depending upon the nature of the alkoxide, the alkyne and the mole ratio of the reactants. The products include alkylidyne complexes, $L_n(RO)_3W{\equiv}CR'$ ($n = 1$ or 0) (Schrock *et al.*, *Organometallics* 1985, **4**, 74), alkyne adducts, $W_2(OR)_6(py)_n(\mu\text{-}C_2R'_2)$, alkylidyne-capped tritungsten complexes, $W_3(\mu_3\text{-}CR')(OR)_9$, and $W_2(OR)_6(L)(\mu\text{-}C_4R'_4)$ or $W_2(OR)_6(\mu\text{-}C_4R'_4)(\eta^2\text{-}C_2R'_2)$ compounds. Evidence for equilibria involving alkyne adducts and alkylidyne species is found for certain combinations of R and R′. (1) The alkylidyne complexes $(Bu^tO)_3W{\equiv}CMe$ and $(py)_2(Pr^iO)_3W{\equiv}CNMe_2$ react with CO (1 atm, 22°C, in hexane) to yield alkyne adducts $W_2(OBu^t)_6(\mu\text{-}C_2Me_2)(CO)$ and $W_2[(OPr^i)_6(CO)_2(\eta^2\text{-}C_2(NMe_2)_2]$, respectively. (2) The alkylidyne complexes $[(Pr^iO)_2(HNMe_2)(R'C{\equiv})W(\mu\text{-}OPr^i)]_2$ react with alkynes R′C≡CR′ (>2 equiv, hexane, 22°C) to give $W_2(OPr^i)_6(\mu\text{-}C_4R'_4)(\eta^2\text{-}C_2R'_2)$ compounds (R′ = Me or Et). (3) The alkyne adducts $W_2(ONp)_6(py)_n(\mu\text{-}C_2R'_2)$ (R′ = Et or Ph, $n = 1$; R′ = Me, $n = 2$) react with $W_2(ONp)_6(py)_2$ in a 1:2 mole ratio at 22°C in hexane to yield $W_3(\mu_3\text{-}CR')(ONp)_9$ compounds. In related reactions involving 1,2-bishydrocarbyltetraalkoxides, $W_2(CH_2R'')_2(OR)_4$, and alkynes (R′C≡CR′) (2 equiv), alkyne adducts of formula $W_2(CH_2R'')_2(\eta^2\text{-}C_2R'_2)_2(OPr^i)_4$ and $W_2(CH_3)_2(\mu\text{-}C_2R'_2)(OBu^t)_4(py)$, alkylidyne-bridged complexes $HW_2(\mu\text{-}CR'')(\mu\text{-}C_4R'_4)(OPr^i)_4$ and products of W≡W and C≡C metathesis have been isolated for various combinations of R, R′ and R″.

The reactivity of multiple bonds between metal atoms represents a new chapter in inorganic chemistry. The classic text[1] on inorganic reaction mechanisms makes no mention of this topic, not surprisingly since the discovery of multiple bonds between metal atoms by Cotton and his coworkers came only in the mid-to-late 1960s.[2] The original emphasis was on determining the electronic structure of the bonds that held metal atoms so close together. There too was the ensuing flourish of activity directed toward determining the propensity for metal atoms to form such compounds and even this has not yet been unequivocally established.[3]

The reactivity of M–M multiple bonds was not given specific attention until the mid-to-late 1970s. One of us speculated about the general patterns of reactivity for triple bonds between molybdenum and tungsten atoms and noted that the different modes of reactivity of the M≡M bond in compounds of formula $M_2(OR)_6$ and $Cp_2M_2(CO)_4$ could be traced to their different electronic configurations and their different sets of attendant ligands.[4] These two factors make the chemistry of M–M triple bonds (M = Mo or W) much more varied than that of C–C triple bonds. The latter always have $\sigma^2\pi^4$ MO configurations and are only somewhat perturbed by substituent effects. By contrast M–M triple bonds may have one of a variety of valence MO configurations, $\sigma^2\pi^4$, $\pi^4\delta^2$, $\sigma^2\pi^4\delta^2\delta^{*2}$

*Author to whom correspondence should be addressed.

and $\sigma^2\pi^2\delta^2$, and are greatly influenced by the supporting ligands.

Over the past 10 years the reactivity of the M≡M bonds in $M_2(OR)_6$ and $Cp_2M_2(CO)_4$ compounds has been extensively and systematically studied. Several reviews dealing with various aspects of the chemistry of these compounds are to be found in the literature.[4–8] In this article we describe results from our laboratory, together with those reported by Professors Schrock and Cotton and their coworkers, dealing with reactions between W–W triple bonds and C–C triple bonds. The supporting ligands on tungsten are alkoxides or alkoxide–alkyl combinations. Comparisons with the reactivity observed for $Mo_2(OR)_6$ and $Cp_2M_2(CO)_4$ compounds are only briefly described.

METATHESIS-LIKE SCISSION OF C–C AND W–W TRIPLE BONDS

Schrock and co-workers[9] first noted the remarkable scission of C–C and W–W triple bonds and the formation of alkoxy-supported alkylidyne complexes [eqn (1)]:

$$W_2(OBu^t)_6 + R'C{\equiv}CR' \xrightarrow[\text{hexane}]{22^\circ C} 2(Bu^tO)_3W{\equiv}CR' \qquad (1)$$

R′ = Me, Et or Pr

Subsequent work[10] showed that this type of reaction could be used for the synthesis of a large group of compounds which were tolerant of a variety of organic functionalities (R′). The simple cleavage of C≡C bonds for symmetrically substituted alkynes was limited by steric factors and reactions employing PhC≡CPh and $Bu^tC{\equiv}CBu^t$ did not yield $(Bu^tO)_3W{\equiv}CR'$ compounds, though other routes could be found for their synthesis. The major thrust of this work was directed toward the utility of the tris-tert-butoxy tungsten alkylidyne complexes as alkyne-metathesis catalysts.[11]

In later work, Cotton and coworkers[12] studied reactions involving PhC≡CPh and EtC≡CEt at somewhat elevated temperatures (60–80°C) and with differing mole ratios of alkyne to $W_2(OBu^t)_6$, but with this ratio always being less than 1. Under these conditions some cleavage of the C≡C bond was observed although alkoxide group scrambling and ligand breakdown also occurs.

Crystalline products that have been structurally characterized from the Cotton reactions include $(Bu^tO)_3W{\equiv}CPh$[12(c)] (**I**), $W_2(OBu^t)_4(\mu\text{-}CPh)_2$,[12(a)] $W_2(OBu^t)_4(\mu\text{-}C_2Ph_2)_2$[12(a)] and $[W_3(OBu^t)_5(\mu\text{-}O)(\mu\text{-}CEt)O]_2$.[12(b)] In our laboratory we have also examined the crystal and molecular structures of $[(Bu^tO)_3W{\equiv}CX]_2$ (**II**) (X = Me[13] or NMe_2[14]), and $(py)_2(Pr^iO)_3W{\equiv}CNMe_2$[15] (**III**). The benzylidyne compound (**I**) is monomeric, while for X = Me and NMe_2 there is loose association to the dimeric structure shown in **II** below. The pyridine adduct (**III**) contains a pseudo octahedral tungsten atom. In each structural type the W≡C bond distance is *ca* 1.76 Å and is little perturbed by groups trans to itself. The terminal alkoxide ligands have fairly short W–O distances (*ca* 1.88–1.90 Å) while bonds *trans* to the W≡C bond in **II** and **III** are extremely long, e.g. W–O = 2.484(4) Å in **II** (X = Me) and W–N = 2.457(12) Å in **III**.

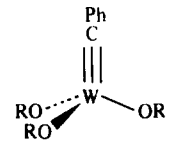

I

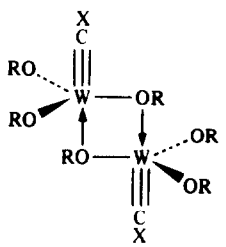

II

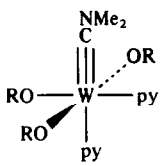

III

ALKYNE ADDUCTS

Reactions between $W_2(OBu^t)_6$ or $W_2(OR)_6(py)_2$ and alkynes (1 equiv) in hydrocarbon solvents in the presence of excess pyridine have allowed the isolation of an extensive series of alkyne adducts of formula $W_2(OR)_6(py)_n(\mu\text{-}C_2R'_2)$.[7,16] For R = Bu^t[16(a)] and Pr^i[16(a)] only ethyne adducts (R′ = H) can be isolated, whilst for the less sterically demanding neopentoxide ligands R′ may be H,[16(b)] Me,[16(a)] Et[16(b)] or Ph.[16(b)] However, attempts to prepare adducts where R′ = Bu^t or $SiMe_3$ failed even for R = Np.[16(b)] Three structural types have been observed in the solid state for these compounds and these are depicted in **IV–VI** below.

Table 1. Selected bond distances (Å) for $W_2(OR)_6(py)_n(\mu\text{-}C_2R'_2)$ compounds (n = 1 or 2)

Compound	Structure type	M–M	C–C	M–C(av)	Reference
$W_2(OPr^i)_6(py)_2(\mu\text{-}C_2H_2)$	IV	2.567(1)	1.39(2)	2.09(2)	16(b)
$W_2(ONp)_6(py)_2(\mu\text{-}C_2H_2)$	V	2.610(1)	1.39(2)	2.12(4)	16(c)
$W_2(ONp)_6(py)_2(\mu\text{-}C_2Me_2)$	V	2.602(1)	1.37(2)	2.14(5)	16(b)
$W_2(ONp)_6(py)(\mu\text{-}C_2Et_2)$	VI	2.572(1)	1.40(2)	2.14(6)	16(c)
$W_2(OBu^t)_6(py)(\mu\text{-}C_2H_2)$	VI	2.665(1)	1.44(1)	2.10(2)	16(b)

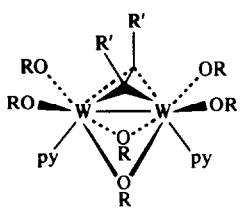

R = Pr^i R′ = H

IV

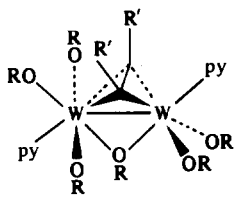

R = Np R′ = H or Me

V

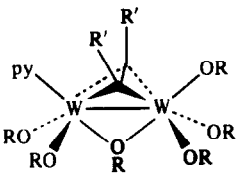

R = Bu^t R′ = H
R = Np R′ = Et or Ph

VI

In each there is a cross-wise or perpendicular alkyne bridge supported by either one or two alkoxide bridges. As a trend one can see that as the combined steric bulk of R and R′ increases so: (i) the number of pyridine ligands decreases, and (ii) the structures having only one alkoxide bridge are favored. It is also interesting to note that the W–W and μ-(C–C) distances are around 2.60 and 1.40 Å, respectively, with the longest W–W and C–C distances being found for $W_2(OBu^t)_6(py)(\mu\text{-}C_2H_2)$. Pertinent structural data are summarized in Table 1.

In solution a number of these compounds are fluxional at room temperature and all are labile toward pyridine dissociation. One must therefore recognize that in solution other structural types are energetically accessible at ambient temperatures and one can only speculate about their structural forms. At low temperatures, however, in toluene-d_8, the ^{1}H NMR data are entirely consistent with expectations based on the observed solid-state structures. Only in the case of the compound $W_2(ONp)_6(py)_2(\mu\text{-}C_2H_2)$ is there evidence[16(b)] for the presence of another structural type in solution and, in this instance, an equilibrium mixture involving the bis-alkoxide-bridged structure (IV) and the mono-alkoxide-bridged structure (V) can reliably be established.

A point of interest arises from a consideration of the spectra of $W_2(\mu\text{-}{}^*C_2H_2)$-containing compounds (*C represents 92 mol % ^{13}C). The ^{1}H and ^{13}C spectra associated with the μ-C_2H_2 moiety are each part of a AA′XX′ spectrum with additional satellites arising from coupling to ^{183}W (I = 1/2, 14.5% natural abundance). The magnitude of $^1J_{^{13}C-^{13}C}$ is very small, falling in the range 11–19 Hz.[7,16(a),17] For related $Mo_2(\mu\text{-}C_2H_2)$-containing compounds, $^1J_{^{13}C-^{13}C}$ values of 23–29 Hz[7,17] are found while in the carbonyl-containing compounds $Cp_2Mo_2(CO)_4(\mu\text{-}C_2H_2)$ and $Co_2(CO)_6(\mu\text{-}C_2H_2)$, $^1J_{^{13}C-^{13}C} = 43$[17] and 56[18]* Hz, respectively (see Table 2). For these alkyne adducts there exists an approximate linear inverse correlation between the magnitude of $^1J_{^{13}C-^{13}C}$ and the C–C bond distance.[17] The smallest value of $J_{^{13}C-^{13}C}$ is seen for the compound $W_2(OBu^t)_6(py)(\mu\text{-}C_2H_2)$ which also has the longest W–W and C–C distance. In solution this compound exists in equilibrium with $(Bu^tO)_3W{\equiv}CH$,[16(a)] as we describe later, and it appears that the magnitude of $J_{^{13}C-^{13}C}$ provides an indication of the likelihood for C–C and M–M cleavage to give alkylidyne species. For a comparison we note that the values of $^1J_{^{13}C-^{13}C}$ in ethyne, ethylene and ethane are 171.5, 67.2 and 34.6 Hz,[19] respectively, with C–C distances of *ca* 1.21, 1.34 and 1.54 Å.[20] Only in small organic rings have such small values of $^1J_{^{13}C-^{13}C}$ been seen; $^1J_{^{13}C-^{13}C}$ = 9.4 Hz[21] and d_{C-C} = 1.48 Å[22] recently reported for the central C_4 tetrahedral unit in $C_4Bu^t_4$ is particularly worthy of mention. On the basis of W–W, C–C and W–C bond distances and $^1J_{^{13}C-^{13}C}$ coupling constants, we formulate these $W_2(\mu\text{-}C_2H_2)$-containing compounds as ditungstatetrahedranes. The presence of a W–W single bond allows one to formally ascribe oxidation states +5 to each tungsten atom. In other words, the addition of an alkyne across the W≡W bond leads to a

Table 2. NMR data for the bridging ethyne ligand in selected transitional-metal complexes

Compound	Structure type	δ^a	$J_{W-C}{}^b$	$^1J_{CH}{}^b$	$^2J_{CH}$	$^1J_{CC}$	$^3J_{HH}$	Reference
$Mo_2(ONp)_6(py)_2(\mu\text{-}C_2H_2)$	IV	166.7[c]	—	201.4	4.7	26.9	0	17
$Mo_2(OPr^i)_6(py)_2(\mu\text{-}C_2H_2)$	IV	163.4[d]	—	200.6	4.0	28.2	0	17
$Mo_2(OBu^t)_6(\mu\text{-}C_2H_2)$	[e]	127.1[f]	—	196.2	2.1	23.2	3.3	17
$W_2(ONp)_6(py)_2(\mu\text{-}C_2H_2)$	V	133.2[f]	44.8 32.8	189.7	1.0	19.0	2.9	17
$W_2(OPr^i)_6(py)_2(\mu\text{-}C_2H_2)$	IV	166.3[g]	42.0	191.6	1.4	11.4	2.4	16(a)
$W_2(OBu^t)_6(py)(\mu\text{-}C_2H_2)$	VI	121.9[d]	47.0[h]	185.3	−1.5	11	2	16(a)
$Co_2(CO)_6(\mu\text{-}C_2H_2)$	$\mu_2\text{-}\eta^2$	71.1[i]	—	225.2	15.7	56.0	0.6	18
$Cp_2Mo_2(CO)_4(\mu\text{-}C_2H_2)$	$\mu_2\text{-}\eta^2$	61.9[i]	—	214.2	7.3	43.4	0	17

[a]Chemical shift in ppm relative to Me_4Si.
[b]All coupling constants are in Hz.
[c]−65°C, C_7D_8.
[d]−40°C, C_7D_8.
[e]Structure unknown.
[f]−20°C, C_7D_8.
[g]25°C, C_7D_8.
[h]$J_{W-C} \sim J_{W-C}$.
[i]25°C, C_6D_6.

W_2^{6+} to W_2^{10+} transformation. Along the same line of reasoning by counting an alkylidyne as a 3-ligand, the metathesis-like reaction (1) may be viewed as an oxidative cleavage of the W≡W bond: $W_2^{6+} \rightarrow 2W^{6+}$.

C–C COUPLING REACTIONS

In all cases where $W_2(OR)_6(py)_n(\mu\text{-}C_2R'_2)$ compounds are isolable and in some instances where such compounds are not (see later) the addition of more alkyne leads to products of C–C coupling, specifically $W_2(OR)_6(L)(\mu\text{-}C_4R'_4)$ and/or $W_2(OR)_6(\mu\text{-}C_4R'_4)(\eta^2\text{-}C_2R'_2)$.[23] These reactions parallel those originally discovered by Rothwell[24] in these laboratories for $Mo_2(OR)_6$ compounds in their reactions with alkynes. The isolation of $M_2(OR)_6(\mu\text{-}C_4R'_4)(\eta^2\text{-}C_2R'_2)$ compounds was possible only for M = W, though related molybdenum analogues are probably involved in the catalytic cyclotrimerization of alkynes by $Mo_2(OR)_6$ compounds. By contrast, $W_2(OR)_6(\mu\text{-}C_4R'_4)(\eta^2\text{-}C_2R'_2)$ compounds (R = Pr^i; R′ = H,[23] Me[23] or Et:[25] R = Np, R′ = H[23] or Me[23]) do not readily eliminate benzenes, and therefore $W_2(OR)_6$ compounds are not catalytically active in the cyclotrimerization of alkynes. This difference in the chemistry of $M_2(OR)_6$ compounds reflects the general truism: reductive elimination is easier from Mo_2 centers than W_2 centers while oxidative addition occurs in the inverse order. This is a reflection of thermodynamic factors and not the mechanism or mechanisms involved.

Addition of ethyne (2 equiv) to $W_2(OBu^t)_6$ in the absence of py leads to $W_2(OBu^t)_6(\mu\text{-}C_4H_4)$[23] which, though rather thermally unstable, can be isolated as a carbonyl adduct, $W_2(OBu^t)_6(\mu\text{-}C_4H_4)(CO)$,[23] in a crystalline state and has been shown to adopt the structure depicted by **VII** below.

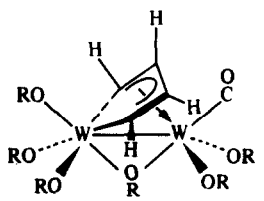

R = Bu^t

VII

Presumably $W_2(OBu^t)_6(\mu\text{-}C_2H_2)$ is a reactive intermediate in the formation of **VII** but such a compound has not been detected. If only 1 equiv of C_2H_2 is added to a solution of $W_2(OBu^t)_6$, **VII** and unreacted $W_2(OBu^t)_6$ are all that are detectable by NMR spectroscopy.[23] Ethyne polymerization to shiny grey metallic $(C_2H_2)_n$ is always competitive with formation of isolable tungsten-containing compounds. It is worth noting that an unstable compound $Mo_2(OBu^t)_6(\mu\text{-}C_2H_2)$ was detected in analogous reactions employing $Mo_2(OBu^t)_6$ and we have confirmed this claim by Schrock and coworkers[26] in our measurement of $^1J_{^{13}C-^{13}C}$ for the central $Mo_2(\mu\text{-}C_2H_2)$ moiety (see Table 2).

* The original values were obtained using a 60-MHz NMR. The compound was synthesized and analyzed in our labs using a 360-MHz NMR. The values were found to correlate well with the originally reported values; however, for the sake of consistency, our values are entered in Table 2.

The molecular structure found for $W_2(OR)_6(\mu\text{-}C_4R'_4)(\eta^2\text{-}C_2R'_2)$ compounds is shown diagramatically in **VIII** below.

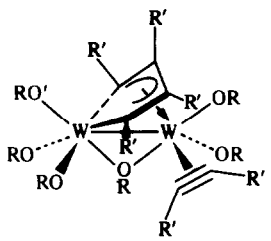

VIII

In both **VII** and **VIII** the coordination about one tungsten atom approximates to octahedral whilst the other tungsten may be viewed as trigonal bipyramidal with the μ-C_4 ligand being π-bonded to one of the equatorial sites. The W–W distances are long, in the range 2.85–2.88 Å, representing single bonds between the metal atoms. The M–M bond can be viewed as a dative bond formed by electron pair donation from the π-C_4-bonded tungsten atom to the six-coordinate W(6+) center. Of course, this is only a simplistic picture.

ALKYLIDYNE-CAPPED TRITUNGSTEN COMPOUNDS

The first member of the $W_3(\mu_3\text{-}CR')(OR)_9$ series to be discovered was for R′ = Me and R = Pr^i.[27] This was obtained from the reaction between $W_2(OPr^i)_6(py)_2$ and MeC≡CMe in a hydrocarbon solvent at room temperature. The tritungsten compound was found together with $W_2(OPr^i)_6(\mu\text{-}C_4Me_4)(\eta^2\text{-}C_2Me_2)$ and some unreacted $W_2(OPr^i)_6(py)_2$. Evidently competitive reactions were occurring and the desired compound $W_2(OPr^i)_6(py)_n(\mu\text{-}C_2Me_2)$ was in some way too reactive to be isolated.

A logical comproportionation route to the above compound, suggested by analogy with reactions of Stone and his coworkers[28] and previous results in this lab involving the formation of oxo-capped tritungsten compounds,[29] proved successful as shown in eqn (2):

$$W_2(OPr^i)_6(py)_2 + (Bu^tO)_3W{\equiv}CMe \xrightarrow[\text{hexane–}Pr^iOH]{22^\circ C} W_3(\mu_3\text{-}CMe)(OPr^i)_9. \quad (2)$$

Extensions of this type of reaction have allowed the synthesis of $W_3(\mu\text{-}CR')(OR)_9$ compounds (R′ = Me,[27] R = Pr^i, R′ = Me[16(b)] or Et,[16(b)] R = Np). In most cases it is important that the added alcohol not be in excess to prevent an initial reaction leading to $W(OR)_6$ and alkane. Consequently, addition of ROH is subsequent to the mixing fo the inorganic compounds and is kept to a minimum (3 equiv). Steric factors are apparently important and prevent any comproportionation involving $W_2(OBu^t)_6$ and $(Bu^tO)_3W{\equiv}CR'$ compounds.

The compound where R′ = Me and R = Pr^i has been characterized by a full X-ray study.[27] ^1H and ^{13}C NMR data for all compounds are consistent with the maintenance of the capped, tris-RO-bridged structure depicted by **IX** below. In solution, bridge-terminal RO group exchange is slow on the NMR time-scale.

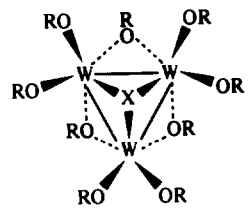

X = CR′

IX

EQUILIBRIA INVOLVING ALKYNE ADDUCTS AND ALKYLIDYNE COMPLEXES

During the course of our characterization of $W_2(OBu^t)_6(py)(\mu\text{-}{}^*C_2H_2)$[16(a)] we discovered in the ^{13}C and ^1H NMR spectra a persistent impurity which could only reasonably be formulated as the methylidyne complex $(Bu^tO)_3W{\equiv}{}^*CH$. When the ^{13}C NMR spectra were recorded on samples prepared from mixtures of the separately labeled compounds $W_2(OBu^t)_6(py)(\mu\text{-}{}^*C_2H_2)$ and $W_2(OBu^t)_6(py)(\mu\text{-}C_2D_2)$, the appearance of a new signal in the ^{13}C NMR spectra was present and assignable to a $W_2(\mu\text{-}H{}^*CCD)$ moiety. When the analogous experiment was carried out for each of the compounds $W_2(OPr^i)_6(py)_2(\mu\text{-}C_2H_2)$[16(a)] and $W_2(ONp)_6(py)_2(\mu\text{-}C_2H_2)$[16(b)] in their labeled forms, no new signal assignable to a $W_2(\mu\text{-}H{}^*CCD)$ moiety was present. It should also be mentioned that no C–H/C–D scrambling was observed in any of the above experiments.

A plausible interpretation of the above was that the μ-ethyne and methylidyne complexes were, in the case of the Bu^tO ligated system, in equilibrium:

$W_2(\mu\text{-}C_2H_2) \rightleftharpoons 2W{\equiv}CH$. If this were the case then at room temperature the position of equilibrium favored the ethyne adduct by *ca* 5:1. The temperature dependence of the equilibrium constant could not reliably be established since the samples were thermally unstable, decomposing over a period of hours at room temperature and within minutes at +60°C. One could not be sure that at any given temperature the sample was at equilibrium and all spectra were recorded by rapidly cooling the sample to −40°C. The frustrating situation then arises in as much as the labelling study does not prove the existence of the equilibrium, it is merely a plausible explanation. However, since that time a number of other chemical reactions and spectroscopic characterizations lead us to the general conclusion that alkyne adducts of formula $W_2(OR)_6(py)_n(\mu\text{-}C_2R'_2)$ and alkylidyne species $(RO)_3W{\equiv}CR'$ are commonly in equilibrium with one another and that the position of equilibrium is dependent on the nature of R and R'. Bulky R and R' combinations favor the alkylidyne species and of the two groups the position of equilibrium is most sensitive to R. We summarize here the basis for our conclusion.

(1) The spectroscopic characterization of the compounds formed in the reaction between $W_2(OCMe_2Et)_6$ and $*C_2H_2$ (1 equiv) in benzene-d_6 in the presence of pyridine indicate a $W_2(\mu\text{-}*C_2H_2)$: $W{\equiv}*CH$ ratio of *ca* 1:5[30] which is roughly the inverse of that found for R = CMe_3.

(2) The compounds $W_2(ONp)_6(py)_n(\mu\text{-}C_2R'_2)$ (R' = Me, $n = 2$; R' = Et or Ph, $n = 1$) act as alkylidyne sources in their reactions with $W_2(ONp)_6(py)_2$ according to eqn (3):[16(b),31]

$$W_2(ONp)_6(py)_n(\mu\text{-}C_2R'_2) + 2W_2(ONp)_6(py)_2 \xrightarrow[\text{hexane}]{22°C} 2W_3(\mu_3\text{-}CR')(ONp)_9 + (n+4)py. \quad (3)$$

A direct preparation of $W_3(\mu_3\text{-}CR')(ONp)_9$ involves the reaction between $W_2(ONp)_6(py)_2$ and $R'C{\equiv}CR'$ in a mole ratio of 3:1.[16(b),31]

(3) The addition of CO (1 atm) to a pale yellow solution of $(Bu^tO)_3W{\equiv}CMe$ causes the solution to turn blue with the formation of $W_2(OBu^t)_6(\mu\text{-}C_2Me_2)(CO)$.[31] The latter compound is stereochemically rigid on the NMR time-scale and has a strongly bond CO ligand [ν(CO) = 1918 cm^{-1}]. The data are consistent with the maintenance of the structure found in the solid state depicted by X below for which W–W = 2.633(1) Å and C–C (μ-C_2Me_2) = 1.36(1) Å.

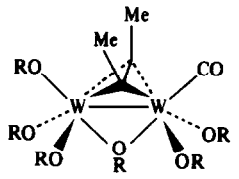

R = Bu^t

X

Our interpretation of (3) is that CO reacts with $W_2(OBu^t)_6(\mu\text{-}C_2Me_2)$, which is a reactive species in equilibrium with the more stable alkylidyne species $(Bu^tO)_3W{\equiv}CMe$. In a similar way, $(py)_2(Pr^iO)_3W{\equiv}CNMe_2$ reacts with CO (1 atm, 22°C) in toluene to yield $W_2(OPr^i)_6(CO)_2(\eta^2\text{-}C_2(NMe_2)_2)$.[15] It is apparent that the π-acceptor properties of the CO ligand drain electron density away from the metal and this displaces an equilibrium between $W_2(\mu\text{-}C_2R'_2)$ and $W{\equiv}CR$ species toward the alkyne adduct. But it should be emphasized that not all $(RO)_3W{\equiv}CR'$ compounds react in the same manner and a competing reaction involving alkylidyne carbon–carbonyl carbon coupling can occur.[15,32]

(4) Addition of alkynes ($R'C{\equiv}CR'$) to $[(Pr^iO)_2(HNMe_2)(R'C{\equiv})W(\mu\text{-}OPr^i)]_2$,[25] which has a structure closely related to that shown in **III** involving μ-OPr^i ligands *trans* to the $W{\equiv}CR'$ moiety, leads to formation of $W_2(OPr^i)_6(\mu\text{-}C_4R'_4)(\eta^2\text{-}C_2R'_2)$ compounds (**VIII**) (R = Me or Et).[25] The reaction is rapid in hydrocarbon solvents at room temperature. When $*C_2H_2$ is added to $[(Pr^iO)_2(HNMe_2)(EtC{\equiv})W(\mu\text{-}OPr^i)]_2$, $W_2(\mu\text{-}C_2{*}C_2H_2Et_2)$ ligands are formed that have the *CH and CEt groups scrambled over all possible sites as determined by ^{13}C NMR spectroscopy. Fractional crystallization of the products derived from the analogous reaction employing ethyne which was not labeled gave the specific isomeric form shown in Fig. 1.[30] This implies that alkyne metathesis is more rapid than μ-C_4R_4 formation; the latter, however, shuts off the former reaction.

(5) Addition of 2.5 equiv of Quin (Quin = quinuclidine) to a toluene-d_8 solution of $W_2(OBu^t)_6(py)(\mu\text{-}C_2H_2)$, which shows two resonances in the ^1H NMR assignable to a bridging ethyne compound and a methylidyne compound, cleanly converts[30] both species to the $(Quin)(Bu^tO)_3W{\equiv}CH$ compound.[10] Conversely, addition of CO (1 equiv) to an equilibrium mixture of $W_2(OBu^t)_6(py)(\mu\text{-}C_2H_2)$ and its methylidyne counterpart in toluene-d_8 leads to the formation of $W_2(OBu^t)_6(\mu\text{-}C_2H_2)(CO)$, an analogue of **X**. Thus, for an equilibrium mixture, $W_2(\mu\text{-}C_2R_2) \rightleftharpoons 2W{\equiv}CR$, supported by alkoxide ligands,

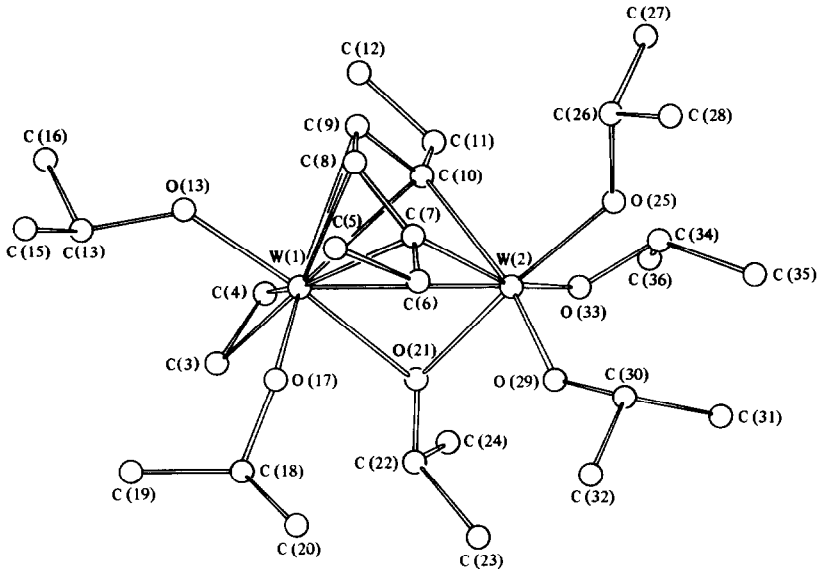

Fig. 1. A ball-and-stick drawing of the $W_2(OPr^i)_6(\mu\text{-}C_4H_2Et_2)(\eta^2\text{-}C_2H_2)$ molecule. Pertinent bond distances (Å) are: W(1)–W(2) = 2.8741(16), W(2)–C(7), W(2)–C(10) = 2.151(16), 2.167(15); W(1)–C(7), W(1)–C(8), W(1)–C(9), W(1)–C(10) = 2.417(16), 2.389(15), 2.407(16), 2.411(16); W(1)–C(3), W(1)–C(4) = 2.110(17), 2.072(16). The W–O distances fall within the range of W–OR distances (terminal and μ_2) reported in Ref. 6.

addition of neutral donor ligands may displace the equilibrium to either the left or the right. The strong σ-donor quinuclidene stabilizes the W(6+) W≡CR species while the π-acceptor CO traps the $W_2(\mu\text{-}C_2R_2)$ species by competing with the alkyne for π-electron density.

REACTIONS BETWEEN 1,2-DIALKYLTETRAALKOXIDES OF DITUNGSTEN AND ALKYNES

Alcoholysis reactions involving 1,2-$W_2(CH_2R'')_2(NMe_2)_4$ compounds[33] have allowed the preparation and isolation of stable compounds of formula 1,2-$W_2(CH_2R'')_2(OR)_4$ (R = Bu^t, R'' = H: R = Pr^i; R'' = Ph, $SiMe_3$ or Bu^t) together with other combinations for R and R'' where CH_2R'' contains no accessible β-hydrogen atoms.[34] These compounds display a variety of reactions with alkynes.[29(b),35] For the sake of brevity we shall focus only on those tungsten compounds specified above and their reactions with MeC≡CMe and EtC≡CEt.

The $W_2(CH_2R'')_2(OPr^i)_4$ compounds react with MeC≡CMe (2 equiv) in hydrocarbon solvents according to eqn (4):

$$W_2(CH_2R'')_2(OPr^i)_4 + 2MeC{\equiv}CMe \rightarrow HW_2(\mu\text{-}CR'')(\mu\text{-}C_4Me_4)(OPr^i)_4 + R''CH_3. \quad (4)$$

The structures of these alkylidyne bridged ditungsten compounds are depicted by **XI** below. The hydride ligand, which was not located by X-ray

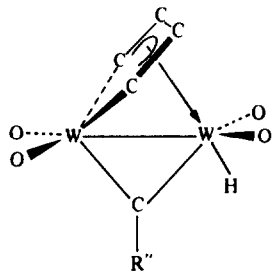

XI

diffraction[35] in the study of the benzylidyne compound $HW_2(\mu\text{-}CPh)(\mu\text{-}C_4Me_4)(OPr^i)_4$, was detected by NMR spectroscopy. The magnitude of J_{W-H} (125 Hz) and more importantly the integral intensity of the satellites relative to the central hydride resonances indicate a terminal W–H moiety. Also, the chemical shift for the hydride at +20.4 ppm is nearly 10 ppm downfield of $W_2(\mu\text{-H})$ signals commonly found with alkoxide-supported, hydrido-bridged W_2 and W_4 species.[36] The actual location of the terminal H ligand was established from NOE difference spectroscopy based on reciprocal NOEs of the hydride with the ortho-hydrogen atoms of the benzylidyne ligand and the adjacent OPr^i methine hydrogens.[29(b)]

The relative rate of reaction (4) is dependent on the steric bulk of R'' following the order R'' = Bu^t -> $SiMe_3$ > Ph and, for R'' = $SiMe_3$ and Ph, inter-

mediates of formula $W_2(CH_2R'')_2(\eta^2\text{-}C_2Me_2)_2(OPr^i)_4$ have been fully characterized. These compounds adopt a common structure based on **XII** and this has been determined crystallographically for R″ = Ph.[35]

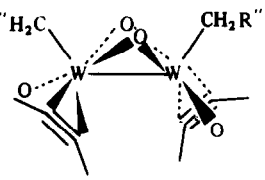

XII

Each tungsten atom is in a square based pyramidal environment with the CH_2R'' ligand in the apical position. The $\eta^2\text{-}C_2Me_2$ ligand can be viewed as a 2- ligand, a metallacyclopropene, and the W–W distance [2.668(1) Å] is representative of a single bond. On the NMR time-scale rotation about the $W\text{–}C_2$ alkyne vector can be monitored, and based on coalescence temperatures, the activation energy was calculated to be 9.9(2) kcal mol^{-1}.

The rate of conversion of **XII** to **XI** in benzene-d_6 [eqn (5)]:

$$W_2(CH_2R'')_2(\eta^2\text{-}C_2Me_2)_2(OPr^i)_4 \xrightarrow{k} HW_2(\mu\text{-}CR'')(\mu\text{-}C_4Me_4)(OPr^i)_4 + R''CH_3 \quad (5)$$

has been followed by NMR spectroscopy as a function of temperature for R″ = Ph and $SiMe_3$.

The reactions obey first-order kinetics beyond four half-lives over the temperature ranges studied, and cross-over experiments employing $W_2(CD_2C_6D_5)_2(\eta^2\text{-}C_2Me_2)_2(OPr^i)_4$ (**XIII**) indicated an intramolecular reaction: no scrambling of H/D was observed in the formation of toluene and toluene-d_8 in eqn (5). Activation parameters were determined to be $\Delta H\dagger = 24 \pm 1$ kcal mol^{-1} and $\Delta S\dagger = -9 \pm 2$ eu for R″ = Ph, and $\Delta H\dagger = 21 \pm$ kcal mol^{-1} and $\Delta S\dagger = -9 \pm 2$ eu for R″ = $SiMe_3$. A comparison of rate constants (k) for **XII** (R″ = Ph) and **XIII** revealed a small primary kinetic isotope ($k_H/k_D = 1.4$ at 60°C).[29(b)]

Interpretation of these data must be speculative at this point since a number of individual reaction steps must occur in eqn (5), and the specific order of C–C coupling to generate the $\mu\text{-}C_4Me_4$ ligand and $C\text{–}H_\alpha$ activation leading to elimination of CH_3R'' remains to be established. The latter presumably involves a 1,2-alkyl shift forming a 1,1-$W_2(CH_2R'')_2$ reactive intermediate prior to $C\text{–}H_\alpha$ activation. Such a shift is observed in a related reaction between 1,2-$W_2Me_2(OBu^t)_4(py)_2$ and MeC≡CMe, forming the thermally unstable compound 1,1-$W_2Me_2(\mu\text{-}C_2Me_2)(OBu^t)_4py$.[29(b)] The solid-state structure of this alkyne-bridged 1,1-dialkyl compound is shown in Fig. 2.

Reactions involving EtC≡CEt and $W_2(CH_2R'')_2(OPr^i)_4$ compounds are more complex and an analogue of **XI** with R′ = Et has not been well characterized. However, the bis-alkyne adducts analogous to **XII** have been fully characterized for R″ = Pr and $SiMe_3$, and are more thermally stable toward $R''CH_3$ elimination than their dimethylacetylene analogues. In the case of R″ = Bu^t, a competing reaction leading to propylidyne formation is extremely rapid [eqn (6)]:

$$W_2(CH_2Bu^t)_2(OPr^i)_4 + EtC{\equiv}CEt \xrightarrow[\text{hexane}]{22°C} [W({\equiv}CEt)(OPr^i)_2(CH_2Bu^t)]_2 \quad (6)$$

and no intermediates have been detected thus far.[29(b)]

The molecular structure of the propylidyne complex is shown in Fig. 3 and reveals that each tungsten atom is in a trigonal bipyramidal environment. The structure is a derivative of **II** in which a pair of terminal OR ligands, one on each tungsten atom, is replaced by a pair of CH_2Bu^t ligands. It is worth noting here that when 1 equiv of alkyne is used in reaction (4), only bis-alkyne compounds (**XII**) or their derivatives (**XI**) and unreacted $W_2(CH_2R'')_2(OPr^i)_4$ are isolated. Evidently in the reaction between EtC≡CEt and $W_2(CH_2Bu^t)_2(OPr^i)_4$, the C≡C and W≡W bond metathesis reaction is faster than any possible C–C coupling or C–H activation reactions.

RELATED REACTIONS INVOLVING C≡C AND W≡W BONDS

Alkynes are known to add to $Cp_2M_2(CO)_4$ compounds to give 1:1 alkyne adducts.[37(a)] No alkylidyne formation has been reported but at elevated temperatures where CO dissociation becomes favored other C–C coupling reactions have been documented: $M_2(\mu\text{-}C_2R_2) \rightarrow M_2(\mu\text{-}C_4R_4) \rightarrow M_2(\mu\text{-}C_8R_8)$.[37(b)]

Though neither $W_2(CH_2SiMe_3)_6$ nor $W_2(NMe_2)_6$ appear to react with alkynes,[9] at least under the conditions employed for the alkoxides, the mixed chlorodimethylamide $W_2Cl_2(NMe_2)_4$ is reactive and a number of alkyne adducts supported by pyridine ligands have been isolated having formula $W_2Cl_x(NMe_2)_{6-x}(\mu\text{-}C_2RR')(py_2)$ ($x = 2$, 3 or 4; R and R′ are one of H, Me or Ph).[38] Phosphine adducts have also been isolated for some of the above, and the conversion of $W_2Cl_3(NMe_2)_3(\mu\text{-}C_2H_2)L_2$ to $W_2Cl_3(NMe_2)_2(\mu\text{-}N(CH_2)CH_3)$

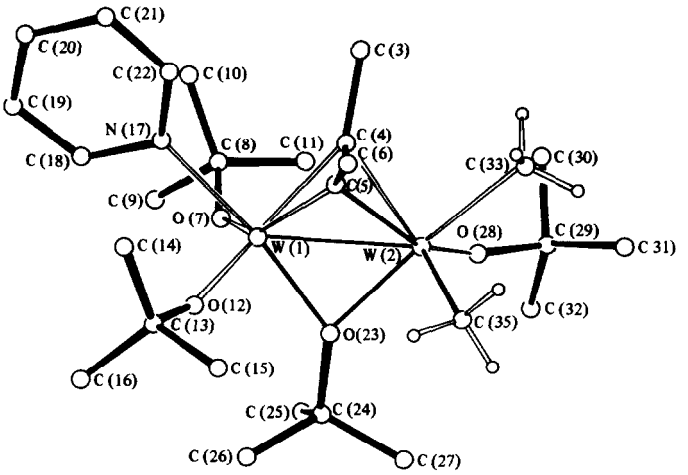

Fig. 2. A ball-and-stick drawing of the 1,1-$W_2Me_2(\mu\text{-}C_2Me_2)(OBu^t)_4(py)$ molecule. Pertinent bond distances (Å) and angles (°) averaged where appropriate: W(1)–W(2) = 2.6223(12); C(4)–C(5) = 1.412(19); W(2)–C(33) = 2.233(16); W(2)–C(35) = 2.162(16); W–O(23) = 2.05(3); W(2)–O(28) = 1.873(11); W(1)–O(terminal) = 1.91(3); W(1)–N(17) = 2.216(12); C–C–C(alkyne) = 133(3); W(2)–O(28)–C(29) = 158.7(11); W(1)–O–C(terminal) = 150(5).

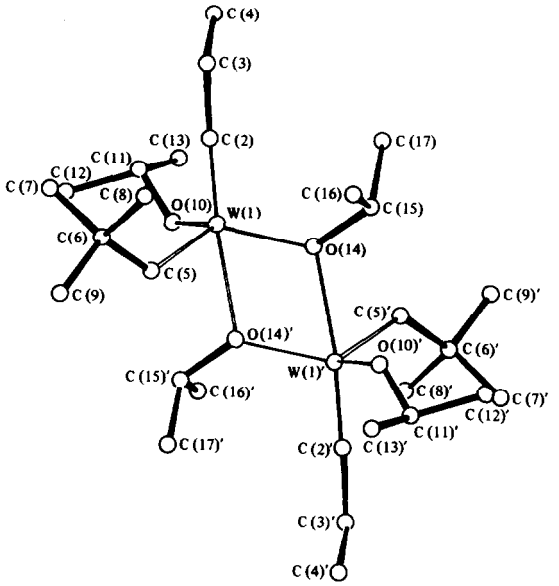

Fig. 3. A ball-and-stick drawing of the $[W(\equiv CEt)(CH_2Bu^t)(OPr^i)_2]_2$ molecule. Pertinent bond distances (Å) and angles (°): W(1)–C(2) = 1.765(7); W(1)–C(5) = 2.105(7); W(1)–O(14) = 1.961(5); W(1)–O(14)′ = 2,365(5); W(1)–O(10) = 1.882(5), W(1)–W(1)′ = 3.514(1); W(1)–O(10)–C(1) = 134.6.

$(\mu\text{-}CHCH_2)L_2$ has been studied for L = PMe_3 and PMe_2Ph.[38(a)] No cleavage of the C–C bond has yet been noted in these studies.

CONCLUSIONS

The reactions between alkynes and $W_2(OR)_6$ compounds highlight the fascinating chemistry surrounding the W≡W bond supported by alkoxide ligands. The latter provide ancillary ligands (spectator ligands) which can tune the reactivity of the W≡W moiety in terms of both its electronic properties and its steric accessibility. This allows one to enter a realm of reactivity not accessible from mononuclear chemistry, though some of the compounds described here, notably the $(RO)_3W{\equiv}CR'$ compounds, can be made from other routes.[39] Many of the detailed reaction pathways at the ditungsten center remain to be established. These matters are of continuing interest to us in our efforts to unravel the chemistry of triple bonds between molybdenum and tungsten atoms supported by alkoxide ligands.

Acknowledgements—We thank the National Science Foundation, the Department of Energy, Office of Basic Research, Chemical Sciences Division and the Wrubel Computing Center at Indiana University for financial support. MHC wishes to thank Professor Sir Jack Lewis and his inorganic colleagues for providing a stimulating environment for the preparation of this article.

REFERENCES

1. F. Basolo and R. G. Pearson, *Mechanisms of Inorganic Reactions*, 2nd Edn. John Wiley, New York (1967).
2. F. A. Cotton, N. F. Curtis, C. B. Harris, B. F. G. Johnson, S. J. Lippard, J. T. Mague, W. R. Robinson and J. S. Wood, *Science* 1964, **145**, 1305.
3. F. A. Cotton, R. A. Walton, *Multiple Bonds between Metal Atoms*. John Wiley, New York (1982).
4. M. H. Chisholm and F. A. Cotton, *Acc. Chem. Res.* 1978, **11**, 356.
5. M. H. Chisholm (Ed.), *Reactivity of Metal–Metal Bonds*. ACS Symposium Series, Vol. 155 (1981).
6. M. H. Chisholm, *Polyhedron* 1983, **2**, 681.
7. M. H. Chisholm, D. M. Hoffman and J. C. Huffman, *Chem. Soc. Rev.* 1985, **14**, 69.
8. M. H. Chisholm, *Angew. Chem. Int. Ed. Engl.* 1986, **25**, 21.
9. R. R. Schrock, M. L. Listemann and L. G. Sturgeoff, *J. Am. Chem. Soc.* 1982, **104**, 4291.
10. R. R. Schrock and M. L. Listemann, *Organometallics*
11. (a) R. R. Schrock, J. H. Wengrovius and J. Sancho, *J. Am. Chem. Soc.* 1981, **103**, 3932; (b) R. R. Schrock and J. Sancho, *J. Mol. Catal.* 1982, **15**, 75.
12. (a) F. A. Cotton, W. Schwotzer and E. S. Shamshoum, *Organometallics* 1983, **2**, 1167; (b) F. A. Cotton, W. Schwotzer and E. S. Shamshoum, *Organometallics* 1983, **2**, 1340; (c) F. A. Cotton, W. Schwotzer and E. S. Shamshoum, *Organometallics* 1984, **3**, 1770.
13. M. H. Chisholm, D. M. Hoffman and J. C. Huffman, *Inorg. Chem.* 1983, **22**, 2903.
14. M. H. Chisholm, J. C. Huffman and N. S. Marchant, *J. Am. Chem. Soc.* 1983, **105**, 6162.
15. M. H. Chisholm, J. C. Huffman and N. S. Marchant, manuscript in preparation.
16. (a) M. H. Chisholm, K. Folting, D. M. Hoffman and J. C. Huffman, *J. Am. Chem. Soc.* 1984, **106**, 6794; (b) M. H. Chisholm, B. K. Conroy, K. Folting, D. M. Hoffman and J. C. Huffman, *Organometallics* 1986, **5**, 2457.
17. M. H. Chisholm, D. L. Clark, B. K. Conroy, D. M. Hoffman and J. C. Huffman, results to be published.
18. S. Aime, D. Osella, E. Giamello and G. Granozzi, *J. Organomet. Chem.* 1984, **262**, C1.
19. A. T. Blomquist and H. Wasserman, *Organic Chemistry: Carbon-13 NMR Spectroscopy*, Vol. 24, p. 370. Academic Press, New York (1972).
20. A. L. Ternay, Jr, *Contemporary Organic Chemistry*, p. 46 W. B. Saunders, Philadelphia, PA (1979).
21. W. Luttke, T. Loerzer, R. Machinek, L. H. Franz, K. D. Malsch and G. Maier, *Angew. Chem. Int. Ed. Engl.* 1983, **22**, 878.
22. H. Irngartinger, A. Goldmann, R. Jahn, M. Nixdorf, H. Rodewald, G. Maier, K. D. Malsch and R. Emrich, *Angew. Chem. Int. Ed. Engl.* 1984, **23**, 993.
23. M. H. Chisholm, D. M. Hoffman and J. C. Huffman, *J. Am. Chem. Soc.* 1984, **106**, 6806.
24. M. H. Chisholm, K. Folting, J. C. Huffman and I. P. Rothwell, *J. Am. Chem. Soc.* 1982, **104**, 4389.
25. M. H. Chisholm, B. K. Conroy and J. C. Huffman, *Organometallics* 1986, **5**, 2384.
26. R. R. Schrock and H. Strutz, *Organometallics* 1984, **3**, 1600.
27. (a) M. H. Chisholm, D. M. Hoffman and J. C. Huffman, *Inorg. Chem.* 1984, **23**, 3683; (b) M. H. Chisholm, K. Folting, J. A. Heppert, D. M. Hoffman and J. C. Huffman, *J. Am. Chem. Soc.* 1985, **107**, 1234.
28. F. G. A. Stone, *Angew. Chem., Int. Ed. Engl.* 1984, **23**, 89.
29. (a) M. H. Chisholm, K. Folting, J. C. Huffman and E. M. Kober, *Inorg. Chem.* 1985, **24**, 241; (b) M. H. Chisholm, B. W. Eichhorn and J. C. Huffman, unpublished results.
30. M. H. Chisholm and B. K. Conroy, unpublished results.
31. M. H. Chisholm, B. K. Conroy, J. C. Huffman and N. S. Marchant, *Angew. Chem. Int. Ed. Engl.* 1986, **25**, 446.
32. R. R. Schrock, M. R. Churchill, H. J. Wasserman and S. J. Holmes, *Organometallics* 1982, **104**, 1739.
33. M. H. Chisholm, D. A. Haitko, K. Folting and J. C. Huffman, *J. Am. Chem. Soc.* 1981, **103**, 4046; (b) M. J. Chetcuti, M. H. Chisholm, K. Folting, D. A. Haitko, J. C. Huffman and J. Janos, *J. Am. Chem. Soc.* 1983, **105**, 1163.
34. M. H. Chisholm, B. W. Eichorn, K. Folting, J. C. Huffman and R. J. Tatz, *Organometallics* 1986, **5**, 1599.
35. M. H. Chisholm, B. W. Eichhorn and J. C. Huffman, *J. Chem. Soc., Chem. Commun.* 1985, 861.
36. (a) M. H. Chisholm, J. C. Huffman and C. A. Smith, *J. Am. Chem. Soc.* 1986, **108**, 222; (b) M. Akiyama, M. H. Chisholm, F. A. Cotton, M. W. Extine, D. A. Haitko, J. Leonelli and D. Little, *J. Am. Chem. Soc.* 1981, **103**, 779.
37. (a) D. S. Ginley, C. R. Bock, M. S. Wrighton, B. Fischer, D. L. Tipton and R. Bau, *J. Organomet. Chem.* 1978, **157**, 41; (b) S. A. Knox, R. F. D. Stansfield, F. G. A. Stone, M. J. Winter and P. J. Woodward, *J. Chem. Soc., Chem. Commun.* 1978, 221.
38. (a) K. J. Ahmed, M. H. Chisholm, K. Folting and J. C. Huffman, *J. Am. Chem. Soc.* (in press); (b) K. J. Ahmed, M. H. Chisholm, K. Folting and J. C. Huffman, *Inorg. Chem.* 1985, **24**, 4039; (c) K. J. Ahmed, M. H. Chisholm, K. Folting and J. C. Huffman, *J. Chem. Soc., Chem. Commun.* 1985, 152.
39. (a) R. R. Schrock, D. N. Clark, J. Sancho, J. H. Wengrovius, S. M. Rocklage and S. F. Pedersen, *Organometallics* 1982, **1**, 1645; (b) J. H. Freudenberger, S. F. Pedersen and R. R. Schrock, *Bull. Soc. Chim. Fr.* 1985, 349.

Polyhedron Vol. 6, No. 4, pp. 793–801, 1987
Printed in Great Britain

0277–5387/87 $3.00+.00
Pergamon Journals Ltd

THE SYNTHESIS AND PROPERTIES OF COMPLEXES CONTAINING HETERONUCLEAR QUADRUPLE BONDS

ROBERT H. MORRIS

Department of Chemistry and the Scarborough Campus, University of Toronto, 80 St George St., Toronto, Ontario, Canada M5S 1A1

Abstract—The complexes $CrMo(O_2CMe)_4$, $CrMo(mhp)_4$, $MoW(mhp)_4$ (mhp = 2-hydroxy-6-methylpyridine anion), $MoW(O_2CCMe_3)_4$, $MoWCl_4(PMe_3)_4$, $MoWCl_4(PMePh_2)_4$ and $Cl_2(PMe_3)_2MoWCl_2(PMePh_2)_2$ are the only ones known to contain heteronuclear quadruple bonds. The synthesis and properties of these complexes are reviewed and compared to analogous complexes containing homonuclear quadruple bonds. The complexes containing bridged Mo–W bonds appear to have enhanced stability relative to their homonuclear congeners whereas complexes containing bridged Cr–Mo bonds or unbridged Mo–W bonds have properties close to the average of their corresponding homonuclears.

Some of the strongest metal–metal bonds found in coordination complexes are the heteronuclear quadruple bonds formed between Mo and W.[1,2] Cotton's group reported that the compound $MoW(mhp)_4$ (mhp = 2-hydroxy-6-methylpyridine anion) has a higher force constant for its quadruple bond and a formally shorter bond than its homonuclear analogues, $Mo_2(mhp)_4$ and $W_2(mhp)_4$.[1,2] Katovic *et al.* in McCarley's laboratory synthesized the pivalate-bridged dimer $MoW(O_2CCMe_3)_4$[3,4] and were surprised to find that it has a shorter bond than the corresponding complex $Mo_2(O_2CMe)_4$.[5] The electronegativity difference between W and Mo is small ($\Delta\chi < 0.1$) and thus the excess bond energy and bond shortening as originally defined by Pauling might not have been expected to be as large as had been observed in these intriguing compounds.

The two other well-characterized compounds known to contain mixed-metal quadruple bonds which are spanned by bridging ligands are $CrMo(O_2CCMe_3)_4$[6,7] and $CrMo(mhp)_4$.[1] The former was the first example of a heteronuclear quadruple bond to be reported; the Cr–Mo spacing appeared to be at the distance predicted by a sum of quadruple-bond covalent radii for Cr and Mo.[7] However other physical properties (Table 1) of the hydroxymethylpyridine-bridged dimers were not at the average of the properties of the Cr_2 and Mo_2 congeners but instead fell closer to the Mo_2 values.[1] The complexes $Cr_2(mhp)_4$ and $Mo_2(mhp)_4$ are examples of complexes containing "supershort" quadruple bonds.[1]

The recent syntheses of some unbridged complexes $MoWCl_4(PR_3)_4$ by Rudy Luck in my lab[8,9] (PR_3 = $PMePh_2$, PMe_2Ph or PMe_3) and independently by Carlin and McCarley[10] ($PR_3 = PMe_3$) have provided valuable information on the properties of the first unbridged Mo–W bonds. The study of these complexes should in principle allow the evaluation of the contribution of bridging ligands to the apparently deviant properties of these heteronuclear dimers. It should be noted that the crystal-structure determinations reported to date for all of these heteronuclears have the problem of disorder of the two metal atoms M and M′ since the two ends of the molecules are so similar; usually a site occupancy of 0.5 for each of M and M′ is observed.[2,4,7] We have recently overcome this problem by making the unbridged complex $Cl_2(PMePh_2)_2WMoCl_2(PMe_3)_2$ where the two centers are quite different[8] (see below).

SYNTHETIC ROUTES TO HETERONUCLEAR QUADRUPLE BONDS

Compounds containing the strong Mo–Mo bond are quite stable relative to their Cr_2 and W_2 congeners. Thus synthetic routes to CrMo and MoW compounds must either avoid the formation of Mo_2 or must include a separation step which can distinguish between these very similar compounds. Successful methods are described in Table 2. No preparation for complexes containing a Cr–W bond has been discovered. It should be noted that

Table 1. A comparison of properties of complexes containing homonuclear and heteronuclear quadruple bonds

Property	Ligands	CrCr	CrMo	MoMo	MoW	WW
$\lambda(\delta^2 \rightarrow \delta\delta^*)$ (nm)	$(mhp)_4$	444[36]		490[36]		535[36]
	$Cl_4(PMe_3)_4$			582[23]	635[9]	657[23]
	$Cl_4(PMePh_2)_4$			596[41]	650[8]	
$E_{1/2}$(ox) (V vs SCE)	$(mhp)_4$	1.01[a1]	0.35[1]	0.20[1]	−0.16[1]	−0.35[1]
	$(O_2CCMe_3)_4$			0.38[14]		−0.37[14]
	$Cl_4(PR_3)_4$			0.64 (R = Bu)[24]	0.42 (R = Me)[9]	0.04 (R = Bu)[24]
$E_{1/2}$(red) (V vs SCE)	$Cl_4(PR_3)_4$			−1.92 (Bu)[24]	−1.86 (Me)[9]	−2.16 (Bu)[24]
IP δ(eV)	$(mhp)_4$	6.8[1]	6.0[1]	5.89[1]	5.60[1]	5.3[1]
	$Cl_4(PMe_3)_4$			6.44[28]	6.11[25]	5.81[28]
	$(O_2CCMe_3)_4$			6.75[14]	6.34[14]	5.93[14]
	$(OAc)_4$	8.65[37]	7.06[37]	6.92[37]		
$D(M\overset{4}{—}M')$ (kJ mol^{-1})	$(OAc)_4$	205[31]	249[31]	334[31]		
	$Cl_4(PH_3)_4$	153[34]		524[34]		428[34]
$k(M\overset{4}{—}M')$(mdyne Å^{-1})	$(mhp)_4$	1.77[b36], 4.73[1]	5.04[1]	5.10[1]	5.47[1]	4.71[1]
	$(OAc)_4$		3.08[c7]	4.63[27]		
	$Cl_4(PR_3)_4$			3.44 $(PMePh_2)$[c41]		3.66 (PBu_3)[c24]
$r(M\overset{4}{—}M')$(Å)	$(mhp)_4$	1.889(1)[35]		2.065(1)[2]	2.091(1)[2]	2.161(1)[2]
	$(OAc)_4$	[2.288(2)][d42]	2.050(1)[7]	2.093(1)[43]		
	$(O_2CCMe_3)_4$			2.088(1)[5]	2.080(1)[4]	
	$(O_2CC_6H_2Me_3)_4$					2.176(1)[15]
	$Cl_4(PMe_3)_4$			2.130(0)[23]	2.209(1)[9]	2.262(1)[23]
					2.218(2)[10]	

[a]Irreversible oxidation.[1]

[b]More reliable value calculated from Ref. 36.

[c]Value calculated from literature $\nu(M\overset{4}{—}M)$ frequency using the harmonic oscillator approximation.

[d]Axial coordination of H_2O[13].

Table 2. Preparative routes to heteronuclear quadruple bonds

Ligands	CrMo	MoW
$(OAc)_4$	Add $Mo(CO)_6$ in HOAc–AcOAc–CH_2Cl_2 to excess $Cr_2(OAc)_4(H_2O)_2$ in HOAc–AcOAc at 118°C CrMo ~ 30%, some Mo_2 and $Cr(OAc)_3$ Purification by sublimation[7]	—
$(O_2CCMe_3)_4$	—	$16HO_2CCMe_3 + Mo(CO)_6 + 3W(CO)_6$ (reflux o-$Cl_2C_6H_4$) MoW 70% of product, Mo_2 30% Selective oxidation with I_2 gives MoW^+ which is then reduced with Zn[3]
$(mhp)_4$	$4Hmhp + Cr(CO)_6 + Mo(CO)_6$ (reflux diglyme–heptane) CrMo ⩽ 1%, equal amounts of Cr_2 and Mo_2[2] Or $CrMo(OAc)_4$ + excess Na(mhp) in ethanol[13]	$4Hmhp + 1.5Mo(CO)_6 + W(CO)_6$ (reflux diglyme–heptane) MoW > 50%, Mo_2 ~ 20%, W_2 ~ 0% Selective oxidation gives MoW^+ which is then reduced with Zn[2]
$Cl_4(PMePh_2)_4$	—	Mo(η^6-PhPMePh)$(PMePh_2)_3 + 3WCl_4(PPh_3)_2$ in C_6H_6 at 22°C MoW > 60%, Mo_2 ⩽ 5%, W_2 0%[8]
$Cl_4(PMe_3)_4$	—	$MoW(O_2CCMe_3)_4$ + excess PMe_3 + excess Me_3SiCl[10] or $MoWCl_4(PMePh_2)_4$ + excess PMe_3 in C_6H_6 at 60°C for 3 h[9]

only a few complexes are known to contain CrW bonds (single in these cases).[11,12]

The method of choice for the synthesis of bridged Cr–Mo bonds is that of Garner and Senior.[6] The mechanistic pathway to $CrMo(O_2CMe)_4$ formation is postulated to involve the attack of reactive $Cr(O_2CMe)_2$ on a low oxidation state (0, I or II) carbonyl complex of Mo to initiate metal–metal bond formation. The carbonyl ligands are lost as a result of the high temperatures of the reaction (>100°C). The Cr reagent is present in excess to avoid the formation of Mo–Mo compounds. The acetate bridges can be replaced by other bridging ligands [trifluoroacetate[7] and mhp[13] (Table 2)] but not by chloride ions.[7] The reaction with Cl^-/HCl results in the cleavage of the Cr–Mo bond.[7]

Complexes containing Mo–W bonds bridged by pivalate or mhp are prepared by reacting a mixture of the hexacarbonyls with the acid form of the ligands at high temperature (>100°C) as in Table 2. Usually a mixture of Mo_2 and MoW dimers are obtained. Under the acidic conditions of the pivalic acid reaction, $W_2(O_2CCMe_3)_4$ would not be stable,[14,15] and thus it is not found in the reaction mixture. Ditungsten complexes are readily oxidized as indicated by their negative oxidation potentials (Table 1). Because of the similar molecular dimensions and structures of the Mo_2 and MoW dimers it is not possible to separate the mixtures by crystallization or chromatography. Instead the MoW complexes can be selectively oxidized with iodine to give $[MoW(O_2CCMe_3)_4]I$[3] or $MoW(mhp)_4I_3$.[2] This is possible because of the more negative potential, $E_{1/2}(ox)$, of the MoW complexes [~ −0.2 V (Table 1)]. These insoluble compounds are then readily separated from the corresponding Mo_2 complexes. The oxidized complexes can then be reduced by Zn to give pure samples of $MoW(O_2CCMe_3)_4$ or $MoW(mhp)_4$.

Complexes of the type $MoWCl_4(PR_3)_4$ which contain unbridged Mo–W bonds can be made either by reacting molybdenum(0) complexes containing η^6-arylphosphine ligands with tungsten(IV) complexes (see below) or by substitution reactions on complexes which already contain Mo–W bonds. Examples are listed in Table 2. McCarley has unpublished work involving the removal of the bridging ligands from $MoW(O_2CCMe_3)_4$ by use of $SiMe_3Cl$ and PMe_3 to give $MoWCl_4(PMe_3)_4$.[10] Trimethylsilylchloride is a mild and selective reagent for similar reactions with homonuclear complexes.[16,17] The Mo–W distance[10] (see Table 1) and the ^{31}P NMR spectrum[8,10] of $MoWCl_4(PMe_3)_4$ have been reported. Preparative routes

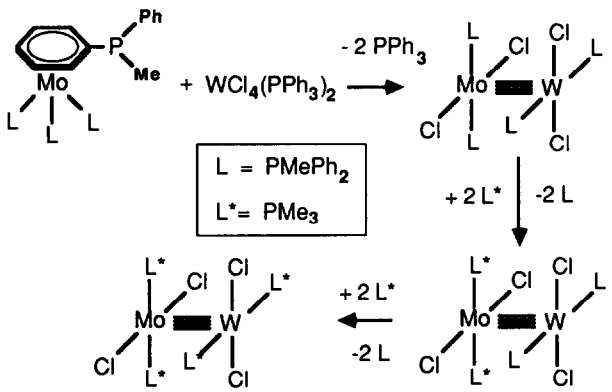

Scheme 1. Preparation and substitution reactions of $MoWCl_4(PMePh_2)_4$.

to $MoWCl_4(PMePh_2)_4$ and its derivatives have been developed in the author's laboratory and are discussed in more detail in the next section.

PREPARATION AND REACTIONS OF $MoWCl_4(PMePh_2)_4$

A particularly direct synthetic route to the green complex $MoWCl_4(PMePh_2)_4$ and its derivatives is outlined in Scheme 1. The preparation of $MoWCl_4(PMePh_2)_4$ differs from the other preparations listed in Table 2 in two respects.

The first difference is the redox reaction involved. In our case molybdenum in the zero oxidation state as $Mo(\eta^6\text{-PhPMePh})(PMePh_2)_3$ ($E_{1/2}(ox) = -0.44$ V)[9] is used to reduce the tungsten(IV) complex $WCl_4(PPh_3)_2$, whereas, in the other methods of M–M′ formation, the acidic ligands are involved in the oxidation of the zero-valent metal carbonyls. Despite its seemingly exotic structure, the complex $Mo(\eta^6\text{-PhPMePh})(PMePh_2)_3$ is a useful starting material as it can be synthesized in one step in 75% yield from commercially available materials (Mo_2Cl_{10}–$PMePh_2$–Mg–THF).[18]

The other main difference is the course of the reaction. The preparations of the bridged Mo–W complexes invariably yield mixtures containing significant amounts ($\geq 20\%$) of the stable Mo_2 complex. These reactions which occur at elevated temperatures may be under thermodynamic control so that the factors favoring the formation of Mo–W would be the ratio of Mo to W employed in the preparation and the slightly greater bond strength of the heteronuclear. By contrast the formation of $MoWCl_4(PMePh_2)_4$ takes place rapidly at 22°C in quite a regiospecific reaction, and thus could be under kinetic control. The fact that $Mo(\eta^6\text{-PhPMePh})(PMePh_2)_3$ gives a much cleaner reaction with $WCl_4(PPh_3)_2$ than does $Mo(N_2)_2(PMePh_2)_4$[8] suggests that precoordination of the η^6-phosphine phosphorus atom to the W is the favoured pathway. Roberts and Geoffroy have classified this type of heternuclear bond formation as a "bridge-assisted" reaction and have reviewed many examples.[12] We have demonstrated elsewhere that a variety of η^6-phosphine complexes of molybdenum(0) can be used as phosphine-like ligands in complexes of rhodium(I),[19] molybdenum(0)[20] and group VI carbonyls.[21] The phosphine ligands in $WCl_4(PPh_3)_2$ are known to be rapidly substituted by a variety of phosphines, and therefore coordination of the η^6-phosphine complex is quite feasible.

The use of η^6-phosphine complexes of molybdenum(0) for the formation of other heteronuclear quadruple bonds may be limited in scope. The reaction of $WCl_4(PPh_3)_2$ with $Mo(\eta^6\text{-PhPMe}_2)P\text{-Me}_2Ph)_3$ does yield $MoWCl_4(PMe_2Ph)_4$[8] but its reaction with $Mo(\eta^6\text{-PhPMePh})(PPh_2CH_2CH_2PPh_2)(PMePh_2)$ does not give a mixed-ligand Mo–W complex as might be expected. In addition, reactions of $Mo(\eta^6\text{-PhPMePh})(PMePh_2)_3$ with other metal chlorides such as $NbCl_4(THF)_2$, $[Nb\text{-}Cl_3(THF)_2]_2(\mu\text{-}N_2)$, $CrCl_3$ and $ReCl_5$ do not yield identifiable products.

Other heteronuclear dimers can be prepared by substitution of the phosphine ligands of complex $MoWCl_4(PMePh_2)_4$ with smaller phosphine ligands. Scheme 1 outlines the substitution reactions involving PMe_3. At 22°C only the phosphines on Mo are replaced to give blue-green $Cl_2(PMe_3)_2Mo\text{-}WCl_2(PMePh_2)_2$. The selectivity of this reaction probably stems from the fact that the Mo–P bonds are weaker than the W–P bonds. As Scheme 1 indicates all of the $PMePh_2$ ligands are displaced by PMe_3 ligands at 60°C and blue-green $Mo\text{-}WCl_4(PMe_3)_4$ can be isolated although the yield of pure material is low ($\sim 10\%$) because the complex partly decomposes during work-up when the free $PMePh_2$ is distilled away. Substitution of $MoWCl_4(PMePh_2)_4$ by excess $PPh_2CH_2CH_2PPh_2$ also yields heteronuclear products which are currently being characterized. Isocyanide ligands on the other hand cleave the Mo–W bond to give mononuclear isocyanide complexes; Walton's group has demonstrated the generality of reactions involving the cleavage of quadruple bonds by isocyanides.[22] Attempts to replace the chloride ligands in our complexes by methyl groups have not succeeded.

PROPERTIES OF COMPLEXES CONTAINING UNBRIDGED Mo–W BONDS

The complexes which have had their structures determined by single-crystal X-ray diffraction are $MoWCl_4(PMePh_2)_4$,[9] $Cl_2(PMe_3)_2MoWCl_2(PMePh_2)_2$[8,9] and $MoWCl_4(PMe_3)_4$.[9,10] Figure 1 shows

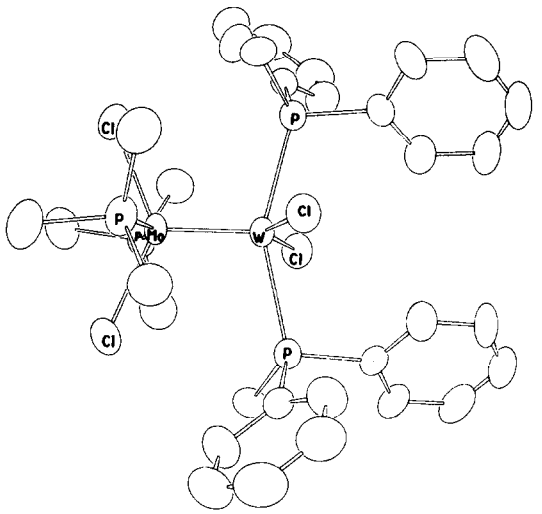

Fig. 1. ORTEP view of the complex $Cl_2(PMe_3)_2Mo$-$WCl_2(PMePh_2)_2$.

an ORTEP view of the second complex. All of the complexes have similar geometries with two pseudo-square-planar MCl_2P_2 fragments eclipsed with respect to one another and separated by a short metal–metal distance of ~2.207(1) Å (Table 3). As is usual for $M_2X_4L_4$ complexes the halide ligands are next to phosphine ligands across the metal–metal bond to minimize steric interactions. Another feature in common with homonuclear $M_2X_4L_4$ complexes[23] is the bending away from the M≡M′ bond of the Cl–M—Cl vectors (angle ~133–141°) and the P–M–P vectors (angle ~153–158°). No intermolecular ligand–metal interactions *trans* to the quadruple bond are possible for these molecules.

The structure determined for $Cl_2(PMe_3)_2Mo$-$WCl_2(PMePh_2)_2$ is significant as it is the only heteronuclear M≡M′ complex which is not disordered with respect to the placement of the metal ions. In this case the two metals are "labelled" with different phosphine ligands and so the two ends of the molecule are quite different. The metal–ligand distances are thus accurately determined in this case: d(Mo–P) = 2.532(2), d(W–P) = 2.539(2), d(Mo–Cl) = 2.424(2), d(W–Cl) = 2.378(2) Å. These are similar to values observed for homonuclear congeners $M_2Cl_4(PMe_3)_4$.[23] The metal–phosphorus distances are the longest ones known for complexes of Mo or W with pseudo-*trans* PMe_3 ligands perhaps indicating a labilization of these ligands by the *cis*-M≡M bond. Phosphine ligands in these complexes can indeed be substituted as indicated in Scheme 1.

Approximate covalent—radii for unbridged quadruple bonds can be derived from the structures of the homonuclear complexes $M_2Cl_4(PMe_3)_4$ (M = Mo or W):[23] r≡(Mo) = 1.065 Å, r≡(W) = 1.131 Å. Therefore the observed Mo–W distances [~2.207(1) Å] for our heteronuclear complexes which are listed in Table 3 are just slightly longer than the sum of these radii [2.196(1) Å] and there is no evidence for extra shortening of the bond with respect to bond distances of the homonuclear complexes. This contrasts with the structural features of bridged MoW complexes (Table 1). The covalent bond radii for bridged quadruple bonds with small or no axial interactions range from 0.92 to ~1.0 Å for Cr,[13] 1.03–1.05 Å for Mo, and 1.08–1.09 Å for W (Table 1), so that the Mo–W distances in $MoW(O_2CCMe_3)_4$ [2.080(1) Å] and MoW $(mhp)_4$ [2.091(1) Å] fall short of the sum of these radii (2.11–2.14 Å). Clearly the bridging ligands in these complexes must be responsible for the unexpectedly large shortening. The reported Cr–Mo distance in $CrMo(O_2CMe)_4$ of 2.050(1) Å is not shorter but appears closer to the sum of the covalent radii; the reason for this is not clear.

The ^{31}P NMR spectra of the complexes $MoWCl_4(PR_3)_4$ are diagnostic of their solution structures. Two equivalent phosphine ligands on Mo couple to two equivalent ligands on W to give an overall spectrum consisting of two sets of triplets with $^3J(^{31}P–^{31}P)$ couplings (Table 3). The resonance for phosphines on W has characteristic satellite triplets corresponding to a coupling $^1J(^{31}P–^{183}W)$ of the $Mo^{183}W$ isotopomer. A $^2J(^{31}P–^{183}W)$ coupling of 43 Hz was resolved for the $Mo^{183}W$ isotopomer of $MoWCl_4(PMePh_2)_4$.[8]

Some other spectroscopic and electrochemical properties of the heteronuclears are listed in Tables 1 and 3. In general these properties are intermediate between those of the corresponding homonuclear complexes. The $\delta^2 \rightarrow \delta\delta^*$ transitions of the complexes $MoWCl_4(PR_3)_4$ (PR_3 = PMe_3 or $PMePh_2$)[8,9] fall between the energies of the Mo_2 and W_2 congeners[23] but closer to the W_2 values (Tables 1 and 3). Replacing $PMePh_2$ ligands by the more basic and smaller PMe_3 ligands shifts this transition to higher energy for the homonuclears $Mo_2Cl_4(PR_3)_4$ (Table 1) and the heteronuclear series (Table 3). This shift is paralleled by a decrease in the energies of both reversible redox couples $MoW^+ \leftrightarrow MoW$ [$E_{1/2}$(ox)] and $MoW \leftrightarrow MoW^-$ [$E_{1/2}$(red)], which indicates that the complexes with more PMe_3 ligands are more electron-rich. The redox products (MoW^+ and MoW^-) which should have the electron configurations $\sigma^2\pi^4\delta$ and $\sigma^2\pi^4\delta^2\delta^*$, respectively, have not yet been isolated. The $E_{1/2}$(ox) value for $MoWCl_4(PMe_3)_4$ falls between the values for related homonuclears with PBu_3 ligands (Table 1).[24]

The ionization energy of the δ-electrons of

Table 3. Properties of complexes containing unbridged Mo–W bonds

Property	$MoWCl_4(PMePh_2)_4$[9]	$(PMe_3)_2Cl_2MoWCl_2(PMePh_2)_2$[8,9]	$MoWCl_4(PMe_3)_4$[9]	$W_2Cl_4(PMe_3)_4$[23]	$Mo_2Cl_4(PMe_3)_4$[23]
$\lambda(\delta^2 \rightarrow \delta\delta^*)$ (nm)	650	643	635	657	582
$E_{1/2}$(ox) (V vs SCE, in THF)	0.47	0.43	0.42		
$E_{1/2}$(red) (V vs SCE, in THF)	−1.72	−1.73	−1.86		
$^1J(^{31}P—^{183}W)$ (Hz)	266	273	271	236[24]	
$^3J(^{31}P—^{31}P)$ (Hz)	23.5	24.4	25.6	28[24]	
r(MoW)(Å)	2.208(4) (av.)	2.207(1)	2.209(1)	2.262(1)[a]	2.130(0)[b]
r(MoP) (Å)	2.58(2) (av.)	2.532(2)	2.529(2)		2.545(1) (av.)
r(WP) (Å)	2.58(2) (av.)	2.539(2)	2.522(2)	2.507(2) (av.)	
r(MoCl) (Å)	2.38(2) (av.)	2.424(2)	2.406(2)		2.414(1) (av.)
r(WCl) (Å)	2.38(2) (av.)	2.378(2)	2.395(2)	2.392(3) (av.)	

[a] r(WW).
[b] r(MoMo).

$MoWCl_4(PMe_3)_4$ has been determined by photoelectron spectroscopy to be 6.11 eV.[25] This value is approximately the average of the homonuclear energies (Table 1). Similarly the π and σ ionization energies at 7.35 and 7.67 eV, respectively, are close to the averages of energies assigned to the Mo_2 and W_2 congeners.[25] These data were useful in demonstrating that the σ and π ionization energies tend to overlap for Mo_2 quadruply bonded compounds[25,26] and were useful in explaining discrepancies in earlier assignments of the σ(M–M) ionization peaks of Mo_2[26–28] and W_2[28–30] PES spectra. The stretching frequency ν(MoW) has not been located[8] so that a comparison of bond force constant with those of the homonuclears (Table 1) is not possible.

A COMPARISON OF PROPERTIES AND REACTIONS OF COMPLEXES CONTAINING HETERONUCLEAR vs HOMONUCLEAR QUADRUPLE BONDS

The question of interest is whether the M–M′ fragment has enhanced stability above that expected from the average of the properties of the homonuclear congeners M–M and M′–M′.

The evidence is sketchy for CrMo complexes since only two complexes are known and both contain bridging ligands (Table 1). However it appears that the heteronuclear bond strength is close to the average of those of the homonuclears in this case. A thermochemical study has allowed the estimation of the quadruple bond dissociation energy for the complexes $Cr_2(O_2CMe)_4$, $CrMo(O_2CMe)_4$ and $Mo_2(O_2CMe)_4$.[31] The energy for Cr–Mo (249 kJ mol^{-1}) was found to be slightly less than the average of the energies of the homonuclears. Note however that these estimates may be consistently low[32] since spectral[33] and computational[34] determinations give values in the range 500–700 kJ mol^{-1} for Mo–Mo compounds. The Cr–Mo distance in $CrMo(O_2CMe)_4$ is at or above the sum of the covalent radii derived from the homonuclear species as discussed above. The force constants for the mhp complexes listed in Table 1 were based on preliminary assignments of complex vibrational spectra.[1,35] A more extensive low-temperature electronic absorption and emission study of $Cr_2(hmp)_4$ indicated that the ground-state vibration ν(Cr–Cr) is 340 cm^{-1} [36] so that the force constant is much lower than had been initially thought (1.77 vs 4.73 mdyne $Å^{-1}$). Thus the determination of the Cr–Mo force constant may also need more work. The δ ionization energies for both $CrMo(O_2CMe)_4$[37] and CrMo-$(mhp)_4$[1] are closer to those of the analogous Mo_2 compounds (Table 1).

The homonuclears Cr_2 and Mo_2 are the greatly favored products when mixtures of the metal carbonyls are refluxed with the ligands in attempts to synthesize the mixed-metal compounds (see Table 2); however it is not known whether this is a kinetic or a thermodynamic effect. The Cr–Mo bond of $CrMo(O_2CMe)_4$ is disrupted when treated with aqueous HCl whereas the Mo–Mo bond of $Mo_2(O_2CMe)_4$ remains intact when it is converted to $Mo_2Cl_8^{4-}$ in a similar reaction.[7] However this CrMo complex can be converted to $CrMo(mhp)_4$ (Table 2) under basic conditions.[13] Thus there is no evidence for enhanced stability of the Cr–Mo bond.

The available data for complexes containing bridged Mo–W bonds suggest that such bonds do have enhanced stability. The bonds are shorter than the sum of the covalent radii of the metals as discussed above. The Mo–W force constant of $MoW(mhp)_4$ is actually higher than those of both homonuclears (Table 1)[1] although the validity of force constants of bonds with bridging groups is questionable. Certainly the mixed-metal products $MoW(mhp)_4$ and $MoW(O_2CCMe_3)_4$ do predominate when the metal carbonyls are heated with the acid forms of their respective ligands (Table 2). The MoW fragment usually does remain intact during reactions. The reaction of HCl with the pivalate complex yields the anion $MoWCl_8H^{3-}$ which contains a formal triple bond.[4,38] The pivalate ligands of $MoW(O_2CCMe_3)_4$ can be replaced by phosphine and chloride ligands by use of trimethylsilylchloride in the presence of excess phosphine ligands (Table 2). It has been reported that in the presence of Me_3SiCl and reduced amounts of PMe_3, the tetramer $Mo_2W_2Cl_8(PMe_3)_4$ forms by a reaction that can be viewed as the cycloaddition reaction of the two Mo–W units.[10] A similar cycloaddition of Mo–Mo units to produce the rectangular cluster $Mo_4Cl_8(PEt_3)_4$ has been reported.[39] The details of the structure of this complex are yet to be published. Such a complex could also be pictured as an intermediate in the (unknown) metathesis reaction of Mo–W bonds to Mo–Mo- and W–W-bonded species. The metathesis of the Mo–Mo and W–W bonds in $M_2(\eta^5\text{-}C_5H_5)_2(CO)_4$ to give the heteronuclear $MoW(\eta^5\text{-}C_5H_5)_2(CO)_4$ has been reported.[40]

The complexes $MoWCl_4(PR_3)_4$ containing unbridged Mo–W bonds appear to have properties at the average of those of the homonuclear complexes. The bond lengths are close to the sum of the covalent radii derived from the homonuclear species. The properties listed in Tables 1 and 3 fall close to the average and slightly nearer to the properties of the W_2 complexes. The Mo–W bond remains

intact in substitution reactions with PMe_3 and $PPh_2CH_2CH_2PPh_2$ but fragments with isocyanide ligands.[8,9] When heated the complexes do not metathesize to homonuclear species.[8]

CONCLUSIONS

The limited data available to date indicate that the Cr≡Mo bond bridged by acetate or mhp does not have extra stabilization with respect to homonuclear congeners and its energy is near or slightly less than the average of the Cr_2 and Mo_2 bond energies. The enhanced stability noted for the bridged Mo≡W complexes may be due to the favorable geometry of the sterically unhindered bridging ligands that allows the metal–metal bond to achieve optimum overlap. The small amount of information available on the unbridged Mo≡W complexes of the type $MoWCl_4(PR_3)_4$ suggests that this heteronuclear bond has properties which are close to the average of the homonuclear properties. More experiments and calculations are needed to verify these interesting observations. Further research into the synthesis of new complexes containing heteronuclear bonds, both bridged and unbridged, could involve pairwise combinations of Tc, Re, Mo, W, Nb and Ta where high quadruple-bond energies are expected.

Acknowledgements—I thank Rudy Luck for his excellent synthetic work and Dr Jeffery Sawyer for the crystal structure determinations. This research was supported by an operating grant from NSERC (Canada).

REFERENCES

1. B. E. Bursten, F. A. Cotton, A. H. Cowley, B. E. Hanson, M. Lattman and G. G. Stanley, *J. Am. Chem. Soc.* 1979, **101**, 6244.
2. F. A. Cotton and B. E. Hanson, *Inorg. Chem.* 1978, **17**, 3237.
3. V. Katovic, J. L. Templeton, R. J. Hoxmeier and R. E. McCarley, *J. Am. Chem. Soc.* 1975, **97**, 5300.
4. V. Katovic and R. E. McCarley, *J. Am. Chem. Soc.* 1978, **100**, 5586.
5. F. A. Cotton, M. Extine and L. D. Gage, *Inorg. Chem.* 1978, **17**, 172.
6. C. D. Garner and R. G. Senior, *J. Chem. Soc., Chem. Commun.* 1974, 580.
7. C. D. Garner, R. G. Senior and T. J. King, *J. Am. Chem. Soc.* 1976, **98**, 3526.
8. R. L. Luck and R. H. Morris, *J. Am. Chem. Soc.* 1984, **106**, 7978.
9. R. L. Luck, R. H. Morris and J. F. Sawyer, *Inorg. Chem.* 1987, in press.
10. (a) R. T. Carlin and R. E. McCarley, INOR 198, 184th ACS Meeting, Kansas City, 1982; (b) R. T. Carlin, Ph.D. Thesis, Iowa State University, 1982.
11. (a) T. Madach and H. Vahrenkamp, *Z. Naturforsch.* 1979, **34B**, 573; (b) M. J. Chetcuti, M. Green, J. C. Jeffery, F. G. A. Stone and A. A. Wilson, *J. Chem. Soc., Chem. Commun.* 1980, 948; (c) G. Huttner, B. Sigwarth, J. von Seyerl and L. Zsolnai, *Chem. Ber.* 1982, **115**, 2035.
12. D. A. Roberts and G. L. Geoffroy, In *Comprehensive Organometallic Chemistry* (Edited by G. Wilkinson, F. G. A. Stone and E. Abels), Chapter 40. Pergamon Press, London (1982).
13. F. A. Cotton and R. A. Walton, *Multiple Bonds between Metal Atoms*, p. 134. Wiley, New York (1982).
14. D. J. Santure, J. C. Huffman and A. P. Sattelberger, *Inorg. Chem.* 1985, **24**, 371.
15. F. A. Cotton and W. Wang, *Inorg. Chem.* 1984, **23**, 1604.
16. R. E. McCarley, T. R. Ryan and C. C. Torardi, *ACS Symp. Ser.* 1981, **155**, 41.
17. M. L. H. Green, G. Parkin, J. Bashkin, J. Fail and K. Prout, *J. Chem. Soc., Dalton Trans.* 1982, 2519.
18. R. L. Luck, R. H. Morris and J. F. Sawyer, *Organometallics* 1984, **3**, 247.
19. R. L. Luck and R. H. Morris, *J. Organomet. Chem.* 1983, **255**, 221.
20. R. L. Luck, R. H. Morris and J. F. Sawyer, *Organometallics* 1984, **3**, 1009.
21. R. L. Luck, Ph.D. Thesis, University of Toronto, 1987.
22. L. B. Anderson, T. J. Barder and R. A. Walton, *Inorg. Chem.* 1985, **24**, 1421 (and references therein).
23. F. A. Cotton, M. W. Extine, T. R. Felthouse, B. W. Kolthammer and D. G. Lay, *J. Am. Chem. Soc.* 1981, **103**, 4040.
24. R. R. Schrock. L. G. Sturgeoff and P. R. Sharp, *Inorg. Chem.* 1983, **22**, 2801.
25. G. M. Bancroft, J. Bice, R. H. Morris and R. L. Luck, *J. Chem. Soc., Chem. Commun.* 1986, 898.
26. T. Ziegler, *J. Am. Chem. Soc.* 1985, **107**, 4453.
27. Reference 13, p. 419.
28. F. A. Cotton, J. L. Hubbard, D. L. Lichtenberger and I. Shim, *J. Am. Chem. Soc.* 1982, **104**, 679.
29. G. M. Bancroft, E. Pellach, A. P. Sattelberger and K. W. McLaughlin, *J. Chem. Soc., Chem. Commun.* 1982, 752.
30. E. M. Kober and D. L. Lichtenberger, *J. Am. Chem. Soc.* 1985, **107**, 7199.
31. K. J. Cavell, D. D. Garner, G. Pilcher and S. Parkes, *J. Chem. Soc., Dalton Trans.* 1979, 1714.
32. Reference 13, p. 351.
33. W. C. Trogler, C. D. Cowman, H. B. Gray and F. A. Cotton, *J. Am. Chem. Soc.* 1977, **99**, 2993.
34. T. Ziegler, *J. Am. Chem. Soc.* 1984, **106**, 5901.
35. F. A. Cotton, P. E. Fanwick, R. H. Niswander and J. C. Sekutowski, *J. Am. Chem. Soc.* 1978, **100**, 4725.
36. M. C. Manning and W. C. Trogler, *J. Am. Chem. Soc.* 1983, **105**, 5311.
37. A. W. Coleman, J. C. Green, A. J. Hayes, E. A. Seddon, R. D. Lloyd and Y. Niwa, *J. Chem. Soc., Dalton Trans.* 1979, 1057.
38. V. Katovic and R. E. McCarley, *Inorg. Chem.* 1978,

17, 1268.
39. R. N. McGinnis, T. R. Ryan and R. E. McCarley, *J. Am. Chem. Soc.* 1978, **100**, 7900.
40. M. H. Chisholm, M. W. Extine, R. L. Kelly, W. C. Mills, C. A. Murillo, L. A. Rankel and W. W. Reichert, *Inorg. Chem.* 1978, **17**, 1673.
41. E. Carmona-Guzman and G. Wilkinson, *J. Chem. Soc., Dalton Trans.* 1977, 1716.
42. F. A. Cotton, B. G. DeBoer, M. D. LaPrade, J. R. Pipal and D. A. Ucko, *Acta Cryst.* 1971, **B27**, 1664.
43. F. A. Cotton, Z. C. Mester and T. R. Webb, *Acta Cryst.* 1974, **B30**, 2768.

Polyhedron Vol. 6, No. 5, pp. 803–835, 1987
Printed in Great Britain

0277-5387/87 $3.00+.00
Pergamon Journals Ltd

POLYHEDRON REPORT NUMBER 20

THE ORGANOMETALLIC CHEMISTRY OF THE LANTHANIDE ELEMENTS IN LOW OXIDATION STATES

WILLIAM J. EVANS

Department of Chemistry, University of California, Irvine, Irvine, CA 92717, U.S.A.

CONTENTS

I. INTRODUCTION

In the three decades following the discovery of ferrocene,[1] organometallic chemistry was investigated extensively and became a major field of chemical research. During this period, research efforts were focused primarily on the transition metals and the organometallic chemistry of the lanthanide elements received comparatively little attention. This situation is understandable when one considers

how the chemistry of the lanthanides was viewed during the time in which organometallic chemistry was being developed.

The early studies on organolanthanide complexes suggested that their chemistry was limited. For example, the first well-documented reports in this area, which concerned the simple cyclopentadienyl complexes $(C_5H_5)_3Ln$,[2] showed that these compounds were rather ionic and suggested that organolanthanide complexes would merely be trivalent versions of alkali and alkaline earth metal organometallic species.

In general, all of the lanthanide elements traditionally were thought to have a very similar chemistry, in contrast to the diverse chemistry observed for a row of transition elements. Furthermore, most lanthanide chemistry centered on a single oxidation state, the trivalent state. Of the few lanthanide elements which had readily accessible non-trivalent oxidation states, Ce^{4+}, Sm^{2+}, Eu^{2+} and Yb^{2+}, none had both the +4 and the +2 oxidation state readily available on the same metal. Hence, the diversity of oxidation states found with transition metals was not present in the lanthanide series and the two-electron processes common in transition-metal chemistry, such as oxidative addition and reductive elimination, were not possible at a single lanthanide metal center. In addition, many reagents of interest to organometallic chemists, e.g. CO, unsaturated hydrocarbons, hydrogen, phosphines, isocyanides, nitrogen etc., were not thought to have a substantial chemistry with these ionic metal complexes. Finally, many reaction pathways important in organometallic synthesis and catalysis were not thought to be available to these elements. All of these factors suggested that lanthanide chemistry would not be as interesting as transition-metal chemistry.

In addition to the problem of an anticipated limited chemistry, the organolanthanide complexes were experimentally more difficult than many transition-metal systems. Almost all organolanthanides are extremely air- and moisture-sensitive and even the metal trihalide starting materials are hydrolytically unstable. Purification and isolation of organolanthanide compounds is difficult because the complexes decompose on chromatographic supports, generally cannot be sublimed in high yield, and frequently undergo ionic redistribution reactions giving mixtures during crystallization attempts. Moreover, the paramagnetism of many of the metals precluded characterization by NMR spectroscopy, the organometallic chemist's most common method of analysis.

Despite the limitations and difficulties described above, it was realized that the lanthanides had the potential for some unique chemistry distinct from anything possible with main-group or transition metals.[3] The basis for this contention was that the lanthanide elements have a special combination of physical properties, including size, type of valence orbital, ionization potential, electron affinity etc., which is not duplicated anywhere else in the periodic table. Hence, a lanthanide element, if placed in the proper oxidation state and coordination environment, could display an unusual chemistry.

In the past few years, the status of organolanthanide chemistry has changed dramatically. The goal of demonstrating a unique organometallic chemistry with these metals has been realized in terms of unusual compounds, unprecedented structures, and spectacular reactivity.[4-7] Increasing numbers of investigators are turning their attention to 4*f*-element chemistry and it is currently one of the most rapidly developing areas of organometallic chemistry.

The most extensively developed area of organolanthanide chemistry has involved trivalent complexes and a substantial body of experimental data is now available. Principles regarding structure and reactivity are emerging for trivalent species as outlined in a recent review[5] and in Section II.

This Report focuses on the organometallic chemistry of the lanthanides in oxidation states less than +3. This area is at that exciting stage of development in which many unusual structures and reactions have been observed, but the general principles governing this chemistry have yet to be determined. The field is in that frontier stage of exploration in which each new piece of data has the potential of providing key insights into general principles.

Low oxidation state organolanthanide chemistry is described in parts of other reviews of organolanthanide chemistry,[4,5,7-10] but only one of these concentrates solely on this topic.[7] In that review, the emphasis was on applications of divalent ytterbium and samarium chemistry to organic synthesis. This review will concentrate on the synthesis and reactivity of divalent and zero-valent organometallic systems and will start with a background section describing basic principles of the chemistry of these elements and their trivalent complexes.

II. TRADITIONAL PRINCIPLES OF ORGANOLANTHANIDE CHEMISTRY

II.1. *Properties of the elements*

The main factor which distinguishes the lanthanide elements from other metallic elements is that their valence orbitals are the 4*f* orbitals. The main factor which differentiates the 4*f* orbitals from valence orbitals of other metallic elements is their relatively limited radial extension. Calculations on lanthanide ions, which have [Xe]$4f^n$ electron configurations, suggest that the 4*f* orbitals do not extend significantly beyond the filled $5s^25p^6$ orbitals of the xenon inert gas core.[11] Consequently, a trivalent lanthanide ion looks like a closed-shell inert-gas electron cloud with a tripositive charge, a situation which has a major effect on the chemical and physical properties of these metals and their complexes.

One effect of the small radial extension of the lanthanides' valence orbitals is that the metals' orbital interactions with ligands are smaller than those in transition-metal complexes. This is the traditional explanation of why the chemistry tends to be much more ionic.[12] Electrostatic factors appear to be more important in determining the stability, structure and chemistry of lanthanide complexes than orbital generalizations. Consistent with this, the physical properties arising from a given $4f^n$ configuration for a lanthanide ion, e.g. the optical spectrum and the magnetic moment, are relatively similar regardless of the nature of the attached ligand.[12-13]

Another consequence of the limited radial extension of the 4*f* orbitals is that the chemistry of the trivalent lanthanide ions can be similar in many systems regardless of the $4f^n$ configuration.[12] Hence, a single symbol, Ln, often has been used in the past to describe the chemistry of all the elements in the series. For example, one similarity in the chemistry of the lanthanide metals is that for each element the +3 oxidation state is the most stable. Another example is the similarity in structure and reactivity of the $(C_5H_5)_3Ln(thf)$ complexes[2,15,16] (except for the single radioactive system, Ln = Pm). This contrasts sharply with the large variation in structure and stability of transition-metal $(C_5H_5)_2M$ complexes as M is varied across a row of the periodic table.[17]

Some differences in the chemistry of the individual lanthanides are observed due to the variations in the radial size of the metals. Radial size diminishes gradually from La^{3+} (1.061 Å) to Lu^{3+} (0.848 Å) as the series is crossed.[18] The other basis for differences in chemistry between the metals arises with the four elements for which non-trivalent oxidation states are accessible under normal reaction conditions: Ce^{4+} ($4f^0$), Eu^{2+} ($4f^7$), Yb^{2+} ($4f^{14}$), and Sm^{2+} ($4f^6$). Differences in trivalent chemistry arise for these elements primarily under strongly oxidizing or reducing conditions. Differences in lower oxidation state chemistry will be discussed in Section III.

Two other important general features of the lanthanide metals are their size and electronegativity. Compared to transition metals the lanthanides are quite large. High coordination numbers of 8–12 are common in lanthanide complexes.[12] The lanthanides are also rather electropositive compared to transition metals[19] and are quite oxophilic.

II.2. *Stability principles for trivalent species*

Given these physical properties, two generalizations on organolanthanide stability traditionally have been followed in order to obtain isolable organolanthanide complexes. First, electrostatic interactions must be optimized by using stable organic anions to balance the charge of the metal cation. Second, additional stability often can be gained by choosing large, bulky anions which can completely occupy the coordination sphere of the metal and sterically block decomposition pathways. The polyhapto anions $C_5H_5^-$ and $C_8H_8^{2-}$ meet both of these requirements and, not coincidentally, they are the most prevalent ligands in organolanthanide chemistry. The reason the smaller metals later in the lanthanide series, Lu, Yb and Er, have been investigated most extensively is that their small size makes steric saturation of the metal coordination sphere less difficult and hence provides more tractable complexes.

Since the electrostatic charge balance requirement for stability must always be met in organolanthanide complexes, the determining factor in stability/reactivity is often steric. Recent results in trivalent organolanthanide chemistry suggest emerging patterns of structure and reactivity which depend on the relative sizes of the ligands vs the metals.[5] Quantitative assessment of this steric saturation is also under development.[20]

Several basic generalizations appear to apply to trivalent organolanthanides based on the data currently available.[5] High reactivity and limited stability are associated with free coordination sites, i.e. steric unsaturation, and with terminal, as opposed to bridging, ligands. High reactivity/limited stability can be caused by insufficient ligand bulk around the metal (steric unsaturation) or by excessive ligand bulk (steric oversaturation) when it leads to structures with open coordination positions and terminal ligands. Examples of these ideas follow. Since trivalent Y displays chemistry much like that of the late lanthanide ions of similar size [Ho(III) and Er(III)],[21-24] examples from Y chemistry will also be included.

The importance of terminal ligands and open coordination positions to organolanthanide reactivity can be readily seen from hydrogenolysis studies [reactions (1)–(4)]. For example, the bridged species $[(C_5H_5)_2Ln(\mu\text{-}CH_3)]_2$ (Ln = Y, Er, Yb or Lu) react slowly with H_2 in arene solvents in which they are fully bridged [reaction (1)]:[23,25]

$$(C_5H_5)_2Ln\begin{matrix}\diagup CH_3 \diagdown \\ \diagdown CH_3 \diagup\end{matrix}Ln(C_5H_5)_2 + H_2 \overset{\text{toluene}}{\rightarrow} \text{very slow.} \quad (1)$$

In contrast, the *tert*-butyl complexes, $(C_5H_5)_2Ln(CMe_3)$ (thf), which do not form bridged dimers, react rapidly with hydrogen in toluene to form the hydride dimers $[(C_5H_5)_2Ln(\mu\text{-}H)(thf)]_2$ [reaction (2)].[22]

$$2(C_5H_5)_2Ln(CMe_3)(thf) + 2H_2 \underset{\text{rapid}}{\overset{\text{toluene}}{\rightarrow}} [(C_5H_5)_2Ln(\mu\text{-}H)(thf)]_2 + 2HCMe_3. \quad (2)$$

This demonstrates the higher reactivity available to terminal ligands.[23]

In thf however, the *tert*-butyl complexes $(C_5H_5)_2Ln(CMe_3)$ (thf) are unreactive to hydrogen [reaction (3)]:[26]

$$(C_5H_5)_2Ln(CMe_3)(thf) + H_2 \overset{\text{thf}}{\rightarrow} \text{no reaction.} \quad (3)$$

The difference in reactivity in toluene vs thf presumably arises because in toluene some dissociation of thf occurs to give a free coordination position, whereas in thf the metal center is constantly solvated. Hence, even with the small reagent hydrogen and the large lanthanide metals, an open coordination position is needed for high reactivity.

These steric effects are subtle, however.[26] For example, hydrogenolysis in thf is possible when the alkyl group is methyl rather than *tert*-butyl [reaction (4)]:

$$2(C_5H_5)_2Ln(CH_3)(thf) + 2H_2 \overset{\text{thf}}{\rightarrow} [(C_5H_5)_2Ln(\mu\text{-}H)(thf)]_2 + 2CH_4. \quad (4)$$

Hence, $(C_5H_5)_2Ln(CH_3)$ (thf) reacts readily with H_2 in thf when Ln = Y or Er. Based on crystal structures of $(C_5H_5)_2Lu(CMe_3)$ (thf)[27] and $(C_5H_5)_2Yb(CH_3)$ (thf),[26] one can estimate that the main difference between a methyl and a *tert*-butyl $(C_5H_5)_2LnR(thf)$ complex for a given Ln is that the *tert*-butyl complex has a Ln—C bond approximately 0.1 Å longer than the Ln—C bond in the methyl complex. The longer distance presumably occurs because the *tert*-butyl complex is sterically too crowded to form a shorter "normal" Ln—C bond.[26,28] Since the *shorter* Ln—C methyl bond is the Ln—C unit which is more reactive to hydrogen, the difference in reactivity appears to be steric.

Although hydrogenolysis of $(C_5H_5)_2Ln(CH_3)$ (thf) is facile in thf for Ln = Er and Y, for Ln = Yb and Lu the reactivity is very low.[26] This presumably occurs because of the increased steric crowding in the coordination environment around these smaller metals. Hence, a change in metallic radius of just 0.03 Å can significantly affect reactivity.

Steric factors can affect structure as well as reactivity, a fact which is well illustrated by the many examples of dicyclopentadienyl lanthanide halide complexes characterized by X-ray diffraction. These complexes exist as symmetrically bridged dimers, $[(C_5H_4R)_2Ln(\mu\text{-}Cl)]_2$, when Ln is one of the smaller metals Sm–Lu and Y, and when the cyclopentadienyl ligand is C_5H_5 or $CH_3C_5H_4$.[29-31] Such complexes are generally considered sterically saturated. For the larger

lanthanides earlier in the series, La, Ce, Pr and Nd, $[(C_5H_5)_2Ln(\mu\text{-}Cl)]_2$ complexes are reported to be unstable with respect to ligand redistribution to the sterically more saturated $(C_5H_5)_3Ln$ species.[9,30] These early lanthanide $[(C_5H_5)_2Ln(\mu\text{-}Cl)]_2$ complexes are sterically unsaturated and therefore less stable. To obtain an isolable bis(cyclopentadienyl) lanthanide halide complex of a large early lanthanide metal, the steric bulk of the ligand set must be increased. This can be done with a substituted cyclopentadienyl ligand, as demonstrated in the structure $\{[(Me_3Si)_2C_5H_3]_2Pr(\mu\text{-}Cl)\}_2$,[32] or by adding an "extra" ligand to the coordination sphere, as found in $[(C_5H_5)_2Nd(thf)(\mu\text{-}Cl)]_2$.[33]

When sterically bulky ligands such as C_5Me_5 are used with the small metals late in the series, complexes such as $[(C_5Me_5)_2Ln(\mu\text{-}Cl)]_2$ are too sterically crowded to form. These sterically oversaturated systems distort from a symmetrical structure to accommodate the ligand–metal size imbalance. For Ln = Y, a monobridged structure, $[(C_5Me_5)_2Y(\mu\text{-}Cl)YCl(C_5Me_5)_2]$, is observed.[34] For the methyl and hydride Lu derivatives $[(C_5Me_5)_2LuZ]_n$ (Z = H or CH_3; n = 1 or 2), an equilibrium is reported to exist between a monobridged structure, $(C_5Me_5)_2Lu(\mu\text{-}Z)LuZ(C_5Me_5)_2$ and the monomer $(C_5Me_5)_2LuZ$.[6,35]

The three classes of organolanthanide complexes, i.e. sterically saturated, sterically unsaturated, and sterically oversaturated compounds, display different types of reactivity due to the differences in terminal vs bridging groups and the relative availability of open coordination positions. This point is illustrated well by the metalation reactivity of organolanthanide hydrides with ethers, hydrocarbons and pyridine. The sterically saturated hydrides $[(C_5H_4R)Ln(\mu\text{-}H)(thf)]_2$ (R = H or CH_3; Ln = Er, Y or Lu) are stable to ethers, metalate only rather acidic hydrocarbons such as terminal alkynes, and do 1,2-LnH addition rather than metalation when reacted with pyridine.[23] In contrast, the sterically oversaturated $[(C_5Me_5)_2LuH]_n$ complex decomposes ethers, metalates pyridine to form a $(C_5Me_5)_2Lu(\eta^2\text{-}NC_5H_4)$ complex, and is such a powerful metalation reagent that not only benzene and Me_4Si are metalated, but even CH_4.[36,37] The sterically unsaturated $[(C_5Me_5)_2Sm(\mu\text{-}H)]_2$[38] has intermediate reactivity—it decomposes ether and metalates pyridine, but metalates arenes only slowly.[39]

Given that all of this reactivity involves the same, nominally ionic, Ln—H bond, it is clear that steric factors influence trivalent organolanthanide chemistry to a great extent. Obviously, the thermodynamic differences in bond strengths and the differences in the charge: radius ratio from one metal to another will also affect the chemistry. However, in many cases these factors are likely to be sufficiently similar that it is the steric parameters which will govern the observed variations in reactivity.

III. DIVALENT ORGANOLANTHANIDE CHEMISTRY

Divalent organolanthanide complexes are the most fully characterized and investigated of the available low oxidation state lanthanide organometallics. Consequently, this is the first class of low-valent species which will be presented in detail. This section is organized into three parts: a brief description of divalent-metal properties, a discussion of synthesis and structure organized according to ligand, and a discussion of reactivity.

III.1. *Background*

Although divalent lanthanide ions for almost all of the elements in the series have been generated by irradiating trivalent ions doped into CaF_2,[40–42] only three elements have divalent states which are chemically accessible in organometallic systems under normal conditions: Eu, Yb and Sm. It is only for these elements that X-ray crystallographic structures of divalent organolanthanide complexes are available. A report of a Ce(II) complex formed by K reduction is in the literature,[43,44] but this result remains to be structurally confirmed.

The aqueous reduction potentials for the Ln^{3+}–Ln^{2+} couple are reported to be −0.35 V for Eu, −1.1 V for Yb and −1.5 V for Sm (vs NHE)[45,46] indicating that Eu^{2+} should be the most stable and Sm^{2+} the most reactive in terms of reducing power. As described in Section II, complexes of the smaller Yb^{2+} ion could be the most stable in terms of steric saturation of the metal coordination sphere and Sm^{2+} could be the most reactive in this regard.

Sm(II) is most desirable not only in terms of high reactivity, but also when NMR characterization

is considered. Sm provides the only Ln(II)–Ln(III) system in which both oxidation states have complexes which are NMR-accessible.[47] Despite room-temperature magnetic moments of 3.4–3.8 μ_B for Sm(II) and 1.3–1.9 μ_B for Sm(III), ^{1}H NMR resonances are reasonably sharp and are found within $\pm$10 ppm of the normal 0–10-ppm region where diamagnetic resonances are located. This is not true for Eu(II), Eu(III) or Yb(III), which have room temperature magnetic moments in the ranges 7.4–8.0, 3.4–4.2 and 4.2–4.9 μ_B, respectively.[48,49] Of course, diamagnetic Yb(II) provides NMR-observable complexes.

Divalent organolanthanide complexes differ in appearance from trivalent species in that their colors are more intense and these colors vary as the ligand set is changed. For trivalent species, the colors arise from Laporte-forbidden $4f \rightarrow 4f$ transitions.[12,13] Due to the limited radial extension of the $4f$ orbitals, crystal field splitting is very small and hence the colors vary little as the ligand set is changed. Another consequence of the limited radial extension is that little vibronic coupling occurs to relax the Laporte-forbidden nature of the transitions. Hence, the colors of the complexes are pale. In contrast, the colors of the divalent lanthanide ions are attributed to Laporte-allowed $4f \rightarrow 5d$ transitions.[14,40] The energies of these transitions change as the ligand set varies. The variation in color with ligand environment is greatest with Sm(II) and Yb(II). Organometallic Sm(II) compounds can be green or purple and Yb(II) species can be yellow, red, blue, green or purple. Eu(II) organometallics, on the other hand, are almost always yellow, orange or red.

III.2. *Synthesis and structure*

III.2(a) *Cyclooctatetraenyl complexes.* The first divalent organolanthanide complexes were prepared by taking advantage of the fact that Eu and Yb dissolve in liquid ammonia to form highly reducing solutions of $[Ln(NH_3)_x^{2+}]$ $[e^-(NH_3)_4]_2$.[50] The cyclooctatetraenyl species, EuC_8H_8 and YbC_8H_8, were obtained by adding 1,3,5,7-cyclooctatetraene to solutions of Eu and Yb in liquid ammonia [reaction (5)]:

$$Ln + 1,3,5,7\text{-}C_8H_8 \xrightarrow{NH_3(l)} LnC_8H_8. \tag{5}$$

The compounds precipitate from the ammonia solution and are insoluble in hydrocarbons and ethers. Soluble adducts are formed in pyridine and dimethylformamide, but have never been fully characterized. C_8H_8Yb can also be prepared by metal vapor methods from zero-valent Yb and 1,3,5,7-C_8H_8.[51] Reduction of [K(glyme)] $[Ce(C_8H_8)_2]$ in glyme with excess K is reported to form $[K(glyme)]_2[Ce(C_8H_8)_2]$, the only organocerium(II) complex in the literature.[43] Neither structural characterization nor reaction chemistry have been reported for any of the divalent cyclooctatetraenyl species.

III.2(b) *Complexes containing unsubstituted cyclopentadienyl ligands.* Divalent cyclopentadienyl complexes were also originally obtained from liquid-ammonia reactions. For Eu, an NH_3 solvate is initially formed [reaction (6)]:

$$Eu + 3C_5H_6 \xrightarrow{NH_3(l)} (C_5H_5)_2Eu(NH_3) + C_5H_8 \tag{6}$$

which can be desolvated by heating to 120–200°C *in vacuo*.[15] This complex is not soluble in hydrocarbons and common ethers, but dissolves in liquid ammonia and dimethylformamide.

For Yb, which has a less stable divalent oxidation state, the reaction analogous to 6 is more complex. The trivalent complex $(C_5H_5)_3Yb(NH_3)$ is obtained in the reaction despite the reducing conditions and sublimation gives trivalent products as well as $(C_5H_5)_2Yb$.[15,52,53] This exemplifies in part the general trend in divalent lanthanide chemistry that Eu(II) complexes are least difficult to obtain in pure form, Yb(II) chemistry is more complex, and Sm(II) chemistry is the most difficult.

A variety of ammonia-free synthetic routes to $(C_5H_5)_2Yb$ are known. One type of reaction involves reduction of $[(C_5H_5)_2YbCl]_2$ with Na,[53] Yb[53] or *tert*-butyllithium[26,27] [reactions (7)–(9) the $(C_5H_5)_2Yb$ product in these and the following reactions is generally isolated as an ether adduct]:

$$[(C_5H_5)_2YbCl]_2 + 2Na \rightarrow 2(C_5H_5)_2Yb + 2NaCl, \tag{7}$$

$$3[(C_5H_5)_2YbCl]_2 + 2Yb \rightarrow 6(C_5H_5)_2Yb + 2YbCl_3, \quad (8)$$

$$[(C_5H_5)_2YbCl]_2 + 2LiCMe_3 \rightarrow 2(C_5H_5)_2Yb + HCMe_3 + H_2C{=}CMe_2 + 2LiCl. \quad (9)$$

Reduction of $(C_5H_5)_3Yb$ with Na[53] or Yb[54,55] also gives $(C_5H_5)_2Yb$ [reactions (10) and (11)]:

$$(C_5H_5)_3Yb + Na \rightarrow (C_5H_5)_2Yb + NaC_5H_5, \quad (10)$$

$$2(C_5H_5)_3Yb + Yb \rightarrow 3(C_5H_5)_2Yb. \quad (11)$$

$(C_5H_5)_2Yb(thf)$ can be obtained by decomposition of $[(C_5H_5)_2Yb(\mu\text{-}H)(thf)]_2$ and $\{[(C_5H_5)_2Yb(\mu\text{-}H)]_3(\mu_3\text{-}H)\}\{Li(thf)_4\}$ although this is not a preparatively desirable synthesis.[26]

Recently, syntheses have been reported which start from Yb metal, which is a more convenient starting material than the $YbCl_3$ reagent needed for reactions (7)–(11). For example, $(C_5H_5)_2Yb$ can be prepared from the reaction of C_5H_5Tl with excess Yb metal,[54] a reaction which is reported to have $(C_5H_5)_3Yb$ as an intermediate [reaction (12)]:

$$6C_5H_5Tl + 3Yb \rightarrow 6Tl + 2(C_5H_5)_3Yb + Yb \rightarrow 3(C_5H_5)_2Yb + 6Tl. \quad (12)$$

Yb metal, which has been activated with $HgCl_2$ to form an amalgam, is also reported to be successful [reaction (13)]:[55]

$$(C_5H_5)_2Hg + Yb \rightarrow Hg + (C_5H_5)_2Yb. \quad (13)$$

$YbI_2(thf)_x$ prepared from Yb metal and ICH_2CH_2I in thf also can be used as a precursor to $(C_5H_5)_2Yb$ [reaction (14)]:[56]

$$YbI_2 + 2C_5H_5Na \rightarrow (C_5H_5)_2Yb + 2NaI. \quad (14)$$

The acid–base reaction of cyclopentadiene with $(C_6F_5)_2Yb$ and $(C_6F_5)_2Eu$, both obtainable from the elemental metal [see Section III.2(g.)], have also been used to form $(C_5H_5)_2Yb(MeOCH_2CH_2OMe)$ and $(C_5H_5)_2Eu(thf)$.[57]

$(C_5H_5)_2Sm(thf)$ was first prepared from $(C_5H_5)_3Sm$ by reduction with $KC_{10}H_8$ [cf. reaction (10)].[58] A more recent synthesis employs the divalent precursor $SmI_2(thf)_x$, in a reaction analogous to reaction (14).[56] A reported synthesis[59] of $(C_5H_5)_2Sm(thf)_2$ from $Hg(C_5H_5)_2$ and Sm according to reaction (13) has been subsequently shown to give only $(C_5H_5)_3Sm(thf)$.[60] Unfortunately, since $(C_5H_5)_2Sm(thf)$ is insoluble in common solvents, the chemistry of this organometallic complex of the most reactive divalent lanthanide metal was not explored. A subsequent study of the $(C_5H_5)_3Sm$–K system in the presence of benzophenone indicates that extraction of the insoluble product with dimethoxyethane (dme) gives a soluble material characterized by elemental analysis as divalent $KSm(C_5H_5)_3$.[60]

Recently, a bis(cyclopentadienyl) Yb complex was characterized by X-ray diffraction as a dme adduct, $(C_5H_5)_2Yb(MeOCH_2CH_2OMe)$.[61] The structure (Fig. 1) is typical of a bent metallocene with two additional ligands. A summary of structural data on all of the crystallographically characterized divalent organolanthanide complexes discussed in this review is presented in Table 1.

III.2(c) *Complexes containing monosubstituted cyclopentadienyl ligands.* Although the first divalent organolanthanide complexes were prepared in 1965,[15] no structural data on any low-valent organolanthanides were reported until 1980. The first X-ray structure determination of a divalent organolanthanide complex involved the methyl-substituted derivative $(CH_3C_5H_4)_2Yb(thf)$.[25] This complex can be synthesized by alkali metal reduction of $[(CH_3C_5H_4)_2YbCl]_2$ [cf. reaction (7)], by transmetalation with $TlC_5H_4CH_3$[54] [cf. reaction (12)], by reaction of $CH_3C_5H_5$ with $Yb(C{\equiv}CC_6H_5)_2$[57] and by thermolysis, photolysis or hydrogenolysis of $[(CH_3C_5H_4)_2YbCH_3]_2$ [(15)–(17)]:[25]

Table 1. Structural data on divalent organolanthanide complexes, $(C_5R_5)_xLnL_y$[a]

Complex	Formal coordination number	Average Ln—C(C_5R_5) distance (Å)	Range of Ln—C(C_5R_5) distances (Å)	Ln—L distance (Å) donor atom of L	Ring centroid–Ln–ring centroid angle[b] (°)	L—Ln—L angle[b] (°)	References
$(C_5H_5)_2Yb(dme)$	8	2.72	2.60(3)–2.91(5)	2.45(3), O 2.50(3), O	129	67.2(9)	61
$[(MeC_5H_4)(thf)Yb(\mu\text{-}MeC_5H_4)]_n$	10	2.76 2.87[c] 2.91[c]	2.75(3)–2.77(3) 2.79(3)–2.94(3) 2.88(3)–2.94(3)	2.53(2), O	—	—	25
$[(Me_3Si)C_5H_4]_2Yb(thf)_2$	8	2.75	2.64(4)–2.84(4)	2.42(2), O 2.39(3), O	133	85	63
$(C_5Me_5)_2Yb(thf)\cdot 0.5CH_3C_6H_5$[d]	7	2.66(2)	2.643(7)–2.694(8)	2.412(5), O	143.5(3)	—	69
$(C_5Me_5)_2Yb(NC_5H_5)_2$	8	2.74(4)	2.692(7)–2.770(8)	2.586(7), N 2.544(6), N	136.3(3)	82.5(2)	72
$(C_5Me_5)_2Yb(thf)(NH_3)$	8	2.77(4)	2.70(4)–2.83(4)	2.46(3), O 2.55(3), N	139.31	87.5(9)	73
$(C_5Me_5)_2Sm(thf)_2$	8	2.86(3)	2.81(1)–2.91(1)	2.61(2), O 2.65(2), O	136.7	82.6(4)	47, 75, 79
$(C_5Me_5)_2Sm$	6	2.79(1)	2.775(6)–2.815(6)	—	140.1	—	78, 79
$(C_5Me_5)_2Eu(OEt_2)$	7	2.795(7)	[e]	2.594(4), O	[e]	[e]	[f]
$(C_5Me_5)_2Eu$	6	2.79(1)	2.765(10)–2.822(9)	—	140.3	—	79
$[(C_5Me_5)(thf)_2Eu(\mu\text{-}C{\equiv}CPh)]_2$	7	2.82(2)	[e]	2.62(1), O	—	—	92
$[(C_5Me_5)(thf)_2Sm(\mu\text{-}I)]_2$	7	2.81(2)	2.77(2)–2.84(3)	2.62(2), O 2.66(2), O	—	—	75

[a] $[(C_5Me_5)_2Yb(\mu\text{-}C{\equiv}CPh)_2]_2Yb$, in which the unique ytterbium is divalent [coordination number 4, Yb—C = 2.52(1) Å][92] is not included in this table.
[b] For $(C_5R_5)_2LnL_2$ complexes.
[c] These distances are for the bridging MeC_5H_4 ligands which are coordinated to ytterbium atoms on each side.
[d] The toluene is not coordinated to the metal.
[e] Not reported.[f]
[f] Unpublished results cited in Ref. 92.

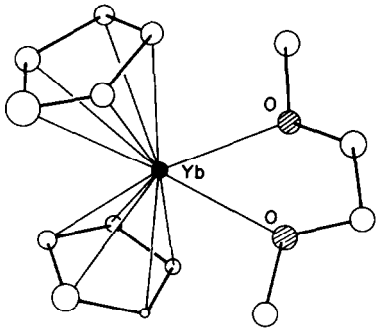

Fig. 1. Structure of $(C_5H_5)_2Yb(CH_3OCH_2CH_2OCH_3)$. White circles are carbon atoms.

$$[(CH_3C_5H_4)_2YbCH_3]_2 \xrightarrow[80°C]{\text{pentane–}Et_2O} 2(CH_3C_5H_4)_2Yb, \tag{15}$$

$$[(CH_3C_5H_4)_2YbCH_3]_2 \xrightarrow[\text{toluene, } 5°C]{h\nu} 2(CH_3C_5H_4)_2Yb, \tag{16}$$

$$[(CH_3C_5H_4)_2YbCH_3]_2 + 2H_2 \xrightarrow[50°C]{\text{toluene}} 2[(CH_3C_5H_4)_2YbH] \rightarrow 2(CH_3C_5H_4)_2Yb. \tag{17}$$

These latter three reactions are significant in divalent organolanthanide chemistry in that they demonstrate that access to the reactive Yb(II) oxidation state is possible without using strongly reducing conditions (e.g. alkali metal present). These reactions may provide the basis for interesting catalytic cycles involving the Yb(III)–Yb(II) couple.

The actual crystals used in the X-ray study of $(CH_3C_5H_4)_2Yb(thf)$[25] were prepared in an attempt to derivatize an Yb–3-hexyne cocondensation product[62] [reaction (18) (see Section IV)]:

$$YbC_6H_{10} + 2CH_3C_5H_5 \xrightarrow{thf} (CH_3C_5H_4)_2Yb(thf). \tag{18}$$

As shown in Fig. 2, $(CH_3C_5H_4)_2Yb(thf)$ is polymeric in the solid state forming a chain structure in which the monomeric $(\mu\text{-}CH_3C_5H_4)(CH_3C_5H_4)Yb(thf)$ units are linked by bridging methylcyclopentadienyl groups.[25] Apparently, a monomeric $(CH_3C_5H_4)_2Yb(thf)$ unit is sterically unsaturated and polymerizes to increase steric saturation in the solid state. Isopiestic molecular-weight studies indicate that in thf, $(CH_3C_5H_4)_2Yb(thf)$ also increases its coordination number and exists as a disolvate in solution.

The trimethylsilyl-substituted cyclopentadienyl complex $(Me_3SiC_5H_4)_2Yb(thf)_2$ was prepared from $[(Me_3SiC_5H_4)_2YbCl]_2$ according to reaction (7) using Na(Hg) as the reductant in thf.[63] The thf of solvation can be displaced by $Me_2NCH_2CH_2NMe_2$ (tmeda) to form $(Me_3SiC_5H_4)_2Yb$ (tmeda) and the solvent-free $(Me_3SiC_5H_4)_2Yb$ can be obtained by sublimation at 308°C. In contrast to the polymeric nature of $(CH_3C_5H_4)_2Yb(thf)$, $(Me_3SiC_5H_4)_2Yb(thf)_2$ crystallizes as a monomer with a bent metallocene structure analogous to that of $(C_5H_5)_2Yb(dme)$ in Fig. 1.

The divalent methylcyclopentadienyl Sm complex $(CH_3C_5H_4)_2Sm$ can be made from $[(CH_3C_5H_4)_2SmCl]_2$ by reduction, but, like the unsubstituted analog, it is insoluble in common solvents.[64]

The indenyl complexes $(C_9H_7)_2Yb(thf)_2$ and $(C_9H_7)_2Eu(thf)$ have been prepared from indene and $Yb(C_6F_5)_2$ and $Eu(C_6F_5)_2$ [Section III.2(g.)], respectively.[57]

III.2(d) *Solvated pentamethylcyclopentadienyl complexes.* The pentamethylcyclopentadienyl ligand, C_5Me_5, has proven to be of great importance in organometallic chemistry. As demonstrated by Bercaw and co-workers with Ti and Zr complexes[65,66] and as subsequently shown by Marks *et al.* for actinide complexes,[67,68] the C_5Me_5 ligand provides solubility and crystallinity to systems difficult to fully characterize using simple unsubstituted C_5H_5 ligands. Utilization of this ligand in divalent organolanthanide chemistry has had similarly spectacular results.

Bis(pentamethylcyclopentadienyl) complexes of all three readily accessible divalent lanthanides are known. $(C_5Me_5)_2Eu(thf)$ was prepared from trivalent $EuCl_3$ and three equivalents of NaC_5Me_5

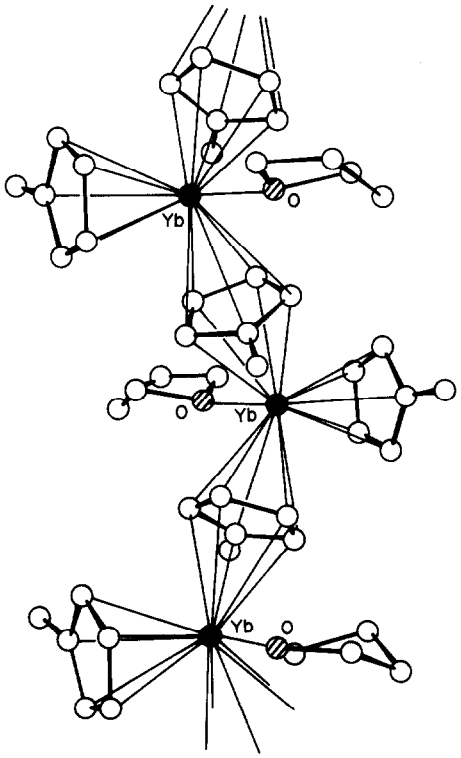

Fig. 2. Structure of $[(CH_3C_5H_4)(thf)Yb(\mu\text{-}CH_3C_5H_4)]_n$. Three units of the continuous chain are shown. White circles are carbon atoms.

in a reaction in which NaC_5Me_5 functions as a reducing agent [reaction (19)]:[69]

$$EuCl_3 + 3NaC_5Me \xrightarrow[\text{reflux}]{\text{thf}} (C_5Me_5)_2Eu(thf). \tag{19}$$

This is not an efficient use of the NaC_5Me_5 reagent, but the simple reaction of two equivalents of NaC_5Me_5 with $EuCl_2$ fails to generate the desired product. Reaction (19) is quite sensitive to specific conditions: using LiC_5Me_5 instead of NaC_5Me_5 or toluene instead of thf fails to give $(C_5Me_5)_2Eu(thf)$. Depending on crystallization conditions, the europium complex can be isolated as the mono-thf solvate or as $(C_5Me_5)_2Eu(thf)(OEt_2)$.

$(C_5Me_5)_2Yb(thf)$ can be prepared from YbI_2 by the route of reaction (14), but the success of the reaction depends on the specific reagents used. $YbBr_2(thf)_2$–KC_5Me_5–ethers[70] and $YbCl_2(thf)_x$–NaC_5Me_5–thf[69] are productive combinations whereas $YbCl_2$–NaC_5Me_5–Et_2O and $YbCl_2$–LiC_5Me_5–thf are not.[69] In addition to the mono-thf solvate, $(C_5Me_5)_2Yb(OEt_2)$,[69] $(C_5Me_5)_2Yb(thf)\cdot\frac{1}{2}CH_3C_6H_5$,[69] $(C_5Me_5)_2Yb(thf)_2$,[70] and $(C_5Me_5)_2Yb(CH_3OCH_2CH_2OCH_3)$[70] have been isolated by varying the conditions of crystallization. In a variation of reaction (7), bis(pentamethylcyclopentadienyl) complexes of Yb can also be prepared by reduction of the trivalent KCl adducts $(C_5Me_5)_2YbCl_2K(solvent)_x$ in CH_3CN or $CH_3OCH_2CH_2OCH_3$ [reaction (20)]:[71]

$$(C_5Me_5)_2YbCl_2K(solvent)_x + Na(Hg) \rightarrow (C_5Me_5)_2Yb(solvent)_y. \tag{20}$$

This reaction was found to be solvent-dependent with thf being a less desirable solvent than dme. Reaction (20) is an inferior synthesis in general for $(C_5Me_5)_2Yb(solvent)$ complexes when compared to reaction (14). $(C_5Me_5)_2Yb(dme)$ can also be prepared by reduction of trivalent $(C_5Me_5)_2Yb(dme)(PF_6)$ with KH or $LiCH_2CMe_3$ [cf. reactions (17) and (9), respectively].[70] $(C_5Me_5)_2Yb(NC_5H_5)_2$ has been obtained by displacing Et_2O from $(C_5Me_5)_2Yb(OEt_2)$ with pyridine.[72] The mono-thf and bis-pyridine adducts have both been structurally characterized as typical bent metallocene structures (cf. Fig. 1).

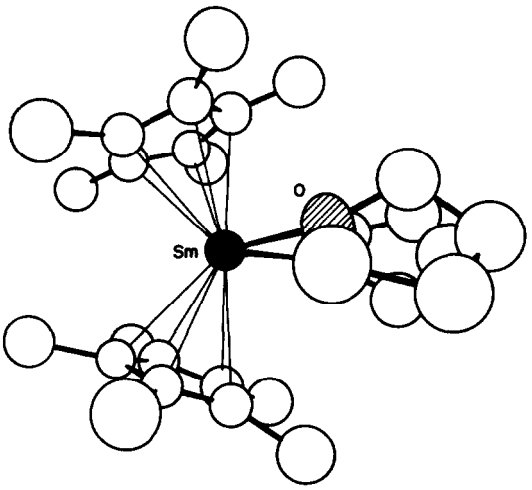

Fig. 3. Side view of the structure of $(C_5Me_5)_2Sm(thf)_2$. The two thf molecules overlap such that only one oxygen atom can be seen from this perspective.

C_5Me_5H reacts with liquid-ammonia solutions of Eu and Yb at low temperature over a 24–36-h period to form bis(pentamethylcyclopentadienyl) products.[73] Crystallization of these products from thf gives $(C_5Me_5)_2Eu(thf)$ and $(C_5Me_5)_2Yb(thf)(NH_3)$. The latter complex has been characterized by X-ray crystallography.[73]

Mono (pentamethylcyclopentadienyl) Yb complexes such as $(C_5Me_5)YbI$ and $[(C_5Me_5)YbI_2]^-$ are thought to be intermediates in the YbI_2–$C_5Me_5^-$ and YbI_2–$(C_5Me_5)_2Yb$ reaction mixtures, but no details on these species were reported.[70,71] Interestingly, YbI_2 has not been mentioned in the literature as a precursor to $(C_5Me_5)_2Yb(solvent)_x$.

The greatest impact of the C_5Me_5 ligand on divalent organolanthanide chemistry has been with Sm. The initially synthesized Sm(II) organometallics, $[(C_5H_5)_2Sm(thf)]_n$ and $[(CH_3C_5H_4)_2Sm(thf)]_n$, are insoluble in common solvents, possibly because with the larger radial size of the metal, more extensive oligomerization/polymerization occurs in the solid state than in the analogous Yb case (cf. Fig. 2). A consequence of this insolubility was that the organometallic chemistry of Sm(II), the most reactive of the divalent lanthanides, could not be investigated with the $(C_5H_4R)_2Sm(thf)$ systems. With the C_5Me_5 ligand, Sm(II) complexes are soluble and a rich and varied chemistry has developed as a consequence.

The initial synthesis of $(C_5Me_5)_2Sm(thf)_2$ was achieved via metal vapor methods [reaction (21) (cf. Section IV)]:[47,74]

$$2Sm + 2C_5Me_5H \xrightarrow{thf} 2[(C_5Me_5)SmH(thf)_2] \rightarrow (C_5Me_5)_2Sm(thf)_2. \quad (21)$$

The bracketed intermediate Sm(II) hydride was not isolated in a pure form. The metal vapor method was also used to synthesize $(C_5Me_4Et)_2Sm(thf)_2$.[74] This species is similar to $(C_5Me_5)_2Sm(thf)_2$ in most respects except that $(C_5Me_4Et)_2Sm(thf)_2$ is more soluble. Like other bis(cyclopentadienyl) bis(ligand) divalent lanthanide complexes (e.g. Fig. 1), the structure of $(C_5Me_5)_2Sm(thf)_2$ has canted cyclopentadienyl rings and the oxygen atoms of the solvating thf molecules lie in a plane which bisects the (ring centroid)–metal–(ring centroid) angle (Fig. 3).

$(C_5Me_5)_2Sm(THF)_2$ subsequently was prepared by solution methods according to reaction (14) using $SmI_2(thf)_x$ and two equivalents of KC_5Me_5.[75] This is a much more convenient synthesis and readily allows the preparation of multigram quantities of this interesting complex. The SmI_2–KC_5Me_5 system contains several species including a mono(pentamethylcyclopentadienyl) complex, $[(C_5Me_5)(thf)_2Sm(\mu\text{-}I)]_2$, which can be best isolated by reacting $SmI_2(thf)_x$ with one equivalent of KC_5Me_5 [reaction 2)]:[75]

$$2SmI_2(thf)_x + 2KC_5Me_5 \rightarrow [(C_5Me_5)(thf)_2Sm(\mu\text{-}I)]_2. \quad (22)$$

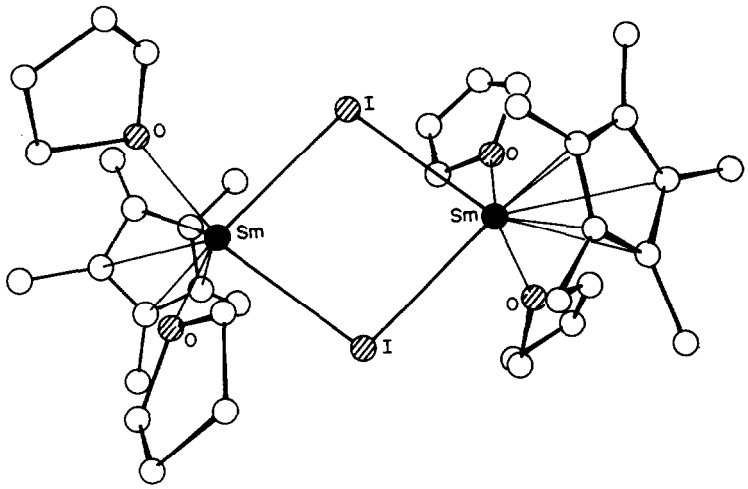

Fig. 4. Structure of $[(C_5Me_5)(thf)_2Sm(\mu\text{-}I)]_2$.

Crystallographic characterization of this complex reveals an iodide-bridged structure as shown in Fig. 4.

III.3(e) *Unsolvated pentamethylcyclopentadienyl complexes.* Almost all lanthanide complexes containing two cyclopentadienyl rings have one to three additional ligands in the coordination sphere of the metal. This is consistent with the large size of these metals and their tendency toward steric saturation in stable complexes. For many years, no structurally characterized simple bis(cyclopentadienyl) system analogous to ferrocene was known. Instead, stable bis(ring) *f*-element sandwich complexes were known only when the larger cyclooctatetraenyl rings were present as in $U(C_8H_8)_2$[76] and $[Ln(C_8H_8)_2]^-$.[77] Although compounds of formula $(C_5H_5)_2Eu$[15] $(C_5H_5)_2Yb$[15,52,53] and $(Me_3SiC_5H_4)_2Yb$[63] could be obtained by high-temperature sublimation, no structural data were available on these systems. Based on the low ether solubility of $(C_5H_5)_2Eu$[15] and the polymeric 10-coordinate structure found for $[(CH_3C_5H_4)_2Yb(thf)]_n$ (Fig. 2),[25] it seemed likely that these unsolvated complexes might be oligomeric in the solid state.

The potential for isolating a monomeric unsolvated divalent bis(cyclopentadienyl) lanthanide complex seemed greater with C_5Me_5 ligands. The first such complex was made by metal vapor methods as a byproduct in the synthesis of $(C_5Me_5)_2Sm(thf)_2$ [reaction (23)]:[47,74]

$$Sm + \text{excess } C_5Me_5H \rightarrow (C_5Me_5)_2Sm. \tag{23}$$

This product was recovered in low yield from the alkane soluble fraction of the metal vapor reaction mixture. Unsolvated $(C_5Me_4Et)_2Sm$ was obtained in a similar manner.[74]

Following the development of a high-yield solution synthesis of $(C_5Me_5)_2Sm(thf)_2$,[75] this species was examined as a precursor to $(C_5Me_5)_2Sm$. Direct desolvation was the obvious synthetic route, but data in the literature did not suggest this would be successful. For example, $[(C_5H_5)_2Sm(thf)]_n$ was reported to decompose on heating[58] and attempts to desolvate $(C_5Me_5)_2Yb(thf)_2$ at 90°C gave only $(C_5Me_5)_2Yb(thf)$.[70] Surprisingly, desolvation of $(C_5Me_5)_2Sm(thf)_2$ is rather facile and occurs at 75°C [reaction (24)]:[78]

$$(C_5Me_5)_2Sm(thf)_2 \xrightarrow[\text{vacuum}]{75^\circ C} (C_5Me_5)_2Sm + 2thf. \tag{24}$$

The desolvated product is soluble in arenes and can be sublimed to give X-ray quality crystals.

The surprising structure of $(C_5Me_5)_2Sm$ is shown in Fig. 5.[78,79] The molecule crystallizes as a monomer with a (ring centroid)–metal–(ring centroid) angle of 140.1°, rather than the 180° angle anticipated for a parallel-ring structure analogous to that found for ferrocene[80] and decamethylferrocene, $(C_5Me_5)_2Fe$.[81] The (ring centroid)–metal–(ring centroid) angle in $(C_5Me_5)_2Sm$ is only slightly larger than the 136.7° angle found in $(C_5Me_5)_2Sm(thf)_2$ (Fig. 3). It is as though

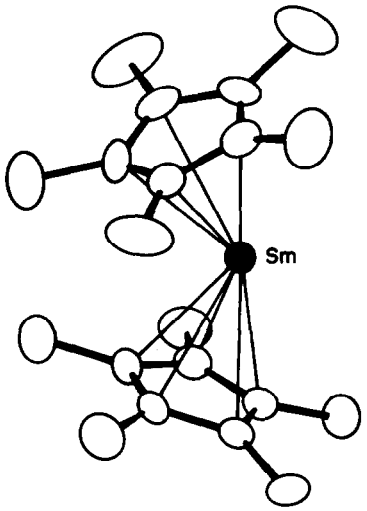

Fig. 5. Structure of $(C_5Me_5)_2Sm$.

removal of the two thf ligands had no effect on this structural feature.

For a predominantly ionic complex governed by electrostatic factors, a parallel-ring structure would be optimal for $(C_5Me_5)_2Sm$ since the anionic ligands would be as far apart as possible. Based on steric considerations a parallel-ring ferrocene-like structure would also be favored over the bent metallocene arrangement. A molecular orbital analysis also suggests that the parallel-ring structure is most stable, although it predicted that distortions would not be energetically costly.[82]

The possibility that the bent structure was due to intermolecular interaction was carefully examined.[78] One methyl group of each $(C_5Me_5)_2Sm$ unit points toward a Sm atom of another unit, but the distances are too long for a substantial interaction (Sm—C, 3.22 Å; Sm—H, 2.75 Å). Moreover, this interaction comes from the side of the bent metallocene unit, not through the sterically most accessible, open, "front" part of the $(C_5Me_5)_2Sm$ unit. Attempts to obtain the gas-phase electron diffraction structure of $(C_5Me_5)_2Sm$ were unsuccessful due to the limited thermal stability of this complex.[83]

To determine if the $4f^6$-electron configuration of Sm^{2+} affected the structure, the structure of the $4f^7$-system $(C_5Me_5)_2Eu$ was also determined.[79] $(C_5Me_5)_2Eu$ is isostructural with $(C_5Me_5)_2Sm$ although the desolvation of $(C_5Me_5)_2Eu(thf)$ was found to be significantly more difficult (multiple desolvation/sublimation reactions were necessary to get the solvate-free species).

The facile synthesis and unusual structure of $(C_5Me_5)_2Sm$ suggest that the principles of divalent organolanthanide chemistry may differ substantially from those of the trivalent species discussed in Section II. A reaction such as reaction (24), in which an oxygen donor adduct is removed to form an isolable sterically much less saturated species (eight-coordinate → six-coordinate), does not follow the expected reactivity patterns for ionic, electropositive oxophilic trivalent lanthanides. The observed structures of $(C_5Me_5)_2Sm$ and $(C_5Me_5)_2Eu$ follow neither the traditional electrostatic nor steric principles.

The best current explanation for the bent structures is the polarization argument used to explain why some heavy alkaline earth metal dihalides, MX_2, are bent rather than linear in the gas phase.[18,84,85] In a parallel-ring $(C_5Me_5)_2Ln$ structure analogous to a linear MX_2 structure, polarization of the cation by one C_5Me_5 anion could diminish the electrostatic interaction between the cation and the second C_5Me_5 anion directly opposite. A bent structure may optimize the polarization of a large cation by two anions and may give better total electrostatic bonding for the two rings. This argument provides an electrostatic rationale for the bent structures of $(C_5Me_5)_2Sm$ and $(C_5Me_5)_2Eu$ without involving 4*f*-orbital participation and without invoking high-energy 5*d* and 6*s* orbitals (via a stereochemically active lone pair argument).[86] If these polarization effects are generally valid for divalent organolanthanides, this may be an important differentiating factor between divalent and trivalent lanthanide chemistry.

III.2(f) *Alkynide complexes.* Several divalent organolanthanide complexes involving alkynyl ligands, —C≡CR, have been reported in the literature. Transmetalation with Hg reagents has been

used to obtain $Yb(C{\equiv}CC_6H_5)_2$ and $Eu(C{\equiv}CC_6H_5)_2(thf)_{0.25}$ [reaction (25)]:[87]

$$Yb + Hg(C{\equiv}CC_6H_5)_2 \rightarrow Yb(C{\equiv}CC_6H_5)_2 + Hg. \tag{25}$$

$Yb(C{\equiv}CCMe_3)_2$ has been prepared in solution by the same method but was not isolated. Divalent Yb alkynides can also be obtained from $Yb(C_6F_5)_2(thf)_4$ (see next section) by an acid–base reaction:[87]

$$Yb(C_6F_5)_2(thf)_4 + 2HC{\equiv}CC_6H_5 \rightarrow Yb(C{\equiv}CC_6H_5)_2 + 2C_6F_5H. \tag{26}$$

Attempts to repeat reaction (26) with $HC{\equiv}CCMe_3$ gave an explosive product.[87] The reaction of methylcyclopentadiene with $Yb(C_6F_5)_2(thf)_4$ similarly gives an explosive material.[57] On the basis of ebulliometric measurements, $Yb(C{\equiv}CC_6H_5)_2$ is associated into a trimer or tetramer in boiling thf.[87]

Eu in liquid ammonia is reported to react with propyne to form a divalent complex [reaction (27)]:

$$Eu + \text{excess } HC{\equiv}CCH_3 \xrightarrow{NH_3(l)} Eu(C{\equiv}CCH_3)_2, \tag{27}$$

but the analogous Yb reaction does not give a pure product presumably due to contamination by $Yb(NH_2)_2$.[88] Structural information has not yet been obtainable on these alkynide products.

Divalent alkynides can also be made from terminal alkynes by metal vapor methods. Hence, reaction of Yb metal with 1-hexyne forms complexes of general formula $[HYb_2(C{\equiv}CC_4H_9)_3]_n$.[89] Isopiestic molecular-weight studies indicated that this species is highly associated in solution and no X-ray quality single crystals of this oligomer were obtainable. Based on the structures of $[(C_5H_5)_2Er(\mu\text{-}C{\equiv}CCMe_3)]_2$[90] and $[(CH_3C_5H_4)_2Sm(\mu\text{-}C{\equiv}CCMe_3)]_2$,[91] oligomerization via alkynide bridges is quite possible. A possible route to the observed product is given in reactions (28)–(30) (R = C_4H_9):

$$Yb + HC{\equiv}CR \rightarrow HYbC{\equiv}CR, \tag{28}$$

$$HYbC{\equiv}CR + HC{\equiv}CR \rightarrow Yb(C{\equiv}CR)_2 + H_2, \tag{29}$$

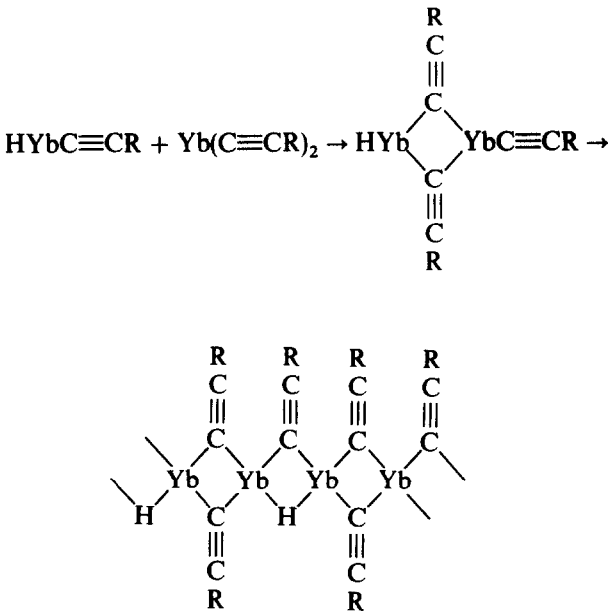

Reaction (28) is a basic oxidative addition of a C—H bond. Reaction (29), a hydride-based

metalation, is well precedented in organolanthanide and organoyttrium hydride chemistry.[23,87] The oligomerization shown in reaction (30) is expected based on the steric unsaturation of the mono- and bimetallic precursors (cf. Fig. 2).

Using the C_5Me_5 ligand, structures of the type shown above have been confirmed crystallographically. The complexes $(C_5Me_5)_2Ln(OEt_2)$ (Ln = Yb or Eu) react with $HC{\equiv}CC_6H_5$ to give mixed-valent and divalent alkynide-bridged species [reactions (31) and (32), R = C_6H_5]:[92]

$$+ (C_5Me_5)_2Yb(OEt_2) + 4HC{\equiv}CR \rightarrow 2C_5Me_5H + H_2$$

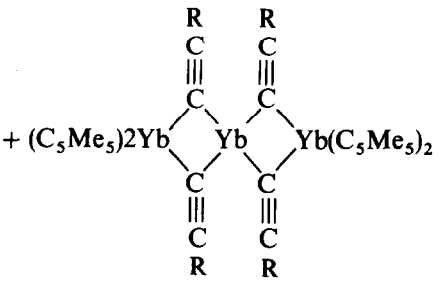

(31)

$$2(C_5Me_5)_2Eu(OEt_2) + 2HC{\equiv}CR \xrightarrow{thf} 2C_5Me_5H + [(C_5Me_5)(thf)_2Eu(\mu\text{-}C{\equiv}CR)]_2. \quad (32)$$

In both reactions the terminal alkyne gives up a proton to C_5Me_5,[93] but with the more strongly reducing Yb system some oxidation of the metal occurs. Magnetic studies show no exchange in the mixed-valent trimetallic Yb system. The Eu dimer has a structure analogous to that of $[(C_5Me_5)(thf)_2Sm(\mu\text{-}I)]_2$[75] shown in Fig. 4.

III.2(g) *Alkyl and aryl complexes.* Reactions of alkyl and aryl iodides with Eu, Yb and Sm metal have been reported to form divalent alkyl and aryl lanthanide halide complexes.[94] These are complex systems, however, and a variety of both trivalent and divalent products may be present including RLnI, LnI_2,[71] $RLnI_2$ etc. The reaction mixtures behave like Grignard reagents. No structural data has been obtainable on these systems.

Subsequent studies of the RX–Ln system using Yb and C_5Me_5I in the presence of LiI led to the identification of the trivalent complexes $(C_5Me_5)YbI_3Li(Et_2O)_2$ and $(C_5Me_5)_2YbI_2Li(Et_2O)_2$ as well as YbI_2.[70,71] The complexity of RX–Ln systems in general is demonstrated well by this case. For example, $(C_5Me_5)YbI_3Li(Et_2O)_2$ is obtained in 30% yield in 15 h but subsequently is converted to $(C_5Me_5)_2YbI_2Li(Et_2O)_2$, which is obtained in 30% yield in 24–48 h. In addition, no organometallic products are isolated in the absence of LiI. The LiI-free reaction of ytterbium metal and C_5Me_5I gives only $C_{10}Me_{10}$, YbI_3 and YbI_2.[71]

Divalent lanthanide aryl complexes can be obtained using fluorinated aryl mercury reagents [reaction (33)]:[95,96]

$$(C_6F_5)_2Hg + Yb \xrightarrow{thf} (C_6F_5)_2Yb(thf)_4 + Hg. \quad (33)$$

$(C_6F_5)_2Yb(thf)_4$ is not very stable thermally and $(2,3,5,6\text{-}F_4C_6H)_2Yb$, prepared in the same way, is less stable. $(2,3,4,5\text{-}C_6F_4H)_2Hg$ reacts with Yb but gives a product too unstable to isolate. Neither $(C_6H_5)_2Hg$ nor $(C_6Cl_5)_2Hg$ are reported to react with Yb. Recently, however, NMR and hydrolytic data have been cited to suggest that $(C_6H_5)_2Hg$–Yb does form $Yb(C_6H_5)_2(thf)_n$.[97] Sm reactions with $(C_6F_5)_2Hg$ and $(C_6F_4H)_2Hg$ are more complex and a mixture of products is formed. The course of reactions such as reaction (33) have been followed by quenching with acid and identifying the products.[98]

Transmetalation as shown in reaction (33) also reportedly can be used to make divalent derivatives of ferrocene,[99] $C_5H_5Mn(CO)_3$,[99] and carboranes.[100] Hence, $(C_5H_5FeC_5H_4)_2Yb$, $[(CO)_3MnC_5H_4]_2Yb$ and $(\eta^1\text{-}C_2B_{10}R)_2Yb$ (R = CH_3 or C_6H_5) are obtained from the reaction of Yb with $Hg(C_5H_4FeC_5H_5)_2$, $Hg[C_5H_4Mn(CO)_3]_2$ and $Hg(C_2B_{10}R)_2$, respectively. $(C_5H_4I)Fe(C_5H_5)$ and $(C_5H_4I)Mn(CO)_3$ are reported to react with Yb metal to form $C_5H_5FeC_5H_4YbI$ and $(CO)_3MnC_5H_4YbI$, respectively.[99] Reaction of $LiC_2B_{10}C_6H_5$ with LnI_2 (Ln = Eu, Yb or Sm) is said to form $[\eta^1\text{-}C_2B_{10}(C_6H_5)]LnI$. Metalation of $C_2B_{10}C_6H_5$ with

"CH_3YbI" forms similar products.[101] Transmetalation of Eu, Sm and Yb with $Hg[C_6H_5Cr(CO)_3]_2$ is reported to form divalent complexes, $[(CO)_3CrC_6H_5]_2Ln(thf)_n$.[97] Lowered ν_{CO} absorptions in the IR spectra suggest Ln—O—C coordination. The only ^1H NMR resonance cited for the phenyl protons was δ 5.645, $J(^{171}Yb-^1H) = 80$ Hz. This is unusual since coupling to ^{171}Yb, which has a natural abundance of only 14.3%, has not been observed previously for divalent Yb organometallic species.

The formation of a divalent methyl complex $(C_5Me_5)Yb(CH_3)_2Li$ by displacement of $C_5Me_5^-$ in $(C_5Me_5)_2Yb$ by CH_3^- has been mentioned in the literature but no details of this reaction were revealed [reaction (34)]:[70]

$$(C_5Me_5)_2Yb + 2CH_3Li \rightarrow (C_5Me_5)Yb(CH_3)_2Li + LiC_5Me_5. \quad (34)$$

An additional class of divalent lanthanide complexes which have some metal hydrocarbon interactions involves the bis(trimethylsilyl) amido ligand, $—N[Si(CH_3)_3]_2$. Although these complexes do not possess formal metal carbon σ-bonds, the conformations of the $(Me_3Si)_2N$ groups are such that long-distance metal–CH interactions are observed. Reaction of EuI_2 or YbI_2 with $NaN(SiMe_3)_2$ gives either $Ln[N(SiMe_3)_2]_2(R_2O)_x$ or $NaLn[N(SiMe_3)_2]_3$, depending on the ether solvent used and the manner of recrystallization.[102] Crystal structures of $NaLn[N(SiMe_3)_2]_3$ (Ln = Eu or Yb) and $Yb[N(SiMe_3)_2]_2(Me_2PCH_2CH_2PMe_2)$ (obtained by displacing the R_2O of solvation with the diphosphine) show that some of the methyl groups are oriented to bring the carbon atoms within 2.86–3.04 Å of Yb and 2.97–3.14 Å of Eu. Similarly, $Yb[N(SiMe_3)_2(AlMe_3)]_2$ has six methyl groups within 2.756(2)–3.202(3) Å of Yb(II).[103]

III.3 *Reactivity*

Although the reactivity of divalent organolanthanide complexes is only beginning to be explored, some general types of reactivity are discernible. An attempt to organize these reactions into general classes is made in the following subsections. The first three subsections deal with reactions which might be expected for complexes which are one-electron reducing agents and which contain electropositive lanthanide metal centers. In each of these cases, the metal gets oxidized and forms a sterically saturated complex containing a new bond or bonds to the most electronegative ligands available in the system. Subsequent sections deal with less traditional lanthanide reactivity patterns and ultimately to unprecedented types of reactivity. Applications of divalent lanthanide chemistry to organic chemistry will not be discussed here since they recently have been comprehensively reviewed elsewhere.[7]

III.3(a) *Oxidation reactions involving halide, pseudohalide and aryl ligands.* Bis(cyclopentadienyl) Yb and Sm complexes react with a variety of alkyl halides to form dicyclopentadienyl halide complexes. Many systems have been observed to have this reactivity including: (a) $(CH_3C_5H_4)_2Yb(thf)$ and $(CH_3C_5H_4)_2Sm(thf)$ with CH_3I, Me_3CCl and $H_2C{=}CHCH_2Br$,[104] (b) $(C_5Me_5)_2Yb(dme)$ with CH_2Cl_2,[70,105] (c) $(C_5Me_5)_2Sm(thf)_2$ with Me_3CCl and ICH_2CH_2I,[106] and (d) $(C_5Me_5)_2Yb(OEt_2)$ with n-C_4H_9Cl and $C_6H_5CH_2Cl$.[107] The trivalent halide complexes $(C_5R_5)_2LnX(solvent)$ are generally the main products of these reactions. $(C_5Me_5)_2SmCl(thf)$ and $(C_5Me_5)_2SmI(thf)$ have been made preparatively by route (c) above and have been crystallographically characterized.[106] The $(C_5Me_5)_2Yb(OEt_2)$–$C_6H_5CH_2Cl$ system has been studied in detail and found to give a variety of products in the presence of a slight excess of RX [reaction (35)]:[107]

$$(C_5Me_5)_2Yb(OEt_2) + 1.52C_6H_5CH_2Cl \rightarrow 0.48(C_5Me_5)_2YCl + 0.52(C_5Me_5)YbCl_2 + Et_2O + 0.52C_5(CH_3)_5(CH_2C_6H_5) + 0.5(C_6H_5CH_2)_2. \quad (35)$$

The reactivity of $(C_5H_5)_2Yb$ in thf or dme with metal halides and pseudohalides has also been studied. Reactions of the divalent ytterbium species with HgX_2, TlX, AgX_2 and CuX salts where

X = O_2CMe, $O_2CC_6F_5$, $O_2CC_5H_4N$, Cl, Br, I, C_6F_5, C≡CPh, $CH(OCMe)_2$ or $CH(OCPh)_2$ have been examined [reactions (36) and (37)]:[108]

$$(C_5H_5)_2Yb(solvent) + MX \rightarrow (C_5H_5)_2YbX(solvent) + M(M = Tl\,or\,Cu), \quad (36)$$

$$2(C_5H_5)_2Yb(solvent) + MX_2 \rightarrow 2(C_5H_5)_2YbX(solvent) + M\,(M = Hg\,or\,Ag). \quad (37)$$

The crystal structure of the $O_2CC_6F_5$ reaction product has been determined to be the dimer $(C_5H_5)_2Yb(O—C(C_6F_5)—O)_2Yb(C_5H_5)_2$. Similarly, $(CH_3C_5H_4)_2Sm(thf)$ can be oxidized with HgI_2 or I_2 to give $(CH_3C_5H_4)_2SmI(thf)$.[104] A toluene suspension of $YbCl_3$ can be used as an oxidant to transform $(C_5Me_5)_2Yb(thf)$ into $(C_5Me_5)_2YbCl(thf)$.[105] $(C_5Me_5)_2Yb(dme)$ can be oxidized by the ferricinium ion [reaction (38)]:[70]

$$(C_5Me_5)_2Yb(dme) + [(C_5H_5)_2Fe][PF_6] \rightarrow (C_5Me_5)_2Yb(dme)(PF_6) + (C_5H_5)_2Fe. \quad (38)$$

$(C_5Me_5)_2Sm(thf)_2$ reacts with $Hg(C_6H_5)_2$ to provide a halide-free synthesis of a trivalent phenyl complex [reaction (39)]:[74]

$$2(C_5Me_5)_2Sm(thf)_2 + Hg(C_6H_5)_2 \rightarrow 2(C_5Me_5)_2Sm(C_6H_5)(thf) + Hg. \quad (39)$$

Oxidation of the mono(pentamethylcyclopentadienyl) anion $[C_5Me_5YbI_2]^-$ by C_5Me_5I is also reported to occur [reaction (40)]:[70]

$$(C_5Me_5)YbI_2Li + C_5Me_5I \rightarrow (C_5Me_5)YbI_3Li + C_5Me_5. \quad (40)$$

The aryl complexes[95] $(C_6F_5)_2Yb(thf)_4$ and $(p\text{-}HC_6F_4)Yb(thf)_4$ generated *in situ* in thf, react with the transition-metal halides $Rh(CO)Cl(PPh_3)_2$, $NiCl_2(bipy)$ (bipy = 2,2′-bipyridine), $NiCl_2(PPh_3)_2$ and $PtCl_2(bipy)$ to form complexes in which the halide ligands have been replaced by fluorinated aryl groups, i.e. $RRh(CO)(PPh_3)_2$, $R_2Ni(bipy)$ (R = C_6F_5 or $p\text{-}HC_6F_4$), $(C_6F_5)_2Ni(PPh_3)_2$ and $(C_6F_5)_2Pt(bipy)$.[96] $YbCl_2$ is the presumed byproduct. The $(C_6F_5)_2Yb(thf)_4$ complex also transfers C_6F_5 to Ph_3SnCl to form $Ph_3SnC_6F_5$. At low temperature I_2 reacts with $(C_6F_5)_2Yb(thf)_4$ to form C_6F_5I. With $HgCl_2$, some oxidation of $(C_6F_5)_2Yb(thf)_4$ occurs giving Hg metal as well as $(C_6F_5)_2Hg$. $(C_6F_5)_2YbCl$ or $YbCl_3$ were possible byproducts.[96] The decomposition of the divalent Yb fluoro-aryl complexes with CO_2[96] and the decomposition of the divalent Yb alkynides with H_2O have also been studied.[87]

III.3(b) *Oxygen abstraction reactions.* $(C_5Me_5)_2Sm(thf)_2$ reacts with a variety of oxygen-containing substrates including $CH_3CH_2\overline{CHCH_2O}$, NO, N_2O and C_5H_5NO to form the trivalent oxide complex $[(C_5Me_5)_2Sm]_2(\mu—O)$ (Fig. 6).[109] The epoxide system [reaction (41)]:

$$(C_5Me_5)_2Sm(thf)_2 + CH_3CH_2\underset{\diagdown\,\diagup}{\overset{O}{CH}}CH_2 \rightarrow (C_5Me_5)_2Sm—O—Sm(C_5Me_5)_2 + CH_3CH_2CH{=}CH_2 \quad (41)$$

and the pyridine *N*-oxide reaction give the oxide product in approximately 50% yield. The other reactions are much more complicated and give mixtures of many products of which the oxide is just one component. The oxide complex is structurally interesting in that the Sm—O—Sm unit is crystallographically linear.

III.3(c) *Reduction of transition-metal carbonyl complexes.* Divalent Yb and Sm organometallics are strong enough reducing agents to react with many transition-metal carbonyl complexes to form anions.[110] Although the simple unsubstituted cyclopentadienyl complexes like $(C_5H_5)_2Yb$ will react with transition-metal carbonyls,[111] reactions with C_5Me_5 derivatives give products which are easier to characterize. The reactivity of $(C_5Me_5)_2Yb(OEt_2)$ has been extensively studied in this regard.[112–115]

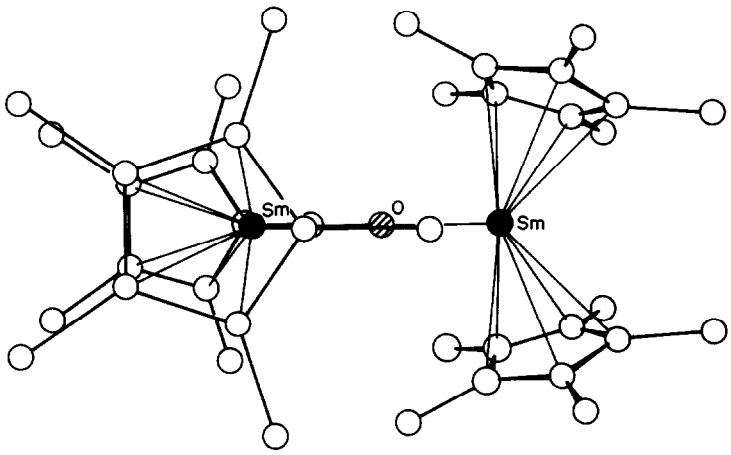

Fig. 6. Structure of $[(C_5Me_5)_2Sm]_2(\mu\text{-}O)$.

Reaction (42):

$$2(C_5Me_5)_2Yb(OEt_2) + Co_2(CO)_8 \xrightarrow{thf} (C_5Me_5)_2(thf)Yb(\mu\text{—}OC)Co(CO)_3 \qquad (42)$$

shows a simple reduction sequence in which the metal–metal bond in $Co_2(CO)_8$ is cleaved to generate the anion $[Co(CO)_4]^-$.[112] The product exists as a tight ion pair in which an isocarbonyl linkage, Yb—O—C—Co, is present. This reactivity is typical in that the divalent lanthanide gets oxidized and gets an additional electronegative ligand. The $Mn_2(CO)_{10}$ system is similar in that trivalent Yb and $Mn(CO)_5^-$ anions are formed. However, the structure of the product is complex and contains dimers, $[(C_5Me_5)_2Yb]$ $[(\mu\text{—}OC)Mn(CO)_3(\mu\text{—}CO)]_2$ $[Yb(C_5Me^5)_2]$, as well as a polymeric chain, $\{[(C_5Me_5)_2Yb]$ $[(\mu\text{-}OC)_3Mn(CO)_2]\}_n$.[113]

$Fe(CO)_5$ reacts with $(C_5Me_5)_2Yb(OEt_2)$ to form an analog of $Na_2Fe(CO)_4$ [reaction (43)]:[114]

$$2(C_5Me_5)_2Yb(OEt_2) + Fe(CO)_5 \rightarrow (CO)_3Fe[(\mu\text{-}CO)Yb(C_5Me_5)_2(thf)]_2. \qquad (43)$$

However, when the trinuclear transition-metal carbonyl $Fe_3(CO)_{12}$ was reacted with $(C_5Me_5)_2Yb(OEt_2)$, an iron–iron bond was broken, a carbonyl ligand was lost, and an $Fe_3(CO)_{11}^{2-}$ unit was formed which was attached to two $[(C_5Me_5)_2Yb]^+$ moieties via four isocarbonyl linkages [reaction (44)]:[114]

$$2(C_5Me_5)_2Yb(OEt_2) + Fe_3(CO)_{12} \rightarrow$$

$$(C_5Me_5)_2Yb\begin{matrix} O\text{–}C \\ \\ O\text{–}C \end{matrix}\begin{matrix} Fe(CO)_3 \\ C\text{–}O \\ Fe\text{–}CO \\ C\text{–}O \\ Fe(CO)_3 \end{matrix}Yb(C_5Me_5)_2 + CO. \qquad (44)$$

Reductive formation of tight ion pairs containing isocarbonyl connections has also been reported for $(C_5Me_5)_2Yb(OEt_2)$ with $(C_5H_5)_2Fe_2(CO)_4$, $(C_5H_5)_2Mo_2(CO)_6$ and $(C_5H_5)Co(CO)_2$.[115]

$(C_5Me_5)_2Sm(thf)_2$ reduces $Co_2(CO)_8$ to form a $(C_5Me_5)_2SmCo(CO)_4$ complex, but the structure of the compound is unknown because a refinable solution to the X-ray data was not readily obtainable. Interestingly, when $SmI_2(thf)_x$ reduces $Co_2(CO)_8$, a $Co(CO)_4^-$ product is obtained which *does not* have isocarbonyl connections. The product of this reaction, $[SmI_2(thf)_5]$ $[Co(CO)_4]$, has discrete $[SmI_2(thf)_5]^+$ and $Co(CO)_4^-$ units.[116]

III.3(d) *Substitution reactions.* As described in Section III.2(d), the solvating ether ligands in $(C_5Me_5)_2YbL_x$ and $(C_5Me_5)_2EuL_x$ ($x = 1$ or 2) can be readily substituted with other ethers.[69]

Hence, depending on crystallization conditions, complexes with L_x = thf, $(thf)_2$, Et_2O, (thf) (Et_2O) or dme can readily be obtained. These complexes have not been formed by deliberate substitution reactions, but rather by specific crystallization procedures.[69] Therefore, a definitive pattern of substitution reactivity has yet to be reported. The direct substitution of Et_2O from $(C_5Me_5)_2Yb(OEt_2)$ by pyridine in toluene has been studied however [reaction (45)]:[72]

$$(C_5Me_5)_2Yb(OEt_2) + 4C_5H_5N \rightarrow (C_5Me_5)_2Yb(NC_5H_5)_2 + 2NC_5H_5 + Et_2O. \quad (45)$$

Given the lability of the solvating ligands in solution, this type of substitution reactivity is expected.

Displacement of C_5Me_5 ligands from $(C_5Me_5)_2LnL_x$ complexes has also been reported. SmI_2 reacts with $(C_5Me_5)_2Sm(thf)_2$ in a ligand redistribution reaction to form a structurally characterized dimer [reaction (46) (Fig. 4)]:[75]

$$(C_5Me_5)_2Sm(thf)_2 + SmI_2 \rightarrow [(C_5Me_5)(thf)_2Sm(\mu\text{-}I)]_2. \quad (46)$$

Displacement of C_5Me_5 from an unspecified solvate of $(C_5Me_5)_2Yb$ by LiI [reaction (47)]:

$$(C_5Me_5)_2Yb + 2LiI \rightarrow (C_5Me_5)YbI_2Li + LiC_5Me_5 \quad (47)$$

and MeLi [reaction (34)] has been reported to give $(C_5Me_5)YbI_2Li$ and $(C_5Me_5)YbMe_2Li$, respectively.[70] If the Yb in these products is not solvated and is therefore formally five-coordinate, this would be an unusual reaction. When Li and I are replaced by K and Br in reaction (47), the reverse reaction is preferred.[70]

III.3(e) CO *reduction.* The reduction of CO by $(C_5Me_5)_2Sm(thf)_2$[47,117] provides an excellent example of the unique reactivity available through this divalent lanthanide oxidation state. $(C_5Me_5)_2Sm(thf)_2$ reacts under a variety of conditions with CO to give complex mixtures of products. Under 90 psi of CO in THF, a crystalline product separates which was crystallographically characterizable [reaction (48)]:

$$4(C_5Me_5)_2Sm(thf)_2 + 6CO \rightarrow \text{[structure]} + 6thf. \quad (48)$$

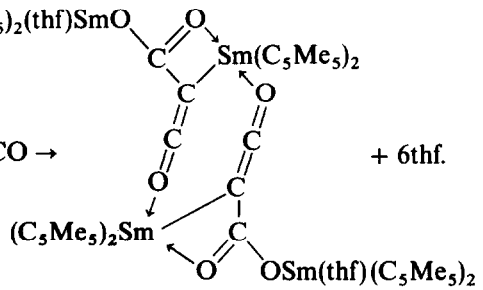

The remarkable dimeric product contains four Sm(III) centers and the equivalent of six CO molecules. Hence, in reaction (48) six CO units have been reduced by four electrons and the reductive homologation has formed two ketenecarboxylate units.

The most interesting feature in the formation of the ketenecarboxylate complex is that complete cleavage of one CO triple bond must have occurred to give the central, oxygen-free carbon of the C=C—C skeleton. Although CO cleavage is thought to occur in heterogeneous Fischer–Tropsch systems,[118] this rarely occurs in homogeneous systems. Complete CO cleavage is not observed in the extensive studies of CO reduction by molecular early transition-metal,[65,119] actinide[120] and lanthanide[121] hydride systems.

Although metal hydride reduction of CO has been heavily investigated, hydrogen-free reduction of CO using one-electron reducing agents as in reaction (48) has received much less attention. The closest related system is the two-electron reduction of two CO molecules by alkali metals which is reported to form an insoluble alkyne diolate [reaction 49)]:[122]

$$2K + 2CO \rightarrow 2[KOC{\equiv}COK]. \quad (49)$$

The relationship between reactions (48) and (49) can be seen by comparing KOCCOK with the

atom connectivity on the right hand (or left hand) side of the ketenecarboxylate dimer, $SmO\overset{O}{\overset{\|}{C}}CCOSm$. Both the K and Sm systems contain MOCCOM units involving two-electron reduction of two CO molecules. The samarium system, a two-electron–three-CO system, has an extra CO formally "inserted" between a C and O bond. The insolubility of the KOC≡COK product may be responsible for the lack of further homologation in this system compared to the Sm system. Hence, $(C_5Me_5)_2Sm(thf)_2$, although strongly reducing like the alkali metals, is differentiated from those reducing agents by its solubility. The C_5Me_5 ligands provide solubility to the reducing agent as well as to intermediate reduction products and allow $(C_5Me_5)_2Sm(thf)_2$ to accomplish chemistry different from that of the alkali metal.

The reactivity of $(C_5Me_5)_2Sm(thf)_2$ with CO can also be compared with that of $(C_5Me_5)_2Ti$. Both organometallic reagents are soluble, strongly reducing complexes of oxophilic metals. As shown in reaction (50):

$$(C_5Me_5)_2Ti + 2CO \rightarrow (C_5Me_5)_2Ti(CO)_2, \tag{50}$$

decamethyltitanocene forms a carbonyl[123] complex rather than reducing the CO. Since the 4*f* valence orbitals of Sm(II) are not as suitable for carbonyl complex formation as those of Ti(II), this is less likely for Sm and reduction occurs.

Considering the comparisons above and the fact that neither $(C_5Me_5)_2Yb$[70,92] nor $(C_5Me_5)_2Eu(thf)$ react with CO, $(C_5Me_5)_2Sm(thf)_2$ appears to be a unique reducing agent in the periodic table. The combination of strong reducing power, oxophilicity, solubility and lack of *d* valence orbitals is not duplicated by any other reducing agent presently available.

$(C_5Me_5)_2Sm(thf)_2$ is not the only Sm(II) reagent which reacts with CO, however. Both $(C_5Me_5)_2Sm$ and $[(C_5Me_5)(thf)_2Sm(\mu\text{-}I)]_2$ reduce CO.[117,124] Again, mixtures of complex products are obtained. The reaction of $(C_5Me_5)_2Sm$ with CO provides X-ray quality crystals but the molecule is so complex that a solution to the X-ray data has not been found.

III.3(f) *Reduction of internal alkynes and azobenzene.* $(C_5Me_5)_2Sm(thf)_2$ reacts with $C_6H_5C{\equiv}CC_6H_5$ instantaneously to form a black product characterized by elemental analysis as $[(C_5Me_5)_2Sm]_2C_2(C_6H_5)_2$.[38] A possible formation pathway and structure are shown in reaction (51):

$$(C_5Me_5)_2Sm(thf)_2 + C_6H_5C{\equiv}CC_6H_5 \rightarrow [(C_5Me_5)_2Sm](C_6H_5)C{=}\dot{C}(C_6H_5) + 2\,thf$$

$$\xrightarrow{(C_5Me_5)_2Sm(thf)_2}$$

$$(C_5Me_5)_2Sm\diagdown \quad \diagup C_6H_5 \qquad\qquad (51)$$

$$\quad\quad C{=}C \qquad + 4thf.$$

$$C_6H_5\diagup \quad \diagdown Sm(C_5Me_5)_2$$

This reaction has some precedent in reactions of alkali metals with arylalkynes, except that in the heterogeneous alkali metal systems, polymerization or dimerization of the radical generally occurs.[125] The more soluble $(C_5Me_5)_2Sm(thf)_2$ may more readily trap the radical to give the bimetallic product. Once again the solubility of $(C_5Me_5)_2Sm(thf)_2$ may be responsible for chemistry different from that of the alkali metals.

$[(C_5Me_5)_2Sm]_2C_2(C_6H_5)_2$ is unusual in several respects.[38] Room-temperature magnetic-susceptibility measurements indicate that it contains Sm(III) centers. Given this oxidation state, the black color of this complex is abnormal since virtually all Sm(III) complexes are pale orange, yellow or red. Also unexpected is the fact that the complex reacts with excess thf to regenerate $(C_5Me_5)_2Sm(thf)_2$ and $C_6H_5C{\equiv}CC_6H_5$. Given the strongly reducing nature of Sm(II), this Sm(III) to Sm(II) conversion under mild conditions was unanticipated. The structure shown in reaction (51) is unproven but is consistent with spectroscopic data, hydrolysis to *trans*-stilbene, and the structure of the azobenzene complex described below.

$(C_5Me_5)_2Sm(thf)_2$ reacts with $C_6H_5N{=}NC_6H_5$ to form an intensely colored product which also has unusual properties [reaction (52)]:[126]

$$2(C_5Me_5)_2Sm(thf)_2 + C_6H_5N{=}NC_6H_5 \rightarrow \begin{array}{l}(C_5Me_5)_2Sm \quad\quad C_6H_5\\ \quad\quad\quad\quad\quad\quad N{=}N\\ C_6H_5 \quad\quad\quad\quad\quad Sm(C_5Me_5)_2\end{array} + 4thf. \qquad (52)$$

The complex has an overall structure like that proposed for $[(C_5Me_5)_2Sm]_2C_2(C_6H_5)_2$ and, given the N for C change, could be viewed as an azobenzene base adduct of $(C_5Me_5)_2Sm(II)$. However, room-temperature magnetic-susceptibility measurements indicate that the metal is in the trivalent oxidation state and the Sm—N distances, 2.40(1) and 2.41(1) Å, are consistent with single σ-bonds. This suggests the presence of a $[(C_6H_5)NN(C_6H_5)]^{2-}$ dianion. However, the 1.25(1) Å NN distance is the same as the N=N double-bond distances in a variety of azobenzene structures. As shown in Fig. 7, the molecule is distorted in that the N—C (phenyl) distances are stretched from a normal 1.42 Å to 1.56–1.61 Å. In addition, the Sm atoms are displaced asymmetrically such that both come within 2.29–2.34 Å of the *ortho* hydrogens of a single phenyl ring in a bonafide agostic[127] Sm–H interaction. The ability of Sm(II) to structurally distort azobenzene in this way is remarkable.

Attempts to get $(C_5Me_5)_2Yb(OEt_2)$ to react with $C_6H_5C{\equiv}CC_6H_5$ in analogy to reaction (51) were unsuccessful.[92]

In the presence of hydrogen, $(C_5Me_5)_2Sm(thf)_2$ reacts with alkynes such as $C_6H_5C{\equiv}CC_6H_5$ and $CH_3CH_2C{\equiv}CCH_2CH_3$ to form systems which are active hydrogenation catalysts.[38] Formation of an enediyl-like structure [cf. reaction (51)] followed by hydrogenolysis of the Sm—C bond, a well-established reaction[22,23] may give the SmH unit which could be the active catalyst [reactions (53)–(55), $(Cp^5{=}C_5Me_5)$]:

$$2Cp^5_2Sm(thf)_2 + RC{\equiv}CR \rightarrow \begin{array}{l}Cp^5_2Sm \quad\quad R\\ \quad\quad C{=}C\\ R \quad\quad\quad SmCp^5_2\end{array} \xrightarrow{H_2} 2[Cp^5_2SmH], \qquad (53)$$

$$[Cp^5_2SmH] + RC{\equiv}CR \rightarrow \begin{array}{l}Cp^5_2Sm \quad\quad H\\ \quad\quad C{=}C\\ R \quad\quad\quad R\end{array} \xrightarrow{H_2} [Cp^5_2SmH] + \begin{array}{l}H \quad\quad H\\ \quad\quad C{=}C\\ R \quad\quad\quad R\end{array} \qquad (54)$$

$$[Cp^5_2SmH] + RHC{=}CHR \rightarrow Cp^5_2SmCHRCH_2R \xrightarrow{H_2} [Cp^5_2SmH] + RCH_2CH_2R. \qquad (55)$$

This scheme is supported by the isolation of the structurally characterized dimer $[(C_5Me_5)_2$

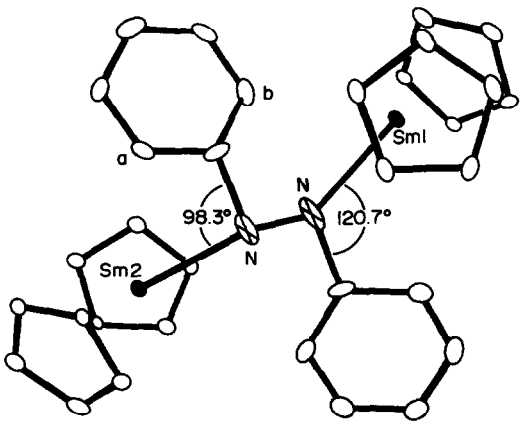

Fig. 7. Structure of $[(C_5Me_5)_2Sm]_2N_2(C_6H_5)_2$. Sm2 is 2.36 Å from the hydrogen atom on phenyl carbon atom a. Sm1 is 2.32 Å from the hydrogen atom on phenyl carbon atom b.

$Sm(\mu\text{-}H)]_2$ from a stoichiometric reaction like reaction (53).[38] In addition, the *cis* addition and hydrogenolysis sequence [reactions (54) and (55)] has been demonstrated for other lanthanide and yttrium hydrides.[23] A subsequent mechanistic study of lanthanide-based hydrogenation catalysis reconfirms the above result.[128]

III.3(g) *Productive* CH *and* CO *activation via* Sm(II). The reaction of the $(C_5Me_5)_2Sm(thf)_2$–$C_6H_5C{\equiv}CC_6H_5$ reaction product with CO has led to a remarkably facile stereospecific synthesis of a tetracyclic hydrocarbon [reaction (56)]:[129]

$$2(C_5Me_5)_2Sm(thf)_2 + C_6H_5C{\equiv}CC_6H_5 \xrightarrow{-4\,thf} [(C_5Me_5)_2Sm]_2C_2(C_6H_5)_2 \xrightarrow{2CO} \text{(56)}$$

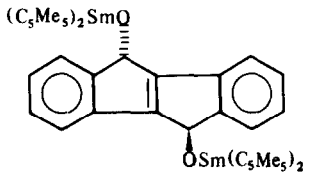

Based on the proposed structure of the product of the $(C_5Me_5)_2Sm(thf)_2$–$C_6H_5C{\equiv}CC_6H_5$ reaction [see reaction (51)] and earlier studies of CO insertion into lanthanide–carbon σ-bonds,[130] the scheme shown below was proposed to explain this synthesis [$(C_5Me_5)_2Sm$ is shown as Sm in a box].

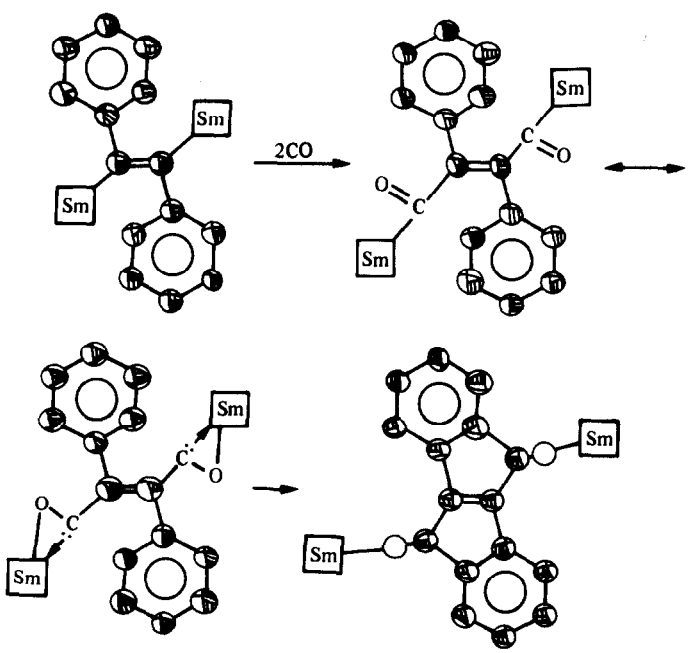

Activation of CO by insertion into the Sm—C bonds could give two dihaptoacyl units with considerable Sm–O interaction and carbene character on the acyl carbon atoms. Insertion of these carbene-like centers into *ortho* C—H bonds would give the two five-membered rings. The proximity of the *ortho* C—H bonds to the samarium-containing moiety in the agostic hydrogen structure of $[(C_5Me_5)_2Sm]_2N_2(C_6H_5)_2$ [reaction (52)] gives support for this possible mode of CH activation. If this synthesis is generally applicable, it would be a valuable way to make polycyclic hydrocarbons in a stereospecific manner from simple starting materials, namely alkynes and CO.

III.3(h) *Reactions with alkenes and dienes.* Attempts to make ethene or butadiene complexes of $(C_5Me_5)_2Yb(thf)$ failed,[70] a result which was not surprising in view of the traditional picture of lanthanides as oxophilic hard acids which have little affinity for unsaturated hydrocarbons. However, $(C_5Me_5)_2Sm(thf)_2$ was found to polymerize ethene.[47,131] Further studies of the catalytic

activity of $(C_5Me_5)_2Yb(OEt_2)$ and $(C_5Me_5)_2Eu(OEt_2)$ in ethene polymerization reactions have shown that these complexes do have low activity.[131]

$(C_5Me_5)_2Sm(thf)_2$ also interacts with other alkenes. It readily isomerizes *cis*-stilbene to the *trans* isomer.[132] It reacts with cyclohexene in a complex reaction which gives a product which on the basis of preliminary X-ray data contains a short 3.03-Å Sm—Sm distance.[133] It reacts readily with cyclohexadienes and with cyclopentadiene. In the latter case, $(C_5Me_5)_2SmC_5H_5$ is formed.[133] In addition, $(C_5Me_5)_2Sm(thf)_2$ in the presence of hydrogen and alkenes leads to a catalytic hydrogenation system [see reactions (53)–(55)].[134]

III.4. *Principles of structure and reactivity for divalent organolanthanides*

Since only 13 divalent organolanthanide complexes have been structurally characterized (Table 1), any firm structural conclusions may be premature at this point. However, 10 of the structures do follow traditional principles of organolanthanide chemistry. The $(C_5R_5)_2Ln(solvent)_x$ systems have typical "bent metallocene plus x ligand" structures in the cases in which the steric bulk of the ligand set is sufficient to confer steric saturation on the complex. When this is not the case, e.g. with $(CH_3C_5H_4)_2Yb(thf)$ (Fig. 2),[25] oligomerization occurs to increase the steric saturation around the metal. Similarly, the monocyclopentadienyl systems such as $[(C_5Me_5)Sm(thf)_2(\mu\text{-}I]_2$ (Fig. 4)[75] and $[(C_5Me_5)Eu(thf)_2(\mu\text{-}C{\equiv}CC_6H_5)]_2$[92] form bridged structures to gain a higher coordination number.

Although the majority of divalent organolanthanide structures follow traditional principles, the remarkable $(C_5Me_5)_2Ln$ complexes ((Ln = Sm or Eu)[78,79] do not. The bent, sterically unsaturated structures are unexpected on the basis of both electrostatic and steric arguments and this structure occurs regardless of the 4*f*-electron configuration or reduction potential of the metal [a differentiating factor in reactivity (see below)].

The unusual geometry of the $(C_5Me_5)_2Ln$ complexes may signal the existence of an entire series of unanticipated structural possibilities for divalent organolanthanides. These complexes strongly indicate that the traditional principles of trivalent organolanthanide chemistry will not carry over directly to divalent systems. One of the exciting questions currently being explored in this area is how generally available are such sterically unsaturated divalent species.

Like the structural features discussed above, the reactivity of divalent complexes follows traditional organolanthanide principles in many cases. For example, there are numerous examples in Sections III.3(a)–(c) in which the metal gets oxidized and forms a sterically saturated trivalent complex which contains a new ligand involving the most electronegative of the donor atoms available in the system. As expected, reactivity parallels reduction potential, with Sm(II) more reactive than Yb(II) which is more reactive than Eu(II). The substitution reactions in Section III.3(d) are also expected considering the lability of solvating species and the tendency toward ligand redistribution reactions found for trivalent species.

Most of the unusual chemical reactivity observed for divalent organolanthanides is found with Sm(II) species. In many cases, what distinguishes Sm(II) from Yb(II) and Eu(II) is its greater reducing power. This opens up avenues of reactivity to Sm(II) which are unavailable to the other divalent lanthanide systems. Prime examples are the reductions of CO and $C_6H_5C{\equiv}CC_6H_5$ which succeed for Sm(II) and fail for Yb(II). Sm(II) has proven to be a unique one-electron reductant due to its special combination of physical properties. Hence, the Sm(II)-based reductive homologation of CO to $O_2C{-}C{=}C{=}O$ is a non-traditional unprecedented CO reduction. However, the reaction follows traditional organolanthanide principles in that sterically saturated oxygen-bound products are formed. Likewise the unusual distortions rendered to $C_6H_5N{=}NC_6H_5$ in the reaction with $(C_5Me_5)_2Sm(thf)_2$ can be traditionally explained given the formation of a highly reduced organic species. An electropositive lanthanide with a strong tendency to achieve a high coordination number will coordinate to whatever electron rich species are available. Hence, in the azobenzene complex the short Sm—N distance and agostic Sm—H interactions occur. The productive CH and CO activations discussed in III.3(g) are seen to follow traditional principles of organolanthanide–CO chemistry given the unusual features of $[(C_5Me_5)_2Sm]_2C_2(C_6H_5)_2$.

There is, however, an observed Sm(II) chemistry which does not follow traditional organolanthanide principles. The facile desolvation of $(C_5Me_5)_2Sm(thf)_2$ to form the sterically unsaturated $(C_5Me_5)_2Sm$ was unexpected. The difference in the desolvation tendencies of $(C_5Me_5)_2Sm(thf)_2$

and $(C_5Me_5)_2Eu(thf)$ is also unusual given the adjacent position of Sm and Eu in the periodic table. The facile reversal of the $(C_5Me_5)_2Sm(thf)_2$ reduction of $C_6H_5C{\equiv}CC_6H_5$ by thf, i.e. the formation of Sm(II) from Sm(III) under very mild conditions, was unanticipated. The unusual reactivity of $(C_5Me_5)_2Sm$ with cyclohexene is another example of non-traditional chemistry. These results, like the unusual structure of the $(C_5Me_5)_2Ln$ complexes, suggest there may be a major part of divalent organolanthanide reactivity which will not follow the traditional principles of the trivalent metals.

IV. ZERO OXIDATION STATE CHEMISTRY: THE CHEMISTRY OF THE METALS

In the mid-1970s, when only a limited amount of trivalent organolanthanide chemistry was known and almost no divalent organolanthanide chemistry was explored, there was an impetus to do rather speculative, highly exploratory synthetic studies in oxidation states other than +3 or +2.[135] The goal was to demonstrate a broader chemistry for the lanthanides than had previously been observed. It was anticipated that by taking a non-traditional approach to lanthanide chemistry, new areas in the field would be opened up and a greater potential for these elements in all oxidation states would be demonstrated.

An intriguing non-trivalent lanthanide oxidation state suitable for non-traditional exploration and available to all of the metals was the formally zero oxidation state of the metals. Although some reactivity was accessible from the bulk metal (see Section IV.3), a much more reactive form of the metal was available in the vapor phase. The metal vapor technique, in which a metal is vaporized from a resistively-heated tungsten container under high vacuum and is cocondensed with a potential ligand at −125 to −196°C, had proven useful in the synthesis of a variety of unusual low-valent transition-metal complexes.[136-140] This method provided the opportunity to study zero-valent lanthanide chemistry and also had the potential to generate zero-valent lanthanide complexes.

IV.1. *Background*

The stability of zero oxidation state complexes of transition metals depends in large part on the transfer of the excess electron density on the metal center back to the ligands via back bonding. Given the limited radial extension of the 4*f* orbitals, the possibility of stabilizing a zero-valent lanthanide complex by backbonding of the 4*f* electron density seemed remote. However, the atomic spectra of the lanthanides show that *in low oxidation states*, the 5*d* orbitals are close in energy to the 4*f* levels and that a variety of mixed 4*f*–5*d*–6*s* electron configurations are low in energy.[13,141] Hence, it is possible that the valence electrons of a low-valent lanthanide metal would possess 5*d* as well as 4*f* character. This electronic situation would be unique among metals and might provide the basis not only for new lanthanide chemistry but also for new types of metal-centered chemistry in general. As an example, zero-valent Er in a neutral complex could have single-electron approximation configurations such as $4f^{13}5d^1$, $4f^{12}5d^2$ and $4f^{11}5d^26s^1$ as well as the $4f^{12}6s^2$ configuration of the elemental metal. The chemistry of an uncharged $5d^1$ or $5d^2$ metal would certainly be unusual.

IV.2. *Lanthanide metal vapor reactivity*

IV.2(a) *Reactions with* CO. One of the early studies of zero-valent lanthanide metal vapor chemistry involved the matrix isolation reaction of the metals with CO.[142] Based on IR data, a variety of metal carbonyl complexes, $Ln(CO)_n$ (n = 1–6), were postulated. This was not a preparative-scale experiment, however, and the postulated complexes were not stable except at very low temperature. Hence, unambiguous confirmation of the formula and structure of these complexes could not be obtained.

IV.2(b) *Reactions with substituted alkynes and alkenes.* One major focus of the study of zero oxidation state lanthanide chemistry on a preparative scale involved reactions with unsaturated hydrocarbons.[3,143,144] Although alkenes and alkynes were not known as ligands or reactants with the trivalent lanthanides at that time, it was important to explore the potential of the zero-valent lanthanide metals to interact with such substrates given the importance of unsaturated hydrocarbon reactions in organometallic chemistry.

These exploratory studies demonstrated that the lanthanide metals have an extensive chemistry with unsaturated hydrocarbons and generated some of the most unusual organolanthanide species currently known. The lanthanide metal vapor reactions (57)–(61):

$$Ln + H_2C{=}CH{-}CH{=}CH_2 \rightarrow Ln(C_4H_6)_3 \quad (Nd, Sm \text{ or } Er), \quad (57)^{135}$$

$$Ln + H_2C{=}C(CH_3){-}C(CH_3){=}CH_2 \rightarrow Ln(C_6H_{10})_2 \quad (La, Nd, Sm \text{ or } Er), \quad (58)^{135}$$

$$Ln + CH_3CH = CH_2 \rightarrow Ln(C_3H_6)_3 \quad (Er), \quad (59)^{145}$$

$$Ln + CH_3CH_2C{\equiv}CCH_2CH_3 \rightarrow Ln_2(C_6H_{10})_3 \quad (Nd \text{ or } Er), \quad (60)^{62}$$

$$\rightarrow Ln(C_6H_{10}) \quad (Sm \text{ or } Yb) \quad (61)^{62}$$

illustrate the main features of this chemistry. In each case, the metal was vaporized at temperatures ranging from 500–1600°C depending on the specific lanthanide involved and cocondensed with the unsaturated hydrocarbon at −196°C. The product was isolated on a preparative scale in an inert-atmosphere glove box and the product formula was determined by complete elemental analysis. Yields varied depending on the specific metal–ligand combination, but as much as 2–3 g of isolated product were obtained in some of the systems.[3,144]

The metal vapor reaction products differed from traditional organolanthanide complexes in many ways. First, the observed stoichiometries had low ligand: metal ratios. For example, the Yb– and Sm–3-hexyne products [reactions (60) and (61)] had formal ligand: metal ratios of 1:1, whereas most organolanthanides are commonly 9- or 10-coordinate. Second, the stoichiometries varied in an unusual manner depending on the ligand and metal. For example, 2,3-dimethyl substitution of the butadiene ligand changed the ligand: metal ratio from 3:1 [reaction (57)] to 2:1 [reaction 58)]. In the 3-hexyne system, changing from Nd and Er to Yb and Sm changed the ratio from 1.5:1 [reaction (60)] to 1:1 [reaction (61)]. Traditionally, the stoichiometries of organolanthanide complexes are invariant to minor substitutional changes on the ligand and are similar for each lanthanide in the series. Third, in contrast to traditional organolanthanides, which have pale colors (see Section III.1), the metal vapor products were intensely colored materials which displayed strong charge transfer absorptions in the near IR and visible regions. Fourth, the room-temperature magnetic moments for these complexes were often outside the range of "free-ion" values previously reported for organolanthanide compounds. Consistent with this, the NMR spectra of the La, Sm and Lu products were broad and uninformative whereas these metals, when trivalent, provide sharp interpretable spectra. The lanthanum butadiene product displayed an EPR absorption (La^{3+} is $4f^0$). Finally, the solution behavior of these complexes was unusual. For example, the 3-hexyne product $[ErC_9H_{15}]_n$ was dimeric in arenes, i.e. $n = 2$ [e.g. $Er_2(C_6H_{10})_3$], but in concentrated solution or in thf it was highly associated with $n > 10$. This is just the opposite of the trend found for traditional organolanthanides which are more highly associated in arenes than in thf.[21,30] Unfortunately, because these metal vaporization products oligomerized rather than crystallized in concentrated solution, these species were not structurally characterized by X-ray diffraction.

Analysis of possible zero-valent reaction pathways suggested three conceivable structural types for these products and initiated further experimental studies to verify them.[144] For the Er–3-hexyne product, $(ErC_9H_{15})_n$, one possibility was a π-complex as shown in **A** below:

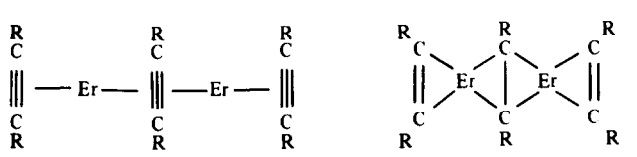

A **A'**

This structure has an alternate cyclometallopropene form (**A'**) which may be more reasonable for

these complexes considering the electropositive nature of the lanthanides. No π-complexes of lanthanides have yet been observed. However, η^2-coordination of C=N double bonds to trivalent Er and Y centers has been structurally characterized in formimidoyl complexes[145,146] and numerous examples of unsaturated hydrocarbons participating in lanthanide reactions are now known.[5,6,23,128,133]

Alternatively, the lanthanide may not interact with the unsaturated bond at all, but instead could insert into C—H bonds by oxidative addition as in **B**:

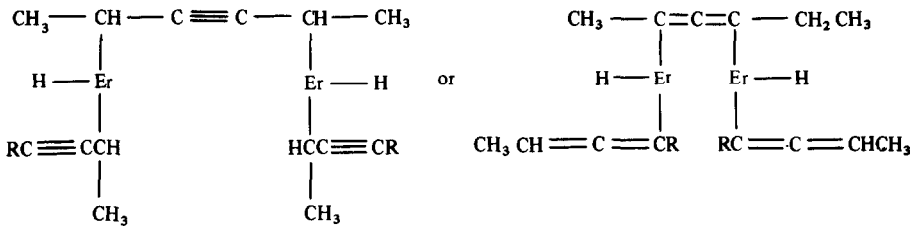

B

This type of C—H activation reaction subsequently was demonstrated in lanthanide metal vapor reactions with terminal alkynes[89] and C_5Me_5H.[47]

A third possibility for the reaction of a lanthanide metal with an alkyne is radical formation (structure **C**) as has been postulated for the Al–HC≡CH system based on matrix EPR spectroscopy.[147] If the monovalent Er in the initially formed radical oxidatively inserts into a C—H

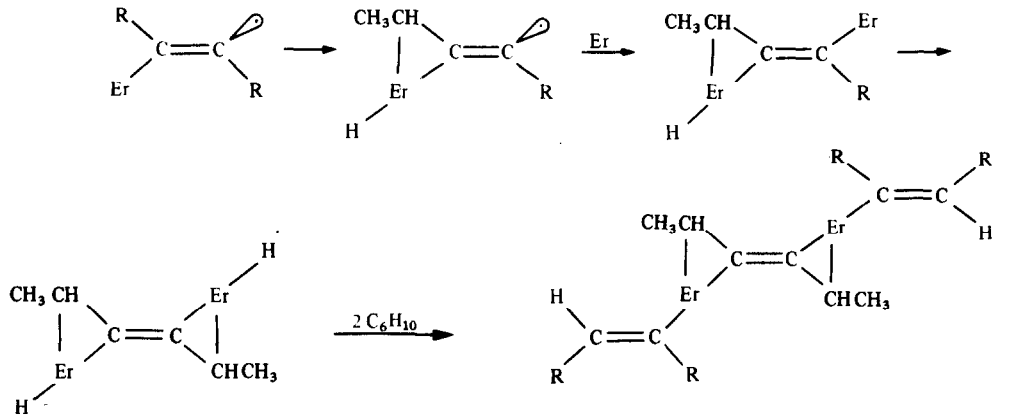

C

linkage and the resulting Er—H adds to excess 3-hexyne in the matrix, the radical-forming reaction can be rationalized to form a product with the exact formula determined experimentally (in contrast to structure **B** which is low in hydrogen). Subsequent studies of the reduction of $C_6H_5C{\equiv}CC_6H_5$[38] and $C_6H_5N{=}NC_6H_5$[126] by $(C_5Me_5)_2Sm(thf)_2$ [see reactions (51) and (52)] support this reaction pathway. Interestingly, the diphenylethyne and azobenzene products are intensely colored like the metal vapor reaction products. Structure **C** fits the available data best, but remains to be structurally established.

IV.2(c) *Reactions with unsubstituted alkenes and cyclopropane.* Since the reactions leading to structures **B** and **C** in the previous section required that substituents attached to the multiply-bonded carbon contain hydrogen for C—H activation, it was of interest to investigate metal vapor reactions involving smaller unsaturated hydrocarbons which lacked these potentially reactive sites. Accordingly, the reactions of ethene and 1,2-propadiene were surveyed with Sm, Yb and Er. The reactivity of two other small hydrocarbons, propene and cyclopropane, was also studied for comparison. These studies indicated an even wider range of reactivity was possible for the lanthanides.[148]

In contrast to the reactions discussed in the previous section, lanthanide metal vapor reactions with these smaller hydrocarbons did not provide soluble products (with the exception of the erbium product, $Er(C_3H_6)_3$ [reaction (59)]). Information on reaction pathways was obtained primarily by analyzing the products of hydrolysis of the metal vapor reaction product.

In ethene reactions, these data indicated that simple stable π-complexes (type A in the previous section) were not predominant products and that σ-bonded linkages, such as 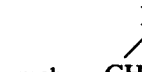 (type A' in the previous section) or $LnCH_2CH_2Ln$ were more likely.[148] The data suggested that alkene insertion and polymerization were occurring as in organolithium chemistry.[149] Lanthanide-based alkene polymerization[150] has been heavily studied subsequently.[151,152] Hydrolytic formation of CH_4 and homologated three-carbon products from the ethene reaction products suggested that the lanthanides had the capacity to break and reform C—C bonds. The presence of Ln—H moieties was also indicated and was consistent with activation of C—H bonds by oxidative addition.

The major reactivity patterns observed in ethene reactions were also found in reactions of lanthanide metal vapor with 1,2-propadiene, propene and cyclopropane, although the larger hydrocarbons gave less complex reaction products.[147] With 1,2-propadiene as the substrate, oxidative addition of CH and the formation of  appeared to be the major routes of reaction. Propene reacted with lanthanide metal vapor primarily by CH oxidative addition to form insoluble allyl hydride complexes. With Er, however, $[Er(C_3H_6)_3]_n$, was obtained. Hydrolysis products also included propyne which indicated that extensive dehydrogenation of propene occurred in this system.

In the cyclopropane–Er system, oxidative addition of C—H to form cyclopropyl Er hydride groups as well as ring cleavage and dehydrogenation reactions were inferred from the hydrolytic data. The fact that the relatively inert C—H bonds in cyclopropane could be activated by a lanthanide metal testifies to the high reactivity found in these systems.[148]

IV.2(d) *Reactions with readily reducible or acidic hydrocarbons.* The metal vapor reactions described in this section involve substrates which are readily convertible to stable organic anions. As described in Section III.2(a), YbC_8H_8 can be prepared by reacting Yb metal vapor with 1,3,5,7-C_8H_8.[51] When this reaction is carried out with lanthanide metals which do not have a readily accessible divalent state, for example, La, Ce, Nd or Er, a different type of product is obtained. Extraction with thf gives trivalent species consisting of a tight ion pair of $[(C_8H_8)Ln(thf)_2]^+$ and $[(C_8H_8)_2Ln]^-$.[51] Hence, complete oxidation of the metal can occur under these conditions with the proper reducible substrate.

When hydrocarbon substrates containing acidic hydrogen are used, oxidative addition of CH readily occurs. As described in Section III.2(f), ytterbium reacts with 1-hexyne to form alkynide hydride complexes $[HYb_2(C{\equiv}CC_4H_9)_3]_n$.[89] With Sm, trivalent alkynide hydride complexes are formed and may involve some dimetalated as well as monometalated alkynide ligands. The Er reaction also forms trivalent alkynide hydrides and is even more complex than the Sm system.[89] The complexity of these systems increases as the stability of the divalent oxidation state decreases.

The reactions of Sm metal vapor with C_5Me_5H and C_5Me_4EtH also give C—H oxidative addition products [see Sections III.2(d) and (e)].[47,74] For C_5Me_5H, a thf workup gives an unstable divalent hydride, $[(C_5Me_5)SmH(thf)_2]$, which transforms to $(C_5Me_5)_2Sm(thf)_2$.[47] Again, oxidative addition of C—H explains this result. When a thf-free workup of the Sm—C_5Me_5H reaction mixture was carried out, an interesting alkane-soluble product was isolated which contained nitrogen by elemental analysis. Addition of toluene to this product liberated N_2 gas and left $(C_5Me_5)_2Sm$. Unfortunately, definitive identification of the nitrogen complex was not possible.[74]

In a similar reaction to those above, Yb metal vapor reacts with C_5H_6 to form $(C_5H_5)_2Yb$.[153]

IV.2(e) *Catalytic activity of metal vapor products.* In the course of characterizing the lanthanide metal vapor 3-hexyne products, it was discovered that these complexes had the capacity to initiate catalytic hydrogenation of alkynes to alkenes and alkanes.[62] A variety of lanthanide metal vapor products have been found to generate catalytic hydrogenation systems. Not only the 3-hexyne

reaction products, but also the products of lanthanide metal cocondensations with 1-hexyne, 2,3-dimethylbutadiene, $(CH_3)_3SiC{\equiv}CSi(CH_3)_3$ and $P(C_6H_5)_3$ are able to do this.[154] Using 3-hexyne as a substrate, these catalytic systems generally give high yields of *cis*-3-hexene, many with >95% stereospecificity.

Although catalytic hydrogenation of alkynes can be accomplished in many other ways, this catalytic system was significant because it was the first time an *f*-element complex had been observed to catalytically activate hydrogen in homogeneous solution.[62] The result had additional importance because the metal hydride complexes presumably involved in the catalyses provided the first evidence for the existence of discrete molecular lanthanide hydrides. The existence of lanthanide hydride complexes subsequently was demonstrated crystallographically[22] and fully characterized lanthanide hydrides were shown to have catalytic activity in hydrogenation reactions.[38] High levels of catalytic hydrogenation activity have subsequently been observed under optimized conditions.[128]

IV.3. *Bulk metal, metal amalgam, and activated metal reactions*

Lanthanide metals in the form of powders, filings or ingots have been used in a variety of systems as reagents. In some cases, the metal is "activated" by addition of Hg or $HgCl_2$ to form an amalgam. When ytterbium is used, divalent products are often obtained and many of these reactions have been discussed in Section III.2. These include oxidation reactions using alkyl and cyclopentadienyl halide reagents, transmetalation reactions with cyclopentadienyl, aryl, alkynyl, carboranyl, transition-metal, mercury and thallium reagents, and reductions of $(C_5H_5)_2YbCl$ and $(C_5H_5)_3Yb$ with Yb. The latter two reductions and some of the transmetalations can give clean reactions, whereas the RX reactions are generally complex. Extension of these reactions to samarium tends to give more complex results due to the formation of Sm(III) products. As is observed in metal vapor reactions with terminal alkynes, the complexity of these oxidations often increases with decreasing stability of the divalent oxidation state.

Lanthanide elements which do not have a readily accessible divalent oxidation state also participate in oxidations of the type described above to give trivalent products. The reactions of Ce and La with alkyl and aryl iodides[94] and Pr, Nd, Gd and Ho with triphenylmethylchloride, benzyl chloride and phenyl bromide[155] have been studied. Mixtures of colored products corresponding to R_aLnX_{3-a} are thought to be present. In a related approach the reactions of La, Tm and Yb with C- and B-mercuriocarboranes have been investigated.[100] Tris(cyclopentadienyl) complexes of Ce, Nd, Gd and Er have been prepared from the metals and thallous cyclopentadienides.[54]

A variety of lanthanide metals have been reacted with transition-metal reagents including $Hg[Co(CO)_4]_2$,[156] $Mn(CO)_5Br$,[157] $C_3H_5Fe(CO)_3I$,[157] $C_5H_5Cr(CO)_3HgCl$[157] and $[(C_5H_5)Mo(CO)_3]_2$.[157,158] These are complex reactions and only recently has a product been crystallographically characterized. The reaction of "lanthanum amalgam" with $[(C_5H_5)Mo(CO)_3]_2$ forms $(thf)_5La[(\mu\text{-}OC)Mo(CO)_2(C_5H_5)]_3 \cdot (thf)$.[158]

Reduction of $PrCl_3$ with K in thf gives an activated reduced form of praseodymium which has an organometallic chemistry. Treatment of the reduced praseodymium with 1,5-cyclooctadiene at room temperature gives products from which 1,3,5,7-cyclooctatetraene can be isolated upon oxidation.[159] The exact oxidation state of the lanthanide was not determined. The C_8H_{12} to $C_8H_8^{2-}$ conversion which apparently occurs led to the development of a high-temperature K-based preparation of 1,3,5,7-C_8H_8 from 1,5-C_8H_{12}.[160]

IV.4. *General principles governing zero-valent lanthanide chemistry*

Since little structural evidence is available on most of the products reported in Section IV, this area of low-valent lanthanide chemistry cannot be analyzed as precisely as was done for trivalent and divalent systems in Sections II.2 and III.4, respectively. The identity of many of the products discussed in Section IV remains unknown. Given what we now know about the reactivity/stability of sterically unsaturated trivalent organolanthanides (Section II.2), and strongly reducing divalent lanthanides (Section III.3) it is not surprising that the zero-valent lanthanide systems would be difficult to fully characterize. However, the goal of much of this chemistry, namely to broaden

organolanthanide chemistry in general, has been achieved.

These studies demonstrated several key aspects about the capacity of the lanthanides to participate in organometallic chemistry. The lanthanides were clearly shown to interact with the unsaturated hydrocarbons, a class of ligands previously uncommon in lanthanide chemistry. The lanthanides were shown to have the potential to effect a variety of interesting transformations on hydrocarbon substrates including C—H activation by oxidative addition, two-electron reduction of unsaturated C—C bonds, C—C cleavage, oligomerization, dehydrogenation, homologation and catalytic hydrogenation. The metal vapor reactions generated products which could catalytically activate hydrogen and which could probably generate molecular lanthanide hydride complexes.

The metal vapor syntheses in particular generated a variety of unusual organolanthanide complexes and "defined a set of conditions under which a variety of remarkable hydrocarbon activation reactions take place in the presence of the lanthanide metals".[148] These studies demonstrated the potential of the lanthanide metals and indicated areas where further development should take place in the field. As stated previously "the challenge in this area is to control this reactivity so that it can be used selectively"[148] and this is being done.

V. CONCLUSIONS

The organometallic chemistry of the lanthanide metals in low oxidation states has grown enormously since the isolated reports of the first complexes of this type appeared in the 1960s. The greatest development has occurred in the past few years and the rate of growth shows no signs of diminishing. The field is still too young to have a definable scope and potential at the present time, although recent results are starting to provide a basis for developing general principles.

The utility of the elemental metals in organolanthanide chemistry has been clearly shown in terms of demonstrating reactivity and the potential of lanthanides in general. The value of zero-valent lanthanide chemistry in forming isolable complexes has yet to be realized.

Although only three of the lanthanide elements have accessible divalent oxidation states, it is clear that divalent chemistry will be an important component of the organolanthanide field. The strong reducing capacity of Sm(II) will continue to distinguish it not only as a special lanthanide, but also as a special reducing reagent in chemistry in general. Clearly, low oxidation state lanthanide complexes have much to offer the field of organometallic chemistry.

Acknowledgements—The research results from my laboratory described in this Report were achievable through the support of the National Science Foundation, the donors of the Petroleum Research Fund administered by the American Chemical Society, and the Division of Basic Energy Sciences of the Department of Energy. I am grateful to those agencies, to the Camille and Henry Dreyfus Foundation for a Teacher–Scholar Grant, and to the Alfred P. Sloan Foundation for a Research Fellowship. I am also grateful to all of the students who participated in my research program.

REFERENCES

1. T. J. Kealy and P. L. Pauson, *Nature (London)* 1951, **168**, 1039; S. A. Miller, J. A. Tebboth and J. F. Tremaine, *J. Chem. Soc.* 1952, 632–3; G. Wilkinson, M. Rosenblum, M. C. Whiting and R. B. Woodward, *J. Am. Chem. Soc.* 1952, **74**, 2125; E. O. Fischer and W. Pfab, *Z. Naturforsch.* 1952, **7B**, 377.
2. J. M. Birmingham and G. Wilkinson, *J. Am. Chem. Soc.* 1956, **78**, 42.
3. W. J. Evans, S. C. Engerer, P. A. Piliero and A. L. Wayda, In *Fundamental Research in Homogeneous Catalysis* (Edited by M. Tsutsui) Vol. 3, p. 941. Plenum Press, New York (1979).
4. J. H. Forsberg and T. Moeller, In *Gmelin Handbook of Inorganic Chemistry, 8th Edn*, Sc, Y, La–Lu, *Part D6* (Edited by T. Moeller, U. Kruerke and E. Schleitzer-Rust), p. 137 (and references therein). Springer, Berlin (1983).
5. W. J. Evans, *Adv. Organomet. Chem.* 1985, **24**, 131 (and references therein).
6. P. L. Watson and G. W. Parshall, *Acc. Chem. Res.* 1985, **18**, 51 (and references therein).
7. H. B. Kagan and J. L. Namy, In *Handbook on the Physics and Chemistry of Rare Earths* (Edited by K. A. Gschneidner, Jr and L. Eyring), Vol. 6, Chap. 50. Elsevier, Amsterdam (1984).
8. T. J. Marks and R. D. Ernst, In *Comprehensive Organometallic Chemistry* (Edited by G. Wilkinson, F. G. A. Stone and E. W. Abel), Chap. 21. Pergamon Press, Oxford (1982).
9. T. J. Marks, *Prog. Inorg. Chem.* 1978, **24**, 51.

10. W. J. Evans, In *The Chemistry of the Metal–Carbon Bond* (Edited by F. R. Hartley and S. Patai), Chap. 12. Wiley, New York (1982).
11. A. J. Freeman and R. E. Watson, *Phys. Rev.* 1976, **9**, 217; H. M. Crosswhite and A. P. Paszek, personal communication.
12. T. Moeller, In *Comprehensive Inorganic Chemistry* (Edited by J. C. Bailar, Jr), Vol. 4, Chap. 44. Pergamon Press, Oxford (1973).
13. G. H. Dieke, In *Spectra and Energy Levels of Rare Earth Ions in Crystals* (Edited by H. M. Crosswhite and H. Crosswhite). Wiley, New York (1968).
14. W. T. Carnall, In *Handbook on the Physics and Chemistry of Rare Earths* (Edited by K. A. Gschneidner, Jr and L. Eyring), Vol. 3, Chap. 24. Elsevier, Amsterdam (1979).
15. E. O. Fischer and H. Fischer, *J. Organomet. Chem.* 1965, **3**, 181.
16. S. Manastyrskyj and M. Dubeck, *Inorg. Chem.* 1964, **3**, 1647.
17. C. M. Lukehart, *Fundamental Transition Metal Organometallic Chemistry*. Brooks/Cole, Belmont, CA (1985).
18. F. A. Cotton and G. Wilkinson, *Advanced Inorganic Chemistry*, 4th Edn. Wiley. New York (1980).
19. J. E. Huheey, *Inorganic Chemistry*, 3rd Edn, p. 146 (and references therein). Harper & Row, New York (1983).
20. R. D. Fischer and L. Xing-Fu, *J. Less Common Met.* 1985, **112**, 303.
21. J. Holton, M. F. Lappert, D. G. H. Ballard, R. Pearce, J. L. Atwood and W. E. Hunter, *J. Chem. Soc., Dalton Trans.* 1979, 54.
22. W. J. Evans, J. H. Meadows, A. L. Wayda, W. E. Hunter and J. L. Atwood, *J. Am. Chem. Soc.* 1982, **104**, 2008.
23. W. J. Evans, J. H. Meadows, W. E. Hunter and J. L. Atwood, *J. Am. Chem. Soc.* 1984, **106**, 1291.
24. W. J. Evans, J. H. Meadows and T. P. Hanusa, *J. Am. Chem. Soc.* 1984, **106**, 4454.
25. H. A. Zinnen, J. J. Pluth and W. J. Evans, *J. Chem. Soc. Chem. Commun.* 1980, 810.
26. W. J. Evans, R. Dominguez and T. P. Hanusa, *Organometallics* 1986, **5**, 263.
27. W. J. Evans, A. L. Wayda, W. E. Hunter and J. L. Atwood, *J. Chem. Soc., Chem. Commun.* 1981, 292.
28. H. Schumann, W. Genthe, N. Bruncks and J. Pickardt, *Organometallics* 1982, **1**, 1194.
29. E. C. Baker, L. D. Brown and K. N. Raymond, *Inorg. Chem.* 1975, **14**, 1376.
30. R. E. Maginn, S. Manastryskyj and M. Dubeck, *J. Am. Chem. Soc.* 1963, **85**, 672.
31. H. G. Brittain, J. H. Meadows and W. J. Evans, *Organometallics* 1985, **4**, 1585.
32. M. F. Lappert, A. Singh, J. L. Atwood and W. E. Hunter, *J. Chem. Soc., Chem. Commun.* 1981, 1190.
33. Z. Jin, Y. Lui and W. Chen, personal communication.
34. W. J. Evans, T. T. Peterson, M. D. Rausch, W. E. Hunter, H. Zhang and J. L. Atwood, *Organometallics* 1985, **4**, 554.
35. P. L. Watson and D. C. Roe, *J. Am. Chem. Soc.* 1982, **104**, 6471.
36. P. L. Watson, *J. Chem. Soc., Chem. Commun.* 1983, 276.
37. P. L. Watson, *J. Am. Chem. Soc.* 1983, **105**, 6491.
38. W. J. Evans, I. Bloom, W. E. Hunter and J. L. Atwood, *J. Am. Chem. Soc.* 1983, **105**, 1401.
39. W. J. Evans and J. W. Grate, unpublished results.
40. Chapter 12 in Ref. 13.
41. D. S. McClure and Z. Kiss, *J. Chem. Phys.* 1963, **39**, 3251; Z. J. Kiss and P. N. Yocom, *J. Chem. Phys.* 1964, **41**, 1511.
42. N. B. Mikheev, *Inorg. Chim. Acta* 1984, **94**, 241.
43. A. Greco, S. Cesca and G. Bertolini, *J. Organomet. Chem.* 1976, **113**, 321.
44. H. R. Bronstein, *J. Phys. Chem.* 1969, **73**, 1320.
45. L. R. Morss, *Chem. Rev.* 1976, **76**, 827 (and references therein); S. G. Bratsch and J. J. Lagowski, *J. Phys. Chem.* 1985, **89**, 3317.
46. P. G. Varlashkin and J. R. Peterson, *J. Less-Common Met.* 1983, **94**, 333.
47. W. J. Evans, I. Bloom, W. E. Hunter and J. L. Atwood, *J. Am. Chem. Soc.* 1981, **103**, 6507.
48. S. A. Cotton and F. A. Hart, *The Heavy Transiton Elements*. Wiley, New York (1975).
49. W. J. Evans and M. A. Hozbor, in preparation.
50. R. G. Hayes and J. L. Thomas, *J. Am. Chem. Soc.* 1969, **91**, 6876.
51. C. W. DeKock, S. R. Ely, T. E. Hopkins and M. A. Brault, *Inorg. Chem.* 1978, **17**, 625.
52. R. G. Hayes and J. L. Thomas, *Inorg. Chem.* 1969, **8**, 2521.
53. F. Calderazzo, R. Pappalardo and S. Losi, *J. Inorg. Nucl. Chem.* 1966, **28**, 987.
54. G. B. Deacon, A. J. Koplick and T. D. Tuong, *Polyhedron* 1982, **1**, 423; G. B. Deacon, A. J. Koplick and T. D. Tuong, *Aust. J. Chem.* 1984, **37**, 517.
55. G. Z. Suleimanov, L. F. Rybakova, Ya. A. Nuriev, T. Kh. Kurbanov and I. P. Beletskaya, *J. Organomet. Chem.* 1982, **235**, C19.
56. J. L. Namy, P. Girard and H. B. Kagan, *Nouv. J. Chim.* 1981, **5**, 479.

57. G. B. Deacon and R. H. Newnham, *Aust. J. Chem.* 1985, **38**, 1757.
58. G. W. Watt and E. W. Gillow, *J. Am. Chem. Soc.* 1969, **91**, 775.
59. G. Z. Suleimanov, T. Kh. Kurbanov, Ya. A. Nuriev, L. F. Rybakova and I. P. Beletskaya, *Dokl. Chem.* 1982, **265**, 254.
60. G. B. Deacon, G. N. Pain and T. D. Tuong, *Polyhedron* 1985, **4**, 1149.
61. G. B. Deacon, P. I. MacKinnon, T. W. Hambley and J. C. Taylor, *J. Organomet. Chem.* 1983, **259**, 91.
62. W. J. Evans, S. C. Engerer, P. A. Piliero and A. L. Wayda, *J. Chem. Soc., Chem. Commun.* 1979, 1007.
63. M. F. Lappert, P. I. W. Yarrow, J. L. Atwood, R. Shakir and J. Holton, *J. Chem. Soc., Chem. Commun.* 1980, 987.
64. W. J. Evans and H. A. Zinnen, unpublished results.
65. P. T. Wolczanski and J. E. Bercaw, *Acc. Chem. Res.* 1980, **13**, 121 (and references therein).
66. J. M. Manriquez, D. R. McAlister, R. D. Sanner and J. E. Bercaw, *J. Am. Chem. Soc.* 1978, **100**, 2716 (and references therein).
67. P. J. Fagan, J. M. Manriquez, E. A. Maata, A. M. Seyam and T. J. Marks, *J. Am. Chem. Soc.* 1981, **103**, 6650.
68. T. J. Marks, *Science* 1982, **217**, 989.
69. T. D. Tilley, R. A. Andersen, B. Spencer, H. Ruben, A. Zalkin and D. H. Templeton, *Inorg. Chem.* 1980, **19**, 2999.
70. P. L. Watson, *J. Chem. Soc., Chem. Commun.* 1980, 652.
71. P. L. Watson, J. F. Whitney and R. L. Harlow, *Inorg. Chem.* 1981, **20**, 3271.
72. T. D. Tilley, R. A. Andersen, B. Spencer and A. Zalkin, *Inorg. Chem.* 1982, **21**, 2647.
73. A. L. Wayda, J. L. Dye and R. D. Rogers, *Organometallics* 1984, **3**, 1605.
74. W. J. Evans, I. Bloom, W. E. Hunter and J. L. Atwood, *Organometallics* 1985, **4**, 112.
75. W. J. Evans, J. W. Grate, H. W. Choi, I. Bloom, W. E. Hunter and J. L. Atwood, *J. Am. Chem. Soc.* 1985, **107**, 941.
76. A. Streitwieser, Jr, U. Muller-Westerhoff, G. Sonnichsen, F. Mares, D. G. Morrell, K. O. Hodgson and C. A. Harmon, *J. Am. Chem. Soc.* 1973, **95**, 8644.
77. K. O. Hodgson, F. Mares, D. F. Starks and A. Streitwieser, Jr, *J. Am. Chem. Soc.* 1973, **95**, 8650.
78. W. J. Evans, L. A. Hughes and T. P. Hanusa, P. *J. Am. Chem. Soc.* 1984, **106**, 4270.
79. W. J. Evans, L. A. Hughes and T. P. Hanusa, *Organometallics* 1986, **5**, 1285.
80. J. D. Dunitz, L. E. Orgel and A. Rich, *Acta Cryst.* 1956, **9**, 393.
81. D. P. Freyberg, J. L. Robbins, K. N. Raymond and J. C. Smart, *J. Am. Chem. Soc.* 1979, **101**, 892.
82. J. V. Ortiz and R. Hoffmann, *Inorg. Chem.* 1985, **24**, 2095.
83. A. Haaland, personal communication.
84. A. Buchler, J. L. Stauffer and W. Klemperer, *J. Am. Chem. Soc.* 1964, **86**, 4544.
85. M. Guido and G. Gigli, *J. Chem. Phys.* 1976, **65**, 1397.
86. P. Jutzi, F. Kohl, P. Hofmann, C. Krüger and Y.-H. Tsay, *Chem. Ber.* 1980, **113**, 757; J. L. Atwood, W. E. Hunter, A. H. Cowley, R. A. Jones and C. A. Stewart, *J. Chem. Soc., Chem. Commun.* 1981, 925.
87. G. B. Deacon and A. J. Koplick, *J. Organomet. Chem.* 1976, **146**, C43; G. B. Deacon, A. J. Koplick and T. D. Tuong, *Aust. J. Chem.* 1982, **35**, 941.
88. E. Murphy and G. E. Toogood, *Inorg. Nucl. Chem. Lett.* 1971, **75**, 755.
89. W. J. Evans, S. C. Engerer and K. M. Coleson, *J. Am. Chem. Soc.* 1981, **103**, 6672.
90. J. L. Atwood, W. E. Hunter, A. L. Wayda and W. J. Evans, *Inorg. Chem.* 1981, **20**, 4115.
91. W. J. Evans, I. Bloom, W. E. Hunter and J. L. Atwood, *Organometallics* 1983, **2**, 709.
92. J. M. Boncella, T. D. Tilley and R. A. Andersen, *J. Chem. Soc., Chem. Commun.* 1984, 710.
93. R. D. Fischer and G. Bielang, *J. Organomet. Chem.* 1980, **191**, 61.
94. D. F. Evans, G. V. Fazakerley and R. F. Phillips, *J. Chem. Soc. A* 1971, 1931.
95. G. B. Deacon and D. G. Vince, *J. Organomet. Chem.* 1976, **112**, C1; G. B. Deacon, W. D. Raverty and D. G. Vince, *J. Organomet. Chem.* 1977, **135**, 103.
96. G. B. Deacon, P. I. Mackinnon and T. D. Tuong, *Aust. J. Chem.* 1983, **36**, 43.
97. G. Z. Suleimanov, V. N. Khandozhko, P. V. Petrovskii, R. Yu. Mekhdrev, E. K. Nadezda and I. P. Beletskaya, *J. Chem. Soc., Chem. Commun.* 1985, 596.
98. G. B. Deacon, A. H. Koplick, W. D. Raverty and D. G. Vince, *J. Organomet. Chem.* 1979, **182**, 121 (and references therein).
99. G. Z. Suleimanov, P. V. Petrovskii, Y. S. Bogachev, I. L. Zhuravleva, E. I. Fedin and I. P. Beletskaya, *J. Organomet. Chem.* 1984, **262**, C35.
100. G. Z. Suleimanov, V. I. Bregadze, N. A. Koval'chuk and I. P. Beletskaya, *J. Organomet. Chem.* 1982, **235**, C17.
101. G. Z. Suleimanov, V. I. Bregadze, N. A. Koval'chuk, Kh. S. Khalilov and I. P. Beletskaya, *J. Organomet. Chem.* 1983, **255**, C5.
102. T. D. Tilley, R. A. Andersen and A. Zalkin, *J. Am. Chem. Soc.* 1982, **104**, 3725.

103. T. D. Tilley, R. A. Andersen and A. Zalkin, *Inorg. Chem.* 1984, **23**, 2271.
104. H. A. Zinnen and W. J. Evans, unpublished results; H. A. Zinnen, Ph.D. dissertation, University of Chicago (1982).
105. T. D. Tilley and R. A. Andersen, *Inorg. Chem.* 1981, **20**, 3267.
106. W. J. Evans, J. W. Grate, K. R. Levan, I. Bloom, T. T. Peterson, R. J. Doedens, H. Zhang and J. L. Atwood, *Inorg. Chem.* 1986, **25**, 3614.
107. R. G. Finke, S. R. Keenan, D. A. Schiraldi and P. L. Watson, *Organometallics* 1986, **5**, 598.
108. G. B. Deacon, G. D. Fallon, P. I. MacKinnon, R. H. Newnham, G. N. Pain, T. D. Tuong and D. L. Wilkinson, *J. Organomet. Chem.* 1981, **277**, C21.
109. W. J. Evans, J. W. Grate, I. Bloom, W. E. Hunter and J. L. Atwood, *J. Am. Chem. Soc.* 1985, **107**, 405.
110. R. E. Dessy, R. B. King and M. Waldrop, *J. Am. Chem. Soc.* 1966, **88**, 5112.
111. W. J. Evans and W. M. Cwirla, unpublished results.
112. T. D. Tilley and R. A. Andersen, *J. Chem. Soc., Chem. Commun.* 1981, 985.
113. J. M. Boncella and R. A. Andersen, *Inorg. Chem.* 1984, **23**, 432.
114. T. D. Tilley and R. A. Andersen, *J. Am. Chem. Soc.* 1982, **104**, 1772.
115. R. A. Andersen, INOR 10, 190th American Chemical Society National Meeting, Chicago, IL (1985).
116. W. J. Evans, I. Bloom, J. W. Grate, L. A. Hughes, W. E. Hunter and J. L. Atwood, *Inorg. Chem.* 1985, **24**, 4620.
117. W. J. Evans, J. W. Grate, L. A. Hughes, H. Zhang and J. L. Atwood, *J. Am. Chem. Soc.* 1985, **107**, 3728.
118. H. H. Storch, N. Golumbic and R. B. Anderson, *The Fischer–Tropsch Reaction and Related Syntheses.* Wiley, New York (1951). V. Ponec, *Catal. Rev.—Sci. Eng.* 1978, **18**, 1515; C. Masters, *Adv. Organomet. Chem.* 1979, **17**, 61; H. H. Kung, *Catal. Rev.—Sci. Eng.* 1980, **22**, 235; K. Klier, *Adv. Catal.* 1982, **31**, 243; B. D. Dombek, *Adv. Catal.* 1983, **322**, 325.
119. G. Erker, *Acc. Chem. Res.* 1984, **17**, 103.
120. D. A. Katahira, K. G. Moloy and T. J. Marks, *Organometallics* 1982, **1**, 1723 (and references therein).
121. W. J. Evans, J. W. Grate and R. J. Doedens, *J. Am. Chem. Soc.* 1985, **107**, 1671.
122. W. Büchner, *Chem. Ber.* 1966, **99**, 1485; W. Büchner, *Helv. Chim. Acta* 1963, **46**, 2111.
123. J. E. Bercaw, R. H. Marvich, L. G. Bell and H. H. Brintzinger, *J. Am. Chem. Soc.* 1972, **94**, 1219; M. Bottrill, P. D. Gavens and J. McMeeking, In *Comprehensive Organometallic Chemistry* (Edited by G. W. Wilkinson, F. G. A. Stone and E. W. Abel), Chap. 22.2. Pergamon Press, Oxford (1982).
124. W. J. Evans, D. K. Drummond and T. A. Ulibarri, unpublished results.
125. H. O. House, *Modern Synthetic Reactions*, p. 205 (and references therein). W. A. Benjamin, Menlo Park, CA (1972).
126. W. J. Evans, D. K. Drummond, S. G. Bott and J. L. Atwood, *Organometallics*, in press.
127. M. Brookhart and M. L. H. Green, *J. Organomet. Chem.* 1983, **250**, 395.
128. G. Jeske, H. Lauke, H. Mauermann, H. Schumann and T. J. Marks, *J. Am. Chem. Soc.* 1985, **107**, 8111.
129. W. J. Evans, D. K. Drummond, L. A. Hughes, H. Zhang and J. L. Atwood, *J. Am. Chem. Soc.* 1986, **108**, 1722.
130. W. J. Evans, A. L. Wayda, W. E. Hunter and J. L. Atwood, *J. Chem. Soc., Chem. Commun.* 1981, 706.
131. P. L. Watson and T. Herskovitz, *ACS Symp. Ser.* 1983, **212**, 459.
132. W. J. Evans and T. P. Hanusa, unpublished results.
133. W. J. Evans, T. A. Ulibarri and T. P. Hanusa, unpublished results.
134. W. J. Evans and R. E. King, III, unpublished results.
135. W. J. Evans, S. C. Engerer and A. C. Neville, *J. Am. Chem. Soc.* 1978, **100**, 331.
136. P. A. Skell and M. J. McGlinchey, *Angew. Chem., Int. Ed. Engl.* 1975, **14**, 195.
137. P. L. Timms and T. W. Turney, *Adv. Organomet. Chem.* 1977, **15**, 53.
138. K. J. Klabunde, *Chemistry of Free Atoms and Particles.* Academic Press, New York (1980).
139. J. R. Blackborow and D. Young, *Metal Vapor Synthesis in Organometallic Chemistry.* Springer, Berlin (1979).
140. M. Moskovits and G. A. Ozin (Eds), *Cryochemistry.* Wiley, New York (1976).
141. W. C. Martin, R. Zalubas and L. Hogan, *Atomic Energy Levels. The Rare Earth Elements.* National Standard Reference Data Series, No. 60, National Bureau of Standards (U.S.), Washington, DC (1978).
142. R. K. Sheline and J. L. Slater, *Angew. Chem., Int. Ed. Engl.* 1975, **14**, 309 (and references therein).
143. M. J. McGlinchey and P. S. Skell, in Ref. 140; P. S. Skell, *Proc. Int. Congr. Pure Appl. Chem.* 1971, **23**, 215.
144. W. J. Evans, In *The Rare Earths in Modern Sciences and Technology* (Edited by G. J. McCarthy, J. J. Rhyne and H. E. Silber), Vol. 3, p. 61. Plenum Press, New York (1982).
145. W. J. Evans, J. H. Meadows, W. E. Hunter and J. L. Atwood, *Organometallics* 1983, **2**, 1252.
146. W. J. Evans, T. P. Hanusa, J. H. Meadows, W. E. Hunter and J. L. Atwood, *Organometallics*, in press.
147. P. H. Kasai, D. McLeod, Jr and T. Watanabe, *J. Am. Chem. Soc.* 1977, **99**, 3521.
148. W. J. Evans, K. M. Coleson and S. C. Engerer, *Inorg. Chem.* 1981, **20**, 4320.

149. V. Rautenstrauch, *Angew. Chem., Int. Ed. Engl.* 1975, **14**, 259.
150. D. G. Ballard, A. Courtis, J. Holton, J. McMeeking and R. Pearce, *J. Chem. Soc., Chem. Commun.* 1978, 994.
151. P. L. Watson, *J. Am. Chem. Soc.* 1982, **104**, 337.
152. P. L. Watson and D. C. Roe, *J. Am. Chem. Soc.* 1982, **104**, 6471.
153. W. J. Evans and S. C. Engerer, unpublished results.
154. W. J. Evans, I. Bloom and S. C. Engerer, *J. Catal.* 1983, **84**, 468.
155. B. A. Dolgoplosk, E. I. Tinyakova, I. N. Markevich, T. V. Soboleva, G. M. Chernenko, O. K. Sharaev and V. A. Yakovlev, *J. Organomet. Chem.* 1983, **255**, 71.
156. R. S. Marianelli and M. T. Durney, *J. Organomet. Chem.* 1971, **32**, C41.
157. A. E. Crease and P. Legzdins, *J. Chem. Soc., Chem. Commun.* 1973, 775.
158. A. A. Pasynskii, I. L. Eremenko, G. Z. Suleimanov, Yu. A. Niriev, I. P. Beletskaya, V. E. Shklover and Yu. T. Struchkov, *J. Organomet. Chem.* 1984, **266**, 45.
159. W. J. Evans, A. L. Wayda, C. W. Chang and W. M. Cwirla, *J. Am. Chem. Soc.* 1978, **100**, 333.
160. W. J. Evans, D. J. Wink, A. L. Wayda and D. A. Little, *J. Org. Chem.* 1981, **46**, 3925.

Polyhedron Vol. 6, No. 5, pp. 837–839, 1987
Printed in Great Britain

0277–5387/87 $3.00+.00

SYNTHESIS AND CHARACTERIZATION OF DICHLORODICARBONYLRUTHENIUM(II) COMPLEXES OF OXYGEN, SULPHUR AND NITROGEN DONOR LIGANDS

A. O. BAGHLAF,* M. ISHAQ and A. K. A. RASHED

King Abdulaziz University, College of Science Department of Chemistry, P.O. Box 9028, Jeddah 21413, Kingdom of Saudi Arabia

(*Received* 7 *April* 1986; *accepted after revision* 27 *June* 1986)

Abstract—Complexes of dichlorodicarbonylruthenium(II) of formula $[RuCl_2(CO)_2L_2]$ (L = tetramethylthiourea, monomethylthiourea, dimethylthiourea, pyridine 2-thiol, piperidine or pyridine) and $[RuCl_2(CO)_2L']$ (L' = 1,2-diaminoethane or tetramethylurea), have been prepared. The complexes were characterized by their IR, NMR and elemental analyses.

Dihalodicarbonylruthenium(II) compounds were first reported by Manchot and Konig[1] in 1924. Wilkinson[2,3] first reported compounds of type $[RuCl_2(CO)_2L_2]$ (L = PPh_3 or $AsPh_3$). Colton and Farthing[4] and later Cleare and Griffith[5] have reported that refluxing $RuCl_3 \cdot xH_2O$ with formic acid produced $[RuCl_2(CO)_2]_n$ almost quantitatively. Since then halocarbonylruthenium(II) $\{[RuX_2(CO)_2]_n\}$ has proved to be a very useful precursor for the synthesis of a variety of complexes.[6] Here we report the synthesis of dichlorodicarbonylruthenium(II) complexes of type $[RuCl_2(CO)_2L_2]$ [L = tetramethylthiourea (TMTU), monomethylthiourea (MMTU), dimethylthiourea (DMTU) or pyridine 2-thiol (PYT)]. These ligands are monodentate and it has been suggested on the basis of IR spectroscopic data that coordination of these ligands to the metal is through the S atom.[7] In the case of $[RuCl_2(CO)_2(PIP)_2]$, (PIP = piperidine), $[RuCl_2(CO)_2(PY)_2]$ (PY = pyridine) and $[RuCl_2(CO)_2(en)]$, (en = 1,2-diaminoethane), the coordination to the metal is through the N atom. All the complexes were insoluble in common organic solvents such as benzene, petroleum ether and carbon tetrachloride, but are soluble or slightly soluble in chloroform, ethanol, acetonitrile and tetrahydrofuran (THF). All the complexes were stable, yellow or pale yellow solids except for complex **3**, which was a waxy solid, and all can be handled in air for a short time.

EXPERIMENTAL

The salt "$RuCl_3 \cdot xH_2O$" and substituted urea, thioureas and amines were purchased from Fluka Inc. and were used without further purification.

IR spectra were measured (KBr pellets) using a Zeiss Model IMR-16 spectrophotometer. Proton magnetic resonance spectra were recorded on a Varian EM 390–90-MHz NMR spectrometer.

Elemental analyses were carried out by the microanalysis laboratory of King Abdulaziz University, Jeddah.

$[RuCl_2(CO)_2]_n$ was prepared as reported.[4]

Preparation of $[RuCl_2(CO)_2(TMTU)_2]$

A typical reaction is described.

To a solution of $[RuCl_2(CO)_2]_n$ (0.5 g, 2.2 mmol) dissolved in THF (30 cm^3) was added tetramethylthiourea (0.6 g, 4.5 mmol). The mixture was refluxed for 1 h. During this period some orange yellow crystals separated out. The contents were then cooled and the addition of petroleum ether separated out the orange yellow crystals of the product $\{[RuCl_2(CO)_2 \cdot (TMTU)_2]\}$ almost quantitatively. This was washed twice with petroleum ether, and dried *in vacuo*. Yield 1.08 g (98%). M.p. 243°C.

*Author to whom correspondence should be addressed.

All the complexes shown in Table 1 were prepared by the same general method from $[RuCl_2(CO)_2]_n$ and a monodentate ligand in a 1:2 mole ratio and a bidentate ligand in a 1:1 mole ratio, respectively. The preparation of complex **8** using a different method has been reported.[9]

RESULTS AND DISCUSSION

The reaction of $[RuCl_2(CO)_2]_n$ with TMTU or other monodentate ligands in a 1:2 mole ratio gives stable yellow crystalline solids.

IR spectra of all the complexes were determined as KBr pellets and the low value of the terminal metal–carbonyl (M–CO) stretching frequencies observed in all the complexes (Table 1) may be attributed to a flow of electron density from the ligand to the metal causing a decrease in the M.⊳CO stretching frequencies. The presence of only two strong CO bands indicates that the two CO groups are *cis*.[8]

The ambidentate nature of substituted thiourea and its mode of coordination with transition metals has been a subject of controversy. Schafer and Curran[7] have suggested for TMTU complexes that an increase in the frequency to 1504 cm^{-1} (which they claim is mainly due to the N.C.N antisymmetrical stretching vibration) and a decrease to 1126 cm^{-1} (which is mainly due to C=S band) means that ligand–metal coordination is through the S atom. Therefore complexes **2**, **4** and **5** also show a lower C=S value ($\sim$10–20 cm^{-1}) compared to the free ligands. A similar behaviour has been noticed in the case of the pyridine 2-thiol complex (**6**). We have shown earlier a similar trend for these ligands with molybdenum carbonyl[10] and uranyl[11] complexes.

The low N.H stretching frequencies of PIP (acting as a monodentate ligand) in complex **7** and en (a bidentate ligand) in complex **9** suggest that these ligands are coordinated to the metal through N atoms.

The NMR spectrum (Table 2) of the dichlorodicarbonylruthenium(II)–TMTU amplex in $CDCl_3$ shows only a single peak at δ 3.3 for the four methyl groups. If bonding of the ligand to the metal occurred through an N atom rather than an S atom then the methyl protons of the complexed dimethylamino group should have a chemical shift different from that of the methyl protons of the uncomplexed dimethylamino group. On the other hand, the NMR spectrum of the dichlorodicarbonylruthenium(II)–TMU complex in $CDCl_3$ shows a low-field chemical shift and splitting of the methyl protons of the complexed dimethylamino group, showing that they are not equivalent. However, the IR spectrum of this complex shows a decrease of $\sim$100 cm^{-1} in ν(C=O) compared to the free ligand. This may be attributed to the fact that the ligand is coordinated to the metal through both an O atom and an N atom.

The NMR spectra of complexes **7** and **8** are given in Table 2.

The low-field shift is indicative of a strong

Table 1. Analytical data and IR spectra[a]

No.	Compound	Expected C	Expected H	Expected N	Found C	Found H	Found N	ν(N—H)	ν(M—CO)	ν(C=S)
1	$[RuCl_2(CO)_2]_n$	10.5	—	—	10.8	—	—	—	2145[w], 2075, 2020 (2080, 2020)[b]	—
2	$[RuCl_2(CO)_2(TMTU)_2]$	29.2	4.8	11.3	28.9	4.7	11.2	—	2035, 1955	1112 (1226)[c]
3	$[RuCl_2(CO)_2(TMU)_2]$	24.4	3.4	8.1	24.2	3.2	8.2	—	2071, 1998	—
4	$[RuCl_2(CO)_2(DMTU)_2]$	22.0	3.6	12.8	22.6	3.9	12.1	3490, 3260	2070, 1995	1040 (1030)[c]
5	$[RuCl_2(CO)_2(MMTU)_2]$	18.7	3.1	14.5	18.9	3.7	14.2	3300, 3180	2060, 1990	1100 (1120)[c]
6	$[RuCl_2(CO)_2(PYT)_2]$	31.9	2.3	6.2	32.0	2.3	6.7	3200 (3155, 3040)[c]	2060, 1982	1128 (1140)[c]
7	$[RuCl_2(CO)_2(PIP)_2]$	36.0	5.5	7.0	36.7	5.8	7.2	3180 (3280)[c]	2056, 1988	—
8	$[RuCl_2(CO)_2PY)_2]$	37.2	2.5	7.2	37.4	2.6	7.4	—	2045, 1985	—
9	$[RuCl_2(CO)_2(en)]$	16.6	2.8	9.7	16.8	2.9	9.9	3290, 3230, 3140 (3360, 3280)[c]	2060, 1982	—

[a]In KBr discs.
[b]In chloroform solution (2080, 2020).
[c]Value for free ligand.

Table 2. Proton magnetic resonance spectra

Compound	Chemical shift (δ)	Relative intensity (ratio)	Multiplicity	Assignment
$[RuCl_2(CO)_2(TMTU)_2]$ (in $CDCl_3$)	3.3		1	4(CH_3) group
$[RuCl_2(CO)_2(TMU)_2]$ (in $CDCl_3$)	3.1 (centre) (2.85)[a]		Broad doublet 1	4(CH_3) group
$[RuCl_2(CO)_2(PYT)_2]$ (in CD_3CN)	8.05	1	Multiplet	
	7.7	2	Multiplet	
	7.2	2	Multiplet	
$[RuCl_2 \cdot (CO)_2(PIP)_2]$ (in CD_3CN)	7.5	1	Broad multiplet	NH
	3.4	10		5(CH_2)
$[RuCl_2(CO)_2(PY)_2]$ (in CD_3COCD_3)	8.9 (8.55)[a]	2	Doublet	α-Protons
	8.15 (7.6)[a]	1	Multiplet	γ-Proton
	7.6 (7.2)[a]	2	Multiplet	β-Proton
$[RuCl_2(CO)_2(en)]$ (in deuterated DMSO)	2.85 (2.65)[a]	1	1	2(CH_2)
	4.65 (2.20)[a]	1	1	2(CH_2)

[a]Value for free ligand.

complexing of the ligand to the metal which results in a net transfer of electron density towards the metal atom.

Thus the NH_2 protons in complex **9** appear at low field (δ 4.65) compared to uncomplexed NH_2 protons. A similar trend was noticed in the case of complex **8** (see Table 2).

The elemental analyses of all the complexes are given in Table 1 and are consistent with the proposed formulation.

Acknowledgements—We thank KAAU for financial support and A. K. A. Rashed wishes to thank the Chemistry Department, KAAU, for Chem. 491 research facilities.

REFERENCES

1. W. Manchot and J. Konig, *Ber. Dtsch. Chem. Ges.* 1924, **57**, 2131.
2. T. A. Stephenson and G. Wilkinson, *J. Inorg. Nucl. Chem.* 1966, **28**, 945.
3. J. V. Kingston, T. W. S. Jamieson and G. Wilkinson, *J. Inorg. Nucl. Chem.* 1967, **29**, 133.
4. R. Colton and R. H. Farthing, *Aust. J. Chem.* 1967, **20**, 1283.
5. M. J. Cleare and W. P. Griffith, *J. Chem. Soc. A* 1969, 372.
6. A. R. Joseph, *Chem. Rev.* 1985, **85**, 1 (and references therein).
7. M. Schafer and C. Curran, *Inorg. Chem.* 1966, **5**, 265.
8. J. M. Jenkins, M. S. Lupin and B. L. Shaw, *J. Chem. Soc. A* 1966, 1787.
9. M. I. Bruce and F. G. A. Stone, *J. Chem. Soc. A* 1967, 1238.
10. A. O. Baghlaf, M. Ishaq and A. S. Daiffullah, *Polyhedron* 1984, **3**, 235.
11. A. O. Baghlaf, M. Ishaq, O. A. S. Ahmed and M. A. Al-Julani, *Polyhedron* 1985, **4**, 853.

Polyhedron Vol. 6, No. 5, pp. 841–844, 1987
Printed in Great Britain

0277-5387/87 $3.00+.00

TWO NEW VANADYL(IV) COMPLEXES CONTAINING BIURET

ENRIQUE J. BARAN,* SUSANA B. ETCHEVERRY and DIANA S. M. HAIEK

Departamento de Química, Facultad de Ciencias Exactas, Universidad Nacional de La Plata, 1900-La Plata, Argentina

(*Received* 17 *June* 1986; *accepted* 24 *July* 1986)

Abstract—Two new biuret/vanadyl(IV) complexes, a normal bis(biuret) oxygen-bonded $VO(biur)_2Cl_2 \cdot 3H_2O$ and a polymeric one, with bridging-bidentate sulfato groups, $VO(biur)SO_4 \cdot 3H_2O$, have been prepared. They were characterized by their IR and electronic spectra and by TG and DTA measurements. One water molecule is strongly bonded to the cation in both compounds.

Vanadium is an essential trace element in both plants and animals[1–3] with numerous physiological effects. There is ample evidence that in living organisms, vanadium exists primarily as the vanadyl(IV), VO^{2+}, cation complexed with proteins and other cellular components.

In order to obtain a deeper insight into some basic aspects of the inorganic biochemistry of vanadium, we have begun the study of different model systems, containing this metal, which are relevant for a better understanding of its biochemical properties and effects.[4–6]

In this context we have now investigated the interaction of the VO^{2+} cation with biuret, which constitutes a good simple model for studies of the coordination properties of amide bonds (cf. for example, Ref. 7). Two new VO^{2+} complexes, $VO(biur)_2Cl_2 \cdot 3H_2O$ and $VO(biur)SO_4 \cdot 3H_2O$, containing the neutral biuret as ligand, were obtained and thoroughly characterized during these studies.

EXPERIMENTAL

Preparation of $VO(biur)_2Cl_2 \cdot 3H_2O$

A solution of vanadyl chloride was prepared by reacting 0.455 g (2.5 mmol) of V_2O_5 with 5 cm^3 of concentrated HCl in the presence of a few drops of ethanol on a water bath until all the pentoxide dissolved giving a clear blue solution.[8] After a dilution of 30 cm^3 of water, another solution containing 1.031 g (10 mmol) of biuret dissolved in 80 cm^3 of ethanol was slowly added. The resulting mixture was left to evaporate slowly at room temperature until a greenish-blue precipitate was obtained. The fine crystalline mass was filtered, washed with small portions of absolute ethanol and dried in a vacuum desiccator over P_4O_{10}. *Analysis*: Found: V, 13.0; N, 21.0%; C, 11.9; H, 3.9%. Calc. for $VO(C_2H_5O_2N_3)_2Cl_2 \cdot 3H_2O$: V, 12.8; N, 21.1; C, 12.1; H, 4.0%.

Preparation of $VO(biur)SO_4 \cdot 3H_2O$

1.256 g (5 mmol) of $VOSO_4 \cdot 5H_2O$ were dissolved in a solution of 35 cm^3 ethanol + 5 cm^3 water. To this solution, 1.031 g (10 mmol) of biuret, dissolved in 80 cm^3 of ethanol, was added dropwise. A fine crystalline clear-blue powder precipitated after a few minutes. It was filtered and handled in the same way as above. *Analysis*: Found: V, 15.8; N, 13.4; C, 7.8; H, 3.3%. Calc. for $VO(C_2H_5O_2N_3)SO_4 \cdot 3H_2O$: V, 15.9; N, 13.1; C, 7.5; H, 3.4%.

Physicochemical measurements

The electronic spectra of the solid samples were recorded with the reflectance attachment of a Shimadzu UV-600 spectrophotometer, using MgO as a standard. The IR spectra were obtained with a Perkin–Elmer 580 B instrument employing the KBr pellet technique. The thermal behavior was investigated on a Rigaku thermoanalyzer (type YLDG/CN 8002 L2) using a chromel–alumel thermoelement and working under a flowing N_2 stream, at a heating rate of 10°C min^{-1}. Al_2O_3 was used as a DTA standard; sample weight ranged between 25–30 mg.

*Author to whom correspondence should be addressed.

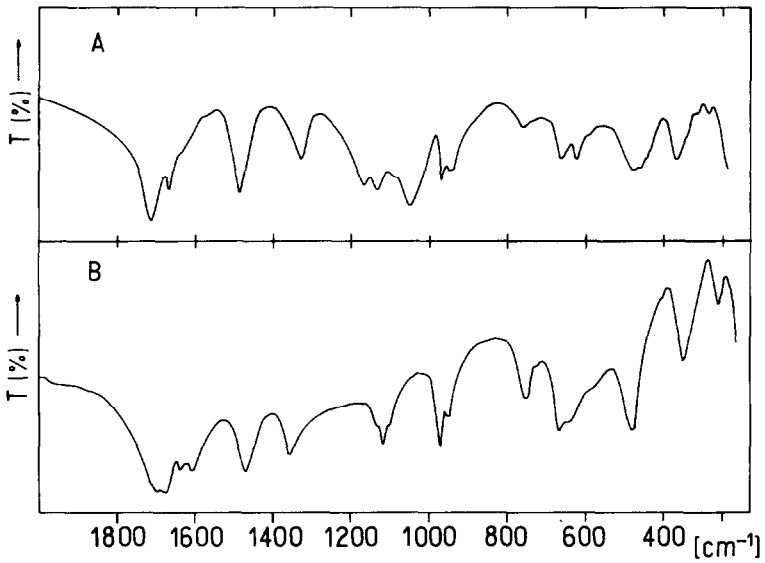

Fig. 1. IR spectra of $VO(biur)SO_4 \cdot 3H_2O$ (A) and $VO(biur)_2Cl_2 \cdot 3H_2O$ (B).

RESULTS AND DISCUSSION

It is known that biuret ($NH_2CONHCONH_2$) can form two types of chelate rings,[7,9,10] coordinated to the metal ions through both carbonyl oxygens or to the two, single deprotonated, NH_2 groups.

The stoichiometry found for the two new vanadyl(IV) complexes indicated the formation of C=O coordinated complexes but two different environments, which depend on the starting vanadyl salt, are found. In the case of the sulfate, this anion is incorporated as a bidentate ligand and a polymeric complex (see below) is probably generated. Starting with the chloride, a normal bis(biuret) cationic complex is obtained.

The IR spectra of both complexes in the range 2000–250 cm^{-1} (Fig. 1) and their assignment shown in Table 1, support the above suppositions. The spectrum of $VO(biur)_2Cl_2 \cdot 3H_2O$ is similar to that of $Cu(biur)_2Cl_2$[11,12] in which the C=O coordination is supported by a structural[13] as well as by a complete normal coordinate analysis.[11]

The $VO(biur)SO_4 \cdot 3H_2O$ spectrum is more complex, due to the presence of the coordinated SO_4-ligand. The spectral features and band positions of these SO_4^{2-} vibrations indicate the presence of bridging bidentate sulfato groups,[12,14,15] which strongly suggest the presence of a polymeric complex, an assumption which is also supported by the rapid precipitation of this species after mixing the biuret and the vanadyl sulfate solutions.

The symmetric stretching and bending vibrations (ν_1 and ν_2) of the sulfate groups apparently are too weak in intensity to be detected or they may be overlapped by stronger bands lying in the same spectral range. Also the antisymmetric bending (ν_4) is clearly overlapped by a $\rho(NH_2)$ biuret vibration.

The characteristic V=O stretching vibration lies in the same range for both complexes, although it shows a small shift to higher wavenumbers and also a somewhat higher intensity in the case of the chloro-compound. The V—O stretching mode which originated in the interaction of the cation with the carbonyl oxygens should lie in the lower frequency region of the spectra. We have tentatively assigned this mode to the band found around 350 cm^{-1}, although in the bis(biuret) copper(II) dichloride and in the nickel(II) analog it was found below 300 cm^{-1}.[11] Notwithstanding, in vanadyl(IV) acetate a band lying at 442 cm^{-1} was assigned to this stretching mode.[16]

The electronic reflectance spectra of both compounds are very similar as can be seen from Fig. 2. They show a very strong and broad band and a well-defined shoulder on its higher energy side. The first band is found at 760 nm (13,757 cm^{-1}) in the bis(biuret) complex and at 750 nm (13,333 cm^{-1}) in the sulfato complex. The shoulder is located at 635 nm (15,748 cm^{-1}) in the first case and at ~600 nm (16,666 cm^{-1}) in the second one.

According to the well known Ballhausen and Gray energy level diagram[17] the main peak can be assigned to the $^2E \leftarrow {}^2B_2$ and the shoulder to the $^2B_1 \leftarrow {}^2B_2$ transitions, respectively. The value for the crystal field splitting parameter $10Dq$ is given directly by the last transition. The observed values are in good agreement with those obtained for other vanadyl complexes with a similar VO^{2+} environment.[18] The small differences in color arise from the relative displacements of the shoulders and from the different form and extension of the 'window' located between the shoulder and the

Table 1. Assignment of the IR spectra of $VO(biur)_2Cl_2 \cdot 3H_2O$ and $VO(biur)SO_4 \cdot 3H_2O$ in the 2000–250 cm^{-1} region (values in cm^{-1})

$VO(biur)_2Cl_2 \cdot 3H_2O$	$VO(biur)SO_4 \cdot 3H_2O$	Assignment
1700 1672	1712	$\nu(C{=}O) + \delta(NH_2)$
1640 1605	1665 1630 sh	$\delta(H_2O) + \delta(NH_2)$
1470	1481	$\nu(CN)$
1335	1326	$\delta(N{-}H)$
1132 1118 1102		$\rho_r(NH_2)$
	1165 1129 1043	$\nu_3(SO_4) + \rho_r(NH_2)$
972	965	$\nu(VO)$
952	946	$\nu(CN) + \nu(C{-}NH_2)$
750	760	Ring deformation
678 643		$\rho(NH_2)$
	673 626 591 sh	$\rho(NH_2) + \nu_4(SO_4)$
480	480, 471, 450	Ring deformations
350	370	$\nu(V{-}O) + \delta(C{-}NH_2)$

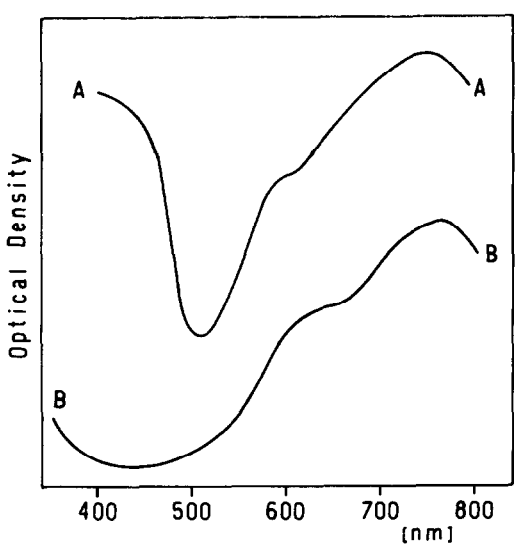

Fig. 2. Electronic reflectance spectra of $VO(biur)SO_4 \cdot 3H_2O$ (A) and $VO(biur)_2Cl_2 \cdot 3H_2O$ (B).

beginning of the strong charge-transfer band, located at higher energies, and not seen in Fig. 2.

The thermal analysis gives more information about the characteristics of the coordination sphere of both complexes.

The thermogram of $VO(biur)SO_4 \cdot 3H_2O$ shows four well-defined endothermic DTA signals, the first of which appears in a doublet form. This doublet (96° and 111°C) corresponds to the loss of two water molecules and the release of the third one occurs at 192°C. After this loss the thermogravimetric curve shows a continuous but irregular weight decrease, related to the other two endothermic peaks. One of them, located at 258°C, is associated with the release of the organic ligand. The last one, at 420°C, corresponds to the generation of SO_3. Further heating, up to 700°C, gives neither mass changes nor thermal effects. From these results, the thermal degradation can be formulated as follows:

$$VO(biur)SO_4 \cdot 3H_2O \rightarrow VO(biur)SO_4 \cdot H_2O + 2H_2O \quad (1)$$

$$VO(biur)SO_4 \cdot H_2O \rightarrow VO(biur)SO_4 + H_2O \quad (2)$$

$$VO(biur)SO_4 \rightarrow VOSO_4 + biur \quad (3)$$

$$VOSO_4 \rightarrow VO_2 + SO_3. \quad (4)$$

The theoretical total weight loss [addition of equa-

tions (1)–(4)] gives 74.06% which correlates with the value of 73.8% found experimentally.

In the case of $VO(biur)_2Cl_2 \cdot 3H_2O$ the release of the first two water molecules is associated with a strong and well-defined endothermic DTA peak centered at 141°C, whereas the release of the third one corresponds to a second endothermic peak, located at 200°C. After the loss of water a continuous weight decrease is observed. Between 220° and 500°C, the observed weight change corresponds to the release of the two biuret molecules. In this range two not well-defined and weak endothermic DTA signals at 260° and 378°C are observed. At 500°C a clear inflexion is observed in the TG curve, and a further weight loss begins and continues slowly until the maximum temperature (700°C) is reached. In this case, the formation of $VOCl_2$ as an intermediate can be expected, but pure $VOCl_2$ decomposes into VOCl and $VOCl_3$ at temperatures above 380°C.[19] The total conversion of the complex to VOCl requires a weight loss of 74.27% in good agreement with the experimentally found values, which always lie around 75%.

Therefore, the degradation of $VO(biur)_2Cl_2 \cdot 3H_2O$ can be formulated as follows:

$$VO(biur)_2Cl_2 \cdot 3H_2O \rightarrow VO(biur)_2Cl_2 \cdot H_2O + 2H_2O \quad (5)$$

$$VO(biur)_2Cl_2 \cdot H_2O \rightarrow VO(biur)_2Cl_2 + H_2O \quad (6)$$

$$VO(biur)_2Cl_2 \rightarrow VOCl_2 + 2biur \quad (7)$$

$$2VOCl_2 \rightarrow VOCl(s) + VOCl_3(g). \quad (8)$$

The most important result obtained from the thermal analysis is the clear evidence of the presence of one strongly bonded water molecule in both complexes. This molecule is probably coordinated directly to the vanadium atom in the *trans* position to the vanadyl oxygen.

The formation of these complexes is another example of the particularly high stability of vanadyl complexes with oxygen donors[21] and suggests a preferential interaction of the VO^{2+} cation with C=O oxygens in the presence of amide groups in biological environments.

Acknowledgements—This research was supported by CONICET (Programa QUINOR) and CIC-Provincia de Buenos Aires. It is also a part of a special program devoted to the chemistry and biochemistry of vanadium, which is sponsored by the Foundation 'Volkswagenwerk' (Hannover, F.R.G.).

REFERENCES

1. K. Kustin and I. G. Macara, *Comments Inorg. Chem.* 1982, **2,** 1.
2. N. D. Chasteen, *Struct. Bonding* 1983, **53,** 105.
3. E. J. Baran, *Química Bio-Inorgánica.* Ediciones Faba, La Plata, Argentina (1984).
4. E. J. Baran, S. B. Etcheverry, E. Diemann and R. Jostes, *An. Asoc. Quím. Argent.* 1984, **72,** 27.
5. S. B. Etcheverry, M. C. Apella and E. J. Baran, *J. Inorg. Biochem.* 1984, **20,** 269.
6. E. J. Baran, *J. Inorg. Biochem.* 1985, **23,** 73.
7. H. Sigel and R. B. Martin, *Chem. Rev.* 1982, **82,** 385.
8. D. N. Sathyanarayana and C. C. Patel, *Indian J. Chem.* 1965, **3,** 486.
9. F. Kurzer, *Chem. Rev.* 1956, **56,** 95.
10. A. W. McLellan and G. A. Melson, *J. Chem. Soc. A* 1967, 137.
11. B. B. Kedzia, P. X. Armendarez and K. Nakamoto, *J. Inorg. Nucl. Chem.* 1968, **30,** 849.
12. K. Nakamoto, *Infrared and Raman Spectra of Inorganic and Coordination Compounds,* 3rd edn. Wiley, New York (1978).
13. H. C. Freeman, J. E. W. L. Smith and J. C. Taylor, *Acta Cryst.* 1961, **14,** 407; M. Nardelli, G. Fava and G. Giraldi, *Acta Cryst.* 1963, **16,** 343.
14. W. R. McWhinnie, *J. Inorg. Nucl. Chem.* 1964, **26,** 21.
15. M. E. Baldwin, *Spectrochim. Acta* 1963, **19,** 315.
16. A. T. Casey and J. R. Thackeray, *Austral. J. Chem.* 1969, **22,** 2549.
17. C. J. Ballhausen and H. B. Gray, *Inorg. Chem.* 1962, **1,** 111.
18. A. B. P. Lever, *Inorganic Electronic Spectroscopy,* 2nd edn. Elsevier, Amsterdam (1984).
19. H. Oppermann, *Z. Anorg. Allg. Chem.* 1967, **351,** 113.
20. N. Mabiala, J. P. Barbier and R. P. Hugel, *Polyhedron* 1984, **3,** 99.
21. N. D. Chasteen, In *Biological Magnetic Resonance* (Edited by L. E. Berliner and J. Reuben), Vol. 3, p. 53. Plenum Press, New York (1981).

Polyhedron Vol. 6, No. 5, pp. 845–848, 1987
Printed in Great Britain

0277–5387/87 $3.00+.00
Pergamon Journals Ltd

SYNTHESIS OF TERNARY COPPER(II) COMPLEXES OF PHENANTHROLINES AND L-DOPA AND RELATED LIGANDS

NEELA A. EMANUEL and PABITRA K. BHATTACHARYA*

Department of Chemistry, Faculty of Science, M.S. University of Baroda, Baroda 390 002, India

(*Received* 22 *November* 1985; *accepted after revision* 13 *May* 1986)

Abstract—The series of ternary complexes of type [CuAL] where A = 1,10-phenanthroline or 5-nitro-1,10-phenanthroline and L = catechol, 2,3-dihydroxynaphthalene, dopamine, phenylalanine, tyrosine or L-dopa have been synthesized and characterized by spectral and magnetic moment studies.

Tyrosine and L-3,4-dihydroxyphenylalanine (L-dopa) are compounds of biochemical importance in the neurotransmission process.[1] Dopa is also used as a drug and is administered orally in the treatment of Parkinson's disease. However, during the passage through the intestine or liver, dopa is converted into dopamine.

It was shown[1] that coordination of L-dopa with a metal ion from the aminocarboxylate end reduces the decarboxylation caused by pyridoxal and a greater portion of L-dopa is transported to the brain.

L-dopa is also interesting because of its ambidentate nature,[2–8] coordinating with Cu(II) from the amino-acid end at low pH and from the catechol end at higher pH. However, it has been shown[8] that in mixed ligand complexes [Cu 2,2′-dipyridyl dopa], the chelation of dopa is from amino-acid end up to higher pH ($\sim$ 7.0). The chelate is similar to that in phenylalanine, tyrosine or tryptophan.

The solution study of these complexes [Cu dipy aminoacid with side groups] shows that the formation constant of the mixed ligand complex is much higher than expected. This has been attributed[9] to hydrophobic interaction of the side group in the axial direction of the metal ion in the ternary complexes.

Following from our study of ternary complexes in solution involving 1,10-phenanthroline or 5-nitro-1,10-phenanthroline[10] and aminoacids with aromatic side chains, this paper presents an account of the isolation of two series of ternary complexes of Cu(II) containing 5-nitro-1,10-phenanthroline or 1,10-phenanthroline (A) and one of the following secondary ligands (L): phenylalanine, tyrosine, L-dopa, catechol, 2,3-dihydroxynaphthalene and dopamine. The structures of the complexes have been characterized by IR spectral, electronic spectral and magnetic studies.

EXPERIMENTAL

Preparation of [Cu A aminoacid] complexes

An aqueous solution of copper acetate (8 mmol) in 20 cm^3 distilled water was added to 20 cm^3 of ethanolic solution of 1,10-phenanthroline or 5-nitro-1,10-phenanthroline (8 mmol). A blue solid was formed immediately. As the mixture was stirred magnetically the appropriate amount of aminoacid (10 mmol) in 10 cm^3 0.1 M hydrochloric acid was slowly added, followed by 1 M ammonium hydroxide solution until a clear blue solution was obtained. The solution was warmed and stirred for a further 45 min, heated until its volume was reduced by approximately half and then a 0.1 M solution of sodium tetraphenylborate was added. The solid immediately separated out and was filtered, washed with small portions of cold water followed by ethanol and then dried *in vacuo*.

Preparation of [CuA $O^- - O^-$] complexes

An aqueous solution of catechol, 2,3,-dihydroxynaphthalene or dopamine (10 mmol) in 20 cm^3 distilled water was slowly added to an ethanolic solution of 1,10-phenanthroline or 5-nitro-1,10-phenanthroline (8 mmol). This ligand mixture was then slowly added to an aqueous solution of copper

* Author to whom correspondance should be addressed.

Table 1. Magnetic susceptibility measurements and analytical data of Cu(II) ternary complexes

Name of complex	Experimental				Theoretical					
	%C	%H	%N	%Cu	%C	%H	%N	%Cu	μ_{eff}	λ_{max}
[Cu(phen)(phenylalal)]BPh_4	73.9	6.0	5.5	8.4	73.4	6.4	5.7	8.6	1.75	606
[Cu(phen)(tyrosine)]BPh_4	72.1	4.5	5.6	8.8	71.8	4.9	5.6	8.4	1.75	606
[Cu(phen)(L-dopa)]BPh_4	70.0	4.5	5.1	8.0	70.3	4.8	5.5	8.3	1.7	606
[Cu(phen)(cat)]	61.6	3.4	8.2	18.3	61.4	3.4	7.9	18.1	1.75	470
[Cu(phen)(2,3-dihydroxynaphthalene)]	64.9	3.0	6.8	15.7	65.9	2.9	6.9	15.9	1.7	495
[Cu(phen)(dopamine)] acetate	56.1	4.3	8.8	13.1	56.3	4.2	8.9	13.6	1.8	450
[Cu(5-nitro-phen)(phenylalal)]BPh_4	69.7	4.6	7.1	7.9	69.1	4.7	7.2	8.1	1.75	598
[Cu(5-nitro-phen)(tyrosine)]BPh_4	68.5	4.8	7.1	8.0	67.9	4.6	7.1	7.9	1.7	598
[Cu(5-nitro-phen)(L-dopa)]BPh_4	66.4	4.4	6.9	7.8	66.1	4.2	6.9	7.7	1.65	598
[Cu(5-nitro-phen)(cat)]	54.4	2.7	11.7	16.4	54.5	2.8	10.6	16.0	1.65	530
[Cu(5-nitro-phen)(2,3-dihydroxynaphthalene)]	57.2	3.1	9.5	13.9	59.1	2.9	9.4	14.2	1.7	540
[Cu(5-nitro-phen)(dopamine)] acetate	49.4	3.8	10.9	12.3	51.1	3.9	10.9	12.3	1.65	520

acetate (8 mmol) in 20 cm^3 distilled water followed by 1 M ammonium hydroxide solution in order to raise the pH to 6.0, where upon the complex was formed immediately. This was filtered, washed with distilled water followed by ethanol and then dried *in vacuo*.

Copper(II) was estimated gravimetrically. Percentages of nitrogen, carbon and hydrogen were estimated on Coleman Analyzer Models 29 and 33, respectively. TLC analysis were done on a silica gel G (Sichem) plates using ethanol as solvent.

IR spectra were recorded on a Perkin–Elmer Model 638 spectrometer. KBr and Nujol mulls were employed. Electronic spectra were run at a concentration of 10^{-2} mol dm^{-3} in freshly prepared aqueous dioxan (1 : 1, v/v) solvent. A Carl Zeiss specord UV–vis spectrometer with 1-cm quartz cells was used for these measurements.

Magnetic susceptibilities were determined at room temperature only by Gouy's method using a Mettler balance and electromagnet working at a constant current strength of 3 A in all cases. The balance was calibrated with $Hg[Co(NCS)_4]$.

RESULTS AND DISCUSSION

TLC of all the complexes, using ethanol as solvent, show a single spot confirming their purity. The elemental analysis of the ternary complexes isolated in the present study are given in Table 1 along with the values of their magnetic moments. The analysis is consistent with the structure suggested. As proposed earlier on the basis of solution studies, L-dopa is found to be coordinating from aminocarboxylate end. Hence [CuA L-dopa] has one positive charge and one $(Bph_4)^-$ is present as a counter ion. In the case of the ternary complex involving dopamine, the complex was immediately formed when metal and two ligands were added and the pH was raised to 6.0. Dopamine coordinates from two phenolic groups, and amino group remains protonated. Hence the ligand contains effectively one negative charge. The complex ion is left with one positive charge and hence one counter ion (acetate ion) is found to be present.

The complex exhibits slightly lower magnetic moment than expected for one unpaired electron.

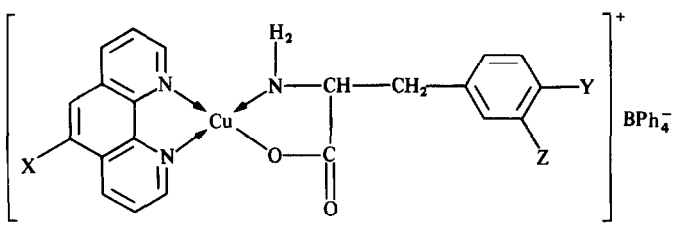

X = H or NO_2, Y = H or OH, Z = H or OH

[CuA (aminoacid)]

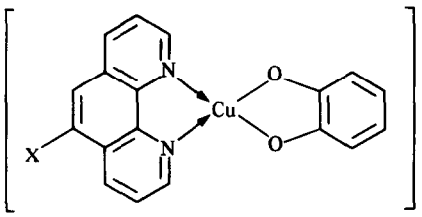

X = H or NO_2
[CuA(catechol)]

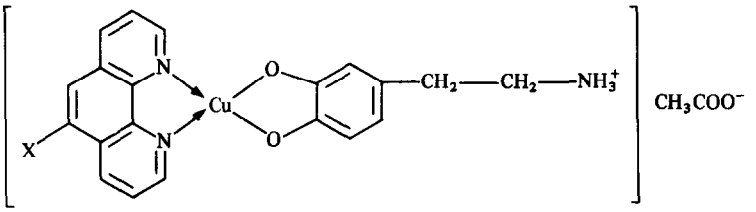

X = H or NO_2
[CuA(dopamine)] acetate

IR spectral studies

The ternary complexes exhibit IR absorptions typical of coordinated ligands (phen: 1625, 1575, 1420, 840, 700 cm^{-1} and 5-nitro-1,10-phen: 1625, 1515, 1420, 840, 720 cm^{-1}). Furthermore in the case of aminoacid complexes remarkable similarities are observed among these ternary complexes in the absorption regions due to the amino and the carboxyl groups, which are found to occur at (a) 3450–3200 cm^{-1}, 1640–1600 cm^{-1}, 1420–1380 cm^{-1} and 600–610 cm^{-1} and (b) 1640–1600 cm^{-1} and 490–460 cm^{-1}, respectively.[11–14]

The mode of coordination of the ambidentate ligands L-dopa, tyrosine and dopamine can be inferred from the IR spectral data of these metal complexes. The uncoordinated unionised phenolic O—H stretching band occurs at 3500 cm^{-1} in the [CuA L-dopa] complex indicating that it is coordinating from the aminoacid end.

In the cases of catechol or 2,3-dihydroxynaphthalene, the coordination is from phenolic groups and hence no unionised phenolic stretching frequencies of phenolic groups (ν_{OH} = 3550–3450 cm^{-1}) are observed. In the case of the dopamine ternary complexes, there are no un-ionised phenolic stretching frequencies of phenolic groups and moreover there are uncoordinated protonated amino stretching frequencies (ν_{NH} = 3450–3400 cm^{-1}) present indicating that the coordination is from phenolic group and amino group is remaining protonated.

Electronic spectral studies

The electronic spectra of these ternary Cu(II) complexes in solution and in the solid state exhibit broad absorption bands in the visible region due to the overlap of three possible transitions $d_{x^2-y^2} \rightarrow d_{xy}$, $d_{x^2-y^2} \rightarrow d_{xz}$, $d_{x^2-y^2} \rightarrow d_{yz}$. The electronic spectra of complexes involving tyrosine and L-dopa are similar to those containing phenylalanine, showing that coordination is from the aminoacid site of all the aminoacids.

The ternary complexes of [CuAL] where L = catechol, 2,3-dihydroxynaphthalene or dopamine exhibit intense broad charge-transfer bands in the visible region (~500 nm), with its tail overlapping the *d–d* absorption bands.

REFERENCES

1. K. S. Rajan, S. Mainer and J. M. Davis, *Bioinorg. Chem.* 1978, **9**, 187.
2. J. E. Gorton and R. F. Jameson, *J. Chem. Soc.* (*A*) 1968, 2615.
3. J. E. Gorton and R. F. Jameson, *J. Chem. Soc.* (*A*) 1972, 304.
4. J. E. Gorton and R. F. Jameson, *J. Chem. Soc.* (*A*) 1972, 310.
5. Whei-hu-Kwick, E. Purdy and E. I. Stiefel, *J. Am. Chem. Soc.* 1974, **96**, 1638.
6. J. R. Pilbow, S. G. Carr and T. D. Smith, *J. Chem. Soc.* (*A*) 1970, 723.

7. S. G. Carr, J. R. Pilbow and T. D. Smith, *J. Chem. Soc. (A)* 1971, 2569.
8. K. S. Rajan, A. A. Manian, J. M. Davis and H. Dekimejian, *Brain Res.* 1976, **107**, 317.
9. V. K. Patel and P. K. Bhattacharya, *J. Inorg. Biochem.* 1984, **21**, 169.
10. N. Emanuel and P. K. Bhattacharya, *J. Indian Chem. Soc.* (in press).
11. R. A. Cordrate and K. Nakamoto, *J. Chem. Phys.* 1965, **42**, 2570.
12. J. F. Jackouitz, J. A. Durkin and J. L. Walters, *Spectrochim. Acta* 1967, **23A**, 67.
13. I. Nakagawa, R. J. Hooper, J. L. Walters and T. J. Lane, *Spectrochim. Acta* 1965, **21**, 1.
14. J. F. Jackouitz and J. L. Walters, *Spectrochim. Acta* 1966, **22**, 1393.

Polyhedron Vol. 6, No. 5, pp. 849–853, 1987
Printed in Great Britain

0277–5387/87 $3.00+.00

BROMO- AND CHLORO-SELENATE(II) COMPOUNDS

J. B. MILNE

Ottawa-Carleton Institute for Research and Graduate Studies in Chemistry, University of Ottawa Campus, Ottawa, Canada, K1N 9B4

(*Received* 6 *July* 1986; *accepted* 4 *August* 1986)

Abstract—Addition of R_4NX (R = Et, *n*-Pr, *n*-Bu) to solutions of SeX_2 (X = Cl, Br) in acetonitrile results in the formation of tri- and tetra-haloselenate(II) complexes (SeX_3^- and SeX_4^{2-}). Raman spectroscopic characterization of these solutions and solids, R_4NSeX_3 and $(R_4N)_2SeX_4$, which may be crystallized from them, are reported. R_4NSeCl_3 compounds are shown to be relatively unstable; they are readily destroyed by laser light,

$$2R_4NSeCl_3 = (R_4N)_2SeCl_6 + Se(0)$$

and especially sensitive to hydrolysis,

$$2SeCl_3^- + H_2O = SeOCl_3^- + 2HCl + Cl^- + Se(0).$$

The Raman spectra of solutions of SeX_3^- and SeX_4^{2-} are consistent with T-shaped and square planar structures, respectively.

Compounds of selenium in the +2 oxidation state are relatively uncommon. A few reports of selenium dihalides have been made. Their existence in the gas phase at elevated temperatures has been known for a long time[1] and recent Raman work has confirmed the existence of $SeCl_2$ in the vapour phase over $SeCl_4$ at 350°C.[2] Selenium difluoride has been studied by matrix isolation.[3] The existence of $SeCl_2$ and $SeBr_2$ in non-aqueous media has been demonstrated[4–6] and the presence of $SeCl_2$ in equilibrium with Se_2Cl_2 and other Se(IV) species in solutions of elemenetal selenium and SeO_2 in aqueous HCl has been established.[7] Several chloro-, bromo- and cyano-complex anions of Se(II) have been described.[8] These three-coordinate complexes dimerize in the solid state in a manner similar to that of the oxotrihaloselenate(IV) anions[9,10] and, since this indicates that the coordination shell of Se(II) is not completely filled in these compounds, it seemed likely that tetrahaloselenate(II) complexes might be prepared. Indeed since this work was started $(Ph_4P)_2SeBr_4$ has been prepared and its crystal structure reported.[11] The oxotetrachloro- and oxotetra-bromoselenate(IV) compounds have both been synthesized.[12,13] Moreover, there is a remarkable similarity between the spectra reported for $SeCl_3^-$ in acetonitrile and that for solid Et_4NSeCl_3 with the reported spectra for the $SeOCl_3^-$ and $(Et_4N)_2SeCl_6$,[14,15] respectively. In view of these similarities and in order to extend our understanding of Se(II) chemistry, a study of chloro- and bromo-selenate(II) compounds was carried out.

EXPERIMENTAL

Materials

Acetonitrile (MeCN) and nitromethane($MeNO_2$) were purified by refluxing over P_4O_{10} for 1 h and distilling (b.p. 81–82°C and 100–101°C, respectively). Selenium (Baker AR) was ground before use. Bromine (Baker AR) was distilled (b.p. 59–60°C) before use. Chlorine (Matheson) was used directly. All quaternary ammonium halides (Aldrich) were dried at 100°C under high vacuum and analysed before use. Selenium tetrabromide and tetrachloride were prepared by standard methods.[16,17]

Preparations

All compounds and solutions were handled under dry conditions. The haloselenate(II) compounds were prepared from a stoichiometric solution of quaternary ammonium halide, selenium tetrahalide and selenium in acetonitrile.

$$2R_4NX + Se(0) + SeX_4 = 2R_4NSeX_3 \quad (1)$$

$$4R_4NX + Se(0) + SeX_4 = 2(R_4N)_2SeX_4 \quad (2)$$

In general ~ 0.4 M, or less, solutions of Se(II) complex were soluble at room temperature and reasonable recoveries could be achieved by cooling in dry ice to the point of crystallization followed by rapid filtration. For instance, 663 mg Et_4NCl, 79 mg Se(0) and 221 mg $SeCl_4$ were combined in 7.4 g MeCN. Sufficient time and mixing were allowed to permit complete dissolution of the elemental selenium and the solution was then cooled and filtered. In the case of the chloro-compounds there appeared to be initial formation of hexachloroselenate(IV) which was insoluble, then slow reaction to give the desired product. Found: Se, 24.8; Cl, 33.4. Calc. for $(Et_4N)SeCl_3$: Se, 25.0; Cl. 33.7%. Found: Cl, 29.3. Calc. for $(Et_4N)_2SeCl_4$: Cl, 29.5%. Found: Cl, 24.1. Calc. for $(Bu_4N)SeCl_3$: Cl, 24.9%. Found: Cl, 20.0. Calc. for $(Bu_4N)_2SeCl_4$: Cl, 20.1%. Found: Br, 53.2. Calc. for $(Et_4N)SeBr_3$: Br, 53.4%. Found: Br, 48.8. Calc. for $(Et_4N)_2SeBr_4$: Br, 48.5%. Found: Br, 47.2. Calc. for $(n\text{-}Pr_4N)SeBr_3$: Br, 47.5%. The trichloro-complexes were orange in colour, the tetrachloro-, yellow while the bromo-complexes were red-orange. All products were very moisture sensitive, turning opaque red on exposure to water. The tetra-*n*-butyl ammonium compounds were very difficult to crystallize and could only be isolated by pumping to dryness. $(Et_4N)_2SeCl_6$ was prepared as described previously.[14]

Melting points

$(Et_4N)_2SeCl_6$ dec. p. 220–225°C; Et_4NSeCl_3 dec. p. 50–51°C; $(Et_4N)_2SeCl_4$ dec. p. 174–182°C.

Raman spectroscopy

Raman spectra were taken with a Jobin–Yvon grating monochromator in conjunction with PAR photon counting. All spectra were excited with a Spectra Physics Model 160 Kr ion laser. The spectra of the solids were excited at low power levels (40 mW at 647.1 nm for Et_4NSeCl_3). In general the Raman lines due to the R_4N^+ ions were very weak or not observed.

RESULTS AND DISCUSSION

The previous preparations of trihaloselenate(II) complexes in acetonitrile were done by redox reactions of selenocyanate with sulphur chloride or bromine[8] or by reaction of tetraphenylphosphonium bromide with the decomposition products of $SeOBr_2$ or $SeBr_4$ in acetonitrile. The recent demonstration of the existence of high concentrations of SeX_2 (X = Cl, Br) in 1 : 1 Se/X_2 mole ratio mixtures in acetonitrile[6] suggested that direct addition of quaternary ammonium halides to such solutions would yield haloselenate(II) complexes.

Chloroselenates

Addition of Et_4NCl to a nitromethane or acetonitrile solution of $SeCl_2$ results in the disappearance of the characteristic strong peak of $SeCl_2$ at 412 cm^{-1}[6] and the appearance of the spectrum shown in Fig. 1(A), which corresponds to 1 : 1 $Et_4NCl/SeCl_2$ stoichiometry. Further addition of Et_4NCl results in a weakening of the band at 346 cm^{-1} and a broadening and strengthening of the band at 261 cm^{-1}, indicating the formation of another species [Fig. 1(C)]. The changes are accounted for by the formation of the $SeCl_3^-$ and $SeCl_4^{2-}$ anions according to,

$$SeCl_2 + Cl^- = SeCl_3^- \quad (3)$$

$$SeCl_3^- + Cl^- = SeCl_4^{2-}. \quad (4)$$

The spectrum of the 2 : 1 $Et_4NCl/SeCl_2$ mole ratio solution has a small peak at 347 cm^{-1} indicating that some $SeCl_3^-$ ion is still present. This peak persists in solution up to 5 : 1 $Et_4NCl/SeCl_2$ where $SeCl_4^{2-}$ dissociation is finally repressed. Cooling of 1 : 1 and 2 : 1 $Et_4NCl/SeCl_2$ mixtures yielded orange and yellow crystals respectively, which analysed correctly for Et_4NSeCl_3 and $(Et_4N)_2SeCl_4$. The spectrum of the $SeCl_3^-$ ion in solution reported by Wynne and Golen shows a band at 231 cm^{-1}, which is not observed in this work. This band is probably due to the presence of $SeOCl_3^-$ ion. Addition of water to, or exposure to moisture of, solutions of $SeCl_3^-$ ion resulted in a darkening of the solutions accompanied by a growth of bands in the Raman spectrum at 950 and 231 cm^{-1}. The growth of these bands and the colour change may be accounted for by the reactions,

$$3Et_4NSeCl_3 + H_2O = Se_2Cl_2 + Et_4NSeOCl_3 + 2Et_4NCl + 2HCl \quad (5)$$

$$2Et_4NSeCl_3 + H_2 = Se(0) + Et_4NSeOCl_3 + Et_4NCl + 2HCl. \quad (6)$$

The bands at 231 and 950 cm^{-1} are due to the $SeOCl_3^-$ ion, which has a Raman spectrum similar to that reported[8] for $SeCl_3^-$. However, the absence of peaks at 139 and 291 cm^{-1} as well as the constant size of the weak Et_4N^+ cation band at 410 cm^{-1}, which is nearly coincident with an Se_2Cl_2 band, and the solvent band at 370 cm^{-1}, which is coincident with the strongest Se_2Cl_2 Raman band,[6] indicates

that Se_2Cl_2 is not formed. Moreover, Se_2Cl_2 undergoes disproportionation in the presence of Cl^- ion. An attempt was made to prepare chloro-anions of Se_2Cl_2 in acetonitrile. Addition of Et_4NCl to a solution of Se_2Cl_2 (1 : 1 mole ratio) resulted in an immediate darkening of the solution and precipitation of elemental selenium and a Raman spetrum of the supernatant showed bands for the $SeCl_3^-$ anion

$$Se_2Cl_2 + Cl^- = Se(0) + SeCl_3^-. \qquad (7)$$

Thus reaction (6) is favoured in the hydrolysis of the $SeCl_3^-$ ion. It should further be noted that although the Cl^- to Se(IV) stoichiometric ratio for the products of reaction (6) is high, the $SeOCl_4^{2-}$ anion is not observed in significant concentration because the Se(IV) concentration is low.[12]

The spectra of solid Et_4NSeCl_3 and $(Et_4N)_2SeCl_4$ are shown in Fig. 1 and listed in Table 1. While the tetrachloroselenate(II) was stable to 647.1 nm laser irradiation at 50 mW power, the trichloroselenate(II) decomposed rapidly as shown by the change in colour from orange to black. This change was accompanied by a change in the Raman spectrum from that of Et_4NSeCl_3 to that of $(Et_4N)_2SeCl_6$. Apparently a disproportionation occurs according to

$$2Et_4NSeCl_3 = (Et_4N)_2SeCl_6 + Se(0). \qquad (8)$$

The characteristic Se(0) band at 240 cm^{-1}[18] is masked by the strong E_g stretch of the $SeCl_6^{2-}$ ion at 241 cm^{-1}.[14] The Raman spectrum of the decomposition product is identical with that observed by Wynne and Golen[8] for their solid Et_4NSeCl_3. But their spectrum cannot be the result of laser decomposition, since their product was yel-

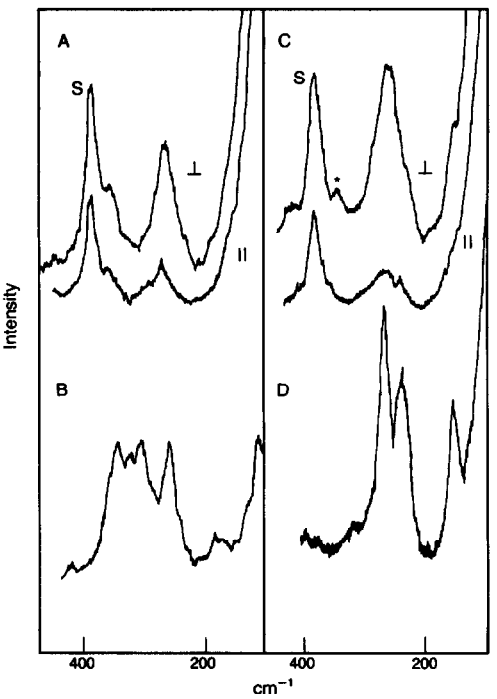

Fig. 1. Raman spectra of chloroselenate(II)s: (A) Et_4NSeCl_3 in CH_3CN (0.25 M), (B) solid Et_4NSeCl_3, (C) $(Et_4N)_2SeCl_4$ in CH_3CN (0.25 M), and (D) solid $(Et_4N)_2SeCl_4$. S = solvent band; * = $SeCl_3^-$ band.

Table 1. Raman spectra of chloroselenate(II)s

$(Et_4N)SeCl_3$ solid	$SeOCl_3^-$ [a] in MeCN	$SeCl_3^-$ [b] in MeCN	Mode description
335(5)	336(3,p)	350(5,p)	$\nu(SeCl_{eq})$
310(4)	—	—	—
292(4)	287(1,dp)	268(5,sh)	$\nu_a(SeCl_{ax})$
251(2)	—	—	—
175(2)	228(7,p?)	260(10,p)	$\nu_s(SeCl_{ax})$
100(1)	—	—	—
72(9)	—	—	—
52(9)	—	—	—
$(Et_4N)_2SeCl_4$ solid	$SeCl_4^{2-}$ [c] in MeCN		Mode description
265(10)	262(10,p)		$\nu_1(A_{1g})$
235(7)	240(1)		$\nu_4(B_{2g})$
150(5)	157(1)		$\nu_3(B_{1g})$

[a] Ref. 14.
[b] Et_4N^+ and n-Bu_4N^+ salts.
[c] Et_4N^+ and n-Pr_4N^+ salts.

low in colour and had a high decomposition point (243–244°C) not unlike that of $(Et_4N)_2SeCl_6$ (220–225°C) but very different from that of Et_4NSeCl_3 (50–51°C). The nature of their product, which analysed correctly for Et_4NSeCl_3, is unknown.

The solution spectra for the anions are listed in Table 1. The observed spectrum of the $SeCl_3^-$ anion is consistent with that expected for the stretching modes of an anion with shape based upon a trigonal bipyramid with two Cl axial and one Cl equatorial[14,15]

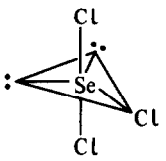

The spectrum is similar to that of the $SeOCl_3^-$ ion, where the SeCl stretching modes are the strongest observed. The $SeCl_3$ skeleton shape is predicted to be the same (T-shaped) by VSEPR theory for both ions and the substitution of an oxygen for a lone pair in the equatorial position has only a small effect on the SeCl stretching modes. There is an increase in the mean of the SeCl stretching frequencies on going from $SeOCl_3^-$ to $SeCl_3^-$, which parallels the change in SeCl stretching frequencies and force constants observed for $SeOCl_2$ and $SeCl_2$.[6]

The Raman spectrum of $SeCl_3^-$ in solution is distinctly different from that in solid Et_4NSeCl_3, which supports the proposal that $SeCl_3^-$ is dimerized in the solid.[5]

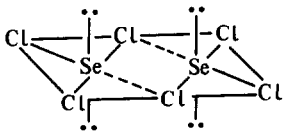

There, is however, a similarity between the spectrum of the $SeCl_4^{2-}$ ion in solid and solution. VSEPR theory predicts that the $SeCl_4^{2-}$ anion will have D_{4h} symmetry ($\Gamma(D_{4h}) = A_{1g}+A_{2u}+B_{1g}+B_{2g}+B_{2u}+2E_u$) and the spectra are consistent with this. Three strong peaks are observed in the Raman spectrum of solid $(Et_4N)_2SeCl_4$, two in the SeCl stretching region, 265 and 235 cm^{-1} and one in the deformation region, 150 cm^{-1}. Of these, the peak at 265 cm^{-1} is strongly polarized ($\rho \sim 0.2$) and may be assigned to the A_{1g} stretching mode. The remaining two peaks are the B_{2g} stretching and B_{1g} deformation modes. There is a weak peak at 310 cm^{-1}, which is not a cation band and is unlikely to be due to any impurity in view of the analysis and the high crystallinity of the product. This may be the forbidden E_u stretching band, which appears due to a distortion from exact D_{4h} symmetry. Such a distortion has been observed in the case of the $SeBr_4^{2-}$ ion in $(Ph_4P)_2SeBr_4$.[11]

Bromoselenates

The strong characteristic peaks of $SeBr_2$ in CH_3CN at 290 and 266 cm^{-1}[16] decrease in intensity on addition of Et_4NBr to the solution and are replaced by strong peaks at 258 and 159 cm^{-1}. The spectrum of a 1 : 1 $SeBr_2/Et_4NBr$ solution is shown in Fig. 2 and the frequencies are listed in Table 2. The spectrum is very similar to that reported for Et_4NSeBr_3 in nitromethane[8] except for the presence of a small peak at 285 cm^{-1} no doubt due to the presence of a small amount of $SeBr_2$ as a result of incomplete formation of the $SeBr_3^-$ ion at these concentrations ($C_{Se(IV)} = 0.09$ M). Further addition of Et_4Br up to 1 : 6 mole ratio $SeBr_2/Et_4NBr$ with the same $C_{Se(IV)}$ results in a progressive increase in the intensity of the peak near 160 cm^{-1} and a decrease in that at 258 cm^{-1} (Fig. 2). These changes are due to further complexation according to

$$SeBr_3^- + Br^- = SeBr_4^{2-}. \qquad (9)$$

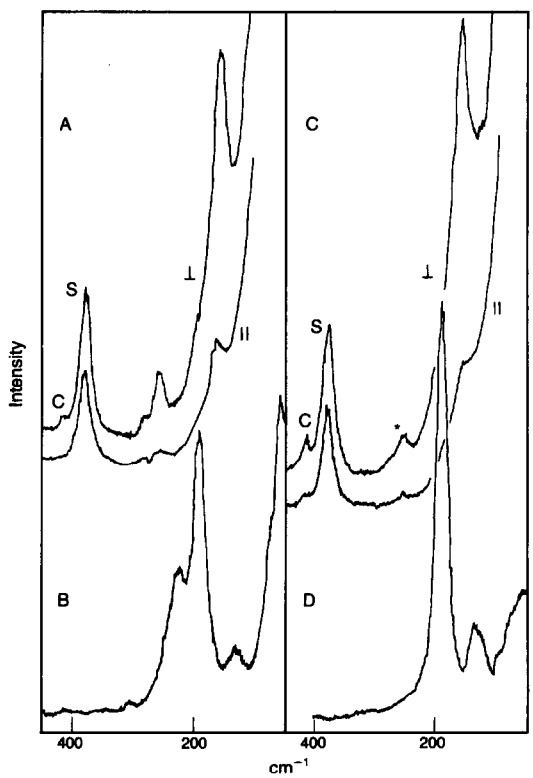

Fig. 2. Raman spectra of bromoselenate(II)s: (A) Et_4NSeBr_3 in CH_3CN (0.09 M), (B) solid Et_4NSeBr_3, (C) 6 : 1 Et_4NBr–Et_4NSeBr_3 [$c_{Se(IV)} = 0.09$ M], and (D) solid $(Et_4N)_2SeBr_4$. S = solvent band; c = cation band; * = $SeBr_3^-$ band.

Table 2. Raman spectra of bromoselenate(II)s

Et_4NSeBr_3 solid	$(Ph_4P)SeBr_3$[a] solid	$SeOBr_3^-$[b] in MeCN	$SeBr_3^-$[c] in MeCN	Mode description
222(6,br)	236 230	261	258(4,p)	$\nu(SeBr_{eq})$
189(10)	178	163	190(0)	$\nu_a(SeBr_{ax})$
127(2,br)	130	135	159(10,p)	$\nu_s(SeBr_{ax})$
54(2)	95			deformations and lattice modes

$(Et_4N)_2SeBr_4$ solid	$(Ph_4P)_2SeBr_4$[a] solid	$SeBr_4^{2-}$[d] in MeCn	Mode description
191(10)	160(10)	162(10,p)	$\nu_1(A_{1g})$
139(2)	149(7)	—	$\nu_4(B_{2g})$
93(1,sh)	88(8)	—	$\nu_3(B_{1g})$
75(2,sh)	—	—	deformations and
60(2,sh)	—		lattice modes

[a] Ref. 11.
[b] SeBr stretches only, Ref. 15.
[c] *n*-Pr_4N^+ and Et_4N^+.
[d] Et_4N^+.

Cooling of 1 : 1 and 1 : 2 $SeBr_2/Et_4NBr$ solutions results in crystallization of the corresponding tribromo- and tetrabromo-salts, Et_4NSeBr_3 and $(Et_4N)_2SeBr_4$. The Raman spectra of these compounds are shown in Fig. 2 and listed in Table 2. The spectrum of Et_4NSeBr_3 corresponds well with that reported for $(Ph_4P)SeBr_3$,[11] which is known to contain the dimeric anion with Br bridging similar to that of $Se_2Cl_6^{2-}$ above. The solution spectrum of tribromo-selenate(II) ion differs significantly from that of the solid. In solution the monomeric solvated $SeBr_3^-$ ion is present.[8] The Raman spectrum of this ion parallels closely that of the $SeOBr_3^-$ ion, ignoring the SeO stretching and deformation modes, as expected where the '$SeBr_3$' skeletons in both anions are T-shaped.

Only one band is observed in the solution spectrum of the $SeBr_4^{2-}$ ion. This band at 162 cm^{-1} is strongly polarized and lies very close to the A_{1g} band observed for solid $(Ph_4P)_2SeBr_4$.[11] However, the Raman spectrum of solid $(Et_4N)_2SeBr_4$ is more complex than that reported for $(Ph_4P)_2SeBr_4$[11] and the strongest peak is 31 cm^{-1} higher than that observed for the latter compound. The spectrum suggests that some anion–anion interaction may occur in the compound with the smaller cation and further work will be necessary to confirm this.

Acknowledgements—The National Science and Engineering Research Council of Canada is thanked for financial support. Lisa Frost and Pierre LaHaie are thanked for technical assistance.

REFERENCES

1. D. M. Yost and C. E. Kircher, *J. Am. Chem. Soc.* 1930, **52**, 4680.
2. G. A. Ozin and A. Van der Voet, *J. Chem. Soc. D* 1970, 896.
3. H. Willner, *Zeit. Anorg. Allgem. Chem.* 1981, **481**, 117.
4. N. W. Tideswell and J. D. McCullough, *J. Am. Chem. Soc.* 1956, **78**, 3026.
5. K. Katsaros and J. W. George, *Inorg. Chem.* 1969, **8**, 759.
6. J. B. Milne, *Polyhedron* 1985, **4**, 65.
7. M. Mahadevan and J. B. Milne, *Inorg. Chem.* 1983, **22**, 1648.
8. K. J. Wynne and J. Golen, *Inorg. Chem.* 1974, **13**, 185.
9. B. Krebs, A. Schaffer and M. Hucke, *Z. Naturforsch.* 1982, **37b**, 1410.
10. B. Krebs, M. Hucke, M. Hein and A. Schaffer, *Z. Naturforsch.* 1983, **38b**, 20.
11. B. Krebs and A. Schaffer, *Z. Naturforsch.* 1984, **39b**, 1633.
12. J. Milne, *Inorg. Chem.* 1979, **18**, 2924.
13. P. LaHaie, Ph.D. Dissertation, University of Ottawa, Ottawa, Canada (1981).
14. P. LaHaie and J. B. Milne, *Inorg. Chem.* 1979, **18**, 632.
15. J. B. Milne and P. LaHaie, *Inorg. Chem.* 1983, **22**, 2425.
16. G. Brauer, *Handbook of Preparative Inorganic Chemistry*, Vol. 1, p. 427. Wiley, New York (1963).
17. *Inorganic Syntheses*, Vol. 5, p. 1525. McGraw-Hill. New York (1957).
18. J. Milne, *Inorg. Chem.* 1978, **17**, 3592.

Polyhedron Vol. 6, No. 5, pp. 855–861, 1987
Printed in Great Britain

0277–5387/87 $3.00+.00

METAL–PHENOXYALKANOIC ACID INTERACTIONS—XXIII.* COMPLEXES OF COPPER(II) WITH THE PHENOXYISOBUTYRIC ACIDS. THE CRYSTAL STRUCTURES OF TETRA-μ-[2-METHYL-2-(4-CHLOROPHENOXY)PROPANOATO-*O*,*O*′)]-BIS[(2-AMINOPYRIMIDINE)COPPER(II)] AND TWO POLYAQUACOPPER(II) TRI-μ-[2-METHYL-2-PHENOXYPROPANOATO-*O*,*O*′]-BIS[(2-METHYL-2-PHENOXYPROPANOATO)COPPER(II)] POLYMORPHS

THOMAS C. W. MAK

Department of Chemistry, The Chinese University of Hong Kong, Shatin, New Territories, Hong Kong

COLIN H. L. KENNARD

Department of Chemistry, University of Queensland, Brisbane, 4067, Australia

and

GRAHAM SMITH,† ERIC J. O'REILLY, DALIUS S. SAGATYS **and** JANELLE C. FULWOOD

Department of Chemistry, Queensland Institute of Technology, Brisbane, 4000, Australia

(*Received* 16 *June* 1986; *accepted* 4 *August* 1986)

Abstract—The crystal structures of three copper(II) complexes with phenoxyisobutyric acid (PIBAH) and *p*-chlorophenoxyisobutyric acid (PCIBAH) have been determined by X-ray diffraction. Tetra-μ-[2-methyl-2-(4-chlorophenoxy)-propanoato-*O*,*O*′]-bis[2-aminopyrimidine)copper(II)], $[Cu_2(PCIBA)_4(2\text{-aminopyrimidine})_2]_2$ (**1**) is a centrosymmetric tetracarboxylate bridged dimer [Cu···Cu, 2.689(2) Å] with the nitrogens of the 2-aminopyrimidine molecules occupying the axial positions [Cu—N, 2.198(7) Å]. Tetraaquacopper(II) tri-μ-[2-methyl-2-phenoxypropanoato-*O*,*O*′]-bis[(2-methyl-2- phenoxypropanoato(copper(II)], $[Cu(H_2O)_4]^{2+}$ $\{[Cu_2(PIBA)_5]^-\}_2$, (**2**), is a disordered precursor of the stable structure (**3**), $[Cu(H_2O)_5]^{2+}$ $\{[Cu_2(PIBA)_5]^-\}\cdot 4H_2O$, consisting of centrosymmetric square planar $[Cu(H_2O)_4]^{2+}$ cations and tris(carboxylate)-bridged dimer anions [Cu···Cu, 2.85(1) Å] (**2**). The fourth position of each square planar dimer 'end' is occupied by a carboxylate oxygen of a PIBA molecule which also provides the ether oxygen capping each axial dimer site [Cu—O, 2.15(4), 2.19(5) Å]. This completes a five-membered chelate ring. A symmetrical array of eight hydrogen bonds link the four waters of the $[Cu(H_2O)_4]^{2+}$ cation to the carboxyl oxygens of both the capping PIBA ligands of the two dimeric anions. Structure (**3**) has essentially identical $[Cu_2(PIBA)_5]^-$ dimer anions [Cu···Cu, 2.929(1) Å] and hydrogen-bonding interactions with the tetraaquacopper(II) cations. However, water molecules partially occupy the octahedral sites of these cations [Cu—O, 2.46(1) Å], as well as a number of lattice sites in the crystal.

---

*Part XXII. The structure of silver(I) (2-carbamoyl)phenoxyacetate.

†Author to whom correspondence should be addressed.

Phenoxyisobutyric acid (PIBAH) has been shown to form unusual complexes with divalent metal ions. With zinc, a novel polymeric complex $[Zn_5(PIBA)_{10}(H_2O)_2]_n$ is formed, having three independent complex centres, two octahedral and one trigonal bipyramidal.[2] Reaction of copper(II) carbonate with PIBAH in aqueous ethanol gave several polymorphs. An early formed green triclinic form (**2**) showed the unusual stoichiometry $\{[Cu_5(PIBA)_{10}(H_2O)_4]\}$, while digestion of the reaction mixture for longer periods gave stable dark green monoclinic crystals. Single crystal preliminaries indicated that a disorder problem decreased with the digestion period, giving finally complex (**3**) with an analysis consistent with the formula $[Cu_5(PIBA)_{10}(H_2O)_9]$.

When *p*-chlorophenoxyisobutyric acid (clofibric acid or PCIBAH) was used instead of PIBAH, a green microcrystalline complex was formed which, on digestion with 2-aminopyrimidine, gave the dark green adduct $[Cu_2(PCIBA)_4(2\text{-aminopyrimidine})_2]$ (**1**). The structures of all three complexes were determined to help clarify the anomalous behaviour of these acids towards copper(II).

EXPERIMENTAL

Preparation

The complexes were prepared as previously described by reacting PIBAH or PCIBAH respectively with excess copper(II) carbonate in boiling aqueous ethanol. Digestion of copper(II) *p*-chlorophenoxyisobutyrate with 2-aminopyrimidine in ethanol gave (**1**) as dark green needles. Complex (**3**) was obtained as the final product in the crystallization of copper(II) phenoxyisobutyrate after a minimum of 2 h digestion on a steam bath.

Analysis

$[Cu_5(PIBA)_{10}(H_2O)_4]$, (**2**). Found: C, 54.2; H, 5.5. Calc. for $C_{100}H_{118}Cu_5O_{34}$: C, 55.0; H, 5.5%.

$[Cu_5(PIBA)_{10}(H_2O)_9]$, (**3**). Found: C, 52.6; H, 5.3. Calc. for $C_{100}H_{128}Cu_5O_{39}$: C, 52.8; H, 5.6%.

Crystal data

(**1**) $[Cu_2(PCIBA)_4(2\text{-aminopyrimidine})_2]$, $C_{48}H_{50}Cl_4Cu_2N_6O_{12}$, $Mr = 1171.3$, triclinic, $a = 8.848(1)$, $b = 12.358(4)$, $c = 12.844(3)$ Å, $\alpha = 102.66(2)$, $\beta = 12.358(4)$, $\gamma = 96.10(2)°$, $V = 1333.0(6)$ Å^3, $Z = 1$, $D_c = 1.459$, $D_f = 1.43$ g cm^{-3}, $F(000) = 602$, $\lambda = 0.71069$ Å, μ(Mo-K_α) = 10.9 cm^{-1}, space group $P\bar{1}$.

(**2**) $[Cu_5(PIBA)_{10}(H_2O)_4]$, $C_{100}H_{118}Cu_5O_{34}$, $Mr = 2181.7$, triclinic, $a = 14.32(1)$, $B = 10.950(8)$, $c = 19.67(1)$ Å, $\alpha = 99.17(4)$, $\beta = 90.32(4)$, $\gamma = 117.22(4)°$,‡ $V = 2697(2)$ Å^3, $Z = 1$, $D_c = 1.343$, $D_f = 1.35$ g cm^{-3}, $F(000) = 1135$, $\lambda = 0.71069$ Å, μ(Mo-K_α) = 10.9 cm^{-1}, space group $P\bar{1}$.

(**3**) $[Cu_5(PIBA)_{10}(H_2O)_9]$, $C_{100}H_{128}Cu_5O_{39}$, $Mr = 2271.7$, monoclinic, $a = 41.90(1)$, $b = 12.135(4)$, $c = 21.501(3)$ Å, $\beta = 91.13(2)°$, $V = 10930(5)$ Å^3, $Z = 4$, $D_c = 1.380$, $D_f = 1.38$ g cm^{-3}, $F(000) = 4740$, $\lambda = 0.71069$ Å, μ(Mo-K_α) = 10.4 cm^{-1}, space group $C2/c$.

X-ray data collection, structure solution and refinement

Data for compounds (**1**)–(**3**) were collected at 293 K on a Nicolet R3m four-circle diffractometer using monochromated Mo-K_α radiation. 4662, 5699 and 4211 unique reflections were collected up to $2\theta_{max} = 50$, 42 and 40° respectively, from crystals measuring $0.40 \times 0.24 \times 0.05$ mm (**1**), $0.46 \times 0.10 \times 0.08$ mm (**2**) and $0.36 \times 0.32 \times 0.18$ mm (**3**). Of these, 2935, 1922 and 3211 respectively, with $I > 2.5\sigma(I)$ were considered observed and used in structure analysis. Data were processed using the learnt profile fitting procedure of Diamond[4] and used without corrections for absorption or extinction. The structure of (**1**) was solved by direct methods[5] and refined by blocked matrix least-squares with unit weights to $R(= \Sigma \|F_o - F_c\| / \Sigma |F_o|) = 0.082$ with anisotropic temperature factors for only the atoms of the coordination sphere and the two chlorines. A number of hydrogens were located in a difference-Fourier synthesis and included in the refinement at fixed positions with their isotropic U values fixed at 0.05 Å^2. The high residual is attributed to considerable thermal motion in evidence in certain of the ring atoms and the attached chlorines, possibly due to disorder in these systems. With (**2**) and (**3**), sharpened Patterson syntheses gave the positions of three copper atoms, one at (0, 0, ½) (**2**) or (0, 0, 0) (**3**) the other two at general positions, separated by ~ 2.8 Å. The latter distance, although long compared with typical values for tetracarboxylate bridged copper(II) dimers, e.g. 2.69 Å for (**1**) and a range of 2.56–2.89 Å for 43 dimers,[6] suggested dimeric species. Subsequent weighted difference-Fourier syntheses gave for (**2**) well-defined coordination polyhedra for both a square planar $[Cu(H_2O)_4]^{2+}$ monomer about (0, 0, ½) and a dimer. However, atoms of the phenoxyisobutyrate ligands of (**2**) were

‡ Reduced cell: $a = 10.94(1)$, $b = 13.47(1)$, $c = 19.67(°)$ Å, $\alpha = 82.21(4)$, $\beta = 80.82(4)$, $\gamma = 70.93(4)°$.

not located with any degree of accuracy, indicative of considerable disorder throughout the structure. Because of the size of the molecule, resolution of the problem in space group $P\bar{1}$ was not attempted and the results are therefore presented in the discussion for the structure at $R = 0.17$, with only the copper atoms being refined anisotropically.

Unlike (**2**), the ring disorder problem was not found in (**3**) and blocked matrix least-squares refinement with anisotropic thermal parameters for the coppers, the oxygens of the PIBA ligands and the coordinated waters, was used. In addition, a number of disordered lattice water molecules, consistent with the formula derived from chemical analyses and density measurements were included in the refinement with the appropriate site occupancy. This gave a final $R = 0.088$ and $Rw = 0.098$. A value of $w = 3.51$ $(\sigma^2 F_o + 1.23 \times 10^{-3} F_o^2)$ was obtained. No hydrogens were located or added to the refinement. For all analyses, neutral atom scattering factors were used, corrected where appropriate for the effects of anomalous dispersion.[7] Bond distances and angles about the coordination polyhedra for (**1**), (**2**) and (**3**) are listed in Table 1. Atomic coordinates, anisotropic thermal parameters, hydrogen atom coordinates (**1**), and observed and calculated structure factors have been deposited with the Editor as supplementary material; copies are available on request. Atomic coordinates have also been deposited with the Cambridge Crystallographic Data Centre.

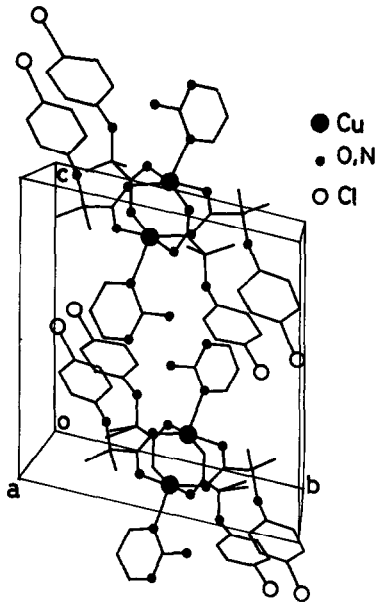

Fig. 2. Packing of (**1**) in the unit cell.

DISCUSSION

$[Cu_2(PCIBA)_4(2\text{-}aminopyrimidine)_2]$ (**1**)

Compound (**1**) forms discrete centrosymmetric tetracarboxylate bridged dimers (Fig. 1), analogous to the 2-aminopyrimidine adduct of copper(II) 4-fluorophenoxyacetate, $[Cu_2(4\text{-FPA})_4(2\text{-aminopyrimidine})_2]$.[8] The bond distances and angles about the dimer cage (mean Cu—O, Cu—N and Cu···Cu) are similar [1.968(7), 2.198(7), 2.689(2) Å (**1**) and 1.977(3), 2.176(3), 2.710(1) Å respectively]. Bonding of the pyrimidine molecules is also via one of the hetero nitrogens while the 2-amino groups provide stabilization to the structure through intradimer hydrogen bonding associations with carboxyl oxygens of one of the coordinated ligands [N(21)···O(11)B, 2.85 Å]. This structure contrasts with that for the 2-aminopyrimidine adduct of copper(II) 2-chlorophenoxyacetate, $[Cu_2(2\text{-CPA})_4(2\text{-aminopyrimidine})]_n$ which forms polymer chains through the *meta*-related hetero nitrogens of the pyrimidine ring.[9] With (**1**), there are no interdimer associations involved in the packing of the molecules in the unit cell (Fig. 2). However, the packing does appear to influence the conformations

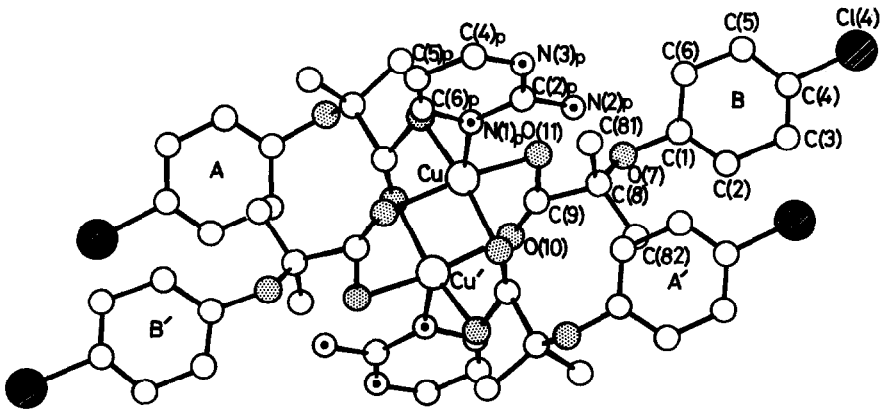

Fig. 1. Molecular configuration and atom naming scheme for (**1**).

Table 1. Bond distances (Å) and angles (degrees) about the coordination spheres for $[Cu_2(PCIBA)_2(aminopyrimidine)_2]$ (**1**), $[Cu_5(PIBA)_{10}(H_2O)_4]$, (**2**) and $[Cu_5(PIBA)_{10}(H_2O)_9]$, (**3**)

(**1**) Distances

Cu—O(10)A	1.961(6)	Cu—O(11)B	1.979(7)
Cu—O(10)B	1.973(7)	Cu—N(1)p	2.198(7)
Cu—O(11)A	1.961(7)	Cu—Cu′	2.689(2)

Angles

N(1)p—Cu—O(10)A	101.5(3)	O(10)B—Cu—O(11)B′	166.8(3)
N(1)p—Cu—O(10)B	97.3(3)	O(11)A′—Cu—O(11)B′	91.2(3)
N(1)p—Cu—O(11)A′	92.3(3)	Cu—N(1)p—C(6)p	114.8(6)
N(1)p—Cu—O(11)B′	95.8(3)	Cu—N(1)p—C(2)p	129.6(6)
O(10)A—Cu—O(10)B	88.8(3)	Cu—O(10)A—C(9)A	122.5(5)
O(10)A—Cu—O(11)A′	166.2(3)	Cu—O(10)B—C(9)B	120.5(6)
O(10)A—Cu—O(11)B′	89.2(3)	Cu—O(11)A—C(9)A	125.4(5)
O(10)B—Cu—O(11)A′	87.8(3)	Cu—O(11)B—C(9)B	125.1(5)

(**2**) and (**3**)

Distances

	(2)	(3)		(2)	(3)
Cu(1)—Ow(1)	1.92(4)	1.97(1)	Cu(3)—O(7)B	2.15(4)	2.220(9)
Cu(1)—Ow(2)	1.92(4)	1.92(1)	Cu(3)—O(11)B	1.94(3)	1.971(9)
Cu(1)—Ow(3)	—	2.46(1)	Cu(3)—O(11)C	1.91(4)	1.953(10)
Cu(2)—O(7)A	2.19(5)	2.201(9)	Cu(3)—O(11)D	1.89(3)	1.984(4)
Cu(2)—O(11)A	1.98(4)	1.917(9)	Cu(3)—O(10)E	1.93(4)	1.960(9)
Cu(2)—O(10)C	2.03(3)	2.025(10)	Cu(2)—Cu(3)	2.85(1)	2.929(1)
Cu(2)—O(10)D	2.08(3)	1.974(9)			
Cu(2)—O(11)E	1.97(3)	1.910(8)			

Angles

	(2)	(3)		(2)	(3)
Ow(1)—Cu(1)—Ow(2)	89(2)	89.2(3)	O(7)B—Cu(3)—O(11)B	78(1)	75.8(4)
Ow(1)—Cu(1)—Ow(3)	—	74.1(3)	O(7)B—Cu(3)—O(11)C	76(1)	97.1(4)
O(7)A—Cu(2)—O(11)A	78(2)	76.1(3)	O(7)B—Cu(3)—O(10)D	103(2)	94.4(4)
O(7)A—Cu(2)—O(10)C	97(2)	90.7(4)	O(7)B—Cu(3)—O(10)E	98(2)	106.9(4)
O(7)A—Cu(2)—O(11)D	105(1)	120.8(4)	O(11)B—Cu(3)—O(11)C	95(1)	89.1(4)
O(7)A—Cu(2)—O(11)E	95(1)	92.8(3)	O(11)B—Cu(3)—O(10)D	84(1)	88.0(4)
O(11)A—Cu(2)—O(10)C	92(1)	91.8(4)	O(11)B—Cu(3)—O(10)E	174(1)	176.6(4)
O(11)A—Cu(2)—O(11)D	89(1)	85.9(4)	O(11)C—Cu(3)—O(10)D	160(2)	167.1(4)
O(11)A—Cu(2)—O(11)E	173(1)	166.4(4)	O(11)C—Cu(3)—O(10)E	90(2)	92.5(4)
O(10)C—Cu(2)—O(11)D	158(2)	146.6(4)	O(10)D—Cu(3)—O(10)E	91(1)	89.8(4)
O(10)C—Cu(2)—O(11)E	90(1)	95.7(4)	Cu(3)—O(7)B—Cu(2)	173(1)	171.3(2)
O(11)D—Cu(2)—O(11)E	91(1)	93.8(4)	Cu(3)—O(7)B—C(1)B	126(3)	124.4(8)
O(7)A—Cu(2)—Cu(3)	174(1)	160.9(2)	Cu(3)—O(7)B—C(8)B	117(3)	113.8(8)
Cu(2)—O(7)A—C(1)A	119(2)	121.9(8)	Cu(3)—O(11)B—C(9)B	121(4)	121.0(10)
Cu(2)—O(7)A—C(8)A	110(2)	114.9(7)	Cu(3)—O(11)C—C(9)C	136(3)	119.2(9)
Cu(2)—O(11)A—C(9)A	118(3)	123.1(8)	Cu(3)—O(10)D—C(9)D	121(3)	120.6(9)
Cu(2)—O(10)C—C(9)C	133(3)	131.7(10)	Cu(3)—O(10)E—C(9)E	133(6)	123.8(9)
Cu(2)—O(11)D—C(9)E	113(2)	128.6(9)			
Cu(2)—O(11)E—C(9)E	116(2)	128.6(8)			

assumed by the ligands which tend to orientate so as to acheive parallelism in the phenoxy groups. This is consistent with observations for other copper(II) phenoxyalkanoate dimers. The comparative torsion angles for ligands A and B in (**1**) [C(2)—C(1)—O(7)—C(8): −84.8, +98.8°; C(1)—O(7)—C(8)—C(9): +80.3, +179.9°; O(7)—C(8)—C(9)—O(10): +10.7, −172.8°] indicate that B is extended while A is twisted. The ligands consequently assume gross conformations with the ether oxygen and one of the carboxyl oxygens synplanar but with significantly different

O(ether)···O(carboxyl) distances [2.719 Å; 2.536 Å]. These values compare with 2.723 Å found for the acid itself.[10]

$[Cu_5(PIBA)_{10}(H_2O)_4]$ (2) *and* $[Cu_5(PIBA)_{10}(H_2O)_9]$ (3)

Although the structure of (2) was not well refined ($R = 0.17$), disorder appears to be confined to the peripheral regions of the complex while the core, consisting of the three copper(II) polyhedra, is quite well defined and allows a meaningful comparison with (3). The net formula of both (2) and (3) [the cell contents in complex (2)] comprises two $[Cu_2(PIBA)_5]^-$ anionic dimers and a square planar $[Cu(H_2O)_4]^{2+}$ cation, lying at a centre of inversion [(0, 0, $\frac{1}{2}$) (2) and (0, 0, 0) (3)]. The Cu—Ow distances in the monomers are 1.92, 1.92(4) Å (2) and 1.92, 1.96(1) Å (3). The occurrence of a discrete square planar tetraaquacopper(II) species is very unusual since the aquated ion more readily gives a rhombic distorted octahedral $[Cu(H_2O)_6]^{2+}$ cation, such as found in Tutton's salts,[11,12] $[Cu^{II}(H_2O)_6SO_4 \cdot M^I_2SO_4]$ and where $M^I = K^+$, Rb^+ or Cs^+. In this isomorphous series, the Cu—O distances in the centrosymmetric 'square' plane range from 1.943(2), 2.069(2) Å in $[Cu(H_2O)_6SO_4 \cdot K_2SO_4]$[13] to 1.966(5), 2.004(4) Å in $[Cu(H_2O)_6SO_4 \cdot Cs_2SO_4]$ neutron).[14] The situation is approached in (3) with a water molecule [Ow(4)] partially occupying the tetragonal sites of the distorted octahedron [Cu—O, 2.46(1) Å]. Some distortion is also apparent in the Cu—O (equatorial) distances compared to those in (2). This axial water forms only a very weak bond to copper since the Cu—O (axial) distance in the Tutton's salts is typically 2.26(1) Å.[13]

The $[Cu_2(PIBA)_5]^-$ dimers in both complexes represent the first examples of tris-carboxylate bridged copper(II) dimeric species, instead of the usual tetra-carboxylate bridging mode. However, the usual dimer core is essentially retained with the fourth position on each square planar 'end' occupied by a carboxylate oxygen of a non-bridging phenoxyisobutyrate ligand, giving mean Cu—O (equatorial) distances of 1.98(4) Å (2) and 1.96(1) Å (3). These same two non-bridging ligands also provide ether oxygens to cap the axial positions of the dimer [Cu—O, 2.15(4), 2.19(5) Å (2) and 2.201, 2.220(9) Å] (Figs 3 and 4) forming five-membered chelate rings. These axial Cu—O bonds are close to colinear in (2) [O(7)A—Cu(2)···Cu(3), 174.3(9)°; O(7)B—Cu(3)···Cu(2), 172.8(8)°]; and for ligand B in (3) [171.3(2)°] but deviate for ligand A, [160.9(2)°]. This is accompanied by a shortening of the Cu—O(11)A distance to 1.917(9) Å. In addition, the carboxylato-*O,O'* bridges are twisted in some of the ligands (Fig. 5), presumably because of the steric imposition of the bulky PIBA ligands.

All bond distances are in agreement with those

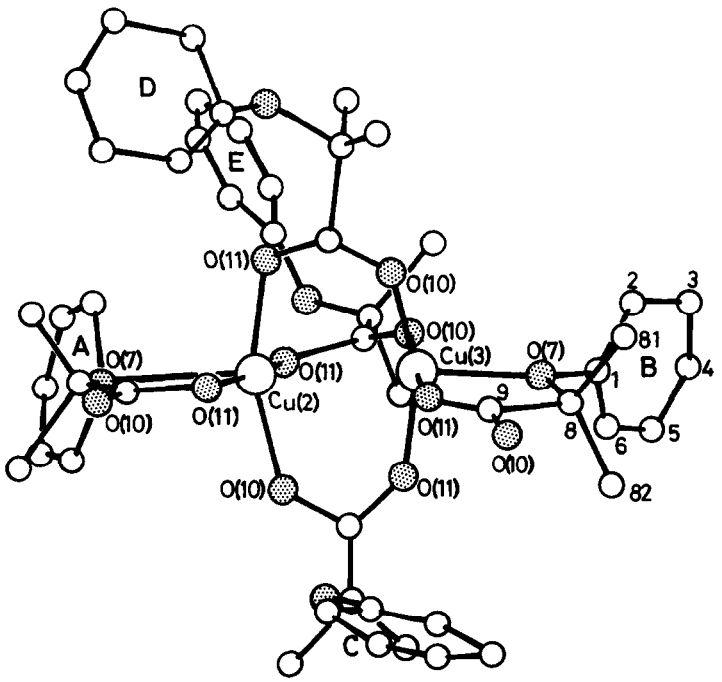

Fig. 3. Molecular configuration of the anionic dimer unit in the structure of (2).

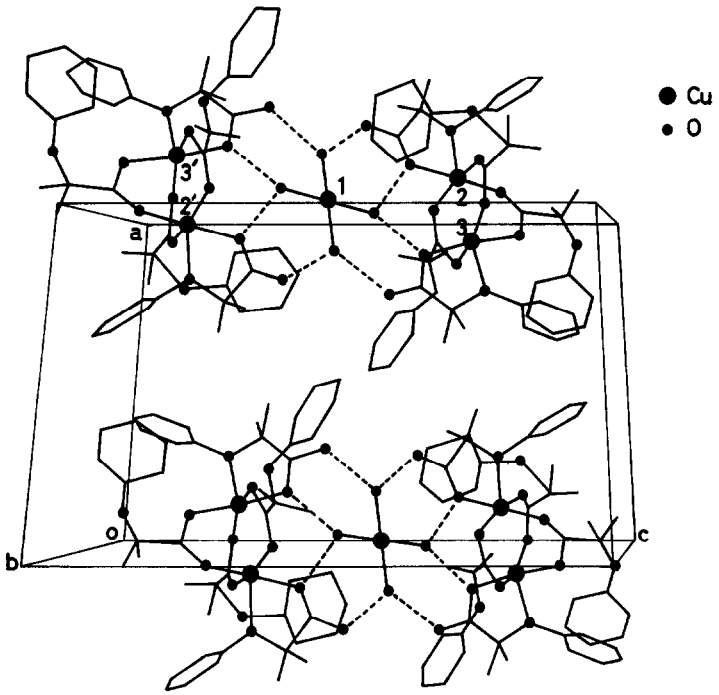

Fig. 4. Packing of (**2**) in the unit cell.

of the conventional copper(II) dimers[6] although the Cu···Cu separation for (**2**) [2.85(1) Å] approaches, or for (**3**) [2.929(1) Å] exceeds the maximum known {2.89 Å in $[Cu_2(CF_3COO)_4(quin)_2]$.[15] The occupancy of the axial positions of the dimer by ether oxygens is consistent with the usual formation in monomeric tetragonally distorted octahedral copper(II) phenoxyacetates of bis-chelate species having ether oxygens at the tetragonally elongated sites.[3] However, these Cu—O distances in (**2**) and (**3**) are considerably shorter than those in the copper(II) monomers which are typically 2.47 Å $[Cu(4\text{-fluorophenoxyacetato})_2(H_2O)_2]$.[8]

In both (**2**) and (**3**), the two complex anions are linked to the waters of the $[Cu(H_2O)_4]^{2+}$ cation by a symmetrical network of eight hydrogen bonds with the carboxyl oxygens of the terminal PIBA ligands (A and B) (Fig. 4). Both the coordinated and uncoordinated oxygens [O(11) and O(10), respectively] are involved [Ow(1)···O(10)A, 2.72 Å (**2**) 2.62 Å (**3**); ···O(10)B, 2.53 Å (**2**), 2.58 Å (**3**); Ow(2)···O(11) A. 2.58 Å (**2**), 2.61 Å (**3**);

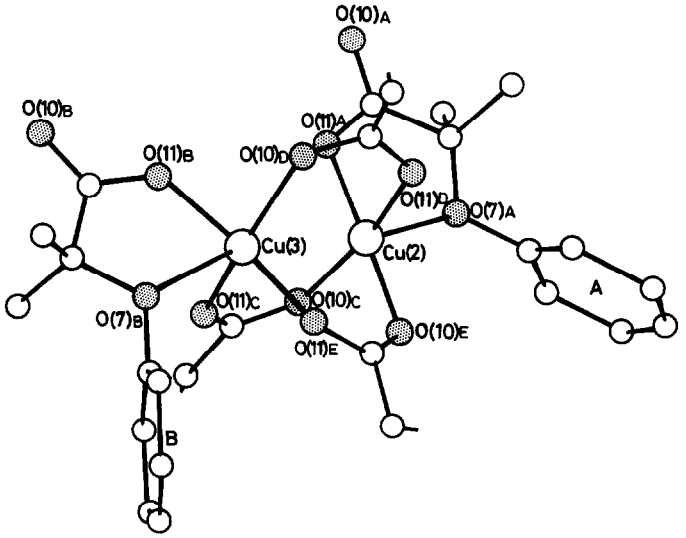

Fig. 5. Molecular configuration of the anionic dimer in (**3**).

···O(11)B, 2.63 Å (**2**), 2.65 Å (**3**)], resulting in discrete $[Cu_5(PIBA)_{10}(H_2O)_4]$ units centred about crystallographic inversion centres in their respective cells. No inter-unit associations are found. The ligands show considerable conformational variation, but as for the majority of the phenoxyalkanoic acids and their ligands found in metal complexes, the O(ether)···O(carboxyl) interactive distances are relatively constants [2.59–2.77 Å (**2**); 2.55–2.77 Å (**3**)]. The shorter distances are found in the ligands A and B of both complexes [2.59, 2.63 Å (**2**) and 2.55, 2.58 Å (**3**)] and are a consequence of the chelate ring formation in each. Comparable O···O distances are found for the analogous chelate rings in the tetragonally distorted monomeric copper(II) phenoxyalkanoate complexes.[8] With the bridging ligands the O···O distances are closer to that of the parent acid PIBAH (2.71 Å).[10]

Lattice stability in the case of (**3**) appears to be derived to some degree from the incorporation of additional water molecules in the lattice. The majority of these waters have only partial site occupancy and are either inter-associated or form hydrogen-bonding interactions with the waters of the $[Cu(H_2O)_4]^{2+}$ complex or with the carboxylate oxygens of the dimers. Of greater importance is the stability achieved through the hydrogen bonding between the $[Cu(H_2O)_4]^{2+}$ cations and the $[Cu_5(PIBA)_{10}]^-$ dimer anions. This is emphasized by the presence of the well-defined complex core even in the disordered triclinic crystals of (**2**), which may be considered as a disordered precursor of the stable monoclinic form (**3**). It might be reasonable to postulate that a more stable form than (**3**) was possible via full site occupancy by the lattice waters, without change in the unit cell. However, there is no evidence that any product other than (**3**) is formed even when prolonged digestion and crystallization conditions are employed.

Acknowledgements—The authors acknowledge financial assistance from the University of Queensland and the Queensland Institute of Technology. The Chinese University of Hong Kong is thanked for providing X-ray diffraction facilities.

REFERENCES

1. T. C. W. Mak, W.-H. Yip, C. H. L. Kennard, G. Smith and E. J. O'Reilly, *Aust. J. Chem.* 1986, **39**, 541.
2. G. Smith, E. J. O'Reilly, C. H. L. Kennard and T. C. W. Mak, *Inorg. Chem.* 1985, **24**, 2321.
3. G. Smith, E. J. O'Reilly, C. H. L. Kennard, K. Stadnicka and B. Oleksyn, *Inorg. Chim. Acta* 1981, **47**, 11.
4. R. Diamond, *Acta Cryst., Sect. A.* 1969, **25**, 43.
5. G. M. Sheldrick, *'SHELX-76', Program for Crystal Structure Determination*, University of Cambridge, England (1976).
6. M. Melnik, *Coord. Chem. Rev.* 1982, **42**, 259.
7. *International Tables for X-ray Crystallography*, Vol. 4 (Edited by J. A. Ibers and W. C. Hamilton). Kynoch Press, Birmingham (1974).
8. E. J. O'Reilly, G. Smith and C. H. L. Kennard, *Inorg. Chim. Acta* 1984, **90**, 63.
9. G. Smith, E. J.. O'Reilly, C. H. L. Kennard and A. H. White, *J. Chem. Soc., Dalton Trans.* 1985, 243.
10. C. H. L. Kennard, G. Smith and A. H. White, *Acta Cryst., Sect B* 1982, **38**, 868.
11. A. E. H. Tutton, In *Crystalline Structure and Chemical Composition*, p. 99. Macmillan, London (1910).
12. J. M. Whitnall and C. H. L. Kennard, *J. Solid State Chem.* 1977, **22**, 379.
13. D. J. Robinson and C. H. L. Kennard, *Cryst. Struct. Commun.* 1972, **1**, 185.
14. K. G. Shields and C. H. L. Kennard, *Cryst. Struct. Commun.* 1972, **1**, 189.
15. J. A. Moreland and R. J. Doedens, *J. Am. Chem. Soc.* 1975, **97**, 508.

Polyhedron Vol. 6, No. 5, pp. 863–870, 1987
Printed in Great Britain

0277–5387/87 $3.00+.00

THE SYNTHESIS, STRUCTURE AND SPECTROSCOPIC PROPERTIES OF THE DI- AND TRI-NUCLEAR Ni(II) THIOLATE COMPLEXES

JOHN R. NICHOLSON, GEORGE CHRISTOU,* JOHN C. HUFFMAN and KIRSTEN FOLTING

Department of Chemistry and the Molecular Structure Center, Indiana University, Bloomington, IN 47405, U.S.A.

(*Received* 15 *May* 1986; *accepted* 4 *August* 1986)

Abstract—The anions $[Ni_2(edt)_3]^{2-}$ (edt = ethane-1,2-dithiolate) and $[Ni_3(edt)_4]^{2-}$ have been prepared by the reaction of $Na_2(edt)$ with $NiCl_2 \cdot 6H_2O$ and, with subsequent work-up, isolated as their $[PPh_4]^+$ salts. For the first time, the structure of di- and tri-nuclear Ni(II) thiolates with identical ligands can be compared. The complex $[PPh_4]_2[Ni_2(edt)_3]$ (**1**) crystallizes in the triclinic space group $P\bar{1}$ with unit cell parameters (at −152°C) $a = 12.861(7)$, $b = 21.057(14)$, $c = 10.324(5)$ Å, $\alpha = 96.03(3)°$, $\beta = 109.88(3)°$, $\gamma = 76.82(3)°$, and $Z = 2$, while $[PPh_4]_2[Ni_3(edt)_4]$ (**2**) crystallizes in the monoclinic space group $P2_1/c$ with (at −60°C) $a = 13.713(3)$, $b = 13.255(3)$, $c = 15.754(5)$ Å, $\beta = 96.53(2)°$ and $Z = 2$. The structures were solved by direct methods and Fourier techniques from 4576 and 2671 diffractometer data, respectively, and refined to respective R values of 0.0552 and 0.0649. In the anion of **1**, one of the ligands provides two terminal thiolate-groups, and the other two each provide one terminal and one μ-thiolate-group such that each Ni(II) has an approximately square planar coordination geometry. The central NiS_2Ni unit is not planar, being folded along the vector joining the two bridging sulphur atoms. The anion of **2** is best considered as chelation of two identical $[Ni(edt)_2]^{2-}$ units to a third, central Ni(II) atom. The anion has a crystallographically observed centre of symmetry, with the central nickel atom thus lying in a perfect plane formed by its four coordinated sulphur atoms. The outer two nickel atoms are approximately square planar and the $Ni(NiS_4)_2$ core exists in a chair conformation. Both of the anions described have short Ni···Ni distances [2.9414(22) in (**1**) and 2.8301(13) Å in (**2**)]. The structures and the spectroscopic properties achieved for these complexes are described and discussed herein.

Our interest in the thiolate chemistry of nickel was stimulated by reports that in several reduced and oxidized hydrogenases the primary coordination sphere of nickel contains several sulphur atoms[1,2] and by the paucity of well-characterized compounds of this type in the literature which might be considered useful structural analogues. Although nickel is found in its +3 oxidation level in the resting state of the hydrogenases,[1,2] the +2 level is involved in the catalytic cycle. Hence the synthesis and characterization of some nickel(II) thiolates was considered to be of importance as a necessary first step in a modelling approach.

Prior to this work being undertaken, a few structurally characterized homoleptic nickel(II) thiolates had been reported[3–9] but none with edt. In our investigation of this area the bidentate ligand ethane-1,2-dithiolate was employed because this ligand has recently found much utility in the thiolate chemistry of the first row transition metals[10,11,13–16] and has been shown to stabilize some of these metals in what is regarded as high oxidation levels.[11,13,16]

Herein, we report the preparation, spectroscopic, and structural characterization of the two title complexes, $[PPh_4]_2[Ni_2(edt)_3]$ and $[PPh_4]_2[Ni_3(edt)_4]$, which contribute to the structural diversity already established for existing nickel thiolates[3–9,12] and allow for the first time direct structural comparison

* Author to whom correspondence should be addressed.

of di- and tri-nuclear Ni(II) thiolates with identical ligands.

EXPERIMENTAL

All manipulations were performed using standard inert-atmosphere techniques. Acetonitrile was distilled from CaH_2 under a dinitrogen atmosphere and ethanol was dried over molecular sieves and degassed before use. Ethane-1,2-dithiol was used as received.

Proton NMR spectra were measured for concentrated solutions in $(CD_3)_2SO$ at 300 and 360 MHz on Varian XL-300 and Nicolet NT-360 instruments. Electronic spectra were obtained in CH_3CN or DMF solution on a 8450A Hewlett Packard UV–Vis spectrophotometer interfaced with a Hewlett Packard 7470A Plotter. IR spectra were recorded, with Nujol mulls between CsI plates, in the range 4000–200 cm^{-1} on a Perkin–Elmer 283 spectrometer. Electrochemical measurements were performed in the cyclic voltammetric mode with an IBM model EEC 25 voltammetric analyser in conjunction with a glassy carbon working electrode, a platinum-wire auxiliary electrode, and an SCE reference electrode. The supporting electrolyte was 0.1 M tetra-*n*-butylammonium perchlorate (TBAP), and concentrations of electroactive species were in the *c.* 5 mM range. Measurements were performed in MeCN solution, and potentials are quoted vs the normal hydrogen electrode (NHE) with ferrocene as an internal standard ($E_{1/2}$ = 0.400 V vs NHE).

Preparation of $[PPh_4]_2[Ni_2(SCH_2CH_2S)_3]$

Sodium metal (0.77 g, 34.0 mmol) was dissolved in EtOH (60 cm^3) and ethane-1,2-dithiol (1.40 cm^3, 17 mmol) added followed by solid $NiCl_2 \cdot 6H_2O$ (2.0 g, 8.4 mmol). Stirring at room temperature resulted in the formation of a white precipitate (NaCl) in a dark green solution within 0.5 h. The solution was filtered into a Schlenk tube containing PPh_4Br (7.4 g, 18 mmol). Intensely green coloured microcrystals of the product began precipitating almost immediately and after storage at room temperature for 24 h this product was collected by filtration, washed with two portions of an $EtOH/Et_2O$ mixture (10 cm^3, 1 : 1 composition) and dried *in vacuo*. The crude yield obtained was 2.8 g (52% with respect to nickel). After several days a further 0.55 g of product was isolated from the filtrate as very large chunky crystals which are intensely green coloured. The crude material is analytically and spectroscopically pure and crystals of a suitable size and quality for X-ray diffraction can be obtained from a slightly more dilute solution. Found: C, 60.7; H, 4.6; S, 18.5. $C_{54}H_{52}Ni_2P_2S_6$ requires C, 60.4; H, 4.9; S, 17.9%.

The crude product can be recrystallized by extracting with hot MeCN followed by slow cooling to room temperature, though this significantly reduces the overall yield (32%).

Employing a Ni : edt^{2-} ratio of 2 : 3 and following the procedure described above leads to the isolation of the same product in lower yield (1.7 g, 32%, crude product). Recrystallization from hot MeCN affords rhomb-shaped crystals which appear red-brown to transmitted light. [Found: C, 59.9; H. 5.0; S, 18.7%.) [Note: Although crystals of $[PPh_4]_2[Ni_2(edt)_3]$ obtained from reactions employing 2 : 1 and 3 : 2 ligand to metal ratios consistently lead to crystals which have different colours, their fully refined X-ray crystal structures are identical.

Preparation of $[PPh_4]_2[Ni_3(SCH_2CH_2S)_4]$

Sodium metal (0.58 g, 25 mmol) was dissolved in EtOH (60 cm^3) and ethane-1,2-dithiol (1.06 cm^3, 12.6 mmol) added followed by solid $NiCl_2 \cdot 6H_2O$ (1.50 g, 6.3 mmol). After *c.* 0.5 h the white precipitate (NaCl) was separated by filtration and PPh_4Br (5.55 g, 13.0 mmol) was added to the dark green filtrate to incipient crystallisation. The Schlenk tube was allowed to stand at room temperature for 36 h before the product was collected by filtration. The product was washed with two portions of an $EtOH/Et_2O$ mixture (8 cm^3, 1 : 1 composition) and dried *in vacuo*. The identity of this product was established as $[PPh_4]_2[Ni_2(edt)_3]$ (1.0 g, 29.6% yield). The filtrate from this product was then exposed to the atmosphere for 24 h by removing the septum cap and leaving the flask undisturbed. A mixture of black crystalline material and white solid was precipitated from solution. Anaerobic conditions were re-established and the mixture was collected by filtration and then extracted with either hot EtOH or hot MeCN. Brown crystals were obtained from the EtOH solution upon standing at room temperature for one week and from the MeCN solution upon storage in a freezer (*c.* −20°C) for three weeks. Crystals from the latter recrystallization were of a suitable quality for X-ray diffraction studies. The non-optimized yield of recrystallized material was 0.3 g (12% with respect to nickel). Found: C, 54.4; H, 4.7; S, 21.6. $C_{65}H_{56}Ni_3P_2S_8$ requires C, 55.0; H, 4.6; S, 21.0%.

Crystal structure determination

Crystal data are summarized in Table 1; details of the diffractometry, low-temperature facilities,

Table 1. Data for crystal structure analyses of $[PPh_4]_2[Ni_2(SCH_2CH_2S)_3]$ (**1**) and $[PPh_4]_2[Ni_3(SCH_2CH_2S)_4]$ (**2**)

	1	**2**
Molecular formula	$C_{54}H_{52}Ni_2P_2S_6$	$C_{56}H_{56}Ni_3P_2S_8$
M	1072.73	1131.44
Crystal system	triclinic	monoclinic
Space group	$P\bar{1}$	$P2_1/n$
Temperature (°C)	−152	−60
a, Å	12.861(7)[a]	13.713(3)[b]
b, Å	21.057(14)	13.255(3)
c, Å	10.324(5)	15.754(5)
α, deg	96.03(3)	
β, deg	109.88(3)	96.53(2)
γ, deg	76.82(3)	
Z	2	2
U, Å^3	2558.75	2844.95
D_c, g cm^{-3}	1.392	1.321
Radiation	Mo-K_α(0.71069 Å)	Mo-K_α(0.71069 Å)
μ, cm^{-1}	10.711	12.871
Method	θ–2θ	θ–2θ
Crystal size, mm	0.28 × 0.24 × 0.20	0.20 × 0.30 × 0.34
Scan speed, deg min^{-1}	4.0	4.0
Scan width, deg	1.8 + dispersion	2.0 + dispersion
Scan range, deg	$6 \leqslant 2\theta \leqslant 45$	$6 \leqslant 2\theta \leqslant 45$
No. of reflections collected	6988	4360
No. of unique intensities	6714	3734
No. of observed intensities	4576	2671
Criterion for observed, $n[I \geqslant n\sigma(I)]$	3	3
Solution method	Direct	Direct
Final R	0.0552	0.0649
Final R_w	0.0537	0.0594
Goodness of fit	0.820	1.075

[a] 40 reflections at −152°C.
[b] 30 reflections at −60°C.

and computational procedures employed by the Molecular Structure Center are available elsewhere.[17] For **1** a systematic search of a limited hemisphere of reciprocal space yielded a set of reflections which exhibited no symmetry or extinctions. The choice of the centrosymmetric space group $P\bar{1}$ was confirmed by the subsequent solution and refinement of the structure. For **2** a similar search located a set of diffraction maxima with monoclinic symmetry and systematic absences corresponding to space group $P2_1/n$. The structures were solved by a combination of direct methods and Fourier techniques and refined by full-matrix least-squares.

All non-hydrogen atoms of $[PPh_4]_2[Ni_2(edt)_3]$ (**1**) were readily located and the hydrogen atoms were located after initial refinement. However, there is a slight disorder problem in the anion at atoms C(12) and C(13). During refinement the hydrogen atoms moved to positions which gave unreasonable distances. A check of the root mean square displacements of the anisotropic atoms showed that the ellipsoids for C(12) and C(13) were quite elongated (.16.24.39) compared to the rest of the atoms. In the subsequent cycles of refinement the C(12) and C(13) atoms were kept isotropic and the hydrogen atoms associated with them were fixed. The structure refinement was completed using full-matrix least-squares with anisotropic thermal parameters on all non-hydrogen atoms (except C(12) and C(13)) and all hydrogen atoms were refined with isotropic thermal parameters (except H(9) to H(12)). The final difference map was essentially featureless except for a few peaks of c. 1e Å^{-3} in the vicinity of C(12) and C(13).

In the refinement of $[PPh_4]_2[Ni_3(edt)_4]$, non-

hydrogen atoms were assigned anisotropic thermal parameters whilst hydrogens were allowed to vary isotropically. A final difference Fourier was essentially featureless, with the largest peak being 0.50 e $Å^{-3}$.

Final values of atomic positional and thermal coefficients and lists of F_o/F_c values have been deposited as Supplementary data with the Editor, from whom copies are available on request. Atomic coordinates have also been deposited with the Cambridge Crystallographic Data Centre.

RESULTS AND DISCUSSION

The structure of the anions of $[PPh_4]_2[Ni_2(edt)_3]$ (**1**) and $[PPh_4]_2[Ni_3(edt)_4]$ (**2**) are shown in Figs 1 and 2, respectively. In the anion of **1**, one of the ligands provides two terminal thiolate groups, and the other two each provide one terminal and one μ-thiolate group such that each Ni(II) has an approximately square planar coordination geometry. The central NiS_2Ni unit is not planar, being folded along the vector joining the two bridging sulphur atoms. The anion of **2** is best considered as chelation of two identical $[Ni(edt)_2]^{2-}$ units to a third, central Ni(II) atom. The anion has a crystallographically observed centre of symmetry, with the central nickel atom thus lying in a perfect plane formed by its four coordinated sulphur atoms.

In order to describe the detailed structure of these anions a consideration of the Ni—S bond lengths given in Table 2 is necessary. It can be seen that a simple classification of these bond lengths into 'terminal' and 'bridging' is not entirely adequate. Those Ni—S bonds which form part of a Ni—S—C—C—S—Ni five-membered chelate ring are, on average, significantly shorter than those Ni—S bonds which are not within this chelate, and yet the former group contains ostensibly bridging *and* terminal ligation. Therefore, the $[Ni_2(edt)_3]^{2-}$

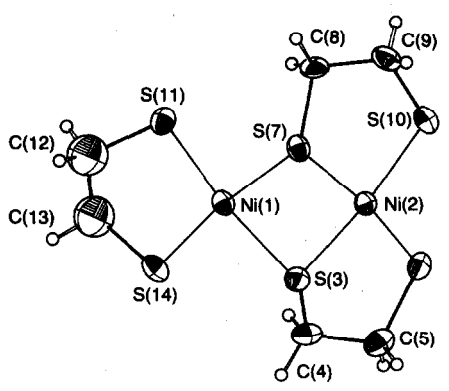

Fig. 1. Structure of $[Ni_2(edt)_3]^{2-}$ (in **1**) showing the atom-labelling scheme.

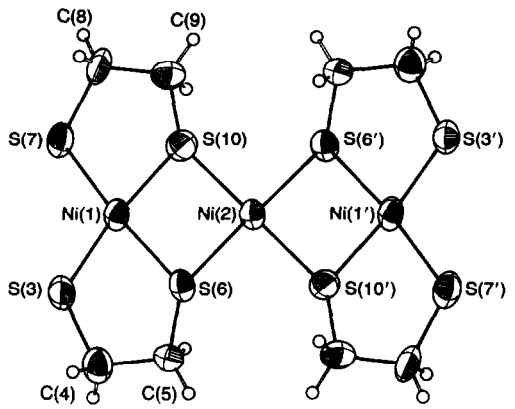

Fig. 2. Structure of $[Ni_3(edt)_4]^{2-}$ (in **2**) showing the atom-labelling scheme.

anion may best be thought of as arising from the chelation of a $[Ni(edt)_2]^{2-}$ monomeric unit to a Ni(edt) fragment with a folding of the two square planes thus formed along the common S···S edge. Similarly, $[Ni_3(edt)_4]^{2-}$ may be viewed as the chelation of a central Ni(II) atom by two $[Ni(edt)_2]^{2-}$ units in such a way as to generate a chair-like configuration of the Ni_3S_8 core. This Ni_3S_8 fragment closely conforms to C_{2h} symmetry, there being a mirror plane passing through the three nickel atoms and the mid-points of the sulphur atoms and a C_2 axis perpendicular to this. Inclusion of the methylene groups in the anion lowers the symmetry from C_{2h} to the crystallographically observed C_i-1. There are precedents for the kind of description given above, viz., the trimeric complexes $[Ni_3(S_2\text{-}o\text{-xyl})_4]^{2-}$ [4] and $[Ni(Ni(NH_2CH_2CH_2S)_2)_2]^{2+}$.[5] The former comprises the chelation of a central $[Ni(S_2\text{-}o\text{-xyl})_2]^{2-}$ unit to two $Ni(S_2\text{-}o\text{-xyl})$ fragments whilst the latter is analogous to $[Ni_3(edt)_4]^{2-}$.

Grouping the Ni—S bonds in the manner described above, i.e. within and without a chelate ring, gives the following average distances: $[Ni_2(edt)_3]^{2-}$, 2.181(14) and 2.216(13) Å; $[Ni_3(edt)_4]^{2-}$, 2.183(8) and 2.217(9) Å; $[Ni_3(S_2\text{-}o\text{-xyl})_4]^{2-}$,[4] 2.192(10) and 2.226(5) Å; $[Ni(Ni(NH_2CH_2CH_2S)_2)_2]^{2+}$,[5] 2.155(1) and 2.212 Å. With the exception of the two Ni—S bond distances within the Ni—S—C—C—N—Ni chelate ring of the latter being slightly shorter than the corresponding distances in the edt and S_2-*o*-xyl complexes, there are no significant differences between the four complexes with respect to their Ni—S bond lengths. The Ni—S bond lengths in the $[Ni_2(SEt)_6]^{2-}$ anion are comparable to those lying outside a chelate ring in the four complexes above [Ni—S_b = 2.220(6), Ni—S_t = 2.208(8) Å].[12]

There are several notable differences between the $[Ni_2(edt)_3]^{2-}$ and $[Ni_2(SEt)_6]^{2-}$ [12] anions.

Table 2. Selected interatomic distances (Å) and angles (deg) for the anions in $[PPh_4]_2[Ni_2(S_2C_2H_4)_3]$ (1) and $[PPh_4]_2[Ni_3(S_2C_2H_4)_4]$ (2)

$[Ni_2(edt)_3]^{2-}$ (1)		$[Ni_3(edt)_4]^{2-}$ (2)	
	Ni—S_t		
Ni(2)—S(6)	2.2032(25)	Ni(1)—S(3)	2.189(3)
Ni(2)—S(10)	2.1894(24)	Ni(1)—S(7)	2.1893(28)
Ni(1)—S(11)	2.1680(25)		
Ni(1)—S(14)	2.1774(25)		
	Ni—S_b		
Ni(2)—S(3)	2.1673(24)	Ni(1)—S(6)	2.1773(26)
Ni(2)—S(7)	2.1778(25)	Ni(1)—S(10)	2.175(3)
Ni(1)—S(7)	2.2250(25)	Ni(2)—S(6)	2.2232(23)
Ni(1)—S(3)	2.2071(24)	Ni(2)—S(10)	2.2102(26)
	Ni···Ni		
Ni(1)···Ni(2)	2.9414(22)	Ni(1)···Ni(2)	2.8301(13)
	S···S		
S(3)···S(7)	2.820(3)	S(6)···S(10)	2.862(3)
	S_b—Ni—S_b		
S(3)—Ni(1)—S(7)	79.01(9)	S(6)—Ni(1)—S(10)	82.23(10)
S(3)—Ni(2)—S(7)	80.92(9)	S(6)—Ni(2)—S(10)	99.59(9)
		S(6)—Ni(2)—S(10′)	80.41
	S_t—Ni—S_t		
S(11)—Ni(1)—S(14)	92.19(10)[a]	S(3)—Ni(1)—S(7)	91.29(11)
S(6)—Ni(2)—S(10)	93.74(10)		
	Ni—S_b—Ni		
Ni(1)—S(7)—Ni(2)	83.83(9)	Ni(1)—S(6)—Ni(2)	80.04(8)
Ni(1)—S(3)—Ni(2)	84.50(8)	Ni(1)—S(10)—Ni(2)	80.38(9)
	S_b—Ni—S_t		
S(7)—Ni(1)—S(11)	93.83(10)	S(3)—Ni(1)—S(6)	93.10(10)
S(3)—Ni(1)—S(14)	95.28(10)	S(7)—Ni(1)—S(10)	93.02(11)

[a] This is the only S—Ni—S angle that occurs *inside* a chelate ring in either (1) or (2).

$[Ni_2(SEt)_6]^{2-}$ is centrosymmetric and is formed by edge sharing of two planar units to generate an Ni_2S_2 *planar* rhomb.[12] In $[Ni_2(edt)_3]^{2-}$ there is no centre of symmetry and the Ni(1,2)S(3,7) core is not planar, there being a folding along the S(3)···S(7) vector. There is a dihedral angle of 119.07° at the intersection of the two NiS_4 planes. This has the effect of bringing the two Ni atoms closer together than in $[Ni_2(SEt)_6]^{2-}$ [2.9414(22) vs 3.355(2) Å] and to make the Ni—S—Ni bond angle in the bridge more acute [83.83(9) and 84.50(8) ° vs 98.2(1)°]. In $[Ni_2(edt)_3]^{2-}$, Ni(1) lies in the least squares plane formed by S(3,7,11,14) (maximum deviation, S(7) 0.085 Å) and Ni(2) is perpendicularly displaced by −0.08 Å from the least squares plane S(3,6,7,10) (maximum deviation, S(3,7) 0.048 Å).

The central nickel atom Ni(2) and the four attached sulphur atoms are required by the crystallographic centre of symmetry, located at Ni(2), to be exactly planar in $[Ni_3(edt)_4]^{2-}$. There is a deviation, though, from perfect square planarity of these sulphur atoms as evidenced by the S(6)—Ni(2)—S(10) angle of 99.59(9)°. Each of the two outer nickel atoms is perpendicularly displaced from its S(3,6,7,10) and S(3′,6′,7′,10′) least squares plane by 0.0874 Å in the direction opposite to the side of the central nickel atom Ni(2). In $Ni(Ni(NH_2CH_2CH_2S)_2)_2^{2+}$ the two outer nickel atoms are similarly displaced, by 0.12 Å.[5] Ni(2) is 1.556 Å from the least squares plane formed by S(3,6,7,10) (maximum deviation by S(10), 0.00979 Å).

In order to try and rationalize the degree of folding along the S···S vector and the Ni···Ni distances observed in this and other, similar complexes, Table 3 was compiled. This gives a selec-

Table 3. Comparison of selected distances (Å) and angles (deg) in some thiolate-bridged complexes of nickel(II)

	Ni···Ni	Ni—S—Ni	S···S	Dihedral[18] angle	Ref.
$[Ni_2(SEt)_6]^{2-}$	3.355(2)	98.2(1)	2.906(4)	180	12
$[Ni_3(SEt)_8]^{2-}$	3.04	87		< 180	12
$[Ni_3(S_2\text{-}o\text{-xyl})_4]^{2-}$	3.016(1) 3.131(1)	85.66(7)– 90.26(7)	2.735(2) 2.687(2)	< 180	4
$[Ni_2(edt)_3]^{2-}$	2.9414(22)	83.83(9) 84.50(8)	2.820(3)	119.07	[a]
$[Ni_3(edt)_4]^{2-}$	2.8301(13)	80.04(8) 80.38(9)	2.862(3)	113.19	[a]
$[Ni_2(SBz)_2(Bzttc)_2]$[b]	2.795(3)	79.5	2.826(5)	114.3	19
$[Ni_2(SEt)_2(Etttc)_2]$[c]	2.763	78.4	*c.* 2.84[d]	110.2	20
$Ni(Ni(NH_2CH_2CH_2S)_2)_2^{2+}$	2.733(7)	77.5	2.89(1)	109	5

[a] This work.
[b] SBz = $SCH_2C_6H_5$; Bzttc = $S_2CSCH_2C_6H_5$.
[c] Etttc = $S_2CSC_2H_5$.
[d] Distance approximated.

tion of distances and bond angles in some thiolate-bridged nickel complexes. The most notable feature is a variation in Ni···Ni distances of more than 0.6 Å. There appear to be a number of factors which might be responsible for the specific metal–metal distances found. These include, (i) direct, net positive, Ni···Ni interaction, (ii) the stereochemistry at the bridging sulphur atom (any chelate constraints will be manifested in this), (iii) the total charge provided by the ligand set, (iv) the S···S separation of the bridging sulphur atoms, and (v) ligand–ligand steric interactions. Crystal packing may or may not be an important additional factor. It is quite clear that no one factor dominates over all of the others and it would appear that they are capable of assuming different relative importances.

The nickel–nickel separation in $[Ni_2(edt)_3]^{2-}$ and $[Ni_3(edt)_4]^{2-}$ is certainly short enough to permit some kind of a net weak positive interaction, though its nature is not clear. Dahl has proposed that this is due to overlap of the filled $3d_z^2$ orbitals on Ni.[5] Similarly, the bridging S···S separation is *c* 0.4 Å shorter than would be expected for a non-bonding interaction, but there is nothing to suggest that it is optimal in these two complexes. Chelate constraints alone cannot be responsible for the resulting Ni···Ni distances, because a difference of 0.6 Å exists between the two dimers[12,20] which both have unconstrained $C_2H_5S^-$ as bridging ligands.

From a consideration of the two trimeric complexes $[Ni_3(edt)_4]^{2-}$ and $Ni(Ni(NH_2CH_2CH_2S)_2)_2^{2+}$ we can make some interesting observations. The similarities between them indicate that of those factors (i)–(v) listed, (iii) should be the one most responsible for the difference in observed Ni···Ni distance. As noted earlier in this section, the Ni—S bonds found within the Ni—S—C—C—N—Ni chelate rings are the shortest (2.155 Å) Ni—SR bonds of any in the complexes under discussion. A reason for this might be that the aminoethanethiolate effectively provides two neutral and two negatively charged ligands for the outer nickel atoms, whereas the edt provides four negatively charged ligands. This results in a larger net positive charge in the nickel in the former which consequently leads to shorter Ni—S distances. As a result, the Ni···Ni separation is decreased. Indeed, of the compounds listed in Table 3, $Ni(Ni(NH_2CH_2CH_2S)_2)_2^{2+}$ has the shortest Ni···Ni distance and is the only one to have a neutral donor atom in its nickel coordination sphere. Pursuing this idea a little further, it could be argued that the trithiocarbonate ligands in $[Ni(CS_3C_2H_5)(SC_2H_5)]_2$[20] and $[Ni(CS_3CH_2Ph)(SCH_2Ph)]_2$[19] have only a uninegative charge which allows the Ni—S bonds in the bridge to shorten (to 2.186 and 2.189 Å) with respect to those average distances found in the compounds having purely thiolate coordination. This then leads to the shorter Ni···Ni distances found in these two complexes. Having said this, however, the effect of total charge provided by the ligand set cannot explain the difference in Ni···Ni separation observed for the $[Ni_2(edt)_3]^{2-}$ and $[Ni_3(edt)_4]^{2-}$ anions. In these two anions, the mean of four Ni—S_b bond distances are identical. The shorter Ni···Ni separation in the trimer is a net result of more acute Ni—S—Ni and dihedral angles and larger S···S separation. All three changes are con-

sistent with a shortening of the Ni···Ni separation, given no variation in Ni—S_b lengths, but it is impossible to categorize them as cause or consequence.

The data in Table 3 do show that, without exception, a shortening of the Ni···Ni distance results in a more acute Ni—S—Ni angles in the bridge and a more acute dihedral angle. The S—Ni—S bond angles within the bridging unit tend to lie in the range 79–84° for the complexes listed in Table 5. Exceptions to this are one of the angles in the $[Ni_3(edt)_4]^{2-}$ anion which is exceptionally large (99.59(9)°) and the angle in $[Ni_2(SB_z)_2(S_2CSCH_2C_6H_5)_2]$ (98.3°).[19] [The data provided[4] for the $[Ni_3(S_2\text{-}o\text{-}xyl)_4]^{2-}$ anion do not permit a definitive comparison.]

^{1}H NMR, IR, UV–VIS AND ELECTROCHEMICAL STUDIES

^{1}H NMR spectroscopy proved to be a very effective analytical tool in this work. Integration of the ligand methylene protons vs those of the PPh_4^+ cation accurately determines the ligand to cation ratio. Also, the spectrum of $[PPh_4]_2[Ni_3(edt)_4]$ is quite distinctly different from and more complex than, that of $[PPh_4]_2[Ni_2(edt)_3]$ in the methylene proton chemical shift region. In the $[Ni_2(edt)_3]^{2-}$ anion, the proton resonances appear as two multiplets having an approximate relative intensity of 1 : 5 centred at 1.72 and 1.95 ppm respectively. The room temperature spectrum of the $[Ni_3(edt)_4]^{2-}$ complex appears to be much more complicated than one would expect from the solid state structure. The methylene proton resonances are found between 1.65 and 2.70 ppm. Within this region there are two reasonably well-resolved multiplets each having six lines centered at 1.7 and 2.65 ppm; the remaining features are relatively broad. It is conceivable that fluxional processes are in effect in the DMSO solvent; this might involve breaking the weaker Ni—S bonds or the existence of different isomers in solution. For both compounds the PPh_4^+ proton resonances are centered around 8.0 ppm as expected.

On the basis of their IR spectra, recorded between 4000 and 200 cm^{-1}, compounds **1** and **2** are essentially indistinguishable.

The UV–Vis spectra were recorded for **1** and **2** on solutions prepared and maintained under an inert atmosphere. **1** dissolves to give a green coloured solution in MeCN and **2** gives a red/brown coloured solution in MeCN and in DMF. Within *c.* 2 h a solution of **2** in MeCN will turn cloudy. The spectrum of **1** has $\lambda_{max}(\varepsilon_m)$ at 468 nm (3,459) and 624 nm (954) which agree reasonably well with the data reported previously for this complex anion.[10] The spectrum of **2** was recorded for both MeCN and DMF solutions and λ_{max} were found at 297(sh) nm (15,561), 325(sh) (13,225), 424 (3818) and 538 (2806) in MeCN and at 432 nm (6775), 542 (4944), and 720 (1576) in DMF. These spectra show a slight shift in band position in CH_3CN vs DMF and both clearly differ from the values reported[10] for putative $[NEt_4]_2[Ni_3(edt)_4]$ in CH_3CN [392 nm (2200) and 468 (1280)]. Unfortunately, neither **1** nor **2** displayed electrochemically reversible behaviour when studied by cyclic voltammetry. **1** gave three oxidation peaks, at $E_{p,a} = -0.32$, -0.03 and $+0.73$ V vs NHE and **2** gave two oxidation peaks, at $E_{p,a} = -0.06$ and $+0.73$ V.

In conclusion, use of the edt^{2-} ligand has allowed nickel(II) thiolate complexes of differing nuclearity to be prepared. Structural characteristics of di- and tri-nuclear products can be compared for the first time under identical ligation. Unfortunately, use of the edt^{2-} ligand does not result in easier accessibility of the nickel(III) oxidation level, as judged by our electrochemical results are least, a situation we had hoped might result given the stabilization by this ligand of manganese(III)[13,16] and cobalt(III).[11] However, the continuing desire for nickel(III) species with sulphur ligation to model the nickel(III) sites of hydrogenases demands further effort in this area, perhaps with mixed ligation around the metal center.

Acknowledgements—J.R.N. is a recipient of a U.K. SERC NATO Postdoctoral Fellowship. We thank the Bloomington Academic Computing Center for a gift of computer time.

REFERENCES

1. P. A. Lindahl, M. Kojimer, R. P. Hausinger, J. A. Fox, B. K. Teo, C. T. Walsh and W. H. Orme-Johnson, *J. Am. Chem. Soc.* 1984, **106**, 3062.
2. R. A. Scott, S. A. Wallin, M. Czechowski, D. V. DerVartanian, J. LeGall, H. D. Peck, Jr and I. Moura, *J. Am. Chem. Soc.* 1984, **106**, 6864.
3. D. Swenson, N. C. Baenziger and D. Coucouvanis, *J. Am. Chem. Soc.* 1978, **100**, 1932.
4. W. Tremel, B. Krebs and G. Henkel, *Angew. Chem., Int. Ed. Engl.* 1984, **23**, 634.
5. C. H. Wei and L. F. Dahl, *Inorg. Chem.* 1970, **9**, 1878.
6. W. Gaete, J. Ros, X. Solans, M. Font-Altaba and J. L. Brianso, *Inorg. Chem.* 1984, **23**, 39.
7. P. Woodward, L. F. Dahl, E. W. Abel and B. C. Crosse, *J. Am. Chem. Soc.* 1965, **87**, 5251.
8. R. O. Gould and M. H. Harding, *J. Chem. Soc. A.* 1970, 875.

9. H. Barrera, J. C. Bayon, J. Suades, C. Germain and J. P. Declerq, *Polyhedron* 1984, **3**, 969.
10. T. Yamamura, H. Miyamae, Y. Katayama and Y. Sasaki, *Chem. Lett.* 1985, 269.
11. J. R. Dorfman, Ch. P. Rao and R. H. Holm, *Inorg. Chem.* 1985, **24**, 453.
12. A. D. Watson, Ch. P. Rao, J. R. Dorfman and R. H. Holm, *Inorg. Chem.* 1985, **24**, 2820.
13. (a) G. Christou and J. C. Huffman, *J. Chem. Soc., Chem. Commun.* 1983, 558; (b) T. Costa, J. R. Dorfman, K. S. Hagen and R. H. Holm, *Inorg. Chem.* 1983, **22**, 4091.
14. (a) R. W. Wiggins, J. C. Huffman and G. Christou, *J. Chem. Soc., Chem. Commun.* 1983, 1313; (b) J. R. Dorfman and R. H. Holm, *Inorg. Chem.* 1983, **22**, 3179; (c) D. Szeymies, B. Krebs and G. Henkel, *Angew. Chem., Int. Ed. Engl.* 1983, **22**, 885.
15. J. K. Money, J. C. Huffman and G. Christou, *Inorg. Chem.* 1985, **24**, 3297.
16. J. L. Seela, J. C. Huffman and G. Christou, *J. Chem. Soc., Chem. Commun.* 1985, 58.
17. J. C. Huffman, L. N. Lewis and K. G. Caulton, *Inorg. Chem.* 1980, **19**, 2755.
18. The dihedral angle is defined here as the angle between the two NiS_4 planes which share a common S···S edge.
19. J. P. Fackler, Jr. and W. J. Zegarski, *J. Am. Chem. Soc.* 1973, **95**, 8566.
20. A. C. Villa, A. G. Manfredotti, M. Nardelli and C. Pelizzi, *J. Chem. Soc., Chem. Commun.* 1970, 1322.

Polyhedron Vol. 6, No. 5, pp. 871–879, 1987
Printed in Great Britain

0277–5387/87 $3.00+.00

STRUCTURES OF THE DIVALENT METAL COMPLEXES WITH BENZENE-1,2-DIOXYDIACETIC ACID

GRAHAM SMITH* and ERIC J. O'REILLY

Department of Chemistry, Queensland Institute of Technology, Brisbane, 4000, Australia

and

COLIN H. L. KENNARD

Department of Chemistry, University of Queensland, Brisbane, 4067, Australia

(*Received* 8 *April* 1986; *accepted* 8 *August* 1986)

Abstract—The divalent calcium, manganese, zinc, cobalt, magnesium and nickel complexes of benzene-1,2-dioxydiacetic acid ($BDDAH_2$) have been prepared and their structures determined by X-ray diffraction. Complexes $[Ca(BDDA)(H_2O)_2]_n \cdot nH_2O$ and $[Mn(BDDA)(H_2O)_2]_n \cdot nH_2O$ are isomorphous and isostructural. There is a pentagonal bipyramidal seven-coordination about each metal, involving four oxygens of the BDDA ligand, two axial waters and a fifth bridging carboxyl oxygen giving a polymer structure. In contrast, $[Zn(BDDA)(H_2O)_3] \cdot 3.5H_2O$ (and the cobalt and magnesium isomorphs) is discretely monomeric with the bridging position of the Ca/Mn structure replaced by a water. The nickel complex with formula $[Ni(BDDAH)_2(H_2O)_4] \cdot H_2O$ is monomeric and six-coordinate, bonded through only one carboxyl group of each of two *trans*-related BDDAH ligands.

Benzene-1,2-dioxydiacetic acid ($BDDAH_2$) [*O,O'*-catecholdiacetic acid, $CDAH_2$] is a multidentate chelating reagent, analogous to EDTA. However, stability constants for the metal complexes with

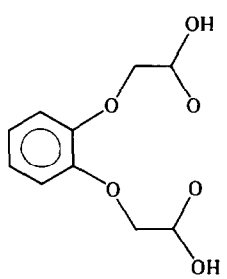

$BDDAH_2$ are substantially smaller than for the corresponding EDTA complexes.[1]

It is possible to modify the basic molecule to produce other acidic complexones with varying selectivities towards cations.[2] An unusual property of $BDDAH_2$ is its ability to form a crystalline precipitate with potassium ion, but not with lithium, sodium, caesium or ammonium ions.[3] The higher precipitimetric selectivity of $BDDAH_2$ towards K^+ compared to $NaBPh_4$ is probably due to the more compatible size of the potassium ion and a more favourable mode of coordination (or electrostatic interaction). The crystal structure of the K complex has an adducted species with formula $[K(BDDAH)(BDDAH_2)]$, with a pentagonal antiprismatic 'coordination' about the metal, one of the known stereochemistries by which K achieves solid state stabilization.[3] This is also seen in the related closed-chain polyether systems; e.g. di-benzo-18-crown-6 or 2,3,11,12-(bis-1,2-acenaptho)-18-crown-6, the latter giving with K^+ a regular 'hexagonal' interaction.[4]

$BDDAH_2$ has also been used to complex trivalent lanthanum as a model for a lanthanide shift ^1H and ^{13}C NMR study[5] since it forms both 1:1 and 1:2 complexes. Earlier, thermodynamic data indicated that the ligand was tetradentate and approximately planar,[6] in contrast with the skew conformation proposed for the ligands on the basis of the NMR solution spectra. The crystal structure of the complex $Na[La(BDDA)_2(H_2O)_2] \cdot 4H_2O$ showed an *s*-

*Author to whom correspondence should be addressed.

capped square antiprismatic deca-coordinate stereochemistry about La with two essentially planar BDDA ligands.[7]

A study of the structural systematics of divalent metal complexes of the phenoxyalkanoic acids,[8,9] which include the commercial herbicides 2,4-dichlorophenoxyacetic acid (2,4-D), 2,4,5-trichlorophenoxyacetic acid (2,4,5-T) and 4-chloro-2-methylphenoxyacetic acid (MCPA), has been extended to include the complexes of certain difunctional acids. These have been prepared and characterized using X-ray diffraction. The acids include 4-carboxyphenoxyacetic acid ($PCPAH_2$), 2-carboxyphenoxyacetic acid ($OCPAH_2$) and benzene-1,2-dioxydiacetic acid. The manganese complex $[Mn(PCPA)_2(H_2O)_4]_n$ is a polymer bridged through both carboxyl groups in *cis*-related octahedral coordination sites, in contrast to the isomorphous Ni and Co complexes which have the formula $[M(PCPAH)_2(H_2O)_4]$ and are discretely monomeric octahedral with *trans*-related unidentate phenoxyacetate ligands.[9] The two copper(II)–$OCPAH_2$ complex polymorphs, $[Cu(OCPA)(H_2O)]_n$, (A) and $[Cu(OCPAH)_2(H_2O)_2]$, (B)[10] also differ markedly. Complex (A) is a step-polymer based on square pyramidal repeating units with tridentate OCPA occupying positions in the complex square plane while in (B), Cu is square planar with *trans*-related OCPA ligands, each having its carboxy group monoprotonated.

The divalent metal complexes of $BDDAH_2$ were prepared and characterized using elemental analysis, infrared spectroscopy and where applicable, X-ray diffraction. Structural results are reported for:

(1) $[Ca(BDDA)(H_2O)_2]_n \cdot nH_2O$

(2) $[Mn(BDDA)(H_2O)_2]_n \cdot nH_2O$

(3) $[Zn(BDDA)(H_2O)_3] \cdot 3.5H_2O$

(4) $[Ni(BDDAH)_2(H_2O)_4] \cdot H_2O$

Complexes (1) and (2) are isostructural and isomorphous. Isomorphism also exists between (3) and $[Co(BDDA)(H_2O)_3] \cdot 3.5H_2O$, (**3a**) and $[Mg(BDDA)(H_2O)_3] \cdot 3.5H_2O$ (**3b**).

EXPERIMENTAL

Preparation of complexes

All complexes were prepared using a previously described method[9] which involved mixing at 80°C, aqueous solutions of the ammonium salt of $BDDAH_2$ and an equimolar quantity of the appropriate metal acetate. An alternative procedure,[8] digesting at *c.* 80°C an aqueous ethanolic solution of $BDDAH_2$ with an excess of the metal carbonate, followed by removal of the unreacted excess by filtration, was also used. Crystals were obtained as colourless prisms [except (**4**) (pale green) and (**3a**) (red)] after partial room temperature evaporation of the filtrate. Because of insufficient sample, no carbon and hydrogen analyses were obtained for **3(a)** and **3(b)**. IR spectra were recorded on Perkin Elmer model 457 or Jasco IR-810 spectrometers using Nujol mulls on KBr discs. Single crystal X-ray preliminaries were completed on an Enraf-Nonius Weissenberg goniometer using nickel filtered Cu-K_α radiation. Unique intensity data sets were collected on a Nicolet R3m four-circle diffractometer at 20°C using graphite crystal monochromated Mo-K_α radiation and were corrected for Lorentz and polarization effects but not for absorption.

Structure solution and refinement

Details of unit cell parameters, data acquisition and structure solution for compounds (**1**)–(**4**) are given in Table 1. Data were recorded using a Nicolet R3m diffractometer and Mo-K_α radiation ($\lambda = 0.7107$ Å); structures were solved and refined via the heavy atom method using the SHELXTL[11] structure solution package on the Nicolet R3m. All structures were refined by blocked-matrix least-squares with anisotropic temperature factors on all non-hydrogen atoms. Three water molecules in the zinc structure (**3**) were found to have only partial site occupancy and were subsequently refined at half weights. This is consistent with its elemental analysis [Found: C, 29.6; H, 5.15. Calc. for $C_{10}H_{21}O_{12.5}Zn$, $\{[Zn(BDDA)(H_2O)_3] \cdot 3.5H_2O\}$: C, 29.5; H, 5.20%]. Neutral atom scattering factors and the f′, f″ terms for anomalous dispersion were taken from Ref. 12. Cell data and details of the structure analyses are given in Table 1 while bond distances and angles about the coordination polyhedra for the four complexes are listed in Table 2.

Tables of atomic coordinates, anisotropic thermal parameters, intraligand bond distances and angles, hydrogen atom coordinates, observed and calculated structure factors and IR spectra have been deposited with the Editor as supplementary material; copies are available on request from the Editor or the Authors. Atomic coordinations have also been deposited with the Cambridge Crystallographic Data Centre.

DISCUSSION

Series A complexes

The structures of complexes of the type $[M(BDDA)(H_2O)]_n \cdot nH_2O$, where M = Ca (**1**) or

Table 1. Cell data for $[Ca(BDDA)(H_2O)_2]_n \cdot nH_2O$ (1), $[Mn(BDDA)(H_2O)]_n \cdot nH_2O$ (2), $[Zn(BDDA)(H_2O)_3] \cdot 3.5H_2O$ (3), and $[Ni(BDDAH)_2(H_2O)_4] \cdot H_2O$ (4)

	(1)	(2)	(3)[a]	(4)
Formula	$C_{10}H_{14}CaO_9$	$C_{10}H_{14}MnO_9$	$C_{10}H_{21}O_{12.5}Zn$	$C_{20}H_{30}NiO_{17}$
M_r	318.8	333.1	406.6	601.2
a (Å)	7.158(4)	7.574(4)	29.343(2)	32.45(3)[b]
b (Å)	7.135(1)	7.151(3)	6.7294(9)	4.987(3)
c (Å)	23.240(9)	23.031(3)	17.259(4)	28.23(1)
β (deg)	93.25(4)	93.65(3)	109.17(5)	146.92(5)
V (Å^3)	1284.3(9)	1244.9(8)	3218.9(9)	2493.4(9)
Z	4	4	8	4
D_c (g cm^{-3})	1.645	1.777	1.677	1.601
D_m (g cm^{-3})	1.64	1.79	1.66	1.58
$F(000)$	664	684	1688	1256
μ (cm^{-1})	5.19	11.59	16.38	8.66
Space group	$P2_1/n$	$P2_1/n$	$C2/c$	$C2/c$
Data collection				
Diffractometer	Nicolet R3m	Nicolet R3m	Nicolet R3m	Nicolet R3m
Radiation	Mo-K_α	Mo-K_α	Mo-K_α	Mo-K_α
2θ range (deg)	2–45	3–45	3–45	3–45
Unique reflections measured (*hkl*)	2048 (±8, 7, 24)	1960 (±8, 7, 24)	1752 (±27, 7, 17)	1642 (±34, 5, 30)
Crystal size (mm)	0.50 × 0.40 × 0.13	0.35 × 0.14 × 0.05	0.38 × 0.28 × 0.05	0.38 × 0.12 × 0.12
Structure solution refinement				
Method used	Patterson	Patterson	Patterson	Heavy atom
R	0.058	0.061	0.082	0.053
Rw	0.063	0.063	0.089	0.057
w^c A	1.2×10^{-3}	2.1×10^{-3}	3.4×10^{-3}	1.5×10^{-3}
Data used	1676	808	1450	1052
Discrimination	$I > 2.5\sigma(I)$	$I > 2.5\sigma(I)$	$I > 2.5\sigma(I)$	$I > 2.5\sigma(I)$

[a] Cell data, obtained on single crystals of $[Co(BDDA)(H_2O)_3] \cdot 3.5H_2O$ (**3a**) and $[Mg(BDDA)(H_2O)_3 \cdot 3.5H_2O$ (**3b**) using a Nicolet R3m diffractometer are: (**3a**), $a = 29.5(4)$, $b = 6.75(1)$, $c = 17.4(2)$ Å, $\beta = 110.0(1)°$, $V = 3264(3)$ Å^3, $D_m = 1.63$ g cm^{-3}, $Z = 8$, $D_c = 1.634$ g cm^{-3} space group, $C2/c$. (**3b**) $a = 29.17(1)$, $b = 6.758(2)$, $c = 17.347(8)$ Å, $\beta = 108.99(3)°$, $V = 3234(2)$ Å^3, $D_m = 1.51$ g cm^{-3}, $Z = 8$, $D_c = 1.507$ g cm^{-3}, space group, $C2/c$.

[b] Reduced cell: $a = 28.23(3)$, $b = 4.987(3)$, $c = 17.74(4)$ Å, $\beta = 93.36(5)°$.

[c] $w = (\sigma^2 F_o + A F_o^2)^{-1}$.

Mn (**2**) have been determined. Single crystal X-ray diffraction methods have confirmed that complexes (**1**) and (**2**) are isomorphous and isostructural. Isomorphism has been observed for a number of Mn and Mg phenoxyacetates, but (**1**) represents the first reported example of a Ca phenoxyacetate. Moreover, Ca is not known to behave in a similar manner to the other two metals. Because the BDDA ligand is essentially planar, as observed in the La complex[7] and the K complex adduct,[3] its donor sites are fixed relative to the metal ion. Therefore the ligand would be expected to exert a strong influence on the stereochemistry assumed by the metal ion. The structures of (**1**) and (**2**) are therefore based upon pentagonal bipyramidal repeating units (Fig. 1), which form into one-dimensional polymer structures. The pentagonal plane comprises four oxygens from the BDDA ligand, with the bonds to the ether oxygens elongated relative to those of the carboxyl oxygen [mean M—O(ether); 2.541(4) Å (**1**); 2.441(9) Å (**2**); mean—O(carboxyl); 2.322(4) Å (**2**)]. The fifth position is occupied by a bridging oxygen [2.451(3) Å (**1**); 2.271(8) Å (**2**) while in the axial positions are two water ligands [mean M—Ow, 2.366(3) Å (**1**); 2.248(8) Å (**2**).] Complex systems involving Ca(II) and Mn(II) with analogous tetra-oxygen donor ligands, the neutral noncyclic ionophores

* TPBDD = *N,N,N′,N′* - tetrapropyl - 1,2 - benzodioxydiacetamide.

† TPCDD = *N,N,N′,N′* - tetrapropyl - 1,2 - cyclohexanediacetamide.

‡ TPDOD = *N,N,N′,N′* - tetrapropyl - 3,6 - dioxyoctanediamide.

Table 2. Bond distances (Å) and angles (deg) about the coordination spheres for complexes (**1**), (**2**), (**3**) and (**4**)

	(1)	(2)	(3)	(4)	
(a) Distances					
M—O(71)	2.521(1)	2.472(8)	2.481(7)	Ni—O(101)	2.064(10)
M—O(72)	2.516(3)	2.410(8)	2.469(7)	Ni—Ow(1)	2.092(7)
M—O(101)	2.336(3)	2.181(9)	2.115(8)	Ni—Ow(2)	2.047(7)
M—O(102)	2.308(4)	2.167(9)	2.184(4)		
M—O(111)′	2.451(3)	2.271(8)	—		
M—Ow(1)	2.334(3)	2.197(9)	2.053(8)		
M—Ow(2)	2.398(3)	2.229(9)	2.022(8)		
M—Ow(3)	—	—	2.112(7)		
(b) Angles					
O(71)—M—O(72)	61.2(1)	62.4(3)	61.2(2)	O(101)—Ni—Ow(1)	92.9(3)
O(71)—M—O(101)	65.0(1)	66.2(4)	67.6(2)	O(101)—Ni—Ow(2)	86.2(3)
O(71)—M—O(102)	126.1(1)	130.6(4)	129.0(2)	Ow(1)—Ni—Ow(2)	88.2(2)
O(71)—M—Ow(1)	82.0(1)	83.4(3)	87.5(3)	Ni—O(101)—C(91)	130.2(6)
O(71)—M—Ow(2)	81.6(1)	86.2(3)	84.1(3)		
O(71)—M—Ow(3)	—	—	149.1(3)		
O(71)—M—O(111)′	140.0(1)		—		
O(72)—M—O(101)	126.2(1)	128.4(3)	128.4(2)		
O(72)—M—O(102)	65.1(1)	68.4(3)	67.9(2)		
O(72)—M—Ow(1)	91.3(1)	88.6(3)	80.9(3)		
O(72)—M—Ow(2)	86.3(1)	91.3(3)	85.3(3)		
O(72)—M—Ow(3)	—	—	149.4(3)		
O(72)—M—O(111)′	149.6(1)	152.0(3)	—		
O(101)—M—O(102)	168.4(1)	161.8(3)	163.0(3)		
O(101)—M—Ow(1)	86.6(1)	89.1(3)	91.4(3)		
O(101)—M—Ow(2)	80.8(1)	81.8(3)	95.7(3)		
O(101)—M—Ow(3)	—	—	82.2(3)		
O(101)—M—O(111)′	79.3(1)	78.2(3)	—		
O(102)—M—Ow(1)	86.6(1)	99.2(3)	91.4(3)		
O(102)—M—Ow(2)	80.8(1)	91.6(3)	90.5(3)		
O(102)—M—Ow(3)	—	—	81.7(3)		
O(102)—M—O(111)′	91.0(1)	86.8(3)	—		
Ow(1)—M—Ow(2)	162.5(1)	168.3(3)	166.0(3)		
Ow(1)—M—Ow(3)	—	—	99.7(3)		
Ow(1)—M—O(111)′	78.3(1)	82.7(3)	—		
Ow(2)—M—Ow(3)	—	—	93.2(3)		
Ow(2)—M—O(111)′	110.9(1)	102.5(3)	—		
M—O(71)—C(1)	123.8(3)	122.7(7)	125.7(7)		
M—O(71)—C(81)	118.9(2)	118.5(7)	116.6(5)		
M—O(72)—C(2)	124.4(2)	124.5(7)	125.6(6)		
M—O(72)—C(82)	118.8(2)	119.1(7)	115.7(5)		
M—O(101)—C(91)	126.2(3)	129.4(7)	128.3(6)		
M—O(102)—C(92)	128.7(3)	126.1(8)	126.3(5)		
M—O(111)′—C(91)′	102.5(2)	114.5(7)	—		

TPBDD,* TPCDD† and TPDOD,‡ [13] show similar bond weakening towards the ether oxygen, although the metals do not have pentagonal bipyramidal stereochemistries in these complexes.

Both the pentagonal bipyramidal stereochemistry and the observed Ca—O bond distances in (**1**) are quite normal for calcium carboxylates, even when the acid ligand has less rigidity than BDDA. A strong tendency also exists for Ca to participate in α-chelation (more so than for other divalent metals).[14] Calcium di-DL-glycerate dihydrate[15] is very similar to (**1**), having two bidentate glycerate ligands and a bridging carboxyl—O in the pentagonal plane while the two waters occupy the axial positions of the bipyramid [mean Ca—O, 2.381 Å]. In calcium malonate dihydrate,[16] the structure is also polymeric but with the two waters in the pentagonal plane [mean Ca—O, 2.528 Å (X-ray) and 2.430 Å (neutron)]. Other variations are found in anhydrous calcium hydrazinecarboxylate[17]

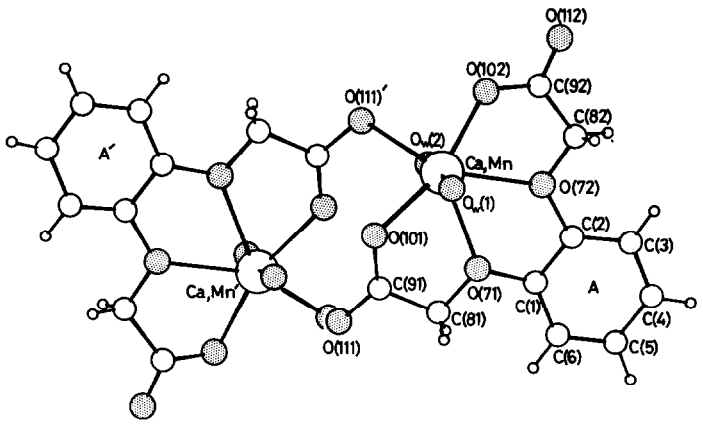

Fig. 1. $[Ca(BDDA)(H_2O)_2]_n \cdot nH_2O$ (**1**) and $[Mn(BDDA)(H_2O)_2]_n \cdot nH_2O$ (**2**).

$[CaO_5N_2$; mean Ca—O, 2.35 Å] and calcium hydrazinecarboxylate monohydrate[18] which is similar in most respects to the anhydrous complex but has a monocapped trigonal bipyramidal stereochemistry $[CaO_6N_2$; mean Ca—O, 2.44 Å]. However, the Mn complex has no precedent among the phenoxyalkanoates which tend to form polymer structures based on octahedral metal centres. Mn—O bond distances are considered normal for manganese carboxylates.

The comparative Ca—O(ether) and Ca—O (amide) distances for $[Ca(TPBDD)_2 \cdot Br_2]$ and $[Ca(TPDOD)_2 \cdot Cl_2]$ are 2.487, 2.327 Å (mean) and 2.462, 2.365 Å respectively while those for Mn—O in the complexes $[Mn(TPBDD)_2 \cdot MnBr_4]$ and $[Mn(TPCDD)_2 \cdot MnBr_4]$ are 2.380, 2.168 and 2.370, 2.185 Å respectively.[13] Mean distances for La—O bonds in $Na[La(BDDA)_2(H_2O)_2] \cdot 4H_2O$[7] (2.689, 2.504 Å), where the lanthanum stereochemistry approximates to an *s*-capped square antiprism and the equivalent values in $[K(BDDAH)(BDDAH_2)]$ (2.89, 2.75 Å) (irregular pentagonal antiprismatic stereochemistry), show similar bond length differences.

The $[M(BDDA)(H_2O)_2]$ repeating units in (**1**) and (**2**) are centrosymmetrically related in step-stack polymer chains which form down the *b* direction in their respective unit cells (Fig. 2). The lattice water [Ow(3)] is involved in hydrogen bonding interactions with the bridging carboxyl oxygen [O(111)]; 2.853 Å (**2**)] and with both coordinated waters [···Ow(1): 2.874 Å (**1**); 2.844 Å (**2**). ···Ow(2): 2.820 Å (**1**); 2.955 Å (**2**)]. Other significant intermolecular hydrogen bonding contacts are: Ow(1)···O(112), 2.683 Å (**1**); 2.696 Å (**2**) and Ow(1)···O(111), 3.023 Å (**1**); 2.952 Å (**2**). The most significant difference between the two polymorphs involve the long contacts between the metal and an *n* glide related carboxylate oxygen [O(101)]* which is considerably shorter in (**1**) (Ca—O, 2.863 Å) than in (**2**) (Mn—O, 3.132 Å). This may be due to a greater tendency for Ca cf. Mn to expand its coordination polyhedron, although the Ca—O distance is not intepreted as a formal bond.

Series B complexes

The complexes of BDDA with zinc(II) (**3**), cobalt(II) (**3a**) and magnesium(II) (**3b**) have been confirmed as isomorphous and isostructural on the basis of single crystal X-ray diffraction preliminaries and IR spectra. Elemental analysis and the X-ray determination for (**3**) is consistent with a

* Symmetry operation $(\frac{1}{2}-x, \frac{1}{2}+y, \frac{1}{2}-z)$.

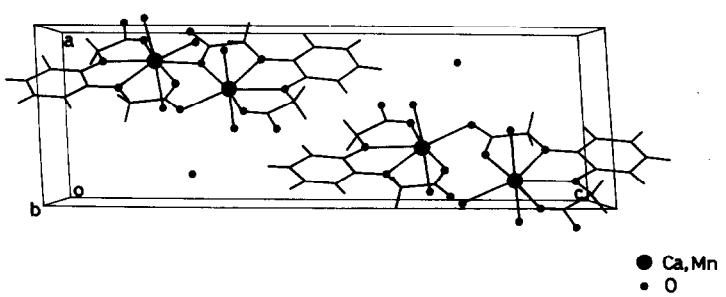

Fig. 2. Packing of (**1**) or (**2**) in the unit cell viewed perpendicular to *ac*.

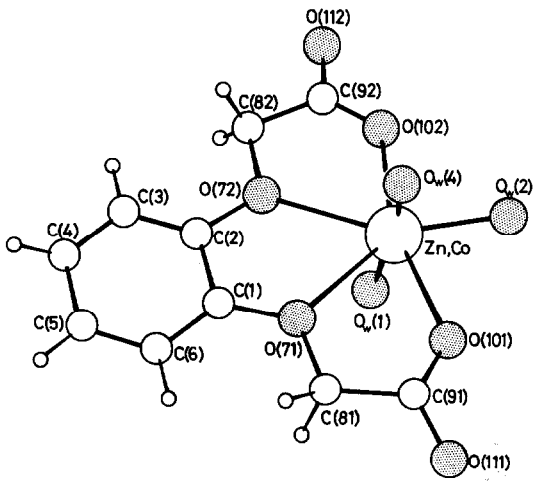

Fig. 3. $[Zn(BDDA)(H_2O)_3]\cdot 3.5H_2O$ (**3**).

formula $[Zn(BDDA)(H_2O)_3]\cdot 3.5H_2O$, with partial occupancy for the lattice water molecules [Ow(6), Ow(7)A, Ow(7)B], which may have significant lability in the solid state. The slight variations in the water absorption bands of the IR spectra for complexes (**3**) and (**3a**) are also probably a consequence of this lability.

In contrast to the Series A complexes, complex (**3**) is discretely monomeric (Fig. 3). However, the stereochemistry about zinc is similarly pentagonal bipyramidal. The planar BDDA ligand is quadridentate with the bonds to zinc similarly elongated towards the ether oxygens [Zn—O, 2.475(7) Å] compared to the carboxyl oxygens [Zn—O, 2.149(7) Å]. The remaining three meridional positions of the pentagonal bipyramid are occupied by waters [mean Zn—Ow, 2.061(7) Å]. This metal stereochemistry has no precedent among the zinc phenoxyalkanoates nor among zinc carboxylates generally, although there are examples with seven-coordination. However, the phenoxyalkanoates have previously shown only four, five and six-coordination, with tetrahedral trigonal bipyramidal, octahedral and skew trapezoidal stereochemistries.[8,19] Pentagonal bipyramidal coordination has been found for the isomorphous diaquanitratopurpuratozinc(II) and cobalt(II) dihydrates.[20] The ligand in this complex is similar to BDDA but with a tridentate O,N,O donor array (Zn—N, 2.229; Zn—O, 2.112, 2.114 Å) which, with an asymmetric bidentate nitrate group (Zn—O, 2.266, 2.511 Å) complete the coordination positions about the square plane. The axial positions are occupied by water molecules (Zn—O, 2.014, 2.138 Å). The stability constants for the zinc, cobalt and magnesium complexes [log K_1, 2.0 (**3**), 1.1 (**3a**) and < 1.5(**3b**)[1]] are also consistent with the isostructurality observed.

Packing of the complex molecules in the unit cell involves the lattice waters in interactive associations with carboxyl oxygens, coordinated waters and with other lattice waters in a complex network (Fig. 4).

These intermolecular O···O contacts are as follows: Ow(1)···O(5), 2.75 Å. Ow(2)···O(111), 2.67 Å. Ow(3)···Ow(6), 2.66, 2.80 Å. Ow(4)···Ow(7), 2.76 Å; ···Ow(8), 2.76 Å; ···O(102), 2.93 Å. Ow(5)···Ow(6), 2.68 Å; ···Ow(8), 2.81 Å; ···O(111), 2.90 Å. Ow(6)···Ow(7), 2.64 Å, Ow(7)···Ow(7)′, 2.77 Å; ···Ow(8), 2.90 Å; ···O(112), 2.83 Å. Ow(8)···Ow(8)′, 2.58 Å; ···O(112), 2.82 Å.

Series C complexes

To date, only nickel(II) forms a complex with $BDDAH_2$ with the formula $[Ni(BDDAH)_2(H_2O)_4]\cdot H_2O$ (**4**). This form, in which the second carboxyl group is protonated, is the product of either the neutral salt method (via the ammonium salt from aqueous solution) or by the carbonate method (from aqueous ethanol). The latter method,

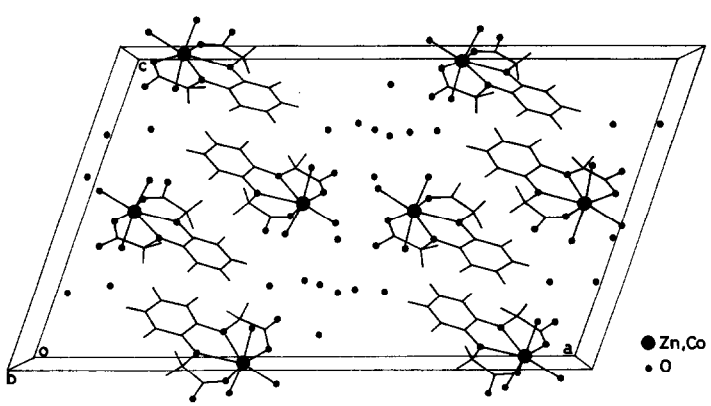

Fig. 4. Packing of (**3**) in the unit cell viewed perpendicular to *bc*.

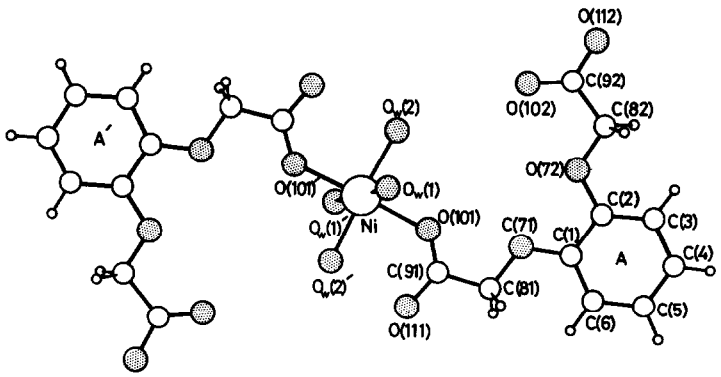

Fig. 5. $[Ni(BDDAH)_2(H_2O)_4]\cdot H_2O$ (**4**).

in which some free unreacted carboxylic acid is often present in the crystallizing mixture, often results in formation of acid adducts of complexes of the phenoxyalkanoates.[21] Although this is not the case in the present instance, the pH may be sufficiently low to protonate the first carboxylate group after which the conventional octahedral nickel complex proceeds to form from solution. The pK_{a1} and pK_{a2} values for the two carboxyl protons are 2.40 and 3.45 respectively for $BDDAH_2$.[1] A similar effect is observed with the complexes $[Ni(PCPAH)_2(H_2O)_2]$[9] and $[Cu(OCPAH)_2(H_2O)_4]$.[10] Complex (**4**) is centrosymmetric six-coordinate with the nickel at the centre of an almost regular octahedron comprising four waters [Ni—Ow, 2.047, 2.092(7) Å] and two carboxylate oxygens from unidentate BDDAH ligands [Ni—O, 2.064(10) Å] (Fig. 5). Unlike previous Series A or B complexes, the ether oxygens are not involved in coordination to the metal. Despite being unidentate, the BDDAH ligand is essentially planar, a conformational state probably maintained by the presence of hydrogen bonding interactions between the uncoordinated carboxyl oxygen [O(102)] and a coordinated water [Ow(1); O···O, 2.765 Å], between O(111) and the second coordinated water [Ow(1); O···O, 2.718 Å] and in addition, a very short contact (2.528 Å) between the protonated carboxyl oxygen [O(112)] and an adjacent carboxyl oxygen [O(111)'] (Fig. 6). This is analogous to the formation of inter-complex cyclic hydrogen bonding contacts found in $[Ni(PCPAH)_2(H_2O)_4]$[9] (2.59 Å) and in $[Cu(OCPAH)_2(H_2O)_2]$ (2.92 Å).[10]

The lattice water [Ow(3)], which lies on a crystallographic two-fold axis is also associated at considerably longer range with the protonated carboxyl oxygen [O(112)] (3.109 Å), the uncoordinated carboxyl oxygen [O(111)] (3.478 Å) and with the coordinated water molecule Ow(2) [3.197 Å].

The BDDA ligand

The important structure parameters of the BDDA ligands in each of the complexes (**1**)–(**4**) are listed in Supp. Table 5. The essentially planar conformation of the ligand in all complexes, as well as in the K^{+3} and La^{3+7} complexes is consistent with the contention that energetically this conformation is preferred for the oxyacetic acid side-chain in the free monofunctional phenoxyalkanoic

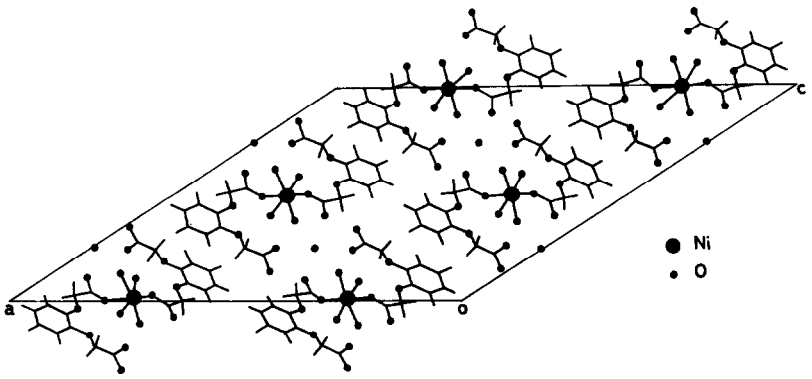

Fig. 6. Packing of (**4**) in the unit cell viewed perpendicular to *ac*.

acids.[22] In addition, other significant structural features generally shared with both the free acids and their metal complexes are

(1) The *exo*-C(1) and C(2) angles are considerably distorted compared with the expected trigonal value, being enlarged away from C(6) and C(3) respectively [mean C(2)—C(1)—O(71)/C(1)—C(2)—O(72), 115(1)°; C(6)—C(1)—O(71)/C(3)—C(2)—O(7), 125(1)°]. These values compare with means of 115° and 125° for equivalent angles in a series of 22 phenoxyalkanoic acids.[22] This indicates that little distortion results from the insertion of the metal ion in the ionosphore cavity during complexation.

(2) In these acids, the side-chain conformation with the carbonyl oxygen [O(10)] synplanar with respect to the ether oxygen [O(7)] is always found. This conformation is also found without exception for C—C—C=O among the α,β-saturated acids.[23] For the phenoxy acids, this results in a relatively constant O···O interactive distance [acid series mean (19 examples), 2.711 Å].[24] Furthermore, this interactive distance is retained on complexation, irrespective of the mode, i.e. unidentate, bidentate, bidentate-chelate. The observation is also true for the complex series (**1**)–(**4**) [mean O···O, 2.60(1) Å], the BDDA complexes of K^+ (2.62 Å),[3] La^{3+} (2.62 Å)[8] and the diacetamide complexes (2.56 Å).[13] The comparable O(71)···O(72) distance [series mean, 2.55 Å, cf. 2.57 Å (K^+); 2.60 Å (La^{3+}); 2.60 Å (diacetamide)] also shows little variation. From this observation for the known phenoxyalkanoate complexes, it is considered that the O···O non-bonded interactions (comparable in length to quite strong OH···O hydrogen bonding interactions) is instrumental in conferring planarity on these side-chains. This does not apply to the analogous (phenylthio)acetic acid complexes[24] in which there is no regularity in the S···O distance, nor any tendency for the thioacetate side-chain to remain planar. This is tenable on the basis of weaker S···O vs O···O interactions.

(3) The significant differences associated with the C—C—O ('carbonyl') and the C—C—O ('hydroxyl') angles, a phenomenon known for carboxylic acids generally [typically 123°, 113° respectively[23] and 125°, 112(1)° for the protonated ligand (**4**)]. Although this was expected to disappear on complexation, it is actually retained in most cases giving their distinctive angular features. This allows labelling of the oxygen either as 'carbonyl' or 'hydroxyl'. Thus in complexes (**1**)–(**4**), complexation of the metal involves the 'carbonyl' oxygen rather than the 'hydroxyl', with retention of the side-chain conformation expected to be found in the free acid.

CONCLUSION

It could be concluded that the free acid $BDDAH_2$ would be essentially planar in the solid state and that the *synplanar* conformation [as for the protonated oxoacetic acid side-chain in complex (**4**)] would be found in both residues in the diprotic acid. Complexation results in little change to the structural features of the BDDA ligand, with the divalent Ca, Mn, Mg, Zn and Co ions providing a compatible fit into the molecular pore-space. In fact, it would appear that ionic radius is not an important determinative factor in predicting the stability of the metal complex. A correlation of stability constants with ionic radii for this series 'shows some anomalous relationships'.[1] The cadmium complex of BDDA ($\log K_1$, 3.8; $r = 0.97$ Å) represents the first example of a Cd chelate in which the stability constant is larger than that of the corresponding Cu complex (3.3; 0.73 Å). With the exception of Cu (high) and Co (low) (1.1; 0.74 Å), the values of the stability constants increase steadily from Mg through Zn and Mn (2.8; 0.82 Å) to Cd, then decrease through Ca (3.1; 0.99 Å) to Ba (2.0; 1.35 Å). Suzuki *et al.* indicate that the unusual order is probably due to the structure of the BDDA ligand. This study confirms that Series A types (Ca, Mn) and Series B types (Zn, Co, Mg) are respectively isostructural and that both structure types are based on the pentagonal bipyramidal stereochemistry, it would appear that the ligand imposes a greater influence on the metal stereochemistry than vice versa. The structures of the Cd and Cu complexes are similar (from IR spectra) despite their different stoichiometries $[Cd(BDDA)(H_2O)_3]$;* $Cu(BDDA)(H_2O)_5$]† and are probably based on the pentagonal plane, although Cu^{II} shows little tendency to give this stereochemistry. More often the stereochemistry ranges from tetragonally distorted octahedral six-coordinate through trigonal bipyramidal or square pyramidal five-coordinate [polymorph A, $Cu(OCPA)(H_2O)$[10]], to square planar four-coordinate [polymorph B, $Cu(OCPAH)_2(H_2O)_4$[10]]. It is also suggested that structurally, Series A and Series B complexes are very similar, the stability constants being marginally enhanced with the formation of

* $[Cd(BDDA)(H_2O)_3]$; Found: C, 30.8; H, 3.62. Calc. for $C_{10}H_{14}CdO_9$; C, 30.7; H, 3.59%.

† $[Cu(BDDA)(H_2O)_5]$; Found: C, 31.7; H, 4.72. Calc. for $C_{10}H_{18}CuO_{11}$: C, 31.8; H, 4.77%.

the polymer structure. Morphologically, both forms are also similar. Consequently, it may be possible to form both modifications with all metal ions under suitable conditions. Nickel(II) usually assumes octahedral $[ML_2(H_2O)_4]$ coordination. It does this with BDDA only when the ligand is monoprotonated and unidentate.

Acknowledgements—The authors thank the University of Queensland and the Queensland Institute of Technology Research and Development Fund for financial assistance while Professor B. R. Penfold and Dr W. J. Robinson of the University of Canterbury, Christchurch, New Zealand are thanked for the use of data collection and structure solution facilities.

REFERENCES

1. K. Suzuki, T. Hatori and K. Yamasaki, *J. Inorg. Nucl. Chem.* 1968, **30**, 161.
2. R. Leppkes and F. Vögtle, *Angew. Chem. Int. Ed. Engl.* 1981, **20**, 396.
3. E. A. Green, W. L. Duax, G. M. Smith and F. Wudl, *J. Am. Chem. Soc.* 1975, **97**, 6689.
4. G. Weber, G. M. Sheldrick, A. Merz and F. Dietl, *Inorg. Chim. Acta* 1984, **90**, L1.
5. L. Kullberg and G. R. Choppin, *Inorg. Chem.* 1977, **16**, 2926.
6. Y. Hasegawa and G. R. Choppin, *Inorg. Chem.* 1977, **16**, 2931.
7. H. B. Kerfoot, G. R. Choppin and T. J. Kistenmacher, *Inorg. Chem.* 1979, **18**, 787.
8. Part 1: G. Smith, E. J. O'Reilly, C. H. L. Kennard, K. Stadnicka and B. Oleksyn, *Inorg. Chim. Acta* 1981, **47**, 111. Part 15: T. C. W. Mak, W.-H. Yip, E. J. O'Reilly, G. Smith and C. H. L. Kennard, *Inorg. Chim. Acta* 1985, **100**, 267 (and references therein).
9. C. H. L. Kennard, G. Smith, E. J. O'Reilly and P. T. Manoharan, *Inorg. Chim. Acta* 1984, **82**, 35.
10. C. H. L. Kennard, G. Smith and E. J. O'Reilly, *Inorg. Chim. Acta* 1986, **112**, 47.
11. G. M. Sheldrick, *SHELXTL User Manual*, Revision 3, 1981. Nicolet XRD Corporation Cupertino, California.
12. J. A. Ibers and W. C. Hamilton, *International Tables for X-ray Crystallography*, Vol. IV. Kynoch Press, Birmingham (1974).
13. K. Neupert-Laves and M. Dobler, *J. Cryst. Spect. Res.* 1982, **12**, 271.
14. H. Einspahr and C. E. Bugg, *Calcium Binding Proteins and Calcium Function* (Edited by R. H. Waaserman, R. A. Corradino, E. Carafoli, R. H. Kretsinger, D. H. MacLennan and F. L. Siegel), pp. 13–20. Elsevier North Holland, New York (1977).
15. E. J. Meehan and H. Einspahr, *Acta Cryst. Sect. B.* 1979, **35**, 828.
16. J. Albertsson, A. Oskarsson and C. Svensson, *Acta Cryst. Sect. B.* 1978, **34**, 2737.
17. A. Braibanti, A. M. Manotti-Lanfredi, M. A. Pellighelli and A. Tiripicchio, *Acta Cryst. Sect. B* 1971, **27**, 2448.
18. A. Braibanti, A. M. Manotti-Lanfredi, M. A. Pellighelli and A. Tiripicchio, *Acta Cryst. Sect. B* 1971, **27**, 2261.
19. G. Smith, E. J. O'Reilly, C. H. L. Kennard and T. C. W. Mak, *Inorg. Chem.* 1985, **24**, 2321. C. H. L. Kennard, G. Smith, E. J. O'Reilly, K. M. Stadnicka and B. J. Oleksyn, *Inorg. Chim. Acta* 1982, **59**, 241. C. H. L. Kennard, S. W. Stewart, E. J. O'Reilly, G. Smith and A. H. White, *Polyhedron* 1985, **4**, 697.
20. A. H. White and A. C. Willis, *J. Chem. Soc., Dalton Trans.* 1977, 1377.
21. C. H. L. Kennard, G. Smith, E. J. O'Reilly and K. E. Brown, *Inorg. Chim. Acta* 1981, **52**, 55. E. J. O'Reilly, G. Smith and C. H. L. Kennard, *Inorg. Chim. Acta* 1984, **90**, 63.
22. C. H. L. Kennard, G. Smith and A. H. White, *Acta Cryst. Sect. B.* 1982, **38**, 868. G. Smith, C. H. L. Kennard, A. H. White and B. W. Skelton, *J. Agric. Food Chem.* 1981, **29**, 1046.
23. L. Leiserowitz, *Acta Cryst. Sect. B.* 1976, **32**, 775.
24. T. C. W. Mak, W.-H. Yip, G. Smith, E. J. O'Reilly and C. H. L. Kennard, *Inorg. Chim. Acta* 1984, **84**, 57. E. J. O,Reilly, G. Smith, C. H. L. Kennard, T. C. W. Mak and W.-H.Yip, *Inorg. Chim. Acta* 1984, **83**, L63. T. C. W. Mak, W.-H.Yip, G. Smith, E. J. O'Reilly and C. H. L. Kennard, *Inorg. Chim. Acta* 1984, **88**, 35.

Polyhedron Vol. 6, No. 5, pp. 881–889, 1987
Printed in Great Britain

0277–5387/87 $3.00+.00

METAL–(PHENYLTHIO)ALKANOIC ACID INTERACTIONS—VII.* THE CRYSTAL AND MOLECULAR STRUCTURES OF DIAQUABIS[(BENZYLTHIO)ACETATO]-ZINC(II), *CATENA*-[DIAQUA-TETRA[(BENZYLTHIO)ACETATO]-BIS[CADMIUM(II)], *CATENA*-TETRA-μ-{2-METHYL-3-(PHENYLTHIO)PROPIONATO-*O,O'*]-BIS[COPPER(II)]} AND TETRA-μ-[2-METHYL-2-(PHENYLTHIO)PROPIONATO-*O,O'*]-BIS[ETHANOLCOPPER(II)]

WING-HONG CHAN

Department of Chemistry, Hong Kong Baptist College, Kowloon, Hong Kong

THOMAS C. W. MAK and WAI-HING YIP

Department of Chemistry, The Chinese University of Hong Kong, Shatin, New Territories, Hong Kong

GRAHAM SMITH† and ERIC J. O'REILLY

Department of Chemistry, Queensland Institute of Technology, Brisbane, 4000, Australia

and

COLIN H. L. KENNARD†

Department of Chemistry, University of Queensland, Brisbane, 4067, Australia

(*Received* 27 *May* 1986; *accepted* 8 *August* 1986)

Abstract—The crystal structures of diaquabis[(benzylthio)acetato]zinc(II), $[Zn(BTA)_2(H_2O)_2]$ (**1**), *catena*-[diaqua-tetra[(benzylthio)acetato)]-bis[cadmium(II)], $[Cd_2(BTA)_4H_2O)_2]_n$ (**2**), *catena*-{tetra-μ-[2-methyl-3-(phenylthio)propionato-*O,O'*]-bis[copper(II)]}, $[Cu_2(MPTP)_4]_n$ (**3**) and tetra-μ-[2-methyl-2-(phenylthio)propionato-*O,O'*]-bis[ethanol copper(II)], $[Cu_2(PTIBA)_4(EtOH)_2]$ (**4**) have been determined using X-ray diffraction techniques. Complex (**1**) is monomeric with distorted octahedral stereochemistry and lies on a two-fold rotational axis. The MO_6 coordination involves four oxygens from two slightly asymmetric bidentate BTA carboxyl groups [Zn—O, 2.138(3), 2.28(3) Å] and two *cis*-related waters [Zn—Ow, 1.996(3) Å]. The cadmium complex (**2**) is best described in terms of a polymer with the repeating unit consisting of two different centres, one seven, the other six-coordinate. With the first, the distorted MO_6S coordination sphere has four oxygens from two asymmetric bidentate carboxylate groups (ligands B and C) [Cd—O, 2.36, 2.56(1) Å; 2.26, 2.67(1) Å], an oxygen and a sulphur from a bidentate chelate ligand (A) [Cd—O, 2.36(1) Å; Cd—S, 2.773(4) Å] and an oxygen from a bridging carboxyl group (ligand D) [Cd—O, 2.28(1) Å]. Ligands C and D also bridge two Cd centres through

* Part VI, Ref. 1.

† Authors to whom correspondence should be addressed.

sulphurs [Cd—S, 2.739, 2.723(4) Å]. The second carboxyl oxygen of ligand A also forms a bridge to the second Cd [(Cd—O, 2.30(1) Å], while the distorted octahedral MO_4S_2 stereochemistry is completed by two waters [Cd—O, 2.25(1), 2.49(1) Å] and a sulphur from ligand D [Cd—S, 2.723(4) Å] giving a polymer structure. Complexes (**3**) and (**4**) are centrosymmetric tetra-carboxylate bridged dimers [for (**3**) Cu···Cu, 2.586(3) Å; mean Cu—O(equatorial), 1.957(11) Å; for the two independent dimers in (**4**), Cu···Cu, 2.596(1), 2.616(1) Å; Cu—O (equatorial), 1.952(4), 1.968(4) Å mean]. The axial positions of the dimer in (**3**) are occupied by carboxyl oxygens of adjacent dimers [Cu—O, 2.280(9) Å] forming a polymer structure. In contrast, these positions in (**4**) are occupied by ethanol molecules with Cu—O, 2.222(3) and 2.177(4) Å respectively for the two independent dimers.

In the course of this current investigation into metal (phenylthio)alkanoic acid interactions, some unusual and unexpected coordination systems have emerged. In the hope of finding some unusual examples, this work has now been extended to include complexes of (benzylthio)acetic acid (BTAH), (phenylsulphinyl)acetic acid (PSAH), 2-methyl-3-(phenylthio)propionic acid (MPTPH) and 2-methyl-2-(phenylthio)propionic acid (PTIBAH). Copper complexes with the first two ligands bis[(benzylthio) - acetato] - bis(pyridine)copper(II) and diaquabis[(phenylsulphinyl)acetato]-bis-pyridine)copper(II) have already been reported.[1] The object of this study is to determine what effect additional carbon atoms in the aliphatic acid side-chain have on Zn(II) and Cd(II) complexes with BTAH, $[Zn(BTA)_2(H_2]_2]$ (**1**) and $[Cd_2(BTA)_4(H_2O)_2]_n$ (**2**) which together with the Cu(II) complexes $[Cu_2(MPTP)_4]_n$ (**3**) and $[Cu_2(PTIBA)_4(EtOH)_2]$ (**4**) are reported here.

EXPERIMENTAL

Preparations

Complexes (**1**), (**2**), (**3**) and (**4**) were prepared by reacting aqueous ethanolic solutions of BTAH, MPTPH or PTIBAH with a suspension of excess metal carbonate (in aqueous ethanol) and digesting for *c.* 1 h at 70–90°C. After removal of the excess carbonate by filtration, standing at room temperature resulted in deposition of crystals which were recrystallised from absolute ethanol as colourless prisms [(**1**) and (**2**)] and dark green needles [(**3**) and (**4**)]. The acid PTIBAH was prepared by the Gilman and Wilder[2] modification of the Galimberti and Defranceschi procedure[3] by reacting thiophenol (0.1 mol) in 100 cm^3 of ethanol with NaOH (0.44 mol) and chloroform (0.11 mol) under reflux for 4 h. After acidification, the acid was obtained in 34% yield as colourless crystals (m.p. 67°C) after recrystallisation from petroleum ether. The crystals of complex (**4**) were found to lose crystallinity rapidly in air, presumably due to loss of ethanol solvate. Consequently, data collection was carried out with the specimen sealed in a glass capillary under an atmosphere of ethanol.

Crystal data, X-ray data collection and structure refinement

Table 1 lists information about unit cell parameters, data acquisition and structure solution for compounds (**1**), (**2**), (**3**) and (**4**). Data were processed using a profile fitting procedure.[4] Structures were solved by the heavy atom method and refined using the SHELX-76 set of programs.[5] Refinement was by blocked-matrix least-squares, with all heavy atoms anisotropic for (**1**) and (**4**) but with only those for Cd and S in (**2**) and Cu, S and O in (**3**) anisotropic. Hydrogens were located from difference Fourier syntheses and included in the respective refinements at fixed positions with their isotropic *U*s set invariant at 0.05 Å.[2]

Data for (**2**) were corrected for absorption. Neutral atom scattering factors were used with the metal and sulphur being corrected for anomalous dispersion.[6] Final atomic parameters, lists of hydrogen atom coordinates, anisotropic thermal parameters intraligand bond distances and angles and observed and calculated structure factors are available from the Editor or the authors.* Bond distances and angles about the coordination spheres for complexes (**1**)–(**4**) are given in Table 2.

DISCUSSION

(**1**) $[Zn(BTA)_2(H_2O)_2]$

The structure of (**1**) consists of very distorted octahedral six-coordinate monomers (Fig. 1), with

*Atomic coordinates have also been deposited with the Cambridge Crystallographic Data Centre.

Table 1. Comparative cell data for $[Zn(BTA)_2(H_2O)_2]$, (1), $[Cd_2(BTA)_4(H_2O)_2]_n$, (2), $[Cu_2(MPTP)_4]_n$, (3) and $[Cu_2(PTIBA)_4(EtOH)_2]$, (4)

	(1)	(2)	(3)	(4)
Formula	$C_{18}H_{22}O_6S_2Zn$	$C_{36}H_{40}Cd_2O_{10}S_2$	$C_{40}H_{44}Cu_2O_8S_4$	$C_{44}H_{56}Cu_2O_{10}S_4$
M_r	463.9	985.8	908.2	1000.3
a (Å)	38.17(1)	8.968(2)	39.71(2)	13.313(4)
b (Å)	5.140(1)	11.596(3)	5.268(2)	14.281(4)
c (Å)	10.604(3)	18.887(5)	21.68(1)	15.446(4)
α (deg)		95.67(2)		116.64(2)
β (deg)	94.30(1)	91.33(2)	114.66(2)	99.63(2)
γ (deg)		90.25(2)		101.16(2)
V (Å^2)	2075(1)	1954(1)	4122(2)	2465(1)
Z	4	2	4	2
D_c (g cm^{-3})	1.484	1.675	1.462	1.347
D_f (g cm^{-3})	1.480	1.696	1.474	1.372
μ (Mo-K_α) (cm^{-1})	14.4	13.4	13.2	11.1
$F(000)$	960	992	1880	1044
Space group	$C2/c$	$P\bar{1}$	$C2/c$	$P\bar{1}$
Data collection				
Diffractometer	Nicolet R3m	Nicolet R3m	Nicolet R3m	Nicolet R3m
Radiation	Mo-K_α	Mo-K_α	Mo-K_α	Mo-K_α
Wavelength (Å)	0.71069	0.71069	0.71069	0.71069
$2\theta_{max}$ (deg)	52	42	45	50
Unique data	1508	4045	2612	7364
Crystal size (mm)	$0.25\times0.25\times0.10$	$0.30\times0.24\times0.05$	$0.24\times0.20\times0.08$	$0.40\times0.40\times0.16$
Structure refinement				
R^a	0.054	0.074	0.081	0.058
Rw^b	0.057	0.081	0.081	unit weights
w^c (A)	1.17	1.38	2.08	—
(B)	1.47×10^{-3}	5.00×10^{-3}	1.04×10^{-3}	—
Data used	1344	2759	1143	6086
Discrimination	$I>2.5\sigma(I)$	$I>2.5\sigma(I)$	$I>2.5\sigma(I)$	$I>2.5\sigma(I)$

[a] $R = [\Sigma||F_o|-|F_c||/\Sigma|F_o|$.
[b] $Rw = [(\Sigma w||F_o|-|F_c||^2/\Sigma w|F_o|^2)^{1/2}]$.
[c] $w = A/(\sigma^2F_o+BF_o^2)$.

two-fold rotational symmetry coincident with crystallographic symmetry. In this respect, (1) is similar to zinc acetate dihydrate,[7] zinc salicylate dihydrate,[8] zinc phenoxyacetate dihydrate,[9] zinc(phenylthio)acetate dihydrate[10] and zinc (2-formyl-6-methoxyphenoxy)acetate dihydrate.[11] The carboxyl oxygens of the two (benzylthio)acetate ligands in (1) form asymmetric bidentate links to Zn [2.139(3), 2.227(3) Å, O—Zn—O, 58.8(1)°] with two waters [Zn—Ow, 1.996(3) Å] completing the coordination sphere. The degree of asymmetry in (1) is intermediate between symmetric zinc acetate dihydrate (2.17, 2.17 Å), and zinc (phenylthio(acetate dihydrate[10] (2.18, 2.20 Å) and zinc salicylate dihydrate[8] (2.03, 2.52 Å). Examples such as zinc phenoxyacetate dihydrate[9] (2.12, 2.34 Å) and zinc 2-ethoxybenzoate dihydrate[12] (2.05, 2.31 Å) are also intermediate. The substituted benzoate complexes[8,12] were considered tetrahedral but on the basis of repulsion energy calculations,[13] complexes of the type [M(bidentate)$_2$(unidentate)$_2$], with small normalized ligand 'bite', distortion of the six-coordinate *trans*-related octahedral structure occurs, giving a skew-trapezoidal bipyramidal structure. Thus these examples, together with (1), are best described on this basis, with the extreme case being the undistorted octahedral species in $[Zn(2,4\text{-}D)_2(H_2O)_4\cdot Zn(2,4\text{-}D)_2(H_2O)_2]$[14] (2,4-D = 2,4-dichlorophenoxyacetate) and in zinc 2-chlorophenoxyacetate tetrahydrate,[11] where the carboxylate ligands are unidentate.

The (benzylthio)acetate ligand in (1) is significantly distorted [torsion angle about the S(7)—C(8) vector c. 90°], in common with the phen-

Table 2. Bond distances (Å) and angles (deg) about the coordination spheres for (**1**), (**2**), (**3**) and (**4**), including these for the ethanol ligand in (**4**)

(a) Distances

(**1**)

Zn—O(10)	2.138(3)		
Zn—O(11)	2.228(3)		
Zn—Ow(1)	1.996(3)		

(**2**)

Cd(1)—S(7)A	2.773(4)	Cd(2)—O(10)A[c]	2.297(10)
Cd(1)—O(11)A	2.360(9)		
Cd(1)—O(10)B	2.362(9)	Cd(2)—S(7)C	2.739(4)
Cd(1)—O(11)B	2.561(10)	Cd(2)—O(11)C	2.256(9)
Cd(1)—O(11)C[a]	2.673(10)	Cd(2)—S(7)D	2.723(4)
Cd(1)—O(10)C[a]	2.259(9)	Cd(2)—Ow(1)	2.489(9)
Cd(1)—O(10)D[b]	2.276(10)	Cd(2)—Ow(2)	2.245(9)

(**3**)

Cu—O(10)A	1.968(9)	Cu[d]—O(11)B	1.947(13)
Cu[d]—O(11)A	2.013(9)	Cu—O(11)A[e]	2.280(9)
Cu—O(10)B	1.971(13)	Cu—Cu[d]	2.586(3)

(**4**)

Cu(1)—O(10)A	1.954(4)	Cu(2)—O(10)C	1.957(4)
Cu(1)[f]—O(11)A	1.940(4)	Cu(2)[f]—O(11)C	1.966(4)
Cu(1)—O(10)B	1.959(5)	Cu(2)—O(10)D	1.977(4)
Cu(1)[f]—O(11)B	1.956(5)	Cu(2)[f]—O(11)D	1.973(5)
Cu(1)—O(1)D	2.222(3)	Cu(2)—O(1)F	2.177(4)
Cu(1)—Cu(1)[f]	2.596(1)	Cu(2)—Cu(2)[f]	2.616(1)
O(1)E—C(2)E	1.45(1)	O(1)F—C(2)F	1.46(1)
C(2)E—C(3)E	1.43(2)	C(2)F—C(3)F	1.47(2)

(b) Angles

(**1**)

O(10)—Zn—O(11)	58.8(1)	S(7)A—Cd(1)—O(11)A	71.0(3)
O(10)—Zn—Ow(1)	144.4(1)	S(7)A—Cd(1)—O(10)B	111.5(3)
O(10)—Zn—O(10)[g]	90.1(1)	S(7)A—Cd(1)—O(11)B	84.6(3)
O(10)—Zn—O(11)[g]	113.4(1)	S(7)A—Cd(1)—O(11)C[a]	84.3(4)
O(10)—Zn—Ow(1)[g]	93.3(2)	S(7)A—Cd(1)—O(10)C[a]	91.7(4)
O(11)—Zn—Ow(1)	87.6(1)	S(7)A—Cd(1)—O(10)D[b]	139.9(4)
O(11)—Zn—O(11)[g]	170.2(1)	O(11)A—Cd(1)—O(10)B	91.0(3)
O(11)—Zn—Ow(1)[g]	98.5(1)	O(11)A—Cd(1)—O(11)B	124.5(4)
Ow(1)—Zn—Ow(1)[g]	103.7(1)	O(11)A—Cd(1)—O(11)C[a]	103.1(3)
Zn—O(10)—C(9)	93.3(2)	O(11)A—Cd(1)—O(10)C[a]	151.8(3)
Zn—O(11)—C(9)	89.1(2)	O(11)A—Cd(1)—O(10)D[b]	75.3(3)
		O(10)B—Cd(1)—O(11)B	52.5(3)

(**2**)

O(10)A[c]—Cd(2)—S(7)C	90.1(3)		
O(10)A[c]—Cd(2)—O(11)C	86.7(4)		
O(10)A[c]—Cd(2)—S(7)D	92.9(3)		
O(10)A[c]—Cd(2)—Ow(1)	165.3(3)		
O(10)A[c]—Cd(2)—Ow(2)	116.9(3)		
S(7)C—Cd(2)—O(11)C	76.6(3)		
S(7)C—Cd(2)—S(7)D	90.2(4)		
S(7)C—Cd(2)—Ow(1)	75.3(3)		
S(7)C—Cd(2)—Ow(2)	150.3(3)		
O(11)C—Cd(2)—S(7)D	166.7(3)		
O(11)C—Cd(2)—Ow(1)	90.6(4)		
O(11)C—Cd(2)—Ow(2)	92.1(3)		

		O(10)B—Cd(1)—O(11)C[a]	161.8(4)	S(7)D—Cd(2)—Ow(1)	86.5(3)
		O(10)B—Cd(1)—O(10)C[a]	116.4(3)	S(7)D—Cd(2)—Ow(2)	99.9(3)
		O(10)B—Cd(1)—O(10)D[b]	90.1(3)	Ow(1)—Cd(2)—Ow(2)	77.5(3)
		O(11)B—Cd(1)—O(11)C[a]	123.6(4)		
		O(11)B—Cd(1)—O(10)C[a]	73.6(3)		
		O(11)B—Cd(1)—O(10)D[b]	133.6(3)		
		O(11)C—Cd(1)—O(10)C[a]	51.7(3)		
		O(11)C—Cd(1)—O(10)D[b]	82.6(3)		
		O(10)C—Cd(1)—O(10)D[b]	109.0(3)		
(3)				**(4)**	
O(10)A—Cu—O(11)A[d]	168.4(4)	O(10)A—Cu(1)—O(11)A[f]	169.3(2)	O(10)C—Cu(2)—O(11)C[f]	168.4(2)
O(10)A—Cu—O(10)B	88.7(5)	O(10)A—Cu(1)—O(10)B	88.8(2)	O(10)C—Cu(2)—O(10)D	89.5(2)
O(10)A—Cu—O(11)B[d]	89.2(5)	O(10)A—Cu(1)—O(11)B[f]	90.3(2)	O(10)C—Cu(2)—O(11)D[f]	88.2(2)
O(10)A—Cu—O(11)A[e]	112.5(4)	O(10)A—Cu(1)—O(1)E	97.1(2)	O(10)C—Cu(2)—O(1)F	95.5(2)
O(11)A[d]—Cu—O(10)B	90.1(4)	O(11)A[f]—Cu(1)—O(10)B	91.1(2)	O(11)C[f]—Cu(2)—O(10)D	91.2(2)
O(11)A[d]—Cu—O(11)B[d]	89.9(5)	O(11)A[f]—Cu(1)—O(11)B[f]	87.9(2)	O(11)C[f]—Cu(2)—O(11)D[f]	88.8(2)
O(11)A[d]—Cu—O(11)A[e]	79.1(4)	O(11)A[f]—Cu(1)—O(1)E	93.5(2)	O(11)C[f]—Cu(2)—O(1)F	95.8(2)
O(10)B—Cu—O(11)B[d]	168.8(5)	O(10)B—Cu(1)—O(11)B[f]	169.7(2)	O(10)D—Cu(2)—O(11)D[f]	168.6(2)
O(10)B—Cu—O(11)A[e]	96.8(5)	O(10)B—Cu(1)—O(1)E	92.9(2)	O(10)D—Cu(2)—O(1)F	98.5(2)
O(11)B[d]—Cu—O(11)A[e]	94.1(5)	O(11)B[f]—Cu(1)—O(1)E	97.3(2)	O(11)D[f]—Cu(2)—O(1)F	92.8(2)
Cu—O(10)A—C(9)A	124.8(9)	Cu(1)—O(10)A—C(9)A	123.5(3)	Cu(2)—O(10)C—C(9)C	121.9(3)
Cu—O(11)A[d]—C(9)A[d]	124.7(9)	Cu(1)—O(11)A[f]—C(9)A[f]	121.6(3)	Cu(2)—O(11)C[f]—C(9)C[f]	124.7(3)
Cu—O(10)B—C(9)B	122.7(9)	Cu(1)—O(10)B—C(9)B	123.9(4)	Cu(2)—O(10)D—C(9)D	126.4(3)
Cu—O(11)B[d]—C(9)B[d]	120.4(9)	Cu(1)—O(11)B[f]—C(9)B[f]	121.2(3)	Cu(2)—O(11)D[f]—C(9)d[f]	121.6(3)
O(11)C—Cu—Cu[d]	162.6(3)	Cu(1)—O(1)E—C(2)E	117.5(4)	Cu(2)—O(1)F—C(2)F	121.4(5)
		O(1)E—C(2)E—C(3)E	110.9(9)	C(1)F—C(2)F—C(3)F	108.6(7)

[a] $1-x, 1-y, 1-z$.
[b] $1-x, 1-y, 1-z$.
[c] $-1+x, -y, -z$.
[d] $-x, -y, -z$.
[e] $-x, 1-y, -z$.
[f] $-x, -y, -z$.
[g] $-x, -y, z$.

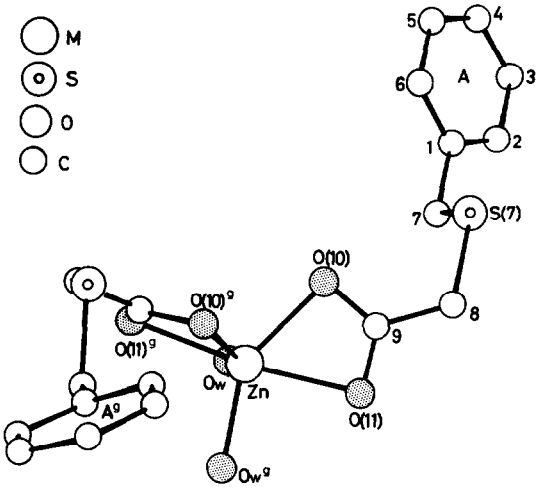

Fig. 1. Molecular configuration and atom naming scheme for (1).

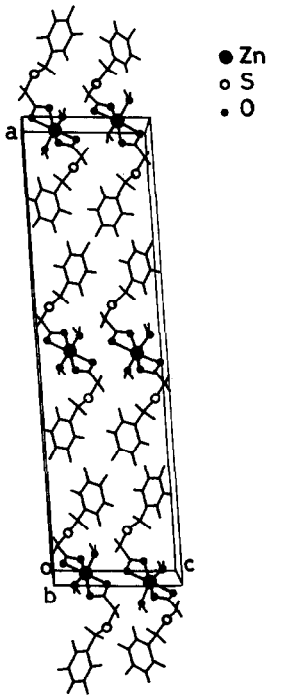

Fig. 2. Packing of (1) in the unit cell viewed down *b*.

ylthio ligand in the Zn and Cd complexes[10] but contrasting with (phenylthio)acetic acid (PTAH)[10] and the Ba and K complexes of PTA[15] (torsion angles *c.* 180°). This is the case even when the thioether-S is not coordinated to the metal as with the Zn,[11] Ba, K[15] and Cu complexes[1] but not the Cd examples, $[Cd_2(PTA)_4(H_2O)]_n$[10] and $[Cd_2(BTA)_4(H_2O)_2]_n$ [example (2), this work]. The non-bonding S···O(carboxylate) distance of 3.03 Å is maintained while the only significant intermolecular contact is a relatively short hydrogen bonding contact (2.67 Å) between the carboxyl oxygen O(10) and a coordinated water (Fig. 2).

(2) $[Cd_2(BTA)_4(H_2O)_2]_n$

Complex (2) is a polymer in which the repeating unit comprises two independent Cd centres, one seven-coordinate, the other six (Fig. 3). The first, Cd(1) has an irregular MO_6S coordination, with two asymmetric bidentate carboxylate groups from ligands B and C [Cd—O: 2.36, 2.56(1) Å; 2.26, 2.67(1) Å respectively], together with a bidentate O, S chelated ligand A (Cd—O(11), 2.36(1) Å; Cd—S, 2.773(4) Å]. The seventh coordination position is occupied by a bridging oxygen [O(10)D^b, 2.28(1) Å] $(1-x, 1-y, 1-z)$. Ligands C and D also provide two O—S bridges between the two Cd centres [Cd(2)—S(7)C, 2.739(4) Å; Cd(2)—S(7)D, 2.723(4) Å] while O(11)C also bridges two centres

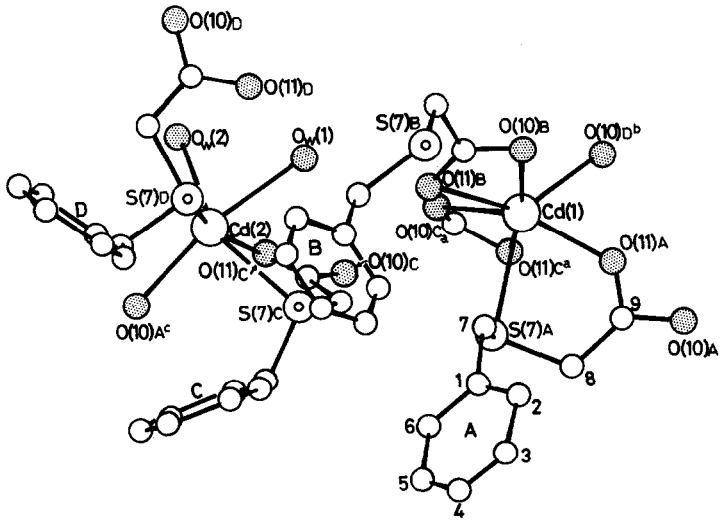

Fig. 3. Molecular configuration and atom naming scheme for (2).

[Cd(2)—O(11)C, 2.61(1) Å]. The second Cd has very distorted octahedral $MO_2Ow_2S_2$ six-coordination, with *cis*-angles varying from 75.3° [Ow(1)—Cd—S(7)C] to 116.9° [O(10)A—Cd—Ow(2)] while the minimum *trans* angle is 150.3° [S(7)C—Cd—Ow(2)]. The two *cis*-related waters are also bound to Cd(2) by unequal bonds [2.25(1), 2.49(1) Å]. Longer Cd—O distances are also found in the structure, but Cd(1)—O(11)D (2.83 Å) and Cd(2)—O(11)A (2.88) Å are not considered as formal bonds.

Although $Cd_2(PTA)_4(H_2O)]_n$[10] is also a polymeric dimer with two independent but different Cd centres, it is quite unlike (**2**) both in the nature of the coordination about each Cd centre and in the bridging mode. In addition, the analogous phenoxyacetate complexes $[Cd(PA)_2(H_2O)_2]$ (PA = phenoxyacetate)[9] and $[Cd(2\text{-}CPA)_2(H_2O)_3]\cdot 2H_2O$ (2-CPA = 2-chlorophenoxyacetate)[11] are different in all respects. Both are monomeric, $[Cd(PA)_2(H_2O)_2]$ being isomorphous with the zinc analogue[9] but with no asymmetry in the Cd—O(carboxyl) distances [2.363, 2.365 Å].[16] $[Cd(2\text{-}CPA)_2(H_2O)_3]\cdot 2H_2O$ is seven-coordinate, with asymmetric bidentate carboxylates [Cd—O, 2.26, 2.49(2) Å] and three waters [Cd—O, 2.27, 2.27, 2.34(2) Å], one on a two-fold axis.[11] At this stage of the work, no general rules for Cd complexes can be formulated as a consistent pattern has yet to emerge.

The packing of the polymer chains of (**2**) in the unit cell (Fig. 4) involves few inter-dimer associations, via the two waters attached to Cd(2): Ow(1)···O(11)B, (2.74 Å); Ow(1)···O(11)B, (2.82 Å); Ow(1)···O(10)D, 2.72 Å and Ow(2)···O(10)D, (2.69 Å).

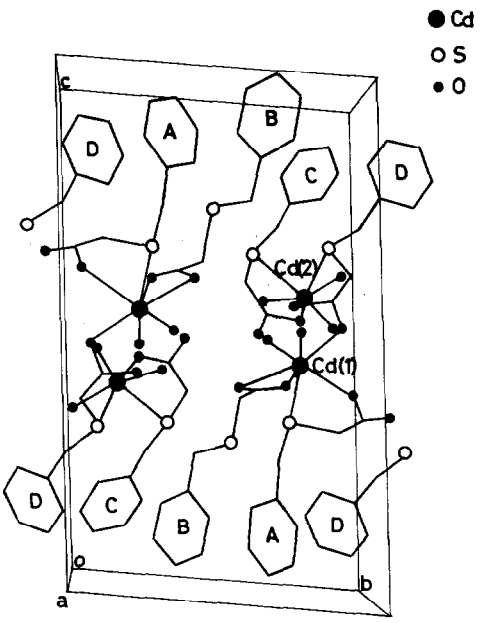

Fig. 4. Packing of (**2**) in the unit cell.

(3) $[Cu_2(MPTP)_4]_n$ *and* (4) $[Cu_2(PTIBA)_4(EtOH)_2]$

The structures of both (**3**) and (**4**) are based on centrosymmetric tetracarboxylate bridged dimers of the copper acetate hydrate type $[Cu_2(Ac)_4(H_2O)_2]$.[17] However, in the anhydrous complex (**3**), the axial water molecules of the copper acetate monomer are replaced by carboxyl oxygens of adjacent dimer units (Fig. 5). This extends the structure into a two-dimensional step polymer which extends down the *b* direction of the unit cell (Fig. 6). In this respect it is similar to other anhydrous examples such as copper(II) propionate,[18] copper(II) butyrate[19] and copper(II) 2-chlorophenoxyacetate.[20] In all these complexes, the structural features of the respective tetracarboxylate cages are generally comparable: Cu—Cu, mean Cu—O (equatorial) and Cu—O (axial) distances are 2.568(3), 1.975(9), 2.280(9) Å (**3**); 2.578(4), 1.94(1), 2.28(1) Å (propionate); 2.565, 1.982, 2.245 Å (butyrate); 2.583(2), 1.965(5), 2.169(5) Å (2-chlorophenoxyacetate). It has been previously noted[20] that these examples exhibit some of the shortest known Cu—Cu separations among the 55 known dimeric copper(II) carboxylates which range up to 2.886 Å $[Cu_2(CF_3COO)_4(quinoline)_2]$.[21] In the only three known copper(II) (phenylthio)carboxylate dimers $[Cu_2(PTA)_4(py)_2]$[22] [PTA = (phenylthio)acetate], $[Cu_2(DCMPTA)_4(acetone)_2]$[23] [(DCMPTA) = (2,4-dichloro-5-methyl-phenylthio)acetate and $[Cu_2(DCMPTA)_4$

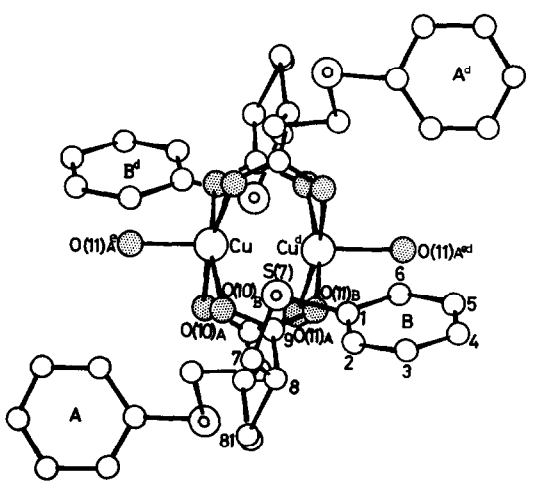

Fig. 5. Molecular configuration and atom naming scheme for (**3**).

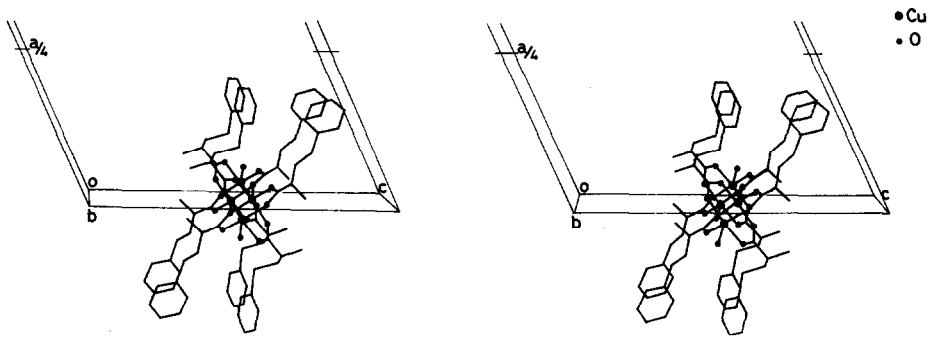

Fig. 6. Stereoview of the packing of part of the unit cell for (3), showing the polymer structure.

$(H_2O)_2]\cdot 2$ acetone[24] the comparative distances are 2.685(1), 1.984(4), 2.151(4) Å (Cu—N); 2.646(1), 1.961(4), 2.206(3) Å; 2.639(5), 1.99(2), 2.13(2) Å respectively. Furthermore the polymer motif of (3) contrasts with the more stereotypical distorted octahedral stereochemistries for the pyridine adducts of copper(II) (benzylthio)acetate and (phenylsulfinyl)acetate.[1]

Structure (4), is also different from that of (3), being discretely dimeric but having two independent, but similar centrosymmetric dimers (A and B) in the asymmetric unit. These lie at inversion centres in the unit cell (Fig. 7). The Cu—Cu and mean Cu—O (equatorial) distances [2.596(1) 1.952(4) Å (A) and 2.616(1), 1.968(4) Å (B) respectively] are within what is considered a normal range for copper(II) dimers.[25] In the axial sites of the dimers are found ethanol molecules [Cu—O, 2.177(4) Å (A); 2.222(3) Å (B)]. This is a reasonably common phenomenon among copper(II) dimers, but (4) represents the first occurrence for either the copper(phenylthio)alkanoates or the (phenoxy)alkanoates. However, the only known example of a dimer with acetone molecules in the axial sites is

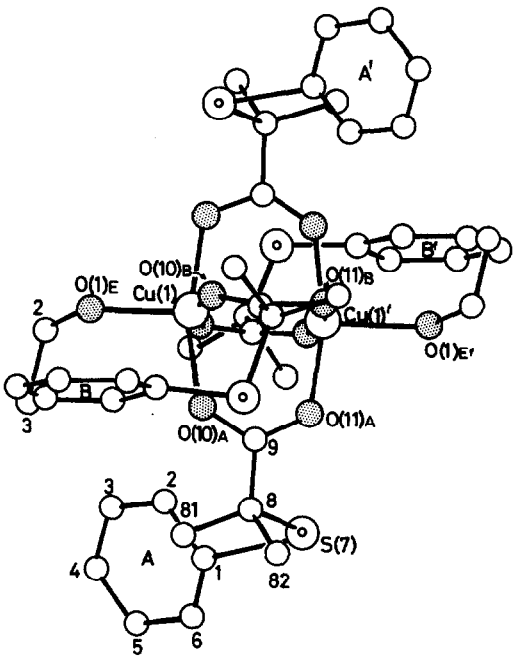

Fig. 7. Molecular configuration and atom naming scheme for (4).

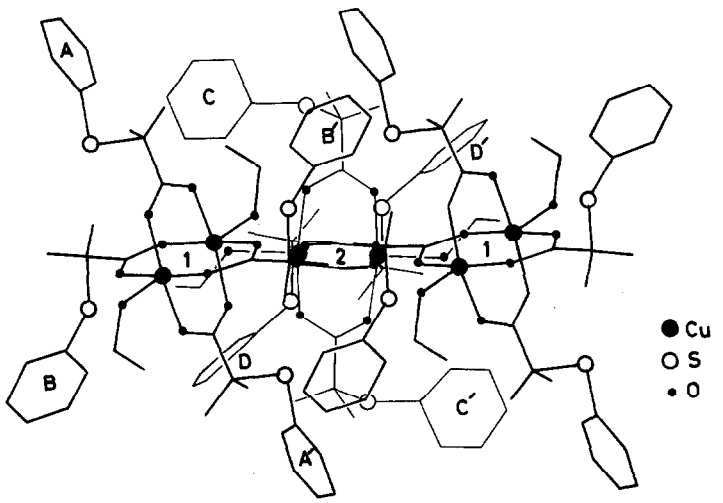

Fig. 8. Packing of (4)

one of the current series, $[Cu_2(DCMPTA)_4(acetone)_2]$.[23] In this example, the acetone molecules were strongly coordinated [Cu—O, 2.206(3) Å], presumably due to the greater steric freedom allowed by the longer (phenylthio)acetate side-chains of the acid.

With (**4**), few inter-dimer associations are found, the most significant being a hydrogen bond between the ethanol molecules, O(1)E···O(1)F, 2.880 Å. This links the two independent dimer units, stabilizing the packing in the unit cell (Fig. 8).

The (phenylthio)alkanoate ligands

The thioacetate (**1**,**2**), 3-thiopropionate (**3**) and thiobutyrate (**4**) side-chains in the four reported complexes vary markedly in formation. This is consistent with previous observations.[1,10,15,16] The introduction of an additional methylene group into the chain (BTAH) or up to two α-methyl groups into the acid (MPTPH or PTIBAH) adds to the conformational possibilities imposed by the coordination and packing modes for the complexes. Previously, conformation has not been a predictable quantity for this series, unlike the observations for the analogous metal phenoxyalkanoates. The much weaker non-bonding S···O cf. O···O interactions are considered the mean causative factor in this respect. For this series, the S···O distances are 3.03 Å (**1**); 2.83, 3.00, 3.12, 3.33 Å (**2**); > 4.0, 3.78 Å (**3**) and 3.11, 3.14, 3.20, 3.33 Å (**4**).

Furthermore, only in the Cd complex (**2**) does the thioether-S enter into coordination with the metal {as is also the case with $[Cd_2(PTA)_4(H_2O)]_n$[10]}. This parallels the lesser affinity of the ether-O of the phenoxyalkanoates towards metals compared to the carboxylate oxygen. With the Cd examples, bonding probably is the result of the greater tendency for Cd to expand its coordination sphere to give irregular stereochemistries through polymerization compared with copper(II) which is more predictable in its coordination in giving monomeric, dimeric or polymeric forms. Even in the zinc complex of (phenylthio)isobutyric acid, $[Zn_2(PTIBA)_4]_n$,[26] which involves a tris-carboxylate bridged dimer with tetrahedral zinc centres, forming a chain polymer through the fourth carboxylate group, only one very weak Zn—S interaction if found (Zn—S, 2.98 Å).

Acknowledgements—The authors thank the Chinese University of Hong Kong for provision of X-ray diffraction data collection facilities, the University of Queensland and the Queensland Institute of Technology for financial assistance and for provision of data preparation services.

REFERENCES

1. W.-H. Chan, T. C. W. Mak, G. Smith, E. J. O'Reilly and C. H. L. Kennard, *Polyhedron* 1985, **4**, 1443.
2. H. Gilman and G. R. Wilder, *J. Am. Chem. Soc.* 1955, **77**, 6644.
3. P. Galimberti and A. Defranceschi, *Gazz. Chim. Ital.* 1947, **77**, 431.
4. R. Diamond, *Acta Cryst.* 1969, **A25**, 43.
5. G. M. Sheldrick, *SHELX-76 Program for Crystal Structure Determination*, University of Cambridge (1976).
6. *International Tables for X-ray Crystallography*, Vol. 4 (Edited by J. A. Ibers and W. C. Hamilton). Kynoch Press, Birmingham (1974).
7. J. N. van Niekerk, F. R. L. Schening and J. H. Talbot, *Acta Cryst.* 1953, **6**, 720.
8. K. P. Klug, L. E. Alexander and G. G. Sumner, *Acta Cryst.* 1958, **11**, 41.
9. G. Smith, E. J. O'Reilly, C. H. L. Kennard, K. Stadnicka and B. Oleksyn, *Inorg. Chim. Acta* 1980, **47**, 111.
10. T. C. W. Mak, W.-H. Yip, G. Smith, E. J. O'Reilly and C. H. L. Kennard, *Inorg. Chim. Acta* 1984, **84**, 57.
11. C. H. L. Kennard, G. Smith and E. J. O'Reilly, *Aust. J. Chem.* 1987, (in press).
12. S. Natarajan, S. S. Sake Gowda and L. Cartz, *Acta Cryst.* 1974, **B30**, 401.
13. D. L. Kepert, *Progress in Inorganic Chemistry* (Edited by S. J. Lippard), Vol. 23, p. 1. John Wiley, New York (1977).
14. C. H. L. Kennard, G. Smith, E. J. O,Reilly, K. M. Stadnicka and B. J. Oleksyn, *Inorg. Chem. Acta* 1982, **59**, 241.
15. T. C. W. Mak, W.-H. Yip, G. Smith, E. J. O'Reilly and C. H. L. Kennard, *Inorg. Chim. Acta* 1984, **88**, 35.
16. T. C. W. Mak, W.-H. Yip, E. J. O'Reilly, G. Smith and C. H. L. Kennard, *Inorg. Chim. Acta* 1985, **100**, 267.
17. J. N. van Niekerk and F. R. L. Schoening, *Acta Cryst.* 1953, **6**, 227.
18. A. V. Ablov, Y. A. Simonov and T. I. Malinovskii, *Sov. Phys. Dokl.* 1967, **11**, 1029.
19. M. J. Bird and T. R. Lomer, *Acta Cryst.* 1972, **B28**, 242.
20. G. Smith, E. J. O'Reilly, C. H. L. Kennard and A. H. White, *J. Chem. Soc., Dalton Trans.* 1985, 243.
21. J. A. Moreland and R. J. Doedens, *J. Am. Chem. Soc.* 1975, **97**, 508.
22. E. J. O'Reilly, G. Smith, C. H. L. Kennard, T. C. W. Mak and W.-H. Yip, *Inorg. Chim. Acta* 1984, **83**, L63.
23. G. Smith, E. J. O'Reilly, C. H. L. Kennard, T. C. W. Mak and W.-H. Yip, *Polyhedron* 1985, **4**, 451.
24. C. H. L. Kennard, G. Smith, E. J. O'Reilly, T. C. W. Mak and W.-H. Yip, *Inorg. Chim. Acta* 1985, **98**, L31.
25. M. Melnik, *Coord. Chem. Rev.* 1982, **42**, 259.
26. C. H. L. Kennard, T. C. W. Mak, W.-H. Yip, W. H. Chan, G. Smith and E. J. O'Reilly, *Aust. J. Chem.* 1987, (accepted).

Polyhedron Vol. 6, No. 5, pp. 891–896, 1987
Printed in Great Britain

0277–5387/87 $3.00+.00

TROPOLONATO COMPLEXES OF OSMIUM, IRIDIUM, PLATINUM, MOLYBDENUM AND TUNGSTEN, AND THE X-RAY CRYSTAL STRUCTURE OF MoO_2trop_2

WILLIAM P. GRIFFITH,* CAROL A. PUMPHREY and ANDRZEJ C. SKAPSKI*

Chemical Crystallography and Inorganic Chemistry Laboratories, Imperial College, London SW7 2AY, U.K.

(*Received* 16 *June* 1986; *accepted* 12 *August* 1986)

Abstract—The new tropolonato (trop) complexes $Os(trop)_3$, $Ir(trop)_3$, $[Pt(trop)(PPh_3)_2]BPh_4$, $OsO_2(trop)_2$, $MoO_2(trop)_2$ and $W_2O_5(trop)_2$ are reported. The vibrational, ^1H and ^{13}C NMR spectra of the complexes have been measured and the X-ray crystal structure of MoO_2trop_2 has been determined. The crystals are monoclinic with $a = 15.485(3)$, $b = 13.583(3)$, $c = 14.211(3)$ Å, $\beta = 117.74(1)°$, space group $C2/c$, $Z = 8$; and the structure has been refined to $R = 0.033$.

We have reported the preparation and characterisation of catecholato (cat) complexes of osmium[1,2] and, more recently, of catecholato complexes of other second and third row elements.[3] The tropolonato ligand $(C_7H_5O_2)^-$ is the seven-membered ring analogue of the benzenoid catecholato ligand $(C_6H_4O_2)^{2-}$; like the latter[4] it is a good chelating ligand for transition metals, lanthanides and actinides.[5,6] Tropolonato complexes of all the first-row transition elements have been isolated[6,7] but there are very few such complexes known of the second and third row elements, and no structural or spectroscopic data on such species. We present here the results of a study of complexes of this ligand with the platinum group metals and with molybdenum and tungsten, complementing our earlier work on catecholato complexes of these metals.

Tropolonato complexes of the platinum metals

The complexes $Rh(trop)_3$[5] and $Pd(trop)_2$[6] are well-characterised; the published preparation of $Ru(trop)_3$[7] involves complex separational procedures. The only reported iridium complex seems to be $Ir(trop)(\pi\text{-}C_3H_7)_2$.[8]

We find that $Os(trop)_3$ can be made by reaction of $[OsCl_6]^{3-}$ with tropolone under basic conditions, and $OsO_2(trop)_2$ can, like its catecholato analogue, be made from *trans*-$K_2[OsO_2(OH)_4]$ and the ligands. Despite many attempts we failed to prepare the unknown $Pt(trop)_2$, but $[Pt(trop)(PPh_3)_2]^+$ was made by an adaptation of the procedure used[9] to make $Pt(cat)(PPh_3)_2$.

Oxo-molybdenum and oxo-tungsten tropolonato complexes

Although there are many oxo-molybdenum and oxo-tungsten complexes with catecholato ligands[3,4,10,11] the only tropolonato complexes of these metals to have been reported are $MoO(trop)_2Cl$[5] and $W(trop)(\pi\text{-}C_3H_7)(CO)_2Cl$.[12]

We find that reaction of ammonium molybdate with tropolone gives yellow crystals of $MoO_2(trop)_2$, the structure of which is discussed below, but similar reaction of tungstates gives a white complex which analyses as $W_2O_5(trop)_2$.

Physico-chemical studies on the complexes

X-ray crystal structure of $MoO_2(trop)_2$. Although there is a number of X-ray crystal structure determinations on *tris*-[13] and *tetrakis*-[14] tropolonato complexes, none has been reported on complexes also containing an oxo ligand. We therefore grew crystals of $MoO_2(trop)_2$ and carried out an X-ray study (see experimental section); attempts to obtain single crystals of $W_2O_5(trop)_2$ were not successful.

* Authors to whom correspondence should be addressed.

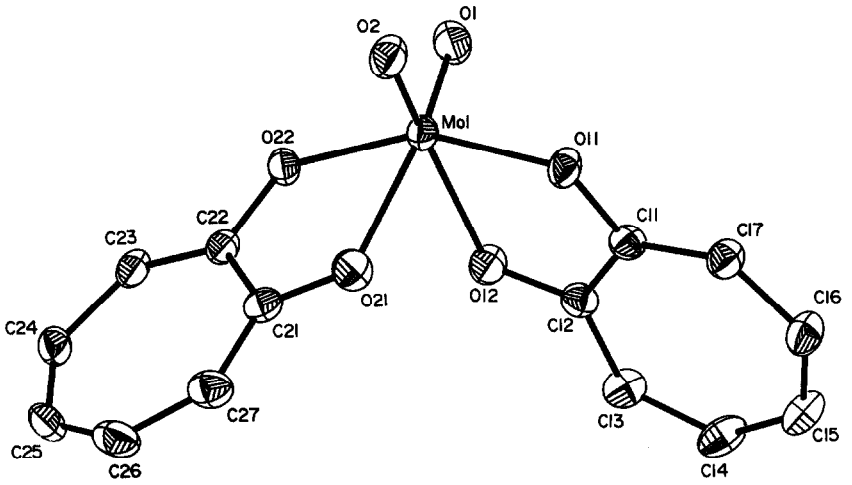

Fig. 1. Molecular structure of $MoO_2(trop)_2$. Thermal vibration ellipsoids are scaled to enclose 50% probability.

Figure 1 shows the molecular structure, and the more important bond lengths and bond angles are given in Tables 1 and 2, respectively. The molecule has approximate C_2 symmetry, and coordination about the molybdenum atom is distorted octahedral with *cis* oxo ligands [mean Mo—O 1.694 Å, O(1)—Mo—O(2) angle 103.4(2)°]. The two Mo—O distances *trans* to these oxo ligands are significantly longer (mean 2.178 Å) than the other two Mo—O distances (mean 2.012 Å); a similar *trans*-weakening effect has been noted in *cis*-$K_2[MoO_2(cat)_2 \cdot 2H_2O$[15] [mean Mo—O(cat) distance *trans* to oxo ligand 2.15(2) Å, mean Mo—O(cat) distance *cis* to oxo ligands 2.05(2) Å].

Within each coordinated tropolonato ligand the two C—O distances are significantly different (mean of 1.322 and 1.279 Å), consistent with the short and the long adjacent Mo—O distances respectively. This 'knock-on' effect persists in the ring systems though becoming slightly less clear-cut further from the Mo—O bonds. The longest bond length in the ring is between the carbon atoms bonded to the two oxygen atoms in each ligand.

IR and Raman spectra. The IR and Raman spectra[16] of tropolone have been measured and assigned, and also the IR spectra of a number of *bis* and *tris* tropolonato complexes[17] and those of normal and ^{18}O-substituted $Cu(trop)_2$.[18] The spectra of tropolonato complexes above 750 cm^{-1} are similar to those of the ligand; there is a small shift

Table 1. Bond lengths (Å) in $MoO_2(trop)_2$ with estimated standard deviations in parentheses

				Mean
Mo(1)—O(1)	1.689(4)	Mo(1)—O(2)	1.699(4)	1.694
Mo(1)—O(11)	2.005(3)	Mo(1)—O(22)	2.018(3)	2.012
Mo(1)—O(12)	2.169(3)	Mo(1)—O(21)	2.186(3)	2.178
O(11)—C(11)	1.321(6)	O(22)—C(22)	1.322(6)	1.322
O(12)—C(12)	1.277(6)	O(21)—C(21)	1.281(6)	1.279
C(11)—C(12)	1.444(7)	C(21)—C(22)	1.451(8)	1.448
C(12)—C(13)	1.410(7)	C(21)—C(27)	1.404(8)	1.407
C(13)—C(14)	1.376(8)	C(27)—C(26)	1.362(9)	1.369
C(14)—C(15)	1.372(8)	C(26)—C(25)	1.389(10)	1.381
C(15)—C(16)	1.373(8)	C(25)—C(24)	1.357(10)	1.365
C(16)—C(17)	1.394(7)	C(24)—C(23)	1.394(8)	1.394
C(17)—C(11)	1.367(7)	C(23)—C(22)	1.368(7)	1.368

Table 2. Bond angles (deg) in $MoO_2(trop)_2$ with estimated standard deviations in parentheses

O(1)—Mo(1)—O(2)	103.4(2)	O(12)—Mo(1)—O(21)	78.1(2)
O(11)—Mo(1)—O(12)	73.2(1)	O(21)—Mo(1)—O(22)	73.2(1)
O(1)—Mo(1)—O(11)	103.7(2)	O(2)—Mo(1)—O(22)	106.3(2)
O(1)—Mo(1)—O(12)	93.5(2)	O(2)—Mo(1)—O(21)	88.6(2)
O(1)—Mo(1)—O(21)	161.6(2)	O(2)—Mo(1)—O(12)	159.5(2)
O(1)—Mo(1)—O(22)	89.9(2)	O(2)—Mo(1)—O(11)	91.4(2)
O(11)—Mo(1)—O(21)	89.7(1)	O(12)—Mo(1)—O(22)	84.9(1)
O(11)—Mo(1)—O(22)	154.7(1)		
Mo(1)—O(11)—C(11)	122.2(3)	Mo(1)—O(22)—C(22)	121.8(3)
Mo(1)—O(12)—C(12)	117.0(3)	Mo(1)—O(21)—C(21)	117.0(3)
O(11)—C(11)—C(12)	112.8(4)	O(22)—C(22)—C(21)	113.7(4)
O(11)—C(11)—C(17)	118.9(4)	O(22)—C(22)—C(23)	118.4(5)
C(12)—C(11)—C(17)	128.3(5)	C(21)—C(22)—C(23)	127.9(5)
O(12)—C(12)—C(11)	114.7(4)	O(21)—C(21)—C(22)	114.3(5)
O(12)—C(12)—C(13)	119.9(5)	O(21)—C(21)—C(27)	120.5(5)
C(11)—C(12)—C(13)	125.5(5)	O(22)—C(21)—C(27)	125.1(5)
C(12)—C(13)—C(14)	129.3(5)	C(21)—C(27)—C(26)	129.9(6)
C(13)—C(14)—C(15)	130.7(5)	C(27)—C(26)—C(25)	130.3(6)
C(14)—C(15)—C(16)	127.3(5)	C(26)—C(25)—C(24)	127.2(6)
C(15)—C(16)—C(17)	129.2(5)	C(25)—C(24)—C(23)	129.4(5)
C(10)—C(17)—C(11)	129.8(5)	C(24)—C(23)—C(22)	129.9(6)

to lower wavenumber of the ν(C—C) stretches near 1615 and 1555 cm^{-1}, and a slight shift to higher wavenumber and considerable increase in intensity of the ν(C═O) mode at 1330 cm^{-1} on co-ordination.[17,18]

We observe these features in the spectra of our complexes and note only the ν(C═O) band in Table 3. In addition to bands arising from the tropolonato ligand there are strong bands in the infrared at 931 and 900 cm^{-1} for $MoO_2(trop)_2$; these bands, observed also in the Raman, are assigned to the symmetric and asymmetric $\nu^s(MoO_2)$ and

Table 3. Spectroscopic data for tropolonato complexes

	IR and Raman data[a]			NMR data[b]				
	ν(C—O)	$\nu^s(MO_2)$	$\nu^{as}(MO_2)$	^1H	$C_{1,2}$	$C_{3,7}$ or $C_{4,6}$		C_5
Tropolone	1308s			6.87–7.55m	172.4	137.6	123.8	128.1
Na(trop)	1363m			7.14m	184.7	139.9	128.1	125.5[c]
$Os(trop)_3$	1353m							
$Ru(trop)_3$	1338s							
$Ir(trop)_3$	1339s			7.16–7.32m	188.6	134.8	129.0	129.6
$Rh(trop)_3$	1330s			7.20–7.40m	187.9	136.8	128.6	128.0
$BPh_4[Pt(trop)(PPh_3)_2]$	1340s				183.6	[d]	[d]	[d]
$OsO_2(trop)_2$	1310s	(884s)	845vs	7.47m				
$MoO_2(trop)_2$	1315s	931s	900vs	7.50–8.06m	192.3	141.3	128.0	132.8
		(931vs)	(900m)		177.6			
$W_2O_5(trop)_2$	1360s	940vs	902vs					
$UO_2(trop)_2$				7.09–7.81m[e]	187.2	139.5	127.4	127.2[e]

[a] Frequencies in cm^{-1}; Raman bands in parentheses.
[b] All δ values are quoted relative to tetramethylsilane on its low-field side.
[c] In ^2H_2O.
[d] Obscured by phenyl resonances.
[e] In d_6-DMSO; other spectra in C^2HCl_3.

$\nu^{as}(MoO_2)$ modes, respectively. The greater intensity of the 931 cm^{-1} band in the Raman suggests it to be the symmetric stretch; similar bands are observed in *cis*-$K_2[MoO_2(cat)_2]$[3] and in other *cis* molybdenum(VI) dioxo species.[19] The IR spectrum of $W_2O_5(trop)_2$ is similar to that for $(NH_4)_2[Mo_2O_5(cat)_2]$;[3] the two bands at 940 and 902 cm^{-1} are likely to arise from the *cis*-WO_2 moiety, while the band at 740 cm^{-1} may be due to a W—O—W asymmetric stretch. A similar band at 733 cm^{-1} is observed in $(NH_4)_2[Mo_2O_5(cat)_2]$;[3] the anion in the latter contains a bridging oxo ligand and also one oxygen atom from each catecholato ligand has a bridging role.[20] It is possible that $W_2O_5(trop)_2$ has a similar structure.

The strong IR band at 845 cm^{-1} in $OsO_2(trop)_2$ has no Raman counterpart and is likely to be $\nu^{as}(OsO_2)$ of a centrosymmetric *trans* O=Os=O 'osmyl' grouping; likewise the strong Raman band at 884 cm^{-1}, not found in the IR, is likely to be the symmetric $\nu^{s}(OsO_2)$, as in other osmyl complexes.[19]

^1H and ^{13}C NMR spectra. The ^1H NMR spectrum of tropolone in C^2HCl_3 shows a complex multiplet from δ 6.87 to 7.55 ppm, with sodium tropolonate in ^2H_2O giving an even broader multiplet, and the diamagnetic complexes show a slight downfield shift. There are few data in the literature on ^1H spectra of tropolonato complexes, but broad multiplets near δ 7.0 ppm have been noted for M(trop)(π-$C_3H_7)_2$[8] and Rh(trop)(diene) complexes.[21]

No ^{13}C NMR data on tropolonato complexes have been published. The ^{13}C NMR (proton-decoupled) spectra of liquid tropolone shows four resonances,[22] close to those found by us for the solution of the ligand. The peak of lowest intensity we tentatively assign to C(n5), the unique carbon atom; the other three are resonances time-averaged by hydroxylic proton exchange, and arise from C(n1, n2), C(n3, n7) and C(n4, n6). The resonance at δ 172.4 ppm is the one most affected by coordination, shifting to higher field in the complexes and in sodium tropolonate, and so may arise from C(n1, n2), the atoms bound to oxygen. This shift could be a consequence of the increased ring current induced in the C_7 ring by coordination; it is interesting to note that two resonances are observed near 175 ppm for $MoO_2(trop)_2$ since, as discussed in the X-ray section above, the chemical environments of C(11, 22) and C(12, 21) are somewhat different.

Mass spectra. We have measured the mass spectra of M(trop)$_3$ (M = Os, Ru, Ir, Rh). These behave in a similar fashion to Cr(trop)$_3$ and Fe(trop)$_3$:[23] the complexes show the molecular ion $[M(trop)_3]^+$ which fragments exclusively by loss of a ligand radical to give $[M(trop)_2]^+$. No peak was found for $[M]^+$ however, although weak peaks were observed for Cr(trop)$_3$ and Fe(trop)$_3$.[23] This may reflect the stability of the trivalent state for the metals studied here, and is indeed analogous to the situation observed for the mass spectra of M(acac)$_3$ (M = Os, Ir, Rh).[24]

EXPERIMENTAL

Tris *tropolonato complexes*

Tris (*tropolonato*)*osmium*(*III*), Os(trop)$_3$. The general method used was similar to that described for the preparation of Os(acac)$_3$.[25]

Silver powder (1.1 g, 0.01 mol) in water (50 cm^3) with 36% hydrochloric acid (10 cm^3), was degassed with nitrogen for 30 min. Solid $Na_2[OsCl_6]\cdot 2H_2O$ (4.5 g, 0.01 mol) was added, and the reddish solution was stirred under nitrogen overnight. To the resulting pale yellow-green solution, potassium bicarbonate (0.6 g, 6 mmol) was added, followed by addition of tropolone (3.67 g, 0.03 mol). The solution was boiled for 15 min. Further potassium bicarbonate (0.4 g, 4 mmol) was then added to the resulting very dark solution which was then heated gently for 2 h. After cooling, it was extracted twice with chloroform, and the chloroform solution washed twice with 2% aqueous sodium hydroxide solution. The resulting red chloroform solution was reduced on the rotary evaporator and the red-brown solid recrystallised from ethanol.

Found: C, 45.4; H, 3.0; $C_{21}H_{15}O_6Os$ requires: C, 45.6; H, 2.7%.

Tris (*tropolonato*)*iridium*(*III*), Ir(trop)$_3$. Sodium acetate trihydrate (0.19 g, 2 mmol) was dissolved in water (10 cm^3). Hydrated iridium trichloride (0.12 g, 0.3 mmol) was added and the solution warmed to give a dark green solution. Tropolone (0.25 g, 2 mmol) was added, with stirring. As the solid tropolone dissolved, the solution became brick red in colour. It was warmed and strirred for a few hours. After cooling, the oily precipitate was filtered off and washed with water, ethanol, and diethyl ether. The resulting red powder was dried over concentrated sulphuric acid.

Found: C, 45.0; H, 2.9; $C_{21}H_{15}IrO_6$ requires: C, 45.4; H, 2.7%, Yield = 40%.

Tris(*tropolonato*)*rhodium*(*III*) *and ruthenium*(*III*), M(trop)$_3$. The literature method was used for Rh(trop)$_3$.[5] The preparation of Ru(trop)$_3$ was attempted by adapting the method used for Ir(trop)$_3$ (above) and Rh(trop)$_3$.[5] It was successful only once and could not be repeated.

Found: C, 54.0; H, 3.6; $C_{21}H_{15}O_6Ru$ requires: C, 54.3; H, 3.3%.

Substituted tropolonato complexes

Bis(*tropolonato*) trans-*dioxo-osmium*(*VI*), $OsO_2(trop)_2$. Potassium osmate, *trans*-$K_2[OsO_2(OH)_4]$ (0.37 g, 1 mmol) was dissolved in water (30 cm^3) by stirring. Tropolone (0.25 g, 2 mmol) in ethanol (5 cm^3) was added, and immediately a mustard coloured precipitate came down. It was filtered off after standing for 30 min, washed with water, ethanol, and diethyl ether, and dried under vacuum.

Found: C, 36.7; H, 2.3; $C_{14}H_{10}O_6Os$ requires: C, 36.2; H, 2.2%; Yield = 90%.

Bis(*tropolonato*) cis - *dioxomolybdenum*(*VI*), $MoO_2(trop)_2$. Tropolone (0.25 g, 2 mmol), in ethanol (5 cm^3) was added to a solution of ammonium molybdate (0.19 g, 1 mmol) in water (10 cm^3). A light yellow precipitate immediately formed. After standing for 30 min it was filtered off, washed with water, ethanol, and diethyl ether. It was dried under vacuum.

Found: C, 44.9; H, 2.7; $C_{14}H_{10}MoO_6$ requires: C, 45.4; H, 2.7%; Yield = 70%.

Bis(*tropolonato*) - μ - *oxo* - bis (cis - *dioxotungsten*(*VI*)), $W_2O_5(trop)_2$. Tropolone (0.25 g, 2 mmol) in ethanol (5 cm^3) was added to a solution of sodium tungstate (0.29 g, 1 mmol) in water (10 cm^3). A pale yellow colour was seen immediately on mixing. After standing for 2 h, the resulting pale yellow solid was filtered off, washed with water and ethanol, and diethyl ether, and dried under vacuum. (The solid may be obtained more quickly by precipitation with ethanol, after mixing the two reactant solutions.)

Found: C, 24.7; H, 1.7; $C_{14}H_{10}O_9W_2$ requires: C, 24.4; H, 1.5%; Yield = 60%.

Mono (*tropolonato*) bis (*triphenylphosphine*) *platinum*(*II*) *tetraphenylboronate* $[Pt(PPh_3)_2(trop)](BPh_4)$. This complex was prepared using the method described for $Pt(PPh_3)_2(cat)$,[9] i.e. via the intermediates $Pt(PPh_3)_4$ and $Pt(PPh_3)_2(O_2)$. All manipulations were carried out under nitrogen, and all solvents were degassed before use. Tropolone (0.06 g, 0.5 mmol) in ethanol (5 cm^3) was added slowly, with stirring, to a solution of $Pt(PPh_3)_2(O_2)$ (0.6 g, 1 mmol) in toluene (10 cm^3) kept in an ice/water bath. The solution became yellow and was left to stir for 1 h. Sodium tetraphenylboronate (0.17 g, 0.05 mmol) in ethanol (8 cm^3) was added to the clear yellow solution, and the pale yellow precipitate which formed immediately was filtered off, washed with ethanol and diethyl ether and left to dry under nitrogen. The solid was stable in air.

Sodium tropolonate was prepared as described by Sasada and Nitta.[26]

IR spectra were measured on a Perkin-Elmer 683 instrument as liquid paraffin mulls between CsI plates, and Raman spectra on a Spex Ramalog 5 instrument as spinning disks on KBr, using a Coherent Radiation Model 52 krypton-ion laser. ^1H NMR spectra were measured on a Perkin-Elmer R32 90 MHz instrument and ^{13}C spectra on a 67.9 MHz Jeol FX 90Q Fourier transform spectrometer at 22.51 MHz. Mass spectra were measured on a VG-Micromass 7070E-HS.

Crystallographic studies

A prismatic crystal of $MoO_2(trop_2)$ of approximate dimensions $0.11 \times 0.075 \times 0.056$ mm was used for intensity data collection. Measurements were carried out on a Nicolet R3m/Eclipse S140 diffractometer system with graphite-monochromated Cu-K_α radiation. Unit-cell dimensions were determined by least-squares refinement of the angular settings of 21 automatically centred reflections.

Crystal data. $C_{14}H_{10}O_6Mo$, $M = 346.3$, monoclinic, $a = 15.485(3)$, $b = 13.583(3)$, $c = 14.211(3)$ Å, $\beta = 117.74(1)^\circ$, $U = 2645.5$ Å^3 (at 20°C), space group $C2/c$, $Z = 8$, $D_c = 1.74$ g cm^{-3}, $F(000) = 1472$, μ(Cu-K_α) = 85.1 cm^{-1}.

Integrated intensities in one quadrant were measured using the ω scan technique. Two reflections (022 and 220) were monitored every 50 measurements, and showed no significant variation in their intensities. A total of 1789 unique reflections were measured (to $\theta = 57^\circ$), of which 360 were judged to be 'unobserved' [$I < 3\sigma(I)$]. The data were scaled using the reference reflections and were corrected for Lorentz and polarisation effects. At a later stage of refinement an analytical absorption correction was applied.[27] All calculations and drawings were made using the SHELXTL program system,[27] and the atomic scattering factors and anomalous dispersion corrections were taken from ref. 28.

The coordinates of the molybdenum atom were derived from an initial Patterson synthesis and the positions of all the other atoms were found from subsequent difference Fourier syntheses. Least-squares refinement was by the block cascade method, typical of the SHELXTL system. All non-hydrogen atoms are refined with anisotropic temperature parameters, while the positions of the hydrogen atoms were tied to those of the parent carbon atoms. A weighting scheme was applied so that $\omega = 1/[\sigma(F_o)^2 + 0.00005F_o^2]$ for the last cycle. R reduced to 0.033, and $R_w = (\Sigma w|\Delta F|^2/\Sigma w|F_o|^2)^{1/2}$ was 0.030. The final difference Fourier synthesis was featureless, with a highest remaining peak of

0.3 e/Å^2 in the immediate vicinity of the metal atom.*

Acknowledgements—We thank the SERC for a grant to one of us (C.A.P.) and for the Nicolet diffractometer, and thank Johnson, Matthey Ltd. for loans of platinum metals.

REFERENCES

1. A. J. Nielson and W. P. Griffith, *J. Chem. Soc., Dalton Trans.* 1978, 1501.
2. M. B. Hursthouse, T. Fram, L. New, W. P. Griffith and A. J. Nielson, *Trans. Met. Chem.* 1978, **3**, 253.
3. W. P. Griffith, C. A. Pumphrey and T. A. Rainey, *J. Chem. Soc., Dalton Trans.* 1986, 1125.
4. C. G. Pierpoint and R. M. Buchanan, *Coord. Chem. Rev.* 1981, **38**, 45.
5. E. L. Muetterties and C. M. Wright, *J. Am. Chem. Soc.* 1965, **87**, 4706.
6. E. L. Muetterties, H. Roesky and C. M. Wright, *J. Am. Chem. Soc.* 1966, **88**, 4856.
7. S. S. Eaton, G. R. Eaton, R. H. Holm and E. L. Muetterties, *J. Am. Chem. Soc.* 1973, **95**, 1116.
8. M. Green and G. J. Parker, *J. Chem. Soc., Dalton Trans.* 1974, 333.
9. S. Muto, K. Tasaka and Y. Kamiya, *Bull. Chem. Soc. Japan* 1977, **50**, 2493.

* Tables of atomic positional and thermal parameters have been deposited as Supplementary Data with the Editor, from whom copies are available on request. Atomic coordinates have also been deposited with the Cambridge Crystallographic Data Centre.

10. R. F. Weinland and F. Gaisser, *Z. Anorg. Chem.* 1919, **108**, 231.
11. R. F. Weinland, A. Babel, K. Gross and H. Mai, *Z. Anorg. Chem.* 1926, **150**, 177.
12. G. Doyle, *J. Organomet. Chem.* 1977, **132**, 243.
13. A. Avdeef, J. A. Costamanga and J. P. Fackler, *Inorg. Chem.* 1974, **13**, 1854, and references therein.
14. A. R. Davis and F. W. B. Einstein, *Acta Cryst.* 1978, **B34**, 2110.
15. V. V. Tkachev and L. O. Atovmyan, *Soviet J. Coord. Chem.* 1975, **1**, 715.
16. Y. Ikegami, *Bull. Chem. Soc. Japan* 1963, **36**, 1118.
17. L. G. Hulett and D. A. Thornton, *Spectrochim. Acta* 1971, **27A**, 2089.
18. H. Junge, *Spectrochim. Acta* 1968, **24A**, 1957.
19. W. P. Griffith, *J. Chem. Soc.(A)* 1969, 211.
20. V. V. Tkachev and L. O. Atovmyan, *Soviet J. Coord. Chem.* 1975, **2**, 89.
21. M. Valderrama, H. Rafart and L. A. Ovo, *Trans. Met. Chem.* 1981, **6**, 221.
22. N. M. Szeverenyi, A. Box and G. E. Maciel, *J. Am. Chem. Soc.* 1983, **105**, 2579.
23. J. Charalambous, *Inorg. Chim. Acta* 1976, **18**, 241.
24. C. G. MacDonald and J. S. Shannon, *Aust. J. Chem.* 1966, **19**, 1545.
25. F. P. Dwyer and A. M. Sargeson, *J. Am. Chem. Soc.* 1955, **77**, 1285.
26. Y. Sasada and I. Nitta, *Acta Cryst.* 1956, **9**, 205.
27. G. M. Sheldrick, *SHELXTL—an Integrated System for Solving, Refining and Displaying Crystal Structures from Diffraction Data*, Revision 4, Nicolet Instruments Ltd., Warwick (1983).
28. *International Tables for X-ray Crystallography*, Vol. 4. The Kynoch Press, Birmingham, (1974).

Polyhedron Vol. 6, No. 5, pp. 897–905, 1987
Printed in Great Britain

0277–5387/87 $3.00+.00

PREPARATION, CHARACTERIZATION, REACTIVITIES AND ELECTROCHEMISTRY OF SOME HOMO- AND HETERODINUCLEAR COMPLEXES OF 2-HYDROXY-5-METHYLBENZENE-1,3-DICARBALDEHYDE AND 1,3-DIACETYL-2-HYDROXY-5-METHYLBENZENE*

BIBHUTOSH ADHIKARY, AMAL K. BISWAS and KAMALAKSHA NAG†

Department of Inorganic Chemistry, Indian Association for the Cultivation of Science, Calcutta 700032, India

and

PIERO ZANELLO† and ARNALDO CINQUANTINI

Dipartimento di Chimica, Universita di Siena, Piano dei Mantellini, 44-53100 Siena, Italy

(*Received* 22 *July* 1986; *accepted* 15 *August* 1986)

Abstract—Homo- and heterodinuclear complexes of composition $[M_2L_2](ClO_4)_2 \cdot 4H_2O$, $[CuML_2](ClO_4)_2 \cdot nH_2O$ (M = Ni, Co or Mn; L = L^1 or L^2) and $[CuML^2Cl_2] \cdot 2H_2O$ (M = Ni or Co) have been synthesized with the dinucleating ligands 2-hydroxy-5-methylbenzene-1,3-dicarbaldehyde (HL^1) and 1,3-diacetyl-2-hydroxy-5-methylbenzene (HL^2). These compounds have been characterized and their chemical reactivities investigated. The electrochemical behaviour of $[M_2L_2^2](ClO_4)_2 \cdot 4H_2O$ and $[CuML_2^2](ClO_4)_2 \cdot nH_2O$ complexes have been examined in acetonitrile and dimethyl sulfoxide using Hg and Pt electrodes. The cyclic voltammograms obtained with a Hg electrode show quasi-reversible electron transfers for both metal centres that often get complicated due to decomplexation of metal ions and adsorption phenomena. On a Pt electrode irreversible electron transfers occur at more negative potentials.

Recent studies on dinuclear metal complexes in which the two metal centres are held in close proximity have addressed ligand environment, redox behaviour, magnetic exchange interactions and spectroscopic properties.[1–12] Considerable interest has also been focussed on synthesis and biomimetic reactions of model systems[13–21] related to copper enzymes.[22–25] For obvious reasons, dinucleating ligands are often used as the building blocks for designing such molecules. While the use of symmetric dinucleating ligands almost invariably lead to the formation of homodinuclear species [see, however, Ref. 6(b) for an exception], heterodinuclear complexes, on the other hand, are generally obtained from ligands containing two non-equivalent co-ordination sites. Frequently, one metal is in an N_2O_2 co-ordination site and the other occupies an O_4 site. Synthesis of heterodinuclear complexes from symmetric dinucleating ligands, therefore, remains to be an important task. We have previously reported chemistry and electrochemical behaviour of phenoxo-bridged acyclic and macrocyclic dicopper(II) complexes.[26–30] Herein we report the synthesis, characterization and electrochemistry of homo- and heterodinuclear complexes of copper(II), nickel(II), cobalt(II) and manganese(II) from 2-hydroxy-5-methylbenzene-1,3-dicarbaldehyde [HL^1 (**1a**)] and 1,3-diacetyl-2-hydroxy-5-methylbenzene [HL^2 (**1b**)].

* Part 5 of the series: Dinuclear metal complexes.

† Authors to whom correspondence should be addressed.

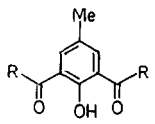

(a) : R=H
(b) : R=Me
(1)

EXPERIMENTAL

Materials

All reagents and solvents were purchased from commercial sources and used as such unless otherwise described. Methanol, ethanol and acetone were dried according to standard methods.[31] HL^1 and HL^2 were prepared as reported earlier.[27] Dried and purified nitrogen gas was used for the preparation of compounds containing cobalt(II) and manganese(II).

Preparation of the complexes

$ML_2 \cdot H_2O$ (M = Cu, Ni, Co *or* Mn; L = L^1 *or* L^2). The copper(II) complexes were obtained as described earlier.[26] The following method was used for the preparation of other complexes. The ligand (4 mmol) was dissolved in ethanol (100 cm^3) and treated with an aqueous solution (400 cm^3) of NaOH (4 mmol). To this was added with stirring an aqueous solution of hydrated metal chloride (2 mmol). The mixture was heated on a steam bath for *ca* 1 h. The compound separated was collected by filtration, washed several times with water, and dried over $CaCl_2$ *in vacuo*. The compound was then dissolved in required amount of chloroform, filtered, concentrated to half of its volume, and allowed to crystallize by adding an equal volume of petroleum ether (b.p. 40–60°C).

$[M_2L_2](ClO_4)_2 \cdot 4H_2O$ (M = Ni, Co *or* Mn; L = L^1 *or* L^2). The preparation of dicopper(II) complexes, $[Cu_2L_2](ClO_4)_2 \cdot 2H_2O$ was reported earlier.[26] Other homodinuclear complexes were obtained according to the method given below. To a boiling suspension of the mononuclear complex, $ML_2 \cdot H_2O$ (1 mmol) in dry ethanol (25 cm^3) corresponding metal perchlorate hexahydrate (1.2 mmol) was added. In a short period, most of the material went into solution and a colour change took place. The mixture was refluxed for *ca* 0.5 h. It was then centrifuged to remove a small amount of slimy residue that tends to pass through filtering glass frit. The centrifugate was concentrated to about 5 cm^3 and kept in a desiccator over $CaCl_2$ for several hours. The crystals that deposited during this period were collected by filtration, washed with a dry ethanol–chloroform (1 : 10) mixture, and dried over $CaCl_2$.

$[CuML_2](ClO_4)_2 \cdot nH_2O$ (M = Ni, Co *or* Mn; L = L^1 *or* L^2). $CuL_2 \cdot H_2O$ (1 mmol) was suspended in dry ethanol (20 cm^3) and solid $M(ClO_4)_2 \cdot 6H_2O$ (1.3 mmol) was added. The mixture was heated under reflux for 1 h. The clear solution that resulted was filtered hot and the filtrate on concentration gave crystals of the desired complex, which were collected and treated as above.

$[CuML^2_2Cl_2] \cdot 2H_2O$ (M = Ni *or* Co). These compounds were prepared in the same way as described above using $MCl_2 \cdot 6H_2O$ instead of the perchlorate salts.

Analytical data for a few representative complexes are given in Table 1.

Physical measurements

Elemental analysis were performed on a Perkin–Elmer model 240C elemental analyzer. IR spectra

Table 1. Analytical data for the dinuclear complexes

Complex	Colour	Analysis[a] (%) C	H	M_1	M_2
$[Ni_2L^1_2](ClO_4)_2 \cdot 4H_2O$	Green	30.6 (30.2)	3.4 (3.1)	16.6 (16.4)	
$[Ni_2L^2_2](ClO_4)_2 \cdot 4H_2O$	Green	34.5 (34.2)	3.9 (3.9)	15.1 (15.2)	
$[Co_2L^2_2](ClO_4)_2 \cdot 4H_2O$	Red	34.5 (34.2)	4.1 (3.9)	15.0 (15.3)	
$[Mn_2L^2_2](ClO_4)_2 \cdot 4H_2O$	Yellow	34.2 (34.6)	3.8 (3.9)	14.6 (14.4)	
$[CuNiL^2_2](ClO_4)_2 \cdot 2H_2O$	Green	36.3 (35.7)	3.35 (3.5)	8.4 (8.6)	7.8 (7.9)
$[CuCoL^2_2](ClO_4)_2 \cdot 2H_2O$	Green	35.4 (35.7)	3.3 (3.5)	8.4 (8.6)	8.1 (7.9)
$[CuMnL^2_2](ClO_4)_2 \cdot H_2O$	Dark green	37.2 (36.8)	3.25 (3.3)	8.65 (8.8)	7.8 (7.6)
$[CuNiL^2_2Cl_2] \cdot 2H_2O$	Green	43.4 (43.2)	4.1 (4.2)	10.2 (10.4)	9.7 (9.6)
$[CuCoL^2_2Cl_2] \cdot 2H_2O$	Green	43.1 (43.2)	4.1 (4.2)	10.5 (10.4)	9.4 (9.6)

[a] Calculated values are given in parentheses.

were recorded on a Perkin–Elmer model 783 IR spectrophotometer in the range 4000–200 cm^{-1} using KBr discs. Electronic spectra were obtained either with a Cary 17d or a Pye–Unicam SP8-150 spectrophotometer with 1-cm quartz cells for solution studies and as Nujol mulls on filter paper for solids. X-ray powder diffraction measurements were carried out on a Philips PW1051 diffractometer using Cu-K_α radiation. Magnetic measurements were made with a PAR model 155 vibrating sample magnetometer at room temperature employing $Hg[Co(SCN)_4]$ as a calibrant. Diamagnetic corrections were made by using Pascal's constants. The electrochemical measurements were made with a previously described[32] apparatus. All potentials refer to an aqueous saturated calomel electrode (s.c.e.). The temperature was controlled at 20 ± 0.1°C. Cyclic voltammograms were recorded using both Pt and Hg working electrodes. The solvents used were dimethyl sulfoxide (dmso) and acetonitrile (MeCN) (Burdick & Jackson u.v. grade). Tetraethyl ammonium perchlorate (Carlo Erba) dried in a vacuum oven was used as the supporting electrolyte. Nitrogen gas (99.99%) was employed to remove dissolved oxygen from the solutions.

RESULTS AND DISCUSSION

Synthesis and reactivities of the complexes

We previously reported[26] that $CuL_2 \cdot H_2O$ complexes are readily formed when copper(II) acetate is reacted with HL. This method, however, is not applicable for the preparation of other mononuclear complexes. $ML_2 \cdot H_2O$ (M = Ni, Co or Mn; $L = L^1$ or L^2) compounds are obtained by reacting one equivalent of the metal salt with two equivalents of the ligand and two equivalents of sodium hydroxide in an ethanol–water medium. Water should be present in large proportion in order to obtained the desired complex. In the case of nickel(II), when the reaction was carried out in ethanol alone, a green insoluble compound of apparent composition NiL_2 was obtained. This compound appears to have a tetrahedral configuration and does not react further to produce dinuclear species. $ML_2 \cdot H_2O$ complexes react smoothly with corresponding metal perchlorates in dry methanol or ethanol to form homodinuclear complexes, $M_2L_2(ClO_4)_2 \cdot 4H_2O$ (M = Ni, Co or Mn; $L = L^1$ or L^2). The heterodinuclear complexes $[CuML_2](ClO_4)_2 \cdot nH_2O$ (M = Ni, Co or Mn; $L = L^1$ or L^2) and $[CuML_2^2Cl_2] \cdot 2H_2O$ are also similarly obtained when a suspension of $CuL_2 \cdot H_2O$ in ethanol is treated with appropriate metal salts. Conversely, if $ML_2 \cdot H_2O$ is reacted with $Cu(ClO_4)_2 \cdot 6H_2O$, the product is always $[Cu_2L_2](ClO_4)_2 \cdot 2H_2O$. This reaction demonstrates that copper(II) has much greater affinity for O_4 co-ordination sites than the other metals. Attempts to prepare heterodinuclear complexes other than copper were unsuccessful. For example, reactions involving $NiL_2 \cdot H_2O$ and $Co(ClO_4)_2 \cdot 6H_2O$ or $CoL_2 \cdot H_2O$ and $Ni(ClO_4)_2 \cdot 6H_2O$ caused scrambling of metal ions in the heterodinuclear species ($2NiCoL_2^{2+} \rightarrow Ni_2L_2^{2+} + Co_2L_2^{2+}$), and the product isolated was a mixture of homodinuclear species. It should be noted that the dinuclear complexes are stable in solution only when the solvent is perfectly dry; moisture in the solvent causes hydrolytic cleavage of the phenoxo bridge and liberates a metal ion. In the case of $[CuML_2](ClO_4)_2 \cdot 2H_2O$ complexes, bridge splitting occur invariably at the M^{2+} site, showing again that the Cu—O linkages have greater bond strengths. The dinuclear complexes of HL^1 are more susceptible to hydrolysis than those of HL^2.

An interesting aspect of the dinuclear metal complexes of the ligand HL^1 is that one of the formyl groups is more susceptible to nucleophilic attack. For example, $[Cu_2L_2^1](ClO_4)_2 \cdot 2H_2O$ complex generated *in situ* undergoes aldol type condensation with a number of ketones containing α-methyl and methylene groups. Working up of the reaction product followed by removal of the metal ion leads to the isolation of 2-hydroxy-3-formyl-5-methyl-1-benzal ketone (**2**) in fairly high yield. By contrast,

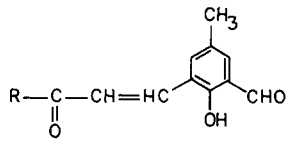

(2)

no such reaction takes place with the mononuclear complex, $CuL_2^1 \cdot H_2O$. The free ligand, HL^1, on the other hand, undergoes self- and polycondensation reactions in the presence of a base producing non-characterized resinous products. The mechanism of the regioselective aldol condensation of $[Cu_2L_2^1](ClO_4)_2 \cdot 2H_2O$ has been investigated in detail,[33] and the reaction has been used to synthesize various derivatives of **2**.

Characterization of the complexes

The IR spectral features of the homo- and heterodinuclear complexes are similar. They are characterized by a broad band centred at about 3450 cm^{-1} due to the constituent water molecules, two strong bands at about 1650 and 1630 cm^{-1} due to

Table 2. X-ray powder diffraction data for some dinuclear complexes

$[CuNiL_2^2](ClO_4)_2 \cdot 2H_2O$		$[CuCoL_2^2](ClO_4)_2 \cdot 2H_2O$		$[Ni_2L_2^2](ClO_4)_2 \cdot 4H_2O$	
d (Å)	I/I_0	*d* (Å)	I/I_0	*d* (Å)	I/I_0
5.37	60	5.28	35	5.33	45
4.72	55	4.62	60	4.64	80
4.52	60	4.43	50	4.38	30
4.09	60				
3.88	100	4.00	100	4.15	100
3.63	55	3.70	50	3.74	60
3.37	50	3.37	30	3.33	25
3.13	30	3.11	25	3.10	25
2.93	20	2.88	20	2.91	20
2.75	25	2.74	15	2.76	25
2.51	20	2.51	10	2.53	20
2.39	10	2.43	20	2.45	15
2.14	20	2.16	20	2.18	20
2.07	15			2.07	10
2.00	15	2.01	20	2.02	10

the metal bound carbonyl (C=O) stretchings, and another strong band at *ca* 1530 cm^{-1} due to metal-bonded phenolic ν(C···O) vibration. The ν(C=C) vibration appears at about 1610 cm^{-1}, often in the form of a shoulder. The most important feature, that the two ν(C=O) vibrations are about 20 cm^{-1} apart, implies that the two metal atoms are not equally strongly bound by the carbonyl groups.

The X-ray powder data for $[CuNiL_2^2](ClO_4)_2 \cdot 2H_2O$, $[CuCoL_2^2](ClO_4)_2 \cdot 2H_2O$ and $[Ni_2L_2^2](ClO_4)_2 \cdot 4H_2O$ are compared in Table 2. It may be noted that these complexes have similar *d*-spacings and intensities, indicating that they have related crystal structures.

The room-temperature magnetic moments (Table 3) of $ML_2 \cdot H_2O$ complexes (M = Ni, Co or Mn) are consistent with high-spin octahedral or square pyramidal stereochemistries, and do not support square planar or tetrahedral arrangements. Similar steric configurations are expected for the homodinuclear complexes, although the observed moments per metal ion for these compounds are

Table 3. Electronic spectral data and magnetic moments for the mono- and dinuclear complexes

Complex	Electronic spectral data: $\tilde{\nu}$ (cm^{-1}) [ε ($dm^3\ mol^{-1}\ cm^{-1}$)]	μ_{eff}[a] (BM)
$NiL_2^1 \cdot H_2O$	7300(4), 9260(12), 13,330(sh), 16,130(22), 24,390(3800)[b]	3.26
$NiL_2^2 \cdot H_2O$	7500(sh), 9260(12), 13,330(sh), 15,870(40), 24,390(5680)[b]	3.28
$CoL_2^1 \cdot H_2O$	7530(6), 13,900(sh), 24,390(3000)[b]	5.16
$CoL_2^2 \cdot H_2O$	9900(5), 15,620(32), 17,100(40), 23,530(4200)[b]	5.20
$[Ni_2L_2^2](ClO_4)_2 \cdot 4H_2O$	9100(16), 13,800(12), 15,870(8)[c]	3.08
$[Co_2L_2^2](ClO_4)_2 \cdot 4H_2O$	8630(14), 18,520(60)[c]	4.88
$[Mn_2L_2^2](ClO_4)_2 \cdot 4H_2O$		5.78
$[CuNiL_2^2](ClO_4)_2 \cdot 2H_2O$	10,000, 13,800, 16,000[d]	2.98
$[CuCoL_2^2](ClO_4)_2 \cdot 2H_2O$	9000, 15,700, 18,200[d]	4.06
$[CuNiL_2^2Cl_2] \cdot 2H_2O$	7020(9), 8470(15), 13,300(sh), 15,150(14), 24,100(8120)[b]	3.04
$[CuCoL_2^2Cl_2] \cdot 2H_2O$	14,700, 15,500, 17,200, 25,000[d]	4.06

[a] At 298 K.
[b] In dimethylformamide.
[c] In ethanol.
[d] Nujol mull.

less than the corresponding mononuclear species, indicating magnetic exchange interactions between two metal ions. In the case of heterodinuclear complexes also the observed moments are less than the expected spin-only values (Cu–Ni, 3.73 BM; Cu–Co, 4.24 BM; Cu–Mn, 6.17 BM) in the absence of such magnetic interactions. However, we presently could not investigate the magnetic properties in detail.

The electronic spectral data of the compounds are given in Table 3. The spectral features of $NiL_2 \cdot H_2O$ and $CoL_2 \cdot H_2O$ complexes provide evidences in favour of a square pyramidal environment[34,35] around the metal ions. $MnL_2 \cdot H_2O$ species lack absorption peaks in the visible range presumably because the weak *d–d* bands are submerged in the tail of the charge transfer band appearing at about 25,000 cm^{-1}.

Concerning the dinuclear complexes $[CuML_2Cl_2] \cdot 2H_2O$, both the metal atoms are likely to have a square pyramidal environment. Their spectral characteristics (Table 3) show a resemblance to $ML_2 \cdot H_2O$ species and are reminiscent of the chloro-bridged dinuclear macrocyclic complexes[35] obtained by condensing HL^1 with 1,3-diaminopropane. Similar to the macrocyclic systems, the chlorine atoms are also believed to be apically bound to the metal atoms. Less clear, however, is the steric environment around metal ions in the dinuclear complexes containing perchlorate ions. In these compounds it is possible to interpret the bands due to nickel(II) and cobalt(II) ions in terms of a pseudo-octahedral symmetry. However, considering the facts that $ML_2 \cdot H_2O$ complexes have C_{4v}-symmetry, and $[CuML_2](ClO_4)_2 \cdot 2H_2O$ and $[Ni_2L_2](ClO_4)_2 \cdot 4H_2O$ complexes are isostructural, it seems more likely that the two metal atoms in both homo- and heterodinuclear species have two different coordination environments. In $[M_2L_2](ClO_4)_2 \cdot 4H_2O$ complexes, one of the metals is probably having a square pyramidal arrangement and in the other two water molecules are axially bound. Similarly in $[CuML_2](ClO_4)_2 \cdot 4H_2O$ complexes, the metal ion M(II) appears to be hexacoordinated.

Electrochemistry

As mentioned earlier the dinuclear complexes of the ligand HL^2 are more stable with respect to solvolytic decomposition; consequently, their electrochemical behaviour was investigated. Cyclic voltammetric studies were made with MeCN and dmso solutions of the complexes using Hg and Pt electrodes.

The typical electrochemical responses for the compounds $[CuML_2^2](ClO_4)_2 \cdot nH_2O$ (**I–III**) and $[M_2L_2^2](ClO_4)_2 \cdot 4H_2O$ (**IV–VI**) are those shown in Fig. 1, which refer to the voltammograms of $[CuCoL_2^2](ClO_4) \cdot 2H_2O$ (**II**) in MeCN (a) and dmso (b), respectively, at an Hg electrode. In MeCN [Fig. 1(a)], the observed electrochemical features of **II** can be explained as follows. The cathodic–anodic peak system, *A/H*, is due to Cu(II) → Cu(I) electron transfer followed by re-oxidation in the reverse scan. The peak, *B*, which is irreproducible in height, is due to adsorption electrode-poisoning phenomena that made it necessary to clean the electrode mechanically after each cycle. The peak, *C*, is due to the subsequent reduction of the copper site [Cu(I) → Cu(0)], as indicated by the appearance of the characteristic stripping peak, *I*, in the reverse scan. The peak system *D/G* is due to the reduction of the second metal centre, Co(II) → Co(I). Finally, the peak system *E/F* is due to ligand-based electron transfer.

Analysis of the metal-centred responses with scan rates reveals that the first cathodic process, Cu(II) → Cu(I) is a quasi-reversible charge transfer followed by a chemical reaction. When the scan rate (v) was varied from 20 mV s^{-1} to 5 V s^{-1}, the following features hold:[36] (i) the anodic to cathodic peak ratio, $i_{p(H)}/i_{p(A)}$, increases from 0.56 to 0.8, (ii) the difference between the peak potentials ($\Delta E_p = E_H - E_A$) increases from 90 to 220 mV, (III) the ratio between the peak current of the cathodic sweep and the square root of the scan rate, $i_{p(A)}/v^{1/2}$, tends to increase, in agreement with the adsorption phenomenon. It is likely that the chemical complication following the electron transfer involves decomplexation of the electrogenerated copper(I) centre giving rise to free Cu^+ ions, as evidenced by the appearance of a reoxidation peak at about +1 V on scan reversal using a Pt electrode (see below). The Co(II) → Co(I) electron transfer appears to be a quasi-reversible process on the basis of the increase of ΔE_p with scan rate (from 65 to 130 mV). However, the study of the relevant electrode kinetics could not be made due to the presence of the pre-peak *C*.

In dmso, the electrochemical response from **II** is more simplified [Fig. 1(b)]. Here, the peak systems present are: *A/H* [Cu(II) → Cu(I)], *D/G* [co(II) → Co(I)], and *E/F* (ligand-based). Moreover, these responses are better reproducible because of the absence of adsorption phenomena; $i_{p(A)}/v^{1/2}$ remains substantially unchanged with the variation in scan rate. However, in this case also the ratio $i_{p(H)}/i_{p(A)}$ remains less than unity, indicating that the species $[Cu(I)Co(II)L^2]^+$ is not a stable product. As regards the Co(II) → Co(I) electron transfer, which can be better tested here with scan rate than in MeCN,

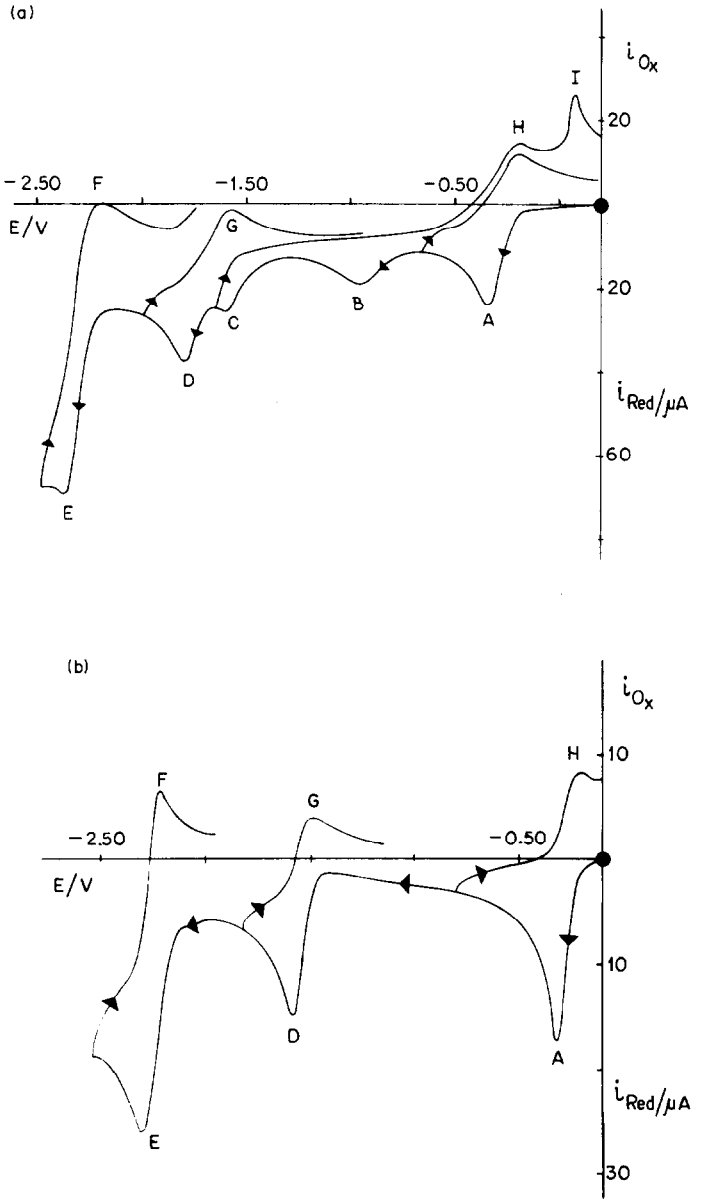

Fig. 1. (a) Cyclic voltammogram of $[CuCoL_2^2](ClO_4)_2 \cdot 2H_2O$ (**II**) in MeCN on an Hg electrode at a scan rate of 200 mV s^{-1}. Concentration of **II** = 1.3×10^{-3} mol dm^{-3}; concentration of supporting electrolyte, $[Et_4N](ClO_4)$ = 0.1 mol dm^{-3}. (b) Cyclic voltammogram of **II** in dmso on an Hg electrode at a scan rate of 200 mV S^{-1}. **II** = 1.3×10^{-3} mol dm^{-3}; $[Et_4N](ClO_4)$ = 0.1 mol dm^{-3}.

appears to have the same characteristic as the Cu(II) → Cu(I) reduction, i.e. a quasi-reversible process followed by a chemical reaction (in the scan rate range 20 mV s^{-1} to 5 V s^{-1}, the $i_{p(G)}/i_{p(D)}$ ratio increases from 0.4 to 0.8, ΔE_p increases from 70 to 150 mV, and the ratio $i_{p(D)}/v^{1/2}$ remains constant). These data indicate that the reduction of cobalt(II) to cobalt(I) leads to its decomplexation.

At a Pt electrode the voltammetric behaviour of the heterodinuclear complexes are quite different in both solvents, in particular for the cathodic reduction of the copper moiety. It appears as a totally irreversible process at a significantly more negative potential. In both solvents this step is followed by electrodeposition of copper metal.[37] The appearance of different responses at different electrode materials is not unusual, and can be attributed either to the occurrence of inner-sphere electrode mechanisms,[38] or to the formation of mercury-stabilized intermediates at the Hg electrode surface.[39]

Table 4 summarizes the electrochemical results obtained for compounds **I–VI**. We believe that the

Table 4. Electrochemical data[a] for the dinuclear complexes in MeCN and dmso media using Hg and Pt electrodes

	Complex	MeCN	dmso	
		Hg, E' (V)	Hg, E' (V)	Pt, E' (V)
I	$[CuNiL_2^2](ClO_4)_2 \cdot 2H_2O$	Cu(II)–Cu(I) = −0.27 Ni(II)–Ni(I) = −1.84	Cu(II)–Cu(I) = −0.27 Ni(II)–Ni(I) = −1.55	Cu(II)–Cu(I) = −0.92 (E_p) Ni(II)–Ni(I) = −1.57
II	$[CuCoL_2^2](ClO_4)_2 \cdot 2H_2O$	Cu(II)–Cu(I) = −0.28 Co(II)–Co(I) = −1.78	Cu(II)–Cu(I) = −0.27 Co(II)–Co(I) = −1.55	Cu(II)–Cu(I) = −0.93 (E_p) Co(II)–Co(I) = −1.57
III	$[CuMnL_2^2](ClO_4)_2 \cdot H_2O$	Cu(II)–Cu(I) = −0.27 Mn(II)–Mn(I) = −1.89	Cu(II)–Cu(I) = −0.26 Mn(II)–Mn(I) = −1.73	Cu(II)–Cu(I) = −0.93 (E_p) Mn(II)–Mn(I) = −1.74
IV	$[Ni_2L_2^2](ClO_4)_2 \cdot 4H_2O$	Ni(II)–Ni(I) = −1.13 (E_p) Ni(I)–Ni(I) = −1.78 (E_p)	Ni(II)–Ni(I) = −1.23 (E_p) Ni(I)–Ni(I) = −1.59 (E_p)	Ni(II)–Ni(I) = −1.52 (E_p) Ni(I)–Ni(I) = −1.66 (E_p)
V	$[Co_2L_2^2](ClO_4)_2 \cdot 4H_2O$		Co(II)–Co(I) = −1.54 Co(I)–Co(I) = −1.54	Co(II)–Co(I) = −1.62 (E_p) Co(I)–Co(I) = −1.62 (E_p)
VI	$[Mn_2L_2^2](ClO_4)_2 \cdot 4H_2O$	Mn(II)–Mn(I) = −1.28 Mn(I)–Mn(I) = −1.58	Mn(II)–Mn(I) = −1.47 (E_p) Mn(I)–Mn(I) = −1.77 (E_p)	Mn(II)–Mn(I) = −1.50 (E_p) Mn(I)–Mn(I) = −1.77 (E_p)

[a] Potentials are measured against a s.c.e. $E' = 0.5(E_p^c + E_p^a)$ · E_p values refer to peak potentials at a scanning rate of 200 mV s^{-1}.

E values obtained by averaging the cathodic and anodic peak potentials provide a good approximation of the formal electrode potentials, albeit the experimental conditions prevented us reaching the $i_{p(c)}/i_{p(a)} = 1$ requirement. In those cases where, even at the highest scan rates, it was not possible to reveal the presence of a peak directly associated to a response in the reverse scan, the E_p value is given. To make the results comparable in the two solvents one may recall that for the nominally solvent independent ferrocene–ferrocenium couple[40] the E^o value is +0.38 V in MeCN and +0.44 V in dmso. Therefore, differences in potentials greater than 60 mV should be considered as the solvent effect.

The results given in Table 4 for the heterodinuclear compounds **I–III** show that the electrochemistry occurring at the second metal ion, M^{2+}, is well out of the redox activity at the copper site. More importantly, within experimental error, the Cu(II) → Cu(I) reduction potentials in these systems when measured with an Hg electrode are independent of the metal ion M^{2+}. This observation finds analogy to the reported electrochemical behaviour of some heterodinuclear macrocyclic complexes.[6(b)] In a previous study we reported[26] that in $[Cu_2L_2^2](ClO_4)_2 \cdot 2H_2O$ complex, the reduction of both the copper sites occurs at the same potential (−0.05 V) in dimethylformamide on an Hg electrode. In the present work we note that, although reduction of both the Co^{2+} ions occurs at the same potential (−1.54 V) in dmso for $[Co_2L_2^2]^{2+}$ species, in the case of dinickcl(II) and diamanganese(II) complexes irreversible reductions occur at two different potentials.

Acknowledgements—K.N. thanks the CSIR, India, for financial support and for awarding a research associateshipe to A.K.B. P.Z. thanks the CNR, Italy, for financial assistance.

REFERENCES

1. K. D. Karlin and J. Zubieta (Eds), *Biological and Inorganic Copper Chemistry*. Adenine Press, New York (1985).
2. D. E. Fenton, In *Advances in Inorganic and Bioinorganic Reaction Mechanisms* (Edited by A. G. Sykes), Vol. 2, p. 187. Academic Press, New York (1983).
3. F. L. Urbach, In *Metal Ions in Biological Systems* (Edited by H. Sigel), Vol. 13, p. 73. Marcel Dekker, New York (1981).
4. U. Casellato, P. A. Vigato, D. E. Fenton and M. Vidali, *Chem. Soc. Rev.* 1979, **8**, 199.
5. S. E. Groh, *Isr. J. Chem.* 1976–1977, **15**, 277.
6. (a) R. R. Gagne, C. A. Koval, T. J. Smith and M. C. Cimolino, *J. Am. Chem. Soc.* 1979, **101**, 4571; (b) R. R. Gagne, C. L. Spiro, T. J. Smith, C. A. Hamann, W. R. Thies and A. K. Shiemke, *J. Am. Chem. Soc.* 1981, **103**, 4073.
7. R. L. Lintvedt and L. S. Kramer, *Inorg. Chem.* 1983, **22**, 796.
8. R. C. Long and D. N. Hendrickson, *J. Am. Chem. Soc.* 1983, **105**, 1513.
9. R. S. Drago, M. J. Desmond, B. B. Corden and K. A. Miller, *J. Am. Chem. Soc.* 1983, **105**, 2287.
10. C. L. Spiro, S. M. Lambert, T. J. Smith, E. N. Duesler, R. R. Gagne and D. N. Hendrickson, *Inorg. Chem.* 1981, **20**, 1229.
11. M. Melnik, *Coord. Chem. Rev.* 1982, **42**, 257.
12. O. Kahn, *Angew. Chem., Int. Ed. Engl.* 1985, **24**, 834.
13. K. D. Karlin and J. Zubieta (Eds), *Copper Coordination Chemistry: Biochemical and Inorganic Perspectives*. Adenine Press, New York (1983).
14. (a) K. D. Karlin, J. C. Hayes, Y. Gultneh, R. W. Cruse, J. W. McKown, J. P. Hutchinson and J. Zubieta, *J. Am. Chem. Soc.* 1984, **106**, 2121; (b) K. D. Karlin, R. W. Cruse, Y. Gultneh, J. C. Hayes and J. Zubieta, *J. Am. Chem. Soc.* 1984, **106**, 3372; (c) K. D. Karlin, M. S. Haka, R. W. Cruse and Y. Gultneh, *J. Am. Chem. Soc.* 1985, **107**, 5828.
15. (a) S. M. Nelson, *Inorg. Chim. Acta* 1982, **62**, 39; (b) S. M. Nelson, P. Esho, A. Lavery and M. G. B. Drew, *J. Am. Chem. Soc.* 1983, **105**, 5693.
16. (a) T. N. Sorrell, M. R. Malachowski and D. L. Jameson, *Inorg. Chem.* 1982, **21**, 3250; (b) T. N. Sorrell and A. S. Borovik, *J. Chem. Soc., Chem. Commun.* 1984, 1489.
17. (a) C. L. Merrill, L. J. Wilson, T. J. Thamman, T. M. Loehr, N. S. Ferris and W. H. Woodruff, *J. Chem. Soc., Dalton Trans.* 1984, 2207; (b) M. G. Simmons, C. L. Merrill, L. J. Wilson, L. A. Bottomley and K. M. Kadish, *J. Chem. Soc., Dalton Trans.* 1980, 1827.
18. L. Casella and L. Rigoni, *J. Chem. Soc., Chem. Commun.* 1985, 1668.
19. J. S. Thompson, *J. Am. Chem. Soc.* 1984, **106**, 4057, 8308.
20. H. M. J. Hendriks, P. J. M. W. L. Birker, J. van Rijn, G. C. Verschoor and J. Reedijk, *J. Am. Chem. Soc.* 1982, **104**, 3607.
21. V. McKee, M. Zvagulis, J. V. Dagdigian, M. G. Patch and C. A. Reed, *J. Am. Chem. Soc.* 1984, **106**, 4765.
22. R. Lontie (Ed.), *Copper Proteins and Copper Enzymes*, Vols 1–3. CRC Press, Boca Raton, FL (1984).
23. T. G. Spiro (Ed.), *Metal Ions in Biology*, Vol. 3. Wiley, New York (1981).
24. C. A. Owen, Jr., *Biochemical Aspects of Copper*. Noyes, Park Ridge, NJ (1982).
25. J. A. Ibers and R. H. Holm, *Science* 1980, **209**, 223.
26. S. K. Mandal and K. Nag, *Inorg. Chem.* 1983, **22**, 2567.
27. (a) S. K. Mandal and K. Nag, *J. Chem. Soc., Dalton Trans* 1983, 2429; (b) *J. Chem. Soc., Dalton Trans* 1984, 2141; (c) *J. Chem. Soc., Dalton Trans.* 1984, 2839.

28. B. Adhikary, S. K. Mandal and K. Nag, *Transition Met. Chem.* 1984, **9**, 454.
29. S. K. Mandal, B. Adhikary and K. Nag, *J. Chem. Soc., Dalton Trans.* 1986, 1175.
30. (a) P. Zanello, P. A. Vigato, Y. Casellato, S. Tamburini and G. A. Mazzochin, *Transition Met. Chem.* 1983, **8**, 294; (b) P. Zanello, S. Tamburini, P. A. Vigato and G. A. Mazzochin, *Transition Met. Chem.* 1984, **9**, 176.
31. A. I. Vogel, *A. Textbook of Practical Organic Chemistry*, 4th Edn, pp. 268, 269 and 275. The English Language Book Society and Longman, London (1978).
32. P. Zanello, R. Seeber, A. Cinquantini, G. A. Mazzochin and L. Fabbrizi, *J. Chem. Soc., Dalton Trans.* 1982, 893.
33. B. Adhikary, A. K. Biswas, R. V. Venkateswaran and K. Nag, *J. Org. Chem.* (submitted for publication).
34. R. Morassi, I. Bertini and L. Sacconi, *Coord. Chem. Rev.* 1973, **11**, 343.
35. N. H. Pilkington and R. Robson, *Aust. J. Chem.* 1970, **23**, 2225.
36. E. R. Brown and R. F. Large, In *Physical Methods of Chemistry, Part* IIA (Edited by A. Weissberger and B. W. Rossifer), Vol. 2, pp. 423–530. Wiley Interscience, New York (1971).
37. P. Zanello, P. A. Vigato and G. A. Mazzochin, *Transition Met. Chem.* 1982, **7**, 291.
38. V. I. Kravatsov, *J. Electroanal. Chem.* 1976, **69**, 125.
39. S. W. Blanch, A. M. Bond and R. Colton, *Inorg. Chem.* 1981, **20**, 755.
40. R. R. Gagne, C. A. Koval and G. C. Lisensky, *Inorg. Chem.* 1980, **19**, 2854.

Polyhedron Vol. 6, No. 5, pp. 907–913, 1987
Printed in Great Britain

0277–5387/87 $3.00+.00

MONONUCLEAR RHENIUM(III) AND RHENIUM(II) COMPLEXES OF 1,2-BIS(DIPHENYLPHOSPHINO)ETHYLENE: THE STRUCTURE OF *TRANS*-$ReCl_2(dppee)_2$

MOHAMMED BAKIR, PHILLIP E. FANWICK and RICHARD A. WALTON*

Department of Chemistry, Purdue University, West Lafayette, IN 47907, U.S.A.

(*Received* 24 *July* 1986; *accepted* 1 *September* 1986)

Abstract—The mononuclear rhenium(III) complexes *trans*-$[ReX_2(dppee)_2]X \cdot nH_2O$ (X = Cl or Br, dppee = $Ph_2PCH{=}CHPPh_2$) have been prepared by the reaction of $(n\text{-}Bu_4N)_2Re_2X_8$ with dppee in methanol–conc. HX; in the case of X = Cl, ethanol may also be used as the reaction solvent. These salts undergo anion exchange reactions with ClO_4^- and/or PF_6^-. The rhenium(II) complex *trans*-$ReCl_2(dppee)_2$ can be prepared by the cobaltocene reduction of *trans*-$[ReCl_2(dppee)_2]Cl \cdot 4H_2O$ and the reaction of $Re_2Cl_6(PBu^n_3)_2$ with dppee in refluxing ethanol. The spectroscopic and electrochemical properties of $[ReX_2(dppee)_2]^+$ have been investigated. Cyclic voltammetry (in 0.1 M tetra-*n*-butylammonium hexafluorophosphate–CH_2Cl_2 with a Pt-bead electrode) shows reversible redox processes at $E_{1/2}$(ox) *ca* +1.5 V, $E_{1/2}$(red) *ca* −0.2 V, and $E_{1/2}$(red) *ca* −1.4 V vs Ag–AgCl that correspond to the Re(IV)–Re(III), Re(III)–Re(II) and Re(II)–Re(I) couples, respectively. The single-crystal X-ray crystal structure of *trans*-$ReCl_2(dppee)_2$ has confirmed its octahedral geometry. This complex crystallizes in the monoclinic space group $P2_1/c$ with the following unit-cell dimensions: $a = 11.321(2)$ Å, $b = 13.011(2)$ Å, $c = 17.242(3)$ Å, $\beta = 95.79(2)°$, $V = 2527(1)$ Å^3, and $Z = 2$. The structure was refined to $R = 0.041$ ($R_w = 0.070$) for 2430 data with $F^2 > 3.0\sigma(F^2)$. The Re—Cl and Re—P distances are 2.422(2) and 2.405(2) Å, respectively.

A few instances are known where reactions of the quadruply bonded octahalodirhenate(III) anions $[Re_2X_8]^{2-}$ (X = Cl or Br) with phosphine ligands give rise to magnetically dilute rhenium(III) complexes rather than the more usually encountered multiply bonded dirhenium complexes that possess the Re_2^{6+}, Re_2^{5+} or Re_2^{4+} cores.[1,2] Examples include the di-μ-halo bridged complexes $Re_2(\mu\text{-}X)_2X_4(LL)_2$, where LL = $Ph_2PCH_2CH_2PPh_2$ or $Ph_2PCH_2CH_2AsPh_2$,[3–5] and $[ReCl_2(dppa)_2]PF_6$, where dppa = $Ph_2PNHPPh_2$.[6] In recent studies dealing with the synthesis and characterization of the α- and β-isomers of the triply bonded dirhenium(II) complexes $Re_2X_4(dppee)_2$ [dppee = 1,2-bis(diphenylphosphino)ethylene],[7] we have isolated salts of the mononuclear rhenium(III) cations $[ReX_2(dppee)_2]^+$ and the neutral rhenium(II) analogue *trans*-$ReCl_2(dppee)_2$. In this paper we describe the synthesis and properties of these complexes together with details of the crystal structure of the rhenium(II) complex, the latter species being a rare example of a neutral mononuclear compound containing this rather uncommon oxidation state.

EXPERIMENTAL

Starting materials

The following compounds were prepared by standard literature procedures: $(n\text{-}Bu_4N)_2Re_2X_8$ (X = Cl or Br)[8,9] and $Re_2Cl_6(PBu^n_3)_2$.[10] The *cis*-isomer of dppee was obtained from Strem Chemicals and used as received.

All reactions were carried out under a dry nitrogen atmosphere, and all solvents were deoxygenated by purging with N_2 gas for at least 15 min prior to use.

Syntheses

(*A*) $[ReX_2(dppee)_2]X$. (i) $[ReCl_2(dppee)_2]Cl \cdot nH_2O$. A mixture of $(n\text{-}Bu_4N)_2Re_2Cl_8$ (0.20 g,

* Author to whom correspondence should be addressed.

0.175 mmol), dppee (0.60 g, 1.51 mmol) and 10 cm^3 of methanol that contained 8 drops of conc. hydrochloric acid was refluxed for 22 h, cooled to room temperature and then filtered in air. The yellow filtrate was evaporated to dryness, the yellow solid recrystallized from CH_2Cl_2–diethyl ether, and the crystals washed with water, hexanes and diethyl ether, and then vacuum dried: yield 0.09 g (46%). Found: C, 53.8; H, 4.3. Calc. for $C_{52}H_{52}Cl_3O_4P_4Re$ (i.e. $[ReCl_2(dppee)_2]Cl \cdot 4H_2O$): C, 54.0; H, 4.2%. The presence of water of crystallization was confirmed by IR spectroscopy (Nujol mull) which showed ν(OH) at 3295w and 3190w cm^{-1}, and an additional weak, sharp feature at *ca* 3660 cm^{-1}.

When the preceding reaction was carried out using ethanol as the reaction solvent in place of methanol–conc. HCl, work-up of the reaction filtrate gave the same product (based upon spectroscopic and electrochemical measurements) although it analysed closer to a dihydrate. Found: C, 55.3; H, 4.0. Calc. for $C_{52}H_{48}Cl_3O_2P_4Re$ (i.e. $[ReCl_2(dppee)_2]Cl \cdot 2H_2O$): C, 55.7; H, 4.3%. A conductivity measurement on an acetonitrile solution of this complex (1.5×10^{-4} M) showed that it behaved as a 1:1 electrolyte ($\Lambda_m = 167\ \Omega^{-1}\ cm^2\ mol^{-1}$).

Further proof as to the identity of these salts was provided by anion exchange reactions with KPF_6 and $NaClO_4$. A small quantity of $[ReCl_2(dppee)_2]Cl \cdot 4H_2O$ (0.10 g) was mixed with a three-fold excess of KPF_6 (0.05 g) and 10 cm^3 of methanol, and the mixture stirred at room temperature for 2 h. The bright yellow solid was filtered off, washed with methanol, hexanes and diethyl ether, and dried under vacuum: yield 0.095 g (86%). This product was identified on the basis of its spectroscopic and electrochemical properties; its IR spectrum (Nujol mull) showed the ν(P—F) mode of PF_6^- at *ca* 850s cm^{-1}. A similar synthetic procedure was used to prepare the related perchlorate salt: yield 90%. The IR spectrum (Nujol mull) of this orange-yellow solid showed ν(Cl—O) of ClO_4^- at 1090s cm^{-1}.

(ii) $[ReBr_2(dppee)_2]Br$. A mixture of $(n\text{-}Bu_4N)_2Re_2Br_8$ (0.10 g, 0.067 mmol), dppee (0.23 g, 0.580 mmol) and 10 cm^3 of methanol (to which eight drops of 48% hydrobromic acid had been added) was refluxed for 2 days, cooled to room temperature and filtered. The filtrate was allowed to evaporate slowly at room temperature to low volume (*ca* 2 cm^3) and the orange crystals that resulted were filtered off, washed with water, a small volume of methanol, hexanes and diethyl ether, and vacuum dried: yield 0.036 g (22%). Found: C, 50.5; H, 3.8; Br, 19.3. Calc. for $C_{52}H_{46}Br_3OP_4Re$ (i.e. $[ReBr_2(dppee)_2]Br \cdot H_2O$): C, 50.5; H, 3.75; Br, 19.4%. A solution of this complex in acetonitrile (1.0×10^{-3} M) had a conductivity typical of a 1:1 electrolyte ($\Lambda_m = 119\ \Omega^{-1}\ cm^2\ mol^{-1}$). Its IR spectrum (Nujol mull) showed ν(OH) at *ca* 3350w and *ca* 3200w cm^{-1}.

An exchange reaction with a methanol solution of KPF_6, similar to that described in A(i), gave the yellow salt $[ReBr_2(dppee)_2]PF_6$: yield 73%. Its IR spectrum (Nujol mull) showed the ν(P—F) mode of PF_6^- at 853s cm^{-1}.

(*B*) $ReCl_2(dppee)_2$. This complex was isolated by two different procedures. The yellow complex $[ReCl_2(dppee)_2]Cl \cdot 4H_2O$ (0.1 g, 0.086 mmol) was mixed with cobaltocene (0.03 g, 0.159 mmol) and this mixture stirred in 10 cm^3 of CH_2Cl_2 for 30 min at room temperature. The orange-yellow solid was filtered off, washed with CH_2Cl_2, water, methanol, hexanes and diethyl ether, and vacuum dried: yield 0.08 g (83%). Found: C, 54.3; H, 4.3; Cl, 16.5. Calc. for $C_{53.75}H_{47.5}Cl_{5.5}P_4Re$ (i.e. $ReCl_2(dppee)_2 \cdot 1.75CH_2Cl_2$): C, 53.9; H, 4.1; Cl, 16.3%. This reaction proceeded similarly when acetone was used as the reaction solvent, but in this instance gave a product that contained acetone of crystallization; IR spectrum (Nujol mull) with ν(C=O) at 1713m cm^{-1}.

This same complex was obtained as a by-product of the reaction between $Re_2Cl_6(PBu^n_3)_2$ (0.10 g, 0.10 mmol) and dppee (0.26 g, 0.656 mmol) in refluxing ethanol (10 cm^3) for 4 days. The yellow-green insoluble product was filtered off, washed with hexanes and diethyl ether, and dried. It was then washed with CH_2Cl_2 to leave insoluble orange-yellow $ReCl_2(dppee)_2$: yield *ca* 30%.

X-ray structure determination on $ReCl_2(dppee)_2$

A batch of $[ReCl_2(dppee)_2]Cl \cdot 4H_2O$ was dissolved in methanol and diethyl ether carefully layered over this solution. Diffusion afforded primarily yellow crystals of this rhenium(III) complex, together with a few orange-yellow crystals. The yellow crystals lost solvent of crystallization and were unsuitable for crystal structure analysis. The orange-yellow crystals proved to be those of the more interesting complex $ReCl_2(dppee)_2$ and were of a quality adequate for a single crystal X-ray structure analysis.

A single crystal of $ReCl_2(dppee)_2$ of dimensions $0.18 \times 0.14 \times 0.07$ mm was mechanically separated and mounted on a glass fiber with epoxy resin. The crystal was indexed, and data were collected on an Enraf–Nonius CAD 4 diffractometer, equipped with a graphite monochromator and a standard focus molybdenum X-ray tube. The crystal data and information relating to data collection and structure refinement are listed in Table 1. Further

Table 1. Crystallographic data and data collection parameters for $ReCl_2(dppee)_2$[a]

Formula	$ReCl_2P_4C_{52}H_{44}$
Formula weight	1049.93
Space group	$P2_1/c$
a (Å)	11.321(2)
b (Å)	13.011(2)
c (Å)	17.242(3)
β(°)	95.79(2)
V (Å^3)	2527(1)
Z	2
$d_{calc.}$ (g cm^{-3})	1.380
Crystal dimensions (mm)	$0.18 \times 0.14 \times 0.07$
Temperature (°C)	22.0
Radiation (wavelength)	Mo-K_α (0.71073 Å)
Monochromator	Graphite
Linear absorption coefficient (cm^{-1})	26.99
Absorption correction applied	Empirical[b]
Diffractometer	Enraf–Nonius CAD4
Scan method	θ–2θ
h, k, l limits	−12–12, 0–13, 0–18
2θ range (°)	4.00–45.00
Scan width (°)	$0.75+0.35 \tan\theta$
Take-off angle (°)	4.90
Programs used	Enraf–Nonius SDP
F_{000}	1050.0
p-Factor used in weighting	0.070
Unique data	3470
Data with $I > 3.0\sigma(I)$	2430
Number of variables	271
Largest shift/esd in final cycle	0.00
R[c]	0.041
R_w[d]	0.070
Goodness of fit[e]	1.751

[a] Numbers in parentheses following certain data are estimated standard deviations occurring in the least significant digit.

[b] N. Walker and D. Stuart, *Acta Cryst.* 1983, **A39**, 158.

[c] $R = \Sigma ||F_o| - |F_c|| / \Sigma |F_o|$.

[d] $R_w = [\Sigma w(|F_o| - |F_c|)^2 / \Sigma w|F_o|^2]^{1/2}$; $w = 1/\sigma^2(F_o)$.

[e] Goodness of fit $= [\Sigma w(|F_o| - |F_c|)^2 / (N_{obs} - N_{parameters})]^{1/2}$.

details of the crystal data collection and reduction methods are described elsewhere.[11]

The structure was refined in the monoclinic space group $P2_1/c$. Three standard reflections were monitored after every hour of beam exposure during data collection and displayed no systematic variation in intensity. The Re, P, Cl and C atoms were refined anisotropically. Hydrogen atoms were not included in the final least-squares refinement. The final residuals were $R = 0.041$ and $R_w = 0.070$ and the final-difference Fourier map displayed no peaks of chemical significance.

All calculations were performed on a PDP 11/34 computer using the Enraf–Nonius structure determination package. An empirical absorption correction was applied,[12] and the linear absorption coefficient was 26.99 cm^{-1}. The least-squares program minimized the function $w(|F_o| - |F_c|)^2$, where w is a weighting factor defined as $w = 1/\sigma^2(F_o)$. Corrections for anomalous dispersion were applied to all atoms. Further details of the data set and the structure solution and refinement may be obtained from Dr P. E. Fanwick. Table 2 lists selected intramolecular bond distances and angles. Tables listing atomic positional parameters (S1), thermal parameters (S2), a complete listing of bond distances (S3) and bond angles (S4) are available as supplementary material.

Table 2. Some important bond distances (Å) and angles (°) for $ReCl_2(dppee)_2$[a]

Re—Cl(1)	2.422(2)
Re—P(1)	2.405(2)
Re—P(2)	2.404(2)
P(1)—C(1)	1.840(8)
P(2)—C(2)	1.821(8)
C(1)—C(2)	1.36(1)
Cl(1)—Re—Cl(1)	180.0
Cl(1)—Re—P(1)	99.39(7)
Cl(1)—Re—P(1)	80.61(7)
Cl(1)—Re—P(2)	92.13(7)
Cl(1)—Re—P(2)	87.87(7)
P(1)—Re—P(1)	180.0
P(1)—Re—P(2)	78.75(7)
P(1)—Re—P(2)	101.25(7)
P(2)—Re—P(2)	180.0

[a] Numbers in parentheses are estimated standard deviations in the least significant digits.

Physical measurements

IR spectra were recorded as Nujol mulls using IBM Instruments IR/32 and 9198 FTIR spectrometers for the regions 4000–400 and 400–200 cm^{-1}, respectively. Electronic absorption spectra were recorded as CH_2Cl_2 solutions on a HP8451A or IBM 9420 spectrophotometer and as Nujol mulls on the IBM 9420. Electrochemical measurements were made in CH_2Cl_2 containing tetra-*n*-butylammonium hexafluorophosphate (TBAH) as supporting electrolyte. $E_{1/2}$ values were determined as $(E_{p,a}+E_{p,c})/2$ and were referenced to the silver–silver chloride (Ag–AgCl) electrode at room temperature, and are uncorrected for junction potentials. Voltammetric experiments were performed using a Bioanalytical Systems Inc. Model CV-1A instrument in conjunction with a Hewlett–Packard model 7035 x–y recorder. Conductivity measurements were performed on acetonitrile solutions using an Industrial Instruments Inc. Model RC-16B2 conductivity bridge. Elemental microanalyses were performed by Dr H. D. Lee of the Purdue University Microanalytical Laboratory.

RESULTS AND DISCUSSION

Synthesis and properties of $[ReX_2(dppee)_2]^+$ (X = Cl *or* Br) *and* $ReCl_2(dppee)_2$

The reaction of $(n\text{-}Bu_4N)_2Re_2X_8$ (X = Cl or Br) with the phosphine ligand $Ph_2PCH{=}CHPPh_2$ (abbreviated as dppee) in methanol–conc. HX or ethanol solution affords the yellow-orange mononuclear rhenium(III) species $[ReX_2(dppee)_2]X\cdot nH_2O$. These results provide further evidence as to the proclivity of bidentate phosphines to cleave the quadruple bond of the $[Re_2X_8]^{2-}$ anions to give six-coordinate magnetically dilute rhenium(III) complexes. This has previously been demonstrated in the case of the ligands $Ph_2PCH_2CH_2PPh_2$ (dppe) and $Ph_2PNHPPh_2$ (dppa) which have been found to produce $[ReX_2(dppe)_2]^+$ (X = Cl or Br),[13] $Re_2(\mu\text{-}Cl)_2Cl_4(dppe)_2$[3–5] and $[ReCl_2(dppa)_2]^+$[6] under certain conditions. The formulation of these complexes is supported by their conversion to the ClO_4^- and/or PF_6^- salts via simple anion exchange reactions with $NaClO_4$ and KPF_6, by their behavior as 1 : 1 electrolytes in acetonitrile solution, and by the close similarity of their electronic absorption spectra (see Table 3) to the related spectral data published pre-

Table 3. Cyclic voltammetric and electronic absorption spectra data for rhenium(III) complexes of dppee

Complex	Electronic absorption spectra[a] (nm)	Voltammetric half-wave potentials[b]		
		$E_{1/2}$(ox)	$E_{1/2}$(red)(1)	$E_{1/2}$(red)(2)
$[ReCl_2(dppee)_2]Cl\cdot 4H_2O$	455sh, 424 (2750)	+1.55	−0.22	−1.40
$[ReCl_2(dppee)_2]PF_6$	455sh, 424 (2610)	+1.55	−0.24	−1.40
$[ReCl_2(dppee)_2]ClO_4$	455sh, 424 (2990) ~480sh, 428[c]	+1.58	−0.22	−1.40
$[ReBr_2(dppee)_2]Br\cdot H_2O$	450 (5170) 510sh, 460[c]	+1.53	−0.12	−1.26
$[ReBr_2(dppee)_2]PF_6$	450 (4230)	+1.50	−0.16	−1.30

[a] Recorded in CH_2Cl_2 solutions (unless otherwise stated) in the region 900–350 nm: ε_{max} values are given in parentheses.

[b] In V (Ag–AgCl). Recorded on solutions in 0.1 M TBAH–CH_2Cl_2 using a Pt-bead electrode. Data obtained at $v = 200$ mV s^{-1}.

[c] Nujol mull spectrum.

viously for $[ReX_2(dppe)_2]X$ (X = Cl or Br),[13] $[ReCl_2(dppa)_2]PF_6$[6] and *trans*-$[ReCl_2(dmpe)_2]Cl$ (dmpe = $Me_2PCH_2CH_2PMe_2$);[14] for example, λ_{max} values for a solution of $[ReCl_2(dppa)_2]Cl$ in CH_2Cl_2 are 470 (ε = 1800) and 425 (ε = 2500) nm.[6]

Of the compounds isolated in the present study only $[ReCl_2(dppee)_2]Cl$ has been reported previously.[15,16] In the previous partial characterization of this compound, which has been formulated as the *trans*-isomer,[16] it was found to have a solid-state magnetic moment of 2.0 BM. In the present study we find that the hydrate has μ_{eff} = 2.3 BM for a solution in CH_2Cl_2.[17] The low-frequency IR spectrum (Nujol mull) of a sample of $[ReCl_2(dppee)_2]PF_6$ shows a single ν(Re—Cl) mode at 338s cm^{-1} which supports its assignment as the *trans*-isomer; similar results have been reported previously for *trans*-$[ReCl_2(dppa)_2]PF_6$ [ν(Re—Cl) at 333 cm^{-1}][6] and *trans*-$[ReCl_2(dmpe)_2]Cl$ [ν(Re—Cl) at 315 cm^{-1}].[14]

The close relationship between these dppee complexes is revealed by cyclic voltammetric measurements on solutions in 0.1 M TBAH–CH_2Cl_2 (see Fig. 1). The $E_{1/2}$ values (vs Ag–AgCl) for the processes that are assigned to the Re(IV)–Re(III), Re(III)–Re(II) and Re(II)–Re(I) couples are listed in Table 3. In the case of $[ReCl_2(dppee)_2]Cl \cdot 4H_2O$ and $[ReBr_2(dppee)_2]Br \cdot H_2O$, irreversible processes associated with the oxidation of the outer-sphere halide ion are seen at $E_{p,a}$ = +1.13 V (for Cl^-), and $E_{p,a}$ = +0.85 and +1.05 V (for Br^-) vs Ag–AgCl. For the metal-based couples we find that the $i_{p,a}/i_{p,c}$ ratios are close to unity. The values of $E_{p,a} - E_{p,c}$ are *ca* 100 mV at scan rate (ν) = 200 mV s^{-1}, and increased slightly with an increase in sweep rate. These properties are (with our cell configuration) and this solvent system consistent with electron transfer processes that approach reversibility.[18] These electrochemical redox properties are very similar to those exhibited by the previously characterized complex $[ReCl_2(dppa)_2]PF_6$.[6] Using a sample available from our earlier study, we find that a solution of this complex in 0.1 M TBAH–CH_2Cl_2 displays processes at $E_{p,a}$ = +1.38 V, $E_{1/2}$(red)(1) = −0.22 V, and $E_{1/2}$(red)(2) = −1.61 V vs Ag–AgCl. Cyclic voltammetric measurements on 0.5 M *n*-Bu_4NClO_4–DMF solutions of *trans*-$[ReCl_2(dmpe)_2]Cl$ have established[14] that the Re(III)–Re(II) and Re(II)–Re(I) couples occur at −0.398 and −1.548 V vs Ag–AgCl, respectively.

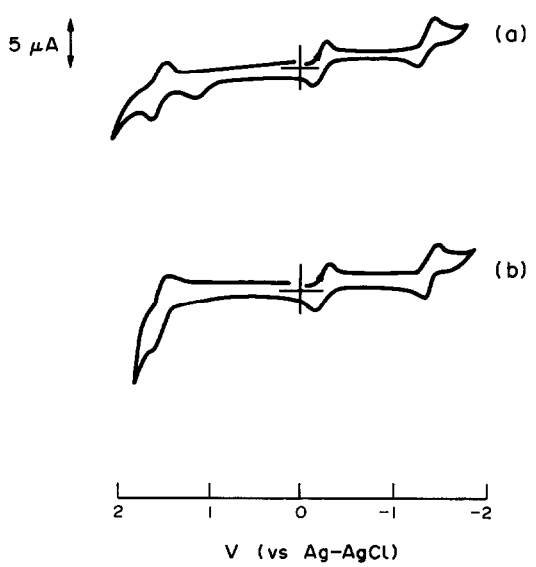

Fig. 1. Cyclic voltammograms (recorded at ν = 200 mV s^{-1} using a Pt-bead electrode) for 0.1 M TBAH–CH_2Cl_2 solutions of: (a) $[ReCl_2(dppee)_2]Cl \cdot 4H_2O$, and (b) $[ReCl_2(dppee)_2]ClO_4$.

In the case of $[ReCl_2(dppee)_2]Cl \cdot xH_2O$, the accessibility of the Re(III)–Re(II) couple has been demonstrated by its chemical reduction to $ReCl_2(dppee)_2$ using cobaltocene dissolved in CH_2Cl_2 or acetone. This rhenium(II) complex has also been isolated as one of the products of the reaction between $Re_2Cl_6(PBu^n_3)_2$ and dppee in refluxing ethanol and was obtained, in single-crystal form, as a minor contaminant in batches of crystalline $[ReCl_2(dppee)_2]Cl \cdot nH_2O$. It is not very soluble in polar and nonpolar solvents although it was sufficiently soluble in 0.1 M TBAH–CH_2Cl_2 to show that it displayed similar cyclic voltammetric behavior to that of $[ReCl_2(dppee)_2]Cl \cdot nH_2O$, with the exception that the process at *ca* −0.2 V now corresponds to an oxidation of the bulk complex and the wave ($E_{p,a}$ = +1.13 V) due to free Cl^- is no longer present. The electronic absorption spectrum of $ReCl_2(dppee)_2$ recorded as a Nujol mull shows λ_{max} at 398 nm as the most intense lower-energy feature.

Structural characterization of trans-$ReCl_2(dppee)_2$

The correspondence between the cyclic voltammetric behavior of $[ReCl_2(dppee)_2]Cl \cdot nH_2O$ and $ReCl_2(dppee)_2$ implies that no isomerization process follows this one-electron redox change, i.e. that both species possess a *trans*octahedral structure. This has been confirmed by a single-crystal X-ray structure analysis of a sample of $ReCl_2(dppee)_2$ that was found, by chance, to be present in a batch of crystalline $[ReCl_2(dppee)_2]Cl \cdot 4H_2O$ (see Experimental).

An ORTEP view of the $ReCl_2(dppee)_2$ molecule is shown in Fig. 2. The crystallographic data are contained in Table 1, while Table 2 lists the key

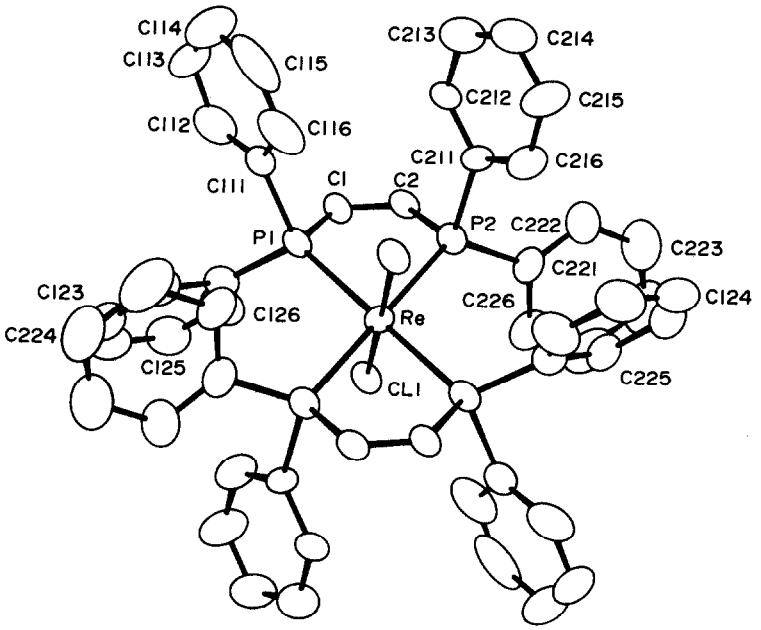

Fig. 2. ORTEP representation of $ReCl_2(dppee)_2$ in which atoms are given as their 50% probability ellipsoids. Unlabeled Cl, P and C atoms are related to the corresponding labeled atoms by an inversion center.

bond distances and angles.* The structure is clearly that of the *trans*-isomer as had been inferred from the previously discussed electrochemical data. The complex contains two chelating dppee ligands in which the C(1)—C(2) bond distance [1.36(1) Å] remains that of a typical C=C bond which is uncoordinated to a metal center. The Re—P distances [2.405(2) Å] are a little shorter than those found for the rhenium(III) complex *trans*-$[ReCl_2(dmpe)_2]Cl$ [2.438(2) Å];[14] this may reflect a slight shortening due to some small measure of Re-to-P π-bonding in the case of the rhenium(II) complex $ReCl_2(dppee)_2$. It is difficult to make informative comparisons with Re—P distances in dirhenium(II) complexes of the type $Re_2X_4(LL)_2$ (X = halide, LL = bidentate phosphine), since even in the cases where the ligands LL are chelating, e.g. α-$Re_2Cl_4(dmpe)_2$[19] and α-$Re_2Cl_4(dppp)_2$ [dppp = $Ph_2P(CH_2)_3PPh_2$],[20] these bond lengths show considerable variability [2.337(2) and 2.401(2) Å in these two instances]. The Re—Cl distance of 2.422(2) Å is, as expected, significantly longer than the comparable distance in the *trans*-$[ReCl_2(dmpe)_2]^+$ cation [2.337(1) Å]. While the Cl—Re—Cl unit is perfectly linear, some distortion in the equatorial ReP_4 plane is reflected by the range of Cl—Re—P angles that are observed (80–99°); this clearly reflects the conformational demands of the Re—P—CH=CH—P chelate rings.

Acknowledgements—We thank the National Science Foundation for support of this research (Grant No. CHE85-06702 to R.A.W.). The PDP 11/34 computer and X-ray Structure Solution Package in the Department of Chemistry were purchased with funds from the NSF Chemical Instrumentation Program (CHE-8204994) and the Monsanto Fund.

REFERENCES

1. F. A. Cotton and R. A. Walton, *Multiple Bonds Between Metal Atoms*. John Wiley, New York (1982).
2. F. A. Cotton and R. A. Walton, *Struct. Bonding (Berlin)* 1985, **62**, 1.
3. J. A. Jaecker, D. P. Murtha and R. A. Walton, *Inorg. Chim. Acta* 1975, **13**, 21.
4. J. A. Jaecker, W. R. Robinson and R. A. Walton, *J. Chem. Soc., Dalton Trans.* 1975, 698.
5. J. R. Ebner, D. R. Tyler and R. A. Walton, *Inorg. Chem.* 1976, **15**, 833.
6. T. J. Barder, F. A. Cotton, D. Lewis, W. Schwotzer, S. M. Tetrick and R. A. Walton, *J. Am. Chem. Soc.* 1984, **106**, 2882.
7. M. Bakir, P. E. Fanwick and R. A. Walton, *Polyhedron*, submitted for publication.
8. T. J. Barder and R. A. Walton, *Inorg. Chem.* 1982, **21**, 2510.

*Atomic positional parameters, thermal parameters, a complete listing of bond distances and angles (Tables S1–S4), and observed and calculated structure factors have been deposited with the Editor as supplementary data.

9. F. A. Cotton, N. F. Curtis, B. F. G. Johnson and W. R. Robinson, *Inorg. Chem.* 1965, **4**, 326.
10. K. R. Dunbar and R. A. Walton, *Inorg. Chem.* 1985, **24**, 5.
11. P. E. Fanwick, W. S. Harwood and R. A. Walton, *Inorg. Chim. Acta* 1986, **122**, 7.
12. N. Walker and D. Stuart, *Acta Cryst.* 1983, **A39**, 158.
13. F. A. Cotton, N. F. Curtis and W. R. Robinson, *Inorg. Chem.* 1965, **4**, 1696.
14. J.-L. Vanderheyden, M. J. Heeg and E. Deutsch, *Inorg. Chem.* 1985, **24**, 1666.
15. J. Chatt and G. A. Rowe, *J. Chem Soc.* 1962, 4019.
16. H. P. Gunz and G. J. Leigh, *J. Chem. Soc.* 1971, 2229.
17. This measurement was carried out on a CH_2Cl_2 solution of the complex by the Evans method (see D. F. Evans, *J. Chem. Soc.* 1959, 2003).
18. T. C. Zietlow, D. D. Klendworth, T. Nimry, D. J. Salmon and R. A. Walton, *Inorg. Chem.* 1981, **20**, 947.
19. T. J. Barder, F. A. Cotton, K. R. Dunbar, G. L. Powell, W. Schwotzer and R. A. Walton, *Inorg. Chem.* 1985, **24**, 2550.
20. N. F. Cole, F. A. Cotton, G. L. Powell and T. J. Smith, *Inorg. Chem.* 1983, **22**, 2618.

Polyhedron Vol. 6, No. 5, pp. 915–919, 1987
Printed in Great Britain

0277–5387/87 $3.00+.00

STRUCTURAL STUDIES ON BULKY PHOSPHINES: X-RAY CRYSTAL STRUCTURES OF [2,4,6-(*t*-Bu)$_3$C$_6$H$_2$P(SiMe$_3$)$_2$] AND [2,4,6-(*t*-Bu)$_3$C$_6$H$_2$POCH$_2$CH$_2$O]

A. H. COWLEY* and M. PAKULSKI

Department of Chemistry, University of Texas at Austin, Austin, TX 78712, U.S.A.

and

N. C. NORMAN

Department of Inorganic Chemistry, University of Newcastle upon Tyne, Newcastle upon Tyne, NE1 7RU, U.K.

(*Received* 7 *July* 1986; *accepted* 1 *September* 1986)

Abstract—The crystal and molecular structures of two bulky phosphines containing the 2,4,6-(*t*-Bu)$_3$C$_6$H$_2$ group are reported. Compound **1**, [2,4,6-(*t*-Bu)$_3$C$_6$H$_2$P(SiMe$_3$)$_2$], crystallizes in the monoclinic space group $P2_1/c$; $a = 9.450(8)$, $b = 17.154(6)$, $c = 17.790(5)$ Å, $\beta = 101.19(5)°$. *Compound* **2**, [2,4,6-(*t*-Bu)$_3$C$_6$H$_2$POCH$_2$CH$_2$O], also crystallizes in the monoclinic space group $P2_1/c$: $a = 18.224(5)$, $b = 9.394(2)$, $c = 12.321(2)$ Å, $\beta = 107.28(2)°$. Structural features resulting as a consequence of the bulky 2,4,6-(*t*-Bu)$_3$C$_6$H$_2$ group, in particular the geometry at phosphorus, are discussed.

There is currently considerable interest in phosphorus compounds containing the 2,4,6-(*t*-Bu)$_3$C$_6$H$_2$ group, since, by virtue of its large steric bulk, a range of unusual low-coordinate complexes may be stabilized. Examples of two-coordinate phosphorus include diphosphenes (**A**)[1] and

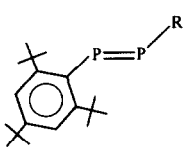

A

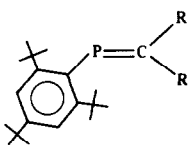

B

phospha-alkenes (**B**),[2] whilst many novel three-coordinate species have also been isolated such as the dithio- and methyleneoxophosphoranes (**C**[3] and **D**[4]). In addition, this degree of steric protection has enabled compounds such as primary phosphine sulphides and oxides (**E** and **F**)[5] and RP(H)(halogen) type phosphines (**G**)[6] to be prepared and characterized. Herein we report the structural characterization of two phosphines containing the 2,4,6-(*t*-Bu)$_3$C$_6$H$_2$ group: [2,4,6-(*t*-Bu)$_3$C$_6$H$_2$P(SiMe$_3$)$_2$] (**1**) and [2,4,6-(*t*-Bu)$_3$C$_6$H$_2$POCH$_2$CH$_2$O] (**2**).

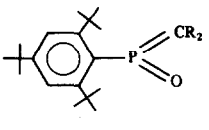

C

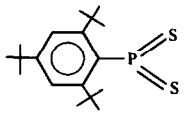

D

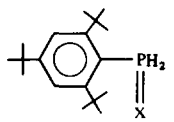

E X = S
F X = O

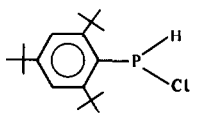

G

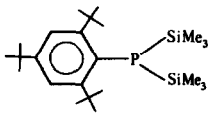

1

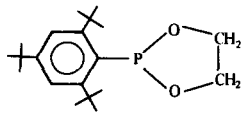

2

* Author to whom correspondence should be addressed.

RESULTS AND DISCUSSION

The bis(trimethylsilyl)-substituted phosphine (**1**) can be prepared by sequential lithiation and silylation of the primary phosphine, 2,4,6-(t-Bu)$_3$C$_6$H$_2$PH$_2$, and is a key intermediate in the synthesis of the only known, stable phosphaketene (**3**) reported by Appel and Paulen[7,8] via its reaction

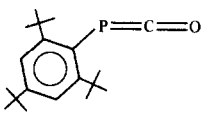

3

with phosgene ($COCl_2$). However, the apparent unreactivity of **1** towards other main-group element dichlorides, for example R_2SiCl_2[9] *vis-à-vis* phosphasilene synthesis,[10] was indicative of severe steric congestion at the phosphorus centre. In order to probe this hypothesis further, an X-ray crystal structure determination of **1** was undertaken. The results are shown in Fig. 1 whilst pertinent bond distance and angle data are collected in Table 1.

Examination of Fig. 1 reveals that the phosphorus centre is indeed sterically well-shielded both by the *ortho* t-Bu and Me$_3$Si groups. Most notable, however, is the geometry at phosphorus. The sum of angles at phosphorus [343.2(1)°] indicates a close-to-planar configuration, although this is somewhat distorted from an idealized (albeit rather flattened) trigonal pyramid as evidenced by the widely disparate C(1)—P(1)—Si bond angles [C(1)—P(1)—Si(1) = 127.0(1) and C(1)—P(1)—Si(2) = 105.2(1)°]. One factor which may contribute to a flattened geometry at phosphorus is partial delocalization of the P lone pair into vacant silicon 3d orbitals. However, the P—Si bond lengths [P(1)—Si(1) = 2.238(1) and P(1)—Si(2) = 2.255(1) Å] are in accord with a single-bond value predicted from the sum of the covalent radii of P and Si, i.e. 2.23 Å. There is therefore no evidence for P → Si π-donation. We suggest that the primary factor responsible for both the above observations is intramolecular steric congestion.

Table 1. Selected bond distances (Å) and angles (°) for **1**

Bond distances	
P(1)—Si(1)	2.238(1)[a]
P(1)—Si(2)	2.255(1)
P(1)—C(1)	1.844(3)
Bond angles	
Si(1)—P(1)—Si(2)	111.03(6)
Si(1)—P(1)—C(1)	127.0(1)
Si(2)—P(1)—C(1)	105.2(1)

[a] Numbers in parentheses are estimated standard deviations in the least significant digit.

The use of models indicates that the observed conformation about the P(1)—C(1) bond is the only one that is sterically tenable in that it minimizes close contacts between the Me$_3$Si and *ortho* t-Bu groups. Moreover these contacts are further reduced by a flattening of the geometry at phosphorus. The reason for the asymmetry in the angles

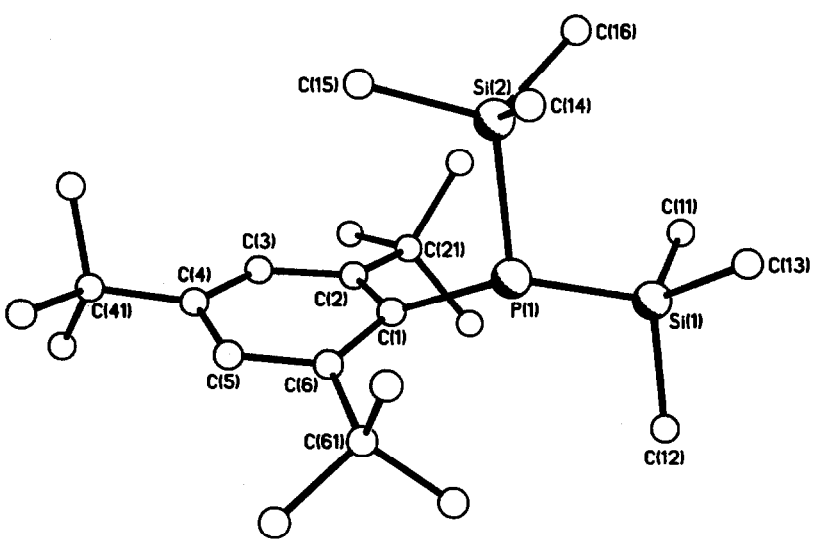

Fig. 1. Molecular structure of **1** showing the atom-numbering scheme. Hydrogen atoms omitted for clarity.

at phosphorus is less clear but is probably also steric in origin. It is possibly associated with the observation that the phosphorus atom is significantly out of the arene ring mean plane (0.85 Å), a factor which has been noted previously in phosphorus compounds containing this arene group[11] and discussed in terms of the large intramolecular strain associated with the *t*-Bu groups.

The synthesis of **2** was mentioned previously in a communication.[12] However, here we provide details of the synthesis. Under flash vacuum pyrolysis conditions, the phosphonite (**2**) eliminates ethene to produce the phosphinate (**4**) *via* a proposed dioxophosphorane intermediate (**5**).[12]

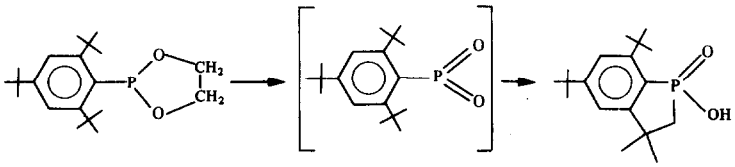

2 **5** **4**

The molecular structure of **2** is illustrated in Fig. 2 and selected bond distances and angles are collected in Table 2. In contrast to **1**, the geometry at phosphorus is markedly pyramidal [sum of angles = 291.4(1)°]. While this is undoubtedly due to the constraint imposed by incorporation into the PO_2C_2 ring, the assymetry in the C(1)—P(1)—O bond angles is considerably less than that for the corresponding C(1)—P(1)—Si angles in **1** [C(1)—P(1)—O(1) = 100.7(1), C(1)—P(1)—O(2) = 97.8(1)°]. Since the $O_2(CH_2)_2$ group in **2** is much smaller than the two Me_3Si groups in **1**, this supports the contention that the asymmetry in **1** is steric in origin. Note, however, that, in **2**, the phosphorus atom is also significantly removed from the arene ring mean plane (0.82 Å). Further structural and synthetic studies on phosphorus compounds containing this bulky arene are in progress.

EXPERIMENTAL

Synthesis

All manipulations were performed under a dry nitrogen atmosphere employing standard inert atmosphere techniques. All solvents were dried prior to use.

[2,4,6-(*t*-Bu)$_3$C$_6$H$_2$P(SiMe$_3$)$_2$] (**1**). This compound was prepared according to the method of Appel and Paulen.[7,8]

[2,4,6-(*t*-Bu)$_3$C$_6$H$_2$POCH$_2$CH$_2$O] (**2**). A THF solution (80 cm^3) of Li[2,4,6-(*t*-Bu)$_3$C$_6$H$_2$][13] (5.0 g, 20 mmol) was added dropwise to an Et_2O solution (20 cm^3) of 2-chloro-1,3,2-dioxaphospholane[14] (2.66 g, 21 mmol) at 0°C. After stirring the reaction mixture for an additional 12 h at room temperature, the solvents were removed *in vacuo*, and the residue extracted with *n*-hexane. Filtration followed by sol-

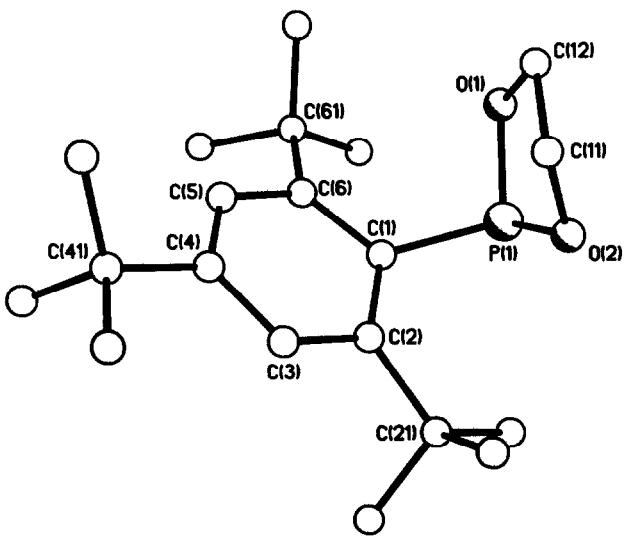

Fig. 2. Molecular structure of **2** showing the atom-numbering scheme. Hydrogen atoms omitted for clarity.

Table 2. Selected bond distances (Å) and angles (°) for **2**

Bond distances	
P(1)—O(1)	1.643(2)
P(1)—O(2)	1.647(2)
P(1)—C(1)	1.874(3)
Bond angles	
O(1)—P(1)—O(2)	92.9(1)
O(1)—P(1)—C(1)	100.7(1)
O(2)—P(1)—C(1)	97.8(1)
P(1)—O(1)—C(12)	113.2(2)
P(1)—O(2)—C(11)	109.4(2)
O(2)—C(11)—C(12)	106.0(3)
O(1)—C(12)—C(11)	106.4(3)

vent stripping afforded crude **2** which was purified by recrystallization from Et_2O. Yield of white, crystalline **2** = 5.3 g (79%), m.p. 76–78°C. The $^{31}P-\{^1H\}$ NMR spectrum of **2** (32.384 MHz) comprised a singlet at δ +169.

X-ray studies

General operating procedures and listings of programs used in the crystallographic studies reported herein have been given previously.[15] Crystal data for the structures of **1** and **2** are presented in Table 3.

Suitable single colourless crystals of **1** and **2** were mounted on an Enraf–Nonius CAD4-F diffractometer. Initial lattice parameters were determined from a least-squares fit to 25 accurately centred reflections, $15 \leqslant 2\theta \leqslant 20°$, and subsequently refined using higher-angle data. These indicated a monoclinic lattice for which data were collected for one independent quadrant, $+h+k\pm l$. Systematic absences observed were $0k0$ absent for k odd and $h0l$ absent for l odd, thus uniquely determining the space group as $P2_1/c$ (No. 14).

Data were corrected for the effects of Lorentz, polarization and decay, but not for absorption. Both structures were solved by direct methods using MULTAN[16] which revealed the location of most non-hydrogen atoms. All others were revealed by subsequent difference Fourier analysis and refined by full-matrix least squares with anisotropic thermal parameters. Hydrogen atoms were placed in calculated positions 0.95 Å from their respective carbon atoms, and were included in the structure factor calculation. Final refinements converged smoothly and revealed no chemically significant peaks in the final-difference map.

Table 3. Crystal data **1** and **2**

	1	**2**
Formula	$C_{24}H_{47}PSi_2$	$C_{20}H_{33}PO_2$
Formula weight	422.79	336.46
Crystal system	Monoclinic	
Space group	$P2_1/c$ (No. 14)	
a (Å)	9.450(8)	18.224(5)
b (Å)	17.154(6)	9.394(2)
c (Å)	17.790(5)	12.321(2)
β (°)	101.19(5)	107.28(2)
Volume (Å^3)	2829(3)	2014(1)
Z (molecules/cell)	4	4
ρ(calc.) (g cm^{-3})	0.992	1.110
λ(Mo-K_α) (Å)	0.71069	
μ(Mo-K_α) (cm^{-1})	1.85	1.4
Data collection time (h)	29.7	47.2
% decay	41.6	4.4
2θ limits (°)	$2.0 \leqslant 2\theta \leqslant 40.0$	$2.0 \leqslant 2\theta \leqslant 50.0$
	ω–2θ	ω–2θ
ω scan angle	$0.8+0.35 \tan\theta$	
No. of unique data measured	2544	3597
No. of data observed	1988	2166
Data cutoff	$I > 2.0\sigma(I)$	$I > 2.5\sigma(I)$
R	0.0504	0.0571
R_w	0.0764	0.0902

Acknowledgement—We thank the U.S. Army Research Office for financial support.

Supplementary material available. Tables of fractional coordinates for **1** and **2** have been deposited with the Cambridge Crystallographic Data Centre. Complete structural information is available from the Editor.

REFERENCES

1. (a) A. H. Cowley, *Polyhedron* 1984, **3**, 389; (b) A. H. Cowley, *Acc. Chem. Res.* 1984, **17**, 386; (c) A. H. Cowley and N. C. Norman, *Prog. Inorg. Chem.* 1986, **34**, 1.
2. A. H. Cowley, R. A. Jones, J. G. Lasch, N. C. Norman, C. A. Stewart, A. L. Stuart, J. L. Atwood, W. E. Hunter and H.-M. Zhang, *J. Am. Chem. Soc.* 1984, **106**, 7015.
3. R. Appel, F. Knoch and H. Kunze, *Angew. Chem.* 1984, **96**, 159; *Angew. Chem., Int. Ed. Engl.* 1984, **23**, 157.
4. (a) J. Navech, J. P. Majoral and R. Kraemer, *Tetrahedron Lett.* 1983, **24**, 5885; (b) M. Yoshifuji, K. Toyota, K. Ando and N. Inamoto, *Chem. Lett.* 1984, 317; (c) R. Appel, F. Knoch and H. Kunze, *Angew. Chem.* 1983, **95**, 1008; *Angew. Chem., Int. Ed. Engl.* 1983, **22**, 1004.
5. M. Yoshifuji, K. Shibayama, K. Toyota and N. Inamoto, *Tetrahedron Lett.* 1983, **24**, 4227.
6. (a) J. Escudié, C. Couret, H. Ranaivonjatovo, J. Satgé and J. Jaud, *Phosphorus and Sulphur* 1983, **17**, 221; (b) A. H. Cowley, J. E. Kilduff, N. C. Norman and M. Pakulski, *J. Chem. Soc., Dalton Trans.* 1986, 1801.
7. W. paulen, Ph.D. dissertation, Universität Bonn, West Germany (1983).
8. R. Appel and W. Paulen, *Angew. Chem.* 1983, **95**, 807; *Angew. Chem., Int. Ed. Engl.* 1983, **22**, 785.
9. A. H. Cowley and M. Pakulski, unpublished observations.
10. A. phosphasilene, $RP{=}SiR_2$, has been reported *via* another synthetic route: C. N. Smit, F. M. Lock and F. Bickelhaupt, *Tetrahedron Lett.* 1984, **25**, 3011.
11. M. Yoshifuji, I. Shima, N. Inamoto, K. Hirotsu and T. Higuchi, *Angew. Chem.* 1980, **92**, 405; *Angew. Chem., Int. Ed. Engl.* 1980, **19**, 399.
12. J. I. G. Cadogan, A. H. Cowley, I. Gosney, M. Pakulski and S. Yaslak, *J. Chem. Soc., Chem. Commun.* 1983, 1408.
13. M. Yoshifuji, I. Shima and N. Inamoto, *Tetrahedron Lett.* 1979, **20**, 3963.
14. H. J. Lucas, F. W. Mitchell, Jr and C. N. Scully, *J. Am. Chem. Soc.* 1950, **72**, 5491.
15. A. H. Cowley, J. E. Kilduff, J. G. Lasch, S. K. Mehrotra, N. C. Norman, M. Pakulski, B. R. Whitlesey, J. L. Atwood and W. E. Hunter, *Inorg. Chem.* 1984, **23**, 2582.
16. P. Main, MULTAN 82, University of York, York, England (1982).

Polyhedron Vol. 6, No. 5, pp. 921–929, 1987
Printed in Great Britain

0277–5387/87 $3.00+.00

SOME TRANSITION METAL COMPLEXES OF NEW TERDENTATE LIGANDS: BIS[2-(DIPHENYLPHOSPHINO)ETHYL]BENZYLAMINE AND BIS[2-(DIPHENYLARSINO)ETHYL)BENZYLAMINE

M. M. TAQUI KHAN,* V. VIJAY SEN REDDY and H. C. BAJAJ

Discipline of Coordination Chemistry and Homogeneous Catalysis, Central Salt and Marine Chemicals Research Institute, Bhavnagar 364002, Gujarat, India

(*Received* 29 *April* 1986; *accepted* 4 *September* 1986)

Abstract—Complexes of the terdentate ligands bis[2-diphenylphosphino)ethyl]benzylamine (DPBA) and bis[2-(diphenylarsino)ethyl]benzylamine (DABA) with Co(II), Ni(II), Pd(II), Pt(II), Rh(III), Ir(III), Rh(I) and Ir(I) are reported. The ligand DPBA reacts with Co(II) ion to form two types of complexes: a high-spin, paramagnetic, tetrahedral Co(II) complex of composition [CoCl(DPBA)]Cl and a low-spin, paramagnetic, square-planar complex of composition [CoBr(DPBA)]$B(C_6H_5)_4$. The reaction of DPBA with Ni(II) ion in methanol yields low-spin, diamagnetic, square-planar complexes of type [NiX(DPBA)]Y [X = Cl, Br or I; Y = Cl or $B(C_6H_5)_4$]. Four-coordinate, square-planar, cationic complexes of type $[MY(L)]^+$ [M = Pd(II), Pt(II), Rh(I) or Ir(I); Y = Cl or $P(C_6H_5)_3$; L = DPBA or DABA], were obtained on reaction of L with various starting materials containing these metal ions. Reaction of DPBA and DABA with rhodium and iridium trichlorides gave octahedral, neutral complexes of general formula $[MCl_3(L)]$ (M = Rh or Ir, L = DPBA or DABA). All the complexes were characterized on the basis of their elemental analysis, molar-conductance data, magnetic susceptibilities, electronic spectra, IR spectral measurements, and ^1H and $^{31}P-\{^1H\}$ NMR spectral data.

During the past few years, transition metal complexes of tertiary phosphines and arsines have been studied extensively, because of their chemistry and utility as catalysts in a number of reactions.[1,2] The chemistry of the metal complexes is governed[3–13] by the electronic and steric properties of the ligands and the oxidation state and coordination number of the metal ion.

The metal complexes of mixed donor ligands containing N, P, As and O have also gained considerable importance due to their catalytic activity in various homogeneous reactions.[14–16]

In our earlier communication[17] we reported the synthesis of two new terdentate ligands containing N and P or As as donor atoms, bis[2-(diphenylphosphino)ethyl]benzylamine (DPBA) and bis [2-(diphenylarsino)ethyl]benzylamine(DABA) and their complexes with Ru(II) and (III). These ligands which have a hard donor amino group confer the necessary nucleophilicity and the soft donor phosphino or arsino groups stabilize the low-valent metal centers. Both of these properties are very important in homogeneous catalytic reactions.[18,19]

In the present paper the synthesis and characterization of complexes of Co(II), Ni(II), Pd(II), Pt(II), Rh(III), Ir(III), Rh(I) and Ir(I) with the ligands DPBA and DABA are reported.

RESULTS AND DISCUSSION

Reaction of the ligand DPBA with cobalt(II) salt in a 1:1 ratio in methanol gave stable, paramagnetic, tetracoordinate complexes of formulation [CoX(DPBA)]Y [X = Cl, Y = Cl(**1**); X = Br, Y = $B(C_6H_5)_4$(**2**)]. The molar-conductance values (Table 1) of complexes **1** and **2** are indicative of 1:1 electrolytes,[20] suggesting a four-coordinate geometry for Co(II) in these complexes.

The far-IR spectrum of complexes **1** and **2** exhibit intense bands at 310 and 265 cm^{-1}, respectively, for

* Author to whom correspondence should be addressed.

Table 1. Analytical and other physical data of the complexes

	Complex[a]	Colour	M.p.[b] (°C)	μ_{eff}[c] (BM)	Elemental analysis (%)[d] C	H	N	Others	Conductivity[e] (λ_∞) (Ω^{-1} cm^{2}mol^{-1})
1	[CoCl(DPBA)]Cl	Bluish-green	105–110	4.40	63.3 (63.5)	5.3 (5.3)	2.0 (2.1)	—	84
2	[CoBr(DPBA)]B(C_6H_5)$_4$	Maroon-red	170–175	2.51	70.0 (71.6)	5.5 (5.6)	1.5 (1.4)	—	137(A)
3	[NiCl(DPBA)]B(C_6H_5)$_4$	Saffron-red	160–165	Diamag.	74.8 (75.0)	5.8 (5.8)	1.4 (1.5)	—	133(A)
4	[NiBr(DPBA)]B(C_6H_5)$_4$	Red	155–160	Diamag.	71.0 (71.5)	5.5 (5.6)	1.4 (1.4)	8.0(Br) (8.1)	141(A)
5	[NiI(DPBA)]B(C_6H_5)$_4$	Blackish-red	175–177	Diamag.	67.7 (68.3)	5.4 (5.3)	1.4 (1.3)	11.9(I) (12.2)	126(A)
6	[NiCl(DPBA)]Cl	Dark red	90–95	Diamag.	63.1 (63.6)	5.3 (5.3)	2.1 (2.1)	—	100(A)
7	[PdCl(DPBA)]B(C_6H_5)$_4$	Yellow	120–125	Diamag.	71.8 (71.4)	6.0 (6.0)	1.3 (1.3)	—	71
8	[PdCl(DABA)]B(C_6H_5)$_4$	Yellow	110–120	Diamag.	66.0 (65.6)	5.1 (5.1)	1.2 (1.3)	—	85
9	[PtCl(DPBA)]Cl	Creamish-white	178–180	Diamag.	51.9 (52.7)	4.4 (4.4)	1.8 (1.7)	—	70
10	[PtCl(DABA)]Cl	Creamish-white	200–205	Diamag.	47.0 (47.5)	3.9 (3.9)	1.6 (1.6)	—	70
11	[$RhCl_3$(DPBA)]	Yellow	>240	Diamag.	56.4 (56.7)	4.6 (4.7)	1.8 (1.9)	—	15
12	[$RhCl_3$(DABA)]	Yellow	220–224	Diamag.	50.2 (50.7)	4.3 (4.2)	1.6 (1.7)	—	5
13	[$IrCl_3$(DPBA)]	Green	>240	Diamag.	49.9 (50.6)	4.3 (4.2)	1.7 (1.7)	—	4(D)
14	[$IrCl_3$(DABA)]	Green	>200	Diamag.	45.6 (45.8)	3.9 (3.8)	1.5 (1.5)	—	2(D)
15	[Rh(PPh_3)(DPBA)]Cl	Yellow	120–126	Diamag.	67.7 (68.2)	5.6 (5.7)	1.5 (1.5)	—	66
16	[Rh(PPh_3)(DABA)]Cl	Yellow	100–105	Diamag.	62.4 (62.4)	4.9 (4.9)	1.3 (1.4)	—	65
17	[Ir(PPh_3)(DPBA)]Cl	White	160–164	Diamag.	62.0 (62.2)	4.8 (4.9)	1.4 (1.4)	—	90

[a] DPBA = bis[2-(diphenylphosphino)ethyl]benzylamine, DABA = bis[2-(diphenylarsino)ethyl]benzylamine.
[b] Decomposition temperature.
[c] BM values are after diamagnetic corrections.
[d] Calculated values are in parentheses.
[e] Conductivity measured in DMF except where mentioned: A = acetone, D = DMSO.

ν(Co—Cl) and ν(Co—Br) stretching frequencies, respectively, supporting the above formulation. The band at 540 cm^{-1} in both complexes **1** and **2** can be assigned to the ν(Co—P) frequency. From the conductivity and far-IR data, it can be proposed that all the three donor atoms of the ligand DPBA are coordinated to the metal ion with one of the halides inside the coordination sphere of the metal ion. This is in contrast to the earlier observation made by Sacconi and Morassi[10] on complexes containing similar ligands.

The ^{31}P–$\{^1H\}$ NMR spectra (Table 2) of complexes **1** and **2** exhibit resonances at 40.38 and 33.18 ppm, respectively, indicating that the two ends of the coordinated phosphorus atoms of DPBA are magnetically equivalent. The downfield coordination chemical shift in both the complexes is considerable compared to the free ligand (Table 2).

The electronic spectrum of **1** in dichloromethane is consistent with a tetrahedral structure. The band in the visible region at 629 nm is assigned[10,21,22] to the $^4A_2(F) \rightarrow {}^4T_1(P)$ (ν_3) transition. This band is further split into a number of components, indicating the presence of considerable deviation from T_d-symmetry. The fine structure is caused[23] by spin–orbit coupling which both splits the $^4T_1(P)$ state and allows the transitions to the neighboring doublet states to gain some intensity. The magnetic moment (Table 1) also corroborates a tetrahedral, Co(II) complex, with paramagnetism near to the spin-only value.[24,25] Complex **1** is therefore a tetrahedral Co(II) species.

The electronic spectrum of **2** in dichloromethane in the visible region shows only a broad band at 500 nm. The magnetic moment of 2.51 BM suggests **2** to be a low-spin Co(II) complex with considerable spin–orbital contribution. Taking the magnetic moment and the colour of the complex into consideration, complex **2** can be tentatively assigned a square-planar geometry with two ends of the phosphorus atoms *trans* to each other.

Reaction of DPBA with Ni(II) halides gave diamagnetic, cationic complexes of formulation $[NiX(DPBA)]^+$ [X = Cl (**3**), Br (**4**) or I (**5**)], best isolated as tetraphenyl borate complexes. Complexes **3–5** are air-stable and behave as 1 : 1 electrolytes[20] in acetone (Table 1), indicating a four-coordinate geometry for Ni(II). The far-IR spectra show bands due to ν(Ni—X) (X = Cl, Br or I) frequencies at 340, 255 and 250 cm^{-1} in complexes **3–5**, respectively, suggesting the presence of one halide group inside the coordination sphere of the metal ion and the coordination of all the donor atoms of the ligand DPBA to the metal ion. The far-IR spectra of complexes **3–5** also show ν(Ni—P) stretching frequencies at 535, 510 and 500 cm^{-1}, respectively.

The ^{31}P–$[^1H]$ NMR spectra (Table 2) of complexes **3–5** show sharp singlets at 22.10, 26.76 and 35.84 ppm, respectively, with a considerable downfield shift upon coordination of DPBA to form five-membered rings, indicating the magnetic equivalency of the two *trans* phosphorus atoms of the ligand DPBA. The downfield shift decreases in the order I > Br > Cl, in line with the decreasing po-

Table 2. ^{31}P–$\{^1H\}$ NMR data[a] of the complexes

	Complex	Solvent	Chemical shifts[b] [δ (ppm)] DPBA	PPh_3	J(M–P)	$J(P_A–P_B)$
	DPBA	$CHCl_3$	−19.25(s)	—	—	—
1	[CoCl(DPBA)]Cl	CH_2Cl_2	40.38(s)	—	—	—
2	[CoBr(DPBA)]$B(C_6H_5)_4$	CH_2Cl_2	33.18(s)	—	—	—
3	[NiCl(DPBA)]$B(C_6H_5)_4$	$CHCl_3$	22.10(s)	—	—	—
4	[NiBr(DPBA)]$B(C_6H_5)_4$	$CHCl_3$	26.76(s)	—	—	—
5	[NiI(DPBA)]$B(C_6H_5)_4$	$CHCl_3$	35.84(s)	—	—	—
7	[PdCl(DPBA)]$B(C_6H_5)_4$	$CHCl_3$	32.23(s)	—	—	—
9	[PtCl(DPBA)]Cl	$CHCl_3$	28.16	—	2722.16	—
11	[$RhCl_3$(DPBA)]	$CH_2Cl_2/CHCl_3$	35.20(d)	—	119.6	—
13	[$IrCl_3$(DPBA)]	DMSO	29.31(s)	—	—	—
15	[Rh(PPh_3)(DPBA)]Cl	CH_3OH	25.03(d) 21.52(d)	41.29(d) 37.96(d) 35.48(d)	119.60, 119.62	24.42
16	[Rh(PPh_3)(DABA)]Cl	CH_3OH	—	34.09(d)	118.19	—
17	[Ir(PPh_3)(DPBA)]Cl	CH_3OH	35.69(d)	3.75(t)	—	~24

[a] Positive chemical shifts downfield from 85% H_3PO_4.
[b] s = singlet, d = doublet, t = triplet.

larizability of the coordinated halide ions. This unusual downfield shift may be explained on the basis of the increased π-acidity of the coordinated halide group in passing through Cl to I. Because of the increased π-acidity of coordinated halide the σ-basicity of the coordinated phosphine increases due to a synergic effect causing an increase in the downfield shift with an increase in the π-acidity of the halogen.

The electronic spectra of complexes **3–5** in dichloromethane contain a single strong band at 490 nm (20,408 cm^{-1}), 505 nm (19,802 cm^{-1}) and 540 nm (18,518 cm^{-1}), respectively, in the visible region. This absorption refers to transitions which have *d*-orbital character $d_{xy} - d_{x^2-y^2}$, and confirms the square-planar geometry of the complexes.[26,27] The energy of the band increases in the order $I^- < Br^- < Cl^-$ as expected from the spectrochemical series for the halides. Complexes **3–5** are thus square-planar and analogous to the complexes with the ligands bis(2-diphenylphosphinoethyl)sulphide[28] and bis(2-diphenylphosphinoethyl)cyclohexylamine[10] with a *trans* arrangement of the phosphorus atoms.

Complex **6** is hygroscopic and behaves as a 1 : 1 electrolyte in acetone (Table 1). The far-IR spectrum shows bands at 310 and 540 cm^{-1}, which can be assigned to ν(Ni—Cl) and ν(Ni—P) stretching frequencies. Complex **6** displays an electronic spectrum identical to that of complex **3**, due to the presence of the same cationic species, $[NiCl(DPBA)]^+$, being present in both complexes. The complex shows a band at *ca* 20,000 cm^{-1}, which is characteristic of a square-planar geometry. The geometry assigned to complex **6** is similar to that of complex **3**.

The terdentate ligand DABA failed to react with Co(II) and Ni(II) metal salts.

Reactions of DPBA and DABA with palladium dichloride in a 1 : 1 mole ratio in methanol gave cationic species of the formulation $[PdClL]^+$ [L = DPBA (**7**) or DABA (**8**)], best isolated as tetraphenyl borate salts. The complexes have conductance values in accord with the presence of a 1 : 1 electrolyte (Table 1). The far-IR spectra of **7** and **8** exhibit ν(Pd—Cl) frequencies at 345 and 330 cm^{-1}, respectively. Bands at 545 and 470 cm^{-1} are due to stretching modes of ν(Pd—P) and ν(Pd—As), respectively.

The $^{31}P-\{^1H\}$ NMR spectrum (Table 2) of complex **7** exhibits a single resonance at 32.23 ppm, indicating the magnetic equivalence of the two phosphorus ends of the ligand DPBA and also suggests a square-planar geometry for the complex with phosphorus atoms *trans* to each other. Based on the above data, complexes **7** and **8** can be assigned a square-planar geometry similar to other known Pd(II) complexes,[7,29] with mono- and terdentate tertiary phosphine ligands. The electronic spectral data of complexes **7** and **8** are discussed along with complexes **9** and **10**.

Treatment of K_2PtCl_4 with DPBA and DABA in a 1 : 1 mole ratio gave four-coordinate, cationic complexes of type $[PtClL]^+$ [L = DPBA (**9**) or DABA (**10**)]. These complexes appear to be square-planar, analogous to the other known complexes of similar type of tridentate ligands reported earlier.[7] Both the complexes exhibit molar conductance values in accord with their formulation as 1 : 1 electrolytes (Table 1).

The far-IR spectra of **9** and **10** show peaks at 330 and 318 cm^{-1}, respectively, corresponding to the ν(Pt—Cl) stretching frequency.[30] The strong peaks at 520 and 470 cm^{-1} in **9** and **10** are due to ν(Pt—P) and ν(Pt—As) vibrational modes, respectively.

The electronic spectra of complexes **7–10** are consistent with a square-planar geometry of the complexes. Complexes of Pd(II) and Pt(II) which are pale yellow and creamish white, respectively, show the bands characteristic of *d–d* transition of square-planar cations. Complex **7** exhibits a band at 341 nm (29,326 cm^{-1}), whereas complex **8** shows a shoulder at 360 nm (27,778 cm^{-1}). Similarly, complexes **9** and **10** exhibit bands at 322 nm (31,056 cm^{-1}) and 359 nm (27,855 cm^{-1}) respectively. The molar extinction coefficient values are slightly higher than the conventional values for *d–d* transitions due to the LMCT character of these bands. A comparison of the energies of the lowest-energy *d–d* band in the corresponding complexes of DPBA and DABA showed that the expected spectrochemical order is observed, i.e. the bands in the DABA complexes are shifted to a lower energy compared to the DPBA ligand, as envisaged from ligand field considerations whenever a phosphorus donor is replaced by an arsenic donor.[31] Comparison of the electronic spectra of complexes **3**, **7** and **9** show that as the size of the metal ion increases in the triad Ni < Pd < Pt the lowest-energy *d–d* transition decreases in the order Pt > Pd > Ni. This hypsochromic shift to larger wavenumbers is due to the increase in the covalency of the complexes because of the increase in the size of the *d*-orbitals of the metal ions. Such a higher degree of metal–ligand bonding can be established in square complexes, by means of the non bonding d_{xz}, d_{yz} and p_z orbitals. The intense bands in all the complexes, around 250 nm can be assigned to the π–π^* transitions of the phenyl rings.

The $^{31}P-\{^1H\}$ NMR spectrum of complex **9** exhibits a singlet (with ^{195}Pt satellites) at 28.16 ppm. The platinum–phosphorus coupling constant was calculated from its ^{195}Pt satellites. The spectrum

shows the two-coordinated phosphorus ends of the DPBA ligand are magnetically equivalent and *trans* to each other confirming the above formulation. A ^1J(Pt–P) coupling constant value of 2722.16 Hz has been observed for complex **9**, which is appreciably higher when compared to those of earlier reports for similar phosphorus atoms *trans* to other phosphorus atoms in square-planar Pt(II) complexes[32] of types *trans*-L_2PtCl_2 and $[L_3PtCl]^+$ [$L = R_n(C_6H_5)_{3-n}P$, where $n = 1$, 2 or 3, and R = alkyl]. It has been reported in these complexes that the coupling constant value increases in every case in both the *cis* and *trans* series in going from trialkyl- to dialkylphenyl-, and to the alkyldiphenylphosphines. This corresponds to the increasing π-acceptor character of the phosphines as the number of phenyls on the phosphorus increases. Thus, the high coupling constant of complex **9** can be ascribed to the increased $d\pi$–$d\pi$ bonding between P and Pt due to the presence of phenyl groups on the two phosphorus atoms.

The reaction of rhodium trichloride with the ligands DPBA and DABA in 1 : 1 mole ratios in boiling methanol gave diamagnetic, yellow Rh(III) complexes of formulation $[RhCl_3L]$ [L = DPBA (**11**) or DABA (**12**)]. Complexes **11** and **12** have low molar-conductivity values in DMF solutions[20] (Table 1), indicating the nonelectrolytic nature of the complexes. Hence, an octahedral geometry has been assigned to complexes **11** and **12**. Such complexes can exist as facial or meridional isomers. The far-IR spectrum of **11** shows bands due to ν(Rh—Cl) stretching frequencies at 316, 295 and 262 cm^{-1}, whereas complex **12** exhibits ν(Rh—Cl) frequencies at 312, 293 and 281 cm^{-1}. These frequencies are in much closer agreement with the ν(Rh—Cl) frequencies for a facial type of isomer.[6,7,33] The far-IR spectra of **11** and **12** also show bands due to ν(Rh—P) and ν(Rh—As) frequencies at 540 and 480 cm^{-1}, respectively.

The ^{31}P–$\{^1H\}$ NMR spectrum of complex **11** shows a doublet centered at 35.20 ppm, with ^1J(Rh–P) = 119.6 Hz, suggesting the magnetic equivalence of the two phosphorus ends of the ligand DPBA.

The electronic spectra of complexes **11** and **12** show bands at 411 nm (24,331 cm^{-1}), 429 nm (23,310 cm^{-1}) and 377(sh) nm (26,525 cm^{-1}), respectively, in conformity with an octahedral Rh(III) species.[34] These *d–d* bands with LMCT character can be assigned to the transitions from the $^1A_{1g}$ ground state to the $^1T_{1g}$ and $^1T_{2g}$ upper states. The intense bands in the UV region can be assigned to the π–π^* transitions and LMCT bands. A facial configuration with *cis* phosphorus or arsenic atoms of the ligands is proposed for complexes **11** and **12**.

Treatment of hydrated iridium trichloride with DPBA and DABA in methanol gave neutral, octahedral complexes of type $[IrCl_3L]$ [L = DPBA (**13**) or DABA (**14**)]. Both the complexes exhibit very low conductance values (Table 1) in DMSO, indicative of a non-ionic nature of the complexes. Hence, they appear to be octahedral, iridium(III) complexes with the ligands occupying three coordination positions. Here also, such complexes can exist either in facial or meridional configurations.

The far-IR spectra of both the complexes show a broad intense signal at 320 cm^{-1} due to ν(Ir—Cl) mode. Peaks at 510 and 475 cm^{-1} in **13** and **14** can be assigned to ν(Ir—P) and ν(Ir—As) frequencies, respectively.

The ^{31}P–$\{^1H\}$ NMR spectrum of complex **13** exhibits a single peak at 29.31 ppm, confirming the equivalency of the phosphorus atoms of the ligand DPBA.

Due to solubility reasons, the electronic spectra of concentrated solutions of **13** and **14** could not be taken.

A meridional configuration or a facial configuration of the ligands is proposed for **13** and **14**.

Square-planar, cationic complexes of type $[Rh(PPh_3)L]^+$ [L = DPBA (**15**) or DABA (**16**)] were synthesized by reacting the Rh(I) complex $RhCl(CO)(PPh_3)_2$ with the ligands DPBA and DABA, respectively. The reaction in boiling acetone or methanol resulted in displacement of one of the coordinated triphenylphosphine groups and carbon monoxide from the starting complex, to give diamagnetic complexes of the above formulation. The molar-conductance values (Table 1) of both the complexes are in accord with their formulation as 1 : 1 electrolytes. The far-IR spectra of the complexes do not show any band around 300 cm^{-1}, indicating the total absence of the chloride ion inside the coordination sphere of the metal ion. Both the complexes show bands characteristic of a ν(Rh—P) stretch, due to the coordinated PPh_3 at 510 cm^{-1}. The complexes also display strong bands at 540 and 470 cm^{-1}, due to ν(Rh—P) and ν(Rh—As) modes, respectively.

The ^{31}P–$\{^1H\}$ NMR spectrum of complex **15** gave a well-resolved spectrum (Fig. 1), consistent with a square-planar, four-coordinate $[Rh(PPh_3)(DPBA)]^+$ cation. It exhibits a pair of doublets centered at 25.03 and 21.52 ppm, which can be assigned to the two equivalent *trans* phosphorus atoms (P_A) (structure **I**) of the ligand DPBA, with $^1J(Rh–P_A)$ = 119.62 Hz. The doublet of doublet can be explained on the basis of the splitting of two equivalent phosphorus atoms (P_A) by a rhodium nucleus ($I = 1/2$) to give a doublet which in turn is split again by the phosphorus atom (P_B) into

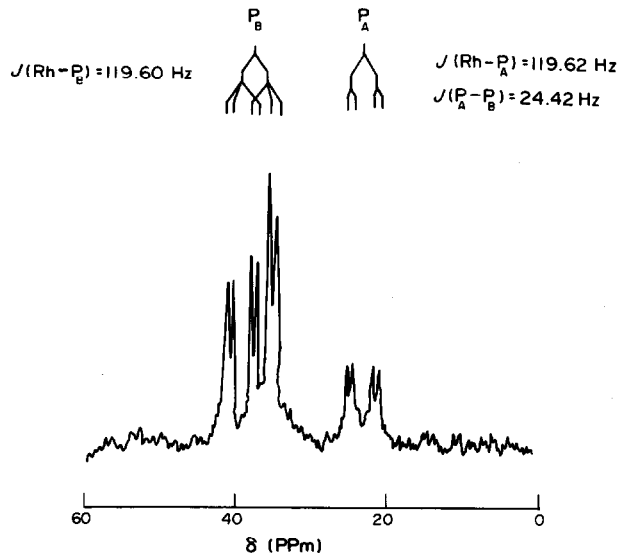

Fig. 1. The $^{31}P-\{^{1}H\}$ NMR spectrum of complex $[Rh(PPh_3)(DPBA)]Cl$.

two doublets. There are three more doublets in the downfield region centered at 41.29, 37.96 and 35.48 ppm, that are assigned to the phosphorus atom (P_B), which is first split by the rhodium nucleus and in turn by the two equivalent phosphorus atoms (P_A) of the ligand (Fig. 1). The coupling constants are $J(Rh–P_B) = 119.60$ Hz and $^{2}J(P_A–P_B) = 24.42$ Hz. The chemical shifts are in agreement with the earlier reported work.[35]

The $^{31}P-\{^{1}H\}$ NMR spectrum of complex **16** exhibits a doublet centered at 34.09 ppm (Table 2) with $^{1}J(Rh–P) = 118.19$ Hz, which can be assigned to the coordinated phosphorus atom of the lone triphenylphosphine group.

The spectra in and near the visible region of **15** and **16** show weak *d–d* transition bands with LMCT character at 384 nm (26,042 cm^{-1}) and 451 nm (22,172 cm^{-1}), and 364 nm (27,510 cm^{-1}) and 299 nm (33,388 cm^{-1}), respectively, which are typical[36] of many d^8 complexes. A similar trend of the band shifting to the longer wavelengths has been observed in the case of DABA complex. The bands in the high-energy region can be attributed to the $\pi–\pi^*$ and charge-transfer bands.

The proposed structures of **15** and **16** are shown in **I**.

Reactions of DPBA with $IrCl(CO)(PPh_3)_2$ in boiling acetone resulted in displacement of one of the two coordinated triphenylphosphine groups and CO, to give a cationic Ir(I) complex of type $[Ir(PPh_3)(DPBA)]^+$ (**17**). The molar conductance of **17** (Table 1) is indicative of a 1 : 1 electrolyte. The cationic formulation of complex **17** is also supported by the complete absence of the ν(Ir—Cl) stretching frequency around 300 cm^{-1} in the far-

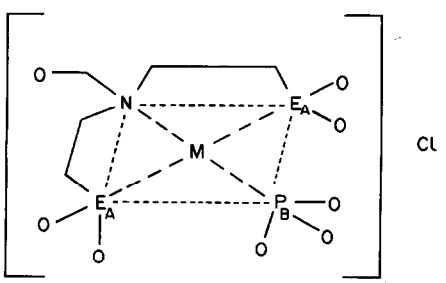

M = Rh or Ir, E = P or As

I

IR spectrum of the complex. The intense peaks at 515 and 545 cm^{-1} can be assigned to the ν(Ir—P) modes of coordinated $PPh_3$and the ligand DPBA, respectively.

The $^{31}P-\{^{1}H\}$ NMR spectrum of complex **17** also corroborates the above formulation. The spectrum exhibits two resonances, a downfield doublet centered at 35.69 ppm, and a triplet centered at 3.75 ppm. The doublet due to the splitting of a P_A by P_B (structure **I**) is assigned to the equivalent phosphorus atoms (P_A) of the ligand DPBA. The appearance of a triplet, which can be assigned to the phosphorus atom (P_B) of the triphenylphosphine, is due to the splitting of P_B by the two equivalent phosphorus atoms (P_A). The small coupling constant $J(P_A–P_B)$ of $\sim$ 24 Hz, may be due to the presence of P_A and P_B *cis* to each other. The proposed structure of **17** is shown as structure **I**.

The ^{1}H NMR spectra of complexes **7–12**, **16** and **17** could be obtained satisfactorily in $CDCl_3$. All the complexes exhibited broadened resonance signals due to phenyl and methylene protons, with

considerable downfield shift, when compared to those of free ligand[17] [DPBA: phenyl = 7.2δ(m); —CH_2CH_2— = 2.58δ(m), 2.10δ(m) and —CH_2— = 3.56δ(s): DABA: phenyl = 7.0(m); —CH_2CH_2— = 2.60δ(m), and 2.05δ(m) —CH_2 = 3.50δ(s)]. The phenyl resonances in the complexes occur as an asymmetric multiplet between 7.2 and 7.5δ. The methylene protons of the benzyl group occur as a singlet between 3.6 and 4.9δ. The methylene protons of CH_2CH_2 bridges occur as broadened, complex asymmetric multiplets, between 2.8 and 3.9 and 2.3 and 2.9δ, corresponding to the methylene protons attached to diphenylphosphino or arsino group and amine center, respectively. The complex asymmetric multiplets are possibly due to the interaction of neighbouring methylene protons followed by the coupling of the ^{31}P nuclear spin (in DPBA). For the remaining complexes the ^1H NMR could not be obtained satisfactorily owing to either the paramagnetic nature of the complexes or insufficient solubility.

Some of the earlier workers[37] have observed a large downfield chemical shift, upon coordination of tertiary phosphines to form five-membered chelate rings, in ^{31}P NMR. A similar effect of a large downfield shift has been observed upon coordination of the ligand DPBA to form five-membered chelate rings in the present work. By ^{31}P–$\{^1H\}$ NMR studies it has been confirmed that both the phosphorus ends of the ligand DPBA coordinate to the metal atom in all the complexes.

EXPERIMENTAL

The compounds $CoX_2 \cdot xH_2O$ (X = Cl or Br) and $NiX_2 \cdot xH_2O$ (X = Cl, Br or I) used were BDH Analar grade. Rhodium trichloride, iridium trichloride trihydrate, palladium dichloride and potassium tetrachloroplatinate were purchased from Strem Chemicals (U.S.A.). The complexes $RhCl(CO)(PPh_3)_2$ and $IrCl(CO)(PPh_3)_2$ were prepared by published procedures.[38] All solvents used in this work were of reagent grade, and were purified and dried before use. All preparations were carried out in an atmosphere of dry nitrogen.

The ligands DPBA and DABA were synthesized as reported earlier.[17] Microanalysis, melting points, conductivity and magnetic-susceptibility measurements were done as reported,[39,40] and are given in Table 1. Far-IR spectra of the complexes in the 600–100-cm^{-1} region were obtained using Nujol mulls pressed between polyethylene plates. The IR spectra were recorded on a Nicolet FT-IR model 200SX spectrometer. The electronic spectra (900–190 nm) were recorded in dichloromethane and chloroform using Shimadzu UV 240 and Beckman DU-7 spectrophotometers. Proton NMR spectra in $CDCl_3$ were recorded at 100 MHz on a JEOL FX-100 spectrometer using tetramethyl silane as reference. The proton-decoupled ^{31}P NMR spectra were taken in the indicated solvents (Table 2) using a JEOL FX-100 spectrometer operating at 40.3 MHz in the Fourier transform mode. The samples were placed in a 10-mm NMR tube and a capillary of deuterium oxide for the lock. 85% phosphoric acid was used as an external standard.

Preparation of the metal complexes

Chlorobis(2 - (*diphenylphosphino*)*ethyl*)*benzyl* - *aminecobalt*(II)*chloride*, [CoCl(DPBA)]Cl. To a refluxing methanolic solution of $CoCl_2 \cdot 6H_2O$ (0.10 g, 0.42 mM), the ligand DPBA (0.22 g, 0.42 mM) was added under a nitrogen atmosphere to get a green solution. After refluxing the reaction contents for 4–5 h, the solution was evaporated to dryness by a roto-evaporator *in vacuo*, to get a bluish-green precipitate, which was then washed with water and CCl_4, and dried over P_4O_{10} *in vacuo*. The compound was recrystallized from an acetone–*n*-hexane mixture. Yield 0.161 g (58%).

Bromobis(2 - (*diphenylphosphino*)*ethyl*)*benzyl* - *aminecobalt*(II)*tetraphenylborate*, [CoBr(DPBA)]B$(C_6H_5)_4$. To a refluxing methanolic solution of $CoBr_2$ (0.10 g, 0.45 mM) the ligand DPBA (0.24 g, 0.92 mM) was added, when a maroon-red solution was formed. After 4–5 h of refluxing 2 mol of $NaBPh_4$ was added to the cooled solution, when a shining red precipitate was obtained. The product was filtered, washed with methanol and diethyl ether, and recrystallized from an acetone–methanol mixture. Yield 0.130 g (60%).

Chlorobis(2 - (*diphenylphosphino*)*ethyl*)*benzyl* - *aminenickel*(II)*tetraphenylborate*, [NiCl(DPBA)]B$(C_6H_5)_4$, *bromobis*(2-(*diphenylphosphino*)*ethyl*)*benzylaminenickel*(II)*tetraphenylborate*, [NiBr(DPBA)]$B(C_6H_5)_4$, *and iodobis* (2-(*diphenylphosphino*)*ethyl*) *benzylaminenickel*(II)*tetraphenylborate*, [NiI(DPBA)]$B(C_6H_5)_4$. To refluxing methanolic solutions of $NiCl_2 \cdot 6H_2O$ (0.10 g, 0.42 mM), $NiBr_2 \cdot 3H_2O$ (0.10 g, 0.46 mM), and NiI_2 (0.10 g, 0.32 mM), the ligand DPBA was added, 0.22 g (0.42 mM) in the case of the chloride, 0.24 g (0.46 mM) in the case of the bromide, and 0.17 g (0.32 mM) in the case of the iodide, under an N_2 atmosphere and further refluxed for 4–5 h. To the cooled solutions a 2-mol excess of $NaB(C_6H_5)_4$ was added to get a saffron-red compound in the case of the chloro complex **3**, shining red in the case of the bromo complex **4**, and blackish-red in the case of the

iodo complex **5**. The products were filtered, washed with methanol and ether, and dried. The complexes **3–5** were recrystallized from an acetone–methanol mixture. Yield 0.31 g (78%) in the case of **3**, 0.36 g (80%) in the case of **4**, and 0.28 g (83%) in the case of **5**.

Chlorobis(2 - (*diphenylphosphino*)*ethyl*)*benzyl* - *aminenickel*(II)*chloride*, [NiCl(DPBA)]Cl. The procedure adapted for this complex is analogous to that described above for complexes **3–5**, except that after refluxing the reaction contents for 4–5 h the solution was evaporated to dryness to get a red precipitate, which was washed and dried and stored in a vacuum desiccator because of its hygroscopicity. Yield 0.18 g (65%).

Chlorobis(2 - (*diphenylphosphino*)*ethyl*)*benzyl* - *aminepalladium*(II)*tetraphenylborate*, [PdCl(DPBA)]$B(C_6H_5)_4$, *and chlorobis*(2-(*diphenylarsino*) *ethyl*) *benzylaminepalladium* (II) *tetraphenylborate*, [PdCl(DABA)]$B(C_6H_5)_4$. After refluxing the yellow methanolic solutions of $PdCl_2$ (0.10 g, 0.56 mM) and the ligands [DPBA (0.30 g, 0.56 mM) or DABA (0.35 g, 0.56 mM)] for 4–5 h, the reaction contents were cooled and a 2-mol excess of $NaB(C_6H_5)_4$ in methanol was added, when a yellow precipitate was obtained in both cases. The complexes were filtered, washed with hot methanol and diethyl ether, and recrystallized from a dichloromethane–methanol mixture. Yield 0.29 g (52%) (DPBA), and 0.3 g (51%) (DABA).

Chlorobis(2 - (*diphenylphosphino*)*ethyl*)*benzyl* - *amineplatinum*(II)*chloride*, [PtCl(DABA)]Cl, *and chlorobis*(2 - (*diphenylarsino*)*ethyl*)*benzylamineplatinum* (II) *chloride*, [PtCl(DABA)]Cl. To an acetone solution of the ligand [DPBA (0.128 g, 0.24 mM) and DABA (0.149 g, 0.24 mM)] the compound K_2PtCl_4 (0.100 g, 0.24 mM) in 2–3 cm^3 of water was added, and the solution slightly warmed for 2–3 h. The resulting pale yellow solutions in both the cases were concentrated to a small volume and the complexes precipitated by the addition of diethyl ether to get a creamish white precipitate in both cases. The complexes were filtered, washed, dried and recrystallized from an acetone–diethyl ether mixture. Yield 0.192 g (88%) (DPBA), and 0.180 g (88%) (DABA).

Trichlorobis(2 - (*diphenylphosphino*)*ethyl*) *benzyl aminerhodium*(III), [$RhCl_3$(DPBA)], *and trichlorobis*(2 - (*diphenylarsino*)*ethyl*)*benzylaminerhodium* (III), [$RhCl_3$(DABA)]. To the refluxing methanolic solution of $RhCl_3$ (0.10 g, 0.47 mM), the ligand [DPBA (0.253 g, 0.47 mM) or DABA (0.294 g, 0.47 mM)] in 5 cm^3 benzene was added slowly over a period of 1 h, under an N_2 atmosphere. A silky yellow precipitate settled down in both the cases after refluxing for 4–5 h. The precipitates were filtered, washed and recrystallized from a dichloromethane–diethyl ether mixture. Yield 0.14 g (40%) (DPBA), and 0.158 g (40%) (DABA).

Trichlorobis(2 - (*diphenylphosphino*)*ethyl*)*benzyl* - *amineiridium*(III), [$IrCl_3$(DPBA)], *and trichlorobis*(2 - (*diphenylarsino*)*ethyl*)*benzylamineiridium* (III), [$IrCl_3$(DABA)]. To a refluxing methanolic solution of the ligand [DPBA (0.302 g, 0.56 mM), or DABA (0.35 g, 0.56 mM)] was added $IrCl_3 \cdot 3H_2O$ (0.10 g, 0.28 mM), and the solution further refluxed for 4–5 h, when a greyish green complex was obtained in the case of **13** and a greenish complex in the case of **14**. The products were filtered, washed with methanol and diethyl ether, and recrystallized from hot dimethylsulphoxide. Yield 0.10 g (45%) (DPBA), and 0.115 g (44%) (DABA).

Triphenylphosphinebis(2 - (*diphenylphosphino*) *ethyl*)*benzylaminerhodium*(I)*chloride*, [Rh(PPh_3) (DPBA)]Cl, *and triphenylphosphinebis* (2- (*diphenyl arsino*)*ethyl*)*benzylaminerhodium*(I) *chloride*, [Rh (PPh_3)(DABA)]Cl. To a refluxing acetone solution of the ligand DPBA (0.125 g, 0.21 mM) and a methanolic solution of DABA (0.130 g, 0.21 mM), was added the Rh(I) complex $RhCl(CO)(PPh_3)_2$ (0.150 g, 0.21 mM). After 3–4 h of refluxing the yellow homogeneous solutions in both the cases were concentrated to a small volume and the complexes precipitated by diethyl ether. The yellow products were filtered, washed with diethyl ether and recrystallized from a methanol–diethyl ether mixture. Yield 0.180 g (89%) (DPBA), and 0.125 g (57%) (DABA).

Triphenylphosphinebis(2 - (*diphenylphosphino*) *ethyl*)*benzylamineiridium*(I)*chloride*, [Ir(PPh_3) (DPBA)]Cl. $IrCl(CO)(PPh_3)_2$ (0.100 g, 0.12 mM) was added to a refluxing methanolic solution of DPBA (0.068 g, 0.12 mM) and further refluxed for 3–4 h. The solution was then concentrated and diethyl ether added to get a creamish white precipitate which was filtered, washed with ether and recrystallized from a dichloromethane–diethyl ether mixture. Yield 0.055 g (57%).

Acknowledgement—One of us (V.V.S.R.) thanks CSIR, New Delhi, India, for financial support.

REFERENCES

1. C. A. McAuliffe and W. Levason, *Phosphine, Arsine and Stibine Complexes of the Transition Elements*. Elsevier, Amsterdam (1979) (and references therein).
2. M. M. Taqui Khan and A. E. Martell, *Homogeneous Catalysis by Metal Complexes*, Vols I and II. Academic Press, New York (1974).

3. G. Booth, *Advances in Inorganic Chemistry and Radiochemistry*, Vol. 6. Academic Press, New York (1964).
4. L. M. Venanzi, *Angew. Chem., Int. Ed. Engl.* 1964, **3**, 453.
5. R. B. King, *Acc. Chem. Res.* 1972, **5**, 177 (and references therein).
6. R. B. King, R. N. Kapoor, M. S. Saran and P. N. Kapoor, *Inorg. Chem.* 1971, **10**, 1851.
7. R. B. King, P. N. Kapoor and R. N. Kapoor, *Inorg. Chem.* 1971, **10**, 1841.
8. M. M. Taqui Khan and A. E. Martell, *Inorg. Chem.* 1975, **14**, 676.
9. M. M. Taqui Khan and A. E. Martell, *Inorg. Chem.* 1974, **13**, 2961.
10. L. Sacconi and R. Morassi, *J. Chem. Soc. A* 1968, 2997.
11. L. Sacconi, I. Bertini and F. Mani, *Inorg. Chem.* 1968, **7**, 1417.
12. L. Sacconi, *J. Chem. Soc. A* 1970, 248.
13. L. Sacconi, G. P. Speroni and R. Morassi, *Inorg. Chem.* 1968, **7**, 1521.
14. M. M. Taqui Khan, B. T. Khan, Safia and Md. K. Nazeeruddin, *J. Mol. Catal.* 1984, **26**, 207.
15. D. M. Roundhill, R. A. Bechtold and S. G. N. Roundhill, *Inorg. Chem.* 1980, **19**, 284 (and references therein).
16. G. K. Anderson and Ravi Kumar, *Inorg. Chem.* 1984, **23**, 4064.
17. M. M. Taqui Khan and V. Vijay Sen Reddy, *Inorg. Chem.* 1986, **25**, 208.
18. J. P. Collman, *Acc. Chem. Res.* 1968, **1**. 136.
19. G. N. Schrauzer, *Transition Metals in Homogeneous Catalysis*. Marcel Dekker, New York (1971).
20. W. J. Geary, *Coord. Chem. Rev.* 1971, **7**, 81.
21. D. M. L. Goodgame and M. Goodgame, *Inorg. Chem.* 1965, **4**, 139.
22. A. D. Liehr, *J. Phys. Chem.* 1963, **67**, 1314.
23. F. A. Cotton and G. Wilkinson, *Advanced Inorganic Chemistry*, 2nd Edn. Wiley Eastern, New York (1972).
24. B. N. Figgis and R. S. Nyholm, *J. Chem. Soc.* 1959, 338.
25. F. A. Cotton, D. M. L. Goodgame and M. Goodgame, *J. Am. Chem. Soc.* 1961, **83**, 4690.
26. C. R. C. Coussmaker, M. H. Hutchinson, J. R. Mellor, L. E. Sutton and L. M. Venanzi, *J. Chem. Soc.* 1961, 2705.
27. N. D. Sadanani, A. Walia, P. N. Kapoor and R. N. Kapoor, *J. Coord. Chem.* 1981, **11**, 39.
28. G. Degischer and G. Schwarzenbach, *Helv. Chim. Acta* 1966, **49**, 1927.
29. H. C. Clark and K. R. Dixon, *J. Am. Chem. Soc.* 1969, **91**, 596.
30. H. C. Clark, K. R. Dixon and W. J. Jacobs, *J. Am. Chem. Soc.* 1968, **90**, 2259.
31. G. Dyer, M. O. Workman and D. W. Meek, *Inorg. Chem.* 1967, **6**, 1404.
32. S. O. Grim, K. L. Keiter and W. McFarlane, *Inorg. Chem.* 1967, **6**, 1133.
33. J. Chatt, G. J. Leigh and D. M. P. Mingos, *J. Chem. Soc. A* 1969, 1674.
34. W. Levason and C. A. McAuliffe, *J. Chem. Soc., Dalton Trans.* 1974, 2238.
35. K. D. Tau, D. W. Meek, T. Sorrel and J. A. Ibers, *Inorg. Chem.* 1978, **17**, 3454.
36. L. Vaska, L. S. Chen and W. V. Miller, *J. Am. Chem. Soc.* 1971, **93**, 6671.
37. P. E. Garrou, *Chem. Rev.* 1981, **81**, 229 (and references therein).
38. W. L. Jolly, Ed., *Inorganic Synthesis*, Vol. XI. McGraw Hill Inc., 1968.
39. M. M. Taqui Khan and K. Veera Reddy, *J. Coord. Chem.* 1982, **12**, 71.
40. M. M. Taqui Khan and Rafeeq Mohiuddin, *Polyhedron* 1983, **2**, 1243.

Polyhedron Vol. 6, No. 5, pp. 931–937, 1987
Printed in Great Britain

0277-5387/87 $3.00+.00

THE CRYSTAL STRUCTURES OF TWO HETEROPOLYTUNGSTATE SALTS CONTAINING ANIONS DERIVED FROM α-OCTADECATUNGSTODIPHOSPHATE(6−): $(NH_4)_{10}[\alpha_2\text{-}P_2W_{17}O_{61}]\cdot 8H_2O$ AND $(Me_2NH_2)_8[\alpha_2\text{-}P_2Co(H_2O)W_{17}O_{61}]\cdot 11H_2O$

TIMOTHY J. R. WEAKLEY

Department of Chemistry, Dundee University, Dundee DD1 4HN, U.K.

(*Received* 18 *May* 1986; *accepted* 4 *September* 1986)

Abstract—The anions in $(NH_4)_{10}[\alpha_1\text{-}P_2W_{17}O_{61}]\cdot 8H_2O$ (I) and $(Me_2NH_2)_8[\alpha_2\text{-}P_2Co(H_2O)W_{17}O_{61}]\cdot 11H_2O$ (II) both have the $[\alpha\text{-}P_2W_{18}O_{62}]^{6-}$ structure with one "cap" W atom and its terminal oxygen atom missing (I), and a $Co(H_2O)^{2+}$ group in place of one "cap" W atom and its terminal oxygen (II). Both anions have approximate mirror symmetry but are disordered in the crystal; in I the anion lies on a crystal inversion centre in two equally-weighted orientations, and in II the Co atom appears as two $Co_{0.5}W_{0.5}$ composite atoms on either side of a crystallographic mirror plane. Crystal data include [diffractometer, Mo radiation, and $|F| \geqslant 3\sigma(F)$]: I, *Cmca*, $a = 18.080(8)$, $b = 17.945(7)$, $c = 21.546(8)$ Å, $Z = 4$, $R = 0.067$ for 1384 data; II, *Pnam*, $a = 28.052(11)$, $b = 15.069(12)$, $c = 20.638(17)$ Å, $Z = 4$, $R = 0.069$ for 3057 data.

The $[\alpha\text{-}P_2W_{18}O_{62}]^{6-}$ anion contains two α-$A\text{-}PW_9O_{34}$ units (each derived from the well-known $[\alpha\text{-}PW_{12}O_{40}]^{3-}$ anion by the removal of a set of three corner-sharing WO_6 octahedra) which are linked through corner-sharing with the elimination of six oxygen atoms.[1,2] The anion has point symmetry D_{3h}, and contains only two structurally-distinct types of W atoms: six "cap" atoms on vertical mirror-planes, grouped in two sets of three, and 12 "belt" atoms which do not lie on mirror-planes and are grouped in two sets of six. Nevertheless base attack in aqueous solution at pH > 6 initially removes just one W atom and its terminal oxygen to give $[\alpha_2\text{-}P_2W_{17}O_{61}]^{10-}$.[3,4] This can then react[5,6] with various $Z^{x+}(aq)$ cations to give products $[P_2Z(OH_y)W_{17}O_{61}]^{(12-x-y)-}$ in which Z is believed to occupy a W site of the original $[\alpha\text{-}P_2W_{18}O_{62}]^{6-}$ anion. It will also form bonds to larger cations through, presumably, the outer four oxygens adjacent to the vacant W site to give complexes of type $[Ce(P_2W_{17}O_{61})_2]^{16-}$.[7,8] The precise location, cap or belt, of the vacancy in $[\alpha_2\text{-}P_2W_{17}O_{61}]^{10-}$ has been disputed. The ^{31}P NMR spectrum of this anion[9] and the results of polarographic studies of the anion and some derived species[10] have been taken to indicate a belt vacancy. However, the presence of a cap vacancy was deduced from ESR measurements on the derivative $[\alpha_2\text{-}P_2V(IV)W_{17}O_{61}]^{8-}$;[11] from the incomplete ($R = 0.19$) crystal structure analysis of $K_{16}[Ce(P_2W_{17}O_{61})_2]\cdot aq$;[8] and from the pattern of line intensities, consistent only with mirror symmetry, in the ^{183}W NMR spectrum of $[\alpha_2\text{-}P_2W_{17}O_{61}]^{10-}$.[12] Also, it has been briefly reported[13] that the Sn atom in $[\alpha_2\text{-}P_2(Bu^nSn)W_{17}O_{61}]^{7-}$ occupies a cap position. The X-ray structural analyses reported in this paper show that a cap atom is missing in $(NH_4)_{10}[\alpha_2\text{-}P_2W_{17}O_{61}]\cdot 8H_2O$ (I) and that a cap substituent is present in $(Me_2NH_2)_8[\alpha_2\text{-}P_2Co(II)(H_2O)W_{17}O_{61}]\cdot 11H_2O$ (II).

EXPERIMENTAL

Preparation of I *and* II

The preparation of I was exactly analogous to the procedure[4] for the K^+ salt. The compound was recrystallized from hot (70°C) water to give tablets bounded by {001} and {110} faces. Compound II was prepared as described previously,[6] or by the reaction of equimolar $[P_2W_{17}O_{61}]^{10-}$ and Co^{2+} in aqueous solution at 40°C followed by the addition of excess $(Me_2NH_2)Cl$; the crude product was redissolved in water, reprecipitated, and finally recrystallized twice from hot water to give prisms

with prominent {011} faces. Crystals of both compounds suitable for X-ray work were obtained by allowing slightly supersaturated aqueous solutions to stand at room temperature.

Crystallographic studies

The choice of salts for structural study was restricted not only by the availability of well-diffracting crystals of suitable size (eliminating, for instance, $K_{10}[P_2W_{17}O_{61}]\cdot aq$ which is always obtained as tiny laths) but by the requirement that the space-group and number of anions in the cell be consistent with a disorder-free structure. The K^+ and Rb^+ salts of $[X_2Z(II)(H_2O)W_{17}O_{61}]^{8-}$ (X = P or As; Z = Mn, Co, Ni or Zn), for example, are rhombohedral (R3 or $R\bar{3}$) with one anion in the primitive cell;[6,14] consequently, if the anion has the $[\alpha\text{-}P_2W_{18}O_{62}]^{6-}$ structure the Co atom must be disordered over three or six sites. Preliminary Weissenberg photographs of **II** indicated space-groups *Pnam* or $Pna2_1$ which for $Z = 4$ respectively impose mirror-symmetry or no symmetry on the anion. In the case of **I**, the possible space-groups *Cmca* or $C2_1ca$ respectively impose C_{2h}- or C_2-symmetry on the anion ($Z = 4$), neither of which is consistent with a well-ordered "defect" P_2W_{18}-type anion. Moreover, Weissenberg photographs showed a number of additional diffuse reflections at positions forbidden by the C-centering, and also regions of diffuse background scattering. Despite these indications of disorder, the structural analysis of **I** was undertaken in the hope that the heavy-atom framework at least could be distinguished.

Crystal data

I, $(NH_4)_{10}[P_2W_{17}O_{61}]\cdot 8H_2O$. Orthorhombic, *Cmca*, $a = 18.080(8)$, $b = 17.945(7)$, $c = 21.546(8)$ Å, $Z = 4$, $d_{calc.} = 4.26$ g cm^{-3}; Mo radiation ($\lambda = 0.71069$ Å), $\mu = 286$ cm^{-1}.

II, $(Me_2NH_2)_8[P_2Co(H_2O)W_{17}O_{61}]\cdot 11H_2O$. Orthorhombic, *Pnam*, $a = 28.052(11)$, $b = 15.069(12)$, $c = 20.638(17)$Å, $Z = 4$, $d_{calc.} = 3.66$ g cm^{-3}; Mo radiation ($\lambda = 0.71069$ Å), $\mu = 230$ cm^{-1}.

Data collection

Data for **I** and **II** were collected on an Enraf–Nonius CAD-4 diffractometer by ω–2θ scans in the 2θ ranges 2–40° (**I**) and 2–48° (**II**), after the refinement of cell parameters from the setting angles of 25 reflections in the 2θ ranges 22–24° (**I**) and 24–26° (**II**). In neither case was there evidence of crystal deterioration during data collection. The numbers of reflections for **I** were: total, 3635; unique, 1702; reflections with $|F| \geqslant 3\sigma(F)$, 1384. The corresponding figures for **II** are: 7603, 6962 and 3057 reflections.

Structure solution and refinement

The SHELX-76 program[15] was used for all calculations other than absorption correction. Approximate positions of the P and W atoms were readily obtained in each case by use of the direct-methods sub-programs EEES and TANG on the assumption that the centrosymmetric choice of space group (**I**, *Cmca*; **II**, *Pnam*) indicated by the *E* statistics was the correct one. The oxygen atoms of the anions were located in difference syntheses alternating with cycles of least-squares refinement. The presence of the Co atom in **II** as two composite atoms, $M = Co_{0.5}W_{0.5}$, related by the crystallographic mirror-plane was suggested by the appreciably larger value of U_{iso} for M when treated as W, and by the short M..M^i distance compared with other W..W distances. Separate Co and W positions at the M site could not be distinguished. After isotropic refinement of the P, Co and W atoms in **I**, and all anion atoms in **II**, the original set of unmerged $|F|$ values was subjected to an empirical absorption correction by means of the program DIFABS,[16] and refinement was continued after remerging the data. *Ab initio* structure solutions were also attempted with assumption of the alternative non-centrosymmetric space-groups, $C2_1ca$ for **I** and $Pna2_1$ for **II**. Essentially the same structures appeared [and in particular the same kinds of disorder (see Discussion)], with numerous strong correlations between the parameters for atoms related by symmetry in the original space-groups. Therefore the centrosymmetric space-groups were retained. A number of inter-anion atoms were located; but in the case of **II** it was clear that the $Me_2NH_2^+$ cations and lattice H_2O molecules were highly disordered, no C_2N units being clearly discernible, and only the strongest difference peaks were included (arbitrarily, as N) in the last cycles of refinement. Convergence was reached for **I** at $R = 0.067$, wR $(= [\Sigma w\Delta^2/\Sigma wF^2]^{1/2}) = 0.091$ for 1384 data, 180 parameters, full matrix, $w = [\sigma^2(F) + 0.0016F^2]^{-1}$ in the last cycle; and for **II** at $R = 0.069$, $wR = 0.090$ for 3057 data, 247 parameters, blocked matrix, $w = [\sigma^2(F) + 0.0026F^2]^{-1}$ in the last cycle.

DISCUSSION

Bond lengths and other intra-anion distances are shown in Table 1 for **I**, and in Table 2 for **II**. Atomic

Table 1. Bond lengths and other interatomic distances (Å) for **I**, $(NH_4)_{10}[P_2W_{17}O_{61}]\cdot 8H_2O$

P—OP(11)	1.54(7)	W(3)—O(33)	1.87(2)
P—OP(12)	1.51(4)	W(3)—O(35)	1.88(3)
P—OP(23)	1.55(5)	W(3)—O(13)	1.90(4)
P—OP(33)	1.53(7)	W(3)—OP(23)	2.39(5)
P—OP(46)	1.55(4)	W(3)—OP(33)	2.40(7)
W(1)—O(1)	1.68(3)	W(4)—O(24)	1.95(3)
W(1)—O(11)	1.87(4)	W(4)—O(14)	1.95(3)
W(1)—O(11A)	2.07(5)	W(4)—O(4)	1.72(6)
W(1)—O(12)	1.81(4)	W(4)—O(44)	1.87(3)
W(1)—O(13)	1.95(4)	W(4)—O(46)	2.03(8)
W(1)—O(14)	1.83(3)	W(4)—OP(46)	2.35(4)
W(1)—OP(11)	2.45(7)	W(5)—O(35)	2.07(3)
W(1)—OP(12)	2.45(5)	W(5)—O(24)	2.05(3)
W(2)—O(2)	1.68(3)	W(5)—O(5)	1.65(7)
W(2)—O(12)	1.93(4)	W(5)—O(57)	1.80(6)
W(2)—O(23)	1.76(4)	W(5)—O(55)	1.91(6)
W(2)—O(22)	1.88(4)	W(5)—OP(46)	2.38(4)
W(2)—O(24)	1.92(3)	W(6)—O(6)	1.68(4)
W(2)—OP(12)	2.29(5)	W(6)—O(35)	1.99(3)
W(2)—OP(23)	2.29(5)	W(6)—O(46)	2.02(7)
W(3)—O(3)	1.70(3)	W(6)—OP(46)	2.27(4)
W(3)—O(23)	1.89(3)		
W(1)..W(1^{i})[a]	3.489(4)	W(3)..W(6)	3.640(6)
W(1)..W(2)	3.505(4)	W(4)..W(4^{i})	3.379(6)
W(1)..W(3^{ii})	3.820(4)	W(4)..W(6)	3.361(6)
W(1)..W(4)	3.576(5)	W(5)..W(5^{i})	3.328(6)
W(2)..W(2^{ii})	3.760(4)	W(1)..P	3.485(16)
W(2)..W(3)	3.478(4)	W(2)..P	3.515(16)
W(2)..W(4)	3.668(5)	W(3)..P	3.502(16)
W(2)..W(5)	3.757(5)	W(4)..P	3.451(17)
W(3)..W(3^{i})	3.529(4)	W(5)..P	3.521(17)
W(3)..W(5)	3.757(5)	W(6)..P	3.383(15)

[a] i = $-x, y, z$; ii = $-x, -y, -z$.

coordinates and thermal parameters have been deposited as supplementary data.

The heavy-atom framework in the parent $[\alpha\text{-}P_2W_{18}O_{62}]^{6-}$ anion[2] is retained in the anion of **I**, but with a vacancy at one cap position. The anion has symmetry m (C_s), but occupies a site of crystallographic symmetry $2/m$(C_{2h}) in two equally-weighted orientations related by the inversion centre midway between the P atoms (or equivalently, by the crystal diad axis normal to the P..P vector). This disorder is illustrated in Fig. 1. The act of inversion brings each belt W atom into near coincidence with an atom of the other belt, to give "composite" belt atoms W(1,2,3) whose components could not be resolved. In $[\alpha\text{-}P_2W_{18}O_{62}]^{6-}$, WO_6 octahedra in the same belt share edges and corners alternately,[2] with averaged W..W distances of 3.36 and 3.68 Å, respectively; in **I**, the apparent W..W distances within each belt have intermediate values, 3.48–3.53 Å. The other W..W distances (Table 1) are clearly consistent with edge-sharing between WO_6 octahedra in the same cap, with corner-sharing between adjacent cap and belt octahedra, and with corner-sharing between octahedra in different belts. The composite belt atoms W(1,1^{i},2,2^{i},3,3^{i}), where "i" denotes reflection at $x = 0$, are coplanar [maximum deviation 0.020 Å for W(2,2^{i}), towards centre of anion]. Their mean plane is parallel to the plane of the atoms of the unbroken cap, W(4,4^{i},6) (dihedral angle 0.16°). Distortions arising from the removal of a W atom from the other cap are shown by the displacement of the remaining atoms W(5,5^{i}) from the W(4,4^{i},6) plane by 0.14 Å (away from the centre of the anion), and by the angles between the P..P vector and the normals to the W(1,1^{i},2,2^{i},3,3^{i}) and W(4,4^{i},6) planes, respectively 1.1 and 1.3°. Oxygen atoms of the anion were also located, with the restriction that a number of oxygen atoms in one orientation of the anion nearly coincide with oxygens in the superimposed inverse orientation (par-

Table 2. Bond lengths and other interatomic distances (Å) for **II**, $(Me_2NH_2)[P_2Co(H_2O)W_{17}O_{61}]\cdot 11H_2O$

W(1)—O(1)	1.62(6)	W(6)—O(23)	2.32(3)
W(1)—O(2)	2.33(4)	W(6)—O(24)	1.93(3)
W(1)—O(3)	1.92(4)	W(6)—O(25)	1.90(3)
W(1)—O(4)	1.88(4)	W(7)—O(16)	1.96(4)
W(2)—O(2)	2.37(4)	W(7)—O(25)	1.88(3)
W(2)—O(4)	1.98(4)	W(7)—O(26)	1.70(4)
W(2)—O(5)	1.91(3)	W(7)—O(27)	1.92(3)
W(2)—O(6)	1.74(4)	W(7)—O(28)	2.36(3)
W(2)—O(7)	1.93(3)	W(7)—O(29)	1.93(3)
W(2)—O(8)	1.93(2)	W(8)—O(12)	1.91(3)
W(3)—O(3)	1.89(4)	W(8)—O(27)	1.86(3)
W(3)—O(9)	1.69(4)	W(8)—O(28)	2.24(3)
W(3)—O(10)	1.91(2)	W(8)—O(30)	1.66(3)
W(3)—O(11)	1.79(4)	W(8)—O(31)	1.88(1)
W(3)—O(12)	1.91(3)	W(8)—O(32)	1.85(3)
W(3)—O(13)	2.35(3)	M(9)—O(24)	1.85(3)
W(4)—O(5)	1.92(3)	M(9)—O(29)	1.92(4)
W(4)—O(11)	1.98(4)	M(9)—O(33)	2.35(3)
W(4)—O(13)	2.38(4)	M(9)—O(34)	1.66(5)
W(4)—O(14)	1.64(4)	M(9)—O(35)	1.88(3)
W(4)—O(15)	1.90(3)	M(9)—O(36)	1.97(3)
W(4)—O(16)	1.87(4)	W(10)—O(32)	1.98(3)
W(5)—O(7)	1.93(3)	W(10)—O(33)	2.35(4)
W(5)—O(15)	1.86(3)	W(10)—O(36)	1.90(3)
W(5)—O(17)	1.74(3)	W(10)—O(37)	1.68(5)
W(5)—O(18)	1.96(3)	P(1)—O(2)	1.58(4)
W(5)—O(19)	2.31(3)	P(1)—O(13)	1.49(4)
W(5)—O(20)	1.90(3)	P(1)—O(19)	1.61(5)
W(6)—O(20)	1.93(6)	P(2)—O(23)	1.56(4)
W(6)—O(21)	1.62(4)	P(2)—O(28)	1.60(3)
W(6)—O(22)	1.90(2)	P(2)—O(33)	1.54(4)
W(1)..W(2)	3.373(5)	W(7)—M(9)	3.713(4)
W(1)..W(3)	3.709(4)	W(8)..W(8^{i})	3.651(3)
W(2)..W(2^{i})[a]	3.373(4)	W(8)..W(10)	3.720(4)
W(2)..W(4)	3.702(4)	M(9)..M(9^{i})	3.244(5)
W(2)..W(5)	3.696(4)	M(9)..W(10)	3.342(5)
W(3)..W(3^{i})	3.648(3)	P(1)..W(1)	3.511(18)
W(3)..W(4)	3.356(4)	P(1)..W(2)	3.498(17)
W(3)..W(8)	3.761(3)	P(1)..W(3)	3.494(17)
W(4)..W(5)	3.656(3)	P(1)..W(4)	3.512(17)
W(4)..W(7)	3.778(3)	P(1)..W(5)	3.519(17)
W(5)..W(5^{i})	3.359(3)	P(2)..W(6)	3.488(17)
W(5)..W(6)	3.768(3)	P(2)..W(7)	3.509(17)
W(6)..W(6^{i})	3.361(3)	P(2)..W(8)	3.504(17)
W(6)..W(7)	3.634(3)	P(2)..M(9)	3.455(18)
W(6)..M(9)	3.680(4)	P(2)..W(10)	3.507(19)
W(7)..W(8)	3.349(3)		

[a] i = $x, y, \frac{1}{2}-z$.

ticularly atoms shared between WO_6 octahedra in the same belt or in different belts); in such cases only composite atoms could be located, except for O(11) and O(11A) which are shared between W(1) and W(1^{i}). Therefore too much significance should not be attributed to the apparent bond lengths (Table 1). Oxygen atoms in PO_4 tetrahedra and in cap WO_6 octahedra were clearly resolved. It was possible to disentangle the superimposed structures, and a view of a single orientation of the anion is shown in Fig. 2.

The $[P_2Co(H_2O)W_{17}O_{61}]^{8-}$ anion in **II** is shown

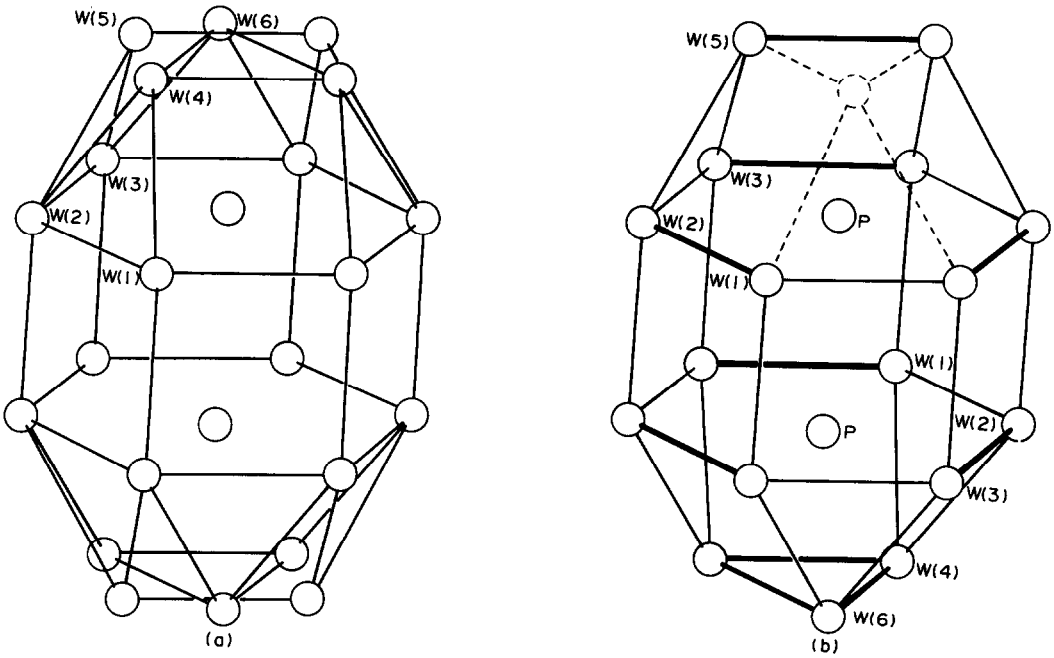

Fig. 1. $[\alpha_2\text{-}P_2W_{17}O_{61}]^{10-}$ anion in **I**. (a) The heavy-atom framework ($2/m$ symmetry) apparent from diffraction data. (b) The anion framework (m-symmetry) in one of the two superimposed orientations. Thick lines imply that WO_6 octahedra share edges, and thin lines that they share corners. The dashed lines indicate the missing W atom and its connections.

in Fig. 3. As expected from the results for **I**, the Co substituent occupies a cap position, on one of the vertical mirror-planes of the parent $[\alpha\text{-}P_2W_{18}O_{62}]^{6-}$ anion of D_{3h}-symmetry.[2] However, this mirror-plane does not coincide with the crystallographic mirror-plane which bisects the anion in **II**, passing through P(1), P(2), W(1) and W(10); instead, the Co atom is distributed equally over the sites M(9) and M(9^i) related by the crystallographic mirror-

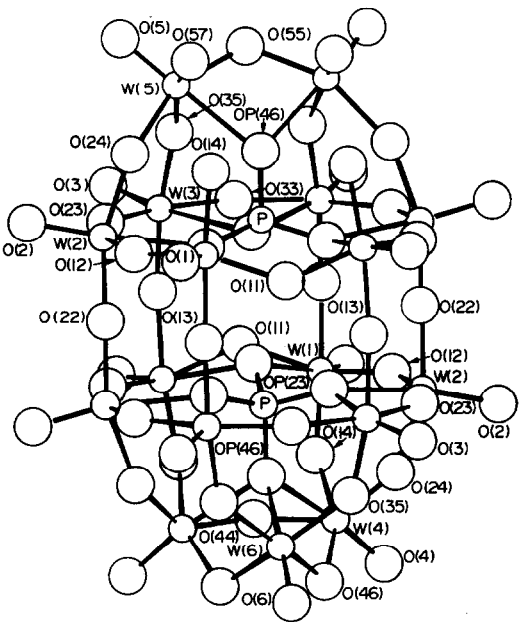

Fig. 2. W—O and P—O bond network in $[\alpha_2\text{-}P_2W_{17}O_{61}]^{10-}$.

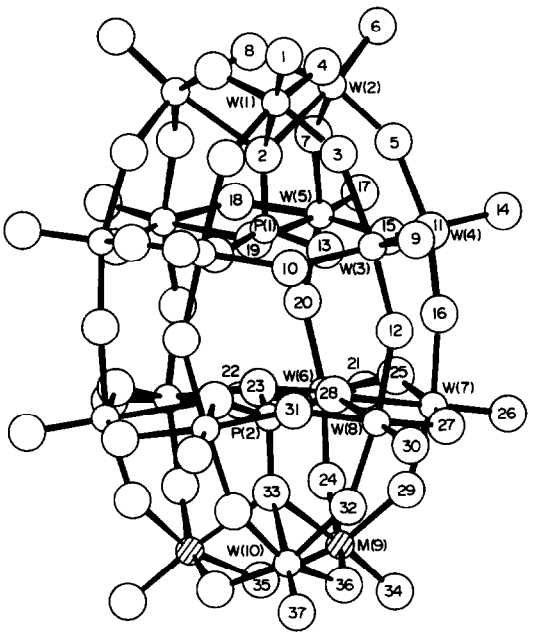

Fig. 3. $[\alpha_2\text{-}P_2Co(H_2O)W_{17}O_{61}]^{8-}$ anion in **II**. Atoms P(1), P(2), W(1) and W(10) lie on a crystal mirror plane. Each hatched atom [M(9)] is composite ($Co_{0.5}W_{0.5}$).

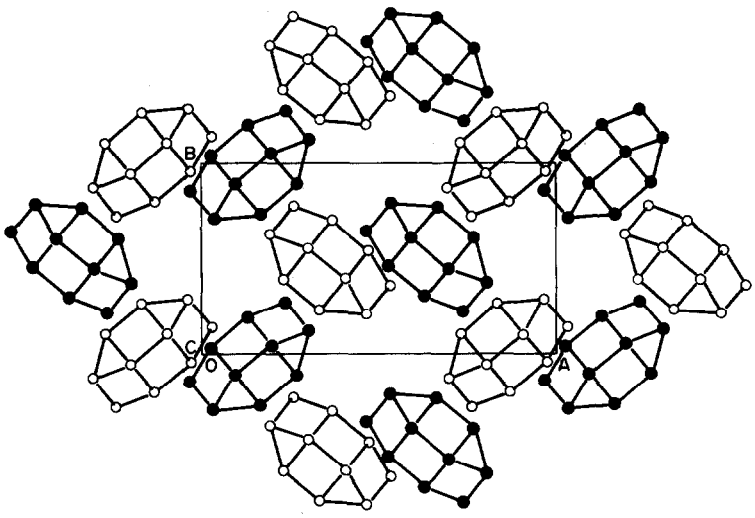

Fig. 4. Packing of anions (represented by their heavy-atom frameworks) in **II**. Filled and open circles denote anions lying on mirror planes at $z = \frac{1}{4}$ and $z = \frac{3}{4}$, respectively. The view is down the *c*-axis.

plane as composite atoms M = $Co_{0.5}W_{0.5}$. The situation is analogous with that in $Na_2(NMe_4)_4[\alpha\text{-}HPW_{11}O_{39}]\cdot 7H_2O$,[17] whose anion has a defect $[\alpha\text{-}PW_{12}O_{40}]^{3-}$ structure; there the tungsten vacancy is observed as two half-vacancies related by a crystallographic mirror-plane which does not coincide with the true mirror-plane of the anion. In **II**, the M(9)..M(9^i) distance of 3.24 Å is significantly shorter than the W(10)..M(9) distance in the same cap (3.34 Å) and the W..W distances in the other cap (3.37 Å), and approaches the shorter Co..Co distances found for edge-sharing CoO_6 groups in $[P_5Co_9W_{27}O_{119}H_{17}]^{16-}$ (3.20–3.21 Å)[18] and $[P_2Co_4W_{18}O_{70}H_4]^{10-}$ (3.16 and 3.19 Å).[19] Other W..W distances and W—O bond lengths in $[\alpha_2\text{-}P_2Co(H_2O)W_{17}O_{61}]^{8-}$ (Table 2) are similar to corresponding distances in $[\alpha\text{-}P_2W_{18}O_{62}]^{6-}$. The terminal oxygen atom O(34) on M(9) is H_2O for M = Co and is unprotonated for M = W. The former assignment is supported by the observation[20] that changes in the solution spectrum of the anion in the region of the ligand-field band of Co at 18,300 cm^{-1} are seen in the presence of potential ligands such as N_3^-, NCS^-, pyridine and methylpyridines, and in mixed solvents (H_2O–MeCN and H_2O–dmso); similar changes have been observed for $[PCo(H_2O)W_{11}O_{39}]^{5-}$ and interpreted[21] as showing the replacement of ligand H_2O at Co.

The packing of the anions in and near one unit cell of **II** is shown in Fig. 4. The anions form layers normal to *c*, in a loose approximation of hexagonal packing, the distances between centroids of neighbouring anions ranging from 13.6 to 16.4 Å. There are voids above and below each anion in the *c*-direction, and also channels extending parallel to *c*. The $Me_2NH_2^+$ cations and lattice water molecules, few of whose atoms could be located, are disordered in these spaces.

Acknowledgements—I thank the Science and Engineering Research Council for access to the X-ray Crystallographic Service, and Dr A. J. Welch for collecting the intensity data.

REFERENCES

1. B. Dawson, *Acta Cryst.* 1953, **6**, 113.
2. H. D'Amour, *Acta Cryst.* 1976, **B32**, 729.
3. M. T. Pope, *Heteropoly and Isopoly Oxometalates*, p. 70. Springer, Berlin (1983).
4. P. Souchay, *Ions Minéraux Condensés*, p. 107. Masson, Paris (1969).
5. C. Tourné, *C. R., Ser. C.* 1968, **266**, 702.
6. S. A. Malik and T. J. R. Weakley, *J. Chem. Soc., Dalton Trans.* 1968, 2647.
7. R. D. Peacock and T. J. R. Weakley, *J. Chem. Soc., Dalton Trans.* 1971, 1836.
8. V. N. Molchanov, L. P. Kazanskii, E. A. Torchenkova and V. I. Simonov, *Kristallografiya* 1978, **24**, 167.
9. R. Massart, R. Contant, J. M. Fruchart, J.-P. Ciabrini and M. Fournier, *Inorg. Chem.* 1977, **16**, 2916.
10. R. Contant and J.-P. Ciabrini, *J. Chem. Res.* 1977, (S) 222, (M) 2601.
11. L. P. Kazanskii, *Koord. Khim.* 1976, **2**, 719.
12. R. Acerete, S. Harmalker, C. F. Hammer, L. C. W. Baker and M. T. Pope, *J. Chem. Soc., Chem. Commun.* 1979, 777.
13. R. L. Firor, unpublished work; quoted by F. Zonnevijlle and M. T. Pope, *J. Am. Chem. Soc.* 1979, **101**, 2731.
14. C. M. Tourné and G. Tourné, *C. R., Ser. C.* 1968, **266**, 1363.

15. G. M. Sheldrick, *SHELX-76 Program for Crystal Structure Determination*. Cambridge University (1975).
16. N. Walker and D. Stuart, *Acta Cryst.* 1983, **A39**, 158.
17. J. Fuchs, A. Thiele and R. Palm, *Z. Naturforsch.* 1981, **36B**, 544.
18. T. J. R. Weakley, *J. Chem. Soc., Chem. Commun.* 1984, 1406.
19. H. T. Evans, C. M. Tourné, G. F. Tourné and T. J. R. Weakley, *J. Chem. Soc., Dalton Trans.* (in press).
20. T. J. R. Weakley, unpublished work.
21. T. J. R. Weakley, *J. Chem. Soc., Dalton Trans.* 1973, 341.

Polyhedron Vol. 6, No. 5, pp. 939–941, 1987
Printed in Great Britain

0277–5387/87 $3.00+.00

COCONDENSATION REACTION OF DISULPHURDINITRIDE WITH NICKEL ATOMS: THE PREPARATION OF $Ni(S_2N_2H)_2$

J. DEREK WOOLLINS*

School of Chemical Sciences, University of East Anglia, Norwich NR4 7TJ, U.K.

(*Received* 4 *July* 1986; *accepted* 4 *September* 1986)

Abstract—The utility of metal atom vapour synthesis in the preparation of metalla-sulphur–nitrogen compounds has been investigated. Reaction of nickel atoms with disulphurdinitride, S_2N_2, gave, after extraction with methanol, $Ni(S_2N_2H)_2$ in *ca* 15% yield.

Cocondensation reactions between metal vapours and organic ligands have become widely accepted for the preparation of organometallic compounds and the advantages of this method have been discussed.[1,2] We are involved in the preparation of metalla-sulphur–nitrogen compounds[3–5] and one important area is the development of rational, general syntheses. A particularly important group of compounds are those which involve the disulphurdinitrido dianion or its protonated analogue $S_2N_2H^-$ since they can adopt[6] stacking structures in, for example, compounds of type $[Pt(S_2N_2H)(PR_3)_2]X$. We have developed a number of wet chemical routes to these complexes but, to date, attempts to extend the range of metals have been unsuccessful. An alternative strategy is the direct reaction of disulphurdinitride with metal atoms. Here we report on the first successful preparation of an M–S–N complex $[Ni(S_2N_2H)_2$ (**1**)] by metal vapour synthesis.

EXPERIMENTAL

CARE: the procedure described involves S_4N_4 and S_2N_2, both of which are known to be explosive.

The apparatus used (Fig. 1) consisted of a section for the preparation of S_2N_2 based on the design of Mikulski[7] and a reactor similar to that used by Timms.[8] Youngs stopcocks and greaseless taps were used throughout. The nickel vapour was generated using a multifilament consisting of two 15-cm strands of 0.4-mm tungsten wire and 5 cm of 0.3-mm nickel wire; this could be used for three or four runs before becoming too brittle to handle.

Preparation of S_2N_2

In a typical experiment the apparatus was charged with S_4N_4 (0.7 g, freshly recrystallized from benzene) and silver wool (1.0 g BDH MAR grade). After evacuating the system to 10^{-5}–10^{-6} torr overnight the temperature of the furnace around the silver wool was brought to 300°C and an oil bath was placed around the lower part of the apparatus (with only 0.5 cm between the top of the oil bath and the bottom of the furnace). The temperature of the oil bath was raised to 90°C and the cold finger filled with liquid nitrogen. Within a few minutes a light tan coloured coating could be seen on the cold finger. The reaction was maintained until no S_4N_4 remained, usually 8–10 h. After this time tap (a) was closed, U-tube (1) surrounded by liquid N_2 and the liquid N_2 in the cold finger was blown out with a stream of N_2. Pumping overnight (with U-tube (1) surrounded by liquid N_2) gave pure S_2N_2 in the U-tube. In a typical run *ca* 0.4 g of S_2N_2 was obtained. At this stage if the taps on the U-tube are closed and it is surrounded by a salt–ice bath polymerization occurs and lustrous bronze crystals of $(SN)_x$ are obtained after 2–3 days.

NOTE: S_2N_2 is extremely explosive and can spontaneously detonate at room temperature!

Preparation of $Ni(S_2N_2H)_2$

The W/Ni filament was slowly warmed to its operating temperature (*ca* 1350°C) and the reactor

* Present address: Department of Chemistry, Imperial College of Science and Technology, South Kensington, London SW7 2AY, U.K.

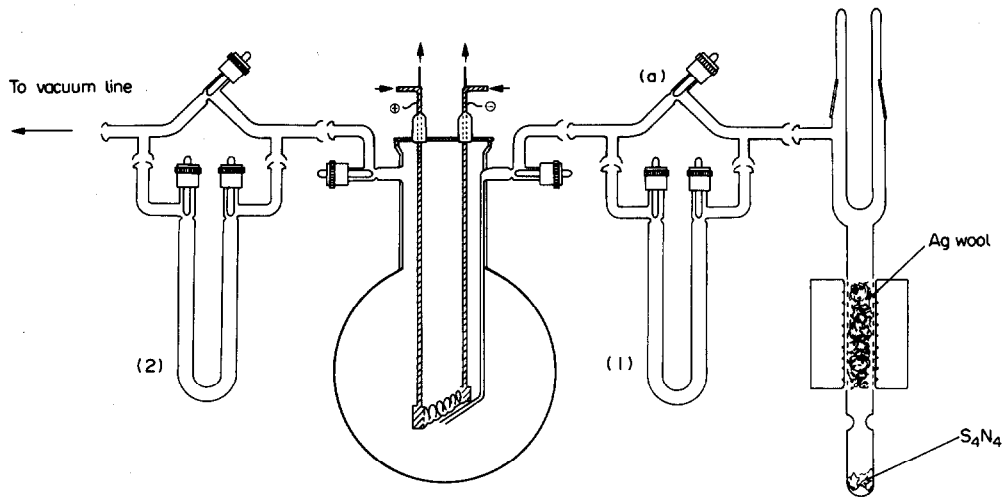

Fig. 1. Apparatus used for the preparation and reaction of S_2N_2 with nickel vapour.

surrounded by liquid N_2 whereupon the liquid N_2 trap surrounding U-tube (1) was replaced by a salt–ice bath allowing S_2N_2 to sublime over into the reaction vessel. At these temperatures in 2 h all of the S_2N_2 sublimed into the reactor and *ca* 45 mg of nickel was evaporated. At the end of the reaction the liquid N_2 was removed from around the reactor and U-tube (2) cooled to enable excess S_2N_2 to be sublimed off overnight.

Attempts to sublime the remaining dark coloured solid in the reactor onto a liquid-N_2 cold finger were unsuccessful. However, it was possible to obtain a violet solution by extraction of the solid with cold methanol. Evaporation of this methanol solution gave **1**, which was identified by UV–VIS and IR spectroscopy.[9,10] Yields varied between 15 and 30 mg of product, depending on the weight of nickel evaporated but were never less than 10% and were generally *ca* 15%.

RESULTS AND DISCUSSION

Cocondensation reaction of nickel atoms with S_2N_2 proceeds to give a dark solid which did not sublime at 10^{-4} torr and 90°C. This material may be a polymeric S_2N_2 adduct and is probably similar to the intractable solid reported[11] from the reaction of $Ni(CO)_4$ and S_4N_4. On treatment with methanol the known complex **1** is obtained:

$$Ni(g) + S_2N_2 \rightarrow [Ni(S_2N_2)]_x \xrightarrow{MeOH} Ni(S_2N_2H)_2.$$

It has been reported[12] that reaction of finely divided nickel powder with S_2N_2 in methanol also gives rise to **1** in low yield and so as to ascertain if this process was occurring here we performed some blank experiments. Thus we condensed nickel vapour followed by S_2N_2 and did not sublime away any S_2N_2 at the end of the process. Extraction with methanol did not result in immediate formation of **1** with the UV spectrum consisting of a single band (λ_{max} 268 nm) due to S_2N_2. If the unfiltered extract, which contained flakes of nickel, was allowed to stand after 5 days a UV–VIS spectrum corresponding to *ca* 5 mg of **1** was observed. In the vapour synthesis procedure excess S_2N_2 was sublimed out of the reactor before addition of methanol. Also we observed an immediate colouration of the alcohol on its addition in the cocondensation reactions and the alcohol was filtered directly after extraction in this case. Clearly, the product obtained derives from the cocondensation reaction and not a simple reaction between nickel and a solution of S_2N_2.

Although the yield obtained here using a relatively complex procedure is not as good as the traditional wet chemical method the results obtained do suggest that the vapour synthesis technique may offer some potential in the preparation of metalla-sulphur–nitrogen compounds and further studies would be worthwhile.

Acknowledgements—I am grateful to Johnson Matthey for support and to Dr R. Grinter and Prof A. J. Thomson for their keen interest.

REFERENCES

1. P. L. Timms, *Adv. Inorg. Radiochem.* 1972, **14**, 122.
2. M. Moskovitz and G. A. Ozin, Eds, *Cryochemistry*. Wiley Interscience, New York (1976).
3. P. F. Kelly and J. D. Woollins, *Polyhedron* 1986, **5**, 607.

4. R. Jones, P. F. Kelly, D. J. Williams and J. D. Woollins, *Polyhedron* 1985, **4**, 1947.
5. J. D. Woollins, *Polyhedron* 1984, **3**, 1365.
6. R. Jones, P. F. Kelly, C. P. Warrens, D. J. Williams and J. D. Woollins, *J. Chem. Soc., Chem. Commun.* 1986, 711.
7. C. M. Mikulski, P. J. Russo, M. S. Saran, A. G. MacDiarmid, A. F. Garito and A. J. Heeger, *J. Am. Chem. Soc.* 1975, **97**, 6358.
8. P. L. Timms, *J. Chem. Ed.* 1972, **49**, 783.
9. J. D. Woollins, R. Grinter, M. K. Johnson and A. J. Thomson, *J. Chem. Soc., Dalton Trans.* 1980, 1910.
10. D. B. Powell and J. D. Woollins, *Spectrochim. Acta* 1980, **A36**, 447.
11. M. Goehring and A. Debo, *Z. Anorg. Allg. Chem.* 1953, **273**, 319.
12. M. Goehring and D. Voigt, *Naturwissenschaften* 1953, **40**, 482.

Polyhedron Vol. 6, No. 5, pp. 943–946, 1987
Printed in Great Britain

0277–5387/87 $3.00+.00

ELECTRON-TRANSFER REACTIONS OF COPPER(II) COMPLEXES CONTAINING THIOETHER SULFUR AND PYRIDYL NITROGEN DONORS WITH FERROCENE AND 1,1′-DIMETHYLFERROCENE

NOBUO AOI, GEN-ETSU MATSUBAYASHI and TOSHIO TANAKA*

Department of Applied Chemistry, Faculty of Engineering, Osaka University, Yamadaoka, Suita, Osaka 565, Japan

(*Received* 21 *July* 1986; *accepted* 4 *September* 1986)

Abstract—Kinetic studies were carried out for the electron-transfer reactions of [Cu(II)L][ClO_4]$_2$ [L = 1,6-bis(2-pyridyl)-2,5-dithiahexane, 1,7-bis(2-pyridyl)-2,6-dithiaheptane, or 1,8-bis(2-pyridyl)-3,6-dithiaoctane] with ferrocene (fc) and 1,1′-dimethylferrocene (Me_2fc), and of [Cu(II)L′$_2$][ClO_4]$_2$ [L′ = 4-(alkylmercaptomethyl)imidazole; alkyl = Me, Et, Pr^n, CH_2Ph or Bu^t] with fc in acetonitrile at 25°C. The electron-transfer reactions are suggested to proceed via a precursor complex, [Cu(II)L · Red], existing in an equilibrium state:

$$[Cu(II)L]^{2+} + Red \rightleftharpoons[Cu(II)L \cdot Red]^{2+} \xrightarrow{k_{et}} [Cu(I)L]^{+} + Red^{+} \quad (Red = fc \text{ or } Me_2fc).$$

In a previous paper dealing with the electron-transfer reactions of Cu(II)N_2S_2 type complexes, bis[(4-alkyl- and phenylmercaptomethyl)imidazole] copper(II) diperchlorate (alkyl = Pr^n, CH_2Ph or Bu^t) and 1,6-bis(4-imidazolyl)-2,5-dithiahexanecopper(II) diperchlorate, as a model of an active site of blue copper (Type I) proteins with ferrocene, we reported the formation of a precursor complex prior to the electron transfer.[1] In order to further understand the mechanism for the electron-transfer reaction of the Cu(II)N_2S_2 type complexes, we have undertaken a study of the reactions of the copper(II) complexes coordinated by pyridyl nitrogen and thioether sulfur atoms with ferrocene (fc) and 1,1′-dimethylferrocene (Me_2fc).

This paper reports the kinetics of the electron-transfer reactions of [Cu(II)L][ClO_4]$_2$ [L = 1,6-bis(2-pyridyl)-2,5-dithiahexane (**1**), 1,7-bis(2-pyridyl)-2,6-dithiaheptane (**2**), and 1,8-bis(2-pyridyl)-3,6-dithiaoctane (**3**)] with fc and Me_2fc, and of [Cu(II)L′$_2$][ClO_4]$_2$ [L′ = 4-(alkylmercaptomethyl)-imidazole; alkyl = Me (**4**), Et (**5**), Pr^n (**6**), CH_2Ph (**7**) and Bu^t (**8**)] with fc in acetonitrile.

* Authors to whom correspondence should be addressed.

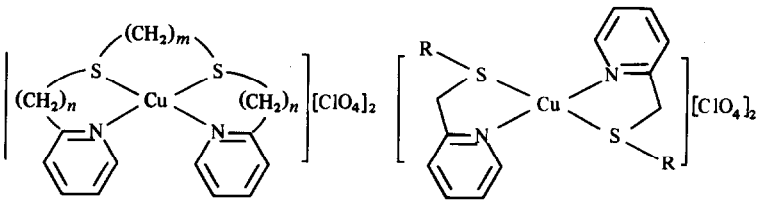

[Cu(II)L][ClO_4]$_2$
m = 2, n = 1 (**1**)
m = 3, n = 1 (**2**)
m = 2, n = 2 (**3**)

[Cu(II)L′$_2$][ClO_4]$_2$
R = Me (**4**), Et (**5**), Pr^n (**6**), CH_2Ph (**7**), or Bu^t (**8**)

Scheme 1.

EXPERIMENTAL

Materials

The Cu(II)N_2S_2 type complexes **1–3**[2,3] and **4–8**[4] were prepared according to the literature. Commercially available fc and Me_2fc were purified by sublimation and recrystallization before use, respectively.

Kinetic measurements

Reaction rates were determined by monitoring the decay of absorbance at a wavelength in the 300–400-nm range absorbed by the copper(II) complexes in acetonitrile using a Union RA-103 stopped-flow spectrophotometer equipped with a 0.2- or 1.0-cm quartz cell in a cell-holder thermostatted at 25±0.2°C. All the kinetic measurements were carried out under pseudo-first-order conditions with at least five-fold excess amounts of fc or Me_2fc relative to the copper(II) complexes (9.7×10^{-5}–1.2×10^{-4} mol dm^{-3}) under a nitrogen atmosphere. Observed pseudo-first-order rate constants, k_{obsd}, were obtained by the least-squares curve fitting using a Union System 77 microcomputer.

RESULTS AND DISCUSSION

Complexes **1–3** exhibit a strong absorption band due to the sulfur-to-copper charge-transfer transition at 330–370 nm.[4] When either the copper(II) complex was mixed with fc or Me_2fc in acetonitrile, the charge-transfer band was weakened in intensity and a band due to the ferrocenium (fc^+) or 1,1′-dimethylferrocenium cation (Me_2fc^+) concurrently appeared at 618 (fc^+) or 652 nm (Me_2fc^+). This is indicative of the occurrence of the redox reaction [eqn (1)]:

$$[Cu(II)L]^{2+} + Red \rightarrow [Cu(I)L]^{+} + Red^{+}, \quad Red = fc \text{ or } Me_2fc \quad (1)$$

being similar to the reaction of bis[4-(alkyl- and phenylmercaptomethyl)imidazole]copper(II) diperchlorates (alkyl = Pr^n, Bu^t or CH_2Ph) and 1,6-bis(4-imidazolyl)-2,5-dithiahexanecopper(II) diperchlorate with fc.[1]

The pseudo-first-order rate constants, k_{obsd}, obtained in the reaction of **1** with excess amounts of fc are listed in Table 1. No linear relation can be seen between the k_{obsd} value and the initial concentration of fc ([fc]), as depicted in Fig. 1. This is suggestive of the existence of a pre-equilibrium process [eqn (2)] prior to the electron-transfer reaction [eqn (3)]:

Table 1. k_{obsd} for the reaction of complex **1** (1.08×10^{-4} mol dm^{-3}) with fc in acetonitrile containing $[Bu^n_4N][BF_4]$ (0.1 mol dm^{-3}) at 25°C

[fc] (mol dm^{-3})	k_{obsd} (s^{-1})
1.06×10^{-3}	1.28±0.02
1.76×10^{-3}	2.08±0.09
2.64×10^{-3}	2.69±0.10
3.52×10^{-3}	3.36±0.19
5.28×10^{-3}	4.61±0.16

$$[Cu(II)L]^{2+} + fc \overset{K}{\rightleftharpoons} [Cu(II)L\cdot fc]^{2+}, \quad (2)$$

$$[Cu(II)L\cdot fc]^{2+} \xrightarrow{k_{et}} [Cu(I)L]^{+} + fc^{+}, \quad (3)$$

where K is the formation constant of a precursor complex, $[Cu(II)L\cdot fc]^{2+}$, and k_{et} is the rate constant of the electron-transfer process. According to this scheme, the k_{obsd} value in the presence of large excess amounts of fc can be expressed by eqn (4), which is transformed to eqn (5):

$$k_{obsd} = \frac{k_{et}K[fc]}{1+K[fc]}, \quad (4)$$

$$\frac{1}{k_{obsd}} = \frac{1}{k_{et}K[fc]} + \frac{1}{k_{et}}. \quad (5)$$

This equation predicts a linear relation between k_{obsd}^{-1} and $[fc]^{-1}$. In fact, there can be seen a linear relation between these values, as shown in Fig. 2, supporting the reaction mechanism of eqns (2) and (3). The K and k_{et} values determined from the slope

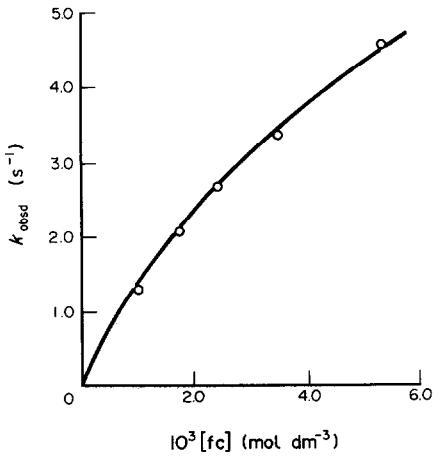

Fig. 1. Plot of k_{obsd} against [fc] for the reaction of complex **1** with fc in acetonitrile at 25°C.

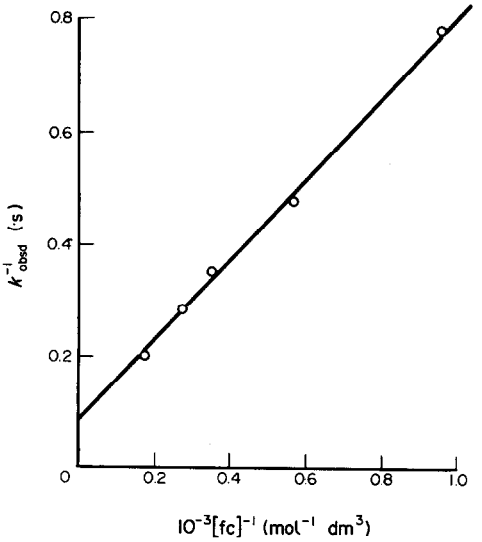

Fig. 2. Plot of k^{-1}_{obsd} against [fc]$^{-1}$ for the reaction of complex **1** with fc in acetonitrile at 25°C.

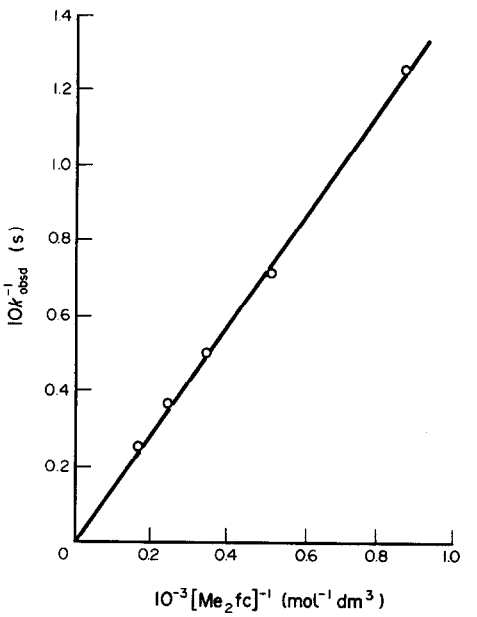

Fig. 3. Plot of k^{-1}_{obsd} against [Me$_2$fc]$^{-1}$ for the reaction of complex **1** with Me$_2$fc in acetonitrile at 25°C.

of the straight line and the intercept, respectively, are shown in Table 2, together with those values obtained similarly for the reactions of **2** and **3** with fc.

In the reaction of **1** with Me$_2$fc, however, there exists a linear relation between k^{-1}_{obsd} and the reciprocal of the initial concentration of Me$_2$fc, [Me$_2$fc]$^{-1}$, as shown in Fig. 3. This result may be explained in terms of the relation $K \ll k_{et}$, which may arise either from a K value small enough to be neglected or from a sufficiently large k_{et} value so that the reciprocal value can be neglected in eqn (5), under the assumption of the mechanism shown by eqns (2) and (3). Reactions of **2** and **3** with Me$_2$fc were similarly analyzed. Kinetics of the reactions of **4**–**8** with fc in acetonitrile were also analyzed in the same manner as those of the reactions of **1**–**3** with Me$_2$fc. The k_2 ($= k_{et}K$) values for the reactions of **1**–**3** with Me$_2$fc and of **4**–**8** with fc are listed in Table 3.

Another mechanism for the electron-transfer reaction without the formation of any precursor complexes may be considered as reported for the reaction of bis[2,9-dimethyl-4,7-bis(sulfonyloxyphenyl)-1,10-phenanthroline]copper(II) diperchlorate with sodium hexacyanoferrate(II) in water.[5] This reaction has been formulated as eqns (6) and (7):

$$[\text{Cu(II)L}]^{2+} \underset{k_{-1}}{\overset{k_1}{\rightleftharpoons}} [\text{Cu(II)L}]^{2+*} \qquad (6)$$

Table 2. K and k_{et} values for the reactions of the copper(II) complexes with fc in acetonitrile containing [Bu$^n_4$N][BF$_4$] (0.1 mol dm^{-3}) at 25°C

Complex	K (mol^{-1} dm^3)	k_{et} (s^{-1})
1	110±10	12±1
2	42±9	50±11
3	66±15	860±200

Table 3. k_2 ($= k_{et}K$) values for the reactions of the copper(II) complexes with fc and Me$_2$fc, and $E^{0\prime}$ values of the copper(II) complexes[a]

Complex	$10^{-4}k_2$ (mol^{-1} dm^3 s^{-1})	$E^{0\prime}$[b] (V)
	For the reactions with fc	
1	0.698±0.008	0.49
2	1.75±0.01	0.55
3	16.5±0.2	0.64
	For the reactions with Me$_2$fc	
4	8.22±0.28	0.66
5	11.0±0.6	0.68
6	12.5±0.3	0.69
7	32.0±2.3	0.72
8	44.2±4.0	0.73

[a] In acetonitrile containing [Bu$^n_4$N][BF$_4$] (0.1 mol dm^{-3}) at 25°C.

[b] $E^{0\prime} = (E_{pc} + E_{pa})/2$ (Ref. 4).

$$[Cu(II)L]^{2+*} + Red \xrightarrow{k_{et}} [Cu(I)L]^{+} + Red^{+}. \quad (7)$$

where $[Cu(II)L]^{2+}$ and $[Cu(II)L]^{2+*}$ stand for the solvated species and the desolvated, active species for the electron transfer, respectively. When the condition $[[Cu(II)L]^{2+}] \ll [Red]$ is satisfied, one can derive eqn (8) from eqns (6) and (7):

$$\frac{1}{k_{obsd}} = \frac{k_{-1}}{k_1 k_{et}[Red]} + \frac{1}{k_1}. \quad (8)$$

Under such a reaction scheme, both plots of k_{obsd}^{-1} against $[fc]^{-1}$ and of k_{obsd}^{-1} against $[Me_2fc]^{-1}$ for the reactions of a copper(II) complex with fc and Me_2fc should give the same intercept. In the reaction of **1** with Me_2fc, however, a plot of k_{obsd}^{-1} against $[Me_2fc]^{-1}$ has an intercept with nearly zero (Fig. 3), which is in contrast to the appreciable non-zero intercept in the reaction of **1** with fc (Fig. 2). Similar results have been obtained for the reactions of **2** and **3** with Me_2fc. In view of these facts, the mechanism shown by eqns (6) and (7) for the electron-transfer reaction is not applicable for the present reactions of the copper(II) complexes with fc and Me_2fc.

The K values (42–110 mol^{-1} dm^3) for the present copper(II)–fc precursor complexes are larger than those (9.7–32.3 mol^{-1} dm^3)[1] for the corresponding precursor complexes formed in the reactions of the $Cu(II)(N_{imidazole})_2S_2$ complex with fc. This result may be explained in terms of the higher electron-accepting abilities of the present $Cu(II)(N_{pyridine})_2S_2$ complexes, which involve the pyridyl group having more effective π-acceptor property than the imidazolyl group.[6] This is consistent with the fact that the redox potentials of **1–3** (0.49–0.64 V vs SCE in acetonitrile) are positively higher than those of the $Cu(II)(N_{imidazole})_2S_2$ complexes (0.23–0.37 V vs SCE in acetonitrile).[1] The k_{et} value also increases with raising the redox potential of the $Cu(II)(N_{pyridine})_2S_2$ complex. The same tendency was seen in the reactions of $Cu(II)(N_{imidazole})_2S_2$ with fc.[1]

The formation of a precursor complex has not been detected not only in the reactions of complexes **1–3** with Me_2fc but also in those of **4–8** with fc. In the former reactions, a steric hindrance of the methyl groups of Me_2fc may cause fairly small K values. Such a steric hindrance, however, may not be significant in the latter reactions concerned with fc. Since complexes **4–8** exhibit sufficiently positive redox potentials (0.66–0.73 V vs SCE in acetonitrile) (Table 3), K values can be expected as large as those observed for the reactions of **1–3** with fc and fairly large k_{et} values are deduced for the reactions of **4–8** with fc.

REFERENCES

1. N. Aoi, G. Matsubayashi and T. Tanaka, *J. Chem. Soc., Dalton Trans.* 1983, 1059.
2. S. E. Livingstone and J. D. Nolan, *Aust. J. Chem.* 1960, **23**, 1553.
3. H. A. Goodwin and F. Lions, *J. Am. Chem. Soc.* 1960, **82**, 5013.
4. N. Aoi, G. Matsubayashi and T. Tanaka, *Inorg. Chim. Acta* 1985, **85**, 123.
5. N. Al-Shatti, A. G. Lappin and A. G. Sykes, *Inorg. Chem.* 1981, **20**, 1466.
6. R. S. Sundberg and R. B. Martin, *Chem. Rev.* 1974, **74**, 471.

Polyhedron Vol. 6, No. 5, pp. 947–955, 1987
Printed in Great Britain

0277–5387/87 $3.00+.00

LIGAND FIELD ANALYSIS OF TRIS(AMINOACIDATO)COBALT(III) COMPLEXES WITH GLYCINATO(N,O) AND β-ALANINATO(N,O) METAL CHELATE RINGS

S. R. NIKETIĆ* and W. URLAND†

Max-Planck Institut für Festkörperforschung, D-7000 Stuttgart-80, F.R.G.

(*Received* 29 *July* 1986; *accepted* 4 *September* 1986)

Abstract—In addition to showing a well-known demarcation between facial and meridional configurations the ligand field spectra of $Co(\beta Ala)_x(Gly)_{3-x}$ ($x = 1$ or 2) [βAla = β-alaninato(N,O) ring, and gly = glycinato(N,O) ring] complexes provide a rare example of a marked difference in the observed splitting pattern of the $^1T_{1g}(O_h)$ level among the three possible meridional isomers generated by cyclic permutation of chelate rings with respect to the pseudo three-fold axis. Angular overlap calculations which consider an anisotropy of the metal–carboxylate oxygen donor interaction reproduce fairly well the ligand field spectra of the complete series of $Co(\beta Ala)_x(Gly)_{3-x}$ ($x = 0$, 1, 2 or 3) complexes.

From their first description at the beginning of this century[1] tris(aminoacidato)cobalt(III) complexes have frequently been a focus of current chemical research: in connection with optical-activity studies,[2–5] proton[3] and ^{13}C NMR studies,[6] characterization of the species with three six-membered β-alaninato chelate rings,[7] "mixed" glycinato–β-alaninato species,[8] and α-hydrogen exchange reactions.[9]

An interesting feature of these systems is the influence of the chelate ring enlargement (from five-membered glycinato to six-membered β-alaninato) on their electronic[8] and circular dichroic‡ spectra.

The complete series of complexes $Co(\beta Ala)_x(Gly)_{3-x}$ [$x = 0$, 1, 2 or 3; βAla = β-alaninato(N,O) ring; and Gly = glycinato(N,O) ring] included in this investigation consists of the following 12 geometrical isomers (Fig. 1). For each of the species containing the rings of the same kind (i.e. $x = 0$ and 3) there are two isomers: facial (*fac*) and meridional (*mer*). The "mixed" complexes with two Gly and one βAla ring ($x = 1$), or vice versa ($x = 2$), comprise one *fac* and three *mer* forms, the

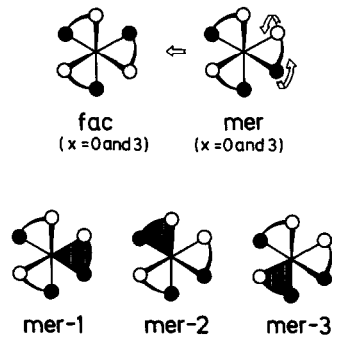

Fig. 1. Isomerism in tris(aminoacidato)cobalt(III) complexes. *First row*: facial and meridional configurations of $Co(Gly)_3$ or $Co(\beta Ala)_3$. The arrows indicate the "*trans*" ring inversion that changes the meridional into the facial configuration. *Second row*: three possible meridional isomers for "mixed" $Co(\beta Ala)_x(Gly)_{3-x}$ ($x = 1$ or 2) structures. The hatched ring indicates the one which is different from the other two: βAla(N,O) for $x = 1$ or Gly(N,O) for $x = 2$. They can be uniquely labelled by the *trans* pair of donor atoms from the rings of the same type as, for example, *mer*(N,O), *mer*(N,N) and *mer*(O,O).

*Author to whom correspondence should be addressed at: Chemistry Department, Faculty of Science, University of Belgrade, POB 550, YU-11001 Belgrade, Yugoslavia.

†Present address: Institut für Anorganische Chemie der Universität Hannover, Callinstrasse 9, D-3000 Hannover-1, F.R.G.

‡Unpublished work carried out at the Chemistry Department A, The Technical University of Denmark, Lyngby, with Olav Overgaard Nielsen, Torben Steen Nielsen and Kirsten Vilholm, in 1971. In part presented at the 21st Meeting of the Serbian Chemical Society, Belgrade, 1978.

latter being generated by cyclic permutation of the chelate rings with respect to the pseudo three-fold axis.

All the isomers are known. Geometrical configurations of tris(glycinato)cobalt(III) complexes have been deduced from their electronic spectra[10] and later reconfirmed.[2-6] X-ray crystal analysis of the *mer* isomer is available.[9] Tris(β-alaninato)cobalt(III) isomers were assigned in a similar way[7] and the crystal structure of the *mer* isomer was also reported.[11] For the "mixed" complexes ($x = 1$ and 2) the electronic spectra[8] distinguish *fac* from *mer* isomers and, in addition, show the subtle but distinct differences among the *mer* isomers within both series ($x = 1$ and 2).*

The present study was initiated in order to find out how well a complete ligand field analysis based on the angular overlap model (AOM)[12-14] formalism may explain the electronic structures of tris(aminoacidato)cobalt(III) complexes. The AOM approach, through its principles of additivity and transferability of σ- and π-contributions of individual ligators, appears to be particularly well suited for this study which aims at explaining the effect of substituting a five-membered Gly with a six-membered βAla chelate ring, and the differences among the triads of *mer* isomers in "mixed" species (for $x = 1$ and 2).

METHODOLOGY

Wave functions

In the present treatment a complete basis of 210 Russell–Saunders free-ion functions $|d^6; \alpha LSJM_J\rangle$ was used. Since (as will be shown below) all the perturbations are applied simultaneously, the choice between a strong- and a weak-field basis was immaterial, and the free-ion basis was chosen for computational convenience.

Hamiltonian

Omitting the spherically symmetric central-field terms, as usually, the Hamiltonian consisted of three terms: ligand field potential $\hat{V}_{LF}$, electron repulsion operator $\Sigma\, e^2/r_{ij}$, and spin–orbit coupling operator $\Sigma\, \xi(t_i)\hat{l}_i \cdot \hat{s}_i$.

Matrix elements

Many-electron matrix elements of the ligand field potential are expanded by expressing $\hat{V}_{LF}$ as a superposition of spherical harmonics $\hat{Y}_k^q$ and evaluated using the standard methods of tensor operator algebra.[15,16] Coefficients of the expansion $R_k c_{kq}$ are expressed as linear combinations of one-electron matrix elements (transformed from the complex into the real *d*-basis). Finally, each of the 15 distinct one-electron matrix elements is parametrized as a sum of σ-, π- etc. contributions from each ligator atom according to the AOM formalism.[12-14] Matrix elements of electron repulsion and spin–orbit coupling operators are also evaluated using the standard tensor operator methods.[15,16] The former are parametrized with Slater–Condon parameters F_2 and F_4 (or Racah parameters B and C), and the latter with the one-electron spin–orbit coupling constant ζ.[15] All reduced matrix elements needed for these calculations were taken from Nielson and Koster's tables.[17]

Energy level calculation

Basic perturbation matrices are set up for each parameter value and summed to form the total (generally complex) Hamiltonian matrix which is diagonalized to give the perturbed eigenvalues. A symmetry analysis of eigenvectors is then performed yielding the composition of the levels expressed in percentage of the free-ion terms which is needed for intensity calculations (see below).

Spectra simulation

Individual spectral bands are assumed to be Gaussian on the wavenumber scale. In order to reconstruct actual spectral profiles three parameters (position, intensity and half-width) are required for each component band. Intensities were calculated using the "spin-only" formula of Schroeder.[18] This very crude approach considers only the spin-allowedness of a transition and expresses a transition probability as a sum of squared products of the components from ground- and excited-state eigenvectors having the same spin multiplicity. Intensities were assumed to be proportional to transition probabilities normalized to match the sum of oscillator strengths of the components of $^1T_{1g}$. Band half-widths were kept constant at about 1700 cm^{-1}. This value is within the range suggested by Jørgensen[19] and indeed gives the best fit to the spectra of *fac* isomers having the unresolved band of $^1T_{1g}$ parentage.

Parameter optimization

The search for the optimum ligand field parameters was carried out in two stages. First, the

* Characteristic differences were also observed in IR, proton and ^{13}C NMR spectra. Unpublished results of N. M. Kostić and S. R. Niketić. In part presented at the 21st Meeting of the Serbian Chemical Society, Belgrade, 1978.

parameters were varied (one or two at a time, in 100- and 50-cm^{-1} steps) in sufficiently large domains. During this preliminary optimization process intensities were estimated using Schroeder's formula (as described above) and simulated spectral profiles compared qualitatively to the experimental ones. The aim of this coarse adjustment of parameters was two-fold: (i) to locate the most probable narrow ranges for each parameter, and (ii) to identify plausible positions of the overlapped bands in experimental spectral profiles.

Final optimization was performed using the SPIRAL algorithm of Jones.[20] The method was devised for non-linear least-squares problems and is claimed[20] to be superior to the standard (Marquardt's and Powell's) algorithms. Only the band positions were fitted (including the overlapped bands positioned according to the results of the preliminary optimization). Computed band profiles were generated using the Schroeder's model to obtain relative intensities from the eigenvectors calculated with the "best-fit" parameter set. This overall tactic was imposed by the quality of experimental data (therefore, spectral deconvolution was not attempted) as well as by the limitations of the theoretical model (therefore, point-by-point fitting was not tried).

PARAMETRIZATION

As a starting point we considered the Hamiltonian parameters for the CoN_6 chromophore. Initial values for the electron repulsion parameters ($F_2 = 1141.3$ and $F_4 = 104.46$ cm^{-1}) as well as the AOM parameter for ammine nitrogen [$e_\sigma(N) = 8000$ cm^{-1}] were taken from the best-fit parameters* which reproduce the low-temperature high-resolution polarized single-crystal spectrum of the $[Co(NH_3)_6]^{3+}$ ion.[21] These parameters were subjected to the optimization procedure as described below. The choice of other AOM parameters was of prime importance. Namely, from the outset, two equally justifiable parametrization schemes appeared to be possible: one based on distinction between ligators from five- and six-membered metal chelate rings leading to the two sets of parameters for nitrogen and oxygen, and the other based on the assumption that AOM parameters for nitrogen and oxygen donors are the same irrespective of the ring size, and that any differences in the interaction with metal *d*-orbitals is due to geometrical factors. In the latter case we need only three AOM parameters: $e_\sigma(N)$, $e_\sigma(O)$ and $e_\pi(O)$. As usual, an π-interaction of ammine nitrogen is not involved so that $e_\pi(N) = 0$ is assumed throughout.

In addition to being more in the spirit of AOM, the second parametrization scheme was selected on the basis of the similarity between the internuclear metal–ligand M–L distances in five- and six-membered aminoacidato metal chelate rings. From eight crystal structure determinations[22] furnishing data on 13 crystallographically distinct isolated cobalt(III) glycinato(N,O) chelate rings the mean M—N distance is 1.96(2) Å and the mean M—O distance is 1.91(2) Å.† Similar data but from a smaller available collection[22] of six unique isolated cobalt(III) β-alaninato(N,O) chelate rings from four crystal structure reports yield for mean M—N and M—O distances values 1.95(2) and 1.91(1) Å, respectively.†

The assumed equivalence between the corresponding metal–ligand distances in five- and six-membered rings is further corroborated, in case of M—N, by the similarity in M—N stretching frequencies in vibrational spectra of $[Co(en)_3]^{3+}$ and $[Co(tn)_3]^{3+}$ ions[24] (en = ethylenediamine, tn = trimethylenediamine) and by the values of ^{59}Co NMR parameters[25] for tris(diamine) cobalt(III) complexes with chelate rings of various sizes. Molecular-orbital calculations are not available for aminoacidato complexes of cobalt(III), but analogous studies[26] of copper(II) and nickel(II) complexes show that differences in the average bond overlap densities of M—L bonds in five- and six-membered aminoacidato complexes are of the same order of magnitude as between different α-aminoacidato complexes (i.e. within the series of five-membered chelate ring structures).

Therefore, as a starting value, the $e_\sigma(O)$ parameter was set at 7000 cm^{-1} in line with the postulated lower ligand field strength of oxygen compared to ammine nitrogen coordinated to cobalt(III). However, the variation of this parameter over a wide range (6000–8000 cm^{-1}) was investigated. In contrast to a nitrogen donor, carboxylate oxygen may be involved in M–L π-bonding requiring an $e_\pi(O) \neq 0$ in AOM analysis. Such a possibility has already been anticipated.[8] Moreover, as will be demonstrated below, the anisotropy

* Table III of Ref. 21 gives *Dq*, *B* and *C* values which were here converted into the corresponding $e_\sigma(N)$, F_2 and F_4.

† However, when the internuclear distances from individual structure determinations are treated as mean values and their estimated standard deviations taken into consideration, we obtain, after Hamilton,[23] the following results: 1.955(1) and 1.907(1) Å for M—N and M—O distances, respectively in five-membered glycinato(N,O) rings, and 1.945(2) and 1.913(2) Å for M—N and M—O distances, respectively, in six-membered β-alaninato(N,O) rings.

of metal–oxygen (M–O) π-interaction has been found to be essential for explaining the characteristic splitting patterns in the spectra of *mer*-isomers of tris(aminoacidato)cobalt(III) complexes with "mixed" Gly–βAla coordination spheres. To our knowledge, the anisotropy of the carboxylate oxygen–metal bond has not been examined hitherto in cobalt(III) complexes. In a recent similar AOM study[27] of tris(glycinato)chromium(III) the M—O bond was treated as if it had axial symmetry, but a concurrent study[28] of cobalt(II) complexes with oxygen donor ligands did consider M—O bond anisotropy. Therefore, we have experimented with $e_{\pi\perp}(O)$ in the range 600–1800 cm^{-1} and set $e_{\pi\parallel}(O) = 0$ with the reference plane for each oxygen donor defined by itself, M and N of the same chelate ring.

Arguments in support of this parametrization stem also from structural evidence. The bond angle on the oxygen donor is 129.2(21) and 115.9(10)° for six-membered βAla rings (from crystal structure data on six individual rings) and five-membered Gly rings (from crystal structure data on 13 individual rings), respectively.[22] These angles together with bond lengths and angles around the carbonyl carbon and torsional angles involving coordinated carboxylate in Gly and βAla chelate rings[22] define a local geometry which is consistent with a simple bonding picture comprising a formally sp^2 oxygen donor (with its p-orbital perpendicular to the σ-framework) which is engaged in a partly delocalized π-system of the carbonyl group.

The effective one-electron spin–orbit coupling constant for cobalt(III) is not known but has been estimated[29] to be in the range 500–600 cm^{-1}. The ζ value of 580 cm^{-1} has been quoted both in a textbook[30] and in a more recent paper.[31] We have followed Wilson and Solomon[21] and adopted an upper limit value of 600 cm^{-1} which was kept fixed in all computations.

GEOMETRIES

Of 12 complex species studied in this work two have been previously characterized by X-ray structural analysis: *mer*-$Co(Gly)_3$[9] and *mer*-$Co(\beta Ala)_3$.[11] For the AOM analysis positions and orientations of donor atoms in these two *mer* isomers were taken from the crystal structure coordinates and M–L torsional angles, respectively. The corresponding *fac* isomers were generated by transposing the "*trans*" N–M–O rings of *mer* structures (rotation by 180° around the axis bisecting the N—M—O bite angle) and averaging to C_3-symmetry (cf. Fig. 1).

Insofar as the chelate-ring size did not have substantial influence on individual M—L bond characteristics enabling one to use the common set of AOM parameters, it is critical in defining the donor atom positions in the coordinate frame of the central metal atom. The N—M—O angle ("bite angle") is 85.3(8)° for five-membered Gly rings and 94.3(6)° for six-membered βAla chelate rings.[22] Using the simple formulae of solid trigonometry pertaining to the rectangular tetrahedron defined by one ligator position in the coordinate frame of the metal atom (Fig. 2) it is possible to relate the bite angle to other geometrical descriptions[32–35] which define the coordination octahedron in a trigonal tris (bidentate) structure. Two independent geometry descriptors are needed to fully specify the coordination octahedron in a tris(bidentate) structure. In addition to the bite angle it is, therefore, common to define, for example either the twist angle (ω)[32] or the tilt angle (θ)[33] or the ratio s/h[34] (here s = octahedron edge, and h = octahedron height along the molecular C_3-axis). From the above-mentioned crystal structures[9,11] we note that an increase in the bite angle is concurrent with an increase in ω and a decrease in θ and the s/h ratio. In other words, the change from five-membered Gly to six-membered βAla rings in tris(aminoacidato)cobalt(III) complexes gives rise to a trigonal elongation of the coordinate octahedron. A similar phenomenon is well-established both experimentally[35] and computationally[36,37] in tris(diamine)cobalt(III) complexes (Table 1).

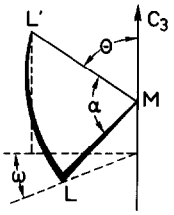

Fig. 2. Definition of bite (α), twist (ω) and tilt (θ) angles in an octahedral trigonal tris(bidentate) structure.

These structural regularities are observed in the construction of the *fac* structures (for $x = 0$ and 3) and the composite structures of "mixed" Gly–βAla complexes ($x = 1$ and 2). The latter eight structures were composed by placing the appropriate chelate ring (Gly or βAla) in the required sequence with respect to the (pseudo) three-fold molecular axis. Since the AOM analysis requires only the ligator coordinates this step was simplified by constructing three coplanar lines radiating from the centre, $2\pi/3$ apart from each other, which are taken as bisectors of the bite angles, and by fixing ligator positions with respect to these lines according to chosen bite and twist angles (cf. Fig. 2).

Table 1. Deformations of coordination octahedra in tris(bidentate)cobalt(III) complexes with five- and six-membered metal chelate rings

Structure[a]	Ring size	Bite angle (α) (°)	Twist angle (ω) (°)	Reference
Octahedron		90.0	60.0	
$[Co(en)_3]^{3+}$	5	85.44	52.69	32, 35
$[Co(tn)_3]^{3+}$	6	94.51	62.34	32, 35
$Co(Gly)_3$	5	85.93	55.25	9
$Co(\beta Ala)_3$	6	94.16	61.83	11

[a] Averaged to C_3-symmetry. Abbreviations: en = 1,2-diaminoethane(N,N), tn = 1,3-diaminopropane(N,N), Gly = glycinato(N,O) ring, βAla = β-alaninato(N,O) ring.

DISCUSSION

The ligand field spectra of tris(aminoacidato)cobalt(III) complexes consist of two broad bands.[2-5,7,8,10] There is no doubt about their assignment to the two spin-allowed singlet transitions. However, like the majority of room-temperature solution spectra of cobalt(III) complexes the low-symmetry components of the $^1T_1$ and $^1T_2$ parentage overlap to such an extent that the spectra are of very little use for detailed analysis. In spite of the low information content of the available experimental data the present analysis did reach conclusions concerning the questions raised in the introduction, demonstrating the utility (but also the limitation) of the AOM approach in a frequently encountered situation with respect to the available spectroscopic evidence.

In an attempt to overcome the lack of sufficiently accurate information about the component peak positions in the observed spectra, we have supplemented the initial (exploratory) optimization of ligand field parameters by introducing qualitative comparison between the observed and computed spectral profiles. Although, such an approach required an introduction of additional degrees of freedom in the model, the fact that we are dealing with a complete set of 12 members of the $Co(\beta Ala)_x(Gly)_{3-x}$ ($x = 0$, 1, 2 or 3) system enabled us to rely not only on the transferability of ligand field (and AOM) parameters within the series but also on the transferability of these additional variables required for spectra simulation (i.e. relative intensities and band half-widths), thus eliminating some of the uncertainty inherent in the analysis.

Parameter optimization was carried out by gradually increasing the number of structures taken into the study simultaneously. It consisted of the following steps. We have first considered the simplest of the structures, namely *fac*-$Co(Gly)_3$, and have varied F_2, F_4 and AOM parameters for nitrogen and oxygen donors, one at a time, mapping the parameter space in sufficiently wide intervals for each parameter.

Parameter fitting was not attempted at this stage because the number of parameters exceeded by far the experimental information. However, this search disclosed various patterns of dependence of calculated band positions on ligand field parameters which, in combination with general physico-chemical experience, such as $e_\sigma(N) > e_\sigma(O) > e_\pi(O)$, helped in defining the most probable narrow ranges for each of the parameters. With a moderately good parameter set the analysis was extended to *mer*-$Co(Gly)_3$ and, upon further (but not complete) refinement, to both *fac*- and *mer*-$Co(\beta Ala)_3$. The analysis showed that the basic spectral features[7,10] (e.g. greater splitting of the $^1T_1$ and $^1T_2$ levels, and a greater splitting of both levels in *mer* than in *fac* isomers) are well reproduced. We look at this well-known result as a starting point for the further analysis of spectral features which are not easily explainable within a conventional ligand field treatment: namely, at this stage we were not able to reproduce the significant difference in the splitting pattern of $^1T_1$ level between *mer*-$Co(Gly)_3$ and *mer*-$Co(\beta Ala)_3$.[7] Different mode of deformation of the coordination octahedron in these two systems obviously does not exert sufficient influence on the electronic energy levels of cobalt(III) ion to account for the observed spectral properties.

However, the other principal difference between five- and six-membered aminoacidato chelates is the conformational flexibility of βAla rings in the latter systems. Experimental* and computational† results show sufficient grounds to argue that six-membered βAla metal chelate rings may adopt conformations having different endocyclic torsional angles. Looking at the M–O interaction, the range of energetically accessible ring conformations are char-

* Mainly the results of crystal structure analyses of β-alaninato(N,O) chelates including the systems with substituted and fused rings. Cf. Ref. 22.

† A conformational analysis of tris(aminoacidato)cobalt(III) complexes based on the consistent force field (CFF) approach[36-38] is being carried out in parallel. Preliminary results show that βAla rings are very flexible and that with conventional[38] parametrization equilibrium conformations do not always correspond to those which emerge from crystal structure studies. A full account of this work will be presented elsewhere.

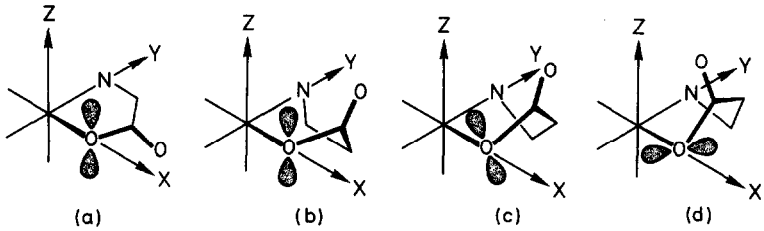

Fig. 3. Simplified sketches of Gly(N,O) and βAla(N,O) metal chelate rings showing: (a) an almost planar Gly(N,O) ring with oxygen-donor *p*-orbital perpendicular to the ring (in this case *XY*) plane; and (b), (c) and (d) a range of βAla(N,O) ring conformations spanning a $\pi/2$ interval of torsional angles around the M—O bond. The energetically favourable "twist-boat" form (c) is intermediate between two "boat" forms, (b) and (d).

acterized with a substantial variation in the M–O torsional angle and, therefore, in the M–O π-interaction. If the M–O torsional angle in an almost planar Gly ring is taken as zero, its value (and thus the orientation of the oxygen donor *p*-orbital with respect to the metal atom coordinate system) in the βAla ring may vary in the range of $-60°$ to $+60°$ (Fig. 3).

The adopted AOM parametrization [$e_{\pi\perp}(O) \neq 0$ and $e_{\pi\parallel}(O) = 0$] together with the consideration of torsional angles around the M—O bond in *mer*-Co(βAla)$_3$ taken from the result of crystal structure analysis[11] do in fact predict the differences in the splitting of the octahedral $^1T_1$ state between *mer*-Co(Gly)$_3$ and *mer*-Co(βAla)$_3$ which accord with the experimental data.

In the next step a full optimization of ligand field parameters was performed *simultaneously* on all four "non-mixed" species using the SPIRAL algorithm. This was necessary in order to ensure that the number of parameters be less than the number of observable band positions to be fitted. The resultant best-fit parameters are given in Table 2.

With calculated band positions and intensities and a constant band half-width the simulated spectra are in full agreement with the experimental ones (Table 3 and Fig. 4).

In order to apply the concept of anisotropy of the M–O interaction in our AOM scheme the orientation of the oxygen donor with respect to the M—O bond axis has to be specified. As this information is lacking for the *fac* isomer of Co(βAla)$_3$ we have attempted to look at the variation of calculated energy levels of *fac*-Co(βAla)$_3$ for a range of plausible ring conformations within the approximation of C_3 molecular symmetry. The results (Fig.

Table 2. "Best-fit" parameter set[a] optimized on four non-mixed isomers of Co(βAla)$_x$(Gly)$_{3-x}$ ($x = 0$ and 3) (in $cm^{-1} \times 10^3$)

$e_\sigma(N) = 8.0$[b]	
$e_\sigma(O) = 7.4$	$e_{\pi\perp}(O) = 1.7$
$F_2 = 1.12$	$F_4 = 0.102$
$\zeta = 0.6$[c]	

[a] Parameters not shown were zero. See Parametrization.

[b] Optimization did not change significantly the value of this parameter (initially taken from Ref. 21).

[c] Kept constant in this work. Cf. Ref. 21.

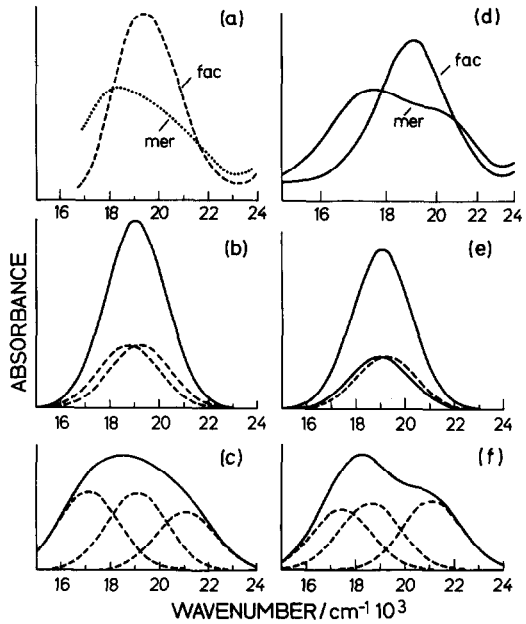

Fig. 4. Comparison of the experimental band shape for the $^1T_{1g} \leftarrow {}^1A_{1g}$ transition of: (a) *fac*- and *mer*-Co(Gly)$_3$ (Refs 2 and 11), and (d) *fac*- and *mer*-Co(βAla)$_3$ (Ref. 7), with the simulated band shape for: (b) *fac*- and (c) *mer*-Co(Gly)$_3$; and (e) *fac*-, and (f) *mer*-Co(βAla)$_3$. Note the nonlinearity of the wavenumber scale in (d) (Ref. 7).

Table 3. Comparison of the observed (Obs.) and calculated (Calc.) energies of ligand field transitions of $Co(\beta Ala)_x(Gly)_{3-x}$ ($x = 0$ and 3) isomers (in $cm^{-1} \times 10^3$)

	$^1T_{1g} \leftarrow {}^1A_{1g}$ transition				$^1T_{2g} \leftarrow {}^1A_{1g}$ transition			
Isomer	Obs.	Calc.	P^a	Assignment[b]	Obs.	Calc.	P	Assignment
$x = 0$, *fac*		18.77	0.87	A_2	26.7	26.85	0.82	A_1
	19.2	19.21	1.73	E_a		27.01	1.64	E_b
$x = 0$, *mer*	18.6	17.12	0.86	A_2		25.93	0.82	A_1
		19.08	0.86	B_1	26.9	27.03	0.82	B_2
	≃20[c]	21.09	0.65	B_2		27.91	0.82	B_1
$x = 3$, *fac*	19.0	18.99	1.73	E_a		26.59	0.82	A_1
		19.25	0.87	A_2	27.0	27.13	1.65	E_b
$x = 3$, *mer*	17.6	17.46	0.76	A_2		25.90	0.81	A_1
		18.64	0.84	B_1	27.0	27.01	0.82	B_2
	≃20[c]	21.11	0.87	B_2		27.96	0.82	B_1

[a] P is a transition probability calculated with the "spin-only" formula of Schroeder (cf. Ref. 18).
[b] The predominent C_{3v} and C_{2v} parentage for *fac* and *mer* configurations, respectively.
[c] Shoulder.

5) obtained with the "best-fit" parameter set (Table 2) show that although A and E components of the $^1T_1$ and $^1T_2$ octahedral parentage are sensitive to the variation in the M–O torsional angle their baricenter changes only slightly. It is close to the experimentally observed value for a range of ring conformations. Variation in the difference in energy between baricenters from $^1T_1$ and $^1T_2$ is too small to be used for comparison with the observed spectrum.

Reversal in the order of A and E levels on an energy scale as a function of chelate ring conformation (cf. Fig. 5) is of no consequence for the interpretation of electronic spectrum under the assumption of the O_h holohedrized symmetry of the *fac* isomer but might be of interest in optical-activity studies.

As a final step, the "best-fit" parameter set (Table 2) was used to calculate the energy levels of "mixed" tris(aminoacidato)cobalt(III) complexes. Again having no experimental indication about the βAla ring conformations in the "mixed" species the twist-boat form [cf. Fig. 3(c)], being one of the energetically favourable forms,* was assumed in all cases. Immediate results were encouraging: they showed that simulated spectra of the triads of *mer* isomers in both series (i.e. for $x = 1$ and 2) are indeed different. Moreover, the differences are—in a qualitative way—similar to the observed ones in most cases (Fig. 6).

CONCLUSIONS

An ultimate justification for the present analysis would be the possibility of assigning geometrical configurations to the *mer* isomers of "mixed" $Co(\beta Ala)_x(Gly)_{3-x}$ species ($x = 1$ or 2). However, the available spectroscopic data are not sufficiently informative to provide the required degree of reliability in such assignment. Furthermore, it

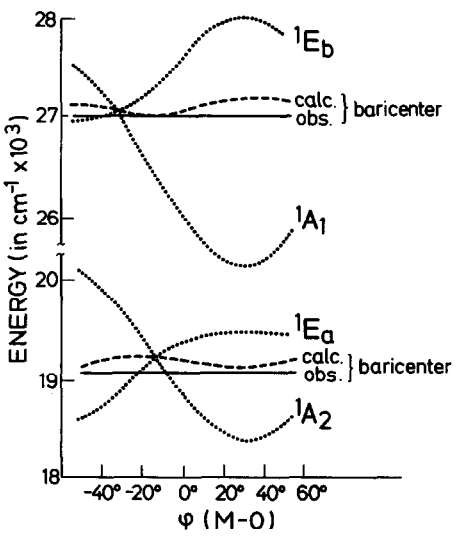

Fig. 5. Variation of energy levels with M–O torsional angle in *fac*-$Co(\beta Ala)_3$ having C_3 molecular symmetry. Zero torsional angle is defined for a conformation in which the *p*-orbital on the oxygen donor is perpendicular to the plane defined by the O, M and N of that ring.

* See footnote † on p. 951.

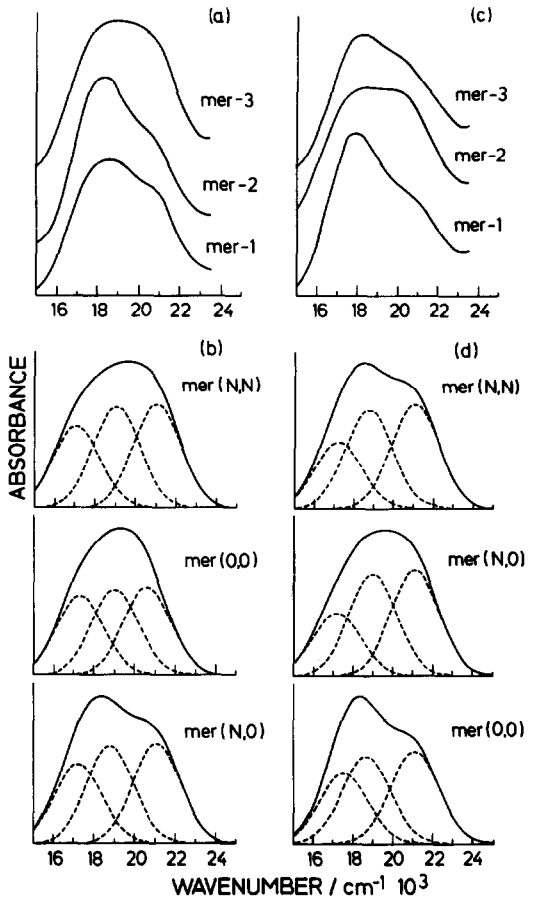

Fig. 6. Comparison of the experimental band shape for the ${}^1T_{1g} \leftarrow {}^1A_{1g}$ transition of: (a) three *mer* isomers of $Co(Gly)_2(\beta Ala)$ numbered in the elution order (Ref. 8), and (c) three *mer* isomers of $Co(\beta Ala)_2(Gly)$ numbered in the elution order (Ref. 8), with the simulated band shape for: (b) *mer*(N,N)-, *mer*(O,O)- and *mer*(N,O)-$Co(Gly)_2(\beta Ala)$, and (d) *mer*(N,N)-, *mer*(N,O)- and *mer*(O,O)-$Co(\beta Ala)_2(Gly)$. For the nomenclature of *mer* isomers see caption to Fig. 1. For the comment on assignment see Conclusion.

would be rational to base the assignment on combined data from different experimental techniques together with the AOM modelling. The results discussed above are, in fact, not intended to offer an assignment, but rather to demonstrate that a compact AOM parametrization related in a natural way to the local features of the ligand field of the cobalt (III) ion in those systems is indeed able to account for the *d–d* spectral pattern and differences among the 12 isomers of $Co(\beta Ala)_x(Gly)_{3-x}$. This parametrization is built on the idea of metal–carboxylate π-anisotropy which is proved to be successful in providing the link between chelate ring conformation and electronic properties, and convenient with respect to the transferability among the related systems. At least two possible lines of further development of this AOM approach are envisaged. One is to refine the conformational analysis of βAla chelate rings in order to reduce the range of possible ring conformations, and hence the interval for plausible M–O torsional angles. The other is to strive to obtain more information from *d–d* spectra (e.g. at low temperature) and thus to improve the accuracy in the refinement of AOM parameters. By extending this kind of analysis to other systems (in particular to conformationally restricted ones) we hope to accumulate the body of knowledge about AOM parameters necessary for the AOM to become an efficient complementary tool for stereochemical studies in transition metal chemistry.

Acknowledgements—This work was supported by the Serbian Research Fund (contract No. 2885 and travel grant to SRN) and by the Max-Planck-Institute for Solid State Research. One of us (SRN) would like to thank M. L. Ellzey (El Paso, Texas), Mme. Faucher (Paris), M. Kibler (Villeurbanne), E. Larsen (Copenhagen), J. R. Perumareddi (Boca Raton, Florida), and C. E. Schäffer (Copenhagen) who kindly provided computer programs, unpublished documentation, valuable counsel, or stimulating discussions at various occasions during the past few years. Major computations were done on the Cray-1* of Max-Planck Institute for Plasma Physics in Garching. Program development, data analysis and other computations were done on the IBM 3031 and 4381 of the Serbian State Institute of Statistics in Belgrade.

REFERENCES

1. H. Ley and H. Winkler, *Ber.* 1909, **42**, 3894; *ibid.* 1912, **45**, 372.
2. B. E. Douglas and S. Yamada, *Inorg. Chem.* 1965, **4**, 1561.
3. R. G. Denning and T. S. Piper, *Inorg. Chem.* 1966, **5**, 1056.
4. E. Larsen and S. F. Mason, *J. Chem. Soc. A* 1966, 313.
5. J. H. Dunlop and R. D. Gillard, *J. Chem. Soc.* 1965, 6531.
6. H. Gerlach and K. Müllen, *Helv. Chim. Acta* 1974, **57**, 2234.
7. M. B. Ćelap, S. R. Niketić, T. J. Janjić and V. N. Nikolić, *Inorg. Chem.* 1967, **6**, 2063.
8. N. M. Kostić and S. R. Niketić, *J. Chem. Soc., Chem. Commun.* 1977, 676.
9. A. Miyanaga, U. Sakaguchi, Y. Morimoto, Y. Kushi and H. Yoneda, *Inorg. Chem.* 1982, **21**, 1387.
10. F. Basolo, C. J. Ballhausen and J. Bjerrum, *Acta Chem. Scand.* 1955, **9**, 810.
11. H. Soling, *Acta Chem. Scand.* 1978, **A32**, 361.

*One complete ligand field calculation with 210 wavefunctions requires 4 s of CPU on the Cray-1.

12. C. E. Schäffer and C. K. Jørgensen, *Mat. Fys. Medd. K. Dan. Vid. Selsk.* 1965, **34**, No. 13.
13. C. E. Schäffer, *Struct. Bonding (Berlin)* 1968, **5**, 68.
14. M. Gerloch, *Magnetism and Ligand Field Analysis.* Cambridge University Press, Cambridge (1983).
15. P. E. Caro, *Structure électronique des éléments de transition.* Presses Universitaires de France, Paris (1973).
16. W. Urland, *Chem. Phys. Lett.* 1977, **46**, 457.
17. C. W. Nielson and G. F. Koster, *Spectroscopic Coefficients for the* p^n, d^n, *and* f^n *Configurations.* MIT Press, Cambridge, Massachusetts (1963).
18. K. A. Schroeder, *J. Chem. Phys.* 1962, **37**, 2553; H. H. Patterson, W. J. DeBerry, J. E. Byrne, M. T. Hsu and J. A. LoMenzo, *Inorg. Chem.* 1977, **16**, 1698.
19. C. K. Jørgensen, *Absorption Spectra and Chemical Bonding in Complexes.* Pergamon Press, Oxford (1962).
20. A. Jones, *Computer J.* 1970, **13**, 301.
21. R. B. Wilson and E. I. Solomon, *J. Am. Chem. Soc.* 1980, **102**, 4085.
22. Structural data obtained through a Cambridge Crystallographic Data Base search. *Cf.* S. Bellard, *Comput. Phys. Commun.* 1984, **33**, 71.
23. W. C. Hamilton, *Statistics in Physical Sciences.* Ronald Press, New York (1964).
24. Kj. Rasmussen, *Spectrochim. Acta* 1974, **30A**, 1763.
25. N. Juranić, *Inorg. Chem.* 1983, **22**, 521; R. Bramley, M. Brorson, A. M. Sargeson and C. E. Schäffer, *J. Am. Chem. Soc.* 1985, **197**, 1780.
26. A. Gupta, G. Loew and J. Lawless, *Inorg. Chem.* 1983, **22**, 111.
27. W. M. Wallace and P. E. Hoggard, *Inorg. Chem.* 1983, **22**, 491.
28. A. Bencini, C. Benelli, D. Gatteschi and C. Zanchini, *Inorg. Chem.* 1983, **22**, 2123.
29. T. M. Dunn, *Trans. Faraday Soc.* 1961, **57**, 1441.
30. B. N. Figgis, *Introduction to Ligand Fields.* Wiley Interscience, New York (1966).
31. E. König, R. Schakig and B. Kanellakopulos, *J. Chem. Phys.* 1975, **62**, 3907.
32. Y. Saito, *Coord. Chem. Rev.* 1974, **13**, 305.
33. L. H. Pignolet, *Top. Curr. Chem.* 1975, **56**, 91.
34. E. I. Stiefel and G. F. Brown, *Inorg. Chem.* 1972, **11**, 434.
35. Y. Saito, *Inorganic Molecular Dissymetry.* Springer, Berlin (1979).
36. S. R. Niketić and Kj. Rasmussen, *Acta Chem. Scand.* 1978, **A32**, 391.
37. S. R. Niketić and Kj. Rasmussen, *Acta Chem. Scand.* 1981, **A35**, 623.
38. N. Raos, S. R. Niketić and V. Simeon, *J. Inorg. Biochem.* 1982, **16**, 1.

Polyhedron Vol. 6, No. 5, pp. 957–962, 1987
Printed in Great Britain

0277–5387/87 $3.00+.00

SOLVENT EFFECT ON THE SYNERGIC EXTRACTION OF PRASEODYMIUM(III) AND NEODYMIUM(III) WITH 1-PHENYL-3-METHYL-4-BENZOYL-5-PYRAZOLONE AND 1,10-PHENANTHROLINE

LUO MINGRUN,* CAO ZIQING and ZHANG FENGMEI

Department of Chemistry, Anhui Normal University, Wuhu, Anhui, People's Republic of China

(*Received* 29 *July* 1986; *accepted* 4 *September* 1986)

Abstract—The solvent effect on the synergic extraction of praseodymium(III) and neodymium(III) with 1-phenyl-3-methyl-4-benzoyl-5-pyrazolone (HPMBP, HA) and 1,10-phenanthroline (phen, B) from a nitric acid medium have been studied by two-phase titration and the slope analysis method. It is found that the synergic reaction in the organic phase (denoted by subscript *o*) can be expressed as follows:

$$LnA_3HA_o + B_o = LnA_3B_o + HA_o.$$

The synergic equilibrium constants (K_s^x) in four different solvents were determined by experiment and calculated on the basis of the regular-solution theory. By comparing the theoretical and experimental values of ln K_s^x, good agreements were observed in the π-donor solvent series of benzene, toluene and xylene, but not in carbon tetrachloride.

Recently the solvent effect on the synergic extraction with acetylacetone (acac-H) and 1,10-phenanthroline (phen) has been quantitatively discussed on the basis of the regular-solution theory by Nakamura *et al.*[1] Li and Xu have also studied the solvent effect on the synergic extraction with 1-phenyl-3-methyl-4-benzoyl-5-pyrazoline (HPMBP, HA) and neutral ligands by the two-phase titration method, but they have announced that the regular-solution theory is too simple to be extensively applicable.[2] In this paper, we try to apply the regular-solution theory to the synergic extraction system with HPMBP and phen in four inert organic solvents—benzene, toluene, xylene and CCl_4. We found that, when extracting with HPMBP alone, the extracted chelate complex forms a self-adduct in the organic phase and the synergic agent phen competes with the undissociated form of the chelating acid HA in the synergic extraction equilibrium just as reported elsewhere.[3] In the system studied the regular-solution theory can be applied satisfactorily to the benzene, toluene and xylene solvent series, but with some restrictions to CCl_4.

* Author to whom correspondence should be addressed.

EXPERIMENTAL

Reagents

HPMBP was obtained in A.R. grade and purified by recrystallization from 1:3 chloroform–petroleum ether (m.p. 91–92°C). phen of A. R. grade was used as obtained.

The rare earth stock solution was prepared by dissolving a known amount of neodynium or praseodymium oxide (99.99%) in concentrated nitric acid, evaporating to near dryness and diluting to a certain volume. The accurate concentration of rare earth ions was determined by titration with EDTA using xylenol orange as indicator. The working solutions were buffered with 0.01 M NaAc, the pH value adjusted to about 4 and the rare earth concentration was diluted to 1×10^{-4} M with 0.1 M $NaNO_3$ solution.

The four organic solvents were purified by ordinary methods[4] and the purity was checked by index of refraction. The experimental values (1.4970 for xylene, 1.4965 for toluene, 1.5010 for benzene and 1.4593 for CCl_4) were very close to that in the literature.[5]

Apparatus

The concentration of rare earth ions in the aqueous phase was determined with a 721 spectrophotometer.

The pH value was measured with a pH S-3C pH meter.

Determination of the partition coefficiency (P_s) *and the acid dissociation constant* (K_{HS}) *of phen*

We adopted the two-phase titration method of Dyressen[6] to determine P_s by titrating a mixture of a 0.025 M phen organic solution and a 0.1 M $NaNO_3$ aqueous solution with a 0.1000 M standard HNO_3 solution (N_2 protected) potentiometrically. K_{HS} was determined by titrating similarly a saturated solution of phen in a 0.1 M $NaNO_3$ solution but in the absence of the organic phase. The end point was determined by Gran's method.[7]

Extraction of Pr(III) *and* Nd(III)

Equal volumes (10 cm^3) of the aqueous and organic solutions were placed in a 50-cm^3 stoppered beaker and stirred with magnetic stirrer for 10 min. (It has been proved by experiment that the result is just the same with shaking in an equilibrium tube for 1 h and the equilibrium can be achieved.) The concentration in the aqueous phase was determined spectrophotometrically[8] and the concentration in the organic phase was determined by the subtraction method.

RESULTS AND DISCUSSION

P_s *and* K_{HS} *of phen*

We have adopted all the symbols used by Li and Xu,[6] but made some modifications to the expressions to suit the phen system.

In the following expressions ( ) and [ ] indicate concentration and activity, respectively, subscript *o* denotes species in the organic phase, and no subscript denotes species in the aqueous phase. For simplicity the charge symbols are omitted.

$$pK_{HS} = pH - \log\frac{(phen)}{(phenH)}, \quad (1)$$

$$(phenH) = \frac{V_{HNO_3}C_{HNO_3} - V_{NaOH}C_{NaOH}}{V} + (OH) - (H), \quad (2)$$

$$C_H = (H) + (phenH), \quad (3)$$

$$\bar{n} = \frac{V_{HNO_3}C_{HNO_3} + V(OH) - V(H)}{V_o^o C_{phen}^o}, \quad (4)$$

$$\log(1+P_s) = pK_{HS} + \log\left(\frac{1-\bar{n}}{\bar{n}}\right) - pH. \quad (5)$$

In the absence of the organic phase:

$$C_{phen} = (phen) + (phenH),$$

$$pK_{HS} = pH - \log\frac{C_{phen}V^o - V_{HNO_3}C_{HNO_3} + V(H) - V(OH)}{C_{HNO_3}V_{HNO_3} - V(H) + V(OH)}. \quad (6)$$

The dissociation constant (pK_{HS}) of phenH can be calculated from eqn (6) to be 5.00, just between the literature values of 5.04[1] and 4.96.[9] The P_s can be calculated from eqns (4) and (5). The results are shown in Table 1. Those of xylene and toluene were first determined in this paper, and those of CCl_4 and benzene are very close to the literature values.[1]

The solubility parameter of phen (δ_s) was calculated according to the relationships deduced by Li and Xu based on the Hildebrand regular-solution theory.[6]

$$Q_s = \log\lambda' + \frac{V_s\delta_o^2}{4.575T} = \frac{2V_s\delta_s}{4.575T}\delta_o + K, \quad (7)$$

where $\lambda' = P_s/(1000d/M)$, V_s is the molar volume of phen (142 ml mol^{-1}),[1] and δ_o is the solubility parameter of the solvent. We plotted Q_s against δ_o and by linear regression the intercept $b = -14.06$, the slope $m = 2.45$ and the correlation coefficient

Table 1. Partition coefficients and other parameters of phen

Solvent	δ_o	Log P_s	Log λ'	$\frac{V_s\delta_o^2}{4.575T}$	Q_s
Benzene	9.15	0.51	−0.5411	8.87	8.33
Toluene	8.9	0.32	−0.6535	8.40	7.74
Xylene	8.8	0.20	−0.7106	8.21	7.50
CCl_4	8.6	0.16	−0.8555	7.84	6.98

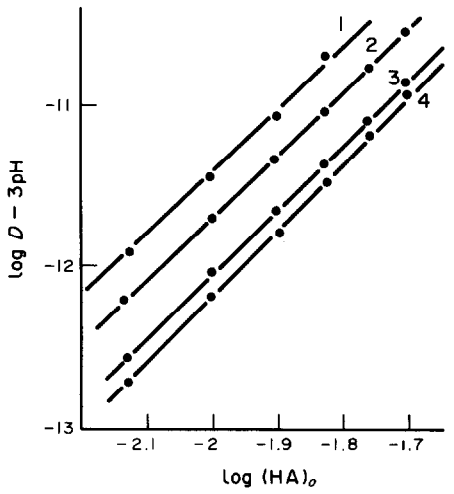

Fig. 1. Extraction of Pr(III) with various C_{HA} in different organic solvents: (1) CCl_4, (2) benzene, (3) toluene, and (4) xylene.

$r = 0.9996$. From eqn (7):

$$\delta_s = \frac{m4.575T}{2V_s}.$$

The calculated δ_s of phen equals 11.56 (at 20°C), slightly lower than that in the literature.[1]

Exraction of Pr(III) *and* Nd(II) *with HPMBP*

We had studied the extraction of rare earth ions by HPMBP in chloroform[10] and the results agreed with those of Roy and Nag.[11] In this paper we have changed the solvent to CCl_4, benzene, toluene and xylene. The results are shown in Figs 1 and 2.

By the slope analysis method the composition of the extracted complex is proved to be LnA_3HA. The extraction equilibrium can be expressed as

$$Ln^{3+} + 4HA_o = LnA_3HA_o + 3H^+, \quad (8)$$

$$K_{ex} = \frac{(LnA_3HA)_o(H^+)^3}{(Ln^{3+})(HA)_o^4},$$

$$\log K_{ex} = \log D - 3pH - 4\log (HA)_o.$$

In the presence of acetate ions, $\log D$ must be corrected by

$$\log D = \log D_{(expl.)} + \log Y,$$

$$\log Y = 1 + \sum_1^n \beta_i (Ac^-)^i.$$

We treat our data according to the following expressions[2] to calculate the solubility parameters (δ_{MA}) of LnA_3HA:

$$\log \beta^o_{310} = \log K_{ex} + 3pK_{aE} + \log K_d, \quad (9)$$

$$Q_{310} = \log \beta^o_{310} + \log \frac{M_1 d_2}{d_1 M_2} + \frac{V_{HA}\delta_o^2}{4.575T}$$

$$= \frac{2\delta_{MA}V_{MA}}{4.575T}\delta_o + K, \quad (10)$$

where $V_{MA} = V_{LnA_3HA}$. V_{MA} can be calculated by comparing with that of $Dy(acac)_3$ and $Y(acac)_3$ (269 $cm^3\ mol^{-1}$),[1] $V_{HA} = 241\ cm^3 mol^{-1}$,[6] and $V_{acac} = M/d = 102.57\ cm^3\ mol^{-1}$.

$$V_{acac} : V_{HA} = V_{Ln(acac)_3} : V_{LnA_3}.$$

Substituting the known values into the above equation, we get $V_{LnA_3} = 632\ cm^3\ mol^{-1}$. Then:

$$V_{MA} = V_{LnA_3} + V_{HA} = 873\ cm^3\ mol^{-1}.$$

The calculated $\log \beta^o_{310}$ and Q_{310} of PrA_3HA and NdA_3HA are shown in Table 2.

When we plot Q_{310} against δ_o we get two nearly straight lines. The slope of each line calculated by linear regression equals 14.77 and 14.69 for PrA_3HA and NdA_3HA, respectively. From expression (10) the slope equals $2V_{MA}\delta_{MA}/4.575T$, so we can get the δ_{MA} of PrA_3HA and NdA_3HA. The values are 11.34 and 11.28, respectively.

We also plot $\log \beta^o_{310}$ against $3pK_{aE} + \log K_d$, when the relationship between benzene, toluene and xylene is nearly linear.

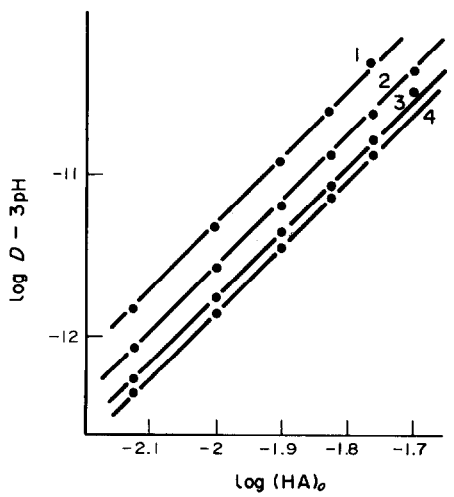

Fig. 2. Extraction of Nd(III) with various C_{HA} in different organic solvents: (1) CCl_4, (2) benzene, (3) toluene, and (4) xylene.

Synergic extraction of Pr(III) *and* Nd(III) *with HBMBP and phen*

By the slope analysis method, the compositions of the synergic extracted complexes are proved to be PrA_3B and NdA_3B, the same as in the chloroform system (see Figs 3–6).

Table 2. Log β^o_{310} and Q_{310} of PrA_3HA and NdA_3HA

Solvent	HA		PrA_3HA		NdA_3HA	
	$pK_{aE}{}^a$	$\log K_d{}^a$	$\log \beta^o_{310}$	Q_{310}	$\log \beta^o_{310}$	Q_{310}
Benzene	7.53	3.43	22.27	77.49	22.42	77.64
Toluene	7.43	3.33	21.57	73.92	21.87	74.22
Xylene	7.21	3.11	20.56	71.82	20.97	72.23
CCl_4	7.30	3.20	21.66	70.56	21.80	70.70

[a] From Ref. 6.

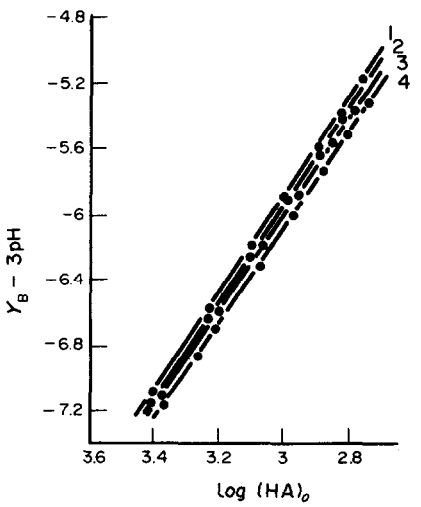

Fig. 3. Synergic extraction of Pr(III) with various C_{HA} and constant C_B in different organic solvents. (1) benzene, (2) toluene, (3) xylene, and (4) CCl_4. $C_B = 1 \times 10^{-4}$ M, $Y_B = \log D - \log (B)_o$.

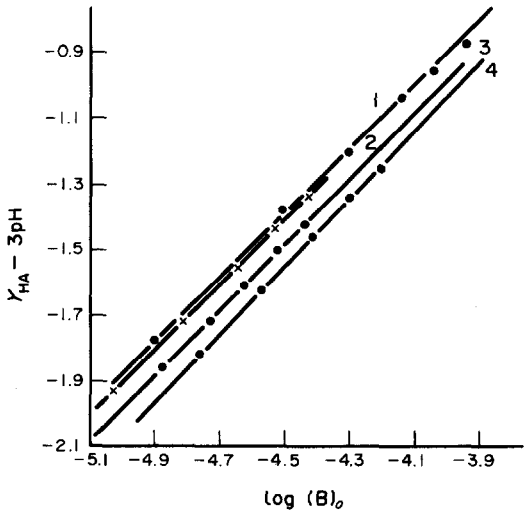

Fig. 5. Synergic extraction of Pr(III) with constant C_{HA} and various C_B in different organic solvents: (1) benzene, (2) toluene, (3) xylene, and (4) CCl_4. $C_{HA} = 5 \times 10^{-4}$ M, $Y_{HA} = \log D - 3 \log (HA)_o$.

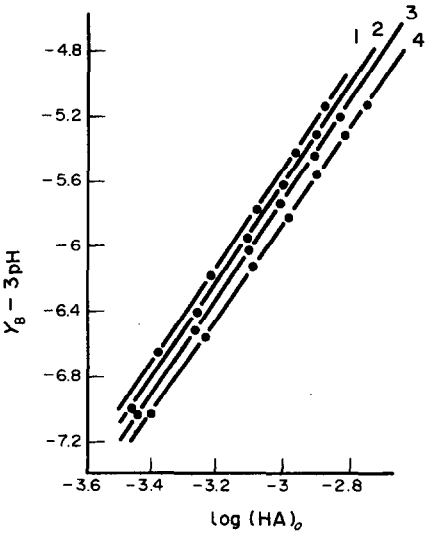

Fig. 4. Synergic extraction of Nd(III) with various C_{HA} and constant C_B in different organic solvents: (1) xylene, (2) toluene, (3) benzene, and (4) CCl_4. $C_B = 1 \times 10^{-4}$ M, $Y_B = \log D - \log (B)_o$.

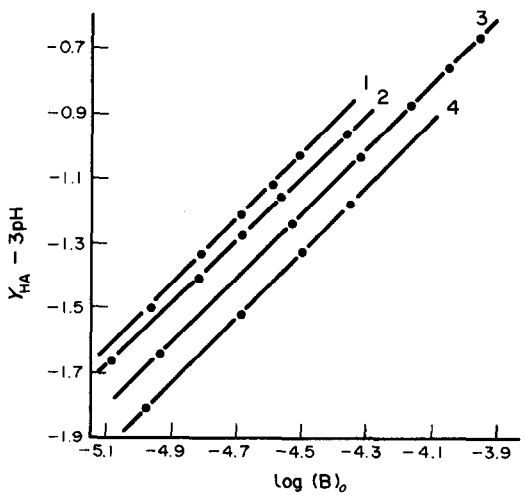

Fig. 6. Synergic extraction of Nd(III) with constant C_{HA} and various C_B in different organic solvents: (1) xylene, (2) toluene, (3) benzene, and (4) CCl_4. $C_{HA} = 5 \times 10^{-4}$ M, $Y_{HA} = \log D - 3 \log (HA)_o$.

The synergic extraction equation can be written as:

$$Ln^{3+} + 3HA_o + B_o = LnA_3B_o + 3H^+, \quad (11)$$

$$K_{s.e.} = \frac{(LnA_3B)_o(H^+)^3}{(Ln^{3+})(HA)^3(B)_o},$$

$$\frac{DY[H^+]^3}{(HA)_o^3(B)_o}$$

$$\log K_{s.e.} = \log D - 3pH - 3\log(HA)_o - \log(B)_o,$$

$$\log D = \log D_{(exp)} + \log Y.$$

Let $[Ln(III)]_o$ be the concentration of combined Pr(III) or Nd(III) in the organic phase. Then the equilibrium concentration of HA and B in the organic phase can be calculated from the following expressions:

$$(HA)_o = \frac{C_{HA} - 3[Ln(III)]_o}{1/K_d(1 + K_a/[H])}, \quad (12)$$

$$(B)_o = \frac{C_B - [Ln(III)]_o}{1 + (1 + [H]/K_{HS})P_s}. \quad (13)$$

We can use the same method to get the solubility parameters for the extracted complex from the following expressions:

$$\log \beta^o_{301} = \log K_{s.e.} + 3pK_{aE} + \log P_s, \quad (14)$$

$$Q_{301} = \log \beta^o_{301} + \log \frac{M_1 d_2}{d_1 M_2} + \frac{V_{MS}\delta_o^2}{4.575T}$$

$$= \frac{2\delta_{MS}V_{MS}}{4.575T}\delta_o + K, \quad (15)$$

where V_{MS} is the molar volume of the synergic extracted complex:

$$V_{MS} = V_{LnA_3} + V_s = 774\,cm^3\,mol^{-1}.$$

The calculated $\log \beta^o_{301}$ and Q_{301} of PrA_3B and NdA_3B are shown in Table 3.

When we plot Q_{301} against δ_o we also get two nearly straight lines. By linear regression we get the slope $m = 12.58$ for PrA_3B and $m = 12.46$ for NdA_3B. From the slope expression we get $\delta_{MS} = 10.89$ for PrA_3B and $\delta_{MS} = 10.79$ for NdA_3B. When we plot $\log \beta^o_{301}$ against $3pK_{aE} + \log P_s$, the relationship between benzene, toluene and xylene is also linear.

Synergic extraction in the organic phase

The synergic extraction reaction in the organic phase can be assumed to be:

$$LnA_3HA_o + B_o = LnA_3B_o + HA_o \quad (16)$$

or

$$MA_o + S_o = MS_o + A_o,$$

and the constant of the synergic extraction reaction can be expressed as $\log K_s$. Since:

$$\text{eqn (16)} = \text{eqn (11)} - \text{eqn (8)},$$

$$\log K_s = \log K_{s.e.} - \log K_{ex}. \quad (17)$$

The solvent effect on this synergic extraction can be quantitatively discussed by considering the activity coefficients of the different species in the four solvents. A thermodynamic equilibrium constant (K_s^o) is defined as follows:

$$K_s^o = \frac{X_{MS}X_A}{X_{MA}X_S}\frac{\gamma_{MS}\gamma_a}{\gamma_{MA}\gamma_s} = K_s^x\frac{\gamma_{MS}\gamma_a}{\gamma_{MA}\gamma_s}. \quad (18)$$

The activity coefficient γ can be calculated from the equation based on the Hildebrand regular-solution theory for a very dilute solution.[1]

$$\ln \gamma_c = \frac{V_c}{RT}(\delta_c - \delta_o)^2. \quad (19)$$

From the molar volume and solubility parameters of the four species in eqn (16) the activity coefficient can be calculated according to eqn (19). When we plot $\ln K_s^x$ against $\ln(\gamma_{MS}\gamma_A/\gamma_{MA}\gamma_S)$ the intercept equals the thermodynamic equilibrium constant ($\ln K_s^o$) and the theoretical $\ln K_s^x$ can be calculated from the following equation:

$$\ln K_s^x = \ln K_s^o + \ln \frac{\gamma_{MA}\gamma_S}{\gamma_{MS}\gamma_A}. \quad (20)$$

The results are shown in Tables 4 and 5.

Table 3. Log β^o_{301} and Q_{301} of PrA_3B and NdA_3B

		PrA_3B		NdA_3B	
Solvent	$3pK_{aE} + \log P_s$	$\log \beta^o_{301}$	Q_{301}	$\log \beta^o_{301}$	Q_{301}
Benzene	23.10	26.22	75.25	26.41	75.44
Toluene	22.61	25.69	72.20	26.03	72.54
Xylene	21.83	24.86	70.40	25.32	70.86
CCl_4	22.06	25.01	68.45	25.23	68.67

Table 4. Extraction equilibrium constants of Pr(III)

Solvent	log K_{ex}	log $K_{s.c.}$	log K_s	ln K_s^x(exp)	ln $\frac{\gamma_{MS}\gamma_A}{\gamma_{MA}\gamma_S}$	ln K_s^x(calc.)
CCl_4	−3.44	2.95	6.39	14.72	−5.21	17.01
Xylene	−4.18	3.03	7.21	16.60	−4.78	16.58
Toluene	−4.05	3.08	7.13	16.42	−4.56	16.36
Benzene	−3.75	3.12	6.87	15.82	−4.01	15.81

Linear regression: $b = 11.70$, $m = -1.028$, $r = -0.9983$ (except for CCl_4). Adjusted $\ln K_s^o = 11.80$.

Table 5. Extraction equilibrium constants of Nd(III)

Solvent	log K_{ex}	log $K_{s.c.}$	log K_s	ln K_s^x(exp)	ln $\frac{\gamma_{MS}\gamma_A}{\gamma_{MA}\gamma_S}$	ln K_s^x(calc.)
CCl_4	−3.30	3.17	6.47	14.90	−5.31	17.18
Xylene	−3.77	3.49	7.26	16.72	−4.87	16.74
Toluene	−3.75	3.42	7.17	16.51	−4.65	16.52
Benzene	−3.60	3.31	6.91	15.91	−4.07	15.92

Linear regression: $b = 11.77$, $m = -1.017$, $r = -0.9999$ (except for CCl_4). Adjusted $\ln K_s^o = 11.87$.

The plots of $\ln K_s^x$ against $\ln(\gamma_{MS}\gamma_a/\gamma_{MA}\gamma_S)$ are close to a straight line with a slope of −1 for xylene, toluene and benzene, but not for CCl_4. Again the calculated values of $\ln K_s^x$ are in good agreement with the experimental constants for xylene, toluene and benzene, but not for CCl_4 (Tables 4 and 5). The abnormal behavior in CCl_4 can be rationalized by the following comparison.

In the extraction by HPMBP, the values of $\log K_{ex}$ are in such order: CCl_4 > benzene > toluene > xylene. However, in the synergic extraction the $\log K_s$ of the reaction in the organic phase are in the reverse order: xylene > toluene > benzene > CCl_4. This experimental fact confirms that in the synergic reaction phen competes with HA. The more stable the self-adducts LnA_3HA, the more difficult is the formation of LnA_3B. But why the LnA_3HA self-adduct is most stable in CCl_4 is a question to be further investigated. We can conclude that, in the system studied, the regular-solution theory can be applied to the π-donor solvent series of benzene, toluene and xylene, but not to CCl_4. We agree with Li and Xu in saying that the Hildebrand regular-solution theory is too simple to be widely applicable but it is still useful for systems in different inert solvents which are very similar in structure.

Acknowledgement—We gratefully acknowledge the support and instruction from Professor Zhang Dingrong of Chemistry Department, Anhui Normal University.

REFERENCES

1. S. Nakamura, H. Imura and N. Suzuki, *Inorg. Chim. Acta* 1985, **109**, 157.
2. L. Li and G. Xu, *Acta Chim. Sin.* (in Chinese) 1982, **40**, 1.
3. T. Sekine and Y. Hasagawa, *Solvent Extraction Chemistry*, p. 203. Marcel Dekker, New York (1977).
4. J. A. Riddick and W. B. Bunger, *Technique of Chemistry, Vol.* II. *Organic Solvents*, 3rd Edn. Wiley Interscience, London (1970).
5. R. C. Weast, *Handbook of Chemistry and Physics*, 64th Edn. CRC Press, Cleveland, OH (1983–1984).
6. L. Li and K. H. Hsu, *Acta Chim. Sin.* (in Chinese) 1978, **36**, 239.
7. G. Gran, *Acta Chim. Scand.* 1950, **4**, 559.
8. C. Hsu, C. S. Hu, X. P. Jia and J. M. Pan, *Anal. Chim. Acta* 1981, **124**, 177.
9. G. Anderegg and S. E. Rasmussen, *Stability Constants*—I. *Organic Ligands*, No. 6. The Chemical Society, London (1957).
10. M. Luo, L. Cheng, L. Song and D. Zhang, *J. Inorg. Chem.* (in Chinese) 1986, **2**, 39, published by the Editorial Staff of *Inorganic Chem.*, Chinese Chemical Society.
11. A. Roy and K. Nag, *J. Inorg. Nucl. Chem.* 1978, **40**, 331.

Polyhedron Vol. 6, No. 5, pp. 963–968, 1987
Printed in Great Britain

0277–5387/87 $3.00+.00

SYNERGIC EXTRACTION OF Cd(II) WITH MIXTURES OF 4-METHYL-*N*-8-QUINOLINYLBENZENESULPHONAMIDE AND TRI-*n*-BUTYLPHOSPHATE OR TRI-*n*-OCTYLPHOSPHINE OXIDE DISSOLVED IN TOLUENE

J. M. CASTRESANA* and M. P. ELIZALDE

Departamento de Química, Universidad del País Vasco, Apartado 644, 48080 Bilbao, Spain

M. AGUILAR

Departamento de Química, E.T.S.I.I.B., Universidad Politécnica de Cataluña, Diagonal 647, Barcelona 02028, Spain

and

M. COX

Division of Chemistry, The Hatfield Polytechnic, Hertfordshire, U.K.

(*Received* 7 *August* 1986; *accepted* 4 *September* 1986)

Abstract—The distribution equilibria of Cd(II) from 0.1 mol dm^{-3} KNO_3 with mixtures of 4-methyl-*N*-8-quinolinylbenzenesulphonamide and the organophosphorus compounds tri-*n*-butylphosphate (TBP) or tri-*n*-octylphosphine oxide (TOPO) dissolved in toluene have been investigated. The composition of the extracted species and values of the corresponding stoichiometric extraction constants have been deduced following both graphical and numerical treatments of experimental data. Synergic effects are bigger with TOPO than with TBP in agreement with its greater ability to displace water molecules from the coordination sphere of the metal ion.

The commercial extractant reagent LIX 34 (Henkel Corp.) was introduced by Kordosky *et al.*[1] and its chemical structure, an 8-alkarylsulphonamidoquinoline, and synthesis were disclosed by Virnig[2] in 1977. Although more emphasis has been given to the LIX 34–Cu(II) system, including equilibria, kinetic studies and pilot plant evaluations,[1,3–5] the extraction of some other metals including Zn(II), Cd(II), Pb(II) and Hg(II) has also been reported.[6–11] Synergic effects on the extraction of Zn in the presence of neutral donors have been claimed although no data on the composition of the extracted species has been indicated.[9] No synergism was found when mixtures of LIX 34 and carboxylic or alkylphosphoric acids were employed.[3,8] The present work was undertaken in order to explore the existence of synergism on the extraction of Cd(II) with mixtures of 8-sulphonamidoquinoline derivatives and neutral donors. The synthesized reagent 4-methyl-*N*-8-quinolinylbenzenesulphonamide was chosen as a model compound closely related to the active component in LIX 34[12] but available in a higher state of purity, and therefore allowing the determination of significant constant values, which are of paramount importance in the design of any liquid–liquid extraction procedure. Some chemical and extractive properties of the reagent have been published elsewhere.[12–15] The organophosphorus compounds tri-*n*-butylphosphate (TBP) and tri-*n*-octylphosphine oxide (TOPO) have been chosen since their interaction equilibria with the reagent are known.[16] On the other hand their different basic properties allow one to study the influence of the basicity of the neutral donor on the extraction equilibria.

* Author to whom correspondence should be addressed.

EXPERIMENTAL

Reagents and solutions

4-Methyl-*N*-8-quinolinylbenzenesulphonamide was synthesized and purified as described previously.[17] TBP (Merck p.a.), TOPO (Eastman–Kodak p.a.) and toluene (Scharlau p.a.) were used as received. Stock solutions containing Cd(II) were prepared in distilled deionized water from $Cd(NO_3)_2 \cdot 4H_2O$ (Merck p.a.) and its ionic content was checked by evaporating an aliquot and weighing the residue. All other chemicals used were of analytical-reagent quality and used without further purification.

Experimental technique

Equal volumes (10 cm^3) of both organic and aqueous phases were mechanically shaken in special stoppered test tubes at 293 ± 2 K for at least 40 min. Preliminary experiments had shown that equilibrium was reached in about 20 min with both synergic mixtures. The aqueous phase contained 5.0×10^{-4} mol dm^{-3} Cd(II) in 0.1 mol dm^{-3} KNO_3. The concentration of 4-methyl-*N*-quinolinylbenzenesulphonamide was 1.0×10^{-2} mol dm^{-3} whereas the concentration of the organophosphorus compounds was varied in the ranges 2.3×10^{-2}–7.8×10^{-1} mol dm^{-3} for TBP and 2.0×10^{-3}–1.0×10^{-2} mol dm^{-3} for TOPO. Organic mixtures had been preconditioned with the proper nitrate solution prior to use in order to avoid volume changes. After phase separation by centrifugation, the H^+ concentration in the aqueous phase was evaluated potentiometrically using a combined glass electrode. The distribution coefficient (D), defined as the ratio between the total organic and aqueous metal concentration, was determined after removing aliquots of both phases for analysis of Cd(II) by A.A.S. The copper content of the organic phase was measured by stripping the metal into 1.0 mol dm^{-3} sulphuric acid. All the data which did not fulfill the mass balance for cadmium within 4% were rejected.

RESULTS AND DATA TREATMENT

The extraction of Cd(II) from nitrate medium with the synergic mixtures of 4-methyl-*N*-8-quinolinylbenzenesulphonamide (HR) and the organophosphorus compounds TBP or TOPO (generically denoted as S), can be represented by the following general equilibrium:

$$Cd^{2+} + rNO_3^- + pHR_{org} + qS_{org} \rightleftharpoons Cd(NO_3)_rR_pS_{q,org} + pH^+, \quad (1)$$

where the absence of polynuclear metal complexes and molecules of the chelating agent solvating the extracted species has been implied. Both facts have been proved in a former work[18] when studying the extraction of several metal ions, including Cd(II), from the same ionic medium using the chelating reagent in toluene.

The distribution coefficient of the metal ion can be expressed as:

$$D = \sum_r \sum_p \sum_q K'_{rpq}[HR]^p_{org}[S]^q_{org}[NO_3^-]^r h^{-p}, \quad (2)$$

where h stands for $[H^+]$ and K'_{rpq} is a conditional extraction constant defined by:

$$K'_{rpq} = K_{rpq}\alpha_{Cd}^{-1}, \quad (3)$$

K_{rpq} being the stoichiometric equilibrium constant for reaction (1) and α_{Cd} the side-reaction coefficient of the metal ion due to the formation of nitrate complexes in the aqueous phase.

Experimental data of type $\log D = f(\text{pH})$ obtained at constant chelating agent concentration and different concentration levels of the two organophosphorus compounds are shown in Figs 1 and 2, respectively. From the slope values (ranging from 1.84 to 1.90) of the straight lines obtained, and taking into account the electroneutrality condition of the extracted species in the organic phase, it can be inferred that the stoichiometric coefficients of the predominant extracted complex have the values $p = 2$ and $r = 0$.

According to eqn (2), values of the stoichiometric coefficient q can be deduced from the plots of the function $\log D - p \log [HR] = f(\log [S]_{org})$ obtained at constant pH values. Distribution coefficient data for the plots were obtained from the intercepts of the experimental $\log D = f(\text{pH})$ with straight lines par-

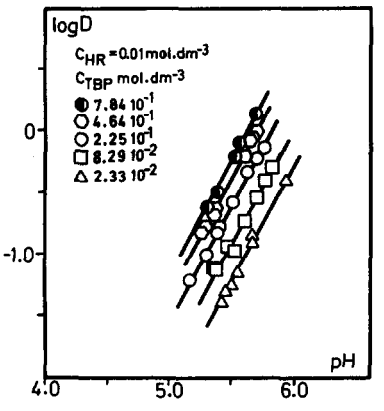

Fig. 1. $\log D$ vs pH for Cd(II) extraction at constant chelating reagent and different TOPO concentrations. Continuous lines were drawn using constants given in Table 1.

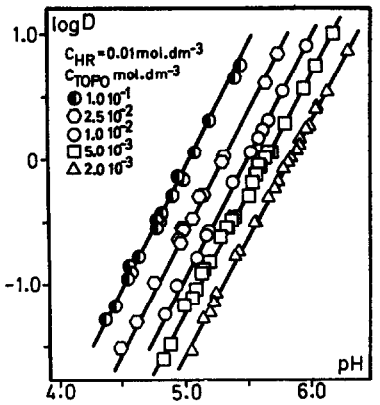

Fig. 2. $\log D$ vs pH for Cd(II) extraction at constant chelating reagent and different TBP concentrations. Continuous lines were drawn using constants in Table 1.

allel to the abscissa axis. Taking into account the proved monomeric behaviour of the reagent in toluene,[17] the free-extractant concentration used in the plots was calculated from the mass balance of the reagents:

$$C_S = [S]_{org}(1+\beta_{11}[HR]_{org}), \quad (4)$$

$$C_{HR} = [HR]_{org}(1+K_D^{-1}+K_{a1}^{-1}K_D^{-1}h + K_{a2}K_D^{-1}h^{-1}+\beta_{11}[S]_{org}), \quad (5)$$

where K_D, K_{a1} and K_{a2} are, respectively, the distribution and acidity constants of the chelating reagent, and β_{11} represents the equilibrium constant for the formation of the 1:1 adduct between the chelating agent and the organophosphorus compounds in the organic phase. Values of these constants had been previously determined.[16,19] In the above mass balances, the concentration of the extractants bound to the metal ion has been disregarded since a high extractant/metal concentration ratio was used in the experiments.

Figure 3 shows that the plots of the experimental function $\log D - 2\log[HR]_{org} = f(\log[S]_{org})$ at different pH values follow, in both systems, an upward curve when increasing the concentration of the organophosphorus compounds, having a limiting slope value of 1. Consequently, the main extracted species seems to have the stoichiometries CdR_2 and CdR_2S, respectively.

In order to confirm the validity of this extraction model, and determine the values of the extraction constants, a grahical curve fitting treatment was carried out. According to the model eqn (1) will take the form:

$$D = K'_{020}[HR]_{org}^2 h^{-2} + K'_{021}[HR]_{org}^2[S]_{org}h^{-2}. \quad (6)$$

Equation (6) can be rearranged and reduced to:

$$Y = 1 + X, \quad (7)$$

Y and X being the following normalized variables:

$$Y = DK'^{-1}_{020}[HR]^{-2}_{org}h^2, \quad (8)$$

$$X = K'_{021}K'^{-1}_{020}[S]_{org}. \quad (9)$$

Since the experimental function $\log D - 2\log[HR]_{org} = f(\log[S]_{org})_{pH}$ and the theoretical $\log Y = \log(1+X) = f(\log X)$ only differ in constant values:

$$(\log D - 2\log[HR]_{org}) - \log Y = \log K'_{020} + 2pH, \quad (10)$$

$$\log X - \log[S]_{org} = \log K'_{021}K'^{-1}_{020}, \quad (11)$$

from the differences in both axes in the position of best fit between the functions (Fig. 3), values of $\log K'_{020} + 2pH$ and $\log K'_{020}K'^{-1}_{021}$ were, respectively, deduced. The straight lines, slopes close to 2 and 0, respectively, obtained when plotting the former differences as a function of pH are in agreement with the proposed model. As an example of

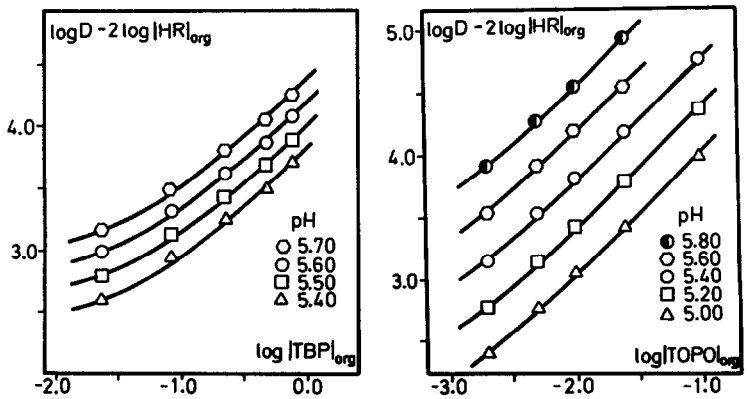

Fig. 3. Position of best fit between the theoretical $\log Y = f(\log X)$ (continuous lines) and experimental data $\log D - 2\log[HR]_{org} = f(\log[S]_{org})$ at different constant pH values in the presence of TBP or TOPO.

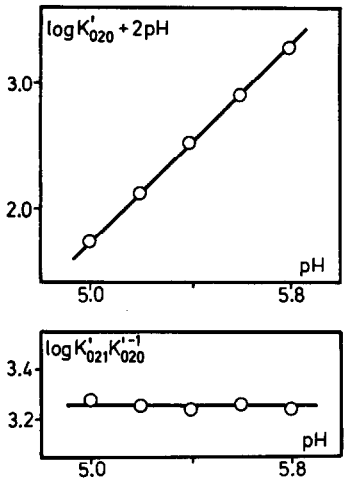

Fig. 4. Differences on both axes between experimental and theoretical functions in Fig. 3 as a function of pH.

the plots, Fig. 4 shows the ones obtained for the extraction of Cd(II) in the presence of TOPO. Graphical values of the stoichiometric extraction constants were calculated from the conditional values derived in the former treatment and published cadmium nitrate complex constants.[20] Table 1 shows the values of the extraction constants graphically derived.

The experimental data were finally treated numerically by means of the LETAGROP–DISTR program[21] in order to refine the values of the extraction constants as well as to look for new models of species which could improve the goodness of the fit. The error square sum (U) extended to the total number of experimental data (N_p) and defined as:

$$U = \sum_{N_p} (\log D_{\text{calc.}} - \log D_{\text{exp}})^2, \qquad (12)$$

was used in the minimization process. D_{exp} represent the experimental distribution coefficient and $D_{\text{calc.}}$ the corresponding value calculated by the program for the model tested after solving the mass balance equations of the components of the system. Therefore, the best model is the one which gives the lowest values of both U and the mean standard deviation $\sigma(\log D) = (U/N_p)^{1/2}$.

The calculations were performed taking the set of species and extraction constants graphically derived as the starting input and considering the influence on the minimized function when partially varying or adding new species to the model. The results obtained are summarized in Table 2.

Table 1. Values of the stoichiometric equilibrium constants for the extraction of Cd(II) with mixtures of 4-methyl-*N*-8-quinolinylbenzenesulphonamide (HR) and the organophosphorus compounds TBP or TOPO dissolved in toluene

System	Method of calculation	log K_{020}	log K_{021}	log K_{110}
Cd/HR–TBP	Graphical	−8.33	−6.93	—
	LETAGROP	−8.44±0.22	−6.89±0.04	−5.57 (max −5.05)
Cd/HR–TOPO	Graphical	−8.13	−4.87	—
	LETAGROP	−8.50 (max −8.30)	−4.90±0.02	−5.31 (max −4.99)

Table 2. Results of the numerical calculations with the LETAGROP–DISTR program for the different models tested

Species $Cd(NO_3)_rR_pS_q$ (r,p,q)	S = TBP		S = TOPO	
	U_{min}	$\sigma(\log D)$	U_{min}	$\sigma(\log D)$
(0,2,0), (0,2,1)	0.043	0.036	0.122	0.037
(0,2,0), (0,2,2)	0.727	0.146	4.780	0.230
(0,2,0), (1,1,1)	0.495	0.121	0.192	0.046
(0,2,0), (0,2,1), (1,1,0)[a]	0.041	0.035	0.112	0.035
(0,2,0), (0,2,1), (1,1,1)	0.043	0.036	0.121	0.037
(0,2,0), (0,2,1), (1,1,0), (1,1,1)	0.043	0.036	0.120	0.037

[a] Proposed model.

Two species models different to the one graphically derived give rise, in both systems, to worse fits of the experimental data. However, the inclusion in the model of the mixed complex $Cd(NO_3)R$ improves the fit to the data and eliminates systematic errors. The existence of the mixed species can explain the slight deviations to lower values than 2 of the slopes of the $\log D = f(\text{pH})$ data for all the concentrations of TBP and TOPO studied. The values of the equilibrium extraction constants calculated by the program are shown in Table 1 and are in good agreement with the values graphically deduced.

CONCLUSIONS

The extraction of Cd(II) from nitrate medium by mixtures of 4-methyl–*N*-quinolinylbenzenesulphonamide and the organophosphorus compounds TBP or TOPO dissolved in toluene takes place mainly by the formation of the chelate CdR_2 and the adduct CdR_2S. Experimental data in both systems are better explained by the inclusion in the model of the mixed species $Cd(NO_3)R$. Although support by independent methods should be desirable to conclude about its presence, it should be pointed out that mixed species of this type have been also postulated in the extraction of several metal ions, including Cd(II) with 8-sulphonamidequinoline derivatives.[18,22] Moreover, a similar complex has been proved to be even predominant in the extraction of Cu(II) with 4-methyl–*N*-8-quinolinylbenzenesulphonamide in the presence of TBP.[23] On the other hand, a fairly good agreement between the values of its extraction constant have been found in the present work in the two systems studied.

On the basis of the extraction data, the constants for the adduct formation in the organic phase (β_s) represented by the reaction:

$$CdR_{2,org} + S_{org} \rightleftharpoons CdR_2S_{org} \qquad (13)$$

mainly responsible of the synergic effect in the systems, were calculated taking into account that:

$$\beta_s = K_{021}K_{020}^{-1}. \qquad (14)$$

A higher constant value and consequently a larger synergic effect was obtained with TOPO ($\log \beta_s = 3.60$) than in the presence of TBP ($\log \beta_s = 1.55$). The result is in agreement with the order of basicity and the capacity of water displacement of the organophosphorus compounds. The different synergic efficiency can be appreciated in Fig. 5, where the percentage of Cd(II) extraction as a function of pH has been plotted in the absence and presence of the solvating extractants.

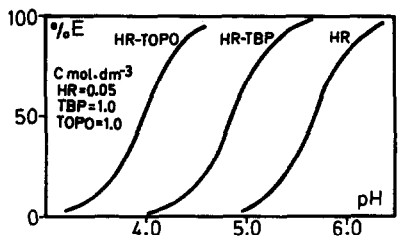

Fig. 5. Percentage extraction of Cd(II) as a function of pH with the chelating reagent and the synergic mixtures.

REFERENCES

1. G. A. Kordosky, K. D. Mackay and M. J. Virnig, 105th AIME Annual Meeting. Las Vegas (1976)
2. M. J. Virnig, *Proceedings of the International Solvent Extraction Conference ISEC'77*, CIM Special Volume 1979, **21**, 535.
3. I. L. Dukov and S. Guy, *Hydrometallurgy* 1982, **8**, 77.
4. F. Nakashio, K. Kondo, M. Matsumoto and K. Yoshizuka, *Proceedings of the International Solvent Extraction Conference ISEC'83*. Denver, p. 22 (1983).
5. D. S. Flett and J. Melling, *Hydrometallurgy* 1979, **10**, 135.
6. Y. C. Hoh and W. K. Wang, *Proceedings of the International Solvent Extraction Conference ISEC'80*, No. 80-92. Liege (1980).
7. C. H. Wang and Y. C. Hoh, *Hydrometallurgy* 1982, **8**, 161.
8. Y. C. Hoh and W. K. Wang, *J. Chem. Technol. Biotechnol.* 1981, **31**, 345.
9. Y. C. Hoh, N. P. Chou and W. K. Wang, *Ind. Eng. Chem. Process Des. Dev.* 1982, **21**, 12.
10. V. Arenas, H. Lizama, R. Schrebler and I. Gardiazabal, *Proceedings of the International Solvent Extraction Conference ISEC'83*, Denver, p. 253 (1983).
11. Y. C. Hoh and W. S. Chuang, *Hydrometallurgy* 1983, **10**, 123.
12. M. Cox and W. J. van Bronswijk, *Proceedings of the International Solvent Extraction Conference ISEC'80*, No. 80-15. Liege (1980).
13. S. U. Kreingol'd, E. A. Bozheevol'nov and G. V. Serebryakova, *Tr. Vses. Nauchno-Issled. Inst. Khim. Reaktivov* 1963, **25**, 422.
14. M. Tagaki, T. Omori, S. Matsuo, K. Ueno and S. Ide, *Chem. Lett.* 1980, 387.
15. S. Ide, T. Yoshida, S. Matsuo, M. Tagaki and K. Ueno, *Anal. Chim. Acta* 1983, **149**, 235.
16. J. M. Castresana, M. P. Elizalde, M. Aguilar and M. Cox, *20th Meeting of the Royal Spanish Chemical Society*, No. 8-140. Castellón (1984).
17. M. P. Elizalde, J. M. Castresana, M. Aguilar and M. Cox, *Chem. Scr.* 1985, **25**, 300.
18. J. M. Castresana, M. P. Elizalde, M. Aguilar and M. Cox, *Chem. Scr.* 1986, **26**, 325.
19. J. M. Castresana, M. P. Elizalde, M. Aguilar and M. Cox, *Quim. Anal.* (in press).

20. R. M. Smith and A. E. Martell, *Critical Stability Constants*, Vol. 4: *Inorganic Ligands*. Plenum Press, New York (1977).
21. D. H. Liem, *Acta Chem. Scand.* 1971, **25**, 1521.
22. G. Sandström, L. Hummelstedt and M. Hagström, *Ion Exchange and Solvent Extraction*, Oslo, Symposium SCI (1982).
23. J. M. Castresana, J. L. Aparicio, M. P. Elizalde, M. Aguilar and M. Cox, *Hydrometallurgy*, 1986, **15**, 363.

Polyhedron Vol. 6, No. 5, pp. 969–974, 1987
Printed in Great Britain

0277–5387/87 $3.00+.00

IRON(III) AMINO ACID COMPLEXES: EVIDENCE FOR THE EXISTENCE OF A SPIN EQUILIBRIUM

J. MARY ELIZABATHE and P. S. ZACHARIAS*

School of Chemistry, University of Hyderabad, Hyderabad 500134, India

(*Received* 26 *February* 1986; *accepted after revision* 16 *September* 1986)

Abstract—Iron(III) amino acid complexes of general composition Fe(amino acid)(OH)Cl · $2CH_3OH$ were synthesized and investigated. The analytical and other physical data support this formulae. The spectral, variable-temperature magnetic and Mössbauer data suggest the presence of a spin equilibrium involving $S = \frac{1}{2}$ and $S = \frac{3}{2}$ spin states, and this is attributed to the large distortions in the compounds.

Investigations on iron(III) amino acid complexes have been very few compared to other transition metals, probably due to the preparative difficulties of these compounds. Of the few iron(III) amino acid complexes known, DL-methionine has been reported to yield either 1 : 1 or 1 : 3 compounds.[1,2] Trimeric iron(III) compounds have been reported for some other amino acids.[3,4] Since the available structural data on either 1 : 1 or 1 : 3 type amino acid complexes are very limited, it was decided to investigate them systematically as part of our general investigations on the amino acid complexes.[5–7] Attempts to repeat the synthesis of 1 : 3 type complexes by the procedure given earlier[2] were unsuccessful, an observation made previously also.[1] This paper describes the syntheses of and investigations on 1 : 1 type iron(III) complexes by spectral, magnetic and Mössbauer methods.

EXPERIMENTAL

Methanol and ether were distilled over $Mg(OMe)_2$ and $LiAlH_4$, respectively, before use. All the preparative work was carried out under dry nitrogen. Preparation of all the complexes was carried out by a general procedure as given below.[1]

Preparation of the lithium salts of amino acids

A mixture of amino acid (10 mmol) and lithium hydroxide (12 mmol) in methanol (30 cm^3) was stirred at 50°C for 30 min. The unreacted lithium hydroxide was filtered off and the filtrate on cooling gave the lithium salt as a white solid. This was filtered and dried *in vacuo*.

Preparation of the iron(III) *complexes*

To a stirred solution of the lithium salt of amino acid (5 mmol) in methanol (20 cm^3) was added anhydrous iron(III) chloride (5 mmol) in methanol (10 cm^3). On addition of ether (100 cm^3) to the resultant reddish brown solution a pale yellow complex separated out, which was filtered and dried. The complex was purified from methanol and ether. Some compounds are highly hygroscopic and hence some of the physical measurements could not be done on them. The variable-temperature magnetic-moment data on some selected compounds are given below. The compounds are represented by their composition with the abbreviated form of the amino acid. These abbreviations are explained in Table 1.

Variable-temperature magnetic-moment data (T *in* K, μ_{eff} *in* BM)

Fe(met)(OH)Cl · $2CH_3OH$: 295, 3.49; 240, 3.3; 200, 3.10; 160, 2.89; 110, 2.59; 86, 2.47; 44, 2.37; 28, 2.22; 14, 2.12.

Fe(leu)(OH)Cl · $2CH_3OH$: 297, 3.49; 260, 3.30; 220, 3.04; 190, 2.83; 165, 2.63; 140, 2.43; 120, 2.25; 100, 2.06; 88, 1.92; 78, 1.90.

Fe(his)(OH)Cl · $2CH_3OH$: 297, 3.49; 240, 3.43; 200, 3.28; 160, 3.15; 130, 3.00; 110, 2.89; 85, 2.75; 60, 2.59; 40, 2.56; 30, 2.40; 22, 2.31; 16, 2.26.

* Author to whom correspondence should be addressed.

Table 1. Analytical, TGA and conductance data of Fe(amino acid)(OH)Cl·$2CH_3OH$ compounds

Compound[a]	Analytical data[b]					TGA data[b]	
	% C	% H	% N	% Cl	Fe	(% wt change)	Conductance[c]
Fe(met)(OH)Cl·$2CH_3OH$	26.4	5.2	4.8	11.4	17.4	21	63
	(26.2)	(6.0)	(4.4)	(11.1)	(17.2)	(20)	
Fe(leu)(OH)Cl·$2CH_3OH$	31.5	6.8	4.3	11.5	18.4	21.1	65
	(31.7)	(7.0)	(4.6)	(11.7)	(18.5)	(20.8)	
Fe(val)(OH)Cl·$2CH_3OH$	29.5	6.6	4.1	12.5	19.5	22.1	60
	(29.1)	(6.6)	(4.9)	(12.3)	(19.4)	(20.6)	
Fe(his)(OH)Cl·$2CH_3OH$	29.1	5.3	12.6	10.7	16.9	19.6	[d]
	(29.4)	(5.3)	(12.8)	(10.9)	(17.1)	(18.8)	
Fe(asn)(OH)Cl·$2CH_3OH$	23.5	5.4	9.8	11.3	18.7	21.1	[d]
	(23.7)	(5.3)	(9.2)	(11.7)	(18.4)	(20.4)	
Fe(phe)(OH)Cl·$2CH_3OH$	39.6	5.2	4.4	10.2	16.6	19.0	60
	(39.2)	(5.7)	(4.2)	(10.5)	(16.6)	(19.7)	
Fe(trp)(OH)Cl·$2CH_3OH$	[d]				14.3	17.0	54
					(14.9)	(16.0)	
Fe(ala)(OH)Cl·$2CH_3OH$	[e]					24.8	79
						(23.8)	
Fe(pro)(OH)Cl·$2CH_3OH$	[e]					22.3	64
						(21.5)	

[a] met = methionine, leu = leucine, val = valine, his = histidine, asn = asparagine, phe = phenylalanine, trp = tryptophan, ala = alanine, pro = proline.

[b] Numbers in parentheses correspond to theoretical values.

[c] In mho cm^2 mol^{-1}.

[d] Not done.

[e] Hygroscopic and hence not measured.

Fe(asn)(OH)Cl·$2CH_3OH$: 297, 3.21; 244, 3.10; 200, 2.98; 160, 2.72; 130, 2.58; 110, 2.48; 84, 2.29; 60, 2.12; 40, 2.02; 30, 1.96; 25, 1.95; 16, 1.90.

Fe(phe)(OH)Cl·$2CH_3OH$: 297, 3.49; 238, 3.32; 204, 3.14; 160, 2.94; 130, 2.78; 110, 2.66; 85, 2.46; 40, 2.12; 32, 2.05; 18, 1.94.

C, H, N and Cl analyses were done by the Australian Microanalytical Service and Fe content was estimated gravimetrically by the oxine method. Room-temperature magnetic-susceptibility measurements were done on a Bruker BM-6 susceptibility set up and variable-temperature measurements using a Sartorius microbalance. IR spectra were recorded on a Perkin–Elmer Model 297 Spectrophotometer and ESR spectra using a JEOL JES FE-3X spectrometer. A PARC 6001 Photo Acoustic Spectrometer was used for electronic spectra of solids whereas solution measurements were carried out on a Cary 17D Spectrophotometer. Mössbauer spectra were recorded employing a constant-acceleration Elscint drive in conjunction with a multichannel analyzer (Promeda). Differential scanning calorimetry was done using a Perkin–Elmer DSC-4.

RESULTS AND DISCUSSION

The analytical data are presented in Table 1 on some selected compounds only since other compounds are highly hygroscopic. The data agree with a general composition of Fe(amino acid)(OH)Cl·$2CH_3OH$, where amino acid stands for the corresponding monoanion. The presence of chlorine is confirmed from the analytical data. The conductances of these complexes in methanol is of the order ~ 60 mho cm^2 mol^{-1}, and are given in Table 1. A reasonable range of conductance values for 1:1 electrolytes[8] is 80–115 mho cm^2 mol^{-1}. Thermogravimetric analysis showed a weight loss corresponding to two molecules of methanol. The TGA data are given in Table 1. Differential scanning calorimetric experiments on a few selected compounds support the TGA results. There is a broad band at ~ 3400 cm^{-1} in the IR spectra of the complexes. Although such bands are associated with OH groups, this cannot be considered as a conclusive proof for its presence since the OH groups of the solvent CH_3OH molecules can also give a band at this position. The overall com-

position satisfies the +3 oxidation state of the metal ion in the complexes.

The room- and low-temperature magnetic-moment values are collected in Table 2. The room-temperature magnetic-moment values are in the range 3.2–3.5 BM. The two known compounds Fe(met)(OH)$NO_3 \cdot 2CH_3OH$ and Fe(met)(OH)Cl·$2CH_3OH$ are reported to have μ_{eff} values of 6.39 and 4.21 BM, respectively.[1] On the basis of this observation, the nitrato compound was assigned an octahedral geometry with iron in the +3 oxidation state. No explanation was given for the low μ_{eff} value of the chloride complex. The trimeric iron(III) amino acid systems of general composition $[Fe_3O(\text{amino acid})_6(H_2O)_3](NO_3)_7$ have μ_{eff} values in the range 2.8–3.6 BM. The Fe^{3+} centre in these compounds is in octahedral geometry and hence μ_{eff} values of ~ 5.9 BM would have been expected for them. The low μ_{eff} values have been attributed to the antiferromagnetic interactions in these trinuclear systems.[4] The 1:3 complexes of type Fe(amino acid)$_3$ have been reported to be octahedral high-spin complexes with μ_{eff} values of ~ 5.6 BM.[2]

The room-temperature μ_{eff} values of 3.2–3.5 BM reported in Table 2 for the present compounds are too small for high spin ($S = \frac{5}{2}$) complexes ($\mu_{eff} \sim 5.9$ BM) or too large for low spin ($S = \frac{1}{2}$) iron(III) complexes ($\mu_{eff} \sim 2.00$ BM). For iron(III) compounds of intermediate spin ($S = \frac{3}{2}$), the expected μ_{eff} value is ~ 4.0 BM. The intermediate μ_{eff} values observed for the present iron(III) amino acid complexes can result from: (i) antiferromagnetic type interactions assuming a trimeric structure, (ii) a spin equilibrium between the low- and high-spin states, and (iii) a quantum mechanical mixing of spin states. However, a trimeric structure[4] of type $[Fe_3O(\text{amino acid})_6(H_2O)_3]Cl_7$ does not fit with the analytical data and hence is not considered for discussion. The second and third alternatives differ in that the spin equilibrium systems contain molecules which have two magnetically distinguishable pure spin states,[9] whereas the spin-admixed system contains only a

Table 2. Magnetic-moment, electronic and Mössbauer spectral data of Fe(amino acid)(OH)Cl·$2CH_3OH$ compounds

Compound	μ_{eff}[a] (M) RT (~ 297 K)	μ_{eff}[a] (M) LT (~ 15 K)	Electronic spectral data[b] [ν (ε)] Solid	Electronic spectral data[b] [ν (ε)] Solution	Mössbauer spectral data[c] δ (mm s^{-1})	Mössbauer spectral data[c] ΔE (mm s^{-1})
Fe(met)(OH)Cl·$2CH_3OH$	3.49	2.12	10,900	10,500 (1)	0.79	0.60
	(74)	(12)	21,500	21,500 (105)	(0.92)	(0.73)
Fe(leu)(OH)Cl·$2CH_3OH$	3.49	1.9	11,000	10,500 (1)	0.77	0.64
	(74)		21,700	21,300 (180)	(0.94)	(0.75)
Fe(val)(OH)Cl·$2CH_3OH$	3.19	[d]	11,000	10,500 (1)	0.75	0.65
	(56)		21,300	21,500 (175)	(0.80)	(0.79)
Fe(his)(OH)Cl·$2CH_3OH$	3.49	2.26	11,100	[e]	0.75	0.66
	(74)	(13)	21,500			
Fe(asn)(OH)Cl·$2CH_3OH$	3.21	1.90	10,500	[e]	0.72	0.64
	(58)		21,300			
Fe(phe)(OH)Cl·$2CH_3OH$	3.49	1.94	10,900	10,500 (1)	0.71	0.68
	(74)	(1)	21,500	21,500		
Fe(trp)(OH)Cl·$2CH_3OH$	3.40	[d]	11,100	[f]	0.79	0.63
	(68)		21,500	21,500 (165)		
Fe(ala)(OH)Cl·$2CH_3OH$	[g]		10,700	10,300 (1)	0.75	0.65
			21,500	21,500 (175)		
Fe(pro)(OH)Cl·$2CH_3OH$	[g]		10,200	10,500	0.79	0.63
			21,300	21,500 (255)		

[a] Values in parentheses correspond to percentage high spin. RT = room temperature, LT = low temperature.
[b] ν in cm^{-1}, ε in l mol^{-1}.
[c] At 297 K. Numbers in parentheses correspond to values at 88 K.
[d] Not measured.
[e] Insoluble.
[f] Not observed.
[g] Highly hygroscopic.

single magnetic species with magnetic properties different from those of either of the pure spin states.[9-11] The variable-temperature magnetic and other spectral data do not favour a spin-admixed system and hence will not be considered in detail. The spin equilibrium may involve the low-spin ($S = \frac{1}{2}$) and high-spin ($S = \frac{5}{2}$) forms, the low-spin ($S = \frac{1}{2}$) and intermediate-spin ($S = \frac{3}{2}$) forms, an intermediate-spin ($S = \frac{3}{2}$) and high-spin ($S = \frac{5}{2}$) forms, or all the three forms. The possibility of an equilibrium between spin states $S = \frac{3}{2}$ and $S = \frac{5}{2}$ can be easily eliminated from the low-temperature μ_{eff} values. At the lowest temperature investigated (14 K), the systems tend to approach a lower limit value of ~ 2.0 BM. Such limiting values are possible only for an $S = \frac{1}{2}$ ground state. Therefore, an equilibrium involving $S = \frac{3}{2}$ and $S = \frac{5}{2}$ spin forms for these complexes does not appear to be satisfactory. The limiting low-temperature μ_{eff} values for some selected compounds are given in Table 2 and the complete low-temperature data are presented in Experimental.

The second alternative is to consider an equilibrium between low- and high-spin states. Equilibria of the type $S = \frac{1}{2} \rightleftharpoons S = \frac{5}{2}$ are well-characterized for several iron(III) compounds. Tris(dithiocarbamato) iron(III) compounds,[12] tris(monothiocarbamato) iron(III) complexes,[13,14] tris(monothio-β-diketonato) iron(III) complexes,[15,16] $[Fe(X\text{-}Sal)_2trien]^+$ and $[Fe(AcacX)_2 trien]^+$ complexes,[17,18] $[Fe(X\text{-}Salmeen)_2]^+$,[19] $[Fe(SalAPA)_2]ClO_4$[20] and $[Fe(3\text{-}X\text{-}Salbenz)_2]^+$ complexes[21] are some examples of these well-studied systems. For systems containing Fe—S or Fe—Se bonds, the large reduction in the Racah interelectronic repulsion parameters produces strong enough ligand fields to produce spin-crossover phenomena.[22] For the $[Fe(X\text{-}Salmeen)_2]^+$ series and their hexadentate analogues with Fe—N and Fe—O bonds, the large tetragonal distortion is mainly responsible for their equilibrium behaviour.[19] For $[Fe(3\text{-}X\text{-}Salbenz)_2]^+$ complexes, two cation sites, one in a low-spin state and another as a mixture of low- and high-spin states cause the spin-crossover phenomenon.[21]

In addition, in systems like tris(4-morpholinecarbodithioato) iron(III), the equilibrium properties are considerably altered due to the presence or change in the solvent molecules in the lattice of the compounds in much the same way as varying the temperature or pressure.[23] For the unsolvated complex (FeM), the equilibrium is between low- and high-spin forms whereas for the dichloromethane solvated complex (FeMDc), the equilibrium changes to a quartet state ($S = \frac{3}{2}$) and the high-spin ($S = \frac{5}{2}$) state. For the benzene solvated complex (FeMBz), the low-temperature magnetic moment corresponds to that of the low-spin ($S = \frac{1}{2}$) ground state and it increases with increase in temperature, attaining a highest value of 3.5 BM at 300 K, representing an equilibrium situation between low- and intermediate-spin forms. Such a change in equilibrium induced by solvent molecules is possible when $S = \frac{1}{2}$, $S = \frac{3}{2}$ and $S = \frac{5}{2}$ states are all low-lying so that a small perturbation of the metal–ligand bond alters the balance between the states. In this example, the trigonal distortion causes the $^2T_2$ ($S = \frac{1}{2}$) state to split into $^2A_1$ and ^2E levels, and the $^4T_1$ ($S = \frac{3}{2}$) state into ^4E and $^4A_2$ levels. The ^4E component falls below the $^6A_1$ level. This makes the $S = \frac{3}{2}$ state thermally more accessible with respect to ^6A ($S = \frac{5}{2}$) state, thereby inducing an equilibrium between low- and intermediate-spin states.

In an analogous manner, it can be visualized that it is the large distortions from the idealized geometry that are mainly responsible for spin-crossover situations in the amino acid complexes. The reasons mentioned earlier for the $S = \frac{1}{2} \rightleftharpoons S = \frac{5}{2}$ spin equilibrium of other well-studied systems do not appear to be applicable in the present case. Such large solvent-induced distortions are very likely for these compounds of general composition Fe(amino acid)(OH)Cl·$2CH_3OH$. These distortions can split the $^2T_2$ and $^4T_1$ states and the $S = \frac{3}{2}$ state becomes thermally more accessible than the $S = \frac{5}{2}$ state. In other words, the spin equilibrium can be assumed to involve the states $S = \frac{1}{2}$ and $S = \frac{3}{2}$ rather than the states $S = \frac{1}{2}$ and $S = \frac{5}{2}$. The μ_{eff} vs T plots (Fig. 1) of these compounds resemble very closely those of iron(III) systems distorted by the presence of solvent molecules.[23,24] Assuming a μ_{eff} value of 1.9

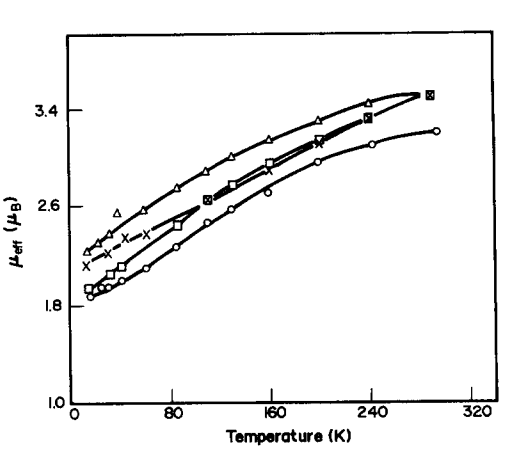

Fig. 1. μ_{eff} vs T plots of the iron(III) amino acid complexes: (—×—) Fe(met)(OH)Cl·$2CH_3OH$, (—○—) Fe(asn)(OH)Cl·$2CH_3OH$, (—□—) Fe(phe)(OH)Cl·$2CH_3OH$, and (—△—) Fe(his)(OH)Cl·$2CH_3OH$.

BM for the low-spin state ($S = \frac{1}{2}$) configuration and 3.9 BM for the intermediate-spin state ($S = \frac{3}{2}$), the room-temperature μ_{eff} value of 3.49 BM for Fe(met)(OH)Cl·CH_3OH would suggest 26% of $S = \frac{1}{2}$ and 74% of $S = \frac{3}{2}$ spin population. For other compounds also, the percentage composition is of the same order.

The electronic spectra were recorded both in the solid phase and in methanol solution. In general, the electronic transitions for iron(III) systems are spin-forbidden and hence weak, and are often masked by charge-transfer bands. However, in several spin-equilibrium systems, the high-spin ($S = \frac{5}{2}$) form has been characterized by a transition at ~ 18,000–20,000 cm^{-1} and the low-spin ($S = \frac{1}{2}$) form by another transition at ~ 14,000–16,000 cm^{-1}.[17,18,25] For a few cases with $S = \frac{3}{2}$ ground state a band at ~ 10,000 cm^{-1} is reported.[26] For the equilibrium $S = \frac{1}{2} \rightleftharpoons S = \frac{5}{2}$, the broad electronic band at ~ 10,000 cm^{-1} can be of $^4E \rightarrow {}^6A$ origin[26] and the ~ 20,000 cm^{-1} shoulder can be tentatively assigned to the $^2T_2 \rightarrow {}^2T_1$, ^2A transition of the low-spin system.[24,27]

Mössbauer spectra have been investigated for all complexes to further characterize their structures. Representative Mössbauer spectra are presented in Fig. 2. The isomer shift (δ) and quadrupole splitting (ΔE) values at room temperature are collected in Table 2. The δ values are ~ 0.6 mm s^{-1} (wrt SNP) and the ΔE value ~ 0.78 mm s^{-1}. These compounds show one quadrupole doublet at all temperatures. For systems with equilibrium, two types of Mössbauer spectral pattern can arise, depending on the relaxation time relative to the effective quadrupole period. If the time required for relaxation from one spin state to the other is larger compared to the quadrupole period, then a spectrum characteristic of individual spin states is observed. If the relaxation time is less than the effective quadrupole period, an averaged spectrum results.

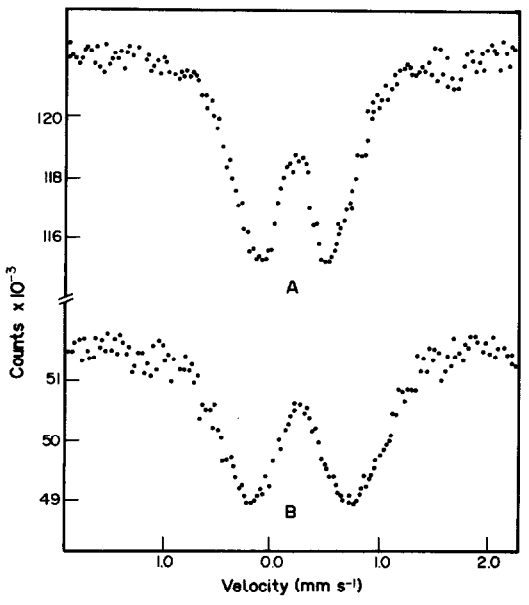

Fig. 2. Mössbauer spectra of Fe(met)(OH)Cl·$2CH_3OH$: (A) at 297 K, and (B) at 88 K.

Several iron(III) dithiocarbamato complexes, shown to be cases of low-spin–high-spin equilibrium, show an averaged Mössbauer spectrum.[24,28,29] This has been explained on the basis of distortion in the compounds. For instance, in a ligand field of perfect cubic symmetry, the energy levels simply cross and, since there is no interaction between the states, Mössbauer spectra should be a superimposition of the spectra of two individual states. When the ligand field has a lower than cubic symmetry, spin–orbit coupling allows the states to mix, resulting in rapid exchange between the low- and high-spin states. An averaged Mössbauer spectrum results from this.[28] Alternatively, a single mixed spin state can also provide an averaged Mössbauer spectrum. However, Mössbauer data cannot distinguish between them.[24]

It should be pointed out that the ΔE values for these compounds are relatively low compared to ΔE values of 2–3 mm s^{-1} reported for several $S = \frac{1}{2}$ or $S = \frac{3}{2}$ systems.[30,31] However, there are also several known cases of low and intermediate spin with ΔE values of less than 1 mm s^{-1} and values ranging from 1 to 2 mm s^{-1}.[13,30,31] When the temperature is lowered, the quadrupole interaction increases and there is an increase in the linewidth of the peaks (ΔE ~ 0.9 mm s^{-1}). The low-temperature Mössbauer data are also shown in Table 2. In fact, ΔE is expected to increase as the population of the low-spin state increases at low temperatures. The broadening of the linewidths results from the increased spin–lattice relaxation times. At liquid-nitrogen temperature (88 K), Fe(met)(OH)Cl·$2CH_3OH$ contains about 84% of the low-spin form and 16% of the $S = \frac{3}{2}$ form (deduced from μ_{eff} values).

The ESR spectrum of a polycrystalline sample of Fe(met)(OH)Cl·$2CH_3OH$ gave a line with an effective g value of 4.21 and another very broad line at a g value of 1.99. The g values for a few other compounds are: Fe(val)(OH)Cl·$2CH_3OH$, 4.35 and 2.04; and Fe(leu)(OH)Cl·$2CH_3OH$, 4.28 and 2.05. For iron(III) systems with an $S = \frac{3}{2}$ ground state in axial symmetry, ESR lines are observed,[32,33] with effective g values of 4.61 and 2.0. Although for the Fe(met)(OH)Cl·$2CH_3OH$ type compounds, $S = \frac{3}{2}$ is not the ground state, it is inferred to be

energetically close to the ground state. This might induce ESR transitions similar to those with $S = \frac{3}{2}$ ground states.

Thus the experimental results can be summarized to suggest the existence of an $S = \frac{3}{2}$ state thermally accessible to $S = \frac{1}{2}$, which is the ground state configuration, thereby providing the spin-crossover possibility. This results from the large distortions in the complexes.

Acknowledgements—We gratefully acknowledge the assistance from Prof. Erik Pedersen of the Copenhagen University and Prof. S. Mitra of TIFR, Bombay, for the low-temperature magnetic measurements, and the Special Assistance Programme in Organic Chemistry of the School. ME thanks the UGC for financial assistance.

REFERENCES

1. E. J. Halbert and M. J. Rogerson, *Aust. J. Chem.* 1972, **25**, 421.
2. C. A. McAuliffe, J. V. Quagliano and L. M. Vallarino, *Inorg. Chem.* 1966, **5**, 1996.
3. W. F. Tucker, R. O. Asplund and S. L. Holt, *Arch. Biochem. Biophys.* 1975, **166**, 433.
4. R. N. Puri and R. O. Asplund, *Inorg. Chim. Acta* 1981, **54**, L187.
5. G. Thomas and P. S. Zacharias, *Polyhedron* 1985, **4**, 811.
6. G. Thomas and P. S. Zacharias, *Transition Met. Chem.* 1984, **9**, 377.
7. G. Thomas and P. S. Zacharias, *Polyhedron* 1985, **4**, 299.
8. W. J. Geary, *Coord. Chem. Rev.* 1971, **7**, 81.
9. A. K. Gregson, *Inorg. Chem.* 1981, **20**, 81.
10. M. M. Maltempo, *J. Chem. Phys.* 1974, **61**, 2540.
11. S. Mitra, V. R. Marathe and R. Birdy, *Chem. Phys. Lett.* 1983, **96**, 103.
12. G. R. Hall and D. N. Hendrickson, *Inorg. Chem.* 1973, **12**, 2269.
13. K. R. Kunze, D. L. Perry and L. J. Wilson, *Inorg. Chem.* 1977, **16**, 594.
14. H. Nakajima, T. Tanaka, H. Kobayashi and I. Tsujikawa, *Inorg. Nucl. Chem. Lett.* 1976, **12**, 689.
15. M. Cox, J. Darken, B. W. Fitzsimmons, A. W. Smith, L. F. Larkworthy and K. A. Rogers, *J. Chem. Soc., Dalton Trans.* 1972, 1191.
16. B. F. Hoskin and C. D. Panna, *Inorg. Nucl. Chem. Lett.* 1975, **11**, 409.
17. E. V. Dose, K. M. M. Murphy and L. J. Wilson, *Inorg. Chem.* 1976, **15**, 2622.
18. M. F. Tweedle and L. J. Wilson, *J. Am. Chem. Soc.* 1976, **98**, 4824.
19. R. H. Petty, E. V. Dose, M. F. Tweedle and L. J. Wilson, *Inorg. Chem.* 1978, **17**, 1064.
20. W. D. Federer and D. N. Hendrickson, *Inorg. Chem.* 1984, **23**, 3861.
21. M. D. Timken, D. N. Hendrickson and E. Sinn, *Inorg. Chem.* 1985, **24**, 3947.
22. C. K. Jorgenson, *Adv. Chem. Phys.* 1965, **8**, 47 (and references therein).
23. R. J. Butcher and E. Sinn, *J. Am. Chem. Soc.* 1976, **98**, 2440, 5159.
24. R. J. Butcher, J. R. Ferraro and E. Sinn, *J. Chem. Soc., Chem. Commun.* 1976, 910.
25. Y. Maeda, N. Tsutsumi and Y. Takashima, *Inorg. Chem.* 1984, **23**, 2440.
26. W. M. Reiff, W. A. Baker, Jr and N. E. Erickson, *J. Am. Chem. Soc.* 1968, **90**, 4794.
27. A. H. Ewald, R. L. Martin, E. Sinn and A. H. White, *Inorg. Chem.* 1969, **8**, 1837.
28. R. Rickards, C. E. Johnson and H. A. O. Hill, *J. Chem. Phys.* 1968, **48**, 5231.
29. E. Frank and C. R. Abeledo, *Inorg. Chem.* 1966, **5**, 1453.
30. S. Mitra, In *Iron Porphyrins* (Edited by A. B. P. Lever and H. B. Gray). Addison-Wesley, Reading, MA (1982) (and references therein).
31. G. M. Bancroft and R. H. Platt, In *Advances in Inorganic Chemistry and Radiochemistry* (Edited by H. J. Emeleus and A. G. Sharp), Vol. 1. Academic Press, New York (1972).
32. M. M. Maltempo, *Chem. Phys. Lett.* 1979, **60**, 441.
33. B. J. Kennedy, G. Brain and K. S. Murray, *Inorg. Chim. Acta* 1984, **81**, L29.

Polyhedron Vol. 6, No. 5, pp. 975–986, 1987
Printed in Great Britain

0277–5387/87 $3.00+.00
Pergamon Journals Ltd

STRUCTURE AND STABILITY OF SOLID AND MOLTEN COMPLEXES IN THE $MgCl_2$–$AlCl_3$ SYSTEM

M.-A. EINARSRUD, H. JUSTNES, E. RYTTER* and H. A. ØYE

Institute of Inorganic Chemistry, The Norwegian Institute of Technology, University of Trondheim, N-7034 Trondheim-NTH, Norway

(*Received* 10 *April* 1986; *accepted* 20 *September* 1986)

Abstract—A visual determination of the phase diagram of the $MgCl_2$–$AlCl_3$ system reveals the formation of two intermediate compounds. One of these compounds is $MgAl_2Cl_8$ crystallizing with a monoclinic unit cell, space group $I2/c$, with dimensions $a = 12.873(1)$ Å, $b = 7.8959(7)$ Å, $c = 11.617(1)$ Å, $\beta = 92.348(8)°$ and $z = 4$. The two crystal modifications of anhydrous magnesium chloride and the lattice parameters of aluminium chloride have been reexamined. Lattice energies for α- and β-$MgCl_2$ have been measured, respectively, as 661(1) and 646(4) kcal mol^{-1}. The liquidus curve on the acidic side has been used to estimate the activity of aluminium chloride. Fourier-transform IR spectra of melts with compositions ranging from 0 to 30 mol% $MgCl_2$ have been interpreted in terms of Al_2Cl_6, strongly perturbed $Al_2Cl_7^-$ and $AlCl_4^-$ entities. In particular, the tetrachloroaluminate ion acts as both a tri- and a bidentate ligand towards Mg^{2+}. Neutral species, e.g. $Mg(AlCl_4)_2$ and $Mg(Al_2Cl_6)(AlCl_4)Cl$, dominate in the melt. *Ab initio* molecular-orbital calculations have been performed to obtain a better understanding of the $Mg^{2+} \cdots AlCl_4^-$ interaction.

The $MgCl_2$–$AlCl_3$ system is of considerable fundamental and industrial importance. Anhydrous $MgCl_2$ is used as a support material in third-generation Ziegler–Natta catalysts for production of stereoregular polypropylene. More recent $MgCl_2$ supports have been modified with $AlCl_3$,[1,2] whereas the chloroaluminate species in the molten and gaseous states are related to new aluminium processes.[3] As part of a more general spectroscopic investigation of the complex formation of $AlCl_3$ in molten chlorides,[4–6] the present system represents an extension to a highly polarizing counterion.

A previous investigation of the phase diagram of $MgCl_2$–$AlCl_3$ (0–30 mol% $MgCl_2$) by Kendall *et al.*[7] indicated the formation of a 1:2 compound. However, the narrow range and limited number of data prompted the present redetermination of the liquidus curve. Belt and Scott[8] confirmed the formation of magnesium chloroaluminate ($MgAl_2Cl_8$) by X-ray powder diffraction and pointed out a possible isomerism with $CoAl_2Cl_8$.[9]

Anhydrous $MgCl_2$ has been known to exhibit two different crystal modifications, a high-temperature form[10] (α-$MgCl_2$) made from thermal decomposition of hydrates and a low-temperature modification[11] (β-$MgCl_2$) produced by chemical dehydration. An extensively milled $MgCl_2$, as employed for the support material of third-generation Ziegler–Natta catalysts, may be looked upon as a mixture of the two forms. Action therefore was taken to determine any difference in the closest coordination sphere of magnesium and to measure accurate lattice parameters.

EXPERIMENTAL

The high-temperature α-form of $MgCl_2$ was prepared by decomposition of magnesium chloride hexahydrate (99%, E. Merck AG, F.R.G.) in a flow of HCl gas (25–600°C) followed by 3 times vacuum distillation (1000°C) in quartz cells. β-$MgCl_2$ was produced by chemical dehydration of $MgCl_2 \cdot 6H_2O$ in refluxing thionyl chloride (75°C) for 3 days. Excess $SOCl_2$ was distilled off, and the product dried *in vacuo* $AlCl_3$ (99%, Fluka AG, Switzerland) was purified by 3 times distillation in sealed quartz tubes.

Needle-shaped crystals of $MgAl_2Cl_8$ were synthesized by fractional crystallization. A mixture of

* Author to whom correspondence should be addressed.

25 mol% α-$MgCl_2$ in $AlCl_3$ was kept at 190°C for 12 h and then melted at 250°C in a tilting furnace to ensure a homogeneous mixture. The quartz tube with the melt was quenched in ice-water. The mixture was again melted in a zone refinement furnace, and $MgAl_2Cl_8$ was solidified as the cell was lowered at a rate of 0.6 mm h^{-1} through the furnace. Alternatively, single crystals were made from a 1 : 3 mixture of $MgCl_2$ and $AlCl_3$ by gas-phase transportation from 230 to 170°C. Crystallization times were 12–80 h. Attempts to prepare the compound $MgAlCl_5$ by these methods failed.

The liquidus in the $MgCl_2$–$AlCl_3$ phase diagram was determined by visual inspection. The melting points in the acidic region of the diagram were observed while the quartz tubes with the mixtures were shaken in a nitrate bath. The temperature in the bath was increased by 0.2–0.5°C and allowed to stabilize for 5–6 h when approaching the melting point. On the basic side of the diagram, however, the melting points were observed visually in a shaking quartz furnace, giving a considerably larger uncertainty, particularly in the 50–70 mol% $AlCl_3$ region.

Neutron powder diffractograms were obtained by the OPUS III diffractometer accommodated at a radial channel of the JEEP II reactor (2 MW, central thermal flux 3×10^{13}) at the Institute of Energy Technology, Kjeller. The monochromatic beam is produced by reflection from the (111) planes of a squashed Ge crystal, and has a wavelength of 1.877(1) Å. The instrument utilizes a multidetector system consisting of five ^3He detectors spaced 10° apart, and each of these covers a range of 80° for the diffraction angle (2θ). The detectors are cylindrical with diameter 5 cm and an active length of 20 cm. They are filled with ^3He gas to a pressure of 4 atm. Each detector has a Soller collimator of 10′ opening angle with plates made of gadolinium oxide coated Mylar foils. The diffractometer is operated through a Mycron microcomputer which allows programming of both the temperature variation of the sample and the scanning procedure. A step length of 0.05° was used, and a range of 5–80° for the diffraction angle was recorded. The sample holder was an aluminium cylinder with inner diameter 12 mm, wall thickness 1 mm and length 40 mm. The lid was sealed with Araldite glue.

IR transmission spectra of the solid samples were recorded in the frequency range 300–800 cm^{-1} with a Perkin–Elmer 580B ratio recording IR spectrophotometer. The samples were Nujol suspensions between CsI windows. The resolution of the spectra is about 5 cm^{-1}. Far-IR spectra to 50 cm^{-1} were recorded with a Bruker IFS 113v Fourier-transform IR spectrometer. The radiation source was an Hg lamp, the beam splitter a 6.0 μm Mylar film, and the detector a He-cooled Ge bolometer. For the low-frequency spectra, the samples were in a Nujol suspension between polyethylene windows. The spectra were recorded with 96 scans, mirror velocity 0.235 cm s^{-1}, resolution 1 cm^{-1}, and a triangular apodization function.

The specular reflection spectra of the molten mixtures were obtained with the Bruker IFS 113v Fourier-transform instrument. The spectra were recorded of thin films (*ca* 1 μm) pressed against a diamond window (type IIA, D. Drukker & Zn., Amsterdam, Netherlands) by a gold-plated nickel piston. Details of the cell and procedure have been described previously.[6,12] Thick samples (2–3 mm) were used as reference to avoid false band splitting.[13,14] The averaged spectra consisted of 500 single scans obtained with a DTGS detector at a resolution of 8 cm^{-1}. A 3.5-μm Mylar beam splitter was used in the frequency range 150–700 cm^{-1}, whereas a 12-μm Mylar was employed between 90 and 210 cm^{-1}.

RESULTS

The phase diagram of $MgCl_2$–$AlCl_3$ is drawn in Fig. 1 together with detail of the acidic region ($X_{AlCl_3} > 0.67$). The diagram indicates the formation of two intermediate compounds. The presence of $MgAl_2Cl_8$ was verified by X-ray and neutron powder diffraction, chemical analysis, morphology, IR and Raman spectroscopy and X-ray investigations

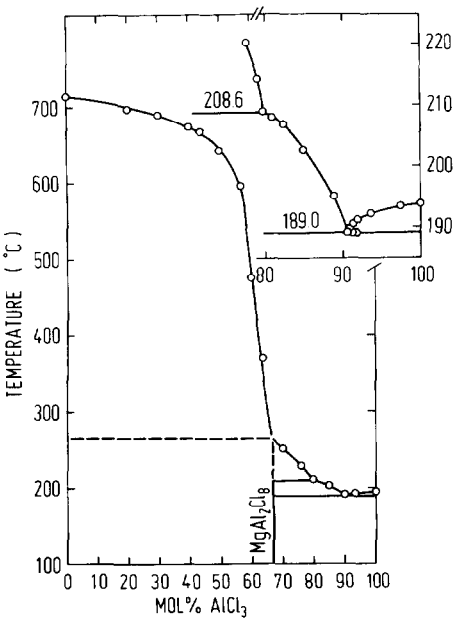

Fig. 1. The $MgCl_2$–$AlCl_3$ phase diagram.

of single crystals. Attempts to prepare $MgAlCl_5$ failed. Neither could the possible existence of both a high- and a low-temperature modification of $MgAl_2Cl_8$ be verified. The melting point of $AlCl_3$ under its own equilibrium pressure was determined to be 193.8°C.

The refinement of the crystal structures is based on a Rietveld analysis of the individual neutron powder diffraction patterns shown in Fig. 2. The calculations were performed by a computer program developed by Wiles and Young.[15] In all analyses, the 2° ranges 46–48 and 54–56° were excluded to avoid contribution from the sample holder. Listings of diffraction angles and calculated and observed integral intensities of the reflections can be obtained from the authors. The complete profiles also are available.

Solid $MgCl_2$

Fourteen reflections with diffraction angles between 16 and 77° were the basis for the refinement of α-$MgCl_2$. The final *R*-factors were $R_B = 0.038$ (the error of fit for the integral intensities of all the considered reflections) and $R_p^w = 0.121$ (the error of fit for each measured point in the intensity profile weighted by the inverse square of their standard deviations). The obtained unit-cell parameters are given in Table 1. In this structure, the magnesium atom is placed at the origin, while the chlorine atom is in the special position $(0, 0, z)$. The final atomic position and isotropic temperature factors refined to $z = 0.2551(2)$, $B(\mathrm{Mg}) = 1.9(2)$ and $B(\mathrm{Cl}) = 1.4(1)$ Å^2. These values correspond to the scale factor $C = 0.118(2)$, half-width parameters $u = 3.2(1)$, $v = -1.8(1)$ and $w = 0.34(2)$, preferred orientation parameter $G = 0.27(1)$ and an asymmetry parameter applied for the first reflection $A = 2.0(2)$. The preferred-orientation parameter is necessary in the structure determination of this compound because of the pronounced flake shape of the crystallites.

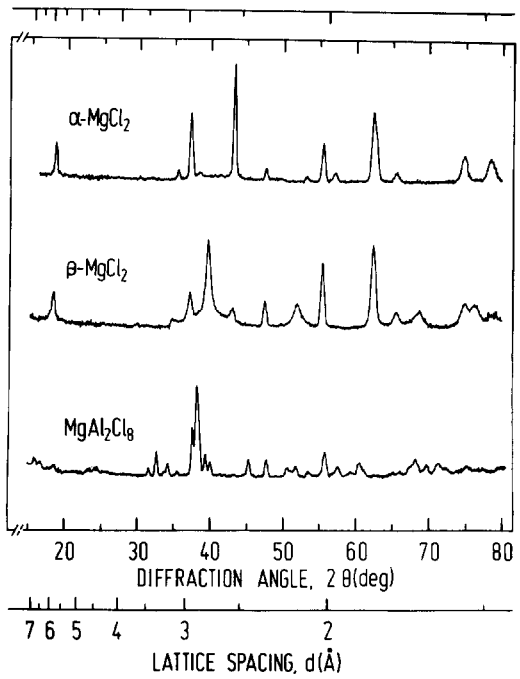

Fig. 2. Neutron powder diffraction patterns of the two crystal modifications of $MgCl_2$ and $MgAl_2Cl_8$.

The intensity profile of β-$MgCl_2$ in Fig. 2 shows that this compound is contaminated by a small amount of the α-phase. The refinement was performed by using separate scale factors for the two modifications and the already obtained structural parameters for α-$MgCl_2$. The two scale factors refined to $C(\beta) = 0.114(3)$ and $C(\alpha) = 0.0040(2)$. Because of the structural similarities, it was possible to calculate the amount of α-$MgCl_2$ as 9.5 mol%. The refinement of β-$MgCl_2$ is based on 17 independent reflections in the 2θ range 16–80°, and the *R*-factors refined to $R_B = 0.061$ and $R_p^w = 0.337$. The unit cell parameters have been included in Table 1. In the structure of β-$MgCl_2$, the magnesium atom is placed at the origin, while the chlorine atom is in the special position $(1/3, 2/3, z)$. The final atomic position $z = 0.235(3)$ was obtained.

Table 1. Unit cell parameters for the two modifications of $MgCl_2$

	α-$MgCl_2$		β-$MgCl_2$	
Parameter	Neutron	X-ray[16]	Neutron	X-ray[11]
a (Å)	3.6435(1)	3.640(4)	3.6376(5)	3.641(3)
c (Å)	17.689(2)	17.673(15)	5.897(2)	5.927(6)
V (Å^3)	203.4	202.8[a]	67.58	68.05
$\rho_{calc.}$ (g cm^{-3})	2.332	2.339	2.339	2.323
Z	3	3	1	1
Space group	$R\bar{3}m$	$R\bar{3}m$	$P\bar{3}m$	$P\bar{3}m$

[a] Recalculated, different from the value given in Ref. 16.

The isotropic temperature factors were transferred from α-$MgCl_2$ as attempts to refine them gave preposterous values because of the diffuse reflections in the diffractogram due to the small crystallites in the sample. The positional parameter and the temperature factors match the half-width parameters $u = 14(2)$, $v = -16(2)$ and $w = 5.3(4)$, and the preferred-orientation parameter $G = 0.31(2)$. No significant improvement or change in structural parameters and R_p^w were obtained by using a Lorentzian profile function instead of the standard Gaussian one, although the half-width parameters were reduced to *ca* $\frac{1}{3}$.

The lattice energies for α- and β-$MgCl_2$ were measured to 661(1) and 646(4) kcal mol^{-1}, respectively. The low-temperature β modification was found by differential scanning calorimetry to be metastable with a transition temperature of *ca* 520°C at a heating rate of 20°C min^{-1}.

The IR spectra of the two modifications of anhydrous magnesium chloride (Fig. 3) are virtually identical. The frequencies, relative intensities and assignments in terms of the D_{3d} factor group are 407 m ($\nu_1+\nu_4$, E_u), 372 m ($\nu_2+\nu_3$, E_u), 329 sh ($\nu_1+\nu_2-\nu_3$, E_u), 276 sh ($\nu_1+\nu_4-\nu_3$, $A_{1u}+A_{2u}E_u$), 248 vs (ν_2, A_{2u}), 185 m (ν_4, E_u), 140 w ($\nu_2+\nu_3-\nu_1$, E_u) and 126 w ($\nu_2-\nu_3$, E_u). It cannot be excluded, however, that some of the shoulders and weak bands appear due to traces of oxychlorides.

Solid $MgAl_2Cl_8$ *and* $MgCl_2$–$AlCl_3$ *melts*

The suggested structure of $MgAl_2Cl_8$ is based on *c*-axis oscillation and zero-level Weissenberg X-ray photographs of a single crystal. This crystal was not suitable for a complete single-crystal analysis because of extended mosaic structure. The unit-cell axes obtained from the X-ray photographs are comparable with the values for $CoAl_2Cl_8$ obtained by Ibers.[9] Furthermore, the systematic extinctions ($h00$ and $0k0$ for h, k = odd and $hk0$ for $h-k$ = odd) can be explained by the space group for the cobalt compound, and the symmetry elements of the space group are reflected in the observed Laue symmetry. $MgAl_2Cl_8$ thus was assumed to be isomorphous with cobalt(II) tetrachloroaluminate ($CoAl_2Cl_8$), and the trial model was given atomic coordinates from this compound.

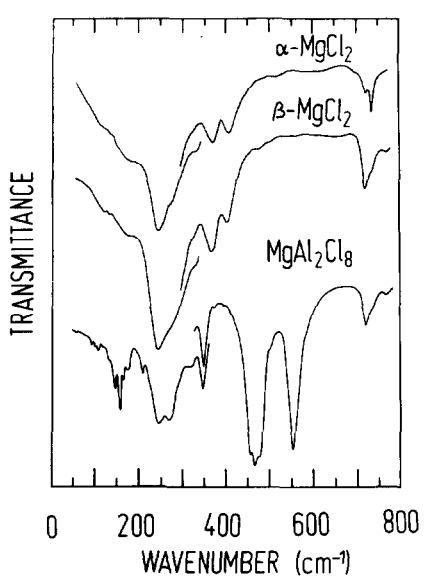

Fig. 3. IR spectra of the two crystal modifications of $MgCl_2$ and $MgAl_2Cl_8$.

The analysis of the neutron diffraction pattern for $MgAl_2Cl_8$ (Fig. 2) was complicated by a rather large contribution from $AlCl_3$. The combined analysis of the total diffraction pattern for the two phases was initially based on the structural data for $AlCl_3$ taken from Ketelaar *et al.*[17] Since, however, their unit-cell dimensions gave calculated peaks displaced from the observed ones, it was necessary to refine the axes of $AlCl_3$ as well. In addition, the preferred-orientation parameter of $AlCl_3$ had to be varied independently. The refinement took into account 194 reflections for $MgAl_2Cl_8$ and 73 reflections for $AlCl_3$ in the 2θ range 15–80°. The final *R*-factors were $R_B = 0.018$ for $MgAl_2Cl_8$, $R_B = 0.011$ for $AlCl_3$ and $R_p^w = 0.163$. The parameters for the monoclinic unit cell of $MgAl_2Cl_8$ with space group $I2/c$ and four formula units are given in Table 2 together with results obtained for several isomorphous compounds.[9,18,19] Monoclinic unit-cell dimensions of $AlCl_3$ with space group $C2/m$ and four formula units are $a = 5.933(2)$ Å, $b = 10.255(3)$ Å, $c = 6.180(4)$ Å and $\beta = 108.24(3)°$.

The derived atomic positions for $MgAl_2Cl_8$ are given in Table 3. The *y*-coordinates of magnesium and aluminium were fixed in their ideal positions (0.00 and 0.25, respectively) during the refinement. Otherwise they would arrive at values (0.04 and 0.22) leading to unlikely bonding distances without a significant better fit ($R_p^w = 0.159$). The applied set of atomic coordinates corresponds to scale factors $C(MgAl_2Cl_8) = 0.058(1)$ and $C(AlCl_3) = 0.073(4)$, common half-width parameters $u = 3.3(2)$, $v = -1.8(2)$ and $w = 0.36(4)$, common overall isotropic temperature factor $B = 4.0(1)$ Å^2 and preferred-orientation parameters $G(MgAl_2Cl_8) = 0.19(1)$ and $G(AlCl_3) = 0.34(3)$.

Because of the ill-conditioned *y*-coordinates of magnesium and aluminium compared with $CoAl_2Cl_8$ [$y(Co) = 0.0017(12)$ and $y(Al) = 0.2516(18)$], another model, with the chain in the middle of the *ab* plane of the unit cell (Fig. 6)

Table 2. Unit cell parameters for isomorphous MAl_2Cl_8 compounds (M = Mg, Co, Ni or Ti)

Parameter	Mg	Co[a]	Ni[b]	Ti[c]
a (Å)	12.873(1)	12.81(2)	12.72(1)	13.000(3)
b (Å)	7.8959(7)	7.75(1)	7.672(7)	7.711(2)
c (Å)	11.617(1)	11.50(2)	11.47(2)	11.772(3)
β (°)	92.348(8)	92.2(2)	92.2(1)	92.2[d]
V (Å^3)	1179.8	1141	1119	1179(1)
$\rho_{calc.}$ (g cm^{-3})	2.037	2.308	2.353	2.171

[a] Reference 9.
[b] Reference 18.
[c] Reference 19.
[d] Not reported, but calculated from the given volume.

translated one-half of the repetition length along the c-axis, was tried out. It turns out that only the y-coordinate of aluminium is altered. The new model has the space group $C2/c$, which explains equally well the observed systematic extinctions and Laue symmetry. However, the fit for the unit-cell axes was less satisfactory and the R-factors, standard deviations and overall temperature factor increased. Hence, the first model was assumed to be correct, although some mixing of the two or lack of stoichiometry is possible.

The IR spectra of solid $MgAl_2Cl_8$ and $MgCl_2$ are compared in Fig. 3. The IR reflectances of the different molten compositions are shown in Fig. 4, whereas the wavenumbers of melts and solid $MgAl_2Cl_8$ are listed in Table 4.

DISCUSSION

Solid $MgCl_2$

The unit-cell dimensions for α–$MgCl_2$ obtained by neutron diffraction in this work compare excellently with the recent reinvestigation by X-ray diffraction (Table 1). This agreement gives us confidence in the somewhat less well defined wavelength of the neutrons compared to X-rays. For β-$MgCl_2$, the discrepancy is larger. In particular, the c-axis (and volume) found by Bassi *et al.*[11] seems too large. In this context it is pertinent to point out that a comparison between the Debye–Scherrer results of these authors with the lattice spacings calculated from the present unit cell axes, gives as good a fit as for the unit cell parameters from the literature.

Table 3. Atomic coordinates for $MgAl_2Cl_8$

Atom	x	y	z
Mg	0	0.0000(—)	1/4
Al	0.0874(20)	0.2500(—)	0.5494(24)
Cl(1)	0.1597(9)	0.4818(29)	0.6127(10)
Cl(2)	0.1579(8)	0.0187(27)	0.6317(11)
Cl(3)	0.0956(7)	0.2369(27)	0.3672(9)
Cl(4)	−0.0625(9)	0.2263(22)	0.6145(9)

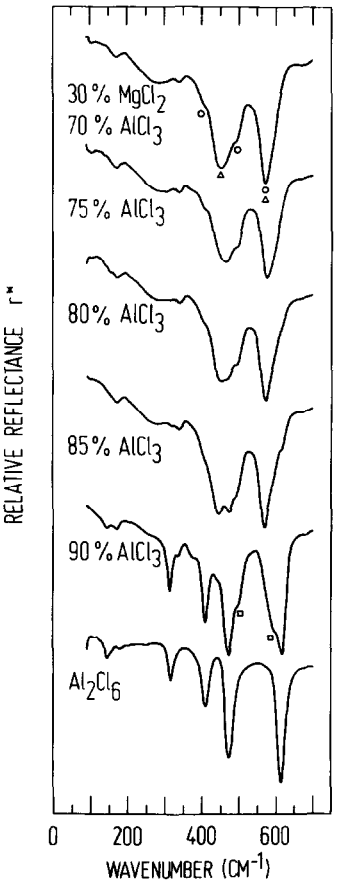

Fig. 4. IR reflectance spectra of molten mixtures in the $MgCl_2$–$AlCl_3$ system at 260–200°C. (△) $AlCl_4^-$ (C_{3v}), (○) $AlCl_4^-$ (C_{2v}), and (□) $Al_2Cl_7^-$.

Table 4. Observed IR frequencies (cm^{-1}) for solid $MgAl_2Cl_8$ and molten magnesium chloroaluminates[a]

Solid $MgAl_2Cl_8$	70% $AlCl_3$ 260°C	75% $AlCl_3$ 250°C	80% $AlCl_3$ 250°C	85% $AlCl_3$ 250°C	90% $AlCl_3$ 200°C	$AlCl_3$ 200°C	Interpretation of melt spectra[b]
			617 sh	617 sh	615 vs	614 vs	Al_2Cl_6 (ν_8)
			599 sh	595 sh	596 sh		$Al_2Cl_7^-$ (ν_{11})
						579 vw	Al_2Cl_6($\nu_{12}+\nu_{16}$)
552 vs	573 vs	575 vs	573 vs	571 vs			$Mg(Al_2Cl_6)\ldots$, $AlCl_4^-$ (ν_3; C_{2v}, C_{3v})
502 sh	498 sh	500 sh	497 sh	497 sh	500 sh		$Al_2Cl_7^-$ (ν_{11}), $AlCl_4^-$ (ν_3; C_{2v})
476 sh			470 s	475 vs	472 vs	473 vs	Al_2Cl_6 (ν_{16})
468 vs		465 s					
457 vs	452 s		453 s	447 s	442 sh		$Mg(Al_2Cl_6)\ldots$, $AlCl_4^-$ (ν_3; C_{3v})
	404 sh	409 sh	410 sh	407 sh	410 s	410 s	Al_2Cl_6 (ν_{13}), $AlCl_4^-$ (ν_3; C_{2v})
		374 sh	370 sh	374 sh	376 sh	383 sh	Al_2Cl_6 ($\nu_3+\nu_9$), $Al_2Cl_7^-$ (ν_5)
347 m	341 m	340 m	341 m	340 m	339 m		$Al_2Cl_7^-$ (ν_6), $AlAlCl_4^{2-}$ (ν_1)
318 w			316 m	320 m	315 m	316 m	Al_2Cl_6(ν_{17})
271 s	288 m	294 m	291 m	280 m			$Mg^{2+}\ldots AlCl_4^-$, Cl^-, Al_2Cl_6
245 s					265 sh	251 vw	Al_2Cl_6 ($\nu_3+\nu_{10}$)
211 w							
176 w	172 w	172 w	174 w	173 w	170 w	178 w	Al_2Cl_6 (ν_9), $Al_2Cl_7^-$ (ν_7), $AlCl_4^-$ (ν_4)
165 w							
157 s							
140 m		146 w	148 w	147 sh	149 w	145 w	Al_2Cl_6 (ν_{18}), $Al_2Cl_7^-$ (ν_{12})
134 sh							
122 vw							
108 w							
103 vw							
94 w							

[a] vs = very strong, s = strong, m = medium, w = weak, vw = very weak, sh = shoulder.

[b] The numbering of fundamentals refers to the idealized T_d- and D_{3d}-symmetries of $AlCl_4^-$ and $Al_2Cl_7^-$, respectively (see Ref. 6). For Al_2Cl_6, see Ref. 25. Ionic entities are parts of neutral species.

The layer structures ($CdCl_2$ and CdI_2) of the two modifications of anhydrous $MgCl_2$ both contain a two-dimensional net as a common structural unit. This unit, a Cl–Mg–Cl sandwich, has D_{3d}-symmetry around magnesium. Distances and angles for α-$MgCl_2$ are Mg—Cl = 2.518(2), Cl—Cl = 3.643(1) within a closed-packed layer, Cl—Cl = 3.477(2) between layers in a sandwich, Cl—Cl = 3.771(3) Å between sandwiches and Cl—Mg—Cl = 87.31(7)° in a sandwich. The values for the β-compound are within $2\sigma(\alpha)$ with the exception Cl—Cl(within layer) = 3.638(1) Å. Thus, the difference between the two modifications is mainly due to the stacking of the Cl–Mg–Cl sandwiches along the *c*-axes; α-$MgCl_2$ consists of a cubic close packing of anions, while β-$MgCl_2$ is based on a hexagonal close packing. Both modifications have the magnesium atoms placed in all octahedral holes between every second chlorine layer.

The $CdCl_2$ stacking arrangement found in the high-temperature α-modification gives a more ionic character because of closer secondary Mg^{2+}–Cl^- interactions. However, the ionic part of the lattice energy has been calculated by Hoppe[20] to be 589.7 (α-$MgCl_2$) and 589.8 kcal mol^{-1} (β-$MgCl_2$). These values correspond to Madelung constants of 4.486 and 4.481, respectively. In order to determine the influence of the packing sequence on the Madelung constant, a calculation was made on β-$MgCl_2$ where the shape of the sandwiches, and the distance between them, were as determined for α-$MgCl_2$. The resulting Madelung constant is 4.472, which means that the cubic close packing has about 0.3% higher ionic character than the hexagonal arrangement. Even though the standard deviations of the structural parameters for β-$MgCl_2$ are rather large, it may look as if the structure of this modification is adjusted to achieve a higher ionic lattice energy. The considerably larger difference[21] in the Madelung constants for $CdCl_2$ (4.489) and CdI_2 (4.382) using idealized structures is probably due to a different *z*-parameter.

The interpretation of the IR spectra in Fig. 2 of $MgCl_2$ can be understood from the correlation

Table 5. Correlation diagram for α- and β-$MgCl_2$[a]

Basis	Site	Sandwich	Factor group	Acoustic mode	Optical mode
Mg	D_{3d}	D_{3d}	D_{3d}		
T_z	A_{2u}	A_{1g}	A_{1g}		T''_z
$T_{x,y}$	E_u	E_g	E_g		$T''_{x,y}$
2Cl	C_{3v}				
$2T''_z$	A_1	A_{2u}	A_{2u}	T_z	T''_z (248)
$2T''_{x,y}$	E	E_u	E_u	$T_{x,y}$	$T''_{x,y}$ (185)

[a] Selected representations. IR activity is indicated by underlined symmetry species and Raman activity by underdashed species.

diagram in Table 5. The same diagram is applicable for α- and β-$MgCl_2$ as both have site symmetry D_{3d} for magnesium, site symmetry C_{3v} for chlorine, D_{3d}-symmetry for the structural unit (sandwich) and factor group D_{3d}. There is only one formula unit in the Bravais cell, and thus a total of six optical and three acoustic modes are expected. An examination of the correlation diagram shows that two IR-active and two Raman-active vibrations are predicted. The observed far-IR frequencies for α- and β-$MgCl_2$ are equal within the uncertainty limits, as expected from the structure determinations. The assignments in terms of IR-active fundamentals, $\nu_2(A_{2u}) = 248$ and $\nu_4(E_u) = 185$ cm^{-1}, and combination bands lead to the Raman-active fundamentals $\nu_1(A_{1g}) = 223$ and $\nu_3)(E_g) = 125\,cm^{-1}$. These values may be compared with the results of Anderson *et al.*,[22] 243 (A_{1g}), 225 (A_{2u}) and 176 cm^{-1} (E_u). Note the apparent interchange of the A_{1g} and A_{2u} values. The Raman-active E_g mode was not observed for $MgCl_2$, but other isomorphous chlorides were reported to have the E_g frequency in the range 130–170 cm^{-1}.[22]

Solid $MgAl_2Cl_8$

The structure of $MgAl_2Cl_8$ can be described within a hexagonal close packing of the chlorine atoms. Magnesium and aluminium atoms are placed, respectively, in one-eighth of the octahedral and tetrahedral holes between alternating layers. The atoms are arranged in such a way that infinite chains of composition $(MgAl_2Cl_8)_n$ are formed with propagation direction along the *c*-axis of the unit cell. The site symmetry of the magnesium is C_2, which is the symmetry of the infinite chain as well. The two-fold rotation axis is perpendicular to the chain, and intersects it through the magnesium atom. A drawing of the chain is shown in Fig. 5

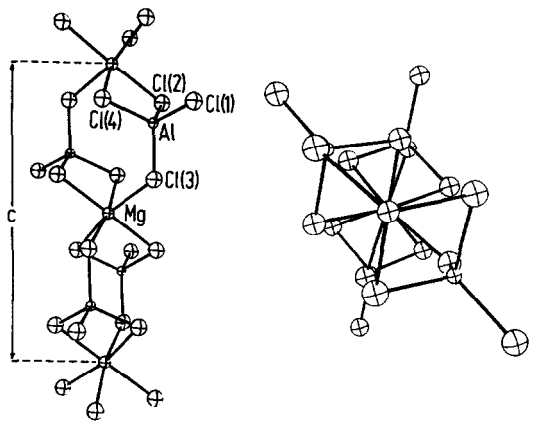

Fig. 5. The repeating part, C, of the infinite chain in $MgAl_2Cl_8$. The right drawing is turned 90° compared to the left and lacks the three upper and the three lower chlorine atoms for clarity.

and interatomic distances are given in Table 6. The bonding distances comply well with the corresponding values for $CoAl_2Cl_8$:[5] Co—Cl 3.45(1)–3.47(1) and Al—Cl 2.11(2)–2.19(2) Å. The standard deviations do not allow elaborate discussions of the bonding within the $MgCl_6$ and $AlCl_4$ units. It is noteworthy, however, that the rather short chlorine–chlorine contact distance of 3.28 Å is across the double chlorine bridge between Al and Mg (3.30 Å for $CoAl_2Cl_8$).

Table 6. Interatomic distances (Å) in $MgAl_2Cl_8$

Bonding distances			
Mg—Cl(2)	2.50(1)	Al—Cl(1)	2.17(4)
Mg—Cl(3)	2.59(3)	Al—Cl(2)	2.24(4)
Mg—Cl(4)	2.49(3)	Al—Cl(3)	2.13(3)
		Al—Cl(4)	2.11(3)

Non-bonding distances within the chain			
$AlCl_4$ group		Between groups	
Cl(1)—Cl(2)	3.66(3)	Cl(2)—Cl(3)	3.52(2)
Cl(1)—Cl(3)	3.52(2)	Cl(2)—Cl(3)	3.84(2)
Cl(1)—Cl(4)	3.50(2)	Cl(2)—Cl(4)	3.63(2)
Cl(2)—Cl(3)	3.58(2)	Cl(2)—Cl(4)	3.63(2)
Cl(2)—Cl(4)	3.28(2)	Cl(3)—Cl(3)	3.60(1)
Cl(3)—Cl(4)	3.59(2)	Cl(3)—Cl(4)	3.69(3)
		Cl(4)—Cl(4)	3.48(1)

Non-bonding distances between chains			
Cl(1)—Cl(2)	3.71(2)	Cl(1)—Cl(3)	3.82(2)
Cl(1)—Cl(2)	3.77(2)	Cl(1)—Cl(4)	3.68(2)
Cl(1)—Cl(3)	3.74(2)	Cl(2)—Cl(3)	3.88(2)

The chains are kept together by interactions between electron-deficient bridging chlorines and electron-rich terminal chlorines from neighbouring chains. It is seen from the stereographic drawing in Fig. 6 that one might expect van der Waals' forces between bridging chlorines from different chains as well. However, the non–bonding distances shorter than 3.90 Å within and between chains given in Table 6, show that only one bridge–bridge distance is below this limit and that terminal–bridge distances are significantly shorter.

The vibrational correlation digram for the infinite chain in $MgAl_2Cl_8$ is given in Table 7. The basis is taken in the 15 degrees of freedom of the unperturbed ligand $AlCl_4$ with T_d-symmetry. Fundamental frequencies of the $AlCl_4$ unit as found[23] in NH_4AlCl_4 have been included in Table 7. The ν_1-mode is the symmetric stretch, ν_2 is a Cl–Al–Cl deformation, ν_3 is the antisymmetric stretch and ν_4

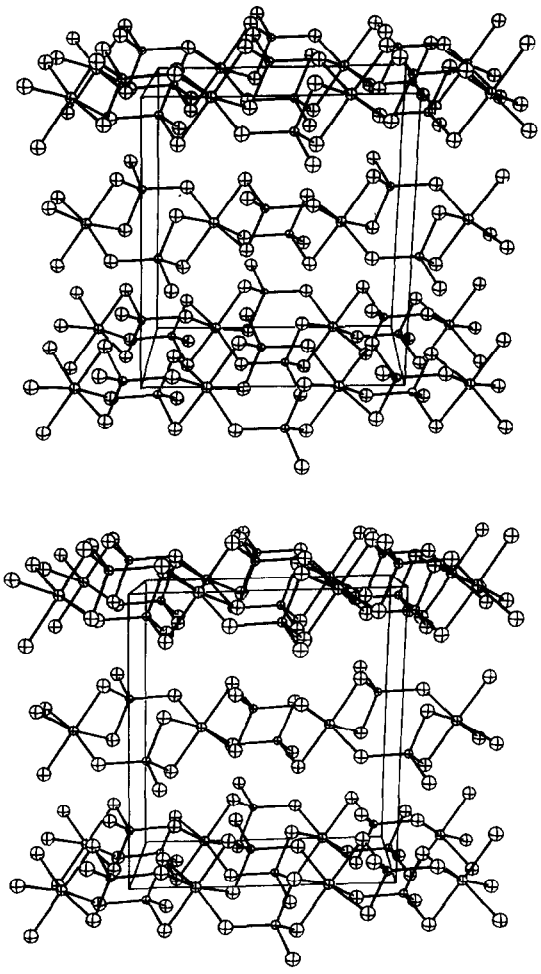

Fig. 6. A stereographic plot of the unit cell of $MgAl_2Cl_8$. The viewer looks along the *b*-axis, and the *a*-axis points upwards in the paper plane.

Table 7. Correlation diagram for the vibrations of an $MgAl_2Cl_8$ chain[a]

Basis	Free $AlCl_4^-$	Perturbed $AlCl_4^-$	$AlCl_4^-$ site	$(MgAl_2Cl_8)_{2n}$ factor	Ligand modes	Ligand vibrations	Skeletal	
	T_d[b]	C_{3v}[b]	C_1	C_2				C_2
$4\nu_1$ (356)	A_1	A_1		A	$2\nu_1, 4\nu_2, 6\nu_3, 6\nu_4$	$6\nu^R$	$5\nu^T, T'$	$\nu^T T'_{Mg}$
$4\nu_2$(126)	E	A_2	R					
$4R$	F_1	E		B	$2\nu^1, 4\nu_2, 6\nu_3, 6\nu_4$	$6\nu^R$	$6\nu^T$	$2\nu^T 2T'_{Mg}$
$4\nu_3(485), \nu_4(184), T$	F_2		$\nu_1(347), \nu_3(552), \nu_4(211), T$					
			$\nu_2(146), \nu_3(468), \nu_4(157), T, R$					

[a] Selected representations.

[b] IR-active species are underlined, Raman-active species underdashed. The acoustic modes are crossed out.

is a deformation. However, since the $AlCl_4^-$ group in the chain has three chlorines bridged to magnesium and one terminal chlorine, the T_d-symmetry is strongly perturbed to a C_{3v}-symmetry as shown in the first part of the diagram. This "chemical correlation" is in turn correlated to the site symmetry (C_1) of the $AlCl_4$ group and then to the symmetry of the chain (C_2). Even though both the *A*- and *B*-representations of the factor group are IR-active, the main effect probably is the "chemical perturbation" of the $AlCl_4$ ligand.

Five bands with their origin in the antisymmetric stretch (ν_3) are observed at 552, 502, 476, 468 and 457 cm^{-1}. The characteristics split into two groups by the chemical perturbation of the $AlCl_4$ entity, as previously found for $TiAl_2Cl_8$,[24] is clearly seen in Fig. 3. The band at 347 cm^{-1} (and possibly 318 cm^{-1}) is the symmetric stretch, IR-inactive for the free ligand (T_d), but activated by the "chemical perturbation" (C_{3v}). Bending modes (ν_4) are observed at 211, 176, 165 and 157 cm^{-1}, whereas ν_2 occur at 146, 134 and 122 cm^{-1}. Two of the Mg—Cl stretching fundamentals appear at 271 and 245 cm^{-1}, and further skeletal modes (librations) are found at 108, 103 and 94 cm^{-1}.

Because of the fine splitting of the absorption band at 468 cm^{-1} into three or four components, we conclude that this frequency corresponds to the *E*-representation and 552 cm^{-1} to the A_1-representation (C_{3v}). These assignments are confirmed by force field calculations. The calculations also show that the frequencies of 211 and 157 cm^{-1} belong to the A_1- and *E*-representations (C_{3v}), respectively, of the ν_4-mode.

Molten $MgCl_2$–$AlCl_3$

Vibrational spectra of molten alkali chloride–$AlCl_3$ mixtures show the presence of the anions $AlCl_4^-$ and $Al_2Cl_7^-$, with some evidence for cation–anion interactions, particularly for Li^+.[4,6] Accordingly, it is expected that the IR reflectance spectra of the acidic $MgAl_2Cl_8$ melts can be interpreted in terms of perturbed anionic entities. If the polarizing power of magnesium is high enough to cause directional Mg—Cl bonds, ion pairs, clusters etc. may be formed. The spectra are interpreted in terms of both the perturbed anion and cluster models.

The magnesium cation can distort the $AlCl_4^-$ group from T_d to C_{3v}- or C_{2v}-symmetry depending on its action as a tri- (mono-) or bidentate ligand. Figure 4 shows that both configurations seem to be present. First it may be noted that the appearance of the totally symmetric stretch, $\nu_1(A_1)$, at 341 cm^{-1} verifies that distortions do take place. The frequencies of 573, 498 and 404 cm^{-1} may reflect the splitting of the antisymmetric stretch, $\nu_3(F_2)$, of tetrahedral $AlCl_4^-$, upon perturbation from T_d to C_{2v}, and the strong bands at 573 and 452 cm^{-1} have their origin in the descent in symmetry from T_d to C_{3v}.

The latter two frequencies may be compared with the solid values 552 and 468 cm^{-1}. Evidently, the interactions are stronger in the melt. A partial explanation of this fact is a lower coordination number of Mg^{2+} in the molten state. Prevalence of smaller entities like $(AlCl_4)Mg(AlCl_4)$, where all bridging chlorine atoms of a given tetrachloroaluminate ion ate bonded to the same magnesium atom, also may contribute to the increased splitting. The accidental degeneracy at 573 cm^{-1} deserves a comment. A parallel situation is found for solid $TiAl_2Cl_8$ and $TiAl_2Cl_8 \cdot C_6H_6$ where C_{3v}-symmetry gives rise to bands at 552 and 466 cm^{-1}, whereas C_{2v} gives 554, 504 and 442 cm^{-1}.[24]

In analogy with Li^+–$Al_2Cl_7^-$ melts,[6] it is proposed that the strong polarizing power of the magnesium cation stabilizes a bent (C_s) rather than a linear (D_{3d}) structure of $Al_2Cl_7^-$. This interaction is manifested by the observed splitting of $\nu_{11}(E_u)$ from 525 cm^{-1} for molten[6] KAl_2Cl_7 to 596 and 500 cm^{-1} upon perturbation from D_{3d} to C_s-symmetry. The corresponding values for $LiAl_2Cl_7$ are 570 and 514 cm^{-1}. Thus, the counterions with high charge/radius ratios strongly perturb both the symmetric Cl–$AlCl_3$ tops of $Al_2Cl_7^-$. Other absorptions in the magnesium system at 376 and 339 cm^{-1} are Al—Cl stretching fundamentals of the $Al_2Cl_7^-$ group, whereas the band at 170 cm^{-1} is a bending mode. The broad band at 280–290 cm^{-1} probably is a direct observation of $Mg^{2+} \cdots AlCl_4^-$ interaction, cf. the Mg—Cl frequency situated at 271 cm^{-1} for solid $MgAl_2Cl_8$. At higher $AlCl_3$ contents, strong bands of Al_2Cl_6 at 615, 472, 410 and 315 cm^{-1} appear.

Although the above interpretation in terms of Al_2Cl_6 and the distorted anions $Al_2Cl_7^-$ and $AlCl_4^-$ is perfectly valid, auxiliary information discussed below together with intensity considerations give further insight into the melt structure. It is seen that the spectra in Fig. 4 essentially are superpositions of $Mg(AlCl_4)_2$ and Al_2Cl_6 with a small contribution from $Al_2Cl_7^-$. Simply, Mg^{2+} destabilizes any $Al_nCl_{3n+1}^-$ ($n \geqslant 2$) polymer. At intermediate compositions, 80 and 85 mol% $AlCl_3$, the seemingly abrupt disappearance of Al_2Cl_6 and the frequency variations in the terminal Al—Cl stretching region around 450 cm^{-1}, point to distortions of Al_2Cl_6 as the Mg^{2+} concentration is increased. The interaction between a magnesium ion and a chloroaluminate species may be formulated in terms of

molecular complexes as

mol% $AlCl_3$	
50	Mg^{2+}, $AlCl_4^-$, Cl^-
67	$Mg(AlCl_4)_2$
80	$Mg(Al_2Cl_6)(AlCl_4)_2$, $Mg(Al_2Cl_6)_2Cl_2$.

Similar complexes obtained by substitution of $Al_2Cl_7^-$ for $AlCl_4^-$ exist in low concentrations. Furthermore, it is possible that more lattice like structures to some extent are formed by polymerization, cf. the $Mg(AlCl_4)_2$ chain in the solid. Some dissociation into ionic species is expected.

This melt model is supported by the following additional information:

(a) Due to a strong, polarized band characteristic for each of the species $AlCl_4^-$, $Al_2Cl_7^-$ and Al_2Cl_6, Raman spectroscopy is better suited than IR spectroscopy to estimate concentrations.[26,27] Comparison of relative concentrations with stoichiometric restrictions leads to the conclusion for the similar acidic $MgCl_2$–$GaCl_3$ system, that some chlorine atoms must be bonded to magnesium only.[27] The same results may be inferred from a preliminary Raman study of the present system.[28]

(b) Raman spectra show that the amount of $Al_2Cl_7^-$ ($Ga_2Cl_7^-$) relative to $AlCl_4^-$ ($GaCl_4^-$) and Al_2Cl_6 (Ga_2Cl_6) is reduced when the polarizing power of the counterion increases.[4,14,27,28] The following series of diminishing $Al_2Cl_7^-$ concentration may be constructed: Cs > K > Li > Mg > Zn.

(c) The terminal IR-active Al—Cl stretching vibrations of C_{2v} perturbed $AlCl_4^-$ follow a smooth trend which may be correlated with polarizing power. Giving the antisymmetric and the symmetric mode, the frequencies (cm^{-1}) are:

	"$[Al(AlCl_4)]^{2+}$"	$[Zn(AlCl_4)]^+$ [5,14]	$[Mg(AlCl_4)]^+$	$[Ti(AlCl_4)]^+$(s)
Asymmetric	614	585	573	554
Symmetric	473	482	498	504

The hypothetical ion $[Al(AlCl_4)]^{2+}$ is part of Al_2Cl_6. The titanium values[24] for solid $Ti(AlCl_4)_2(C_6H_6)$ are in the molten state expected to become close to the $[Mg(AlCl_4)]^+$ data.

(d) Contrary to the alkali chloride[29] and calcium chloride[30] mixtures with $AlCl_3$, no indication of an immiscibility gap was found in the present phase diagram investigation of the $MgCl_2$ system. As Al_2Cl_6 can dissolve less than 1 mol% ionic species, there is a strong case for the prevalence of neutral entities in acidic $MgCl_2$–$AlCl_3$ melts.

(e) Attempts by vapour pressure studies on acidic $MgCl_2$–$AlCl_3$ mixtures failed to establish any liquid phase in the range $0.67 < X_{AlCl_3} < 1$ for vapour pressures of 1 atm or less. This observation is also contrary to the mixture with alkali chloride (and calcium chloride) and show that $MgCl_2$ does not donate Cl^- as easily to $AlCl_3$, forming an ionic melt, as alkali chloride and calcium chloride.

Activity of acidic melts

As discussed above, the $AlCl_3$ vapour pressure and corresponding activity could not be obtained from boiling point method studies. Such information can, however, be calculated from the lowering of the $AlCl_3$ freezing point. The change in freezing point is so small that the difference in C_p can be neglected. The following equation is valid for the liquidus line to the right in Fig. 1:

$$\ln a_{AlCl_3} = -\Delta H^o_{fus}(AlCl_3)\left[\frac{\Delta T}{RT_{liq}T_{fus}}\right],$$

where ΔT is the freezing point depression. Further:

$$a_{Al_2Cl_6} = P_{Al_2Cl_6}/P^o_{Al_2Cl_6} = a^2_{AlCl_3}.$$

From the ΔT values of 0.6 and 1.6°C at $X_{AlCl_3} = 0.974$ and 0.936, respectively, and setting $\Delta H_{fus}(AlCl_3) = 8450$ cal, Al_2Cl_6 activities of 0.980 and 0.943 are found.

Based on these data the activity coefficient function:

$$\gamma_{AlCl_3} = 1 + 0.6(1 - X_{AlCl_3}) \quad (X_{AlCl_3} > 0.7),$$

is proposed. This equation gives for instance $a_{Al_2Cl_6} = 0.74$ for 75 mol% $AlCl_3$. It is hence understood that the vapour pressures above the $MgCl_2$–$AlCl_3$ liquids were higher than 1 atm.

It is concluded that the activity of $AlCl_3$ in $MgCl_2$–$AlCl_3$ mixtures show a positive deviation from ideality, but the deviation is not so strong that liquid–liquid immiscibility occurs. When, however, the composition $Mg(AlCl_4)_2$ is approached, negative deviation may prevail as the Al^{3+} ion is saturated with respect to Cl^-.

Molecular-orbital calculations

In order to gain a clearer understanding of the energetics when $AlCl_4^-$ and Mg^{2+} interact, molecular-orbital calculations on the *ab initio* Hartree Fock level were performed on $[MgAlCl_4]^+$ (C_{3v})

Table 8. *Ab initio* calculated properties of $[MgAlCl_4]^+$ and $MgAlCl_5$[a]

Parameter	$[MgAlCl_4]^+$ (C_{3v})	$[MgAlCl_4]^+$ (C_{2v})	$MgAlCl_5$ (C_{2v})
Al—Cl_t	2.028	2.046	2.062
Al—Cl_b	2.213	2.289	2.207
Mg—$Cl_{t'}$	—	—	2.086
Mg—Cl_b	2.280	2.181	2.274
Mg—Al	2.734	3.203	3.231
Cl_t—Al—Cl_t	—	130.2	122.1
Cl_t—Al—Cl_b	126.4	108.0	110.2
Cl_b—Al—Cl_b	88.4	85.8	89.1
E	−2254.75994	−2254.74218	−2709.63293

[a] Units: bond lengths in Å, angles in degrees and energies in Hartrees.

[b]

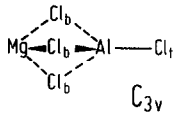

C_{3v}

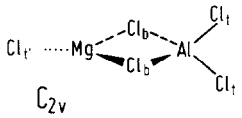

C_{2v}

with tridentate Mg, $[MgAlCl_4]$ (C_{2v}) and $MgAlCl_5$ (C_{2v}). The computations were done with the gradient program GAUSSIAN 80 employing a minimal STO-3G basis.[31] The results after optimizing all geometrical parameters are given in Table 8. It may be of interest to compare the bond lengths in Table 8 with the calculated values for $AlCl_4^-$ (T_d), 2.113 Å, and $MgCl_2$ ($D_{\infty h}$), 2.090 Å.

The two $[MgAlCl_4]^+$ structures probably correspond to the only energy minima when Mg^{2+} is moved around the $AlCl_4^-$ ion.[32] The C_{3v} structure is favoured by 11.1 kcal mol^{-1} relative to C_{2v}. These results agree with the conclusions from the IR spectroscopic investigations; both modifications are present in the melt, but with a higher concentration of the C_{3v} structure. In a calculation on $LiAlCl_4$ it was verified that the alternative C_{3v} structure with a monodentate counterion is unstable.[32]

The geometrical parameters seem to be reasonable, both the absolute values and, in particular, terminal–bridge differences and the shifts from species to species. For instance, Al—Cl_t < Al—Cl_b (cf. 2.065 and 2.252 Å observed in Al_2Cl_6[33]), Cl_t—Al—Cl_t > Cl_b—Al—Cl_b (123.4 and 91.0° in Al_2Cl_6[33]) and one terminal bond (2.028 Å in Table 8) is stronger than two adjacent terminal bonds (2.046 Å). The latter effect also is seen in the Al—Cl_b bonds.

Due to the low coordination number imposed on magnesium in the models, the Mg—Cl_b distances are short compared to the observed bond lengths in $MgAl_2Cl_8$(s) (see Table 6). Naturally, bidentate magnesium give stronger Mg—Cl_b than tridentate magnesium, mainly because of the reduced Mg–Al repulsion. Adding another terminal chlorine to magnesium forming $MgAlCl_5$ gives the expected reduction in the counterion influence on $AlCl_4^-$.

Acknowledgements—Financial support from NTNF and Norges Tekniske Høgskoles Fond gratefully is acknowledged. The phase diagram work was sponsored by ALCOA laboratories through Dr Ed. Martin. Special thanks go to Professor J. Lützow Holm for DSc, Professor H. J. Seifert for calorimetry, Dr A. F. Andresen for recording the neutron diffractograms, and to B. M. Faanes for phase diagram measurements.

REFERENCES

1. T. Tanaka, T. Asanuma, T. Shiomura and A. Ito, U.S. Patent 4,220,745 (1980).
2. J. A. Loontjens and D. I. L. Jacomen, Ger. Offen. 3,012,376 (1980).
3. K. Grjotheim. C. Krohn and H. A. Øye, *Aluminium* 1975, **51**, 697.
4. E. Rytter, H. A. Øye, S. J. Cyvin, B. N. Cyvin and P. Klæboe, *J. Inorg. Nucl. Chem.* 1973, **35**, 1185.
5. P. Klæboe, E. Rytter and C. E. Sjøgren, *J. Mol. Struct.* 1984, **113**, 213.
6. J. Hvistendahl, P. Klæboe, E. Rytter and H. A. Øye, *Inorg. Chem.* 1984, **23**, 706.
7. K. Kendall, E. D. Crittenden and H. K. Miller, *J. Am. Chem. Soc.* 1923, **45**, 963.
8. R. F. Belt and H. Scott, *Inorg. Chem.* 1964, **3**, 1785.
9. J. A. Ibers, *Acta Cryst.* 1962, **15**, 967.
10. A. Ferrari, A. Briabanti and G. Bigliardi, *Acta Cryst.* 1963, **16**, 846.
11. I. W. Bassi, F. Polato, M. Calcaterra and J. C. J. Bart, *Z. Krist.* 1982, **159**, 297.
12. E. Rytter, J. Hvistendahl and T. Tomita, *J. Mol. Struct.* 1982, **79**, 323.
13. J. Hvistendahl, E. Rytter and H. A. Øye, *Appl. Spectroc.* 1983, **37**, 182.

14. E. Rytter, Extended Abstract, 163rd Meeting, The Electrochemical Society, San Francisco (1983).
15. D. B. Wiles and R. A. Young, *J. Appl. Cryst.* 1981, **14**, 149.
16. I. Dorrepaal, *J. Appl. Cryst.* 1984, **17**, 483.
17. J. A. A. Ketelaar, C. H. McGillavry and P. A. Renes, *Rec. Trav. Chim., Pays-Bas* 1947, **66**, 501.
18. J. Brynestad, H. L. Yakel and G. P. Smith, *Inorg. Chem.* 1970, **9**, 686.
19. J. Brynestad, S. von Winbush, H. L. Yakel and G. P. Smith, *Inorg. Nucl. Chem. Lett.* 1970, **6**, 889.
20. R. Hoppe, Inst. Anorganische Chemie Institut der Universitat Giessen, B.R.D., private communication.
21. Q. C. Johnson and D. H. Templeton, *J. Chem. Phys.* 1961, **34**, 2004.
22. A. Anderson, Y. W. Lo and J. P. Todoeschuck, *Spectrosc. Lett.* 1981, **14**, 105.
23. G. Mairesse, P. Barbier and J. P. Wignacourt, *Can. J. Chem.* 1978, **56**, 764.
24. H. Justnes, E. Rytter and A. F. Andresen, *Polyhedron* 1982, **1**, 393.
25. T. Tomita, C. E. Sjøgren, P. Klæboe, G. N. Papatheodorou and E. Rytter, *J. Raman Spectrosc.* 1983, **14**, 415.
26. H. A. Øye, E. Rytter, P. Klæboe and S. J. Cyvin, *Acta Chem. Scand.* 1971, **25**, 559.
27. E. Rytter, thesis No. 26, Institute of Inorganic Chemistry, University of Trondheim (1974).
28. T. Kirkerud, E. Rytter and H. A. Øye, unpublished results.
29. A. A. Fannin, L. A. King, D. W. Seegmiller and H. A. Øye, *J. Chem. Eng. Data* 1982, **27**, 114; R. A. Carpio, A. A. Fannin, F. C. Kibler, L. A. King and H. A. Øye, *J. Chem. Eng. Data* 1983, **28**, 34.
30. I. I. Ivanov, E. N. Ryabov, R. A. Sandler and G. V. Bazheeva, *Russ. J. Inorg. Chem.* 1981, **26**, 443; *Zh. Neorg. Khim.* 1981, **26**, 825.
31. J. S. Binkley, R. A. Whiteside, R. Krishnan, R. Seeger, D. J. Defrees, H. B. Schlegel, S. Topiol, L. R. Kahn and J. A. Pople, *GAUSSIAN-80*, Quantum Chemistry Program Exchange 1981, **13**, 406.
32. E. Rytter, unpublished results.
33. Q. Shen, Ph.D. thesis, Oregon State University (1974).

Polyhedron Vol. 6, No. 5, pp. 987–993, 1987
Printed in Great Britain

0277–5387/87 $3.00+.00

X-RAY CRYSTALLOGRAPHIC AND SOLUTION STUDIES OF THE PENTAMETHYLDIETHYLENETRIAMINE AND TETRAMETHYLETHYLENEDIAMINE ADDUCTS OF LITHIUM DIPHENYLPHOSPHIDE

ROBERT E. MULVEY*† and KENNETH WADE

Chemistry Department, Durham University Science Laboratories, South Road, Durham DH1 3LE, U.K.

DAVID R. ARMSTRONG, GORDON T. WALKER and RONALD SNAITH

Department of Pure and Applied Chemistry, University of Strathclyde, 295 Cathedral Street, Glasgow G1 1XL, U.K.

WILLIAM CLEGG

Department of Inorganic Chemistry, The University, Newcastle upon Tyne NE1 7RU, U.K.

and

DAVID REED

Department of Chemistry, University of Edinburgh, West Mains Road, Edinburgh EH9 3JJ, U.K.

(*Received* 15 *July* 1986; *accepted* 20 *September* 1986)

Abstract—X-ray crystallographic studies on the lithium diphenylphosphide adducts $(Me_2NCH_2CH_2)_2NMe \cdot LiPPh_2$ (**1**) and $Me_2NCH_2CH_2NMe_2 \cdot LiPPh_2$ (**2**) are reported. **1** is monomeric, with a terminal PPh_2 unit containing a pyramidally coordinated phosphorus atom attached to the four-coordinate metal atom by a Li—P bond of length 2.567(6) Å. **2** crystallizes as dimers, $(Me_2NCH_2CH_2NMe_2 \cdot LiPPh_2)_2$, with bridging PPh_2 units containing (distorted) tetrahedrally coordinated phosphorus atoms: their planar $(LiP)_2$ rings are roughly square-shaped (mean P—Li—P angle 91°, mean Li—P distance 2.61 Å). Discussion of features of these structures is facilitated by *ab initio* MO calculations on the model systems $LiPH_2$ and $(LiPH_2)_2$. Cryoscopic molecular mass measurements and high-field $^7Li/^{31}P$ NMR spectroscopic studies on solutions of **1** and **2** indicate that both solid-state structures are retained in arene solution, though some dissociation of **2** into monomers is apparent.

Lithium diphenylphosphide, $LiPPh_2$, which has long been a key reagent for the synthesis of diphenylphosphido-bridged metallic and metalloidal systems,[1] has recently been receiving attention in its own right. Interest has centred on its states of association and structures in both the crystal and solution phases. Three adducts have been structurally characterized by X-ray crystallography. The crown ether adduct $(12\text{-crown-4})_2 \cdot LiPPh_2$[2] is of interest in crystallizing in the ionic form $[Li \cdot (12\text{-crown-4})_2]^+[PPh_2]^-$. The two crown ether molecules sandwiching each metal ion generate an unusual eight-coordinate environment for the metal and prevent significant lithium–phosphorus bonding. By contrast, the diethyl ether and tetrahy-

* Author to whom correspondence should be addressed.

† Present address: Department of Pure and Applied Chemistry, University of Strathclyde, 295 Cathedral Street, Glasgow G1 1XL, U.K.

drofuran adducts $Et_2O \cdot LiPPh_2$ and $(THF)_2 \cdot LiPPh_2$ crystallize with zig-zag lithium–phosphorus chain structures in which the formally two-centre two-electron Li—P bonds have mean lengths of 2.49 and 2.63 Å, respectively.[3] NMR studies on their solutions suggest that they may dissolve as cyclic dimers or tetramers.[4,5] In 1,4-dioxane, $(LiPPh_2)_n$ appears from cryoscopic studies[6] to exist as monomers and dimers.

Hitherto, studies of $LiPPh_2$ complexes have been confined to those containing donor molecules which attach through oxygen. In this work, we report on the effects of complexation by nitrogen donors, specifically the chelating amines pentamethyldiethylenetriamine {PMDETA [$(Me_2NCH_2CH_2)_2$ NMe]} and tetramethylethylenediamine [TMEDA ($Me_2NCH_2CH_2NMe_2$)]. Accordingly, crystals of both $(PMDETA \cdot LiPPh_2)_n$ (**1**) and $(TMEDA \cdot LiPPh_2)_n$ (**2**) have been synthesized, isolated and subjected to X-ray diffraction studies which have, for the first time, established unequivocally that the lithium diphenylphosphide can, when complexed, adopt both monomeric ($n = 1$ for **1**) and dimeric ($n = 2$ for **2**) structures. *Ab initio* MO calculations have been performed on the related *uncomplexed* hypothetical species, $LiPH_2$ and $(LiPH_2)_2$, in order to gauge the influence the donor molecules exert on the geometry of **1** and **2**.

In addition, high-field $^7Li/^{31}P$ NMR spectroscopic and cryoscopic relative molecular mass (crmm) studies have been carried out in an attempt to shed light on the natures of the new complexes in aromatic hydrocarbon solutions.

EXPERIMENTAL

Lithium diorganophosphides, in common with most other lithium organic derivatives, are extremely air- and moisture-sensitive. Accordingly, all syntheses and manipulations of products were carried out using standard inert atmosphere techniques.

Synthesis of $(PMDETA \cdot LiPPh_2)_n$ (1)

n-Butyl-lithium (5.0 cm^3 of a 2.0 mol dm^{-3} solution in hexane, 10 mmol) was added to a frozen solution of diphenylphosphine (1.86 g, 10 mmol) in toluene (5.0 cm^3). Warming to room temperature produced a yellow solid, which dissolved on addition of PMDETA (3.0 cm^3, 14.4 mmol). Slow cooling then afforded pale orange crystals of **1** which were recrystallized from toluene; yield 85%, m.p. 128°C (Found: C, 69.1; H, 9.2; Li, 1.9; N, 11.2; P, 8.5. $C_{21}H_{33}LiN_3P$ requires: C, 69.0; H, 9.0; Li, 1.9; N, 11.5; P, 8.5%). ^7Li NMR: (20°C) singlet, δ −0.96 ppm; (−80°C) singlet, δ −0.94 ppm. ^{31}P NMR: (20°C) singlet, δ −22.11 ppm; (−80°C) singlet, δ −23.63 ppm. Crmm measurements: $n = 0.96 \pm 0.08$ for a 0.01 mol dm^{-3} solution.

Synthesis of $(TMEDA \cdot LiPPh_2)_n$ (2)

n-Butyl-lithium (5.0 cm^3 of a 2.0 mol dm^{-3} solution in hexane, 10 mmol) was added to a chilled solution of diphenylphosphine (1.86 g, 10 mmol) in TMEDA (3.0 cm^3, 20 mmol). Warming to room temperature gave a yellow solution. Refrigeration then afforded pale yellow crystals of **2** which were recrystallized from a hexane–toluene mixture; yield 88%, decomp. from 196°C (Found: C, 70.0; H, 8.4; Li, 2.2; N, 9.1; P, 10.1. $C_{18}H_{26}LiN_2P$ requires: C, 70.1; H, 8.4; Li, 2.3; N, 9.1; P, 10.1%). ^7Li NMR: (20°C) singlet, δ −0.39 ppm; (−80°C) 1:2:1 triplet, δ −0.19 ppm; $J(^{31}P–^7Li)$ 45 Hz. ^{31}P NMR: (20°C) broad singlet, δ −30.17 ppm; (−80°C) 1:2:3:4:3:2:1 septet, δ −33.34 ppm; $J(^{31}P–^7Li)$ 45 Hz. Crmm measurements: $n = 1.67 \pm 0.08$ for a relatively concentrated solution, 0.04 mol dm^{-3}; $n = 1.05 \pm 0.08$ for a relatively dilute solution, 0.02 mol dm^{-3}.

High-field ^7Li (139.96-MHz) and ^{31}P (145.78-MHz) NMR spectra were recorded on a Bruker WH360 NMR spectrometer. Samples were prepared in [$^2H_8$]toluene, made up in a glove box and sealed under nitrogen prior to examination. ^7Li chemical shifts (δ) are quoted relative to external phenyl-lithium in [$^2H_8$]toluene (*E* value 38.863 882 MHz). ^{31}P chemical shifts are quoted relative to external 85% H_3PO_4.

Relative molecular mass measurements in benzene were carried out cryoscopically with a Beckmann-type apparatus which was modified slightly to handle air-sensitive materials.

Crystallography

(**1**) $C_{21}H_{33}LiN_3P$, $M = 365.4$, orthorhombic, *Pbca*, $a = 8.5590(4)$, $b = 16.3324(7)$, $c = 32.357(2)$ Å, $V = 4523.1$ Å^3, $Z = 8$, $D_c = 1.073$ g cm^{-3}, $F(000) = 1584$, $\mu = 1.11$ mm^{-1} for Cu-K_α radiation ($\lambda = 1.54184$ Å). Of 6413 reflections measured with a Siemens AED2 diffractometer at 295 K ($2\theta_{max} = 125°$), 3597 were unique ($R_{int} = 0.033$), and 2412 with $F > 4\sigma(F)$ were used for structure determination by automatic direct methods.[7] Blocked-cascade refinement to minimize $\Sigma w\Delta^2$ [$\Delta = |F_o| - |F_c|$, $w^{-1} = \sigma^2(F) + 0.00049F^2$] with anisotropic thermal parameters for non-H atoms and constrained H atoms [C—H = 0.96 Å, aromatic H on ring external bisectors, H—C—H = 109.5°

for aliphatic H, $U(H) = 1.2U$ eq (C)] gave $R = 0.068$, $R' = (\Sigma w\Delta^2/\Sigma wF_o^2)^{1/2} = 0.078$, a satisfactory analysis of variance, and no significant features in a final-difference map.

(**2**) $C_{36}H_{52}Li_2N_4P_2$, $M = 616.7$, triclinic, $P\bar{1}$, $a = 15.960(2)$, $b = 19.791(2)$, $c = 21.090(2)$ Å, $\alpha = 71.628(5)$, $\beta = 77.242(5)$, $\gamma = 67.525(4)°$, $V = 5803.5$ Å^3, $Z = 6$ (two dimers and two half-dimers in the asymmetric unit), $D_c = 1.059$ g cm^{-3}, $F(000) = 1992$, $\mu = 1.21$ mm^{-1} for Cu-K_α radiation. 14,988 reflections measured, 14,542 unique ($R_{int} = 0.029$), 6583 with $F > 4\sigma(F)$. Structure solution by direct methods $w^{-1} = \sigma^2(F) + 0.00246F^2$ in refinement; phenyl rings constrained as ideal rigid hexagons (C—C = 1.395 Å), no H atoms included because of program memory restrictions; $R = 0.111$, $R' = 0.145$.

Tables of atomic coordinates and other crystallographic data have been deposited with the Editor and with the Cambridge Crystallographic Data Centre.

DISCUSSION

Figure 1 shows the molecular structure of **1**, which is monomeric. The terminal PPh_2 unit is bonded to the four-coordinate metal atom by a two-centre two-electron Li—P bond of length 2.567(6) Å. Such terminal PR_2 units are expected in phosphide adducts, $(donor)_nLiPR_2$, where association is prohibited by either excessively bulky R substituents or by suitable Lewis bases such as PMDETA. However, at present only one other such system appears to have been structurally characterized, namely $(THF)_3 \cdot LiP(PPh_2)_2C_6H_4$,[8] in which the Li—P distance [2.580(7) Å] like that in **1** exceeds slightly the sum of the normal covalent radii for Li (1.34 Å) and P (1.10 Å).[9] In the chelate compounds TMEDA·$Li(PPh_2)_2CH$[10] and TMEDA·$Li(PMe_2CH_2)_2AlMe_2$,[11] which each contain a pair of four-coordinate phosphorus atoms (cf. three-coordinate in **1**), the P → Li dative linkages are similar in length, being 2.582 and 2.606(5) Å, respectively.

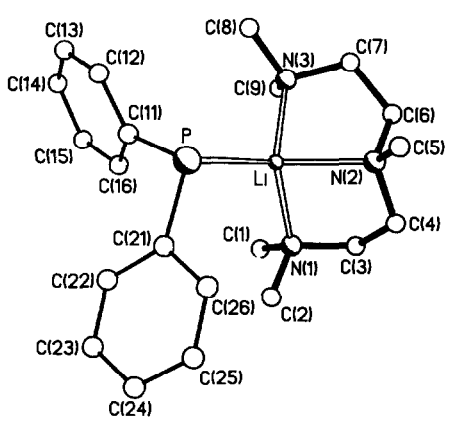

Fig. 1. Molecular structure of (PMDETA·$LiPPh_2$) (**1**). H atoms have been omitted for clarity.

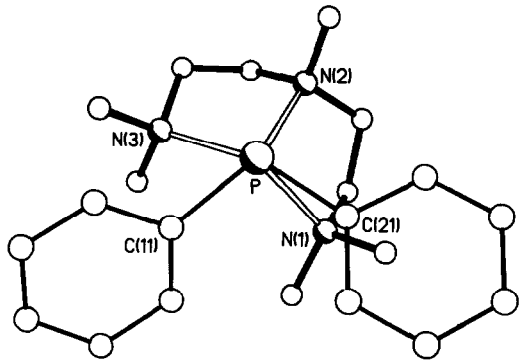

Fig. 2. An alternative view of **1** looking down the P—Li bond.

The geometry about the phosphorus atom in **1** is pyramidal while about the lithium it is pseudo-tetrahedral. From Fig. 2, which shows an alternative view looking down the P—Li bond, it can be seen that the PC_2 and LiN_3 units are neither eclipsed nor fully staggered with respect to each other. The characteristic "embrace" of PMDETA fills three of the four metal valence-shell atomic orbitals leaving one available for the binding of the phosphido ligand. The N → Li bond lengths and N—Li—N bond angles (given with other selected bond lengths and bond angles in Table 1) show no significant differences from those in the related systems PMDETA·$Li[CH(SiMe_3)_2]$[12] and PMDETA·$Li(C_2B_{10}H_{10}Me)$.[13]

Ab initio calculations[14–18] on the uncomplexed $LiPH_2$ using geometry optimization procedures show that a pyramidal conformation is favoured over a planar form by 5.6 kcal mol^{-1} (66-31G**). This is an interesting result on comparison with the optimized geometries of lithiated ammonia $LiNH_2$[19,20] for which planar conformations are preferred over the corresponding pyramidal geometries. Such a difference can be rationalized by examining the electronic distribution of $LiNH_2$ and $LiPH_2$, where the main electronic difference is that in $LiNH_2$ the hydrogen atoms are positively charged (+0.20 e) and thus coupled with the highly positive Li (+0.58 e), causing $LiNH_2$ to adopt a planar conformation, while in $LiPH_2$ the hydrogens carry a slight negative charge (−0.06 e) and hence a pyramidal arrangement of $LiPH_2$ is stabilized by the interactions between them and the highly positive

Table 1. Selected bond lengths (Å) and angles (°) for **1**

Li—P	2.567(6)	Li—N(1)	2.150(6)
Li—N(2)	2.091(6)	Li—N(3)	2.126(6)
P—C(11)	1.829(4)	P—C(21)	1.803(4)
P—Li—N(1)	118.6(2)	P—Li—N(2)	124.9(2)
P—Li—N(3)	114.9(2)	N(1)—Li—N(2)	85.0(2)
N(2)—Li—N(3)	87.5(2)	N(1)—Li—N(3)	119.0(3)
Li—P—C(11)	91.5(2)	Li—P—C(21)	108.1(2)
C(11)—P—C(21)	105.1(2)		

lithium (+0.47 e). The calculated Li—P bond distance is 2.391 Å so a comparison with the crystal structure data on complex **1** shows that the effect of the ligands is to lengthen the Li—P bond by *ca* 0.18 Å.

In the X-ray structure analysis of **2**, four independent dimeric (i.e. $n = 2$) molecules were found; these are shown in Fig. 3. There are, as discussed below, differences in their respective bond lengths and bond angles, but their gross structural features are the same. The basic molecular structure, a planar four-membered ring system, is well known in $(donor \cdot LiX)_n$ chemistry, where X is a first-row element. Examples are: X = C, $(TMEDA \cdot LiPh)_2$[21] and $(TMEDA \cdot LiCH_2SCH_3)_2$;[22] X = N, $(HMPA \cdot LiN{=}CBu^t_2)_2$[23] [HMPA = $(Me_2N)_3P{:}O$] and $[Et_2O \cdot LiN(CH_2Ph)_2]_2$;[24] X = O, $(THF \cdot LiOCBu^t_3)_2$[25] and $[(H_2O)_2 \cdot Li \cdot (\mu_2\text{-}HMPA)]_2^{2+} \cdot 2Cl^-$.[26] This is the first time, however, that a lithio-phosphine coordination complex has been found to have a $(LiP)_2$ ring structure. Although the uncomplexed, sterically crowded, phosphidolithium $\{LiP[CH(SiMe_3)_2]_2\}_2$[27] contains a similar ring, it fails to retain such on complexation; addition of TMEDA leads to monomer formation.

Both the Li and P atoms in each of the molecules of **2** are in distorted tetrahedral environments. The metal coordination sphere accommodates the two N atoms of bidentate TMEDA and a pair of μ_2-P atoms. Table 2 lists the important bond lengths and bond angles in the four crystallographically distinct molecules. Considering all four molecules the mean ring angle at Li is 91° while at P it is 89° and the mean Li—P ring distance is 2.61 Å. Unfortunately, the rather high R value (0.111) negates a com-

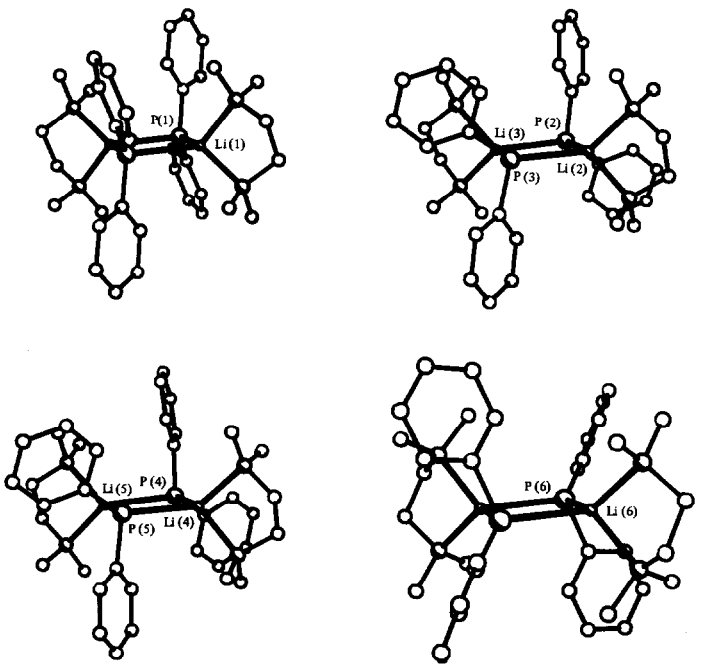

Fig. 3. Structures of the four crystallographically distinct molecules of $(TMEDA \cdot LiPPh_2)_2$ (**2**). H atoms have been omitted for clarity.

Table 2. Selected bond lengths (Å) and angles (°) for **2**[a]

Li(1)—P(1)	2.615(16)	Li(6)—P(6)	2.573(19)
Li(1a)—P(1)	2.614(17)	Li(6b)—P(6)	2.575(16)
Li(1)—N(11)	2.113(24)	Li(6)—N(61)	2.195(22)
Li(1)—N(12)	2.113(21)	Li(6)—N(62)	2.144(26)
P(1)—C(111)	1.856(8)	P(6)—C(611)	1.856(10)
P(1)—C(121)	1.829(13)	P(6)—C(621)	1.863(9)
Li(2)—P(2)	2.630(16)	Li(3)—P(3)	2.610(19)
Li(3)—P(2)	2.582(18)	Li(2)—P(3)	2.665(16)
Li(2)—N(21)	2.130(20)	Li(3)—N(31)	2.226(28)
Li(2)—N(22)	2.094(25)	Li(3)—N(32)	2.092(22)
P(2)—C(211)	1.846(9)	P(3)—C(311)	1.852(12)
P(2)—C(221)	1.834(11)	P(3)—C(321)	1.848(9)
Li(4)—P(4)	2.574(19)	Li(5)—P(5)	2.607(18)
Li(5)—P(4)	2.623(19)	Li(4)—P(5)	2.629(20)
Li(4)—N(41)	2.117(25)	Li(5)—N(51)	2.114(24)
Li(4)—N(42)	2.136(19)	Li(5)—N(52)	2.162(19)
P(4)—C(411)	1.846(9)	P(5)—C(511)	1.847(10)
P(4)—C(421)	1.873(9)	P(5)—C(521)	1.823(11)
P(1)—Li(1)—P(1a)	91.3(5)	N(11)—Li(1)—N(12)	87.8(7)
P(1)—Li(1)—N(11)	115.6(10)	P(1)—Li(1)—N(12)	127.9(8)
P(1a)—Li(1)—N(11)	120.4(8)	P(1a)—Li(1)—N(12)	117.1(9)
Li(1)—P(1)—Li(1a)	88.7(5)	C(111)—P(1)—C(121)	106.2(4)
Li(1)—P(1)—C(111)	135.3(5)	Li(1)—P(1)—C(121)	108.6(6)
Li(1a)—P(1)—C(111)	109.1(5)	Li(1a)—P(1)—C(121)	104.0(6)
P(2)—Li(2)—P(3)	91.7(5)	N(21)—Li(2)—N(22)	88.7(8)
P(2)—Li(2)—N(21)	115.7(9)	P(2)—Li(2)—N(22)	119.4(8)
P(3)—Li(2)—N(21)	127.0(8)	P(3)—Li(2)—N(22)	117.3(9)
Li(2)—P(2)—Li(3)	87.7(6)	C(211)—P(2)—C(221)	105.1(4)
Li(2)—P(2)—C(211)	110.2(5)	Li(2)—P(2)—C(221)	105.5(5)
Li(3)—P(2)—C(211)	137.7(6)	Li(3)—P(2)—C(221)	106.3(7)
P(2)—Li(3)—P(3)	94.1(6)	N(31)—Li(3)—N(32)	85.9(8)
P(2)—Li(3)—N(31)	117.4(11)	P(3)—Li(3)—N(31)	117.5(8)
P(2)—Li(3)—N(32)	123.5(9)	P(3)—Li(3)—N(32)	121.0(11)
Li(2)—P(3)—Li(3)	86.4(5)	C(311)—P(3)—C(321)	104.0(4)
Li(2)—P(3)—C(311)	108.9(6)	Li(3)—P(3)—C(311)	102.0(6)
Li(2)—P(3)—C(321)	139.2(5)	Li(3)—P(3)—C(321)	109.8(6)
P(4)—Li(4)—P(5)	89.7(6)	N(41)—Li(4)—N(42)	88.5(8)
P(4)—Li(4)—N(41)	120.4(11)	P(4)—Li(4)—N(42)	117.0(7)
P(5)—Li(4)—N(41)	116.5(7)	P(5)—Li(4)—N(42)	128.1(12)
Li(4)—P(4)—Li(5)	90.9(6)	C(411)—P(4)—C(421)	106.4(4)
Li(4)—P(4)—C(411)	115.9(6)	Li(4)—P(4)—C(421)	108.5(6)
Li(5)—P(4)—C(411)	133.7(5)	Li(5)—P(4)—C(421)	98.8(5)
P(4)—Li(5)—P(5)	89.2(5)	N(51)—Li(5)—N(52)	88.6(8)
P(4)—Li(5)—N(51)	117.6(7)	P(5)—Li(5)—N(51)	119.0(11)
P(4)—Li(5)—N(52)	129.1(11)	P(5)—Li(5)—N(52)	116.7(7)
Li(4)—P(5)—Li(5)	90.1(6)	C(511)—P(5)—C(521)	105.5(4)
Li(4)—P(5)—C(511)	137.2(6)	Li(5)—P(5)—C(511)	114.7(6)
Li(4)—P(5)—C(521)	102.8(6)	Li(5)—P(5)—C(521)	101.4(5)
P(6)—Li(6)—P(6b)	91.0(5)	N(61)—Li(6)—N(62)	85.5(8)
P(6)—Li(6)—N(61)	127.1(10)	P(6)—Li(6)—N(62)	121.3(10)
P(6b)—Li(6)—N(61)	120.1(9)	P(6b)—Li(6)—N(62)	114.6(9)
Li(6)—P(6)—Li(6b)	89.0(5)	C(611)—P(6)—C(621)	102.9(4)
Li(6)—P(6)—C(611)	96.0(6)	Li(6)—P(6)—C(621)	130.5(5)
Li(6b)—P(6)—C(611)	111.7(6)	Li(6b)—P(6)—C(621)	123.7(6)

[a] Symmetry operators: (a) $1-x, 1-y, -z$; (b) $-x, -y, 2-z$.

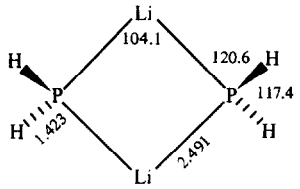

Fig. 4. 66-31G optimized geometry of $(LiPH_2)_2$: angles in degrees, distances in Å.

parison of the angles/lengths within individual dimers.

It is quite clear that complexation greatly influences the size and shape of the $(LiP)_2$ ring; the dimensions of the uncomplexed systems $\{LiP[CH(SiMe_3)_2]_2\}_2$[27]—measured experimentally from a crystal structure determination—and $(LiPH_2)_2$— theoretically determined by our *ab initio* MO calculation—bear this out. The former adopts a slightly asymmetric rhomboidal structure with Li—P—Li angles of 72.0(3) and 72.4(3)° and P—Li—P angles of 108.1(3) and 107.5(3)°; the Li—P bond lengths are significantly shorter than those in **2** and range from 2.456 to 2.481 Å. As noted earlier, the groups attached to phosphorus in this compound are exceptionally bulky, in contrast to the smaller phenyl groups in **2**. Therefore, for more direct comparison we have carried out an *ab initio* geometry-optimized calculation (at the 66-31G level) on the $(LiPH_2)_2$ cyclic dimer. The dimensions of the resulting D_{2h} structure (shown in Fig. 4) agree reasonably well with those of $\{LiP[CH(SiMe_3)_2]_2\}_2$[27] (the P—Li—P angles and Li—P distances optimize to 104.1° and 2.491 Å, respectively), indicating that the steric natures of the *exo* ligands have no pronounced bearing on ring geometry. From angle considerations one could visualize the "complexed" ring being converted to its uncomplexed form by "pulling-out" the structure along the P...P axis, and thereby causing an elongation of the ring bonds. The fact that such bonds actually shorten, however, can be attributed to the lower coordination numbers of the uncomplexed metal atoms (i.e. 2, cf. 4 in the TMEDA adduct) and so a greater *s* character of the Li—P bonds. From energy considerations we calculate the energy of dimerization of $LiPH_2$ to be 55 kcal mol^{-1} and so less favourable than the corresponding association of isovalent $LiNH_2$ units by 19 kcal mol^{-1}.[20] This arises from a less polarized charge distribution in $LiPH_2$ where the Li and P atoms have a charge of +0.47 and −0.36 e, respectively, compared to that in $LiNH_2$ where Li and N carry +0.58 and −0.98 e charges, respectively.

As alluded to earlier, the propensity of lithium to form dimeric ring structures extends to its organonitrogen derivatives. A number of examples could be cited but the most apt for comparison is the lithium amide $[TMEDA \cdot LiN(Ph)Me]_2$.[28] Here the ring angles at Li and N span 90° much more markedly, being 97.6 and 82.4°, respectively, while the mean Li—N bond length is only 2.19 Å, cf. 2.61 Å for the Li—P bonds in **2**. Two-centre bonds to phosphorus atoms are generally about 0.4 Å longer than analogous bonds to nitrogen atoms.

Recently a further link between LiN and LiP structural chemistry was established by the independent X-ray crystallographic characterizations of $\{PMDETA \cdot [LiN(CH_2)_3CH_2]_3\}_2$[29] and $\{THF \cdot [Li_2(\mu_3\text{-}Bu^t_2P) \cdot (\mu_2\text{-}Bu^t_2P)]\}_2$[30] which display both μ_2- and μ_3-type bonding interactions: the essential feature common to both compounds is a ladder-type framework generated by the lateral association of two $(LiN)_2/(LiP)_2$ rings. On the basis of these observations it is highly likely that laddered structures of infinite lengths will prevail in the total absence of donors. Lithium diphenylphosphide itself may well possess this type of polymeric structure (the possible framework of which is illustrated in Fig. 5); its physical properties (i.e. high melting point and arene insolubility) support this. Furthermore, it is particularly noteworthy that starting from such a "parent" structure one can visualize, by breakage of selected numbers of Li—P bonds in the presence of donors, the formation of the zig-zag chains, the ladders, and the dimers and monomers referred to in this paper.

Finally, we have employed crmm measurements and high-field $^7Li/^{31}P$ NMR spectroscopic studies to shed light on the solution natures of **1** and **2** in aromatic solvents. The results obtained are detailed in Experimental.

For **1**, the cryoscopic data (measured in benzene) are compatible with a monomeric structure as its mean solution state of association (*n*) is 0.96. The NMR spectra (recorded in $[^2H_8]$toluene at 20 and −80°C) are consistent with this interpretation showing the singlet ^7Li and ^{31}P resonances expected for a pyramidal phosphorus system. Conversely, the corresponding low-temperature spectra of adduct **2** exhibit well-resolved 1:2:1 triplet (^7Li) and 1:2:3:4:3:2:1 septet (^{31}P) patterns, indi-

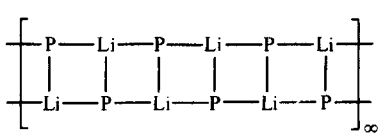

Fig. 5. Framework of the proposed structure of $(LiPPh_2)_\infty$.

cating that the solid-state dimeric structure is probably retained in relatively concentrated solutions. However, cryoscopic studies reveal that under more dilute conditions (indeed, too dilute for meaningful NMR spectra to be obtained in a reasonable time) **2** dissociates appreciably: n falls dramatically from 1.67 to 1.05 on halving the solution concentration (from 0.04 to 0.02 mol dm^{-3}), implying a substantial preponderance of monomer at the lower concentration.

Acknowledgement—We thank the SERC for financial support including a research grant towards crystallographic apparatus and for the provision of NMR facilities.

REFERENCES

1. F. A. Cotton and G. Wilkinson, *Advanced Inorganic Chemistry*, 4th Edn. p. 150. Wiley Interscience, New York (1980); (and references therein); M. Thornton-Pett, M. A. Beckett and J. D. Kennedy, *J. Chem. Soc., Dalton Trans.* 1986, 303.
2. H. Hope, M. M. Olmstead, P. P. Power and X. Xu, *J. Am. Chem. Soc.* 1984, **106**, 819.
3. R. A. Bartlett, M. M. Olmstead and P. P. Power, *Inorg. Chem.* 1986, **25**, 1243.
4. I. J. Colquhoun, H. C. E. McFarlane and W. McFarlane, *J. Chem. Soc., Chem. Commun.* 1982, 220.
5. A. Zschunke, E. Bauer, H. Schmidt and K. Issleib, *Z. Anorg. Allg. Chem.* 1982, **495**, 115.
6. K. Issleib and A. Tzschach, *Chem. Ber.* 1959, **92**, 1118.
7. G. M. Sheldrick, *SHELXTL*: an integrated system for solving, refining and displaying crystal structures from diffraction data. Revision 5. University of Göttingen (1985).
8. A. Schmidpeter, G. Burget and W. S. Sheldrick, *Chem. Ber.* 1985, **118**, 3849.
9. L. Sutton, Ed., *Tables of Interatomic Distances and Configurations in Molecules and Ions*. Special Publication Nos 11 and 18, The Chemical Society, London (1958) and (1965).
10. D. J. Brauer, S. Hietkamp and O. Stelzer, *J. Organomet. Chem.* 1986, **299**, 137.
11. H. H. Karsch, A. Appelt and G. Müller, *J. Chem. Soc., Chem. Commun.* 1984, 1415.
12. M. F. Lappert, L. M. Engelhardt, C. L. Raston and A. H. White, *J. Chem. Soc., Chem. Commun.* 1982, 1323.
13. W. Clegg, D. A. Brown, S. J. Bryan and K. Wade, *Polyhedron* 1984, **3**, 307.
14. M. Dupuis, D. Spangler and J. J. Wendoloski, *GAMESS*, N.R.C.C. Software Catalogue, Vol. 1, Program No. 2G01 (1980).
15. M. F. Guest, J. Kendrick and S. A. Pope, *GAMESS Documentation*, Daresbury Laboratory (1983).
16. M. S. Gordon, J. S. Binkley, J. A. Pople, W. J. Pietro and W. J. Hehre, *J. Am. Chem. Soc.* 1982, **104**, 2797.
17. M. M. Franci, W. J. Pietro, W. J. Hehre, J. S. Binkley, M. S. Gordon, D. J. Defrees and J. A. Pople, *J. Chem. Phys.* 1982, **77**, 3654.
18. W. J. Hehre, R. Ditchfield and J. A. Pople, *J. Chem. Phys.* 1972, **56**, 2257.
19. E. U. Würthwein, K. D. Sen, J. A. Pople and P. v. R. Schleyer, *Inorg. Chem.* 1983, **22**, 496.
20. D. R. Armstrong, P. G. Perkins and G. T. Walker, *J. Mol. Struct. (Theochem.)* 1985, **122**, 189.
21. U. Schümann, J. Kopf and E. Weiss, *Angew. Chem., Int. Ed. Engl.* 1985, **24**, 215.
22. R. Amstutz, T. Laube, W. B. Schweizer, D. Seebach and J. D. Dunitz, *Helv. Chim. Acta* 1984, **67**, 224.
23. D. Barr, W. Clegg, R. E. Mulvey, D. Reed and R. Snaith, *Angew. Chem., Int. Ed. Engl.* 1985, **24**, 328.
24. D. Barr, W. Clegg, R. E. Mulvey and R. Snaith, *J. Chem. Soc., Chem. Commun.* 1984, 285.
25. T. Fjeldberg, P. B. Hitchcock, M. F. Lappert, S. J. Smith and A. J. Thorne, *J. Chem. Soc., Chem. Commun.* 1985, 939.
26. D. Barr, W. Clegg, R. E. Mulvey and R. Snaith, *J. Chem. Soc., Chem. Commun.* 1984, 974.
27. P. B. Hitchcock, M. F. Lappert, P. P. Power and S. J. Smith, *J. Chem. Soc., Chem. Commun.* 1984, 1669.
28. D. Barr, Ph.D. thesis, University of Strathclyde (1984).
29. D. R. Armstrong, D. Barr, W. Clegg, R. E. Mulvey, D. Reed, R. Snaith and K. Wade, *J. Chem. Soc., Chem. Commun.* 1986, 869.
30. R. A. Jones, A. L. Stuart and T. C. Wright, *J. Am. Chem. Soc.* 1983, **105**, 7459.

Polyhedron Vol. 6, No. 5, pp. 995–1001, 1987
Printed in Great Britain

0277–5387/87 $3.00+.00

HALOGEN- AND PHENOXY-SUBSTITUTED QUADRIDENTATE SCHIFF BASES: THEIR Co(III) COMPLEXES AND REACTIVITY OF THE Co—C BOND IN RELATED ALKYL COMPLEXES

JEAN-PIERRE COSTES and GERARD CROS*

Laboratoire de Chimie de Coordination du CNRS, Unité n° 8241 liée par Convention à l'Université Paul Sabatier, 205, route de Narbonne, 31077 Toulouse Cedex, France

and

FRANCOIS MURATET and MARIE-HELENE DARBIEU

Laboratoire de Chimie de Coordination du CNRS and UER de Sciences Pharmaceutiques, Toulouse, France

(*Received* 21 *July* 1986 ; *accepted* 20 *September* 1986)

Abstract—Introduction of halogeno and phenoxy substituents onto the methine carbons of the symmetrical and unsymmetrical Schiff bases, bis-(acetylacetone)ethylenediimine, salicylaldehydeacetylacetoneethylenediimine, and *o*-hydroxyacetophenoneacetylacetoneethylenediimine, has been performed through the use of halogenosuccinimides and sodium phenoxide. The related [Co(Chel),2py]ClO_4 and RCo(Chel), H_2O (Chel = quadridentate ligand) complexes have been synthesized and characterized. The influence of these substituents on the electrochemical properties and behaviour of the Co—C bond have been investigated. It appears that halogen-substituted complexes exhibit less negative potential values for the Co(III)–Co(II) couple than do unsubstituted complexes. However, all alkylated complexes are reactive toward CH_3SnCl_3 while ^1H NMR and EPR measurements point to the occurrence of the homolytic cleavage of the Co—C bond.

Small organocobalt complexes have played an important role in giving insight into many aspects of the processes involving B_{12}-dependent enzymes. Within the framework of this model approach, we have focused our attention on the study of alkyl transfer reactions between cobalt and tin centres.[1–3] Although no direct evidence has been given so far that tin compounds may be alkylated under biotic conditions,[4,5] the factors which may influence this transfer have received considerable study and speculation, due to the large increase in use of organotin compounds over the last 20 years.[6–11]

We have previously considered model systems involving, on the one hand, some alkyl cobalt complexes, RCo(Chel) (Chel is a quadridentate ligand such as BAE, DMG, Salen† ...) and, on the other hand, CH_3SnCl_3 or $(CH_3)_2SnCl_2$.[1–3] The resulting data have shown that the behaviour of the Co—C bond strongly depends on the nature of the equatorial ligand Chel and, therefore, may be altered by introducing suitable substituents onto the ligand framework.

It is well known that electrophilic and nucleophilic substitution may be achieved on the methine carbons of complexed H_2BAE.[12,13] For instance, we succeeded in preparing [Co(X_2BAE), 2Py]ClO_4 complexes[14] from the parent complex [Co(H_2BAE), 2Py]ClO_4, but all attempts to introduce substituents onto the corresponding alkylated complexes RCo(H_2BAE) have failed due to the instability of the Co—C bond.

Recently,[15] we have shown that this difficulty

* Author to whom correspondence should be addressed.

† BAE, bis-(acetylacetone)ethylenediimine; DMG, bis(dimethylglyoxime); Salen, *N*,*N*′-bis-(salicylaldehyde)ethylenediimine.

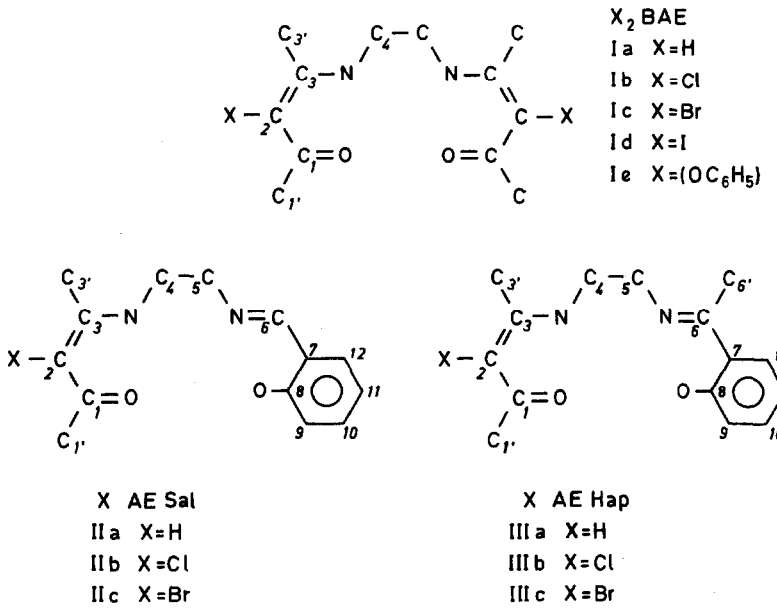

Fig. 1. Schematic representation of ligands.

may be overcome by making use of Schrauzer's method.[16] This implies that the free substituted ligands may be prepared. In some instances,[17] they have been obtained by demetallation of the related nickel(II) or copper(II) complexes but this process is tedious and results in low yield.

In the present paper, we report on the possibility of preparing three types of substituted ligands, i.e. X_2BAE, XAESal and XAEHap (Fig. 1). Of particular importance is the fact that the use of non-symmetrical ligands (HAESal and HAEHap) allows the preparation of monosubstituted species which are expected to give a smooth modulation of the properties of the derived cobalt complexes.

RESULTS AND DISCUSSION

As described in Experimental, halogeno substituents are easily introduced onto the methine carbons of H_2BAE, HAESal and HAEHap by reacting these unsubstituted ligands with the suitable halogenosuccinimides. The X-substituted ligands are stable compounds except the iodo derivatives which are light-sensitive and must be stored at low temperature. The results of elemental analyses are quoted in Table 1. The ligands have been further characterized by NMR (^{1}H and ^{13}C) spectroscopy. The relevant data are collected in Tables 2 and 3. The spectral patterns (chemical shift and multiplicity of the signals) confirm the nature of the species and, more particularly, the occurrence of substitutions on the methine carbons. The influence of the substituents is clearly perceptible in the ^{1}H spectra but it may be recognized that only the BAE moiety of the molecule is significantly perturbed. No attempt has been made to analyse fully the complex spectra of the Salen moiety but the ^{1}H nuclei of the benzenoid ring give two sets of signals with maxima at 7.30 and 6.90 ppm for XAESal, and 7.35 and 6.80 for XAEHap, irrespective of the nature of the X-substituent. Returning to the BAE moiety, it appears that the two $C\underline{H}_3$ are shifted to lower magnetic fields in the order (H, Cl, Br, I) expected on the basis of simple electronegativity arguments.

These ligands have been used to prepare the complexes [Co(Chel), 2Py]ClO_4 and RCo(Chel), R being CH_3 or C_2H_5. Due to the instability and/or low solubility, ^{13}C spectra could only be obtained for nonalkylated complexes. The NMR data are quoted in Tables 4–7. As was the case for the free ligands, the effects of the substituents are restricted to the BAE part of the molecules.

In previous papers,[2,3] we have shown that the redox potentials of the Co(III)–Co(II) couple affords a convenient evaluation of the inductive effects of the ligands onto the cobalt centre. However, it is known that in the alkyl complexes, RCo(Chel), difficulties in measuring the redox potential may arise from cleavage of the Co—C bond and/or cobalt–axial base bond upon reduction and, eventually, from the irreversible nature of the reduction process.[18,19] For these reasons, it is more advisable to consider the nonalkylated complexes which are readily soluble in pyridine and lead, in this solvent, to a one-electron reversible (or quasi-reversible) reduction process. Thus they give more

Table 1. Analytical data

	C		H		N		Co	
	Found	Calc.	Found	Calc.	Found	Calc.	Found	Calc.
Ligand								
Ib	49.1	49.1	6.3	6.2	10.1	9.5		
Ic	38.1	37.7	4.7	4.7	7.2	7.3		
Ie	69.8	70.6	6.7	6.9	6.8	6.9		
IIb	59.3	59.3	6.1	6.1	10.9	10.0		
IIc	51.7	51.7	5.4	5.3	9.1	8.6		
IIIb	61.4	61.1	6.4	6.5	10.1	9.5		
IIIc	53.6	53.1	5.6	5.6	8.3	8.3		
[Co(Chel), 2py]ClO_4								
Ie	56.4	56.5	4.9	5.0	7.6	7.7	8.7	8.1
IIb	47.9	48.4	4.3	4.2	9.0	9.4	10.1	9.9
IIc	45.0	45.0	4.1	3.9	8.4	8.8	8.9	9.2
IIIb	49.0	49.2	4.5	4.5	9.0	9.2	10.3	9.7
IIIc	46.5	45.9	4.5	4.2	8.8	8.6	9.9	9.0
RCo(Chel), H_2O								
R = CH_3								
Ib	39.9	40.7	4.9	5.5	7.0	7.3	16.0	15.4
Ic	33.4	33.1	4.5	4.5	5.9	5.9	12.6	12.5
IIb	48.8	48.5	5.3	5.4	7.3	7.5	16.5	15.4
IIc	44.0	43.4	4.7	4.9	6.8	6.7	14.5	14.2
IIIb	50.2	49.9	5.7	5.8	7.0	7.3	15.1	15.3
IIIc	45.4	44.7	5.8	5.2	5.8	6.5	14.2	13.7
R = C_2H_5								
Ib	42.9	42.3	5.9	5.8	6.8	7.0	15.2	14.8
Ic	35.2	34.6	4.7	4.8	6.2	5.8	12.3	12.1
IIb	50.5	49.9	5.6	5.8	7.1	7.3	16.2	15.3
IIc	44.8	44.8	4.7	5.2	6.8	6.5	13.3	13.7
IIIb	50.6	51.2	6.2	6.1	7.0	7.0	15.8	14.8
IIIc	45.3	46.1	5.3	5.5	6.2	6.3	14.0	13.3

Table 2. ^1H chemical shifts for ligands (ppm vs TMS in $CDCl_3$): the numbering scheme is indicated in Fig. 1[a]

	H'_1 H'_3	H_2	N—H	H_4H_5	H_6	H'_6
Ia	2.00(s), 1.93(s)	4.98(s)	11.4(s)	3.47(m)		
Ib	2.27(s), 2.15(s)		11.4(s)	3.46(m)		
Ic	2.34(s), 2.20(s)		11.7(s)	3.47(m)		
Id	2.57(s), 2.34(s)		12.2(s)	3.56(m)		
Ie	1.93(s), 1.98(s)		10.8(s)	3.50(m)		
IIa	2.15(s), 1.90(s)	5.00(s)	10.9(s)	3.73(m)	8.41(s)	
IIb	2.24(s), 2.17(s)		11.4(s)	3.76(m)	8.36(s)	
IIc	2.32(s), 2.22(s)		11.7(s)	3.76(m)	8.36(s)	
IIIa	2.00(s), 1.93(s)	5.04(s)	11.0(s)	3.30(m)		2.36(s)
IIIb	2.25(s), 2.14(s)		11.45(s)	3.73(m)		2.33(s)
IIIc	2.32(s), 2.25(s)		11.75(s)	3.73(m)		2.32(s)

[a] m = multiplet, d = doublet, s = singlet (same abbreviations in Tables 4, 6 and 7).

Table 3. ^{13}C chemical shifts for ligands (ppm vs TMS): the numbering scheme is indicated in Fig. 1

	C_1	C'_1	C_2	C_3	C'_3	C_4	C_5	C_6	C'_6	C_7	C_8	C_9	C_{10}	C_{11}	C_{12}
Ia	195.3	28.6	95.9	162.7	18.4	43.3									
Ib	193.8	28.3	103.0	160.4	16.1	46.8									
Ic	194.3	30.2	92.4	161.7	19.0	44.3									
Ie	193.8	25.6	126.6	159.3	12.6	41.9									
IIa	195.3	28.8	95.9	162.9	18.7	43.4	59.9	167.2	—	118.8	161.0	117.0	131.5	118.8	132.6
IIb	193.5	28.3	—	160.8	16.4	44.3	59.5	167.1	—	118.8	160.8	116.9	131.6	118.4	132.6
IIc	193.9	30.1	92.1	162.1	19.3	44.7	59.3	167.0	—	118.6	160.7	116.8	131.6	118.6	132.5
IIIa	195.2	28.7	95.8	162.8	18.7	43.3	49.9	173.1	14.5	118.3	162.8	117.4	128.2	118.8	132.4
IIIb	193.4	28.2	102.4	160.9	16.3	44.3	49.6	173.1	14.6	118.3	162.5	117.5	128.1	119.3	132.4
IIIc	194.0	30.1	92.1	162.2	19.3	44.8	49.7	173.2	14.7	118.2	162.5	117.6	128.1	119.4	132.5

Table 4. ^1H chemical shifts for [Co(Chel), 2Py]ClO_4 complexes (pmm vs TMS in $CDCl_3$)

	H'_1 H'_3	H_2	H_4	H_6	H'_6
Ia	2.33(s), 2.11(s)	5.02(s)	3.86(m)	—	
Ib	2.71(s), 2.44(s)	—	4.07(m)	—	
Ic	2.80(s), 2.56(s)	—	4.11(m)	—	
Id	2.97(s), 2.67(s)	—	3.87(m)		
Ic	2.30(s), 2.08(s)				
IIa	2.36(s), 2.20(s)	5.11(s)	4.13(s)	8.15(s)	
IIb	2.61(s), 2.42(s)	—	4.11(s)	8.20(s)	
IIc	2.69(s), 2.51(s)	—	4.11(s)	8.21(s)	
IIIa	2.40(s), 2.15(s)	5.09(s)	4.11		3.35(s)
IIIb	2.60(s), 2.35(s)	—	4.12–4.04(m)		2.84(s)
IIIc	2.61(s), 2.35(s)	—	4.12–4.04(m)		2.83(s)

Table 5. ^{13}C chemical shifts for [Co(Chel), 2Py]ClO_4 complexes (ppm vs TMS in $CDCl_3$)

	C_1	C'_1	C_2	C_3	C'_3	C_4	C_5	C_6	C'_6	C_7	C_8	C_9	C_{10}	C_{11}	C_{12}
Ia	178.9	25.8	97.7	171.2	22.9	52.3	52.3								
Ib	176.0	26.9	103.3	171.2	22.5	53.7	53.7								
Ic	177.7	29.9	94.0	172.1	26.3	54.7	54.7								
Id	179.8	33.6	n.o.	172.9	29.7	55.3	55.3								
IIa	179.3	26.2	96.9	171.7	23.4	50.0	59.3	169.5	—	119.0	165.3	116.4	135.0	123.4	135.8
IIb	176.3	27.2	102.9	171.3	22.2	51.9	58.4	169.3	—	118.6	164.6	116.4	134.7	123.4	135.7
IIc	178.0	29.8	n.o.	n.o.	25.1	52.5	n.o.	169.4	—	n.o.	n.o.	116.5	134.8	123.2	135.8
IIIa	179.0	26.1	97.0	171.4	22.9	50.9	55.6	176.5	20.6	122.1	165.6	116.1	130.6	124.3	134.0
IIIb	176.4	26.8	103.2	170.8	21.5	52.6	54.9	176.0	20.3	121.5	164.8	116.7	139.4	124.0	133.9
IIIc	177.3	29.3	93.0	171.4	24.4	53.2	54.9	176.4	20.3	121.5	164.8	116.2	130.4	124.0	134.0

Table 6. ^{1}H chemical shifts for $CH_3Co(Chel)$ complexes (ppm vs TMS in $CDCl_3$)

	H'_1 H'_3	H_2	H_4	H_6	H'_6	Co—CH_3
Ia	2.09(s), 2.03(s)	5.12(s)	3.40(s)			2.25(s)
Ib	2.30(s), 2.30(s)		3.49(s)			2.30(s)
Ic	2.34(s), 2.26(s)		3.47(s)			2.33(s)
IIa	2.17(s), 2.05(s)	5.17(s)	3.50(m)	8.02(s)		2.37(s)
IIb	2.37(s), 2.32(s)		3.60(m)	7.95(s)		2.32(s)
IIc	2.42(s), 2.30(s)		3.60(m)	7.90(s)		2.30(s)
IIIa	2.12(s), 2.06(s)	5.16(s)	3.40(m)		2.50(s)	2.26(s)
IIIb	2.33(s), 2.30(s)		3.80(m)		2.51(s)	2.33(s)
IIIc	2.40(s), 2.35(s)		3.70(m)		2.47(s)	2.24(s)

reliable data as regards the effect of changing the equatorial ligand than the alkylated complexes do. Furthermore, we have observed in several instances that the data related to the two series of complexes show very similar trends.[2]

The $E_{1/2}$ values obtained for the Co(XAESal) and Co(XAEHap) complexes are reported in Table 8 together with some pertinent results available in the literature. Looking first at the unsubstituted complexes, it appears that the nonsymmetrical complex **IIa** lies between the symmetrical {$E_{1/2}$ Co(III)–Co(II) for [Co(III)(Salen), 2py]ClO_4 = −0.39 V}[20] ones so that use of nonsymmetrical ligands leads to a modulation of the redox properties of the metal centre. Further modulation results from introducing substituents onto the ligand framework. As expected on the basis of inductive arguments, the halogen-substituted complexes exhibit potential values less negative than do the unsubstituted complexes. On decreasing the overall donor power of the equatorial ligand the Co(III)–Co(II) polarographic wave shifts towards less negative values in agreement with a reduction in the electron density on the cobalt atom. The most important variations of $E_{1/2}$ are observed for the Co(X_2BAE) complexes where substitutions occur on both halves of the equatorial ligand. The effects are reduced by half in going to the Co(XAESal) series where only the BAE moiety is substituted. Feeble variations are observed for the Co(XAEHap) complexes. The difference between these two series may result from the electron-releasing effect of the third methyl group in the XAEHap ligands.

Of particular importance is the fact that two complexes, namely Co(BrAESal) and Co(ClAESal), are characterized by potential values greater than −0.4 V. We have previously observed that the behaviour of the Co—C bond in various types of RCo(Chel) complexes was correlated with the $E_{1/2}$ [Co(III) → Co(II)] values and, as regards the $MeSnCl_3$–RCo(Chel) systems, that $E_{1/2} \cong -0.4$ V was a limiting value.[3] On the basis of this empirical correlation, both RCo(XAESal) complexes would be unreactive towards $MeSnCl_3$. Surprisingly, they are found to be reactive. A study (^{1}H NMR, spin-trapping EPR, and chromatography) of $MeSnCl_3$–MeCo(XAESal) (X = Cl or Br) shows that homolytic cleavage of the Co—C bond occurs in both cases.

This abnormal behaviour may originate in a lengthening of the Co—B bond (B being the axial

Table 7. ^{1}H chemical shifts for $C_2H_5Co(Chel)$ complexes (ppm vs TMS in $CDCl_3$)

	H'_1 H'_3	H_2	H_4	$CoCH_2$	$CoCH_2$—CH_3
Ia	2.07(s), 2.01(s)	5.08(s)	3.40(s)	3.44(q)	−0.29(t)
Ib	2.28(s), 2.27(s)		3.41(s)	3.45(q)	−0.31(t)
Ic	2.38(s), 2.35(s)		3.47(s)	3.47(q)	−0.29(t)
IIa	2.61(s), 2.01(s)	5.14(s)	3.50(m)	3.54(q)	−0.31(t)
IIb	2.33(s), 2.14(s)		3.60(m)	3.53(q)	−0.33(t)
IIc	2.45(s), 2.33(s)		3.60(m)	3.53(q)	−0.33(t)
IIIa	2.10(s), 2.04(s)	5.16(s)	3.70(m)	3.40(q)	−0.35(t)
IIIb	2.33(s), 2.26(s)		3.80(m)	3.44(q)	−0.39(t)
IIIc	2.41(s), 2.33(s)		3.68(m)	3.42(q)	−0.40(t)

Table 8. Electrochemical data for [Co(III)(Chel), 2py]ClO_4 complexes

Complex[a]	Polarography		Cyclic voltammetry[b]				
	$E_{1/2}$[c] (V)	Slope	E_{p_c}	E_{p_a}	I_{p_c}/I_{p_a}	$E_{1/2}$ (V)	nb e^- exchanged
Ia	-0.56_8[d]	70					1
	-0.61[e]						
Ib	-0.41_4	69	-0.43_9	0.37_3	1.10	-0.40_6	1
Ic	-0.40[f]		-0.49_6	-0.36_3	0.98	-0.42_9	1
Id	-0.44[f]						1
Ie	-0.51_5	65	-0.57_4	-0.47_2	0.88	-0.52_3	1
IIa	-0.44[f]						1
IIb	-0.35_8	102.7	-0.38_7	-0.25_7	1.56	-0.32_2	1
IIc	-0.34_4	92	-0.37_3	-0.23_0	0.96	-0.30_1	
IIIa	-0.52[g]						1
IIIb			-0.48_7	-0.46_5	0.93	-0.45_1	1
IIIc	-0.50_2	109	-0.56_3	-0.41_4	1.15	-0.48_8	1

[a] Complex (10^{-3} M) in pyridine, Bu_4NClO_4 (0.1 M).
[b] Cyclic voltammetry at 0.1 V s^{-1}.
[c] Vs $Ag–Ag^+$.
[d] See Ref. 15.
[e] Vs SCE, see Ref. 20.
[f] Vs SCE, see Ref. 14.
[g] Vs SCE, see Ref. 21.

base, i.e. pyridine) which would favour the reduction Co(III) → Co(II) since Co—B bond lengths in Co(II) complexes are expected to be longer than in Co(III) complexes.[22–24] Another possibility would be related to an increased flexibility of the XAESal ligands which could adopt a nonplanar conformation resulting in an increased stability for the Co(II) form. Alternatively, one may suggest that the reactivity of the Co—C bond would be enhanced by some structural particularities. For instance, steric interactions between the alkyl group axially coordinated to the cobalt atom and the equatorial ligand could be responsible for the observed abnormality. Recent theoretical work[25] supports the view that the Co—C linkage is particularly susceptible to angular distortion and/or steric hindrance. However, at this point we can only speculate as to the reasons for the seemingly abnormal behaviour of the Co(XAESal) complexes. Structural determinations are needed to clarify this point. Work is in progress to obtain suitable crystals of RCo(AESal) complexes.

EXPERIMENTAL

Synthesis

Ligands. BAE was prepared following the procedure reported by Martell *et al.*[26] We have previously described the synthesis of AESal and AEHap ligands.[21]

X_2BAE, XAESal and XAEHap (X = Cl, Br, I or OC_6H_5) have been obtained through a method similar to that used recently to prepare X_2BAE-substituted compounds with X = C_6H_5NHCO and C_6H_5NHCS.[15] In a typical run, bromosuccinimide (2×10^{-2} mol) was added to a solution of BAE (10^{-2} mol) in acetonitrile at 10°C. The mixture was stirred for 2 h. The white precipitate of Br_2BAE was filtered out, dried and recrystallized in a chloroform–ethanol mixture. I_2BAE, BrAESal and BrAEHap were obtained in a similar way. For X = Cl, it was necessary to add water (60 cm^3) to obtain complete precipitation. The iodo derivative was very light-sensitive.

$(C_6H_5O)_2$BAE was prepared by addition of sodium phenoxide (2×10^{-2} mol) to Br_2BAE (2×10^{-2} mol) dispersed in acetonitrile (40 cm^3), with magnetic stirring for 48 h. Solvent evaporation afforded an oily product. A white precipitate was obtained on adding water and acetone (20 cm^3). The white product was filtered off and dried in dynamic vacuum.

Complexes. [Co(III)(Chel), 2py]ClO_4 complexes were synthesized according to Costa's procedure[27] modified by Averill and Broman.[28]

The brown-red alkylated complexes, RCo(Chel), H_2O, were prepared according to Schrauzer's

procedure.[16] In chloroform, they gave the characteristic green coloration of pentacoordinated RCo-Chel species. Almost all these species were light-sensitive and unstable at room temperature, specifically the iodo and the phenoxy derivatives which could not be obtained pure.

Measurements

Electrochemical measurements were carried out as previously described.[29] A platinium auxiliary electrode and an Ag–AgCl reference electrode were used in conjunction with a dropping mercury electrode. ^{1}H and ^{13}C NMR spectra were recorded on a Bruker WH90 spectrometer using $CDCl_3$ as internal reference.

Acknowledgement—We are grateful to D. de Montauzon for electrochemical measurements.

REFERENCES

1. G. Cros, M.-H. Darbieu and J.-P. Laurent, *Inorg. Nucl. Chem. Lett.* 1980, **16**, 349.
2. J.-P. Costes, G. Cros, M.-H. Darbieu and J.-P. Laurent, *Transition Met. Chem.* 1982, 7, 219.
3. M.-H. Darbieu and G. Cros, *J. Organomet. Chem.* 1983, **252**, 327.
4. P. J. Craig, *Environ. Technol. Lett.* 1980, **1**, 225.
5. P. J. Craig, *Inorg. Chim. Acta* 1985, **107**, 39.
6. L. E. Hallas, J. C. Means and J. J. Cooney, *Science* 1982, **295**, 1505.
7. L. J. Dizikes, W. P. Ridley and J. M. Wood, *J. Am. Chem. Soc.* 1979, **101**, 1442.
8. J. S. Thayer, *Inorg. Chem.* 1978, **18**, 1171.
9. Y. T. Fanchiang, W. P. Ridley and J. M. Wood, *J. Am. Chem. Soc.* 1979, **101**, 1442.
10. Y. T. Fanchiang and J. M. Wood, *J. Am. Chem. Soc.* 1981, **103**, 5100.
11. J. S. Thayer and F. E. Brinckman, *Adv. Organomet. Chem.* 1982, **40**, 313.
12. R. K. Kluiber, *J. Am. Chem. Soc.* 1960, **82**, 4839.
13. L. F. Lindoy, H. C. Lip and W. E. Moody, *J. Chem. Soc., Dalton Trans.* 1974, 44.
14. M.-H. Darbieu, G. Cros, D. de Montauzon and J.-P. Laurent, *Transition Met. Chem.* 1982, **7**, 149.
15. M.-H. Darbieu, G. Cros and J.-P. Laurent *Polyhedron* 1986, **5**, 711.
16. G. N. Schrauzer, J. W. Sibert and R. J. Windgassen, *J. Am. Chem. Soc.* 1968, **90**, 6681.
17. J. W. Kenney and J. H. Nelson, *J. Chem. Soc., Chem. Commun.* 1973, 690.
18. R. G. Finke, B. L. Smith, M. W. Droege, C. M. Elliott and E. Hershenhart, *J. Organomet. Chem.* 1980, **202**, C25.
19. C. M. Elliott, E. Hershenhart, R. G. Finke and B. L. Smith, *J. Am. Chem. Soc.* 1981, **103**, 5558.
20. G. Costa, G. Mestroni, A. Puxeddu and E. Reisenhofer, *J. Chem. Soc.* 1970, 2870.
21. J.-P. Costes, G. Cros, M.-H. Darbieu and J.-P. Laurent, *Inorg. Chim. Acta* 1982, **60**, 111.
22. R. L. Courtright, R. S. Drago, J. A. Nusz and M. S. Nozari, *Inorg. Chem.* 1973, **12**, 2809.
23. D. G. Brown and R. B. Flay, *Inorg. Chim. Acta* 1982, **57**, 63.
24. L. G. Marzilli, N. Bresciani-Pahor, L. Randaccio, E. Zangrado, R. G. Finke and S. A. Myers, *Inorg. Chim. Acta* 1985, **107**, 139.
25. D. W. Christianson and W. N. Lipscomb, *J. Am. Chem. Soc.* 1985, **107**, 2683.
26. A. E. Martell, R. L. Belford and M. Calvin, *J. Inorg. Nucl. Chem.* 1968, **5**, 170.
27. G. Costa, G. Mestroni, G. Thauzer and L. Stephani, *J. Organomet. Chem.* 1964, **6**, 181.
28. D. F. Averill and R. F. Broman, *Inorg. Chem.* 1978, **17**, 3381.
29. J.-P. Costes, G. Cros and J.-P. Laurent, *Inorg. Chim. Acta* 1985, **97**, 211.

Polyhedron Vol. 6, No. 5, pp. 1003–1007, 1987
Printed in Great Britain

0277–5387/87 $3.00+.00

CYCLOMETALLATION—III.* REGIOSELECTIVITY IN Pd(II) CYCLOMETALLATED COMPLEXES

J. M. VILA, A. SUAREZ, M. T. PEREIRA, E. GAYOSO and M. GAYOSO†

Departamento de Química Inorgánica, Facultad de Química, Universidad de Santiago de Compostela, Spain

(*Received* 1 *May* 1986; *accepted* 16 *September* 1986)

Abstract—Cyclometallated complexes derived from organic ligands where two initial metallation sites are present have been synthesized. The preferred palladation position is discussed on the basis of electronic and steric effects, and the regioselectivity of the cyclometallation is characterized by means of IR and ^{1}H NMR spectroscopy. The spectral studies show that the less favored position is not attached to the metal atom. Acetato- and halogeno-bridged dimers, as well as phosphine monomers derived from the latter, have been obtained and studied by spectroscopical methods.

Cyclometallation reactions have aroused great interest in the past,[2–5] not only because of their importance in themselves but also because they provide good starting materials in organic synthesis.[6–8] The question of regioselectivity in these complexes has arisen before[9–11] in those cases where two cyclometallation sites are possible. As a continuation of our studies on cyclometallated compounds[12–14] we now report the preparation and characterization of the complexes derived from *N*-(3,4-dimethoxybenzylidene)-2,4,6-trimethylaniline (**I**), *N*-(4-methoxy-3-methylbenzylidene)-2,4,6-trimethylaniline (**II**) and *N*-(3,4-methylenedioxobenzylidene)-2,4,6-trimethylaniline (**III**). We discuss the preferred cyclometallation site which can be well defined by means of IR and ^{1}H NMR spectroscopy.

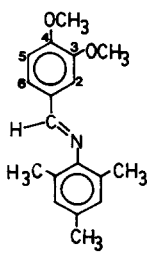

I

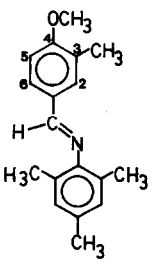

II

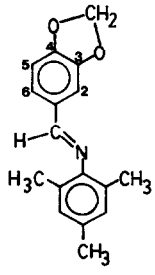

III

* For Part II see Ref. 1.

† Author to whom correspondence should be addressed.

EXPERIMENTAL

Solvents were purified by the standard methods.[15] Chemicals were reagent grade. Palladium(II) acetate was purchased from Fluka. Elemental analyses were carried out in a Perkin–Elmer Elemental analyzer 240-B. Palladium was analyzed by atomic absorption in a Varian Techtron AA-G spectrophotometer. The syntheses of the acetato-bridged dimers were carried out under dry N_2. IR spectra were recorded on a Perkin–Elmer 180 spectrophotometer. ^{1}H NMR spectra were obtained in $CDCl_3$ solutions, with $(CH_3)_4Si$ as the standard ($\delta = 0$ ppm), and were recorded on either a Varian CFT-20 or a Bruker WM-250 spectrometer.

Preparation of the complexes

$[Pd\{4'\text{-}CH_3O\text{-}5'\text{-}CH_3C_6H_2C(H)=N\text{-}2,4,6\text{-}(CH_3)_3C_6H_2\}(CH_3COO)]_2$. In a 100-cm^3 round-bottomed flask, 0.39 g (1.46 mmol) of **II** and 0.3 g (1.34 mmol) of palladium acetate were added in 25 cm^3 of glacial acetic acid, to give a clear solution. After refluxing for 2 h the solution was cooled and the acetic acid removed *in vacuo*. The residue was diluted with water and extracted with dichloromethane. The combined extract was dried with anhydrous sodium sulphate, filtered and then concentrated *in vacuo* to give a yellow solid, which was column chromatographed on silica gel, eluting with

dichloromethane to remove any unchanged starting materials. Elution with dichloromethane–ethanol (1%) gave the desired complex, which was recrystallized from dichloromethane–*n*-hexane, giving a yellow powder. Attempts to produce crystals were unsuccessful.

$[Pd\{4'\text{-}CH_3O\text{-}5'\text{-}CH_3C_6H_2C(H)=N\text{-}2,4,6\text{-}(CH_3)_3C_6H_2\}X]_2$ (X = Cl *or* Br). To 0.1 g of the acetato-bridged dimer dissolved in acetone, giving a clear solution, a solution of sodium chloride or sodium bromide in water ($\simeq 10^{-2}$ M) was added. A solid immediately precipitated. After stirring for 1 h at room temperature, the solid was filtered off and dried *in vacuo*.

$[Pd\{4'\text{-}CH_3O\text{-}5'\text{-}CH_3C_6C(H)=N\text{-}2,4,6\text{-}(CH_3)_3C_6H_2\}(X)P(C_6H_5)_3]$ (X = Cl *or* Br). To a suspension of 0.05 g of the halogeno-bridged dimer in 10 cm^3 of acetone, $P(C_6H_5)_3$ was added in a dimer–phosphine (1 : 2) molar ratio to give a clear solution. After stirring for 2 h, a solution of acetone-water (1 : 3) was added and a solid precipitated. The solid was filtered off and dried *in vacuo*.

The analogous complexes were prepared in the form described above. The amounts used in their preparation can be seen in Table 1. The analytical data, color and yield for the complexes are collected in Table 2.

RESULTS AND DISCUSSION

We have previously studied the preparation and characterization of cyclometallated complexes[1,12–14] in which the organic ligand presented only one possible cyclometallation site, or two equivalent ones which would afford the same product no matter which carbon atom of the phenyl ring was attacked by the metal atom. We are now interested in studying ligands that may give rise to different compounds depending on the carbon atom to which the metal atom is attached in the final product; by means of IR and ^1H NMR spectroscopies we have achieved this. In the complexes derived from **I** the halogeno-bridged dimers were too insoluble for the determination of their NMR spectra; nevertheless, we can assume that what can be said regarding the cyclometallation site of the phenyl ring for the **I** acetato-bridged complex holds in the halogeno-bridged ones, since the latter derive from the former by a metathesis reaction which should render the same complexes save for the bridging ligands. Furthermore, this also applies to the phosphine monomers, which are synthesized from the halogeno-bridged dimers.

Two possible cyclometallation sites, 2 and 6, are present in the mentioned ligands, the electrophilic attack[16] of the palladium atom on either one of them being influenced by both electronic and steric effects. In ligand **I** the C(6) atom was preferred. The methoxy group at C(4) decreases the value of electrophilic palladation at C(2) and C(6). Furthermore, the C(2) position is deactivated by the electron-withdrawing inductive effects of the adjacent methoxy group, which, on the other hand, activates the C(6) position by its strongly *para* directing mesomeric effect. Added to this a steric effect of the C(3) methoxy group, it all accounts for metallation

Table 1. Amounts of products used in the preparation of the complexes

	$Pd(CH_3COO)_2$		Schiff base		Acetato-bridged dimer		NaX solution	X-bridged dimer		$P(C_6H_5)_3$	
	g	mmol	g	mmol	g	mmol		g	mmol	g	mmol
Ia	0.3	1.34	0.41	1.46							
Ib					0.1	0.112	10^{-2} M				
Ic					0.1	0.112	10^{-2} M				
Id								0.05	0.073	0.038	0.146
Ie								0.05	0.068	0.036	0.136
IIa	0.3	1.34	0.39	1.46							
IIb					0.1	0.116	10^{-2} M				
IIc					0.1	0.116	10^{-2} M				
IId								0.05	0.061	0.032	0.122
IIe								0.05	0.055	0.029	0.110
IIIa	0.3	1.34	0.39	1.46							
IIIb					0.1	0.116	10^{-2} M				
IIIc					0.1	0.116	10^{-2} M				
IIId								0.05	0.061	0.032	0.122
IIIe								0.05	0.055	0.029	0.110

Table 2. Analytical data, color and yield for the complexes, and IR data for the ligands and complexes

Compound	Color	Yield (%)	Analytical data found (calc.) (%) C	H	N	Pd	IR data
I							1638s[a]
Ia	Yellow	91	53.6 (53.6)	5.1 (5.2)	3.0 (3.1)	22.9 (23.8)	1612sh,w,[a] 1590m, b,[b] 1420m[b]
Ib	Yellow	79	50.9 (50.9)	4.8 (4.8)	3.0 (3.3)	24.4 (25.1)	1612m,[a] 290m,[c] 268m[c]
Ic	Yellow	83	46.5 (46.1)	4.3 (4.3)	2.7 (3.0)	22.4 (22.7)	1615m,[a] 176sh,m,[c] 166m[c]
Id	Yellow	92	62.9 (62.9)	5.0 (5.1)	1.9 (2.1)	15.0 (15.5)	1610sh,m,[a] 298m[d]
Ie	Yellow	90	58.4 (59.1)	4.9 (4.8)	1.6 (1.9)	14.0 (14.5)	1611m,[a] 184sh,m[d]
II							1635m[a]
IIa	Yellow	83	55.4 (55.6)	5.7 (5.4)	3.1 (3.2)	24.1 (24.6)	1605m,[a] 1582s,[b] 1412m[b]
IIb	Yellow	81	53.5 (53.0)	5.2 (5.0)	3.2 (3.4)	25.7 (24.6)	1611m,[a] 307m,[c] 280m[c]
IIc	Yellow	84	47.5 (47.8)	4.7 (4.5)	3.1 (3.1)	23.0 (23.5)	1611sh,m,[a] 190m,[c] 164m[c]
IId	Light yellow	> 95	64.0 (64.5)	5.1 (5.3)	2.0 (2.1)	15.7 (15.9)	1610m,[a] 306m[d]
IIe	Light yellow	> 95	59.9 (60.5)	4.9 (4.9)	1.7 (2.0)	14.5 (14.9)	1605sh,m,[a] 200m[d]
III							1639m[a]
IIIa	Orange-yellow	85	53.1 (52.9)	5.0 (4.4)	3.3 (3.2)	24.3 (24.6)	1611m,[a] 1580m,[b] 1432m[b]
IIIb	Yellow	78	50.5 (50.0)	4.6 (4.0)	2.9 (3.4)	25.8 (26.1)	1611s,[a] 250m,[c] 224m[c]
IIIc	Yellow	83	45.9 (45.1)	3.7 (3.6)	2.8 (3.1)	23.1 (23.5)	1611s,[a] 192m,[c] 142m-w[c]
IIId	Yellow	90	62.4 (62.7)	4.8 (4.7)	1.5 (2.1)	15.5 (15.9)	1620m,[a] 306m[d]
IIIe	Yellow	> 95	58.4 (58.8)	4.5 (4.4)	1.6 (2.0)	14.7 (14.9)	1615m,[a] 200m-w[d]

[a] CN.
[b] CH_3COO.
[c] PdX_b.
[d] PdX_t.

not ocurring at the C(2) position, but rather at C(6). As we have described before,[1] attempts to prepare cyclometallated complexes where a methoxy group *ortho* to the metallation site is present have been unsuccessful. For reasons given there we think that it is mainly a strong steric effect by the methoxy group that prevents metallation of the carbon atom *ortho* to it.

In ligand **II**, also the C(6) site is preferred. Again the C(4) methoxy group has a deactivating effect on the C(2) and C(6) atoms, whereas the 3-methyl group is expected to highly activate electrophilic attack at the *para* C(6) position. We do not believe that the methyl group has a strong steric effect so as to prevent palladation at C(2) because, as we have already shown,[14] complexes with a methyl group *ortho* to the metallation site can be obtained in high yield. In this case it is only a matter of electronic effects which favor the C(6) site for palladation.

For ligand **III** we see no reason why palladation should not occur on any one of the C(2) and C(6) atoms; in fact, a mixture of isomers might be possible. However, in contrast to the complexes obtained by Barr and Dyke[9,17] where cyclopalladation occurred at the 6-position, we have obtained complexes in which it takes place through the 2-position, and no isomer with the metal bound to the C(6) atom was found.

The ^1H NMR spectra for the **I** and **II** dimer complexes show two H(1) singlets due to the H(6′) and H(3′) protons. The initial double doublet of protons H(5) and H(6) disappears, upon metallation to the C(6) atom, as is expected. For the **III** dimer complexes, the initial double doublet of H(5) and H(6) protons still holds, and the H(2) singlet disappears. In the phosphine monomers the great amount of phenyl protons does not allow a correct assignment in this region. The data are shown in Table 3.

Further evidence for these situations can be obtained from the IR spectra of the complexes, by studying the bands in the 900–800-cm^{-1} region, and which are due to the different substitution pattern of the phenyl ring.

In the **I** and **II** complexes the band at 825–805 cm^{-1} due to two adjacent protons in a 1,2,4-substituted phenyl ring disappears, as is expected if the metallation takes place at the C(6) atom, leaving two solitary protons on the ring. The 1,2,3,4-phenyl substitution produced by palladation at the C(2) atom in the **III** complexes leaves two adjacent protons on the ring which gives rise to a band at 810–

Table 3. ^{1}H NMR data for the ligands and dimer complexes

	H_{imine}	H6(2′)[a]	H2(6′)[a]	H5(3′)[a]	OCH_2O	CH_3O	CH_3	CH_3COO
I	7.95s	7.11d ($J_{6,5}$ = 8.2, $J_{6,2}$ = 1.7)	7.53d ($J_{2,6}$ = 1.7)	6.75d ($J_{5,6}$ = 8.2)		3.83, 3.77	2.14, 1.99[b]	
Ia	7.52s		6.85s	6.19s		3.88, 3.76	2.51, 2.25[b]	1.70s
Ib	7.52s		n.o.	n.o.		3.76[b]	2.26,[b] 2.19	
Ic	7.61s		n.o.	n.o.		3.85, 3.81	2.31,[b] 2.27	
II	8.08s	7.63dd ($J_{6,5}$ = 8, $J_{6,2}$ = 2)	7.77s	6.85d ($J_{5,6}$ = 8)		3.89s	2.28, 2.27, 2.11[b]	
IIa	7.49s		7.04s	6.10		3.67s	2.52, 2.26, 2.19, 2.18	1.71s
IIb	7.49s		7.04s	6.10		3.67s	2.30, 2.27, 2.19, 2.11	
IIc	7.59s		7.07s	n.o.		3.79s	2.32,[b] 2.27, 2.10	
III	7.98s	7.11dd ($J_{6,5}$ = 8, $J_{6,2}$ = 2)	7.49d ($J_{2,6}$ = 2)	6.79d ($J_{5,6}$ = 8)	5.94s		2.19, 2.02	
IIIa	7.44s	6.86dd ($J_{6,5}$ = 8)		6.50dd ($J_{5,6}$ = 8)	5.62s		2.17,[b] 2.12	1.63s
IIIb	7.52s	6.99dd ($J_{6,5}$ = 8)		6.61dd ($J_{5,6}$ = 8)	5.98s		2.24,[b] 2.20	
IIIc	7.50s	6.92dd ($J_{6,5}$ = 8)		6.55dd ($J_{5,6}$ = 8)	5.91s		2.24,[b] 2.14	

[a] The numbers in parentheses apply only to the **I** and **II** complexes. J in Hz.

[b] This signal integrates for six protons.

CH_3O signals in the phosphine monomers: **Id** 3.81 and 2.88, **Ie** 3.71 and 2.82, **IId** 2.85, and **IIe** 2.84.

800 cm^{-1} in the IR spectrum that would otherwise be absent.

With this in mind, and as we have discussed before,[1,12-14] the complexes may be formulated as follows with a d^8 palladium atom in a 2+ oxidation state:

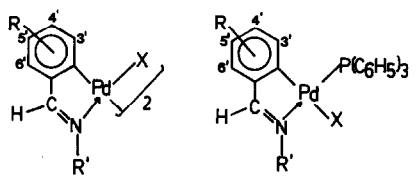

a: X = CH_3COO d: X = Cl

b: X = Cl e: X = Br

c: X = Br

I: R = 4′,5′-$(CH_3O)_2$; R′ = 2,4,6-$(CH_3)_3C_6H_2$

II: R = 4′-CH_3O-5′-CH_3; R′ = 2,4,6-$(CH_3)_3C_6H_2$

III: R = 3,4-OCH_2O; R′ = 2,4,6-$(CH_3)_2C_6H_2$

The numbers on the phenyl rings apply only to the I and II complexes; for the III complexes the notation of the free ligand holds.

The present compounds are all remarkably air-stable solids ranging in color from orange-yellow to light yellow. Except for the halogeno-bridged dimers, which are only sparingly soluble in chloroform and dichloromethane and totally insoluble in alcohols, the complexes are soluble in the more common organic solvents, and insoluble in water.

They all show a shift of the νCN band towards lower wavenumbers (Table 2) with respect to the parent organic ligand, the magnitude of which shows that the metal atom is bound through the nitrogen lone pair[14,18-20] and not to the C=N double bond. Further evidence of this is the 0.43–0.57-ppm upfield shift of the azomethine proton signal,[14,21] as is depicted in Table 3.

The acetato-bridged ligands have characteristic bands in the IR spectrum at 1590m and 1420m cm^{-1} (**Ia**), 1582s and 1412m cm^{-1} (**IIa**), and 1580m and 1432m cm^{-1} (**IIIa**), the separations between them show the acetato ligand to be bridging between the metal atoms[14,22] (Table 2).

In the ^{1}H NMR spectra an H(6) singlet, 1.70 (**Ia**), 1.71 (**IIa**) and 1.63 (**IIIa**), is found in each case (Table 3). This peak has been assigned to the two acetate-methyl groups, so that they are equivalent, therefore rendering the organic ligands in a *trans* disposition.[23,24] The upfield shift of this signal, compared to that of palladium(II) acetate (δ 2.04 ppm) may be due to the through-space shielding environment of the unmetallated phenyl ring.[1,14]

The chloro-bridged dimers have a *trans* geometry as have been shown by IR[25] and X-ray studies;[26] they show two $\nu PdCl_b$ bands in the IR spectrum. The higher-frequency band is attributed to the Pd—Cl bond *trans* to nitrogen, and the lower frequency one to the Pd—Cl bond *trans* to the phenyl

carbon atom, owing to the higher *trans* influence of a phenyl carbon atom than that of a nitrogen atom.[27,28]

In the phosphine monomers, as we have shown before[1,12–14] the phosphine ligand is *trans* to the nitrogen atom, and the halogen ligand to the carbon atom. The high *trans* influence of the latter weakens the Pd—Cl bond and thus the $\nu PdCl_t$ vibration frequency appears at lower wavenumbers than could be expected should the halogen atom be *trans* to a weak *trans* influence ligand[27] (Table 2). Further proof can be drawn from the ^1H NMR spectra of the monomer complexes. The C(4) methoxy group signal suffers an upfield shift with respect to its position in the free ligand and the dimer complexes due to the aromatic shielding cone of the phosphine ligand (Table 3), which can only take place with this ligand *trans* to the nitrogen atom.[1] In complexes **Ia**, **IIa** and **IIb** the H5(3′) proton signal is shifted upfield by 0.59–0.75 ppm compared to the parent free ligand, whereas in **IIIa–c** it is only shifted 0.18–0.29 ppm. This could be due to a flow of charge from the d^8 palladium atom[29] which would be more notorious in the **I** and **II** complexes as in them H5(3′) is *ortho* to the σPd—C bond, whereas in the **III** complexes H(5) would be *para* to this bond, and hence farther away, so that the effect would be less intense in these cases.

Acknowledgement-We wish to thank the Comisión Asesora de Investigación Científica y Técnica for financial support of this work.

REFERENCES

1. J. M. Vila, M. T. Pereira, E. Gayoso and M. Gayoso, *Transition Met. Chem.* 1986, **11**, 342.
2. I. Omae, *Chem. Rev.* 1979, **79**, 289.
3. I. Omae, *Coord. Chem. Rev.* 1980, **32**, 235.
4. I. Omae, *Coord. Chem. Rev.* 1979, **28**, 97.
5. I. Omae, *Coord. Chem. Rev.* 1982, **42**, 245.
6. R. A. Holton, *J. Am. Chem. Soc.* 1977, **99**, 8083.
7. S. I. Murahashi, Y. Tauba, M. Yamamura and I. Moritani, *Tetrahedron Lett.* 1974, **43**, 3749.
8. A. D. Ryabov, *Synthesis* 1985, **3**, 233.
9. S. F. Dyke and S. N. Quessy, *Transition Met. Chem.* 1982, **7**, 233.
10. R. A. Holton and R. G. Davis, *J. Am. Chem. Soc.* 1977, **99**, 4175.
11. J. M. Vila, M. T. Pereira, A. Suárez, J. Filgueira, E. Gayoso and M. Gayoso, 7° *Encontro Anual da S.P.Q.* Lisboa, 1984, PB6.
12. A. Suárez, J. M. Vila, E. Gayoso and M. Gayoso, *An. Quím.* 1985, **81**, 251.
13. A. Suárez, J. M. Vila, E. Gayoso and M. Gayoso, *Rev. Port. Quím.* 1984, **26**, 21.
14. J. M. Vila, M. T. Pereira, A. Suárez, E. Gayoso and M. Gayoso, *Synth. React. Inorg. Met.-Org. Chem.* 1986, **16**, 499.
15. D. D. Perrin, W. L. F. Armarego and D. R. Perrin, *Purification of Laboratory Chemicals*, 1st Edn. Pergamon Press, Oxford (1966).
16. G. W. Parshall, *Acc. Chem. Res.* 1970, 139.
17. N. Barr and S. F. Dyke, *J. Organomet. Chem.* 1983, **243**, 223.
18. S. P. Molnar and M. Orchin, *J. Organomet. Chem.* 1969, **16**, 196.
19. H. Onoue and I. Moritani, *J. Organomet. Chem.* 1972, **43**, 431.
20. H. Onoue, K. Minami and K. Nakagawa, *Bull. Chem. Soc. Jpn* 1970, **43**, 3480.
21. Y. A. Ustynyuk, V. A. Chertov and I. V. Barniov, *J. Organomet. Chem.* 1971, **29**, C53.
22. K. Nakamoto, *IR and Raman Spectra of Inorganic and Coordination Compounds*, 3rd Edn, p. 232. Wiley Interscience, New York (1978).
23. J. Selbin, K. Abboud, S. F. Watkins, M. A. Gutiérrez and F. R. Fronczek, *J. Organomet. Chem.* 1983, **241**, 259.
24. W. Hiller, A. Castiñeiras, J. M. Vila, A. Suárez, M. T. Pereira and M. Gayoso, *Acta Cryst.* 1986, **C42**, 1136.
25. J. Dehand, M. Pfeffer and J. Shamir, *Spectrochim. Acta* 1977, **33A**, 1101.
26. R. C. Elder, R. D. P. Cruea and R. F. Morrison, *Inorg. Chem.* 1976, **15**, 1623.
27. B. Crociani, T. Boschi, R. Pietropaolo and U. Belluco, *J. Chem. Soc. A* 1970, 531.
28. F. R. Hartley, *The Chemistry of Platinum and Palladium*. Applied Science Publications, London (1973).
29. M. A. Gutiérrez, G. R. Newkome and J. Selbin, *J. Organomet. Chem.* 1980, **202**, 341.

Polyhedron Vol. 6, No. 5, pp. 1009–1015, 1987
Printed in Great Britain

0277–5387/87 $3.00+.00

MIXED-LIGAND COMPLEXES OF Ru(III) AND Rh(III): ESR STUDIES ON SOME Ru(III) COMPLEXES

H. K. GUPTA and S. K. DIKSHIT*

Department of Chemistry, Indian Institute of Technology, Kanpur 208016 (UP), India

(*Received* 6 *May* 1986; *accepted after revision* 16 *September* 1986)

Abstract—Reactions of 2-mercapto-3-phenyl-4-quinazolinone (LH) with $RuCl_3 \cdot xH_2O$ and $RhCl_3 \cdot xH_2O$ afforded the compounds $[RuL_2Cl(H_2O)]H_2O$, $[RuL_2Cl \cdot DMF]$ and $RhL(LH)Cl_2 \cdot 2H_2O$. Reactions of LH with $RuCl_3 \cdot xH_2O$ in the presence of *N*-heterocyclic bases led to the formation of complexes of type $[RuL_2ClB] \cdot H_2O$ (B = pyridine, 3-picoline or imidazole) and $[RuLCl_2(o\text{-phen})]H_2O$ (*o*-phen = 1,10-phenanthroline). These complexes were characterized on the basis of analytical, conductivity, magnetic, IR and electronic spectral and ESR studies. Tentative structures for the complexes are proposed.

Studies on the complexing behaviour of biologically active ligands containing thioamide group have been the subject of investigations in our laboratory.[1–3] Recently the complexes of Pd(II), Pt(II) and Ru(II) with ligands containing a thioamide group reported from our laboratory have been selected for anticancer screening by the National Cancer Institute, Bethesda, Maryland, U.S.A. The effect of various ligands and metal ions on metal–ligand covalency, *d*-orbital splitting and distortion of complexes have been of considerable interest in the field of coordination chemistry. The low-spin d^5-configuration is a good probe of molecular structure and bonding since *g* values of such complexes vary widely, owing to the structure of the complex and the degree of metal–ligand covalency. Although a large number of $d^5(t_{2g}^5)$ complexes have been studied, the application of ESR was mainly limited to the first-row transition series. Only a few Ru(III) complexes have been subjected to ESR studies.[4–8] In view of the biological activity of the complexes and diverse coordinating ability of the ligand 2-mercapto-3-phenyl-4-quinazolinone (LH) we were prompted to study the Ru(III) and Rh(III) complexes. Recently, we have reported the interaction of LH with Co(II), Ni(II), Pd(II), Pt(II) and Pt(IV) ions in the presence and absence of various *N*-heterocyclic bases.[9,10] The ligand (LH) has been used for the estimation of copper[11] and Dave *et al.* have reported the interaction with Cu(II), Co(III) and Ni(II).[12]

The IR spectrum of LH in the solid state displays a ν(NH) absorption band at *ca* 3250 cm^{-1} but no ν(SH) absorption band at *ca* 2500 cm^{-1}, indicating that, in the solid state, the ligand exists as a thione (**1**) and not as a thiol (**2**) tautomer.

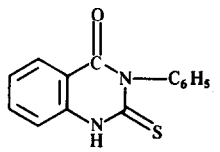

1

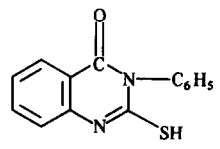

2

EXPERIMENTAL

All the chemicals used were either AR or chemically pure grade. Sulphur and chloride were estimated gravimetrically. Ruthenium was estimated on a IL-751 atomic absorption spectrophotometer after the complex had been decomposed by heating with a mixture of H_2SO_4 and HNO_3. Electronic spectra were recorded on a Cary model 17D UV–visible spectrophotometer. The IR spectra were obtained on a Perkin–Elmer 580 spectrophotometer in KBr in the range 4000–250 cm^{-1}. Melting points of the complexes were recorded on a Fisher–John melting-point apparatus and are uncorrected. The ESR spectra were recorded on 109E-line century series EPR spectrometer at *X*-band frequencies at 293 K using DPPH ($g = 2.0036$) as internal stan-

* Author to whom correspondence should be addressed.

Table 1. Analytical and magnetic data of complexes

Compound	Colour	M.p. (°C)	μ_{eff}[a] (BM)	Found (calc.) (%) M	S	C	H	N	Cl
$RhL(LH)Cl_2 \cdot 2H_2O$	Yellow	> 290	DM[b]	—	9.1	46.8	3.1	8.0	10.0
				(14.4)	(8.9)	(46.9)	(3.2)	(7.8)	(9.9)
$[RuL_2Cl \cdot DMF]$	Violet	232d[c]	1.75	14.4	9.1	51.8	3.4	9.6	4.8
		250		(14.1)	(8.9)	(52.0)	(3.5)	(9.8)	(5.0)
$[RuL_2Cl(H_2O)]H_2O$	Black	> 290	1.82	15.1	9.2	50.3	3.3	8.5	5.0
				(14.9)	(9.4)	(50.0)	(3.2)	(8.3)	(5.2)
$[RuL_2Cl(py)]H_2O$	Greenish black	> 290	2.10	13.4	8.6	53.5	3.5	9.3	5.0
				(13.7)	(8.7)	(53.6)	(3.4)	(9.5)	(4.8)
$[RuL_2Cl(3\text{-pic})]H_2O$	Brown black	210	2.07	13.6	8.4	54.3	3.4	9.1	4.9
				(13.4)	(8.5)	(54.1)	(3.6)	(9.3)	(4.7)
$[RuLCl_2(o\text{-phen})]H_2O$	Reddish brown	212	1.73	16.5	5.3	50.3	3.2	9.1	11.3
				(16.2)	(5.1)	(50.1)	(3.0)	(8.9)	(11.4)
$[RuL_2Cl(imid)]H_2O$	Sea-green	215	1.94	13.8	9.0	52.0	3.7	11.8	5.1
				(14.0)	(8.9)	(51.8)	(3.6)	(11.7)	(4.9)

[a] At 20°C and uncorrected for diamagnetism.
[b] DM = diamagnetic.
[c] d = decomposes.

dard. Magnetic susceptibilities were measured by a parallel-field vibrating sample magnetometer (VSM) model 150A at 293 K.

The ligand LH was prepared by a literature method.[13,14]

Preparation of complexes

$RhL(LH)Cl_2 \cdot 2H_2O$. A solution of $RhCl_3 \cdot xH_2O$ (0.26 g, 1 mmol) in DMF (10 cm^3) was added to a filtered solution of LH (0.508 g, 2 mmol) in DMF (25 cm^3). The resulting solution was heated under reflux with constant stirring for an hour. The solution was allowed to cool at room temperature. Addition of excess ammonia solution to it precipitated a yellow complex which was centrifuged, washed with water, alcohol and ether, and dried at 80°C.

$[RuL_2Cl \cdot DMF]$. A solution of $RuCl_3 \cdot xH_2O$ (0.26 g, 1 mmol) in DMF (10 cm^3) was added to a filtered solution of LH (0.5 g) in DMF (25 cm^3). The resulting solution was refluxed for an hour. The solution was concentrated to about 5 cm^3 on a water bath: on cooling a violet precipitate resulted which was filtered, washed with alcohol and ether, and dried at 80°C.

General method of preparation of $[RuL_2ClB]H_2O$ [B = H_2O, *pyridine* (py), 3-*picoline* (3-pic) *or imidazole* (imid)] *and* $[RuLCl_2(o\text{-phen})]H_2O$ (*o*-phen = 1,10-*phenanthroline*). A filtered alkaline (pH 9–10) ethanolic solution (25 cm^3) of LH (0.5 g, 2 mmol)* was added to an aqueous solution (50 cm^3) of $RuCl_3 \cdot xH_2O$ (0.26 g, 1 mmol) containing the appropriate heterocyclic base† solution. The resulting solution was heated under reflux for 15 h. The resultant precipitates were filtered, washed thoroughly with water, a little amount of alcohol and ether. The compounds were recrystallized from methanol.

RESULTS AND DISCUSSION

Microanalytical data as well as sulfur, metal and chloride estimations are in good agreement with stoichiometry proposed for complexes (Table 1). All complexes were found to be nonconducting in methanol.

IR spectra

The ligand LH contains a thioamide group (H—N—C=S) and gives rise to four characteristic thioamide bands, namely, I, II, III and IV, in the region of 1500, 1300, 1000 and 800 cm^{-1}, and have contributions from $\delta(C—H)+\delta(N—H)$, $\nu(C=S)+\nu(C=N)+\nu(C—H)$, $\nu(C—N)+\nu(C—S)$,

* 0.25 g of LH in the case of $[RuLCl_2(o\text{-phen})]H_2O$.

† 5 cm^3 of pyridine, 3-picoline, 5 cm^3 of an ethanolic solution of 1,10-phenanthroline (0.2 g, 1 mmol) or 5 cm^3 of an aqueous solution of imidazole (0.07 g, 1 mmol).

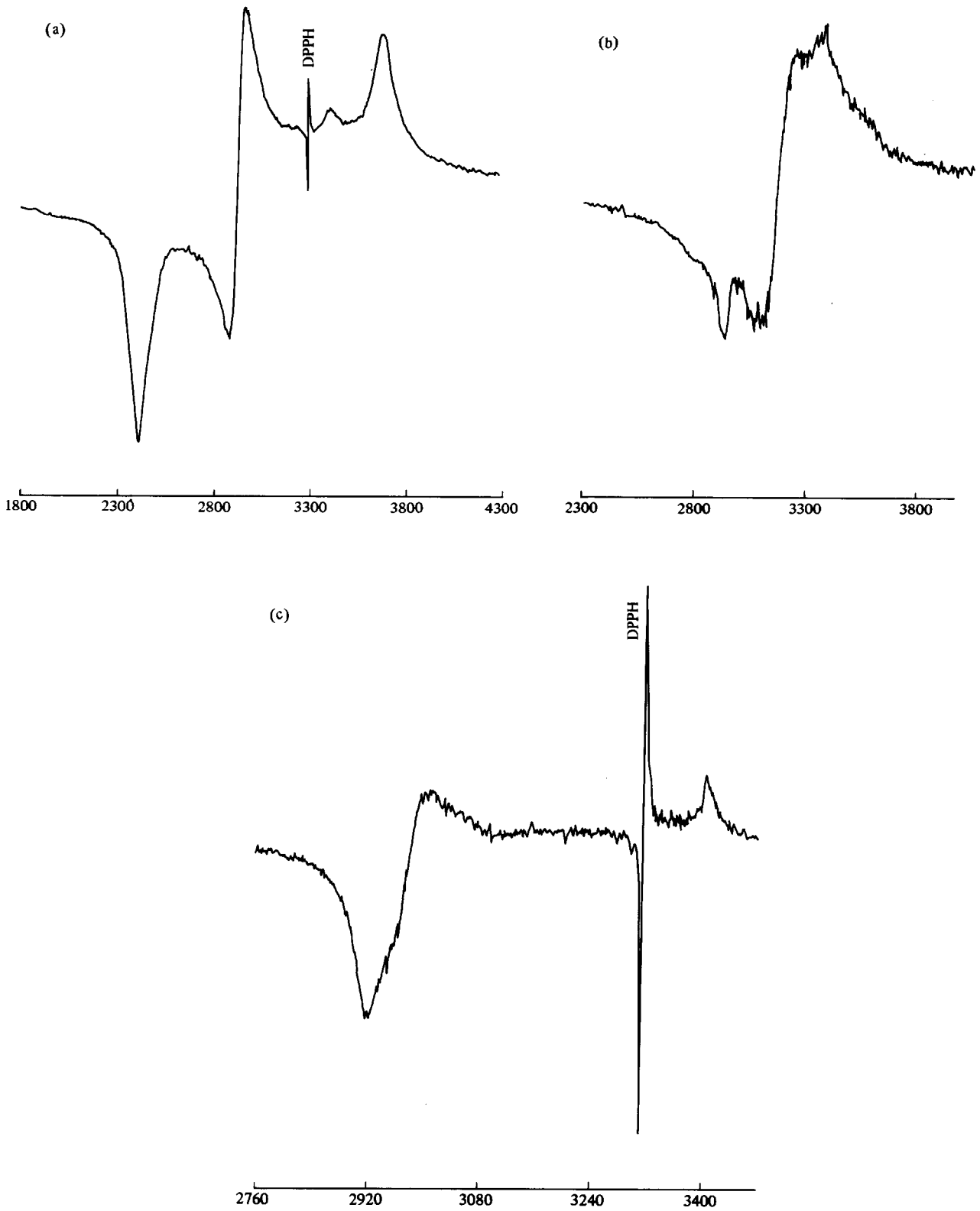

Fig. 1. Solid-state ESR spectra at 293 K (field H in Gauss): (a) $[RuL_2Cl \cdot DMF]$, (b) $[RuL_2Cl(py)] \cdot H_2O$, and (c) $[RuLCl_2(o\text{-phen})] \cdot H_2O$.

Table 2. Comparison of IR bands of ligand (LH) and metal complexes (in cm^{-1})

Compound	ν(NH)	ν(OH)	ν(C=O)	Thioamide bands I	II	III	IV
LH	3250	—	1660s	1540s	1345s	1000s 980m	770s
$RhL(LH)Cl_2 \cdot 2H_2O$	3240–3260w	3500br	1700s	1520m	1330s 1340w	1000w	770s
$[RuL_2Cl \cdot DMF]$	—	—	1690s	1520m	1330m	1000m	780s
$[RuL_2Cl(H_2O)]H_2O$	—	3460br	1700s	1510m 1320s	1330s 1320s	1030w 990w	770s
$[RuL_2Cl(py)]H_2O$	—	3460br	1680s	1510s	1320s	1010m 990m	770s
$[RuL_2Cl(3\text{-pic})]H_2O$	—	3400br	1690s,br	1505s	1310s	980m	790m 760s
$[RuLCl_2(o\text{-phen})]H_2O$	—	3400br	1690s	1510s	1320m	990w	770s
$[RuL_2Cl(imid)]H_2O$	3340–3420br		1700s	1510m	1330m 1320m	1000w	770s

and ν(C⋯S) modes of vibrations, respectively[15–18] (Table 2).

The disappearance of the ν(NH) band of the ligand at 3250 cm^{-1} from the spectra of all complexes except $RhL(LH)Cl_2 \cdot 2H_2O$ indicates the displacement of N—H hydrogen by Ru(III) and Rh(III), and formation of a metal–nitrogen bond. The presence of weak broad band at 3240–3260 cm^{-1} in the IR spectrum of $RhL(LH)Cl_2 \cdot 2H_2O$ indicates that one ligand is present as LH.

The weakening and broadening of ν(NH) after complexation can be tentatively assigned to Rh(III)—N bond formation.

The presence of a broad band in the region of 3400–3500 cm^{-1} in the spectra of complexes is assigned as ν(OH) of water. The broad band at 3360–3420 cm^{-1} in the spectra of $[RuL_2Cl(imid)] \cdot H_2O$ may be assigned as mixed band of ν(NH) of imidazole and ν(OH) of water.

The ν(C=O) band of the ligand at 1660 cm^{-1} shifts towards a higher wavenumber by 10–30 cm^{-1} in the spectra of complexes, indicating the non-involvement of the C=O group in metal bonding. The ν(C=O) of DMF in the $[RuL_2Cl \cdot DMF]$ complex is probably merged with the band present at 1690 cm^{-1} in the IR spectrum of the complex. ν(C=O)[19] in DMF appears at 1683 cm^{-1}, hence coordination of DMF through its N atom is likely.

The thioamide band I of the ligand at 1540 cm^{-1} shifts to a lower wavenumber by 20–35 cm^{-1} in the spectra of the complexes. This indicates M—N bond formation as the thioamide band I has its principal contribution from δ(C—H)+δ(N—H).

The thioamide band II of the ligand at 1345 cm^{-1} either splits or shifts to a lower wavenumber as a result of coordination as band II has a contribution from ν(C=S)+ν(C=N)+ν(C—H).

The thioamide band III [ν(C—N)+ν(C—S)] is relatively weak in the spectra of the complexes. The thioamide band IV ν(C⋯S) of the ligand at 770 cm^{-1} changes its position by ± 10 cm^{-1} in the spectra of the complexes. A red shift of 25–55 cm^{-1} in band IV usually indicates bonding through sulphur and a blue shift of 40–90 cm^{-1} in this band indicates bonding through nitrogen. However, if there is simultaneous coordination through nitrogen and sulphur, there may not be much of a shift in band IV.[20] Hence the small shift of band IV is attributed to simultaneous coordination through nitrogen and sulphur. In contrast with soft metal ions, similar ligands are reported to coordinate through sulphur only.[21]

New bands of weak to medium intensity in the region 250–500 cm^{-1} in the spectra of the complexes may be assigned to the coupled vibrations ν(M—Cl), ν(M—N) and ν(M—S).[22]

In the spectra of the complexes, there seems to be extensive mixing between the bands of the ligand and those of the bases, hence the characteristic frequencies of *N*-heterocycles did not occur at their standard positions.

Magnetic moments and electronic spectra

The magnetic-susceptibility measurements at room temperature show that the magnetic moments of ruthenium complexes lie in the range 1.7–2.1 BM (Table 1) corresponding to one unpaired electron. The rhodium complex was found to be diamagnetic.

The electronic spectrum of LH in DMF exhibits

a strong peak at 295 nm and a weak shoulder at 262 nm which are assigned to a $\pi \rightarrow \pi^*$ intraligand (IL) transition.[23]

The electronic spectra of the Ru(III) complexes show bands in the 645–655-, 525–565- and 415–465-nm regions (Table 3) which may be assigned to $^2T_{2g} \rightarrow {}^4T_{1g}$, $^2T_{2g} \rightarrow {}^4T_{2g}$ and $^2T_{2g} \rightarrow {}^2A_{2g}$, $^2T_{1g}$ transitions,[24] respectively.

In the spectra of Ru(III) complexes, some of these transitions could not be observed, probably because of masking by a strong charge-transfer (CT) and/or an IL transition. A band or shoulder around 295–310 nm is assigned to the IL transition. Another band at 330 nm in the spectrum of $[RuL_2Cl(py)]H_2O$ may be assigned to an M → L or L → M CT transitions.

The rhodium complex shows only IL transitions. All other expected transitions[24] were probably masked by IL bands.

ESR spectra

To interpret the ESR data, we have used the theory as described by Bleaney and O'Brien which has been successfully applied to many complexes.[4–6]

The ESR measurement does not determine the sign of g_i components, nor the correspondence of g_1, g_2 or g_3 to g_x, g_y or g_z. It only gives the absolute principal g values. Therefore, we considered all possible combinations for acceptable results. For axially symmetric molecules g_z is assigned to the unique component and only eight possible sign combinations were taken, whereas for molecules with lower symmetry 48 possible combinations were considered.

A Fortran IV computer program on a DEC-1090 system was used for all these calculations. The experimental g values and approximate values of the starting vector (approximate values of A, B, C and k, keeping the normalization condition $A^2+B^2+C^2 = 1$, in mind) were fed into the program. For each set in turn, values of A, B, C and k were found by use of the Newton–Raphson method. The computer program was then tested by using literature-reported[5] data.

For all of the possible combinations the values of A, B, C, k, Δ/λ and V/λ were obtained, and reasonable combinations were selected (Table 4) by considering the following conditions. (1) Solutions with $0.75 < k < 2.0$ were examined while a defi-

Table 3. Electronic spectra of complexes in methanol and typical g values of some of the Ru(III) complexes

Compound	Band position λ_{max} (nm)	Assignment	ESR spectra			
			g_1	g_2	g_3	g^b
Ligand (LH)[a]	262	$\pi \rightarrow \pi^*$				
	295	$\pi \rightarrow \pi^*$				
$RuL(LH)Cl_2 \cdot 2H_2O$	265	IL				
	310sh	IL or CT				
$[RuL_2Cl \cdot DMF]$[a]	265	IL	2.74	2.25	1.79	2.29
	306	IL				
	465	$^2T_{2g} \rightarrow {}^2A_{2g}$, $^2T_{1g}$				
	525	$^2T_{2g} \rightarrow {}^4T_{2g}$				
$[RuL_2Cl(H_2O)]H_2O$	295	IL				
	555	$^2T_{2g} \rightarrow {}^4T_{2g}$				
$[RuL_2Cl(py)]H_2O$	300	IL	2.32	2.14	2.01	2.16
	330	CT				
	415	$^2T_{2g} \rightarrow {}^2A_{2g}$, $^2T_{1g}$				
$[RuL_2Cl(3\text{-pic})]H_2O$	295	IL				
	430	$^2T_{2g} \rightarrow {}^2A_{2g}$, $^2T_{1g}$				
	655	$^2T_{2g} \rightarrow {}^4T_{1g}$				
$[RuLCl_2(o\text{-phen})]H_2O$	295	IL	2.23	2.23	1.95	2.14
	485	$^2T_{2g} \rightarrow {}^2T_{1g}$				
$[RuL_2Cl(imid)]H_2O$	300	IL				
	565	$^2T_{2g} \rightarrow {}^4T_{2g}$				
	645	$^2T_{2g} \rightarrow {}^4T_{1g}$				

[a] Spectra taken in DMF solvent.
[b] $g = (\frac{1}{3}g_1^2+\frac{1}{3}g_2^2+\frac{1}{3}g_3^2)^{1/2}$.

Table 4. g Values, ground-state wave function parameters, orbital reduction factors and energy level splitting parameters of Ru(III) complexes

Compound	Fit	g_x	g_y	g_z	k	A	B	C	V/λ	Δ/λ
$[RuL_2Cl\cdot DMF]$	(1)	−2.25	2.74	1.79	1.209	0.768	0.639	0.047	0.193	0.243
	(2)	−2.74	2.25	1.79	1.209	0.768	0.639	−0.047	−0.193	0.243
$[RuL_2Cl(py)]H_2O$	(1)	−2.14	2.32	2.01	1.119	0.802	0.598	0.018	0.067	0.074
	(2)	−2.32	2.14	2.01	1.119	0.802	0.598	−0.018	−0.067	0.074
$[RuLCl_2(o\text{-phen})]H_2O$	(1)	−2.23	2.23	−1.95	0.953	0.902	0.996	0.0	0.0	0.640
	(2)	−2.23	2.23	1.95	1.104	0.798	0.603	0.0	0.0	0.099

nition of k requires $0.75 < k < 1.0$ as a large value of k can be obtained if the assumptions made in the theory are not strictly valid.[4,25–27] (2) Kramer's doublets obtained from the knowledge of A, B and C should be coincident with those of the ground state obtained from the matrix of spin–orbit coupling and low-symmetry field, for the observed ESR spectra were due to the lowest Kramer's doublets. (3) For molecules showing three featured spectra, 48 combinations usually lead to six solutions with identical k values. These solutions differ only in their ordering of real one-electron d-functions and in the value of the coefficients A, B, and C. In such cases we made a choice by taking the pair corresponding to $g_z \approx 2.0$. (4) The tetragonal distortion (Δ) is assumed to be larger than the rhombic distortion (V), which seems reasonable if we consider the structure of the complexes examined.

As a consequence, two possible fits (Table 4) for $[RuL_2Cl\cdot DMF]$ and $[RuL_2Cl(py)]H_2O$ were limited to the following: $g_1 = -g_x$, $g_2 = g_y$, $g_3 = g_z$; or $g_1 = g_y$, $g_2 = -g_x$, $g_3 = g_z$. These solutions are equivalent with each other, differing only in the choice of the x- and y-axes, in other words, differing in the signs of both the coefficient C and V/λ values, and it is difficult to reject either of the two, although assignments giving a negative V/λ value were chosen and reported for $[RuX(NH_3)_5]^{2+}$ (X = Cl or Br).[28]

For an axially symmetric molecule, $[RuLCl_2(o\text{-phen})]H_2O$ there are two acceptable fits. Both fits produce a small Δ/λ ($\Delta < \lambda$) corresponding to a small axial distortion. The value of k is in the range 0.95–1.10, and the estimated energy of electronic transitions between Kramer's doublet lies in the range 1400–1800 cm^{-1}. [Here we assume $\Delta \approx 1000$ cm^{-1}, arbitrarily considering a reduction from the free-ion value of 1180 cm^{-1} for Ru(III).] These transitions fall in the IR range of the spectrum and may get obscured by vibrational transitions.

The fit (1) for $[RuL_2Cl(o\text{-phen})]H_2O$ is chosen here, the sign of g_y is positive and both g_x and g_z are negative ($B > A$, C) and the results show that the hole is in the t_2^o (d_{xy}) orbital. Similar assignments have been reported for β-diketonate complexes of Ru(III).[5] The ordering of the one-electron real functions is one where the doubly degenerate level $t_2^{\pm}$ ($d_{xz} \pm d_{yz}$) lies the lowest. The orbital energies of some of the complexes are given in Table 5. For the compounds with three distinct components, two fits were found and results are not very much different from each other. The highest lying orbital is d_{xy} and the ground state may be either: (a) d_{yz}, or (b) d_{xz}. It is difficult to decide between the two possibilities. The positive value of Δ/λ found in this work means that the d_{xy}-orbital lies at a higher energy than the d_{xz}- and d_{yz}-orbitals, thus supporting the order of d-orbital energies listed in Table 5.

Table 5. Energies of three Kramer's eigenstates and calculated d-orbital energies for the complexes[a]

Compound	E/λ	E_1/λ	E_2/λ	$\Delta E_1/\lambda$	$\Delta E_2/\lambda$	d-Orbital order	Energies (λ cm^{-1})
$[RuL_2Cl\cdot DMF]$	−1.093	0.326	0.525	1.419	1.618	$YZ < XZ < XY$	−0.177, 0.015, 0.162
						$XZ < YZ < XY$	−0.177, 0.015, 0.162
$[RuL_2Cl(py)]H_2O$	−1.026	0.444	0.508	1.470	1.534	$YZ < XZ < XY$	−0.058, 0.009, 0.050
						$XZ < YZ < XY$	−0.058, 0.009, 0.050
$[RuLCl_2(o\text{-phen})]H_2O$	−1.281	0.141	0.5	1.422	1.781	$e(XZ,YZ) < b_2(XY)$	−0.21, 0.42
	−1.035	0.436	0.5	1.471	1.535	$e(XZ,YZ) < b_2(XY)$	−0.33, 0.66

[a] E is lowest energy of ground-state Kramer's doublet.

For the complexes studied the value of k is in the range 0.95–1.21. The 0.953 value for the orbital reduction factor k for the compound $[RuLCl_2(o\text{-phen})]H_2O$ is as expected since *o*-phenanthroline is known to behave as a π-bonding ligand and forms strong metal–ligand covalent bonds. The value of k greater than 1.0 is also not surprising as many other factors besides covalency are responsible for the variation in the value of k[4,25–27] and moreover the complexes of π-bonding ligands such as PPh_3 and $AsPh_3$ are reported to have k values greater than 1.0.[5] An important contribution to the large values of k is, probably, the presence of low-lying CT states. Since 4*d* and 5*d* electrons are less tightly bound to the metal atom, the molecular-orbital formation occurs readily and as a result the CT states have a lower energy than most crystal field states.[29]

Thus the ESR study of $[RuL_2Cl \cdot DMF]$ and $[RuL_2Cl(py)]H_2O$ compounds indicates the rhombic distortion, $g_x \neq g_y \neq g_z$, for these complexes and axial symmetry, $g_x = g_y \neq g_z$ for the $[RuLCl_2(o\text{-phen})]H_2O$ complex.

On the basis of analytical, conductivity, magnetic, spectroscopic and ESR data, a distorted octahedral geometry is assigned to Ru(III) and Rh(III) complexes, assuming that LH is bidentate and coordinated through the nitrogen and sulphur of the thioamide group.

REFERENCES

1. R. Saheb, U. C. Agarwala and S. K. Dikshit, *Indian J. Chem.* 1981, **20A**, 1196.
2. R. Saheb, S. K. Dikshit and U. C. Agarwala, *Indian J. Chem.* 1983, **22A**, 24.
3. R. Saheb, S. K. Dikshit and U. C. Agarwala, *Indian J. Chem.* 1983, **22A**, 1050.
4. A. Hudson and M. J. Kennedy, *J. Chem. Soc. A* 1969, 1116.
5. O. K. Medhi and U. Agarwala, *Inorg. Chem.* 1980, **19**, 1381 (and references therein).
6. S. Sakai, Y. Yanase, N. Hagiwara, T. Takeshita, H. Naganuma and K. Ohkubo, *J. Phys. Chem.* 1982, **86**, 1038.
7. S. Sakai, N. Hagiwara, Y. Yanase and A. Ohyoshi, *J. Phys. Chem.* 1978, **82**, 1917.
8. J. B. Raynor and B. G. Jeliazkowa, *J. Chem. Soc., Dalton Trans.* 1982, 1185.
9. H. K. Gupta and S. K. Dikshit, *Indian J. Chem.* 1986, **25A**, 842.
10. H. K. Gupta and S. K. Dikshit, *Transition Met. Chem.* 1985, **10**, 469.
11. G. R. Dave, G. S. Mewada and G. C. Amin, *Colour Age* 1967, **16**, 49.
12. L. D. Dave, Cherian Mathew and Varughese Oommen, *Indian J. Chem.* 1983, **22A**, 420.
13. Suman Mehrotra, J. P. Barthwal, A. K. Saxena, K. P. Bhargava and S. S. Parmar, *J. Heterocycl. Chem.* 1981, **18**, 1157.
14. P. N. Bhargava and M. R. Chawrasia, *J. Med. Chem.* 1968, **11**, 405.
15. C. N. R. Rao and R. Venkataraghavan, *Spectrochim. Acta* 1962, **18**, 541.
16. C. N. R. Rao, R. Venkataraghavan and T. Kasturi, *Can. J. Chem.* 1964, **42**, 36.
17. I. Suzuki, *Bull. Chem. Soc. Jpn* 1962, **35**, 1286, 1449, 1456.
18. B. Singh, M. M. P. Rukhaiyar and R. J. Sinha, *J. Inorg. Nucl. Chem.* 1977, **39**, 29.
19. R. N. Haszeldine, *J. Chem. Soc.* 1954, 4145.
20. B. Singh and R. Singh, *J. Inorg. Nucl. Chem.* 1977, **39**, 25.
21. K. K. Pandey, M. Noltemeyer, G. M. Sheldrick and R. Saheb, *Z. Naturforsch.* 1984, **39b**, 586.
22. D. M. Adams, *Metal Ligand and Related Vibrations*, pp. 249, 284 and 316. St. Martins Press, New York (1968).
23. S. F. Mason, *Q. Rev.* 1961, **15**, 287.
24. S. K. Sengupta, S. K. Sahni and R. N. Kapoor, *Polyhedron* 1983, **2**, 317 (and references therein).
25. R. E. Desimone, *J. Am. Chem. Soc.* 1973, **95**, 6238.
26. S. A. Cotton and J. F. Gibson, *J. Chem. Soc. A* 1971, 803.
27. M. Gerloch and J. R. Miller, *Prog. Inorg. Chem.* 1968, **10**, 1.
28. D. Kaplan and G. Navon, *J. Phys. Chem.* 1974, **78**, 700.
29. C. J. Ballhausen, *Introduction to Ligand Field Theory*, p. 273, McGraw-Hill, New York (1962).

Polyhedron Vol. 6, No. 5, pp. 1017–1020, 1987
Printed in Great Britain

0277–5387/87 $3.00+.00

Ni(II) COMPLEXES OF SOME POLYFUNCTIONAL *N*-NAPHTHYLIDENEAMINO ACIDS

M. R. MAHMOUD* and S. A. EL-GYAR

Chemistry Department, Faculty of Science, Assiut University, Assiut, Egypt

and

A. A. MOUSTAFA and A. SHAKER

Chemistry Department, Faculty of Science, Sohag, Egypt

(*Received* 3 *June* 1986; *accepted* 16 *September* 1986)

Abstract—A new series of amino acid Schiff base Ni(II) complexes of 2-hydroxy-1-naphthaldehyde with glycine, L-alanine, L-valine, L-leucine, DL-isoleucine, DL-norleucine, L-serine and L-aspartic acid has been prepared by constituent combination. The structure of the complexes is investigated by microanalysis, conductance, electronic and IR spectral measurements. It is concluded that the bivalent anions of the Schiff bases coordinated to Ni(II) as a tetradentate ligand (O–N–O–O), in the case of the aspartic acid moiety, or as a tridentate ligand (O–N–O) in the case of the other amino acid moieties. The structure of the Ni(II) complexes is suggested to be square planar.

Though much attention has been paid to metal complexes of Schiff bases derived from salicylaldehyde and amino acids,[1–10] there is little in the literature on using 2-hydroxy-1-naphthaldehyde (naph). Only MacDonald *et al.*[11] investigated the Cu(II) complexes of naphthylidene polyfunctional amino acids. Accordingly, the work of this paper describes the synthesis as well as elucidation of the chemical structure of a series of new Ni(II) complexes of Schiff bases derived from naph and some bi- and tridentate α-amino acids. The amino acids applied in this investigation are glycine (gly), L-alanine (ala), L-valine (val), L-leucine (leu), DL-isoleucine (isoleu), DL-norleucine (norleu), L-serine (ser), and L-aspartic acid (asp).

EXPERIMENTAL

All chemicals used were A.R. products and were used without further purification.

Preparation of complexes

The general method used for preparation of the different complexes under investigation is the constituent combination method which has proved to be an excellent synthetic procedure. Quantitative yields of the Ni(II)–*N*-naphthylideneamino acid complexes were obtained by adding an alcoholic solution of Ni(II) chloride to an alcoholic solution of stoichiometric amounts of both naph and amino acid. Sodium carbonate was added to the reaction mixture and then it was gently refluxed on a water bath for 3 h. After cooling a crystalline product obtained. The collected solid complexes were washed with water and ethanol, and then dried. The analytical data of the different Ni(II) complexes synthesized along with their decomposition temperatures are given in Table 1.

Physical measurements

The electrolytic conductances were measured at 25°C using a Pye conductance bridge. The UV and visible electronic spectra were carried out using matched 1-cm^3 stoppered silica cells on a Pye–Unicam SP 100 spectrophotometer. The IR spectra of the complexes were recorded in potassium bromide using a Perkin–Elmer 599 B IR spectrophotometer.

* Author to whom correspondence should be addressed.

Table 1. Characterization data of Ni(II)–naphthylideneamino acids complexes

Complex	Decomposition temperature (°C)	Appearance of crystals	Molar conductance (Ω^{-1} cm^2 mol^{-1})	Analysis (%)[a] C	N
[Ni(naph-gly)]H_2O	265	Brown	2.6[b]	51.1 (51.2)	4.4 (4.6)
[Ni(naph-ala)]H_2O	> 300	Dark yellow	2.3[b]	52.5 (52.7)	4.3 (4.4)
[Ni(naph-val)]H_2O	155	Yellowish-green	7.2[b]	55.2 (55.4)	4.0 (4.0)
[Ni(naph-leu)]H_2O	288	Dark yellow	9.2[b]	56.4 (56.6)	3.6 (3.8)
[Ni(naph-isoleu)]H_2O	> 300	Yellow	4.3[b]	56.4 (56.6)	3.6 (3.8)
[Ni(naph-norleu)]H_2O	284	Yellow	6.0[b]	56.6 (56.5)	3.7 (3.8)
[Ni(naph-ser)]H_2O	274	Yellowish-green	5.0[b]	49.9 (50.1)	3.9 (4.1)
[Ni(naph-asp)]H	248	Brown	[c]	49.4 (49.6)	3.8 (3.8)

[a] Calculated values are given in parentheses.
[b] Measured in DMF.
[c] Insoluble in ethanol or DMF.

RESULTS AND DISCUSSION

Chemical analysis and molar-conductance measurements

The results of microanalysis of the prepared Ni(II) naphthylideneamino acid complexes (Table 1) suggest the general molecular formula [Ni (II)(naph)(amino acid)] for the synthesized complexes. This reveals the behaviour that the divalent anions of the naphthylideneamino acids are coordinated to the central Ni(II) ion. Except in the case of Ni(II)–naphthylideneaspartic acid complexes which is insoluble in ethanol or DMF, the measured molar-conductance values for the DMF or ethanolic solutions of the other prepared Ni(II) complexes are very low (< 10.0 Ω^{-1} cm^2 mol^{-1}) as given in Table 1. This suggests a non-electrolytic nature for these complexes.

Electronic spectra

The recorded visible spectra of the different Ni(II)–naphthylideneamino acid complexes in DMF (Fig. 1) show two main bands at 408 and 396 nm (ε_{max} = 3000–12,200 and 6200–13,000 l mol^{-1} cm^{-1}, respectively). Furthermore a broad weak band or shoulder is observed in the range 560–530 nm (ε_{max} = 40–800 l mol^{-1} cm^{-1}). This spectral behaviour suggests a square planar structure for the different Ni(II)–naphthylideneamino acid complexes since it was reported before that the visible spectra of square planar Ni(II) complexes are characterized by an absorption band in the 666–400-nm region (ε_{max} = 50–500 l mol^{-1} cm^{-1}) followed by a more intense one in the 434–330-nm region.[12] The high excitation energy visible band observed in the spectra of the Ni(II) complexes (λ_{max} = 396 nm) can be presumably ascribed to an intramolecular charge-transfer transition liable to take place in the complexed ligand, naphthylideneamino acid.

IR spectra

The IR of all Ni(II) complexes show a broad band at 3300 cm^{-1}, supporting the presence of a water molecule in each complex as indicated by the chemical-analysis data listed in Table 1. The broad band appearing in the 1630–1615-cm^{-1} region in the IR spectra of all complexes can be considered as an overlapped band due to two stretching vibrations, antisymmetric coordinated COO^- and C=N. Since it has been reported that the stretching vibration of the phenolic C—O usually appears near 1530 cm^{-1} [13] the band that appeared in the IR spectra of all complexes in the 1540–1525-cm^{-1} region can be attributed to phenolic C—O stretching.

The IR spectrum of the synthesized Ni(II)–naphthylideneaspartic acid complex does not show

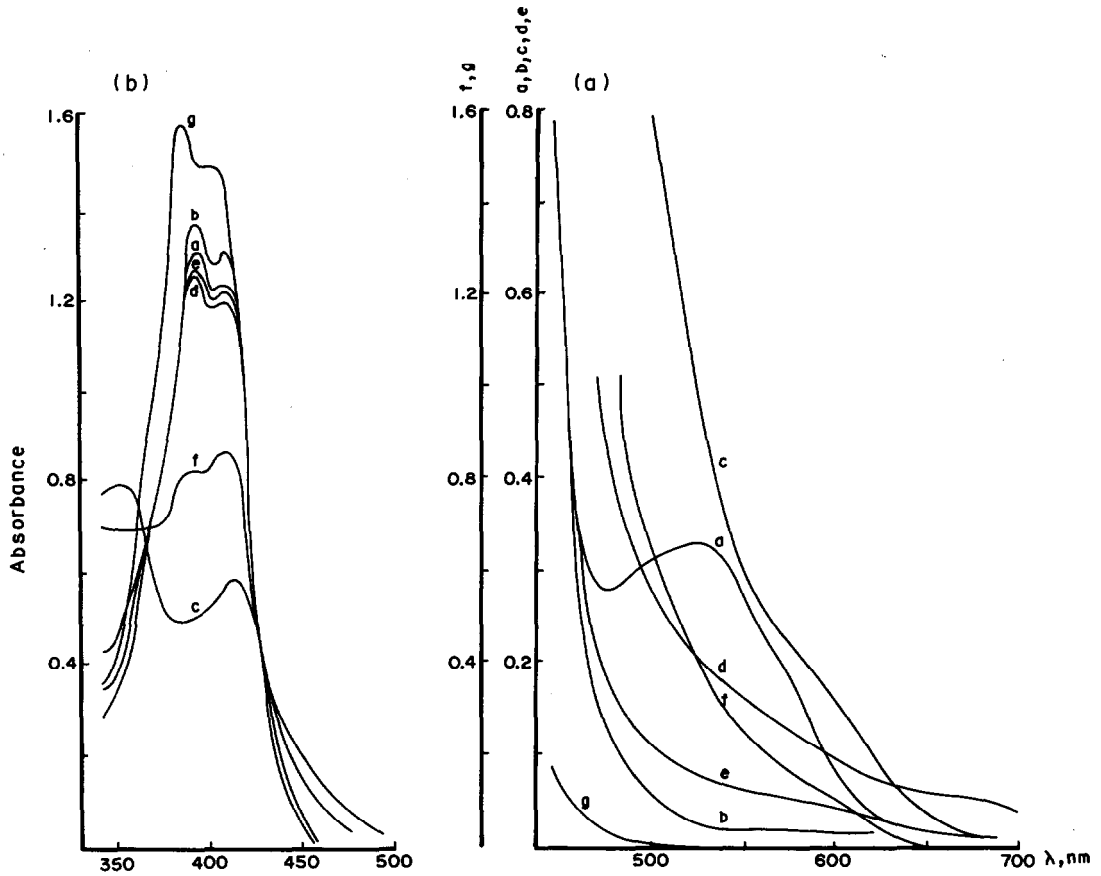

Fig. 1. Visible electronic absorption spectra of 2×10^{-3} M (700–500 nm) (a) and 1×10^{-4} M (500–340 nm) (b) Ni(II)–*N*-naphthylideneamino acid complexes in DMF: (a) gly, (b) ala, (c) val, (d) leu, (e) isoleu, (f) norleu, and (g) ser.

an absorption band due to unionized uncoordinated COO stretching which usually appears at 1750–1700 cm^{-1}.[14] This indicates that the Schiff base naphthylideneaspartic acid coordinated to Ni(II) as a trivalent anion tetradentate (O–N–O–O) ligand. With respect to the amino acid serine, the binding ability of the alcoholic oxygen was estimated to be comparatively weak in an acid or neutral medium.[15] Accordingly, in the case of the Schiff base naphthylideneserine the possibility that the serine moiety OH group takes part in complex formation can be ruled out. This is what is observed since the molar-conductance measurement of the Ni(II)–naphthylideneserine complex shows the nonelectrolytic nature of such a complex i.e. it behaves as a bivalent anion tridentate (O–N–O) ligand.

Conclusions

The important conclusions that can be drawn from this study can be summarized as follows:

(i) Except for the Schiff base naphthylideneaspartic acid, the other naphthylideneamino acids studied coordinate to the central Ni(II) as bivalent anion tridentate O–N–O ligands where two five- and six-chelated rings are formed. The bonding sites are the oxygens of the *o*-hydroxy and α-carboxyl groups belonging to the naphthylideneamino acid moieties. The third bonding site is the azomethine nitrogen atom. The structure of such complexes can be represented schematically (Fig. 2).

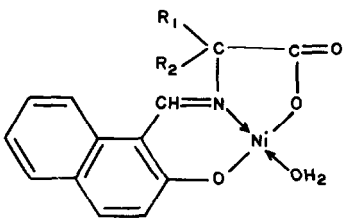

Fig. 2. Ni(II)–naphthylideneamino acid complexes (square planar structure) $R_1 = H$; $R_2 = H$ (gly), CH_3 (ala), $CH(CH_3)_2$ (val), $CH_2CH(CH_3)_2$ (leu), $CH(CH_3)CH_2CH_3$ (isoleu), $CH_2CH_2CH_2CH_3$ (norleu), or CH_2OH (ser).

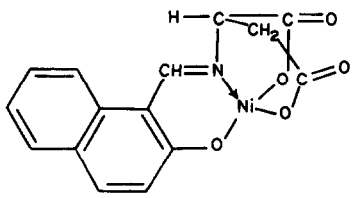

Fig. 3. Ni(II)–naphthylideneaspartic acid complex (square planar structure).

(ii) The dianions of naphthylideneaspartic acid are coordinated to Ni(II) as a O–N–O–O tetradentate ligand where three chelated rings are formed. The additional fourth bonding site is the oxygen β-carboxyl group of the aspartic acid moiety. The structure of this complex can be represented as in Fig. 3.

REFERENCES

1. G. L. Eichhorn and N. D. Marchand, *J. Am. Chem. Soc.* 1956, **78**, 2688.
2. R. C. Burrows and J. C. Bailar, *J. Am. Chem. Soc.* 1966, **88**, 4150.
3. L. N. Sakurai and A. Nakahara, *Bull. Chem. Soc. Jpn* 1967, **46**, 1536.
4. G. O. Carlisle and L. J. Theriot, *J. Inorg. Nucl. Chem.* 1973, **55**, 2093.
5. L. J. Theriot, G. O. Carlisle and H. Hu, *J. Inorg. Nucl. Chem.* 1969, **31**, 3303.
6. L. J. Theriot, G. O. Carlisle and H. J. Hu, *J. Inorg. Nucl. Chem.* 1969, **31**, 2841.
7. L. J. Theriot, G. O. Carlisle and H. J. Hu, *J. Inorg. Nucl. Chem.* 1969, **31**, 2891.
8. R. L. Dutta and R. K. Ray, *J. Inorg. Nucl. Chem.* 1977, **39**, 1848.
9. M. R. Mahmoud, A. K. El-Shafei and A. M. Abdel-Mawgoud, *J. Chem. Technol. Biotechnol.* 1982, **32**, 933.
10. M. R. Mahmoud, A. A. El-Samahy, R. Abdel-Hamid and A. M. Abdel-Mawgoud, *Bull. Soc. Chem. Belg.* 1981, **10**, 1023.
11. L. G. MacDonald, D. H. Brown, J. D. Morris and W. E. Smith, *Inorg. Chim. Acta* 1982, **67**, 7.
12. A. B. P. Lever, *Inorganic Electronic Spectroscopy*, p. 343. Elsevier, New York (1968).
13. S. J. Gruber, C. M. Harris and E. Sinn, *J. Inorg. Nucl. Chem.* 1968, **30**, 1805.
14. K. Nakamoto, *Infrared and Raman Spectra of Inorganic and Coordination Compounds*, 3rd Edn, p. 311. John Wiley, New York (1978).
15. A. Nakahara, H. Yamamoto and H. Matsumoto, *Sci. Rep., Coll. Gen. Educ., Osaka Univ.* 1963, **12**, 11.

Polyhedron Vol. 6, No. 5, pp. 1021–1025, 1987
Printed in Great Britain

0277–5387/87 $3.00+.00

MONONUCLEAR AND BINUCLEAR LANTHANUM(III) COMPLEXES OF MACROCYCLIC LIGANDS DERIVED FROM 2,6-DIACETYLPYRIDINE

O. P. PANDEY

Department of Chemistry, Gorakhpur University, Gorakhpur 273009, India

(*Received* 10 *June* 1986 ; *accepted* 16 *September* 1986)

Abstract—Two novel series of complexes of types $[La(DAPCH)X_2]X$ and $[La(DAPTC)X_2]X$ (DAPCH = a potentially pentadentate ligand derived from 2,6-diacetylpyridine and carbohydrazide; DAPTC = a potentially tridentate ligand derived from 2,6-diacetylpyridine and thiocarbohydrazide; X = Cl, Br or NO_3) have been synthesized and characterized by elemental analyses, conductance measurements and IR spectral data. All these complexes contain terminal hydrazinic nitrogen atoms with an unshared electron pair and may take part in nucleophilic condensations. Therefore, the reactions of these complexes with 2,6-diacetylpyridine have also been studied which cause ring closure and formation of macrocyclic ligand complexes. Two types of cyclic products, viz. mononuclear $[La(mac)X_2]X$, $[La(mac')X_2]X$ and binuclear $[La_2(mac)X_4]X_2$, $[La_2(mac')X_4]X_2$ (mac- = macrocyclic ligand derived from DAPCH and 2,6-diacetylpyridine; mac′ = macrocyclic ligand derived from DAPTC and 2,6-diacetylpyridine; X = Cl, Br or NO_3) have been isolated by carrying out the reactions by different methods. The IR spectra of these cyclic products are reported.

Much research on macrocyclic complexes has been focused on species containing a first-row transition metal ion and a tetradentate ligand.[1] The majority of the ligands contain nitrogen donor atoms and are coordinated in a planar manner to the metal ion.[2–11] The formation of macrocyclic complexes depends significantly on the dimension of the internal cavity, on the rigidity of the macrocycle, on the nature of its donor atoms and on the complexing properties of the anion involved in the coordination.[1,12,13] These ligands are also of theoretical interest since they are capable of furnishing an environment of controlled geometry and ligand field strength.[5,6]

The coordination chemistry of polyaza macrocyclic ligands towards lanthanides has been studied[14–19] and papers have appeared on crown ether and cryptand complexes of lanthanide ions.[20–24]

In this paper, the synthesis and characterization of lanthanum(III) macrocyclic complexes derived from the condensation of 2,6-diacetylpyridine, carbohydrazide or thiocarbohydrazide is reported.

RESULTS AND DISCUSSION

The condensation reactions of 2,6-diacetylpyridine with carbohydrazide or thiocarbohydrazide in ethanol in the presence of sodium acetate give rise to the ligands DAPCH or DAPTC:

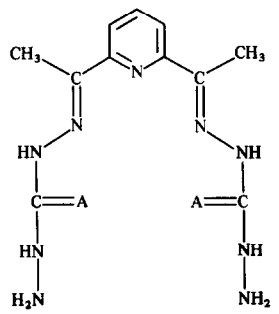

A=O (DAPCH) or S (DAPTC)

These ligands react with a lanthanum salt in a 1 : 1 molar ratio and form ring-opened complexes:

$$LaX_3 + DAPCH \rightarrow [La(DAPCH)X_2]X,$$

$$LaX_3 + DAPTC \rightarrow [La(DAPTC)X_2]X.$$

It appears that, in the above complexes, the two terminal amino groups remain uncoordinated and can take part in condensation reactions with diketones, and, therefore, the reactions of above complexes with 2,6-diacetylpyridine have been carried out which result in the formation of complexes with the following types of macrocyclic ligand:

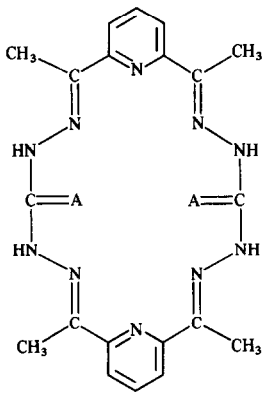

A = O (mac) or S (mac')

However, if the reactions are carried out *in situ*, i.e. the metal salt, carbohydrazide or thiocarbohydrazide and 2,6-diacetylpyridine are mixed together in ethanol and refluxed, an entirely different binuclear product is obtained. The reaction is proposed as follows:

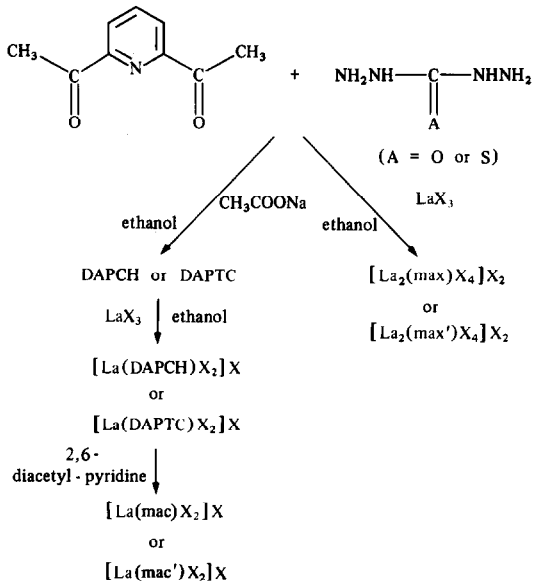

The metal to ligand stoichiometry of all these products has been established on the basis of elemental analysis (Table 1). The complexes have high melting points. The mononuclear lanthanum complexes behave as 1 : 1 electrolytes and binuclear complexes as 1 : 2 electrolytes in dimethylformamide. Since these cyclic products could not be isolated in the absence of metal ion, lanthanum(III) appear to act as a kinetic "template".

IR spectra of parent DAPCH or DAPTC complexes

These ligands show bands due to the pyridine ring, amine groups, hydrazine or azomethine groups, and amide groups (DAPCH) or thioamide groups (DAPTC).

The IR spectrum of the ligand DAPCH shows bands at 1675, 1500, 1260, 660 and 530 cm^{-1} which may be assigned[25,26] to amide-I [ν(C=O)], amide-II [ν(CN)+δ(NH)], amide-III [δ(NH)], amide-IV [ϕ(C=O)] and amide-VI [π(C=O)] vibrations, respectively. In the lanthanum complexes, all these bands except amide-I show upward shifts ($\sim$ 60–30 cm^{-1}), whereas amide-I band shows a downward shift ($\sim$ 35–20 cm^{-1}). These changes in amide group vibrations indicate that the amide oxygen (ketonic) takes part in coordination to the metal atom.[25] This has further been confirmed by the appearance of new bands at *ca* 490–70 cm^{-1} assignable[27] to ν(La—O). The IR spectrum of the ligand DAPTC shows bands at *ca* 1560, 1210, 1080 and 770 cm^{-1} which are assigned[28] to thioamide-I, -II, -III and -IV vibrations, respectively. The ligands containing an HN—C=S group can undergo thione $\rightleftharpoons$ thiol tautomerism. However, the appearance of four thioamide bands in DAPTC indicates the existence of the ligand in the thione form. The thioamide-IV band has been found to have a maximum ν(C=S) contribution.[28] In the lanthanum complexes, all these bands remain at the same position, indicating the non-coordination of the thioamide sulphur to the lanthanum atom.

Both the ligands show a weak band at *ca* 1640 cm^{-1} which can be assigned to the ν(C=N) vibration of the azomethine linkage. The appearance of a weak ν(C=N) band is in accord with the observations of several other workers.[29,30] The band due to ν(C=N) appears at slightly lower wavenumbers ($\sim$ 1625–1610 cm^{-1}) in the complexes, suggesting[29] that nitrogen atoms of the azomethines are coordinated to the lanthanum atom. The bands appearing in the 400–350 cm^{-1} region may be assigned[27] to ν(La—N) vibrations.

The pyridine ring vibrations most affected by pyridine nitrogen coordination to a metal atom are 8a (pyridine ring deformation), 6a (in-plane ring defor-

Table 1. Analytical data of the complexes[a]

Complex	Colour	Found (calc.) (%)					
		C	H	N	S	La	Cl/Br
$[La(DAPCH)Cl_2]Cl$	Light yellow	23.8 (23.8)	3.0 (3.0)	22.7 (22.8)	— —	25.1 (25.1)	19.2 (19.2)
$[La(DAPCH)Br_2]Br$	Light yellow	19.2 (19.2)	2.4 (2.4)	18.3 (18.3)	— —	20.1 (20.2)	34.9 (34.9)
$[La(DAPCH)(NO_3)_2]NO_3$	Light brown	20.8 (20.8)	2.6 (2.6)	26.4 (26.5)	— —	21.9 (21.9)	— —
$[La(mac)Cl_2]Cl$	Dark yellow	35.2 (35.3)	3.1 (3.2)	20.6 (20.6)	— —	20.4 (20.4)	15.6 (15.6)
$[La(mac)Br_2]Br$	Brown	29.4 (29.5)	2.6 (2.7)	17.1 (17.2)	— —	17.0 (17.0)	29.4 (29.4)
$[La(mac)(NO_3)_2]NO_3$	Orange	31.5 (31.6)	2.8 (2.8)	23.9 (23.9)	— —	18.2 (18.3)	— —
$[La_2(mac)Cl_4]Cl_2$	Brown	25.9 (25.9)	2.3 (2.3)	15.1 (15.1)	— —	30.0 (30.0)	23.0 (23.0)
$[La_2(mac)Br_4]Br_2$	Brown	20.1 (20.1)	1.8 (1.8)	11.7 (11.7)	— —	23.3 (23.3)	40.2 (40.2)
$[La_2(mac)(NO_3)_4](NO_3)_2$	Yellowish brown	22.1 (22.1)	1.9 (2.0)	20.6 (20.6)	— —	25.6 (25.6)	— —
$[La(DAPTC)Cl_2]Cl$	Light yellow	22.5 (22.5)	2.8 (2.9)	21.5 (21.5)	10.9 (10.9)	23.7 (23.7)	18.2 (18.2)
$[La(DAPTC)Br_2]Br$	Light brown	18.3 (18.3)	2.2 (2.3)	17.5 (17.5)	8.8 (8.9)	19.3 (19.3)	33.2 (33.4)
$[La(DAPTC)(NO_3)_2]NO_3$	Light brown	19.8 (19.8)	2.5 (2.5)	25.2 (25.3)	9.6 (9.6)	20.9 (20.9)	— —
$[La(mac')Cl_2]Cl$	Brown	33.6 (33.7)	3.0 (3.0)	19.6 (19.6)	8.9 (8.9)	19.5 (19.5)	14.9 (14.9)
$[La(mac')Br_2]Br$	Brown	28.4 (28.4)	2.5 (2.6)	16.5 (16.5)	7.5 (7.5)	16.4 (16.4)	28.3 (28.3)
$[La(mac')(NO_3)_2]NO_3$	Yellowish brown	30.3 (30.3)	2.7 (2.7)	23.0 (23.0)	8.0 (8.0)	17.4 (17.5)	— —
$[La_2(mac')Cl_4]Cl_2$	Dark yellow	25.0 (25.0)	2.1 (2.2)	14.6 (14.6)	6.6 (6.6)	29.0 (29.0)	22.2 (22.2)
$[La_2(mac')Br_4]Br_2$	Chocolate	19.6 (19.6)	1.7 (1.7)	11.3 (11.4)	5.1 (5.2)	22.7 (22.7)	39.1 (39.1)
$[La_2(mac')(NO_3)_4](NO_3)_2$	Orange	21.5 (21.5)	1.9 (1.9)	20.0 (20.0)	5.7 (5.7)	24.8 (24.8)	— —

[a] DAPCH = 2,6-diacetylpyridine-bis(carbohydrazone), DAPTC = 2,6-diacetylpyridine-bis(thiocarbohydrazone), mac = macrocyclic ligand derived from DAPCH and 2,6-diacetylpyridine, mac' = macrocyclic ligand derived from DAPTC and 2,6-diacetylpyridine.

mation) and 16b (out-of-plane deformation).[31,32] These vibrations appear at *ca* 1580, 620 and 410 cm^{-1}, respectively, in the free ligands. In all the complexes, these bands show a shift to a higher energy ($\sim$ 30–10 cm^{-1}), indicating coordination of the pyridine nitrogen to the lanthanum atom.[30] The ν(La–Py) vibrations are located at *ca* 280–250 cm^{-1}.

The ligands also show a broad band at *ca* 3250 cm^{-1} along with two shoulders at *ca* 3300–3280 and 3230–3220 cm^{-1} which may be due to ν[sym(NH)] and ν[asym(NH)] vibrations. In the complexes, these bands persist, indicating non-coordination of the terminal amino groups to the metal atom.

IR spectra of macrocyclic products

The IR spectra of the macrocyclic complexes show few significant changes compared with the products. The $\nu(NH_2)$ bands disappear. Only one band is observed in the ν(NH) region at *ca* 3200 cm^{-1} which may be due to secondary amino group,

establishing the condensation of the primary amino group with 2,6-diacetylpyridine. This is further supported by the appearance of a very weak band at *ca* 1635 cm^{-1} in the $[La(mac)X_2]X$ or $[La(mac')X_2]X$ complexes, establishing the formation of an azomethine linkage. In the binuclear macrocyclic complexes, this band disappears, which may be taken as evidence of the coordination of the azomethine nitrogen to another metal atom. Further, the medium or weak bands appearing at *ca* 1570, 620, and 420 cm^{-1} in the $[La(mac)X_2]X$ or $[La(mac')X_2]X$ complexes may be due to[31] 8a, 6a and 16b vibrations of the non-coordinated pyridine moiety. In binuclear mactrocyclic complexes, these bands shift to a higher frequency and overlap with the coordinated pyridine ring vibrations of the first metal. As a result broad bands appear at *ca* 1590, 630 and 425 cm^{-1}. This confirms the coordination of the second pyridine nitrogen to another metal. The spectral features in conjunction with the intense colour of the complexes support the formation of macrocyclic ligand complexes. The intense colour originates from a high degree of conjugation present in macrocyclic systems.

In addition to the above bands, the nitrato complexes of lanthanum show bands at *ca* 1550–1535, 1270–1260 and 1040–1025 cm^{-1} due to $\nu[asym(NO_2)]$, $\nu[sym(NO_2)]$ and $\nu(NO)$, indicating the presence of coordinated nitrate groups in the complexes. In the chloro and bromo complexes, the bands appearing at *ca* 350–330 and 310–300 cm^{-1} may be assigned to ν(La—Cl) and ν(La—Br) vibrations, respectively.

EXPERIMENTAL

The ligands 2,6-diacetylpyridine-bis(carbohydrazone) (DAPCH) and 2,6-diacetylpyridine-bis(thiocarbohydrazone) (DAPTC) were prepared as reported in the literature.[33] Lanthanum salts were procured from B.D.H. Ltd.

Preparation of complexes of DAPCH and DAPTC, $[La(DAPCH)X_2]$ *and* $[La(DAPTC)X_2]X$ (X = Cl, Br *or* NO_3)

A general procedure was adopted to synthesize these complexes. The procedure involves the addition of the appropriate ligand (0.02 mol) to an aqueous ethanolic (60%) solution of the appropriate metal salt (0.02 mol). The mixture was refluxed for *ca* 6–8 h on a water bath. Light yellow or light brown masses which appeared immediately in the case of halo complexes, or on keeping the solution overnight in the case of nitrato complexes, were filtered, washed with ethanol and dried *in vacuo* at room temperature.

Preparation of mononuclear complexes of the macrocyclic ligand, $[La(mac)X_2]X$ *and* $[La(mac')X_2]X$ (*mac = macrocyclic ligand derived by condensation of DAPCH and 2,6-diacetylpyridine; mac' = macrocyclic ligand derived by condensation of DAPTC and 2,6-diacetylpyridine;* X = Cl, Br *or* NO_3)

A common procedure was followed to synthesize these complexes. 2,6-Diacetylpyridine dissolved in aqueous ethanol (60%) (0.02 mol in 50 cm^3) was added to the appropriate DAPCH or DAPTC complexes (0.02 mol) and refluxed for *ca* 18–20 h. The colour of the mixture was intensified and the precipitate obtained was filtered, washed with ethanol and hot water, and dried *in vacuo* at room temperature.

Preparation of binuclear complexes of the macrocyclic ligand, $[La_2(mac)X_4]X_2$ and $[La_2(mac')X_4]X_2$ (X = Cl, Br *or* NO_3)

A general procedure adopted to synthesize these complexes involved the addition of an excess of the appropriate metal salt to an aqueous ethanolic solution of 2,6-diacetylpyridine (0.01 mol) and carbohydrazide or thiocarbohydrazide (0.01 mol). The solution was refluxed for *ca* 20–24 h, when dark yellow, brown or orange coloured precipitates appeared which were filtered, washed thoroughly with ethanol and dried *in vacuo* at room temperature.

Microanalyses for carbon and hydrogen were performed by the C.D.R.I., Lucknow, and by the Department of Chemistry, B.H.U., Varanasi. Nitrogen was estimated by Kjeldahl's method, sulphur as $BaSO_4$, and chloride and bromide as their silver salts. Lanthanum was estimated gravimetrically as its oxide.

The details of physical measurements are the same as described earlier.[34]

Acknowledgements—I am grateful to Prof. S.C. Tripathi and Dr S. K. Sengupta, Chemistry Department, Gorakhpur University, Gorakhpur, India, for helpful discussions.

REFERENCES

1. G. A. Melson, *Coordination Chemistry of Macrocyclic Compounds*. Plenum, New York (1979).
2. N. F. Curtis, *Coord. Chem. Rev.* 1968, **3**, 3.

3. N. F. Curtis, *J. Chem. Soc., Dalton Trans.* 1974, 347.
4. V. B. Rana, P. Singh, D. P. Singh and M. P. Teotia, *Transition Met. Chem.* 1982, **7**, 174.
5. S. Chandra and K. K. Sharma, *Transition Met. Chem.* 1983, **8**, 1.
6. W. U. Malik, R. Bembi and R. Singh, *Transition Met. Chem.* 1983, **8**, 62.
7. Y. Bhoon and R. P. Singh, *J. Coord. Chem.* 1981, **11**, 99.
8. R. W. Hay, D. P. Piplani and B. Jeragh, *J. Chem. Soc., Dalton Trans.* 1977, 1951.
9. L. F. Lindoy and D. H. Busch, *Prep. Inorg. React.* 1971, **6**, 1.
10. D. E. Douglas, *Inorg. Synth.* 1978, **18**, 1.
11. M. G. B. Drew, J. D. Cabral, M. P. Cabral, E. S. Esho and S. M. Nelson, *J. Chem. Soc., Chem. Commun.* 1979, 1033.
12. J. J. Christensen, D. J. Eatough and R. M. Izatt, *Chem. Rev.* 1974, **74**, 351.
13. G. Newkome, J. D. Sauer, J. M. Roper and D. C. Hager, *Chem. Rev.* 1977, **77**, 513.
14. C. J. Pedersen, *J. Am. Chem. Soc.* 1967, **89**, 7017.
15. S. Gurrieri, A. Seminara, G. Siracusa and A. Cassol, *Thermochim. Acta* 1975, **11**, 433.
16. W. Radecka-Paryzek, *Inorg. Chim. Acta* 1979, **34**, 5.
17. W. Radecka-Paryzek, *Inorg. Chim. Acta* 1979, **35**, L349.
18. W. Radecka-Paryzek, *Inorg. Chim. Acta* 1980, **45**, L147.
19. W. Radecka-Paryzek, *Inorg. Chim. Acta* 1981, **52**, 261.
20. R. B. King and P. R. Hockley, *J. Am. Chem. Soc.* 1974, **96**, 3118.
21. J. Massaux, J. F. Desreux, C. Delchambre and G. Duyckaerts, *Inorg. Chem.* 1980, **19**, 1893.
22. M. Ciampolini, C. Mealli and N. Nardi, *J. Chem. Soc., Dalton Trans.* 1980 376.
23. G. L. Eichhorn, *Inorganic Biochemistry*. Elsevier, London (1973).
24. J. Reuben, In *Handbook on the Physics and Chemistry of Rare Earths*, Vol. 4, p. 515 (1979).
25. S. K. Sahni, S. P. Gupta, S. K. Sangal and V. B. Rana, *J. Inorg. Nucl. Chem.* 1977, **39**, 1098.
26. U. Casellato, M. Videli and P. A. Vigato, *Inorg. Nucl. Chem. Lett.* 1974, **10**, 437.
27. J. R. Ferraro, *Low Frequency Vibrations of Inorganic and Coordination Compounds*. Plenum, New York (1971).
28. S. K. Sengupta, S. K. Sahni and R. N. Kapoor, *Synth. React. Inorg. Met.–Org. Chem.* 1980, **10**, 269, *Indian J. Chem.* 1980, **19A**, 703.
29. S. Kher, S. K. Sahni, V. Kumari and R. N. Kapoor, *Inorg. Chim. Acta* 1979, **37**, 121.
30. S. K. Sahni, *Transition Met. Chem.* 1979, **4**, 73.
31. D. P. Maddan, M. M. da Mota and S. M. Nelson, *J. Chem. Soc. A* 1970, 890.
32. D. P. Maddan and S. M. Nelson, *J. Chem. Soc. A* 1968, 2342.
33. S. K. Sengupta and S. Kumar, *Synth. React. Inorg. Met.–Org. Chem.* 1983, **13**, 929.
34. O. P. Pandey, S. K. Sengupta and S. C. Tripathi, *Polyhedron* 1984, **3**, 695.

Polyhedron Vol. 6, No. 5, pp. 1027–1032, 1987
Printed in Great Britain

0277–5387/87 $3.00+.00

THE INTERACTION OF PENTACARBONYL IRON(0) WITH SELECTED 1,2-QUINONE MONO-OXIMES (2-NITROSOPHENOLS) IN THE PRESENCE OR ABSENCE OF ANILINE

JOHN CHARALAMBOUS,* L. IAN B. HAINES, JACKIE S. MORGAN and DAVID S. PEAT

School of Chemistry, The Polytechnic of North London, London N7 8DB, U.K.

MICHAEL J. M. CAMPBELL

School of Chemistry, Thames Polytechnic, London SE18 6PF, U.K.

and

JOE BAILEY

Kodak Ltd, Harlow, Middlesex HA1 4TY, U.K.

(*Received* 20 *June* 1986; *accepted* 16 *September* 1986)

Abstract—Reaction of pentacarbonyl iron(0) with 1,2-quinone mono-oximes (qoH) gives the $Fe(qo)_2$ complexes as the main products together with various organic products. In the presence of aniline the main products are again the complexes $Fe(qo)_2$ which are accompanied by the formation of organic products and complexes of type $Fe(qo\text{-}A)_2$ where qo-A is a species arising from the coupling of the qo ligand with aniline. The formation of the latter type of complex and of the organic products is rationalized in terms of deoxygenation of the qo ligand. The complexes $Fe(qo)_2$ and $Fe(qo\text{-}A)_2$ have oligomeric structures as indicated by their magnetic properties and Mössbauer spectra. Both these types of complex react with pyridine to give dipyridine adducts.

Reactions of pentacarbonyl iron(0) with oximino, nitro and nitroso compounds have been described in several publications.[1–12] Nitro and nitroso compounds undergo deoxygenation to give products whose nature is generally accounted for in terms of nitrene intermediates.[5–9] For oximino compounds both deoxygenation and deoximation behaviour has been reported.[6,12] A number of reactions have been reported in which pentacarbonyl iron(0) reacts with a chelating ligand to give rise to an iron(II) complex,[13–20] e.g. the reaction of acetylacetone gives rise to bis(acetylacetonato)iron(II).[13] Hence, reaction of pentacarbonyl iron(0) with 1,2-quinone mono-oximes could also give rise to chelates in addition to products arising from reactions such as those indicated above involving the oxime group.

In this paper we report on the reactions of pentacarbonyl iron(0) with 1,2-naphthoquinone-2-oxime (**1a**), 1,2-naphthoquinone-1-oxime (**1b**) and 5-methoxy-1,2-quinone-2-oxime (**1c**). We also report on the interaction of **1a** and **1b** with pentacarbonyl iron(0) in the presence of aniline and on the interaction of pentacarbonyl iron(0) with the iron(III) complexes, $Fe(qo)_3$(qoH = **1a–1c**).

Interaction of pentacarbonyl iron(0) with the quinoneoximes (**1a–1c**) in refluxing tetrahydrofuran gave, in each case, the corresponding iron(II) 1,2-quinone mono-oximato complex, $Fe(qo)_2$ (**2**), as the main product and a mixture of small amounts of organic products (Scheme 1). The organic products isolated from the reaction of **1a** included 2-amino-N^4(1-hydroxy-2-naphthyl)-1,4-naphthoquinone 4-imine and 5-hydroxy-dibenzo[b,i]phenazin-12(6*H*)-one. For the reaction involving **1c** the predominant

* Author to whom correspondence should be addressed.

organic product was 2-amino-7-methoxy-3*H*-phenoxazin-3-one. The complexity of the mixture of organic products arising from 1*b* hindered characterization.

In the presence of aniline **1a** and **1b** again reacted with pentacarbonyl iron(0) to give the $Fe(qo)_2$ complex as the main product. In addition, iron(II) complexes of type $Fe(qo\text{-}A)_2$ (**3** and **4**), where qo-A is a species arising from the coupling of the qo ligand with aniline and various organic products, were formed. The predominant organic product isolated from both of these systems was 2-phenylamino-N^4-phenyl-1,4-naphthoquinone-4-imine. Other products isolated from the reaction involving **1a** were 2-amino-N^4-phenyl-1,4-naphthoquinone 4-imine, N^4-phenylamino-1,2-naphthoquinone and

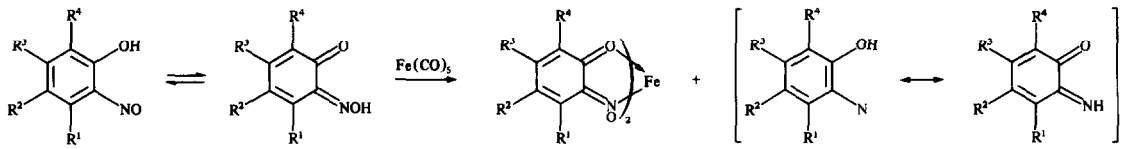

1 **2** **8**

a $R^1 = R^2 = H$, $R^3, R^4 = -HC{=}CH-CH{=}CH-$
b $R^3 = R^4 = H$, $R^1, R^2 = -HC{=}CH-CH{=}CH-$
c $R^1 = R^2 = R^4 = H$, $R^3 = OMe$

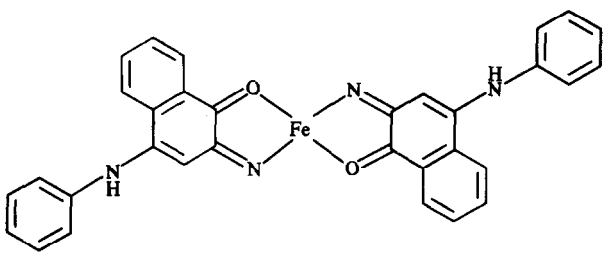

3

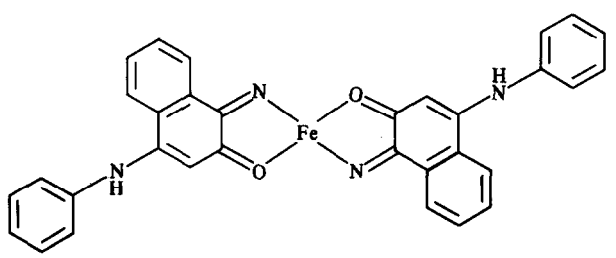

4

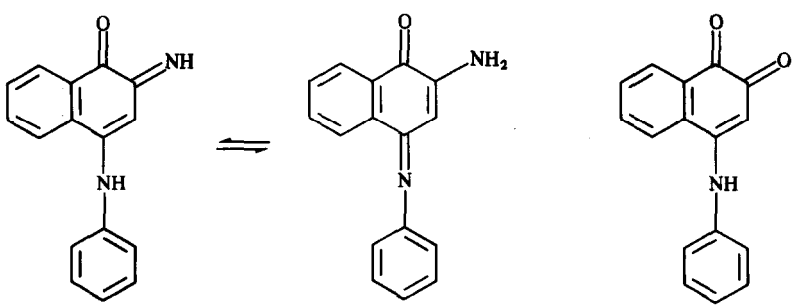

5a **5b** **6**

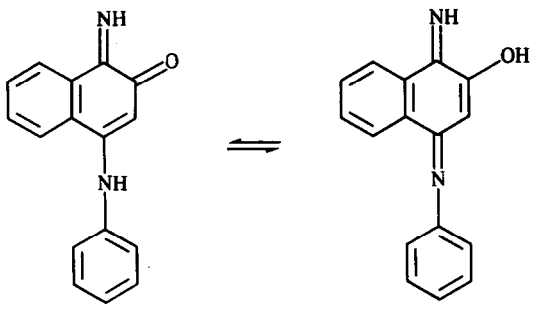

7a **7b**

5-hydroxy-dibenzo-[b,i]phenazin-12(6*H*)-one. For the system involving **1b**, N^4-phenylamino-1,2-naphthoquinone was also isolated. The nature of the ligands in the Fe(qo-A)$_2$ complexes **3** and **4** was established by isolating and characterizing the organic products formed from the reaction of the complexes with aqueous hydrochloric acid. In the case of the complex **3** the acidolysis led to the protonated ligand **5a**, which exists mainly as the amino tautomer **5b**. In contrast, acidolysis of complex **4** led to the quinone **6**. Similar behaviour was observed earlier for the analogous copper(II) complex which was obtained from the reaction of aniline with Cu(qo)$_2$ (qoH = **1b**).[21]

The iron(III) complexes Fe(qo)$_3$ (qoH = **1a–1c**) reacted readily with pentacarbonyl iron(0) in refluxing tetrahydrofuran to give the respective Fe(qo)$_2$ complexes in quantitative yield. No organic products were formed in these reactions.

The Fe(qo)$_2$ complexes obtained from the above reactions are oligomeric, as indicated by their magnetic properties and Mössbauer spectra, and as suggested previously for such complexes obtained by other routes.[22] By analogy, oligomeric structures (Fig. 1) are also suggested for the Fe(qo-A)$_2$ complexes. These compounds exhibit two doublets in their Mössbauer spectra and the values of their room-temperature magnetic moments (*ca* 3 BM) (Table 1) are in accord with the presence of both high-spin five-coordinate and low-spin six-coordinate iron atoms. The pyridine adducts of the Fe(qo-A)$_2$ complexes are six-coordinate diamagnetic species which lose pyridine at 160°C/0.3 mmHg to give the respective bischelates.

The formation of the complexes Fe(qo)$_2$ as the major products from the reactions between pentacarbonyl iron(0) and the quinoneoximes probably reflects their high insolubility in tetrahydrofuran and organic solvents in general. The organic products obtained from these reactions parallel closely those arising from reactions of the copper(II) complexes of these quinone oximes with aniline[21] or triphenylphosphine.[23] They can be accounted for in terms of deoxygenation of the protonated ligands to give the quinoneimine/nitrene **8** followed by hydrogen abstraction and/or coupling reactions. Their formation through deoxygenation of the chelated anionic ligands is unlikely, as suggested by the absence of any organic products in the reactions between the complexes Fe(qo)$_3$ and pentacarbonyl iron(0), and by the inertness of the Fe(qo)$_2$ complexes towards pentacarbonyl iron(0). When aniline is involved, products arising from coupling reactions of the quinoneimine/nitrene with aniline are also obtained. The formation of 2-phenylamino-N^4-phenyl-1,4-naphthoquinone-4-imine from both the reaction involving **1a** and that involving **1b** probably arises as a result of interaction of aniline with N^4-phenylamino-1,2-naphthoquinone.

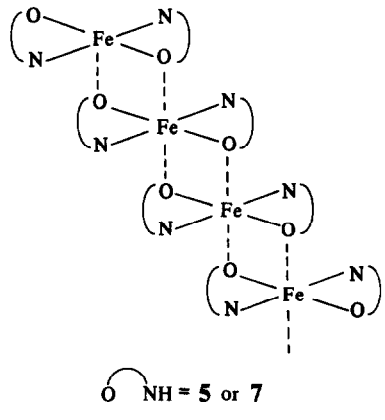

Fig. 1.

Table 1. Mössbauer parameters and room-temperature magnetic moments of iron(II) complexes derived from the mono-oximes of 1,2-naphthoquinone[a]

Complex	Δ (mm s^{-1})	δ(Fe) (mm s^{-1})	μ_{eff} (BM)
Fe(1-nqo)$_2$·2py	0.92	0.19	0.50
Fe(2-nqo)$_2$·2py	0.88	0.20	0.60
Fe(1-nqo)$_2$	0.79	0.08	3.08
	4.00	1.22	
Fe(2-nqo)$_2$	0.71	0.05	3.04
	3.99	1.22	
Fe(1-qo-A)$_2$ (**4**)	0.88	0.12	3.12
	3.27	0.47	
Fe(2-qo-A)$_2$ (**3**)	0.77	0.08	3.13
	3.40	0.92	

[a] All spectra were recorded at room temperature. No significant differences were observed when recording spectra at liquid-nitrogen temperature (77 K).

EXPERIMENTAL

Magnetic-susceptibility data, and also IR, NMR, electronic and Mössbauer spectra, were obtained as described earlier.[21,22]

Reaction between pentacarbonyl iron(0) *and* 1,2-*naphthoquinone*-1-*oxime*

Pentacarbonyl iron(0) (2.0 g, 10.2 mmol) and the mono-oxime (5.2 g, 30.0 mmol) were heated under reflux in dry tetrahydrofuran (50 cm^3) under nitrogen for 24 h. The mixture was filtered and the residue washed with tetrahydrofuran (2 × 10 cm^3) and dried at 100°C/0.1 mmHg to give green bis(1,2-naphthoquinone-1-oximato)iron(II) (2.56 g, 64%) (Found: C, 59.6; H, 3.2; Fe, 13.8; N, 6.9. Calc. for $C_{20}H_{12}FeN_2O_4$: C, 60.0; H, 3.0; Fe, 14.0; N, 7.0%).

Reaction between pentacarbonyl iron(0) *and* 1,2-*naphthoquinone*-2-*oxime*

Similarly, pentacarbonyl iron(0) (2.0 g, 10.2 mmol) and 1,2-naphthoquinone-2-oxime (5.2 g, 30.0 mmol) gave green bis(1,2-naphthoquinone-2-oximato)iron(II) (3.28 g, 82%) (Found: C, 59.8; H, 3.1; Fe, 13.9; N, 6.9. Calc. for $C_{20}H_{12}FeN_2O_4$: C, 60.0; H, 3.0; Fe, 14.0; N, 7.0%). The combined filtrate and washings were evaporated under reduced pressure to give a brown oil which was chromatographed on silica gel. Toluene eluted unreacted 1,2-naphthoquinone-2-oxime (0.42 g, 8% recovery) followed by 5-hydroxy-dibenzo[b,i]-phenazin-12(6*H*)-one (0.19 g, 4%), m.p. 280–283°C (decomp), *m/z* 312 (M^+) (identical TLC and IR to an authentic sample[21]). Toluene–ethyl acetate (1 : 1) eluted 2-amino-N^4-)1-hydroxy-2-naphthyl)-1,4-naphthoquinone 4-imine (0.28 g, 68%) m.p. 274–276°C, *m/z* 314 (M^+) (identical TLC and IR to an authentic sample[23]).

Reaction between pentacarbonyl iron(0) *and* 5-*methoxy*-1,2-*quinone*-2-*oxime*

Similarly, pentacarbonyl iron(0) (2.0 g, 10.2 mmol) and the mono-oxime 5-methoxy-1,2-quinone-2-oxime (4.6 g, 30.0 mmol) gave green bis(5-methoxy-1,2-quinone-2-oximato)iron(II) (1.8 g, 50%) (Found: C, 46.4; H, 3.6; Fe, 15.2; N, 7.3. Calc. for $C_{14}H_{12}FeN_2O_6$: C, 46.6; H, 3.8; Fe, 15.5; N, 7.6%). The combined filtrate and washings were evaporated under reduced pressure to give a brown oil which was chromarographed on silica gel. Toluene eluted 2-amino-7-methoxy-3*H*-phenoxazin-3-one (0.91 g, 25%) (identical TLC and IR to an authentic sample[23]).

Reaction between pentacarbonyl iron(0) *and* 1,2-*naphthoquinone*-1-*oxime in the presence of aniline*

Pentacarbonyl iron(0) (2.0 g, 10.2 mmol) and the mono-oxime (5.0 g, 29.0 mmol) were heated under reflux with aniline (4.4 g, 47.0 mmol) in dry tetrahydrofuran (100 cm^3) under nitrogen for 24 h. The mixture was stirred at ambient temperature for a further 16 h and filtered to give a green solid (2.7 g) which was stirred in pyridine for 72 h and chromatographed on silica gel. Light petrol (b.p. 30–40°C)–toluene (1 : 1) eluted 2-phenylamino-N^4-phenyl-1,4-naphthoquinone-4-imine (0.66 g, 7%); (Found: C, 81.5; H, 5.0; N, 8.6. $C_{22}H_{16}N_2O$ requires: C, 81.5; H, 4.9; N, 8.6%); ν_{max}(KBr) 1660 (C═O), and 3360 (N—H) cm^{-1}; δ[$(CD_3)_2So$] 181.8 (1C, CO), 6.6 (1H, s), and 6.7–8.7 (15H, br, m); *m/z* 324 (M^+). Toluene–ethyl acetate (3 : 1) eluted bis(1,2-naphthoquinone-1-oximato)dipyridineiron(II) (1.86 g, 33%) (Found: C, 63.8; H, 3.9; Fe, 9.9; N, 10.0. Calc. for $C_{30}H_{22}FeN_4O_4$: C, 64.5; H, 3.9; Fe, 10.0; N, 10.0%). Ethyl acetate eluted bis(4-phenylamino-1-imino-1,2-naphthoquinone)dipyridineiron(II) (1.08 g, 15%) (Found: C, 71.5; H, 4.0; Fe, 7.5; N, 11.7. $C_{42}H_{32}FeN_6O_2$ requires: C, 71.2; H, 4.5; Fe, 7.9; N, 11.9%.) Evaporation of the filtrate under reduced pressure gave a brown tar (8.0 g) which was chromatographed on silica gel. Light petrol (b.p. 30–40°C)–toluene (1 : 1) eluted 2-phenylamino-N^4-phenyl-1,4-naphthoquinone–4–imine (1.66 g, 18%) (identified by TLC). Toluene eluted N^4-phenylamino-1,2-naphthoquinone (0.53 g, 7.3%), m.p. 257–259°C (lit. 254–256°C[24]) (Found: C, 77.9; H, 3.9; N, 6.0. Calc for $C_{16}H_{11}NO_2$: C, 77.1; H, 4.4; N, 5.6%); *m/z* 249 (M^+).

Pyrolysis of bis(4-*phenylamino*-1-*imino*-1,2-*naphthoquinone*)*dipyridine iron*(II)

This bis(pyridine) iron(II) complex (1.0 g) was heated at 160°C and 0.3 mmHg for 1 h. The residue was green *bis*(4-*phenylamino*-1-*imino*-1,2-*naphthoquinone*)*iron*(II) (0.79 g) (Found: C, 69.4; H, 3.9; Fe, 10.1; N, 10.5. $C_{32}H_{22}FeN_4O_2$ requires: C, 69.8; H, 3.9; Fe, 10.2; N, 10.2%). The distillate, collected in a trap cooled in a solid carbon dioxide–ethanol bath, was shown to be pyridine (IR).

Reaction between bis(4-*phenylamino*-1-*imino*-1,2-*naphthoquinone*)*iron*(II) *and hydrochloric acid*

The bis(pyridine) iron(II) complex (0.2 g) was shaken with aqueous hydrochloric acid (15%, 50 cm^3) for 10 min. After neutralisation ($NaHCO_3$) chloroform was added and the mixture shaken for 5 min. The chloroform layer was separated from the

aqueous layer, which was then further extracted with chloroform. The combined chloroform extracts were dried ($MgSO_4$), filtered and evaporated under reduced pressure to give N^4-phenylamino-1,2-naphthoquinone (0.16 g, 90%) (identified by TLC).

Reaction between pentacarbonyl iron(0) and 1,2-naphthoquinone-2-oxime in the presence of aniline

Pentacarbonyl iron(0) (2.0 g, 10.2 mmol) and the mono-oxime (5.3 g, 31.0 mmol) were heated under reflux with aniline (4.6 g, 49.0 mmol) in dry tetrahydrofuran (100 cm^3) under nitrogen for 24 h. The mixture was stirred at ambient temperature for a further 16 h and filtered to give a green solid (2.3 g), which was stirred in pyridine for 72 h and chromatographed on silica gel. Light petrol (b.p. 30–40°C)–toluene (1 : 1) eluted 2-phenylamino-N^4-phenyl-1,4-naphthoquinone-4-imine (0.17 g, 2%) (identified by TLC). Toluene–ethyl acetate (3 : 1) eluted bis(1,2-naphthoquinone-2-oximato)dipyridine iron(II) (2.96 g, 52%) (Found: C, 65.1; H, 4.5; Fe, 10.6; N, 9.6. Calc. for $C_{30}H_{22}FeN_4O_4$: C, 64.5; H, 3.9; Fe, 10.0; N, 10.0%). Ethyl acetate eluted *bis(4-phenylamino-2-imino-1,2-naphthoquinone)dipyridineiron*(II) (0.48 g, 7%) (Found: C, 70.5; H, 4.1; Fe, 8.2; N, 12.2. $C_{42}H_{32}FeN_6O_2$ requires: C, 71.2; H, 4.5; Fe, 7.9; N, 11.9%). Evaporation of the filtrate under reduced pressure gave a brown tar (9.8 g) which was chromatographed on silica gel. Light petrol (b.p. 30–40°C)–toluene (1 : 1) eluted 2-phenylamino-N^4-phenyl-1,4-naphthoquinone-4-imine (2.7 g, 27%); identified by TLC, Ir and NMR) Toluene eluted 2-amino-N^4-phenyl-1,4-naphthoquinone-4-imine (1.1 g, 14.0%) (Found: C, 77.3; H, 4.1; N, 11.5. Calc. for $C_{16}H_{12}N_2O$: C, 77.4; H, 4.8; N, 11.3%); ν_{max}(KBr) 3495, 3380, 1660, 1620 and 1600 cm^{-1}; λ_{max}($CHCl_3$) 247 nm (log ε 4.25), 299 nm (log ε 4.06), 345 nm (log ε 3.72), and 445 nm (log ε 3.70); *m/z* 248 (M^+); followed by N^4-phenylamino-1,2-naphthoquinone (0.23 g, 3%); m.p. 256–259°C (lit. 254–256°C[24]) (identical by comparison with the sample isolated above; TLC and IR). Toluene–ethyl acetate (3 : 1) eluted 5-hydroxy-dibenzo[b,i]-phenazin-12(6*H*)-one (0.18 g, 4%) (identical TLC and IR to an authentic sample[21]).

Pyrolysis of bis(4-phenylamino-2-imino-1,2-naphthoquinone)dipyridine iron(II)

The bis(pyridine) iron(II) complex (1.0 g) was heated at 160°C/0.3 mmHg for 1 h. The residue was green *bis(4-phenylamino-2-imino-1,2-naphthoquinone)iron*(II) (0.8 g) (Found: C, 69.3; H, 3.8; Fe, 10.3; N, 9.8. $C_{32}H_{22}FeN_4O_2$ requires: C, 69.8; H, 4.0; Fe, 10.2; N, 10.2%). The distillate, collected in a trap cooled in a solid carbon dioxide–ethanol bath, was shown to be pyridine (IR).

Reaction between bis(4-phenylamino-2-imino-1,2-naphthoquinone)iron(II) *and hydrochloric acid*

The bis iron(II) complex (0.2 g) was shaken with aqueous hydrochloric acid (15%, 50 cm^3) for 10 min. After neutralization ($NaHCO_3$) chloroform was added and the mixture shaken for 5 min. The chloroform layer was separated from the aqueous layer, which was then further extracted with chloroform. The combined chloroform extracts were dried ($MgSO_4$), filterd and evaporated under reduced pressure to give 2-amino-N^4-phenyl-1,4-naphthoquinone-4-imine (0.12 g, 67%) (identified by TLC).

Reaction of pentacarbonyl iron(0) with tris(1,2-quinone mono-oximato)iron(III)

Pentacarbonyl iron(0) (*ca* 1.0 g, 1 mol. equiv.) and tris(1,2-quinone mono-oximato(iron)(III) [fe(qo)$_3$; qoH = **1a**, **b** or **c**] (1 mol. equiv.) were heated under reflux in dry tetrahydrofuran (50 cm^3) under nitrogen for 24 h. Bis(1,2-quinone mono-oximato)iron(II) was filtered off, washed with tetrahydrofuran (2 × 10 cm^3) and dried at 100°C/0.1 mmHg.

Product	% yield	Found (%) C	H	Fe	N
2a	98	59.5	3.2	13.9	6.9
2b	97	59.8	3.2	14.1	6.8
2c	98	46.3	3.2	15.2	7.3

Acknowledgements—We thank the S.E.R.C., Kodak Ltd and Filtrona Ltd for C.A.S.E. Awards to D.S.P. and J.S.M., and Dr H. D. Mathewson for many useful discussions.

REFERENCES

1. S. A. C. Gervasio, L. M. R. Rossetti and P. L. Stanghellini, *J. Chem. Soc., Chem. Commun.* 1976, 370.
2. H. Alper and C. H. Keung, *Tetrahedron Lett.* 1970, 53.
3. H. Alper, *Inorg. Chem.* 1972, **11**, 976.
4. J. Eeekhof, H. Hogeveen and R. M. Kellogg, *J. Chem. Soc., Chem. Commun.* 1966, 657.
5. M. Dekker and G. R. Knox, *J. Chem. Soc., Chem. Commun.* 1967, 1243.

6. H. Alper and J. T. Edward, *Can. J. Chem.* 1970, **48**, 1543.
7. J. E. Kmiecik, *J. Org. Chem.* 1965, **30**, 2014.
8. M. J. Barrow and O. S. Mills, *Angew. Chem., Int. Ed. Engl.* 1969, **8**, 879.
9. S. Horie and S. Murahashi, *Bull. Chem. Soc. Jpn* 1960, **33**, 88.
10. S. Horie and S. Murahashi, *J. Am. Chem. Soc.* 1956, **78**, 4816.
11. P. A. S. Smith and B. B. Brown, *J. Am. Chem. Soc.* 1951, **73**, 2435.
12. A. Dondoni and G. Barbara, *J. Chem. Soc., Chem. Commun.* 1975, 761.
13. T. G. Dunne and F. A. Cotton, *Inorg. Chem.* 1963, **2**, 263.
14. W. R. McClelland and R. E. Benson, *J. Am. Chem. Soc.* 1966, **88**, 5165.
15. F. Calderazzo, C. Floriani, R. Henzi and F. L'Eplatteniers, *J. Chem. Soc. A* 1969, 1378.
16. M. Tsutsui, R. A. Velapodi, K. Suzuki, F. Vohwinkel, M. Ichikawa and T. Koyano, *J. Am. Chem. Soc.* 1969, **91**, 6292.
17. K. D. Karlin and S. J. Lippard, *J. Am. Chem. Soc.* 1976, **98**, 6951.
18. A. L. Balch, I. G. Dance and R. L. Holm, *J. Am. Chem. Soc.* 1968, **90**, 1139.
19. J. Miller and A. L. Balch, *Inorg. Chem.* 1971, **101**, 1410.
20. C. J. Jones, J. A. McCleverty and D. G. Orchard, *J. Chem. Soc., Dalton Trans.* 1972, 1109.
21. R. G. Buckley, J. Charalambous and E. G. Brain, *J. Chem. Soc., Perkin* I 1982, 1075.
22. D. K. Allen, J. Charalambous, M. H. Johri, R. Sims, J. Bailey, H. D. Mathewson and D. Cunningham, *Inorg. Chim. Acta* 1978, **29**, L235.
23. R. G. Buckley, J. Charalambous, M. J. Kensett, M. McPartlin, D. Mukergee, E. G. Brain and J. M. Jenkins, *J. Chem. Soc., Perkin* I 1983, 693.
24. I. D. Biggs and J. M. Tedder, *Tetrahedron* 1978, **34**, 1377.

Polyhedron Vol. 6, No. 5, pp. 1033–1035, 1987
Printed in Great Britain

0277–5387/87 $3.00+.00

COMPLEXES OF COPPER(II) WITH MONONITROSO- AND DINITROSORESORCINOLS

JOHN CHARALAMBOUS,* COLIN W. NEWNHAM, F. BRIAN TAYLOR, MARTIN J. WHELEHAN, KEITH W. P. WHITE and IVAN G. H. WILSON

Polytechnic of North London, Holloway, London N7 8DB, U.K.

(*Received* 20 *June* 1986 ; *accepted* 16 *September* 1986)

Abstract—Polymeric complexes of the type Cu(X-dnr)·H_2O (X-dnrH_2 = 2,4 - dinitrosoresorcinol and 4 - ethyl -, 4 - chloro- or 5 - methyldinitrosoresorcinol) have been prepared by nitrosation of resorcinol, 4-ethylresorcinol, 4-chlororesorcinol and 5-methylresorcinol with sodium nitrite–acetic acid in the presence of copper(II) chloride. Nitrosation of 2 - methylresorcinol gives Cu(2 - Memnr)$_2$·$4H_2O$ (2 - MemnrH = 2 - methyl - 4 - nitrosorcinol). Reaction of the complexes Cu(X-dnr)·H_2O (X = H, 6-Et or 6-Cl) with hot pyridine gives the respective Cu(X-dnr)·py complexes. Magnetic-susceptibility studies indicate antiferromagnetic interaction through the X-dnr^{2-} ligand in the complexes Cu(X-dnr)·L (L = H_2O or py) and association of Cu(2-Memnr)$_2$ units in the complex Cu(2-Memnr)$_2$·$4H_2O$.

Metal complexes of 1,2 - quinonemono - oximes (2 - nitrosophenols) have synthetic, analytical and other uses.[1–3] We have previously reported that polymeric complexes of the type Ni(X-dnr)·$2H_2O$ where X-dnrH_2 (**1**) is 2,4 - dinitrosoresorcinol, 6 - ethyl - 2,4 - dinitrosoresorcinol or 5 - methyl - 2,4 - dinitrosoresorcinol are obtained by nitrosation of resorcinol, 4 - ethylresorcinol and 5 - methylresorcinol, respectively, in the presence of nickel chloride.[4] In contrast nitrosation of 2 - methylresorcinol in the presence of nickel chloride gives a bischelated complex derived from the mononitrosated resorcinol **2**.[4] In this paper we describe the preparation, characterization and magnetic properties of analogous copper(II) complexes.

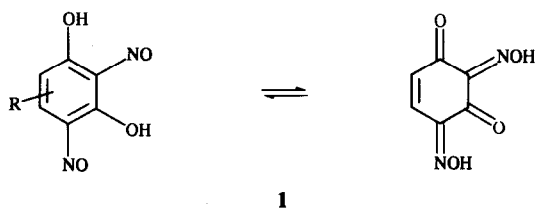

1

2

EXPERIMENTAL

Elemental analyses were carried out by the microanalytical laboratory of the Polytechnic of North London. Copper was determined by atomic absorption with a Pye–Unicam SP9 spectrophotometer, after decomposing the complexes with concentrated sulphuric acid and hydrogen peroxide. IR spectra, magnetic susceptibilities and thermal gravimetric data were obtained as described earlier.[5] Magnetic moments were corrected for the diamagnetic effect of the ligands.[6]

Preparation of the complexes Cu(X-dnr)·H_2O (X = H, 6-Et, 6-Cl *or* 5-Me) *and* Cu(2-Memnr)$_2$·$4H_2O$ *by nitrosation of resorcinols*

The resorcinol (0.05 mol) in ethanol (100 cm^3) was added to a solution of copper(II) chloride dihydrate (8.5 g, 0.05 mol), acetic acid (20 cm^3) and sodium acetate (20 g) in water (120 cm^3). Sodium

* Author to whom correspondence should be addressed.

Table 1. Analytical and room-temperature magnetic data for Cu(II) complexes of nitrosoresorcinols

Phenol	Product formula	No.	Yield (%)	Found (%) C	H	N	Cu	Required (%) C	H	N	Cu	μ_{eff} (BM) (*ca* 295 K)
Resorcinol	Cu(dnr)·H_2O	**1**	87	29.1	1.8	10.2	25.9	29.1	1.6	11.3	25.7	1.00
4-Ethylresorcinol	Cu(6-Etdnr)·H_2O	**2**	61	34.1	2.8	9.8	22.8	34.8	2.3	10.1	23.0	1.40
4-Chlororesorcinol	Cu(6-Cldnr)·H_2O	**3**	79	25.2	1.5	8.8	22.8	25.5	1.1	9.9	22.5	1.25
5-Methylresorcinol	Cu(5-Mednr)·H_2O	**4**	62	31.4	2.1	10.7	23.9	32.1	2.3	10.7	24.3	1.33
2-Methylresorcinol	Cu(2-Memnr)$_2$·$4H_2O$	**5**	50	37.5	4.0	6.4	14.6	38.2	4.6	6.3	14.7	1.48
	Cu(dnr)·py	**6**	62	42.9	2.7	13.2	21.2	42.8	2.3	13.6	20.6	1.34
	Cu(6-Etdnr)·py	**7**	65	45.1	3.0	10.6	18.7	46.3	3.3	12.5	18.9	1.55
	Cu(6-Cldnr)·py	**8**	56	38.4	1.9	12.4	18.8	38.5	1.8	12.3	18.5	1.37

nitrite (10 g) in water (60 cm^3) was added with stirring. The resulting mixture was stirred at 20°C for 1 week and then the *product* was filtered off, washed thoroughly by stirring with water (3 × 100 cm^3) and ethanol (3 × 100 cm^3) for several hours and dried at 50°C/0.1 mm (see Table 1 for analysis and other data).

Interaction of the complexes Cu(X - dnr) · H_2O (X = H, 6-Et *or* 6-Cl) *with pyridine*

The hydrated complex (*ca* 3 g) was heated under reflux in pyridine (100 cm^3) for 1 h. The reaction mixture was filtered hot, the filtrate was evaporated to dryness at 60°C/0.1 mm and the resultant residue of the *pyridine adduct* was washed with ethanol and ether, and dried at 50°C/0.1 mm.

RESULTS AND DISCUSSION

Bottei and McEachern[7] have reported that the interaction of copper sulphate pentahydrate with 2,4 - dinitrosoresorcinol in aqueous ethanol gave a polymeric product which they formulated as Cu(dnr). In contrast, Hunter and Webb[8] formulated the product of a similar reaction in methanol as [Cu(dnrH)$_2$(H_2O)$_2$] · $2H_2O$. We have obtained a polymeric complex of formula Cu(dnr) · H_2O by nitrosation of resorcinol in the presence of copper chloride. The analogous complexes Cu(5 - Mednr) · H_2O, Cu(6 - Etdnr) · H_2O and Cu(6 - Cldnr) · H_2O have been obtained similarly by nitrosation of 5 - methylresorcinol, 4 - ethylresorcinol and 4 - chlororesorcinol, respectively. Nitrosation of 2-methylresorcinol in the presence of copper(II) chloride, leads to mononitrosation and formation of the complex Cu(2 - Memnr)$_2$ · $4H_2O$. The formulation of the complexes was established by elemental analysis and IR spectroscopy. The position of nitrosation has been established as described previously.[4]

The complexes Cu(X - dnr) · H_2O (X = H, 6-Et, 6-Cl or 5-Me) were insoluble in ethanol, acetone, chloroform and diethyl ether, but dissolved in refluxing pyridine to give 1 : 1 adducts as shown by the isolation and characterization of the pyridine

Table 2. Thermal gravimetric analysis

Compound[a]	Weight of sample (mg)	T[b,c] (°C)	Weight loss (mg) Found	Calc.[d]	Decomposition temperature (°C) of M(X-dnr)[c]
1	107	100	8	8	170
2	103	142	8	7	175
3	103	115	7	7	185
4	114	132	9	8	162

[a] Nos from Table 1.
[b] Temperature of loss of water.
[c] Maxima on the rate of weight loss against temperature curve.
[d] Calculated for 1 mol equiv. of water.

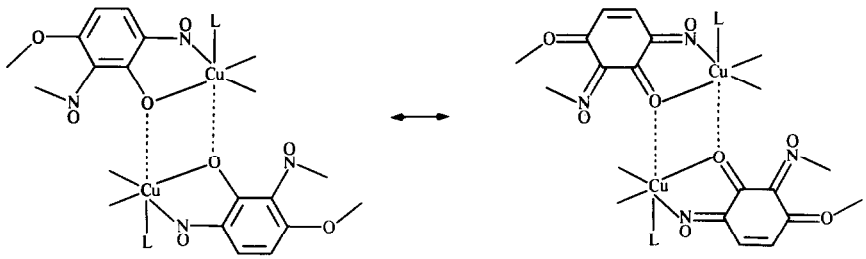

3

Table 3. Variable-temperature magnetic data for Cu(6-Cldnr)·py

T (K)	293	273	253	233	213
$10^6 \times A$	810	845	906	960	1016
μ_{eff}	1.38	1.36	1.36	1.34	1.32
$-\theta$ (K)	75				

adducts when X = H, 6-Et or 6-Cl. Thermal gravimetric analysis (Table 2) on all the hydrates showed that water was lost quantitatively between 100 and 150°C to give Cu(X-dnr) which decomposed between 160 and 190°C.

Magnetic susceptibilities for the complexes Cu(X - dnr)·H_2O (X = H, 6-Et, 6-Cl or 5-Me) and Cu(X-dnr)py (X = H, 6-Et or 6-Cl) were measured at room temperature and the calculated magnetic moments are given in Table 1. The magnetic moments at room temperature for both the hydrates and the pyridine adducts of Cu(X-dnr) studied fall in a range (1.0–1.6 BM) which is well below the limits expected for magnetically dilute copper(II) complexes. Generally, copper complexes have moments in the range 1.8–2.1 BM, independent of the co-ordination number.[6] A deviation from simple paramagnetic behaviour therefore is indicated for these copper complexes. A variable-temperature study of magnetic moments was carried out on Cu(6 - Cldnr) · py. The decreasing magnetic moment with temperature (Table 3) and the negative Weiss constant observed for the complex suggests antiferromagnetic behaviour. This may arise either through the bridging X-dnr^{2-} ligand or through association involving copper atoms in different chains of the polymer (**3**). The latter possibility is less likely because: (i) antiferromagnetic behaviour is also shown by the corresponding six-coordinate nickel(II) complexes Ni(X - dnr)·$2H_2O$ which have X-dnr bridges, and (ii) the pyridine adducts of analogous copper(II) complexes of 2-nitrosophenols are known to exhibit five-co-ordination.[5,9]

The relatively low magnetic moment of Cu(2-Memnr)$_2$·$4H_2O$ would suggest some association between Cu(2-Memnr)$_2$ units as found in related nickel complexes.[10]

REFERENCES

1. R. G. Buckley, J. Charalambous, M. J. Kensett, M. McPartlin, D. Mukerjee, E. G. Brain and J. M. Jenkins, *J. Chem. Soc., Perkin Trans.* I 1983, 693.
2. C. B. Castellani and R. Millini, *J. Chem. Soc., Dalton Trans.* 1984, 1461.
3. J. Charalambous, L. I. B. Haines and J. S. Morgan, B.P. Application 83 31464.
4. R. G. Cawthorne, J. Charalambous, W. M. Shutic, F. B. Taylor and A. Betts, *Inorg. Chim. Acta* 1979, **37**, 245.
5. J. Charalambous, M. J. Frazer and F. B. Taylor, *J. Chem. Soc. A* 1969, 2787.
6. A. Earnshaw, *Introduction to Magnetochemistry*. Academic Press, London (1968).
7. R. S. Bottei and C. P. McEachern, *J. Inorg. Nucl. Chem.* 1971, **33**, 9.
8. P. W. W. Hunter and G. A. Webb, *J. Inorg. Nucl. Chem.* 1970, **32**, 1386.
9. M. McPartlin, *Inorg. Nucl. Chem. Lett.* 1973, **9**, 1207.
10. J. Charalambous, M. J. Kensett and J. M. Jenkins, *Inorg. Chim. Acta* 1976, **16**, 213.

Polyhedron Vol. 6, No. 5, pp. 1037–1039, 1987
Printed in Great Britain

0277–5387/87 $3.00+.00

^{119}Sn NMR STUDY OF THE EQUILIBRIUM OF FORMATION OF TRIORGANOTIN(IV) CHLORIDE COMPLEXES IN COORDINATING SOLVENTS

J. HOLEČEK,* K. HANDLÍŘ, V. ČERNÝ and M. NÁDVORNÍK

Department of General and Inorganic Chemistry, Institute of Chemical Technology, 53210 Pardubice, Czechoslovakia

and

A. LYČKA

Research Institute of Organic Syntheses, 532 18 Pardubice-Rybitví, Czechoslovakia

(*Received* 26 *March* 1985; *accepted* 25 *September* 1986)

Abstract—The temperature and concentration dependences of ^{119}Sn chemical shifts of triorganotin(IV) chlorides [R_3SnCl (R = *n*-butyl, benzyl or phenyl)] in deuteriochloroform and three coordinating solvents [S (S = pyridine, dimethyl sulphoxide or hexamethylphosphortriamide)] have been studied. The values of ^{119}Sn chemical shifts of the complexes $R_3SnCl.S$ formed have been determined from the temperature dependence, and the values of the thermodynamic parameters K_x, ΔG, ΔH and ΔS of these complexes have been calculated. The stability of complexes increases in the R-substituent series: *n*-butyl < benzyl < phenyl, and in the solvent series: pyridine < dimethyl sulphoxide < hexamethylphosphortriamide.

For the description of the equilibrium of formation of triorganotin(IV) complexes in solutions of coordinating solvents, which occurs only when the molar ratio of the components is 1:1, the simple equation[1] based on the knowledge of the concentration dependence of the chemical shift $\delta(^{119}Sn)$ was derived. The $\delta(^{119}Sn)$ of pure components of the equilibrium system, necessary for the calculation of the equilibrium constant, are obtained as limiting values by the extrapolation of this concentration dependence. In some systems it is difficult to implement such an extrapolation, because experimental data are limited to a narrow concentration range due to the specific physical properties of the system. In this paper we report on the $R_3SnCl(S)$ systems, where R is *n*-butyl (Bu), phenyl (Ph) or benzyl (Bz), and (S) is pyridine (py), dimethyl sulphoxide (dmso) or hexamethylphosphortriamide (hmpa), respectively, so that in such cases the necessary data can be obtained from the temperature dependences of the $\delta(^{119}Sn)$ parameter.

EXPERIMENTAL

Tri-*n*-butyl-, tribenzyl- and triphenyltin(IV) chlorides were prepared by known methods.[2,3] The ^{119}Sn NMR spectra were measured on a JNM-FX 100 spectrometer (JEOL, Japan) at 37.14 MHz. The ^{119}Sn chemical shifts were measured at $\pm$0.1-ppm digital resolution at various temperatures, and referred to external neat tetramethylstannane. The positive $\delta(^{119}Sn)$ values denote downfield shifts. An external ^{2}H lock was used in the measurements using py, dmso and hmpa. The temperature was measured with an accuracy of $\pm$1 K.

RESULTS AND DISCUSSION

Due to the limited sensitivity of the experimental equipment and the physical properties of the $R_3SnCl(S)$ system (R = Bu, Ph or Bz) studied the $\delta(^{119}Sn)$ values can be determined in the concentration region x (mole fraction) of the order of $\sim 10^{-2}$ and in the temperature regions 240–320 K with S = $CDCl_3$, 300–360 K (S = dmso or hmpa)

* Author to whom correspondence should be addressed.

and 240–300 K (S = py). The changes in $\delta(^{119}Sn)$ in the studied concentration range are very small (1–3 ppm) and therefore it is not possible to extrapolate to infinite dilution. The temperature dependences of $\delta(^{119}Sn)$ for all the studied triorganotin(IV) chlorides in $CDCl_3$ solution are also small, but in the coordination solvents they are sufficiently high, and in the temperature region studied the observed changes in $\delta(^{119}Sn)$ are ~60–100 ppm. This is manifested in Fig. 1 where the temperature dependences of $\delta(^{119}Sn)$ are shown for the $Bz_3SnCl(py)$ system with two concentrations ($x = 1.35 \times 10^{-2}$ and 5.11×10^{-2}, respectively) and for the $Bz_3SnCl(CDCl_3)$ system with $x = 2.12 \times 10^{-2}$.

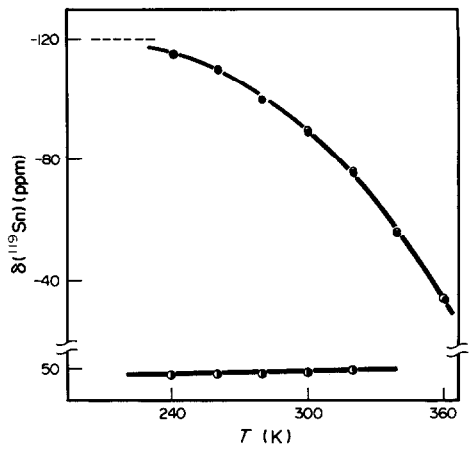

Fig. 1. Temperature dependence of ^{119}Sn chemical shifts of tribenzyltin(IV) chloride in pyridine (py) and $CDCl_3$. Concentration (mole fraction): (○) 1.35×10^{-2} (py), (●) 5.11×10^{-2} (py), (◑) 2.12×10^{-2} ($CDCl_3$).

The equilibrium constants (K_x) of the complex formation according to the reaction:

$$R_3SnCl + S \rightleftharpoons R_3SnCl(S)$$

were calculated from the original Hunter and Reeves equation[1] transferred to the form:

$$K_x = \frac{(\delta_o - \delta_A)[(\delta_{AB} - \delta_A) - x(\delta_o - \delta_A)]}{(\delta_{AB} - \delta_o)[(1-x)(\delta_{AB} - \delta_A) - x(\delta_o - \delta_A)]}$$

where x is the concentration of R_3SnCl (mole fraction), δ_o is the observed $\delta(^{119}Sn)$, and δ_A and δ_{AB} are the $\delta(^{119}Sn)$ of components R_3SnCl and $R_3SnCl(S)$, respectively.

For the $\delta(^{119}Sn)$ of the pure R_3SnCl component the value of $\delta(^{119}Sn)$ measured in a $CDCl_3$ solution was used. The $\delta(^{119}Sn)$ of the complex $R_3SnCl(S)$ was obtained by the optimalizing process for the parameter δ_{AB} supposing the linear dependence of $\ln K_x$ on T^{-1}, resp. ΔG on T. This presumption is consistent with the complex formation $R_3SnCl(S)$ with a component ratio of 1 : 1 and was justified in Ref. 4. Using a simple computer program, the selected values of $\delta(^{119}Sn)$ for complexes $R_3SnCl(S)$ (with a 0.5-ppm step) were gradually introduced into the expression for the equilibrium constant with the aim of finding the best correlation coefficient (r) of the linear regression of the function $\ln K \sim T^{-1}$. The values of r for the optimum linear regressions for the systems studied varied within the limits 0.985–0.999. The optimum values of $\delta(^{119}Sn)$ for the correlation of the individual systems are taken as the values for $R_3SnCl(S)$ complexes. The calculated values of K_x and the other thermodynamic quantities of the systems under study are given in Table 1.

The values obtained in this way correspond well with those obtained by another method.[5,6] The value of $\Delta H = -41.0$ kJ mol^{-1} obtained by Graddon and Rana[5] for the $Ph_3SnCl(py)$ system seems to be very high, which could be caused by an incorrect method used for its determination. The value of -33 kJ mol^{-1} for the heat of mixing for the $Ph_3SnCl(py)$ system[6] is clearly distorted by the heat of crystallization.

From our measurements we can conclude that in the studied group of complexes their stability increases (in agreement with K_x and/or ΔG values)

Table 1. Thermodynamic data for formation of $R_3SnCl(S)$ complexes at 300 K

System	K_x	$-\Delta G$ (kJ mol^{-1})	$-\Delta H$ (kJ mol^{-1})	$-\Delta S$ (J mol^{-1} K^{-1})
Bu_3SnCl–py	4.1±0.3	3.5±0.2	18.0±0.7	49±2
Bu_3SnCl–dmso	20.4±1.0	7.5±0.1	18.8±0.2	38±1
Bu_3SnCl–hmpa	25.2±2.2	8.0±0.2	14.5±0.1	21±1
Bz_3SnCl–py	4.7±0.0	3.9±0.0	20.1±0.6	54±2
Bz_3SnCl–dmso	23.8±0.7	7.9±0.1	18.1±0.1	34±1
Bz_3SnCl–hmpa	35.6±0.1	8.9±0.0	19.0±0.2	33±1
Ph_3SnCl–py	10.9±0.0	6.0±0.0	18.6±0.8	43±3
Ph_3SnCl–dmso	35.5±2.0	8.9±0.1	14.9±0.6	20±2
Ph_3SnCl–hmpa	176.1	12.9	21.9±0.3	30±1

in the series of substituents Bu < Bz < Ph, and in the series of coordinating solvents py < dmso < hmpa. Therefore, the most stable complexes are formed in systems with Ph_3SnCl and hmpa. The conversion into the complex is almost complete in this case.

REFERENCES

1. B. K. Hunter and L. W. Reeves, *Can. J. Chem.* 1968, **46**, 1399.
2. G. J. M. van der Kerk and J. G. A. Luijten, *J. Appl. Chem.* 1956, **6**, 93.
3. K. Sisido, Y. Taketa and Z. Kinugawa, *J. Am. Chem. Soc.* 1961, **83**, 538.
4. J. D. Kennedy, W. McFarlane, P. J. Smith, R. F. M. White and L. Smith, *J. Chem. Soc., Perkin Trans.* II 1973, 1785.
5. D. P. Graddon and B. A. Rana, *J. Organomet. Chem.* 1976, **105**, 51.
6. V. G. Tsvetkov, K. P. Zabotin, A. N. Shmeleva, A. N. Bryukhanov, B. V. Sul'din and Yu. A. Aleksandrov, *Zh. Obshch. Khim.* 1982, **53**, 388.

Polyhedron Vol. 6, No. 5, pp. 1041–1048, 1987
Printed in Great Britain

0277–5387/87 $3.00+.00

THE PACKING SATURATION RULE AND THE PACKING CENTRE RULE: STRUCTURAL CHARACTERISTICS IN LANTHANIDE COORDINATION COMPOUNDS

FENG XI-ZHANG, GUO AO-LING, XU YING-TING, LI XING-FU*

Application Department, The Institute of High Energy Physics, Beijing, P.O. Box 2732, China

and

SUN PENG-NIAN

Biology Department, The Univeristy of Science and Technology of China, Hofei, Anhwei, China

(*Received* 16 *October* 1985; *accepted after revision* 25 *September* 1986)

Abstract—The concepts of the Cone Packing Model, namely the Solid Angle Factor (SAF), Fan Angle (FA), Coordination Vector ($\mathbf{r}$), Gap and Hole have been introduced to describe steric packing around the metal centre. In a treatment of more than 160 structures of lanthanide coordination compounds, it was found that the sums of the ligand SAFs (SAS) are mainly in the region SAS = 0.78, $\sigma = 0.05$. This result provides concrete evidence that "coordination saturation" in the lanthanide compounds is actually saturation in the coordination space. The Packing Centre Rule has shown for the first time that the vector sum of the ligand SAFs, i.e. $\Sigma \mathrm{SAF} \cdot \mathbf{r}$, of each structure closely approaches zero with an average $\Sigma \mathrm{SAF} \cdot \mathbf{r}$ of 0.02 and a standard deviation of 0.015. The Packing Centre Rule indicates that there is a clear tendency for the ligands to distribute themselves so that the non-bonding repulsions are at a minimum.

Two major problems remain unclarified in lanthanide and actinide chemistry. Firstly, although "coordination saturation" is a well-accepted concept in coordination and organometallic chemistry and is extensively used as a criterion for the thermal stability and chemical reactivity of *d*-transition metal compounds, the concept is not clearly defined for the *f*-group analogues. There are two plausible arguments, of which the first refers to saturation in the valence orbital shell of the metal ion. Coordination saturation is achieved if the electron count reaches a certain limit (the electron configuration attains the "next inert gas" configuration, e.g. the 18- or 16-electron rules). Another argument is based on the occupation of the coordination space by the ligands. There is altogether a 4π solid angle around the metal ion and, when the metal is coordinated to enough ligands to prevent the entry of further more ligands into the coordination sphere, the space is believed to be saturated. The second interesting problem is concerned with the decisive factors in the molecular structure of coordination and organometallic compounds. In *d*-transition metal coordination compounds, the problem can be analysed in terms of the Crystal Field Stabilization Energy (CFSE). The structure which has the higher CFSE will be more stable than those with a lower CFSE. However, the CFSE is minimal in *f*-group metal compounds. There is a considerable flexibility in the coordination geometry adopted by their complexes whereas there is little gain or loss in CFSE. We have recently suggested that the structure of lanthanide and actinide coordination compounds is very similar to the packing in an ionic lattice so that the size of the ions plays a dominant role in their arrangement.[1]

The two approaches to the above problems are

* Author to whom correspondence should be addressed.

based on different models. The first approach is based on metal–ligand orbital interactions whereas the second is based on the geometrical packing. Since Tolman made the first attempt to describe steric crowding quantitatively,[2] there has been continued interest[3,4] in this subject. The idea of the solid angle was introduced by several authors[5–8] almost simultaneously to describe steric packing around the metal centre. Although we have reported many applications of the Cone Packing Model[9–13] in inorganic preparations and in explaining bonding in the products, a detailed treatment of the model itself has not yet been published. In the present paper we report our work on the structural characteristics of lanthanide coordination compounds and report the Packing Saturation and Uniform Packing Rules that we have determined.

A FEW CONCEPTS OF THE CONE PACKING MODEL

In dealing with a monomeric structure, a unit sphere of radius 1 Å is drawn with the metal ion as the centre. The ligands are centripetally projected onto the surface of the unit sphere in the first and second order, respectively. The first-order steric effect is due to the directly coordinating atoms and the second-order steric effect is due to the next layer of non-coordinating atoms which is usually at a distance of 3.5–4.5 Å from the metal ion (Fig. 1). The Solid Angle Factor (SAF) is defined as the solid angle of the ligand cone comprising the metal at the apex and the primary coordinating atom or group (the first-order SAF) or the whole ligand (the second-order SAF) divided by 4π. Geometrically, it refers to the ratio of the projected area to 4π, i.e. the area of the sphere surface. It actually represents the size of the ligand as viewed from the metal centre towards the ligand. The sum of the values of SAF of all the ligands coordinated to the metal centre represents the total occupancy of the ligands in the coordination sphere. It is apparent that this occupancy should not reach unity because there are gaps and holes among the ligands. Previously we have used the symbols c.a.f. and Σc.a.f. to express the SAF and the overall occupancy.[8] The symbols were later changed to SAF and SAS in order to avoid confusion with Tolman's Cone Angle concept.

The fan angle (FA) is defined as one-half of the angle subtended by the primary coordinating atom or group (the first-order FA) or the whole ligand (the second-order FA) in different symmetry planes using the van der Waals' sphere concept. In practice the FA of the second-order steric effect has the same meaning as the term "Cone Angle" as defined by Toman. Irregular ligands have more than one FA, so that the FA could be used to describe he shape of a ligand.

Coordination Vector ($\vec{r}$): this is a unit vector directed from the metal ion towards the primary coordinating atom. $\vec{r}$ is used to define the position of a ligand. The product of the ligand SAF and $\vec{r}$, i.e. $4\pi\text{SAF}\cdot\vec{r}$, expresses not only the projectional area of a specified ligand on the unit sphere but also indicates the location of that area.

It should be remarked here that the $\vec{r}$ of a chelating ligand is described by each of the individual vectors

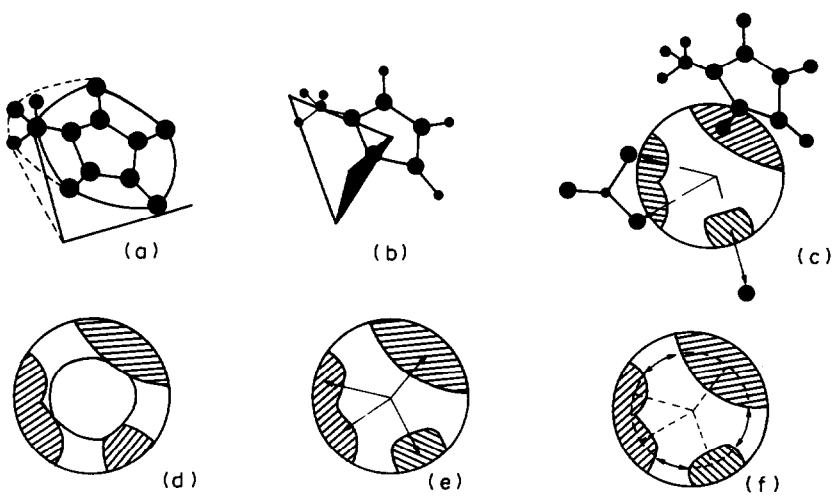

Fig. 1. Geometrical description of concepts of Cone Packing Model: (a) Solid Angle, (b) Fan Angle, (c) projection of ligands to the unit sphere, (d) hole among the ligands, (e) Coordination Vector ($\vec{r}$), and (f) gap between two ligands.

of the coordinating atoms rather than by their sum. For example, the $\vec{r}$ of bidentate nitrate is $\vec{r}_{O1}+\vec{r}_{O2}+\vec{\Delta}$, where $\vec{r}_{O1}$ and $\vec{r}_{O2}$ are the coordination vectors of the two oxygen atoms and $\vec{\Delta}$ is the coordination area of the overlapping part of the two atoms. The coordination vector of a plate-like ligand, e.g. cyclopentadienyl, is directed towards the centre of the ligand.

The vector sum of the values of SAF of all the coordinating ligands, $\Sigma \mathrm{SAF}_i \cdot \vec{r}_i$ throughout the metal ion, indicates the distribution of the areas in the sphere surface. If the ligands are concentrated at one side of the sphere and the other side is empty, the vector sum of the ligand SAF will be significantly high in this direction. Since $\Sigma \mathrm{SAF}_i \cdot \vec{r}_i$ of the most popular coordination geometry are always zero, we adopt it as one, but not a unique, criterion of uniformity in the packing of the ligands around the metal ion.

The Gap between two neighbouring ligands A and B is defined as the difference between the bond angle AMB and their FA sum, $G_{AB} = \measuredangle \mathrm{AMB} - (\mathrm{FA_A}+\mathrm{FA_B})$.

When the van der Waals' spheres of the coordinating atoms separate from each other the Gap is positive, when they are in contact the Gap is zero, and when they overlap the Gap is negative.

Holes among the ligands: The Hole is defined as the largest cone which could be inserted among the ligands present. Since it is an empty site for an incoming ligand, it is also described by SAF and $\vec{r}$. The Hole expresses the vacancy among the ligands discussed above. The steric packing in a reported structure could be studied using the above concepts by the following approach.

MATHEMATICAL TREATMENT

The published atomic lattice coordinates are transformed into rectangular coordinates by means of the following equations:

$$X = ax\sin\beta + by\sin\alpha\cos\phi,$$

$$Y = by\sin\alpha\sin\phi,$$

$$Z = cz + by\cos\alpha + ax\cos\beta,$$

$$\phi = \cos^{-1}\left(\frac{\cos\gamma - \cos\alpha\cos\beta}{\sin\alpha\sin\beta}\right),$$

where a, b and c and α, β and γ are the lattice parameters, and x, y and z the atomic lattice coordinates. $\vec{r}$ may be calculated from:

$$\vec{r} = (\vec{X}+\vec{Y}+\vec{Z})/R$$

$$R = (X^2+Y^2+Z^2)^{1/2}.$$

The distance between any two atoms may then be calculated. The FA $\theta = \sin^{-1}(v/l)$, where v is the van der Waals' radius of a specific atom and l is the bond length between metal ion and the coordination atom.

$$\mathrm{SAF} = \tfrac{1}{2}(1-\cos\theta).$$

The first-order packing refers to the packing in the primary coordination sphere.

Correction must be made for bidentate ligands for overlapping according to the following equation:

$$\Delta\mathrm{SAF} = (\pi v^2\psi/180 - dv\sin\psi)/(2\pi l^2\cos^2\eta)$$

where η is one-half of the angle L—M—L′ (L and L′ are the two coordinating atoms in one ligand): d is one-half the distance between the two atoms (Fig. 2) and $\psi = \cos^{-1}(d/v)$. The approximation comes from the shaded area when the two atoms are identical and are equidistant from the metal. More accurate corrections can be made if the two atoms are not identical or they are not equidistant from the metal ion.[8(b)]

The second-order steric packing has only been

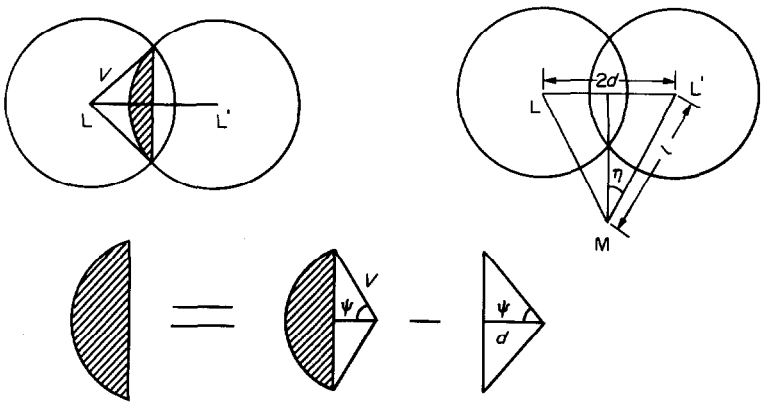

Fig. 2. Correction for overlapping of bidentate ligands.

Table 1. Calculation of steric packing for lanthanide coordination compounds

Coordination atom	Bond length	SAF	FA (°)	SAF·$\hat{X}$/R	SAF·$\hat{Y}$/R	SAF·$\hat{Z}$/R	SAS = ΣSAF$_i$	ΣSAF$_i$·$\hat{r}_i$
				(a) Example A : La[N(SiMe$_3$)$_2$]$_3$PPh$_3$O[14]				
N(1)	2.419	0.1078	38.3	−0.0865	−0.0355	0.0536		
N(2)	2.392	0.1105	38.8	0.0817	0.0191	0.0719		
N(3)	2.381	0.1117	39.1	0.0328	−0.0609	−0.0878		
O	2.405	0.0934	35.6	−0.0217	0.0837	−0.0354		
				SAF$_i$·($\hat{X}$/R)$_i$ = 0.0063	SAF$_i$·($\hat{Y}$/R)$_i$ = 0.0064	SAF$_i$·($\hat{Z}$/R)$_i$ = 0.0023	0.423	0.009
				(b) Example B : Yb(acac)$_3$(CH$_3$COOCH=C(NH$_2$)CH$_3$)[15]				
O(1) acacl	2.289	0.104	37.7	0.0693	0.0242	−0.0737		
O(2) acacl	2.197	0.117	40.0	0.0961	−0.0612	0.0267		
O(3) acac2	2.265	0.107	38.2	−0.0512	−0.0071	−0.0937		
O(4) acac2	2.210	0.113	39.3	−0.0984	0.0530	0.0164		
O(5) acac3	2.202	0.114	39.5	−0.0496	−0.1025	0.0043		
O(6) acac3	2.238	0.110	38.7	−0.0150	−0.0134	0.1082		
O(7)	2.239	0.110	38.7	0.0384	0.0956	0.0386		
				SAF$_i$($\hat{X}$/R)$_i$ = −0.010	SAF$_i$($\hat{Y}$/R)$_i$ = −0.011	SAF$_i$($\hat{Z}$/R)$_i$ = 0.027	0.775	0.031

Table 2. Steric packing of selected structures for lanthanide coordination compounds[a]

No.	Pattern	Compounds	Formal coordination number	$\lvert\Sigma SAF\cdot\vec{r}\rvert$	SAS	Reference
1	MB_3	$Dy\{(C_6H_{11})_2PS_2\}_3$	6	0.001	0.767	16
2	$MA_3A'_3$	$Pr[OP\{N(CH_3)_2\}_3]_3Cl_3$	6	0.008	0.699	17
3	MA_6	$[(C_6H_5)_3HP]_3[PrCl_6]$	6	0.009	0.736	18
4	$MA_3MA'_3$	$Sc(C_4H_8O)_3Cl_3$	6	0.009	0.841	19
5	MAB_3	$Yb(acac)_3(H_2O)$	7	0.011	0.710	20
6	MA_7	$[Er(dmp)_7](ClO_4)_3$	7	0.008	0.737	21
7	MB_4	$NH_4Pr(tta)_4(H_2O)$	8	0.021	0.714	22
8	MB_4	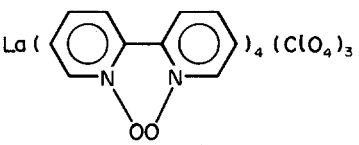	8	0.006	0.683	23
9	MB_4	$Er(PF_6)_3\cdot 4L$, $L = CH_2(CON(CH_3)_2)_2$	8	0.012	0.811	24
10	$M_2D_3A_4$	$Yb_2(C_2O_4)_3(H_2O)_6$	8	0.022	0.788	25
11	MC_3	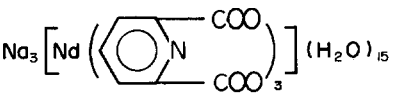	9	0.004	0.779	26
12	MA_9	$Y(H_2O)_9(C_2H_5SO_4)_3$	9	0.00	0.826	27
13	MA_5B_3	$[La(NO_3)_3(H_2O)_5](H_2O)$	11	0.014	0.797	28
14	MB_3F	$La(NO_3)_3$(18-crown-6)	12	0.010	0.842	29
15	MFA_2B	$Sm(ClO_4)_3$(dbc-6)	10	0.005	0.834	30

[a]A full list for Table 2 is deposited as supplementary data.

treated for a few structures. The second-order SAS value is the sum of the SAFs of all atoms in the layer from 3.5 to 4.5 Å from the metal ion.

We have given two examples to show the calculation (Table 1). The values of SAS and $\Sigma SAF\cdot\vec{r}$ of some selected structures are listed in Table 2.

RESULTS AND DISCUSSION

Ligand packing around the metal centre is very similar to the packing of an ionic lattice in which:

(1) The SAS of all anions around a cation stays approximately constant regardless of the lattice character.

(2) The vector sum of the value of the SAF of all anions around a cation tends to be zero.

(3) The anions are in contact with each other in the lattice.

All three characteristics remain approximately true in structures of lanthanide coordination compounds.

The purpose of our work is to demonstrate that steric packing plays a dominant role in the molecular structures of lanthanide coordination compounds. Fluctuations in both the coordination number and the SAS values are analysed as follows: if the coordination saturation in *f*-group chemistry is explained on the basis of filling the valence orbitals with electrons, the formal coordination number in these structures should be distributed around certain electron counts with few exceptions. On the other hand, if coordination saturation is explained on the basis of filling up coordination space, the sum of the ligand SAFs will be concentrated around a value which represents the criterion of the proper packing. One ligand more in the coordination sphere will lead to steric overcrowding and one ligand less will lead to steric undercrowding. It is expected that the standard deviation of the ligand packing should therefore be within the SAF of one ligand (see Table 3).

In fact, we have found that the sum of the ligand SAFs are quite constant in spite of the change in the formal coordination number from 4 to 12 (Fig. 3). Steric packing increases steadily and slowly with

Table 3. Average steric packing and deviations for 164 structures[a]

Coordination number	Number of structures	$\Sigma SAF \cdot \vec{r}$	SAS
6	15	0.008 ± 0.009	0.742 ± 0.053
7	14	0.024 ± 0.009	0.729 ± 0.033
8	58	0.012 ± 0.009	0.766 ± 0.051
9	48	0.009 ± 0.01	0.793 ± 0.038
10	19	0.016 ± 0.008	0.812 ± 0.032
11	6	0.018 ± 0.007	0.814 ± 0.020
12	4	0.008 ± 0.005	0.891 ± 0.037

[a] General: $\Sigma SAF \cdot \vec{r} = 0.02 \pm 0.015$, $SAS = 0.78 \pm 0.05$*. The standard deviation is less than the SAF of the smallest ligand in our calculation.

the increasing formal coordination number. This phenomenon is very similar to the phenomenon in the packing of balls in a box in that the smaller the balls the higher the space occupancy. The values of SAS reach about 0.90 for structures of high coordination number, although the electron count has not yet achieved the inert-gas formalism. It was noticed that the gaps between the neighbouring ligands were almost zero or even negative, indicating a very crowded steric packing. It is definitely the steric repulsion that prevents more ligands entering the coordination space. Thus equilibrium is established and the CFSE is compensated for by the ligand non-bonding repulsions.

It is found that the structures of compounds with relatively lower SAS values always contain ligands which are bulky in the second order. A typical example is $LA[N(SiMe_3)_2]_3PPh_3O$. Although there are only four coordinating atoms in the first order with an SAS value of 0.423 [Table 1(a)], in the second-order steric crowding there are six silicon atoms, six carbon atoms and a phosphorus atom at distances from 3.45 to 3.91 Å around the lanthanum ion. The calculated SAS value in the second layer is 0.78. The second- and first-order steric effects have a cooperative effect with respect to each other. That is, if all the ligands in a molecule have little steric effect in the second order, then steric crowding in the first order would be higher then the average value of SAS e.g. $LnCl_6^{3-}$, $[Ln(NO_3)_6]^{3-}$ and $[Ln(NO_3)_5]^{2-}$ whereas ligands which are bulky in the second order always form complexes in which the SAS value is less than the average (e.g. with ligands containing $-Ph^-$, $-CMe_3^-$, $-NMe_2^-$ or $-SiMe_3^-$).

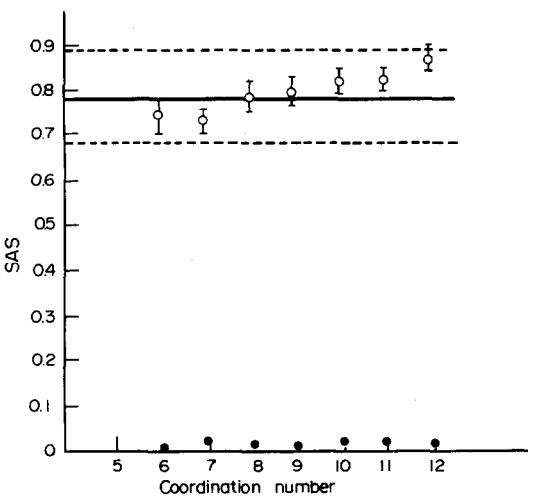

Fig. 3. The Packing Saturation Rule and the Packing Centre Rule. The stable region is described with a centre line at the SAS equal to the average steric crowding and two border lines of either gain or loss of one ligand with an SAF of 0.1.

The Packing Centre Rule: in a box filled with balls, in spite of the different sizes and different arrangements of the balls, the centre of gravity of the balls moves very little and it always coincides approximately with the centre of the box. We have found a similar result in studying the structures of lanthanide coordination compounds. The vector sums of the first-order ligand SASs in all the structures without exception approach zero (Table 3) regardless of the molecular geometries and the formal coordination numbers. This also occurs in ionic latice, for the lattice will change with the variation in the ionic radii of the anions around a cation, as well as vice versa. This behaviour is in clear contrast to the structures of main-group element compounds such as water and ammonia where the centres of gravity of the hydrogen atoms are apparently not close to the central atoms due to the lone pair of electrons. Thus the structures of lanthanide coordination compounds, being individual molecular structures, obviously retain the properties of ionic lattices. Since the crystal field stabilization energy is at a minimum and the molecular geometry is

Table 4. Molecular geometry of the coordination pattern MA_3B

Compound	Ligand	SAF	Reference	Bond angle (°) (thf/Cp)	Reference	Bond angle (°) (calc.) (thf/Cp)
$LaCp_3thf$				99.5 117.7	30	
$PrCp_3thf$	Cp	0.215		99.0 117.6	31	97.8
$NdCp_3thf$	thf	0.087		100.2 117.0	31	118.2
$GdCp_3thf$			12, 13	99.2 117.5	32	
YCp_3thf				99.1 117.4	30	

very flexible, the bonds between the metal and the ligands are almost undirectional. Steric and static repulsion among the ligands lead to a uniform distribution of ligands.

The Packing Centre Rule is further proved by its application in predicting the molecular structures. For example, for the molecular geometry of MA_3B compounds, according to the rule (Fig. 4):

$$3SAF_A \cos(180-\theta) - SAF_B = 0,$$

the bond angle AMB is thus derived from the reported SAF values,[12(a)] and another bond angle is derived according to the sphere triangle function:

$$\phi = \cos^{-1}(\tfrac{3}{2}\cos^2\theta - \tfrac{1}{2}).$$

Some of the results are shown in Table 4. The calculated results are in good agreement with the reported ones.

Finally, non-bonding distances of the coordination polyhedron were calculated for many structures. In most cases, the distances are close to or less than the sums of the van der Waals' radii of the corresponding atoms in the neighbouring ligands. When the atoms are not in contact in the primary coordination sphere, the ligands would then be in either contact in the secondary layer or in contact with ligands in the other molecules. This phenomenon offers an explanation for the geometrical flexibility of the molecular structure and for the question how the ligands are fixed at their positions. Favourable orbital interaction seems to play no significant role in molecular geometry. A ligand remains at its position simply because its drifting is interlocked by other ligands in the neighbourhood.

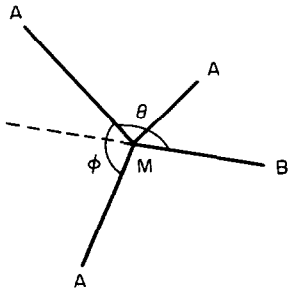

Fig. 4. Application of the Packing Centre Rule in calculating the molecular geometry of the structural pattern MA_3B ($\theta = \measuredangle AMB$, $\phi = \measuredangle AMA$): the vector sum must be zero along the MB direction.

Acknowledgement—This work was supported by the Science Fund of the Chinese Academy of Science. We gratefully thank Professor R. D. Fischer for helpful discussion and Professor K. W. Bagnall for help in preparing this paper.

REFERENCES

1. Li Xing-fu, Feng Xi-zhang, Xu Ying-ting, Shu Peng-nian and Shi Jie, *Acta Chim. Sin.* 1985, **43**, 502.
2. (a) C. A. Tolman, *J. Am. Chem. Soc.* 1970, **92**, 2956; (b) C. A. Tolman, *Chem. Rev.* 1977, **77**, 313.
3. J. D. Smith and J. D. Oliver, *Inorg. Chem.* 1978, **77**, 2585.
4. G. Ferguson, P. J. Robert, E. C. Alyea and M. Khan, *Inorg. Chem.* 1978, **17**, 2965.
5. A. J. Smith, *Proceedings of the* 11 *émes Journées des Actinides*, p. 64. Lido de Jesolo, CNR, Padua, Italy (1982).
6. S. N. Titova, V. T. Bychkov, . A. Domrachev, G. A. Razuvaev, L. N. Zakharov, G. G. Alexandrov and Yu. T. Struchkov, *Inorg. Chim. Acta* 1981, **50**, 71.
7. E. B. Lobkovskii, *Zh. Strukt. Khim.* 1983, **24**, 66.
8. (a) Li Xing-fu, Ph. D. qualification report, The University of Manchester (1980); (b) Li Xing-fu, Ph.D. thesis, The Univeristy of Manchester (1982); (c) K. W. Bagnall and Li Xing-fu, *J. Chem. Soc., Dalton Trans.* 1982, 1365; (d) K. W. Bagnall and Li Xing-

fu, *Abstracts of Actinides*—1981, LBL-12441, 188 (1981).
9. K. W. Bagnall, Li Xing-fu, Pao Po-jung and A. G. M. Al-daher, *Can. J. Chem.* 1983, **61**, 708.
10. K. W. Bagnall, A. V̄. Lopez and Li Xing-fu, *J. Chem. Soc., Dalton Trans.* 1983, 1153.
11. I. Ahmed, K. W. Bagnall, Li Xing-fu and Pao Po-jung, *J. Chem. Soc., Dalton Trans.* 1984, 19.
12. (a) Li Xing-fu and R. D. Fischer, *Inorg. Chim. Acta*, **94**, Abstracts of the First International Conference on Lanthanides and Actinides, P. 50, 1983; (b) G. Bombieri, F. Benetollo, U. Croatto, K. W. Bagnall and Li Xing-fu, *Inorg. Chim. Acta* 1983, **94**, 50.
13. Li Xing-fu, S. Eggers, J. Kopf, W̄. Jahn, R. D. Fischer, C. Apostolidis, B. Kanellakopulos, F. Benetollo, A. Polo and G. Bombieri, *Inorg. Chim. Acta* 1985, **100**, 183.
14. D. C. Bradley, J. S. Ghotra, F. A. Hart, M. B. Hursthours and P. R. Raithby, *J. Chem. Soc., Dalton Trans.* 1977, 1166.
15. M. F. Richardson, P. W. R. Corfield, D. E. Sands and R. E. Sievers, *Inorg. Chem.* 1970, **9**, 1632.
16. A. A. Pinkerton and D. Schwarzenbach, *J. Chem. Soc., Dalton Trans.* 1980, 1300.
17. L. J. Radonovich and M. D. Glick, *J. Inorg. Nucl. Chem.* 1973, **35**, 2745.
18. R. J. Majeste, D. Chriss and L. M. Trefonas, *Inorg. Chem.* 1977, **16**, 188.
19. J. L. Atwood and K. D. Smith, *J. Chem. Soc., Dalton Trans.* 1974, 921.
20. E. F. Korytnii, L. A. Aslanov, M. A. Porai-koshits and O. M. Petrukhin, *Zh. Strukt. Khim.* 1970, **11**, 311.
21. C. Castallani Bisi, A. Coda and V. Tazzoli, *Cryst. Struct. Commun.* 1981, **10**, 703.
22. R. A. Lalancethe, M. Cefola, W. C. Hamilton and S. J. Laplace, *Inorg. Chem.* 1969, **6**, 2127.
23. A. R. Al-karaghouli, R. O. Day and J. S. Wood, *Inorg. Chem.* 1978, **17**, 3702.
24. E. E. Castellano and R. W. Becher, *Acta Cryst.* 1981, **B37**, 61.
25. E. Hansson, *Acta Chem. Scand.* 1973, **27**, 823.
26. J. Albertsson, *Acta Chem. Scand.* 1972, **26**, 1023.
27. D. R. Fitzwater and R. E. Rundle, *Z. Krist.* 1959, **112**, 362.
28. B. Eriksson, L. O. Larsson and L. Ninistö, *Inorg. Chem.* 1980, **19**, 1207.
29. I. Grenthe, *Acta Chem. Scand.* 1971, **25**, 3347.
30. R. D. Rogers, J. L. Atwood, A. Emad, D. J. Sikara and M. D. Rausch, *J. Organomet. Chem.* 1981, **216**, 383.
31. Fan Yuguo, Lü Pinzhe, Jin Zhongsheng and Chen Wenqi, *Sci. Sin.* 1984, **B27**, 994.
32. R. D. Rogers, R. D. Bynum and J. L. Atwood, *J. Organomet. Chem.* 1980, **192**, 65.

Polyhedron Vol. 6, No. 5, pp. 1053–1058, 1987
Printed in Great Britain

0277–5387/87 $3.00+.00

SPECTROSCOPIC STUDIES ON THREE MIXED-LIGAND COPPER(II) COMPLEXES

B. A. SASTRY,* B. BALAIAH, K. V. G. REDDY and B. MADHU

Department of Physics, Osmania University, Hyderabad 500007, India

and

G. PONTICELLI and M. MASSACESSI

Istituto Chimica Generale, Inorganica Ed Analitica, Universita di Cagliari, Via Ospedale 72, 09100 Cagliari, Italy

(*Received* 6 *January* 1986; *accepted after revision* 25 *September* 1986)

Abstract—The mixed-ligand complexes $[Cu(den)en](ClO_4)_2$, $[Cu(den)Pn](ClO_4)_2$ and $[Cu(den)tn](ClO_4)_2$ (where den = diethylenetriamine, en = ethylenediamine, Pn = 1,2-diaminopropane, and tn = 1,3-diaminopropane) have been synthesized, and their IR, electronic and ESR spectral properties have been studied to understand the stereochemistry of these complexes both in the solid state and in DMF (dimethylformamide) or pyridine solutions. The metal appears to be five-coordinate in the solid state, formed with five nitrogens of the mixed ligand, and is found to change in solution, probably due to the attachment of a solvent molecule in the sixth coordination position. The equatorial and axial bond strengths are estimated in the solutions.

It is well known that IR and optical absorption spectra can be used to obtain information regarding the nature and number of ligating atoms in a metal complex, and that the ESR technique in most of the cases can easily detect the point symmetry and bond nature in copper(II) complexes.[1–7] Mixed-ligand complexes were found to be interesting due to the fact that the arrangement of ligating atoms around copper(II) was found to change as one goes from the solid to the solution state.[8] Therefore the authors have undertaken the synthesis of three mixed-ligand complexes with general formula $[Cu(den)L](ClO_4)_2$ [where den = diethylenetriamine, and L = en (ethylenediamine), Pn (1,2-diaminopropane) or tn (1,3-diaminopropane)] and carried out spectroscopic studies on them using IR, optical absorption and ESR techniques with the aim of understanding the stereochemistry of these complexes in both the solid and the solution state.

* Author to whom correspondence should be addressed.

EXPERIMENTAL

Materials

En, tn, Pn and den were commercially available. $CuBr_2$ and $Cu(ClO_4)_2 \cdot 6H_2O$ were prepared according to literature methods.

Preparation of the complexes

All complexes were prepared by the following method.

To a hot solution of the appropriate salt (10 mmol) in methanol (150 cm^3) a hot solution of tridentate amine (10 mmol) and one of the bidentate amine (10 mmol) in the same solvent were slowly added. Isopropyl alcohol was added to the concentrated solution in order to promote crystallization.

All the complexes were filtered and dried *in vacuo* over P_4O_{10}.

Analysis

Nitrogen, carbon and hydrogen were analysed with a Perkin–Elmer 240 Elemental Analyser.

Physical measurements

The room-temperature electronic spectra of the solid compounds were recorded on a Schimadezer MPS 50L spectrophotometer. The IR spectra on CsI discs with Nujol mulls were recorded on a Perkin–Elmer 325 spectrophotometer.

ESR spectra of these complexes in polycrystalline and solution forms were recorded using Varian E-4, *X*-band and E-112 *Q*-band spectrometers having a 100- and 70-KHz magnetic field modulation, respectively. DPPH was used as a *g* marker. The errors in *g* and *A* (hyperfine line separation) are about ± 0.001 and ± 2 G, respectively.

RESULTS AND DISCUSSION

IR and electronic spectra studies

The analytical data and physical properties of these complexes are reported in Table 1. The compounds are microcrystalline or powder-like, intensely coloured, and they are very soluble in MeOH, H_2O, DMF (dimethylformamide) and pyridine. The principal near- and far-IR bands are reported in Table 2. The single band (occasionally doublet) of the amino groups at 3350–3320 cm^{-1} can be assigned to symmetric $\nu(NH_2)$, and the bands in the 3290–3225-cm^{-1} region to asymmetric $\nu(NH_2)$. A single band near 3200–3170 cm^{-1} is usually assigned to the ν(NH) stretching of a secondary amino group [possibly plus an uncoupled ν(NH) of the primary amino group] and the band near 1580 cm^{-1} is assigned to $\delta(NH_2)$. It appears that all the amino groups are coordinated to copper(II). The bands assigned to the perchlorate group are: ν_3 at 1080–1070 cm^{-1} and ν_4 at 625–620 cm^{-1}, which are typical of compounds with free ClO_4. The ν(Cu—N) stretching band occurs in the range 485–427 cm^{-1}, which confirms that the polyamines are coordinated by the nitrogens to the copper(II) ion.

The electronic spectra of solid compounds have a large asymmetric *d–d* band in the range 12,800–16,600 cm^{-1}, and a shoulder at a lower wavenumber in the range 11,600–12,800 cm^{-1}. This pattern is similar to that presented by the diffuse-reflectance spectra of $[Cu(dpt)L]X_2$ (where L = en or tn; dpt = 3,3′-diaminodipropylamine; X = Cl^-, Br^-, I^- or ClO_4^-) which have a five-coordinate distorted square pyramidal structure.[9].

ESR data

Polycrystalline spectra. Figure 1 shows the ESR spectra of the polycrystalline mixed-ligand copper(II) complexes at *Q*-band microwave frequencies. The principal *g* values are calculated using the Kneubuhl procedure[10] from which the useful parameters G $\{(g_3-2)/[(g_1+g_2/2)-2]\}$ and R $[(g_2-g_1)/(g_3-g_2)]$ are also calculated. These parameters for the three complexes are given in Table 3. The G value (4.97) of $[Cu(den)en](ClO_4)_2$ lies between 3.5 and 5.0, indicating that the *g* values obtained in the polycrystalline sample are near to the molecular *g* values, and hence the unit cell of this complex contains magnetically equivalent sites.[11–14] In the case of other two complexes the G values are found to be less than 3.5, indicating an exchange interaction among magnetically inequivalent copper(II) ions in the unit cell, and hence the *g* values obtained in polycrystalline samples will be different from the molecular *g* values.[15] It is also found that for values of R less than 1 the ground state of copper(II) will be either $d_{x^2-y^2}$ or d_{xy}. A d_{z^2} ground state for copper(II) is indicated by values of R greater than 1.[14] From Table 3 it is evident that the ground state of copper(II) in $[Cu(den)en](ClO_4)_2$ is either $d_{x^2-y^2}$ or d_{xy}, which indicates that this five-coordinate complex may have a square-based pyramidal structure. This ground state is supported by the fact that the low-field side of the spectrum is less intense than the high-field side of

Table 1. Analytical data of the mixed-ligand copper(II) complexes

Complex	Colour	M.p. (°C)	Analysis (%)[a] C	H	N
$[Cu(den)en](ClO_4)_2$	Periwinkle-azure	221–227 (dec)	17.2 (16.9)	5.0 (5.0)	16.6 (16.5)
$[Cu(deb)Pn](ClO_4)_2$	Sky-blue	227–234 (dec)	19.6 (19.1)	5.4 (5.3)	16.1 (15.9)
$[Cu(den)tn](ClO_4)_2$	Azure	197–205 (dec)	19.4 (19.1)	5.3 (5.3)	17.6 (16.6)

[a] Calculated values are given in parentheses.

Table 2. IR and electronic spectra of the mixed-ligand copper(II) complexes

Complex	IR (cm^{-1}) Symmetric $\nu(NH_2)$	Asymmetric $\nu(NH_2)$	ν(NH)	$\delta(NH_2)$	ClO_4 ν_3	ν_4	ν(M—N)	Electronic spectra (cm^{-1})
$[Cu(den)en](ClO_4)_2$	3320vs	3270vs, 3235vs	3135vs	1575	1080	625vs	435s	12,500sh, 16,600
$[Cu(den)Pn](ClO_4)_2$	3340vs	3280vs	3150m	1575	1085vsbr	620vs	442m	11,600sh, 12,800 16,100sh
$[Cu(den)tn](ClO_4)_2$	3350vs	3290vs	3170vs	1575	1070vsbr	620vs	485m	11,800sh, 13,800

the spectrum.[8] Since R is greater than 1 in the case of the other two complexes the ground state appears to be d_{z^2}, indicating a compressed trigonal bipyramidal symmetry for these five-coordinate complexes, which is also supported by the fact that the low-field side of the spectrum is more intense than the high-field side of the spectrum.[16]

Solution spectra. The room-temperature spectra of these complexes in DMF and pyridine solutions of four hyperfine lines of copper(II) with a spin-dependent linewidth due to the tumbling motion of the microcrystalline unit in solution.[17] In frozen solutions the ESR spectra consists of four hyperfine lines as parallel features and an unresolved line as

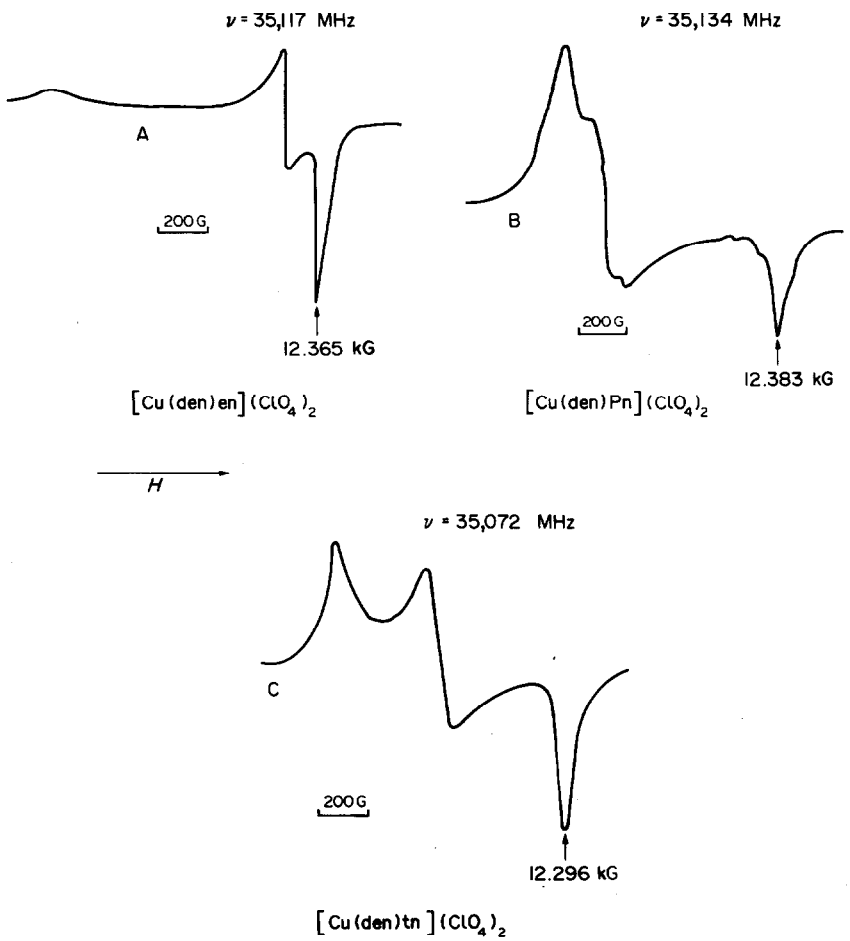

Fig. 1. ESR spectra of the polycrystalline mixed-ligand copper(II) complexes at Q-band (A, B and C) microwave frequencies.

Table 3. g Values of polycrystalline mixed–ligand copper(II) complexes

Complex	g_1	g_2	g_3	G	R	Ground state
$[Cu(den)en](ClO_4)_2$	2.029	2.055	2.209	4.97	0.124	$d_{x^2-y^2}$
$[Cu(den)Pn](ClO_4)_2$	2.027	2.137	2.167	2.03	3.00	d_{z^2}
$[Cu(den)tn](ClO_4)_2$	2.037	2.115	2.159	2.09	1.77	d_{z^2}

the perpendicular feature of the spectrum as shown in Fig. 2. The variation in the hyperfine line intensities of the parallel features of the spectrum can be due to the superposition of the perpendicular features over the parallel features of the spectrum. Low-intensity lines as the parallel features of the spectrum can also be seen which arise most probably due to the presence of a second species with a low population. The g and A values are calculated from the spectra following the usual procedure[18] for the highly populated species, and these values are given in Table 4. It can be seen from Tables 3 and 4 that the g values obtained in the polycrystalline sample of $[Cu(den)en](ClO_4)_2$ are not much different from those in the pyridine solution, indicating that the structure of the chromophore around the solid copper(II) is not disturbed much in pyridine solutions. From Table 4 it is evident that in the case of the DMF solution of $[Cu(den)tn](ClO_4)_2$ the $g_\parallel$ values are smaller and $A_\parallel$ are larger than the corresponding values in the pyridine solution. This is an indication that the solute–solvent interaction in pyridine is greater compared to DMF for the compound $[Cu(den)tn](ClO_4)_2$. The g and A values in both solutions are characteristic of nitrogen coordination.[19] Due to solute–solvent interactions the solvent molecules have probably occupied the sixth coordination position, converting the five-coordinate complexes into six-coordinate ones.

In the presence of axial bonds, $4s$ mixing will be present in the ground state and also the equatorial bonds will be weakened.[20] The σ-bond parameter (α^2) and the fraction of $3d$ character in the $3d$ $4s$ ground state of copper(II) (f^2), which give the strengths of the equatorial and axial bonds, respectively, can be obtained from the following equations:[21]

$$\alpha^2 f^2 = \frac{7}{4}\left[\frac{A_\parallel}{P} - \frac{|A|}{P} + \frac{2}{3}g_\parallel - \frac{5}{21}g_\perp - \frac{6}{7}\right], \quad (1)$$

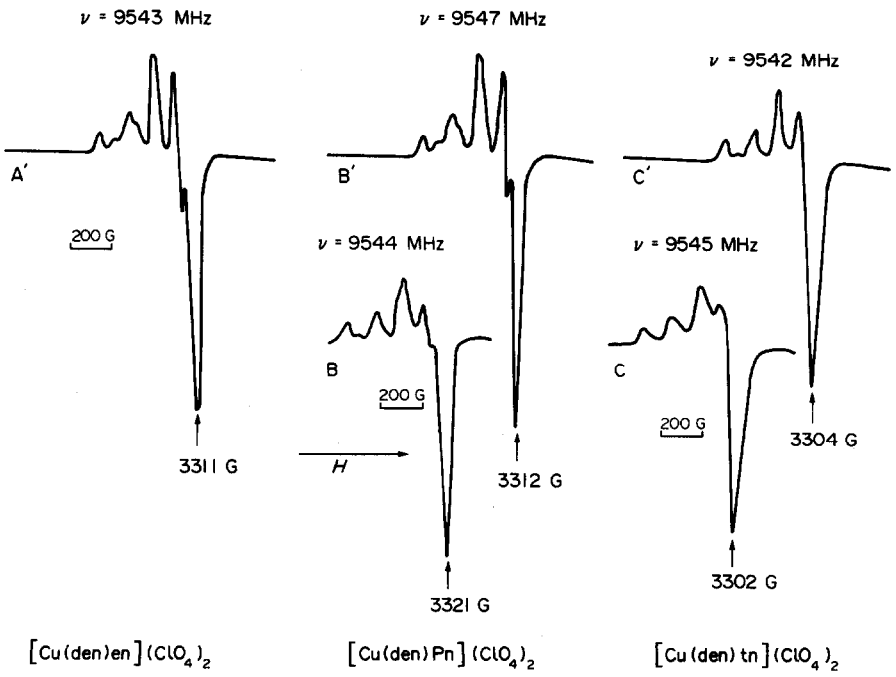

Fig. 2. ESR spectra of the mixed-ligand copper(II) complexes in frozen DMF (B and C) and pyridine (A′, B′ and C′) solutions.

Table 4. Spin-Hamiltonian constants of mixed-ligand copper(II) complexes in DMF and pyridine solutions

Complex	Solvent	g	A ($\times 10^{-4}$ cm^{-1})	$g_\parallel$	$g_\perp$	$A_\parallel$ ($\times 10^{-4}$ cm^{-1})	$A_\perp$ ($\times 10^{-4}$ cm^{-1})
$[Cu(den)en](ClO_4)_2$	Pyridine	2.106	64.7	2.200	2.059	173.9	10.10
$[Cu(den)Pn](ClO_4)_2$	DMF	2.099	64.4	2.190	2.053	176.2	8.6
	Pyridine	2.104	69.5	2.194	2.059	173.3	17.6
$[Cu(den)tn](ClO_4)_2$	DMF	2.103	66.5	2.179	2.065	172.2	13.6
	Pyridine	2.107	78.3	2.194	2.063	170.0	25.8

$$\alpha^2 = \frac{|A|}{PK_o} + \frac{\Delta g}{K_o} + \frac{0.0975(1-f^2)}{PK_o}, \qquad (2)$$

where P is a dipolar term ($2.0023 g_N \beta_e \beta_N \langle r^{-3} \rangle_{av} = 1194$ MHz[22]), and $K_o = 0.43$. In eqn(2) an electron in the 4s orbital has been assigned a value of 0.0975 cm^{-1}.[21,23] The values of α^2 and f^2 for all the complexes are given in Table 5. The value of α^2 in the case of the pyridine solution of $[Cu(den)tn](ClO_4)_2$ is found to be less and its f^2 value more than that of the corresponding values of the other complexes in solutions, indicating strong equatorial and weak axial bonds. On the other hand the α^2 values are more and f^2 values are less in the case of the pyridine solution of $[Cu(den)en](ClO_4)_2$ and the DMF solution of $[Cu(den)Pn](ClO_4)_2$, indicating weak equatorial bonds and strong axial bonds compared to the other cases.

Conclusions

Mixed-ligand copper(II) complexes with general formula $[(Cu(den)L](ClO_4)_2$ have been synthesized, and the IR, electronic and ESR spectral studies of the polycrystalline and solution forms show that:

(a) IR and electronic spectral studies indicate that these mixed-ligand copper(II) complexes are nitrogen-bonded five-coordinate complexes in solid state.

(b) ESR studies of polycrystalline samples indicate that $[Cu(den)en](ClO_4)_2$ has a square-based pyramidal CuN_5 chromophore and the unit cell contains all magnetically equivalent ions, whereas the complexes $[Cu(den)Pn](ClO_4)_2$ and $[Cu(den)tn](ClO_4)_2$ have compressed trigonal bipyramidal CuN_5 chromophores and the unit cell contains magnetically inequivalent ions with a strong exchange interaction among them.

(c) The solute–solvent interaction in the pyridine solutions of all these complexes is found to be more than that of the DMF solutions of these complexes. The chromophore of solid $[Cu(den)en](ClO_4)_2$ is found to be less disturbed in the pyridine solution of this complex. The equatorial bonds of $[Cu(den)tn](ClO_4)_2$ in a pyridine solution is stronger than other complexes in that solution. Except in the above case, in all the other solutions of these complexes, the presence of a 4s orbital in the ground state indicates axial bonds.

Table 5. Bond parameters of mixed-ligand copper(II) complexes

Complex	Solvent	α^2	f^2
$[Cu(den)en](ClO_4)_2$	Pyridine	0.76	0.98
$[Cu(den)Pn](ClO_4)_2$	DMF	0.76	0.98
	Pyridine	0.71	0.997
$[Cu(den)tn](ClO_4)_2$	DMF	0.70	0.997
	Pyridine	0.65	1.000

REFERENCES

1. J. Reedijk, J. C. A. Windhorst, N. H. M. Van Ham and W. L. Groneveld, *Recueil* 1971, **111**, 234.
2. J. Reedijk and J. A. Smith, *Recueil* 1971, **90**, 1135.
3. J. Reedijk, *Recueil* 1971, **90**, 117.
4. B. J. Hathaway, *Coord. Chem. Rev.* 1982, **41**, 423.
5. I. Bertini, D. Gatteschi and A. Scozzafava, *Coord. Chem. Rev.* 1979, **29**, 67.
6. J. Kohout, M. Havastijova and J. Gazo, *Coord. Chem. Rev.* 1978, **27**, 141.
7. D. Reinen and C. Freibel, *Struct. Bonding* 1979, **37**, 1.
8. B. A. Sastry, S. Md. Asadullah, G. Ponticelli and G. Devoto, *J. Mol. Struct.* 1981, **71**, 343.
9. G. Ponticelli, *Inorg. Chimi. Acta* 1971, **5**, 461.
10. F. K. Kneubuhl, *J. Chem. Phys.* 1960, **33**, 1074.
11. I. M. Proctor, B. J. Hathaway and P. Nicholis, *J. Chem. Soc. A* 1968, 1678.
12. M. J. Beu, B. J. Hathaway and R. J. Fereday, *J. Chem. Soc. A* 1972, 1229.
13. A. A. G. Tomlinson and B. J. Hathaway, *J. Chem. Soc. A* 1968, 1905.
14. B. J. Hathaway, *J. Chem. Soc., Dalton Trans.* 1972, 1196.

15. I. M. Procter, B. J. Hathaway and P. G. Hodgson, *J. Inorg. Nucl. Chem.* 1972, **34**, 3689.
16. B. A. Sastry, M. N. Chary, G. Ponticelli and R. Pinna, *J. Mol. Struct.* 1980, **66**, 319.
17. H. M. McConnel, *J. Chem. Phys.* 1956, **25**, 709.
18. B. A. Sastry, S. Md. Asadullah, G. Ponticelli and M. Massacesi, *J. Chem. Phys.* 1979, **70**, 2834.
19. A. A. G. Tomlinson and B. J. Hathaway, *J. Chem. Soc. A* 1985, 1685.
20. R. Barbucci, P. Paoletti and M. J. M. Campbell, *Inorg. Chim. Acta* 1974, **10**, 69.
21. H. A. Kuska, M. T. Rogers and R. E. Drullinger, *J. Phys. Chem.* 1967, **71**, 109.
22. J. A. MacMillan, N. S. Dixson and T. Halpern, *J. Chem. Phys.* 1971, **55**, 452.
23. A. J. Freeman and R. E. Watson, *Phys. Rev.* 1961, **41**, 2027.

Polyhedron Vol. 6, No. 5, pp. 1053–1058, 1987
Printed in Great Britain

0277–5387/87 $3.00+.00

SPECTROSCOPIC STUDIES ON THREE MIXED-LIGAND COPPER(II) COMPLEXES

B. A. SASTRY,* B. BALAIAH, K. V. G. REDDY and B. MADHU

Department of Physics, Osmania University, Hyderabad 500007, India

and

G. PONTICELLI and M. MASSACESSI

Istituto Chimica Generale, Inorganica Ed Analitica, Universita di Cagliari, Via Ospedale 72, 09100 Cagliari, Italy

(*Received* 6 *January* 1986; *accepted after revision* 25 *September* 1986)

Abstract—The mixed-ligand complexes $[Cu(den)en](ClO_4)_2$, $[Cu(den)Pn](ClO_4)_2$ and $[Cu(den)tn](ClO_4)_2$ (where den = diethylenetriamine, en = ethylenediamine, Pn = 1,2-diaminopropane, and tn = 1,3-diaminopropane) have been synthesized, and their IR, electronic and ESR spectral properties have been studied to understand the stereochemistry of these complexes both in the solid state and in DMF (dimethylformamide) or pyridine solutions. The metal appears to be five-coordinate in the solid state, formed with five nitrogens of the mixed ligand, and is found to change in solution, probably due to the attachment of a solvent molecule in the sixth coordination position. The equatorial and axial bond strengths are estimated in the solutions.

It is well known that IR and optical absorption spectra can be used to obtain information regarding the nature and number of ligating atoms in a metal complex, and that the ESR technique in most of the cases can easily detect the point symmetry and bond nature in copper(II) complexes.[1–7] Mixed-ligand complexes were found to be interesting due to the fact that the arrangement of ligating atoms around copper(II) was found to change as one goes from the solid to the solution state.[8] Therefore the authors have undertaken the synthesis of three mixed-ligand complexes with general formula $[Cu(den)L](ClO_4)_2$ [where den = diethylenetriamine, and L = en (ethylenediamine), Pn (1,2-diaminopropane) or tn (1,3-diaminopropane)] and carried out spectroscopic studies on them using IR, optical absorption and ESR techniques with the aim of understanding the stereochemistry of these complexes in both the solid and the solution state.

* Author to whom correspondence should be addressed.

EXPERIMENTAL

Materials

En, tn, Pn and den were commercially available. $CuBr_2$ and $Cu(ClO_4)_2 \cdot 6H_2O$ were prepared according to literature methods.

Preparation of the complexes

All complexes were prepared by the following method.

To a hot solution of the appropriate salt (10 mmol) in methanol (150 cm^3) a hot solution of tridentate amine (10 mmol) and one of the bidentate amine (10 mmol) in the same solvent were slowly added. Isopropyl alcohol was added to the concentrated solution in order to promote crystallization.

All the complexes were filtered and dried *in vacuo* over P_4O_{10}.

Analysis

Nitrogen, carbon and hydrogen were analysed with a Perkin–Elmer 240 Elemental Analyser.

Physical measurements

The room-temperature electronic spectra of the solid compounds were recorded on a Schimadezer MPS 50L spectrophotometer. The IR spectra on CsI discs with Nujol mulls were recorded on a Perkin–Elmer 325 spectrophotometer.

ESR spectra of these complexes in polycrystalline and solution forms were recorded using Varian E-4, *X*-band and E-112 *Q*-band spectrometers having a 100- and 70-KHz magnetic field modulation, respectively. DPPH was used as a *g* marker. The errors in *g* and *A* (hyperfine line separation) are about ± 0.001 and ± 2 G, respectively.

RESULTS AND DISCUSSION

IR and electronic spectra studies

The analytical data and physical properties of these complexes are reported in Table 1. The compounds are microcrystalline or powder-like, intensely coloured, and they are very soluble in MeOH, H_2O, DMF (dimethylformamide) and pyridine. The principal near- and far-IR bands are reported in Table 2. The single band (occasionally doublet) of the amino groups at 3350–3320 cm^{-1} can be assigned to symmetric $\nu(NH_2)$, and the bands in the 3290–3225-cm^{-1} region to asymmetric $\nu(NH_2)$. A single band near 3200–3170 cm^{-1} is usually assigned to the ν(NH) stretching of a secondary amino group [possibly plus an uncoupled ν(NH) of the primary amino group] and the band near 1580 cm^{-1} is assigned to $\delta(NH_2)$. It appears that all the amino groups are coordinated to copper(II). The bands assigned to the perchlorate group are: ν_3 at 1080–1070 cm^{-1} and ν_4 at 625–620 cm^{-1}, which are typical of compounds with free ClO_4. The ν(Cu—N) stretching band occurs in the range 485–427 cm^{-1}, which confirms that the polyamines are coordinated by the nitrogens to the copper(II) ion.

The electronic spectra of solid compounds have a large asymmetric *d–d* band in the range 12,800–16,600 cm^{-1}, and a shoulder at a lower wavenumber in the range 11,600–12,800 cm^{-1}. This pattern is similar to that presented by the diffuse-reflectance spectra of $[Cu(dpt)L]X_2$ (where L = en or tn; dpt = 3,3′-diaminodipropylamine; X = Cl^-, Br^-, I^- or ClO_4^-) which have a five-coordinate distorted square pyramidal structure.[9].

ESR data

Polycrystalline spectra. Figure 1 shows the ESR spectra of the polycrystalline mixed-ligand copper(II) complexes at *Q*-band microwave frequencies. The principal *g* values are calculated using the Kneubuhl procedure[10] from which the useful parameters G $\{(g_3-2)/[(g_1+g_2/2)-2]\}$ and R $[(g_2-g_1)/(g_3-g_2)]$ are also calculated. These parameters for the three complexes are given in Table 3. The G value (4.97) of $[Cu(den)en](ClO_4)_2$ lies between 3.5 and 5.0, indicating that the *g* values obtained in the polycrystalline sample are near to the molecular *g* values, and hence the unit cell of this complex contains magnetically equivalent sites.[11–14] In the case of other two complexes the G values are found to be less than 3.5, indicating an exchange interaction among magnetically inequivalent copper(II) ions in the unit cell, and hence the *g* values obtained in polycrystalline samples will be different from the molecular *g* values.[15] It is also found that for values of R less than 1 the ground state of copper(II) will be either $d_{x^2-y^2}$ or d_{xy}. A d_{z^2} ground state for copper(II) is indicated by values of R greater than 1.[14] From Table 3 it is evident that the ground state of copper(II) in $[Cu(den)en](ClO_4)_2$ is either $d_{x^2-y^2}$ or d_{xy}, which indicates that this five-coordinate complex may have a square-based pyramidal structure. This ground state is supported by the fact that the low-field side of the spectrum is less intense than the high-field side of

Table 1. Analytical data of the mixed-ligand copper(II) complexes

Complex	Colour	M.p. (°C)	Analysis (%)[a] C	H	N
$[Cu(den)en](ClO_4)_2$	Periwinkle-azure	221–227 (dec)	17.2 (16.9)	5.0 (5.0)	16.6 (16.5)
$[Cu(deb)Pn](ClO_4)_2$	Sky-blue	227–234 (dec)	19.6 (19.1)	5.4 (5.3)	16.1 (15.9)
$[Cu(den)tn](ClO_4)_2$	Azure	197–205 (dec)	19.4 (19.1)	5.3 (5.3)	17.6 (16.6)

[a] Calculated values are given in parentheses.

Table 2. IR and electronic spectra of the mixed-ligand copper(II) complexes

Complex	IR (cm^{-1}) Symmetric $\nu(NH_2)$	Asymmetric $\nu(NH_2)$	ν(NH)	$\delta(NH_2)$	ClO_4 ν_3	ν_4	ν(M—N)	Electronic spectra (cm^{-1})
$[Cu(den)en](ClO_4)_2$	3320vs	3270vs, 3235vs	3135vs	1575	1080	625vs	435s	12,500sh, 16,600
$[Cu(den)Pn](ClO_4)_2$	3340vs	3280vs	3150m	1575	1085vsbr	620vs	442m	11,600sh, 12,800 16,100sh
$[Cu(den)tn](ClO_4)_2$	3350vs	3290vs	3170vs	1575	1070vsbr	620vs	485m	11,800sh, 13,800

the spectrum.[8] Since R is greater than 1 in the case of the other two complexes the ground state appears to be d_{z^2}, indicating a compressed trigonal bipyramidal symmetry for these five-coordinate complexes, which is also supported by the fact that the low-field side of the spectrum is more intense than the high-field side of the spectrum.[16]

Solution spectra. The room-temperature spectra of these complexes in DMF and pyridine solutions of four hyperfine lines of copper(II) with a spin-dependent linewidth due to the tumbling motion of the microcrystalline unit in solution.[17] In frozen solutions the ESR spectra consists of four hyperfine lines as parallel features and an unresolved line as

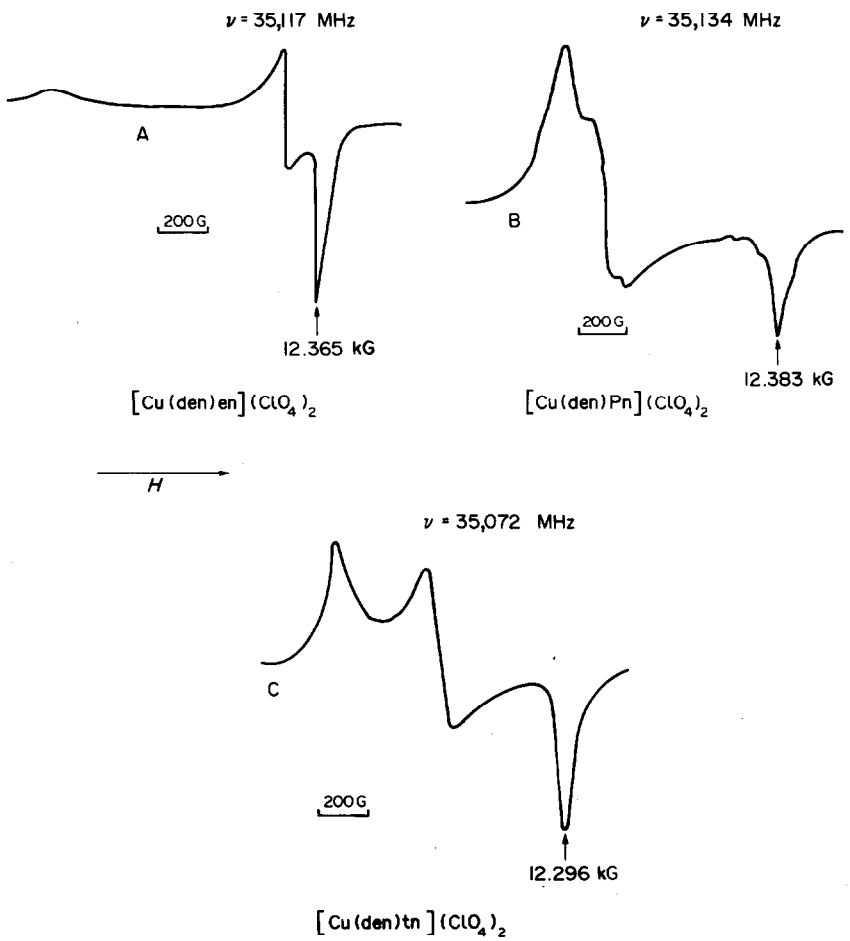

Fig. 1. ESR spectra of the polycrystalline mixed-ligand copper(II) complexes at Q-band (A, B and C) microwave frequencies.

Table 3. g Values of polycrystalline mixed–ligand copper(II) complexes

Complex	g_1	g_2	g_3	G	R	Ground state
$[Cu(den)en](ClO_4)_2$	2.029	2.055	2.209	4.97	0.124	$d_{x^2-y^2}$
$[Cu(den)Pn](ClO_4)_2$	2.027	2.137	2.167	2.03	3.00	d_{z^2}
$[Cu(den)tn](ClO_4)_2$	2.037	2.115	2.159	2.09	1.77	d_{z^2}

the perpendicular feature of the spectrum as shown in Fig. 2. The variation in the hyperfine line intensities of the parallel features of the spectrum can be due to the superposition of the perpendicular features over the parallel features of the spectrum. Low-intensity lines as the parallel features of the spectrum can also be seen which arise most probably due to the presence of a second species with a low population. The g and A values are calculated from the spectra following the usual procedure[18] for the highly populated species, and these values are given in Table 4. It can be seen from Tables 3 and 4 that the g values obtained in the polycrystalline sample of $[Cu(den)en](ClO_4)_2$ are not much different from those in the pyridine solution, indicating that the structure of the chromophore around the solid copper(II) is not disturbed much in pyridine solutions. From Table 4 it is evident that in the case of the DMF solution of $[Cu(den)tn](ClO_4)_2$ the $g_\parallel$ values are smaller and $A_\parallel$ are larger than the corresponding values in the pyridine solution. This is an indication that the solute–solvent interaction in pyridine is greater compared to DMF for the compound $[Cu(den)tn](ClO_4)_2$. The g and A values in both solutions are characteristic of nitrogen coordination.[19] Due to solute–solvent interactions the solvent molecules have probably occupied the sixth coordination position, converting the five-coordinate complexes into six-coordinate ones.

In the presence of axial bonds, $4s$ mixing will be present in the ground state and also the equatorial bonds will be weakened.[20] The σ-bond parameter (α^2) and the fraction of $3d$ character in the $3d$ $4s$ ground state of copper(II) (f^2), which give the strengths of the equatorial and axial bonds, respectively, can be obtained from the following equations:[21]

$$\alpha^2 f^2 = \frac{7}{4}\left[\frac{A_\parallel}{P} - \frac{|A|}{P} + \frac{2}{3}g_\parallel - \frac{5}{21}g_\perp - \frac{6}{7}\right], \quad (1)$$

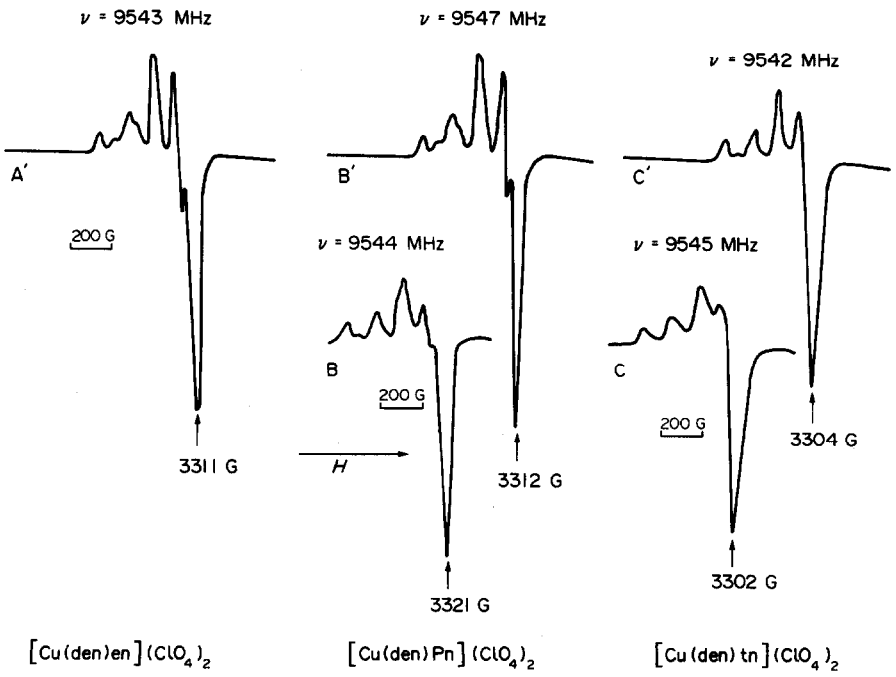

Fig. 2. ESR spectra of the mixed-ligand copper(II) complexes in frozen DMF (B and C) and pyridine (A′, B′ and C′) solutions.

Table 4. Spin-Hamiltonian constants of mixed-ligand copper(II) complexes in DMF and pyridine solutions

Complex	Solvent	g	A ($\times 10^{-4}$ cm^{-1})	$g_\parallel$	$g_\perp$	$A_\parallel$ ($\times 10^{-4}$ cm^{-1})	$A_\perp$ ($\times 10^{-4}$ cm^{-1})
$[Cu(den)en](ClO_4)_2$	Pyridine	2.106	64.7	2.200	2.059	173.9	10.10
$[Cu(den)Pn](ClO_4)_2$	DMF	2.099	64.4	2.190	2.053	176.2	8.6
	Pyridine	2.104	69.5	2.194	2.059	173.3	17.6
$[Cu(den)tn](ClO_4)_2$	DMF	2.103	66.5	2.179	2.065	172.2	13.6
	Pyridine	2.107	78.3	2.194	2.063	170.0	25.8

$$\alpha^2 = \frac{|A|}{PK_o} + \frac{\Delta g}{K_o} + \frac{0.0975(1-f^2)}{PK_o}, \qquad (2)$$

where P is a dipolar term ($2.0023 g_N \beta_e \beta_N \langle r^{-3} \rangle_{av} = 1194$ MHz[22]), and $K_o = 0.43$. In eqn(2) an electron in the 4s orbital has been assigned a value of 0.0975 cm^{-1}.[21,23] The values of α^2 and f^2 for all the complexes are given in Table 5. The value of α^2 in the case of the pyridine solution of $[Cu(den)tn](ClO_4)_2$ is found to be less and its f^2 value more than that of the corresponding values of the other complexes in solutions, indicating strong equatorial and weak axial bonds. On the other hand the α^2 values are more and f^2 values are less in the case of the pyridine solution of $[Cu(den)en](ClO_4)_2$ and the DMF solution of $[Cu(den)Pn](ClO_4)_2$, indicating weak equatorial bonds and strong axial bonds compared to the other cases.

Conclusions

Mixed-ligand copper(II) complexes with general formula $[(Cu(den)L](ClO_4)_2$ have been synthesized, and the IR, electronic and ESR spectral studies of the polycrystalline and solution forms show that:

(a) IR and electronic spectral studies indicate that these mixed-ligand copper(II) complexes are nitrogen-bonded five-coordinate complexes in solid state.

(b) ESR studies of polycrystalline samples indicate that $[Cu(den)en](ClO_4)_2$ has a square-based pyramidal CuN_5 chromophore and the unit cell contains all magnetically equivalent ions, whereas the complexes $[Cu(den)Pn](ClO_4)_2$ and $[Cu(den)tn](ClO_4)_2$ have compressed trigonal bipyramidal CuN_5 chromophores and the unit cell contains magnetically inequivalent ions with a strong exchange interaction among them.

(c) The solute–solvent interaction in the pyridine solutions of all these complexes is found to be more than that of the DMF solutions of these complexes. The chromophore of solid $[Cu(den)en](ClO_4)_2$ is found to be less disturbed in the pyridine solution of this complex. The equatorial bonds of $[Cu(den)tn](ClO_4)_2$ in a pyridine solution is stronger than other complexes in that solution. Except in the above case, in all the other solutions of these complexes, the presence of a 4s orbital in the ground state indicates axial bonds.

Table 5. Bond parameters of mixed-ligand copper(II) complexes

Complex	Solvent	α^2	f^2
$[Cu(den)en](ClO_4)_2$	Pyridine	0.76	0.98
$[Cu(den)Pn](ClO_4)_2$	DMF	0.76	0.98
	Pyridine	0.71	0.997
$[Cu(den)tn](ClO_4)_2$	DMF	0.70	0.997
	Pyridine	0.65	1.000

REFERENCES

1. J. Reedijk, J. C. A. Windhorst, N. H. M. Van Ham and W. L. Groneveld, *Recueil* 1971, **111**, 234.
2. J. Reedijk and J. A. Smith, *Recueil* 1971, **90**, 1135.
3. J. Reedijk, *Recueil* 1971, **90**, 117.
4. B. J. Hathaway, *Coord. Chem. Rev.* 1982, **41**, 423.
5. I. Bertini, D. Gatteschi and A. Scozzafava, *Coord. Chem. Rev.* 1979, **29**, 67.
6. J. Kohout, M. Havastijova and J. Gazo, *Coord. Chem. Rev.* 1978, **27**, 141.
7. D. Reinen and C. Freibel, *Struct. Bonding* 1979, **37**, 1.
8. B. A. Sastry, S. Md. Asadullah, G. Ponticelli and G. Devoto, *J. Mol. Struct.* 1981, **71**, 343.
9. G. Ponticelli, *Inorg. Chimi. Acta* 1971, **5**, 461.
10. F. K. Kneubuhl, *J. Chem. Phys.* 1960, **33**, 1074.
11. I. M. Proctor, B. J. Hathaway and P. Nicholis, *J. Chem. Soc. A* 1968, 1678.
12. M. J. Beu, B. J. Hathaway and R. J. Fereday, *J. Chem. Soc. A* 1972, 1229.
13. A. A. G. Tomlinson and B. J. Hathaway, *J. Chem. Soc. A* 1968, 1905.
14. B. J. Hathaway, *J. Chem. Soc., Dalton Trans.* 1972, 1196.

15. I. M. Procter, B. J. Hathaway and P. G. Hodgson, *J. Inorg. Nucl. Chem.* 1972, **34**, 3689.
16. B. A. Sastry, M. N. Chary, G. Ponticelli and R. Pinna, *J. Mol. Struct.* 1980, **66**, 319.
17. H. M. McConnel, *J. Chem. Phys.* 1956, **25**, 709.
18. B. A. Sastry, S. Md. Asadullah, G. Ponticelli and M. Massacesi, *J. Chem. Phys.* 1979, **70**, 2834.
19. A. A. G. Tomlinson and B. J. Hathaway, *J. Chem. Soc. A* 1985, 1685.
20. R. Barbucci, P. Paoletti and M. J. M. Campbell, *Inorg. Chim. Acta* 1974, **10**, 69.
21. H. A. Kuska, M. T. Rogers and R. E. Drullinger, *J. Phys. Chem.* 1967, **71**, 109.
22. J. A. MacMillan, N. S. Dixson and T. Halpern, *J. Chem. Phys.* 1971, **55**, 452.
23. A. J. Freeman and R. E. Watson, *Phys. Rev.* 1961, **41**, 2027.

Polyhedron Vol. 6, No. 5, pp. 1059–1064, 1987
Printed in Great Britain

0277–5387/87 $3.00+.00

REACTIONS OF PALLADIUM(II) CHLORIDE WITH 1,4 - DIPHENYL - 2,3 - DIMETHYL - 1,4 - DIAZABUTADIENE AND 1,4-DI(*p*-METHOXYPHENYL)-2,3-DIMETHYL-1,4 - DIAZABUTADIENE

M. C. NAVARRO-RANNINGER,* M. J. CAMAZON, A. ALVAREZ-VALDES and J. R. MASAGUER

Departamento de Química Inorgánica, Facultad de Ciencias, Universidad Autónoma de Madrid, 28049 Madrid, Spain

and

S. MARTÍNEZ-CARRERA and S. GARCÍA-BLANCO

Departamento de Rayos X, Consejo Superior de Investigaciones Científicas, Serrano, 119, 28006 Madrid, Spain

(*Received* 24 *March* 1986 ; *accepted after revision* 25 *September* 1986)

Abstract—The reactions of palladium(II) chloride with 1,4 - diphenyl - 2,3 - dimethyl - 1,4 - diazabutadiene and 1,4 - di(*p* - methoxyphenyl) - 2,3 - dimethyl - 1,4 - diazabutadiene are described. With 1,4 - diphenyl - 2,3 - dimethyl - 1,4 - diazabutadiene diimine fission is produced, giving rise to a product identified by elemental analysis, IR and Raman spectra, and X-ray diffraction, as *trans*-dichlorobis(aniline) palladium(II). The complex is soluble in dimethylformamide and crystallizes with two molecules of solvent. The substance crystallizes in the monoclinic space group $P2_1/n$. The X-ray data were refined to $R = 0.047$ and $R_w = 0.046$. Final distances are Pd—N = 2.060(5) Å and Pd—Cl = 2.299(2) Å. There are two bifurcated intermolecular N—H.... Cl and C—H.... Cl hydrogen bonds which, together with one more intermolecular hydrogen bond N—H....O, are responsible for the packing of the molecules. However, when 1,4 - di(*p* - methoxyphenyl) - 2,3 - dimethyl - 1,4 - diazabutadiene was treated with palladium chloride under the same conditions *cis* - dichloro - 1,4 - di(*p* - methoxyphenyl) - 2,3 - dimethyl - 1,4 - diazabutadiene was formed, as deduced from elemental analysis, and IR and Raman spectra.

As a part of our investigation of ligand systems containing N donor atoms we recently reported the synthesis, spectroscopic data and crystal structure of two diimines.[1]

Diimines are bidentate ligands and can coordinate two metallic centers, giving rise to highly interesting compounds.[2] The most likely reaction of these compounds would be, however, the chelation of a single metal ion by the bidentate ligand.[3–5]

The donating capacity of the nitrogen atoms of compounds similar to 1,4 - diphenyl - 2,3 - dimethyl - 1,4 - diazabutadiene can be modified by the presence of *para* substituents on the phenyl ring. These substituents increase the ring charge, favouring the bidentate complex.

In this work the formation of a stable complex of $PdCl_2$ with 1,4 - di(*p* - methoxyphenyl) - 2,3 - dimethyl - 1,4 - diazabutadiene was studied. In the resulting compound the ligand was bidentate. Likewise, we have studied the reaction between 1,4 - diphenyl - 2,3 - dimethyl - 1,4 - diazabutadiene and $PdCl_2$ in a methanol solvent.

* Author to whom correspondence should be addressed.

EXPERIMENTAL

Starting materials

Solvents of commercial quality were purified and dried by standard methods. $PdCl_2$ (Merck, anhydrous) with a minimum Pd of 59% was used without further purification. The ligands 1,4 - diphenyl - 2,3 - dimethyl - 1,4 - diazabutadiene and 1,4 - di(*p* - methoxyphenyl) - 2,3 - dimethyl - 1,4 - diazabutadiene were kindly supplied by Drs J. Plumet and R. Alvarez-Osorio of the Universidad Complutense de Madrid.

Compound preparations

A stoichiometric amount of the diimine (molar ratio 2.3 : 1) was added to a suspension of $PdCl_2$ in MeOH at room temperature. The mixture was stirred for 13 h. The precipitate was then collected by filtration, washed with methanol followed by diethyl ether, and finally vacuum dried at room temperature.

The analytical composition of the product obtained with 1,4 - di(*p* - methoxyphenyl) - 2,3 - dimethyl - 1,4 - diazabutadiene was: C, 45.9; N, 5.9; H, 4.3. Calc. for $PdCl_2(C_{18}N_2O_2H_{20})$: C, 45,4; N, 5.9; H, 4.2%.

For the product obtained from 1,4 - diphenyl - 2,3 - dimethyl - 1,4 - diazabutadiene the composition was: C, 39.7; N, 7.7; H, 4.0. Calc. for $PdCl_2(C_{12}N_2H_{14})$: C, 39.9; N, 7.7; H, 4.0%. The product $PdCl_2(C_{12}N_2H_{14})$ was recrystallized from dimethylformamide for crystallographic structural determination.

Physical methods

Chemical analyses were carried out using standard methods. IR spectra were run in hexachlorobutadiene mulls in the range 4000–1300 cm^{-1} between NaCl windows, and in Nujol mulls in the range 1650–200 cm^{-1} between CsI windows. The Raman spectra were measured with a Jarrell–Ash 25–300 using a Kr^+ laser as a source of excitation.

Crystallography and structure determination

Recrystallization of $PdCl_2(C_{12}N_2H_{14})$ from dimethylformamide produced the compound $PdCl_2(C_{12}N_2H_{14})\cdot 2C_3NOH_7$, whose X-ray structure analysis is reported here. There crystals, light yellow needles, decomposed in air through loss of solvent, and the crystal used for data collection was mounted in a sealed 0.3-mm Lindemann glass capillary tube in the manner commonly used for proteins.[6] One crystal of dimensions $0.10\times0.30\times0.10$ mm^3 was chosen for the preliminary work of orientation, lattice constants, and space group determination, and finally for data collection.

Precise geometric and intensity data were collected at room temperature on an automated four-circle diffractometer (Enraf–Nonius CAD-4), equipped with an Mo X-ray tube and a graphite monochromator ($\lambda = 0.7093$ Å). The unit-cell parameters and orientation of the crystal with respect to the goniometer reference frame were determined by a least-squares fit to the angular positions of 25 reflections. The compound was found to be monoclinic with space group $P2_1/n$. The cell constants were determined (at *ca* 22°C) as: $a = 13.783(3)$ Å, $b = 5.977(5)$ Å, $c = 14.878(4)$ Å; $\beta = 111.87(1)°$, $Z = 2$, $V = 1137.0(9)$ Å^3, $d_x = 1.49$ g cm^{-3}. The data were collected using the θ–2θ scan technique in the range $2\theta(Mo-K_\alpha) \leqslant 60°$. Standard reflections which were periodically remeasured during the course of data collection showed a decline in intensity. Of the 3614 independent data, 2605 with $I > 2\sigma(I)$ were considered to be observed; only these data were used in the subsequent calculations. The usual Lorentz and polarization corrections were applied to the raw data. No absorption correction was applied, however, as the linear absorption coefficient of this compound is small (~ 10.6 cm^{-1} for $Mo-K_\alpha$).

Structure solution and refinement

The structure was solved by the heavy-atom technique. Dimethylformamide molecules were located from a difference Fourier map. The function $\Sigma w(|F_o|-|F_c|)^2$ was minimized, with the weighting scheme $w = 1$. In the calculations of F_c, the neutral atom scattering factors for Pd, Cl, N and C were taken from Ref. 7(a). The effects of the anomalous dispersion of Pd and Cl were included. The values of $\Delta f'$ and $\Delta f''$ were taken from Ref. 7(b). Anisotropic refinement of these atomic positions gave $R = 0.050$ and $R_w = 0.049$. The H atom positions were located from a difference synthesis. Each H atom was assigned the $B_{eq.}$ of the atom to which it was attached and included in all further calculations, but the parameters were not refined. The final cycle gave $R = 0.047$ and $R_w = 0.046$ with 124 variables.

Calculations were carried out with the X-ray system[8] and program PARST[9] on a Univac 1100/80 computer. The maximum residual on a difference map was 1.14 *e* Å^{-3}, near the Pd atom.

Atom positional parameters, observed and calculated structure factors, as well as final anisotropic thermal parameters and coordinates for the H

atoms are listed in supplementary material deposited with the Editor.

Atomic coordinates have also been deposited with the Cambridge Crystallographic Data Centre.

RESULTS AND DISCUSSION

The preparation of $PdCl_2(C_{12}N_2H_{14})$ may proceed by the route given in Scheme 1.

The complex is soluble in dimethylformamide, acetone, slightly soluble in methanol, dichloromethane and cyclohexane, and insoluble in benzene and heptane.

In the case of the *cis* compound, $PdCl_2(C_{18}N_2O_2H_{20})$, the electron-donating characteristics of the methoxy group in the *para* position make the N atom negative. This increases the donating capacity of the N atom with respect to the Pd(II) ion. In this way, the attack of the methanol molecules after forming the complex is avoided and the adduct can be formed. On the other hand, in the absence of the electron-donating methoxy group, the positive charge appearing on the N atom after formation of the complex would give some electrophilic characteristics to be double bond, so that the nucleophilic methanol molecules would attack and split the bond of the azomethine group. The compound formed in this case is insoluble in dichloromethane, cyclohexane and ether, slightly soluble in acetone, and soluble in dimethylformamide. Unfortunately, no crystal suitable for X-ray analysis could be obtained.

IR and Ramana spectra

The IR and Raman spectra are discussed, particularly the metal–halogen and metal–ligand vibrations.

In order to interpret the IR spectra, we have divided these into two groups. From 4000 to 600 cm^{-1} all the bands are ligand bands.

In $PdCl_2(C_{18}N_2O_2H_{20})$ the bands at 2830 cm^{-1} (corresponding to the $-OCH_3$ group and 1632 cm^{-1} (corresponding to the —C=N— group) are shifted *ca* 10 cm^{-1} to lower frequencies with respect to those observed for the free ligand.

The product obtained in the reaction of $PdCl_2$ with 1,4 - diphenyl - 2,3 - dimethyl - 1,4 - diazabutadiene, $PdCl_2(C_{12}N_2H_{14})$, does not show a band corresponding to the —C=N— group, as well as three more bands corresponding to the C—H vibration in $-CH_3$.

Below 600 cm^{-1} the bands correspond to Pd—N and Pd—C vibrations. We attempted to assign the

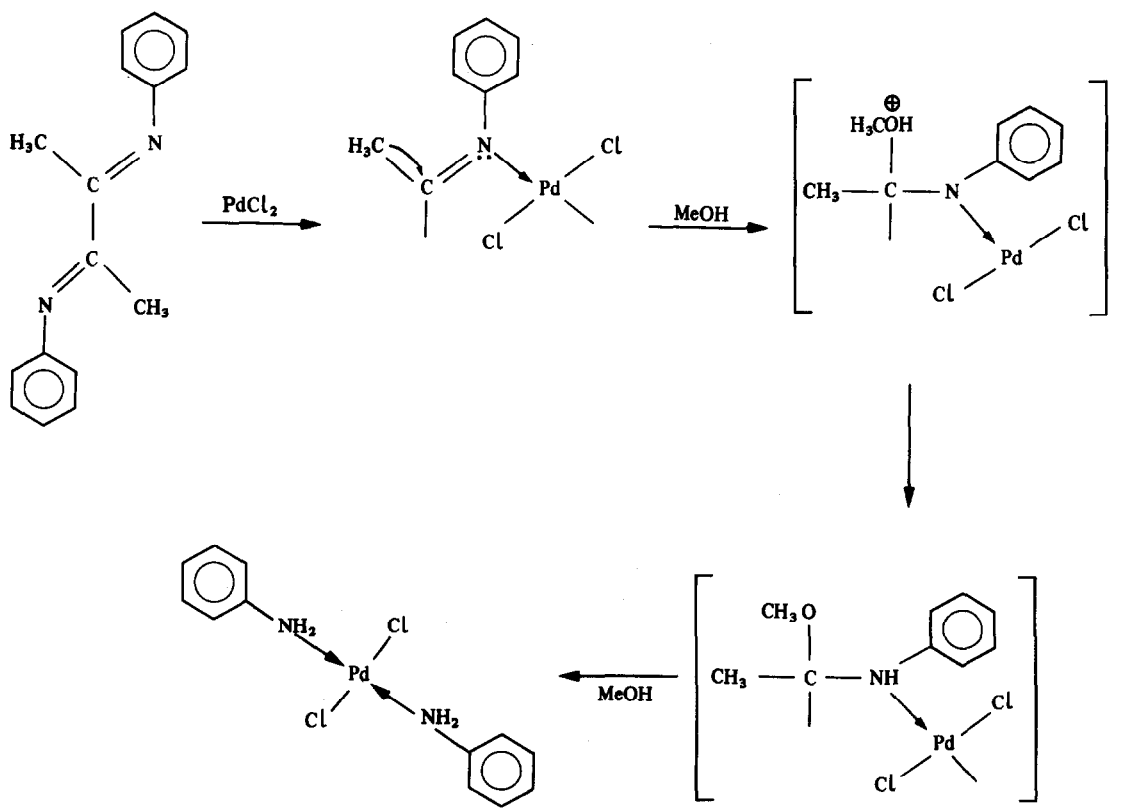

Scheme 1.

bands observed in the IR spectra, taking into account the limitations imposed by the lack of a crystal structure for $PdCl_2(C_{18}N_2O_2H_{20})$.

Structural determination of *cis*- and *trans*-PdL_2Cl_2 or $PdL'Cl_2$ (where L and L' are mono- or bidentate ligands containing N donor atoms), shows that they have a square-planar coordination with bond angles of very nearly 90° about the Pd(II) ion. The selection rules for C_{2v} (*cis*) and D_{4h} (*trans*) symmetry may, therefore, reasonably be expected to apply, i.e. two ν(Pd—N) and two ν(Pd—Cl) IR-active bands for the *cis*-isomer and one of each for the *trans* isomer, and one ν(Pd—N) and one ν(Pd—Cl) Raman-active band in both isomers. The corresponding bending vibrations are expected to occur below 250 cm^{-1}.

The metal–halogen stretching vibrations are the most readily assigned. Often, it is particularly difficult to assign bands to the metal–nitrogen stretching. Although the Pd—N stretching frequency has been extensively investigated, the intensity of this vibration if often very weak and this frequency has not been reported by some authors who studied similar compounds.[10,11] Furthermore, a second difficulty in assigning the Pd—N frequencies arises from the overlap of the fundamental vibrations of the ligands with the Pd—N vibrations of the complex.

In *trans*-diammine dichloro-palladium, it would be expected that two prominent bands would appear in the Raman spectra of the complexes,[12] one near 500 cm^{-1} due to the symmetric metal–nitrogen stretching mode of vibration (B_{2g}) and the other the metal–chlorine symmetric stretching mode (B_{3g}) near 320 cm^{-1}. In the IR spectrum, the metal–nitrogen asymmetric stretching mode (B_{2u}) has a frequency close to that of the Raman-active metal–halogen stretching vibration.

In *cis*-diammine dichloro-palladium, as mentioned previously, two stretching vibrations of each type are expected in the IR spectra (A_1 and B_1 in C_{2v}-symmetry). The antisymmetric stretching vibration is the higher frequency of the two bands observed in the *cis* complexes for both the Pd—N stretching and Pd—X stretching modes.[13] In Raman spectra two vibrations (B_1) are expected.

The wavenumbers of the absorption bands in the far-IR region (600–250 cm^{-1}) are listed in Table 1. A "splitting" is observed in the bands near 300 cm^{-1} in the IR spectrum. The splitting may be due to an intermolecular crystal effect.

The Pd—Cl symmetrical vibration could be responsible for the band at 304 cm^{-1}. This vibration is theoretically Raman-inactive, but could become active as a consequence of certain geometrical distortions in the proximity of the Pd(II). Such distortions have been observed by means of X-ray diffraction in some Pd complexes.[14]

In the IR the broad band at 328 probably includes the ν_s(Pd—Cl).

Description of the structure

The complex consists of monomeric $PdCl_2(C_6H_7N)_2$ units and molecules of dimethylformamide as solvate.

The stereochemistry of the molecules is shown in Fig. 1.

The Pd atom is coordinated in a square-planar fashion to the Cl atoms and the N atoms. The Pd—N(1) and Pd—Cl distances of 2.054(5) and 2.300(2) Å, respectively, are comparable with values found in related complexes.[15–17]

Table 2 shows relevant interatomic distances and bond angles. Dimethylformamide molecules were found to be disordered.

The dihedral angle between the plane of the ring and the square plane around Pd is 109.1(1)°.

Crystal packing and hydrogen bonding

The packing of the molecules is completely determined by the N—H....Cl, C—H....Cl and N—H....O intermolecular hydrogen bonding.

Table 1. IR and Raman (R) assignments in the range 600–200 cm^{-1}

trans-$PdCl_2(C_{12}N_2N_{12})$			*cis*-$PdCl_2(C_{18}N_2O_2H_{20})$		
IR	R	Assignment	IR	R	Assignment
450		B_{3u} [ν_{as}(Pd—N)]	523	541	B_1 [ν_{as}(Pd—N)]
328			328		
		B_{2u} [ν_{as}(Pd—Cl)]		333	B_1 [ν_{as}(Pd—Cl)]
323			323		
	—	B_{3g} [ν_s(Pd—N)]	463		A_1[ν_s(Pd—N)]
	297	B_{2g} [ν_s(Pd—Cl)]		304	A_1 [ν_s(Pd—Cl)]

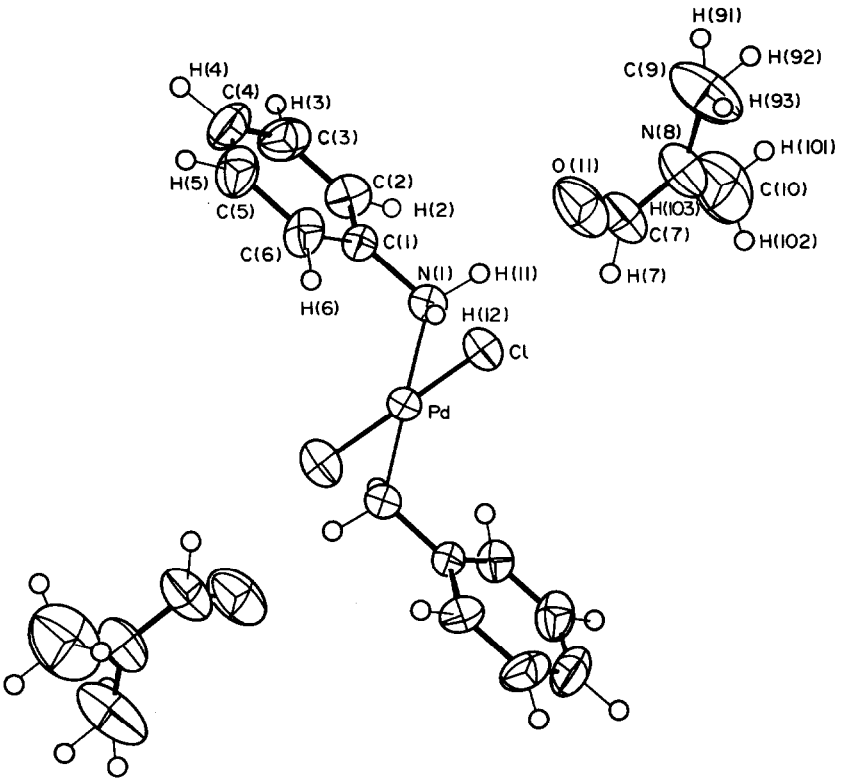

Fig. 1. ORTEP view of the complex showing the numbering scheme used.

Table 2. Intramolecular bond distances (Å) and angles (°) (esds in parentheses)

Pd—Cl	2.300(2)	Cl—Pd—N(1)	90.2(1)
Pd—N(1)	2.054(5)	Cl*—Pd—N(1)	89.8(1)
N(1)—C(1)	1.436(5)	Pd—N(1)—C(1)	113.4(3)
C(1)—C(2)	1.384(8)	N(1)—C(1)—C(2)	119.2(4)
C(2)—C(3)	1.386(7)	C(1)—C(2)—C(3)	119.3(5)
C(3)—C(4)	1.38(1)	C(2)—C(3)—C(4)	120.6(6)
C(4)—C(5)	1.38(1)	C(3)—C(4)—C(5)	119.9(6)
C(5)—C(6)	1.385(8)	C(4)—C(5)—C(6)	120.2(6)
C(6)—C(1)	1.389(7)	C(5)—C(6)—C(1)	119.8(6)
		C(6)—C(1)—N(1)	120.6(4)
	Solvate molecule		
O(11)—C(7)	1.22(1)	O(11)—C(7)—N(8)	125.7(9)
C(7)—N(8)	1.31(1)	C(7)—N(8)—C(9)	121.9(9)
N(8)—C(9)	1.46(1)	C(7)—N(8)—C(10)	122.7(7)
N(8)—C(10)	1.45(1)	C(9)—N(8)—C(10)	115.2(9)

Table 3. Hydrogen bond distances (Å) and angles (°)[a]

Donor (D)—H.... acceptor (A)	D—H	D....A	H....A	D—H....A	
N(1)—H(11)....O(11)	0.999(5)	2.911(8)	1.929(7)	166.7(3)	(0)
N(1)—H(12)....Cl*	0.836(4)	3.332(4)	2.512(2)	167.3(3)	(0)
N(1)—H(12)....Cl	0.836(4)	3.332(4)	2.512(2)	167.3(3)	(1)
C(7)—H(7)....Cl*	1.177(10)	3.480(10)	2.571(2)	132.8(4)	(2)
C(7)—H(7)....Cl	1.177(10)	3.480(10)	2.571(2)	132.8(4)	(3)

[a] Symmetry code: (0) x, y, z; (1) $-x+1, -y+1, -z+1$; (2) $-x+1, -y, -z+1$; and (3) $+x, +y-1, +z$.

There are two bifurcated hydrogen bonds, one involving H(12) which is shared by N(1) and Cl ($+x, +y-1, +z$) and Cl* ($-x+1, -y, -z+1$), and another involving H(7) which is shared by C(7) and Cl (x, y, z) and Cl* ($-x+1, -y+1, -z+1$). Another intermolecular hydrogen bond involves H(11) (see Table 3).

The distances of these hydrogen bonds agree well with the values published for other $PdCl_2$ complexes with ligands containing N donor atoms.[17,18]

Acknowledgements—We thank Professor García Ruano, of the Departamento de Química Organica de la Universidad Autónoma de Madrid, for many useful discussions, the Instituto de Química Inorgánica "Elhuyar" del C.S.I.C., Madrid, for recording the IR spectra, and Dr Fernández Herrero for recording the Raman spectra.

REFERENCES

1. M. C. Navarro-Ranninger, M. A. Hoyos, G. Escobar, J. Plumet, S. Martínez-Carrera and S. García-Blanco, private communication.
2. V. Castellato, P. A. Vigato and M. Vivaldi, *Coord. Chem. Rev.* 1977, **23**, 31.
3. G. R. Newkome, D. K. Kohli, F. R. Fronczek, B. J. Hales, E. E. Case and G. Chiari, *J. Am. Chem. Soc.* 1980, **102**, 7608.
4. R. L. Bodner and D. G. Hendricker, *Inorg. Chem.* 1973, **12**, 33.
5. P. Singh, A. Clearfield and I. Bernal, *J. Coord. Chem.* 1971, **1**, 29.
6. T. L. Blundell and L. N. Johnson, *Protein Crystallography*, *p.* 81. Academic Press, London (1976).
7. *International Tables for X-ray Crystallography*, Vol. 4, Kynoch Press, Birmingham (1974): (a) Table 2.2 A; (b) Table 2.3.1.
8. J. M. Stewart, *The XRAY 76 System.* Technical Report TR-446, Computer Science Center, University of Maryland, College Park, MD (1976).
9. M. Nardelli, *Comput. Chem.* 1983, **7**, 95.
10. B. Crociani, T. Boschi, R. Pietropaolo and U. Belluco, *Inorg. Phys. Theor. J. Chem. Soc.* 1970, **A**, 531.
11. J. Reedijk and J. K. de Rieder, *Inorg. Nucl. Chem. Lett.* 1976, **17**, 585.
12. P. J. Hendra, *Spectrochim. Acta* 1967, **23A**, 1275.
13. C. H. Perry, D. P. Athans, E. F. Young, J. R. Durig and B. R. Mitchell, *Spectrochim. Acta* 1967, **23A**, 1137.
14. K. V. Deuten and G. Klar, *Cryst. Struct. Commun.* 1976, **5**, 387.
15. G. R. Newkome, F. R. Fronczek, V. K. Grupta, W. E. Puckett, D. C. Pantaleo and G. E. Kiefer, *J. Am. Chem. Soc.* 1982, **104**, 1782.
16. J. D. Bell, D. Hall and T. N. Waters, *Acta Cryst.* 1966, **21**, 440.
17. M. C. Navarro-Ranninger, S. Martínez-Carrera and S. García-Blanco, *Acta Cryst.* 1983, **C39**, 186; 188.
18. G. Reck, B. Heyn and H. P. Schröer, *Cryst. Struct. Commun.* 1982, **11**, 179.

Polyhedron Vol. 6, No. 5, pp. 1065–1070, 1987
Printed in Great Britain

0277–5387/87 $3.00+.00

COORDINATION COMPOUNDS OF Pd(II) AND Pt(II) WITH THIODIACETIC ACID

I. A. ZAKHAROVA,* A. P. KURBAKOVA, Z. V. BELYAKOVA

N. S. Kurnakov Institute of General and Inorganic Chemistry, Academy of Sciences of the USSR, Moscow, U.S.S.R.

Kh. I. GASANOV and T. Kh. KURBANOV

Institute of Inorganic and Physical Chemistry of the Azerbaijan Academy of Sciences, Baku, U.S.S.R.

and

G. PONTICELLI

Istituto di Chimica Generale, Inorganica ed Analitica, Università di Cagliari, Via Ospedale 72, 09124 Cagliari, Italy

(*Received* 29 *April* 1986; *accepted after revision* 2 *September* 1986)

Abstract—The coordination compounds of Pd(II) and Pt(II) with thiodiacetic acid $[(H_2L)_2MX_2]$ [$H_2L = S(CH_2COOH)_2$, M = Pd or Pt, X = Cl or Br] were synthesized. Independently of the reaction conditions (aqueous or non-aqueous media) the complexes produced had the same structure. The vibrational spectroscopic data suggested that in the square-planar complexes of Pd(II) and Pt(II) the thiodiacetic acid is coordinated as a monodentate ligand through the sulphur atom and the oxygen atoms do not take part in the coordination to the central metal atom. The palladium complexes contain terminal metal–halogen bonds in the *trans* position but in the platinum complexes the *cis* configuration is more probable.

There is a growing interest in chelate sulphur-containing ligands which can be considered as simple models of biological systems. Studies on the complex formation between metal ions and these ligands can show how the direct synthesis of platinum and palladium complexes with coordination spheres of different stability can be carried out.

Studies on platinum and palladium coordination compounds with chelate ligands containing C—SH and COOH groups (such as cysteine[1–3]) showed that the ligand coordination depended on the reaction conditions.

Thiodiacetic acid is one of the simplest representatives of chelate ligands containing the S-donor functional group.[4] In complex formation thiodiacetic acid can be coordinated to a metal atom: (a) as a monodentate ligand through the sulphur atom or one of the oxygen atoms of the carboxylic group, (b) as a bidentate ligand through the sulphur atom and the oxygen atom of the carboxylic group, or (c) as a terdentate ligand through one sulphur and two oxygen atoms.

A number of thiodiacetic acid complexes with first-row transition metals (V, Cr, Mn, Fe, Co or Ni) are known.[5–6] The behaviour of thiodiacetic acid towards the ions of these metals has been studied in aqueous solution[5] and, according to the potentiometric and spectrophotometric data, the formation of 1:1 and 1:2 (metal: ligand) complexes has been established. Solid 1:1 complexes of type $ML \cdot nH_2O$ (M = Cr, Mn or Co, $n = 1$; M = Ni, $n = 3$) and the 1:2 complex Na_2NiL_2 have been prepared and characterized.[6] In these complexes thiodiacetic acid in the form of the thio-

* Author to whom correspondence should be addressed.

diacetate anion acts as a tridentate ligand, giving solid complexes of pseudo-octahedral symmetry.

The reaction of $K_2[PtCl_4]$ with 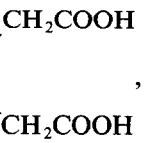 ,

yielding the compound 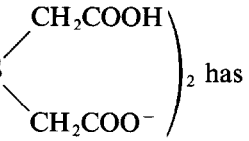 has been described,[7] but the authors did not discuss the structure of this complex and the bonding character of the ligand. Palladium complexes with thiodiacetic acid have never been reported previously.

The present work has involved the synthesis and investigations of IR and Raman spectra of some new Pd(II) and Pt(II) complexes with thiodiacetic acid.

EXPERIMENTAL

Materials

Starting substances for the preparation of Pd(II) and Pt(II) complexes with thiodiacetic acid were synthesized by methods described elsewhere: $S(CH_2COOH)_2$,[8] *trans*-$(C_6H_5CN)_2PdX_2$ (X = Cl or Br),[9] *cis*-$[(C_6H_5CN)_2PtCl_2]$,[10] and $K_2[MX_4]$ (M = Pt or Pd, X = Cl or Br).[11] All other chemicals were of analytical-reagent grade.

Spectra measurements

The IR spectra of the solid starting compounds and of complexes **I–VI** in the form of Nujol and Fluorolube mulls between CsI or KBr plates, or polyethylene windows, were obtained in the range 100–4000 cm^{-1} using a Bruker Fourier Spectrometer "IFS-113V". The Raman spectra of the powders H_2L and Na_2L, and of complexes **I** and **III** were obtained in the range 20–4000 cm^{-1} using a Raman or HG-2S spectrometer with an Ar^+-ion laser excitation at 5145 Å. The laser power varied from 50 to 200 mW.

Preparation of the complexes

All the complexes studied in this work were synthesized as follows.

$[(S(CH_2COOH)_2)_2PdCl_2]$ (**I**). Powdered thiodiacetic acid (0.0905 g, 0.6 mmol) was added to a filtered solution of *trans*-$[C_6H_5CN)_2PdCl_2]$ (0.1156 g, 0.30 mmol) in 15 cm^3 of benzene. The reaction mixture was stirred at room temperature for 3–4 h. The resulting yellow precipitate was filtered, washed in benzene and ethyl ether, and dried in air and *in vacuo*. The yield was 0.1342 g (93%).

$[(S(CH_2COOH)_2)_2PdBr_2]$ (**II**). 0.1418 g (0.94 mmol) of thiodiacetic acid was added to a filtered solution of *trans*-$[C_6H_5CN)_2PdBr_2]$ (0.2232 g, 0.47 mmol) in 15 cm^3 of benzene. The reaction mixture was stirred at room temperature for 3–4 h. The brown precipitate formed in the reaction was filtered, washed in benzene and ethyl ether, and dried *in vacuo*. The yield was 0.2497 g (93%).

$[(S(CH_2COOH)_2)_2PtCl_2]$ (**III**). 0.1281 g (0.27 mmol) of *cis*-$[C_6H_5CN)_2PtCl_2]$ was dissolved in 20 cm^3 of benzene for 2.5 h to complete dissolution and then filtered. 0.0842 g (0.54 mmol) of thiodiacetic acid was added to this solution. The reaction mixture was allowed to stir for 12 h. It was heated to 35–40° every 2 h. The yellow compound thus formed was filtered, washed in benzene and ethyl ether, and dried in air and *in vacuo*. The yield was 0.1228 g (79%).

$[(S(CH_2COOH)_2)_2PdCl_2]$ (**IV**). A solution containing 0.3109 g (0.95 mmol) of $K_2[PdCl_4]$ in 15 cm^3 of water was filtered and mixed with a filtered solution of 0.2859 g (1.90 mmol) of thiodiacetic acid in 10 cm^3 of water. Ten minutes after mixing, the resulting solution became green-yellow. It was evaporated under reduced pressure at 35–40°C, yielding a greenish-brown solid. This solid was dissolved in acetone, giving a potassium chloride precipitate which was filtered. The filtrate was left for slow crystallization and a pale-yellow compound was isolated. The yield was 0.3561 g (78%).

$[(S(CH_2COOH)_2)_2PdBr_2]\cdot 5H_2O$ (**V**). Filtered solutions of 0.5263 g (1.04 mmol) of $K_2[PdBr_4]$ in 15 cm^3 of water and 0.3133 g (2.08 mmol) of thiodiacetic acid in 10 cm^3 of water were mixed together. The colour of the resulting solution was unchanged. The solution was stirred at room temperature for 30 min and then evaporated under reduced pressure, forming a cherry-brown solid. The product was dissolved in acetone and the precipitated potassium bromide was removed by filtration. Slow crystallization of the filtrate gave a pale-brown powder. The yield was 0.5773 g (97%).

$[(S(CH_2COOH)_2)_2PtBr_2]$ (**VI**). A filtered solution of 0.3392 g (2.26 mmol) of thiodiacetic acid in 10 cm^3 of water was added to a filtered solution containing 0.6713 g (1.13 mmol) of $K_2[PtBr_4]$ in 15 cm^3 of water. The resulting solution became dark-red. After stirring and heating to 35–40°C for 5 min it became pale-yellow. The solution was evaporated dry under reduced pressure at 35–40°C. The solid was dissolved in acetone and the precipitated KBr was filtered off. Slow crystallization of the filtrate gave an orange product which was recrystallized from hot acetone. The product isolated after

removal of the solvent was dried in air and *in vacuo*. The yield was 0.4726 g (63%).

RESULTS AND DISCUSSION

Both aqueous and non-aqueous media were used to show the influence of the reaction conditions on the character of the H_2L interaction with Pd(II) and Pt(II) derivatives.

The reactions of *trans*-$[(C_6H_5CN)_2PdX_2]$ (X = Cl or Br) and *cis*-$[(C_6H_5CN)_2PtCl_2]$ with thiodiacetic acid (H_2L) using a 1:2 molar ratio in benzene solution produced the complexes $[(H_2L)_2PdCl_2]$ (**I**); $[(H_2L)_2PdBr_2]$ (**II**) and $[(H_2L)_2PtCl_2]$ (**III**). $[(H_2L)_2PdCl_2]$ (**IV**); $[(H_2L)_2PdBr_2]\cdot 5H_2O$ (**V**) and $[(H_2L)_2PtBr_2]$ (**VI**) were obtained in aqueous media using $K_2[PdX_4]$ (X = Cl or Br) and H_2L as starting compounds. An attempt to obtain a palladium complex containing four molecules of H_2L in the coordination sphere of palladium was not successful. The reaction of H_2L with *trans*-$[(C_6H_5CN)_2PdCl_2]$ in a 4:1 molar ratio only yields the product $[(H_2L)_2PdCl_2]$.

Analytical data for complexes **I–VI** are presented in Table 1.

All these complexes are thin, crystalline, coloured solids readily soluble in water and acetone, and insoluble in chloroform, carbon tetrachloride, ether and benzene.

A thermographic analysis of complexes **I, II, III** and **VI** showed that the complexes decompose before melting when heated in air (heating rate = 10°C min^{-1}). Decomposition of these complexes starts at 120°C for **I** and **III**, and at 170°C for **II** and **VI**, and is followed by endothermal effects.

The molecular weight of $[(H_2L)_2PdCl_2]$ was determined in aqueous solution using reverse ebullioscopy. The molecular weight value found is 480 (calc. 477.61) and suggested a monomeric structure for complex **I**.

The structure of complexes **I–VI** was established using vibrational spectroscopy. Spectra changes on going from the free ligand H_2L to complexes **I–VI** have been examined. The IR spectra of complexes **I** and **IV** and **II** and **V** are similar, showing that the structure of the complexes is the same whatever the method of synthesis.

The type of coordination of thiodiacetic acid to the metal atom was determined from the spectral changes obtained on going from the free ligand to complexes **I–VI**.

In the IR spectrum of H_2L the strong band of the asymmetric stretching vibration of the carboxylic group $\nu_{as}(COOH)$ at 1692 cm^{-1} was observed. The asymmetric stretching vibration of the deprotonated carboxylic group $\nu_{as}(CO_2^-)$ in thiodiacetate anion was found at 1592 cm^{-1} for the thiodiacetic acid sodium salt Na_2L. In the IR spectra of **I–VI** the $\nu_{as}(COOH)$ band at a frequency of about 1700 cm^{-1}, which is the same in H_2L and in complexes **I–VI**. This fact proves that the oxygen atoms of the carboxylic groups do not partake in the coordination with the central metal atom. Table 2 shows $\nu_{as}(COOH)$ as observed in the IR spectra of complexes **I–VI**.

The most pronounced changes in the IR spectra of **I–VI** and Raman spectra of **I** and **III** are observed in the low-frequency region (100–500 cm^{-1}), were metal–ligand and metal–halogen vibrations are manifest. Figures 1 and 2 show IR and Raman spectra in the low-frequency region of the ligand H_2L and of complexes **I** and **III**. In comparison with the free-ligand spectra, two new bands at 308 and 362 cm^{-1}, absent in the IR spectrum, were observed in the Raman spectrum of **I**.

A strong Raman line at 308 cm^{-1} is assigned to

Table 1. Elemental analysis of Pd(II) and Pt(II) complexes with thiodiacetic acid: H_2L = 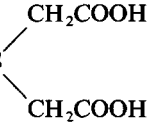

Compound		Yield (%)	M = Pd or Pt(%)		X = Cl or Br (%)		S (%)		C (%)		H (%)	
			Calc.	Found	Calc.	Found	Calc.	Found	Calc.	Found	Calc.	Found
$(H_2L)_2PdCl_2$	(I)	93	22.3	22.3	14.8	14.4	13.4	13.9	20.1	20.6	2.5	2.4
$(H_2L)_2PdBr_2$	(II)	93	18.7	18.3	28.2	28.4	11.3	11.7	17.0	17.6	2.1	2.2
$(H_2L)_2PtCl_2$	(III)	79	34.4	34.2	12.5	12.3	11.3	12.1	17.0	17.6	2.1	2.3
$(H_2L)_2PdCl_2$	(IV)	78	22.2	22.1	14.8	14.5	13.4	13.8	20.1	—	2.5	—
$(H_2L)_2PdBr_2\cdot 5H_2O$	(V)	97	16.2	16.3	24.3	24.5	9.8	9.9	14.6	14.7	3.3	3.5
$(H_2L)_2PtBr_2$	(VI)	63	29.9	30.0	24.3	24.0	9.8	10.0	14.7	—	1.8	—

Table 2. Some characteristic frequencies [ν (cm^{-1})] observed in IR and Raman spectra of thiodiacetic acid and complexes **I–VI**[a]

Compound	Vibration [ν (cm^{-1})]							
	ν_{as}(COOH)		$\nu_{as}(CO_2^-)$		ν(M—X)		ν(M—S)	
	IR	Raman	IR	Raman	IR	Raman	IR	Raman
H_2L ($=S(CH_2COOH)_2$)	1692 s	1640	—	—	—	—	—	—
Na_2L	—	—	1592 s	1630 w,br	—	—	—	—
$(H_2L)_2PdCl_2$ (I)	1698 s	—	—	—	350 m	—	370 m	—
					—	308 s	—	362 w,br
$(H_2L)_2PdBr_2$ (II)	1700 s	—	—	—	253 m		368 m	
$(H_2L)_2PtCl_2$ (III)	1692 s	—	—	—	342 s,br	338 s,br	378 m	373 w,br
							368 m	
$(H_2L)_2PdCl_2$ (IV)	1698 s	—	—	—	350 m	—	370 m	—
$(H_2L)_2PdBr_2 \cdot 5H_2O$ (V)	1700 s	—	—	—	253 m	—	368 m	—
$(H_2L)_2PtBr_2$ (VI)	1697 s	—	—	—	251 m	—	378 m	—
							368 m	

[a] Abbreviations: s, strong; m, medium; w, weak; br, broad.

the symmetric stretching vibration ν_s(PdCl), and the line at 362 cm^{-1} to the symmetric stretching vibration ν_s(PdS). The new bands at 350 and 370 cm^{-1}, observed in the IR spectrum and absent in the Raman spectrum, correspond to the asymmetric stretching vibrations ν_{as}(PdCl) and ν_{as}(PdS) respectively. The assignment is proved by the fact that on replacement of the chlorine atom by bromine, the band ν_{as}(PdCl) at 350 cm^{-1} in the IR spectrum of complex **II** disappears and a new band corresponding to ν_{as}(PdBr) appears at 253 cm^{-1}. The band of the Pd—S stretching vibration remains at 368 cm^{-1}.

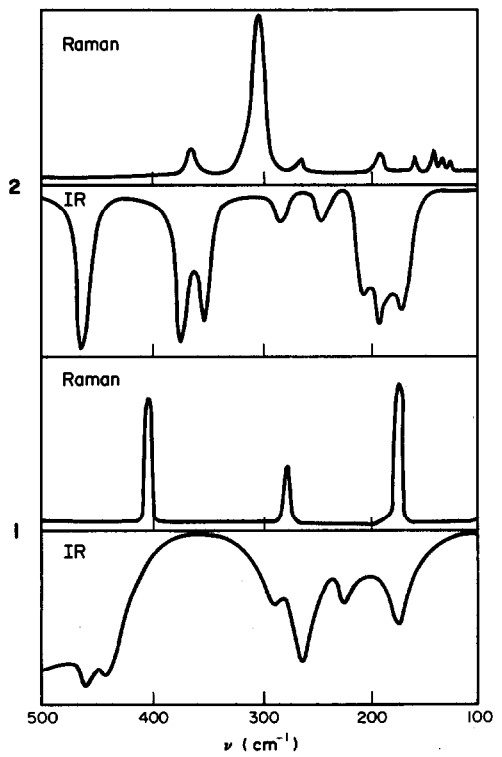

Fig. 1. Vibrational spectra of thiodiacetic acid (H_2L) (**1**) and of the complex $[(H_2L)_2PdCl_2]$ (**2**).

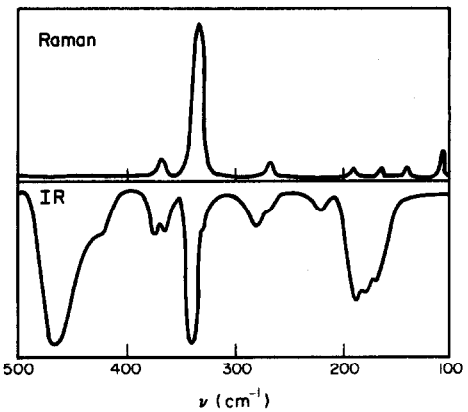

Fig. 2. Vibrational spectra of the complex $[(H_2L)_2PtCl_2]$.

A comparison between IR and Raman spectral data solves the problem of geometric isometry for complex **I**. In the case of the *trans* configuration of metal–halogen bonds in square-planar complexes of type $[ML_2Cl_2]$(D_{2h}-symmetry), the symmetric metal–halogen vibration must appear only in the

Raman spectrum and is forbidden in the IR spectrum. On the other hand, the asymmetric metal–halogen vibration must be present only in the IR spectrum and is forbidden in the Raman spectrum (mutual exclusion rule). In the case of the *cis* configuration, moreover, the complexes $[ML_2Cl_2]$ have C_{2v}-symmetry and the metal–halogen vibrations are active both in the IR and in the Raman spectrum. The same is true for metal–sulphur vibrations. As follows from the data given in Table 2 and Fig. 1, complex **I** contains terminal metal–halogen bonds located in the *trans* position with respect to each other.

We have no Raman data for complex **II**, but its IR spectrum contains only one Pd—Br and only one Pd—S stretching band, from which we can conclude that this complex also shows a *trans* configuration.

In the case of the platinum complexes the situation is more difficult. Both in the IR spectrum of **III** and in the Raman spectrum only Pt—Cl stretching vibrations were found (Fig. 2). But the frequency of the strong Raman line at 338 cm^{-1} is near the strong IR band at 342 cm^{-1}. Due to the presence of the heavy Pt central atom, the separation distance between symmetric and asymmetric Pt—Cl vibrations is small.[11] We cannot be sure whether the second band is absent or present in the spectrum, because the bands are superimposed. The Pt—S stretching vibrations appear as the doublet 368/378 cm^{-1} in the IR spectrum. In consideration of this fact and also of the method of the synthesis of complex **III** from *cis*-$[Pt(C_6N_5CN)_2Cl_2]$ the *cis*-configuration seems to be more probable.

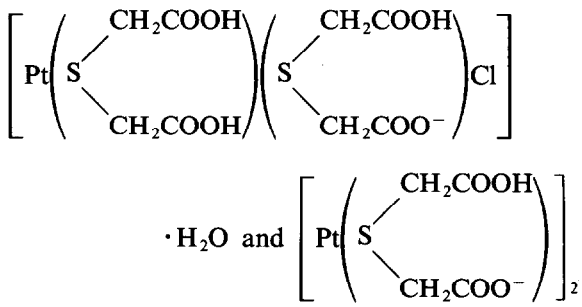

The *cis* configuration is also confirmed by the synthesis of the *cis* complexes when we used **III** as a starting compound (data to be published).

The IR spectrum of the complex **VI** is similar to the spectrum of **III**. The assignment of M—X (M = Pd or Pt, X = Cl or Br) and M—S (M = Pd or Pt) stretching vibrations proposed by us are in good agreement with literature data[12–15] for the related Pd(II) and Pt(II) complexes.

Thus, from the available spectral data we can conclude that, in the square-planar complexes **I–VI**, thiodiacetic acid is coordinated as a monodentate ligand through the sulphur atom and that chelate formation does not occur. This way of thiodiacetic acid coordination was unknown before.

It was interesting to compare the stability of the coordination sphere for the complexes $[(H_2L)_2MX_2]$ (M = Pd or Pt, X = Cl or Br) with that for triphenylphosphine (PPh_3) complexes. For this purpose the reaction of $[(H_2L)_2PdBr_2]$ (**II**) with PPh_3 was carried out. The aqueous solution of $[(H_2L)_2PdBr_2]$ (0.49 mmol) was stirred with the solution of PPh_3 (0.98 mmol) in ethyl alcohol and complex **VII** was produced. The yield was 81.62%.

In the IR spectrum of complex **VII**, the bands corresponding to the vibrations of thiodiacetic acid disappear and instead new bands due to the vibrations of the PPh_3 fragment of the emerging compound appear. The IR spectrum of complex **VII** in the region 400–4000 cm^{-1} is similar to that for *trans*-$[(PPh_3)_2PdCl_2]$. The band of the stretching Pd—Br vibration at 253 cm^{-1} remains in the IR spectrum of **VII**. All these results prove that PPh_3 replaces thiodiacetic acid in the inner coordination sphere yielding the complex *trans*-$[(PPh_3)_2PdBr_2]$, in agreement with the electron acceptor ability of neutral ligands.[16]

Thus, we have synthesized the unknown coordination compounds of Pd(II) and Pt(II) with thiodiacetic acid $[(H_2L)_2MX_2]$ (where H_2L =

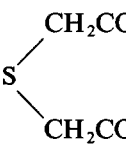

, M = Pd or Pt, X = Cl or Br).

Independently of the reaction conditions (aqueous or non-aqueous media) the complexes produced are of the same structure. From the vibrational spectroscopy data we can conclude that in the above-mentioned square-planar complexes of Pd(II) and Pt(II) the thiodiacetic acid is coordinated as a monodentate ligand through the sulphur atom, and the oxygen atoms of the carboxylic groups do not take part in the coordination to the central metal atom. The palladium complexes **I**, **II**, **IV** and **V** contain metal–halogen bonds in the *trans* position. For the platinum complexes **III** and **VI** the *cis* configuration seems to be more probable.

REFERENCES

1. L. M. Volshtein and L. F. Krilova, *Zh. Neorg. Khim.* 1976, **21**, 2250.
2. W. Levason, C. A. McAuliffe and D. M. Johns, *Inorg. Nucl. Chem. Lett.* 1977, **13**, 123.
3. H. Sigel, Ed., *Metal Ions in Biological Systems*, Vol.

9, *Aminoacids and Derivatives as Ambivalent Ligands.* Marcel Dekker, New York (1979).
4. S. Paul, *Acta Cryst.* 1967, **23**, 490.
5. J. Podlaha and J. Podlahova, *Inorg. Chim. Acta* 1970, **4**, 521.
6. J. Podlaha and J. Podlahova, *Inorg. Chim. Acta* 1970, **4**, 549.
7. L. Ramberg, *Z. Anorg. Chem.* 1906, **50**, 439.
8. D. G. Danielyan, N. V. Tsirulnicova and V. Ja. Temkina, *Tr. IREA* 1984, **46**, 1.
9. F. R. Hartley, *The Chemistry of Platinum and Palladium.* Applied Science Publications, Barking, U.K. (1973).
10. I. I. Chernyaev, Ed., *The Synthesis of Complex Compounds of Platinum Group Metals.* Nauka, Moscow (1964).
11. C. James, L.Lock and M. Zvagulis, *Inorg. Chem.* 1981, **20**, 1817.
12. J. R. Durig, R. Layton, D. W. Sink and B. R. Mitchell, *Spectrochim. Acta* 1965, **21**, 1367.
13. R. Roy, S. H. Mondal and K. Nag, *J. Chem. Soc., Dalton Trans.* 1983, 1935.
14. U. A. Jayasoriya and D. W. Powell, *Inorg. Chem.* 1982, **21**, 1054.
15. R. J. H. Clark, G. Natile, U. Belluco, L. Cattalini and C. Filippin, *J. Chem. Soc. A* 1970, 659.
16. V. I. Nefedov, *Structure of Molecules and Chemical Bond*, Vol. 1, p. 115. Viniti, Moscow (1973).

Polyhedron Vol. 6, No. 5, pp. 1071–1074, 1987
Printed in Great Britain

0277–5387/87 $3.00+.00

VISIBLE ABSORPTION SPECTRAL MEASUREMENTS OF THE FORMATION OF THE COBALT PORPHYRIN DIOXYGEN COMPLEX USING A HIGH-PRESSURE CELL

KIAKI FUSE, TOSHIHIRO GOTO, KOICHI HASEGAWA, TAIRA IMAMURA* and MASATOSHI FUJIMOTO*

Department of Chemistry II, Faculty of Science Hokkaido University, Sapporo 060, Japan

(*Received* 17 *June* 1986 ; *accepted* 25 *September* 1986)

Abstract—The 1:1 complex formation between dioxygen and the *meso*-tetraphenylporphinatocobalt(II)pyridine complex in toluene was followed spectrophotometrically using a high-pressure cell. The values of the equilibrium constant K_p obtained are 0.0278, 0.0513, 0.0840, 0.157 and 0.278 atm^{-1} at −30, −36, −42, −48 and −54°C, respectively. The thermodynamic data are $\Delta H^{\ominus} = -10.1 \pm 0.6$ kcal mol^{-1} and $\Delta S^{\ominus} = -49 \pm 3$ eu at a standard pressure of 1 atm.

Studies of the reactions of metal complexes with molecular gases, O_2, N_2, CO_2 etc., are very interesting in relation to reactions such as oxygenation reactions, nitrogen fixation, and C_1 chemistry.

However, the gas adducts expected in the initial stages of the reactions are usually unstable or at very low concentration at room temperature, which causes difficulty in the characterization of those adducts. The concentrations of gas adducts are expected to be increased under the reaction conditions of high gas pressure and low temperature. In the present study a high-pressure cell was made for the trial and applied to the visible spectral measurements of the 1:1 complex formation between dioxygen and the *meso*-tetraphenylporphinatocobalt(II)pyridine complex, py·Co(II)TPP, in toluene.

EXPERIMENTAL

Co(II)TPP was synthesized by the literature method[1] and purified using a Soxhlet extractor. The complex was crystallized from the extracted ether solution and stored in a Schlenk tube under argon. Toluene, purified by successive treatments with H_2SO_4, H_2O, 5% NaOH and H_2O, and dried with $CaCl_2$ and 4A molecular sieves,[2] was distilled under argon before use. The volumes of the toluene solutions at low temperatures were corrected by extrapolations of the density–temperature linear relation obtained from the data[2] at 10, 20, 25 and 30°C to the low-temperature region. Pyridine was dried with 4A molecular sieves and distilled under argon. Absorption spectra were recorded on a Hitachi 808 spectrophotometer equipped with double-beam double monochromators.

The high-pressure cell (stainless steel, SUS 304)† with two optical windows was designed to measure the visible spectra of the solutions under a 150-atm pressure at low temperatures (> −80°C). The high-pressure cell system is illustrated schematically in Fig. 1. The Almax 1 glasses (Hoya glass works), usually used for adjustment of water level of a boiler, were used for the optical windows (33 mm in diameter × 16 mm thick) which withstand a 250 kg cm^{-2} (242 atm) high pressure. The transmittance of the glass were 27, 82 and 86% at 350, 400 and 450 nm, respectively. This tough window glass was used to avoid a sudden burst at high pressure.‡ The cell was dipped in a Dewar vessel (150-mm i.d.), with two optical windows (Pyrex), which is filled with dry ice–ethanol (4 l) as the cold source. Cloth bags containing dry ice were hung in the Dewar vessel from the edge of the vessel for the measure-

* Authors to whom correspondence should be addressed.

† Stainless steels such as SUS 410 which has a lower thermal expansion coefficient than SUS 304 must be of more practical use for avoiding gas leakage from the apparatus at low temperatures.

‡ Bengelsdijk and Drago[3] who measured the oxygenation reaction of Co(II)(PIXDME) using a similar high-pressure cell, have advised that the apparatus must be well-shielded and the oxygen pressure must never be increased rapidly.

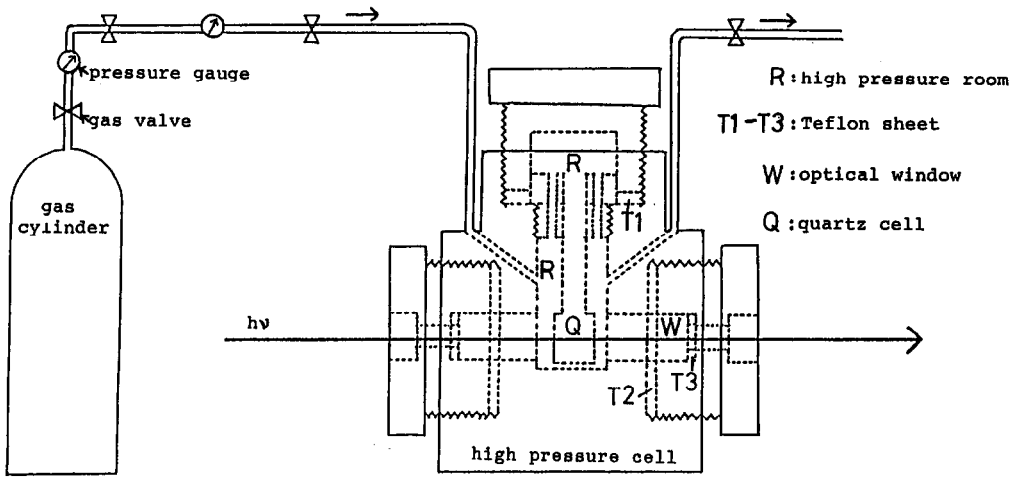

Fig. 1. Schematic diagram of the high-pressure cell system.

ments at −72°C. If dry ice was on the bottom of the vessel, many small bubbles from the dry ice interfered with the spectrophotometric measurements. When the spectral measurements were performed in the range of −72 to 0°C, the cold source of the bath was heated to an appropriate temperature. The bath was agitated continuously to maintain a constant temperature without a local temperature gradient. The high-pressure cell was connected to an oxygen cylinder with tubings (4-mm o.d.) through the pressure gauge [0–150 kg cm^{-2} (YR-506-2, Yamato Sangyo Co.)]. The valves (250K-1/4, CARP-316) for purging and stopping the oxygen gas were supplied by Fujikinzoku Kogyo. The temperature of the bath was monitored continuously using a copper–constantan thermocouple which was dipped in the middle portion of the Dewar vessel.

Measurements of the spectral changes using the high-pressure cell were performed as follows. Toluene was degassed by several freeze–pump–thaw cycles before the preparations of sample solutions in a glove bag filled with 1-atm pure dioxygen gas (>99.9% Nippon Sanso). The sample solutions containing Co(II)TPP and 1% (v/v) pyridine were prepared as quickly as possible to avoid any oxidation of the cobalt porphyrin before the measurements of the oxygenation reaction. The optical cuvette (10-mm path length) containing the sample solution was set up in the high-pressure cell, through which was passed dioxygen gas from a gas cylinder through tubings during the setting of the cuvette. It took about 1 h to equilibrate the reaction of the sample solution at a given pressure and temperature, and it needed about 2 h to measure a spectrum.

RESULTS AND DISCUSSION

Spectral measurements

Absorption spectrum of Co(II)TPP in toluene at −72°C has bands at 412 and 526 nm, and these bands shift to 410 and 535 nm when the solution contains 1% (v/v) (0.124 M) pyridine. This spectral change is due to the formation of a 1 : 1 pyridine adduct.[4] The equilibrium constants K_1 and the thermodynamic data have been reported to be $K_1 = 759$ M^{-1}† for py·Co(II)TPP and $K_1 = 485 \pm 29$ M^{-1}, $\Delta H^{\ominus} = -8.5$ kcal mol^{-1} and $\Delta S^{\ominus} = -16$ eu (cal mol^{-1} deg^{-1}) for py·Co(II)(*p*-CH_3)TPP[4] in toluene at 25°C. From these data, almost all (≃ 100%) the Co(II)TPP in 1% (v/v) pyridine–toluene was estimated to be the 1 : 1 pyridine adduct at lower temperatures than 0°C. The equilibrium constant K_2 for the 2 : 1 complex is much smaller than 1.[4] When oxygen gas was introduced into the sample solution at −72°C, the absorption spectrum showed new bands due to py·CoTPP·O_2 at 422 and 546 nm. The absorbance at 410 nm due to py·Co(II)TPP decreased with increasing oxygen pressure. The bands due to the pyridine adduct were recovered at −72°C when the solution was deoxygenated by freeze–pump–thaw cycles. If it takes a long time for the deoxygenation, the absorbance at 410 nm recovered is a little lower than that of the original solution, indicating the oxidation of a small amount of Co(II) porphyrin complex to the Co(III) complex.

The spectral changes in the visible region with

† Calculated from other data.[5]

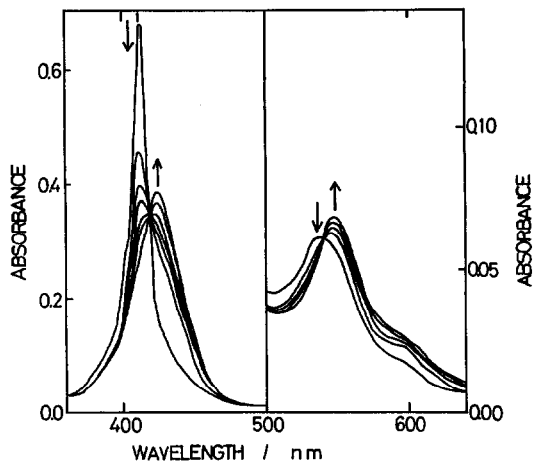

Fig. 2. Visible spectral changes accompanied by oxygen uptake at −40°C. First and final traces are the spectra at 1 and 60 atm, respectively.

increasing dioxygen pressure at −40°C are shown in Fig. 2. The absorbances at 410 and 535 nm due to py·Co(II)TPP decreased with a concomitant increase in the absorbances at 422 and 546 nm. More than 80% of complex is converted to the dioxygen adduct at 60 atm. This spectral changes showed isosbestic points. The diminution of the oxygen pressure from 60 to 1 atm caused the inverse spectral change, i.e. the absorbances at 422 and 546 nm decreased due to the deoxygenation reaction.

ESR spectra. The complex py·Co(II)TPP in toluene at −72°C shows an ESR spectrum ($g = 2.36$) analogous to the spectrum of B·Co(II)(p-OCH_3)TPP.[6] The signal height decreased on exposure to oxygen gas with the simultaneous appearance of a new spectrum at $g = 2.01$. The latter spectrum is similar to the spectrum of the dioxygen complex of the cobalt(II) protoporphyrin 1X-dimethyl ester.[7]

Thermodynamic data

For a general equilibrium reaction (1):

$$M + nL \rightleftharpoons ML_n \quad (K), \qquad (1)$$

if L has no absorption, the absorbance change can be expressed by $\log \{(A-A_0)/(A_\infty-A)\} = n \log [L] + \log K$, where A is the absorbance of the reaction system at a given wavelength, A_0 the absorbance due to the initial complex when [L] = 0, and A_∞ the limiting absorbance due to pure ML_n. The equation shows that n and $\log K$, respectively, can be evaluated from the slope and intercept of the linear plots, $\log \{(A-A_0)/(A_\infty-A)\}$ vs $\log [L]$, at a given temperature. In the following reaction (2):

$$py \cdot CoP + O_2 \rightleftharpoons py \cdot CoP \cdot O_2 \quad (K_p), \qquad (2)$$

A_0 and A_∞ are the absorbances of py·Co(II)TPP and py·CoTPP·O_2, respectively, and [L] can be expressed by pO_2, the equilibrium partial pressure of dioxygen. When A_∞ could not be obtained for a relatively high temperature system, e.g. at −30°C, the molar absorptivity of the dioxygen adduct evaluated at −72°C was used to determine the limiting absorbance. The absorbances for the plots were measured at 5–10 different pressures within the 10–90-atm range. The slope n obtained from the least-square plots fell in the range 0.96–1.03. The equilibrium constants obtained from the intercepts are summarized in Table 1, indicating a large dependence of the equilibrium constant K_p on the temperature. Thermodynamic data, $\Delta H^\ominus = -10.1 \pm 0.6$ kcal mol^{-1} and $\Delta S^\ominus = -49 \pm 3$ eu,† determined from the slope and the intercept of the van't Hoff plots (Fig. 3)

Table 1. Equilibrium constants and thermodynamic data for reversible O_2 binding to tetraphenylporphinatocobalt(II)pyridine in 1% (v/v) pyridine–toluene solution

Temperature (°C)	K_p (atm^{-1})	ln K_p
−30	2.78×10^{-2}	−3.58
−36	5.13×10^{-2}	−2.97
−42	8.40×10^{-2}	−2.48
−48	1.57×10^{-1}	−1.85
−54	2.78×10^{-1}	−1.28

$\Delta H^\ominus = -10.1 \pm 0.6$ kcal mol^{-1}
$\Delta S^\ominus = -49 \pm 3$ eu at standard pressure of 1 atm

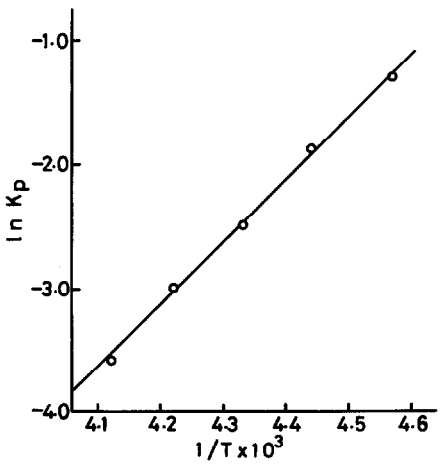

Fig. 3. van't Hoff plot for the oxygenation reaction of py·Co(II)TPP.

† Standard pressure is 1 atm. To convert to a standard pressure of 1 torr the quantity R ln 760 must be subtracted from this value. $\Delta S^\ominus = -62$ eu at a standard pressure of 1 torr.

do not differ significantly from the values of the cobalt(II) protoporphyrin 1X-dimethyl ester system[8,9] and cobalt(II) tetra(*p*-methoxyphenyl)porphyrin.[6] If the thermodynamic data, $\Delta H^{\ominus}$ and $\Delta S^{\ominus}$, are extrapolated back to 25°C, the value of K_p is estimated to be 5.8×10^{-4} atm^{-1}, i.e. almost all the cobalt complexes exist as deoxygenated complexes at 1-atm dioxygen pressure. The K_p value for the system at −72°C is estimated to be 2.2 atm^{-1}, indicating at least 68% of cobalt(II). tetraphenylporphyrin exists as the dioxygen adduct at 1-atm pressure. Thus the equilibrium constants and the thermodynamic data of the 1 : 1 complex between dioxygen and α,β,γ,δ - *meso* - tetraphenylporphinatocobalt(II) in toluene were evaluated successfully by spectral methods using the high-pressure cell. We think the high-pressure cell is useful for spectrophotometric measurements of gas-participating reactions.

Acknowledgement—We thank Mr M. Kohiyama in the workshop of the Faculty of Science for his technical assistance.

REFERENCES

1. P. Rothemund and A. R. Menotti, *J. Am. Chem. Soc.* 1948, **70**, 1808.
2. J. A. Riddick and W. B. Bunger, Eds, *Organic Solvents*, Vol. 2. Wiley, New York (1970).
3. T. J. Beugelsdijk and R. S. Drago, *J. Am. Chem. Soc.* 1975, **97**, 6466.
4. F. A. Walker, *J. Am. Chem. Soc.* 1973, **95**, 1150.
5. F. A. Walker, D. Berioiz and K. M. Kadish, *J. Am. Chem. Soc.* 1976, **98**, 3484.
6. F. A. Walker, *J. Am. Chem. Soc.* 1973, **95**, 1154.
7. H. C. Stynes and J. A. Ibers, *J. Am. Chem. Soc.* 1972, **94**, 5125.
8. D. V. Stynes, H. C. Stynes, B. R. James and J. A. Ibers, *J. Am. Chem. Soc.* 1973, **95**, 1796.
9. J. A. Ibers, D. V. Stynes, H. C. Stynes and B. R. James, *J. Am. Chem. Soc.* 1974, **96**, 1358.

Polyhedron Vol. 6, No. 5, pp. 1075–1080, 1987
Printed in Great Britain

0277–5387/87 $3.00+.00

TRANSITION-METAL COMPLEXES OF HYDRAZONES DERIVED FROM 1,4-DIFORMYL- AND 1,4-DIACETYLBENZENES

JANINE A. ANTEN and DAVID NICHOLLS*

Donnan Laboratories, The University, Liverpool L69 3BX, U.K.

JOHN M. MARKOPOULOS

Department of Chemistry, University of Athens, Greece

and

OLGA MARKOPOULOU

Department of Chemistry, National Technical University, Athens, Greece

(*Received* 22 *August* 1986; *accepted* 25 *September* 1986)

Abstract—The new ligands 1,4-diformylbenzene bishydrazone (DFBH) and 1,4-diacetylbenzene bishydrazone (DABH) have been prepared. DFBH forms complexes with transition metal(II) ions of types MX_2(DFBH) (M = Co, Ni, Mn, Zn or Cd, X = Cl; M = Co or Ni, X = SCN; M = Ni, X = Br) and $MX_2(DFBH)_2$ (M = Co, Ni, Mn, Zn, Cd or Hg, X = Cl; M = Ni or Mn, X = Br). DABH forms complexes of types $MX_2(DABH)_2$ (M = Co, Ni or Zn, X = Cl or Br; M = Co or Ni, X = Cl, Br or SCN) and $MX_2(DABH)_3$ (M = Co, X = Br or SCN; N = Ni X = Cl or SCN; M = Zn, X = Cl, Br or SCN). Electronic spectra, magnetic moments and IR spectra have been used to deduce probable structures of the complexes. All contain six co-ordinated metals in high-spin configurations except $ZnCl_2$(DFBH) and possibly $CdCl_2$(DFBH) which are tetrahedral. The reactions between cobalt(II) halides and DABH in acetone yield the tetrahedral complexes CoX_2(DABAZ), where DABAZ = the acetone azine of 1,4-diacetylbenzene hydrazone.

In order to use bishydrazones as chelating agents we have in recent years characterized complexes of the bishydrazones of 1,2-dicarbonyl compounds. Thus tetrahedral chelates are obtained from diacetylbisdimethylhydrazone[1] and diacetyl bismonomethylhydrazone[2] with several transition metal (II) ions while the bishydrazone of diacetyl forms octahedral chelates.[2] The resemblance between complexes of dimethylhydrazine [giving, for example,[3] tetrahedral $CoCl_2(Me_2NNH_2)_2$] and of hydrazine [giving[3] octahedral $CoCl_2(N_2H_4)_6$] with these bishydrazone complexes leads us to suspect that steric factors are largely responsible for the different co-ordination numbers. In contrast with the chelating bishydrazones, the bishydrazone of benzil forms pseudo-octahedral complexes, e.g.[4] $CoCl_2(PhC:NNH_2C:NNH_2Ph)_2$ which are probably polymeric with bidentate *N*-methine co-ordination of the ligand. All of these ligands contain the —N=C—C=N— grouping which is the characteristic group of some of the best known chelating agents, e.g. dimethylglyoxime, 2,2′-bipyridyl and 1,10-phenanthroline. The co-ordination chemistry of bishydrazones of 1,3-dicarbonyl compounds has not been studied because the reaction between these diketones and hydrazines leads to cyclization and the formation of pyrazoles. By increasing the carbonyl group separation, however, the bishydrazones can once again be obtained. In this paper we report on the ligands formed by reaction between hydrazine and 1,4-diformyl- and 1,4-diacetyl benzenes, i.e. DFBH (**1**) and DABH (**2**).

* Author to whom correspondence should be addressed.

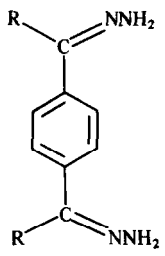

1 R = H
2 R = CH_3

EXPERIMENTAL

Experimental techniques were as described previously[5] except that reflectance spectra were measured on a Perkin–Elmer 330 instrument over the range 40,000–6,6000 cm^{-1}. The anhydrous metal halides of cobalt, nickel and manganese were prepared by dehydration of the hydrated salts at 100°C *in vacuo*. The ligands 1,4-diformylbenzene bishydrazone (DFBH) and 1,4-diacetylbenzene bishydrazone (DABH) were prepared, by heating under reflux for 4 h, a mixture of the diketone (10 g) in absolute ethanol (250 cm^3) with an excess of hydrazine hydrate (25 cm^3). The bishydrazones crystallized on cooling to room temperature. Their analytical data are presented in Tables 1 and 2, and some of their IR bands in Table 4. DFBH was soluble in hot ethanol from which it could be recrystallized; DABH however had a very low solubility in ethanol but was more soluble in hot methanol. The ligands were further characterized by their melting points (DFBH, m.p. 157±1°C; DABH, m.p. 176±1°C) and NMR spectra in dimethylsulphoxide-d_6. [DFBH showed singlets at 6.85 ppm (NH_2 protons), 7.53 ppm (C_6H_4 protons) and 7.80 ppm (CH protons) from TMS with relative intensities 4:4:2; DABH showed singlets at 2.03 ppm (CH_3), 6.35 ppm (NH_2) and 7.63 ppm (C_6H_4) with relative intensities 6:4:4].

The preparation of complexes of DFBH was straightforward. The anhydrous metal salt and the ligand were dissolved in hot absolute ethanol, the solutions mixed and the mixture heated under reflux for 15 min. The mixture was filtered hot and the precipitate washed with hot ethanol and ether before being dried *in vacuo*. All reactions were carried out using reaction ratios of 4:1 and 1:4 (metal salt:ligand). For complexes of DABH, however, the low solubility of the ligand necessitated the use of a soxhlet apparatus. The metal salt was dissolved in methanol (which was a better solvent for DABH than ethanol) and the ligand contained in the thimble of a soxhlet extractor was continually extracted with hot methanol for several hours so that the extracts ran into the metal salt solution. For nickel and zinc complexes, precipitation occurred in the hot while the cobalt-containing solutions had to be cooled somewhat to achieve precipitation. The complexes were isolated as before.

The best solvent for DABH was acetone. Consequently, $CoCl_2$ (0.35 g, 2.7×10^3 mol) dissolved in hot acetone (25 cm^3) was added to DABH (2.05 g, 11×10^{-3} mol) dissolved in acetone (100 cm^2) and the mixture heated under reflux for 30 min. Upon cooling, a dark green precipitate formed; this was filtered off, washed with acetone and ether, and dried *in vacuo*. A similar reaction with $CoBr_2$ gave a dark blue-green precipitate but no compound precipitated when $Co(SCN)_2$ was used. Analytical data on these compounds were as follows. $CoCl_2$ complex—Found: C, 46.6; H, 5.44; N, 12.7. $CoCl_2C_6H_{22}N_4$ requires: C, 48.0; H, 5.55; N, 14.0%. $CoBr_2$ complex—Found: C, 39.4; H, 4.53; N, 10.9. $CoBr_2C_{16}H_{22}N_4$ requires: C, 39.3; H, 4.54; N, 11.5%.

RESULTS AND DISCUSSION

The addition–elimination reactions between hydrazine and 1,4-diformylbenzene and 1,4-diacetylbenzene produce the new ligands DFBH and DABH respectively, as crystalline solids. These have low solubilities in non-co-ordinating solvents but complexes have been prepared using hot ethanol as solvent for DFBH and hot methanol for DABH.

Complexes of DFBH have been prepared from Co(II), Ni(II), Mn(II), Zn(II), Cd(II) and Hg(II), and are of types MX_2(DFBH) and MX_2(DFBH)$_2$; their colours, analytical data and magnetic moments are given in Table 1. Complexes of DABH, however, have been isolated having the formulae MX_2(DABH)$_2$ (M = Co, Ni or Zn; X = Cl or Br; M = Co or Ni, X = NCS) and ; MX_2(DABH)$_3$ (M = Co, Ni or Zn, X = Cl; M = Co or Zn, X = Br; M = Ni or Zn, X = NCS); they are listed in Table 2. Unfortunately the complexes are insoluble in solvents such as chloroform and nitromethane so that measurements of solution spectra and molar conductivity have been precluded. The magnetic moments of the cobalt, nickel and manganese complexes of both ligands show that the complexes are all high-spin; the moments for the cobalt and nickel complexes are in the regions expected for six-co-ordinate metal ions, with much orbital contribution in the $t_{2g}^5 e_g^2$ cobalt(II) case and little in the $t_{2g}^6 e_g^2$ nickel(II) case. The electronic spectra of the cobalt (II) and nickel(II) complexes can also be assigned to transitions in pseudo-octahedral structures

Table 1. Complexes of 1,4-diformylbenzene bishydrazone (DFBH): colours, analytical data and magnetic moments

Complex	Colour	Elemental analysis[a] (%)			μ_{eff} (BM) (20°C)
		C	H	N	
DFBH	White	59.9 (59.3)	6.4 (6.2)	34.9 (34.6)	
$CoCl_2(DFBH)$	Pink	32.5 (32.9)	3.4 (3.4)	19.0 (19.2)	5.1
$CoCl_2(DFBH)_2$	Yellow	42.4 (42.3)	4.9 (4.4)	25.0 (24.7)	4.9
$CoBr_2(DFBH)_2$	Green	35.0 (35.4)	3.7 (3.7)	21.1 (20.6)	5.2
$Co(SCN)_2(DFBH)$	Yellow	35.9 (35.6)	2.5 (3.0)	25.3 (24.9)	5.1
$NiCl_2(DFBH)$	Yellow	32.3 (32.9)	3.1 (3.4)	19.3 (19.2)	3.3
$NiCl_2(DFBH)_2$	Green	42.4 (42.3)	4.1 (4.4)	24.6 (24.7)	3.2
$NiBr_2(DFBH)$	Yellow	25.0 (25.2)	2.8 (2.6)	14.3 (14.7)	2.7
$NiBr_2(DFBH)_2$	Yellow	35.7 (35.4)	3.8 (3.7)	20.6 (20.6)	2.9
$Ni(SCN)_2(DFBH)$	Brown	35.2 (35.6)	2.9 (3.0)	24.9 (24.9)	2.8
$MnCl_2(DFBH)$	Orange	34.1 (33.4)	3.9 (3.5)	17.9 (19.4)	5.9
$MnCl_2(DFBH)_2$	Yellow	42.0 (42.7)	4.5 (4.5)	25.0 (24.9)	5.9
$MnBr_2(DFBH)_2$	Yellow	35.6 (35.6)	3.5 (3.7)	19.3 (20.8)	5.9
$ZnCl_2(DFBH)$	Yellow	32.3 (32.2)	3.7 (3.3)	18.4 (18.8)	Diamagnetic
$ZnCl_2(DFBH)_2$	Yellow	41.9 (41.7)	4.6 (4.3)	24.5 (24.4)	Diamagnetic
$CdCl_2(DFBH)$	Yellow	27.9 (27.8)	3.0 (2.9)	16.0 (16.2)	Diamagnetic
$CdCl_2(DFBH)_2$	Yellow	38.1 (37.8)	4.2 (3.9)	21.9 (22.1)	Diamagnetic
$HgCl_2(DFBH)_2$	Yellow	32.2 (32.2)	3.5 (3.3)	18.6 (18.8)	Diamagnetic

[a] Theoretical values in parentheses.

(Table 3). The obvious tetragonality of the complexes is shown in the nickel(II) compounds where the $^3T_{1g}(F)$ level is often split into the two components ^3E_g and $^3A_{2g}$ of D_{4h}-symmetry. The band positions in the nickel complexes indicate[6] that the ligand field increases from N_2Cl_4 in $NiCl_2(DFBH)$ to N_4Cl_2 in $NiCl_2(DFBH)_2$ and to N_6 in $Ni(NCS)_2(DFBH)$. Unfortunately the *d–d* bands above 20,000 cm^{-1} are often obscured by the intense charge-transfer band which gives the com-

Table 2. Complexes of 1,4-diacetylbenzene bishydrazone (DABH): colours, analytical data and magnetic moments

Complex	Colour	Elemental analysis[a] (%)			μ_{eff} (BM) (20°C)
		C	H	N	
DABH	Beige	63.5 (63.1)	7.6 (7.4)	29.4 (29.4)	
$CoCl_2(DABH)_2$	Yellow	48.7 (47.1)	5.9 (5.4)	19.7 (21.9)	5.1
$CoBr_2(DABH)_2$	Yellow	41.0 (40.1)	4.5 (4.7)	18.4 (18.7)	4.8
$Co(NCS)_2(DABH)_2$	Yellow	48.0 (47.6)	5.0 (5.1)	24.8 (25.2)	4.7
$CoBr_2(DABH)_3$	Yellow	45.8 (45.6)	5.2 (5.4)	21.1 (21.3)	5.2
$Co(NCS)_2(DABH)_3$	Yellow	51.8 (51.5)	5.2 (5.7)	21.6 (21.6)	4.8
$NiCl_2(DABH)_2$	Pale green	47.2 (47.1)	5.7 (5.5)	20.9 (22.0)	3.1
$NiBr_2(DABH)_2$	Pale green	40.1 (40.1)	4.7 (4.7)	18.7 (18.7)	3.0
$Ni(NCS)_2(DABH)_2$	Pale green	48.0 (47.6)	5.2 (5.1)	24.8 (25.2)	3.0
$NiCl_2(DABH)_3$	Pale green	52.1 (52.5)	6.0 (6.0)	20.4 (20.5)	3.1
$Ni(NCS)_2(DABH)_3$	Pale green	51.8 (51.5)	5.8 (5.7)	25.8 (26.3)	3.0
$ZnCl_2(DABH)_2$	Yellow	47.5 (46.5)	5.6 (5.5)	20.5 (21.7)	Diamagnetic
$ZnBl_2(DABH)_2$	Yellow	41.5 (39.7)	4.8 (4.7)	18.4 (18.5)	Diamagnetic
$ZnCl_2(DABH)_3$	Yellow	51.1 (51.0)	5.9 (6.0)	22.9 (23.8)	Diamagnetic
$ZnBr_2(DABH)_3$	Yellow	45.4 (45.3)	5.2 (5.3)	20.8 (21.1)	Diamagnetic
$Zn(NCS)_2(DABH)_3$	Yellow	51.1 (51.1)	5.6 (5.6)	25.8 (26.1)	Diamagnetic

[a] Theoretical values in parentheses.

Table 3. Electronic spectra ($cm^{-1} \times 10^3$) (diffuse-reflectance) of complexes of the bishydrazones of 1,4-diformylbenzene (DFBH) and 1,4-diacetylbenzene (DABH)

	$^4T_{1g}$			$^3A_{2g}$		
Cobalt complex	$^4A_{2g}$, $^4T_{1g}$	$^4T_{2g}$	Nickel complex	$^3T_{1g}(P)$	$^3T_{1g}(F)$	$^3T_{2g}$
$CoCl_2(DFBH)$	19.0, 18.0, 17.0	7.2	$NiCl_2(DFBH)$	Obscured, 20.0sh	13.6	8.0
$CoCl_2(DFBH)_2$	19.2, 18.3	9.2	$NiCl_2(DFBH)_2$	Obscured	17.2, 14.9	8.4
$CoCl_2(DABH)_2$	17.4, 16.0	8.3	$NiCl_2(DABH)_2$		17.4	8.7
$CoBr_2(DFBH)_2$	20.0, 17.9	9.0	$NiCl_2(DABH)_3$		17.4	8.7
$CoBr_2(DABH)_2$	16.7, 15.6, 14.5	8.9	$NiBr_2(DFBH)$	24.3	13.4	7.9
$CoBr_2(DABH)_3$	18.2, 16.7, 15.4	9.5	$NiBr_2(DFBH)_2$	Obscured, 20.8sh	17.2, 13.6	8.1
$Co(NCS)_2(DFBH)$	19.8sh, 17.8sh	9.9	$NiBr_2(DABH)_2$	Obscured	17.4, 14.3	8.0
$Co(NCS)_2(DABH)_2$	Obscured	10.0	$Ni(NCS)_2(DFBH)$	25.0	16.9sh	10.5
$Co(NCS)_2(DABH)_3$	17.5, 16.3	9.3	$Ni(NCS)_2(DFBH)_2$	Obscured	17.5sh	10.5

plexes their yellow colour or tinge. Similar ligand field changes are observable in the cobalt complexes but with less certainty because of the multiplicity of bands in the 18,000-cm^{-1} region. The spectra thus give evidence for co-ordination of the anions; the isothiocyanato complexes showing higher transition energies than their chloro analogues, which in turn show higher transition energies than the bromo analogues. The ligand field strengths of the two ligands being studied here are very similar to that of benzildihydrazone.[4]

Some important features of the IR spectra of the ligands and some of their complexes are shown in Table 4. The use of chloro, bromo and thiocyanato anions has enabled the identification of the mode of bonding of these moieties. Thus ν(M—Cl) in $ZnCl_2(DFBH)$ indicates terminal Zn—Cl bonds in a tetrahedral structure with bridging DFBH. In $ZnCl_2(DFBH)_2$ ν(Zn—Cl) moves to 225 cm^{-1} in the region expected[7] for terminal Zn—Cl bonds in an octahedral structure with two DFBH bridges between each zinc atom. Similarly the other MCl_2L_2 (L = DFBH or DABH) complexes show spectra consistent with their containing terminal M—Cl octahedral bonds. The absence of ν(M—Cl) in the mono-ligand complexes $CoCl_2(DFBH)$ and $NiCl_2(DFBH)$ is consistent with them containing bridging chlorides, the frequency of which is usually to be found below 200 cm^{-1}. The cadmium complex $CdCl_2(DFBH)$ shows a ν(Cd—Cl) at 275 cm^{-1} which is not present in $CdCl_2(DFBH)_2$ so that the mono-ligand complex might be the only other tetrahedrally coordinated complex with these ligands. The thiocyanato complexes all show ν(CN),

Table 4. Some important IR bands in complexes of the bishydrazones of 1,4-diformylbenzene (DFBH) and 1,4-diacetylbenzene (DABH)

Compound	$\nu(CN)_{NCS}$	ν(C=N)	ν(N—N)	ν(CS)	δ(NCS)	ν(M—X)
DFBH		1580	1110			
$CoCl_2(DFBH)$		1579	1160			
$CoCl_2(DFBH)_2$		1571	1161			222
$Co(NCS)_2(DFBH)$	2079	1570	1152	793	478, 468	
$Ni(NCS)_2(DFBH)$	2085	1578	1164	788	470	
$ZnCl_2(DFBH)$		1570	1180			315, 295
$ZnCl_2(DFBH)_2$		1570	1180			225
DABH		1586	1070			
$CoCl_2(DABH)_2$		1578	1170			220
$Co(NCS)_2(DABH)_2$	2080	1575	1160	800	482, 475	
$NiCl_2(DABH)_2$		1580	1175			238
$NiCl_2(DABH)_3$		1575	1165			
$Ni(NCS)_2(DABH)_2$	2080	1568	1160	795	480, 470	238
$ZnCl_2(DABH)_2$		1568	1170			221
$Zn(NCS)_2(DABH)_3$	2070	1575	1155	790	480, 470	

ν(CS) and δ(NCS) absorptions in the regions characteristically found for complexes containing terminal *N*-bonded isothiocyanate groups.[8] The ν(CS) band, being in the 788–800-cm^{-1} region, is probably too high in frequency for bridging thiocyanates which normally[9] give a band only a little higher than the free-ion value of *ca* 750 cm^{-1}. Further, bridging thiocyanates give[8,9] ν(CN) well above 2100 cm^{-1}. The occurrence of terminal *N*-bonded isothiocyanates is also in keeping with the electronic spectra in which no splitting of ν_1 or ν_2 is observed in the nickel complexes, and the ligand field is that of six N donor atoms around the metal with little distortion from octahedral symmetry.

The IR bands of principal interest in the ligands are ν(C=N) and ν(N—N) since the shift in these bands on complexing is often indicative of the mode of bonding of the ligand. We locate ν(C=N) in the ligands at 1580 cm^{-1} (DFBH) and 1586 cm^{-1} (DABH) this being the only band between 1500 cm^{-1} and the $\delta(NH_2)$ vibration at *ca* 1620 cm^{-1}. Very little shift in ν(C=N) occurs on complexing with the metal salts. A slight increase in ν(C=N) is usually observed[4,10] when the nitrogen atom of this bond (N^1) is bonded to a metal. The absence of such a shift in our complexes implies bonding of the ligand to metal via the aminic nitrogen atom (N^2). The N—H stretching modes ν_{as} and ν_s in the free ligands are at 3335 and 3158 cm^{-1} (DFBH), and 3328 and 3188 cm^{-1} (DABH). Upon co-ordination to the metal these frequencies are decreased; typically $CoCl_2$(DFBH) has ν_{as} at 3259 cm^{-1} and ν_s at 3115 cm^{-1}. Coordination by N^2 is again therefore implied. The N—N stretch in the ligands has been assigned to the bands at 1110 cm^{-1} (DFBH) and 1070 cm^{-1} (DABH) in accordance with the assignment in hydrazine[11] and other hydrazones.[1,2,4] The observed shift of ν(N—N) to higher frequencies upon bonding of the ligands is similar to that found in other hydrazone complexes.[1,2,4] Whilst bonding of hydrazone ligands to metals more usually occurs via N^1, coordination from N^2 is known to occur when bulky substituents occur on the imimic carbon atom.[12] It is noteworthy that, in complexes of benzildihydrazone, coordination by the azomethine nitrogen atom is favoured by the five-membered ring formation formed by the —N=C—C=N— grouping with the metal atom. No such possibility occurs with the present ligands. In the *mono-* and *bis*-ligand complexes prepared here then we believe the ligand to be bridging via the two —NH_2 groups, each —NH_2 group being bonded to a different metal atom. Curiously DABH forms *tris*-ligand complexes also. These do not appear to be *tris* chelates because there are no differences in the spectra of, for example, $NiCl_2(DABH)_2$ and $NiCl_2(DABH)_3$. The IR spectra of the *bis* and *tris* complexes are also similar and show no evidence of the presence of free ligand in the *tris* complexes. One possibility is that in the *tris* complexes the metal atoms are bonded to two anions, two nitrogen atoms from bridging hydrazones and two nitrogen atoms from unidentate hydrazones.

Whilst the inductive effect of the methyl groups in DABH would be expected to increase the basicity of the hydrazone over that of DFBH, the hydrazone of 1,4-dibenzoylbenzene would be expected to be appreciably less basic. We prepared this latter hydrazone and found that no complexes with cobalt(II) could be isolated even after many hours of heating the ligand and salt together in refluxing methanol.

The use of acetone as a solvent for DABH led to dark coloured cobalt complexes whose analytical data indicate them to be 1 : 1 complexes of the diacetone azine of DABH, i.e. the hydrazone has undergone an addition-elimination reaction with the acetone to give the azine DABAZ (**3**).

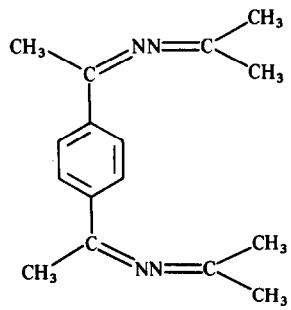

3

The magnetic moments of $CoCl_2$(DABAZ) and $CoBr_2$(DABAZ) are 4.6 and 4.5 BM, respectively, and their reflectance spectra confirm their tetrahedral structure, bands at 16,700 cm^{-1} (Cl^- complex) and 15,400 cm^{-1} (Br^- complex) being assigned to the $^4A_2 \rightarrow {}^4T_1(P)$ transition, and the bands at 9090 cm^{-1} (Cl^- complex) and 8700 cm^{-1} (Br^-) to the $^4A_2 \rightarrow {}^4T_1(F)$ transition. The IR spectra show ν(Co—X) at 340 and 315 cm^{-1} (X = Cl) and 264 cm^{-1} (X = Br), again clearly showing the halide ions to be terminal in tetrahedral structures. These complexes were unfortunately insoluble in organic solvents so other structural studies could not be undertaken; they may be polymeric with bridging and bidentate azines.

REFERENCES

1. C. N. Elgy, M. R. Harrison and D. Nicholls, *Inorg. Chim. Acta* 1982, **57**, 21.
2. M. R. Harrison and D. Nicholls, *Transition Met. Chem.* 1984, **9**, 144.

3. D. Nicholls, M. Rowley and R. Swindells, *J. Chem. Soc.* 1966, 950.
4. S. P. Perlepes, D. Nicholls and M. R. Harrison, *Inorg. Chim. Acta* 1985, **102**, 137.
5. C. N. Elgy and D. Nicholls, *J. Inorg. Nucl. Chem.* 1981, **43**, 2025.
6. A. B. P. Lever, *Inorganic Electron Spectroscopy*, 2nd Edn. Elsevier, Amsterdam (1984).
7. J. R. Ferraro, *Low Frequency Vibrations of Inorganic and Coordination Compounds*. Plenum, New York (1971).
8. R. A. Bailey, S. L. Kazak, T. W. Michelsen and W. N. Mills, *Coord. Chem. Rev.* 1971, **6**, 407.
9. A. V. Butcher, D. J. Phillips and J. P. Redfern, *J. Chem. Soc. A* 1971, 1640.
10. R. C. Stoufer and D. H. Busch, *J. Am. Chem. Soc.* 1960, **82**, 3491.
11. D. N. Sathyanarayana and D. Nicholls, *Spectrochim. Acta* 1978. **34A**, 263.
12. B. Galli, F. Gasparrini, L. Maresca, G. Natile and G. Palmieri, *J. Chem. Soc., Dalton Trans.* 1983, 1483.

Polyhedron Vol. 6, No. 5, pp. 1081–1087, 1987
Printed in Great Britain

0277–5387/87 $3.00+.00

OXO METHYLS OF MOLYBDENUM(V), TUNGSTEN(V) AND RHENIUM(V): X-RAY CRYSTAL STRUCTURE OF $(Me_4WO)_2Mg(thf)_4$

PERICLES STAVROPOULOS and GEOFFREY WILKINSON*

Chemistry Department, Imperial College of Science and Technology, London SW7 2AY, U.K.

and

MAJID MOTEVALLI and MICHAEL B. HURSTHOUSE*

Chemistry Department, Queen Mary College, London E1 4NS, U.K.

(*Received* 1 *September* 1986; *accepted* 25 *September* 1986)

Abstract—The interaction of $MgMe_2$ or MeLi with $MOCl_4$ (M = W or Mo) leads to the paramagnetic (d^1) complexes $(Me_4MO)_2Mg(thf)_4$ and $(Me_4MO)Li(thf)_2$, respectively. The structure of $(Me_4WO)_2Mg(thf)_4$ has been determined by X-ray crystallography and shown to consist of Mg^{2+} co-ordinated by thf and square pyramidal Me_4WO^- units. The preparation of the diamagnetic rhenium(V) compound $(Me_4ReO)Li(thf)_2$ is also reported.

Prior to 1974 the only σ-bonded alkyl derivatives of high oxidation state tungsten that had been isolated were the methyl-, ethyl- and butyl-tungsten pentachlorides[1] and hexamethyl tungsten.[2] Increasing interest in the preparation of organo tungsten and molybdenum complexes, especially with the presence of an oxo ligand on the metal, is related to the reactivity of WCl_6[3] and $WOCl_4$[4] in combination with various alkylating agents as catalyst precursors in the alkene methathesis reaction. There are still relatively few tungsten and molybdenum oxo alkyls. These include the trigonal bipyramidal $MO(neopentyl)_3X$ (M = Mo or W, X = Cl or OR), prepared by the intereaction of $WOCl_4$ and dineopentylmagnesiumdioxane;[5] $W_2O_3(CH_2CMe_3)_6$ and WO_3R^- (R = CH_2CMe_3 or CH_2SiMe_3), prepared by hydrolysis of relevant alkylidyne complexes;[6] compounds of type $MoO_2R_2(bipy)$ (R = Me,[7] CH_2CMe_3[8] or CH_2Ph[9]); and MoO_3R^- species (R = Me, Et or Pr) observed in solutions.[10] Some oxo alkyls with a supporting cyclopentadienyl group, $(\eta^5\text{-}C_5H_5)W(O)_2(CH_2SiMe_3)(\eta^5\text{-}C_5H_5)W(O)(CH_2SiMe_3)_3$ and $(\eta^5\text{-}C_5H_5)W(O)(CHSiMe_3)(CH_2SiMe_3)$, have also been described,[11] the latter being the first instance of an oxoalkylidene complex prepared from an oxo alkyl complex. Tungsten alkyl and alkylidene compounds containing imido, neopentylidyne or cyclopentadienyl groups proved to be more readily accessible.[12]

All the above oxo alkyl complexes have M(VI) and the only compounds with a formal oxidation state (V) (d^1) are the metallabicyclic derivatives $\{[C_6H_4(CH_2)_2\text{-}o]_2WO\}_2Mg(thf)_4$[13] and $\{[(C_6H_4CH_2\text{-}2)]_2WO\}_2Mg(thf)_4$[14] prepared from the interaction of $WOCl_4$ and the appropriate di-Grignard reagent. Although the formation of such compounds has been initially attributed to the strong reducing properties of the relevant dianions we have shown that similar oxo complexes of rhenium(V) with unidentate alkyls[15] and aryls[16] can be easily obtained. We now extend our studies to methyl compounds of molybdenum, tungsten and rhenium.

Analytical data for the various compounds are collected in Table 1.

RESULTS AND DISCUSSION

Oxo methyl compounds of tungsten(V) *and rhenium*(V)

The alkylation of $WOCl_4$ by various methylating agents, including $HgMe_2$, $ZnMe_2$, $ZnMe_2$, $MgMe_2$ and MgMeI, has been thoroughly investigated by both Santini-Scampucci and Riess,[17] and Muetterties and Band[18] and $MeWOCl_3 \cdot OEt_2$ has been

* Authors to whom correspondence should by addressed.

Table 1. Properties and analyses for molybdenum, tungsten and rhenium oxo methyl compounds

Compound	Colour	M.p.[a] (°C)	Analysis (%)[b] C	H	O
$(Me_4MoO)_2Mg(thf)_4$	Orange-red	100	43.1 (43.9)	8.4 (8.6)	15.1 (14.6)
$(Me_4MoO)Li(thf)_2$	Red	105	44.6 (44.6)	8.6 (8.7)	14.0 (14.8)
$(Me_4WO)_2Mg(thf)_4$	Orange-red	120	34.4 (34.6)	6.7 (6.8)	11.6 (11.5)
$(Me_4WO)Li(thf)_2$	Orange-red	110	34.5 (35.1)	6.7 (6.9)	11.5 (11.7)
$(Me_4ReO)Li(thf)_2$	Orange-red	175	35.2 (34.9)	6.7 (6.8)	11.8 (11.6)

[a] Decomposition without melting.
[b] Found (required).

isolated and characterized at low temperatures. It is surprising that no other species were obtained although when an excess of $MeMe_2$ was used the formation and subsequent decomposition of polymethylated tungsten derivatives was postulated.

The intereaction of $WOCl_4$ with three equivalents of $MgMe_2$ or six equivalents of MeMgCl in thf leads to good yields of a paramagnetic, orange-red crystalline complex of stoicheiometry $(Me_4WO)_2Mg(thf)_4$ that can be crystallized from toluene provided that a small amount of thf is always present. There are clearly several intermediates as indicated by colour changes from the early stages of the reaction at −78°C up to room temperature that are similar to those reported in the preparation of the chelating alkyl analogs.[13,14] The pale greenish solution formed initially at −78°C could be due to a reduced oxo (chloro)tungsten(V) species $[WCl_4O]^-$; the solution rapidly becomes reddish possibly due to $[WCl_5O]^{2-}$, and as the temperature approaches ambient levels turns to the final orange-red colour of the isolated product.

The IR spectrum of the compound shows peaks at 1030s.br, 1010sh, 945s, 920s.br and 880s.br cm^{-1} that can be assigned to skeletal vibrations of thf[19] and the $\nu(W{=}O)$ stretch—probably at 945 cm^{-1} by comparison with the rhenium analogue.[15] The broad band at 500 cm^{-1} is assigned to W—C vibrations,[13] and the bands at 360 and 310 cm^{-1} to Mg—O stretches.[20]

The compound is thermally stable—decomposition starts at *ca* 120°C—though less so than the rhenium analogue; it is exceedingly air-sensitive both in the solid state and in solutions, giving almost colourless products. Attempts to isolate the product from oxidation, possibly $WOMe_4$ whose rhenium analogue $ReOMe_4$ has long been known,[21] by regulating the oxidation step under various conditions were unsuccessful.

A diagram of the molecular structure is shown in Fig. 1; selected bond lengths and angles are given in Table 2. The molecule is isostructural with those of the analogous rhenium(V) complex,[15] and the definition of the structure is similarly affected by significant disorder in the orientation of the $Me_4W{=}O$ groups and the conformations of the thf molecules (see Experimental). Accordingly, the

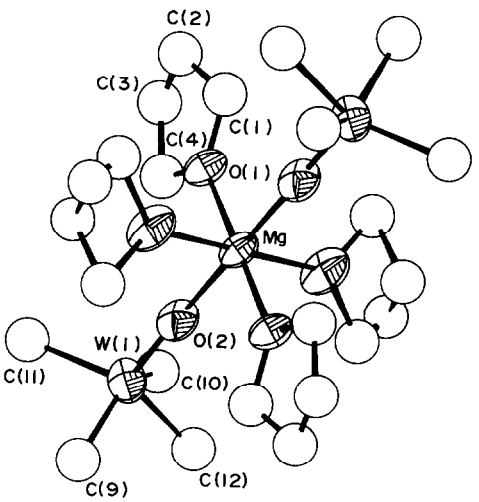

Fig. 1. Structure of $(Me_4WO)_2Mg(thf)_4$.

Table 2. Selected bond lengths (Å) and angles (°) for $(Me_4WO)_2Mg(thf)_4$

	Bond lengths		
O(1)—W(1)	1.733(6)	C(9)—W(1)	2.052(14)
C(9A)—W(1)	2.233(17)	C(10)—W(1)	2.115(18)
C(10A)—W(1)	2.333(16)	C(11)—W(1)	2.083(14)
C(11A)—W(1)	2.259(17)	C(12)—W(1)	2.133(17)
C(12A)—W(1)	2.329(15)		
O(1)—Mg(1)	2.010(6)	O(2)—Mg(1)	2.102(7)
O(3)—Mg(1)	2.110(7)		
	Bond angles		
C(9)—W(1)—O(1)	116.4(5)	C(9A)—W(1)—O(1)	109.6(5)
C(10)—W(1)—O(1)	110.5(5)	C(10)—W(1)—C(9)	117.3(7)
C(10A)—W(1)—O(1)	106.4(4)	C(10A)—W(1)—C(9A)	130.8(5)
C(11)—W(1)—O(1)	116.3(5)	C(11)—W(1)—C(9)	108.2(6)
C(11)—W(1)—C(10)	84.1(7)	C(11A)—W(1)—O(1)	109.7(5)
C(11A)—W(1)—C(9A)	53.9(6)	C(11A)—W(1)—C(10A)	82.9(7)
C(12)—W(1)—O(1)	111.8(4)	C(12)—W(1)—C(9)	86.5(7)
C(12)—W(1)—C(11)	114.1(7)	C(12A)—W(1)—O(1)	107.0(4)
C(12A)—W(1)—C(9A)	76.5(7)	C(12A)—W(1)—C(10A)	122.8(7)
C(12A)—W(1)—C(11A)	125.4(6)		
O(2)—Mg—O(1)	90.3(3)	O(3)—Mg—O(1)	90.3(3)
O(3)—Mg—O(2)	89.9(3)		
Mg—O(1)—W(1)	178.5(3)		

geometry parameters for some parts of the molecule, especially the Me_4W and thf fragments, are very unreliable. The W—O—Mg and MgO_6 geometries are reasonable, however, and compare in an expected manner with the equivalent fragments in the Re compound. In particular, the W=O bond is some 0.04(1) Å greater than the Re=O distance.

The paramagnetic (d^1) $[WOMe_4]^-$ unit retains the square pyramidal geometry found for other similar d^1 or d^2 species, $ReOR_4$ (R = Me, CH_2SiMe_3, 2,4,6-Me_3-C_6H_2 or *o*-MeO-C_6H_4),[16,21] $ReOR_4^-$ [R = Me, CH_2SiMe_3 or *o*-$(CH_2O_2—C_6H_4]$,[15] and $W(\eta^5\text{-}C_5Et_3Me_2)Me_4$[12] from crystallographic studies or from ESR spectra; whereas d^0 cases, MO(neopentyl)$_3$X (M = Mo or W, X = Cl or OR),[5] $[W(\eta^5\text{-}C_5Me_5)Me_4]^+$,[22] $W(NPh)R_3X$ (R = Me, CH_2SiMe_3, CH_2CMe_3 or CH_2Ph; X = Cl or OR)[12] and the unstable $W(NPh)R_4$ (R = Me, CH_2SiMe_3),[12] all have been assigned trigonal bipyramidal structures. Although the two geometries are subject to facile interconversion[23] the tendency can be easily explained since the presence of non-bonding *d*-electrons on the equatorial plane forces the equatorial alkyl ligands below the plane to a square pyramidal geometry whereas the absence of *d*-electrons alows a trigonal bipyramidal geometry. On these grounds the d^0 complex $WOMe_4$ could be expected to be less stable than the d^1 species $[WOMe_4]^-$ or $ReOMe_4$ since in the former case the axial alkyl group *trans* to oxygen would be weakly bound; this is also clearly indicated by the relative instability of $W(NPh)R_4$ complexes compared to $W(NPh)R_3X$ (X–halide or alkoxide) compounds.

The interaction of $WOCl_4$ with six equivalents of MeLi in thf yields an orange-red, paramagnetic complex of stoichiometry $(Me_4WO)Li(THF)_2$ that can be crystallized from light petroleum as fine needles which collapse to a red powder *in vacuo* losing thf. The compound is soluble in aliphatic and aromatic hydrocarbons and ethers, but shows slow decomposition in halogenated solvents even in absence of air. The thermal stability of the complex is comparable to the magnesium solvate—decomposition starts at *ca* 110°C—but exhibits greater air sensitivity to, as yet, unidentified colourless products.

The IR spectrum shows broad bands at 1042s.br and 900s.br cm^{-1} that can be assigned to ν(W=O) and skeletal vibrations of the co-ordinated thf, but due to the broadness of the peaks further multiplicity is obscured and specific assignments cannot be made. The ν(W—C) stretch appears at 500 cm^{-1} and the Li—O vibrations at 420m and 380 cm^{-1}. The ESR spectrum is discussed below.

A thf-solvated lithium complex of identical stoicheiometry can also be obtained for rhenium by the interactionof $[Me_3NH][ReO_4]$ or Re_2O_7 with seven equivalents of MeLi per rhenium. This solvent-dependent compound crystallizes from light petroleum as orange-red needles. Rigorous exclusion of oxygen in the reaction mixture is essential since the compound oxidizes readily to the volatile, paramagnetic complex $ReOMe_4$.[21] the thermal stability of the rhenium compound is higher ($d > ca$ 175°C) only than the tungsten or molybdenum analogues.

The IR spectrum is uninformative in the ν(Re=O) stretch region due to the broadness of the co-ordinated thf peaks. The ν(Re—C) stretch appears at 518m cm^{-1} and the Li—O vibrations at 425 m and 360m cm^{-1}.

In contrast to the tungsten analogue the rhenium complex is diamagnetic; however, its ^1H NMR spectrum displays an unusual and not fully understood behaviour. At room temperature the methyl peaks are not observed but on lowering the temperature a very broad peak appears at *ca* 0°C which rapidly sharpens with decreasing temperature to give only a sharp singlet at δ 3.12 ppm at −60°C. The values for the co-ordinated thf are at δ 3.45 and 1.33 ppm. Even lower temperatures are needed in order to detect the methyl peak in the ^{13}C–$\{^1H\}$ spectrum; at −60°C only a weak band is observed for the methyl carbon at δ 27.84 ppm, whereas the co-ordinated thf appears at δ 67.97 and 25.53 ppm. Although in the case of the magnesium analogue[15] we attributed the broadening to non-rigid behaviour for the five-co-ordinate Me_4ReO grouping it now seems possible that the broadening could be attributed to unusually short spin–lattice relaxation times (T_1) probably due to coupling with the quadrupolar rhenium isotopes (^{185}Re and ^{187}Re, $I = \frac{5}{2}$). This has recently been shown to be the main relaxation pathway for Re–C interactions in $[Re_3(\mu\text{-}H)_4(CO)_{10}]^-$.[24] It has also been shown for this case that relaxation times increase with decreasing temperature, which might account for the sharpening of the peak at lower temperatures.

Oxo methyl compounds of molybdenum(V)

The interaction of $MoOCl_4$ with three equivalents of $MeMe_2$ or six equivalents of MeMgCl in thf affords good yields of an orange-red, paramagnetic complex of stoicheiometry $(Me_4MoO)_2Mg(thf)_4$. The compound can be obtained from toluene as fine orange-red plates; unlike the other thf-solvated magnesium complexes previously described, this compound is not particularly stable in aromatic hydrocarbons, and since toluene seems to be the only convenient solvent for crystallization there are obvious difficulties in its isolation. However, if the procedure of dissolving the extracts of the reaction and crystallizing the product from toluene is kept below 0°C the decomposition is minimal and the complex can be obtained pure as large plates; these can be separated from any black residue by hand picking under inert atmosphere. Once isolated the compound is thermally stable to *ca* 100°C and is soluble without decomposition in ethers and thf, though it is insoluble in aliphatic hydrocarbons and decomposes in halogenated solvents.

The reaction pathway is far from clear but reduction to molybdenum(V) probably precedes alkylation as it is known that $MeOCl_4$ decomposes rapidly to $MoOCl_3$[25] even at 25°C. The binding of four methyl groups is probably due to the small size of the ligand since a bulkier substituting aryl has been reported to yield a $MoOR_3$ complex (R = mesityl).[26] It is not thus surprising that the chelating *o*-xylenediyl ligand which gave isolable products in the case of tungsten[13] and rhenium[15] failed to yield analogous complexes for molybdenum. Schrock was also unable to prepare methylated species from the interaction of $(\eta^5\text{-}C_5Me_5)MoCl_4$ with various methylating agents,[12] whereas the tungsten analogue gave easily $(\eta^5\text{-}C_5Me_5)WMe_4$.

The IR spectrum shows the usual pattern of bands with the ν(Mo=O) stretch probably at 930s cm^{-1}, the ν(Mo—C) at 510 cm^{-1} and the Mg—O bands at 370 and 320 cm^{-1}.

When traces of oxygen were added to solutions of this very air-sensitive complex, a yellow-orange, extremely volatile and thermally unstable product could be detected, but could not be obtained in any substantial yield without extensive decomposition; it is probably $MoOMe_4$.

The interaction of $MoOCl_4$ with six equivalents of MeLi leads to the paramagnetic complex $(Me_4MoO)Li(thf)_2$ as red needles from light petroleum. The compound is stable in aliphatic hydrocarbons, ether and thf, though unstable in aromatic and halogenated hydrocarbons.

The thermal stability and air sensitivity of the complex is similar to that for the magnesium solvate.

Attempts to prepare tungsten and molybdenum complexes with the bulkier alkyls, neopentyl, trimethylsilylmethyl and benzyl, gave only oily thermally unstable materials.

ESR spectra of molybdenum and tungsten complexes

The ESR spectrum of $(Me_4WO)_2Mg(thf)_4$ at 98 K in a frozen toluene solution is characteristic of a

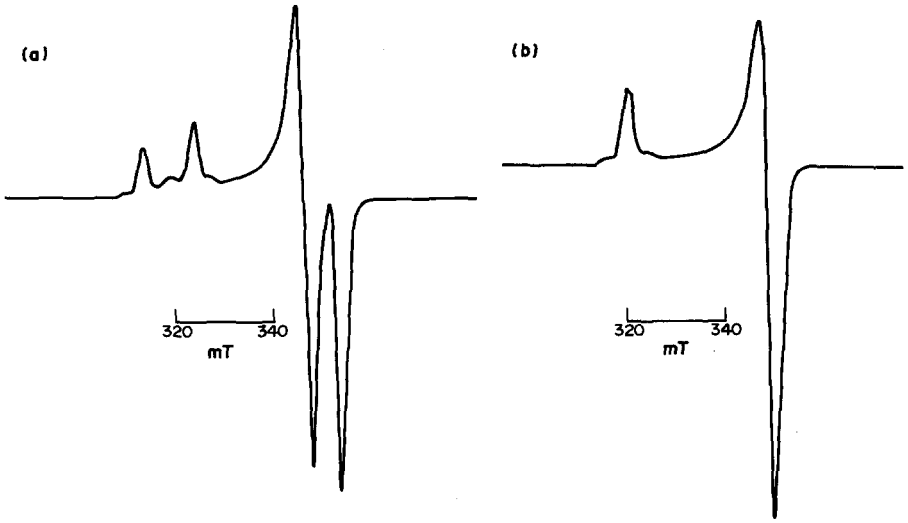

Fig. 2. ESR spectra (*X*-band) of: (a) $(Me_4WO)_2Mg(thf)_4$, and (b) $(Me_4WO)Li(thf)_2$ in toluene at 98 K.

square pyramidal molecule with $S = \frac{1}{2}$ (Fig. 2). The orientations in this axially symmetric spectrum are well separated, $g_{\parallel} = 2.075, g_{\perp} = 1.891$, but the most interesting feature is the splitting of the bands on each axis due to long range magnetic dipole–dipole interaction[27] between the two tungsten atoms in the molecule that give rise to a separation of *ca* 100 and 60 G for the parallel and perpendicular orientations, respectively. If this interaction is assumed to be of a purely dipole–dipole nature, the difference in the splitting along each axis can be roughly explained due to the term $3\cos^2 v - 1/r^3$, where v is the angle formed by the line joining the two tungstens and the external magnetic field, and r the tungsten–tungsten distance; for $v = 0°$ (parallel orientation) the interaction is expected to be twice as strong as that along the perpendicular axis ($v = 90°$). Hyperfine splitting due to ^{183}W ($I = \frac{1}{2}$, 14.40%) is also observed on both sides of the peaks for the parallel orientation but, due to the low natural abundance of the isotope, an accurate calculation of the hyperfine splitting cannot be made.

The ESR spectrum of $(Me_4WO)Li(thf)_2$ recorded under identical conditions (Fig. 2) suggests that the compound is a monomer at least in solution. The main features observed for the solvated magnesium analogue are once again evident in this spectrum, with a band appearing on each axis ($g_{\parallel} = 2.065$, $g_{\perp} = 1.902$) but no further splitting, due to interspace interaction, is observed. Hyperfine splitting with the ^{183}W isotope can also be seen while the substantial broadening of the bands—and probably four distinct unsymmetrical features on the shape of the curve at the parallel orientation—can be attributed to interaction with the ^{7}Li isotope ($I = \frac{3}{2}$, 92.58%).

Spectra of the molybdenum complexes appears to be more complicated since the parallel and perpendicular orientations are very closely spaced (the separation is estimated to be *ca* 100 G), and the hyperfine splitting arising from interaction with molybdenum isotopes (^{95}Mo: $I = \frac{5}{2}$, 15.72%; ^{97}Mo: $I = \frac{5}{2}$, 9.46%) has to be considered. However, the appearance of four dominant peaks in the spectrum of both the magnesium and the lithium solvate correlates better with the case of $(Me_4WO)_2Mg(thf)_4$, and both molybdenum complexes might be expected to be dimers in solution.

EXPERIMENTAL

Microanalyses were by Pascher, Bonn. Spectrometers: IR, Perkin–Elmer 683 (spectra in Nujol mulls, in cm^{-1}); NMR, Bruker WM-250 and JEOL FX-90Q (data in ppm relative to $SiMe_4$); ESR, Varian E12 (X-Band).

$WOCl_4$,[28] $MoOCl_4$,[29] $[Me_3NH][ReO_4]$[15] and Re_2O_7[30] were prepared by literature procedures. The tungsten and molybdenum oxo tetrachlorides were sublimed prior to use. Solvents were refluxed over sodium or sodium–benzophenone under argon, and distilled before use. The petroleum used has a b.p. of 40–60°C. All operations were carried out *in vacuo* or purified argon.

Tetrakis(tetrahydrofuran)magnesium bis[oxotetramethyl tungstate(VI)]

To a stirred solution of $WOCl_4$ (0.82 g, 2.40 mmol) in thf (30 cm^3) at −78°C was added MeMgCl (15 cm^3 of a 0.96 mol dm^{-3} solution in Et_2O, 14.4 mmol). The mixture was allowed to

warm to room temperature and stirring was continued for *ca* 1 h. The resulting orange-red solution was evaporated and the residue extracted with toluene (3×20 cm^3); the filtered extract was reduced to 40 cm^3 and cooled to -20°C to give orange-red polyhedra. The compound can be recrystallized from toluene–thf (1:1). Yield 0.28 g (28%). IR: ν(W=O), 945s; other, 1290m, 1240w, 1185m, 1170m, 1030s.br, 1010sh, 920s.br, 880s.br, 670m, 600m, 500m.br, 360m and 310m.

Bis(tetrahydrofuran)lithium[oxotetramethyl tungstate(V)]

To a solution of $WOCl_4$ (0.70 g, 2.05 mmol) in thf (30 cm^3) at -78°C with stirring was added MeLi (16.20 cm^3 of a 0.76 mol dm^{-3} solution in Et_2O, 12.31 mmol). The mixture was slowly allowed to warm to room temperature; the orange-red solution was evaporated and the residue extracted with light petroleum (3×20 cm^3). Filtration of the extracts, reduction to *ca* 40 cm^3, and cooling at -20°C gave orange-red needles. The compound can be recrystallized by dissolving the thf, followed by evaporation and extraction in light petroleum. Yield 0.22 g (26%). IR: 1290m, 1260w, 1240w, 1190m, 1170m, 1042s.br, 900s.br, 670m, 600m, 500m, 420m and 380m.

Tetrakis(tetrahydrofuran)magnesium bis[oxotetramethyl molybdate(V)]

To a stirred solution of $MoOCl_4$ (0.67 g, 2.64 mmol) in thf (30 cm^3) at -78°C was added MeMgCl (16.50 cm^3 of a 0.96 mol dm^{-3} solution in Et_2O, 15.84 mmol); the solution was allowed to warm and held at room temperature for *ca* 0.5 h. Evaporation and extraction of the residue at 0°C with pre-cooled toluene (3×20 cm^3) followed by filtration of the extracts at low temperature and reduction to *ca* 30 cm^3 led to orange-red plates on cooling at -20°C. The crystals are of analytical purity and can be separated from any black precipitate by hand picking. Yield 0.19 g (22%). IR: ν(Mo=O), 930s; other, 1290m, 1230w, 1180m, 1165w, 1035s, 1010sh, 920s.br, 880m.br, 675m, 600w, 510m, 370m and 320m. ESR: $g_\parallel = 1.967$, $g_\perp = 1.907$.

Bis(tetrahydrofuran)lithium[oxotetramethyl molybdate(V)]

To a stirred solution of $MoOCl_4$ (0.57 g, 2.25 mmol) in thf (30 cm^3) at -78°C was added MeLi (177 cm^3 of a 0.76 mol dm^{-3} solution in Et_2O, 13.45 mmol). The mixture was slowly allowed to warm to room temperature; the red solution was evaporated and the residues extracted with light petroleum (3×20 cm^3). Filtration of the extracts, reduction of *ca* 30 cm^3 and cooling at -20°C gave red needles, which were collected dissolved in thf. Evaporation and extraction in light petroleum gave the pure product on cooling. Yield 0.17 g (24%). IR: 1295m, 1250m, 1185m, 1160m, 1035s.br, 910s.br, 670m, 600m, 490m.br, 400m and 360m. ESR: $g_\parallel = 2.009$, $g_\perp = 1.924$.

Bis(tetrahydrofuran)lithium[oxotetramethyl rhenate(V)]

To a stirred suspension of $[Me_3NH][ReO_4]$ (1.0 g, 3.22 mmol) in thf (30 cm^3) at -78°C was added MeLi (29.7 cm^3 of a 0.76 mol dm^{-3} solution in Et_2O, 22.56 mmol). The mixture was allowed to warm up to room temperature and the resulting orange-red solution evaporated and the residues extracted with light petroleum (4×20 cm^3). Filtration of the extracts, reduction to *ca* 30 cm^3, and cooling at -20°C gave orange-red needles. Yield 0.31 g (23.5%). IR: 1290w, 1210w, 1170m.br, 1140sh, 1038s.br, 900s.br, 670m, 518m, 428m.br and 360m.br.

NMR (C_7D_8, -60°C): ^{1}H, 3.12 (3H, s, Me), 3.49 (2H, m, thf), and 1.33 (2H, m, thf); ^{13}C–{^{1}H}: 27.84 (s, Me), 67.97 (s, thf), and 25.53 (s, thf).

X-ray diffraction studies

The specimen used for structure analysis of $(Me_4WO)_2Mg(thf)_4$ was sealed under argon in a thin-walled capillary. All X-ray measurements were made on a CAD-4 diffractometer operating in the ω–2θ scan mode with graphite-monochromated Mo-K_α radiation ($\lambda = 0.71069$ Å), following procedures previously described.[31] The structure was refined using full-matrix least squares, with the coordinates of the isomorphous rhenium compound as a starting point.[15] The same difficulties as those encountered with the rhenium compound were met—*viz.* disorder in the position of the set of four methyl groups attached to a tungsten and severe conformational disorder in the thf groups. The occupancies of the two sets of methyl carbons were fixed at 0.55 and 0.45, which gave comparable isotropic temperature factor coefficients for atoms of the two sets. A similar procedure was used to treat the carbons of the thf groups, each of which was split between two sites. The same occupancy factors were found to apply. Following the settled choice of occupancy factors, the partial carbons were allowed to refine anisotropically and, although some ellipsoids adopted rather anisotropic shapes,

all atoms remained positive definite and a significant reduction in the R value was achieved. Accordingly this model was considered to be acceptable. No hydrogen atoms were included, however. Details of the analysis are as follows:

Crystal data. $C_{24}H_{56}O_6MgW_2$, $M = 832.80$, triclinic, $a = 9.959(5)$, $b = 9.959(3)$, $c = 10.517(2)$ Å, $\alpha = 63.95(2)$, $\beta = 116.20(3)$, $\gamma = 104.09(3)°$, $V = 839.3$ Å^3, space group $P\bar{1}$, $Z = 1$, $D_c = 1.65$ g cm^{-3}, μ(Mo-K_α) = 66.03 cm^{-1}.

Data collection. $1.5 \leqslant \theta \leqslant 25°$, $T = 291$ K, 3251 data measured, 2941 unique, 2304 observed $[I > 2\alpha(I)]$; empirical absorption correction.

Refinement. 260 parameters, unit weighting scheme, $R = 0.032$. All calculations made on a DEC VAX 11/750 computer with programs as specified in Ref. 31.

Final atomic positional and thermal parameters, bond lengths and angles, and F_o/F_c values have been deposited as supplementary material with the Editor, from whom copies are available on request. Atomic coordinates have also been submitted to the Cambridge Crystallographic Data Centre.

Acknowledgements—We thank the British Council for a studentship (P.S.) and the S.E.R.C. for X-ray facilities.

REFERENCES

1. W. Grahlert and K.-H. Thiele, *Z. Anorg. Allg. Chem.* 1971, **383**, 144.
2. A. J. Shortland and G. Wilkinson, *J. Chem. Soc., Dalton Trans.* 1973, 872.
3. E. L. Muetterties and M. A. Busch, *J. Chem. Soc., Chem. Commun.* 1974, 754; E. L. Muetterties, *Inorg. Chem.* 1975, **14**, 951; R. H. Grubbs and C. R. Hoppin, *J. Chem. Soc., Chem. Commun.* 1977, 634.
4. M. T. Mocella, R. Rovner and E. L. Muetterties, *J. Am. Chem. Soc.* 1976, **98**, 4689.
5. J. R. M. Kress, M. J. M. Russell, M. G. Wesolek and J. A. Osborn, *J. Chem. Soc., Chem. Commun.* 1980, 431.
6. I. Feinstein-Jaffe, S. F. Pedersen and R. R. Schrock, *J. Am. Chem. Soc.* 1983, **105**, 7176; I. Feinstein-Jaffe, J. C. Dewan and R. R. Schrock, *Organometallics* 1985, **4**, 1189.
7. G. N. Schrauzer, L. A. Hughes, N. Strampach, P. Robinson and E. O. Schlemper, *Organometallics* 1982, **1**, 44.
8. G. N. Schrauzer, L. A. Hughes, N. Strampach, F. Ross, D. Ross and E. O. Schlemper, *Organometallics* 1983, **2**, 481.
9. G. N. Schrauzer, L. A. Hughes, E. O. Schlemper, F. Ross and D. Ross, *Organometallics* 1983, **2**, 11.
10. G. N. Schrauzer, L. A. Hughes and N. Strampach, *Z. Naturforsch.* 1982, **37B**, 380; L. A. Hughes, L. N. Hui and G. N. Schrauzer, *Organometallics* 1983, **2**, 486.
11. P. Legzdins, S. J. Rettig and L. Sánchez, *Organometallics* 1985, **4**, 1470.
12. S. F. Pedersen and R. R. Schrock, *J. Am. Chem. Soc.* 1982, **104**, 7483; R. R. Schrock, D. N. Clark, J. Sancho, J. H. Wengrovius, S. M. Rocklage and S. F. Pedersen, *Organometallics* 1982, **1**, 1645; R. C. Murray, L. Blum, A. H. Liu and R. R. Schrock, *ibid.* 1985, **4**, 953; S. J. Holmes and R. R. Schrock, *ibid.* 1983, **2**, 1463.
13. M. F. Lappert, C. L. Raston, G. L. Rowbottom, B. W. Skelton and A. M. White, *J. Chem. Soc., Dalton Trans.* 1984, 883.
14. L. M. Engelhardt, R. I. Papasergio, C. L. Raston, G. Salem and A. H. White, *J. Chem. Soc., Dalton Trans.* 1986, 789.
15. P. Stavropoulos, P. G. Edwards, G. Wilkinson, M. Motevalli, K. M. A. Malik and M. B. Hursthouse, *J. Chem. Soc., Dalton Trans.* 1985, 2167.
16. P. Stavropoulos, P. G. Edwards, T. Behling, G. Wilkinson, M. Motevalli and M. B. Hursthouse, *J. Chem. Soc., Dalton Trans.* 1987 (in press).
17. C. Santini-Scampucci and J. G. Riess, *J. Chem. Soc., Dalton Trans.* 1976, 195; *J. Organomet. Chem.* 1974, **73**, C13.
18. E. L. Muetterties and E. Band, *J. Am. Chem. Soc.* 1980, **102**, 6572.
19. A. Palm and E. R. Bissell, *Spectrochim. Acta* 1960, **16**, 459; J. M. Eyster and E. W. Prohotsky, *ibid.* 1974, **30A**, 2041.
20. H. Wieser and P. J. Krueger, *Spectrochim. Acta* 1970, **26A**, 1349.
21. K. Mertis, D. H. Williamson and G. Wilkinson, *J. Chem. Soc., Dalton Trans.* 1975, 607.
22. R. C. Murray and R. R. Schrock, *J. Am. Chem. Soc.* 1985, **107**, 4557.
23. A. R. Rossi and R. Hoffmann, *Inorg. Chem.* 1975, **14**, 365.
24. T. Beringhelli, H. Molinari and A. Pastore, *J. Chem. Soc., Dalton Trans.* 1985, 1899.
25. M. L. Larson and F. W. Moore, *Inorg. Chem.* 1966, **5**, 801.
26. B. Heyn and R. Hoffmann, *Z. Chem.* 1976, **16**, 407.
27. T. D. Smith and J. R. Pilbrow, *Coord. Chem. Rev.* 1974, **13**, 173.
28. R. Colton and I. B. Tomkins, *Aust. J. Chem.* 1965, **18**, 447.
29. R. Colton, I. B. Tomkins and P. W. Wilson, *Aust. J. Chem.* 1964, **17**, 496.
30. A. D. Melaven, J. N. Fowle, W. Bricknell and C. F. Hiskey, *Inorg. Synth.* 1950, **3**, 188.
31. M. B. Hursthouse, R. A. Jones, K. M. A. Malik and G. Wilkinson, *J. Am. Chem. Soc.* 1979, **101**, 4128.

Polyhedron Vol. 6, No. 5, pp. 1089–1095, 1987
Printed in Great Britain

0277–5387/87 $3.00+.00

ORGANONITRILE COMPLEXES OF IRON(II) AND RUTHENIUM(II): X-RAY CRYSTAL STRUCTURE OF TRANS-$[Fe(NCMe)_2(dmpe)_2](BPh_4)_2$

ANDREW R. BARRON and GEOFFREY WILKINSON*

Department of Chemistry, Imperial College, London SW7 2AY, U.K.

and

MAJID MOTEVALLI and MICHAEL B. HURSTHOUSE*

Department of Chemistry, Queen Mary College, London E1 4NS, U.K.

(*Received* 16 *September* 1986; *accepted* 10 *October* 1986)

Abstract—The interaction of $FeCl_2(dmpe)_2$ [dmpe = 1,2-bis(dimethylphosphino)ethane] with RCN (R = Me or Et) gives the partially substituted complex *trans*-$[FeCl(NCR)(dmpe)_2]Cl$ at room temperature, but in refluxing RCN in the presence of $NaBPh_4$ the product is *trans*-$[Fe(NCR)_2(dmpe)_2](BPh_4)_2$. The X-ray crystal structure of the acetonitrile complex has been determined. No reaction is observed between $RuCl_2(dmpe)_2$ and MeCN, although the disubstituted complex can be made in a similar way to the iron analogue. The interaction of *trans*-$[M(NCMe)_2(dmpe)_2][BPh_4)_2$ (M = Fe or Ru) with H_2 leads to the amine complexes *trans*-$[M(H_2NEt)_2(dmpe)_2](BPh_4)_2$. Although the ethylamine can be removed on refluxing in MeCN the complexes do not act as catalysts. Addition of MeCN to $FeCl_2(PMe_3)_2$ yields only the complex $[FeCl(NCMe)(PMe_3)_2]Cl$; $RuCl_2(PMe_3)_4$ reacts in refluxing MeCN in the presence of $NaBPh_4$ to give *trans*-$[Ru(NCMe)_2(PMe_3)_4](BPh_4)_2$.

We have recently reported the synthesis and reactivity of the Cr(II) nitrile complexes *trans*-$[CrCl(NCR)(dmpe)_2]^+$ and *trans*-$[Cr(NCR)_2(dmpe)_2]^{2+}$ [R = Me or Et, dmpe = 1,2-bis(dimethylphosphino)ethane].[1,2]

We now report the synthesis and characterization of the analogous complexes of Fe(II) and Ru(II), including the products of hydrogenation.

RESULTS AND DISCUSSION

1,2-*Bis*(*dimethylphosphino*)*ethane complexes*

Interaction of $FeCl_2(dmpe)_2$[3] with MeCN at room temperature leads to a pink solution of *trans*-$[FeCl(NCMe)(dmpe)_2]Cl$ (**1**) which can be isolated as bright pink crystals. A similar reaction has been reported for the complex $FeCl_2(depe)_2$ [depe = 1,2-bis(diethylphosphino)ethane],[4] where replacement of the second chloride could readily be accomplished by addition of $NaBPh_4$ at room temperature. If $NaBPh_4$ is added to a MeCN solution of **1** only *trans*-$[FeCl(NCMe)(dmpe)_2]BPh_4$ (**1b**) is isolated. Reaction of **1b** with excess $NaBPh_4$ in refluxing MeCN yields the bright yellow *trans*-$[Fe(NCNe)_2(dmpe)_2](BPh_4)_2$ (**2**), whose structure has been confirmed by X-ray crystallography (see below).

Unlike the analogous chromium complexes,[2] **1** and **2** are unaffected by air and methanol, and are 1 : 1 and 1 : 2 electrolytes, respectively, in MeCN.

The IR spectra of **1** and **2** are similar to their depe analogues, where the monosubstituted complex (**1**) shows a decrease in the C≡N stretch (2240 cm^{-1}) compared to "free" MeCN (2255 cm^{-1}). The decrease in the ν(C≡N) upon coordination may be due to decreased CN bond order caused by π-bonding between the metal *d*-orbitals and the π^*-orbitals of the CN group.[5] This π-bonding is pre-

* Authors to whom correspondence should be addressed.

sumably minimal for the disubstituted complex (**2**) as no change in the C≡N stretch is observed (2255 cm^{-1}).

Both **1** and **2** are diamagnetic, low-spin d^6, showing sharp ^1H NMR spectra with a slight down-field (more positive δ) shift of the methyl signal for the coordinated MeCN, compared to free MeCN.

Complex **2** has been made previously by the reduction of $FeCl_2(dmpe)_2$ with sodium naphthalide followed by addition of HSO_3CF_3 in MeCN.[6]

The use of proprionitrile leads to the formation of *trans*-[FeCl(NCEt)(dmpe)$_2$]X (**3**) (X = Cl or BPh_4) and *trans*-[Fe(NCEt)$_2$(dmpe)$_2$](BPh_4)$_2$ (**4**) (see Experimental).

The bright yellow complex *trans*-[Ru(NCMe)$_2$(dmpe)$_2$](BPh_4)$_2$ (**5**) can be prepared similarly. However no ionic species were observed when $RuCl_2(dmpe)_2$[7] was dissolved in MeCN (Λ_M = 34 ohm cm^2 mol^{-1}). Spectroscopically **5** is similar to the iron complex (see Experimental and Table 1).

X-ray crystallography

A diagram of the cation structure is shown in Fig. 1; selected bond lengths and angles are given in Table 2. The structure is analogous to that of the Cr(II) complex, the structure of which has been determined as the $CH_3CO_2^-$ salt.[1] The most interesting features of the geometry relate to the comparison between this structure and that of the Cr(II) complex which is low-spin d_2^4 paramagnetic. The M—N (nitrile) distances are essentially equal at 1.905(7) (Fe) and 1.906(6) Å (Cr), but the Fe—P distances [2.264 and 2.270(4) Å] are significantly shorter than the Cr—P distances [2.364–2.392(3) Å]. All other things being equal, we would expect Fe(II)—X distances to be considerably smaller than Cr(II)—X distances just on the basis of trends in bond radii. Additionally, we would expect M$d\pi \rightarrow$ P$d\pi$ back bonding to be maximized for the Fe(II) t_{2g}^6 system and thus further shorten the Fe—P bond relative to the Cr—P bond. It is possible therefore that some of the Fe—P shortening is due to π-bonding, and that perhaps the acetonitrile ligand in the Fe complex which appears not to be involved in any $d\pi$–$p\pi$ backbonding (see above) is also being squeezed out along the axis by the tighter packing of the two dmpe ligands.

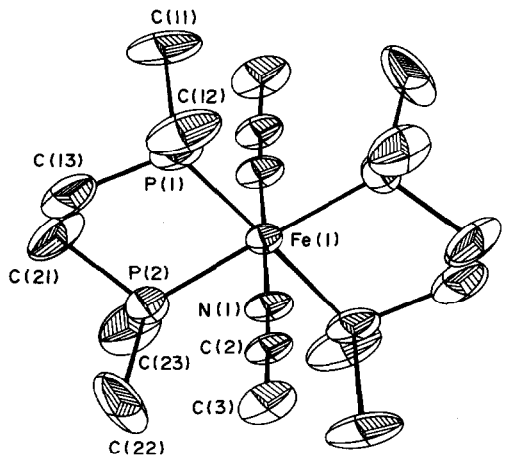

Fig. 1. Structure of the cation $[Fe(NCMe)_2(dmpe)_2]^{2+}$.

trans-[M(NCMe)$_2$(dmpe)$_2$](BPh_4)$_2$ (M = Fe or Ru) react readily with H_2 (3 atm) at room temperature in MeCN, to give the ethylamine complexes *trans*-[M(H_2NEt)$_2$(dmpe)$_2$](BPh_4)$_2$ [M = Fe (**6**) or Ru (**7**)].

The IR spectra show broad ν(N—H) bands about 3220 cm^{-1}. In addition to dmpe and BPh_4 peaks (Table 1) the ^1H NMR show a quartet [δ 3.30 ppm, J(H–H) = 7.0 Hz (**6**); 3.26 ppm, J(H–H) = 7.1 Hz (**7**)] and a triplet [δ 1.09 ppm, J(H–H) = 7.0 Hz (**6**); δ 1.09 ppm, J(H–H) = 7.1 Hz (**7**)] due to the ethyl group. The signal due to the amine N—H protons appears as a singlet partly overlapping the phosphine methylene signal.

The coordinated ethylamine can be liberated from **6** and **7** on refluxing in MeCN. We have, however, been unable to find suitable conditions for the catalytic hydrogenation of MeCN using **2** or **5** as catalysts, even under thermal (150°C, 1500 psi) or photochemical conditions (254 nm, 80 psi).

There has been considerable study of non-catalytic hydrogenation of nitriles using cluster complexes of iron, ruthenium and osmium.[8] Although direct hydrogenation of nitrile and imine groups has been observed,[8(c),9] the majority of these transformations have involved the formation of metal hydride intermediates. Catalytic reduction has recently been observed for $(C_5H_5)_2ScH$[10] and $[RuCl(dppb)(MeCN)_3]^+$ [dppb = 1,4-bis(diphenylphosphino)butane].[11]

Trimethylphosphine complexes

Addition of MeCN to $FeCl_2(PMe_3)_2$[12] at room temperature leads to an orange solution of [FeCl(NCMe)(PMe_3)$_2$]Cl (**8**) which can be isolated as bright orange crystals. Refluxing $FeCl_2(PMe_3)_2$ in MeCN with an excess of $NaBPh_4$ does not substitute the second chloride but forms the tetraphenylboron salt (**8b**). The complex is air-stable and a 1 : 1 electrolyte.

The IR spectrum of **8** contains two weaks bands in the C≡N stretch region. One is the ν(CN) band (2300 cm^{-1}) and the other (2310 cm^{-1}) a com-

Table 1. ^{1}H and $^{31}P-\{^{1}H\}$ NMR data (298 K) for organonitrile complexes[a]

Compound	^{1}H	Assignment	$^{31}P-\{^{1}H\}$
(1) $[FeCl(NCMe)(dmpe)_2]X$[b]	2.17m	8H P—C<u>H</u>$_2$	59.60
	2.01s	3H NC—C<u>H</u>$_3$	
	1.49m	24H P—C<u>H</u>$_3$	
(2) $[Fe(NCMe)_2(dmpe)_2](BPh_4)_2$	7.20m, 6.93m	40H BPh_4	64.00
	2.20m	8H P—C<u>H</u>$_2$	
	2.01s	6H NCC<u>H</u>$_3$	
	1.41m	24H P—C<u>H</u>$_3$	
(3) $[FeCl(NCEt)(dmpe)_2]X$[b]	2.35q, J(H–H) = 7.6	2H C<u>H</u>$_2$CH$_3$	60.02
	2.11m	8H P—C<u>H</u>$_2$	
	1.42m	24H P—C<u>H</u>$_3$	
	1.18t, J(H–H) = 7.6	3H CH$_2$C<u>H</u>$_3$	
(4) $[Fe(NCEt)_2(dmpe)_2](BPh_4)_2$	7.30m, 6.94m	40H BPh_4	64.17
	2.35q, J(H–H) = 7.6	4H C<u>H</u>$_2$CH$_3$	
	2.11m	8H P—C<u>H</u>$_2$	
	1.43m	24H P—C<u>H</u>$_3$	
	1.18t, J(H–H) = 7.6	6H CH$_2$C<u>H</u>$_3$	
(5) $[Ru(NCMe)_2(dmpe)_2](BPh_4)_2$	7.25m, 6.95m	40H BPh_4	42.94
	2.10m	8H P—C<u>H</u>$_2$	
	2.10s	6H NCC<u>H</u>$_3$	
	1.49m	24H P—C<u>H</u>$_3$	
(6) $[Fe(H_2NEt)_2(dmpe)_2](BPh_4)_2$	7.15m, 6.90m	40H BPh_4	66.00
	3.30q, J(H–H) = 7.0	4H C<u>H</u>$_2$CH$_3$	
	2.10s	4H N<u>H</u>$_2$	
	2.05m	8H P—C<u>H</u>$_2$	
	1.49m	24H P—C<u>H</u>$_3$	
	1.09t, J(H–H) = 7.0	6H CH$_2$—C<u>H</u>$_3$	
(7) $[Ru(H_2NEt)_2(dmpe)_2](BPh_4)_2$	7.14m, 6.90m	40H BPh_4	47.31
	3.33q, J(H–H) = 7.1	4H C<u>H</u>$_2$CH$_3$	
	2.10s	4H N<u>H</u>$_2$	
	2.01m	8H P—C<u>H</u>$_2$	
	1.50m	24H P—C<u>H</u>$_3$	
	1.08t, J(H–H) = 7.1	6H CH$_2$C<u>H</u>$_3$	
(8) $[FeCl(NCMe)(PMe_3)_2]X$[b]	2.13br.s	3H NCC<u>H</u>$_3$	
	1.50br.s	18H P—C<u>H</u>$_3$	
(9) $[Ru(NCMe)_2(PMe_3)_4](PBh_4)_2$	7.46m, 7.08m	40H BPh_4	−1.16
	2.36s	6H NCC<u>H</u>$_3$	
	1.63m	36H P—C<u>H</u>$_3$	

[a] δ in ppm relative to $SiMe_4$ (^{1}H) and 85% H_3PO_4 external (^{31}P), J values in Hz.
[b] X = Cl or BPh_4. For BPh_4 salts spectra also include multiplets *ca* δ 7.2 and 6.9 ppm.

Table 2. Selected bond lengths (Å) and bond angles (°) for $[Fe(CH_3CN)_2(dmpe)_2](BPh_4)_2$

P(1)—Fe(1)	2.270(4)	P(2)—Fe(1)	2.264(4)
N(1)—Fe(1)	1.905(7)	C(11)—P(1)	1.817(10)
C(12)—P(1)	1.813(9)	C(13)—P(1)	1.822(10)
C(21)—P(2)	1.827(11)	C(22)—P(2)	1.812(11)
C(23)—P(2)	1.849(10)	C(1)—N(1)	1.129(7)
C(2)—C(1)	1.463(10)	C(23)—C(13)	1.476(11)
P(2)—Fe(1)—P(1)	84.8(2)	N(1)—Fe(1)—P(1)	89.0(2)
N(1)—Fe(1)—P(2)	90.1(2)	C(11)—P(1)—Fe(1)	122.5(4)
C(12)—P(1)—Fe(1)	116.7(4)	C(12)—P(1)—C(11)	101.4(6)
C(13)—P(1)—Fe(1)	109.1(4)	C(13)—P(1)—C(11)	100.4(6)
C(13)—P(1)—C(12)	104.4(6)	C(21)—P(2)—Fe(1)	116.8(4)
C(22)—P(2)—Fe(1)	120.5(5)	C(22)—P(2)—C(21)	105.5(8)
C(23)—P(2)—Fe(1)	107.8(3)	C(23)—P(2)—C(21)	102.3(6)
C(23)—P(2)—C(22)	101.3(6)	C(1)—N(1)—Fe(1)	178.1(5)
C(2)—C(1)—N(1)	177.9(7)	C(23)—C(13)—P(1)	110.1(7)
C(13)—C(23)—P(2)	110.0(6)		

bination band resulting from the symmetrical CH_3 deformation and the C—C stretch which borrows intensity from the ν(CN) band.[13] If CD_3CN is used the band at 2310 cm^{-1} is not present and the C≡N stretch becomes more intense. The complex is paramagnetic showing a broad ^1H NMR spectrum.

No reaction is observed between $RuCl_2(PMe_3)_4$[14] and MeCN; however on refluxing in the presence of two equivalents of $NaBPh_4$ *trans*-$[Ru(NCMe)_2(PMe_3)_4](BPh_4)_2$ (**9**) is formed.

Besides bands due to the phosphine and tetraphenylborate the IR spectrum contains a strong band at 2270 cm^{-1} due to coordinated MeCN. The ^1H NMR shows a down-field shift of the methyl CH_3 peak, whilst the *trans* configuration is confirmed by a singlet in the ^{31}P–$\{^1H\}$ NMR spectrum (δ −1.16 ppm).

No reaction is observed between **8** and **9** with hydrogen (100°C, 180 psi).

None of the above complexes show any evidence of reduction of the metal and the concurrent formation of the $(H \cdot MeCN)^+$ species, as has been found for the chromium complex.[2]

EXPERIMENTAL

Microanalyses were by Imerial College Laboratories. Melting points were determined in sealed capillaries and are uncorrected. IR spectra were recorded on a Perkin–Elmer 683 grating spectrometer in Nujol mulls (4000–400 cm^{-1}). NMR spectra (in CD_3CN) were recorded on a JEOL FX90Q spectrometer, and data are given in Table 1. Conductivities were determined in MeCN on a Data Scientific PT1-18 instrument. High-pressure reactions were carried out in a Berghof Autoclave. All manipulations were carried out under argon. Solvents were distilled and degassed before use. Analytical data are collected in Table 3.

trans - *Acetonitrile* - *bis*[1,2 - *bis*(*dimethylphosphino*)*ethane*] *chloroiron*(II) *chloride* (**1**)

To $FeCl_2(dmpe)_2$ (0.46 g, 1.08 mmol) was added MeCN (30 cm^3). As the solid dissolved the colour changed from green to pink. Stirring was continued until all the solid had dissolved. The solution was filtered, concentrated and cooled to −20°C to yield pink crystals. Yield 0.45 g (90%), m.p. 180°C.

IR : 2240m, 1420s, 1300m, 1285s, 1245m, 1145w, 1140w, 1075m, 1035m, 940vs, 895s, 840s, 800m, 740s, 705s, 645s.

Conductivity (MeCN): $\Lambda_M = 156\ \Omega\ cm^2\ mol^{-1}$.

The tetraphenylborate salt (**1b**) was obtained by the addition of one equivalent of $NaBPh_4$ to a MeCN solution of **1**. Filtration followed by removal of the solvent yielded a pink solid. Yield *ca* 100%, m.p. 217°C (dec.).

IR: 3060m, 3040m, 2240m, 1900w, 1880w, 1845w, 1750w, 1580m, 1425m, 1305m, 1280w, 1270m, 1105br.m, 1090s, 1040m, 935vs, 875m, 845m, 755m, 740s, 710s, 615s, 410m.

Conductivity (MeCN): $\Lambda_M = 151\ \Omega\ cm^2\ mol^{-1}$.

trans - *Bis*(*acetonitrile*)*bis*[1,2 - *bis*(*dimethylphosphino*)*ethane*]*iron*(II)*bis*(*tetraphenylborate*) (**2**)

To $FeCl_2(dmpe)_2$ (0.56 g, 1.31 mmol) in MeCN (80 cm^3), was added $NaBPh_4$ (0.90 g, 2.63 mmol). The solution was refluxed vigorously for 18 h then

Table 3. Analytical data for nitrile complexes[a]

Compound	Analysis (%)		
	C	H	N
(1) $[FeCl(NCMe)(dmpe)_2]Cl$	32.8 (35.9)	7.2 (7.4)	2.6 (2.9)
(1b) $[FeCl(NCMe)(dmpe)_2]BPh_4$	62.1 (60.7)	7.3 (7.3)	1.8 (1.8)
(2) $[Fe(NCMe)_2(dmpe)_2](BPh_4)_2$	71.3 (71.4)	7.0 (7.1)	2.6 (2.6)
(3) $[FeCl(NCEt)(dmpe)_2]Cl$	37.5 (37.3)	7.8 (7.7)	2.9 (2.9)
(3b) $[FeCl(NCEt)_2(dmpe)_2]BPh_4$	61.0 (61.1)	7.4 (7.4)	1.9 (1.8)
(4) $[Fe(NCEt)_2(dmpe)_2](BPh_4)_2$	60.2 (59.7)	7.5 (7.4)	2.0 (2.5)
(5) $[Ru(NCMe)_2(dmpe)_2](BPh_4)_2$	69.0 (68.5)	7.6 (7.0)	2.6 (2.5)
(6) $[Fe(H_2NEt)_2(dmpe)_2](BPh_4)_2$	70.7 (70.8)	7.7 (7.9)	2.6 (2.6)
(7) $[Ru(H_2NEt)_2(dmpe)_2](BPh_4)_2$	68.3 (68.0)	7.7 (7.6)	2.5 (2.5)
(8) $[FeCl(NCMe)(PMe_3)_2]Cl$	29.6 (30.0)	6.1 (6.6)	4.6 (4.3)
(8b) $[FeCl(NCMe)(PMe_3)_2]BPh_4$	53.0 (53.0)	6.7 (6.8)	2.1 (2.3)
(9) $[Ru(NCMe)_2(PMe_3)_4](BPh_4)_2$	69.2 (68.2)	7.2 (7.3)	2.5 (2.4)

[a] Required values in parentheses.

cooled and the bright yellow solution filtered. Concentration and cooling (−20°C) the solution gives yellow crystals. Yield 1.32 g (93%), m.p. 210°C (dec.).

IR: 3050m, 3030m, 2255m, 1950w, 1890w, 1740w, 1580m, 1420m, 1305s, 1290m, 1260m, 1150br.m, 1140m, 1070w, 1060w, 935vs, 885m, 840s, 750s, 745s, 730s, 710s, 700w, 620s.

Conductivity (MeCN): $\Lambda_M = 190\ \Omega\ cm^2\ mol^{-1}$.

trans-*Bis*[1,2-*bis*(*dimethylphosphino*)*ethane*] *chloroproprionitrile iron*(II) *chloride* (**3**)

This complex was prepared as for **1** but using EtCN to give pink solid. Yield 74%, m.p. 193°C.

IR: 2240m, 1440m, 1430m, 1320m, 1295m, 1280s, 1235m, 1130w, 1080s, 1035m, 940s, 895s, 840s, 800m, 740m, 710m, 640m, 550w.

Conductivity (MeCN): $\Lambda_M = 142\ \Omega\ cm^2\ mol^{-1}$.

Addition of $NaBPh_4$ in MeCN yields the tetraphenylborate salt (**3b**).

IR: 3040m, 3020m, 2240m, 1950w, 1870w, 1820w, 1580m, 1430m, 1320m, 1290s, 1275s, 1250m, 1235m, 1130w, 1080s, 1040s, 945s, 900m, 840s, 800s, 740s, 710m, 640s, 615s, 605s, 545w.

Conductivity (MeCN): $\Lambda_M = 137\ \Omega\ cm^2\ mol^{-1}$.

trans - *Bis*[1,2 - *bis*(*dimethylphosphino*)*ethane*] *bisproprionitrile iron*(II) *bis*(*tetraphenylborate*) (**4**)

Prepared as for **2** but using EtCN to give yellow solid. Yield 58%, m.p. 230° (dec.).

IR: 3050m, 3030m, 2250m, 1950w, 1870w, 1820w, 1580m, 1420m, 1305s, 1290s, 1275s, 1250m, 1240m, 1130w, 1080s, 1045s, 945s, 900m, 840s, 805s, 740s, 710m, 640s, 615m, 600m.

Conductivity (MeCN): $\Lambda_M = 205\ \Omega\ cm^2\ mol^{-1}$.

trans - *Bis*(*acetonitrile*)*bis*[1,2 - *bis*(*dimethylphosphino*)*ethane*] *ruthenium*(II) *bis*(*tetraphenylborate*) (**5**)

As for **2** but using $RuCl_2(dmpe)_2$ to give a yellow solid. Yield *ca* 70%, m.p. 240°C (dec.).

IR: 3040m, 3020m, 2280m, 1950w, 1870w, 1820w, 1580m, 1425m, 1290s, 1275s, 1250m,

1150m, 1135m, 1045s, 945s, 900m, 845m, 735vs, 705vs, 650m, 615s, 605s.

Conductivity (MeCN): $\Lambda_M = 240\ \Omega\ cm^2\ mol^{-1}$.

trans - *Bis*[1,2 - *bis*(*dimethylphosphino*)*ethane*] *bis*(*ethylamine*)*iron*(II) *bis*(*tetraphenylborate*) (**6**)

A MeCN (50 cm^3) solution of **2** (0.40 g, 0.37 mmol) was pressurized with H_2 (3 atm) in an autoclave. The solution was stirred at room temperature for 12 h. After releasing the pressure, the solution was transferred to a flask and cooled (−20°C) to give bright yellow crystals, further crystals were obtained on reducing of the filtrate. Yield 0.29 g (73%), m.p. 187°C (dec.).

IR: 3220w, 3060m, 3040m, 1950w, 1890w, 1835w, 1750w, 1580m, 1420m, 1310m, 1295s, 1270m, 1150m, 1140m, 1075m, 1065m, 1035m, 940s, 930s, 890s, 845m, 795m, 750m, 735s, 715s, 705m, 650m, 615s, 465w, 435m.

Conductivity (MeCN): $\Lambda_M = 210\ \Omega\ cm^2\ mol^{-1}$.

trans - *Bis*[1,2 - *bis*(*dimethylphosphino*)*ethane*] *bis*(*ethylamine*)*ruthenium*(II) *bis*(*tetraphenylborate*) (**7**)

As for **6** but using **5**. Yield *ca* 90%. m.p. 193°C (dec.).

IR: 3220w, 3020m, 1950w, 1870w, 1820w, 1575m, 1435m, 1300w, 1270m, 1185m, 1155m, 1150m, 1030s, 950m, 850m, 745vs, 730vs, 705vs, 620m, 610s, 605vs, 490m, 465m.

Conductivity (MeCN): $\Lambda_M = 217\ \Omega\ cm^2\ mol^{-1}$.

Acetonitrile chlorobis(*trimethylphosphine*) *iron*(II) *chloride* (**8**)

To solid $FeCl_2(PMe_3)_2$ (2.50 g, 139 mmol) was added MeCN (100 cm^3). The solution rapidly became bright orange and orange solid was deposited on stirring for 2 h. The solid was filtered and dried *in vacuo*. Further solid can be obtained on cooling the supernatant. Yield 1.98 g (65%), m.p. 145°C (dec.).

IR: 2310w, 2300w, 1440m, 1310m, 1290s, 1275w, 1100m, 1045m, 985m, 955vs, 945sh, 870m, 730s, 675m, 435w.

Conductivity (MeCN): $\Lambda_M = 123\ \Omega\ cm^2\ mol^{-1}$.

Refluxing a MeCN solution of **8** in the presence of $NaBPh_4$ (1 equivalent) yields the tetraphenylborate salt (**8b**). Yield *ca* 60%, m.p. 161°C (dec.).

IR: 3030m, 3020m, 2315w, 2300w, 1950w, 1890w, 1820w, 1750w, 1585m, 1425m, 1405w, 1305m, 1290m, 1265m, 1150s, 1100w, 1065m, 1040m, 1015w, 955m, 950s, 860m, 745vs, 735vs, 710vs, 630m, 620s, 605s, 490m, 470w.

Conductivity (MeCN): $\Lambda_M = 120\ \Omega\ cm^2\ mol^{-1}$.

trans - *Bis*(*acetonitrile*)*tetrakis*(*trimethylphosphine*) *ruthenium*(II) *bis*(*tetraphenylborate*) (**9**)

To a solution of $RuCl_2(PMe_3)_4$ (0.30 g, 0.63 mmol) in MeCN (100 cm^3) was added solid $NaBPh_4$ (0.43 g, 1.26 mmol). The solution was gently refluxed for 12 h, then cooled and the colourless solution filtered, concentrated and cooled to −20°C giving colourless crystals. Yield 0.46 g (65%), m.p. 148°C (dec.).

IR: 3035m, 2270m, 1950w, 1905w, 1835w, 1755w, 1570m, 1430m, 1425m, 1300m, 1290m, 1265s, 1150m, 1085m, 1025m, 940s, 845m, 740vs, 700vs, 625m, 610s, 600s, 505m, 500m, 470w.

Conductivity (MeCN): $\Lambda_M = 235\ \Omega\ cm^2\ mol^{-1}$.

X-ray crystallography

The crystal of $[Fe(NCMe)_2(dmpe)_2]BPh_4$ used for structure analysis was sealed under argon in a thin-walled glass capillary. All X-ray measurements were made on a CAD-4 diffractometer operating in the ω–2θ scan mode with graphite monochromated Mo-K_α radiation ($\lambda = 0.71069$ Å), following procedures previously described in detail.[15] The structure was solved and refined via the heavy-atom method and full-matrix least squares in a routine manner. All non-hydrogen atoms were refined anisotropically and, although most hydrogen atoms were located in difference maps, those on the phenyl and methylene groups were included in idealized positions and refined as parts of rigid groups with group isotropic U values; methyl hydrogens, however, were located experimentally and freely refined isotropically. Crystallographic details are as follows.

Crystal data. $[C_{16}H_{38}N_2P_4Fe]^+[C_{24}H_{20}B]^-_2$, $M_w = 1076.69$, triclinic, space group $P\bar{1}$, $a = 12.239(2)$, $b = 13.129(4)$, $c = 12.207(4)$ Å, $\alpha = 63.62(2)$, $\beta = 118.96(2)$, $\gamma = 117.10(2)°$, $V = 1463.4$, $Z = 1$, $D_c = 1.22$ g cm^{-3}, μ(Mo-K_α) = 4.03 cm^{-1}.

Data collection. $1.5 \leqslant \theta \leqslant 25$, $T = 293$, 3999 data recorded, 3777 unique, 2597 observed [$I > 1.5\sigma(I)$]. Empirical absorption correction.

Refinement. 349 parameters, unit weights, $R = 0.054$, $R_G = 0.0545$. All calculations were made on a DEC VAX11/750 computer using standard programs.[15]

Final atomic positional and thermal parameters, bond lengths and angles and F_o/F_c values have been deposited as supplementary material with the Editor, from whom copies are available on request. Atomic coordinates have also been submitted to the Cambridge Crystallographic Data Centre.

Acknowledgements—We thank the S.E.R.C. for a studentship (A.R.B.) and for the provision of diffractometer and computing facilities, and Johnson Matthey PLC for the loan of the ruthenium.

REFERENCES

1. J. E. Salt, G. Wilkinson, M. Motevalli and M. B. Hursthouse, *J. Chem. Soc., Dalton Trans.* 1986, 1141.
2. A. R. Barron, J. E. Salt, G. Wilkinson, M. Motevalli and M. B. Hursthouse, *J. Chem. Soc., Dalton Trans.* 1987, in press.
3. G. S. Girolami, G. Wilkinson, A. M. R. Galas, M. Thornton-Pett and M. B. Hursthouse, *J. Chem. Soc., Dalton Trans.* 1985, 1339.
4. J. M. Bellerby and M. J. Mays, *J. Chem. Soc., Dalton Trans.* 1975, 1281.
5. R. E. Clarke and P. C. Ford, *Inorg. Chem.* 1970, **9**, 227.
6. J. E. Salt, Thesis, Imperial College, University of London (1985).
7. J. Chalt and R. G. Hayter, *J. Chem. Soc.* 1961, 896.
8. (a) M. A. Andrews and H. D. Kaesz, *J. Am. Chem. Soc.* 1979, **101**, 7255; (b) M. A. Andrews, G. van Buskirk, C. B. Knobler and H. D. Kaesz, *J. Am. Chem. Soc.* 1979, **101**, 7245; (c) R. D. Adams and I. T. Horvath, *Prog. Inorg. Chem.* 1985, **33**, 128.
9. J. Banford, Z. Dawoodi, K. Henrick and M. J. Mays, *J. Chem. Soc., Chem. Commun.* 1982, 554.
10. J. E. Bercaw, D. L. Davies and P. T. Wolczanski, *Organometallics* 1986, **5**, 443.
11. I. S. Thorburn, S. J. Retting and B. R. James, *J. Organomet. Chem.* 1985, **296**, 103.
12. T. V. Harris, J. W. Rathke and E. L. Muetterties, *J. Am. Chem. Soc.* 1978, **100**, 6966.
13. J. B. Milne, *Can. J. Chem.* 1970, **48**, 75.
14. R. A. Jones, F. Mayor Real, G. Wilkinson, A. M. Galas, M. B. Hursthouse and K. M. Abdul-Malik, *J. Chem. Soc., Dalton Trans.* 1980, 551.
15. M. B. Hursthouse, R. A. Jones, K. M. A. Malik and G. Wilkinson, *J. Am. Chem. Soc.* 1979, **101**, 4128.

Polyhedron Vol. 6, No. 5, pp. 1097–1101, 1987
Printed in Great Britain

0277–5387/87 $3.00+.00

AZOMETHINE DERIVATIVES OF ALUMINIUM CONTAINING Al—O—$SiMe_3$ GROUPS

K. K. CHATURVEDI, R. V. SINGH and J. P. TANDON*

Department of Chemistry, University of Rajasthan, Jaipur 302004, India

(*Received* 7 *May* 1986; *accepted after revision* 7 *October* 1986)

Abstract—The synthesis of azomethine derivatives of aluminium containing Al—O—$SiMe_3$ groups and resistant to hydrolysis is described. These have been prepared either by the equimolar reactions of bibasic tridentate or bibasic tetradentate azomethines, viz. *N*-(2-mercaptoethyl) salicylaldimine, *N*-(2-mercaptophenyl) salicylaldimine, salicylaldehyde sulphisoxazole, salicylaldehyde azine, salicylaldehyde semicarbazone, salicylaldehyde thiosemicarbazone, *o*-hydroxyacetophenone azine *N*,*N*′1,3-propylene-bis(salicylaldimine) and diacetyl bis(2-mercaptoanil), or of 1 : 2 molar reactions of monobasic bidentate imines viz. *N*-(2-mercaptophenyl) benzaldimine, benzaldehyde semicarbazone and benzaldehyde thiosemicarbazone with Me_3Si—O—$Al(OPr^i)_2$ in the medium of dry benzene. The resulting derivatives are coloured solids with sharp m.ps, non-volatile, non-electrolytes, soluble in chloroform, dimethylformamide and dimethylsulphoxide, and monomeric in nature. Their IR, ^1H NMR and electronic spectral data have been presented in support of the proposed structures.

Frisch[1] synthesized some binuclear compounds of arsenic containing the Si—O—As linkage by the interaction of alkyl or aryl chlorosilanes with arsonic acids, and which on hydrolysis yield polymers containing arsenic and silicon in the molar ratio 1 : 2. A number of patents concerning the complexes having Si—O—As type bonding appear in the literature.[2,3] Bradley and Thomas[4] were the first to utilize the transesterification method for the preparation of silyloxides of Ti(IV), Zr(IV), Nb(V) and Ta(V). A few reactions of alkoxides of lanthanides and trimethyl acetoxysilane with a variety of tridentate azomethines, possessing the O⌒N⌒S donor sequence have been reported from these laboratories.[5] However, reactions of aluminium isopropoxide and trimethylacetoxysilane with azomethins having N⌒S, O⌒N, O⌒N⌒S, O⌒N⌒N, O⌒N⌒N⌒O and S⌒N⌒N⌒S donor sequences do not seem to have been studied earlier. The present paper describes the synthesis and characterization of a few heteronuclear derivatives of type, Me_3Si—O—Al(SB), Me_3Si—O—Al(S′B′) and Me_3Si—O—$Al(S''B'')_2$ (where SB^{2-}, $S'B'^{2-}$ and $S''B''^{1-}$ = anions of different Schiff bases).

RESULTS AND DISCUSSION

The equimolar reaction of trimethylacetoxysilane $Me_3SiOOCCH_3$ with aluminium isopropoxide $Al(OPr^i)_3$ can be represented by the following equation:

$$(CH_3)_3SiOOCCH_3 + Al(OPr^i)_3 \rightarrow (CH_3)_3Si—O—Al(OPr^i)_2 + OPr^iOCCH_3.$$

The liberated isopropylacetate in the above reaction was simultaneously fractionated off as an azeotrope with cyclohexane and its estimation at regular intervals oxidimetrically indicated the extent to which the reaction had proceeded.

To the resulting solution of silyloxide of aluminium, an appropriate amount of azomethine [equimolar in the case of bibasic tri- (HO⌒N⌒XH) or tetradentate (HX⌒N⌒N⌒XH), and 1:2 in the case of monobasic bidentate (N⌒XH) was added. The liberated isopropanol was again fractionated

* Author to whom correspondence should be addressed.

off till the reaction was complete (8–12 h):

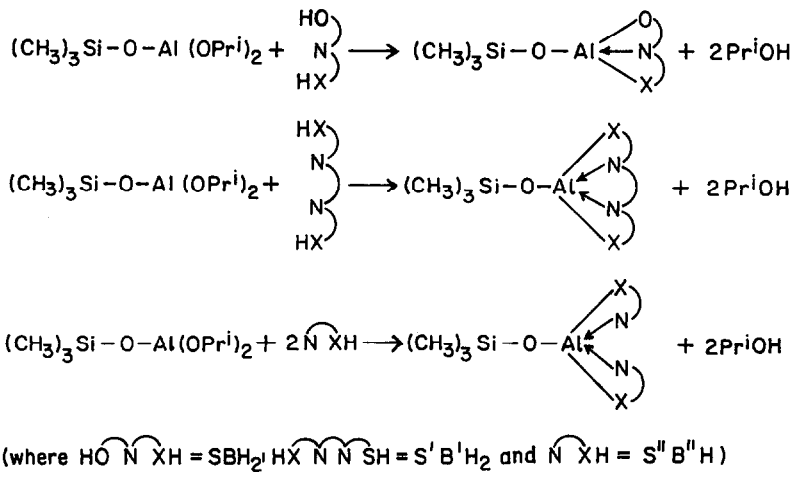

These reactions take place in two consecutive steps and the following reaction mechanism can possibly be advanced.

(i) The first step involving the reaction between aluminium isopropoxide and trimethylacetoxysilane is almost similar to the one suggested for the transesterification reaction and it may be illustrated as below:

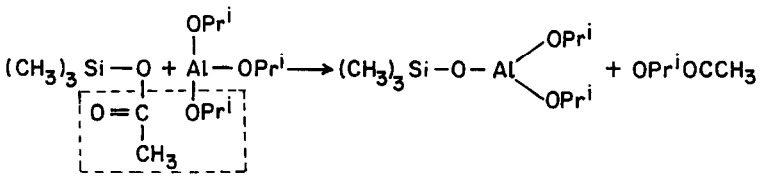

(ii) The trimethylsilyloxide of aluminium diisopropoxide subsequently reacts with a bibasic tri- or tetradentate azomethine probably by an SN^2 type of mechanism as depicted below:

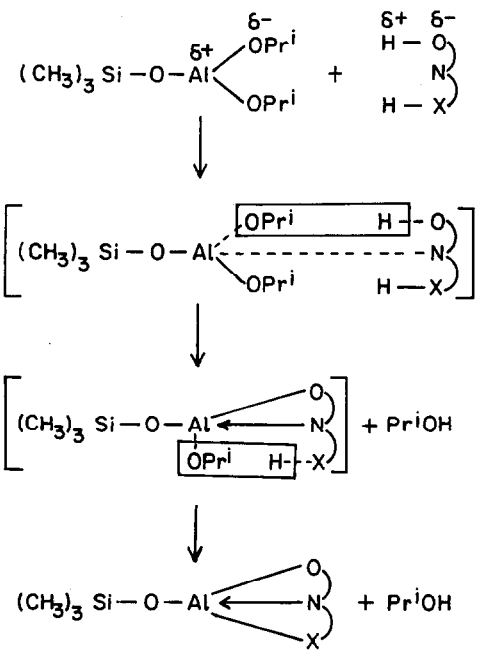

The resulting complexes are coloured solids, non-volatile and soluble in chloroform, dimethylformamide and dimethylsulphoxide. Their resistance to hydrolysis may be due to the water repellent properties of the organo-silicon group present in these derivatives. The molar conductance in dry dimethylformamide has been found to be below 15 Ω^{-1} cm^2 mol^{-1} at 10^{-3} M concentration, which is indicative of the non-ionic nature of these derivatives. The molecular-weight determinations indicate their monomeric nature.

It may, therefore, be inferred that in these newly synthesized complexes, the silicon atom is in the tetracoordinated environment,[5] whereas the aluminium atoms possibly are in tetra- or penta-coordination states as shown at top of next column.

The proposed structures of the imine complexes are further supported by the IR, electronic and ^{1}H NMR spectral studies.

A strong and broad band in the 3400–3100-cm^{-1} region is observed in the IR spectra of the ligands and this may be due to the hydrogen-bonded OH or NH stretching vibrations. Further, the absence of ν(SH) in the 2600–2500-cm^{-1} region along with a ν(C=N) band at $\sim$ 1600 cm^{-1} in the ligands *N*-(2-mercaptoethyl) salicylaldimine ($C_9H_{11}ONS$), *N*-(2-mercaptophenyl)salicylaldimine ($C_{13}H_{11}ONS$) and diacetylbis(2-mercaptoanil) ($C_{16}H_{16}N_2S_2$) is strong evidence for the existence of benzothiazoline ring and not the imine form in these ligands.[6]

The IR spectra of aluminium complexes do not

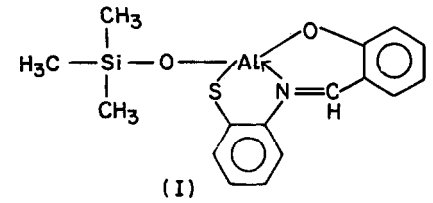

(I)

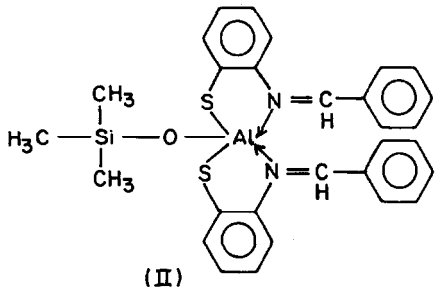

(II)

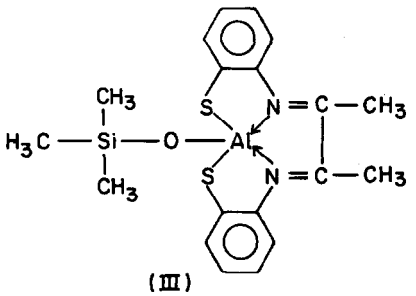

(III)

show any band in the 3400–3100-cm^{-1} region, indicating the chelation of the phenolic oxygen and azomethine nitrogen of the ligands to the aluminium atom.[5] Further, the >C=N stretching vibration at 1635 cm^{-1} in the case of the ligand salicylaldehyde azine shifts towards a lower wavelength in the corresponding aluminium complex, which suggests the coordination of the azomethine nitrogen to the aluminium atom.[7]

In the case of complexes derived from *N*-(2-mercaptophenyl) salicylaldimine and diacetylbis(2-mercaptoanil), a strong band appearing at 1600 cm^{-1} may be assigned to the coordinated >C=N group which supports very well the fact that the resulting complexes are metal–imine complexes due to the rearrangement of the benzothiazoline structure[8] to give the imine form, which finally acts as a bibasic tri- or tetradentate ligand.

The C—O stretching modes of the phenolimine form of the ligands occur at ~ 1280 cm^{-1} and shift towards a higher frequency (~ 1300 cm^{-1}) due to complexation through the phenolic oxygen of the ligand moiety.

A band of medium intensity is observed in all the trimethylsilyloxide aluminium-bonded imine complexes in the 1250–1260-cm^{-1} region which may be assigned to the presence of a $-Si(CH_3)_3$ group, as also reported by Barraclough[9] in the case of trimethylsilanol.

The appearance of some new bands of strong to weak intensities in the spectra of metal imine complexes in the 900–920(s)-, 760–620(m,s)-, 570–430(m,w)- and 410–300(w)-cm^{-1} regions are due to ν(Si—O—Al), ν(Al—O),[10] ν(Al←N)[10-12] and ν(Al—S),[13] respectively. Barraclough *et al.*[9] have similarly assigned a strong band at 900 cm^{-1} in the case of a number of monomeric metal trialkylsilyloxides to Si—O stretching vibrations.

The electronic spectra of ligands derived from *o*-aminothiophenol show two bands at 250 and 310 nm, and these are fully consistent with the typical spectrum of benzothiazolines.[14] These transitions, which arise due to ϕ–ϕ^* and π–π^* benzenoid rings, remain unchanged in all the silyloxide aluminium-bonded imine complexes, whereas an additional band is also observed at ~ 415 nm due to n–π^* electronic transitions of the azomethine group, indicating the isomerization of the ligand on complexation.

However, the electronic spectra of other azomethines used in these investigations exhibit three bands around 245, 295 and 400 nm. The bands around 245 and 295 nm are possibly due to ϕ–ϕ^* and π–π^* transitions of the benzenoid ring in conjugation with the double bond of the azomethine group, and the band around 400 nm may be due to n–π^* transitions of bonding electrons present on the nitrogen of the azomethine group. In the corresponding complexes, there is no shift in the positions of the first two bands. However, the band around 400 nm undergoes a bathochromic shift of 20 nm in the complexes and this may be due to the coordination of the nitrogen of the azomethine group to the central aluminium atom.

Further, to confirm the bonding modes in these complexes, the ^1H NMR spectra of salicylaldehyde azine and its 1 : 1 complex with metal silyloxide have been recorded in $CDCl_3$ and the chemical-shift values [δ (ppm)] for different protons reveal the following salient point.

In the ligand, the hydrogen-bonded NH proton signal appears as a broad signal centred at δ 13.40 ppm which disappears in the corresponding azinate complex, showing the chelation of both phenolic oxygens of the ligand moiety to the aluminium atom after the deprotonation of both phenolic groups.

The proton signal for the azomethine proton (—C(H)=N) is observed at δ 7.95 ppm in the ligand, and it shifts downfield to δ 8.40 ppm in the spectrum of the aluminium complex due to the deshielding as

Table 1. Reactions of $Al(OPr^i)_3$ with Me_3SiOAc and azomethines

No.	Me_3SiOAc (g)	$Al(OPr^i)_3$ (g)	Ligand (g)	Molar ratio	Compound formed, characteristics and yield (g)	AcOH, Pr^iOH (g) Found (calc.)	Analyses (%) Si Found (calc.)	Al Found (calc.)	N Found (calc.)
1	0.75	1.16	$C_9H_{11}ONS$ (1.02)	1:1:1	Me_3Si—O—$Al(C_9H_9ONS)$, brown solid, 1.52	0.34, 0.68 (0.34, 0.68)	9.6 (9.5)	9.1 (9.2)	4.8 (4.8)
2	0.64	0.99	$C_{13}H_{11}ONS$ (1.11)	1:1:1	Me_3Si—O—$Al(C_{13}H_9ONS)$, yellow solid, 1.49	0.28, 0.58 (0.29, 0.58)	8.1 (8.2)	7.9 (7.0)	4.1 (4.0)
3	0.52	0.80	$C_{16}H_{17}O_4N_3S$ (1.46)	1:1:1	Me_3Si—O—$Al(C_{16}H_{15}O_4N_3S)$, dark yellow solid, 1.65	0.23, 0.45 (0.23, 0.46)	5.8 (5.7)	5.4 (5.5)	8.7 (8.6)
4	0.60	0.94	$C_{14}H_{12}O_2N_2$ (1.10)	1:1:1	Me_3Si—O—$Al(C_{14}H_{10}O_2N_2)$, shining yellow solid, 1.45	0.27, 0.54 (0.27, 0.54)	8.0 (7.9)	7.5 (7.6)	7.9 (7.9)
5	1.18	1.82	$C_8H_9O_2N_2$ (0.69)	1:1:1	Me_3Si—O—$Al(C_8H_7O_2N_3)$, light yellow solid, 1.57	0.51, 1.05 (0.53, 1.06)	9.6 (9.5)	9.1 (9.2)	14.1 (14.3)
6	0.88	1.36	$C_8H_9ON_3S$ (0.67)	1:1:1	Me_3Si—O—$Al(C_8H_7ON_3S)$, light brown solid, 1.36	0.39, 0.81 (0.40, 0.80)	9.1 (9.0)	8.8 (8.7)	13.5 (13.6)
7	0.56	0.86	$C_{16}H_{16}O_2N_2$ (1.13)	1:1:1	Me_3Si—O—$Al(C_{16}H_{14}O_2N_2)$, yellow solid, 1.45	0.25, 0.50 (0.25, 0.50)	7.4 (7.3)	6.9 (7.0)	7.2 (7.3)
8	0.76	1.17	$C_{17}H_{18}O_2N_2$ (0.84)	1:1:1	Me_3Si—O—$Al(C_{17}H_{16}O_2N_2)$, dim yellow solid, 1.46	0.34, 0.68 (0.34, 0.68)	7.1 (7.0)	6.6 (6.8)	7.0 (7.0)
9	0.67	1.03	$C_{16}H_{16}N_2S_2$ (0.94)	1:1:1	Me_3Si—O—$Al(C_{16}H_{14}N_2S_2)$ yellow solid, 1.44	0.29, 0.61 (0.30, 0.60)	5.8 (5.9)	5.6 (5.7)	8.9 (8.8)
10	0.44	0.68	$C_{13}H_{11}NS$ (1.55)	1:1:2	Me_3Si—O—$Al(C_{13}H_{10}NS)_2$, brownish yellow solid, 1.68	0.19, 0.38 (0.19, 0.38)	4.9 (4.7)	4.5 (4.6)	4.8 (4.8)
11	0.52	0.80	$C_8H_9ON_3$ (1.28)	1:1:2	Me_3Si—O—$Al(C_8H_8ON_3)_2$, light brown solid, 1.80	0.23, 0.46 (0.23, 0.46)	6.6 (6.4)	6.0 (6.1)	18.9 (19.1)
12	0.72	1.11	$C_8H_9N_3S$ (1.50)	1:1:2	Me_3Si—O—$Al(C_8H_8N_3S)_2$, yellow solid, 1.5	0.32, 0.64 (0.32, 0.64)	6.0 (5.9)	5.6 (5.7)	17.6 (17.8)

[a] Satisfactory carbon and hydrogen analyses were also obtained. Ligands **1**, **2**, **3**, **4**, **5**, **6**, **7**, **8**, **9**, **10**, **11** and **12** are *N*-(2-mercaptoethyl) salicylaldimine, *N*-(2-mercaptophenyl) salicylaldimine, salicylaldehyde sulphisoxazole, salicylaldehyde azine, salicylaldehyde semicarbazone, salicylaldehyde thiosemicarbazone, *o*-hydroxyacetophenone azine, *N*,*N*′-1,3-propylanebis(salicylaldimine), diacetylbis(2-mercaptoanil), *N*-(2-mercaptophenyl)benzaldimine, benzaldehyde semicarbazone and benzaldehyde thiosemicarbazone, respectively.

a result of coordinate bond formation between the nitrogen and aluminium.

The signal observed at δ 1.05 ppm in the complex is attributable to the methyl protons of the —$Si(CH_3)_3$ groups. Further, a downfield shift in the resonance signal of aromatic protons of the ligand has also been observed in the case of the metal complex as a result of the deshielding of the aromatic protons due to the coordination of the azomethine nitrogen to the aluminium atom.

EXPERIMENTAL

Throughout these investigations, a glass apparatus fitted with interchangeable standard ground joints was used.

The different Schiff bases used as ligands in the present investigations were prepared by the usual condensation[6,7] of a carbonyl compound (ketone/aldehyde) with the appropriate amine, aminothiol, sulphonamide or diamine. The ligands were further purified either by recrystallization or by distillation under reduced pressure.

Aluminium isopropoxide was prepared by the direct reaction of aluminium metal with isopropanol in the presence of mercuric chloride as a catalyst and distilled before use (85°C/0.6 mm). Found: Al, 13.2; OPr^i, 86.7. Calc.: Al, 13.2; OPr^i, 86.8%.

Trimethylacetoxysilane was obtained by the reaction between anhydrous sodium acetate and trimethyl chlorosilane in ether. The product was distilled before use (b.p. 103°C/740 mm). Found: Si, 21.1; OAc, 44.3, Calc.: Si, 21.2; OAc, 44.7%.

The binuclear Schiff base complexes of aluminium containing Al—O—$SiMe_3$ groups were synthesized by the reactions of aluminium isopropoxide in an equimolar ratio with trimethylacetoxysilane, $(CH_3)_3SiOOCCH_3$, in dry cyclohexane medium. The aluminium isopropoxide was refluxed under a fractionating column and the calculated amount of trimethylacetoxysilane diluted with dry cyclohexane was added. The reaction led to the liberation of isopropylacetate, $C_3H_7^iCOOCH_3$ which was continuously fractionated off azeotropically with cyclohexane at regular intervals for 8–10 h. When the liberated isopropanol/acetic acid corresponded to 1 mol, an equimolar amount of bibasic tri- or tetradentate azomethine was added to the resulting product, $(CH_3)_3Si$—O—$Al(OC_3H_7^i)_2$. However, in the case of monobasic bidentate ligands, the azomethine was added in a 1 : 2 molar ratio.

The reaction mixture was further refluxed for 8–14 h and the isopropanol liberated was again fractionated off and estimated oxidimetrically. The liberation of almost the theoretical amount of isopropanol in the azeotrope is an indication of the completion of the reaction. The excess of the solvent was then stripped off by distillation and the last traces of the volatile materials were removed under reduced pressure. The solid products so obtained were washed several times with anhydrous *n*-hexane and finally dried at 50–60°C/0.25 mm for about 4 h. The experimental details of these reactions along with the analyses of the products are recorded in Table 1.

The apparatus and instruments used for conductance measurements, molecular-weight determinations and electronic, IR and ^1H NMR spectral studies were the same as reported in our previous communications.[5,7] Silicon and aluminium were estimated gravimetrically as silicon dioxide and aluminium oxinate, respectively. Isopropanol was estimated oxidimetrically.[15] For the determination of the acetoxy group, a weighed amount of the compound was hydrolyzed and then titrated against a 0.05 N solution of sodium hydroxide using phenolphthalein as an indicator.

Acknowledgement—One of us (K.K.C) thanks the U.G.C., New Delhi, for financial support.

REFERENCES

1. R. M. Kary and K. G. Frisch, *J. Am. Chem. Soc.* 1957, **79**, 2140.
2. Y. Hirota and H. Oda, Japanese Patent 1964, **10**, 912.
3. M. Magasawa and F. Yamamoto, *Chem. Abstr.* 1964, **60**, 4185.
4. D. C. Bradley and I. M. Thomas, *Chem. Ind.* 1958, **17**, 1231; *J. Chem. Soc.* 1959, 3404.
5. J. P. Tandon, R. V. Singh, M. N. Mookerjee and S. P. Mital, *Curr. Sci.* 1982, **51**, 333.
6. R. V. Singh and J. P. Tandon, *Inorg. Nucl. Chem. Lett.* 1979, **15**, 319.
7. K. K. Chaturvedi, R. V. Singh and J. P. Tandon, *J. Prakt. Chem.* 1985, **327**, 144.
8. F. John, E. Kitchen and C. Elizabeth, *J. Am. Chem. Soc.* 1983, **105**, 2175.
9. C. G. Barraclough, D. C. Bradley, J. Lewis and I. M. Thomas, *J. Chem. Soc.* 1961, 2601.
10. R. N. Prasad and J. P. Tandon, *J. Inorg. Nucl. Chem.* 1974, **36**, 1473.
11. G. W. Fraser, N. N. Greenwood and B. P. Straughan, *J. Chem. Soc.* 1963, 3472.
12. C. A. Smith and M. G. H. Wattbridge, *J. Chem. Soc.* 1967, 7.
13. M. Agarwal, J. P. Tandon and R. C. Mehrotra, *J. Inorg. Nucl. Chem.* 1979, **41**, 1405.
14. K. K. Chaturvedi, R. V. Singh and J. P. Tandon, *Synth. React. Inorg. Met–Org. Chem.* 1983, **13**, 155.
15. D. C. Bradley, F. M. A. Halim and J. Wardlaw, *J. Chem. Soc.* 1950, 3050.

Polyhedron Vol. 6, No. 5, pp. 1103–1110, 1987
Printed in Great Britain

0277–5387/87 $3.00+.00

MOLECULAR STRUCTURE AND DYNAMICAL BEHAVIOR OF SEVEN-COORDINATE $Mo(CO)_3X_2(Ar_2POPAr_2)$ COMPLEXES

FONTAINE C. BRADLEY and EDWARD H. WONG*

Department of Chemistry, University of New Hampshire, Durham, NH 03824, U.S.A.

and

ERIC J. GABE, FLORENCE L. LEE and Y. LEPAGE

Chemistry Division, National Research Council of Canada, Ottawa, Canada K1A OR9

(*Received* 9 *July* 1986; *accepted* 7 *October* 1986)

Abstract—Direct reaction of elemental halogens with $Mo(CO)_4(R_2POPR_2)$ yielded seven-coordinate Mo(II) complexes of type $Mo(CO)_3X_2(R_2POPR_2)$ (R = phenyl or *p*-tolyl, X = I or Br). The structures of $Mo(CO)_3I_2(Ph_2POPPh_2)$ (**I**) and $Mo(CO)_3Br_2(tolyl_2POPtolyl_2)$ (**II**) have been determined by X-ray diffraction methods. Crystal data: $MoI_2P_2O_4C_{27}H_{20}\cdot C_2H_2Cl_4$, complex **I**, triclinic space group $P\bar{1}$; $a = 10.019(1)$, $b = 11.876(1)$, $c = 15.342(2)$ Å; $\alpha = 73.96(1)°$, $\beta = 79.12(1)°$, $\gamma = 78.19(1)°$, $Z = 2$, $D_{calc.} = 1.88$ Mg m^{-3}. The structure was solved by MULTAN on the basis of 5169 reflections to a final *R* value of 0.035. Crystal data: $MoBr_2P_2O_4C_{31}H_{28}$, complex **II**, monoclinic space group $P2_1/c$, $a = 15.932(2)$, b = 9.847(1), c = 21.360(2) Å, $\beta = 106.58(1)°$, $Z = 4$, $D_{calc.} = 1.62$ Mg m^{-3}. The structure was solved using MULTAN on the basis of 1588 reflections to a final *R* value of 0.097. Both structures approximate a pentagonal bipyramidal coordination geometry around the metal center. This stereochemistry is in accord with Kepert's prediction for chelate normalized bites of less than 1.1 (1.03 and 1.05, respectively, for the POP ligands). The equatorial plane contains both halides, the two phosphorus donors, and a carbonyl. The axial carbonyls are distorted from linearity by 8.5(2) and 13(2)°, respectively. Variable-temperature ^{31}P NMR studies of these and the related $Mo(CO)_3I_2(Ph_2PCH_2PPh_2)$ complex confirmed fluxional behavior. Furthermore, for each of the iodo complexes, equilibration with a second solution isomer was observed.

Coordination number seven remains a fascinating one since no uniquely favored stereochemistry exists.[1] Kepert has presented theoretical ligand–ligand repulsion energy caculations for structural preference in a variety of seven-coordinate metal complexes.[2] For the family of M(bidentate ligand)(unidentate ligand)$_5$ complexes, he predicted that a capped trigonal prismatic (**A**) or a pentagonal bipyramidal (**B**) structure should be favored where the chelate's normalized bite ($b = 2\sin\alpha/2$) is less than 1.1. Above this value, there are four stereochemistries of comparable energies including capped octahedrons (A–D).[1,2] Lippard has reported stereochemistry B (pentagonal bipyramid) for cationic $[Mo(\text{chelating phosphine})(CNR)_5]^{2+}$ complexes in spite of the range of normalized bites for dppm [bis(diphenylphosphino)-methane, $b = 1.06$] and dppe [bis(diphenylphosphino)-ethane, $b = 1.27$].[3] We have been interested in the coordination chemistry of the diphosphoxane (POP) ligand known to have an even smaller normalized bite than dppm. For example, $Mo(CO)_4(Ph_2POPPh_2)$ with $b = 1.06$ can be compared to a value of 1.11 in $Mo(CO)_4$(dppm).[4] Upon halogenation, the seven-coordinate $Mo(CO)_3X_2$(diphosphine) product may be expected to have an even smaller *b* value due to increased steric congestion. Furthermore, the geometries of several $Mo(CO)_3X_2$(diphosphine) complexes with higher *b* values are already known.[5] Of these, $Mo(CO)_3(Ph_2P(CH_2)_3PPh_2)I_2$ ($b = 1.33$) and $Mo(CO)_3(Ph_2P(CH_2)_2PPh_2)I_2$ ($b = 1.24$) have iodo-capped

* Author to whom correspondence should be addressed.

trigonal prismatic geometries (D). Unforunately the structure of $Mo(CO)_3I_2$(dppm) could not be determined though the W analogue was found to have stereochemistry B (pentagonal bipyramid), albeit in a disordered structure.[5]

We report here the halogenation reaction of $Mo(CO)_4(Ar_2POPAr_2)$ (Ar = phenyl or tolyl) and the solid-state structures of $Mo(CO)_3I_2(Ph_2POPPh_2)$ (**I**) and $Mo(CO)_3Br_2(tolyl_2POPtolyl_2)$ (**II**). In accord with Kepert's predictions, both of these were found to be pentagonal bipyramidal (stereochemistry B) with **I** featuring a very low diphosphine *b* value of 1.03 and a POP angle of only 99.9(2)°.

While detailed delineation of solution stereochemical processes for several classes of seven-coordinate complexes have appeared,[6] surprisingly little is known about the dynamical ^{31}P NMR behavior of the $M(CO)_3X_2$(diphosphine) family. We report here the variable-temperature ^{31}P NMR of complexes **I**, **II** and $Mo(CO)_3I_2$(dppm), a previously prepared compound.[5] In all three cases, fluxionality was confirmed. We also present evidence for the presence of a second solution isomer in the iodo complexes. Colton and coworkers have reported the existence of two $M(CO)_3I_2$(dppm) isomers in the solid state for both molybdenum and tungsten. These are all nonelectrolytes. The yellow (α) isomer is probably the expected seven-coordinate product while the orange (β) isomer has been postulated to be a six-coordinate complex with a monodentate dppm ligand.[5]* It was also mentioned that in solution IR data supported the presence of both species in equilibrium.[7-9] We present here NMR evidence that in solution at least, both major isomers are most likely seven-coordinate.

RESULTS AND DISCUSSION

Iodination and bromination of $Mo(CO)_4(Ar_2POPAr_2)$ proceeded readily at room temperature or below liberating CO to yield seven-coordinate complexes of type $Mo(CO)_3X_2(Ar_2POPAr_2)$ (X = Br or I, Ar = Ph or *p*-tolyl). These orange or orange-yellow solids are of limited stability as evident from CO loss and formation of black powders after several days of storage.

Iodination of $Mo(CO)_4(Ar_2POPAr_2)$ at room temperature afforded orange solids. X-ray quality crystals of complex **I** were grown from $C_2H_2Cl_4$ and CH_2Cl_2 solutions. IR carbonyl stretches are at 2038(w), 1970(s) and 1923(m) cm^{-1}. Asymmetric and symmetric POP stretches can be found at 815 and 760 cm^{-1}.[10] The *p*-tolyl analogue has Co stretches at 2046(w), 1956(s) and 1860(m) cm^{-1}. Its POP stretches are at 820 and 746 cm^{-1}.

Bromination of $Mo(CO)_4(Ph_2POPPh_2)$ at 0°C afforded a yellow and an orange solid. Their IR spectra are significantly different in both the carbonyl and POP regions. The yellow solid has bands at 2027(w), 1960(s) and 1890(s) cm^{-1} assignable to CO stretches in addition to a medium band at 847 cm^{-1} assigned to the asymmetric POP stretch. The orange product has CO bands at 1975(s) and 1883(s) cm^{-1} with POP stretches at 803 and 760 cm^{-1}. Unfortunately neither solid is sufficiently soluble for more detailed structural characterization. Bromination of the more soluble $Mo(CO)_4(tolyl_2POPtolyl_2)$ afforded a yellow-orange complex which can recrystallized from CH_2Cl_2. Complex **II** has CO stretches at 2049(w), 1975(sh) and 1961(s) cm^{-1}. The POP stretches are at 819 and 749 cm^{-1}.

Description of the structures

The structures of complexes **I** and complex **II** both feature seven-coordinate molybdenum atoms. The geometry about each metal is best described as a distorted pentagonal bipyramid (Figs 1 and 2). This stereochemistry has been reported in a series of $[Mo(CNR)_5(diphosphine)]^{2+}$ salts but has not been confirmed for $Mo(CO)_3X_2$(diphosphine) complexes. The equatorial plane in each case comprises one carbonyl carbon, C(3), both halogen atoms, and the two chelating phosphorus atoms, P(1) and P(2). Least-squares calculations for the equatorial atoms in complex **I** indicated significant distortions form planarity. Most serious is that of P(2) which is 0.734(3) Å out of the plane of the other four atoms. The pentagon in **II** is essentially planar with the maximum out-of-plane distance at only 0.06(2) Å for P(2). Each MoP(1)—O—P(2) chelate ring is also close to planarity with deviations of less than 0.04(3) Å. The apical positions are occupied by the remaining two carbonyl carbons, C(1) and C(2). There is no crystallographically required symmetry imposed on either structure.

The P—Mo—P angles in **I** and **II** are 61.96(4) and 63.0(4)°, respectively. The bite angles (*b*) are 1.03 for **I** and 1.05 for **II**. Thus the observed pentagonal bipyramids (stereochemistry **B**) are in accord with Kepert's prediction for ligands with small bites. In fact, complex **I** possesses the smallest such value known for a diphosphine ligand. Its diphosphoxane angle at 99.9(2)° is also remarkably

* A second solution isomer in low concentration has been suggested to account for the line-shape of the proton NMR in $TaH(CO)_2(Me_2PCH_2CH_2PMe_2)_2$.[7] Unsymmetrical diphosphines gave *cis*/*trans* isomers of $MX(CO)_2(PP')_2$.[8]

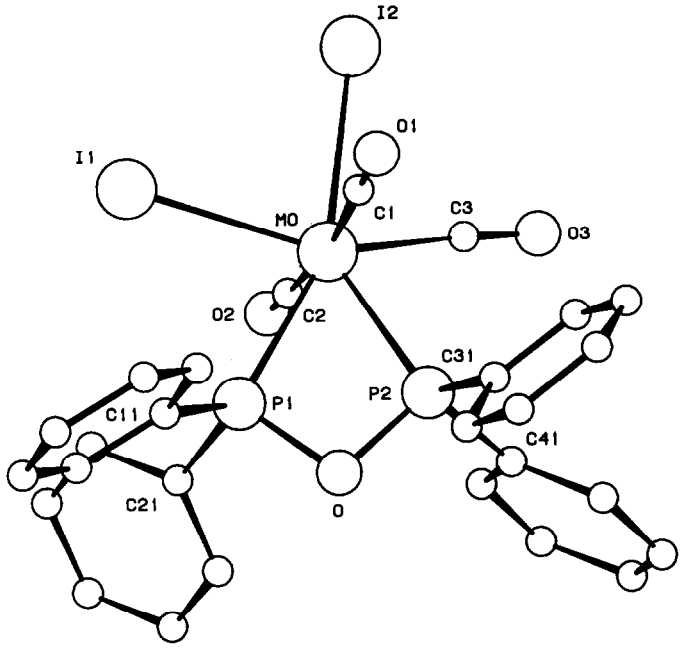

Fig. 1. Molecular structure of complex I.

low for a P—O—P group. This is consistent with a strained chelate ring crowded into the pentagonal equatorial region. The P—O distances in I are accordingly long at 1.638(3) and 1.668(3) Å, indicative of low multiple-bond character due to the unfavorable P—O—P angle. The corresponding POP angle in II of 106(1)° and P—O distances at 1.59(3) and 1.62(3) Å reflect some relief of this strain in the bromo structure.

There appears to be slight differences in the two types of metal–carbonyl distances in each structure. The apical Mo—C bonds are 2.04(1) and 2.05(1) Å in complex I while the corresponding values in II are 2.08(4) and 2.01(4) Å. The equatorial Mo—C bond in each case is marginally shorter at 2.02(1) and 1.93(4) Å, respectively. Apical C—Mo—C angles are 171.5(2)° in I and 167(2)° in II.

Values of the two Mo—P distances in I differ

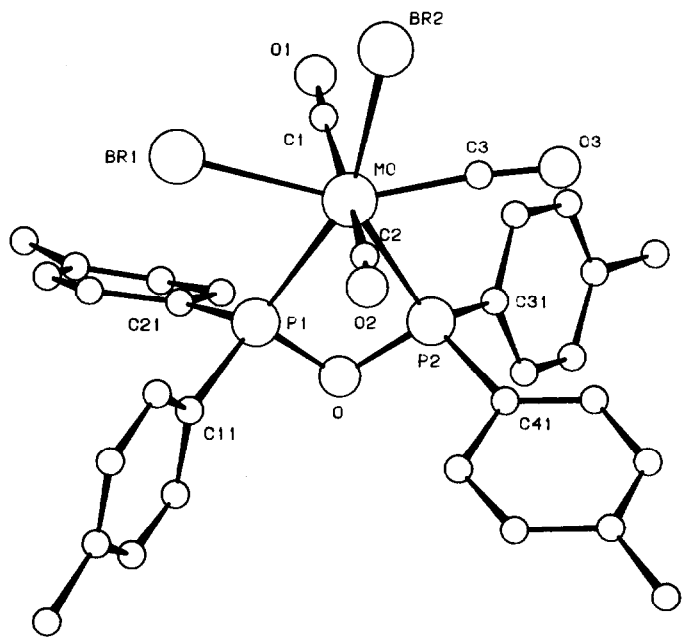

Fig. 2. Molecular structure of complex II.

Table 1. Comparisons of experimental angular coordinates of complexes **I** and **II** with calculated values for stereochemistries A and B

Ligand atom	Calculated[a] for stereochemistry B ϕ/θ	Calculated for stereochemistry A ϕ/θ	Complex **I** ϕ/θ	Complex **II** ϕ/θ
A	30	30	31	32
C	105/0	98/52	101/24	103/6
D	91/90	100/137	93/104	93/97
E	105/180	98/232	104/198	105/180
F	91/270	100/317	94/287	98/278
G	180	180	164/303	167/314

[a] Definitions of ϕ and θ, ligands A–G, and calculated values of angular coordinates for ligand bite $b = 1.0$ are from Table 4, Ref. 2.

significantly, being 2.471(2) and 2.446(1) Å. In **II**, they are closer at 2.46(1) and 2.44(1) Å. This discrepancy in Mo—P distances has been observed in the structures of $Mo(CO)_3I_2(Ph_2P(CH_2)_nPPh_2)$, $n = 2$ or 3, and has been rationalized as originating from the stronger *trans* influence of a carbonyl vs a halide ligand.[5] Such an argument is less persuasive in **I** and **II** since no phosphorus is close to being *trans* to a carbonyl group. Nevertheless the Mo—P bonds most clearly across (at 129.6 and 136°, respectively) from the equatorial carbonyl [C(3)] are indeed longer.

Comparison of stereochemistry with repulsion energy calculations

A comparison of the experimental angular coordinates for complexes **I** and **II** together with those calculated for stereochemistries A (capped trigonal pyramid) and B (pentagonal bipyramid) is tabulated in Table 1.[2]

It can be seen that structure **II** approximates stereochemistry B reasonably well except for ϕ(G) where the deviation is 13°, representing the slight nonplanarity of the Br(2) atom. The angular coordinates for complex **I** show more notable deviations. A major twist distortion for C(2), C(3), C(1) and I(1) (ligands F, C, D and E) can been seen in the θ deviations of 17, 24, 14 and 18°, respectively. This is in the direction towards a capped trigonal prism (stereochemistry A) of the type predicted by Kepert for small-bite ligands.[1] Additionally I(2) or ligand G is distorted away from the pentagonal plane by 16°. The more severe distortions in complex **I** compared to **II** and $W(CO)_3I_2(Ph_2PCH_2PPh_2)$ may be a result of the more congested coordination environment of **I**, consistent with its very low bite (1.03) and narrow POP angle [99.9(2)°].

Variable-temperature ^{31}P-31 *studies*

Temperature dependence of the ^{31}P NMR of complexes **I**, **II** and the related $Mo(CO)_3I_2(tolyl_2POPtolyl_2)$, as well as $Mo(CO)_3I_2(Ph_2PCH_2PPh_2)$, were examined. All were observed to be stereochemically nonrigid at ambient temperature.

The spectra for complex **I** in CH_2Cl_2 are as shown in Fig. 3. At 30°C, a broad singlet at about +92 ppm and a sharp singlet at +70.6 ppm were observed. At −60°C, the broad singlet collapsed into AB doublets at +81 and +112 ppm ($J = 193$ Hz) while the sharp singlet remained unchanged. At temperatures above 30°C, the sharp singlet increasingly broadened but coalescence was not observed as decomposition set in above 120°C. Simulation of the high-temperature spectra predicts an exchange barrier of about 17 kcal mol^{-1} for the two singlets. This spectral behavior is reversible as long as extensive decomposition is avoided. These results suggest the presence of two solution species, **IA** and **IB**, in equilibrium with **IA**:**IB** ratios of 1:0.14 at −60°C, 1:0.32 at 30°C, and 1:0.42 at 70°C. Assignment of the solid-state pentagonal bipyramidal structure featuring inequivalent phosphorus atoms to **IA** is consistent with its limiting AB spectrum. An estimate of its intramolecular rearrangement barrier yields the value 9.8 kcal mol^{-1}. The identity of **IB** can only be speculated upon. One possibility is a second isomer (stereochemistry A, B, C or D) featuring either equivalent phosphine sites or rapidly scrambling inequivalent sites. Another explanation would be dissociation of an iodide to give a six-coordinate cationic complex. This, however, would be contrary to the nonelectrolytic behavior of the complex in chlorinated hydrocarbons. Furthermore, reaction of complex **I** with silver tetrafluoroborate gave a

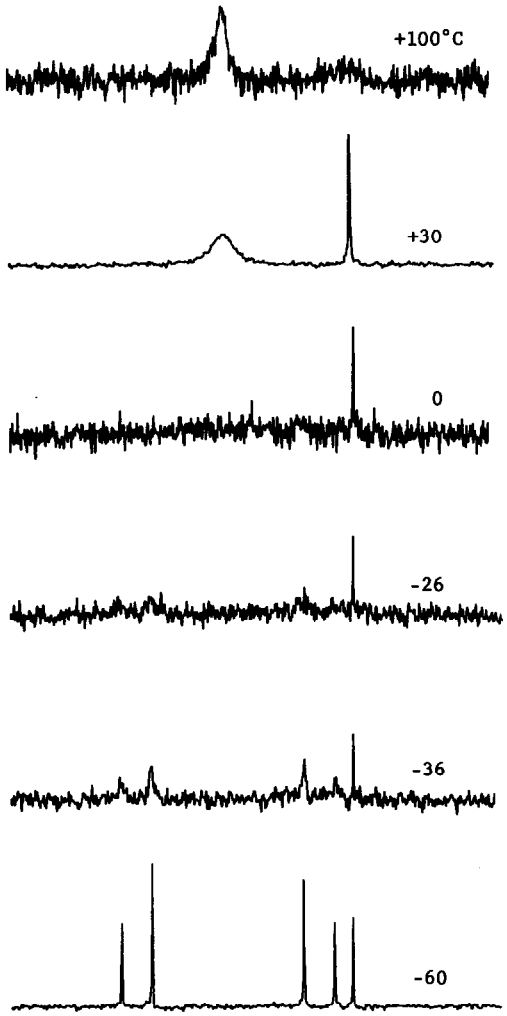

Fig. 3. Variable temperature $^{31}P-\{^1H\}$ NMR spectra of **I**.

cationic complex featuring a ^{31}P signal at +120 instead of +70.6 ppm. A third possibility of **IB** containing a monodentate diphosphoxane similar to that suggested for the β-isomer of $Mo(CO)_3I_2(PPh_2CH_2PPh_2)$ isolated by Colton also seems unlikely in light of its singlet resonance.[5,9] Even if rapid scrambling between the two ends is occurring, the observed average chemical shift of +70.6 ppm would be unreasonable since the known shift of the uncoordinated end of Ph_2POPPh_2 is at +109 ppm.[4,11] A likely structure of **IB** would be the polytopal isomer with stereochemistry A (capped trigonal prism). Observed distortions of the solid-state structure of complex **I** towards this geometry is in line with this hypothesis. An alternate structural assignment of **IB** as a symmetrically substituted pentagonal bipyramid retaining stereochemistry **B** cannot be ruled out.

The variable-temperature ^{31}P spectra of $Mo(CO)_3I_2(tolyl_2POPtolyl_2)$ are very similar with the limiting AB doublets centered at +81 and +111 ppm (J = 193 Hz) and the singlet at +76 ppm.

Complex **II** exhibited a featureless ^{31}P spectrum at 30°C. The slow exchange spectrum at −60°C, however, revealed two AB doublets centered at +91 and +119 ppm (J = 205 Hz). This is entirely consistent with its solid-state structure of a pentagonal bipyramid. Its rearrangement barrier is at 9.9 kcal mol^{-1}. A second solution isomer, if present, would be in much lower abundance.

The complex $Mo(CO)_3I_2(Ph_2PCH_2PPh_2)$ has been known for sometime. Two isomers were reported by Colton in both the solid state and in solution.[5] Their structures have not been determined but at least one is likely to be of stereochemistry **B** by analogy to complexes **I**, **II** and its tungsten analogue.[5] The room-temperature ^{31}P spectrum exhibited a singlet resonance at −22.5 ppm (Fig. 4). This broadened at lower temperatures while a small, sharp singlet appeared at −35.8 ppm. Below −30°C, the major signal collapsed into two sets of AB doublets one of which sharpened at −70°C (−5 and −30 ppm, J = 122 Hz). Below

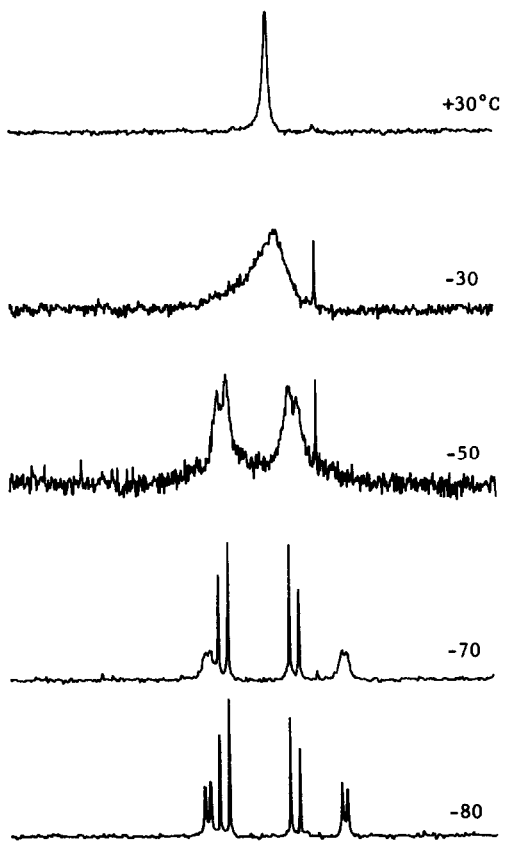

Fig. 4. Variable temperature $^{31}P-\{^1H\}$ NMR spectra of $Mo(CO)_3I_2(Ph_2PCH_2PPh_2)$.

−80°C, the other set eventually resolved into AB doublets at 0 and −47 ppm ($J = 68$ hz). The small singlet at −22.5 ppm, in the meantime, has diminished further into the baseline. Again, these spectra are consistent with the presence of two major solution isomers, both with inequivalent phosphoruses. The barriers to intramolecular scrambling for the two major isomers can be estimated to be 8.4 and 9.5 kcal mol^{-1}. The small singlet suggests presence of a minor third isomer at temperatures above −70°C that is also in equilibrium with the two major isomers. Exact structural assignment of each of these solution species is not yet possible. Nevertheless, the absence of any resonance at around −24 ppm normally assigned to the uncoordinated dppm argues against a six-coordinate geometry featuring a monodentate dppm ligand. We are therefore in favor of both major solution isomers being seven-coordinate with chelating diphosphines.

These data support the presence of significant amounts of a second solution isomer for all three iodo complexes. Interestingly, complex **II**, the bromo analogue of **I**, appears to exist as a single solution species. This along with the much less severe distortions of its solid-state structure from stereochemistry B suggest a higher preference for the pentagonal bipyramidal geometry by complex **II**. Finally, the different slow-exchange spectra for complexes **I**, **II** and $Mo(CO)_3I_2(Ph_2PCH_2PPh_2)$ further illustrate the sensitivity of seven-coordinate stereochemistry to relatively subtle changes in ligand environment.

EXPERIMENTAL

Standard inert-atmosphere techniques were used for reactions, purifications, and other manipulations.

Synthesis of complex **I**

To a stirred solution of 1 g of $Mo(CO)_4(Ph_2POPPh_2)$ (1.68 mmol) in 10 cm^3 CH_2Cl_2 was added dropwise 20.7 cm^3 of a solution of iodine in CH_2Cl_2 (20.6 mg cm^{-3}). Carbon monoxide evolved slowly and after 0.5 h the solution was concentrated *in vacuo* to about 15 cm^3 and 10 cm^3 hexane added slowly. A microcrystalline orange solid deposited over 3 h (0.667 g, 53%). Additional product can be obtained by workup of the mother liquor to give a combined yield of 75%. Found: C, 39.1; H, 2.4. Calc. for $C_{27}H_{20}I_2MoO_4P_2$: C, 39.5; H, 2.5%. X-ray crystals of **I** were grown from $C_2H_2Cl_4$ solution of **I** by layering with hexane.

Synthesis of complex **II**

The same procedure was followed as for **I** except that the bromination was carried out at 0°C. A combined yield of 73% of orange-yellow product was obtained. Found: C, 47.3; H, 3.8. Calc. for $C_{31}H_{28}Br_2MoO_4P_2$: C, 47.6; C, 3.6%. X-ray crystals were obtained by layering of a CH_2Cl_2 solution of **II** with *n*-hexane.

X-ray structural determination of **I**

Crystal data. $C_{27}H_{20}I_2MoO_4P_2 \cdot C_2H_2Cl_4$, triclinic, space group $P\bar{1}$, $a = 10.0185(6)$, $b = 11.8763(10)$, $c = 15.3419(16)$ Å, $\alpha = 73.960(8)°$, $\beta = 79.120(7)°$, $\gamma = 78.193(6)°$, $Z = 2$, $D_{calc.} = 1.88$ Mg m^{-3}. The diffraction intensities of an approximately $0.45 \times 0.3 \times 0.25$ mm crystal were collected with graphite-monochromatized Mo-K radiation using the θ–2θ scan technique with profile analysis to $2\theta_{max} = 50°$.[12] A total of 5965 unique reflections were measured, of which 5169 were considered significant with $I_{net} > 2.5\sigma(I_{net})$. Lorentz and polarization factors were applied but absorption correction was not calculated ($\mu = 2.45$ mm^{-1}). The cell parameters were obtained by least-square refinement of the setting angles of 40 reflections with $2\theta > 45°$(Mo-$K_{1\alpha} = 0.70932$ Å).

The structure was solved by Multan and refined with full-matrix least squares.[13] Where possible, H atom positions were calculated but their parameters were not refined. All heavy atoms were refined anisotropically. The solvent, tetrachloroethane, was located as a disordered molecule, C atoms with occupancy factors as 0.84 and 0.89, and Cl atoms as 0.84, 0.93, 0.83 and 0.83. The final residuals are R_F 0.035 and R_W 0.036 with counting statistics weights. All calculations were performed on the NRCVAX system of programs.[14] Scattering factors were taken from the *International Tables for X-ray Crystallography*.[15] Important distances and angles are listed in Table 2. Atomic positions, anisotropic thermal parameters and structure factors are included in the supplementary material.

X-ray structural determination of **II**

Crystal data. $C_{31}H_{28}Br_2MoO_4P_2$, monoclinic, space group $P2_1/c$, $a = 15.9322(19)$, $b = 9.8466(13)$, $c = 21.3601(22)$ Å, $\beta = 106.58(1)°$, $Z = 4$, $D_{calc.} = 1.62$ Mg m^{-3}. The diffraction intensities of an approximately $0.3 \times 0.2 \times 0.2$ mm crystal were collected as described above for **I**. During data collection, the crystal was observed to split from the display of the profile. The agreement factor

Table 2. Important bond lengths (Å) and angles (°) for I[a]

Mo—I(1)	2.8458(6)	Mo—C(2)	2.047(6)
Mo—I(2)	2.8775(6)	Mo—C(3)	2.020(6)
Mo—P(1)	2.4713(15)	P(1)—O	1.668(3)
Mo—P(2)	2.4462(14)	P(2)—O	1.638(3)
Mo—C(1)	2.039(6)		
I(1)—Mo—I(2)	82.29(2)	C(1)—Mo—C(2)	171.49(22)
I(1)—Mo—P(1)	75.30(3)	C(1)—Mo—C(3)	98.63(24)
I(1)—Mo—P(2)	134.20(4)	C(2)—Mo—C(3)	82.75(24)
I(1)—Mo—C(1)	86.42(15)	Mo—P(1)—O	98.15(12)
I(1)—Mo—C(2)	88.55(16)	Mo—P(2)—O	99.99(12)
I(1)—Mo—C(3)	152.36(17)	P(1)—O—P(2)	99.90(18)
I(2)—Mo—P(1)	157.39(4)	P(1)—Mo—P(2)	61.96(4)
I(2)—Mo—P(2)	140.27(4)	P(1)—Mo—C(1)	100.01(16)
I(2)—Mo—C(1)	81.35(16)	P(1)—Mo—C(2)	85.33(16)
I(2)—Mo—C(2)	91.18(16)	P(1)—Mo—C(3)	129.60(17)
I(2)—Mo—C(3)	71.76(17)		
P(2)—Mo—C(1)	85.54(16)		
P(2)—Mo—C(2)	102.87(16)		
P(2)—Mo—C(3)	73.43(17)		

[a] Numbers in parentheses are standard deviations.

processed between the equivalent sets was 0.13, which probably accounts for the high residual. A total of 4237 unique reflections were measured, of which 1588 were considered significant with $I_{net} > 2.5\sigma(I_{net})$. Lorentz and polarization factors were applied but not absorption correction ($\mu = 2.99$ mm^{-1}). The cell parameters were obtained from least-squares refinement of the setting angles of 50 reflections with $2\theta > 40°$ (Mo-$K_{1\alpha}$ = 0.70932 Å).

The structure was solved by Multan and refined with full-matrix least squares. Where possible, H atom positions were calculated though their parameters were not refined. Due to crystal degradation, all C atoms were refined isotropically, while heavier atoms were refined anisotropically. No attempt was made to locate H atoms of the methyl group. The final residuals are R_F 0.097 and R_W 0.070 for the significant data. Details of calculations are as for I. Important bond distances and angles are given in Table 3. Atomic positions, anisotropic thermal par-

Table 3. Important bond lengths (Å) and angles (°) for II[a]

Mo—Br(1)	2.633(6)	Mo—C(2)	2.01(4)
Mo—Br(2)	2.602(6)	Mo—C(3)	1.93(4)
Mo—P(1)	2.462(11)	P(1)—O	1.59(3)
Mo—P(2)	2.444(11)	P(2)—O	1.62(3)
Mo—C(1)	2.08(4)		
Br(1)—Mo—Br(2)	84.80(18)	C(1)—Mo—C(2)	167.4(19)
Br(1)—Mo—P(1)	73.0(3)	C(1)—Mo—C(3)	97.4(18)
Br(1)—Mo—P(2)	135.9(3)	C(2)—Mo—C(3)	84.3(18)
Br(1)—Mo—C(1)	79.4(12)	Mo—P(1)—O	95.4(9)
Br(1)—Mo—C(2)	93.1(13)	Mo—P(2)—O	95.2(9)
Br(1)—Mo—C(3)	151.3(15)	P(1)—O—P(2)	106.3(13)
Br(2)—Mo—P(1)	157.8(3)	P(1)—Mo—P(2)	63.0(4)
Br(2)—Mo—P(2)	139.2(3)	P(2)—Mo—C(1)	97.2(13)
Br(2)—Mo—C(1)	86.4(12)	P(2)—Mo—C(2)	95.3(15)
Br(2)—Mo—C(2)	82.8(13)	P(2)—Mo—C(3)	72.7(15)
Br(2)—Mo—C(3)	66.5(15)		
P(1)—Mo—C(1)	90.3(11)		
P(1)—Mo—C(2)	97.2(12)		
P(1)—Mo—C(3)	135.7(15)		

[a] Numbers in parentheses are standard deviations.

ameters and structure factors are included in the supplementary material.

Variable-temperature ^{31}P *studies*

A JEOL FX-90Q NMR spectrometer with deuterium lock was used. Samples were studied in CH_2Cl_2 solution in 10-mm tubes. Temperature measurements were made using a thermocouple calibrated with a chemical shift thermometer. All ^{31}P chemical shifts are referenced to 85% phosphoric acid with positive downfields shifts.

Acknowledgement—We thank the National Science Foundation for an instrument grant towards the purchase of the FT-NMR spectrometer.

REFERENCES

1. See, for example, D. L. Kepert, *Inorganic Stereochemistry*, Chap. 11. Springer, Berlin (1982); M. G. B. Drew, *Prog. Inorg. Chem.* 1977, **23**, 67.
2. J. C. Dewan, K. Hendrick, D. L. Kepert, K. R. Trigwell, A. H. White and S. B. Wild, *J. Chem. Soc., Dalton Trans.* 1975, 546.
3. J. C. Dewan, T. E. Wood, R. A. Walton and S. J. Lippard, *Inorg. Chem.* 1982, **21**, 1854; P. W. R. Corfield, J. C. Dewan and S. J. Lippard, *Inorg. Chem.* 1983, **22**, 3424.
4. E. H. Wong, L. Prasad, E. J. Gabe and F. C. Bradley, *J. Organomet. Chem.* 1982, **236**, 321.
5. R. M. Foy, D. L. Kepert, C. L. Raston and A. H. White, *J. Chem. Soc., Dalton Trans.* 1980, 440; R. Colton and J. J. Howard, *Aust. J. Chem.* 1970, **23**, 223.
6. See, for example, F. A. Van-Catledge, S. D. Ittel and J. P. Jesson, *Organometallics* 1985, **4**, 18; E. L. Muetterties and K. J. Packer, *J. Am. Chem. Soc.* 1964, **86**, 293; J. O. Albright, S. Datta, B. Dezube, J. K. Kouba, D. S. Marynick, S. S. Wreford and B. M. Foxman, *J. Am. Chem. Soc.* 1979, **101**, 611; P. J. Domaille, R. L. Harlow and S. S. Wreford, *Organometallics* 1982, **1**, 935; J. L. Templeton and B. C. Ward, *J. Am. Chem. Soc.* 1981, **103**, 3743.
7. P. Meakin, L. J. Guggenberger, F. N. Tebbe and J. P. Jesson, *Inorg. Chem.* 1974, **13**, 1025.
8. L. D. Brown, S. Datta, J. K. Kouba, L. K. Smith and S. S. Wreford, *Inorg. Chem.* 1978, **17**, 729.
9. R. Colton and C. J. Rix, *Aust. J. Chem.* 1969, **22**, 2535.
10. D. E. C. Corbridge, *Top. Phosphorus Chem.* 1969, **6**, 282.
11. E. H. Wong, R. M. Ravanelle, E. J. Gabe, F. L. Lee and L. Prasad, *J. Organomet. Chem.* 1982, **233**, 321.
12. D. F. Grant and E. J. Gabe, *J. Appl. Cryst.* 1978, **11**, 114.
13. G. Germain, P. Main and M. M. Woolfson, *Acta Cryst.* 1971, **A27**, 368.
14. E. J. Gabe, F. L. Lee and Y. LePage, Int. Union Cryst. Summer School on Cryst. Comput., Mulheim, F.R.G. (in press).
15. *International Tables for X-ray Crystallography*. Vol. 4, Table 2.2B, p. 99. Kynoch Press, Birmingham, U.K. (1974).

Polyhedron Vol. 6, No. 5, pp. 1111–1114, 1987
Printed in Great Britain

0277–5387/87 $3.00+.00

METAL COMPLEXES OF POLYCYCLIC TERTIARY AMINES—IX.* X-RAY CRYSTAL STRUCTURE OF HEXAAQUAZINC(II) (1,3,5,7-TETRAAZAADAMANTANE)-TRICHLOROZINCATE(II) HEXAHYDRATE, $[Zn(H_2O)_6][\{(CH_2)_6N_4\}ZnCl_3]_2 \cdot 6H_2O$

THOMAS C. W. MAK†

Department of Chemistry, The Chinese University of Hong Kong, Shatin, New Territories, Hong Kong

and

SHENG-HUA HUANG

Department of Chemistry, Zhongshan University, Guangzhou, China

(*Received* 28 *July* 1986; *accepted* 7 *October* 1986)

Abstract—The title complex has been prepared and characterized by X-ray crystallography [trigonal, $P\bar{3}$, $a = 10.884(1)$, $c = 8.784(1)$ Å, $Z = 1$, $R = 0.036$ for 747 Mo-K_α reflections]. The crystal structure comprises two types of columns: one of quasi tetrahedral $[\{(CH_2)_6N_4\}ZnCl_3]^-$ ions stacked along crystallographic three-fold axes, and a second kind composed of an alternate arrangement of $[Zn(H_2O)_6]^{2+}$ octahedra and chair-shaped hydrogen-bonded $(H_2O)_6$ "spacers" centered at $\bar{3}$ sites, consecutive moieties being linked by "intermolecular" O—H...O hydrogen bonds. Neighboring columns are further interconnected by lateral O—H...N and O—H...Cl hydrogen bonds to form a three-dimensional network.

Several products have been isolated from the reaction of 1,3,5,7-tetraazaadamantane [formula $(CH_2)_6N_4$, commonly known as hexamethylenetetramine and abbreviated as HMT] with zinc(II) halides in aqueous media, with or without the presence of HCl and alcohol. In the older literature, compounds of stoichiometries $(CH_2)_6N_4 \cdot ZnCl_2 \cdot HCl$[2] and $2(CH_2)_6N_4 \cdot 3ZnCl_2 \cdot 6H_2O$[3] were reported. Subsequently, the adducts $(CH_2)_6N_4 \cdot ZnX_2$ (X = Cl or Br) were obtained from crystallization in water–methanol and investigated by X-ray diffraction (lattice constants only)[4] and vibrational spectroscopy.[5] Recently Pickhardt and Dross reported that these two anhydrous complexes are isotypic, forming polymeric chains in the crystal lattice with tetrahedral Cl_2N_2 coordination about each metal atom.[6] In the present paper, we describe the preparation and X-ray crystal structure of the title complex, which can be re-formulated as $2(CH_2)_6N_4 \cdot 3ZnCl_2 \cdot 12H_2O$ for comparison with other related compounds.

EXPERIMENTAL

Preparation of $[Zn(H_2O)_6][\{(CH_2)_6N_4\}ZnCl_3]_2 \cdot 6H_2O$

This compound was obtained from slow evaporation of an aqueous solution of $(CH_2)_6N_4$ and $ZnCl_2$ in a 2 : 3 molar ratio. The crystals effloresced rapidly and turned milky in air, but underwent no apparent change if allowed to remain immersed in the mother liquor.

Crystal data

$C_{12}H_{48}N_8Cl_6O_{12}Zn_3$, $M = 905.38$; prismatic, $0.36 \times 0.32 \times 0.20$ mm sealed in 0.5 mm Lindemann glass capillary; trigonal, $P\bar{3}$ (No. 147),

* Part VII is Ref. 1.

† Author to whom correspondence should be addressed.

$a = 10.884(1)$, $c = 8.784(1)$ Å, $V = 901.2(2)$ Å^3, $D_m = 1.73(1)$ (flotation in CCl_4–$BrCH_2CH_2Br$, crystal turning milky), $D_c = 1.668$ g cm^{-3}, $Z = 1$, $F(000) = 464.76$; Nicolet R3m diffractometer, monochromatized Mo-K_α radiation, $\lambda = 0.71069$ Å, $\mu = 25.35$ cm^{-1}. Accurate unit-cell dimensions were obtained by least-squares refinement of the setting angles of 21 slowly centered reflections in the range $15 < 2\theta < 25°$, and data collection ($2\theta_{max} = 60°$, 783 unique reflections) and reduction followed established procedures in our laboratory.[7] Absorption correction (mean $\mu r = 0.20$, transmission factors 0.763–0.849) was applied using an empirical method based on a pseudo-ellipsoidal fit to azimuthal (ψ) scan data of selected strong reflections.[8]

Structure determination

Statistical distributions of normalized structure factors strongly favored the centrosymmetric space group $P\bar{3}$, which was subsequently confirmed in X-ray analysis. The structure was solved by direct phase determination, and all non-hydrogen atoms were subjected to anisotropic refinement. The methylene H atoms were generated geometrically, and three of the four independent water protons located from a difference Fourier map; these were included in structure-factor calculations with assigned isotropic temperature factors. Convergence was reached at $R = 0.032$, wR (on $|F_o|^2$) $= 0.051$ with $w = [\sigma^2(F_o) + 0.0002|F_o|^2]^{-1}$, and $S = 2.654$ for 63 variables and 747 observed [$|F_o| > 3\sigma(F_o)$] reflections.*

Computations were performed on a Data General Nova 3/12 minicomputer with the SHELXTL program package.[9] Analytic expressions of neutral atomic scattering factors were employed, and anomalous dispersion corrections were incorporated.[10]

RESULTS AND DISCUSSION

It is now well established that the presence of $(CH_2)_6N_4$ as a ligand tends to promote the occurrence of variable coordination geometries about different metal ions of the same kind in the same crystal lattice,[7,11] and the present complex provides yet another illustrative example. Figure 1 shows a perspective view of the discrete $[Zn(H_2O)_6]^{2+}$ and $[\{(CH_2)_6N_4\}ZnCl_3]^{-1}$ ions, which have crystallographically-imposed $\bar{3}$ and 3 molecular symmetries, respectively, and the "lattice" water molecule in the asymmetric unit, together with the system of atom numbering. Bond distances and angles are tabulated in Table 1.

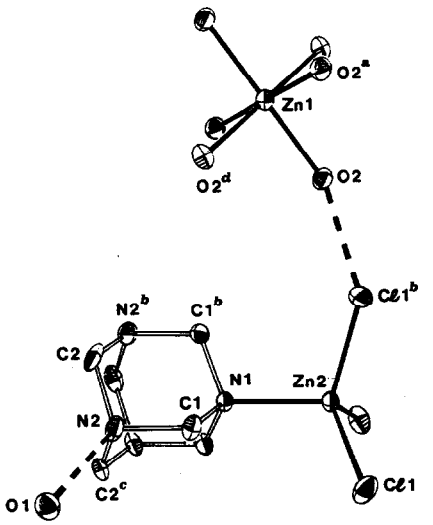

Fig. 1. Perspective view of the discrete molecular ions and lattice water molecule in $[Zn(H_2O)_6][\{(CH_2)_6N_4\}ZnCl_3]_2 \cdot 6H_2O$. Thermal ellipsoids are drawn at the 30% probability level, and hydrogen bonds are represented as broken lines. Atom numbering and symmetry transformations match those given in Table 1.

The $[Zn(H_2O)_6]^{2+}$ octahedron is slightly but significantly flattened along its $\bar{3}$ axis, as shown by the O(2)—Zn—O(2)^a angle of 91.1(1)°; otherwise the Zn(1)—O(2) bond of 2.086(2) Å is normal for the hexaaquazinc(II) moiety, as compared to distances in the range 2.056(2)–2.104(2) Å for the cation in the $[Zn(H_2O)_6]$(isonicotinate *N*-oxide) salt.[12] On the other hand, the quasi tetrahedral $[\{(CH_2)_6N_4\}ZnCl_3]^-$ anion is, to our knowledge, the first reported example of an aminotrichlorozinc(II) species. In fact, discrete tetrahedral anions of the type $[LZnCl_3]^-$ (L = organic ligand) are rare, and cases where L = acetone [Zn—Cl = 2.23 Å][13] and tetrahydrofuran [Zn—Cl = 2.240(3) Å, Cl—Zn—Cl = 112.9(1)–115.9(1)°][14] made their appearance only recently in the literature, whereas dichlorozinc(II) complexes of tetrahedral coordination geometry are commonly encountered. It is evident that the bond lengths and angles around the metal atom in the $[\{(CH_2)_6N_4\}ZnCl_3]^-$ anion (Table 1) are consistent with those in the *O*-donor analogues. As compared to relevant dimensions reported for polymeric $(CH_2)_6N_4 \cdot ZnCl_2$[6] [Zn—N = 2.111(8),

* Final atomic positional and thermal parameters, bond lengths and angles, and F_o/F_c values have been deposited as supplementary material with the Editor, from whom copies are available on request. Atomic coordinates have also been submitted to the Cambridge Crystallographic Data Centre.

Table 1. Bond lengths (Å) and angles (°) with ESDs in parentheses

(1) $[Zn(H_2O)_6]^{2+}$ in Wyckoff position 1(*a*), point system $\bar{3}$			
Zn(1)—O(2)	2.086(2)		
O(2)—Zn(1)—O(2)[a]	91.1(1)	O(2)—Zn(1)—O(2)[d]	88.9(1)
(2) $[\{(CH_2)_6N_4\}ZnCl_3]^-$ in Wyckoff position 2(*d*), point symmetry 3			
Zn(2)—Cl(1)	2.246(1)	Zn(2)—N(1)	2.102(5)
Cl(1)—Zn(2)—Cl(1)[b]	112.6(1)	Cl(1)—Zn(2)—N(1)	106.2(1)
Zn(2)—N(1)—C(1)	110.6(2)		
C(1)—N(1)	1.488(4)	C(1)—N(2)	1.479(5)
C(2)—N(2)	1.473(6)	C(2)[c]—N(2)	1.454(6)
C(1)—N(1)—C(1)[b]	108.3(2)	N(1)—C(1)—N(2)	111.0(3)
C(1)—N(2)—C(2)	107.6(3)	C(1)—N(2)—C(2)[c]	108.9(4)
C(2)—N(2)—C(2)[c]	108.5(5)	N(2)—C(2)—N(2)[b]	112.4(5)
(3) Hydrogen bonding			
O(1)—H...N(2)	2.790(3)	O(1)—H...O(1)[g]	2.732(5)
O(2)—H...O(1)[e]	2.727(4)	O(2)—H...Cl(1)[b]	3.254(5)
N(2)...O(1)...O(1)[g]	122.8(1)	N(2)...O(1)...O(2)[f]	92.4(1)
N(2)...O(1)...O(1)[h]	123.8(1)	O(1)[g]...O(1)...O(1)[h]	88.7(2)
O(1)[h]...O(1)...O(2)[f]	131.1(1)	O(1)[g]...O(1)...O(2)[f]	98.3(1)
O(1)[e]...O(2)...Cl(1)[b]	100.0(2)	Zn(1)—O(2)...O(1)[e]	121.4(2)
Zn(1)—O(2)...Cl(1)[b]	124.8(3)	Zn(2)—Cl(1)[b]...O(2)	120.7(3)
O(1)...N(2)—C(1)	106.3(4)	O(1)...N(2)—C(2)	119.1(4)
O(1)...N(2)—C(2)[c]	106.2(4)		

Symmetry codes: [a] $-x+y, -x, z$; [b] $-x+y, 1-x, z$; [c] $1-y, 1+x-y, z$; [d] $y, -x+y, -z$; [e] $-1+y, -x+y, -z$; [f] $1+x-y, 1+x, -z$; [g] $y, 1-x+y, -1-z$; [h] $1+x-y, x, -1-z$.

Zn—Cl = 2.221(4) Å, Cl—Zn—Cl = 119.3(2)°] and tetrahedral $[Zn(NH_3)_2Cl_2]$[15] [Zn—N = 2.024(2), Zn—Cl = 2.273(1) Å and Cl—Zn—Cl = 109.2(1)°], the present data reflect the difference in number of chloro ligands, and the fact that zinc(II) forms stronger bonds to primary amines than tertiary amines, with concomitant weakening of the Zn—Cl bonds in the former instance.

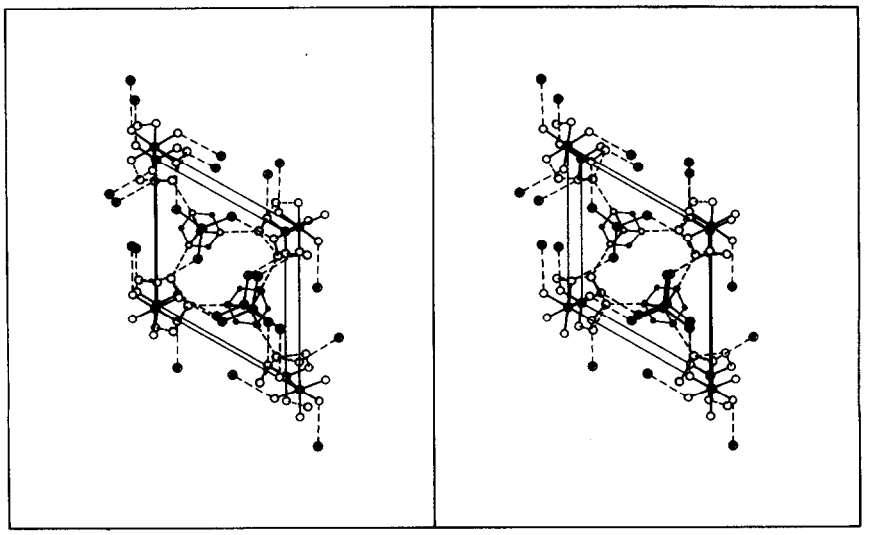

Fig. 2. Stereoview of the molecular packing. The origin of the unit cell lies at the lower left corner, with **a** pointing from left to right at a slant, **b** upwards, and **c** towards the reader. Hydrogen bonds are represented by broken lines, and atom types are differentiated by size and shading.

As illustrated in Fig. 2, the $[\{(CH_2)_6N_4\}ZnCl_3]^-$ ions are stacked in columns along the crystallographic three-fold axes. The $\bar{3}$ symmetry operation on O(1) generates a chair-like aggregate of six water molecules, forming a hydrogen-bonded $(H_2O)_6$ ring which serves as a "spacer" midway between a pair of $[Zn(H_2O)_6]^{2+}$ octahedra. Similar puckered $(H_2O)_6$ rings have been recognized as structural fragments in a variety of crystalline hydrates: well-known examples include the ice polymorphs,[16] polyhedral clathrate hydrates,[17] $(CH_2)_6N_4 \cdot 6H_2O$,[18] and other hydrate inclusion compounds.[19,20] Nevertheless, the occurrence of such a ring in a coordination compound is highly unusual. In the present complex, the $(H_2O)_6$ rings and cations occupying alternate $\bar{3}$ sites are linked by "intermolecular" O—H...O hydrogen bonds, giving rise to a second type of columnar stack. In the resulting crystal structure, the two types of columns interconnect laterally via O—H...N and O—H...Cl hydrogen bonds (involving lattice and ligand water molecules, respectively) to form a three-dimensional network (Fig. 2). Geometrical details of the hydrogen bonding are given in Table 1. It is seen that the bond configuration about the O(1) atom deviates markedly from regular tetrahedral, with O...O...O angles over a wide range of 88.7(2)–131.1(1)°.

The measured dimensions of the organic ligand (Table 1), which utilizes all four nitrogen lone pairs in stabilizing the crystal lattice, are in fairly good agreement with those of crystalline $(CH_2)_6N_4$ [C—N = 1.476(2) Å, C—N—C = 107.2(1)°, N—C—N = 113.6(2)°].[21] Deviation of the present cage system from idealized $\bar{4}3m$ symmetry is manifested by the significantly different C(1)—N(1) and C(2)^c—N(2) bond distances, and involvement in coordinate and hydrogen bonding leads to enlargement of the C—N—C angles in accordance with VSEPR expectations.

Acknowledgements—This work was performed under the auspices of an academic exchange and collaboration programme between the Chinese University of Hong Kong and institutions of higher learning in China. We also thank Wai-Hing Yip for technical assistance.

REFERENCES

1. T. C. W. Mak and Y.-K. Wu, *Inorg. Chim. Acta* 1985, **104**, 149.
2. J. Altpeter, *Das Hexamethylentetramin und seine Verwendung*, p. 42. Knapp, Halle (1931).
3. J. C. Duff and E. J. Bills, *J. Chem. Soc.* 1929, 411.
4. G. Giuseppetti, *Period. Mineral.* 1954, **23**, 177.
5. J. R. Allan, D. H. Brown and M. Lappin, *J. Inorg. Nucl. Chem.* 1970, **32**, 2287.
6. J. Pickardt and P. Dross, *Z. Naturforsch.* 1985, **40b**, 1756.
7. T. C. W. Mak, *Inorg. Chim. Acta* 1984, **84**, 19; 1984, **90**, 153.
8. G. Kopfmann and R. Huber, *Acta Cryst.* 1968, **A24**, 348; A. C. T. North, D. C. Phillips and F. S. Mathews, *Acta Cryst.* 1968, **A24**, 351.
9. G. S. Sheldrick, In *Computational Crystallography* (Edited by D. Sayre), p. 506. Oxford University Press, New York (1982).
10. *International Tables for X-ray Crystallography*, Vol. 4, pp. 55–60, 99–101 and 149–150. Kynoch Press, Birmingham, U.K. (1974). [Now distributed by D. Reidel, Dordrecht.]
11. T.-F. Lai and T. C. W. Mak, *Z. Krist.* 1983, **165**, 105.
12. P. Knuuttila, *Polyhedron* 1984, **3**, 303.
13. V. C. Adam, U. A. Gregory and B. T. Kilbourn, *J. Chem. Soc., Chem. Commun.* 1970, 1400.
14. K. Folting, J. C. Huffman, R. L. Bansemer and K. G. Caulton, *Inorg. Chem.* 1984, **23**, 3289.
15. T. Yamaguchi and O. Lindqvist, *Acta Chem. Scand.* 1981, **A35**, 727.
16. B. Kamb, In *Structural Chemistry and Molecular Biology* (Edited by A. Rich and N. Davidson), p. 507. Freeman, San Francisco (1968).
17. G. A. Jeffrey and R. K. McMullan, *Prog. Inorg. Chem.* 1967, **8**, 43.
18. T. C. W. Mak, *J. Chem. Phys.* 1965, **43**, 2799.
19. G. A. Jeffrey, In *Inclusion Compounds* (Edited by J. L. Atwood, J. E. D. Davis and D. D. MacNicol), Vol. 1, p. 135. Academic Press, London (1984).
20. G. A. Jeffrey, *J. Incl. Phenom.* 1984, **1**, 211.
21. L. N. Becka and D. W. J. Cruickshank, *Proc. R. Soc.* 1963, **A273**, 434.

Polyhedron Vol. 6, No. 5, pp. 1115–1123, 1987
Printed in Great Britain

0277–5387/87 $3.00+.00

A REACTION CONVERTING A W–W TRIPLE BOND TO A DOUBLE BOND: TETRAKIS-DIETHYLDITHIOPHOSPHATE-DISULFIDE-DITUNGSTEN, PREPARATION AND CHARACTERIZATION

MALCOLM H. CHISHOLM,* DOUGLAS M. HO, JOHN C. HUFFMAN and WILLIAM G. VAN DER SLUYS

Department of Chemistry and Molecular Structure Center, Indiana University, Bloomington, IN 47405, U.S.A.

(*Received* 6 *October* 1986; *accepted* 10 *October* 1986)

Abstract—The reaction between $W_2X_2(OR)_4$ compounds [X = CH_2CMe_3 or OBu^t] and $HS_2P(OEt)_2$ (6 equivalents) in hydrocarbon solvents, produces a molecule of formula $W_2S_2[S_2P(OEt)_2]_4$ with corresponding elimination of alkane, alcohol and $[(EtO)_2PS]_2$. This tungsten compound has been characterized by IR, ^1H, ^{13}C, and ^{13}P NMR spectroscopy, electronic absorption spectroscopy and single-crystal X-ray crystallography. The molecule adopts a structure based on an edge-shared bioctahedron, with two bridging sulfides, two chelating dithiophosphate ligands and two dithiophosphate ligands bridging the metal–metal double bond. The W–W distance of 2.5987(11) Å along with the acute W—S—W angles of 67.74(8)°, are consistent with the metal–metal double bond formulation $\sigma^2\pi^2$. This structure is similar to the $W_2S_2(S_2CNEt_2)_4$ molecule prepared by Cotton *et al.* (*Inorg. Chem.* 1978, **17**, 2946).

Of all the compounds containing metal–metal multiple bonds, the group VI (Cr, Mo and W) metals show the most varied and fascinating coordination chemistry. The range of formal bond order extends from M–M single bonds to M–M quadruple bonds.[1] The chemistry of compounds containing M–M single, triple and quadruple bonds is quite extensive, but an exception is seen for M–M double bonds. The list of compounds containing M–M double bonds is comparatively short.[1]

We have been investigating the chemistry of M–M triply bonded compounds of formula M_2X_n (M = Mo or W, X = ligand atom, n = 6–12).[2] Of particular interest has been the higher metal coordination numbers of 5 and 6.[3–5] In this paper we wish to present our results concerning the reactions of $W_2X_2(OR)_4$ (X = alkyl or alkoxide) with dialkyldithiophosphoric acids.

Following our discovery of a general synthesis of compounds with the formula $M_2R_2(O_2CR')_4$ (M = Mo or W) [eqn (1)]:[6]

$$M_2R_2(OPr^i)_4 + 4R'CO_2H \xrightarrow[25°C]{\text{toluene}} M_2R_2(O_2CR')_4 + 4HOPr^i, \quad (1)$$

we wished to extend this series of compounds to include bidentate ligands other than carboxylates. Interest in compounds of formula $M_2R_2(O_2CR')_4$ arises from their unusual valence MO description of the M–M triple bond as $\pi^4\delta^2$.[7] Our choice of dialkyldithiophosphates seemed appropriate in that this ligand has somewhat different steric and electronic properties from carboxylates.

RESULTS AND DISCUSSION

Synthesis

The reaction of $W_2Np_2(OPr^i)_4$ (Np = CH_2CMe_3) with $(EtO)_2PS_2H$ in toluene does not produce a complex with the formula $W_2Np_2[S_2P(OEt)_2]_4$, but does produce a rather interesting molecule of formula $W_2S_2[S_2P(OEt)_2]_4$ (**1**). This green,

* Author to whom correspondence should be addressed.

diamagnetic, crystalline, air-stable, hydrocarbon-soluble compound can be isolated in approximately 60% crystalline yield according to eqn (2):

$$W_2Np_2(OPr^i)_4 + \geqslant 6HS_2P(OEt)_2 \xrightarrow[0°C]{\text{toluene}} W_2S_2[S_2P(OEt)_2]_4 + 2NpH + 4HOPr^i + [(EtO)_2PS]_2. \quad (2)$$

The phosphorus-containing by-product of eqn (2) was identified by ^{31}P NMR spectroscopy and has a chemical shift of δ 89.8 ppm in benzene-d_6.* The volatile product, neopentane, was identified in the ^1H NMR spectrum of the reaction mixture and has a chemical shift of 0.89 ppm in benzene-d_6.

There is some question as to how the neopentane was produced in eqn (2). It could be either produced by: (1) homolytic cleavage of the W—C bonds to produce Np$^\bullet$ radicals, which then abstracted H$^\bullet$; or by (2) acid protonolysis of the alkyl ligands. When the reaction was carried out at −78°C, a turquoise color could be detected before the final deep forest green was formed. When the reaction was monitored by ^1H NMR spectroscopy at −78°C, several intermediates were observed, but it was difficult to definitively assign any of these to $W_2[S_2P(OEt)_2]_6$.

It was also found that **1** can be prepared by the reaction of $W_2(OBu^t)_6$ with $(EtO)_2PS_2H$, according to eqn (3):

$$W_2(OBu^t)_6 + \geqslant 6HS_2P(OEt)_2 \xrightarrow[0°C]{\text{toluene}} \underset{\mathbf{1}}{W_2S_2[S_2P(OEt)_2]_4} + 6HOBu^t + [(EtO)_2PS]_2. \quad (3)$$

This result suggests that the neopentane produced in eqn (2) results from protonation of the alkyl ligands and that $W_2[S_2P(OEt)_2]_6$ is a likely, but not proven, intermediate in reactions (2) and (3).

When **1** was heated to 60°C in a sealed NMR tube, an orange solution was produced. The ^1H NMR spectrum of this product or products is very complicated. The most information is gained from the methylene signals. There are at least four $ABMX_3$ patterns in this region, which suggests that there is no plane of symmetry in this product(s). Perhaps the molecule has undergone further oxidative addition of sulfide ligands, but the thermolysis reaction has not yet been followed up.

*The ^{31}P NMR chemical shift of $(Et_2PS)_2$ is δ 52.5 and $(Ph_2PS)_2$ is δ 37.9 in toluene-d_8; PEt_3 is δ −20 and $P(OEt)_3$ is δ 86.[8]

NMR studies

The ^1H NMR spectrum of **1** at 25°C in benzene-d_6 is shown in Fig. 1. It is evident that this molecule has two different types of dithiophosphate ligands. The methylene protons of the ethyl groups display A_2MX_3 patterns with the slightly different $^3J_{PH}$ coupling of 9.7 and *ca* 7.0 Hz. This gives rise to the doublet of quartets at δ 4.35 ppm and the apparent pentet at δ 3.46 ppm.

The ^{31}P–$\{^1H\}$ spectrum of **1** shows that there are two different types of phosphorus nuclei in a 1:1 ratio. These signals occur at δ 194.0 and 127.4 ppm, and do not show coupling to ^{183}W. The ^1H-coupled spectrum reveals that the signal at δ 127.4 ppm becomes a triplet, with $^3J_{PH}$ = 9.6 Hz. This indicates that the ^{31}P signal at 127.4 ppm and the ^1H NMR signal at 4.35 ppm arise from the same ligand.

The ^{13}C NMR spectra, ^1H-coupled and decoupled, are shown in Fig. 2. It can be seen in the ^{13}C–$\{^1H\}$ spectrum that there are again two types of ethyl resonances. One of the methylene resonances at δ 65.37 ppm shows coupling to phosphorus of $^2J_{PC}$ = 10.4 Hz, while the other resonance at 65.99 ppm does not show coupling. Likewise, the methyl resonances have a similar pattern. The signal at δ 16.08 ppm shows a $^3J_{PC}$ = 8.3 Hz, while the signal at δ 15.75 ppm is a singlet.

We believe that the differences in the coupling constants of the two different ligands can be explained by the differences in the bite angles of the ligands (*vide infra*).

Solid-state and molecular structure

Good-quality crystals of **1** were grown from concentrated hexane solutions at −20°C. An ORTEP view of the molecule showing the atom numbering scheme used in the tables is given in Fig. 3, and a stereo view of the molecule is given in Fig. 4. Bond distances and angles are given in Tables 1 and 2, respectively.

The overall geometry of **1** is quite similar to that of $W_2S_2(S_2CNEt_2)_4$ (**2**) prepared and characterized by Cotton *et al.*[9] The W–W bond distance of **1** is 2.5987(11) Å, and is slightly longer than the W–W bond distance of **2** at 2.530(2) Å. Both of these molecules have two bridging sulfides. There are two significant indications that these molecules must have W–W double bonds: (1) the W–W distances are intermediate between W–W triple bonds, *ca* 2.3 Å, and W–W single bonds, *ca* 2.7 Å; and (2) the W—S—W angles are very acute, being *ca* 68°.

The bonding in d^n–d^n edge-shared bioctahedra of formula $L_4M(\mu\text{-}L)_2ML_4$ was first discussed in detail by Hoffmann and coworkers[10] who

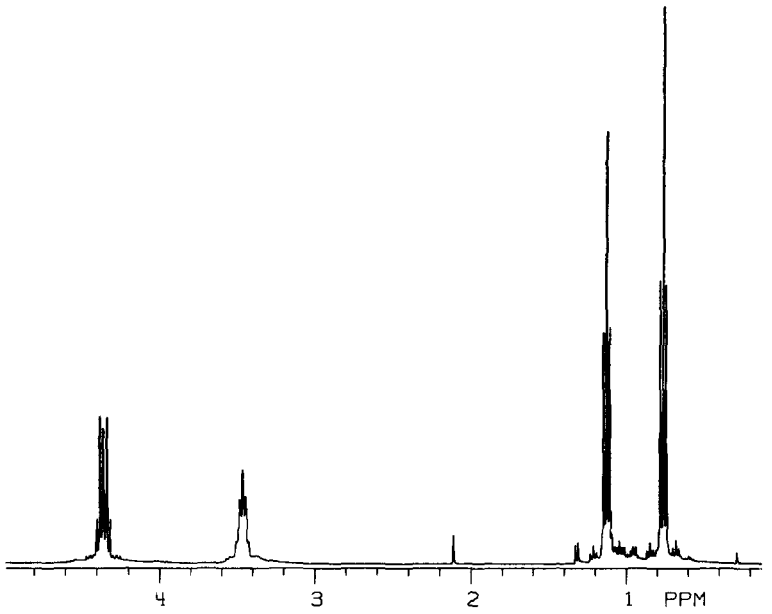

Fig. 1. ^{1}H NMR spectrum of $W_2S_2[S_2P(OEt)_2]_4$ in benzene-d_6 at 22°C (360 MHz).

showed that at certain metal–metal distances and with the μ-L groups having filled π-orbitals, the intuitive ordering of the t_{2g}–t_{2g} interaction $\sigma < \pi < \delta < \delta^* < \pi^* < \sigma^*$ of M–M bonding MOs will not hold. The problem arises most acutely for the δ- and δ^*-levels which may be inverted. In the present case of a d^2–d^2 dimer the M–M configuration of $\sigma^2\pi^2$ will remain. However, it should be noted that the M–M π-orbital will interact to some extent with the sulfur lone pairs of the dithiophosphate ligands. If the latter were dominant, which it clearly is not, then M–M π^* occupation would occur. For example, the M–M distance in **1** is notably shorter than the Mo–Mo distance in $[(HNMe_2)_2(Bu^tS)_2Mo(\mu\text{-}S)]_2$ [2.730(1) Å], which is a d^2–d^2 dinuclear compound having a central planar $[Mo(\mu\text{-}S)]_2$ moiety involving the fusing of trigonal bipyramids along a common axial–equatorial edge.[11] There the M–M MO description is probably $\sigma^2\delta^2$, and at best there is only effectively a single M–M bond at a distance of 2.7 Å. For a comparison with a non-bonding distance one may note the Zn–W distance [2.927(1) Å] in $[Zn(WS_4)_2]^{2-}$, which involves three fused tetrahedra: $S_2W(\mu\text{-}S)_2Zn(\mu\text{-}S)_2WS_2$.[12]

An interesting feature of **1**, not observed in **2**[9] is that the W_2S_2P unit of the bridging phosphate ligands is not planar, whereas the WS_2P unit of the chelated phosphate ligands is planar. This could be the result of the bite angle of the tetrahedral phosphorus not being conducive for forming a planar five-membered ring. It may well be that in the dithiocarbamate ligand, the CS_2 unit is flexible enough to allow for planarity in both the bridging and chelating ligands, and in any event for electronic reasons there is conjugation with the amido lone pair which is not possible for the dithiophosphate ligands.

A final point of interest to us is that the W—S distances to the chelating $S_2P(OEt)_2$ ligands

Table 1. Selected bond distances (Å) for $W_2S_2[S_2P(OEt)_2]_4$

A	B	Distance
W(1)	W(1)′	2.5987(11)
W(1)	S(2)	2.258(3)
W(1)	S(2)′	2.400(3)
W(1)	S(3)	2.561(3)
W(1)	S(5)	2.582(3)
W(1)	S(12)	2.507(3)
W(1)	S(14)′	2.461(3)
S(3)	P(4)	1.988(4)
S(5)	P(4)	2.002(4)
S(12)	P(13)	2.012(4)
S(14)	P(13)	2.009(4)
P(4)	O(6)	1.576(8)
P(4)	O(9)	1.587(9)
P(13)	O(15)	1.569(8)
P(13)	O(18)	1.560(9)
O(6)	C(7)	1.462(15)
O(9)	C(10)	1.460(17)
O(15)	C(16)	1.455(15)
O(18)	C(19)	1.453(15)

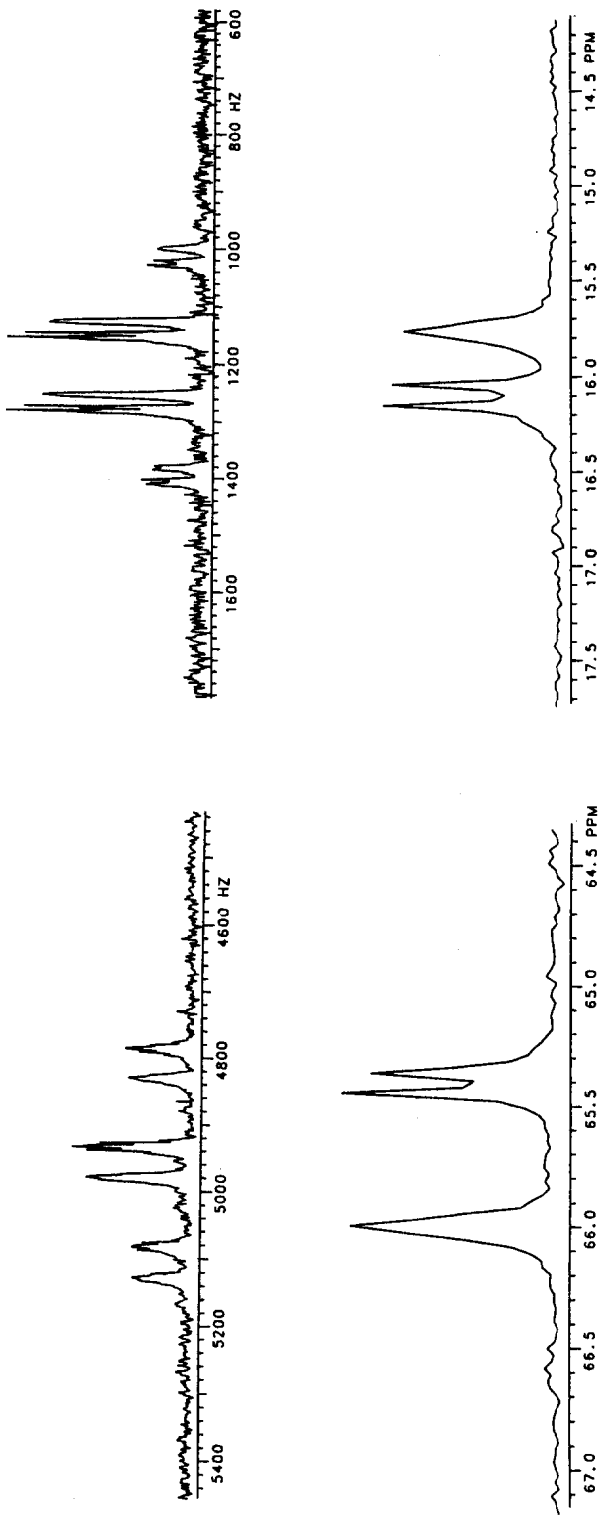

Fig. 2. ^{13}C NMR spectrum of $W_2S_2[S_2P(OEt)_2]_4$ (A), and $^{13}C\{^1H\}$ NMR spectrum (B) recorded in benzene-d_6 at 75 MHz.

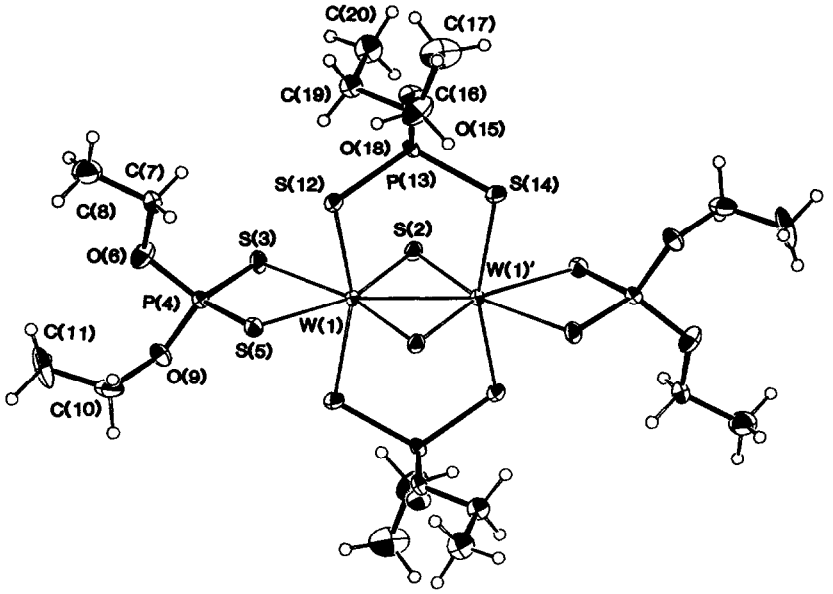

Fig. 3. ORTEP view of the centrosymmetric $W_2S_2[S_2P(OEt)_2]_4$ molecule giving the atom-numbering scheme used in the tables.

are longer than those to the bridging $S_2P(OEt)_2$ ligands. The difference, 2.57 vs 2.48 Å (averaged), is the same as noted for d^1–d^1 dinuclear compounds of formula $W_2(OPr^i)_6(O_2C_2R_2)_2$[13] and $Mo_2(OPr^i)_6(O_2C_6Cl_4)_2$, where $O_2C_6Cl_4$ is *ortho*-tetra-chlorobenzoquinone in its fully reduced form.[14] The reasoning for the differences in M—L_{ax} vs M—L_{eq} distances, though small, could have a similar origin as that invoked previously.[13]

Electronic absorption spectra

The electronic absorption spectra of both **1** and **2** are compared in Fig. 5. Both molecules are dark green and both show several absorption features between 300 and 750 nm. The spectrum of **1** has two well-resolved maxima at 645 nm (1.55×10^4 cm^{-1}) and 443 nm (2.26×10^4 cm^{-1}) as well as a series of absorptions between 400 and 300 nm. The spectrum of **2** is quite similar to **1** except for the inclusion of a new absorption at low energy [693 nm (1.44×10^4 cm^{-1})]. This transition at low energy does not appear to be present in the spectrum of **1** and thus may be due to: (1) a change in point group from C_{2h} in **1** to D_{2h} in **2**, or (2) a difference in the ligands supporting the molecules. A summary of the UV–visible spectral data is given in Table 3.

If it is assumed that the M–M δ- and δ^*-orbitals

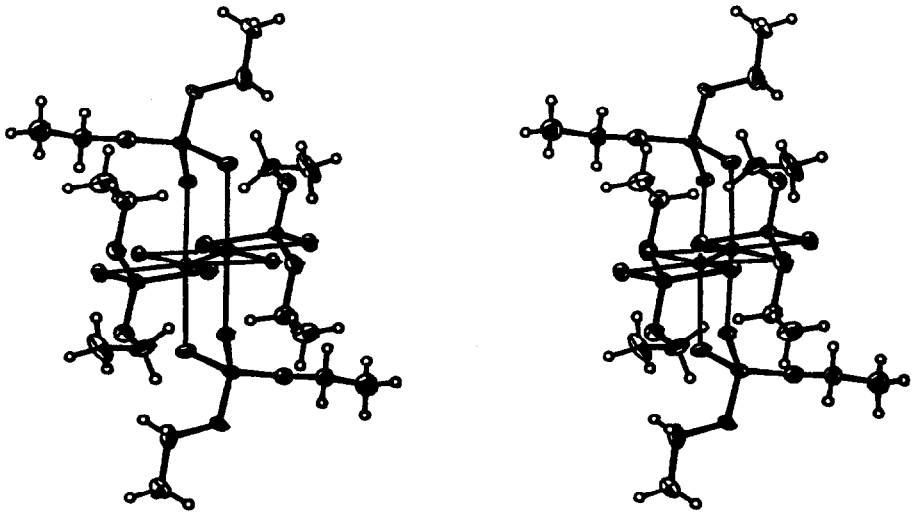

Fig. 4. Stereo view of the $W_2S_2[S_2P(OEt)_2]_4$ molecule emphasizing the nonplanar nature of the bridging W_2S_2P units.

Table 2. Selected bond angles (°) for $W_2S_2[S_2P(OEt)_2]_4$

A	B	C	Angle
W(1)′	W(1)	S(2)′	53.52(7)
W(1)′	W(1)	S(3)	142.93(7)
W(1)′	W(1)	S(5)	139.90(7)
W(1)′	W(1)	S(12)	96.91(7)
W(1)′	W(1)	S(14)′	100.62(8)
S(2)	W(1)	S(2)	112.26(8)
S(2)	W(1)	S(3)′	84.19(10)
S(2)	W(1)	S(5)	160.30(10)
S(2)	W(1)	S(12)	98.36(10)
S(2)	W(1)	S(14)′	99.11(11)
S(2)	W(1)	S(1)′	58.74(11)
S(2)′	W(1)	S(14)′	92.90(11)
S(2)′	W(1)	S(12)	89.62(11)
S(2)′	W(1)	S(3)	163.54(11)
S(2)′	W(1)	S(5)	86.71(11)
S(3)	W(1)	S(5)	76.96(10)
S(3)	W(1)	S(12)	88.23(10)
S(3)	W(1)	S(14)′	83.72(10)
S(5)	W(1)	S(12)	75.63(10)
S(5)	W(1)	S(14)′	84.60(10)
S(12)	W(1)	S(14)′	159.90(10)
W(1)	S(2)	W(1)′	67.74(8)
W(1)	S(3)	P(4)	88.40(14)
W(1)	S(5)	P(4)	87.51(14)
W(1)	S(12)	P(13)	103.96(14)
W(1)	S(14)	P(13)	105.63(16)
S(3)	P(4)	S(5)	106.66(18)
S(3)	P(4)	O(6)	115.6(4)
S(3)	P(4)	O(9)	108.8(3)
S(5)	P(4)	O(6)	111.9(3)
S(5)	P(4)	O(9)	113.8(4)
O(6)	P(4)	O(9)	100.1(5)
S(12)	P(13)	S(14)	114.44(19)
S(12)	P(13)	O(15)	107.0(4)
S(12)	P(13)	O(18)	114.6(3)
S(14)	P(13)	O(15)	108.6(3)
S(14)	P(13)	O(18)	108.8(3)
O(15)	P(13)	O(18)	102.5(5)
P(4)	O(6)	C(7)	122.5(8)
P(4)	O(9)	C(10)	121.2(8)
P(13)	O(15)	C(16)	120.8(8)
P(13)	O(18)	C(19)	122.6(7)
O(6)	C(7)	C(8)	108.3(10)
O(9)	C(10)	C(11)	109.5(11)
O(15)	C(16)	C(17)	109.0(11)
O(18)	C(19)	C(20)	107.7(10)

are occupied and lie to lower energy than the M–M σ- and π-orbitals, because these represent sulfur-based orbitals, then we might look for the lowest-energy transition to be M–M $\pi \rightarrow \pi^*$. However, in the absence of a detailed MO calculation which reliably establishes the ground state electronic

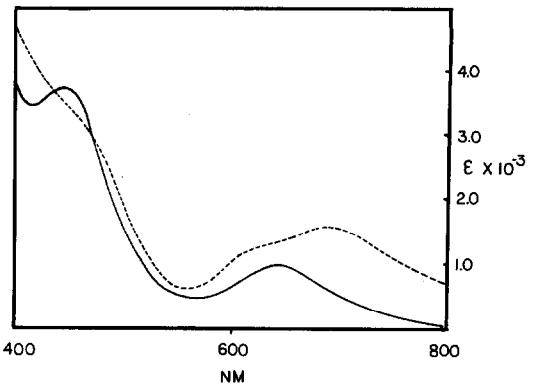

Fig. 5. Electronic absorption spectra of $W_2S_2[S_2P(OEt)_2]_4$ (——) and $W_2S_2(S_2CNEt_2)_4$ (– – –).

structure, we must defer further speculation about such an assignment.

Concluding remarks

Compound **1** provides another example of a compound containing a metal–metal double bond. Since this molecule is quite similar to the **2** molecule,[9] we have been able to compare relatively subtle changes in the physical properties of these molecules. The electronic structure though not well understood, almost certainly has the valence MO configuration of $\sigma^2\pi^2$ for the M–M bond.

EXPERIMENTAL

All operations were carried out using standard Schlenk and Glove-box techniques with dry and oxygen-free solvents and atmospheres. Starting

Table 3. Electronic absorption data for $W_2S_2[S_2P(OEt)_2]_4$ (**1**) and $W_2S_2(S_2CNEt_2)_4$ (**2**) recorded in CH_2Cl_2

Compound	λ (nm)	λ ($\times 10^4$ cm^{-1})	ε (M^{-1} cm^{-1})
1	645	1.55	1000
	443	2.26	3800
	sh 350	2.86	5700
	330	3.03	5800
	300	3.33	5700
2	693	1.44	1600
	sh 600	1.67	1100
	sh 460	2.17	3200
	sh 394	2.54	10,000
	356	2.81	11,000

materials were prepared via published procedures.[15,16] Diethyldithiophosphoric acid and diethyldithiuramdisulfide were purchased from Aldrich and the acid was degassed by two freeze–pump–thaw cycles.

^{1}H NMR spectra were run on a Nicolet NT-360 spectrometer at 360 MHz, and chemical shifts are reported in δ ppm with the ^{1}H impurity of benzene-d_6 set at δ 7.15 ppm. ^{13}C NMR spectra were run on a Varian XL-300 spectrometer at 75 MHz. ^{31}P NMR spectra were run on a Varian XL-100 at 40.5 MHz.

IR spectra were obtained on a Perkin–Elmer 283 spectrophotometer as Nujol mulls, between CsI salt plates and referenced to polystyrene at 1601 cm^{-1}.

Electronic absorption spectra were obtained on a Perkin–Elmer 330 spectrophotometer using matched 1.00- and 0.10-cm quartz cells. Spectral grade solvents were used without further purification, except for degassing.

Elemental analysis was performed by Alfred Bernhardt Microanalytisches Laboratorium, Elbach, West Germany.

Synthesis

$W_2S_2[S_2P(OEt)_2]_4$. In a Schlenk flask, 0.50 g (0.67 mmol) of $W_2Np_2[OPr^i)_4$ was dissolved in 10 cm^3 of toluene. The flask was cooled to 0°C in an ice bath. To this was added via a syringe, 0.69 cm^3 (4.1 mmol, 6 equivalents) of diethyldithiophosphoric acid. The solution immediately turned from yellow to turquoise, and then after several minutes turned dark green. After the solution had turned green the solvent was removed *in vacuo* to give a green waxy microcrystalline solid. Hexane was added and the green solution was filtered. The volume of the solution was reduced until several small crystals began to appear. The flask was then slowly cooled to −20°C. After 24 h large green cubes had formed. The solvent was removed via a cannula to yield 0.48 g of the product (61% yield based on tungsten). This compound is air-stable in the solid state for indefinite periods.

Analysis: Found: C, 16.5; H, 3.3; N, < 0.03; S, 27.4. Calc. for $W_2S_{10}P_4O_8C_{16}H_{40}$: C, 16.4; H, 3.4; N, 0.00; S, 27.3%.

IR (cm^{-1}): 272(mw), 310(mw), 452(w), 523(m), 539(m), 630(ms), 647(ms), 762(ms), 778(ms), 786(s), 948(vs), 957(vs), 970(vs), 999(vs), 1010(vs), 1032(vs), 1099(mw), 1160(mw), 1275(vw).

^{1}H NMR (22°C) (benzene-d_6): δ 4.35 (dq, $^3J_{HH}$ = 7.2 Hz, $^3J_{PH}$ = 9.7 Hz, C$\underline{H}_2$CH$_3$), δ 3.46 (p, $^3J_{HH}$ = 7.2 Hz, $^3J_{PH}$ = 7 Hz), δ 1.12 (t, $^3J_{HH}$ = 7.2 Hz, CH$_2$C$\underline{H}_3$), δ 0.76, (t, $^3J_{HH}$ = 7.2 Hz, CH$_2$C$\underline{H}_3$).

^{31}P–{^{1}H} NMR (22°C) (benzene-d_6): δ 193.96 [s, bridging $S_2P(OEt)_2$], δ 127.37 [s, chelate $S_2P(OEt)_2$].

^{13}C–{^{1}H} NMR (22°C) (benzene-d_6): δ 65.99 (s, $\underline{C}H_2CH_3$), δ 65.37 (d, $^2J_{PH}$ = 10.4 Hz, $\underline{C}H_2CH_3$), δ 16.08 (d, $^3J_{PH}$ = 8.3 Hz, $CH_2\underline{C}H_3$), δ 15.75 (s, $CH_2\underline{C}H_3$).

Melting point: 127–132°C, turns red with decomposition.

An alternative synthesis used $W_2(OBu^t)_6$[16] in place of $W_2Np_2(OPr^i)_4$ with the procedure described above. The yield was 52% based on tungsten.

$W_2S_2(S_2CNEt_2)_4$. The procedure of Cotton *et al.*[9] was used to prepare this compound. $W(CO)_3(NCMe)_3$ (1.0 g, 1.7 mmol), was placed in a Schlenk flask and dissolved in acetone. To this was added 2 equivalents (1.04 g, 3.4 mmol) of diethyldithiuramdisulfide using a solids addition tube. The solution was stirred for 24 h, after which a green powder had precipitated from a red solution. The solid was collected by filtration, to give 0.27 g (15% yield based on tungsten). The red product appeared to be $W(S_2CNEt_2)_4$ based on ^{1}H NMR.

^{1}H NMR (22°C) (benzene-d_6): δ 4.11 (q, $^3J_{HH}$ = 7.2 Hz, C$\underline{H}_2$CH$_3$), δ 3.34 (q, $^3J_{HH}$ = 7.2 Hz, C$\underline{H}_2$CH$_3$), δ 1.47 (t, $^3J_{HH}$ = 7.2 Hz, CH$_2$C$\underline{H}_3$), δ 0.92 (t, $^3J_{HH}$ = 7.2 Hz, CH$_2$C$\underline{H}_3$).

Crystallography. General operating procedures and a listing of programs have been given.[17] Crystal data for **1** are summarized in Table 4. An air-stable green-black crystal with dimensions 0.20 × 0.21 × 0.21 mm was selected and affixed to the end of a glass fiber with silicone grease, and then transferred to a Picker goniostat and cooled to −152°C for characterization and data collection.

A systematic search of a limited hemisphere of reciprocal space located a set of diffraction maxima with systematic absences and symmetry consistent with the monoclinic space group $P2_1/n$. Subsequent solution and refinement confirmed this choice.

Data were collected in the usual manner and Lorentz-polarization and absorption corrections applied yielding a unique set of 2456 reflections. Of these, 2445 reflections had $F > 3.0\,\sigma(F)$. The R on averaging was 0.020 for 644 reflections measured more than once.

The structure was solved by a combination of direct methods (MULTAN78) and Fourier techniques, and was refined by full-matrix least squares. Many of the hydrogen positions were visible in a difference Fourier map phased on the non-hydrogen structure after isotropic refinement. Subsequent refinements with anisotropic parameters for all non-hydrogen atoms and, with hydrogen positional and thermal parameters included as variables, resulted

Table 4. Summary of crystal data for the $W_2S_2[S_2P(OEt)_2]_4$ molecule

Empirical formula	$W_2S_{10}P_4O_8C_{16}H_{40}$
Color of crystal	Green-black
Space group	$P2_1/n$
Cell dimensions	
Temperature (°C)	−152
a (Å)	10.905(3)
b (Å)	13.784(4)
c (Å)	13.360(4)
β (°)	110.48(1)
Z (molecules/cell)	2
Volume (Å^3)	1881.08
Calculated density (g cm^{-3})	2.070
Wavelength (Å)	0.71069
Molecular weight	1172.68
Linear absorption coefficient (cm^{-1})	69.803
Detector to sample distance (cm)	22.5
Sample to source distance (cm)	23.5
Take off angle (°)	2.0
Average ω scan width at half height (°)	0.25
Scan speed (deg min^{-1})	6.0
Scan width (deg + dispersion)	1.8
Aperture size (mm)	3.0 × 4.0
2θ range (°)	6–45
Total number of reflections collected	3290
Number of unique intensities	2456
Number of $F > 3.00\ \sigma(F)$	2445
$R(F)$	0.0455
$R_w(F)$	0.0545
Goodness of fit for the last cycle	2.1136
Maximum δ/σ for last cycle	0.0023

in some of the C—H bonds being observed as uncomfortably long and also indicated that the carbon atoms of one of the ethoxy groups had gone non-positive definite. Attempts to locate a suitable disorder model for this ethoxy group were without success. Refinement was resumed with isotropic temperature factors for these two carbon atoms and anisotropic parameters for all other non-hydrogen atoms. The hydrogens were included in the succeeding cycles of least squares as fixed contributors at calculated positions and with thermal parameters of $1 + B_{iso}$ that of the carbon atoms to which they were bound. The final-difference map was essentially featureless, with the largest peak being 1.0 e Å^{-3} and located 0.3 Å from the tungsten atom.*

*Final atomic positional and thermal parameters, bond lengths and angles and F_o/F_c values have been deposited as supplementary material with the Editor, from whom copies are available on request. Atomic coordinates have also been submitted to the Cambridge Crystallographic Data Centre.

Acknowledgements—We would like to thank the NSF and the Wrubel computing center for financial support. Thanks to J. Pelati for helpful discussions and W. E. Buhro for experimental assistance.

REFERENCES

1. F. A. Cotton and R. A. Walton, *Multiple Bonds Between Metal Atoms*. Wiley, New York (1982).
2. M. H. Chisholm, *Angew. Chem., Int. Ed. Engl.* 1986, **25**, 21.
3. B. Bursten, M. H. Chisholm, D. L. Clark, J. C. Huffman, E. Kober, D. L. Lichtenberger and W. G. Van Der Sluys, *J. Am. Chem. Soc.* in press.
4. M. H. Chisholm, D. L. Clark, J. C. Huffman and W. G. Van Der Sluys, manuscript in preparation.
5. M. H. Chisholm, J. Heppert, D. M. Hoffman and J. C. Huffman, *Inorg. Chem.* 1985, **24**, 3214.
6. (a) M. H. Chisholm, D. M. Hoffman, J. C. Huffman, W. G. Van Der Sluys and S. Russo, *J. Am. Chem. Soc.* 1984, **106**, 5386; (b) M. H. Chisholm, J. C. Huffman and W. G. Van Der Sluys, *Inorg. Chim. Acta* 1986, **116**, L13.
7. M. D. Braydich, B. E. Bursten, M. H. Chisholm and D. L. Clark, *J. Am. Chem. Soc.* 1985, **107**, 4459.
8. V. Mark, J. R. Van Wazer and M. M. Crutchfield, *Top. Phosphorus Chem.* 1967, **5**, 227.

9. A. Bino, F. A. Cotton, Z. Dori and J. C. Setuowski, *Inorg. Chem.* 1978, **17**, 2946.
10. S. Shaik, R. Hoffmann, C. R. Fisel and R. H. Summerville, *J. Am. Chem. Soc.* 1980, **102**, 4555. For a recent review of the structural parameters in edge-shared bioctahedral complexes of the early transition elements see: F. A. Cotton, *Polyhedron* 1986, **5**, 3.
11. M. H. Chisholm, J. F. Corning and J. C. Huffman, *Inorg. Chem.* 1982, **21**, 286.
12. I. Poulat-Boschen, B. Krebs, A. Muller, E. Konger-Alborn, H. Dornfeld and H. Schulz, *Inorg. Chem.* 1978, **17**, 1400.
13. M. H. Chisholm, J. C. Huffman and A. R. Ratermann, *Inorg. Chem.* 1983, **22**, 4100.
14. T. P. Blatchford, Ph.D. thesis, Indiana University, Bloomington, IN (1986).
15. M. H. Chisholm and D. A. Haitko, *J. Am. Chem. Soc.* 1979, **101**, 6784.
16. M. Akiyama, M. H. Chisholm, F. A. Cotton, M. W. Extine, D. A. Haitko, D. Little and P. E. Fanwick, *Inorg. Chem.* 1979, **18**, 2266.
17. M. H. Chisholm, K. Folting, J. C. Huffman and C. C. Kirkpatrick, *Inorg. Chem.* 1984, **23**, 1021.

Polyhedron Vol. 6, No. 5, pp. 1125–1130, 1987
Printed in Great Britain

0277–5387/87 $3.00+.00

EXTRACTION OF Pd FROM ACIDIC HIGH-ACTIVITY NUCLEAR WASTE USING PUREX PROCESS COMPATIBLE ORGANIC EXTRACTANTS

R. G. SHULER, C. B. BOWERS, Jr, J. E. SMITH, Jr, V. VAN BRUNT and M. W. DAVIS, Jr*

Department of Chemical Engineering, University of South Carolina, Columbia, SC 29208, U.S.A.

(*Received* 11 *August* 1986; *accepted* 10 *October* 1986)

Abstract—Purex process compatible organic systems which selectively and reversibly extract Pd from synthetic mixed fission product solutions containing 3 M HNO_3 have been developed. This advance makes the development of continuous solvent extraction processes for its recovery more likely. The matrix solution consists of tributyl phosphate (TBP) and kerosene in a TBP/kerosene ratio of 0.667. The anion exchangers Aliquat 336 and Alamine 336 both selectively extract Pd from the synthetic mixed fission product solution. The most effective Pd extractant appeared to be the tertiary amine Alamine 336. In a concentration of 0.3 M in the organic matrix solution when contacted with an equal volume of aqueous phase containing 0.004514 M Pd a distribution coefficient ($D_{org/aq}$) of 1.95 was observed at 25°C. This was an order of magnitude greater than the distribution coefficient for any of the other species in the solution.

Reprocessing of nuclear fuel from commercial power reactors when combined with the use of breeder reactors would increase the power available from nuclear fuel by a factor of 100 and would also permit recovery of potentially valuable fission products such as Pd. If Pd were recovered from nuclear waste it would serve as a new source of the metal whose producer cost is set by the Soviet Union and the Union of South Africa.

This article summarizes research to define solvent extraction process chemistry that is compatible with the Purex process for reprocessing of commercial nuclear waste and specific for the economic recovery of useful fission products. Military nuclear waste could also be treated before neutralization.

The work reported here is concerned with the treatment of Purex process acidic waste in order to remove elements for which beneficial uses have been or may be found. It is of course understood that the recovery and purification of U and Pu would be an economic justification for commercial reprocessing. This economy results if the U use cycle includes a breeder reactor which allows the conversion of ^{238}U to ^{239}Pu reactor fuel and therefore increases the U power production potential by more than 100-fold over that of natural U which contains only 0.72% ^{235}U.

Using the ORIGEN-2 code (CCC-371) from the Oak Ridge National Laboratory and the conditions of operation for a PWR shown in Table 1, the isotopic composition of the Pd produced in the reactor was obtained.

On a basis of a metric ton of initial U metal 1.380 kg of Pd is produced. The isotropic composition as a function of cooling time is shown in Fig. 1. On

Table 1. Typical commercial power reactor fuel and operational conditions

Fuel	3.2% U-235
Burnup	33,000 MWD metric ton
Exposure	880 days in reactor
Neutron flux (specific power)	3.24×10^{14} cm^2 s^{-1}
Cooling time prior to reprocessing	10 yr

* Author to whom correspondence should be addressed.

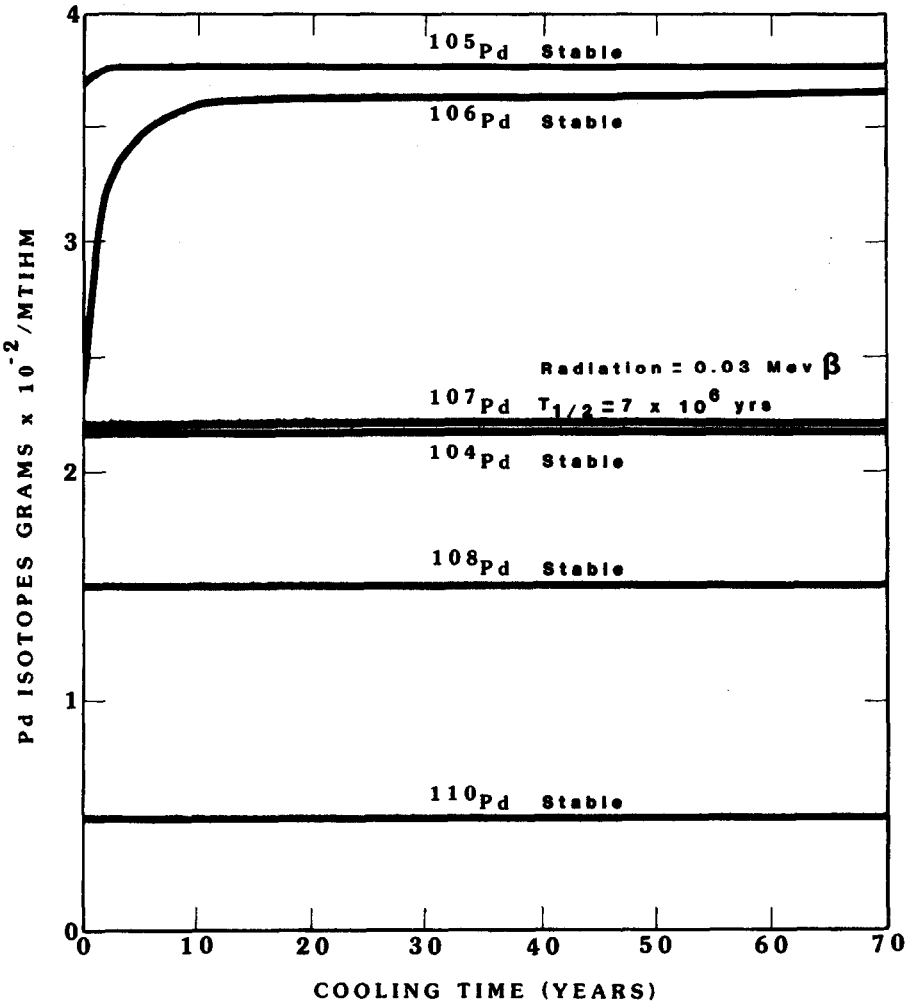

Fig. 1. Pd isotopic mix as a function of fuel cooling time. MTIHM = metric ton of initial heavy metal. Results obtained from the decay of high-level PWR-uranium waste using the ORIGEN-2 code and the conditions shown in Table 1.

the basis of a single commercial reprocessing plant, such as the AGNS plant, operating at 5 metric tons per day or 1500 metric tons per year approximately 7% of the U.S. Pd needs could be met (Moore,[1] Shuler,[2] and Davis and Van Brunt[3]. Of the six Pd isotopes produced only ^{107}Pd is very slightly radioactive, but it could have a restricted use in industrial applications without creating a health hazard.

Pd behavior from reprocessing flowsheets has been studied by Vialard and Germain.[4] They conclude that under certain conditions Pd will precipitate with most reagents used for partitioning. However, it appears in the waste stream at the Savannah River Plant. The basic behavior of most fission products in both nitrate and chloride media is discussed by Orth *et al.*[5] Recovery from waste streams has been performed by ion exchange. Use of liquid ion exchange reagents for selective recovery has been performed by Horwitz and Delphin.[6] As opposed to previous research, this paper focuses on the selective solvent extraction of Pd from a synthetic multielement mixed fission product solution with a Purex process compatible solution.

EXTRACTION OF Pd WITH TRIBUTYL PHOSPHATE (TBP)

The distribution of Pd in TBP–kerosene solutions is important because during primary decontamination in the Purex process, U and Pu are separated from most of the fission products by extraction with an organic solution containing 30 vol% TBP in kerosene. It is necessary to know whether large amounts of the Pd are extracted during this step or whether it remains with the other fission products (Lunichkina *et al.*,[7] De and Sen,[8]

Casey *et al.*,[9] and Gindon *et al.*[9]). Lunichkina *et al.*[7] reported maximum distribution ratios of Pd of about 1.3 and about 0.24 for solutions of 100% TBP and 30% TBP in decane, respectively, when the aqueous phase was at low acidity (0.4–0.8 M HNO_3). A rapid decrease in the $D_{org/aq}$ of Pd was observed when the molarity of HNO_3 exceeded 1 M.

Contacts made between solutions of 0.001 M Pd in varying HNO_3 concentrations (0.5, 1, 2, 3, 4, 6 and 9 M) and TBP–kerosene solutions of varying vol% TBP (30–70, 50–50, 70–80, 80–10 and 100% TBP) formed a fine black precipitate at the interface except for the 6 and 9 M HNO_3 solutions. The percent of Pd extracted increased with increasing TBP content, and it decreased with increasing HNO_3 concentration, although at 1.0 M there appeared to be a slight increase in percent removed over that at 0.5 M. This is in agreement with the maximum observed by Lunichkina *et al.*[7] at HNO_3 concentrations between 0.4 and 0.8 M. After settling for several days, much of the precipitate returned to the solution. Lunichkina *et al.*[7] also reported the formation of a solid phase containing Pd in certain systems. They attributed this to the reduction of Pd(II) to the metallic state due to the formation of TBP degradation products. For example: TBP is subject to hydrolysis (Alcock *et al.*,[11] and Siddall[12]); the reaction of water with TBP gives DBP (di-*n*-butyl phosphate) and butyl alcohol; HNO_3 also reacts directly to give DBP and butyl nitrate; and the formation of DBP is greatly increased if the solvent is held for protracted periods at temperatures above 50°C. DBP can be effectively removed by washing with almost any basic solution.

EXPERIMENTAL

As described in Shuler *et al.*[13] a synthetic mixed fission product solution was developed based on 1.4 M uranium. The mixture is given in Table 2. The experimental procedure for multielement analysis is provided in Shuler *et al.*[13] Utilizing an ICP-5000, inductively coupled plasma, all elements with the exception of Ru and Cs were analyzed. Flame atomic emmission using an Atomic Absorption spectrophotometer was used for the Ru and Cs analysis. Care was taken to optimize the operation conditions and the wavelengths of analysis to minimize interference. The conditions of analysis are given elsewhere (Shuler[2] and Shuler *et al.*[13]).

Alamine 336 and Aliquat 336 were evaluated as organic anion exchangers in this work. Their structures are shown in Fig. 2.

In order to have compatibility with the Purex process it was necessary to convert the Aliquat 336 chloride salt to the nitrate form. This was done by first preparing solutions containing the desired concentration of the chloride salt in TBP and kerosene and then equilibrating this with an equal volume of 3 M HNO_3 in a separatory funnel. The mixture was shaken for 30 min on a wrist action shaker and then allowed to separate. The aqueous layer was decanted and the procedure was then repeated two more times with fresh 3 M HNO_3.

Table 2. Synthetic fission product solution used in these studies excluding acid

Element[a]	Molarity basis: 1.4 M U
Te	0.001302
Ru	0.007448
Pd	0.004514
Rh	0.001582
Zr	0.013097
Y	0.001670
La	0.003051
Nd	0.009683
Ce	0.005851
Pr	0.002760
Sr	0.003048
Sm	0.002008
Ba	0.003759
Rb	0.001424
Cs	0.006038

[a] Initially 3 M HNO_3.

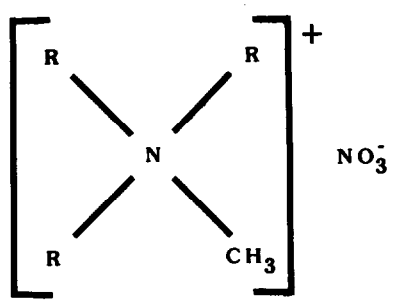

Aliquat 336 (Nitrate)

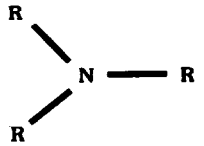

Alamine 336

Fig. 2. Structures of organic anion exchangers.

After initial evaluation of the quarternary- and tertiary-amine extractability with single-element solutions, amine extractability with the synthetic mixed fission product solution was evaluated. The behavior of the quarternary- and tertiary-amine salts used in this work is thought to follow the mechanisms suggested by Koch.[14] Figure 3 shows the effect of temperature on the Pd distribution at the molarity conditions that provided the highest distribution coefficients with the mixed fission product solution. TBP concentration appeared to have little effect on the distribution of the Pd.[2] The high TBP/kerosene ratio of 0.667 was chosen to insure that there was no third-phase formation which had been observed at low TBP/kerosene ratios.[2]

The multielement mixed fission product solution distributions are reported in Tables 3 and 4. The 0.1 M Aliquat 336 (nitrate) solution is selective for Pd over all other components found in the solution. Table 4 shows the behavior of the tertiary amine Alamine 336 at 0.3 M. This solution appears to be highly selective for Pd over the other fission products.

BACK EXTRACTION STUDIES

It was found that the Pd could be recovered from the Alamine solution by back extraction with 8 M HNO_3 in two equal volume contacts. Eighty percent recovery was obtained with three equal volume contacts with a 3 M HNO_3 solution followed by one contact with a 2:1 aq:org volumetric ratio. Ninety-six percent recovery could be obtained from the Aliquat 336 solution. Under these processing conditions only two phase systems were observed.

RECOMMENDED PROCESS CHEMISTRY FOR Pd EXTRACTION

The experimental results indicated that from a synthetic mixed fission product solution, an organic

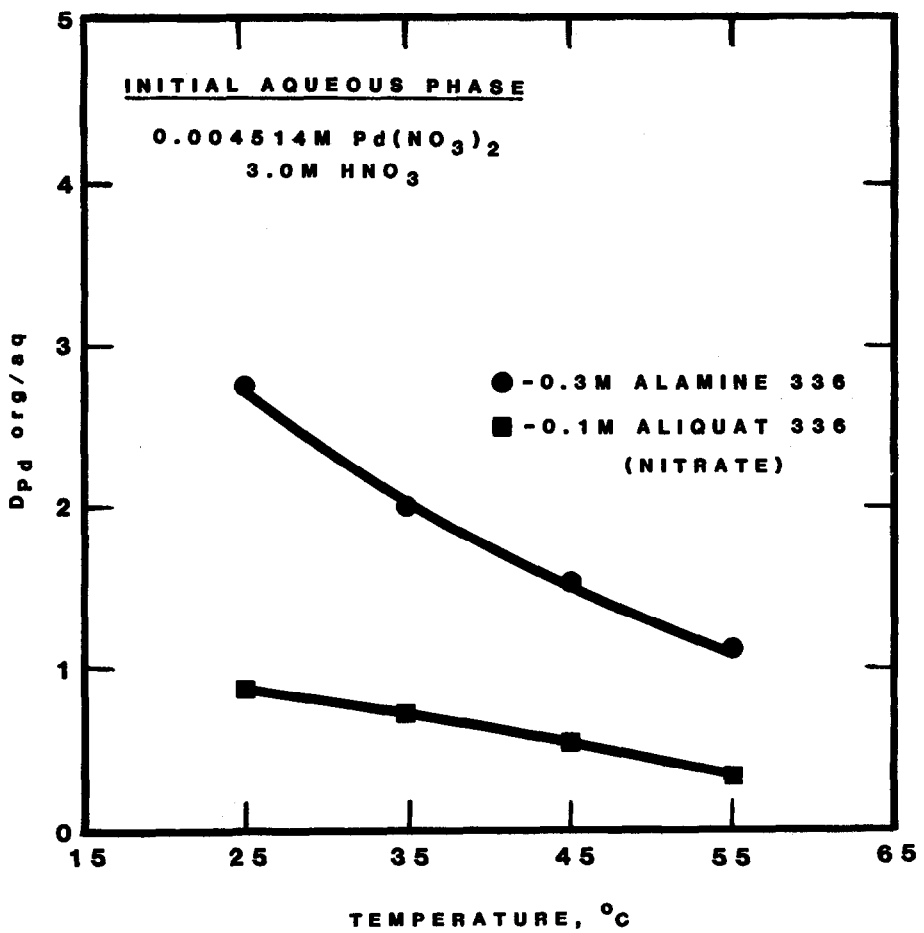

Fig. 3. Pd distribution coefficients as a function of temperature using an extracting solution containing either 0.3 M Alamine 336 or 0.1 M Aliquat 336 (nitrate) with a TBP/kerosene volumetric ratio of 0.667.

Table 3. Distribution coefficients of fission products between aqueous nitric acid[a] and 0.1 M Aliquat 366[b] (nitrate) in TBP and kerosene solutions: temperature = 25°C

Element[c]	Distribution coefficient (org/aq)[d]	Distribution coefficient (org/aq)[e]
Te	0.02	0.01
Ru	0.14	0.18
Pd	0.61	0.61
Rh	0.01	0.02
Zr	0.15	0.22
Y	0.07	0.07
La	0.09	0.08
Nd	0.11	0.10
Cs	0.11	0.11
Pr	0.12	0.11
Sr	0.12	0.03
Sm	0.10	0.12
Ba	0.01	0.02
Rb	0.04	0.03
Cs	0.08	0.03

[a] Initially 3 M HNO_3.
[b] Nitrate salt formed by equilibrating with 3 M HNO_3.
[c] See Table 2 for initial molarity.
[d] TBP/kerosene ratio = 0.538.
[e] TBP/kerosene ratio = 0.667.

Table 4. Distribution coefficients of fission products between aqueous nitric acid[a] and 0.3 M Alamine 336 in an organic matrix with a TBP/kerosene volumetric ratio of 0.667: temperature = 25°C

Element[b]	Distribution coefficient (org/aq)
Te	0.00
Ru	0.01
Pd	1.95
Rh	0.00
Zr	0.02
Y	0.00
La	0.03
Nd	0.11
Ce	0.06
Pr	0.07
Sr	0.00
Sm	0.04
Ba	0.00
Rb	0.00
Cs	0.00

[a] Initially 3 M HNO_3.
[b] See Table 2 for initial molarity.

phase consisting of 0.3 M Alamine 336 in a 33 vol% TBP–66 vol% kerosene matrix would extract Pd with a $D_{org/aq}$ of 1.95. The Pd can be recovered from the solvent by back extraction with aqueous nitric acid.

CONCLUSION

This work has resulted in a Purex compatible organic solution that is highly selective for Pd recovery from mixed fission product solutions. Two phase systems without precipates were observed with the recommended process chemistry.

It appears that Pd can be selectively and reversibly extracted from commercial nuclear fuel if reprocessing is ever considered. This would involve treating the high-activity nuclear acidic waste after uranium and plutonium removal and prior to neutralization.

Acknowledgement—This research was sponsored by the Department of Energy, Savannah River Operations Office, Aiken, SC 29801, under Contract No. DE-AS09-81SR10714.

REFERENCES

1. C. M. Moore, *Platinum-Group Metals*. Preprint from the 1980 Bureau of Mines Minerals Yearbook.
2. R. G. Shuler, M.S. thesis, University of South Carolina (1982).
3. M. W. Davis, Jr and V. Van Brunt, D.O.E. Report for contract DE-AS09-81SR10714 (1984).
4. E. Vialard and M. Germain, *I Chem. E Symp. Ser.* 1984, **88**, 19.
5. D. A. Orth, R. M. Wallace and D. G. Karraker, In *Science and Technology of Tributyl Phosphate* (Edited by W. W. Schulz, J. D. Navratil and A. E. Talbot), Vol. 1, Chap. 6. CRC Press, Boca Raton, FL (1984).
6. E. P. Horwitz and H. Delphin, U.S. Patent 4,162,231 (1979).
7. K. P. Lunichkina, E. V. Renard and V. B. Shevchenko, *Zh. Neorg. Khim.* 1974, **19**, 205.
8. A. K. De and A. K. Sen, In *Solvent Extraction Chemistry* (Edited by D. Dyrssen *et al.*), p. 343. John Wiley, Amsterdam (1967).
9. A. T. Casey, E. Davies, T. L. Meek and E. S. Wagner, In *Solvent Extraction Chemistry* (Edited by D. Dyrssen *et al.*), p. 327. John Wiley, Amsterdam (1967).
10. L. M. Gindon, S. N. Ivanova, A. A. Mazurova, A.

A. Vasilyeva, L. Ya. Mirovova, A. P. Sokolov and P. P. Smirnov, In *Solvent Extraction Chemistry* (Edited by D. Dyrssen *et al.*), p. 433. John Wiley, Amsterdam (1967).
11. D. Alcock, S. S. Grimley, T. V. Healy, J. Kennedy and H. A. C. McKay, *Trans. Farad Soc.* 1956, **52**, 39.
12. T. H. Siddall III, In *Chemical Processing of Reactor Fuels* (Edited by J. F. Flagg), Chap. 5. Academic Press, New York (1961).
13. R. G. Shuler, C. B. Bowers, Jr, J. E. Smith, Jr, V. Van Brunt and M. W. Davis, Jr, *Solv. Extr. Ion Exch.* 1985, **3**, 567.
14. G. Kock, In *Solvent Extraction Chemistry of Metals* (Edited by H. A. C. McKay *et al.*), p. 247, MacMillan (1965).

Polyhedron Vol. 6, No. 5, pp. 1131–1134, 1987
Printed in Great Britain

0277–5387/87 $3.00+.00

PREPARATION AND STRUCTURAL CHARACTERIZATION OF Os(II) AND Ru(II) COMPLEXES, $MCl_2(vdpp)_2$ [M = Os OR Ru, vdpp = 1,1-BIS(DIPHENYLPHOSPHINO)ETHENE]

F. A. COTTON,* M. P. DIEBOLD and M. MATUSZ

Department of Chemistry and Laboratory for Molecular Structure and Bonding, Texas A&M University, College Station, TX 77843, U.S.A.

(*Received* 15 *July* 1986; *accepted* 15 *August* 1986)

Abstract—A reaction between $Os_2(O_2CCH_3)_4Cl_2$ and vdpp [vdpp = 1,1-bis(diphenylphosphino)ethene] was investigated. When the reactants, in the presence of LiCl, were heated in toluene $OsCl_2(vdpp)_2$, **1**, was formed. In a similar reaction $Ru_2(O_2CCH_3)_4Cl$ with vdpp afforded $RuCl_2(vdpp)_2$, **2**. The molecular structures of **1** and **2** were elucidated using X-ray crystallography. Single crystals of **1** and **2** grown from dichloromethane–hexane crystallize in the space group $P2_1/c$ with these cell dimensions: $a = 11.046(2)$ Å, $b = 18.168(3)$ Å, $c = 12.678(3)$ Å, $\beta = 110.24(2)°$ and $V = 2387(2)$ Å^3 for **1** and $a = 11.055(1)$ Å, $b = 18.199(3)$ Å, $c = 12.693(2)$ Å, $\beta = 110.16(1)°$, $V = 2392(1)$ Å^3 for **2**. The molecules of **1** and **2** are isostructural. Metal atoms reside on inversion centers relating the two halves of the molecules. The complexes are six-coordinate with two four-membered chelate rings and *trans* chlorine atoms. For $RuCl_2(vdpp)_2$ the P–M–P angle in the chelate ring is 73.13(2)° and the P–C–P angle in the chelate ring is 98.6(1)°. These values are 72.74(3)° and 97.9(2)°, respectively, for $OsCl_2(vdpp)_2$. There is a disordered dichloromethane solvent molecule present in the lattice and there are no unusual intermolecular contacts.

In our continuing effort to investigate the chemistry of multiple bonds between osmium and ruthenium atoms[1–3] we turned our attention to exploring the possibility of forming multiply bridged dimers with diphosphine ligands acting as the bridges. Initial experiments with dppe and dppm[4–5] indicated that only monomers were formed under a variety of conditions. We decided to employ vdpp [vdpp = 1,1-bis(diphenylphosphino)ethene] as a bridging ligand in the hope that the phosphine would favor a bridging mode of coordination because of the presumed strain a four-membered chelate ring would impose on the sp^2 carbon atom.

Our hope was not fulfilled and instead of dinuclear $M_2X_4(LL)_2$ type species we obtained the quasi-octahedral $MX_2(LL)_2$ (M = Os or Ru) complexes. These belong to a familiar class of M(II) compounds, some of which has been previously structurally characterized.[6] Rather than inventing any fictitious or *ex post facto* justification for the synthesis of **1** and **2**, we candidly report it as a failure to synthesize the desired dimers, albeit still a worthwhile chemical finding.

EXPERIMENTAL

All reactions were carried out in an inert atmosphere using standard Schlenk techniques. $Os_2(O_2CCH_3)_4Cl_2$ and $Ru_2(O_2CCH_3)_4Cl$ were prepared according to the literature procedures.[4,7] Vdpp was prepared as described previously.[8] All solvents were freshly distilled from appropriate drying agents.

Preparation of $OsCl_2(vdpp)_2$, 1

A round-bottomed flask was charged with 0.60 g (14 mmol) anhydrous LiCl and dried at 110–115°C for 2 h. The flask was removed from the oven and placed under vacuum for 15–20 min while it cooled. $Os_2(O_2CCH_3)_4Cl_2$ (0.10 g, 0.145 mmol), vdpp (0.40 g, 1.0 mmol) and toluene (10 cm^3) were added to the flask. The reaction mixture was refluxed with stirring for 2 days. It was cooled and filtered. The solid residue was extracted with dichloromethane and filtered to give a red colored

* Author to whom correspondence should be addressed.

solution. The volume of the solution was reduced to *ca* 10 cm^3 and hexane was layered on top of it. After several days a crop of dark red crystals was collected. Yield: *ca* 80 mg (52%).

Preparation of $RuCl_2(vdpp)_2$, **2**

A synthetic procedure analogous to that described above was used. The reaction was carried out in 30 cm^3 of toluene. From the filtrate a small crop of needle-shaped orange crystals was collected. From the dichloromethane solution a crop of block-shaped dark red crystals was collected. Yield, *ca* 60 mg (30%).

X-ray crystallography

Single crystals of **1** and **2** were mounted on the tip of a glass fiber. Cell constants were refined on a set of 25 high angle reflections and axial lengths were confirmed by partial rotation photographs. In the case of the osmium complex, **1**, empirical absorption corrections based on azimuthal scans near $\chi = 90°$ were applied. Data were corrected for Lorentz and polarization factors and processed according to procedures routine to this laboratory.[9] Heavy atom positions in **1** were determined from a Patterson map, and the solution of **2** was initiated by using the coordinates of heavy atoms from the structure of **1**. In each case remaining atoms (including hydrogen atoms on the phosphine ligand) were found by an alternating series of least-squares refinements and difference Fourier maps. Hydrogen atoms were included in the last refinement cycles and were allowed to refine freely. All atoms except hydrogen atoms were refined with anisotropic displacement parameters. All pertinent crystallographic data are presented in Table 1.*

RESULTS AND DISCUSSION

The reasons for conducting the reactions that lead to the formation of $OsCl_2(vdpp)_2$ and $RuCl_2(vdpp)_2$ were stated above. Both complexes belong to the well-known group of $MX_2(LL)_2$ compounds were LL is a chelating diphosphine (see Ref. 10 for reviews of Ru complexes and Ref. 11 for reviews of Os complexes).

Two isomers, *cis* and *trans*, are possible for these types of compounds and it is interesting that only the *trans* isomer was formed in the case of osmium. In the preparation of $RuCl_2(vdpp)_2$, there was also a small amount of an orange crystalline material, which might be the *cis* isomer.

Lithium chloride was included in these syntheses because of our recent success in synthesizing $Os_2(fhp)_4Cl$ (fhp = fluorohydroxypyridinato) in high yields when LiCl is present.[12] The formation of **1** is accompanied by the reduction of Os(III,III) to Os(II) and the formation of **2** is accompanied by the reduction of Ru(III,II) to Ru(II). Excess phosphine is the most likely reducing agent. One could suggest a more rational method of preparing **1** and **2** but we have made no attempt to explore alternative syntheses or to refine our present procedure.

As expected for Os(II) and Ru(II) complexes in octahedral environments, complexes **1** and **2** are diamagnetic, showing ^1H NMR spectra in $CDCl_3$ solution that consist of a multiplet centered at 7.24 ppm (C_6H_5) and a triplet at 5.93 ppm (CH_2) for **1** and 6.17 ppm for **2** ($J = J_{HP} + J_{HP'} = 9$ Hz for Os and 12 Hz for Ru). Both complexes crystallize in the monoclinic space group $P2_1/c$. In both cases a disordered molecule of dichloromethane is present in the lattice and located near an inversion center. There are two orientations of the CH_2Cl_2 molecule (related by the inversion center) and one orientation was chosen and assigned 0.5 occupancy. The positional parameters as well as isotropic-equivalent displacement parameters are given in the

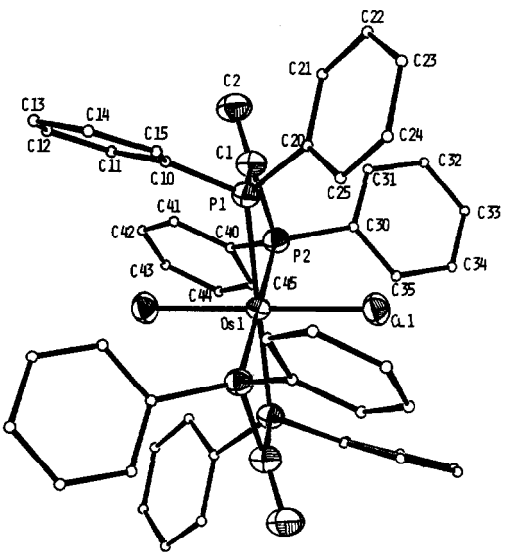

Fig. 1. An ORTEP view of $OsCl_2(vdpp)_2$ at 50% probability level. Phenyl carbons were assigned arbitrarily small size for the sake of clarity.

* Atomic positional and thermal parameters, full lists of bond lengths and angles and F_o/F_c values have been deposited as supplementary material with the Editor, from whom copies are available on request. Atomic coordinates have also been deposited with the Cambridge Crystallographic Data Centre.

Table 1. Crystal data for $OsCl_2(vdpp)_2 \cdot CH_2Cl_2$, **1** and $RuCl_2(vdpp)_2 \cdot CH_2Cl_2$, **2**

Formula	$OsCl_4P_4C_{53}H_{46}$	$RuCl_4P_4C_{53}H_{46}$
Formula weight	1138.87	1049.77
Space group	$P2_1/c$	$P2_1/c$
Systematic absences	$0k0$, $k = 2n+1$	$0k0$, $k = 2n+1$
	$h0l$, $l = 2n+1$	$h0l$, $l = 2n+1$
a (Å)	11.046(2)	11.055(1)
b (Å)	18.168(3)	18.199(3)
c (Å)	12.678(3)	12.693(2)
α (°)	90.0	90.0
β (°)	110.24(2)	110.16(1)
γ (°)	90.0	90.0
V (Å^3)	2387(2)	2392(1)
Z	2	2
d_{calc} (g cm^{-3})	1.584	1.457
Crystal size (mm)	0.5 × 0.4 × 0.3	0.5 × 0.4 × 0.2
μ(Mo-K_α) (cm^{-1})	30.687	6.536
Data collection instrument	CAD-4	CAD-4
Radiation (monochromated in incident beam)	Mo-K_α (λ_α^- = 0.71073 Å)	
Orientation reflections [number, range (2θ)]	25, $18 < 2\theta < 38$	25, $21 < 2\theta < 40$
Temperature (°C)	23	23
Scan method	ω–2θ	ω–2θ
Data collection range [2θ (°)]	$4 < 2\theta < 50$	$5 < 2\theta < 45$
Number of unique data, total with $F_o^2 > 3\sigma(F_o^2)$	4187, 3349	2898, 2566
Number of parameters refined	368	368
Transmission factors (max, min)	0.9996, 0.5915	—
R*	0.0237	0.0292
R_w†	0.0339	0.0416
Quality-of-fit indicator‡	1.112	1.391
Largest shift/esd, final cycle	0.65	0.15
Largest peak (e Å^{-3})	0.92	0.63

* $R = \Sigma ||F_o| - |F_c|| / \Sigma |F_o|$.
† $R_w = [\Sigma w(|F_o| - |F_c|)^2 / \Sigma w|F_o|^2]^{1/2}$; $w = 1/\sigma^2(|F_o|)$.
‡ Quality-of-fit = $[\Sigma w(|F_o| - |F_c|)^2 / (N_{obs} - N_{parameters})]^{1/2}$.

supplementary material. In Table 2 selected bond distances and angles of both compounds are presented. A complete listing of bond distances and angles as well as general displacement parameters and calculated and observed structure factors is available as supplementary material. An ORTEP drawing of $OsCl_2(vdpp)_2$, **1**, is presented in Fig. 1.

Our original hope that the sp^2 bridging carbon would not permit the formation of a four-membered chelate ring was not realized. The P–C–P angles are 97.9(2)° and 98.6(1)° for **1** and **2**, respectively. These angles are larger than those found in the dppm complexes[6] (e.g. the P–C–P angle in *trans*-$RuCl_2(dppm)_2$ is 93.4(4)° and that in *cis*-$OsCl_2(dppm)_2$ is 94.4°), which would be expected when going from sp^3 to sp^2 carbon. It is uncertain whether this is related to increased strain of the four-membered ring since the corresponding angles in the free phosphine are not known. The Cl–M–P angles do not deviate significantly from 90°. Metal–chlorine distances range from 2.42–2.43 Å and metal–phosphorus distances range from 2.33–2.34 Å in both complexes. All other distances and angles are within expected ranges and require no further comment.

This study demonstrates that the formation of four-membered chelate rings is common, especially with the later transition metals. We are also exploring the significance of using LiCl in substituting carboxylate ligands with a variety of other ligands.

Table 2. Selected bond distances (Å) and bond angles (°) for $OsCl_2(vdpp)_2$, **1** and $RuCl_2(vdpp)_2$, **2**

	1	2
	Bond distances	
M(1)–Cl(1)	2.431(1)	2.419(1)
M(1)–P(1)	2.343(1)	2.344(1)
M(1)–P(2)	2.330(1)	2.331(1)
P(1)–C(1)	1.831(4)	1.834(3)
P(2)–C(1)	1.845(3)	1.840(3)
C(1)–C(2)	1.314(5)	1.316(4)
	Bond angles	
C(1)–M(1)–P(1)	91.65(3)	91.99(3)
Cl(1)–M(1)–P(2)	92.81(3)	93.11(3)
P(1)–M(1)–P(2)	72.74(3)	73.13(2)
M(1)–P(1)–C(1)	94.0(1)	93.30(9)
M(1)–P(2)–C(1)	94.0(1)	93.55(9)
P(1)–C(1)–P(2)	97.9(2)	98.6(1)
P(1)–C(1)–C(2)	131.8(3)	131.4(3)
P(2)–C(1)–C(2)	129.6(3)	129.4(3)

Acknowledgements—We are grateful to the U.S. National Science Foundation for support. M.P.D. is a National Science Foundation Predoctoral Fellow and also holds a Texaco–IUCCP Fellowship from this department.

REFERENCES

1. F. A. Cotton, K. R. Dunbar and M. Matusz, *Polyhedron*, in press.
2. F. A. Cotton, K. R. Dunbar and M. Matusz, *Inorg. Chem.* 1986, **25**, 1585.
3. F. A. Cotton, K. R. Dunbar and M. Matusz, *Inorg. Chem.* 1986, **25**, 1589.
4. T. Behling, G. Wilkinson, T. A. Stephenson, D. A. Tocher and M. D. Walkinshaw, *J. Chem. Soc., Dalton Trans.* 1983, 2109.
5. F. A. Cotton and A. R. Chakravarty, unpublished results.
6. A. R. Chakravarty, F. A. Cotton and W. Schwotzer, *Inorg. Chim. Acta* 1984, **84**, 179.
7. T. A. Stephenson and G. Wilkinson, *J. Inorg. Nucl. Chem.* 1966, **28**, 2285.
8. I. J. Colquhoun and W. McFarlane, *J. Chem. Soc., Dalton Trans.* 1982, 1915.
9. Calculations were done on a departmental VAX 11-780 with a SDP package software.
10. *Gmelin Handbook der Anorganischen Chemie, Ruthenium*, p. 435 (1970).
11. *Gmelin Handbook of Inorganic Chemistry, Osmium*, p. 320, supplement, Vol. 1 (1980).
12. F. A. Cotton and M. Matusz, unpublished results.

Polyhedron Vol. 6, No. 5, pp. 1135–1142, 1987
Printed in Great Britain

0277–5387/87 $3.00+.00

REACTIONS BETWEEN $W_2I_4(CO)_8$ AND PHOSPHINES UNDER FORCING CONDITIONS: ATTEMPTED DECARBONYLATION TO TUNGSTEN(II) DIMERS WITH QUADRUPLE METAL–METAL BOND—X-RAY MOLECULAR STRUCTURE OF $WI_2(CO)(dppm)_2$

F. ALBERT COTTON,* LARRY R. FALVELLO and RINALDO POLI

Department of Chemistry and Laboratory for Molecular Structure and Bonding, Texas A&M University, College Station, TX 77843, U.S.A.

(*Received* 18 *July* 1986; *accepted* 24 *October* 1986)

Abstract—The reactions of $W_2I_4(CO)_8$ with bis(diphenylphosphino)methane (dppm) and PMe_3 have been studied under forcing conditions. From the dppm reaction a monocarbonyl compound has been isolated, which crystallizes as $3WI_2(CO)(dppm)_2 \times 2$ toluene. Crystal data: space group $C2/c$, $a = 31.141(8)$, $b = 25.447(7)$, $c = 20.135(6)$ Å, $\beta = 104.89(4)°$, $V = 15420(20)$ Å^3, $Z = 4$, $R = 0.0538$ for 4367 data with $F_o^2 > 3\sigma(F_o^2)$. The PMe_3 reaction afforded $WI_2(CO)_2(PMe_3)_3$ as the major product. No derivatives containing a metal–metal quadruple bond were detected in solution.

Recent investigations carried out in this Laboratory[1–4] led to the discovery of a new reaction, namely thermal decarbonylation of $Mo_2I_4(CO)_8$ in the presence of phosphines, which is at the same time a new reactivity path for compounds of the $Mo_2X_4(CO)_8$ type and a new synthetic method for $Mo_2X_4L_4$ or $Mo_2X_4(L–L)_2$ compounds with a metal–metal bond.

In an attempt to extend this method to the analogous tungsten complexes, the thermal reaction of $W_2I_4(CO)_8$[5] with selected phosphines was carried out. PMe_3 and bis(diphenylphosphino)methane (dppm), i.e. the phosphines which gave the best results with the molybdenum system,[1,2] were chosen. Quadruply bonded tungsten dimers could not be obtained and the isolated products were carbonyl complexes related to intermediates of the molybdenum reactions. These products and the mechanism of their formation are discussed here.

EXPERIMENTAL

All operations were carried out by standard Schlenck tube techniques under an atmosphere of purified argon. Solvents were dehydrated by conventional methods and distilled under dinitrogen. Instruments used were: IR, Perkin–Elmer mod 783; UV–visible, Cary 17. Solution IR spectra were recorded on expanded abscissa and calibrated with both $CO_{(g)}$ and $H_2O_{(g)}$. Elemental analyses were by Galbraith Laboratories Inc., Knoxville, Tennessee. $W_2I_4(CO)_8$[5] and PMe_3[6] were prepared by known procedures. Dppm was purchased from Strem Chemicals and used without further purification.

Reaction of $W_2I_4(CO)_8$ *with dppm*

$W_2I_4(CO)_8$ (0.52 g, 0.47 mmol) and dppm (0.40 g, 1.04 mmol) were dissolved in 50 cm^3 of toluene to produce, after gas evolution, an orange solution with IR bands at 2035m, 1962s, 1938m, 1908m and 1856w cm^{-1}. The solution was then refluxed and the reaction monitored by IR in the carbonyl stretching region. After *ca* 24 h all of the bands had practically disappeared and a new, weak band at *ca* 1775 cm^{-1} had grown. The mixture was filtered while hot and slowly cooled to room temperature. The red crystals that formed (compound **1**, *ca* 72 mg) were decanted, washed with *n*-hexane and dried *in vacuo*. Found: C, 50.4; H, 3.8. Calc. for $C_{167}H_{148}I_6O_3P_{12}W_3$: C, 51.6; H, 3.8%. IR (Nujol mull) (cm^{-1}): 1765s,

* Author to whom correspondence should be addressed.

1590w, 1575w, 1435m, 1355w, 1315w, 1160w, 1085m, 1030w, 1005w, 975w, 845w, 790m, 745s, 735s, 720m, 690s, 615w, 595w, 520m, 505m, 480m, 450w, 420m; (CH_2Cl_2 solution) (cm^{-1}): 1778. Subsequent work-up of the mother solution did not lead to the isolation of any pure crystalline material. UV–visible spectroscopy on this solution did not show any band in the 600–900-nm region.

Reaction of $W_2I_4(CO)_8$ *with* PMe_3

$W_2I_4(CO)_8$ (0.75 g, 0.69 mmol) was treated in 20 cm^3 of toluene with 0.30 cm^3 of PMe_3 (3.0 mmol). A yellow solution and a flocculent yellow precipitate were obtained after gas evolution. The solution had IR bands at 2071w, 2046w, 2014s, 1936s, 1907s and 1888vs cm^{-1}. The mixture was then warmed to reflux and at the same time irradiated with a UV-mercury lamp. The solid gradually dissolved and the color changed to red within 12 h. This solution had IR bands at 2017w, 1926vs, *ca* 1900w (sh), 1827vs and 1731m cm^{-1}. Color and IR spectrum did not change upon further treatment for an additional 24 h. UV–visible spectroscopy did not show any band in the 600–900-nm region. After evaporation to dryness, the residue was washed several times with hot *n*-hexane to give red solutions whose prominent IR band was at 1730 cm^{-1}, and to leave a yellow microcrystalline material. This was recrystallized by dissolution in toluene and slow diffusion of *n*-hexane to give large orange crystals (compound **2**, yield 0.33 g). Found: C, 18.7; H, 3.8. Calc. for $C_{11}H_{27}I_2O_2P_3W$: C, 18.3; H, 3.8%. IR (Nujol mull) (cm^{-1}): 1915s, 1820vs, 1430m, 1425m, 1415w, 1305m, 1300w, 1285m, 1275ms, 950s, 870w, 860w, 730m, 670w, 585w, 570w, 515w, 490w, 445w; (toluene solution) (cm^{-1}): 1925s, 1830s (asymmetric).

X-ray crystallography for compound **1**

Data collection and reduction were carried out by routine procedures. A semi-empirical absorption correction was applied according to the method described by North *et al.*[7] The structure solution and the early stages of refinement were performed with the Enraf–Nonius SDP software. On the basis of systematic absences, the space group could be either *Cc* or *C2/c*. Direct methods on the non-centrosymmetric space group showed three independent and equivalent arrangements of heavy atoms, which were initially assigned the WI_3 formulation. The positional parameters were in agreement with an extra symmetry element, this being a C_2-axis passing through a W and an I atom of one of the three WI_3 groupings. Refinement was thus attempted in the *C2/c* space group, which led to correct development of the structure. All iodine atoms which were not in a special position were first refined at full occupancy but I(2), I(3) and I(4) refined with unusually high thermal parameters. Chemical information and elemental analyses suggested that this compound might be a di-iodide derivative of tungsten; we therefore considered the possibility of having, in each independent molecule, one iodide atom disordered over two mutually *trans* positions. Assignment of a 0.5 occupancy factor to the above mentioned iodine atoms led to correct refinement. Subsequent alternate difference Fourier maps and least-squares full-matrix refinements showed the positions of all the atoms of the dppm ligands and the carbonyl carbon atoms. The latter ones were refined at half occupancy. The *R* factor was 0.070. The carbonyl oxygen atoms were not located on the difference Fourier map. Since they were expected to be at about the same position as the iodine atoms, they were introduced in the atom list starting with the same positions as those of the iodine atoms. Subsequent refinement was performed with the SHELX-76 package of programs. The phenyl rings were constrained to be perfect hexagons (C—C = 1.395 Å) and the C—O distances were restrained to a value of 1.14(2) Å, which is the distance found for the same bond in $MoI_2(CO)(dmpm)_2$[dmpm = bis(dimethylphosphino)methane], having a geometry similar to that of the present compound.[3] Isotropic refinement converged to $R = 0.068$. All the atoms were then allowed to behave anisotropically and refined. The carbonyl carbon and oxygen atoms did not refine well, most probably because of high correlation with the iodine atoms, and they were therefore left isotropic. At this point, the difference Fourier map showed peaks ascribable to a toluene molecule in a general position of the lattice, with the methyl groups disordered over two positions at bonding distance to two *ortho* carbons of the ring. Independent refinement of all parameters led to instability. To avoid this, the toluene ring was constrained to be a perfect hexagon (C—C = 1.395 Å), the methyl groups restrained at 1.47(10) Å from the corresponding ring atoms and with a constraint on their occupancies such that the sum of these be equal to 1. Finally the isotropic thermal parameters of all the carbon atoms of the toluene molecule were constrained to the same value, which was refined. Final refinement converged to $R = 0.0538$ ($R_w = 0.0670$). Significant crystal data are reported in Table 1, while selected bond distances and angles are reported in Table 2.

Table 1. Crystal data for $3WI_2(CO)(dppm)_2 \times 2$ toluene

Formula	$C_{167}H_{148}I_6O_3P_{12}W_3$
Formula weight	3887.7
Space group	$C2/c$
Systematic absences	$h0l$: $l \neq 2n$; hkl: $h+k \neq 2r$
a (Å)	31.141(18)
b (Å)	25.447(7)
c (Å)	20.135(6)
α (°)	90
β (°)	104.89(4)
γ (°)	90
V (Å^3)	15420(20)
Z	4
d_{calc} (g cm^{-3})	1.675
Crystal size (mm)	$0.1 \times 0.2 \times 0.4$
μ(Mo-K_α) (cm^{-1})	36.437
Data collection instrument	CAD-4
Radiation (monochromated in incident beam)	Mo-K_α (λ_α^- = 0.71073 Å)
Orientation reflections, number, range (2θ)	25, 18–25
Temperature (°C)	20
Scan method	ω
Data collection range [2θ (°)]	4–45
Number of unique data, total with $F_o^2 > 3\sigma(F_o^2)$	4367
Number of parameters refined	679
Transmission factors (max, min)	99.94, 91.80
R^a	0.0538
R_w^b	0.0670
Quality-of-fit indicator^c	1.383
Largest shift/esd, final cycle	0.255
Largest peak (e Å^{-3})	0.764

[a] $R = \Sigma \| F_o| - |F_c \| / \Sigma |F_o|$.
[b] $R_w = [\Sigma w(|F_o| - |F_c|)^2 / \Sigma w |F_o|^2]^{1/2}$; $w = 1/\sigma^2(|F_o|)$.
[c] Quality-of-fit = $[\Sigma w(|F_o| - |F_c|)^2 / (N_{obs} - N_{parameters})]^{1/2}$.

RESULTS AND DISCUSSION

The reaction of $W_2I_4(CO)_8$ with phosphines and diphosphines had already been the subject of several studies.[5,8,9] Dppm was one of the ligands employed:[8] its reaction was shown to lead to the formation of $WI_2(CO)_3(dppm)$ and $WI_2(CO)_2(dppm)_2$ with 2 and 4 equivalents, respectively, per tungsten dimer at room temperature, and a reflux treatment of the dicarbonyl derivative in $CHCl_3$ gave rise to the formation of *trans*- and *cis*-$[WI(CO)_2(dppm)_2]I$.[9]

We used, for our reaction, a solvent (toluene) with a higher boiling point and less polarity than that used by Colton and Rix.[9] In agreement with their findings, we obtained a mixture of $WI_2(CO)_3(dppm)$ (bands at 2035m, 1962s and 1908m cm^{-1}; cf. with 2030m, 1960s, 1935m and 1910m cm^{-1} in acetone[9]) and small amounts of $WI_2(CO)_2(dppm)_2$ (bands at 1938m and 1856w cm^{-1}; cf. with 1940s and 1855s in CH_2Cl_2 or $CHCl_3$[8]) at room temperature; the appearance of the dicarbonyl derivative is presumably due to the small excess of the diphosphine over the 1:2 stoichiometry. When, however, the solution was refluxed, we obtained neutral compounds. $WI_2(CO)(dppm)_2$ (**1**), not previously reported, was obtained in low yields; other toluene-soluble, non-carbonyl-containing materials were also present but we were not able to isolate them in crystalline form. The lack of a visible absorption band in the 600–900-nm region, however, rules out the possibility

Table 2. Selected bond distances (Å) and angles (°), and their estimated standard deviations, for $3WI_2(CO)(dppm)_2 \times 2$ toluene[a]

Atom 1	Atom 2	Distance	Atom 1	Atom 2	Distance	Atom 1	Atom 2	Distance
W1	I1	2.876(2)	W2	P6	2.543(6)	P4	C70	1.86(2)
W1	I2	2.980(7)	W2	C6	1.73(6)	P4	C80	1.82(2)
W1	I3	2.984(5)	P1	C1	1.86(2)	P5	C5	1.88(2)
W1	P1	2.546(7)	P1	C10	1.81(2)	P5	C90	1.82(2)
W1	P2	2.562(6)	P1	C20	1.80(2)	P5	C100	1.78(2)
W1	P3	2.560(6)	P2	C1	1.87(2)	P6	C5	1.80(2)
W1	P4	2.552(7)	P2	C30	1.83(2)	P6	C110	1.90(3)
W1	C3	1.79(5)	P2	C40	1.829(15)	P6	C120	1.78(2)
W1	C4	1.85(5)	P3	C2	1.85(2)	O3	C3	1.08(7)
W2	I4	2.985(6)	P3	C50	1.82(2)	O4	C4	1.11(11)
W2	I5	2.876(3)	P3	C60	1.800(15)	O6	C6	1.09(9)
W2	P5	2.551(6)	P4	C2	1.86(2)			

Atom 1	Atom 2	Atom 3	Angle	Atom 1	Atom 2	Atom 3	Angle	Atom 1	Atom 2	Atom 3	Angle
I1	W1	I2	85.5(1)	P4	W1	C3	97.(2)	W1	P3	C2	96.0(6)
I1	W1	I3	85.0(1)	P4	W1	C4	89.(2)	W1	P3	C50	124.1(6)
I1	W1	P1	75.2(1)	I4	W2	I5	85.2(1)	W1	P3	C60	124.3(7)
I1	W1	P2	138.7(1)	I4	W2	P5	84.2(2)	C2	P3	C50	104.(1)
I1	W1	P3	139.0(2)	I4	W2	P5′	93.3(2)	C2	P3	C60	104.(1)
I1	W1	P4	75.3(1)	I4	W2	P6	87.2(2)	C50	P3	C60	100.8(9)
I1	W1	C3	91.(1)	I4	W2	P6′	100.1(2)	W1	P4	C2	96.0(7)
I1	W1	C4	89.(1)	I4	W2	C6′	171.(2)	W1	P4	C70	127.3(8)

I2	W1	P1	94.1(2)	I5	W2	P5	75.2(2)	W1	P4	C80	119.4(6)
I2	W1	P2	99.9(2)	I5	W2	P6	138.8(1)	C2	P4	C70	105.(1)
I2	W1	P3	86.9(2)	I5	W2	C6	87.(2)	C2	P4	C80	103.6(9)
I2	W1	P4	84.4(2)	P5	W2	P5′	150.5(2)	C70	P4	C80	102.(1)
I2	W1	C3	176.(2)	P5	W2	P6	63.7(2)	W2	P5	C5	94.7(7)
I3	W1	P1	83.4(2)	P5	W2	P6′	145.7(2)	W2	P5	C90	118.7(6)
I3	W1	P2	87.2(2)	P5	W2	C6	88.(2)	W2	P5	C100	126.6(7)
I3	W1	P3	100.3(2)	P5	W2	C6′	90.(2)	C5	P5	C90	104.(1)
I3	W1	P4	93.4(2)	P6	W2	P6′	82.4(2)	C5	P5	C100	105.4(9)
I3	W1	C3	7.(1)	P6	W2	C6	89.(2)	C90	P5	C100	104.(1)
I3	W1	C4	173.(1)	P6	W2	C6′	96.(2)	W2	P6	C5	97.0(7)
P1	W1	P2	63.6(2)	W1	P1	C1	97.9(7)	W2	P6	C110	123.1(6)
P1	W1	P3	145.6(2)	W1	P1	C10	126.5(8)	W2	P6	C120	124.8(7)
P1	W1	P4	150.5(2)	W1	P1	C20	118.0(7)	C5	P6	C110	103.(1)
P1	W1	C3	82.(2)	C1	P1	C10	103.8(9)	C5	P6	C120	102.2(9)
P1	W1	C4	91.(2)	C1	P1	C20	102.(1)	C110	P6	C120	102.(1)
P2	W1	P3	82.3(2)	C10	P1	C20	104.6(9)	P1	C1	P2	92.3(9)
P2	W1	P4	145.8(2)	W1	P2	C1	97.1(7)	P3	C2	P4	93.8(9)
P2	W1	C3	81.(1)	W1	P2	C30	125.4(8)	W1	C3	O3	159.(5)
P2	W1	C4	95.(2)	W1	P2	C40	122.9(8)	W1	C4	O4	165.(6)
P3	W1	P4	63.9(2)	C1	P2	C30	103.3(9)	P5	C5	P6	93.7(9)
P3	W1	C3	97.(2)	C1	P2	C40	103.(1)	W2	C6	O6	162.(6)
P3	W1	C4	87.(1)	C30	P2	C40	101.(1)				

[a] Numbers in parentheses are estimated standard deviations in the least significant digits.

that the quadruply bonded dimer $W_2I_4(dppm)_2$ was present.*[10]

Although not certain, it would seem that, upon reflux, $WI_2(CO)_3(dppm)$ gives rise to the unidentified non-carbonyl materials, presumably containing a dppm/W ratio of 1, while $WI_2(CO)_2(dppm)_2$ produces compound **1**. A few complexes with a stoichiometry similar to that of $WI_2(CO)_2(dppm)_2$ have been structurally characterized {e.g. $MoCl_2(CO)_2(dpam)_2$,[11] $MoBr_2(CO)_2(dpam)_2$,[12] [dpam = bis(diphenylarsino)methane], $MoCl_2(CO)_2(dppm)_2$[11] and $MoI_2(CO)_2(dppm)_2$[13]} and found to be seven-coordinate with one chelating and one monodentate phosphine. By assuming that $WI_2(CO)_2(dppm)_2$ also has such a structure, the formation of **1** can easily take place by chelation of the second diphosphine *via* preliminary dissociation of a CO ligand (see Scheme 1). In the thermal treatment carried out by Colton and Rix,[8] on the other hand, the substitution of one iodide ligand occurs, presumably because of the higher polarity of the solvent.

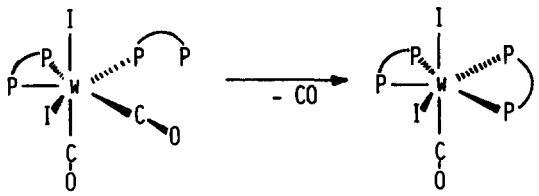

Scheme 1.

The crystal structure of compound **1** exhibits two independent molecules of $WI_2(CO)(dppm)_2$, one in a general position and one located on a C_2-axis, which passes through W(2) and I(5). One molecule of toluene is also present in the asymmetric unit, so that the composition of the crystalline material is $3WI_2(CO)(dppm)_2 \times 2$ toluene. Figure 1 shows a view of the molecule which is on the general position. Both independent molecules show the same geometry around tungsten, which is fairly close to that of an ideal pentagonal bipyramid, and have identical structural parameters within the experimental error. One iodide ion and the two diphosphine ligands are in the equatorial plane, and the second iodide ion and the carbonyl ligand are in the axial positions. The symmetry imposes a 50:50 disorder of the axial iodide and carbonyl ligands in the molecule lying on the C_2-axis. In the other molecule, although this is not required by symmetry, the same ligands were also found to be 50:50 disordered among the two axial positions. Figure 1 shows only one of the two orientations, for clarity. This result can be easily explained by considering the presence of eight bulky phenyl groups which completely surround the I–W–CO core of the molecule. The packing of the molecules in the crystal is expected to be dominated by the van der Waals' interactions of the phenyl groups. The random disorder of the two possible orientations shows that the arrangement of the axial I–W–CO system does not appreciably influence the energy of the crystal.

The molecular structure is the same as that found[3] for $MoI_2(CO)(dmpm)_2$. The "bite" angles of the diphosphines in **1** are a little smaller [63.6(2), 63.9(2) and 63.7(2)°, compared with 65.7(2) and 66.1(2)° for $MoI_2(CO)(dmpm)_2$[3]], perhaps because of steric repulsion between the phenyl groups. The W—I distance, as expected,[14] is larger for the axial bonds [2.980(7), 2.984(5) and 2.985(6) Å] than for the equatorial ones [2.876(2) and 2.876(3) Å]. The W—P bond lengths are all close to 2.55 Å, which is *ca* 0.05 Å longer than those of the corresponding Mo–dmpm complex.[3]

It is interesting to compare the reactivity of $W_2I_4(CO)_8$ towards dppm with that of the corresponding molybdenum system. The reaction of $Mo_2I_4(CO)_8$ with dppm (1:2 molar ratio) under forcing conditions afforded $Mo_2I_4(dppm)_2$ (Mo—Mo) in high yields.[2] No similar compound appears to be formed from $W_2I_4(CO)_8$. Also, $MoI_2(CO)_2(dppm)_2$ was found to decompose in refluxing toluene and no formation of $MoI_2(CO)(dppm)_2$, analogous to **1**, could be observed.[3,13] Instead, such a decomposition reaction seemed to produce $Mo_2I_4(dppm)_2$ upon loss of diphosphine and CO. In the tungsten reaction, on the other hand, compound **1** was produced, which seemed to be rather stable in such conditions. It might be that the presumably higher energies of the W—P, W—I and W—CO bonds with respect to those of the Mo—P, Mo—I and Mo—CO bonds are capable of thermodynamically or kinetically stabilizing a highly crowded structure such as that of compound **1**. The same may not be true in the molybdenum system. It is worth noting in this respect that when the more basic and less sterically demanding dmpm ligand was employed, $MoI_2(CO)(dmpm)_2$ was obtained, and this was found to be fairly stable in refluxing toluene.[3]

The room-temperature reaction of $W_2I_4(CO)_8$

* $W_2Cl_4(PMe_3)_4$ has the $\delta \rightarrow \delta^*$ absorption at 657 nm, *ca* 80 nm red-shifted with respect to the same band of $Mo_2Cl_4(PMe_3)_4$.[10] Since $Mo_2I_4(dppm)_2$ has the $\delta \rightarrow \delta^*$ maximum at 707 nm,[2] the hypothetical $W_2I_4(dppm)_2$ compound is expected to have the same band at a higher wavelength, around 800 nm.

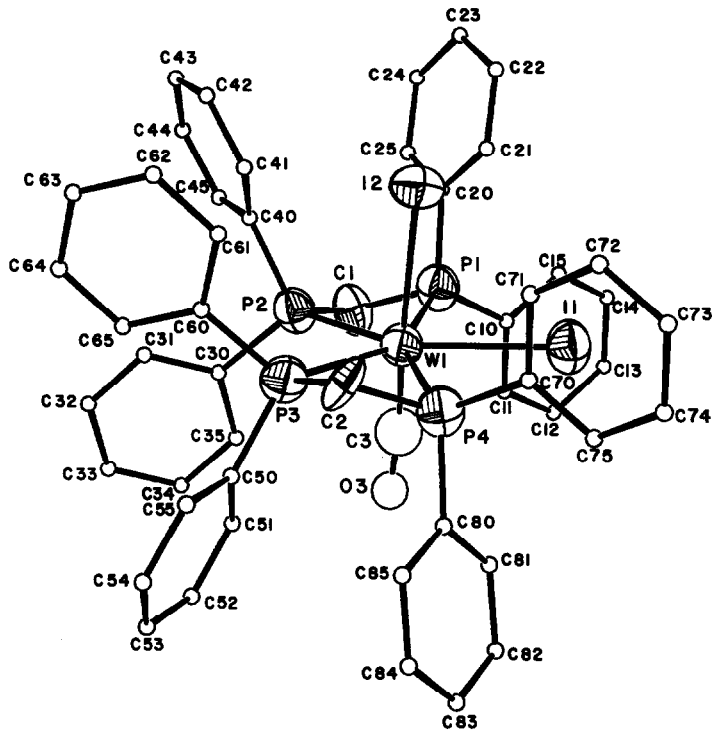

Fig. 1. ORTEP view of the molecule of compound **1** which lies in a general position. Atoms I(3), C(4) and O(4) have been omitted for the sake of clarity. For the same reason, the phenyl carbon atoms have been drawn with arbitrary radii.

with PMe_3 produced a solution containing several products, as judged from the complexity of the IR spectrum. Some of the bands could presumably be assigned to $WI_2(CO)_3(PMe_3)_2$ [the room-temperature interaction of $W_2I_4(CO)_8$ with PPh_3 was reported[5] to afford the tricarbonyl derivative, $WI_2(CO)_3(PPh_3)_2$]. After prolonged reflux with simultaneous UV irradiation, $WI_2(CO)_2(PMe_3)_3$ (**2**) was the major product, isolated in *ca* 33% yield with respect to tungsten (49.5% with respect to PMe_3). The fate of the rest of the tungsten is unknown, although small amounts of a more soluble material, having an IR band at 1731 cm^{-1}, were detected by IR spectroscopy; the position of the IR band suggests that this compound may be a monocarbonyl derivative of tungsten(II). Again, visible absorption bands in the 600–900-nm region were not detected in the final solution, which means that tungsten(II) dimers with a quadruple bond between the metals did not form. This is again in contrast with the results of the same reaction on molybdenum systems.[1,4]

The formation of tungsten–tungsten quadruple bonds by decarbonylation of tungsten(II) carbonyl derivatives proves then to be a difficult, if not impossible, reaction, contrary to what was found for the analogous molybdenum systems. One factor contributing to this might be the higher stability of the tungsten(II) carbonyls with respect to those of molybdenum(II), as suggested by higher W—CO bond energies, at least for M(0) derivatives.[15] Also, the molybdenum–molybdenum quadruple bond is generally less reactive than the same bond between tungsten(II) ions, and thus more likely to remain intact once formed. Both these factors should cause the decarbonylation of tungsten(II) carbonyls to be more difficult and, in turn, the reaction of $W_2X_4L_4$ (W—W) systems with CO to be easier. A few reactions of $W_2Cl_4(PR_3)_4$ systems with CO have actually been studied and reported to be more facile than those of the corresponding molybdenum(II) dimers.[16]

Acknowledgement—This work was supported by the National Science Foundation.

REFERENCES

1. F. A. Cotton and R. Poli, *J. Am. Chem. Soc.* 1986, **108**, 5628.
2. F. A. Cotton, K. R. Dunbar and R. Poli, *Inorg. Chem.* 1986, **25**, 3700.
3. F. A. Cotton and R. Poli, *Inorg. Chem.* 1986, **25**, 3703.

4. F. A. Cotton and R. Poli, *Inorg. Chem.* 1986, **25**, 3624.
5. R. Colton and C. J. Rix, *Aust. J. Chem.* 1969, **22**, 305.
6. H. H. Murray, J. D. Basil and J. P. Fackler, Jr, private communication.
7. A. C. T. North, D. C. Phillips and F. S. Mathews, *Acta Cryst.* 1968, **A24**, 351.
8. M. W. Anker, R. Colton, C. J. Rix and I. B. Tomkins, *Aust. J. Chem.* 1969, **22**, 1341.
9. R. Colton and C. J. Rix, *Aust. J. Chem.* 1969, **22**, 2535.
10. F. A. Cotton, M. W. Extine, T. R. Felthouse, B. W. S. Kolthammer and D. G. Lay, *J. Am. Chem. Soc.* 1981, **103**, 4040.
11. M. G. B. Drew, A. P. Wolters and I. B. Tomkins, *J. Chem. Soc., Dalton Trans.* 1977, 974.
12. M. G. B. Drew, *J. Chem. Soc., Dalton Trans.* 1972, 626.
13. F. A. Cotton and M. Matusz, *Polyhedron* 1987, **6**, 000.
14. M. G. B. Drew, *Prog. Inorg. Chem.* 1977, **23**, 67.
15. J. A. Connor, *Top. Curr. Chem.* 1977, **71**, 71.
16. F. A. Cotton, D. J. Darensbourg and B. W. S. Kolthammer, *J. Organomet. Chem.* 1981, **217**, C14.

Polyhedron Vol. 6, No. 5, pp. 1143–1145, 1987
Printed in Great Britain

0277–5387/87 $3.00+.00
Pergamon Journals Ltd

COMMUNICATION

SYNTHESIS OF DIVALENT ARYLOXY- AND DIORGANOAMIDO-LANTHANIDES FROM BIS(PENTAFLUOROPHENYL)LANTHANIDE(II) COMPLEXES

G. B. DEACON,* C. M. FORSYTH and R. H. NEWHAM

Chemistry Department, Monash University, Clayton, Victoria 3168, Australia

(*Received* 2 *February* 1987; *accepted* 23 *February* 1987)

Abstract—The complexes $M(OR)_2(thf)_3$ (M = Yb or Eu, R = 2,6-Bu^t_2-4-MeC_6H_2; M = Yb, R = 2,4,6-$Bu^t_3C_6H_2$ or 2,6-$Bu^t_2C_6H_3$; thf = tetrahydrofuran) and $M(NR_2)_2(thf)_4$ (M = Yb or Eu, R_2N = carbazol-9-yl; M = Yb, R_2N = 2-phenylindol-1-yl) have been prepared by reactions of $(C_6F_5)_2M$ (M = Yb or Eu) with substituted phenols, carbazole, or 2-phenylindole.

Lanthanide(III) aryloxides, alkoxides and diorganoamide complexes are well established,[1–7] but much less is known of the lanthanide(II) derivatives. Complexes of bis[bis(trimethylsilyl)amido]-europium(II) and -ytterbium(II)[8–10] and anionic derivatives $Na\{M[N(SiMe_3)_2]_3\}$(M = Yb or Eu)[10] have been characterized crystallographically, whilst $Yb[N(SiMe_3)_2]_3^-$ has been generated electrochemically.[5] Recently $M[N(SiMe_3)_2]_2$(dme) (M = Yb, Eu, or Sm; dme = 1,2-dimethoxyethane) have been prepared by redox transmetallation from $Hg[N(SiMe_3)_2]_2$ and the ytterbium complex converted into $(Bu^tO)_2Yb$ by alcoholysis.[11] Divalent ethoxides of ytterbium and samarium have been prepared by metathesis from the diiodides.[12]

We now report facile syntheses of some bis-(aryloxy)- and bis(diorganoamido)-ytterbium(II) and -europium(II) compounds by acidolysis of the corresponding bis(pentafluorophenyl)lanthanides[13,14] with bulky phenols and secondary amines [reactions (1) and (2)]. The preparations were carried out in purified tetrahydrofuran (thf) under purified nitrogen.

$$(C_6F_5)_2M + 2ROH \xrightarrow{thf} M(OR)_2 + 2C_6F_5H \quad (1)$$

(M = Yb or Eu, R = 2,6-Bu^t_2-4-MeC_6H_2;

M = Yb, R = 2,4,6-$Bu^t_3C_6H_2$ or 2,6-$Bu^t_2C_6H_3$)

$$(C_6F_5)_2M + 2R_2NH \xrightarrow{thf} M(NR_2)_2 + 2C_6F_5H \quad (2)$$

(M = Yb or Eu, R_2N = carbazol-9-yl;

M = Yb, R_2N = 2-phenylindol-1-yl)

Solutions of the organolanthanide reactants were obtained by redox transmetallation between $(C_6F_5)_2Hg$ and the lanthanide metal[13,14] and were filtered before addition of stoichiometric amounts of the phenols or amines as solids or solutions in tetrahydrofuran. Rapid reaction generally occurred but the reaction mixtures were stirred for 16–24 h at room temperature. Some complexes, $Yb(OR)_2$ (R = 2,6-Bu^t_2-4-MeC_6H_2, 2,4,6-$Bu^t_3C_6H_2$ or 2,6-$Bu^t_2C_6H_3$) and bis(2-phenylindol-1-yl)ytterbium(II), were also prepared by reaction between bis(pentafluorophenyl)mercury, the phenol or 2-phenylindole (R_2NH), and an excess of ytterbium

* Author to whom correspondence should be addressed.

metal in tetrahydrofuran at room temperature.

$$(C_6F_5)_2Hg + 2ROH\,(\text{or } 2R_2NH) + Yb$$

$$Yb(OR)_2\,[\text{or } Yb(NR_2)_2] + 2C_6F_5H + Hg\downarrow. \quad (3)$$

The initial step is presumably the redox transmetallation synthesis of $(C_6F_5)_2Yb$, and it has been shown that ytterbium does not react with 2-phenylindole or 2,6-di-*t*-butyl-4-methylphenol in the absence of $(C_6F_5)_2Hg$.

The products precipitated from solution in the case of the sparingly soluble bis(carbazol-9-yl)lanthanides. In other cases, the compounds were isolated by evaporation to dryness [after filtration where reaction (3) was used] or by evaporation to low volume, addition of hexane and crystallization. All were obtained as highly air-sensitive yellow solids and had the analytical compositions, $M(OR)_2(thf)_3$ and $M(NR_2)_2(thf)_4$. The infrared spectra of the complexes showed no absorption above 3100 cm^{-1} establishing loss of the OH and NH protons in reactions (1)–(3). Intense absorption at 1035–1020 cm^{-1} and 880–860 cm^{-1} in the spectrum of each complex is attributable to ring stretching modes of tetrahydrofuran, shifted from the free ligand values, 1070 and 912 cm^{-1}, as expected on coordination.[15] The UV/Vis/near IR spectra (300–1500 nm) of the bis(carbazol-9-yl)lanthanides in 1,2-dimethoxyethane show intense bands (ε 2000–9000) at 300–400 nm attributable to 5d ← 4f transitions and L ← M charge transfer.[16–18] There was no absorption near 1000 nm for the ytterbium complex, hence the presence of ytterbium(III) can be eliminated. Brief exposure to air generated absorption of free carbazole and ytterbium(III). The UV/Vis/near IR spectra of $M(OR)_2(thf)_3$ (M = Yb or Eu; R = 2,6-Bu^t_2-4-MeC_6H_2) in tetrahydrofuran also show intense absorption at 300–400 nm. Unusually, complexes of lanthanide(III) ions with bulky aryloxide ligands are soluble in petroleum ether,[6] but the present bis(aryloxy)lanthanide(II) complexes are insoluble. Whilst this may indicate associated structures by contrast with the monomeric lanthanide(III) aryloxides,[6] it may simply be a reflection of greater ionic character for lanthanide(II) derivatives; see e.g. the hydrides.[19]

Reactions (1)–(3) further indicate the synthetic value of bis(pentafluorophenyl)lanthanide(II) reagents, which have previously been used in C-acid displacements with phenylacetylene[20] and cyclopentadiene[21] to give the corresponding diorganolanthanides, as well as in organic synthesis.[22,23] The present reactions reflect greater acidity for phenols[24] and carbazole[25] than pentafluorobenzene.[26]

Acknowledgements—We are grateful to the Australian Research Grants Scheme for support, to Rare Earth Products for a gift of REACTON ytterbium and europium, and for a Commonwealth Postgraduate Research Award to C.M.F.

REFERENCES

1. K. C. Malhotra and R. L. Martin, *J. Organomet. Chem.* 1982, **239**, 159.
2. D. C. Bradley, R. C. Mehrotra and D. P. Gaur, *Metal Alkoxides*. Academic Press, London (1978).
3. D. C. Bradley and M. H. Chisholm, *Acc. Chem. Res.* 1976, **9**, 273.
4. M. F. Lappert, P. P. Power, A. R. Sanger and R. C. Srivastava, *Metal and Metalloid Amides*, Ch. 8. Ellis Horwood, Chichester (1980).
5. D. C. Bradley and M. Ahmed, *Polyhedron* 1983, **2**, 87.
6. P. B. Hitchcock, M. F. Lappert and A. Singh, *J. Chem. Soc., Chem. Comm.* 1983, 1499.
7. K. S. Kharia, S. Mathur, M. Singh and B. S. Sankhla, *J. Nepal Chem. Soc.* 1981, **1**, 33. (*Chem. Abstr.* 1986, **104**, 101117q).
8. T. D. Tilley, A. Zalkin, R. A. Andersen and D. H. Templeton, *Inorg. Chem.* 1981, **20**, 551.
9. T. D. Tilley, R. A. Andersen and A. Zalkin, *J. Am. Chem. Soc.* 1982, **104**, 3725.
10. T. D. Tilley, R. A. Andersen and A. Zalkin, *Inorg. Chem.* 1984, **23**, 2271.
11. Yu. F. Radkov, E. A. Fedorova, S. Ya. Khorshev, G. S. Kalinina, M. N. Bochkarev and G. A. Razuvaev, *J. Gen. Chem. U.S.S.R.* 1985, **55**, 1911.
12. J. L. Namy, P. Girard and H. B. Kagan, *Nouv. J. Chim.* 1981, **5**, 479.
13. G. B. Deacon, W. D. Raverty and D. G. Vince, *J. Organomet. Chem.* 1977, **135**, 103.
14. G. B. Deacon, A. J. Koplick, W. D. Raverty and D. G. Vince, *J. Organomet. Chem.* 1979, **182**, 121.
15. J. Lewis, J. R. Miller, R. L. Richards and A. Thompson, *J. Chem. Soc.* 1965, 5850.
16. F. D. S. Butement, *Trans. Faraday Soc.* 1948, **44**, 617; D. S. McLure and Z. Kiss, *J. Chem. Phys.* 1963, **39**, 3251.
17. F. A. Hunt and Wenxiang Zhu, *Rare Earths Mod. Sci. Technol.* 1982, **3**, 95.
18. F. Calderazzo, R. Pappalardo and S. Losi, *J. Inorg. Nucl. Chem.* 1966, **28**, 987.
19. G. G. Libowitz and A. J. Maeland, *Hydrides* in K. A. Gschneidner and L. Eyring eds., *Handbook of the Chemistry and Physics of Rare Earths*, Vol. 13, Ch. 26. North Holland, Amsterdam (1971).
20. G. B. Deacon, A. J. Koplick and T. D. Tuong, *Aust. J. Chem.* 1982, **35**, 941.
21. G. B. Deacon and R. H. Newnham, *Aust. J. Chem.* 1985, **38**, 1757.
22. G. B. Deacon and T. D. Tuong, *J. Organomet. Chem.* 1981, **205**, C4.

23. G. B. Deacon and P. I. MacKinnon, *Tetrahedron Lett.* 1984, **25**, 783.
24. G. Kortüm, W. Vogel and K. Andrussow, *Dissociation Constants of Organic Acids in Aqueous Solution*. Butterworth, London (1961).
25. F. G. Bordwell, G. E. Drucker and H. E. Fried, *J. Org. Chem.* 1981, **46**, 632.
26. A. Streitwieser, P. J. Scannon and H. M. Niemeyer, *J. Am. Chem. Soc.* 1972, **94**, 7936.

Polyhedron Vol. 6, No. 5, pp. 1147–1148, 1987
Printed in Great Britain

0277-5387/87 $3.00+.00
Pergamon Journals Ltd

COMMUNICATION

THE SOLUTION CONSTITUTION OF THE ROUSSIN ESTER $Fe_2(SBu\text{-}t)_2(NO)_4$

ANTHONY R. BUTLER, CHRISTOPHER GLIDEWELL* and IAN L. JOHNSON

Chemistry Department, University of St Andrews, St Andrews, Fife KY16 9ST, U.K.

(*Received* 27 *August* 1986; *accepted after revision November* 1986)

Abstract—The ^1H and ^{15}N NMR spectra of the Roussin ester $Fe_2(SBu\text{-}t)_2(NO)_4$ show that in solution it exists as a mixture of two isomeric forms (**I** and **II**), of C_{2h}- and C_{2v}-symmetry, respectively. Unlike other similar esters, $Fe_2(SR)_2(NO)_4$, the isomers are present in non-equal proportions: the equilibrium constant $K = [\mathbf{II}]/[\mathbf{I}]$ is unchanged in the temperature range 220–298 K, indicating that entropy factors are primarily responsible for the unequal abundance of **I** and **II**.

The X-ray structure analysis of the ethyl ester of Roussin's red salt, $Fe_2(SEt)_2(NO)_4$, showed[1] the molecule to be centrosymmetric, having approximate C_{2h} molecular symmetry. However, in solution a series of esters $Fe_2(SR)_2(NO)_4$ (R = Me, Et, *n*-Pr, CH_2Ph[2] or Ph[3]) were shown by ^1H NMR spectroscopy to exist in solution as an equimolar mixture of two isomeric forms, and activation parameters were measured[2] for their interconversion for R = Me, Et, *n*-Pr, *i*-Pr and CH_2Ph. In the cases of R = Me and *i*-Pr, the identities of the isomers as having C_{2h}- and C_{2v}-symmetry **I** and **II**, respectively, were rigorously established[4] using ^{15}N NMR spectroscopy on 99% ^{15}N-enriched samples.

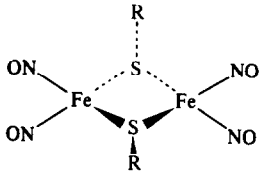

I

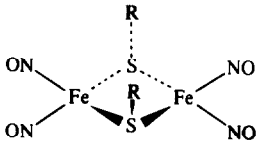

II

However in the case of R = *t*-Bu, we did not in our earlier work[2] observe any splitting of the single even at 223 K, and the question of the solution structure of $Fe_2(SBu\text{-}t)_2(NO)_4$ could not be resolved. Here we present results from ^1H and ^{15}N NMR spectroscopy which establish the solution structure of $Fe_2(SBu\text{-}t)_2(NO)_4$.

The ^{15}N NMR spectrum of $Fe_2(SBu\text{-}t)_2(^{15}NO)_4$ consists of a singlet, and a pair of doublets which comprise an AX spin system (Table 1). As previously,[4] the singlet is assigned to the C_{2h} isomer (**I**) in which all the nitrosyl ligands are identical: the AX spectrum is assigned to the C_{2v} isomer (**II**), in which two nitrosyl ligands bound to each iron are in different environments: no long range $^4J(^{15}NFeSFe^{15}N)$ was resolved, consistent with earlier observations[4] on $Fe_2(SMe)_2(^{15}NO)_4$ and $Fe_2(SPr\text{-}i)_2(^{15}NO)_4$.

For $Fe_2(SMe)_2(^{15}NO)_4$ and $Fe_2(SPr\text{-}i)_2(^{15}NO)_4$, the integrated intensities showed[4] that the C_{2h} and C_{2v} isomers exist in equal abundance at 298 K, as deduced[2] earlier from the ^1H spectra. In the ^{15}N spectrum of $Fe_2(SBu\text{-}t)_2(^{15}NO)_4$, however, the intensities show that the C_{2h} isomer (**I**) is very much the minor isomer, present in 26 ± 1% abundance at both 298 and 220 K. The constancy of the equilibrium constant $K = [\mathbf{II}/\mathbf{I}]$ over this temperature range implies that for the isomerization **I** → **II** $\Delta H^\ominus$ is effectively zero: a K value of 2.85 ± 0.15 gives $\Delta S^\ominus$ for isomerization as 8.7 ± 0.4 J K^{-1} mol^{-1}. The entropy differences which give rise to the unequal abundance of **I** and **II** presumably arises from a differential solvation of the two isomers: specific solvation of Roussin esters $Fe_2(SR)_2(NO)_4$ has been invoked[5] previously to rationalize ASIS observations. If this is so, then the two isomers should exhibit equal abundances in the vapour phase.

In the ^1H spectrum of $Fe_2(SBu\text{-}t)_2(^{14}NO)_4$ in

*Author to whom correspondence should be addressed.

Table 1. ^{15}N NMR data for $Fe_2(SR)_2(^{15}NO)_4$

Compound	T (K)	C_{2h} isomer δ (ppm)	C_{2v} isomer δ (ppm)	J (Hz)
$Fe_2(SMe)_2(^{15}NO)_4$[a]	298	30.5(s)	23.1(d), 36.2(d)	2.8
$Fe_2(SPr\text{-}i)_2(^{15}NO)_4$[a]	298	30.2(s)	26.7(d), 35.7(d)	2.6
$Fe_2(SBu\text{-}t)_2(^{15}NO)_4$	298	38.8(s)	31.1(d), 37.1(d)	3.0
	220	36.6(s)	28.8(d), 35.6(d)	3.1

[a] Data from Ref. 4.

$CDCl_3$ solution, there is a single resonance at $\delta = 1.43$ ppm, which shows no perceptible broadening until the freezing point of the solvent is approached. Hence in this solvent the protons in the two isomers are fortuitously isochronous. In toluene-d_8 solution, the ASIS phenomenon shifts the sharp ($\nu_{1/2} = 0.5$ Hz) room-temperature resonance to $\delta = 1.22$ ppm. However, on cooling, the spectrum was resolved into two peaks separated at 80 MHz by 1.2 Hz at 260 K and 1.7 Hz at 240 K. Because of the small peak separation, accurate integration was not possible, but an approximate estimate of the peak areas was consistent with the value of K deduced from the ^{15}N spectrum. The coalescence temperature was determined as 289 K.

EXPERIMENTAL

Samples of $Fe_2(SBu\text{-}t)_2(^{14}NO)_4$ and $Fe_2(SBu\text{-}t)_2(^{15}NO)_4$ were prepared from $Fe_2(SBu\text{-}t)_2(CO)_6$ by use of ^{14}NO gas in $CHCl_3$ solution and $Na[^{15}NO_2]$ in DMF solution, according to published procedures.[2,4] $Fe_2(SBu\text{-}t)_2(^{14}NO)_4$ was identified and characterized by mass spectrometry, ^1H and ^{13}C NMR spectroscopy, and IR spectroscopy: $\nu(^{14}NO)$, 1770, 1743 cm^{-1}. $Fe_2(SBu\text{-}t)_2(^{15}NO)_4$ was characterized by ^{15}N NMR and IR-spectroscopy: $\nu(^{15}NO)$, 1739, 1712 cm^{-1}. ^{15}N NMR spectra were recorded relative to external $CH_3{}^{15}NO_2$ in the FT mode on the Brüker WH-360 spectrometer of the Science and Engineering Research Council regional NMR service at the University of Edinburgh, using spectral conditions and parameters as previously described.[4]

Acknowledgements—We thank the Ministry of Agriculture, Fisheries and Food for financial support, and Dr R. K. Mackie for valuable discussions.

REFERENCES

1. J. T. Thomas, J. H. Robertson and E. G. Cox, *Acta Cryst.* 1958, **11**, 599.
2. A. R. Butler, C. Glidewell, A. R. Hyde, J. McGinnis and J. E. Seymour, *Polyhedron* 1983, **2**, 1045.
3. T. B. Rauchfuss and T. D. Weatherill, *Inorg. Chem.* 1982, **21**, 827.
4. A. R. Butler, C. Glidewell, A. R. Hyde and J. McGinnis, *Inorg. Chem.* 1985, **24**, 2931.
5. C. Glidewell and A. R. Hyde, *Polyhedron* 1985, **4**, 1155.

Polyhedron Vol. 6, No. 5, pp. 1149–1151, 1987
Printed in Great Britain

0277–5387/87 $3.00+.00

COMMUNICATION

A NOVEL SIX-VERTEX COORDINATION POLYHEDRON IN THE CRYSTAL STRUCTURE OF THE $CuBr_2$ COMPLEX OF 1,6-BIS(BENZIMIDAZOL-2-YL)-2,5-DIOXAHEXANE

WILLIAM CLEGG* and JOYCE C. LOCKHART

Department of Inorganic Chemistry, The University, Newcastle upon Tyne NE1 7RU, U.K.

(*Received* 8 *September* 1986; *accepted* 1 *December* 1986)

Abstract—A novel polyhedron has been discovered in the coordination geometry of the $CuBr_2$ complex of 1,6-bis(benzimidazol-2-yl)-2,5-dioxahexane. A rhombus or lozenge-shaped base (BrNBrN) shares its edges with four BrNO triangles and its Br vertices with two BrOO triangles, all six triangles lying on one side of the base. The polyhedron may be derived from an octahedron (with a *trans*-Br_2, *cis*-O_2, *cis*-N_2 arrangement of vertices) by breaking the N...N edge and bringing the N atoms into coplanarity with the Br atoms.

We have previously reported the preparation of some polydentate and macrocyclic ligands incorporating benzimidazole, and of complexes of these with transition-metal ions.[1] The determination of one of these complexes, formed from $CuBr_2$ and the ligand 1,6-bis(benzimidazol-2-yl)-2,5-dioxahexane (**1**) has revealed a novel coordination polyhedron for the Cu atom.

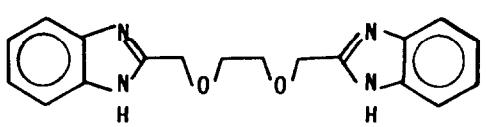

1

EXPERIMENTAL

The preparation of the complex has already been described.[1] It was recrystallized from a methanol–chloroform mixture.

Crystallography

$C_{18}H_{18}Br_2CuN_4O_2$, $M_r = 545.7$, orthorhombic, *Pccn*, $a = 8.940(1)$, $b = 10.634(1)$, $c = 20.455(2)$ Å, $V = 1944.6$ Å^3, $Z = 4$, $D_c = 1.864$ g cm^{-3}, $F(000) = 1076$, $\mu = 5.22$ mm^{-1} for Mo-K_α radiation ($\lambda = 0.71073$ Å). Of 2828 reflections measured with a Stoe–Siemens AED2 diffractometer at 295K ($2\theta_{max} = 50°$), and corrected for absorption by semi-empirical methods, 1725 were unique ($R_{int} = 0.034$), and 1068 with $F > 4\sigma(F)$ were used for structure determination by automatic direct methods.[2] Blocked-cascade refinement to minimize $\Sigma w\Delta^2$ [$\Delta = |F_o| - |F_c|$, $w^{-1} = \sigma^2(F)$] with anisotropic thermal parameters for non-H atoms, constrained H atoms [C—H = 0.96 Å, aromatic H on external ring angle bisectors, H—C—H = 109.5° for aliphatic H, $U(H) = 1.2U_{eq}(C)$] and an isotropic extinction correction [$F_c' = F_c/(1 + xF_c^2/\sin 2\theta)^{1/4}$, $x = 6.4(6) \times 10^{-7}$] gave $R = 0.066$, $R' = (\Sigma w\Delta^2/\Sigma wF_o^2)^{1/2} = 0.043$, a satisfactory analysis of variance, and no significant features in a final difference synthesis.

RESULTS AND DISCUSSION

The molecular structure is shown in Fig. 1, and the bond lengths and angles for the coordination of Cu are given in Table 1. A crystallographic C_2-axis passes through the Cu atom, bisecting the C(12)—C(12′) bond. The Cu atom is coordinated by the oxygen and two nitrogen atoms of ligand **1** and by two bromine atoms. The six-vertex polyhedron thus formed has a geometry never documented

*Author to whom correspondence should be addressed.

Table 1. Selected bond lengths (Å) and angles (°)[a]

Cu—Br	2.465(1)	Cu—N(1)	1.987(7)
Cu—O(11)	2.743(6)		
Br—Cu—N(1)	90.7(2)	Br—Cu—O(11)	90.8(1)
N(1)—Cu—O(11)	67.2(3)	Br—Cu—Br′	168.2(1)
N(1)—Cu—Br′	88.2(2)	O(11)—Cu—Br′	99.6(1)
N(1)—Cu—N(1′)	168.9(5)	O(11)—Cu—N(1′)	123.8(3)
O(11)—Cu—O(11′)	57.6(3)		

[a]The prime denotes an atom generated by the two-fold rotation axis passing through Cu (symmetry operator $\frac{1}{2} - x, \frac{1}{2} - y, z$).

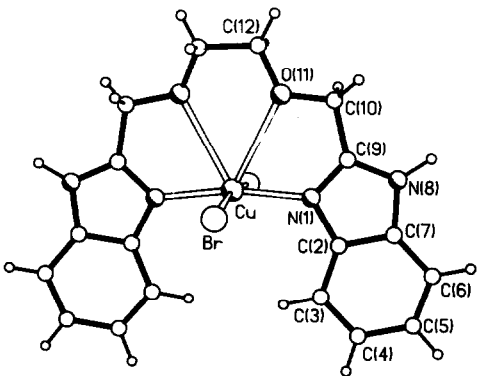

Fig. 1. Molecular structure with the numbering scheme.

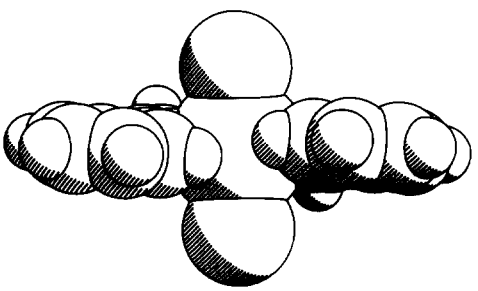

Fig. 3. Space-filling representation; view direction along the C_2-axis [opposite direction to Fig. 2(b)].

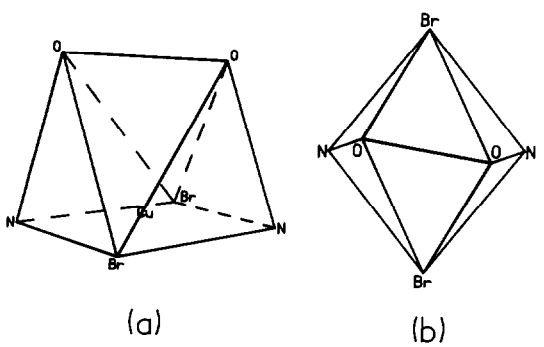

Fig. 2. Coordination polyhedron: (a) view direction as in Fig. 1; (b) seen along the C_2-axis.

previously, and *outré* even in Cu(II) chemistry (Fig. 2). The Cu atom is bonded strongly to two N and two Br atoms which form a basal plane with essentially a rhombus or lozenge shape (Br and N atoms deviate by only ±0.03 Å from their mean plane; N...Br edges are 3.12 and 3.18 Å long, the axes of the rhombus are a shorter N...N of 3.96 Å and a longer Br...Br of 4.90 Å). The Cu atom lies 0.22 Å above this basal plane, displaced towards the two O atoms, to which it is more weakly bonded. The O...O line is approximately parallel to the N...N line, forming six triangular faces, all above the basal rhombus: four BrNO triangles share one BrN edge each with the rhombus, while the two BrOO triangles, with a common O...O edge, share only their Br vertices with the rhombus (Fig. 2). The O...N edges are 2.69 Å long, O...O is 2.64 Å, and the Br...O edges group as two at 3.71 Å and two slightly longer at 3.98 Å.

The relationship between the observed polyhedron (with six vertices, 11 edges and seven faces) and an octahedron (six vertices, 12 edges and eight faces) may be seen by reference to Figs 1 and 2(a). If both N atoms are displaced downwards from the basal plane (away from the O atoms), the N—Cu—N angle and N...N distance decrease; with sufficient displacement, a N...N edge may be considered to form and the rhombus is converted to two NBrN triangular faces of an actahedron.

The long Cu—O distance, forced by the ligand architecture, is reminiscent of the even longer Cu—O bond (3.08 and 3.14 Å in two independent molecules) notable in the most recent (1.8 Å resolution) determination of an azurin structure,[3] in which a peptide oxygen (of GLY45) is held in a peptide loop over a planar arrangement of imidazole nitrogens (HIS46 and HIS117) and cysteinyl sulphur (CYS112) around copper, the trigonal bipyramid in this case being completed by a long Cu—S (MET121) of 3.13 Å *trans* to Cu—O.

In the present structure, the coordination geometry is such as to leave one side of the Cu atom

essentially unligated. This vacant side is, however, protected by the bulky benzimidazole groups protruding on the same side as is shown by the space-filling representation in Fig. 3.

Future extensions of this work will be concerned with exploiting the pocket formed on one side of the lozenge-shaped basal coordination plane (which may be compared with the lacunar complexes of Busch *et al.*[4]), with a view to new host–guest formulations.

Acknowledgement—We thank SERC for a research grant towards crystallographic equipment.

REFERENCES

1. W. Clegg, J. C. Lockhart and F. H. Musa, *J. Chem. Soc., Dalton Trans.* 1986, 47.
2. G. M. Sheldrick, *SHELXTL*: an integrated system for solving, refining and displaying crystal structures from diffraction data. Revision 5, University of Göttingen (1985).
3. G. E. Norris, B. F. Anderson and E. N. Baker, *J. Am. Chem. Soc.* 1986, **108**, 2784.
4. B. Korybut-Daszkiewicz, M. Kojima, J. H. Cameron, N. Herron, M. Y. Chavan, A. J. Jircitano, B. K. Coltrain, G. L. Neer, N. W. Alcock and D. H. Busch, *Inorg. Chem.* 1984, **23**, 903.

Polyhedron Vol. 6, No. 5, pp. 1153–1155, 1987
Printed in Great Britain

0277-5387/87 $3.00+.00

COMMUNICATION

THE REACTIONS OF SOME PENTAAMMINE(*o*-SUBSTITUTED BENZOATO)CHROMIUM(III) CATIONS IN PERCHLORIC ACID AND WATER

RODNEY L. WILLIAMSON and JAMES C. CHANG*

Department of Chemistry, University of Northern Iowa, Cedar Falls, IA 50614, U.S.A.

(*Received* 7 *July* 1986; *accepted after revision* 1 *December* 1986)

Abstract—The reactions of pentaammine(*o*-fluorobenzoato)-, pentaammine(*o*-bromobenzoato)- and pentaammine(*o*-nitrobenzoato)chromium(III) cations in 0.01 M perchloric acid solution and water have been studied at 21°C. It was found that the reaction in acid was the release of ammonia but in water it was aquation to the pentaammineaquachromium(III) cation. The aquation rates in water decrease in the order *o*-fluorobenzoate, *o*-bromobenzoate and *o*-nitrobenzoate complexes, suggesting an associative mechanism.

The mechanism of the aquation of some pentaammine- and pentaaqua complexes of chromium(III) has been suggested to be I_a, based upon studies of pressure effects.[1,2] Since one of the chemical methods to distinguish between dissociative and associative mechanisms is by changing the size of the leaving group,[3] we have undertaken a study of the aquation of some pentaammine (*o*-substituted benzoato)chromium(III) cations in order to see whether any difference in the aquation rates could be detected with different size substituents.

EXPERIMENTAL

Pentaammine(*o*-fluorobenzoato)chromium(III), pentaammine(*o*-bromobenzoato)chromium(III) and pentaammine (*o*-nitrobenzoato)chromium(III) perchlorates were prepared by a method similar to that used by Jackman *et al.*[4] and Chang *et al.*[5] In a typical preparation, 10 mmol of an acid in 10 cm^3 of dimethylformamide (dmf) and 5 mmol of dicyclohexylcarbodiimide in 5 cm^3 of dmf were stirred for 30 min, after which the white precipitate of dicyclohexylurea was filtered off. To the filtrate was added 1.0 mmol of pentaammineaquachromium(III) perchlorate in 10 cm^3 of dmf, pretreated with 5 mmol of *N*,*N*-dimethylbenzylamine. The solution was stirred for 20 min at room temperature, then 50 cm^3 of absolute ethanol and 300 cm^3 of diethyl ether were added to the mixture to produce a red oil. The solvent was decanted, and the oil was dissolved in 20 cm^3 of a 1:1 ethanol–acetone mixture. Again 200 cm^3 of diethyl ether was added to this mixture, and a solid compound precipitated upon vigorous stirring. The percentage yield was about 20%. Found: C, 18.6; H, 4.4; N, 13.4. Calc. for $CrC_7H_5O_2(NH_3)_5$: C, 18.6; H, 4.2; N, 14.8%. Found: C, 16.3; H, 4.0; N, 12.5. Calc. for $CrC_7H_5O_2Br(NH_3)_5$: C, 15.7; H, 3.5; N, 13.0%. Found: C, 18.2; H, 3.9; N, 15.6. Calc. for $CrC_7H_5NO_4(NH_3)_5$: C, 16.7; H, 3.8; N, 16.7%.

All visible absorption spectra were measured using a Cary 14 recording spectrophotometer. The rate of aquation was followed by observing the decrease in the absorbance of aqueous solutions of the complexes at 490 nm. The rate of release of NH_3 in 0.01 M $HClO_4$ was followed by the analysis of NH_3, eluted from Dowex AG50W-X8 columns, with Nessler's reagent.

RESULTS AND DISCUSSION

It was observed that the pentaammine(*o*-substituted benzoato)chromium(III) cations reacted in 0.01 M $HClO_4$ by the release of NH_3. Actually, the odor of NH_3 could be detected from the solid

*Author to whom correspondence should be addressed.

Table 1. Rate constants for the hydrolysis of $[Cr(X\text{-}C_6H_5COO)(NH_3)_5]^{2+}$ cations in perchloric acid (k_{NH_3}) and water (k_{aq}) at 21°C

X	k_{NH_3} (s^{-1})	k_{aq} (s^{-1})
F	1.87×10^{-5}	8.32×10^{-4}
Br	1.89×10^{-5}	4.10×10^{-4}
NO_2	2.50×10^{-5}	1.35×10^{-4}

compounds, upon storage, even in the dark. This loss of NH_3 in the solid state resulted in the fairly poor elemental analyses. Other Cr(III) complexes undergoing Cr—N bond rupture in solution have been reported. $[Cr(ox)(en)_2]^+$ hydrolyzed in acidic solution to give $[Cr(ox)(H_2O)(en)(enH)]^{2+}$,[6] and α-$[Cr(ox)(trien)]^+$ hydrolyzes to give $[Cr(ox)(H_2O)(trienH)]^{2+}$.[7] House[8] has found that $[Cr(ox)(NH_3)_4]^+$ aquates in dilute $HClO_4$ to give $[Cr(ox)(H_2O)(NH_3)_3]^+$, and Linck[9] has found that some bis(1,2-ethanediamine)chromium(III) complexes also undergo Cr—N bond rupture in acidic solutions. The rate constants of the NH_3 release (k_{NH_3}) for the three complexes studied were about the same at 21°C (see Table 1); therefore it seemed that a common intermediate was involved in the Cr—N bond rupture process. Several mechanisms for the bond rupture have been proposed,[10-12] but our data are insufficient to favor any mechanism.

The visible absorption spectra of the three complexes in water all resemble the spectrum of the acetatopentamminechromium(III) cation[10] with maxima at 488 ± 2 and 366 ± 1 nm, and a minimum at 423 ± 1 nm. A repeated scan of the spectra showed isosbestic points, and the spectra of all three complexes changed to one that resembled the spectrum of $[Cr(H_2O)(NH_3)_5]^{3+}$; therefore in aqueous solutions these complexes aquate to the pentaammineaquachromium(III) cation. The observed isosbestic points [listed as wavelength (nm) and molar absorptivity (in parentheses) ($dm^3\ mol^{-1}\ cm^{-1}$)] are as follows: *o*-fluorobenzoate complex, 555 (19), 442 (25), 399 (22); *o*-bromobenzoate complex, 556 (20), 434 (26), 329 (22); o-nitrobenzoate complex, 555 (18), 452 (34). Plots of $\ln(A_t - A_\infty)$ vs time gave good straight lines from which the rate constants of aquation (k_{aq}) at 21°C were evaluated (see Table 1).

The rate constants of aquation in water showed a decreasing trend from the *o*-fluorobenzoate complex to the *o*-bromobenzoate complex to the *o*-nitrobenzoate complex. Since the acid dissociation constants of the three *o*-substituted benzoic acids are of the same order of magnitude, the difference in the aquation rates must not be caused by the base strength of the benzoates. Also, the aquation occurs in water but not in acid so that the base strength of the benzoate anions probably had little effect on the reaction rates. The inductive effects of the three substituents are in the increasing order F^- to Br^- to NO_2^- as the Taft substituent constants are 0.17, 0.29 and 0.83, respectively, evaluated from the reaction rates of substituted naphthoic acids and naphtholates.[13] This order of the inductive effect predicts that the *o*-nitrobenzoate complex should react the fastest and the *o*-fluorobenzoate complex the slowest, but the observed rates are just the reverse. However, the steric effect of these substituents are in the increasing order NO_2^- to Br^- to F^- as the steric substituent constants are −0.75, 0.00 and +0.49, respectively.[14] This order of the steric effect predicts that the *o*-fluorobenzoate complex should react the fastest and the *o*-nitrobenzoate complex the slowest, and this is the order found in our study. Thus we have found that a larger leaving group reacted slower than a smaller leaving group in these pentaammine(carboxylato)chromium(III) complexes, and an associative mechanism is indicated.

Several complexes of type *cis*-$[Cr(A)_2(en)_2]^+$ (A^- = propionate, isobutyrate or pivalate) have been prepared,[15] and preliminary studies have indicated that the complexes with a large leaving group (pivalate or 2,2-dimethylpropionate) aquate slower than that with a small leaving group (propionate). Details of this study will be reported later.

REFERENCES

1. G. Guastalla and T. W. Swaddle, *Can. J. Chem.* 1973, **51**, 821.
2. M. C. Weekes and T. W. Swaddle, *Can. J. Chem.* 1975, **53**, 3697.
3. F. Basolo and R. G. Pearson, *Mechanisms of Inorganic Reactions*, 2nd Edn, p. 137. John Wiley, New York (1958).
4. L. M. Jackman, R. M. Scott, R. H. Portman and J. F. Dormish, *Inorg. Chem.* 1979, **18**, 1497.
5. J. C. Chang, L. E. Gerdom, N. C. Baenziger and H. M. Goff, *Inorg. Chem.* 1983, **22**, 1739.
6. H. Gausman, Dissertation, Johann Wolfgang Goethe Universität, Frankfurt am Main, F.R.G. (1964) (quoted in Ref. 8).
7. J. M. Veigel, *Inorg. Chem.* 1968, **7**, 69.
8. D. A. House, *Acta Chem. Scand.* 1972, **26**, 2847.
9. R. G. Linck, *Inorg. Chem.* 1977, **16**, 3143.
10. E. Zinato, R. Lindholm and A. W. Adamson, *J. Inorg. Nucl. Chem.* 1969, **31**, 449.
11. M. V. Olsen, *Inorg. Chem.* 1973, **12**, 1416.
12. T. Ramasami, R. K. Wharton and A. G. Sykes, *Inorg. Chem.* 1975, **14**, 359.

13. P. R. Wells, S. Ehrenson and R. W. Taft, In *Progress in Physical Organic Chemistry* (Edited by A. Streitwieser and R. W. Taft), Vol. 6, p. 150. Interscience, New York (1968).
14. R. W. Taft, In *Steric Effects in Organic Chemistry* (Edited by M. S. Newman), p. 598. John Wiley, New York (1956).
15. J. C. Chang, *Inorg. Chem.* 1986, **25**, 1725.

Polyhedron Vol. 6, No. 5, pp. 1157–1159, 1987
Printed in Great Britain

0277-5387/87 $3.00+.00
Pergamon Journals Ltd

COMMUNICATION

MOLECULAR STRUCTURE OF TETRAKIS[BENZENETHIOLATOTRIMETHYLPLATINUM(IV)], $(\mu_3\text{-SPh})_4(PtMe_3)_4$

DON C. CRAIG and IAN G. DANCE*

School of Chemistry, University of New South Wales, PO Box 1, Kensington, NSW 2033, Australia

(*Received* 17 *September* 1986; *accepted* 22 *December* 1986)

Abstract—The crystal structure of the title compound is reported, and the geometry and symmetry of the three-fold bridging by the arylthiolate ligand with two-fold symmetry is assessed. Pt—S bond lengths are differentiated by only 0.04 Å. Crystal data: $C_{36}H_{56}Pt_4S_4$, $M = 1897.4$, tetragonal, space group $P4_32_12$, $a = 14.187(1)$, $c = 40.399(6)$ Å, $U = 8131.11$ Å^3, $Z = 8$.

In the substantial number of metal thiolate complexes now characterized structurally[1] some abnormal geometries have appeared around triply-bridging thiolate ligands. For instance, in the crowded molecule $Ag_6(SC_6H_4Cl)_6(PPh_3)_5$ (**1**),[2] two of the S atoms have two S—Ag bonds and the S—C bond virtually coplanar, with the third S—Ag bond inclined at an angle of 67 or 63°. A similar stereochemistry occurs in $(\mu_3\text{-SPh})_2(\mu\text{-SPh})_2(CuPPh_3)_4$ (**2**).[3] In **1** even further deviation from the expected tetrahedral stereochemistry for $M_3(\mu_3\text{-SR})$ occurs with some S atoms lying *outside* their Ag_3C coordination polyhedra. In some cases the thiolate S atom primarily bridges two metal atoms, pyramidally, with a longer secondary connection to another metal atom.[1]

This abnormal non-three-fold geometry at triply-bridging thiolate is observed for aryl substituents, which confer non-three-fold (mirror) symmetry on the ligand. The question arises as to whether electronic (or steric) factors in the arylthiolate ligands could be responsible for dissymmetric triple bridging. Arguments have been presented for the occurrence of M—SAr π-bonding in $(ArS)_2(Pr^iO)MoMo(OPr^i)(SAr)_2$,[4] which could cause such dissymmetry.

The $(\mu_3\text{-SR})_4(PtMe_3)_4$ series of high-symmetry cubanes[5] provide a good test of these questions, and therefore we have determined the molecular structure of the compound with R = Ph (**3**). The structure of the member with R = Me, (**4**), in which the substituent need not break the molecular symmetry, has been reported.[5]

RESULTS AND DISCUSSION

The molecular structure of **3** is shown in Fig. 1, and dimensions are provided in Table 1. The molecular symmetry is close to S_4, the highest possible, with the virtual S_4 axis bisecting the Pt1--Pt4 and Pt2--Pt3 vectors. Dimensions averaged under this symmetry (standard deviation of the sample in parentheses) are: Pt—S 2.51(2) Å, Pt--Pt 3.83(1) Å, S--S 3.20(2) Å, Pt—C 2.09(2) Å, S—Pt—S 79.4(6)°, C—Pt—C 88(2)°, S—Pt—C(*cis*) 96(3)°; the value of S—Pt—S is indistinguishable from that of **4**, but the values of Pt—S and Pt--Pt are *ca* 0.03 Å larger.

Close examination of the molecular structure reveals minor but significant metrical features associated with the orientations of the phenyl rings. The plane of each phenyl ring can be twisted at most by 30° from a Pt—S bond, when viewed along the C—S bond as shown in Fig. 2: that is the smallest Pt—S—C—C torsional angle (ϕ) must lie in the range 0–30°. It can be seen from Table 1 that these angles range from 3 to 15°, indicating a

*Author to whom correspondence should be addressed.

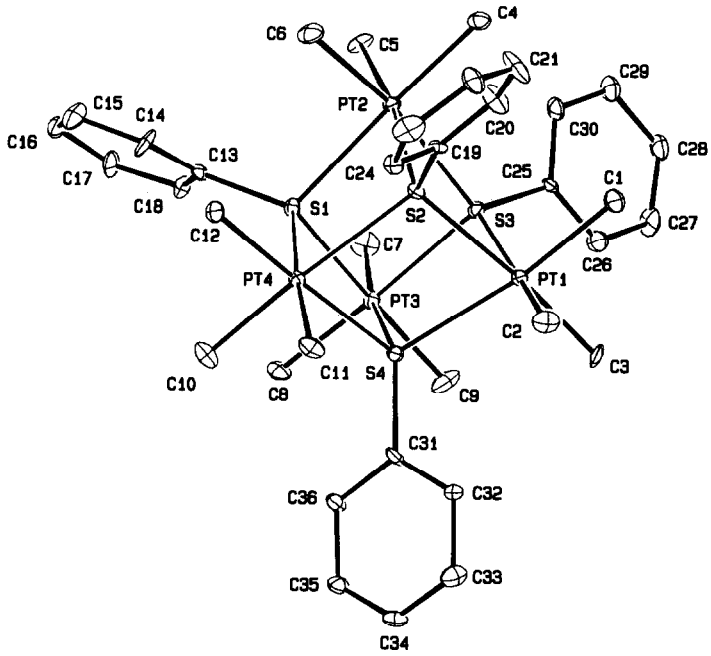

Fig. 1. Molecule of $(\mu_3\text{-SPh})_4(PtMe_3)_4$ (3) showing the atom labelling and thermal ellipsoids at 10% probability.

Table 1. Selected interatomic distances (Å) and angles (°) for $(\mu_3\text{-SPh})_4(PtMe_3)_4$

S1—Pt2	2.480(5)	Pt2—S1—Pt3	100.4(2)	Pt2—S1—C13	115.0(6)
S1—Pt3	2.519(5)	Pt2—S1—Pt4	100.4(2)	Pt3—S1—C13	117.7(7)
S1—Pt4	2.509(5)	Pt3—S1—Pt4	99.2(2)	Pt4—S1—C13	120.8(6)
S2—Pt1	2.487(5)	Pt1—S2—Pt2	99.5(2)	Pt1—S2—C19	116.5(6)
S2—Pt2	2.512(4)	Pt1—S2—Pt4	99.8(2)	Pt2—S2—C19	119.1(6)
S2—Pt4	2.537(5)	Pt2—S2—Pt4	98.7(2)	Pt4—S2—C19	119.4(6)
S3—Pt1	2.503(5)	Pt1—S3—Pt2	98.4(2)	Pt1—S3—C25	117.6(7)
S3—Pt2	2.537(5)	Pt1—S3—Pt3	100.1(2)	Pt2—S3—C25	120.8(7)
S3—Pt3	2.483(5)	Pt2—S3—Pt3	99.8(2)	Pt3—S3—C25	116.3(7)
S4—Pt1	2.533(5)	Pt1—S4—Pt3	98.5(2)	Pt1—S4—C31	118.8(7)
S4—Pt3	2.512(5)	Pt1—S4—Pt4	100.6(2)	Pt3—S4—C31	118.4(7)
S4—Pt4	2.462(5)	Pt3—S4—Pt4	100.7(2)	Pt4—S4—C31	116.5(8)
Pt1--Pt2	3.817	S2—Pt1—S3	80.6(1)		
Pt1--Pt3	3.822	S2—Pt1—S4	78.9(2)		
Pt1--Pt4	3.843	S3—Pt1—S4	79.3(2)		
Pt2--Pt3	3.841	S1—Pt2—S2	80.0(1)		
Pt2--Pt4	3.832	S1—Pt2—S3	78.9(2)		
Pt3--Pt4	3.830	S2—Pt2—S3	79.5(2)		
S1--S2	3.209	S1—Pt3—S3	79.2(2)		
S1--S3	3.190	S1—Pt3—S4	78.5(2)		
S1--S4	3.182	S3—Pt3—S4	80.1(2)		
S2--S3	3.228	S1—Pt4—S2	79.0(1)		
S2--S4	3.188	S1—Pt4—S4	79.6(2)		
S3--S4	3.214	S2—Pt4—S4	79.2(2)		

Torsional angles (ϕ)

Pt1—S4—C31—C32	14.8(22)
Pt3—S1—C13—C18	−10.0(20)
Pt2—S3—C25—C30	−6.0(21)
Pt4—S2—C19—C24	3.3(19)

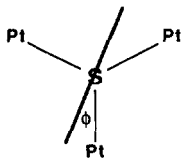

Fig. 2. Conformations and torsional angle (ϕ) for triply-bridging arylthiolate, viewed along the C—S bond. The thick line represents the plane of the arylthiolate ligand.

weak tendency of the ligand plane to adopt the "eclipsed" symmetrical conformation with $\phi = 0$ rather than the "staggered" symmetrical conformation with $\phi = 30°$. The Pt—S bond which is closest to the plane of the ligand substituent is slightly longer than the other two: the mean of the four close Pt—S bond lengths is 2.532(9) Å, and of the other eight Pt—S lengths is 2.494(19) Å. Note that the four longer Pt—S bonds follow the pseudo S_4 molecular symmetry. There is no significant expansion of the Pt—S—C angles in the plane closest to the ligand plane.

Therefore we conclude that any inherent (intramolecular) reduction in threefold symmetry of bonding at triply-bridging arylthiolate is virtually insignificant, being not more than a 0.04-Å elongation of the M—S bond almost coplanar with the aryl group.

EXPERIMENTAL

A sample of **3** provided by Dr Appleton was crystallized from $CHCl_3$.

Crystallographic studies

$C_{36}H_{56}Pt_4S_4$, $M = 1897.4$, tetragonal, space group $P4_32_12$, $a = 14.187(1)$, $c = 40.399(6)$ Å, $U = 8131.11$ Å^3, $Z = 8$, $D_c = 2.28\,g\,cm^{-3}$, $\mu_{Mo} = 140.9\,cm^{-1}$. Crystal size: 0.15 by 0.17 by 0.20 mm.

Intensities for 6294 reflections were measured with an Enraf–Nonius CAD-4 diffractometer in θ–2θ scan mode ($2\theta_{max} = 46°$) using graphite-monochromatized molybdenum radiation ($\lambda = 0.71069$ Å). Data were corrected for absorption. After determination of the space group, 3314 data with $h \leqslant k$ were selected for structure solution and refinement. Of these, 2725 with $I > 3\sigma(I)$ were considered observed. The structure was solved in space group $P4_12_12$ using MULTAN-80[6] and Fourier methods. Phenyl hydrogens were included in calculated positions and assigned temperature factors equal to those of the atom to which bonded; methyl hydrogens did not appear in a difference Fourier and were omitted. Least-squares refinement of positional and anisotropic thermal parameters for the non-hydrogen atoms converged to give R (R_W) = 0.041 (0.053). Reflection weights used were $1/\sigma^2(F_o)$ with $\sigma(F_o)$ being derived from $\sigma(I_o) = [\sigma^2(I_o) + (0.04I_o)^2]^{1/2}$. Atomic scattering factors and anomalous dispersion parameters were from *International Tables for X-ray Crystallography*.[7]

The structure was subsequently refined in the enantiomorphous space group $P4_32_12$, and gave $R(R_W) = 0.034$ (0.046), indicating this to be the correct assignment.*

Acknowledgments—This research was supported by the Australian Research Grants Scheme. We thank Dr Appleton for provision of the sample of **3**.

REFERENCES

1. I. G. Dance, *Polyhedron* 1986, **5**, 1037.
2. I. G. Dance, L. J. Fitzpatrick and M. L. Scudder, *Inorg. Chem.* 1984, **23**, 2276.
3. I. G. Dance, M. L. Scudder and L. J. Fitzpatrick, *Inorg. Chem.* 1985, **24**, 2547.
4. M. H. Chisholm, J. F. Corning and J. C. Huffman, *Inorg. Chem.* 1984, **23**, 754.
5. G. Smith, C. H. L. Kennard and T. C. W. Mak, *J. Organomet. Chem.* 1985, **290**, C7.
6. P. Main, *MULTAN* 80. University of York, U.K. (1980).
7. J. A. Ibers and W. C. Hamilton (Eds), *International Tables for X-ray Crystallography*, Vol. 4. Kynoch Press, Birmingham, U.K. (1974).

*Atomic coordinates, thermal parameters, bond lengths and angles, and lists of F_o/F_c have been deposited with the Editor as supplementary data. Atomic coordinates and molecular dimensions have also been deposited with the Cambridge Crystallographic Data Centre.

Polyhedron Vol. 6, No. 5, pp. 1161–1163, 1987
Printed in Great Britain

0277-5387/87 $3.00+.00
Pergamon Journals Ltd

COMMUNICATION

SYNTHESIS AND CHARACTERIZATION OF NOVEL MACROCYCLIC ANTIMONY CARBOXYLATES CONTAINING DISULFIDE BONDS

RYOKI NOMURA,* MASATAKA YAMAMOTO, AKIHISA TAKABE and HARUO MATSUDA

Department of Applied Chemistry, Faculty of Engineering, Osaka University, Yamada-Oka, Suita, Osaka 565 (Japan)

(*Received* 9 *December* 1986; *accepted* 12 *January* 1987)

Abstract—Novel 18- and 22-membered ring cyclic antimony carboxylates which contained two S—S bonds were synthesized in the one-pot oxidative-coupling/condensation reaction of triphenylstibine oxide with thioglycolic or β-thiopropionic acids, respectively.

Recently, much attention has been given to the preparation of organoantimony heterocycles. For example, the reactions of several classes of organoantimony(V) compounds with glycolic acid derivatives,[1] phenols and related compounds,[2–4] dibasic acids,[5] glycols[6] and dioxetanes[7] produced organoantimony heterocycles in which chalcogen atoms (O or S) were directly bonded to the central antimony atom. However, the reported heterocycles contain less than 14-membered rings. In this communication, we describe the preparation and characterization of novel cyclic antimony carboxylates which have two S—S moieties and possess the largest ring among the antimony heterocycles reported, and their complexability with alkaline picrates.

A mixture of triphenylstibine oxide [Ph_3SbO (10 mmol)] and thioglycolic or β-thiopropionic acid (10 mmol) was heated at 80°C for 6 h in benzene (20 cm^3) and unexpected macrocyclic antimony carboxylates (**Ia** and **b**) were obtained in 98 and 95% yields, respectively. The molecular-weight measurement (VPO, $CHCl_3$) revealed that **I** were 2:4 (based on the starting carboxylic acid) cyclocondensates. Spectral and analytical data† are also consistent with the proposed macrocyclic structure.

The C=O stretching frequency was so high as to suggest that the central antimony atom was bound to a COO group by an ester type linkage. Signals of methylene protons in **Ib** split into a characteristic $A_2A'_2$ type dd pattern which resembled those of dithiodipropionic acid (**IIb**). In general, triorganoantimony(V) compounds are known to react with thioglycolic acid or *o*-aminophenols to give a stable 1,3,2λ^5-oxathiastibolane[1] or 1, 3, 2λ^5-oxazastibolane[4] ring (a 1:1 or 2:2 condensate), respectively. Consequently, it is very interesting that the reactions selectively gave 2:4 condensates but not 1:1 or 2:2 ones.

Previously, we have found that Ph_3SbO oxidizes thiols to the corresponding disulfides and also

*Author to whom correspondence should be addressed.

†Selective analytical data; (**Ia**) m.p. 59–62°C. IR (cm^{-1}, KBr): ν(C=O) 1660, ^1H NMR (90 MHz, $CDCl_3$): δ 3.09s (8H, CH_2); 7.40 and 7.93m (30H, *Ph*—Sb). ^{13}C NMR {^1H} (22.6 MHz, $CDCl_3$): δ 172.1s (*C* = O), 136.6s (*ipso*), 133.9d (*o*), 131.4d (*p*), 129.4d (*m*), 12.9t (CH_2). Found: C, 49.6; H, 3.6%, Mw (VPO, $CHCl_3$) 1044. Calc. for $C_{44}H_{38}O_8S_4Sb_2$: C, 49.1; H, 3.7%, Mw 1067. (**Ib**) m.p. 91°C. IR (cm^{-1}, KBr): ν(C=O) 1640. ^1H NMR (90 MHz, $CDCl_3$): δ 2.50dd (16H, $A_2A'_2$ type, J 6.7 Hz); 7.40 and 7.92 m (30H, *Ph*—Sb). ^{13}C NMR {^1H} (22.6 MHz, $CDCl_3$): δ 175.4s (*C*=O), 138.1s (*ipso*), 134.0d (*o*), 131.3d (*p*), 129.4d (*m*), 35.6t [$CH_2C(O)O$], 34.4t (CH_2S). Found: C, 49.9; H, 4.3%, Mw (VPO, $CHCl_3$) 1123. Calc. for $C_{48}H_{46}O_8S_4Sb_2$: C, 51.3; H, 4.1%, Mw 1123.

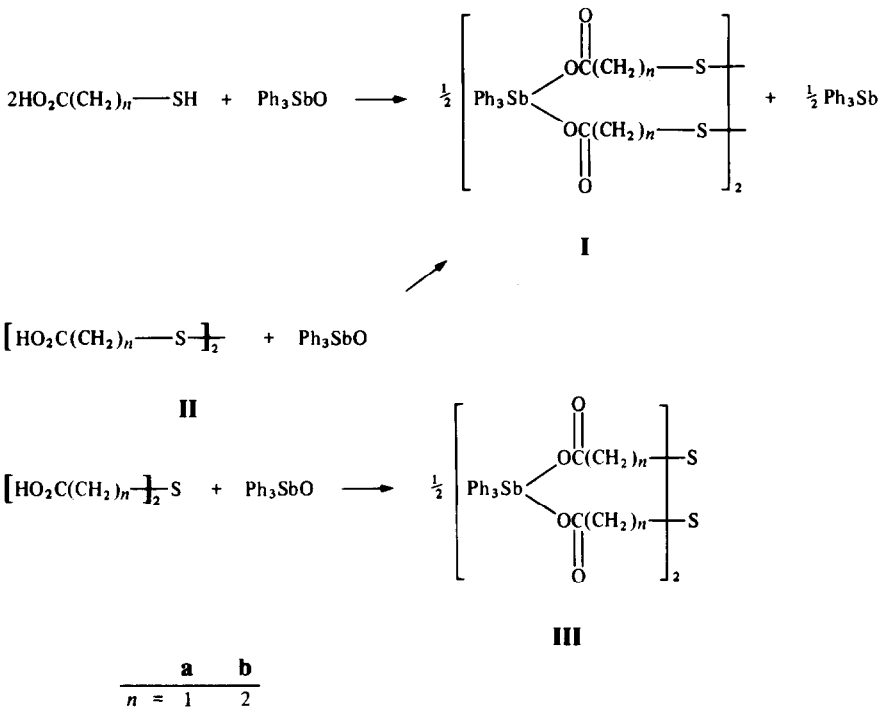

catalyzes the oxidative coupling.[8,9] The functionalized thiol, β-thiopropionic acid (10 mmol), was selectively converted to **IIb** in 95% yield at 80°C for 2 h in the presence of Ph_3SbO (1 mmol). Accordingly, it is presumed that a chemoselective condensation of Ph_3SbO with thiol groups gave triphenylantimony dimercaptides which underwent reductive-elimination to afford **IIb** in the initial stage of the reaction. The controlled reactions of Ph_3SbO with one equivalent amount of dithiodiglycolic acids **IIa** or **IIb** gave the 2:2 (based on the starting diacids) condensates quantitatively even at room temperature. Similarly, thiodiglycolic and thiodipropionic acids gave corresponding antimony heterocycles having two sulfide bonds (**III**) quantitatively in CH_2Cl_2 at room temperature. Although organoantimony(III) is known to give 2:2 cyclocondensates containing up to a 14-membered ring,[10] the isolation of such 2:2 condensates is reported here for the first time for organoantimony(V) derivatives.

Because **I** possessed several donating sites such as two disulfide bonds and four carboxylate linkage in their 18- or 22-membered ring structures and are soluble in most organic solvents, **I** can be expected to be effective host molecules. Thus, we attempted to investigate their complexability with alkaline metal ions by means of the picrate method.[11] The results are shown in Table 1. It was found that **Ib** showed very large values of K_e, namely, the values of log K_e were larger than 7 for Na^+, K^+ and Rb^+.[12] Just a small difference among K_es for individual ions was observed. However, since the formation of any alkaline metal carboxylates was not detected with ^1H and ^{13}C NMR spectra both in aqueous and organic layers during the complexation runs, the Sb–OC(O) linkage did not cleave under these conditions. The detailed investigation is currently under way.

Table 1. Extraction equilibrium constants (K_e) at 25°C[a]

	Na^+	K^+	Rb^+
Log K_e	7.19	7.33	7.39

[a]Extraction conditions: MtOH, 1.0×10^{-4} mol l^{-1}; picric acid, 7.0×10^{-5} mol l^{-1}; **Ib**, 2.8×10^{-5}–1.4×10^{-4} mol l^{-1}; H_2O–$CHCl_3$ = 10–10 cm^3, 20 min.

Acknowledgement—This research was financially supported by Grant-in-Aids for Scientific Research No. 60750787.

REFERENCES

1. Y. Matsumura, M. Shindo and R. Okawara, *J. Organomet. Chem.* 1971, **27**, 357.
2. Yu. A. Sokolova, O. A. D'yachenko, L. O. Atovmyan, N. I. Liptuga and M. O. Lozinskii, *Izv. Akad. Nauk SSSR, Ser. Khim.* 1980, 1446.

3. M. Hall and D. B. Sowerby, *J. Am. Chem. Soc.* 1980, **102**, 628.
4. G. Bauer, K. Scheffler and H. B. Stegmann, *Chem. Ber.* 1976, **109**, 2231.
5. B. Milewsky-Mahrla and H. Schmidtbauer, *Z. Naturforsch.* 1982, **37B**, 1393; H. Schmidtbauer and K.-H. Mitschke, *Angew. Chem., Int. Ed. Engl.* 1971, **10**, 36.
6. M. Wieber and N. Baumann, *Z. Anorg. Allg. Chem.* 1975, **418**, 279.
7. A. L. Baumstork, M. E. Landis and P. J. Brooks, *J. Org. Chem.* 1979, **44**, 4251.
8. R. Nomura, M. Kori and H. Matsuda, *Chem. Lett.* 1985, 579.
9. R. Nomura, A. Takabe and H. Matsuda, *Chem. Express* 1986, **1**, 375.
10. M. Wieber, D. Wirth and C. Burschka, *Z. Naturforsch.* 1984, **39B**, 600; M. Wieber and I. Fetzer-Kremling, *ibid.* 1984, **39B**, 754.
11. K. Kimura, T. Maeda and T. Shono, *Talanta* 1979, **26**, 945.
12. R. M. Izatt, J. S. Bradshaw, S. A. Nielsen, J. D. Lamb and J. J. Christensen, *Chem. Rev.* 1985, **85**, 271.

Polyhedron Vol. 6, No. 6, pp. 1165–1182, 1987
Printed in Great Britain

0277-5387/87 $3.00+.00

POLYHEDRON REPORT NUMBER 21

ORGANOMETALLIC OXIDES: THE EXAMPLE OF TRIOXO-(η^5-PENTAMETHYLCYCLOPENTADIENYL)RHENIUM(VII)*

WOLFGANG A. HERRMANN†, EBERHARDT HERDTWECK, MARTINA FLÖEL, JÜRGEN KULPE, ULRICH KÜSTHARDT and JUN OKUDA

Anorganisch-chemisches Institut der Technischen Universität München, Lichtenbergstraß 4, D-8046 Garching, F.R.G.

CONTENTS

1. INTRODUCTION

When the title compound trioxo(η^5-pentamethylcyclopentadienyl)rhenium(VII) (1) was discovered in our laboratory by Ricardo Serrano 2 years ago,[1] there was much surprise about the existence and stability of this material. In addition, nobody would have predicted such a pleasant and versatile chemistry as has developed since. Some basic, synthetically useful reactions have been described in a number of publications,[2–15] and a first comprehensive review was given recently.[16] The present up-dated account is aimed at the disclosure of novel key results that we have obtained since the above-mentioned review article was submitted (12 August 1985).[16] It is our declared intention to focus our peers' eyes to a field that, as we feel, shall turn out to gain extensively in

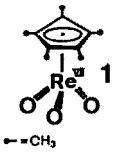

1

importance within the scopes of both organometallic and inorganic chemistry in future years. Not only synthetic uses of "organometallic oxides" can be thought of (e.g. construction of unprecedented heterocycles involving metal oxide structural entities, stabilization of high-valent transition metals etc.) but there are also obvious applications in the field of catalysis such as oxidation of unsaturated organic molecules (e.g. olefins and acetylenes) as well as olefin metathesis type reactions. Since it is always demanding to first investigate the chemistry of a given key compound before laborious

*Communication 34 of the series "Multiple bonds between main group elements and transition metals". Preceding paper: W. A. Herrmann, Ch. Hecht, E. Herdtweck and H.-J. Kneuper, *Angew. Chem.* (in press); *Angew. Chem., Int. Ed. Engl.* (in press).

†Author to whom correspondence should be addressed.

catalytic studies are done, we have decided to provide ourselves with as clear a picture as possible of the title compound's chemistry and the further chemical transformations of derivatives arising therefrom.

2. HISTORICAL SKETCH

A remark regarding the history of compounds such as (**1**)[1,17] should be made at this point. Oxides and oxohalides of transition metals (vanadium, chromium, molybdenum and tungsten) stabilized by π-aromatic ligands such as the unique cyclopentadienyl ligand have occasionally been observed from time to time for more than 20 years. Thus, Fischer's Munich laboratory reported on the synthesis of the vanadium compounds $(\eta^5\text{-}C_5H_5)VOX_2$ (X = Cl or Br) way back in 1958,[18] before Green *et al.* got hold of related molybdenum derivatives such as $(\eta^5\text{-}C_5H_5)MoO_2$ *and* $(\eta^5\text{-}C_5H_5)MoO_2Cl$.[19] Other organometallic oxides exhibiting terminal oxo functionalities have been made since then but their number is still quite small:

$(\eta^5\text{-}C_5H_5)_2Mo_2O_4$ (*cis*)[a]	Green (1964)[19]
$(\eta^5\text{-}C_5H_5)_2Mo_2O_5$	Green (1964)[19]
$(\eta^5\text{-}C_5H_5)_2WO$	Green (1972)[20]
$(\eta^5\text{-}C_5Et_5)WO_2(O^tBut)$	Schrock (1984)[21]
$(\eta^5\text{-}C_5Me_5)_2Cr_2O_4$ (*trans*)[a]	Herberhold (1985)[22]
$(\eta^5\text{-}C_5Me_5)_2Mo_2O_4$ (*cis*)[a]	Herrmann (1985),[23,24] Arzoumanian (1985)[25]
$(\eta^5\text{-}C_5Me_5)_2Mo_2O_5$	Herberhold (1985)[22]
$(\eta^5\text{-}C_5Me_5)_2W_2O_4$	Herrmann (1985)[23,24]
$(\eta^5\text{-}C_5H_4CH_3)_2MoO$[a]	Green (1972),[20] Tyler (1985)[26]
$(\eta^5\text{-}C_5H_5)WO(\pi\text{-}C_2H_2)R$ [R = Me or C(=O)Me]	Alt (1985)[27]
$(\eta^5\text{-}C_5H_5)WOR_3$ and $(\eta^5\text{-}C_5H_5)WO_2R$[a] (R = CH_2SiMe_3)	Legzdins (1985)[28]
$[\{\eta^5\text{-}(\text{-}CH_2C_5Et_4)\}WO_2(O\text{-}^tC_4H_9)]_2$	Schrock (1985)[29]
$[\{\eta^5\text{-}(\text{-}CH_2C_5Et_4)\}WOCl_3]_2$	

[a]X-ray structurally confirmed compounds.

Other organometallic oxorhenium complexes that have appeared in the literature are $ReO(\pi\text{-}C_2H_2)_2I$,[30] $Re(CH_3)_4O$,[31] $Re(CH_3)_3O_2$,[32] $Re(CH_3)O_3$,[33] $Re(CH_2SiMe_3)_4O$,[31] $Re_2(CH_2SiMe_3)_6O_3$,[31,34] $Re_2(CH_3)_6O_3$,[34] and $Re(O^tBut)O_3$.[34] The siloxy derivative $Re(OSiMe_3)O_3$[35] may prove to be starting material for new organometallic rhenium(VII) compounds. Wieghardt's recent compound $[(\eta^3\text{-}C_6N_3H_{12})ReO_3]^+BF_4^-$[36] looks like a "more inorganic" congener of our title complex **1**. High-nuclearity organometallic oxides are not considered here (cf. review in Ref. 37), with the remarkable compounds $(\eta^5\text{-}C_5H_5)_4$,[38] $(\eta^5\text{-}C_5H_5)_5V_5O_6$,[39] and $(\eta^5\text{-}C_5H_5)_6Ti_6O_6$[40] representing special highlights in this field.

If we are willing to disregard oxohalide and other mixed-ligand compounds for a moment, then it becomes evident that we really were lucky to trace down the title compound **1**: together with its manganese and technetium congeners, it is the only mononuclear compound in the series $(C_5R_5)MO_x$ that one might believe to show reasonable stability, provided the metal center is assumed to be present in its highest possible oxidation state according to the rules of the Periodic Table (Chart 1). Thus, for the scandium, yttrium and lanthanum compounds, the general composition $(C_5R_5)MO$ would be the logical extrapolation of compound **1**'s stoichiometry but it is quite clear that aggregation of this monomeric species that has a total of only two ligands would occur. The situation with respect to the vanadium, niobium and tantalum monomers of composition $(C_5R_5)MO_2$ is not yet clear; the vanadium compound $(\eta^5\text{-}C_5H_5)VO_2$ was described in a hardly available journal in 1974[41] but its true existence is still a questionable one since convincing synthetic, spectroscopic and structural data never became available. Three-coordinate, pentavalent Group-V transition metals may be achievable; they are expected to be structural analogues of the low-valent carbonyl series $(\eta^5\text{-}C_5R_5)M(CO)_2$, with M representing the elements cobalt, rhodium and iridium. However, the electronic nature of the oxo ligands could also give rise to dimerization of the monomeric species. By way of contrast, transition metals of the even-numbered groups do not provide us with diamagnetic monomeric compounds of composition $(C_5R_5)MO_x$ in their

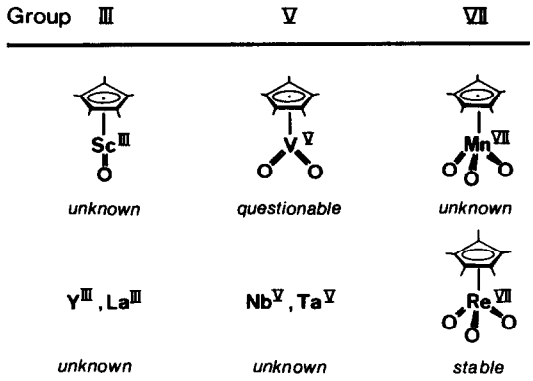

Chart 1.

highest possible oxidation states; here, only dimers or oligomers are possible, and the well-established compound $(\eta^5\text{-}C_5Me_5)_2Mo_2O_5$ containing an additional oxo ligand in a bridging function may be quoted in this context.[22]

From what has been said in this brief section, it becomes quite obvious that clear lines are still missing in organometallic metal oxide chemistry from all possible points of view. Hence, this field deserves systematic investigations with respect to synthesis, chemical reactivity, structural chemistry, and bonding theory. Only a very few steps directed towards these areas have been made up to the present.

3. SYNTHESIS OF TRIOXO(η^5-PENTAMETHYLCYCLOPENTADIENYL)RHENIUM(VII)

Construction of metal oxide structures in inorganic coordination or organometallic compounds (monomeric or oligomeric species) follows treatment of appropriate precursors (e.g. metal carbonyls and alkyls) with various reagents such as elemental oxygen, hydrogen peroxide, nitrous and nitric oxide, trimethylamine oxide, nitrobenzene, *t*-butyl hydroperoxide, or the nickel complex $[^t\text{But-NC}]_2\text{Ni}(\eta^2\text{-}O_2)$. Another possible strategy involves introduction of stabilizing organic ligands such as cyclopentadienyl (η^5) or benzene (η^6) into precursors like transition metal oxides or halides. However, this method has not yet been very successful, probably due to uncontrolled redox reactions occurring at the high-valent metal (reduction) and at the organic ligand (oxidation) (e.g. reaction of ReO_3Cl with $M^+C_5R_5^-$).[15]

The title complex **1** is nowadays easily accessible according to Scheme 1 by treatment of the low-valent carbonyl precursor species $(\eta^5\text{-}C_5Me_5)Re(CO)_3$ with concentrated aqueous hydrogen

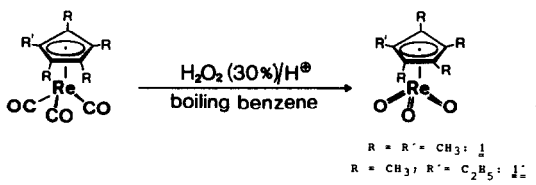

Scheme 1.

peroxide in a boiling two-phase water–benzene system; yields as high as 80% can be reached, depending a little on the purity of the starting materials and the reaction conditions. Purification of **1** is commonly achieved by means of column chromatography on silica and subsequent recrystallization from *n*-hexane–methylene chloride solutions at below ambient temperatures. The closely related derivative trioxo(η^5-ethyltetramethylcyclopentadienyl)rhenium(VII) (**1'**) has just been synthesized by Jun Okuda along exactly the same lines (see Experimental). In this particular case, suitable single crystals could be obtained, in contrast to what we had experienced for the title compound **1**.

The molecular geometry of **1'** is depicted in Fig 1(a) and (b), giving proof that we are indeed dealing with a mononuclear species containing short rhenium–oxygen bonds. The three ReO

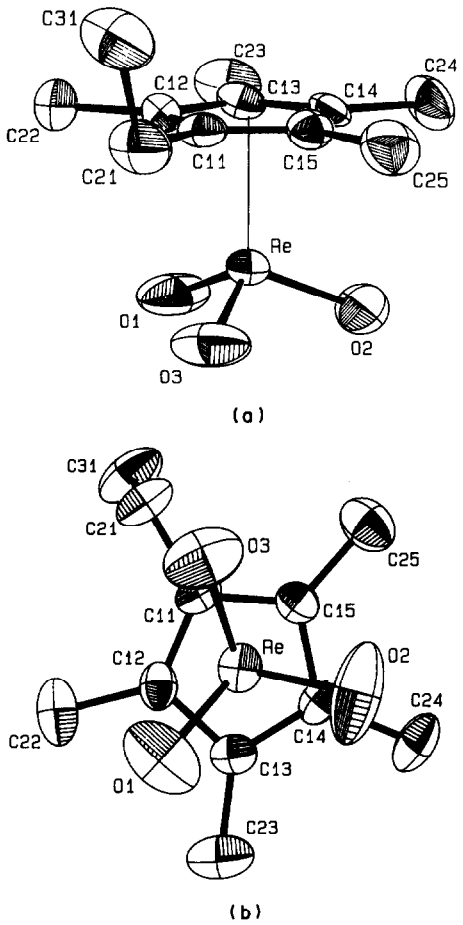

Fig. 1. Molecular structure [ORTEP representation, projection view down the five-membered π-ligand] of the trioxorhenium(VII) compound (η^5-C_5Me_4Et)ReO_3 (1'). Thermal ellipsoids correspond to 50% probability. Selected bond lengths (pm) and angles (°): Re—O(1) 166.4(4), Re—O(2) 171.6(4) Re—O(3) 170.7(3), Re—C(11) 239.2(3), Re—C(12) 239.2(3), Re—C(13) 243.0(4), Re—C(14) 241.8(3), Re—C(15) 238.5(4); 0(1),Re—O(2) 106.7(2), O(2)—Re—O(3) 104.7(2), O(1)—Re—O(3) 105.6(2); sum of angles within the ReO_3 core 317.0°.

interatomic distances of *ca* 170 pm are consistent with ordinary double bonds. It thus appears that terminal oxo groups act as powerful π-donor ligands in this particular case too. The overall geometry of the compound is best described as a slightly distorted trigonal pyramid if the five-membered π-ligand is considered to be the apex of this polyhedron.

No oxygen–oxygen contacts are present according to the recorded distances; the O, Re, O angles amount to approximately 105°, and the sum of these three angles is 317.0°. In contrast to the structures described below, the π-bonded hydrocarbon ligand is coordinated to the metal atom in a symmetrical fashion but the metal–carbon distances warrant a comment: they are *all* rather long compared to structurally related compounds (see Section 6 and Table 1). Whether this rhenium–carbon bond lengthening in compounds of type **1** does result in any significant weakening of the bond towards an easier replacement of the cyclopentadienyl ligand remains an issue to be pursued in the future. Cycloaddition reactions at the ReO_3 fragment and reductions to lower-valent derivatives do not involve replacement of this π-ligand. The only cases in which we have observed at least partial elimination of this ligand are limited to the synthesis of the trinuclear, ionic cluster compound [(η^5-C_5Me_5)$ReO(\mu$-$O)_2(\eta^5$-C_5Me_5)] containing two perrhenate counter-ions, the formation of the tetranuclear species [(η^5-C_5Me_5)$ReO(\mu$-$O)_2(\eta^5$-C_5Me_5)$Re(OReO_3)_2$].[5] and the synthesis of the glykolato complex [($\eta^5C_5Me_5$)$Re(OCH_2CH_2O)(\mu$-$O)_2(\eta^5C_5Me_5$)$Re(OReO_3)_2$].[48]

4. OXOHALIDE DERIVATIVES OF RHENIUM(V)

Most effective and useful is the reduction of the title compound **1** to the oxohalide complexes of composition $(\eta^5\text{-}C_5Me_5)ReOX_2$. Several synthetic routes have been worked out in our laboratory. Most elegantly, Flöel has exploited the high thermodynamic stability of germanium dioxide when she treated the title compound **1** with the dioxane adduct of germanium dichloride ($GeCl_2 \cdot C_4H_8O_2$) to make the dichloro rhenium(V) complex **3b** in 75% yield (Scheme 2). An indirect but

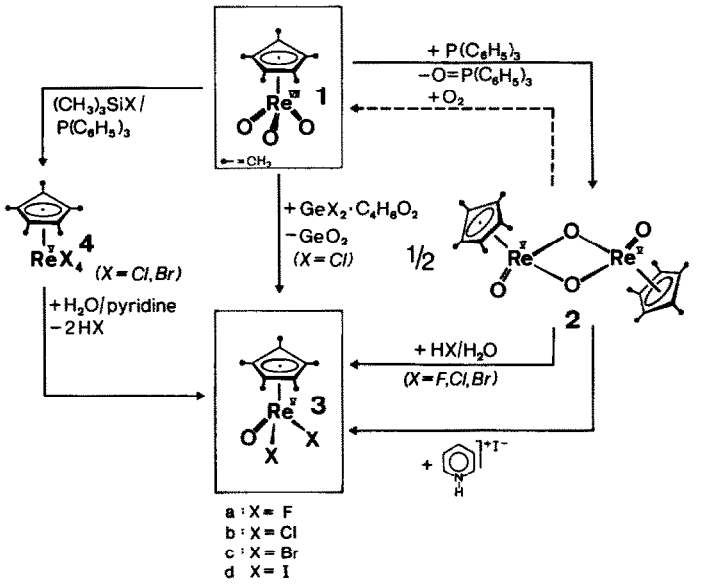

Scheme 2.

nevertheless high-yield access to compounds **3a–d** involves the isolable dinuclear intermediate **2** that is reportedly obtained via reductive deoxygenation of **1** with triphenylphosphane in the absence of oxygen. Due to the achievements of Küsthardt, compound **2** is quantitatively converted in fast reactions to the mononuclear difluoro, dichloro and dibromo derivatives **3a–c** when treated with aqueous hydrogen fluoride, chloride and bromide, respectively, at room temperature. According to Kulpe, the diiodo compound **3d** is best obtained by using pyridinium hydrochloride ($C_5H_6N^+I^-$), starting from the same precursor **2** (Scheme 2).

A further two-step synthetic procedure towards the oxohalide complexes of type **3** involves the intermediates **4** of composition $(C_5Me_5)ReX_4$. These latter compounds have been isolated for X = Cl and Br [**4b** and **c** (Scheme 3)] but their exact nature has not yet been resolved since solutions appear to contain at least two species, suggesting the existence of both monomeric and dimeric units.[42] In any case, hydrolysis with stoichiometric amounts of water and pyridine (formation of pyridinium chloride and bromide, respectively) at room temperature straightforwardly yields the desired mononuclear oxohalide derivatives **3b** and **3c** according to Scheme 2. It is obvious that the tetrahalides of type **4** are subject to partial hydrolysis only (replacement of *two* halide ligands by *one* oxo ligand). Complete hydrolysis occurs, however, when these tetrahalides are treated with a large excess of water in an acetone solution, yielding the dimer $(\eta^5\text{-}C_5Me_5)_2Re_2O_4$ (**2**). As established by Okuda, the best and most convenient way of making compounds **4** is simultaneous treatment of the title compound **1** with chloro- and bromotrimethylsilane, respectively, plus triphenylphosphane (Scheme 2). Keeping in mind that the action of the Lewis base triphenylphosphane upon **1** gives the reduced dimer **2** [Re(V)], this intermediate is likely to be formed in the synthesis of **4**, too. This proposal has been confirmed by the observed clean transformation of **2** into **4** effected by the $(CH_3)_3SiX$ reagents. In other words, both the phosphane and the halosilanes are responsible for stepwise deoxygenation of the precursor compound **1**. Compounds **4** are also formed from **1** in the absence of triphenylphosphane but the yields are not so good.

Further hydrolysis of the mononuclear oxohalides **3** may be achieved under basic conditions: treatment of the dichloro derivative **3b** with magnesium oxide in the presence of water gives the unusual dimer **5**, as has been established by Kulpe (Scheme 3).[43] The formation of this particular

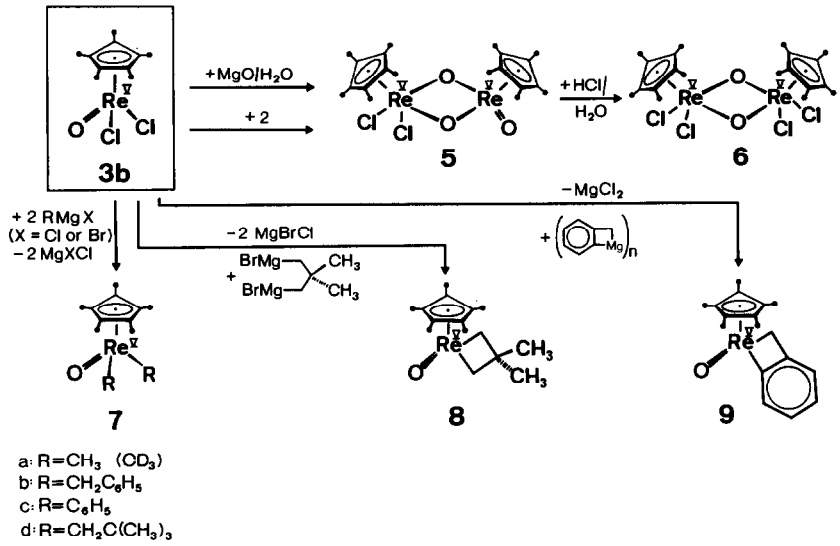

Scheme 3.

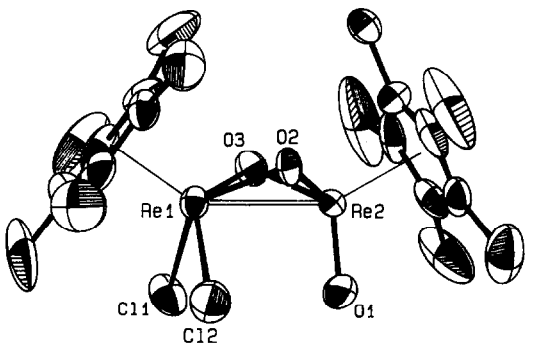

Fig. 2. ORTEP drawing of the molecular structure of the dinuclear oxohalide complex $(\eta^5\text{-}C_5Me_5)_2Re_2O_3Cl_2$ (**5**). Thermal ellipsoids correspond to 50% probability. Selected bond distances (pm) and angles (°): Re(1)—Re—(2) 269.1(<1), Re(1)—Cl(1) 239.5(1), Re(1)—Cl(2) 239.7(1), Re(1)—O(3) 202.0(3), Re(2)—O(1) 168.1(3), Re(2)—O(2) 185.9(3), Re(2)—O(3) 186.5(3), Re(1)—O(2) 202.1(3); Re(1),O(2),Re(2) 87.7(1), Re(1),O(3),Re(2) 87.6(1). The coordination geometry of the π-bonded ring ligands is discussed in Section 6 (see also Table 1).

compound may be viewed as a result of the condensation of unchanged $(\eta^5\text{-}C_5Me_5)ReOCl_2$ (**3b**) with its (hypothetical) hydroxy derivative $(\eta^5\text{-}C_5Me_5)ReO(OH)_2$. [The methoxy derivative $(\eta^5\text{-}C_5Me_5)ReO(OMe)_2$ of this latter species, however, proved stable under ordinary conditions.[16]] It is interesting to note that **5** does also result from the combination of **3b** with the highly reactive dimer **2** in the sense of a metathesis-type reaction; it has in fact repeatedly been observed that the dimeric rhenium(V) compound **2** is a useful synthetic source for the $(\eta^5\text{-}C_5Me_5)ReO_2$ fragment. Compound **5** is a straightforward (quantitative) coupling product between these two species (Scheme 3).

The terminal oxo ligand remaining in compound **5** can be effectively replaced by two chloro ligands by means of hydrochloric acid, without any breakdown of the dinuclear Re_2O_2 core structure. An X-ray crystallographic study carried out by Herdtweck revealed the *cis* stereochemistry of this molecule (approximate C_s-symmetry). The metal centers adopt distorted tetragonal-pyramidal [Re(1)] and trigonal-pyramidal [Re(2)] coordination geometries (Fig. 2). Small distortion of the π-bonded ring ligand at Re(1) only is evident from Fig. 3 and will be discussed separately in Section 6.

Similar reductive deoxygenation reactions have been carried out by Jun Okuda with the ethyltetramethylcyclopentadienyl compound **1'**, as summarized in Scheme 4. Once again, exhaustive deoxygenation occurs by means of the reagent combination $(CH_3)_3SiX/P(C_6H_5)_3$, yielding the

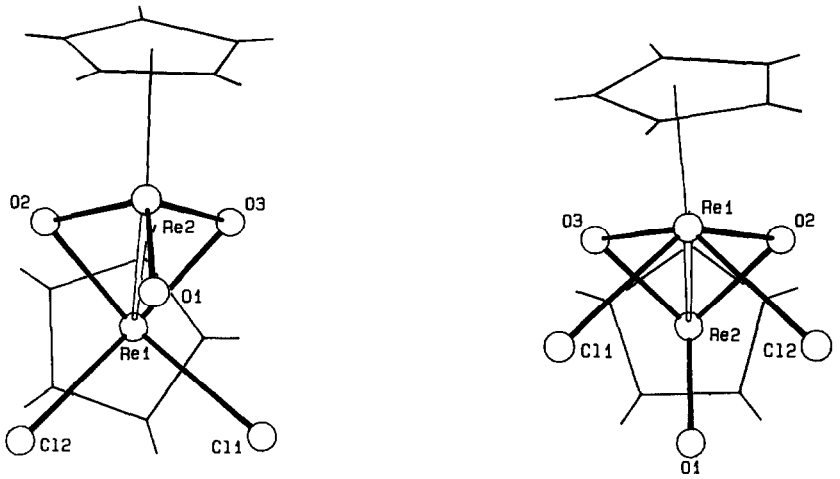

Fig. 3. Schematic drawings of compound **5**'s molecular structure. *Right*: Projection view onto the C_5Me_5 ring of the $(C_5Me_5)ReO_3$ core. *Left*: Projection view onto the C_5Me_5 ring of the $(C_5Me_5)ReO_2Cl_2$ core; this picture shows out-of-centroid distortion of the π-bonding between the metal atom and the five-membered ring ligand.

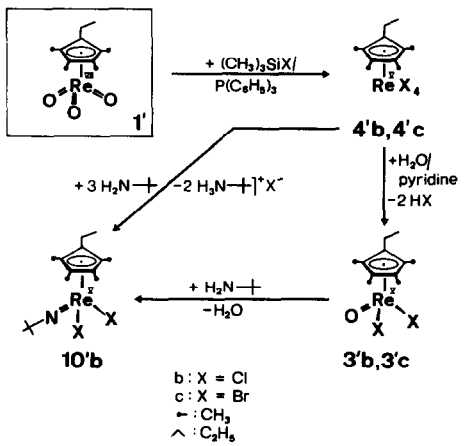

Scheme 4.

tetrahalide derivatives **4'b** (X = Cl) and **4'c** (X = Br). In contrast to the observations made with the pentamethylcyclopentadienyl congeners **4b** and **c**, these latter compounds are much more soluble in common organic solvents; for this simple reason, they promise a broader variety of chemical reactions. Hydrolysis with water and pyridine cleanly results in the formation of the rhenium(V) oxohalides **3'b** and **3'c**, respectively. Furthermore, the novel imido derivative (η^5-C_5Me_4Et-$ReCl_2(N^tBut)$) (**10'b**) is obtained in virtually quantitative yield when **4'b** is treated with excess *t*-butylamine in a toluene solution (see Experimental). Since imido (NR) groups, like oxo ligands, are capable of stabilizing metal centers in high oxidation states by virtue of their pronounced π-donation, one can expect another field of extensive chemistry here.[44] Imido complexes of the present type may not only be synthesized by the above methodology ($L_xMX_2 + H_2NR \rightarrow L_xM{=}NR + 2HX$) but also by decarboxylative coupling of organometallic oxides with isocyanates ($L_xM{=}O + (\eta^5\text{-}C_5Me_5)_2Mo_2(N^tBut)_4$.[45] with a recent example being the molybdenum compound $(\eta^5\text{-}C_5Me_5)_2Mo_2(N^tBut)_4$.[45]

5. OXOALKYL COMPOUNDS OF RHENIUM(V)

The oxohalide compounds of type **3** offered a unique possibility to further extend our work on oxoalkyl rhenium(V) compounds (Scheme 3). Whilst the parent dimethyl derivative **7a** is accessible through reductive deoxygenation of the title compound **1** by means of trimethylaluminium or

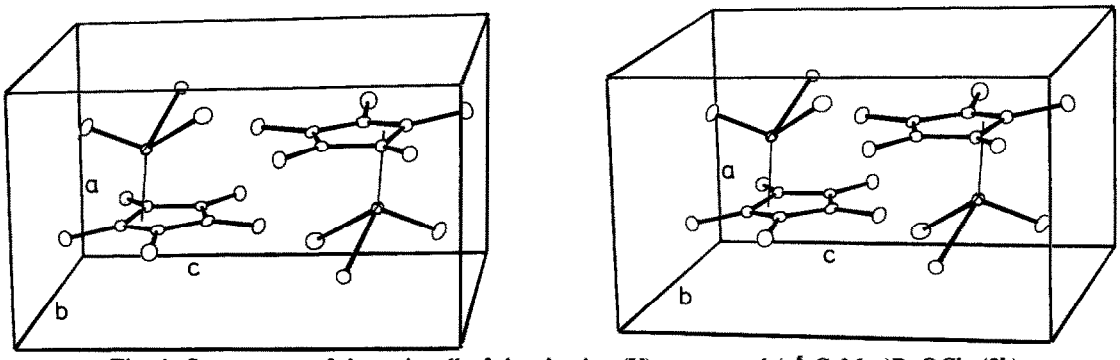

Fig. 4. Stereo view of the unit cell of the rhenium(V) compound $(\eta^5\text{-}C_5Me_5)ReOCl_2$ (**3b**).

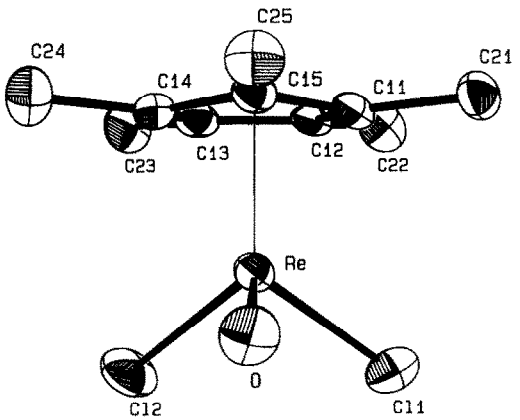

Fig. 5. ORTEP drawing of the molecular structure of compound **3b** (thermal ellipsoids at 50% probability). Bond lengths (pm) and angles (°): Re—O 170.0(4), Re—Cl(1) 234.8(2), Re—Cl(2) 234.5(2), Re—C(11) 222.5(5), Re—C(12) 247.7(6), Re—C(13) 247.5(6), Re—C(14) 222.5(6), Re—C(15) 218.0(6), Re—Cp* 195.5, C(11)—C(12), 146.2(8), C(12)—C(13) 139.3(8), C(13)—C(14) 145.4(9), C(14)—C(15) 144.5(8), C(15)—C(11) 143.8(8), Cl(1),Re,Cl(2) 85.4(1), Cl(1),Re,Cp* 123.0, Cl(1),Re,O 105.3(2), Cl(2),Re,Cp* 124.2, Cl(2),Re,O 106.2(2), O,Re,Cp* 109.5. The sum of angles within the $ReOCl_2$ core amounts to 296.9°. Cp* marks the center of C(11), C(14) and C(15).

dimethylzinc,[16] several homologues of this series, including the benzyl (**7b**), phenyl (**7c**), and neopentyl derivatives (**7d**) were synthesized in isolated yields around 70% by Martina Flöel using the Grignard approach. This synthetic route requires much experimental care because the precursor compound **3b** is also susceptible to messy reactions at the oxo ligand if the reactions with the Grignard compounds are not carried out carefully enough; thus, very clean Grignard compounds in the right stoichiometry must be used in these preparations. The novel metallacycles **8** and **9** became accessible in a collaborative effort with the Bickelhaupt group (Amsterdam).[46] Scrupulously dried glassware and starting materials are the crucial prerequisites for the successful preparation of these latter compounds too.[46,47]

6. STRUCTURAL AND ELECTRONIC CONSIDERATIONS

Although we are dealing here with rather handy compounds, some intriguing structural aspects are to be considered. In an extensive series of accurate X-ray structural determinations,[48] Herdtweck has accumulated ample evidence for highly distorted π-coordination of the five-membered ring ligands in several key compounds under discussion. This effect has been documented in all $(\pi\text{-}C_5Me_5)Re$ complexes in which the metal atom exhibits an additional set of *different* ligands with distorted tetrahedral coordination, e.g. $(C_5Me_5)ReL(L')_2$. One prominent example is the oxohalide compound $(\eta^5\text{-}C_5Me_5)ReOCl_2$ (**3b**) presented in Figs 4–6. The stereoview of Fig. 4 gives an excellent

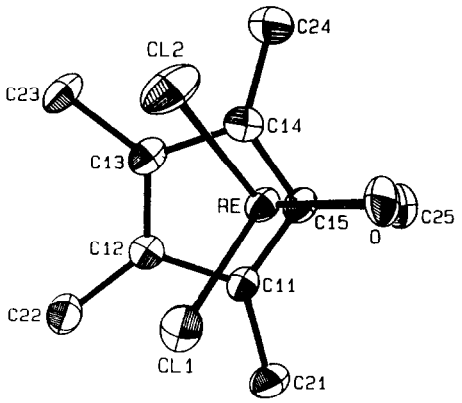

Fig. 6. ORTEP projection of compound **3b**'s molecular structure down the orthonormal vector between the plane of C(11), C(14), C(15) and the metal atom (thermal ellipsoids at 50% probability).

impression of how enormously the π-coordination of the pentamethylcyclopentadienyl ligand is distorted from the center of gravity. The two molecules present in the triclinic unit cell are arranged such that the out-of-centroid shift of the π-ligands is intermolecularly counterbalanced. If we disregard this peculiarity for a moment, then the basic structure of each molecule is described as a distorted trigonal pyramid, with two chlorine and one oxo ligand occupying the basal positions. The angle between the two chlorine ligands is much smaller [85.4(1)°] than the Cl(1/2), Re, O angles [105.3(2) and 106.2(2)°], with the sum of angles within the pyramidal $ReOCl_2$ entity amounting to 296.9°. This geometry is rather trivial but nevertheless entails distortion of π-coordination at the opposite ring ligand. It becomes clear from Fig. 5 that, unlike the architecture of the trioxo compound **1'** [Fig. 1(b)], the metal atom is no longer situated below the centroid of a regular pentagon but is rather shifted approximately parallel to the best plane of this ligand so that the carbon atoms C(15), C(11) and C(14) are much closer to the metal [218.0(6), 222.5(5) and 222.5(6) pm, respectively] than the two remaining ring atoms C(12) and C(13) [247.7(6) and 247.5(6) pm, respectively]. Taking into account that the bond between the more distant carbon atoms C(12) and C(13) is significantly shorter [139.3(8) pm] than the four other inter-ring distances (143.8–146.2 pm), a η^3-allyl/η^2-olefin-type coordination of the pentamethylcyclopentadienyl ring must be concluded.

Where does this acentric π-coordination arise from? Structural comparison with related compounds listed in Table 1 provides some help in answering this question. It is to be noted that: (i) the distances between rhenium and the attached pentamethylcyclopentadienyl ligand are generally somewhat shorter in low-valent compounds such as $(\eta^5\text{-}C_5Me_5)Re(CO)_2Br_2$ and $(\eta^5\text{-}C_5H_4SiMe_3)Re(CO)_3$ (Table 1),[49–55] and that (ii) substantial out-of-centroid coordination only occurs in rhenium compounds that display *different* ligands around the metal atom.

Structural details of the low-valent reference compound tricarbonyl(η^5-pentamethylcyclopentadienyl)rhenium(I) have not yet become available but rhenium–carbon distances of roughly 230–235 pm seem to be a pretty good extrapolation from the data of closely related compounds (cf. Table 1). If we now compare with the recorded rhenium–carbon distances of the structurally analogous high-valent oxo derivative **1'**, then we encounter a significant bond lengthening in this latter case (Fig. 1(a) and (b), Table 1). The rhenium–carbon distances of 238–243 pm are close to the set of *longer* distances in the unsymmetrical rhenium(V) derivatives $(\eta^5\text{-}C_5Me_5)ReOR_2$ (R = Cl, I, CH_3 or $CH_2C_6H_5$), while the π-bonded organic ligand, however, is rather symmetrically attached to the metal atom in the case of **1'** [Fig. 1(a) and (b)].

The conclusion to be drawn from these findings is quite obvious now: The oxo ligand, like nitrido ("naked" N) and carbyne (CR) groups, is a notorious π-donor ligand which property results in a strong *trans* effect, primarily labilizing the bonds on the opposite side of a given polyhedron. The selected compounds $(\eta^5\text{-}C_5Me_4Et)ReO_3$ (ReO_3-fragment) and $(\eta^5\text{-}C_5Me_5)ReOCl_2$ ($ReOCl_2$-fragment) demonstrates how dramatic this *trans* effect of terminal oxo ligands can be. Future studies have to show as to whether these architectural distortions of π-coordination within the class of compounds considered here do entail chemical consequences.

Table 1. Intramolecular distances between π-bonded cyclopentadienyl ligands and the metals attached to them [compounds containing (π-C_6Me_5)Re groups]

Compound	M[x]	No. of ligands[a]	d(M-C_5Me_5)[b] (pm)	Reference
(A) C_5Me_5 complexes				
(η^5-C_5Me_5)$_2$Re$_2$(CO)$_4$O	Re^{II}	5[c]	225–236	2
(η^5-C_5Me_5)Re(CO)$_2$[C$_2$(C$_6$H$_5$)$_2$O$_2$]	Re^{III}	5	227–237	11
(η^5-C_6Me_5)ReO[C$_6$H$_5$)$_2$O$_2$]	Re^{V}	4	219(1) 241( ) 223(1) 244(1) 225(1)	10
(η^5-C_5Me_5)ReO[C$_2$(C$_6$H$_5$)$_2$O$_3$]	Re^{V}	4	221(1) 239(2) 224(2) 241(1) 226(1)	10
(η^5-C_5Me_5)ReO[C$_2$O$_2$NC$_6$H$_5$]	Re^{V}	4	221(1) 242(1) 224(1) 244(1) 225(1)	10
[(η^5-C_5Me_5)$_3$Re$_3$O$_6$][ReO$_4$]$_2$	$Re^{V_{2/3}}$ (cation)	5 (cation)	219(3) 237(3) 219(4) 229(4) 231(3)	5
(η^5-C_5Me_5)$_2$Re$_2$O$_3$(OReO$_3$)$_2$	Re^{V}	4/5	219–238	5
(η^5-C_5Me_4Et)ReO$_3$	Re^{VII}	4	238–243	48
(η^5-C_5Me_5)ReOCl$_2$	Re^{V}	4	218 247 222 247 222	12
(η^5-C_5Me_5)ReOI$_2$	Re^{V}	4	219 252 224 254 225	This work; 68 68
(η^5-C_5Me_5)$_3$Re$_2$O$_3$Cl$_2$	Re^{V}	4	232–236	48
	Re^{V}	5	217 235 221 235 231	
(η^5-C_5Me_5)ReCl$_4$(PMe$_3$)	Re^{V}	6	225 237 226 240 247	8
(η^5-C_5Me_5)ReO(CH$_3$)$_2$	Re^{V}	4	214 250 223 250 223	48
(η^5-C_5Me_5)ReO(CH$_2$C$_6$H$_5$)$_2$	Re^{V}	4	216 25 226 252 227	This work; 68 68
(η^5-C_5Me_5)Re[O$_2$C$_6$Cl$_4$]$_2$	Re^{V}	5	(221–234)[c]	7
trans-(η^5-C_5Me_5)Re(CO)$_2$Br$_2$	Re^{III}	5	225–236	49
(B) C_5H_5 complexes				
(η^5-$C_5H_4SiMe_3$)Re(CO)$_2$	Re^{I}	4	230 (av.)	50
(η^5-$C_5H_4COCH_3$)Re(CO)$_3$	Re^{I}	4	228 (av.)	51
(η^5-C_5H_7)Re(CO)$_3$	Re^{I}	4	228(3) (av.)	52
(η^5-C_5H_5)Re(NO)(CHO)[P(C$_6$H$_5$)$_3$]	Re^{I}	4	231(1) (av.)	53
(η^5-C_5H_5)$_2$Re$_2$(CO)$_5$	Re^{I}	5[d]	224–234	54
trans-(η^5-C_5H_5)Re(CO)$_2$H(CH$_2$C$_6$H$_5$)	Re^{III}	5	229 (av.)	55

[a]The π-bonded C_5 ring ligands are assigned *one* position around the metal.

[b]Standard deviations refer to the least significant digit(s). If no entry is made, the standard deviation is less than 1 in the last given digit.

[c]Distorted pentamethylcyclopentadienyl ligand.

[d]Including ReRe bond.

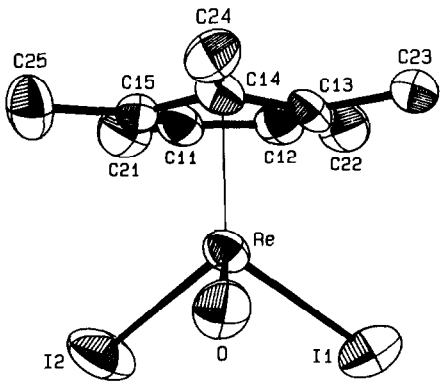

Fig. 7. The diiodo derivative (η^5-C_5Me_5)$ReOI_2$ (**3d**): ORTEP representation, with the thermal ellipsoids being at 50% probability. Selected bond lengths (pm) and angles (°): Re—O 168.7(3), Re—I(1) 268.1(< 1), Re—I(2) 267.6(< 1), Re—C(11) 253.5(4), Re—C(12) 251.7(4), Re—C(13) 223.7(4), Re—C(14) 218.6(4), Re—C(15) 225.4(4); I(1),Re,I(2), 88.8(< 1), I(1),Re,O 99.4(1), I(2),Re,O 101.7(4). The sum of angles within the $ReOI_2$ core amounts to 289.9°.

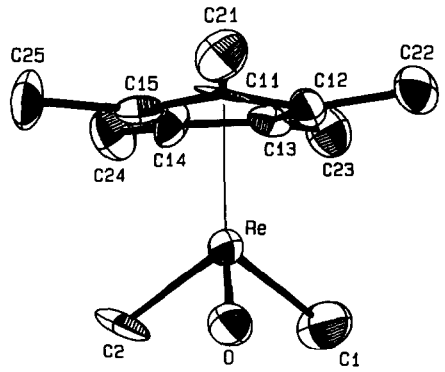

Fig. 8. The dimethyl derivative (η^5-C_5Me_5)$ReO(CH_3)_2$ (**7a**): ORTEP representation, with the thermal ellipsoids being at 50% probability. Selected bond lengths (pm) and distances (°): Re—C(1) 212.9(12), Re—C(2) 216.1(10), Re—O 168.1(7), Re—C(11) 213.7(9), Re—C(12) 223.1(9), Re—C(13) 249.9(9), Re—C(14) 249.7(9), Re—C(15) 223.5(9); C(1),Re,C(2) 81.7(5), C(1),Re,O 97.0(4), C(2),Re,O 99.8(4); sum of angles within the $ReOC_2$ core 278.5°. The C(13)—C(14) bond [137.3(13) pm] is shorter than the other four CC bonds within the five-membered π-ligand (143–145 pm).

The picture does not basically change as we move to related compounds of composition (C_5Me_5)$ReOR_2$:[48] thus, the diiodo derivative (η^5-C_5Me_5)$ReOI_2$ (**3d**) shown in Fig. 7 just adds to the conclusions drawn from the above-mentioned structures (Figs 1 and 4–6). The differences in rhenium–carbon bond lengths are again around 30 pm (!), with the two longer ReC distances being *trans* to the Re=O group. Although the bulkier iodo ligands (compared with Cl) may contribute to this effect by steric (through space) repulsions a little bit, the dominating reason is due to the electronic properties of the terminal oxo ligand. Otherwise, the Re—C(13) and Re—C(15) bonds [223.7(4) and 225.4(4) pm] should be about as long as the Re—C(11) and Re—C(12) bonds [253.5(4) and 251.7(4) pm, respectively]. Figures 9 and 11 should be compared with Figs 1(b) (title compound) and 8 (oxodichloro complex **3b**).

The same findings and interpretations apply to the dialkyl series (C_5Me_5)$ReOR_5$ [R = CH_3 (**7a**) or $CH_2C_6H_5$ (**7b**)]. Boths compounds (Figs 8–11) adopt the same overall geometry, with the distortion of the hydrocarbon π-ligand being even more pronounced than what we have observed for the dichloro and diiodo derivatives **3b** and **3d**. The bond length difference is as high as 37 pm (compound **7b**), and the five-membered ligand is no longer planar! Still, halogen vs alkyl substituents at the rhenium atom do not appear to greatly influence the structural details in compounds of analogous composition.

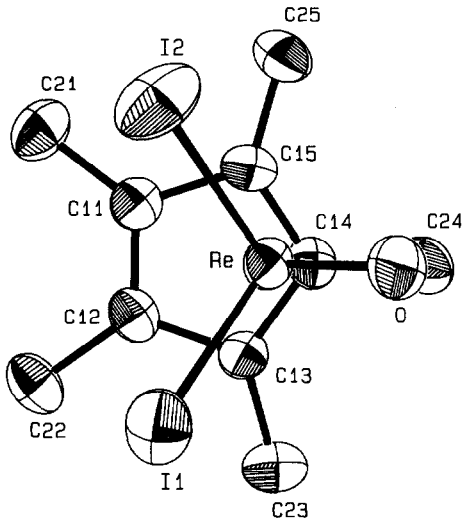

Fig. 9. Projection of compound **7a**'s molecular structure viewed down onto the best plane of the π-bonded pentamethylcyclopentadienyl ligand.

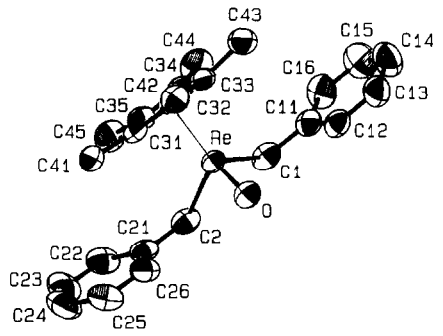

Fig. 10. The dibenzyl derivative $(\eta^5\text{-}C_5Me_5)ReO(CH_2C_6H_5)_2$ (**7b**): ORTEP representation, with the thermal ellipsoids being at 50% probability. Selected bond lengths (pm) and distances (°): Re—C(1) 217.5(3), Re—C(2) 216.3(3), Re—O 168.6(2), Re—C(31) 226.8(3), Re—C(32) 215.6(3), Re—C(33) 225.9(3), Re—C(34) 252.2(3), Re—C(35) 252.2(3); C(1),Re,C(2) 83.1(2), C(1),Re,O 98.6(1), C(2),Re,O 98.4(1); sum of angles within the $ReOC_2$ core 280.1°. The C(34)—C(35) bond length [139.0(4) pm] is shorter than the other four CC bonds within the five-membered π-ligand [143.4(4)–144.7(4) pm].

The comparative compilation of structural data presented in Table 1 gives the following general information:

(i) There are two arbitrary sets of rhenium–carbon (C_5Me_5 ring ligand) bond distances, smaller or larger than *ca* 235 pm.

(ii) The longer bonds are approximately *trans* to oxorhenium (ReO) groups. There is not too much of a difference, however, as to whether we are dealing with terminal or bridging oxo groups to cause this *trans* effect; in this respect, comparison may be drawn between compounds of type $(\eta^5\text{-}C_5Me_5)ReOX_2$ on the one hand, and the dimer $(\eta^5\text{-}C_5Me_5)_2Re_2(\mu\text{-}O)_2OCl_2$ (**5**) on the other hand.

(iii) The stronger the *trans* effect comes to the fore, the shorter are the remaining rhenium–carbon distances. The latter ones may then even be much shorter [e.g. 214–223 pm in compound **7a** (Figs 10 and 11)] than in low-valent compounds containing exclusively π-acceptor ligands such as carbon monoxide [e.g. 230 pm (*average*) in $(\eta^5\text{-}C_5H_4SiMe_3)Re(CO)_3$ (Table 1)].

(iv) The *trans* effect is not an additive one, because otherwise the rhenium–carbon bond lengthening in the title compound's congener **1'** (*d*Re—C 238–243 pm) should be even stronger, approaching *ca* 250 pm (cf. Table 1).

(v) The kind of distortion of the rhenium–cyclopentadienyl bonding depends on the coordination

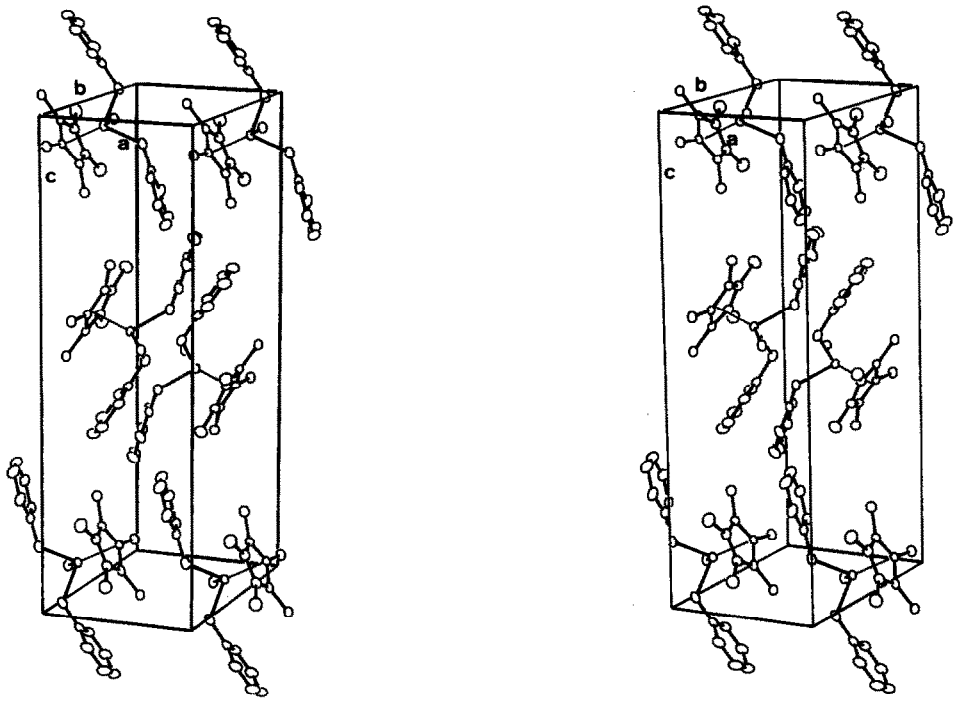

Fig. 11. Stereoview of compound **7b**'s unit cell.

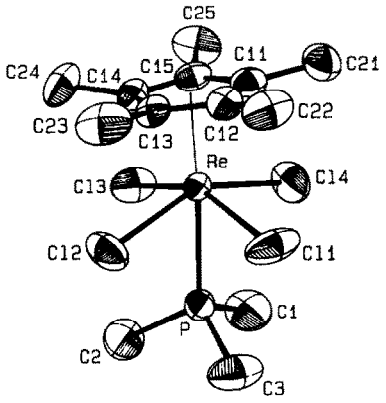

Fig. 12. Structure of the rhenium(V) compound $(\eta^5\text{-}C_5Me_5)ReCl_4(PMe_3)$ in the crystal (ORTEP representation, thermal ellipsoids at 50% probability). Selected bond distances (pm) and angles (°): Re—Cl(1) 238.5(2), Re—Cl(2) 239.4(2), Re—Cl(3) 243.6(2), Re—Cl(4) 240.6(2), Re—P 260.6(2), Re—C(11) 236.9(6), Re—C(12) 246.7(6), Re—C(13) 240.3(6), Re—C(14) 225.9(6), Re—C(15) 225.4(6); Cl(1),Re,Cl(2) 85.9(1), Cl(1),Re,Cl(4) 85.8(1), Cl(1),Re,P 78.6(1), Cl(2),Re,P 72.7(1). The sum of the angles within the $ReCl_4$ core amounts to 323.0°. The CC bond lengths within the five-membered π-ligand vary between 139.9 and 144.4 pm.

number (c.n.). Thus, in compounds of type $(\eta^5\text{-}C_5Me_5)ReL(L')_2$ (c.n. 4) the out-of-centroid distortion is directed towards one ring carbon atom (η^3-allyl/η^2-olefin coordination; *two* short and *three* long ReC bonds), while in compounds of type $(\eta^5\text{-}C_5Me_5)ReL_4$ (c.n. 5) two ring carbon atoms are closest to the metal (*one* short and *four* long ReC bonds).

Not yet clear is the origin of the asymmetry of π-bonding observed for the rhenium(V) compound $(\eta^5\text{-}C_5Me_5)ReCl_4(PMe_3)$. The overall structure is derived from an octahedron, with the five-membered ring ligand and the trimethylphosphane occupying positions *trans* to each other. The four chlorine ligands are skipped towards the phosphane, probably because of the bigger steric

requirements of the C_5Me_5 ligand (Fig. 12, Table 1).

The terminal rhenium–oxygen bond lengths are in the order of 168–172 pm in all compounds considered here. For the sake of comparison, some compounds may be quoted:

$KReO_4$	172.3(4) pm	Ref. 56
ReO_3Cl	170 pm	Ref. 57
$ReO_3(OSiMe_3)$	165 pm	Ref. 58
$Cs_2[ReO_3Cl_3]$	170(2) pm	Ref. 59
$(L_3)ReO_3^+$ (L_3 = *cyclo*-$C_6H_{12}N_3$)	175.6(5) pm	Ref. 60

The mononuclear rhenium(V) compounds of composition $(\eta^5\text{-}C_5Me_5)ReR_4$ (R = halogen or alkyl) contain rhenium in a d^2 electronic configuration. The possible singlet and triplet spin states are present in a temperature-dependent equilibrium, as we have demonstrated by means of ^1H NMR spectroscopy: the signal of the methyl groups (at the ring ligand and/or at the metal) experiences a paramagnetic (low-field) shift upon going from low to high temperatures, indicating a higher paramagnetic spin population at increasing temperatures.[14,43,47] A particularly nice example to amplify this is the square-pyramidal rhenium(V) derivative $(\eta^5\text{-}C_5Me_5)ReBr_2Me_2$.[14] Further attempts are being made to determine the energetics of these spin equilibrium phenomena. Another elegant tool for determining both the electronic situation within organometallic Re_xO_y cores and for establishing possible fluctionality within those metal oxide structures is available through ^{17}O NMR, particularly of ^{17}O-labelled compounds.[43]

7. FURTHER PERSPECTIVES

We have stumbled into an ostensibly rich field of research which once again holds promise of furnishing strong interlinks between inorganic (metal oxide) and organometallic chemistry.[61] High oxidation states of the participating transition metals is not at all the pivotal prerequisite of approaching compounds that contain both organic ligands and oxo groups. Low and high oxidation numbers of the metals are attainable for π-aromatic functionalities as well as for oxo groups, and a plethora of possible ligand combinations lies between the extremes. It is good to know that a potent oxidizing agent such as rhenium(VII) "doesn't chew up the organic ligand".[62] The title compound **1** convincingly amplifies this statement.

Where are we heading to? Further extension of our preparative work warrants high priority, including the "relatives" of rhenium: vanadium and niobium likewise are quite oxophilic and thus promise new "organometallic oxides", related and certainly surprising ones too. First attempts along this perspective have already been made in our research group. On the other hand, the synthetic future of rhenium compounds reviewed in this paper has just begun. Suffice to say that products like the amazing hexahydrido(η^5-pentamethylcyclopentadienyl)rhenium(VII), $(\eta^5\text{-}C_5Me_5)ReH_6$, synthesized by Okuda[63] from $(\eta^5\text{-}C_5Me_5)ReCl_4$ and $LiAlH_4$ presents another new key compound in high-valent organorhenium chemistry. It will be of interest to see how various oxidation states of rhenium interconvert with each other, both electrochemically (cyclovoltammetry) and on a preparative scale. Finally, the major perspective is directed towards catalysis. Do alkylrhenium(V) compounds such as $(\eta^5\text{-}C_5Me_5)ReO(CH_3)_2$ produce species containing alkylidenerhenium(V) ($Re{=}CH_2$) fragments upon thermolysis and can such units be generated by other means? If yes, is olefin metathesis[64] feasible at such fragments? Note that rhenium like molybdenum and tungsten is known to constitute the most effective olefin metathesis metal![64] Moreover, what is the fate of alkynes once coordinated to rhenium in high and intermediate oxidation states? Shall we find ourselves in a position of modelling organometallic oxides related to the mechanistically completely unclear SOHIO "ammonoxidation" process? A further possible utilization of oxorhenium and related compounds may be found in the functionalization of unsaturated organic compounds; reactivity patterns known from osmium tetroxide chemistry could arise here (e.g. glycols from olefins).[65] Upon considering the broad range of organometallic oxides landmarked by "david" $(\eta^5\text{-}C_5Me_5)ReO_3$ and "goliath" $[\{(\eta^5\text{-}C_7H_8)Rh\}_5(cis\text{-}Nb_2W_4O_{19})_2]^{3-}$,[66] then a rich harvest is to be expected during the years to come.

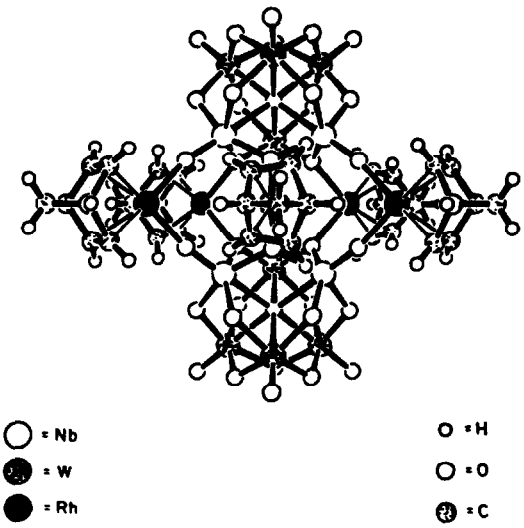

Fig. 13. SCHAKAL drawing of the C_{2v} structure of Klemperer's "organometallic oxide" $[\{(\eta^5\text{-}C_7H_8)Rh\}_5(cis\text{-}Nb_2W_4O_{19})_2]^{3-}$ [taken from Ref. 66(a)].

8. EXPERIMENTAL

Trioxo(η^5-1-ethyl-2,3,4,5-tetramethylcyclopentadienyl)rhenium(VII) (1')

A mixture of $(\eta^5\text{-}C_5Me_4Et)Re(CO)_3$* (1.00 g, 2.38 mmol) in benzene (35 cm^3) and conc. sulfuric acid (0.5 cm^3) in aqueous hydrogen peroxide (30%, 25 cm^3) was refluxed for 7 h under vigorous stirring. After approximately 2 h the organic layer turned dark red, and more hydrogen peroxide (5 cm^3) was added. The yellow organic phase was separated from the bluish-green aqueous layer, the latter one being extracted with toluene (3 × 5 cm^3). The combined extracts were washed with $NaHCO_3$ solution (5%) and water, and then dried over anhydrous $MgSO_4$. The solvent was removed *in vacuo* and the crude product recrystallized from toluene–*n*-hexane (1:2) at *ca* −30°C as bright yellow needles. Yield 400 mg (44%). From the aqueous phase *ca* 35% of Re was recovered as $KReO_4$ by concentrating this solution and subsequent addition of excess potassium hydroxide. Compound 1' melts at 145°C under decomposition.

Spectroscopic characterization. IR (KBr, cm^{-1}): 920 s (νReO_3 sym.), 887 vs (νReO_3 asym.), and 405 m (δReO_3). ^1H NMR (C_6D_6, 28°C): δ 2.17 (q, 2H, J_{HH} = 7.7 Hz, CH_3CH_2), 1.76 (s, 6H_3, CH_3) 1.62 (s, 6H, CH_3), and 0.74 (t, 3H, J_{HH} = 7.7 Hz, CH_3CH_2). ^{13}C NMR (C_6D_6, 28°C): δ 122.0 (CH_3CH_2C), 120.0 (CH_3C), 119.9 (CH_3C), 18.8 (CH_3CH_2), 13.2 (CH_3CH_2), 9.94 (CH_3), and 9.68 (CH_3). EI-MS (70°C, 70 eV): *m/z* 384 (M^+, parent ion).

Elemental analysis. Found: C, 34.3, H, 4.5, O, 12.4, Re, 47.0%. Calc. for $C_{11}H_{17}O_3Re$ (383.45): C, 34.5, H, 4.5, O, 12.5, Re, 48.6%.

(t-Butylimido)dichloro(η^5-pentamethylcyclopentadienyl)rhenium(V)

$(C_5Me_5)ReCl_4$ (225 mg, 0.49 mmol) was added as a solid to a solution of *t*-butyl amine (1.50 g, 20.5 mmol) in 5 cm^3 of toluene at room temperature. A dirty green solution formed from which a colorless solid separated. After filtration, the solvent was removed *in vacuo* to leave a dark brown oil which was extracted with pentane (2 × 3 cm^3). The olive-green residue was then recrystallized repeatedly from tetrahydrofuran–*n*-hexane (1:4) at *ca* −30°C to give blue-green, well-shaped crystals. Yield 125 mg (56%). M.p. 133–134°C.

*This starting compound was prepared by analogy with $(\eta^5\text{-}C_5Me_5)Re(CO)_3$ from $Re_2(CO)_{10}$ (Strem Chemicals) and 1-ethyl-2,3,4,5-tetramethylcyclopentadiene according to the procedure given in Refs 14, 15, 43, 67. Characterization: elemental analysis, ^1H and ^{13}C NMR, IR, and EI-MS [J. Okuda, unpublished results, Technische Universität München (1986)].

Spectroscopic characterization. IR (KBr, cm^{-1}): 1249 s [$(CH_3)_3C$], 338 and 332 m (νReCl). ^1H NMR (C_6D_6, 28°C): δ 1.83 (s, 15H, C_5Me_5), and 1.18 [s, 9H, $(CH_3)_3C$]. ^{13}C NMR (C_6D_6, 28°C): δ 107.9 (C_5Me_5), 76.0 [$(CH_3)_3C$], 31.4 [$(CH_3)_3C$] and 12.7 (C_5Me_5). EI-MS (90°C, 70 eV): *m/z* 463 (M^+, 21%), 407 ($M^+ - C_4H_8$, 100%), 390 ($M^+ - C_4H_{11}N$, 20%), 371 ($M^+ - C_4H_9 - Cl$, 65%), and 354 ($M^+ - C_4H_{11}N - Cl$, 24%).

Elemental analysis. Found: C, 36.3, H, 5.3, N, 3.0, Cl, 15.0, Re, 40.3%. Calc. for $C_{14}H_{24}Cl_2NRe$ (463.46): C, 36.3, H, 5.2, N, 3.0, Cl, 15.3, Re, 40.2%.

Dichloro(oxo)(η^5-1-ethyl-2,3,4,5-tetramethylcyclopentadienyl)rhenium(V) (**3'b**)

A suspension of $(C_5Me_4Et)ReCl_4$ (350 mg, 0.73 mmol) in 75 cm^3 of toluene was treated in a dropwise manner with a mixture of water (15 mg, 0.8 mmol), pyridine (140 mg, 1.6 mmol), and tetrahydrofuran (2 cm^3). The purple starting material rapidly dissolved and a green solution formed with concomitant deposition of a pale, greenish precipitate consisting of pyridinium hydrochloride and traces of $[(\eta^5\text{-}C_5Me_5Et)ReOCl_2]_2$. After filtration, the solvent was removed *in vacuo*. The crude product was then recrystallized at *ca* −30°C from methylene chloride–diethyl ether (1:5) as green platelets. Yield 200 mg (65%). M.p. 175°C.

Spectroscopic characterization. IR (KBr, cm^{-1}): 957 s (νReO), 353, and 338 mw (νReCl). ^1H NMR (C_6D_6, 28°C): δ 1.96 (q, 2H, CH_2, J_{HH} = 7.7 Hz), 1.66 (s, 6H, CH_3), 1.61 (s, 6H, CH_3), and 0.73 (t, 3H, CH_3, J_{HH} = 7.7 Hz). EI-MS (100°C, 70 eV): *m/z* 422 (M^+, 100%), and 386 (M^+ − HCl, 82%).

Elemental analysis. Found: C, 31.2, H, 4.1, Cl, 16.5%. Calc. for $C_{11}H_{17}Cl_2ORe$ (422.36): C, 31.3, H, 4.0, Cl, 16.8%.

Tetrachloro(η^5-1-ethyl-2,3,4,5-tetramethylcyclopentadienyl)rhenium(V) (**4'b**)

To a solution of $(\eta^5\text{-}C_5Me_4Et)ReO_3$ (300 mg, 0.8 mmol) in 5 cm^3 of toluene triphenylphosphane (205 mg, 0.8 mmol) followed by chlorotrimethylsilane (1.30 g, 12 mmol) was added at room temperature. The color of the mixture changed over a period of 1 h from brown to green, and finally to purple. The black purple crystals deposited were isolated by decanting off the supernatant solution which was discarded. The crystals were washed with toluene and diethyl ether. Yield 325 mg (85%). Analytically pure samples were obtained by repeated recrystallization from methylene chloride–diethyl ether (1:1) at *ca* −30°C. M.p. 145°C (dec.).

Spectroscopic characterization. IR (KBr, cm^{-1}): 330 ms (νReCl). EI-MS (100°C, 70 eV): *m/z* 476 (M^+ − Cl), 406 (M^+ − 2Cl), and 371 (M^+ − 3Cl).

Elemental analysis. Found: C, 27.7, H, 3.6, Cl, 29.9, Re, 38.7%. Calc. for $C_{11}H_{17}Cl_4Re$ (477.27): C, 27.7, H, 3.6, Cl, 29.7, Re, 39.0%.

Acknowledgements—The work summarized here would not have been possible without the active and continuous support of the Fonds der Chemischen Industrie, HOECHST Aktiengesellschaft, DEGUSSA AG, Chemische Werke Hüls AG, the BASF Aktiengesellschaft and the German Bundesministerium für Forschung und Technologie. We express our gratitude for the financial help that we have been receiving from these companies and institutions. Miss Juliane Geisler (text) and Mister Krebs (drawings) gratefully acknowledged for the preparation of this manuscript.

REFERENCES

1. W. A. Herrmann, R. Serrano and H. Bock, *Angew. Chem.* 1984, **96**, 364; *Angew. Chem., Int. Ed. Engl.* 1984, **23**, 383. See also: *Nachr. Chem. Techn. Labor. (Weinheim/Germany)* 1984, **32**, 202.
2. W. A. Herrmann, R. Serrano, A. Schäfer, M. L. Ziegler and E. Guggolz, *J. Organomét. Chem.* 1984, **272**, 55.
3. W. A. Herrmann, R. Serrano, U. Küsthardt, M. L. Ziegler, E. Guggolz and Th. Zahn, *Angew. Chem.* 1984, **96**, 498; *Angew. Chem., Int. Ed. Engl.* 1984, **23**, 515.
4. W. A. Herrmann, R. Serrano, M. L. Ziegler, H. Pfisterer and B. Nuber, *Angew. Chem.* 1985, **97**, 50; *Angew. Chem., Int. Ed. Engl.* 1985, **24**, 50.
5. W. A. Herrmann, R. Serrano, U. Küsthardt, E. Guggolz, B. Nuber and M. L. Ziegler, *J. Organomet. Chem.* 1985, **287**, 329.
6. W. A. Herrmann, U. Küsthardt, M. L. Ziegler and Th. Zahn, *Angew. Chem.* 1985, **97**, 857; *Angew. Chem.*,

Int. Ed. Engl. 1985, **24**, 860.
7. W. A. Herrmann, U. Küsthardt and E. Herdtweck, *J. Organomet. Chem.* 1985, **294**, C33.
8. W. A. Herrmann, E. Voss, U. Küsthardt and E. Herdtweck, *J. Organomet. Chem.* 1985, **294**, C37.
9. W. A. Herrmann, E. Vos and M. Flöel, *J. Organomet. Chem.* 1085, **297**, C5; W. A. Herrmann and J. Okuda, *J. Mol. Catal.* (in press).
10. U. Küsthardt, W. A. Herrmann, M. L. Ziegler, Th. Zahn and B. Nuber, *J. Organomet. Chem.* (in press).
11. W. A. Herrmann, U. Küsthardt and E. Herdtweck, *Angew. Chem.* (in press).
12. W. A. Herrmann, U. Küsthardt, M. Flöel, J. Kulpe, E. Herdtweck and E. Voss. *J. Organomet. Chem.* 1986, **314**, 151.
13. W. A. Herrmann, T. Cuenca and U. Küsthardt, *J. Organomet. Chem.* 1986, **309**, C15.
14. E. Voss, Ph.D. thesis, Technische Universität München (1986).
15. U. Küsthardt, Ph.D. thesis, Technische Universität München (1986).
16. W. A. Herrmann, *J. Organomet. Chem.* 1986 **300**, 111.
17. This compound was also reported by another research group: A. H. Klahn-Oliva and D. Sutton, *Organometallics* (1984) **3**, 1313.
18. (a) E. O. Fischer and S. Vigoureux, *Chem. Ber.* 1958 **91**, 1342; (b) E. O. Fischer, S. Vigoureux and P. Kuzel, *Chem. Ber.* 1960, **93**, 701.
19. M. Cousins and M. L. H. Green, *J. Chem. Soc. A* 1964, 1567. For structure of $(\eta^5\text{-}C_5H_5)_2Mo_2O_4$ see Ref. 22.
20. M. L. H. Green, A. H. L. Lynch and M. G. Swanwick, *J. Chem. Soc., Dalton Trans.* 1972, 1445.
21. R. R. Schrock, S. F. Pedersen, M. R. Churchill and J. W. Ziller, *Organometallic* 1984 **3**, 1574.
22. M. Herberhold, W. Kremnitz, A. Razavi, U. Schöllhorn and U. Thewalt, *Angew. Chem.* 1985 **97**, 603; *Angew. Chem., Int. Ed. Engl.* 1985 **24**, 601.
23. W. A. Herrmann, G. Ihl and D. Mandon, unpublished results, cf. W. A. Herrmann in Ref. 16.
24. G. Ihl, Ph.D. thesis, Technische Universität München (1986).
25. Structure of $(\eta^5\text{-}C_5Me_5)_2Mo_2O_4$: H. Arzoumanian, A. Baldy, M. Pierrot and J.-F. Petrignani, *J. Organomet. Chem.* 1985 **294**, 327.
26. N. D. Silavwe, M. Y. Chiang and D. R. Tyler, *Inorg. Chem.* 1985 **24**, 4219.
27. H. G. Alt and H. I. Hayen, *Angew Chem.* 1985, **97**, 506; *Angew. Chem., Int. Ed. Engl.* 1985, **24**, 497.
28. P. Legzdins, S. J. Rettig and L. Sanchez, *Organometallics* 1985, **4**, 1479.
29. J. H. Wengrovius, J. Sancho and R. R. Schrock, *J. Am. Chem. Soc.* 1981, **103**, 3932.
30. (a) J. M. Mayer and T. H. Tulip, *J. Am. Chem. Soc.* 1984, **106**, 3878; (b) J. M. Mayer, D. L. Thorn and T. H. Tulip, *J. Am. Chem. Soc.* 1985, **107**, 7454.
31. (a) J. F. Gibson, K. Mertis and G. Wilkinson, *J. Chem. Soc., Dalton Trans.* 1975, 1093; (b) K. Mertis, D. H. Williamson and G. Wilkinson, *ibid.* 1975, 607.
32. J. F. Gibson, G. M. Lack, K. Mertis and G. Wilkinson, *J. Chem. Soc., Dalton Trans.* 1976, 1490.
33. I. R. Beattie and P. J. Jones, *Inorg. Chem.* 1979, **18**, 2318.
34. P. Stavropoulos, P. G. Edwards, T. Behling, G. Wilkinson, M. Motevalli and M. B. Hursthouse, *J. Chem. Soc., Dalton Trans.* 1985, 2167; P. Edwards and G. Wilkinson, *ibid.* 1984, 2695.
35. M. Schmidt and H. Schmidbaur, *Inorg. Synth.* 1967, **9**, 149.
36. K. Wieghardt, C. Pomp, B. Nuber and J. Weiss, *Inorg. Chem.* 1986, **25**, 1659.
37. Cf. Ref. 24, p. 52ff.
38. (a) Synthesis: E. O. Fischer, K. Ulm and H. P. Fritz, *Chem. Ber.* 1960, **93**, 2167; (b) structure: F. Bottomley, D. E. Paez and P. S. White, *J. Am. Chem. Soc.* 1981, **103**, 5581; *ibid.* 1982, **104**, 5651.
39. (a) F. Bottomley and P. White, *J. Chem. Soc., Chem. Commun.* 1981, 28; (b) F. Bottomley, D. Paez and P. White, *J. Am. Chem. Soc.* 1985, **107**, 7226.
40. J. Huffman, J. Stone, W. Krusell and K. G. Caulton, *J. Am. Chem. Soc.* 1977, **99**, 5829.
41. V. N. Latyaeva, V. V. Pereshein and A. N. Lineva, *Tr. Khim. Khim. Tekhnol.* 1974, 32.
42. J. Okuda and W. A. Herrmann, unpublished results (1986).
43. J. Kulpe, Diploma thesis, Universität Frankfurt/Main (1986); K. Jung, Diploma thesis, Technische Universität München (1986); H.-J. Kneuper, Ph.D. Thesis, Technische Universität München (1986).
44. Cf. B. L. Haymore, E. A. Maatta and R. A. D. Wentworth, *J. Am. Chem. Soc.* 1979, **101**, 2063 (and reference quoted therein).
45. M. L. H. Green and K. J. Moynihan, *Polyhedron*, 1986, **5**, 921.
46. F. Bickelhaupt, W. A. Herrmann *et al.*, *Angew. Chem.* (1987), in press.
47. M. Flöel and W. A. Herrmann, unpublished results (1986).
48. E. Herdtweck and W. A. Herrmann, unpublished results (1985–1986).
49. F. W. B. Einstein, A. H. Klahn-Oliva, D. Sutton and K. G. Tyers, *Organometallics*, 1986, **5**, 53.
50. W. Harrison and J. Trotter, *J. Chem. Soc., Dalton Trans.* 1972, 678.
51. T. L. Khotsyanova, S. I. Kuznetsov, E. V. Bryukhova and Y. V. Makarov, *J. Organomet. Chem.* 1975, **88**, 351.

52. K. K. Joshi, R. H. B. Mais, F. Nyman, P. G. Owston and A. M. Wood, *J. Chem. Soc. A* 1968, 318.
53. W.-K. Wong, W. Tam, C. E. Strouse and J. A. Gladysz, *J. Chem. Soc., Chem. Commun.* 1979, 530.
54. A. S. Foust, J. Hoyano and W. A. G. Graham, *J. Organomet. Chem.* 1971, **32**, C65.
55. E. O. Fischer and A. Frank, *Chem. Ber.* 1978, **111**, 3740.
56. C. J. Lock and G. Turner, *Acta Cryst.* 1975, **B31**, 1764.
57. J. F. Lotspeich, A. Jaran and A. Englebrecht, *J. Chem. Phys.* 1959, **31**, 633.
58. G. M. Sheldrick and W. S. Sheldrick, *J. Chem. Soc. A* 1969, 2160.
59. T. Lis, *Acta Cryst.* 1983, **B39**, 961.
60. K. Wieghardt, C. Pomp, B. Nuber and J. Weiss, *Inorg. Chem.* 1986, **25**, 1659.
61. W. A. Herrmann, *Angew. Chem.* 1986, **98**, 57; *Angew. Chem., Int. Ed. Engl.* 1986, **25**, 56.
62. R. Dagani, *Chem. Eng. News* 1984, **62**, 28.
63. W. A. Herrmann and J. Okuda, *Angew. Chem.* (in press, December 1986); *Angew. Chem., Int. Ed. Engl.* (in press).
64. R. H. Grubbs, In *Comprehensive Organometallic Chemistry* (Edited by G. Wilkinson, F. G. A. Stone and E. W. Abel), Vol. 8, Chap. 54, pp. 499ff. Pergamon Press, Oxford (1982).
65. C. C. Hinckley and P. A. Kibala, *Polyhedron* 1986, **5**, 119 (and references quoted therein). *cf* A. O. Chong, K. Oshima and B. L. Sharpless, *J. Am. Chem. Soc.* 1977, **99**, 3420.
66. (a) C. J. Besecker, W. G. Klemperer and V. W. Day, *J. Am. Chem. Soc.* 1982, **104**, 6158; (b) C. Besecker and W. G. Klemperer, *J. Am. Chem. Soc.* 1980, **102**, 7598; (c) V. W. Day, M. F. Frederick, M. R. Thompson, W. G. Klemperer, R.-S. Liu and W. Shum, *J. Am. Chem. Soc.* 1981, **103**, 3597.
67. A. T. Patton, C. E. Strouse, C. B. Knobler and J. A. Gladysz, *J. Am. Chem. Soc.* 1983, **105**, 5804.
68. Compound **7a**: Green crystals obtained from diethylether/dichlormethane; $P\bar{1}$, $Z = 2$, $a = 715.4(1)$pm, $b = 839.5(1)$pm, $c = 1194.1(1)$pm, $\alpha = 83.30(1)°$, $\beta = 82.85(1)°$, $\gamma = 82.61(1)°$; $V = 702.10^6$pm^3; D(calc) = 2.797 gcm^{-3}; Enraf-Nonius CAD4, 294 K, 4870 reflexions messured, 2305 reflexions unique $I > 1\sigma(I)$; 128 parameters; corrections for absorption and extinction; weighting scheme $1/\sigma^2$(Fo); Hydrogen atoms included to calculations but not refined; $R = 0.032$, $R_w = 0.039$, GOF = 5.205; Program STRUX-II. Compound **7b**: Red brown crystals obtained from pentan; $P2_1/n, Z = 4$, $a = 751.9(1)$pm, $b = 2368.0(5)$pm, $c = 1201.8(2)$pm, $\beta = 90.74(2)°$; $V = 2140.10^6$pm^3; D(calc) = 1.613 gcm^{-3}; Enraf-Nonius CAD4, 294 K, 7626 reflexions messured, 3082 reflexions unique $I > 1\sigma(I)$; 351 parameters; corrections for absorption and decomposition; weighting scheme $1/\sigma^2$(Fo); Hydrogen atoms located and refined; $R = 0.022$, $R_w = 0.019$, GOF = 2.154; Programm STRUX-II.
Further details of the crystal structure determination can be obtained from the Fachinformationszentrum Energie Physik Mathematik, D-7514 Eggenstein-Leopoldshafen 2, F.R.G., by quoting the depository number CSD 52 223, the name of the authors and the journal citation.

Polyhedron Vol. 6, No. 6, pp. 1183–1189, 1987
Printed in Great Britain

0277–5387/87 $3.00+.00

CAPTURE OF BORANE IN AQUEOUS MEDIA: ROLE OF THE METAL ION IN THE FORMATION OF AROMATIC 2-AMINO-*N*-HETEROCYCLE BORANE COMPLEXES

YOSHIHISA OKAMOTO,* KUNIYOSHI OGURA and TOSHIO KINOSHITA

School of Pharmaceutical Sciences, Kitasato University, 5-9-1, Shirokane, Minato-ku, Tokyo 108, Japan

and

MICHIKO SHIRAI and YOSHIO MATSUMOTO

Department of Chemistry, Faculty of Hygienic Sciences, Kitasato University, 1-15-1, Kitasato, Sagamihara-shi, Kanagawa-ken 228, Japan

(*Received* 30 *June* 1986; *accepted after revision* 24 *October* 1986)

Abstract—The reasons why borane is captured by aromatic 2-amino-*N*-heterocycles in water are described. The key intermediate is found to be a chelate complex which contains borane, an amine and a metal ion.

Although amine–borane complexes are prepared by several methods,[1,2] the preparations are done under absolutely anhydrous conditions and sometimes in an atmosphere of dry nitrogen. In a previous communication,[3] we reported the first method for synthesizing an aromatic 2-amino-*N*-heterocycle borane in aqueous media. The reaction required a metal salt whose role we would like to describe in this paper.

RESULTS AND DISCUSSION

Borane adducts of some nitrogen heterocyclic compounds such as 2-aminopyridine and 2-amino-4-methylpyridine were prepared by the reaction of a Lewis base with trimethylamine–borane (and dimethylsulfide–borane), thereby resulting in a base displacement.[4,5] This transfer may also be possible by use of borane in tetrahydrofuran solution (BH_3–THF). However, these reactions require both anhydrous and nitrogen atmospheric conditions which sometimes are inconvenient for the organic chemist. On the other hand, amine–borane complexes are synthesized using a metal borohydride according to eqns (1)[1,2] and (2)[6] which should be worked up under anhydrous conditions. In contrast, we synthesized 2-aminopyridine–borane (**2a**) and its analogs (**2b–2f**) in aqueous solutions [eqn (3)].[3] When compared with eqn (2), there is the presence of a particular metal ion in eqn (3) in the place of a hydrochloride in eqn (2), and the presence of the 2-amino group in aromatic *N*-heterocycles. These two factors were examined to see whether they were involved in the reaction of eqn (3).

The results of the test for the ability of the one factor, namely the presence of amino group, are summarized in Table 1. Neither 4-aminopyridine nor 8-aminoquinoline would form their borane complexes; however, 8-amino-1,2,3,4-tetrahydroquinoline was obtained in a trace amount from the latter compound. It has already been reported that amidine compounds such as benzamidine and 1,5-benzodiazepine derivative were readily deaminated by this method, even without using a metal salt,[7] and that 2-aminomethylpyridine was converted to pyrazine and oxazole derivatives.[8] On the basis of the results described in Table 1, it is apparent that the 2-amino group in aromatic *N*-heterocycles is essential to the formation of the corresponding amine–borane complexes in

* Author to whom correspondence should be addressed.

Table 1. Reaction of $NaBH_4$–$CoCl_2$ with various amines in aqueous media

Starting material (SM)	Products
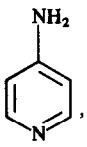 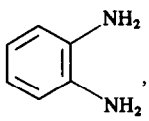 $H_2N(CH_2)_2NH_2$	SM
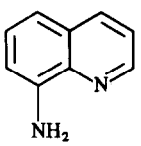	SM + 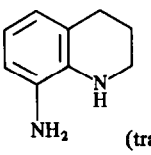 (trace)
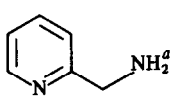	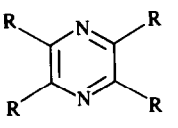 (48%) + 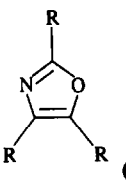 (trace) (R = 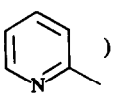)
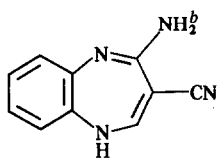	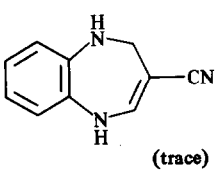 (trace) + 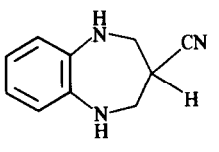 (37%)
$R—C(=NH)NH_2$ ($R = CH_3, C_2H_5$, Ph or tolyl)[b]	$R—CH_2NHCH_2—R$ (11–23%)

[a] Reference 8.
[b] Reference 7.

eqn (3). Meanwhile, 2-amino-6-methylpyridine (**1e**) afforded the corresponding borane complex (**2e**) in a very low yield though it is a stronger base than 2-aminopyridine (**1a**). This fact clearly indicates that the methyl substituent at the 6-position in pyridine ring causes great steric hindrance to the coordination between the boron and the ring nitrogen. Similar phenomena have already been observed by Brown *et al.*[9]

Next, many metal ions were evaluated as the

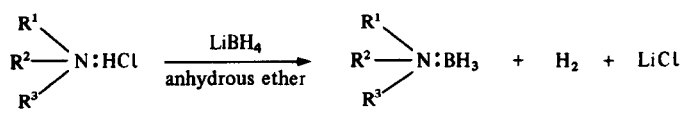

(1)

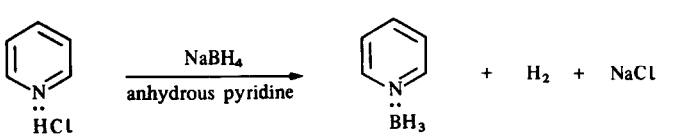

(2)

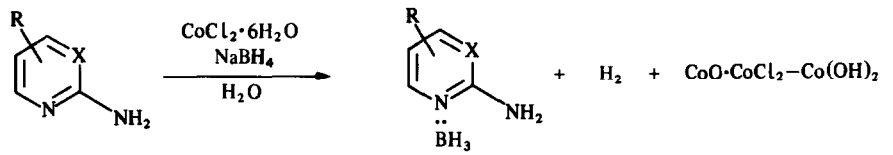

(3)

1a–f **2a–f**

X = C: R = H (**1a**) X = C: R = H (**2a**)
R = 3-CH_3 (**1b**) R = 3-CH_3 (**2b**)
R = 4-CH_3 (**1c**) R = 4-CH_3 (**2c**)
R = 5-CH_3 (**1d**) R = 5-CH_3 (**2d**)
R = 6-CH_3 (**1e**) R = 6-CH_3 (**2e**)
X = N: R = H (**1f**) X = N: R = H (**2f**)

other one of the two factors, and it was found that Ni^{2+} and Co^{2+} ions were much more effective than other metal ions (Scheme 1). Although nickel nitrate was best to yield 2-amino-4-methylpyridine–borane (**2c**), we selected cobalt chloride as the metal ion source for studying the reaction mechanisms because the reactions of cobalt chloride with sodium borohydride in several solvents have been investigated. For example, there are mainly three kinds of reaction solvent, i.e. water [eqn (4)],[10] ethanol [eqn (5)],[11] and tetrahydrofuran [eqn (6)].[12] These reactions gave cobalt borohydride, a complicated cobalt hydride (LnCoH), and cobalt boride or cobalt metal in eqns (4) and (5). It was only in the latest study [eqn (6)] that the formation of borane was recognized under anhydrous conditions and a nitrogen stream. It has also been reported that the reactions of sodium borohydride with chlorides of Fe(III),[13] Hg(I),[14] Sb(III),[14] Bi(III)[15] and Sn(II)[16] gave borane. These reactions, however, were carried out in diglyme or without a solvent, but not in water or alcohol. Our results as shown in eqn (3) suggested that borane could be generated by the reaction of cobalt chloride with sodium borohydride even in aqueous media. The borane was presumably captured by both 2-aminopyridine (or its analogs) and the metal ion through a stabilized intermediate. We attempted to clarify this presumption by isolating the intermediate from the reaction. When a solution of cobalt chloride in water was added to a solution of 2-amino-4-methylpyridine (**1c**) and sodium borohydride in water, a black powder immediately appeared, part of which was filtered off, washed with water and dried in a vacuum desiccator. During the drying the black powder turned gray. It was found that the gray powder contained 2-amino-4-methylpyridine–borane (**2c**) and 3% of cobalt, but no chlorine. On stirring the above reaction mixture (pH 9.5) for 3 h, the black precipitates were hydrolyzed to **2c** and green gelatinous precipitates which were found to be the products obtained by hydrolysis of cobalt chloride at pH 9.5 under air, presumably a mixture of cobaltous hydroxide and cobaltous oxychloride.[17] On the other hand, when nickel nitrate was used in place of cobalt chloride in the above reaction, a similar black powder was obtained and was not readily hydrolyzed. When dried in a vacuum desiccator, the black powder was also converted to a gray one which contained **2c** and nickel. The elemental ratio of the gray powder was Ni : C : N = 1 : 6 : 2 which indicated that the Ni^{2+} ion might be coordinated with at least one molecule of **2c**. The amine–borane complex **2c** was readily isolated from these intermediates by extraction with chloroform. The difference between the nickel-containing intermediate and the cobalt-containing intermediate is observed in their stability towards water, namely the former is more stable than the latter. On the basis of these results, we proposed a possible structure for the intermediate as shown in Scheme 2 where all requirements for eqn (3) were filled.

It is clear in Scheme 2 that a metal ion must coordinate to a nitrogen of an amidine moiety of a *N*-heterocycle. In order to confirm this kind of chelation, we utilized adenine (**3a**) and its 9-methyl derivative (**3b**) because interactions between metal

(Ni^{2+}), Co^{2+}, $(Co^{2+}) \gg Mg^{2+}$, Al^{3+}, Ca^{2+}, (Cr^{3+}), (Mn^{2+}), Fe^{2+}, (Cu^{2+}), Zn^{2+}, (Ag^{+}), Sn^{2+}, Sb^{3+},

(Ce^{3+}), Tl^{3+}, (Pb^{2+}), (Th^{4+})

Scheme 1. Effect of metal ions: chlorides (nitrates).

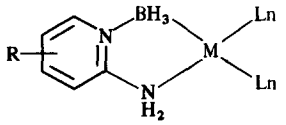

Scheme 2.

ions and these nucleic acid bases have extensively been studied. When 9-methyladenine (**3b**) was reacted with cobalt chloride in ethanol, a 9-methyladenine–cobalt chloride complex [a blue polymer (**6**)] was obtained, where the adenine nucleus utilizes N(1) and N(7) sites in binding to the metal ion.[18] Complex **6** reacted with sodium borohydride in water to give 9-methyladenine–borane (**8**). The possible structure of the intermediate of **8** might be **7** as shown in Scheme 3. On the other hand, adenine (**3a**) whose most preferred binding site for Co^{2+} ion coordination is the N(9) position[19] did not afford adenine–borane (**4**), but the 9-deprotonated adenine salt (**5**) (Scheme 4).

Coordination sites of borane to **1a** and **3b** were studied by UV (Table 2) and ^{1}H NMR spectral analyses. It has already been found that the protonation site is N(1) in both **1a**[20] and **3b**.[21] These protonated amines showed the bathochromic shifts in **1a**, and the blue shifts in **3b** in their UV spectra. Since **2a** showed similar shifts to those of the protonated compound of **1a**, the borane would coordinate to N(1) of the ring nitrogen.[5] On the other hand, **8** did not show the blue shifts. Moreover, the signal of amino protons of **2a** in ^{1}H NMR was observed at 5.67 ppm which was 1 ppm lower than that of **1a**. In contrast, the signal of amino protons of **8** was observed at 8.93 ppm which was 1.87 ppm lower than that of **3b**. This larger shift observed in **8** (about twice that of **2a**) indicates that the amino nitrogen might directly contact with borane. Therefore, the borane does not coordinate to the ring nitrogen N(1) of **3b**, but to the amino nitrogen.

$$CoCl_2\cdot 6H_2O \xrightarrow[H_2O]{NaBH_4} Co(BH_4)_2 + Co_nB_m + LnCoH \quad (4)$$

$$CoCl_2\cdot 6H_2O \xrightarrow[EtOH]{NaBH_4} LnCoH,\ Co\ \text{and/or}\ Co(BH_4)_2 \quad (5)$$

$$CoCl_2 \xrightarrow[\text{anhydrous THF}]{NaBH_4} CoH_2 + BH_3 + NaCl \quad (6)$$

As Scheme 5 shows, there are three kinds of bonding between a metal ion and borohydride anion,[22] and only one example has been reported

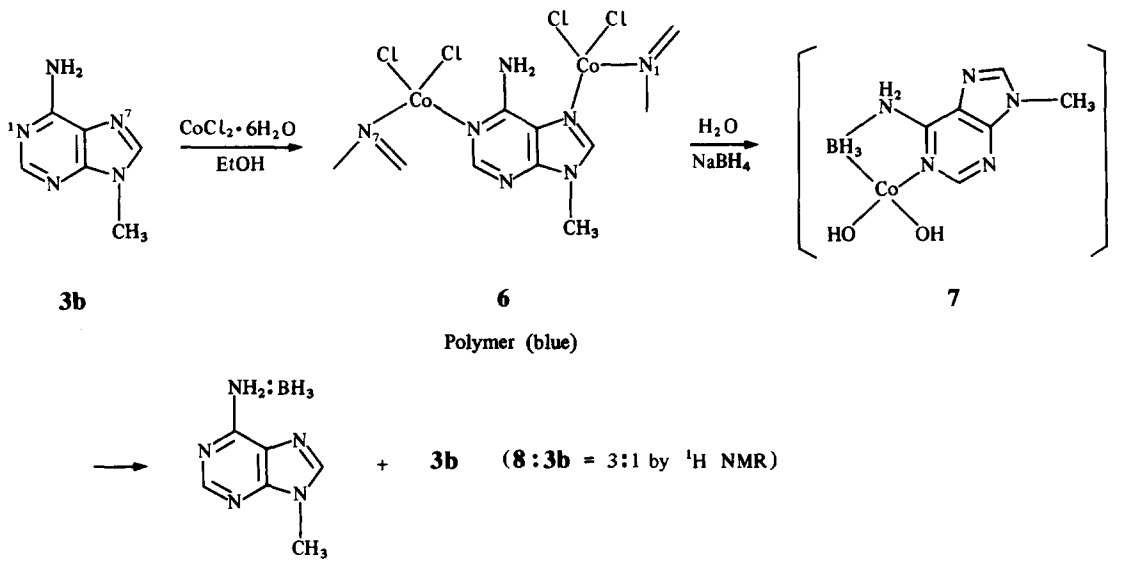

Scheme 3.

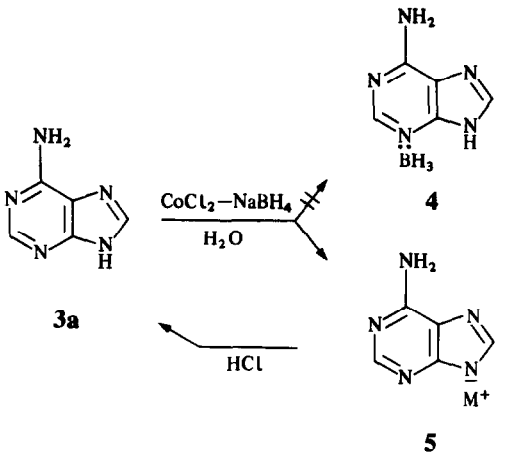

Scheme 4.

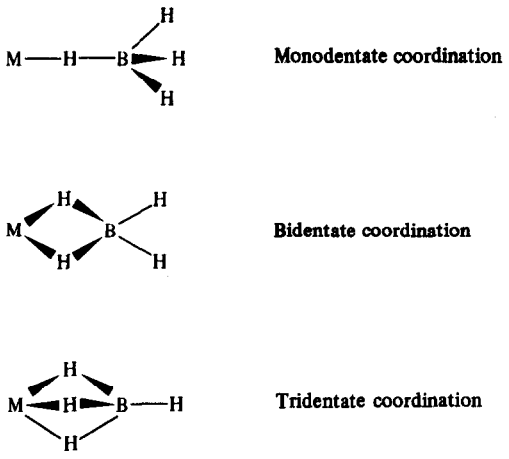

Scheme 5.

Table 2. UV spectral measurement [$\lambda_{max}^{H_2O}$ (nm)] (log ε)

Compound	Neutral solution		Acidic solution[a]	
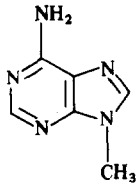	210.5 (4.25)	262.0 (4.12)	207.0 (4.27)	260.5 (4.13)
Mixture of **8** and **3b** (3 : 1)	211.5	262.0		
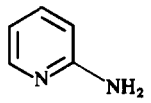	230.0 (3.87)	292.0 (3.55)	231.0 (4.09)	301.0 (3.94)
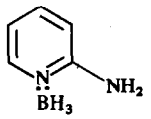	231.5 (3.89)	299.0 (3.70)		

[a] pH = 0.3.

for cobalt metal which has the bidentate coordination.[23] Since it is thought that an amine–borane complex is equivalent to the borohydride anion, the bonding between the metal and the borane which is coordinated with the amine would be similar to that described above.

In conclusion, the role of the metal ion in eqn (3) is both to produce borane from sodium borohydride and to form a chelate complex with the aromatic 2-amino-*N*-heterocycle which is able to capture borane in aqueous media. The amine–boranes listed in Table 1 were found to have properties of both the primary amine–borane and pyridine–borane,[24] namely the former is very effective for stereo- and chemoselective reductions of aldehyde and ketons,[25] and the latter shows many interesting reactions in acid media.[26]

EXPERIMENTAL

Melting points were determined by using a Yamato Scientific stirred liquid apparatus and are uncorrected. IR* and UV spectra were recorded on JASCO IR-G and Hitachi 200-20 spectrophotometers, respectively. ^{1}H NMR spectra

* All amine–borane complexes obtained here showed their characteristic absorption bands in the 2250–2400-cm^{-1} region.

were run on Varian EM-90 and T-60 spectrometers with $(CH_3)_4$ Si as the internal standard. The mass spectra were run on JEOL OlS and DX-300 (equipped with JMA-3100) spectrometers. Elemental analyses were performed on a Perkin–Elmer 240B instrument, and the results were within ± 0.36 of theoretical values of C, H and N. The X-ray fluorescence analyses (Cl and metals) were performed on a Rigaku Geiger Flex 3063P instrument. Metals were also determined on a Shimadzu Atomic Absorption/Flame Emission spectrophotometer (AA-630-02).

*General procedure for the reaction of amine with sodium borohydride in the presence of cobalt chloride**

A solution of $CoCl_2 \cdot 6H_2O$ in 10 cm^3 of water was gradually added to a mixed solution of 1 g of amine and 1 g of $NaBH_4$ in 100 cm^3 of water with stirring. After 3 h, the reacted solution was extracted with chloroform (40 $cm^3 \times 3$), and the extract was dried with Na_2SO_4. The dried solution was evaporated at 30–40°C under a reduced pressure to give products which were purified by column chromatography ($CHCl_3$ as eluant).

8-*Amino*-1,2,3,4-*tetrahydroquinoline*

m/z 148.101 [M^+], calc. for $C_9H_{12}N_2$, 148.100 [M].

2-*Aminopyridine–borane* (**2a**)

Yield 71%; m.p. 36–38°C (lit.,[5] 38–40°C), mass analysis, *m/z* 107.078 [$M^+ - 1$]; calc. for $C_5H_8BN_2$, 107.078 [$M^+ - H$]; ^1H NMR ($CDCl_3$) δ† 2.25 (3H, bq, $J = 93$ Hz, BH_3), 5.67(4.67) (2H, b, NH_2), 6.67(6.44) (1H, dd, 3-H), 6.60(6.58) (1H, dq, 5-H), 7.53(7.36) (1H, dq, 4-H), 8.07(8.03) (1H, dd, 6-H).

2-*Amino*-3-*methylpyridine–borane* (**2b**)

Yield 72%; m.p. 65–66°C; mass analysis, *m/z* 121.098 [$M^+ - 1$], calc. for $C_6H_{10}BN_2$, 121.094 [M−H]; ^1H NMR ($CDCl_3$) δ† 2.20(2.12) (3H, s, CH_3), 2.33 (3H, bq, $J = 93$ Hz, BH_3), 5.60(4.68) (2H, b, NH_2), 6.58(6.58) (1H, q, 5-H), 7.42(7.23) (1H, dd, 4-H), 8.03(7.93) (1H, dd, 6-H).

2-*Amino*-4-*methylpyridine–borane* (**2c**)

Yield 71% [80% when used $Ni(NO_3)_2$ in place of $CoCl_2$]; m.p. 88–89°C; mass analysis, *m/z* 121.000 [$M^+ - 1$], calc. for $C_6H_{10}BN_2$, 121.094 [M−H]; ^1H NMR ($CDCl_3$) δ† 2.18 (3H, bq, $J = 93$ Hz, BH_3), 2.35(2.22) (3H, s, CH_3), 6.48(6.45) (1H, dd, 5-H), 6.52(6.30) (1H, d, 3-H), 7.98(7.92) (1H, d, 6-H).

2-*Amino*-5-*methylpyridine–borane* (**2d**)

Yield 75%; m.p. 94–95°C; mass analysis, *m/z* 121.098 [$M^+ - 1$], calc. for $C_6H_{10}BN_2$, 121.094 [M−H]; ^1H NMR [$CDCl_3 + (CD_3)_2SO$] δ 2.13 (3H, s, CH_3), 2.60 (3H, bq, $J = 55$ Hz, BH_3), 6.20 (2H, b, NH_2), 6.60 (1H, d, 3-H), 7.23 (1H, dd, 4-H), 7.70 (1H, d, 6-H).

2-*Amino*-6-*methylpyridine–borane* (**2e**)

Yield 2%; m.p. 51–52°C; mass analysis, *m/z* 121.096 [$M^+ - 1$], calc. for $C_6H_{10}BN_2$, 121.094 [M−H].

2-*Aminopyrimidine–borane* (**2f**)‡

Yield 43%; m.p. 111–112°C; mass analysis, *m/z* 108.076 [$M^+ - 1$], calc. for $C_4H_7BN_3$, 108.073 [M−H].

Cobalt-containing intermediate

A solution of $NaBH_4$ (0.5 g, 13 mmol) of 50 cm^3 of water was added to a solution of $CoCl_2 \cdot 6H_2O$ (0.5 g, 2.1 mmol) and **1c** (0.45 g, 4.2 mmol) in 50 cm^3 of water with stirring. A black powder simultaneously appeared with bubbling. The powder was collected, washed with water and dried in vacuum desiccator over P_4O_{10} to give a gray powder. Elemental analysis: C, 53.4; H, 8.4; N, 21.1; Co, 3.0; Cl, o%. C:H:N = 5.8:11:2. The gray powder (100 mg) was treated with chloroform, and the mixture was filtered off. The filtrate was evaporated to give **2c** (90 mg).

Nickel-containing intermediate

A black powder was obtained by use of $Ni(NO_3)_2 \cdot 6H_2O$ in place of $CoCl_2 \cdot 6H_2O$ in the above experiment. When dried over P_4O_{10} in a vacuum desiccator, a gray powder was obtained. Elemental analysis: C, 32.7; H, 5.5; N, 12.7; Ni, 24.0%. C:(H):N:Ni = 6:(12):2:0.9.

* The optimum molar ratio for the reaction was determined as $CoCl_2$:**1c**:$NaBH_4 = 1:2:6$ from the viewpoint of the yield of **2c**.

† The values in parentheses are the corresponding chemical shifts of the starting amine.

‡ Bubbles occurred during ^1H NMR measurement in $(CD_3)_2SO$.

9-Methyladenine–borane (**8**)

The cobalt chloride–9-methyladenine complex (**6**) (260 mg) was dissolved in 40 cm^3 of water to give a pink solution. $NaBH_4$ (260 mg) was gradually added to the solution with stirring. After 3 h, the mixed solution was extracted with chloroform (30 $cm^3 \times 4$). The extract was dried with Na_2SO_4, and evaporated below 30°C under reduced pressure to give a powder (70 mg) which was decomposed at 257°C. TLC ($CHCl_3 : CH_3OH = 9 : 1$), two spots (**8** and 9-methyladenine); mass analysis, *m/z* 162.094 [$M^+ - 1$], calc. for $C_6H_9BN_5$, 162.095 [M − H]; ^1H NMR [$(CD_3)_2SO$] δ* 3.78(3.69) (3H, s, CH_3), 8.30(8.03) (1H, s, 8-H), 8.43(8.12) (1H, s, 2-H), 8.93(7.03) (2H, b, NH_2). BH_3 signals could not be determined clearly because of both very diluted solution and broadening. The powder was decomposed on a silica gel column.

9-Deprotonated adenine salt (**5**)

Adenine (1 g) and $CoCl_2 \cdot 6H_2O$ (1 g) were dissolved in 100 cm^3 of water. $NaBH_4$ (1 g) was gradually added to the mixture with stirring. After 3 h, the reaction mixture was filtered off, and the filtrate was extracted with chloroform, but nothing was obtained. The residues were treated with 100 cm^3 of hot ethanol and the mixture was filtered off. The filtrate was evaporated to give 170 mg of powder. Elemental analysis: Co, 1.2%. ^1H NMR [$(CD_3)_2SO$] δ* 6.93(6.97) (2H, b, NH_2), 8.02(8.05) (1H, s, 8-H), 8.06(8.10) (1H, s, 2-H), (12.50) (1H, b, NH). The powder was readily converted to adenine by hydrolysis.

REFERENCES

1. G. W. Schaeffer and E. R. Anderson, *J. Am. Chem. Soc.* 1949, **71**, 2143.
2. H. Nöth and H. Beyer, *Chem. Ber.* 1960, **93**, 928.
3. Y. Okamoto, T. Osawa and T. Kinoshita, *Synthesis* 1982, 462.
4. C. E. May and K. Niedenzu, *Synth. React. Inorg. Met.-Org. Chem.* 1977, **7**, 509.
5. C. J. Foret, M. A. Chiusano, J. D. O'Brien and D. R. Martin, *J. Inorg. Nucl. Chem.* 1980, **42**, 165.
6. M. D. Taylor, L. R. Grant and C. A. Sands, *J. Am. Chem. Soc.* 1955, **77**, 1506.
7. Y. Okamoto and T. Kinoshita, *Chem. Pharm. Bull.* 1981, **29**, 1165.
8. Y. Okamoto, K. Ogura and T. Kinoshita, *Polyhedron* 1984, **3**, 635.
9. H. C. Brown, H. I. Schlesinger and S. Z. Cardon, *J. Am. Chem. Soc.* 1942, **64**, 325.
10. T. Hirai and K. Takahashi, *Denki Kagaku*, 1967, **35**, 886.
11. S.-K. Chung, *J. Org. Chem.* 1979, **44**, 1014; R. A. Shunn, *Transition Metal Hydrides*, Vol. 1, p. 203. Marcel Dekker, New York (1971); E. Wiberg and E. Amberger, *Hydrides*, p. 136. Elsevier, Amsterdam (1971).
12. N. Satyanarayana and M. Periasamy, *Tetrahedron Lett.* 1984, **25**, 2501.
13. W. H. Schechter and R. H. Shakely, 1959, U.S.P. 2888326 (*C.A.* 53, 19324).
14. G. F. Freeguard and L. H. Long, *Chem. Ind.* 1965, 471.
15. S. J. Chiras, 1961, U.S.P. 2967760 (*C.A.* 55, 13789).
16. W. Jeffers, *Chem. Ind.* 1961, 431.
17. J. W. Mellor, *A Comprehensive Treatise on Inorganic and Theoretical Chemistry*, Vol. 14, p. 628. Longmans, Green, London (1957).
18. P. De Meester, D. M. L. Goodgame, A. C. Skapski and Z. Warnke, *Biochim. Biophys. Acta* 1973, **324**, 301.
19. W. Saenger, *Principles of Nucleic Acid Structure*, p. 201. Springer, Berlin (1983).
20. A. Albert, In *Physical Methods in Heterocyclic Chemistry* (Edited by A. R. Katritzky), p. 33. Academic Press, New York (1963).
21. K. Shikata, T. Ueki and T. Mitsui, *Acta Cryst.* 1973, **B29**, 31.
22. T. J. Marks and J. R. Kolb, *Chem. Rev.* 1977, **77**, 263.
23. M. Nakajima, H. Moriya, A. Kobayashi, T. Saito and Y. Sasaki, *J. Chem. Soc., Chem. Commun.* 1975, 80.
24. Y. Okamoto, T. Osawa, T. Kurasawa, T. Kinoshita and K. Takagi, *J. Heterocyclic Chem.* 1986, **23**, 1383.
25. G. C. Andrews and T. C. Crawford, *Tetrahedron Lett.* 1980, **21**, 693; G. C. Andrews, *ibid.* 1980, **21**, 697.
26. Y. Kikugawa, *Ventron Alembic* **1**, No. 29 (1983).

*The values in parentheses are the corresponding chemical shifts of the starting amine.

Polyhedron Vol. 6, No. 6, pp. 1191–1195, 1987
Printed in Great Britain

0277–5387/87 $3.00+.00

THE REACTIONS OF IRON(III) BROMIDE AND IRON(II) THIOCYANATE WITH AMMONIA AND THEIR REDUCTIONS WITH ALKALI METALS IN LIQUID-AMMONIA SOLUTIONS OF ALKALI METAL CYANIDES

ELAINE S. DODSWORTH, PETER J. O'GRADY, DAVID NICHOLLS* and DAVID ROBERTS

Donnan Laboratories, The University, Liverpool L69 3BX, U.K.

(*Received* 29 *August* 1986; *accepted* 24 *October* 1986)

Abstract—Iron(II) thiocyanate dissolves in liquid ammonia to form ammines $Fe(NCS)_2 \cdot 8NH_3$, $Fe(NCS)_2 \cdot 7NH_3$ and $Fe(NCS)_3 \cdot 5NH_3$; these evolve ammonia at room temperature to form the diammine $Fe(NCS)_2(NH_3)_2$ which has a tetragonal structure with thiocyanate bridges. Iron(III) bromide is also soluble in ammonia but with partial ammonolysis. Reduction of these compounds, and of iron(II) bromide, with potassium or caesium in ammonia solutions of the appropriate alkali metal cyanide yields cyanoferrates(0). Only $Cs_4Fe(CN)_4$ has been isolated in a pure state; it is oxidized by ammonium cyanide in ammonia to $Cs_4[Fe(CN)_6]$.

One of the most fascinating features of liquid ammonia as a solvent lies in its ability to dissolve alkali metals without reaction and thereby to produce solutions which act as very strong and homogeneous reducing agents. Whilst metal carbonyl chemistry is extensive, compounds containing transition metals in zero oxidation state bonded to cyanide ion have only been isolated using alkali metal solutions in liquid ammonia. The first of these, potassium tetracyanonickelate(0), $K_4Ni(CN)_4$, was prepared by Eastes and Burgess[1] in 1942 and subsequently many other cyanometallates(0) have been isolated. In recent years these have included compounds of the early transition elements e.g. $K_4Ti(CN)_4$,[2] $K_2V(CN)_2 \cdot 0.5NH_3$[3] and $K_5Zr(CN)_5$,[4] and indeed low oxidation state cyanides have now been isolated for all of the first-row transition elements except iron and copper. We report here our attempts to prepare an iron(0) cyano complex. One of the problems encountered in preparing such compounds is the availability of suitable starting materials. Complex cyanides in high oxidation states are not usually reducible to cyanometallates(0) by an alkali metal in ammonia solutions, so that simple salts of the metal (for solubility reasons these are usually bromides or thiocyanates) must be used as starting materials. It is then desirable to know how these salts react themselves with liquid ammonia so that the nature of the species present is understood. We here thus also report on the reactions of iron(II) thiocyanate and iron(III) bromide with ammonia.

The reactions of the iron(II) halides with liquid ammonia have been well studied,[5,6] they form the ammines $FeCl_2 \cdot 10$, 6, 2 and $1NH_3$, $FeBr_2 \cdot 6$, 2 and $1NH_3$, and $FeI_2 \cdot 6$ and $2NH_3$. Unfortunately these have very limited solubilities in ammonia. Iron(III) chloride and bromide are reported[7] to be considerably more soluble in ammonia but the authors report that this is probably accompanied by some ammonolysis. We chose to study the reactions of iron(II) thiocyanate and iron(III) bromide with ammonia, these being the two most likely soluble starting materials for preparing iron compounds in liquid ammonia.

RESULTS AND DISCUSSION

Iron(II) thiocyanate gives a brown solution in liquid ammonia at −36°C. The vapour pressure–composition isotherm in this system at −36°C is shown in Fig. 1. Apart from a saturated solution dissociation vapour pressure (~ 430 mmHg), the

* Author to whom correspondence should be addressed.

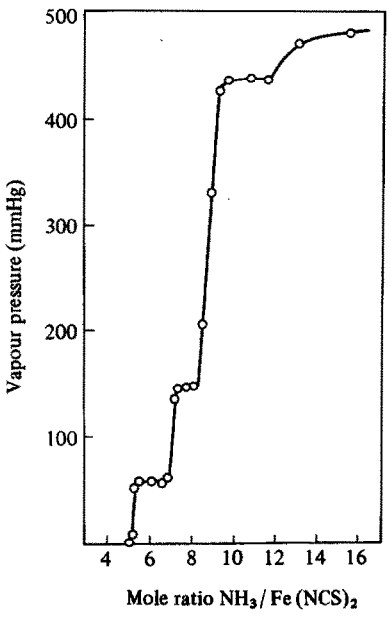

Fig. 1. Vapour pressure–composition isotherm for the $Fe(NCS)_2$–NH_3 system at −36°C.

isotherm shows univariant portions at 140 and 50 mmHg. These two plateaux correspond to the dissociations:

$$Fe(NCS)_2 \cdot 8NH_3(s) \rightleftharpoons Fe(NCS)_2 \cdot 7NH_3(s) + NH_3(g),$$

$$Fe(NCS)_2 \cdot 7NH_3(s) \rightleftharpoons Fe(NCS)_2 \cdot 5NH_3(s) + 2NH_3(g).$$

By measuring the ammonia vapour pressure over each of these systems at various temperatures and using the integrated form of the van't Hoff isochore, we calculate the enthalpies of these dissociations to be 34.9 and 85.9 kJ mol^{-1}. Such heats of dissociation show that the ammonia molecules being evolved are only held by weak ion-dipole type forces. At −36°C, the stable phase is $Fe(NCS)_2 \cdot 5NH_3$; on warming this phase to room temperature, three further molecules of ammonia are evolved to give the diammine $Fe(NCS)_2 \cdot 2NH_3$. This has a magnetic moment of 5.1 BM, showing it to contain high-spin iron(II); its solid-state reflectance spectrum shows bands at 13,300 and 7300 cm^{-1}, which we assign to the $^5B_{2g} \rightarrow {}^5A_{1g}$ and $^5B_{2g} \rightarrow {}^5B_{1g}$ transitions in a tetragonal structure. Such large splittings of the ^5E_g (O_h) state are common[8] in tetragonal iron(II) complexes; our band positions are very close to those found[9] for $Fe(py)_2(NCS)_2$, which is known to have a tetragonal structure with bridging thiocyanates. The IR spectra of $Fe(NCS)_2$ and $Fe(NCS)_2 \cdot 2NH_3$ are assigned in Table 1. The spectrum of the diammoniate again resembles that of $Fe(NCS)_2(py)_2$ in so far as the thiocyanate modes are concerned and is consistent[10] with linear bridging thiocyanates. We do not locate the ν(Fe—SCN) band; this is expected[9] to be below 200 cm^{-1}.

Iron(III) bromide gives a brown solution in ammonia at −36°C; the vapour pressure–composition isotherm for this system is shown in Fig. 2. This clearly shows the presence of ammonium bromide in the mixture, the univariant portions at 40 and 30 mmHg corresponding[11] to the dissociations:

$$NH_4Br \cdot 3NH_3(s) \rightleftharpoons NH_4Br \cdot 1.5NH_3(s) + 1.5NH_3(g),$$

$$NH_4Br \cdot 1.5NH_3(s) \rightleftharpoons NH_4Br(s) + 1.5NH_3(g).$$

The overall length of these steps is approximately one molar ratio of ammonia to iron(III) bromide, i.e. there is thus approximately one-third of a mole of ammonium bromide present per mole of starting iron(III) bromide. The composition of the orange-brown mixture when all ammonia is removed at −36°C is $FeBr_3 \cdot 6.3NH_3$; this represents a mixture of approximately $\frac{2}{3}[Fe(NH_3)_6]Br_3 + \frac{1}{3}[Fe(NH_3)_5(NH_2)]Br_2 + \frac{1}{3}NH_4Br$ which has deposited from the equilibrium:

$$[Fe(NH_3)_6]Br_3 + NH_3 \rightleftharpoons [Fe(NH_3)_5(NH_2)]Br_2 + NH_4Br.$$

The orange-brown powder has a composition close to $FeBr_3 \cdot 6NH_3$ at room temperature; the IR spectrum of this solid clearly shows the presence of ammonium ions. We thus confirm the assumption

Table 1. IR spectra of $Fe(NCS)_2$ and $Fe(NCS)_2 \cdot 2NH_3$

$Fe(NCS)_2$	$Fe(NCS)_2 \cdot 2NH_3$	Assignment
	3360(m)	$\nu_{as}(NH_3)$
	3260(m)	$\nu_s(NH_3)$
2138(s)	2098(s)	ν(CN)
	1600(m)	δ(HNH)
	1260(m)	$\delta(NH_3)$
	1165(s)	$\delta(NH_3)$
912(w)	916(w)	2δ(NCS)
	801(m)	$\rho(NH_3)$
770(m)	770(m)	ν(CS)
720(m)	720(m)	ν(CS)
	581(s)	$\rho(NH_3)$
452(m)	458(m)	δ(NCS)
	368(m)	ν(Fe—NH_3)
270(m)	240(m)	ν(Fe—NCS)

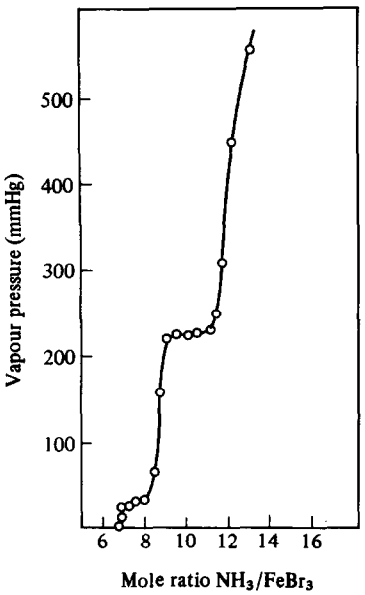

Fig. 2. Vapour pressure–composition isotherm for the $FeBr_3$–NH_3 system at −36°C.

of earlier workers[7] that iron(III) bromide dissolves in liquid ammonia with partial ammonolysis.

In our efforts to isolate an iron(0) cyanide complex we chose initially to attempt the reduction of potassium hexacyanoferrate(II). Watt[12] has reported that reduction of potassium hexacyanoferrate(III) by potassium in liquid ammonia proceeds only as far as the hexacyanoferrate(II). We confirm that no reduction of hexacyanoferrate(II) by potassium occurs in liquid ammonia at temperatures up to −40°C. The reaction of iron(III) bromide with an excess of potassium cyanide and potassium in liquid ammonia proceeds rapidly even at −78°C with the vigorous evolution of hydrogen and the formation of a dark coloured precipitate in a yellow solution. After filtration and washing of the precipitate, a black, pyrophoric powder was obtained. Although numerous experiments were performed with widely varying $K:KCN:FeBr_3$ ratios, no consistent stoichiometric formula could be derived from the analytical data which showed in every case only K, Fe, C and N to be present with up to 1% H [with an average stoichiometry of approximately $K_2Fe(CN)_2$]. The IR spectra of the black solids were the same, showing ν(CN) at 2040(w), 2000(s) and 1960(s) cm^{-1}, and ν(Fe—C) at 582(m) and 568(m) cm^{-1}. The solids were however ferromagnetic and the electronic spectrum (diffuse reflectance) showed only increasing absorption between 9000 and 30,000 cm^{-1}, so that no *d–d* bands could be observed. Clearly a low oxidation state cyanide complex of iron arises in this reaction. The vigorous effervescence in the reaction probably arises initially from the reaction of ammonium bromide (ammonolysis product of $FeBr_3$) with potassium but the continued decoloration of the alkali metal solution must occur through catalysis by one of the products. The ferromagnetism suggests that the catalyst may be iron metal and/or iron nitride. Iron and Fe_3N are known[14] to be the reduction products of iron(II) bromide with potassium in ammonia. A very similar product [of stoichiometry $K_{1.5}Fe(CN)_{1.5}$] was obtained when either iron(II) bromide or iron(II) thiocyanate was used as the starting material so that the ammonolysis of iron(III) bromide was not solely responsible for the vigorous effervescence and non-integral stoichiometry of the product.

The reaction of caesium with iron(II) or iron(III) bromide or with iron(II) thiocyanate in the presence of excess caesium cyanide proceeds with less hydrogen evolution to give a green-grey precipitate of $Cs_4Fe(CN)_4$. Unlike the black precipitates obtained when potassium is the reductant, this product is air- and moisture-sensitive, but not pyrophoric, suggesting that the pyrophoricity of the black compounds may be due to the presence of finely divided iron. The caesium compound has ν(CN) at 2040, 1995 and 1950 cm^{-1}, and ν(Fe—C) at 560 cm^{-1}; the spectrum is very similar to those obtained in the potassium reductions. When the sample was exposed to the atmosphere and the spectrum rerun, the peak at 2040 cm^{-1} grew and the other cyanide stretches disappeared. It is possible, therefore, that the 2040-cm^{-1} band in "$Cs_4Fe(CN)_4$" may be due to the presence of $Cs_4[Fe(CN)_6]$ formed during handling of the sample. The occurrence of ν(CN) at 1995 and 1950 cm^{-1} is indicative of much back bonding to π^*-orbitals on CN^-, and these bands are in the region found for other metal(0) cyanide complexes, e.g. $K_4Ti(CN)_4$ (1943 cm^{-1})[2] and $K_4Ni(CN)_4$ (1985 cm^{-1}),[13] so that we believe our green-grey product to be caesium tetracyanoferrate(0). Its electronic spectrum showed a band at 11,800 cm^{-1} with a shoulder on the high-frequency side (12,700 cm^{-1}), with intense change-transfer absorption above 30,000 cm^{-1}. We cannot assign this spectrum presently but hope to continue structural studies on $Cs_4Fe(CN)_4$ in due course. Unfortunately, this compound is also ferromagnetic.

It is interesting that caesium reduction has produced a stoichiometric compound. Caesium is the strongest reducing agent that can be used for this work; its electrode potential in ammonia is only slightly more negative[15] than that of potassium. The metals with more negative potential, however,

e.g. lithium, all have ammonia-insoluble amides, so that contamination of the insoluble product with amides is inevitable. We believe that the products obtained in the potassium reduction are mixtures of $K_4Fe(CN)_4$ with iron metal and possibly iron nitride.

The reaction of $Cs_4Fe(CN)_4$ with an excess of ammonium cyanide in ammonia proceeds with effervescence to give insoluble caesium hexacyanoferrate(II). The iron(0) compound is thus oxidized according to:

$$Cs_4Fe(CN)_4 + 2NH_4CN \rightarrow Cs_4[Fe(CN)_6] + H_2 + 2NH_3.$$

This oxidation is similar to that observed with other[16] cyanometallates(0) except that chromium(0) and cobalt(0) are oxidized to the +3 state by ammonium cyanide. In the iron case the +2 state is stabilized (as is the +3 state in cobalt) by the t_{2g}^6 configuration which gives the maximum propensity for π-bonding to the vacant π^*-orbitals on CN^-.

EXPERIMENTAL

Reactions, tensimetric studies and manipulations in liquid ammonia were carried out in vacuum apparatus as described elsewhere.[15] Magnetic and spectroscopic methods were as previously described.[3] Iron(II) thiocyanate was prepared in aqueous solution from iron(II) sulphate and barium thiocyanate under a nitrogen atmosphere in a Schlenk apparatus. The filtrate was evaporated, extracted with ethanol, and the filtered extract evaporated. The product was extracted with ether to remove the red colour of iron(III) thiocyanate and the remaining grey-green solid evacuated at 100°C (Found: C, 14.7; N, 16.6; S, 36.9; IR shows H_2O absent; $Fe(NCS)_2$ requires: C, 14.0; N, 16.3; S, 37.3%). Iron(II) and iron(III) bromides were ex Aldrich. Ammonium cyanide was prepared as described previously.[16] Caesium cyanide was prepared by passing hydrogen cyanide through a 50 wt % solution of caesium hydroxide to which an equal volume of ethanol had been added. An extraction with a small amount of ether removed brown oily contaminants, and then further ether was added to precipitate the caesium cyanide which was filtered off, washed with ether and dried *in vacuo* at 100°C (Found: CN^-, 16.2; IR shows H_2O and –OH absent; CsCN requires: CN^-, 16.4%).

Reaction of $Fe(NCS)_2$ *with ammonia*

A measured excess of ammonia was condensed on to a weighed quantity of $Fe(NCS)_2$ *in vacuo* and the vapour pressure–composition isotherm constructed at −36°C. After removal of all ammonia at 20°C, the brown product was removed from the vacuum apparatus under an atmosphere of dry nitrogen (Found: C, 11.8; H, 3.0; N, 29.9; S, 31.3; $Fe(NCS)_2(NH_3)_2$ requires: C, 11.7; H, 2.9; N, 27.2; S, 31.1%).

Reaction of $FeBr_3$ *with ammonia*

Similarly the orange-brown product obtained in this system at room temperature was analysed for ammonia as a check on the values obtained in the vapour pressure–composition isotherm (Found: NH_3, 25.6; $FeBr_3 \cdot 6NH_3$ requires: NH_3, 25.7%; IR spectrum shows in addition to NH_3 modes, bands at 1730 and 1400 cm^{-1} assignable to NH_4^+).

Reduction of $FeBr_3$ *with caesium in the presence of caesium cyanide*

$FeBr_3$. Liquid ammonia (~ 100 cm^3) was condensed on to a mixture of $FeBr_3$ (1.6 g, 5.4×10^{-3} mol) and CsCN (7.7 g, 4.8×10^{-2} mol); caesium (5g, 3.8×10^{-2} mol) was then added under an atmosphere of argon and the mixture cooled to −78°C and re-evacuated. Effervescence occurred and the blue colour of the solution disappeared after about 10 min to leave a green-grey precipitate in a colourless solution. The mixture was filtered and the precipitate washed 8 times with liquid ammonia (~ 50 cm^3) until no further white solids (CsCN, $CsNH_2$ and CsBr) were being extracted. The residue was then evacuated at room temperature before being removed from the apparatus under dry argon.

$FeBr_2$ *and* $Fe(NCS)_2$. Similar products were obtained using $FeBr_2$ (0.69 g, 3.2×10^{-3} mol), CsCN (5.86 g, 3.7×10^{-2} mol) and caesium (5 g, 3.8×10^{-2}), or $Fe(NCS)_2$ (0.58 g, 3.4×10^{-3} mol), CsCN (6.18 g, 3.9×10^{-2} mol) and caesium (5 g, 3.8×10^{-2} mol). Effervescence occurred also in these reactions but the blue solutions remained for longer periods than in the $FeBr_3$ reactions. Analytical data on these products are given in Table 2.

Table 2. Analytical data (%) on $Cs_4Fe(CN)_4$

Starting materials	Cs	Fe	C	N	H
$FeBr_3$, Cs and CsCN	76.2	8.5	6.8	8.3	0.2
$FeBr_2$, Cs and CsCN	74.7	7.7	6.7	7.8	0.3
$Fe(NCS)_2$, Cs and CsCN	78.5	7.8	6.6	7.1	0.3
$Cs_4Fe(CN)_4$ requires	76.9	8.1	6.9	8.1	0

Reaction of $Cs_4Fe(CN)_4$ *with* NH_4CN

An excess of ammonium cyanide (~ 5 g) was sublimed into the reaction vessel containing liquid ammonia (~ 100 cm^3) and a sample of $Cs_4Fe(CN)_4$ (~ 1 g) which had been prepared *in situ*. The reaction was maintained at −78°C for several hours with intermittent agitation. A green-yellow solution slowly formed with mild effervescence. The mixture was then allowed to warm to −33°C and then filtered. The yellow insoluble product was washed several times with liquid ammonia before being dried by evacuation at room temperature and removed from the apparatus under dry nitrogen [Found: C, 10.1; N, 11.1; H, absent; $Cs_4Fe(CN)_6$ requires: C, 9.7; N, 11.3%; IR spectrum showed ν(CN) at 2095(sh), 2065(sh) and 2040 cm^{-1}, ν(Fe—C) at 580 cm^{-1}, and δ(FeCN) at 400 cm^{-1}. Vacuum-dried $K_4Fe(CN)_6$ has ν(CN) at 2092, 2070 and 2040 cm^{-1}, ν(Fe—C) at 578 cm^{-1} and δ(FeCN) at 410 cm^{-1}].

REFERENCES

1. J. W. Eastes and W. M. Burgess, *J. Am. Chem. Soc.* 1942, **64**, 1187.
2. D. Nicholls and T. A. Ryan, *Inorg. Chim. Acta* 1980, **41**, 233.
3. E. S. Dodsworth and D. Nicholls, *Inorg. Chim. Acta* 1982, **61**, 9.
4. D. Nicholls and T. A. Ryan, *Inorg. Chim. Acta* 1977, **21**, L17.
5. W. Biltz, *Z. Anorg. Chem.* 1923, **130**, 93.
6. W. Biltz and E. Rahlfs, *Z. Anorg. Chem.* 1925, **148**, 145.
7. A. Schneider and R. Gehrke, *Naturwissenschaften* 1962, **49**, 467.
8. A. B. P. Lever, *Inorganic Electronic Spectroscopy*, 2nd Edn. Elsevier, Amsterdam (1984).
9. W. M. Rieff, R. B. Frankel, B. F. Little and G. J. Long, *Inorg. Chem.* 1974, **13**, 2153.
10. R. J. H. Clark and C. S. Williams, *Spectrochim. Acta* 1966, **22**, 1081.
11. E. Bannister and G. W. A. Fowles, *J. Chem. Soc.* 1958, 4374.
12. G. W. Watt, *Chem. Rev.* 1950, **46**, 289.
13. G. W. Watt, J. L. Hall, G. R. Choppin and P. S. Gentile, *J. Am. Chem. Soc.* 1954, **76**, 373.
14. G. W. Watt, G. R. Choppin and J. L. Hall, *J. Electrochem. Soc.* 1954, **101**, 229.
15. D. Nicholls, *Inorganic Chemistry in Liquid Ammonia*. Elsevier, Amsterdam (1979).
16. E. S. Dodsworth, J. P. Eaton, M. P. Ellerby and D. Nicholls, *Inorg. Chim. Acta* 1984, **89**, 143.

Polyhedron Vol. 6, No. 6, pp. 1197–1202, 1987
Printed in Great Britain

0277–5387/87 $3.00+.00

NITRILOTRIACETIC ACID, THIOUREA AND CYSTEINE LIGANDS IMMOBILIZED ON CELLULOSE FOR THE UPTAKE OF TRACE METAL IONS

E. MENTASTI,* C. SARZANINI, M. C. GENNARO and V. PORTA

Dipartimento di Chimica Analitica, Università di Torino, Via P. Giuria, 5, 10125 Torino, Italy

(*Received* 8 *September* 1986; *accepted* 24 *October* 1986)

Abstract—Functionalized celluloses containing nitrilotriacetic acid, thiourea and cysteine have been prepared for the uptake of a series of trace metal ions, namely Al(III), Ca(II), Cd(II), Co(II), Cu(II), Fe(III), Hg(II), Mg(II), Ni(II), Pb(II) and Zn(II). The recovery has been evaluated as a function of pH, and the capacities determined at the pH of maximum yield. The experimental yields obtained for the metal recoveries have been compared with the ones calculated with the aid of the computed distribution of metal–ligand species. The materials obtained may be utilized for the enrichment of trace metals, for the demetalization of solutions, and for speciation studies.

Many papers have been published regarding the use of chelating agents bound to cellulose for the concentration and removal of trace metal ions in solution.[1–4] In previous work from this laboratory the suitability of iminodiacetic acid (IDA),[5] *N*-methyliminodiacetic acid (MIDA)[6] and EDTA[7] to concentrate a large number of cations has been investigated.

The reactions to graft nitrilotriacetic acid (NTA), thiourea (THIO) and cysteine (CYS) onto commercial cellulose filters have been optimized for the application of chelating materials in concentration and speciation studies.

The uptake, capacity, recovery and enrichment of a series of metal ions such as Al(III), Ca(II), Cd(II), Co(II), Cu(II), Fe(III), Hg(II), Mg(II), Ni(II), Pb(II) and Zn(II) was evaluated. Matrix interferences were investigated using chloride, nitrate, phosphate and sulphate ions, competition between bound and free ligands was studied.

With the aid of a computer program and by comparison with the experimental data, the apparent stability constants of the complexes between metals and ligands grafted to the functionalized filters were evaluated. The degree of interaction between each of the metal ions and free or bound ligand on cellulose was calculated according to a described procedure.

The results showed a satisfactory agreement with the experimental values obtained in the competition reactions.

EXPERIMENTAL

Reagents and equipment

Metal stock solutions [1,000 mg l^{-1} (C. Erba) for atomic absorption] were diluted as required. High-purity water (HPW) prepared in a Milli Q Millipore equipment was used. NTA sodium salt, THIO, CYS and all other chemicals were analytical reagent-grade products.

All laboratory glassware, polyethylene and polypropylene equipments, were cleaned in 6 M nitric acid and repeatedly rinsed with HPW.

A d.c. plasma emission spectrometer Spectraspan IV (SMI, Andover, MA) and an ICP emission spectrometer Plasma-300 (Allied Analytical Systems, Waltham, MA) have been used for the metal measurements. Standard solutions and blanks were run in the same manner as the samples.

The pH measurements were made with an Orion 811 pH-meter equipped with a combined glass calomel electrode.

Adjustable Eppendorf pipettes were used to pre-

* Author to whom correspondence should be addressed.

pare the solutions. A Millipore 47-mm glass-frit filtration unit was employed to ensure reproducible placement of the prepared filters.

Preparation of the filters

The chelating agents, NTA, THIO and CYS, were attached to cellulose according to the method described by Smits and Van Grieken.[8] The preparation reaction proceeds through preliminary chlorination with phosphorus oxychloride ($POCl_3$):

$$\text{Cell-OH} \xrightarrow[\text{DMF}]{POCl_3} \text{Cell-Cl}$$

where Cell-OH represents the cellulose filters and DMF is the solvent *N*,*N*-dimethylformamide. Whatman 41 cellulose filter discs (47 mm diam., 165 mg) were conditioned for 60 min in dry DMF. To maximize the chlorination yield the solvent was dehydrated with molecular sieves. The filters were successively added to a solution of $POCl_3$ in DMF [3% (v/v)] heated on a water bath to 90°C. Heating was continued for about 30 min. The brown filters obtained were washed with DMF, HPW, 5% NaOH, HPW, 5% HAc, HPW and DMF in that order. The filters again white, were then treated at 105–110°C for about 150 min in a saturated solution of NTA, THIO or CYS in DMF and HPW [3 : 1 (v/v)]. The filters were washed with HPW and air dried. In such conditions the following reactions occur:

$$\text{Cell-Cl} \begin{cases} \text{—N(CH}_2\text{COOH)}_3 \rightarrow \text{Cell-}\overset{+}{\text{N}}\text{(CH}_2\text{COOH)}_3 \\ \text{—SC(NH}_2\text{)}_2 \rightarrow \text{Cell-NH—CS—NH}_2 \\ \text{—HSCH}_2\text{CH(NH}_2\text{)} \rightarrow \text{Cell-NH—CHCH}_2\text{CH}_2\text{SH} \\ \qquad\qquad\qquad\qquad\quad | \qquad\qquad\qquad\qquad\quad | \\ \qquad\qquad\qquad\qquad \text{COOH} \qquad\qquad\qquad\quad \text{COOH} \end{cases}$$

RESULTS AND DISCUSSION

The chelating ability of the ligands grafted on cellulose has been evaluated by conducting a systematic concentration study as a function of pH. The functionalized filters were fitted in the filtering unit and conditioned at the desired pH. 100.0 cm^3 of 1.00 $\mu g\ cm^{-3}$ solution of each metal (previously brought to the desired pH between 1.0 and 8.0) were then filtered.

The metal uptake was then evaluated by releasing the metal from the filter with 10.0 cm^3 of 2.0 M HCl and determining each metal in the final solution by atomic emission spectrometry.

Table 1 reports the results obtained for all the functionalized celluloses with the investigated metals. Each entry is the mean of triplicate measurements, and independent replicates showed the standard deviation estimate to be within 5% for each entry in Table 1. Analysis of the metal fraction filtered through the filters gave values in agreement, again within 5%, with the fraction not recovered by the filters, proving that: (i) irreversible uptake by the filters was not operating, and (ii) systematic errors in the procedure were absent.

The values reported in Table 1 show a general trend with a sharp increase of recovery yield with increasing pH, followed by a nearly constant and almost quantitative uptake. Such behaviour parallels the coordinating ability of the investigated ligands as shown by their formation constants,[9(a)–(c)] the higher values corresponding to the larger high-yield portion. A somewhat reduced coordination ability was expected for the NTA ligand since after grafting on cellulose the nitrogen atom of the ligand becomes quaternary and therefore without coordinating ability.

As an example, Cu(II), which has a log β of 13.3 has a recovery > 92% between pH 3 and 8. Fe(III) and Hg(II) show a less favourable recovery yield due to the high tendency to hydrolyse which competes with the uptake by the filters.

Table 2 reports the evaluated capacities of the filters for each metal. They have been determined from the amount of retained metal when equilibrated with 100.0 cm^3 of solution containing 100.0 $\mu g\ cm^{-3}$ of each metal ion at the pH of maximum-uptake yield. Table 2 reports, for comparison purposes, also the results obtained for other functionalized celluloses previously investigated in our laboratory. As it can be seen a similar capacity is shown by ligands of different coordinating ability such as IDA, MIDA, EDTA and NTA; the values for THIO and CYS were somewhat lower with respect to the corresponding value for NTA, showing either a lower efficiency in the grafting reaction of the chlorinated filters or a decrease in the coordinating ability of the ligands after grafting on the filters.

The similar values within the polyaminocarboxylic ligand family support a similar coordinating behaviour for each member; in fact, as has been previously suggested, two IDA, MIDA and here NTA units anchored on cellulose may act

Table 1. Percent uptake yields as a function of pH for the investigated metals (100.0-cm^3 solutions containing 1.00 ppm for each metal) on NTA, THIO and CYS filters

	pH							
	1.0	2.0	3.0	4.0	5.0	6.0	7.0	8.0
				NTA filters				
Al(III)	22.0	23.4	68.2	72.0	91.1	95.1	79.0	81.9
Ca(II)	0.0	56.3	89.7	100.8	100.7	98.0	100.0	100.0
Cd(II)	78.3	87.5	90.2	97.0	98.4	98.5	99.7	99.6
Co(II)	20.8	40.6	76.4	86.6	89.1	92.8	96.2	93.5
Cu(II)	0.2	1.9	92.2	96.5	99.6	98.4	98.5	83.0
Fe(III)	72.0	72.0	73.0	59.1	52.6	50.9	98.7	97.0
Hg(II)	3.1	10.4	84.0	97.4	84.8	72.0	80.5	91.0
Mg(II)	78.1	82.4	91.0	97.4	93.5	96.7	98.3	96.9
Ni(II)	4.6	7.2	81.1	87.1	94.7	81.7	87.8	90.7
Pb(II)	0.1	41.3	93.7	92.5	97.3	86.2	71.5	49.9
Zn(II)	10.9	58.2	88.8	96.6	89.5	86.4	96.6	78.2
				THIO filters				
Ca(II)	10.6	16.4	80.8	89.1	88.0	85.0	89.5	95.1
Cd(II)	44.0	57.5	65.8	72.4	73.7	74.6	80.9	91.1
Co(II)	9.6	35.3	86.5	93.4	95.1	95.2	96.4	94.3
Cu(II)	1.0	60.1	80.8	97.1	93.6	88.2	92.8	100.1
Hg(II)	25.5	60.7	81.8	93.6	96.5	97.8	97.7	98.9
Mg(II)	10.7	22.2	83.0	86.8	87.9	88.7	90.0	87.8
Ni(II)	4.0	8.1	80.8	85.4	86.6	87.3	87.2	98.0
Pb(II)	5.0	27.8	83.1	95.8	96.2	95.8	96.2	98.1
Zn(II)	2.2	33.9	83.8	87.3	89.5	90.4	89.9	97.4
				CYS filters				
Ca(II)	4.7	19.1	87.1	87.5	88.6	82.8	74.2	67.0
Cd(II)	15.8	39.3	71.6	78.6	94.3	83.7	77.9	74.0
Co(II)	0.5	35.0	74.9	91.2	96.3	100.0	95.4	92.6
Cu(II)	0.1	0.6	59.5	80.2	89.3	87.8	87.2	87.4
Hg(II)	29.0	73.2	89.5	94.8	99.0	100.1	100.0	100.3
Mg(II)	15.7	25.9	86.7	88.2	88.6	89.1	89.7	90.1
Ni(II)	7.5	11.6	72.2	86.2	94.3	88.2	95.0	99.6
Pb(II)	2.0	13.1	79.0	80.7	80.6	88.0	96.2	98.0
Zn(II)	2.0	2.1	83.1	88.6	92.2	99.0	98.7	98.6

as an EDTA-like molecule with full saturation of the octahedral ligand field of the metals.[6,7]

The release of each metal has been investigated and the results for all metals were similar to the ones reported in Fig. 1 for Pb(II) and Cu(II). A 10.0-cm^3 portion of 2.0 M HCl proved to be adequate for the complete recovery of all metals from the filters. In order to characterize the mechanism of the uptake reaction between the bound ligand and metal ions, the experimental uptake yield has been compared with the one which can be theoretically computed according to the following model. If coordination is the only interaction responsible for the metal uptake on the filters, the uptake yield should be equal to the fraction of metal in a complex form in an homogeneous solution of the same volume as the one submitted to concentration and containing a number of micromoles of ligand as that present in the filter during the uptake experiments (this last quantity has been assumed to be equal to the one derived from the highest capacity showed by each filter with the investigated metals).[5-7]

Figure 2(a)–2(f) report, as examples, the experimental behaviour for Cu(II) and Pb(II) together with the behaviour computed with a computer program acording to the model reported above and using the complex formation stability constants and hydrolysis constants reported in Table 3 (the values reported have been chosen from the published

Table 2. Capacities of a series of functionalized chelating filters for a series of metal ions (47-mm Whatman 41 functionalized filters; 1 filter = 165 mg)

	Capacity (μmol per filter)					
	NTA[a]	THIO[a]	CYS[a]	IDA[b]	MIDA[c]	EDTA[d]
Al(III)	17					
Ca(II)	21	11	13	18	18	54
Cd(II)	19	13	15	28	18	33
Co(II)	24	21	27	28	9	33
Cu(II)	37	14	34	34	18	56
Hg(II)	4	3	3	15	14	17
Mg(II)	30	27	37	30	22	28
Na(I)	84					
Ni(II)	62	14	18			
Pb(II)	14	13	16	36	21	27
Zn(II)	50	18	17	26	12	35

[a] This work.
[b] Reference 5.
[c] Reference 6.
[d] Reference 7.

values to be as close as possible to the conditions of the present paper).

Since the shape of computed behaviour does not closely fit in all cases the experimental data, the immobilization on cellulose alters the behaviour displayed by the ligands in homogeneous solution; thus, as a result, increasing ligand rigidity after bonding to the substrate, and substrate interaction with the bound metal alters the stability constants reported in Table 3. In order to account for this effect, apparent stability constants for Cu(II) and Pb(II) have been used which gave the best agreement between experimental and computed points in Fig. 2(a)–2(f). The derived $*\beta$ values are reported in Table 3 together with the literature values.

As can be seen from Fig. 2, a good agreement was obtained in all cases and three different situations may be evidenced: (i) the recomputed values for the NTA filter are lower than the literature data; this can be explained considering that in the immobilized NTA a quaternary positive nitrogen is formed and consequently the chelating ability of the grafted ligand is reduced. (ii) The optimization of the data of Cu(II) with the THIO filters is more difficult. This is because only one cumulative stability constant ($\beta_{1,4}$) is available, while intermediate complex species are probably favoured with the immobilized ligand. (iii) The CYS filters show an improved affinity for the metals. This fact can be explained if one considers that two or more CYS groups can be immobilized in such a position so that they can bind simultaneously to the metals.

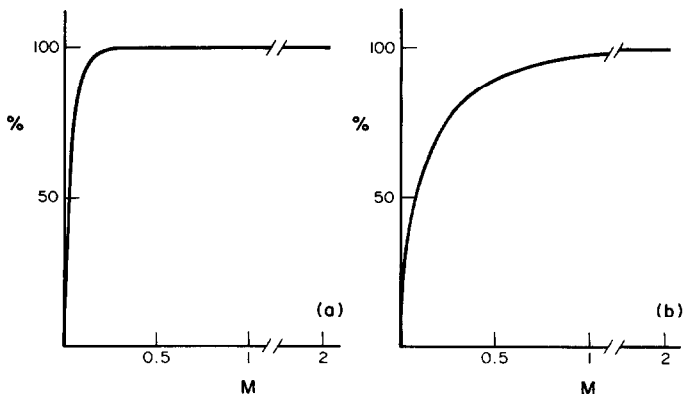

Fig. 1. Percent recovery yield for Pb(II) (a) and Cu(II) (b) from NTA filters as a function of the concentration of the stripping agent, 10.0 cm^3 HCl.

Table 3. Stability constants (β) and apparent constants ($*\beta$) (see Ref. 9 and text)[a]

Complex	Log β	Log $*\beta$
PbNTA	12.4	11.0
PbHNTA	13.5	13.5
CuNTA	13.3	10.5
Cu(OH)NTA	3.7	3.7
PbTHIO	0.4	3.0
$PbTHIO_2$	0.6	6.0
$PbTHIO_3$	1.2	10.0
$PbTHIO_4$	1.8	16.0
$CuTHIO_4$	14.7	18.0
PbCYS	13.2	17.0
$PbCYS_2$	19.2	19.2
CuHCYS	17.4	19.0
CuH_2CYS_2	34.4	38.0
Cu_2HCYS_2	31.7	31.7
Cu_2CYS_2	28.1	28.1
Cu_2CYS	14.0	14.0
$Cu_2H_2CYS_2$	48.8	48.8

[a] Expressed as log $\beta^{M_nH_{\pm p}L_q}{}_{nM,\pm pH,qL}$ values, where log β = literature value, and log $*\beta$ = computed apparent value.

This is evidenced in Table 3 since the greatest modification adopted for the $*\beta$ stability constants was the one for species CuH_2CYS_2.

All these observations are still valid if one considers the results obtained when the species distribution as a function of pH is computed in the case of competitive experiments. As described above, solutions containing Pb(II) or Cu(II) were fluxed through the functionalized filters in the presence of free NTA, THIO and CYS, alternatively, at different concentrations.

Table 4 reports, as an example, for Pb(II), the NTA filter and NTA, THIO or CYS free-ligand systems, the experimental and computed data obtained by taking into account, for the bound ligands, the assumption previously described and the apparent stability constants.

Experimental uptake data show that the chelating ability of NTA when bound to cellulose is practically maintained even in the presence of interfering ligands. The NTA filter is in fact able to fix > 90% of the total Pb(II) even from solutions containing cysteine and thiourea at a molar concentration of 2.4×10^{-3} M (i.e. at a molar ratio of 100 : 1 with respect to the metal concentration).

Rather surprising is the behaviour of the NTA filter when the competitive ligand is NTA itself. In fact, although the $*\beta$ value computed for the NTA filter is lower than the β-value reported for an aqueous solution, a recovery of ~ 40% of the total Pb(II) is still achieved from solutions containing an NTA molar concentration equal to about four-fold that assigned to NTA on the filter.

This unexpected behaviour is reflected in the comparison between computed and experimental

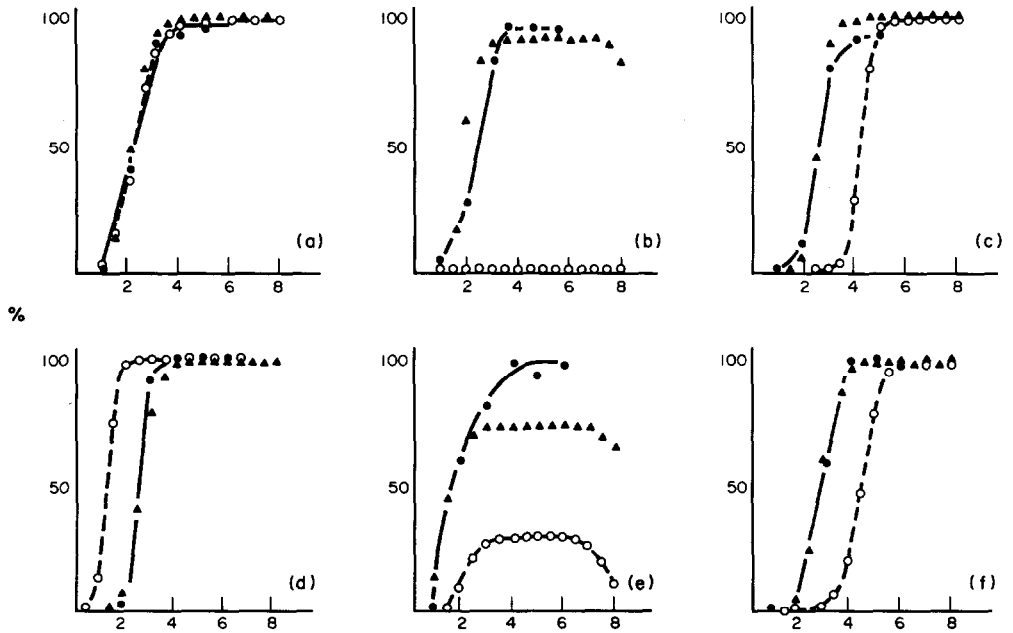

Fig. 2. (a) Experimental and computed percent recovery yield for Pb(II) onto NTA filters as a function of pH: (●) experimental, (○) computed with literature stability constants β of Table 3, (▲) computed with the apparent stability constants $*\beta$ of Table 3. (b) Pb(II), THIO filters; (c) Pb(II), CYS filters; (d) Cu(II), NTA filters; (e) Cu(II), THIO filters; (f) Cu(II), CYS filters.

Table 4. Comparison of computed (Comp.) and experimental (Exp.) (%) Pb(II) recovery (5.00 $\mu g\ cm^{-3}$ solutions) onto NTA filters in the presence of competitive species

L:M[a] molar ratio	% Recovery in the presence of					
	NTA		THIO		CYS	
	Comp.	Exp.	Comp.	Exp.	Comp.	Exp.
1:1	62.0	92.2	99.5	100.0	99.5	96.5
5:1	19.8	86.0	99.5	100.0	99.5	95.1
20:1	5.1	42.1	99.5	96.2	99.4	87.8
100:1	1.0	40.6	99.4	94.0	99.0	89.0

[a] L:M = competitive free ligand:metal molar ratio.

data (see Table 3). An explanation for this discrepancy could be the formation of mixed 1:2 metal:ligand complexes with one bound and one unbound NTA unit; this would still make possible the metal uptake even in the presence of excess free ligand in solution.

On the other hand, a good agreement is observed when THIO and CYS are the interfering ligands; both experimental and computed uptake values reported in Table 4 show the higher coordinating efficiency of these ligands when bound to cellulose, in agreement with previous findings for other systems.

Similar results were obtained also for the uptake of Cu(II). Competitive experiments obtained using THIO and CYS filters and, in turn, all the three free ligands as competitors, showed results parallel to those described above for the NTA filters.

Also interferences in the uptake of Pb(II) and Cu(II) from chloride, nitrate, sulphate and phosphate ions, present in concentrations ranging between 0.001 and 0.1 M, have been tested with all the three investigated filters. No significative differences in the uptake efficiencies were observed for the lower part of the investigated range, while uptake reductions of *ca* 5% for chloride and nitrate, *ca* 10% for sulphate, and *ca* 30% for phosphate ions were observed for concentrations of 0.1 M. Such uptake reductions are practically not relevant if one considers that the concentration range of such interfering species is, in real samples, much lower.

In conclusion, the prepared filters show a good efficiency for the uptake, recovery and enrichment of trace metal ions and may be conveniently used for speciation studies of transition-metal species.[10]

REFERENCES

1. D. E. Leyden and W. Wegscheider, *Anal. Chem.* 1981, **53**, 1059.
2. J. A. Smits and R. Van Grieken, *Anal. Chem.* 1980, **52**, 1479.
3. G. Reggers and R. Van Grieken, *Fresenius' Z. Anal. Chem.* 1984, **317**, 520.
4. M. Forster and K. H. Lieser, *Fresenius' Z. Anal. Chem.* 1981, **309**, 352 (and references therein).
5. M. C. Gennaro, C. Baiocchi, E. Campi, E. Mentasti and R. Aruga, *Anal. Chim. Acta* 1983, **151**, 339.
6. M. C. Gennaro, C. Sarzanini, E. Mentasti and C. Baiocchi, *Talanta* 1985, **32**, 961.
7. M. C. Gennaro, E. Mentasti and C. Sarzanini, *Nouv. J. Chim.* 1986, **10**, 107.
8. J. A. Smits and R. Van Grieken, *Angew. Makrom. Chem.* 1978, **72**, 105.
9. (a) L. G. Sillén and A. E. Martell, *Stability Constants of Metal Ion Complexes*. Special Publications No. 17 (1964) and 25 (1971), The Chemical Society, London; (b) A. E. Martell and R. M. Smith, *Critical Stability Constants*, Vol. 1 (1974). Plenum Press; D. D. Perrin, *Stability Constants of Metal Ion Complexes*, Part B. Pergamon Press, New York (1979).
10. M. C. Gennaro, E. Mentasti, C. Sarzanini and C. Baiocchi, *Anal. Chim. Acta* 1985, **174**, 259.

Polyhedron Vol. 6, No. 6, pp. 1203–1207, 1987
Printed in Great Britain

0277–5387/87 $3.00+.00

PROPERTIES OF α-BROMOVALERIC ACID AS EXTRACTING AGENT FOR COPPER(II)

YUKIO FUJII,* HIROMICHI YAMADA and MASATERU MIZUTA

Faculty of Engineering, Gifu University, 1-1 Yanagido, Gifu 501-11, Japan

(*Received* 9 *September* 1986; *accepted* 24 *October* 1986)

Abstract—Copper(II) was extracted with α-bromovaleric acid in benzene from 0.1 mol dm^{-3} (Na, H)ClO_4 aqueous solution at 25°C. The acid dissociation constant of the extracting agent was determined to be $K_a = 10^{-2.79}$ in aqueous solution at 25°C. The partition constant of the acid (HA) between the aqueous phase and benzene, and the dimerization constant of the acid in benzene were evaluated to be 2.6 and 56 in molarity, respectively. The dimeric copper(II) α-bromovalerate is responsible for the extraction:

$$2Cu^{2+} + 3(HA)_{2,o} \overset{K_{ex}}{\rightleftharpoons} Cu_2A_4(HA)_{2,o} + 4H_3O^+, \quad (\text{subscript } o = \text{organic phase})$$

with $\log K_{ex} = -7.87$. The complex formation of cupric ion with the acid anion observed in the aqueous phase was taken into consideration for calculation of the extraction constant. It was proved that the formation of dimeric copper(II) species is not prevented by the bromine at the α-position in the valeric acid.

Solvent extraction of metal carboxylates has been considerably studied in the past three decades.[1] Extraction of copper(II) alkanoates has received most attention for their extraction characteristics: the species extracted in nonpolar organic solvent has a dimeric form given by $Cu_2A_4(HA)_2$, where HA denotes the alkanoic acid.[2–5]

From the view point of solution chemistry and hydrometallurgy, α-halogenoalkanoic acids are of particular interest among many substituted homologues. The presence of the halogen at the α-position in a carboxylic acid modifies its properties.[6,7] However, the properties as an extracting agent are not known. More studies are, therefore, necessary for a full understanding of the effect of a halogen introduced in the α-position of a carboxylic acid on the coordination and extraction properties.

In this paper we report the results for the extraction of copper(II) with α-bromovaleric acid in benzene. The dimeric copper(II) α-bromovalerate, $Cu_2A_4(HA)_2$, was found to be extracted in benzene.

EXPERIMENTAL

Reagent

The extracting agent, α-bromovaleric acid (R.G.), was purified by distillation under reduced pressure. The purity of the middle fraction was 99.6±0.3% as determined by titration with standard alkaline solution.

Sodium perchlorate, copper(II) perchlorate and benzene were the same as presented previously.[6]

Procedure

Partition was carried out at 0.5×10^{-3}–1×10^{-3} mol dm^{-3} initial concentration of copper(II) in the aqueous phase and 0.1–1 mol dm^{-3} α-bromovaleric acid in the organic phase. 15 cm^3 of the aqueous and organic solutions were introduced into a 50-cm^3 stoppered centrifuge tube. The ionic strength in the aqueous phase was kept constant at 1.0 mol dm^{-3} so as to hold the activity coefficients of α-bromovalerate, cupric and hydrogen ions constant. The tube was shaken for 1 h in a water bath thermostatted at 25.0±0.2°C. This shaking time was

* Author to whom correspondence should be addressed.

found to be sufficient for complete equilibration. The acid concentration in the organic phase was determined by a two-phase titration with a standard alkaline solution. The copper(II) concentrations in the organic and/or aqueous phases were determined by complexiметry or spectrophotometry. The complex formation of cupric ion with α-bromovaleric acid in the aqueous solution was evaluated by e.m.f. measurements using a cupric ion selective electrode, Orion No. 94-24.

Apparatus

Measurements of pH were carried out with an Orion research microprocessor ionalyzer, M-901. Spectrophotometric measurements were performed on a Shimadzu double-beam spectrophotometer, M-UV210A.

RESULTS AND DISCUSSION

Liquid–liquid distribution of α-bromovaleric acid

In the extraction of a metal ion with a carboxylic acid HA, it is indispensable to have information about the following equilibria, the acid dissociation in the aqueous solution:

$$HA + H_2O \overset{K_a}{\rightleftharpoons} H_3O^+ + A^-,$$

$$K_a = [H_3O^+][A^-]/[HA], \quad (1)$$

the partition of carboxylic acid defined by the ratio of the concentration of the acid in a monomeric form in the organic phase to its concentration in the same form in the aqueous phase at equilibrium:

$$HA \overset{K_d}{\rightleftharpoons} HA_o, \quad K_d = [HA]_o/[HA], \quad (2)$$

and the dimerization of the monomeric acid in the organic phase:

$$2HA_o \overset{K_2}{\rightleftharpoons} (HA)_{2,o}, \quad K_2 = [(HA)_2]_o/[HA]_o^2, \quad (3)$$

where subscript *o* denotes the organic phase.

When the acid is distributed between the two phases, the analytical acid concentration in the aqueous and organic phases are, respectively, given by:

$$C_{HA} = [A^-] + [HA] \quad (4)$$

and

$$C_{HA,o} = [HA]_o + 2[(HA)_2]_o. \quad (5)$$

The distribution ratio measured at equilibrium is given by:

$$D = C_{HA,o}/C_{HA}$$

$$= (K_d + 2K_d^2K_2[HA])/(1 + K_a/[H_3O^+]). \quad (6)$$

By pH-metric titration the acid dissociation constant was determined to be $\log K_a = -2.79$ in the aqueous solution, 1.0 mol dm^{-3} (Na, H)ClO_4 at 25°C. According to eqn (6), a plot of $D(1 + K_a/[H_3O^+])$ vs [HA] should yield a straight line with intercept K_d and slope $2K_d^2K_2$. Figure 1 is the plot of the experimental data. The constants thus obtained are given in Table 1 together with those of some α-bromoalkanoic acids for comparison. These values of α-bromovaleric acid were used for calculation of the equilibrium concentrations: $[A^-]$, [HA], $[HA]_o$ and $[(HA)_2]_o$.

Extraction of copper(II) with α-bromovaleric acid

The chemical species of copper(II) carboxylate extracted in benzene being denoted as $(CuA_2(HA)_x)_j$, the extraction constant K_{ex} can be written as:

$$jCu^{2+} + j\left(1 + \frac{x}{2}\right)(HA)_{2,o}$$

$$\overset{K_{ex}}{\rightleftharpoons} (CuA_2(HA)_x)_{j,o} + 2jH_3O^+,$$

$$K_{ex} = [(CuA_2(HA)_x)_j]_o[H_3O^+]^{2j}$$

$$\times [Cu^{2+}]^{-j}[(HA)_2]_o^{-j(1+(x/2))}, \quad (7)$$

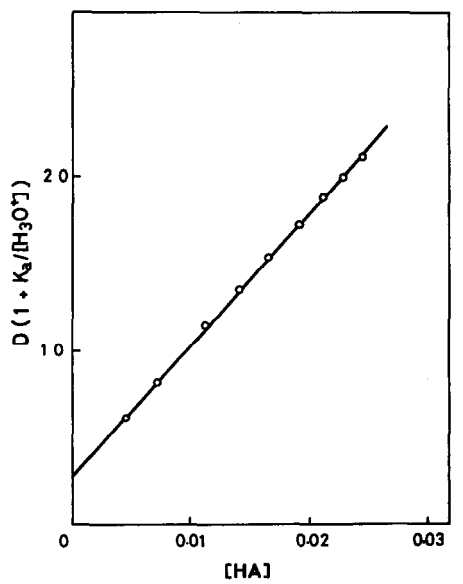

Fig. 1. Distribution of α-bromovaleric acid between benzene and 1.0 mol dm^{-3} (Na,H)ClO_4 solution as a function of the acid concentration in the aqueous solution.

Table 1. Equilibrium constants for α-bromoalkanoic acids at 25°C

Acid	pK_a	Log K_d[a]	Log K_2[a]	Log K_{CuA}
Bromoacetic	2.86[bc]	−1.54[d]	1.49[d]	1.59[c]
α-Bromopropionic	2.97[bd]	−0.79[d]	1.51[d]	—
α-Bromobutyric	2.97[bc]	−0.24[d]	1.70[d]	1.46[c]
α-Bromovaleric	2.99[bd]	0.30[d]	1.77[d]	—
	2.79[ef]	0.41[ef]	1.75[f]	1.50[ef]
α-Bromostearic	—	—	1.90[g]	—

[a] Organic phase: benzene, saturated with water.
[b] Extrapolated to zero ionic strength.
[c] Reference 8.
[d] Reference 6.
[e] Ionic strength: 1.0(Na,H)ClO_4.
[f] This work.
[g] Evaluated from the IR data in Ref. 17.

where x denotes the number of HA coordinated to the CuA_2 unit.

Now the analytical copper(II) concentration in the aqueous solution is given by:

$$C_{Cu,w} = [Cu^{2+}]\alpha_{Cu}, \quad (8)$$

where α_{Cu} refers to the side-reaction coefficient of formation of water soluble complex of copper: $\alpha_{Cu} = 1 + K_{CuA}[A^-]$. The plot used for the determination of K_{CuA} is shown in Fig. 2. The formation constant was found to be $\log K_{CuA} = 1.50$. This value is in agreement with the values for copper(II) bromoacetate and α-bromobutyrate[8] (see Table 1).

If the species of copper(II) carboxylate in benzene is denoted as $(CuA_2(HA)_x)_j$, the copper concentration in the organic phase is given by:

$$C_{Cu,o} = jK_{ex}[(HA)_2]_o^{j(1+(x/2))}(C_{Cu,w}\alpha_{Cu}^{-1}[H_3O^+]^{-2})^j. \quad (9)$$

As anticipated from eqn (9), the plot of $\log C_{Cu,o}$ vs $\log(C_{Cu,w}/\alpha_{Cu}) - 2\log[H_3O^+]$ should give a straight line with slope j at a certain concentration of dimeric α-bromovaleric acid in the organic phase. The plot is shown in Fig. 3. The slope of the straight lines is 2.0 providing the copper species in the organic phase is $Cu_2A_4(HA)_{2x}$. It is noteworthy that the dimeric species persists in the organic solvent down to $C_{Cu,o} = 10^{-4}$ mol dm^{-3}.

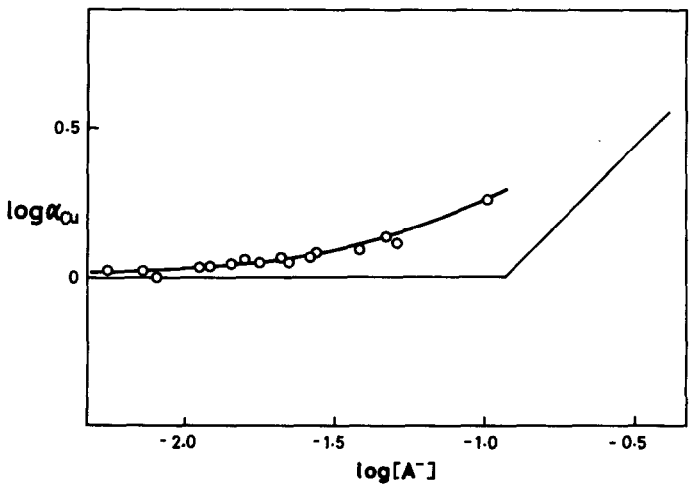

Fig. 2. Determination of the formation constant of copper(II) α-bromovalerate complex in the aqueous solution. Ionic strength: 1.0 (Na,H)ClO_4. α_{Cu} was obtained from e.m.f. measurement by using a cupric ion selective electrode. The solid curve denotes the theoretical one calculated by using $\log K_{CuA} = 1.50$. The straight lines are the asymptotes for the curve.

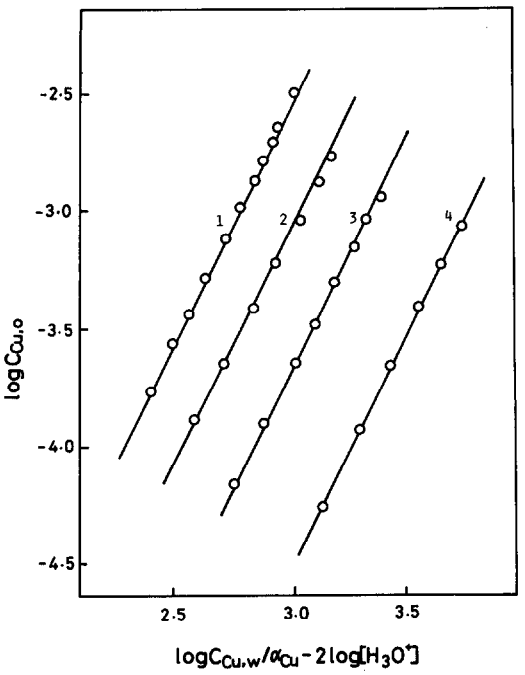

Fig. 3. Identification of the degree of polymerization of Cu(II) α-bromovalerate extracted in benzene. Aqueous ionic strength: 1.0 (Na,H)ClO_4. $C_{HA,o}$ (mol dm^{-3}): (1) 0.93, (2) 0.70, (3) 0.45, and (4) 0.23.

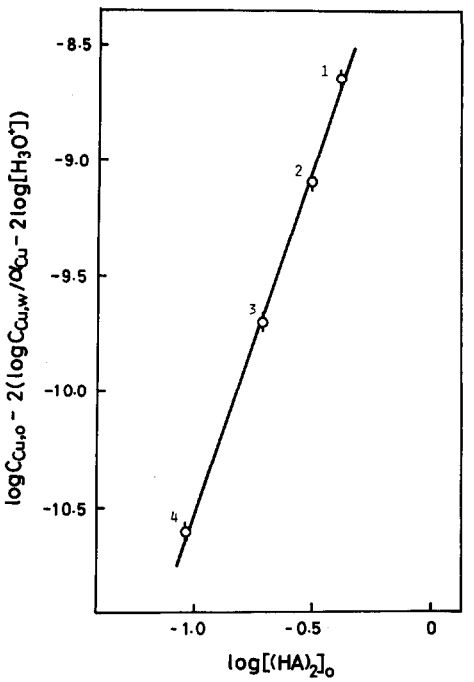

Fig. 4. Determination of the number of α-bromovaleric acid involved in the extracted species. Labelling as in Fig. 3.

Therefore eqn (9) can be rewritten as follows:

$$\log C_{Cu,o} - 2\{\log (C_{Cu,w}/\alpha_{Cu}) - 2\log [H_3O^+]\} = (x+2)\log [(HA)_2]_o + \log 2K_{ex}. \quad (10)$$

When the value of the left-hand side of eqn (10) is plotted against $\log[(HA)_2]_o$, the number of acid molecules participating in the extraction will be given by the slope. Figure 4 is the plot of the experimental data. The points were fitted to a straight line with slope 3.0, implying that the species $Cu_2A_4(HA)_2$ is correct. The corresponding extraction equilibrium is described as follows:

$$2Cu^{2+} + 3(HA)_{2,o} \underset{}{\overset{K_{ex}}{\rightleftharpoons}} Cu_2A_4(HA)_{2,o} + 4H_3O^+, \quad (11)$$

with $\log K_{ex} = -7.87$.

Absorption spectra in UV region

Copper(II) alkanoates have three absorption bands at about 300, 375 (shoulder) and 700 nm.[9,10] The second band at about 375 nm, which is characteristic of the dimeric copper(II) alkanoates, was also observed for the copper(II) α-bromovalerate extracted in benzene.

The band was then used to verify the extraction equilibrium given by eqn (11). The following equation is anticipated for the absorbance (A) at 375 nm:

$$A = \varepsilon[Cu_2A_4(HA)_2]_o = \varepsilon C_{Cu,o}/2, \quad (12)$$

where ε denotes the molar absorptivity per two copper atoms.

The plot of A against $C_{Cu,o}/2$ leads to a linear relation, down to $C_{Cu,o} = 10^{-4}$ mol dm^{-3}, with a slope of $\varepsilon = 126 \pm 10$. The absorptivity is comparable with that for copper(II) acetate in acetic acid ($\varepsilon = 102$),[11] copper(II) propionate in chloroform ($\varepsilon = 120$)[3] and copper(II) octanoate in heptane ($\varepsilon = 120$).[12] Our results indicate that the absorbance at 375 nm is directly proportional to the dimeric copper concentration. The results also suggests that the molar absorptivity is not significantly influenced by the bromine at the α-position.

Extracted species and extraction constant

Copper(II) alkanoates are extracted as a dimer, $Cu_2A_4(HA)_2$ in nonpolar organic solvents. The stability is so high that no appreciable amount of monomeric copper species can be detected in most nonpolar solvents, except for some system of sterically crowded carboxylic acids such as cyclohexanecarboxylic acid,[13] cyclopentylacetic acid,[14] tri-

Table 2. Extraction constant for copper(II) alkanoate, $Cu_2A_4(HA)_2$, at 25°C

Acid	Aqueous phase (mol dm^{-3})	Log K_{ex}[a]	Reference
Butyric	0.1 $(Na,H)ClO_4$	−11.50	4
Pentanoic	0.1 $(Na,H)ClO_4$	−11.56	4
Hexanoic	0.1 $(Na,H)ClO_4$	−11.48	4
Heptanoic	0.1 $(Na,H)ClO_4$	−11.58	4
Octanoic	0.1 $(Na,H)ClO_4$	−11.65	4
Nonanoic	0.1 $(Na,H)ClO_4$	−11.56	4
Decanoic	0.1 $(Na,H)ClO_4$	−11.58	4
		−11.52	Unpublished
Palmitic	1.0 $(Na,H)ClO_4$	−12.0	[b]
Stearic	0.1 $NaNO_3$	−12.6	[c]
α-Bromovaleric	1.0 $(Na,H)ClO_4$	−7.87	This work
α-Bromostearic	0.1 $NaNO_3$	−8.1	[c]

[a] Organic phase: benzene.
[b] E. Grzegrzolka, Z. Chodowska and G. Maciejko, *Chem. Anal. (Warsaw)* 1979, **24**, 1019.
[c] Calculated from the data in Ref. 17.

methylacetic acid[15] and versatic acid.[16] When such a bulky acid is used, monomeric copper species is found together with the dimer.

Bold and Bălușescu[17] proposed the monomeric copper(II) α-bromostearate, $CuA_2(HA)_2$, in the extraction of copper(II) with α-bromostearic acid in benzene. However, recalculation of their data using eqns (9) and (10) leads us to the dimeric copper species, $Cu_2A_4(HA)_2$. We, therefore, conclude that the formation of dimeric copper species is not prevented by the bromine at the α-position.

As shown in Table 2, the logarithmic extraction constants fell in region from −12.6 to −11.5 for a series of nonsubstituted acids and from −8.1 to −7.9 for α-bromoalkanoic acids. The constants for the latter have higher values than the former by a factor of about $10^{3.6}$. This implies that the extraction of copper(II) with α-bromoalkanoic acid starts from a lower pH region by about 0.9 pH units than the nonsubstituted acid systems. In addition, it is useful to consider the relation between the extraction constant and the acid dissociation constant. The relationship is formulated as:

$$\log K_{ex} = 1.7 \log K_a - 3.2. \qquad (13)$$

This equation indicates that the extraction constant becomes progressively higher as the acidity of the acid, K_a, increased. Equation (13) should be applicable in predicting the extraction constant of copper(II) carboxylate, $Cu_2A_4(HA)_2$, in the case when benzene is used as the organic solvent.

REFERENCES

1. H. Yamada and M. Tanaka, *Advances in Inorganic Chemistry and Radiochemistry*, Vol. 29, p. 143. Academic Press, London (1985).
2. D. P. Graddon, *J. Inorg. Nucl. Chem.* 1959, **11**, 337.
3. D. P. Graddon, *Nature* 1960, **186**, 715.
4. I. Kojima, M. Uchida and M. Tanaka, *J. Inorg. Nucl. Chem.* 1970, **32**, 1333.
5. H. Yamada and M. Tanaka, *J. Inorg. Nucl. Chem.* 1976, **38**, 1501.
6. Y. Fujii and M. Tanaka, *J. Chem. Soc., Faraday Trans.* 1 1977, **73**, 788.
7. Y. Fujii, Y. Kawachi and M. Tanaka, *J. Chem. Soc., Faraday Trans.* 1 1981, **77**, 63.
8. M. Lloyd, V. Wycherley and C. B. Monk, *J. Chem. Soc.* 1951, 1786.
9. M. Kato, H. E. Jonassen and J. C. Fanning, *Chem. Rev.* 1964, **64**, 99.
10. L. Dubicki and R. L. Martin, *Inorg. Chem.* 1966, **5**, 2203.
11. K. Sawada, H. Ohtaki and M. Tanaka, *J. Inorg. Nucl. Chem.* 1972, **34**, 625.
12. M. J. Jaycock, A. D. Jones and C. Robinson, *J. Inorg. Nucl. Chem.* 1974, **36**, 887.
13. Z. Brózka and Rózycki, *Chem. Anal. (Warsaw)* 1983, **28**, 585.
14. C. Rózycki, *Chem. Anal. (Warsaw)* 1981, **26**, 37.
15. W. J. Haffenden and G. J. Lawson, *J. Inorg. Nucl. Chem.* 1967, **29**, 1133.
16. W. J. Haffenden and G. J. Lawson, *J. Inorg. Nucl. Chem.* 1967, **29**, 1499.
17. A. Bold and L. Bălușescu, *Rev. Roum. Chim.* 1978, **23**, 1631.

Polyhedron Vol. 6, No. 6, pp. 1209–1214, 1987
Printed in Great Britain

0277–5387/87 $3.00+.00

SOLVENT EXTRACTION STUDIES OF Hg(II) AND Zn(II) WITH DINONYL NAPHTHALENE SULFONIC ACID IN THE PRESENCE OF IMIDAZOLES

SUNG-MAO WANG* and JI-JEN CHIOU

Department of Chemistry, National Tsing Hua University, Hsinchu, Taiwan 30043, Republic of China

(*Received* 10 *September* 1986; *accepted* 24 *October* 1986)

Abstract—The extractions of Zn(II) and Hg(II) from hydrochloric acid solution using dinonylnaphthalene sulfonic acid (HD) as the cation exchanger have been studied. Zn(II) can be extracted from HCl solution by the following reaction:

$$Zn^{2+} + (HD)_{x,0} = (ZnH_{x-2}D_x)_0 + 2H^+,$$

where x is the number of aggregation of a HD micelle and the subscript 0 denotes the organic phase. However, the Hg(II) cannot be extracted because it predominantly forms an anionic complex, $HgCl_4^{2-}$, in the HCl solution. In the presence of an imidazole (Im), 2-methyl imidazole (2MIm), or histidine (His) ligand with the condition [L] < [HCl], Zn(II) forms a 1:1 complex, ZnL^{2+}, with the ligand, and thus the distribution ratio of Zn(II) decreases. The formation constants for $Zn(Im)^{2+}$, $Zn(2MIm)^{2+}$ and $Zn(His)^{2+}$ were calculated to be 4.32×10^7, 3.46×10^8 and 1.56×10^8, respectively. When [L] > [HCl], the pH of the solution rises and a rapid increase in the distribution ratio is observed for both Zn(II) and Hg(II) ions. The metal ions form ML_n^{2+} complexes, which in turn can be solubilized into the HD micelles by the following equation:

$$ML_n^{2+} + (HD)_{x,0} = (ML_nH_{x-2}D_x)_0 + 2H^+.$$

For Hg(II) insoluble complexes precipitate at pH > 4.5. The solid substances were isolated and analyzed to be $Hg(C_3H_3N_2)Cl$, $Hg(C_4H_5N_2)Cl$ and $Hg(C_6H_8N_3O_2)Cl\cdot 2H_2O$ for Im, 2MIm and His complexes, respectively. The precipitate dissociates to become soluble HgL_2^{2+} when the solution is shaken with HD in hexane solution. The extraction behavior of Hg(II) from HCl solution with HD in the presence of 2MIm has also been proved by NMR measurements.

A solution of dinonylnaphthalene sulfonic acid (hereafter denoted as HD) in non-polar organic solvents forms micelles and has been shown to serve as an analogue of a cross-linked resinous strong acid cation-exchanger.[1–4] The exchange reaction between M^{b+} and HD can be represented by the equation:

$$M_a^{b+} + (HD)_{x,0} = (MH_{x-b}D_x)_0 + bH_a^+ \quad (1)$$

where x is the number of aggregation of a HD micelle, and the subscripts a and 0 denote the aqueous and organic phases, respectively. The distribution ratio (D) is related to the equilibrium constant (K_{ex}) by:

$$D = K_{ex}\frac{[HD]_x}{[H^+]^b}. \quad (2)$$

From the logarithmic form of eqn (2), the log D vs log $[H^+]$ plot is expected to be a straight line with a slope of $-b$, which indicates the charge of the species extracted. However, the deviation from the expected slope was found when the metallic ion forms complexes in the solution.[2,3]

It is known that the Hg(II) ion forms anionic complexes with halide ions, and in this paper studies

*Author to whom correspondence should be addressed.

of the extraction behavior of Hg(II) and Zn(II) from HCl solution with HD and the effect of imidazole (Im), 2-methyl imidazole (2MIm) and histidine (His) on the extraction will be reported.

EXPERIMENTAL

Materials

HD was obtained as a 39% solution in *n*-heptane from R. T. Vanderbilt Co. (U.S.A.). Im was obtained from E. Merck (Darmstadt), 2MIm from Kokyo Kasei Co. (Japan), and His from Nutritional Biochemicals Corporation (U.S.A.). The *n*-hexane and all the other inorganic reagents were of highest-purity grade.

Preparation of radioisotopes

The high-activity radioisotopes ^{179}Hg and ^{65}Zn were prepared in the form of perchlorate by irradiating their oxides in the Tsing Hua Open Pool Reactor using a pneumatic tube system. The purity of radioisotopes was confirmed by γ-ray spectrometery.

Procedures

In solvent extraction experiments the aqueous phase normally was prepared to contain the cation (radioisotope) in a concentration of the order of 10^{-6} M and varying concentrations of acid solution. The organic phase contained HD in *n*-hexane with concentrations of the order of 10^{-3} formula weight per liter. Equal volumes (10 cm^3) of aqueous and organic phases were then mixed in polyethylene flasks, shaken at 25 ± 1°C for 1 h, and allowed to settle for 30 min. Aliquots of both phases were taken for the measurements of the radioactivity with an ORTEC model 1431 well-type γ scintillation counter. D is defined as:

$$D = \frac{\text{activity of tracer metal in organic phase}}{\text{activity of tracer metal in aqueous phase}}.$$

The pH titrations were carried out with a standard pH meter PHM62 Radio meter Copenhagen. ^1H NMR spectra were obtained using a JEOL-C60 NMR spectrometer.

RESULTS AND DISCUSSION

Extractions of Hg(II) *and* Zn(II) *from* HCl *solution*

The results of distribution measurements for ^{65}Zn and ^{197}Hg between HD in *n*-hexane and HCl solution are shown in Fig. 1. The slope of log D vs log $[H^+]$ plot was found to be -2 as expected for Zn(II). The extraction constant for Zn(II) was calculated to be 1.64 which is less than the value of 2.9 reported for the extraction of Zn(II) from $HClO_4$ solution.[2] The smaller value obtained from HCl solution may be ascribed to the formation of anionic complexes, $ZnCl_n^{2-n}$.

The Hg(II) ion was not to be extracted with HD from HCl solution at all as seen in Fig. 1. Since it is known that the Hg(II) in HCl forms $HgCl_n^{2-n}$ complexes and the stability constants β_2, β_3 and β_4 were reported to be 1.66×10^{13}, 1.17×10^{14} and 0.17×10^{15}, respectively,[5] the Hg(II) exists mostly as $HgCl_4^{2-}$ in HCl solution and naturally could not be extracted by a cationic exchanger such as HD.

Extraction of Zn(II) *from* HCl *solution in the presence of Im, 2MIm and His*

Zn(II) exists largely as aquated Zn^{2+} in HCl solution as indicated in Fig. 1, and it forms complexes, $Zn(HL)_n^{2+}$, with the ligand, HL, added to the solution. Since only Zn^{2+} ion is extracted into the HD phase, the D of Zn(II) may be expressed by:

$$D = \frac{[ZnH_{x-2}D_x]_0}{[Zn^{2+}]+[Zn(HL)^{2+}]+\cdots+[Zn(HL)_n^{2+}]} = \frac{[HD]_0K_{ex}}{[H^+]^2(1+K_1[HL]+K_1K_2[HL]^2+\cdots K_1K_2\ldots K_n[HL]^n)}, \quad (3)$$

where K_{ex} is the extraction constant and K_1, K_2, ... and K_n are the formation constants for $Zn(HL)^{2+}$, $Zn(HL)_2^{2+}$, ... and $Zn(HL)_n^{2+}$. Equation (3) may be rewritten as:

$$\frac{[HD]}{D[H^+]^2[HL]} = \frac{1}{K_{ex}[HL]} + \frac{K_1}{K_{ex}} + \cdots + \frac{K_1K_2\ldots K_n}{K_{ex}}[HL]^{n-1}. \quad (4)$$

Figure 2 shows the results of distribution measurements for Zn(II) between HD in *n*-hexane and HCl solution, varying the concentration of Im, 2MIm and His at constant HD and acid concentrations. When the total concentration of ligand is smaller than that of acid, $[HL]_{total} < [HCl]$ (the pH values are 1.05–1.50 for Im and 2MIm and 1.30–1.70 for His solutions, respectively), D decreases

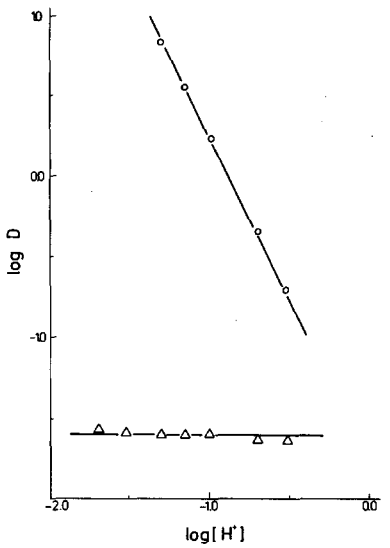

Fig. 1. Acid concentration dependency of D at [HD] = 1.05×10^{-2} F. (○) Zn(II), (△) Hg(II).

gradually with increase in ligand concentration, while it increases rapidly to reach the maximum value when the total concentration of ligand exceeds the acid concentration, $[HL]_{total} > [HCl]$ (the pH values are 7.10–7.70 for Im, 8.00–8.50 for 2MIm, and 5.60–6.00 for His solutions, respectively).

For Im, 2MIm and His in acidic solution, the following protonation reaction occurs:

$$HL + H_3O^+ = H_2L^+ + H_2O. \quad (5)$$

The values of the protonation constant (K_H) were reported to be 1.29×10^7 at $\mu = 0.16$ for Im,[6] 1.35×10^8 at $\mu = 1.0$ for 2MIm,[7] and 1.00×10^6 for His.[8] The concentration of free ligand ([HL]) can be estimated using the values of K_H and the measured values of pH of the solution.

When $[HL]_{total} < [HCl]$, Zn^{2+} forms complexes with the ligand in acidic solution and the concentration of free Zn^{2+} ion extracted into the HD phase decreases. Figure 3 shows plots of log $[HD]/D[H^+]^2[HL]$ vs log [HL], and it is seen that slopes of the plot become zero when $[Im] < 5 \times 10^{-7}$ M, $[2MIm] < 10^{-8}$ M, and $[His] < 5 \times 10^{-6}$ M, which implies that only the second term becomes important in eqn (4). This in turn indicates that only the 1 : 1 complex exists under the experimental conditions. Thus at constant [HD] and $[H^+]$, eqn (4) can be simplified as:

$$\frac{1}{D} = \frac{1}{D_0} + \frac{K_1}{D_0}[L], \quad (6)$$

where D_0 is the distribution ratio of Zn(II) in the absence of ligand.

Plots of $1/D$ vs [HL] gave straight lines, and from the slopes and intercepts the values of K_1 were calculated to be 4.32×10^7, 3.46×10^8 and 1.56×10^8 for Im, 2MIm and His, respectively. It is of interest to note that at constant concentrations of HD and ligand under the experimental conditions, $[HL]_{total} < [HCl]$, plots of log D vs log $[H^+]$ gave straight lines with a slope of -2, which indicated that the only species Zn^{2+} was extracted into the organic phase.

When $[HL]_{total} > [HCl]$, because of the larger values of protonation constant for Im, 2MIm and His, concentration of protonated species becomes approximately the same as that of the acid, and the free-ligand concentration in the solution would be $[HL] = [HL]_{total} - [HCl]_{total}$. Accordingly the pH of

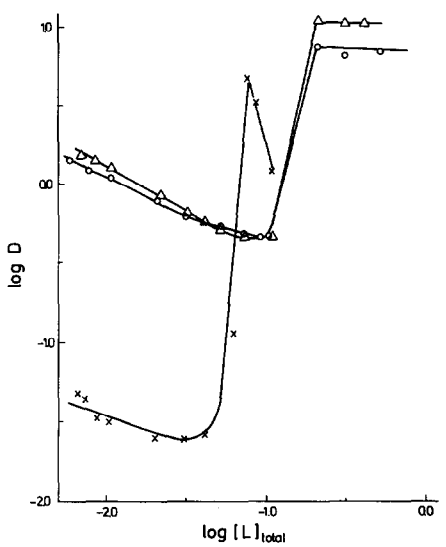

Fig. 2. D of Zn(II) vs total ligand concentration at [HD] = 1.05×10^{-2} F. (○) Im, [HCl] = 0.10 M; (△) 2MIm, [HCl] = 0.10 M; (×) His, [HCl] = 0.05 M.

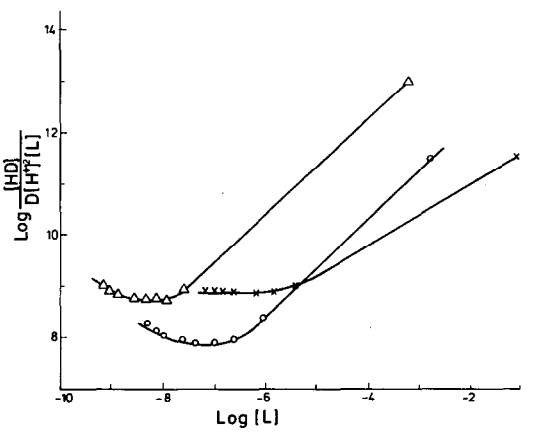

Fig. 3. Extraction of Zn(II) in the presence of ligand with [HL] < [HCl], [HD] = 1.05×10^{-2} F. (○) Im, [HCl] = 0.10 M; (△) 2MIm, [HCl] = 0.10 M; (×) His, [HCl] = 0.05 M.

the solution rises and the mixture behaves as a buffer solution. Edsall *et al.*[6] reported by a pH titration method that Zn(II) forms stable complexes with log $K_1 = 1.98$, log $K_2 = 2.19$, log $K_3 = 2.41$ and log $K_4 = 2.62$ for Im, and Li and Manning[9] found the log K_1 and log K_2 for His to be 6.67 and 5.11, respectively. Thus it is believed that, when $[HL]_{total} > [HCl]$, Zn(II) forms predominantly complex ions, $Zn(HL)_n^{2+}$, which would then be solubilized in the micelle of HD in *n*-hexane by the following reaction:

$$Zn(HL)_n^{2+} + (HD)_{x,0} = [Zn(HL)_n H_{x-2} D_x]_0 + 2H^+. \quad (7)$$

Plots of log D vs log [HD] as shown in Fig. 4 with slopes of +1 indicate that HD exists as micelle with aggregation number x as expected from eqn (7).

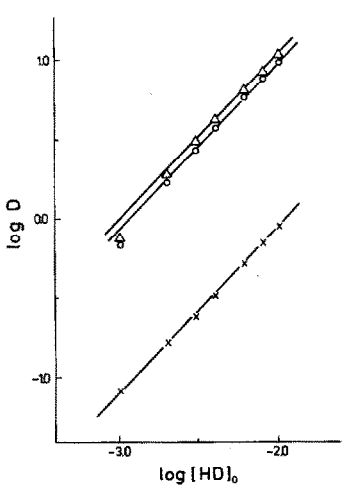

Fig. 4. HD concentration dependency of the D of Zn(II). (○) [Im] = 0.20 M, [HCl] = 0.10 M; (△) [2MIm] = 0.20 M, [HCl] = 0.10 M; (×) [His] = 0.12 M, [HCl] = 0.06 M.

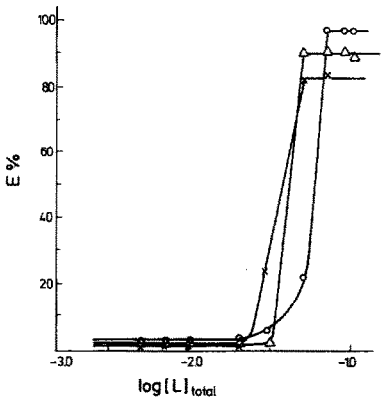

Fig. 5. Extraction of Hg(II) as function of ligand concentrations at [HD] = 1.05×10^{-2} F, [HCl] = 0.03 M. (○) Im, (△) 2MIm, (×) His.

Extraction of Hg(II) *from* HCl *solution in the presence of Im, 2MIm and His*

Figure 5 shows the results of distribution measurements in terms of percent extracted for Hg(II) between HD in hexane and HCl solution, varying the concentration of Im, 2MIm and His at constant HD and acid concentrations. When $[HL]_{total} < [HCl]$, Hg(II) exists predominantly as $HgCl_4^{2-}$ and is not extracted at all by HD into the organic phase. It was found, however, that when the concentration of the added ligand became larger than that of the acid D increased rapidly as observed for the extraction of Zn(II).

When $[HL]_{total} > [HCl]$, the pH of the solution rises to 7.0–7.5, and because of the strong affinity of Hg(II) to nitrogen ligand, the $HgCl_4^{2-}$ ion would react with added ligand to form $Hg(HL)_n^{2+}$ which would then be solubilized in HD:

$$HgCl_4^{2-} + nHL = Hg(HL)_n^{2+} + 4Cl^-, \quad (8)$$

$$Hg(HL)_n^{2+} + (HD)_{x,0} = [Hg(HL)_n H_{x-2} D_x]_0 + 2H^+. \quad (9)$$

When $[HL]_{total} > [HCl]$, keeping the concentrations of HL and acid constant, a plot of log D vs log [HD] gave a slope of +1. Figure 6 shows plots of log D vs log [HCl] at constant concentrations of HD and HL, and varying the concentration of HCl with $[HCl]_{total} < [HL]$. The slope of −2 was obtained for each ligand as expected from eqn (9).

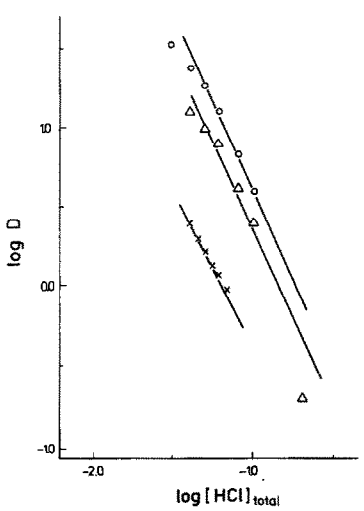

Fig. 6. Acid concentration dependency of the D of Hg(II) at [HL] > [HCl], [HD] = 1.05×10^{-2} F. (○) [Im] = 0.25 M; (△) [2MIm] = 0.25 M; (×) [His] = 0.12 M.

Table 1. Elemental analysis of Hg(II) complexes

Compound	wt% found[a]					
	Hg	C	H	N	Cl	O
Hg(II)–imidazole $Hg(C_3H_3N_2)Cl$	63.3 (66.2)	13.4 (11.9)	1.4 (1.0)	10.1 (9.2)	11.9 (11.7)	
Hg(II)–2-methyl imidazole $Hg(C_4H_5N_2)Cl$	62.1 (63.2)	15.8 (15.2)	2.0 (1.6)	8.8 (8.8)	11.3 (11.2)	
Hg(II)–histidine $Hg(C_6H_8N_3O_2)Cl\cdot 2H_2O$	47.1 (47.1)	15.4 (16.9)	2.3 (2.8)	8.8 (9.9)	9.8 (8.3)	16.6 (15.0)

[a] Calculated values are given in parentheses.

Hg(II) *complexes of Im, 2MIm and His in solvent extraction*

On addition of Im, 2MIm or His (e.g. 0.02 M) to an HCl solution (e.g. 0.01 M) containing a macroamount of $HgCl_2$ (e.g. 2×10^{-3} M), white precipitates formed. When these mixtures were shaken with an equal volume of HD in hexane (e.g. 0.05 F), the white precipitate disappeared immediately.

These precipitates were isolated and analyzed. The results are shown in Table 1.

Brooks and Davidson[10] studied the Hg(II) complexes of Im and His by a potentiometric method and reported that Hg(II) forms $Hg(Im)_2^{2+}$ predominantly at pH 2–4 and a solid substance, $Hg(C_3H_3N_2)ClO_4\cdot H_2O$, precipitates from solutions at pH > 4. They also calculated the formation constant for $Hg(Im)_2^{2+}$ to be $10^{16.74}$ M^{-2} and for $Hg(His)_2^{2+}$ to be $10^{21.22}$ M^{-2}.

The Im, 2MIm and His complexes with Hg(II) becomes insoluble as the pH is raised. The Im complexes precipitate copiously at pH values greater than 4.5, but the His complex is more soluble. Brooks and Davidson[10] presumed that the insoluble mercury compound, obtained from perchlorate solution, $Hg(C_3H_3N_2)ClO_4\cdot H_2O$, contains a linear polymer with one positive charge per polymer unit. A similar structure, $Hg(C_3H_3N_2)Cl$, has been reported by Bottcher.[11]

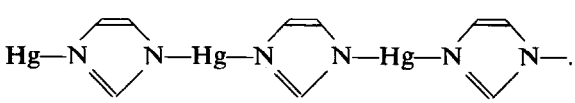

When the aqueous solution (pH > 4) containing insoluble Hg(II) complexes is shaken with HD, the solid substance, $(HgL\cdot Cl)_n$, may react with acid

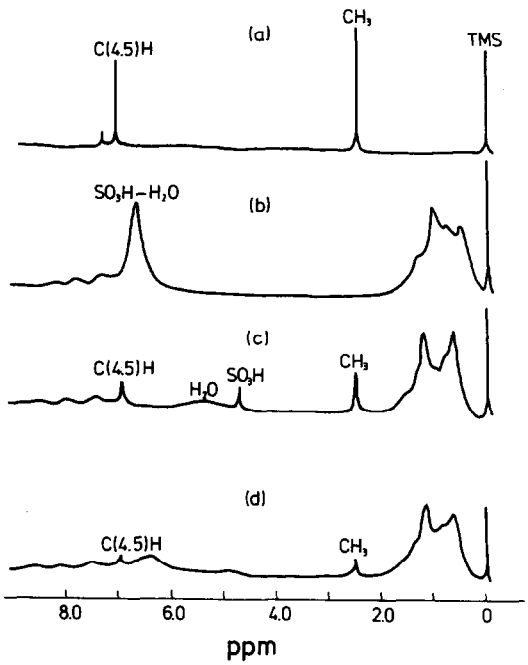

Fig. 7. NMR spectra. (a) 2MIm in $CDCl_3$, (b) HD in CCl_4, (c) organic phase after 2MIm in aqueous solution was extracted into HD in CCl_4, (d) organic phase after 2MIm with $HgCl_2$ in aqueous solution was extracted into HD in CCl_4.

from HD and dissociate to $Hg(HL)_2^{2+}$:

$$2(HgL\cdot Cl)_n + 2nH^+ = nHg(HL)_2^{2+} + nHg^{2+} + 2nCl^- \quad (10)$$

or

$$2[Hg(C_3H_3N_2)]^+ + 2H^+ = [Hg(C_3H_4N_2)_2]^{2+} + Hg^{2+}. \quad (11)$$

Then, the $Hg(HL)_2^{2+}$ complex would be extracted into the organic phase with HD following eqn (9).

In order to investigate whether the Im ligand was extracted into the organic phase, we carried out the following experiments: 2MIm is insoluble in CCl_4, but it becomes soluble in the presence of HD, and this is shown in Fig. 7. Figure 7(a) is the ^1H NMR spectrum of 2MIm in $CDCl_3$ and Fig. 7(b) is that of HD in CCl_4. When an aqueous solution of 2MIm was shaken with CCl_4, no signal of 2MIm was observed. However, when it is shaken with HD in CCl_4 solution, the signals of 2MIm appear as shown in Fig. 7(c). The SO_3H–H_2O proton signal of HD, which solubilized H_2O at 6.78 ppm [Fig. 7(c)] disappears, and new SO_3H and free H_2O signals appear at δ 4.75 and 5.4 ppm, respectively, when 2MIm is solubilized into HD micelles.

On addition of 2MIm into $HgCl_2$ aqueous solution a white precipitate formed, and it disappeared when the mixture in the aqueous phase was shaken with HD in CCl_4. The NMR spectrum of the organic phase was taken, and is shown in Fig. 7(d). The appearance of CH_3 and 4,5C—H signals of 2MIm at δ 2.5 and 6.9 ppm indicates that 2MIm could also be solubilized into the HD micelles in the extraction of Hg(II).

Acknowledgement—We are grateful to the National Science Council of the Republic of China for financial support.

REFERENCES

1. S. Kaufman and C. K. Singleterry, *J. Colloid Sci.* 1955, **10**, 139; *ibid.* 1957, **12**, 465.
2. J. M. White, P. Tang and N. C. Li, *J. Inorg. Nucl. Chem.* 1960, **14**, 255.
3. S. M. Wang and N. C. Li, *J. Inorg. Nucl. Chem.* 1965, **27**, 2093; *ibid.* 1966, **28**, 1091.
4. S. M. Wang, M. N. Chung, C. L. Tseng and P. S. Weng, *Radioisotopes* 1973, **22**, 492.
5. T. Sekine, H. Twaki, M. Sakai, F. Shimada and M. Inarida, *Bull. Chem. Soc. Jpn* 1968, **41**, 1.
6. J. T. Edsall, G. Felsenfeld, D. S. Goodman and F. R. Gurd, *J. Am. Chem. Soc.* 1954, **76**, 3054.
7. S. Nakatsuji, R. Nakajima and T. Hara, *Bull. Chem. Soc. Jpn* 1969, **42**, 3698.
8. W. E. Van Der Liden and C. Beers, *Anal. Chim. Acta* 1973, **68**, 143.
9. N. C. Li and R. A. Manning, *J. Am. Chem. Soc.* 1955, **77**, 5285.
10. P. Brooks and N. Davidson, *J. Am. Chem. Soc.* 1960, **82**, 2118.
11. K. Bottcher, *Chem. Zentralblatt* 1931, **102**, 2757.

Polyhedron Vol. 6, No. 6, pp. 1215–1222, 1987
Printed in Great Britain

0277–5387/87 $3.00 + .00

THEORETICAL STUDIES ON ORGANIC TRANSITION-METAL COMPLEXES—I. PARAMETERIZATION AND CALIBRATION OF AN EXTENDED CNDO/2 METHOD FOR THE CALCULATION OF STABILITY CONSTANTS

JOHN A. HUNTER

Department of Chemistry, Heriot-Watt University, Riccarton, Currie, Edinburgh EH14 4AS, U.K.

and

JOHN O. MORLEY*

Research Department, Imperial Chemical Industries PLC, Organics Division, Hexagon House, Blackley, Manchester M9 3DA, U.K.

(*Received* 5 *August* 1986; *accepted* 27 *October* 1986)

Abstract—An extended CNDO/2 method has been developed for the calculation of stability constants of organic transition-metal complexes. An atom parameterization scheme is described for Mn to Zn using Slater exponents which is found to give a reasonable correlation with the ionization potential of the respective metal. The corresponding bonding parameters have been evaluated by initially deriving the best correlation between the calculated and experimental stability constants of a series of substituted copper bis(salicylaldehydes) and then relating these values to the other transition metals using the bond dissociation energies of simple diatomics as the essential criteria.

A considerable number of molecular-orbital calculations have been carried out on organic transition-metal complexes over the past few years. Most of these studies, however, have been restricted to valence electron semi-empirical methods such as CNDO/2[1] because the very large number of basis functions on the metal coupled with those of the organic ligand usually preclude studies with the more accurate *ab initio* methods. For example, CNDO/2 calculations have been reported recently on complexes of the transition metals with dimethyldithiocarbamic acid and diformylmethane,[2] maleinonitrilodithiolate,[3] phthalocyanines,[4] ammonia[5] and carbon monoxide cluster systems.[6]

In contrast to these studies which deal with the physical properties of the metal complexes themselves, the work described here relates to the development of an extended CNDO/2 method[7] which would be useful in conjunction with molecular graphics for the design of organic ligands for the selective extraction of transition metals from solutions which may contain high concentrations of other metals. In the design of ligands for this purpose, both the stability constants and conformations of the derived metal complexes have been considered. Clearly, the transition-metal parameterization adopted within the CNDO/2 framework must reproduce:

(1) the known effects of substituents on the stability constant;

(2) the Irving–Williams Order;

(3) the known crystallographic conformation of a given complex.

APPROXIMATIONS

The proton ionization constant (K_H) and stability constant (K_S) for a simple stoichiometric reaction

* Author to whom correspondence should be addressed.

of type:

$$LH = L^- + H^+,$$

$$M^{2+} + 2L^- = ML_2,$$

where LH is a selected organic ligand (such as salicylaldoxime or 8-hydroxyquinoline), M^{2+} is a given transition-metal cation, and ML_2 is the resulting complex, are given by:

$$K_H = \frac{[L^-][H^+]}{[LH]},$$

$$K_S = \frac{[ML_2]}{[M^{2+}][L^-]^2}.$$

The free-energy change (ΔG) for these processes is related to the appropriate constant by the equation:

$$\Delta G = -RT \ln K.$$

The calculation of ΔG from first principles is difficult even for gas-phase reactions of the above type because it is dependent on both enthalpy (ΔH) and entropy (ΔS) terms, i.e.:

$$\Delta G = \Delta H - T\Delta S.$$

However, the successful calculation of the proton ionization and stability constants for a series of structurally related complexes by theoretical methods can be accomplished, in principle, if either of the following conditions hold:

(1) the entropy is constant throughout the series,

(2) the entropy is linearly related to the enthalpy.

Provided one of these conditions is met then the calculation of the free energy and hence the stability constant can be achieved by calculating the energy of the reaction using the expression:

$$\Delta E = E(ML_2) - E(M^{2+} + 2L^-),$$

where E is the calculated energy of the molecular components.

Fortunately this relation can be demonstrated in some cases though it is clear that this concept is fraught with difficulties, not the least being that the enthalpy change is often positive and the driving force of the reaction is dependent, therefore, on a large positive entropy. For example, while the high stability of nickel and copper 5-nitro- and 3,5-dinitro-salicylates[8] in water arises from a large positive entropy term, the free-energy change for the formation of substituted silver phenylthioacetates[9] and the formation of copper and nickel complexes of catechol[10] is due mainly to changes in enthalpy. However, in the formation of five or six co-ordinated copper complexes, prepared from Schiff bases of salicylaldehyde and either aliphatic or aromatic amines with pyridine, the entropy of the process shows a linear correlation with the enthalpy over a wide range of substituents.[11] Similar results have been reported for the addition of heterocyclic bases both to a series of transition-metal complexes of salicylaldimines[12] and nickel complexes of diacetylbisbenzoylhydrazones.[13]

Because the enthalpy term appears to be dominant in many reactions of the type described, correlations have been sought between the calculated energy changes (ΔE) and the experimentally observed stability constant. In the present studies, both the parameterization of the extended CNDO/2 method (CINDO54)[7] and the influence of electron-withdrawing and electron-donating substituents on the calculated stability constants of substituted copper bis(salicylaldehydes) are described.

RESULTS AND DISCUSSION

Parameterization and calibration of the extended CNDO/2 method

Various CNDO/2 parameterization schemes have been proposed for the transition metal in these complexes,[14] but the most widely used parameters are those described by Clack *et al.*[15] which are based on the exponents devised by Zerner and Gouterman.[16] These values have been criticized, however, because in a number of cases the effective charge on the metal atom in the complex is found to be negative, the delocalization of spin density in the ligands is too low, and the energies of removal of the ligands are several times too high.[14] Recently Bohm and Gleiter have described an alternative MO formalism for the transition metals which has been used to interpret the photoelectron spectra of transition-metal complexes.[17]

The theoretical requirements for the transition elements at the CNDO/2 level are different from those previously encountered in the original scheme for elements of the second row of the periodic table (sodium to chlorine) since two shells are now involved. In the calculations described here Slater-type orbitals[18] are used for the 3*d*, 4*s* and 4*p* valence shells, and all inner electrons (including the 3*s* and 3*p* electrons) are treated as part of the non-polarizable core. The approximations arising from the complete neglect of, *inter alia*, a large number of two-centre electron repulsion terms are clearly greater than those for second-row elements, and accordingly the calculated results can only be approximate. In the evaluation of integrals for the valence orbitals, the radial part is given by $r^{2.7}e^{-\zeta r}$ when n is 4 which is not suitable for integration by parts.[18] Following Hase and Schweig[19] we have

adopted a radial exponent of 3 for such cases rather than introduce the averaging technique proposed by Jaffé and Doak.[20] When Burns orbitals[21] are used, such a correction is not required, but these orbitals have generally given unsatisfactory results in our hands.

Because the 3*d* orbitals are partially occupied in the transition elements and are heavily involved in bonding, the local core potential (U^A_{kk}) has been modified to take account of the differences in the one-centre repulsion integrals (γ_{AA}) for the 3*d*, 4*s* and 4*p* orbitals using the relation:[6]

$$U_{ss} = -\tfrac{1}{2}(I_s + A_s) - Z_A\gamma_{ds} + \tfrac{3}{2}\gamma_{ds} - \gamma_{ss},$$

$$U_{pp} = -\tfrac{1}{2}(I_p + A_p) - Z_A\gamma_{dp} + \tfrac{5}{2}\gamma_{dp} - \gamma_{sp},$$

$$U_{dd} = -\tfrac{1}{2}(I_d + A_d) - Z_A\gamma_{dd} + \tfrac{5}{2}\gamma_{dp} - \gamma_{sp},$$

where *s*, *p* and *d* represent the 4*s*, 4*p* and 3*d* orbitals only.

The off-diagonal elements of both the extended Huckel matrix and the core Hamiltonian are modified for second-row atoms such that:

$$H^{\text{core}}_{k1} = K(\beta^o_A + \beta^o_B) * S_{k1}/2.$$

K is empirically given the value of 0.75 if either atom A or B is a second-row element. While this modification is found to improve the overall performance of the theory[1] no calibration studies have been reported for the transition elements. In the studies reported here, *K* has been set at unity for all interactions between the transition element and other elements irrespective of whether the latter is a first-, second- or indeed third-row element such as bromine.

Selection of Mulliken electronegativities

The reported values for elements of the first transition series (used as the on-diagonal elements of the Huckel matrix) were adopted for manganese to copper.[15] The values for zinc, however, have not been determined although extrapolated values have been used recently for the calculation of zinc phthalocyanine.[4] Because the electronegativity of zinc is less than that of either cobalt, nickel or copper on either the Allred–Rochow[22] or Pauling[23] scales, the extrapolated values are almost certainly in error.

The orbital electronegativities increase linearly with increasing atomic number along the first row of transition elements with the exception of the 4*s* value for copper which is higher than that expected.[15] A similar trend is observed for the general electronegativities on the Allred–Rochow scale, but the copper value is less than that expected.[22] Because of these apparent anomalies, the zinc value has been derived from the average value of the two preceding elements of the transition elements representing both an open- and closed-shell electronic configuration (cobalt and nickel) using the relation:

$$(I_k + A_k)_{Zn} = \tfrac{1}{2}(I_k + A_k)_{Ni}X_{Zn}/X_{Ni} + \tfrac{1}{2}(I_k + A_k)_{Co}X_{Zn}/X_{Co},$$

where *X* is the Allred–Rochow electronegativity, and *k* represents the 4*s*, 4*p* or 3*d* orbital as appropriate.

An alternative derivation from the Pauling scale is equally valid but the non-linearity of this scale in comparison with the Mulliken scale makes it less attractive.

Electronic configuration of the first transition series

The average configuration energies of the first-row transition elements (M) determined spectroscopically are given by:[6,24]

(1) $3d^{n-2}4s^2$ for the elements Sc to Mn and Zn,

(2) $3d^{n-1}4s^1$ for the elements Fe to Cu.

While these configurations have given satisfactory results for the calculation of cobalt and manganese carbonyl clusters,[6] very poor correlations were obtained in the present work between the calculated ionization $M \rightarrow M^{2+}$, which is required for the calculation of ΔE, and the known ionization potentials of the transition elements Mn to Zn; as a result, subsequent calculations were carried out with the $3d^{n-2}4s^2$ configuration.

The multiplicity of copper(II) in most of its complexes is well established because of its single unpaired electron. The multiplicity of other transition elements is less clearly defined since a number of different spin states may arise. For example, nickel(II) may be paramagnetic with two unpaired electrons or diamagnetic with paired electrons (see Table 1). In contrast, cobalt(II) is always paramagnetic with either one or three unpaired electrons with multiplicities of 2 and 4, respectively. However, iron and manganese have a variety of spin states depending on the oxidation state and the nature of the ligand (Table 1). Because of the wide variation of spin states encountered, the energy of each element was calculated using the simplest multiplicity possible and these values then adopted as parameters for subsequent binding-energy calculations on metal complexes.

Despite the drastic nature of these approximations for the metals themselves, the calculated energy of the ionization $M \rightarrow M^{2+}$ shows a reasonable monatomic correlation with the known ionization potentials of the transition elements (see Fig. 1). The Slater orbital exponents used for these

Table 1. Spin multiplicity of some transition-metal complexes[a]

Metal	Configuration	Representative complex	Conformation	Referenence	U	UE	US	M	Adopted M value
Cu	$3d^9$	Bis(*N*-propylSAL)	Square planar	25	1.86	1	1.73	2	2
		Bis(8-hydroxyquinolinate)	Square planar	26	1.85	1	1.73	2	
Ni	$3d^8$	Bis(*N*-isopropylSAL)	Tetrahedral	27	3.30	2	2.83	3	1
		Bis[*N*-(3-aminopropyl)SAL]	Trigonal bipyramid	28	3.34	2	2.83	3	
		Bis(salicylaldoxime)	Square planar	29	D	0	0	1	
		Bis(*N*-methylSAL)	Square planar	27	D	0	0	1	
Co	$3d^7$	Bis(*N*-methylSAL)	Trigonal bipyramid	27	4.62	3	3.87	4	2
		Bis(anilino)dichloride	Tetrahedral	30	3.96	3	3.87	4	
		Phthalocyanine	Square planar	30	2.22	1	1.73	2	
		SALEN	Square planar	30	2.06	1	1.73	2	
Fe	$3d^5$	SALEN acetate	Distorted octahedral	31	5.24		5.92	6	1
		$[(DAS)_2Cl_2]ClO_4$	Distorted octahedral	32	2.22	1	1.73	2	
	$3d^6$	Dinitrosyliron iodide	Tetrahedral	33	D	0	0	1	
Mn	$3d^5$	Bis[*N*-(3-aminopropyl)SAL]	Trigonal bipyramid	28	5.90	5	5.92	6	2
		$K_4Mn(CN)_6 \cdot 3H_2O$	Octahedral	34	2.03	1	1.73	2	
	$3d^4$	Bis4(SALEN) acetate	Distorted octahedral	35	4.77	4	4.90	5	

[a] U = magnetic moment (BM), UE = number of unpaired electrons, US = theoretical "spin-only" magnetic moment (BM), M = multiplicity $(2S+1)$, SAL = salicylaldimine, SALEN = *N*,*N*′-ethylenebis(salicylaldimine), DAS = *o*-phenylenebis(dimethylarsine), D = diamagnetic.

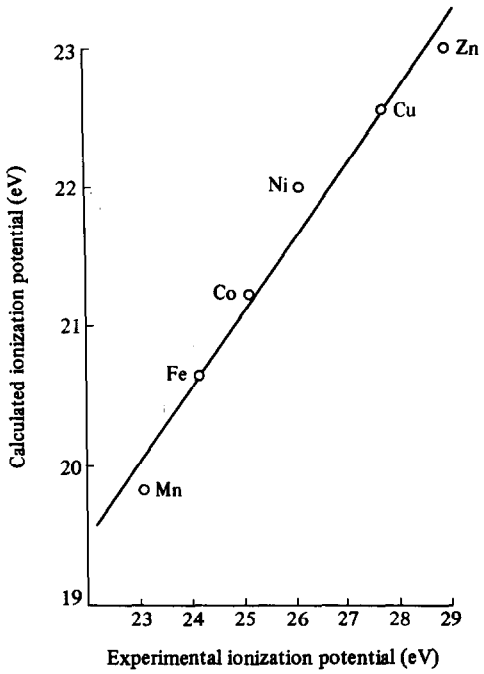

Fig. 1. Plot of calculated vs experimental ionization potentials of transition elements ($M \rightarrow M^{2+}$).

calculations are shown in Table 1 and form the basis for all subsequent calculations reported here.

Selection of bonding parameter values

The values of the bonding parameters (β_k^o) for the transition elements are highly empirical though dependent on the exponents selected. For example, nickel has been assigned the following values:

Metal	$\beta^o(3d)$	$\beta^o(4s, 4p)$	Reference
Ni	19.5	24.6	15
	29.0	32.0	15
	29.0	3.9	14
	10.0	5.0	6

Because of this typically wide variation for the transition elements, calibration studies were carried out with variable β^o values for a series of complexes (see below) so that the resulting binding energies gave the best fit with the experimental stability constants. Salicylaldehyde and its bis complexes with copper(II) were selected for the calibration study for reasons which follow:

(1) Reliable stability constant data are available for a whole range of substituted derivatives which contain both electron-withdrawing and electron-donating groups;

(2) The crystal structure of the copper complex is known[36] (but see below);

(3) The reaction can be represented theoretically by a simple scheme (Scheme 1) which involves a single ionization of the ligand.

However, because the introduction of substituents into a given molecular system usually results in a distortion of the original geometry, standard planar geometries[1] were adopted for calculation purposes except for the angles *a* and *b* which were set at 127.5°, and the metal–oxygen bond length which was set at 1.86 Å, both on the basis of average data from the **A** and **B** forms of copper bis(salicylaldehyde).[36] A wide range of $\beta^o(4s, 4p)$ and $\beta^o(3d)$ values was explored and the binding-energy differences between a given copper complex and the reactants was evaluated and compared with published stability constant data[37,38] using the relation:

$$\Delta E = E_{\text{complex}} - (2E_{\text{anion}} + E_{Cu^{2+}}).$$

Overall, 12 derivatives of salicylaldehyde, its anion, and its copper bis complex were calculated for each β^o value. Selected results from this exercise are shown in Table 2. An analysis of the full data generated (not shown) reveals very complex relationships between the values of β^o adopted and ΔE on the one hand and the correlation coefficients on the other. In summary:

(1) Both the magnitude and the sign of ΔE are determined mainly by the value of $\beta^o(4s, 4p)$ and a linear correlation results at constant $\beta^o(3d)$ values.

(2) Variations in $\beta^o(3d)$ at constant $\beta^o(4s, 4p)$ values cause only small changes in the ΔE values, but the best correlations are obtained at high $\beta^o(3d)$ values.

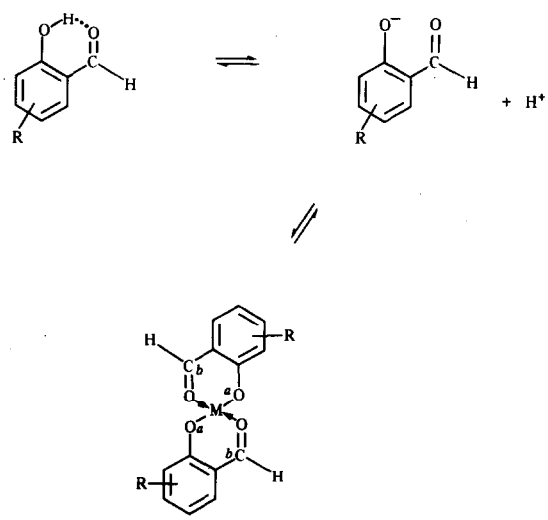

Scheme 1.

Table 2. Correlation coefficients and ΔE values from variable β^o values for copper bis(salicylaldehyde)

$\beta^o(4s, 4p)$	$\beta^o(3d)$	r^a	ΔE^b (eV)	$\beta^o(4s, 4p)/\beta^o(3d)$
30	15	0.673	−25.9199	2.0
15	15	0.488	8.4522	1.0
6	12	0.804	23.5430	0.5
7.5	15	0.501	23.6774	0.5
15	30	0.929	4.3941	0.5
15	7.5	0.487	6.2112	2.0
7.5	30	0.843	19.5992	0.25

[a] Correlation coefficient.
[b] Values for the unsubstituted complex and anion.

The complex relationships observed in the series reflect the varied interactions between the orbitals of the substituents in their relative molecular positions, and the σ- and π-bonding orbitals of the copper atom. Thus, while high $\beta^o(4s, 4p)$ and low $\beta^o(3d)$ values may adequately represent σ-bonded substituents, such as alkyl groups, the reverse may be required to represent the interactions of π-electron acceptors or donors such as the nitro group or amino group.

Because of the complexity of these relationships, the best fit with experiment was selected (see Fig. 2) with $\beta^o(4s, 4p) = 15$ and $\beta^o(3d) = 30$. The $\beta^o(3d)$ value for copper calculated in this way is the same as that reported by Clack for Gouterman orbitals,[15] and accordingly, the $\beta^o(3d)$ values for the other transition elements have been taken from the published data since they all show a curvilinear relationship with atomic number. The zinc value has been derived by extrapolation. However, because the $\beta^o(4s, 4p)$ value for copper differs considerably from that published, the values for the other transition

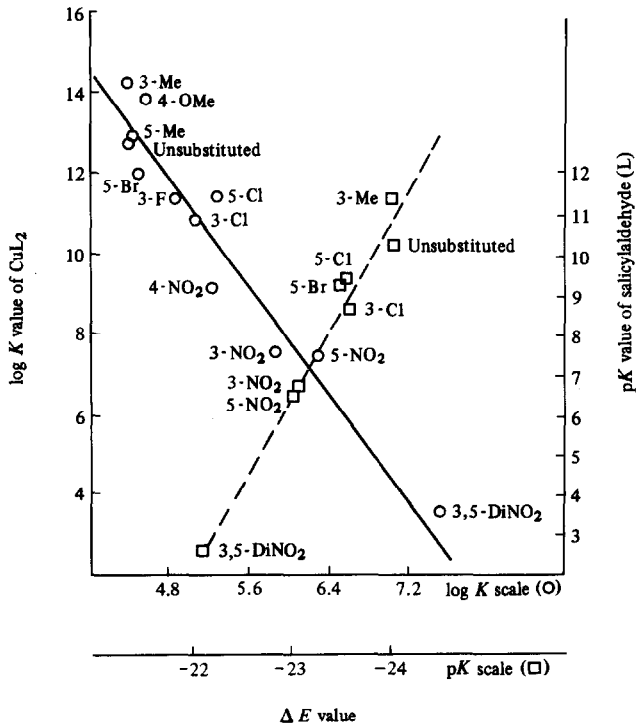

Fig. 2. Plot of calculated binding energies vs experimental proton ionization constants (pK) and stability constants (log K) for substituted salicylaldehydes and their bis complexes with copper.

Table 3. CNDO/2 parameters for the transition elements (in eV)

Transition element	Orbital electronegativity $[-\frac{1}{2}(I_k+A_k)]$			Bonding parameter $(-\beta_k^o)$			Orbital exponent[a] (ζ_k)		
	4s	4p	3d	4s	4p	3d	4s	4p	3d
Mn	3.983	0.975	5.157	16.0	16.0	25.0	0.973	0.973	1.867
Fe	4.120	1.062	5.504	16.0	16.0	27.0	1.014	1.014	2.083
Co	4.170	1.160	5.839	17.0	17.0	28.0	1.054	1.054	1.300
Ni	4.306	1.260	6.182	17.0	17.0	29.0	1.095	1.095	2.517
Cu	4.567	1.347	6.520	15.0	15.0	30.0	1.135	1.135	2.733
Zn	4.080	1.160	5.800	10.0	10.0	31.0	1.176	1.176	2.950

[a] Orbital configurations adopted given by $3d^{n-2}4s^2$.

elements have been derived by relating the bond dissociation energies of a series of simple diatomics (MX) to the corresponding value of the copper system.[39] The resultant energy ratio varies widely over the series depending on whether the atom (X) attached to the transition element (M) possesses:

(1) an *s*-orbital (X = H),
(2) *s*- and *p*-orbitals (X = O or F),
(3) *s*-, *p*- and *d*-orbitals (X = Cl, Br, I or S).

In the last two cases it is evident that the bond dissociation energies will reflect an increasing degree of *d*-orbital interaction associated with increasing atomic number. While the relative value for MH alone should be related to the $\beta^o(4s)$ value (only σ-orbitals are involved), the proportionality does not extend to $\beta^o(4p)$. The full data obtained by this procedure for the elements Mn–Ni and for Zn are shown in Table 3 along with the orbital electronegativities and Slater exponents.

COMPUTER PROGRAM CINDO54

The program used for these calculations was based on the standard CNDO/2 version of Pople *et al.*,[1] but with extensive modifications. These were introduced to deal with problems of portability between different machines, to permit the use of smaller or larger basis sets, and to facilitate the incorporation of third-row (or later) elements so that calculations can be carried out on any element, in principle, up to xenon. While overlap integrals are calculated directly by the method of Mulliken,[40] an option of using Burns atomic functions[21] in place of the more usual Slater ones[18] has been included. Slater functions for orbitals with $n = 4$ have a radial part of the form $r^{2.7}e^{-\zeta r}$ for which the normal process of integration by parts fails. This problem is eliminated by the use of Burns orbitals. However, like Clack *et al.*,[15] we have found Burns orbitals to give less than satisfactory results. Accordingly the calculations involving Slater (or quasi-Slater) coefficients have been performed taking the exponent as 3, rather than introduce the additional complication of Jaffé's device.[20]

Output options include the possible suppression of the printing of various of the larger arrays, output of localized orbitals, dipole moment analysis over such orbitals[41] and the display or Armstrong–Perkins bond orders and valences.[42] The evaluation of the eigenvalues and eigenvectors is performed by an algorithm based on those of Wilkinson.[43] This has the advantage of requiring less temporary workspace than that in the original program. Some attempt has been made to overcome the occasional problem of failure of the self-consistent field section to converge. This is done by an empirical density matrix weighting procedure which seems frequently to be sufficient to get the process back to a state of monotonic convergence.

REFERENCES

1. J. A. Pople and D. L. Beveridge, *Approximate Molecular Orbital Theory*. McGraw-Hill, New York (1970) (and references therein).
2. A. T. Pilipenko, L. I. Savransky, A. I. Zubenko and V. P. Kobylyashny, *J. Mol. Struct.* 1982, **3**, 155.
3. S. Zalis and A. A. Vlcek, *Proc. Conf. Coord. Chem.* 1980, **8**, 461.
4. V. G. Maslov, *Teor. Eksp. Khim.* 1980, **16**, 93.
5. E. Kai and K. Nishimoto, *Int. J. Quantum Chem.* 1980, **18**, 403.
6. H.-J. Freund and G. Hohlneicher, *Theor. Chim. Acta* 1979, **51**, 145.
7. J. A. Hunter and J. O. Morley, Program CINDO54.
8. A. R. Das and V. S. K. Nair, *J. Inorg. Nucl. Chem.* 1975, **37**, 995, 2125.

9. D. Barnes, P. G. Laye and L. D. Pettit, *J. Chem. Soc. A* 1969, 2073; G. J. Ford, P. Gans, L. D. Pettit and C. Sherrington, *J. Chem. Soc., Dalton Trans.* 1972, 1973.
10. R. F. Jameson and M. F. Wilson, *J. Chem. Soc., Dalton Trans.* 1972, 2614, 2617.
11. A. Ewert, K. J. Wannowius and H. Elias, *Inorg. Chem.* 1978, **17**, 1961.
12. L.-T. Ang and D. P. Graddon, *Aust. J. Chem.* 1976, **29**, 565.
13. L. Sacconi, G. Lombardo and P. Paoletti, *J. Chem. Soc.* 1956, 848.
14. N. V. Shokhirev and P. V. Shastnev, *J. Struct. Chem. (U.S.S.R.)* 1978, **19**, 186 (and references therein).
15. D. W. Clack, N. S. Hush and J. R. Yandle, *J. Chem. Phys.* 1972, **57**, 3503.
16. M. Zerner and M. Gouterman, *Theor. Chim. Acta.* 1966, **4**, 44.
17. M. C. Bohm and R. Gleiter, *Theor. Chim. Acta* 1981, **52**, 127, 153.
18. J. C. Slater, *Phys. Rev.* 1930, **36**, 57.
19. H. L. Hase and A. Schweig, *Theor. Chim. Acta* 1973, **21**, 215.
20. H. H. Jaffé and G. O. Doak, *J. Chem. Phys.* 1953, **21**, 196.
21. G. Burns, *J. Chem. Phys.* 1964, **41**, 1521.
22. A. L. Allred, *J. Inorg. Nucl. Chem.* 1961, **17**, 215; A. L. Allred and A. L. Hensley, *ibid.* 1961, **17**, 43; A. L. Allred and E. G. Rochow, *ibid.* 1958, **5**, 264, 269.
23. L. Pauling, *The Nature of the Chemical Bond.* 3rd Edn. Cornell University Press, Ithaca, NY (1960).
24. T. Anno and H. Teruya, *J. Chem. Phys.* 1970, **52**, 2840.
25. L. Sacconi and M. Ciampolini, *J. Chem. Soc.* 1964, 276.
26. G. W. Inman, W. E. Hatfield and R. F. Drake, *Inorg. Chem.* 1972, **11**, 2425.
27. L. Sacconi, P. L. Orioli and M. Di Vaira, *J. Am. Chem. Soc.* 1965, **87**, 3102.
28. L. Sacconi and I. Bertini, *J. Am. Chem. Soc.* 1966, **88**, 5180.
29. E. G. Cox, F. W. Pinkard, W. Wardlaw and K. C. Webster, *J. Chem. Soc.* 1935, 459.
30. B. N. Figgis and R. S. Nyholm, *J. Chem. Soc.* 1959, 338.
31. M. Gerloch, J. Lewis and A. Richards, *J. Chem. Soc. A* 1968, 112.
32. R. D. Feltham, W. Silverthorn, H. Wickman and W. Wesolowski, *Inorg. Chem.* 1972, **11**, 676.
33. L. F. Dahl, E. R. de Gil and R. D. Feltham, *J. Am. Chem. Soc.* 1969, **91**, 1653.
34. B. N. Figgis, *Introduction to Ligand Fields*, p. 287. Interscience, New York (1967).
35. A. Earnshaw, E. A. King and L. F. Larkworthy, *J. Chem. Soc. A* 1968, 1048.
36. A. J. McKinnon, T. N. Waters and D. Hall, *J. Chem. Soc.* 1964, 3290; 1945, 425 (CSSR 6445, 6446).
37. J. G. Jones, J. B. Poole, J. C. Tomkinson and R. J. P. Williams, *J. Chem. Soc.* 1958, 2001.
38. M. Calvin and K. W. Wilson, *J. Am. Chem. Soc.* 1945, **67**, 2003.
39. J. A. Kerr and A. F. Trotman-Dickenson, *CRC Handbook of Chemistry and Physics*, p. F185. CRC Press, Boca Raton, FL (1983).
40. R. S. Mulliken, C. A. Rieke, D. Orloff and H. Orloff, *J. Chem. Phys.* 1949, **17**, 1248.
41. P. M. Kusnesof, F. B. T. Pessine, R. E. Bruns and D. F. Shriver, *Inorg. Chim. Acta* 1974, **14**, 271.
42. D. R. Armstrong, P. G. Perkins and J. J. P. Stewart, *J. Chem. Soc., Dalton Trans.* 1973, 838.
43. R. S. Martin, C. Reinsch and J. H. Wilkinson, *Numer. Math.* 1968, **11**, 181; H. Bowdler, R. S. Martin, C. Reinsch and J. H. Wilkinson, *ibid* 1968, **11**, 293.

Polyhedron Vol. 6, No. 6, pp. 1223–1227, 1987
Printed in Great Britain

0277–5387/87 $3.00+.00

THE FIRST NICKEL(II) *ALLOGON* OF A DITERTIARY PHOSPHINE LIGAND: PREPARATION, SPECTRAL AND CRYSTALLOGRAPHIC CHARACTERIZATION OF SQUARE-PLANAR BIS(DIPHENYLPHOSPHINOMETHYL)DIMETHYL-SILANEDINITRATONICKEL(II)

ELMER C. ALYEA,* GEORGE FERGUSON,* BARBARA L. RUHL and RAM SHAKYA

(GWC)², Guelph Campus, University of Guelph, Guelph, Ontario, Canada N1G 2W1

(*Received* 29 *August* 1986; *accepted* 27 *October* 1986)

Abstract—The reaction of nickel(II) nitrate with bis(diphenylphosphinomethyl)dimethylsilane in ethanol solution gives $Ni(NO_3)_2 \cdot (Ph_2PCH_2)_2SiMe_2$, recrystallized as orange and violet crystals from dichloromethane. Vibrational, electronic spectral and magnetic measurements of the initial product indicate the presence of *allogons*, the first case involving nitrate anions or a ditertiary phosphine ligand. The structure of the orange crystals **1** was determined by single-crystal X-ray diffraction analysis. The crystals are monoclinic, space group $P2_1/c$ with four molecules in a unit cell of dimensions $a = 10.512(2)$, $b = 15.821(5)$, $c = 18.948(8)$ Å, $\beta = 104.87(4)°$. The structure was solved by the heavy-atom method and refined by full-matrix least-squares calculations to $R = 0.029$ for 2563 observed data. In the monomeric molecule the Ni atoms are square planar, with monodentate nitrate groups [Ni—O = 1.926(2) and 1.933(2) Å]. The bidentate phosphine ligand has a bite angle of 94.81(3)° and the Ni—P bond distances are 2.166(1) and 2.170(1) Å. The six-membered NiP_2C_2Si ring adopts a boat conformation.

The coordination chemistry of nickel(II) complexes of phosphine ligands is well-developed, with much interest focusing on the factors influencing the stereochemistry of $NiX_2(PR_3)_2$ complexes.[1,2] The square planar $\rightleftharpoons$ tetrahedral equilibrium observed for many examples [especially for X = Br and $PR_3 = PPh_2R'$ (R′ = alkyl)] are reasonably predictable in that larger phosphines or halide ions, weaker ligand field strength of the phosphine or halide, and more polar solvents favour the adoption of tetrahedral nickel(II) geometry. The actual isolation of both geometric forms, called *allogons*,[3] has however only been possible for a few specific cases. X-ray crystallographic data are available for the interallogon compounds $NiBr_2[PPh_2(CH_2Ph)]_2$[3] and $NiCl_2(PPh_3)_2$,[4] whereas synthetic and spectroscopic characterization data are reported for some isolable isomeric cases involving $PPh_{3-n}Cy_n$ ($n = 0$–3),[5] $PPh_{3-n}Bu_n$ ($n = 1$ or 2)[6] and other PPh_2R' ligands.[7,8]

All known interallogon compounds of nickel(II) involve halide and monodentate phosphines as ligands. With other anions, the complexes with various phosphines are reported to be either square planar (e.g. NCS^-) or tetrahedral (e.g. NO_3^-) only.[2] With ditertiary phosphines, square planar $\rightleftharpoons$ tetrahedral equilibria were observed for nickel(II) halide complexes of bis(diphenylphosphino)propane (dppp), but *allogons* were not isolated.[9] Similarly, electronic spectral data indicated a related isomeric phenomenon for bis(dicyclohexylphosphino)ethane (dcpe), involving diamagnetic square pyramidal $[Ni(NO_3)_2(dcpe)(H_2O)]$ and square planar $[Ni(NO_3)(dcpe)(H_2O)](NO_3)$; in contrast the ligands dmpe and dppe (R = Me and Ph, respectively, instead of Cy) gave only the yellow square planar $[Ni(L\text{–}L)_2](NO_3)_2$ complexes.[10]

* Authors to whom correspondence should be addressed.

As part of the investigation[11] of the coordinating ability of the related silicon-backbone phosphine ligands, $Me_2Si(CH_2PPh_2)(CH{=}CH_2)$($L^1$) and $Me_2Si(CH_2PPh_2)_2$(L^2) we have observed that $NiX_2 \cdot L^2$ complexes are on the square planar $\rightleftharpoons$ tetrahedral threshold.[12] The orange and violet interallogon compounds $Ni(NO_3)_2 \cdot L^2$ are the subject of this report, which includes synthetic, spectral and (for the orange isomer) X-ray crystallographic data. These *allogons* are the first known for Ni(II) with nitrate as the anion and with a ditertiary phosphine ligand.

EXPERIMENTAL

Preparation of bis(diphenylphosphinomethyl)dimethylsilanedinitratonickel(II), $Ni(NO_3)_2 \cdot L^2$

Equimolar amounts of nickel(II) nitrate dissolved in ethanol and dimethoxypropane (1.5 cm^3) and the ligand L^2 dissolved in methylene chloride were mixed, giving a deep purple precipitate. After stirring the reaction mixture for 20 min, the solid was collected by filtration, washed with ethanol and ether, and dried *in vacuo* at room temperature overnight. Found (calc.): C, 52.5 (52.6); H, 4.8 (4.7); N, 4.4 (4.4). Decomposition temperature, 218°C. Recrystallization of the violet product by slow evaporation from a methylene chloride solution gave both violet (major) and orange (minor) crystals. Repeated attempts at recrystallization failed to give either isomer as a pure product or suitable crystals of the violet isomer for an X-ray analysis. The orange crystals were readily separated (though in small quantity) in suitable form on several occasions, with their relative quantity being favoured by faster evaporation of the dichloromethane solvent.

Physical methods

IR spectra were recorded in the range 4000–200 cm^{-1} using a Perkin–Elmer Model 180 double-beam spectrometer and Nujol or halocarbon mulls between KBr or polythene plates. Electronic spectra were recorded on a Cary 14 spectrophotometer with solid transmission spectra being obtained by the filter paper technique. Magnetic-moment measurements were performed on a Varian EM 360 (60 MHz, CW) NMR spectrometer by the Evans method.

Crystal data. $C_{28}H_{30}NiSiN_2O_6P_2$, $M_r = 639.31$, monoclinic, $a = 10.512(2)$, $b = 15.821(5)$, $c = 18.948(8)$ Å, $\beta = 104.87(1)°$, $V = 3045$ Å^3, $D_c = 1.39\,g\,cm^{-3}$, $Z = 4$, $F(000) = 1328$, Mo-K_{α_1} radiation, $\lambda = 0.70926$ Å, μ(Mo-K_α) = 8.2 cm^{-1}. Space group $P2_1/c$ uniquely from the systematic absences.

Structure solution and refinement. Data were collected to a maximum 2θ of 44.0° on an Enraf–Nonius CAD-4 diffractometer by the ω–2θ scan technique using monochromatized Mo-K_α radiation. Following machine location and centering of 25 reflections with θ in the range $10 < \theta < 15°$, accurate cell constants and the orientation matrix were obtained by a least-squares refinement. A total of 4249 reflections were collected of which 3472 were unique (R factor on averaging 0.015). Of these, the 2563 with $I > 3\sigma(I)$ were used in structure solution and refinement. The intensities of three standard reflections monitored at regular intervals did not change significantly over the period of data collection. The data were corrected for Lorentz and polarization factors and for absorption (maximum and minimum transmission coefficients 0.888 and 0.772).

The structure was solved by the heavy-atom method. Initial refinement* was by full-matrix least-squares calculations with isotropic temperature factors for the non-hydrogen atoms. Difference maps calculated at various stages revealed maxima corresponding to the hydrogen atoms; these were then included (but not refined) in the subsequent calculations in geometrically idealized positions (C—H = 0.95 Å) with an overall isotropic thermal parameter ($U = 0.085$ Å^2). In the final cycles of refinement, weights were derived from counting statistics, and the non-hydrogen atoms were allowed anisotropic motion. Scattering factors used in the structure factor calculations were taken from Ref. 13 for non-hydrogen atoms and Ref. 14 for hydrogen atoms, and allowance made for anomalous dispersion.[15] Refinement converged with $R = 0.029$ and $R_w = [\Sigma w\Delta^2/\Sigma wF_o^2]^{1/2} = 0.039$. A difference map calculated at the conclusion of the refinement had maxima less than 0.22 e Å^{-3} and no significant features. Tables of atomic positional parameters and anisotropic thermal vibrational parameters, each with estimated standard deviations, calculated hydrogen coordinates, molecular dimensions and observed structure amplitudes and calculated structure factors have been deposited.†

* All calculations were done on our PDP11/73 computer using the SDP-Plus system, B. Frenz and Associates Inc. (1983), SDP-Plus, College Station, TX 77840, and Enraf–Nonius, Delft, Holland.

† Copies are available from the Editor. Atomic coordinates have also been deposited at the Cambridge Crystallographic Data Centre.

RESULTS AND DISCUSSION

The phenomenon of interallogony, involving the occurrence of two different stereochemical arrangements of the same number of bonds, is well established for nickel(II) phosphine complexes, though the examples are limited to those involving halide anions and monodentate phosphines.[1-9] X-ray structural determinations are only available for the four *allogon* complexes, $NiBr_2[PPh_2(CH_2Ph)]_2$[3] and $NiCl_2(PPh_3)_2$.[4] Our discovery that the complexes $NiX_2 \cdot L^2$ (X = halide)[12] were on the tetrahedral side of the square planar $\rightleftharpoons$ tetrahedral equilibria, as compared to the analogous $NiX_2 \cdot$ dppp complexes previously reported by Van Hecke and DeW. Horrocks,[9] led us to react $Ni(NO_3)_2$ with our new silicon-backbone ligand. The initial product formed in ethanol was a violet powder, but various recrystallizations from dichloromethane solution gave mixtures of orange and violet crystals. Rapid evaporation of the solvent favoured formation of a larger quantity of the orange crystals. Manual separation of a few crystals of the latter allowed their X-ray analysis and verification as the square planar isomer. Numerous attempts to obtain suitable crystals of the violet form for a single-crystal determination were not successful, although it was possible to isolate a product virtually free of the orange crystals by slow evaporation.

Physical measurements on the violet product initially isolated from the ethanol reaction mixture indicated the presence of four-coordinate Ni(II) species having both square planar and tetrahedral geometries. The complex $Ni(NO_3)_2 \cdot L^2$, which is non-conducting in nitromethane ($\Lambda_M = 25.0\ \Omega^{-1}\ cm^2\ mol^{-1}$ for a 10^{-3} M solution, indicating some solvolysis), showed IR bands attributable to monodentate nitrato groups.[16,17] Bands at 1435 and 1350 cm^{-1} (ν_3 splitting of 85 cm^{-1}), 1000 cm^{-1} (ν_1), 820 cm^{-1} (ν_2), and at 760 and 740 cm^{-1} (ν_4), are absent in the corresponding halide complexes.[12] Weak bands in the far IR at 298 and 267 cm^{-1} can tentatively be assigned to ν(Ni—O) and ν(Ni—P) modes, respectively. An attempt to observe the relative intensities of the three highest-frequency Raman shifts attributable to nitrate fundamentals[18] was unsuccessful due to sample decomposition in the laser beam.

In contrast to the $NiX_2 \cdot$ dppp complexes,[9] for which the square planar $\rightleftharpoons$ tetrahedral equilibria lie considerably toward the square planar side (totally in the solid state), our results[12] for $NiX_2 \cdot L^2$ complexes show that formation of the tetrahedral isomer is favoured. For the present $Ni(NO_3)_2 \cdot L^2$ case, the magnetic moment, measured at 303 K in CH_2Cl_2 solution, is 3.4 BM. Assuming that a value of $\mu_{eff} = 3.5$ BM corresponds to the totally tetrahedral value (as found for $NiI_2 \cdot L^2$),[12] this magnetic moment represents a per cent paramagnetism of 94, or alternatively, $K_{eq} = 17.0$ in favour of the tetrahedral isomer. We have determined that $Ni(NO_3)_2 \cdot$ dppp, not previously reported,[9] is diamagnetic, with no indication of formation in solution of the tetrahedral isomer. By comparison, electronic spectroscopy of $Ni(NO_3)_2 \cdot L^2$ shows that the tetrahedral isomer is predominant, both in the solid state (12,200- and 18,000-cm^{-1} bands) and in CH_2Cl_2 solution [bands occur at 9400 (30), 11,100 (40), 16,800 (70) and 22,200 cm^{-1} (200)]. Electronic spectral parameters for several $NiX_2 \cdot L^2$ complexes and comparisons to reported spectral data for the analogous dppp complexes will be discussed in a future paper. This report verifies that the expectedly larger bite of L^2 than dppp as a chelating ditertiary phosphine ligand leads to the existence of *allogons* for the $Ni(NO_3)_2 \cdot L^2$ case.

The molecular structure of the orange isomer of $Ni(NO_3)_2 \cdot L^2$ is shown in Fig. 1. The Ni coordination, with *cis* P and O atoms in the coordination sphere, is slightly distorted from square planar towards square pyramidal [deviations from the NiO_2P_2 plane (Fig. 1) are: Ni, 0.029(1); O(11), −0.028(2); O(21), 0.014(2); P(1), 0.009(1); P(2), −0.024(1) Å]. Selected bond distances and angles are summarized in Table 1. The six-membered NiP_2C_2Si ring adopts a boat conformation with atoms Ni, P(2), Si and C(1) forming a plane to within ±0.09 Å and with P(1)+0.814(1) and C(2)+0.633(4) Å from the plane. This conformation results in the non-equivalence of substituents on P and Si.

The Ni—P bond distances [2.166(1) and 2.170(1) Å] are considerably shorter than the corresponding

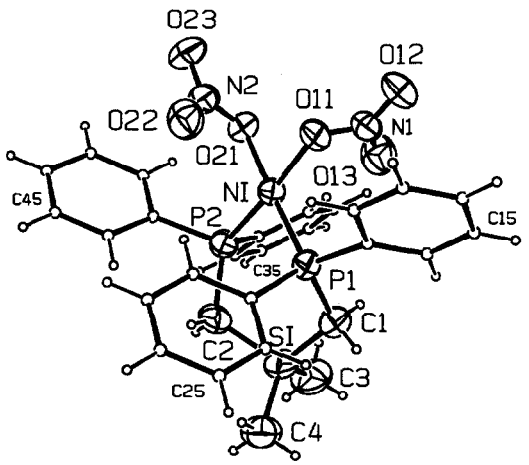

Fig. 1.

Table 1. Principal[a] bond distances (Å) and bond angles (°) of the orange crystal $Ni(NO_3)_2 \cdot L^2$

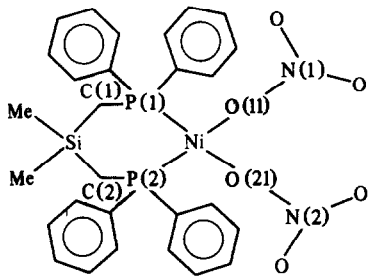

Ni—P(1)	2.166(1)	P(1)—Ni—P(2)	94.81(3)
Ni—P(2)	2.170(1)	P(1)—Ni—O(11)	91.76(7)
Ni—O(11)	1.926(2)	P(1)—Ni—O(21)	178.08(7)
Ni—O(4)	1.933(2)	P(2)—Ni—O(11)	172.70(7)
P(1)—C(1)	1.795(3)	P(2)—Ni—O(21)	86.80(7)
P(2)—C(2)	1.803(3)	O(11)—Ni—O(21)	86.58(9)
Si—C(1)	1.884(4)	Ni—P(1)—C(1)	114.6(1)
		Ni—P(2)—C(2)	121.0(1)
Si—C(2)	1.895(4)	P(1)—C(1)—Si	117.7(2)
Si—C(3)	1.829(4)	P(2)—C(2)—Si	117.5(2)
Si—C(4)	1.843(4)	C(1)—Si—C(2)	107.3(1)

[a] For more detailed information, see supplementary data.

distances in the square planar isomers of $NiCl_2(PPh_3)_2$(2.242(3))[4] and $NiBr_2[PPh_2(CH_2Ph)]_2$ (2.263(7) Å).[3] Ni—P bond distances in the tetrahedral isomers of the latter two interallogon examples are longer still by 0.05 Å. The shortening of Ni—P bond distances for the present square planar *allogon*, compared to the monodentate phosphine cases, can perhaps be attributed to the presence of O (of weaker *trans* influence[19]) rather than P atoms in the *trans* positions. The shorter Ni—P bond length also suggests that a stronger bond than normal results from the chelate ring formation. A shortened Ni—P bond length [2.175(4) Å] in *trans*-$Ni(C{\equiv}CPh)_2(PEt_3)_2$ was explained by electronic effects.[20]

The Ni—O bond distances [1.926(2) and 1.933(2) Å] are shorter than previously reported for the Ni—O monodentate nitrato interaction in octahedral dinitrato[2,6 - diacetylpyridinebis(anil)] nickel(II) [2.027(5) vs 2.104(5) ave. for the bidentate nitrato group in the same molecule].[21] The shorter Ni—O bond in a square planar environment is as expected. In the square planar complex bis-(*N*-isopropyl - 3 - methylsalicylaldiminato)nickel(II), Ni—O equals 1.837(2) Å (ave.).[22] The effect of coordination of the nitrato groups is discernible in the differences of the N—O distances, i.e. N—O (bonded), 1.293(4) and 1.303(4) Å, compared to N—O (terminal), 1.217–1.227(4) Å. Similarly, the O—N—O bond angles are considerably larger to the terminal O atoms, 124.3(3)° ave. compared to 116.7–119.2(3)° when both terminal and bound O are involved.

The P—Ni—O angles [172.70(7) and 178.08(7)°] depart significantly from idealized square planar expectations; consistent with the small square pyramidal distortion noted above. Similarly, the P—Ni—O and O—Ni—O angles are less than the theoretical 90° [86.58(9) and 86.80(7)°]. The P—Ni—P angle of 94.81(3)° shows that the bite angle of L^2 is enhanced by the incorporation of a Si atom in the backbone. For comparison, the bite angle of dppp in $Pd(NCS)_2 \cdot$dppp is 89.3°, while that of dppe in Pd(NCS)(SCN)·dppe is 85°.[23]

The C—P—C angles [103.0–107.8(2)°] are less than the ideal tetrahedral value (109.5°) and the Ni—P—C angles [107.0–121.0(1)°] are larger, as expected for metal–phosphine complexes. Other bond distances, such as P—C(CH_2) [1.795 and 1.803(3)Å] and P—C(phenyl) [1.804–1.818(4) Å], are similar to those in other phosphine complexes. The range of C—Si—C angles [107.3–111.5(2)°] reflects the flexibility of the ligand backbone; the 107.3° angle for C(1)—Si—C(2) compares to 116.7° for the C—C—C backbone angle of dppp in $Pd(NCS)_2 \cdot$dppp.[23] The conformationally flexible nature of the L^2 ligand probably contributes to its coordinating ability with several metal centres,[12] and allows interallogon compounds in the case of $Ni(NO_3)_2 \cdot L^2$.

Acknowledgements—E.C.A. and G.F. thank N.S.E.R.C., Canada for assistance in the form of operating grants and updated computing facilities for the diffractomer system.

REFERENCES

1. L. Sacconi, In *Transition Metal Chemistry* (Edited by R. L. Carlin), Vol. 4, p. 199. Marcel Dekker, New York (1968).
2. C. A. McAuliffe and W. Levason, *Phosphine, Arsine and Stibine Complexes of the Transition Elements*. Elsevier, Amsterdam (1979).
3 B. T. Kilbourn and H. M. Powell, *J. Chem. Soc. A* 1970, 1688.
4. B. Corain, B. Longato, R. Angeletti and G. Valle, *Inorg. Chim. Acta* 1985, **104**, 15.
5. P. J. Stone and Z. Dori, *Inorg. Chim. Acta* 1971, **5**, 434.
6. C. R. C. Coussmaker, H. H. Hutchinson, J. R. Mellor, L. E. Sutton and L. M. Venanzi, *J. Chem. Soc.* 1961, 2705.
7. R. G. Hayter and F. S. Humiec, *Inorg. Chem.* 1965, **4**, 1701.
8. L. H. Pignolet, W. DeW. Horrocks, Jr and R. H. Holm, *J. Am. Chem. Soc.* 1970, **92**, 1855.
9. G. R. Van Hecke and W. DeW. Horrocks, Jr, *Inorg. Chem.* 1966, **5**, 1968.
10. J. A. Connor and P. I. Riley, *Inorg. Chim. Acta* 1975, **15**, 197.
11. E. C. Alyea, R. P. Shakya and A. E. Vougioukas, *Transition Met. Chem.* 1985, **10**, 435.
12. E. C. Alyea and R. Shakya, unpublished results.
13. D. T. Cromer and J. B. Mann, *Acta Cryst.* 1968, **A24**, 321.
14. R. F. Stewart, E. R. Davidson and W. T. Simpson, *J. Chem. Phys.* 1965, **42**, 3175.
15. D. T. Cromer and D. Liberman, *J. Chem. Phys.* 1970, **53**, 1891.
16. N. F. Curtis and Y. M. Curtis, *Inorg. Chem.* 1965, **4**, 804.
17. P. H. Merrell, E. C. Alyea and L. Ecott, *Inorg. Chim. Acta* 1982, **59**, 25.
18. C. C. Addison, N. Logan, S. C. Wallwork and C. D. Garner. *Q. Rev.* 1971, **25**, 289.
19. T. G. Appleton, H. C. Clark and L. E. Manzer, *Coord. Chem. Rev.* 1973, **10**, 335.
20. G. R. Davies, R. H. B. Mais and P. G. Austen, *J. Chem. Soc.* 1967, 1750.
21. E. C. Alyea, G. Ferguson and R. J. Restivo, *Inorg. Chem.* 1975, **14**, 2491.
22. R. L. Braun and E. C. Lingafelter, *Acta Cryst.* 1966, **21**, 546.
23. G. J. Palenik, M. Mathew, W. L. Steffen and G. Beran, *J. Am. Chem. Soc.* 1975, **97**, 1059.

Polyhedron Vol. 6, No. 6, pp. 1229–1233, 1987
Printed in Great Britain

0277–5387/87 $3.00+.00

THE REACTIVITIES OF AMINOARSINES TOWARD DIARSINES

V. K. GUPTA, L. K. KRANNICH and C. L. WATKINS*

Department of Chemistry, University of Alabama at Birmingham, Birmingham, AL 35294, U.S.A.

(*Received* 28 *August* 1986; *accepted after revision* 30 *October* 1986)

Abstract—The reactions of Me_2AsNR_2 with $Et_2AsAsEt_2$, and of Et_2AsNR_2 with $Me_2AsAsMe_2$ (R = Me or Et), were investigated over the temperature range 24–75°C by using ^1H and ^{13}C NMR spectroscopy. The NMR data indicate the initial formation of the unsymmetrical diarsine, $Me_2AsAsEt_2$, and the respective dialkylaminodialkylarsine, Et_2AsNR_2 or Me_2AsNR_2. The $Me_2AsAsEt_2$ then undergoes symmetrization to yield $Me_2AsAsMe_2$ and $Et_2AsAsEt_2$. Additional competitive reactions involving 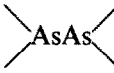 and 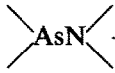 systems also occur in the reaction mixture. In each case, the percentage distribution of products and reactants in the studied systems at equilibrium is independent of temperature within experimental measurement. The reaction rates are dependent upon the nature of R and the alkyl group in the diarsine. In addition, equilibrium constants for several competitive reactions have been determined.

The chemistry of P—P-, As—As-, P—N-, As—N- and As—P-bonded compounds has been of continued interest[1–4] with most of the attention being directed toward the reactivity of P—N-bonded systems.[5–13] During the last 20 years, several studies have focused on the reactivity of the more labile As—N bond.[14–19] This literature establishes the fact that As—As and As—N bonds are more labile than the P—P and P—N bonds, respectively. Recently the synthesis and reactivity of heteroatomic group 15 compounds, which contain multiple bonds, i.e., P═N, P═As and P═Sb, have been reported.[20,21]

Our multinuclear NMR investigations of the Me_2AsNMe_2–Me_2AsH[22] and Me_2AsNMe_2–$MeAsH_2$[23] reaction systems demonstrate that the lability of the As—As and As—N bonds leads to reactions involving the exchange of H—, 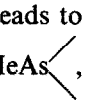 , Me_2As— and Me_2N— units in solution. These exchange processes directly influence the rate of reaction and/or the distribution of products at equilibrium.

There are no reports in the literature on the reactivities of aminoarsines toward As—As-bonded compounds, except our recent observations[22] while studying the reactivity of Me_2AsNMe_2 toward Me_2AsH. Thus, we have undertaken a systematic study of reactions involving the 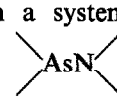 system to elucidate the mechanism of reaction, understand the effect that various substituents have on As—N and As—As bond lability, and characterize and establish the relative importance of competing reactions. In this paper, we report a ^1H and ^{13}C NMR study of the reactions of four dialkylaminodialkylarsines with tetramethyl- and tetraethyl-diarsine in toluene-d_8 solution as a function of temperature and time. Some competing reactions have also been studied to establish their relative significance in the 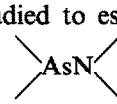 reaction system.

EXPERIMENTAL

Standard high vacuum line techniques and a Vacuum Atmospheres Model HE-43-Dri lab equipped with a Model HE-493 Dri-Train were used for storing and handling of all compounds. Me_2NH

* Author to whom correspondence should be addressed.

(Matheson Gas Products) was dried over sodium metal and was distilled in the vacuum line prior to use. Toluene-d_8 and Me_4Si were purchased from Aldrich Chemical Co. and stored over molecular sieves. Me_2AsNEt_2 (b.p. 80.5°C/90 torr),[15] Et_2AsNEt_2 (58°C/8 torr),[19] Me_2AsNMe_2 (108°C),[24] and $Me_2AsAsMe_2$ (60°C/25 torr)[25] were synthesized by previously reported methods. $Et_2AsAsEt_2$ (185°C) was synthesized[25] by the reaction of Et_2AsCl with Zn dust. Et_2AsNMe_2 (132°C/549 torr) was obtained by the reaction of Et_2AsI with Me_2NH using the procedure[24] analogous to that reported for Me_2AsNMe_2. The purity of all compounds was checked by NMR spectroscopy prior to use.

^1H and ^{13}C NMR spectra were recorded on a Nicolet 300 MHz multinuclear FT NMR spectrometer operating at 300.1 and 75.4 MHz, respectively. The chemical shifts were measured with respect to tetramethylsilane as an internal reference. The reaction mixtures were protected from exposure to light and care was also taken to ensure that the exchange processes were not acid-catalyzed by carrying out reactions in NMR tubes that were not acid washed.

Reactions of $Me_2AsAsMe_2$ *with* Et_2AsNMe_2 *or* Et_2AsNEt_2, *and of* $Et_2AsAsEt_2$ *with* Me_2AsNMe_2 *or* Me_2AsNEt_2

The reactions of $Me_2AsAsMe_2$ (1.0 mmol) with equimolar amounts of Et_2AsNMe_2 or Et_2AsNEt_2, and of $Et_2AsAsEt_2$ (1.0 mmol) with Me_2AsNMe_2 or Me_2AsNEt_2 in a 1:1 mole ratio, were carried out in toluene-d_8 using the following procedure. A stoichiometric amount of the less volatile compound dissolved in toluene-d_8 and a drop of TMS were added to a NMR tube (10 mm × 22.5 cm, pyrex) equipped with a greaseless vacuum stopcock. The tube was degassed using standard vacuum line techniques. An equimolar amount of the more volatile compound was transferred at −196°C into the NMR tube. The total volume of the solution was maintained at 3.0 cm^3. The tube was sealed, agitated gently at −78°C (dry ice–acetone slush), and inserted into the precooled (−60°C) probe of the NMR spectrometer. The reaction was then monitored at the selected temperature by ^1H and ^{13}C NMR spectroscopy as a function of time.

Reactions of Me_2AsNMe_2 *with* Et_2AsNEt_2, Me_2AsNEt_2 *with* Et_2AsNMe_2, *and* $Me_2AsAsMe_2$ *with* $Et_2AsAsEt_2$

Equimolar amounts (1.0 mmol) of the reactants dissolved in toluene-d_8 were mixed to give a total solution volume of 3.0 cm^3 in an NMR tube at room temperature. The progress of the reaction mixture was monitored by ^1H and ^{13}C NMR spectroscopy until equilibrium was attained.

The following is a list of NMR spectral data (values in ppm) independently determined in our laboratory at room temperature in toluene-d_8 solution on synthesized compounds that are identified in the reaction mixture.

^1H *spectral data*

$Me_2AsAsMe_2$: 0.95 (MeAs). $Et_2AsAsEt_2$: 1.17 (CH_3CH_2As, t, $^3J_{HH} = 7.7$ Hz), and 1.56 (CH_3CH_2As, m). $Me_2AsAsEt_2$: 1.02 (MeAs), 1.16 (CH_3CH_2As, t, $^3J_{HH} = 7.7$ Hz), and 1.53 (CH_3CH_2As, m). Me_2AsNMe_2: 0.82 (MeAs), and 2.43 (MeN). Me_2AsNEt_2: 0.87 (MeAs), 0.99 (CH_3CH_2N, t, $^3J_{HH} = 7.0$ Hz), and 2.81 (CH_3CH_2N, q). Et_2AsNEt_2: 1.00 (CH_3CH_2N, t, $^3J_{HH} = 7.1$ Hz), 2.88 (CH_3CH_2N, q), and 1.04–1.50 (Et_2As, m). Et_2AsNMe_2: 1.02–1.54 (Et_2As, m), and 2.56 (MeN).

^{13}C *spectral data*

$Me_2AsAsMe_2$: 5.96 (MeAs, $^1J_{CH} = 132.6$ Hz). $Et_2AsAsEt_2$: 12.78 (CH_3CH_2As, $^1J_{CH} = 125.8$ Hz), and 14.81 (CH_3CH_2As, $^1J_{CH} = 132.4$ Hz). $Me_2AsAsEt_2$: 6.16 (MeAs, $^1J_{CH} = 132.7$ Hz), 12.61 (CH_3CH_2As, $^1J_{CH} = 125.6$ Hz), and 15.28 (CH_3CH_2As, $^1J_{CH} = 132.3$ Hz). Me_2AsNMe_2: 9.92 (MeAs, $^1J_{CH} = 130.6$ Hz), and 41.91 (MeN, $^1J_{CH} = 132.7$ Hz). Me_2AsNEt_2: 12.12 (MeAs, $^1J_{CH} = 130.3$ Hz), 15.73 (CH_3CH_2N, $^1J_{CH} = 125.1$ Hz), and 44.31 (CH_3CH_2N, $^1J_{CH} = 132.2$ Hz). Et_2AsNEt_2: 10.44 (CH_3CH_2As, $^1J_{CH} = 126.4$ Hz), 20.92 (CH_3CH_2As, $^1J_{CH} = 130.6$ Hz), 16.32 (CH_3CH_2N, $^1J_{CH} = 124.9$ Hz), and 44.88 (CH_3CH_2N, $^1J_{CH} = 132.2$ Hz). Et_2AsNMe_2: 10.38 (CH_3CH_2As, $^1J_{CH} = 126.6$ Hz), 19.59 (CH_3CH_2As, $^1J_{CH} = 130.6$ Hz), and 42.61 (MeN, $^1J_{CH} = 132.6$ Hz).

RESULTS AND DISCUSSION

Reaction of Me_2AsNR_2 *with* $Et_2AsAsEt_2$ (R = Me *or* Et)

The ^1H and ^{13}C NMR spectra of a 1:1 mole ratio of Me_2AsNR_2 and $Et_2AsAsEt_2$ in toluene-d_8 solution showed no reaction had occurred at −60°C. As the temperature was raised to 24°C, a reaction occurred to give a mixture of $Me_2AsAsEt_2$, $Me_2AsAsMe_2$, $Et_2AsAsEt_2$, Et_2AsNR_2 and Me_2AsNR_2. Equilibrium was reached within 1 h. No temperature effect was noted on the equilibrium

when the mixture was monitored at 50°C (15 days), 75°C (13 days) and then again at 24°C (10 days). The ^{1}H NMR intensity data gave the following percent distributions at equilibrium for the indicated Me_2AsNR_2–$Et_2AsAsEt_2$ systems: Me_2AsNMe_2–$Et_2AsAsEt_2$ system = 31% $Me_2AsAsEt_2$, 6% $Me_2AsAsMe_2$, 30% Et_2AsNMe_2, 19% Me_2AsNMe_2, and 14% $Et_2AsAsEt_2$; Me_2AsNEt_2–$Et_2AsAsEt_2$ system = 32% $Me_2AsAsEt_2$, 5% $Me_2AsAsMe_2$, 31% Et_2AsNEt_2, 19% Me_2AsNEt_2, and 13% $Et_2AsAsEt_2$.

These results indicate that Me_2AsNR_2 readily reacts with $Et_2AsAsEt_2$ to give the unsymmetrical $Me_2AsAsEt_2$ and Et_2AsNR_2 [eqn (1)]:

$$Me_2AsNR_2 + Et_2AsAsEt_2 \rightleftarrows Me_2AsAsEt_2 + Et_2AsNR_2. \quad (1)$$

The unsymmetrical diarsine, $Me_2AsAsEt_2$, then undergoes symmetrization [eqn (2)]:[22]

$$2Me_2AsAsEt_2 \rightleftarrows Me_2AsAsMe_2 + Et_2AsAsEt_2. \quad (2)$$

This reaction is very facile, with equilibrium being reached within 30 min. Interestingly, the distribution of diarsines is independent of temperature (see discussion below).

Owing to the lability of the As—As and As—N bonds, $Me_2AsAsMe_2$ then reacts with Et_2AsNR_2 according to eqn (3) (see discussion below):

$$Me_2AsAsMe_2 + Et_2AsNR_2 \rightarrow Me_2AsAsEt_2 + Me_2AsNR_2. \quad (3)$$

All other reactions involving the very labile As—N and As—As bonds undoubtedly occur in solution. For example, $Me_2AsAsMe_2$ in eqn (2) would be expected to react with Me_2AsNR_2 [eqn (1)]. However, due to the indistinguishability of reactants and products in these other systems, they could not be studied independently using our NMR techniques.

Since establishment of equilibrium is so fast at 24°C, rate data were collected at −10°C. These data indicate that substitution of an Et for a Me group in the amino moiety of Me_2AsNR_2 does not affect the final equilibrium distribution of species in the reaction mixture. However, the graphs of % Et_2AsNR_2 produced with respect to Me_2AsNR_2 vs time for the Me_2AsNR_2–$Et_2AsAsEt_2$ system [Fig. 1(A)] indicate that substitution of an Et for a Me group in Me_2AsNR_2 does affect the rate of reaction. The Me_2AsNMe_2–$Et_2AsAsEt_2$ reaction is slower than the Me_2AsNEt_2—$EtAsAsEt_2$ reaction. Since these reactions appear to proceed through formation of a concerted four-centered activated intermediate,[26,27] these data suggest that substitution of an Et for a Me group lowers the energy barrier for As—N bond dissociation and leads to a faster reaction.

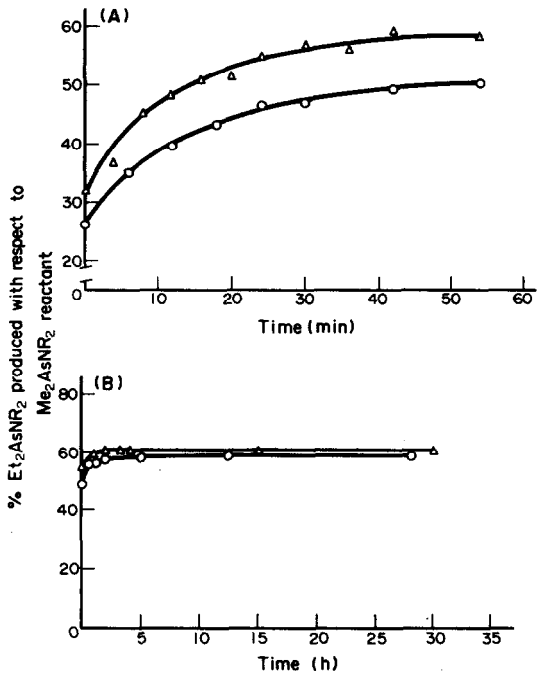

Fig. 1. Percentage of Et_2AsNR_2 formed as a function of time: (A) at −10°C, (B) at 24°C. (△) $Et_2AsAsEt_2$–Me_2AsNEt_2 system, (○) $Et_2AsAsEt_2$–Me_2AsNMe_2 system.

Reaction of Et_2AsNR_2 *with* $Me_2AsAsMe_2$ (R = Me *or* Et)

The ^{1}H and ^{13}C NMR spectra of an equimolar mixture of Et_2AsNR_2 and $Me_2AsAsMe_2$ in toluene-d_8 solution also indicated no reaction at −60°C. At 24°C, resonances assignable to $Me_2AsAsEt_2$, $Et_2AsAsEt_2$, $Me_2AsAsMe_2$, Et_2AsNR_2 and Me_2AsNR_2 were observed. Equilibrium was attained in 29 h for the Et_2AsNMe_2–$Me_2AsAsMe_2$ system and in 6 h for the Et_2AsNEt_2–$Me_2AsAsMe_2$ system. No effect of temperature on the equilibrium was noted when the reaction mixtures were monitored at 50, 75 and then again at 24°C. The ^{1}H NMR intensity data gave the following percent distributions at equilibrium for the indicated Et_2AsNR_2–$Me_2AsAsMe_2$ systems. Et_2AsNMe_2–$Me_2AsAsMe_2$ system: 26% $Me_2AsAsEt_2$, 7% $Et_2AsAsEt_2$, 35% Me_2AsNMe_2, 14% Et_2AsNMe_2, and 18% $Me_2AsAsMe_2$; Et_2AsNEt_2–$Me_2AsAsMe_2$ system: 24% $Me_2AsAsEt_2$, 6% $Et_2AsAsEt_2$, 35% Me_2AsNEt_2, 15% Et_2AsNEt_2, and 20% $Me_2AsAsMe_2$.

These results suggest that Et_2AsNR_2 readily reacts with $Me_2AsAsMe_2$ to yield $Me_2AsAsEt_2$ and Me_2AsNR_2 [eqn (3)]. This reaction, in comparison to that represented by eqn (1), appears to be irreversible, since the reaction of $Me_2AsAsEt_2$ with Me_2AsNR_2 gives indistinguishable reactants and products. $Me_2AsAsEt_2$ undergoes symmetrization via eqn (2) and can also react with Et_2AsNR_2 according to eqn (4):

$$Me_2AsAsEt_2 + Et_2AsNR_2 \rightleftarrows Me_2AsNR_2 + Et_2AsAsEt_2. \quad (4)$$

The $Et_2AsAsEt_2$ produced from the reactions described by eqns (2) and (4) further reacts with the Me_2AsNR_2 [see eqn (1)] formed during the reaction described by eqn (3). Because of the lability of the As—N and As—As bonds, several other reactions involving $\rangle AsAs\langle - \rangle AsAs\langle$,[22] $\rangle AsAs\langle - \rangle AsN\langle$ and $\rangle AsN\langle - \rangle AsN\langle$ systems undoubtedly occur in solution. Due to the indistinguishability of reactants and products in these other systems, they could not be studied independently using our NMR techniques.

The graph of % Me_2AsNR_2 produced with respect to Et_2AsNR_2 vs time for the Et_2AsNR_2–$Me_2AsAsMe_2$ system (Fig. 2) also suggests that substitution of an Et for a Me group in the amino moiety of Et_2AsNR_2 has no effect on the final equilibrium distribution of species. However, the rate of the Et_2AsNEt_2–$Me_2AsAsMe_2$ reaction is much faster than that of the Et_2AsNMe_2–$Me_2AsAsMe_2$ reaction. Also, in this case, substitution of an Et for a Me group appears to lower the energy barrier for As—N bond dissociation.

A comparison of Figs 1(B) and 2 indicates that the rate of reaction for the $Et_2AsAsEt_2$–Me_2AsNR_2 systems is considerably greater than for the analogous $Me_2AsAsMe_2$–Et_2AsNR_2 systems. Thus substitution of an Et for a Me group in the diarsines has a greater influence on the reaction rates than does the substitution in the aminoarsines. This probably is due to the lower As—As bond strength[28] in $Et_2AsAsEt_2$ relative to that in $Me_2AsAsMe_2$, which should lower the energy barrier to As—As bond dissociation in the four-centered intermediate.

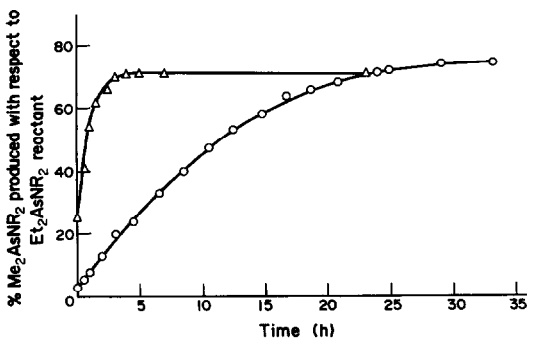

Fig. 2. Percentage of Me_2AsNR_2 formed as a function of time at 24°C: (○) $Me_2AsAsMe_2$–Et_2AsNMe_2 system, (Δ) $Me_2AsAsMe_2$–Et_2AsNEt_2 system.

Reactions of Me_2AsNMe_2 *with* Et_2AsNEt_2, *and of* Me_2AsNEt_2 *with* Et_2AsNMe_2

In both the Me_2AsNR_2–$Et_2AsAsEt_2$ and the Et_2AsNR_2–$Me_2AsAsMe_2$ systems described above, Me_2AsNR_2 and Et_2AsNR_2 are simultaneously present in solution as reactant and/or product. Because the products and the reactants from an exchange reaction represented by eqn (5):

$$Me_2AsNR_2 + Et_2AsNR_2 \rightleftarrows Me_2AsNR_2 + Et_2AsNR_2 \quad (5)$$

are indistinguishable, we could not study this reaction using available NMR techniques. Instead, we established the occurrence of such an exchange by reacting Me_2AsNMe_2 with Et_2AsNEt_2. Within 15 h of mixing a 1:1 stoichiometric ratio of the reactants at 24°C, the ^1H NMR spectrum indicated establishment of an equilibrium to give a mixture containing 24% each of the Me_2AsNEt_2 and Et_2AsNMe_2, and 26% each of Me_2AsNMe_2 and Et_2AsNEt_2:

$$Me_2AsNMe_2 + Et_2AsNEt_2 \rightleftarrows Me_2AsNEt_2 + Et_2AsNMe_2. \quad (6)$$

The calculated equilibrium constant for the reaction represented by eqn (6) is 0.90. The reversibility of this reaction was substantiated by reacting Me_2AsNEt_2 with Et_2AsNMe_2, forming Et_2AsNEt_2 and Me_2AsNMe_2. The calculated equilibrium constant for this reaction is 1.1 at 24°C. These exchange reactions have a low enthalpy of reaction, as evidenced by our findings that the equilibrium constants are invariant with temperature within experimental measurement.

Reaction of $Me_2AsAsMe_2$ *with* $Et_2AsAsEt_2$

The ^1H spectra of a 1:1 mole ratio of $Me_2AsAsMe_2$ and $Et_2AsAsEt_2$ in toluene-d_8 were obtained at 24 and 50°C. The spectra indicate a rapid exchange reaction. The relative concentration of parent and mixed compounds was determined from the integration of the ^1H signals. An equilibrium constant of 1.0 was obtained at each tem-

perature by using the following expression:

$$K = \frac{[Et_2AsAsMe_2]^2}{[Me_4As_2][Et_4As_2]}.$$

These data are consistent with those reported for exchange reactions involving P—As and As—Sb systems. Equilibrium constants of 0.26 and 0.37 were obtained for the Me_2PPMe_2–$Me_2AsAsMe_2$[4] and Ph_2PPPh_2–$Ph_2AsAsPh_2$[3] systems, respectively, in benzene-d_6. In the Ph_2PPPh_2–$Ph_2AsAsPh_2$ system, ΔH^o was very low ($+1.3 \pm 0.3$ kcal mol^{-1}) with a positive entropy contribution ($\Delta S^o = +3.5 \pm 1.0$ eu) and the reaction was rather fast. An equilibrium constant of 0.9 was obtained for the $Me_2SbSbMe_2$–$Me_2AsAsMe_2$ system.[4]

The results of our current study indicate that reactions between As—As- and As—N-bonded compounds occur readily. For the systems studied, the overall reactions involve numerous competing equilibria that are very facile. Preliminary investigations of analogous reactions involving P—P- and As—N-bonded compounds indicate high reactivity, while those involving As—As- and P—N-bonded compounds indicate no reactivity. The reaction of Et_2PPEt_2 and Me_2AsNMe_2 goes to completion within 30 min to yield Et_2PAsMe_2 and Et_2PNMe_2 in solution. Et_2PAsMe_2 then undergoes a slow exchange to give an equilibrium mixture of Et_2PAsMe_2, Et_2PPEt_2 and $Me_2AsAsMe_2$. The 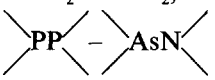 systems are currently being studied to obtain kinetic and thermodynamic data, and to relate these data with those obtained from the 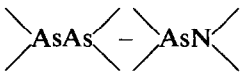 systems.

REFERENCES

1. H. H. Sisler, In *Inorganic Reactions and Methods* (Edited by J. J. Zuckerman), Vol. 7 (and references therein). VCH Publishers, Deerfield Beach, FL (in press).
2. L. K. Krannich, In *Inorganic Reactions and Methods* (Edited by J. J. Zuckerman), Vol. 7 (and references therein). VCH Publishers, Deerfield Beach, FL (in press).
3. A. Belforte, F. Calderazzo, A. Morvillo, G. Pelizzi and D. Vitali, *Inorg. Chem.* 1984, **23**, 1504.
4. A. J. Ashe III and E. G. Ludwig, Jr, *J. Organomet. Chem.* 1986, **303**, 197.
5. H. W. Roesky, J. Lucas, M. Noltemeyer and G. M. Sheldrick, *Chem. Ber.* 1984, **117**, 1583.
6. H. R. O'Neal and R. H. Neilson, *Inorg. Chem.* 1984, **23**, 1372.
7. R. R. Ford, M. A. Goodman, R. H. Neilson, A. K. Roy, U. G. Wettermark and P. Wisian-Neilson, *Inorg. Chem.* 1984, **23**, 2063.
8. D. W. Morton and R. H. Neilson, *Organometallics* 1982, **1**, 289.
9. O. Adler and F. Kober, *J. Organomet. Chem.* 1974, **72**, 351.
10. D. H. Brown, K. D. Crosbie, G. W. Fraser and D. W. A. Sharp, *J. Chem. Soc. A* 1969, 551.
11. A. B. Burg and P. J. Slota, Jr., *J. Am. Chem. Soc.* 1958, **80**, 1107.
12. A. H. Cowley and R. A. Kemp, *Inorg. Chem.* 1983, **22**, 547.
13. A. B. Burg, *J. Am. Chem. Soc.* 1961, **83**, 2226.
14. L. K. Krannich, In *Compounds Containing* As—N *Bonds* (Edited by H. H. Sisler), Vol. 5. Benchmark Papers in Inorganic Chemistry, Dowden Hutchinson & Ross, Stroudsburg, PA (1976).
15. F. Kober, *Z. Anorg. Allg. Chem.* 1973, **400**, 285.
16. O. Adler and F. Kober, *Chem. Ztg.* 1976, **100**, 235.
17. F. Kober, *Z. Anorg. Allg. Chem.* 1973, **398**, 115.
18. F. Kober, *Z. Anorg. Allg. Chem.* 1973, **397**, 97.
19. A. Tzschach and W. Lange, *Z. Anorg. Allg. Chem.* 1964, **326**, 280.
20. A. H. Cowley, *Polyhedron* 1984, **3**, 389.
21. E. Fluck, *Top. Phosphorus Chem.* 1980, **10**, 193.
22. V. K. Gupta, L. K. Krannich and C. L. Watkins, *Inorg. Chem.* 1986, **25**, 2553.
23. V. K. Gupta, L. K. Krannich and C. L. Watkins, *Inorg. Chim. Acta* 1987, **126**, 173.
24. K. Moedritzer, *Chem. Ber.* 1959, **92**, 2637.
25. R. W. Bunsen, *Annalen* 1842, **42**, 14.
26. A. L. Rheingold, J. E. Lewis and J. M. Bellama, *Inorg. Chem.* 1973, **12**, 2845.
27. J. C. Lockhart, *Redistribution Reactions*, p. 158. Academic Press, New York (1970).
28. G. M. Bogolyubov, N. N. Grishin and A. A. Petrov, *J. Gen. Chem. U.S.S.R.* (Engl. Transl.) 1971, **41**, 1717.

Polyhedron Vol. 6, No. 6, pp. 1235–1238, 1987
Printed in Great Britain

0277–5387/87 $3.00+.00

TRANSITION-METAL COMPLEXES WITH DEHYDROACETIC ACID: CRYSTAL STRUCTURE OF BIS(3 - ACETYL - 4 - HYDROXY - 6 - METHYL - 2 - PYRONE)COBALT(II) BIS(DIMETHYLFORMAMIDE)

J. CASABÓ,* J. MARQUET, M. MORENO-MAÑAS, M. PRIOR and F. TEIXIDOR

Department of Chemistry, Universitat Autonoma de Barcelona, Bellaterra, 08193 Barcelona, Spain

and

F. FLORENCIO, S. MARTÍNEZ-CARRERA and S. GARCÍA-BLANCO

Instituto de Química Física "ROCASOLANO" (C.S.I.C.), Serrano 119, 28006 Madrid, Spain

(*Received* 10 *June* 1986; *accepted after revision* 4 *November* 1986)

Abstract—Co(II), Ni(II), Cu(II) and Cr(III) complexes with monoprotic dehydroacetic acid (3 - acetyl - 4 - hydroxy - 6 - methyl - 2 - pyrone) are described. The Co, Ni and Cu compounds present 1 : 2 metal : ligand ratios and the Cr compound a 1 : 3 ratio. All of these compounds are soluble in dimethylformamide and formed adducts with this solvent. One of these solvates, bis(3 - acetyl - 4 - hydroxy - 6 - methyl - 2 - pyrone)cobalt(II) bis(dimethylformamide), afforded crystals suitable for X-ray diffraction analysis, and its crystalline and molecular structures are reported. The crystals are triclinic, space group $P\bar{1}$, with $a = 8.290(1)$, $b = 9.570(2)$, $c = 7.731(1)$ Å, $\alpha = 94.16(2)$, $\beta = 101.52(2)$, $\gamma = 85.15(2)°$, $V = 597.9(2)$ Å^3, $Z = 1$. Least-squares refinement of the structure based on 3088 observations led to final discrepancy indices of $R = 0.075$ and $R_w = 0.049$. The Co atoms lies on a inversion center having distorted octahedral coordination through four O atoms of two 3 - acetyl - 4 - hydroxy - 6 - methyl - 2 - pyrone groups and two O atoms of two dimethylformamide molecules. The 3 - acetyl - 4 - hydroxy - 6 - methyl - 2 - pyrone group is practically planar.

Dehydroacetic acid (3 - acetyl - 4 - hydroxy - 6 - methyl - 2 - pyrone) (**Ia**) is an industrially available product used as a fungicide, a bactericide and also as an important intermediate in organic synthesis. However, little is known on its metal complexes. The Cu and Zn complexes have been reported to be, respectively, a fungicide[1] and a heat stabilizer for vinyl chloride resins.[2] There are some other reports in the patent literature,[3] and also the stability constants of some complexes have been measured.[4,5]

Some of us,[6,7] have described the use of the Co(II) complex (**Ib**) as a substrate to achieve one of the few reactions known to occur at C5 in the dehydroacetic acid. However, nothing was known about **Ib** apart from the most simple spectroscopic characteristics. Therefore, it was considered that a structural study of **Ib** and its congeners **Ic–e**, also prepared for synthetic purposes, could be of interest.

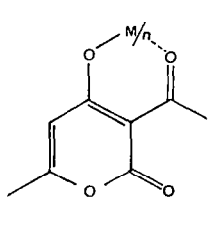

Ia M = H, $n = 1$
Ib M = Co, $n = 2$
Ic M = Ni $n = 2$
Id M = Cu, $n = 2$
Ie M = Cr, $n = 3$

As far as we know the most related molecule studied by X-ray diffraction is the Ni(II) dehydroacetic acid monoimide complex.[8]

*Author to whom correspondence should be addressed.

EXPERIMENTAL

Synthesis of the complexes

Co(II) *complex*. Co(II) chloride hexahydrate (2.3 g, 9.7 mmol) in water (15 cm^3) was added under stirring to a mixture of dehydroacetic acid (3.27 g, 19.4 mmol) in acetone (40 cm^3) and sodium acetate trihydrate (2.63 g, 19.4 mmol) in water (15 cm^3). The stirring was continued for 1 h, after which the solid pink purple precipitate was filtered, washed with water and acetone, mixed with toluene, and evaporated again to afford 3.5 g of the complex. Found: C, 48.9; H, 3.5. Calc. for $C_{16}H_{14}O_8Co$: C, 48.9; H, 3.6%.

Co(II) complex-dimethylformamide solvate. Crystals suitable for X-ray diffraction with formula $C_{16}H_{14}O_8Co \cdot 2$ dmf were obtained by slow diffusion of ethanol in a dmf solution of the aforementioned Co(II) complex.

Cu(II) *complex*. A mixture of copper acetate monohydrate (3.15 g, 16.0 mmol) and sodium acetate trihydrate (4.35 g, 32 mmol) in water (20 cm^3) was added dropwise with stirring to a solution of dehydroacetic acid (5.50 g, 32 mmol) in acetone (80 cm^3). The blue precipitate formed was filtered, washed with water and acetone, and dried to afford 3.97 g of the complex. Yield 65%, m.p. 322°C. Found: C, 48.3; H, 3.6. Calc. for $C_{16}H_{14}O_8Cu$: C, 48.3; H, 3.6%.

Ni(II) *complex*. A mixture of nickel chloride hexahydrate (10.58 g, 45 mmol) and sodium acetate trihydrate (12.11 g, 89 mmol) in water (90 cm^3) was added dropwise with stirring to a solution of dehydroacetic acid (15.0 g, 89 mmol) in acetone (250 cm^3). The stirring was maintained for 1 h, and the green precipitate filtered, washed with water and acetone, and dried to afford 14.1 g of the complex. Yield 72%, m.p. 190°C. Found C, 44.3; H, 4.4. Calc. for $C_{16}H_{14}O_8Ni \cdot 2H_2O$: C, 44.8; H, 4.2%.

Cr(III) *complex*. A mixture of urea (20.0 g, 0.33 mol), chromium trichloride hexahydrate (3.0 g, 11 mmol), dehydroacetic acid (4.54 g, 27 mmol), water (50 cm^3), and acetone (100 cm^3) was refluxed for 20 h. The mixture was then cooled at room temperature and poured into water (100 cm^3). The formed precipitate was filtered, washed with water and acetone, and dried to afford 2.5 g of the complex. Yield 41%, m.p. 172–174°C. Found C, 52.3; H, 4.1. Calc. for $C_{24}H_{21}O_{12}Cr$: C, 52.1; H, 3.8%.

X-ray structure determination

A prismatic crystal of 0.2 × 0.2 × 0.3 mm was used to determine the cell parameters on a Nonius CAD-4 four-circle diffractometer. Intensity data were collected using the same diffractometer from the same crystal with graphite monochromated Mo-K_α radiation for $2 \leqslant \theta \leqslant 30°$ and the ω–2θ scan technique. Two reflections were used as standard and remeasured every 100 reflections. No decomposition was observed. Of the 3485 independent reflections measured, 3088 were considered as observed with $I > 2\sigma(I)$, σ being determined from counting statistics. Lorentz and polarization corrections were applied but no correction was made for absorption.

The structure was solved by direct methods with MULTAN 80[9] program and subsequent difference Fourier synthesis.

Further least-squares refinements, first with isotropic and later with anisotropic temperature factor coefficients for non-H atoms and isotropic for H atoms (located on a difference Fourier synthesis) reduced R to 0.075 and R_w to 0.049.

The final-difference Fourier map had all residual peaks less than 0.15 e $Å^{-3}$. Figure 1 shows a view of the molecule and Co octahedron. The final bond lengths and bond angles involving the non-H atoms are given in Table 1. Atomic positional parameters and thermal coefficients and lists of F_o/F_c values have been deposited as supplementary material with the Editor from which copies are available on request. Atomic coordinates have also been deposited with the Cambridge Crystallographic Data Centre.

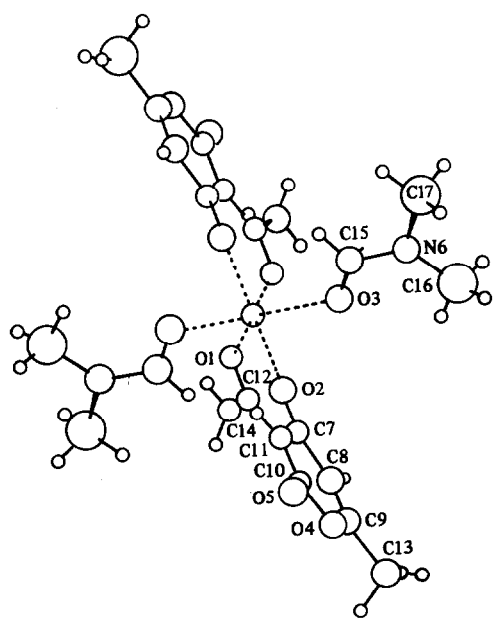

Fig. 1. Molecular structure of bis(3 - acetyl - 4 - hydroxy - 6 - methyl - 2 - pyrone)cobalt(II) bis(dimethylformamide).

Table 1. Selected interatomic distances (Å) and bond angles (°)

Co—O1	2.027(2)	Co—O2	2.002(2)
Co—O3	2.171(2)	O1—C12	1.249(3)
O2—C7	1.264(3)	O3—C15	1.230(4)
O4—C9	1.351(4)	O4—C10	1.405(4)
O5—C10	1.211(4)	N6—C15	1.325(4)
N6—C16	1.445(5)	N6—C17	1.452(5)
C7—C8	1.446(4)	C7—C11	1.431(4)
C8—C9	1.329(4)	C9—C13	1.487(5)
C10—C11	1.440(4)	C11—C12	1.442(4)
C12—C14	1.498(5)		
O2—Co—O3	91.48(9)	O1—Co—O3	91.90(9)
O1—Co—O2	85.53(8)	C9—O4—C10	122.5(2)
C16—N6—C17	117.3(3)	C15—N6—C17	121.2(3)
C15—N6—C16	121.5(3)	O2—C7—C11	125.4(3)
O2—C7—C8	117.0(2)	C8—C7—C11	117.6(2)
C7—C8—C9	121.3(3)	O4—C9—C8	121.7(3)
C8—C9—C13	126.3(3)	O4—C9—C13	112.0(3)
O4—C10—O5	113.2(3)	O5—C10—C11	129.1(3)
O4—C10—C11	117.7(3)	C7—C11—C10	119.2(2)
C10—C11—C12	118.9(2)	C7—C11—C12	121.9(2)
O1—C12—C11	122.7(3)	C11—C12—C14	122.7(3)
O1—C12—C14	114.6(3)	O3—C15—N6	124.3(3)

Weighted least-squares planes through the starred atoms

Plane: $-0.8770(6)X-0.400(1)Y-0.266(1)Z = -0.478(5)$

Atom	Des. (Å)	Atom	Des.	Atom	Des.
C7*	0.018(3)	Co	0.4779(9)	C12	−0.091(3)
C8*	−0.014(3)	O1	−0.020(2)	C13	−0.004(4)
C9*	−0.009(3)	O2	0.045(2)	C14	−0.318(5)
O4*	0.013(2)	O3	−1.553(2)	C15	−2.352(3)
C10*	−0.012(3)	O5	−0.009(3)	C16	−4.130(5)
C11*	−0.008(3)	N6	−3.593(3)	C17	−4.493(5)

The scattering factors were taken from *International Tables for X-ray Crystallography* (1974). The computation was made with programs of the X-ray 80 systems,[10] PARST[11] and PESOS[12] on a Vax 11/750 computer.

Physical measurements

Elemental analyses of the newly prepared complexes were performed in our microanalytical laboratory using a Perkin–Elmer 240 microanalyzer. IR spectra were recorded in a Beckman IR-20A spectrophotometer as KBr pellets. Magnetic measurements were made in a Faraday type equipment in the 300–77 K temperature range. The balance was calibrated with standard $Hg[Co(SCN)_4]$. Pascal tables were used for diamagnetic corrections but no attempts were made to introduce TIP corrections.

RESULTS AND DISCUSSION

Structural description of the Co(II) *complex*

The Co atom lies on a inversion center and it has a distorted octahedral coordination with O1 and O2 atoms in equatorial positions, and the O3 atom from the dimethylformamide molecule occupying the most electronegative elongated axial position (Fig. 1).

The Co—O3 distance [2.171(2) Å], is similar to the value of 2.161(3) Å suggested by Castiñeiras *et al.*,[13] but the Co—O1 [2.027(2) Å] and Co—O2 [2.002(2) Å] distances are shorter. However the dimensions are in good agreement with the value of the Co octahedron found by Florencio *et al.*[14] in a Co(II) benzenesulphonate–ethanol complex and in hexahydrated Co(II) benzenesulphonate.

The asymmetric molecular group forms a planar

six-membered ring. All the exocyclic atoms are practically situated in the same plane (Table 1). The Co atom is situated out of this plane by 0.4779 Å. C8—C9 [1.329(4) Å] has a double-bond character and the other molecule bonds display a conjugation effect. The dimethylformamide molecule shows a normal geometry.

Magnetic and spectroscopic properties

All these compounds are very insoluble in the common solvents but they are slightly soluble in dimethylformamide. From this solvent it is possible to isolate different solvates as in the case of the Co complex. The coordination about the Co(II) ion is octahedral in the disolvated complex as shown by X-ray diffraction, but the geometry for the non-solvated compound is not obvious. Magnetic measurements down to liquid-nitrogen temperature gave us evidence for a tetrahedral coordination in this compound.

The complex follows the Curie–Weiss law in the temperature range tested. The plot of the inverse of the magnetic susceptibility vs temperature is a straight line with a very good approximation (correlation coefficient = 0.9996, slope = 0.337, intercept with the X-axis = -7.2 K).

The magnetic moments are temperature-independent in the range 300–77 K, and their average value is 4.77 BM. This value is characteristic for tetrahedral Co(II) complexes[15] with no orbital contribution in the $^4A_2$ ground state. The g value for the Co(II) ion calculated from the Curie constant assuming a spin value of $\frac{3}{2}$ is 2.5. The negative value of the Weiss constant (θ) could be explained assuming intermolecular antiferromagnetic interactions in the crystalline structure. Orbital contributions to the ground state through the mixing in the $^4T_2$-state by a second-order spin–orbit coupling perturbation or effects due to zero field splitting could also contribute to the θ constant.

Magnetic measurements at room temperature of the other compounds also give information for the geometries about the Ni(II), Cu(II) and Cr(III) ions. The dihydrated Ni compound exhibits a magnetic moment of 3.2 BM, which is characteristic for Ni(II) octahedral complexes, and a similar structure to that found in the Co(II) complex should be assumed. The Cu compound has a magnetic moment of 1.8 BM at room temperature and its coordination geometry could be tetrahedral. On the other hand, the Cr compound is a 1 : 3 complex and its magnetic moment is 3.5 BM, so that an octahedral coordination should be expected.

IR spectra show the coordination of the dehydroacetic acid through the hydroxylic and carbonylic groups. The frequency of the C=O band decreases in the complexes with respect to the free ligand (**Ia**, 1750 cm^{-1}; **Ib**, 1680 cm^{-1}; **Ic**, 1680 cm^{-1}; **Id**, 1700 cm^{-1}; **Ie**, 1715 cm^{-1}).

Acknowledgement—Financial support from C.A.I.C.Y.T. (Ministerio de Educacion y Ciencia of Spain) through research project No. 2014/83 is gratefully acknowledged.

REFERENCES

1. G. Scheuer and H. Pommer, Ger. 1,224,088; *C. A.* 1966, **65**, PC14361.
2. I. Akiba, M. Minagawa and T. Emori, Japan Kokai 76 34,939; *C. A.* 1976, **85**, P47606x.
3. F. H. Norton, U.S. 3,076,834; *C. A.* 1963, **59**, P2719.
4. S. Goto, *Zakugaku Zasshi* 1962, **82**, 26.
5. K. Kadian, I. Singh, B. S. Garg and R. P. Singh, *J. Indian Chem. Soc.* 1983, **60**, 331.
6. J. Marquet and M. Moreno-Mañas, *Chem. Lett.* 1981, 173.
7. P. de March, J. Marquet, M. Moreno-Mañas, R. Pleixats, J. Ripoll and A. Trius, *An. Quim.* 1983, **79C**, 15.
8. S. Kiryu, *Acta Cryst.* 1967, **23**, 392.
9. P. Main, S. J. Fiske, S. El. Hull, L. Lessinger, G. Germain, M. M. Woolfson and J. P. Declerk, *MULTAN 80. A System of Computer Programs for the Automatic Resolution of Crystal Structures from X-ray Diffraction Data.* University of York, U.K., and University of Louvain, Belgium (1980).
10. J. M. Stewart, F. A. Kundell and J. C. Baldwin, *The XRAY 80 system.* Computer Program. Computer Science Center, University of Maryland, College Park, MD (1980).
11. M. Nardelli, *PARST.* Instituto de Chimica Generale, University of Parma, Italy (1980).
12. M. Martinez-Ripoll and F. H. Cano, *PESOS, A Weighting Schemas.* Instituto Rocasolano, CSIC, Madrid, Spain (1975).
13. A. Castiñeiras, W. Hiller, J. Strahle, M. V. Paredes and J. Sordo, *Acta. Cryst.* 1985, **C41**, 41.
14. F. Florencio, S. Martinez-Carrera and S. Garcia-Blanco, private communication.

Polyhedron Vol. 6, No. 6, pp. 1239–1241, 1987
Printed in Great Britain

0277–5387/87 $3.00+.00

NEW PATHWAY TO TRIAMMINE COMPLEXES OF CHROMIUM(III): CRYSTAL STRUCTURE OF 1-CHLORO-2,3-DIAQUO-4,5,6-TRIAMMINECHROMIUM(III) CHLORIDE

J. PONS and J. CASABÓ*

Departament de Química (Unitat de Química Inorgánica), Institut de Ciencia de Materials (C.S.I.C.), Universitat Autonoma de Barcelona, Bellaterra, Barcelona, Spain

and

X. SOLANS and M. FONT ALTABA

Department of Crystallography, Universitat de Barcelona, Barcelona, Spain

(*Received* 15 *July* 1986; *accepted after revision* 4 *November* 1986)

Abstract—A new synthetic method to triammine complexes of Cr(III) is reported, via a hydrolytic process from tetrammine complexes. The crystal and molecular structure of 1 - chloro - 2,3 - diaquo - 4,5,6 - triamminchromium(III) chloride are described. The crystals are orthorombic, space group *Pnma*, with $a = 13.230(2)$, $b = 10.545(1)$, $c = 6.754(1)$ Å, $V = 942.3(3)$, $Z = 4$. Least-squares refinement of the structure based on 529 observations led to final discrepancy indices of $R = 0.047$ and $R_w = 0.056$. The Cr atom is bonded to two water molecules, three ammonia molecules and one chlorine atom in a distorted octahedral coordination showing a *trans* chloro–aquo configuration.

While the hexaamine, pentammine and tetrammine complexes of Cr(III) are very well known in their synthetic, structural and reactivity aspects, the chemistry of the triammine species are not so well documented.

Four types of triammine complexes are known: triaquo complexes, $[Cr(NH_3)_3(H_2O)_3]X_3$; monoacidodiaquo complexes, $[Cr(NH_3)_3(H_2O)_2X]X_2$; diacidoaquo complexes, $[Cr(NH_3)_3(H_2O)X_2]X$; and triacido complexes, $[Cr(NH_3)_3X_3]$.[1]

The classical synthetic pathway to triammine complexes starts with the peroxo Cr(IV) species $[Cr(NH_3)_3(O_2)_2]$.[2] This compound affords different triammine Cr(III) complexes by hydrolytic decomposition, depending on the experimental conditions.[1,2]

As part of our thermomagnetic research plan involving double complexed salts[3] we tried to synthesize *cis*-$[Cr(NH_3)_4(H_2O)_2][FeCl_6]$ by mixing a solution of *cis*-$[Cr(NH_3)_4(H_2O)_2](ClO_4)_3$ in water with a solution of $FeCl_3$ in concentrated HCl. After a few days well-formed red crystals appeared which were shown by analysis and spectrophotometric measurements to be a triammine complex of Cr(III).

There are no examples of triamminecomplexes of Cr(III) fully characterized, so we have undertaken its complete characterization by X-ray analysis. To the best of our knowledge this is the first crystal structure of a triammine complex of Cr(III) reported in the literature. Furthermore we think our synthetic method is an easier pathway to triammine complexes than those already reported.

EXPERIMENTAL

Preparation

$[Cr(NH_3)_3(H_2O)_2Cl]Cl_2$ was prepared by dissolving the compound *cis*-$[Cr(NH_3)_4(H_2O)_2](ClO_4)_3$ (1.5 g) in H_2O (10 cm^3). The solution was filtered, poured on hot concentrated HCl and left to stand at room temperature for 2 days in the

* Author to whom correspondence should be addressed.

dark. The red crystals which formed were filtered, washed with EtOH and dried.

A few crystals suitable for X-ray analysis were collected from the main portion of the product. Chemical analyses were in agreement with the formula proposed.

X-ray crystallography

$[Cr(NH_3)_3(H_2O)_2Cl]Cl_2$, $Mw = 245.5$, orthorhombic, $a = 13.230(2)$, $b = 10.545(1)$, $c = 6.754(1)$ Å, $V = 942.3(3)$ Å^3, *Pnma*, $D_x = 1.730$ g cm^{-3}, $Z = 4$, $F(000) = 500$, $\lambda(\text{Mo-}K_\alpha) = 0.71069$ Å, $\mu(\text{Mo-}K_\alpha) = 20.5$ cm^{-1}. Room temperature.

A red prismatic crystal ($0.07 \times 0.07 \times 0.12$ mm) was selected and mounted on a Philips PW-1100 four-circle diffractometer, and the unit-cell parameters were determined from 25 reflections and refined by least squares. Intensities were collected with graphite-monochromatized Mo-K_α radiation, using the ω-scan technique, (scan width 0.8°, scan speed 0.03 s^{-1}). 529 independent reflections were measured in the range $2 \leqslant \theta \leqslant 25$, 520 of which were assumed as observed by applying the condition $I > 2.5\sigma(I)$: three reflections were measured every 2 h as orientation and intensity control, no significant intensity decay was observed, and Lorentz-polarization corrections were made, but not absorption corrections.

The Cr atom was located from a Patterson synthesis, and the remaining non-hydrogen atoms from a weighted Fourier synthesis. The structure was isotropically and anisotropically refined by a full-matrix least-squares method using SHELX76.[4] The function minimized was $\Sigma w \|F_o| - |F_c\|^2$, where $w = [\sigma^2(F_o) + 0.0046|F_o|^2]^{-1}$. f, f' and f'' were taken from *International Tables of X-ray Crystallography*.[5] The final R factor was 0.047 ($R_w = 0.056$) for all observed reflections.

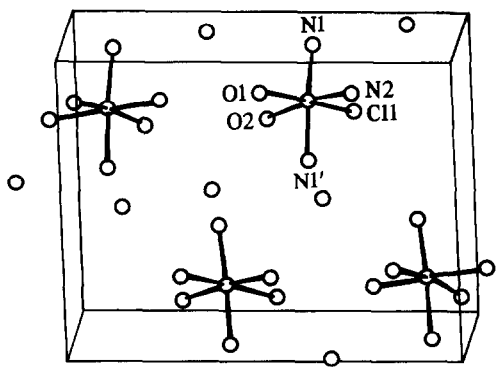

Fig. 1. Crystalline structure of $[Cr(H_2O)_2(NH_3)_3Cl]Cl_2$.

Table 1. Selected bond distances (Å) and angles (°) for $[Cr(H_2O)_2(NH_3)_3Cl]Cl_2$

Cl(1)—Cr	2.314(3)
N(1)—Cr	2.073(7)
N(2)—Cr	2.079(9)
O(1)—Cr	2.066(9)
O(2)—Cr	2.044(8)
N(1)—Cr—Cl(1)	91.2(2)
N(2)—Cr—Cl(1)	90.6(3)
N(2)—Cr—N(1)	89.5(2)
O(3)—Cr—Cl(1)	178.0(3)
O(1)—Cr—N(1)	88.8(2)
O(1)—Cr—N(2)	91.3(4)
O(2)—Cr—Cl(1)	90.5(3)
O(2)—Cr—N(1)	90.5(2)
O(2)—Cr—N(2)	178.9(3)
O(2)—Cr—O(1)	87.6(4)

A diagram of the crystal structure and the numbering scheme used is shown in Fig. 1. Bond distances and bond angles are given in Table 1. Tables of atomic coordinates, anisotropic thermal parameters and the observed and calculated structure factors have been deposited with the Editors. Atomic coordinates and thermal parameters have also been deposited with the Institut für Anorganische Chemie, Bonn, F.R.G.

Electronic spectra

Electronic spectra were recorded in aqueous solution on a Shimadzu UV-240 spectrophotometer.

RESULTS AND DISCUSSION

The structure consists of discrete ions. The Cr atom is bonded to two water molecules, three ammonia molecules and one chlorine atom in a distorted octahedral coordination polyhedron, showing a *mer* configuration (Fig. 1). The Cr, Cl1, O1, O2 and N2 atoms lie on the crystallographic plane, the N and N1′ atoms being located symmetrically with reference to this mirror plane, but not on the axis of the ideal octahedron; their projection is inside the Cr, N2, O1 triangle. The largest deviations from an ideal octahedron are in the N1—Cr—N1′ and O1—Cr—O2 bond angles. The Cr—N distances are essentially equal, bu Cr—O1, *trans* to one chlorine atom, is slightly larger than Cr—O2, *trans* to one nitrogen atom.

There is only one isomer for the complex having a *fac* configuration of the triammine moiety, but two isomers for the *mer* configuration. On the basis

of spectrophotometric and ion-exchange studies Caldwell and House[2] assigned a *mer* configuration to all triammine complexes discussed in their paper: $[Cr(NH_3)_3(H_2O)_3]Cl_3$, $[Cr(NH_3)_3(H_2O)_2Cl]Cl_2$ and $[Cr(NH_3)_3(H_2O)Cl_2]Cl$. In addition a *trans*-chloroaquo and *trans*-dichloro configuration were assigned for the second and third aforementioned complexes, respectively, all of them basically synthesized from the peroxo species $[Cr(NH_3)_3(O_2)_2]$. Our results confirm these predictions, although we have obtained the triammine complex by a very different method, via a hydrolytic process from a tetrammine complex.

Acknowledgement—This work was supported by "Comisión Asesora de Investigación Científica y Técnica" grant 360/82.

REFERENCES

1. C. S. Garner and D. A. House, *Coord. Chem. Rev.* 1969, **60**, 82.
2. S. H. Caldwell and D. A. House, *Inorg. Chem.* 1969, **8**, 151.
3. (a) R. L. Carlin, R. Burriel, J. Casabo and J. Pons, *Inorg. Chem.* 1981, **21**, 2905; (b) R. L. Carlin, R. Burriel, F. Pons and J. Casabo, *Inorg. Chem.* 1983, **22**, 2832; (c) R. Burriel, J. Casabo, J. Pons, D. W. Carnegie, Jr and R. L. Carlin, *Physica B* 1985, **123**, 185; (d) J. Bartolome, F. Lazaro, R. Burriel, J. Pons and J. Casabo, *J. Magn. Magn. Matter.* 1986, **54**, 1503.
4. G. M. Sheldrick, *Shelx: a Computer Program for Crystal Structure Determination.* University of Cambridge, U.K. (1976).
5. *International Tables for X-ray Crystallography* Vol. 3. Kynoch Press, Birmingham, U.K. (1962).

Polyhedron Vol. 6, No. 6, pp. 1243–1245, 1987
Printed in Great Britain

0277–5387/87 $3.00+.00

SYNTHESIS AND COMPLEXATION OF A NEW 1,1′-DISUBSTITUTED FERROCENE WITH TWO PENDANT CHELATING SITES OF AN α,β-UNSATURATED β-KETO AMINE SUBUNIT

MASAYOSHI ONISHI,* KATSUMA HIRAKI, SHUNJI WADA and YUSHICHIRO OHAMA

Department of Industrial Chemistry, Faculty of Engineering, Nagasaki University, Bunkyo-machi, Nagasaki 852, Japan

(*Received* 29 *July* 1986; *accepted* 4 *November* 1986)

Abstract—Condensation of 1,1′-bis(aminomethyl)ferrocene with acetylacetone gave 1,1′-bis(3 - methyl - 5 - oxo - 2 - aza - 3 - hexenyl)ferrocene in a 56% yield. In chloro-bridge splitting reactions of dinuclear cyclopalladated complexes of benzo[*h*]quinoline and *N*,*N*-dimethylbenzylamine, the condensed compound served as a binucleating ligand of an α,β-unsaturated β-keto aminate subunit. These new compounds formed were characterized by means of ^{1}H and ^{13}C NMR and IR spectroscopy. Their electrochemical properties were discussed also.

With the concept of using functionally substituted metallocenes as ligands in coordination compounds, a few ferrocenyl β-diketones were prepared, such as mono- and 1,1′-bis(benzoylacetyl)ferrocenes by Hauser and Cain[1] and (acetoacetyl)ferrocene by Imai and his coworkers,[2] and their coordination properties were examined towards some transition-metal ions. In this paper, we wish to report on the synthesis of a new 1,1′-disubstituted ferrocene with two pendant chelating sites of an α,β-unsaturated β-keto amine subunit, and its complexation as a bridging ligand between two metal centers.

RESULTS AND DISCUSSION

Condensation of 1,1′-bis(aminomethyl)ferrocene with acetylacetone† gave brown microcrystals of 1,1′ - bis(3 - methyl - 5 - oxo - 2 - aza - 3 - hexenyl)ferrocene (**I**) in a 56% yield. Although the solid material was stable in air, it decomposed slowly in halogenated organic solvents on exposure to air. In the mass spectrum of **I**, the parent ion was observed at *m*/*z* 408 in accordance with the proposed structure. The ^{1}H NMR spectrum in CD_2Cl_2 showed a broad singlet at δ *ca* 11.0 for the NH proton and a doublet ($^{3}J = 5.7$ Hz) at δ 4.14 for protons of the ferrocenyl-bonded methylene group on the nitrogen. In the ^{13}C NMR spectrum in CD_2Cl_2, there were signals at δ 194.8 and 162.5, assigned to the α,β-unsaturated carbonyl carbon (5-C) and the olefinic carbon (3-C) bonded to the nitrogen, respectively.‡ These findings indicated the α,β-unsaturated β-keto amine form of **I** in CD_2Cl_2, rather than the β-keto imine and β-imino enol ones. The indicated form was consistent with the IR data of **I** in CH_2Cl_2, showing bands at 1605, 1565, and 1510 cm^{-1}, and similar sets of IR bands were reported previously for some 4 - amino - 3 - penten - 2 - ones[4] with intramolecular hydrogen bonding.

A mixture of **I** and NaOEt in THF–EtOH was treated with chloro-bridged dinuclear cyclopalladated complexes prepared from benzo[*h*]quinoline[5] and *N*,*N*-dimethylbenzylamine,[6] affording complexes **II** and **III**, respectively, where compound **I** served as a binucleating bridging ligand via two pendant chelating sites of an α,β-unsaturated β-keto

* Author to whom correspondence should be addressed.

† Acetylacetone = 2,4-pentanedione.

‡ Carbonyl carbons in alkyl methyl ketones resonate at δ more than 200, whereas those in planar α,β-unsaturated ketones resonate usually at around δ 196. Olefinic carbons bonded to amines are expected to show signals in the *ca* δ 148–165 region.[3]

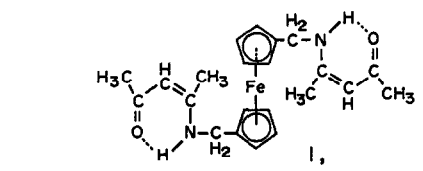

I,

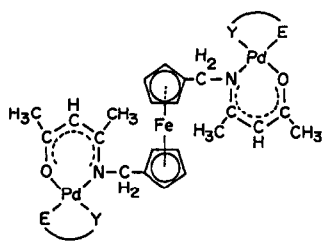

2,

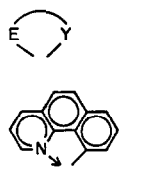

3,

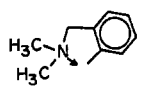

aminate subunit towards two palladium centers. As for **III**, an analytically pure sample was not isolated owing to contamination of **I** in less than a tenth molar amount of **III**. Some decomposition of **III** was observed in the attempt to purify the crude product by column chromatography on silica gel.

Upon complexation with palladium, the NH proton resonance disappeared and the proton signal of the methylene group on the nitrogen turned into a singlet. In addition, the ^{13}C NMR spectrum of **II** showed an up-field shift of the carbonyl carbon resonance by *ca* 16 ppm from that of the free ligand **I**, and the resonance of the methylene carbon on the nitrogen moved down-field by *ca* 14 ppm. These ^{13}C-resonance shifts were due to increased contribution of the β-imino enolate form on chelate complexation with palladium.

Electrochemical experiments using platinum working electrodes were performed with CH_3CN solutions of test compounds containing 0.1 M $(Et_4N)PF_6$ as a supporting electrolyte. The reference electrode was a platinum wire immersed in an CH_3CN solution of 0.01 M $[Fe(C_5H_5)_2]$ and $[Fe(C_5H_5)_2]PF_6$ besides the supporting electrolyte. In the cyclic voltammogram of **I**, we observed an electrochemically reversible redox couple at *ca* 75 mV with a diffusion-controlled one-electron transfer, and attributed it to the Fe(II) ⇄ Fe(III) process

Table 1. ^1H NMR data of **I**, **II** and **III**[a]

	3-Methyl-5-oxo-2-aza-3-hexenyl group					Cyclopentadienyl ring	
Compound	CH_3CN	CH_3CO	CH	CH_2	NH	2- and 5-H	3- and 4-H
I	1.95(s)	1.99(s)	5.00(s)	4.14(d, 5.7)	11.0(bs)	4.25(bs)	
II[b]	1.76(s)	1.97(s)	4.78(s)	5.01(s)	—	4.10(t, 1.0)	3.85(t, 1.0)
III[c]	1.82(s)	1.86(s)	4.75(s)	4.60(s)	—	4.1(m)	

[a] δ Value (ppm) from TMS, measured in CD_2Cl_2; signal shape and coupling constant in Hz are given in parentheses; abbreviations used: s = singlet, bs = broad singlet, d = doublet, t = triplet, m = multiplet.

[b] Benzo[*h*]quinolin-10-yl group, δ 9.05(d, 6), 8.18(d, 8), and 7.3–7.8 for 2-H, 4-H, and other aromatic protons, respectively.

[c] 2-(Dimethylaminomethyl)phenyl group, δ 2.60(s), 3.89 and 6.8–7.3 for CH_3N, CH_2N, and aromatic protons, respectively.

Table 2. ^{13}C NMR data of **I** and **II**[a]

	3-Methyl-5-oxo-2-aza-3-hexenyl group						Cyclopentadienyl ring	
Compound	1-C	3-C	4-C	5-C	6-C	CH_3 on 3-C	1-C	2- and 5-C 3- and 4-C
I	42.2	162.5	95.3	194.8	28.9	19.2	86.4	68.2, 69.3
II[b]	55.7	167.4	100.9	179.1	26.4	21.3	89.0	68.5, 69.4

[a] δ Value (ppm) from TMS. measured in CD_2Cl_2.

[b] Benzo[*h*]quinolin-10-yl group, δ 146.5 for 2-C, δ 136.9 for 4-C, and δ 155.7, 155.2, 142.3, 133.3 and 126.8 for quaternary carbons probably associated with 10b-C, 10-C, 10a-C, 6a-C and 4a-C, respectively.

in the ferrocenyl moiety. A similar redox couple was found at *ca* 20 mV for **II**, and showed the decrease in electron density at the Fe redox center upon complexation with palladium.

EXPERIMENTAL

General procedures and materials

^1H and ^{13}C NMR spectra were run on JEOL model MH-100 and FX-90-Q spectrometers with tetramethylsilane as an internal standard. IR spectra were obtained using a JASCO IRA-1 spectrometer. Melting points were determined on a Yanagimoto MP-S3 microstage apparatus in capillary tubes sealed *in vacuo*, and are uncorrected.

The hydrochloride salt of 1,1′-bis(aminomethyl)ferrocene[7] and chloro-bridged cyclopalladated complexes[5,6] were prepared according to the reported methods. All the experiments were performed under dry nitrogen.

Preparation of 1,1′ - *bis*(3 - *methyl* - 5 - *oxo* - 2 - *aza* - 3 - *hexenyl*)*ferrocene* (**I**)

The hydrochloride salt (1.4 g, 4.4 mmol) of 1,1′-bis(aminomethyl)ferrocene in benzene (50 cm^3) was treated with NaOH in a small quantity of H_2O. The aqueous layer was removed with a separatory funnel, and its pH value was around 12. After drying the benzene layer over anhydrous $MgSO_4$, acetylacetone (4.4 cm^3) was added to the layer and the mixture was heated under reflux for 8 h, at which time the H_2O liberated was removed azeotropically by use of a Dean–Stark trap. Benzene and unreacted acetylacetone were evaporated *in vacuo* at room temperature. After washing the residue with hexane 3 times, recrystallization from diethyl ether and hexane gave a brown powder (1.0 g) (**I**) in a 56% yield. M.p. 85–86°C; IR (CH_2Cl_2) 1605(m), 1565(m), and 1510(w) cm^{-1}.

Found: C, 64.4; H, 7.0; N, 7.0. Calc. for $C_{22}H_{28}N_2FeO_2$: C, 64.7; H, 6.9: N, 6.9%.

Reaction of **I** *with chloro-bridged cyclopalladated complexes*

An EtOH solution (6 cm^3) of NaOEt (1.7 mmol) was added slowly to a THF suspension (50 cm^3) of material **I** (300 mg, 0.73 mmol) and the cyclopalladated complex (470 mg, 0.73 mmol) prepared from benzo[*h*]quinoline. After stirring overnight at room temperature and evaporation to dryness *in vacuo*, the residue was recrystallized from diethyl ether and hexane, affording a yellow powder (420 mg) (**II**) in a 59% yield. M.p. 136–139°C; IR (KBr) 1615(w), 1570(m), and 1503(m) cm^{-1}.

Found: C, 59.2; H, 4.5; N, 5.5. Calc. for $C_{48}H_{42}N_4FeO_2Pd_2$: C, 59.1; H, 4.3; N, 5.7%.

A similar reaction of **I** was performed with another cyclopalladated complex prepared from *N*,*N*-dimethylbenzylamine, and the corresponding complex **III** was obtained as a brown powder in a *ca* 70% yield. M.p. 90°C; IR (KBr) 1608(w), 1570(m), and 1500(m) cm^{-1}.

Electrochemistry

Electrochemical experiments were performed on millimolar concentrations of the ferrocenyl compounds in CH_3CN solutions (20 cm^3) of 0.1 M $(Et_4N)PF_6$ as the supporting electrolyte, using a conventional three-compartment electrochemical cell with a Hokuto Denko HA-301 potentiostat and a HB-104 function generater. The cell involved a Pt-disc or Pt-gauze working electrode, a Pt-wire auxiliary electrode, and a $[Fe(C_5H_5)_2]$–$[Fe(C_5H_5)_2]PF_6$ reference electrode. Scan rate was 100 mV s^{-1}.

REFERENCES

1. C. R. Hauser and C. E. Cain, *J. Org. Chem.* 1958, **23**, 1142.
2. H. Imai and Y. Yaehashi, *Nippon Kagaku Zasshi* 1970, **91**, 452; H. Imai and T. Shiraiwa, *Technol. Rep. Kansai Univ.* 1981, 107.
3. E. Breitmaier and W. Voelter, ^{13}C *NMR Spectroscopy*. Verlag Chemie, Weinheim (1974); F. Toda and T. Oshima, *Handbook of* ^{13}C *NMR Spectra*. Sankyo Shuppan, Tokyo (1981).
4. K. Hiraki, T. Matsumoto, Y. Fuchita and Y. Zegi, *Bull. Chem. Soc. Jpn* 1981, **54**, 1044; K. Hiraki, M. Onishi, M. Hayashida and K. Kurita, *Bull. Chem. Soc. Jpn* 1983, **56**, 1410; H. F. Holtzclaw, Jr, J. P. Collman and R. M. Alire, *J. Am. Chem. Soc.* 1958, **80**, 1100; N. H. Cromwell, F. A. Miller, A. R. Johnson, R. L. Frank and D. J. Wallace, *J. Am. Chem. Soc.* 1949, **71**, 3337.
5. G. E. Hartwell, R. V. Lawrence and M. J. Smas, *J. Chem. Soc., Chem. Commun.* 1970, 912.
6. A. C. Cope and E. C. Friedrich, *J. Am. Chem. Soc.* 1968, **90**, 909.
7. P. E. Cassidy, D. M. Carlton and L. Fogle, *J. Polym. Sci. A* 1971, **9**, 2419.

Polyhedron Vol. 6, No. 6, pp. 1247–1249, 1987
Printed in Great Britain

0277–5387/87 $3.00+.00

COMPLEXING PROPERTIES OF NITRILOTRI(METHYLENEPHOSPHONIC) ACID WITH VARIOUS TRANSITION AND HEAVY METALS IN A 10:90 ETHANOL–WATER MEDIUM

B. SPIESS,* E. HARRAKA, D. WENCKER and P. LAUGEL

Laboratoire de Chimie Analytique, Faculté de Pharmacie 74, route du Rhin, 67048 Strasbourg Cedex, France

(*Received* 23 *September* 1986; *accepted* 4 *November* 1986)

Abstract—The nature and stability of some transition- and heavy-metal cation complexes of nitrilotri(methylenephosphonic) acid have been determined in 0.1 M $NaClO_4$ 10:90 ethanol–water solutions by means of pH metric measurements. In this medium stable 1:1 complexes and protonated species were found.

Among the numerous applications found for nitrilotri(methylenephosphonic) acid (NTP) and its salts is one that is concerned with the demetalization of wines, in particular the elimination of iron and copper.[1–7] Indeed such cations can lead to precipitations which make the wine unsuitable for selling as well as for consumption. These wines have then to be treated and the process recommended in Eastern European Countries uses NTP. An important feature of such a treatment is that all the compound has to be removed at the end of the process. It is therefore interesting to know if complexation can occur with the cations present in the wine, and if soluble complexes can remain in solution.

The purpose of the present work is to study at 25°C in a (10:90) ethanol–water medium ($I = 0.1$ M $NaClO_4$), the complex formation between NTP and some transition- and heavy-metal cations such as Fe^{2+}, Cu^{2+}, Zn^{2+}, Cd^{2+} and Pb^{2+} in order to determine their stability constants.

In the past several authors[8–12] have studied the complexation ability of NTP with some of these cations in aqueous solution. Their results are also reported here and compared with ours.

The nature of the protonated or complexed species and their stability constants are referred to in the following stepwise equilibria:

$$H_{(i-1)}L^{(7-i)-} + H^+ \rightleftharpoons H_iL^{(6-i)-},$$

$$K_{i1} = \frac{[H_iL^{(6-i)-}]}{[H_{(i-1)}L^{(7-i)-}][H^+]};$$

$$MH_{(i-1)}L^{(5-i)-} + H^+ \rightleftharpoons MH_iL^{(4-i)-},$$

$$K_{1i1} = \frac{[MH_iL^{(4-i)-}]}{[MH_{(i-1)}L^{(5-i)-}][H^+]};$$

$$i = 1, 2, 3, \ldots, 6.$$

These constants have been obtained by potentiometric titrations where solutions of the ligand NTP and metallic perchlorates of various stoichiometries have been titrated with NaOH. Details of the experimental procedure, the glass electrode conditioning and the calculation methods using the numerical program SCOGS[13] have been previously reported.[14]

Tables 1 and 2 contain our values of $\log K_{i1}$ and $\log K_{1i1}$, respectively, and those previously determined by several other authors in different media.

As shown in Table 1 only small differences can be observed between our values and those of Hendrickson[8] and Nikitina *et al.*[9] for $\log K_{21}$–$\log K_{51}$. The lower values determined by Carter *et al.*[10] could be due to the ionic strength they used ($I = 1$ M instead of 0.1 M used in the other experiments). Greater differences appear for the first and last con-

* Author to whom correspondence should be addressed.

Table 1. Logarithms of the protonation constants K_{i1} of NTP[a]

Log K_{i1}	10:90 EtOH–H_2O I = 0.1 M $NaClO_4$ t = 25°C Our values	H_2O I = 0.1 M Met_4Cl t = 20°C Reference 8	H_2O I = 0.1 M KCl or KNO_3 t = 25°C Reference 9	H_2O I = 1 M KNO_3 t = 25°C Reference 10
Log K_{11}	$\geqslant$ 12.00	10.90	12.10	12.34
Log K_{21}	7.31 ± 0.02	7.35	7.30	6.66
Log K_{31}	6.13 ± 0.03	5.92	5.86	5.46
Log K_{41}	4.85 ± 0.05	4.60	4.64	4.30
Log K_{51}	1.68 ± 0.06	2.00	1.50	< 2
Log K_{61}	$\leqslant$ 1.00	1.90	0.30	< 2

[a] The confidence interval $+2\sigma$ is given by the program.

stants which are in general more difficult to determine. In our case only upper and lower limits are given.

The values of the logarithms of the stability constants were obtained from a minimum of two experiments for which the ratio of the metal to the ligand concentration was generally about 1 and 0.5. In the calculations the values of the protonation constants were kept constant and $\log \beta_{11}$ was fixed at 12.00. The results show that only the formation of 1:1 complexes and protonated species occur in the pH range studied. Although the determinations were performed in different media, the results are in good agreement with the previous studies of Morozova *et al.*,[11] with the exception of the ZnL complex. On the other hand we were not able to find any evidence of the CuH_4L and ZnH_4L species.

Other results (Table 2) concerning the complexation of transition cations such as Co^{2+}, Ni^{2+} and Fe^{2+} have been collected from the literature.[8,11,12] It would appear, if one considers the whole set of constants, that, except for Ni^{2+}, the cations of the first transition row follow for the ML complexes the Irving–Williams rule.[15] This states that there is an increase in stability from Mn^{2+} to Cu^{2+}, then a decrease for Zn^{2+}. By contrast the complexes of the MH_iL type do not follow this same rule and, moreover, the values of the constants are close together. It seems possible that the selectivity which is observed for the ML complexes is determined by the bonding of the metallic cations and the lone pair on the nitrogen group. Taking into account the high value of $\log K_{11}$ which is related to the protonation of the amine, it is possible that the formation of monoprotonated complexes arises from the fixation of H^+ on the

Table 2. Logarithms of the stability constants K_{1i1} for metallic complexes of NTP

Cation	Log K_{101}	Log K_{111}	Log K_{121}	Log K_{131}	Log K_{141}	pH range
Fe^{2+}	12.60 ± 0.05	7.00 ± 0.04	5.67 ± 0.03	4.36 ± 0.04	—	2.78–6.93
Fe^{3+}	—	—	—	—	—	—
	(14.60)[a] (15.57)[b]	(9.90)[a] (9.88)[b]	(6.00)[a] (6.10)[b]	—	—	—
Co^{2+}	—	—	—	—	—	—
	(14.37)[c]	(6.26)[c]	(5.16)[c]	(4.26)[c]	—	—
Ni^{2+}	—	—	—	—	—	—
	(9.85)[a] (11.05)[c]	(6.90)[a] (8.77)[c]	(5.20)[a] (5.76)[c]	(4.48)[c]	—	—
Cu^{2+}	17.58 ± 0.25	6.56 ± 0.20	4.67 ± 0.12	3.92 ± 0.2	—	2.59–7.36
	(17.40)[c]	(6.40)[c]	(4.70)[c]	(3.50)[c]	—	
Zn^{2+}	14.71 ± 0.05	6.24 ± 0.05	5.19 ± 0.04	4.10 ± 0.04	—	2.67–7.45
	(16.40)[c]	(6.10)[c]	(5.10)[c]	(4.10)[c]	(1.50)[c]	
Cd^{2+}	12.05 ± 0.04	6.99 ± 0.04	5.78 ± 0.04	4.47 ± 0.03	—	2.74–7.24
	(11.60)[c]	(7.00)[c]	(5.70)[c]	(4.80)[c]	(1.70)	
Pb^{2+}	16.22 ± 0.52	6.49 ± 0.19	5.28 ± 0.06	3.57 ± 0.16	—	2.63–7.13

[a] Reference 8.
[b] Reference 12.
[c] Reference 11.

nitrogen atom. This would mask a coordination site and at the same time introduce a positive charge. The only available coordination sites would then be the oxygen atoms of the phosphonic groups for which the transition-metal cations show lower affinities as pointed out in Pearson's HSAB principle.[16]

Concluding our study, it clearly appears that NTP can form stable soluble complexes with some cations present in the wine. It is likely that the same can occur in this medium when it is treated with NTP.

REFERENCES

1. N. A. Mekhuzla, A. L. Panasyuk and V. Y. Temkina, *Vinodel. Vinograd. SSSR* 1976, **3**, 14.
2. N. A. Mekhuzla, A. L. Panasyuk and V. Y. Temkina, *Vinodel. Vinograd. SSSR* 1978, **8**, 15.
3. N. A. Mekhuzla and A. L. Panasyuk, *Otkrytiya, Izobret, Prom. Obraztsy, Tovarnye Znaki* 1979, **29**, 91.
4. N. A. Mekhuzla, A. L. Panasyuk and Yu. N. Dubrov, *Vinodel. Vinograd. SSSR* 1981, **2**, 57.
5. L. M. Romantseva, I. S. Shablovskaya, E. N. Chislova and T. Yu Andriyanova, *Vinodel. Vinograd. SSSR* 1980, **4**, 17.
6. L. M. Romantseva, V. A. Sukhanova and A. M. Sergeeva, *Vinodel. Vinograd. SSSR* 1981, **6**, 24.
7. L. M. Romantseva, V. A. Sukhanova and A. M. Sergeeva, *Izv. Vyssh. Uchebn. Zaved., Pishch. Tekhnol.* 1982, **4**, 40.
8. H. S. Hendrickson, *Anal. Chem.* 1967, **39**, 998.
9. L. V. Nikitina, A. I. Grigor'ev and N. M. Dyatlova, *Zh. Obshch. Khim.* 1974, **44**, 1598.
10. R. P. Carter, R. L. Carroll and R. R. Irani, *Inorg. Chem.* 1967, **6**, 939.
11. S. S. Morozova, L. V. Nikitina, N. M. Dyatlova and G. V. Serebryakova, *Zh. Neorg. Khim.* 1975, **20**, 413.
12. A. Yu. Kireeva, M. Z. Gurevich, N. F. Shugai and V. Ya. Temkina, *Khim. Reaktivov Osobo Chist. Khim. Veshch.* 1982, **44**, 134.
13. I. G. Sayce, *Talanta* 1968, **15**, 1397.
14. B. Spiess, E. Harraka, D. Wencker and P. Laugel, *Analusis* 1984, **6**, 290.
15. H. Irving and R. J. P. Williams, *Nature* 1948, **162**, 746.
16. R. G. Pearson, *Science* 1966, **151**, 172.

Polyhedron Vol. 6, No. 6, pp. 1251–1254, 1987
Printed in Great Britain

0277–5387/87 $3.00+.00

EXTRACTION OF Ni(II) FROM NITRATE MEDIA BY DI-*n*-OCTYLPHOSPHINIC ACID DISSOLVED IN TOLUENE

M. P. ELIZALDE,* J. M. CASTRESANA, M. AGUILAR and M. COX

Departamento de Química, Universidad del País Vasco, Apartado 644, Bilbao 48080, Spain

(*Received* 29 *September* 1986; *accepted* 4 *November* 1986)

Abstract—The extraction of Ni(II) from nitrate media of ionic strength 1.0 mol dm^{-3} by di-*n*-octylphosphinic acid (HR) in toluene solution has been studied over a range of pH and reagent concentrations. The data have been analysed both graphically and numerically to determine the stoichiometry of the extracted complexes and their extraction constants. Evidence was found for the formation of both $NiR_2(HR)_4$ ($\log K_{24} = -9.14 \pm 0.06$) and $NiR_2(HR)_2$ ($\log K_{22} = -7.35 \pm 0.10$), the former being the predominant species although the latter is important at low reagent concentrations and high pH values.

Interest in the extraction of nickel by organophosphorus extractants has recently increased with the introduction of the commercial reagents based on di-(2-ethylhexyl)phosphonic acid (PC88A Daihatchi Chemical Co.) and bis-2,4,4-trimethylpentylphosphinic acid (Cyanex 272 American Cyanamid Inc.). These reagents have found particular application in the separation of cobalt from nickel in sulphate media.[1,2] Fundamental studies of nickel extraction by organophosphorus acids have largely been confined to di-(2-ethylhexyl)phosphoric acid where the stoichiometries $NiR_2(HR)_2$ and NiR_2, $(HR)_2$ representing the dimer of the organophosphorus acid, have been proposed.[3–5] Extraction experiments with the commercial phosphonic acid ester have also indicated from slope analysis the formation of nickel complexes of type $NiR_2(H_2R_2)_{2+x}(H_2O)_{2-x}$, with $x = o$, 1 or 2 depending on the reagent concentration.[1] Recently, Danesi *et al.*[6] studied the extraction equilibria of Ni(II) and Co(II) by purified Cyanex 272 in toluene and postulated the formation of $NiR_2(HR)_4$ species.

However, because of the presence of impurities of unknown composition and concentration in these industrial reagents it is essential to use pure synthesized reagents in any fundamental studies of metal extraction. This paper is therefore concerned with the complexes involved in the extraction of nickel by di-*n*-octylphosphinic acid (HR) and represents an intermediate step in the interpretation of the distribution data in the Ni(II)–LIX 63–HR system. The object of the work is to determine the composition of the metallic species extracted as well as their extraction constants.

EXPERIMENTAL

Reagents

HR was prepared according to Peppard *et al.*[7] by the reaction of octene-1 and hypophosphorous acid using benzoyl peroxide as catalyst. The product after extraction from the reaction mixture was recrystallized several times from hexane as white crystals, m.p. 84°C (literature 84°C[7]). Nickel nitrate, $Ni(NO_3)_2 \cdot 6H_2O$ (Carlo Erba p.a.), was from twice distilled water. Sodium nitrate, toluene, sodium hydroxide and nitric acid (Merck, p.a.) were used as supplied.

Experimental procedure

Experimental data of the distribution coefficient were collected for several total HR concentrations as a function of pH. Organic solutions of HR in toluene in the concentration range 0.020 up to 0.200 mol dm^{-3} were mixed with aqueous phases consisting of 0.5×10^{-3} mol dm^{-3} Ni(II), 1.0 mol dm^{-3} $NaNO_3$ and pH varied from 4 to approximately 7.

Equal volumes (10 cm^3) of organic and aqueous phases were mechanically shaken in special stoppered tubes until equilibrium had been attained (less than 15 min). The pH was measured using a Radio-

* Author to whom correspondence should be addressed.

meter pHM 64 meter, fitted with a GK2322C Radiometer combined glass electrode, standardized with buffer solutions of pH 4.00 and 7.00 at 293 K. Nickel concentration in both phases was measured by atomic absorption spectroscopy (Perkin–Elmer 560). In order to determine the organic metal concentration the nickel was first stripped from organic phases with 1.0 mol dm^{-3} nitric acid solutions.

GRAPHICAL TREATMENT OF THE DATA

The extraction of NI(II) by HR dissolved in toluene may be described by the following general equation:

$$Ni^{2+} + \tfrac{1}{2}(p+q)(HR)_{2org} \rightleftharpoons NiR_p(HR)_{q\,org} + pH^+, \quad (1)$$

where HR stands for the organic acid which behaves as a dimer in aromatic solvents.[7]

K_{pq} being the stoichiometric equilibrium constant for reaction (1), the distribution coefficient of Ni(II) can be expressed as:

$$D = \sum_p \sum_q K_{pq} \alpha_{Ni}^{-1} [(HR)_2]_{org}^{(p+q)/2} [H^+]^{-p}, \quad (2)$$

where α_{Ni} represents the side-reaction coefficient due to the formation of nitrate complexes in the aqueous phase.[8] Taking into account the experimental conditions used, the formation of hydroxo complexes of Ni(II) can be considered as negligible.

Experimental data in the form $\log D$ vs pH at several HR concentrations are illustrated in Fig. 1, where straight lines of slope value 2.0 are obtained. If the extraction of a single species is assumed, eqn (2) becomes:

$$\log D = \log K_{pq} \alpha_{Ni}^{-1} + \tfrac{1}{2}(p+q) \log [(HR)_2]_{org} + p\text{pH}. \quad (3)$$

Experimental functions, $\log D = f(\text{pH})$, defined by eqn (3) have been compared with the theoretical model function:

$$\log D = -p \log V = f(\log V) \quad (4)$$

for different values of the parameter p, V being a normalized variable defined by:

$$V = (K_{pq} \alpha_{Ni}^{-1} [(HR)_2]_{org}^{(p+q)/2})^{-1/p} [H^+]. \quad (5)$$

The best fit between both functions was obtained for $p = 2$, as can be seen in Fig. 1. The differences on the X-axis are functions of $\log [(HR)_2]_{org}$ according to:

$$\log V + \text{pH} = -\frac{1}{p} \log K_{pq} \alpha_{Ni}^{-1} - \frac{p+q}{2p} \log [(HR)_2]_{org}, \quad (6)$$

which are represented in Fig. 2. The value of the slope of the straight line obtained, -1.5, indicates that $q = 4$. From the intercept on Y-axis the value $\log K_{24} = -7.33$ was determined for the extraction of the species $NiR_2(HR)_4$.

As it can be noticed in Fig. 2, it seems that the experimental points at the lowest HR concentrations deviate from the straight line. This can be interpreted in terms of the formation of metallic species with a different solvation number in the organic phase. In order to determine if q can take values other than 4, a curve-fitting analysis has been

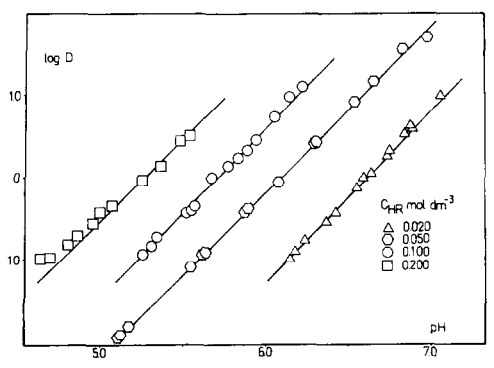

Fig. 1. Variation of the distribution coefficient of Ni(II) with pH at several total concentrations of di-*n*-octylphosphinic acid (HR). Continuous lines represent the normalized function $\log D = f(\log V)_p$ in the best-fit position ($p = 2$).

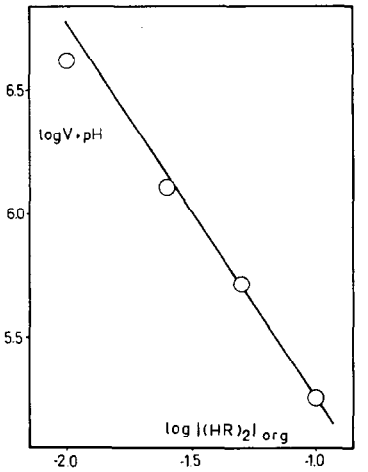

Fig. 2. Differences on X-axis from Fig. 1 as a function of $\log [(HR)_2]_{org}$.

made assuming the formation of species $NiR_2(HR)_n$ as well as the main species $NiR_2(HR)_4$.

With K_{24} and K_{2n} being the respective extraction constants of the above species, the distribution coefficient of Ni(II) can be expressed as:

$$D = K_{24}\alpha_{Ni}^{-1}[(HR)_2]_{org}^3[H^+]^{-2} + K_{2n}\alpha_{Ni}^{-1}[(HR)_2]_{org}^{(n+2)/2}[H^+]^{-2}, \quad (7)$$

which can be rearranged to give:

$$D[H^+]^2\alpha_{Ni}^{-1}K_{24}^{-1}[(HR)_2]_{org}^{-3} = 1 + K_{2n}K_{24}^{-1}[(HR)_2]_{org}^{(n-4)/2}. \quad (8)$$

Defining the new normalized variables:

$$Y = D[H^+]^2\alpha_{Ni}^{-1}K_{24}^{-1}[(HR)_2]_{org}^{-3}, \quad (9)$$

$$X = (K_{2n}K_{24}^{-1})^{(n-4)/2}[(HR)_2]_{org}, \quad (10)$$

and the parameter:

$$i = (n-4)/2, \quad (11)$$

the experimental functions $\log D - 2pH - 3\log[(HR)_2]_{org} = f(\log[(HR)_2]_{org})$ have been compared with the model function:

$$\log Y = \log(1+X^i) = f(\log X) \quad (12)$$

for different values of the parameter i. The experimental functions were obtained from Fig. 1 at different constant values corresponding to 25, 50 and 75% extraction at the different total reagent concentrations. Figure 3 shows the comparison of the experimental functions (it can be noticed that data for each concentration coincide) and the theoretical ones at different i values. The best fit was obtained for $i = -1$; that means, according to eqn (11), $n = 2$.

From the position of best fit in Fig. 3, differences on both axes, according to eqns (9) and (10), let us determine the values of the extraction constants, yielding the values $\log K_{24} = -7.37$ and $\log K_{22} = -9.22$.

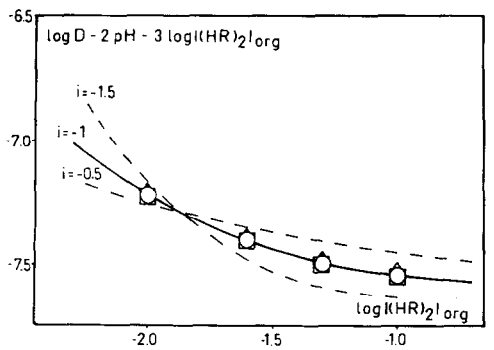

Fig. 3. Comparison of the experimental function defined by eqn (8) and the theoretical functions defined by eqn (12) for different values of the parameter i.

NUMERICAL TREATMENT OF THE DATA

In order to refine the equilibrium constant values graphically obtained and to search for a new combination of species which could improve the fit to the experimental data, a numerical treatment was carried out using the LETAGROP-DISTR program.[9] In this treatment the function to be minimized was the error square sum (U) defined by:

$$U = \sum_{N_p}(\log D_{calc} - \log D_{exp})^2, \quad (13)$$

where D_{exp} represents the experimental distribution coefficient, D_{calc} the corresponding magnitude calculated by the program assuming a certain set of species and constants, and N_p the number of experimental data. For each combination of species tried the program calculates both U_{min} and the mean standard deviation $[\sigma(\log D)]$.

Table 1 summarizes the results of the numerical calculations, being the best fit obtained with the model of species graphically ascertained. In Table 2 values of the stoichiometric extraction constants are given and the uncertainties in the constants refer to $\pm 3\sigma(\log K)$. The fit to the data is illustrated in Fig. 4, where the standard deviation for each experimental point is plotted as a function of pH, showing the absence of systematic deviations.

Table 1. Results of the numerical calculations

Species $NiR_p(HR)_q$	U_{min}	$\sigma(\log D)$
(2,4)	0.888	0.149
(2,2), (2,4)	0.128	0.057[a]
(2,4), (2,1)	0.138	0.059
(2,4), (2,0)	0.151	0.062
(2,4), (2,3)	0.175	0.062
(2,4), (2,2), (2,0)	0.138	0.060

[a] Proposed model.

Table 2. Proposed stoichiometric equilibrium constants for the extraction of Ni(II) from nitrate media by di-*n*-octylphosphinic acid (HR) in toluene

$$Ni^{2+} + 2(HR)_{2org} \rightleftharpoons NiR_2(HR)_{2org} + 2H^+$$
$$\log K_{22} = -7.35 \pm 0.10$$
$$Ni^{2+} + 3(HR)_{2org} \rightleftharpoons NiR_2(HR)_{4org} + 2H^+$$
$$\log K_{24} = -9.14 \pm 0.06$$

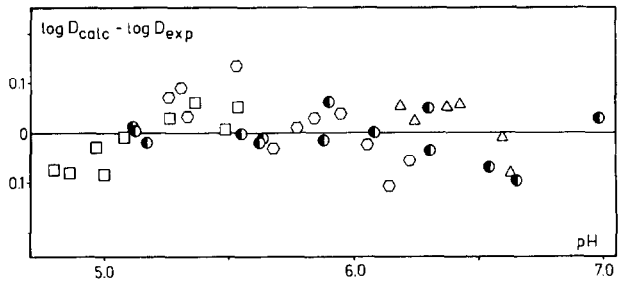

Fig. 4. Deviations $\log D_{calc} - \log D_{exp}$ obtained by the LETAGROP-DISTR program as a function of pH.

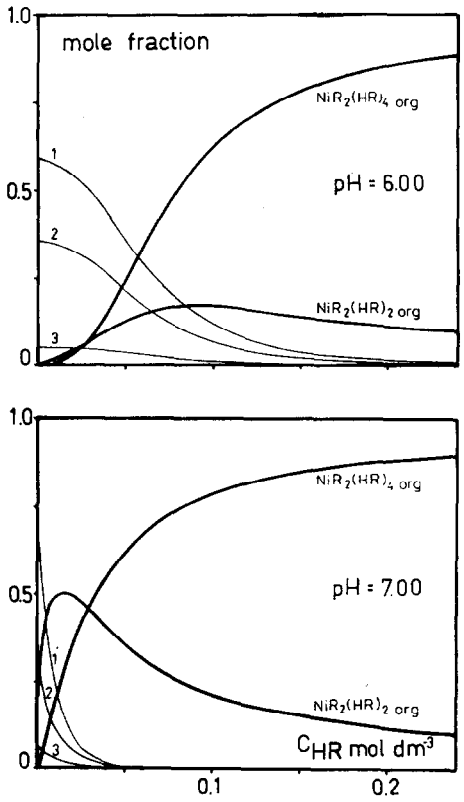

Fig. 5. Nickel distribution diagrams as a function of the total concentration of di-*n*-octylphosphinic acid (HR) at two selected pH values. Lines 1, 2 and 3 represent, respectively, Ni^{2+}, $NiNO_3^+$ and $Ni(NO_3)_2$ species in the aqueous phase.

CONCLUSIONS

The results of the work indicate that the extraction of Ni(II) from nitrate medium by HR dissolved in toluene can be explained assuming the formation of the species $NiR_2(HR)_4$ and $NiR_2(HR)_2$. If compared with the extraction of Ni(II) by di-(2-ethylhexyl)phosphoric acid (DEHPA)[5] it must be pointed out that the extractant ability of HR is lower than that from DEHPA since the extraction occurs at higher pH values under the same conditions. On the other hand, the composition of the extracted species is similar in both cases although there is a difference in the solvation number, HR having more solvating ability than DEHPA.

Figure 5 shows the distribution diagram of Ni(II) species as a function of the total reagent concentration at selected pH levels. It can be seen that $NiR_2(HR)_4$ is the predominant species extracted, but the contribution of the species $NiR_2(HR)_2$ is important at high pH levels and low HR concentration.

REFERENCES

1. J. S. Preston, *Hydrometallurgy* 1985, **9**, 115.
2. V. A. Rickelton, D. S. Flett and D. W. West, *Solv. Extn Ion Exch.* 1984, **2**, 815.
3. R. Grimm and Z. Kolarik, *J. Inorg. Nucl. Chem.* 1974, **36**, 189.
4. Z. Kolarik and R. Grimm, *J. Inorg. Nucl. Chem.* 1976, **38**, 121.
5. L. A. Fernández, M. P. Elizalde, J. M. Castresana, M. Aguilar and S. Wingefors, *Solv. Extn Ion Exch.* 1985, **3**, 807.
6. P. R. Danesi, L. Reichley-Yinger, C. Cianetti and P. G. Rickert, *Solv. Extn Ion Exch.* 1984, **2**, 781.
7. D. F. Peppard, G. W. Mason and S. Lewey, *J. Inorg. Nucl. Chem.* 1965, **27**, 2065.
8. V. A. Fedorov, I. I. Shmyd'ko, A. M. Robov, L. S. Simaeva, V. A. Kukhtina and V. E. Mironov, *Russ. J. Inorg. Chem.* 1973, **18**, 673.
9. D. H. Liem, *Acta Chem. Scand.* 1971, **25**, 1521.

Polyhedron Vol. 6, No. 6, pp. 1255–1259, 1987
Printed in Great Britain

0277–5387/87 $3.00+.00

SULPHUR–ARSENIC LIGANDS: SYNTHESIS AND CHARACTERIZATION OF SOME RHENIUM(I), RUTHENIUM(II), RHODIUM(III) AND GOLD(I) COMPLEXES OF BIS(DIMETHYLARSINO)SULPHIDE($Me_2AsSAsMe_2$) AND DIMETHYL(METHYLTHIO)ARSINE(Me_2AsSMe)

EDWARD W. ABEL* and MICHAEL A. BECKETT

Department of Chemistry, University of Exeter, Exeter EX4 4QD, U.K.

(*Received* 23 *October* 1986; *accepted* 4 *November* 1986)

Abstract—The complexes $[\{RuCl_2(CO)_3\}_2(Me_2AsSAsMe_2)]$, $[RuCl_2(CO)_2(Me_2AsSAsMe_2)_2]$, $[RuCl_2(CO)_2(Me_2AsSMe)_2]$, $[ReX(CO)_3(Me_2AsSAsMe_2)]$ (X = Cl, Br or I), $[RhCl_2(C_5Me_5)(Me_2AsSMe)]$, $[AuCl(Me_2AsSMe)]$ and $[(AuCl)_2(Me_2AsSAsMe_2)]$ have been synthesized from the electron-rich ligands $Me_2AsSAsMe_2$ and Me_2AsSMe. IR and NMR spectrometry along with mass spectra have given sufficient data to indicate structures for all of these products. In all complexes of both ligands, binding to metal is invariably via arsenic and not sulphur. $Me_2AsSAsMe_2$ has now been shown to be capable of monodentate, bridging and chelating modes of complexation.

The use of bis(dimethylarsino)sulphide, $Me_2AsSAsMe_2$ (dmas) and dimethyl(methylthio) arsine, Me_2AsSMe (dmmta) as ligands has received little reported attention. Earlier work on both $Me_2AsSAsMe_2$[1] and Me_2AsSMe[2–5] was restricted to group VI metal pentacarbonyl derivatives, and we have recently investigated reactions with Pt(IV)[6] and Re(I)[6,7] compounds. Despite the availability of potential ligand electrons on both arsenic and sulphur atoms, all products characterized to date have been exclusively arsenic-bound. Herein we have extended our investigation of these two arsenic ligands to report the action of $Me_2AsSAsMe_2$ and Me_2AsSMe upon $[\{RuCl_2(CO)_3\}_2]$, $[\{RhCl_2(C_5Me_5)\}_2]$ and $[AuCl(SMe_2)]$, and the action of $Me_2AsSAsMe_2$ upon the $[ReX(CO)_5]$ halides.

EXPERIMENTAL

General

Reactions were carried out using standard Schlenk conditions under nitrogen, with solvents distilled under nitrogen from an appropriate drying agent. Dmas and dmmta were prepared by reported methods.[7–9] $[AuCl(SMe_2)]$,[10] $[ReX(CO)_5]$[11] and $[\{RhCl_2(C_5Me_5)\}_2]$[12] were also prepared by standard techniques and $[\{RuCl_2(CO)_3\}_2]$ was used as supplied by Johnson–Matthey. The methods used in the syntheses of the metal complexes were very similar and are typified by the examples below. Reaction times, yields, m.ps and analytical data for the products are summarized in Table 1.

Preparation of $[RuCl_2(CO)_2(Me_2AsSAsMe_2)_2]$

To a solution of $[\{RuCl_2(CO)_3\}_2]$ (200 mg, 0.39 mmol) in thf (5 cm^3) was added $Me_2AsSAsMe_2$ (430 mg, 1.78 mmol). After *ca* 1 min a white precipitate had formed (this was the binuclear $[\{RuCl_2(CO)_3\}_2(Me_2AsSAsMe_2)]$ which could be isolated by rapid filtration at this stage and characterized), but subsequent heating under reflux (2 h) produced a clear yellow solution. Low-pressure removal of solvent left a yellow deposit which was extracted at 40°C with 60–80°C light petroleum. Cooling of the filtered extract overnight to −20°C gave pale yellow crystals of the product $[RuCl_2(CO)_2(Me_2AsSAsMe_2)_2]$ (110 mg, 20%).

Preparation of $[ReBr(CO)_3(Me_2AsSAsMe_2)]$

To a solution of $[ReBr(CO)_5]$ (250 mg, 0.61 mmol) in thf (5 cm^3) was added $Me_2AsSAsMe_2$

*Author to whom correspondence should be addressed.

Table 1. Preparation and characterization of metal complexes of Me_2AsSMe and $Me_2AsSAsMe_2$

Complex	Yield (%)	Reaction time[a] (h)	M.p.[b] (°C)	Analysis[c] C	Analysis[c] H
$[\{RuCl_2(CO)_3\}_2(Me_2AsSAsMe_2)]$[d]	40	0.1[e]	175 dec.[f]	16.3 (15.9)	1.7 (1.6)
$[RuCl_2(CO)_2(Me_2AsSAsMe_2)_2]$	20	2	90–92 dec.	17.1 (16.9)	3.5 (3.4)
$[RuCl_2(CO)_2(Me_2AsSMe)_2]$	50	2	138–140	18.1 (18.1)	3.6 (3.4)
$[ReCl(CO)_3(Me_2AsSAsMe_2)]$	49	24	110–112	15.5 (15.3)	2.2 (2.2)
$[ReBr(CO)_3(Me_2AsSAsMe_2)]$	51	24	128–132	14.3 (14.2)	2.0 (2.0)
$[ReI(CO)_3(Me_2AsSAsMe_2)]$	38	240	130 dec.	13.2 (13.2)	1.9 (1.9)
$[RhCl_2(C_5Me_5)(Me_2AsSMe)]$	73	0.5[eg]	153–155	33.8 (33.9)	5.2 (5.3)
$[AuCl(Me_2AsSMe)]_n$?	46	0.1[eg]	95 dec.[f]	7.9 (9.4)	2.0 (2.4)
$[\{AuCl\}_2(Me_2AsSAsMe_2)]_n$?	55	0.1[eg]	120 dec.[f]	7.0 (6.8)	1.8 (1.7)

[a] Under reflux in thf unless otherwise stated.
[b] Yellow or pale yellow solids unless otherwise stated.
[c] Calculated values in parentheses.
[d] As and Cl analysed: As, 20.8 (19.9); Cl, 18.6 (18.8).
[e] At room temperature.
[f] White solid.
[g] In chloroform solution.

(170 mg, 0.70 mmol), and the reaction mixture placed under reflux for 24 h. Solvent was removed at low pressure and the residue redissolved in chloroform (2 cm^3). Subsequent addition of 60–80°C light petroleum (5 cm^3) produced a precipitate of the crude product, which was then redissolved in $CHCl_3$ 60–80°C petrol and cooled to −20°C overnight to yield yellow crystals (180 mg, 51%).

NMR studies

^1H and ^{13}C experiments were performed on a Bruker AM 250 instrument at 250 and 62.8 MHz, respectively. All samples were dissolved in $CDCl_3$ and spectra were recorded at ambient temperature.

RESULTS AND DISCUSSION

Reactions and syntheses

The ruthenium(II) dimer $[\{RuCl_2(CO)_3\}_2]$ undergoes reaction with $Me_2AsSAsMe_2$ at room temperature without evolution of carbon monoxide to break the halogen bridges and, in effect, become inserted between the two halves of the dimer. The IR spectrum of this product in the metal carbonyl region shows three distinct bands suggesting a *fac* orientation of the three carbonyl groups about the ruthenium(II) centres. If the binuclear product is not isolated from the cold reaction mixture, heating under reflux causes the precipitate to redissolve with evolution of carbon monoxide. From the resulting yellow solution *cis, cis, trans*-$[RuCl_2(CO)_2(Me_2AsSAsMe_2)_2]$ may be isolated. The metal carbonyl stretching region now shows two bands, indicating the mutually *cis* nature of the carbonyl groups, and the ^1H NMR spectrum is consistent with two arsenic-bonded monodentate $Me_2AsSAsMe_2$ ligands mutually *trans* on the ruthenium(II) centre (*vide infra*). When $[RuCl_2(CO)_2(Me_2AsSAsMe_2)_2]$ was heated under reflux in thf further carbon monoxide was evolved. This was presumably due to carbon monoxide displacement by non-bonding arsenic atoms. The hope that what would be formed was the bis chelate complex, $[RuCl_2(Me_2AsSAsMe_2)_2]$, was not realized. The product was polymeric, presumably with $Me_2AsSAsMe_2$ linkages between $RuCl_2$ units.

$[\{RuCl_2(CO)_3\}_2]$ and Me_2AsSMe in thf undergo reaction in 4 days at room temperature to produce $[RuCl_2(CO)_2(Me_2AsSMe)_2]$ in good yield. The reaction is complete in 2 h under reflux and no other product was isolated.

The configuration of the product as *cis, cis, trans*-$[RuCl_2(CO)_2(Me_2AsSMe)_2]$ is evident from IR and ^1H NMR data. This *trans*-Me_2AsSMe complex underwent no decomposition or rearrangement upon prolonged heating under reflux in thf. ^1H NMR measurements indicated bonding of the ligand via arsenic, with no indication that the sulphur could be brought into coordination.

Me_2AsSMe has already been reported to displace carbon monoxide from rhenium pentacarbonyl halides[7] with the formation of *fac*-$[ReX(CO)_3$

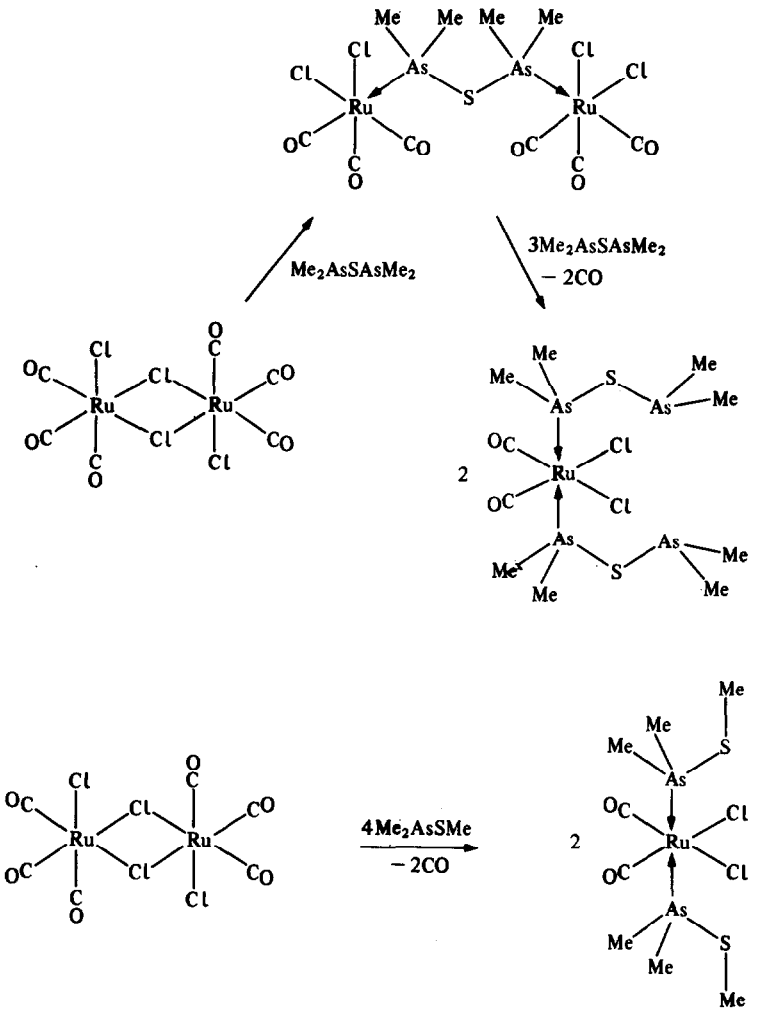

$(Me_2AsSMe)_2$] complexes. We have now reacted the rhenium carbonyl halides with $Me_2AsSAsMe_2$ in thf to produce crystalline air-stable products with stoichiometry $[ReX(CO)_3(Me_2AsSAsMe_2)]$. IR spectra indicate a *fac* configuration about rhenium, and the mass spectrum of $[ReCl(CO)_3(Me_2AsSAsMe_2)]$ shows a strong M^+ at *m/z* 550 (^{37}Cl, ^{187}Re) with a total absence of any signal at *m/z ca* 1100. This along with ^1H NMR evidence points to a *fac* mononuclear type of complex.

The halogen bridge in $[\{RhCl_2(C_5Me_5)\}_2]$ undergoes rapid fission at room temperature upon treatment with Me_2AsSMe in chloroform.

The $[RhCl_2(C_5Me_5)(Me_2AsSMe)]$ produced is again characterized as having arsenic coordinated to the rhodium centre.

$Me_2AsSAsMe_2$ also underwent rapid reaction at room temperature in chloroform, but we have been unable to isolate and purify a stable product.

Monometallic and bimetallic gold(I) complexes

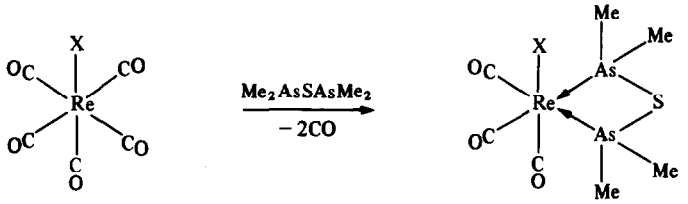

To date transition-metal complexes of $Me_2AsSAsMe_2$ have been reported in which the ligand has either a monodentate or a bridging role. These rhenium complexes are the first to demonstrate that $Me_2AsSAsMe_2$ is capable of chelation at a metal centre.

of formulae [ClAuL] and [ClAuL–LAuCl] are conveniently prepared[10] by the reaction of a monodentate or bidentate ligand, respectively, upon $[AuCl(SMe_2)]$. Accordingly, we have investigated the reactions of both $Me_2AsSAsMe_2$ and Me_2AsSMe upon the gold compound. In both reac-

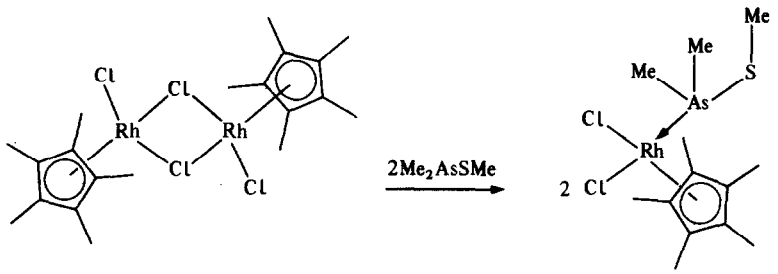

tions there was rapid production of air- and light-sensitive white insoluble precipitates. Persistent washing and vacuum drying gave complexes whose analyses (Table 1) corresponded closely to [AuCl(Me_2AsSMe)] and [ClAu($Me_2AsSAsMe_2$)AuCl]. The insoluble and amorphous nature of the products prevented further characterization, and suggested that they were polymers.

NMR studies

The ^1H NMR data for the rhenium(I), ruthenium(II) and rhodium(III) complexes of Me_2AsSMe and $Me_2AsSAsMe_2$ are listed in Table 2. The use of this information for the ascertainment of product structures is outlined below.

The mononuclear complexes [$RuCl_2(CO)_2(Me_2AsSMe)_2$] and [$RuCl_2(CO)_2(Me_2AsSAsMe_2)_2$] have *cis* carbonyl groups and one sharp resonance for the coordinated arsenic-methyl protons. This is inconsistent with the arsenic and chlorine ligands being in the *cis*, *cis* configuration. Either two halogens or two arsines are mutually *trans*. The problem is analogous to the corresponding dimethylphenylphosphine complex [$RuCl_2(CO)_2(PMe_2Ph)_2$] where the assignment *cis* dichloro, *cis* dicarbonyl and *trans* diphosphine was arrived at[13] by virtual coupling arguments. On this basis we favour the analogous configuration for both of our arsenic complexes.

These arsine complexes both show a single ^1H signal for the coordinated arsenic-methyl protons and one signal for the free $AsMe_2$ or SMe protons. The coordinated arsenic-methyl protons resonate *ca* 0.5 ppm downfield from the free-ligand values, whilst the uncoordinated $AsMe_2$/SMe protons are deshielding by only *ca* 0.1 ppm. This behaviour has been noted previously,[6,7] and does enable the ligand bonding mode via arsenic to be clearly defined. The binuclear complex [$Cl_2(CO)_3Ru(Me_2AsSAsMe_2)Ru(CO)_3Cl_2$] has extremely low solubility, but did give one ^1H signal only at δ 2.37 ppm. This was assignable to the protons of the four identical methyl groups where the presence of two metal atoms causes a larger deshielding than observed in the mononuclear complexes, an observation already noted[1] for analogous binuclear metal pentacarbonyl derivatives.

The ^1H NMR spectra of the *fac*-[$ReX(CO)_3(Me_2AsSAsMe_2)$] complexes all show a doublet centred at *ca* 0.5 ppm downfield from the free ligand, suggesting that both arsenic centres are co-ordinated to rhenium in a chelate structure. The two different methyl environments of the doublet lie, respectively, on the halogen and carbonyl sides of the ReAsSAs plane of the molecule. There is a

Table 2. IR and NMR data for metal complexes of Me_2AsSMe and $Me_2AsSAsMe_2$

Complex	ν_{CO}[a] (cm^{-1})	^1H (ppm)		
		Coordinated Me_2As	Free Me_2As	MeS
[{$RuCl_2(CO)_3$}$_2(Me_2AsSAsMe_2)$]	2142, 2088, 2045[b]	2.37		
[$RuCl_2(CO)_2(Me_2AsSAsMe_2)_2$]	2057, 1992	2.05	1.52	
[$RuCl_2(CO)_2(Me_2AsSMe)_2$]	2058, 1992	2.00		2.44
[$ReCl(CO)_3(Me_2AsSAsMe_2)$]	2032, 1950, 1905	2.09, 1.96		
[$ReBr(CO)_3(Me_2AsSAsMe_2)$]	2030, 1952, 1905	2.10, 2.02		
[$ReI(CO)_3(Me_2AsSAsMe_2)$]	2030, 1953, 1906	2.15, 2.14		
[$RhCl_2(C_5Me_2)(Me_2AsSMe)$][c]		1.81		2.32

[a] In chloroform solution unless otherwise stated.

[b] Nujol mull.

[c] ^1H: C_5Me_5, δ 1.74; $\delta(^{13}C)$: +97.4 [^1J(Rh–C) 7.5 Hz], C_5Me_5; +9.1, C_5Me_5; +12.9 [^2J(Rh–As–C), 1.5 Hz], $AsMe_2$; +12.0, SMe.

notable *cis* effect in these complexes, where the methyl protons are shifted increasingly downfield on progressing along the series Cl, Br, I. This trend has been similarly noted for the corresponding *fac*-$[ReX(CO)_3(Me_2AsSMe)_2]$ complexes.[7]

The ^1H NMR spectrum of $[RhCl_2(C_5Me_5)(Me_2AsSMe)]$ consists of the three expected singlets of relative intensity 15 : 6 : 3 from high to low field, respectively. The arsenic-methyl protons are shifted by coordination further downfield (relative to the free ligand than are the sulphur-methyl protons suggesting an arsenic–rhodium-bound ligand. Further, whilst ^{103}Rh coupling is not observed to any of the protons in the molecule, our $^{13}C-\{^1H\}_{sel}$ experiments correlate the arsenic-methyl protons with a carbon resonance coupled to ^{103}Rh (^2J *ca* 1.5 Hz), in the absence of a comparable (^3J) coupling to the sulphur-methyl carbon.

REFERENCES

1. E. W. Ainscough, A. M. Brodie and G. Leng-Ward, *J. Chem. Soc., Dalton Trans.* 1974, 2437.
2. W. Ehrl and H. Vahrenkamp, *Chem. Ber.* 1970, **103**, 3563.
3. J. Grobe and D. Le Van, *Z. Naturforsch.* 1979, **34B**, 1653.
4. J. Grobe and D. Le Van, *Z. Naturforsch.* 1980, **35B**, 694.
5. J. Grobe and D. Le Van, *J. Fluorine Chem.* 1984, **24**, 25.
6. E. W. Abel, M. A. Beckett, P. A. Bates and M. B. Hursthouse, *J. Organomet. Chem.* (in press).
7. E. W. Abel and M. A. Beckett, *J. Chem. Soc., Dalton Trans.* (in press).
8. R. A. Zingaro, K. J. Irgolic, D. H. O'Brien and L. J. Edmonson, Jr, *J. Am. Chem. Soc.* 1971, **93**, 5677.
9. W. R. Cullen, *Can. J. Chem.* 1963, **41**, 2424.
10. F. Bonati and G. Minghetti, *Gazz. Chim. Ital.* 1973, **103**, 373.
11. G. Dolcetti and J. R. Norton, *Inorg. Synth.* 1976, **16**, 35.
12. J. W. Kang, K. Moseley and P. M. Maitlis, *J. Am. Chem. Soc.* 1969, **91**, 5970.
13. J. M. Jenkins, M. S. Lupin and B. L. Shaw, *J. Chem. Soc. A* 1966, 1787.

Polyhedron Vol. 6, No. 6, pp. 1261–1272, 1987
Printed in Great Britain

0277–5387/87 $3.00+.00

NMR STUDIES OF STEREOCHEMICAL NON-RIGIDITY IN DINUCLEAR THIOLATO-BRIDGED COMPLEXES OF PLATINUM(IV) WITH PLATINUM(II) AND PALLADIUM(II): THE STRUCTURE OF [Pt(dppe)(μ_2-SMe)$_2$PtClMe$_3$]

EDWARD W. ABEL,* NEIL A. COOLEY, KENNETH KITE, KEITH G. ORRELL and VLADIMIR ŠIK

Department of Chemistry, The University, Exeter EX4 4QD, U.K.

and

MICHAEL B. HURSTHOUSE and HELEN M. DAWES

Department of Chemistry, Queen Mary College, Mile End Road, London E1 4NS, U.K.

(*Received* 11 *September* 1986; *accepted* 13 *November* 1986)

Abstract—The complexes [M(dppe)(μ_2-SMe)$_2$PtXMe$_3$] [M = Pd or Pt; X = Cl, Br or I; dppe = 1,2-bis(diphenylphosphino)ethane] have been synthesized, and by means of ^{1}H and ^{31}P variable-temperature NMR studies are shown to have several different fluxional modes. Where possible, accurate activation parameters for the processes have been determined. The unexpected trends of these values demonstrate the consequences of the presence of the four-membered Pt(IV)—S—M(II)—S ring. The structure of a representative member of this novel range of complexes, [Pt(dppe)(μ_2-SMe)$_2$PtClMe$_3$], has been determined by X-ray diffraction methods.

Since the earliest observations[1] of fluxionality in transition-metal complexes the field has greatly proliferated.[2–4] In many cases the occurrence of stereochemical non-rigidity is facilitated by or dependent upon the presence of the transition metal(s). Large numbers of these species exhibit transitions with values of activation free energy change $\Delta G^{\ddagger}$ in the range 35–100 kJ mol^{-1}, which enables them to be conveniently studied by DNMR techniques. The organochalcogen complexes of the trimethylplatinum halides fall into this category and have been studied extensively.[4] Pyramidal chalcogen atom inversion is commonly observed in such compounds, along with, in many cases, higher-energy processes which involve very considerable bond reorganization. As a further step in our investigation of the factors influencing the stereodynamics and energetics of such systems we have prepared and studied the thiolato complexes [M(dppe)(μ_2-SMe)$_2$PtXMe$_3$], (M = Pd or Pt; X = Cl, Br or I).

Mononuclear metal thiolato complexes have been utilized in the preparation of a range of heteronuclear transition-metal complexes,[5] and in some of these species stereochemical non-rigidity has been observed, and comparisons made between thiolato complex metalloligands and thioethers.[6] Quantitative studies of fluxionality of these thiolato-bridged species are to date rare, and we have now examined them by full DNMR bandshape analysis.

EXPERIMENTAL

Materials

The following were prepared using previously reported procedures: [M(dppe)(SMe)$_2$] (M = Pd or Pt),[6] [{PtXMe$_3$}$_4$][7,8] (X = Cl, Br or I), [Pd(dppe)Cl$_2$],[9] and [Pt(PPh$_3$)$_4$].[10]

* Author to whom correspondence should be addressed.

Complexes

$[M(dppe)(\mu_2\text{-}SMe)_2PtXMe_3]$ (M = Pd *or* Pt; X = Cl, Br *or* I). All of these complexes were prepared in a similar manner and a representative example is described.

A benzene (10 cm^3) suspension of $[Pt(dppe)(SMe)_2]$ (0.11 g, 0.16 mmol) was treated with $[\{PtClMe_3\}_4]$ (0.47 g, 0.042 mmol). The mixture was stirred for 4 h until the solution lost all trace of the yellow $[Pt(dppe)(SMe)_2]$. The resulting white precipitate was collected by decantation. This crude product was recrystallized from chloroform (14 cm^3) and hexane (20 cm^3) by layer diffusion at −10°C, giving colourless prisms of $[Pt(dppe)(\mu_2\text{-}SMe)_2PtClMe_3]$ (**1**) (0.13 g, 84%).

Complexes **2**–**6** were prepared by the same procedure, with the following reaction times and yields:

Complex	Reaction time (h)	Yield (%)
$[Pt(dppe)(\mu_2\text{-}SMe)_2PtBrMe_3]$ (**2**)	5	89
$[Pt(dppe)(\mu_2\text{-}SMe)_2PtIMe_3]$ (**3**)	8	94
$[Pd(dppe)(\mu_2\text{-}SMe)_2PtClMe_3]$ (**4**)	3	91
$[Pd(dppe)(\mu_2\text{-}SMe)_2PtBrMe_3]$ (**5**)	10	63
$[Pd(dppe)(\mu_2\text{-}SMe)_2PtIMe_3]$ (**6**)	16	36

All of the complexes were isolated as air-stable crystals. The compounds were only moderately soluble in benzene and toluene, but were very soluble in dichloromethane, chloroform and nitrobenzene. Solutions of the compounds in chlorohydrocarbon solvents tended to react over a period of days to produce $[\{PtMe_3(SMe)\}_4]$ and $[M(dppe)Cl_2]$.

Characterization data for complexes **1**–**6** are given in Table 1.

Preparation of [PdS—CH(Me)—CH_2—S(dppe)]. A suspension of $[Pd(dppe)Cl_2]$ (0.50 g, 0.87 mmol) in toluene (50 cm^3) was stirred with 1,2-propanedithiol (2 cm^3) and triethylamine (4 cm^3) for 3 h. Diethylether (200 cm^3) was added to this mixture and the precipitated triethylamine hydrochloride was removed by filtration. The resulting yellow solution was cooled to −5°C yielding large yellow needles of [PdS—CH(Me)—CH_2—S(dppe)] (**7**) (0.48 g, 98%) ^{31}P NMR ($CDCl_3$): δ (ppm) = 49.7 and 50.1, relative to 85% H_3PO_4 (ext.), J(P–P) (Hz) = 32.1.

Preparation of [PtS—CH(Me)—CH_2—S$(Ph_3P)_2$]. 1,2-Propanedithiol (1.0 cm^3) was added to a solution of $[Pt(PPh_3)_4]$ in dichloromethane (10 cm^3). The solution immediately turned pale yellow and after 3 min stirring was discontinued. The mixture was triturated with diethylether (30 cm^3) and cooled to −20°C. The product [PtS—CH(Me)—CH_2—S$(Ph_3P)_2$] (**8**) (0.27 g, 76%) was isolated as pale yellow prisms.

^{31}P NMR ($C_6D_5NO_2$): δ (ppm) = 21.4 and 22.1, relative to 85% H_3PO_4 (ext.), J(P–P) (Hz) = 23.8.

NMR spectra

^1H and ^{31}P spectra were recorded on a Brüker AM250 spectrometer operating at 250 and 36.2 MHz, respectively. Measurement of ^1H and ^{195}Pt NMR spectra was also performed for certain compounds at the SERC High Field NMR Service

Table 1. Characterization of the $[M(dppe)(\mu_2\text{-}SMe)_2PtXMe_3]$ complexes

Complex	M	X	M.p. (°C)	Colour	Analysis			
					% C[a]	% H[a]	% C[b]	% H[b]
1	Pt	Cl	216–217(d)	Colourless	38.6	4.1	38.7	4.1
2	Pt	Br	227–229(d)	Colourless	37.1	3.9	36.9	3.9
3	Pt	I	225–226(d)	Colourless	35.3	3.8	35.3	3.7
4	Pd	Cl	205–208(d)	Yellow	41.2	4.3	42.5	4.5
5	Pd	Br	198–201(d)	Yellow	40.5	4.3	40.5	4.3
6	Pd	I	235–239(d)	Yellow	38.4	4.1	38.5	4.1
7[c]			225–227(d)	Yellow/orange	57.5	5.5	56.7	5.4
8[d]			292–295	Yellow	56.7	4.3	56.7	4.4

[a] Obtained.
[b] Calculated.
[c] [PdS—CH(Me)—CH_2—S(dppe)].
[d] [PtS—CH(Me)—CH_2—S$(Ph_3P)_2$].

at Warwick University. Computer simulation of spectra was carried out using previously reported procedures.[4]

X-ray crystallography

All crystallographic measurements were made on a crystal sealed under nitrogen in a glass capillary, using a CAD-4 diffractometer operating in the ω–2θ scan mode with graphite-monochromated Mo-K_α radiation ($\lambda = 0.71069$ Å) as described previously.[11]

Crystal data. $C_{31}H_{39}ClS_2Pt_2P_2 \cdot CHCl_3$, formula weight = 1082.732, monoclinic, $a = 10.298(1)$, $b = 20.189(5)$, $c = 18.209(2)$ Å, $\beta = 92.41(1)°$, $V = 3782.2$ Å^3, space group $P2_1/c$, $Z = 4$, $D_{calc} = 1.87$ g cm^{-3}, μ(Mo-K_α) = 73.6 cm^{-1}. Data were collected in the range $1.5 \leqslant \theta \leqslant 23°$, giving 5612 measured, 5243 unique and 3904 with $I > 1.5\sigma(I)$.

The structure was solved via the heavy-atom method, developed and refined by ΔF syntheses and full-matrix least squares. A disordered molecule of chloroform was found to be present. An absorption correction was applied using DIFABS.[12] Non-hydrogen atoms were refined anisotropically; hydrogens on phenyl rings were freely refined isotropically, those on the CH_2 groups were included with free positional refinement but a common group isotropic U value, whilst methyl hydrogens were inserted in idealized positions and refined as part of a rigid group, with a group U_{iso} for each methyl. The chloroform molecule was represented by one C atom and six half-Cl atoms. The final R and R_ω values were 0.0338 and 0.0342 for 320 parameters. The weighting scheme $\omega = 1/[\sigma^2(F_o) + 0.0002F_o^2]$ was applied. Structure solution and refinement computations were made using SHELX[13] on a VAX 11/780 computer; scattering factor data were taken from Ref. 14. Lists of atomic positional and thermal parameters for all atoms, full lists of bond lengths and angles, and F_o/F_c values have been deposited as supplementary data with the Editor from whom copies are available on request. Atomic co-ordinates have also been deposited with the Cambridge Crystallographic Data Centre.

RESULTS AND DISCUSSION

X-ray studies

The structure of [Pt(dppe)(μ_2-SMe)$_2$PtClMe$_3$] has been determined by X-ray crystallography, and is illustrated in Fig. 1, along with selected bond distances and angles in Table 2.

The two platinum atoms have co-ordination numbers of four and six and oxidation states II and IV for Pt(1) and Pt(2), respectively. The platinum–platinum interatomic distance is 3.482 Å which is not indicative of metal–metal bonding. The bond angles S(1)—Pt(1)—S(2) and S(1)—Pt(2)—S(2) are 83.0(2) and 79.2(2)°, respectively, showing the strained nature of the Pt_2S_2 ring. The dihedral angle between the square plane of Pt(1) and the equatorial plane (containing both sulphur atoms) of Pt(2) is approximately 154°. This angle compares with angles between the square planes in the thiolato-bridged Pt(II) dimers [{Pt(PMePh$_2$)(SCH$_2$Ph)(μ_2-SCH$_2$Ph)}$_2$][15] and *cis* - [{Pt(PPr$^n_3$)Cl(μ_2 - SEt)}$_2$][16] of 138.8 and 130°, respectively. In [Pt(dppe)(μ_2-SMe)$_2$PtClMe$_3$] the sulphur atoms are pseudo-tetrahedral in character and the methylthio groups adopt an *anti* configuration, thereby minimizing steric crowding. The Pt(II)—S bonds at 2.358(4) and 2.386(4) Å are notably shorter than the Pt(IV)—S bonds at 2.461(4) and 2.468(4) Å.

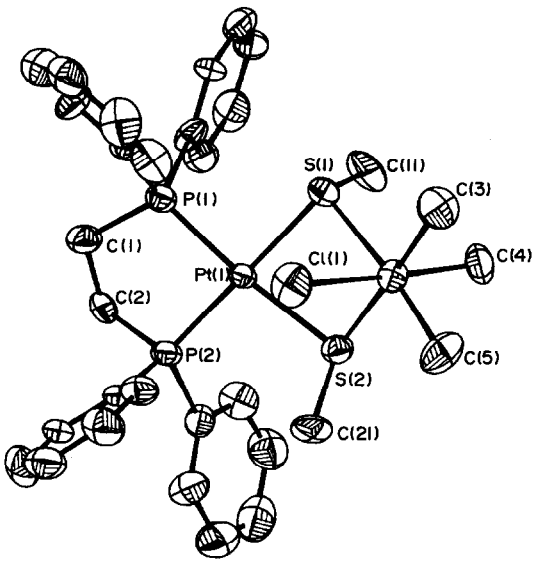

Fig. 1. ORTEP drawing of the X-ray structure of [Pt(dppe)(μ_2-SMe)$_2$PtClMe$_3$] with atom labelling.

Low-temperature NMR studies

The two important relevant structural features of these complexes are the folded nature of the Pt_2S_2 ring and the pyramidal configuration of the bridging sulphur atoms, as revealed by the X-ray diffraction studies. Thus, in principle in solution, a total of eight configurational and conformational isomers are possible, with interconversions occurring by the two processes of ring reversal and pyramidal inversion about sulphur. Ring reversal will convert

Table 2. Selected bond distances (Å) and angles (°) for [Pt(dppe)(μ_2-SMe)$_2$PtClMe$_3$]

Pt(2)—Pt(1)	3.482(4)	S(1)—Pt(1)	2.386(4)
S(2)—Pt(1)	2.358(4)	P(1)—Pt(1)	2.249(4)
P(2)—Pt(1)	2.252(4)	S(1)—Pt(2)	2.468(4)
S(2)—Pt(2)	2.461(4)	Cl(1)—Pt(2)	2.492(4)
C(3)—Pt(2)	2.049(13)	C(4)—Pt(2)	2.036(12)
C(5)—Pt(2)	2.089(14)	C(11)—S(1)	1.819(13)
C(21)—S(2)	1.817(12)	C(1)—P(1)	1.832(12)
C(111)—P(1)	1.816(10)	C(121)—P(1)	1.821(12)
C(2)—P(2)	1.823(12)	C(211)—P(2)	1.823(11)
C(221)—P(2)	1.812(10)		
S(2)—Pt(1)—S(1)	83.0(2)	P(1)—Pt(1)—S(1)	92.6(2)
P(1)—Pt(1)—S(2)	172.3(1)	P(2)—Pt(1)—S(1)	177.0(1)
P(2)—Pt(1)—S(2)	97.9(2)	P(2)—Pt(1)—P(1)	86.1(2)
S(2)—Pt(2)—S(1)	79.3(2)	Cl(1)—Pt(2)—S(1)	84.8(2)
Cl(1)—Pt(2)—S(2)	90.8(2)	C(3)—Pt(2)—S(1)	96.0(4)
C(3)—Pt(2)—S(2)	174.9(3)	C(3)—Pt(2)—Cl(1)	90.7(4)
C(4)—Pt(2)—S(1)	96.3(4)	C(4)—Pt(2)—S(2)	92.7(4)
C(4)—Pt(2)—Cl(1)	176.5(3)	C(5)—Pt(2)—S(1)	173.5(3)
C(5)—Pt(2)—S(2)	96.9(4)	C(5)—Pt(2)—Cl(1)	90.0(4)
C(4)—Pt(2)—C(3)	85.8(5)	C(5)—Pt(2)—C(3)	87.9(5)
C(5)—Pt(2)—C(4)	89.2(5)	Pt(2)—S(1)—Pt(1)	91.7(2)
C(11)—S(1)—Pt(1)	103.1(5)	C(11)—S(1)—Pt(2)	108.4(5)
Pt(2)—S(2)—Pt(1)	92.5(2)	C(21)—S(2)—Pt(1)	109.5(4)
C(21)—S(2)—Pt(2)	107.5(5)	C(1)—P(1)—Pt(1)	109.6(4)
C(111)—P(1)—Pt(1)	119.9(4)	C(111)—P(1)—C(1)	103.3(5)
C(121)—P(1)—Pt(1)	110.0(4)	C(121)—P(1)—C(1)	107.5(5)
C(121)—P(1)—C(111)	105.7(5)	C(2)—P(2)—Pt(1)	106.4(4)
C(211)—P(2)—Pt(1)	115.2(4)	C(211)—P(2)—C(2)	104.5(5)
C(221)—P(2)—Pt(1)	115.8(4)	C(221)—P(2)—C(2)	106.7(5)
C(221)—P(2)—C(211)	107.5(5)		

exo-methylthio groups to *endo* and vice versa, and independent pyramidal sulphur inversion will exchange *syn* to *anti* configurations of the complex. Both the conformational and configurational changes would be required to fully interconvert all of the possible isomers.

The room-temperature methyl ^{1}H spectral data for all six complexes are collected in Table 3. The ^{1}H spectrum of **1** [Fig. 2(a)] consists of a doublet signal with ^{195}Pt satellites (in addition to a singlet due to a trace of water in the solvent CD_2Cl_2). The doublet splitting is due to four-bond coupling to

Table 3. Selected ^{1}H NMR chemical shifts and coupling constants for [M(dppe)(μ_2-SMe)$_2$PtXMe$_3$] (M = Pd or Pt; X = Cl, Br or I)

Complex	Solvent	T (°C)	Platinum–methyl (*trans* to S) δ^a	Platinum–methyl (*trans* to S) $^2J^b$	Platinum–methyl (*trans* to X) δ^a	Platinum–methyl (*trans* to X) ^2J	Sulphur–methyl δ^a
1	CD_2Cl_2	25	0.68	69.4	0.90	77.6	1.52
2	$CDCl_3$	25	0.98	69.3	1.16	77.2	1.69
3	$CDCl_3$	25	1.08	70.1	1.28	76.4	1.79
4	$C_6D_5NO_2$	25	1.37	69.5	1.40	80.9	1.73
5	$C_6D_5NO_2$	25	1.48	69.5	1.52	78.0	1.73
6	$C_6D_5NO_2$	25	1.51	71.9	1.59	76.2	1.73

[a] Chemical shifts (ppm).
[b] $^2J(^{195}Pt-^1H)$ (Hz).

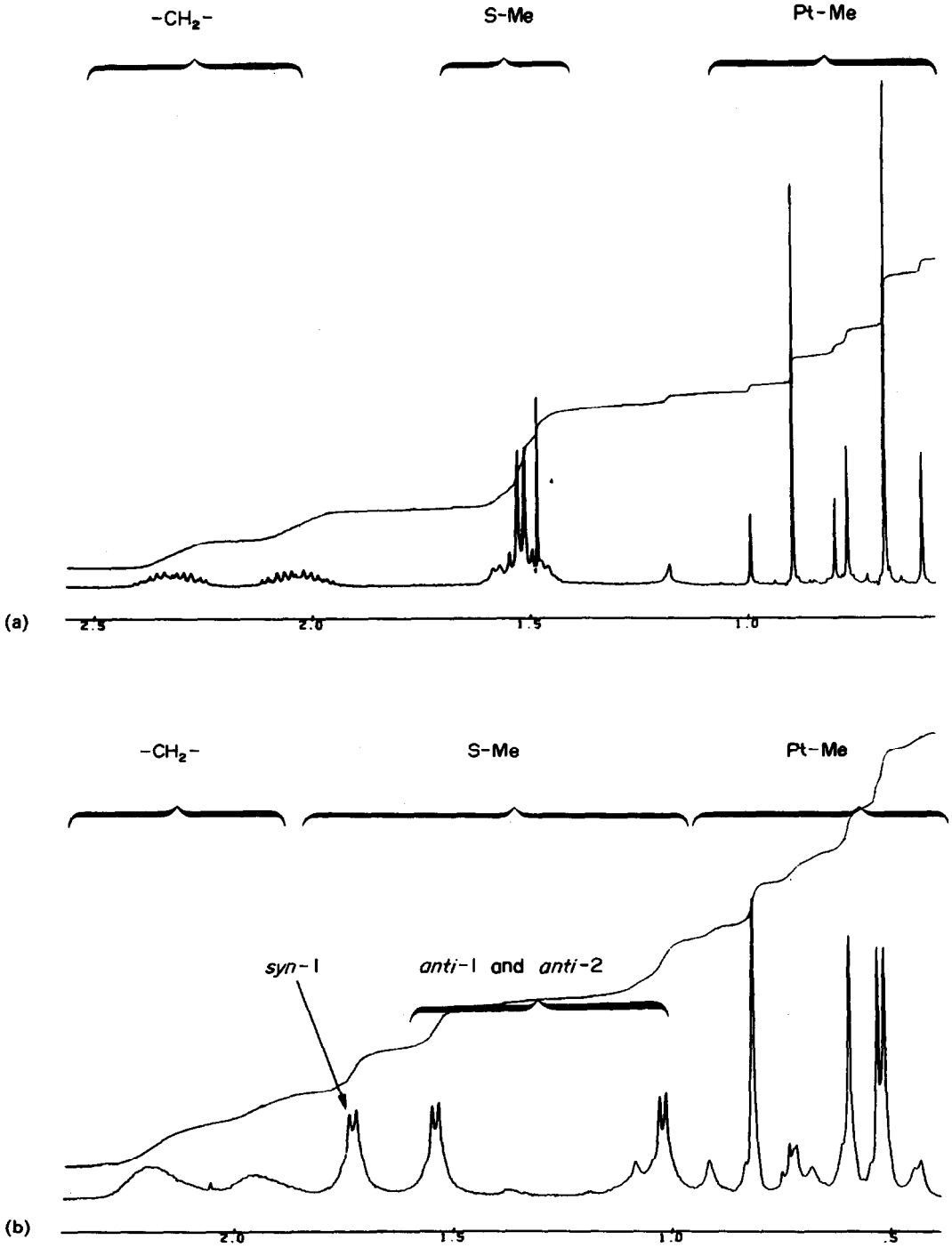

Fig. 2. ^{1}H NMR spectra of [Pt(dppe)(μ_2-SMe)$_2$PtClMe$_3$] at: (a) 25°C, and (b) −105°C.

the ^{31}P nucleus *trans* to the methylthio group. The ^{195}Pt satellite spectrum shows six of the eight expected signals due to the methylthio protons coupling to one Pt(II) and one Pt(IV) nucleus with different magnitudes. Thus, the total SMe proton absorption clearly shows only one environment for methylthio groups, but on cooling changes occur in all of the spectral regions. At −105°C three signals of approximately equal intensity are observed for the methylthio resonances [Fig. 2(b)]. These changes are interpretable as the slowing down of the pyramidal sulphur inversions on the NMR time-scale; but not unexpectedly ring reversal is still very rapid, and the *endo* and *exo* conformers are not separately observable.

In the solid state complex **1** is in the *anti* con-

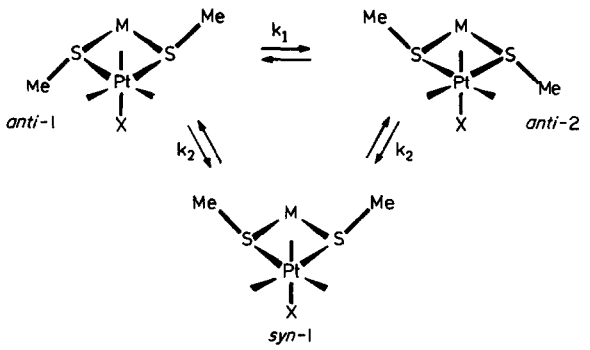

Fig. 3. Interconversion of isomers in complexes **1–6**.

figuration, and the solution spectrum is dominated by the presence of these two diastereoisomers, as illustrated in Fig. 3. These are in equilibrium with the *syn* form, which is thought to be *syn*-1 by virtue of the population dependence of this structure upon halogen type. The populations of these invertomers (Table 4) increase with halogen size, namely Cl < Br < I in accordance with previous findings for the complexes $[PtXMe_3(MeEZEMe)]$ [E = S or Se; X = Cl, Br or I; Z = —CH_2—CH_2— or —CH=CH—).[4]

These conclusions from the ^1H spectra are confirmed by ^{195}Pt NMR spectroscopy (Table 5), which at low temperature shows resonances indicative of only two environments for both Pt(II) and Pt(IV) atoms.[17] For both Pt(II) and Pt(IV) the separate signals are in an intensity ratio of approximately 2:1. The two *anti* isomers are optical antimers and not separately observable by NMR, but from these data we can say that the isomers *anti*-1, *anti*-2 and *syn*-1 in Fig. 3 are all present in approximately equal amounts.

At 25°C the ^{195}Pt spectrum of **1** is averaged to give only one signal each for Pt(II) and Pt(IV) as a result of the onset of rapid sulphur inversion.

The ^{31}P NMR spectra of complexes **1–6** are similar (Table 4), with room-temperature spectra again confirming rapid sulphur inversions. At −80°C "static" spectra are observable with the mirror-image invertomers *anti*(1) and *anti*-(2) producing AB or AX patterns when the two phosphorus environments are anisochronous (complexes **1**, **3** and **6**), and a broad singlet in the other cases (complexes **2**, **4** and **5**). In all cases a singlet due to the *syn*-1 species is additionally observed.

Activation parameters for sulphur inversion

The rate constants in Fig. 3 represent two distinct processes, but the experimental spectra were found

Table 4. ^{31}P NMR spectroscopic data for $[M(dppe)(\mu_2\text{-}SMe)_2PtXMe_3]$ (M = Pd or Pt, X = Cl, Br or I)

Complex	T (°C)	δ^a (ppm)	Invertomer	% Population
1	25	43.2[b]		
1	−80	44.5	*syn*-1	29.6
		43.9, 42.7	*anti*-1/2	70.4
2	25	42.8[c]		
2	−80	42.4	*syn*-1	35.2
		43.9	*anti*-1/2	64.8
3	25	42.6[c]		
3	−80	42.3	*syn*-1	38.7
		44.3, 43.6	*anti*-1/2	61.3
4	25	52.6		
4	−80	52.6	*syn*-1	24.8
		54.4	*anti*-1/2	75.2
5	−5	52.4		
5	−100	52.9	*syn*-1	27.9
		54.5	*anti*-1/2	62.1
6	0	52.1		
6	−80	52.2	*syn*-1	33.3
		54.4, 53.2	*anti*-1/2	66.7

[a] Shifts relative to 85% H_3PO_4 (ext). Solvent CD_2Cl_2.
[b] $^1J(^{195}Pt\text{–}^{31}P) = 2873$ Hz; $^3J(^{195}Pt\text{–}^{31}P) = 116$ Hz.
[c] $^1J(^{195}Pt\text{–}^{31}P) = 2880$ Hz; $^3J(^{195}Pt\text{–}^{31}P) = 117$ Hz.

Table 5. ^{195}Pt–{^{1}H} chemical shift data for [Pt(dppe)(μ_2-SMe)$_2$PtClMe$_3$][a]

Nucleus	T (°C)	Chemical shift[b] (δ) (ppm)	
Pt(II)	25	−9	
Pt(IV)	25	1995	
		anti-1/2	*syn*-1
Pt(II)	−40	−21	4
Pt(IV)	−40	1954	1870

[a] In CD_2Cl_2.
[b] Shifts relative to $\Xi(^{195}Pt) = 21.4$ MHz.

to be virtually insensitive to k_1, the rate constant for a double-site inversion. Only complex **6** exhibited appreciable sensitivity to this parameter, and the experimental and computer synthesized spectra based on the ^{31}P spin problem (Scheme 1) for this complex are illustrated in Fig. 4. The ^{31}P-determined activation parameters for pyramidal inversion about sulphur in compounds **1–6** are noted in Table 6.

Extensive studies of organo-sulphur and organo-selenium ligands co-ordinated to transition metals have demonstrated the dramatic lowering of the barriers to pyramidal inversion.[4] Among many factors recognized, the two that predominate in the current context are metal electronegativity and π-conjugation effects. In the present complexes, the sulphur inversion barriers ΔG^+ are in the range 40–50 kJ mol^{-1}. These represent among the lowest values which have been obtained to date for complexes of the trimethylplatinum halide unit. Such low energies presumably reflect the co-ordination of each inverting sulphur atom to two transition metals.

Complexes **1–6** show two distinctive trends in their values of ΔG^+ for pyramidal inversion, namely:

$$\Delta G^+, \text{Pd(II)} > \text{Pt(II)}$$

and

$$\Delta G^+, \text{I} > \text{Br} > \text{Cl}^*$$

Both trends are unusual.

In general,[4] the variation of halogen in trimethylplatinum halide complexes has very little effect upon the barriers to inversions and is attributed to the negligible influence of ligands in the *cis* position with respect to inverting atoms. As evidenced by the direction of halogen dependence of the invertomer populations in these complexes, the steric effect of halogen on the ground state of the complexes is not the major effect, or the order would be reversed. We would therefore consider that the order of energies is possibly due to a halogen-dependent destabilization of the transition states, possibly associated with the special nature of the inversion in the constrained four-membered ring.

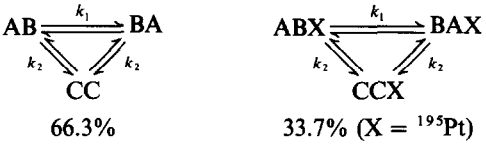

Scheme 1.

The lower values of ΔG^+ for sulphur inversion in the Pt(II) complexes compared to the Pd(II) complexes is unexpected and unprecedented, as both on electronegativity and conjugation arguments the reverse order would be predicted.

In the transition state for pyramidal sulphur inversion the M—S—M′ bond angle should become 120°, and it would appear that access to this ideal transition-state geometry is more restricted for the Pd(II)—S—Pt(IV)—S ring than for the corresponding Pt(II)—S—Pt(IV)—S system.

High-temperature ^{1}H *NMR studies*

Platinum–methyl equilibration. Warming solutions of complexes **1–6** in either *d*-chloroform or d_5-nitrobenzene caused the ^{1}H NMR signals of the methyl–platinum protons to broaden and eventually coalesce to a sharp singlet at 100°C, with associated Pt(IV) satellites retained. Further, while these changes were taking place, no alteration of the methyl–sulphur resonances occurred and all ^{195}Pt(IV)–S–C–^{1}H couplings were retained unaltered. These spectral variations are fully temperature-reversible, although some decomposition of **6** does take place at the higher temperatures.

The above changes are indicative of intramolecular scrambling of the platinum methyl groups, and the variable temperature spectra can be simulated using the ^{1}H spin problem described in Scheme 2, where the labels R and S refer to

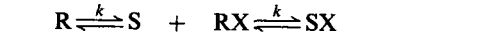

Scheme 2.

* The ΔG^+ value for complex **4** does not fully accord with this trend, but the large value of ΔS^+ and the low $\log_{10} A$ values quoted for this case suggest that our band-shape fittings were less reliable here.

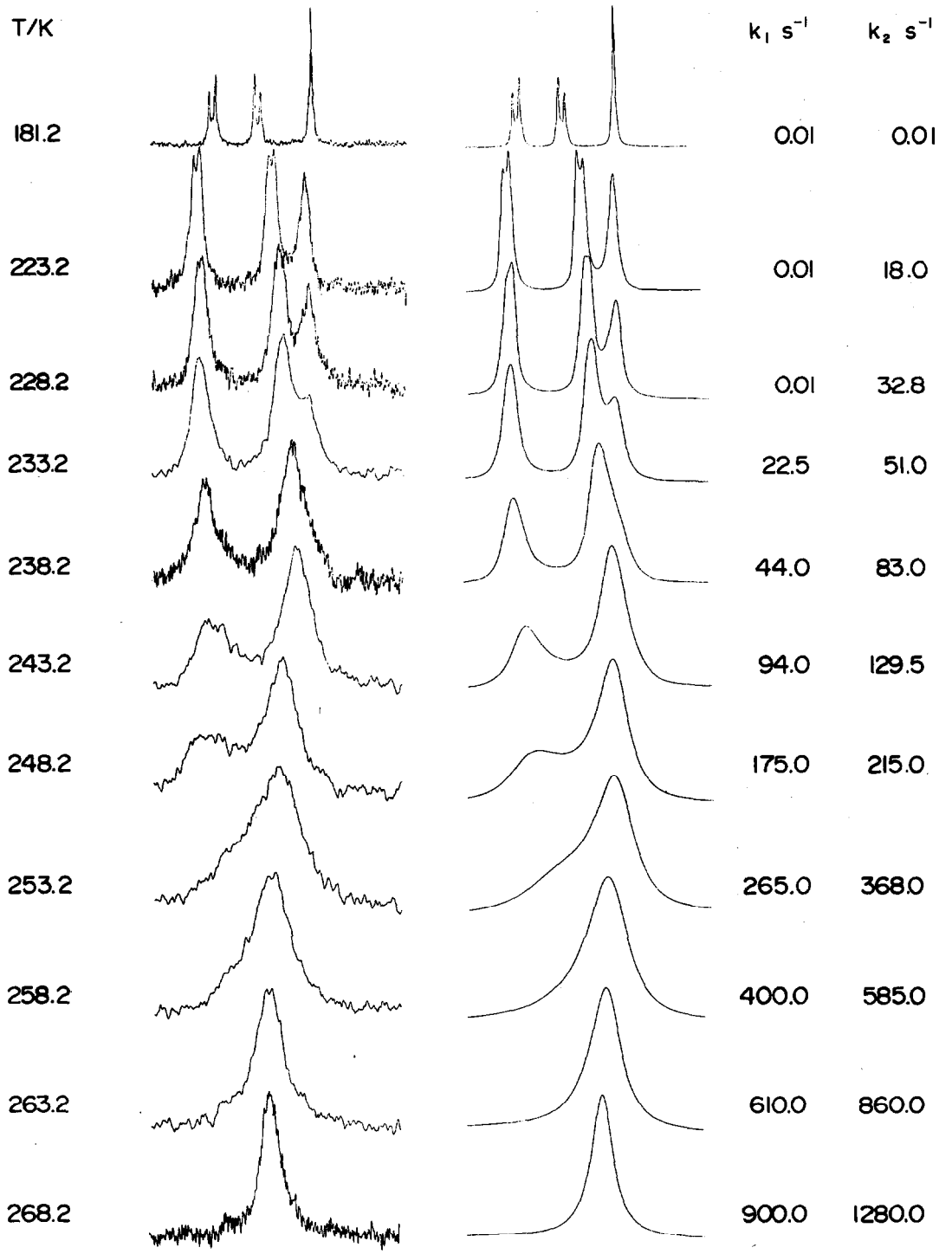

Fig. 4. Variable-temperature experimental and computer-simulated ^{31}P NMR spectra of $[Pd(dppe)(\mu_2\text{-}SMe)_2PtBrMe_3]$ showing the effects of pyramidal sulphur atom inversion.

Table 6. Arrhenius and Eyring activation parameters for pyramidal sulphur inversion

Complex	Inversion[a]	E_a (kJ mol^{-1})	$\log_{10}[A\ (s^{-1})]$	ΔG^{+} (kJ mol^{-1})	ΔH^{+} (kJ mol^{-1})	ΔS^{+} (J K^{-1} mol^{-1})
1	S^1	41.8±0.9	12.4±0.2	44.0±0.3	40.0±0.9	−13.5±4.2
2	S^1	46.5±0.3	13.1±0.1	44.5±0.1	44.7±0.3	0.4±1.5
3	S^1	46.5±0.8	12.9±0.2	45.6±0.2	44.6±0.8	−3.2±3.5
4[b]	S^1	40.9±1.2	11.3±0.3	49.6±0.4	39.0±1.2	−35.6±5.1
5	S^1	47.8±1.0	12.7±0.2	48.5±0.2	45.9±1.0	−8.8±4.1
6	S^1	47.3±0.8	12.3±0.2	50.0±0.2	45.2±0.7	−16.1±3.1
7	S^2	53.5±2.9	13.4±0.6	49.8±0.6	51.4±3.0	5.4±11.9

[a] S^1 = [*anti*-1/2] → [*syn*-1]; S^2 = [*anti*-2] → [*anti*-1].
[b] The data here are considered less reliable.

the axial and equatorial platinum methyls and are population-weighted in a 1 : 2 ratio.

Figure 5 shows the experimental and computer-simulated ^{1}H NMR spectra of **4** in the temperature range of the platinum–methyl fluxions, and the activation parameters for the process are recorded in Table 7. The ΔG^{+} values are of comparable magnitude to those found[18] for other Pt(IV) chelate complexes, e.g. [$PtXMe_3(MeSCH_2SCH_2SMe)$] (X = Cl, Br or I), but unlike the previous study show a small but consistent halogen dependence. In Pt(IV)-chelated thioether complexes[19] the analogous platinum–methyl fluxions are believed to be associated with, in effect, a concurrent 180° rotation of the chelating ligand.[4] The symmetry of complexes **1–6** prevents full evidence of such a movement here, but it seems probable that some such comparable relative motion between the $M(dppe)(\mu_2\text{-}SMe)_2$ moiety and the $PtXMe_3$ unit is taking place in a non-dissociative manner in order to produce such spectral changes.

Palladium thiolato moiety rotation. Whilst the NMR signals for the methylthio hydrogens of Pt(II)–Pt(IV) complexes (**1–3**) remained essentially unchanged over the temperature range 25–150°C, this was not the case for the Pd(II)–Pt(IV) complexes (**4–6**). The bandshape changes of complex **5** are illustrated in Fig. 6 along with computer simulations.

These changes are indicative of an equilibration of the magnetic environments of the two methylthio groups with respect to the phosphorus atoms of the dppe ligand. At ambient temperature each methylthio hydrogen is coupled strongly [^4J(P–Pd–S–C–H) ≃ 14 Hz] to the phosphorus atom mutually *trans*, and only very weakly [^4J(P–Pd–S–C–H) < 1 Hz] to the mutually *cis* phosphorus. At higher temperatures (Fig. 6) the methylthio hydrogens are coupled equally to both of the phosphorus atoms in dppe. The signal essentially changes from a doublet to a triplet, with a halving of the phosphorus–hydrogen coupling, but the full retention of the Pt(IV) satellites.

We perceive two possible processes which could explain these spectral changes in compounds **4–6**. The first would involve successive 180° "rotations" of the dppe ligand about the palladium, whereas the second possibility could involve the entire (dppePd) moiety with respect to the rest of the molecule (Fig. 7). The first of these processes seems unlikely as studies of [$PtClMe_3$dppe] have shown no such rotational process up to 150°C. However, presumably due to the availability of extra lone pairs of electrons on sulphur ligands as opposed to phosphorus ligands, such rotations about metal–sulphur systems have been reported and well characterized.[4] We would therefore propose that these spectral changes occur as a result of a rotation of the (dppePd) moiety through 180° which affects the transposition of the mutually *cis* and *trans* MeS groups with respect to each phosphorus. The activation parameters for this proposed rotation are noted in Table 8.

Complexes **7** and **8** were prepared in order to examine the possibility of comparable rotations in these species. In both complexes the ^{31}P AB quartet was retained up to a temperature of 150°C, indicating an absence of rotation. So it would appear that the rotation of the (dppePd) moiety in complexes **4–6** is aided by the presence of a bimetallic system.

In order to explain the occurrence of methyl scrambling about the Pt(IV) centre, it would appear that both the Pd(II) and Pt(IV) moieties are each undergoing independent "rotations" relative to the central methylthio bridges in complexes **4–6**. In the Pt(II)–Pt(IV) complexes (**1–3**), the unchanged nature of the SMe signal at high temperatures

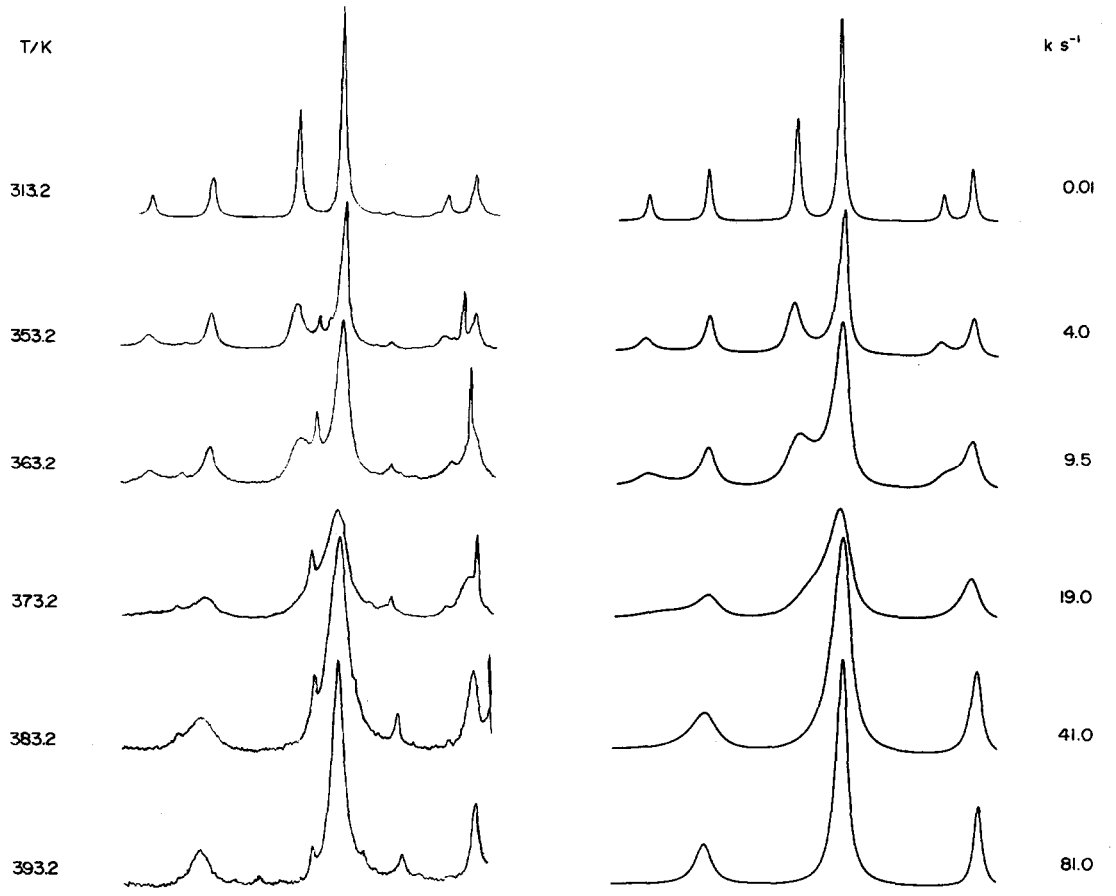

Fig. 5. Variable-temperature experimental and computer-simulated ^1H NMR spectra of [Pd(dppe)(μ_2-SMe)$_2$PtBrMe$_3$] showing the effects of platinum–methyl group scrambling.

Table 7. Arrhenius and Eyring activation parameters for platinum-methyl scrambling

Complex	E_a (kJ mol^{-1})	$\log_{10}[A\ (s^{-1})]$	ΔG^+ (kJ mol^{-1})	ΔH^+ (kJ mol^{-1})	ΔS^+ (J K^{-1} mol^{-1})
1	79.6±3.0	12.4±0.4	81.7±0.8	76.4±3.0	−17.5±8.0
2	81.2±1.7	13.0±0.2	79.7±0.3	78.2±1.7	−5.2±4.7
3	77.4±0.5	12.6±0.1	78.4±0.1	74.3±0.6	−13.6±1.7
4	89.5±1.9	13.4±0.3	86.1±0.4	86.4±1.9	1.0±5.0
5	86.4±1.2	13.4±0.2	82.9±0.2	83.3±1.2	1.1±3.1
6	79.0±1.4	13.0±0.2	77.7±0.2	76.0±1.3	−5.7±3.7

Table 8. Arrhenius and Eyring activation parameters for ligand rotation in [Pd(dppe)(μ_2-SMe)$_2$PtXMe$_3$] complexes

Complex	E_a (kJ mol^{-1})	$\log_{10}[A\ (s^{-1})]$	ΔG^+ (kJ mol^{-1})	ΔH^+ (kJ mol^{-1})	ΔS^+ (J K^{-1} mol^{-1})
4	75.0±1.2	12.8±0.2	74.9±0.2	72.0±1.2	−9.9±3.2
5	69.3±1.4	11.9±0.2	74.5±0.2	66.4±1.4	−27.2±4.1
6[a]	60.0±3.5	11.4±0.5	68.3±0.5	57.2±3.5	−37.0±10.2

[a] These parameters only approximate, due to the overlap of the sulphur–methyl signal with the H_2O resonance.

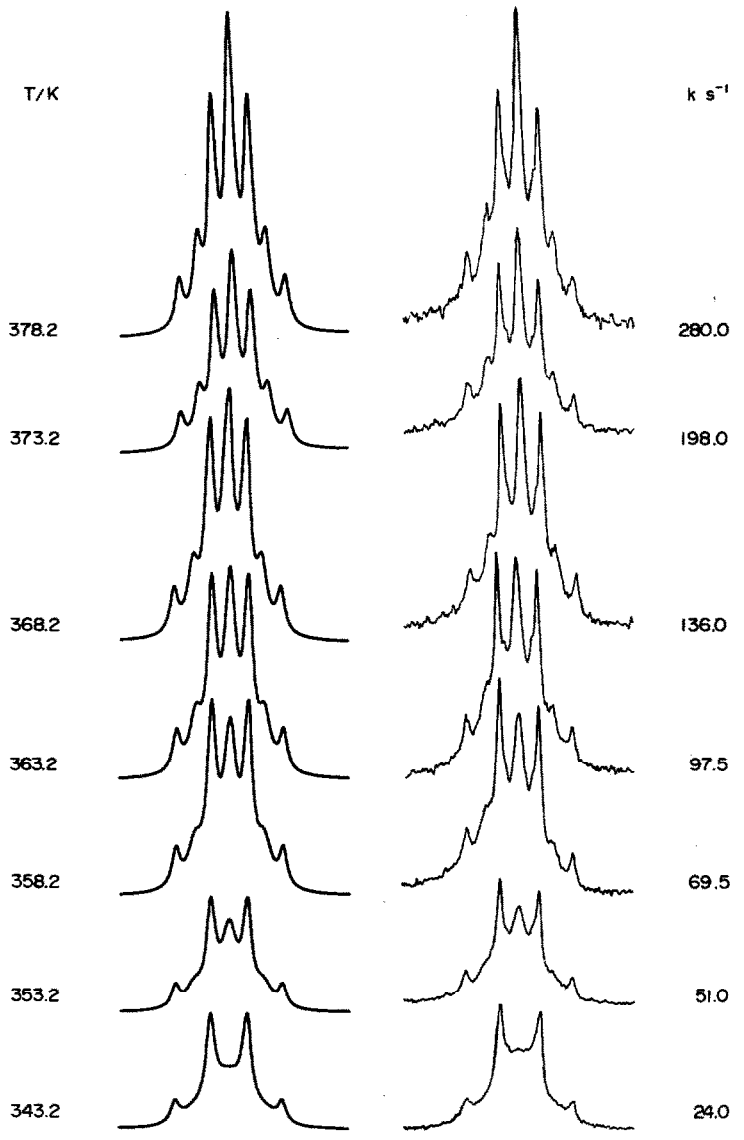

Fig. 6. Variable-temperature experimental and computer-simulated ^{1}H NMR spectra of [Pd(dppe)(μ_2-SMe)$_2$PtClMe$_3$] showing the effects of the rotation of the Pd(dppe) moiety.

implies that any rotation of the [dppePt(II)] fragment is slow on the NMR time scale, even at 150°C. The energies of the ligand rotation fluxion for the Pd(II)–Pt(IV) complex are 8–11 kJ mol^{-1} lower than for the methyl scrambling process, suggesting that the two fluxions are non-concerted and involve different transition states (Fig. 7).

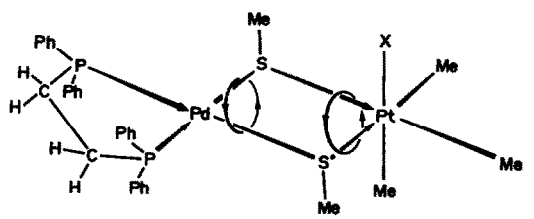

Fig. 7. Individual metal moiety"rotations" about the μ_2-SMe bridges.

Acknowledgements—We thank the S.E.R.C. for a research studentship (to N.A.C.) and for use of the High Field NMR facility at the University of Warwick.

REFERENCES

1. T. S. Piper and G. Wilkinson, *J. Inorg. Nucl. Chem.* 1956, **3**, 104.
2. L. M. Jackman and F. A. Cotton (Eds.), *Dynamic Nuclear Magnetic Resonance Spectroscopy*. Academic Press, New York (1975).
3. J. W. Faller, *Adv. Organomet. Chem.* 1978, **16**, 211.

4. E. W. Abel, S. K. Bhargava and K. G. Orrell, *Prog. Inorg Chem.* 1984, **32**, 1.
5. T. B. Rauchfuss and C. J. Ruffing, *Organometallics* 1985, **4**, 524 (and references therein).
6. P. S. Braterman, V. A. Wilson and K. K. Joshi, *J. Organomet. Chem.* 1971, **31**, 123.
7. D. E. Clegg and J. R. Hall, *Inorg. Synth.* 1967, **10**, 71.
8. D. H. Goldsworthy, Ph.D. thesis, Exeter University (1980).
9. R. G. Hayter and F. S. Humiec, *J. Inorg. Nucl. Chem.* 1964, **26**, 807.
10. R. Ugo, F. Cariati and G. La Monica, *Inorg. Synth.* 1968, **11**, 105.
11. M. B. Hursthouse, R. A. Jones, K. M. A. Malik and G. Wilkinson, *J. Am. Chem. Soc.* 1979, **101**, 4128.
12. N. Walker and D. Stuart, *Acta Cryst.* 1983, **A39**, 159.
13. G. M. Sheldrick, SHELX76, University of Cambridge (1976).
14. *International Tables for X-ray Crystallography*, Vol. 4. Kynoch Press, Birmingham (1974).
15. P. H. Bird, U. Sirwardane, R. D. Sai and A. Shaver, *Can. J. Chem.* 1982, **60**, 2075.
16. M. C. Hall, J. A. J. Jarvis, B. T. Kilbourn and P. G. Owston, *J. Chem. Soc., Dalton Trans.* 1972, 1544.
17. P. S. Pregosin, *Coord. Chem. Rev.* 1982, **44**, 247.
18. E. W. Abel, M. Z. A. Chowdhury, K. G. Orrell and V. Šik, *J. Organomet. Chem.* 1983, **258**, 109.
19. E. W. Abel, S. K. Bhargava, K. Kite, K. G. Orrell, V. Šik and B. L. Williams, *J. Chem. Soc., Dalton Trans.* 1982, 583.

Polyhedron Vol. 6, No. 6, pp. 1273–1277, 1987
Printed in Great Britain

0277–5387/87 $3.00+.00

SYNTHESIS AND SOLID-STATE STRUCTURAL CHARACTERIZATION OF BIS (THIOCYANATEMERCURY)TETRACARBONYLIRON

A. E. MAURO*

Instituto de Química de Araraquara, UNESP, C.P. 174, 14800, Araraquara, S.P. Brasil

and

R. H. A. SANTOS, M. T. P. GAMBARDELLA and R. H. P. FRANCISCO

Instituto de Física e Química de São Carlos, USP, C.P. 396, 13560, São Carlos, S. P. Brasil

(*Received* 23 *May* 1986; *accepted after revision* 13 *November* 1986)

Abstract—The bis (thiocyanatemercury)tetracarbonyliron, $[Fe(CO)_4(HgSCN)_2]$, was prepared from $[Fe(CO)_5]$ and $Hg(SCN)_2$, and studied by IR spectroscopy and X-ray diffraction. The compound crystallizes in the tetragonal space group $I4_1/a$. The unit cell, with dimensions of $a = 13.778(3)$, $c = 13.234(3)$ Å, $V = 2512.3(9)$ Å^3, contains four molecules. The iron atom is octahedrally coordinated by four carbonyl groups and two mercury atoms in *cis* positions. The coordination of the mercury atoms is distorted square-planar, since, besides mercury–iron and mercury–sulphur bonds, there are also mercury–mercury and mercury-nitrogen interactions. The Fe—Hg distance is 2.506(5) Å and the Hg—Fe—Hg angle is 78.0(1)°.

Reactions of transition-metal complexes with mercury salts have yielded a number of complexes in which there are metal–mercury bonds. Among the first ones described in the chemistry of metal carbonyls are those compounds with Fe—Hg bonds, like $[HgFe(CO)_4]$,[1] a typical example of a cluster. It has been suggested that this compound has a structure analogous to that of $[CdFe(CO)_4]$, which consists of an almost square-planar centrosymmetric eight-membered ring of alternating Cd and $[Fe(CO)_4]$ units.[2] An other important example is given in the series $[Fe(CO)_4(HgX)_2]$ (X = Cl, Br or I), prepared by Hock and Stuhlmann,[3] and subjected to investigations by Lewis,[4,5] who have also shown that these complexes react with amines, without displacement of the CO groups, giving adducts where the nitrogen ligands are coordinated to the mercury atoms. Metal–metal interactions also occur in the series $[Fe(CO)_3L_2HgX_2]$ (L = PPh_3, $AsPh_3$ or $SbPh_3$; X = Cl or Br) obtained from reactions of $[Fe(CO)_3L_2]$ with HgX_2.[6] We are interested in the chemistry of carbonyls containing this type of bonding, and in continuing the studies with compounds that have Fe—M bonds (M = Zn, Cd or Hg)[7–9] we now wish to report our results concerning the synthesis and structure of $[Fe(CO)_4(HgSCN)_2]$. The coordination geometry of the iron atom is *cis*-octahedral, but that of the mercury is not simple because of strong interactions involving the HgSCN groups.

EXPERIMENTAL

Synthesis

All operations involved in the synthesis, except the weighings, were carried out in an atmosphere of purified nitrogen in a Schlenk apparatus. To a solution of 0.236 g (0.745 mmol) of $Hg(SCN)_2$ in 12 cm^3 of H_2O, containing a small amount of NH_4SCN to facilitate the dissolution of the salt, 0.1 cm^3 (0.745 mmol) of $[Fe(CO)_5]$ was added. The mixture was stirred for 3 h at room temperature causing a yellow solid to appear. The insoluble product was filtered off, washed thoroughly with water and diethylether, and then dried *in vacuo*.

* Author to whom correspondence should be addressed.

IR spectrum

The IR spectrum, at room temperature, was recorded as a Nujol mull between CsI plates on a Carl Zeiss Specord 75 IR spectrophotometer.

Determination of the crystal and molecular structure of $[Fe(CO)_4(HgSCN)_2]$

Yellow single crystals, suitable for X-ray analysis, were obtained from acetone solution. They were found to be stable to air and X-ray exposure. The elemental analysis results were in agreement with the formula.

Crystals of $[Fe(CO)_4(HgSCN)_2]$ are tetragonal, $a = 13.778(3)$, $c = 13.234(3)$ Å, $V = 2512.3(9)$ Å^3, space group $I4_1/a$, $Z = 4$, $d_{calc} = 1.812$ Mg m^{-3}.

The cell parameters were determined by least-squares fit from 2θ values of 25 reflexions, using a Nonius CAD-4 diffractometer. Three-dimensional intensity data were collected using graphite-monochromated Mo-K_α radiation ($\lambda = 0.71069$ Å) up to $2\theta = 46°$.

The ω–2θ scanning mode with varying intervals was used. Of the 863 recorded independent reflections, 559 were observed above background [$I \geqslant 3\sigma(I)$, where $\sigma(I)$ was based on counting statistics]. The data were reduced to structure factors with absorption corrections ($\mu = 124.58$ mm^{-1}).

A Patterson map showed the Fe atom to be in the special position (0, $\frac{1}{4}$, z) on the two-fold axis, and the Hg atom in a general position. All the remaining atoms appeared clearly on the difference Fourier map. Refinement was carried out by full-matrix least-squares calculations with anisotropic thermal parameters for all atoms. The function minimized was $\Sigma w_i(k|F_o| - |F_c|)^2$ where $w_i = 1$ for the observed and $w_i = 0$ for the unobserved reflections. The atomic scattering factors used was taken from *International Tables*.[10] The final refinement cycle gave $R = 0.059$ for the observed reflections and $R = 0.076$ with inclusion of the unobserved.

Lists of atomic parameters, observed and calculated structure factors, and anisotropic thermal coefficients for all atoms have been deposited with the Editor as supplementary material.*

RESULTS AND DISCUSSION

The metal–metal-bonded species of general formula $[Fe(CO)_4(MX)_2]$ (X = Cl, Br or I) are well known for M = Hg;[4,5] only one was reported for M = Zn, $[Fe(CO)_4(ZnCl)_2]$,[11] and none containing cadmium have yet been described. In this paper we report our data concerning with the IR and X-ray diffraction studies of $[Fe(CO)_4(HgSCN)_2]$. The CO stretching vibrations are generally the most characteristic ones for the carbonyl compounds and while four IR-active modes ($2A_1 + B_1 + B_2$) are expected on the basis of group theory for the *cis*-$[Fe(CO)_4(HgSCN)_2]$ structure only one (E_u) is expected for the *trans* structure.

The *cis* structure with C_{2v}-symmetry around the iron atom is in agreement with the experimental data, since, as expected, four ν(CO) are observed in the IR spectrum (Fig. 1) of $[Fe(CO)_4(HgSCN)_2]$ at 2083(m-s), 2025(m-s), 2008(m-s) and 1980(sh) cm^{-1} (m = medium, s = strong, sh = shoulder). Taking the average ν(CO) stretching frequencies of the compounds $[Fe(CO)_4(HgSCN)_2]$ (mean 2024 cm^{-1}) and $[Fe(CO)_4(HgI)_2]$ (mean 2042 cm^{-1}) it is shown that the HgSCN group has a lower electronegativity than HgI. The strong band at 595 cm^{-1} in the IR spectrum is assigned to the bending mode δ(FeCO), which in the IR spectrum of $[Fe(CO)_4Hg]$ appears at 599 cm^{-1}.[8]

The three characteristic modes of the thiocyanate[12] were assigned to the bands observed at 2118(m-s) [ν(CN)], 765(w) [ν(CS)] and 495 cm^{-1} (w) [δ(SCN)] (w = weak).

The solid-state structure of $[Fe(CO)_4(HgSCN)_2]$ determined by X-ray diffraction shows that the iron atom is coordinated by the four carbonyl groups and the two mercury atoms in *cis* positions, in a slightly distorted octahedral arrangement. The iron atom lies on a crystallographic two-fold axis and thus the complete molecule has a two-fold symmetry. The structure of the compound with the atom-numbering scheme is shown in Fig. 2. Pertinent bond lengths and angles are given in Table 1.

Within experimental error, average Fe—C [1.85(5) Å] and CO [1.14(5) Å] distances *cis* and *trans* to mercury atoms are identical. The average Fe—C—O angle is 176(1)°.

The Fe—Hg distances are equal to 2.506(5) Å, and it is interesting to compare this value with those of related compounds. In the $[Fe(CO)_4(HgBr)_2]$ molecule two different Fe—Hg bond lengths (2.44 and 2.59 Å) were observed.[13] For the $[Fe(CO)_4(HgCl)_2]$ four independent molecules were observed[14] in the asymmetric unit with different Fe—Hg distances, the average value being 2.49(8) Å. A greater value, 2.552(8) Å, was found in $[Fe(CO)_4(HgCl)_2(py)_2]$, and this may be a consequence of the higher coordination number of the mercury atom in this compound.[15]

The coordination of the mercury atoms is not simple because there are other interactions besides their bonding to the iron and sulphur atoms. The

* Atomic coordinates have also been deposited with the Cambridge Crystallographic Data Centre.

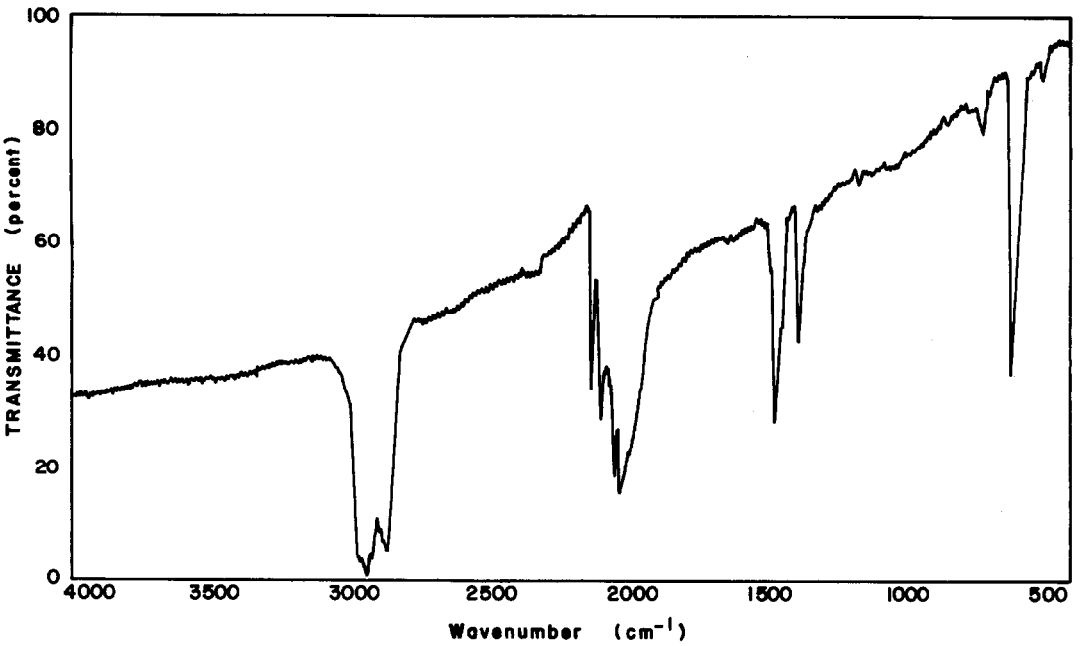

Fig. 1. IR spectrum of $[Fe(CO)_4(HgSCN)_2]$.

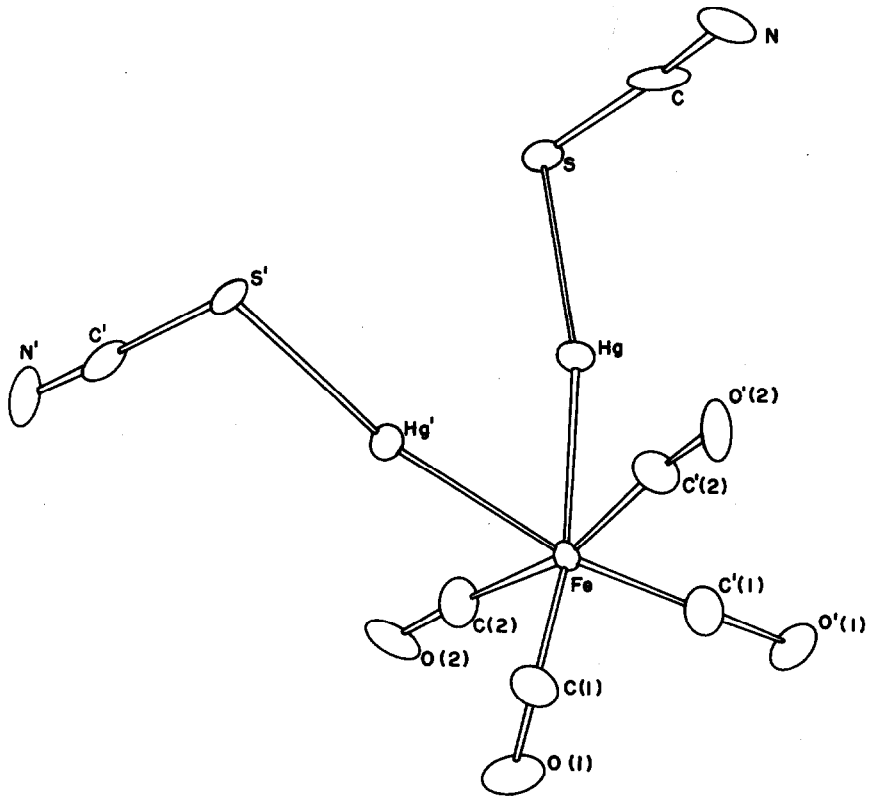

Fig. 2. Molecular structure of $[Fe(CO)_4(HgSCN)_2]$.

Table 1. Relevant distances (Å) and angles (°) for $[Fe(CO)_4(HgSCN)_2]$[a]

Hg—Fe	2.506(5)	Hg—S	2.48(1)
S—C	1.70(4)	C—N	1.13(6)
Fe—C1	1.83(5)	Fe—C2	1.87(4)
C1—O1	1.16(6)	C2—O2	1.12(5)
Hg—Hg^{i}	3.154(2)	Hg—N^{ii}	2.66(3)
Hg—Fe—Hg^{i}	78.0(1)	S—Hg—N^{ii}	85.9(8)
Hg—Fe—C1^{i}	91(1)	Fe—Hg—N^{ii}	105.2(8)
Hg—Fe—C2^{i}	85(1)	Hg^{i}—Hg—Fe	51.0(1)
Hg—Fe—C1	168(1)	Hg^{i}—Hg—N^{ii}	149.1(8)
Hg—Fe—C2	85(1)	Hg^{i}—Hg—S	118.5(2)
C1—Fe—C2	95(1)	Hg—S—C	98(1)
C2—Fe—C2^{i}	166(1)	S—C—N	172(1)
C1—Fe—C1^{i}	101(1)	Fe—C1—O1	176(1)
C1—Fe—C2^{i}	94(1)	Fe—C2—O2	175(1)
Fe—Hg—S	168.9(2)		

[a] Symmetry codes: (i) $-x, \frac{1}{2}-y, z$; and (ii) $\frac{3}{4}-y, \frac{1}{4}+x, \frac{1}{4}+z$.

distance between the mercury atoms in the molecule of $[Fe(CO)_4(HgSCN)_2]$ is 3.154(2) Å, which agrees well with the distances observed in other clusters: 3.142 Å in $[Hg_6Rh_4(PMe_3)_{12}]$,[16] and 3.171(4) Å in $[Fe(CO)_4(HgCl)_2(py)_2]$.[15] This suggests a metal–metal bond involving the mercury atoms and is reinforced by the small Hg—Fe—Hg angle [78.0(1)°] in the $[Fe(CO)_4(HgSCN)_2]$ molecule.

In the solid state the molecular packing can allow interactions between atoms of neighbour molecules. In this compound each mercury atom has, at 2.66(3) Å, a nitrogen atom of a thiocyanate group of another molecule ($\frac{3}{4}-y, \frac{1}{4}+x, \frac{1}{4}+z$ symmetry operation). This suggests a Hg—N bond, since this distance is 2.81(1) Å in $Hg(SCN)_2$, where this bond is believed to exist.[17]

Thus the effective coordination number of the mercury atoms is four and its coordination polyhedron is distorted square-planar, as shown in Fig. 3. The mean plane is defined by the constants

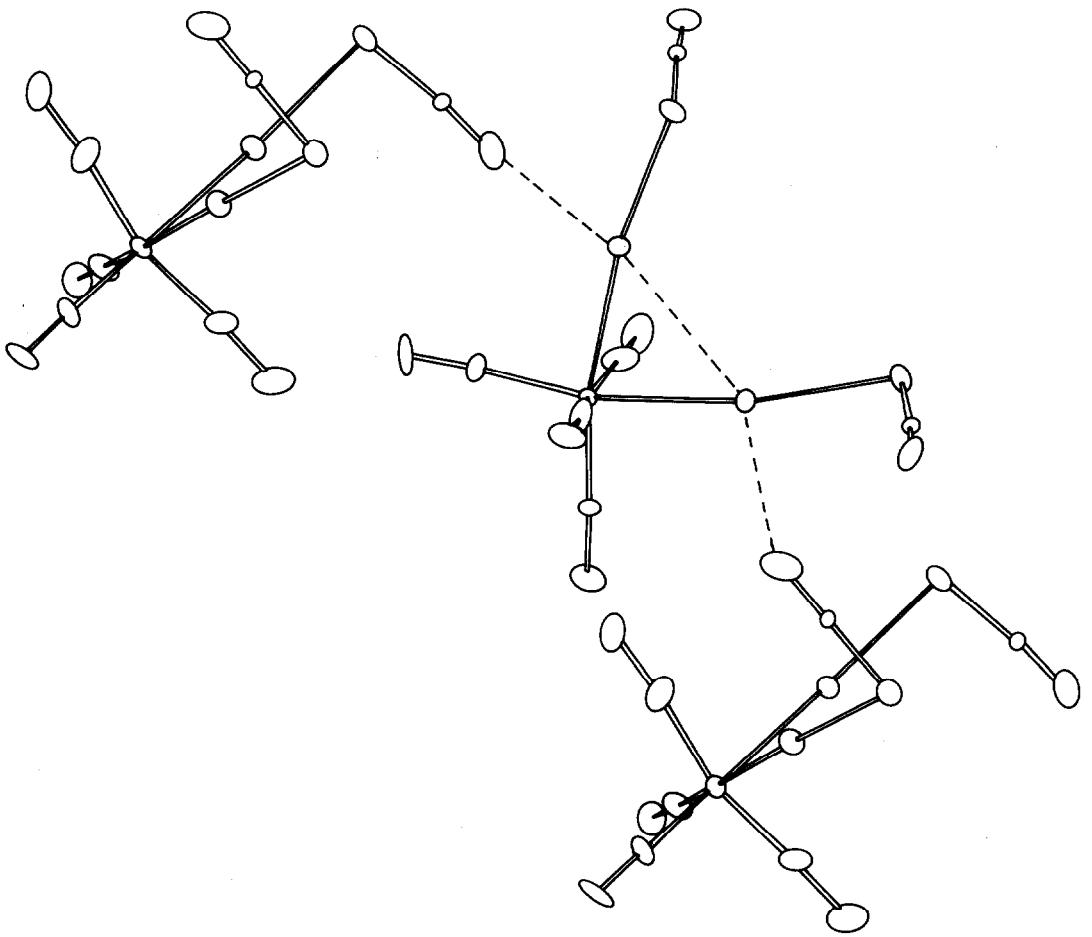

Fig. 3. Coordination of the mercury in the crystal of $[Fe(CO)_4(HgSCN)_2]$.

$A = -0.4940$, $B = 0.8506$, $C = -0.1802$ and $D = 2.1904$, the largest distance to this plane being 0.304(2) Å for the mercury ($\bar{x}$, $\frac{1}{2}-y$, z symmetry operation) atom.

The angle S—C—N is 177.5(13)° in $Hg(SCN)_2$ and 172(1)° in $[Fe(CO)_4(HgSCN)_2]$. The distortion from linearity may be due to the strong intermolecular interactions between mercury and nitrogen atoms. Thus the compound $[Fe(CO)_4(HgSCN)_2]$ can be considered as an infinite polymer due to these Hg—N bonds in the direction of the *c*-axis of the crystal, which is the developed needle axis.

Acknowledgements—We thank CNPq, FAPESP and FINEP for financial support.

REFERENCES

1. H. Hock and H. Stuhlmann, *Ber.* 1929, **62**, 431.
2. R. D. Ernst, T. J. Marks and J. A. Ibers, *Inorg. Chem.* 1977, **99**, 2090.
3. H. Hock and H. Stuhlmann, *Ber.* 1928, **61**, 2097.
4. J. Lewis and S. B. Wild, *J. Chem. Soc. A* 1966, 69.
5. A. A. Chalmers, J. Lewis and S. B. Wild, *J. Chem. Soc. A* 1968, 1013.
6. D. M. Adams, D. J. Cook and R. D. Kemmitt, *J. Chem. Soc. A* 1968, 1067.
7. A. E. Mauro, O. Sala and Y. Hase, *J. Mol. Struct.* 1978, **48**, 199.
8. A. E. Mauro, Y. Hase and O. Sala, *J. Mol. Struct.* 1979, **51**, 9.
9. A. E. Mauro and M. N. G. Mancini, *Polyhedron* 1984, **3**, 1333.
10. *International Tables for X-ray Crystallography*, Vol. 4. Kynoch Press, Birmingham (1974).
11. J. M. Burlitch and R. C. Winterton, *Inorg. Chem.* 1979, **18**, 2309.
12. K. Nakamoto, *Infrared Spectra of Inorganic and Coordination Compounds*. Wiley Interscience, New York (1970).
13. H. W. Baird and L. F. Dahl, *J. Organomet. Chem.* 1967, **7**, 503.
14. C. L. Raston, A. H. White and S. B. Wild, *Aust. J. Chem.* 1976, **29**, 1905.
15. R. W. Baker and P. Pauling, *J. Chem. Soc., Chem. Commun.* 1970, 573.
16. R. A. Jones, F. M. Real, G. Wilkinson, A. M. Galas and M. B. Hursthouse, *J. Chem. Soc., Dalton Trans.* 1981, 126.
17. A. L. Beauchamp and D. Goutier, *Can. J. Chem.* 1972, **50**, 977.

Polyhedron Vol. 6, No. 6, pp. 1279–1282, 1987
Printed in Great Britain

0277–5387/87 $3.00+.00

LIGAND COMPLEXES OF Ni(II) WITH ALCOHOLAMINES

J. M. ANTELO, F. ARCE,* F. REY and A. VARELA

Departamento de Quimica Fisica, Facultad de Quimica, E-Santiago de Compostela, Spain

(*Received* 21 *October* 1986; *accepted* 13 *November* 1986)

Abstract—The stability constants of Ni(II) complexes containing alcoholamines were determined by potentiometric titration in aqueous solutions at several ionic strengths. The influence of temperature and ligand substituents are examined.

Studies of the formation of Ni(II)–alcoholamine complexes in aqueous solution have been relatively common.[1–9] The results have nevertheless been contradictory as regards the composition of the complexes, their stability constants, and the effects of variables such as ionic strength, temperature or the nature of the ligand substituents. This article reports the equilibria in aqueous solution of Ni(II) complexes with alcoholamines of form $HOCH_2CH_2NR_1R_2$ (R_1 and $R_2 = CH_3$ or CH_2CH_3).

EXPERIMENTAL

Reagents

Merck p.a. ethanolamine (MEA), *N*-methylethanolamine (NMEA), *N*-ethylethanolamine (EMEA), *N,N*-dimethylethanolamine (NNMEA) and *N,N*-diethylethanolamine (EEMEA) were purified by standard procedures. Alcoholamine solutions were prepared with CO_2-less water and protonated by adding Merck p.a. HCl solution, and their concentration was determined by titration against mercury oxide.

Ni(II) solutions were prepared from the nitrate (Merck p.a.) and their concentration determined by titration against EDTA.

Ionic strength was maintained at 1.0, 0.7, 0.5, 0.3 or 0.2 with Merck p.a. KNO_3 desiccated at 100°C for at least 24 h.

Method

The formation constants of the metal complexes were determined by potentiometric titration in a 250-cm^3 glass cell thermostatted by a Crison Viscobath 54 at 298.0, 305.5 or 313.0 K. Nitrogen purified by Fieser solutions[10] was used to provide an inert atmosphere within the cell and to stir the complex solution during titration. The pH of solution was measured with a Beckman 4500 pH-meter equipped with a Radiometer GK 4501B electrode and calibrated using standard buffers of pH 7.0 and 10.0 (experimental points lay within this range).

The solutions determined contained known quantities of metal ion, alcoholamine, acid (enough to guarantee the total protonation of the alcoholamine) and KNO_3 (to control ionic strength). The ranges of initial concentrations of the various components are listed in Table 1 (solutions with various [Ni(II)]/[alcoholamine] ratios were studied). The titration agent was the same alcoholamine as in the complex being studied, but a concentration some 25–30 times its initial concentration in the cell, and was 0.01 cm^3 added at a time from a Crison 738 microburette equipped with a 1-cm^3 Hamilton syringe accurate to an estimated ± 0.005 cm^3. Each titration was performed at least twice, and the replicate values differed in each case by less than 0.01 pH units. In no case did the fall in ionic strength during titration exceed 2%.

Table 1. Initial concentrations of solutions of Ni(II)–alcoholamine complexes

	Ligand	Ni(II)
MEA	0.1561	7.549E−3–3.020E−2
NMEA	0.1561	7.549E−3–3.020E−2
EMEA	0.1057	4.529E−3–9.814E−3
NNMEA	0.1015	4.529E−3–9.814E−3
EEMEA	0.0818	2.265E−3–7.549E−3

* Author to whom correspondence should be addressed.

Table 2. Influence of ionic strength on the stability constants of the complex system

System	T	I	p	q	$\log\beta$	S	χ^2	R	n	pH range
MEA	298.0	1.0	1	1	3.22	0.44E−04	98.9	0.0022	133	6.90–9.39
			1	2	5.65					
			1	3	7.40					
		0.7	1	1	3.18	0.32E−04	40.6	0.0018	134	6.90–9.40
			1	2	5.66					
			1	3	7.21					
			1	4	8.12					
		0.5	1	1	3.17	0.40E−04	75.1	0.0021	134	6.80–9.40
			1	2	5.65					
			1	3	7.18					
			1	4	8.27					
		0.3	1	1	3.09	0.60E−04	166.5	0.0021	135	6.85–9.40
			1	2	5.53					
			1	3	6.97					
			1	4	8.02					
		0.2	1	1	3.24	0.42E−05	26.9	0.0008	86	6.48–9.32
			1	2	5.60					
			1	3	7.15					
NMEA	298.0	1.0	1	1	2.96	0.11E−04	8.2	0.0018	86	6.58–9.53
			1	2	5.08					
			1	3	5.85					
		0.7	1	1	3.12	0.67E−04	19.8	0.0035	90	6.58–9.43
			1	2	5.11					
		0.5	1	1	2.95	0.12E−04	15.7	0.0019	82	6.43–9.38
			1	2	4.82					
		0.3	1	1	2.91	0.13E−04	18.3	0.0018	91	6.50–9.36
			1	2	4.77					
		0.2	1	1	2.88	0.20E−04	22.7	0.0025	75	6.90–9.40
			1	2	4.88					
EMEA	298.0	1.0	1	1	2.53	0.20E−05	80.2	0.0010	94	6.79–8.61
			1	2	5.03					
		0.7	1	1	2.49	0.20E−05	92.9	0.0010	94	6.58–8.59
			1	2	4.98					
		0.5	1	1	2.49	0.74E−06	142.7	0.0010	39	6.55–8.62
			1	2	4.73					
		0.3	1	1	2.42	0.97E−06	127.9	0.0006	121	6.63–8.51
			1	2	4.99					
		0.2	1	1	2.37	0.31E−06	49.9	0.0004	109	6.55–8.56
			1	2	4.90					
NNMEA	298.0	1.0	1	2	2.94	0.80E−04	167.7	0.0057	116	6.50–8.65
		0.7	1	1	0.50	0.73E−04	157.4	0.0054	116	6.52–8.65
			1	2	2.84					
		0.5	1	1	0.85	0.83E−04	191.3	0.0055	125	6.45–8.80
			1	2	3.16					
		0.3	1	1	0.48	0.95E−04	138.8	0.0062	114	6.57–8.69
EEMEA	298.0	1.0	1	1	2.03	0.22E−04	70.0	0.0005	76	6.39–8.62
			1	1	1.76	0.48E−06	53.0	0.0009	53	6.70–8.63

For each ionic strength, the stability constants of the complexes were determined using the program MINIQUAD 75.[11] For each set of curves, various models chosen on the basis of published data for similar systems were tested and refined until total convergence was achieved. Criteria such as minimum χ^2 (chi-square) value, R (crystallographic) factor or sum of square residuals were used to identify the correct model. All calculations were performed on a Univac 1100 computer.

RESULTS AND DISCUSSION

The aim of this study was to establish the stoichiometry of the various Ni(II)–alcoholamine complexes formed, to determine their stability constants, and to investigate the influence of ionic strength, temperature and substituents on these constants. In order to achieve the first of these goals, the experimental results were compared with those predicted by various different stoichiometries considered to be possible *a priori*, i.e. with those expected for various different equilibria of form:

$$pM + qL + rOH \rightleftharpoons M_pL_q(OH)_r, \qquad (1)$$

where M is the metal ion and L the alcoholamine ligand.

For none of the alcoholamines studied were any except mononuclear complexes observed ($p = 1$), hypothetical complexes with $p \geqslant 1$ being rejected by the program, and the stability constants determined separately from each of the pertinent curves were in all cases identical. It was also found that r was in all cases zero. Thus under the conditions of the present study, only simple ML_q complexes are formed, with q depending on the nature of the ligand, the temperature and the ionic strength of the medium.

Table 2 shows that the value of K_1 falls with increasing substitution in alcoholamines, in the order MEA > NMEA ≃ EMEA > NNMEA ≃ EEMEA, which may be attributed to increasing steric hindrance as the space occupied by the ligand grows. For a given degree of substitution, however, stability is not determined by the size of the ligand, but rather by its basicity, as is shown by the fact that whereas the stability constants of NMEA and EMEA are, like their K_{H^+}, very similar, those of NNMEA and EEMEA differ considerably, again like their K_{H^+}.

Table 3. Thermodynamic stability constants of Ni(II)–alcoholamine complexes

	1–1	1–2	1–3	1–4
MEA	2.98	5.59	7.02	8.10
NMEA	2.83	4.80	5.85	
EMEA	2.34	4.89		
NNMEA	(0.50)	2.90		
EEMEA	1.50			

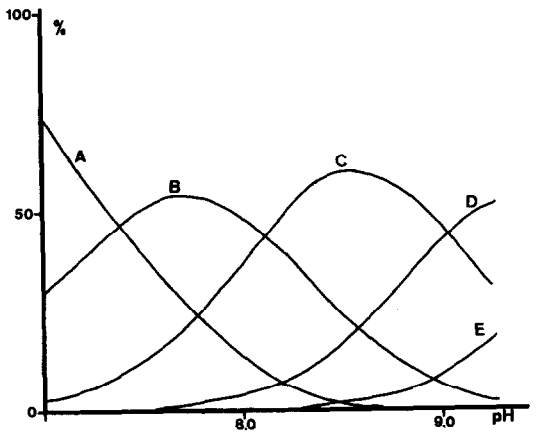

Fig. 1. Variation with pH of the distribution of the several species present in aqueous solution of Ni(II)–MEA $I = 0.70$: (A) Ni(II), (B) Ni–MEA, (C) Ni–$(MEA)_2$, (D) Ni–$(MEA)_3$, (E) Ni–$(MEA)_4$.

In all the systems studied the stability of the complexes increased with the degree of coordination. At the same time, the constants of the successive steps $ML_{n-1} \rightleftharpoons ML_n$ decreased. Thus the increase in steric hindrance with increasing coordination tended increasingly to offset the gain in stability due to the formation of successive metal–ligand bonds.

Reducing the ionic strength of the medium also reduced the stability of the complexes. Although its cause is not known for sure this effect has been observed in various kinds of metal–ligand system.[12] Table 3 lists the thermodynamic constants obtained by extrapolating to $I = 0$ and using the expression $pK = \text{constant} \cdot I^{1/2}$, which is derived from the Debye–Huckel equation and has proved useful in similar systems.[13]

The stability constants of Ni(II)–MEA complexes were calculated at three different temperatures. The differences being within the experimental error, it is not possible to use them to calculate the thermodynamic parameters of the complexation process. This agrees with the results of others,[1,14] and confirms that the potentiometric method is not suitable for determining such parameters for systems like those of the present study.

Figure 1 shows the changing distribution of the various complexes observed as pH varies. As pH rises, the degree of coordination of predominant species increased as the result of the shift in the

equilibrium:

$$LNR_1R_2H^+ \overset{OH^-}{\rightleftharpoons} LNR_1R_2 + OH_2$$
$$\Big\downarrow\uparrow \text{Ni(II)}$$
$$(LNR_1R_2)Ni \rightleftharpoons (LNR_1R_2)_2Ni \rightleftharpoons \cdots$$

REFERENCES

1. A. Y. Sychev and A. P. Gerbeleu, *Russ. J. Inorg. Chem.* 1962, **7**, 138.
2. U. V. Udovenko and Y. S. Duchinskii, *Russ. J. Inorg. Chem.* 1967, **12**, 517.
3. G. A. Bhat and R. S. Subrahamanya, *J. Inorg. Nucl. Chem.* 1971, **33**, 3487.
4. G. A. Bhat and R. S. Subrahamanya, *Indian J. Chem.* 1973, **11**, 584.
5. G. I. Galkina and E. G. Timofeeva, *Russ. J. Inorg. Chem.* 1969, **14**, 1745.
6. J. M. Antelo, F. Arce, J. Casado and A. Varela, *Ann. Chim.* 1980, **70**, 267.
7. J. Bjerrum and P. Djurjevic, *J. Indian Chem. Soc.* 1982, **59**, 595.
8. B. Agarwala and J. Bjerrum, *Acta Chem. Scand.* 1982, **36A**, 459; 1983, **37A**, 88.
9. G. N. Rao, C. S. R. Murthy and A. Prakash, *Indian J. Chem.* 1982, **203**, 21.
10. A. Albert and P. Serjeant, *Ionization Constants of Acids and Bases*, Chap. 2. J. Wiley, New York (1966).
11. P. Gans, A. Sabbatini and A. Vacca, *Inorg. Chim. Acta* 1976, **18**, 237.
12. P. G. Daniele, C. Rigano and S. Sammartano, *Talanta* 1983, **30**, 81; *Transition Met. Chem.* 1982, **7**, 109; *Ann. Chim.* 1983, **73**, 741.
13. J. M. Antelo, F. Arce, J. Casado, M. Sastre and A. Varela, *J. Chem. Eng. Data* 1984, **29**, 10.
14. T. G. Marchenkova, O. P. Nesterova and E. G. Timofeeva, Deposited document, Moscow (1980).

Polyhedron Vol. 6, No. 6, pp. 1283–1290, 1987
Printed in Great Britain

0277–5387/87 $3.00+.00

THE HYDROLYSIS OF THE La(III) ION IN AQUEOUS PERCHLORATE SOLUTION AT 60°C†‡

LIBERATO CIAVATTA,§ MAURO IULIANO and RAFFAELLA PORTO

Dipartimento di Chimica dell'Università, Via Mezzocannone, 4, 80134 Napoli, Italy

(*Received* 30 *October* 1986; *accepted* 13 *November* 1986)

Abstract—The hydrolysis equilibria of the La(III) ion have been studied at 60°C by measuring, with a glass electrode, the hydrogen ion concentration of a series of lanthanum perchlorate solutions. The [La(III)] of the test solutions, which were made to contain 3 m (molal) ClO_4^- by adding $LiClO_4$, varied from 0.03 to 1 m. Hydrolyzed solutions were prepared by generating OH^- by constant-current coulometry. The potentiometric data, which indicate that at most 3% of the metal ion can be transformed to reaction products without the formation of a precipitate, can be explained by assuming the mononuclear $LaOH^{2+}$ ion and the polynuclear La_2OH^{5+}, $La_2(OH)_3^{3+}$ and $Le_3(OH)_3^{6+}$ ions. Their formation constants in the inert 3 m $LiClO_4$ medium are reported and the effects of medium changes, caused by the replacement of Li^+ with La^{3+}, estimated by the specific interaction theory.

The evidence of numerous, accurate investigations[1,2] on the hydrolysis of Me^{z+} cations suggests the formation of polynuclear $Me_q(OH)_p^{zq-p}$ species with $q > 1$. Though, in principle, the array of (p, q) values may vary in a wide range, in each of the investigated systems the number of polynuclear complexes has been found to be small, usually not greater than 2 or 3, and often the complexes have a high nuclearity: $Bi_6(OH)_{12}^{6+}$, $Pb_4(OH)_4^{4+}$, $Pb_6(OH)_8^{4+}$, $Ce_3(OH)_5^{4+}$ and $Al_{13}(OH)_{32}^{7+}$. Of course we cannot exclude the existence of intermediate species. These are present in undetectable amounts in the solutions studied, most often at 25°C in a 3 M $NaClO_4$ ionic medium; however, they may become important under different experimental conditions of temperature, pressure, or ionic medium.

The objective of the present work was that of exploring at 60°C the intermediate species of the La(III) ion hydrolysis which at 25°C in 3 M $(Li)ClO_4$ has been interpreted[3] in terms of $LaOH^{2+}$, La_2OH^{5+}, $La_5(OH)_9^{6+}$ or $La_6(OH)_{10}^{8+}$. The starting point was Arnerk's[4] systematic investigation on the enthalpies of hydrolytic reactions. For $qMe^{z+} + pOH^- \leftrightarrows Me_q(OH)_p^{zq-p}$ Arnek found $\Delta H_{pq} < 0$ and, moreover, for a given cation $\Delta H_{pq}/p$ is a constant to within $\mp$ 1.7 kJ. It is easily shown by applying the vant'Hoff equation that of two complexes (p', q') and (p'', q'') with $p' < p''$, the (p', q') one is favoured by a temperature increase.

As to the choice of temperature, we were guided by the results of a previous study on the hydrolysis of the Be(II) ion at 60°C.[5] At this temperature we found evidence for $Be_2(OH)_2^{2+}$, a species not detected at 25°C,[6,7] where the predominating complex is $Be_3(OH)_3^{3+}$.

METHOD

To study the hydrolysis equilibria the hydrogen ion concentration of lanthanum perchlorate sol-

† This work is dedicated *in memoriam* of the late Professor Georg Biedermann, K.T.H., Stockholm.

‡ Notation used in this paper: a_w, water activity; A, concentration of Cl^-; B, concentration of La(III); b, concentration of La^{3+}; ${}^*\beta_{pq}$, equilibrium constant for the formation of $La_q(OH)_p^{3q-p}$, regarding H_2O and not OH^- as the reagent; γ_B, γ_H and γ_{pq}, activity coefficients of La^{3+}, H^+ and $La_q(OH)_p^{3q-p}$, respectively; H, proton analytical excess $([ClO_4^-]+A-[Li^+]-3B)$; h, equilibrium concentration of H^+; Δ^*H_{pq}, formation enthalpy of $La_q(OH)_p^{3q-p}$ considering H_2O and not OH^- as the reagent; K_p, formation constant of all species containing p OH^- groups [eqn (8)]; Z, average number of OH^- bound per lanthanum atom. Concentrations and equilibrium constants are expressed on the molal scale {m [mol (kg of water)$^{-1}$]}.

§ Author to whom correspondence should be addressed.

utions was measured with a glass half-cell. The [La(III)] varied between 0.03 and 1 m. At each [La(III)] the acidity was decreased from a level, where the hydrolysis is negligible, to low enough values for solid lanthanum hydroxide to start to form. All of the test solutions were prepared to contain 3 m ClO_4^- by adding $LiClO_4$. This salt has been preferred to the more popular $NaClO_4$ because it is conveniently purified by recrystallization.

As exploratory experiments indicated, the hydrolysis is negligible at $\log h > -5.5$ and less than 3% of B can be transformed into reaction products before precipitation. Thus we were confronted with the problem of investigating poorly buffered solutions, and considerable effort had to be taken to keep protolytic contamination to a minimum. The experience gained in previous studies[3,8,9] on the hydrolysis of cations, which behave as weak acids, was of great value. Test solutions in a state of high purity were prepared by generating OH^- by coulometric methods. Stable and reproducible EMF data could be measured even in solutions where the concentration of OH^- bound to hydrolytic species was as low as 5×10^{-5} m.

The test solutions, abbreviated in the following as TS, had the general composition:

$$B \text{ m La(III)}, H \text{ m } H^+, A \text{ m } Cl^-, (3-3B-H+A) \text{ m } Li^+, 3 \text{ m } ClO_4^-.$$

The auxiliary chloride ion, whose concentration ranged from 5×10^{-3} and 0.05 m, was chosen, first, as a reference in cells without liquid junction for measurements of h and, second, to enable us to decrease the acidity of TS by electrolysis cells using no bridges. It is easily imaginable what sort of experimental difficulties bridges cause when operating at values higher than room temperature.

The hydrogen ion concentration in TS was determined with cell (I):

$$-\text{Ag–AgCl/TS/GE}+ \qquad \text{(I)}$$

where GE denotes glass electrode. At 60°C the EMF of (I) is expressed as:

$$E = E_o' + 66.10 \log (hA) + 66.10 \log \gamma_{HCl}^2, \qquad (1)$$

where E_o' is a constant and γ stands for the activity coefficient. The standard states are so defined that activity coefficients tend to unity as the composition of TS approaches 3 m $LiClO_4$. In each series of measurements, where B was constant, since only low Z values were available, we may neglect variations of γ_{HCl} and calculate h with the simplified form of eqn (1):

$$E = E_o + 66.10 \log (hA). \qquad (2)$$

The value of E_o, which is constant at constant B, must be determined in each experiment, by potentiometric titration, by measuring E in solutions where the hydrolysis is negligible and, consequently, h can be set equal to H. The E_o as well as the H of the starting solution were simultaneously assessed by constructing a Gran diagram.[10] In each case E_o could be calculated to within ± 0.1 mV, while the initial H was evaluated with an uncertainty of less than 0.3%.

The presence of chloride ions enabled us to alkalify TS by constant-current coulometry. For this purpose two additional electrodes were immersed into TS giving rise to the electrolysis circuit (II)

$$-\text{Pt/TS/Ag}+, \qquad \text{(II)}$$

which was connected to a constant-current supply. By electrolysis reaction (3) occurs on the right:

$$\text{Ag(s)} + H_2O + Cl^- \rightarrow \text{AgCl(s)} + OH^- + 0.5H_2\text{(g)}. \qquad (3)$$

Though the test solution contains the redox couples H^+–H_2 and Ag(I)–Ag, no spontaneous reaction seems to take place between H_2 and AgCl as indicated by the constancy within ± 0.1 mV of the EMF of cell (I) for 24 h or more.

The current efficiency was studied by potentiometric acid–base titration of exactly standardized 2×10^{-3} m $HClO_4$. Several analyses, carried out with current intensities between 1 and 5 mA, showed results higher than 1%. After inspection of various factors the origin of the error was identified in the reduction on the cathode of small amounts of silver. These turned out to be nearly proportional to the electrolysis duration but almost independent of chloride in the $5 \times 10^{-3} \leqslant A \leqslant 0.05$ m range.

At the end of each titration, the cathode was withdrawn from TS and the silver deposited on it analysed so that the moles of silver reduced per second (χ) could be ascertained. In experiments with lanthanum two or three platinum gauze electrodes were immersed into TS and each was employed as a cathode in different stages of the electrolysis. In this way the unappreciable influence of acidity on χ could be established.

The χ values were found to fall between 3×10^{-10} and 5×10^{-10} mol s^{-1}. Therefore a 99.9% efficiency can be achieved only with current intensities exceeding 50 mA. On the other hand, high intensities make problematic the avoidance of a local excess of base which might promote the premature precipitation of lanthanum hydroxide. As a compromise, we employed current intensities between 2 and 10 mA,

and corrected the moles of electrons, passed during the electrolysis time t, as χt. For χ we assumed the value found in the same experiment. The results of $HClO_4$ analyses coincided, then, to 0.3% or better with the values calculated from dilution of the stock solution.

The lanthanum titrations hitherto presented were performed by decreasing gradually the acidity of TS. Doubts may, therefore, arise whether a true equilibrium was attained. To answer this essential question a series of measurements was made by acidification of partially hydrolysed solutions: 0.1 m La(III), -1.5×10^{-3} m H^+, 5×10^{-3} m Ag^+, 2.697 m Li^+, 3 m ClO_4^-. Acid was generated coulometrically according to the electrolysis reaction (4):

$$2Ag^+ + H_2O \rightarrow 2Ag(s) + 0.5O_2(g) + 2H^+. \quad (4)$$

The results (back titration in Table 1) are seen in Fig. 1 to agree, within the limits of experimental uncertainty, with data obtained by alkalification. This fact also demonstrates, besides a real equilibrium, the negligible effect of chloride ions on the hydrolysis reaction.

EXPERIMENTAL

Materials and analysis

Lanthanum perchlorate solutions were prepared from lanthanum oxide (99.99% purity), furnished by K.E.K., and $HClO_4$ (p.a. Merck). The oxide was added in a slight excess to a concentrated (3.2 M) $HClO_4$ solution and the pH of the resulting suspension was adjusted to 7. Consequently, the heavy metal ions present in $HClO_4$ precipitated as a

Table 1. $Z(\log h)_B$ data

$B = 0.9946$ m

$Z\times10^3(-\log h)$ series a: 2.02(6.840); 3.27(6.053); 5.32(6.215); 6.62(6.267); 8.56(6.336); 10.2(6.397); 11.9(6.435); 13.6(6.462); 15.3(6.500); 17.2(6.525); 19.2(6.543); 23.1(6.575).
Series b: 2.58(5.966); 4.24(6.132); 5.96(6.266); 7.98(6.321); 10.0(6.384); 12.0(6.436); 14.3(6.485); 18.6(6.534); 21.15(6.560).

$B = 0.6274$ m

$Z\times10^3(-\log h)$: 0.84(5.637); 1.37(5.900); 2.03(6.066); 5.16(6.375); 7.00(6.450); 8.84(6.515); 13.8(6.615); 16.6(6.658); 19.6(6.696); 22.5(6.722); 25.45(6.743); 28.4(6.759); 28.8(6.761); 31.4(6.771).

$B = 0.4008$ m

$Z\times10^3(-\log h)$: 1.36(6.026); 2.23(6.240); 3.33(6.379); 4.295(6.462); 5.67(6.530); 7.16(6.591); 8.66(6.642); 10.5(6.685); 12.9(6.727); 15.7(6.760).

$B = 0.2004$ m

$Z\times10^3(-\log h)$: 0.975(6.034); 2.21(6.383); 3.45(6.521); 5.12(6.623); 7.21(6.700); 9.305(6.772); 11.4(6.813); 14.0(6.862); 16.5(6.898); 19.1(6.924); 21.65(6.945); 24.2(6.956).

$B = 0.1002$ m

$Z\times10^3(-\log h)$ series a: 1.58(6.333); 2.55(6.501); 2.92(6.576); 4.57(6.716); 6.485(6.797); 8.73(6.864); 11.5(6.931); 14.6(6.983); 18.2(7.025); 22.4(7.056).
Series b: 1.26(6.230); 2.13(6.480); 3.25(6.632); 4.61(6.728); 5.99(6.789); 7.36(6.831); 8.97(6.871); 10.6(6.911); 12.7(6.947); 14.75(6.979); 16.8(7.006); 18.9(7.030).
Series c (back titration): 14.9(7.005); 13.5(6.972); 11.4(6.924); 9.26(6.869); 7.16(6.825); 5.29(6.757); 3.90(6.669); 3.75(6.657); 3.34(6.619); 2.92(6.578); 2.51(6.526); 2.11(6.456); 1.70(6.372); 1.30(6.249); 0.89(6.168).

$B = 0.03004$ m

$Z\times10^3(-\log h)$: 2.97(6.690); 4.56(6.855); 7.13(6.970); 10.2(7.045); 13.8(7.109); 18.15(7.172); 22.8(7.221); 27.3(7.262); 31.8(7.282).

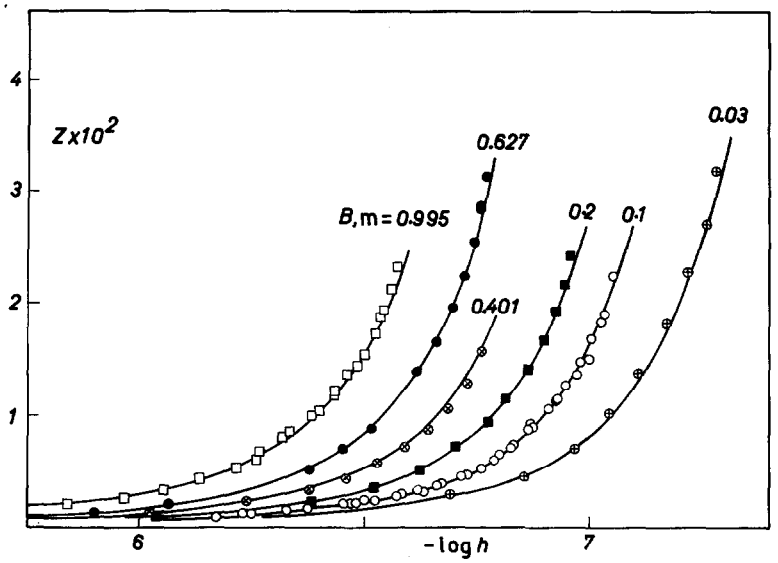

Fig. 1. Z, the average number of OH^- bound per lanthanum atom, as a function of $\log h$. The curves were calculated using the constants given in Table 3 and expressions (12) and (13) for medium changes.

hydroxide or silicate. The excess La_2O_3 was removed by filtration and the acidity was regulated at 10^{-2} m to minimize absorption of CO_2. The exact hydrogen ion concentration was analysed by coulometric titration, the end-point being determined by potentiometry with a glass electrode.

The [La(III)] was established both by titration with EDTA, using xylenol orange as visual indicator,[11] and by precipitating the oxalate which then was oxidized with $KMnO_4$.[12] The results coincided to 0.1%.

Perchloric acid solutions were standardized against $KHCO_3$ and Tl_2CO_3 which are considered primary standards in this laboratory. The analyses, performed with methyl red, agreed better than 0.1%.

Lithium chloride was obtained as described previously.[13]

To prepare *lithium perchlorate* the method described earlier[9] was employed with the modification that small amounts of protolytic impurities, contaminating the final product, were determined with the following potentiometric procedure. Solutions of composition 10^{-2} m H_3BO_3, H m H^+, A m Cl^-, $(3-H+A)$ m Li^+, 3 m ClO_4^-, were alkalified at 60°C with cell (II) while h was measured with cell (I). From data with $h > 10^{-4.5}$ m, E_o and H_o, the initial H, were established as usual on the basis of Gran plots. The data in the $10^{-6} \geqslant h \geqslant 10^{-7.5}$ m interval were employed to get a preliminary value of the dissociation constant of H_3BO_3 (K_a) and, then, to construct the graph $1/(h+K_a)$ vs moles of OH^- generated. Since the result is linear for all the h available, it was concluded that weak acids (HB) present as impurities are almost completely protolyzed at $h < 10^{-6}$ m. Extrapolation to $1/(h+K_a) \to 0$ gave $H_o+[HB]_{tot}$, and consequently $[HB]_{tot}$. The impurities in 3 m $LiClO_4$ amounted to $(34\pm3)\times10^{-6}$ m, in substantial agreement with previous preparations.[14]

The $Z(\log h)_B$ data in lanthanum solutions were corrected for the impurity by assuming its complete protolysis in solutions with $\log h < -6$. This correction makes the Z values of the lowest B uncertain to $\pm10^{-4}$ units.

Experimental details

The EMF measurements were carried out in a silicone oil thermostat at 60.00 ± 0.05°C. The Ag–AgCl electrodes were prepared according to Brown.[15] Pt gauze electrodes (2 × 2 cm) were boiled in 1 : 1 HNO_3 and ignited in alcohol flame. Ag-coated Pt nets, used for electrolysis with cell (II), were prepared by cathodic reduction from 0.03 m AgCl in 16 m LiCl. The silver layers were washed with concentrated ammonia and then they were soaked for several days with water. Glass electrodes, manufactured by Jenaer Glasswerk, were employed. The E values were read with a precision of 0.01 mV with a Keithley 195 System DMM multimeter. To measure the potential of the membrane electrode a preamplifier (Analog Device 309K) had to be used. The constant-current source was a 220 Programable Current Source (Keithley). This instrument furnished intensities constant and accurate to within 0.02%.

Prior to each experiment with cell (I) a stream of

purified and presaturated nitrogen gas was passed overnight through TS, kept at room temperature, to purge it of dissolved oxygen. Throughout the measurements at 60°C the solution was protected by atmospheric contamination by placing it in a six-necked vessel fitted with high-vacuum ground glass stoppers. If the vessel is not hermetically closed, oxygen from the atmosphere may cause drifts in the potential of the Ag–AgCl half-cell. With our apparatus the EMFs of cell (I) remained constant to within 0.1 mV for several hours. The reproducibility of $E-E_o$ was within 0.1 mV.

To analyse silver deposited on Pt cathodes of cell (II), it was anodically stripped in 50 cm^3 3 m $LiClO_4$. The Ag^+ that formed was potentiometrically titrated with Ag^+ generated coulometrically, while the end-point was localized on the basis of Gran plots. Metal (1 μmol) was analysed with error of 2%, which is sufficient for our purposes.

DETERMINATION OF THE COMPOSITION OF THE HYDROLYSIS PRODUCTS

The $Z(\log h)_B$ data, which are the basis of the following calculations, are collected in Table 1 and are graphically represented in Fig. 1. Since less than 3% of La(III) can be transformed into reaction products, the determination of the hydrolysis mechanism may be carried out in two steps. In the first [Section (1)] each set of data, pertaining to a particular B level, was treated with the self-medium approach of Hietanen and Sillén.[16] By this method one obtains the number of OH^- (p) bound to the hydrolysis products and the homoligand equilibrium constants (K_p). Subsequently [Section (2)] the number of lanthanum ions in the complexes (q) and the equilibrium constants ($^*\beta_{pq}$) were determined by analysing the $K_p(B)$ functions. Medium changes caused by the replacement of Li^+ with La^{3+} were estimated by the specific interaction theory (SIT).[17]

Finally [Section (3)] in order to check whether any significant error was introduced by a number of approximations in Sections (1) and (2), all the data were treated by numerical procedures founded on the principle of the least-squares method.

(1) *Evaluation of the prevailing* p *values*

When we consider data at constant B and of Z values not exceeding 0.03, then, without introducing an appreciable error, we may simplify the preliminary calculations by putting:

$$[La^{3+}] = b \sim B. \tag{5}$$

Assuming the formation of a series of hydrolysis products, $La_q(OH)_p^{3q-p}$, the concentration of hydrogen ions set free by hydrolysis (BZ) is expressed by:

$$BZ = h - H = \Sigma p[La_q(OH)_p^{3q-p}]$$
$$= \Sigma p^*\beta_{pq} b^q h^{-p} \gamma_B^q \gamma_H^{-p} \gamma_{pq}^{-1} a_w^{4p}, \tag{6}$$

where the exponent $4p$, to which a_w is elevated, stems from the assumption that H^+ in solution is solvated by $4H_2O$, as suggested by experimental[18,19] as well as theoretical[20] evidence, and that La^{3+} maintains its coordination unchanged in the hydrolysis complexes. At constant B the activity coefficients and water activity may be regarded as constant; consequently, eqns (5) and (6) can be written as:

$$BZ = \Sigma p K_p h^{-p}, \tag{7}$$

where for brevity:

$$K_p = \Sigma B^q {}^*\beta_{pq} \gamma_B^q \gamma_H^{-p} \gamma_{pq}^{-1} a_w^{4p}. \tag{8}$$

We attempted, first, to explain the data in the simplest way by assuming a single p value. This hypothesis was tested by comparing the experimental $BZ(\log h)$ data with model functions calculated on the basis of eqn (7). In the entire BZ range no satisfactory agreement was found with any p between 1 and 5. The shape of the $BZ(\log h)$ graphs was intermediate between model curves calculated with $p = 1$ and 3. Then the family of $Y(\log u)_P$ curves [eqns (9) and (10)] was calculated for $P = 2$, 3 and 4:

$$Y = \log(BZh) - \log K_1 = \log(1 + Pu^{P-1}), \tag{9}$$

$$\log u = [1/(P-1)]\log(K_P/K_1) - \log h. \tag{10}$$

The experimental data could satisfactorily be fitted to the model function with $P = 3$, whereas systematic deviations were found with both $P = 2$ and 4. Therefore data of the present level of accuracy can be explained by the complexes $(1, q)$ and $(3, q')$.

The K_1 and K_3 values, given in Table 2, were calculated from the $\log h + \log u$ and $\log(BZh) - Y$ differences read off in the position of best agreement. The errors represent maximum deviations from mean values.

The results so far presented rest on the validity of eqn (5). To gain an idea of the uncertainty introduced by this approximation the computations were repeated putting $p = q$, hence:

$$b = B(1 - Z). \tag{11}$$

It is evident from Table 2 that the constants evaluated using eqn (5) or (11) are very similar. The

Table 2. Survey of determined K_1 and K_3 values

B (m)	$-\log K_1$	$-\log K_3$	$-\log K_1$	$-\log K_3$
	$b = B$		$b = B(1-Z)$	
0.030	10.81±0.03	25.51±0.03	10.83±0.03	25.46±0.03
0.100	10.19±0.03	24.48±0.03	10.19±0.02	24.49±0.03
0.200	9.78±0.03	23.84±0.03	9.79±0.03	23.80±0.03
0.401	9.34±0.03	23.20±0.03	9.35±0.03	23.17±0.03
0.627	8.98±0.03	22.68±0.02	8.99±0.03	22.64±0.02
0.995	8.57±0.02	22.11±0.03	8.58±0.02	22.07±0.03

Table 3. Calculated values of the equilibrium constants

Method	$-\log {}^*\beta_{11}$	$-\log {}^*\beta_{12}$	$-\log {}^*\beta_{32}$	$-\log {}^*\beta_{33}$
Dependence on B of K_p	9.29±0.03	8.93±0.05	22.47±0.05	22.9±0.2
Least-squares	9.28±0.015	8.92±0.02	22.47±0.02	22.87±0.06

values obtained from eqn (11) were selected for the following treatment.

(2) *Estimation of the most probable* q *values*

To evaluate q in the hydrolysis products the dependence on B of K_1 and K_3 was examined. Clearly, correct conclusions on q and ${}^*\beta_{pq}$ depend on the estimation of changes in the activity coefficients as well as of the water activity caused by the substitution of Li^+ with La^{3+}. Corrections for medium effects were based on SIT.[17] According to the theory, since all participants to the hydrolytic equilibria are positively charged and the anionic composition of the medium remains essentially unchanged, the activity coefficient of a species "i" of charge z_i, defined so that $\gamma_i \to 1$ as $[i] \to 0$ in 3 m $LiClO_4$, may be expressed as a function of the ionic strength (I) as:

$$\log \gamma_i = -z_i^2[0.5452I^{0.5}/(1+1.5I^{0.5})-0.2624] = -z_i^2 D. \quad (12)$$

Concerning the water activity the theory predicts a linear variation between the values relevant in 3 m $LiClO_4$ and 1 m $La(ClO_4)_3$ at 60°C. On the medium scale $a_w \to 1$ as the composition of TS tends to 3 m $LiClO_4$. We estimate from data published by Pitzer[21] that:

$$\log a_w = 0.0199B. \quad (13)$$

With these assumptions eqn (8) for $p = 1$ may be written as eqn (14):

$$K_1 = {}^*\beta_{11}B \times 10^{-4D}a_w^4 + {}^*\beta_{12}B^2 \times 10^{8D}a_w^4. \quad (14)$$

We consider improbable the species with 3 La^{3+} so that no higher terms were included in the series (14). The plot $K_1 \times 10^{4D}B^{-1}a_w^{-4}$ against $B \times 10^{12D}$ is shown in Fig. 2. It is seen that the points lie, within the limits of experimental error, on a straight line. This means that the $LaOH^{2+}$ and La_2OH^{5+} ions are formed with equilibrium constants given in Table 3.

Equation (8) for $p = 3$ can be rearranged to:

$$K_3 = {}^*\beta_{32}B^2 \times 10^{-6D}a_w^{12} + {}^*\beta_{33}B^3 \times 10^{12D}a_w^{12} + \cdots \quad (15)$$

In writing eqn (15) the formation of $La(OH)_3$ was assumed to be negligible. From the plot of $K_3 \times 10^{6D}$

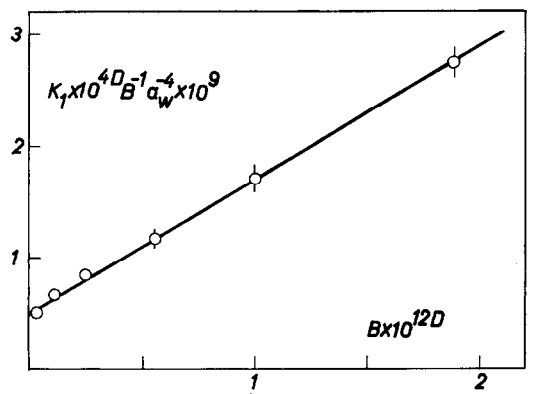

Fig. 2. $K_1B^{-1}a_w^{-4} \times 10^{4D}$ [eqn (14)] as a function of $B \times 10^{12D}$. The line represents: $5.13 \times 10^{-10} + 1.17 \times 10^{-9}B \times 10^{18D}$.

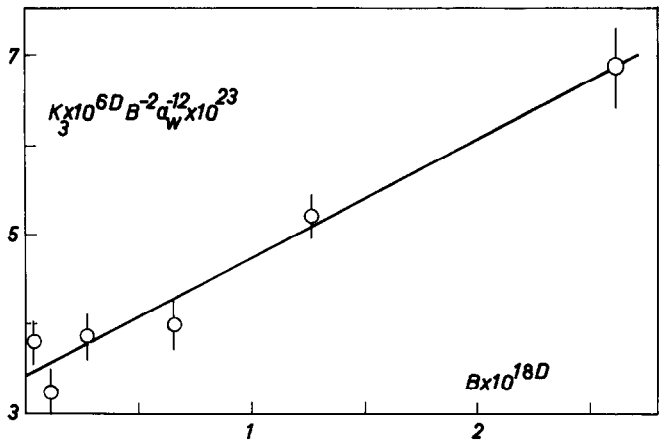

Fig. 3. $K_3 B^{-2} a_w^{-12} \times 10^{6D}$ [eqn (15)] as a function of $B \times 10^{18D}$. The straight line was calculated with: $3.39 \times 10^{-23} + 1.26 \times 10^{-23} B \times 10^{18D}$.

$a_w^{-12} B^{-2}$ against $B \times 10^{18D}$, shown graphically in Fig. 3, it appears that the points fall, within the limits of estimated error, on a straight line, indicating the presence of $La_2(OH)_3^{3+}$ and $La_3(OH)_3^{6+}$. The intercept and slope of the best line through the points gave the constants in Table 3. The error of the slope is fairly large due to the fact that $La_3(OH)_3^{6+}$ is a minor species.

(3) *Refinement of the equilibrium constants*

The calculations of the previous sections have furnished evidence for the formation of $LaOH^{2+}$, La_3OH^{5+}, $La_2(OH)_3^{3+}$ and $La_3(OH)_3^{6+}$. The results were attained by methods based on eqns (5) and (11) which are of approximate validity. It was therefore desirable to refine the constants with more exact procedures.

The experimental data were treated by numerical approaches founded on the principle of least squares. The computation consisted in the minimization of the sum:

$$U = \Sigma (((BZ)_i - (BZ)_{ic})/(BZ)_i)^2, \qquad (16)$$

where $(BZ)_i$ denotes an experimental datum and $(BZ)_{ic}$ a calculated value with a certain set of $*\beta_{pq}$. Medium effects were accounted for by eqns (12) and (13).

The minimum was found with the constants given in Table 3. These are seen to agree well with the graphical evaluation. The uncertainty represents 3 times the standard deviation, as defined by the D-boundary,[22] and is lower than the maximum error estimated by curve fitting.

As a measure of the fit between experimental data and the proposed model we may consider the distribution of the relative error $[1-(BZ)_{ic}/(BZ)_i]$. From a total 103 points 50 are found to have a positive deviation while 53 have a negative deviation. The average of the positive ones amounts to 4.1%, the average of the negative ones to 3.5%. The magnitude and sign of the deviations do not exhibit an appreciable trend with B and Z.

DISCUSSION

We may summarize the results of this work by saying that the La^{3+} hydrolysis at 60°C is explainable in terms of La_2OH^{5+}, $La_2(OH)_3^{3+}$, $La_3(OH)_3^{6+}$ and $LaOH^{2+}$ which link the simple La^{3+} ion with the final hydrolysis products, colloidal lanthanum hydroxide. According to expectation the intermediate species $La_2(OH)_3^{3+}$ and $La_3(OH)_3^{6+}$, that escaped detection at 25°C, are present. The absence of $La_5(OH)_9^{6+}$ or $La_6(OH)_{10}^{8+}$ is readily understood on the basis of the arguments that follow.

From the $*\beta_{11}$ and $*\beta_{12}$ of Table 3 and those determined at 25°C in 3 M $LiClO_4$[3] we estimate the heats associated with the formation of $LaOH^{2+}$ and La_2OH^{5+}, $\Delta^*H_{11} = 40.6 \pm 7.1$ kJ mol^{-1} and $\Delta^*H_{12} = 56 \pm 8$ kJ mol^{-1}. If the mentioned hypothesis, namely Δ^*H_{pq}/p is constant for a given cation, is valid we calculate $\Delta^*H_{95} = 377$ kJ mol^{-1}, which gives at 60°C $\log *\beta_{95} = -64.2$. $La_5(OH)_9^{6+}$ with such an equilibrium constant would reach, at the highest Z studied, a concentration influencing BZ by less than 1%.

The formation of polynuclear complexes may be easier to visualize when it is expressed in terms of polymerization from the mononuclear species. We obtain:

$$LaOH^{2+} + La^{3+} \leftrightarrows La_2OH^{5+}$$

$$[\log(*\beta_{12} \times *\beta_{11}^{-1}) = 0.4 \pm 0.1],$$

$$3LaOH^{2+} \leftrightarrows La_2(OH)_3^{3+} + La^{3+}$$

$$[\log(*\beta_{32} \times *\beta_{11}^{-3}) = 5.37 \pm 0.15],$$

$$3LaOH^{2+} \leftrightarrows La_3(OH)_3^{6+}$$

$$[\log(*\beta_{33} \times *\beta_{11}^{-3}) = 4.9 \pm 0.3].$$

From comparison of these with values of various cations[1,2] it may be inferred that, within the large limits of error, $*\beta_{pq} \times *\beta_{1}^{-p}$ is approximately constant, independent of the nature of the metal. Therefore polymerization is primarily a property of the oxygen atom and the hydroxide ion.

In any case, the question arises why $Me_2(OH)_2^{4+}$ is readily formed by cations of the same 3a group, Sc^{3+} and Y^{3+}, but not by La^{3+}. Presumably the greater stability of $La_2(OH)_3^{3+}$ than of $La_2(OH)_2^{4+}$ is attributable to the effect of charge distribution. Pauling's postulate of the essential neutrality of atoms[23] suggests that charges on atoms in stable substances are generally near zero or at least between $-\frac{1}{2}$ and $+\frac{1}{2}$. Therefore the La^{3+} ion would not reach in $La_2(OH)_2^{4+}$ a sufficient electrical neutrality for stability as, on the contrary, the more electronegative Y^{3+} ion does. Obviously, the introduction of another OH^- bridge in $La_2(OH)_2^{4+}$ further neutralizes charges on the metal and, consequently, causes the resulting $La_2(OH)_3^{3+}$ to be stable. On the other hand, in the attempt to make $Y_2(OH)_3^{3+}$, a more negative charge will pass to Y(III) which is apparently more than required for stability.

The tendency to electrical neutrality may also account for the higher stability of La_2OH^{5+} than of Y_2OH^{5+}. If one tries to replace in La_3OH^{5+} the more electronegative Y^{3+}, in the attempt to render less negative the oxygen atom, more charge will be transferred to Y(III). This, evidently, is more than can be accepted for Y_2OH^{5+} to be stable.

Acknowledgement—This work has been financially supported by the Ministero della Pubblica Istruzione, Rome.

REFERENCES

1. (a) L. G. Sillén and E. A. Martell, *Stability Constants*, The Chemical Society, London, Special Publication No. 17 (1964), and No. 25 (1971); (b) E. Högfeldt, *Stability Constants*. Pergamon Press, Oxford (1982).
2. C. F. Baes and R. E. Mesmer, *The Hydrolysis of Cations*, J. Wiley, New York (1976).
3. G. Biedermann and L. Ciavatta, *Acta Chem. Scand.* 1961, **15**, 1347.
4. R. Arnek, *Ark. Kemi* 1970, **32**, 55.
5. L. Ciavatta and M. Grimaldi, *Gazzetta* 1973, **103**, 731.
6. H. Kakihana and L. G. Sillén, *Acta Chem. Scand.* 1956, **10**, 985.
7. B. Carell and Å. Olin, *Acta Chem. Scand.* 1961, **15**, 1875.
8. G. Biedermann and L. Ciavatta, *Acta Chem. Scand.* 1962, **16**, 2221.
9. G. Biedermann and L. Ciavatta, *Ark. Kemi* 1964, **22**, 253.
10. G. Gran, *Analyst* 1952, **77**, 661.
11. I. M. Kolthoff and P. J. Elving, *Treatise on Analytical Chemistry*, Part 2, Vol. 8, p. 57. J. Wiley, New York (1963).
12. I. M. Kolthoff and R. Elmquist, *J. Am. Chem. Soc.* 1931, **53**, 1225.
13. L. Ciavatta, D. Ferri and G. Riccio, *Polyhedron* 1985, **4**, 15.
14. L. Ciavatta, *Ark. Kemi* 1963, **20**, 417.
15. A. S. Brown, *J. Am. Chem. Soc.* 1934, **56**, 646.
16. S. Hietanen and L. G. Sillén, *Acta Chem. Scand.* 1959, **13**, 533.
17. L. Ciavatta, *Ann. Chim.* 1980, **70**, 551.
18. D. G. Tuck and R. M. Diamond, *J. Phys. Chem.* 1961, **65**, 193.
19. D. S. Terekhova, *Zh. Strukt. Khim.* 1970, **11**, 530.
20. R. Grahn, *Ark. Fys.* 1962, **21**, 13.
21. K. S. Pitzer, In *Activity Coefficients in Electrolyte Solutions* (Edited by R. M. Pytkowicz), Vol. 1. CRC Press, Boca Raton, FL (1979).
22. L. G. Sillén, *Acta Chem. Scand.* 1962, **16**, 159.
23. L. Pauling, *J. Chem. Soc.* 1948, 1461.

Polyhedron Vol. 6, No. 6, pp. 1291–1294, 1987
Printed in Great Britain

0277–5387/87 $3.00+.00

MACROCYCLIC TETRAAMINES FROM REACTION OF THE (1,10-DIAMINO-4,7-DIAZADECANE)COPPER(II) CATION WITH FORMALDEHYDE AND THE CARBON ACIDS NITROETHANE AND DIETHYLMALONATE: VARIABILITY IN REACTIVITY

GEOFFREY A. LAWRANCE* and MARGARET A. O'LEARY

Department of Chemistry, The University of Newcastle, New South Wales 2308, Australia

(*Received* 13 *October* 1986; *accepted* 13 *November* 1986)

Abstract—Reaction of (1,10-diamino-4,7-diazadecane)copper(II) in basic methanol with formaldehyde and the carbon acid nitroethane leads to the facile and high-yielding synthesis of the (10-methyl-10-nitro-1,4,8,12-tetraazacyclopentadecane)copper(II) cation. The similar reaction with diethylmalonate, a weaker carbon acid, yields the (10,10-dicarboxyethyl-1,4,8,12-tetraazacyclopentadecane)copper(II) cation in only low yield.

Recently, metal-directed syntheses of multidentate and macrocyclic ligands employing formaldehyde and nitroalkane carbon acids around labile metal ions have been developed.[1,2] These studies supplement earlier studies of inert octahedral amine complexes, where similar reactions have led to the development of a range of macrobicyclic hexaamine ligands.[3–5] In each case, the nitro group introduced into the new ligand from the nitroalkane carbon acid can be chemically or electrochemically reduced to a pendant amine. This produces a new class of macromonocyclic amine ligands, some of which are capable of penta- or hexa-coordination by employing the pendant primary amine group(s) as donor atoms.[2,6] In addition to the chemistry based on nitroalkanes, it was of some interest to us to investigate similar condensation reactions with other carbon acids. While nitroethane is a strong carbon acid ($pK_a \sim 8.6$),[7] it is apparent that other simple organic molecules may be sufficiently acidic to participate in similar reactions. We have noted that diethylmalonate is acidic ($pK_a \sim 13.3$),[7] and may be reactive. With the latter carbon acid, there is the prospect of forming cyclic molecules with pendant acid groups.

The general reaction with nitroalkanes [eqn (1)] is currently being explored in detail for a range of chelate ring sizes and metal ions, and one particular example is described here.

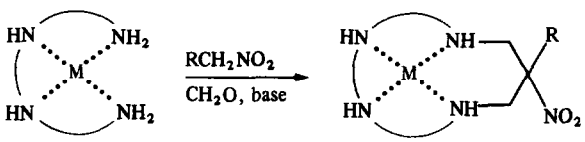

(1)

With diethylmalonate, there is the initial opportunity for macrocyclization [eqn (2)] although hydrolysis and decarboxylation reactions involving the formed *gem* diester, as well as alternate initial reactions, suggest that the reaction may be complicated. Details of this reaction are described and compared with the nitroethane reaction.

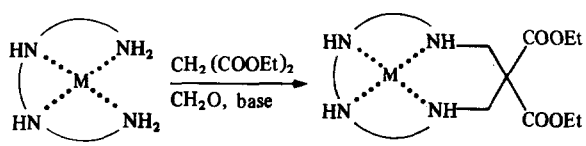

(2)

EXPERIMENTAL

Syntheses

$[Cu(L_1)](NO_3)_2$. The tetraamine 1,10-diamino-4,7-diazadecane (35 g, 0.2 mol) was added to $Cu(NO_3)_2 \cdot 3H_2O$ (48 g, 0.2 mol) in methanol (1.5 l). The resulting dark blue solution was warmed, and triethylamine (22 g, 0.22 mol), nitroethane (37 g, 0.49 mol) and formaldehyde (100 cm^3, 37% aq,

* Author to whom correspondence should be addressed.

1.34 mol) were added. After heating at ~ 55°C for 30 min, the solution was left to crystallize at room temperature overnight. Filtration gave glistening blue crystals of the complex (68 g, 74%). Found: C, 31.1; H, 6.0; N, 21.0. Calc. for $C_{12}H_{27}CuN_7O_8$: C, 31.3; H, 5.9; N, 21.3%. IR (KBr disc): $\nu_{as}(NO_2)$ 1530 cm^{-1}, $\nu_s(NO_2)$ 1340 cm^{-1}. Electronic spectrum (water): λ_{max} 572 nm (ε 99 M^{-1} cm^{-1}), 263 (ε 7440). The complex can be readily recrystallized from water as perchlorate or chloride salts. Found (chloride salt): C, 32.8; H, 7.2; N, 16.3. Calc. for $C_{12}H_{27}Cl_2CuN_5O_2 \cdot 1\frac{1}{2}H_2O$: C, 33.1; H, 6.9; N, 16.1%.

$[Cu(L_2)](ClO_4)_2$. The tetraamine 1,10-diamino-4,7-diazadecane (3.5 g, 0.02 mol) was added to $Cu(NO_3)_2 \cdot 3H_2O$ (4.8 g, 0.02 mol) in methanol (200 cm^3). The resulting dark blue solution was warmed, then diethylmalonate (3.2 g, 0.02 mol), triethylamine (3 cm^3, 0.02 mol) and formaldehyde (10 cm^3, 37% aq, 0.13 mol) were added. After heating for a further 1 h, the solution was left at room temperature overnight. The solution was diluted with water, sorbed onto SP Sephadex C-25 resin (25 cm × 4 cm column) and eluted with 0.25 M $NaClO_4$ adjusted to pH ~ 3. Three significant blue bands were collected. The first failed to crystallize readily, proved to be acid-sensitive and hence non-cyclic, and was discarded. The third band on concentration and standing gave a blue powder (1.44 g). Rapid and essentially complete loss of colour of a solution of this material on acid addition is indicative of a non-cyclic product; the diester macrocycle does not decolourize readily in aqueous acid. Spectroscopy (IR and UV–vis) indicated a similarity to the precursor, and the microanalysis indicated a C : N ratio of 9 : 4, although an acceptable fit for all elements to presumed structures was not forthcoming. Clearly, this material does not arise from a condensate involving diethylmalonate, and complete identification was not pursued. The second band, on concentration, gave blue needles which were collected, washed with alcohol and ether, and air dried to give the diester product (40 mg, < 2%). Found: C, 31.9; H, 5.4; N, 8.9. Calc. for $C_{17}H_{34}Cl_2CuN_4O_{12} \cdot H_2O$: C, 31.9; H, 5.7; N, 8.8%. IR (KBr disc): 1726 cm^{-1} (ester). Electronic spectrum (water): λ_{max} 568 nm (ε 105 M^{-1} cm^{-1}), 268 (ε 7030).

Physical methods

Electronic spectra were recorded in aqueous solution using a Hitachi 220A spectrophotometer. IR spectra were recorded on complexes dispersed in KBr discs using a Nicholet MX-1 Fourier-transform spectrometer. Electrochemical measurements were performed with either a Bioanalytical Systems Inc. CV-27 controller and a glassy carbon working electrode, or with an AMEL Model 473 controller linked to an EG&G PAR Model 303A static mercury drop electrode. A conventional three-electrode system, with Ag–AgCl reference electrode and argon or nitrogen purge gas was employed.

RESULTS AND DISCUSSION

Reaction of copper(II) nitrate, 1,10-diamino-4,7-diazadecane, formaldehyde and nitroethane proceeds readily in warm methanol containing triethylamine as a non-coordinating base, with the product macrocycle 10-methyl-10-nitro-1,4,8,12-tetraazacyclopentadecane (L_1) actually crystallizing as the copper(II) complex during reaction. Without any extensive attempts to refine conditions, yields of the isolated solid of ~ 75% have been obtained routinely. Chromatography of a reaction mixture on SP-Sephadex C-25 cation exchange resin indicated that $[Cu(L_1)]^{2+}$ accounts for ⩾ 90% of copper in the product mixture. The product exhibits characteristic IR vibrations for the nitro group, with ν_{as} at 1530 cm^{-1} and ν_s at 1340 cm^{-1}. Voltammetry in water defined a Cu(II)–(I) couple at −0.67 V (vs Ag–AgCl) and a multielectron irreversible nitro group reduction at −0.94 V. The product is also extremely resistant to dissociation in aqueous acid. Spectroscopic and electrochemical properties are similar to those reported for other well-characterized analogues,[1,2] and preliminary results of an X-ray crystal structure analysis confirm the structure assigned. Evidently, reaction via Scheme 1 proceeds to the essential exclusion of

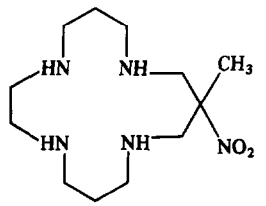

L_1

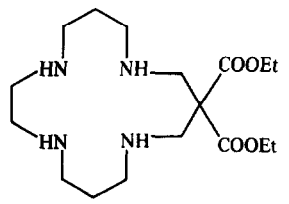

L_2

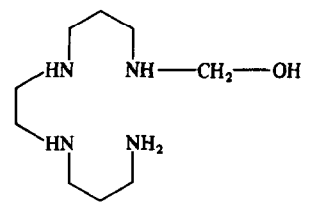

L_3

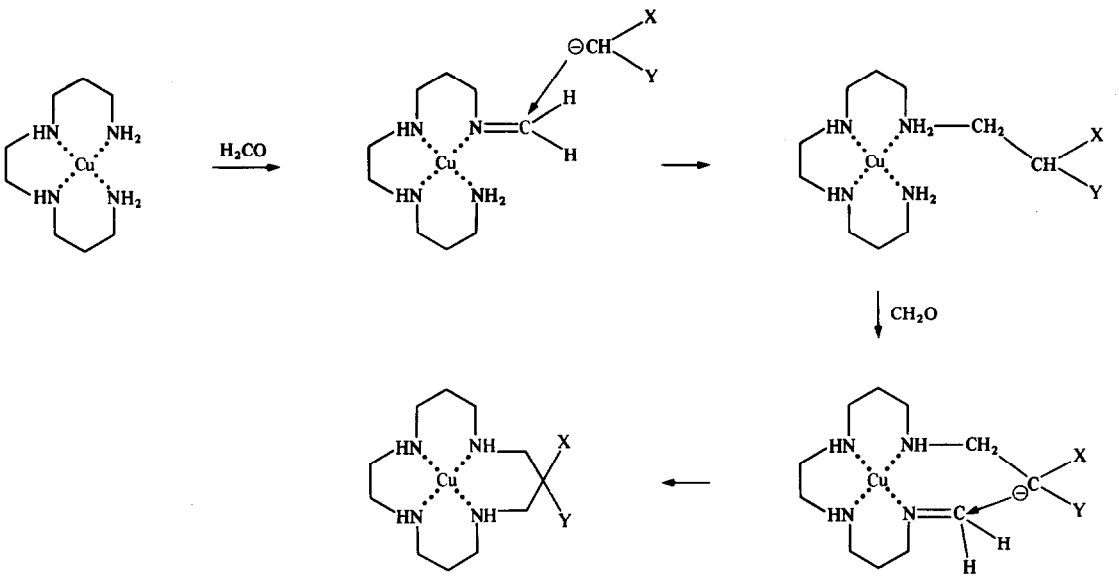

Scheme 1.

other reactions, the formation of the new six-membered ring being favoured entropically. We are currently pursuing this type of reaction with a range of nitroalkanes and amine complexes, as well as looking at complexes of the pendant amine ligands resulting from nitro group reduction. It is clear that the experimental method represents a facile and probably general route to a new range of macromonocyclic ligands.

When the identical reaction to that described above was performed with diethylmalonate as carbon acid, it was not possible to crystallize any product directly. Chromatography on SP-Sephadex C25 resin indicated that several products were present. The major band, from which a blue solid was crystallized, did not contain a cyclic ligand, decomposing readily in aqueous acid. Spectroscopy and microanalysis best fit a simple structure such as L_3, rather than the required compound L_2. A complex of the latter compound was isolated in low yield from a second band; despite attempts to vary the outcome by altering reaction conditions, the result was always similar. The only macrocyclic complex isolated, which amounted to less than 10% of total copper and was crystallized in no better than 2% yield, proved to contain the macrocycle L_2. The IR spectrum showed a strong band at 1726 cm^{-1} characteristic of an ester. The complex was stable in aqueous acid, indicative of a macrocyclic complex. Voltammetry yielded a well-defined reversible Cu(II)–(I) couple at a potential of −0.82 V, with an irreversible wave at −1.34 V associated with electron addition to the ester substituents and in a similar position to waves assigned to this process in several macrobicyclic cobalt(III) complexes with ester substituents.[8] There was no evidence for any amide species such as L_4, analogues of which have appeared in similar reactions around inert cobalt(III) amines.[9] The diamide L_5 which can form by condensation in the absence of metal ion

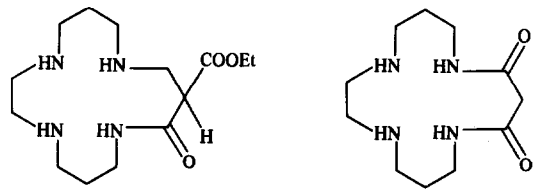

L_4 L_5

and formaldehyde[10] was also absent. While decarboxylation or hydrolysis of the *gem* diester isolated had been anticipated, neither apparently occurred under the experimental conditions employed.

The likely reaction of the putative monoimine intermediate (product of the first step in Scheme 1) with hydroxide ion to ultimately form L_3, rather than reaction with the $(EtOOC)_2CH^-$ nucleophile, is not unreasonable since there was no attempt to exclude water from the reaction mixture. The pK_a of $(EtOOC)_2CH_2$ is about 5 units higher than that of $CH_3CH_2NO_2$, strictly limiting the concentration of the anion in the former case. Even assuming like nucleophilicity for the two carbon acid reactants, there will clearly be far greater opportunity for com-

petition by OH^- in the case of the diethylmalonate reaction. Possibly in stringently anhydrous conditions, reactions involving carbon acids with higher pK_a values may prove more successful. We are pursuing this prospect. Evidently nitroalkane carbon acids are far more successful reactants than diester alkane carbon acids under the conditions described.

Acknowledgement—Support of this research by the Australian Research Grants Scheme is gratefully acknowledged.

REFERENCES

1. P. Comba, T. W. Hambley and G. A. Lawrance, *Helv. Chim. Acta* 1985, **68**, 2332.
2. P. Comba, N. F. Curtis, G. A. Lawrance, A. M. Sargeson, B. W. Skelton and A. H. White, *Inorg. Chem.* 1986, **25**, 4260.
3. R. J. Geue, T. W. Hambley, J. M. Harrowfield, A. M. Sargeson and M. R. Snow, *J. Am. Chem. Soc.* 1984, **106**, 5478.
4. H. A. Boncher, G. A. Lawrance, P. A. Lay, A. M. Sargeson, A. M. Bond, D. F. Sangster and J. C. Sullivan, *J. Am. Chem. Soc.* 1983, **105**, 4652.
5. J. MacB. Harrowfield, A. J. Herlt, P. A. Lay, A. M. Sargeson, A. M. Bond, W. A. Mulac and J. C. Sullivan, *J. Am. Chem. Soc.* 1983, **105**, 5503.
6. N. F. Curtis, G. J. Gainsford, T. W. Hambley, G. A. Lawrance, K. R. Morgan and A. Siriwardena, *J. Chem. Soc., Chem. Commun.*, 1987, in press.
7. W. P. Jencks and J. Regenstein, In *Ionization Constants of Acids and Bases* (Edited by H. A. Sober), "Handbook of Biochemistry", 2nd Edn. Chemical Rubber, Cleveland (1970).
8. A. M. Bond, G. A. Lawrance, P. A. Lay and A. M. Sargeson, *Inorg. Chem.* 1983, **22**, 2010; P. A. Lay, doctoral dissertation, Australian National University (1981).
9. A. M. Sargeson, *Pure Appl. Chem.* 1984, **56**, 1603; *Chem. Br.* 1979, **15**, 23.
10. I. Tabushi, Y. Taniguchi and H. Kato, *Tetrahedron Lett.* 1977, 1049.

Polyhedron Vol. 6, No. 6, pp. 1295–1307, 1987
Printed in Great Britain

0277-5387/87 $3.00+.00

PREPARATION OF *ORTHO*-SUBSTITUTED ARYLDIFLUOROPHOSPHINES, 2-$XC_6H_4PF_2$ (X = MeO OR Me_2N), AND SOME OF THEIR DERIVATIVES. X-RAY CRYSTAL STRUCTURE DETERMINATION OF (2-$MeOC_6H_4P)_4$ AND OF THE PLATINUM COMPLEX, $Cl_2Pt(2\text{-}MeOC_6H_4PF_2)_2$

LUTZ HEUER, MICHAEL SELL and REINHARD SCHMUTZLER*

Institut für Anorganische und Analytische Chemie der Technischen Universität, Hagenring 30, 3300 Braunschweig, F.R.G.

and

DIETMAR SCHOMBURG

Gesellschaft für Biotechnologische Forschung mbH, Mascheroder Weg 1, 3300 Braunschweig-Stöckheim, F.R.G.

(*Received* 12 *August* 1986; *accepted* 10 *November* 1986)

Abstract—The preparation of the *ortho*-substituted aryldifluorophosphines 2-$MeOC_6H_4PF_2$ and 2-$Me_2NC_6H_4PF_2$ by chlorine–fluorine exchange from the corresponding dichlorophosphines using sodium fluoride in acetonitrile in the presence of a crown ether is described. The *ortho*-substituted aryldichlorophosphines 2-$MeOC_6H_4PCl_2$ and 2-$Me_2NC_6H_4PCl_2$ were prepared from the respective bis(*N*,*N*-dimethylamino)phosphines by cleavage of the P—N bonds with hydrogen chloride. The reaction of 4-fluoroanisole and 2-methoxyphenyllithium with phosphorus trichloride did not yield the expected chlorophosphines, i.e. 2-MeO-5-F-$C_6H_3PCl_2$ and 2-$MeOC_6H_4PCl_2$, but led to formation of 4-fluorophenyldichlorophosphite in the former, and to tris(2-methoxyphenyl)phosphine in the latter case. The difluorophosphine 2-$MeOC_6H_4PF_2$ was found to undergo a spontaneous oxidation–reduction reaction with formation of the tetrafluorophosphorane 2-$MeOC_6H_4PF_4$, and the cyclotetraphosphine (2-$MeOC_6H_4P)_4$. A single-crystal X-ray structure determination of the latter indicated the presence of a strongly puckered four-membered ring with P—P bond lengths ranging between 222 and 223 pm, and endocyclic bond angles of 84°. Vicinal $MeOC_6H_4$ groups were found arranged *trans* to each other. Dichloroplatinum(II) complexes were prepared, involving the two new fluorophosphines, 2-$XC_6H_4PF_2$ (X = MeO or Me_2N), as ligands. In neither case was any evidence found for coordination between platinum and oxygen or nitrogen, and the fluorophosphines were found to function solely as phosphorus donors. The absence of interaction between platinum and the oxygen atom in the *ortho* position of the ligand 2-$MeOC_6H_4PF_2$ was confirmed in a single-crystal X-ray determination of the complex $Cl_2(2\text{-}MeOC_6H_4PF_2)_2Pt$. The compound was found to exist as a planar, *cis*-coordinated species with Pt—Cl bond lengths between 232 and 234 pm, and a Pt—P bond length of 218 pm. All compounds were characterized by NMR spectroscopy (^1H, ^{31}P and ^{19}F, where applicable).

Phosphorus(III) compounds, involving aromatic groups bearing an *ortho* substituent with potential donor atoms, e.g. N, O or Sb, have been known for some time.

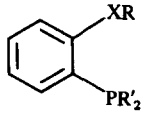

X = O, NR, SbR, etc; R, R′ = alkyl or aryl groups.

* Author to whom correspondence should be addressed.

Numerous coordination compounds involving such ligands, displaying interesting catalytic properties in some cases, have been synthesized.[1-4]

Phosphorus(III) compounds of the above type are expected to coordinate, primarily, via the phosphorus atom, but may give rise to chelate formation on account of the potential donor function of the heteroatom. Even though in many cases a proper bond between the metal and the heteroatom may not exist, evidence has been obtained which suggests that, in the course of catalytic reactions, a weak interaction between platinum and the heteroatom may serve to stabilize vacant coordination sites.

In our own previous work concerning the coordinating potential of *ortho*-substituted aryl- and alkyl-phosphines with metals such as Rh(I) or Ir(I),[5] or Pd(II) and Pt(II),[6] such interactions were demonstrated. Thus, it was shown that phosphorus (III) ligands, involving 2-*N*,*N*-dimethylamino substituents in an aromatic group form chelate complexes of composition $(L)PtCl_2$ (M = Pd or Pt), involving coordination of the ligand to the metal via phosphorus as well as nitrogen.[7] In contrast, the related complexes with *ortho*-alkoxy-phenyl groups seem to be bonded to the metal solely via phosphorus. These findings are in agreement with reports by other authors.[2,8] Oxygen does get involved in bonding or interacts strongly with the metal in the case of metallic centres of higher oxidation number.[4(b),9]

The coordinating ability of a heteroatom in the *ortho* position of an aromatic substituent at phosphorus(III) is strongly affected by its basicity, according to the concept of Pearson: nitrogen, as a "softer" atom is expected to coordinate to a "soft" metallic centre, rather than the "hard" oxygen. In addition, the +*I*-effect of a further methyl group at nitrogen was found to be favourable.[5] In an attempt to affect the interaction between the metal and the *ortho* substituent in an aryl group at phosphorus, the following possibilities were considered: (a) Elimination of ligands, e.g. chlorine, using silver salts, generating vacant coordination sites, or coordination sites to which solvent molecules are loosely bound. (b) Increase of the electrophilic character of the metal through the introduction of ligands which reduce the electron density at the metal, e.g. CO, PF_3 or PF_2O^-, isoelectronic to PF_3. (c) Modification of the phosphorus ligand, e.g. through the introduction of fluorine. The considerations listed under (b) also apply.

A ligand of the general type

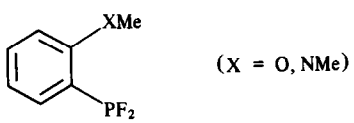

(X = O, NMe)

on account of the superior back-bounding qualities of the PF_2 grouping is expected to be capable of withdrawing electron density from the metal, in contrast to a PR_2 group (R = alkyl or aryl). Thus, an increase in the electrophilic character will result, facilitating the coordination of a heteroatom. The compounds under discussion are considered to represent novel ligand systems which provide access to a variety of interesting coordination compounds.

An additional feature of difluorophosphines, RPF_2 (R = alkyl or aryl), is their pronounced tendency to undergo oxidation–reduction reactions, with formation of tetrafluorophosphoranes and cyclopolyphosphines.[10,11] The synthesis of two *ortho*-substituted difluorophosphines, their coordination compounds with platinum(II), and the redox disproportionation of one of the two compounds, $2\text{-}MeOC_6H_4PF_2$, will be described in what follows.

RESULTS AND DISCUSSION

Preparation of substituted aryldichlorophosphines

According to Michaelis,[12] anisole and *N*,*N*-dimethylaniline may be converted to the corresponding *para*-substituted dichlorophosphines under Friedel–Crafts conditions. It is known[13] that, in the case of substituted aryl precursors, mixtures of isomers (predominantly *para*, and some *ortho*) may be formed.

First, the synthesis of 2-methoxy-5-fluorophenyldichlorophosphine was attempted via the reaction of 4-fluoroanisole with phosphorus trichloride in the presence of aluminium chloride. Cleavage of the intermediate complex formed initially with phosphorus oxychloride,[14] however, only furnished 4-fluorophenyldichlorophosphite (**1**) as a result of the cleavage of the ether linkage [eqn (1)], **1** has not previously been described in the literature and was characterized by elemental analysis and NMR spectroscopy.

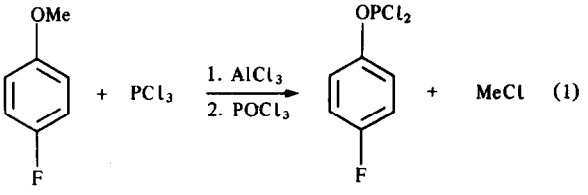

1

Next, an attempt was made at synthesizing 2-methoxyphenyldichlorophosphine by the reaction of 2-lithioanisole with phosphorus trichloride at low temperature [eqn (2)]. The main reaction product here was the tertiary phosphine, tris(2-methoxy-

phenyl)phosphine, which has previously been reported by Mann and Chaplin.[15]

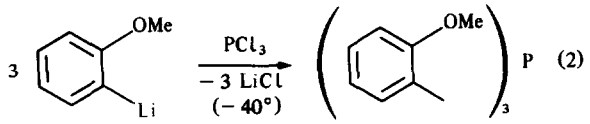

(2)

The synthesis of 2-methoxyphenyldichlorophosphine in a yield of 10%, using a diazonium intermediate, was first reported by Quin.[16] It was thought that a more efficient route to this dichlorophosphine might be the cleavage of the appropriate bis(*N*,*N*-diethylamino)phosphine with dry hydrogen chloride. A number of *para*-substituted aryldichlorophosphines have previously been obtained by this route.[17] The same principle has been employed by Shaw[18] and, later, by McEwen,[19] in the synthesis of *ortho*-substituted aryldichlorophosphines.

The synthesis of the dichlorophosphines required in the present research was accomplished in accordance with eqns (3) and (4).

The aryl compounds, **2b** and **3b**, react with bis(diethylamino)chlorophosphine according to eqn (3b). The P—N bond in the aminophosphines, **4** and **5**, is cleaved by anhydrous hydrogen chloride with formation of the dichlorophosphines, **6** and **7**, in good yield. The NMR data for compounds **4**–**7** are listed in Table 1.

Preparation of 2-*methoxy- and* 2-N,N-*dimethylaminophenyldifluorophosphine*, **8** *and* **9**

It has been demonstrated that the unsubstituted compound, $C_6H_5PF_2$, may be obtained in good yield by chlorine–fluorine exchange with sodium fluoride from the dichlorophosphine.[20]

It was found that the 2-substituted aryldichlorophosphines, **6** and **7**, may be converted into the corresponding difluorophosphines, **8** and **9**, using sodium fluoride in acetonitrile, in the presence of catalytic quantities of crown ether (15-crown-5), in accordance with eqn (5).

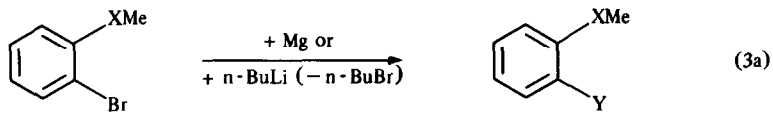

(3a)

2a X = O
3a X = NMe

2b X = O; Y = MgBr
3b X = NMe; Y = Li

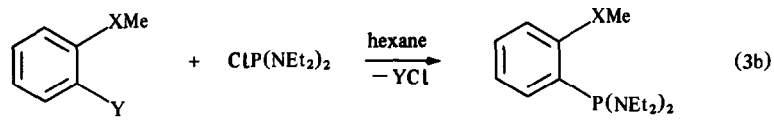

(3b)

4 X = O
5 X = NMe

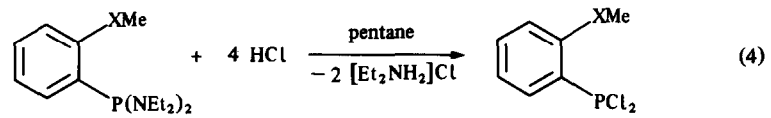

(4)

6 X = O
7 X = NMe

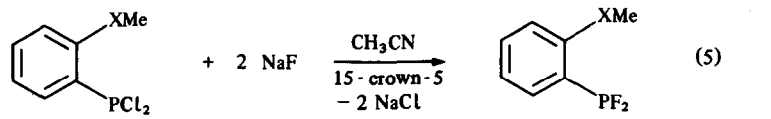

(5)

8 X = O
9 X = NMe

All the compounds are distillable liquids which were characterized by elemental analysis, and by NMR spectroscopy (Table 1).

The possibility was considered that compounds **8** and **9** may result from the direct reaction of PF_2Cl[21] with a suitable aryllithium compound. Thus, 2-methoxyphenyllithium was allowed to react with PF_2Cl at low temperature in a sealed, heavy-wall glass tube [eqn (6)].

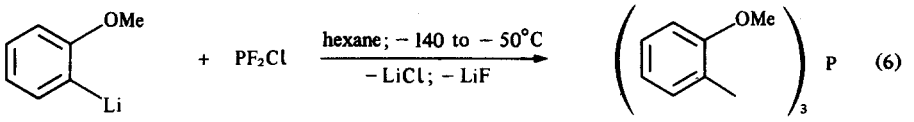

(6)

It was found, however, that both P—F bonds and the P—Cl bond in PF_2Cl reacted, with formation of the tertiary phosphine $(2\text{-}MeOC_6H_4)_3P$ as the only product which could be isolated. Chlorodifluorophosphine does not, therefore, react more selectively than phosphorus trichloride [cf. eqn (2)]. Part of the PF_2Cl was recovered unreacted.

Spontaneous oxidation–reduction reaction of 2-*methoxyphenyldifluorophosphine* (**8**)

The difluorophosphine (**8**) could be kept unchanged over periods of several months at −30°C. It was found, however, that a spontaneous disproportionation reaction commences at room temperature, and is accelerated at elevated temperature. Thus, a sample of **8** kept in a sealed NMR

Table 1. ^1H, ^{19}F and ^{31}P NMR data for compounds **4–9**

Compound		^1H NMR	^{19}F NMR	^{31}P NMR
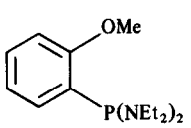	**4**[ab]	$\delta_{CH_3} = 1.4$ (t, 12 H); $^3J(HH) = 7$ Hz $\delta_{CH_2} = 3.4$ (dq, 8 H); $^3J(HP) = 9$ Hz $^3J(HH) = 7$ Hz $\delta_{OCH_3} = 3.9$ (s, 3 H) $\delta_{C_6H_4} = 6.9$–7.8 (m, 4 H)		$\delta = 92.3$
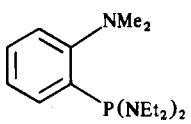	**5**[ab]	$\delta_{CH_3} = 1.0$ (t, 12 H); $^3J(HH) = 7$ Hz $\delta_{CH_2} = 2.9$ (dq, 8 H); $^3J(HP) = 9$ Hz $^3J(HH) = 7$ Hz $\delta_{NCH_3} = 2.7$ (s, 6H) $\delta_{C_6H_4} = 6.7$–7.5 (m, 4 H)		$\delta = 96.9$
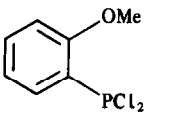	**6**[ab]	$\delta_{OCH_3} = 4.0$ (s, 3 H) $\delta_{C_6H_4} = 6.9$–8.2 (m, 4 H)		$\delta = 163.3$
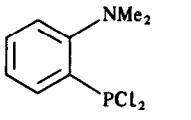	**7**[ab]	$\delta_{NCH_3} = 2.4$ (s, 6 H) $\delta_{C_6H_4} = 6.8$–7.8 (m, 4 H)		$\delta = 150.2$
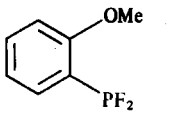	**8**[de]	$\delta_{OCH_3} = 3.90$ (s, 3 H) $\delta_{C_6H_4} = 6.94$ (dd, 1 H); $J = 4.8$ Hz $= 7.06$ (t, 1 H); $J = 7.5$ Hz 7.47–7.55 (m, 2 H)	$\delta = -99.5$ (d), $^1J(FP) = 1166$ Hz	$\delta = 208.3$ (t), $^1J(FP) = 1176$ Hz
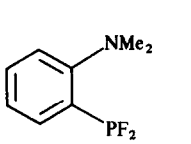	**9**[cd]	$\delta_{NCH_3} = 2.80$ (s, 6 H) $\delta_{C_6H_4} = 7.32$ (dt, 1 H); $J = 4, 7.5$ Hz $= 7.41$ (br, t, 1 H); $J = 7.5$ Hz $= 7.59$–7.72 (m, 1 H), $= 7.77$ (ddd, 1 H); $J = 2, 7.5, 16$ Hz	$\delta = -100.5$ (d), $^1J(FP) = 1143$ Hz	$\delta = 197.1$ (t), $^1J(PF) = 1147$ Hz

[a] ^1H NMR; instrument JEOL JNMC-60.
[b] ^{19}F and ^{31}P NMR; instrument JEOL JNMC-60 HL.
[c] ^1H NMR, in $CDCl_3$; instrument Bruker AM 300.
[d] ^{31}P NMR; instrument Bruker WM 400.
[e] ^1H NMR, in $CDCl_3$; instrument Bruker WM 400.

tube for 48 h at 80°C was found to be converted into the corresponding cyclotetraphosphine (**10**) and tetrafluorophosphorane (**11**) in a yield of 90% [eqn (7)].

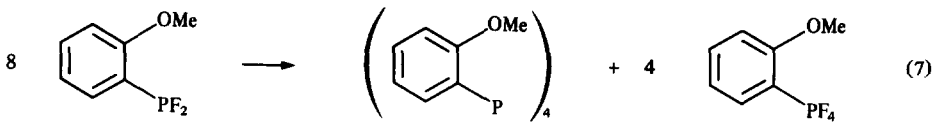

8 **10** **11**

Oxidation–reduction reactions of the above type have been known for a few years, and were first observed in the case of methyldifluorophosphine.[10,22] Such reactions will be catalytically affected by traces of hydrogen fluoride, formed in the presence of moisture.[23]

Besides tetrafluorophosphoranes, cyclopolyphosphines $[(RP)_n$ (n = usually 4, 5 or 6)] are formed.[24,25] The number n depends on the size and electronegativity of the organic group.[25,26] From mass-spectroscopic (parent ion, m/z 552) and NMR spectroscopic investigations the presence of the four-membered ring $(2\text{-}MeOC_6H_4P)_4$ is clearly indicated. The high-field shift, $\delta_P = -55.6$, in **10** is considered typical of cyclopolyphosphines $(RP)_4$.[25]

The ^1H NMR spectrum of **10** suggests that the state of the compound in solution is not simple. Several δ_H values for the protons of the CH_3O groups ($\delta_H = 3.7$–3.9); besides, unresolved multiplets in the phenyl region are observed. It is assumed, therefore, that the orientation of the phenyl rings (and the methoxy groups connected to them) is different, and/or that the molecule dissociates or rearranges in solution.

The second product, formed during the disproportionation of the difluorophosphine **8**, 2-methoxyphenyltetrafluorophosphorane (**11**) was also formed in the oxidative fluorination reaction of the dichlorophosphine **6** with antimony trifluoride, in analogy to the unsubstituted parent compound, $C_6H_5PF_4$.[27]

The separation of **11** from $SbCl_3$ by distillation proved difficult, and **11** could not be obtained in a pure state. It was, however, characterized unambiguously by its NMR data. Further evidence for its identity has been provided by the hydrolysis of **11** [eqn (9)].

The phosphonic acid, previously reported in the literature,[28] has been characterized by analysis and by its melting point. NMR data could not be obtained, on account of its poor solubility.

Syntheses of the platinum(II) *complexes*, **13** *and* **14**

Dichloro-(1,5-cyclooctadiene)platinum(II)[29] was found to react in dichloromethane solution with two equivalents of the difluorophosphines **8** and **9** with displacement of the cyclooctadiene ligand. The complexes *cis*-dichloro-bis{(2-methoxyphenyl) difluorophosphine}platinum(II) (**13**) and *cis*-dichloro - bis{(2 - dimethylaminophenyl)difluoro - phosphine}platinum(II) (**14**) are thus readily obtained.

The *cis* structure of complexes **13** and **14** is suggested by their IR and NMR spectra; it has also been established by a single-crystal X-ray diffraction study of **13** (*vide infra*).

In the IR spectra of both complexes, **13** and **14**, a weak absorption due to ν_{Pt-Cl} is observed at 280 and 335 cm^{-1}, respectively; this is typical of *cis*-chlorine substitution at platinum.[30] Furthermore,

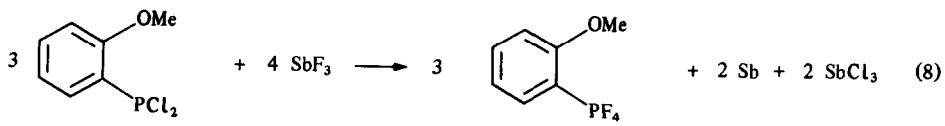

6 **11**

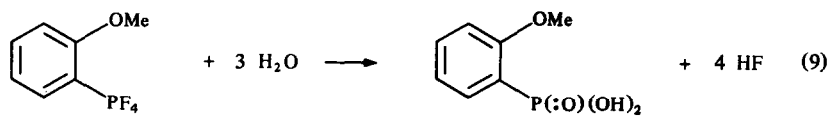

11 **12**

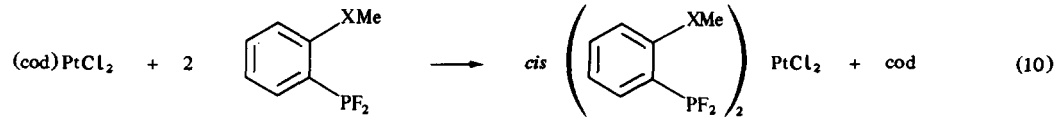

8 X = O
9 X = NMe

13 X = O
14 X = NMe

cod = cyclooctadiene - 1.5

two characteristic strong bands for ν_{P-F}[31] at 770 and 845–865 cm^{-1} are observed.

The NMR spectra (cf. Table 2) display symmetrical higher-order spin systems of type $A_2XA'_2X'M$ (A and A′ = ^{19}F, X and X′ = ^{31}P, M = Pt). In the ^1H NMR spectra single lines are observed for the $-OCH_3$ and $-N(CH_3)_2$ groups *ortho* to phosphorus. This confirms that the heteroatom, O or N, is not coordinated with platinum, as otherwise platinum satellites should be observed. The platinum–phosphorus coupling constants ^1J(PPt) (5268 Hz for **13** and 5613 Hz for **14**) are of a magnitude expected for PF ligands bonded to platinum.[32] They indicate the presence of *cis* compounds, the Pt–P coupling constants of *trans* complexes being smaller, because of the larger *trans* effect of phosphine ligands compared to chloride. From the ^{19}F and ^{31}P NMR spectra only the sum of the PF coupling constants [$|^1J(PF)+{}^3J(PF)| = 1136$ for **13** and 1117 for **14**] can be obtained directly. The situation in these spin systems involving ^{19}F and ^{31}P nuclei, of which "virtual coupling"[33] is characteristic, is different than for systems with ^1H and ^{31}P nuclei. In the *cis* complexes which are under investigation here the coupling constant ^2J(PP′) is large, because of the very large coupling constant ^1J(PPt). Further, the "virtual coupling" between fluorine of one of the PF ligands to the phosphorus of the second (*cis*) ligand [^3J(FP′)] must be rather large. A simulation of this spectrum should be informative but could not be realized, thus far, because of the difficulty of assigning the coupling constants.

Single-crystal X-ray structure determination of compounds **10** *and* **13**

The cyclotetraphosphine **10** has a geometry very similar to that of the other cyclotetraphosphine derivatives that can be found in the literature. The P—P bond lengths (mean 222.5 pm) compare well with 221.7 pm in $(t\text{-BuP})_4$,[34] 222.4 pm in $(H_{11}C_6P)_4$,[35] 222.2 pm in $(F_3CP)_4$,[36] and 223.4 pm in $(F_5C_6P)_4$.[37] As in these compounds the four-membered ring in **10** is not planar. This is reflected in the mean P—P—P bond angle of 84.1°. While

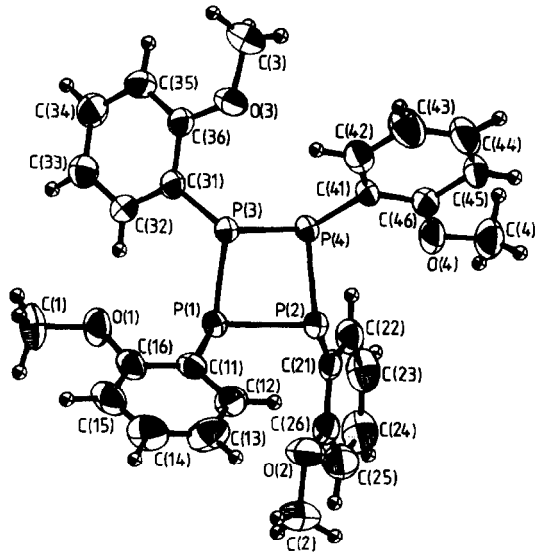

Fig. 1. Molecular structure of tetra(2-methoxyphenyl)-cyclotetraphosphine.

Table 2. ^1H, ^{19}F and ^{31}P NMR data of complexes **13** and **14**

Compound	^1H NMR[a]	^{19}F NMR[b]	^{31}P NMR[a]
13	$\delta_{OCH_3} = 3.93$ (s, 6 H) $\delta_{C_6H_4} = 7.02$–7.96 (m, 8 H)	$\delta = -67.0$, ^2J(FPt) = 501 Hz	$\delta = +133.5$, ^1J(PPt) = 5268 Hz J(PF)[c] = 1136 Hz
14	$\delta_{NCH_3} = 2.89$ (s, 12 H) $\delta_{C_6H_4} = 7.25$–8.42 (m, 8 H)	$\delta = -71.4$, ^2J(FPt) = 518 Hz	$\delta = +122.7$, ^1J(PPt) = 5613 J(FP)[c] = 1117 Hz

[a] ^1H NMR, ^{31}P NMR in $CDCl_3$; instrument Bruker WM 400.
[b] ^{19}F NMR in CH_2Cl_2; instrument Varian EM 390.
[c] $|J(PF)| = |{}^1J(PF)+{}^3J(PF)|$.

Table 3. Bond lengths (Å) in compound **10**

P(1)—P(2)	2.226(1)	P(1)—P(3)	2.232(1)
P(1)—C(11)	1.834(3)	P(2)—P(4)	2.221(1)
P(2)—C(21)	1.830(3)	P(3)—P(4)	2.222(1)
P(3)—C(31)	1.832(3)	P(4)—C(41)	1.825(3)
C(11)—C(12)	1.383(5)	C(11)—C(16)	1.388(4)
C(12)—C(13)	1.396(5)	C(13)—C(14)	1.371(6)
C(14)—C(15)	1.369(6)	C(15)—C(16)	1.384(5)
C(16)—O(1)	1.372(4)	O(1)—C(1)	1.421(4)
C(21)—C(22)	1.391(4)	C(21)—C(26)	1.404(5)
C(22)—C(23)	1.384(5)	C(23)—C(24)	1.356(7)
C(24)—C(25)	1.382(6)	C(25)—C(26)	1.379(6)
C(26)—O(2)	1.359(4)	O(2)—C(2)	1.415(5)
C(31)—C(32)	1.387(4)	C(31)—C(36)	1.395(5)
C(32)—C(33)	1.382(5)	C(33)—C(34)	1.351(6)
C(34)—C(35)	1.383(5)	C(35)—C(36)	1.385(5)
C(36)—O(3)	1.368(4)	O(3)—C(3)	1.433(5)
C(41)—C(42)	1.382(5)	C(41)—C(46)	1.392(4)
C(42)—C(43)	1.389(5)	C(43)—C(44)	1.367(6)
C(44)—C(45)	1.373(6)	C(45)—C(46)	1.394(5)
C(46)—O(4)	1.363(4)	O(4)—C(4)	1.427(4)

the lengths of the P—C_{sp^3} bonds in these compounds are around 187 pm the P—C_{sp^2} bond lengths in **10**, and in the pentafluorophenyl derivative, $(F_5C_6P)_4$[37] are near 183 pm (mean value of the P—C bond length in **10**, 183.0 pm).

The bonding geometry at the platinum atom in **13** is distorted square planar with bond angles between 85° (P—Pt—Cl) and 99° (P—Pt—P) (sum of the angles between *cis* bonds 359.9°). The observed distances between platinum and the methoxy-oxygen atoms (347 and 349 pm) prove that there is no increase in the coordination number of platinum.

Whereas the Pt—Cl bond distances of 232 and 234 pm in **13** are very close to similar values found in the literature[36] (e.g. terminal Pt—Cl in $[Pt(Cl)\{P(:O)F_2\}(PEt_3)]_2$, the Pt—P bonds in the molecule are amongst the shortest such bonds described in the literature. Very short bond lengths between phosphorus and the transition metal are generally found in complexes of fluoro-substituted phosphines with transition metals. In the complex $[Pt(Cl)\{P(:O)F_2\}(PEt_3)]_2$ the Pt—$P(Et)_3$ bond length is 225.7 pm whereas the Pt–$P(:O)F_2$ bond length is only 216.8 pm.[39]

The *ortho* substitution at the phenyl ring causes rather short non-bonded distances between the methoxy oxygen and the phosphorus atoms in both compounds (276–283 pm). These values are about 50 pm shorter than the sum of the van der Waals' radii (332 pm). The fact that such a short non-bonding distance is possible is probably due to a certain degree of acceptor character of the phosphorus atom. This interaction causes changes in the bonding geometry around phosphorus. The equivalence of the P—P—C_{sp^2} angles which is found in the other cyclotetraphosphines is lost in **10** where two groups of such angles can be found, one with a mean value of 104.7(7)°, the other with a mean

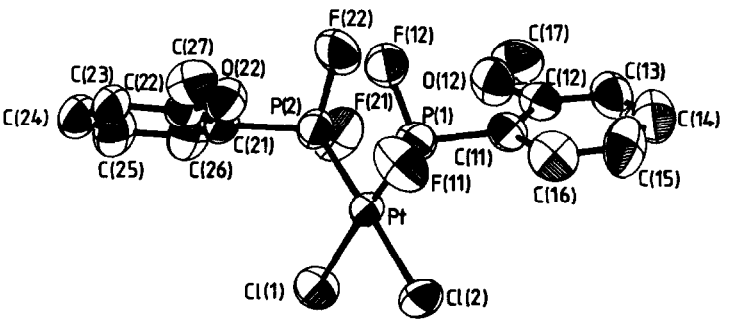

Fig. 2. Molecular structure of *cis*-dichloro-bis{(2-methoxyphenyl)difluorophosphine}platinum(II), **10**.

Table 4. Bond angles (°) in compound **10**

P(3)—P(1)—P(2)	84.1(0)	C(11)—P(1)—P(2)	104.9(1)
C(11)—P(1)—P(3)	102.1(1)	P(4)—P(2)—P(1)	84.1(0)
C(21)—P(2)—P(1)	100.6(1)	C(21)—P(2)—P(4)	103.9(1)
P(4)—P(3)—P(1)	83.9(0)	P(3)—P(4)—P(2)	84.4(0)
C(31)—P(3)—P(1)	104.3(1)	C(31)—P(3)—P(4)	100.4(1)
C(41)—P(4)—P(2)	101.9(1)	C(41)—P(4)—P(3)	105.6(1)
C(12)—C(11)—P(1)	124.9(2)	C(16)—C(11)—P(1)	116.2(2)
C(16)—C(11)—C(12)	118.6(3)	C(13)—C(12)—C(11)	120.1(3)
C(14)—C(13)—C(12)	120.0(4)	C(15)—C(14)—C(13)	120.6(4)
C(15)—C(16)—C(11)	121.2(3)	C(16)—C(15)—C(14)	119.4(4)
O(1)—C(16)—C(11)	114.6(3)	O(1)—C(16)—C(15)	124.2(3)
C(1)—O(1)—C(16)	119.7(3)	C(22)—C(21)—P(2)	125.3(2)
C(26)—C(21)—P(2)	116.8(2)	C(26)—C(21)—C(22)	117.8(3)
C(23)—C(22)—C(21)	121.3(3)	C(24)—C(23)—C(22)	119.4(4)
C(25)—C(24)—C(23)	121.3(4)	C(25)—C(26)—C(21)	120.6(3)
C(26)—C(25)—C(24)	119.5(4)	O(2)—C(26)—C(21)	114.5(3)
O(2)—C(26)—C(25)	124.9(3)	C(2)—O(2)—C(26)	119.7(3)
C(32)—C(31)—P(3)	124.5(2)	C(36)—C(31)—P(3)	117.4(2)
C(36)—C(31)—C(32)	118.1(3)	C(33)—C(32)—C(31)	120.8(3)
C(34)—C(33)—C(32)	119.8(4)	C(35)—C(34)—C(33)	121.7(4)
C(35)—C(36)—C(31)	121.1(3)	C(36)—C(35)—C(34)	118.4(3)
O(3)—C(36)—C(31)	114.6(3)	O(3)—C(36)—C(35)	124.2(3)
C(3)—O(3)—C(36)	118.6(3)	C(42)—C(41)—P(4)	124.6(2)
C(46)—C(41)—P(4)	117.3(2)	C(46)—C(41)—C(42)	118.0(3)
C(43)—C(42)—C(41)	121.0(3)	C(44)—C(43)—C(42)	119.7(4)
C(45)—C(44)—C(43)	121.3(4)	C(45)—C(46)—C(41)	121.3(3)
C(46)—C(45)—C(44)	118.7(3)	O(4)—C(46)—C(41)	114.7(3)
O(4)—C(46)—C(45)	124.0(3)	C(4)—O(4)—C(46)	118.9(3)

value of 101.3(9)°. A similar observation can be made in the platinum complex where two groups of C—P—F and C—P—Pt angles are found. The O···P—P angles involving the phosphorus atoms most nearly *trans* to O···P are all between 153 and 158°, whereas to the *cis*-P—P bonds they are between 84 and 90°.

These values can be explained by the fact that the bonding geometry at phosphorus is between the normal pyramid and a pseudo-trigonal bipyramid where one of the equatorial positions is occupied by the non-bonding electron pair and the oxygen donor atom is at an axial position. Similarly the O···P—F angles in **13** are 156.0 and 156.4°. The

Table 5. Bond lengths (Å) in compound **13**

		Pt—Cl(1)	2.339(5)
Pt—Cl(2)	2.315(4)	Pt—P(1)	2.180(5)
Pt—P(2)	2.181(4)	P(1)—F(11)	1.546(11)
P(1)—F(12)	1.551(11)	P(1)—C(11)	1.745(14)
C(11)—C(12)	1.402(21)	C(11)—C(16)	1.435(21)
C(12)—O(12)	1.350(20)	C(12)—C(13)	1.366(23)
O(12)—C(17)	1.459(21)	C(13)—C(14)	1.378(28)
C(14)—C(15)	1.400(33)	C(15)—C(16)	1.360(25)
C(16)—H(16)	1.080(25)	P(2)—F(21)	1.559(12)
P(2)—F(22)	1.551(15)	P(2)—C(21)	1.788(14)
C(21)—C(22)	1.390(21)	C(21)—C(26)	1.341(24)
C(22)—O(22)	1.379(21)	C(22)—C(23)	1.397(21)
O(22)—C(27)	1.439(24)	C(23)—C(24)	1.324(28)
C(24)—C(25)	1.410(27)	C(25)—C(26)	1.403(23)

Table 6. Bond angles (°) in compound **13**

Cl(2)—Pt—Cl(1)	91.4(2)	P(1)—Pt—Cl(1)	175.9(2)
P(1)—Pt—Cl(2)	84.5(2)	P(2)—Pt—Cl(1)	84.9(2)
P(2)—Pt—Cl(2)	176.1(2)	P(2)—Pt—P(1)	99.1(2)
F(11)—P(1)—Pt	113.1(5)	F(12)—P(1)—Pt	115.7(5)
F(12)—P(1)—F(11)	98.6(7)	C(11)—P(1)—Pt	118.8(5)
C(11)—P(1)—F(11)	103.2(7)	C(11)—P(1)—F(12)	104.9(7)
C(12)—Cl(1)—P(1)	119.5(12)	C(16)—C(11)—P(1)	123.8(12)
C(16)—C(11)—C(12)	116.7(14)	O(12)—C(12)—C(11)	112.7(14)
C(13)—C(12)—C(11)	122.4(15)	C(13)—C(12)—O(12)	124.9(15)
C(17)—O(12)—C(12)	120.2(14)	C(14)—C(13)—C(12)	119.1(18)
C(15)—C(14)—C(13)	121.4(20)	C(15)—C(16)—C(11)	121.2(17)
C(16)—C(15)—C(14)	119.1(20)	H(16)—C(16)—C(11)	119.4(18)
H(16)—C(16)—C(15)	119.4(20)	F(21)—P(2)—Pt	111.9(5)
F(22)—P(2)—Pt	116.9(5)	F(22)—P(2)—F(21)	97.5(7)
C(21)—P(2)—Pt	121.7(5)	C(21)—P(2)—F(21)	100.5(7)
C(21)—P(2)—F(22)	104.5(7)	C(22)—C(21)—P(2)	115.5(11)
C(26)—C(21)—P(2)	122.6(12)	C(26)—C(21)—C(22)	121.8(15)
O(22)—C(22)—C(21)	114.8(13)	C(23)—C(22)—C(21)	119.3(14)
C(23)—C(22)—O(22)	125.9(14)	C(27)—O(22)—C(22)	118.9(13)
C(24)—C(23)—C(22)	119.6(16)	C(25)—C(24)—C(23)	121.6(17)
C(25)—C(26)—C(21)	118.9(16)	C(26)—C(25)—C(24)	118.8(17)

geometry around the phosphorus atom is between tetrahedral and trigonal bipyramidal, with axial P—O and P—F bonds, where the bond angles between the pseudo-equatorial Pt—P and C—P bonds, respectively, and the pseudo-equatorial P—F bond [to F(12) and F(22)] are about 3–4° larger than those to the pseudo-axial P—F bond.

EXPERIMENTAL

All manipulations were carried out in an atmosphere of dry oxygen-free nitrogen, using standard techniques. Magnetic stirring was employed throughout. Literature procedures were employed for the synthesis of 2-bromo-*N*,*N*-dimethylaniline,[40] bis(diethylamino)chlorophosphine[41] and dichloro-1,5-cyclooctadieneplatinum.[29]

NMR spectra were recorded using the following instruments and conditions:

JEOL JNMR-60 HL: ^1H (60 MHz), ^{19}F (56.4 MHz), ^{31}P (24.3 MHz);
Varian EM 390: ^{19}F (84.6 MHz);
Bruker WM 400: ^1H (400 MHz), ^{31}P (162.0 MHz);
Bruker AM 300: ^1H (300 MHz).
References: TMS internal (^1H), CCl_3F external (^{19}F), 85% H_3PO_4 external (^{31}P).
Mass spectra: A.E.I. instruments MS 9 and MS 902 S at 70 eV.

Attempts directed at the synthesis of 2-methoxyphenyldichlorophosphine

Reaction of 4-fluoroanisole with phosphorus trichloride: formation of 4-fluorophenyldichlorophosphite (**1**). 4-Fluoroanisole (26 g, 0.2 mol) was added to 30 g (0.23 mol) of aluminium trichloride at such a rate that the temperature of the mixture was kept below 90°C (4 h). Over a period of 30 min, 30 g (0.23 mol) of phosphorus trichloride was then added, so that the temperature was kept between 60 and 100°C, and that the mixture remained liquid. Stirring was continued for 5 h at 60°C and for 12 h at room temperature. A white solid was precipitated upon addition of 51 g (0.33 mol) of phosphorus oxychloride. The mixture was subsequently kept for 1 h at 100–110°C. Upon cooling and addition of 100 cm^3 of petroleum ether (40–60) the mixture was refluxed for 2 h. Fractional distillation of the liquid product remaining after removal of the solid yielded 11.5 g (27%) of **1** [b.p. 70°C (0.5 mm)].

NMR spectra: ^1H, $\delta_{C_6H_3} = 6.7–7.1$ (m, 3H); CH_2Cl_2 as an internal reference. δ ^1H (TMS) = δ ^1H (CH_2Cl_2) -5.35; ^{19}F, $\delta = -111.5$ (s), $CFCl_3$ as an external reference; ^{31}P, $\delta = 178.2$ (s).

Analysis: $C_6H_3Cl_2FOP$ (211.97). Found: C, 34.0; H, 1.9; P, 14.8. Calc.: C, 34.0; H, 1.4; P, 14.6%.

Reaction of 2-methoxyphenyllithium with phosphorus trichloride: preparation of tris(2-methoxyphenyl)phosphine.[15] A solution of *n*-butyllithium (0.134 mol as 57.3 g of a 1.38 M solution in hexane) was added to 25 g (0.134 mol) of 2-bromoanisole. After the mixture had been stirred at room temperature for 8 h, it was cooled to −78°C and stirred for 2 h at this temperature, after addition of 18.3 g (0.134 mol) of phosphorus trichloride. After the mixture had been allowed to warm up to room temperature the lithium chloride precipitated was removed by filtration. Tris(2-methoxyphenyl) phosphine was precipitated upon slow evaporation of the remaining liquid *in vacuo* (12 mm). The product was recrystallized from dichloromethane. Yield 9.8 g (71%) (m.p. 186°C).

NMR spectra: ^1H, $\delta_{OMe} = 3.85$ (s, 9H); $\delta_{Ar} = 6.8–7.5$ (m, 12H) in $CDCl_3$; CH_2Cl_2 as an internal reference; ^{31}P, δ P = −36.5 (CH_2Cl_2 as solvent).

Preparation of 2-methoxyphenyl-bis(N,N-diethylamino)phosphine (**4**)

A Grignard reagent was prepared from 28.1 g (0.15 mol) of 2-bromoanisole (**2a**) and 3.65 g (0.15 mol) of magnesium in 50 cm^3 of diethylether. After 2 h reflux bis(diethylamino)chlorophosphine (31.6 g; 0.15 mol) was added over a period of 0.5 h at −15°C. The mixture was refluxed for 6 h, and the magnesium halide mixture formed was separated by filtration. Distillation of the liquid product furnished 24.9 g (59%) of **4** [b.p. 115°C (0.2 mm)].

Analysis: $C_{15}H_{27}N_2OP$ (282.36). Found: C, 63.8; H, 9.7. Calc.: C, 63.8; H, 9.6%.

Preparation of 2-N,N-dimethylaminophenyl-bis(diethylamino)phosphine (**5**)

A mixture of 0.115 mol of *n*-butyllithium (as 60 g of a 1.38 M solution in hexane) and 23.1 g (0.115 mol) of 2-bromo-*N,N*-dimethylaniline (**3a**) was prepared at −10°C, and was stirred for 12 h at room temperature. Upon cooling to −30°C 24 g (0.115 mol) of bis(diethylamino)chlorophosphine in 20 cm^3 of hexane was added over a period of 0.5 h. The mixture was subsequently refluxed for 5 h. The lithium chloride was removed by centrifugation at room temperature, and the supernatant liquid was fractionally distilled. The product (**5**) was obtained in a yield of 21.8 g (64%) [b.p. 138–140°C (1.0 mm)].

Analysis: $C_{16}H_{30}N_3OP$ (295.41). Found: C, 65.1; H, 10.5. Calc.: C, 65.0; H, 10.2%.

Preparation of 2-methoxyphenyldichlorophosphine (**6**)

A solution of 14.5 g (0.05 mol) of 2-methoxyphenyl-bis(*N,N*-diethylamino)phosphine (**4**) in 40 cm^3 of petroleum ether (40–60) was placed in a 200-cm^3 heavy wall glass tube, fitted with a TEFLON® stopcock, and was cooled to −196°C. Anhydrous hydrogen chloride (7.8 g, 0.21 mol) was than condensed onto the mixture via a vacuum line. The sealed reaction tube was allowed to reach room temperature with continuous shaking over a period of 1 h. The tube was opened in an atmosphere of nitrogen, and the diethylammonium chloride precipitated was filtered off, using a sintered glass disc, and was washed repeatedly with small portions of petroleum ether (40–60), totalling 50 cm^3. The clear liquid product was fractionally distilled, and **6** was obtained in a yield of 8.69 g (82%) [b.p. 83–85°C (0.3 mm)].

Analysis: $C_7H_7Cl_2OP$ (290.01). Found: C, 40.2; H, 3.4. Calc.: C, 40.2; H, 3.4%.

Preparation of 2-N,N-dimethylaminophenyldichlorophosphine (**7**)

As described in the preceding experiment, a mixture of 18.8 g (0.064 mol) of the aminophosphine **5** and 9.65 g (0.265 mol) of dry hydrogen chloride was allowed to react, yielding 10.5 g (74%) of **7** [b.p. 71°C (0.1 mm)].

Analysis: $C_8H_{10}Cl_2NP$ (222.05). Found: C, 43.1; H, 4.6. Calc.: C, 43.3; H, 4.5%.

Preparation of 2-methoxyphenyldifluorophosphine (**8**)

A suspension of 3.8 g (0.09 mol) of carefully dried sodium fluoride in 30 cm^3 of acetonitrile and 8.0 g (0.038 mol) of the chlorophosphine **6** to which two drops of the crown ether 15-crown-5 had been added, was stirred for 24 h at room temperature. The solids were removed by filtration, using a sintered glass disc, and were washed with 5 cm^3 of acetonitrile. Fractional distillation of the liquid product furnished the fluorophosphine **8** in a yield of 5.1 g (76%) [b.p. 62–64°C (1.5 mm)].

Analysis: $C_7H_7F_2OP$ (176.10). Found: C, 46.1; H, 3.9; F, 22.6. Calc.: C, 47.7; H, 4.0; F, 21.6%.

The deviation of the analytical data from the calculated values may be accounted for as a result of the presence of some 2-methoxyphenyltetrafluorophosphorane (**11**) resulting from the disproportionation of **8**.

Preparation of 2-N,N-*dimethylamino-phenyldifluorophosphine* (**9**)

As described in the preceding experiment, 6.0 g (0.027 mol) of the dichlorophosphine **7** were fluorinated during a reaction time of 3 days, employing 3.0 g (0.073 mol) of sodium fluoride, in the presence of two drops of the crown ether 15-crown-5. Distillation furnished **9** as a colourless liquid of b.p. 63–66°C (2.0 mm). Yield 4.2 g (82%).

Analysis: $C_8H_{10}F_2NP$ (189.14). Found: C, 50.6; H, 5.4; P, 16.6. Calc.: C, 50.8; H, 5.3; P, 16.4%.

Oxidation–reduction reaction of **8**

NMR experiment. A mixture of 0.53 (0.003 mol) of **8** with *ca* the same amount of $CDCl_3$ was sealed into a 5-mm NMR tube, and was maintained at 80°C for 2 days. Inspection of the ^{31}P NMR spectrum revealed that **8** had been transformed to a mixture of the cyclotetraphosphine **10** and the tetrafluorophosphorane **11**.

On a preparative scale, the reaction was conducted as follows. A sample of *ca* 1.3 g of the difluorophosphine **8** was found to change to a crystalline solid on standing at room temperature over a period of 3–4 weeks. The crude product was first washed with small amounts of dichloromethane, followed by recrystallization from acetonitrile [solubility of **10** *ca* 1 mg (1 cm^3 of acetonitrile)$^{-1}$]. M.p. 253–255°C.

Analysis: $(C_7H_7OP)_n$ (552.42 for $n = 4$). Found: C, 59.4; H, 5.1; P, 22.4. Calc.: C, 60.9; H, 5.1; P, 22.4%.

Mass spectrum: M^+, 552; base peak 107 ($C_6H_4OMe^+$).

Preparation of 2-*methoxyphenyltetrafluorophosphorane* (**11**)

A mixture of 7.3 g (0.035 mol) of the dichlorophosphine **6** and 9.8 g (0.055 mol) of carefully dried antimony trifluoride was stirred for 3 h at 50°C. The liquid product thus formed was collected by pumping *in vacuo* (*ca* 20 mm), and was subsequently redistilled to give 4.5 g (60%) of the tetrafluorophosphorane [b.p. 84°C (15 mm)]. Elemental analysis (C, H, Cl and P) revealed that the sample contained *ca* 12% of antimony trichloride which proved unseparable by fractionation from **11**. It may be assumed that, as an alternative, AsF_3 should be the reagent to be preferred over SbF_3.

Hydrolysis of **11**: *preparation of* 2-*methoxyphenylphosphonic acid* (**12**)

A mixture of 1.5 g (0.007 mol) of **11** and 1.0 g (0.056 mol) of water was stirred for 1 h. The resulting white solid was dried *in vacuo* (1 mm) and 10 cm^3 of hot water was added. After 2 days at room temperature the product (**12**) crystallized as needles from the filtered solution (m.p. 207°C).

No NMR data were obtained because of the poor solubility of the product.

Analysis: $C_7H_9O_4P$ (188.12). Found: C, 43.5; H, 4.7; P, 16.3. Calc.: C, 44.7; H, 4.8; P, 16.5%.

Preparation of cis-*dichloro-bis*(2-*methoxyphenyldifluorophosphino*)*platinum*(II) (**13**)

To a solution of 0.722 g (0.0019 mol) of the complex, dichlorobis-(1,5-cyclooctadiene)platinum in 8 cm^3 of dichloromethane was added a solution of 0.680 g (0.0039 mol) of **8** in 2 cm^3 of dichloromethane. The mixture was stirred at room tem perature for 10 min. A white precipitate was formed which was removed by filtration and was repeatedly washed with 5-cm^3 portions of ether and pentane. The precipitate was dissolved in *ca* 30 cm^3 of dichloromethane. Subsequently, a 1:1 mixture of toluene and methylcyclohexane was added until the solution remained clear (*ca* 10 cm^3). During a period of 5 days the formation of a crystalline product was observed when a gentle stream of nitrogen was passed over the solution at room temperature. Upon further evaporation of the solid–liquid mixture, a total of 1.04 g (87%) of **13** was obtained (m.p. 221–223°C).

Analysis: $C_{14}H_{14}Cl_2F_4O_2P_2Pt$ (618.20). Found: C, 27.6; H, 2.4; P, 10.4. Calc.: C, 27.2; H, 2.3; P, 10.0%.

Preparation of cis-*dichloro-bis*(2-N,N-*dimethylaminophenyldifluorophosphine*)*platinum*(II) (**14**)

As described in the preceding experiment 0.680 g (0.0018 mol) of dichloro-(1,5-cyclooctadiene) platinum was dissolved in 5 cm^3 of dichloromethane. To this solution a solution of 0.690 g (0.0037 mol) of the fluorophosphine **7** in 4 cm^3 of dichloromethane was added. The solid product formed after 15 min of stirring at room temperature was collected and washed with *ca* 10 cm^3 of pentane. A total of 1.13 g (96%) of complex **13** (m.p. 185–187°C) was obtained.

Analysis: $C_{16}H_{20}Cl_2F_4N_2P_2Pt$ (644.28). Found: C, 29.6; H, 3.3; P, 9.9. Calc.: C, 29.8; H, 3.1; P, 9.6%.

X-ray analysis

Crystals of **13** obtained by recrystallization from CH_2Cl_2–toluene–methylcyclohexane have triclinic symmetry, space group $P\bar{1}$. The unit cell which has the parameters $a = 765.1(2)$, $b = 1037.0(2)$, $c = 1242.5(2)$ pm, $\alpha = 93.32(3)$, $\beta = 92.67(3)$, $\gamma = 104.02(2)°$ contains two molecules, yielding a calculated density of 2.154 g cm^{-3}.

Crystals of **10** obtained by recrystallization from CH_3CN have monoclinic symmetry, space group $P2_1/n$. The unit cell which has the parameters $a = 1192.27(11)$, $b = 1517.16(13)$, $c = 1541.74(16)$ pm, $\beta = 100.303(13)°$ contains four molecules, yielding a calculated density of 1.337 g cm^{-3}.

The data were collected at room temperature on a Syntex $P2_1$ diffractometer using graphite-monochromated Cu-K_α radiation ($\lambda = 154.178$ pm) in the θ–2θ mode in the range $3° \leqslant 2\theta \leqslant 135$, at a scan speed between 2.93 and 29.30° min^{-1}, depending on the intensity of the reflection.

The data were corrected for Lorentz, polarization and absorption effects [$\mu = 18.47(2.675)$ mm^{-1}].* The structures were solved by direct methods and difference-Fourier syntheses. The refinement using 3070 (3389) out of 3411 (4247) measured independent reflections [$I \geqslant 2.0\sigma(I)$] converged at $R = 0.075$ (0.049). A final difference map displayed no electron density higher than 0.36 (0.98) $\times 10^6$ e pm^{-3}. The program SHELX-76[37] and our own programs were used. Complex atom-scattering factors[43] were employed.†

Acknowledgements—We are indebted to Bayer AG Chemmetall, and DEGUSSA for gifts of chemicals. The support of Fonds der Chemischen Industrie is gratefully acknowledged. M.S. acknowledges a studentship awarded by Verband der Chemischen Industrie. Thanks are due to Drs L. Ernst and V. Wray (Stöckheim) for some NMR spectra.

REFERENCES

1. W. S. Knowles, M. J. Sebacky and B. D. Vineyard, *Am. Chem. Soc., Adv. Chem. Ser.* 1974, **132**, 274.
2. T. B. Rauchfuss, F. T. Patino and D. M. Roundhill, *Inorg. Chem.* 1975, **14**, 652.
3. J. C. Jeffrey and T. B. Rauchfuss, *Inorg. Chem.* 1979, **18**, 2658.
4. (a) R. Graziani, G. Bombieri, L. Volponi, C. Panattoni and R. J. H. Clark, *J. Chem. Soc.* 1969, 1236; (b) M. Visinkin, G. Bombieri, L. Volponi, C. Panattoni and R. J. H. Clark, *J. Mol. Catal.* 1984, **24**, 277.
5. E. Meintjies, E. Singleton, R. Schmutzler and M. Sell, *S. Afr. J. Chem.* 1985, **38**, 112.
6. M. Sell and R. Schmutzler, unpublished results.
7. H. P. Fritz, I. R. Gordon, K. E. Schwarzhans and L. M. Venanzi, *J. Chem. Soc.* 1965, 5210.
8. B. Zarli, L. Volponi and G. DePaoli, *Inorg. Nucl. Chem. Lett.* 1973, **9**, 997.
9. M. M. de V. Steyn, R. B. English, T. V. Ashworth and E. Singleton, *J. Chem. Res.* 1981, 3146.
10. V. N. Kulakova, Yu. M. Zinov'ev and L. Z. Soborovskii, *Zh. Obshch. Khim.* 1959, **29**, 3957.
11. L. Maier, *Fortschr. Chem. Forsch.* 1967, **8**, 1.
12. (a) A. Michaelis, *Liebigs Ann. Chem.* 1896, **293**, 249; (b) A. Michaelis and A. Schenk, *Liebigs Ann. Chem.* 1890, **260**, 1.
13. G. M. Kosolapoff, *J. Am. Chem. Soc.* 1952, **74**, 4119.
14. B. Buchner and L. B. Lockhardt, *J. Am. Chem. Soc.* 1951, **73**, 755.
15. F. G. Mann and E. J. Chaplin, *J. Chem. Soc.* 1937, 527.
16. L. D. Quin and J. S. Humphrey Jr, *J. Am. Chem. Soc.* 1961, **83**, 4124.
17. K. S. Yudina, T. Ya. Medved' and M. I. Kabachnik, *Izv. Akad. Nauk. S.S.S.R., Ser. Khim.* 1966, 154.
18. E. M. Miller and B. L. Shaw, *J. Chem. Soc., Dalton Trans.* 1974, 480.
19. W. E. McEwen and B. D. Beaver, *Phosphorus and Sulfur* 1985, **24**, 259.
20. R. Schmutzler, *Chem. Ber.* 1965, **98**, 552.
21. (a) W. Krüger, M. Sell and R. Schmutzler, *Z. Naturforsch.* 1983, **38B**, 1074; (b) W. Albers, W. Krüger, W. Storzer and R. Schmutzler, *Synth. React. Inorg. Met.-Org. Chem.* 1985, **15**, 187.
22. F. Seel and K. Rudolph, *Z. Anorg. Allg. Chem.* 1968, **363**, 233.
23. R. Schmutzler, O. Stelzer and J. F. Liebman, *J. Fluorine Chem.* 1984, **25**, 289.
24. H. G. Ang and R. Schmutzler, *J. Chem. Soc.* 1969, 702.
25. E. J. Wells, H. P. K. Lee and L. K. Peterson, *J. Chem. Soc., Chem. Commun.* 1967, 894.
26. L. R. Smith and J. L. Mills, *J. Chem. Soc., Chem. Commun.* 1974, 808.
27. R. Schmutzler, *Inorg. Synth.* 1967, **9**, 63.
28. V. L. Bell Jr and G. M. Kosolapoff, *J. Am. Chem. Soc.* 1953, **75**, 4901.
29. H. C. Clark and L. E. Manzer, *J. Organomet. Chem.* 1973, **59**, 411.
30. D. A. Dudell, P. L. Goggin, P. J. Goodfellow, M. G. Norton and J. G. Smith, *J. Chem. Soc.* 1970, 545.
31. J. F. Nixon, *Endeavour* 1973, **32**, 19.
32. (a) J. Grosse and R. Schmutzler, *J. Chem. Soc., Dalton Trans.* 1976, 405; (b) S. Hietkamp and R. Schmutzler, *Z. Naturforsch.* 1980, **35B**, 548.

* Values for compound **10** in parentheses.

† Final atomic positional and thermal parameters, bond lengths and angles and F_o/F_c values have been deposited as supplementary material with the Editor, from whom copies are available on request. Atomic coordinates have also been submitted to the Cambridge Crystallographic Data Centre.

33. (a) J. G. Verkade, *Coord. Chem. Rev.* 1972/1973, **9**, 1; (b) P. S. Pregosin and R: W. Kunz, In *NMR Basic Principles and Progress*, Vol. 16, p. 40. Springer, Berlin (1979).
34. W. Weigand, A. W. Cordes and P. N. Swepston, *Acta Cryst.* 1981, **B37**, 1631.
35. J. C. J. Bart, *Acta Cryst.* 1969, **B25**, 762.
36. G. J. Palenik and J. Donohue, *Acta Cryst.* 1962, **15**, 564.
37. F. Sanz and J. J. Daly, *J. Chem. Soc.* (*A*) 1971, 1083.
38. S. Neumann, D. Schomburg and R. Schmutzler, *J. Chem. Soc. Chem. Comm.* 1979, 848.
39. D. Schomburg, unpublished.
40. H. Gilman and I. Banner, *J. Am. Chem. Soc.* 1940, **62**, 344.
41. J. R. van Wazer and L. Maier, *J. Am. Chem. Soc.* 1964, **86**, 811.
42. G. M. Sheldrick, unpublished.
43. D. T. Cromer and J. T. Waber, in *International Tables for Crystallography*, Vol. IV, pp. 99ff and 149. Kynoch Press, Birmingham (1974).

Polyhedron Vol. 6, No. 6, pp. 1309–1311, 1987
Printed in Great Britain

0277–5387/87 $3.00+.00

SYNTHESIS AND PROPERTIES OF TETRAGONAL SILVER(I,III) OXIDE, AgO

P. TISSOT

Département de Chimie Minérale, Analytique et Appliquée, Université de Genève, 30, quai E. Ansermet, 1211 Genève 4, Suisse

(*Received* 26 *September* 1986; *accepted* 10 *November* 1986)

Abstract—The pure tetragonal AgO modification was obtained by ozonation of a suspension of Ag_2O or Ag in stirred water. The oxidation proceeds in two steps from Ag, with the intermediary formation of Ag_2O. An oxygen content corresponding to the formula $AgO_{1.15}$ is obtained when the bubbling of ozone is maintained for a long time. The thermal decomposition of tetragonal AgO is complex and has been studied by thermogravimetry and differential thermal analysis.

In a previous article[1] we have described the synthesis of monoclinic AgO by oxidation with ozone of a suspension of Ag or Ag_2O in an aqueous solution of sodium hydroxide. The same procedure, using a suspension of Ag or Ag_2O in pure water instead of a sodium hydroxide solution, affords an other form of AgO. The structure of this silver(I,III) oxide has been determined by neutron powder diffraction;[2] all reflexions could be indexed on a body-centered tetragonal cell with $a = 6.833$ Å and $c = 9.122$ Å.

The existence of a second AgO modification was a matter of controversy for a long time. Early X-ray diffraction data on samples which were synthesized by oxidation of Ag by ozone[3] were interpreted in terms of a tetragonal structure built up by an unusual combination of Ag(I), Ag(II), O_2^{2-} and O^{2-} atoms.[4] Its existence was questioned by some workers[5] but confirmed by others on samples obtained by electrochemical oxidation of silver with asymmetrical current.[6–8] Its structure and properties, however, were never investigated in detail, presumably because of difficulties to obtain samples of sufficient quantity and quality.

EXPERIMENTAL

The experimental details of the synthesis and the analytical methods have been described previously.[1] As already mentioned, the only difference consists in the substitution of the 2 N sodium hydroxide solution by distilled water.

RESULTS AND DISCUSSION

Figure 1 shows the evolution of the concentration of Ag, Ag_2O and AgO as a function of time during the synthesis. From the outset of the oxidation, the tetragonal modification of AgO is formed; only traces of the monoclinic form (less than 3%) have been detected by X-ray analysis at the end of the synthesis. Figure 1 clearly demonstrates that the oxidation proceeds in two successive steps. The maximum concentration of Ag_2O reached is about 18%; this is much less than the 50% obtained in the case of the monoclinic form.[1]

After 22 h, all the silver is oxidized in AgO, but the oxygen content of the product increases slowly when the bubbling of ozone is continued; after 40 h, a maximum excess of oxygen of 10–15% with respect to the stoichiometry of AgO is reached. The thermogravimetry of the compound obtained after 40 h is shown in Fig. 2, and is compared with the monoclinic AgO. The tetragonal AgO decomposes to Ag_2O at a lower temperature than the monoclinic form. All the oxygen in excess is released during this first step, which correspond to a complex reaction as shown in Fig. 3. The DTA curves seems to correspond to the superposition of an endothermic reaction over the exothermic decomposition of AgO to Ag_2O. This endotherm could be due to the decomposition of an oxygen-rich phase, since it increases with the oxygen content; however, diffraction methods have not allowed to see an impurity phase, and this point remains to be clari-

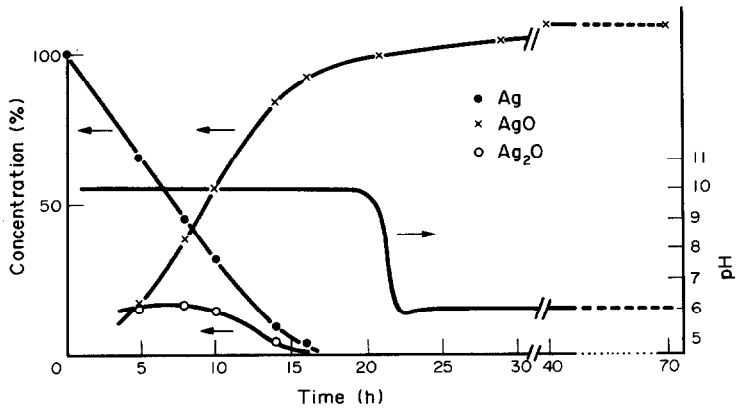

Fig. 1. Evolution of the concentrations and pH during the synthesis. Total flow (O_2+O_3), 150 l h^{-1}; flow of O_3, 2.6 g h^{-1}; temperature, 20°C; reaction mixture, 100 g of Ag in 10 l of water.

fied. The small endothermic effect at 190–200°C is due to the decomposition of Ag_2CO_3 which is formed progressively with the CO_2 contained in the air.

Figure 4 shows a scanning electron microphotograph of the tetragonal AgO; it appears as homogeneous small crystals of 1–3 μm, and is completely different from the large flakes obtained in the sodium hydroxide solution.[1] The poor stability of the tetragonal AgO in hot 7 N KOH solution is probably due to the small size of the particles.

The comparison of the structure of the two modifications of AgO shows that no single shear operation appears to exist which allow to transform one structure into the other;[2] as a matter of fact, we have not observed a transformation after 1 week at 60°C and 1 b, nor after 2 h at 25°C and 10 kb.

CONCLUSIONS

The oxidation of several silver salts in aqueous solution with ozone has been studied by Selbin and Usategui,[9] who obtained either pure monoclinic AgO or a complex compound which decomposes to monoclinic AgO in water. The oxidation by ozone of a suspension of silver in an aqueous solution of sodium hydroxide leads also to monoclinic AgO.[1] On the other hand, this work shows that pure tetragonal AgO is obtained when water is used instead of an alkaline solution. In both cases the oxidation takes place in two steps, with the intermediary formation of Ag_2O. Now this compound is amphoteric; it is slightly soluble as Ag^+ below pH = 12 and as AgO^- above pH = 12.[10] The pH of water saturated with Ag_2O is 10.1 (see Fig. 1), so that the

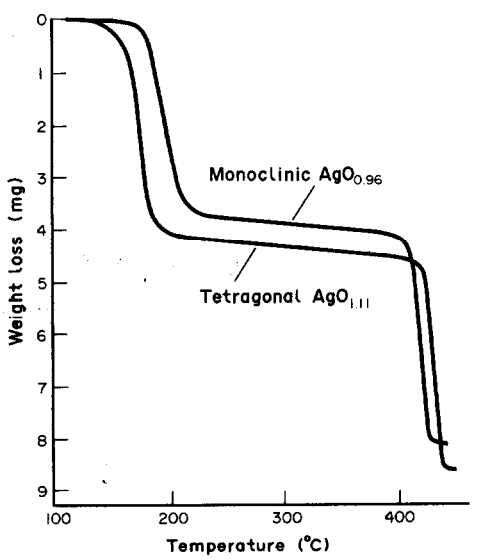

Fig. 2. Thermogravimetry of AgO. Sample weight, 61.5 mg; heating rate: 4°C min^{-1}; atmosphere: static air.

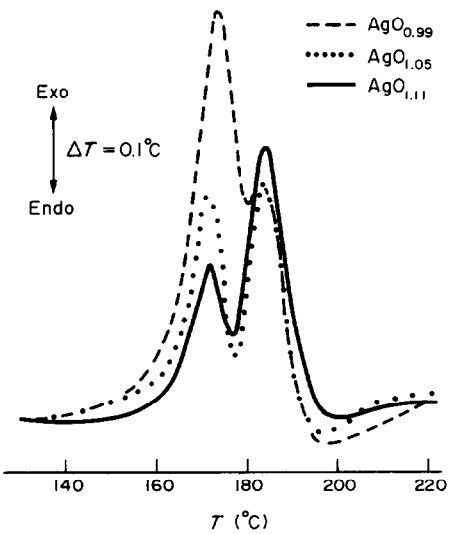

Fig. 3. Differential thermal analysis of tetragonal AgO. Samples weight, 46 mg; heating rate, 6°C min; atmosphere, static air.

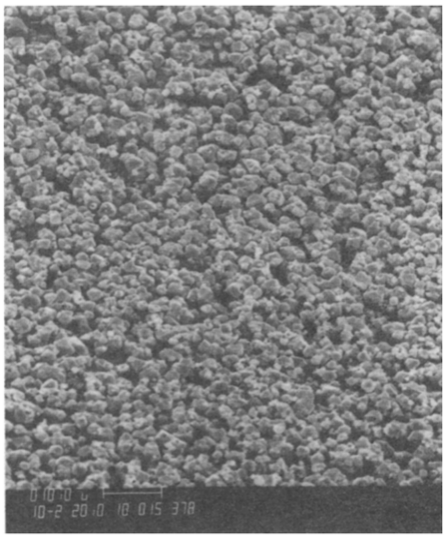

Fig. 4. Scanning electron microscope photography of tetragonal AgO.

main species present in these conditions is Ag^+. Though the mechanism of formation of both modifications of AgO is not known, the two following equations can be written:

$$Ag^+ \xrightarrow{O_3} \text{tetragonal AgO},$$

$$AgO^- \xrightarrow{O_3} \text{monoclinic AgO}.$$

From the low concentration of Ag_2O (Fig. 1) one can deduce that the first reaction is faster than the second.

Acknowledgement—We are grateful to Miss H. Lartigue, and to Mr J. Painot and Mr. R. Dallenbach for their collaboration.

REFERENCES

1. R. Dallenbach, J. Painot and P. Tissot, *Polyhedron* 1982, **1**, 183.
2. K. Yvon, A. Bezinge, P. Tissot and P. Fischer, *J. Solid State Chem.* 1986, **65**, 225.
3. G. M. Schwab and G. Hartmann, *Z. Anorg. Allg. Chem.* 1955, **281**, 183.
4. A. S. McKie and A. P. Clark, *Batteries*, p. 285. Pergamon Press, Oxford (1963).
5. J. A. McMillan, *Chem. Rev.* 1962, **62**, 65.
6. G. Z. Kazakevich, I. E. Yablokova and U. S. Bagotskii, *Sov. Electrochem.* 1966, **2**, 969.
7. G. Z. Kazakevich, V. A. Kirkinskii and I. E. Yablokova, *Sov. Electrochem.* 1970, **6**, 355.
8. G. P. Ereiskaya, T. A. Lozouskaya, V. I. Goncharov, N. P. Gaivoronskaya and F. I. Kukoz, *Sov. Electrochem.* 1974, **10**, 1236.
9. J. Selbin and M. Usategui, *J. Inorg. Nucl. Chem.* 1961, **20**, 91.
10. M. Pourbaix, *Atlas d'équilibres électrochimiques*, p. 393. Gauthier-Villars, Paris (1963).

Polyhedron Vol. 6, No. 6, pp. 1313–1317, 1987
Printed in Great Britain

0277–5387/87 $3.00+.00

DIALKYL SULFOXIDES COMPLEXES WITH NICKEL(II) NITRATE AND PERCHLORATE

DENISE DE OLIVEIRA and VIKTORIA K. LAKATOS OSORIO*

Instituto de Química, Universidade de São Paulo, Caixa Postal 20.780, São Paulo, Brasil

(*Received* 12 *August* 1986; *accepted after revision* 10 *November* 1986)

Abstract—Nickel(II) perchlorate and nitrate complexes containing dimethyl, di-*n*-propyl, di-*n*-butyl, di-*i*-butyl and di-*t*-butyl sulfoxides have been synthesized and characterized by IR and electronic spectroscopies, magnetic-susceptibility and electrolytic-conductance measurements. In the complexes containing perchlorate, the metal : sulfoxide molar ratio is 1 : 6 and the perchlorate groups are ionic. In the nitrate compounds, the molar ratio decreases from 1 : 6 to 1 : 2 according to the increase in the steric bulk of the alkyl group from methyl to *t*-butyl. The nitrate group may either be non-coordinating or behave as a monodentate or bidentate ligand. All the complexes contain O-bonded sulfoxide molecules and are characterized as high-spin, with an octahedral or distorted octahedral geometry. The dialkyl sulfoxides studied in this work fall in the same position as dimethyl sulfoxide in the spectrochemical and nephelauxetic series. Electrolytic conductivities suggest that the compounds containing ionic nitrate exhibit sulfoxide–nitrate exchange in nitromethane solutions.

Reports of nickel(II) dimethyl sulfoxide (Me_2SO) complexes are extremely numerous.[1] Little attention, however, has been focused in nickel(II) coordination by dialkyl sulfoxides different from Me_2SO. Currier and Weber[2] have synthesized complexes of type $[NiL_6](ClO_4)_2$, where L = di-*n*-propyl or di-*n*-butyl sulfoxide, while Kolosnitsyn *et al.*[3] have obtained the compounds $Ni(NO_3)_2 \cdot xL$, where L = di-*n*-hexyl sulfoxide and $x = 2$ or 4.

This paper deals with nickel(II) nitrate complexes of the sulfoxides R_2SO, where R = methyl, *n*-propyl, *n*-butyl, *i*-butyl or *t*-butyl. These sulfoxides were selected for study owing to their different basicities and stereochemistries. A nickel(II) perchlorate complex of *i*-Bu_2SO was obtained for the first time and the corresponding compounds with *n*-Pr_2SO and *n*-Bu_2SO, described by Currier and Weber,[2] were prepared in order to determine the ligand field spectroscopic parameters.

EXPERIMENTAL

Chemicals

Me_2SO (Carlo Erba) was dried over 4 Å molecular sieves. Me_2SO-d_6 (Aldrich, isotopic purity 99.5%), *n*-Pr_2SO and *n*-Bu_2SO (K & K Laboratories) were used as such. *t*-Bu_2SO was prepared by oxidation of the corresponding sulfide with H_2O_2 in methanol,[4] the reaction time being 15 h.

The hydrated nickel nitrate was obtained from Merck and nickel perchlorate was prepared from the metal carbonate (Carlo Erba) and perchloric acid.

Nitromethane and diethyl ether were purified by conventional procedures.

Preparation of the complexes

All the complexes were prepared by dissolving the hydrated nickel salt in triethylorthoformate (molar ratio 1 : 10 or more) and adding the sulfoxide in slight excess (neat when liquid or dissolved in a minimum amount of triethylorthoformate and ethanol when solid). The nickel perchlorate complexes with Me_2SO and *n*-Pr_2SO precipitated at room temperature. In the other cases, crystallization was achieved by adding anhydrous diethyl ether and cooling off or by concentrating the solution in a rotatory evaporator, adding anhydrous ether and cooling. The solid obtained after a few days was collected, washed with anhydrous ether and dried at room temperature over silica gel and paraffin, until constant weight. Typical yields ranged from 70 to 90%.

* Author to whom correspondence should be addressed.

Analysis

The Ni content was estimated by titration with EDTA.[5] Analyses for C and H were carried out by the Microanalytical laboratory at this Institute.

Instrumentation

The IR spectra were recorded with a Perkin–Elmer model 180 spectrophotometer, using Nujol mulls of all the solid compounds, films of the liquid ligands between KBr and polyethylene plates and Fluorolube mulls of the nitrate complexes between NaCl plates. The electronic spectra were obtained as described in an earlier paper.[6]

The magnetic-susceptibility measurements (solid samples) were carried out at room temperature, $25 \pm 5°C$, by Gouy's method.

Conductance measurements were carried out on 10^{-3} M solutions of the complexes in nitromethane, at $25.0 \pm 0.5°C$, with a bridge composed of a resistance box No. 4760 and an A.C. galvanometer No. 2370, both from Leeds and Northrup Co., and a conventional cell calibrated with aqueous KCl solution.

The compounds were handled in a dry box, owing to their hygroscopic nature.

RESULTS AND DISCUSSION

Perchlorate compounds

As can be seen from Table 1, the metal–sulfoxide molar ratio is 1:6 for these compounds. The IR spectral features associated with the perchlorate group (unsplitted bands at 620 and 1090 cm^{-1}) as well as the electrolytic-conductance data in nitromethane solutions (Table 1) are indicative of the ionic nature of the complexed nickel–perchlorate bond. The lower frequencies of ν_{SO} (Table 2) relative to the corresponding free sulfoxide indicate the coordination of sulfinyl group to Ni(II) ion by the oxygen atom. The observed magnetic moments and electronic spectra (Table 2) are typical of Ni(II) compounds in high-spin octahedral stereochemistries. The ligand field parameters (Table 2) were calculated[8] from the σ_2-band (at about 13,000 cm^{-1}) and the σ_3-band (at about 24,000 cm^{-1}). The σ_1-band, which gives directly the $10Dq$ value, was hampered by ligand overtones. In spite of the different basicities and stereochemical requirements of the sulfoxides investigated, they are placed at about the same position in the spectrochemical and nephelauxetic series. During the synthesis of the complexes, however, sterical hindrance plays an important role. The general procedure described in Experimental gave products with *n*-Bu_2SO/Ni and *i*-Bu_2SO/Ni ratios of about 5.5. Only after recrystallization in the presence of a 10-fold excess of R_2SO (Table 1) could the hexakis(sulfoxide)nickel complexes be obtained. In the case of Me_2SO and *n*-Pr_2SO, the use of a slight excess of R_2SO (5–15%) in the synthesis was enough to produce directly the stoichiometric 1:6 complexes. Moreover, all the attempts to obtain nickel perchlorate complexes with the bulkier di-*i*-propyl, di-*s*-butyl and di-*t*-butyl sulfoxides were unsuccessful.

Table 1. Analytical results, conductivity data and melting points of the complexes

Complex	R_2SO[a] Ni	Analysis: found (calc.) (%) Ni	C	H	Λ_M[b]	M.p. (°C)
$Ni(Me_2SO)_6(ClO_4)_2$	7.0	8.1 (8.1)	20.3 (19.8)	5.2 (5.0)	171	[c]
$Ni(n\text{-}Pr_2SO)_6(ClO_4)_2$	6.3	5.5 (5.5)	41.2 (40.7)	8.0 (8.0)	164	142–147
$Ni(n\text{-}Bu_2SO)_6(ClO_4)_2$[d]	11.1	4.9 (4.8)	46.2 (46.9)	9.3 (8.9)	147	85–93
$Ni(i\text{-}Bu_2SO)_6(ClO_4)_2$[d]	10.1	4.7 (4.8)	46.7 (46.9)	9.3 (8.9)	169	110–125
$Ni(Me_2SO)_6(NO_3)_2$	6.1	9.1 (9.0)	20.7 (22.1)	6.0 (5.6)	14	40–64
$Ni(Me_2SO)_4(NO_3)_2$	5.0	11.6 (11.9)	18.6 (19.4)	5.0 (4.9)	12	[c]
$Ni(Me_2SO)_3(NO_3)_2$	4.1	14.1 (14.1)	16.5 (17.3)	5.0 (4.4)	11	88–93
$Ni(Me_2SO\text{-}d_6)_3(NO_3)_2$[d]	4.0	13.6 (13.5)	16.3 (16.6)	—	9	87–93
$Ni(n\text{-}Pr_2SO)_2(NO_3)_2$[d]	2.2	13.0 (13.0)	32.4 (32.0)	6.5 (6.3)	11	58–74
$Ni(n\text{-}Bu_2SO)_3(NO_3)_2$	4.8	8.8 (8.8)	42.8 (43.1)	8.2 (8.1)	14	44–70
$Ni(i\text{-}Bu_2SO)_2(NO_3)_2$	4.0	11.5 (11.6)	38.3 (37.9)	7.6 (7.2)	5	93–99
$Ni(i\text{-}Bu_2SO)_3(NO_3)_2$	10.0	9.0 (8.8)	43.7 (43.1)	8.6 (8.1)	7	30–87
$Ni(t\text{-}Bu_2SO)_2(NO_3)_2$	6.0	11.7 (11.6)	37.4 (37.9)	7.2 (7.2)	3	148–155 (dec)

[a] Molar ratio employed in the synthesis or recrystallization of the compound.
[b] Molar conductance (S cm^2 mol^{-1}) of 10^{-3} M solution in nitromethane.
[c] The compound did not melt up to 250°C.
[d] Obtained after recrystallization.

Table 2. Magnetic susceptibilities, IR data, electronic spectral bands and ligand field parameters of the complexes $[NiL_6](ClO_4)_2$ in solid state

Complex L	μ_{eff} (BM)	IR bands (cm^{-1}) in ν_{MO} region	IR bands (cm^{-1}) in ν_{SO} region	Electronic bands (cm^{-1})	Possible assignments[a]	$10Dq$ (cm^{-1})	B (cm^{-1})	β
Me_2SO	3.4	440m	990s, 940s	~ 8000[b]	σ_1	786	920	0.89
				13,170, 14,770[c]	σ_2, σ_4			
				20,810, 24,210[c]	σ_5, σ_3			
n-Pr_2SO	3.4	447m	975s	~ 7800[b]	σ_1	779	910	0.88
				13,050, 14,740[c]	σ_2, σ_4			
				22,630, 24,040[c]	σ_5, σ_3			
n-Bu_2SO	3.1	455m	970s	~ 7800[b]	σ_1	778	910	0.88
				13,010, 14,710[c]	σ_2, σ_4			
				20,450, 23,750[c]	σ_5, σ_3			
i-Bu_2SO	3.3	455m	975s	~ 7800[b]	σ_1	788	890	0.86
				13,150, 14,720[c]	σ_2, σ_4			
				20,580, 23,830[c]	σ_5, σ_3			

[a] $\sigma_1 = {}^3T_{2g} \leftarrow {}^3A_{2g}$; $\sigma_2 = {}^3T_{1g}(F) \leftarrow {}^3A_{2g}$; $\sigma_3 = {}^3T_{1g}(P) \leftarrow {}^3A_{2g}$; $\sigma_4 = {}^1E_g \leftarrow {}^3A_{2g}$; $\sigma_5 = {}^1T_{2g} \leftarrow {}^3A_{2g}$.
[b] Band hampered by ligand overtones.
[c] Band positions determined after decomposition of the spectrum by a SPECSOLV program.[7]

Fredrick and Johnson[9] reported perchlorate compounds with Me_2SO/metal ratios > 6, which they attributed to the incorporation of additional quantities of Me_2SO and $HClO_4$. We did not observe such incorporation even by intentionally adding $HClO_4$ to the reaction medium. We could neither obtain an adduct between Me_2SO and $HClO_4$. The protonated Me_2SO cation, $[(Me_2SO)_2H]^+$, is known[10–12] to form compounds with anions such as $[AuCl_4]^-$, $[RhCl_4(Me_2SO)_2]^-$ and $[ClHCl]^-$, but none with ClO_4^-. However, excess of Me_2SO can be held, as solvation molecules, in complexes. In fact, the compound $Ni(ClO_4)_2 \cdot 8Me_2SO$ has been known since 1960,[13] the same year of the publication of Cotton's systematic study of Me_2SO complexes,[14] reporting the compound $Ni(ClO_4)_2 \cdot 6Me_2SO$. By heating the 1 : 8 compound *in vacuo*, at 50°C, the 1 : 6 complex can be obtained.[15]

Nitrate compounds

In the case of these compounds, a variety of stoichiometries were observed (Table 1) as a result of the competitive ligand abilities of the neutral sulfoxide molecules and the nitrate ions. In some instances, products with no integer R_2SO/Ni ratios were obtained and recrystallization was necessary in order to obtain compounds of definite composition.

The decreasing of the steric bulk of the alkyl radical from t-Bu_2SO to Me_2SO promotes an increase of the Ni : R_2SO molar ratio from 1 : 2 to 1 : 6.

Complexes with Ni : Me_2SO ratios of 1 : 8[13,15] and 1 : 4[16] have already been synthesized, as well as the compounds with 1 : 6[17] and 1 : 3[15,18] ratios, which were obtained by decomposition of the 1 : 8 compound, *in vacuo*, instead of by a direct crystallization as reported here.

The results of magnetic measurements and electronic spectra (Table 3) indicate that octahedral symmetry is closely approximated in all the compounds. IR spectral data (Table 3) show that the sulfoxide molecules are O-bonded to the Ni(II) ion. The NO_3 bands are not easily assigned, since IR spectra of these complexes are highly complicated. Table 3 shows some fundamental bands while Table 4 gives the combination bands in the 1700–1800-cm^{-1} region, useful as a criterion of the mode of coordination of the nitrate group.[19]

The nitrate complexes with Ni : sulfoxide molar ratios of 1 : 2 and 1 : 3 are non-conducting in nitromethane (Table 1) and contain bidentate nitrate and both mono- and bidentate nitrate, respectively, as evidenced by IR data (Tables 3 and 4).

The Me_2SO complex of 1 : 4 stoichiometry contains both ionic and bidentate nitrate, instead of only monodentate groups as previously suggested,[16] and can be formulated as $[Ni(Me_2SO)_4(NO_3)]NO_3$. The non-conducting nature of this compound and of $[Ni(Me_2SO)_6](NO_3)_2$ in nitromethane (Table 1) is, therefore, anomalous

Table 3. Magnetic susceptibilities, electronic bands and IR spectral data of the complexes $NiL_x(NO_3)_2$ in solid state

Complex L	x	μ_{eff} (BM)	Electronic bands[a] (cm^{-1})	ν_{SO} bands (cm^{-1})	Tentative assignment of NO_3 bands (cm^{-1})
Me_2SO	6	3.5	13,200, 14,780, 24,290	1000vs, 955vs	1340vs, br, 1040sh, 833m[b]
	4	3.1	13,200, 14,670, 24,290	998vs, 955vs	1338vs, 830w[b] 1470sh, 1288sh, 810w[c]
	3	3.2	12,800, 14,170, 24,390	995vs, 955vs	1435sh, 1320sh, 815sh[d] 1468s, 1285sh, 810m[c]
Me_2SO-d_6	3	3.3	12,670, 14,230, 24,220	965vs	1435s, 1315vs, 815sh[d] 1468m, 1295sh, 808m[c]
n-Pr_2SO	2	3.7	12,740, 14,450, 24,220	985s, 965vs	1485s, 1278vs, 1020w, 808m[c]
n-Bu_2SO	3	3.1	12,860, 14,450, 23,740	1008s, 967vs	1483m, 1350m, 812m[d] 1518sh, 1280s, 808sh[c]
i-Bu_2SO	2	3.2	12,450, 13,990, 23,530	998s, 975s	1513vs, 1270vs, 1020sh, 808m[c]
	3	3.4	12,690, 14,310, 23,530	998s, 978vs	1502s, 1350m, 805m[d] 1513vs, 1272vs, 805m[c]
t-Bu_2SO	2	3.3	12,770, 14,390, 23,530	985s, 968s	1495s, 1275vs, 1020m, 805w[c]

[a] Band positions at 12,000–15,000 cm^{-1} determined after decomposition of the spectra by a SPECSOLV program.[7]
[b] Ionic NO_3^-.
[c] Bidentate nitrate mode.
[d] Monodentate nitrate mode.

and most likely arises as a result of sulfoxide–nitrate exchange. The exchange reaction can be reversed by adding Me_2SO to the solution. The molar conductances of mM solutions of both complexes in 90:10 (v/v) $MeNO_2$–Me_2SO rise to 150–160 S cm^2 mol^{-1}, falling therefore in the accepted range for 2:1 electrolytes in nitromethane.[20] Electronic spectra (Table 5) give further support for the above hypothesis. The spectrum of the nitrate complex in Me_2SO solution approaches those of the perchlorate complex in Me_2SO and $MeNO_2$ solutions, which contain the $[Ni(Me_2SO)_6]^{2+}$ species, while the nitrate complexes in $MeNO_2$ solution exhibit higher values of extinction coefficients, in accordance with the decrease in symmetry accomplished by the presence of Me_2SO and nitrate groups in the Ni(II) coordination sphere. The replacement of monodentate ligands by ionic nitrate, in solution, has already been observed with other ligands.[21,22]

CONCLUSIONS

One can conclude that the ease of formation of non-stoichiometric products in the synthesis of sulfoxide complexes is a general characteristic of the coordination chemistry of this class of ligand. This feature has been more emphasized in the literature about 4*f* metal complexes,[23,24] but it also occurs with O-bonded sulfoxide complexes with 3*d* metals. Several factors can contribute to it, e.g. the weak-

Table 4. IR bands of representative nitrate complexes in the 1700–1800-cm^{-1} region

Complex	ν (cm^{-1})	$\Delta\nu$ (cm^{-1})	Nitrate mode
$[Ni(Me_2SO)_6](NO_3)_2$	1738w	—	Ionic
$[Ni(Me_2SO)_4(NO_3)]NO_3$	1738w	—	Ionic
	1720vw, 1755sh (or 1770sh)	35 (or 50)	Bidentate
$[Ni(Me_2SO)_3(NO_3)_2]$	1723w, 1748vw	25	Monodentate
	1723w, 1778vw	55	Bidentate
$[Ni(n\text{-}Pr_2SO)_2(NO_3)_2]$	1700w, 1715w, 1765sh, 1770vw	65, 55	Bidentate
$[Ni(t\text{-}Bu_2SO)_2(NO_3)_2]$	1713w, 1770vw	57	Bidentate

Table 5. Visible spectral data for dimethyl sulfoxide–nickel complexes in solution

Complex	Molar concentration	Solvent	Band position (cm^{-1}) and extinction coefficient (in parentheses)		
			σ_2[a]	σ_4[a]	σ_3
$[Ni(Me_2SO)_6](ClO_4)_2$	0.0950	Me_2SO	12,940 (3.1)	14,630 (1.2)	24,040 (10.2)
	0.0990	$MeNO_2$	13,060 (3.7)	14,730 (1.8)	24,100 (10.6)
$[Ni(Me_2SO)_6](NO_3)_2$	0.0705	Me_2SO	12,960 (3.4)	14,680 (1.4)	23,810 (10.9)
	0.0260	$MeNO_2$	12,910 (8.2)	14,530 (4.7)	24,110 (29.2)
$[Ni(Me_2SO)_4(NO_3)]NO_3$	0.0487	$MeNO_2$	12,970 (9.0)	14,550 (5.7)	24,100 (33.5)

[a] Component position and extinction coefficient determined after decomposition of the spectra by a SPECSOLV program.[7]

ness of the metal–ligand interaction, the competition between sulfoxide and anions or solvent molecules in the coordination sphere of the metal, the incorporation of sulfoxide as solvation molecules, the possibility of sulfoxide molecules acting as bridging ligands, or the possibility of crystallization of a mixture of complexed species. The synthetic procedure plays, therefore, an important role in obtaining well-defined compounds.

Acknowledgements—A grant from FAPESP to D. de O. is gratefully acknowledged. Thanks are also due to Dr K. Sone from Ochanomizu University, Tokyo, for his kind interest in this work and to L. A. Morino for valuable help.

REFERENCES

1. J. A. Davies, *Adv. Inorg. Chem. Radiochem.* 1981, **24**, 115.
2. W. F. Currier and J. H. Weber, *Inorg. Chem.* 1967, **6**, 1539.
3. V. S. Kolosnitsyn, Yu. I. Murinov and Yu. E. Nikitin, *Russ. J. Inorg. Chem.* 1980, **25**, 1216.
4. J. Drabowicz and M. Mikolajczyk, *Synth. Commun.* 1981, **11**, 1025.
5. H. A. Flaschka, *EDTA Titrations*. Pergamon Press, London (1959).
6. O. A. Serra, M. Perrier, V. K. L. Osorio and Y. Kawano, *Inorg. Chim. Acta* 1976, **17**, 135.
7. H. S. Gold, C. E. Rechsteiner and R. P. Buck, *Anal. Chem.* 1976, **48**, 1540.
8. A. B. P. Lever, *Inorganic Electronic Spectroscopy*, 2nd Edn. Elsevier, Amsterdam (1984).
9. F. C. Fredrick and K. E. Johnson, *J. Inorg. Nucl. Chem.* 1981, **43**, 1483.
10. R. A. Potts, *Inorg. Chem.* 1970, **9**, 1284.
11. B. R. James and R. H. Morris, *J. Chem. Soc., Chem. Commun.* 1980, 31.
12. A. Bertoluzzi, S. Bonora, G. Fini, M. A. Bataglia and P. Monti, *J. Raman Spectrosc.* 1981, **11**, 430.
13. H. L. Schläfer and W. Schaffernicht, *Angew. Chem.* 1960, **72**, 618.
14. F. A. Cotton and R. Francis, *J. Am. Chem. Soc.* 1960, **82**, 2986.
15. H. L. Schläfer and H. P. Opitz, *Z. Anorg. Allg. Chem.* 1961, **313**, 178.
16. F. A. Cotton and R. Francis, *J. Inorg. Nucl. Chem.* 1961, **17**, 62.
17. M. W. Suwalsky and D. M. Moneva, *Bol. Soc. Chil. Quim.* 1965, **15**, 21.
18. C. C. Addison and D. Sutton, *J. Chem. Soc. A* 1966, 1524.
19. A. B. P. Lever, E. Mantovani and B. S. Ramaswamy, *Can. J. Chem.* 1971, **49**, 1957.
20. W. J. Geary, *Coord. Chem. Rev.* 1971, **7**, 81.
21. S. L. Holt and R. L. Carlin, *J. Am. Chem. Soc.* 1964, **86**, 3017.
22. E. S. Raper and I. W. Nowell, *Inorg. Chim. Acta* 1980, **43**, 165.
23. V. K. L. Osorio, A. de Oliveira and E. Giesbrecht, *J. Inorg. Nucl. Chem.* 1980, **42**, 930.
24. L. C. Thompson, In *Handbook on the Physics and Chemistry of Rare Earths* (Edited by K. A. Gschneider and L. Eyring), Vol. 3, Chap. 25. North-Holland, Amsterdam (1979).

Polyhedron Vol. 6, No. 6, pp. 1319–1323, 1987
Printed in Great Britain

0277–5387/87 $3.00+.00

REACTIONS OF CYANOACETYLHYDRAZINE COMPLEXES WITH SALICYLALDEHYDE AND CONSEQUENT METAL-PROMOTED REACTIONS

M. S. SOLIMAN, A. M. SHALLABY, R. M. EL-SHAZELY and M. M. MOSTAFA*†

Chemistry Department, Faculty of Science, Mansoura University, Mansoura, Egypt

(*Received* 14 *January* 1986; *accepted after revision* 17 *November* 1986)

Abstract—The reactions of salicylaldehyde with a suspension of cyanoacetylhydrazine and/or malonic acid amido-hydrazide complexes in aqueous ethanolic solutions afford novel complexes. The structures of the isolated complexes have been elucidated by conventional physical and chemical measurements. The absence of the cyano group band at 2270 cm^{-1} in the IR spectra of all complexes, except those of Co(II) and Ni(II) complexes, suggests the promotion of H_2O to the cyano group (C≡N) forming amido group. Several structures have been proposed in which salicylaldehyde behaves differently toward the cyanoacetylhydrazine complexes. Also, 1-salicylhydrazo-3-imino-3-(*o*-formyl) phenoxy propionic acid hydrazide is synthesized either by extraction from the isolated solid complexes using disodium ethylene-diaminetetraacetate or during refluxing of Co(II) and/or Fe(II) complexes with salicylaldehyde. This novel compound is confirmed by elemental analysis, spectra (IR and ^1H NMR) and mass spectra.

The synthesis and characterization of some metal complexes derived from cyanoacetylhydrazine and some divalent metal ions have been reported earlier.[1] Also, the role of metal ions and salicylaldehyde on the promotion of water to the cyano group was discussed.[1–5] As a consequence of our interest in the complexes containing cyano group, we report herein some studies on cyanoacetylhydrazine and/or malonic acid amido-hydrazide complexes with salicylaldehyde in aqueous ethanolic solution. Also, the action of salicylaldehyde on the promotion process was studied. Moreover, the condensating products of salicylaldehyde with cyanoacetylhydrazine and/or malonic acid amidohydrazide complexes were isolated and elucidated. Accordingly, several structures have been proposed and discussed in which salicylaldehyde behaves differently.

* Author to whom correspondence should be addressed.
† Present address: Institut National De L'Enseignement, Superieur De L'Hydraulique De Tlemcen, B.P. 119, Algerie.

EXPERIMENTAL

The starting complexes of cyanoacetylhydrazine and malonic acid amido-hydrazide are described in Ref. 1. The complexes under investigation were synthesized by refluxing a suspension of the starting complexes in aqueous ethanol solution with excess salicylaldehyde for 2 h. The reaction mixture was dissolved completely at the beginning of reflux and the new solid complexes started to precipitate at the end of the reaction. The structures of the isolated solid complexes depend on the type of starting compound, the preparation conditions and the type of metal ion present. Analytical data, together with colours and magnetic moments, are given in Table 1. Different structures of complexes were isolated according to the following procedures:

(i) The complexes with formulae $[Ni(H_2L)_2(H_2L'')]Ac_2 \cdot H_2O$ and $[Co(HL^+)_2(H_2L'')]$ (H_2L = cyanoacetylhydrazine, HL^+ = malonic acid amido-hydrazide, H_2L'' = salicylaldehyde) were isolated from the reactions of $[Ni(H_2L)_2(Ac)_2]H_2O^1$ and/or $[Co(HL)_2(H_2O)_2]H_2O^1$ with salicylaldehyde in ethanol. Salicylaldehyde

Table 1. Elemental analyses and some physical properties of the isolated complexes

Compound[a]	M.p. (°C)	Colour	% Calc. C	% Calc. H	% Calc. M	% Calc. X (Cl or Br)	% Found C	% Found H	% Found M	% Found X (Cl or Br)	Λ_m[b] in DMSO	μ_{eff} (BM)
H_2L^{**}	236	Yellow	62.8	4.7	—	—	63.1	4.6	—	—	—	—
$[Cd(H_2L^{**})_4Cl_2]$	252	Yellow	55.0	4.1	7.6	4.8	55.4	3.8	7.9	5.0	18.0	Diamagnetic
$[Zn(HL^*)_2]$	284	Pale-brown	47.7	3.6	13.0	—	46.8	4.2	12.3	—	20.0	Diamagnetic
$[UO_2(HL^*)_2]C_2H_5OH$	> 290	Orange	34.9	3.5	31.5	—	35.7	2.9	30.7	—	1.0	Diamagnetic
$[Cu(HL^*)H_2O]Cl$	> 290	Deep-green	35.6	3.6	18.8	10.5	35.4	3.5	18.8	10.3	35.0[c]	1.72
$[Cu_2L^*H_2O\cdot\frac{1}{2}C_2H_5OH]Br_2$	> 290	Reddish-brown	24.1	2.6	23.2	29.2	23.6	2.2	24.1	30.0	90.0[c]	0.78
$[Co(HL^+)_2(H_2L'')]$	> 290	Brown	37.8	4.4	14.3	—	37.9	4.4	14.7	—	—	3.27
$[Ni(H_2L)_2(H_2L'')]Ac_2\cdot H_2O$	> 290	Brick-red	39.6	4.6	11.4	—	39.5	4.0	11.3	—	7.5[c]	2.12

[a] H_2L^{**} = 1-salicylhydrazo-3-imino-3-(*o*-formyl) phenoxy propionic acid hydrazide, H_2L^* = malonic acid amido-salicoylhydrazone, H_2L = cyanoacetylhydrazine, H_2L'' = salicylaldehyde.
[b] In Ω^{-1} cm^2 mol^{-1}.
[c] In DMF.

behaves as a mixed ligand towards Co(II) and Ni(II) complexes together with cyanoacetylhydrazine. Also, salicylaldehyde affords an amido group in the case of the Co(II) complex only.

(ii) The reactions of salicylaldehyde with the complexes of Zn(II), $[Zn(HL)_2(H_2O)_2]H_2O$,[1] and U(VI)O_2, $[UO_2(HL)_2]$,[1] gave complexes with formulae $[Zn(HL^*)_2]$ and $[UO_2(HL^*)_2C_2H_5OH]$ [H_2L^* = malonic acid amido-salicoylhydrazone (**1**)]. The analyses of those two complexes showed that salicylaldehyde has been condensed with the amino graoup of the hydrazide moiety together with the promotion of H_2O to the cyano-forming amido group.

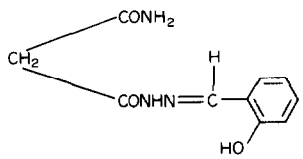

1 (H_2L^*)

(iii) 1-Salicylhydrazo-3-imino-3-(*o*-formyl) phenoxy propionic acid hydrazide (**2**) was obtained from the reaction of $[Co(H_2L)_2(H_2O)_2]Cl_2$[1] and/or $[Fe(H_2L)_2(H_2O)_2]Cl_2$[1] with excess salicylaldehyde. The yellow shiny crystals (m.p. = 236°C) were isolated in a very pure state (structure **2**). The analysis and spectral measurements (IR and ^{1}H NMR) confirm structure **2**.

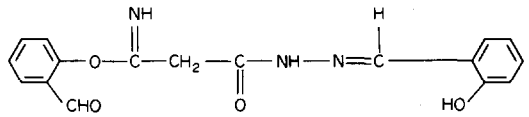

2 (H_2L^{**})

(iv) The Cd(II) complex, $[Cd(H_2L^{**})_4Cl_2]$, was obtained from the reaction of $[Cd(H_2L)_2)Cl_2]$[1] with excess salicyaldehyde in ethanol. On mixing $[Cd(H_2L^{**})_4Cl_2]$ with a suspension of disodium ethylenediaminetetraacetate in water, a yellow precipitate was formed on the surface of the reaction mixture. The product was filtered off and crystallized from acetonitrile. All physicochemical analyses indicate that the yellow material is similar to compound **2** synthesized by method (iii).

(v) The reaction of $[Cu(H_2L^+)Cl]$ (H_2L^+ = malonic acid amido-hydrazide) with salicylaldehyde gave a new solid complex with formula $[Cu(H_2L^*)H_2O]Cl$ in which the coordinated ligand (H_2L^*) is similar to those obtained from method(II) but differs in its mode of complexation. On the other hand, the complex with formula $[Cu_2(L^*)H_2O\cdot\frac{1}{2}C_2H_5OH]Br_2$ was obtained from

the reaction of $[Cu(H_2L)Br]$[1] with excess salicylaldehyde. The reaction of the Cu(I) chloride and bromide complexes with salicylaldehyde is followed by oxidation to Cu(II). The existence of Cu(II) is confirmed from the values of magnetic moments and the appearance of a *d–d* transition band.

All the isolated solid complexes were filtered hot, washed several times with hot ethanol, and dried in a vacuum desiccator over anhydrous calcium chloride.

Physical measurements

The preparative techniques of the starting compounds as well as the instruments used in this study were identical to our previous work.[1]

RESULTS AND DISCUSSION

The new solids prepared in this study are shown in Table 1. The complexes are microcrystalline or powder-like, and stable in atmospheric conditions. They are insoluble in common organic solvents but quite soluble in DMF and DMSO. The molar conductivities of the complexes in DMF at 25°C are in the 1–20 Ω^{-1} cm^2 mol^{-1} range, indicating a non-electrolytic nature[6] for all complexes except $[Cu(HL^*)H_2O]Cl$ and $[Cu_2L^*H_2O \cdot \frac{1}{2}C_2H_5OH]Br_2$, which have values of 35 and 90 Ω^{-1} cm^2 mol^{-1}, suggesting 1 : 1 and 1 : 2 electrolytes,[6] respectively.

1-Salicylhydrazo-3-imino-3-(*o*-formyl) phenoxy propionic acid hydrazide (structure **2**, H_2L^{**}, m.p. = 236°C) has not been reported before. This novel compound was synthesized during the attempt to prepare the hydrazone complexes of $[Co(H_2L)_2(H_2O)_2]Cl_2$[1] or $[Fe(H_2L)_2(H_2O)_2]Cl_2$[1] with salicylaldehyde. Also, compound **2** was obtained by warming the Cd(II) complex $[Cd(H_2L^{**})_4Cl_2]$ with a suspension of disodium ethylenediaminetetraacetate in water. The solution became yellow and a yellow precipitate appeared on the surface of the reaction mixture. The yellow compound was filtered off, washed with hot ethanol, crystallized from acetonitrile and preserved in a vacuum desiccator over anhydrous $CaCl_2$. The products (compound **2**) from both methods are identical and have the same melting point (236°C) and IR spectra.

The IR spectrum of compound **2** shows characteristic bands at 1615, 1580 and 1320 cm^{-1} assignable to the azomethine (C=N) of imidate[7] and hydrazone, and C—O—C moieties,[8,9] respectively. The observation of a broad band centred at 3440 cm^{-1} indicates the existence of the OH of salicylaldehyde group. Also, the broadness of this band suggests the presence of a hydrogen bond between the azomethine nitrogen of the hydrazone and the OH groups (structure **3**). Moreover, the two strong bands at 1710 and 1685 cm^{-1} were assigned to the carbonyl oxygen of the hydrazide and salicylaldehyde groups, respectively. Those two bands are strong enough to suggest that the carbonyl groups are free from hydrogen bonding (structure **3**).

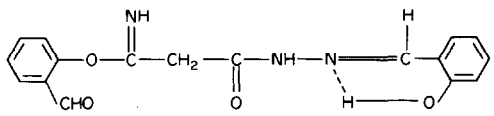

3

The ligand H_2L^{**} contains several coordination sites but the IR spectrum of the Cd(II) complex indicates that the ligand behaves as a monodentate via the carbonyl oxygen of the hydrazide moiety. Undoubtedly the negative shift (20 cm^{-1}) of the carbonyl group of the hydrazide moiety indicates the participation of this group in bonding. All of the other bands remain more or less unchanged. The presence of only one band at 330 cm^{-1}, due to Cd—Cl,[10] suggests that the two chloride ions are *trans* to each other.

The IR spectra of the Co(II), $[Co(HL^*)_2(H_2L'')]$, and Ni(II), $[Ni(H_2L)_2(H_2L'')]Ac_2 \cdot H_2O$, complexes show that both the carbonyl and the OH groups of salicylaldehyde are coordinated to the metal ion beside the bidentate nature of H_2L and HL^+ in the Co(II) and Ni(II) complexes as reported in Ref. 1. The appearance of new bands at 1720, 1240 and 1155 cm^{-1}, attributable to ν(C=O), ν(C—O)[11] and δ(OH)[11] vibrations, respectively, can be taken as evidence for the participation of salicylaldehyde in bonding. The existence of the OH (phenolic) was checked qualitatively using fresh $FeCl_3$ solution which gives a brown colouration. Salicylaldehyde replaces two water molecules in the original Co(II) complex,[1] but it replaces two acetate ions in the Ni(II) complex.[1]

The stereochemistries of those two complexes, $[Co(HL^+)_2(H_2L'')]$ and $[Ni(H_2L)_2(H_2L'')]Ac_2 \cdot H_2O$, are identical to the original complexes which were prepared from them[1] but different from each other. The differences between the two structures are that the Ni(II) complex exists in the keto form and the Co(II) complex in the enol form. Also, the former shows the cyano group which has disappeared in the latter.

The electronic spectrum of the Co(II) complex $[Co(HL^+)_2(H_2L'')]$ in Nujol mulls shows two bands at 18,900 and 16,900 cm^{-1}, assigned to $^4T_{1g} \rightarrow {}^4T_{1g}(P)$ and $^4T_{1g} \rightarrow {}^4A_{2g}$, suggesting an octahedral structure around the cobalt ion.[12] The magnetic-moment value (3.27 BM) is lower than those

reported for the octahedral structure but similar to $[Co(PBI)_2]I_2$[13,14] [PBI = pyridine-2,6-dialdehyde bis(benzylimine)] which is reported as an octahedral structure with an anomalous magnetic moment (3.72 BM). The spectrum of the Ni(II) complex $[Ni(H_2L)_2(H_2L'')]Ac_2 \cdot H_2O$ in Nujol mulls shows two bands at 26,300 and 18,500 cm^{-1}, assigned to $^3A_{2g}(F) \rightarrow {}^3T_{1g}(F)$ and $^3A_{2g}(F) \rightarrow {}^3T_{1g}(P)$, respectively, in an octahedral symmetry.[15] Also, the band at 20,800 cm^{-1} may be assigned to the $^1A_{1g} \rightarrow {}^1A_{2g}$ transition in a square planar geometry.[12] The anomalous magnetic moment (2.12 BM) is also reported for Ni(II) complexes with a mixed stereochemistry.[16,17]

The reaction of salicylaldehyde with the Zn(II) and U(VI)O_2 complexes, $[Zn(HL)_2(H_2O)_2]H_2O$[1] and $[UO_2(HL)_2]$[1], affords new complexes with formulae $[Zn(HL^*)_2]$ and $[(UO_2(HL^*)_2]C_2H_5OH$, respectively, with promotion of water to the cyano group, forming an amido group. Also salicylaldehyde condensed to the NH_2 hydrazide group forming hydrazone. The condensation product (H_2L^*) coordinates to the Zn(II) and U(VI)O_2 ions in a tridentate manner via the azomethine nitrogen, the carbonyl oxygen of the amide group and the enolized carbonyl oxygen of the hydrazide moiety with displacement of a proton from the latter group.

The IR spectra of those two complexes are identical and show no bands at 2270 cm^{-1}, indicating the promotion of water to the cyano group. The new bands at 1710 and 1615 cm^{-1} were assigned to the ν(CO) and $\beta(NH_2)$ vibrations of the amide group formed from the promotion of water to the cyano group. Also, the existence of a broad band centred at 3480 cm^{-1} due to the ν(OH) vibration of salicylaldehyde may indicate the presence of hydrogen-bonded structure between the azomethine of the hydrazone and the OH groups. Moreover, the new bands at 1445, 1410 and 1240 cm^{-1} are assigned to ν_{as}(C—O),[18] ν_s(C—O)[18] and δ(OH) vibrations, respectively.

The band at 930 cm^{-1} assigned to the asymmetric stretching frequency (ν_3) of the dioxouranium ion[19] in the U(VI)O_2 complex before condensation, $[UO_2(HL)_2]$, is shifted to a lower wavenumber (900 cm^{-1}) after condensation, $[UO_2(HL^*)_2]C_2H_5OH$, with salicylaldehyde. The negative shifts (30 cm^{-1}) may suggest the participation of a third coordination site in the bonding in the latter case and coordination via N, O and O instead of N and O before condensation. Also, it suggests the formation of coordination number 8 around the uranium in the case of $[UO_2(HL^*)_2]C_2H_5OH$ but 6 in the case of $[UO_2(HL)_2]$.

The ^{1}H NMR spectrum of the U(VI)O_2 complex $[UO_2(HL^*)_2]C_2H_5OH$ shows signals at δ 10.25, 9.35, 8.65 and 3.4 ppm (downfield of TMS) in d_6-DMSO at room temperature (25°C). These signals are assigned to the protons of OH (phenolic), NH, CH and OH (ethanolic), respectively. Also, the existence of ethanol is confirmed by the observation of the characteristic ethyl resonances.

Finally, the reaction of salicylaldehyde with the diamagnetic Cu(I) complexes, $[Cu(H_2L')Cl]$[1] and $[Cu(H_2L')Br]$, affords new complexes in which Cu(I) is oxidized to Cu(II), and at the same time the condensation of salicylaldehyde on the amino group of the hydrazide group occurs.

The IR spectrum of the Cu(II) complex $[Cu(HL^*)H_2O]Cl$ suggests that HL* coordinates in a tridentate manner via OH (phenolic), azomethine nitrogen (C=N) and the enolized carbonyl oxygen with displacement of a hydrogen atom from the latter group. The observation of a very strong broad band centred at 3350 cm^{-1} suggests the existence of strong hydrogen bonding, probably between the coordinated water and the carbonyl oxygen of the amide and/or the OH phenolic. The bands at 1540, 1460, 1445, 1290, 710, 550, 470 and 340 cm^{-1} are assigned to ν(C=N), ν_{asy}(C—O), ν_s(C—O), δ(OH), ν(Cu—O)[18] (H_2O), ν(Cu—O)[11] (phenol), (Cu—O) (carbonyl) and ν(M—N),[10] respectively. The electronic spectrum in Nujol mulls shows two bands at 18,800 and 13,600 cm^{-1}, indicating a pseudo-tetrahedral geometry[20] around the Cu(II) ion. The bands at 23,800 and 21,700 cm^{-1} are assigned to d–π^* and Cl–Cu charge transfer.[21,22] The magnetic moment (1.72 BM) is in a good agreement with those reported for a d^9-configuration[23] and shows no Cu–Cu interaction. The molar-conductance value (35.0 Ω^{-1} cm^2 mol^{-1}) for the complex $[Cu(HL^*)H_2O]Cl$ in DMF at room temperature (25°C) indicates a 1 : 1 electrolyte.[6]

The electronic spectrum of the Cu(II) bromide complex $[Cu_2L^* \cdot H_2O \cdot \frac{1}{2}C_2H_5OH]Br_2$ in a Nujol mull shows two bands at 18,200 and 15,600 cm^{-1}, indicating a pseudo-tetrahedral geometry around the Cu(II) ion. The subnormal magnetic moment (0.78 BM) is accounted for by assuming the existence of a polymeric structure in the solid state and considerable interaction between the Cu(II) due to spin exchange.[23] Also, the low magnetic moment of the complexes containing the bromide ion compared with the chloride has been reported earlier.[23] Finally, the molar conductivity in DMF is 90.0 Ω^{-1} cm^2 mol^{-1}, suggesting a 1 : 2 electrolyte.[6]

REFERENCES

1. A. M. Shallaby, M. S. Soliman, R. M. El-Shazely and M. M. Mostafa, *Polyhedron* (submitted for publication).

2. G. D. Diana, E. S. Zalay and R. A. Cuter, Jr, *J. Org. Chem.* 1965, **30**, 298.
3. R. L. Dutta and P. Ray, *J. Indian Chem. Soc.* 1959, **36**, 499.
4. G. B. Payne, *J. Org. Chem.* 1961, **26**, 668.
5. R. L. Dutta and A. M. Singh, *J. Inorg. Nucl. Chem.* 1978, **40**, 417.
6. W. J. Geary, *Coord. Chem. Rev.* 1971, **7**, 81.
7. D. Hadži and D. Prevoršek, *Spectrochim. Acta* 1957, **10**, 38.
8. R. L. Dutta and A. Syamal, *J. Indian Chem. Soc.* 1967, **44**, 571.
9. R. Silverstein and G. C. Bassler, *Spectrometric Identification of Organic Compounds*. Wiley, New York (1967).
10. J. R. Ferraro, *Low Frequency Vibrations of Inorganic and Coordination Compounds*. Plenum Press, New York (1971).
11. L. J. Bellamy, *The Infrared Spectra of Complex Molecules*. Methuen, London (1966).
12. A. B. P. Lever, *Inorganic Electronic Spectroscopy*. Elsevier, Amsterdam (1968).
13. R. C. Stoufer, D. H. Busch and W. B. Hadley, *J. Am. Chem. Soc.* 1961, **83**, 3732.
14. R. C. Stoufer, D. W. Smith, E. A. Clevenger and T. E. Norris, *Inorg. Chem.* 1966, **5**, 1167.
15. C. K. Jørgensen, *Acta Chim. Scand.* 1956, **10**, 887.
16. G. Maki, *J. Chem. Phys.* 1958, **28**, 651.
17. D. Liehr and C. J. Ballhausen, *J. Am. Chem. Soc.* 1959, **81**, 538.
18. K. Nakamoto, *Infrared Spectra of Inorganic and Coordination Compounds*. Wiley, New York (1970).
19. L. H. Jones, *Spectrochim. Acta* 1959, **11**, 409.
20. L. Sacconi, *Coord. Chem. Rev.* 1966, **1**, 126.
21. J. C. T. Rendell and L. K. Thompson, *Can. J. Chem.* 1979, **1**, 57.
22. B. Bosnich, *J. Am. Chem. Soc.* 1968, **90**, 627.
23. M. Kato, H. B. Jonassen and J. C. Fanning, *Chem. Rev.* 1964, **64**, 99.

Polyhedron Vol. 6, No. 6, pp. 1325–1327, 1987
Printed in Great Britain

0277–5387/87 $3.00+.00

CHEMISTRY OF IRON COMPLEXES—VII. SPECTROSCOPIC (IR AND UV–VIS), MAGNETIC AND OTHER STUDIES OF IRON(II) COMPLEXES WITH BIS(TERTIARYPHOSPHINE/ARSINE OXIDES)

T. S. LOBANA* and S. S. BHATTI

Department of Chemistry, Guru Nanak Dev University, Amritsar 143005, India

(*Received* 21 *July* 1986; *accepted after revision November* 1986)

Abstract—A series of iron(II) complexes with bis(tertiaryphosphine/arsine oxides), $Ph_2E(O)(CH_2)_nE(O)Ph_2$, of general formula $[FeX_2(L–L)(H_2O)_2]\cdot mH_2O$ [X = Cl, Br or SCN; m = 0 or 1; E, n, L–L: P, 1, mdpo; P(As), 2, edpo (edao); P(As), 4, bdpo (bdao); P, 6, hdpo] have been studied using analytical, spectroscopic (IR, far-IR and UV–VIS), magnetic, TGA, conductance and molecular-weight data. All of these compounds have been assigned octahedral structures and are high-spin.

Bis(tertiaryphosphine/arsine oxides) (L–L) (**I**), $Ph_2E(O)(CH_2)_nE(O)Ph_2$ (E = P or As; n = 1, 2, 4 or 6) are known to interact with iron(III) salts forming ionic complexes, $[Fe(L–L)_2X_2][FeX_4]$ (X = Cl or Br), or neutral complexes, $[Fe(L–L)(NCS)_3]$.[1–9] In the case of iron(II), there is one paper dealing with the interaction of iron(II) iodide and iron(II) tetracarbonyl iodide with the above ligands.[10]

In this paper, the reactions of these ligands (**I**) have been extended to iron(II) chloride, bromide and isothiocyanate. In order to overcome the possibility of air oxidation of iron(II), the iron(II) salt solution was obtained from an iron(III) salt by reducing with the minimum amount of ascorbic acid in ethyl alcohol/isopropyl alcohol followed by its interaction with a suitable ligand. The complex once formed was stable and remained unaffected even when exposed to air for several hours.

EXPERIMENTAL

Ligands

The ligands were prepared by the oxidation of bis(tertiaryphosphines/arsines) using 30% H_2O_2 or $KMnO_4$ as the oxidants.[1,11]

Preparation of complexes

Iron(II) chloride solution was refluxed with a ligand solution in a 1 : 1 mole ratio for a period of 15–30 min to ensure completion of the reaction. It was then filtered and washed several times with isopropyl alcohol. Iron(II) bromide complexes were obtained similarly: the refluxing time was 2 h. The volume was reduced to nearly one-half its original volume and the solid complex separated on cooling was filtered and washed with isopropyl alcohol.

Iron(II) isothiocyanate solution [obtained from treatment of iron(II) chloride with KSCN in a 1:2 mole ratio in ethyl alcohol/isopropyl alcohol] and the ligand solution in ethyl alcohol were refluxed for about 2 h. and the volume reduced to nearly one-half its original volume. The complex was separated either on cooling or after the addition of diethyl ether. It was filtered and washed with an ethyl alcohol–diethyl ether mixture.

All the complexes were dried *in vacuo*. An inert atmosphere was maintained during synthesis.

Analytical data and spectroscopic techniques

Carbon, hydrogen and nitrogen analyses were obtained from the University College of Science, Calcutta, India. Iron was estimated by the phenanthroline method.[12] The halogens were estimated by Volhard's method. The techniques used for molar conductivities (nitrobenzene), reflectance spectra (MgO as the standard reflector), thermogravimetric analysis and magnetic-susceptibility measurements were the same as described earlier.[1–8,10] The IR and far-IR spectra of the complexes (as KBr pellets) were recorded in the

* Author to whom correspondence should be addressed.

range 4000–200 cm^{-1} with a Pye–Unicam SP-300 spectrophotometer. The molecular weights of some of the iron(II) isothiocyanate complexes (in nitrobenzene) were determined cryoscopically using a Beckmann thermometer.

RESULTS AND DISCUSSION

The analysis shows that the complexes have a metal : ligand ratio of 1 : 1 (Table 1). The colour of the complexes varies from green to red or brown. The melting or decomposition points of the complexes lie in the range 128–296°C. The complexes are soluble in many common organic solvents.

In the IR spectra of the complexes, the ν(PO) and ν(AsO) decrease on complexation by 25–67 and 38–53 cm^{-1}, respectively. Usually, ν(PO) peaks appear as two peaks while ν(AsO) appears as single peak. The low-energy shifts support coordination by both (EO) groups of the bidentate ligands.[1,7] The ν(E–C_{Phenyl}) (E = P or As) peaks remain essentially unchanged. It is interesting to note that the analogous high-spin iron(III) complexes, $[Fe(L–L)_2X_2][FeX_4]$ (X = Cl, Br, L–L = mdpo, edpo, etc.), showed downward shifts in ν(E–C_{Phenyl}) on coordination.[1,7] Further all these iron(II) halides

Table 1. Analytical data, magnetic moments and other physical data[a–k]

	Complex	Found (calc.) (%) C	H	Fe	N/X	μ_{eff} (BM)
(1)	$[FeCl_2(mdpo)(H_2O)_2]$[c]	51.2 (51.8)	4.9 (4.5)	10.1 (9.7)	12.7 (12.3)	5.66
(2)	$[FeCl_2(bdpo)(H_2O)_2]$[c]	55.2 (54.1)	4.8 (5.2)	9.1 (9.0)	11.9 (11.4)	5.47
(3)	$[FeCl_2(bdao)(H_2O)_2]$[a]$\cdot H_2O$	45.2 (46.2)	4.7 (4.7)	7.1 (7.7)	10.1 (9.8)	5.62
(4)	$[FeBr_2(bdpo)(H_2O)_2]$[e]$\cdot H_2O$	46.2 (46.1)	3.9 (4.7)	8.0 (7.7)	22.6 (22.0)	5.29
(5)	$[FeBr_2(edao)(H_2O)_2]$[f]$\cdot H_2O$	38.9 (39.6)	3.9 (3.6)	7.7 (7.1)	20.0 (20.3)	5.20
(6)	$[FeBr_2(bdao)(H_2O)_2]$[c]$\cdot H_2O$	41.9 (41.2)	3.8 (3.4)	7.1 (6.9)	19.1 (19.6)	4.90
(7)	$[Fe(NCS)_2(mdpo)(H_2O)_2]$[g]	52.6 (52.0)	4.3 (4.2)	8.6 (9.0)	4.7 (4.5)	5.28
(8)	$[Fe(NCS)_2(edpo)(H_2O)_2]$[f]$\cdot 2H_2O$	49.8 (49.9)	3.9 (4.7)	8.5 (8.3)	4.8 (4.2)	5.47
(9)	$[Fe(NCS)_2(bdpo)(H_2O)_2]$[h]$\cdot H_2O$	53.5 (52.6)	5.0 (5.0)	8.1 (8.2)	4.7 (4.1)	5.35
(10)	$[Fe(NCS)_2(hdpo)(H_2O)_2]$[g]$\cdot H_2O$	53.9 (53.9)	5.2 (5.3)	7.3 (7.9)	4.5 (3.9)	5.29
(11)	$[Fe(NCS)_2(edao)(H_2O)_2]$[i]	46.9 (46.3)	4.0 (3.9)	7.1 (7.7)	—	5.31
(12)	$[Fe(NCS)_2(bdao)(H_2O)_2]$[j]	47.3 (47.7)	4.1 (4.2)	7.7 (7.4)	3.4 (3.7)	5.29

[a] Λ_m are 26, 18, 25, 18, 18, 28, 13, 13, 12, 14, 13 and 13 Ω^{-1} cm^2 mol^{-1}, respectively.

[b] M.p. (°C) 296(d), 203–208(d), 135(d), 165, 158, 178, 298d, 140d, 131d, 128d, 160d and 225, respectively.

[c] Greenish yellow.

[d] Light yellow.

[e] Brick red.

[f] Light brown.

[g] Intense red.

[h] Maroon.

[i] Reddish brown.

[j] Yellowish brown.

[k] Molecular weights found (required) for **7**, **9**, **10** and **12** are: 534 (624), 564 (684), 737 (712) and 766 (754).

complexes show different line positions with respect to ν(EO) compared to those shown by the iron(III) halide complexes, $[Fe(L\text{–}L)_2X_2][FeX_4]$.[1,7]

In the far-IR region, the chloride complexes show medium to strong peaks in the range 355–370 cm^{-1}, while the bromide complexes show similar peaks in the range 270–285 cm^{-1}.[13–15] The presence of H_2O is shown by the elemental analysis and IR spectral bands [ν(OH) (3400–3440 cm^{-1}) and δ(HOH) (1635–1660 cm^{-1})]. The rocking mode of coordinated H_2O at 790 cm^{-1} was detected in the complexes of bdpo only.[16] Tentative assignments to ν(FeO) peaks (weak) have been made in the range 350–428 cm^{-1}.

In the thiocyanate complexes, the ν(CN) peaks (sharp and single) lie in the range 2010–2055 cm^{-1}, indicating the formation of Fe(II)–NCS instead of Fe(II)–SCN or Fe(II)–NCS–Fe(II) bonds. The S-bonded or bridged SCN groups show absorptions for ν(CN) in the 2090–2110- and 2110–2175-cm^{-1} regions, respectively.[17] It is significant to note that the analogous complexes $[Fe(NCS)_3(L\text{–}L)]$ (L–L = edpo, bdpo etc.] and $[Fe(mdpo)_2(NCS)_2](NCS)\cdot 3H_2O$ showed $\nu(C{\equiv}N)$ peaks at a somewhat higher energy [2040–2058 cm^{-1}] and the peaks were broad.[8] The bending modes, δ(NCS), occur in the range 462–492 cm^{-1} in the Fe(II) complexes. The edpo and hdpo complexes show ν(CS) peaks at 840 and 855 cm^{-1}, respectively, and this peak in other complexes has either been obscured (ligand bands) or merged with ν(AsO) peaks (835–840 cm^{-1}). The low-energy ν(Fe–NCS) bands of weak to medium intensity occur in the 245–300-cm^{-1} region.[17] The range for ν(Fe–O) in the isothiocyanate complexes is 380–385 cm^{-1}. The presence of H_2O is shown by IR and elemental analysis.

The molar conductance values (Table 1) suggest the formulation $[FeX(L\text{–}L)(H_2O)_2]^+X^-$ for the halide complexes, but, in view of considerable conductance values of isothiocyanate complexes (< than for a 1 : 1 electrolyte), it is believed that the conductance values are due to possible ionization of the complexes in the solution phase, the halide complexes registering greater values than isothiocyanate complexes [eqn (1)]:

$$[FeX_2(L\text{–}L)H_2O)_2] \rightleftharpoons [FeX(L\text{–}L)(H_2O)_2]^+X^- \quad (X = Cl, Br \text{ or } NCS). \quad (1)$$

Magnetic moments (μ_{eff}) of the complexes (5.20–5.66 BM) are characteristic of high-spin iron(II) complexes (Table 1).[18] The complex $[FeBr_2(bdao)(H_2O)_2]\cdot H_2O$, however, showed a lower value of 4.90 BM which may be attributed to the quenching of the orbital contribution, possibly due to a lower site symmetry. It may be noted that the analogous iron(III) complexes, $[Fe(NCS)_3(L\text{–}L)]$ (L–L = mdpo etc.), reported earlier showed lower μ_{eff} values (5.34–5.58 BM).[8] This lends support to the earlier observation that the FeN_3O_2 chromophores in the iron(III) complexes have a relatively larger ligand field effect due to three nitrogen atoms. The FeN_2O_4 chromophores in iron(II) complexes, however, show a normal magnetic behaviour.[17] The molecular weights of some of the isothiocyanate complexes show their monomeric nature (Table 1).

The solid-phase electronic spectra of the complexes show *d–d* and charge-transfer transitions in the range 12,000–28,000 cm^{-1} supporting octahedral structures.[17] The TGA of the complexes containing coordinated and uncoordinated H_2O molecules showed loss of H_2O in the range 100–180°C; the range was 130–170°C in the case of the complexes containing only coordinated H_2O.

Acknowledgement—One of us (SS Bhatti) is thankful to the Guru Nanak Dev University for research facilities.

REFERENCES

1. T. S. Lobana, H. S. Cheema and S. S. Sandhu, *J. Chem. Soc., Dalton Trans.* 1983, 2039.
2. T. S. Lobana, H. S. Cheema and S. S. Sandhu, *Transition Met. Chem.* 1984, **9**, 119.
3. T. S. Lobana, H. S. Cheema and S. S. Sandhu, *Transition Met. Chem.* 1984, **9**, 330.
4. T. S. Lobana, H. S. Cheema and S. S. Sandhu, *Polyhedron* 1984, **3**, 911.
5. T. S. Lobana, H. S. Cheema and S. S. Sandhu, *J. Indian Chem. Soc.* 1982, **59**, 799.
6. T. S. Lobana, H. S. Cheema and S. S. Sandhu, *Indian J. Chem.* 1985, **24A**, 516.
7. T. S. Lobana, H. S. Cheema and S. S. Sandhu, *Spectrochim. Acta* 1986, **42A**, 399.
8. T. S. Lobana, H. S. Cheema and S. S. Sandhu, *Spectrochim. Acta* 1986, **42A**, 735.
9. S. A. Cotton, *Coord. Chem. Rev.* 1972, **8**, 185.
10. T. S. Lobana, H. S. Cheema and S. S. Sandhu, *Polyhedron* 1985, **4**, 717.
11. T. S. Lobana, H. S. Cheema and S. S. Sandhu, *J. Chem. Sci. (Guru Nanak Dev Univ.)* 1981, **7**, 58; *Chem. Abstr.* 1983, **99**, 204979e.
12. A. I. Vogel, *A Text Book of Quantitative Inorganic Analysis*, p. 781. ELBS and Longman, London (1973).
13. T. E. Nappier, R. O. Feltham, J. H. Enemark, A. Kruse and M. Cooke, *Inorg. Chem.* 1975, **14**, 806.
14. C. D. Burbridge and D. M. L. Goodgame, *J. Chem. Soc. A* 1968, 1074.
15. R. B. King, R. N. Kapoor, P. N. Kapoor and M. S. Saran, *Inorg. Chem.* 1971, **10**, 1851.
16. H. Meider and P. Bronzan, *Polyhedron* 1983, **2**, 69.
17. P. P. Singh, *Coord. Chem. Rev.* 1980, **32**, 33.
18. P. Gutlich, *Struct. Bonding* 1981, **44**, 84.

Polyhedron Vol. 6, No. 6, pp. 1329–1335, 1987
Printed in Great Britain

0277–5387/87 $3.00+.00

PREPARATION AND CATALYTIC ACTIVITY OF CATIONIC RHODIUM(I) AND IRIDIUM(I) COMPLEXES WITH PHOSPHINE SULPHIDE LIGANDS

C. CLAVER,* F. GILI, J. VIÑAS and A. RUIZ

Departamento de Química, Facultad de Ciencias Químicas, Universidad de Barcelona, Pl. Imperial Tarraco 1, 43005 Tarragona, Spain

(*Received* 2 *October* 1986; *accepted* 17 *November* 1986)

Abstract—The preparation and properties of cationic rhodium and iridium complexes of types $[M(diolefin)L_2](ClO_4)$ and $[M(diolefin)L(PPh_3)](ClO_4)$ [M = Rh, diolefin = 1,5-cyclooctadiene (COD) or 2,5-norbornadiene; M = Ir, diolefin = COD; L = phosphine sulphide] are described. The complexes have been characterized by IR, ^1H NMR and ^{31}P NMR spectroscopy. The use of $[M(diolefin)L_2](ClO_4)$ as catalyst precursors in homogeneous hydrogenation of olefins has been studied.

Studies conducted in this laboratory have focused on the synthesis, characterization and reactivity of rhodium and iridium complexes containing S-donor ligands, thioethers and dithioethers.[1–6] In this paper synthetic details and characterization data for several rhodium(I) and iridium(I) cationic complexes with phosphine sulphide as ligands are presented. Although some related neutral and cationic rhodium and iridium complexes with phosphine sulphide have been previously reported[7] different synthetic methods to those reported here were used.

Single-crystal X-ray studies on different complexes have indicated that tertiary phosphine sulphides are moderate σ-donors with minimal π-acceptor properties.[7–9] We have studied the ability of the phosphine sulphide to displace a diolefin in $[M(diolefin)_2]^+$ complexes as well as the stability and reactivity of the isolated complexes.

In the other hand, there have been many studies of the homogeneous hydrogenation of olefins catalyzed by rhodium cationic complexes, and the catalytic activity of some iridium(I) cationic complexes is also known. $[Rh(COD)(PR_3)_2]^+$ and $[Ir(COD)(PR_3)_2]^+$ (COD = 1,5-cyclooctadiene) are active precursors in homogeneous hydrogenation of olefins.[10–13] Nevertheless, the catalytic activity of complexes with sulphur ligands has been studied to a much lesser extent. Recently Kalck *et al.* have shown that hydrogenation and hydroformylation of olefins and other substrates are catalyzed at low pressure and temperature (5 bar, 80°C) by dinuclear complexes of rhodium(I) with a thiolato ligand.[14–16] In this paper we describe the catalytic activity of some cationic complexes with phosphine sulphide in the homogeneous hydrogenation of 1-heptene.

RESULTS AND DISCUSSION

$[Rh(diolefin)L_2](ClO_4)$ *and* $[(diolefin)Rh\{\mu\text{-}(L\text{–}L)\}_2Rh(diolefin)](ClO_4)_2$ *complexes* (L *and* L–L = *phosphine sulphide*)

The addition to dichloromethane solutions of $[Rh(diolefin)_2](ClO_4)$ [diolefin = COD[17] or 2,5-norbornadiene (NBD)[18]] of a stoichiometric amount (or a slight excess) of L gives the $[Rh(diolefin)L_2](ClO_4)$ derivatives:

$$[Rh(diolefin)_2](ClO_4) + 2L \rightarrow [Rh(diolefin)L_2](ClO_4) + diolefin, \quad (1)$$

where diolefin = COD or NBD, and L = Me_3PS, Et_3PS or Ph_3PS.

When an equimolecular amount of the bidentate ligand $Me_2P(S)(S)PMe_2$ was added to dichloromethane solutions of $[Rh(diolefin)_2](ClO_4)$, the C, H and S elemental analyses of the complexes obtained correspond to the formulation $[Rh(COD)(L\text{–}L)]_n(ClO_4)_n$.

* Author to whom correspondence should be addressed.

Measurements of the equivalent conductivities of the complexes with this ligand at different concentrations in nitromethane solutions gave plots of the Onsager equation $\Lambda_e = \Lambda_o - A\sqrt{c}$, for which A values are characteristic of 2:1 electrolytes,[19] in accordance with the formation of dinuclear complexes [Rh(diolefin)Rh{μ-(L–L)}$_2$Rh(diolefin)] $(ClO_4)_2$, where the ligand is bidentate, bonding two metal atoms.[1,2]

The analytical results, conductivities values,[19,20] IR data and melting points for the complexes are listed in Table 1.

The nuclearity of the complexes [Rh(diolefin)L]$_n(ClO_4)_n$ was found to be n = 1 in the cases of L = Me_3PS, Et_3PS or Ph_3PS, according to the sulfur elemental analyses, in accordance with the behaviour of the phosphine sulphides as monodentate ligands.

The complexes are yellow and moderately air-stable solids. IR spectra show the P=S stretching frequencies to have decreased in the usual manner on coordination,[7] together with those due to the coordinated diolefins, and uncoordinated perchlorate anion (1100s and 620s cm^{-1}).[21]

The ^1H NMR data are given in Table 2. For [Rh(COD)L_2](ClO_4) (L = Me_2PS or Ph_2PS) the spectra in $CDCl_3$ show the resonances corresponding to coordinated COD and the corresponding at sulphur ligand. In the spectrum of the complex with L = Me_3PS, the signal corresponding to Me–P shows a doublet at 2.10 ppm downfield compared to the free ligand (1.79d ppm), with ^2J(P–H) = 13 Hz.

The complex [Rh(COD)$(Me_3PS)_2$](BPh_4) has been previously published by Ainscough *et al.*, but NMR data were not reported.[7]

[Rh(diolefin)L(PPh_3)](ClO_4) *complexes* (L = Me_3PS *or* Ph_3PS)

The addition of a stoichiometric amount of sulphur phosphine ligand and triphenylphosphine

Table 1. Analytical results, conductivity data, melting points and IR data for complexes [Rh(diolefin)L_2](ClO_4), [(diolefin)Rh{μ-(L–L)}$_2$Rh(diolefin)]$(ClO_4)_2$ and [Rh(diolefin)L(PPh_3)](ClO_4)

Complex	Analysis: Found (Calc.) (%) C	H	S	Conductivity data Λ_M[a]	A[b]	M.p.[c] (°C)	IR data ν(P=S) (cm^{-1})
[Rh(COD)$(Ph_3PS)_2$](ClO_4)	57.7 (58.8)	4.9 (4.8)	7.2 (7.1)	148	—	130–134	595(h)
[Rh(COD)$(Me_3PS)_2$](ClO_4)	31.7 (31.9)	5.6 (5.7)	11.6 (12.1)	145	—	122–126	532(f)
[Rh(COD)$(Et_3PS)_2$](ClO_4)	38.5 (39.3)	6.8 (6.9)	—	147	—	125–128	555(d)
[(COD)Rh{μ-(L–L)}$_2$Rh(COD)]$(ClO_4)_2$	28.1 (29.0)	4.9 (4.8)	12.8 (12.9)	142	386[d]	135–138	582(m)
[Rh(NBD)$(Ph_3PS)_2$](ClO_4)	58.7 (58.5)	4.0 (4.3)	8.0 (7.2)	145	—	137–141	592(m)
[Rh(NBD)$(Me_3PS)_2$](ClO_4)	29.00 (30.5)	5.6 (5.1)	11.8 (12.5)	132	—	92–95	530(m)
[(NBD)Rh{μ-(L–L)}$_2$Rh(NBD)]$(ClO_4)_2$	26.5 (27.4)	4.2 (4.2)	13.7 (13.4)	145	280[d]	131–134	580(m)
[Rh(COD)$(Ph_3PS)(PPh_3)$](ClO_4)	60.8 (60.9)	4.9 (4.8)	3.6 (3.7)	128	—	144–149	590(m)
[Rh(COD)$(Me_3PS)(PPh_3)$](ClO_4)	50.8 (51.1)	5.2 (5.2)	5.1 (4.8)	134	—	134–138	528(f)
[Rh(NBD)$(Ph_3PS)(PPh_3)$](ClO_4)	60.3 (60.6)	4.8 (4.5)	4.5 (3.8)	146	—	128–132	595(m)
[Rh(NBD)$(Me_3PS)(PPh_3)$](ClO_4)	49.0 (50.5)	5.0 (4.8)	7.2 (6.7)	137	—	76–80	545(m)

[a] Measured in acetone solution (Ω^{-1} cm^2 mol^{-1}).
[b] Slope found for Onsager's equation $\Lambda_e = \Lambda_o - A\sqrt{c}$.
[c] Decomposes.
[d] Measured in nitromethane solution.

Table 2. ^{1}H NMR data [δ (ppm)] for complexes [Rh(COD)L_2](ClO_4), [Ir(COD)L_2](ClO_4) and [Ir(COD)(Me_3PS)(PPh_3)](ClO_4)

Complex[a]	COD		PPh_3	Ph_3PS	Me_3PS
	HC=CH	CH_2—C			
[Rh(COD)(Ph_3PS)$_2$](ClO_4)	5.40	3.12	—	7.80–7.20	—
[Rh(COD)(Me_3PS)$_2$](ClO_4)	4.46	2.85	—	—	2.10(d)
[Ir(COD)(Ph_3PS)$_2$](ClO_4)	4.18	2.35	—	7.80–7.20	—
[Ir(COD)(Me_3PS)$_2$](ClO_4)	4.10	3.30	—	—	1.95(d)
[Ir(COD)(Me_3PS)(PPh_3)](ClO_4)	4.22	3.30	7.80–7.30	—	1.96(d)

[a] $CDCl_3$ as solvent, T^a = 20°C, external reference TMS.

(PPh_3) to dichloromethane solutions of [Rh(diolefin)$_2$](ClO_4) (diolefin = COD or NBD)[17,18] gives derivatives of formula [M(diolefin)L(PPh_3)](ClO_4). The complexes can also be prepared by adding a stoichiometric amount of triphenylphosphine to a dichloromethane solution of [Rh(diolefin)L_2](ClO_4) (L = Me_3PS or Ph_3PS):

$$[Rh(diolefin)_2](ClO_4) + L + PPh_3 \rightarrow [Rh(diolefin)L(PPh_3)](ClO_4), \quad (2)$$

$$[Rh(diolefin)L_2](ClO_4) + PPh_3 \rightarrow [Rh(diolefin)L(PPh_3)](ClO_4), \quad (3)$$

where diolefin = COD or NBD, and L = Me_2PS or Ph_3PS.

The isolated yellow or orange complexes are air-stable. The C, H and S elemental analyses, molar conductivities in acetone, melting points and IR data are listed in Table 1. The IR spectra show bands due to the sulphur ligand and coordinated triphenylphosphine, and bands corresponding to the uncoordinated perchlorate ion.[21]

The ^{1}H NMR spectrum of [Rh(COD)(Ph_3PS)(PPh_3)](ClO_4) shows two signals corresponding to the olefinic proton CH=C resonance and two signals corresponding to the methylenic CH_2—C from the COD, together with a large signal from the aromatic protons at 7.80–7.20 ppm. These data suggest redistribution reactions in solution for [Rh(COD)(Ph_3PS)(PPh_3)](ClO_4). The ^{31}P NMR (Table 3) spectrum of $CDCl_3$ solutions of this complex shows a doublet at 26.1 ppm [^1J(Rh–P) = 147 Hz], together with two signals at 28.15 and 29.85 ppm corresponding to coordinated Ph_3PS. The doublet characteristic of square-planar rhodium(I) complexes[22] is coincident with the signal from the [Rh(COD)(PPh_3)$_2$]$^+$ complex, suggesting redistribution reactions in solution:

$$2[Rh(COD)L(PPh_3)](ClO_4) \rightleftarrows [Rh(COD)(PPh_3)_2](ClO_4) + [Rh(COD)L_2](ClO_4). \quad (4)$$

In contrast, the ^{31}P NMR spectrum of a $CDCl_3$ solution of [Rh(COD)(Me_3PS)(PPh_3)](ClO_4) shows a doublet at 29.5 ppm [^1J(Rh–P) = 147 Hz], charac-

Table 3. ^{31}P NMR data [δ (ppm)] for complexes [Ir(COD)L_2](ClO_4) and [Rh(COD)L(PPh_3)](ClO_4)

Compound[a]	Ph_3PS	PPh_3	^1J(Rh–P) (Hz)
Ph_3PS	43.4	—	—
[Rh(COD)(Ph_3PS)(PPh_3)](ClO_4)	28.15, 29.85	26.1	147
[Rh(COD)(Me_3PS)(PPh_3)](ClO_4)	39.14	29.5	147
[Ir(COD)(Ph_3PS)$_2$](ClO_4)	31.7	—	—

[a] $CDCl_3$ as solvent, T^a = 20°C, external reference H_3PO_4.

teristic of square-planar rhodium(I) complexes and a resonance at 39.14 ppm that could be attributed to coordinated Me_3PS, in accordance with the stability of the complex in solution. The ^{31}P NMR data published for the complex $[Rh(COD)(PPh_3)(Ph_3PO)](ClO_4)$ present similar resonances and $^2J(Rh–P)$ is not observed.[23]

Iridium complexes

The reaction in dichloromethane of $[Ir(COD)_2](ClO_4)$[24] with a stoichiometric amount or a slight excess of phosphine sulphide ligand (L = Me_3PS or Ph_3PS) gave derivatives whose C, H and S elemental analyses, conductivity and IR data are in accordance with the formulation $[Ir(COD)L_2](ClO_4)$:

$$[Ir(COD)_2](ClO_4)+2L \rightarrow [Ir(COD)L_2](ClO_4]+COD. \quad (5)$$

When, under the same conditions, the ligand used was $Me_2P(S)(S)PMe_2$, the equivalent conductivities measured at different concentrations in nitromethane solutions of the complex obtained, gave values of A in Onsager's equation $\Lambda_e = \Lambda_o - A\sqrt{c}$[19,20] characteristic of 2:1 electrolytes (Table 4) in accordance with eqn (6):

$$2[Ir(COD)_2](ClO_4)+2L–L \rightarrow [(COD)Ir\{\mu\text{-}(L–L)\}_2Ir(COD)](ClO_4)_2 +2COD. \quad (6)$$

As in the case of rhodium complexes the reactivity of $[Ir(COD)L_2](ClO_4)$ towards PPh_3 gives mixed complexes, $[Ir(COD)L(PPh_3)](ClO_4)$:

$$[Ir(COD)L_2](ClO_4)+PPh_3 \rightarrow [Ir(COD)L(PPh_3)](ClO_4)+L, \quad (7)$$

where L = Ph_3PS or Me_3PS.

The same reaction for the iridium complexes $[Ir(COD)L_2](ClO_4)$ (L = thioether, tetrahydrothiophen or trimethylene sulphide gave pentacoordinated iridium(I) complexes, $[Ir(COD)L_2(PPh_3)](ClO_4)$[2], and no pentacoordinated mixed complexes were obtained with phosphine sulphide ligands.

All the isolated complexes are moderately stable in the solid state but decompose in solutions exposed to air. The C, H and S elemental analyses, conductivity data and melting points of the complexes are listed in Table 4.

The ^1H NMR spectrum of $[Ir(COD)(Ph_3PS)_2](ClO_4)$ in $CDCl_3$ shows the signal at 7.80–7.20 ppm corresponding to Ph_3PS, together with several signals in the region corresponding to COD. However when excess Ph_3PS was added to the $CDCl_3$ solution, the spectrum showed only single signals characteristic of the coordinated COD at 4.18 ppm for olefinic protons, and at 2.35 ppm for methylenic protons.[25–27] The results described could be attributed to the displacement of the Ph_3PS ligand in solution (Table 2).

In order to obtain further information the ^{31}P spectrum in $CDCl_3$ was obtained, showing a major single signal at 31.7 ppm attributed to the coor-

Table 4. Analytical results, conductivity data, melting points and IR data for complexes $[Ir(COD)L_2](ClO_4)$, $[(COD)Ir\{\mu\text{-}(L–L)\}_2Ir(COD)](ClO_4)_2$ and $[Ir(COD)L(PPh_3)](ClO_4)$

Complex	Analysis: Found (Calc.) (%)			Conductivity data		M.p.[d] (°C)	IR data ν(P=S) (cm^{-1})
	C	H	S	Λ_M[a]	A[b]		
$[Ir(COD)(Ph_3PS)_2](ClO_4)$	53.1 (53.4)	4.3 (4.2)	6.1 (6.4)	148	—	96–99	586(m)
$[Ir(COD)(Me_3PS)_2](ClO_4)$	26.0 (27.3)	4.9 (4.8)	9.8 (10.4)	125	—	100–104	520(d)
$[(COD)Ir\{\mu\text{-}(L–L)\}_2Ir(COD)](ClO_4)_2$	24.5 (24.6)	4.2 (4.1)	13.0 (10.9)	225	622[d]	111–114	575(m)
$[Ir(COD)(Ph_3PS)(PPh_3)](ClO_4)$	57.0 (55.3)	4.5 (4.4)	3.2 (3.3)	126	—	136–140	540(m)
$[Ir(COD)(Me_3PS)(PPh_3)](ClO_4)$	43.5 (45.2)	4.4 (4.6)	5.4 (4.2)	133	—	120–124	522(d)

[a] Measured in acetone solution (Ω^{-1} cm^2 mol^{-1}).
[b] Slope found for Onsager's equation $\Lambda_e = \Lambda_o - A\sqrt{c}$.
[c] Decomposes.
[d] Measured in nitromethane solution.

dinated Ph_3PS and a minor single signal at 44.0 ppm corresponding to uncoordinated Ph_3PS (Table 3).

For the $[Ir(COD)(Me_3PS)_2](ClO_4)$ complex the ^1H NMR spectrum in $CDCl_3$ indicated the stability of the complex in solution, showing single signals for coordinated COD at 4.10 ppm (CH=C) and 3.30 ppm (CH_2—C), together with the signal assigned to coordinated Me_3PS at 1.95 ppm with $^2J(P–H) = 13$ Hz, characteristic of this ligand, and downfield compared to the free ligand (Table 2).

The ^1H NMR spectrum of $[Ir(COD)(Me_3PS)(PPh_3)](ClO_4)$ in $CDCl_3$ shows the signal corresponding to PPh_3 at 7.80–7.30 ppm, those due to the coordinated COD, 4.22 ppm (CH=C) and 3.30 ppm (CH_2—C), characteristic of this type of complex and a doublet signal at 1.96 ppm [$^2J(P–H) = 11$ Hz] assigned to the coordinated Me_3PS ligand, in accordance with the stability of the complex in solution (Table 2).

Catalytic activity

During recent years a number of rhodium(I) and iridium(I) complexes have proved to be effective hydrogenation catalysts for multiple carbon–carbon bonds. Osborn *et al.* have studied the catalytic activity of cationic $[M(diolefin)L_2]^+$ species (M = Rh or Ir, L = PR_3) in coordinating solvents such as ethanol, acetone or tetrahydrofuran.[10,11,28,29] On the other hand, Crabtree *et al.* have shown that dichloromethane solutions of cationic diolefin iridium(I) complexes in the presence of an olefin constitute hydrogenation catalysts of unprecedented activity for iridium(I) complexes.[12,30] Oro *et al.* have studied the catalytic activity of different cationic rhodium(I) and iridium(I) complexes, $[M(diolefin)L_2]^+$, with different donor ligands and different diolefins.[31,32] The catalytic activities of complexes with sulfur ligands have not been studied. It is known that rhodium(III) complexes containing SEt_2 are active in homogeneous hydrogenation[33,34] and Maitlis *et al.* prepared some complexes with thioethers, but, when 2,5-dimethylthiophene or tetramethylthiophene were used as ligands, the isolated complexes were of type $[Rh(diolefin)(\eta^5\text{-}L)](PF_6)$. The latter complexes are the only ones studied showing catalytic activity for hydrogenation of olefins, but they rapidly deposited rhodium metal.[35] Simultaneously with this work, the catalytic activity of the related $[M(diolefin)L_2](ClO_4)$ and $[(diolefin)M(\mu\text{-}L)_2M(diolefin)](ClO_4)_2$ complexes (L = thioether or dithioether ligand) are being studied in our laboratory.

The $[Rh(diolefin)(Ph_3PS)_2](ClO_4)$ complexes (diolefin = COD or NBD) dissolve in ethanol at 25°C under 1 atm of hydrogen to give catalytically active solutions for the hydrogenation of 1-heptene. In the same way dichloromethane solutions of $[Ir(COD)(Ph_3PS)_2](ClO_4)$ containing 1-heptene react with hydrogen at atmospheric pressure to form species which catalyze the homogeneous hydrogenation of this substrate.

The molar catalyst : 1-heptene ratio was 1 : 100 and isomerization to *cis*-2-heptene was observed in all cases. The $[Rh(COD)(Ph_3PS)_2](ClO_4)$ complexes provide higher conversion rates of 1-heptene than the $[Rh(NBD)(Ph_3PS)_2](ClO_4)$ complex, probably due to the π-acceptor character[36] of NBD in comparison with 1,5-COD (Table 5).

It is noteworthy that in this type of complex the Ir(I) complex provides higher activities than the corresponding Rh(I) complexes (Table 5 and Fig. 1). Figure 1 shows a faster initial rate for the Ir(I) compound, probably due to the rapid formation of active species in this case. The reactivity of the complexes toward molecular hydrogen was studied by bubbling H_2 through solutions of the complexes, and no reaction was found for $[Rh(diolefin)(Ph_3PS)_2](ClO_4)$ complexes (1 atm, 25°C). In contrast, the $[Ir(COD)(Ph_3PS)_2](ClO_4)$ complex reacts rapidly with molecular hydrogen under the

Table 5. Hydrogenation of 1-heptene[a]

Catalyst precursor	Reaction time (min)	% heptane	% 1-heptene	% *cis*-2-heptene	Turnover rate (min^{-1})[b]
$[Rh(COD)(Ph_3PS)_2](ClO_4)$	500	54.2	35.7	10.1	0.90
$[Rh(NBD)(Ph_3PS)_2](ClO_4)$	450	19.7	67.1	13.2	0.15
$[Ir(COD)(Ph_3PS)_2](ClO_4)$	500	68.2	26.5	5.3	7.00

[a] Reaction conditions : [1-heptene] : [Rh] = 100 : 1, pH_2 = 1 atm, T^a = 25°C, solvent = 20 cm^3.

[b] Turnover rate is defined as the ratio of the number of moles of 1-heptene converted to the number of moles of species per time unit.

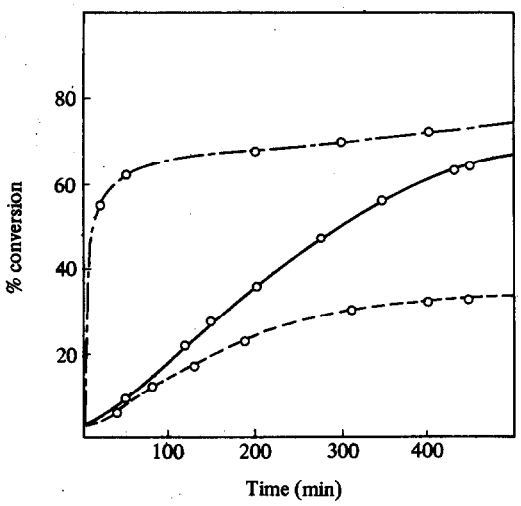

Fig. 1. Conversion of 1-heptene as function of the time catalyzed by $[Rh(COD)(Ph_3PS)_2](ClO_4)$ (O——O), $[Rh(NBD)(Ph_3PS)_2](ClO_4)$ (O---O) and $[Ir(COD)(Ph_3PS)_2](ClO_4)$ (O-·-·-O).

same conditions. The ^1H NMR spectra of $CDCl_3$ solutions show signals at -13 and -20 ppm characteristic of Ir—H protons, in accordance with the Ir(I) tendency to undergo oxidative addition.[5,12,26] This reactivity probably contributes to the easy formation of active hydride species.

EXPERIMENTAL

All preparations were carried out under a nitrogen atmosphere using Schlenk techniques. All the solvents were distilled and deoxygenated before use. The elemental analyses were carried out with a Perkin–Elmer 240 B microanalyzer. The IR spectra were recorded on a Beckman IR 4260 spectrophotometer, using Nujol mulls between polyethylene sheets. Conductivities were measured in acetone or nitromethane solutions in the concentration range *ca* 1×10^{-4}–5×10^{-4} M, with a Radiometer CDM 3 conductimeter. Values of A were determined from Onsager's equation $\Lambda_c = \Lambda_o - A\sqrt{c}$, using several concentrations in nitromethane solutions in the 10^{-3}–10^{-5} M range. The ^1H NMR and ^{31}P NMR spectra were measured on an XL-200 Varian spectrometer using $CDCl_3$ as solvent, and $SiMe_4$ and H_3PO_4 as references. Melting points were determined with a Buchi 510 Melting Point apparatus. The starting materials were prepared as previously reported.[17,18,24] $RhCl_3\cdot xH_2O$ was obtained from Johnson Matthey and phosphine sulphide ligands were purchased from Maybridge Co.

Catalytic activity experiments were performed in a conventional hydrogenation apparatus. The order of introduction of reactants into the hydrogenation flask was: 0.03 mmol of the catalyst precursor, 3 mmol of the substrate in 15 cm^3 of ethanol or dichloromethane, freshly distilled and dried, and finally hydrogen. The mixture was stirred in a thermostat bath at 25°C. The hydrogenation rate were determined by analyzing the products with a Hewlett–Packard 5840 A chromatograph. The peak areas were obtained with a Hewlett–Packard 5840A GC computing integrator.

Preparation of $[Rh(diolefin)L_2](ClO_4)$ (L = Ph_3PS, Me_3PS *or* Et_3PS) *and* $[(diolefin)Rh\{\mu\text{-}(L\text{–}L)\}_2Rh(diolefin)](ClO_4)_2$ [L–L = $Me_2P(S)(S)PMe_2$]

Upon addition of slightly more than the stoichiometric amount of ligand (0.18 mmol L, 0.09 mmol L–L) to dichloromethane solutions of $[Rh(COD)_2](ClO_4)$ or $[Rh(NBD)_2](ClO_4)$ (0.08 mmol) an immediate reaction was observed. The resulting complexes were precipitated by adding ether, and were filtered off, washed with ether and vacuum dried. Yields 85–90%.

Preparation of $[Ir(COD)L_2](ClO_4)$ (L = Ph_3PS *or* Me_3PS) *and* $[(COD)Ir\{\mu\text{-}(L\text{–}L)\}_2Ir(COD)](ClO_4)_2$ [L–L = $Me_2P(S)(S)PMe_2$]

The phosphine sulphide ligand (0.15 mmol L, 0.075 mmol L–L) was added to a dichloromethane solution of $[Ir(COD)_2](ClO_4)$ (0.07 mmol) and an immediate reaction was observed. Subsequent addition of ether precipitated out the complexes, which were filtered off, washed with cold ether, and vacuum dried. Yields 70–75%.

Preparation of $[M(diolefin)L(PPh_3)](ClO_4)$ *complexes* (M = Rh, diolefin = COD *or* NBD; M = Ir, diolefin = COD; L = Ph_3PS *or* Me_3PS)

The compounds were prepared by two routes as described below:

(i) The addition of a slight excess of ligand (0.065 mmol L) and a stoichiometric amount of PPh_3 (0.06 mmol) to dichloromethane solutions of $[M(diolefin)_2](ClO_4)$ (0.06 mmol) produced an immediate reaction. The resulting complex was precipitated out by adding ether and then filtered off, washed with ether, and vacuum dried. Yields *ca* 80%.

(ii) The addition of a stoichiometric amount of PPh_3 (0.06 mmol) to dichloromethane solutions of $[M(diolefin)L_2](ClO_4)$, previously prepared, produced an immediate reaction. The resulting complexes were precipitated by adding ether, and were filtered off, washed with ether, and vacuum dried. Yields 70–80%.

REFERENCES

1. A. Tiripicchio, M. Tiripicchio Camellini, C. Claver, A. Ruiz and L. A. Oro, *J. Organomet. Chem.* 1983, **241**, 77.
2. C. Claver, J. C. Rodriguez and A. Ruiz, *J. Organomet. Chem.* 1983, **251**, 369.
3. C. Claver, J. C. Rodriguez and A. Ruiz, *Transition Met. Chem.* 1984, **9**, 83.
4. A. Ruiz, C. Claver, J. C. Rodriguez, M. Aguiló, X. Solans and M. Font-Altaba, *J. Chem. Soc., Dalton Trans.* 1984, 2665.
5. J. C. Rodriguez, C. Claver and A. Ruiz, *J. Organomet. Chem.* 1985, **293**, 115.
6. J. C. Rodriguez, A. Ruiz and C. Claver, *Transition Met. Chem.* 1984, **9**, 237.
7. E. W. Ainscough, A. M. Brodie and E. Mentzer, *J. Chem. Soc., Dalton Trans.* 1973, 2167.
8. P. G. Eller and P. W. R. Lorfield, *J. Chem. Soc., Chem. Commun.* 1971, 105.
9. P. C. McMorran, M.Sc. thesis, University of Canterbury (1972).
10. R. R. Schrock and J. A. Osborn, *J. Am. Chem. Soc.* 1976, **98**, 2143.
11. R. R. Schrock and J. A. Osborn, *J. Am. Chem. Soc.* 1976, **98**, 4450.
12. R. H. Crabtree, *Acc. Chem. Res.* 1979, **12**, 331.
13. R. Uson, L. A. Oro and M. J. Fernandez, *J. Organomet. Chem.* 1980, **193**, 127.
14. Ph. Kalck, R. Poilblanc, R. P. Martin, A. Rovera and A. Gaset, *J. Organomet. Chem.* 1980, **195**, C9.
15. Ph. Kalck, J. M. Frances, P. M. Pfister, J. G. Southern and A. Thorez, *J. Chem. Soc., Chem. Commun.* 1983, 510.
16. J. M. Frances, A. Thorez and Ph. Kalck, *Nouv. J. Chim.* 1984, **8**, 213.
17. J. Chatt and L. M. Venanzi, *J. Chem. Soc.* 1957, 4735.
18. E. W. Abel, M. A. Bennett and C. Wilkinson, *J. Chem. Soc.* 1959, 3178.
19. R. D. Feltham and R. G. Hayter, *J. Chem. Soc.* 1964, 4587.
20. W. J. Geary, *Coord. Chem. Rev.* 1971, **7**, 81.
21. B. J. Hathaway and A. E. Underhill, *J. Chem. Soc.* 1961, 3091.
22. P. S. Pregosin and R. W. Kunz, *NMR Basic Principles and Progress*, Vol. 16, p. 110. Springer, Berlin (1979).
23. R. Uson, L. A. Oro, M. A. Ciriano, F. J. Lahoz and M. C. Bello, *J. Organomet. Chem.* 1982, **234**, 205.
24. G. Pannetier, R. Bonnaire, P. Fougeroux and P. Alepee, *J. Less-Common Met.* 1970, **21**, 105.
25. G. Winkhaus and H. Singer, *Chem. Ber.* 1966, **99**, 3610.
26. R. H. Crabtree, H. Felkin, T. Fillebeen-Khan and G. E. Morris, *J. Organomet. Chem.* 1979, **168**, 183.
27. R. H. Crabtree and G. E. Morris, *J. Organomet. Chem.* 1977, **135**, 395.
28. J. R. Shapley, R. R. Schrock and J. A. Osborn, *J. Am. Chem. Soc.* 1969, **91**, 2816.
29. R. R. Schrock and J. A. Osborn, *J. Am. Chem. Soc.* 1976, **98**, 4450.
30. R. H. Crabtree, H. Felkin and G. E. Morris, *J. Organomet. Chem.* 1977, **141**, 205.
31. R. Uson, L. A. Oro and M. J. Fernandez, *J. Organomet. Chem.* 1980, **193**, 127.
32. R. Uson, L. A. Oro, R. Sariego, M. Valderrama and C. Rebullida, *J. Organomet. Chem.* 1980, **197**, 87.
33. B. R. James and F. T. T. Ng, *J. Chem. Soc. A* 1972, 355.
34. B. R. James and F. T. T. Ng, *J. Chem. Soc. A* 1972, 1321.
35. M. J. H. Russell, C. White, A. Yates and P. M. Maitlis, *J. Chem. Soc., Dalton Trans.* 1978, 857.
36. K. Vrieze, H. C. Volger and A. P. Praat, *J. Organomet. Chem.* 1968, **14**, 185.

Polyhedron Vol. 6, No. 6, pp. 1337–1342, 1987
Printed in Great Britain

0277-5387/87 $3.00+.00

PREFERENTIAL SOLVATION AND ASSISTED SUBSTITUTION OF CHLOROPENTAAMMINECOBALT(III) ION IN WATER-DIMETHYL SULFOXIDE MEDIA

W. L. REYNOLDS*

Chemistry Department, University of Minnesota, Minneapolis, MN 55455, U.S.A.

and

MIRA GLAVAŠ **and** YU YUAN

Chemistry Department, University of Sarajevo, Sarajevo, Yugoslavia

(*Received* 21 *October* 1986; *accepted* 17 *November* 1986)

Abstract—The composition of the solvent cage of chloropentaamminechromium(III) ion was determined in water–dimethyl sulfoxide media using proton NMR line-broadening methods and the approach of Covington and coworkers. The number of solvent molecules in the solvent cage was found to be 10. The stepwise formation constants for the substitution of 10 water molecules by 10 dimethylsulfoxide molecules in this solvent cage were calculated. After the first such substitution each successive substitution becomes 1027 J mol^{-1} more difficult, exclusive of statistical factors, than the preceding substitution. The solvent cage composition was assumed to apply to the chloropentaamminecobalt(III) ion. Mercury(II)-assisted removal of chloride ion from the latter complex gave $[Co(NH_3)_5\{OSMe_2\}]^{3+}$/$[Co(NH_3)_5(H_2O)]^{3+}$ product ratios which did not correlate with either the solvent cage composition or the activity ratio of the two solvent components in the bulk phase of the solvent.

The solvent cage of a metal complex ML_p which has a well-defined first coordination shell of ligands L occupying p coordination sites, may be thought of as a more labile and less well-ordered second coordination shell around the ion. The number, n_o, of solvent molecules in, and the composition of, the solvent cage in binary solvent mixtures is known for a few complexes but this information is important in the interpretation of the properties and reactions of the complexes. The Covington[1] theory provides a means of determining n_o and the composition by treating the solvent cage as a coordination shell in which substitution of one solvent by a second occurs in a stepwise manner, as shown in reaction (1), with a stepwise formation constant given by eqn (2):

$$ML_p \cdot W_{n_o-i+1}D_{i-1} + D \overset{K_{iD}}{\rightleftharpoons} ML_p \cdot W_{n_o-i}D_i + W, \quad (1)$$

$$K_{iD} = \frac{[ML_p \cdot W_{n_o-i}D_i]a_W}{[ML_p \cdot W_{n_o-i+1}D_{i-1}]a_D}. \quad (2)$$

Reynolds *et al.*[2,3] have applied this theory to proton magnetic resonance line broadenings measured in water–dimethyl sulfoxide solutions of $[Cr(NH_3)_5\{OSMe_2\}]^{3+}$ and $[Cr(NH_3)_5(H_2O)]^{3+}$. For the former complex ion $n_o = 10$ and for the latter $n_o = 12$. Values of the stepwise constants for both complexes were also reported. The compositions of the solvent cages were quantiatively and simply related to the first-order rate constants

* Author to whom correspondence should be addressed.

for solvent interchange in reaction (3):

$$[Co(NH_3)_5(H_2O)]^{3+} + OSMe_2 \underset{k_w}{\overset{k_s}{\rightleftharpoons}} [Co(NH_3)_5\{OSMe_2\}]^{3+} + H_2O. \quad (3)$$

Frankel *et al.*[4] had previously shown that Cr(III) and Co(III) complexes with like first coordination shells had like solvent cages within experimental error.

Langford and coworkers[5-10] have determined compositions of solvent cages of a number of Cr(III) and Co(III) complexes by NMR techniques and found that frequently the solvent cages were considerably richer in one solvent component than was the solution as a whole. The term "preferential solvation" has been used in the literature to describe this situation; if no "preferential solvation" occurred the fraction of the solvent cage sites occupied by a solvent component would be the same as the mole fraction X_s of that component in the solution as a whole. It would be more accurate when ascertaining whether a solvent is preferentially solvating a complex to compare the ratio n_1/n_2, where n_1 is the number of solvent cages sites around a complex occupied by component 1 and n_2 is the number of these sites occupied by component 2, with the ratio a_1/a_2 of the activities of the two solvent components. When there are large deviations from Raoult's law it may be that:

$$\frac{a_1}{a_2} > \frac{n_1}{n_2} > \frac{X_1}{X_2}$$

or that

$$\frac{a_1}{a_2} < \frac{n_1}{n_2} < \frac{X_1}{X_2}.$$

In the former case the solvent cage is richer in component 1 than is the solution as a whole but not as rich as it should be given the high activity of 1 relative to 2; in this case it is incorrect to regard the complex as preferentially selecting component 1 to occupy solvent cage sites. In the second case the solvent cage is richer in component 2 than is the solution as a whole but not as rich as it should be given the high activity of 2 relative to 1; again it is incorrect to regard the complex as preferentially selecting component 2 for solvent cage sites. However there is frequently a lack of quantitative data concerning the activities of components in solvent mixtures and the only comparison which can be made is of n_1/n_2 with respect to X_1/X_2.

The water (W)–dimethyl sulfoxide (D) mixture exhibits very non-ideal behaviour. At $X_D \leqslant 0.3$ the activities, a_D, of dimethyl sulfoxide show large negative deviations from ideal behavior and $a_D/a_W < X_D/X_W$ but $n_D/n_W > X_D/X_W$ for the solvent cages of aquo- and (dimethyl sulfoxide)pentaamminechromium(III) ions. Also the mole ratio (n_D/n_W) remained greater than the activity ratio (a_D/a_W) up to $X_D = 0.9$. The complexes preferred dimethyl sulfoxide in the solvent cage and, in effect, extracted dimethyl sulfoxide from its low activity state in the bulk solvent phase into the solvent cage. This result is consistent with the view that a complex ion has a second coordination shell in which one ligand (dimethyl sulfoxide) can replace another ligand (water).

Here we report on the solvation number and the solvent cage composition of $Cr(NH_3)_5Cl^{2+}$ in water–dimethyl sulfoxide solvents and compare the results with the ratio of the products formed from the Hg^{2+}-assisted removal of Cl^- from $Co(NH_3)_5Cl^{2+}$ in the same media.

EXPERIMENTAL

Chemicals

Aquo-,[11] (dimethyl sulfoxide)-[12] and chloropentaamminecobalt(III)[13] perchlorates were prepared by literature methods. Chloro- and bromopentaamminechromium(III) dihalides were synthesized from $[Cr(NH_3)_5(OH_2)](NO_3)_3 \cdot NH_4NO_3$ by the method of Zinato *et al.*[14] The dihalides were converted to the perchlorates by precipitation from aqueous solution with concentrated $HClO_4$. All the other chemicals were reagent grade and were used as supplied.

Solvent cage studies

These studies were made as described in detail[3] previously only $[Cr(NH_3)_5Cl](ClO_4)_2$ and $[Cr(NH_3)_5Br](ClO_4)_2$ were used in place of the corresponding aquo and dimethyl sulfoxide complexes. Line widths were obtained by magnifying the lines many times on a screen and then measuring the screen image with a millimeter scale.

The viscosities of the solvent mixtures at 40°C were used to correct the measured line broadenings as previously described.[3] The viscosity-corrected increases in line width were then used to calculate the ratio n_i/n_o for solvent i from eqn (4):

$$\frac{n_i}{n_o} = \frac{\Delta\nu_i}{\Delta\nu_{oi}} \times \frac{N_i}{N_{oi}}. \quad (4)$$

In eqn (4) n_i is the number of molecules of solvent i in a total of n_o solvent molecules in a solvent cage, N_i and N_{oi} are the total number of molecules of the same solvent in the solvent mixture and in the

neat solvent, respectively, and $\Delta\nu_i$ and $\Delta\nu_{oi}$ are the proton line broadenings (corrected for viscosity effect) of solvent i in the mixture and in the neat solvent, respectively. The ratio n_i/n_o is the fraction of the solvent cage sites occupied by solvent i.

Kinetic studies

A known amount of the halo complex (usually 0.150 mmol) was dissolved in a predetermined volume of water–dimethyl sulfoxide solvent mixture of predetermined ionic strength thermostatted at a desired temperature. An excess of concentrated $Hg(ClO_4)_2$ was added quickly by syringe and the assisted removal of the halide ion allowed to go to completion. The reaction mixture was treated as described previously[15] and, as then, the reaction mixture was analysed sometimes by chromatographic separation of the aquo and dimethyl sulfoxide complexes, and sometimes by spectrophotometric methods. Only these two products were formed in the studies reported here.

RESULTS AND DISCUSSION

The solvent cage of $[Cr(NH_3)_5X]^{2+}$

The fractions of the solvent cage sites occupied by dimethyl sulfoxide (n_D/n_o) and water (n_W/n_o) were calculated from eqn (4) and are given in Table 1 along with the activities of dimethyl sulfoxide and water, the activity ratio $Y = a_D/a_W$, and the excess free energy of mixing (ΔG^E).

The enthalpies of mixing and the excess entropies of mixing water and dimethyl sulfoxide at 25 and 70°C measured by Kenttamaa and Lindberg[16] are nearly independent of temperature. Their averages were used to calculate values of ΔG^E at 40°C which were then fit to eqn (5) used by Scott *et al.*[17] by the method of least squares:

$$\Delta G^E = RTX_DX_W(\ln 10)[A + B(2X_D - 1) + C(2X_D - 1)^2] \quad (5)$$

The values of A–C determined from the least-squares fit were used to calculate ΔG^E values for the many solvent mixtures of interest; a few of these are listed in Table 1.

The activities of water and dimethyl sulfoxide at 0.001 mole fraction intervals were calculated from the excess free energies given by eqn (5) and the Duhem–Margules equation. The successive approximations to the correct activities of the two solvents at each mole fraction were repeated until the activities were constant to 16 significant figures to reduce accumulation of error. Previously[3] the successive approximations had been repeated until constancy to 10 significant figures had been achieved. Comparison of the Y values in Table 1 with those previously obtained[3] shows that, with the exception of $X_D = 0.1$, the activity ratios were changed by much less than 1% by the increased rigour of the calculations. It cannot be stressed too strongly that good values of this ratio are needed; Y varies by a factor (29.706/0.0176) = 1688 from $X_D = 0.1$ to $X_D = 0.9$ and, when $n_o = 10$, Y^{10} can range over a factor of 2×10^{32} and other powers of Y over a lesser, but still large, range. Poor Y values

Table 1. Values of the activities of dimethyl sulfoxide (a_D) and water (a_W), the activity ratio $Y = a_D/a_W$, the excess free energy of mixing (ΔG^E), the fractions of the solvent cage sites occupied by dimethyl sulfoxide (n_D/n_o) and water (n_D/n_o), and the stepwise formation constants for replacing water by dimethyl sulfoxide in the solvent cage of $Cr(NH_3)_5Cl^{2+}$

X_D[a]	a_D	a_W	Y	ΔG^E (cal)	n_D/n_o	n_W/n_o	K'[b]
0	0	1.0	0	0	0	1.0000	—
0.1	0.0154	0.8580	0.0176	−144.0	0.2234	0.8093	33.4477
0.2	0.0590	0.6791	0.0869	−232.9	0.3850	0.6193	29.1701
0.3	0.1395	0.5116	0.2726	−278.8	0.5356	0.5315	24.0084
0.4	0.2506	0.3740	0.6701	−291.9	0.6871	0.4236	24.8712_5
0.5	0.3784	0.2674	1.4149	−280.3	0.7883	0.2922	30.1622_5
0.6	0.5103	0.1857	2.7474	−250.3	0.8501	0.1972	33.9287
0.7	0.6401	0.1219	5.2516	−206.0	0.9404	0.1481	31.7129_5
0.8	0.7663	0.0707	10.840	−149.6	1.0345	0.0991	30.0375
0.9	0.8878	0.0299	29.706	−81.5	0.9682	0.0406	29.3718
1.0	1.0	0	—	0	1.0000	0	—

[a] Mole fraction of dimethyl sulfoxide based on solvents only.
[b] For $n_o = 10$, $k = 0.66092$.

would make it impossible to fit the experimental data with one value of K' in eqn (6) over the whole solvent composition range. In eqn (6) the powers of Y appear as coefficients in terms involving K', the first stepwise equilibrium constant for $i = 1$ in eqn (2) with the statistical factor removed, and k, a constant related to the incremental free energy increase in the stepwise substitutions. Equation (6) relates chemical-shift or line-broadening data to the solvent cage parameters n_o, K' and k. The final equation derived by Covington and Thain [eqn (6) in Ref. 1] contains a typographical error; the power of k should read $i(i-n)/2$, not $(i(i-1)/2)-((n-1)/2)$ (the expression given).[1] When the correct power of k is used the equation is readily converted to a more convenient form, namely:

$$\frac{\delta_j}{\delta_{oj}} = \frac{\sum_{i=1}^{n_o} \frac{(n_o-1)!}{(n_o-i)!(i-1)!} Y^i (K')^i k^{i(i-1)/2}}{1+\sum_{i=1}^{n_o} \frac{(n_o!}{(n_o-i)!i!} Y^i (K')^i k^{i(i-1)/2}}. \tag{6}$$

Here $\delta_j/\delta_{oj} = n_j/n_{oj}$ for solvent j.

The solvent cage parameters in eqn (6) are fitted to the n_j/n_{oj} ratios obtained from line-broadening data in the following manner. It is assumed that n_o, K' and k are constant over the whole range of solvent compositions. For a given solvent composition the value of Y is inserted into eqn (6) for (say) dimethyl sulfoxide and an equation of the form given in eqn (7a) is obtained:

$$\frac{n_D}{n_o} = \frac{A'}{B} \quad \text{or} \quad 1 = \frac{A}{B}, \tag{7a}$$

where $A = n_o A'/n_D$. For the other solvent component (say water) there is an analogous equation related to n_W/n_o and insertion of the Y value gives an equation of the form:

$$\frac{n_W}{n_o} = \frac{C'}{D} \quad \text{or} \quad 1 = \frac{C}{D}, \tag{7b}$$

where $C = n_o C'/n_W$. For a given value of n_o the denominators B and D are, and must be, equal. Therefore $A = C$ or, as given in eqn (8):

$$A - C = 0. \tag{8}$$

For a given n_o and solvent composition there are an infinite number of sets of (k, K') values which will satisfy eqn (8). Most of these sets do not remotely satisfy eqn (8) when applied to other compositions with other Y values; the large range in the values of the Y^i coefficients can rapidly make $A-C$ unequal to zero when the (k, K') set of values does not fit that solvent composition. One (k, K') set should fit eqn (8) for *all* solvent compositions. However, because of experimental error one (k, K') set will not be found which satisfies eqn (8) exactly for all solvent compositions. Instead a (k, K') set is found which will minimize the sum of the squared residuals given in eqn (9) for the solvent compositions studied:

$$\sum (A_i - C_i)^2 = \sum \rho_i^2. \tag{9}$$

The smallest sum indicates the best fit of the parameters (k, K') for the assumed n_o. The process is repeated for other n_o values until the best set of (n_o, k, K') values giving the best fit is found.

For 40°C, the ambient temperature at which the NMR spectra were taken, the best set of values was:

$$n_o = 10, \; k = 0.66092, \; K' = 29.8931.$$

When $k = 0.66092$ was used in eqn (8) for $n_o = 10$ and eqn (8) solved for the value of K' for each of nine solutions the K' values given in Table 1 were obtained. The average value of K' and the standard deviation for determination of K' from a single solution are 29.6 ± 3.4. Thus the standard deviation in the solvent range $0.1 \leqslant X_D \leqslant 0.9$ is 11.5%, which is very good considering the very large range covered by the coefficients of k and K' in eqn (6). From Table 1 it is seen that there is no trend in the K' values with change of solvent composition; this result supports the assumption that n_o and k do not change significantly over the solvent range studied.

It can also be seen from Table 1 that the sum of n_D/n_o and n_W/n_o is unity or slightly greater, but does not indicate any significant trend. This result supports the assumption that n_o is constant over the solvent range studied. The tendency for the sum to be somewhat greater than unity may result from the viscosity corrections but the deviation is not serious.

The k and K' values obtained can be used[1] to give the stepwise equilibrium constants defined in eqn (2). For dimethyl sulfoxide replacing water these are: $K_{D1} = 296$, $K_{D2} = 88.1$, $K_{D3} = 34.5$, $K_{D4} = 15.0$, $K_{D5} = 6.79$, $K_{D6} = 3.11$, $K_{D7} = 1.4$, $K_{D8} = 0.612$, $K_{D9} = 0.240$, and $K_{D10} = 0.0713$.

The value $k = 0.66092$ means that on average it becomes more difficult by 1027 J mol^{-1} to replace a water molecule by a dimethyl sulfoxide molecule after each such substitution occurs.

It is seen from Table 1 that at $X_D = 0.1(n_D/n_W) > (X_D/X_W) > (a_D/a_W)$. Because $a_D \ll X_D$ the dimethyl sulfoxide appears to be bonded in the bulk solvent phase in a manner that greatly lowers its activity from that expected on the basis of ideal behavior. Despite this decrease in a_D the mole ratio n_D/n_W for the solvent cage is considerably greater than X_D/X_W

and much greater then a_D/a_W. We can conclude that $Cr(NH_3)_5Cl^{2+}$ is strongly preferentially solvated by dimethyl sulfoxide. The data of Table 1 show that n_D/n_W remains greater than a_D/a_W up to approximately $X_D = 0.8$ and that thereafter the ratio of the solvents in the solvent cage approximately parallels the activity ratio of the solvent in the bulk phase.

A few line-broadening measurements for $Cr(NH_3)_5Br^{2+}$ at $X_D = 0.20$, 0.50 and 0.80 showed that this complex closely paralleled the chloro complex in the composition of the solvent cage. The studies were discontinued and it was concluded that dimethyl sulfoxide preferentially solvated this complex also at $X_D \leqslant 0.5$.

The composition of the solvent cage of the chloro complex can be related to the solvent composition X_D by the following equation:

$$\frac{n_D}{n_o} = \sum_{i=0}^{8} C_i X_D^i,$$

where $C_0 = -8.7646 \times 10^{-6}$, $C_1 = 1.79640$, $C_2 = 17.3356$, $C_3 = -209.2838$, $C_4 = 1021.5398$, $C_5 = -2563.0867$, $C_6 = 3451.8270$, $C_7 = -2368.6495$, and $C_8 = 649.5212$. We are not aware that other equations exist in the literature giving the composition of a solvent cage in terms of mole fractions of solvents.

Hg^{2+}-assisted substitution of $Cr(NH_3)_5X^{2+}$ in water–dimethyl sulfoxide solutions

The Hg^{2+}-assisted release of X^- ($X^- = Cl^-$ or Br^-) from the first coordination shell of $Co(NH_3)_5X^{2+}$ in water–dimethyl sulfoxide solutions leads to formation of $Co(NH_3)_5S^{3+}$ (S = water or dimethyl sulfoxide) as in reaction (10):

$$Co(NH_3)_5X^{2+} + Hg^{2+} + S \rightarrow Co(NH_3)_5S^{3+} + HgX^+. \quad (10)$$

It was of interest in the mechanism of substitution of S for X^- to determine whether the product ratio $[Co(NH_3)_5\{OSMe_2\}^{3+}]/[Co(NH_3)_5(H_2O)]^{3+}$ formed was the same as the n_D/n_W ratio in the solvent cage around the reactant halo complexes. [It was assumed that the $Cr(NH_3)_5X^{2+}$ and $Co(NH_3)_5X^{2+}$ complexes have very similar solvent cages.] In the solvent interchange reaction (3) it has been found[3] that k_S is strictly second-order in n_D/n_o, and that k_W is strictly first-order in n_W/n_o where n_D/n_o and n_W/n_o were for the aquo- and (dimethyl sulfoxide)pentaamminechromium(III) complexes, respectively. This finding strongly supports the I_d mechanism[18] which has previously been assigned to the unassisted thermal substitution reactions of pentaamminecobalt(III) complexes. The mechanism of the assisted substitution reactions of these complexes is less certain and a comparison of the product ratios with solvent cage compositions is desirable.

Table 2. Percentages of $[Co(NH_3)_5OSMe_2]^{3+}$ (p_D) and $[Co(NH_3)_5(H_2O)]^{3+}$ (p_W) formed in the Hg^{2+}-assisted removal of Cl^- and Br^- from $Co(NH_3)_5X^{2+}$ in water–dimethyl sulfoxide solutions as functions of the mole fraction (X_D) of dimethyl sulfoxide: 20.0°C < t < 60.0°C

X^-	X_D	p_D	p_W	p_D/p_W	n_D/n_W
Cl^-	0.1	9.3±0.4	89.6±0.7	0.104	0.276
	0.2	14.3±0.3	84.3±0.6	0.169	0.622
	0.3	19.5±0.8	78.7±0.8	0.247	1.01
	0.4	28.8±0.6	69.3±0.7	0.416	1.62
	0.5	34.5±0.8	64.0±0.7	0.540	2.70
	0.6	41.8±0.7	56.0±0.9	0.739	4.31
	0.7	49.6±0.7	48.8±0.6	1.02	6.35
	0.8	56.7±0.8	42.0±1.1	1.36	10.4
	0.9	64.5±0.5	33.8±0.5	1.91	23.8
Br^-	0.1	9.6±0.4	88.4±1.1	0.108	
	0.2	20.6±0.6	78.0±1.2	0.265	
	0.3	30.5±0.8	67.8±0.5	0.450	
	0.4	39.9±0.8	58.6±0.9	0.680	
	0.5	50.0±1.1	49.0±1.1	1.02	
	0.6	60.0±0.9	38.7±0.7	1.55	
	0.7	69.0±0.8	29.0±0.9	2.34	
	0.8	79.0±0.7	20.0±0.7	3.93	
	0.9	87.7±0.8	10.6±0.6	8.24	

The percentages of the dimethyl sulfoxide (p_D) and aquo (p_W) complexes formed in reaction (10) are given in Table 2 for 20, 40 and 60°C for the solvent range $0.1 \leqslant X_D \leqslant 0.9$ for $X^- = Cl^-$ or Br^-. The percentages listed in Table 2 were determined 4 times each at each of the three temperatures at each solvent composition. The percentage of each product at each solvent composition remained the same within the experimental error of less than 3% in the 20–60°C temperature range so that only the average and the standard deviation for a single determination are listed.

When the values of the product ratio p_D/p_W for Cl^- in Table 2 are compared with the solvent cage ratios (n_D/n_W) in the last column of Table 2 it is readily seen that the composition of the solvent cage of $Co(NH_3)_5Cl^{2+}$ does not determine the product ratio of reaction (10). Likewise when the product ratios for Cl^- are compared with the corresponding Y values in Table 1 it is readily seen that the solvent activity ratio does not determine the product ratio. A possible explanation of these results is that formation of a dinuclear complex such as $(NH_3)_5Co\,ClHg^{4+}$ prior to the rate-determining loss of Cl^-

very markedly changes the composition of the solvent cage or at least makes water more available near the departing $HgCl^+$ group. It is very unlikely that the five-coordinate intermediate $Co(NH_3)_5^{3+}$ was formed in the major pathway of reaction (10). Firstly, if it were formed and if it reacted in a first-order step with the solvent in its solvent cage then the product ratio p_D/p_W values would be expected to parallel the n_D/n_W values. This is because the chloro-, bromo-, aquo- and (dimethyl sulfoxide) pentaamminechromium(III) complexes are all strongly preferentially solvated by dimethyl sulfoxide, and it seems likely that the five-coordinate pentaammine complex would be also if it existed.

Secondly, if $Co(NH_3)_5^{3+}$ were formed as an intermediate which reacted in a second-order (but pseudo first-order) step with the bulk solvent components then the p_D/p_W values would be expected to parallel the Y values. This is because the rate of formation of the dimethyl sulfoxide product would be proportional to the product $a_{Co(NH_3)_5^{3+}} \times a_D$, the rate of formation of the aquo product would be proportional to the product $a_{Co(NH_3)_5^{3+}} \times a_W$, and the product ratio would be approximately proportional to a_D/a_W. But this proportionality was not observed.

Likewise the product ratios for Br^- in Table 2 show that they are not determined by n_D/n_W or a_D/a_W. Again these results are readily explained by a dinuclear complex as in the case of Cl^- but not by the formation of the five-coordinate intermediate $Co(NH_3)_5^{3+}$.

It is concluded that the results of the product ratio and solvent cage studies furnish rather strong evidence against the formation of $Co(NH_3)_5^{3+}$ as an intermediate with a lifetime sufficiently long to equilibrate its solvent cage and to undergo diffusional collisions with the major solvent components in a major pathway in reaction (10).

REFERENCES

1. A. K. Covington and J. M. Thain, *J. Chem. Soc., Faraday Trans.* 1 1974, **70**, 1879 (and earlier papers referred to therein).
2. W. L. Reynolds, L. Reichley-Yinger and Yu Yuan, *J. Chem. Soc., Chem. Commun.* 1985, 526.
3. W. L. Reynolds, L. Reichley-Yinger and Yu Yuan, *Inorg. Chem.* 1985, **24**, 4273.
4. L. S. Frankel, C. H. Langford and T. R. Stengle, *J. Phys. Chem.* 1970, **74**, 1376.
5. L. S. Frankel, T. R. Stengle and C. H. Langford, *J. Chem. Soc., Chem. Commun.* 1965, 393.
6. C. H. langford and J. F. White, *Can. J. Chem.* 1967, **45**, 3049.
7. V. S. Sastri, R. W. Henwood, S. Behrendt and C. H. Langford, *J. Am. Chem. Soc.* 1972, **94**, 753.
8. S. Behrendt, C. H. Langford and L. S. Frankel, *J. Am. Chem. Soc.* 1969, **91**, 2236.
9. V. S. Sastri and C. H. Langford, *J. Phys. Chem.* 1970, **74**, 3945.
10. C. H. Langford, R. Scharfe and R. Jackson, *Inorg. Nucl. Chem. Lett.* 1973, **9**, 1033.
11. E. S. Gould and H. Taube, *J. Am. Chem. Soc.* 1964, **86**, 1318.
12. C. R. P. Mac-Coll and L. Beyer, *Inorg. Chem.* 1973, **12**, 7.
13. G. G. Schlessinger, *Inorg. Synth.* 1967, **9**, 160.
14. E. Zinato, R. Lindholm and A. W. Adamson, *J. Inorg. Nucl. Chem.* 1969, **31**, 451.
15. W. L. Reynolds, M. Glavaš and E. Dželilović, *Inorg. Chem.* 1982, **22**, 1946.
16. J. Kenttamaa and J. J. Lindberg, *Suom. Kemi. B*, 1960, **33**, 98.
17. L. P. Scott, T. J. Weeks, Jr, D. E. Bracken and E. L. King, *J. Am. Chem. Soc.* 1969, **91**, 5219.
18. C. H. Langford and H. B. Gray, *Ligand Substitution Processes*. Benjamin Press, New York (1965).

Polyhedron Vol. 6, No. 6, pp. 1343–1345, 1987
Printed in Great Britain

0277–5387/87 $3.00+.00

SYNTHESIS OF Co(III) MOLYBDOHETEROPOLYANIONS USING CARBONATO-AMMINE Co(III) COMPLEXES AS STARTING MATERIALS

KENJI NOMIYA, MINORU WADA, HIROYUKI MURASAKI and MAKOTO MIWA*

Department of Industrial Chemistry, Faculty of Engineering, Seikei University, Musashino, Tokyo 180, Japan

(*Received* 8 *September* 1986; *accepted* 19 *November* 1986)

Abstract—The preparation of two cobalt(III) molybdoheteropolyanions, $[CoMo_6O_{24}H_6]^{3-}$ and $[Co_2Mo_{10}O_{38}H_4]^{6-}$, was systematically studied using some carbonato-ammine cobalt(III) complexes as starting materials. The selectivity and yields of products were significantly influenced by the number of ammine ligands and the charge on the complexes.

Two molybdoheteropolyanions containing a Co(III) ion as the heteroatom, Anderson-type $[CoMo_6O_{24}H_6]^{3-}$ and Evans-Showell-type $[Co_2MO_{10}O_{38}H_4]^{6-}$ polyanions, are well-known.[1] The former, with D_{3d}-symmetry, has also been called a 1:6 salt and the Co(III) ion is located in an octahedral cavity of a crown of six MoO_6 octahedra formed by edge sharing.[2] The latter, with D_2-symmetry, has appeared as a by-product in the preparation of the former and has the dimeric nature of the former.[3] Polyhedral models of them are shown in Fig. 1. These compounds have been directly prepared from reaction of a boiling solution of ammonium heptamolybdate with an aqueous mixture of the Co(II) salt and hydrogen peroxide (the direct method).[4] On the other hand, there are only a few examples of the preparation of such polyanions using Co(III) complexes as a source of the heteroatom. For instance, there are the preparation from $[CoCO_3(NH_3)_4]^+$ reported by Baker *et al.*[5] and Shibata's method using a cold green solution containing the $[Co(CO_3)_3]^{3-}$ complex.[6] We have been interested in the preparation of heteropoly compounds using a transition-metal complex as the starting material.[7] In this work, we have systematically studied the preparation of two Co(III) molybdoheteropolyanions from carbonato-ammine Co(III) complexes such as $[CoCO_3(NH_3)_4]^+$ (**1**), $[CoCO_3(NH_3)_5]^+$ (**2**) and $[Co(CO_3)_2(NH_3)_2]^-$ (**3**), and compared them with the results by the direct method and Shibata's method.

RESULTS AND DISCUSSION

The yields of the two heteropolymolybdates by the preparations studied are shown in Table 1. From complex **2** with five ammine ligands, neither of the two polymolybdates are obtained. In this case, pink undissolved precipitates only are produced, which are probably due to an adduct between the complex cation and the heptamolybdate anion. On the other hand, from complex **1** with four ammines two polymolybdates are obtained with higher yields than by the direct method. Moreover, by prolonging the boiling after the addition of the complex solution to the boiled solution of heptamolybdate, only an Evans–Showell-type molybdate can be isolated.

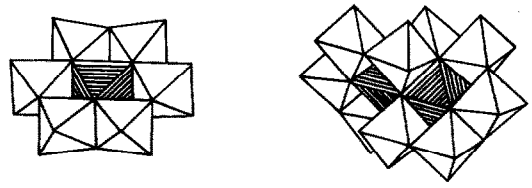

Fig. 1. Polyhedral models of Anderson- (left) and Evans–Showell-type (right) heteropolyanions. Striped octahedra represent the Co(III) ion as a heteroatom.

* Author to whom correspondence should be addressed.

Table 1. Yields of two Co(III) heteropolymolybdates

Starting materials	Yields (%)[a] Anderson-type	Evans–Showell-type
$[CoCO_3(NH_3)_4]^+$ (1)	16.8[b]	Trace[b]
	Trace[c]	42.4[c]
$[CoCO_3(NH_3)_5]^+$ (2)	—	—
$[Co(CO_3)_2(NH_3)_2]^-$ (3)	—	20.8
$CoSO_4 \cdot 7H_2O + 30\%\ H_2O_2$[d]	14.4	11.8
$[Co(CO_3)_3]^{3-}$[e]	33.5	17.2

[a] Yields with respect to the molar number of starting Co(III) ion.

[b] The boiling time after the final drop was less than 2 min.

[c] The boiling time was more than 20 min.

[d] The direct method.

[e] Shibata's method.

These facts imply that carbonato-ammine complexes containing a lower number of ammine ligands are more reactive. In fact, complex **3** with two ammines produces only an Evans–Showell-type molybdate in a very short reaction time. An Anderson-type molybdate is not obtained from complex **3** even if the solution of heptamolybdate is mildly heated. Shibata's method is a preparation using a tricarbonato Co(III) complex without an ammine ligand. As a matter of fact, this complex is so active and unstable even at room temperature that the starting solution should be ice-cooled. The preparation from complex **1** takes a relatively long time. It is likely that the decomposition of an adduct between a complex cation and the heptamolybdate anion takes extra time.

From a synthetic point of view, it should be noted that yields and selectivity of desired heteropoly compounds can be changed by choosing the ligand in the starting complex.

EXPERIMENTAL

Electronic absorption and IR spectra were recorded with a Hitachi 340 spectrophotometer and a JASCO IR-G spectrophotometer, respectively.

Matrials

The starting complexes $[CoCO_3(NH_3)_4]NO_3 \cdot \frac{1}{2}H_2O$ (**1**), $[CoCO_3(NH_3)_5]NO_3 \cdot \frac{1}{2}H_2O$ (**2**) and $K[Co(CO_3)_2(NH_3)_2] \cdot 3H_2O$ (**3**) were prepared according to the literature, and identified by IR and absorption spectra.[6,8,9] All reagents were of analytical grade.

Preparations

An aqueous solution of complex **1** (6 g, 0.023 mol in 1000 cm^3 of water) was added through a dropping funnel into a boiling solution of ammonium heptamolybdate (28.8 g, 0.023 mol in 200 cm^3 of water). The dropping rate was balanced between the loss of water by evaporation and addition from the funnel. If the dropping rate was fast, reddish precipitates were formed and the reaction was inhibited. The colour of the solution became purple via reddish purple during the first 30 min of dropping and deep green until after 1 h of dropping. The whole addition took about 5 h. After the final drop, the solution was boiled further for a few minutes. Insoluble material was filtered and solid ammonium chloride (3.7 g) was added to the filtrate. On standing the solution overnight at room temperature, bluish green crystals of the Anderson-type heteropolymolybdate $(NH_4)_3[CoMo_6O_{24}H_6] \cdot 7H_2O$ were deposited. From the filtrate, dark olive green crystals of an Evans–Showell-type polymolybdate, $(NH_4)_6\ [Co_2Mo_{10}O_{38}H_4] \cdot 7H_2O$, were obtained. The two polymolybdates were recrystallized twice from water.

The boiling time after the final drop in the above procedure significantly influenced the yields of the two polymolybdates. When the boiling time was prolonged, the yield of the Anderson-type molybdate was lowered and that of the Evans–Showell-type molybdate was raised. From the solution boiled for more than 20 min, only the Evans–Showell-type molybdate was formed.

The two polymolybdates were characterized by IR and electronic absorption spectra.[10–13] The first and second *d–d* absorption bands of the Anderson-type molybdate were measured at 16,500 ($\varepsilon = 18.9$) and 24,300 cm^{-1} ($\varepsilon = 19.4$), respectively. The first *d–d* absorption band of the Evans–Showell-type molybdate was observed at 16,600 cm^{-1} ($\varepsilon = 89.1$). IR bands were measured at 937(s), 920(m), 880(vs), 830(sh), 680(sh), 665(sh), 640(vs), 580(m), 550(br m) and 445(m) cm^{-1} for the Anderson-type molybdate, and at 940(vs), 900(vs), 850(s), 735(sh), 675(s), 665(s), 650(s), 620(m), 600(vs), 560–550(br) and 520(m) cm^{-1} for the Evans–Showell-type compound.

From an aqueous solution of complex **2**, only a pink undissolved solid was produced and neither of the desired polymolybdates were obtained. IR spectra suggested that the pink solid was an adduct of a complex cation with the heptemolybdate anion.

From a dark blue solution of complex **3**, only the Evans–Showell-type polymolybdate was obtained. An aqueous solution of complex **3** (3.14 g, 0.01 mol in 100 cm^3 of water) was added dropwise to a boiling solution of ammonium heptamolybdate (12.6 g, 0.01 mol in 100 cm^3 of water). On dropping, it became effervescent and the dark blue of the complex solution changed to green. The reaction was over within 30 min. The resulting solution was evaporated to a volume of about 30 cm^3 on a steam bath and insoluble material was filtered. By cooling the filtrate to room temperature, dark olive green crystals were produced.

The direct method. An aqueous mixture of $CoSO_4 \cdot 7H_2O$ (4.2 g, 0.015 mol in 30 cm^3 of water) and 30% hydrogen peroxide (2 cm^3) was added to a boiling solution of ammonium heptamolybdate (30.9 g, 0.025 mol in 260 cm^3 of water). The hot solution was filtered once and cooled to room temperature. Bluish green crystals were deposited in the solution. By evaporating the filtrate on a steam bath, dark olive green crystals were obtained.

Shibata's method.[6] A cold mixture of an aqueous solution (4 cm^3) containing $CoCl_2 \cdot 6H_2O$ (6 g, 0.025 mol) and 30% hydrogen peroxide (9 cm^3) was added dropwise to an ice-cooled slurry of potassium hydrogen carbonate (18 g, 0.18 mol in 18 cm^3 of water), and the resulting green solution was filtered quickly. The filtrate was again cooled in an ice bath and used as a starting solution.

The starting solution was added dropwise to an aqueous solution of ammonium heptamolybdate (60 g, 0.049 mol in 200 cm^3 of water) with stirring at room temperature. The resulting mixture was further stirred for 2 h. Bluish green crystals of the Anderson-type molybdate were produced and recrystallized twice from water. To the filtrate the starting solution was added, the pH of the solution was quickly adjusted to 4 with glacial acetic acid, and the solution was stirred for 1 h. After filtration, the dark green filtrate was concentrated to half volume at 60–65°C. On standing at room temperature, the Anderson-type molybdate as a by-product was removed and ammonium chloride (5 g) was added to the filtrate. Dark olive green crystals were produced and recrystallized twice from water.

REFERENCES

1. M. T. Pope, *Heteropoly and Isopoly Oxometalates*, p. 81. Springer, New York (1983).
2. A. Perloff, *Inorg. Chem.* 1970, **9**, 2228.
3. H. T. Evans, Jr and J. S. Showell, *J. Am. Chem. Soc.* 1969, **91**, 6881.
4. R. D. Hall, *J. Am. Chem. Soc.* 1907, **29**, 692.
5. L. C. W. Baker, B. Loev and T. P. McCutcheon, *J. Am. Chem. Soc.* 1950, **72**, 2374.
6. M. Shibata, *Nippon Kagaku Zasshi* 1966, **87**, 771.
7. K. Nomiya, M. Wada, H. Murasaki and M. Miwa, 52nd National Meeting of Chemical Society of Japan, Kyoto, April 1986, Abstract No. 3K36.
8. G. Schlessinger, *Inorg. Synth.* 1960, **6**, 173.
9. F. Basolo and R. K. Murmann, *Inorg. Synth.* 1953, **4**, 171.
10. Y. Shimura, H. Ito and R. Tsuchida, *Nippon Kagaku Zasshi* 1954, **75**, 560.
11. T. Ama, J. Hidaka and Y. Shimura, *Bull. Chem. Soc. Jpn* 1970, **43**, 2654.
12. K. Nomiya, R. Kobayashi and M. Miwa, *Polyhedron* 1985, **4**, 149.
13. K. Nomiya, T. Takahashi, T. Shirai and M. Miwa, *Polyhedron* 1987, **6**, 213.

Polyhedron Vol. 6, No. 6, pp. 1347–1350, 1987
Printed in Great Britain

0277–5387/87 $3.00+.00

SYNTHESES OF (IMIDAZOLE)PENTAAMMINEMETAL(III) AND μ-IMIDAZOLATODECAAMMINEDIMETAL(III) COMPLEXES FROM TRIFLUOROMETHANESULFONATO PRECURSORS

PAUL V. BERNHARDT and GEOFFREY A. LAWRANCE*

Department of Chemistry, The University of Newcastle, N.S.W. 2308, Australia

and

NEVILLE J. CURTIS

Propulsion and Ballistics Division, Weapons Systems Research Laboratory, Defence Science and Technology Organization, GPO Box 2151, Adelaide 5001, Australia

(*Received* 5 *November* 1986; *accepted* 28 *November* 1986)

Abstract—The $[M(NH_3)_5(imidH)]^{3+}$ complex ions (M = Co, Rh or Ir; imidH = imidazole) can be readily prepared by reaction of $[M(NH_3)_5(OSO_2CF_3)]^{2+}$ ions with imidazole in sulfolane. Subsequent reaction of $[M'(NH_3)_5(OSO_2CF_3)]^{2+}$ with $[M(NH_3)_5(imidH)]^{3+}$ in sulfolane in the presence of a non-coordinating base permits synthesis of the binuclear imidazolate-bridged complexes $[(NH_3)_5M(imid)M'(NH_3)_5]^{5+}$ (M = M′ = Co or Rh; M = Co, M′ = Rh), characterized by spectroscopic, chromatographic and voltammetric methods, and by reactivity.

Imidazole is a biologically important heterocycle which is known as the anion to bridge Cu(II) and Zn(II) in bovine erythrocyte superoxide dismutase,[1] for example. Bridging through the two equivalent heteroatoms in the anion has also been achieved in several model complexes.[2] Crystal structure analysis has defined a "bent" geometry (**I**) in the dimers.[3] Imidazole, as a neutral molecule, is also well known as a monodentate ligand (**II**).

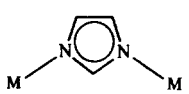

I

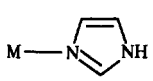

II

The simple (imidazole)pentaammines of the inert metal ions Co(III), Cr(III) and Ru(III), as well as impure Rh(III) and Ir(III) species, are now known.[4–6] We have found that all of the triad $[M(NH_3)_5(imidH)]^{3+}$ (M = Co, Rh or Ir; imidH = imidazole) can be prepared simply and in high purity from the $[M(NH_3)_5(OSO_2CF_3)]^{2+}$ ions by displacing the labile $CF_3SO_3^-$ group by imidazole. Further, these labile precursors have permitted us to explore the synthesis of the dimers $[(NH_3)_5M(imid)M'(NH_3)_5]^{5+}$ by reaction of $[M(NH_3)_5(imid)]^{2+}$ with $[M'(NH_3)_5(OSO_2CF_3)]^{2+}$, and the results of these investigations are reported herein. Routes to the simple decaamminedimetal(III) species have not been explored much previously. During the course of this work, synthesis of the dicobalt(III) dimer was reported.[7] However, the reaction conditions employed led also to the formation of a trinuclear complex with two bridging imidazolates and to the hexaamminecobalt(III) ion. The different conditions reported here appear to permit synthesis without ligand rearrangement, and can be extended to permit formation of a range of dimetal and mixed-metal compounds.

* Author to whom correspondence should be addressed.

EXPERIMENTAL

Syntheses

$[Ir(NH_3)_5(imidH)](ClO_4)_3 \cdot H_2O$. A solution of $[Ir(NH_3)_5(OSO_2CF_3)](CF_3SO_3)_2$[8] (3.0 g) and imidazole (1.5 g) in dry sulfolane (20 cm^3) was heated at 90°C for 4 h. The colourless solution was cooled and washed into a flask with ~ 20 cm^3 of ethanol. Slow addition of diethyl ether (~ 900 cm^3), with stirring, produced a precipitate which was collected and dried. The product was dissolved in 10 cm^3 of water at ~ 40°C, filtered, and a solution of 5 g of $LiClO_4$ in 10 cm^3 of ethanol added. A precipitate began to form near the end of the addition. After refrigeration overnight the product was collected, washed with 1 : 1 ethanol–water (2 × 20 cm^3) and ether (20 cm^3), and dried *in vacuo* (2.0 g, 75%). Found: C, 5.2; H, 3.3; N, 14.6; S, 0.0. Calc. for $C_3H_{21}Cl_3IrN_7O_{13}$: C, 5.5; H, 3.2; N, 14.8; S, 0.0%.

$[Rh(NH_3)_5(imidH)](ClO_4)_3$. A solution of $[Rh(NH_3)_5(OSO_2CF_3)](CF_3SO_3)_2$[8] (5.0 g) and imidazole (2.5 g) in dry sulfolane (50 cm^3) was heated at 80°C for 2 h. The solution was cooled and washed into a flask with ethanol (50 cm^3), from which a white precipitate was isolated following ether addition (~ 900 cm^3) with stirring. The product was dissolved in water (20 cm^3), filtered, warmed to ~ 40°C and a solution of 10 g of $LiClO_4$ in 20 cm^3 of ethanol added slowly. The absence of any initial precipitate when commencing $LiClO_4$ addition indicates the absence of any hexaamminerhodium(III), which is very insoluble as a perchlorate salt. The solution was refrigerated overnight, and the white powder collected, washed with 1 : 1 ethanol–ether (2 × 20 cm^3), then ether (20 cm^3), and dried *in vacuo* (3.25 g, 75%). Found: C, 6.6; H, 3.6; N, 17.3. Calc. for $C_3H_{19}Cl_3N_7O_{13}Rh$: C, 6.5; H, 3.6; N, 17.7%.

$[Co(NH_3)_5(imidH)](ClO_4)_3$. This compound was prepared from $(Co(NH_3)_5(OSO_2CF_3)](CF_3SO_3)_2$ and imidazole in sulfolane essentially as described for the rhodium analogue above. This complex has been reported before.[4]

$\{[Co(NH_3)_5]_2(imid)\}(ClO_4)_5 \cdot 3H_2O$. A solution of $[Co(NH_3)_5(imidH)](ClO_4)_3$ (1.02 g) and $[Co(NH_3)_5(OSO_2CF_3)](CF_3SO_3)_2$[8] (1.18 g) in 20 cm^3 of dry sulfolane was treated with triethylamine (0.5 g), and stirred at 80°C for 1 h. After cooling, the reaction mixture was treated with ethanol (100 cm^3) and ether (200 cm^3) to precipitate a brown solid. This was dissolved in water (20 cm^3) and $NaClO_4$ (2.5 g) added. On standing in a refrigerator for 2 days, an orange powder was obtained (0.4 g, 25%). Found: C, 3.8; H, 4.1; N, 18.3; Cl, 19.3. Calc. for $C_3H_{39}Cl_5Co_2N_{12}O_{23}$: C, 4.0; H, 4.4; N, 18.6; Cl, 19.6%. The reaction mixture may also be chromatographed on Dowex 50W × 2 H^+-form resin. Dilution of the reaction mixture with water (~ 500 cm^3) prior to loading onto the column was required. Elution with 1.0 and 3.0 M HCl removed chloro- and imidazolepentaammine monomers, with the orange dimer being removed with 5.0 M HCl. Evaporation under reduced pressure to ~ 20 cm^3, followed by ethanol addition (~ 50 cm^3), precipitated a brown-orange product (0.7 g, 65%) which can be recrystallized as the perchlorate salt as described above. Electronic spectrum (water), λ_{max} (nm) [ε_{max} (M^{-1} cm^{-1})]: 475 (157), 335 (220).

$[(NH_3)_5Co(imid)Rh(NH_3)_5](ClO_4)_5 \cdot 3H_2O$. A solution of $[Rh(NH_3)_5(imidH)](ClO_4)_3$ (1.1 g) and $[Co(NH_3)_5(OSO_2CF_3)](CF_3SO_3)_2$[8] (1.2 g) in 20 cm^3 of dry sulfonate was treated with triethylamine (0.5 cm^3), and stirred at 80°C for 3 h. The solution was cooled, 1 g of $LiClO_4$ was added, followed by ethanol (~ 100 cm^3). Refrigeration overnight separated an oil. The solvent was decanted, and the oil dissolved in water (25 cm^3), with warming. A solution of $LiClO_4$ (2 g) in ethanol (25 cm^3) was added slowly, and a precipitate formed on chilling overnight. This was collected, washed with ethanol (2 × 10 cm^3) and ether (10 cm^3), and air dried. It was recrystallized from water (20 cm^3) by addition of $LiClO_4$ (2 g) in ethanol (25 cm^3), followed by chilling overnight, and isolated as above (0.9 g, 50%). Found: C, 3.7; H, 3.7; N, 17.2; Cl, 18.4. Calc. for $C_3H_{39}Cl_5CoN_{12}O_{23}Rh$: C, 3.8; H, 4.1; N, 17.7; Cl, 18.7%. Electronic spectrum (water), λ_{max} (nm) [ε_{max} (M^{-1} cm^{-1})]: 475 (50), 340 (100).

$\{[Rh(NH_3)_5]_2(imid)\}(ClO_4)_5 \cdot C_2H_5OH$. A solution of $[Rh(NH_3)_5(imidH)](ClO_4)_3$ (1.0 g) and $[Rh(NH_3)_5(OSO_2CF_3)](CF_3SO_3)_2$ (1.2 g) in 20 cm^3 of dry sulfolane with triethylamine (0.5 cm^3) added was stirred at 80°C for 3 h. After cooling, ethanol (10 cm^3) and ether (~ 500 cm^3) were added to precipitate an oily white solid. The supernatant was decanted, the oil dried in a desiccator, then redissolved in water (25 cm^3) and filtered. Following addition of 1 g of $LiClO_4$ and 25 cm^3 of ethanol, the solution was chilled overnight and the near white powder was collected, washed with ethanol (5 × 20 cm^3) and ether (20 cm^3), and air dried (1.0 g, 60%). Found: C, 5.4; H, 3.8; N, 16.1; Cl, 16.6. Calc. for $C_5H_{44}Cl_5N_{12}O_{24}Rh_2$: C, 5.8; H, 4.2; N, 16.2; Cl, 17.0%. Electronic spectrum (water), λ_{max} (nm) [ε_{max} (M^{-1} cm^{-1})]: 300 (420), 230sh (2650).

Physical methods

Electronic spectra were recorded using an Hitachi 220A spectrophotometer. IR spectra of compounds dispersed in KBr discs were recorded using a Nic-

olet MX-1 FT-IR. NMR spectra were collected using a JEOL FNM FX200 spectrometer in D_2O solution. Voltammetry was performed using an AMEL Model 473 or PAR Model 170 controller linked to an EG&G PAR Model 303A static mercury drop electrode or conventional dropping mercury electrode, and a three-electrode configuration with a platinum wire auxiliary electrode and an Ag–AgCl or saturated calomel reference electrode, with argon as purge gas. Measurements were made on 10^{-3} M solutions of complex in 0.1 M $NaClO_4$ or $NaCF_3SO_3$ as supporting electrolyte.

RESULTS AND DISCUSSION

The value of trifluoromethanesulfonato complexes as synthetic precursors for a range of inert mononuclear complexes has been established earlier.[9] However, few examples employing such compounds in the synthesis of simple binuclear complexes have appeared. In view of the known role of imidazolate as a bridging ligand, it was appropriate to pursue molecules with this anion linking the metal ions, and this has now been achieved for several decaamminedimetal(III) complexes.

The synthetic route developed required the prior synthesis of imidazolepentaamminemetal(III) complexes, and this was achieved from the trifluoromethanesulfonatopentaamminemetal (III) precursors. The complete triad $[M(NH_3)_5(OSO_2CF_3)]^{2+}$ (M = Co, Rh or Ir) were simply prepared in high yield and purity. While Cr(III) and Co(III) complexes were previously known,[4,5] the Ir(III) and Rh(III) complexes had been prepared before only as impure mixtures of imidazole and aqua pentaammines, with as much as 35% aqua complex present.[6] The pure complexes of the cobalt triad are best characterized by their ^1H NMR spectra in d_6-dimethylsufoxide. Apart from the single broad signal from the ammine protons at δ 3.59 (Co), 3.80 (Rh), and 4.39 (Ir), three separate signals from the non-equivalent imidazole ring carbon protons occur at δ 7.31, 7.69 and 8.28 (Co), δ 7.20, 7.52 and 8.14 (Rh), and δ 7.17, 7.45 and 8.05 (Ir). As has been reported previously,[7] the signal changes to two peaks (ratio 1 : 2) on forming a symmetric dimer.

Characterization of the apparently binuclear complexes is conveniently performed initially by ion chromatography. Mixtures of the binuclear complexes and imidazolepentaamminemetal(III) precursors elute from SP Sephadex C-25 (Na^+-form) or Dowex 50W × 2 (H^+-form) cation exchange resin as two separate bands, with the higher charged binuclear complex eluting more slowly than its precursor. Chromatography can permit convenient separation on a synthetic scale. Further, the symmetric dimer $\{[Co(NH_3)_5]_2(imid)\}^{5+}$ exhibits a ^1H NMR spectrum in 0.1 M DCl [δ 3.6 (broad, NH), 7.08, 7.54 (2 : 1, imidazolate)] like that reported earlier for this molecule.[7] The IR spectra of the molecules also provide evidence for the structural assignments of the molecule as $[(NH_3)_5M(imid)M'(NH_3)_5]^{5+}$ complexes. All monomer precursors and binuclear products show weak but characteristic bands for imidazole throughout the 3000–450-cm^{-1} region, and characteristic ammine vibrations. Further, certain multiplicities absent in the symmetric dimers $\{[M(NH_3)_5]_2(imid)\}^{5+}$ (M = Co or Rh) appear in the mixed complex $[(NH_3)_5Co(imid)Rh(NH_3)_5]^{5+}$; apparent M–N stretching vibrations at 315 and 279 cm^{-1} for the dicobalt and dirhodium complexes, respectively, are replaced by two vibrations at 313 and 282 cm^{-1} in the mixed-metal molecule, whereas ammine resonances at 1350 cm^{-1} (dicobalt) and 1385 cm^{-1} (dirhodium) are replaced by overlapping bands at 1340 and 1390 cm^{-1} in the mixed-metal species. These physical characterizations, in composite, define the existence of binuclear complexes synthesized from imidazolepentaammine and trifluoromethanesulfonatopentaammine precursors in combination.

Further characterization comes from the kinetic behaviour of the binuclear complexes. The $[(NH_3)_5Co(imid)Rh(NH_3)_5]^{5+}$ molecule is stable in 0.01 M OH^-, with no change in optical spectrum observed after 3 h at 25°C, but in 12 M HCl it undergoes slow decomposition ($k_{obs} = 3.5 \times 10^{-5}$ s^{-1}). The rate of electron transfer of this molecule when reacted with VO^{2+} in 0.5 M base at 25°C ($k = 0.020$ M^{-1} s^{-1}) is markedly slower than that reported for $[Co(NH_3)_5(imid)]^{2+}$ under identical conditions ($k = 1.3$ M^{-1} s^{-1}),[10] and presumably results partly from electrostatic considerations in briging together the cationic reductant and the cationic oxidants of different charge and size.

The voltammetry of the complexes is also indicative of the binuclear nature of the products. Metal-centred reduction potentials for complexes determined polarographically are collected in Table 1. The $[M(NH_3)_5(imidH)]^{3+}$ precursors exhibit a single irreversible reduction with $E_{1/2}$ pH-dependent as a consequence of protonation/deprotonation of the imidazole ligand.[11] The dimers display a complex pattern of two sequential one-electron irreversible reductions. No reversible character is shown even at scan rates of 50 V s^{-1} in cyclic voltammograms at a hanging mercury drop electrode. Reduction waves in the mixed cobalt–rhodium molecule are well-separated, but sequential

Table 1. Reduction potentials determined by polarography in aqueous solution at ambient temperature of imidazolepentaammine complexes

Complex	$E_{1/2}$ [V (vs SCE)]
$[(NH_3)_5Co(imid)]^{2+}$	−0.47
$[(NH_3)_5Co(imidH)]^{3+}$	−0.30
$[(NH_3)_5Rh(imid)]^{2+}$	−1.17
$[(NH_3)_5Rh(imidH)]^{3+}$	−1.10
$[(NH_3)_5Co(imid)Co(NH_3)_5]^{5+}$	−0.12, −0.40
$[(NH_3)_5Co(imid)Rh(NH_3)_5]^{5+}$	−0.11, −1.20
$[(NH_3)_5Rh(imid)Rh(NH_3)_5]^{5+}$	−1.02, −1.20

processes can even be distinguished in the d.c. polarograms of the dicobalt and dirhodium complexes. Further, a.c. polarography of the complexes clearly defines two sequential reduction steps in each case. It is notable that the first reduction, assigned to electron addition to one metal ion of the binuclear compound, occurs at a potential of up to 350 mV more positive than in the deprotonated imidazole monomer complex, and some 200 mV more positive than in the protonated monomer complex. Clearly, the reduction potential is shifted to a more positive value as the charge on the opposite side of the imidazole ring increases. While imidazole is apparently not a good mediator of electronic influences,[12] these shifts may be related most simply to overall complex charge. The appearance of two waves in the dimers is probably a consequence of the known rapid dissociation of pentaamminemetal(II) complexes;[11] if reduction and the following dissociation in the first step are very fast, then the second reduction step in the double layer may approximate that of the deprotonated monomer. The observed potentials for the second process (Table 1) do approach those of definitive monomers closely, in support of this view.

It is presumed that the synthetic approach developed here for formation of μ-imidazolato complexes may have general applicability when linking inert metal ions is involved. We are pursuing other reactions employing trifluoromethanesulfonato complexes as synthons with a view to forming other small polymeric metal complexes.

Acknowledgement—We are grateful for provision of and access to facilities at the Research School of Chemistry, The Australian National University, during early stages of this work.

REFERENCES

1. J. S. Richardson, K. A. Thomas, B. H. Rubin and D. C. Richardson, *Proc. Natl Acad. Sci. U.S.A.* 1975, **72**, 1349.
2. M. S. Haddad, E. N. Duesler and D. M. Hendrickson, *Inorg. Chem.* 1979, **18**, 141 (and references therein).
3. C.-L. O'Young, J. C. Dewan, H. R. Lilienthal and S. J. Lippard, *J. Am. Chem. Soc.* 1978, **100**, 7291.
4. J. M. Harrowfield, V. Norris and A. M. Sargeson, *J. Am. Chem. Soc.* 1976, **98**, 7282.
5. N. J. Curtis and G. A. Lawrance, *Inorg. Chim. Acta* 1985, **100**, 275.
6. M. F. Hoq and R. E. Shepherd, *Inorg. Chem.* 1984, **23**, 1851.
7. C. J. Hawkins, E. Horn, J. Martin, J. A. L. Palmer and M. R. Snow, *Aust. J. Chem.* 1986, **39**, 1213.
8. N. E. Dixon, G. A. Lawrance, P. A. Lay and A. M. Sargeson, *Inorg. Chem.* 1984, **23**, 2940.
9. G. A. Lawrance, *Chem. Rev.* 1986, **86**, 17.
10. H. A. Boucher, G. A. Lawrance, A. M. Sargeson and D. F. Sangster, *Inorg. Chem.* 1983, **22**, 3482.
11. N. J. Curtis, G. A. Lawrance and A. M. Sargeson, *Aust. J. Chem.* 1983, **36**, 1327.
12. S. S. Isied and C. B. Kuehn, *J. Am. Chem. Soc.* 1978, **100**, 6754.

Polyhedron Vol. 6, No. 6, pp. 1351–1360, 1987
Printed in Great Britain

0277–5387/87 $3.00+.00

SYNTHESIS AND REACTIONS OF *TRANS*-DICARBONYL BIS-[1,2-BIS(DIMETHYLPHOSPHINO)ETHANE] VANADIUM(0): X-RAY CRYSTAL STRUCTURES OF *TRANS*-$V(CO)_2(dmpe)_2$ [*CIS*-$V(CO)_2(dmpe)_2(CH_3CN)]BPh_4$ AND *CIS*-$V(CO)_2(dmpe)_2(O_2CEt)$

FIONNA J. WELLS and GEOFFREY WILKINSON*

Chemistry Department, Imperial College, London SW7 2AY, U.K.

and

MAJID MOTEVALLI and MICHAEL B. HURSTHOUSE

Chemistry Department, Queen Mary College, London E1 4NS, U.K.

(*Received* 10 *November* 1986; *accepted* 28 *November* 1986)

Abstract—Interaction of *trans*-$VCl_2(dmpe)_2$ with sodium amalgam in tetrahydrofuran under CO gives *trans*-$V(CO)_2(dmpe)_2$. The latter is oxidized by Ag^+ in acetonitrile to give [*cis*-$V(CO)_2(dmpe)_2(CH_3CN)]^+$, isolated as the tetraphenylborate. Interactions with acids (HX) gives neutral complexes of the type $V(CO)_2(dmpe)_2X$ (X = Cl, $MeCO_2$, $EtCO_2$, CF_3CO_2, $PhPO_2H$ or NH_2SO_3); the chloride can be exchanged with N_3^- or CN^- in methanol. X-ray structural studies confirm the *trans* stereochemistry for $V(CO)_2(dmpe)_2$ and the seven-coordination of V^I in both $[V(CO)_2(dmpe)_2(CH_3CN)][BPh_4]$ and $V(CO)_2(dmpe)_2(O_2CEt)$, which have a pseudo octahedral geometry with the two carbonyls occupying a "split" axial site. ^{51}V NMR and other spectra are reported.

Phosphine-substituted carbonyls of vanadium[1] have commonly been prepared from $V(CO)_6$ or $[V(CO)_6]^-$ but for dicarbonyls with bidentate chelating phosphines, only $V(CO)_2(dppe)_2$ [dppe = 1,2-bis(diphenylphosphino)ethane] is known. The characterization of *trans*-$VCl_2(dmpe)_2$[2] now allows the synthesis of *trans*-$V(CO)_2(dmpe)_2$ by the same method used for the preparation of *cis*-$Cr(CO)_2(dmpe)_2$.[3] Some reactions of *trans*-$V(CO)_2(dmpe)_2$ are discussed. Analytical data for new compounds are given in Table 1, and IR and NMR data in Tables 2 and 3.

RESULTS AND DISCUSSION

Synthesis of trans-$V(CO)_2(dmpe)_2$

The interaction of *trans*-$VCl_2(dmpe)_2$ in tetrahydrofuran with excess sodium amalgam under CO (5 atm) gives an orange solution from which air-sensitive crystals of the dicarbonyl complex can be isolated. Although the IR spectrum in hexane shows only a single band at 1763 cm^{-1} as expected for a *trans* stereochemistry, the solid-state spectrum (Nujol mull) shows two bands, which are presumably due to solid-state splitting. The *trans* structure is confirmed by the X-ray crystal structure analysis.

A diagram of the molecule is given in Fig. 1; selected bond lengths and angles are given in Table 4. The V—C distances are *ca* 0.1 Å longer than the Cr—C distances in *cis*-$Cr(CO)_2(dmpe)_2$ and the V—P bonds are also *ca* 0.1Å longer than the two mutually *trans* Cr—P bonds in that complex,[3] and the Cr—P bonds in the analogous Cr^0 complex, $Cr(N_2)_2(dmpe)_2$.[3] However, the V—C distances are only 0.05 Å greater than the Cr—N distances, an indication of the greater π-acceptor capability of the carbonyl ligand. Interestingly, the volume per molecule of this vanadium compound is *ca* 20 $Å^3$ *less* than that of the dinitrogen complex. Although

* Author to whom correspondence should be addressed.

Table 1. Analytical data for vanadium compounds

Compound	Colour	M.p. (°C)	Analysis[a] C	H	P	Other	*M*
trans-$V(CO)_2(dmpe)_2$	Orange-red	247d	41.1 (41.3)	8.1 (7.9)	28.4 (30.4)		*m/z*, 408 54.2% M^+
[*cis*-$V(CO)_2(dmpe)_2(MeCN)][BPh_4]$	Orange-red	170d	62.4 (62.6)	7.3 (7.2)	16.2 (16.2)	N, 1.9 (1.8) O, 3.7 (4.2)	
cis-$V(CO)_2(dmpe)_2Cl$	Red	200d	37.8 (38.0)	7.3 (7.2)	27.7 (27.7)	Cl, 8.1 (8.0) O, 7.5 (7.2)	*m/z*, 442 0.1% M^+
cis-$V(CO)_2(dmpe)_2(MeCO_2)$	Red	130d	41.3 (41.2)	7.6 (7.5)	24.2 (26.6)	O, 13.8 (13.7)	
cis-$V(CO)_2(dmpe)_2(EtCO_2)$	Red	135d	42.6 (42.5)	7.9 (7.7)	25.2 (25.8)	O, 12.9 (13.3)	
cis-$V(CO)_2(dmpe)_2(CF_3CO_2)$	Red	140d	36.3 (36.9)	6.1 (6.2)	22.8 (23.8)	O, 13.1 (12.3) F, 11.5 (11.0)	
cis-$V(CO)_2(dmpe)_2N_3$	Orange-red	140d	37.9 (37.4)	7.1 (7.1)		N, 8.7 (9.3)	
cis-$V(CO)_2(dmpe)_2CN$	Yellow	200d	41.9 (41.6)	7.6 (7.9)	28.5 (28.6)	N, 3.3 (3.2) O, 7.4 (7.4)	*m/z*, 434 6.8% M^+
cis-$V(CO)_2(dmpe)_2(PhPO_2H)$	Red	140d	44.0 (43.8)	6.7 (6.9)	27.9 (28.3)	O, 11.4 (11.7)	
cis-$V(CO)_2(dmpe)_2(NH_2SO_3)$	Red	150d	33.6 (33.4)	6.9 (6.8)	24.5 (24.7)	O, 16.0 (15.9) N, 2.8 (2.8)	

[a] Found (required).

the thermal ellipsoids for atoms of the dmpe ligands indicate considerable thermal motion or disorder in the vanadium compound, it would seem that the crystal packing in this monoclinic structure is better than that for the dinitrogen chromium structure which is triclinic.

The difference between the *trans* dicarbonyl structure found here and *cis*-$Cr(CO)_2(dmpe)_2$ can be rationalized by MO calculations[4] which suggest that for 18e species such as the chromium complex the *cis* isomer is more stable but for 17e complexes the *trans* isomer is thermodynamically preferred.

The compound is a paramagnetic, low-spin d^5-species ($\mu_{eff} = 1.5$ BM*) from magnetic-sus-

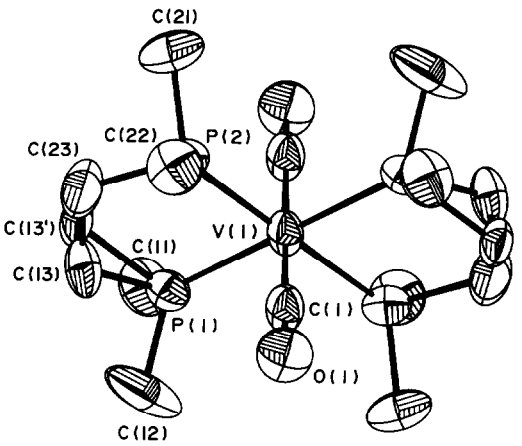

Fig. 1. Structure of *trans*-$V(CO)_2(dmpe)_2$.

* Non-SI units employed: $\mu_B = ca\ 9.27 \times 10^{-24}$ A m^{-2}.

Table 2. IR[a] spectra for vanadium compounds

Compound	ν(CO) (cm^{-1})	Other bands (cm^{-1})
trans-$V(CO)_2(dmpe)_2$	1820s, 1760s 1763[b]	
[*cis*-$V(CO)_2(dmpe)_2(MeCN)$][BPh_4]	1836s, 1779s 1839s, 1776s[c]	2250w [ν(C≡N)]
cis-$V(CO)_2(dmpe)_2Cl$	1811s, 1748s 1838s, 1777s[b]	
cis-$V(CO)_2(dmpe)_2(MeCO_2)$	1809s, 1741s	1624 [$\nu(CO_2)$(asym)] 1323 [$\nu(CO_2)$(sym)]
cis-$V(CO)_2(dmpe)_2(EtCO_2)$	1808s, 1750s	1602 [$\nu(CO_2)$(asym)]
cis-$V(CO)_2(dmpe)_2(CF_3CO_2)$	1816s, 1752s 1828s, 1767s[d]	1696s [$\nu(CO_2)$(asym)] 1698s[d]
cis-$V(CO)_2(dmpe)_2N_3$	1800s, 1745s	2060s [ν(N≡N)]
cis-$V(CO)_2(dmpe)_2CN$	1815s, 1765s	2070m [ν(C≡N)]
cis-$V(CO)_2(dmpe)_2(PhPO_2H)$	1808s, 1743s	2268m [ν(P—H)] 1200s [ν(P=O)]
cis-$V(CO)_2(dmpe)_2(NH_3SO_3)$	1816s, 1750s	3370w [$\nu(NH_2)$(asym)] 3260w [$\nu(NH_2)$(sym)] 1570w [$\delta(NH_2)$] 1182s [ν(S=O)]

[a] In Nujol mulls unless otherwise stated.
[b] In hexane.
[c] In MeCN.
[d] In toluene.

ceptibility measurements by Evans' NMR method.[5] The ESR spectrum (X-band) appears to be an overlapping of three sets of eight lines (^{51}V, $I = \frac{7}{2}$, 100%) corresponding to the interaction of the single electron spin with the nuclear spin of ^{51}V.

By contrast with *trans*-$CrCl_2(dmpe)_2$,[3] reduction of *trans*-$VCl_2(dmpe)_2$ under either dihydrogen or dinitrogen does not give isolatable complexes.

Table 3. ^{31}P and ^{51}V NMR data for *cis*-$V(CO)_2(dmpe)_2X$ complexes

X	$\delta(^{31}P)$[a] (ppm)	J(P–V) (Hz)	$\delta(^{51}V)$[a] (ppm)	J(V–P) (Hz)
Cl	53.7	153	−1134	157
CF_3CO_2	54.0	153	−1009	158
$MeCO_2$	52.9	161	−1074	159
$EtCO_2$	56.7	158	−1083	161
N_3	53.6	153	−1161	161
CN	57.4[b]	*ca* 117	−1248[b]	*ca* 135
$PhHPO_2$	53.9[c]	157	−975	160
NH_2SO_3	52.6	164	−906	161

[a] In d^6-benzene.
[b] Broad signal due to increased quadrupolar relaxation.
[c] Additional singlet at 17.2 ppm attributed to the P atom in the O_2PHPh group.

Reactions of trans-$V(CO)_2(dmpe)_2$

Oxidation by Ag^+. Interaction of the complex in acetonitrile at −30°C with $AgSO_3CF_3$ leads to the formation of the cation [*cis*-$V(CO)_2(dmpe)_2(MeCN)]^+$, which can be readily isolated as the orange tetraphenylborate salt, a 1 : 1 electrolyte in MeCN. The spectroscopic properties of the complex (Table 2) are in accordance with the structure determined by X-ray crystallography (see below).

Attempts to isolate an ion $[V(CO)_2(dmpe)_2]^+$ comparable to octahedral *trans*-$[Cr(CO)_2(dmpe)_2]^+$[6] by other types of oxidation were unsuccessful. The coordination of acetonitrile to give the seven-coordinate cation gives an 18e complex which is obviously more stable than an unsolvated 16e species.

Oxidation by HX. *trans*-$V(CO)_2(dmpe)_2$ reacts with HX (X = Cl, $MeCO_2$, $EtCO_2$, CF_3CO_2, $PhPO_2H$ or NH_2SO_3) in diethylether, tetrahydrofuran or toluene to give hydrogen and neutral non-conducting V^I complexes of form *cis*-$V(CO)_2(dmpe)_2X$. These can be recrystallized from hexane or diethylether as red needles. The spectroscopic data are collected in Tables 2 and 3.

Table 4. Selected bond lengths (Å) and angles (°) for $V(CO)_2(dmpe)_2$

P(1)—V(1)	2.377(4)	P(2)—V(1)	2.378(5)
C(1)—V(1)	1.891(11)	C(11)—P(1)	1.787(15)
C(12)—P(1)	1.808(15)	C(13)—P(1)	1.776(23)
C(13′)—P(1)	1.954(20)	C(21)—P(2)	1.833(14)
C(22)—P(2)	1.809(13)	C(23)—P(2)	1.883(14)
C(1)—O(1)	1.184(10)	C(13′)—C(13)	1.018(27)
C(23)—C(13)	1.424(28)	C(23)—C(13′)	1.256(20)
P(2)—V(1)—P(1)	78.6(2)	C(11)—P(1)—V(1)	122.0(6)
C(1)—V(1)—P(2)	90.7(4)	C(12)—P(1)—C(11)	98.7(8)
C(12)—P(1)—V(1)	121.5(6)	C(13)—P(1)—C(11)	111.5(10)
C(13)—P(1)—V(1)	111.7(8)	C(13′)—P(1)—V(1)	110.2(6)
C(13)—P(1)—C(12)	85.4(12)	C(13′)—P(1)—C(12)	110.6(11)
C(13′)—P(1)—C(11)	89.0(9)	C(21)—P(2)—V(1)	121.8(6)
C(22)—P(2)—V(1)	119.6(5)	C(22)—P(2)—C(21)	102.2(7)
C(23)—P(2)—V(1)	112.0(5)	C(23)—P(2)—C(21)	96.5(8)
C(23)—P(2)—C(22)	100.6(8)	O(1)—C(1)—V(1)	179.5(8)
C(23)—C(13′)—P(1)	111.2(13)	C(23)—C(13)—P(1)	113.2(15)
C(13)—C(23)—P(2)	109.7(12)	C(13′)—C(23)—P(2)	116.8(13)
C(1)—V(1)—P(1)	89.4(4)		

The structure of the molecule $[V(CO)_2(dmpe)_2(O_2CEt)]$ and the cation $[V(CO)_2(dmpe)_2(NCMe)]^+$ are essentially analogous, and may be described as "pseudo octahedral", with "equatorial" *bis* -dmpe groups and one axial site occupied by the acetonitrile or unidentate propionate ligands and the other being "split" and accommodating the two carbonyls. Diagrams of the two structures are given in Figs 2 and 3; selected bond lengths and angles are in Tables 5 and 6. The near equality of the C—V—N and C—V—O angles between the "axial" sites preclude the possibility of using a capped octahedral description. One particular feature of this bonding of the two carbonyls is the very narrow C—V—C angle in both structures (*ca* 68°) and the resulting very close non-bonded approach of the two carbon atoms (*ca* 2.1 Å).

The V—C and V—P distances are very similar in both complexes. The former are *ca* 0.05 Å smaller than in the *trans* V^0 dicarbonyl described above, but the V—P distances are *ca* 0.1 Å greater. This difference again probably reflects the greater π-acceptor activity of the carbonyls, especially in a non-*trans* arrangement and bonded to an 18e metal

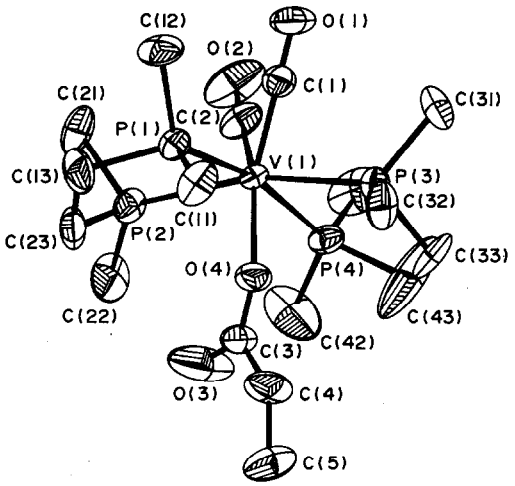

Fig. 2. Structure of $V(CO)_2(dmpe)_2(O_2CEt)$.

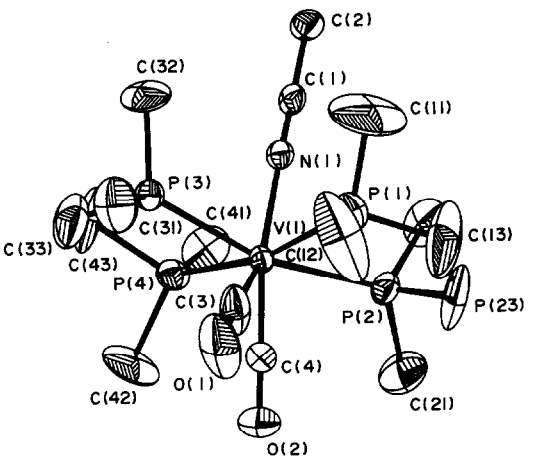

Fig. 3. Structure of the cation $[V(CO)_2(dmpe)_2(NCMe)]^+$.

Table 5. Selected bond lengths (Å) and angles (°) for $V(CO)_2(C_2H_5COO)(dmpe)_2$

P(1)—V(1)	2.507(6)	P(2)—V(1)	2.479(5)
P(3)—V(1)	2.481(5)	P(4)—V(1)	2.478(5)
O(4)—V(1)	2.141(9)	C(1)—V(1)	1.858(14)
C(2)—V(1)	1.854(13)	C(11)—P(1)	1.852(14)
C(12)—P(1)	1.850(13)	C(13)—P(1)	1.828(15)
C(21)—P(2)	1.874(14)	C(22)—P(2)	1.860(15)
C(23)—P(2)	1.820(17)	C(31)—P(3)	1.866(15)
C(32)—P(3)	1.829(14)	C(33)—P(3)	1.888(14)
C(41)—P(4)	1.830(18)	C(42)—P(4)	1.790(18)
C(43)—P(4)	1.749(21)	C(1)—O(1)	1.201(14)
C(2)—O(2)	1.189(14)	C(3)—O(3)	1.245(16)
C(3)—O(4)	1.191(14)	C(4)—C(3)	1.518(20)
C(5)—C(4)	1.451(21)	C(23)—C(13)	1.503(20)
C(43)—C(33)	1.429(24)		
P(2)—V(1)—P(1)	74.3(2)	P(3)—V(1)—P(1)	103.8(2)
P(3)—V(1)—P(2)	163.0(1)	P(4)—V(1)—P(1)	165.6(1)
P(4)—V(1)—P(2)	102.0(2)	P(4)—V(1)—P(3)	75.6(2)
O(4)—V(1)—P(1)	81.1(3)	O(4)—V(1)—P(2)	86.7(3)
O(4)—V(1)—P(3)	76.4(3)	O(4)—V(1)—P(4)	84.8(3)
C(1)—V(1)—P(1)	78.4(4)	C(1)—V(1)—P(2)	118.9(5)
C(1)—V(1)—P(3)	76.3(5)	C(1)—V(1)—P(4)	114.9(4)
C(1)—V(1)—O(4)	140.6(4)	C(2)—V(1)—P(1)	115.2(5)
C(2)—V(1)—P(2)	76.4(6)	C(2)—V(1)—P(3)	118.5(6)
C(2)—V(1)—P(4)	76.5(4)	C(2)—V(1)—O(4)	151.3(4)
C(2)—V(1)—C(1)	67.9(7)	C(11)—P(1)—V(1)	116.3(5)
C(12)—P(1)—V(1)	121.2(5)	C(12)—P(1)—C(11)	101.4(7)
C(13)—P(1)—V(1)	115.1(6)	C(13)—P(1)—C(11)	101.6(8)
C(13)—P(1)—C(12)	97.8(8)	C(21)—P(2)—V(1)	114.1(7)
C(22)—P(2)—V(1)	121.4(6)	C(22)—P(2)—C(21)	103.5(8)
C(23)—P(2)—V(1)	110.7(5)	C(23)—P(2)—C(21)	101.0(8)
C(23)—P(2)—C(22)	103.7(9)	C(31)—P(3)—V(1)	121.1(6)
C(32)—P(3)—V(1)	117.8(5)	C(32)—P(3)—C(31)	99.8(8)
C(33)—P(3)—V(1)	112.5(6)	C(33)—P(3)—C(31)	101.1(8)
C(33)—P(3)—C(32)	101.5(8)	C(41)—P(4)—V(1)	119.0(7)
C(42)—P(4)—V(1)	119.8(7)	C(42)—P(4)—C(41)	104.4(12)
C(43)—P(4)—V(1)	113.8(8)	C(43)—P(4)—C(41)	97.4(14)
C(43)—P(4)—C(42)	98.6(14)	C(3)—O(4)—V(1)	147.7(8)
O(1)—C(1)—V(1)	175.9(12)	O(2)—C(2)—V(1)	174.8(13)
O(4)—C(3)—O(3)	120.5(13)	C(4)—C(3)—O(3)	119.1(14)
C(4)—C(3)—O(4)	120.3(14)	C(5)—C(4)—C(3)	121.7(15)
C(23)—C(13)—P(1)	109.9(11)	C(13)—C(23)—P(2)	109.7(12)
C(43)—C(33)—P(3)	111.2(12)	C(33)—C(43)—P(4)	121.0(14)

centre. The V—N and V—O distances are very similar at 2.15 Å.

Azido and cyano complexes can be made from *cis*-$V(CO)_2(dmpe)_2Cl$ by interaction of NaN_3 or KCN in methanol. The azido compound is also formed when *trans*-$V(CO)_2(dmpe)_2$ is treated with Me_3SiN_3 in hexane.

The IR spectra of the complexes are as expected—all showing two strong CO stretching frequencies for the *cis* carbonyls and appropriate bands for the other ligands (Table 2). The carboxylates show the asymmetric and symmetric $\nu(CO_2)$ stretches and the $\Delta\nu$ value (301 cm^{-1}) for the acetate indicates η^1-binding.[7] The ^{31}P–$\{^1H\}$ NMR spectra all show an octet resulting from the coupling of the equivalent phosphorus atoms to the ^{51}V nucleus (Table 3).

The ^{51}V NMR spectra (Table 3) of the $V(CO)_2(dmpe)_2X$ complexes all show a quintet due to the splitting of the ^{51}V resonance by the four equivalent P atoms. The resonances lie between −906 and −1248 ppm in the region expected for V^I

Table 6. Selected bond lengths (Å) and angles (°) for $[V(CO)_2(NCMe)(dmpe)_2]B(Ph)_4$

P(1)—V(1)	2.479(5)	P(2)—V(1)	2.475(5)
P(3)—V(1)	2.477(6)	P(4)—V(1)	2.459(6)
N(1)—V(1)	2.166(10)	C(3)—V(1)	1.851(15)
C(4)—V(1)	1.831(15)	C(11)—P(1)	1.793(17)
C(12)—P(1)	1.801(16)	C(13)—P(1)	1.775(19)
C(21)—P(2)	1.876(16)	C(22)—P(2)	1.826(14)
C(23)—P(2)	1.771(16)	C(31)—P(3)	1.858(16)
C(32)—P(3)	1.809(15)	C(33)—P(3)	1.756(17)
C(41)—P(4)	1.865(15)	C(42)—P(4)	1.857(15)
C(43)—P(4)	1.849(14)	C(1)—N(1)	1.123(12)
C(3)—O(1)	1.172(13)	C(4)—O(2)	1.196(14)
C(2)—C(1)	1.477(17)	C(23)—C(13)	1.478(21)
C(43)—C(33)	1.518(19)		
P(2)—V(1)—P(1)	75.1(2)	P(3)—V(1)—P(1)	98.6(2)
P(3)—V(1)—P(2)	164.6(1)	P(4)—V(1)—P(1)	166.3(1)
P(4)—V(1)—P(2)	106.5(2)	P(4)—V(1)—P(3)	76.3(2)
N(1)—V(1)—P(1)	84.1(3)	N(1)—V(1)—P(2)	83.4(3)
N(1)—V(1)—P(3)	82.0(3)	N(1)—V(1)—P(4)	82.5(3)
C(3)—V(1)—P(1)	78.0(5)	C(3)—V(1)—P(2)	115.7(5)
C(3)—V(1)—P(3)	75.8(5)	C(3)—V(1)—P(4)	112.4(5)
C(3)—V(1)—N(1)	148.9(6)	C(4)—V(1)—P(1)	117.3(5)
C(4)—V(1)—P(2)	74.1(5)	C(4)—V(1)—P(3)	120.9(5)
C(4)—V(1)—P(4)	75.7(5)	C(4)—V(1)—N(1)	142.4(6)
C(4)—V(1)—C(3)	68.7(8)	C(11)—P(1)—V(1)	119.7(7)
C(12)—P(1)—V(1)	119.7(6)	C(12)—P(1)—C(11)	101.9(12)
C(13)—P(1)—V(1)	112.6(7)	C(13)—P(1)—C(11)	98.4(12)
C(13)—P(1)—C(12)	101.0(12)	C(21)—P(2)—V(1)	122.5(6)
C(22)—P(2)—V(1)	116.5(5)	C(22)—P(2)—C(21)	97.1(9)
C(23)—P(2)—V(1)	113.0(6)	C(23)—P(2)—C(21)	100.9(9)
C(23)—P(2)—C(22)	103.9(8)	C(31)—P(3)—V(1)	121.9(6)
C(32)—P(3)—V(1)	119.2(6)	C(32)—P(3)—C(31)	97.1(9)
C(33)—P(3)—V(1)	112.0(6)	C(33)—P(3)—C(31)	100.4(9)
C(33)—P(3)—C(32)	103.0(10)	C(41)—P(4)—V(1)	115.9(6)
C(42)—P(4)—V(1)	120.6(6)	C(42)—P(4)—C(41)	101.6(8)
C(43)—P(4)—V(1)	111.5(6)	C(43)—P(4)—C(41)	105.2(7)
C(43)—P(4)—C(42)	99.8(9)	C(1)—N(1)—V(1)	176.3(9)
C(2)—C(1)—N(1)	177.6(12)	O(1)—C(3)—V(1)	175.6(15)
O(2)—C(4)—V(1)	176.6(12)	C(23)—C(13)—P(1)	117.4(12)
C(13)—C(23)—P(2)	109.2(12)	C(43)—C(33)—P(3)	108.3(12)
C(33)—C(43)—P(4)	108.3(10)		

compounds (−870 to −1540 ppm).[8] The observed resonances lie towards the high-frequency end of this range because of the electron-donating ability of the methyl groups on the dmpe ligands. There is indeed a tendency for an increase in ^{51}V deshielding as the bulk of the phosphine increases and the electronegativities of the substituent groups on phosphorus decrease.[9] The small $^1J(V-P)$ values (*ca* 160 Hz) are also in accord with those for vanadium alkyl-phosphine complexes.[10] Finally the ^{51}V shielding increases in the order $X = CN > N_3 > Cl > EtCO_2 > MeCO_2 > CF_3CO_2 > PhPO_2H > NH_2SO_3$; this agrees with Rehder's magnetochemical series of ligands.[11]

Protonation to hydrido species. Interaction of *trans*-$V(CO)_2(dmpe)_2$ with 1 equivalent of tetrafluoroboric acid in methanol at −78°C gives a red solution; on warming to room temperature, an orange solution is obtained from which orange crystals can be isolated. Analytical and spectroscopic data for the BF_4^- and $PhC(SO_2CF_3)_2^-$ salts given in Table 7 indicate that the cation has $[HV(CO)_2(dmpe)]^+$ stoichiometry. The conductivity corresponds to that of a 1 : 1 electrolyte.

The mull IR spectrum shows two strong bands at 1865 and 1827 cm^{-1} attributable to *cis* carbonyls. A relatively weak, sharp band is also observed at 1952 cm^{-1} which is assigned to ν(V—H). However

Table 7. Analytical and spectroscopic data for salts of the $[V_2H_2(CO)_4dmpe_4]^{2+}$ ion

	BF_4^-			$PhC(SO_2CF_3)_2^-$		
Analysis	C, 34.4 (34.2)	H, 6.4 (7.0)	P, 33.7 (23.5)	C, 36.0 (36.2)	H, 4.6 (5.0)	P, 14.7 (16.2)
	O, 9.0 (9.1)	F, 14.6[a] (14.4)		F, 15.2 (14.9)		
IR[b] (cm^{-1})	ν(C≡O) 1865, 1827			ν(C≡O) 1860, 1828		
	ν(C≡O) 1875, 1850[c]			ν(C≡O) 1875, 1850[c]		
	ν(M—H) 1952			ν(M—H) 1949		
	ν(M—H) 1960, 1942[c]			ν(M—H) 1960, 1945[c]		
^{31}P[d]	55.8br					
^{51}V[d]	−1311br					
^{19}F[d]	−152s					
^{1}H[d]	1.63s [3H], 2.06t[e] [1H]					

[a] For methanol solvate (1 : 1).
[b] In Nujol mulls.
[c] In CH_2Cl_2.
[d] In CD_2Cl_2 at 298 K, δ values in ppm.
[e] Virtually coupled triplet.

in CH_2Cl_2 solution two bands are observed in the terminal hydride stretching region at 1960 and 1942 cm^{-1}, although the number of ν(CO) bands does not change. The presence of V—H bands is confirmed by essentially quantitative formation (GLC) of $CHCl_3$ on refluxing the compound with CCl_4.

However, magnetic-susceptibility and ESR measurements show that the cation is diamagnetic, thus eliminating the possibility that the ion is analogous to $[MH(CO)_2(dmpe)_2]^+$ (M = Cr,[6] Mo or W[12]). The ^{31}P–{^1H} and ^{51}V–{^1H} NMR spectra in CD_2Cl_2 do not provide any useful structural information, showing only broad resonances at +55.8 ppm and −1311 ppm, respectively. This broadening of the resonances can be ascribed to quadrupolar relaxation caused by the presence of the vanadium nucleus, and thus cooling the NMR sample merely broadens the signals. This quadrupolar relaxation probably also accounts for the fact that no resonance for the hydride proton can be seen in the ^1H NMR.

The diamagnetism of the cation suggests that dimerization of a paramagnetic $VVH(CO)_2(dmpe)_2^+$ species has occurred, presumably with the formation of a V—V bond. The IR spectra shows that there are no bridging CO or hydrido groups; since there are two V—H stretches in solution spectra, this could indicate isomers or some lack of symmetry in solution.

Despite repeated attempts to obtain X-ray quality crystals with different anions, none were obtained; the crystals form as thin mica-like platelets. In the absence of structural data we can only speculate on the structure on the basis of the above data and a reasonable possibility is I shown as the "*trans*" isomer where there is a supported metal–metal bond. V—V bonds have been discussed;[13] there is a precedent for bridging dmpe in the compound $Rh_2(CH_2SiMe_3)_2dmpe_3$[14] which has a single dmpe bridge.

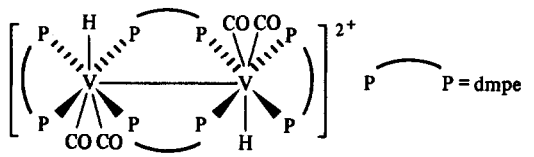

I

EXPERIMENTAL

Microanalyses were performed by Pascher (Bonn) and Imperial College Laboratories.

Instruments

IR: Perkin–Elmer 683, spectra in Nujol mulls unless otherwise stated. NMR: JEOL FX90Q and Bruker WM 250; δ values in ppm relative to Me_4Si (^1H), 85% H_3PO_4 external (^{31}P) and $VOCl_3$ external (^{51}V). ESR: Varian E-12 (X-band). Mass: VG Micromass 7070 and MS9. Conductivities: Data Scientific PT1-18, data in $\Omega^{-1}\,cm^2\,mol^{-1}$. Magnetic

susceptibilities in solution were determined using a modification of Evans' method. Melting points (uncorrected) were determined in sealed capillaries. All manipulations were carried out under argon or nitrogen, and all solvents were dried, distilled and degassed before use.

trans-*Dicarbonyl bis*-[1,2-*bis*(*dimethylphosphino*)*ethane*] *vanadium*(0)

A pressure bottle containing sodium amalgam (5 equivalents of Na per V) and *trans*-$VCl_2(dmpe)_2$ (0.5 g, 1.23 mmol), in tetrahydrofuran (70 cm^3) at −78°C, was pressurized with CO to 5 atm. The mixture was vigorously stirred and allowed to warm to room temperature. The initial purple solution became red and finally orange. The solution was filtered, evaporated and the residue extracted with hexane (40 cm^3). Filtration, concentration to *ca* 10 cm^3 and cooling to −20°C gave small orange-red prisms which were collected, and dried *in vacuo*. Yield 0.25 g (50%).

ESR (toluene, 97 K): $g_x = 2.1563$, $g_y = 2.0523$, $g_z = 1.8379$. Magnetic susceptibility (CH_2Cl_2, 25°C): $\mu_{eff} = 1.53$ BM.

cis-*Dicarbonyl bis*-[1,2-*bis*(*dimethylphosphino*)*ethane*] *acetonitrile vanadium*(I) *tetraphenylborate*

To *trans*-$V(CO)_2(dmpe)_2$ (0.4 g, 0.98 mmol), in acetonitrile (30 cm^3) at −30°C, was added $AgSO_3CF_3$ (1 equivalent, 0.98 mmol) in the dark. After *ca* 15 min. the resultant red-brown solution was filtered and the solvent removed *in vacuo*. Addition of a methanolic solution of $NaBPh_4$ gave an orange precipitate which was collected, washed with methanol (2 × 10 cm^3) and dried. Subsequent extraction into acetonitrile (30 cm^3) gave an orange-brown solution, which was stirred with a small amount of mercury to collect the finely-divided silver suspended in solution. After several minutes the orange solution was filtered, concentrated and cooled to −20°C yielding orange-red prisms. Yield 0.5 g (50%).

NMR [^1H (CD_2Cl_2)]: 7.3s, 7.0s, 6.9s (phenyl); 1.95 (CH_2). 1.5 (CH_3). Conductivity (MeCN, 25°C): $\Lambda_M = 61\ \Omega^{-1}\ cm^2\ mol^{-1}$.

cis-*Dicarbonylchloro bis*-[1,2-*bis*(*dimethylphosphino*)*ethane*] *vanadium*(I)

To *trans*-$V(CO)_2(dmpe)_2$ (0.3 g, 0.74 mmol), in diethylether (40 cm^3) at 78°C, was added HCl (1.47 mmol, 0.9 M in Et_2O). After stirring for *ca* 1 h at room temperature, the red solution was evaporated and the residue extracted into diethylether. Filtration, concentration and cooling to −20°C gave red needles which were collected and dried *in vacuo*. Yield 0.2 g (60%).

NMR [^1H (C_6D_6)]: 1.32s (dmpe).

cis-*Dicarbonyltrifluoroacetato bis*-[1,2-*bis*(*dimethylphosphino*)*ethane*] *vanadium*(I)

To *trans*-$V(CO)_2(dmpe)_2$ (0.26 g, 0.64 mmol), in tetrahydrofuran (50 cm^3) at −78°C, was added CF_3CO_2H (1.28 mmol, 1.5 M in Et_2O). The mixture was stirred and allowed to warm to room temperature. Removal of the solvent and extraction of the residue into hexane (50 cm^3) gave a red solution. Filtration, concentration and cooling to −20°C yielded small red crystals. Yield 0.17 g (50%).

NMR [^1H (C_6D_6)]: 1.26s (dmpe).

cis-*Dicarbonylacetato bis*-[1,2-*bis*(*dimethylphosphino*)*ethane*] *vanadium*(I)

To *trans*-$V(CO)_2(dmpe)_2$ (0.34 g, 0.84 mmol), in tetrahydrofuran (50 cm^3) at −78°C, was added CH_3CO_2H (3.95 mmol, 2.6 M in Et_2O). After stirring for 24 h at room temperature, the solvent was removed *in vacuo*, and the residue extracted and crystallized from diethylether, yielding red crystals. Yield 0.2 g (50%).

NMR [^1H (C_6D_6)]: 1.69s (CH_3), 1.32s (dmpe).

cis-*Dicarbonylpropionato bis*-[1,2-*bis*(*dimethylphosphino*)*ethane*] *vanadium*(I)

To *trans*-$V(CO)_2(dmpe)_2$ (0.48 g, 1.18 mmol), in diethylether (50 cm^3) at −78°C, was added $EtCO_2H$ (2.5 mmol, 1.8 M in Et_2O). After stirring for 24 h at room temperature, the solvent was removed *in vacuo*, and the residue extracted and crystallized from hexane, yielding red needles. Yield 0.28 g (50%).

NMR [^1H (C_6D_6)]: 1.88q (CH_2), 1.13s (dmpe), 1.08t (CH_3).

cis-*Dicarbonylcyano bis*-[1,2-*bis*(*dimethylphosphino*)*ethane*] *vanadium*(I)

(i) To *trans*-$V(CO)_2(dmpe)_2$ (0.47 g, 1.15 mmol), in hexane (50 cm^3) at −78°C, was added Me_3SiN_3 (3 mmol, 0.5 M in hexane). After stirring at room temperature for 24 h, the resulting yellow precipitate was collected, washed with hexane (2 × 10 cm^3), filtered and dried. Subsequent extraction into diethylether (50 cm^3), filtration and cooling to −20°C gave orange needles which were collected and dried *in vacuo*. Yield 0.2 g (40%).

(ii) A methanolic solution of NaN_3 (0.1 g, 1.54

mmol) was added to *cis*-$V(CO)_2(dmpe)_2Cl$ (0.31 g, 0.7 mmol) in methanol (30 cm^3) at −78°C. After stirring for 24 h at room temperature, the solvent was removed and the residue extracted into diethylether (50 cm^3). Crystallization as above gave orange needles. Yield 0.25 g (80%).

NMR [^1H (C_6D_6)]: 1.25s (dmpe).

cis-*Dicarbonylcyano bis*-[1,2-*bis*(*dimethylphosphino*) *ethane*] *vanadium*(I)

A methanolic solution of KCN (0.084 g, 1.29 mmol) was added to *cis*-$V(CO)_2(dmpe)_2Cl$ (0.15 g, 1.15 mmol) in methanol (50 cm^3) at −78°C. After stirring at room temperature for 24 h, the solvent was removed and the residue extracted into acetonitrile (60 cm^3). Subsequent filtration, concentration and cooling to −20°C gave yellow needles. Yield 0.37 g (75%).

NMR [^1H (C_6D_6)]: 1.28s (dmpe).

cis-*Dicarbonylphenylphosphinato bis*-[1,2-*bis*(*dimethylphosphino*)*ethane*] *vanadium*(I)

To *trans*-$V(CO)_2(dmpe)_2$ (0.16 g, 0.39 mmol), in toluene (40 cm^3) at −78°C, was added $PhPO_2H_2$ (56.6 mg, 0.4 mmol). After stirring for 24 h at room temperature, the solvent was removed *in vacuo* and the residue extracted and recrystallized from diethylether, yielding red crystals. Yield 0.13 g (65%).

NMR [^1H (C_6D_6)]: 1.34s (dmpe).

cis-*Dicarbonylsulphamato bis*-[1,2-*bis*(*dimethylphosphino*)*ethane*] *vanadium*(I)

To *trans*-$V(CO)_2(dmpe)_2$ (0.39 g, 0.96 mmol), in thf (60 cm^3) at room temperature, was added NH_2SO_3H (97.4 mg, 1 mmol). After stirring for 24 h, the solvent was evaporated and the residue extracted into toluene (40 cm^3). Concentration and cooling to −20°C of the solution gave red needles. Yield 0.35 g (70%).

Table 8. Crystallographic data

(a) Crystal data			
Formula	$C_{14}H_{32}O_2P_4V$	$C_{17}H_{37}O_4P_4V$	$C_{40}H_{55}BNO_2P_4V$
M_r	407.242	480.313	767.527
Crystal system	Monoclinic	Orthorhombic	Monoclinic
a (Å)	8.936(1)	17.867(3)	18.444(7)
b (Å)	12.540(2)	8.787(1)	15.325(2)
c (Å)	10.039(3)	15.772(2)	15.011(2)
α (°)	90	90	90
β (°)	95.87(2)	90	94.89(2)
γ (°)	90	90	90
U (Å^3)	1119.05(40)	2476.16(59)	4227.48(1.79)
Space group	$P2_1/n$	$P2_12_12_1$	$P2_1/a$
D_c (g cm^{-3})	1.21	1.29	1.21
Z	2	4	4
F(000)	430	1016	1624
μ(Mo-K_α) (cm^{-1})	7.12	6.59	4.70
(b) Data collection			
θ (min, max) (°)	1.5, 25	1.5, 25	1.5, 23
Total data measured	2269	2627	6594
Total data unique	1967	2490	5860
Total data observed	926	1675	2508
Significant test	$F_o > 4\sigma(F_o)$	$F_o > 3\sigma(F_o)$	$F_o > 3\sigma(F_o)$
(c) Refinement			
No. of parameters	155	239	414
Weighting scheme parameters g[a]	0.0005	0.0005	0.0005
Final R[b]	0.0690	0.0571	0.0738
Final R_G[c]	0.0807	0.0656	0.0765

[a] $W = 1/[\sigma^2(F_o) + gF_o^2]$.
[b] $R = \Sigma|\Delta F|/\Sigma|F_o|$.
[c] $R_G = [\Sigma w(\Delta F)^2/\Sigma w|F_o^2|]^{1/2}$.

NMR [^{1}H (C_6D_6)]: 1.22m, 0.88m (dmpe); 4.29s (NH_2).

Salts of the cation $[HV(CO)_2(dmpe)_2]_2^{2+}$

(a) To *trans*-$V(CO)_2(dmpe)_2$ (0.24 g, 0.59 mmol), in methanol (40 cm^3) at −78°C, was added tetrafluoroboric acid (0.67 M in Et_2O, 0.6 mmol). After allowing the red solution to warm with stirring at room temperature for 24 h the final orange solutions was filtered, concentrated and cooled to −20°C, yielding orange crystals of the tetrafluoroborate as methanol solvate. Yield 0.25 g (42%), m.p. 135°C(d). Conductivity (MeOH, 25°C): $\Lambda_M = 90\ \Omega^{-1}\ cm^2\ mol^{-1}$.

(b) To *trans*-$V(CO)_2(dmpe)_2$ (0.22 g, 0.54 mmol), in toluene (40 cm^3) at room temperature, was added a toluene solution of $HCPh(SO_2CF_3)_2$ (0.19 g, 0.54 mmol) giving an orange precipitate. The reaction mixture was stirred for about 2 h and the solid collected, washed with toluene (2×20 cm^3), and dried *in vacuo*. Yield 0.6 g (79%). $\Lambda_M = 79\ \Omega^{-1}\ cm^2\ mol^{-1}$.

(c) The tetrafluoroborate can be converted to the tetraphenylborate by the addition of $NaBPh_4$ in methanol. However, attempts to recrystallize this salt from acetonitrile lead to the isolation of $[V(CO)_2(dmpe)_2(MeCN)][BPh_4]$.

It has also been noted that on standing in dichloromethane the hydrido species slowly gives $V(CO)_2(dmpe)_2Cl$ as shown by IR.

Crystallography

Crystals were sealed under argon in thin-walled-glass capillaries. All crystallographic measurements were made using a CAD4 diffractometer, operating in the ω–2θ scan mode with graphite-monochromated Mo-K_α radiation ($\lambda = 0.71069$ Å) in a manner described previously.[15] Details are given in Table 8. The structures were solved using routine heavy-atom methods and refined by full-matrix least squares, non-hydrogen atoms anisotropically, hydrogens isotropically. One of the bridging methylenes in the unique dmpe ligands of $V(CO)_2(dmpe)_2$ is disordered over two sites which refine to have 47/53 occupancies. Details of the crystal data, intensity measurement and refinement are given in Table 8.

Sources of scattering factor data and computer programs used are given in Ref. 15; all calculations were made on a DEC VAX 11/750 computer.

Acknowledgements—We thank the SERC for a studentship (F.J.W.) and for X-ray facilities. We also thank Dr A.R. Siedle of Minnesota Mining and Manufacturing for a generous gift of fluoro acids.

REFERENCES

1. N. G. Connelly, In *Comprehensive Organometallic Chemistry* (Edited by G. Wilkinson, F. G. A. Stone and E. W. Abel), Vol. 3, Chap. 24. Pergamon Press, Oxford (1982).
2. G. S. Girolami, G. Wilkinson, A. M. R. Galas, M. Thornton-Pett and M. B. Hursthouse, *J. Chem. Soc., Dalton Trans.* 1985, 1339.
3. J. E. Salt, G. S. Girolami, G. Wilkinson, M. Motevalli, M. Thornton-Pett and M. B. Hursthouse, *J. Chem. Soc., Dalton Trans.* 1985, 685.
4. D. M. P. Mingos, *J. Organomet. Chem.* 1979, **179**, C29.
5. D. F. Evans, *J. Chem. Soc.* 1959, 2003.
6. J. E. Salt, G. Wilkinson, M. Motevalli and M. B. Hursthouse, *J. Chem. Soc., Dalton Trans.* 1986, 1141.
7. R. C. Mehrotra and R. Bohra, *Metal Carboxylates.* Academic Press, London (1983).
8. R. Garth Kidd, *Annual Reports on NMR Spectroscopy*, Vol. 10A. Academic Press, New York (1980).
9. K. Ihmels and D. Rehder, *Organometallics* 1985, **4**, 1334.
10. D. Rehder, W. L. Dorn and J. Schmidt, *Transition Met. Chem. (Weinheim)* 1976, **1**, 233.
11. K. Ihmels and D. Rehder, *Organometallics* 1985, **4**, 1340.
12. J. A. Connor, P. I. Riley and C. J. Rix, *J. Chem. Soc., Dalton Trans.* 1977, 1317.
13. F. A. Cotton, M. P. Diebold and I. Shim, *Inorg. Chem.* 1985, **24**, 1510.
14. R. P. Tooze, Ph.D. thesis, p. 110. University of London (1985).
15. M. B. Hursthouse, R. A. Jones, K. M. A. Malik and G. Wilkinson, *J. Am. Chem. Soc.* 1979, **101**, 4128.

Polyhedron Vol. 6, No. 6, pp. 1361–1364, 1987
Printed in Great Britain

0277–5387/87 $3.00+.00

KINETIC STUDY OF THE REACTION OF *meso*-TETRAKIS(*p*-TRIMETHYLAMMONIUMPHENYLPORPHINATO)DIAQUOCHROMATE(III) WITH THIOCYANATE IONS

J. G. LEIPOLDT* and H. MEYER

Department of Chemistry, University of the Orange Free State, Bloemfontein, Republic of South Africa

(*Received* 2 *January* 1985; *accepted* 1 *December* 1986)

Abstract—The reaction of *meso*-tetrakis(*p*-trimethylammoniumphenylporphinato)-diaquochromate(III), $[CrTAPP(H_2O)_2]^{5+}$, with NCS^-, has been studied at 15, 25 and 35°C in 0.1 M H^+ with $\mu = 1.00$ M ($NaNO_3$). The reaction is first-order in anion concentration up to 0.9 M. The value of the second-order rate constant at 25°C is 4.2×10^{-3} $M^{-1}\,s^{-1}$ with $\Delta H^{\ddagger}$ and $\Delta S^{\ddagger}$ having values of 16.2 kcal mol^{-1} and -15.3 cal (deg mol)$^{-1}$, respectively. The porphine ligand greatly labilizes the chromium(III) toward substitution. High-pressure kinetic data ($\Delta V^{\ddagger}_{exp} = 9.2$ cm^3 mol^{-1}) indicate that the reaction proceeds via an I_d-mechanism.

It is well-known that the porphine ligand labilizes the axial positions in complexes of cobalt(III), rhodium(III) and chromium(III).[1–7] The extent of labilization is dependent upon the other metal complex to which it is being compared. If the reactivity of the porphine complex is compared with the reactivity of the pentaammineaquo complexes, it is found that the labilization is about 10^9, 10^3 and 10^2 for the TPPS [TPPS = *meso*-tetra(*p*-sulphonatophenyl)porphine] complexes of cobalt(III),[3,8] rhodium(III)[4,8] and chromium(III),[5,8] respectively.

The extent of labilization depends not only on the particular central metal ion, but also on the particular porphine. The anation reactions of $[CoTPPS(H_2O)_2]^{3-}$ are, for example, about 100 times faster than those of $[CoTMPP(H_2O)_2]^{5+}$ [TMPP = *meso*-tetra(4-*N*-methylpyridyl)porphine],[1,3] while the anation reactions of $[CrTPPS(H_2O)_2]^{3-}$ are only about 6 times faster than those of $[CrTMPP(H_2O)_2]^{5+}$.[5,6]

It has been suggested that the anation reactions of $[CrTPPS(H_2O)_2]^{3-}$ and $[CrTMPP(H_2O)_2]^{5+}$ proceed via an I_d-mechanism.[5,6] Strong support for this view was recently obtained from a high-pressure kinetic study of the reaction between $[CrTPPS(H_2O)_2]^{3-}$ and NCS^-.[9]

In an effort to gain more insight into the mechanism of the substitution reactions of chromium(III) porphines, we have decided to extend this work to the anation reactions of another water-soluble porphine, the [*meso*-tetrakis(*N*-trimethylammoniumphenyl)porphine (TAPP)] complex of chromium(III).

EXPERIMENTAL AND RESULTS

The iodide salt of TAPP was synthesized as described by Krishnamurthy.[10] The chromium complex of this porphine was synthesized in the same way as $[CrTPPS(H_2O)_2]_3^{3-}$: 100 mg of the iodide salt of TAPP was dissolved in 100 cm^3 dimethylformamide. While the solution was refluxed and purged with nitrogen gas, about 200 mg of chromium hexacarbonyl (an excess) was added in small portions over a period of about 2 h, until all the free porphine were converted into the chromium complex as indicated by the visible spectrum. The solution was allowed to cool to room temperature and 500 cm^3 of diethylether was added to precipitate the chromium(III) complex. The precipitate $\{[CrTAPP(H_2O)_2]I_5\}$ was washed with ether and allowed to dry in the atmosphere at room temperature.

The wavelength of the Soret band for this complex in an acidic medium is at 444 nm with a molar

* Author to whom correspondence should be addressed.

absorptivity of 1.59×10^4 M^{-1} cm^{-1}, and in an alkaline medium at 445 nm with a molar absorptivity of 1.053×10^4 M^{-1} cm^{-1}.

The acid dissociation constants were determined by means of a pH titration. Taking into account the mass balance, Beer's law, and the definition of K_{a1} and K_{a2}, we can write the following equation:

$$A = \frac{A_b K_a + A_a[H^+]}{K_a + [H^+]}, \quad (1)$$

where A is the absorbance at a particular pH, A_b the absorbance of the deprotonated form, A_a the absorbance of the protonated form, and K_a is either K_{a1} or K_{a2} in Scheme 1. K_{a1} was obtained by fitting the absorbance vs $[H^+]$ data, by using a nonlinear least-squares program,[11] to eqn (1). The value of K_{a1} was determined as $4.68\ (\pm 0.76) \times 10^{-8}$ M at 25°C and $\mu = 1.00$ M ($NaNO_3$). This value is a good agreement with the corresponding value for $[CrTPPS(H_2O)_2]^{3-}$,[5] and significantly lower than K_{a1} for $[CrTMPP(H_2O)_2]^{5+}$.[6] We were unable to determine the value of K_{a2} due to the small change in the absorbance with pH in the pH region of the expected value for K_{a2}.

It was not possible to determine the equilibrium constant for the reaction of this complex with NCS^- due to the formation of a precipitate during the reaction. One would expect a value of about 2 M^{-1} for K_1 (Scheme 1) as was the case for the complexes $[CrTPPS(H_2O)_2]^{3-}$ and $[CrTMPP(H_2O)_2]^{5+}$.[5,6]

The anation reactions of $[CrTAPP(H_2O)_2]^{5+}$ by NCS^- were studied at 15, 25 and 35°C in 0.1 M HNO_3 and $\mu = 1.00$ M ($NaNO_3$). It was established that the reaction rates are $[H^+]$-independent at $[H^+] > 10^{-3}$ M. This clearly indicates that $[CrTAPP(H_2O)_2]^{5+}$ is the only reactive species under the experimental conditions.

The rate law for the anation reactions at low pH values is

$$-\frac{d[CrTAPP(H_2O)_2^{5+}]}{dt} = (k_1[NCS^-] + k_{-1})[CrTAPP(H_2O)_2^{5+}]. \quad (2)$$

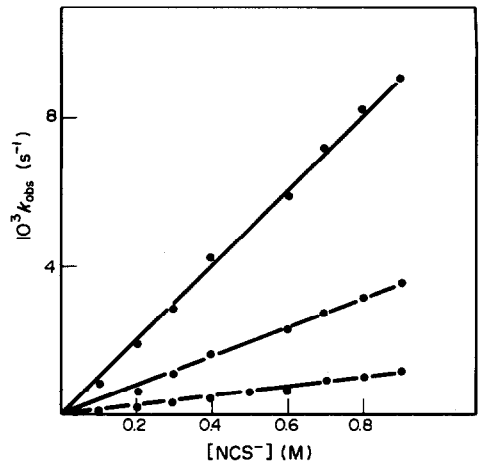

Fig. 1. Plot of k_{obs} vs $[NCS^-]$ at $[H^+] = 0.1$ M ($\mu = 1.0$ M).

All kinetic studies were performed under pseudo-first-order conditions with:

$$k_{obs} = k_1[NCS^-] + k_{-1}. \quad (3)$$

Figure 1 is a plot of k_{obs} vs $[NCS^-]$. The values of k_1 are reported in Table 1. The values of k_1, and particularly those of k_{-1}, were not as accurate as one would like as a result of the formation of a precipitate near the completion of the reaction. The activation parameters (ΔH^+ and ΔS^+) were calculated by means of a nonlinear least-squares fit[11] of the values of k_1 vs temperature to the Eyring–Polanyi equation. These values are given in Table 1.

The high-pressure kinetic data were obtained in a thermostated (± 0.1°C) high-pressure cell[12] coupled to a Zeiss PMQ II spectrophotometer. The results are summarized in Tables 1 and 2.

DISCUSSION

The data in Table 1 clearly indicate that labilization of the chromium(III) ion has been effected by the porphine. The extent of labilization due to TAPP is dependent on the comparison reaction and is, for example, 2700 and 100 compared to $[Cr(H_2O)_6]^{3+}$[13] and $[Cr(NH_3)_5H_2O]^{3+}$,[14] respect-

$$[CrTAPP(H_2O)_2]^{5+} + NCS^- \underset{k_{-1}}{\overset{K_1, k_1}{\rightleftharpoons}} [CrTAPP(H_2O)(NCS)]^{4+} + H_2O$$

$$K_{a1}, -H^+ \Big\| \Big\uparrow +H^+$$

$$[CrTAPP(H_2O)(OH)]^{4+}$$

$$K_{a2}, -H^+ \Big\| \Big\uparrow +H^+$$

$$[CrTAPP(OH)_2]^{3+}$$

Scheme 1.

Table 1. Kinetic parameters for the anation by NCS^- for selected compounds at 25°C and an ionic strength of 1.0 M

	k_1 ($M^{-1}s^{-1}$)	$\Delta H^{\neq}$ (kcal mol^{-1})	$\Delta S^{\neq}$ [cal (deg mol)$^{-1}$]	$\Delta V^{\neq}_{exp}$ (cm^3mol^{-1})
$[CrTAPP(H_2O)_2]^{5+}$	4.2×10^{-3}[a]	16.2	−15.3	9.2
$[CrTPPS(H_2O)_2]^{3-}$	4.7×10^{-3}	16.8	−12.8	7.4
$[CrTMPP(H_2O)_2]^{5+}$	7.4×10^{-4}	20.1	−5.5	
$[Cr(NH_3)_5(H_2O)]^{3+}$	3.0×10^{-5}	24.2	3.0	−4.9

[a] k_1 is 1.38×10^{-3} $M^{-1}s^{-1}$ at 15°C, and 1.06×10^{-2} $M^{-1}s^{-1}$ at 35°C.

ively. This is clearly not as great as the labilization effect in the case of the cobalt(III) complexes.[3,8]

The anation reaction rate constant for the reaction between $[CrTAPP(H_2O)_2]^{5+}$ and NCS^- is about the same as for the corresponding reaction of $[CrTPPS(H_2O)_2]^{3-}$,[5] and about 6 times faster than the corresponding reaction of $[CrTMPP(H_2O)_2]^{5+}$ [6] (see Table 1). The overall charge on the complex thus plays a minor role in the reaction process. In this respect it is important to note that the overall charge is spread over a large planar surface area, and that the negatively charged sulphonato groups and the positively charged trimethylammonium groups are removed far from the reaction metal centre. The values of $\Delta H^{\neq}$ and $\Delta S^{\neq}$ are about the same for the three different porphine complexes of chromium(III). The similarity of the activation parameters and the rate constants for the three porphine complexes (see Table 1) clearly indicate a common reaction mode.

The value of the volume of activation for the reaction between $[CrTAPP(H_2O)_2]^{5+}$ and NCS^- (9.2 cm^3 mol^{-1}) is also about the same as for the corresponding reaction of $[CrTPPS(H_2O)_2]^{3-}$, and may be interpreted as evidence for a dissociative interchange mechanism. This reaction mechanism may be represented as follows:

$$[CrTAPP(H_2O)_2]^{5+} + NCS^- \underset{}{\overset{K}{\rightleftharpoons}} [CrTAPP(H_2O)_2^{5+}, NCS^-], \quad (4)$$

$$[CrTAPP(H_2O)_2^{5+}, NCS^-] \xrightarrow{k_2} [CrTAPP(H_2O)(NCS)]^{4+} + H_2O.$$

The pseudo-first-order reaction rate constant for this mechanism is given by eqn (5):

$$k_{obs} = k_2K[NCS^-]/(1+K[NCS^-]). \quad (5)$$

This relationship between k_{obs} and NCS^- simplifies to:

$$k_{obs} = k_2K[NCS^-] \quad (6)$$

because no curvature in the k_{obs} vs $[NCS^-]$ plot was observed (see Fig. 1) and K is expected to be small.

It follows from eqns (3) and (6) that:

$$k_1 = k_2K.$$

According to this equation:

$$\Delta V^{\neq}_{exp} = \Delta V^{\neq}(k_2) + \Delta V(K)$$

$\Delta V(K)$ is expected to be close to zero: although there is an overall reduction of charges, the positive charges are very far removed from the negative charge on the NCS^- ligand, so that it is not expected that this formal overall reduction of charges would have a significant influence on $\Delta V(K)$. This charge reduction during the pre-equilibrium, in contrast to the charge concentration in the case of the $[CrTPPS(H_2O)_2]^{3-}$ reaction, may be used to explain the slightly higher value of $\Delta V^{\neq}_{exp}$ for the $[CrTAPP(H_2O)_2]^{5+}$ reaction.

The activation volume for the reaction between $[Cr(NH_3)_5H_2O]^{3+}$ and NCS^- [8] points to {in contrast to the activation volume for the anation reaction of $[CrTAPP(H_2O)_2]^{5+}$} an associative acti-

Table 2. k_{obs} as a function of pressure for the anation of $[CrTAPP(H_2O)_2]^{5+}$ by NCS^- at 15°C, $[H^+] = 0.1$ M and $[NCS^-] = 0.9$ M

P (bar)	20	250	500	750	1000
10^4k_{obs} ($M^{-1}s^{-1}$)	13.7	12.7	11.3	10.5	9.39

vation (see Table 1). These results indicate that the labilization of the axial water molecules is accompanied by promoting a dissociative activation. The labilization effect of the porphine ligand, and its capability to promote a dissociative activation, may be explained by its capability to donate electron density to the central metal ion making the chromium(III) d^3, more like a labile d^4 chromium(II) ion, and also stabilizes the five-coordinate intermediate in a dissociative reaction mode.

This phenomenon of promoting a dissociative mechanism (with the corresponding labilization) was also observed in the case of the rhodium(III) and cobalt(III) complexes of TPPS.[9] The high-pressure kinetic data clearly point to a D- and a I_d-mechanism for the anation reactions of $[CoTPPS(H_2O)_2]^{3-}$ and $[RhTPPS(H_2O)_2]^{3-}$, respectively, while an I_d- and an I_a-mechanism were proposed for the anation reaction of the penta-ammineaquo complexes of cobalt(III) and rhodium(III), respectively.[8,9,15]

Acknowledgements—We thank the South African C.S.I.R. and the research fund of this university for financial support, and Dr R. van Eldik of the University of Frankfurt am Main, F.R.G., who made it possible for us to do the high-pressure study.

REFERENCES

1. R. F. Pasternack, M. A. Cobb and N. Sutin, *Inorg. Chem.* 1975, **14**, 866.
2. K. R. Ashley and S. Au-Young, *Inorg. Chem.* 1976, **15**, 1937.
3. K. R. Ashley and J. G. Leipoldt, *Inorg. Chem.* 1981, **20**, 2326.
4. K. R. Ashley, Shaw-Bey Shyu and J. G. Leipoldt, *Inorg. Chem.* 1980, **19**, 1613.
5. K. R. Ashley, J. G. Leipoldt and V. K. Joshi, *Inorg. Chem.* 1980, **19**, 1608.
6. J. G. Leipoldt, S. S. Basson and D. R. Rabie, *J. Inorg. Nucl. Chem.* 1981, **43**, 3239.
7. J. G. Leipoldt, S. S. Basson, G. J. Lamprecht and D. R. Rabie, *Inorg. Chim. Acta* 1981, **51**, 67.
8. R. van Eldik, D. A. Palmer and H. Kelm, *Inorg. Chem.* 1979, **18**, 1520.
9. J. G. Leipoldt, R. van Eldik and H. Kelm, *Inorg. Chem.* 1983, **22**, 4146.
10. M. Krishnamurthy, *Indian J. Chem.* 1977, **15B**, 964.
11. R. H. Moore, Report No. LA2367, Los Alamos Scientific Laboratory (1960) [and addendum (1963)].
12. F. K. Fleischmann, E. G. Conze, D. R. Strantis and H. Kelm, *Rev. Sci. Instrum.* 1974, **45**, 1427.
13. D. Thusius, *Inorg. Chem.* 1971, **10**, 1106 (and references within).
14. N. V. Duffy and J. E. Earley, *J. Am. Chem. Soc.* 1967, **89**, 272.
15. T. W. Swaddle and D. R. Stranks, *J. Am. Chem. Soc.* 1972, **94**, 8357.

Polyhedron Vol. 6, No. 6, pp. 1365–1373, 1987
Printed in Great Britain

0277-5387/87 $3.00+.00

EQUILIBRIA IN AQUEOUS SOLUTION BETWEEN Be(II) AND NITRILOTRIACETIC, METHYL-*C*-NITRILOTRIACETIC, NITRILODIACETICPROPIONIC, NITRILOACETICDIPROPIONIC AND NITRILOTRIPROPIONIC ACIDS

A. MEDEROS,* S. DOMÍNGUEZ and A. M. MEDINA

Departamento de Química Inorgánica, Universidad de La Laguna, Tenerife, Canary Islands, Spain

and

F. BRITO, E. CHINEA and K. BAZDIKIAN

Laboratorio de Equilibrios en Solución, Escuela de Química, Facultad de Ciencias, Universidad Central de Venezuela, Caracas, Venezuela

(*Received* 28 *October* 1986; *accepted* 1 *December* 1986)

Abstract—The complex species formed in aqueous solution between Be(II) and nitrilotriacetic acid (NTA), methyl-*C*-nitrilotriacetic acid (MNTA), nitrilodiaceticpropionic acid (NDAP), nitriloaceticdipropionic acid (NADP) and nitrilotripropionic acid (NTP) were studied at 25°C and ionic strength 0.5 M in $NaClO_4$. The application of the calculus program LETAGROP to the experimental potentiometric data, taking into account hydrolysis of the ion Be(II), indicates that, upon varying the ligand–metal relationships, the following complex species are formed (H_3C ligands): NTA($[BeC]^-$, $\log K = 6.84$); MNTA ($[BeC]^-$, $\log K = 7.39$; BeHC, $\log K = 1.79$); NDAP ($[BeC]^-$, $\log K = 8.10$; BeHC, $\log K = 1.96$; $[BeH_2C]^+$, $\log K = 1.37$); NADP ($[BeC]^-$, $\log K = 9.25$; BeHC, $\log K = 2.37$); and NTP ($[BeC]^-$, $\log K = 9.23$). The values of the stability constants ($[BeC]^-$, $\log K$) indicate the following order of coordinating capacity: NTA < MNTA < NDAP < NADP ≃ NTP. This order is attributed to the increase in propionic groups. It has been confirmed that six-membered ring chelates are the most stable for Be(II), in a similar manner to other elements of the first short period, such as boron and carbon, while Cu(II), Ni(II), lanthanides and other heavier elements prefer five-membered ring chelates.

In our studies in aqueous solution of the EDTA–Be(II)[1,2] (EDTA = ethylenediaminetetraacetic acid) and IDA–Be(II)[3] (IDA = iminodiacetic acid) systems we have found upon analysing the experimental potentiometric data by means of the NERNST/LETA/GRAFICA[4] version of the LETAGROP[5] program, that the species resulting from the hydrolysis of Be(II) must be taken into consideration in the calculations in order to determine the complex species present in the solution and to obtain correct values of the stability constants. Otherwise, the values obtained are higher than the true ones, since the acidity due to hydrolysis of the non-complexed Be(II) is included in the value of the stability constants obtained.

Be(II) tends to tetracoordination.[6] EDTA,[1,2] a potentially hexadentate ligand, forms the complexes $[BeHC]^-$ and $[BeC]^{2-}$ (H_4C ligand). IDA,[3] a potentially tridentate ligand, only forms the monohydroxide complex $[Be(OH)C]^-$ (H_2C ligand) in significant amounts, OH^- occupying the fourth place in coordination. Nitrilotriacetic acid (NTA), a potentially tetradentate ligand, fulfils the coor-

* Author to whom correspondence should be addressed.

dination requirements of Be(II). However, the data available in the literature are contradictory: Dyatlova *et al.*[7,8] affirm that the species BeHC, $[BeC]^-$ and $[BeC(HC)]^{3-}$ (H_3C ligand) are formed with NTA. Stary,[9] by extraction with oxine in $CHCl_3$, found $\log K = 7.11$, at $I = 0.1$ M in $NaClO_4$ and 20°C, for the stability constants of the complex $[BeC]^-$. Other authors[10–12] also determined the stability constant of the complex $[BeC]^-$ from potentiometric measurements in aqueous solution, but the results are contradictory and no reference is made to whether or not the hydrolysis of Be(II) was taken into account in the calculations involved. Votava and Bartušek[10] also studied the NTP–Be(II) (NTP = nitrilotripropionic acid) system and found that the complex $[BeC]^-$ is slightly more stable with NTP than with NTA, contrary to the general belief,[13] still upheld,[14] that five-membered chelate rings provide greater stability than any other size of chelate ring.

It therefore seemed worthwhile to study the influence of the length of the chelate rings on the stability of complexes with Be(II). As well as re-examining the NTA–Be(II) and NTP–Be(II) systems, the MNTA–Be(II) (MNTA = methyl-*C*-nitrilotriacetic acid), NDAP–Be(II) (NDAP- = nitrilodiaceticpropionic acid), and NADP–Be(II) (NADP = nitriloaceticdipropionic acid) systems were also studied. The studies were carried out in aqueous solution at 25°C and $I = 0.5$ M in $NaClO_4$. The only work known on the NTP–Be(II) system is the above-mentioned report of Votava and Bartušek.[10] No reference was found in the literature to the MNTA–Be(II) and NADP–Be(II) systems.

Be(II) is perhaps the most toxic of metallic cations[15] and ligands containing propionic groups may be better sequestering agents.

EXPERIMENTAL

Reagents

NTA. The product used was supplied by Merck, of analytical grade and previously recrystallized.

MNTA. The method of preparation by Irving and Miles[16] was very slow and gave a low yield. It was therefore modified as follows: a solution of α-alanine in a small amount of water was made to react with previously neutralized chloroacetic acid, by heating to 90°C and maintaining the pH between 8 and 9 with NaOH. After addition of NaOH, magnetic stirring was continued for 4 h and the Cd(II) salt was precipitated by adding a theoretical amount of $Cd(NO_3)_2$, aided by ethanol. The Cd(II) salt was filtered and washed with a 50% water–ethanol mixture, suspended in a small amount of water and through this a current of H_2S was then passed. The CdS was separated by filtration. The solution was concentrated in a steam bath, through which a current of argon was passed in order to remove the excess of H_2S, concentrated in a rotavaporator and left to crystallize. The acid was purified by recrystallization in water–ethanol mixtures. This procedure afforded the acid in a high state of purity and within a short period (3–4 days), although the yields were also low.

NDAP. The method of Pratt and Smith[17] was modified in order to obtain the acid in a high degree of purity, following the method employed by Souchay *et al.*[18] in the preparation of some derivatives of iminodiacetic acid: β-alanine was made to react with previously neutralized chloroacetic acid. After formation of the Ba(II) salt, the acid was obtained with conc. H_2SO_4 in good yield.

NTP. This was prepared by reacting β-alanine with β-chloropropionic acid, according to the procedure indicated by Chaberek and Martell,[19] adapted by Votava and Bartušek.[10] The yield was good.

NADP. This acid was prepared analogously to NTP, by reacting glycine with β-chloropropionic acid, again with a good yield.

The acids were identified by their potentiometric equivalents, ^1H NMR and mass spectra.

The solution of $Be(ClO_4)_2$ was prepared by reacting metallic Be (Spex Industries Inc.) with an excess of $HClO_4$ (Merck, analytical grade), its free acidity[20] being determined, as well as the concentration of Be(II) in aqueous solution which was evaluated gravimetrically.[21,22] A carbonate-free sodium hydroxide solution was prepared according to the School of Sillén[23] and standardized against potassium hydrogen phthalate. $NaClO_4$ was prepared by recrystallization of $NaClO_4$ (Merck, analytical grade).

Apparatus and titration procedures

The potentiometric titrations were carried out in inert argon atmosphere, at 25±0.05°C, $I = 0.5$ M in $NaClO_4$, using a Radiometer Type PHM-64 potentiometer, a Radiometer G 202 B glass electrode and a K 401 calomel electrode. The cell constants were determined according to the method of Biedermann and Sillén,[24] the liquid junction potentials being found to be negligible within the margins of $[H^+]$ studied. It was found that $pK_w = 13.72$, in excellent agreement with reported data.[25]

Measurements were taken of the ligands alone at the following concentrations: NTA ($C_L = 5$ mM), MNTA($C_L = 3.7$ and 4.7 mM), NDAP ($C_L = 10$

and 20 mM), NADP (C_L = 4.7 and 5.2. mmM), and NTP (C_L = 2.1 and 2.5 mM); and the ligands in the presence of Be(II) at the following concentrations and ligand : metal ratios : C_M = 0.8 and 1.2 mM, ratios 1 : 1, 2 : 1, 4 : 1 and 6 : 1, for NTA; C_M = 1.5, 3.2 and 12.0 mM, ratios 2 : 1, 1 : 1 and 1 : 2, for MNTA; C_M = 10, 15 and 20 mM, ratios 2 : 1, 1 : 1 and 1 : 2, for NDAP; C_M = 2.0, 5.0 and 9.7 mM, ratios 2 : 1, 1 : 1 and 1 : 2, for NADP; and C_M = 2.3 mM, ratios 2 : 1 and 1 : 1, for NTP.

The normal titration procedure could not be employed for the potentiometric titrations of NTP acid in the presence of Be(II) because of the long time required to reach the equilibria (up to 3 h between two consecutive additions of NaOH). This problem was overcome by preparing individual beakers with solutions of the NTP–Be(II) system at different pH values (25°C and I = 0.5 M in $NaClO_4$), shaking each solution for 24 h and then measuring the potentials when equilibrium was reached in each titration cell.

Data treatment

The experimental potentiometric data were analysed by means of the NERNST/LETA/GRAFICA version[4] of the LETAGROP program,[5] based on a generalized form of the least-squares method that establishes the best model and best values of the β_{pqr} constants, minimizing the function $U = \Sigma(Z_{exp} - Z_{calc})^2$, Z being the average number of dissociated protons for the concentration of ligand (Z_C) or for the total concentration of metal (Z_B). The LETAGROP calculations also give standard deviations $\sigma(Z)$ and $\sigma(\log \beta_{pqr})$.[26] The computations were performed on a Burroughs 6700 computer (Facultad de Ciencias, Universidad Central de Venezuela, Caracas).

Hydrolysis of Be(II) was previously studied under the same experimental conditions.[3]

RESULTS

Ionization constants of the acids

From the values obtained for the constants β_{pr} corresponding to equilibrium (1):

$$pH^+ + rH_3C \rightleftharpoons [H_p(H_3C)_r]^{p+}, \qquad (1)$$

the ionization constants of the acids (K_i) given in Table 1 could readily be determined.

The values of pK_1, pK_2 and pK_3 are in good agreement with those found for NTA at 25°C and I = 0.5 M,[27–29] and with those found for MNTA at 25[30] and 20°C,[16,31] and I = 0.1 M; for NDAP at 25,[30,32] 20[33] and 30°C,[19] and I = 0.1 M; for NADP at 30°C and I = 0.1 M;[19] and NTP at 25,[34] 20[10] and 30°C,[19] and I = 0.1 M. The value of pK_0

Table 1. Ionization constants of MNTA, NTA, NDAP, NADP and NTP (25°C, I = 0.5 M in $NaClO_4$)

	$-\text{Log } \beta_{pr}$				
pr	MNTA	NTA	NDAP	NADP	NTP
11	−0.5[a]	−0.7[a]	−1.07±0.03	−1.95±0.03	−2.71±0.05
−11	1.60±0.03	1.82±0.05	2.22±0.01	3.12±0.02	3.77±0.05
−21	3.96±0.02	4.20±0.02	5.87±0.02	7.12±0.02	8.05±0.04
−31	13.65±0.03	13.25±0.01	15.16±0.02	16.67±0.03	17.64±0.05
[b]/[c]	2/115	1/125	3/169	2/102	2/60
[d]	0.020	0.005	0.014	0.015	0.025
[e]	1.6–11.5	2.0–10.4	1.4–10.5	1.7–11.3	1.8–10.9
Equilibrium			pK_i		
H_4C^+–H_3C	0.5[a]	0.7[a]	1.07	1.95	2.71
H_3C–H_2C^-	1.60	1.82	2.22	3.12	3.77
H_2C^-–HC^{2-}	2.36	2.38	3.65	4.00	4.28
HC^{2-}–C^{3-}	9.69	9.05	9.29	9.55	9.59

[a] Values estimated from the linear correlations pK_0 vs pK_1.
[b] Number of titrations.
[c] Number of experimental points.
[d] Standard deviation [$\sigma(Z)$].
[e] −Log [H^+] range.

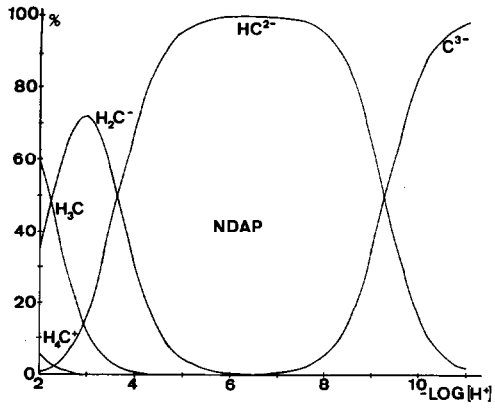

Fig. 1. Species distribution as a function of $-\log[H^+]$ for NDAP.

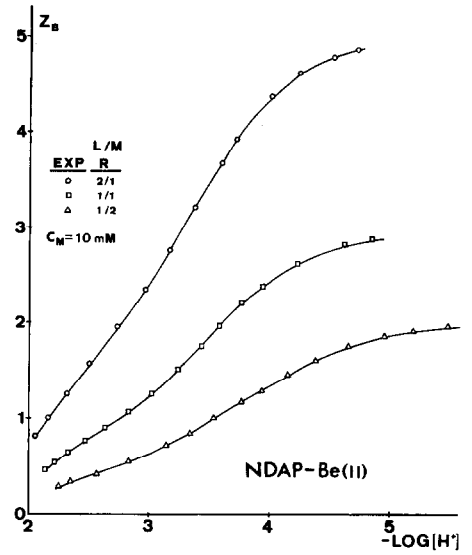

Fig. 2. Z_B vs $-\log[H^+]$ curves for the NDAP–Be(II) system. Full curves have been calculated using the β_{pqr} constants in Table 2.

(H_4C^+–H_3C equilibrium) is in good agreement with that for NTP.[34] For NDAP and NADP the values of pK_0 are obtained for the first time. For NTA at 20°C and $I = 0.1$ M in KCl, $pK_0 = 0.8 \pm 0.2$.[35]

The order of basicity NTA < NDAP < NADP < NTP is in agreement with the substitution of acetic groups by propionic groups having a greater inductive electron donor effect because of another CH_2 group.[18] The values of pK_0, pK_1 and pK_2 correspond to fundamentally carboxylic protons.[19] The values of pK_3 (HC^{2-}–C^{3-} equilibrium) for all the ligands are in agreement with the protonation of the N atom in aqueous solution.[36] The order of basicity for pK_3 (MNTA > NTA) is explained by the inductive electron donor effect of the methyl radical on the N atom in MNTA. The diagrams of the distribution of species as a function of $-\log[H^+]$, calculated in accordance with the values of $-\log\beta_{pr}$ given in Table 1, show that the monoprotonated species HC^{2-}, with a betaine structure, is the most stable species and occupies the greatest field, and also that the species containing protonated carboxylic groups improve the stability as the number of propionic groups increases. The diagram corresponding to NDAP is represented in Fig. 1.

Stability constants of the complexes formed

The analysis of the experimental data of the Be–ligand systems studied by the NERNST/LETA/GRAFICA version[4] of the LETAGROP program[5] allowed us to calculate the β_{pqr} constants for the complex species formed for each ligand, defined by means of equilibrium (2):

$$pH^+ + qBe^{2+} + rH_3C \rightleftharpoons [H_pBe_q(H_3C)_r]^{(p+2q)+}. \quad (2)$$

Taking into account the species resulting from the massive ionizations of the ligand (H_4C^+, H_3C, H_2C^-, HC^{2-} and C^{3-}) as well as the hydrolytic species of Be(II) existing in the area of calculus, i.e. $[Be_2(OH)]^{3+}$ and $[Be_3(OH)_3]^{3+}$ (whose formation constants at this temperature and ionic strength have been calculated by us in a previous work[3]), the results that best fit the experimental results are those given in Table 2. Although models were tested that included the possible presence of the hydroxy complex $[Be(OH)C]^{2-}$, and complex species with excess of ligand and excess of metal, the results indicate that they are not present in significant amounts. The validity of this analysis can be checked in Fig. 2 for the NDAP–Be(II) system, where an excellent fit can be observed between the experimental Z_B vs $-\log[H^+]$ curves and those calculated from the values of β_{pqr} given in Table 2. Analogous curves are obtained for the other four systems. In Fig. 2 it can be observed that the limit values of Z_B ($Z_B \rightarrow$ 5, 3 and 2, respectively, for ligand : metal ratios of 2 : 1, 1 : 1 and 1 : 2) are those expected for the formation of the complex $[BeC]^-$ and the non-formation of the complex $[Be(OH)C]^{2-}$.

The values of $\log K$ corresponding to the stability constants of the complex species found for the different ligands studied are also given in Table 2, being readily obtained from the values of the β_{pqr} in Table 2, and taking into account the values of the β_{pr} constants of the acids presented in Table 1.

The data in tables 1 and 2 also readily afford the

Table 2. Stability constants of the complexes of MNTA, NTA, NDAP, NADP and NTP with Be(II) (25°C, $I = 0.5$ M in $NaClO_4$)

	$-\text{Log } \beta_{pqr}$				
pqr	MNTA	NTA	NDAP	NADP	NTP
−111			0.85±0.06		
−211	2.17±0.07		3.91±0.05	4.75±0.08	
−311	6.26±0.08	6.41±0.03	7.06±0.02	7.42±0.01	8.41±0.06
[a]/[b]	9/246	4/99	9/364	9/311	2/28
[c]	0.038	0.013	0.023	0.026	0.068
[d]	1.9–5.3	2.3–5.9	1.9–5.8	2.5–6.5	3.2–5.1
Equilibrium			Log K		
$Be^{2+} + H_2C^- - [BeH_2C]^+$			1.37		
$Be^{2+} + HC^{2-} - BeHC$	1.79		1.96	2.37	
$Be^{2+} + C^{3-} - [BeC]^-$	7.39	6.84	8.10	9.25	9.23
		7.11[e]			7.90[f]
		7.64[f]			
		7.82[g]			
		7.86[h]			

[a] Number of titrations.
[b] Number of experimental points.
[c] Standard deviation [$\sigma(Z)$].
[d] $-\text{Log } [H^+]$ range.
[e] 20°C, $I = 0.1$ M in $NaClO_4$.[9]
[f] 20°C, $I = 0.11$ M in KNO_3.[10]
[g] 25°C, $I = 0.4$ M in $NaClO_4$.[12]
[h] 25°C, $I = 0.1$ M in KNO_3.[11]

pK_i values corresponding to the ionization of the protonated complex species:

	MNTA	NDAP	NADP
pK BeHC	4.09	3.15	2.67
pK $[BeH_2C]^+$		3.06	

The values found in the literature for log K of the complex $[BeC]^-$ in the case of NTA and NTP are also given in Table 2. The values obtained for NTA by Votava and Bartušek,[10] Fraústo da Silva[11] and Dubey *et al.*[12] are approximately one unit of log K greater than those found by us, probably attributable to the fact that the hydrolysis of Be(II) was not taken into account by these authors. The value found by Stary,[9] although somewhat greater, is the closest to our own, which is explained perfectly by the lower ionic strength (0.1 M in $NaClO_4$) and temperature (20°C). Moreover, the method used by Stary was extraction in oxine with $CHCl_3$, operating at pH ≃ 6, taking care that hydrolysis of Be(II) exerted a negligible influence. For NTP, the value found by Votava and Bartušek[10] is much smaller than that obtained by us. These authors did not take into account the hydrolysis of Be(II) in their calculations and affirm that the constant of the complex $[BeC]^-$ was calculated within a very small range of pH values. However, we consider that the much lower value of log K found by Votava and Bartušek[10] is due to the kinetic process that takes place in the NTP–Be(II) system in aqueous solution, which compelled us to operate in a different manner in order to achieve the equilibria, as indicated in Experimental. Votava and Bartušek do not report in their work[10] that the kinetic process takes place and probably performed the potentiometric measurements without the equilibrium having been reached.

DISCUSSION

In comparison with IDA and analogues[3] (tridentate coordinating agents) that form the

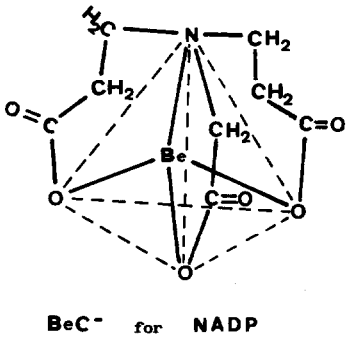

Fig. 3. Structure proposed for the complex $[BeC]^-$ with NADP.

monohydroxycomplex $[Be(OH)C]^-$ (H_2C ligands) as the most stable species, the formation of the species $[BeC]^-$ as the most stable in NTA and analogues (H_3C ligands) implies that these ligands act vs Be(II) as tetradentate coordinating agents, coordinating the N atom and the three carboxylate groups. The tendency of Be(II) to attain tetrahedral coordination[6] is totally fulfilled. The complex $[BeC]^-$ for NADP acid is represented in Fig. 3. Tetrahedrons are analogous for the other ligands. The coordination of the N atom of NTA acid to Be(II) has been manifested by Grigor'ev[37] upon analysing the IR spectrum of the complex $BeHC \cdot 2H_2O$, obtained in a crystalline state.

The following order of stability (Table 2), NTA < MNTA < NDAP < NADP ≃ NTP, is found for the complex $[BeC]^-$. The order NTA < MNTA is explained in that the electron donor nature of the radical CH_3 exerts a positive inductive effect that is superimposed on the steric repulsion exerted by the same radical on the coordinated Be(II), thus strengthening the N—Be bond in an overall manner. The sequence that follows implies an increase in the stability of the complex $[BeC]^-$ as the number of propionic groups coordinated to Be(II) increases, and is analysed below.

The diagrams of the distribution of species of Be(II) as a function of $-\log[H^+]$ was calculated from the values of β_{pr} given in Table 1, β_{pqr} in Table 2, and β_{pq} presented in an earlier work.[3]

The distributions of species of Be(II) as a function of $-\log[H^+]$ are presented in Figs 4–6 for NTA, NDAP and NADP, respectively ($C_{Be} = 1$ mM, ligand : metal ratios 1 : 1 and 3 : 1). The diagram corresponding to MNTA is analogous to that of NTA, with the sole difference that the monoprotonated species BeHC is present in a small amount. The diagram corresponding to NTP is identical with that of NADP, with the exception of the negligible formation of the species BeHC for NTP.

An analysis of the diagrams shows that the complex species are formed directly from the $[Be(H_2O)_4]^{2+}$, which is the non-hydrolysed species present in aqueous solution.[6,38,39] If these diagrams are compared with those of the acids alone (Fig. 1) it is found that the complex species are fundamentally

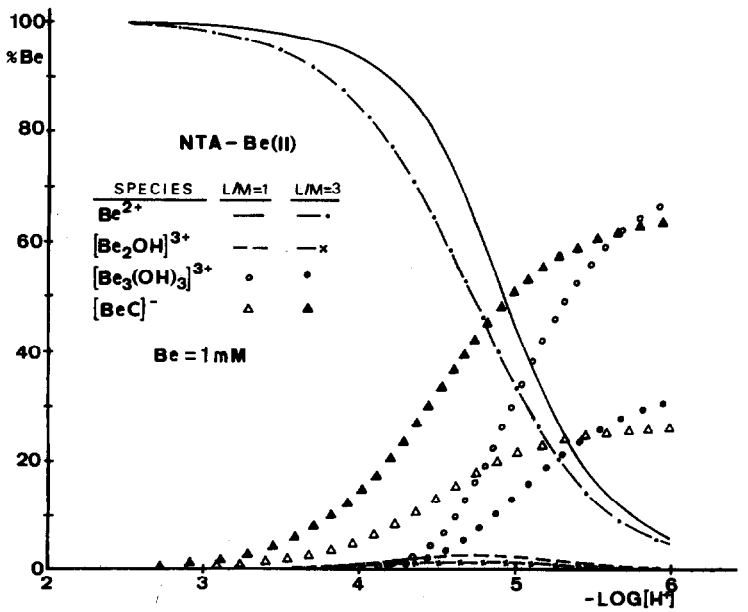

Fig. 4. Species distribution as a function of $-\log[H^+]$ for the NTA–Be(II) system.

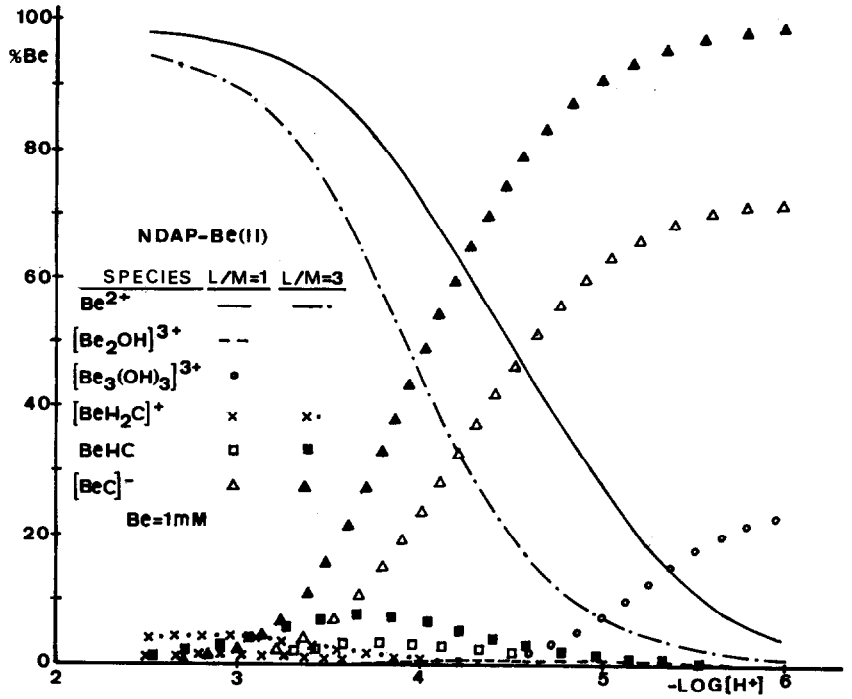

Fig. 5. Species distribution as a function of $-\log[H^+]$ for the NDAP–Be(II) system.

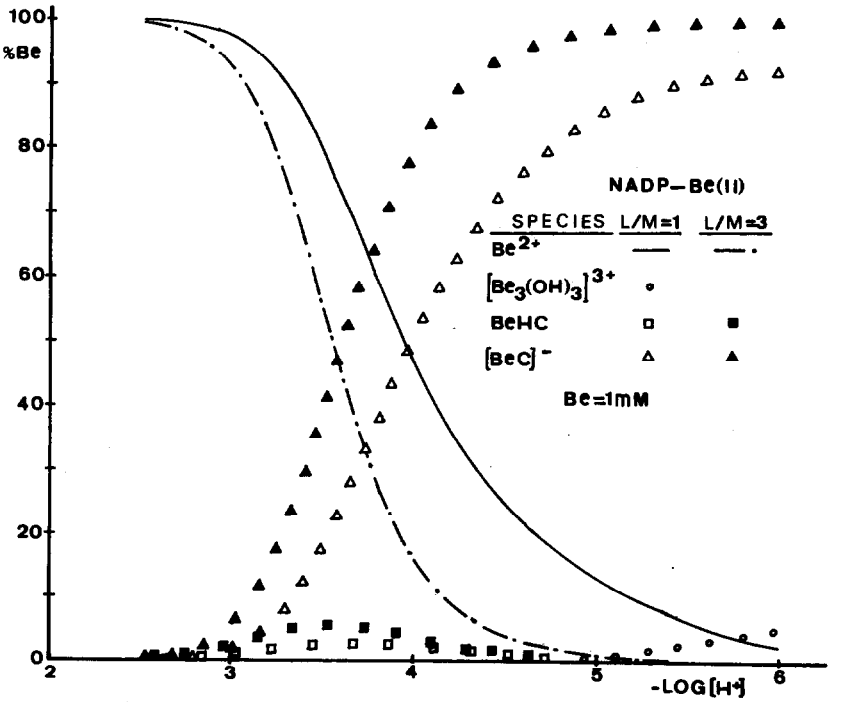

Fig. 6. Species distribution as a function of $-\log[H^+]$ for the NADP–Be(II) system.

formed from the equilibria:

$$[Be(H_2O)_4]^{2+} + H_3C \rightleftharpoons [Be(H_2C)(H_2O)_2]^{+} + H^{+} + 2H_2O, \quad (3)$$

$$[Be(H_2O)_4]^{2+} + H_2C^{-} \rightleftharpoons Be(HC)(H_2O) + H^{+} + 3H_2O, \quad (4)$$

$$[Be(H_2O)_4]^{2+} + HC^{-} \rightleftharpoons [BeC]^{-} + H^{+} + 4H_2O. \quad (5)$$

Equilibrium (5) gives $Z \rightarrow 3$ when the complex $[BeC]^{-}$ is formed (Fig. 2), implying also the coordination of the N atom upon displacement by Be of the betaine proton of the most stable protonated species of the ligand HC^{2-}, accounting in turn for the much greater stability of the complex species $[BeC]^{-}$. In the species $[BeH_2C]^{+}$ and BeHC, the ligand is bidentate and tridentate, respectively, bonding only carboxylate groups to the metal and maintaining the betaine proton, which explains the low stability of these protonated species and the fact also that these are practically not formed by the more symmetric ligands NTA and NTP. Upon raising the pH, of course, the species $[BeH_2C]^{+}$ is transformed into BeHC and the latter into $[BeC]^{-}$.

The species distribution diagrams (Figs 4–6) explain the order of stability of the species $[BeC]^{-}$ in more detail: at a 1 mM concentration of Be(II) and in a ligand: metal ratio of 1:1 for NTA only 25% is complexed at pH 5–6, reaching 65% at a 3:1 ratio. Figure 4 thus justifies the study of the NTA–Be(II) system in Experimental, with ligand: metal ratios of up to 6:1. For NDAP (Fig. 5), under the same experimental conditions, 70% of Be(II) is complexed at pH 5–6 at a ratio of 1:1, attaining almost 100% at a ratio of 3:1. These percentages rise for NADP (Fig. 6) to 90% at a ratio of 1:1, and 100% at a ratio of 3:1. NTP behaves in an identical manner. The non-complexed Be(II) undergoes hydrolysis to form mainly the species $[Be_3(OH)_3]^{3+}$. The practical disappearance of this species at a ligand: metal ratio of 3:1 can be observed in Figs 5 and 6.

The stability sequence found in this work for Be(II), NTA < MNTA < NDAP < NADP ~ NTP, is precisely the opposite of that generally found for other heavier cations such as Cu(II) and Ni(II), as manifested by the data given in Table 3.

These and other results for 3*d* transition and alkaline earth cations led to the conclusion that the decrease in stability upon passing from five- to six-membered chelate rings was a general phenomenon for all metals and polydentate ligands,[13] a belief which is still widespread.[14] This phenomenon was also found to take place in the case of lanthanide chelates with NTA, MNTA and NDAP,[43] as well as in other polyaminocarboxylic acids.[44]

However, contrary to general belief, this phenomenon whereby five-membered chelate rings are more stable than six-membered ones is not common. Indeed, it seems to hold true for central atoms with atomic numbers greater than 10, in which coordination numbers greater than 4 predominate. It has been found that first short period elements, among which Be and B readily form complexes, prefer six-membered chelate rings, in a similar manner to organic compounds having a tetrahedral carbon. Evidence of this phenomenon has been found for complexes of B(III)[45,46] and Be(II).[10,47,48] The present work confirms that for Be(II) six-membered chelate rings are more stable than five-membered ones, analogously to B and C. With regard to the small central atom belonging to the first short period, which is coordinated with a tetrahedral geometry, six-membered chelate rings are puckered with tetrahedral links, and are submitted to fewer strains than five-membered rings. The opposite occurs for larger atoms, such as Ni: structural and ^1H NMR studies indicate that six-membered rings are puckered much more and are submitted to more steric strains than five-membered rings.[17] The step from a tetrahedral to an octahedral geometry, when the volume of the central cation increases, must exert an influence on this change in the stability of the chelate rings. The results obtained in this work show that the stability of the complex $[BeC]^{-}$ is practically the same for NADP and NTP. That is, the third six-membered ring no longer increases

Table 3. Stability constants of the complexes of NTA, NDAP, NADP and NTP with Cu(II) and Ni(II)

	NTA[a]	NDAP[a]	NADP[b]	NTP[b]	NTP[c]
Log *K*, Cu(II)	13.1	12.6	11.9	9.1	8.83
Log *K*, Ni(II)	11.5	11.4	9.1	5.8	5.64

[a] 25°C, $I = 0.1$ M.[27,40 42]
[b] 30°C, $I = 0.1$ M in KCl.[19]
[c] 25°C, $I = 0.1$ M in KNO_3.[34]

the stability with respect to the five-membered ring (Fig. 3, complex $[BeC]^-$ with NADP). This must be attributed to the fact that the third ethylene group (CH_2—CH_2) in the case of NTP undergoes steric repulsion on the part of the other two, that compensate the increase in stability which would correspond to the third six-membered ring. In the case of a ligand : metal ratio of 1 : 1 with NTA, models show that when all three carboxylate groups are bonded (the rings are now five-membered), the three chelate rings are not all equivalent, and one at least is strained.[17]

REFERENCES

1. A. Mederos, S. Domínguez, M. Hernández-Padilla, F. Brito and E. Chinea, *Bol. Soc. Quim. Peru* 1984, **50**, 277.
2. A. Mederos, J. M. Felipe, M. Hernández-Padilla, F. Brito, E. Chinea and K. Bazdikian, *J. Coord. Chem.* 1986, **14**, 277.
3. A. Mederos, S. Domínguez, M. J. Morales, F. Brito and E. Chinea, *Polyhedron* 1987, **6**, 000.
4. F. Brito and J. M. Gonçalves, Project No. 51.78.31-S1-1228. CONICIT, Caracas, Venezuela (1981).
5. R. Arnek, L. G. Sillén and B. Warnqvist, *Ark. Kemi* 1969, **31**, 341.
6. J. Burgess, *Metal Ions in Solution*. Ellis Horwood, Chichester (1978).
7. N. M. Dyatlova, M. I. Kabachnik, T. Y. Medved, M. V. Rudomino and Y. F. Belugin, *Dokl. Akad. Nauk S.S.S.R.* 1965, **161**, 607.
8. N. M. Dyatlova, V. V. Medyntsev and B. V. Zhadanov, *Chem. Abstr.* 1968, **68**, 16594 m; 1968, **69**, 6572 j.
9. J. Stary, *Anal. Chim. Acta* 1963, **28**, 132.
10. J. Votava and M. Bartušek, *Coll. Czech. Chem. Commun.* 1975, **40**, 2050.
11. J. J. R. Fraústo da Silva and M. C. T. Abreu Vaz, *J. Inorg. Nucl. Chem.* 1977, **39**, 613.
12. S. N. Dubey, A. Singh and D. M. Puri, *J. Inorg. Nucl. Chem.* 1981, **43**, 407.
13. H. Irving, R. J. P. Williams, D. J. Ferret and A. E. Williams, *J. Chem. Soc.* 1954, 3494.
14. C.-S. Chung, *J. Chem. Educ.* 1984, **61**, 1062.
15. E. Ochiai, *Bioinorganic Chemistry*. Allyn & Bacon, Boston (1977).
16. H. M. N. H. Irving and M. G. Miles, *J. Chem. Soc. A* 1966, 1268.
17. L. Pratt and B. B. Smith, *Trans. Faraday Soc.* 1969, **75**, 915.
18. P. Souchay, N. Israily and P. Gouzerh, *Bull. Soc. Chim. Fr.* 1966, 3917.
19. S. Chaberek, Jr and A. E. Martell, *J. Am. Chem. Soc.* 1953, **75**, 2888.
20. G. Gran, *Analyst* 1952, **77**, 661.
21. J. Huré, M. Kremer and F. Bequer, *Anal. Chim. Acta* 1952, **7**, 37.
22. R. Pribil, *Analytical Applications of EDTA and Related Compounds*. Pergamon Press, Braunschweig (1972).
23. F. Brito and N. Ingri, *An. Quím.* 1960, **56B**, 165.
24. G. Biedermann and L. G. Sillén, *Ark. Kemi* 1953, **5**, 425.
25. G. Lagerström, *Acta Chem. Scand.* 1959, **13**, 722.
26. L. G. Sillén, *Acta Chem. Scand.* 1962, **16**, 159; L. G. Sillén and B. Warnqvist, *Ark. Kemi* 1969, **31**, 341.
27. A. E. Martell and R. M. Smith, *Critical Stability Constants*, Vol. 5: *First Supplement*. Plenum Press, New York (1982).
28. A. Napoli, *J. Inorg. Nucl. Chem.* 1977, **39**, 463.
29. M. Morin and J. P. Scharff, *Anal. Chim. Acta* 1973, **66**, 113.
30. S. González García and J. Niclós Gutiérrez, *Ars Pharm.* 1981, **22**, 429.
31. E. Riekanska, J. Mayer, A. Bumbalova and M. Kalina, *Chem. Zvesti* 1974, **28**, 332, 768.
32. S. H. Eberle and S. A. Ali, *Z. Anorg. Allg. Chem.* 1968, **361**, 1.
33. G. Schwarzenbach, H. Ackermann and P. Ruckstuhl, *Helv. Chim. Acta* 1949, **32**, 1175.
34. S. González García, M. T. Fernández Martínez, F. J. Sánchez Santos and J. Niclós Gutiérrez, XVIII Reunión Bienal de la Real Sociedad Española de Química, Burgos (1980), Com. 22.5, Book M; XIX Reunión Bienal, Santander (1982), Com. 16.44, Book G.
35. H. M. Irving, M. G. Miles and L. D. Pettit, *Anal. Chim. Acta* 1967, **38**, 475.
36. K. Nakamoto, Y. Morimoto and A. E. Matell, *J. Am. Chem. Soc.* 1962, **84**, 2061.
37. A. I. Grigor'ev, N. D. Mitrofanova and L. I. Martinenko, *Zh. Neorg. Khim.* 1955, **10**, 1409.
38. C. F. Baes and R. E. Mesmer, *The Hydrolysis of Cations*. John Wiley, New York (1976).
39. P. L. Brown, J. Ellis and R. N. Sylva, *J. Chem. Soc., Dalton Trans.* 1983, 2001.
40. A. E. Martell and R. M. Smith, *Critical Stability Constants, Vol 1: Amino Acids*. Plenum Press, New York (1974).
41. E. Uhlig and R. Krannich, *J. Inorg. Nucl. Chem.* 1967, **29**, 1164.
42. A. Martín and E. Uhlig, *Z. Anorg. Allg. Chem.* 1970, **375**, 166.
43. S. González García and J. Niclós Gutiérrez, *An. Quím.* 1983, **79B**, 572.
44. P.-K. Tse, J. E. Powell, M. W. Potter and H. R. Burkholder, *Inorg. Chem.* 1984, **23**, 1437.
45. M. Bartušek and L. Havelkova, *Coll. Czech. Chem. Commun.* 1967, **32**, 3853; 1968, **33**, 4189.
46. J. Havel, L. Havelkova and M. Bartušek, *Chem. Zvesti* 1969, **23**, 582.
47. H. J. Debrin, D. Kairatis and R. B. Temple, *Aust. J. Chem.* 1952, **15**, 457.
48. N. T. Athavole, N. Mahadevan, P. K. Mather and R. M. Satne, *J. Inorg. Nucl. Chem.* 1967, **29**, 1947.

Polyhedron Vol. 6, No. 6, pp. 1375–1381, 1987
Printed in Great Britain

0277–5387/87 $3.00+.00

COPPER(II) AND IRON(III) COMPLEXES OF *N*-NITROSO-*N*-ALKYLHYDROXYLAMINES, AND THE X-RAY CRYSTAL STRUCTURES OF BIS(*N*-NITROSO-*N*-ISOPROPYLHYDROXYLAMINATO)COPPER(II) AND TRIS(*N*-NITROSO-*N*-PROPYLHYDROXYLAMINATO)IRON(III)

MICHAEL H. ABRAHAM, JOSEPH I. BULLOCK,* JOHN H. N. GARLAND, ANDREW J. GOLDER, GRAHAME J. HARDEN, LESLIE F. LARKWORTHY,* DAVID C. POVEY, MICHAEL J. RIEDL and GALLIENUS W. SMITH

Department of Chemistry, University of Surrey, Guildford GU2 5XH, U.K.

(*Received* 1 *September* 1986; *accepted* 5 *December* 1986)

Abstract—*N*-nitroso-*N*-alkylhydroxylamines have been prepared by hydrolysis of the mixture obtained by reaction of nitric oxide with Grignard reagents, and stabilized as their copper(II) or iron(III) complexes, $Cu(RN_2O_2)_2$ and $Fe(RN_2O_2)_3$, where R is, for example, Me, Et, Pr^i, Bu^{iso}, Ph, n-C_8H_{17} or n-$C_{12}H_{25}$. The complexes have been characterized by analytical, magnetic and spectroscopic measurements. By single-crystal X-ray methods $Cu(Pr^iN_2O_2)_2$ has been found to be *trans*-planar and $Fe(Pr^nN_2O_2)_3$ has a facial octahedral structure; in each complex the N—O bond lengths are equal with no significant variation between the copper and iron complexes.

The action of nitric oxide on alkyl compounds of diamagnetic metal atoms usually yields[1–16] the corresponding *N*-nitroso-*N*-alkylhydroxylamine derivative [eqn (1)]:

$$R—M+2NO \rightarrow (RN_2O_2)M. \quad (1)$$

As with cupferron (R = phenyl) complexes,[17–19] the hydroxylamate ligand is chelated and coordinates through the two oxygen atoms in the X-ray crystallographic structures reported[8,10,11,13,16–19] to date. Diamagnetic metals in eqn (1) include zinc,[1,2,12] magnesium,[2–6] cadmium,[2] boron,[2] aluminium,[2,7,8] gallium,[8] zirconium,[9,10] tungsten,[11,12] copper(I),[12] niobium,[13,14] tantalum,[13,14] titanium,[9,15] rhenium(III)[16] and rhodium(I).[12] For some paramagnetic metal ions, for example, vanadium(IV),[14] and titanium(III),[14] the *N*-nitroso-*N*-alkylhydroxylamine derivatives cannot be prepared directly through eqn (1) while the reaction[20] of a low-valent cobalt nitrosyl with an alkyl halide afforded the nitrosoalkane complex.

Chemical identification of the products in eqn (1) was first carried out by Sand and Singer.[3] They showed that the action of nitric oxide on phenylmagnesium bromide followed by hydrolysis gave the free acid *N*-nitroso-*N*-phenylhydroxylamine (cupferron), identified because its reactions were the same as those of the product[21] obtained by the action of nitrous acid on *N*-phenylhydroxylamine. The free acid could not be isolated on hydrolysis of the nitric oxide–methylmagnesium iodide reaction mixture, but Sand and Singer[3] did obtain a copper(II) complex, $Cu(MeN_2O_2)_2$, on treatment of the product with copper(II) oxide. There are scattered references to copper(II) complexes of various other *N*-nitroso-*N*-alkylhydroxylamines, but little other than their preparation[1,3,5,9,12] and fungicidal properties[22] have been reported.

We present here a convenient route to *N*-nitroso-*N*-alkylhydroxylamine derivatives of copper(II) and iron(III) which is based on the early work of Sand and Singer.[3] As far as we know complexes of iron(III) have not been characterized previously.

EXPERIMENTAL

Preparation of the complexes

The ligands were first isolated as the magnesium complexes from the appropriate Grignard reagent.

* Authors to whom correspondence should be addressed.

For example, magnesium turnings (1.25 g, 0.051 mol) were converted into the methyl Grignard by the slow addition of methyl iodide (7.1 g, 0.05 mol) in dry ether (80 cm^3). When the ethereal solution had been added the contents of the flask were refluxed for 1 h, the flask cooled in ice, evacuated, and nitric oxide admitted. The solution was stirred in nitric oxide until gas uptake ceased (gas burette). The solvent was removed under reduced pressure, and the resulting pale yellow and hygroscopic *N*-nitroso Grignard complex was stored over calcium chloride.

To prepare the copper(II) complex, half by weight of the product was suspended in water (100 cm^3), cooled, and acidified with dilute sulphuric acid to give the free *N*-nitroso-*N*-methylhydroxylamine which was then extracted into ether (5×20 cm^3 portions). Copper(II) oxide in excess was stirred with the combined extract for several hours, and the suspension left to stand overnight. The deep blue liquor was filtered from the copper(II) oxide which was washed with acetone. The ether and acetone solutions were evaporated to dryness, and the solid recrystallized from methylated spirits. The blue crystals were dried in vacuum.

To prepare the iron(III) complex, iron(III) alum in excess was added to a cooled aqueous suspension of the remaining *N*-nitroso Grignard complex and after stirring for half an hour the iron(III) complex was extracted into chloroform (6×20-cm^3 portions). The extract was dried with calcium chloride, filtered, and taken to dryness. The solid was recrystallized from methylated spirits and the orange crystals dried *in vacuo*.

Complexes of other *N*-nitroso-*N*-substituted hydroxylamines were similarly prepared (Table 1). They were obtained in 20–40% yield based on the mass of magnesium.

The *N*-methyl derivatives were also prepared from *N*-methyl hydroxylamine hydrochloride. This was dissolved in water, acidified with hydrochloric acid, cooled to 0°C, and iron(III) alum and sodium nitrite added with stirring. The iron(III) complex was extracted with chloroform as above. The copper(II) complex was prepared by continuous extraction of the *N*-nitroso-*N*-methylhydroxylamine into a suspension of the oxide in ether. The *N*-phenyl-substituted complexes were also prepared from cupferron in aqueous solution. These methods gave 80–90% yields.

Physical measurements

Diffuse-reflectance electronic spectra were recorded using powdered samples with lithium fluoride as reference material on a Beckman Acta MIV spectrophotometer. Relative molecular masses were measured using a calibrated Mechrolab vapour phase osmometer model 301A (solvent chloroform).

Crystallography

Crystals of $Fe(Pr^nN_2O_2)_3$ and $Cu(Pr^iN_2O_2)_2$ suitable for X-ray investigation were obtained from methylated spirits.

Crystal data. $C_9H_{21}N_6O_6Fe$(**I**), $M = 365.15$, orthorhombic, $a = 9.059(1)$, $b = 11.492(1)$, $c = 15.988(2)$ Å, $U = 1664.5$ Å^3, space group $P2_12_12_1$, $Z = 4$, $D_c = 1.457$ g cm^{-3}, $F(000) = 764$, μ(Mo-K_α) = 9.4 cm^{-1}.

$C_6H_{14}N_4O_4Cu$(**II**), $M = 269.74$, monoclinic, $a = 22.789(2)$, $b = 4.865(1)$, $c = 11.400(1)$ Å, $U = 1106.6$ Å^3, space group $C2/c$, $Z = 4$, $D_c = 1.619$ g cm^{-3}, $F(000) = 556$, μ(Mo-K_α) = 19.8 cm^{-1}.

Data collection and processing. Numbers in brackets refer to structure **II**. Intensity data were collected using graphite-monochromated Mo-K_α radiation ($\lambda = 0.71069$ Å) on an Enraf–Nonius CAD4 four-circle diffractometer in a ω–2θ scan mode. 1896 (1253) reflexions were measured [$\sin\theta/\lambda \leqslant 0.62$], which reduced to 1875 (1111) unique reflexions with 1537 (926) reflexions having $I \geqslant 3\sigma(I)$. Following Lp correction, analysis of a standard reflexion showed no significant decay.

Structure analysis and refinement. The heavy-atom method was used to solve and develop the structures. In structure **II** it was noted that $(k+l)$ and $(h+l)$ even were systematically strong and the volume indicated four molecules per unit cell implying that copper is on a centre of symmetry, at ($\frac{1}{4}$, $\frac{1}{4}$, 0) and related positions. When phased on copper alone the $(k+l)$, l = odd reflexions will have zero calculated F_cs causing two peaks per atom on the F_o map. Correct selection of atom positions overcame this. Full-matrix least-squares refinement was carried out using isotropic thermal parameters and an empirical absorption correction, DIFABS[23] was applied [1768 (1039) reflexions corrected, minimum absorption correction 0.822 (0.851), maximum 1.168 (1.256), average 0.987 (0.989)] prior to refinement with anisotropic thermal parameters. The positions of hydrogen atoms were calculated geometrically and the weighting scheme $w = 1/[\sigma^2(F_o)+0.05(F_o)^2]$ gave satisfactory agreement analysis. Final R and R_w values are 0.043 (0.025) and 0.056 (0.034). All crystallographic programs used were from the SDP package.[24]

Selected bond lengths and angles are given in Table 2. Fractional atomic coordinates, anisotropic temperature factor coefficients and F_o/F_c values

Table 1. Analytical, spectroscopic and related data

Complex[a]	M.p. (°C)	RMM[bc]	Analysis (%)[b] C	H	N	μ_{eff}[d] (BM)	Reflectance[e] spectrum absorption[f] maxima (cm^{-1})	
$Cu(MeN_2O_2)_2$	196 196[g]	212[h] (214)				1.93[i]		
$Cu(EtN_2O_2)_2$[j]	113	261[h] (241)				1.93		
$Cu(Pr^iN_2O_2)_2$	131 133[g]	274[h] (270)	27.9 (26.7)	5.6 (5.2)	20.6 (20.8)	1.87[i]	15,600	17,900
$Cu(Bu^nN_2O_2)_2$	73		32.5 (32.3)	6.0 (6.1)	18.8 (18.8)		16,000	(17,900)
$Cu(Bu^{iso}N_2O_2)_2$	79 80–83[k]		32.4 (32.3)	6.7 (6.1)	18.6 (18.8)		16,000	17,900
$Cu(Bu^{sec}N_2O_2)_2$[j]	115 122[g]	297[h] (296)	32.3 (32.3)	6.1 (6.1)	18.5 (18.8)		15,900	(17,900)
$Cu(Bu^tN_2O_2)_2$	152		32.6 (32.3)	6.0 (6.1)	18.6 (18.8)		16,000	(18,900)
$Cu(n\text{-}C_8H_{17}N_2O_2)_2$	106	410 (434)	46.4 (46.9)	8.1 (8.4)	13.5 (13.7)	2.02[j]	16,000	17,900
$Cu(n\text{-}C_{12}H_{25}N_2O_2)_2$	99		55.7 (55.2)	10.0 (9.7)	10.6 (10.7)	1.97	16,000	17,900
$Cu(allylN_2O_2)_2$	73		27.3 (27.1)	3.7 (3.8)	21.0 (21.1)		15,700	17,700
$Cu(PhN_2O_2)_2$	197					2.02		
$Fe(MeN_2O_2)_3$[j]	150	297 (281)	12.9 (12.8)	3.2 (3.2)	29.6 (29.9)	6.00		
$Fe(EtN_2O_2)_3$	85	350 (323)	23.1 (22.3)	5.0 (4.7)	25.0 (26.0)	5.94		
$Fe(Pr^nN_2O_2)_3$	61		29.7 (29.6)	5.8 (5.8)	22.7 (23.0)	5.81		
$Fe(Bu^{sec}N_2O_2)_3$	64		34.3 (35.4)	6.6 (6.7)	19.0 (20.6)			
$Fe(n\text{-}C_{12}H_{25}N_2O_2)_3$	42	760 (744)	58.8 (58.2)	10.2 (10.3)	11.5 (11.3)	6.03		
$Fe(PhN_2O_2)_2$	141	510 (470)	46.5 (46.3)	3.1 (4.2)	17.2 (18.0)	5.96		

[a] Cu(II) complexes of cyclohexyl[5] and trimethylsilylmethyl[12] also known. Complexes are new except Cu, R = Me, Pr^i, Bu^{iso}, Bu^{sec}, Ph; Fe, R = Ph.

[b] Calculated values in parentheses.

[c] Vapour pressure osmometry ($CHCl_3$).

[d] At room temperature, 1 BM = 9.274×10^{-24} A m^2.

[e] Also a shoulder near 13,200 cm^{-1}.

[f] Parentheses indicate ill-defined maximum.

[g] Reference 22.

[h] Parent ions observed in mass spectra.

[i] The Me derivative[9] has $\theta = 8°$, the $n\text{-}C_8H_{17}$ derivative has $\theta = 10°$, and the Pr^i derivative obeys the Curie law [μ_{eff} (90 K) = 1.88 BM] with $1/\chi = C(T+\theta)$.

[j] Non-conducting in acetone at 25°C.

[k] Reference 5.

Table 2. Selected bond distances (Å) and angles (°)

(i) $Fe(Pr^nN_2O_2)_3$

Atom 1	Atom 2	Distance	Atom 1	Atom 2	Distance
Fe	O	2.001(10)	O	N	1.313(11)
N	N	1.266(10)	N	C	1.468(6)
C	C	1.498(16)			

Atom 1	Atom 2	Atom 3	Angle
O(11)	Fe	O(12)	76.2(2)
O(11)	Fe	O(32)	91.7(2)
O(11)	Fe	O(22)	162.4(2)
O(11)	N(11)	N(12)	122.8(4)
O(11)	N(11)	C(11)	118.3(4)
N(22)	N(21)	C(21)	120.3(5)

(ii) $Cu(Pr^nN_2O_2)_2$

Atom 1	Atom 2	Distance	Atom 1	Atom 2	Distance
Cu	O	1.906(4)	O	N	1.316(4)
N	N	1.273(3)	N	C	1.473(3)
C	C	1.514(4)			

Atom 1	Atom 2	Atom 3	Angle
O(1)	Cu	O(1′)	180.0(1)
O(1)	Cu	O(2)	81.99(6)
Cu	O(1)	N(1)	108.6(1)
Cu	O(2)	N(2)	113.4(1)
O(1)	N(12)	N(2)	122.5(2)
N(2)	N(1)	C(1)	119.7(2)

have been deposted as supplementary data with the Editor.*

RESULTS AND DISCUSSION

The three methods of preparation of the copper(II) and iron(III) complexes are outlined in Schemes 1–3.

The *N*-methyl-substituted copper(II) and iron(III) complexes whether prepared by Scheme 1 or 2 had identical melting points and IR and mass spectra. The same is true for the *N*-phenyl derivatives from Schemes 1 and 3. The constitution of the complexes is therefore clearly established although the structure of the *N*-nitroso Grignard intermediate remains uncertain. Although alkylmagnesium bromides and iodides are monomeric in ether at low concentration (less than about 3×10^{-2} mol dm^{-3}),[25,26] at concentrations used in preparative studies they are mostly dimeric and exist either as **III** or **IV**.[26]

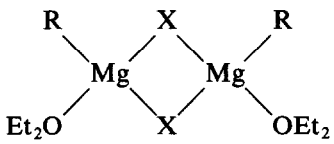

III

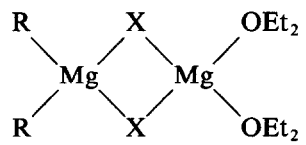

IV

It is possible that the action of nitric oxide on **III** or **IV** in ether would initially yield species **I** or **II**, respectively, but in either case hydrolysis will give RN(NO)OH and complex formation with, e.g. Cu^{2+} will give $[Rn(NO)O]_2Cu$. Since neither the active species in the Grignard reagent nor the initial

* Atomic coordinates have also been deposited with the Cambridge Crystallographic Data Centre.

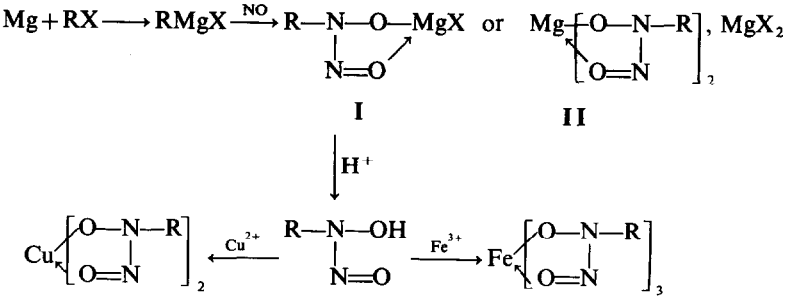

Scheme 1. For R, see Table 1.

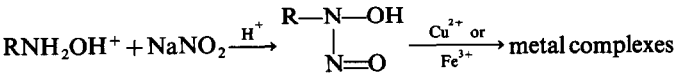

Scheme 2.

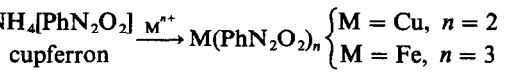

Scheme 3.

magnesium complex produced is known, the simplest schematic formulation that is stoichiometrically correct is given below:

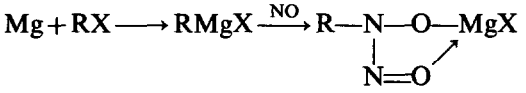

I

Molecular structures

The molecular structure and the atom-numbering scheme for $Cu(Pr^iN_2O_2)_2$ are shown in Fig. 1. The molecule excluding the alkyl substituents is planar, and the ligands are *trans* as in the *N*-phenyl analogue.[17] The Cu—O bond distances are equal (Table 2) within experimental error but the small bite of the ligand leads to angles significantly below 90° subtended at the metal atom (O(1)—Cu—O(2) = 81.99°). The nearest neighbours axially to the copper(II) ion are N(2) atoms at 3.2 Å, which is much greater than the sum of the radii of Cu^{2+} and nitrogen (*ca* 2.3 Å). Thus there is no intermolecular interaction and the copper(II) ions are in essentially planar coordination.

The atom-numbering scheme and the molecular structure of $Fe(Pr^nN_2O_2)_3$ are presented in Fig. 2. The six O atoms form a distorted octahedron around the iron(III) ion, and the Fe—O distances (Table 2) are the same (2.00 Å) as in the phenyl derivative.[18] The ligands are in a facial arrangement. As in the copper(II) complex, the ligands

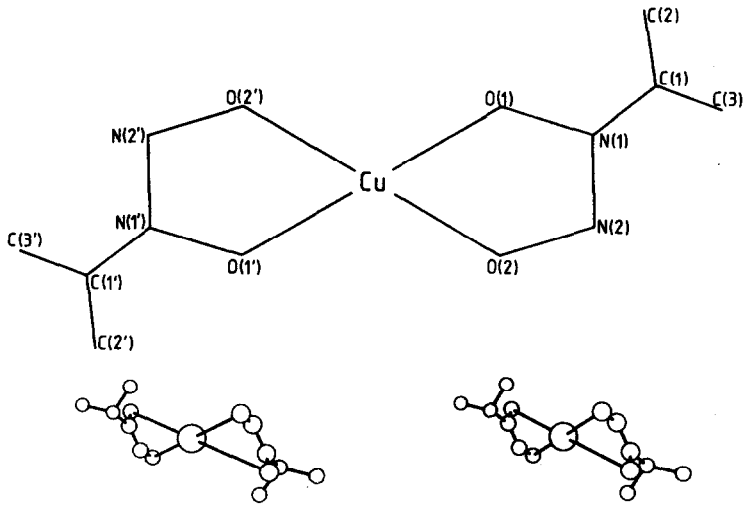

Fig. 1. Atom-numbering scheme, structure, and stereoscopic view of $Cu(Pr^iN_2O_2)_2$.

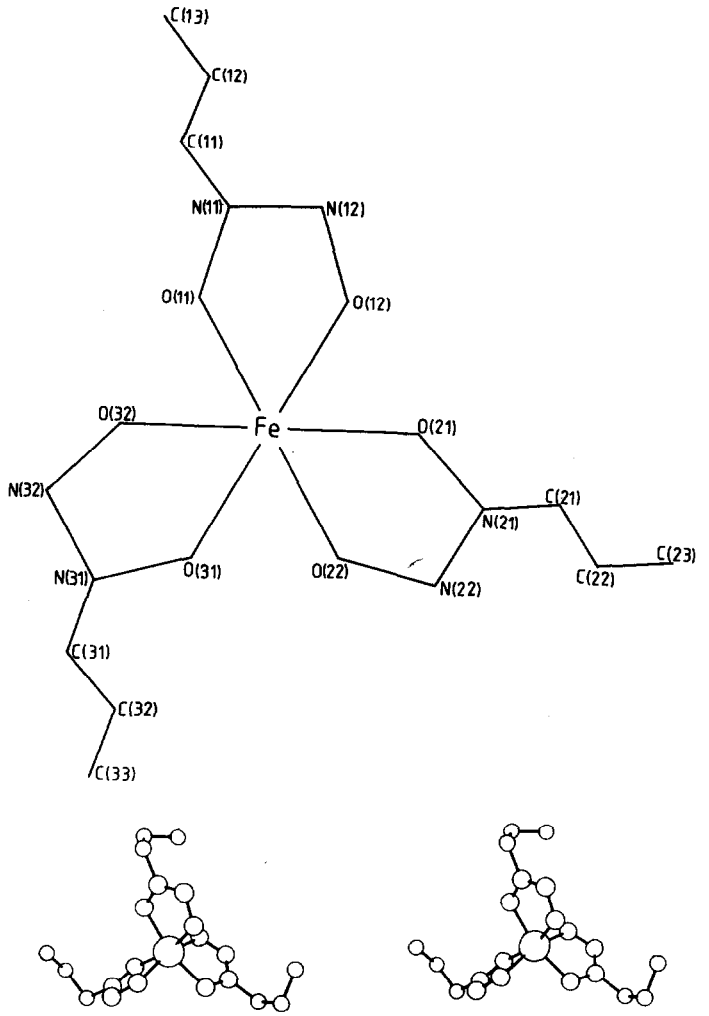

Fig. 2. Atom-numbering scheme, structure, and stereoscopic view of $Fe(Pr^nN_2O_2)_3$.

subtend small angles at the metal ion (76.2°). The ligand dimensions are the same in the two complexes within the stated standard deviations. The N—O bond lengths in the copper(II) and iron(III) complexes are almost equal [Cu, 1.316(4) Å; and Fe, 1.313(11) Å]. Those for Cu(II) are much better refined than any [8,10,11,13,16–19] previously reported. On reviewing the available structures of *N*-nitroso-*N*-alkyl- or *N*-nitroso-*N*-arylhydroxylaminato complexes we find no compelling evidence, as judged by the reported standard deviations in the N—O bond lengths, to support the claim[10] that significantly different N—O bond lengths occur within a single ligand in any given complex. Our values are intermediate between those expected[10] for single (*ca* 1.37 Å) and double (*ca* 1.23 Å) bonds. Our N–N bond lengths are short[10] and invariant with clear evidence for significant double-bond character. The C—N bond distances are normal for single bonds (Table 2).

Magnetic measurements

The effective magnetic moments (μ_{eff}) of the copper(II) complexes (Table 1) are a little above the spin-only value (1.73 BM) as expected for planar or tetragonally-distorted, six-coordinate complexes; and the moments of $Cu(Pr^iN_2O_2)_2$ and $Cu(n\text{-}C_8H_{17}N_2O_2)_2$ are almost independent of temperature (Table 1) as expected for monomeric complexes. The iron(III) complexes are high-spin (for the $t_{2g}^3e_g^2$ configuration moments close to the spin-only value of 5.92 BM are expected); thus the *N*-nitroso-*N*-alkylhydroxylamines are weak field ligands.

Electronic spectroscopic measurements on the copper(II) complexes

The electronic spectra of copper(II) complexes have been extensively reviewed.[27,28] Potentially π-bonding ligands such as acetylacetonate (acac) and

its derivatives appear to favour square planar CuO_4 geometry. The electronic spectra of this chromophore, recorded by diffuse reflectance from powdered samples or by polarized measurements from single crystals, exhibit three or four bands in the visible region with no absorption maxima below 10,000 cm^{-1}. The polarized spectrum of Cu(3-ϕacac)$_2$ is typical with maxima at 15,400, 16,900, 19,000 and 20,600 cm^{-1}, while in other cases, e.g. $CaCuSi_4O_{10}$ and Cu(3-Meacac)$_2$, the spectrum is shifted to lower energy by 2500–1000 cm^{-1}.

These complexes have T (a corrected ratio of the in-plane bond lengths to axial contacts) in the range 0.56–0.66. Semi-coordination need not be considered. If the in-plane bond lengths are about 2 Å then the close contacts in the axial directions are at least 2.8–3 Å for true square planar CuO_4 chromophores. The bond lengths in the solid state are not temperature-dependent.

The diffuse-reflectance spectra of powdered samples of our blue/violet copper(II) complexes (Table 1) are all very similar. A broad envelope centred near 16,700 cm^{-1} has two ill-resolved maxima near 15,600 and 17,800 cm^{-1}, with a low-energy shoulder at about 13,200 cm^{-1}. The complex Cu(Pr^{i}N$_2$O$_2$)$_2$ is square planar with T (uncorrected) = 0.59 as determined by the in-plane Cu—O distances and the closest contacts to Cu from N(2) above and below the plane at 3.205 Å. The spectra show that all of the copper(II) complexes reported here are square planar and confirm the established structure–spectral correlations for such chromophores. It would appear that the olefinic function in Cu(allylN$_2$O$_2$)$_2$ does not interact with the copper(II) atom.

REFERENCES

1. E. Frankland, *Phil. Trans.* 1857, **147**, 59.
2. M. H. Abraham, J. H. N. Garland, J. A. Hill and L. F. Larkworthy, *Chem. Ind. (London)* 1962, 1615.
3. J. Sand and F. Singer, *Liebigs Ann. Chem.* 1903, **329**, 190.
4. T. E. Stevens, *J. Org. Chem.* 1964, **29**, 311.
5. E. H. White and D. W. Grisley, *J. Am. Chem. Soc.* 1961, **83**, 1191.
6. E. Muller and H. Metzger, *Chem. Ber.* 1956, **89**, 396.
7. E. B. Baxter and H. H. Sisler, *J. Am. Chem. Soc.* 1953, **75**, 5193.
8. S. Amirkhalili, P. B. Hitchcock, J. D. Smith and J. G. Stamper, *J. Chem. Soc., Dalton Trans.* 1980, 2493.
9. P. C. Wailes, H. Weigold and A. P. Bell, *J. Organomet. Chem.* 1972, **34**, 155.
10. G. Fochi, C. Floriani, A. Chiesei-Villa and C. Guastini, *J. Chem. Soc., Dalton Trans.* 1986, 445.
11. S. R. Fletcher and A. C. Skapski, *J. Organomet. Chem.* 1973, **59**, 299.
12. A. R. Middleton and G. WIlkinson, *J. Chem. Soc., Dalton Trans.* 1981, 1898.
13. J. D. Wilkins and M. G. B. Drew, *J. Organomet. Chem.* 1974, **69**, 111.
14. A. R. Middleton and G. Wilkinson, *J. Chem. Soc., Dalton Trans.* 1980, 1888.
15. R. J. H. Clark, J. A. Stockwell and J. D. Wilkins, *J. Chem. Soc., Dalton Trans.* 1976, 120.
16. P. Edwards, K. Mertis, G. Wilkinson, M. B. Hursthouse and K. M. A. Malik, *J. Chem. Soc., Dalton Trans.* 1980, 334.
17. L. M. Shkolnikova and E. A. Shugam, *J. Struct. Chem.* 1963, **4**, 350.
18. D. van der Helm, L. L. Merritt, R. Degeilh and C. H. MacGillavry, *Acta Cryst.* 1965, **18**, 355.
19. W. Mark, *Acta Chem. Scand.* 1970, **24**, 1398.
20. W. P. Weiner and R. G. Bergman, *J. Am. Chem. Soc.* 1983, **105**, 3922.
21. E. Bamberger, *Chem. Ber.* 1894, **27**, 1553.
22. British Patent 815,537 (1959).
23. N. Walker and D. Stuart, *Acta Cryst.* 1983, **A39**, 158.
24. B. A. Frenz, *Structure Determination Package (SDP) Program System.* Enraf–Nonius, Delft, Netherlands (1982).
25. A. D. Vreugdenhil and C. Blomberg, *Recl. Trav. Chim.* 1963, **82**, 453.
26. E. C. Ashby, *Q. Rev.* 1967, **21**, 259; E. C. Ashby and R. B. Smith, *J. Am. Chem. Soc.* 1964, **86**, 4363; E. C. Ashby, *Bull. Soc. Chim. Fr.* 1972, 2133.
27. B. J. Hathaway and D. E. Billing, *Coord. Chem. Rev.* 1970, **5**, 143.
28. B. J. Hathaway, *Coord. Chem. Rev.* 1982, **41**, 423.

Polyhedron Vol. 6, No. 6, pp. 1383–1390, 1987
Printed in Great Britain

0277–5387/87 $3.00+.00

SUBSTITUTION REACTION OF η^5-CYCLOPENTADIENYLRUTHENIUM(II) COMPLEXES WITH NITROGEN, OXYGEN AND SULFUR DONOR LIGANDS

KOLLIPARA MOHAN RAO, LALLAN MISHRA* and UMESH CHANDRA AGARWALA†

Department of Chemistry, Indian Institute of Technology, Kanpur 208016, India

(*Received* 15 *July* 1986; *accepted after revision* 8 *December* 1986)

Abstract—The heterocycles pyridine, γ-picoline, 2,2′-bipyridine and 1,10-phenanthroline react with $[(\eta^5\text{-}C_5H_5)Ru(MPh_3)_2X]$ (M = P, As or Sb) and $[(\eta^5\text{-}C_5H_5)Ru(AsPh_3)(PPh_3)X]$ (X = Cl, Br, I, CN, NCS or $SnCl_3$) to form complexes of types $[(\eta^5\text{-}C_5H_5)(MPh_3)(L\text{–}L)^+X^-$ (L–L = 2,2′-bipyridine or 1,10-phenanthroline; X = Cl, Br, I, CN, NCS or $SnCl_3$) and $[(\eta^5\text{-}C_5H_5)Ru(MPh_3)LX]$ (M = As or Sb; L = pyridine or γ-picoline; X = Cl, Br, I, CN, NCS or $SnCl_3$). Interactions of dithiocarbamate (DTC) with $[(\eta^5\text{-}C_5H_5)Ru(SbPh_3)_2X]$ (X = Cl, Br or I) and acetylacetonate (acac) with parent compounds $[(\eta^5\text{-}C_5H_5)Ru(MPh_3)_2X$ (M = P or Sb; X = Cl, Br or I) yielded $[(\eta^5\text{-}C_5H_5)Ru(MPh_3)L]$ (where L = DTC or acac). The reaction products have been characterized by magnetic, spectral and microanalytical data.

The unusual chemistry of cyclopentadienyl ruthenium complexes, $[(Cp)Ru(MR_3)_2X]$ (Cp = η^5-C_5H_5; M = P, As or Sb; R = Ph, Me or OPh), have captured the attention of many investigators for several years.[1–12] In continuation of our previous work[10] we wished to examine the reactions of $[(Cp)Ru(MPh_3)_2X]$ (M = As or Sb) and $[(Cp)Ru(AsPh_3)(PPh_3)X]$ (X = Cl, Br, I, CN, NCS or $SnCl_3$) towards heterocyclic bases like pyridine (py), γ-picoline (γ-pic), 2,2′-bipyridine (bipy) and 1,10-phenanthroline (1,10-phen) and towards sodium diethyl-dithiocarbamate (DTC) and acetylacetone (acac). This paper reports the results of such a study.

EXPERIMENTAL

All of the chemicals used were chemically pure or Analar grade. Solvents were distilled and dried before use. The complexes $[(Cp)Ru(AsPh_3)(PPh_3)X]$ and $[Ru(Cp)(MPh_3)_2X]$ (M = As or Sb; X = Cl, Br, I, CN, NCS or $SnCl_3$) were prepared by the literature procedures.[11,12]

Typical methods of synthesizing the complexes

Preparation of the complexes $[(Cp)Ru(MPh_3)LX]$ (M = As *or* Sb) *and* $[(Cp)Ru(MPh_3)L\text{-}L]^+X^-$ (M = P, As *or* Sb) (X = Cl, Br, I, CN, NCS, $SnCl_3$, DTC *or* acac). The complexes were synthesized by refluxing $[(Cp)Ru(MPh_3)_2X]$ (*ca* 1.2×10^{-4} mol) in 20 cm^3 ethanol with the corresponding substrate for several hours. After concentrating the resulting solution to nearly 5 cm^3‡ a slight excess of diethyl ether (*ca* 20 cm^3) was added yielding a microcrystalline product. It was separated by centrifugation and recrystallized from the appropriate solvent. The recrystallized product was washed with light petroleum, and air dried.

Attempts to synthesize the corresponding arsine complexes having DTC or acac as coligands were unsuccessful.

Preparation of $[(Cp)Ru(MPh_3)L\text{–}L]^+Y^-$ (L = As *or* Sb; Y = BPh_4, BF_4, ClO_4^-, $HgCl_3$ *or* $\frac{1}{2}$ Zn_2Cl_6). These were synthesized by metathesis reactions. The complex $[(Cp)Ru(MPh_3)L\text{–}L]^+X^-$ (*ca* 1.0×10^{-4} mol) in 15 cm^3 of ethanol on mixing with equimolar quantity of Y^- in ethanol (5 cm^3) yielded an immediate orange red precipitate. (Perchlorates of these cations could also be isolated by the addition of a few drops of perchloric acid to their alcoholic solutions. **CAUTION:** One should be careful in their syntheses because of their highly explosive nature.) The precipitated residue was

* Department of Chemistry, S.C.P.G. College, Ballia 277001, India.

† Author to whom correspondence should be addressed.

‡ The solution was concentrated to get a better yield of the complex. It also appeared without concentration, but the yield was poor.

separated by filtration, washed with diethyl ether and recrystallized from a chloroform–methanol mixture.

Using ethanol as solvent no stable product was obtained by the reaction of bipy or 1,10-phen with $[(Cp)Ru(MPh_3)_2H]$ (M = As or Sb). However, in the presence of the anions BPh_4^-, BF_4^-, ClO_4^-, $HgCl_3^-$ and $Zn_2Cl_6^{2-}$ the same reaction mixture yielded the stable cationic salts $[(Cp)Ru(MPh_3)L–L]^+$ (M = As or Sb, L–L = bipy or 1,10-phen). The same reactions carried out in halohydrocarbons such as CH_2Cl_2, CHX_3 etc. gave the corresponding halide salts $[(Cp)Ru(MPh_3)L–L]^+X^-$ (X = Cl or Br) which in the presence of a large anion (Y^-) afforded the corresponding salt of Y^-.

Physical measurements

Carbon, hydrogen and nitrogen analyses were carried out by the Microanalytical laboratory of the Indian Institute of Technology, Kanpur, India. The percentages of halides and sulfur in the complexes were determined by the standard methods[13] in the filtrate obtained after fusing the sample with the fusion mixture (1 : 8 $NaNO_3$–NaOH), extracting it with distilled water and filtering it. IR, UV and visible, ^1H NMR spectroscopic and magnetic measurements were carried out by the methods described elsehwere.[10,11] The results are given in Table 1.

The specific reaction conditions, the analytical data, and other physical properties are given in Table 1.

RESULTS AND DISCUSSION

The empirical formulae of the complexes formed by the substitution reactions of *N*-heterocyclic bases, $[Na(C_2H_5)_2NCS_2]$, or acac with the complexes $[(Cp)Ru(MPh_3)_2X]$ (M = As or Sb; X = Cl, Br, I, CN, NCS or $SnCl_3$) are listed in Table 1. These are air-stable, highly soluble in organic polar solvents like CH_2Cl_2, $CHCl_3$ etc., and relatively less soluble in methanol and ethanol.

The formation of identical substitution products from both $[(Cp)Ru(AsPh_3)_2X]$ with heterocyclic bases is not surprising, because of the substitution of a larger molecule (PPh_3, cone angle 145°) in the latter by a smaller one ($AsPH_3$ cone angle)[14] due to steric hindrance.

An interesting aspect of these reactions is the formation of cationic complexes with bipy and 1,10-phen while py and γ-pic gave neutral ones. Under our reaction conditions we were not able to isolate the cationic complexes with py or γ-pic similar to those reported by Uson *et al.*[15] Although one could have anticipated the formation of the cationic complexes $[(Cp)RuL_2(MPh_3)]^+X^-$ (M = As or Sb; L = py or γ-pic), in the case of py and γ-pic also, seemingly the chelate effect of the ligands L–L plays a significant role in stabilizing the cationic complexes. The cationic nature of the complexes has been confirmed: (a) by exchange reactions using cationic and anionic exchangers (Dowex 50W-XB and Dowex 1-XB), and (b) by synthesizing various salts of the cations with a number of large anions (Table 1). It has been shown here that the bipy and 1,10-phen complexes are cationic $\{[(Cp)Ru(MPh_3)L–L]^+$ (M = As or Sb)$\}$. Although it was previously reported[10] that the corresponding triphenylphosphine complexes have the formula $[(Cp)Ru(PPh_3)L–L_{0.5}X]$, it was later shown that even the PPh_3 complexes gave $[(Cp)Ru(PPh_3)L–L]^+$ on prolonged refluxing (24 h), while on refluxing for a shorter time a mixture of the latter with the starting material was obtained.

The complexes $[(Cp)Ru(MPh_3)L–L]^+Cl^-$ (M = As or Sb) were converted to $[(Cp)Ru(MPh_3)L–L]^+X^-$ (X = Br, I, NCS, CN or $SnCl_3$) by refluxing in methanol with a molar excess of KBr, KI, KCN, KNCS and $SnCl_2$, respectively, with the intermediate $[(Cp)Ru(MPh_3)(MeOH)L–L]^+$ probably being formed during these reactions.[16]

The IR spectra of all the complexes exhibited sharp bands of medium intensity in the 840–850-cm^{-1} region and relatively broader bands at 420 cm^{-1}. These bands have been assigned to the out-of-plane bending and skeletal modes of the C_5H_5 ring, respectively. In addition to these, the characteristic bands of triphenylarsine and triphenylstibine (530s, 1100s, 1440 and 1490 cm^{-1}), together with those of the heterocyclic bases pyridine (1590 and 735 cm^{-1}), γ-picoline (1600, 1505 and 720–730 cm^{-1}), 2,2′-bipyridine (720–740, 840, 1430–1435 and 1600–1590 cm^{-1}) were also observed.[17–20] Further, in all the spectra the characteristic pattern of three bands of decreasing intensity lying in the 540–500-cm^{-1} region suggested the presence of only one coordinated triphenylarsine or triphenylstibine analogue.[15]

The presence of medium-intensity bands due to ν(CS) around 1000 cm^{-1} in the spectra of the DTC complexes,[5] and broad and intense bands around 1600 cm^{-1}, assigned to the mixed vibration having contributions from ν(C═O) and ν(C═C) in the acac complexes[21] suggested the presence of the respective ligands in their complexes.

The cyanide and thiocyanato complexes showed absorption bands at 2050 and 2100 cm^{-1}, respectively, indicating the presence of CN and NCS group.[22–24] The spectra of the cationic complexes having BF_4^- (1050 cm^{-1}), BPh_4^- (1100 cm^{-1})

Table 1. Special conditions for the synthesis of the complexes and their characterization data

Sl. No.	Complex [M.p. (°C),[a] color,[b] yield (%)]	Reaction conditions[c] [A/B, S (mg), T (h), R^1 other conditions]	Analyses [found (calc.)] (%) C	H	N	Halide/ sulfur	IR bands C_5H_5 (cm^{-1})	C_5H_5 ^1H NMR [δ (ppm)][d]
1	$[(Cp)Ru(PPh_3)(bipy)]^+I^-$ (240, O, 60)	A, bipy (50), 14, ethanol, diethyl ether	55.4 (55.7)	4.5 (3.9)	3.7 (3.9)	18.5 (17.9)	835	4.6
2	$[(Cp)Ru(PPh_3)(o\text{-phen})]^+I^-$ (245, OR, 60)	A, *o*-phen (50), 14, EtOH–ether	56.9 (57.1)	3.3 (3.8)	3.5 (3.8)	17.7 (17.3)	830	4.6
3	$[(Cp)Ru(PPh_3)(bipy)]^+CN^-$ (250, OY, 60)	A, bipy (50), 20, CH_2Cl_2–light petroleum	66.5 (66.9)	4.2 (4.6)	7.1 (6.9)	—	850 ν(CN) 2080	4.35
4	$[(Cp)Ru(PPh_3)(o\text{-phen})]^+CN^-$ (265, OY, 65)	A, *o*-phen (50), 20, CH_2Cl_2–light petroleum	67.8 (68.1)	4.7 (4.1)	6.3 (6.6)	—	850 ν(CN) 2055	4.25
5	$[(Cp)Ru(PPh_3)(bipy)]^+NCS^-$ (193, OY, 70)	A, bipy (60), 20, $CHCl_3$–light petroleum	63.1 (63.5)	4.9 (4.4)	6.2 (6.5)	5.7 (5.0)	832 ν(CN) 2050	4.4
6	$[(Cp)Ru(PPh_3)(o\text{-phen})]^+NCS^-$ (203. OY. 70)	A, *o*-phen (55), 20, $CHCl_3$–light petroleum	64.3 (64.9)	4.5 (4.2)	6.1 (6.3)	5.5 (4.8)	832 ν(CN) 2040	4.4
7	$[(Cp)Ru(PPh_3)(bipy)]^+SnCl_3^-$ (210, O, 50)	A, bipy (60), 24, $CHCl_3$–light petroleum	48.5 (48.7)	3.7 (3.5)	3.3 (3.5)	13.6 (13.1)	852	4.5
8	$[(Cp)Ru(PPh_3)(o\text{-phen})]^+SnCl_3^-$ (206, O, 55)	A, *o*-phen (60), 24, $CHCl_3$–light petroleum	50.1 (50.3)	3.9 (3.4)	3.2 (3.4)	13.5 (12.7)	850	4.55
9	$[(Cp)Ru(AsPh_3)(py)Cl]$ (106d,[e] Y, 50)	A, py (0.5–1 cm^3), 10, evaporation under reduced pressure, CH_2Cl_2–light petroleum	57.0 (57.4)	4.0 (4.2)	2.3 (2.4)	6.5 (6.0)	850	4.4
10	$[(Cp)Ru(AsPh_3)(\gamma\text{-pic})Cl]$ (130, Y, 50)	A, γ-pic (0.5–1 cm^3), 10, CH_2Cl_2–light petroleum evaporated under reduced pressure	58.4 (58.0)	4.7 (4.5)	2.2 (2.3)	6.6 (5.8)	840	4.4
11	$[(Cp)Ru(AsPh_3)(bipy)]^+Cl^-$ (230, OY, 70)	A, bipy (50), 13, ethanol–ether	59.2 (59.7)	4.5 (4.2)	4.0 (4.2)	5.6 (5.3)	845	4.6
12	$[(Cp)Ru(AsPh_3)(o\text{-phen})]^+Cl^-$ (235, OY, 75)	A, *o*-phen (70), 13, ethanol–ether	61.6 (61.1)	3.9 (4.1)	4.0 (4.2)	5.5 (5.1)	847	4.7
13	$[(Cp)Ru(AsPh_3)(py)Br]$ (108, Y, 50)	A, py (1 cm^3), 10, evaporation under reduced pressure, CH_2Cl_2–light petroleum	53.1 (53.3)	3.5 (4.0)	2.1 (2.2)	13.2 (12.7)	840	4.5

Table 1. (*Contd*)

Sl. No.	Complex [M.p. (°C),[a] color,[b] yield (%)]	Reaction conditions[c] [A/B, S (mg), T (h), R^1 other conditions]	Analyses [found (calc.)] (%) C	H	N	Halide/ sulfur	IR bands C_5H_5 (cm^{-1})	C_5H_5 ^1H NMR [δ (ppm)][d]
14	[(Cp)Ru($AsPh_3$)(γ-pic)Br] (136d, Y, 50)	A, γ-pic (1 cm^3), 11, evaporation under reduced pressure, CH_2Cl_2–light petroleum	54.3 (54.0)	4.1 (4.3)	2.0 (3.2)	12.8 (12.4)	840	4.5
15	[(Cp)Ru($AsPh_3$)(bipy)]$^+Br^-$ (250, OY, 65)	A, bipy (50), 15, ethanol–ether	55.5 (55.9)	4.2 (4.0)	4.1 (4.0)	11.7 (11.3)	845	4.63
16	[(Cp)Ru($AsPh_3$)(*o*-phen)]$^+Br^-$ (250, Y, 70)	A, *o*-phen (50), 15, ethanol–ether	57.0 (57.4)	3.5 (3.8)	4.0 (3.8)	11.3 (10.9)	850	5.0
17	[(Cp)Ru($AsPh_3$)(py)I] (165d, OY, 50)	A, py (1 cm^3), 13, CH_2Cl_2–diethyl ether	49.2 (49.6)	3.9 (3.7)	2.0 (2.1)	19.4 (18.8)	840	4.5
18	[(Cp)Ru($AsPh_3$)(bipy)]$^+I^-$ (250, O, 70)	A, bipy (60), 15, $CHCl_3$–diethyl ether	52.7 (52.5)	4.2 (3.7)	3.4 (3.7)	16.0 (16.8)	845	4.65
19	[(Cp)Ru($AsPh_3$)(*o*-phen)]$^+I^-$ (250, O, 75)	A, *o*-phen (50), 15, $CHCl_3$–diethyl ether	53.6 (53.9)	3.4 (3.6)	3.9 (3.6)	16.8 (16.3)	847	5.0
20	[(Cp)Ru($AsPh_3$)(py)CN] (225, YG, 65)	A, py (1 cm^3), 12, CH_2Cl_2–light petroleum	60.1 (60.4)	4.7 (4.3)	4.6 (4.9)	—	840	4.6
21	[(Cp)Ru($AsPh_3$)(γ-pic)CN] (235d, YG, 55)	A, γ-pic (1 cm^3), 12, CH_2Cl_2–light petroleum	62.0 (61.1)	4.5 (4.6)	5.1 (4.8)	—	840 ν(CN) 2050	4.6
22	[(Cp)Ru($AsPh_3$)(bipy)]$^+CN^-$ (250. OY, 60)	A, bipy (60), 20, $CHCl_3$–light petroleum	62.0 (62.4)	4.1 (4.3)	6.5 (6.4)	—	845 ν(CN) 2060	4.8
23	[(Cp)Ru($AsPh_3$)(*o*-phen)]$^+CN^-$ (250, OY, 68)	A, *o*-phen (60), 20, $CHCl_3$–light petroleum	63.2 (63.7)	4.3 (4.1)	6.2 (6.1)	—	845 ν(CN) 2060	4.8
24	[(Cp)Ru($AsPh_3$)(py)$SnCl_3$] (185, Y, 40)	A, py (1 cm^3), 14, $CHCl_3$–light petroleum	43.6 (43.3)	3.5 (3.2)	2.0 (1.8)	14.2 (13.7)	845	4.5
25	[(Cp)Ru($AsPh_3$)(bipy)]$^+SnCl_3^-$ (225, OY, 50)	A, bipy (60), 20, $CHCl_3$–light petroleum	46.7 (46.2)	3.5 (3.3)	3.0 (3.3)	12.7 (12.4)	845	4.5
26	[(Cp)Ru($AsPh_3$)(*o*-phen)]$^+SnCl_3^-$ (227, OY, 60)	A, *o*-phen (60), 20, $CHCl_3$–light petroleum	47.4 (47.9)	3.1 (3.2)	3.5 (3.2)	12.5 (12.0)	850	4.6
27	[(Cp)Ru($SbPh_3$)(py)Cl] (185, 4, 50)	A, py (1 cm^3), 10, evaporation under reduced pressure, CH_2Cl_2–petroleum ether	53.1 (53.2)	4.1 (4.0)	2.2 (2.0)	5.3 (5.5)	845	4.67

28	$[(Cp)Ru(SbPh_3)(\gamma\text{-pic})Cl]$ (260, Y, 50)	A, γ-pic (1 cm^3), 10, evaporation under reduced pressure, CH_2Cl_2–petroleum ether	53.7 (53.8)	4.4 (4.2)	2.3 (2.2)	6.0 (5.4)	845	4.65
29	$[(Cp)Ru(SbPh_3)(bipy)]^+Cl$ (250, OY, 70)	A, bipy (50), 15, $CHCl_3$–ether	55.3 (55.8)	3.5 (3.9)	4.0 (3.9)	5.2 (4.9)	850	4.6
30	$[(Cp)Ru(SbPh_3)(o\text{-phen})]^+Cl$ (255, O, 75)	A, *o*-phen (50), 15, ethanol–ether	57.6 (57.2)	3.8 (3.8)	4.0 (3.8)	4.2 (4.8)	850	4.77
31	$[(Cp)Ru(SbPh_3)(py)Br]$ (185d, Y, 40)	A, py (1 cm^3), 12, CH_2Cl_2–light petroleum	49.1 (49.6)	3.2 (3.7)	2.0 (2.1)	12.4 (11.8)	845	
32	$[(Cp)Ru(SbPh_3)(bipy)]^+Br^-$ (250, Y, 60)	A, bipy (50), 15, ethanol–ether	51.7 (52.4)	4.5 (3.7)	3.6 (3.7)	11.1 (10.6)	850	4.7
33	$[(Cp)Ru(SbPh_3)(o\text{-phen})]^+Br^-$ (240, OR, 70)	A, *o*-phen (50), 15, $CHCl_3$–ether	54.1 (53.9)	3.4 (3.6)	3.7 (3.6)	11.0 (10.3)	850	4.8
34	$[(Cp)Ru(SbPh_3)(py)I]$ (160d, Y, 50)	A, py (1 cm^3), 12, CH_2Cl_2–light petroleum	46.9 (46.4)	4.2 (3.4)	2.2 (1.9)	18.2 (17.5)	850	4.51
35	$[(Cp)Ru(SbPh_3)(bipy)]^+I^-$ (235d, O, 60)	A, bipy (50), 15, $CHCl_3$–light petroleum	49.0 (49.3)	4.1 (3.5)	3.7 (3.5)	16.6 (15.8)	850	4.8
36	$[(Cp)Ru(SbPh_3)(o\text{-phen})]^+I^-$ (225, OR, 60)	A, *o*-phen (50), 15, $CHCl_3$–light petroleum	50.2 (50.8)	4.0 (3.4)	3.2 (3.4)	16.2 (15.4)	850	4.8
37	$[(Cp)Ru(SbPh_3)(py)CN]$ (225, Y, 60)	A, py (1 cm^3), 13, CH_2Cl_2–light petroleum	55.3 (55.8)	4.5 (4.0)	4.5 (4.5)	—	845	4.5
38	$[(Cp)Ru(SbPh_3)(bipy)]^+CN^-$ (242, OY, 70)	A, bipy (50), 20, $CHCl_3$–diethyl ether	58.0 (58.2)	3.5 (4.0)	6.2 (6.4)	—	850	4.6
39	$[(Cp)Ru(SbPh_3)(o\text{-phen})]^+CN^-$ (240, OY, 70)	A, *o*-phen (50), 20, $CHCl_3$–diethyl ether	60.1 (59.6)	4.2 (3.9)	5.6 (5.8)	—	850	4.3
40	$[(Cp)Ru(SbPh_3)(py)NCS]$ (193, OY, 50)	A, py (1 cm^3), 12, CH_2Cl_2–light petroleum	52.8 (53.0)	4.2 (3.8)	4.1 (4.3)	5.5 (4.9)	850 ν(CN) 2030	4.5
41	$[(Cp)Ru(SbPh_3)(bipy)]^+NCS^-$ (195, OY, 40)	A, bipy (60), 15, $CHCl_3$–light petroleum	55.3 (55.7)	4.3 (3.8)	5.9 (5.7)	5.0 (4.4)	850 ν(CN) 2030	4.66
42	$[(Cp)Ru(SbPh_3)(o\text{-phen})]^+NCS^-$ (205, O, 60)	A, *o*-phen (60), 15, $CHCl_3$– diethyl ether	56.7 (57.1)	4.1 (3.7)	5.4 (5.5)	4.8 (4.2)	850 ν(CN) 2040	4.7
43	$[(Cp)Ru(SbPh_3)(py)(SnCl_3)]$ (215, Y, 50)	A, py (2 cm^3), 15, CH_2Cl_2–light petroleum	41.2 (40.9)	3.2 (3.1)	2.1 (1.7)	13.5 (12.8)	845	4.5
44	$[(Cp)Ru(SbPh_3)(bipy)]^+SnCl_3^-$ (225, OY, 70)	A, bipy (50), 24, $CHCl_3$–diethyl ether	44.2 (44.0)	3.5 (3.1)	3.0 (3.1)	12.4 (11.8)	850	4.6

Table 1. (*Contd.*)

Sl. No.	Complex [M.p. (°C),[a] color,[b] yield (%)]	Reaction conditions[c] [A/B, S (mg), T (h), R^1 other conditions]	Analyses [found (calc.)] (%) C	H	N	Halide/ sulfur	IR bands C_5H_5 (cm^{-1})	C_5H_5 ^1H NMR [δ (ppm)][d]
45	$[(Cp)Ru(SbPh_3)(o\text{-phen})]^+SnCl_3^-$[f] (180, OY, 60)	A, *o*-phen (60), 24, $CHCl_3$–diethyl ether	44.8 (45.5)	3.5 (3.0)	3.2 (3.0)	12.0 (11.5)	850	4.57
46	$[(Cp)Ru(AsPh_3)(bipy)]^+BPh_4^-$ (250, OY)	B, $NaBPh_4$ (50), $CHCl_3$–ethanol	71.5 (72.2)	5.7 (5.1)	3.0 (2.9)	—	850	
47	$[(Cp)Ru(AsPh_3)(bipy)]^+BF_4^-$ (260, OR)	B, $NaBF_4$ (40), $CHCl_3$–ethanol	55.0 (55.4)	5.2 (3.9)	4.0 (3.9)	—	847	
48	$[(Cp)Ru(AsPh_3)(bipy)]^+HgCl_3^-$ (260, R)	B, $HgCl_2$ (50, *ca* 0.2 mmol), refluxed for 10 min, $CHCl_3$–ethanol	42.6 (42.3)	3.7 (3.0)	3.1 (3.0)	11.7 (11.3)	850	
49	$[(Cp)Ru(AsPh_3)(bipy)]_2^{2+}Zn_2Cl_6^{2-}$ (280, R)	B, $ZnCl_2$ (50), refluxed for 10 min, $CHCl_3$–ethanol	49.3 (49.5)	4.1 (3.5)	3.4 (3.5)	14.0 (13.3)	845	
50	$[(Cp)Ru(AsPh_3)(o\text{-phen})]^+BPh_4^-$ (260, OR)	B, $NaBPh_4$ (50), $CHCl_3$–ethanol	72.2 (72.9)	5.6 (5.0)	3.1 (2.9)	—	850	
51	$[(Cp)Ru(AsPh_3)(o\text{-phen})]^+BF_4^-$ (250, R)	B, $NaBF_4$ (40), $CHCl_3$–ethanol	56.7 (56.8)	4.2 (3.8)	3.6 (3.8)	—	847	
52	$[(Cp)Ru(AsPh_3)(o\text{-phen})]^+HgCl_3^-$ (270, R, 80)	B, $HgCl_2$ (30), refluxed 10 min, $CHCl_3$–ethanol	43.5 (43.8)	3.5 (2.9)	3.2 (2.9)	11.7 (11.1)	850	
53	$[(Cp)Ru(AsPh_3)(o\text{-phen})]_2^{2+}Zn_2Cl_6^{2-}$ (280, R, 80)	B, $ZnCl_2$ (40), refluxed for 10 min, $CHCl_3$–ethanol	50.3 (51.0)	3.4 (3.4)	3.1 (3.4)	13.5 (12.9)	850	
54	$[(Cp)Ru(SbPh_3)(bipy)]^+BPh_4$ (250, OR)	B, $NaBPh_4$(50), $CHCl_3$–ethanol	67.5 (68.8)	4.7 (4.6)	2.7 (2.8)	—	850	
55	$[(Cp)Ru(SbPh_3)(bipy)]^+(bipy)]^+BF_4^-$ (260, R)	B, $NaBF_4$ (30), $CHCl_3$–ethanol	51.5 (52.0)	3.7 (3.7)	3.6 (3.7)	—	850	
56	$[(Cp)Ru(SbPh_3)(bipy)]^+HgCl_3^-$ (260, R, 80)	B, $HgCl_2$ (50), the reaction mixture was refluxed for 10 min, $CHCl_3$–ethanol	39.7 (40.3)	4.0 (2.8)	3.1 (2.8)	11.2 (10.5)	850	
57	$[(Cp)Ru(SbPh_3)(bipy)_2^{2+}Zn_2Cl_6^{2-}$ (280, R, 80)	B, $ZnCl_2$ (50), the reaction mixture was refluxed for 10 min, $CHCl_3$–ethanol	47.2 (46.7)	3.5 (3.3)	3.2 (3.3)	13.0 (12.5)		
58	$[(Cp)Ru(SbPh_3)(o\text{-phen})]^+BPh_4^-$ (245, R)	B, $NaBPh_4$ (40), $CHCl_3$–ethanol	69.6 (69.5)	5.3 (4.7)	2.5 (2.7)	—		
59	$[(Cp)Ru(SbPh_3)(o\text{-phen})]^+BF_4^-$ (250, R)	B, $NaBF_4$ (30), $CHCl_3$–ethanol	53.1 (53.4)	4.2 (3.6)	3.6 (3.6)	—		

60	$[(Cp)Ru(SbPh_3)(o\text{-phen})]^+HgCl_3^-$ (260, R, 80)	B, $HgCl_2$(40), the reaction mixture was refluxed for 10 min, $CHCl_3$–	41.3 (41.7)	3.0 (2.1)	3.1 (2.8)	11.3 (10.5)			
61	$[(Cp)Ru(PPh_3)(acac)]$ (140d, 80, 50)	A, acac (5 cm^3), CH_2Cl_2–ether; after evaporation of the solvent a red oil was formed: the red oil was washed with light petroleum several times	63.2 (63.7)	5.6 (5.1)	—	—	840		4.3
62	$[(Cp)Ru(SbPh_3)(acac)]$ (160d, R, 50)	A, acac (5 cm^3), CH_2Cl_2–ether	54.6 (54.3)	4.1 (4.5)	—	—	840		4.5
63	$[(Cp)Ru(SbPh_3)(DTC)]$ (155, O, 50)	A, DTC (25 mg), CH_2Cl_2–petroleum ether	50.1 (50.4)	4.4 (4.5)	2.0 (2.1)	10.0 (9.6)	840		4.27

[a] Melting points (uncorrected).
[b] R = red, Y = yellow, O = orange, YG = yellowish green, OR = orange-red, BO = brownish orange.
[c] A/B = method, S = substrate, T = time, R′ = recrystallization of complex.
[d] Solvent $CDCl_3$. Aromatic protons of the other coligands appeared in the δ-7.0–8.5 region as broad multiplets, and in the case of γ-picoline, dithiocarbamate and acetylacetonate complexes additional signal in the δ-1.8–2.5 region were observed due to methyl protons.
[e] d = decomposed.
[f] Found: mass 922, required: 924 (mass spectrometry FD).

ClO_4^- (1100 cm^{-1}), $HgCl_3^-$ (292 cm^{-1}) and $Zn_2Cl_6^{2-}$ (335 and 300 cm^{-1}) exhibited the characteristic bands of the anions.[2,7] The zinc complex showed no bands attributable to the ν(ZnCl) of $ZnCl_3^-$.[2]

^{1}H *NMR spectra*

^{1}H NMR spectra of all the complexes showed sharp resonance in the δ-4.4–5.0 region. In the spectra of the cationic stibine complexes $[(Cp)Ru(SbPh_3)L\text{–}L]^+X^-$ (L–L = bipy or 1,10-phen) three resonances (1:2:2) were observed, whereas for the $[(Cp)Ru(SbPh_3)LX]$ (L = py or γ-pic) complexes a sharp singlet was observed. The aromatic protons of the triphenylarsine, triphenylstibine and the *N*-donor ligands exhibited broad resonances in the range δ 7.0–8.5. The complexes having γ-pic also showed a resonance due to methyl protons around δ 1.8–2.0. DTC- and acac-containing complexes exhibited additional signals in the δ 3.5 (CH_2), δ 2.0 (methyl) region and δ 5.7 (—CH), δ 2.23 (methyl) region, respectively.[5,20] The interesting aspect of these spectra is that the C_5H_5 proton resonances in the complexes having bases as coligands were shifted downfield compared to their parent species (δ 4.2), viz. $[(Cp)Ru(MPh_3)_2X]$ (M = As or Sb). Furthermore, the downfield shift is larger in the cationic species in conformity with those previously observed for other Ru–Cp cationic complexes.[1-10]

The downfield shift in the position of C_5H_5 protons in all the complexes (neutral or cationic) compared to that in the spectra of the complexes having two molecules of MPh_3 linked to the ruthenium could possibly be due to the difference in the π-accepting behaviour of the heterocyclic bases and triphenylarsine or triphenylstibine.[25]

Electronic spectra

The electronic spectra of the complexes showed a fairly intense band around 450 nm, which could be assigned to a metal to ligand charge-transfer (M → L) transition.[26,27] The variation in the position of the (M → L) charge-transfer bands with the nature of the heterocyclic bases was not regular.

On the basis of the results discussed in the preceding paragraphs and on the basis of the previous studies[1-12] a distorted octahedral structure has been assigned to all the complexes.

Acknowledgements—One of us (L.M.) wishes to thank the University Grants Commission, New Delhi, for financial assistance in the form of a National Associateship.

REFERENCES

1. J. D. Gilbert and G. Wilkinson, *J. Chem. Soc.* 1969, 1749.
2. T. Blackmore, M. I. Bruce and F. G. A. Stone, *J. Chem. Soc. A* 1971, 2376.
3. M. I. Bruce and N. J. Windsor, *Aust. J. Chem.* 1977, **30**, 1601 (and references therein).
4. P. M. Treichel and D. A. Komar, *Synth. React. Inorg. Met.-Org. Chem.* 1980, **10**, 205.
5. T. Wilczewski, M. Bochenska and J. F. Biernat, *J. Organomet. Chem.* 1981, **215**, 87.
6. H. Lehmkuhl, J. Grundke, R. Benn, G. Schroth and R. Mynott, *J. Organomet. Chem.* 1981, **217**, CS.
7. M. I. Bruce and R. C. Wallis, *Aust. J. Chem.* 1979, **32**, 1471.
8. M. I. Bruce and R. C. Wallis, *Aust. J. Chem.* 1981, **34**, 209.
9. M. I. Bruce, D. N. Buffy, M. G. Humphrey and A. G. Swincer, *J. Organomet. Chem.* 1985, **282**, 383.
10. R. F. N. Ashok, M. Gupta and U. C. Agarwala, *Inorg. Chim. Acta* 1985, **98**, 161.
11. K. Mohan Rao, L. Mishra and U. C. Agarwala, *J. Organomet. Chem.* (submitted).
12. K. Mohan Rao, L. Mishra and U. C. Agarwala, *Polyhedron* 1986, **5**, 1491.
13. A. I. Vogel, *A Textbook of Quantitative Inorganic Analysis*, 4th Edn., p. 591. Longmans Green, London (1978).
14. (a) C. A. Tolman, *Chem. Rev.* 1977, **77**, 313; (b) C. A. Tolman, *J. Am. Chem. Soc.* 1970, **92**, 2956.
15. R. Uson, L. A. Oro, M. A. Giriano, M. M. Noval, M. C. Apreda, C. F. Foces, F. H. Cano and S. G. Blanco, *J. Organomet. Chem.* 1983, **256**, 331.
16. R. J. Haines and A. L. Du Preez, *J. Organomet. Chem.* 1975, **84**, 357.
17. L. Maier, *Prog. Inorg. Chem.* 1963, **5**, 27.
18. R. L. Bohon, R. Isaac, H. Hofteizer and R. J. Cellner, *Anal. Chem.* 1958, **30**, 245.
19. D. P. Biddiscombe, E. A. Coulson, R. Handley and E. F. G. Herrington, *J. Chem. Soc.* 1954, 1957.
20. A. A. Schilt and R. C. Taylor, *J. Inorg. Nucl. Chem.* 1959, **9**, 211.
21. H. A. Meinema, A. Mackor and J. G. Noltes, *J. Organomet. Chem.* 1972, **37**, 285.
22. S. D. Ross, *Inorganic and Raman Spectra*, p. 136. McGraw-Hill, London (1972).
23. J. J. Veszpremi, J. Nagy, I. A. Barta and G. S. Zscomlok, *J. Organomet. Chem.* 1980, **185**, 323.
24. N. Bertazzi, G. Alonso, A. Silvestri and G. Consiglio, *J. Organomet. Chem.* 1972, **37**, 281.
25. H. G. Alt and H. E. Engelhardt, *Z. Naturforsch.* 1985, **40B**, 1134.
26. A. E. Martell (Ed.), *Coordination Chemistry*, Vol. 1, p. 180. ACS Monograph, Van Nostrand Reinhold, New York (1971).
27. C. R. Johnson and R. E. Shepherd, *Inorg. Chem.* 1983, **22**, 2439.

Polyhedron Vol. 6, No. 6, pp. 1391–1397, 1987
Printed in Great Britain

0277–5387/87 $3.00+.00

PALLADIUM COMPLEXES WITH BIOLOGICAL LIGANDS—III.* KINETICS AND REACTION MECHANISM OF THE INTERACTION OF Pd(II) WITH METHIONINE AND *S*-METHYL-L-CYSTEINE

HAYAT M. MARAFIE, NADYAH SHUAIB and MOHAMED S. EL-EZABY†

Chemistry Department, Faculty of Science, Kuwait University, P.O. Box 5969, Safat, 13060 Safat, Kuwait

(*Received* 22 *September* 1986; *accepted after revision* 8 *December* 1986)

Abstract—Two rate steps have been observed when excess Pd(II) was reacted with methionine (Meth) and *S*-methyl-L-cysteine (SMC) in the pH range 1–3.5. The fast step in both systems was attributed to the formation of a mononuclear chelated complex, and the slow step may be due to the effect of hydrolysis and/or polymerization processes. The mechanism of the fast reaction was discussed in terms of the species $PdCl_4^{2-}$, $[PdCl_3(OH)]^{2-}$, H_2L^+ and HL (L = Meth or SMC). It was concluded that $[PdCl_3(OH)]^{2-}$ was the more reactive species in the complex formation reaction. It was also found that substitution reactions involving Meth were more labile than those involving SMC.

Recent discoveries of the anticarcinogenic properties of some platinum complexes have drawn attention to palladium complexes which in general are chemically similar.[2,3] Although platinum complexes have been shown to be more effective in the treatment of some cancer cases than palladium complexes,[4] yet the latter complexes offer a chemical advantage over the former due to the fact that they are kinetically more labile. This allows a better understanding of the platinum complexes.

In order to study the role of some platinum and palladium complexes in cancer chemotherapy; the interaction of these metal ions should be carefully investigated with ligands commonly found in the biological systems. In this work L-methionine (Meth) and *S*-methyl-L-cysteine (SMC) have been selected as the ligands. Preparative work on Pd(II) complexes with Meth have been reported.[5–8] Among the synthesized complexes are those corresponding to the formulae $[PdCl_2(Meth)]^-$, $[Pd(Meth\text{-}H)_2]^{2+}$, $[Pd(Meth)_2]$, $[Pd(Meth\text{-}H)Cl_2]$ and $[Pd(Meth)H_2O]^+$ {Meth = $[CH_3S(CH_2)_2CH(NH_2)COO]^-$}. The formation constants of $[Pd(Meth)]^+$ and $[Pd(Meth)_2]$ were calculated ($\log\beta_1 = 9.14$ and $\log\beta_2 = 17.00$).[9,10] SMC also interacts with Pd(II) to form several complexes[11–13] having the following formulae $[Pd(SMC\text{-}H)Cl_2]$, $[Pd(SMC)_2]$ and $[Pd_2(SMC\text{-}H)_2Cl_2]^{2+}$ {SMC = $[CH_3SCH_2CH(NH_2)COO]^-$}. The log formation constant of $[Pd(SMC)]^+$ is 9.38.[9]

EXPERIMENTAL

Materials

Meth (Fluka, 99%) and SMC (Fluka, ⩾ 98%) were used without purification. Stock solutions (taken by weight) of the ligands were kept in a dark cool place. A stock solution of Pd(II) chloride (Pierce) was prepared in HCl [which was 10 times the concentration of the Pd(II)]. The concentration of the metal ion was determined by gravimetric methods as Pd(dimethylglyoxime)$_2$.[14]

The kinetic measurements were done using a Union Giken stopped-flow apparatus as previously described.[15] The optical path of the cuvette was 10.0 mm, thermostated at 25°C. The observed rate constants were calculated by a program using the Guggenheim method.

The absorption spectra were obtained using Pye–Unicam SP8-100 and Schimadzu-160 spec-

* For Part II see Ref. 1.

† Author to whom correspondence should be addressed.

trophotometers in the wavelength range 200–500 nm. The pH measurements were obtained by using a Radiometer pH-meter type 62 equipped with a combined glass electrode (GK 2301C). The pH meter was calibrated before use with two buffers at 2.0 and 4.0.

In all measurements, the ionic strength was kept constant at 0.15 M. The Pd(II) concentration (T_{Pd}) ranges from 10^{-3} to 10^{-2} M, and the ligand concentration (T_{Meth} or T_{SMC}) was fixed at 1×10^{-4} M.

RESULTS AND DISCUSSION

The addition of the solution of Meth or SMC to that of Pd(II) almost decolourized it in the pH range 1–5 (when the concentration of ligand is greater than the metal). The spectra show considerable changes where the bands of Pd(II) chloro complexes are shifted to shorter wavelengths with an increase in intensity in the wavelength range 600–200 nm. The ligands themselves have no absorption at wavelengths longer than ~ 220 nm Fig. 1(A)–(C). The spectra are pH-dependent in the pH range used while those of Pd(II) chloro complexes show only a minor change in the intensity with increase in the pH of the solution.

The kinetic runs were monitored at $\lambda_{380\,nm}$ under pseudo-first-order conditions with the con-

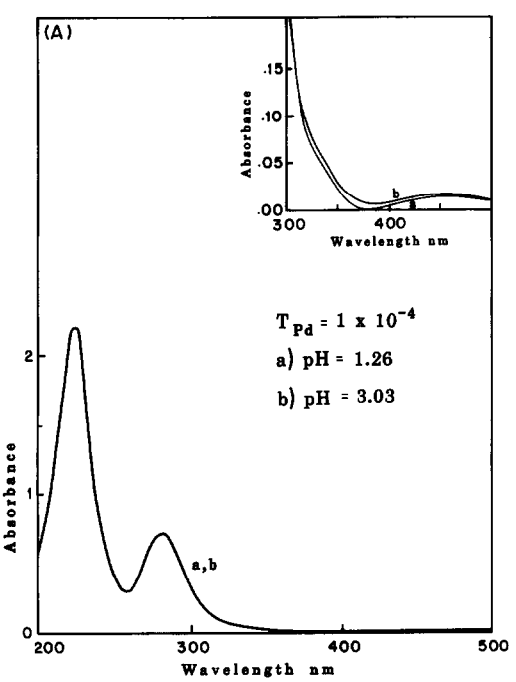

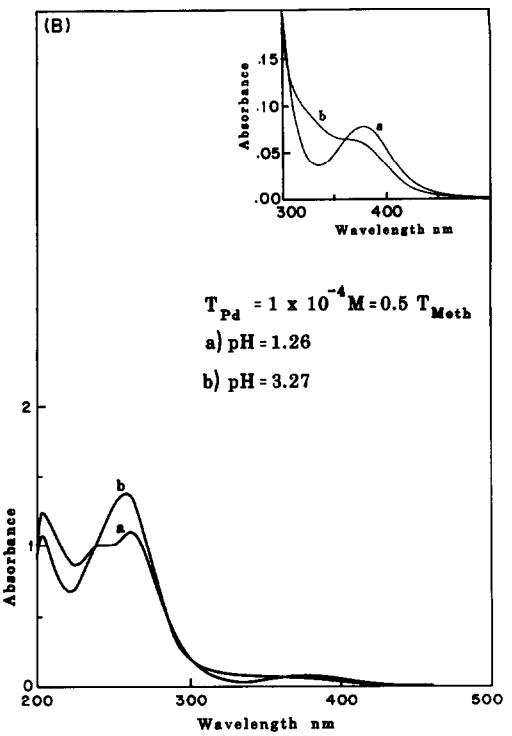

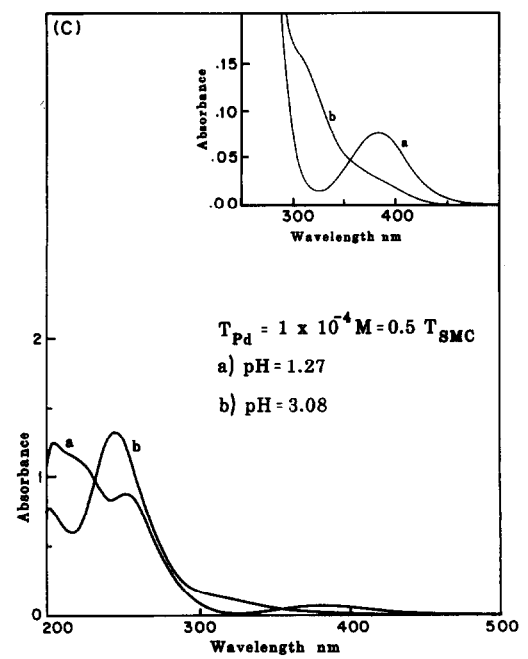

Fig. 1. Spectra of Pd(II)–Meth and Pd(II)–SMC systems at representative pH values. (A) Spectra of Pd(II) at the indicated pH values. (B) Spectra of Pd(II)–Meth at the indicated pH values. (C) Spectra of Pd(II)–SMC at the indicated pH values.

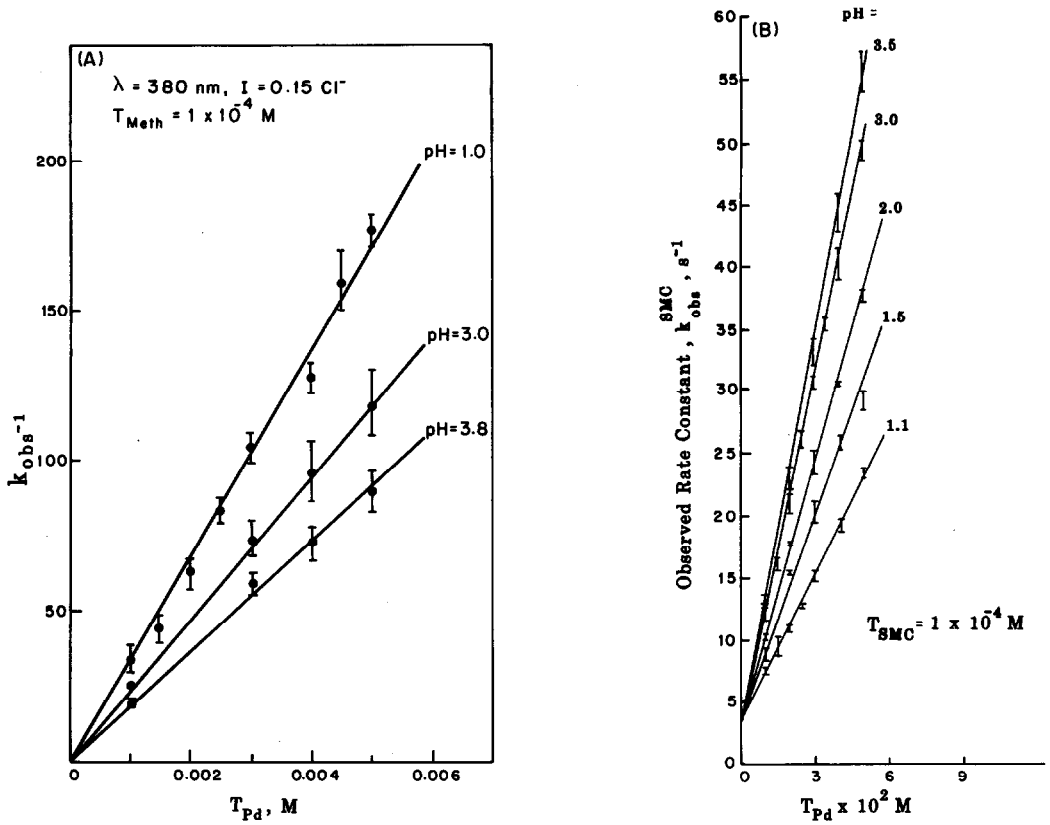

Fig. 2. Dependence of the observed rate constants on pH for: (A) the Pd(II)–Meth system, and (B) the Pd(II)–SMC system.

centration of Pd(II) much greater than that of the ligands. Two rate steps were observed, one in the millisecond range and the other in the second range. The change in absorbance with time for the first fast step was much greater than that for the second slow step which allows a better determination of the first step than the second one. The fast step may be attributed to mononuclear-complex formation, and only that step will be considered, while the slow step may be due to the formation of a polymeric and/or hydrolytic processes. The pseudo-first-order rate constants (k_{obs}) are linearly dependent on the T_{Pd} at constant T_{Meth} or T_{SMC}, and constant pH, Figs 2(A) and (B). These linear relationships are empirically expressed as follows:

$$k_{obs}^{L} = m_i^{L} + m_j^{L} T_{Pd}, \quad (1)$$

where L = Meth or SMC, and m_i^L and m_j^L are the intercepts and slopes at various pH values for both systems. In the Pd(II)–Meth and Pd(II)–SMC systems the intercepts have constant values within experimental errors, in the former the value is 3.5 s^{-1} and in the latter it is zero. On the other hand m_j^{Meth} is inversely proportional to the pH and m_j^{SMC} is directly proportional to the pH. Table 1 records the values of m_j for both systems at various pH values, interpolated from their plots against experimental pH values.

The possible ligand species which may primarily exist in the pH range used (1–3.5) are the protonated and dipolar species since the pK values are 2.24 and 9.17 for Meth,[16] and ~ 2.2* and 8.75 for SMC.[17] The metal species, on the other hand, are the tetrachloro complex of Pd(II) ($PdCl_4^{2-}$, $\log \beta_4 = 11.11$[18]) and likely the species $[PdCl_3(OH)]^{2-}$ ($\log \beta_{1OH} = \log K_{1OH} + \log \beta_{4Cl} = 16.81$[18]†).

The interaction of Pd(II) species with the ligand species may be described by the following reaction

* Estimated value.

† K_{1OH} (= $10^{5.7}$) stands for the equilibrium reaction:

$$PdCl_4^{2-} + OH^- \rightleftarrows [PdCl_3(OH)]^{2-} + Cl^-,$$

and β_{4Cl} stands for the equilibrium reaction:

$$Pd^{2+} + 4Cl^- \rightleftarrows PdCl_4^{2-}.$$

mechanism:

$$PdCl_4^{2-} + LH_2^+ \rightleftarrows PdCl_2LH + 2Cl^- + H^+; \quad k_1, k_{-1} \quad \text{(a)}$$

$$PdCl_4^{2-} + LH_2^+ \rightleftarrows [PdCl_2L]^- + 2Cl^- + 2H^+; \quad k_2, k_{-2} \quad \text{(b)}$$

$$K_{1CH} \Big\uparrow\Big\downarrow$$

$$PdCl_4^{2-} + LH \rightleftarrows PdCl_2LH + 2Cl^-; \quad k_3, k_{-3} \quad \text{(c)}$$

$$PdCl_4^{2-} + LH \rightleftarrows [PdCl_2L] + 2Cl^- + H^+; \quad k_4, k_{-4} \quad \text{(d)}$$

$$K_{1OH} \Big\uparrow\Big\downarrow \qquad K_{1CH} \Big\uparrow\Big\downarrow$$

$$[PdCl_3(OH)]^{2-} + LH_2^+ \rightleftarrows PdCl_2LH + Cl^- + H_2O; \quad k_5, k_{-5} \quad \text{(e)}$$

$$[PdCl_3(OH)]^{2-} + LH_2^+ \rightleftarrows [PdCl_2L]^- + Cl^- + H^+ + H_2O; \quad k_6, k_{-6} \quad \text{(f)}$$

$$[PdCl_3(OH)]^{2-} + LH \rightleftarrows PdCl_2LH + Cl^- + OH^-; \quad k_7, k_{-7} \quad \text{(g)}$$

$$[PdCl_3(OH)]^{2-} + LH \rightleftarrows [PdCl_2L]^- + Cl^- + H_2O; \quad k_8, k_{-8} \quad \text{(h)}$$

Scheme 1.

where k_i and k_{-i} are the forward and backward micro-rate constants, and K_{1CH} and K_{1OH} are the deprotonation constant of $PdCl_2LH$ and the mixed chloro hydroxo complex of Pd(II) $\{PdCl_4^{2+} + OH^- \rightleftarrows [PdCl_3(OH)]^{2-} + Cl^-\}$, respectively. In this mechanism the polymerization processes are ignored if one considers only the fast rate step. The formation of other mononuclear complexes was also neglected due to the presence of excess metal concentration with respect to the ligands.

The rate equation describing the mechanism in

Table 1. Values of m_j obtained at interpolated pH values for the Pd(II)–Meth and Pd(II)–SMC systems[a]

pH	L m_j (10^{-3} $s^{-1}M^{-1}$)	L′ m_j (10^{-2} $s^{-1}M^{-1}$)	L Q_2 ($\times 10^{-8}$)	L′ Q_2 ($\times 10^{-7}$)	L $m_j(Q_1Q_2)$ ($\times 10^{-11}$)	L′ $m_j(Q_1Q_2)$ ($\times 10^{-9}$)
1.0	3.40	—	27.130	—	922	—
1.1	3.35	4.0	17.400	65.730	583	263.0
1.2	—	4.4	—	42.230	—	186.0
1.3	3.25	4.7	7.186	27.180	233	128.0
1.4	—	4.9	—	17.600	—	86.0
1.5	3.15	5.2	3.030	11.460	95	60.0
1.7	3.05	5.7	1.320	5.010	40	28.0
1.8	3.00	—	—	—	26	—
1.9	—	6.2	—	2.260	—	14.0
2.0	2.85	6.6	0.410	1.530	12	10.1
2.1	—	—	—	—	—	—
2.2	2.75	6.9	0.200	0.740	54	5.1
2.4	—	7.4	—	0.380	—	2.8
2.5	2.60	—	0.075	—	20	—
2.6	—	7.9	—	0.200	—	1.6
2.7	2.45	—	0.044	—	11	—
2.8	—	8.4	—	0.120	—	1.0
3.0	2.40	8.9	0.018	0.068	4	0.6
3.2	2.20	9.4	0.010	0.038	2	0.4
3.4	—	9.9	—	0.024	—	0.24
3.5	2.0	10.0	0.005	0.019	1	0.19

[a] L = Meth, and L′ = SMC.

Scheme 1 is as follows:

$$\frac{dC_2}{dt} = \frac{T_{Pd}}{Q_3 Q_2}\left(\frac{T_{Meth} - C_2 Q_3}{Q_1}\right) \times \left(Q_6 + \frac{[OH^-]K_{1OH}Q_7}{[Cl^-]}\right) - \frac{C_2 Q_8}{Q_3}, \quad (2)$$

where:

$C_1 = [PdCl_2LH]$,

$C_2 = [PdCl_2L^-]$,

$$Q_1 = 1 + \frac{[H^+]}{K_{2h}} + \frac{[H^+]^2}{K_{1h}K_{2h}}$$

(K_{1h} and K_{2h} are the deprotonation constants of the ligands),

$$Q_2 = 1 + \frac{K_{1OH}[OH^-]}{[Cl^-]},$$

$$Q_3 = (K_{1CH} + [H^+])/K_{1CH},$$

$$Q_4 = k_{-1}[Cl^-]^2[H^+] + k_{-3}[Cl^-]^2 + k_{-5}[Cl^-] + k_{-7}[Cl^-][OH^-],$$

$$Q_5 = k_{-2}[Cl^-]^2[H^+]^2 + k_{-4}[Cl^-]^2[H^+] + k_{-6}[H^+][Cl^-] + k_{-8}[Cl^-],$$

$$Q_6 = (k_1 + k_2)\frac{[H^+]^2}{K_{1h}K_{2h}} + (k_3 + k_4)\frac{[H^+]}{K_{2h}},$$

$$Q_7 = (k_5 + k_6)\frac{[H^+]^2}{K_{1h}K_{2h}} + (k_7 + k_8)\frac{[H^+]}{K_{2h}},$$

and

$$Q_8 = \frac{[H^+]Q_4}{K_{1CH}} + Q_5.$$

The integrated form of eqn (2)* is:

$$\ln\frac{(C_2)_\infty}{(C_2)_\infty - (C_2)_t} = \ln\frac{A_{s_\infty}}{A_{s_\infty} - A_{s_t}} = k_{obs}^L t \quad (3)$$

where:

$$k_{obs}^L = Q_8/Q_3 + Q_9 T_{Pd}/Q_1 Q_2. \quad (4)$$

The terms Q_8/Q_3 and Q_9/Q_1Q_2 stand for the intercepts and slopes expressed in eqn (1) for the Pd(II)–Meth and Pd(II)–SMC systems.

The intercepts are zero in the Pd(II)–Meth system. Figure 2(A) indicates that the Meth complex of Pd(II) has a large value for the formation constant since it represents the backward rate constant. On the other hand, the intercepts have constant values independent of the pH in the Pd(II)–SMC system. In another way:

$$m_i^{SMC} = Q_8/Q_3 \simeq Q_4 \simeq (k_{-3} + k_{-4}K_{1CH})[Cl^-]^2 + (k_{-5} + k_{-6}K_{1CH})[Cl^-]. \quad (5)$$

Equation (5) is correct if $K_{1CH} \leqslant [H^+]$ and m_i is independent of pH. If one accepts the approximations that $k_{-4}K_{1CH}$ and $k_{-6}K_{1CH}$ are much less than k_{-3} and k_{-5}, respectively ($K_{1CH} \leqslant k_{-4}$ and $K_{1CH} \leqslant k_{-6}$), then:

$$m_i^{SMC} = k_{-3}[Cl^-]^2 + k_{-5}[Cl^-] = 3.5\,s^{-1}.$$

If the term corresponding to the slopes is rearranged, one gets the following equation:

$$m_j Q_1 Q_2 = (k_1 + k_2)[H^+]^2/K_{1h}K_{2h} + \{(k_3 + k_4)/K_{2h} + (k_5 + k_6) \times K_w K_{1OH}/K_{1h}K_{2h}[Cl^-]\}[H^+] + (k_7 + k_8)K_w K_{1OH}/K_{2h}[Cl^-], \quad (6)$$

where K_w is the ionic product of water ($= 10^{-13.78}$ at 25°C) and $Q_1 \simeq 1$.

Table 1 shows the values of $m_j Q_1 Q_2$ at interpolated values of pH for the Pd(II)–Meth and Pd(II)–SMC systems. The plots of this dependence are shown in Fig. 3(A) and (B) for both systems. The dependence on H^+ follows a quadratic relationship, specially in the pH range 1–2.5. The coefficients of eqn (6) are equal to $(8.19 \pm 4.17) \times 10^{10}$, $(9.88 \pm 3.26) \times 10^{12}$ and $(9.11 \pm 0.03) \times 10^{15}$ for the Pd(II)–Meth system, and ~ zero, $(1.08 \pm 0.08) \times 10^{12}$ and $(2.93 \pm 0.1) \times 10^{13}$ for the Pd(II)–SMC system. Table 2 shows a numerical comparison of the rate constants of both systems. It seems from Table 2 that the interactions of Pd(II) with Meth or SMC are identical in the sense that most of the reactions in Scheme 1 are significant

Table 2. Micro-rate constants obtained in this work for the Pd(II)–Meth and Pd(II)–SMC system

Rate constants	Pd(II)–Meth	Pd(II)–SMC
$k_1 + k_2$	3.6×10^4	3.0×10^2
$k_3 + k_4$[a]	6.7×10^3	1.9×10^3
$k_5 + k_6$[a]	6.95×10^8	7.6×10^7
$k_7 + k_8$	1.0×10^9	≈ Zero

*Where A_{s_∞}, A_{s_t}, C_∞ and C_t are the absorbances at infinite time t and time t, concentration at infinite time t and time t, respectively.

[a] In determining these constants, the assumption has been made that either the term $(k_7 + k_8)K_w K_{1OH}/K_{2h}[Cl^-]$ or the term $(k_5 + k_6)K_w K_{1OH}/K_{1h}K_{2h}[Cl^-]$ is equal to zero.

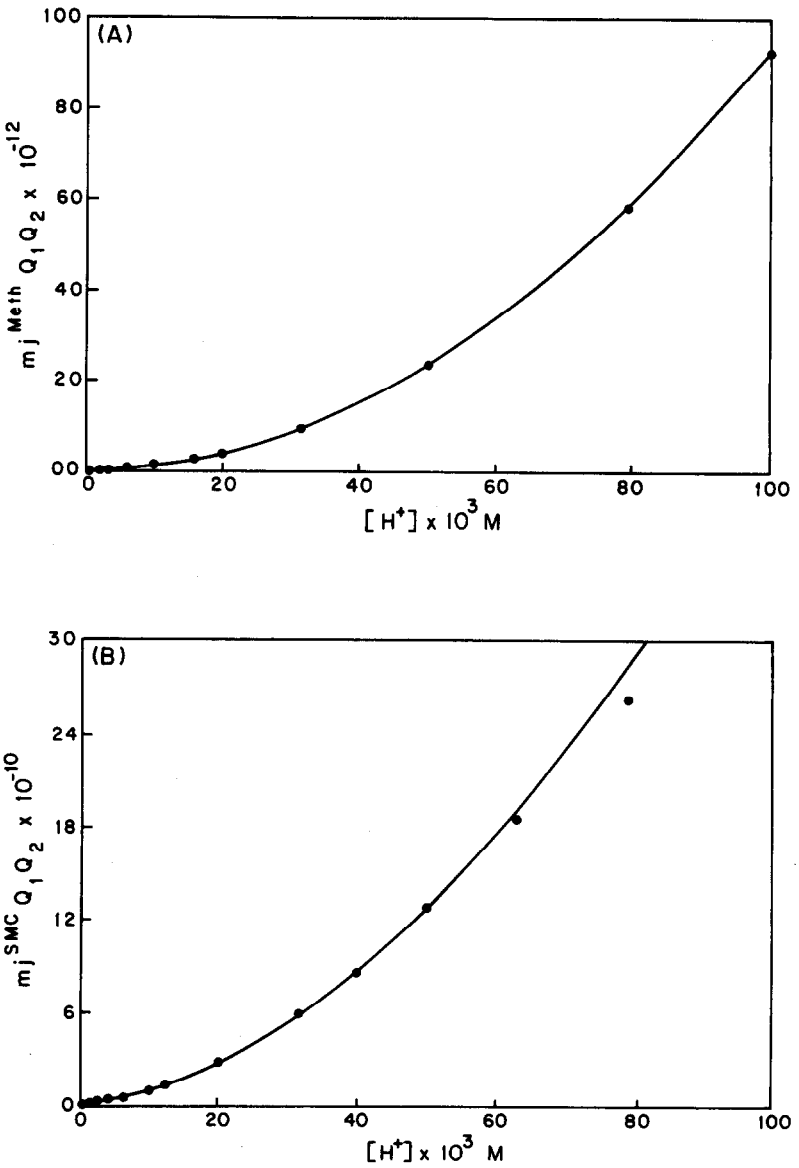

Fig. 3. Dependence of $m_j^L Q_1 Q_2$ on hydrogen ion concentration for: (A) the Pd(II)–Meth system, and (B) the Pd(II)–SMC system.

in the formation of the mononuclear complexes. However, the Pd(II)–Meth system is more labile than the Pd(II)–SMC system despite the fact that a six-membered metal complex is formed in the former and a five-membered complex in the latter, assuming that the amino nitrogen and etherial sulfur are the sites of the ligation. In addition, the substitution reactions involving $[PdCl_3OH]^{2-}$ are more labile than those involving $PdCl_4^{2-}$.

Acknowledgement—The authors thank Kuwait University for the provision of SC021 research grant and SDC 120 and 121.

REFERENCES

1. M. S. El-Ezaby, H. M. Marafie and H. M. Abu-Soûd, *Polyhedron* 1986, **6**, 329.
2. B. Rosenberg, L. Van Camp, J. E. Trosko and V. H. Mansour, *Nature* 1969, **222**, 385.
3. N. M. Moussa, A. Laham, M. S. El-Ezaby, N. A. Al-Salem, M. Abu Zeid, G. S. Mahmoud, A. Kabarity and S. Mazrooei, *J. Inorg. Biochem.* 1982, **17**, 185.
4. M. J. Cleare, In *Recent Results in Cancer Research* (Edited by T. A. Conners and J. J. Roberts), Vol. 48, p. 40. Springer, New York (1974).
5. L. M. Volstein and M. F. Mogilevkina, *Russ. J. Inorg. Chem.* 1963, **8**, 304.

6. C. A. McAuliffe, *J. Chem. Soc. A* 1967, 641.
7. N. N. Chernova and I. G. Kurskii, *Russ. J. Inorg. Chem.* 1978, **23**, 561.
8. O. Vicol, N. Hurduc and I. A. Schneider, *J. Inorg. Nucl. Chem.* 1979, **41**, 309.
9. O. Farooq, N. Ahmad and A. V. Malik, *J. Electroanal. Chem.* 1973, **48**, 475.
10. M. C. Lim, *J. Chem. Soc., Dalton Trans.* 1978, 726.
11. S. E. Livingstone and J. D. Nohan, *Inorg. Chem.* 1968, **7**, 1447.
12. C. A. McAuliffe and S. G. Murray, *Inorg. Chim. Acta, Rev.* 1972, 103.
13. C. A. McAuliffe, *Inorg. Chem.* 1973, **12**, 1699.
14. A. I. Vogel, *Quantitative Inorganic Analysis*, 3rd Edn. Longmans, London (1966).
15. N. M. Shuaib, H. M. Marafie, M. M. Hassan and M. S. El-Ezaby, submitted for publication.
16. D. D. Perrin, *Stability Constants of Metal–Ion Complexes, Part B. Organic Ligands.* IUPAC Chemical Data Series No. 22, Pergamon Press, Oxford (1979).
17. D. P. Wrathall, R. M. Izatt and J. J. Christensen, *J. Am. Chem. Soc.* 1964, **86**, 4779.
18. N. A. Al-Salem, M. S. El-Ezaby, H. M. Marafie and H. M. Abu-Soûd, *Polyhedron* 1986, **5**, 633.

Polyhedron Vol. 6, No. 6, pp. 1399–1405, 1987
Printed in Great Britain

0277–5387/87 $3.00+.00

SPECTROPHOTOMETRIC AND CONDUCTOMETRIC STUDY OF COPPER(II) BROMIDE–*N*,*N*-DIMETHYLFORMAMIDE SOLUTIONS

MICHAŁ PILARCZYK,* WACŁAW GRZYBKOWSKI and LUCYNA KLINSZPORN

Department of Physical Chemistry, Technical University of Gdańsk, 80-952 Gdańsk, Poland

(*Received* 19 *November* 1986; *accepted* 7 *December* 1986)

Abstract—Visible absorption spectra and the molar-conductance curve for $CuBr_2$ in *N*,*N*-dimethylformamide (DMF) as well as the spectra for the $Cu(ClO_4)_2$–Et_4NBr–DMF and $CuBr_2$–DMF–chlorobenzene systems have been studied. The results indicate the formation of the $CuBr_3(DMF)^-$ complex being the predominating bromo complex of copper(II) in the most concentrated solutions of $CuBr_2$ in DMF. The stability constants of the individual bromo complexes of copper(II) have been determined: $\log\beta_1 = 3.35$, $\log\beta_2 = 5.4$, and $\log\beta_3 = 8.8$.

The nonaqueous copper(II) chloride systems have been extensively studied spectrophotometrically by Vierling and coworkers,[1] and the solvent effect on the stability, the electronic spectra, and the structure of copper(II) chloro complexes was discussed. Their results provided quantitative evidence of the well-known facts that the complexes of copper(II) are less stable in better solvating solvents and the solvation of the anion is an effect of minor importance. However, their opinion concerning the exclusive existence of uncomplexed copper(II) in the form of the four-coordinate $Cu(solvent)_4^{2+}$ cations seems to be questionable.

We report here the copper(II) bromide ($CuBr_2$) system in *N*,*N*-dimethylformamide (DMF). The copper(II) chloride complexes in DMF were studied spectrophotometrically by Gutmann,[2] Vierling,[3] and spectrophotometrically and calorimetrically by Ohtaki,[4] providing the experimental evidence for the existence of four chloro complexes of copper(II) in the system. However, there is a lack of quantitative data of non-aqueous $CuBr_2$ solutions. Chmurzyński *et al.*[5] investigated the DMSO–$CuBr_2$ system and identified four consecutive bromo complexes of copper(II) from spectrophotometric data. The corresponding acetonitrile system was studied by Barnes and Hume,[6] who have shown that $CuBr_2$ undergoes reduction, producing CuBr.

The present work was undertaken in order to determine the nature and stability of complexes formed in DMF solutions of $CuBr_2$. In previous papers we reported the study of ionization equilibria of $CoBr_2$ and $NiBr_2$ in this solvent. It has been shown that the most important factor controlling the electrolytic properties of the DMF solutions of $CoBr_2$ is the high stability of the tetrahedral $CoBr_3(DMF)^-$ complex,[7] while the octahedral $NiBr(DMF)_5^+$ complex is the predominating species in DMF solutions of $NiBr_2$.[8]

EXPERIMENTAL

DMF (analytical grade) was dried using a 4A molecular sieve and distilled under reduced pressure at 45–50°C. The specific conductivity of the purified solvent was in the range $3.0–5.0 \times 10^{-8}$ S cm^{-1}.

DMF-solvated $CuBr_2$ and $Cu(ClO_4)_2$ were prepared from the respective hydrates by dissolving them in DMF, followed by removing any excess of the solvent under reduced pressure at *ca* 65°C. The crystalline solids were recrystallized twice from anhydrous DMF. The products were used to prepare the stock solutions immediately before measurements.

The reagent grade tetraethylammonium bromide

* Author to whom correspondence should be addressed.

(Et_4NBr) was recrystallized twice from anhydrous acetonitrile and dried *in vacuo* at elevated temperature.

The stock solutions of $CuBr_2$ and $Cu(ClO_4)_2$ were analysed for copper(II) by standard EDTA titrations. Solutions for measurements were prepared by weighed dilutions, and the concentrations were calculated using the known densities determined independently.

Absorption spectra were measured using a Beckman UV 5270 spectrophotometer. A conductance bridge Beckman RC 18A was used. Details of the procedures for measuring values were identical to those described previously.[5,7,9,13]

RESULTS AND DISCUSSION

It is convenient to start a discussion of the results obtained for DMF solutions of $CuBr_2$ from an analysis of the spectrophotometric results obtained for the three-component $Cu(ClO_4)_2$–Et_4NBr (variable concentration)–DMF solutions. The study of the spectral effects generated by an increasing concentration of Et_4NBr provides the possibility of the identification of consecutive bromo complexes of copper(II) formed.

Our spectrophotometric and conductometric studies[9] have shown six-coordinated $Cu(DMF)_6^{2+}$ to be the only detectable species in DMF solutions of $Cu(ClO_4)_2$. This conclusion is consistent with that derived from X-ray diffraction measurements on the solution of $Cu(ClO_4)_2$ in DMF reported by Ishiguro and Ohtaki.[11] However, four of the six DMF molecules have a shorter Cu—O bond length. This observation explains the behaviour of the solvated Cu^{2+} within the Mn^{2+}–Zn^{2+} series.[9]

Figure 1 shows the electronic absorption spectra (500–1500 nm) of a series of solutions containing $Cu(ClO_4)_2$ at an approximately constant concentration of 0.0050 mol dm^{-3}, and Et_4NBr at a number of different concentrations not exceeding a 3:1 Et_4NBr:$Cu(ClO_4)_2$ mole ratio. The spectrum of copper(II) for pure $Cu(ClO_4)_2$ in DMF is indicated by curve 1. The position and intensity of the band are characteristic of tetragonally distorted octahedral copper(II) complexes.[12] As is seen, addition of Et_4NBr brings about a rapid increase in the intensity of the band accompanied by a regular shift of the maximum from 790 nm towards longer wavelengths. Further changes in the spectrum of copper(II) induced by an addition of Et_4NBr consist in a development of an absorption band with a maximum at 592 nm. The band is observed at $Et_4NBr/Cu(ClO_4)_2$ ratios exceeding 1.0. With increasing Et_4NBr concentration the band changes in intensity only, indicating the presence of one bromo complex of copper(II) absorbing light in this spectral range, while the changes in the long-wavelength range are due to the consecutive bromo complexes of copper(II).

The changes in the spectrum of copper(II) caused

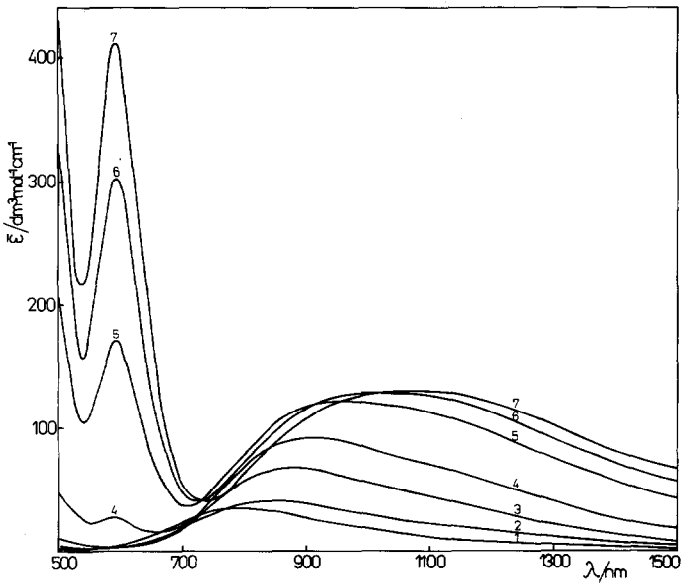

Fig. 1. Absorption spectra of $Cu(ClO_4)_2$–Et_4NBr solutions in DMF at 25°C. The concentrations (mol dm^{-3}) of $Cu(ClO_4)_2$ and Et_4NBr are, respectively: (1) 0.00519, 0.0; (2) 0.00513, 0.00247; (3) 0.00531, 0.00482; (4) 0.00556, 0.00729; (5) 0.00512, 0.00970; (6) 0.00513, 0.01213; (7) 0.00511, 0.01448.

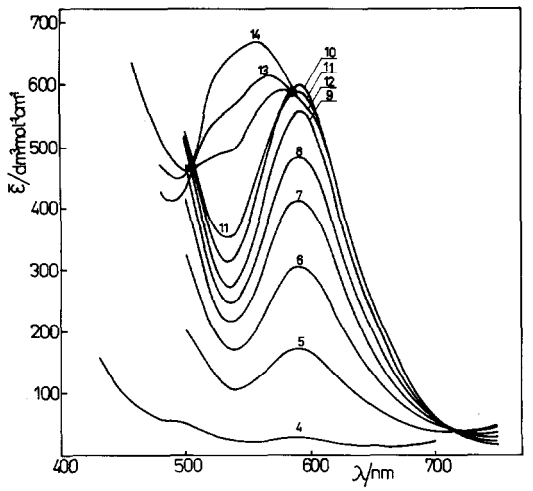

Fig. 2. Absorption spectra of $Cu(ClO_4)_2$–Et_4NBr^- solutions in DMF at 25°C. The concentrations (mol dm^{-3}) of $Cu(ClO_4)_2$ and Et_4NBr are, respectively: (4) 0.00556, 0.00729; (5) 0.00512, 0.00970; (6) 0.00913, 0.01213; (7) 0.00511, 0.01448; (8) 0.00518, 0.01675; (9) 0.00536, 0.02207; (10) 0.00534, 0.03218; (11) 0.00545, 0.05349; (12) 0.00540, 0.10837; (13) 0.00500, 0.13319; (14) 0.00511, 0.17235.

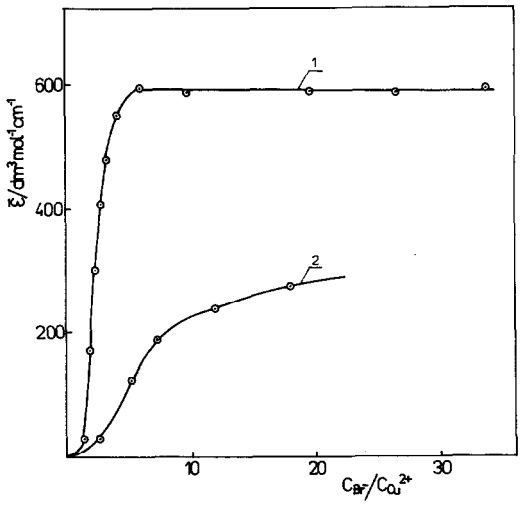

Fig. 3. Plots of the mean absorption coefficient of copper(II) against the $C_{Et_4NBr}/C_{Cu(ClO_4)_2}$ ratio for $Cu(ClO_4)_2$–Et_4NBr solutions in DMF at 25°C for the isosbestic point at 587 nm. (1) $C_{Cu(ClO_4)_2} = 0.005$ mol dm^{-3}, (2) $C_{Cu(ClO_4)_2} = 0.00034$.

by an increasing Et_4NBr concentration are illustrated in Fig. 2 (showing the 592-nm band only). This band seems to be due to the higher bromo complex of copper(II). Moreover, the drastic difference in shape and position suggests a corresponding change in the geometry of the complex. We infer that the band is associated with the presence of a four-coordinate bromo complex of copper(II). At $Et_4NBr/Cu(ClO_4)_2$ ratios from *ca* 1.3 to 4.1 an increase in Et_4NBr concentration results in the gradual growth of this band. When the $Et_4NBr/Cu(ClO_4)_2$ ratio amounts to 19.5 a distinct change in the spectrum of copper(II) is observed. The effect consists in the development of a new band with the maximum shifted toward shorter wavelengths. Subsequently, two well-defined isosbestic points can be observed on the spectra at 504 and 587 nm. Their appearance indicates a two-species equilibrium established within the 19–34 range of the Br^-/Cu^{2+} ratio. Due to the high excess of bromide ion we infer that one of the complexes is the $CuBr_4^{2-}$ complex. The effect of increasing the Et_4NBr concentration becomes more clear when the mean molar absorption coefficient of copper(II) at the wavelength of the isosbestic point is plotted against the Br^-/Cu^{2+} ratio. Figure 3 shows the corresponding plots for the isosbestic point at 587 nm obtained for two series of $Cu(ClO_4)_2$–Et_4NBr solutions markedly differing in $Cu(ClO_4)_2$ concentration. Curve 1 represents the results obtained for the series of solutions containing $Cu(ClO_4)_2$ at a constant concentration of 0.0050 mol dm^{-3}, while curve 2 shows the results obtained in the same range of $Et_4NBr/Cu(ClO_4)_2$ ratios for a lower concentration of $Cu(ClO_4)_2$ (0.00034 mol dm^{-3}). As is seen, the isosbestic point may be observed for the set of spectra corresponding to curve 1, as is indicated by the horizontal section of the plot. Moreover, this fact indicates clearly that the isosbestic points can be observed for more concentrated solutions only. This observation seems to be of practical importance for a study of the analogous systems.

The spectra of a series of solutions of $CuBr_2$ within the concentration range 0.0005–0.06 mol dm^{-3} at 25°C are shown in Fig. 4. The most characteristic feature of the presented set of spectra of copper(II) is the presence of the absorption band with a maximum at 592 nm observed previously for $Et_4NBr/Cu(ClO_4)_2$ ratios exceeding 1.0, but lower than 19.5 (Figs 1 and 2). Inspection of Fig. 4 shows that the band position is independent of salt concentration, while a variation in the intensity with the increase in $CuBr_2$ concentration is observed. The effect of concentration becomes more evident when the mean molar absorption coefficient of copper(II) is plotted against the $CuBr_2$ concentration for the isosbestic point at 587 nm (Fig. 5). The most characteristic feature of this dependence is the sharp increase in the intensity with the increase in $CuBr_2$ concentration below 0.01 mol dm^{-3}, while a further increase in the salt concentration affects the spectrum to a lesser extent.

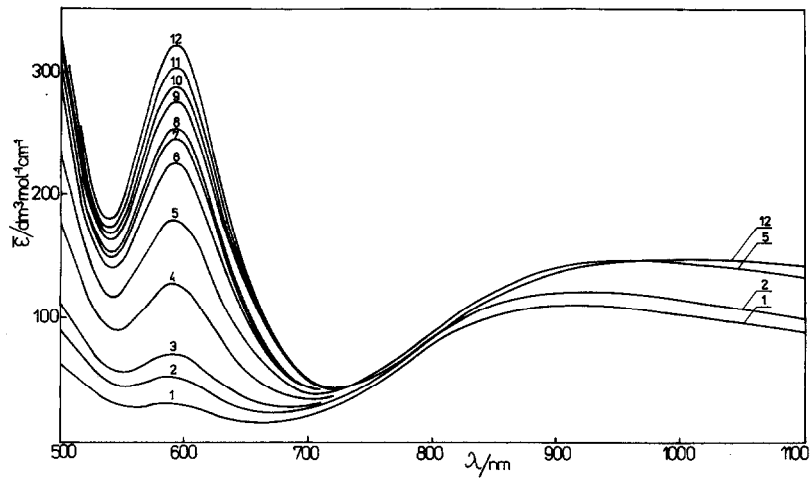

Fig. 4. Visible absorption spectra of $CuBr_2$ solutions in DMF at 25°C. The molar concentrations of $CuBr_2$ are: (1) 0.0004834, (2) 0.0007023, (3) 0.0009793, (4) 0.001953, (5) 0.003644, (6) 0.007327, (7) 0.01022, (8) 0.01319, (9) 0.02021, (10) 0.02682, (11) 0.04020, (12) 0.05536.

This fact may be interpreted in terms of replacing the six-coordinated complexes with the four-coordinated one. The independence of the band position and shape of $CuBr_2$ concentration suggests that only one four-coordinated complex of copper(II) exists in solution. Moreover, an increase in the $CuBr_2$ concentration in the solution brings about an increase in its relative content.

Figure 6 shows the molar-conductance curve of $CuBr_2$ in DMF at 25°C, while the experimental values are listed in Table 1. We may note that the limiting molar conductance of $CuBr_2$ would have

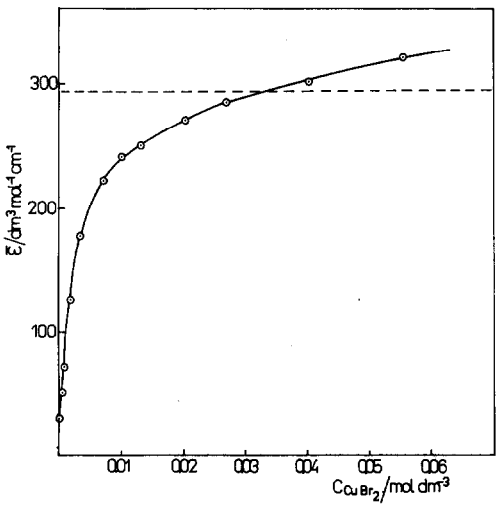

Fig. 5. Plot of the mean molar absorption coefficient of copper(II) for DMF solutions of $CuBr_2$ at 25°C for the isosbestic point at 587 nm. The broken line corresponds to 50% of copper(II) in the form of the $CuBr_3DMF^-$ complex.

the value 187.3 S cm^2 mol^{-1}, calculated from known ionic conductances,[9,10] and this value is significantly higher than the value obtained for the most dilute solution. The solid line in Fig. 6 indicates a fragment of the molar-conductance curve predicted for $CuBr_2$ with the assumption that the solute exists in DMF as a 1 : 1-type electrolyte, i.e. the $CuBr(DMF)_5^+ \cdot Br^-$ complex electrolyte. It becomes clear that extensive complex formation must occur already in the lowest concentration range. Moreover, it can be seen from Fig. 6 that the molar-conductance curve runs almost horizontally at higher $CuBr_2$ concentrations. Such behaviour was found to be characteristic of the formation of ionic species in solution.[7,13] This range of higher concentrations corresponds to the appearance of the band with a maximum at 592 nm in the spectrum of the $CuBr_2$ solution. Thus, we infer that the band is due to the presence of the $CuBr_3(DMF)^-$ complex anion. Formation of this tribromo complex of copper(II) is responsible for the low molar-conductance values. A qualitative confirmation of this conclusion is provided by the effect which the addition of a non-coordinating diluent of low polarity (chlorobenzene) exerts on the spectrum of $CuBr_2$ dissolved in DMF. The spectra of copper(II) observed at a high chlorobenzene content are shown in Fig. 7 along with the spectrum of $CuBr_2$ in pure DMF. As is seen, the addition of diluent results in the disappearance of the band with a maximum at 592 nm. However, this effect is accompanied by the development of a new absorption band with a maximum at *ca* 652 nm (curve 4, 95 mol % of chlorobenzene). It may be expected that the decrease in the dielectric constant of the medium

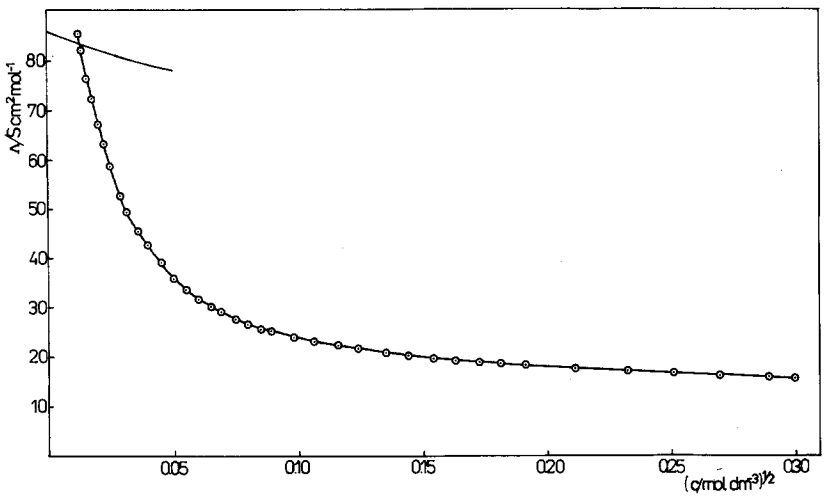

Fig. 6. Plot of the molar conductance of $CuBr_2$ in DMF solutions against the square of concentration at 25°C. The solid line represents the conductometric curve predicted for the 1 : 1-type $CuBr^+ \cdot Br^-$ complex electrolyte.

favours the formation of a neutral species. Thus, it seems to be evident that the light-absorbing complex of copper(II) existing in a DMF solution of $CuBr_2$ is the $CuBr_3(DMF)^-$ complex anion, while the species responsible for the absorption band at 652 nm is a neutral dibromo complex of copper(II), i.e. the pseudotetrahedral $CuBr_2(DMF)_2$ complex. Further conformation of this conclusion arises from the influence of temperature on the intensity of the band at 652 nm. Figure 8 shows the spectra of the $CuBr_2$–DMF–chlorobenzene (95 mol %) solution determined at three different temperatures. As is seen, an increase in the temperature brings about a distinct increase in the band intensity. This temperature variation of the spectrum is consistent with the conclusion mentioned above. The increase in temperature results in a liberation of the coordinatively active solvent from the six-coordinated

Table 1. Molar conductances of $CuBr_2$ in DMF at 25°C

C ($\times 10^{-4}$ mol dm^{-3})	Λ_m (S cm^2 mol^{-1})	C ($\times 10^{-4}$ mol dm^{-3})	Λ_m (S cm^2 mol^{-1})
1.3828	85.32	72.494	25.62
1.6595	82.03	77.072	25.23
2.1907	76.36	95.236	23.95
2.8365	72.20	112.26	23.00
3.7884	67.12	134.58	22.15
4.7733	63.36	153.29	21.56
5.8648	58.63	182.83	20.76
7.7872	53.48	206.90	20.27
9.8036	49.30	236.46	19.53
12.666	45.52	265.57	19.16
15.507	42.79	297.71	18.78
20.266	39.06	329.96	18.54
25.090	35.70	364.78	18.17
30.041	33.45	446.27	17.62
35.597	31.75	536.95	17.08
41.703	30.12	631.74	16.60
47.426	28.97	724.54	16.25
55.574	27.56	833.89	15.90
63.248	26.68	905.28	15.68

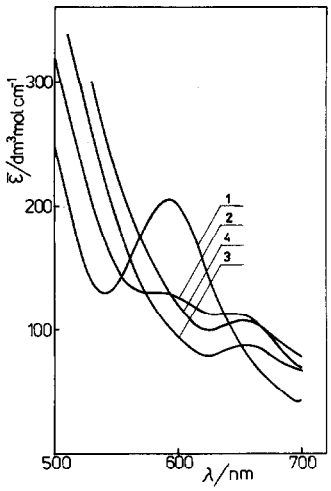

Fig. 7. Absorption spectra of copper(II) for $CuBr_2$–DMF–chlorobenzene solutions at 25°C for constant $CuBr_2$ concentration (0.00512 mol dm^{-3}) and variable chlorobenzene mole fraction: (1) 0.0, (2) 0.638, (3) 0.862, (4) 0.945.

species and the non-ionic $CuBr_2(DMF)_2$ complex is formed. Additional manifestations of this process are the changes observed at longer wavelengths consisting of a decrease in intensity and a blue-shift of the broad band with a maximum between 920 and 940 nm.

The most important feature of the spectra obtained at 25°C for the DMF solutions of $CuBr_2$ is the band due to the presence of the $CuBr_3(DMF)^-$ complex located in the spectral range where absorption due to the six-coordinate species can be ignored. Thus, the band intensity is directly related to the mole fraction of copper(II) existing as the tribromo complex. Figure 5 shows the concentration dependence of the mean molar absorption coefficient of copper(II) in DMF solutions of $CuBr_2$ ($\bar{\varepsilon}$) at the isosbestic point at 587 nm where the molar absorption coefficients of $CuBr_3(DMF)^-$ and $CuBr_4^{2-}$ have a common value of $\varepsilon_{34} = 588$ dm^3 mol^{-1} cm^{-1}. The above results permit the calculation of the equilibrium concentration of the $CuBr_3(DMF)^-$ complex. Thus, ignoring absorption due to other species, the mole fraction of the tribromo complex may be calculated as:

$$\frac{C_3}{C} = \frac{\bar{\varepsilon}}{\varepsilon_{34}}. \tag{1}$$

Inspection of the plot presented in Fig. 5 shows that the value of $\bar{\varepsilon}$ approaches 320 dm^3 mol^{-1} cm^{-1} in the more concentrated solution. Taking into account the value of ε_{34} the mole fraction of $CuBr_3(DMF)^-$ amounts to 0.54. It means that more than 50% of the copper(II) exists as the $CuBr_3(DMF)^-$ complex in more concentrated solutions of $CuBr_2$. It should be noted that the value of 0.54 is lower than the value of $\frac{2}{3}$ expected for complete binding of bromide to the $CuBr_3(DMF)^-$ complex. However, we infer that such a situation is possible for the most concentrated solutions of $CuBr_2$. It corresponds to the formation of a complex electrolyte of type $ML_6^{2+} \cdot 2MX_3L^-$ (L denotes the solvent molecule) known to be one of the most common coordination forms of the transition-metal halides in donor solvents.[7,13,14]

The results presented above provide the possibility of calculating stability constants of all the complexes assumed to be formed in DMF solutions of $CuBr_2$. In the computer analysis performed we assumed the formation of the $CuBr^+$, $CuBr_2$ and $CuBr_3^-$ formal complexes, the corresponding formation constants being defined as:

$$K_n = \frac{C_n}{C_{n-1}[Br^-]} Y_n, \tag{2}$$

where $n = 1$, 2 or 3, and Y_n is the quotient of the respective activity coefficients. Variations in the activity coefficients were assumed to follow the Debye–Hückel equation involving the ion-size parameter *Bå*, the latter being estimated from conductance data[9] as 3.3. Taking into account the equations

$$C = C_0 + C_1 + C_2 + C_3, \tag{3}$$

$$2C = C_1 + 2C_2 + 3C_3 + [Br^-], \tag{4}$$

arising from the material balance for the cation and anion we attempted to find the best values of K_n describing the properties of the DMF solutions of $CuBr_2$ for the range of concentrations in which the absorption due to $CuBr_3(DMF)^-$ was measured. The resulting values of the logarithms of the formation constants are: $\log K_1 = 3.35$ (± 0.10), $\log K_2 = 2.05$ (± 0.05) and $\log K_3 = 3.40$ (± 0.05). The equilibrium concentrations of the single com-

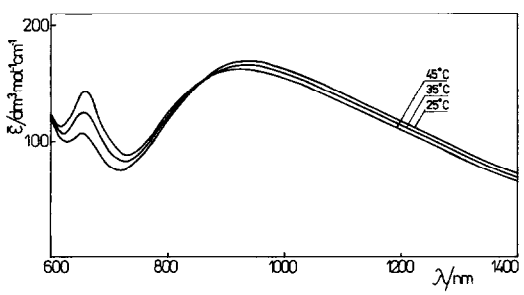

Fig. 8. The influence of temperature on the absorption spectrum of copper(II) for $CuBr_2$–DMF–chlorobenzene solution ($C_{CuBr_2} = 0.0051$, $X_{chlorobenzene} = 0.945$).

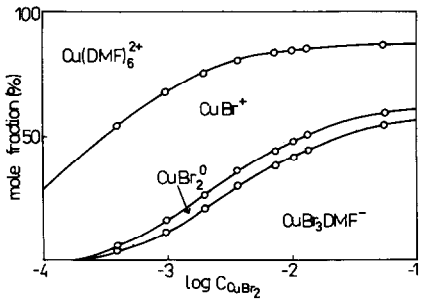

Fig. 9. Formation diagram for the copper(II) complexes in DMF solutions of $CuBr_2$ at 25°C.

plexes found for different concentrations of the solute have been used for preparing the distribution diagram shown in Fig. 9. As is seen, the dominating bromo complexes of copper(II) are the mono- and tribromo species while the formation of the dibromo complexes is an effect of minor importance for the $CuBr_2$–DMF system as well as for the $CuBr_2$–DMF–chlorobenzene solutions. The established sequence of the formation constants, $K_1 > K_2 < K_3$, reflects properly the change in the coordination number of the central metal atom upon coordinating the third bromide anion.

It seems to be of interest to compare the data obtained with results reported by Vierling for the chloro complexes of copper(II) in DMF.[1] The formation constants obtained correspond to values of 3.35, 5.40 and 8.8 for the logarithms of the stability constants of the mono-, di- and tribromo complexes of copper(II), respectively, while the values for the corresponding chloro complexes are 4.4, 9.0 and 12.0. It seems to be obvious that the higher stability of the chloro complexes is a consequence of the better donicity of chloride anion. The order of donor strength found by Gutmann[15] is as follows: $\ldots I^- < Br^- < DMF \leqslant Cl^- < DMSO \ldots$

Acknowledgement—This work was supported by Program No. 86-0293, Poland.

REFERENCES

1. C. Amuli, M. Elleb, J. Muellemeestre, M.-J. Schwing and F. Vierling, *Inorg. Chem.* 1986, **25**, 856 (and references therein).
2. H. Hubacek, B. Stancie and V. Gutmann, *Monatsh. Chem.* 1963, **94**, 1118.
3. M. Elleb, J. Muellemeestre, M.-J. Schwing-Weill and F. Vierling, *Inorg. Chem.* 1980, **19**, 2699.
4. S. Ischiguro, B. G. Jeliazkova and H. Ohtaki, *Bull. Chem. Soc. Jpn* 1985, **58**, 1143.
5. L. Chmurzyński, M. Kluczkowski and M. Pilarczyk, *Electrochim. Acta* 1984, **29**, 373.
6. J. C. Barnes and D. N. Hume, *Inorg. Chem.* 1963, **2**, 444.
7. M. Pilarczyk and L. Klinszporn, *Electrochim. Acta* 1986, **31**, 185.
8. M. Pilarczyk and L. Klinszporn, *Bull. Acad. Pol. Sci., Ser. Sci. Chim.* 1986, **34**, 53.
9. W. Grzybkowski and M. Pilarczyk, *J. Chem. Soc., Faraday Trans.* 1 1983, **79**, 2319.
10. J. E. Prue and P. J. Sherrington, *Trans. Faraday Soc.* 1961, **57**, 1795.
11. S. Ishiguro and H. Ohtaki, *Thermodynamics and Structures of Metal Complexes in Various Solvents.* Tokyo Institute of Technology, Tokyo (1985).
12. C. K. Jørgensen, *Absorption Spectra and Chemical Bonding in Complexes.* Pergamon Press, London (1962).
13. W. Grzybkowski and M. Pilarczyk, *J. Chem. Soc., Faraday Trans* 1 1986, **82**, 1703.
14. W. Grzybkowski, *J. Chem. Soc., Dalton Trans.* 1987 (in press).
15. V. Gutmann and U. Mayer, *Monatsh. Chem.* 1968, **99**, 1383.

Polyhedron Vol. 6, No. 6, pp. 1407–1413, 1987
Printed in Great Britain

0277–5387/87 $3.00+.00

NICKEL(II) COMPLEXES OF METHYLPHOSPHINEDIACETIC ACID

J. PODLAHOVÁ,* F. HARTL, J. PODLAHA and F. KNOCH†

Department of Inorganic Chemistry, Charles University, 128 40 Prague, Czechoslovakia

(*Received* 19 *August* 1986; *accepted* 22 *December* 1986)

Abstract—Methylphosphinediacetic acid (H_2G) is coordinated to nickel(II) in two different ways, depending on whether its carboxyl groups are protonated or dissociated. The acid behaves as a monodentate tertiary phosphine in that it yields a series of *trans*-square planar $NiX_2(H_2G)_2$ complexes (X = Cl, Br, NCS or CN) which are stable in the solid state and as solutions in polar non-aqueous solvents. In neutral aqueous solution the NiG_2^{2-} complex is the predominant species ($\log\beta_2 = 8.24$ at 25°C and $I = 0.1$) even in excess nickel(II). Solid $NiG \cdot 4H_2O$ is the nickel salt of this anion, $Ni[NiG_2] \cdot 8H_2O$. The X-ray structural determination of the barium salt, $BaNiG_2 \cdot NaClO_4 \cdot 5H_2O$, revealed the uncommon *cis*-square planar arrangement around nickel with the G^{2-} anions acting as chelating P,O-bidentate to nickel and as O-monodentate to barium. Sodium and perchlorate ions are located between the complex units and, surprisingly, cannot be removed on recrystallization.

Phosphineacetic acids belong to the class of functionalized phosphines which are capable of coordinating metal ions through the soft or hard donor or through both donors simultaneously as chelating or bridging ligands. Depending on the metal ion type and the structure of the particular phosphineacetate, all these coordination modes have been demonstrated for complexes studied in this laboratory.[1] From the ligands investigated, those with the general formula $RP(CH_2CO_2H)_2$ represent a series which offers a possibility of studying the influence of the R substituent on the coordination properties of the potentially terdentate $-P(CH_2CO_2)^{2-}$ group. As expected, the coordination behaviour has been shown to change drastically from $R = C_6H_5$[2] to $R = C_2H_5$.[3] Hence, a program was developed to synthesize and study several ligands containing R groups with very different steric and/or electronic parameters. The present paper describes nickel(II) complexes of methylphosphinediacetic acid[4] (H_2G) as the ligand involving the sterically undemanding methyl substituent with a marked $+I$ effect.

EXPERIMENTAL

The synthesis of the ligand[4] and most of the experimental techniques[3–5] have been described. All manipulations with solutions were carried out in a dry argon atmosphere; the solids are air-stable.

Preparation of the complexes

$NiCl_2(H_2G)_2$: 1 mmol $NiCl_2 \cdot 6H_2O$ and 2 mmol $H_2G \cdot HCl$ were dissolved in a small amount of water and repeatedly evaporated *in vacuo* to dryness with excess acetic acid–benzene (1 : 1 vol.) until a red crystalline material separated. This was dissolved in hot acetic acid, filtered and allowed to cool slowly. Recrystallization from acetic acid and drying at 80°C/0.2 kPa gave the product in 55% yield.

$NiX_2(H_2G)_2$ (X = Br, NCS or CN) were obtained by metathesis of the chlorocomplex with stoichiometric amounts of KX in acetic acid, filtration of KCl and crystallization (for X = CN, crystallization was induced by addition of benzene). Yields of the recrystallized (acetic acid) and dried complexes varied between 40 and 70%. The iodo complex could not be obtained pure because of irreversible precipitation of anhydrous NiI_2. For measurements in solution, the complex was freshly prepared by metathesis and removal of KCl by filtration where necessary.

* Author to whom correspondence should be addressed.

† Anorganisch-Chemisches Institut der Universität Bonn. Present address: Institut für anorganische Chemie II, Egerlandstrasse 1, 8520 Erlangen, F.R.G.

$NiG \cdot 4H_2O$: 1 mmol $H_2G \cdot HCl$ was dissolved in 4 cm^3 water, neutralized by 1.5 mmol Li_2CO_3 and mixed with 1.02 mmol hydrated nickel(II) perchlorate. The product was precipitated by slow addition of excess ethanol. After washing with ethanol and drying at 25°/0.2 kPa the yield was 85%.

$BaNiG_2 \cdot NaClO_4 \cdot 5H_2O$: 4.00 mmol $H_2G \cdot HCl$, 2.00 mmol hydrated nickel(II) perchlorate and 2.00 mmol hydrated barium(II) perchlorate were dissolved in 6.00 cm^3 2.00 M NaOH. After addition of 6 cm^3 ethanol at 60°C and cooling, the product suddenly crystallized out. It was recrystallized twice from 50% (vol.) aqueous ethanol and dried at 25°C/0.2 kPa with an overall yield of 65%.

CAUTION: the compound detonates violently on heating above 230°C.

Numerous attempts to obtain a product of this type in the absence of sodium and/or perchlorate ions failed.

The samples containing ^{64}Ni were prepared from ^{64}NiO (Tekhsnabeksport, U.S.S.R.) by scaling down the procedures outlined.

Analytical data for all the new compounds (C, H, Ni, P, halogens, N, Na, Ba and H_2O where appropriate) agreed with the calculated values within ± 0.5 relative %.

Crystal structure determination

The preparation of single crystals of $BaNiG_2 \cdot NaClO_4 \cdot 5H_2O$ involved considerable difficulty, mainly because of the notorious tendency of needle-like crystals to aggregate along the needle axis. Finally, 0.2 mmol $NiBr_2(H_2G)_2$ dissolved in 1 cm^3 water was neutralized with 0.4 cm^3 2 M NaOH, and the solution was poured into a long 5-mm internal diameter test tube and mixed with 1.4 cm^3 of a freshly prepared 5% gelatine solution in 50 vol. % aqueous ethanol. After formation of the gel, a solution of 0.2 mmol $Ba(ClO_4)_2 \cdot 3H_2O$ in 2 cm^3 ethanol was carefully layered on the top, the tube was sealed and left undisturbed for 2 weeks at room temperature. Crystals which formed in the gel layer were isolated by thorough decantation with 70 vol. % and then absolute ethanol. Their identity and quality was confirmed by Weissenberg photographs. The sample chosen for X-ray measurement was about $1.0 \times 0.15 \times 0.04$ mm^3. 6898 reflections were collected for $3° < 2\theta < 54°$. 5244 asymmetric data yielded a final number of 4386 strong reflections with $F > 4\sigma$. The symmetry is triclinic, space group $P\bar{1}$, $a = 6.991(2)$, $b = 11.470(3)$, $c = 15.341(3)$ Å, $\alpha = 102.09(2)°$, $\beta = 91.60(2)°$, $\gamma = 90.47(2)°$, $V = 1202.2(5)$ $Å^3$, $d_m = 1.99$ (flotation in bromoform–benzene), $d_x = 2.02$ g cm^{-3}, $Z = 2$, $R = 0.045$, $R_w = 0.040$, and the number of refined parameters is 331. The measurement was carried out on a Nicolet R3m diffractometer. The radiation was Mo-K_α, the unit cell was refined using 16 reflections, and the Wykoff scan from 2.0 to 29.3° min^{-1}, scan width 1.0°. Structure determination using direct methods (SHELXTL), anisotropic refinement of non-hydrogen atoms, the hydrogen atoms were calculated for ideal tetrahedra and refined in rigid groups. Isotropic hydrogens, water hydrogen atoms with a fixed temperature factor of 0.1. The last refinement used a weighting scheme with $w = 1/\sigma^2[R_w]$. Final atomic coordinates, thermal parameters and a list of bond lengths and angles have been deposited with the Cambridge Crystallographic Data Centre.

RESULTS AND DISCUSSION

The properties of the complexes are summarized in Table 1.

H_2G as the ligand

Analogously to other monophosphineacetic acids, H_2G in non-aqueous solvents of medium polarity coordinates to nickel(II) as a monodentate phosphine forming complexes of the $NiX_2(H_2G)_2$ type. Their properties in the solid state and in solution are consistent[6] with the familiar *trans*-square planar structure and with uncoordinated, strongly hydrogen-bonded ligand carboxyl groups. The *trans* geometry follows unambiguously from the number of isotope-substitution-sensitive bands in the far-IR spectra.[5,7] As is usual for nickel(II) complexes, the thiocyanate is N-bonded.[8]

With the exception of the cyano complex, all members of the series decompose instantaneously in water to yield H_2G and NiX_2. The solutions in non-aqueous solvents contain monomeric molecules of the complexes, are non-conducting, and their UV–VIS spectra are identical with the solid-state spectra. The conductivity of the aqueous solution of $Ni(CN)_2(H_2G)_2$ can be explained by a partial dissociation of carboxyl protons as indicated[9] by the solution IR spectrum. In contrast, the Ni—CN bond persists even in a strong acid. All the complexes are kinetically labile as indicated by their NMR spectra consisting of broad bands. The spectra become sharper on cooling but remain unresolved at −40°C which is the temperature where the solubility of the samples becomes impractically low. Hence, the only information from the NMR spectra is the coordination shifts which exhibit usual trends suggesting a strong P → Niσ-interaction.

Table 1. Properties of the compounds prepared

Compound	Colour [m.p. (°C)]	UV–VIS[a] $\tilde{\nu}_{max}$ (10^{-3} cm^{-1}) (ε_M)	IR[b] $\tilde{\nu}_{max}$ (cm^{-1})	NMR[c] δ (ppm)	Remarks
$NiCl_2(H_2G)_2$	Red [152 (dec)]	17.1sh, 18.6 (115), 20.9 (320), 28.1 (8900), 34.8sh, 37.3sh, 41.0 (15,600)	3170vs, 1693vs, 1292s COOH 407m [11] ν(Ni—Cl) 260w [14] ν(Ni—P)	^{1}H: 1.70, 3.22, 9.20 ^{31}P: 6.2	[d]
$NiBr_2(H_2G)_2$	Purple [150 (dec)]	15.1sh, 17.5 (970), 20.7 (440), 26.0 (6530), 32.2sh, 36.4sh, 40.3 (23,700)	3170sb, 1693vs, 1293s COOH 383m [11] ν(Ni—Br) 259w [16] ν(Ni—P)	^{1}H: 1.67, 2.62, 10.60 ^{31}P: 5.1	[d]
$NiI_2(H_2G)_2$[e]	Olive green	16.5 (270), 22.2 (1890), 26.6 (3520), 31.5 (3890), 35.4 (11,600), 39.4 (5820)		^{1}H:[f] 1.76, 2.58, 10.71 ^{31}P:[f] 4.7	[d]
$Ni(NCS)_2(H_2G)_2$	Orange [159–161 (dec)]	19.5sh, 20.9sh, 27.3 (1470) 35.0 (4710), 37.3sh, 42.2 (5950)	3170sb, 1714vs, 1290s COOH 2090vs ν(C≡N), 445w δ(NCS) 418m [11] ν(Ni—N) 256w [8] ν(Ni—P)	^{1}H: 1.69, 3.11, 10.72 ^{31}P: 8.3	[d]
$Ni(CN)_2(H_2G)_2$	Yellow [210–230 (dec)]	22.2sh, 24.3 (1400), 33.7sh, 36.6sh, 40.5 (18,600)	3170sb, 1712vs, 1299s COOH 1710vs, 1588m COOH+COO[h] 2110m ν(C≡N) 255vw [9] ν(Ni—P)	^{1}H: 1.73, 3.21m 10.80 2.05, 3.53[h] ^{31}P: 11.8, 14.2[h]	[g]
$NiG \cdot 4H_2O$	Greenish yellow [260–270 (dec)]	9.8 (5), 16.2 (8), 24.5 (200), 26.2sh, 37.0 (2210), 41.5 (6800)	3360vs, 3275s, 1640m H_2O 1600vs, 1370vs COO 249w [6] ν(Ni—P)		[i]
$BaNiG_2 \cdot NaClO_4 \cdot 5H_2O$	Golden yellow[j]	24.6 (365). 37.6 (4400), 42.0 (13,900)	3420vs, 1635sh H_2O 1610vs, 1380s COO 1144m, 1086s, 912m, 624w ClO_4 251w [8] ν(Ni—P) 1588vs, 1630sh COO[h]	^{1}H:[h] 1.98, 3.72 ^{31}P:[h] 23.0	[k]

[a] Band positions in THF solutions (except where stated otherwise).
[b] Only bands of diagnostic value are given; bands sensitive to isotopic substitution with $\tilde{\nu}$(Ni)–$\tilde{\nu}$(^{64}Ni) in brackets.
[c] In d_8-THF unless stated otherwise; all bands are broad singlets.
[d] Diamagnetic; non-conducting in solution.
[e] Solution properties in acetic acid.
[f] In CD_3CO_2D.
[g] Diamagnetic; Λ_M = 82 (H_2O, 0.01 M).
[h] Dried samples in D_2O solution.
[i] μ_{eff} = 2.9 BM per two formula units.
[j] **Decomposes explosively at 235°C.**
[k] Diamagnetic; Λ_M = 190 (H_2O, 0.01 M).

G^{2-} as the ligand

In aqueous solution, the G^{2-} anion coordinates to nickel(II) with the formation of the NiG_2^{2-} complex anion. The $Ni(ClO_4)_2$–G^{2-}–H^+ system was studied potentiometrically with a glass electrode at 25°C, $I = 0.1$(Na)ClO_4, total G = 0.002 and 0.003 M, 0.0004 < total Ni < 0.006 M, 1.8 < log H^+ < 12.5, and the stability constants obtained by the standard data treatment[10] are:

$$\log \beta_{120} = \log [NiG_2]/([Ni][G]^2) = 8.24(6),$$

$$\log \beta_{121} = \log [NiHG_2]/([Ni][H][G]^2) = 12.5(2),$$

$$\log \beta_{122} = \log [NiH_2G_2]/([Ni][H]^2[G]^2) = 16.1(2)$$

(charges omitted). Interestingly, no detectable amounts of 1 : 1 complexes are formed in the system under the given experimental conditions.

The properties of the complexes containing the NiG_2^{2-} anion suggest a square-planar arrangement involving the ligand as bidentate P,O-chelating with one carboxylate group free and thus easily protonated. Further protonation destroys the NiG_2 core completely. The formally 1 : 1 solid compound, $NiG \cdot 4H_2O$, should be certainly formulated as $Ni[NiG_2] \cdot 8H_2O$: the nickel(II) ion outside the NiG_2 core seems to be coordinated by water molecules and/or intra- and intermolecular carboxyl oxygens in a pseudo-octahedral arrangement, analogous to dinickel(II) ethylenediphosphinetetraacetate.[1(e),5] The structure of the barium salt of the complex anion represents a problem of special interest. Firstly, the compound contains the stoichiometric amount of sodium perchlorate which cannot be removed on recrystallization from aqueous ethanol. The IR spectrum indicates that the perchlorate is present as the ionic species. Secondly, the geometry of the (presumably planar) nickel coordination environment remains unclear on the basis of the spectral data: down to the temperature where measurements in aqueous methanol are possible, the complex is NMR-labile and the spectra thus yield no information about the P–CH_2 virtual coupling;[11] further, the IR spectrum is obscured by ligand bands in the region where the isotopic shifts of ν(Ni—O) should be of diagnostic value. However, the solution IR spectrum clearly shows the presence of two types of COO groups.[9] Consequently, an X-ray structural determination was undertaken.

The perspective view of the structure together with the atom numbering is depicted in Fig. 1 and the stereoview of the unit cell in Fig. 2. Table 2 summarizes the important distances and angles. The structure consists of NiG_2^{2-} complex anions with P,O-chelating ligands; the uncoordinated carboxyls form ionic bonds to barium(II). Hence, the G^{2-} anion should be formally considered as a simultaneously chelating and bridging terdentate ligand, which is a novel bonding type among phosphineacetates. The interspace available permits almost exact accommodation of perchlorate and sodium ions, thus probably explaining why analogous compounds without sodium perchlorate could not be prepared.

The conformation of the chelate rings and, consequently, the pertinent bonding distances and angles differ from one ring to another but are all unexceptional. As usual,[1] the main distortion of the ligand resulting from its coordination is located on the phosphorus atom with bonding angles varying between 97.4 and 125.8°. For the carboxylate

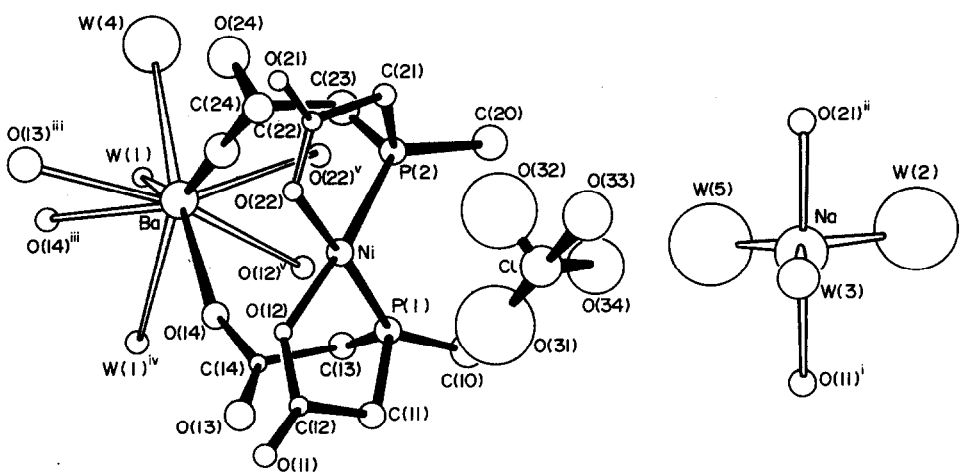

Fig. 1. Perspective view of the structure of $BaNiG_2 \cdot NaClO_4 \cdot 5H_2O$ with closest intermolecular contacts. Hydrogen atoms (omitted for clarity) are given the numbers of their bonding partners. W denotes the oxygen atom of a water molecule. For symmetry code, see Table 2.

Table 2. Important bond distances (Å) and angles (°) with esds in parentheses[a]

		(a) Ni environment	
Ni—P(1)	2.139(2)	P(1)—Ni—P(2)	100.8(1)
Ni—P(2)	2.137(1)	P(1)—Ni—O(12)	85.9(1)
Ni—O(12)	1.903(3)	P(1)—Ni—O(22)	173.1(1)
Ni—O(22)	1.907(4)	P(2)—Ni—O(12)	172.8(1)
		P(2)—Ni—O(22)	86.1(1)
		O(12)—Ni—O(22)	87.2(2)
		(b) Ba environment	
Ba—O(14)	2.695(5)	Ba—O(13)^{iii}	2.805(5)
Ba—O(23)	2.687(5)	Ba—O(14)^{iii}	2.888(5)
Ba—W(1)	2.861(4)	Ba—O(12)^{v}	2.905(4)
Ba—W(1)^{iv}	2.901(4)	Ba—O(22)^{v}	2.853(5)
Ba—W(4)	2.855(7)		
		(c) Na environment	
Na—W(2)	2.264(12)	W(2)—Na—W(3)	118.5(4)
Na—W(3)	2.440(8)	W(2)—Na—W(5)	109.6(5)
Na—W(5)	2.320(13)	W(3)—Na—W(5)	131.8(4)
Na—O(11)^{i}	2.345(4)	O(11)^{i}—Na—O(21)^{ii}	168.3(2)
Na—O(21)^{ii}	2.332(4)	O(11)^{i}—Na—W, O(21)^{ii}—Na—W(mean)	90(5)
		(d) Cl environment	
Cl—O(31)	1.332(9)	O(31)—Cl—O(32)	109.6(7)
Cl—O(32)	1.327(13)	O(31)—Cl—O(33)	111.0(6)
Cl—O(33)	1.409(7)	O(31)—Cl—O(34)	109.7(6)
Cl—O(34)	1.420(8)	O(32)—Cl—O(33)	110.1(6)
		O(32)—Cl—O(34)	107.2(6)
		O(33)—Cl—O(34)	109.1(5)
		(e) Intermolecular contacts	
W(1)—Ba^{iv}	2.901(4)	Ba—W(1)—Ba^{iv}	110.3(1)
W(1)—O(11)^{iii}	2.791(6)	Ba—W(1)—O(11)^{iii}	105.6(2)
W(1)—O(23)^{v}	2.846(7)	Ba—W(1)—O(23)^{v}	122.3(2)
		Ba^{iv}—W(1)—O(11)^{iii}	90.8(1)
		Ba^{iv}—W(1)—O(23)^{v}	112.8(2)
		O(11)^{iii}—W(1)—O(23)^{v}	110.1(2)
W(2)—O(24)^{vi}	2.882(12)	Na—W(2)—O(24)^{vi}	138.2(5)
W(3)—O(13)^{i}	2.797(8)	Na—W(3)—O(13)^{i}	108.3(2)
W(3)—O(24)^{ii}	2.763(8)	Na—W(3)—O(24)^{ii}	111.6(2)
		O(13)^{i}—W(3)—O(24)^{ii}	124.5(3)
W(4)—O(21)^{v}	2.842(8)	Ba—W(4)—O(21)^{v}	88.1(2)
W(5)—O(33)^{v}	2.786(14)	Na—W(5)—O(33)^{v}	173.3(4)[b]

[a] W denotes the oxygen atom of a water molecule. Symmetry code: i, $1-x$, $-y$, $1-z$; ii, $1-x$, $1-y$, $1-z$; iii, $2-x$, $-y$, $-z$; iv, $3-x$, $-y$, $-z$; v, $x+1$, y, z; vi, x, y, $z+1$.

[b] Not assumed to be hydrogen bonding.

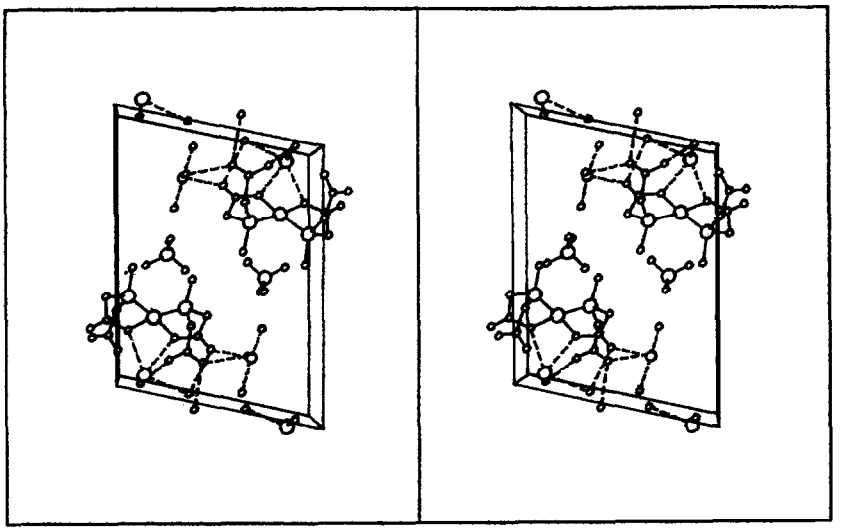

Fig. 2. Stereoview of the unit cell down the *a*-axis.

groups bonded to nickel, the carbonyl and hydroxyl C—O distances can be safely distinguished (1.218, 1.206, 1.306, 1.317 Å, respectively), suggesting a high degree of covalency of the Ni—O bond. In contrast, the carboxylate bonds to barium are ionic with a mean C—O distance of 1.238(7) Å.

The environments of all three cations are more or less unusual. The nickel(II) coordination polyhedron represents a rare example of the *cis*-square planar monophosphine complex for which, to our knowledge, only one other representative has been safely authenticated.[12] The NiP_2O_2 moiety is planar within ± 0.04 Å and the distortion of the angles from an ideal square is attributable to the bulkiness of phosphorus. The available data suggest that there is a general tendency for P,O-chelating phosphineacetates to assume the P,P-*cis* arrangement in complexes of Group VIII metals,[1(b),(c),(e)] forming chelate rings of very similar envelope conformations irrespective of the metal ion type.

The environment of barium(II) includes nine oxygen atoms from water molecules and intra- and intermolecular carboxylate groups. As expected, the intramolecular bonding distances to O(14) and O(23) are considerably shorter than the remaining Ba–O contacts; consequently, the geometrical arrangement is distorted and does not seem to be simply related to any of the ideal polyhedrons calculated for the hard-sphere model.[13] Roughly stated, the BaO_9 moiety can be approximated as a pentagonal bipyramid with doubled axial positions and barium in the centre: the O(14) and O(23) atoms together with three water molecules constitute an approximate equatorial plane (within ± 0.34 Å including barium) yielding, probably by chance, the exact theoretical O—Ba—O angle of 72(6)°. Four intermolecular carboxylate oxygens arranged as two couples, $O(13)^{iii}+O(14)^{iii}$ and $O(12)^{v}+O(22)^{v}$, complete the arrangement at the two doubled axial positions. The straight line connecting the centers of gravity of the two couples of oxygen atoms intersects the mean equatorial plane at an acceptable angle of 85.7° and at a distance of only 0.25 Å from barium. The two pairs of axial oxygens adopt a staggered conformation with a dihedral angle of 45.8° between the Ba–$O(13)^{iii}$–$O(14)^{iii}$ and Ba–$O(12)^{v}$–$O(22)^{v}$ planes.

The environment of sodium(I) is a distorted trigonal bipyramid with three water molecules forming an equatorial plane (within ± 0.03 Å including sodium) and with two intermolecular carboxylate oxygens at the axial positions.

The water molecules are coordinated at barium and sodium; W(1) acts as a bridge between two adjacent barium ions. The hydrogen atoms of the water molecules could not be located precisely but, according to the geometry of O...O contacts,[14] are likely to be involved in hydrogen bonding to carboxylate oxygens (Table 2). The various degrees of participation of the water molecules in coordination and hydrogen bonding conform to the temperature factors of the water oxygen atoms.

REFERENCES

1. Representative examples include: (a) J. Podlahová, J. Loub and J. Ječný, *Acta Cryst.* 1979, **B35**, 328; (b) S. Civiš, J. Podlahová, J. Loub and J. Ječný, *Acta Cryst.* 1980, **B36**, 1395; (c) A. Jegorov, B. Kratochvíl, V. Langer and J. Podlahová, *Inorg. Chem.* 1984, **23**, 4288; (d) J. Podlahová, B. Kratochvíl, J. Podlaha and J. Hašek, *J. Chem. Soc., Dalton Trans.* 1985,

2393; (e) J. Podlahová, B. Kratochvíl, V. Langer and J. Podlaha, *Polyhedron* 1986, **5**, 799.
2. J. Podlahová, *Coll. Czech. Chem. Commun.* 1978, **43**, 57; *ibid.* 1978, **43**, 64.
3. D. Nosková and J. Podlahová, *Polyhedron* 1983, **2**, 349.
4. J. Podlahová and F. Hartl, *Coll. Czech. Chem. Commun.* 1984, **49**, 568.
5. J. Podlahová, L. Kavan, J. Šilha and J. Podlaha, *Polyhedron* 1984, **3**, 963.
6. K. K. Chow, W. Levason and C. A. McAuliffe, In *Transition Metal Complexes of Phosphorus, Arsenic and Antimony Ligands* (Edited by C. A. McAuliffe), p. 134. Macmillan, London (1973).
7. C. Udovich, J. Takemoto and K. Nakamoto, *J. Coord. Chem.* 1971, **1**, 89.
8. R. A. Bailey, S. L. Kozak, T. W. Michelsen and W. N. Mills, *Coord. Chem. Rev.* 1971, **6**, 407.
9. K. Nakamoto, Y. Morimoto and A. E. Martell, *J. Am. Chem. Soc.* 1962, **84**, 2081; *ibid.* 1963, **85**, 309.
10. J. Podlahová and J. Podlaha, *Coll. Czech. Chem. Commun.* 1982, **47**, 1078.
11. J. J. MacDougall, J. H. Nelson, F. Mathey and J. J. Mayerle, *Inorg. Chem.* 1980, **19**, 709 (and references therein).
12. R. A. Palmer, H. F. Giles and D. R. Whitcomb, *J. Chem. Soc., Dalton Trans.* 1978, 1671.
13. M. G. B. Drew, *Coord. Chem. Rev.* 1977, **24**, 179.
14. M. Falk and O. Knop, In *Water—A Comprehensive Treatise* (Edited by F. Franks), Vol. 2, p. 70. Plenum Press, New York (1973); R. Taylor and O. Kennard, *J. Am. Chem. Soc.* 1982, **104**, 5063.

Polyhedron Vol. 6, No. 6, pp. 1415–1420, 1987
Printed in Great Britain

0277–5387/87 $3.00+.00

STABILITY CONSTANTS OF BORATE COMPLEXES OF OLIGOSACCHARIDES

J. F. VERCHERE* and M. HLAIBI

Laboratoire de Chimie Macromoléculaire, U.A. 500 du C.N.R.S., Faculté des Sciences de Rouen, B.P. 67, 76130 Mont-Saint-Aignan, France

(*Received* 28 *November* 1986; *accepted* 22 *December* 1986)

Abstract—The formation of borate complexes of several mono-, di- and trisaccharides in aqueous solution [$t = 25°C$, $I = 0.1$ M (KCl)] was studied by the potentiometric method. Values of the stability constants β_1 and β_2 of the 1 : 1 and 1 : 2 species were calculated for all compounds, using an extended version of the Antikainen equation. Raffinose, melezitose, saccharose and other fructose-containing oligosaccharides gave complexes of low stability, whereas lactulose and fructose gave very stable complexes. It is concluded that fructose moieties in oligosaccharides complex the borate anion by their 2- and 3-OH groups, in agreement with recent work by ^{11}B NMR.

The complexation of borate ion by polyhydroxy compounds has been widely studied, most of all for analytical purposes, and many polyols and sugars have been tested for the potentiometric determination of boric acid. Another interest of this reaction can be found in the field of bioinorganic chemistry, since many biological molecules contain hydroxyl groups in positions favourable for complexation. As a result, many sugars can be separated as borate complexes on anion-exchange resins,[1,2] and the use of a boric acid solution as an eluent permits the determination of several carbohydrates by HPLC with conductimetric detection.[3] We had begun the determination of the stability constants of the species involved in such experiments when a preliminary paper[4] by Lajunen *et al.* appeared on the same subject. These authors published stability constants for several borate–sugar complexes, most of which were assigned 1 : 1 stoichiometries. However, we have detected both 1 : 1 and 1 : 2 borate–sugar ratios for all the sugars we have studied. Examination of earlier literature revealed other discrepancies of the same type. For example, two papers[5,6] reported that all the sugars investigated formed 1 : 1 as well as 1 : 2 species, while the 1 : 1 complex was claimed[7] to be absent in the case of arabinose.

This prompted us to publish this account of our work in progress, using a modified treatment of the data obtained by the classical potentiometric method. Numerical calculations (assisted by a micro-computer) were performed instead of the traditional graphical methods, in order to avoid the problems encountered when the 1 : 1 and 1 : 2 complexes are of similar stabilities. It allowed the first determination of the stability constants of the complexes of two trisaccharides.

Principle

The principle of the potentiometric determination of the stability constants of borate–polyol complexes has been widely described.[4–10] It is well known that the acidity of boric acid, according to eqn (1), increases when complexation by a polyol occurs, as represented in eqn (2). One can therefore consider the new ionization equilibrium (3) of acidity constant $K'a$:

$$HB \rightleftharpoons B^- + H^+, \quad (1)$$

$$B^- + nL \rightleftharpoons BL_n^-, \quad (2)$$

$$HB + nL \rightleftharpoons BL_n^- + H^+, \quad (3)$$

where HB stands for boric acid, B^- for the borate ion, and BL_n^- for the 1 : n complex formed with the neutral ligand L. The acidity constants are K_a for boric acid alone and K'_a in the presence of ligand at concentration [L].

The values of pK'_a can easily be obtained by titrat-

* Author to whom correspondence should be addressed.

ing HB+L mixtures with a strong base. A more convenient method has been described[8] in which the ligand is added to a solution of borax. Attention must be paid to avoid: (i) the formation of polyborates, by using a low total boron concentration; and (ii) the protonation of the complexes, by working in neutral or slightly acidic media. Using these assumptions, Antikainen[9] derived the relationship known as the "Antikainen equation":

$$K'_a = k_n[L]^n + K_a, \quad (4)$$

in which k_n, the equilibrium constant for eqn (3), can be related to the stability constant β_n:

$$\beta_n = [BL_n^-]/[B^-][L]^n = k_n/K_a. \quad (5)$$

Subsequent studies have developed various formulations of this equation. When the complex is unique, a graphical treatment leads to a straight line, the slope and intercept of which determine the values of n and k_n. The intervention of a second species causes a curvature of the graphs, which are then treated anew so as to show two segments of slopes 1 and 2, respectively.

This method was found of little accuracy when applied to sugars which form two complexes of comparable stabilities. It made us look for a method which would not rest on the assumption of only one predominant species, but would take into account the simultaneous formation of several complexes. As a matter of fact, an extensive study[10] of the well-known borate–mannitol system[8] showed that, although small contributions of several other complexes could be demonstrated, a satisfactory description of the system in neutral media was possible by considering only the anionic 1:1 and 1:2 complexes. This conclusion was assumed to be true in every borate–sugar system, allowing us to write thus the analytical borate concentration:

$$c_B = [B^-] + [BL^-] + [BL_2^-]. \quad (6)$$

The concentrations of complexes BL^- and BL_2^- can be calculated as a function of $[B^-]$ using the stability constants β_1 and β_2:

$$c_B = [B^-](1 + \beta_1[L] + \beta_2[L]^2). \quad (7)$$

Using the notion of the conditional stability constant[11] which is basically identical to the apparent acidity constant K'_a used by Antikainen, we can write:

$$K'_a = c_B[H^+]/[HB]. \quad (8)$$

Finally, combining eqns (7) and (8) yields eqn (9):

$$K'_a = K_a(1 + \beta_1[L] + \beta_2[L]^2), \quad (9)$$

which is a more general form of the Antikainen equation.

EXPERIMENTAL

Chemicals

All the sugars, of the highest available commercial grade (Aldrich or Fluka), were used without further purification. The borax solutions were prepared from disodium tetraborate (Prolabo) and their concentrations were checked by titration with sodium hydroxide in the presence of sorbitol.[12] The borax concentration was kept very low to avoid any formation of polyborate ions (50 mg in 100 cm^3, corresponding to $c_B = 2.62 \times 10^{-3}$ M). The ionic strength was always 0.1 M (KCl).

In order to prevent any chemical or microbial degradation, the sugars were added in solid form in the borax solutions. It had the further advantage of minimizing the dilution effect of their introduction.

Apparatus

The measurements were made in a cell thermostated at 25°C by a water bath. The pH-metre was a Metrohm E 632, fitted with a Metrohm combined glass electrode, calibrated with commercial buffers (Prolabo Normadose). With some sugars, it was necessary to wait about 15 min before the stabilization of the pH values. However, we verified in several runs that the final values were reproducible.

Calculations

The experimental pH values of the borax–sugar mixtures (equivalent to pK'_a values) were compared to values calculated from eqn (9) on a micro-computer, using a laboratory-made BASIC routine. An iteration was then performed on the β_1 and β_2 parameters until the observation of the closest agreement between the two sets of values.

RESULTS

The complexes formed by the borate ion and 12 carbohydrates, including mono-, di- and trisaccharides, were studied by the potentiometric method. The values of the conditional acidity constants of boric acid, K'_a, were determined vs the concentration [L] of the ligand. Generally, we used the method[8] based on the measurement of the pH of borax–ligand mixtures, but when the complexation was fast, we checked that identical values of K'_a were obtained from the titration curves of boric acid by a base in the presence of ligand. For most sugars, however, the reaction was slow and the readings of pH were made after complete stabilization. It was

verified by duplicating the runs that the final pH values were highly reproducible, showing the observed pH drifts to be a slow conformational evolution to a definite equilibrium state.

The pK_a value for uncomplexed boric acid in our experimental conditions was checked in each experiment for [L] = 0. The mean value was $pK_a = 9.04 \pm 0.02$.

Typical sets of data and calculations are presented in Tables 1–4. The parameters β_1 and β_2 were adjusted in eqn (9) until complete agreement between calculated and experimental pK'_a values. For a given run, the accuracy on $\log \beta_n$ was ± 0.02. The comparison of several runs showed the values to have a mean standard deviation of ± 0.08. The values of the stability constants are collected in Table 5 and compared with literature values of different origins.

List of di- and trisaccharides[a]

Lactose	4-O-β-D-galactopyranosyl-D-glucose
Maltose	4-O-α-D-glucopyranosyl-D-glucose
Saccharose	α-D-glucopyranosyl-β-D-fructose
Lactulose	4-O-β-D-galactopyranosyl-D-fructose
Melibiose	6-O-α-D-galactopyranosyl-D-fructose
Turanose	3-O-α-D-glucopyranosyl-D-fructose
Raffinose	O-α-D-galactopyranosyl-(1 → 6)-α-D-glucopyranosyl-β-D-fructofuranoside
Melezitose	O-α-D-glucopyranosyl-(1 → 3)-β-D-fructofuranosyl-α-D-glucopyranoside

[a] The formulae are represented in Figs 1 and 2.

Table 1. Borate–raffinose complexes: data for calculation of stability constants [$t = 25°C$, $I = 0.1$ M (KCl)][a]

Mass of ligand [g (100 cm^3)$^{-1}$]	[L] (mol l^{-1})	pK'_a of boric acid	
		Calc.[b]	Exp
1	0.0168	8.90	8.89
2	0.0336	8.78	8.78
3	0.0505	8.69	8.69
4	0.0673	8.61	8.61
5	0.0841	8.53	8.54
6	0.1009	8.47	8.47
7	0.1177	8.41	8.41
8	0.1346	8.35	8.35
9	0.1514	8.30	8.30
10	0.1682	8.26	8.25
12	0.2018	8.17	8.17

[a] Concentration of borax = 1.31×10^{-3} mol l^{-1}. [L] = concentration of ligand, $M = 594.52$ g mol^{-1}.
[b] Calculated using eqn (9) with parameters: $\beta_1 = 22$, $\beta_2 = 47$.

Table 2. Borate–melezitose complexes: data for calculation of stability constants [$t = 25°C$, $I = 0.1$ M (KCl)][a]

Mass of ligand [g (100 cm^3)$^{-1}$]	[L] (mol l^{-1})	pK'_a of boric acid	
		Calc.[b]	Exp
1	0.0185	8.92	8.92
2	0.0370	8.84	8.84
3	0.0555	8.78	8.78
4	0.0740	8.72	8.72
5	0.0925	8.67	8.67
6	0.1110	8.62	8.62
7	0.1295	8.57	8.57
8	0.1480	8.53	8.53
9	0.1665	8.49	8.49
10	0.1850	8.45	8.45
12	0.2220	8.38	8.38

[a] Concentration of borax = 1.31×10^{-3} mol l^{-1}. [L] = concentration of ligand, $M = 540.47$ g mol^{-1}.
[b] Calculated using eqn (9) with parameters: $\beta_1 = 11$, $\beta_2 = 14$.

DISCUSSION

For all the oligosaccharides studied, we could determine the values of the stability constants β_1 *and* β_2, contrary to the results[4] of Lajunen *et al.*, who generally reported only β_1 values for disaccharides. Nevertheless, all of these β_1 values agreed

Table 3. Borate–lactulose complexes: data for calculation of stability constants [$t = 25°C$, $I = 0.1$ M (KCl)][a]

Mass of ligand [g (100 cm^3)$^{-1}$]	[L] (mol l^{-1})	pK'_a of boric acid	
		Calc.[b]	Exp
0.4	0.0117	7.57	7.57
0.6	0.0175	7.28	7.27
0.8	0.0234	7.06	7.04
1	0.0292	6.89	6.86
1.5	0.0438	6.56	6.52
2	0.0584	6.32	6.30
3	0.0876	5.99	5.97
4	0.1169	5.74	5.74
5	0.1461	5.55	5.55
6	0.1753	5.40	5.40
7	0.2045	5.27	5.26
8	0.2337	5.15	5.15

[a] Concentration of borax = 1.31×10^{-3} mol l^{-1}. [L] = concentration of ligand, $M = 342.30$ g mol^{-1}.
[b] Calculated using eqn (9) with parameters: $\beta_1 = 813$, $\beta_2 = 1.3804 \times 10^5$.

Table 4. Borate–erythritol complexes: data for calculation of stability constants [$t = 25°C$, $I = 0.1$ M (KCl)][a]

Mass of ligand [g (100 cm^3)$^{-1}$]	[L] (mol l^{-1})	pK'_a of boric acid	
		Calc.[b]	Exp
0.2	0.0164	8.73	8.74
0.3	0.0246	8.60	8.60
0.4	0.0328	8.49	8.49
0.5	0.0409	8.39	8.39
0.7	0.0573	8.22	8.22
1	0.0819	8.02	8.02
1.5	0.1228	7.77	7.77
2	0.1638	7.57	7.57
2.5	0.2047	7.41	7.41
3	0.2457	7.28	7.28
3.5	0.2866	7.17	7.17
4	0.3275	7.06	7.07

[a] Concentration of borax = 1.31×10^{-3} mol l^{-1}. [L] = concentration of ligand, $M = 122.12$ g mol^{-1}.

[b] Calculated using eqn (9) with parameters: $\beta_1 = 71$, $\beta_2 = 813$.

well. It is of interest to note that our values for lactose confirm those[6] of Evans *et al.*, who also found evidence for the formation of two complexes. Similarly, our results for arabinose concord with two earlier studies[5,6] on the existence of two complexes, although another paper[7] considered only the 1 : 2 species.

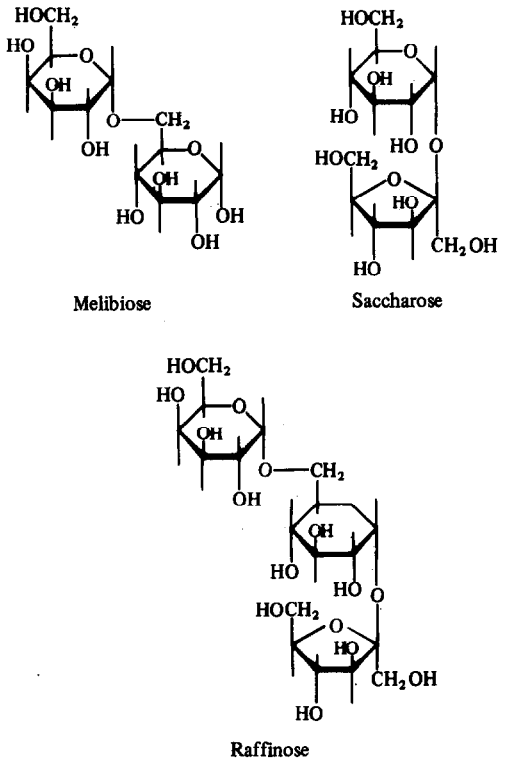

Fig. 1.

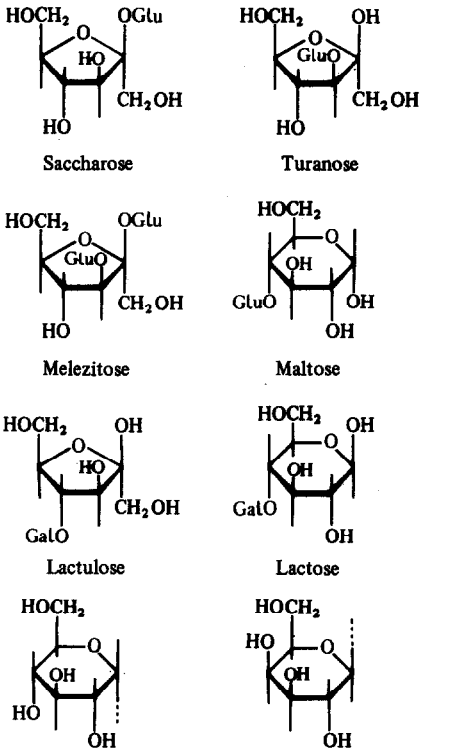

Fig. 2.

We first thought that the method employed by Lajunen *et al.*[4] did not allow the determination of low β_2 values, because this paper did not report values lower than $\log\beta_2 = 2.44$. It would have explained the absence of β_2 for lactose, maltose and saccharose. Besides, it could not account for the discrepancy on erythritol, for which we found $\log\beta_2 = 2.91$, with a β_1 value close to that given by Lajunen *et al.*

Therefore, we decided to check the validity of our method by studying three aldoses, glucose, galactose and mannose, for which the literature values were in good concordance. It can be seen in Table 5 that our results are close to previous ones, and we infer then that our procedure is as reliable as those used earlier. The results for arabinose lead to the same conclusion. Since the complexes of erythritol and arabinose appear to have stabilities comparable to those of the aldoses, there does not seem to exist any fundamental difference in the complexing behaviours of these monosaccharides, and hence any reason for their complexes displaying different stoichiometries. It makes the origin of the discrepancies even more puzzling.

This study allows interesting comparisons of the

Table 5. Stability constants of borate–sugar complexes: $t = 25°C$, $I = 0.1$ M (KCl)

	This work		Reference 4		Other references	
Compound	Log β_1	Log β_2	Log β_1	Log β_2	Log β_1	Log β_2
D-galactose	1.99	2.56	1.97	2.52	2.10	2.47 (5)
					2.09	2.62 (6)
D-glucose	1.80	3.05	2.07	2.80	1.90	2.89 (5)
					2.11	2.87 (6)
D-mannose	2.01	2.74	NS		1.70	2.69 (5)
					1.76	2.60 (6)
L-arabinose	2.14	2.99	NS		2.11	2.83 (5)
					ND	3.55 (7)
D-arabinose	NS		NS		2.19	3.02 (6)
Erythritol	1.85	2.91	1.99	ND		
D-fructose	2.82	4.97	NS		3.16	5.07 (6)
Lactose	1.43	2.17	1.51	ND	1.36	2.05 (6)
Maltose	1.41	1.89	1.36	ND		
Saccharose	0.86	0.70	0.75	ND		
Melibiose	NS		1.82	2.44		
Turanose	NS		1.91	2.47		
Lactulose	2.91	5.14	NS			
Raffinose	1.35	1.67	NS			
Melezitose	1.05	1.14	NS			

[a] ND = value not determined, NS = compound not studied.

stabilities of mono- and disaccharide complexes. The complexes of maltose (made of two glucose moieties) are weaker than those of glucose itself, and the complexes of lactose are weaker than those of its two constituents, glucose and galactose. This loss of complexing ability of glucose and galactose when they are engaged in disaccharides is probably due to the formation of the glycosidic link, which makes one anomeric hydroxyl group no longer available for complexation.

The case of fructose-containing oligosaccharides (Figs 1 and 2) appears much more complicated. Fructose is known[6,13] to give complexes of much higher stability than aldoses. However, saccharose forms complexes which present the lowest stabilities of all those investigated in this work. Moreover, the formation of the 1:2 complex from the 1:1 complex is thermodynamically unfavourable, since $\beta_2 < \beta_1$. In the same way, the complexes of turanose (3-O-α-D-glucopyranosyl-D-fructose) were reported[4] to be much weaker than those of fructose.

The results obtained for the trisaccharides can now be used to rationalize this difference. Raffinose (Fig. 1) can be considered as a combination, either of galactose and saccharose, or of melibiose and fructose. Lajunen *et al*'s results[4] and ours give the following order of stability of the complexes:

fructose ≫ melibiose > raffinose > saccharose.

Thus the addition of galactose to saccharose, to form raffinose, *increases* the complex stability. On the other hand, the addition of fructose to melibiose, to form raffinose, *decreases* the complex stability. It can be concluded that the complexation sites of raffinose and saccharose are not located on the fructose moiety. In the case of raffinose, these facts even suggest that the galactose moiety contains the complexation site.

Similarly, melezitose (Fig. 2) can be considered as a combination, either of saccharose and glucose, or of turanose and glucose. Since the order of stability of the complexes is:

fructose ≫ glucose > turanose

> melezitose > saccharose,

it is clear that the complexation sites of saccharose, turanose and melezitose are not situated on the fructose moiety, but on the glucose moieties. It can be noticed that the addition of glucose to saccharose, which forms melezitose, *increases* the stability of the borate complexes.

By contrast, other fructose-containing disaccharides form complexes as stable as those of fructose. This is the case[13] for isomaltulose (6-O-α-D-glucopyranosyl-D-fructose) and lactulose, as shown in Table 3. It clearly indicates that the borate ion is bound to the fructose moiety of the molecule since

the other moiety, which is an aldose, would form complexes of much lower stability. Further evidence is given by the comparison with lactose, which only differs from lactulose (Fig. 2) by a glucose moiety replacing the fructose moiety. Lactose gives only weak complexes, showing that the presence of a fructose moiety is indeed necessary for the formation of complexes of high stability.

We can conclude that the complexing properties of the fructose moiety in disaccharides dramatically depend on the location of the glycosidic link. This is obviously related to the fact that the complexation with a borate ion requires[14] two adjacent hydroxyl groups in adequate positions. The above discussion revealed that substitution of the 6-OH group (example of isomaltulose) and of the 4-OH group (example of lactulose) had almost no effect on the complexes stabilities. On the other hand, substitution of the 3-OH group (in the case of turanose), of the 2-OH group (in saccharose and raffinose), or of both groups (in melezitose), strongly decreased the affinity of fructose towards the borate ion. These conclusions are in perfect agreement with those of a recent ^{11}B and ^{13}C NMR study,[13] which deduced from the variations of the chemical shifts through complexation that borate was bound to the 2- and 3-OH groups of fructose, either free or combined to glucose in isomaltulose. The present study provides evidence that an extended version of the Antikainen equation allows an accurate calculation of the stability constants of borate–carbohydrate complexes, even with large ligands like di- or trisaccharides. Such determinations offer a basis for the establishment of structure–reactivity correlations, as examplified for a series of fructose-containing oligosaccharides. A demonstration of their usefulness can be found in a recent study[3] devoted to the conductimetric detection of carbohydrates, in which the observed order of sensitivity was exactly the same as the order of complex stability shown in Table 5.

Acknowledgement—We thank Mrs E. Leconte for her assistance in part of the experimental work.

REFERENCES

1. J. X. Khym and L. P. Zill, *J. Am. Chem. Soc.* 1952, **74**, 2090.
2. L. P. Zill, J. X. Khym and G. M. Cheniae, *J. Am. Chem. Soc.* 1953, **75**, 1339.
3. T. Okada and T. Kuwamoto, *Anal. Chem.* 1986, **58**, 1375.
4. K. Lajunen, P. Hakkinen and S. Purokoski, *Finn. Chem. Lett.* 1986, **13**, 21.
5. G. L. Roy, A. L. Laferriere and J. O. Edwards, *J. Inorg. Nucl. Chem.* 1957, **4**, 106.
6. W. J. Evans, E. J. McCourtney and W. B. Carney, *Anal. Biochem.* 1979, **95**, 383.
7. P. J. Antikainen and K. Tevanen, *Suom. Kemistil.* 1959, **B32**, 214.
8. J. Knoeck and J. K. Taylor, *Anal. Chem.* 1969, **41**, 1730.
9. P. J. Antikainen, *Ann. Acad. Sci. Fenn., Ser. A2* 1954, **56**, 3; *Acta Chem. Scand.* 1955, **9**, 1008; *ibid.* 1959, **13**, 312.
10. J. J. Kankare, *Anal. Chem.* 1973, **45**, 2050.
11. A. Ringbom, *Complexation in Analytical Chemistry* (French translation), p. 32. Dunod, Paris (1967).
12. R. Belcher, G. W. Tully and G. Svehla, *Anal. Chim. Acta* 1970, **50**, 261.
13. M. Makkee, A. P. G. Kieboom and H. van Bekkum, *Recl Trav. Chim. Pays-Bas* 1985, **104**, 230.
14. R. E. Moore, J. J. Barchi and G. Bartolini, *J. Org. Chem.* 1985, **50**, 374.

Polyhedron Vol. 6, No. 6, pp. 1421–1425, 1987
Printed in Great Britain

0277–5387/87 $3.00+.00

CYCLIC VOLTAMMETRIC STUDIES INTO THE REDUCTION OF A SERIES OF TRIS(1,3-DIKETONATO)IRON(III) COMPOUNDS IN DICHLOROMETHANE AND DIMETHYLSULPHOXIDE

HOLLY J. McCARTHY and DEREK A. TOCHER*

Department of Chemistry, University College London, 20 Gordon Street, London WC1H 0AJ, U.K.

(*Received* 5 *December* 1986; *accepted* 22 *December* 1986)

Abstract—A series of seven tris(1,3-diketonato)iron(III) chelates were prepared and studied using cyclic voltammetry in dichloromethane and dimethylsulphoxide. In the former solvent only a single reduction wave is observed and is assigned to the Fe(III)–Fe(II) couple. Despite the metal-based redox chemistry the formal potential is strongly influenced by the substituent groups on the chelating ligands and can be linearly correlated with the sum of the Taft inductive parameters for these substituents. In dimethylsulphoxide the reduced monoanion $[Fe(1,3\text{-diketonate})_3]^-$ undergoes a following chemical reaction which is interpreted as the extrusion of one 1,3-diketonate ligand. That reaction is an equilibrium and the position of the equilibrium is observed to depend upon the electronic effect of the substituent groups on the chelating ligands. For the strongly withdrawing trifluoroacetylacetonate ligand the dissociation of that ligand is essentially quantitative.

Transition-metal 1,3-diketonato complexes have been known for many years and have been subjected to study by numerous techniques.[1,2] Much research effort continues to be devoted to this topic. For example there are several recent literature reports into the catalytic properties of the compound $Ru(acac)_3$.[3–6]

Several years ago the polarographic reduction potentials of extended series of chromium(III) tris(1,3-diketonato) and ruthenium(III) tris(1,3-diketonato) compounds were reported in the literature.[7,8] A significant variation in these half-wave potentials was observed. That variation was rationalized on the basis of the relative electronic effects of the substituent groups on the 1,3-diketonato rings.

For many other transition metals only the parent compound, $M(acac)_2$ or $M(acac)_3$, has been examined electrochemically.[9] A case in point is that the redox chemistry of $Fe(acac)_3$† has been studied by several authors.[9–12] This compound undergoes a reversible reduction, assigned to a metal-based Fe(III)–Fe(II) couple, and an irreversible oxidation.[9] The reduction product, $[Fe(acac)_3]^-$, is observed to undergo a coordinative relaxation reaction with lithium ions in acetonitrile solution.[10]

In the present investigation seven tris(1,3-diketonato)iron(III) chelates were prepared and investigated using cyclic voltammetry in dichloromethane and dimethylsulphoxide.

EXPERIMENTAL

The Fe(III) chelates were prepared by established methods.[13]

Cyclic voltammetric studies were performed in dichloromethane and dimethylsulphoxide solutions, containing 0.2 and 0.1 mol dm^{-3}, respectively, of tetra-*n*-butylammonium tetrafluoroborate as supporting electrolyte, using the instrumentation and cell geometry previously described.[14]

* Author to whom correspondence should be addressed.

† The following ligand abbreviations are employed: acac, acetylacetonate; tfp, trifluoroacetylacetonate; dbm, dibenzoylmethanide; bzac, benzoylacetonate; paa, 3-phenylacetylacetonate; tmh, tetramethyl-3,5-heptanedionate; maa, 3-methylacetylacetonate.

RESULTS AND DISCUSSION

Iron complexes are particularly suitable for electrochemical studies because of the existence of two well-defined oxidation states (II and III) of the metal ion. It was therefore not unexpected that the Fe(III)tris(1,3-diketonates) exhibited uncomplicated voltammetric behaviour in dichloromethane solution with current–voltage curves indicative of near reversible one-electron transfer reactions:

$$[Fe(R_1COCR_2COR_3)_3]+e^- \rightleftharpoons [Fe(R_1COCR_2COR_3)_3]^-, \quad (1)$$

and half-wave potentials strongly influenced by the nature of the chelate ring substituents. The reversibility of the electrode reactions was investigated in several ways. Plots of $i_p/v^{1/2}$ and $i_{p,c}/i_{p,a}$ vs v are linear in the range 20–500 mV s^{-1}, consistent with reversible electron transfer. The potentials $E_{p,c}$ and $E_{p,a}$ were observed to be independent of scan rate below 200 mV s^{-1}, and the peak-to-peak separations (ΔE_p) to be 60 ± 5 mV at 100 mV s^{-1}. Table 1 contains the voltammetric data on the electroreductions of this series of tris-chelate complexes.

Inspection of the data in Table 1 for the electrode reactions in dichloromethane solution immediately reveals the qualitative behaviour of the half-wave potentials with the nature of the substituent. Potentials become more positive [i.e. increasing ease of reduction of the Fe(III) species] as the number and type of electron-releasing substituents are decreased. Because these complexes can be assumed to possess similar trigonal geometries and a common redox active centre, the mechanism of electron transfer at the electrode surface should be the same, and linear free-energy relationships may be sought. Earlier two groups[7,8] explored such relationships in series of ruthenium and chromium tris(1,3-diketonato) complexes, and arguments were advanced for the use of both σ_m and σ_p Hammett parameters in such correlations. We have chosen to avoid the controversy as to which of Hammett's parameters is more appropriate in these systems by correlating our electrode potentials with the one-ligand sum of the Taft inductive parameters, which are independent of the stereochemical relationship between metal centre and position of the substituent group on the metallocyclic ring.

A plot of the potential for the one-electron reduction of the Fe(1,3-diketonato)$_3$ complexes against the one-ligand sum of Taft's inductive parameters is presented in Fig. 1. Free-energy relationships of this type have previously been described for other metal tris- and bis-chelate complexes,[15] though a firm theoretical justification has frequently been lacking. Thus for the present series of complexes such a relationship is best regarded as an empirical observation on the substituent effects on the Fe(1,3-diketonato)$_3$ $\rightleftharpoons$ [Fe(1,3-diketonato)$_3$]$^-$ redox couples.

It was pointed out several years ago that in order to correlate $E_{1/2}$ of Cu(1,3-diketonates)$_2$ to the electronic effect of the substituent groups on the ligands the chelates must be similarly substituted, i.e. all aliphatic, all aromatic, or all mixed aliphatic–aro-

Table 1. Cyclic voltammetric results in dichloromethane and dimethylsulphoxide solutions

Compound	Solvent: Dichloromethane		Solvent: Dimethylsulphoxide			
	$E_{1/2}$[a]	ΔE_p[b] (mV)	$E_{p,c}$	$E^1_{p,a}$	$E^2_{p,a}$	$I^1_{p,a}/I_{p,c}$[b]
(1) Fe(tfp)$_3$	+0.02	60±5	+0.12	—	+0.35	0.00
(2) Fe(dbm)$_3$	−0.50	65±5	−0.36	−0.30	+0.01	0.32
(3) Fe(bzac)$_3$	−0.53	65±5	−0.41	−0.35	−0.03	0.59
(4) Fe(paa)$_3$	−0.65	55±5	−0.56	−0.32	−0.08	0.37
(5) Fe(acac)$_3$	−0.62	65±5	−0.48	−0.38	−0.19	0.66
(6) Fe(maa)$_3$	−0.78	60±5	−0.73	−0.53	−0.21	0.78
(7) Fe(tmh)$_3$	−0.97	60±5	—[c]	—	—	—

[a] Potentials measured in V vs Ag–AgCl and referenced to the $FeCp_2$–$FeCp_2^+$ couple at +0.60 V.

[b] Measured at a scan rate of 100 mV s^{-1}.

[c] Response complicated by additional waves at more negative potentials.

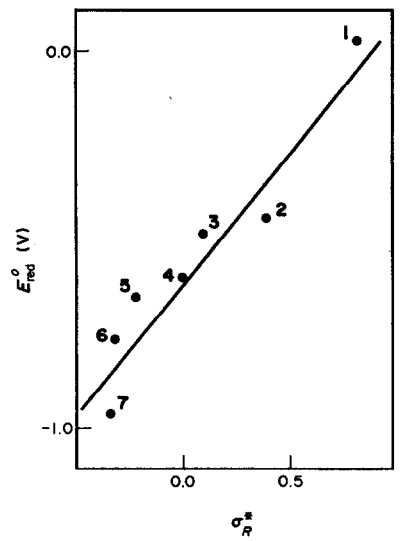

Fig. 1. Plot of half-wave potentials vs one-ligand sum of Taft inductive parameters for tris(1,3-diketonato) iron(III,II) complexes in dichloromethane. Complexes are numbered as in Table 1.

matic substituents.[16] Correlations between different classes of these Cu(II) chelates are not straightforward. The same is not true, however, for the Cr(III)[7] or Ru(III)[8,17] 1,3-diketonate complexes, or for the Fe(III) 1,3-diketonate complexes discussed in this paper. For each of these three series of compounds strong correlations exist between the reduction potentials and the electronic effect of the substituent group(s), regardless of its identity. The other obvious difference between the copper complexes and those of the other three metals is the geometry of the diketonate ligands about the metal ion. It is likely that the electrode surface can interact more directly with the chelated Cu(II) than with the chelated M(III) ions on simple stereochemical grounds. Although the details of such interactions are unknown the consequences are clearly important in determining the nature of the ligands' influence on reduction potentials.

The potentials which we have obtained for the electroreduction of the Fe(III) tris(1,3-diketonate) compounds can be compared with those obtained earlier for the related ruthenium compounds. The potential range encompassed by the series of compounds described in this paper is some 0.99 V, with $Fe(tfp)_3$ being the easiest to reduce ($E_{1/2} = +0.02$ V), while $Fe(tmh)_3$ is the most difficult to reduce ($E_{1/2} = -0.97$ V). The potential interval for the related ruthenium complexes is 1.03 V (−0.36 to −1.39 V).[17] A detailed comparison of the reduction potentials for pairs of compounds with the same ligating groups clearly shows that in every instance the iron compound is substantially easier to reduce (by *ca* 0.1 V, after having made an appropriate correction for the different reference electrodes employed in the various studies). These observations are in keeping with the higher oxidation state becoming more favourable down the triad. Clearly the MO to which the electron is being added must contain substantial ligand character. Inasmuch as the t_{2g} metal orbitals can mix with the π ligand MOs a variation in substituent group will of necessity alter the energies of these orbitals[18] and hence a degree of substituent dependence of $E_{1/2}$ is expected. The ligand contribution to the redox-active MOs is difficult to quantify solely on the basis of electrochemical measurements. Nevertheless a recent report on the electrochemical properties of a series of Ni, Pd and Pt bis(dithio-1,3-diketonate) compounds[15] reached the conclusion that for these compounds the redox-active MOs are ligand-based, a deduction subsequently confirmed for $[Ni(MeCS \cdot CHCS \cdot Me)_2]^-$ by ESR spectroscopy.[19] Although the ligand participation in the redox-active MOs in this series of compounds is substantial we do not feel, at this time, that there is sufficient evidence to describe the electron-transfer reaction in dichloromethane as anything other than an Fe(III)–Fe(II) couple.

We turn now to the electrochemical behaviour in dimethylsulphoxide solution. Figure 2 illustrates the voltammagrams obtained for the compounds $Fe(acac)_3$ and $Fe(tfp)_3$ in dimethylsulphoxide solution, while Table 1 contains the pertinent data on the potentials for the electron-transfer reactions. The voltammagram for $Fe(acac)_3$ is characterized

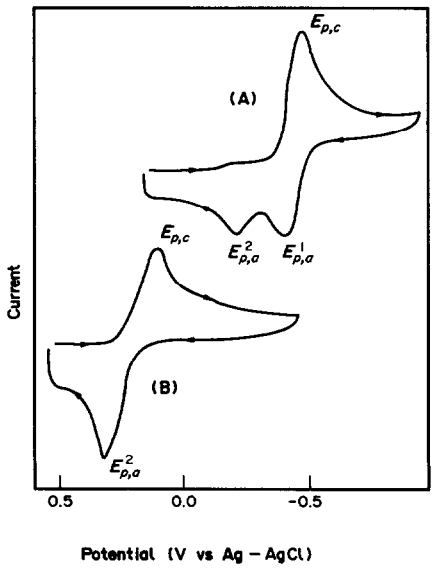

Fig. 2. Cyclic voltammograms of: (A) $Fe(acac)_3$, and (B) $Fe(tfp)_3$, in dimethylsulphoxide solution. Scan rate 100 mV s^{-1}.

by a clean forward wave at −0.48 V. On reverse scan two responses are observed. The one at more negative potential, −0.38 V, can be attributed to the reoxidation of the $[Fe(acac)_3]^-$ formed initially. The second wave occurs at a significantly less cathodic potential, −0.19 V, and can most likely be assigned to the oxidation of $Fe(acac)_2(DMSO)_2$, as discussed below. At a scan rate of 100 mV s^{-1} the current ratio $I^l_{p,a}/I_{p,c}$ is *ca* 0.66. Surprisingly this current ratio *decreases* with increasing scan rate, and is observed to be a maximum (*ca* 0.90) at the slowest scan rate, 20 mV s^{-1}, which we have employed. At the same time it is observed that the peak attributed to $Fe(acac)_2(DMSO)_2$ is a maximum at fast scan rates. The voltammetric peak at less cathodic potentials, −0.19 V, is completely suppressed by addition of an excess of acac anions, in the form of Na(acac), to the electrochemical cell. This is indicative of the dissociative nature of the chemical reaction coupled to the electron transfer. Thus we believe that reaction to be of the form:

$$[Fe(acac)_3]^- \underset{}{\overset{DMSO}{\rightleftharpoons}} Fe(acac)_2(DMSO)_2 + [acac]^- . \quad (2)$$

There are a number of precedents for the dissociation of the acac ion from a reduced metal acetonate complex, usually, though not always, in the presence of an alkali metal ion.[10,11,17,20–22] The less cathodic oxidative response can be attributed to the removal of an electron from $Fe(acac)_2(DMSO)_2$. As the cation $[Fe(acac)_2(DMSO)_2]^+$ was not detected in subsequent scans that cation must rapidly recombine with the free $[acac]^-$ ion, reforming $Fe(acac)_3$. The unusual current response on varying the scan rate can best be explained by invoking a fast forward reaction and slow back reaction in eqn (2). The mechanism for the electroreduction/electrooxidation and coupled chemical reactions is fully illustrated in Scheme 1. The voltammetric behaviour of $Fe(dbm)_3$, $Fe(bzac)_3$, $Fe(paa)_3$ and $Fe(maa)_3$ is similar to that described for

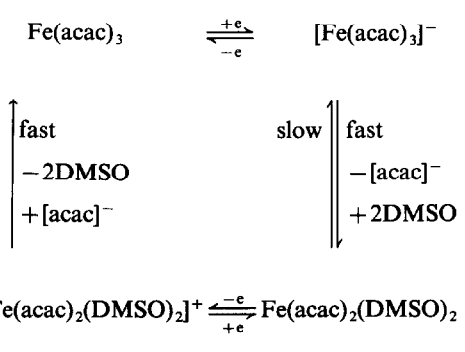

Scheme 1. A mechanism for the behaviour of $Fe(acac)_3$ in dimethylsulphoxide solution.

$Fe(acac)_3$ although the details of the analysis differ. In particular it would appear that the position of the chemical equilibrium is significantly influenced by the electronic effects of the various substituents on the chelating ligands. The data which we have available suggest that the more electron-withdrawing are the chelating ligands' substituents the further to the right lie the equilibria of the type illustrated in eqn (2) (see Table 1). In the limiting case of $Fe(tfp)_3$ only a single reoxidation wave is observed. When Na[tfp] is added to the electrochemical cell the position of that wave shifts to a value *ca* 100 mV more cathodic and now occurs close to the potential at which we would expect to observe the oxidation of $[Fe(tfp)_3]^-$. Thus the voltammetric peak initially observed at +0.35 V must be due to the oxidation of $Fe(tfp)_2(DMSO)_2$, i.e. the redox behaviour of $Fe(tfp)_3$ in dimethylsulphoxide can also be rationalized on the basis of the scheme described earlier.

CONCLUSIONS

We have shown that the $[Fe(1,3\text{-diketonate})_3]^{0/-}$ couple is strongly influenced by substituent groups on the ligand, yielding an approximately linear plot of $E_{1/2}$ vs Taft inductive parameter (σ^*_R). The substituent dependence is very similar to that for the $[Ru(1,3\text{-diketonate})_3]^{0/-}$ couple, and is interpreted as the redox-active orbital having appreciable ligand character. The assignment from electrochemical studies alone of a redox process as being substantially metal- or ligand-based in character must be treated with caution. However, the systematic shifting in potentials on changing the metal centre from ruthenium to iron argues strongly for metal-based processes.

Measurements in dimethylsulphoxide solutions indicate that the reduced monoanions are activated towards substitution in the strongly coordinating solvent. The ability of the metal ion to participate in such coupled chemical reactions is a function of the substituent groups on the ligand and can be suppressed by addition of the free 1,3-diketonate anion. Parallels have been drawn between these reactions and the coordinative relaxation reactions of reduced metal 1,3-diketonates.

REFERENCES

1. J. P. Fackler, Jr, *Prog. Inorg. Chem.* 1966, **7**, 361.
2. R. C. Mehrotra, R. Bohra and D. P. Gaur, *Metal-β-diketonates and Allied Derivatives*. Academic Press, New York (1978).
3. J. F. Knifton, *J. Chem. Soc., Chem. Commun.* 1983, 729.

4. H. Kheradmond, A. Kiennemann and A. Jenner, *J. Organomet. Chem.* 1983, **251**, 339.
5. A. Doyle, *J. Mol. Catal.* 1983, **18**, 251.
6. B. Marciniec, J. Gulinski and W. Urbanisk, *Pol. J. Chem.* 1982, **56**, 287.
7. R. F. Handy and R. L. Lintvedt, *Inorg. Chem.* 1974, **13**, 893.
8. G. S. Patterson and R. H. Holm, *Inorg. Chem.* 1972, **11**, 2285.
9. J. H. Tocher and J. P. Fackler, Jr, *Inorg. Chim. Acta* 1985, **102**, 211 (and references therein).
10. R. W. Murray and L. K. Hiller, Jr, *Anal. Chem.* 1967, **39**, 1221.
11. W. R. Heineman, J. N. Burnett and R. W. Murray, *Anal. Chem.* 1968, **40**, 1970.
12. B. D. Beaver, L. C. Hall, C. M. Lukeheart and L. D. Preston, *Inorg. Chim. Acta* 1981, **47**, 25.
13. D. T. Farrar and M. M. Jones, *J. Phys. Chem.* 1964, **68**, 1717.
14. D. A. Tocher and J. H. Tocher, *Polyhedron* 1986, **5**, 1615.
15. G. A. Heath and J. H. Leslie, *J. Chem. Soc., Dalton Trans.* 1983, 1587 (and references therein).
16. R. L. Lindvedt, H. D. Russell and H. F. Holtzclaw, Jr, *Inorg. Chem.* 1966, **5**, 1603.
17. A. Endo, *Bull. Chem. Soc. Jpn* 1983, **56**, 2733.
18. K. DeArmond and L. S. Forster, *Spectrochim. Acta* 1963, **19**, 1393.
19. G. A. Bowmaker, P. D. W. Boyd, M. Zvagulis, K. J. Cavell and A. F. Masters, *Inorg. Chem.* 1985, **24**, 401.
20. S. Misumi, M. Aihara and Y. Nonaka, *Bull. Chem. Soc. Jpn* 1970, **43**, 774.
21. M. K. Kalinowski and A. Cmiel, *Inorg. Chim. Acta* 1981, **49**, 179.
22. J. N. Burnett, L. K. Hiller, Jr and R. W. Murray, *J. Electrochem. Soc.* 1970, **117**, 1028.

Polyhedron Vol. 6, No. 6, pp. 1427–1431, 1987
Printed in Great Britain

0277–5387/87 $3.00+.00

RHODIUM(I) COMPLEXES WITH THE 2,2′-BIPYRIMIDINE LIGAND

MARIA P. GARCIA, JOSE L. MILLAN, MIGUEL A. ESTERUELAS and LUIS A. ORO*

Departamento de Química Inorgánica, Instituto de Ciencia de Materiales de Aragón, Universidad de Zaragoza—Consejo Superior de Investigaciones Científicas, 50009 Zaragoza, Spain

(*Received* 5 *December* 1986; *accepted* 22 *January* 1987)

Abstract—Mono- and dinuclear rhodium(I) complexes of formulae $[Rh(L_2)(bipym)]^+$ and $[\{Rh(L_2)\}_2(\mu\text{-bipym})]^{2+}$ [L_2 = diolefin or $(CO)_2$] have been prepared and their catalytic activity in hydrogen-transfer reactions explored. The heterodinuclear $[Cl_2Pd(\mu\text{-bipym})Rh(tfb)]ClO_4$ complex was obtained by reacting $[Rh(tfb)(bipym)]^+$ with $[PdCl_2(cod)]$ or alternatively from $[Rh(tfb)(acetone)_x]^+$ with $[PdCl_2(bipym)]$. Ion-pair complexes of formulae $[Rh(diolefin)(bipym)]^+[RhCl_2(diolefin)]^-$ (diolefin = cod, nbd or tfb) were prepared by adding bipym to acetone suspensions of $[RhCl(diolefin)]_2$.

The preparation and properties of cationic rhodium(I) complexes with chelating nitrogen donor ligands are of growing interest;[1–3] in particular, some of them, containing diolefins as ancillary ligands, are active catalyst precursors for hydrogen-transfer reactions.[4–7] There is also an increasing interest in the synthesis of mixed-valence or homo- and heterobinuclear complexes with bidentate bridging ligands,[8] due to the possibility of exploring their electronic interactions in a fundamental way and also utilizing such complexes for multielectron transfer catalysis; very recently a cationic ruthenium(II)–palladium(II) binuclear complex, and binuclear platinum(II) complexes bridged by 2,2′-bipyrimidine (bipym) have been reported.[9]

In this paper we describe some neutral and cationic rhodium(I) complexes, as well as a rhodium(I)–palladium(II) complex, with the bipym ligand which can potentially act as a chelate or "bidentate" bridging ligand between two metal centers.

RESULTS AND DISCUSSION

A general route for the synthesis of cationic species of the type $[Rh(L_2)(bipym)]^+$ [L_2 = tetrafluorobenzobicyclo(2,2,2)octatriene (tfb), bicyclo(2,2,1)heptadiene (nbd), 1,5-cyclooctadiene (cod) or $(CO)_2$] (compounds **1–4**) involves the reaction of the solvated $[Rh(L_2)(Me_2CO)_x]ClO_4$ intermediate with bipym, in the stoichiometric ratio 1:1. Compound **4** was also obtained by bubbling carbon monoxide through a dichloromethane solution of any of the $[Rh(diolefin)(bipym)]ClO_4$ complexes, or by reaction of $[Rh(acac)(CO)_2]$ (acac = acetylacetonate) with bipym in the presence of perchloric acid. After working up the compounds were isolated as air-stable microcrystalline solids in good yield; they are 1:1 electrolytes in acetone or nitromethane, and their IR spectra show bands due to the uncoordinated perchlorate anion at *ca* 1100s and 620s cm^{-1}. Complex **4** shows, in dichloromethane solution, two strong $\nu(CO)$ bands at 2105 and 2050 cm^{-1} typical of *cis*-dicarbonyl derivatives,[10] suggesting an electron density on the rhodium atom similar to that found for related 2,2′-bipyridine or 1,10-phenanthroline cationic complexes.[10,11] The coordinated bipym ligand in these complexes has two prominent bands near 1570 and 1550 cm^{-1} assigned to ring-stretching modes, a strong band at *ca* 745–750 cm^{-1}, due to the C—H bending mode, and one near 660 ascribed to the ring-bending mode of the phenyl groups. The low solubility of these compounds, in most solvents, prevented the obtaining of NMR spectra.

Most probably, the mononuclear $[Rh(L_2)(bipym)]^+$ complexes are square-planar with the bipym ligand acting in a bidentate way. Thus, these

* Author to whom correspondence should be addressed.

rhodium complexes have the capability of acting as N-donor ligands for metals, and could be considered as "metalloligands". So, homobinuclear rhodium complexes of formula $[\{Rh(diolefin)\}_2(\mu\text{-bipym})](ClO_4)_2$ (**5–7**) can be prepared by reacting $[Rh(diolefin)(Me_2CO)_x]^+$ species with the mononuclear $[Rh(diolefin)(bipym)]ClO_4$ complexes, or more directly by treating the solvated species with bipym in the ratio 2:1; they are obtained as air-stable black or brown microcrystalline solids, which are insoluble in diethylether or hexane, and only slightly soluble in acetone or dichloromethane. These products are 1:2 electrolytes in acetone and their IR spectra show bands of the uncoordinated perchlorate anion at *ca* 1100s and 620s cm^{-1} which are split, in the solid state, for complex **5**, may be indicating a coordination of the perchlorate anion in the solid state; a possible formulation could be $[Rh(OClO_3)(tfb)(bipym)Rh(tfb)]ClO_4$.* The coordinated bipym in these homobinuclear compounds presents, in the IR spectrum, differences from their monometallic precursors;[12] so, the 1550-cm^{-1} band, assigned to ring-stretching modes in the monometallic complexes is absent in the bimetallic derivatives; there is also an invariable decrease in energy, by *ca* 15–20 cm^{-1}, of the C—H bending mode, and finally the addition of the second metal leads to loss of the band near 600 cm^{-1}.

The mononuclear $[Rh(L_2)(bipym)]^+$ compounds can also act as N-donor ligands for other metals, so, reaction of the "metalloligand" complex **1** with $[PdCl_2(cod)]$, in acetone, gave the heterobinuclear $[Cl_2Pd(\mu\text{-bipym})Rh(tfb)]ClO_4$ (**8**). An alternative synthesis of this heterobinuclear complex was by the reaction of $[PdCl_2(bipym)]$ (**9**) {obtained from $[PdCl_2(cod)]$ or $[PdCl_2(tht)_2]$ (tht = tetrahydrothiophene)} with the solvated species $[Rh(tfb)(Me_2CO)_x]^+$; compound **8** was prepared as a brown, air-stable solid and it is a 1:1 electrolyte in acetone solution. Its IR spectrum shows bands due to the uncoordinated perchlorate anion at 1100s and 625s cm^{-1}; the coordinated bipym bands are similar to that found for the homobinuclear complexes, that is 1580s cm^{-1} (ring-stretching) and 735s cm^{-1} (C—H bending); there are also two ν(Pd—Cl) at 335 and 360 cm^{-1}, corresponding to two chlorine atoms *cis* to the palladium atom.

Attempts at preparing neutral dinuclear rhodium complexes containing the "RhCl(diolefin)" moiety and bipym as a bridging ligand, prompted us to explore the reaction of $[RhCl(diolefin)]_2$ with bipym (Rh : bipym ratio 2 : 1). With the diolefin cod, a red, very insoluble solid was obtained, in acetone (**10a**); analytical results revealed the presence of only one molecule of bipym for two rhodium atoms, and its IR spectrum in the solid state showed an absorption characteristic of a M—Cl terminal band *trans* to a C=C double bond in the species "MCl(cod)L".[19] These data suggested the formulation of the complex as a binuclear square-planar compound of formula $[\{RhCl(COD)\}_2(\mu\text{-bipym})]$. Stirring this red compound in chloroform caused the colour to change to green (**10b**), the 260-cm^{-1} band disappeared, and the product was slightly more soluble than the red solid. An ^1H NMR spectrum of compound **10b** shows two different types of cod: vinyl resonances at 4.27 (br, 8H), aliphatic resonances at 2.50 (br, 2H), 2.40 (br, 2H) and 1.76 (br, 2H), and 1.27 (br, 2H) ppm. This spectrum is characteristic of species of type $[Rh(cod)(bipym)][RhCl_2(cod)]$.[20]

When the diolefin was nbd or tfb, compounds **11** and **12** were obtained; they are dark-green solids, with IR spectra similar to that found for compound **10b**, so we formulated them as ion-pair species.

The reaction of $[RhCl(diolefin)]_2$ with bipym (Rh : bipym ratio 1 : 1) in acetone gave, for the diolefins cod and nbd, compounds **10a** and **11**, while, for tfb, a mononuclear rhodium compound was prepared (**13**). This compound did not show the ν(Rh—Cl) absorption band present in square-planar rhodium(I) chlorine complexes, indicating that the compound is probably five-coordinated, but in acetone solution it shows some conductivity (20 Ω^{-1} cm^2 mol^{-1}) which suggests an equilibrium between neutral five-coordinated and ionic square-planar species, with ionic chlorine.[21]

Finally, we have used the related 2,4,6-tris(2-pyridyl)-s-triazine (tpt) which has six nitrogen atoms and could potentially coordinate to three metallic centers. Thus, reacting this ligand with the solvated species $[Rh(nbd)(Me_2CO)_x]^+$ in the ratio 1:3 gave the cationic trinuclear complex $[\{Rh(nbd)\}_3(tpt)](ClO_4)_3$ (**14**).

Catalytic activity

The above-mentioned similarity of bipym to 2,2′-bipyridine or 1,10-phenanthroline prompted us to explore the ability of the diolefin complexes as catalyst precursors for hydrogen transfer from isopropanol to acetophenone in the presence of potassium hydroxide. Thus, after 1 h of reaction the extent of conversion (%), using 2,5-norbor-

* In this context, it is interesting to mention that, while the pentacoordinated tetrafluorobenzobarrelene complex of formula $[Ir(OClO_3)(tfb)(diolefin)]$ (diolefin = tfb[13] or cod[14]) and $[Rh(OClO_3)(tfb)_2]$[15] have been reported, only square-planar $[M(diolefine)_2]ClO_4$(M = Ir or Rh) compounds were obtained for diolefin = cod,[16] Me_3tfb[17] or nbd.[18]

nadiene rhodium precursors, decreased in the sequence $[\{Rh(nbd)\}_2(bipym)](ClO_4)_2$ (**52**) > $[Rh(nbd)(bipym)][RhCl_2(nbd)]$ (**8**) > $[Rh(nbd)(bipym)]ClO_4$ (**4**), whilst under similar conditions the well-known complex $[Rh(nbd)(phen)]ClO_4$[4] converted 60%. Interestingly 81% conversion was observed using $[\{Rh(nbd)\}_3(tpt)](ClO_4)_3$ as the catalyst precursor.

EXPERIMENTAL

C, H and N analyses were carried out with a Perkin–Elmer 240-B microanalyzer. Conductivities were measured at 20°C in *ca* 5×10^{-4} M acetone or nitromethane solutions using a 9501/01 conductometer. IR spectra were recorded on a Perkin–Elmer 599 spectrophotometer over the range 4000–200 cm^{-1}, using Nujol mulls between polyethylene sheets or in dichloromethane solution between NaCl plates. The GLC analyses were performed on a Perkin–Elmer 3920B chromatograph connected to a Perkin–Elmer M-2 integrator. The starting materials, $[RhCl(cod)]_2$,[22] $[RhCl(nbd)]_2$,[23] $[RhCl(tfb)]_2$,[24] $[Rh(acac)(CO)_2]$[25] and $[PdCl_2(cod)]$[26] were prepared by published methods.

$[Rh(diolefin)(bipym)]ClO_4$ (**1–3**)

An acetone solution (15 cm^3) of $[Rh(diolefin)(OCMe_2)_x]^+$ (diolefin = tfb, cod or nbd) {prepared by treating the appropriate $[RhClL_2]_2$ (0.1 mmol) with $AgClO_4$ (42 mg, 0.2 mmol) in acetone for 30 min and filtering off the AgCl formed} was added to a solution of bipym (32 mg, 0.2 mmol) in acetone. Evaporation of the solution to *ca* 1 cm^3 and addition of diethyl ether (15 cm^3) gave compounds **1–3** as microcrystalline solids which

Table 1. Color, analytical results, conductance and yields for the new complexes

Compound		Color	Analyses [found (calc.) (%)] C	H	N	Λ_M[a]	Yield (%)
$[Rh(tfb)(bipym)]ClO_4$	(**1**)	Orange	41.2 (40.9)	2.3 (2.0)	9.1 (9.5)	110	85
$[Rh(nbd)(bipym)]ClO_4$	(**2**)	Brown	37.1 (37.9)	3.5 (3.0)	12.4 (12.6)	131	80
$[Rh(cod)(bipym)]ClO_4$	(**3**)	Brown	40.2 (41.0)	3.5 (3.8)	11.4 (11.5)	121	85
$[Rh(CO)_2(bipym)]ClO_4$	(**4**)	Yellow	27.9 (28.8)	1.5 (1.4)	13.2 (13.4)	79[b]	86
$[\{Rh(tfb)\}_2(bipym)](ClO_4)_2$	(**5**)	Black	38.0 (37.8)	1.9 (1.7)	5.9 (5.5)	317	72
$[\{Rh(nbd)\}_2(bipym)](ClO_4)_2$	(**6**)	Brown	35.2 (35.3)	3.2 (3.2)	7.4 (7.5)	223	88
$[\{Rh(cod)\}_2(bipym)](ClO_4)_2$	(**7**)	Brown	36.7 (36.9)	3.8 (3.8)	7.4 (7.2)	239	74
$[Cl_2Pd(bipym)Rh(tfb)]ClO_4$	(**8**)	Brown	31.0 (31.4)	1.4 (1.4)	7.6 (7.3)	151	70
$[PdCl_2(bipym)]$	(**9**)	Yellow	28.6 (28.6)	1.8 (1.8)	17.3 (16.7)	—	93
$[Rh(cod)(bipym)][RhCl_2(cod)]$	(**10**)	Dark-green	44.8 (44.3)	4.4 (4.6)	9.0 (8.6)	—	84
$[Rh(nbd)(bipym)][RhCl_2(nbd)]$	(**11**)	Dark-green	41.5 (42.4)	3.5 (3.7)	9.0 (9.0)	—	92
$[Rh(tfb)(bipym)][RhCl_2(tfb)]$	(**12**)	Dark-green	42.1 (43.3)	2.0 (2.1)	6.2 (6.3)	—	93
$[RhCl(tfb)(bipym)]$	(**13**)	Red	44.3 (45.2)	2.5 (2.7)	9.5 (9.4)	20	67
$[\{Rh(nbd)\}_3(tpt)](ClO_4)_3$	(**14**)	Brown	38.5 (39.0)	3.5 (3.0)	7.4 (7.0)	—	72

[a] Acetone solvent (in Ω^{-1} cm^2 mol^{-1}).
[b] Nitromethane solvent. ν(CO) for complex **4**: 2105 and 2050 cm^{-1} (in dichloromethane).

were filtered, washed with diethyl ether and dried *in vacuo*.

$[Rh(CO)_2(bipym)]ClO_4$ (**4**)

This complex was prepared by two different routes:

(i) To a solution of $[Rh(acac)(CO)_2]$ (80 mg, 0.31 mmol) in acetone (20 cm^3) were added successively $HClO_4$ (0.31 mmol) and solid bipym (0.31 mmol). A slow precipitation of a yellow solid began immediately. After stirring the suspension for 30 min, diethyl ether (15 cm^3) was added and then the solid was filtered off, washed with diethyl ether and dried *in vacuo*.

(ii) Carbon monoxide was bubbled through a solution of $[Rh(diolefin)(bipym)]ClO_4$ (diolefin = tfb, cod or nbd) (0.10 mmol) in 5 cm^3 dichloromethane for 15 min, at room temperature. The resulting solution was vacuum concentrated to *ca* 0.5 cm^3. Slow addition of diethyl ether led to precipitation of required complex, which was filtered off, washed with diethyl ether, and vacuum dried.

$[\{Rh(diolefin)\}_2(bipym)](ClO_4)_2$ (**5–7**)

An acetone solution (20 cm^3) of $[Rh(diolefin)(OCMe_2)_x]^+$ (diolefin = tfb, cod or nbd) (0.26 mmol) was added to a solution of bipym (20.5 mg, 0.13 mmol) in acetone (5 cm^3). The initial yellow colour of the solution changed immediately to dark red and a black solid was formed. The mixture was stirred for 30 min, and then the solid was filtered off, washed with diethyl ether and air dried.

$[Cl_2Pd(bipym)Rh(tfb)]ClO_4$ (**8**)

This complex was prepared by two different routes:

(i) To an acetone suspension (30 cm^3) of complex **1** (0.15 mmol) solid $[PdCl_2(cod)]$ (0.15 mmol) was added. The mixture was stirred for 24 h giving a brown solid and a brown-reddish solution. After removing part of the acetone and adding diethyl ether, the solid was filtered off, washed with diethyl ether and air dried.

(ii) An acetone solution (20 cm^3) of $[Rh(tfb)(OCMe_2)_x]ClO_4$ (0.14 mmol) was added to a suspension of $[PdCl_2(bipym)]$ (**9**) (0.14 mmol) in acetone (10 cm^3). Precipitation of a brown solid began immediately. The mixture was stirred for 30 min. Diethyl ether was added, and then the solid was filtered off, washed with diethyl ether and air-dried.

$[PdCl_2(bipym)]$ (**9**)

This complex was prepared by two different routes:

(i) To an acetone solution (20 cm^3) of bipym (159 mg, 1.0 mmol) solid $[PdCl_2(cod)]$ (1.0 mmol) was added. The suspension was stirred for 12 h, yielding a light yellow solid which was filtered off, washed with acetone and vacuum dried.

(ii) Slow addition of a solution of $[PdCl_2(tht)_2]$ (353.0 mg, 1.0 mmol) in 10 cm^3 of acetone, to a solution of bipym (170.0 mg, 1.0 mmol) in 10 cm^3 of acetone led to instantaneous precipitation of a yellow solid. After 30 min, the solid was filtered off, washed with acetone and vacuum dried.

$[\{RhCl(cod)\}_2(bipym)]$ (**10a**)

Addition of bipym (35.0 mg, 0.22 mmol) to a suspension of $[RhCl(cod)]_2$ (54 mg, 0.11 mmol) in 20 cm^3 of acetone led to instantaneous precipitation of a red solid, which was filtered off, washed with acetone and vacuum dried.

$[Rh(cod)(bipym)][RhCl_2(cod)]$ (**10b**)

A suspension of $[\{RhCl(cod)\}_2(bipym)]$ (65.1 mg, 0.10 mmol) in 10 cm^3 of chloroform was stirred for 30 min. The green solid formed was filtered off and vacuum dried.

$[Rh(nbd)(bipym)][RhCl_2(nbd)]$ (**11**)

Addition of bipym (37.9 mg, 0.24 mmol) to a suspension of $[RhCl(nbd)]_2$ (55.2 mg, 0.12 mmol) in 20 cm^3 of acetone led to instantaneous precipitation of dark-green solid, which was filtered off, washed with acetone and vacuum dried.

$[Rh(tfb)(bipym)][RhCl_2(tfb)]$ (**12**)

The precedure described for preparation of **11** was used, but starting from $[RhCl(tfb)]_2$ (50.0 mg, 0.07 mmol) and bipym (10.8 mg, 0.07 mmol). A dark-green solid was obtained.

$[RhCl(tfb)(bipym)]$ (**13**)

The procedure described for preparation of **12** was used, but starting from $[RhCl(tfb)]_2$ (100.0 mg, 0.14 mmol) and bipym (48.4 mg, 0.31 mmol). A red solid was obtained.

$[\{Rh(nbd)\}_3(tpt)](ClO_4)_3$ (**14**)

An acetone solution (20 cm^3) of $[Rh(nbd)(OCMe_2)_x]ClO_4$ (0.1 mmol) was added to a sol-

ution of tpt (0.06 mmol) in acetone (10 cm^3). The initial yellow colour of the solution changed immediately to red. The mixture was stirred for 30 min. Evaporation of the solution to *ca* 2 cm^3 and addition of diethyl ether gave a brown solid which was filtered off, washed with diethyl ether and vacuum dried.

Table 1 collects analytical results, conductance and yields for the reported complexes.

Catalytic activity

The hydrogen-transfer reactions were carried out under argon in refluxing isopropanol with magnetic stirring. The equipment consisted of a 50-cm^3 round bottomed flask, fitted with a condenser and provided with a secum cap. The catalysts were prepared by adding potassium hydroxide (0.1 mmol) in isopropanol (1 cm^3) to an isopropanol solution (8 cm^3) of precursor complex (0.02 mmol referred to rhodium). The resulting solution was refluxed for 1 h, and 2 mmol of the substrate in isopropanol (1 cm^3) were injected. Reactions were followed by GLC using FFAP on Chromosorb GHP 80/100 mesh (3.6 m × $\frac{1}{8}$ in.) at 120°C.

REFERENCES

1. R. S. Dickson, *Organometallic Chemistry of Rhodium and Iridium*, p. 117. Academic Press, New York (1982).
2. R. P. Hughes, In *Comprehensive Organometallic Chemistry* (Edited by G. Wilkinson, F. G. A. Stone and E. W. Abel), Vol. 5, p. 288. Pergamon Press, Oxford (1982).
3. S. Trofimenko, *Prog. Inorg. Chem.* 1986, **34**, 115.
4. R. Usón, L. A. Oro, R. Sariego and M. A. Esteruelas, *J. Organomet. Chem.* 1981, **214**, 399.
5. L. A. Oro, M. P. Lamata and M. Valderrama, *Transition Met. Chem.* 1983, **8**, 48 (and references therein).
6. G. Zassinovich, G. Mestroni and A. Camus, *J. Organomet. Chem.* 1979, **168**, C37.
7. R. Spogliarich, G. Zassinovich, G. Mestroni and M. Graziani, *J. Organomet. Chem.* 1979, **179**, C45.
8. (a) R. Usón, L. A. Oro and J. A. Cabeza, *J. Organomet. Chem.* 1983, **247**, 105; (b) S. Lanza, *Inorg. Chim. Acta* 1983, **75**, 131.
9. (a) R. Sahai and P. Rillema, *Inorg. Chim. Acta* 1986, **118**, L35; (b) J. D. Scott and R. J. Puddephatt, *Organometallics* 1986, **5**, 1538.
10. R. Usón, L. A. Oro, C. Claver and M. A. Garralda, *J. Organomet. Chem.* 1976, **105**, 365.
11. G. Mestroni, A. Camus and G. Zassinovich, *J. Organomet. Chem.* 1974, **65**, 119.
12. V. F. Sutcliffe and G. B. Young, *Polyhedron* 1984, **3**, 87.
13. R. Usón, L. A. Oro, D. Carmona and M. A. Esteruelas, *J. Organomet. Chem.* 1984, **263**, 109.
14. R. Usón, L. A. Oro, D. Carmona and M. A. Esteruelas, *Inorg. Chim. Acta* 1983, **73**, 275.
15. M. Esteban, Ph.D. dissertation, Universidad de Zaragoza (1984).
16. (a) R. R. Schrock and J. A. Osborn, *J. Am. Chem. Soc.* 1971, **93**, 3089; (b) R. Usón, L. A. Oro and F. Ibañez, *Rev. Acad. Cienc. Zaragoza* 1975, **31**, 169.
17. L. A. Oro, D. Carmona, M. A. Esteruelas, C. Foces-Foces and F. H. Cano, *J. Organomet. Chem.* 1986, **307**, 83.
18. R. Usón, L. A. Oro, J. A. Cuchi and M. A. Garralda, *J. Organomet. Chem.* 1976, **116**, C35.
19. (a) R. N. Haszeldine, R. J. Lunt and R. V. Parish, *J. Chem. Soc. A* 1971, 3711; (b) R. Usón, L. A. Oro, D. Carmona and M. Esteban, *J. Organomet. Chem.* 1981, **220**, 103.
20. M. A. Garralda and L. Ibarlucea, *J. Organomet. Chem.* 1986, **311**, 225.
21. M. P. García, J. A. Manero, L. A. Oro, M. C. Apreda, F. H. Cano, C. Foces-Foces, J. G. Haasnoot, R. Prins and J. Reedijk, *Inorg. Chim. Acta* 1986, **122**, 235.
22. G. Giordano and R. H. Crabtree, *Inorg. Synth.* 1979, **19**, 218.
23. E. W. Abel, M. A. Bennett and G. Wilkinson, *J. Chem. Soc.* 1959, 3178.
24. D. M. Roe and A. G. Massey, *J. Organomet. Chem.* 1971, **28**, 273.
25. Yu. S. Varshavski and T. G. Cherkasova, *Russ. J. Inorg. Chem.* 1967, **12**, 899.
26. J. Chatt, M. Vallarino and L. M. Venanzi, *J. Chem. Soc.* 1957, 3413.

Polyhedron Vol. 6, No. 6, pp. 1433–1437, 1987
Printed in Great Britain

0277–5387/87 $3.00+.00

PREPARATION AND STRUCTURES OF THE BINUCLEAR VANADIUM(II) COMPLEXES $[L_3V(\mu\text{-}Cl)_3VL_3]BPh_4$ (L = TETRAHYDROFURAN OR 3-METHYLTETRAHYDROFURAN)

JO ANN M. CANICH, F. ALBERT COTTON,* STAN A. DURAJ and WIESLAW J. ROTH

Department of Chemistry and Laboratory for Molecular Structure and Bonding, Texas A&M University, College Station, TX 77843, U.S.A.

(*Received* 6 *October* 1986; *accepted* 7 *January* 1987)

Abstract—Two compounds of the general formula $[L_3V(\mu\text{-}Cl)_3L_3]BPh_4$ [L = tetrahydrofuran (**1**) or 3-methyltetrahydrofuran (**2**)] were prepared and investigated via single-crystal X-ray studies. Compound **1**, tris(μ-chloro)hexakis(tetrahydrofuran)divanadium(II) tetraphenylborate, crystallizes in space group $P2_1/c$ with unit-cell dimensions: a = 16.636(6) Å, b = 16.771(5) Å, c = 19.158(5) Å, β = 110.71(4)°, V = 5000(6) Å^3, Z = 4. Compound **2**, tris(μ-chloro)hexakis(3-methyltetrahydrofuran)divanadium(II) tetraphenylborate, forms monoclinic crystals (space group Cc) with a = 18.376(5) Å, b = 10.843(3) Å, c = 29.317(6) Å, β = 103.02(2)°, V = 5691(5) Å^3, Z = 4. Refinement, by least-squares methods, using a data to parameter ratio of 6.1 for **1** and 9.1 for **2**, converged with an unweighted discrepancy index of 7.46 and 5.31% for **1** and **2**, respectively. The V—V′ distances are: 2.978(3) Å for **1** and 2.976(1) Å for **2**. The use of 3-methyltetrahydrofuran as a supporting ligand is discussed since such substituted THF molecules reduce the tendency to disorder in the $[V_2(\mu\text{-}Cl)_3(THF)_6]^+$ cations.

The reduction of $VCl_3(THF)_3$ in tetrahydrofuran (THF) with Zn or $AlR_2(OR)$ affords novel, vanadium(II), face-sharing bioctahedral complexes, $[V_2(\mu\text{-}Cl)_3(THF)_6]_2Zn_2Cl_6$ or $[V_2(\mu\text{-}Cl)_3(THF)_6]AlR_2Cl_2$, respectively.[1,2] These compounds proved to be useful starting materials for a variety of unusual dinuclear and polynuclear vanadium complexes.[3–7] However, crystallographic studies of $[V_2(\mu\text{-}Cl)_3(THF)_6]_2Zn_2Cl_6$, and in particular those of $[V_2(\mu\text{-}Cl)_3(THF)_6]AlR_2Cl_2$ (R = C_2H_5), were very difficult because of an extensive disorder in the THF ligands at room temperature. For $[V_2(\mu\text{-}Cl)_3(THF)_6]_2Zn_2Cl_6$ the quality of the intensity data was greatly improved by collection at −100°C and the structure was satisfactorily refined (the unweighted discrepancy index was 0.045).[1] Crystals of $[V_2(\mu\text{-}Cl)_3(THF)_6]AlEt_2Cl_2$ diffracted poorly (even at −100°C) and the structure could not be satisfactorily refined because of additional severe disorder in the diethyldichloroaluminate anion.[2]

In order to overcome these problems we decided to substitute 3-methyltetrahydrofuran for THF to see whether such substitution would improve the quality of the intensity data and result in a better crystallographic structure of the $[V_2(\mu\text{-}Cl)_3L_6]^+$ cation.

We report here the preparation of a new compound, $[L_3V(\mu\text{-}Cl)_3L_3]BPh_4$ (**2**) (L = 3-methyltetrahydrofuran), and its complete X-ray analysis. The crystallographic data are further compared with those for the THF analog (**1**), and it is demonstrated that a more accurate and nondisordered structure was obtained for the 3-methyltetrahydrofuran derivatives.

EXPERIMENTAL

All operations were performed under an atmosphere of argon by using standard Schlenk techniques and a double-manifold vacuum line. THF, 3-methyltetrahydrofuran and hexane were freshly

* Author to whom correspondence should be addressed.

distilled from benzophenone ketyl prior to use. Solutions were transferred via stainless steel cannulae and/or syringes. Anhydrous VCl_3 was purchased from Strem Chemicals, Inc. and 3-methyltetrahydrofuran and $AlEt_2(OEt)$ (as a 25 wt % solution in toluene) were purchased from Aldrich Chemical Co. $NaBPh_4$ was deaerated *in vacuo* at room temperature.

$[V_2(\mu\text{-}Cl)_3(THF)_6]BPh_4$ (1)

This compound was prepared from $[V_2(\mu\text{-}Cl)_3(THF)_6]_2(Zn_2Cl_6)$ according to our earlier published procedure.[1(b)] Better X-ray quality crystals were obtained by the following modified procedure. Several solutions of different concentration of **1** in THF were prepared and each of them was carefully covered with hexane at room temperature. The solutions were allowed to stand undisturbed for several weeks, after which period good-quality crystals of **1** were obtained from the most dilute solution.

$[V_2(\mu\text{-}Cl)_3(3\text{-methyltetrahydrofuran})_6]BPh_4$ (2)

A solution of VCl_3 (0.6 g, 0.8 mmol) in 10 cm^3 of freshly distilled 3-methyltetrahydrofuran was refluxed for 12 h under argon in a 50-cm^3 round-bottomed three-neck flask equipped with a magnetic stirrer and a reflux condenser. The solution became clear and red-orange in color. To this solution of $VCl_3(3\text{-methyltetrahydrofuran})_3$ in 3-methyltetrahydrofuran was added 7.5 cm^3 of a 25 wt % solution of $AlEt_2(OEt)$ in toluene via a syringe. The solution was stirred for 7 days at room temperature during which time the color changed to a bright green. This solution of $[V_2(\mu\text{-}Cl)_3(3\text{-methyltetrahydrofuran})_6]AlCl_2Et_2$ was then filtered through Celite 545 (Fisher Scientific Co.) onto 1.0 g (2.9 mmol) of $NaBPh_4$. The solution was stirred for 12 h at room temperature and filtered through Celite to a Schlenk tube. Freshly distilled hexane (25 cm^3) was carefully placed on top of this solution and the Schlenk tube was allowed to stand undisturbed for several days. Green X-ray quality crystals of **2** were isolated by filtration, washed with hexane and dried *in vacuo* [yield 1.5 g, 1.4 mmol (83%)].

X-ray crystallography

General procedures that have already been fully described elsewhere were used to determine the crystal structures.[8] Information about data collection and structure refinement for **1** and **2** is given in Table 1. The intensity data were corrected for Lorentz and polarization effects. The positions of vanadium atoms in the unit cell of **1** (space group $P2_1/c$) and **2** (space group Cc) were determined by direct methods using program MULTAN 84. A series of isotropic least-squares refinements and Fourier syntheses then revealed the rest of the structure. Two THF rings in **1** were assigned a disordered model with a fractional occupancy factor 0.5 for each carbon atom. Taking into account the number of observed reflections for **1** it was reasonable to limit anisotropic refinement to the V, Cl and O atoms only. In the case of **2** all atoms could be refined anisotropically. Since the 3-methyltetrahydrofuran derivative crystallized in a non-centrosymmetric space group the enantiomorph giving lower residuals was chosen for refinement.

Tables of positional and isotropic equivalent thermal parameters, anisotropic thermal parameters, *B*s, observed and calculated structure factors, as well as full lists of bond distances and angles for both compounds have been deposited as supplementary material with the Editor at Queen Mary College.

RESULTS AND DISCUSSION

Figures 1 and 2 show the two divanadium(II) cations, **1** and **2**, respectively, and define the atomic numbering scheme used in the tables and the following discussion. Tables 2 and 3 list important interatomic dimensions for **1** and **2**, respectively.

The structure of tris(μ-chloro)hexakis(tetrahydrofuran)divanadium(II) tetraphenylborate (**1**) has already been described by us in 1985.[1(b)] At that time, however, we were not able to obtain good-quality crystals of this compound so the reported structural determination was not very accurate. Since that time we have learnt more about complexes containing the $[(THF)_3V(\mu\text{-}Cl)_3V(THF)_3]^+$ cation and not only were we able to obtain better-quality single crystals of **1** (which still exhibit disorder in the THF ligands) but we have also prepared a new compound in this area which possesses non-disordered 3-methyltetrahydrofuran ligands, namely tris(μ-chloro)hexakis(3-methyltetrahydrofuran)divanadium(II) tetraphenylborate (**2**).

The immediate coordination sphere of the two vanadium centers in both cations is that of a bioctahedron sharing a face comprised of three chlorine atoms. The V—V distance of 2.978(3) Å in **1** and 2.976(1) Å in **2** is *ca* 3 Å, a value very similar to those in other compounds containing the $V(\mu\text{-}Cl)_3V$ unit which we have reported, e.g. 2.993(1) Å in $[(THF)_3V(\mu\text{-}Cl)_3V(THF)_3]_2Zn_2Cl_6$.[2] As expected the metal–ligand distances are practically the same in both compounds.

Table 1. Crystallographic data

Formula	$V_2Cl_3O_6C_{48}H_{68}B$	$V_2Cl_3O_6C_{54}H_{80}B$
Formula weight	960.13	1044.29
Space group	$P2_1/c$	Cc
Systematic absences	$0k0$, $k \neq 2n$; $h0l$, $l \neq 2n$	hkl, $h+k \neq 2n$; $h0l$, $l \neq 2n$
a (Å)	16.636(6)	18.376(5)
b (Å)	16.771(5)	10.843(3)
c (Å)	19.158(5)	29.317(6)
α (°)	90.0	90.0
β (°)	110.71(4)	103.02(2)
γ (°)	90.0	90.0
V (Å^3)	5000(6)	5691(5)
Z	4	4
d_{calc} (g cm^{-3})	1.275	1.219
Crystal size (mm)	0.35 × 0.30 × 0.20	0.70 × 0.50 × 0.45
μ(Mo-K_α) (cm^{-1})	5.655	5.019
Data collection instrument	Enraf–Nonius CAD-4	Syntex P$\bar{1}$
Radiation (monochromated in incident beam)	Mo-K_α (λ_α^- = 0.71073 Å)	
Orientation reflections, [number, range (2θ)]	25, 6.5–26.9	15, 15.5–29.5
Temperature (°C)	22	5
Scan method	ω–2θ	ω
Data collection range [2θ (°)]	$4 < 2\theta < 45$	$4 < 2\theta < 50$
Number of unique data, total	3334	7135
with $F_o^2 > 3\sigma(F_o^2)$	2001	5408
Number of parameters refined	328	593
R^a	0.0746	0.0531
$R_w{}^b$	0.0867	0.0667
Quality-of-fit indicator[c]	2.076	1.399
Largest shift/esd, final cycle	0.06	0.23
Largest peak (e Å^{-3})	0.388	0.491

[a] $R = \Sigma ||F_o| - |F_c|| / \Sigma |F_o|$.
[b] $R_w = [\Sigma w(|F_o| - |F_c|)^2 / \Sigma w|F_o|^2]^{1/2}$; $w = 1/\sigma^2(|F_o|)$.
[c] Quality-of-fit = $[\Sigma w(|F_o| - |F_c|)^2 / (N_{obs} - N_{parameters})]^{1/2}$.

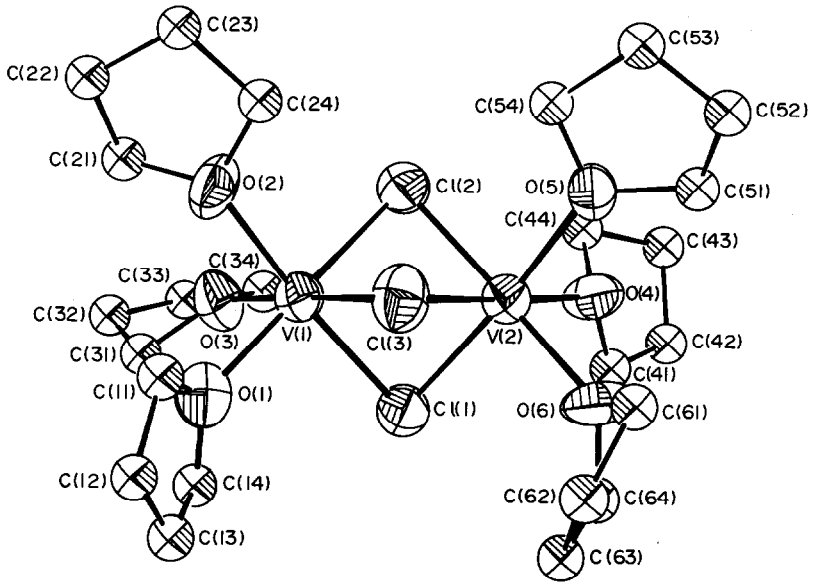

Fig. 1. ORTEP drawing (50% probability level) of the $[V_2Cl_3(THF)_6]^+$ cation. The carbon atoms have been assigned the same isotropic thermal parameter for the sake of clarity.

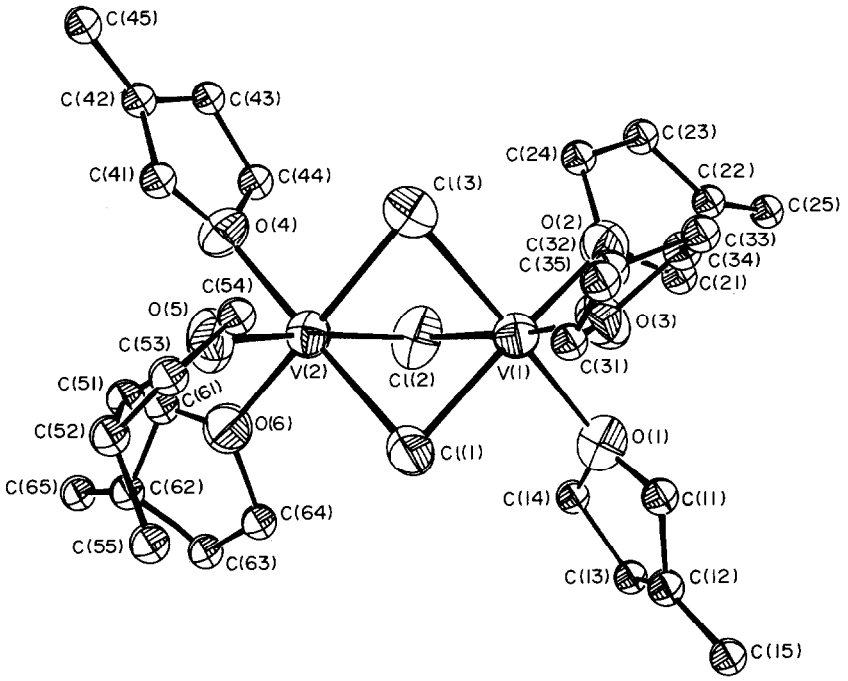

Fig. 2. ORTEP drawing (40% probability level) of the $[V_2Cl_3(3\text{-methyltetrahydrofuran})]^+$ cation. The carbon atoms have been assigned the same isotropic thermal parameter for the sake of clarity.

Table 2. Important interatomic distances (Å) and angles (°) for $[V_2Cl_3(THF)_6]BPh_4$[a]

V(1)—V(2)	2.978(3)	V(2)—Cl(1)	2.469(3)
V(1)—Cl(1)	2.488(4)	V(2)—Cl(2)	2.471(3)
V(1)—Cl(2)	2.479(4)	V(2)—Cl(3)	2.480(4)
V(1)—Cl(3)	2.470(4)	V(2)—O(4)	2.142(8)
V(1)—O(1)	2.161(8)	V(2)—O(5)	2.125(7)
V(1)—O(2)	2.146(7)	V(2)—O(6)	2.162(8)
V(1)—O(3)	2.149(8)		
Cl(1)—V(1)—Cl(2)	85.2(1)	Cl(1)—V(2)—O(4)	94.9(2)
Cl(1)—V(1)—Cl(3)	87.9(1)	Cl(1)—V(2)—O(5)	176.7(2)
Cl(1)—V(1)—O(1)	95.7(3)	Cl(1)—V(2)—O(6)	93.5(2)
Cl(1)—V(1)—O(2)	175.0(2)	Cl(2)—V(2)—Cl(3)	89.1(1)
Cl(1)—V(1)—O(3)	91.2(2)	Cl(2)—V(2)—O(4)	92.3(2)
Cl(2)—V(1)—Cl(3)	89.2(1)	Cl(2)—V(2)—O(5)	91.4(2)
Cl(2)—V(1)—O(1)	177.5(3)	Cl(2)—V(2)—O(6)	179.3(2)
Cl(2)—V(1)—O(2)	90.4(2)	Cl(3)—V(2)—O(4)	176.8(2)
Cl(2)—V(1)—O(3)	92.6(2)	Cl(3)—V(2)—O(5)	90.0(2)
Cl(3)—V(1)—O(1)	88.6(3)	Cl(3)—V(2)—O(6)	90.6(2)
Cl(3)—V(1)—O(2)	89.7(2)	O(4)—V(2)—O(5)	87.0(3)
Cl(3)—V(1)—O(3)	178.0(3)	O(4)—V(2)—O(6)	88.1(3)
O(1)—V(1)—O(2)	88.5(3)	O(5)—V(2)—O(6)	89.2(3)
O(1)—V(1)—O(3)	89.7(3)	V(1)—Cl(1)—V(2)	73.8(1)
O(2)—V(1)—O(3)	91.3(3)	V(1)—Cl(2)—V(2)	74.0(1)
Cl(1)—V(2)—Cl(2)	85.8(1)	V(1)—Cl(3)—V(2)	74.0(1)
Cl(1)—V(2)—Cl(3)	88.1(1)		

[a] Numbers in parentheses are estimated standard deviations in the least significant digits.

Table 3. Important interatomic distances (Å) and angles (°) for $[V_2Cl_3(3\text{-methyltetrahydrofuran})_6]BPh_4$[a]

V(1)—V(2)	2.976(1)	V(2)—Cl(1)	2.483(2)
V(1)—Cl(1)	2.475(2)	V(2)—Cl(2)	2.486(2)
V(1)—Cl(2)	2.483(2)	V(2)—Cl(3)	2.481(2)
V(1)—Cl(3)	2.488(2)	V(2)—O(4)	2.146(4)
V(1)—O(1)	2.184(4)	V(2)—O(5)	2.161(4)
V(1)—O(2)	2.137(4)	V(2)—O(6)	2.131(4)
V(1)—O(3)	2.146(4)		
Cl(1)—V(1)—Cl(2)	87.64(6)	Cl(1)—V(2)—O(4)	175.7(1)
Cl(1)—V(1)—Cl(3)	88.92(6)	Cl(1)—V(2)—O(5)	88.7(1)
Cl(1)—V(1)—O(1)	87.5(1)	Cl(1)—V(2)—O(6)	94.0(1)
Cl(1)—V(1)—O(2)	175.6(1)	Cl(2)—V(2)—Cl(3)	86.93(6)
Cl(1)—V(1)—O(3)	93.7(1)	Cl(2)—V(2)—O(4)	96.0(1)
Cl(2)—V(1)—Cl(3)	86.83(6)	Cl(2)—V(2)—O(5)	175.9(1)
Cl(2)—V(1)—O(1)	94.8(1)	Cl(2)—V(2)—O(6)	89.4(1)
Cl(2)—V(1)—O(2)	90.6(1)	Cl(3)—V(2)—O(4)	88.6(1)
Cl(2)—V(1)—O(3)	175.0(1)	Cl(3)—V(2)—O(5)	94.3(1)
Cl(3)—V(1)—O(1)	176.0(1)	Cl(3)—V(2)—O(6)	175.2(1)
Cl(3)—V(1)—O(2)	95.0(1)	O(4)—V(2)—O(5)	88.0(2)
Cl(3)—V(1)—O(3)	88.4(1)	O(4)—V(2)—O(6)	88.7(2)
O(1)—V(1)—O(2)	88.6(2)	O(5)—V(2)—O(6)	89.5(2)
O(1)—V(1)—O(3)	90.0(2)	V(1)—Cl(1)—V(2)	73.76(5)
O(2)—V(1)—O(3)	88.5(2)	V(1)—Cl(2)—V(2)	73.58(5)
Cl(1)—V(2)—Cl(2)	87.40(6)	V(1)—Cl(3)—V(2)	73.58(5)
Cl(1)—V(2)—Cl(3)	88.90(6)		

[a] Numbers in parentheses are estimated standard deviations in the least significant digits.

As mentioned in the introduction, the disorder in the THF ligands of **1** is extensive. It is associated with the adoption of different conformations by a particular THF ring. In some cases the different carbon atom positions could be resolved and they have been dealt with in a conventional manner by assigning fractional occupancy factors. In general, however, different conformations could not be resolved and the corresponding carbon atoms had relatively high thermal parameters. In contrast, the structure of **2** required no disorder treatment since well-refined carbon atoms of 3-methyltetrahydrofuran ligands were obtained, and this led to a lower unweighted discrepancy index of 5.31%. The estimated standard deviations of the interatomic dimensions are lower, roughly by a factor of 2 in the 3-methyltetrahydrofuran derivative.

The crystallization of **2** in a noncentrosymmetric space group indicates that the introduction of substituted THF leads to the formation and resolution of chiral isomers.

This report clearly shows that substitution of disordered THF ligands by 3-methyltetrahydrofuran results in more accurate X-ray structure determination. We believe that this is an artifice that could profitably be employed in many other cases.

Acknowledgement—We thank the National Science Foundation for support.

REFERENCES

1. (a) F. A. Cotton, S. A. Duraj, M. W. Extine, G. E. Lewis, W. J. Roth, C. D. Schmulbach and W. Schwotzer, *J. Chem. Soc., Chem. Commun.* 1983, 1377; (b) F. A. Cotton, S. A. Duraj and W. J. Roth, *Inorg. Chem.* 1985, **24**, 913; (c) R. J. Bouma, J. H. Teuben, W. R. Beukema, R. L. Bansemer, J. C. Huffman and K. G. Caulton, *Inorg. Chem.* 1984, **24**, 2715.
2. F. A. Cotton, S. A. Duraj, L. E. Manzer and W. J. Roth, *J. Am. Chem. Soc.* 1985, **107**, 3850.
3. F. A. Cotton, G. E. Lewis and G. J. Mott, *Inorg. Chem.* 1982, **21**, 3316.
4. F. A. Cotton, S. A. Duraj and W. J. Roth, *Inorg. Chem.* 1984, **23**, 4113.
5. F. A. Cotton, S. A. Duraj and W. J. Roth, *Inorg. Chem.* 1984, **23**, 4042.
6. F. A. Cotton, S. A. Duraj, W. J. Roth and C. D. Schmulback, *Inorg. Chem.* 1985, **24**, 525.
7. R. J. Bansemer, J. C. Huffman and K. G. Caulton, *J. Am. Chem. Soc.* 1983, **105**, 6163.
8. See, for example, A. Bino, F. A. Cotton and P. E. Fanwick, *Inorg. Chem.* 1979, **18**, 3558.

Polyhedron Vol. 6, No. 6, pp. 1439–1443, 1987
Printed in Great Britain

0277–5387/87 $3.00+.00

SYNTHESIS AND STRUCTURAL CHARACTERIZATION OF A POLAR Os(II, III) COMPLEX, $Os_2(fhp)_4Cl$

F. ALBERT COTTON* and MAREK MATUSZ

Department of Chemistry and Laboratory for Molecular Structure and Bonding, Texas A&M University, College Station, TX 77843, U.S.A.

(*Received* 26 *October* 1986; *accepted* 23 *January* 1987)

Abstract—The title compound was prepared by prolonged reaction of $Os_2(CH_3COO)_4Cl_2$ with Hfhp (Hfhp = 6-fluoro-2-hydroxypyridine) in refluxing toluene in the presence of LiCl. The product, $Os_2(fhp)_4Cl$ (**1**), is a result of ligand displacement with a concomitant core reduction of Os_2^{6+} to Os_2^{5+}. Crystals were grown by slow diffusion of hexane into a dichloromethane solution of **1**. Crystallographic data are as follows: tetragonal crystal system, space group *I*4*mm* (No. 107), $a = b = 11.000(3)$ Å, $c = 13.142(2)$ Å, $V = 1590(1)$ Å^3, $Z = 2$. The molecule possesses crystallographic 4*mm* symmetry, with the Os—Os bonds lying along the four-fold axes. The four fhp ligands are arranged in a polar fashion around the diosmium core, blocking one axial site. The second axial position is occupied by a chloride ion. The principal distances in **1** are: Os(1)—Os(2) = 2.341(1) Å, Os(1)—N = 2.027(12) Å, Os(2)—O = 2.014(5) Å, Os(2)—Cl = 2.487(7) Å. The title compound was also investigated by several physical methods. The electrochemistry as determined by cyclic voltammetry revealed two processes: a reversible, one-electron reduction at $E_{1/2} = -0.63$ V in dichloromethane and an irreversible oxidation at $E_{ox} = +0.95$ V in dichloromethane vs Ag–AgCl at room temperature. The electronic spectrum shows strong bands at 413 nm ($\varepsilon = 4290$ M^{-1} cm^{-1}), 309 nm ($\varepsilon = 23{,}560$ M^{-1} cm^{-1}) and at 294 nm ($\varepsilon = 26{,}500$ M^{-1} cm^{-1}) as well as shoulders at 334 and 261 nm.

In this laboratory we are continuing our investigation of compounds that contain a multiply-bonded Os_2^{n+} ($n = 4$, 5 or 6) core. Early reports suggested that attempted ligand substitution reactions on $Os_2(CH_3COO)_4Cl_2$ usually afford monomeric products,[1] but further investigations in our laboratory[2–5] and elsewhere[6] since then have provided routes to an array of multiply-bonded diosmium complexes. Our synthetic efforts have been focused on compounds containing 6-substituted oxypyridine anions as ligands. These ligands are generally useful in spanning multiply-bonded dimetallic units.[7] The steric demand of the substituent in the 6-position of the 2-hydroxypyridinato ring plays a crucial role in determining the structure and properties of the product. With the relatively bulky chlorine atom as a substituent two interesting molecules have been synthesized. A polar complex,[8] $Os_2(chp)_4Cl$, containing the Os_2^{5+} core is formed in the reaction of diosmium-tetraacetate dichloride with 6-chloro-2-hydropyridine. In the same reaction, a second product is formed,[9] $Os_2Cl_4(chp)_2 \cdot L$ (L = py or H_2O), an Os(III, III) complex with four terminal chloride ions, two *trans* chp ligands and an axial, neutral ligand.

It has been shown previously that 6-fluoro-2-hydroxypyridine (Hfhp) characteristically prefers to form a polar arrangement (also called a 4:0 arrangement) of the four ligands across the dimetal unit. The complexes $M_2(fhp)_4 \cdot THF$ (M = Cr, Mo or W),[10] $Ru_2(fhp)_4Cl$[11] and $Rh_2(fhp)_4 \cdot DMSO$[12] have previously been synthesized, and all have the 4:0 arrangement. The work reported here was undertaken to determine how the diosmium unit would behave toward the same ligand.

* Author to whom correspondence should be addressed.

EXPERIMENTAL

Starting materials

$Os_2(CH_3COO)_4Cl_2$ was prepared by a literature procedure.[1] The ligand, Hfhp, was obtained from Dow Chemical Co. Lithium chloride was dried at 110°C overnight. Dry and deoxygenated solvents were freshly distilled before use.

Preparation of $Os_2(fhp)_4Cl$ (**1**)

$Os_2(CH_3COO)_4Cl_2$ (0.1 g, 0.145 mmol), LiCl (0.6 g, 14 mmol), Hfhp (0.6 g, 5.3 mmol) and 10 cm^3 of toluene were refluxed for 3 days under an argon atmosphere. The crystalline diosmium-tetraacetate dichloride gradually disappeared and a brown precipitate was deposited. The reaction mixture was cooled and filtered. The solid residue was washed several times with diethyl ether to remove unreacted ligand. The remaining solids were extracted with CH_2Cl_2 until the washings were almost colorless. The brown-yellow CH_2Cl_2 solution was concentrated and carefully layered with hexane. In a few days a uniform mass of well-formed, block-shaped crystals was deposited. They were filtered, washed with hexane and air dried. The yield is 70 mg (*ca* 56%). The complex is air-stable in the solid state and in solution.

Found: C, 28.2; H, 1.5. Calc. for $Os_2ClF_4O_4N_4C_{20}H_{12}$: C, 27.8; H, 1.4%. Electronic spectrum (850–250 nm, CH_2Cl_2 solvent): λ_{max} = 413 nm (ε = 4300 M^{-1} cm^{-1}), λ = 334 nm (sh), λ_{max} = 309 nm (ε = 23,600 M^{-1} cm^{-1}), λ_{max} = 284 nm (ε = 26,500 M^{-1} cm^{-1}), λ = 261 nm (sh).

Measurements

Elemental analyses were performed by Galbraith Laboratories Inc. The electronic spectra were measured on CH_2Cl_2 solutions (HPLC grade) using a Cary 17D spectrophotometer. Electrochemical measurements were done with a Bioanalytical Systems Inc., model BAS 100 Electrochemical Analyzer in conjunction with a Bausch & Lomb, Houston Model DMP 40 digital plotter. Experiments were carried out in CH_2Cl_2 containing *ca* 0.2 M tetra-*n*-butylammonium hexafluorophosphate (TBAH) as a supporting electrolyte. A three-electrode cell configuration was used with a platinum disk and a platinum wire as working and auxiliary electrodes, respectively. All potentials are referenced to the Ag–AgCl electrode at 24±2°C with full positive feedback resistance compensation, and are uncorrected for junction potentials. Magnetic measurements were made at room temperature on CH_2Cl_2 solution by the Evans method on a Varian 390 spectrometer. A correction for the diamagnetism of the ligand was applied. X-band ESR spectra were obtained on CH_2Cl_2 frozen solutions using a Varian E-6S spectrometer.

X-ray crystallographic procedures

The structure of a single crystal of **1** was determined by application of general procedures which have been fully described elsewhere.*[13] The pertinent crystallographic data are summarized in Table 1. Important bond distances and angles are given in Table 2. A regular, block-shaped crystal of approximate dimensions 0.3 × 0.4 × 0.6 mm was mounted in a capillary in mother liquor. The diffraction data were collected on a CAD 4 auto-diffractometer equipped with graphite-monochromated Mo-K_α (λ = 0.71073 Å) radiation. Lorentz, polarization and absorption corrections were applied. There are five possible space group choices consistent with the systematic absences. These are *I*422, *I*4*mm*, *I*$\bar{4}$*m*2, *I*$\bar{4}$2*m* and *I*4/*mmm*. Given the cell volume and the expected molecular formula, $Os_2(fhp)_4Cl$, there must be two molecules in the unit cell. With Z = 2 and an ordered model, the only possible space group is *I*4*mm*, with the molecule on a four-fold axis. One Os atom can be placed at the origin, which than allowed us to determine the position of the other Os atom from the Patterson map. The alternating least-squares and difference Fourier cycles revealed positions of all non-hydrogen atoms. As the refinement progressed it became clear that absorption still affected the calculations, despite an earlier empirical absorption correction based on psi scans. The program DIFABS[14] was applied to the data. Successful refinement confirmed our choice of space group. The largest peaks in the final difference Fourier map were ghosts of heavy atoms. In a final cycle, 497 data were used to refine 57 parameters to give R = 0.028 and R_w = 0.054.

RESULTS AND DISCUSSION

Preparation

The $Os_2(fhp)_4Cl$ compound reported here is formed in good yields (*ca* 60%) in the reaction of $Os_2(CH_3COO)_4Cl_2$ with Hfhp in refluxing toluene

* Calculations were done on the VAX-11/780 computer at the Department of Chemistry, Texas A&M University, College Station, Texas with a VAX-SDP software package.

Table 1. Crystal data for $Os_2(fhp)_4Cl$

Formula	$Os_2ClF_4O_4N_4C_{20}H_{12}$
Formula weight	864.19
Space group	*I4mm* (No. 107)
Systematic absences	$h+k+l \neq 2n$, $0kl$ $(k+l \neq 2n)$, hhl $(l \neq 2n)$
a (Å)	11.000(2)
b (Å)	11.000(2)
c (Å)	13.142(4)
α (°)	90.0
β (°)	90.0
γ (°)	90.0
V (Å^3)	1590(1)
Z	2
d_{calc} (g cm^{-3})	1.805
Crystal size (mm)	$0.3 \times 0.4 \times 0.6$
μ(Mo-K_α) (cm^{-1})	81.28
Data collection instrument	CAD-4
Radiation (monochromated in incident beam	Mo-K_α ($\lambda_\alpha^- = 0.71073$ Å)
Orientation reflections [number, range (2θ)]	25, $16° < 2\theta < 35°$
Temperature (°C)	24
Scan method	ω–2θ
Data collection range [2θ (°)]	4–50
Number of unique data, total with $F_o^2 > 3\sigma(F_o^2)$	587, 497
Number of parameters refined	57
Transmission factors (max, min)	0.998, 0.892
R^a	0.0283
$R_w{}^b$	0.0354
Quality-of-fit indicator[c]	1.145
Largest shift/esd, final cycle	0.16
Largest peak (e Å^{-3})	1.5

[a] $R = \Sigma ||F_o| - |F_c|| / \Sigma |F_o|$.
[b] $R_w = [\Sigma w(|F_o| - |F_c|)^2 / \Sigma w|F_o|^2]^{1/2}$; $w = 1/\sigma^2(|F_o|)$.
[c] Quality-of-fit $= [\Sigma w(|F_o| - |F_c|)^2 / (N_{obs} - N_{parameters})]^{1/2}$.

in the presence of LiCl. Attempts to run the reaction in molten Hfhp in a fashion analogous to the previously described syntheses[8,9] of $Os_2(chp)_4Cl$ and $Os_2Cl_4(chp)_2 \cdot L$ did not yield any identifiable products. The use of stoichiometric amounts of $Os_2(CH_3COO)_4Cl_2$ and Hfhp (1 : 2) in the presence of LiCl, in an attempt to obtain $Os_2Cl_4(fhp)_2$, yielded only **1** in lower yields. We have not, under any conditions, seen evidence of the formation of $Os_2Cl_4(fhp)_2$. Also, use of Me_3SiCl, which has been shown to remove acetate ions and other oxygen-containing ligands from the multiply-bonded dimetallic units, has failed in this case. The role of LiCl is unknown (although its use has been reported[16] before) and we do not wish to speculate on the mechanistic aspects of the reaction since the additional complicating factor is the reduction of the diosmium unit.

The reducing agent is most likely Hfhp, but the possibility of disproportionation cannot be excluded in view of the 60% yield of reaction.

Spectroscopic and magnetic properties

The visible region of the electronic spectrum of **1** in CH_2Cl_2 displays one strong band at 413 nm ($\varepsilon = 4300$ M^{-1} cm^{-1}). This is similar to the previously observed band for the $Os_2(chp)_4Cl$ complex ($\lambda_{max} = 412$ nm, $\varepsilon = 3800$ M^{-1} cm^{-1}).

The ground electronic state for this molecule is most likely a spin-quartet derived from the $\sigma^2\pi^4\delta^2\delta^*\pi^{*2}$ electronic configuration, since it has

Table 2. Selected bond distances (Å) and bond angles (°) for $Os_2(fhp)_4Cl$[a]

Atom 1	Atom 2	Distance	
Os(1)	Os(2)	2.341(1)	
Os(1)	N	2.027(12)	
Os(2)	Cl	2.487(7)	
Os(2)	O	2.014(5)	
F	C(5)	1.38(2)	
O	C(1)	1.21(4)	
N	C(1)	1.46(5)	
N	C(5)	1.26(3)	
Atom 1	Atom 2	Atom 3	Angle
Os(2)	Os(1)	N	89(1)
Os(1)	Os(2)	Cl	180.00(0)
Os(1)	Os(2)	O	89.9(6)
Os(2)	O	C(1)	123(2)
Os(1)	N	C(1)	117(2)
O	C(1)	N	120.3(6)

[a] Numbers in parentheses are estimated standard deviations in the least significant digits.

a room-temperature magnetic moment in CH_2Cl_2 solution of 3.70 BM. For $Os_2(chp)_4Cl$ a moment of only 2.90 BM was found, and this was taken to mean that there was substantial population of a spin-doublet derived from a $\sigma^2\pi^4\delta^2\sigma^2*\pi*$ or $\sigma^2\pi^4\delta^2\pi*^3$ configuration. In the present case there would appear to be much less thermal access to such a doublet state. The $Os_2(fhp)_4Cl$ compound exhibits an ESR signal at −196°C (in frozen CH_2Cl_2 solution), but it has a different appearance from the one shown by $Os_2(chp)_4Cl$. We are not certain how to interpret this result. In any case, **1** can be added to the list of diosmium complexes, of both the III, III and II, III types whose magnetic properties require more detailed study.

Electrochemistry

The electrochemical properties of the compound were studied by cyclic voltammetry. CH_2Cl_2 solutions with TBAH as a supporting electrolyte were used. A reversible, one-electron reduction at $E_{1/2} = -0.63$ V and an irreversible oxidation at $E_{ox} = +0.90$ V (Fig. 1) were observed. The presumably metal-based reduction represents the following process:

$$Os_2^{5+} + e^- \rightarrow Os_2^{4+}.$$

For the similar $Os_2(chp)_4Cl$ complex this reduction was observed at −0.60 V. To our surprise the oxidation appears to be irreversible, although the above-mentioned $Os_2(chp)_4Cl$ undergoes reversible oxidation at almost the same potential (+0.90 V).

*Molecular structure**

Selected bond distances and angles are presented in Table 2, and Fig. 2 presents an ORTEP view of the molecule with the atoms labeled. The molecular symmetry is rigorously C_{4v} (*4mm*) with Os(1), Os(2) and Cl lying along a four-fold axis. The four fhp ligands are placed on two perpendicular mirror planes. The asymmetric unit consists of Os(1), Os(2), Cl and one fhp ligand.

The molecule has a polar arrangement with the four fhp ligands pointing in one direction. One axial site, which is unoccupied, is encumbered by the four fluorine atoms. The second axial site is occupied by a chlorine atom. The perfect C_{4v}-geometry is possible in this case because the relatively small fluorine atoms do not come in close contact. In contrast, the polar molecules with chp or mhp as ligands are always twisted from the ideal eclipsed conformation to alleviate repulsive X---X interactions.

The Os—Os distance is 2.341(1) Å. This is the same distance, within experimental error, as found earlier in $Os_2(chp)_4Cl$. Additional distances and angles are at about the expected values.

We wish now to compare some experimental results for **1** to those of the isomorphous and isostructural $Ru_2(fhp)_4Cl$, as summarized in Table 3.

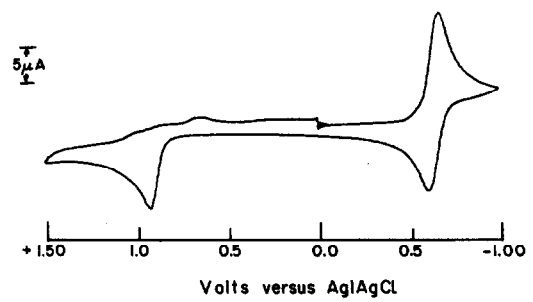

Fig. 1. Cyclic voltammogram of $Os_2(fhp)_4Cl$ (measured at 200 mV s^{-1} in 0.2 M TBAH–CH_2Cl_2 at a Pt-disk electrode).

* *Supplementary material available.* Full listing of bond angles, bond distances, anisotropic displacement parameters and observed and calculated structure factors (6 pages) have been deposited with the Editor. Atomic positional parameters have been deposited with the Cambridge Crystallographic Data Centre.

Table 3. Comparison of selected experimental properties of $Os_2(fhp)_4Cl$ and $Ru_2(fhp)_4Cl$

	$Os_2(fhp)_4Cl$	$Ru_2(fhp)_4Cl$
Visible λ_{max} (ε)	413 (4290)	522 (4720)
$E_{1/2}$ (V)	+0.95,[a] −0.63	+1.68, −0.01
Magnetic moment (BM)	3.70	—
M—M (Å)	2.341(1)	2.284(1)
M—O (Å)	2.014(5)	1.971(2)
M—N (Å)	2.027(12)	2.089(4)
M—Cl (Å)	2.487(7)	2.427(3)

[a] E_{ox}.

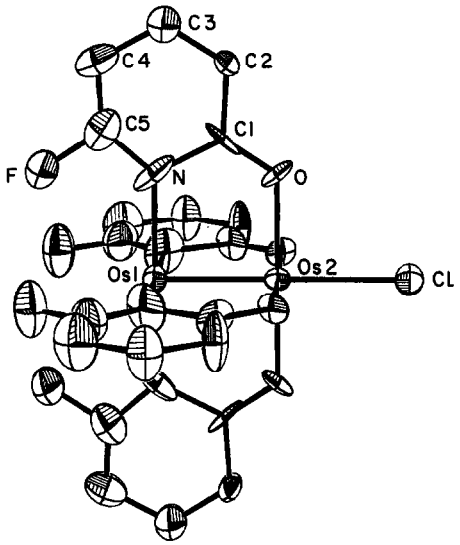

Fig. 2. ORTEP drawing of the $Os_2(fhp)_4Cl$ molecule with the atom-labelling scheme. Atoms are represented by their thermal vibration ellipsoids at the 50% level.

As far as the structural parameters are concerned, the only difference between these two structures can be attributed to the larger size of Os than Ru. This in turn leads to a longer metal–metal bond (by 0.057 Å). The Os—Cl and Os—O distances are also slightly longer than the corresponding Ru ones, but the Os—N distances are shorter (by about 0.06 Å).

As a part of our investigation of diosmium chemistry we have established the formation of a second polar diosmium complex. **1** is formed in reasonable yield from $Os_2(CH_3COO)_4Cl_2$. Ligand substitution is accompanied by a reduction from an Os_2^{6+} to an Os_2^{5+} dimetallic core.

Acknowledgement—We thank the National Science Foundation for support.

REFERENCES

1. T. Behling, G. Wilkinson, T. A. Stephenson, D. A. Tocher and M. D. Walkinshaw, *J. Chem. Soc., Dalton Trans.* 1983, 2109.
2. A. R. Chakravarty, F. A. Cotton and D. A. Tocher, *Inorg. Chem.* 1984, **23**, 4693.
3. A. R. Chakravarty, F. A. Cotton and D. A. Tocher, *Inorg. Chem.* 1985, **24**, 1334.
4. A. R. Chakravarty, F. A. Cotton and D. A. Tocher, *J. Chem. Soc., Chem. Commun.* 1984, 501.
5. K. R. Dunbar, F. A. Cotton and M. Matusz, *Polyhedron* 1986, **5**, 903.
6. (a) P. E. Fanwick, M. K. King, S. M. Tetrick and R. A. Walton, *J. Am. Chem. Soc.* 1985, **107**, 5009; (b) P. A. Agaskar, F. A. Cotton, K. R. Dunbar, L. R. Falvello, S. M. Tetrick and R. A. Walton, *J. Am. Chem. Soc.* 1986, **108**, 4850.
7. F. A. Cotton and R. A. Walton, *Multiple Bonds Between Metal Atoms*. Wiley, New York (1982).
8. K. D. Dunbar, F. A. Cotton and M. Matusz, *Inorg. Chem.* 1986, **25**, 1585.
9. K. D. Dunbar, F. A. Cotton and M. Matusz, *Inorg. Chem.* 1986, **25**, 1589.
10. F. A. Cotton, L. R. Falvello, S. Han and W. Wang, *Inorg. Chem.* 1983, **22**, 4106.
11. A. R. Chakravarty, F. A. Cotton and W. Schwotzer, *Polyhedron* 1986, **5**, 1821.
12. F. A. Cotton, S. Han and W. Wang, *Inorg. Chem.* 1984, **23**, 4762.
13. (a) A. Bino, F. A. Cotton and P. E. Fanwick, *Inorg. Chem.* 1979, **18**, 3358; (b) F. A. Cotton, B. A. Frenz, G. Deganello and A. Shaver, *J. Organomet. Chem.* 1973, **50**, 227; (c) A. C. T. North, D.C. Phillips and F. S. Matthews, *Acta Cryst.* 1968, **A24**, 351.
14. N. Walker and D. Stuart, *Acta Cryst.* 1983, **A39**, 158.
15. S. M. Tetrick, V. T. Coombe, G. A. Heath, T. A. Stephenson and R. A. Walton, *Inorg. Chem.* 1984, **23**, 4567.
16. R. W. Mitchell, A. Spencer and G. Wilkinson, *J. Chem. Soc., Dalton Trans.* 1973, 846.

Polyhedron Vol. 6, No. 6, pp. 1445–1456, 1987
Printed in Great Britain

0277-5387/87 $3.00 + .00

$[Fe_2S_2(CO)_6]^{2-}$ AS A CLUSTER PRECURSOR: SYNTHESIS AND STRUCTURE OF $[MoFe_3S_6(CO)_6]^{2-}$ AND OXIDATIVE DECARBONYLATION TO A PERSULFIDE-BRIDGED $MoFe_3S_4$ DOUBLE CUBANE

JULIE A. KOVACS, JAMES K. BASHKIN* and R. H. HOLM†

Department of Chemistry, Harvard University, Cambridge, MA 02138, U.S.A.

(*Received* 21 *October* 1986; *accepted* 12 *January* 1987)

Abstract—Reactions of $[Fe_2S_2(CO)_6]^{2-}$ (**3**) with $[Cl_2FeS_2MS_2]^{2-}$ [M = Mo (**4**) or W (**6**)] and $[Cl_2FeS_2VS_2FeCl_2]^{3-}$ (**8**) in acetonitrile–THF solutions afford the new clusters $[MFe_3S_6(CO)_6]^{2-}$ (M = Mo (**5**) or W (**7**)] and $[VFe_6S_8(CO)_{12}]^{3-}$ (**9**). $(Et_4N)_2$ (**5**) crystallizes in orthorhombic space group *Pbcn* with $a = 15.314(7)$ Å, $b = 16.627(6)$ Å, $c = 29.971(13)$ Å, and $Z = 8$. Cluster **5** is formed by displacement of chloride from **4** by **3** to yield a species with the $[Fe_2(\mu_3\text{-}S)_2Fe(\mu_2\text{-}S)_2MoS_2]^{2-}$ core arrangement containing one Fe(II) and Mo(VI) in distorted tetrahedral sites. Similar structures are proposed for **7** and **9**, with the latter containing two **3** ligands bound to the $[VFe_2S_4]^{1+}$ core of **8**. Treatment of **5** with RSSR results in oxidative decarbonylation and formation of $[Mo_2Fe_6S_8(S_2)_2(SR)_6]^{4-}$ (**10**) (R = *p*-C_6H_4Cl or *p*-C_6H_4Br), which consists of two $[MoFe_3(\mu_3\text{-}S)_4]^{3+}$ cubane-type subclusters bridged by two $\mu_2\text{-}\eta^3\text{-}S_2^{2-}$ groups. Cluster **10** was also obtained in a direct-assembly system consisting of $[MoS_4]^{2-} + 3FeCl_3 + S_2^{2-} + 7RS^-$ in methanol. Evidence is presented that the solid-state structure of **10** is maintained in solution. The redox change $[MoFe_3(\mu_2\text{-}S)_2(\mu_3\text{-}S)_2S_2]^{2-}$ (**5**) → $[MoFe_3(\mu_3\text{-}S)_4(S_2)]^{1+}$ (**10**) is described as an oxidatively induced core internal conversion in which there is net Fe and S oxidation and Mo reduction. It is argued that the reduction of tetrahedral Mo(VI) to or near Mo(III), stabilized in a six-coordinate site, is a significant factor in the formation of the cubane structure. The formation of the cubane cluster $[VFe_3S_4Cl_3(DMF)_3]^{1-}$ from **8** and $FeCl_2$ is similarly promoted by the reduction of tetrahedral V(V) to or near V(III). The syntheses of **5**, **7**, **9** and **10** illustrate the utility of **3** as a cluster precursor.

At present, the synthetic cluster species most closely related to the native cluster which is the FeMo-cofactor of nitrogenase are those containing one or two cubane-type $MoFe_3(\mu_3\text{-}S)_4$ cores. The leading aspects of these clusters have recently been summarized.[1] Their synthesis is usually achieved by direct cluster assumbly involving the simple reactants $[MoS_4]^{2-}$, $FeCl_3$ and thiolate in an alcohol solvent. In this way the double-cubane clusters $[Mo_2Fe_6S_8(SR)_9]^{3-}$ [2–4] (**1**) and $[Mo_2Fe_7S_8(SR)_{12}]^{3-}$ [5] (**2**), containing the indicated bridge units, have been prepared in good yield. Single cubanes of general types $[MoFe_3S_4(SR)_3(cat)L]^{2-,3-}$ [6–8] [cat = 3,6-disubstituted catecholate(2−)] and $[MoFe_3S_4(SR)_4(dmpe)]^{1-}$ [9] [dmpe = 1,2-bis(dimethylphosphino) ethane] are accessible by bridge cleavage of **2**. The single cubanes exhibit certain electronic features[10] and possess Mo site structural properties[1,11] that bear an apparent resemblance to corresponding aspects of the cofactor.

Recently we have been exploring other routes to Mo–Fe–S and other heterometal Fe–S clusters of possible biological relevance. Noting the chelating ability[12,13] of the Seyferth anion $[Fe_2S_2(CO)_6]^{2-}$ [12] and the possibility of oxidative decarbonylation[14] of reaction products by disulfides leading to new clusters, we have examined the reactions of this anion with Fe(II) complexes derived from the thiometalates of Mo, W and V. Among the results

* National Institutes of Health Postdoctoral Fellow (1984–1985).

† Author to whom correspondence should be addressed.

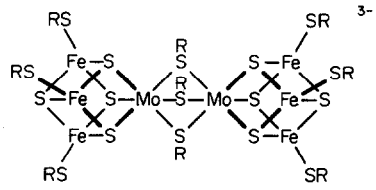

1

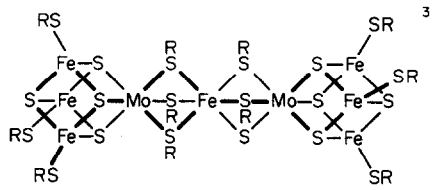

2

presented are the synthesis and structure of a new cluster type exemplified by $[MoFe_3S_6(CO)_6]^{2-}$, and the identity of its decarbonylation product. The information provided here augments earlier brief reports[15,16] of some of the principal findings of this research.

EXPERIMENTAL

Preparation of compounds

All operations were performed under a pure dinitrogen atmosphere. Acetonitrile was purified by distillation from CaH_2 and stored over 3-Å molecular sieves. Methanol and THF were distilled from $Mg(OMe)_2$ and Na–K alloy, respectively. $Fe_2S_2(CO)_6$,[12] Na_2S_2,[17] $(NH_4)_2[MoS_4]$,[18] $(Et_4N)_2[MFeS_4Cl_2]$ (M = Mo[19] or W[20]), and $(Et_4N)_3[VFe_2S_4Cl_4]$[21] were prepared as described. Bis (*p*-chlorophenyl)disulfide was obtained as a white crystalline solid by the iodine oxidation of *p*-ClC_6H_4SH in methanol. Solutions of $Li_2[FeS_2(CO)_6]$ in THF were prepared by the method of Seyferth *et al.*[12]

$(Et_4N)_2[MoFe_3S_6(CO)_6]$ (**5**). A freshly prepared, bright green solution of 5.8 mmol of $Li_2[Fe_2S_2(CO)_6]$ (**3**) in 100 cm^3 of THF at −78°C was treated with an equimolar, red-brown solution of $(Et_4N)_2[MoFeS_4Cl_2]$ (**4**) in 400 cm^3 of acetonitrile. The reaction mixture was slowly warmed over 5 h to ambient temperature, stirred overnight, and filtered to remove LiCl and a black insoluble solid. Ether (~ 200 cm^3) was added to the dark purple filtrate to afford 2.21 g (43%) of crude product as a purple-brown microcrystalline solid. Recrystallization of this material from acetonitrile–ether [3 : 1 (v/v)] afforded 1.80 g (35%) of pure product as purple-brown microcrystals. Found: C, 29.9; H, 4.7; Fe, 18.6; Mo, 10.7; N, 3.2; S, 21.6. Calc. for $C_{22}H_{40}Fe_3MoN_2O_6S_6$: C, 29.9; H, 4.6; Fe, 18.9; Mo, 10.8; N, 3.2; S, 21.7%. IR (MeCN): ν_{CO} 2042 (m), 2004 (s), and 1960 (vs) cm^{-1}. Absorption spectrum (MeCN): λ_{max} (ε_M) 331 (23,600), 410 (sh), and 470 (8960) nm.

$(Et_4N)_2[WFe_3S_6(CO)_6]$ (**7**). A freshly prepared solution of 1.86 mmol of $Li_2[Fe_2S_2(CO)_6]$ in 50 cm^3 of THF at −78°C was treated with an equimolar, bright orange solution of $(Et_4N)_2[WFeS_4Cl_2]$ (**6**) in 200 cm^3 of acetonitrile. Following slow warming over about 12 h to room temperature, the reaction mixture was filtered to remove LiCl and a black insoluble solid. The volume of the orange-brown filtrate was reduced to ~ 75 cm^3, 30 cm^3 of ether were added, and the solution was cooled to −20°C to afford 1.3 g (72%) of crude product as a gold-brown microcrystalline solid. Recrystallization of this material from acetonitrile–ether [2 : 1 (v/v)] gave 1.1 g (61%) of pure product as gold-brown microcrystals. IR (MeCN): ν_{CO} 2043 (m), 2004 (s), and 1959 (vs) cm^{-1}. Absorption spectrum (MeCN): λ_{max} (ε_M) 272 (19,700), 360 (14,800), 415 (8810), 464 (5570), and 524 (5100) nm.

$(Et_4N)_3[VFe_6S_8(CO)_{12}]$ (**9**). To a solution of 2.90 mmol of $Li_2[Fe_2S_2(CO)_6]$ in 100 cm^3 of THF at −78°C was added a solution of 1.19 g (1.45 mmol) of $(Et_4N)_3[VFe_2S_4Cl_4]$ (**8**) in 250 cm^3 of acetonitrile. After the reaction mixture was warmed to room temperature over ~ 12 h, it was filtered to remove LiCl. The volume of the purple filtrate was reduced to ~ 80 cm^3. The solution was cooled to −20°C and filtered to remove additional LiCl. Addition of ether (~ 80 cm^3) to the filtrate caused the separation of 1.1 g (54%) of crude product as a purple-black microcrystalline solid. Recrystallization of this material from acetonitrile–ether [1 : 1 (v/v)] afforded 0.62 g of pure product as a black crystalline solid. Found: C, 31.3; H, 4.5; Fe, 24.8; N, 3.1; S, 18.5; V, 3.8. Calc. for $C_{36}H_{60}Fe_6N_3O_{12}S_8V$: C, 31.6; H, 4.4; Fe, 24.5; N, 3.1; S, 18.7; V, 3.7%. IR (MeCN): ν_{CO} 2035 (m), 1998 (s), and 1955 (vs) cm^{-1}. Absorption spectrum (MeCN): λ_{max} (ε_M) 316 (26,500), 416 (11,500), 526 (sh), and 560 (12,100) nm.

$(Et_4N)_4[Mo_2Fe_6S_8(S_2)_2(S\text{-}p\text{-}C_6H_4Cl)_6]$ (**10**). (i) *By oxidative decarbonylation of* **5**. A solution of 0.65 g (2.26 mmol) of bis(*p*-chlorophenyl)disulfide in 20 cm^3 of ether was added to a stirred solution of 1.00 g (1.13 mmol) of **5** in 100 cm^3 of acetonitrile. The reaction mixture gradually changed from a purple-brown to a yellow-brown color over a period of 1 day. The mixture was stirred at ambient temperature for 4 days, or at 50°C for 10 h, after which no bound CO was detectable (IR). Following reduction of the solvent volume to ~ 40 cm^3, the mixture was filtered to remove disulfide. THF (~ 50 cm^3) was added to the yellow-brown filtrate, the

solution was cooled at −20°C for ~ 4 h, and then filtered to give 0.80 g of crude product as a black microcrystalline solid. The product was separated from the more soluble salts of $[Fe_nS_n(S\text{-}p\text{-}C_6H_4Cl)_4]^{2-}$ ($n = 2$ or 4[14]) by thorough washing with acetone–acetonitrile [3:1 (v/v)]. This procedure afforded 0.48 g (37%) of pure product as a black microcrystalline solid. Found: C, 34.9; H, 4.4; Cl, 9.1; Fe, 15.0; Mo, 8.6; N, 2.4; S, 25.0. Calc. for $C_{66}H_{104}Cl_6Fe_6Mo_2N_4S_{18}$: C, 35.6; H, 4.6; Cl, 9.3; Fe, 14.6; Mo, 8.4; N, 2.4; S, 25.1%. Absorption spectrum (MeCN): λ_{max} (ε_M) 348 (sh), and 437 (30,600) nm. The *p*-bromobenzenethiolate derivative was prepared analogously with use of bis(*p*-bromophenyl)disulfide.

(ii) *Direct synthesis.* A slurry of 2.0 g (7.7 mmol) of $(NH_4)_2[MoS_4]$ in 50 cm^3 of methanol was added to 0.85 g (7.7 mmol) of Na_2S_2 to produce a bright red solution. This was treated with a mixture of NaOMe (5.4 mmol) and *p*-ClC_6H_4SNa (54 mmol) (from 59.4 mmol of NaOMe and 54.0 mmol of the thiol) in 300 cm^3 of methanol. A filtered solution of 3.7 g (23 mmol) of $FeCl_3$ in 100 cm^3 of methanol was added dropwise to the bright red reaction mixture over a period of 30 min. The resultant purple-brown reaction mixture was stirred for 16 h to afford an intense yellow-brown solution. Addition of 2.6 g (15 mmol) of Et_4NCl caused separation of a brown amorphous solid, which was collected by filtration. This material was extracted with 1 l of acetonitrile to effect separation from chloride salts, the extract was filtered, and the solvent was removed *in vacuo*. The solid residue was washed with 5 × 100 cm^3 of acetone, leaving 1.2 g of crude product as a brown amorphous solid. Recrystallization of this material from acetonitrile–THF afforded 1.0 g (11%) of pure product as a black microcrystalline solid. Found: C, 34.9; H, 4.4; Cl, 9.1; Fe, 15.0; Mo, 8.6; N, 2.4; S, 25.0%. The product was spectroscopically identical with that prepared by method (i). The *p*-bromobenzenethiolate derivative was prepared analogously with use of *p*-BrC_6H_4SNa.

Structure determination of $(Et_4N)_2[MoFe_3S_6(CO)_6]$

Collection and reduction of data. Single crystals of **5** were obtained by ether diffusion into a propionitrile solution. A crystal was mounted in glass capillary which was sealed under dinitrogen. Diffraction experiments were performed with a Nicolet R3M four-circle automated diffractometer equipped with a Mo X-ray tube and a graphite monochromator. Data collection parameters are summarized in Table 1. The final orientation matrix and unit-cell parameters were obtained from the least-squares refinement of 25 machine-centered reflections having $20° \leqslant 2\theta \leqslant 25°$. Selected omega scans were symmetrical and exhibited full widths at half-height of 0.37–0.45°. Three standard reflections examined after every 63 observations showed no signs of decay over the course of data collection. The data were corrected for Lorentz and polarization effects and an empirical absorption correction was applied with the programs XTAPE and XEMP of the SHELXTL structure determination package (Nicolet XRD Corporation, Madison, WI). The systematic absences $0k0$ ($k = 2n+1$), $h0l$ ($l = 2n+1$), and $hk0$ ($h+k = 2n+1$) uniquely define the space group as *Pbcn* (No. 60).

Solution and refinement of the structure. The structure was solved by a combination of direct methods (MULTAN) and Fourier techniques. Trial positions of the Mo and Fe atoms were taken from the E-map derived from the phase set with the highest combined figures of merit. The remaining non-hydrogen atoms were located in subsequent Fourier refinement cycles by using the program CRYSTALS. Atom-scattering factors were taken from a standard source.[22] Isotropic refinement converged at 20%. The asymmetric unit consists of two cations and one anion. Both cations displayed thermal parameters sufficiently large to indicate disorder, which was not successfully modeled. The anion and the cation nitrogen atoms were anisotropically refined by using blocked-cascade least-squares refinement. The cation carbon atoms were refined isotropically by using the method of additional observational equations.[23] Several carbonyl groups also have thermal parameters suggestive of disorder. In the final stages of refinement, hydrogen atoms were placed at a distance of 0.98 Å from bonded carbon atoms and assigned an isotropic thermal parameter of 0.05 $Å^2$. Unique data used in the refinement and final R values are given in Table 1. Tables of atom coordinates, thermal parameters, and structure factors have been deposited as supplementary data with the Editor, from whom copies are available on request.*

Other physical measurements

All measurements were performed under strictly anaerobic conditions. ^1H NMR spectra were recorded on a Brüker WM-300 spectrometer. CD_3CN was purified by distillation from CaH_2 and was stored over 3-Å molecular sieves. UV–visible and IR spectra were recorded on a Cary Model 219 and a Perkin–Elmer Model 599B spectrophotometer,

*Atomic coordinates have also been deposited with the Cambridge Crystallographic Data Centre.

Table 1. Summary of crystal data, intensity collection and structure refinement parameters for $(Et_4N)_2[MoFe_3S_6(CO)_6]$

Formula	$C_{22}H_{40}Fe_3MoN_2O_6S_6$
Molecular weight	884.43
a (Å)	15.314(7)
b (Å)	16.627(6)
c (Å)	29.971(13)
Crystal system	Orthorhombic
V (Å^3)	7631(5)
Z	8
d_{calc} (g cm^{-3})	1.64
Space group	*Pbcn*
Crystal dimensions (mm)	$0.12 \times 0.46 \times 0.70$
Radiation	Mo-K_{α_1} ($\lambda = 0.71069$)
Absorption coefficient (μ) (cm^{-1})	18.1
Transmission factors (max/min)	0.94/0.54
Scan speed (deg min^{-1})	2.00–29.3 (θ–2θ scan)
Scan range (°)	$1.25+(2\theta_{K\alpha_1}-2\theta_{K\alpha_2})$
Background/scan time ratio	0.25
Data collected	5–45° ($+h$, $+k$, $+l$)
Total reflections	5820
R_{merge}[a] (%)	2.8
Unique data [$F_o^2 > 3.0\sigma(F_o^2)$]	3220
Number of variables	282
R[b] (%)	8.3
R_w[c] (%)	9.5[d]

[a] R_{merge} is defined by:

$$R_{merge} = \left[\frac{\sum N_i \sum_{j=1}^{N_i} (\bar{F}_j - F_j)^2}{\sum (N_i - 1) \sum_{j=1}^{N_i} F_j^2} \right]^{1/2},$$

where N_i is the number of reflections in a given set, F_j is one member of the set, and $\bar{F}_j$ is the mean.

[b] $R = [\Sigma (|F_o| - |F_c|)/\Sigma |F_o|]$.

[c] $R_w = [\Sigma w(|F_o|^2 - |F_c|^2)/\Sigma w|F_o|^2]^{1/2}$.

[d] Weighting scheme for least-squares refinement: $w = 1/\sigma(F_o)$.

respectively. Solution magnetic moments were determined by the usual NMR method.[24] Electrochemical measurements were made with standard PAR instrumentation; other details are given in a figure legend.

RESULTS AND DISCUSSION

Synthesis and properties of derivatives of $[Fe_2S_2(CO)_6]^{2-}$

Reduction of persulfide-bridged $Fe_2S_2(CO)_6$ affords the highly reactive dianion $[Fe_2S_2(CO)_6]^{2-}$ [12] (**3**). Recent work has shown that the LUMOs of the isostructural compounds $Fe_2E_2(CO)_6$ (E = S[25] or Se[26]) are mainly E–E antibonding in character and that the Se—Se bond is broken upon reduction (EXAFS determination).[27] With its demonstrated ability to chelate a variety of main-group and transition-element halides to form species containing $MFe_2(\mu_3\text{-}S)_2$ and $MFe_4(\mu_3\text{-}S)_4$ cores,[12,13] **3** is a potentially useful precursor in cluster synthesis. The reactions of **3** carried out in this study are shown in Fig. 1. The clusters $[MFe_3S_6(CO)_6]^{2-}$ [M = Mo (**5**) or W (**7**)] were prepared according to reaction (1):

$$[Fe_2S_2(CO)_6]^{2-} + [MFeS_4Cl_2]^{2-} \rightarrow [MFe_3S_6(CO)_6]^{2-} + 2Cl^-, \quad (1)$$

which involves displacement of chloride from the tetrahedral Fe(II) centres of $[MFeS_4Cl_2]^{2-}$ [M = Mo (**4**) or W (**6**)]. These ligands had been shown earlier to be susceptible to substitution by

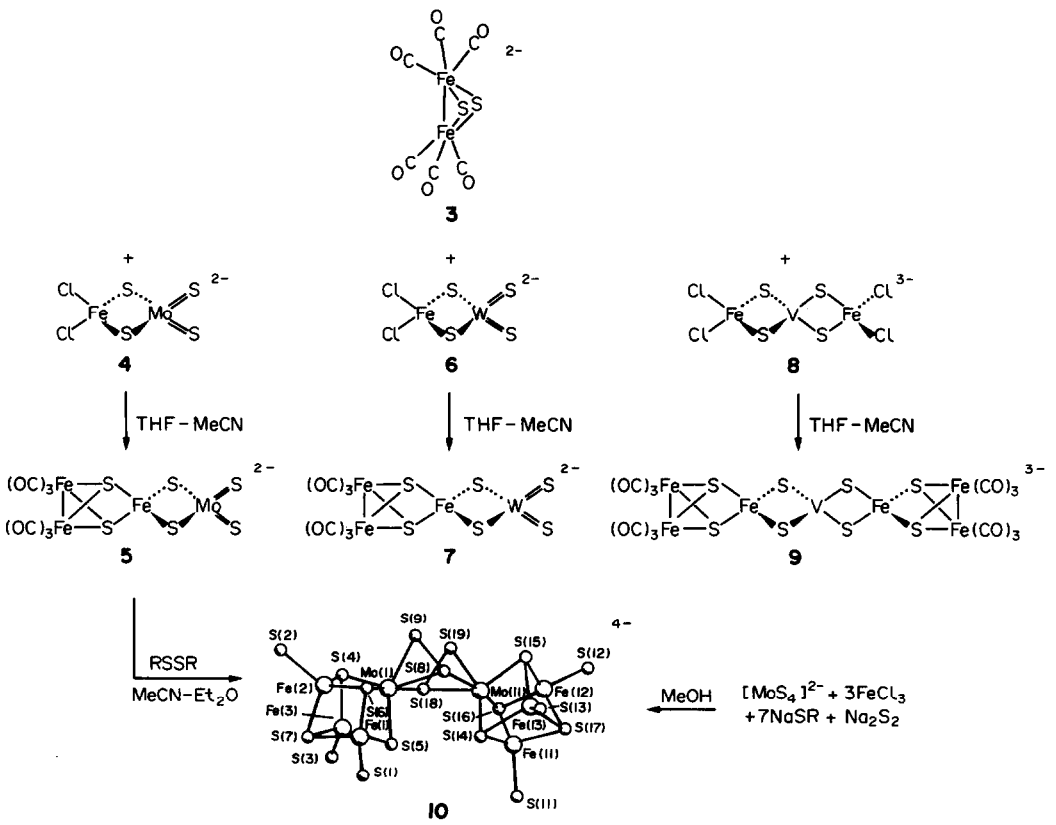

Fig. 1. Scheme showing the synthesis of clusters **5**, **7**, **9** and **10** from the common precursor $[Fe_2S_2(CO)_6]^{2-}$ (**3**) and their established (**5** and **10**) or probable (**7** and **9**) structures.

thiolate.[19] In the related reaction (2):

$$2[Fe_2S_2(CO)_6]^{2-} + [VFe_2S_4Cl_4]^{3-} \rightarrow [VFe_6S_8(CO)_{12}]^{3-} + 4Cl^- \quad (2)$$

the heptanuclear cluster $[VFe_6S_8(CO)_{12}]^{3-}$ (**9**) was derived from the "linear" precursor $[VFe_2S_4Cl_4]^{3-}$ (**8**), whose VFe_2S_4 core is nonlabile.[21] In contrast, the isoelectronic and isostructural clusters $[MFe_2S_4Cl_4]^{2-}$ (M = Mo or W) form an equilibrium mixture with **4**/**6** and $FeCl_2$ in DMF solution. Presumably because of core lability, all attempts to prepare $[MoFe_6S_8(CO)_{12}]^{2-}$ even in acetonitrile–THF solution yielded only **5**.

Clusters **5**, **7** and **9** are most simply recognized by their characteristic LMCT visible spectra, which are shown in Fig. 2. These are perturbed versions of the spectra of the parent $[MS_4]^{2-,3-}$ ions[21] and indicate retention of the M(VI or V) oxidation state. IR spectra in the carbonyl region are nearly identical for the three clusters. The three-band patterns are similar in intensity to that of $Fe_2S_2(CO)_6$ (ν_{CO} 2080, 2038 and 1998 cm^{-1}) but are shifted to lower frequencies by about 40 cm^{-1}, a consistent feature of metal derivatives containing the intact $Fe_2S_2(CO)_6$ group.[12,13,28-30] Diffraction quality crystals of only **5** were obtained. Cluster **7** was not analyzed inasmuch as its preparation, purification and IR spectrum were strictly analogous to those of **5**. The indicated structure of **9** is entirely probable and follows from its composition and IR spectrum, and the structure of **5**.

Structure of $[MoFe_3S_6(CO)_6]^{2-}$

The crystal structure of the Et_4N^+ salt of cluster **5** consists of well-separated anions and cations. The latter are unexceptional and are not further considered. Two perspectives of the structure of **5** are shown in Fig. 3. Selected interatomic distances and angles are collected in Table 2. In addition to $Fe_2S_2(CO)_6$[25] itself, there are other species whose structures are pertinent to a consideration of that of **5**. These formally contain the dianion **3** and include a variety of $Fe_2(\mu_2\text{-}SR)_2(CO)_6$ compounds with $Fe_2(SEt)_2(CO)_6$[31] prototypical, $Fe_2(\mu_2\text{-}SR)(\mu_2\text{-}SHgR)(CO)_6$[32] (R = Me or Et), $Ge[S_2Fe_2(CO)_6]_2$[33] (**11**), $[Fe_6S_6(CO)_{12}]^{2-}$[30] (**12**), and $[MoOFe_5S_6(CO)_{12}]^{2-}$[29] (**13**). The only other structurally characterized derivative of **3** is $[Fe_4S_4(CO)_{12}]^{2-}$, which contains two

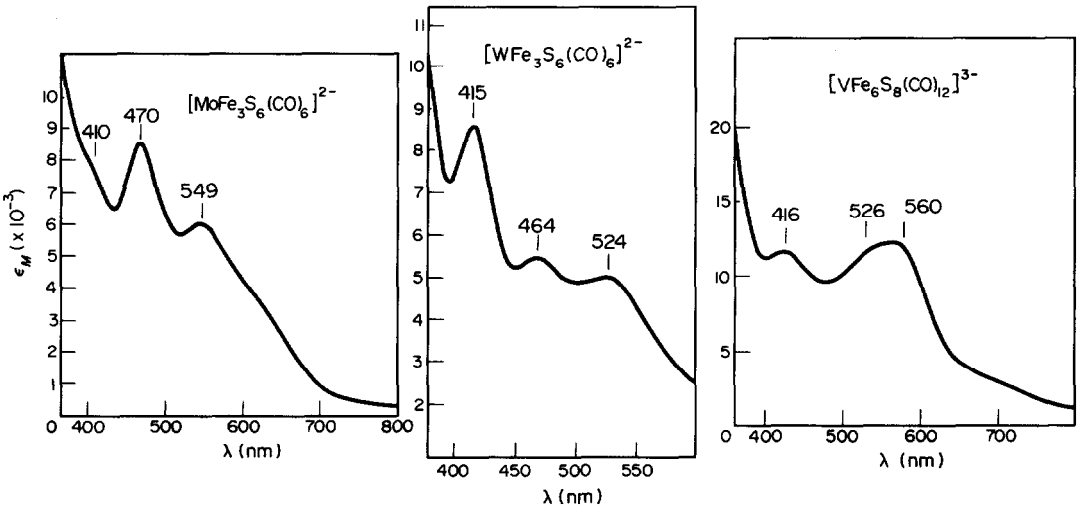

Fig. 2. Visible-absorption spectra of $[MoFe_3S_6(CO)_6]^{2-}$ (**5**), $[WFe_3S_6(CO)_6]^{2-}$ (**7**), and $[VFe_6S_8(CO)_{12}]^{3-}$ (**9**) in acetonitrile solutions.

$[Fe_2S_2(CO)_6]^{1-}$ groups joined by a disulfide bond.[34]

The configuration of cluster **5** approaches C_{2v}-symmetry, with the C_2-axis containing Mo and Fe(1), and is immediately recognizable as a combination of **3** and **4** (Fig. 1) with the anticipated chloride displacement. The $[MoFe_3(\mu_2\text{-}S)_2(\mu_3\text{-}S)_2]^{2+}$ core contains a roughly planar $Mo(\mu_2\text{-}S)_2Fe_3$ portion with atom displacements of ≤ 0.06 Å from

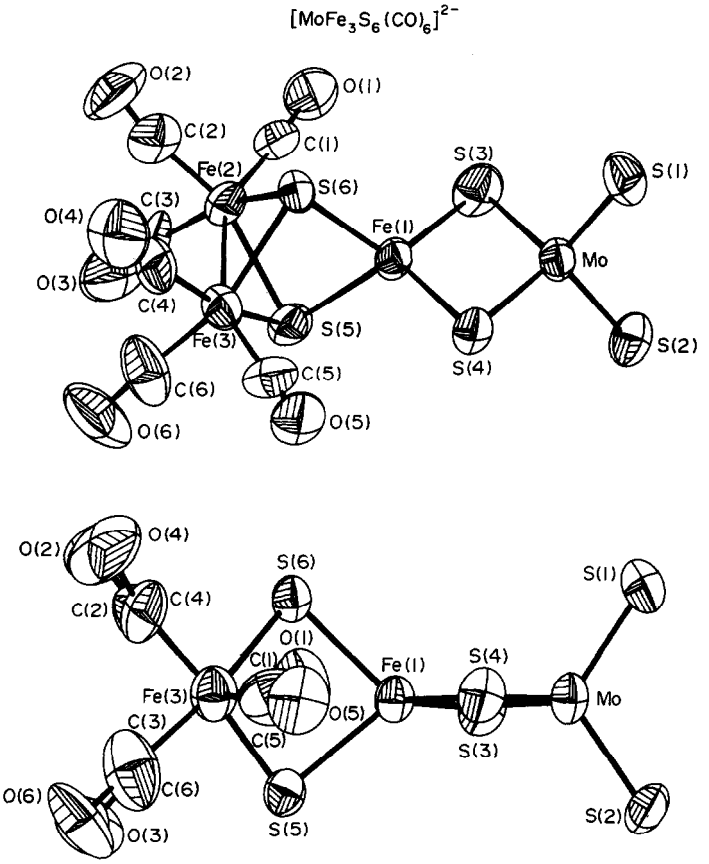

Fig. 3. Two views of the structure of $[MoFe_3S_6(CO)_6]^{2-}$ (**5**) showing 50% probability ellipsoids and the atom-labeling scheme. The views are related by a 45° rotation around the idealized C_2-axis.

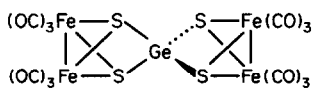

11

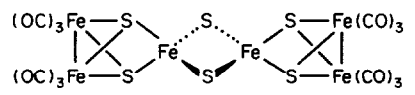

12

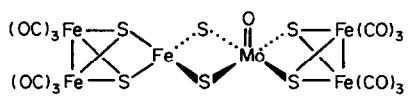

13

the MoS(3,4)Fe(1–3) plane.* The $Fe_3(\mu_3\text{-}S)_2$ fragment consists of two triply bridging atoms S(5,6) equidistant (± 1.55 Å) from the Fe_3 plane. In this sense, the fragment is similar to the $[Fe_3S_2]^{2+}$ core of $[Fe_3S_2(WS_4)_3]^{4-}$,[35] except that the Fe atoms form an isosceles rather than an equilateral triangle. The $S_2Fe(1)S_2MoS_2$ portion consists of two edge-shared irregular MoS_4 and FeS_4 tetrahedra. The dihedral angle MoS(1,2)/MoS(3,4) = 89.6° and Fe(1)S(3,4)/Fe(1)S(5,6) = 92.8°. Chelation of Fe(1) by atoms S(5,6) of subunit **3** is anticipated in **11**–**13**.

The Mo and Fe(1) atoms occupy sites which approach local C_{2v}-symmetry. The expanded terminal S(1)—Mo—S(2) [111.9(2)°] and compressed bridging S(3)—Mo—S(4) angles [104.7(2)°], and the shorter Mo—S terminal (mean 2.16 Å) than bridging distances (mean 2.262 Å), are typical of μ_2-η^2 binding to $[MoS_4]^{2-}$.[1] These effects are well exemplified by $[(PhS)_2FeS_2MoS_2]^{2-}$ [36] in which, for example, the terminal and bridging Mo—S bond lengths (S—Mo—S bond angles) are 2.149 Å [112.2(1)°] and 2.262 Å [105.5(1)°], respectively. As its NH_4^+ salt, $[MoS_4]^{2-}$ is nearly perfectly tetrahedral,[37] with mean bond distances and angles of 2.178(6) Å and 109.5(7)°. The coordination unit of the unique atom Fe(1) is severely distorted from a tetrahedral arrangement. Bond angles range from 85.6(2) to 119.2(1)°, with the lower limit being the chelate bite angle S(5)—Fe(1)—S(6), which corresponds to an S...S bite distance of 3.107(6) Å. This angle at Ge [86.4(2)° (**11**)] and Fe [86.8(1)° (**12**), and 84.1(5)° (**13**)] in other complexes is nearly the same. However, the bite angle of **3** is not constrained from lower values inasmuch as it is decreased to 70.8(3)° at Mo in **13**.[29]

Carbonyl-ligated atoms Fe(2,3) exhibit distorted square pyramidal coordination with basal planes C(2,3)S(5,6) and C(4,5)S(5,6), disposed at a dihedral angle of 66.8°. Atoms Fe(2) and Fe(3) are displaced 0.31 and 0.32 Å, respectively, from their basal planes toward apical carbonyl groups. Atom S(6) nearly symmetrically bridges Fe(1–3), the mean distance being 2.301(3) Å. Bridging by S(5) is less regular [mean 2.302(22) Å] and is the principal feature that degrades core symmetry below C_{2v}. The Fe—Fe distance of 2.491(4) Å is 0.06 Å shorter than that in $Fe_2S_2(CO)_6$, and reflects the consistent but not necessarily monotonic tendency of the metal–metal bond to decrease as the S···S bite is increased. This effect also appears with $Fe_2S_2(CO)_6$ and **3** in THF solution, where from EXAFS results the two Fe—Fe distances differ by 0.03 Å.[27] (With $[Fe_2Se_2(CO)_6]^{0,2-}$ in THF the Fe—Fe bond length increases by about 0.03 Å upon passing to the dianion.[27]) More information is required to establish any relationship between bite distance or Fe_2S dihedral angle and Fe—Fe bond length in derivatives of **3**. Given that the upper occupied MOs of **3** are mainly sulfur in character and the LUMO has a Fe–Fe antibonding component,[38] measurable differences in Fe—Fe and S···S distances in a more extensive series of compounds can be anticipated. These effects notwithstanding, it is evident that fragment **3** retains its essential geometrical and electronic features in the derivatives **5** and **11**–**13**. The structure of **5** is most consistent with the oxidation state assignment Mo(VI)+Fe(II)+2Fe(I) in the $[MoFe_3S_4]^{2+}$ core. The magnetic moment of $4.90\mu_B$ (acetonitrile, 297 K) is due to tetrahedral Fe(II) and is the same as the value for $[(PhS)_2FeS_2MoS_2]^{2-}$ in the solid state.[36]

Oxidative decarbonylation of $[MoFe_3S_6(CO)_6]^{2-}$

Reaction (3) effects the core oxidation $2[Fe_2S_2]^0 \rightarrow [Fe_4S_4]^{2+} + 2e^-$ and affords the product cluster with R = Ph in 65% isolated yield:[14]

$$2Fe_2S_2(CO)_6 + RSSR + 2RS^- \rightarrow [Fe_4S_4(SR)_4]^{2-} + 12CO. \quad (3)$$

Other than with the simpler metal carbonyls, oxidative decarbonylation reactions using disulfides have been little explored. The compositional identity of the $[MoFe_3S_4]^{2+}$ core of **5** and the $[MoFe_3S_4]^{3+}$ cores of **1**, **2** and other cubane-type clusters[1] suggested the core oxidation $[MoFe_3S_4]^{2+} \rightarrow [MoFe_3S_4]^{3+} + e^-$ with structural

* All planes are unweighted least-squares planes.

Table 2. Selected interatomic distances (Å) and angles (°) for $[MoFe_3S_6(CO)_6]^{2-}$

Mo(1)—S(1)	2.142(6)	Fe(1)—S(3)	2.267(6)
Mo(1)—S(2)	2.170(6)	Fe(1)—S(4)	2.256(5)
Mo(1)—S(3)	2.260(5)	Fe(1)—S(5)	2.277(6)
Mo(1)—S(4)	2.265(5)	Fe(1)—S(6)	2.298(6)
Mo(1)···Fe(1)	2.762(5)	Fe(1)···Fe(2)	3.088(6)
		Fe(1)···Fe(3)	3.126(6)
Fe(2)—S(6)	2.303(6)		
Fe(2)—S(5)	2.318(6)	Fe(2)—C(1)	1.752(20)
Fe(3)—S(5)	2.312(7)	Fe(2)—C(2)	1.802(25)
Fe(3)—S(6)	2.301(6)	Fe(2)—C(3)	1.757(25)
		Fe(3)—C(4)	1.755(24)
Fe(2)—Fe(3)	2.491(4)	Fe(3)—C(5)	1.793(28)
		Fe(3)—C(6)	1.801(21)
C(1)—O(1)	1.180(23)	Mean	1.777(24)
C(2)—O(1)	1.156(26)		
C(3)—O(3)	1.186(27)		
C(4)—O(4)	1.158(27)	S(5)···S(6)	3.107(6)[a]
C(5)—O(5)	1.165(30)		
C(6)—O(6)	1.134(22)		
Mean	1.163(19)		
		S(3)—Fe(1)—S(4)	104.8(2)
		S(5)—Fe(1)—S(6)	85.6(2)[b]
S(1)—Mo(1)—S(2)	111.9(2)	S(3)—Fe(1)—S(6)	119.2(2)
S(3)—Mo(1)—S(4)	104.7(2)	S(3)—Fe(1)—S(5)	116.7(2)
S(1)—Mo(1)—S(4)	110.2(3)	S(4)—Fe(1)—S(5)	117.4(2)
S(1)—Mo(1)—S(3)	110.0(3)	S(4)—Fe(1)—S(6)	113.2(2)
S(2)—Mo(1)—S(3)	110.3(2)		
S(2)—Mo(1)—S(4)	109.4(2)		
		Fe(1)—S(5)—Fe(3)	85.9(2)
Mo(1)—S(3)—Fe(1)	75.2(2)	Fe(1)—S(6)—Fe(2)	84.3(2)
Mo(1)—S(4)—Fe(1)	75.3(2)	Fe(1)—S(5)—Fe(2)	84.4(2)
		Fe(1)—S(6)—Fe(3)	85.7(2)
S(5)—Fe(3)—Fe(2)	57.6(2)	S(6)—Fe(2)—Fe(3)	57.2(2)
S(5)—Fe(3)—C(4)	159.0(9)	S(6)—Fe(2)—C(3)	158.8(9)
S(5)—Fe(3)—C(6)	102.3(8)	S(6)—Fe(2)—C(1)	102.6(8)
S(5)—Fe(3)—C(5)	88.0(9)	S(6)—Fe(2)—C(2)	87.1(7)
S(6)—Fe(3)—Fe(2)	57.3(2)	S(5)—Fe(2)—Fe(3)	57.3(2)
S(6)—Fe(3)—C(4)	87.2(8)	S(5)—Fe(2)—C(3)	87.4(8)
S(6)—Fe(3)—C(6)	104.9(8)	S(5)—Fe(2)—C(1)	104.6(7)
S(6)—Fe(3)—C(5)	155.5(9)	S(5)—Fe(2)—C(2)	154.1(7)
C(4)—Fe(3)—C(6)	98.5(1)	C(3)—Fe(2)—C(1)	98.4(11)
C(4)—Fe(3)—C(5)	91.4(12)	C(3)—Fe(2)—C(2)	91.7(9)
C(5)—Fe(3)—C(6)	99.4(12)	C(2)—Fe(2)—C(1)	101.1(10)
Fe(3)—C(4)—O(4)	173.4(24)	Fe(2)—C(3)—O(3)	175.0(21)
Fe(3)—C(5)—O(5)	177.0(20)	Fe(2)—C(2)—O(2)	173.6(22)
Fe(3)—C(6)—O(6)	177.9(30)	Fe(2)—C(1)—O(1)	176.1(22)

[a] $[Fe_2(\mu_2\text{-}S)_2(CO)_6]^{2-}$ chelate "bite" distance.
[b] $[Fe_2(\mu_2\text{-}S)_2(CO)_6]^{2-}$ chelate "bite" angle.

rearrangement, and probable conversion of terminal sulfide to an oxidized form. After some experimentation, reaction (4) was developed by using excess disulfide (R = *p*-C_6H_4Cl or *p*-C_6H_4Br*):

$$2[MoFe_3S_6(CO)_6]^{2-} + 3RSSR \rightarrow [Mo_2Fe_6S_8(S_2)_2(SR)_6]^{4-} + 12CO. \quad (4)$$

Products were obtained in ~ 40% yields as Et_4N^+ salts. Structure **10** (R = *p*-C_6H_4Br) was established by X-ray analysis and has been described.[15] Relatively poor crystal quality led to insufficient data for precise structural determination of these crystals, which have two formula units per asymmetric unit. However, the configuration of the anion was established as the double cubane **10** whose subclusters are joined by two μ_2-η^3 persulfide bridges in bridge unit **14**. Subcluster dimensions are unexceptional.[1] In **14** nonbridging sulfur atoms are in a *syn* arrangement; their MoS_2 groups are roughly parallel (dihedral angle 17°). The bridge is folded such that the two $Mo(\mu_2\text{-}S)_2$ groups are disposed at a dihedral angle of 22°. Mean values (Å) of certain bond lengths are indicated; the Mo···Mo distance of

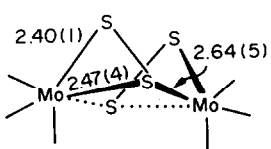

14

3.97(7) Å is nonbonding. The μ_2-η^3 mode of persulfide bridging has been less frequently encountered than other arrangements.[39] Three prior examples are known.[40] Of these, the most relevant is $(Me_5C_5)_2Mo_2(\mu_2\text{-}S_2)_3(S_2)_2$,[40(d)] whose corresponding bridge fragment has dimensions within 0.03 Å of those of **14**. In this molecule the bridge structure also includes a μ_2-η^2-S_2^{2-} group. Cluster **10** provides the only case of an $Mo_2(\mu_2\text{-}\eta^3\text{-}S_2^{2-})_2$ bridge unit.

Attempted oxidative decarbonylation of $[WFe_3S_6(CO)_6]^{2-}$ (**7**) did not proceed analogously to reaction (4). $[(RS)_2FeS_2WS_2]^{2-}$ [36] and $[Fe_4S_4(SR)_4]^{2-}$ were the only identifiable products, suggesting that the usual reducibility order W(VI) < Mo(VI) applies to **5** and **7**. A similar reaction of $[VFe_6S_8(CO)_{12}]^{3-}$ (**9**) afforded mainly $[Fe_nS_n(SR)_4]^{2-}$ (n = 2 or 4) detected by ^{1}H NMR together with a lesser amount of unknown products (δ 4.8, 5.2, 15.2 and 17.3). No VFe_3S_4 cubane cluster was detected, but it is available by another route[16] (*vide infra*).

Direct synthesis and properties of $[Mo_2Fe_6S_8(SR)_6(S_2)_2]^{4-}$

The establishment of the structure of **10** raised the possibility of a direct synthesis of the cluster, i.e. a procedure not requiring isolation of an intermediate. Cluster assembly reaction (5) in methanol conducted with the indicated stoichiometry gave the desired cluster in 11% purified yield:

$$2[MoS_4]^{2-} + 6FeCl_3 + 14RS^- + 2S_2^{2-} \rightarrow [Mo_2Fe_6S_8(S_2)_2(SR)_6]^{4-} + 18Cl^- + 4RSSR. \quad (5)$$

Thus, as all other cubane-type $MoFe_3S_4$ clusters,[1-5] **10** can be prepared from simple reactants in a redox-buffered system that produces the $[MoFe_3S_4]^{3+}$ core oxidation level. The low-yield is offset by the use of inexpensive, readily accessible reagents.

In solution, **10** displays an intense absorption band at 437 nm, in the region typical of thiolate-ligand clusters.[2-7] Retention of the solid-state structure in solution is adequately shown by the electrochemical and NMR results in Fig. 4. The coupled one-electron reductions at $E_{1/2}$ = −1.14 and −1.34 V are entirely typical of double cubanes such as **1** and those with $Mo_2(\mu_2\text{-}OR)_3$ bridges.[3-5] Potential separations of about 200 mV are a common feature of clusters with Mo···Mo distances of 3.2–3.8 Å. This feature extends to **10**, whose Mo···Mo is ~ 0.2 Å longer than the previous upper limit. All other cubane-type $MoFe_3S_4$ clusters have either trigonal (e.g. **1** and **2**) or mirror symmetry,[1] properties clearly reflected in their isotropically shifted NMR spectra. While **10** has overall C_{2v}-symmetry, its subclusters lack symmetry owing to the unsymmetrical nature of the bridge **14**. The occurrence of three *m*-H signals is consistent with retention of this bridge structure in solution.

The presence of persulfide and the unsymmetrical nature of the bridge **14** with the long Mo—S bond of 2.64(5) Å suggest possible ligand-induced cleavage with or without persulfide reduction to single cubanes having $MoL(SH)_2$ or $MoL(\eta^2\text{-}S_2)$ coordination. The former group might also afford a sulfido-bridged double cubane. Reduction of coordinated persulfide by thiol or thiolate is documented.[41] Unfortunately, we have thus far been unable to effect regiospecific bridge reactions. Thiols (*p*-ClC_6H_4SH, PhSH and EtSH), $NaBH_4$

* These substituents afforded disulfides of sufficient oxidizing power and by-product clusters $[Fe_nS_n(SR)_4]^{2-}$ (n = 2 or 4) whose salts were separable from **10**. With R = Ph reaction (4) was much slower, and with R = *p*-$C_6H_4NO_2$ the reaction was nearly complete in 10 h at ambient temperature, but by-product clusters were not readily separable.

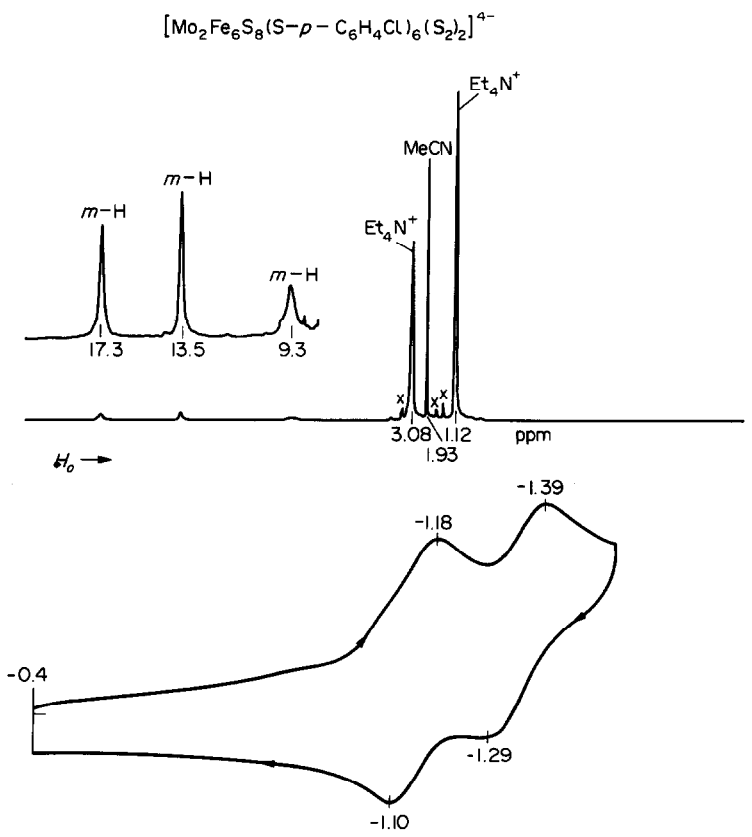

Fig. 4. Upper: ^{1}H NMR spectrum (300 MHz) of $[Mo_2Fe_6S_8(S_2)_2(S\text{-}p\text{-}C_6H_4Cl)_6]^{4-}$ (**10**) in CD_3CN solution at 298 K. Lower: cyclic voltammogram of **10** in acetonitrile solution (0.1 *M* *n*-Bu_4NCl supporting electrolyte, 100 mV s^{-1}, glassy carbon working electrode). Peak potentials vs SCE are given.

and $LiEt_3BH$ proved unreactive, while butane-1,4-dithiol, Et_3P, Et_2PPh and CN^- gave complex mixtures of products usually including $[Fe_4S_4(SR)_4]^{2-}$. Experiments directed toward the attainment of clusters with the above coordination groups are continuing.

Core conversion reactions

If the core composition of **5** is taken to include the terminal sulfides, the overall redox change of oxidative decarbonylation reaction (4) is given by reaction (6):

$$[MoFe_3(\mu_2\text{-}S)_2(\mu_3\text{-}S)_2S_2]^{2-} \rightarrow [MoFe_3(\mu_3\text{-}S)_4(S_2)]^{1+} + 3e^- \quad (6)$$

The product core contains $[MoFe_3S_4]^{3+}$* whose oxidation state descriptions as deduced from structural features and ^{57}Fe isomer shifts of isoelectronic delocalized clusters,[1,3,10] is Mo(III)+3$Fe^{2.67+}$. Reaction (6) involves, in effect, a one-electron oxidation of $[MoFe_3S_4]^{2+}$ with concomitant electron redistribution, and the ligand-based oxidation $2S^{2-} \rightarrow S_2^{2-} + 2e^-$. Given an adequate oxidant, reaction (4) succeeds in part because of two interdependent effects: (i) the Fe atoms become sufficiently oxidized to have no affinity for CO and are therefore free to bind thiolate and adopt the stable tetrahedral $FeS_3(SR)$ coordination of cubane clusters;[1] and (ii) internal electron redistribution affords an oxidation state at or near Mo(III), which concertedly drives the structural rearrangement to a stabilized, six-coordinate Mo site. These effects justify description of reaction (6) as an *oxidatively induced core internal conversion.*[15] It is similar to,

*This and following considerations continue the description of (S_2) as persulfide. Given the formation without exception of the 3+ core in synthesis[1] and the numerous cases of authenticated persulfide binding by Mo(III–VI),[39,40(b)(d),42,43] this description is well-founded. However, the X-ray analysis of **10** yields an S—S distance of 2.0(2) Å, which is insufficiently precise to distinguish between coordinated S_2 (1.89 Å[44]) and S_2^{2-} (2.13 Å[45]), whose bond lengths when uncoordinated are indicated.

but not strictly a member of, a small but growing set of reactions in which an external *oxidant* leads to internal *reduction* of a metal center.[43,46-50] Reactions (7)[43] and (8)[50]:

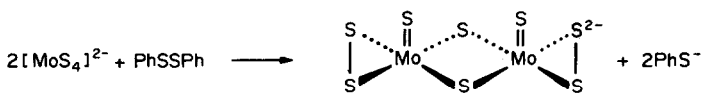

15 (7)

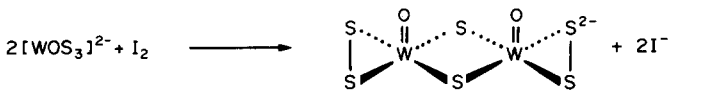

16 (8)

are clear examples, yielding M(V) products **15** and **16**, respectively, with sulfide and persulfide ligands, and no loss of sulfur atoms. These reactions have been termed (without mechanistic implication) *induced internal electron transfers*.[43,46] Reaction (4) differs from them by reason of a net oxidation of the metal atom set. The two reaction types, however, share the characteristics of ligand oxidation, metal atom (partial) reduction, and reduction of the external oxidant, whose reduced form functions as a ligand in reaction (4).

Reduction (or oxidation) of a metal atom to an oxidation state stabilized by a different stereochemistry in product than reactant is a common occurrence. However, in the form of the generalized core component reaction $M_3S_4 + M \rightarrow M_4(\mu_3\text{-}S)_4$, it is an exceptional means of closing metal cluster polyhedra. Indeed, there appear to be only two instances of this type of reaction. One of these, described in (ii) above, is made explicit in reaction (6). The other is reaction (9):[16,51]

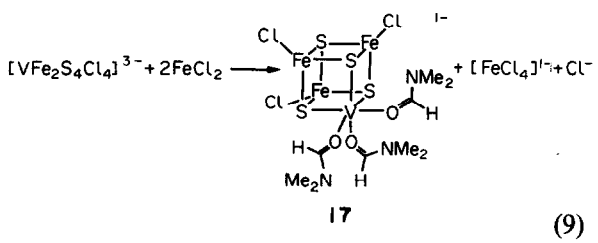

17 (9)

Here linear cluster 8[21] undergoes the core conversion $[VFe_2S_4]^{1+} + e^- + Fe^{2+} \rightarrow [VFe_3S_4]^{2+}$ with incorporation of Fe^{2+}, electron redistribution, and *reduction* of V(V) to or near the V(III) level,[51,52] which is stabilized by six-coordination. Presumably, reduction precedes capture of Fe^{2+}. Note that $[MoFe_3S_4]^{3+}$ and the core of product **17** are isoelectronic and are similarly delocalized.[51] In reactions (4) and (9) closure to the cubane core is strongly driven by the instability of the reduced heterometal in its original tetrahedral site. The same point likely applies to reaction (5) and other direct synthesis of $MoFe_3S_4$ clusters, all of which utilize $[MoS_4]^{2-}$. However, the intermediate(s) immediately prior to cubane formation have not been identified. This concept of cluster closure may be applicable in other systems. The scope of reactions analogous to (9) with other reductants and metal sources remains to be established. Lastly, the preparations of **5**, **7**, **9**, **10**, **12**[30] and **13**[29] illustrate the utility of the Seyferth anion **3** as a precursor in cluster synthesis.

Acknowledgement—This research has been supported by National Science Foundation Grants CHE 81-06017 and CHE 85-21365.

REFERENCES

1. R. H. Holm and E. D. Simhon, In *Molybdenum Enzymes* (Edited by T. G. Spiro), Chap. 1. Wiley Interscience, New York (1985).
2. T. E. Wolff, J. M. Berg, K. O. Hodgson, R. B. Frankel and R. H. Holm, *J. Am. Chem. Soc.* 1979, **101**, 4140.
3. G. Christou, P. K. Mascharak, W. H. Armstrong, G. C. Papaefthymiou, R. B. Frankel and R. H. Holm, *J. Am. Chem. Soc.* 1982, **104**, 2820.
4. G. Christou and C. D. Garner, *J. Chem. Soc., Dalton Trans.* 1980, 2354.
5. T. E. Wolff, P. P. Power, R. B. Frankel and R. H. Holm, *J. Am. Chem. Soc.* 1980, **102**, 4694.
6. W. H. Armstrong, P. K. Mascharak and R. H. Holm, *J. Am. Chem. Soc.* 1982, **104**, 4373.
7. P. K. Mascharak, W. H. Armstrong, Y. Mizobe and R. H. Holm, *J. Am. Chem. Soc.* 1983, **105**, 475.
8. R. E. Palermo, R. Singh, J. K. Bashkin and R. H. Holm, *J. Am. Chem. Soc.* 1984, **106**, 2600.
9. Y.-P. Zhang, J. K. Bashkin and R. H. Holm, *Inorg. Chem.* 1987, **26**, 694.
10. P. K. Mascharak, G. C. Papaefthymiou, W. H. Armstrong, S. Foner, R. B. Frankel and R. H. Holm, *Inorg. Chem.* 1983, **22**, 2851.
11. (a) S. D. Conradson, B. K. Burgess, W. E. Newton, K. O. Hodgson, J. W. McDonald, J. F. Rubinson, S. F. Gheller, L. E. Mortenson, M. W. W. Adams, P. K. Mascharak, W. H. Armstrong and R. H. Holm,

J. Am. Chem. Soc. 1985, **107**, 7935; (b) A. M. Flank, M. Weininger, L. E. Mortenson and S. P. Cramer, *J. Am. Chem. Soc.* 1986, **108**, 1049.
12. D. Seyferth, R. S. Henderson and L.-C. Song, *J. Organomet. Chem.* 1980, **192**, Cl; *Organometallics* 1982, **1**, 125.
13. D. Seyferth, R. S. Henderson and M. K. Gallagher, *J. Organomet. Chem.* 1980, **193**, C75.
14. J. J. Mayerle, S. E. Denmark, B. V. DePamphilis, J. A. Ibers and R. H. Holm, *J. Am. Chem. Soc.* 1975, **97**, 1032.
15. J. A. Kovacs, J. K. Bashkin and R. H. Holm, *J. Am. Chem. Soc.* 1985, **107**, 1784.
16. J. A. Kovacs and R. H. Holm, *J. Am. Chem. Soc.* 1986, **108**, 340.
17. F. Feher and H. J. Berthold, *Z. Anorg. Allg. Chem.* 1953, **273**, 144.
18. J. W. McDonald, G. D. Friesen, L. D. Rosenhein and W. E. Newton, *Inorg. Chim. Acta* 1983, **72**, 205.
19. R. H. Tieckelmann, H. C. Silvis, T. A. Kent, B. H. Huynh, J. V. Waszczak, B.-K. Teo and B. A. Averill, *J. Am. Chem. Soc.* 1980, **102**, 5550.
20. (a) A. Müller, R. Jostes, H.-G. Tölle, A. Trautwein and E. Bill, *Inorg. Chim. Acta* 1980, **46**, L21; (b) D. Coucouvanis, E. D. Simhon, P. Stremple, M. Ryan, D. Swenson, N. C. Baenziger, A. Simopoulos, V. Papaefthymiou, A. Kostikas and V. Petrouleas, *Inorg. Chem.* 1984, **23**, 741.
21. Y. Do, E. D. Simhon and R. H. Holm, *J. Am. Chem. Soc.* 1983, **105**, 6731; *Inorg. Chem.* 1985, **24**, 4635.
22. D. T. Cromer and J. T. Waber, *International Tables for X-ray Crystallography*; Vol. 4. Kynoch Press, Birmingham, U.K. (1974).
23. J. Waser, *Acta Cryst.* 1963, **16**, 1091.
24. D. H. Live and S. I. Chan, *Anal. Chem.* 1970, **42**, 79.
25. C.-H. Wei and L. F. Dahl, *Inorg. Chem.* 1965, **4**, 1.
26. C. F. Campana, F. Y.-K. Lo and L. F. Dahl, *Inorg. Chem.* 1979, **18**, 3060.
27. T. D. Weatherill, T. B. Rauchfuss and R. A. Scott, *Inorg. Chem.* 1986, **25**, 1466.
28. V. W. Day, D. A. Lesch and T. B. Rauchfuss, *J. Am. Chem. Soc.* 1982, **104**, 1290.
29. K. S. Bose, P. E. Lamberty, J. E. Kovacs, E. Sinn and B. A. Averill, *Polyhedron* 1986, **5**, 393.
30. G. L. Lilley, E. Sinn and B. A. Averill, *Inorg. Chem.* 1986, **25**, 1075.
31. L. F. Dahl and C.-H. Wei, *Inorg. Chem.* 1963, **2**, 328.
32. C. Chieh, D. Seyferth and L.-C. Song, *Organometallics* 1982, **1**, 473.
33. N. S. Nametkin, V. D. Tyurin, G. G. Aleksandrov, O. V. Kuz'min, A. I. Nekhaev, V. G. Andrianov, M. Mavlonov and Yu. T. Struchkov, *Bull. Acad. Sci. U.S.S.R., Div. Chem. Sci.* 1979, **28**, 1266.
34. K. S. Bose, E. Sinn and B. A. Averill, *Organometallics* 1984, **3**, 1126.
35. A. Müller, W. Hellmann, H. Bögge, R. Jostes, M. Römer and U. Schimanski, *Angew. Chem., Int. Ed. Engl.* 1982, **21**, 860.
36. D. Coucouvanis, P. Stremple, E. D. Simhon, D. Swenson, N. C. Baenziger, M. Draganjac, L. T. Chan, A. Simopoulos, V. Papaefthymiou, A. Kostikas and V. Petrouleas, *Inorg. Chem.* 1983, **22**, 293.
37. J. Lapasset, N. Chezeau and P. Belougne, *Acta Cryst.* 1976, **B32**, 3087.
38. R. L. DeKock, E. J. Baerends and R. Hengelmohlen, *Organometallics* 1984, **3**, 289.
39. A. Müller, W. Jaegermann and J. H. Enemark, *Coord. Chem. Rev.* 1982, **46**, 245.
40. (a) $(MeCp)_2Fe_2(S_2)CO$: C. Giannotti, A. M. Ducourant, H. Chanaud, A. Chiaroni and C. Riche, *J. Organomet. Chem.* 1977, **140**, 289; (b) $[Mo_4(NO)_4(S_2)_5S_3]^{4-}$: A. Müller, W. Eltzner and N. Mohan, *Angew. Chem., Int. Ed. Engl.* 1979, **18**, 158; (c) $[W_2S_8OH_3]^{1-}$: F. Sécheresse, J. Lefebvre, J. C. Daran and Y. Jeannin, *Inorg. Chim. Acta* 1981, **54**, L175; (d) $(Me_5C_5)_2Mo_2S_{10}$: M. Rakowski DuBois, D. L. DuBois, M. C. Van DerVeer and R. C. Haltiwanger, *Inorg. Chem.* 1981, **20**, 3064.
41. (a) D. Leonard, K. Plute, R. C. Haltiwanger and M. Rakowski DuBois, *Inorg. Chem.* 1979, **18**, 3246; (b) E. I. Stiefel, In *Fourth International Conference on the Chemistry and Uses of Molybdenum* (Edited by H. F. Barry and P. C. H. Mitchell), pp. 56–66. Climax Molybdenum Co., Ann Arbor, MI (1982); (c) T. R. Halbert, K. McGauley, W.-H. Pan, R. S. Czernuszewicz and E. I. Stiefel, *J. Am. Chem. Soc.* 1984, **106**, 1849.
42. A. Müller, *Polyhedron* 1986, **5**, 323.
43. W.-H. Pan, M. A. Harmer, T. R. Halbert and E. I. Stiefel, *J. Am. Chem. Soc.* 1984, **106**, 459.
44. B. Meyer, *Chem. Rev.* 1976, **76**, 367.
45. H. Föppl, E. Busmann and F.-K. Frorath, *Z. Anorg. Allg. Chem.* 1962, **314**, 12.
46. M. A. Harmer, T. R. Halbert, W.-H. Pan, C. L. Coyle, S. A. Cohen and E. I. Stiefel, *Polyhedron* 1986, **5**, 341.
47. E. D. Simhon, N. C. Baenziger, M. Kanatzidis, M. Draganjac and D. Coucouvanis, *J. Am. Chem. Soc.* 1981, **103**, 1218.
48. M. Draganjac, E. Simhon, L. T. Chan, M. Kanatzidis, N. C. Baenziger and D. Coucouvanis, *Inorg. Chem.* 1982, **21**, 3321.
49. S. A. Cohen and E. I. Stiefel, *Inorg. Chem.* 1985, **24**, 4657.
50. S. Sarkar and M. A. Ansari, *J. Chem. Soc., Chem. Commun.* 1986, 324.
51. J. A. Kovacs and R. H. Holm, *Inorg. Chem.* 1987, **26**, 702, 711.
52. M. J. Carney, J. A. Kovacs, Y.-P. Zhang, G. C. Papaefthymiou, R. B. Frankel and R. H. Holm, *Inorg. Chem.* 1987, **26**, 719.

Polyhedron Vol. 6, No. 6, pp. 1457–1461, 1987
Printed in Great Britain

0277–5387/87 $3.00+.00
Pergamon Journals Ltd

NICKEL COMPLEXES OF *N,N,N',N'*-TETRAKIS-(2-BENZIMIDAZOLYLMETHYL)-1,2-DIAMINOETHANE (L) AND THE X-RAY CRYSTAL STRUCTURE OF $\{[NiL]^{2+}[NiCl_2(H_2O)_3(C_2H_5OH)]\}2Cl^-(C_2H_5OH)$

STEPHEN D. HOLT and BRIAN PIGGOTT*

Inorganic Chemistry Research Laboratory, School of Natural Sciences,
The Hatfield Polytechnic, Hatfield AL10 9AB, U.K.

and

MICHAEL B. HURSTHOUSE* and RICHARD L. SHORT

Chemistry Department, Queen Mary College, Mile End Road, London E1 4NS, U.K.

(*Received* 10 *December* 1986; *accepted* 12 *January* 1987)

Abstract—The preparation and properties of Ni(II) complexes of the title ligand (L) are described and the X-ray crystal structure of $Ni_2LCl_4(H_2O)_3(C_2H_5OH)_2$ is reported. The crystal structure shows that the two nickel ions are not bridged but exist as two distinct distorted octahedral species. Six coordination about one nickel ion is produced exclusively by L to give the cationic species $[NiL]^{2+}$. The second nickel ion achieves six coordination through an interesting combination of ligands to produce the novel complex $[NiCl_2(H_2O)_3(C_2H_5OH)]$. Since the two remaining chloride ions are hydrogen bonded to two of the water molecules and the ethanol molecule of $[NiCl_2(H_2O)_3(C_2H_5OH)]$ the entire complex can be considered to be formed by the cocrystallization of the large cation $[NiL]^{2+}$ by the "large anion" $\{[NiCl_2(H_2O)_3(C_2H_5OH)]Cl_2\}^{2-}$.

The ligand *N,N,N',N'*-tetrakis-(2-benzimidazolylmethyl)-1,2-diaminoethane (L) reacts with $Cu(H_2O)_6(BF_4)_2$ to give a six-coordinate $[CuL]^{2+}$ ion of unusual geometry.[1] Reaction with an excess of $Cu(NO_3)_2(H_2O)_3$ has given a ligand- and nitrate-bridged dimer $[Cu_2L(NO_3)_3]^+$,[2] whilst $CuClO_4$ gives the Cu(I) dimer $[Cu_2L]^{2+}$.[2] L is also known to react with $Mo(CO)_6$ to give the ligand-bridged dimer $Mo_2(CO)_6L$.[3] We are particularly interested in dimeric nickel complexes, in which the metal atoms are within approximately 6 Å of each other, as potential models for our EXAFS studies of the enzyme urease.[4] In view of this it was decided to investigate the coordination chemistry of L with a series of Ni(II) salts in the hope of generating suitable EXAFS models.

* Authors to whom correspondence should be addressed.

EXPERIMENTAL

L was synthesized as described previously and characterized using NMR and mass spectroscopy.[5] $NiL(ClO_4)_2 \cdot 2H_2O$, $NiL(NO_3)_2$, $NiLCl_2 \cdot 2H_2O$, $NiLBr_2 \cdot 2(C_2H_5OH)$ and $NiL(SCN)_2$ were all prepared by the same general method, viz. the appropriate metal salt was dissolved in hot ethanol and this was added slowly to a hot ethanolic solution of ligand. The crystalline product which formed rapidly was filtered off, and dried *in vacuo*. A metal : ligand ratio of 2 : 1 was used for these preparations.

$Ni_2LCl_4 \cdot 6H_2O$

$NiCl_2 \cdot 6H_2O$ (0.59 g) was dissolved in the minimum volume of hot ethanol and then diluted with acetone (30 cm^3). To this was added dropwise a

solution of L (0.73 g) in acetone (30 cm^3). A pale blue product formed which could not be recrystallized from acetone. This was filtered off and dried *in vacuo*.

$Ni_2LCl_4(H_2O)_3(C_2H_5OH)_2$

To a stirred hot mixture of $NiCl_2 \cdot 6H_2O$ (0.59 g) and nitromethane (30 cm^3) was added sufficient ethanol to give a clear solution. To this was added dropwise a solution of L (0.73 g) in nitromethane (30 cm^3). The resulting dark green solution was heated and stirred for a few minutes, when a pale blue product formed. On cooling the blue product redissolved, and on standing for 2 weeks the solution gave brown microcrystals in low yield. The crystals used in the X-ray study were obtained by successive filtrations of a crystallizing solution until large single crystals formed.

$Ni_2LBr_4 \cdot 2H_2O \cdot C_2H_5OH$

$NiBr_2 \cdot 3H_2O$ (0.45 g) was dissolved in the minimum volume of hot ethanol, and the solution diluted with 30 cm^3 of acetone. To this was added dropwise a solution of L (0.47 g) in acetone (30 cm^3). A purple product formed which turned blue-grey on filtering and vacuum drying at 70°C.

$Ni_2LBr_4 \cdot 3H_2O$

$NiBr_2 \cdot 3H_2O$ (0.45 g) was dissolved in the minimum volume of hot ethanol and then diluted with hot nitromethane (30 cm^3). To this was added dropwise a hot solution of L (0.47 g) in nitromethane (30 cm^3). A blue product formed which was filtered off and air dried, which caused a colour change to grey on the surface and green in the bulk of the material. The green product was separated and dried at 70°C *in vacuo*.

$Ni_2L(SCN)_4$

$Ni(SCN)_2$ was prepared from KSCN (0.97 g) and $Ni(NO_3)_2 \cdot 6H_2O$ (0.73 g) in ethanol. To an ethanolic solution of $Ni(SCN)_2$ was added 30 cm^3 of nitromethane followed by L (0.73 g) in nitromethane (30 cm^3). The grey product that quickly formed was filtered off and dried *in vacuo*.

The analytical results for the above complexes are given in Table 1.

The diffuse-reflectance spectra were recorded on a Beckmann DK2 spectrophotometer and are given in Table 2.

Magnetic measurements (Table 2) were carried out at room temperature on a Gouy balance of conventional design.

X-ray crystallography

The crystal used for the X-ray study was sealed in a thin-walled glass capillary. All crystallographic measurements were made at 293±2 K using a CAD4 diffractometer operating in the ω–2θ scan mode, with Ni-filtered Cu-K_α radiation (λ = 1.54178 Å) as previously described.[6] The structure was solved via the heavy-atom method and refined using full-matrix least-squares using two blocks, one for atoms in each ion, and with scattering factors taken from Ref. 7. All non-hydrogen atoms were refined anisotropically; hydrogen atoms were inserted in idealized positions, allowed

Table 1.[a]

Complex	Analytical data of the complexes					
	Found (%)			Calc. (%)		
	C	H	N	C	H	N
$NiL(ClO_4)_2 \cdot 2H_2O$	47.0	3.9	15.8	46.7	4.1	16.0
$NiL(NO_3)_2 \cdot 2H_2O$	51.7	4.7	19.9	51.0	4.5	21.0
$NiLCl_2 \cdot 2H_2O$	54.7	5.4	17.4	54.7	4.9	18.8
$NiLBr_2 \cdot 2EtOH$	50.8	4.9	15.5	51.2	5.0	15.7
$NiL(SCN)_2 \cdot 2H_2O$	43.4	3.9	14.5	43.1	4.7	14.8
$Ni_2LCl_4 \cdot 6H_2O$	43.4	3.9	14.5	43.1	4.7	14.8
$Ni_2LCl_4 \cdot 3H_2O \cdot 2EtOH$	46.2	4.9	14.6	46.3	5.1	14.2
$Ni_2LBr_4 \cdot 2H_2O \cdot EtOH$	39.2	3.5	12.9	39.3	3.8	12.7
$Ni_2LBr_4 \cdot 3H_2O$	38.6	3.3	12.9	38.1	3.6	13.1
$Ni_2L(SCN)_4$	48.7	3.9	20.5	49.1	3.5	21.1

[a] EtOH is C_2H_5OH.

Table 2. Diffuse-reflectance spectra and magnetic moments of the complexes

Complex[a]	Spectral peaks[b] ν_1 (cm^{-1})	ν_2 (cm^{-1})	ν_3 (cm^{-1})	Magnetic moment
$NiL(ClO_4)_2 \cdot 2H_2O$	10,750	18,200	27,000	3.80
$NiL(NO_3)_2 \cdot 2H_2O$	10,650	17,900	28,600	3.62
$NiLCl_2 \cdot 2H_2O$	10,200	17,900	27,800	2.98
$NiLBr_2 \cdot 2EtOH$	10,400	17,900	28,600	3.08
$NiL(SCN)_2 \cdot 2H_2O$	10,500	17,900	28,200	3.64
	Spectral peaks (not assigned)			
$Ni_2LCl_4 \cdot 6H_2O$	8000, 11,000, 14,300 sh, 15,600			3.45
$Ni_2LCl_4 \cdot 3H_2O \cdot 2EtOH$	(9100–10,600) br, 18,200 sh, 21,750 sh, 24,400, 30,300			3.48
$Ni_2LBr_4 \cdot 2H_2O \cdot EtOH$	7250, 10,500, 13,300 sh, 14,300, 28,600			3.00
$Ni_2LBr_4 \cdot 3H_2O$	7700, 10,750, 13,500 sh, 14,500, 16,100 sh, 29,400			Insufficient sample
$Ni_2L(SCN)_4$	Insufficient sample			

[a] EtOH = C_2H_5OH.

[b] $\nu_1 = {}^3A_{2g}(F) \rightarrow {}^3T_{2g}(F)$, $\nu_2 = {}^3A_{2g}(F) \rightarrow {}^3T_{1g}(F)$, $\nu_3 = {}^3A_{2g}(F) \rightarrow 3T_{1g}(P)$ (in O_h-symmetry). sh = shoulder, br = broad.

to "ride" on the parent atom and assigned group isotropic thermal parameters. Computer programs used are listed in Ref. 6.

Crystal data. $[C_{34}H_{32}N_{10}Ni]^{2+}[C_2H_{12}O_4Cl_2Ni] \cdot 2Cl^- \cdot (C_2H_6O)$, $M_r = 985.02$, triclinic, $a = 11.342(5)$, $b = 11.611(1)$, $c = 18.770(2)$ Å, $\alpha = 104.50(1)$, $\beta = 74.11\ (2)$, $\gamma = 109.91(3)°$, $V = 2201.2$ Å^3, space group $P\bar{1}$, $Z = 2$, $D_c = 1.49$ g cm^{-3}, $\mu(Cu = K_\alpha) = 34.1$ cm^{-1}, $F(000) = 952$.

Total unique data recorded, 4503 ($1.5° \leqslant \theta \leqslant 50°$), 2850 observed [$I > 1.5\sigma(I)$].

Final $R = 0.0615$, $R_w = 0.0506$, weights = $1/[\sigma^2(F_o) + 0.00002F_o^2]$.

Tables of atomic positional and thermal parameters, bond lengths and angles, and F_o/F_c values have been deposited as supplementary data with the Editor, from whom copies are available on request. Atomic co-ordinates have also been deposited with the Cambridge Crystallographic Data Centre.

RESULTS AND DISCUSSION

The structure of the title compound is shown in Fig. 1 where Cl(3) is hydrogen bonded to hydrogen atoms of water oxygens O(1) and O(2), and Cl(4) is hydrogen bonded to the hydrogen atoms of O(4) (an ethanol molecule) and O(3) (a water molecule). Selected bond lengths and angles are given in Table 3. $[NiCl_2(H_2O)_3(C_2H_5OH)]$ exhibits facial geometry and the interesting feature of the molecule is the unusual combination of ligands utilized to achieve the distorted octahedral stereochemistry. $[NiL]^{2+}$ is also distorted octahedral. The two distances Ni—N(13) (2.051 Å) and Ni—N(33) (2.058 Å) are very similar to the values found for other Ni(II) benzimidazole complexes.[8,9] The other two Ni imino nitrogen distances, Ni—N(23) (2.101 Å) and Ni—N(42) (2.147 Å), are somewhat longer and presumably a consequence of the geometrical requirements of the ligand. The various bond angles centred at Ni range from 78.3 to 122.6° for *cis* groups and from 157.9 to 176.3° for *trans* groups. The most marked deviation from ideal geometry is the N(42)—Ni(1)—N(23) angle of 122.6°, the largest angle less than this being 96.8° for the *cis* N(13)—Ni(1)—N(2).

The complexes of stoichiometry $NiLX_2$ (X^- is ClO_4^-, NO_3^-, Cl^-, Br^- or SCN^-) have electronic spectral and magnetic properties which are consistent with the assignment of a structure similar to that of the cation in the title complex together with the appropriate anion, i.e. $NiL^{2+}2X^-$. The elec-

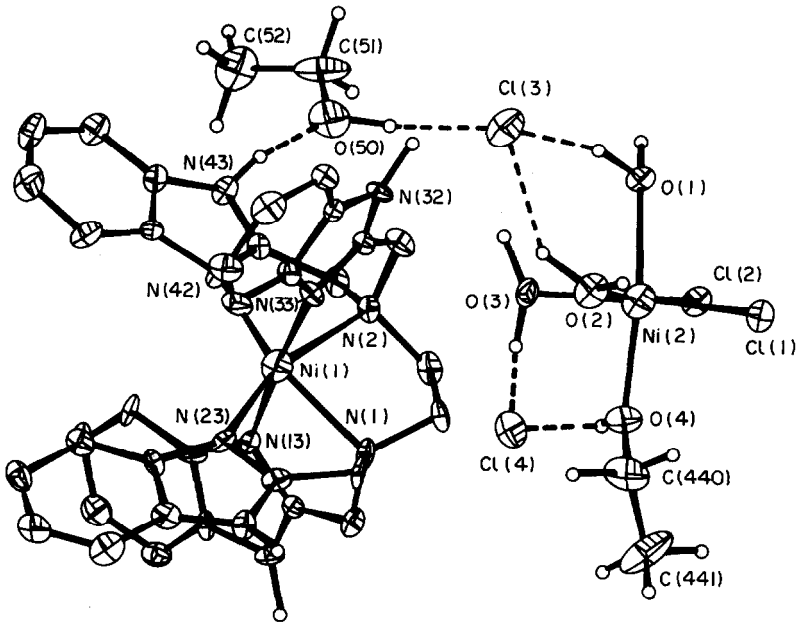

Fig. 1.

tronic spectra of the title complex can be interpreted as the superposition of the spectra due to the two species $[NiL]^{2+}$ and $[NiCl_2(H_2O)_3(C_2H_5OH)]$.

It could be argued that the electronic spectra of $Ni_2LCl_4 \cdot 6H_2O$ and the two forms of Ni_2LBr_4 contain features attributable to Ni(II) ions in octahedral and tetrahedral environments. This would lead to the assignment of the structure $NiX_4^{2-}NiL^{2+}$ to these complexes (X^- is Cl^-, Br^- or SCN^-) but their spectra do not show the relatively high intensity absorption bands associated with tetrahedrally coordinated Ni(II) complexes. In view of this,

Table 3. Selected bond lengths (Å) and angles (°)

Ni(1)—N(1)	2.186(9)	Ni(1)—N(2)	2.179(12)
Ni(1)—N(13)	2.051(9)	Ni(1)—N(23)	2.101(12)
Ni(1)—N(33)	2.058(9)	Ni(1)—N(42)	2.147(10)
Ni(2)—Cl(1)	2.369(5)	Ni(2)—Cl(2)	2.410(6)
Ni(2)—O(1)	2.120(8)	Ni(2)—O(2)	2.090(12)
Ni(2)—O(3)	2.068(8)	Ni(2)—O(4)	2.085(8)
N(2)—Ni(1)—N(1)	81.8(4)	N(13)—Ni(1)—N(1)	81.3(4)
N(13)—Ni(1)—N(2)	96.8(4)	N(23)—Ni(1)—N(1)	78.3(4)
N(23)—Ni(1)—N(2)	157.9(3)	N(23)—Ni(1)—N(13)	89.5(4)
N(33)—Ni(1)—N(1)	95.5(4)	N(33)—Ni(1)—N(2)	80.8(5)
N(33)—Ni(1)—N(13)	176.3(3)	N(33)—Ni(1)—N(23)	91.7(5)
N(42)—Ni(1)—N(1)	158.2(4)	N(42)—Ni(1)—N(2)	78.4(4)
N(42)—Ni(1)—N(13)	92.2(4)	N(42)—Ni(1)—N(23)	122.6(4)
N(42)—Ni(1)—N(33)	90.1(4)		
Cl(1)—Ni(2)—Cl(2)	90.9(1)	Cl(1)—Ni(2)—O(1)	95.7(3)
Cl(2)—Ni(2)—O(1)	89.9(4)	Cl(1)—Ni(2)—O(2)	87.8(3)
Cl(2)—Ni(2)—O(2)	175.4(2)	O(2)—Ni(2)—O(1)	85.9(4)
Cl(1)—Ni(2)—O(3)	172.9(3)	Cl(2)—Ni(2)—O(3)	95.4(4)
O(1)—Ni(2)—O(3)	87.6(4)	O(2)—Ni(2)—O(3)	86.2(4)
Cl(1)—Ni(2)—O(4)	92.1(3)	Cl(2)—Ni(2)—O(4)	87.9(4)
O(1)—Ni(2)—O(4)	171.9(3)	O(2)—Ni(2)—O(4)	96.9(4)
O(3)—Ni(2)—O(4)	84.8(4)		

assignment of a structure to these complexes will not be attempted. However, because of the possibility that some of these complexes might be of the structural type suitable for our EXAFS studies we are currently trying to grow crystals of them suitable for an X-ray crystallographic investigation.

REFERENCES

1. P. J. M. W. L. Birker, H. M. J. Hendriks, J. Reedijk and G. C. Verschoor, *Inorg. Chem.* 1981, **20**, 2408.
2. H. M. J. Hendriks, P. J. M. W. L. Birker, J. van Rijn, G. C. Verschoor and J. Reedijk, *J. Am. Chem. Soc.* 1982, **104**, 3607.
3. S. F. Wong, Personal communication.
4. L. Alagna, S. Hasnain, B. Piggott and D. J. Williams, *Biochem. J.* 1984, **220**, 591.
5. H. M. J. Hendriks, W. O. ten Bokkel Huinink and J. Reedijk, *Recl. Trav. Chim. Pays-Bas* 1979, **98**, 499.
6. M. B. Hursthouse, R. A. Jones, K. M. A. Malik and G. Wilkinson, *J. Am. Chem. Soc.* 1979, **101**, 4128.
7. *International Tables for X-ray Crystallography*, Vol. 4. Kynoch Press, Birmingham, U.K. (1974).
8. B. Piggott and A. C. Skapski, *Inorg. Chim. Acta* 1983, **77**, L171.
9. M. Goodgame, S. D. Holt, B. Piggott and D. J. Williams, *Inorg. Chim. Acta* 1985, **107**, 49.

Polyhedron Vol. 6, No. 6, pp. 1463–1467, 1987
Printed in Great Britain

0277–5387/87 $3.00+.00

SYNTHESIS AND STRUCTURAL STUDIES OF METAL(II) 4,9,16,23-PHTHALOCYANINE TETRAAMINES

B. N. ACHAR,* G. M. FOHLEN,† J. A. PARKER‡ and J. KESHAVAYYA

Department of Post-Graduate Studies and Research in Chemistry, Manasagangotri, Mysore 570006, India

(*Received* 27 *August* 1986; *accepted after revision* 21 *January* 1987)

Abstract—Preparation of pure metal(II) 4,9,16,23-phthalocyanine tetraamine 2-hydrates of copper, cobalt, nickel and zinc are reported. Elemental analysis, electronic spectra, FT-IR spectra, powder X-ray diffraction, magnetic-susceptibility measurements, dynamic thermogravimetric MS and GC–MS spectral studies are carried out to check the purity, structural integrity, thermal stability and mode of fragmentation of these complexes. Magnetic-susceptibility measurements showed a variation in the magnetic moments of these complexes with magnetic field strength, indicating the presence of a co-operative intermolecular effect.

Metal phthalocyanines and their derivatives are of great technological importance for the manufacture of blue-green pigments.[1–3] Currently intensive research is going on in producing phthalocyanine compounds useful for applications[1] as catalysts, photoconductors, photosensitizers, electrical conductors, photovoltaic materials, and thermally stable polymers.[1–7] Incorporation of the phthalocyanine structure either in the polymeric backbone or as curing agent to epoxy resins is expected to increase thermal stability, chemical resistance and fire retardance. The polymers prepared from phthalocyanines did not give the thermal stability expected from the stable phthalocyanine structure.[8–13] The use of phthalocyanine carboxylic acids and copper phthalocyanine to cure epoxy resins has been described in the literature.[14,15] However, those phthalocyanine derivatives and copper phthalocyanine are insoluble, react heterogeneously and remained as discrete particles even after curing. Because of this major disadvantage of insolubility, complete realization of their thermal stability and the chemical resistance of phthalocyanines were not seen in the cured resins. This is because phthalocyanine and its metal derivatives are insoluble in water and most common organic solvents. But the solubility can be altered by substituting suitable functional groups in the peripheral benzene rings of the phthalocyanine structure. Among the thermally stable soluble phthalocyanine compounds, amine groups substituted metal phthalocyanine derivatives are found to be promising. The amine derivatives of metal phthalocyanines have been previously synthesized mostly for the preparation of inks, dyes and pigments.[1,16–21] The procedures described often give impure compounds and these compounds have not given clear solutions in aprotic solvents. An efficient method was developed for the synthesis of analytically pure metal(II) 4,9,16,23-phthalocyanine tetraamines with the structure shown in Fig. 1.

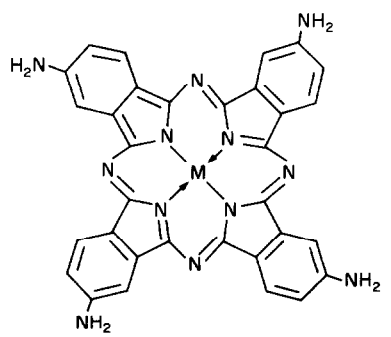

Fig. 1. Structure of metal(II) 4,9,16,23-phthalocyanine tetraamines.

*NRC–NASA Research Associate (1979–1982). Author to whom correspondence should be addressed.

†Present address: Vista Grande 1307, Millbrae, CA 94030, U.S.A.

‡Present address: 1330 McClure Av., Los Altas, CA, U.S.A.

The present work describes the synthesis and structural investigations of pure metal phthalocyanine tetraamines (MPTAs). The synthetic procedure has been adapted from the methods outlined to synthesize various other types of metal phthalocyanine derivatives.[16–25]

EXPERIMENTAL

Materials

4-Nitrophthalic acid, ammonium chloride and ammonium molybdate are A.C.S. reagents from Aldrich Chemical Co., U.S.A. All other chemicals were of analytical grade. Metal(II) 4,9,16,23-phthalocyanine tetraamine 2-hydrates of copper, cobalt, nickel and zinc are prepared as follows.

(1) *Copper*(II) 4,9,16,23-*tetranitrophthalocyanine.* 12.0 g copper sulfate pentahydrate, 37.0 g 4-nitrophthalic acid, 4.5 g ammonium chloride, 0.5 g ammonium molybdate and excess urea (50–60 g) were finely ground and placed in a 500-cm^3 three-necked flask containing 25 cm^3 of nitrobenzene. The temperature of the stirred reaction mixture was slowly increased to 185°C and maintained at 185 ± 5°C for 4.5 h. The solid product was finely ground and washed with alcohol until free from nitrobenzene. The product was added to 500 cm^3 of 1.0 N hydrochloric acid saturated with sodium chloride, boiled for about 5 min, cooled to room temperature and filtered. The resulting solid was treated with 500 cm^3 1.0 N sodium hydroxide containing 200 g sodium chloride and heated at 90°C until the evolution of ammonia ceased. The solid product after filtration was treated with 1.0 N hydrochloric acid and separated by centrifugation. Alternate treatment with hydrochloric acid and sodium hydroxide was repeated twice. The copper(II) 4,9,16,23-tetranitrophthalocyanine was washed with water until chloride-free. The blue complex was dried at 125°C.

(2) *Copper*(II) 4,9,16,23 - *tetraaminophthalocyanine 2-hydrate.* About 10 g of finely ground copper(II) 4,9,16,23-tetranitrophthalocyanine was placed in 250 cm^3 water. To this slurry 50 g of sodium sulfide nonahydrate was added and stirred at 50°C for 5 h. The solid product was separated by centrifuging the reaction mixture and treated with 750 cm^3 of 1.0 N hydrochloric acid. The bulky blue precipitate of copper(II) tetraaminophthalocyanine hydrochloride was separated by centrifugation. It was then treated with 500 cm^3 of 1.0 N sodium hydroxide, stirred for 1 h and centrifuged to separate the dark green solid complex. The product was repeatedly treated with water, stirred and centrifuged until the material was free from sodium hydroxide and sodium chloride. The pure copper complex was dried *in vacuo* over P_2O_5.

Metal(II) tetranitrophthalocyanines of cobalt, nickel and zinc were prepared by the same method using cobalt, nickel and zinc salts in place of the copper salt of procedure (1). The corresponding metal phthalocyanine tetraamines are obtained by using procedure (2) as described above.

Methods

Beckman Model DB spectrophotometer with 1-cm silica cells, from Beckman Instruments Inc., U.S.A., was used for UV and visible spectral studies. IR spectra were recorded using a Nicolet MX-1 FT-IR spectrometer. Carbon, hydrogen and nitrogen elemental analyses were done by Huffman Laboratories Inc. Co., U.S.A. The metal contents in the MPTAs were determined by decomposing a known amount of the complex using a sulphuric acid–nitric acid mixture followed by careful evaporation and calcination to constant weight. Thermogravimetric studies were carried out with a Du Pont Model 990 thermal analyzer and a 951 thermogravimetic module. A heating rate of 10°C min^{-1} was used in air and nitrogen atmospheres with a flow rate of 100 cm^3 min^{-1}. The Gouy magnetic balance consisting of a type NP-53 electromagnet with a DC power supply type MP-1053 and a semimicrobalance supplied by Universal Scientific Co., India, was used. A mercury tetrathiocyanato cobaltate(II) complex was used as the calibration standard. The JDX-8P JEOL X-ray diffractometer was used to study the X-ray diffraction pattern of the samples. The spectra were obtained with the following conditions: target Fe (Mn filter), voltage 30 kV, current 30 mA, time constant 4, chart speed 10 mm min^{-1}, channel width 0.7, and channel center 1.0.

A Hewlett–Packard model 5980 mass spectrometer equipped with a data acquisition system provided mass spectra of the individual components of the pyrolysis products at 70 eV. Two direct inlet probes (DIPs) were used. The low-temperature DIP can heat to 470°C at a heating rate of 50–100°C min^{-1} below 350°C and 10–50°C min^{-1} above 350°C. The high-temperature DIP was attached to a solid pyrolizer. The sample was heated for 1 min at each of the following temperatures: 700, 800, 900 and 1000°C. A Hewlett–Packard model 5830A gas chromatograph was used to study the volatile gaseous products formed during the thermal treatment. A sample of 1–2 mg of MPTA was inserted inside the platinum coil of the pyroprobe. The sample was

Table 1. Elemental, magnetic and spectral data of metal(II) 4,9,16,23-phthalocyanine tetraamine 2-hydrate (MPTA·$2H_2O$)

Name of compound	Field strength (G)	Magnetic susceptibility ($\chi_m \times 10^{-6}$)	μ_{eff} (BM)	UV–visible absorptions: wavelength (ε)	IR spectral data (cm^{-1})	Elemental analyses (%): found (calc.)
CuPTA·$2H_2O$	1024	+1792.60	2.093	214 (5.7776)	3282, 3188, 1604,	C: 57.5 (57.2)
	1960	+1679.54	2.022	300 (5.5267)	1411, 1343, 1303,	H: 3.6 (3.6)
	2816	+1560.42	1.946	382 (5.1547)	1251, 1136, 1098,	N: 24.9 (25.0)
	3584	+1423.13	1.862	749 (5.4678)	1053, 951, 863,	Cu: 9.8 (9.6)
	4352	+1311.42	1.790		833, 744 and 831	
	4792	+1304.42	1.783			
	5632	+1257.58	1.747			
	6144	+1198.64	1.709			
CoPTA·$2H_2O$	1024	+3269.73	2.822	212 (5.6931)	3284, 3180, 1607,	C: 58.1 (57.6)
	1960	+2956.77	2.683	298 (5.5603)	1420, 1345, 1309,	H: 3.3 (3.6)
	2816	+2629.67	2.530	388 (5.1521)	1254, 1134, 1097,	N: 25.2 (25.2)
	3584	+2602.47	2.518	738 (5.2844)	1060, 950, 863,	Co: 8.9 (8.8)
	4352	+2469.46	2.452		822, 780 and 736	
	4792	+2269.30	2.354			
	5632	+2222.47	2.332			
	6144	+2169.67	2.302			
NiPTA·$2H_2O$	6144	−460.782	—	208 (5.6991)	3280, 3186, 1605,	C: 56.8 (57.6)
				302 (5.6212)	1412, 1344, 1308,	H: 3.5 (3.6)
				380 (5.1538)	1251, 1135, 1098,	N: 24.8 (25.2)
				738 (5.5251)	1056, 950, 864,	Ni: 8.9 (8.8)
					822, 748 and 733	
ZnPTA·$2H_2O$	6144	−468.284	—	214 (5.7416)	3279, 3165, 1602,	C: 56.1 (57.0)
				302 (5.5430)	1401, 1340, 1299,	H: 3.7 (3.6)
				384 (5.1515)	1248, 1133, 1095,	N: 24.5 (25.0)
				742 (5.4249)	1045, 936, 864,	Zn: 9.6 (9.4)
					823, 743 and 728	

then kept in the pyrolysis chamber which was kept at 250°C. The sample was pyrolyzed at 900°C for 1 min. The volatile products were flushed with helium carrier gas to the GC separation column. The GC column used was 2 m long with a 2 mm i.d., glass column packed with 3% OV101 on 80/100 supelcoport. During the analyses the column temperature was held at 60–280°C and then maintained at the upper limit for 8 min. The helium gas flow was 20 cm^3 min^{-1}.

RESULTS AND DISCUSSION

The procedures described above are simple, commercially realizable and give pure compounds with almost quantitative yields (≃ 90%) except in the case of the zinc compound where the yield was only 30–40%. In this case the zinc complex seems to undergo degradation when it is heated in the presence of sodium hydroxide solution. These MPTAs have a metallic lustre and a deep greenish black colour. They give clear solutions in aprotic solvents such as dimethylsulphoxide, dimethylformamide and dimethylacetamide. The method of synthesis is applicable to the preparation of MPTAs of metals whose ionic radii[26] are about 0.8 Å. The preferred metals are copper, cobalt, nickel, zinc, iron, platinum, aluminium and vanadium. The most preferred metals are copper, cobalt and nickel. The results of the elemental analyses for carbon, hydrogen, nitrogen and metal agreed fairly well with the calculated values and were consistent with the structures shown in Fig. 1 with two water molecules.

Electronic absorption spectra

Metal(II) 4,9,16,23-tetraaminophthalocyanines of copper, cobalt, nickel and zinc showed absorption bands at 208–218, 288–306 and 732–746 nm in 30 N sulphuric acid (Table 1). In addition, shoulders are observed around 380–384 nm in all the absorption spectra of the complexes. The deep greenish

blue colour of the derivatives may be due to the $e_g \leftarrow a_{2u}$ transitions. A small dependence of the spectrum upon the central metal ion may be due either to the involvement of the $p\pi(a_{2u})$ orbitals in the π-bonding of the phthalocyanine ring system or more probably to the inductive effect.[27] In comparison with the spectra of the corresponding parent phthalocyanines the two peaks in UV regions around 208–218 and 288–306 nm remained almost unaffected in the spectra of the corresponding MPTAs. The peaks in the parent metal phthalocyanines around 424–438 nm appeared as shoulders at 380–384 nm with a blue shift. The peaks in the longer-wavelength region (732–746 nm) showed a bathochromic shift with increasing intensity with respect to the corresponding parent phthalocyanines. This is due to the auxochromic $-NH_2$ group present in the benzene portion of the complexes.

IR spectra

The FT-IR spectral data were recorded in KBr discs and the results are presented in Table 1. Two weak broad absorption bands at 3279–3284 and 3165–3188 cm^{-1} are observed in all the spectra of the MPTAs. These absorptions may be assigned to the ν_{as} and ν_s stretching vibrations of the amino groups. Intense $-NH_2$ group in-plane bending vibrations are observed at 1602–1607 cm^{-1}. Peaks around 1340–1345, 1299–1309 and 1248–1251 cm^{-1} indicated the presence of C—N aromatic stretching. The bands at 1133–1136, 1095–1098, 1045–1060, 936–951, 863–864 and 743–750 cm^{-1} may be assigned to the various phthalocyanine skeletal vibrations.[27]

Dynamic thermogravimetric studies

The nature of the analytical curves (Fig. 2) indicated that these amine derivatives of copper, cobalt, nickel and zinc phthalocyanines are degraded mainly in two steps. The weight loss (5–5.4%) which takes place between 50 and 130°C corresponds to the loss of two water molecules. The second weight loss is very catastrophic in an oxidizing atmosphere and is about 76–77% which is equivalent to the degradation of the unmetallated phthalocyanine structure. The final products in the oxidizing atmospheres are CuO, CoO, NiO and ZnO. The stability of the MPTAs in the oxidizing atmosphere is in the order CoPTA > CuPTA > NiPTA > ZnPTA. The second step of weight loss is very resistant in a nitrogen atmosphere and the weight loss seems to be due to some other mode of degradation. This weight loss is gradual in the temperature range 500–900°C and the char yields vary from 65 to 79%, depending on the MPTA. The stability in the inert atmosphere is found to follow the order NiPTA > CoPTA > CuPTA > ZnPTA.

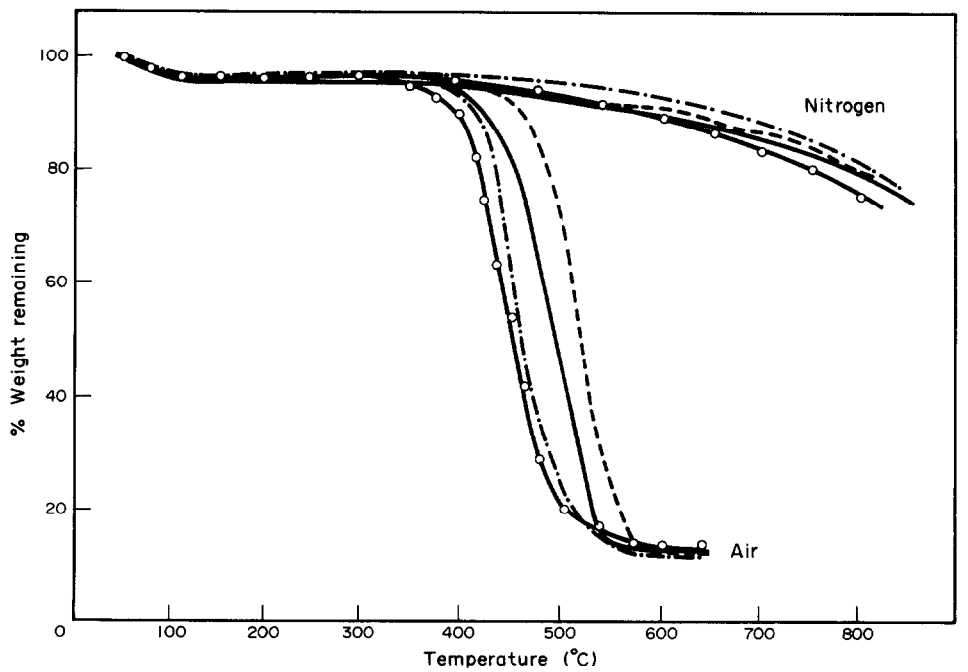

Fig. 2. Dynamic thermogravimetric analytical curves of: (1) $CuPTA \cdot 2H_2O$ (——), (2) $CoPTA \cdot 2H_2O$ (– – – –), (3) $NiPTA \cdot 2H_2O$ (— · — · —), and (4) $ZnPTA \cdot 2H_2O$ (— ○ — ○ —).

Magnetic-susceptibility measurements

The magnetic-susceptibility data for metal(II) 4,9,16,23-phthalocyanine tetraamines of copper, cobalt, nickel and zinc are consistent with the paramagnetic nature of the copper and cobalt complexes and the diamagnetic nature of the nickel and zinc complexes. The complexes are square planar with molecular symmetry D_{4h}. A summary of the magnetic properties over the range of magnetic field strengths 1025–6144 G are reported in Table 1. The magnetic moment parallels that of other spin-paired square planar cobaltous derivatives with a moment considerably above that expected for one unpaired electron. This may be due to the orbital contribution which could arise by mixing the ground state $(b_{2g})^2 (e_g)^4 (a_{1g})^1$ and higher orbitally degenerate states such as $(b_{2g})^2 (e_g)^3 (a_{1g})^2$. CuPTA has a moment corresponding to the spin-only value at a higher magnetic field strength and this value is very close to the 1.9 BM observed in most of the copper complexes. The variation in the magnetic moments with magnetic field strength has also been observed in the case of metal phthalocyanine sulphonic acid and metal phthalocyanine tetracarboxylic acid complexes. The variations in these complexes may also be due to the intermolecular co-operative effect.[25]

Powder X-ray diffraction

X-ray diffraction spectrographs of CuPTA, CoPTA, NiPTA and ZnPTA recorded through a range of angles (5–90°) showed similar patterns. All these complexes showed one broad sufficiently intense diffracted peak and the interplanar spacings calculated based on these data gave values (in Å) of 13.05, 12.32, 12.32 and 12.32 for CuPTA, CoPTA, NiPTA and ZnPTA, respectively.

Mass and GC–mass spectral studies

The mass spectra recorded at various temperatures indicated that the concentrations of the volatile products observed are very low even at a very high temperature. At 500°C, m/z of 18, 14, 64, 91, 118 and 143 appeared in more than 20% relative abundance with $m/z = 118$ being the base peak. At higher temperatures (700–1000°C) m/z of 28, 32, 44, 64, 82, 96, 128, 160, 192 and 256 (base peak) are seen in the mass spectra of the MPTAs. The gas chromatograms of the pyrolysed products of the MPTAs showed only trace quantities of volatile materials. The products identified are N_2, N_2H_4, C_6H_6, $C_6H_5NH_2$, C_6H_5CN, $C_6H_5(CN)_2$ and $C_6H_4(CN)(NH_2)$. The peak corresponding to $m/z = 44$ in mass spectra of MPTAs seems to be unusual. However, this is possible if the tetraamines have the property of adsorbing carbon dioxide gas. The study to support this is under further investigation.

Acknowledgements—We thank NRC–NASA, Washington D.C., and the University of Mysore for support of the work.

REFERENCES

1. F. H. Moser and A. L. Thomas, *Phthalocyanine Compounds*. Reinhold, New York (1963).
2. S. P. Potnis and A. B. Daruwala, *Paintindia* 1969, **21**.
3. K. Venkataraman, *The Chemistry of Synthetic Dyes*, Vol. 2. Academic Press, New York (1952).
4. B. N. Achar, G. M. Fohlen and J. A. Parker, U.S. Pat. 4,450,268 (1984).
5. B. N. Achar, G. M. Fohlen and J. A. Parker, U.S. Pat. 4,499,260 (1985).
6. B. N. Achar, G. M. Fohlen and J. A. Parker, U.S. Pat. 4,537,834 (1985).
7. B. N. Achar, G. M. Fohlen and J. A. Parker, U.S. Pat. accepted.
8. S. P. Potnis and A. B. Daruwala, *Paintindia* 1968, **17**.
9. A. D. Delman, J. J. Kelly and B. B. Simms, *J. Polym. Sci., Part A* 1970, **8**, 111.
10. A. A. Berlin and A. I. Sherle, *Inorg. Macromol. Rev.* 1971, **1**, 235.
11. T. R. Watton, J. R. Griffith and J. G. O'Rear, *Polym. Sci. Technol. (Adhes. Sci. Technol.)* 1975, **9B**, 665.
12. J. R. Griffith and J. G. O'Rear, U.S. Pet. 4,056,560 (1977).
13. K. J. Wynne and J. B. Davidson, U.S. Pat. 4,132,482 (1979).
14. H. L. Parry, *Heat Resistant Adhesives Based on Phthalocyanine Copolymers*. TDC Report ASD-TDR-63-396 (1963).
15. H. L. Parry, U.S. Pat. 3,301,814 (1967).
16. S. Horiguchi, *Shikizai Kyokaishi* 1965, **38**(3), 99.
17. S. Horiguchi, *Shikizai Kyokaishi* 1965, **38**(3), 109.
18. N. H. Haddock, U.S. Pat. 2,280,072 (1942).
19. N. H. Haddock, W. O. Jones, A. Parkinson and G. A. Rowe, Brit. 589,118 (1947).
20. N. H. Haddock, W. O. Jones, A. Parkinson and G. A. Rowe, U.S. Pat. 2,430,052 (1947).
21. N. H. Haddock, W. O. Jones, A. Parkinson and G. A. Rowe, U.S. Pat. 2,47,491 (1949).
22. F. Baumann, U.S. Pat. 2,613,128 (1952).
23. N. Fukuda, *Nippon Kagaku Zasshi* 1954, **75**, 1141.
24. N. Fukuda, *Nippon Kagaku Zaashi* 1959, **79**, 396.
25. J. H. Weber and D. H. Busch, *Inorg. Chem.* 1965, **4**, 469.
26. A. A. Berlin and A. L. Sherle, *Inorg. Macromol. Rev.* 1971, **1**, 175.
27. A. B. P. Lever, *Adv. Inorg. Chem. Radiochem.* 1965, **7**, 27.

Polyhedron Vol. 6, No. 6, pp. 1469–1472, 1987
Printed in Great Britain

0277–5387/87 $3.00+.00

COMPLEXATION OF PROTONS BY MACROCYCLIC POLYETHERS IN ACETONITRILE

HANS-JÜRGEN BUSCHMANN

Physikalische Chemie, Universität-GH Siegen, Postfach 101240, D-5900 Siegen, F.R.G.

(*Received* 19 *November* 1986; *accepted* 21 *January* 1987)

Abstract—The complexation of H^+ by different macrocyclic polyethers in acetonitrile solutions has been studied by means of calorimetric titrations. The most stable complex is observed with 18-crown-6. The measured stability constants decrease when the number of benzo substituents of 18C6 are increased. The stability of the complexes formed with larger macrocyclic polyethers is also smaller in comparison with 18C6. Unfavourable entropic changes during the reaction are responsible. Compared with noncyclic polyethers all ligands studied form more stable complexes. Favourable entropic contributions are mainly responsible.

The interactions of different crown ethers with various cations have been studied very intensively.[1] However, results for the reaction of H^+ with macrocyclic polyethers are very rare.[2] Some stability constants for these reactions have already been reported.[3] Even experimental results for the protonation of noncyclic and macrocyclic polyethers in the gas phase are available from the literature.[4] The gas-phase reactions of H_3O^+ and $CH_3OH_2^+$ with crown ethers have also been studied.[5] These results can not be directly compared with the experimental data obtained in solution due to interactions between solvent molecules and crown ethers.[6]

As a continuation of an earlier work[2] the complexation of H^+ by more crown ethers in acetonitrile solutions is studied to get more information about the factors influencing the experimental results observed.

EXPERIMENTAL

Materials

The different benzo crown ethers shown in Fig. 1 are non-commercial and were provided by Prof. E. Weber (Bonn).[7] All other crown ethers (see Fig. 2) like 21-crown-7 (21C7, Parish), dibenzo-21-crown-7 (DB21C7, Parish), dicyclohexano-27-crown-9 (DC27C9, Parish), dibenzo-30-crown-10 (DB30C10, Parish) and dicyclohexano-30-crown-10 (DC30C10, Parish) were used without further purification.

Trifluoromethanesulfonic acid (Ega) was used as purchased. The dissociation of trifluoromethanesulfonic acid can be considered as complete under experimental conditions.[8] The water content of the solvent acetonitrile (Merck) was less than 0.3%.

Procedure

All stability constants smaller than $10^5\ M^{-1}$ and reaction enthalpies were determined by titration calorimetry using a Tronac Model 450 calorimeter. The procedure used to calculate the stability of the complex formed from the thermogram and the corresponding reaction enthalpy has already been described elsewhere.[9] It has already been shown that even the large crown ethers only form 1:1 complexes:[2]

$$L + H^+ \rightleftharpoons LH^+, \quad K = \frac{[LH^+]}{[L][H^+]}.$$

Therefore it is possible to titrate a solution of trifluoromethanesulfonic acid (0.06–0.08 M) into a ligand solution (5×10^{-3} M). The heat (Q) produced during titration is related to the reaction enthalpy (ΔH) after correction for all non-chemical heat effects as shown by the following equation:

$$Q_t = \Delta H \Delta n_t$$

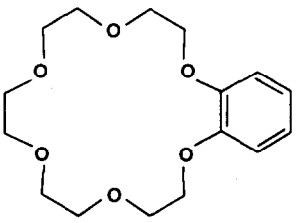

B18C6

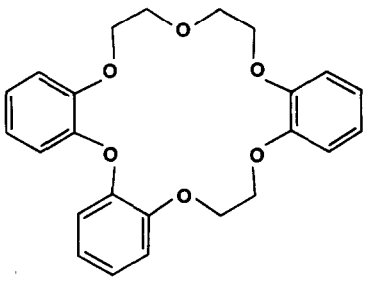

TB18C6

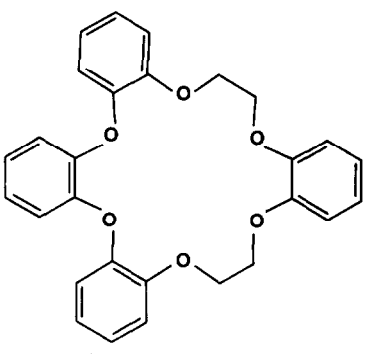

TeB18C6

Fig. 1. Benzo-crown ethers.

where Δn_t is the number of mol of complex formed at time t. For stability constants smaller than 10^5 M^{-1} Δn_t is not constant during titration but is a function of the stability constant of the reaction observed. Also from the experimental data in this investigation no evidence is found of the existence of complexes with compositions other than 1 : 1. The electrostatic repulsion between two protons complexed by one ligand molecule obviously prevents the formation of such complexes in acetonitrile solutions.

RESULTS AND DISCUSSION

The values of $\log K$, ΔH and $T\Delta S$ for the reaction of H^+ with different 18-crown-6 ligands are given in Table 1. With an increasing number of benzo groups attached to 18-crown-6 decreasing values are measured for the reaction enthalpies. These data clearly demonstrate an electron withdrawal effect of the benzo groups. Thus, the electron density at the neighbouring oxygen donor atoms is reduced, directly influencing the reaction enthalpies measured. However, the reaction enthalpies measured for the reaction of 18C6 and B18C6 are almost identical.

Reaction entropies obtained for both ligands differ considerably. This observation is based on several factors. It is known that the ligand 18C6 forms complexes with the solvent acetonitrile.[6] No such information is obtainable for B18C6. If both ligands are not equally solvated in acetonitrile solutions the reaction entropies observed should reflect this situation. Assuming stronger interactions between 18C6 and acetonitrile than between B18C6 and this solvent more solvent molecules are liberated during the complex formation of 18C6 with H^+ compared to B18C6. As a result the com-

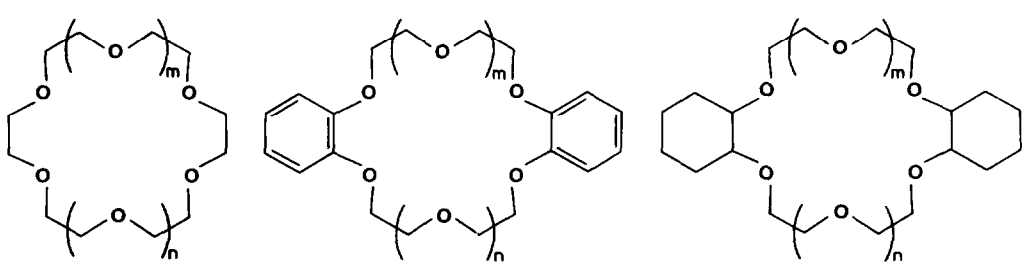

m = 1, n = 1 : 18C6
m = 1, n = 2 : 21C7

m = 1, n = 1 : DB18C6
m = 1, n = 2 : DB21C7
m = 2, n = 2 : DB24C8
m = 3, n = 3 : DB30C10

m = 1, n = 1 : DC18C6
m = 2, n = 2 : DC24C8
m = 2, n = 3 : DC27C9
m = 3, n = 3 : DC30C10

Fig. 2. Macrocyclic ligands.

Table 1. Stability constants (log K, K in M^{-1}) and thermodynamic parameters (ΔH and $T\Delta S$, in kJ mol^{-1}) for the reaction of H^+ with different 18-crown-6 ethers in acetonitrile at 25°C

Value	18C6	B18C6	DB18C6	TB18C6	TeB18C6	DC18C6
Log K	6.5[a]	3.78	3.73[b]	4.08	3.69	8.2[a]
$-\Delta K$	29.0[b]	32.1	19.8[b]	18.7	15.5	42.8[b]
$T\Delta S$	7.9[b]	−10.6	+1.4[b]	4.5	5.5	3.8[b]

[a] From Ref. 3.
[b] From Ref. 2.

plexation of H^+ by 18C6 is favoured by entropic contributions.

The reaction entropies increase from B18C6 with an increasing number of the ligand's benzo groups. The structural flexibility of these ligands during the formation of the H^+ complexes is reduced and an increasing number of donor atoms already possess a fixed position in the ligand. The proton complex formed with the ligand DC18C6 is much stronger in comparison with all other 18-crown-6 ligands. Only enthalpic factors are responsible for this observation which may result from the different solvation of these ligands. This interpretation is also supported by further experimental results measured for the reaction of different 18-crown-6 ligands with alkali ions in acetonitrile solutions.[10]

In Table 2 more results for the reaction of H^+ with crown ethers larger than 18-crown-6 are summarized. Comparing the reaction enthalpies of the unsubstituted crown ethers 18C and 21C7 with one another and also their dibenzo derivatives one finds that they are identical in both cases. The additional oxygen donor atom does not influence the values of the reaction enthalpies. The differences in complex stabilities are only caused by minor entropic changes.

On increasing the size of the macrocyclic ligands further, an enhancement of the measured reaction enthalpies is observed in nearly all cases. The values of the reaction enthalpies for the reaction of all dibenzo-crown ethers are smaller than for the dicyclohexano-crown ethers. These results are in agreement with the influence of the electron withdrawal effect of benzo groups already discussed. This effect vanishes with an increasing number of oxygen donor atoms not attached to benzo groups of the crown ether. Thus, there is the possibility of the complexed proton increasing to interact with "normal" oxygen donor atoms. In contrast, the enhancement of the flexibility of the ligand is responsible for more unfavourable entropic changes during the reaction.

The dicyclohexano-crown ethers show much smaller changes in the reaction enthalpies with a number of donor atoms. The basicity of all oxygen donor atoms is nearly equal. Sterical reasons may therefore be responsible for the observed changes in the reaction enthalpies. Compared with the results for the corresponding dibenzo-crown ethers more of the observed reaction entropies for dicyclohexano-crown ethers are negative. When the size of the ligand increases, all thermodynamic values for the different ligands substituted obviously approach one another. This behaviour is not surprising because the individuality of all crown ethers is expected to vanish if the ligands are large enough.

The values of the reaction enthalpy measured for the reaction of large crown ethers decrease in the

Table 2. Stability constants (log K, K in M^{-1}) and thermodynamic parameters (ΔH and $T\Delta S$, in kJ mol^{-1}) for the reaction of H^+ with monocyclic ligands in acetonitrile at 25°C

Value	21C7	DB21C7	DB24C8	DB30C10	DC24C8	DC27C9	DC30C10
Log K	> 5	4.02	4.03[b]	3.64	3.46[b]	3.95	4.19
	5.3[a]	2.9[a]	3.2[a]	3.6[a]			
$-\Delta H$	29.1	19.9	27.3[b]	37.2	50.1[b]	56.0	44.8
$T\Delta S$	1.0	2.9	−4.4[b]	−16.5	−30.4[b]	−33.6	−21.0

[a] From Ref. 3.
[b] From Ref. 2.

following order as far as experimental data are available:

dicyclohexano-crown ether > crown ether

> dibenzo-crown ether.

An identical sequence was found for different ligands.[2] However, reaction entropies cannot be arranged in a similar way. The values for the reaction of unsubstituted and dibenzo-crown ethers are rather similar. Only larger unfavourable entropic contributions are observed for the complexation reaction of the large dicyclohexano-crown ethers.

The values of the reaction enthalpies measured for the complexation of H^+ by different non-cyclic polyethers are smaller when compared with the values obtained for the dicyclohexano-crown ethers estimated in this work.[2] In methanol solution it was found that the values of the reaction enthalpy for the complexation of alkali ions by non-cyclic polyethers increase with an increasing number of ether oxygen donor atoms.[11] Until further data are published the same behaviour may be presumed for the complexation of H^+.

All crown ether ligands studied in this work form more stable complexes compared with their non-cyclic analogues.[2] With the restriction given above entropic factors are responsible for this observation.

Acknowledgement—The ligands B18C6, TB18C6 and TeB18C6 were kindly donated by Prof. E. Weber. Financial support by the Deutsche Forschungsgemeinschaft is gratefully acknowledged.

REFERENCES

1. R. M. Izatt, J. S. Bradshaw, S. A. Nielsen, J. D. Lamb and J. J. Christensen, *Chem. Rev.* 1985, **85**, 271.
2. H.-J. Buschmann, *Inorg. Chim. Acta* 1986, **118**, 77 (and references therein).
3. J. M. Kolthoff, W.-J. Wang and M. K. Chantooni, *Anal. Chem.* 1983, **55**, 1202.
4. M. Meot-Ner, *J. Am. Chem. Soc.* 1983, **105**, 4906; R. B. Sharma, A. T. Blades and P. Kebarle, *J. Am. Chem. Soc.* 1984, **106**, 510.
5. R. B. Sharma and P. Kebarle, *J. Am. Chem. Soc.* 1984, **106**, 3913.
6. P. A. Mosier-Boss and A. I. Popov, *J. Am. Chem. Soc.* 1985, **107**, 6168.
7. E. Weber, *Chem. Ber.* 1985, **118**, 4439.
8. T. Fujinaga and J. Sakamoto, *Electroanal. Chem.* 1977, **84**, 185.
9. R. M. Izatt, R. E. Terry, D. P. Nelson, Y. Chan, D. J. Eatough, J. S. Bradshaw, L. D. Hansen and J. J. Christensen, *J. Am. Chem. Soc.* 1976, **98**, 7626.
10. H.-J. Buschmann, in preparation.
11. H.-J. Buschmann, *Polyhedron* 1985, **4**, 2039; *Makromol. Chem.* 1986, **187**, 423.

Polyhedron Vol. 6, No. 6, pp. 1473–1476, 1987
Printed in Great Britain

0277–5387/87 $3.00+.00

DINUCLEAR COPPER(II) COMPLEX MEDIATED REGIOSELECTIVE ALDOL-TYPE CONDENSATION OF 2-HYDROXY-5-METHYLBENZENE-1,3-DICARBALDEHYDE*

BIBHUTOSH ADHIKARY, AMAL K. BISWAS and KAMALAKSHA NAG†

Department of Inorganic Chemistry, Indian Association for the Cultivation of Science, Calcutta 700032, India

(*Received* 1 *December* 1986; *accepted* 21 *January* 1987)

Abstract—An aldol-type reaction of one of the carbaldehyde moieties of 2-hydroxy-5-methylbenzene-1,3-dicarbaldehyde (HL) takes place with ketones containing α-methyl and/or α-methylene groups through an *in situ* generated dicopper(II) complex, $Cu_2L_2(ClO_4)_2 \cdot 2H_2O$. The metal-free condensation products are 2-hydroxy-3-formyl-5-methyl-1-benzal ketones. No such reaction takes place with the mononuclear complex $CuL_2 \cdot H_2O$. The ligand (HL) itself undergoes uncontrolled self-condensation and polycondensation.

Although aldol condensation[1] is a versatile method in organic chemistry, its application suffers from the drawback of self-condensation and polycondensation, especially when a cross-coupling reaction is carried out with conventional base or acid catalysts. In recent years considerable attention has been focussed on directed coupling of two carbonyl compounds in a regioselective manner.[2–4] A very useful approach has been the reaction of a carbonyl compound with a suitably reactive metal enolate or enol-ether that is derived regioselectively from the other carbonyl compound. Of the various metal derivatives, boron enolates are found to react most selectively with aldehydes.[5–7] In several cases the desired aldol condensation products have also been obtained by using some transition-metal complexes as catalysts.[8] The present study is concerned with the regioselective addition of α-methyl and/or α-methylene ketones to one of the carbonyl groups of the symmetric molecule 2-hydroxy-5-methylbenzene-1,3-dicarbaldehyde (HL) through its dinuclear copper(II) complex, $Cu_2L_2(ClO_4)_2 \cdot 2H_2O$.

During the course of our studies[9] on the dinuclear metal complexes $M_2L_2(ClO_4)_2 \cdot 2H_2O$ (**1**) (M = Cu, Ni, Co or Mn), we noted that the two metal atoms are not equally strongly bound to the ligand. These complexes are formed when the mononuclear complex species $ML_2 \cdot H_2O$ are reacted with their corresponding metal perchlorate salts in dry EtOH. However, the phenoxo bridge of the dinuclear complexes undergoes hydrolytic cleavage in a wet solvent to regenerate $ML_2 \cdot H_2O$. The IR spectra of **1** show[9(b)] the presence of two C=O stretchings, which are separated by *ca* 20 cm^{-1}. The rationale for these observations is that, since in a dinuclear chelate the drainage of electron density occurs through the phenoxo bridge, the metal atom that was originally bound to the ligand draws more electronic charge from the formyl oxygen co-ordinated to it in order to retain its greater stability, and as a result the C=O stretching vibration of this carbonyl group appears at a lower frequency relative to the other one. We considered that in this situation the activated carbonyl group should be more susceptible to nucleophilic attack, and complex **1** may be directed to undergo regioselective aldol type condensation. We find that such a reaction indeed takes place with ketones containing α-methyl and/or α-methylene groups, and offers a route to the synthesis of 2-hydroxy-3-formyl-5-methyl-1-benzal ketones (**2**). To our knowledge no straightforward method exists for the preparation of compounds of type **2**.

RESULTS AND DISCUSSION

Preliminary studies showed that all the dinuclear complexes react in the same way. However, the

* Part 6 of the series: Dinuclear metal complexes. Part 5 is Ref. 9(b).

† Author to whom correspondence should be addressed.

reactions of **1** with acetone, acetophenone, 2-butanone, 4-methyl-2-pentanone and *trans*-4-phenyl-3-butene-2-one, as reported here, involve the use of the dicopper(II) complex for the sake of convenience.

Typically, the reactions were carried out by heating a mixture of $CuL_2 \cdot H_2O$, $Cu(ClO_4)_2 \cdot 6H_2O$ and a ketone in a molar ratio of 1 : 1.5 : 6 in dry EtOH. The condensation products were isolated and characterized as the mononuclear complex species (**4**), which are the derivatives of α,β-unsaturated ketones rather than those of aldols (**3**). It appears that the dehydration of **3** to **4** is caused by the effect of heat. Although aldol condensation is normally carried at ambient or subambient temperature, in the present study the application of heat was necessary due to the poor solubility of the precursor complex. The removal of the metal from the condensation products yield 2-hydroxy-3-formyl-5-methyl-1-benzal ketones (**2a–f**). It may be noted that, when the condensation is carried out with 2-butanone, two isomeric products, viz. **2c** and **d**, are obtained in a ratio of 5 : 1. In the case of 4-methyl-2-pentanone, however, the reaction takes place only through the α-methyl group.

The overall yield of **2** lies in the range 70–50%. About 10–15% of the parent dialdehyde (HL) is recovered unchanged. Other reaction product(s) obtained as an intractable viscous material remains uncharacterized.

It is important to mention that all these reactions take place with $Cu_2L_2(ClO_4)_2 \cdot 2H_2O$ generated *in situ*, but *not* with a preformed material. This indicates that the aldol condensation taking place here is catalyzed by the trace of free $HClO_4$ present in the perchlorate salt. In fact the pH of an aqueous solution of $Cu(ClO_4)_2 \cdot 6H_2O$ (0.2 M) was found to be *ca* 3.9. It is also important to note that the use of a dry solvent is a prerequisite, and the use of aqueous $HClO_4$ is forbidden on the ground of hydrolytic cleavage of **1**. The aldol type reaction *does not* take place with the mononuclear complex $CuL_2 \cdot H_2O$ under a variety of conditions, including the use of acid and base catalysts. The failure of $CuL_2 \cdot H_2O$ to bring about a cross-coupling reaction underscores the specific role of the dinuclear species (Scheme 1). The free ligand, on the other hand, undergoes uncontrolled self-condensation and poly-condensation in the presence of aqueous NaOH.

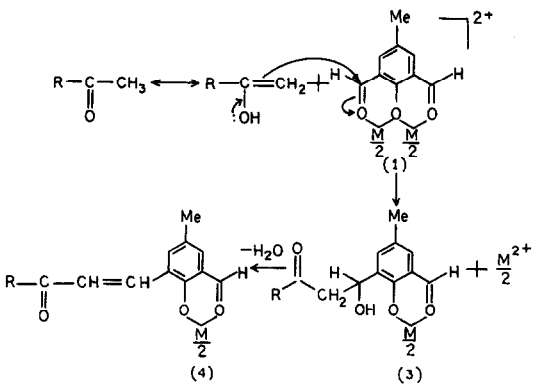

Scheme 1

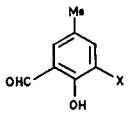

Scheme 1. (**2a**) X = CH=CHCOCH$_3$, (**2b**) X = CH=CHCOC$_6$H$_5$, (**2c**) X = CH=CHCOCH$_2$CH$_3$, (**2d**) X = CH=C(CH$_3$)COCH$_3$, (**2e**) X = CH=CHCOCH$_2$CH(CH$_3$)$_2$, (**2f**) X = CH=CHCOCH=CHC$_6$H$_5$, (**4a**) R = CH$_3$, (**4b**) R = C$_6$H$_5$.

EXPERIMENTAL

Melting points were measured in open capillary tubes and are uncorrected. C and H analyses were performed on a Perkin–Elmer model 240C elemental analyzer. IR spectra were recorded on a Perkin–Elmer model 783 IR spectrophotometer with KBr pellets. UV spectra in $CHCl_3$ solutions were obtained with a Pye–Unicam SP8-150 spectrophotometer. ^{1}H NMR spectra [δ (ppm)] were recorded at 200 MHz on a Varian Associates XL-200 spectrometer in $CDCl_3$ with Me_4Si as an internal standard.

HL was prepared by a method described in the literature.[10] Mono- and dinuclear copper(II) complexes of HL were prepared as described earlier.[9(a)]

Preparation of 2a–f

2a. A mixture of $CuL_2 \cdot H_2O$ (4.08 g, 10 mmol), $Cu(ClO_4)_2 \cdot 6H_2O$ (5.55 g, 15 mmol) and dry Me_2CO (100 cm^3) was heated under reflux. Within a few minutes, bright-green crystals of $Cu_2L_2(ClO_4)_2 \cdot 2H_2O$ deposited, which began to dissolve with the passage of time, and a dark-brown solution was obtained over a period of 10 h. The solution was filtered and slowly added with stirring to 500 cm^3 of water, when a brown precipitate was obtained. This was collected by filtration and dried. The crude complex (**4a**)* thus obtained was dis-

* The crude complex (**4a**) was recrystallized twice from a $CHCl_3$–*n*–hexane mixture and gave satisfactory analytical data for the composition $C_{24}H_{22}O_6Cu \cdot H_2O$. The IR spectra of **4a** and the product obtained by reacting **2a** with $Cu(OAc)_2 \cdot H_2O$ were identical.

solved in $CHCl_3$ (50 cm^3) and shaken with 2 M HCl (3 × 20 cm^3). The organic layer after washing with water was dried over Na_2SO_4. The $CHCl_3$ solution was evaporated to dryness and the residue was repeatedly extracted with light petroleum (b.p. 40–60°C). The combined extracts on concentration gave long light-yellow needles of **2a**, which was further recrystallized from light petroleum (65%) (m.p. 101°C). (Found: C, 70.4; H, 6.0. $C_{12}H_{12}O_3$ requires: C, 70.6; H, 5.9%.) ^{1}H NMR: 2.37 (s, 3H, $ArCH_3$), 2.41 (s, 3H, $COCH_3$), 6.87, 7.83 (q, 2H, J_{AB} = 16.0 Hz, *trans*-CH=CH), 7.42 [d, 1H, J = 2.0 Hz, 3-CH(phenyl)], 7.62 [d, 1H, J = 1.6 Hz, 5-CH(phenyl)], 9.85 (s, 1H, CHO), 11.51 (s, 1H, OH). IR (cm^{-1}): 1675(s), 1645(s), 1625(s). UV (nm) [ε ($dm^3 mol^{-1} cm^{-1}$)]: 370 (7100), 300 (8850), 260 (22,300).

2b. A mixture of $CuL_2 \cdot H_2O$ (3.66 g, 9 mmol), $Cu(ClO_4)_2 \cdot 6H_2O$ (5.0 g, 13.5 mmol) and PhCOMe (6.48 g, 54 mmol) in dry EtOH (100 cm^3) was refluxed for 16 h. A brown solid (**4b**)* formed was collected by filtration and washed with MeOH and $CHCl_3$. This was suspended in MeOH (100 cm^3) and stirred with 4 M HCl (25 cm^3) when it changed to a yellow material. The product was collected by filtration and recrystallized from $CHCl_3$–MeOH (1:2) mixture. Further recrystallization from light petroleum afforded yellow needles of **2b** (70%) (m.p. 106°C). (Found: C, 76.9; H, 5.2. $C_{17}H_{14}O_3$ requires: C, 76.7; H, 5.3%.) ^{1}H NMR: 2.39 (s, 3H, $ArCH_3$), 7.54 (m, 5H, COC_6H_5), 7.86, 7.96 (q, 2H, J_{AB} = 16.7 Hz, *trans*-CH=CH), 8.03 [d, 1H, J = 2.6 Hz, 3-CH(phenyl)], 8.07 [d, 1H, J = 2.4 Hz, 5-CH(phenyl)], 9.84 (s, 1H, CHO), 11.67 (s, 1H, OH). IR (cm^{-1}): 1660(s), 1645(s). UV (nm) [ε ($dm^3 mol^{-1} cm^{-1}$)]: 370 (11,100), 310 (13,600), 270 (26,400).

2c *and* **d**. To a suspension of $CuL_2 \cdot H_2O$ (5.3 g, 13 mmol) in dry EtOH (150 cm^3), $Cu(ClO_4)_2 \cdot 6H_2O$ (7.22 g, 19.5 mmol) and MeCOEt (4.68 g, 65 mmol) were added. A dark brown solution obtained after a 36-h reflux was filtered and evaporated to dryness on a rotary evaporator. The residue dissolved in MeOH (50 cm^3) was poured into water (1 dm^3), when a brown precipitate was obtained. This was collected by filtration, dissolved in $CHCl_3$ and decomposed with HCl (2 M). The $CHCl_3$ layer after drying was evaporated to dryness. The residue was extracted repeatedly with boiling light petroleum and the combined extract was subjected to column chromatography (silica gel, 60–120 mesh). The first fraction separated on elution with light petroleum was HL (10%). The second fraction obtained with a 2:98 (v/v) mixture of $MeCO_2Et$–light petroleum was **2c** (50%). The third fraction (**2d**) (10%) was collected by eluting with the same solvent mixture in a ratio of 5:95.

2c: m.p. 101–102°C. (Found: C, 71.3: H, 6.5. $C_{13}H_{14}O_3$ requires: C, 71.6: H, 6.4%.) ^{1}H NMR: 1.18 (t, 3H, CH_2CH_3), 2.36 (s, 3H, $ArCH_3$), 2.73 (q, 2H, CH_2CH_3), 6.90, 7.80 (q, 2H, J_{AB} = 16.5 Hz, 2H), 7.39 [d, 1H, J = 1.4 Hz, 3-CH(phenyl)], 7.58 [s, 1H, 5-CH(phenyl)], 9.86 (s, 1H, CHO), 11.55 (s, 1H, OH). IR (cm^{-1}): 1690(s), 1660(s), 1635(s). UV (nm) [ε ($dm^3 mol^{-1} cm^{-1}$)]: 370 (8000), 290 (11,500), 260 (25,800).

2d: m.p. 122°C. (Found: C, 71.5: H, 6.3. $C_{13}H_{14}O_3$ requires: C, 71.6: H, 6.4%.) ^{1}H NMR: 1.99 [s, 3H, CH=C(CH_3)], 2.38 (s, 3H, $ArCH_3$), 2.49 (s, 3H, $COCH_3$), 7.41 [s, 1H, 3-CH(phenyl)], 7.46 [s, 1H, CH=C(CH_3)], 7.67 [s, 1H, 5-CH(phenyl)], 9.88 (s, 1H, CHO), 11.32 (s, 1H, OH). IR (cm^{-1}): 1660(s), 1650(s), 1630(s). UV (nm) [ε ($dm^3 mol^{-1} cm^{-1}$)]: 360 (7500), 290 (8200), 260 (26,500).

2e. The reaction was carried out in the same way as described above using 2-methylpentanone. Chromatographic separation of the crude product by eluting with light petroleum [to remove HL (15%)], followed by a 98:2 mixture of light petroleum and $MeCO_2Et$ afforded **2e** (50%) (m.p. 59°C). No further isomer could be separated by increasing the polarity of the solvent mixture. (Found: C, 73.4; H, 7.2. $C_{15}H_{18}O_3$ requires: C, 73.2; H, 7.3%.) ^{1}H NMR: 0.99 [d, 6H, $CH(CH_3)_2$], 2.26 [m, 1H, $CH(CH_3)_2$], 2.36 (s, 3H, $ArCH_3$), 2.56 (d, 2H, CH_2CO), 6.90, 7.78 (q, 2H, J_{AB} = 16.4 Hz, *trans*-CH=CH), 7.39 [d, 1H, J = 1.5 Hz, 3-CH(phenyl)], 7.59 [d, 1H, J = 1.7 Hz, 5-CH(phenyl)], 9.87 (s, 1H, CHO), 11.56 (s, 1H, OH). IR (cm^{-1}): 1680(s), 1645(s), 1625(s). UV (nm) [ε ($dm^3 mol^{-1} cm^{-1}$)]: 370 (8700), 290 (12,300), 260 (28,000).

2f. By using PhCH=CH COMe as the reactant, **2f** was obtained (50%) in the same way as described above (m.p. 96°C). (Found: C, 77.8; H, 5.4. $C_{19}H_{16}O_3$ requires: C, 78.1; H, 5.5%.) ^{1}H NMR: 2.38 (s, 3H, $ArCH_3$), 7.12, 7.94 (q, 2H, J_{AB} = 16.1 Hz, ArCH=CH), 7.33, 7.75 (q, 2H, J_{AB} = 16.0 Hz, PhCH=CH), 7.44, 7.72 (m, 7H, aromatic), 9.89 (s, 1H, CHO), 11.67 (s, 1H, OH). IR (cm^{-1}): 1665(s), 1640(s), 1615(s). UV (nm) [ε ($dm^3 mol^{-1} cm^{-1}$)] 370 (15,500), 325 (24,000), 270 (18,500).

* The analytical data of the crude product showed that it was substantially pure and had desired IR spectral features.

Acknowledgements—K.N. thanks the CSIR, India, for financial support and for awarding a research associateship to A.K.B. Our thanks are due to Professor U. R.

Ghatak and Dr R. V. Venkateswaran of the Department of Organic Chemistry for providing the NMR facility. We are grateful to Dr S. K. Mandal for his participation in the initial phase of the study.

REFERENCES

1. A. T. Wielsen and W. J. Houlihan, *Org. React.* 1968, **16**, 1.
2. T. Mukaiyama, *Org. React.* 1982, **28**, 203.
3. D. A. Evans, J. V. Nelson and T. R. Taber, In *Topics in Stereochemistry* (Edited by N. L. Allinger, E. L. Eliel and S. H. Wilen), Vol. 13, p. 1. John Wiley, New York (1982).
4. C. H. Heathcock, In *Asymmetric Synthesis* (Edited by J. D. Morisson), Vol. 3, p. 111. Academic Press, New York (1983).
5. (a) M. Hirama, D. S. Garvey, L. D.-L. Lu and S. Masamune, *Tetrahedron Lett.* 1979, 3937; (b) T. Inoue and T. Mukaiyama, *Bull. Chem. Soc. Jpn* 1980, **53**, 174; (c) D. A. Evans, J. V. Nelson, E. Vogel and T. R. Taber, *J. Am. Chem. Soc.* 1981, **103**, 3099.
6. (a) C. Gennari, L. Colombo, C. Scolastico and R. Todeschini, *Tetrahedron* 1984, **40**, 4051; (b) H. Hamana, K. Sasakura and T. Sugasawa, *Chem. Lett.* 1984, 1729.
7. H. F. Chow and D. Seebach, *Helv. Chim. Acta* 1986, **69**, 604 (and references cited therein).
8. K. Watanabe, Y. Yamada and K. Goto, *Bull. Chem. Soc. Jpn* 1985, **58**, 1401 (and references cited therein).
9. (a) S. K. Mandal and K. Nag, *Inorg. Chem.* 1983, **22**, 2567; (b) B. Adhikary, A. K. Biswas, K. Nag, P. Zanello and A. Cinquantini, *Polyhedron* 1987, **6**, 897.
10. F. Ulleman and K. Brittner, *Chem. Ber.* 1909, **42**, 2539.

Polyhedron Vol. 6, No. 6, pp. 1477–1482, 1987
Printed in Great Britain

0277–5387/87 $3.00+.00

COMPLEXES OF VITAMIN B_6—XVIII.* TERNARY AND QUATERNARY COMPLEXES INVOLVING PYRIDOXAMINE, GLYCYLGLYCINE AND IMIDAZOLE AND SOME BIVALENT METAL IONS

N. M. MOUSSA†

Department of Biochemistry, Faculty of Science, Kuwait University, P.O. Box 5969, Safat 13060, Kuwait

and

H. M. MARAFIE, M. S. EL-EZABY† and M. RASHAD‡

Department of Chemistry, Faculty of Science, Kuwait University, P.O. Box 5969, Safat 13060, Kuwait

(*Received* 22 *December* 1986; *accepted* 21 *January* 1987)

Abstract—The formation constants of ternary and quaternary complexes containing the ligands pyridoxamine, glycylglycine and imidazole with Co(II), Ni(II), Zn(II) and Cd(II) were determined by pH-metric titration in 0.15 M $NaNO_3$ at 37°C using the MINIQUAD-75 program. It has been shown that the logarithms of the ternary formation constants are linear increasing functions of the sum of the logarithms of the first protonation constants of the ligands, but the $\log K^1$ ($MLH_m + ML'H_m \rightleftharpoons^{K^1} MLL'H_s$) are linear decreasing functions. It has been shown that deprotonation of the peptidic group is prohibited in ternary and quaternary metal complexes. It is also found that the imidazole moiety favourably ligates the ternary complexes rather than the bare metal ions.

The present investigation is a continuation of our efforts to study ternary and quaternary metal complexes of vitamin B_6 compounds and other biological ligands.[2,3] The importance of this study is firstly to prove that ternary and quaternary metal complexes may exist in biological systems in addition to the binary complexes. Secondly, supplementation of trace metal concentrations in nutritive mixtures should take into consideration the interaction between different ligands and metal ions not only to form binary metal complexes but also to form ternary and quaternary metal complexes. Thirdly, the complex equilibria may serve as models for vitamin B_6 dependent enzymatic reactions.

EXPERIMENTAL

Materials

The ligands glycylglycine (Glycyl) (> 99%, BDH) and pyridoxamine dihydrochloride [$Pm(HCl)_2$] (> 99%; Merck) were used without further purification. Imidazole (Imd) (Aldrich) was crystallized from benzene and dried under reduced pressure. Nickel(II), cobalt(II), zinc(II) and cadmium(II) nitrates (> 99%, BDH) were used without purification. Stock solutions of the ligands (L^-) were kept at ~ 5°C in dark. The concentration of stock solutions of the metal ions (M^{2+}) were checked by EDTA complexiometric methods. Potentiometric approaches were used utilizing a Radiometer pH meter model pH M62 provided with a Radiometer cupric selectrode type F1112 Cu as indicator electrode and a Radiometer calomel electrode type K 401 as a reference electrode.[4]

* For Part XVII see Ref. 1.

† Authors to whom correspondence should be addressed.

‡ Present address: Kuwait Institute of Technology, Kuwait.

Measurements

The titrimetric data were acquired using a Orion Research Microprocessor Ionalyzer type 901 using a Radiometer combined glass electrode type GK 2301C. The ionalyzer in the pH mode was calibrated using two Radiometer buffers at pH values of 6.98 and 4.03 at 37°C. All pH-metric titrations were carried out as previously described.[2] The ionic strength was kept constant at 0.15 M $NaNO_3$ and the temperature at 37°C. In ternary systems, the concentrations of each ligand were not more than twice the concentration of the metal ions. In the quaternary systems, the concentration of each ligand was identical to that of the metal ions except for Imd where its concentration was not more than 4 times that of the metal ions. The metal ion concentration was in the range $(0.6–2.0) \times 10^{-3}$ M. The hydrogen ion concentration was taken as 10^{-pH}.

Precipitation usually occurs above pH 7 in most of the titrations when the composition ratio was 1:1 (L:M) in the case of binary systems and above 8 when the ratio was $\geqslant 2:1$. In the ternary and quaternary systems the precipitation occurs at pH not greater than 8.5 in some systems, the Zn(II) and Cd(II) systems in particular.

Methods

Titration data were analyzed by using the MINIQUAD-75 program.[5] Several equilibrium models were tested. The results were assessed as previously described.[2] The pK_w used in the computation is 13.38.[2]

RESULTS AND DISCUSSION

Binary complexes of Ni(II), Co(II), Zn(II) *and* Cd(II)

The formation constants of the binary complexes of Ni(II), Co(II), Zn(II) and Cd(II) with Pm and Imd have been recently studied.[4] Although some of the formation constants of the binary complexes of these metal ions with Glygly have been previously reported,[6] yet they have been reevaluated under the experimental conditions used in this work (Table 1). It is noted that Co(II) and Ni(II) form $1:1:-1$ species ($Glygly^-:M^{2+}:H^+$) similarly to Cu(II) in which the peptidic proton has probably been lost, forming a tridentate ligand.[3] Besides, Ni(II) can also form a $2:1:-2$ species with Glygly which is

Table 1. Formation constants of binary complexes of Glygly with Co(II), Ni(II), Zn(II) and Cd(II) at $I = 0.15$ M ($NaNO_3$) and $T = 37$°C: p, r and s stand for the stoichiometric coefficients of Glygly, M^{2+} and H^+, n is number of titration data points

System	p	r	s	$\log \beta (\pm\sigma)$	S	X_i^2	R	n	pH range	Literature value	Reference, I, T
H	1	0	1	7.98							
	1	0	2	11.09							Ref. 2
Co(II)	1	1	−1[a]	−7.32 (0.49)	9.05E−8	99	0.016	96	7.1–8.6		
	1	1	0	2.97 (0.02)						3.08	(i), 0.15, 25°C
	2	1	0	6.45[b]						5.30	(i), 0.15, 25°C
Ni(II)	2	1	−2[a]	−11.56 (0.03)	3.76E−9	154	0.004	128	6.6–9.2		
	1	1	−1[a]	−4.77 (0.00)							
	1	1	0	3.95 (0.01)						3.34	(ii), 0.10, 25°C
	2	1	0	7.18 (0.01)						7.41	(ii), 0.10, 25°C
Zn(II)	1	1	0	3.37 (0.31)	1.65E−6	24	0.077	86	7.0–8.0	3.40	(iii), 0.15, 25°C
	2	1	0	6.91 (0.12)						6.27	(iii), 0.14, 35°C
Cd(II)	1	1	0	3.75 (0.10)	5.9E−9	202	0.003	150	7.1–8.5	2.95	(iv), 0.15, 25°C
	1	1	1	11.35 (0.12)							(iv), 0.15, 25°C
	2	1	0	6.08 (0.11)							

[a] The negative sign indicates dissociation of a proton from the ligand or the formation of an hydroxy species or both. The formation constants should be corrected by adding the proper number of pK_w.

[b] Estimated from Fig. 1.

(i) M. K. Kim and A. E. Martell, *J. Am. Chem. Soc.* 1967, **89**, 5138; (ii) S. Pelletier, *J. Chim. Phys.* 1972, **69**, 751; (iii) N. C. Li and M. C. M. Chen, *J. Am. Chem. Soc.* 1958, **80**, 5678; (iv) E. V. Sklenskaya and M. Kh. Karapetyants, *Russ J. Inorg. Chem.* 1966, **11**, 1102.

not formed with Co(II) and Cu(II). This has been attributed to the possible formation of stable hexacoordinated species. Zn(II) and Cd(II), similarly to Co(II), Ni(II) and Cu(II), form regular 1 : 1 : 0 and 2 : 1 : 0 species where Glygly is bidentate. These complexes are less stable than the corresponding glycine metal complexes.[4] However, the inability of Zn(II) and Cd(II) to deprotonate the peptidic proton may possibly be due to the precipitation encountered in these systems at pH ~ 8.5.

When $\log\beta_1^{ML}$ of the binary metal complexes (1 : 1 : 0 species) of Glygly, Gly,[4] Pm and Imd were plotted against the log of the first protonation constant of the ligands ($\log\beta_1^{HL}$), linear relationships were obtained (Fig. 1). These linear relationships can be understood on the basis of the following equation:[7]

$$\log\beta_1^{ML} = \log\beta_1^{HL} + \frac{1}{2.303RT}\{[G^o(M) - G^o(H)] + [G^o(HL) - G^o(ML)]\}. \quad (1)$$

This equation implies that the slope should be 1 if the second term on the right is constant. From Fig. 1 all the binary systems studied have slopes of approximately 1 except for the Cu(II) system where the slope was ~ 2. A non-unity slope means that the term $[G^o(HL) - G^o(ML)]$ must also be a linear function of $\log\beta_{1LH}$ since the term $[G^o(M) - G^o(H)]$ is a constant.

Similarly, the plots of $\log\beta_2^{ML_2}$ (for 2 : 1 : 0 species) vs $\log\beta_1^{HL}$ were linear with non-unity slopes. The slopes are greater than 1 with the exception of Cd(II) where it is less than 1. Equation (1) is usually useful in predicting unknown values of the formation constants.

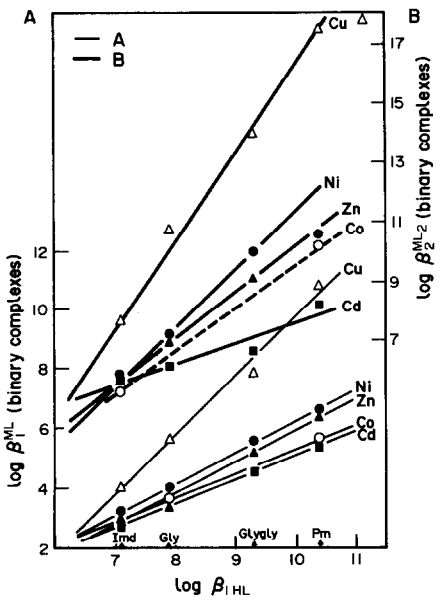

Fig. 1. Dependence of $\log\beta_1^{ML}$ (scale A) and $\log\beta_2^{ML_2}$ (scale B) on the basicity of the ligand exemplified by $\log\beta_{1HL}$ for Co(II), Ni(II), Zn(II) and Cd(II) metal ions.

Ternary and quaternary complexes of Co(II), Ni(II), Zn(II) *and* Cd(II)

The formation constants of the ternary and quaternary complexes of Co(II), Ni(II), Zn(II) and Cd(II) are for the following equilibrium reaction:

$$l\mathrm{Pm}^- + p\mathrm{Glygly}^- + q\mathrm{Imd}^- + r\mathrm{M}^{2+} + s\mathrm{H}^+ \rightleftharpoons (\mathrm{Pm}_l\mathrm{Glygly}_p\mathrm{Imd}_q\mathrm{M}_r\mathrm{H}_s)^z, \quad (2)$$

where l, p, q, r and s are the stoichiometric coefficients, and $z = (2r+s)-(l+p)$.

Many equilibrium models (at least 20 models) have been tried using the MINIQUAD-75 program. The accepted models were based on the values of chi square $[(xi)^2]$, reliability factor (R) and sum of the squared residuals (S) whenever they were the smallest and when the calculated values of the constants had the smallest standard deviations. Furthermore, the effect of variations in the values of protonation constants and binary formation constants of the chosen ternary model (and also ternary formation constants in the case of the chosen quaternary model) were tested. The selected equilibrium models depicted in Tables 2–4 were adopted in which the values of the formation constants did not change on testing within their standard deviations.

Ternary complexes of Co(II), Ni(II), Zn(II) *and* Cd(II). The ternary complexes of Co(II), Ni(II), Zn(II) and Cd(II) involving Pm–Imd have been previously reported.[4] Only the systems involving Pm–Glygly and Glygly–Imd will be discussed in this work. It seems from Tables 2 and 3 that the metal ions under consideration are incapable of deprotonating the peptidic proton in the presence of Pm and Imd contrary to the systems involving Cu(II).[3] This finding may be understood in the cases of the Zn(II) and Cd(II) systems due to early precipitation but not in the cases of the Co(II) and Ni(II) systems. However, it may be rationalized on the basis of ionic potential where the electrostatic interaction between different ligands is greater in the Cu(II) system than in the Co(II) and Ni(II) systems. Another feature can be extracted from Tables 2 and 3, that a number of protonated species appear in the Pm–Glygly systems, similar to the Pm–Imd systems,[4] while none of these complexes appear in the Glygly–Imd system. One should expect that protons are located on the Pm moiety presumably on the pyridinic nitrogen (Pm acts as a bidentate ligand)

Table 2. Formation constants of the ternary complexes of the Pm–Glygly system with Co(II), Ni(II), Zn(II) and Cd(II) at 0.15 M (KNO_3), $T = 37°C$

System	l	p	r	s	log β ($\pm\sigma$)	S	X_i^2	R	n	pH range
H^+	1	0	0	1[a]	10.41					
	1	0	0	2[a]	18.56					
	1	0	0	3[a]	22.06					
Co(II)	1	1	1	0	8.46 (0.04)	4.6E−7	38	0.013	202	7.1–8.6
	1	1	1	1	17.05 (0.04)					
Ni(II)	1	1	1	0	10.55[b]					
	1	1	1	2	26.26 (0.08)	9.8E−7	74	0.024	189	6.1–9.8
	1	2	1	2	29.07 (0.50)					
	2	1	1	2	32.13 (0.20)					
Zn(II)	1	1	1	0	8.95[b]					
	1	2	1	0	13.81 (0.10)	8.4E−7	48	0.028	164	6.7–9.3
	2	1	1	0	15.16 (0.12)					
	2	1	1	4	47.69 (0.11)					
Cd(II)	1	1	1	0	8.80[b]					
	1	1	1	1	17.36 (0.04)	5.7E−8	133	0.005	208	7.0–9.4
	1	2	1	0	11.91 (0.02)					
	1	2	1	1	20.48 (0.06)					
	1	2	1	2	28.48 (0.07)					
	2	1	1	4	47.00 (0.05)					

[a] Reference 3.
[b] Estimated from Fig. 2.

and on the amino group (Pm acts as a monodentate ligand).

The application of an equation similar to eqn (1) on the ternary Pm–Glygly and Glygly–Imd complex systems:

$$\log \beta_{1MLL'H_s} = (\log \beta_1^{HL} + \log \beta_1^{HL'}) + \frac{1}{2.303RT}[G^o(M)2G^o(H)] + [G^o(HL) + G^o(HL')] + G^o(MLL'H_s), \quad (3)$$

where L and L′ are two different ligands, together with the systems previously studied[3,4] reveals a linear relationship between the ternary formation constants (log $\beta_{1MLL'H_s}$) and (log β_1^{HL} + log $\beta_1^{HL'}$) (Fig. 2).

However, the slope is not 1 but less than 1 in the Co(II), Ni(II), Zn(II) and Cd(II) systems, and surprisingly is 1 in the case of the Cu(II) systems. In addition, the plots of log K^1 ($K^1 = \beta_{1MLL'H_s}/\beta_{1MLH_m}\beta_{1ML'H_m}$) vs the sum (log β_1^{HL} + log $\beta_1^{HL'}$) are also linear for the 1 : 1 : 1 : 0 spec-

Table 3. Formation constants of the ternary complexes of the Pm–Glygly system with Co(II), Ni(II), Zn(II) and Cd(II) at 0.15 M (KNO_3), $T = 37°C$: p, q, r and s stand for Glygly, Imd, M^{2+} and H^+, respectively

System	p	q	r	s	log β ($\pm\sigma$)	S	X_i^2	R	n	pH range
H^+	0	0	1	1	7.09[a]					
Co(II)	(a) 1	1	1	0	6.79 (0.40)	7.6E−7	144	0.046	210	7.4–8.6
	1	3	1	0	13.93 (0.15)					
	(b) 1	3	1	0	12.10 (0.04)	4.2E−7	476	0.011	210	7.4–8.6
	2	2	1	0	12.12 (0.06)					
Ni(II)	1	1	1	0	8.82 (0.11)	1.4E−6	520	0.034	194	7.2–8.6
	2	2	1	0	14.30 (0.31)					
Zn(II)	1	1	1	0	6.77 (0.05)	4.8E−7	376	0.012	278	6.5–7.8
	1	3	1	0	12.56 (0.04)					
Cd(II)	1	1	1	0	7.09 (0.10)	1.8E−7	450	0.011	140	7.4–9.0
	1	4	1	0	14.70 (0.18)					

[a] Reference 3.

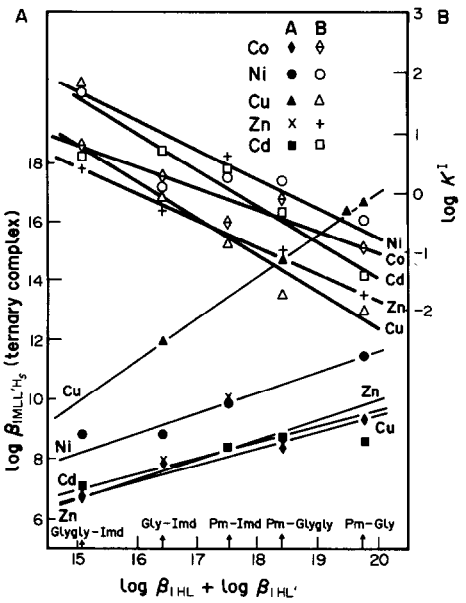

Fig. 2. Dependence of $\log \beta_{1MLL'H_s}$ (scale A) and $\log K^1$ (scale B) for ternary complexes on ($\log \beta_{1HL} + \log \beta_{1HL'}$) of Co(II), Ni(II), Zn(II) and Cd(II) metal ions.

ies (Fig. 2) with negative slopes. This linear dependence may show the bonding strength and, in particular, the extent of the contribution of π-bonding character. It should be kept firmly in mind that the magnitudes of $\log K^1$ is strongly influenced by statistical differences in the formation of each complex as well as differences in bonding. The statistical values of $\log K^1$ depend on the coordination number of the metal ion and denticity of the ligands,[8,9] e.g. for the tetragonal complexes of Cu(II) with bidentate ligands the statistical value is $-\log 4$ (-0.6). For other geometries the statistical values may be less but are always negative. Values of $\log K^1$ greater than -0.6 indicate that ternary metal complex formation is more favored over that of binary metal complexes and reasons other than statistics should be considered. Although $\log K^1$ may be evidence for the formation of the ternary complexes, other approaches may also be considered to indicate its formation in solution.[2]

Quaternary complexes of Co(II), Ni(II), Zn(II) *and* Cd(II). Table 4 shows the formation constants of the quaternary complexes of the Pm–Glygly–Imd system with Co(II), Ni(II), Zn(II) and Cd(II). They are less by one log unit than the Pm–Gly–Imd systems.[4] This may be ascribed to the more steric hindrance exerted by Glygly-containing quaternary complexes over the Pm–Gly–Imd systems. The complexes are mostly protonated: where possible the protons are located on Pm and Glygly (e.g. in the case of 1:1:1:1:2 and 1:1:1:1:3 species).

Table 4. Formation constants of the ternary complexes of the Pm–Glygly–Imd system with Co(II), Ni(II), Zn(II) and Cd(II) at 0.15 M (KNO_3), $T = 37°C$: *l*, *p*, *q*, *r* and *s* stand for Pm, Glygly, Imd, M^{2+} and H^+, respectively

System	*l*	*p*	*q*	*r*	*s*	$\log \beta$ ($\pm\sigma$)	*S*	X_i^2	*R*	*n*	pH range
Co(II)	1	1	1	1	0	11.41 (0.06)	2.7E−7	169	0.002	246	6.6–8.8
	1	1	1	1	1	20.19[a]					
	1	1	1	1	2	27.66 (0.17)					
	1	1	2	1	1	23.34 (0.02)					
	1	1	2	1	2	31.14 (0.04)					
Ni(II)	1	1	1	1	0	13.39[a]					
	1	1	1	1	1	22.17 (0.28)	3.7E−8	45	0.012	148	6.4–9.5
	1	1	1	1	2	30.21 (0.14)					
	1	1	1	1	3	37.34 (0.07)					
	1	1	2	1	1	25.38 (0.14)					
	1	1	2	1	2	33.25 (0.11)					
Zn(II)	1	1	1	1	0	14.58[a]					
	1	1	1	1	1	23.37[a]					
	1	1	1	1	2	29.83[a]					
	1	1	1	1	3	36.71 (0.12)	8.9E−8	62	0.005	152	6.5–7.5
	1	1	2	1	1	25.22 (0.09)					
	1	1	2	1	2	31.96 (0.31)					
Cd(II)	1	1	1	1	0	12.07[a]					
	1	1	1	1	1	22.76[a]					
	1	1	1	1	2	31.54 (0.14)	5.7E−7	218	0.023	118	6.7–9.2
	1	1	1	1	3	39.23 (0.08)					
	1	1	2	1	0	16.82 (0.20)					

[a] Estimated values.

Table 5. Log values of K' and K'' described by eqns (4) and (5), respectively, for Pm–Gly–Imd and Pm–Glygly–Imd systems

Stoichiometry					Pm–Gly–Imd					Pm–Glygly–Imd				
l	*p*	*q*	*r*	*s*	Co	Ni	Cu	Zn	Cd	Co	Ni	Cu	Zn	Cd
1	1	1	1	1	4.21	3.91	5.35	—	3.74	3.14	2.97	5.0	—	5.02
1	1	2	1	1	6.89	6.31	7.47	7.99	6.26	6.29	6.18	8.15	8.0	
0	0	1	1	0	3.03	3.20	4.02	2.98	2.74					
0	0	1	2	0	5.60	5.25	7.55	5.63	—					

Some of the values of the formation constants have been estimated on the assumption that the differences in the log forms of the formation constants, e.g. 1:1:1:1:0 and 1:1:1:1:1 species, are independent of the type of metal ion [Cu(II) systems are exceptions] or the type of ligand system under consideration, i.e. Gly[3] or Glygly quaternary complex systems. This was found to be true to a great extent in these systems.

It is interesting to notice that the metal ions can acquire up to two molecules of Imd in the presence of Pm and Glygly or Gly.[4] In fact, the chelation of these metal ions with Pm and Gly or Glygly facilitates the ligation with Imd. This may be verified by comparing the formation constants of the equilibrium reactions:

$$\text{M(Pm)(Gly)H [or M(Pm)(Glygly)H]} + \text{Imd} \rightleftharpoons \text{M(Pm)(Gly)(Imd)H [or M(Pm)(Glygly)(Imd)H]},$$

$$K' = \beta_{1QH}/\beta_{1TH}; \quad (4)$$

$$\text{M(Pm)(Gly)H [or M(Pm)(Glygly)H]} + 2\text{Imd} \rightleftharpoons \text{M(Pm)(Gly)(Imd)H [or M(Pm)(Glygly)(Imd)}_2\text{H]},$$

$$K'' = \beta_{2QH}/\beta_{1TH} \quad (5)$$

[where β_{1QH} and β_{2QH} are the formation constants of the quaternary 1:1:1:1:*s* and 1:1:2:1:*s* complexes (Pm:Gly or Glygly:Imd:M^{2+}:H^+) and β_{1TH} is the formation constant of the ternary species] with those of the binary complexes of these metal ions with Imd (Table 5).

It it clear from Table 4 that the peptidic proton of Glygly is not dissociated in the quaternary complexes of the metal ions under investigation in contrast to the Cu(II) system previously reported.[1]

CONCLUSION

The aforementioned results may indicate that not only binary and/or ternary complexes could be formed but quaternary complexes may also be formed specially in the pH range 6.5–8.5. Generally, the presence of Pm (specially the protonated forms) in the vicinity of metal ions allows the attack of other nucleophilic ligands leading to the formation of ternary and quaternary species. These complexes are positively charged in most cases, which facilitates their transport in biological fluids but prohibits their transfer through cell membranes since neutral species are preferred.

Acknowledgement—We would like to thank Kuwait University for the provision of the Research Council Grant No. SC021.

REFERENCES

1. M. Makhyoun, N. Al-Salem and M. S. El-Ezaby, *Inorg. Chim. Acta* 1986, **123**, 117.
2. H. M. Marafie, M. S. El-Ezaby, M. Rashad and N. M. Moussa, *Polyhedron* 1984, **3**, 787.
3. M. S. El-Ezaby, M. Rashad and N. M. Moussa, *Polyhedron* 1983, **2**, 245.
4. *Introduction Manual for Cupric Selectrode Type F*1112 Cu. Radiometer A/S, Copenhagen (1972).
5. P. Gans, A. Sabatini and A. Vacca, *Inorg. Chim. Acta* 1976, **18**, 237.
6. (a) L. G. Sillen and A. E. Martell, In *Stability Constants of Metal Ion Complexes*, Special Publication No. 17 (1964), and Supplement No. 1, Special Publication No. 25 (1971). The Chemical Society, London; (b) D. D. Perrin, In *Stability Constants of Metal–Ion Complexes, Part B, Organic Ligands*, IUPAC Chemical Data Series, No. 22, Pergamon Press, Oxford (1979).
7. D. R. Williams (Ed.), *An Introduction to Bioinorganic Chemistry*. Charles C. Thomas, Springfield, IL (1976).
8. B. Ben, *Anal. Chim. Acta* 1962, **27**, 515.
9. V. S. Sharma and T. J. Schubert, *J. Chem. Educ.* 1969, **46**, 506.

Polyhedron Vol. 6, No. 6, pp. 1483–1489, 1987
Printed in Great Britain

0277–5387/87 $3.00+.00

THE ISOLATION AND CHARACTERIZATION OF THE FIRST EXAMPLES OF PAIRS OF α- AND β-ISOMERS OF DIRHENIUM(II) OF TYPE $Re_2X_4(LL)_2$ (X = Cl OR Br, LL = BIDENTATE PHOSPHINE LIGAND)

LORI BETH ANDERSON, MOHAMMED BAKIR and RICHARD A. WALTON*

Department of Chemistry, Purdue University, West Lafayette, IN 47907, U.S.A.

(*Received* 28 *November* 1986; *accepted* 23 *January* 1987)

Abstract—The complexes $Re_2Br_4(depe)_2$ and $Re_2X_4(dppee)_2$ (X = Cl or Br, depe = $Et_2PCH_2CH_2PEt_2$, dppee = *cis*-$Ph_2PCH{=}CHPPh_2$) have been prepared in their α- (eclipsed rotational geometry, chelating phosphine ligands) and β- (staggered rotational geometry, bridging phosphine ligands) isomeric forms. The chloro complex β-$Re_2Cl_4(depe)_2$ has also been isolated. In the case of α- and β- $Re_2Br_4(depe)_2$, the preparations involve the reactions of $Re_2Br_4(P\text{-}n\text{-}Pr_3)_4$ with depe in toluene–ethanol. While α-$Re_2X_4(dppee)_2$ are prepared from the reactions of $(n\text{-}Bu_4N)_2Re_2X_8$ with dppee in various solvents, the β-isomers are obtained upon reacting $Re_2X_4(PR_3)_4$ (R = Et or *n*-Pr) with dppee in benzene. These are the first examples of triply bonded dirhenium(II) complexes that have been isolated in both their α- and β-forms. β-$Re_2X_4(dppee)_2$ (X = Cl or Br) constitute the first examples of complexes of this structural type which contain both C=C and M≡M units within the same fused decalin-like ring system. The isomers β-$Re_2Cl_4(depe)_2$ and β-$Re_2X_4(dppee)_2$ (X = Cl or Br) are oxidized by $NOPF_6$ in acetonitrile to give paramagnetic β-$[Re_2Cl_4(depe)_2]PF_6$ and β-$[Re_2X_4(dppee)_2]PF_6$. These oxidized complexes in turn react with CH_3CN in the presence of $TlPF_6$ to afford β-$[Re_2Cl_3(depe)_2(NCMe)](PF_6)_2$ and β-$[Re_2X_3(dppee)_2(NCMe)](PF_6)_2$, respectively. The cleavage of the Re≡Re bonds of α- and β-$Re_2Cl_4(dppee)_2$ occurs upon their reaction with CCl_4–CH_2Cl_2 to give *cis*-$ReCl_4(dppee)$. The related bromo complex *cis*-$ReBr_4(dppee)$ is formed when β-$Re_2Br_4(dppee)_2$ is reacted with CH_2Cl_2–Br_2.

The existence of the complexes β-$M_2X_4[R_2P(CH_2)_2PR_2]_2$ (M = Mo, W, or Re; X = Cl, Br or I; R = Me, Et or Ph) which contain intramolecular bridging phosphine ligands has sparked considerable interest.[1–4] This bonding mode leads to the formation of two stable six-membered rings that are fused about a common metal–metal quadruple (M = Mo or W) or triple (M = Re) bond. These compounds have proved to be of significance in metal–metal multiple bond chemistry from the point of view of the ring conformations that are present, the rotational geometry (eclipsed or staggered) about the metal–metal multiple bond, and their chirality.[1–3,5] In the case of the complexes where M = Mo or W, the related α-isomers, in which the phosphine ligands are chelating and there is an eclipsed rotational geometry, have also been isolated in some instances.[1–3]

We now report the first cases of dirhenium(II) complexes of this type which have been isolated in both their α- and β-isomeric forms [the phosphine ligands are $Et_2PCH_2CH_2PEt_2$(depe) and *cis*-$Ph_2PCH{=}CHPPh_2$(dppee)]. In the case of β-$Re_2X_4(Ph_2PCH{=}CHPPh_2)_2$ (X = Cl or Br), these complexes constitute the first examples of complexes of this type which contain both C=C and M≡M units within the same fused decaline-like ring system.

EXPERIMENTAL

Starting materials

Samples of the complexes $Re_2Cl_6(P\text{-}n\text{-}Bu_3)_2$,[6] $Re_2Cl_4(PEt_3)_4$,[7] $Re_2X_4(P\text{-}n\text{-}Pr_3)_4$ (X = Cl or Br)[7]

* Author to whom correspondence should be addressed.

and α-$Re_2Cl_4(dmpe)_2$[8] were prepared, according to the literature methods, from $(n\text{-}Bu_4N)_2Re_2X_8$ (X = Cl or Br)[9,10] and the appropriate phosphine in alcohol solution. The $Me_2PCH_2CH_2PMe_2$(dmpe), depe and dppee ligands were purchased from Strem Chemicals. In the case of depe, a 0.606 M solution in toluene was used. The $LiBEt_3H$ reagent was obtained from Aldrich as a 1.0 M solution in THF. Solvents used in the preparation of the complexes were of commercial grade and were thoroughly deoxygenated prior to use.

Reaction procedures

All reactions were performed in a nitrogen atmosphere using standard vacuum line techniques. Chromatographic separations were performed on a silica gel column (60–200-mesh, Davidson Grade 62).

(A) *Preparation of* $Re_2X_4(depe)_2$. (i) β-$Re_2Cl_4(depe)_2$. A quantity of $Re_2Cl_4(P\text{-}n\text{-}Pr_3)_4$ (0.30 g, 0.26 mmol) was suspended in 20 cm^3 of a 1 : 1 mixture (by volume) of toluene and ethanol, and then treated with depe (1.29 cm^3, 0.78 mmol). This reaction mixture was refluxed for 20 h, cooled to room temperature, and ethanol (~ 15 cm^3) was added. The purple crystalline product which precipitated from the purple-brown solution was collected by filtration, washed with ethanol and hexane, then dried *in vacuo*: yield 0.140 g (70%). Found: C, 25.8; H, 5.3. Calc. for $C_{20}H_{48}Cl_4P_4Re_2$: C, 25.9; H, 5.2%.

(ii) α-$Re_2Br_4(depe)_2$. The preparation of this complex involved refluxing a mixture of $Re_2Br_4(P\text{-}n\text{-}Pr_3)_4$ (0.465 g, 0.35 mmol) and depe (1.75 cm^3, 1.1 mmol) in 20 cm^3 of a 1 : 1 mixture (by volume) of toluene and ethanol for 24 h. The reaction mixture was cooled, filtered, and the dark green crystalline solid collected. The purple-brown filtrate was set aside [see A(iii)]. The green product was washed with ethanol and hexane and dried *in vacuo*; yield 0.262 g (68%). Found: C, 22.0; H, 4.4. Calc. for $C_{20}H_{48}Br_4P_4Re_2$: C, 21.7; H, 4.4%.

(iii) β-$Re_2Br_4(depe)_2$. Addition of 20 cm^3 of ethanol to the purple-brown filtrate obtained from A(ii) yielded a purple solid. This was collected, washed with ethanol and hexane and dried *in vacuo*; yield 0.032 g (8%). The identity of this product was based upon its electrochemical and spectroscopic properties (*vide infra*).

(B) *Preparation of* $Re_2X_4(dppee)_2$. (i) α-$Re_2Cl_4(dppee)_2$. A mixture comprising $(n\text{-}Bu_4N)_2Re_2Cl_8$ (0.20 g, 0.175 mmol), dppee (0.60 g, 1.51 mmol), and 10 cm^3 of methanol, to which eight drops of conc. HCl had been added, was refluxed for 24 h. The resulting reaction mixture was cooled to room temperature and filtered to give a green solid and yellow filtrate. The solid was washed with methanol until the washings were colorless, and then with hexanes and finally diethyl ether. It was purified by chromatography (silica gel column with CH_2Cl_2 as eluent) and recrystallized from CH_2Cl_2–diethyl ether; yield 0.035 g (15%). Found: C, 47.9; H, 3.7; Cl, 11.0. Calc. for $C_{52}H_{44}Cl_4P_4Re_2$: C, 47.8; H, 3.4; Cl, 10.8%.

The reaction between $(n\text{-}Bu_4N)_2Re_2Cl_8$ and dppee in refluxing ethanol (4 days) likewise gave α-$Re_2Cl_4(dppee)_2$ in low yield. Work-up of the yellow filtrate from this reaction, and that from the analogous reaction in methanol–conc. HCl (*vide supra*), gave *trans*-$[ReCl_2(dppee)_2]Cl \cdot nH_2O$ as a second product.[11] The reaction of $Re_2Cl_6(P\text{-}n\text{-}Bu_3)_2$ (0.10 g, 0.10 mmol) with dppee (0.26 g, 0.67 mmol) in refluxing ethanol (10 cm^3) for 4 days gave a green-yellow solid which was filtered off, washed with hexanes and diethyl ether, and dried. This product was washed with CH_2Cl_2 to give a green extract [shown to be α-$Re_2Cl_4(dppee)_2$]; the remaining orange-yellow solid was shown to be *trans*-$ReCl_2(dppee)_2$.*

(ii) β-$Re_2Cl_4(dppee)_2$. A mixture of $Re_2Cl_4(PEt_3)_4$ (0.15 g, 0.152 mmol), dppee (0.18 g, 0.454 mmol) and 10 cm^3 of benzene was refluxed for 2 days. The reaction mixture was cooled to room temperature and filtered. A light brown solid was collected, and washed with benzene, methanol, hexanes and diethyl ether. The product was purified by chromatography (silica gel column with CH_2Cl_2 as eluent) and recrystallized from CH_2Cl_2–diethyl ether: yield 0.09 g (45%). Found: C, 47.7; H, 3.4. Calc. for $C_{52}H_{44}Cl_4P_4Re_2$: C, 47.8; H, 3.4%.

β-$Re_2Cl_4(dppee)_2$ was isolated in 35% yield when $Re_2Cl_4(P\text{-}n\text{-}Pr_3)_4$ was used in place of $Re_2Cl_4(PEt_3)_4$ in the above procedure.

(iii) α-$Re_2Br_4(dppee)_2$. The reaction between $(n\text{-}Bu_4N)_2Re_2Br_8$ (0.10 g, 0.067 mmol) and dppee (0.23 g, 0.580 mmol) in 10 cm^3 of methanol that contained eight drops of conc. HBr (48%) was carried out with a procedure similar to that described in B(i) and a reaction time of 2 days. The green insoluble product was found to be the bis-CH_2Cl_2 solvate: yield 0.02 g (20%). Found: C, 39.1; H, 2.9. Calc. for $C_{54}H_{48}Br_4Cl_4P_4Re_2$: C, 39.2; H, 2.9%. The presence and amount of CH_2Cl_2 was confirmed by ^1H NMR spectroscopy in $(CD_3)_2SO$ ($\delta = +5.76$).

The filtrate from this reaction was evaporated to low volume to afford orange crystals of $[ReBr_2(dppee)_2]Br \cdot H_2O$: yield 0.036 g (22%).[11]

* The identity of *trans*-$ReCl_2(dppee)_2$ has been established by an X-ray structure analysis[11] and its independent preparation from the one-electron reduction of *trans*$[ReCl_2(dppee)_2]Cl$.

(iv) β-$Re_2Br_4(dppee)_2$. The reaction between $Re_2Br_4(PR)_3)_4$ (R = Et or *n*-Pr) and dppee in refluxing benzene gave brown β-$Re_2Br_4(dppee)_2$ in yields of 35–50% when a procedure similar to B(ii) was used. Purification was affected by chromatography (silica gel column with CH_2Cl_2 as eluent) and recrystallization from CH_2Cl_2–diethyl ether. Found: C, 42.2; H, 3.2. Calc. for $C_{52}H_{44}Br_4P_4Re_2$: C, 42.1; H, 3.0%.

(C) *Reactions of the* $Re_2X_4(depe)_2$ *complexes.* (i) β-$[Re_2Cl_4(depe)_2]PF_6$. The neutral species β-$Re_2Cl_4(depe)_2$ was oxidized by suspending a quantity of it (0.10 g, 0.11 mmol) in 4 cm^3 of CH_3CN. The suspension was chilled, and a stoichiometric quantity of $NOPF_6$ (0.021 g, 0.12 mmol) added. Following the addition of $NOPF_6$, all of the solid dissolved to yield a red-violet solution. The solution was warmed to room temperature and stirred for 30 min. It was filtered to remove any trace amounts of unreacted $NOPF_6$ and diethyl ether was added to the filtrate. The resulting red-violet solid was collected by filtration, washed with diethyl ether and dried *in vacuo*: yield 0.085 g (74%). Found: C, 22.3; H, 4.7. Calc. for $C_{20}H_{48}Cl_4F_6P_5Re_2$: C, 22.4; H, 4.5%. Addition of an excess of $NOPF_6$ produced the dark purple, air-sensitive dication $[Re_2Cl_4(depe)_2](PF_6)_2$ as evidenced by its electrochemical properties.

(ii) β-$[Re_2Cl_3(depe)_2(NCMe)](PF_6)_2$. The preparation of this complex involved dissolving β-$[Re_2Cl_4(depe)_2]PF_6$ [see C(i)] (0.10 g, 0.093 mmol) and $TlPF_6$ (0.032 g, 0.093 mmol) in 5 cm^3 of acetone and adding 1 cm^3 of CH_3CN. When the reaction mixture was stirred for 12 h, a white precipitate of TlCl formed in the purple-colored reaction medium. This mixture was filtered to remove the TlCl, and diethyl ether was added to the filtrate to precipitate a purple-brown solid. This was collected, washed with diethyl ether and dried *in vacuo*: yield 0.085 g (75%). Found: C, 22.0; H, 4.7. Calc. for $C_{22}H_{51}Cl_3F_{12}NP_6Re_2$: C, 21.6; H, 4.2%.

(iii) β-$[Re_2Cl_3(depe)_2(NCMe)]PF_6$. The reduction of $[Re_2Cl_3(depe)_2(NCMe)](PF_6)_2$ [C(ii)] was accomplished by placing a quantity of it (0.075 g, 0.061 mmol) in 5 cm^3 of THF and adding a solution of $LiBEt_3H$ in THF (0.10 cm^3). The violet suspension turned green-brown within 5 min of stirring the reaction mixture at room temperature. Stirring was continued for a total of 30 min, and diethyl ether added to the green-brown solution to precipitate a light green solid. This solid was collected and recrystallized from CH_2Cl_2–diethyl ether and dried *in vacuo*: yield 0.048 g (73%). Found: C, 24.7; H, 4.8. Calc. for $C_{22}H_{51}Cl_3F_6NP_5Re_2$: C, 24.5; H, 4.8%.

(D) *Reactions of the* $Re_2X_4(dppee)_2$ *complexes.* (i) β-$[Re_2Cl_4(dppee)_2]PF_6$. A mixture of β-$Re_2Cl_4(dppee)_2$ (0.15 g, 0.115 mmol) and $NOPF_6$ (0.022 g, 0.125 mmol) was dissolved in 10 cm^3 of CH_3CN and then stirred for 30 min at room temperature. The solution was reduced in volume and diethyl ether was added to precipitate the product. A pale blue solid was filtered off, washed with hexanes and diethyl ether, and dried *in vacuo*: yield 0.14 g (84%). Found: C, 43.4; H, 3.2. Calc. for $C_{52}H_{44}Cl_4F_6P_5Re_2$: C, 43.0; H, 3.0%.

(ii) $[Re_2Br_4(dppee)_2]PF_6$. A procedure similar to D(i) produced a purple solid; yield 97%. Found: C, 39.0; H, 3.0. Calc. for $C_{52}H_{44}Br_4F_6P_5Re_2$: C, 38.3; H, 2.7%.

(iii) β-$[Re_2Cl_3(dppee)_2(NCMe)](PF_6)_2$. A mixture of β-$[Re_2Cl_4(dppee)_2]PF_6$ (0.09 g, 0.062 mmol) and $TlPF_6$ (0.02 g, 0.06 mmol) was dissolved in 10 cm^3 of CH_3CN. The reaction mixture was stirred at room temperature for 4 h and then evaporated to dryness. The residue was dissolved in CH_2Cl_2 and filtered into a flask containing diethyl ether. The purple insoluble product was filtered off, washed with hexanes and diethyl ether, and dried *in vacuo*: yield 0.075 g (81%). Found: C, 41.9; H, 3.4; Cl, 5.9. Calc. for $C_{54}H_{47}Cl_3F_{12}P_6Re_2$: C, 40.5; H, 3.0; Cl, 6.6%.

(iv) β-$[Re_2Br_3(dppee)_2(NCMe)](PF_6)_2$. A procedure identical to D(iii) produced a purple solid: yield 93%. Found: C, 38.1; H, 3.0. Calc. for $C_{54}H_{47}Br_3F_{12}P_6Re_2$: C, 37.4; H, 2.7%.

(v) *cis*-$ReCl_4(dppee)$. α-$Re_2Cl_4(dppee)_2$ (0.05 g, 0.038 mmol), 5 cm^3 of CH_2Cl_2, and 10 cm^3 of CCl_4 were refluxed for 2 days. The reaction mixture was cooled to room temperature, the solvent evaporated, and the resulting orange residue was extracted into CH_2Cl_2, filtered, and diethyl ether added to the filtrate to crystallize *cis*-$ReCl_4(dppee)$: yield 0.03 g (54%). Found: C, 42.8; H, 3.2; Cl, 19.2. Calc. for $C_{26}H_{22}Cl_4P_2Re$: C, 43.1; H, 3.1; Cl, 19.6%.

When β-$Re_2Cl_4(dppee)_2$ was used in place of the α-isomer, this same mononuclear Re(IV) complex *cis*-$ReCl_4(dppee)$ was isolated in 88% yield.

(vi) *cis*-$ReBr_4(dppee)$. A quantity of β-$Re_2Br_4(dppee)_2$ (0.05 g, 0.034 mmol), was suspended in 10 cm^3 of CH_2Cl_2 and treated with 2 drops of liquid Br_2. This mixture was then stirred at room temperature for 18 h. The solvent was evaporated and the resulting dark red residue was worked-up as described in D(v): yield 0.06 g (98%). Found: C, 34.9; H, 2.7. Calc. for $C_{26}H_{22}Br_4P_2Re$: C, 34.6; H, 2.5%.

Physical measurements

IR spectra were recorded as Nujol mulls using an IBM IR/32 Fourier transform spectrometer (4000–

400 cm^{-1}). Electronic absorption spectra were recorded as CH_2Cl_2 solutions on Cary 17D and IBM 9420 spectrophotometers. Electrochemical experiments were performed by using a Bioanalytical Systems, Inc., Model CV-1A instrument in conjunction with a Hewlett–Packard Model 7035B x–y recorder. CH_2Cl_2 solutions containing 0.1 *M* tetra-*n*-butylammonium hexafluorophosphate (TBAH) as a supporting electrolyte were utilized. $E_{1/2}$ values $[(E_{p,a}+E_{p,c})/2]$ were referenced against an Ag-AgCl electrode at room temperature and were uncorrected for junction potentials. ^{31}P NMR and ^{1}H NMR spectra were recorded with use of a Varian XL-200 spectrometer. The ^{31}P NMR spectra were referenced to H_3PO_4 as an internal standard while for the ^{1}H NMR spectra resonances were referenced internally to the residual protons of the incompletely deuterated solvents.

Analytical procedures

Elemental microanalyses were performed by Dr H. D. Lee of the Purdue University microanalytical laboratory.

RESULTS AND DISCUSSION

Preparation and characterization of $Re_2X_4(depe)_2$ (X = Cl *or* Br)

The complex β-$Re_2Cl_4(depe)_2$ was first prepared and structurally characterized by Cotton and coworkers.[12] However, the reported method for its synthesis produced the desired compound in 20% yield. In order to explore the reaction chemistry of this complex, an improved synthetic route was desirable. We found that by using $Re_2Cl_4(P\text{-}n\text{-}Pr_3)_4$ in place of $(n\text{-}Bu_4N)_2Re_2Cl_8$ and refluxing this, in the presence of depe, in a mixed-solvent system (to enhance the solubility of the starting dirhenium complex), the yield of β-$Re_2Cl_4(depe)_2$ was increased to *ca* 70%. The bromide analogue β-$Re_2Br_4(depe)_2$ could also be isolated using reaction conditions similar to those employed in the preparation of the chloride derivative. The β-isomer, however, was formed in very low yield (< 10%), while the major product of the reaction was α-$Re_2Br_4(depe)_2$. The α-form is insoluble in the reaction mixture and crystallizes during the course of the reaction. This is the first time that α- and β-isomers of a dirhenium(II) complex of this type have been isolated although both isomers are known for certain dimolybdenum(II) and ditungsten(II) species.[1-4]

The identification of the new species α- and β-$Re_2Br_4(depe)_2$* was based upon a comparison of their electrochemical and spectroscopic properties (Table 1) with the related behavior of the structurally characterized complexes α-$Re_2Cl_4(dmpe)_2$,[8] α-$Re_2Cl_4(dppp)_2$ [dppp = $Ph_2P(CH_2)_3PPh_2$],[13] β-$Re_2Cl_4(depe)_2$[12] and β-$Re_2Cl_4(dppe)_2$[dppe = $Ph_2P(CH_2)_2PPh_2$].[14-16] In the case of α-$Re_2Cl_4(dmpe)_2$ and β-$Re_2Cl_4(depe)_2$, these data have not been reported previously and so are included here for the first time (see Table 1). The cyclic voltammograms (CVs) of solutions of these complexes in 0.1 M TBAH–CH_2Cl_2 revealed the presence of two accessible one-electron oxidations (Fig. 1); this property is characteristic of the triply bonded Re_2^{4+} core.[2,17] Oxidation of β-$Re_2Cl_4(depe)_2$ to the paramagnetic monocation was achieved by using 1 equivalent of $NOPF_6$ as the oxidizing agent. Attempts to carry out the analogous oxidation of α-$Re_2Br_4(depe)_2$ led to its decomposition. The oxidized species β-$[Re_2Cl_4(depe)_2]PF_6$ possesses electrochemical processes at $E_{1/2}$ = +0.08 V(red) and $E_{1/2}$ = +0.88 V(ox) vs Ag–AgCl (Fig. 1). The X-band ESR spectrum of the monocation, as measured at −160°C in CH_2Cl_2,

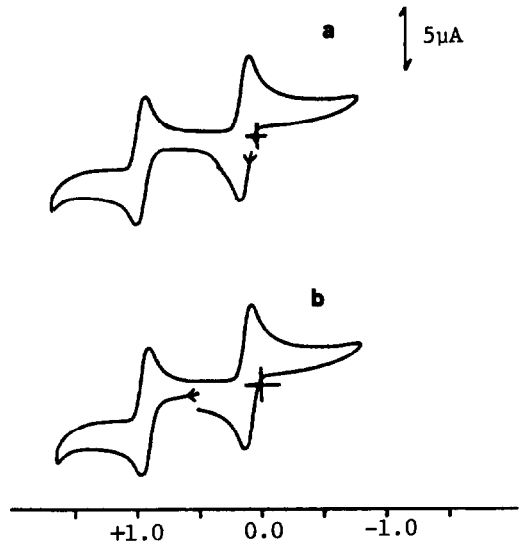

Fig. 1. Cyclic voltammograms (recorded at v = 200 mV s^{-1} using a Pt-bead electrode) for 0.1 M TBAH–CH_2Cl_2 solutions of: (a) β-$Re_2Cl_4(depe)_2$, and (b) β-$[Re_2Cl_4(depe)_2]PF_6$.

* The structure of α-$Re_2Br_4(depe)_2$ has recently been confirmed by a single-crystal X-ray structure analysis with data collected at −150°C. The structure [space group $I4_1/acd$, with a = 13.466(2) Å and c = 36.619(7) Å] is disordered and the Re—Re distance is 2.202(6) Å (L. F. Falvello, unpublished results).

Table 1. Electrochemical properties and electronic absorption spectra

Complex	Half-wave potentials[a]		Electronic absorption spectrum[b]	
	$E_{1/2}$(ox 1)	$E_{1/2}$(ox 2)	λ (nm) (ε)	Reference
β-$Re_2Cl_4(depe)_2$	+0.08	+0.88	~ 580sh, 492 (200), 438 (180)	f
α-$Re_2Br_4(depe)_2$	+0.02	+1.07[c]	842 (130), 545 (150)	f
β-$Re_2Br_4(depe)_2$	+0.13	+0.89	505 (200), 442 (200)	f
α-$Re_2Cl_4(dppee)_2$	+0.30	+1.05	825m, 613m, 445sh[e]	f
β-$Re_2Cl_4(dppee)_2$	+0.24	+1.13	~ 640sh, 474 (300)	f
α-$Re_2Br_4(dppee)_2$	+0.33	~ +1.0[d]	842m, 618m, 465sh[e]	f
β-$Re_2Br_4(dppee)_2$	+0.34	+1.15	~ 650sh, ~ 575sh, 475m-s[e]	f
α-$Re_2Cl_4(dmpe)_2$	+0.21	+1.10[c]	874 (190), 563 (100)	f
α-$Re_2Cl_4(dppp)_2$	—	—	820m-s, 642m, 568w, 432s[e]	13
β-$Re_2Cl_4(dppe)_2$	+0.23	+1.04	625sh, 525 (335), 500sh	15, 16

[a] In V vs Ag–AgCl for 0.1 m TBAH–CH_2Cl_2 solutions recorded at $v = 200$ mV s^{-1}. In the case of the reversible couples, the ΔE_p values ($= E_{p,a} - E_{p,c}$) are in the range 90–130 mV.

[b] Spectra recorded in CH_2Cl_2 unless otherwise stated; ε values are given in parentheses.

[c] $E_{p,a}$ value.

[d] Approximate value since for $E_{p,a} = +1.08$ V and $E_{p,c} = +0.90$ V, $i_{p,a} > i_{p,c}$.

[e] Recorded as Nujol mull. Relative intensities of bands are signified by w = weak, m = medium and s = strong.

[f] This work.

displayed a broad signal between 1000 and 4000 G which is centered at $g = 2.1$. In the presence of an excess of $NOPF_6$, the second oxidation can be accessed to yield the dark purple air-sensitive dication. This species was characterized by cyclic voltammetry in 0.1 M TBAH–CH_2Cl_2 solution; the processes at $E_{1/2} = +0.08$ V and $E_{1/2} = +0.88$ V correspond to reductions.

While β-$Re_2Cl_4(depe)_2$ did not react with CH_3CN, its oxidized congener β-[$Re_2Cl_4(depe)_2$]PF_6 did so to give [$Re_2Cl_3(depe)_2(NCMe)$]$(PF_6)_2$ when $TlPF_6$ was present. This behavior resembles that observed in the case of the formation of the dppe analogues [$Re_2X_3(dppe)_2(NCMe)$]$(PF_6)_2$ (X = Cl or Br).[18] The CV of the paramagnetic dication exhibits $E_{1/2} = +0.35$ V(red) and $E_{p,a} = +1.55$ V vs Ag–AgCl. In this depe-bridged system, the potentials are shifted by at least 1 V to more positive values compared to the dppe analogue.[18] Thus, while the irreversible reduction at ~ −1.5 V in the CV of [$Re_2X_3(dppe)_2(NCMe)$]$(PF_6)_2$ is apparently shifted to a potential below the solvent limit in the CV of [$Re_2Cl_3(depe)_2(NCMe)$]$(PF_6)_2$, an additional oxidation is not accessible (at +1.55 V). These differences presumably reflect the greater σ-donor ability of depe compared to dppe. The complex behaves as a 2:1 electrolyte in acetone ($\Lambda_M = 170$ Ω^{-1} cm^2 mol^{-1}), in accord with its formulation as a dication. The paramagnetism of this species is evidenced by its ESR spectrum measured at −160°C in CH_2Cl_2 ($g \simeq 2.1$). The electronic absorption spectrum of [$Re_2Cl_3(depe)_2(NCMe)$]$(PF_6)_2$ in CH_2Cl_2 has λ_{max} at 1275 nm (ε = 150), 640 nm(sh), 486 nm (ε = 700) and 424 nm (ε = 900).

The dication [$Re_2Cl_3(depe)_2(NCMe)$]$(PF_6)_2$ could be reduced chemically to [$Re_2Cl_3(depe)_2$ (NCMe)]PF_6 by the use of $LiBEt_3H$ in THF solution. The electrochemistry of the resulting monocation displays $E_{1/2} = +0.35$ V(ox), as well as $E_{p,a} = +1.55$ V vs Ag–AgCl. The conductivity of a 1×10^{-3} M acetone solution is consistent with the formulation as a 1:1 salt ($\Lambda_M = 120$ Ω^{-1} cm^2 mol^{-1}). Its electronic absorption spectrum, recorded in CH_2Cl_2 solution exhibits λ_{max} at 645 nm (ε = 120), 506 nm (ε = 200) and a shoulder at 400 nm, while the IR spectrum (Nujol mull) possesses a weak ν(CN) mode at 2269 cm^{-1} due to the coordinated MeCN ligand. Its $^{31}P-\{^1H\}$ NMR spectrum, measured in $(CD_3)_2CO$ solution, is similar to that of [$Re_2X_3(dppe)_2(NCMe)$]PF_6,[18] namely two apparent triplets at δ −4.81 and −5.02 which are the components of an AA′BB′ pattern.

Preparation and characterization of $Re_2X_4(dppee)_2$ (X = Cl *or* Br)

The phosphine ligand dppee reacts with $(n\text{-}Bu_4N)_2Re_2Cl_8$ in refluxing methanol–conc. HCl or ethanol, and with $Re_2Cl_6(P\text{-}n\text{-}Bu_3)_2$ in refluxing ethanol,

to give the green isomer α-$Re_2Cl_4(dppee)_2$ in yields of *ca* 15%. Work-up of the yellow filtrate and washings from the reactions of $(n\text{-}Bu_4N)_2Re_2Cl_8$ with dppee gave *trans*-$[ReCl_2(dppee)_2]Cl \cdot nH_2O$ as an additional reaction product, while *trans*-$ReCl_2(dppee)_2$ is a by-product of the reaction of $Re_2Cl_6(P\text{-}n\text{-}Bu_3)_2$ with dppee. The green bromo analogue α-$Re_2Br_4(dppee)_2$ was formed (yield *ca* 20%) upon heating $(n\text{-}Bu_4N)_2Re_2Br_8$ with an excess of dppee in methanol–conc. HBr (48%) for 2 days. Orange crystalline *trans*-$[ReBr_2(dppee)_2]Br$ was isolated from this reaction filtrate. Upon heating the dirhenium(II) species $Re_2X_4(PR_3)_4$ (X = Cl or Br, R = Et or *n*-Pr) with dppee in benzene, the brown β-isomers of $Re_2X_4(dppee)_2$ precipitated and were isolated in yields of 35–50%.

As shown in Table 1, the distinction between the α- and β-isomers is best seen in the differences between their electronic absorption spectra. The most prominent lowest-energy band is either at ~ 850 nm (α-forms) or at ~ 500 nm (β-forms), with weak lower-energy shoulders also apparent in some of the latter spectra. A further difference is apparent in the case of the low-frequency Nujol mull IR spectra of the chloride complexes in which α-$Re_2Cl_4(dppee)_2$ has ν(Re—Cl) modes at 314s, 282s and 260w cm^{-1}, while for β-$Re_2Cl_4(dppee)_2$ the corresponding bands are at 333s, 320m and 304m cm^{-1}. These data can be compared with that reported for α-$Re_2Cl_4(dppp)_2$ [ν(Re—Cl) at 307s, 292sh and 270m cm^{-1}][13] and β-$Re_2Cl_4(dppe)_2$ [ν(Re—Cl) at 333vs and 303m-s cm^{-1}].[15] These conclusions are further substantiated by differences in the $^{31}P\text{-}\{^1H\}$ NMR spectra of the pairs of α- and β-$Re_2X_4(dppee)_2$ compounds. For the α-isomers, a singlet is observed at δ +29.6 (CD_2Cl_2 solvent) for X = Cl, and at δ +25.9 ($(CD_3)_2SO$ solvent) for X = Br; these chemical shifts are characteristic of five-membered rings formed by chelating phosphines.[5,19] On the other hand, the β-isomers display singlets which are shifted upfield to δ +5.6 (CD_2Cl_2 solvent) and δ −0.2 (CD_2Cl_2 solvent) for X = Cl and Br, respectively. This shift is typical of the greater shielding associated with six-membered rings compared to their five-membered analogues.[19] The ^1H NMR spectra [recorded in CD_2Cl_2 or $(CD_3)_2SO$] showed the expected phenyl resonances along with an AA′XX′ pattern centered between δ +8.2 and +8.8 for the olefinic protons of the dppee ligand.

Although we were able to grow single crystals of β-$Re_2Cl_4(dppee)_2$ for an X-ray structure analysis, a satisfactory structure solution was thwarted by poor crystal quality. While we have not yet been able to obtain better crystals, the preliminary structure analysis is sufficient to clearly define the major structural details of this molecule.*

The reactivity of β-$Re_2X_4(dppee)_2$ towards $NOPF_6$ in CH_3CN resembled that found for β-$Re_2X_4(depe)_2$ (*vide supra*). Oxidation occurred to give β-$[Re_2X_4(dppee)_2]PF_6$ which displayed the expected electrochemical properties (see Table 1), with a one-electron oxidation at $E_{1/2} \simeq +1.1$ V and a one-electron reduction at $E_{1/2} \simeq +0.3$ V vs Ag–AgCl. These complexes behaved as 1 : 1 electrolytes in CH_3CN ($\Lambda_M \sim 125\ \Omega^{-1}\ cm^2\ mol^{-1}$ for $C_M = 1.5 \times 10^{-4}$ M) and had Nujol mull IR spectra with ν(P—F) of PF_6^- at *ca* 850 cm^{-1}. Like their depe analogues, these salts react with acetonitrile in the presence of $TlPF_6$ to give $[Re_2X_3(dppee)_2(NCMe)](PF_6)_2$ whose properties resemble closely those of $[Re_2X_3(depe)_2(NCMe)](PF_6)_2$ (*vide supra*) and $[Re_2X_3(dppe)_2(NCMe)](PF_6)_2$.[18]†

Cleavage of β-$Re_2X_4(dppee)_2$ to give the mononuclear rhenium(IV) complexes *cis*-$ReX_4(dppee)$ occurred upon reaction with CCl_4 (X = Cl) or Br_2 (X = Br). These orange (X = Cl) or dark red (X = Br) colored complexes are almost certainly close structural analogues of *cis*-$ReCl_4(dppe)$.[20] In the case of *cis*-$ReCl_4(dppee)$, its low-frequency IR spectrum showed a pattern for the ν(Re—Cl) modes at 345m, 326s and 305s cm^{-1} that is very characteristic of a *cis*-MCl_4L_2 geometry [i.e. *cis*-$ReCl_4(dppe)$ has ν(Re—Cl) at 346m, 331s and 305s cm^{-1}].[20] Like other complexes of type *cis*-$ReCl_4(LL)$, where LL = dppe, dppm or arphos,[17]

* Crystal data for β-$Re_2Cl_4(dppee)_2$ at 22°C: monoclinic space group $P2_1/n$, $a = 16.684(7)$, $b = 12.869(7)$, $c = 9.766(3)$ Å; $\beta = 106.69(3)°$, $V = 4706(7)$ Å^3, $Z = 4$, $\rho_{calc.} = 1.843$ g cm^{-3}. A preliminary structure analysis was based upon 6458 reflections of which 5431 have $F_o^2 > 5\sigma(F_o^2)$. Like the crystal structures of other multiply bonded dimetal complexes, β-$Re_2Cl_4(dppee)_2$ exhibits a disorder in which there are two orientations of the M_2 unit within the polyhedron defined by the eight donor atoms. The Re—Re distance of 2.24(1) Å (for the major orientation, 76%) is typical of that seen in other complexes that contain Re≡Re bonds.[9,12–14] The staggered rotational geometry about the Re—Re bond is similar to that in β-$Re_2Cl_4(dppe)_2$. In the case of β-$Re_2Cl_4(dppee)_2$ the pairs of Cl—Re—Re—Cl and P—Re—Re—P torsional angles average to approximately 62 and 59°, respectively, while for β-$Re_2Cl_4(dppe)_2$ the corresponding values are 59.6 and 52.4°.[14]

† For example, the CVs of solutions of $[Re_2X_3(dppee)_2(NCMe)](PF_6)_2$ in 0.1 M TBAH–CH_2Cl_2 are as follows: X = Cl, $E_{1/2}(red) = +0.58$ V and $E_{p,c} = -1.67$ V vs Ag–AgCl; X = Br, $E_{1/2}(red) = +0.67$ V and $E_{p,c} \simeq -1.55$ V vs Ag–AgCl. Solutions of these complexes in CH_3CN had $\Lambda_M \simeq 230\ \Omega^{-1}\ cm^2\ mol^{-1}$ for $C_M = 1.2 \times 10^{-4}$ M.

cis-ReX_4(dppee) display a very accessible one-electron reduction in the CVs of their solutions in 0.1 M TBAH–CH_2Cl_2 with $E_{1/2} = +0.13$ V (X = Cl) and $E_{1/2} = +0.21$ V (X = Br) vs Ag–AgCl.

Concluding remarks

The preparation of $Re_2X_4(depe)_2$ and $Re_2X_4(dppee)_2$ is the first time that the α- and β-pairs of the type $M_2X_4(bidentate)_2$ (see **I** and **II**) have been isolated for dirhenium(II), although such pairs are known in the case of the isostructural (but

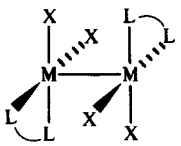

I

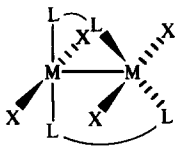

II

not isoelectronic) dimolybdenum(II) and ditungsten(II) cores.[1-4] In contrast to the much studied dimolybdenum(II) complexes of this type,[1,2] we find no evidence for α-⇌β-isomerization in CH_2Cl_2 solutions of these complexes. This surprising result is under further investigation in view of the facility with which this isomerization occurs in the case of α- and β-isomers of $Mo_2X_4(LL)_2$ and the current interest in the mechanism of such transformations.[21,22]

The complexes β-$Re_2X_4(dppee)_2$ are of special interest for they establish the stability of the fused ring system depicted below, and point to the existence of other complexes of this class.*

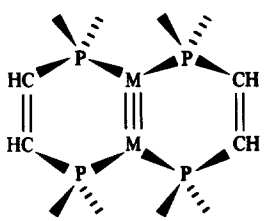

Acknowledgements—We thank the National Science Foundation for support of this research (Grant No. CHE85-06702 to R.A.W.). We are grateful to Dr P. E. Fanwick for carrying out a preliminary study of the crystal structure of β-$Re_2Cl_4(dppee)_2$, and to Dr L. R. Falvello (Texas A&M University) for communicating the results of his attempts to solve the structure of α-$Re_2Br_4(depe)_2$.

* The α- and β-isomers of $Mo_2X_4(dppee)_2$ (X = Cl, Br or I) have now been isolated (M. Bakir, F. A. Cotton, C. Simpson and R. A. Walton, unpublished results).

REFERENCES

1. F. A. Cotton and R. A. Walton, *Multiple Bonds Between Metal Atoms*. Wiley, New York (1982).
2. F. A. Cotton and R. A. Walton, *Struct. Bonding* 1985, **62**, 1.
3. A. C. Price and R. A. Walton, *Polyhedron* 1987, **6**, 729.
4. R. R. Schrock, L. G. Sturgeoff and P. R. Sharp, *Inorg. Chem.* 1983, **22**, 2801.
5. (a) I. F. Fraser and R. D. Peacock, *J. Chem. Soc., Chem. Commun.* 1985, 1727; (b) P. A. Agaskar, F. A. Cotton, I. F. Fraser and R. D. Peacock, *J. Am. Chem. Soc.* 1984, **106**, 1851; (c) I. F. Fraser, A. McVitie and R. D. Peaock, *Polyhedron* 1986, **5**, 39.
6. K. R. Dunbar and R. A. Walton, *Inorg. Chem.* 1985, **24**, 5.
7. J. R. Ebner and R. A. Walton, *Inorg. Chem.* 1975, **14**, 1987.
8. T. J. Barder, F. A. Cotton, K. R. Dunbar, G. L. Powell, W. Schwotzer and R. A. Walton, *Inorg. Chem.* 1985, **24**, 2550.
9. T. J. Barder and R. A. Walton, *Inorg. Chem.* 1982, **21**, 2510.
10. F. A. Cotton, N. F. Curtis, B. F. G. Johnson and W. R. Robinson, *Inorg. Chem.* 1965, **4**, 326.
11. M. Bakir, P. E. Fanwick and R. A. Walton, *Polyhedron* 1987, **6**, 907.
12. F. L. Campbell, III, F. A. Cotton and G. L. Powell, *Inorg. Chem.* 1985, **24**, 4384.
13. N. F. Cole, F. A. Cotton, G. L. Powell and T. J. Smith, *Inorg. Chem.* 1983, **22**, 2618.
14. F. A. Cotton, G. G. Stanley and R. A. Walton, *Inorg. Chem.* 1978, **17**, 2099.
15. P. Brant, H. D. Glicksman, D. J. Salmon and R. A. Walton, *Inorg. Chem.* 1978, **17**, 3203.
16. J. R. Ebner, D. R. Tyler and R. A. Walton, *Inorg. Chem.* 1976, **15**, 833.
17. P. Brant, D. J. Salmon and R. A. Walton, *J. Am. Chem. Soc.* 1978, **100**, 4424.
18. L. B. Anderson, S. M. Tetrick and R. A. Walton, *J. Chem. Soc., Dalton Trans.* 1986, 55.
19. P. E. Garrou, *Chem. Rev.* 1981, **81**, 229.
20. R. E. Myers and R. A. Walton, *Inorg. Chem.* 1976, **15**, 3065.
21. P. A. Agaskar and F. A. Cotton, *Inorg. Chem.* 1986, **25**, 15.
22. S. Christie, I. F. Fraser, A. McVitie and R. D. Peacock, *Polyhedron* 1986, **5**, 35.

Polyhedron Vol. 6, No. 6, pp. 1491–1495, 1987
Printed in Great Britain

0277–5387/87 $3.00+.00

FAST ATOM BOMBARDMENT MASS SPECTROMETRY OF CATIONIC COMPLEXES CONTAINING HOMO- AND HETERO-ATOMIC CYCLIC UNITS *TRIHAPTO*-BONDED TO THE METAL ATOM

GIUSEPPE CETINI, LORENZA OPERTI and GIAN ANGELO VAGLIO*

Istituto di Chimica Generale ed Inorganica, Università, Corso Massimo d'Azeglio 48, 10125 Torino, Italy

and

MAURIZIO PERUZZINI and PIERO STOPPIONI*

Dipartimento di Chimica, Università and Istituto I.S.S.E.C.C., C.N.R., Via Maragliano, 77, 50144 Firenze, Italy

(*Received* 12 *December* 1986; *accepted* 9 *January* 1987)

Abstract—The fast atom bombardment mass spectra of a series of ionic compounds of formula [(triphos)M(η^3-E_2X)]Y (triphos = 1,1,1-tris(diphenylphosphinomethyl)ethane; M = Ni, E = X = P, Y = BF_4 or PF_6; M = Co, E = P, X = S or Se; E = As, X = S, Se or Te; Y = BF_4) are reported. The cations contain a homo- or hetero-atomic trimembered inorganic ring *trihapto* bonded to a metal–triphos unit. Both in glycerol and thioglycerol the complexes exhibit a characteristic fragmentation which involves the stepwise loss of the three atoms of the inorganic ring and the ejection of organic radicals from the triphos ligand. Adduct ions with sulphur atoms or sulphur organic radicals are, furthermore, observed in thioglycerol. Such adducts infer interactions of the matrix with: (a) the atoms of the inorganic ring of the complex cations, and (b) the metal atom of the (triphos)M moiety.

In recent years desorption mass spectrometric methods have been increasingly applied to the characterization of metal-containing compounds of low volatility.[1–16] Field desorption mass spectrometry usually shows only the molecular ion, but fast atom bombardment (FAB) mass spectrometry yields also fragment ions which supply significant information on the structures of the metal complexes.[1–13] Recently the comparison of the solution chemistry of transition-metal compounds and their behaviour when dissolved in appropriate matrices under FAB has provided a powerful new tool for the study of solution dynamics and reactivity.[17]

This paper reports the FAB mass spectra of the following cationic compounds: [(triphos)Ni(η^3-P_3)]BF_4 (**1**), [(triphos(Ni(η^3-P_3)]PF_6 (**2**), [(triphos)Co(η^3-P_2S)]BF_4 (**3**), [(triphos)Co(η^3-P_2Se)]BF_4 (**4**), [(triphos)Co(η^3-As_2S)]BF_4 (**5**), [(triphos)Co(η^3-As_2Se)]BF_4 (**6**), and [(triphos)Co(η^3-As_2Te)]BF_4 (**7**).

This isostructural and isoelectronic series of compounds contain a (triphos)M unit η^3-bound to the homocyclic P_3 ring (M = Ni) or to the heterocyclic triatomic E_2X (E = P; X = S or Se: E = As; X = S, Se or Te) ring (M = Co). The metal and the three unsubstituted main group atoms form a pseudotetrahedral core and the general structure of the cation of the compounds is shown in Fig. 1.

EXPERIMENTAL

Complexes **1**, **2**,[18] **3**, **4**,[19] **5**,[20] **6** and **7**[21] were prepared according to published procedures. The

* Authors to whom correspondence should be addressed.

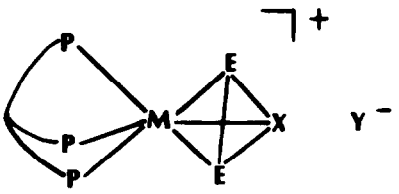

Fig. 1. General structure of the complexes.

compounds crystallize with a molecule of solvent (ethanol for **6** and benzene for the other complexes) which has been omitted for it is not relevant in the present study.

The mass spectra were obtained on a Kratos MS 80 mass spectrometer equipped with a FAB source. Primary argon atoms at an energy of 6–7 keV were generated in an Ion Tech Ltd gun. The samples were dissolved in a small amount of chloroform and one droplet of the solutions was mixed with the matrix (glycerol or thioglycerol) on the copper tip of the FAB probe.

RESULTS AND DISCUSSION

The FAB mass spectra of all compounds have been obtained using glycerol and thioglycerol as matrices. The abundances of the ions are rather low for the samples dissolved in glycerol and the overall ionic yield is significantly lower than in thioglycerol.

FAB spectra with glycerol as matrix

The cations $[C]^+$ display a characteristic fragmentation pathway (Table 1) with stepwise loss of the three phosphorus atoms in compounds **1** and **2** (E = X = P), or of the two pnicogen atoms followed by the chalcogen atom in all the other compounds. $[(triphos)M]^+$ (M = Co or Ni) is the base peak in the spectra of all compounds; it undergoes further breakdown with ejection of organic radicals. In the spectra of **1** and **2** these fragmentation processes give the ions at *m/z* 497, $[(triphos)Ni-PPh_2]^+$; *m/z* 442, $[(triphos)Ni-CH_3CCH_2CH_2PPh_2]^+$; and *m/z* 420, $[(triphos)Ni-Ph-PPh_2]^+$.

Such ions exhibit the typical pattern due to the nickel isotopes. The cobalt complexes present the corresponding peaks at *m/z* 498, 443 and 421. No other ion containing metal are formed.

A comparison of the spectra obtained from $[(triphos)Ni(P_3)]BF_4$ (**1**) and $[(triphos)Ni(P_3)]PF_6$ (**2**) shows that the different anions (Table 1) do not affect appreciably the nature and the relative abundances of the positive ions.

FAB spectra with thioglycerol as matrix

The FAB mass spectra of complexes **1**–**7** in thioglycerol exhibit a higher number of abundant ions and are more complicated than those with glycerol as matrix; such behaviour has to be ascribed to the interactions that occur between the samples and the matrix containing the thio group.

Two remarkable features distinguish the spectra run in thioglycerol from those in glycerol: (a) the intact $[C]^+$ cation is the base peak (Table 2) for all the compounds at variance with glycerol where the most abundant ion is $[(triphos)M]^+$, and (b) several hydrogenated peaks are observed whilst no protonated ion is detected in glycerol.

Table 1. Relative abundances of the most significant ions in the FAB mass spectra of $[(triphos)M(\eta^3\text{-}E_2X)]Y$ complexes[a] with glycerol as matrix

Ion	1	2	3	4	5	6	7
$[C]^+$	55	28	13	8	60	15	16
$[C-E]^+$	11	5	20	10	65	21	12
$[C-2E]^+$	4	2	5	12	37	8	8
$[(triphos)M]^+$	100	100	100	100	100	100	100
$[(triphos)M-Ph]^+$	23	25	10	—	—	—	—
$[(triphos)M-PPh_2]^+$	42	50	41	27	25	40	45
$[(triphos)M-CH_3CCH_2CH_2PPh_2]^+$	—	—	95	87	85	90	96
$[(triphos)M-Ph-PPh_2]^+$	88	96	35	—	15	—	20
$[triphos-Ph]^+$	—	—	25	27	38	32	28
$[triphos-PPh_2]^+$	—	—	—	—	10	25	—

[a] **1** = $[(triphos)Ni(\eta^3\text{-}P_3)]BF_4$, **2** = $[(triphos)Ni(\eta^3\text{-}P_3)]PF_6$, **3** = $[(triphos)Co(\eta^3\text{-}P_2S)]BF_4$, **4** = $[(triphos)Co(\eta^3\text{-}P_2Se)]BF_4$, **5** = $[(triphos)Co(\eta^3\text{-}As_2S)]BF_4$, **6** = $[(triphos)Co(\eta^3\text{-}As_2Se)]BF_4$, **7** = $[(triphos)Co(\eta^3\text{-}As_2Te)]BF_4$.

Table 2. Relative abundances of the most significant ions in the FAB mass spectra of [(triphos)M(η^3-E_2X)]Y complexes[a] with thioglycerol as matrix

Ion	1	2	3	4	5	6	7
$[C-E+2RS+H]^+$	0.4	0.3	—	—	—	—	—
$[C-E+2RS]^+$	—	—	6	—	—	—	—
$[C+H+RS]^+$	2	1	11	—	—	—	—
$[C+RS]^+$	1	1	—	11	2	—	1
$[C-E+RS+H]^+$	—	0.5	12	7	1	—	—
$[C-E+RS]^+$	2	1	25	20	12[b]	8	6
$[C-2E+RS]^+$	—	—	—	—	—	15	—
$[C+S+2H]^+$	1	2	—	—	—	—	—
$[C+S+H]^+$	—	—	3	—	—	—	—
$[C+S]^+$	1	1	10	—	12[b]	—	—
$[C+H]^+$	—	—	55	35	—	—	—
$[C]^+$	100	100	100	100	100	100	100
$[C-E+H]^+$	8	5	16	14	—	9	11
$[C-E]^+$	0.5	2	75	32	36[c]	31	34
$[C-2E+H]^+$	5	3	36	8	1	12	—
$[C-2E]^+$	7	2	54	12	13	40	23
$[C-Ph+H]^+$	5	4	—	—	—	—	—
$[(triphos)M+S+2RS]^+$	—	—	—	—	3	2	—
$[(triphos)M+2RS]^+$	0.2	0.3	2	—	12[b]	4	20
$[(triphos)M+RS]^+$	2	2	1	—	36[c]	—	85
$[(triphos)M+2S+H]^+$	—	—	—	—	3	—	—
$[(triphos)M+2S]^+$	—	—	—	—	16	32	—
$[(triphos)M+S+H]^+$	—	—	—	—	—	77	48
$[(triphos)M+S]^+$	—	—	—	—	—	12	53
$[(triphos)M]^+$	14	11	80	35	15	65	92
$[(triphos)M-CH_2P]^+$	4	2	23	—	12	—	—
$[(triphos)M-Ph]^+$	3	3	4	—	7	6	5
$[(triphos)M-PPh]^+$	7	8	—	—	—	—	—
$[(triphos)M-2Ph+H]^+$	10	4	—	—	3	—	—
$[(triphos)M-2Ph]^+$	8	6	—	—	6	—	—
$[(triphos)M-PPh_2]^+$	—	—	—	—	9	21	13
$[(triphos)M-Ph-PPh_2]^+$	22	20	65	13	—	—	28
$[(triphos)M-CH_3CCH_2CH_2PPh_2]^+$	—	—	95	88	75	95	90
$[(triphos)-CH_2Ph]^+$	7	1	40	42	13	—	37
$[(triphos)-Ph]^+$	6	5	75	36	17	40	31
$[(triphos)-PPh_2]^+$	18	7	21	23	1	65	19

[a] **1** = [(triphos)Ni(η^3-P_3)]BF_4, **2** = [(triphos)Ni(η^3-P_3)]PF_6, **3** = [(triphos)Co(η^3-P_2S)]BF_4, **4** = [(triphos)Co(η^3-P_2Se)]BF_4, **5** = [(triphos)Co(η^3-As_2S)]BF_4, **6** = [(triphos)Co(η^3-As_2Se)]BF_4, **7** = [(triphos)Co(η^3-As_2Te)]BF_4.

[b] $[C+S]^+$, $[C-As+RS]^+$ and $[(triphos)Co+2RS]^+$ show the same nominal mass at *m/z* 897.

[c] $[C-As]^+$ and $[(triphos)Co+RS]^+$ show the same nominal mass at *m/z* 790.

The spectra of the nickel compounds **1** and **2** (Table 2) which have different counterions (BF_4^- for **1** and PF_6^- for **2**, respectively) are practically identical, showing that the nature of the anion does not affect the fragmentation of the compounds when they are dissolved in thioglycerol. The metal-retaining ions have been identified through the typical isotopic pattern for the two nickel derivatives. The composition of the fragments which contain cobalt has been assigned by their mass and by comparison to the corresponding species of the nickel compounds **1** and **2**.

The several ions found in the FAB spectra of compounds **1–7** may be divided into three distinct groups. The largest one consists of ions which do not contain sulphur atoms or RS (RS is the $CH_2OHCHOHCH_2S^{\cdot}$ radical that originates from thioglycerol). Such ions show a mass that ranges between $[C+H]^+$ and $[triphos-PPh_2]^+$ and are present also in the spectra in glycerol (except the

hydrogenated ones). This indicates that a portion of the cations undergo in thioglycerol the same fragmentation pathway as in glycerol.

The second group of ions consists of species, in which one S or RS group is linked to the intact cation, namely $[C+H+RS]^+$, $[C+RS]^+$, $[C+S+2H]^+$, $[C+S+H]^+$ and $[C+S]^+$, or to fragments originating by loss of one or two pnicogen atoms. The peaks due to these ions, which are not very strong and whose intensity changes for the different compounds **1–7**, show an interaction between the complex cation and the matrix. The $[C+S]^+$ and the protonated $[C+H+S]^+$ species suggest that also in the ions formed from $[C]^+$ and the RS radical the interaction between the cation and the matrix occurs through the sulphur atom. It is likely that the sulphur atom and the sulphur-containing radicals bind the inorganic triatomic unit of the complex cations. The metal ions of compounds **1–7** are actually in a six-coordinate environment (Fig. 1) and hence coordinatively saturated; the spectral data furthermore do not contain fragments which originate from thiophilic attack on the triphos ligand. Taking into account that the major decomposition pathway of the cations in glycerol goes through the stepwise loss of pnicogen atoms, the heavier ions, $[C-E+2RS+H]^+$, $[C-E+2RS]^+$, $[C-E+RS+H]^+$, $[C-E+RS]^+$ and $[C-2E+RS]^-$ (Table 2), likely originate from the substitution of a pnicogen atom from the cyclic E_2X unit of the intact cation with sulphur-containing species.

The remaining sulphur- or thioradical-containing ions, namely $[(triphos)M+S+2RS]^+$, $[(triphos)M+2RS]^+$, $[(triphos)M+RS]^+$, $[(triphos)M+2S+H]^+$, $[(triphos)M+2S]^+$, $[(triphos)M+S+H]^+$ and $[(triphos)M+S]^+$ have lost the cyclic triatomic ring P_3 or E_2X. Their presence provides evidence for the ability of the metal–ligand system to interact with thio species of the matrix. This is supported by the following points: the $[(triphos)M]^+$ species is the base peak in glycerol, which does not yield any interaction with metal-containing fragments; the hemioctahedral (triphos)M moiety provides a fragment which has orbitals whose energy and symmetry are well suited to stabilize a wide class of complexes with unsubstituted or substituted sulphur atoms.[22]

All the reactions of these complex ions in thioglycerol (yielding ions which contain RS radicals or other sulphur species) appear to take place at high rate under the fast argon atom beam. The ionic abundances, in fact, do not change noticeably in spectra run at different times after the beginning of the atom bombardment.

The FAB mass spectra of the cations $[(triphos)M(\eta^3\text{-}E_2X)]^+$, which contain the new triatomic units E_2X (E = X = P; M = Ni; E = As; X = S, Se or Te: E = P; X = S or Se; M = Co), in glycerol and thioglycerol provide interesting information on the behavior of the pseudo-tetrahedral ME_2X core which undergoes a demolition by a stepwise loss of the pnicogen and chalcogen atoms.

By comparing the spectra of the cations in glycerol and thioglycerol it appears that in the latter matrix two different kinds of interactions occur at the cations and the related fragments. The sulphur atom and the thio groups from thioglycerol are suggested to bind to: (a) the inorganic units of the intact complex cations, and (b) the (triphos)M fragment. It has been recently found that the (triphos)M (M = Co or Ni) moieties in the presence of the appropriate sulphur species yield a wide group of monomeric and oligomeric complexes in which they are bound to unsubstituted or substituted sulphur atoms.[22] Such behaviour shows a parallelism between the reactivity of (triphos)M both in solution and under FAB.

According to such considerations the presence in the FAB spectra of the ions that originate from the cations and the sulphur-containing species may suggest a reactivity in solution of the intact cations with sulphur-containing species provided that the appropriate reagents and conditions are employed.

Acknowledgement—We thank the Ministero della Pubblica Istruzione for financial support.

REFERENCES

1. J. M. Miller, *Adv. Inorg. Chem. Radiochem.* 1984, **28**, 1.
2. D. E. Games, J. L. Gower, M. Gower and L. A. P. Kane-Maguire, *J. Organomet. Chem.* 1980, **193**, 229.
3. D. E. Games, J. L. Gower and L. A. P. Kane-Maguire, *J. Chem. Soc., Dalton Trans.* 1981, 1994.
4. C. N. McEwen and S. D. Ittel, *Org. Mass Spectrom.* 1980, **15**, 35.
5. M. Barber, R. S. Bordoli, R. D. Sedgwick and A. N. Tyler, *Biomed. Mass Spectrom.* 1981, **8**, 491.
6. R. A. W. Johnstone and I. A. S. Lewis, *Int. J. Mass Spectrom. Ion Proc.* 1983, **46**, 451.
7. I. Tkatchenko, D. Nelbecker, D. Fraisse, F. Gomez and D. F. Barofsky, *Int. J. Mass Spectrom. Ion Phys.* 1983, **46**, 499.
8. R. L. Cerny, B. P. Sullivan, M. M. Bursey and T. J. Meyer, *Anal. Chem.* 1983, **55**, 1954.
9. J. Meili and J. Seibl, *Org. Mass Spectrom.* 1984, **19**, 581.
10. B. Gregory, C. R. Jablonski and Y. P. Wang, *J. Organomet. Chem.* 1984, **269**, 75.
11. R. B. Freas and J. E. Campana, *Inorg. Chem.* 1984, **23**, 4654.

12. B. J. Brisdon and A. J. Floyd, *J. Organomet. Chem.* 1985, **288**, 305.
13. R. L. Cerny, B. P. Sullivan, M. M. Bursey and T. Y. Meyer, *Inorg. Chem.* 1985, **14**, 397.
14. G. Bojesen, *Org. Mass Spectrom.* 1985, **20**, 413.
15. D. Parker, *Org. Mass Spectrom.* 1985, **20**, 26.
16. B. Divisia-Blohorn, G. Kyriakakou and J. Ulrich, *Org. Mass Spectrom.* 1985, **20**, 463.
17. H. T. Kalinoski, U. Hacksell, D. F. Barofsky, E. Barofsky and G. D. Daves, Jr, *J. Am. Chem. Soc.* 1985, **107**, 6476.
18. M. Di Vaira, L. Sacconi and P. Stoppioni, *J. Organomet. Chem.* 1983, **250**, 183.
19. M. Di Vaira, M. Peruzzini and P. Stoppioni, *J. Chem. Soc., Dalton Trans.* 1984, 359.
20. M. Di Vaira, P. Innocenti, S. Moneti, M. Peruzzini and P. Stoppioni, *Inorg. Chim. Acta* 1984, **83**, 161.
21. M. Di Vaira, M. Peruzzini and P. Stoppioni, *Polyhedron* 1986, **5**, 945.
22. F. Cecconi, C. A. Ghilardi and S. Midollini, *Inorg. Chem.* 1983, **22**, 3802 (and references therein).

Polyhedron Vol. 6, No. 6, pp. 1497–1502, 1987
Printed in Great Britain

0277–5387/87 $3.00+.00

ESR STUDIES ON THE INTERMOLECULAR INTERACTIONS OF THE MONONITROSYL CHELATE COMPLEXES OF IRON

V. I. ILIEV* and D. SHOPOV

Institute of Kinetics and Catalysis, Bulgarian Academy of Sciences, 1113 Sofia, Bulgaria

(*Received* 18 *February* 1986; *accepted after revision* 12 *January* 1987)

Abstract—Using ESR the exchange of ligands was studied between mononitrosyl chelate complexes of iron and chelate complexes of nickel with the following ligands: dithiocarbamate (dtc), dithiophosphate (dtp), dithiocarbonate (xant), 8-quinolinethiolate, 8-hydroxyquinoline, acetylacetonate and *o*-hydroxy-benzylideneaniline. For some mixed-ligand complexes the exchange of the covalency of the metal–ligand bond was evaluated. The interaction of the mononitrosyl complexes with Lewis acids (I_2 and Br_2) and bases (pyridine, DMFA and DMSO) was studied in the cases of $Fe(NO)(dtc)_2$, $Fe(NO)(dtp)_2$ and $Fe(NO)(xant)_2$. In both of the latter cases the interactions with Lewis acids and bases led to the formation of paramagnetic dinitrosyl complexes, while with $Fe(NO)(dtc)_2$ hexacoordinated mononitrosyl complexes were formed. A reaction pathway is suggested and discussed for the formation of the dinitrosyl complexes and their composition.

In our previous studies[1] it was shown that the interaction of the tris-chelates of Fe(III) with NO and NO_2 is connected with the splitting of one chelate ligand and the formation of iron nitrosyl complexes. The continuous treatment with NO_2 leads to complete destruction of the nitrosyl complexes.

Although there exists a considerable interest in the mononitrosyl chelate complexes, we have not found data in the literature concerning the possibility of exchange of ligands in the non-charged mononitrosyl chelate complexes and the formation of thermodynamically stable complexes with mixed ligands. Some aspects of the interaction were studied[2,3] for iron mononitrosyl dithiocarbamate complexes with Lewis acids (X), where hexacoordinated complexes are obtained of type $Fe(NO)\cdot X\cdot(dtc)_2$ (dtc = dithiocarbamate) therefore changes occur only in the coordination polyhedron, but the chelate encirclement is not changed.

The purpose of the present investigations was to study the changes in the ligands in iron mononitrosyl chelate complexes with other chelate ligands. The changes taking place in the first coordination sphere during the interactions with some monodentate organic Lewis bases and acids were also studied.

The investigations were carried out with the following mononitrosyl complexes of iron: $Fe(NO)(R_2dtp)_2$, $Fe(NO)(Et_2dtc)_2$, $Fe(NO)(Et\text{-}xant)_2$, $Fe(NO)(tox)_2$ (R_2dtp = dialkyldithiophosphato, Et_2dtc = diethyldithiocarbamato). The basic method of our investigations was ESR spectroscopy.

EXPERIMENTAL

The sodium salt of *O*,*O*-diisopropyldithiophosphoric acid was synthesized according to methods described in the literature.[4] The same applies to *o*-hydroxy-benzylideneaniline (SchB).[5] The rest of the ligands used, $Me_2dtp\cdot NH_4$, $Et_2dtc\cdot Na$, $tox\cdot HCl$ and $ox\cdot H_2SO_4$ (8-hydroxyquinolinesulphate) (Fluka), and Et-xant·K (Merck) were used after filtration of their water solutions.

The mononitrosyl complexes $Fe(NO)L_2$ were obtained according to Ref. 6, from the respective ligands, $FeSO_4$ and $NaNO_2$, with argon bubbled through the solution. The complexes $Fe(NO)(Et\text{-}xant)_2$ and $Ni(SchB)_2$ were obtained by extraction of the aqueous solutions of the respective ligands, and $NiCl_2$ with $CHCl_3$. After that they were recry-

* Author to whom correspondence should be addressed.

stallized from $CHCl_3$ or a $CHCl_3$–toluene mixture in a 1 : 1 ratio. $Ni(acac)_2$ was from Fluka.

$Fe \cdot I \cdot (NO)_2 \cdot H_2O$ was synthesized according to Ref. 7 with the use of NO gas (Merck–Schuhardt).

The ESR spectra were measured on a Brucker ER 200D-SRC spectrometer in the *X*-band. The g factors are determined using diphenylpicrylhydrazyl as a reference.

RESULTS

Exchange of ligands in nitrosyl complexes of iron

Because the mononitrosyl complexes studied gave too similar ESR parameters the exchange of ligands was carried out as follows: (1) between iron mononitrosyl complexes with ligands of one type and diamagnetic chelate complexes of nickel with ligands of the other type (see Table 1); and (2) an exchange at lower temperature (240 K), where the observed bands were considerably narrower. The ESR spectra were registered for 5 min, and after the initial mixing of the starting solutions no change was detected in the ESR parameters and the intensity of the spectra for 2 h.

When solutions of $Fe(NO)(Et_2dtc)_2$, $Fe(NO)(Et\text{-}xant)_2$ and $Fe(NO)(tox)_2$ in chloroform were mixed with $Ni(i\text{-}prdtp)_2$ and the concentration of the latter increased, the ESR spectra of the initial nitrosyl complexes decreased in intensity, and the spectra of new complexes were obtained (Fig. 1). Only in the case when $Fe(NO)(Et_2dtc)_2$ interacted with $Ni(i\text{-}prdtp)_2$ (in 1 : 1 molar ratio of the starting complexes) was formation of $Fe(NO)(i\text{-}prdtp)(Et_2dtc)$ observed as proved by the ESR spectra [Fig. 1(a) and (b)]. The ESR parameters of $Fe(NO)(i\text{-}prdtp)(Et_2dtc)$ in frozen chloroform–toluene solution (volume ratio 1 : 3) were as follows: $g_\parallel = 2.026, g_\perp = 2.043$; ${}^{N}A_\parallel = 15.7$ G; ${}^{N}A_\perp = 12.5$ G, ${}^{P}A = 7.3$ G.

In both of the other cases under the same experimental conditions and ratio of reagents as for the initial $Fe(NO)(Et\text{-}xant)_2$ or $Fe(NO)(tox)_2$, the parameters of the newly formed $Fe(NO)(i\text{-}prdtp)(Et\text{-}xant)$ or $Fe(NO)(i\text{-}prdtp)(tox)$ were observed [see Fig. 1(c) and (d)]. In frozen solutions (mixture of toluene–chloroform) and a $Fe(NO)L_2/Ni(i\text{-}prdtp)_2$ ratio of 1 : 1 in all three cases the presence of $Fe(NO)(i\text{-}prdtp)_2$ was detected. In solution (298 and 240 K) the ESR spectrum of $Fe(NO)(dtp)_2$ was not observed, most probably because the bands are very much expanded.[8]

When solutions in chloroform of $Fe(NO)(tox)_2$ with $Ni(Et\text{-}xant)_2$ or $Ni(Et_2dtc)_2$ were mixed (molar ratio of the initial complexes 1 : 2) the ESR spectra (see Fig. 2) of the initial $Fe(NO)(tox)_2$ were detected, formed as a result of the exchange between $Fe(NO)(tox)(Et\text{-}xant)$ and $Fe(NO)(Et\text{-}xant)_2$ or $Fe(NO)(tox)(Et_2dtc)$ and $Fe(NO)(Et_2dtc)$ mononitrosyl complexes (see Table 1).

During the interaction of $Fe(NO)(Et_2dtc)_2$ with $Ni(Et\text{-}xant)_2$ in chloroform (molar ratio of the complexes from 1 : 1 to 1 : 4) the ESR spectra showed only the formation of $Fe(NO)(Et\text{-}xant)_2$.

When solutions in chloroform–toluene (volume ratio 1 : 3) of $Fe(NO)(Et_2dtc)_2$, $Fe(NO)(Et\text{-}xant)_2$ or $Fe(NO)(tox)_2$ with $Ni(ox)_2$, $Ni(SchB)_2$ or $Ni(acac)_2$ (at molar ratio from 1 : 2 to 4 : 1) were mixed at 298, 240 and 140 K only a decrease in the intensity of the ESR spectra of the initial nitrosyl complexes was observed.

Interaction of $Fe(NO)(Et_2dtc)_2$, $Fe(NO)(Et\text{-}xant)_2$ *and* $Fe(NO)(Me_2dtp)_2$ *with Lewis bases and acids*

When $Fe(NO)(Et_2dtc)_2$ was dissolved in pyridine, dimethylformamide (DMFA) or dime-

Table 1. ESR parameters of $Fe(NO) \cdot L_2$ and $Fe(NO) \cdot L' \cdot L''$ complexes in chloroform at 240 K

Complex	g	${}^{N}A_o$ (G)	${}^{P}A_o$ (G)	C_s^2 ${}^{31}P$
$Fe(NO)(i\text{-}prdtp)_2$	2.045[a]	12.9[a]	8.3[a]	0.0022
$Fe(NO)(Et_2dtc)_2$	2.038	13.0	—	
$Fe(NO)(Et\text{-}xant)_2$	2.041	11.9	—	
$Fe(NO)(tox)_2$	2.035	13.1	—	
$Fe(NO)(i\text{-}rdtp)(Et_2dtc)$	2.040	12.9	7.3	0.0020
$Fe(NO)(i\text{-}prdtp)(Et\text{-}xant)$	2.041	12.0	7.0	0.0019
$Fe(NO)(i\text{-}prdtp)(tox)$	2.041	13.0	6.3	0.0017
$Fe(NO(tox)(Et\text{-}xant)$	2.037	12.3	—	
$Fe(NO)(tox)(Et_2dtc)$	2.036	13.0	—	

[a] $g = (g_\parallel + 2g_\perp)/3$, ${}^{N}A_o = ({}^{N}A_\parallel + 2{}^{N}A_\perp)/3$, and ${}^{P}A_o = ({}^{P}A_\parallel + 2{}^{P}A_\perp)/3$.

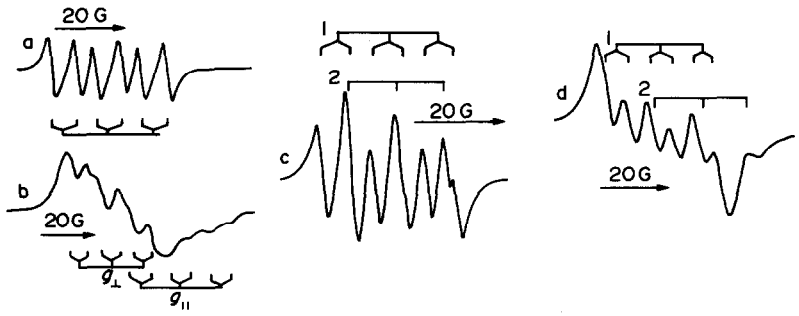

Fig. 1. ESR spectra of mixed-ligand complexes: (a) Fe(NO)(*i*-prdtp)(Et_2dtc) (240 K in chloroform); (b) Fe(NO)(*i*-prdtp)(Et_2dtc) (140 K in toluene–chloroform); (c) (1) Fe(NO)(*i*-prdtp)(Et-xant) and, (2) Fe(NO)(Et-xant)$_2$ (240 K in chloroform); and (d) (1) Fe(NO)(*i*-prdtp)(tox), and (2) Fe(NO)(tox)$_2$ (240 K in chloroform).

thylsuphoxide (DMSO) at ambient temperature, the characteristic triplet ESR spectrum of the mononitrosyl complex was preserved. Only a slight change in the ESR parameters was observed, compared with those in chloroform (Table 2).

The addition at ambient temperature of pyridine, DMFA or DMSO (1–10% by volume) to the solutions in chloroform–toluene of Fe(NO)(Me_2dtp)$_2$ or Fe(NO)(Et-xant)$_2$ led to a decrease in intensity and to the complete disappearance of the ESR spectra of the mononitrosyl complexes after a period of 10–15 min. The ESR spectra were not observed in frozen solutions ($T = 140$ K). The addition of the same amounts of the bases to the solutions of both complexes in *i*-amyl alcohol showed that the decrease in intensity of the ESR spectra of the mononitrosyl complexes is accompanied by the observation of dinitrosyl complexes—Fe(NO)$_2$(Me_2dtp) or Fe(NO)$_2$(Et-xant) (Fig. 3). The solutions of Fe(NO)(Me_2dtp)$_2$ and Fe(NO)(Et-xant)$_2$ in *i*-amyl alcohol gave ESR spectra characteristic only of the mononitrosyl complexes. The addition of Ni(Et_2dtc)$_2$ to the Fe(NO)$_2$(Me_2dtp) or Fe(NO)$_2$(Et-xant) obtained (even in the cases when pure pyridine and DMFA were used as solvents) led to the formation of Fe(NO)(Et_2dtc)$_2$ which was identified by its ESR spectrum (Fig. 3). The addition of Ni(Et-xant)$_2$ under the same conditions, to the Fe(NO)$_2$(Et-xant) did not cause destruction of the dinitrosyl complexes, but only a weak broadening of the lines is observed for the hyperfine splitting from ^{14}N.

When Fe(NO)(Et-xant)$_2$ was dissolved in nitrobenzene, a solvent where no coordination is observed, but which has a dielectric constant ($\varepsilon = 34.8$) close to that of DMFA ($\varepsilon = 36.7$), the ESR spectrum showed that the structure of the mononitrosyl complex was preserved.

The addition of I_2 or Br_2 to the solution of Fe(NO)(Et_2dtc)$_2$ in ethanol (molar ratio 3 : 1) led to a complete disappearance of its spectrum after several minutes. Under the same conditions for Fe(NO)(Me_2dtp)$_2$ or Fe(NO)(Et-xant)$_2$ together

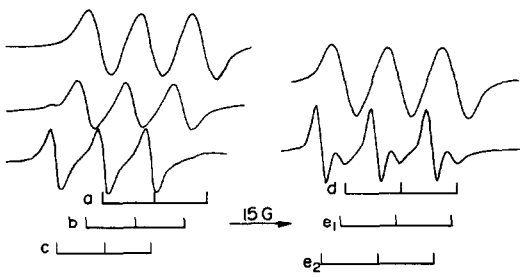

Fig. 2. ESR spectra in chloroform at 240 K of: (a) Fe(NO)(tox)$_2$, (b) Fe(NO)(tox)(Et-xant), (c) Fe(NO)(Et-xant)$_2$, (d) Fe(NO)(tox)$_2$, (e_1) Fe(NO)(tox)(Et_2dtc), and (e_2) Fe(NO)(Et_2dtc)$_2$.

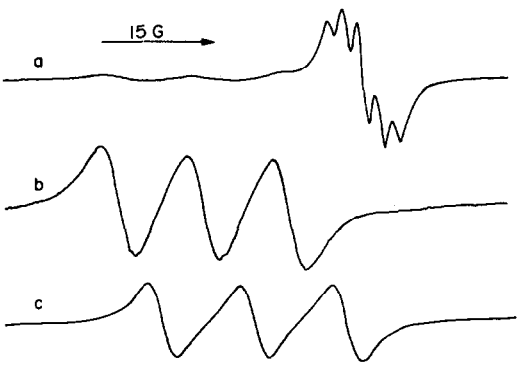

Fig. 3. Typical ESR spectra of the interaction of Fe(NO)·L_2 with bases ($T = 298$ K): (a) Fe(NO)$_2$(Et-xant) [obtained during dissolution of Fe(NO)(Et-xant)$_2$ in *i*-amyl alcohol : pyridine (3 : 1)], (b) Fe(NO)(Et-xant)$_2$ in *i*-amyl alcohol, and (c) Fe(NO)(Et_2dtc)$_2$ [obtained by adding (a) to Ni(Et_2dtc)$_2$].

Table 2. ESR parameters of complexes obtained during the interaction of $Fe(NO)\cdot L_2$ with Lewis bases ($T = 298$ K)

$Fe(NO)\cdot L_2$	Solvent, base (B)	Observed complex	g	$^{N}A_o$ (G)
$Fe(NO)(Et_2dtc)_2$	DMFA	$Fe(NO(Et_2dtc)_2\cdot B$	2.040	12.6
	Pyridine	$Fe(NO)(Et_2dtc)_2\cdot B$	2.040	12.6
$Fe(NO)(Et\text{-}xant)_2$	*i*-Amyl alcohol	$Fe(NO)(Et\text{-}xant)_2$	2.044	11.6
	DMFA	$Fe(NO)_2\cdot Et\text{-}xant$	2.030	2.1
	Pyridine	$Fe(NO)_2\cdot Et\text{-}xant$	2.031	2.1
$Fe(NO)(Me_2dtp)_2$	*i*-Amyl alcohol	$Fe(NO)(Me_2dtp)_2$	[a]	[a]
	DMFA	$Fe(NO)_2\cdot Me_2dtp$	2.033	2.1
	Pyridine	$Fe(NO)_2\cdot Me_2dtp$	2.032	2.1

[a] At 298 K ESR spectrum is not observed.

with the disappearance of the ESR spectra new signals attributed to new complexes were observed (Fig. 4). An ESR spectrum with the same parameters was obtained when thiocarbamide was added to $Fe\cdot I\cdot (NO)_2\cdot H_2O$ (Table 3).

DISCUSSION

Exchange of ligands in the mononitrosyl complexes of iron

In all the cases studied by us, it was found that complete ligand exchange proceeded between the respective $Fe(NO)\cdot L'_2$ and NiL''_2. This fact was confirmed by the observation of ESR spectra of mononitrosyl complexes with composition $Fe(NO)L''_2$. The decrease in the intensity of the ESR spectra of $Fe(NO)(Et_2dtc)_2$, $Fe(NO)(Et\text{-}xant)_2$ and $Fe(NO)(tox)_2$ during the interaction with $Ni(ox)_2$, $Ni(SchB)_2$ and $Ni(acac)_2$ can also be considered as a result of the exchange of ligands between these complexes and the formation of the respective nitrosyl species, for some of which it was supposed[8] that they are high-spin complexes.

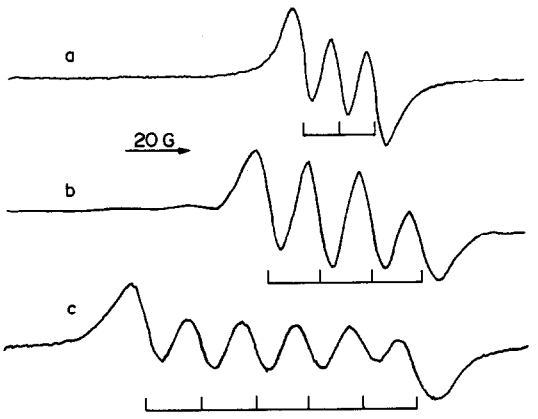

Fig. 4. Typical ESR spectra obtained during the interaction of $Fe(NO)\cdot L_2$ with Lewis acids in ethanol at 298 K: (a) $Fe(NO)(Et\text{-}xant)_2$, (b) $Fe(NO)_2\cdot Br\cdot L$, and (c) $Fe(NO)_2\cdot I\cdot L$. L is coordinated Et-xant.

The ESR spectra obtained during the interaction of $Ni(i\text{-}prdtp)_2$ with $Fe(NO)(Et_2dtc)_2$, $Fe(NO)(Et\text{-}xant)_2$, and $Fe(NO)(tox)_2$, and of the latter with $Ni(Et_2dtc)_2$ and $Ni(Et\text{-}xant)_2$, have different parameters from those of the complexes studied of type $Fe(NO)\cdot L_2$. This fact can be attributed to the formation of mixed-ligand mononitrosyl complexes of the following type—$Fe(NO)\cdot L'\cdot L''$. A synonymous proof for the formation of mixed-ligand complexes with composition $Fe(NO)(i\text{-}prdtp)(Et_2dtc)$, $Fe(NO)(i\text{-}prdtp)(Et\text{-}xant)$ and $Fe(NO)(i\text{-}prdtp)(tox)$ was the superhyperfine structure observed in all three cases due to the interaction of the unpaired electron with one phosphorus nucleus.

An additional indication of the formation of mixed-ligand complexes was the fact that their ESR parameters satisfy the following inequalities: $g^{Fe(NO)\cdot L'_2} \leqslant g^{Fe(NO)\cdot L'\cdot L''} \leqslant g^{Fe(NO)\cdot L''_2}$ and $A^{Fe(NO)\cdot L'_2} \leqslant A^{Fe(NO)\cdot L'\cdot L''} \leqslant A^{Fe(NO)\cdot L''_2}$ (Table 1). A similar dependence was observed for the ESR parameters of the mixed-ligand chelate complexes of copper.[9,10]

For the complexes $Fe(NO)(tox)_2$[1,8] and for its mixed-ligand complexes obtained during the interaction of $Ni(Et\text{-}xant)_2$ and $Ni(Et_2dtc)_2$ the superhyperfine structure from the ^{14}N nuclei of the thiooxine ligands was not observed. However, the fact that the ESR parameters of the complexes obtained fulfil the condition above, i.e. that they are approximately average values of the respective

Table 3. ESR parameters of complexes obtained during the interaction of $Fe(NO)\cdot L_2$ with Lewis acids ($T = 298$ K, solvent = ethanol)

Complex	Lewis acid	g	$^{X}A_o$[b] (G)
$Fe(NO)_2\cdot I_2^-$[a]	—	2.070	20.2
$Fe(NO)_2\cdot I\cdot H_2O$[a]	—	2.055	20.2
$Fe(NO)(Et\text{-}xant)_2$	I_2	2.055	16.8
$Fe(NO)(Me_2dtp)_2$	I_2	2.055	16.8
$Fe(NO)_2\cdot Br_2^-$[a]	—	2.045	19.5
$Fe(NO)_2\cdot Br\cdot H_2O$[a]	—	2.039	19.5
$Fe(NO)(Et\text{-}xant)_2$	Br_2	2.043	16.7
$Fe(NO)(Me_2dtp)_2$	Br_2	2.043	16.7
$Fe(NO)_2\cdot I\cdot H_2O$	Thiocarbamide	2.055	16.8

[a] Reference 7.
[b] X = Br or I.

initial nitrosyl complexes (Table 1), gives us reason to assign them to mixed-ligand complexes having the following compositions: $Fe(NO)(tox)(Et_2dtc)$ and Fe(NO)(tox)(Et-xant).

Most probably, the exchange of ligands between $Fe(NO)(Et_2dtc)_2$ and $Ni(Et\text{-}xant)_2$ proceeds also through the formation of mixed-ligand complexes but, because of the too similar ESR parameters of $Fe(NO)(Et_2dtc)_2$ and $Fe(NO)(Et\text{-}xant)_2$, the latter were not resolved. Mixed-ligand complexes are formed probably during the exchange of ligands between $Fe(NO)(Et_2dtc)_2$, $Fe(NO)(Et\text{-}xant)_2$ and $Fe(NO)(tox)_2$ with $Ni(Ox)_2$, $Ni(SchB)_2$ and $Ni(acac)_2$. The absence of ESR spectra of mixed-ligand complexes can arise as a result of the low equilibrium concentration and/or because they are high-spin complexes.

The formation of mixed-ligand complexes is not thermodynamically favoured in all of the cases we have studied. For example, for a $Fe(NO)\cdot L_2'/Ni\cdot L_2''$ ratio of 1:1 only Fe(NO)(*i*-prdtp)(Et_2dtc) was obtained. In the other cases that we have studied the ratio of the complexes and the equilibrium process of exchange of ligands is drawn in different extent towards the initial complexes. In our previous papers[9,10] a 100% yield of mixed-ligand complexes during the interaction of $Cu(R_2dtc)_2$ with $Cu(R_2dtp)_2$ was observed.

Qualitatively, the same results are obtained when the exchange of ligands is studied between the respective mononitrosyl chelate complexes of iron.

Taking into account the low polarity of the solvents, favouring the exchange of ligands according to an association mechanism,[9] the following most probable scheme for the exchange of ligands in mononitrosyl complexes can be proposed:

$$Fe(NO)\cdot L_2' + Ni\cdot L_2''\,[Fe(NO)\cdot L_2''] \rightleftharpoons$$
$$Fe(NO)\cdot L_2'\ldots No\cdot L_2'', \rightleftharpoons$$
$$Fe(NO)\cdot L'\cdot L'' + Ni\cdot L'\cdot L'' \rightleftharpoons$$
$$Fe(NO)\cdot L_2'' + Ni\cdot L_2'.$$

In our previous study,[1] on the basis of the analysis of $^{57Fe}A_o$ it was found that the covalency of the Fe—L bonds changes in the following order:

$$Fe(NO)(dtp)_2 < Fe(NO)(xant)_2$$
$$< Fe(NO)(dtc)_2 < Fe(NO)(tox)_2.$$

However, in the cases of the mixed-ligand complexes of $Fe(NO)\cdot L\cdot(dtp)$ just the opposite order of covalency change of the dithiophosphate bonds depending on L was observed:

$$tox < Et\text{-}xant \leqslant Et_2dtc < i\text{-}prdtp.$$

The latter is determined by the spin density on the 3*s* orbital of ^{31}P (Table 1). Therefore, the covalency of the bonds of the ligands giving more covalent bonds in $Fe(NO)\cdot L_2$ gets stronger in mixed-ligand complexes and, on the contrary, with the less covalent bonds it gets weaker. The results obtained are in agreement with the theoretical treatment of the question concerning the formation of mixed-ligand complexes of this kind.[11]

In all the other cases that we have studied, the changes in g_o and ^{N}A values were similar within experimental error, and conclusions such as those above can not be drawn.

Interaction of mononitrosyl complexes of iron with Lewis acids and bases

The disappearance of the ESR spectra of Fe(NO)(Me_2dtp)$_2$ and Fe(NO)(Et-xant)$_2$(in chloroform–toluene mixture) when small amounts of pyridine, DMFA or DMSO are added is a result of the low solubility of the dinitrosyl chelate complexes of iron in non-polar solvents. The absence of a dinitrosyl complex when pyridine or DMFA is added to Fe(NO)(Et_2dtc)$_2$ can be explained by its greater stability. This is confirmed by the results of the interaction of Fe(NO)$_2$(Ex-xant) or Fe(NO)$_2$(Me_2dtp) (obtained in the presence of bases) with Ni(Et_2dtc)$_2$, where the formation of Fe(NO)(Et_2dtc)$_2$ was found. At the same time the addition of Ni(Ex-xant)$_2$ did not lead to the destruction of the Fe(NO)$_2$(Et-xant) complex. It should be noted that a dinitrosyldithiocarbamate complex of iron has not been described in the literature.[3]

Although DMFA and nitrobenzene have approximately equal permeativity values (35), the dinitrosyl complex is obtained only in the presence of DMFA which expresses weak coordination properties as a Lewis base. Taking into account this fact, one can draw the conclusion that the coordination properties of the solvents influence this process. One can suggest that the coordination of pyridine, DMFA or DMSO to Fe(NO)(Et-xant)$_2$ and Fe(NO)(Me_2dtp)$_2$ helps the opening of the chelate ring, leading to redistribution of the nitrosyl groups and ligands among the molecules, when Fe(NO)$_2$·L, FeL$_2$·2B and disulphide are obtained from the ligands. The following reasons confirm the possibility of the formation of dinitrosyl complexes in such a way:

(1) It has been shown[12] that the interaction of Fe(III)(xant)$_3$ and Fe(III)(dtp)$_3$ (dithiophosphinato complex) with pyridine leads to splitting of chelate ligands from the complex, when Fe(II)(chel)$_2$·2Py and disulphide are obtained from the ligands.

(2) It was shown that an exchange proceeds in solution between Fe^{15}(NO)(dtc)$_2$ and ^{14}NO.[3]

It is known that when the Fe(NO)(dtc)$_2$ complex interacts with I_2 and Br_2 hexacoordinated diamagnetic nitrosyl complexes [*cis*-I·Fe(NO)(dtc)$_2$ and *cis*-Br·Fe(NO)dtc$_2$] are formed.[2,3] However, during the interaction of Fe(NO)(Et-xant)$_2$ and Fe(NO)(Me_2dtp)$_2$ with I_2 and Br_2 we found the formation of paramagnetic species giving the superhyperfine structure of one iodine or bromine nucleus. The ESR spectra show similar parameters to those described in our experiments and given in[7] for the following species: Fe(NO)$_2$·X_2^- and Fe(NO)$_2$·X·H_2O (X = I or Br) (Table 3). The constants of superhyperfine interaction obtained by us have lower values than those given in the literature (Table 3). The reason for this can be the difference of the ligands from the first coordination sphere of the metallic ion. The observation of an ESR spectrum with the same parameters during the interaction of Fe(NO)·I·H_2O with thiocarbamate suggests that the complexes obtained have the structure described, but in their first coordinate sphere a monodendate-bonded sulphur-containing ligand can be found. Therefore, the interaction of Fe(NO)(Et-xant)$_2$ and Fe(NO)(Me_2dtp)$_2$ with I_2 and Br_2 leads to full destruction of the chelate encirclement of the initial mononitrosyl complexes, and then dinitrosyl complexes are obtained.

REFERENCES

1. N. D. Yordanov, V. Iliev, D. Shopov, A. Jezierski and B. Jezowska-Trzebiatowska, *Inorg. Chim. Acta* 1982, **60**, 9.
2. H. Butner and R. D. Feltham, *Inorg. Chem.* 1972, **11**, 971.
3. O. A. Ileperuma and R. D. Feltham, *Inorg. Chem.* 1977, **16**, 1876.
4. W. A. Forster, P. Brazenall and J. Bridge, *Analyst* 1961, **86**, 408.
5. A. P. Terent'ev and E. G. Rukhadze, *Vestn. Mosk. Univ, Ser. Fiz.-mat. Estestv. Nauk* 1949, **31**, 31.
6. B. Jezowska-Trzebiatowska, N. D. Yordanov, A. Jezierski, H. Kozlowski and D. Shopov, *Inorg. Chim. Acta* 1978, **31**, 31.
7. R. Burlamacchi, G. Martini and E. Tiezzi, *Inorg. Chem.* 1969, **8**, 2021.
8. N. S. Garif'anov and S. A. Lutchkina, *Sb. Stroenie Molekul Kvantovaia Khim., Naukova Dumka, Kiev* 1970, 62.
9. N. D. Yordanov and V. Alexiev, *Commun. Dept. Chem. Bulg. Acad. Sci.* 1983, **16**, 214.
10. V. Iliev and N. D. Yordanov, *J. Mol. Liquids* 1984, **28**, 137.
11. A. I. Zubenko, A. T. Pilipenko and L. I. Savranski, *Coord. Khim.* 1985, **11**, 248.
12. R. Y. Salen and D. K. Straub, *Inorg. Chem.* 1974, **13**, 1559.

Polyhedron Vol. 6, No. 6, pp. 1503–1507, 1987
Printed in Great Britain

0277–5387/87 $3.00+.00

SYNTHESIS AND STRUCTURAL PROPERTIES OF A SERIES OF PENTACOORDINATE RHODIUM NITROSYL COMPLEXES: CRYSTAL AND MOLECULAR STRUCTURES OF *CIS*-DIBROMONITROSYLBIS(METHOXYDIPHENYLPHOSPHINE)RHODIUM AND *TRANS*-DIBROMONITROSYLBIS-(*ISO*-PROPOXYDIPHENYLPHOSPHINE)RHODIUM

ROBIN B. ENGLISH*

Department of Chemistry and Biochemistry, Rhodes University, Grahamstown 6140, Republic of South Africa

MARGOT M. DE V. STEYN

Department of Chemistry, University of South Africa, Pretoria, Republic of South Africa

and

RAYMOND J. HAINES

U.N./C.S.I.R. Research Unit of Metal Cluster Chemistry, Department of Chemistry, University of Natal, Pietermaritzburg, Republic of South Africa

(*Received* 9 *October* 1986; *accepted* 23 *January* 1987)

Abstract—The pentacoordinate rhodium nitrosyl complexes $[RhBr_2(NO)L_2]$ [L = $P(OPh)_2Ph$, $P(OMe)Ph_2$ or $P(OPr^i)Ph_2$] have been synthesized and the structures of $[RhBr_2(NO)\{P(OMe)Ph_2\}_2]$ and $[RhBr_2(NO)\{P(OPr^i)Ph_2\}_2]$ have been determined X-ray crystallographically. Both of these latter compounds are tetragonal pyramidal with the nitrosyl group apical. The methoxydiphenylphosphine ligands in $[RhBr_2(NO)\{P(OMe)Ph_2\}_2]$ are *cis*-disposed whereas the larger *cis*-propoxydiphenylphosphine ligands in $[RhBr_2(NO)\{P(OPr^i)Ph_2\}_2]$ are mutually *trans*. The nitrosyl group in *trans*-$[RhBr_2(NO)\{P(OPr^i)Ph_2\}_2]$ eclipses an Rh-P axis but in *cis*-$[RhBr_2(NO)\{P(OMe)Ph_2\}_2]$ it is staggered with respect to the P–Rh–P linkage. The isomeric behaviour of nitrosyl complexes of type $[RhX_2(NO)L_2]$ (X = halogen, L = phosphorus donor ligand) is rationalized in terms of the size of the ligand L.

It has been established that the pentacoordinate nitrosyl complexes $[MCl_2(NO)(PPh_3)_2]$ (M = Rh or Ir) adopt tetragonal pyramidal geometries with the nitrosyl group in the apical position and the triphenylphosphine ligands *trans*-disposed with respect to each other.[1,2] The nitrosyl bends rather unexpectedly in the more sterically crowded P–M–P plane. We subsequently synthesized the rhodium triphenylphosphite nitrosyl complex $[RhBr_2(NO)\{P(OPh)_3\}_2]$ and established that this compound assumes a related structure but with the triphenylphosphite ligands mutually *cis*.[3] The nitrosyl group again bends towards the phosphorus ligands but is staggered in relation to the P–Rh–P linkage. Hoffman *et al.*,[4] by considering the relative energies of the metal orbitals and those on the nitrosyl group for pentaccordinate nitrosyl complexes, have postulated a set of rules dictating the conditions under which the NO ligand will bend in these complexes

* Present address: Inorganic Chemistry Laboratory, South Parks Road, Oxford OX1 3QR, U.K. Author to whom correspondence should be addressed.

and, if it does, in which direction it will do so. In particular the bending of the NO group along the P–M–P axis in $[MCl_2(NO)(PPh_3)_2]$ (M = Rh or Ir) was rationalized but at the time of publication compounds of type *cis*-$[MX_2(NO)L_2]$ (M = Rh or Ir, X = halogen, L = phosphorus donor ligand) were not known, and as a consequence reference was not made to them.

With the object of elucidating the factors governing the isomeric behaviour of compounds of type $[MX_2(NO)L_2]$, we have synthesized a number of complexes of formula $[RhBr_2(NO)L_2]$ where L has been systematically varied. This paper describes the synthesis and molecular structures of two closely related complexes, $[RhBr_2(NO)\{P(OMe)Ph_2\}_2]$ (**1**) and $[RhBr_2(NO)\{P(OPr^i)Ph_2\}_2]$ (**2**), as well as the investigation of the synthesis of $[RhBr_2(NO)\{P(OPh)_2Ph\}_2]$ (**3**) and $[RhBr_2(NO)\{P(OPh)Ph_2\}_2]$ (**4**) containing phosphorus ligands intermediate between PPh_3 and $P(OPh)_3$.

EXPERIMENTAL

Complexes **1**–**3** were synthesized by treatment of $[\{Rh(NO)Br_2\}_n]$[5] with the appropriate phosphorus ligand following the procedure described in the literature.[6] Compound **1** crystallized as air-sensitive, olive-green platelets [ν(N—O) 1680 cm^{-1}, in Nujol] from methanol at −15°C: yield *ca* 65%. (Found: C, 43.4; H, 3.7; N, 1.9. $C_{26}H_{26}Br_2NO_3P_2Rh$ requires C, 43.1; H, 3.6; N, 1.9.) **2** was obtained as dark red, air-stable chunky crystals [ν(N—O) 1620 cm^{-1}, in Nujol] from acetone–ethanol at −15°C: yield *ca* 30% (the reason for this low yield has been discussed[6]). (Found: C, 46.0; H, 4.3; N, 1.9. $C_{30}H_{34}Br_2NO_3P_2Rh$ requires C, 46.1; H, 4.4; N, 1.8.) Compound **3** was crystallized as air-sensitive, green microcrystals [ν(N—O) 1740 cm^{-1}, in Nujol] from dichloromethane–methanol at 0°C: yield *ca* 65%. (Found: C, 50.3; H, 3.8; N, 1.3. $C_{36}H_{30}Br_2NO_5P_2Rh$ requires C, 49.1; H, 3.4; N, 1.6.) Compounds **1** and **3** decomposed after a few days to oils which were nitrosyl-free according to the IR spectroscopic evidence.

X-ray crystallographic studies

Data collection, structure solution and refinement details have been described previously.[6] In the case of compound **1** all atoms except the phenyl carbons were refined anisotropically, while only the Rh, Br and P atoms of **2** were given anisotropic temperature factors. Anisotropic refinement of the nitrosyl atoms in **2** resulted in improbable temperature factors. The high final value of R (and R_W) in the case of compound **2** is probably a consequence of thermal effects: the average volume per non-hydrogen atom is 21.3 $Å^3$, compared with 19.8 $Å^3$ for **1**.

Crystal data, data collection and refinement details are summarized in Table 1, and selected bond lengths and angles are given in Table 2.

RESULTS AND DISCUSSION

While **1**–**3** were readily synthesized from $[\{Rh(NO)Br_2\}_n]$, attempts to prepare **4** proved unsuccessful. Reaction of $[\{Rh(NO)Br_2\}_n]$ with $P(OPh)Ph_2$ resulted in the formation of $[\{RhBr(NO)\{(Ph_2PO)_2H\}\}_2]$,[6] or intractable oils with no N—O stretching bonds in their IR spectra, depending on whether or not traces of water were present in the reaction mixture. Exchange of the $AsPh_3$ ligands in $[RhBr_2(NO)(AsPh_3)_2]$, another possible route to **4**, was also unsuccessful: stirring of a suspension of the triphenylarsine complex in dry ethanol in the presence of a twice molar excess of $P(OPh)Ph_2$ did not result in ligand substitution (indicated by monitoring by means of IR spectroscopy).

Single crystals suitable for X-ray diffraction studies could only be obtained for two of the three compounds synthesised, viz. **1** and **2**. The molecular structures of these two compounds, as established crystallographically, are illustrated in Figs 1 and 2, respectively. Both compounds are tetragonal pyramidal with bent apical nitrosyl groups. The two phosphorus ligands and the two bromine atoms are mutually *cis* in compound **1** whereas in compound **2**, which exhibits crystallographic two-fold symmetry, they are mutually *trans*. As such the two compounds are structurally analogous to $[RhBr_2(NO)\{P(OPh)_3\}_2]$[3] and $[RhCl_2(NO)(PPh_3)_2]$,[1] respectively.

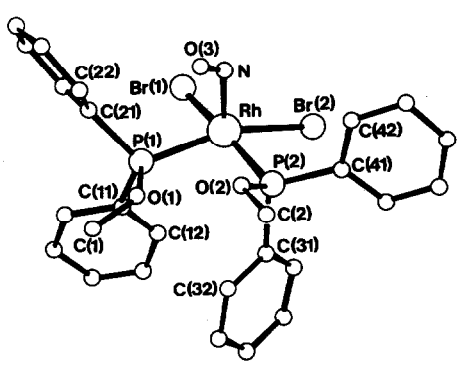

Fig. 1. Molecular stereochemistry of *cis*-$[RhBr_2(NO)\{P(OMe)Ph_2\}_2]$.

Table 1. Crystal data, data collection and refinement details

	$[RhBr_2(NO)\{P(OMe)Ph_2\}_2]$	$[RhBr_2(NO)\{P(OPr^i)Ph_2\}_2]$
Formula	$C_{26}H_{26}Br_2NO_3P_2Rh$	$C_{30}H_{34}Br_2NO_3P_2Rh$
M	725.17	781.29
Space group	$P2_1/c$	$C2/c$
a (Å)	13.451(5)	22.346(5)
b (Å)	11.700(5)	9.354(5)
c (Å)	17.649(5)	17.140(5)
β (°)	90.92(5)	111.76(5)
$F(000)$	1432	1560
U (Å^3)	2777(6)	3327(5)
Z	4	4
D_m (g cm^{-3}) (flotation in CH_3I–hexane)	1.72(5)	1.56(5)
D_c (g cm^{-3})	1.73	1.56
μ (cm^{-1})	35.4	29.3
Crystal size (mm)	$0.05 \times 0.15 \times 0.15$	$0.07 \times 0.1 \times 0.1$
Number of reflections ($3° < \theta < 23°$)	2746 ($\pm h, k, l$)	2143 ($\pm h, k, l$; $h+k = 2n$)
Observed reflections	1596 [$I > 4\sigma(I)$]	1207 [$I > 3\sigma(I)$]
R	0.055	0.091
R_w	0.043	0.091
k and g in $w = k[\sigma^2(F_o)+g\lvert F_o\rvert^2]^{-1}$	1.62, 8×10^{-6}	Unit weights
$N_{parameters}$	Two blocks: 156 in each block, comprising all non-phenyl parameters with parameters for two phenyl rings	70

The σ-donor–π-acceptor properties of $P(OMe)Ph_2$ and $P(OPr^i)Ph_2$ may be assumed to be very similar, so that the different isomeric forms adopted by compounds **1** and **2** are best rationalized in terms of the difference in the steric size of the two ligands. A simple geometrical parameter which is used extensively to rank the steric influence of phosphorus donor ligands is the ligand cone angle.[7] This angle, which is essentially the apical angle of the cone whose apex is the metal atom and which envelopes the van der Waals' volume of the strain-free ligand, has been used to rank ligands in the correct order of the degree of dissociation of $[NiL_4]$ (L = ligand) complexes in solution. The cone angles for those ligands corresponding with crystallographically established structures for the nitrosyl complexes of type $[RhX_2(NO)L_2]$ (X = halogen, L = phosphorus donor ligand) are: $P(OPh)_3$ 121(10)° (the large uncertainty in this cone angle reflects the considerable flexibility of this ligand arising from the P–O–C linkages), $P(OMe)Ph_2$ 132(2)°, $P(OPr^i)Ph_2$ 140°, and PPh_3 145(2)°; the cone angle for $P(OPr^i)Ph_2$ has been estimated by taking the weighted arithmetic mean of the cone angles for $P(OPr^i)_3$ and PPh_3. Although it is accepted that the two phosphorus ligands in the *cis* isomers, $[RhBr_2(NO)L_2]$, may be considerably intermeshed and that the ligand cone angle is not necessarily the sole parameter for ranking ligands in the order of their steric influence it is proposed, nevertheless, that the critical ligand cone angle representing the crossover point between a preferred *cis* and a preferred *trans* configuration for

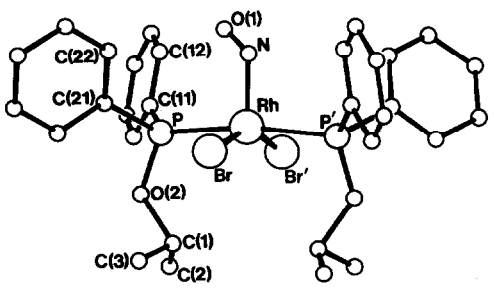

Fig. 2. Molecular stereochemistry of *trans*-$[RhBr_2(NO)\{P(OPr^i)Ph_2\}_2]$.

Table 2. Selected interatomic distances (Å) and angles (°) with estimated standard deviations in parentheses

	(a) $[RhBr_2(NO)\{P(OMe)Ph_2\}_2]$		
Rh—Br(1)	2.518(2)	Br(2)—Rh—P(2)	86.2(1)
Rh—Br(2)	2.525(2)	Br(2)—Rh—N	107.1(4)
Rh—P(1)	2.263(4)	P(1)—Rh—P(2)	95.7(1)
Rh—P(2)	2.275(4)	P(1)—Rh—N	97.2(4)
Rh—N	1.923(15)	P(2)—Rh—N	92.8(4)
N—O(3)	1.14(2)	Rh—N—O(3)	128(1)
P(1)—O(1)	1.596(10)	Rh—P(1)—O(1)	111.9(4)
P(1)—C(11)	1.814(15)	Rh—P(1)—C(11)	111.8(5)
P(1)—C(21)	1.849(15)	Rh—P(1)—C(21)	115.6(5)
O(1)—C(1)	1.43(2)	O(1)—P(1)—C(11)	106.2(6)
P(2)—O(2)	1.595(10)	O(1)—P(1)—C(21)	102.8(6)
P(2)—C(31)	1.820(15)	C(11)—P(1)—C(21)	107.7(7)
P(2)—C(41)	1.804(14)	Rh—P(2)—O(2)	111.5(4)
O(2)—C(2)	1.43(2)	Rh—P(2)—C(31)	109.9(5)
Br(1)—Rh—Br(2)	87.1(1)	Rh—P(2)—C(41)	117.3(5)
Br(1)—Rh—P(1)	85.2(1)	O(2)—P(2)—C(31)	105.8(6)
Br(1)—Rh—P(2)	167.0(1)	O(2)—P(2)—C(41)	101.7(6)
Br(1)—Rh—N	100.0(4)	C(31)—P(2)—C(41)	109.9(7)
Br(2)—Rh—P(1)	155.5(1)	P(1)—O(1)—C(1)	123(1)
		P(2)—O(2)—C(2)	121(1)
	(b) $[RhBr_2(NO)\{P(OPr^i)Ph_2\}_2]$		
Rh—Br	2.454(2)	P—Rh—P′	170.8(2)
Rh—P	2.362(7)	P—Rh—N	94.6(2)
Rh—N	1.85(5)	Rh—N—O(1)	133(4)
N—O(1)	0.88(4)	Rh—P—O(2)	112.0(7)
P—O(2)	1.61(2)	Rh—P—C(11)	116.9(7)
P—C(11)	1.81(2)	Rh—P—C(21)	118.6(7)
P—C(21)	1.81(2)	O(2)—P—C(11)	104(1)
O(2)—C(1)	1.57(4)	O(2)—P—C(21)	103(1)
C(1)—C(2)	1.46(5)	C(11)—P—C(21)	100(1)
C(1)—C(3)	1.58(6)	P—O(2)—C(1)	128(2)
Br—Rh—Br′	152.4(1)	C(2)—C(1)—O(2)	97(4)
Br—Rh—P	88.6(2)	C(3)—C(1)—O(2)	94(3)
Br—Rh—N	103.8(1)	C(2)—C(1)—C(3)	124(4)

$[RhBr_2(NO)L_2]$ lies somewhere between 132 and 140° on the basis of the above angles. The structure of **3** could not be established unequivocally by crystallographic methods (*vide supra*) but on the basis that the compound has the same colour (green) as $[RhBr_2(NO)\{P(OPh)_3\}_2]$ (green) and $[RhBr_2(NO)\{P(OMe)Ph_2\}_2]$ (olive green) it is assumed that it adopts the *cis* configuration. The estimated cone angle for $P(OPh)_2Ph$ (129°) is less than 132°, and thus the structure of **3** is consistent with this cone angle proposal.

Similar to that in $[RhCl_2(NO)(PPh_3)_2]$,[1] the nitrosyl group in compound **2** adopts a bent geometry [Rh—N—O(1) 133(4)°] (*vide supra*) and in so doing eclipses the P–Rh–P axis. As described above, Hoffmann *et al.* have explained[4] this bending in terms of a general molecular orbital scheme for pentacoordinate metal nitrosyl complexes. In particular they showed that the metal d_{xz}- and d_{yz}-orbitals which are degenerate for compounds of the type $[Rh(NO)L_4]$ with C_{4v}-symmetry, are not of the same energy in *trans*-$[RhX_2(NO)L_2]$ as a consequence of the *trans* arrangement of the basal ligands, and that the orbital lying in the same plane as the weaker donor ligands (d_{xz}) is lower in energy. The π^*(NO) orbitals will interact differently with the two *d*-orbitals with the interaction involving d_{yz} being the stronger. Bending will thus take place in the plane of the weaker donor ligands. Extending the proposals of Hoffmann *et al.* it is suggested that the metal d_{xz}- and d_{yz}-orbitals in **1** and $[RhBr_2(NO)\{P(OPh)_3\}_2]$ (see below) will also interact differently with the π^*-orbitals of the NO group with the interaction involving d_{yz} again being the

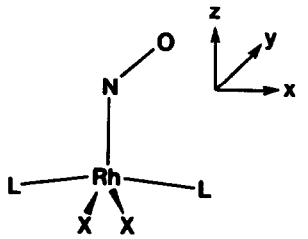

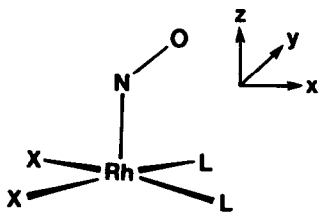

stronger such that bending occurs towards the phosphorus ligands but in a plane (*xz*) which bisects the P—Rh—P angle. Bending in this plane will also minimize steric repulsions.

A more simplistic picture is that the nitrosyl group, free to rotate about the Rh–N vector, will orient itself so that its dipole moment opposes the dipole moment of the rest of the complex. The positive end of the dipole of the *cis*-$RhBr_2L_2$ moiety lies in a direction bisecting the P—Rh—P angle and it is in this direction that the negative end of the NO dipole will orient itself. However the *trans*-RhX_2L_2 moiety has a very small resultant dipole moment, and in this situation one could expect the NO group to orient itself so that the Br...O distances are maximized as indeed observed. Significantly the NO group in the compound $[Rh(O_2CCF_3)_2(NO)(PPh_3)_2]$[8] which has a *trans* structure analogous to $[RhCl_2(NO)(PPh_3)_2]$,[1] is oriented so that it bends in a plane approximately bisecting one of the P—Rh—O angles. An interpretation of this observation is that, for this particular *trans* complex, the steric repulsion effects of the two sets of basal ligands, i.e. the triphenyl phosphines and the trifluoroacetate groups, are very similar, and that as a consequence the nitrosyl group bends in the plane where steric effects are least. Alternatively, in terms of the proposals[4] of Hoffmann *et al.* it could be argued that the powerful electron-withdrawing effect of the CF_3 groups reduces the donor strength of the trifluoroacetate ligands such that the donor properties of the PPh_3 and CF_3COO ligands are similar, and that, as a consequence, steric effects will govern the direction of bending of the nitrosyl group.

A further feature of the nitrosyl complexes under discussion which warrants some comment is that concerning their stability. Whereas the *trans* derivatives $[RhCl_2(NO)(PPh_3)_2]$ and $[RhBr_2(NO)\{P(OPr^i)Ph_2\}_2]$ are stable in solution at ambient temperature the *cis* species $[RhBr_2(NO)L_2]$ [L = $P(OPh)_3$, $P(OMe)Ph_2$ or $P(OPh)_2Ph$] are unstable under similar conditions. It is suggested that although *cis* products are only isolated for the less bulky phosphorus ligands, the steric repulsion between these ligands when *cis*-disposed is sufficient to cause the instability of their complexes. The inability to isolate $[RhBr_2(NO)\{P(OPh)Ph_2\}_2]$ may be attributed to the formation of the *cis* isomer and its inherent instability. The reason as to why the *cis* compounds do not rearrange to the more sterically stable *trans* isomers is not however clear.*

Acknowledgements—We express our sincere thanks to the South African Council for Scientific and Industrial Research, Rhodes University, and the Universities of Cape Town, Natal and South Africa for financial support, Mr J. Albain of the N.P.R.L., C.S.I.R., Pretoria, for the intensity data collection, and Dr I.J. McNaught for helpful discussions.

REFERENCES

1. S. Z. Goldberg, C. Kubiak, C. D. Meyer and R. Eisenberg, *Inorg. Chem.* 1975, **14**, 1650.
2. D. M. P. Mingos and J. A. Ibers, *Inorg. Chem.* 1971, **10**, 1035.
3. R. B. English, L. R. Nassimbeni and R. J. Haines, *Acta Cryst.* 1976, **B32**, 3299.
4. R. Hoffmann, M. M. L. Chen, M. Elian, A. R. Rossi and D. M. P. Mingos, *Inorg. Chem.* 1974, **13**, 2666.
5. G. R. Crookes and B. F. G. Johnson, *J. Chem. Soc. A* 1970, 1662.
6. R. B. English and M. M. de V. Steyn, *S. Afr. J. Chem.* 1984, **37**, 177.
7. C. A. Tolman, W. C. Seidel and L. W. Gosser, *J. Am. Chem. Soc.* 1974, **96**, 53.
8. A. Dobson, D. S. Moore, S. D. Robinson, A. M. R. Galas and M. B. Hursthouse, *J. Chem. Soc., Dalton Trans.* 1985, 611.

* Atomic coordinates, thermal parameters and F_o/F_c data have been deposited with the Editor as supplementary data: atomic coordinates have also been deposited with the Cambridge Crystallographic Data Centre.

Polyhedron Vol. 6, No. 6, pp. 1509–1512, 1987
Printed in Great Britain

0277–5387/87 $3.00+.00

COMPLEXES OF RHODIUM(III) AND IRIDIUM(III) WITH THE MONO-OXIMES OF 1,2-NAPHTHOQUINONE: X-RAY CRYSTAL STRUCTURE OF PYRIDINIUM TRICHLORO(1,2-NAPHTHOQUINONE 1-OXIMATO)(PYRIDINE)IRIDATE(III)

JOHN CHARALAMBOUS,* KIM HENRICK, YUSUF MUSA and RON G. REES

School of Chemistry, The Polytechnic of North London, Holloway, London N7 8DB, U.K.

and

ROBERT N. WHITELEY

Inco Europe Ltd, Bashley Road, Acton, London NW10, U.K.

(*Received* 21 *October* 1986; *accepted* 23 *January* 1987)

Abstract—The complexes $M(1\text{-nqo})_3$ (M = Rh or Ir, 1-nqoH = 1,2-naphthoquinone 1-oxime) and $M(2\text{-nqo})_3$ (M = Rh or Ir, 2-nqoH = 1,2-naphthoquinone 2-oxime) were prepared by the interaction of the quinone oxime with hydrated rhodium(III) chloride or chloroiridic(III) acid. The mixture resulting from the reaction of chloroiridic(III) acid and 1,2-naphthoquinone 1-oxime on treatment with pyridine afforded [pyH][Ir(1-nqo)(py)Cl_3] which was characterized by X-ray crystallography. The complexes $Rh(1\text{-nqo})_3$ and $Rh(2\text{-nqo})_3$ were also obtained by the nitrosation of the respective naphthol in the presence of hydrated rhodium(III) chloride. None of the trischelates showed any tendency to react with pyridine, triphenylphosphine or aqueous hydrochloric acid.

RESULTS AND DISCUSSION

Recently several papers dealing with metal complexes of 1,2-quinone mono-oximes and their structures have been published.[1–3] These complexes have been concerned mainly with first-row transition metals. Complexes of other metals have attracted attention for analytical or extraction purposes, but apart from studies of uranyl,[4] ruthenium,[5] and related platinum[6] complexes, the routes leading to them and their properties and structures have not been investigated. Here we report on the synthesis and properties of the complexes $M(1\text{-nqo})_3$ (M = Rh or Ir, 1-nqoH = 1,2-naphthoquinone 1-oxime), $M(2\text{-nqo})_3$ (M = Rh or Ir, 2-nqoH = 1,2-naphthoquinone 2-oxime) and [pyH][Ir(1-nqo)$pyCl_3$], and on the X-ray crystallographic characterization of the latter.

The complexes $Rh(1\text{-nqo})_3$ and $Rh(2\text{-nqo})_3$ were obtained from the reaction of rhodium(III) chloride with the appropriate 1,2-naphthoquinone mono-oxime or its sodium salt, in buffered aqueous acetone at pH 5–6 under reflux. All reactions afforded mixtures of products from which the trischelates were separated by using column chromatography. Thin-layer chromatographic examination of the trischelates, however, showed the presence of two components suggesting that each product is a mixture of two isomers. The formation of isomers is not unexpected in view of the ambidentate and asymmetric nature of the ligands which can give rise to linkage and/or geometrical isomerism. Similar behaviour has been reported for the analogous cobalt(III) complexes.[7]

The iridium trischelates $Ir(1\text{-nqo})_3$ and $Ir(2\text{-nqo})_3$ were prepared by reacting a solution of chloroiridic(III) acid with the sodium salt of the mono-oxime in buffered aqueous acetone at pH 4–5 under reflux. As in the case of the corresponding rhodium complexes these were separated as mixtures of isomers chromatographically. The reaction of chlo-

* Author to whom correspondence should be addressed.

roiridic(III) acid with either of the 1,2-naphthoquinone mono-oximes in unbuffered aqueous methanol under reflux afforded very complex mixtures which contained some of the respective trischelate. Addition of pyridine to the mixture arising from the reaction of 1,2-naphthoquinone 1-oxime with chloroiridic(III) acid led to the isolation of the complex [pyH][Ir(1-nqo)(py)Cl_3] in low yield.

Mixtures of isomers of Rh(1-nqo)$_3$ and Rh(2-nqo)$_3$ were also obtained from the nitrosation of the appropriate naphthol in the presence of rhodium(III) chloride. However, the yield of the products were lower than those obtained from the direct reaction of the oximes with rhodium(III) chloride. No iridium trischelates resulted from the nitrosation of either of the naphthols in the presence of chloroiridic(III) acid. In both cases the main product was the respective 1,2-naphthoquinone monooxime.

Neither the rhodium nor the iridium trischelates showed any tendency to react with pyridine or triphenylphosphine. This behaviour contrasts with that of the corresponding iron(III), cobalt(III) and chromium(III) complexes which undergo internal redox and/or deoxygenation reactions on treatment with these Lewis bases.[5] All the trischelates showed passivity towards hydrochloric acid, a feature which again contrasts with that of analogous complexes of first transition series metals.

Both the rhodium and iridium trischelates, and the complex [pyH][Ir(nqo)(py)Cl_3] were found to be diamagnetic, which reflects the tendency of both rhodium(III) and iridium(III) to adopt a low-spin t_{2g}^6 arrangement. The IR spectra of all the complexes include strong absorptions in the 1500–1620 cm^{-1} region assignable to ν(C=O) and ν(C=N) stretching vibrations, and which are indicative of the quinone oximic character of the ligand. Evidence for the quinone oximic character is also provided by the X-ray study of the pyridinium trichloro(1,2-naphthoquinone 1-oximato)(pyridine)-iridate(III).

Crystal and molecular structure of [pyH][Ir(1-nqo)(py)Cl_3]

Crystal data. $C_{20}H_{17}IrN_3Cl_3$, monoclinic, $P2_1/c$, $a = 11.403(3)$, $b = 11.977(4)$, $c = 15.155(5)$ Å, $U = 2062.87$ Å^3, $D_c = 1.810$ g cm^{-3}, $Z = 4$. Intensity data were collected on a Phillips PW1100 four-circle diffractometer using graphite-monochromated Mo-K_α radiation. The structure was solved and refined using 2816 unique reflections [$I > 3\sigma(I)$] to a final R factor of 0.0366.* Anisotropic thermal parameters were used for the Ir, N, the carbonyl O and all the Cl atoms. All hydrogen atoms for the compound were found from a subsequent difference map and included in the calculation of the structure factors, but were not refined. The bond lengths and the bond angles are listed in Tables 1 and 2, and the atomic numbering is explained in Fig. 1.

As with other 1,2-quinone oximato-complexes of *d*-block metals the chelate ring in the trichloro(1,2-naphthoquinone 1-oximato)(pyridine)iridate(III) anion is five-membered. The bond lengths in the chelate ring agree well with results for other 1,2-naphthoquinone oximato complexes and the short C_3—C_4 bond length provide additional evidence for the quinone oximic character.[8–10] The Cl—Ir—Cl bond angles [89.5°(av.)] are close to the idealized value of 90° for octahedral complexes. The pyridine molecule completes the distorted octahedral arrangement around Ir.

EXPERIMENTAL

IR spectra were recorded with a Pye–Unicam SP2000 spectrophotometer. Magnetic measurements were made at room temperature using a Gouy balance equipped with a permanent magnet of 3600 Oe. The absorbent used in the chromatography columns was Merk Kieselgel 60 (70–230-mesh) and TLC was carried out using precoated Merck Kieselgel 60 F_{254} plates. Chloroiridic(III) acid was prepared from chloroiridic(IV) acid as described earlier.[11] Hydrated rhodium(III) chloride of 39.0% Rh content was used.

Table 1. Bond lengths (Å) for [pyH][Ir($C_{10}H_6NO_2$)(py)Cl_3]

Ir—Cl(1)	2.343(2)	Ir—Cl(2)	2.350(2)
Ir—Cl(3)	2.364(2)	Ir—O(2)	2.025(5)
Ir—N(1)	1.976(6)	Ir—N(11)	2.099(6)
O(2)—C(2)	1.300(10)	O(1)—N(1)	1.274(8)
N(1)—C(1)	1.352(10)	C(1)—C(2)	1.416(11)
C(1)—C(9)	1.465(11)	C(2)—C(3)	1.421(11)
C(3)—C(4)	1.350(12)	C(4)—C(10)	1.431(12)
C(9)—C(10)	1.426(12)		

* Final atomic positional and thermal parameters, bond lengths and angles and F_o/F_c values have been deposited as supplementary material with the Editor, from whom copies are available on request. Atomic coordinates have also been submitted to the Cambridge Crystallographic Data Centre.

Table 2. Bond angles (°) for [pyH][Ir($C_{10}H_6NO_2$)(py)Cl_3]

Cl(2)—Ir—Cl(1)	175.8(1)	Cl(3)—Ir—Cl(1)	92.1(1)
Cl(3)—Ir—Cl(2)	91.6(1)	O(2)—Ir—Cl(1)	89.1(2)
O(2)—Ir—Cl(2)	87.3(2)	O(2)—Ir—Cl(3)	176.5(2)
N(1)—Ir—Cl(1)	90.2(2)	N(1)—Ir—Cl(2)	91.2(2)
N(1)—Ir—Cl(3)	96.3(2)	N(1)—Ir—O(2)	80.4(2)
N(11)—Ir—Cl(1)	88.8(2)	N(11)—Ir—Cl(2)	89.3(2)
N(11)—Ir—Cl(3)	89.9(2)	N(11)—Ir—O(2)	93.4(2)
N(11)—Ir—N(1)	173.8(3)	C(2)—O(2)—Ir	111.5(5)
O(1)—N(1)—Ir	124.0(5)	C(1)—N(1)—Ir	115.3(5)
C(1)—N(1)—O(1)	120.6(6)	C(11)—N(11)—Ir	120.6(5)
C(15)—N(11)—Ir	119.8(5)		

Reaction of hydrated rhodium(III) *chloride with* 1,2-*naphthoquinone* 1-*oxime or its sodium salt*

A solution of hydrated rhodium(III) chloride (2.09 g, 7.9 mmol) in water (50 cm^3) was added to a solution of 1,2-naphthoquinone 1-oxime (5.24 g, 30.3 mmol) in acetone (100 cm^3) in a sodium acetate–acetic acid buffered medium at pH 5–6, and the mixture was heated under reflux for 2 h. Filtration gave a solid which was washed with water, dried at 60°C/30 mmHg and chromatographed. Elution with toluene gave a mixture of purple isomers of *tris*(1,2-*naphthoquinone* 1-*oximato*)*rhodium*(III) (3.25 g, 67%). (Found: C, 57.8; H, 3.4; N, 6.2; Rh, 16.0%. $C_{30}H_{18}N_3O_6Rh$ requires: C, 58.2; H, 2.9; N, 6.8; Rh, 16.6%.)

Similarly, hydrated rhodium(III) chloride (2.00 g, 7.6 mmol) and sodium 1,2-naphthoquinone 1-oximate (5.50 g, 28.2 mmol) gave tris(1,2-naphthoquinone 1-oximato)rhodium(III) (3.01 g, 64%) (identified by TLC and IR).

Reaction of hydrated rhodium(III) *chloride with* 1,2-*naphthoquinone* 2-*oxime or its sodium salt*

A solution of hydrated rhodium(III) chloride (2.00 g, 7.6 mmol) in water (50 cm^3) was added to a solution of the 1,2-naphthoquinone 2-oxime (5.29 g, 30.8 mmol) in acetone (100 cm^3) in a sodium acetate–acetic acid buffered medium at pH 5–6 and the mixture was heated under reflux for 2 h. Filtration gave a solid which was washed with water, dried at 60°C/30 mmHg and chromatographed. Elution with toluene gave a mixture of isomers of *tris*(1,2-*naphthoquinone* 2-*oximato*)*rhodium*(III) (3.25 g, 69%). (Found: C, 59.0; H, 3.2; N, 6.9; Rh, 16.3. $C_{30}H_{18}N_3O_6Rh$ requires: C, 58.2; H, 2.9; N, 6.8; Rh, 16.6%.)

Similarly, hydrated rhodium(III) chloride (2.00 g, 7.6 mmol) and sodium 1,2-naphthoquinone 2-oximate (5.4 g, 27.7 mmol) gave tris(1,2-naphthoquinone 2-oximato)rhodium(III) (3.15 g, 67%) (identified by TLC and IR).

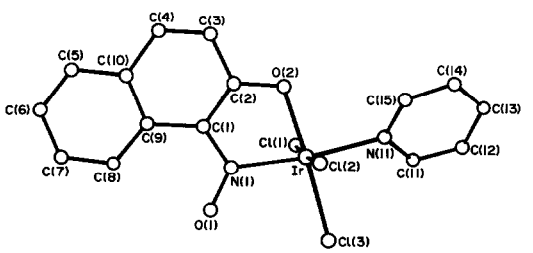

Fig. 1. Structure of the anion of [pyH][Ir($C_{10}H_6NO_2$](py)Cl_3].

Reaction of chloroiridic(III) *acid with the mono-oximes of* 1,2-*naphthoquinone*

Chloroiridic(III) acid (3.00 cm^3, containing 0.40 g Ir, 2.2 mmol) was added to a solution of 1,2-naphthoquinone 1-oxime (5.8 g, 33.5 mmol) in methanol (150 cm^3) and heated under reflux for 3 days. Removal of solvent gave a brown solid (4.93 g) (multicomponent by TLC). A portion of the solid (0.51 g) was stirred with pyridine (100 cm^3) for 2 days. Filtration gave a purple solid which was recrystallized from methanol to give needle-like crystals of pyridinium trichloro(1,2-naphthoquinone 1-oximato)(pyridine)iridate(III) (0.05 g, 4%) (characterized by X-ray crystallography).

Similarly chloroiridic(III) acid (3.00 cm^3, containing 0.40 g Ir, 2.2 mmol) and 1,2-naphthoquinone 2-oxime (5.8 g, 33.5 mmol) gave a brown solid which was shown by TLC to be multicomponent.

Reaction of chloroiridic(III) *acid with sodium* 1,2-*naphthoquinone mono-oximates*

Chloroiridic(III) acid (4.00 cm^3, containing 0.54 g of Ir) was added to a solution of sodium 1,2-

naphthoquinone 1-oximate (7.5 g, 38.5 mmol) in 1 : 1 water–acetone (200 cm^3) buffered at pH 4–5 with sodium acetate–acetic acid and heated under reflux for 5 days. The mixture was filtered to give a dark brown solid (4.28 g) which was dried at 60°C/30 mmHg and chromatographed. Elution with toluene gave *tris*(1,2-*naphthoquinone* 1-*oximato*) *iridium*(III) (0.41 g, 20%). (Found: C, 49.6; H, 3.7; N, 5.4; Ir, 26.7. $C_{30}H_{18}IrN_3O_6$ requires: C, 50.8; H, 3.3; N, 5.9; Ir, 27.1%.)

Similarly *tris*(1,2-*naphthoquinone* 2-*oximato*)*iridium*(III) (18%) (Found: C, 49.3; H, 3.8; N, 5.3; I, 27.5. $C_{30}H_{18}IrN_3O_6$ requires C, 50.8; H, 3.3; N, 5.9; Ir, 27.1%) was obtained when sodium 1,2-naphthoquinone 2-oximate was used.

Nitrosation of 1-*naphthol or* 2-*naphthol in the presence of hydrated rhodium*(III) *chloride*

A solution of sodium nitrite (5.13 g, 74.3 mmol) in water (50 cm^3) was added to a stirred solution of 1-naphthol (4.01 g, 29.9 mmol), hydrated rhodium(III) chloride (1.98 g, 7.5 mmol), acetic acid (10 cm^3) and sodium acetate (10.00 g) in 2 : 1 methanol–water mixture (300 cm^3). After 20 h the mixture was filtered to give a dark purple solid which was washed with water and dried at 60°C/35 mmHg and chromatographed. Elution with toluene gave tris(1,2-naphthoquinone 2-oximato)rhodium(III) (1.9 g, 39%) (identified by TLC and IR).

Similarly, nitrosation of 2-naphthol gave tris(1,2-naphthoquinone 1-oximato)rhodium(III) (1.6 g, 32%) (identified by TLC and IR).

Nitrosation of 1- *or* 2-*naphthol in the presence of chloroiridic*(III) *acid*

Nitrosation of 1-naphthol (3.00 g, 20.8 mmol) in the presence of chloroiridic(III) acid, (3.00 cm^3, containing 0.41 g of Ir, 2.2 mmol) carried out as above, gave unreacted 1-naphthol (32%) and 1,2-naphthoquinone 1-oxime (41%) (identical TLC, IR with an authentic sample). TLC of the filtrate indicated a multicomponent mixture which did not contain $Ir(1\text{-nqo})_3$.

Similarly nitrosation of 2-naphthol (3.00 g, 20.8 mmol) gave unreacted 2-naphthol (26%) and 1,2-naphthoquinone 2-oxime (55%) (identical TLC and IR with an authentic sample). TLC of the filtrate indicated a multicomponent mixture which did not contain $Ir(2\text{-nqo})_3$.

Attempted reactions of the $Rh(1\text{-nqo})_3$, $Rh(2\text{-nqo})_3$, $Ir(1\text{-nqo})_3$ *or* $Ir(2\text{-nqo})_3$ *with concentrated hydrochloric acid, triphenylphosphine or pyridine*

$M(1\text{-nqo})_3$ or $M(2\text{-nqo})_3$ (M = Rh or Ir) (*ca* 0.50 g) was recovered in *ca* 95% yield after being: (i) heated under reflux with pyridine (30 cm^3) for 7 days, or (ii) stirred with triphenylphosphine (1.00 g) in toluene (30 cm^3) for 7 days under reflux, or (iii) heated with concentrated aqueous hydrochloric acid (20 cm^3) for 3 days.

Acknowledgements—We thank the S.E.R.C. for a studentship (to Y.M.) and Inco Europe Ltd for the loan of rhodium and iridium compounds.

REFERENCES

1. J. Charalambous, M. J. Kensett and J. M. Jenkins, *J. Chem. Res.* 1982, **5**, 306.
2. C. B. Castellani and R. Millini, *J. Chem. Soc., Dalton Trans.* 1984, 1461.
3. C. B. Castellani, G. Gatti and R. Millini, *Inorg. Chem.* 1984, **23**, 4004.
4. R. Graziani, U. Casellato, P. A. Vigato, S. Tamburini and M. Vidali, *J. Chem. Soc., Dalton Trans.* 1983, 697.
5. D. Baluch, J. Charalambous, L. I. B. Haines, J. S. Morgan, W. Stoten and G. Soobramanien, unpublished results.
6. E. Lieol, U. Nagel and W. Beck, *Chem. Ber.* 1983, **116**, 1370.
7. J. Charalambous, G. Soobramanien, A. Betts and J. Bailey, *Inorg. Chim. Acta* 1982, **60**, 157.
8. R. G. Buckley, J. Charalambous, M. J. Kensett, M. McPartlin, D. Mukerjee, E. G. Brain and J. M. Jenkins, *J. Chem. Soc., Perkin Trans.* I 1983, 693.
9. H. Saarinen and J. Korvenranta, *Acta Chem. Scand.* 1975, **A29**, 409.
10. P. W. Carreck, J. Charalambous, M. J. Kensett, M. McPartlin and R. Sims, *Inorg. Nucl. Chem. Lett.* 1974, **10**, 749.
11. C. Masters, B. L. Shaw and R. E. Stainbank, *J. Chem. Soc., Dalton Trans.* 1972, 664.

Polyhedron Vol. 6, No. 6, pp. 1513–1515, 1987
Printed in Great Britain

0277–5387/87 $3.00+.00
Pergamon Journals Ltd

COMMUNICATION

A NOVEL PREPARATION OF KEGGIN-TYPE DODECATUNGSTOCOBALTATE(II) USING $[Co(ox)_3]^{3-}$ AND HYDROGEN PEROXIDE AS STARTING MATERIALS

KENJI NOMIYA, TSUNEO OCHIAI and MAKOTO MIWA*

Department of Industrial Chemistry, Faculty of Engineering,
Seikei University, Musashino, Tokyo 180, Japan

(*Received* 1 *December* 1986; *accepted* 9 *February* 1987)

Abstract—A novel rapid route for the preparation of the Keggin-type $[Co(II)W_{12}O_{40}]^{6-}$ heteropolyanion was found by using the $[Co(ox)_3]^{3-}$ complex and 30% aqueous hydrogen peroxide. The intermediate dicobalt species $[Co(II)Co(II)W_{11}O_{40}H_2]^{8-}$ was directly isolated in high yield and the final product was easily and rapidly derived from it.

Dodecatungstocobaltate(II), $[CoW_{12}O_{40}]^{6-}$, one of the Keggin-structure heteropoly tungstopolyanions with transition-metal ions as a heteroatom, was first prepared by Baker and McCutcheon.[1,2] It has been derived from the acid (HCl) hydrolysis of green crystals of an intermediate dicobalt species, $[Co(II)Co(II)W_{11}O_{40}H_2]^{8-}$, which is formed from a boiling mixture of the aqueous solution of sodium tungstate and aqueous Co(II) acetate. One of the Co(II) ions in the dicobalt species occupies the central tetrahedral cavity and the other an exterior octahedral site of the Keggin structure, the latter being coordinated with one water molecule.[3] In the preparation, the purification process of the dicobalt species, by repeated recrystallizations from the aqueous solution acidified with acetic acid, takes a very long time and seriously influences the yield of the final product.[4] To reduce the total time for preparation, we have previously tried an improved version.[5] By adding ether and 6 M sulpuric acid to the aqueous solution of the dicobalt species, which is still crude, the ether adduct of the free acid of the final product is formed as the third layer. The metatungstate obtained as a byproduct in the ether adduct should be removed. The separation is comparatively easy, because the thermal stabilities of the metatungstate and the desired product are quite different. This purification is surely more convenient than the original one. On the other hand, we have been interested in the preparation of heteropoly compounds using transition-metal complexes as the starting material.[6] In this work, we have devised a greatly improved preparation of the pure dicobalt species in high yield using the $[Co(ox)_3]^{3-}$ complex and 30% aqueous hydrogen peroxide as starting materials. In this method, it is surprising that the starting Co(III) state is completely converted to the Co(II) state in spite of the presence of a strong oxidation reagent.

*Author to whom correspondence should be addressed.

EXPERIMENTAL

Spectral measurements were performed by previously reported methods.[4,5] All chemicals used were analytical grade.

Preparations

The starting complex, $K_3[Co(ox)_3]\cdot 3H_2O$, was prepared according to the literature,[7] and identified by IR spectroscopy.[8] $Na_3[Co(ox)_3]\cdot 4H_2O$ was synthesized by using $Na_2C_2O_4$ instead of $K_2C_2O_4$ in the preparation of the corresponding potassium salt.

Dicobalt species. $Na_2WO_4\cdot 2H_2O$ (50 g, 0.15 mol) was dissolved in 100 cm^3 water. The pH of the solution was adjusted to *ca* 6 with glacial acetic acid. A separate solution was prepared by dissolving 6.2 g (0.013 mol) of $K_3[Co(ox)_3]\cdot 3H_2O$ in 100 cm^3 water to which 4.5 cm^3 of 30% aqueous hydrogen peroxide

had been added. The tungstate solution was maintained at above 90°C on a steam bath and the cobalt complex solution was added dropwise with stirring. All of the cobalt solution had been added over about 1.5 h and a deep green solution was formed. After the addition of the final drop, the solution was maintained at above 90°C for about 30 min with stirring. By filtering the hot solution, small amounts of a brown precipitate of Co(II) oxalate were removed. The deep green filtrate was kept overnight in the refrigerator and the green crystals of pure dicobalt species which deposited were collected, washed with ethanol and then ether, and dried *in vacuo* (yield 21 g).

The inital $Na_2WO_4 \cdot 2H_2O$ in the preparation cannot be replaced with K_2WO_4 because sparingly soluble precipitates of paratungstate were produced on the pH adjustment with glacial acetic acid.

$K_6[Co(II)W_{12}O_{40}] \cdot nH_2O$ *and* $K_2(TBA)_4[Co(II)W_{12}O_{40}]$. Twenty grams of the green crystals of the dicobalt species were dissolved in 100 cm^3 of 1 M aqueous HCl. The colour of the solution changed immediately from green to blue and insoluble precipitates were formed, while the dicobalt species were converted to the $[Co(II)W_{12}O_{40}]^{6-}$ ion. After filtering the precipitates, the deep blue filtrate was evaporated to dryness on a steam bath. During the process, the metatungstate present as an impurity was decomposed to an insoluble yellow solid (tungsten trioxide).[5] About 50 cm^3 of water was added, the yellow solid was filtered off and the deep blue filtrate was again evaported to dryness on the steam bath. No more yellow solid appeared. This fact shows contamination by less metatungstate as an impurity and that the obtained blue-green solid is the $[Co(II)W_{12}O_{40}]^{6-}$ compound. The potassium salt was isolated by dissolving the residual solid in about 40 cm^3 aqueous solution containing 4 g of KCl, concentrating the solution on a steam bath, cooling and adding equal amounts of ethanol. This compound was contaminated with *ca* 0.2% Na. Yield 4.1 g.

The precipitated $K_2(TBA)_4[CoW_{12}O_{40}]$ (TBA = tetrabutylammonium) was obtained by adding an aqueous solution containing 10 g of TBABr into an aqueous solution of the potassium salt. Sky-blue crystals (1.6 g) were obtained without any solvation by recrystallizing twice from acetronitrile. In this compound, no Na was detected. Found: C, 19.9; H, 4.0; N, 1.4. Calc. for $K_2[(C_4H_9)_4N]_4[CoW_{12}O_{40}]$: C, 19.5; H, 3.7; N, 1.4%. Electronic absorption bands and their intensities in UV–vis and near-IR regions were identical with the previously described data.[5] IR bands (KBr disk) were observed at 1025 (w), 945 (s), 875 (vs), 765 (vs), 520–580 (w, br) and 445 (m) cm^{-1}, which show the W—O vibrations characteristic of the Keggin structure.[4,5,9]

When the corresponding amounts of an $Na_3[Co(ox)_3] \cdot 4H_2O$–$Na_2WO_4 \cdot 2H_2O$–30% H_2O_2 system as starting materials were used, the sodium salt of dicobalt species was formed. However, this compound was highly soluble and cannot be obtained as crystals. By adding ethanol to the once filtered solution, a deep green paste of the dicobalt species was collected at the bottom of the beaker and was separated by decantation. By repeating the procedures described above, $Na_2(TBA)_4[Co-W_{12}O_{40}]$ was finally formed with a yield of 1.5 g. In this case, the purification, which involves the decomposition of the contaminated metatungstate on a steam bath, must be repeated many times.

RESULTS AND DISCUSSION

The method described here provides the potassium salt, the potassium TBA salt and the sodium TBA salt of $[Co(II)W_{12}O_{40}]^{6-}$ in high yields within a few days. The total time for the preparation of final products is markedly shortened and the yield is superior to the previous methods with the purity retained.

The $[Co(ox)_3]^{3-}$ complex reacts with the tungstate ion in aqueous solution at above 90°C without hydrogen peroxide. The visible absorption spectrum of its reaction mixture showed the formation of tetrahedral Co(II) species. Although the hydrogen peroxide was used with the aim of maintaining the starting Co(III) state, the formation of the Co(II) species was unexpectedly promoted. The amount of hydrogen peroxide did not affect the yield and quality of the dicobalt species. It is probable that in the hot solution the oxalato ligand acts as a reducing reagent for the Co(III) ion and the hydrogen peroxide catalytically promotes the reduction reaction. Instead of hydrogen peroxide, other "oxidation reagents", e.g. potassium peroxodisulphate, gave no dicobalt species, but pink-red precipitates as a main product, which is presumably the Co(II)-substituted species in one of the exterior octahedral tungsten sites of the metatungstate.

The $[Co(III)W_{12}O_{40}]^{5-}$ species with a tetrahedral Co(III) ion as a heteroatom can be derived from the isostructural Co(II) species by oxidation with peroxodisulphate.[1,5] Thus, this work is also useful for such a preparation.

REFERENCES

1. L. C. W. Baker and T. P. McCutcheon, *J. Am. Chem. Soc.* 1956, **78**, 4503.
2. L. C. W. Baker and V. E. Simmons, *J. Am. Chem. Soc.* 1959, **81**, 4744.

3. L. C. W. Baker and J. S. Figgis, *J. Am. Chem. Soc.* 1970, **92**, 3794.
4. K. Nomiya, M. Miwa, R. Kobayashi and M. Aiso, *Bull. Chem. Soc. Jpn* 1981, **54**, 2983.
5. K. Nomiya, R. Kobayashi and M. Miwa, *Bull. Chem. Soc. Jpn* 1983, **56**, 2272.
6. K. Nomiya, M. Wada, H. Murasaki and M. Miwa, *Polyhedron*, 1987, **6**, 1343.
7. J. C. Bailar, Jr and E. M. Jones, *Inorg. Synth.* 1939, **1**, 35.
8. K. Nakamoto, *Infrared and Raman Spectra of Inorganic and Coordination Compounds* 3rd Edn, p. 234. John Wiley, New York (1978).
9. K. Nomiya and M. Miwa, *Polyhedron* 1983, **2**, 955.

Polyhedron Vol. 6, No. 7, pp. 1517–1521, 1987
Printed in Great Britain

0277–5387/87 $3.00+.00
Pergamon Journals Ltd

POTENTIOMETRIC STUDY OF THE Co(II), Ni(II), Cu(II), Zn(II) AND Cd(II) COMPLEXES WITH 3-HYDROXY-2-NAPHTHALENE CARBOXYLIC ACID

E. CASASSAS,* G. FONRODONA and R. TAULER

Department of Analytical Chemistry, Universitat de Barcelona, Diagonal 647, Barcelona 08028, Spain

(*Received* 7 *April* 1986; *accepted* 16 *September* 1986)

Abstract—Formation constants of Co(II), Ni(II), Cu(II), Zn(II) and Cd(II) complexes with 3-hydroxy-2-naphthalene carboxylic acid have been determined potentiometrically in a 50% (v/v) dioxane–water solution at 25°C and 0.2 M KNO_3. Experimental data are analysed using several computer programs. The obtained values for the log of the formation constant of the first 1 : 1 (metal : ligand) complex with the different metals are: Co 7.9, Ni 7.1, Cu 10.44, Zn 7.8 and Cd 7.3. The log of the formation constant for the 1 : 2 copper complex is 18.20. It is to be noted that Ni(II) yields a 1 : 1 complex weaker than expected from the Irving–Williams series.

Metal complex formation with 3-hydroxy-2-naphthalene carboxylic acid (hnca) has not been previously studied in a conclusive way. Sandhu *et al.*[1] studied it under rather limited conditions (for each metal ion all the experiments were performed at the same concentrations and at a unique ratio of metal to ligand, and the potentiometric cell was calibrated externally using aqueous buffer solutions, whereas measurements were made in a dioxane–water medium). Other studies[2,3] refer mainly to hnca complexes with Cu(II) and Zn(II) including a rough evaluation of the formation constants.

Complexation with hnca cannot be studied in aqueous solution by potentiometric methods because of the low solubility of this ligand at neutral pH. In the present work, dioxane–water mixtures [50% (v/v)] were chosen because of the increased solubility of the ligand in this medium, allowing therefore higher total concentrations of both ligand and metal ion in the potentiometric determinations. However hydrolysis of the metal ions disturbs the complex formation near neutral pH, preventing the formation of binary complexes higher than the 1 : 1, except for Cu(II) ion where the complexation is the strongest.

Salicylate and 5-sulphosalicylate ions have the same donor groups and in the same respective positions as the hnca ligand. Their bivalent metal complexes follow the Irving–Williams series of stabilities, but the increase in stability along the series is rather small, as usual when dealing with ligands with only oxygen-donor groups. In their Ni(II) complexes this increase in stability [relative to the cobalt(II) complex] is unusually low. Comparison of hnca with salycilate complexes will allow the evaluation of the influence of a more extended aromatic system. Comparison with aliphatic β-hydroxycarboxylic acids cannot be made, because of the lower acidity of the hydroxy group in these compounds, which act as monodentate ligands through the carboxylate group, leading to much lower values of the constants. Aromatic ortho-hydroxycarboxylic acids form chelates through both oxygen atoms—carboxylate and phenoxide—whereas related aliphatic hydroxycarboxylic acids do not.

In the present work the stability constants of the Cu(II), Ni(II), Zn(II), Cd(II) and Co(II) complexes with hnca have been evaluated within a rather wide concentration range, and using very different metal to ligand concentration ratios, at 25°C, 0.2 M KNO_3 ionic strength and in 50% (v/v) dioxane–water mixtures. Protonation constants of the 3-hydroxy-2-naphthoate ligand under the conditions of the present work are $\log K_1 = 13.54$ and $\log K_2 = 17.17$.[4]

* Author to whom correspondence should be addressed.

EXPERIMENTAL

Reagents and solutions

3-Hydroxy-2-naphthalene carboxylic acid (Merck, synthesis) was recrystallized twice in ethanol and treated with activated carbon. Ni(II) stock solutions were prepared from $Ni(NO_3)_2 \cdot 6H_2O$ (Merck, p.a.) and standardized gravimetrically with dimethylglyoxime; Co(II) stock solutions were prepared from $Co(NO_3)_2 \cdot 6H_2O$ (Merck, p.a.) and standardized volumetrically with EDTA [with hexamethylenetetramine (Carlo Erba, RPE) at pH 6 and 40°C, orange xylenol as indicator];[5] Cu(II) stock solutions were prepared from $Cu(NO_3)_2 \cdot 5H_2O$ (Merck, p.a.) and standardized iodometrically; Zn(II) stock solutions were prepared from $Zn(NO_3)_2 \cdot 4H_2O$ (Merck, p.a.) and standardized gravimetrically with phosphate;[5] Cd(II) stock solutions were prepared from $Cd(NO_3)_2 \cdot 4H_2O$ (Merck, p.a.) and standardized volumetrically with EDTA (with hexamethylenetetramine at pH 5 and orange xylenol as indicator). Stock KOH (Merck, p.a.) solutions were prepared with an ionic exchange resin[6] to avoid carbonation, and were standardized volumetrically with biphthalate. HNO_3 solutions were prepared from HNO_3 (Merck, p.a.) and standardized volumetrically with tris(hydroxymethyl)aminomethane. All these solutions were made 50% (v/v) dioxane–water by mixing doubly distilled freshly boiled water and dioxane (Carlo Erba, purified by the Eigenberger method[7]). The ionic strength was kept at 0.2 M with KNO_3 (Probus, p.a.; recrystallized twice). A flow of N_2 (previously purified with vanadous perchlorate and barium hydroxide) bubbled continuously through the potentiometric solutions.

Apparatus

The potentiometric cell was:

Ag/AgCl/KCl(sat)//test solution

(50% dioxane–water)/GE

The value of the emf of the potentiometric cell was taken with an Orion 701A potentiometer (precision 0.1 mV), a reference Ag–AgCl electrode (Orion 9005 keramic junction type), and a glass electrode (GE) (Orion 9101). The potentiometric cell was thermostatted externally at 25°C. Titrant was added with a Metrohm Multidosimat E415 autoburette equipped with an Exchange Unit 10-cm^3 burette cylinder (552) with an antidiffusion burette tip. All the potentiometric assembly is controlled by an HP 9816 microcomputer via an HP 3421A Data Acquisition Control Unit (see later).

Procedure

The potentiometric method previously described[8] has been adapted to a computer-controlled titration procedure. A BASIC program controls both acquisition of emf readings and addition of titrant volumes. Readings are taken every 90 s; when two successive readings differ by less than 0.1 mV a new addition of a prefixed titrant volume is made (if reading stabilization is not reached in 12 min, a new prefixed titrant volume is added anyway and a warning message is stored). Calibration of the potentiometric cell is carried out by a Gran titration of a diluted mineral acid solution in the same ionic medium with a strong base. The calibration parameters (standard potential of the cell and value of the ionic product of the medium[4,8]), are calculated using a multiparametric data-fitting procedure[9] or Grant plots.[10] Additionally, both procedures can be used to test the Nernstian response of the potentiometric cell. Once the calibration parameters are known the ligand and metal ion are added, and the potentiometric titration is performed. The values of the emf readings and added volumes are recorded on both magnetic and paper media ready for their further treatment. The titration is finished either when there is hydrolysis of the metal ion (easily detected from the hydroxide precipitation or from its effect on the emf readings: instability, acid drift...), or at a prefixed pH value. The followings titrations were performed: Eight titrations of solutions containing Co(II) concentrations in the range 5.56×10^{-4}–4.78×10^{-3} M and ligand concentrations in the range 2.29×10^{-3}–1.92×10^{-2} M (covering a range of ligand/metal ratios from 1.1 to 4.5); 13 titrations of solutions containing Ni(II) concentrations in the range 2.98×10^{-4}–7.14×10^{-3} M and ligand concentrations in the range 2.89×10^{-3}–1.92×10^{-2} M (covering a range of ligand/metal ratios from 1.07 to 20); four titrations of solutions containing Cu(II) concentrations in the range 9.57×10^{-4}–2.69×10^{-3} M and the ligand concentrations in the range 6.34×10^{-3}–2.07×10^{-2} M (covering a range of ligand/metal ratios from 6.6 to 8.5); five titrations of solutions containing Zn(II) concentrations in the range 4.48×10^{-4}–2.88×10^{-3} M, and ligand concentrations in the range 2.58×10^{-3}–2.49×10^{-2} M (covering a range of ligand/metal ratios from 1.6 to 19.7); and five titrations of solutions containing Cd(II) concentrations in the range 5.5×10^{-4}–3.29×10^{-3} M and ligand concentrations in the range 2.40×10^{-3}–4.16×10^{-3} M (covering a range of ligand/metal ratios from 1.0 to 4.5).

For the Co(II), Ni(II) and Cu(II) systems, complexation can be detected by the colour changes.

The absorption spectra show a shift in the maximum of the absorption band to shorter wavelengths, which is related to the stronger ligand field produced by the ligand molecules compared to the solvent molecules. Cu(II) solutions change to green, with bands at $\lambda_{max} = 755$ [ε (cm^{-1} mol^{-1} l) = 114] at pH = 4.4, at $\lambda_{max} = 735$ ($\varepsilon = 95$) at pH = 5.12, and at $\lambda_{max} = 640$ ($\varepsilon = 110$) at pH = 12; Co(II) solutions change to red-orange, with bands at $\lambda_{max} = 507$ ($\varepsilon = 146$) and $\lambda_{max} = 1218$ ($\varepsilon = 293$) at pH = 5.3; Ni(II) solutions change to green with bands at $\lambda_{max} = 660$ ($\varepsilon = 145$), $\lambda_{max} = 725$ ($\varepsilon = 158$), $\lambda_{max} = 1150$ ($\varepsilon = 83$) and $\lambda_{max} = 1190$ ($\varepsilon = 76$) at pH = 6.5. Zn(II) and Cd(II) solutions do not absorb.

Solutions which contain high concentrations of copper ion (e.g. 3.0×10^{-3} M) and excess of ligand gave a red precipitate at neutral pH. Elemental analysis shows that the insoluble product is the 1 : 1 complex. Its low solubility is related to the fact that it has no electrical charge.

RESULTS AND DISCUSSION

Cu(II) *complexes*

The values of the formation constants of the Cu(II) complexes with hnca, obtained from the numerical analysis of the experimental potentiometric data using the computer programs MINIGLASS,[9] MINIQUAD[11] and SUPERQUAD,[12] are given in Table 1.

The same experimental data were used to evaluate the formation curves given in Fig. 1. Independently of which is the minimization function defined by each program, the values obtained for the stability constants are similar. For MINIGLASS the standard deviation of the titre residuals is 0.024 cm^3, (compared to an autoburette resolution of 0.01 cm^3, a reproducibility error of 0.005 cm^3 and an absolute error of 0.02 cm^3); for MINIQUAD the standard deviation of the residuals on the total concentrations is 0.88×10^{-5} M (less than 1% of the analytical concentration); and for SUPERQUAD the ratio of the root mean square of the weighted residuals to the estimated error in our working conditions (0.01 cm^3 for the autoburette and 0.1 mV for the emf readings) is sigma = 2.37.[12] In the additional statistical analysis of the residuals performed by MINIQUAD and SUPERQUAD[11,12] the values obtained for the chi-square satistic with both programs are quite high, reflecting[8,12,13] the difficulties in having a normal distribution of residuals in the least-squares analysis of tiration emf data. This fact is more discernible when the different test solutions are prepared from completely independent stock solutions, in accordance with the findings by Braibanti *et al.*[14] As it is known, moreover, for a given model there is a tendency to yield higher chi-square values when the fit is improved through parameter refinement, reflecting that there is a limit in the consideration of the normal distribution of residuals, which is related to the limit of precision attainable in the usual experimental conditions. Some work is made by us at present to analyse this behaviour, which on the other hand has also been recognized by other authors.[14]

Table 1. Formation constants of Cu(II)–hnca complexes[a]

Treatment	Log of the constants[b,c]	No. of curves (No. of points)	s[d]	χ^2[e]
MINIGLASS	10.42(1)	4	0.024	—
	18.20(3)	(184)		
MINIQUAD	10.42(3)	4	0.88×10^{-5}	125.8
	18.20(3)	(184)		
SUPERQUAD	10.44(2)	4	2.37	52.5
	18.20(3)	(184)		

[a] At 25°C, 50% (v/v) dioxane–water and 0.2 M KNO_3.

[b] Value of the log of the global formation constants for the reactions: Cu(II) + hnca = Cu(hnca) and Cu(II) + 2hnca = $Cu(hnca)_2$.

[c] In parentheses three times the standard deviation of the last figure calculated by program.

[d] Standard deviation of the residuals respect added volumes in MINIGLASS, and all total concentrations in MINIQUAD. Value of sigma for SUPERQUAD.

[e] Value of the residual chi-squares defined as in Refs 12, 13 and 8, respectively.

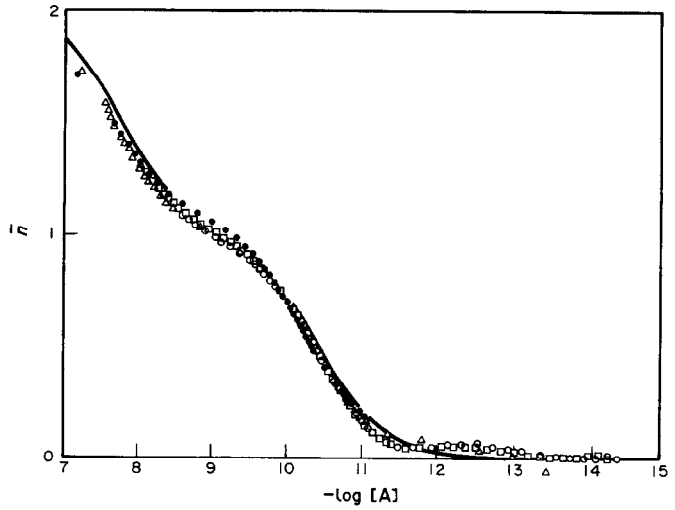

Fig. 1. Complexation of Cu(II) ion with hnca at $I = 0.2$ M KNO_3 and 50% (v/v) dioxane–water medium. In the figure $\bar{n}$ is the average ligand number[8] and $-\log[A]$ is the log of the free ligand concentration. Initial hnca and copper(II) ion concentrations given in millimol: (□) 7.69 and 0.96, (○) 6.34 and 1.06, (△) 8.43 and 0.98, and (●) 20.7 and 2.69. The continuous line is the theoretical curve obtained with the log of the complexation constants (see Table 1) (10.44 and 18.20).

The values obtained for the two formation constants of Cu(II) complexes are of the magnitude to be expected from the values of the Cu(II)–salicylate complexes in aqueous solutions.[8] The second stepwise formation constant ($\log K_2 = 7.76$) is nearly three log units lower than the first one ($\log K_1 = 10.44$), showing the enhancement of the first complexation by neutralization of charge.[15] In Fig. 2 the distribution of species which contain Cu(II) when the pH is changed are given.

Other metal ion complexes

In Table 2 the log values of the first formation constant of the complexes of hnca with Co(II), Ni(II), Zn(II) and Cd(II) are given. As was pointed out (see earlier), for all these metal ions it was only possible to obtain the formation constant of the first complex, since the formation of the second one is disturbed by the hydrolysis and precipitation of the metal ion. Therefore the experimental data including measurements in the pH range where hydrolysis occurs were not taken into account, since data in this pH range would not improve the numerical fit and because, if they are included, the rejection of species becomes arbitrary (e.g. the 1 : 1 complex is discarded by SUPERQUAD when hydroxocomplexes are included in the model). Moreover these data cannot be considered at equilibrium, since the emf readings at this stage showed

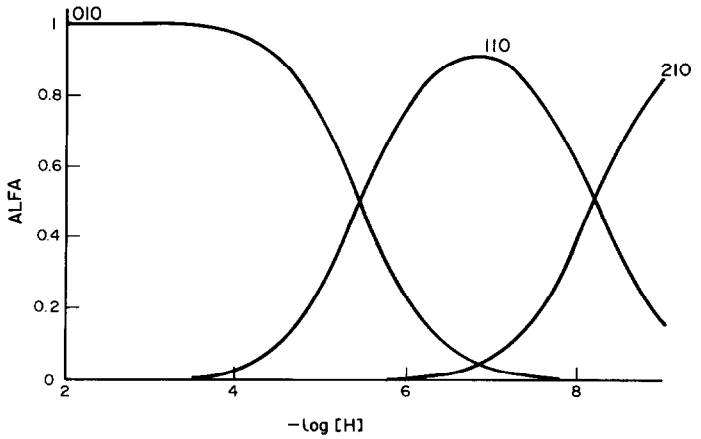

Fig. 2. Distribution plot of the species which contain copper(II). In the figure 010, 110 and 210, refer respectively to Cu(II), Cu(hnca) and $Cu(hnca)_2$. ALFA is the ratio of each species concentration to the total copper(II) concentration.

Table 2. First formation constants of Co(II), Ni(II), Zn(II) and Cd(II) complexes with hnca[ab]

Metal ion	Log of the constant[c]	No. of curves (No. of points)	sigma[d]	χ^{2e}
Co(II)	7.9(1)	8 (70)	4.6	1.09
Ni(II)	7.07(6)	13 (112)	6.5	30.90
Zn(II)	7.8(1)	5 (94)	1.5	32.60
Cd(II)	7.30(9)	5 (41)	4.2	8.76

[a] At 25°C, 50% (v/v) dioxane–water and 0.2 M KNO_3.
[b] Log of the formation constants obtained with the SUPERQUAD (Ref. 12) program.
[c] In parentheses three times the standard deviation of the last figure calculated by program.
[d] See Ref. 12.
[e] Value of the residual chi-squares.[12]

a steady drift (see Experimental). The values of sigma shown in Table 2 for the SUPERQUAD treatment[12] are somewhat higher than expected. In any case we have preferred to maintain the results such as they are given in Table 2, since the improvement of the fit produced by the rejection of "queue" titration points does not yield different values of the constants but decreases the formation extent of the first complex, reducing therefore the precision of its constant. High chi-square values are also here related to the not quite Gaussian behaviour of the weighed queue residuals.

DISCUSSION

Comparison of the values given in Tables 1 and 2 confirms[1] that the formation constants for the 1 : 1 complexes of the metal ions studied here do not follow completely the Irving–Williams sequence.[16] The value of the constant for the Ni(II) complex is the lowest obtained, while according to the Irving–Williams series it should lie between the Cu(II) and Co(II) values. As it was pointed out before (see earlier), the increase in stability from Co(II) to Ni(II) in the Irving–Williams series is rather weak in the case of complexes with oxygen-donor groups.[17] Additionally, the greater stability of the Co(II) complex could be partially explained by a high stabilization due to a high Jahn–Teller distortion of the octahedral low-spin Co(II) complex.[3]

REFERENCES

1. S. S. Sandhu, J. N. Kumaria and R. S. Sandhu, *J. Indian Chem. Soc.* 1976, **53**, 435; 1977, **49**, 675; 1978, **55**, 670.
2. O. Makitie, *Suomen Kemi.* 1966, **B39**, 26.
3. R. M. Sathe and S. Y. Shetty, *J. Inorg. Nucl. Chem.* 1970, **32**, 1383.
4. E. Casassas and G. Fonrodona (to be published).
5. A. I. Vogel, *Textbook of Quantitative Inorganic Analysis*, 4th Edn. Longman, London (1981).
6. J. E. Powell and M. A. Hiller, *J. Chem. Ed.* 1957, **34**, 330.
7. A. I. Vogel, *A Text Book of Practical Organic Chemistry*, p. 177. Longmans Green, London (1961).
8. E. Casassas and R. Tauler, *J. Chim. Phys.* 1984, **81**, 233; 1984, **81**, 557; 1985, **82**, 1067.
9. A. Izquierdo and J. L. Beltran, *Anal. Chim. Acta* 1986, **181**, 87.
10. G. Gran, *Acta Chem. Scand.* 1950, **4**, 559; *Analyst*, 1952, **77**, 661.
11. A. Sabatini, A. Vacca and P. Gans, *Talanta* 1974, **21**, 53; *Inorg. Chim. Acta* 1976, **18**, 237.
12. P. Gans, A. Sabatini and A. Vacca, *J. Chem. Soc., Dalton Trans.* 1985, 1195.
13. L. Bologni, A. Sabatini and A. Vacca, *Inorg. Chim. Acta* 1983, **69**, 71.
14. A. Braibanti, F. Dallavalle, G. Mori and B. Veroni, *Talanta* 1982, **29**, 725.
15. D. D. Perrin, In *Essays on Analytical Chemistry* (Edited by E. Wanninen), p. 181. Pergamon Press, Oxford (1977).
16. H. M. N. Irving and R. J. P. Williams, *J. Chem. Soc.* 1953, 3192.
17. F. A. Cotton and G. Wilkinson, *Advanced Inorganic Chemistry*, p. 783, 4th ed. Wiley Interscience, New York (1980).

Polyhedron Vol. 6, No. 7, pp. 1523–1532, 1987
Printed in Great Britain

0277–5387/87 $3.00+.00

MONO- AND DINITROSYL COMPLEXES OF MOLYBDENUM: CRYSTAL STRUCTURE OF MOLYBDENUM DINITROSYL BIS(2-PICOLINATE)

M. F. PERPIÑÁN,*† L. BALLESTER,† A. SANTOS,‡ A. MONGE,†‡ C. RUIZ-VALERO†‡ and E. GUTIÉRREZ PUEBLA†‡

†Departamento de Química Inorgánica, Facultad de Ciencias Químicas, Universidad Complutense, 28040 Madrid, Spain; and ‡Instituto de Química Inorgánica "Elhúyar" del C.S.I.C., 28006 Madrid, Spain

(*Received* 17 *June* 1986; *accepted after revision* 27 *October* 1986)

Abstract—The reaction of the $[Mo(NO)_2]^{2+}$ moiety with the (X,Y)-donor ligands (X,Y = dithiocarbamates, xanthates, 2-picolinate, *o*-aminophenoxide, *o*-aminothiophenoxide or dithizone) leads fundamentally to formation of complexes of type $Mo(NO)_2(X,Y)_2$. Sometimes secondary products are also formed, as for example the mononitrosyl heptacoordinated complex $Mo(NO)(2\text{-pic})_3$ (5) (2-pic = 2-picolinate). In the reaction with dithizone a complex of composition $Mo(NO)_2(HDtz)_2(H_2Dtz)$ was isolated. The $Mo(NO)_2(R_2dtc)_2$ (R_2dtc = *N*,*N*-dialkyldithiocarbamates) complexes decompose in $CHCl_3$ or by reaction with CO in CH_2Cl_2 to give the mononitrosyl derivatives $Mo(NO)(R_2dtc)_3$. The reaction of complex 6 with PPh_3 yields $Mo(2\text{-pic})_3 \cdot H_2O$. The crystal structure of $Mo(NO)_2(2\text{-pic})_2$ has been determined. The crystals are orthorhombic, space group *Pbca* with $a = 12.502(3)$, $b = 15.15(4)$, $c = 15.296(6)$ Å, $U = 2897(8)$ Å^3, $z = 8$, $D_c = 1.84\ g\ cm^{-3}$ $\mu(Mo\text{-}K_\alpha) = 9.23\ cm^{-1}$, $F(000) = 1584$. The Mo atom presents a distorted octahedral coordination. The atomic parameters have been refined by least-squares analysis of 1845 observed reflexions to $R = 0.025$.

Several examples of molybdenum dinitrosyl derivatives have been described, such as $Mo(NO)_2(L,L)_2$ [L,L = R_2dtc (R = Me or Et),[1–4] or acac[2]], $Mo(NO)_2X_2L_2$,[3–6] $[Mo(II)(NO)_2(NCS)_4]^{2-}$, $[Mo(II)(NO)_2(NHO)(NCS)_4]^{2-}$ and $Mo(II)(NO)_2(NCS)_2(L,L)$[4] (L,L = bipy or phen). These dinitrosyl derivatives can be obtained by three general methods: (1) oxidation by NO^+ or substitution by NO of molybdenum hexacarbonyl or its derivatives;[1,2,5,6] (2) reduction of $MoCl_5$ by nitric oxide;[7] and (3) reductive dinitroxylation of: (a) ammonium hepamolybdate by hydroxylamine in slightly basic or acidic media,[3] or (b) of MoO_4^{2-} by hydroxylamine in the presence of NCS^-. In case (3b) mono- or dinitrosyl species of molybdenum(II) can be obtained too. To date, mononitrosyl molybdenum(II) complexes of formula $Mo(NO)(R_2dtc)_3$ (R = Me, Et, Pr^n or Bu^n),[1,8] $Mo(NO)(NH_2O)(NCS)_2(L,L)$ (L,L = bipy or phen),[4] $Mo(NO)(NH_2O)(Et_2dtc)_2$[4] and $Mo(NO)(NH_2O)(2\text{-pic})_2$[9] have been described in the literature.

Electrochemical and ESR studies of *cis*-$Mo(R_2dtc)_2(NO)_2$ have been reported,[10] as well as the electronic spectra[11] of a wide variety of six-coordinate complexes containing the cis-$[Mo(NO)_2]^{2+}$ moiety.

Activation of a nitrosyl group to give mononitrosyl complexes occurs by reaction of *cis*-$Mo(NO)_2(Et_2dtc)_2$ with strong Lewis bases such as azide, cyanate, cyanide or diethyldithiocarbamate in hot dimethyl sulfoxide.[12]

The dinitrosyl complexes of type $Mo(NO)_2(L,L)_2$ described contain only (S,S)-donor uninegative ligands such as the *N*,*N*-dialkyldithiocarbamates, or (O,O)-donor ligands such as acetylacetonate or oxalate. This fact prompted us to investigate the synthesis and characterization of new dinitrosyl derivatives, obtained by method (3a), with anionic (X,Y)-donor ligands (X,Y = N, O or S) containing donor atoms of different size and basicity. The ligands used were xanthates (Rxant; R = Me or

* Author to whom correspondence should be addressed.

Et), and *N*-alkyldithiocarbamates (RHdtc, R = Me) [(S,S)-donor ligands]; *o*-aminophenoxide (*o*-AP) and 2-picolinate (2-pic) [(N,O)-donor ligands]; *o*-aminothiphenoxide (*o*-ATP) [(N,S)-donor ligand] and dithizone (H_2Dtz) [(potentially S-(S,S) or (N,S)-donor ligand].

A study of the reactivity of the new complexes towards chloroform or Lewis bases (carbon monoxide or triphenylphosphine) has been carried out.

RESULTS AND DISCUSSION

(*a*) *Reaction of the* $[Mo(NO)_2]^{2+}$ *moiety with the* (X,Y)*-donor ligands*

The new derivatives have been prepared by addition of the alkali salt of ligand or of the ligand in basic medium to the reaction mixture which contains the $[Mo(NO)_2]^{2+}$ moiety. The compounds stable to air and atmospheric moisture have been characterized by elemental analysis, electric-conductance and magnetic-susceptibility measurements, and IR and electronic spectroscopy (in solution and diffuse reflectance). The complexes are non-electrolytes and diamagnetic.

The compounds obtained by this type of reaction are hexacoordinated molybdenum(O) complexes of general formula $Mo(NO)_2(X,Y)_2$, although sometimes secondary products are formed which sometimes could not be characterized. So, in the reaction with 2-picolinate a mixture of $Mo(NO)_2(2\text{-pic})_2$ (**1**) (crystalline green solid) and $Mo(NO)(2\text{-pic})_3$ (**5**) (pale yellow solid) is obtained. These compounds can be separated by successive recrystallizations from dichloromethane. The mononitrosyl derivative with this ligand (**5**) is insoluble in all solvents. The heptacoordinated mononitrosyl derivative, $Mo(NO)(NH_2O)(2\text{-pic})_2$, has been described in the literature.[9] The *o*-aminophenoxide ligand reacts with the $[Mo(NO)_2]^{2+}$ moiety to give the $Mo(NO)_2(o\text{-AP})_2$ complex and a mixture of unidentified products, some of which are ligand condensation products.

The reaction with dithizone leads to the formation of a dark purple solid with metallic lustre of formula $[Mo(NO)_2(HDtz)_2(H_2Dtz)]$ where HDtz is the monoanion of the ligand and H_2Dtz the neutral ligand.

The behaviour of the (S,S)-donor ligands towards $[Mo(NO)_2]^{2+}$ is different. When the ligand used is an *N*,*N*-dialkyldithiocarbamate, the reaction leads to formation of a $Mo(NO)_2(R_2dtc)_2$ complex, as described in the literature[3] for other dithiocarbamates. In the case of *N*-methyldithiocarbamate a mixture of $Mo_2O_3(MeHdtc)_4$ (purple) and a dinitrosyl species is obtained, but if the experiment is carried out in an inert atmosphere an orange solid is isolated although with very low yield. The elemental analysis data of this compound are consistent with a formula of type $Mo(NO)(MeHdtc)_3$, but its IR spectrum presents two $\nu(NO)$ vibrations. The presence of oxocomplexes in the reaction medium has been also previously described.[3,4] On the other hand, the alkali xanthates react instantaneously, but no characterizable products could be isolated because of the formation of unstable oils or oil solids and molybdenum oxides or oxocomplexes.

(*b*) *Reaction of the* $Mo(NO)_2(X,Y)_2$ *complexes with chloroform,* CO *or* PPh_3

The $Mo(NO)_2(R_2dtc)_2$ derivatives (R_2 = 2Et or pyr) react with PPh_3 in chloroform to give a mixture of compounds from which the molybdenum(V) oxocomplex, $Mo_2O_3(R_2dtc)_4$, can be isolated. When these dinitrosyl species are stirred in $CHCl_3$ for a prolonged time in an N_2 atmosphere they decompose giving rise to an oxocomplex $[Mo_2O_4(R_2dtc)_2]$ and the mononitrosyl complexes $Mo(NO)(R_2dtc)_3 \cdot \frac{1}{2}CHCl_3$.

As mentioned above, complexes of this type have been previously described,[1,8] but they do not contain the crystallization solvent. The presence of $CHCl_3$ has been shown by IR spectroscopy and Cl analysis by X-ray fluorescence.

The reaction of the *N*-methyldithiocarbamate complex (**6**) with $CHCl_3$ is not reproducible. Sometimes a solid of composition $Mo(NO)(MeHdtc)_3 \cdot \frac{1}{2}CHCl_3$ is isolated.

$Mo(NO)_2(o\text{-AP})_2$ (**2**) and $Mo(NO)_2(o\text{-ATP})_2$ (**3**) do not react with PPh_3 and are stable in $CHCl_3$. However, when an excess of PPh_3 is added to complex **1** in $CHCl_3$ a relatively quick reaction occurs with formation of a molybdenum(III) complex of composition $Mo(2\text{-pic})_3 \cdot H_2O$. Compounds of this type, with (O,O)-donor ligands have been described.[13]

No reaction was observed on bubbling CO through a solution of $Mo(NO)_2(X,Y)_2$ complexes (X,Y = 2-pic, *o*-AP or *o*-ATP) in CH_2Cl_2 and the recovered solids were spectroscopically (IR) identical with the starting compounds. However the formation of $Mo_2O_4(R_2dtc)_2 \cdot xCH_2Cl_2$ and $Mo(NO)(R_2dtc)_3$ occurs upon treatment with CO of $MO(NO)_2(R_2dtc)_2$ species. This process is analogous to the decomposition in $CHCl_3$, but here the oxo complex is obtained pure.

All these results [(a) and (b)] are summarized in Scheme 1. Table 1 lists analytical, physical and IR data for the new complexes.

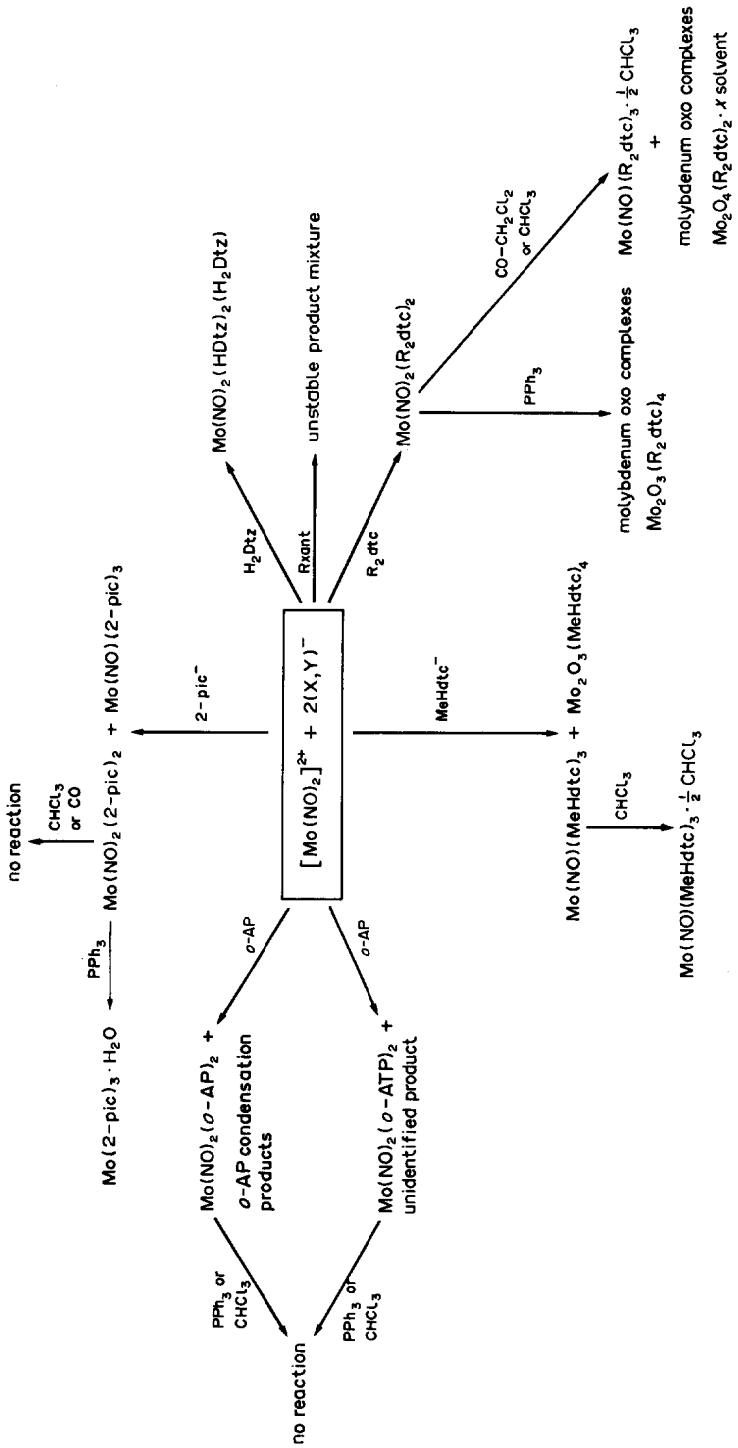
[Mo(NO)2]2+ + 2(X,Y)−
2-pic−
H2Dtz
Rxant
R2dtc
MeHdtc−
Mo(NO)2(2-pic)2 + Mo(NO)(2-pic)3
Mo(NO)2(HDtz)2(H2Dtz)
unstable product mixture
Mo(NO)2(R2dtc)2
Mo2O3(MeHdtc)4
CO–CH2Cl2 or CHCl3
PPh3
Mo(NO)(R2dtc)3 · ½ CHCl3
+
molybdenum oxo complexes
Mo2O4(R2dtc)2 · x solvent
molybdenum oxo complexes
Mo2O3(R2dtc)4
CHCl3
Mo(NO)(MeHdtc)3 · ½ CHCl3
CHCl3 or CO
no reaction
PPh3
Mo(2-pic)3 · H2O
o-AP
Mo(NO)2(o-AP)2 +
o-AP condensation products
o-AP
Mo(NO)2(o-ATP)2 +
unidentified product
PPh3 or CHCl3
PPh3 or CHCl3
no reaction

Scheme 1.

Table 1. Analytical, physicochemical and IR data of the complexes

Complex	Colour	Analysis[a] (%) C	H	N	Λ_m (Ω^{-1} cm^{2}mol^{-1})	IR data (cm^{-1}) ν(NO)	Other bands	
(1) $Mo(NO)_2(2\text{-pic})_2$	Green	35.9 (36.0)	2.0 (2.0)	14.1 (14.0)	3.7[b]	1783vs 1665vs	1695vs	ν(C=O)
(2) $Mo(NO)_2(o\text{-AP})_2$	Green-brown	39.0 (38.7)	3.4 (3.2)	15.0 (15.0)	3.7[b]	1769vs 1644vs	3230s 2490s,br	ν(NH)
(3) $Mo(NO)_2(o\text{-ATP})_2$	Orange-brown	36.0 (35.6)	3.0 (3.0)	13.8 (13.8)	9.6[b]	1760vs 1638vs	3490w 3270–2920,br	ν(NH)
(4) $Mo(NO)_2(HDtz)_2(H_2Dtz)$	Dark purple	50.0 (50.7)	3.7 (3.9)	21.3 (21.2)	1.8[c]	1767vs 1654vs	3260–3120m,br 1517vs 365w 325w	ν(NH) ν(C=N) ν(Mo—S)
(5) $Mo(NO)(2\text{-pic})_3$	Pale-yellow	43.7 (43.9)	2.4 (2.4)	11.1 (11.4)	—	1655m	1695vs	ν(C=O)
(6) $Mo(NO)(MeHdtc)_3$	Orange-yellow	16.6 (16.2)	2.7 (2.7)	12.6 (12.6)	18.3[d]	1760vs 1640vs	1528vs 362m	ν(C=N) ν(Mo—S)
(7) $Mo(NO)(pyrdtc)\cdot\frac{1}{2}HCl_3$	Orange-yellow	29.7 (19.8)	3.9 (3.9)	8.6 (8.9)	15.3[b]	1637vs	1495vs 369m 349m	ν(C=N) ν(Mo—S)
(8) $Mo(NO)(Et_2dtc)_3\cdot\frac{1}{2}CHCl_3$	Yellow	29.2 (29.5)	5.0 (4.8)	9.2 (8.9)	15.0[b]	1630vs	1510vs 370m	ν(C=N) ν(Mo—S)
(9) $Mo(2\text{-pic})_3\cdot H_2O$	Earth-yellow	44.8 (45.0)	3.1 (2.9)	8.8 (8.8)	14.8[b]			

[a] Calculated values are shown in parentheses.
[b] In DMF solution.
[c] In chloroform solution.
[d] In DMSO solution.

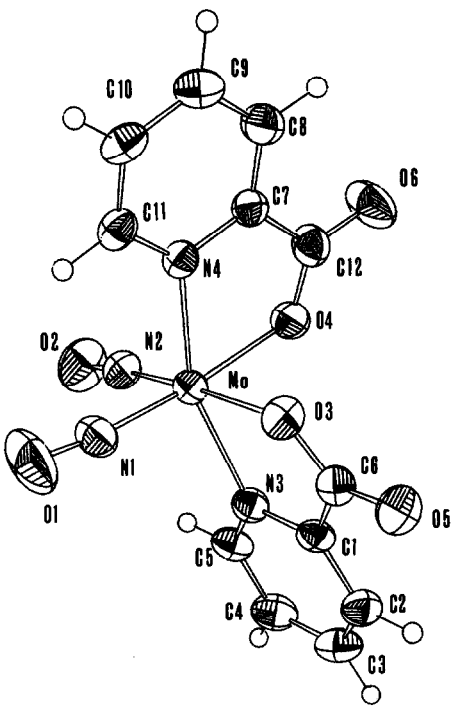

Fig. 1.

Crystal structure of complex 1

Structure. Figure 1 shows the geometry of the structure and the atom labelling.[14] Table 2 lists the bond lengths and angles.

Few X-ray structures are available for $[Mo(NO)_2]^{2+}$ complexes.[15] The present study has confirmed the formation of a new compound, namely $MO(NO)_2(2\text{-pic})_2$. The molybdenum atom is coordinated to two 2-picolinates as (N,O)-donor chelating ligands, and to two NO groups in *cis* positions, forming a distorted octahedron. Both NO groups are almost linear. The ON—Mo—NO angle [87.6(2)] is close to that reported[11] for $Mo(NO)_2(Et_2dtc)_2$ [88.0(4)].

The Mo—N bond lengths are similar to those found by Enemark and Feltham[16] in $Mo(NO)_2Cl_2(PPh_3)_2$. The N—O distances [1.168(6) and 1.173(5) Å] and Mo—N—O angles [173.9(4) and 174.9(4)°] are less than in the above compound but are within the range found for linear nitrosyls in other nitrosyl derivatives.[2,17,18] The bond lengths and bond angles are as expected for the 2-picolinate ligand.[19] The packing of the crystal is determined only by van der Waals' interaction and significative intermolecular interactions have not been observed. This fact is important to explain the magnetic behaviour found in the complex.

IR spectra

In the IR spectra of the dinitrosyl species, two NO stretching frequencies are observed indicating the *cis* coordination of these ligands. The complexes should then exist as optical isomers although these have been not resolved. In all spectra, ν(NO) occurs in the 1783–1630-cm^{-1} region, and, if NO is considered to be coordinated as NO^+, then the $Mo(NO)_2(X,Y)_2$ derivatives could be regarded as hexacoordinated complexes of zerovalent metal ions.

On the basis of observed IR spectra the lower-frequency ν(NO) vibrations have been assigned to $M^{(n+1)+}—N^-=O$ and the higher-frequency vibrations to the $M^{(n-1)+}—N\equiv O^+$ structure, although this rule is misleading because of the great overlap in the ν(NO) frequencies of bent and linear nitrosyls in the 1720–1620-cm^{-1} range.[20]

The NO^+ character of the nitrosyl group in the derivatives can also be deduced from the study of the crystalline structure of complex **1**. The Mo—N—O bond angles (173.9 and 174.9°) are characteristic of octahedral metal linear nitrosyls in which this angle varies from 170 to 180° indicating a straight coordination of the NO^+ group.[20]

In the $Mo(NO)_2(X,Y)_2$ complexes the values of the ν(NO) frequency vary in the order (N,O) > (S,N) > (S,S) with the nature of the (X,Y) ligand. This variation is consistent with the decrease in the π-contribution to the Mo—NO bond and with the electronegativity of the donor atoms of the (X,Y) group. The same variation can be observed in the mononitrosyl derivatives whose stereochemistry and metal environment are comparable.

In the dinitrosyl complexes the (X,Y) ligand is a uninegative bidentate ligand as can be deduced from its characteristic IR vibrations (see Table 1). As mentioned above, the crystal structure of $Mo(NO)_2(2\text{-pic})_2$ shows that the 2-picolinate ligand acts as an (N,O)-donor chelating group.

The assignment of a possible structure to the dithizone derivative is difficult owing to the different coordination modes of this ligand (H_2Dtz) of resonant formulae:

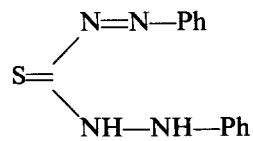

and

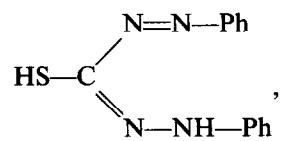

,

which can lose one or two protons behaving as an uninegative group (primary dithizone, HDtz) or binegative group (secondary dithizone, Dtz),

respectively. The primary dithizone can be coordinated by several modes:[21]

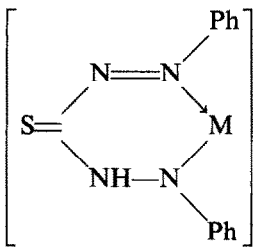

I

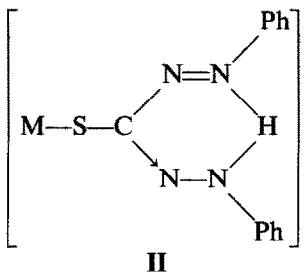

II

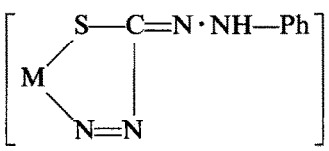

III

The IR spectrum of primary dithizone complexes may be different to the compounds with secondary dithizones because the former present bands are due to the NH, C=N or N=N group, while such vibrations, would disappear in the spectrum of the latter.[22] In our complex, ν(NH) and ν(C=N) bonds are observed so that a formulation of type $Mo(NO)_2(Dtz)_3$ Is discarded. The hydrogen analysis and magnetic moments also do not correspond to this formulation. On the other hand the conductivity measurement and potassium analysis by X-ray fluorescence are not in agreement with a formulation of type $K[Mo(NO)_2(Dtz)_3]$.

According to all the experimental data, the two more possible stereochemistries for the dithizones derivative are $Mo(NO)_2(HDtz)(H_2Dtz)$ or $Mo(II)(NO)_2(Dtz)_2(H_2Dtz)$. The diagmagnetism observed could be consistent with either formula. The ν(NO) values are also in agreement with those corresponding to hexacoordinated molybdenum(O) complexes and with those of heptacoordinated molybdenum(II) complexes of type $Mo(NO)_2(NHO)(NCS)_2(L,L)$ (L,L = bipy or phen) or $[PPh_4][Mo(NO)_2(NHO)(NCS)_4]$,[4] so that it is difficult to distinguish between the possible compounds, although the hydrogen elemental analysis seems to correspond to the molybdenum(O) complex (**4**). The dithizone neutral molecule can act as an S-donor monodentate ligand.

Most metal complexes containing primary dithizonate show an N,S-coordination. In our case the primary dithizone is also probably coordinated as an N,S-ligand (structure **III**).

As mentioned above, the IR spectrum of mononitrosyl complex **4** shows two ν(NO) bands. The separation between the bands of *ca* 120 cm^{-1} can not be attributed to an isomer mixture or to the presence of a symmetrical dimer, but could be due to an asymmetrical dimer with metal atoms in different oxidation states of type $(NO)_2(MeHdtc)Mo(O)(\mu\text{-}MeHdtc)_2Mo(IV)(MeHdtc)_3$. However, in the literature, some examples of monomeric mononitrosyl complexes with two ν(NO) bands have been reported.[23]

The *N*-methyldithiocarbamate derivative $Mo(NO)(MeHdt)_3$ shows a broad ν(NH) band at *ca* 3250 cm^{-1} in the solid-state spectrum, but this vibration appears as a sharp band at higher frequency (*ca* 3450 cm^{-1}) in the solution spectrum (DMSO or acetone). This fact can be attributed to interactions in the solid state between NH groups of different molecules.

The remaining mononitrosyl derivatives show only one NO stretching frequency as expected. The values obtained for this frequency are analogous to those of heptacoordinated molybdenum(II) complexes, $Mo(NO)(R_2dtc)_3$,[1,8] $Mo(NO)(NH_2O)(NCS)_2(L,L)$[4] or $Mo(NO)(NH_2O)(Et_xdtc)_2$.[4]

All nitrosyl complexes prepared of formulae $Mo(NO)_2(X,Y)_2$ and $Mo(NO)(X,Y)_3$ conform to the 18-electron rule, with the NO^+ group and the (X,Y) chelating ligand regarded as a three-electron donor.

The chloroform of crystallization in the $Mo(NO)(X,Y)_3 \cdot \frac{1}{2}CHCl_3$ complexes gives rise to a ν(C—Cl) band at *ca* 750 cm^{-1}.

The ν(C=O) frequencies of all 2-picolinate complexes rule out the existence of interactions through this oxygen atom.

Electronic spectra

Electronic spectra for several products are recorded in DMF or DMSO solution in the 260–900-nm region. Diffuse-reflectance spectra were also measured in the 190–900-nm region. Table 3 summarizes the absorption maxima (λ_{max}), the molar absorptivities values (ε), and a tentative assignment.

We have assigned the spectra on the basis of the data reported by Budge *et al.*[10] and Minelli *et al.*[11] We assign the electronic absorption at 655–800 nm to a transition within the $\{Mo(NO)_2\}^6$ group from the $a_2[d_{xy}, \pi^*(NO)]$ or $b_2[d_{xy}, \pi^*(NO)]$ to the $b_1(\pi^*NO)$ orbital. The more intense absorption at *ca* 450 nm is assigned to a transition from the

Table 2. Bond lengths (Å) and angles (°) with estimated standard deviations in parentheses

Mo—N(1)	1.820(4)	O(4)—C(12)	1.294(5)
Mo—N(2)	1.826(4)	O(5)—C(6)	1.215(5)
Mo—N(3)	2.186(4)	O(6)—C(12)	1.220(6)
Mo—N(4)	2.164(5)	C(1)—C(2)	1.383(6)
Mo—O(3)	2.095(3)	C(1)—C(6)	1.511(7)
Mo—O(4)	2.087(3)	C(2)—C(3)	1.390(7)
N(1)—O(1)	1.168(6)	C(3)—C(4)	1.374(7)
N(2)—O(2)	1.173(5)	C(4)—C(5)	1.373(6)
N(3)—C(1)	1.349(5)	C(7)—C(8)	1.380(6)
N(3)—C(5)	1.347(6)	C(7)—C(12)	1.511(6)
N(4)—C(7)	1.353(5)	C(8)—C(9)	1.390(6)
N(4)—C(11)	1.251(6)	C(9)—C(10)	1.381(7)
O(3)—C(6)	1.289(5)	C(10)—C(11)	1.386(7)
N(1)—Mo—N(2)	87.6(2)	Mo—O(3)—C(6)	119.7(4)
N(1)—Mo—N(3)	97.7(2)	Mo—O(4)—C(12)	119.2(3)
N(1)—Mo—N(4)	96.2(2)	N(3)—C(1)—C(2)	121.9(5)
N(1)—Mo—O(3)	94.7(2)	N(3)—C(1)—C(6)	115.6(4)
N(1)—Mo—O(4)	172.6(2)	C(2)—C(1)—C(6)	122.5(4)
N(2)—Mo—N(3)	98.6(2)	C(1)—C(2)—C(3)	118.6(4)
N(2)—Mo—N(4)	99.5(2)	C(2)—C(3)—C(4)	119.1(5)
N(2)—Mo—O(3)	174.2(2)	C(3)—C(4)—C(5)	119.6(6)
N(2)—Mo—O(4)	93.9(1)	N(3)—C(5)—C(4)	121.9(5)
N(3)—Mo—N(4)	157.6(1)	O(3)—C(6)—O(5)	125.2(6)
N(3)—Mo—O(3)	75.9(1)	O(3)—C(6)—C(1)	114.8(4)
N(3)—Mo—O(4)	89.2(1)	O(5)—C(6)—C(1)	120.0(4)
N(4)—Mo—O(3)	85.6(2)	N(4)—C(7)—C(8)	121.8(4)
N(4)—Mo—O(4)	76.4(1)	N(4)—C(7)—C(12)	115.6(4)
O(3)—Mo—O(4)	84.5(1)	C(8)—C(7)—C(12)	122.5(4)
Mo—N(1)—O(1)	173.9(4)	C(7)—C(8)—C(9)	119.2(4)
Mo—N(2)—O(2)	174.9(4)	C(8)—C(9)—C(10)	118.9(6)
Mo—N(3)—C(1)	113.8(4)	C(9)—C(10)—C(11)	119.6(5)
Mo—N(3)—C(5)	127.2(3)	N(4)—C(11)—C(10)	121.4(4)
C(1)—N(3)—C(5)	118.9(4)	O(6)—C(12)—C(7)	120.3(5)
Mo—N(4)—C(7)	113.4(3)	O(4)—C(12)—C(7)	114.3(4)
Mo—N(4)—C(11)	127.0(3)	O(4)—C(12)—O(6)	125.4(6)
C(7)—N(4)—C(11)	119.1(4)		

$a_1[d_z^2, \pi^*(NO)]$ to the $b_1(\pi^*NO)$ orbital of the $\{Mo(NO)_2\}^6$ group. Our data agree with the results of Minelli *et al.*[11] These authors have emphasized that the ON—Mo—NO angle value is very important so that no interaction between the $b_1(\pi^*NO)$ orbital and the d_{xz} orbital (which also has b_1-symmetry) occurs if this angle is $\simeq 90°$. The value of 87.6(2) found in the case of $Mo(NO)_2(2\text{-pic})_2$ permits the above-mentioned assignment. Likewise the absorption bands at higher energies included $L \leftarrow M$ charge-transfer and/or intraligand transitions.

In the ditizone complexes a high contribution of the ligand bands is present in all maxima observed in the spectrum.

The significant change observed in the solution and solid spectra of complex **3** can be due to the existence of an interaction with the solvent.

Magnetic properties

All the compounds show at room temperature a feeble paramagnetism which can be partially due to a temperature-independent paramagnetism (tip). The corrected molar susceptibilities founded for these compounds are generally higher than those reported for other nitrosyl complexes and are attributed to a tip.[4] However the carbonyl complexes of molybdenum frequently exhibit complicated magnetic properties.[24]

In the case of complex **1**, which exhibits the higher susceptibility values, the susceptibility was measured as a function of field strength at four different temperatures (Table 4) and was found to be dependent of field strength and temperature. However the structural data preclude any spin–spin interaction in this compound.

Table 3. Electronic absorption and magnetic-susceptibility data of the complexes

	Electronic spectra data[a]				Magnetic data		
	Solution		Solid				
Complex	λ_{max} (nm)	ε[c]	λ_{max} (nm)	Assignment	$10^6\chi$ m^6 (cm^3 mol^{-1})	T (K)	μ_{eff} (BM)
1	655	100	655	$d \leftarrow d$	801	293.5	1.38
	433	1544	433	π^*(NO) $\leftarrow$ M CT	861	206	1.20
	296 sh	5372	325		893	151	1.04
			260		941	77	0.76
2	650	179	676	$d \leftarrow d$	270	295	0.80
	475	2667	478	π^*(NO) $\leftarrow$ M CT			
	325 sh	2264	290				
	280 sh	10,798	255	$\pi^* \leftarrow \nu$(2-pic)			
3	800	141	735	$d \leftarrow d$	720	295	1.31
	590	227	495 sh	$d \leftarrow d$			
	425	2039	445	π^*(NO) $\leftarrow$ M CT			
	345	7951	310				
	247	17,365	255				
4	554	57,711	680		207	290	0.69
	465 sh	34,912	490 sh				
	320 sh	27,683	370 sh				
	265	44,706	267				
5			665	$d \leftarrow d$	459	293	1.04
			342 sh				
			298				
			260	$\pi^* \leftarrow \pi$(2-pic)			
6[b]	720	36	720	$d \leftarrow d$			
	478	754	478	π^*(NO) $\leftarrow$ M CT			
	325	6811	325				

[a] In DMF solution (10^{-3}–10^{-5} M).
[b] In DMSO solution.
[c] Values of ε in dm^3 mol^{-1} cm^{-1}.
[d] Corrected molar susceptibilities.

EXPERIMENTAL

All reagents and solvents required for compound preparation were of analytical grade. Sodium *N*-methyldithiocarbamate was prepared by the method described in the literature.[25] The complexes $Mo(NO)_2(R_2dtc)_2$ (R = Et, R_2 = pyr) were obtained by the method described by Sarkar and Subramanian.[3] C, H and N analysis were carried out by Elemental Microanalysis Ltd Laboratories (Devon, U.K.). Conductance measurements were performed at room temperature using a Philips PW 9506120 conductivity bridge. IR spectra in the 4000–200-cm^{-1} region were recorded on a 325 Perkin–Elmer spectrophotometer, using KBr disks. Electronic spectra were scanned in DMF or DMSO solution on a Kontron Uvikon 820 spectrophotometer. The diffuse-reflectance spectra of the solid compounds were recorded on the same spectrophotometer with the standard Kontron diffuse-reflectance accessory and barium sulfate as reference. Sometimes, the solid samples were slightly diluted with $BaSO_4$. The magnetic susceptibilities were measured by the Faraday method.

Crystal data

$C_{12}H_8MoN_4O_6$, $M = 400.07$, orthorhombic, $a = 12.502(3)$, $b = 15.15(4)$, $c = 15.296(6)$ Å, $U = 2897(8)$ Å^3, $Z = 8$, $D_c = 1.84$ g cm^{-3}, $F(000) = 1584$, space group *Pbca*, μ(Mo-K_α) = 9.23 cm^{-1}.

X-ray data collection

A green prismatic crystal of size $0.3 \times 0.2 \times 0.2$ (**1**) was mounted on a Nonius CAD-4-F diffrac-

tometer. The cell dimensions were refined by least-squares fitting on the θ values of 25 reflexions.

The lower precision achieved in the values of the b parameter could be attributed to a mosaic spread in this direction. The intensities of 2816 unique reflexions with $1 < \theta < 25°$, $hkl(000)$ to (15 18 18), were measured at 295 K with monochromatic Mo-K_α radiation ($\lambda = 0.71069$ Å) and a ω–2θ scan technique. There was no appreciable change in the periodically monitored standard reflexions. The intensities were corrected for Lorentz and polarization effects and 1845 of these were considered as observed by the criterion $I > 2\sigma(I)$. Scattering factors for neutral atoms and anomalous dispersion corrections for atom were taken from *International Tables for X-ray Crystallography* (1974).[26]

Solution and refinement

The heavy atom was located from the three-dimensional Patterson map. The positions of the remaining non-hydrogen atoms were obtained for Fourier synthesis. An empirical absorption[27] and extinction correction was applied at the end of the isotropic refinement. The H atom positions were calculated and included. Final refinement minimizing $\Sigma w[|F_o| - |F_c|]^2$ with fixed isotropic temperature factors and coordinates for H atoms gave $R = 0.025$ and $R_w = 0.027$. No trend in ΔF vs $F_o \sin\theta/\lambda$ was observed. Maximum and average shift/error were 0.59 and 0.07, respectively. Most of the calculations were performed with XRAY76.[28]

Final atomic positional and thermal parameters, bond lengths and angles, and F_o/F_c values have been deposited as supplementary material with the Editor, from whom copies are available on request. Atomic coordinates have also been submitted to the Cambridge Crystallographic Data Centre.

Preparation of the complexes

$Mo(NO)_2(2\text{-pic})_2$ (**1**) and $Mo(NO)(2\text{-pic})_3$ (**5**). Ammonium heptamolybdate (0.5 g) and hydroxylamine hydrochloride (0.85 g) were heated in 10 cm^3 of DMF at *ca* 90°C for an hour to get a green solution as described in the literature.[3] A suspension of 2-picolinic acid (0.697 g) in 20 cm^3 methanolic KOH (0.65 g) was added and a lemon green solid was formed immediately. The reaction mixture was refluxed in an inert atmosphere for an hour and poured into 100 cm^3 of boiled water. After keeping at *ca* 90°C for 30 min the mixture was allowed to cool, and the precipitate was filtered off. The solid obtained was recrystallized several times from dichloromethane. Two products were obtained, a green solid soluble in CH_2Cl_2, **1**, and a pale yellow solid insoluble in the solvent **5**.

$Mo(NO)_2(o\text{-AP})_2$ (**2**). To the green solution in DMF obtained as described above a solution of *o*-aminophenol (0.68 g) in 30 cm^3 of methanolic KOH (0.65 g) was added and the resulting reddish-brown mixture was refluxed for 1 h in an inert atmosphere. The mixture was allowed to cool and the precipitate formed was filtered off. The filtrate was poured into 150 cm^3 of boiled water saturated with N_2. A green-brown solid appeared after a few minutes. The mixture was stirred as *ca* 90°C for 20 min and then the precipitate was filtered off, washed with water, and dried over P_4O_{10} *in vacuo* for several hours.

$Mo(NO)_2(o\text{-ATP})_2$ (**3**). To the DMF green solution of $[Mo(NO)_2]^{2+}$ obtained as above a solution of *o*-aminothiophenol (0.71 g) in 30 cm^3 of methanolic KOH (0.65 g) was added and the resulting yellow-brown mixture was refluxed for 1 h in an inert atmosphere. Then, it was allowed to cool and the mixture was poured into 150 cm^3 of boiled water saturated with N_2. The brown solid formed was filtered off, washed with water, and dried over P_4O_{10} *in vacuo*. After the addition of $CHCl_3$ (75 cm^3) to the crude product, the mixture was stirred and the solid resulting was filtered off, washed with $CHCl_3$ and MeOH several times, and dried *in vacuo*.

$Mo(NO)_2(HDtz)_2(H_2Dtz)$ (**4**). A solution of dithizone (1.43 g) in 15 cm^3 methanolic KOH (0.65 g) was added to a green solution of $[Mo(NO)_2]^{2+}$. The mixture was refluxed in an inert atmosphere for 1 h and poured into 100 cm^3 of boiled water. A very dark precipitate was formed. After 1 h of stirring at room temperature the violet-purple solid was filtered off, washed with water, and dried over P_4O_{10} *in vacuo*.

$Mo(NO)(MeHdtc)_3$ (**6**). To the green solution containing the $[Mo(NO)_2]^{2+}$ moiety a suspension of $NaMeHdtc \cdot 2.5H_2O$ (0.986 g) in methanol (40 cm^3) was added under N_2. The reddish-brown reaction mixture was refluxed. After 30 min the solvent was partially evaporated at reduced pressure and the mixture was filtered. The filtrate was poured into 150 cm^3 of boiled and degasified water. The orange gel obtained was centrifuged, washed with water, and dried *in vacuo* over P_4O_{10}. The product was recrystallized from MeOH.

$Mo(NO)(pyrdtc)_3 \cdot \frac{1}{2}CHCl_3$ (**7**). The $Mo(NO)_2(pyrdtc)_2$ complex was stirred in $CHCl_3$ and under N_2 for several days. Then the reaction mixture was filtered and the yellow solution obtained was precipitated with light petroleum ether (b.p. 40–60°C). The orange-yellow solid formed was filtered off, washed with light petroleum ether, and dried *in vacuo*.

$Mo(NO)(Et_2dtc)_3 \cdot \frac{1}{2}CHCl_3$ (**8**). The $Mo(NO)_2$

$(Et_2dtc)_2$ complex was stirred in chloroform and under N_2 for 16 h. Then the brown oil and yellow solution formed are separated by decantation. The addition of light petroleum ether (b.p. 40–60°C) gave rise to the formation of a yellow solid, which was filtered off, washed with light petroleum, and dried *in vacuo*. On the other hand, acetone added to the oil gave rise to a brown solid (product mixture) and a yellow solution from which a yellow solid was obtained by precipitation with light petroleum ether. Both the yellow products were identical.

$Mo(2\text{-pic})_3 \cdot H_2O$ (**9**). The reaction was carried out under N_2. Complex **1** and PPh_3 in a 1 : 1 molar ratio were stirred in $CHCl_3$ for 2 days, during which the colour of the solution became topaz. Diethyl ether was added to precipitate an earth-yellow solid, which was filtered off, washed with ether, and dried *in vacuo*. The same reaction in an excess of PPh_3 occurred much more rapidly and the solution became topaz in 1 h.

Reaction of $Mo(NO)_2(pyrdtc)_2$ *with* CO. Carbon monoxide was bubbled through a solution of the complex $Mo(NO)(pyrdtc)_2$ in CH_2Cl_2 at room temperature for 50 min giving rise to the formation of an $Mo_2O_4(pyrdtc)_2 \cdot xCH_2Cl_2$ complex as a crystalline red solid or an orange powder. This solid was filtered off, washed with the CH_2Cl_2, and dried *in vacuo*. The mononitrosyl derivative $Mo(NO)(pyrdtc)_3$ was precipitated from the filtrate by addition of light petroleum ether (b.p. 40–60°C). Sometimes this compound contained traces of the starting dinitrosyl complex.

REFERENCES

1. B. F. G. Johnson, K. H. Al-Obaidi and J. A. McCleverty, *J. Chem. Soc. A* 1969, 1688.
2. M. Green and S. H. Taylor, *J. Chem. Soc. A* 1972, 2629.
3. S. Sarkar and P. Subramanian, *Inorg. Chim. Acta* 1979, **35**, L357 (and refs therein).
4. R. Bhattacharyya and G. P. Bhattacharjee, *J. Chem. Soc., Dalton Trans.* 1983, 1593.
5. F. A. Cotton and B. F. G. Johnson, *Inorg. Chem.* 1964, **3**, 1609; B. F. G. Johnson, *J. Chem. Soc. A* 1967, 475.
6. F. Canciani, U. Sartorella and F. Cariati, *Ann. Chim. (Rome)* 1964, **54**, 1354; M. W. Anker, R. Colton and I. B. Tomkins, *Aust. J. Chem.* 1968, **21**, 1149.
7. L. Bencze, J. Kohan, B. Hohai and L. Mako, *J. Organomet. Chem.* 1974, **70**, 421.
8. T. F. Brennan and I. Bernal, *Inorg. Chim. Acta* 1973, **7**, 203.
9. K. Weighardt, W. Holzbach, B. Nuber and J. Weiss, *Chem. Ber.* 1980, **113**, 629.
10. J. R. Budge, J. A. Broomhead and P. D. W. Boyd, *Inorg. Chem.* 1982, **21**, 1031.
11. M. Minelli, J. L. Hubbarg and J. H. Enemark, *Inorg. Chem.* 1984, **23**, 970.
12. J. A. Broomhead and J. R. Budge, *Inorg. Chem.* 1978, **17** 2414; J. A. Broomhead, J. R. Budge, W. A. Grumley, T. R. Norman and M. Sterns, *Aust. J. Chem.* 1976, **29**, 275.
13. M. L. Larson and F. W. Moore, *Inorg. Chem.* 1962, **1**, 856; T. G. Dunne and F. A. Cotton, *Inorg. Chem.* 1963, **2**, 263.
14. C. K. Hohnson, ORTEP, Report ORNL-3794, Oak Ridge National Laboratory, Tennessee.
15. R. D. Feltham and J. H. Enemark, *Top. Stereochem.* 1981, **12**, 55.
16. J. H. Enemark and R. D. Feltham, *Coord. Chem. Rev.* 1974, **13**, 339.
17. M. G. Reisner, L. Bernal, H. Brunner and J. Doppelberger, *J. Chem. Soc., Dalton Trans.* 1978, 1664.
18. J. T. Malito, R. Shakir and J. L. Atwood, *J. Chem. Soc., Dalton Trans.* 1980, 1253.
19. I. W. Nowell, J. Brooks, G. Beech and R. Hill, *J. Organomet. Chem.* 1983, **244**, 119.
20. M. M. Taqui Khan and A. E. Martell, *Homogeneous Catalysis by Metal Complexes*, p. 360. Academic Press, New York (1974).
21. H. Irving and J. J. Cos, *J. Chem. Soc.* 1961, 1470.
22. W. Kemula and T. Gaúko, *J. Chem. Soc., Chem. Commun.* 1971, 1063.
23. G. Booth and J. Chatt, *J. Chem. Soc.* 1962, 2099.
24. F. A. Cotton and G. Wilkinson, *Advanced Inorganic Chemistry*, 4th Edn, p. 878. John Wiley, New York (1980).
25. H. L. Klopping and G. J. M. van der Kerk, *Recl Trav. Chim.* 1951, **70**, 917.
26. *International Tables for X-ray Crystallography*. Vol. 4, p. 72. Kynoch Press, Birmingham (1974).
27. N. Walker and D. Stuart, *Acta Cryst.* 1983, **A39**, 158.
28. J. M. Steward, P. A. Machin, C. W. Dickinson, H. L. Ammon, H. Heck and H. Flack, *The XRAY 76 System*. Technical Report TR-446, Computer Science Center, University of Maryland, College Park, MD (1976).

Polyhedron Vol. 6, No. 7, pp. 1533–1539, 1987
Printed in Great Britain

0277–5387/87 $3.00+.00

SYNTHESIS AND CHARACTERIZATION OF MONO- AND BINUCLEAR COPPER(II) COMPLEXES WITH 2,2′:6′,2″-TERPYRIDINE (TERPY) AND CARBOXYLATES: X-RAY CRYSTAL STRUCTURE OF [Cu(terpy)(OOCH)(OH_2)](ClO_4) COMPLEX

JOSÉ V. FOLGADO, EMILIO ESCRIVÁ, AURELIO BELTRÁN-PORTER and DANIEL BELTRÁN-PORTER*

Departament de Química Inorgánica, Facultat de Ciencies Químiques, Universitat de Valencia (Estudi General), Dr. Moliner 50,46100 Burjassot (Valencia), Spain

and

AMPARO FUERTES and CARLES MIRAVITLLES

Instituto de Ciencia de Materiales (C.S.I.C.), Martí i Franqués, s/n. 08028 Barcelona, Spain

(*Received* 13 *October* 1986; *accepted* 23 *January* 1987)

Abstract—Perchlorate and hexafluorophosphate salts of monomeric [Cu(terpy)(OOCH)(OH_2)]$^+$ and dimeric [Cu(terpy)(OOCR)]$_2^{2+}$ cations (terpy = 2,2′:6′,2″-terpyridine, R = CH_3 or C_2H_5) have been synthesized and characterized by IR, electronic and ESR spectra, and analytical data. Spectroscopic results indicate a five-coordinate, close-to-square pyramidal geometry around the copper(II) ion. The half-field absorption in the $\Delta M_s = 2$ region of powdered X-band ESR spectra has been observed for the dimeric species. The crystal structure of [Cu(terpy)(OOCH)(OH_2)](ClO_4) has been determined by X-ray diffraction methods. The compound crystallizes in the space group $P2_1/c$ with unit-cell dimensions: a = 7.341(3), b = 13.919(2), c = 18.081(3) Å, β = 101.68(3)°, V = 1809(1) Å^3, Z = 4. The structure was refined to R = 0.044, R_w = 0.051.

To design synthetic pathways to systems of desired properties is a growing challenge for inorganic chemists.[1,2] Our current interest in this area is focused on copper(II) chemistry. In addition to understanding the factors determining the conformation around copper(II) in the solid state,[3] we intend to gain insight into the chemical and structural effects that govern exchange-coupling interactions in condensed species.[4] Thus, we have reported the synthesis and characterization of a wide set of pentacoordinated Cu(L_{III})XY complexes (L_{III} = tridentate ligand, X = coordinating anion, Y = coordinating or non-coordinating anion) showing a great structural diversity (including mono-, bi- and polynuclear species). Tridentate rigid "quasi-planar" ligands such as terpy (2,2′:6′,2″-terpyridine),[3–8] paphy (pyridine-2-aldehyde-2′-pyridylhydrazone)[9] and TPT [2,4,6-tris(2-pyridyl)-1,3,5-triazine][10] favour the stacking of [Cu(L_{III})X]$^+$ entities to give dimers or other condensed systems (simple or ladder-like chains), but the ultimate nature of the resulting compound depends mainly not only on the concrete ligand but also on the character of the potentially bridging X anion.

We have now synthesized and characterized a family of carboxylate and terpy-containing copper(II) complexes. The ability and adaptability of simple carboxylates as bridging ligands is well-established.[11]

EXPERIMENTAL

Preparation of the complexes

[Cu(terpy)(OOCH)(OH_2)](ClO_4] (A). Solutions of $CuSO_4 \cdot 5H_2O$ (0.061 g, 0.2 mmol) in water (4

* Author to whom correspondence should be addressed.

cm^3), terpy (0.046 g, 0.2 mmol) in acetone (4 cm^3) and NaOOCH (0.027 g, 0.4 mmol) in water (2 cm^3) were mixed in sequence with stirring. The resulting blue solution was filtered and then $NaClO_4 \cdot H_2O$ (0.12 g, 0.8 mmol) in water (4 cm^3) was added to the filtrate with stirring. Slow evaporation at room temperature yields blue prismatic crystals after several hours. Crystals were separated by filtration, washed with cold water and acetone, and stored in a desiccator over silica gel. Found: C, 42.2; H, 3.1; N, 9.1. Calc. for $C_{16}H_{14}ClCuN_3O_7$: C, 41.8; H, 3.1; N, 9.2%.

[Cu(terpy)(OOCH)(OH_2)](PF_6) (**B**). This blue complex was prepared as described for **A** but using KPF_6 instead of $NaClO_4 \cdot H_2O$. Found: C, 38.1; H, 2.5; N, 8.3. Calc for $C_{16}H_{14}PF_6CuN_3O_3$: C, 38.1; H, 2.8; N, 8.3%.

[Cu(terpy)(OOCMe)]$_2$(ClO_4)$_2 \cdot 2H_2O$ (**C**). A solution of terpy (0.046 g, 0.2 mmol) in acetone (3 cm^3) was added to other of $Cu(OOCMe)_2 \cdot H_2O$ (0.040 g, 0.2 mmol) in water (3 cm^3) with stirring. After filtration of the resulting blue solution, $NaClO_4 \cdot H_2O$ (0.112 g, 0.8 mmol) in water (4 cm^3) was added with stirring and the solution allowed to stand at room temperature. The green-bluish needles which appeared after several hours were separated, washed and stored as above. Found: C, 43.2; H, 3.3; N, 8.8. Calc for $C_{17}H_{16}ClCuN_3O_7$: C, 43.1; H, 3.4; N, 8.9%.

[Cu(terpy)(OOCMe)]$_2$(PF_6)$_2 \cdot 2H_2O$ (**D**). Green-bluish needles of this complex were obtained by the same method as for **C** but using KPF_6 instead of $NaClO_4 \cdot H_2O$. Found: C, 39.6; H, 3.1; N, 8.0. Calc. for $C_{17}H_{16}PF_6CuN_3O_3$: C, 39.4; H, 3.1; N, 8.1%.

[Cu(terpy)(OOCEt)]$_2$(ClO_4)$_2$ (**E**). This anhydrous complex was prepared as described for **A** but using HOOCEt instead of NaOOCH. The resulting blue solution was adjusted to pH = 7 by aqueous NaOH solution and then allowed to stand at 60°C. After several hours, green-bluish needles appeared and were separated from the solution by filtration and treated as above. Found: C, 46.3; H, 3.3; N, 9.0. Calc. for $C_{18}H_{16}ClCuN_3O_6$: C, 46.1; H, 3.4; N, 9.0%.

[Cu(terpy)(OOCEt)]$_2$(PF_6)$_2 \cdot 2H_2O$ (**F**). Green-bluish needles of this complex were obtained in the same way as for **E** but using KPF_6 instead of $NaClO_4 \cdot H_2O$, and allowing to stand the solution at room temperature. Found: C, 40.8; H, 3.3; N, 7.9. Calc. for $C_{18}h_{18}PF_6CuN_3O_3$: C, 40.6; H, 3.4; N, 7.9%.

Physical measurements

IR spectra (KBr pellets) were recorded on a Pye-Unicam SP2000 spectrophotometer. Diffuse-reflectance electronic spectra were registered on a Pye-Unicam SP 180 spectrophotometer. ESR spectra were recorded on a Bruker ER 200D *X*-band spectrometer. Water was determined thermogravimetrically using a Setaram B70 simultaneous TGA-DTA thermobalance.

Crystallographic study

Crystal data of A. Blue prismatic crystals of $C_{16}H_{14}ClCuN_3O_7$, $M = 459.3$, monoclinic, $a = 7.341(3)$, $b = 13.919(2)$, $c = 18.081(3)$ Å, $\beta = 101.68(3)°$, $V = 1809(1)$ Å^3, space group $P2_1/c$, $Z = 4$, $D_c = 1.686$ g cm^{-3}, $F(000) = 932$, μ(Mo-K_α) = 14.0 cm^{-1}, λ(Mo-K_α = 0.70926 Å.

Data collection. A well-formed crystal of dimensions $0.14 \times 0.16 \times 0.18$ mm was mounted on an Enraf-Nonius CAD-4 diffractometer equipped with a graphite monochromator. The cell dimensions were obtained by least-squares refinement of 25 well-centered reflections ($22° < 2\theta < 37°$). From systematic absences ($0k0$, k odd; $00l$, l odd; $h0l$, l odd) the space group $P2_1/c$ was assumed. Examination of four standard reflections [(1 7 $\bar{8}$), (0 4 $\bar{10}$), (0 8 0), (0 3 $\bar{9}$)], monitored after each 50 reflections, showed no appreciable intensity decay. 3444 reflections were measured ($2° < 2\theta < 50°$; $-8 < h < 8$, $0 < k < 16$, $0 < l < 21$) with the variable-speed ω-2θ technique, of which 2397 were unique with $I > 2.5\sigma(I)$ and used in the determination of the structure. Lorentz and polarization corrections were applied, but not absorption.

Structure solution and refinement. The position of copper and 15 non-hydrogen atoms were determined by direct methods (MULTAN 11/84).[12] The remaining non-hydrogen atoms were located from successive Fourier syntheses. Refinement of the structure was carried out with the SHELX76 system[13] by weighted anisotropic full-matrix least squares. All hydrogen atoms were located by Fourier difference syntheses and included in the refinement with common fixed isotropic thermal parameters ($U = 0.059$ Å^2). The perchlorate anion is disordered. A difference map calculated at this stage revealed four minor O sites around the central Cl. A model with eight O sites and two sets of complementary occupancies was introduced. The oxygen atoms with minor occupancy factor were isotropically refined and a value of 0.14 was obtained for this parameter. The final R values were $R = 0.044$ and $R_w = 0.051$ (237 parameters refined). $\Sigma w(|F_o| - |F_c|)^2$ minimized with $w = 1/(\sigma^2(F_o) + 0.01455F_o^2)$ with $\sigma^2(F_o)$ from counting statistics. In the final difference map the residual maxima were less than 0.60 e Å^{-3} except for one peak (1.25 e Å^{-3}) around the perchlorate

anion. Atomic scattering factors and corrections for anomalous dispersion for the copper atom were taken from *International Tables for X-ray Crystallography*.[14] The geometrical calculations were performed with XANADU[15] and DISTAN,[16] and molecular illustrations were drawn with PLUTO.[17] Final atomic coordinates, thermal parameters and F_o/F_c values have been deposted with the Editor as supplementary data. Atomic coordinates have also been deposited with the Cambridge Crystallostallographic Data Centre.

RESULTS AND DISCUSSION

Significant aspects guiding the synthetic strategies have been previously reported.[10] Molecular formulae have been written considering all the structural information available (see below). Except for **A**, the thermal dehydration step occurs as a one-stage endothermic process. In the case of **A**, this first step seems more complex, showing an exothermic component. The weight loss involved fits to the evolution of 1 mol CO_2 overlapping with H_2O removal, and the DTA temperature peak is relatively high (see Table 1).

Assignments of the more relevant IR spectral bands in the complexes are listed in Table 1. Bands due to terpy ligand and counterions are not discussed. Notwithstanding, it must be stressed that in no case the bands proper of ClO_4^- and PF_6^- regular groups appear split. We conclude that both anions act as non-coordinating groups.[18] From the data in Table 1 some facts are noteworthy: (1) in both formate complexes, bands assignable to ν_{as}(COO) and ν_s(COO) are located at 1600 and 1330 cm^{-1} ($\Delta\nu = 270$ cm^{-1}), respectively. However, these bands appear around 1580 and 1410 cm^{-1} ($\Delta\nu$ *ca* 170 cm^{-1}) in the remaining complexes spectra (2) Likewise, only the spectra of the formate complexes display a weak band at 425–430 cm^{-1}, which can be associated to Cu—O(water) stretching vibrations.[19] These facts argue in favour of: (1) a different carboxylate coordination mode in formate complexes with respect to the others. Thus, $\Delta\nu$ values are consistent with monodentate formate and bidentate (chelating or bridging) acetate and propionate;[11,20] (2) when considering the anhydrous character of **E**, the lack of ν(Cu—O) in the spectra of **C**, **D** and **F** suggests that water molecule occupies a coordination site only in the formate complexes. However, in all cases, the main component of ν(O—H) band is centered about 3410 cm^{-1}. It can be thought that water is involved in hydrogen bonds of medium strength.[21] This might explain why lattice water removal **C**, **D** and **F** also requires moderately high temperatures (Table 1).

The reflectance electronic spectra of all the solids studied exhibit one broad unresolved band centred around 15,300 cm^{-1} (Table 1). Our previous results on related systems[3–8] indicate that the rigid terpy ligand favours geometries close to square pyramidal around copper(II). This contention is also consistent in the present case and the position of the intensity maximum in the absorption envelope agrees with the Hathaway observations for $[CuN_3O_2]$ chromophores.[22]

X-band ESR spectra of polycrystalline samples show axial-type signals which remain unchanged from room temperature down to 125 K (Fig. 1). The ESR line shapes, leading to $g_\parallel = 2.23$–$2.25 > g_\perp = 2.06$ (Table 1) points towards a mainly copper(II) $d_{x^2-y^2}$ orbital ground state, a result which agrees with the above statements. In addition, it must be noted the appearance at half-field values (i.e. in the $\Delta M_s = 2$ forbidden transition region) of a new weak absorption (Fig. 1, Table 1) in the spectra of the acetate and propionate complexes. This signal implies a magnetic interaction between two copper(II) ions and supports unequivocally the presence of dimeric entities in these complexes (**C**–**F**). IR, visible and ESR spectra data become coherent here, assuming a molecular structure similar to that schematized in Fig. 2 in which the [Cu(terpy)(OOCR)]$^+$ moieties are linked through bidentate bridging carboxylate groups to give the dimeric pentacoordinated unities. Lacking X-ray structural

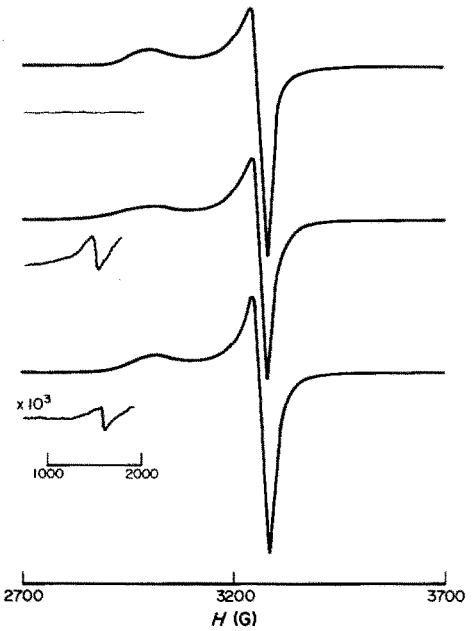

Fig. 1. Polycrystalline *X*-band ESR spectra of complexes **A**, **C** and **E** at room temperature. (frequency = 9.435 GHz).

Table 1. Relevant spectral data for the complexes

Compound	IR (cm^{-1})				Electronic spectra (cm^{-1})		ESR[a]				Dehydration temperature[b] (°C)
	ν(O—H)	ν_{as}(COO)	ν_s(COO)	ν(Cu—O)	$\Delta\nu$	ν_{max}	$g_\parallel$	$g_\perp$	$\Delta M_s = 2$[c]	G	
A	3410m,br	1600vs	1330m	425w	270	15,300	2.25	2.06	—	4.2	165
							(2.25)	(2.06)	—	(4.2)	
B	3410m,br	1600vs	1330m	430w	270	15,300	2.24	2.06	—	4.0	150
							(2.24)	(2.06)	—	(4.0)	
C	3510–3420m,br	1580vs	1400m	—	180	15,300	2.24	2.06	4.2	4.0	122
							(2.23)	(2.03)	(4.2)	(3.8)	
D	3600m, 3400m,br	1575vs	1400m	—	175	15,300	2.23	2.06	4.2	3.8	144
							(2.23)	(2.06)	(4.2)	(3.8)	
E	—	1580vs	1410m	—	170	15,300	2.24	2.06	4.2	4.0	
							(2.24)	(2.06)	(4.2)	(4.0)	
F	3600m, 3400m,br	1580vs	1410m	—	170	15,300	2.23	2.06	4.2	3.8	148
							(2.23)	(2.06)	(4.2)	(3.8)	

[a] Values at 125 K are given in parentheses.
[b] DTA temperature peak.
[c] g values of the half-field signal.

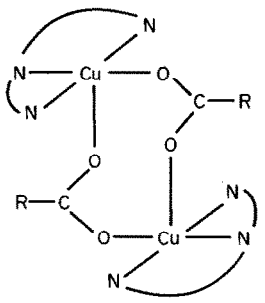

Fig. 2. Schematic view of the proposed approximate geometry for the dimeric species.

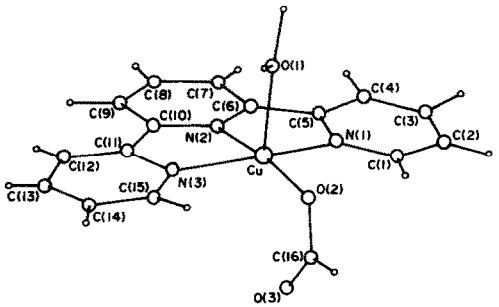

Fig. 3. Perspective view of $[Cu(terpy)(OOCH)(OH_2)]^+$ cation with labelling of atoms.

data (attempts to grow suitable crystals have been not successfully up to date) an *anti–syn* carboxylate coordination mode has been assumed (as the more likely) for pictorial purposes only.

Now, the absence of the $\Delta M_s = 2$ signal in the ESR spectra of the formate complexes may be related to the monodentate character of the carboxylate groups shown by IR. Thus, it has been previously noted that copper(II) formate and its adducts are reluctant to adopt the binuclear copper(II) acetate type structure (which is also found in the higher alkanoates).[11] This behaviour has been associated to the low σ-electron donor efficiency of the $HCOO^-$ group which generally leads to polymeric complex structures.[11] In our case, monodentate formates might yield mononuclear or polymeric (containing mono-oxo-bridging formate anions) species. Although the probable coordination to copper of the water molecule points towards a monomeric formulation for these complexes, the question remains open at this stage. This fact and the availability of single crystals of **A** suitable for X-ray study lead us to approach its structural resolution.

Figure 3 shows a perspective view of the $[Cu(terpy)(OOCH)(OH_2)]^+$ cation with the detailed labelling of the atoms, and Fig. 4 shows a stereoscopic view of the unit cell. Significant bond distances and angles are given in Table 2. The coordination sphere of copper(II) is best described as a square pyramid. The basal positions are occupied by the three nitrogen atoms from the terpy ligand and an oxygen atom of the monodentate formate anion [Cu—N(1) = 2.030(4), Cu—N(2) = 1.947(4),

Table 2. Selected bond distances (Å) and angles (°) for complex **A** : standard deviations are given in parentheses

Cu—O(1)	2.247(3)	C(16)—O(2)	1.266(6)
Cu—O(2)	1.935(3)	C(16)—O(3)	1.237(5)
Cu—O(3)	2.815(4)	C(16)—H(160)	1.020(5)
Cu—N(1)	2.030(4)	O(1)—H(w1)	0.81(6)
Cu—N(2)	1.947(4)	O(1)—H(w2)	1.18(6)
Cu—N(3)	2.056(4)	Cl—O(average)	1.380(5)
O(2)—Cu—O(1)	88.4(1)	O(3)—Cu—O(1)	140.0(1)
O(3)—Cu—O(2)	51.9(1)	N(1)—Cu—O(1)	97.7(1)
N(1)—Cu—O(2)	99.9(1)	N(1)—Cu—O(3)	94.5(1)
N(2)—Cu—O(1)	99.1(1)	N(2)—Cu—O(2)	172.4(1)
N(2)—Cu—O(3)	120.5(1)	N(2)—Cu—N(1)	80.1(1)
N(3)—Cu—O(1)	93.3(2)	N(3)—Cu—O(2)	98.8(1)
N(3)—Cu—O(3)	88.7(1)	N(3)—Cu—N(1)	158.5(1)
N(3)—Cu—N(2)	79.9(2)	O(3)—C(16)—O(2)	125.5(5)
O(3)—C(16)—H(160)	133.1(5)	O(2)—C(16)—H(160)	101.2(4)
H(w1)—O(1)—H(w2)	102(5)	O—Cl—O(average)	109.1(9)
	Hydrogen bonding[a]		
O(1)···O(3)′	2.699(5)	O(1)—H(w2)—O(3)′	175(5)
O(1)···O(5)	3.039(6)	O(1)—H(w1)—O(5)	168(3)

[a] O(3)′ from O(3) after $1+x, y, z$.

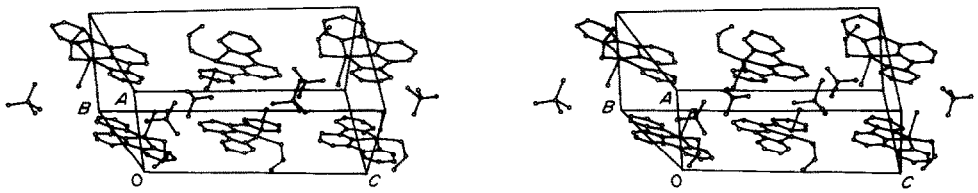

Fig. 4. Stereoscopic view of the unit cell for complex **A**.

Cu—N(3) = 2.056(4), Cu—O(2) = 1.935(3) Å], while the apical site is occupied by the oxygen atom from the water molecule [Cu—O(1) = 2.247(3) Å]. The basal atoms are coplanar within ±0.02 Å and the copper atom is displaced 0.15 Å from the mean plane. The terpy ligand is planar within ±0.13 Å and the plane through the atoms Cu, O(1) and O(2) makes an angle of 87.9° with the basal mean plane. If the second oxygen atom of the formate anion is considered as "semicoordinated"[22] [Cu—O(3) = 2.815(4) Å] the environment of the copper would be described as an elongated and strongly distorted octahedron [the O(2)—Cu—O(3) angle is 51.9(1)°]. This kind of coordination has been also found in other carboxylate, nitro and nitrite copper(II) complexes.[2,22,23]

The interatomic distances and angles in the terpy ligand are in agreement with those found in previously described complexes.[4,7,23,24] As predicted above, the formate group is asymmetric [C(16)—O(2) = 1.266(6) and C(16)—O(3) = 1.237(5) Å] as a consequence of the polarization of the charge density towards the metal-bonded oxygen atom.

The structure of **A** (Fig. 4) consists of double layers which are parallel to the "*bc*" plane. These double layers are built up with pairs of $[Cu(terpy)(OOCH)(OH_2)]^+$ units related by an inversion center; perchlorate anions occupy interlayer empty spaces. Crystal packing of the layers is achieved by intermolecular hydrogen bonding between the water molecule and the "semicoordinated" oxygen atom from the formate anion [O(1)—O(3)′ = 2.699(5) Å, O(1)—H(w2)—O(3)′ = 171(5)°] giving infinite chains $\cdots H_2O—Cu—O—C—O—H_2O—Cu\cdots$ along the (1 0 0) direction [O(3)′ from O(3) after $1+x, y, z$]. The water molecule is also involved in another hydrogen bond with an oxygen atom from the perchlorate anion [O(1)—O(5) = 3.039(4)Å; O(1)—H(w1)—O(5) = 168(3)°].

Based on the results reported, a similar structure can be expected for **B**. Only the hydrogen-bonding scheme must differ from its perchlorate analogue, and this might lay behind the difference observed in the dehydration step.

Lastly, dealing with exchange interactions, we note (Table 1) that the $G = g_{\parallel} - 2/g_{\perp} - 2$ parameter value is near to 4 even for the dimeric species, indicating that exchange interactions are weak.[22] This result is not surprising if the actual geometry of the dimers is that proposed above. The effective overlap between the magnetic orbitals involved in the entity would be very poor.[3–8] Furthermore, bridging carboxylates provide in general a poor support to propagation of the exchange interactions except when the structural function is *syn–syn*, as in the copper(II) acetate.[11]

Accordingly, further structural and magnetic studies could play a key role improving the understanding of the factors controlling exchange-coupling interactions, and are in progress.

Acknowledgements—We gratefully acknowledge the C.A.I.C.Y.T. and C.S.I.C. for support of this research and for fellowships to A.F. and J.V.F.

REFERENCES

1. L. J. de Jongh, In *Magneto-structural Correlations in Exchange-coupled Systems* (Edited by D. Gatteschi, O. Khan and R. D. Willet). NATO Advances Institute Series, Reidel, Dordrecht (1984).
2. A. Fuertes, C. Miravitlles, E. Escriva, E. Coronado and D. Beltran, *J. Chem. Soc., Dalton Trans.* (in press).
3. T. Rojo, J. L. Mesa, M. I. Arriortua and D. Beltran, *An. Quim.* 1980, **80B**, 477 (and references therein).
4. T. Rojo, J. Darriet, G. Villeneuve, M. I. Arriortua, J. Ruiz and D. Beltran, *J. Chem. Soc., Dalton Trans.* 1987, 285.
5. J. V. Folgado, E. Coronado and D. Beltran, *J. Chem. Soc., Dalton Trans.* 1986, 1061.
6. E. Coronado, M. Drillon and D. Beltran, *Inorg. Chim. Acta* 1984, **82**, 13.
7. T. Rojo, J. Darriet, J. M. Dance and D. Beltran, *Inorg. Chim. Acta* 1982, **L105**, 64.
8. J. V. Folgado, E. Coronado, D. Beltran, M. I. Arriotua, T. Rojo and J. M. Savariault, *Proc.* XXIV *Int. Conf. Coord. Chem.* p. A5-262. Athens, Greece (1986).
9. J. L. Mesa, M. I. Arriotua, T. Rojo, J. M. Savariault, J. Galy and D. Beltran, *Proc. Ninth European Crystallographic Meeting* (*I.U.C.*), Vol. 1, p. 189. Torino, Italy (1985).

10. J. V. Folgado, E. Escriva, A. Beltran-Porter and D. Beltran-Porter, *Transition Met. Chem.* 1986, **11**, 485.
11. R. C. Mehrotra and R. Bohra, *Metal. Carboxylates.* Academic Press, New York (1983) (and references therein).
12. P. Main, G. Germain and M. M. Woolfson, *MULTAN* 11/84. *A System of Computer Programs for the Automatic Solutions of Crystals Structures from X-ray Diffraction Data.* University of York, U.K., and Louvain, Belgium (1984).
13. G. M. Sheldrick, *SHELX*76. *Program for Crystal Structure Determination.* University of Cambridge, U.K. (1976).
14. *International Tables for X-ray Crystallography*, Vol. 1. p. 99. Kynoch Press, Birmingham, U.K. (1974).
15. P. Roberts and G. M. Sheldrick, *XANADU. Program for Crystallographic Calculations.* University of Cambridge (1975).
16. J. Burzlaff, V. Bohme and M. Gomm, *DISTAN.* University of Erlangen, F.R.G. (1977).
17. W. D. S. Motherwell and W. Clegg, *PLUTO*78. *Program for Plotting Molecular and Crystal Structures.* University of Cambridge (1978).
18. K. Nakamoto, *Infrared and Raman Spectra of Inorganic and Coordination Compounds.* Wiley, New York (1978).
19. J. R. Ferraro, *Low-frequency Vibrations of Inorganic and Coordination Compounds.* Plenum Press, New York (1971).
20. G. B. Deacon and R. J. Phillips, *Coord. Chem. Rev.* 1980, **33**, 227.
21. E. Escriva, A. Fuertes, J. V. Folgado, E. Martinez-Tamayo, A. Beltran-Porter and D. Beltran-Porter, *Thermochim. Acta* 1986, **104**, 223.
22. B. J. Hathaway, *Struct. Bonding* 1984, **57**, 55 (and references therein); B. J. Hathaway, *Struct. Bonding* 1973, **14**, 49; B. J. Hathaway and D. E. Billing, *Coord. Chem. Rev.* 1970, **5**, 143.
23. J. M. Savariault, T. Rojo, M. I. Arriortua and J. Galy, *C. R. Acad. Sci.* 1983, (II)**297**, 895.
24. T. Rojo, M. Vlasse and D. Beltran-Porter, *Acta Cryst.* 1983, **C39**, 194.

Polyhedron Vol. 6, No. 7, pp. 1541–1545, 1987
Printed in Great Britain

0277–5387/87 $3.00+.00
Pergamon Journals Ltd

THE PREPARATION AND USE OF DISULPHURDINITRIDO COMPLEXES: THE X-RAY STRUCTURE OF $[PPh_4][S_3N_3]$

RAY JONES, PAUL F. KELLY, DAVID J. WILLIAMS and J. DEREK WOOLLINS*

Department of Chemistry, Imperial College of Science and Technology, South Kensington, London SW7 2AY, U.K.

(*Received* 4 *November* 1986; *accepted* 23 *January* 1987)

Abstract—The preparation of $M(S_2N_2)(PR_3)_2$ (M = Pd or Pt) (**1**) complexes by reaction of $MCl_2(PR_3)_2$ with $S_4N_4H_4$ in the presence of diazabicycloundecane is described. A variety of other reagents also give rise to **1**; in particular S_4N_4–BuLi. The reactive intermediate in the latter case appears to be $S_3N_3^-$ which has been characterized by X-ray crystallography as the PPh_4^+ salt: tetragonal, space group $P\bar{4}$, $a = 17.579(5)$, $c = 7.447(2)$ Å. The protonation of **1** to $[M(S_2N_2H)(PR_3)_2]X$ ($X = Cl^-$ or BF_4^-) and the use of **1** in the preparation of S_3N_2O is reported.

Metalla-sulphur–nitrogen chemistry provides access to a number of unusual compounds.[1–3] Apart from the potentially interesting solid-state properties of the stacking compounds[4] many complexes stabilize otherwise unknown anionic sulphur–nitrogen species such as $S_2N_2^{2-}$ and $S_2N_2H^-$. A number of synthetic strategies have been employed in the preparation of $Pt(S_2N_2)(PR_3)_2$ (**1**) and $[Pt(S_2N_2H)(PR_3)_2]X$ ($X = PF_6^-$) complexes. For example, in **1** when $PR_3 = PPh_3$ reaction of $Pt(PPh_3)_3$ with $S_4N_4H_4$ is satisfactory.[5] However this method is not readily extended to other systems. We have successfully used $Na(S_3N_3)$ [eqn (1)]:

$$PtCl_2(PR_3)_2 + 2Na(S_3N_3) \rightarrow Pt(S_2N_2)(PR_3)_2 + S_4N_4 + 2NaCl. \quad (1)$$

but this salt is air-sensitive and **extremely explosive**; clearly an alternative is preferable.

Reaction of $[Me_2Sn(S_2N_2)]_2$ with $PtCl_2(PR_3)_2$ in the presence of $[NH_4][PF_6]$ provides a useful route to **2** but the tin reagent is moderately air-sensitive and probably toxic. We have been investigating alternative routes to **1** and **2**. Here we report on the use of $S_4N_4H_4$–dbu (dbu = diazabicycloundecane) and S_4N_4–RLi as reagents. Both can be reacted with *cis*-$PtCl_2(PR_3)_2$ to give **1**. In the case of S_4N_4–RLi reactions one of the reactive intermediates is the $S_3N_3^-$ anion and the crystal structure of its tetraphenylphosphonium salt is reported. Protonation reactions for the conversion of **1** into **2** are described. The usefulness of **1** as a source of S_2N_2 in ring syntheses has also been studied.

EXPERIMENTAL

General reaction conditions, drying of solvents, preparation of starting materials and spectroscopic measurements were as described previously.[6]

$Pt(S_2N_2)(PMe_2Ph)_2$

To a suspension of $S_4N_4H_4$ (20 mg, 0.1 mmol) in a CH_2Cl_2 (10 cm^3) solution of *cis*-$PtCl_2(PMe_2Ph)_2$ (110 mg, 0.2 mmol) was added excess dbu (six drops). The colourless solution gradually turned pale yellow and the $S_4N_4H_4$ started to dissolve. After 10 min the reaction was a golden yellow colour with only a trace of $S_4N_4H_4$ undissolved. At this point additional dbu (two drops) was added and the reaction was stirred for a further 90 min. The CH_2Cl_2 was removed *in vacuo* leaving an oily pale yellow solid which was washed with degassed water (2×60 cm^3), and then dried *in vacuo*. The final product was obtained as a pale yellow/off white solid by extraction with CH_2Cl_2 followed by precipitation using hexane. Yield 90 mg (79%). The product had indistinguishable IR and ^{31}P NMR properties from those previously reported.[7]

$Pt(S_2N_2)(PEt_3)_2$ *and* $Pt(S_2N_2)(PPh_2Me)_2$

Reactions performed on a ^{31}P NMR scale gave the same products as those previously reported.[7]

* Author to whom correspondence should be addressed.

$Pd(S_2N_2)(PR_3)_2$ (PR_3 = PEt_3, PMe_2Ph, PPh_2Me *or* PPh_3)

Reactions were performed as described for $Pt(S_2N_2)(PMe_2Ph)_2$ but using *trans* or *cis*/*trans* mixtures of the palladium complexes.

For $PR_3 = PMe_2Ph$: Found: C, 40.1; H, 4.5; N, 5.8. Required: C, 40.5; H, 4.7; N, 5.9%. IR: ν(NS) 1070(vs), 605(w) cm^{-1}. $^{31}P-\{^1H\}$: δ −3.8, −9.2 ppm; ^2J = 41.5 Hz.

For $PR_3 = PEt_3$: Found: C, 31.8; H, 6.6; N, 6.6. Required: C, 33.1; N, 6.9; H, 6.4%. IR: ν(NS) 1074(vs), 671(m), 605(w), δ(NS)/ν(PdS) 443(w), 348(w) cm^{-1}. $^{31}P-\{^1H\}$: δ 16.5, 22.5 ppm; ^2J = 37 Hz.

For $PR_3 = PPh_2Me$: $^{31}P-\{^1H\}$: δ 7.9, 11.5 ppm, ^2J = 39 Hz; product not isolated.

For $PR_3 = PPh_3$: reaction did not proceed as for other phosphines. No AX ^{31}P NMR spectrum was observed.

$[Pd(S_2N_2)(PPh_3)]_2$ precipitated out of the reaction mixture.

$[M(S_2N_2H)(PR_3)_2]X$

X = BF_4^-. To a suspension of **1** in thf (0.1 mmol in 10 cm^3) was added $Et_2O \cdot BF_3$ (Aldrich, two drops). Initially **1** dissolved giving an intense green-yellow solution, and after further stirring some precipitate appeared. The volume of thf was reduced *in vacuo* and diethyl ether added to precipitate **2**. The product may be purified by crystallization from Et_2O–CH_2Cl_2. In this way analytically pure $[Pt(S_2N_2H)(PMe_2Ph)_2][BF_4]$ is obtained. In the case of palladium complexes for $PR_3 = PEt_3$: $^{31}P-\{^1H\}$: δ 20.6, 23.9 ppm; ^2J = 29 Hz. $PR_3 = PMe_2Ph$: IR: ν(NH) 3300 cm^{-1}. $^{31}P-\{^1H\}$: δ −3.9, −5.4 ppm; ^2J 34 Hz.

X = Cl^-. To a suspension of $Pt(S_2N_2)(PMe_2Ph)_2$ in thf (0.1 mmol in 10 cm^3) was added a few drops of HCl-saturated CH_2Cl_2. The solvent was removed under *in vacuo* and the gummy solid triturated with hexane. Filtration, extraction of the solid into thf and removal of solvent *in vacuo* gave a green oily solid. The crystalline product was obtained by slow diffusion of hexane into a CH_2Cl_2 solution. Yield 0.08 mmol (80%). Found: C, 29.7; H, 3.5; N, 4.0. Required for $[Pt(S_2N_2H)(PMe_2Ph)_2]Cl \cdot CH_2Cl_2$: C, 29.8; H, 3.7; N, 4.1%. NB: the ^{31}P NMR of the initial crude reaction shows *ca* 20% *cis*-$PtCl_2(PMe_2Ph)_2$ as the side product. No attempt was made to recover this material.

Preparation of S_3N_2O

$Pt(S_2N_2)(PMe_2Ph)_2$ (56 mg, 0.1 mmol) in CH_2Cl_2 (10 cm^3) was treated with excess $SOCl_2$ (two drops) with stirring under N_2. The solution immediately changed from golden yellow to light orange. After stirring for 1 min the solvent was removed *in vacuo*. The resulting red oil was extracted into CH_2Cl_2 (1 cm^3) and this solution chromatographed (Kieselgel 60 Prep. plate) using CH_2Cl_2 as the eluant. The band at R_f = 0.65 was extracted from the silica using CH_2Cl_2 and after removal of this solvent the product was further purified by vacuum sublimation onto a liquid nitrogen cold finger (bath temperature 60°C). Yield 5 mg (35%). IR: 1125(s), 985(m), 912(m), 740(m), 670(m), 510(m) cm^{-1}.

$[PPh_4][S_3N_3]$

A solution of S_4N_4 (0.28 g, 1.5 mmol) in thf (20 cm^3) was treated with ^{n}BuLi [0.56 cm^3, 2.7 M (Aldrich), 1.5 mmol]. The reaction immediately went dark red. The thf solution was reduced *in vacuo* and treated with hexane (50 cm^3) giving an orange-red precipitate. After filtration and drying the remaining solid was extracted into thf and solid $[PPh_4]Cl$ (0.56 g, 1.5 mmol) added. CH_2Cl_2 was added until most of the $[PPh_4]Cl$ had dissolved and the solution was filtered. After standing for a few minutes a yellow solid precipitated. Enough CH_2Cl_2 to dissolve this solid was added and hexane was layered on the resulting red solution. The product was obtained as large orange crystals. Found: C, 59.5; H, 3.4; N, 8.3. Calc. C, 60.4; H, 4.2; N, 8.8%.

X-ray structural analysis of $[PPh_4][S_3N_3]$

Crystal data: $C_{24}H_{20}N_3PS_3$, orange tetragonal sphenoidal crystals, tetragonal, a = 17.579(5), c = 7.447(2) Å, U = 2230 $Å^3$, space group $P\bar{4}$, Z = 4, M = 477.6, D_c = 1.38 g cm^{-3}, μ(Cu-K_α) = 37 cm^{-1}.

Measurements. Crystal dimensions 0.5 × 0.2 × 0.2 mm. Refined unit-cell parameters were obtained by centring 14 reflections on a Nicolet R3m diffractometer, 1807 independent reflections ($\theta \leqslant 58°$) were measured with Cu-K_α radiation (graphite monochromator) using the ω-scan measuring routine. Of these 1652 had $|F_o| > 3\sigma(|F_o|)$, and were considered to be observed. Lorentz, polarization and an analytical absorption correction based on indexed faces were applied.

Structure analysis. The structure was solved by a combination of the heavy-atom method and ΔE map recycling. The positions of the phosphorus atoms, one on the two-fold axis at [(0, $\frac{1}{2}$, z)] and the other two on the $\bar{4}$ special positions [(0, 0, $\frac{1}{2}$) and ($-\frac{1}{2}$, $\frac{1}{2}$, $\frac{1}{2}$)] were determined from the Patterson map. The positions of all the other non-hydrogen atoms

were determined by successive ΔE map recycling. The non-hydrogen atoms were refined anisotropically. The hydrogen atom positions were idealized (C—H = 0.96 Å) assigned isotropic thermal parameters [$U(H) = 1.2U_{eq}(C)$] and allowed to ride on their parent carbons.

Refinement was by block cascade full-matrix least squares to $R = 0.063$, $R_w = 0.074$ [$w^{-1} = \sigma^2(F) + 0.0011F^2$]. The chirality of the structure was established by refinement of a free variable (η) which multiplies all f'' values. This variable converged to a value of 1.1(1). Computations were carried out on an Eclipse S140 computer using the SHELXTL program system.[8]

Final atomic coordinates, including those of the hydrogen atoms, and thermal parameters have been deposited with the Editor as supplementary data. Atomic coordinates have been deposited with the Cambridge Crystallographic Data Centre.

RESULTS AND DISCUSSION

It has been recognized for several years[9] that the S_4N^- anion is in equilibrium with S_7N^- formed by deprotonation of S_7NH [eqn (2)]:

$$S_7N^- = S_4N^- + \tfrac{3}{8}S_8 = S_3N^- + \tfrac{1}{2}S_8. \qquad (2)$$

and we have made use of this equilibrium in the preparation[10] of $AuCl_2(S_3N)$. Surprisingly, reaction of the S_3N^- anion with group VIII metal chlorides gives complexes containing the $S_2N_2H^-$ ligand and this, together with the results of our studies (*vide infra*), suggests the involvement of anions such as $S_2N_2^{2-}$ in solution reactions of a number of sulphur–nitrogen compounds.

Since the deprotonation reaction of S_7NH provides a useful route to M–S–N complexes we have investigated the reactivity of $S_4N_4H_4$ in the presence of the base dbu. Thus treatment of *cis*-$PtCl_2(PR_3)_2$ or *trans*-$PdCl_2(PR_3)_2$ with $S_4N_4H_4$–dbu yields $M(S_2N_2)(PR_3)_2$ (**I**) in good yield [eqn (3)]:

$$2MCl_2(PR_3)_2 + S_4N_4H_4\text{–dbu} \rightarrow 2M(S_2N_2)(PR_3)_2 + 2\text{dbuHCl}. \qquad (3)$$

(NB: only demonstrative examples were isolated; the generality of the reaction was established by ^{31}P NMR). The new palladium complexes gave satisfactory NMR, IR and microanalytical data. An interesting feature of the reaction is the formation of an intermediate compound, observed by ^{31}P NMR (Fig. 1), with $\delta = -13.8$ and -23.0 ppm and $^1J(Pt–P) = 3658$ and 2987 Hz. Attempts to isolate this intermediate were unsuccessful; it is also observed from reaction of dbu with *cis*-$PtCl_2(PR_3)_2$ and the NMR data suggests a complex with two phosphine, one chloro and one dbu ligand. This is somewhat

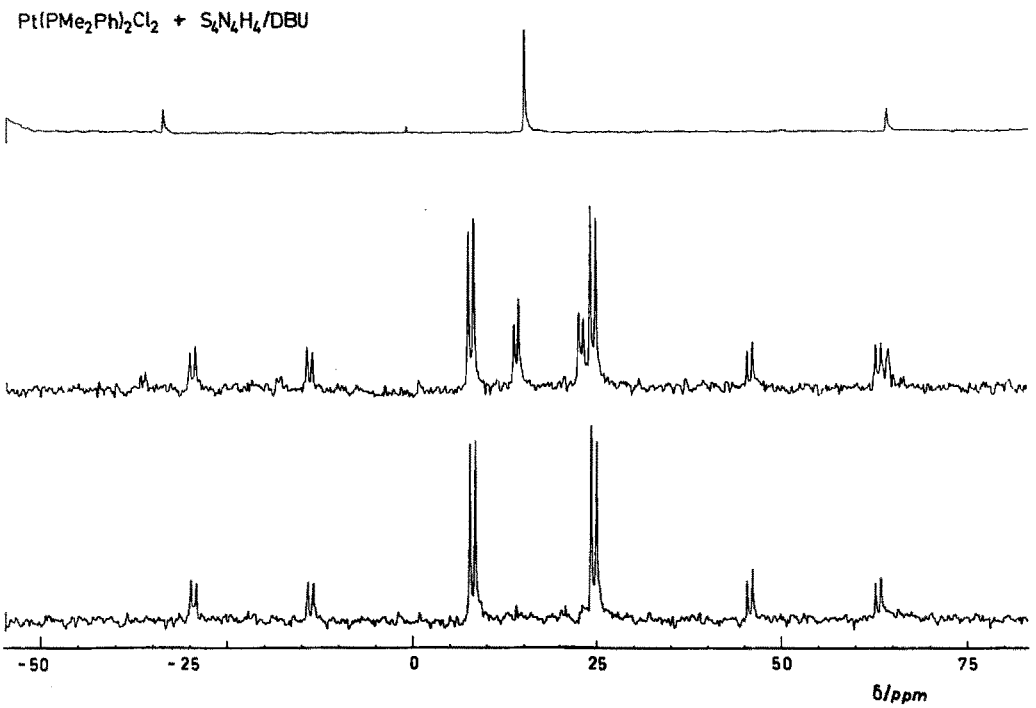

Fig. 1. ^{31}P–{^1H} NMR of the reaction of *cis*-$PtCl_2(PMe_2Ph)_2$ with $S_4N_4H_4$ and dbu. Upper trace shows starting material, middle trace shows $Pt(S_2N_2)(PMe_2Ph)_2$ and intermediate believed to be *cis*-$PtCl(dbu)(PMe_2Ph)_2$, lower trace is after addition of additional dbu.

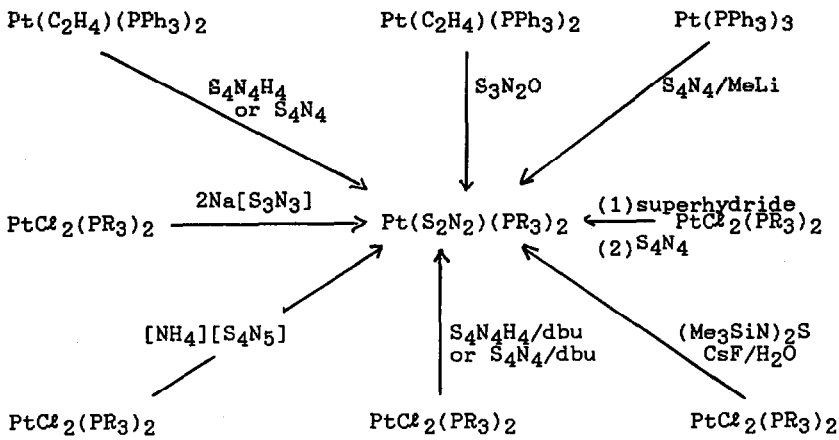

Scheme 1. Reactions in which $Pt(S_2N_2)(PR_3)_2$ is a major product. Note that in some cases the results are from ^{31}P NMR only.

surprising since dbu is considered to be a non-nucleophillic base.

The mechanism of the reaction in eqn (2) is not immediately obvious and two observations appear to rule out a simple equilibrium process involving $S_2N_2^{2-}$. Firstly, the reaction is extremely clean (Fig. 1) with all of the $S_4N_4H_4$ eventually being complexed as $S_2N_2^{2-}$; in other studies[7] on $S_3N_3^-$ we always observed the formation of S_4N_4. Secondly, unlike many of the reactions involving SN species no major colour changes are seen; these would be expected if species such as S_3N^- were involved. It is possible that the reaction proceeds via co-ordination of $S_4N_4H_4$ followed by elimination of HCl to give $Pt(S_4N_4H_2)(PR_3)_2$ which is then attacked by $PtCl(dbu)(PR_3)_2$ to give two molecules of $[Pt(S_2N_2H)(PR_3)]Cl$; this will be deprotonated by dbu to yield **1**.

We have also observed disulphurdinitrido complexes from a number of other routes and these are summarized in Scheme 1. One particularly interesting reaction is that of S_4N_4 with BuLi; a very reactive species is formed. We thought it possible that the intermediate might be $S_2N_2^{2-}$ and thus attempted to crystallize it using $[PPh_4]Cl$. Surprisingly, the product obtained is $[PPh_4][S_3N_3]$, identified by X-ray crystallography, IR and microanalysis. The crystal structure (Fig. 2, Table 1) reveals the expected planar ring for the anion with similar bond distances and angles to those reported for the $[(n\text{-}C_4H_9)_4N]^+$ salt.[11] We do not believe that the variation in S—N bond distances in the ring are a consequence of anion–cation interactions in the solid state as all of the inter-ion distances are con-

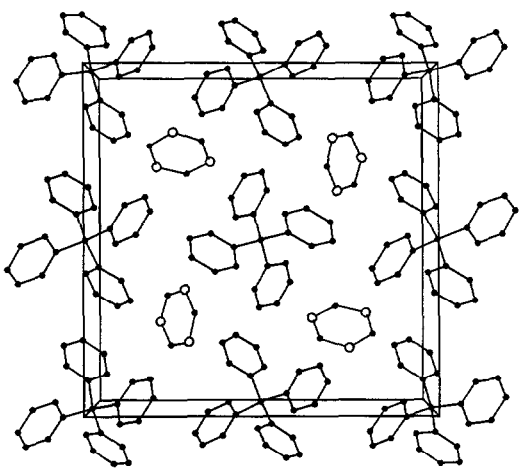

Fig. 2. X-ray structure of $[PPh_4][S_3N_3]$ viewed down the crystallographic *c*-direction. The sulphur atoms are depicted as open circles.

Table 1. Selected bond distance (Å) and angles (°) for $[PPh_4][S_3N_3]$

S(1)—N(1)	1.641(9)	S(1)—N(3)	1.566(8)
S(2)—N(1)	1.601(10)	S(2)—N(2)	1.609(7)
S(3)—N(2)	1.590(7)	S(3)—N(3)	1.628(8)
N(1)—S(1)—N(3)	116.6(4)	N(1)—S(2)—N(2)	116.4(4)
N(2)—S(3)—N(3)	115.6(4)	S(1)—N(1)—S(2)	122.6(5)
S(2)—N(2)—S(3)	124.4(5)	S(1)—N(3)—S(3)	124.3(5)

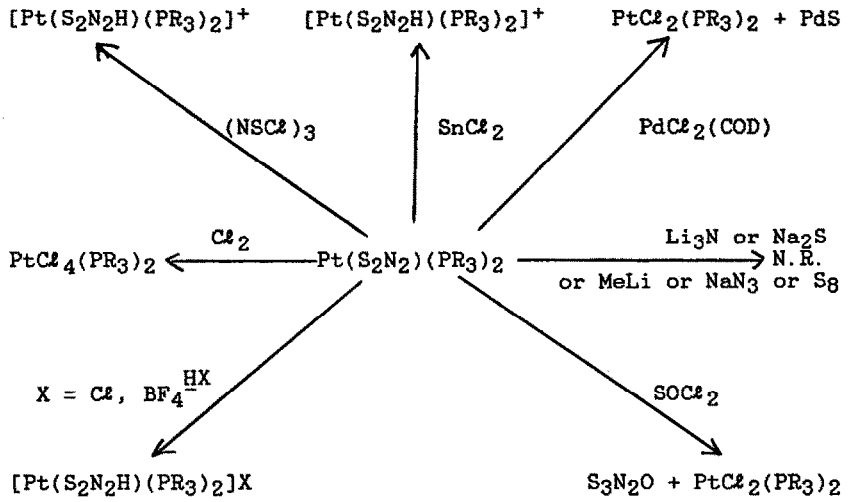

Scheme 2. Reactions of $Pt(S_2N_2)(PR_3)_2$.

sistent with the van der Waals' radii. In contrast to the PPh_4^+ salt reported here and the $[(n\text{-}C_4H_9)_4N]^+$ salt[11] the S—N distances of the $S_3N_3^-$ anion in $Tl_2[S_3N_3][S_4N_5]$[12] show no significant variation.

The wide variety of circumstances in which we have observed $S_2N_2^{2-}$ complexes suggests that this anion is an important species in sulphur–nitrogen chemistry although it may be unstable. The platinum centre appears to be particularly appropriate for trapping and stabilizing the disulphurdinitrido group. The complexes reported here are all reasonably air-stable both as solids and in solution.

The protonation of **1** is readily accomplished using HCl or HBF_4, enabling the isolation of **2** which have stacking structures with columns of cations and anions. Other reactions of **1** are shown in Scheme 2. The majority of the reactions were followed by ^{31}P NMR but we have been able to isolate S_3N_2O by the reaction with $SOCl_2$ [eqn (4)]:

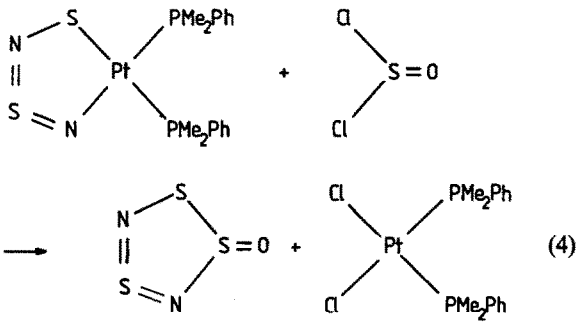

(4)

Reaction of **1** with S_2Cl_2 in attempts to prepare S_4N_2 is less satisfactory; the product decomposing during workup. In the preparation of S_3N_2O the starting *cis*-$PtCl_2(PR_3)_2$ is recyclable and thus **1** appears to have potential as a reagent in the synthesis of sulphur–nitrogen heterocycles.

Acknowledgement—We are grateful to Johnson Matthey for loans of precious metals.

REFERENCES

1. P. F. Kelly and J. D. Woollins, *Polyhedron* 1986, **5**, 607.
2. R. Jones, P. F. Kelly, D. J. Williams and J. D. Woollins, *J. Chem. Soc., Chem. Commun.* 1985, 1325.
3. N. P. C. Walker, M. B. Hursthouse, C. P. Warrens and J. D. Woollins, *J. Chem. Soc., Chem. Commun.* 1985, 227.
4. R. Jones, P. F. Kelly, D. J. Williams and J. D. Woollins, *J. Chem. Soc., Chem. Commun.* 1986, 711.
5. R. Jones, P. F. Kelly, D. J. Williams and J. D. Woollins, *J. Chem. Soc., Dalton Trans.* 1986.
6. R. Jones, C. P. Warrens, D. J. Williams and J. D. Woollins, *J. Chem. Soc., Dalton Trans.* (accepted for publication).
7. P. A. Bates, M. B. Hursthouse, P. F. Kelly and J. D. Woollins, *J. Chem. Soc., Dalton Trans.* 1986.
8. G. M. Sheldrick, SHELXTL, *An Integrated System for Solving, Refining and Displaying Crystal Structures from Diffraction Data.* University of Gottingen, Gottingen F.R.G. (1978), Revision 4.1 (1983).
9. T. Chivers and R. T. Oakley, *Top. Curr. Chem.* 1982, **102**, 117.
10. J. D. Woollins, *Polyhedron* 1984, **3**, 1365.
11. J. Bojes, T. Chivers, W. G. Laidlaw and M. Trsic, *J. Am. Chem. Soc.* 1979, **101**, 4517.
12. H. Martan and J. Weiss, *Acta Cryst.* 1983, **C39**, 959.

Polyhedron Vol. 6, No. 7, pp. 1547–1550, 1987
Printed in Great Britain

0277–5387/87 $3.00+.00

SYNTHESIS AND X-RAY CRYSTAL STRUCTURE OF TETRAETHYLAMMONIUM BIS(1,1-DICYANOETHENE-2,2-DISELENOLATO)OXOTECHNETATE(V), $[Et_4N][TcO(Se_2C{=}C(CN)_2)_2]$

GIULIANO BANDOLI*

Dipartimento di Scienze Farmaceutiche, via Marzolo 5, Università di Padova, 35131 Padova, Italy

ULDERICO MAZZI

Istituto di Chimica e Tecnologia dei Radioelementi del CNR, Corso Stati Uniti 4, 35020 Padova, Italy

and

ULRICH ABRAM, HARTMUT SPIES and RUDOLF MÜNZE

Central Institute of Nuclear Research, Rossendorf, PF 19, Dresden, 8051, G.D.R.

(*Received* 10 *November* 1986; *accepted* 23 *January* 1987)

Abstract—Tetraethylammonium bis(1,1-dicyanoethene-2,2-diselenolato)oxotechnetate(V) has been prepared from Tc(V) gluconate and characterized by single-crystal X-ray structural analysis ($R = 0.064$). In the complex the technetium atom is centred in an approximate square pyramid in which the four selenium atoms form the basal plane and the oxygen is at the apex. The Tc—Se distances average 2.471(4) Å, while Tc=O is 1.67(2) Å.

The widespread use of the nuclide ^{99m}Tc (γ-emitter, γ-energy: 140 keV, $t_{1/2} = 6$ h) in the diagnostic nuclear medicine[1–3] has strongly stimulated the development of the coordination chemistry of technetium. Using the long-lived isotope ^{99}Tc (β^--emitter, $E_{max} = 0.29$ MeV, $t_{1/2} = 2.1 \times 10^5$ years) a series of technetium complexes has been prepared and characterized[4] including oxidation states of the metal from "0" up to "+7".

Oxotechnetium(V) complexes have been studied by X-ray analysis with O-, S-, N- and P-donor atom ligands,[5,6] as well as tetrachlorooxotechnetate(V), $TcOCl_4^-$.[7] Here, the first report dealing with the X-ray structure of a technetium complex with selenium coordinated tetraethylammonium bis(1,1-dicyanoethene - 2,2 - diselenolato)oxotechnetate(V) is presented.

* Author to whom correspondence should be addressed.

EXPERIMENTAL

Potassium 1,1-dicyanoethene-2,2-diselenolate can be prepared from malonitrile and carbon diselenide by literature procedures.[8] All other reagents were analytical grade.

Synthesis of tetraethylammonium bis(1,1-dicyanoethene-2,2-diselenolato)oxotechnetate(V)[9]

A solution of 330 mg (1.1 mmol) potassium salt of the ligand in water (2 cm^3) was added dropwise to a solution of Tc(V) gluconate[10] (0.5 mmol) at pH 6–7. After addition of 0.5 cm^3 of a saturated Et_4NBr solution and cooling, a yellow brown powder was precipitated and collected by suction filtration. Recrystallization from acetone–*i*-propanol gave large brown crystals (175 mg, yield 49% based on Tc). M.p. = 182–184°C. (Found: C, 26.7; H, 2.7; N, 9.3; Se, 44.3; Tc, 13.8. Calc. for $(Et_4N)TcO$-

Table 1. Summary of the crystal data and refinement results

Molecular formula	$C_{16}H_{20}N_5OSe_4Tc$
Molecular weight	713.1
Crystal system	Triclinic
a (Å)	13.394(8)
b (Å)	9.935(6)
c (Å)	9.703(6)
α (°)	107.21(7)
β (°)	95.12(5)
γ (°)	92.89(4)
V (Å^3)	1224.4(14)
Z, $F(000)$, d_{calc} (g cm^{-1})	2, 676, 1.934
Space group	$P\bar{1}$
Crystal dimensions (mm)	$0.20 \times 0.10 \times 0.15$
Linear absorption coefficient (μ) (Mo-K_α) (cm^{-1})	64.8
Scan mode, scan rate (° min^{-1})	θ–2θ, 2.4
Scan range (°)	1.2
Background counting time	7 s at each end
2θ limits (°)	3–48
Total number of independent reflections	3811
Number of reflections used in refinement	1923[a]
Number of variables	134
Weighting scheme	$w = 1$
Anisotropic parameters	Tc and Se
$R(F) = \Sigma \lvert F_o \rvert - \lvert F_c \rvert / \Sigma \lvert F_o \rvert$	0.064

[a] $I > 3\sigma(I)$.

(ligand)$_2$ C, 26.9; H, 2.8; N, 9.8; Se, 44.3; Tc, 13.9%.)

*Structure determination and crystal data**

The collection of X-ray data was carried out at room temperature on an automatic Philips PW 1100 diffractometer, using Mo-K_α radiation ($\lambda = 0.7107$ Å). A summary of the crystallographic data is given in Table 1. An experimental absorption correction based on Ψ scans[11] of three reflections at $\chi = 90°$ was applied to the intensities. Most of the calculations were carried out in the SHELX-76 system.[12]

Relevant bond lengths and angles are contained in Table 2, and the molecular structure and labelling are reported in Fig. 1.

* Final positional thermal parameters, a list of all bond lengths and angles, a table of some geometrical features (least-square planes, torsion angles and interatomic contacts) and a list of the observed and calculated structure factors have been deposited as supplementary materials with the Editor, from whom copies are available on request. Atomic coordinates have also been deposited with the Cambridge Crystallographic Data Centre.

RESULTS AND DISCUSSION

Preparation and spectroscopical behaviour

Tc(V) gluconate[10] has been shown to be a useful precursor for the preparation of technetium oxo complexes. Reaction with 1,1-dicyanoethene-2,2-diselenolate yields a complex anion of the type $[TcO(ligand)_2]^-$, as previously reported for a series of dithiolato ligands,[10,13] which can be isolated in form of its salts with large cations (e.g. tetraethylammonium).

The complex, which represents the first coordination compound of technetium with a $TcOSe_4$ coordination sphere, yields brown crystals, easily soluble in organic solvents like acetone and dichloromethane. In the IR spectrum the typical Tc=O stretching frequency can be observed as an intense band at 965 cm^{-1}. A comparison with the bands in corresponding Tc=O complexes with the stepwise sulphur substituted ligands 1,1-dicyanoethene-2,2-thioselenolate, $[SSeC{=}C(CN)_2]^{2-}$, and 1,1-dicyanoethene-2,2-dithiolate, $[S_2C{=}C(CN)_2]^{2-}$, shows a bathochromic shift depending on the number of selenium atoms in the coordination sphere (see Table 3).[9] The same holds true for the electronic spectra

Table 2. Relevant bond lengths (Å) and angles (°) with esds in parentheses

Tc—O	1.67(2)		
Tc—Se(1)	2.476(4)	Tc—Se(3)	2.475(4)
Tc—Se(2)	2.471(4)	Tc—Se(4)	2.463(4)
Se(1)—C(1)	1.92(2)	Se(3)—C(5)	1.89(2)
Se(2)—C(1)	1.90(2)	Se(4)—C(5)	1.89(2)
C(1)—C(2)	1.32(3)	C(5)—C(6)	1.41(3)
O—Tc—Se(1)	108.1(6)	O—Tc—Se(3)	110.8(6)
O—Tc—Se(2)	112.2(6)	O—Tc—Se(4)	112.4(6)
Se(1)—Tc—Se(2)	76.0(2)	Se(3)—Tc—Se(4)	76.7(6)
Se(1)—Tc—Se(4)	89.6(2)	Se(2)—Tc—Se(3)	88.5(2)
Tc—Se(1)—C(1)	88.4(7)	Tc—Se(3)—C(5)	87.3(7)
Tc—Se(2)—C(1)	88.9(7)	Tc—Se(4)—C(5)	87.8(7)
Se(1)—C(1)—Se(2)	105.8(1.1)	Se(3)—C(5)—Se(4)	108.2(1.1)
Se(1)—C(1)—C(2)	127.2(1.8)	Se(3)—C(5)—C(6)	125.2(1.7)
Se(2)—C(1)—C(2)	127.0(1.8)	Se(4)—C(5)—C(6)	126.2(1.8)

Table 3. Spectroscopical data of $(Et_4N)[TcO(XYC{=}C(CN)_2)_2]$ complexes

	X and Y = Se	X = S, Y = Se	X and Y = S
IR[a] (cm^{-1})			
Tc=O	965	970	980
C=C	1493	1490	1490
C≡N	2222	2220	2225
UV–VIS[b] (nm) (log ε)	361 (4.6)	350 (4.8)	350 (4.9)
	269 (4.5)	269 (4.7)	267 (4.9)

[a] In KBr pellets.
[b] In ethanol.

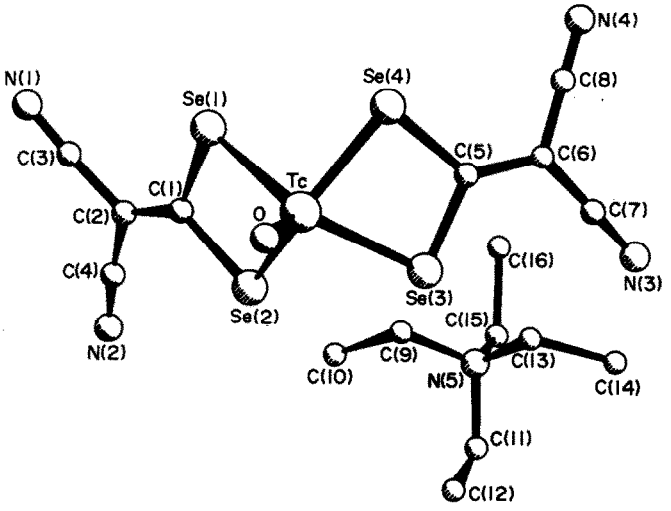

Fig. 1. View along the *c*-axis. Numbering scheme is shown.

as outlined in Table 3, probably caused by the lowering of the ligand field strength by the selenium donors with respect to sulphur. Similar results have been found studying various transition-metal complexes with dichalcogenocarbamates[14] including nitridotechnetium(V) complexes with these ligands[15] and dichalcogenophosphinates.[16]

X-ray analysis

The structure of $(Et_4N)TcO(Se_2C{=}C(CN)_2)_2$ contains well-separated anions and countercations, as shown in Fig. 1. This X-ray analysis confirms the square pyramidal geometry typical of mono-oxo Tc(V) compounds; the tetrahedral tetraethylammonium ion has no unusual features and is not further discussed. In the oxotechnetium anion the four selenium atoms on the base lie roughly in a plane, with the Tc atom 0.88 Å above it, towards the "yl" oxygen atom. The fifth bond, Tc=O, is approximately perpendicular to this plane and its distance of 1.67 Å is similar to that in other mono-oxo technetium complexes.[6] Two features of the structure are worthy of note. Firstly, there appears no prior report of a Tc—Se bond length. The four Tc—Se bond distances are in very close agreement with each other, with a mean value of 2.471 Å. The bond is longer by 0.15 Å than the mean Tc—S value in five-coordinate TcO^{3+} complexes.[17] However, this lengthening is to be expected on the basis of the different covalent radii of Se and S (1.17 and 1.04 Å, respectively).[18] The values for the Se—C bond lie in the narrow range 1.89–1.92 Å, which compares well with the values in the literature,[19] and seems to be normal for a Se—C (sp^2) distance.

Secondly, there is something remarkable about the C=C bond length in the selenolate ligands. In fact, the C(1)—C(2) and C(5)—C(6) lengths [1.32(3) and 1.41(3) Å, respectively] are different and there is no apparent reason for such a difference. A slight mispositioning of C(2) and C(6) atoms could be attributable to anisotropy, but introduction of anisotropic thermal parameters for all the atoms of the anion and/or application of a weighting scheme based on statistics counting did not improve the model (R index lowered to 0.063, but with 199 variables). If we assume the average value (1.36 Å), it parallels those found in $[Ni(Se_2C{=}C(CN)_2)_3]^{3-}$[20] and $[Ni(SeSC{=}C(CN)_2)_2]^{2-}$.[21]

Acknowledgement—We thank Dr W. Dietzsch (Karl-Marx-University, Leipzig) for providing us with the selenium-containing ligands.

REFERENCES

1. G. Subramanian, B. A. Rhodes, J. F. Cooper and V. J. Sodd, *Radiopharmaceuticals*. The Society of Nuclear medicine, New York (1975).
2. S. C. Srivastava and P. Richards, *Radiotracers for Medical Applications*. (Edited by G. V. S. Rayud). CRC Press, Boca Raton, Florida (1981).
3. R. Münze, *Isopenpraxis* 1983, **19**, 401.
4. A. G. Jones and A. Davison, *Int. J. Appl. Radiat. Isot.* 1982, **33**, 867; A. Davison and A. G. Jones, *Int. J. Appl. Radiat. Isot.* 1982, **33**, 881; K. Schwochau, *Radiochim. Acta* 1983, **32**, 139.
5. G. Bandoli, U. Mazzi, E. Roncari and E. Deutsch, *Coord. Chem. Rev.* 1982, **44**, 191.
6. C. Kay Fair, D. E. Troutner, E. O. Schlemper, R. K. Murmann and M. L. Hoffe, *Acta Cryst.* 1984, **C40**, 1544; S. Jurisson, E. O. Schlemper, D. E. Troutner, L. R. Canning, D. P. Novotnik and R. D. Neirinckx, *Inorg. Chem.* 1986, **25**, 513 (and references therein).
7. F. A. Cotton, A. Davison, V. W. Day, L. D. Gage and H. S. Trop, *Inorg. Chem.* 1979, **18**, 3024; L. Golic, I. Leban, U. Abram, K. Köhler, R. Kirmse and R. Böttcher, to be published.
8. K. A. Jensen and L. Hendricksen, *Acta Chim. Scand.* 1972, **24**, 1092.
9. U. Abram and H. Spies, *Z. Chem.* 1984, **24**, 74.
10. H. Spies and B. Johannsen, *Inorg. Chim. Acta* 1979, **33**, L113.
11. A. C. T. North, D. C. Phillips and F. S. Mathews, *Acta Cryst.* 1968, **A34**, 351.
12. G. M. Sheldrick, *A Program for Crystal Structure Determination*. University Chemical Laboratory, Cambridge, U.K. (1976).
13. H. Spies and B. Johannsen, *Inorg. Chim. Acta* 1981, **48**, 255.
14. T. Matsuda, K. Tanaka and T. Tanaka, *Inorg. Chem.* 1979, **18**, 454.
15. U. Abrams, H. Spies, W. Görner, R. Kirmse and J. Stach, *Inorg. Chim. Acta* 1985, **109**, L9.
16. R. Heber, R. Kirmse and E. Hoyer, *Z. Anorg. Allg. Chem.* 1979. **393**, 454.
17. J. E. Smith, E. F. Byrne, F. A. Cotton and J. C. Sekutowski, *J. Am. Chem. Soc.* 1978, **100**, 5571; B. V. DePamphilis, A. G. Jones, M. A. Davis and A. Davison, *J. Am. Chem. Soc.* 1978, **100**, 5570; G. Bandoli, M. Nicolini, U. Mazzi, H. Spies and R. Münze, *Transition Met. Chem.* 1984, **9**, 127.
18. F. A. Cotton and Wilkinson, *Advanced Inorganic Chemistry*, 4th Edn, p. 502. J. Wiley, New York (1980).
19. M. Bonamico and G. Dessy, *J. Chem. Soc. A* 1971, 264 (and references therein).
20. J. Kaiser, W. Dietzsch, R. Richter, L. Golic and J. Shiftar, *Acta Cryst.* 1980, **B36**, 147.
21. W. Dietzsch, J. Kaiser, R. Richter, L. Golic, J. Shiftar and R. Heber, *Z. Anorg. Allg. Chem.* 1981, **477**, 71.

Polyhedron Vol. 6, No. 7, pp. 1551–1557, 1987
Printed in Great Britain

0277–5387/87 $3.00+.00

SYNTHESIS AND REACTIVITY OF COMPOUNDS OF FORMULA W(S)(OR)$_4$

M. H. CHISHOLM,* J. C. HUFFMAN and J. W. PASTERCZYK

Department of Chemistry and Molecular Structure Center, Indiana University, Bloomington, IN 47405, U.S.A.

(*Received* 5 *January* 1987; *accepted* 23 *January* 1987)

Abstract—In ethereal solutions, $WSCl_4$ and 4 equiv LiOR (R = Bu^t or Pr^i) react to form compounds of formula W(S)(OR)$_4$. A single-crystal X-ray diffraction study of W(S)(OBu^t)$_4$ showed it to have a square-based pyramidal geometry with an apical sulfide ligand. Pertinent bond distances (Å) and angles (°) are: W—S = 2.1396(13), W—O(av.) = 1.886(3), S—W—O(av.) = 105.09(10), W—O—C(av.) = 143.47(27). The tert-butoxide compound is stable toward sulfur atom abstraction by phosphines, and neither compound has shown any tendency to undergo comproportionations with $W_2(OR)_6$ (R = Pr^i or CH_2Bu^t) species to form compounds of formula $W_3(\mu_3\text{-}S)(OR)_{10}$, in direct contrast to analogous molybdenum and tungsten oxo alkoxides.

Soluble transition-metal oxide and sulfide clusters have been the subjects of much research as models for both industrially-important heterogeneous catalysts[1] and active sites in metalloenzymes.[2] Particularly common is the family of trinuclear molybdenum and tungsten oxo and sulfido clusters.[3] Efforts in this area in our group have so far focused on metal oxo, imido and alkylidyne alkoxide clusters. For example the compounds $Mo_3(\mu_3\text{-}O)(\mu_3\text{-}OR)(\mu\text{-}OR)_3(OR)_6$ (R = Pr^i or CH_2Bu^t) were recently reported,[4] and the series was extended in further work[5] to include the isostructural species $W_3(O)(OPr^i)_{10}$ and $Mo_2W(O)(OPr^i)_{10}$. Use was made of ligand substitution accompanied by comproportionation in the synthesis of $W_3(\mu_3\text{-}NH)(OPr^i)_{10}$ from $W_2(OPr^i)_6(py)_2$ and $W(N)(OBu^t)_3$ in the presence of isopropanol.[6] Since this synthetic strategy has proven so useful and considering the high affinity that molybdenum and tungsten show for sulfur, we considered the possibility of making sulfido-capped tritungsten decaalkoxide clusters, particularly since the triply-bridging sulfido ligand is such a common entity in both early and late transition metal chemistry.[3,7] This paper describes the synthesis of the necessary monomeric precursors and our efforts to use them in cluster-building reactions.

* Author to whom correspondence should be addressed.

RESULTS AND DISCUSSION

Syntheses

The reaction between $WSCl_4$ and 4 equiv of LiOR (R = Bu^t or Pr^i) in ethereal solutions at −78°C gives W(S)(OR)$_4$ in good isolated yields [eqn (1)]:

$$W(S)Cl_4 + 4LiOR \xrightarrow[-78°C]{\text{ether}} W(S)(OR)_4 + 4LiCl. \quad (1)$$

This simple ligand exchange route is essentially analogous to that used in preparing $W(O)(OPr^i)_4$[5] and $W(O)(NMe_2)_4$[8] from $WOCl_4$ (though the latter product must be prepared via an intermediate methoxide to minimize side reactions). Direct combination of alcohols with $MoOCl_4$ or $WOCl_4$, however, must occur in the presence of ⩾ 4 equiv of an amine to precipitate the HCl liberated as trialkylammonium chloride. In this manner W(O)(OR)$_4$ (R = Me, Et, Pr^n, Pr^i, Bu^n or benzyl) compounds were first prepared over 25 years ago,[9] and the analogous $Mo(O)(OPr^i)_4$ was obtained more recently,[5] though this latter compound can also be prepared via the lithium alkoxide method.[10] Mononuclear Mo(O)(OR)$_4$ (R = Bu^t, Pr^i or CH_2Bu^t) species also result from direct reaction of O_2 with the appropriate Mo(IV) alkoxide.[4]

Comparison with other mononuclear monosulfide species is provided by $[V(S)(edt)_2]^{2-}$ (edt = ethane-1,2-dithiolate dianion), recently reported by two groups.[11,12] Henkel's synthesis involves either a comproportionation and ligand rearrangement of VS_4^{3-} and $V_2(edt)_4^{2-}$ or reaction of the former with excess edt^{2-}. The Christou synthesis, however, occurs via the direct exchange of sulfur for the oxygen atom of $[V(O)(edt)_2]^{2-}$ using hexamethyldisilthiane, $(Me_3Si)_2S$. Other analogs are the $[Re(S)(edt)_2]^-$ anion[13] and the neutral species V(S)(acen) [acen-*N*,*N*′-ethylenebis(acetylacetonylideneaminato) dianion][14] and V(S)(salen) (salen = bis-salicylaldehydeethylenediimine dianion).[15] The latter two Schiff base complexes are obtained from the vanadyl compounds via S for O exchange using B_2S_3.

Physicochemical properties

The new $W(S)(OR)_4$ compounds are pale colored solids which are soluble in common organic solvents. They are air- and moisture-sensitive, particularly the tert-butoxide. Both are readily sublimable and the tert-butoxide can be crystallized from CH_2Cl_2 or Et_2O. Analytical, IR and ^1H NMR data are given in Experimental.

Solid-state and molecular structure of $W(S)(OBu^t)_4$: *bonding considerations*

The sample of $W(S)(OBu^t)_4$ which was used for the X-ray study crystallized from CH_2Cl_2 in the space group $P\bar{1}$. An ORTEP diagram of this molecule is shown in Fig. 1. Selected bond distances and angles are given in Table 1.

Table 1. Selected bond distances (Å) and angles (°) for $W(S)(OBu^t)_4$ (averaged where appropriate)

W—S	2.1396(13)
W—O	1.886(3)
O—C	1.448(6)
S—W—O	105.09(10)
O—W—O *cis*	86.13(13)
O—W—O *trans*	149.83(13)
W—O—C	143.47(27)

The overall coordination geometry consists of a square-based pyramid with the sulfide ligand occupying the axial site and the four alkoxide oxygen atoms lying in the basal sites. The tungsten atom is 0.49 Å above the mean plane of the oxygen atoms. The molecule has a slight distortion such that the two pairs of *trans* O—W—O angles are inequivalent by 2.85° giving the molecule virtual C_2-symmetry, but the ^1H NMR spectrum shows equivalent methyl resonances. Thus rapid O—C bond rotation and scissoring of the *trans* alkoxides must be occurring at room temperature. The solid-state distortion is likely due to crystal packing forces.

In square pyramidal compounds of formula MXL_4 symmetry considerations dictate that M–X π- and M–L $\pi_\parallel$-bonding (L orbitals parallel to the M–X vector) compete for the same metal orbitals, namely the d_{xz} and d_{yz}. In the present compound the W—S distance is shorter than the sum of standard literature covalent radii (1.37+0.94 Å).[16] The W—O distances are also shorter than the sum of the covalent radii (1.37+0.67 Å)* and at the lower end of the W—OR bond length range.[17] The W—O—C angles are also rather large. These data indicate a large amount of O → W and S → W π-

* See discussion of M—OR π-bonding in Ref. 17 for derivation of the oxygen 0.67-Å single-bond radius.

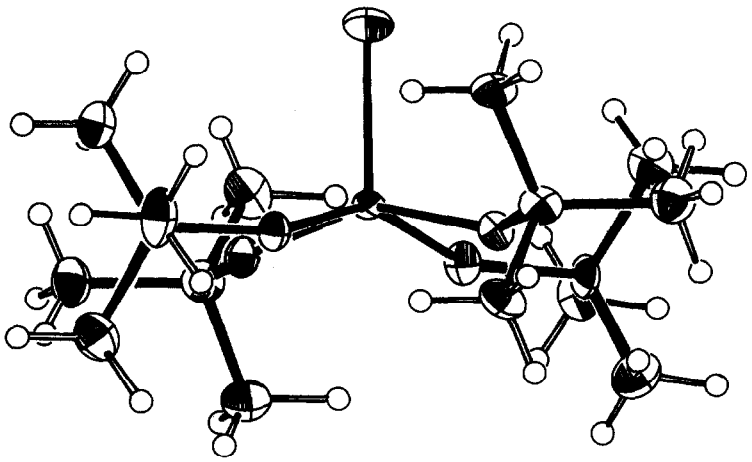

Fig. 1. ORTEP diagram of $W(S)(OBu^t)_4$. Atomic positions are represented by 50% probability thermal ellipsoids.

Table 2. M=S compounds, M=S distances, and M=S stretching bands

Compound	d(M=S) (Å)	$\bar{\nu}$(M=S) (cm^{-1})	Reference
$[WSCl_4]_2$	2.098(8)	569	18, 19
$WSCl_4$[a]	2.086(6)	568	20, 21
$[WSBr_4]_2$	2.079(21)	555	18, 19
$WSBr_4$[a]	—	564	21
$[PPh_4]_2[W_2(S)_2(\mu\text{-}S)_2(edt)_2]$	2.144(2)	504	22
$[NEt_4]_2[W_2(S)_2(\mu\text{-}S)_2(S_4)_2]$	2.116(5)	506	23
V(S)(acen)	2.061(1)	556	14, 15
$[PPh_4]Na[V(S)(edt)_2]$	2.087(1)	502	12
$[NMe_4][Re(S)(edt)_2]$	2.014(2)	517	13
$W(S)(OBu^t)_4$	2.1396(13)	518	This work
$W(S)(OPr^i)_4$	—	540	This work

[a] d(M=S) measured in gas phase, $\bar{\nu}$(M=S) measured in frozen matrix.

bonding, and that the oxygen atoms are hybridized in between sp^2 and sp as their filled p-orbitals donate into vacant tungsten orbitals. Furthermore, the lower value of $\bar{\nu}$(W=S) for the tert-butoxide vs the iso-propoxide (518 vs 540 cm^{-1}, respectively) when combined with the former's greater basicity reflects that the same tungsten orbitals are used for π-bonding by both the sulfide and the alkoxide ligands. Table 2 lists a series of compounds in which the terminal sulfide ligands occupy the axial position in a square-based pyramidal geometry. Note that the M=S distances fall within a fairly narrow range as do the $\bar{\nu}$(M=S) values. Comparing the tungsten compounds, there is a rough inverse relationship between d(W=S) and $\bar{\nu}$(W=S), as expected, and the larger d(W=S) values occur for compounds containing good π-donating equatorial ligands, further supporting the contention that the same metal orbitals accept π-electron density from both equatorial and axial ligands. Considering the formal electronic unsaturation of the metal atom in the present compounds, the high degree of ligand → metal π-bonding should be no surprise. In an Xα-SW calculation on $WSCl_4$, S → W π-bonding is in fact predicted giving rise to a high-lying ligand-centered orbital of e symmetry.[24]

Attempted comproportionation reactions to form compounds of formula $W_3(\mu_3\text{-}S)(\mu_3\text{-}OR)(\mu\text{-}OR)_3(OR)_6$

Synthesis of trinuclear oxo-capped alkoxide clusters proceeds according to eqn (2):[4,5]

$$M_2(OR)_6 + M(O)(OR)_4 \rightarrow M_3(\mu_3\text{-}O)(\mu_3\text{-}OR)(\mu\text{-}OR)_3(OR)_6 \quad (2)$$

M = Mo, R = Pr^i or CH_2Bu^t; M = W, R = Pr^i

Synthesis of isoelectronic imido-capped analogs proceeds similarly, possibly via comproportionation of the metal moieties followed by addition of alcohol [eqn (3)]:[6,25]

$$M_2(OR)_6 + M(N)(OBu^t)_3 \xrightarrow{\text{hexane–ROH}} M_3(\mu_3\text{-}NH)(OR)_{10} \quad (3)$$

M = Mo, R = Pr^i or CH_2Bu^t; M = W, R = Pr^i

Sulfur occurs widely as a four-electron donor in a μ_3-coordination mode[7] and the tungsten sulfide monomers described above are formally isolobal to the M(O)(OR)$_4$ species of eqn (2). These facts led us to believe that a sulfur-capped trinuclear alkoxide cluster could be easily accessible via M(S)(OR)$_4$ precursors.

Attempts to synthesize compounds of formula $W_3(\mu_3\text{-}S)(OR)_{10}$ (R = Pr^i or CH_2Bu^t) are summarized in Table 3. In all cases ^{1}H NMR spectroscopy showed no evidence of a 3 : 3 : 3 : 1 pattern for the four types of different OR ligands expected for products of formula $W_3(\mu_3\text{-}S)(\mu_3\text{-}OR)(\mu\text{-}OR)_3(OR)_6$. Instead W(S)(OR)$_4$ compounds and (in cases where excess alcohol was used) W(OR)$_6$ compounds were observed in the reaction mixtures. The observation of mononuclear hexaalkoxides has precedent in reaction (3) in which addition of alcohol to $(Bu^tO)_3W{\equiv}N$ to form W(OR)$_6$ and ammonia competes with triangle formation.[25] Regardless, it appears that alcoholysis of the starting materials is at least a kinetically favored reaction compared to trimer formation. Unfavourable steric factors arising from the larger sulfido vs oxo ligand could reasonably explain this difference in reactivity. Of note here are the observations that in space-filling diagrams of the related imido-capped complex the imido proton is tightly wedged into the pocket

Table 3. Summary of attempted syntheses of $W_3(\mu_3\text{-}S)(OR)_{10}$ compounds

$W_2(OBu^t)_6 + W(S)(OBu^t)_4 + xsPr^iOH \xrightarrow[2\,days,\,RT]{toluene}$
$W_2(OBu^t)_6 + W(S)(OBu^t)_4 + xsPr^iOH \xrightarrow[2\,days,\,RT]{CH_2Cl_2}$
$W_2(OBu^t)_6 + W(S)(OPr^i)_4 + 6Pr^iOH \xrightarrow[1\,day,\,RT]{toluene}$
$W_2(NMe_2)_6 \xrightarrow[xsPr^iOH]{(1)\ hexane,\ 0°C} \xrightarrow{(2)\ strip} \xrightarrow[toluene]{(3)\ W(S)(OPr^i)}$
$W_2(OPr^i)_6(py)_2 + W(S)(OPr^i)_4 \xrightarrow[reflux]{hexane,\ 6\,h}$
$W(S)(OBu^t)_4 \xrightarrow[4NeOH]{(1)\ toluene} \xrightarrow[50°C,\,1\,day]{(2)\ W_2(ONe)_6(HNMe_2)_2}$
$W_2(ONe)_6(py)_2 \xrightarrow[5\,h,\,RT]{(1)\ W(S)(OBu^t)_4,\ hexane} \xrightarrow[12\,h]{(2)\ 4NeOH}$
$W_2(ONe)_6(HNMe_2)_2 + W(S)(OBu^t)_4 \xrightarrow[28\,h,\,RT]{(1)\ toluene} \xrightarrow[1\,day]{(2)\ 4NeOH}$

formed by the adjacent alkoxide ligands, and that no $M_3X(OR)_{10}$ clusters containing alkoxide ligands bulkier than the iso-propoxy group are known.

Attempted desulfurization/aggregation via phosphines

Trialkyl and triaryl phosphines are widely known to be efficient sulfur atom abstractors. It was thought that desulfurization of $W(S)(OBu^t)_4$ using phosphines would yield a highly reactive $W(OBu^t)_4$ fragment which could possibly react with the tungsten starting material forming a confacial bioctahedral $(Bu^tO)_3W(\mu\text{-}S)(\mu\text{-}OBu^t)_2W(OBu^t)_3$ species. However, no reaction occurs between $W(S)(OBu^t)_4$ and either PPh_3 or PBu^n_3 as confirmed by ^1H NMR spectroscopy.

EXPERIMENTAL

All manipulations were performed under a dry-nitrogen atmosphere using standard Schlenk techniques or a Vacuum Atmospheres drybox. Solvents were dried and deoxygenated by standard methods. $WSCl_4$ was prepared by the sealed tube reaction of WCl_6 and S_8.[26] Lithium alkoxides were prepared by reaction of *n*-butyllithium with the corresponding alcohol. ^1H NMR spectra were obtained on a Nicolet 360 MHz spectrometer; shifts are relative to the 7.15-ppm signal of residual protons in d_6-benzene. IR spectra were obtained on a Perkin–Elmer 283 spectrophotometer. Electron impact mass spectra were obtained on a Kratos MS-80 mass spectrometer. Elemental analyses were performed by Alfred Bernhardt Analytical Laboratories (Elbach, F.R.G.).

$W(S)(OBu^t)_4$

$LiOBu^t$ (1.03 g, 12.8 mmol) was placed in a large Schlenk tube equipped with a stirbar. Diethyl ether (60 cm^3) was added and the solution cooled to $-78°C$. $WSCl_4$ (1.15 g, 3.2 mmol) was added via an addition tube over 10 min with stirring. The solution immediately became red, then faded to yellow within 15 min. The solution was left to stir and warm to room temperature over 4 h. After allowing the LiCl precipitate to settle overnight it was filtered off using a medium frit and the solution stripped to dryness leaving a yellow powder. X-ray quality crystals as yellow plates were grown in 54% yield by cooling a concentrated CH_2Cl_2 solution of this powder to $-15°C$. The product also sublimes at 50°C, 10^{-4} torr onto a water-cooled probe. ^1H NMR data (25°C, d_6-benzene): δ 1.51 ppm. IR data (Nujol mull, CsI plates, cm^{-1}): 1359(s), 1230(m), 1170(s), 1024(w), 940(vs), 906(msh), 784(s), 557(s), 518(s), 478(s), 365(m), 288(m). Analysis for $WSO_4C_{16}H_{36}$ (Calc.): C, 37.6 (37.8); H, 7.0 (7.1); S, 6.5 (6.3)%. The mass spectrum showed a weak molecular ion at $m/z = 508$ and a *t*-butyl$^+$ parent ion at $m/z = 57$ as well as numerous other ions.

$W(S)(OPr^i)_4$

$LiOPr^i$ (1.04 g, 15.7 mmol) was placed in a large Schlenk tube equipped with a stirbar. Diethyl ether (40 cm^3) was added and the solution cooled to −78°C. $WSCl_4$ (1.40 g, 3.9 mmol) was added with stirring over 3 h via an addition tube with the solution changing from colorless to yellow to brown. The solution was allowed to stir 6 h and warmed to room temperature. LiCl was filtered off using a medium frit and the solution evaporated to dryness *in vacuo*, leaving an oily red residue. This was taken up in 20 cm^3 of CH_2Cl_2, allowed to stand for an hour, then the solvent removed *in vacuo*, leaving an orange solid. Sublimation at 50°C, 10^{-4} torr onto a water-cooled probe gave the product as a pale orange powder. ^1H NMR data (25°C. d_6-benzene): δ 1.32 ppm (d, $^3J_{H-H} = 6.14$ Hz, 6H), 5.25 ppm (septet, 1H). IR data (Nujol mull, CsI plates, cm^{-1}): 1320(m), 1258(w), 1164(s), 1126(ssh), 1113(vs), 975(vs), 846(s), 598(vs), 465(mbr), 425(msh), 300(mbr). Solution IR (hexane, KBr cavity cell) also shows $\tilde{\nu}$(W=S) at 540(m) cm^{-1}. Analysis for $WSO_4C_{12}H_{28}$ (Calc.): C, 31.6 (31.9); H, 6.1 (6.2); S, 7.0 (7.1)%. This product can also be obtained substituting $NaOPr^i$ in place of $LiOPr^i$ or by reacting $W(S)(OBu^t)_4$ with 4 equiv isopropanol overnight in toluene. The original method, given above, gave the best yields.

Attempted desulfurization and comproportionation reactions involving $W(S)(OBu^t)_4$

(a) $W(S)(OBu^t)_4$ (0.50 g, 0.98 mmol) was placed in a 50-cm^3 Schlenk flask equipped with a stirbar. Toluene (20 cm^3) was added via syringe, stirring commenced, and PPh_3 (0.129 g, 0.49 mmol) was added via a sidearm addition tube over $\frac{1}{2}$ h. The solution was stirred for 24 h, then heated to 50°C and stirred for an additional 24 h. The solvent was then removed *in vacuo*. ^1H NMR spectroscopy of

Table 4. Summary of crystal data for $W(S)(OBu^t)_4$

Empirical formula	$WC_{16}H_{36}O_4S$
Color of crystal	Pale yellow
Crystal dimensions (mm)	$0.05 \times 0.06 \times 0.06$
Space group	$P\bar{1}$
Cell dimensions	
Temperature (°C)	−160
a (Å)	9.130(2)
b (Å)	14.008(4)
c (Å)	9.217(2)
α (°)	101.49(1)
β (°)	113.48(1)
γ (°)	94.81(1)
Z (molecules/cell)	2
Volume (Å^3)	1041.92
Calculated density (g cm^{-3})	1.620
Wavelength (Å)	0.71069
Molecular weight	508.37
Linear absorption coefficient (cm^{-1})	57.706
Detector to sample distance (cm)	22.5
Sample to source distance (cm)	23.5
Average omega scan width at half height (°)	0.25
Scan speed (deg min^{-1})	4.0
Scan width (deg+dispersion)	2.0
Individual background (s)	4
Aperture size (mm)	3.0×4.0
Two-theta range (°)	6–45
Total number of reflections collected	2832
Number of unique intensities	2728
Number with $F > 3.00\sigma(F)$	2636
$R(F)$	0.0187
$R_w(F)$	0.0215
Goodness of fit for the last cycle	0.833
Maximum delta/sigma for last cycle	0.05

the residue revealed only unreacted $W(S)(OBu^t)_4$ and PPh_3.

(b) $W(S)(OBu^t)_4$ (0.43 g, 0.84 mmol) was placed in a 50-cm^3 Schlenk flask equipped with a stirbar. Hexane (20 cm^3) was added, followed by PBu^n_3 (105 μl, 0.42 mmol). The solution was stirred for 24 h, and then the solvent was removed *in vacuo*. ^1H NMR spectroscopy of the residue showed unreacted $W(S)(OBu^t)_4$.

Attempted comproportionation reactions involving $W(S)(OR)_4$ *and* $W{\equiv}W^{6+}$ *species*

Reactions performed in attempts to synthesize a compound of the formula $W_3(\mu_3\text{-}S)(OR)_{10}$ (R = Pr^i or CH_2Bu^t) are summarized in Table 3. In no case was there ^1H NMR spectroscopic evidence demonstrating the formation of such a species. The only compounds identified in the reaction mixtures (via ^1H NMR spectroscopy) were $W(S)(OR)_4$* and in cases where excess alcohol was used $W(OR)_6$ (R = Pr^i or CH_2Bu^t).

Crystallographic study of $W(S)(OBu^t)_4$

General operating procedures have been described previously.[28] Crystal data for $W(S)(OBu^t)_4$ are summarized in Table 4.

A suitable equidimensional fragment was cleaved from a large plate and transferred to the goniostat using standard inert atmosphere handling techniques and cooled to $-160°C$ for characterization and data collection. The sample remaining in the glovebag darkened rapidly, indicating extreme sensitivity.

A systematic search of a limited hemisphere of reciprocal space yielded a set of diffraction maxima with no systematic absences or symmetry, and was thus indexed as triclinic. The structure was successfully solved via a Patterson function and refined in the centrosymmetric space group $P\bar{1}$. All atoms including hydrogens were located and refined.

A final difference Fourier was featureless, the largest peak being 1.21 e $Å^{-3}$ located at the metal site, the next largest peak being 0.42 e $Å^{-3}$.

Final atomic parameters, full lists of bond distances and angles and F_o/F_c values have been deposited as supplementary materials with the Editor from whom copies are available upon request. Atomic coordinates have also been deposited with the Cambridge Crystallographic Data Center.

Acknowledgements—We thank the National Science Foundation and the Wrubel Computing Center for support.

* Reaction of $W(S)(OBu^t)_4$ and 4 equivalents of neopentanol in toluene gives a very air-sensitive mixture whose major product is believed to be $W(S)(OCH_2Bu^t)_4$ and which displays ^1H NMR resonances at δ = 1.06 and 4.54 ppm, consistent with products obtained in attempted comproportionations using excess neopentanol.[27]

REFERENCES

1. See, for example, A. Gaunt, *Catalysis*, **1**. Special Report, Chemical Society (1977); V. Ponec, *Catal. Rev. Sci. Eng.* 1978, **18**, 151.
2. E. Stiefel, *Prog. Inorg. Chem.* 1977, **22**, 1.
3. A. Müller, R. Jostes and F. A. Cotton, *Angew. Chem., Int. Ed. Engl.* 1980, **19**, 875.
4. M. H. Chisholm, K. Folting, J. C. Huffman and C. C. Kirkpatrick, *Inorg. Chem.* 1984, **23**, 1021.
5. M. H. Chisholm, K. Folting, J. C. Huffman and E. M. Kober, *Inorg. Chem.* 1985, **24**, 241.
6. M. H. Chisholm, D. M. Hoffman and J. C. Huffman, *Inorg. Chem.* 1985, **24**, 796.
7. H. Vahrenkamp, *Angew. Chem., Int. Ed. Engl.* 1975, **14**, 322.
8. D. M. Berg and P. Sharp, 190th Annual Meeting, American Chemical Society, Chicago, Abstract INOR 109 (1985).
9. H. Funk, W. Weiss and G. Mohaupt, *Z. Anorg. Allg. Chem.* 1960, **304**, 128.
10. M. H. Chisholm and J. W. Pasterczyk, unpublished results.
11. D. Szeymies, D. Krebs and G. Henkel, *Angew. Chem., Int. Ed. Engl.* 1984, **23**, 804.
12. J. Money, J. C. Huffman and G. Christou, *Inorg. Chem.* 1985, **24**, 3297.
13. P. Blower, J. Dilworth, J. Hutchinson and J. Zubieta, *Inorg. Chim. Acta* 1982, **65**, L225.
14. M. Sato, K. Miller, J. Enemark, C. Strouse and K. Callahan, *Inorg. Chem.* 1981, **20**, 3571.
15. K. Callahan and P. Durand, *Inorg. Chem.* 1980, **19**, 3211.
16. *Handbook of Chemistry and Physics*, 63rd Edn. CRC Press, Cleveland, OH (1982).
17. M. H. Chisholm, *Polyhedron* 1983, **2**, 681.
18. M. Drew and R. Mandyczewsky, *J. Chem. Soc. A* 1970, 2815.
19. D. Britnell, G. Fowles and R. Mandyczewsky, *J. Chem. Soc., Chem. Commun.* 1970, 608.
20. E. Page, D. Rice, K. Hagen, L. Hedberg and K. Hedberg, *Inorg. Chem.* 1982, **21**, 3280.
21. P. Jones, W. Levason, J. Ogden, J. Turff, E. Page and D. Rice, *J. Chem. Soc., Dalton Trans.* 1983, 2625.
22. W.-H. Pan, T. Chandler, J. Enemark and E. Stiefel, *Inorg. Chem.* 1984, **23**, 4265.
23. S. Cohen and E. Stiefel, *Inorg. Chem.* 1985, **24**, 4657.
24. I. Topol, A. Chesnyi, K. Kovba and N. Stepanov, *Chem. Phys.* 1980, **53**, 63.

25. N. S. Marchant, Ph.D. thesis, Indiana University (1986).
26. D. Britnell, G. Fowles and D. Rice, *J. Chem. Soc., Dalton Trans.* 1974, 2191.
27. M. H. Chisholm and J. W. Pasterczyk, unpublished results.
28. K. G. Caulton, J. C. Huffman and L. N. Lewis, *Inorg. Chem.* 1980, **19**, 2755.

Polyhedron Vol. 6, No. 7, pp. 1559–1562, 1987
Printed in Great Britain

0277–5387/87 $3.00+.00

He I PHOTOELECTRON SPECTROSCOPIC STUDY OF *CLOSO*-DICARBADODECABORANES AND THEIR 9-HALOGENO DERIVATIVES

TOMÁŠ VONDRÁK

ESCA Centre, The J. Heyrovský Institute of Physical Chemistry and Electrochemistry, Czechoslovak Academy of Sciences, Vlašská 9, 11840 Prague, Czechoslovakia

(*Received* 5 *December* 1986; *accepted* 28 *January* 1987)

Abstract—He I photoelectron spectra of the *closo*-carboranes 1,2-$C_2B_{10}H_{12}$ and 1,7-$C_2B_{10}H_{12}$, and their 9-halogeno derivatives are reported. The low ionization energy bands are gathered into two groups. The MNDO quantum chemical method provides the same picture and indicates that these bands correspond predominantly to the B—H (C—H) bonding molecular orbitals. Bromine and iodine bring about an almost uniform increase in ionization energies whereas the shape of the low ionization energy features of the chloro derivatives differ from those of the parent compounds. This effect is interpreted by the conjugative interaction of cluster π-type orbitals with the chlorine non-bonding orbitals.

The *closo*-carboranes form a group of polyhedral molecules of particular interest from the viewpoint of multicentre bonding.[1] The interest in the electronic structure of this class of compounds is stimulated by their analogy with transition-metal cluster compounds through the isolobal principle.[2] Numerous quantum chemical calculations on these compounds have been reported.[3–7] The MNDO calculated MO energies are in reasonably good agreement with those obtained by the *ab initio* method[8] and Stone's tensor surface harmonic approach.[9–11]

To our knowledge no attempt has been made to compare the calculated orbital energies with the energies of ionic states accessible by UV photoelectron (PE) spectroscopy. Fehlner *et al.* used the equatorial-apex model[3] for a discussion of the PE spectra of some thiaboranes and the effect of the exo substituent.[12]

We report here the He I PE spectra of the *closo*-carboranes 1,2-$C_2B_{10}H_{12}$ (**1a**) and 1,7-$C_2B_{10}H_{12}$ (**2a**), as well as the spectra of their 9-chloro derivatives (**1b** and **2b**), 9-iodo derivatives (**1d** and **2d**), and 9-Br-1,2-$C_2B_{10}H_{12}$ (**1c**), together with the results of the MNDO calculations on the non-substituted species.

The PE spectra can be divided into three regions labeled A–C (Figs 1 and 2). In region A four overlapping bands (1–4) and a well-resolved band (5) are found in the spectrum of **1a**. Only four bands are observed within this region in the spectrum of **2a**. Four and three ionization events are observed in region B of the spectrum of the *ortho* and the *meta* isomer, respectively. A vibrational fine structure corresponding to a wavenumber of 720 cm^{-1} is observed in region C of the spectrum of **2a**. The *ortho* isomer has only two broad features in this region.

To interpret the spectral bands we apply Koopmans theorem allowing the correlation of the ionic state energies with the orbital energies of the ground state.[13]

The MNDO calculations on **1a** and **2a** provide the 15 outermost occupied levels gathered into two groups (Table 1). For **1a** the HOMO and five levels are within a 0.6-eV interval. The two nearly degenerate MOs are separated by 0.5 eV and the following MO lies 0.6 eV lower (Table 2). Hence we can tentatively assign bands 1–3 to the $6b_1$, $6b_2$, $10a_1$, $3a_2$, $9a_1$ and $5b_2$ MOs, band 4 to the $2a_2$ and $5b_1$ MOs, and band 5 to the $8a_1$ MO. For **2a** the nine outermost MOs lie in a narrower interval and no level is markedly separated from the others. Thus any detailed assignment of region A is not possible since there is no hint how to assign nine levels to the four observed bands. The six MOs lying between -15 and -17 eV correspond to the bands observed in region B. It follows from the composition of the MOs that the ionizations found in

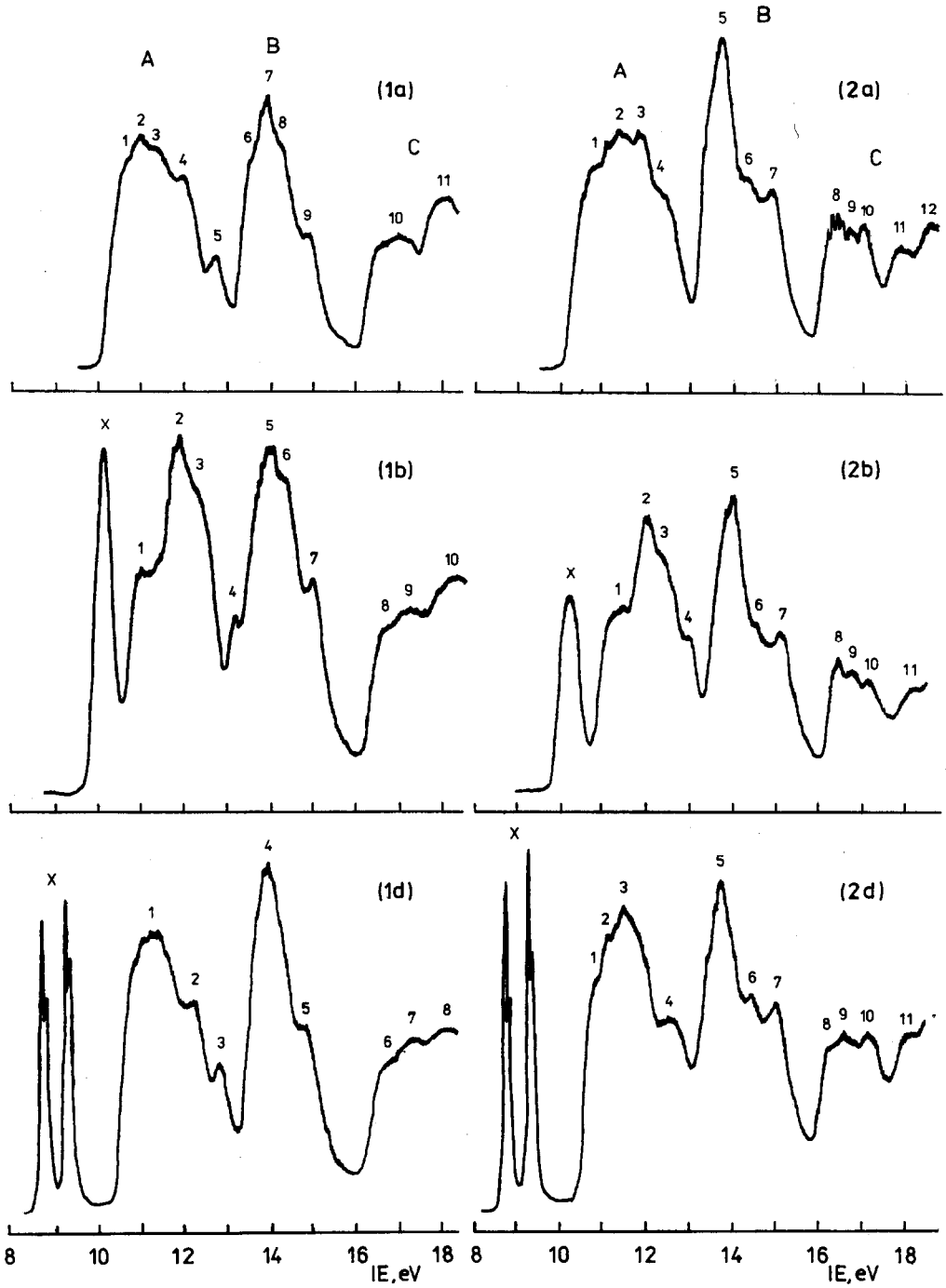

Fig. 1. He I photoelectron spectra of 1,2-$C_2B_{10}H_{12}$ (**1a**), 9-Cl-1,2-$C_2B_{10}H_{11}$ (**1b**), 9-I-1,2-$C_2B_{10}H_{11}$ (**1d**), 1,5-$C_2B_{10}H_{12}$ (**2a**), 9-Cl-1,5-$C_2B_{10}H_{11}$ (**2b**) and 9-I-1,5-$C_2B_{10}H_{11}$ (**2d**).

regions A and B come mainly from the B—H (C—H) bonding MOs. The sharp bands at low ionization energy (IE) which are observed in the spectra of the halogeno derivatives come unambiguously from ionizations of the halogen lone pairs. The spin–orbit splitting of the lone-pair ionization found in the spectra of the iodo derivatives and the bromo derivative amounts to 0.27 and 0.54 eV, respectively. The value of the spin–orbit splitting found for tertiary alkyl iodides is only 0.01 eV higher, and the shape of the peaks is identical. The low IE component of the lone-pair band broadens with increasing conjugative interaction between the halogen and the alkyl.[14] The FWHM of the spin–orbit components in the iodo derivatives are 0.16 and 0.18 eV for the high and the low one, respect-

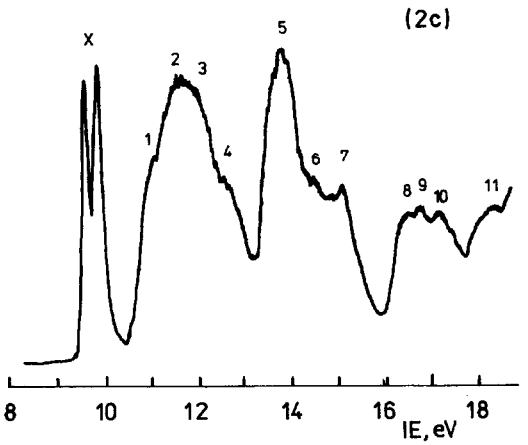

Fig. 2. He I photoelectron spectrum of 9-Br-1,5-$C_2B_{10}H_{11}$ (**2c**).

ively (0.19 and 0.26 eV for tertiary aliphatic alkyl iodides[15]). Hence the degree of conjugation between halogen lone pairs and carborane skeleton π-orbitals* is essentially the same as in the alkyl halogenides. The identical shape of the bands within region A of the spectra of the iodo and bromo derivatives, and an almost uniform shift of all bands to a higher IE, corroborate this conclusion since no carborane MO is markedly stabilized.

Region A of the spectra of the chloro derivatives **1b** and **2b** differs significantly from those of the parent compound. Band 1 is more resolved and band 2 increases in intensity. We believe that this demasking of band 1 is due to the stabilization of the carborane π-orbitals. The HOMO ($6b_1$) and HOMO-3 ($10a_1$) in **1a** and HOMO ($10a_1$) and HOMO-4 ($6b_2$) in **2a** have a significantly higher localization on atom B(9) (Table 1). Thus these MOs can be stabilized by a conjugative interaction. The absence of this effect in the spectra of the bromo and iodo derivatives could be rationalized by a smaller resonance integral and/or by an increase in the energy difference between the interacting orbitals.

For the MNDO calculation the experimental internal coordinates[16] of the heavy atoms have been used and the coordinates for the hydrogen atoms were allowed to relax.

The He I PE spectra were recorded on a VG Scientific UVG 3 spectrometer. The resolution (FWHM) was 30–40 meV through the entire spectrum. An Ar–Xe mixture has been used as the internal calibrant.

* π-Orbitals are composed from the boron *p*-orbitals tangential to the surface of the cluster.

Table 1. Calculated MO energies and composition of MOs for **1a** and **2a**

1,2-$C_2B_{10}H_{12}$ (**1a**)				1,7-$C_2B_{10}H_{12}$ (**2a**)			
C_s	$-\varepsilon$ (eV)	H (%)[a]	B(9) (%)[b]	C_s	$-\varepsilon$ (eV)	H (%)[a]	B(9) (%)[b]
$6b_1$	12.34	18	13	$10a_1$	12.23	2	16
$6b_2$	12.38	1	1	$3a_2$	12.34	14	9
$10a_1$	12.45	23	1	$6b_1$	12.46	23	6
$3a_2$	12.57	23	6	$9a_1$	12.72	30	6
$9a_1$	12.75	36	2	$6b_2$	12.77	23	12
$5b_2$	12.93	35	0	$5b_1$	13.12	16	7
$2a_2$	13.39	35	6	$8a_1$	13.22	39	7
$5b_1$	13.41	21	0	$2a_2$	13.53	21	1
$8a_1$	14.11	16	6	$5b_2$	13.75	12	1
$4b_1$	15.35	27	0	$4b_1$	15.17	40	2
$4b_2$	15.50	31	0	$7a_1$	15.28	40	9
$7a_1$	15.71	34	6	$4b_2$	15.67	38	0
$3b_1$	16.16	43	0	$3b_1$	16.19	42	10
$6a_1$	16.49	41	6	$3b_2$	16.45	41	0
$3b_2$	16.97	39	12	$6a_1$	16.92	41	4
$5a_1$	19.36	35	1	$5a_1$	19.05	27	4

[a] The sum of squares of atomic-orbital coefficients over all hydrogen atoms.

[b] Localization on B atom in position 9.

Table 2. Experimental vertical ionization energies (eV)[a]

Band	Compound						
	1a	**1b**	**1d**	**2a**	**2b**	**2c**	**2d**
X[b]		10.16	8.71[c]		10.12	9.64[c]	8.80[c]
			9.25[c]			9.91[c]	9.34[c]
1	10.62	11.11	11.37	10.78	11.43	11.13	10.93
2	10.93	11.90	12.17	11.36	12.04	11.65	11.23
3	11.35	12.32	12.81	11.82	12.30	12.04	11.61
4	11.92	13.17	13.94	12.29	12.91	12.67	12.64
5	12.64	14.01	14.77	13.74	13.96	13.80	13.77
6	13.48	14.30	16.79	14.35	14.51	14.49	14.48
7	14.14	14.98	17.37	14.89	15.07	15.10	15.07
8	14.77	16.76	18.22	16.29[d]	16.40	15.07	16.32
9	16.88	17.17		16.71	16.74	16.74	16.63
10	17.97	18.39		16.99	17.13	17.14	17.18
11				17.84	18.13	18.24	18.12
12				18.64			

[a] Estimated error 0.05 eV.
[b] Halogen non-bonding orbitals.
[c] Spin–orbit components.
[d] Vibrational fine structure (720 cm^{-1}).

Acknowledgement—I thank J. Dolanský, Institute of Inorganic Chemistry, Czechoslovak Academy of Sciences, for the loan of the samples.

REFERENCES

1. R. N. Grimes, *Carboranes*. Academic Press, New York (1970).
2. R. W. Rudolph, *Acc. Chem. Res.* 1976, **9**, 446.
3. R. Hoffmann and W. N. Lipscomb, *J. Chem. Phys.* 1962, **36**, 2179.
4. R. B. King and D. H. Rowray, *J. Am. Chem. Soc.* 1977, **99**, 7834.
5. D. A. Dixon, D. A. Kleier, T. A. Halgren, J. H. Hall and W. N. Lipscomb, *J. Am. Chem. Soc.* 1977, **99**, 6226.
6. J. Bicerano, D. S. Marinick and W. N. Lipscomb, *Inorg. Chem.* 1978, **17**, 3443.
7. R. B. King and D. M. Rouvray, *J. Am. Chem. Soc.* 1977, **99**, 7834.
8. M. J. S. Dewar, *Inorg. Chem.* 1980, **19**, 2862.
9. P. Brint, J. P. Cronin, E. Seward and T. Whelan, *J. Chem. Soc., Dalton Trans.* 1983, 975.
10. A. J. Stone, *Mol. Phys.* 1980, **19**, 1319.
11. A. J. Stone and M. J. Alderton, *Inorg. Chem.* 1982, **21**, 2297.
12. T. P. Fehlner, M. Wu, B. J. Menengheli and R. W. Rudolph, *Inorg. Chem.* 1980, **19**, 49.
13. T. Koopmans, *Physica* 1934, **1**, 104.
14. F. Brogli and E. Heilbronner, *Helv. Chim. Acta* 1971, **54**, 1423.
15. R. G. Dromey and J. B. Peel, *J. Mol. Struct.* 1974, **23**, 53.
16. R. K. Bohn and M. D. Bohn, *Inorg. Chem.* 1971, **10**, 350.

Polyhedron Vol. 6, No. 7, pp. 1563–1569, 1987
Printed in Great Britain

0277–5387/87 $3.00+.00

POLYMERIZATION REACTIONS IN $[Co(NH_3)_5(H_2O)][CoX(CN)_5]$ AND *CIS*-$[Co(NH_3)_4(H_2O)_2][CoX(CN)_5]$ (X = Cl, Br, I, NO_2 OR N_3) DOUBLE-COMPLEX SALTS

T. FLOR and J. CASABÓ*

Departament de Química, Universitat Autónoma de Barcelona, i Institut de Ciència dels Materials, C.S.I.C., Bellaterra, 08193 Barcelona, Spain

(*Received* 5 *January* 1987; *accepted* 28 *January* 1987)

Abstract—Polymerization reactions of $[Co(NH_3)_5(H_2O)][CoX(CN)_5]$ and *cis*-$[Co(NH_3)_4(H_2O)_2][CoX(CN)_5]$ (X = Cl, Br, I, NO_2 or N_3] have been studied. The compounds undergo aging reactions in the solid state or in solution induced by the ligand X involving solvolytic processes affording polymeric materials with μ-cyano bridges. A mechanistic explanation of these reactions is given and a comparison between both series of compounds together with the parent compound $[Co(NH_3)_6][Co(CN)_6]$ is discussed.

The dehydration–anation reaction of double-complex salts of type:

$$[Co(NH_3)_5(H_2O)][Co(CN)_6] \rightarrow [(NH_3)_5Co—NC—Co(CN)_5]+H_2O \quad (1)$$

is well known.

Many examples of this reaction have been reported in the literature, and a number of μ-CN dinuclear complexes have been synthesized by this method, employing different amminated or aminated cationic aquo complexes and cyanurated anions.[1,2]

The physical and chemical properties of these μ-CN dinuclear complexes have been studied.[3] The kinetic parameters of such reactions have been currently studied in a series of double-complex salts containing different cations but the same anion. The aim of such work is to understand the influence of the varying cation in the kinetic parameters and to propose a realistic mechanism for the reaction.

We have reported a complete kinetic–mechanistic study of the reaction:

$$[Co(NH_3)_5(H_2O)][CoX(CN)_5] \rightarrow [(NH_3]_5Co—NC—CoX(CN)_4]+H_2O$$

in order to understand the influence of the anion.[4] The unit-cell parameters of these double-complex salts are modified by the different X groups; consequently, variation in the lattice free spaces allows a study of their influence in the activation energy and kinetic parameters of the solid-state process, we have proposed an S_N1 mechanism with a Frenkel-type defect and a square-base pyramid as an activated complex according to the House and LeMay nomenclature.[5,6] In the course of these studies, we have observed significant differences in the behaviour of the double-complex salts with the $[CoX(CN)_5]^{3-}$ anions or the simpler one $[Co(CN)_6]^{3-}$, and the $[Co(NH_3)_4(H_2O)_2]^{3+}$ and $[Co(NH_3)_5(H_2O)]^{3+}$ cations. We have, therefore, made a complete comparative study of the corresponding dehydration–anation reaction, the results of which are reported in this paper.

EXPERIMENTAL

Synthesis of the new compounds cis-$[Co(NH_3)_4(H_2O)_2][CoX(CN)_5]$ (X = Cl, Br, I, NO_2, N_3 *or* CN)

Starting materials such as *cis*-$[Co(NH_3)_4(H_2O)_2](ClO_4)_3$,[7] $K_3[CoN_3(CN)_5]$[8] and $K_3[Co(CN)_6]$[9] were prepared by literature methods. Acidopentacyanocobaltates(III) salts of type $K_3[CoX(CN)_5]$ were prepared by a method already reported by us.[10]

Double-complex salts, *cis*-$[Co(NH_3)_4(H_2O)_2]$

* Author to whom correspondence should be addressed.

$[CoX(CN)_5]$ (X = Cl, Br, I, NO_2, N_3 or CN), were synthesized by precipitation from their corresponding compounds. In a typical experiment, $NaClO_4$ (2.0 g) was added to a solution of $K_3[CoCl(CN)_5]$ (1.2 g) in a water–acetic acid mixture (5 : 1, 6 cm^3). $KClO_4$ precipitated immediately and was discarded. To the clear solution *cis*-$[Co(NH_3)_4(H_2O)_2](ClO_4)_3$ (1.2 g) was added in small portions with continuous stirring until all the solid was dissolved. Then glacial acetic acid was added, resulting in the formation of an orange-pink precipitate which was filtered, washed with ethanol, and dried *in vacuo*. Yields were about 65%, and the analytical data were in agreement with the formula proposed in all cases (Table 1).

Synthesis of the compounds $[Co(NH_3)_5(H_2O)][CoX(CN)_5]$ (X = Cl, Br, I, NO_2, N_3 *or* CN)

These compounds were synthesized according to the procedure already reported by us.[4]

Physical measurements

IR spectra were measured on a Beckman IR-20 spectrophotometer as KBr pellets. Electronic spectra were measured in aqueous solution on a Beckman Acta III and a Shimadzu UV-240 spectrophotometer. The electronic spectra of the insoluble compounds were measured as KBr pellets on the Beckman Acta III instrument. Powder X-ray diffraction were done on a Phillips diffractometer. Molar conductivities were measured on a Radiometer CDM-3 conductivitimeter. Thermogravimetric analyses were done on a Perkin–Elmer TGS-2 and a Rigaku Thermoflex system. C, H and N microanalyses were performed on a Perkin–Elmer 240 microanalyzer. Co analyses were done by a complexometric method with EDTA.[12]

RESULTS

Spectral measurements

We have already reported[4] that the compounds $[Co(NH_3)_5(H_2O)][CoX(CN)_5]$ (X = Cl, Br, I, NO_2, N_3 or CN) are isomorphous. The tetrammine series also shows a similar behaviour (Table 2), and both series are isostructural with the parent compound $[Co(NH_3)_6][Co(CN)_6]$, the crystalline structure of which has been resolved by X-ray diffraction method. The latter compound has a trigonally distorted CsCl structure distorted affecting spatial group $R\bar{3}$.[12] The isostructuralism with the aquoammine complexes may be explained assuming a disorder of the water molecules in the coordination sphere of Co(III) ion as has been proved in other cases too.[13]

The electronic spectra of these compounds in aqueous solution are reported in Table 3. All of them show two bands in the visible and near-UV region. The former bands at higher energies are attributed to the first *d–d* transition of the anionic moiety while the latter ones at lower frequencies are assigned to the first *d–d* transition of the cationic moiety. The second band always exhibits less intensity than the first one, and apparently seems to be partially overlapped by this band. It is, therefore, necessary to have a Gaussian analysis of these bands to ascertain the position of the maximum of the less intense band. Both these bands appear to have the same energy as in the simple salts of both anionic and cationic species, showing the presence of the amminated cation and cyanurated anion in the compound without significant interactions between them.

Table 1. Analytical data

Compound	C Calc. (found)	H Calc. (found)	N Calc. (found)	Co Calc. (found)	H_2O^a Calc. (found)
$[Co(NH_3)_5(H_2O)][CoCl(CN)_5]$	15.5 (16.2)	36.2 (36.5)	4.4 (4.5)	30.5 (30.4)	4.7 (4.6)
$[Co(NH_3)_5(H_2O)][CoBr(CN)_5]$	14.0 (14.1)	32.5 (32.8)	4.0 (4.2)	27.4 (27.4)	4.2 (4.1)
$[Co(NH_3)_5(H_2O)][CoI(CN)_5]$	12.5 (12.7)	29.3 (28.7)	3.5 (3.5)	24.7 (25.1)	3.8 (3.5)
$[Co(NH_3)_5(H_2O)][CoN_3(CN)_5]$	15.3 (15.5)	46.3 (46.8)	4.3 (4.3)	30.1 (29.6)	4.6 (4.1)
$[Co(NH_3)_5(H_2O)][CoNO_2(CN)_5]$	15.1 (15.3)	38.8 (38.4)	4.3 (4.3)	29.7 (29.3)	4.5 (4.2)
cis-$[Co(NH_3)_4(H_2O)_2][CoCl(CN)_5]$	15.5 (15.6)	32.5 (31.4)	4.1 (4.3)	30.4 (30.1)	9.3 (8.6)
cis-$[Co(NH_3)_4(H_2O)_2][CoBr(CN)_5]$	13.9 (14.1)	29.2 (28.7)	3.7 (3.8)	27.3 (27.7)	8.3 (8.0)
cis-$[Co(NH_3)_4(H_2O)_2][CoI(CN)_5]$	12.5 (13.5)	26.3 (26.3)	3.3 (3.3)	24.6 (24.6)	— —
cis-$[Co(NH_3)_4(H_2O)_2][CoN_3(CN)_5]$	15.2 (15.4)	42.3 (42.3)	4.1 (4.0)	29.9 (29.3)	9.1 (8.5)
cis-$[Co(NH_3)_4(H_2O)_2][CoNO_2(CN)_5]$	15.1 (15.4)	35.2 (35.0)	4.0 (4.1)	29.6 (29.2)	9.0 (8.3)

[a] H_2O values are measured by thermogravimetric methods.

Table 2. X-ray powder diffraction data for the double-complex salts

Compound	2θ (°)	d (Å)	hkl	$100I/I_o$
$[Co(NH_3)_5(H_2O)][Co(CN)_6]$	16.43	5.40	$10\bar{1}$	95
	18.04	4.92	110	40
	30.25	2.95	$21\bar{1}$	100
$[Co(NH_3)_5(H_2O)][CoCl(CN)_5]$	16.53	5.36	$10\bar{1}$	100
	19.13	4.64	110	50
	30.38	2.94	$21\bar{1}$	65
$[Co(NH_3)_5(H_2O)][CoBr(CN)_5]$	16.40	5.41	$10\bar{1}$	100
	18.95	4.68	110	55
	30.15	2.95	$21\bar{1}$	64
$[Co(NH_3)_5(H_2O)][CoI(CN)_5]$	16.25	5.46	$10\bar{1}$	99
	18.75	4.73	110	80
	28.93	3.09	$21\bar{1}$	100
$[Co(NH_3)_5(H_2O)][CoN_3(CN)_5]$	16.10	5.51	$10\bar{1}$	100
	19.15	4.64	110	73
	29.95	2.98	$21\bar{1}$	78
$[Co(NH_3)_5(H_2O)][CoNO_2(CN)_5]$	16.55	5.36	$10\bar{1}$	100
	18.60	4.77	110	33
	30.25	2.97	$21\bar{1}$	33
cis-$[Co(NH_3)_4(H_2O)_2][CoCl(CN)_5]$	16.70	5.31	$10\bar{1}$	100
	19.30	4.60	110	45
	30.70	2.91	$21\bar{1}$	65
cis-$[Co(NH_3)_4(H_2O)_2][CoBr(CN)_5]$	16.35	5.42	$10\bar{1}$	100
	18.85	4.71	110	70
	30.05	2.97	$21\bar{1}$	90
cis-$[Co(NH_3)_4(H_2O)_2][CoI(CN)_5]$[a]				
cis-$[co(NH_3)_4(H_2O)_2][CoN_3(CN)_5]$	16.20	5.47	$10\bar{1}$	100
	19.20	4.62	110	65
	30.20	2.96	$21\bar{1}$	65
cis-$[Co(NH_3)_4(H_2O)_2][CoNO_2(CN)_5]$	16.60	5.33	$10\bar{1}$	100
	18.75	4.73	110	75
	30.50	2.93	$21\bar{1}$	75

[a] Values for this compound were not found due to fast polymerization.

Table 4 shows the most significant bands in the IR spectra of these compounds. The CN stretching mode is very characteristic, appearing as a strong and narrow band at 2120 cm^{-1}. Sometimes a weak band appearing at slightly higher frequencies is also assigned to the same mode perturbed by hydrogen bonding.[14]

Thermal behaviour of *cis*-$[Co(NH_3)_4(H_2O)_2][CoX(CN)_5]$ (X = Cl, Br, I, NO_2, N_3 *or* CN)

Thermogravimetric measurements show as the first step, for all these compounds, the loss of two water molecules, so a difficulty in isolating dinuclear compounds with a μ-CN ligand of the type indicated in reaction (2) could be expected:

$$[Co(NH_3)_4(H_2O)_2][CoX(CN)_5] \rightarrow [(NH_3)_4(H_2O)Co—NC—CoX(CN)_4] + H_2O. \quad (2)$$

The heating of these double complexed salts in the solid state does not give isolable μ-CN dinuclear compounds, unlike the pentammine series, but insoluble compounds for which IR spectrum displays two bands of equal intensity in the CN stretching mode region. The appearance of two bands in this region is attributed to two different types of CN bonds. Terminal —CN bonds appear at lower frequency while bridging —CN— bonds appear at

Table 3. Electronic spectra for $[Co(NH_3)_5(H_2O)][CoX(CN)_5]$ and *cis*-$[Co(NH_3)_4(H_2O)_2][CoX(CN)_5]$

Compound	Medium	λ (nm)	Assignment
$[Co(NH_3)_5(H_2O)](ClO_4)_3$	H_2O	490 342	$^1A_1 \rightarrow {}^1E\,(C_{4v})$ $^1A_1 \rightarrow {}^1A_2\,(C_{4v})$ $^1A_{1g} \rightarrow {}^1T_{2g}\,(O_h)$
$[Co(NH_3)_5(H_2O)][CoCl(CN)_5]$	KBr (solid)	505 385–390	$^1A_1 \rightarrow {}^1E\,(C_{4v})$ $^1A_1 \rightarrow {}^1A_2\,(C_{4v})$ $^1A_1 \rightarrow {}^1E\,(C_{4v})$
$[Co(NH_3)_5(H_2O)][CoBr(CN)_5]$	KBr (solid)	510 395	$^1A_1 \rightarrow {}^1E\,(C_{4v})$ $^1A_1 \rightarrow {}^1A_2\,(C_{4v})$ $^1A_1 \rightarrow {}^1E\,(C_{4v})$
$[Co(NH_3)_5(H_2O)][CoI(CN)_5]$	H_2O	495 $\simeq$ 440(sh) 329	$^1A_1 \rightarrow {}^1E\,(C_{4v})$ $^1A_1 \rightarrow {}^1A_2\,(C_{4v})$ $^1A_1 \rightarrow {}^1E\,(C_{4v})$ $\pi \rightarrow d_{z^2}$
$[Co(NH_3)_5(H_2O)][CoN_3(CN)_5]$	H_2O	485–490 378	$^1A_1 \rightarrow {}^1E\,(C_{4v})$ $^1A_1 \rightarrow {}^1A_2\,(C_{4v})$ $^1A_1 \rightarrow {}^1E\,(C_{4v})$
$[Co(NH_3)_5(H_2O)][CoNO_2(CN)_5]$	H_2O	490–500 370 280	$^1A_1 \rightarrow {}^1E\,(C_{4v})$ $^1A_1 \rightarrow {}^1A_2\,(C_{4v})$ $^1A_1 \rightarrow {}^1E\,(C_{4v})$ $d\pi \rightarrow \pi^*(NO_2^-)$
cis-$[Co(NH_3)_4(H_2O)_2](ClO_4)_3$	H_2O	505 357	$^1A_{1g} \rightarrow {}^1T_{1g}\,(O_h)$ $^1A_{1g} \rightarrow {}^1T_{2g}\,(O_h)$
cis-$[Co(NH_3)_4(H_2O)_2][CoCl(CN)_5]$	H_2O	500–505 389 $\simeq$ 320(sh)	$^1A_{1g} \rightarrow {}^1T_{1g}\,(O_h)$ $^1A_1 \rightarrow {}^1E\,(C_{4v})$ $^1A_1 \rightarrow {}^1A_2\,(C_{4v})$
cis-$[Co(NH_3)_4(H_2O)_2][CoBr(CN)_5]$	H_2O	500–505 395	$^1A_{1g} \rightarrow {}^1T_{1g}\,(O_h)$ $^1A_1 \rightarrow {}^1E\,(C_{4v})$
cis-$[Co(NH_3)_4(H_2O)_2][CoI(CN)_5]$	H_2O	495–500 $\simeq$ 440(sh) 329	$^1A_{1g} \rightarrow {}^1T_{1g}\,(O_h)$ $^1A_1 \rightarrow {}^1E\,(C_{4v})$ $\pi \rightarrow d_{z^2}$
cis-$[Co(NH_3)_4(H_2O)_2][CoN_3(CN)_5]$	H_2O	500–505 378	$^1A_{1g} \rightarrow {}^1T_{1g}\,(O_h)$ $^1A_1 \rightarrow {}^1E\,(C_{4v})$
cis-$[Co(NH_3)_4(H_2O)_2][CoNO_2(CN)_5]$	H_2O	500–505 $\simeq$ 345(sh) 282	$^1A_{1g} \rightarrow {}^1T_{1g}\,(O_h)$ $^1A_1 \rightarrow {}^1E\,(C_{4v})$ $d\pi \rightarrow \pi^*(NO_2^-)$

higher energies.[1,15] These solids are polymeric materials formulated as $Co_2(NH_3)_4(CN)_5X$.

Reaction (2) in aqueous solution was followed by spectrophotometric methods. As an example, the results for *cis*-$[Co(NH_3)_4(H_2O)_2][CoCl(CN)_5]$ were the following. At first it shows an electronic spectrum with two bands at 505 and 390 nm. The spectrum shifts to higher energies during the heating. When the spectrum remains constant a solid product can be collected by precipitation, showing bands at 490 and 345 nm in the electronic spectra in aqueous solution, and two bands in the CN stretching mode region in the IR spectra.

The first maximum (490 nm) is characteristic of a Co(III) ion in an octahedral environment of five nitrogens and one oxygen as in the $[Co(NH_3)_5(H_2O)]^{3+}$ ion. On the other hand, the second maximum (345 nm) is typical of a Co(III) ion surrounded by five carbons and one nitrogen as is known to occur in $[Co(—NC)(CN)_5]^{3-}$.[16] and $[Co(NH_3)(CN)_5]^{2-}$.[17] These results are identical for all the double salts discussed in this paper.

Table 4. Selected IR bands (cm^{-1})

Assignment	$[Co(NH_3)_5(H_2O)][CoX(CN)_5]$				
	X = Cl	X = Br	X = I	$X = N_3$	$X = NO_2$
$\nu_s(OH)$, $\nu_{as}(OH)$	3450–3500	3400–3500	3400–3600	3400–3500	3400–3600
$\nu(NH)$	3120–3280	3100–3280	3180–3280	3100–3280	3120–3260
$\nu(CN)$	2190	2190	2200	2180	
	2120	2120	2120	2115	2120
$\nu_a(NNN)^a$				2040	
$\delta_d(NH_3)$, $\delta(OH)$	1620	1600	1620	1610	1610
$\delta_s(NH_3)$, $\nu_{as}(NO_2)^b$	1395	1400	1390	1390	1380
$\nu_s(NO_2)$,^{b} $\delta_s(NH_3)$	1345	1350	1340	1340	1310–1340
$\nu_s(NNN)^a$				1290	
$\rho_r(NH_3)$, $\rho_r(H_2O)$, $\delta(ONO)^b$	840	850	840	840	840
$\delta(NNN)^a$			660		
			575		
$\rho_w(NO_2)^b$					600–590
$\nu(Co—C)$	410	410	415	405	410
$\delta(Co—C—N)$	360	360	360	360	360
$\delta(N—Co—N)$	300–310	320	310	310	310
	cis-$[Co(NH_3)_4(H_2O)_2][CoX(CN)_5]$				
	X = Cl	X = Br	X = I	$X = N_3$	$X = NO_2$
$\nu_s(OH)$, $\nu_{as}(OH)$	3360–3500	3340–3480	3360–3600	3360–3500	3360–3500
$\nu(NH)$	3080–3180	3080–3160	3080–3160	3100–3160	3100–3160
$\nu(CN)$	2190	2180	2180	2180	
	2120	2120	2120	2120	2120
$\nu_a(NNN)^a$				2040	
$\delta_d(NH_3)$, $\delta(OH)$	1620	1620	1640	1620	1620
$\delta_s(NH_3)$, $\nu_{as}(NO_2)^b$	1390	1385	1390	1380	1400–1380
$\nu_s(NO_2)$,^{b} $\delta_s(NH_3)$	1345	1340	1340	1340	1340
$\nu_s(NNN)^a$				1295	
$\rho_r(NH_3)$, $\rho_r(H_2O)$, $\delta(ONO)^b$	860	850	860	855	840–855
$\delta(NNN)^a$				670	
				580	
$\rho_w(NO_2)^b$					590–600
$\nu(Co—C)$	410	410	415	410	415
$\delta(Co—C—N)$	360	350	355		355
$\delta(N—Co—N)$	310	310	310	310–330	310–330

[a] For $[Co(NH_3)_5(H_2O)][CoN_3(CN)_5]$ and *cis*-$[Co(NH_3)_4(H_2O)_2][CoN_3(CN)_5]$.
[b] For $[Co(NH_3)_5(H_2O)][CoNO_2(CN)_5]$ and *cis*-$[Co(NH_3)_4(H_2O)_2][CoNO_2(CN)_5]$.

Solid-state reactions in the $[Co(NH_3)_5(H_2O)][CoX(CN)_5]$ *series*

In an earlier paper[4] we have reported the synthesis of dinuclear compounds with a μ-CN ligand according to the following reaction:

$$[Co(NH_3)_5(H_2O)][CoX(CN)_5] \rightarrow [(NH_3)_5Co—NC—CoX(CN)_4] + H_2O \quad (3)$$

(X = Cl, Br, I, NO_2, N_3 or CN). These dinuclear compounds are fairly stable, permitting to isolate, characterize and study them. However, they undergo reactions in the solid state as well as in solution as we have shown by spectrophotometric and ^{59}Co NMR spectroscopy.[4]

As a typical case, $[(NH_3)_5Co—NC—CoCl(CN)_4]$ was chosen. At first this compound shows bands at 388 and 470 nm. After 2 weeks, the compound was recrystallized by discarding the insoluble part. The compound obtained from the clear solution showed bands at 340–345 and 470 nm in the electronic spectrum in aqueous solution. The amminated Co(III)

cation does not change its electronic spectrum, while, on the contrary, the cyanurated Co(III) anion changes its spectrum, being finally similar to $[Co(—NC)(CN)_5]^{3-}$ and $[Co(NH_3)(CN)_5]^{2-}$ species.[16,17] Furthermore, chemical analyses showed a C : H : N ratio identical to the freshly prepared dinuclear compound, indicating that no loss of NH_3, $(CN)_2$ or H_2O had occurred. The compound showed an electrical conductivity of 520 Ω^{-1} mol^{-1} cm^2 and the presence of free chlorine. The IR spectrum was similar to the original complex. These results are similar for all pentamminaquocobalt(III) double salts.

DISCUSSION

It is known that by heating the double-complex salt $[Co(NH_3)_4(H_2O)_2][Co(CN)_6]$ the μ-CN dinuclear compound $[(NH_3)_4(H_2O)Co—NC—Co(CN)_5]$ is obtained,[18] and there is no report of polymerization problems in this case. A similar observation has been made in the case of the dinuclear compound, $[(NH_3)_5Co—NC—Co(CN)_5]$, obtained by controlled heating of $[Co(NH_3)_5(H_2O)][Co(CN)_6]$.[1] It is clear that the presence of the X ligands favours both the solution and solid-state processes with time shown by these compounds, and hence all mechanisms describing them must be taken into account. On the other hand, it is well known that the easy hydrolysis of the $[CoX(CN)_5]^{3-}$ ions gives $[Co(H_2O)(CN)_5]^{2-}$ species,[16] which undergo polymerization even in solution. The aged solutions of this species exhibit one band at 350 nm in its electronic spectrum.

The nature of the aged dinuclear μ-CN compounds in both the pentammine and tetrammine series may be explained by two alternative mechanisms. In the first step a μ-CN dinuclear compound is formed. Such reactions may follow one of the following mechanisms.

(a) The chloride ligand or any of the X ligands is lost by a hydrolytic process and a new intermolecular μ-CN bond is formed with other dinuclear molecule. This mechanism should give to a polymeric material as indicated in **Ia** and **b**, depending on the starting amminated salt:

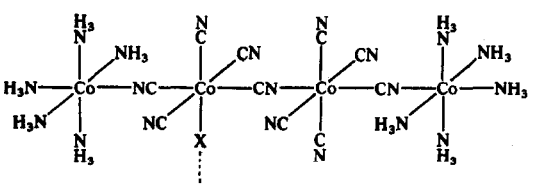

Ia X = Cl^-, Br^- or H_2O

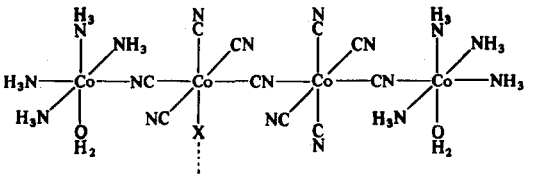

Ib X = Cl^- or H_2O

(b) One X ligand is lost by a migration mechanism of an NH_3 group giving a new intermolecular μ-CN bond, as indicated in **IIa** and **b**. Intramolecular migration of such types in these compounds has been demonstrated to occur by ^{59}Co NMR spectroscopy.[4]

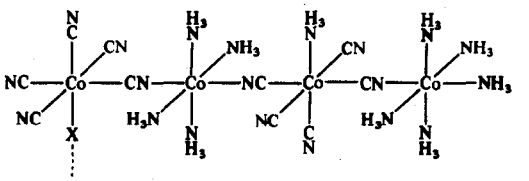

IIa X = Cl^-, Br^- or H_2O

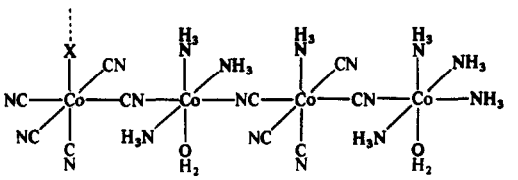

IIb X = Cl^- or H_2O

If the new μ-CN bond formed in the above-mentioned mechanism was intramolecular, dinuclear compounds of formula $[(NH_3)_4Co(NC)_2Co(CN)_3NH_3]X$ or $[(NH_3)_3(H_2O)Co(NC)_2Co(CN)_3NH_3]X$ may be synthesized as reported by several authors.[18,19]

The polymers shown above are similar but with different sequences of the amminated and cyanurated moieties.

CONCLUSIONS

The chemical and spectral characteristics of these polymeric materials are in agreement with the experimental results found. The difference in reactivity between these acidopentacyanocobaltates(III) and the parent hexacyanocobaltate(III) depends on the nature of the ligand X. The easy hydrolysis of these X groups is a critical step in the polymerization process. The rate of polymerization varies in the order Cl < Br < I. The difference between the polymeric materials afforded by aging

of both amminated series of compounds is due only to the presence of coordinated water molecules in the fragments of the polymerization of the tetramminated series as shown in **I** and **II**. The coordinated water molecules are extremely susceptible to polymerization, as has been repeatedly demonstrated in a number of cases involving the synthesis of μ-CN dinuclear compounds.[1,20] Because of this reason, the pentamminated series behaves differently, which permits the isolation of μ-CN dinuclear compounds before undergoing polymerization. On the contrary, the tetramminated series is more sensitive to these processes, and undergoes rapid polymerization, which prevents the isolation of dinuclear complexes.

Acknowledgements—This work was supported by Comisión Asesora de Investigación Científica y Técnica C.A.I.C.Y.T., Ministerio de Educación y Ciencia, Spain (grant No. 360/81).

REFERENCES

1. R. A. Castelló, C. Piriz, N. Egen and A. Haim, *Inorg. Chem.* 1969, **8**, 699.
2. (a) J. Ribas, J. Casabó, J. M. Coronas and M. L. Alvarez, *Ann. Quim.* 1981, **77**, 26; (b) J. Ribas, J. Casabó, M. Montfort, M. L. Alvarez and J. M. Coronas, *J. Inorg. Nucl. Chem.* 1980, **42**, 707; (c) J. Ribas, A. Escuer and M. Montfort, *Thermochim. Acta* 1984, **76**, 201.
3. J. Ribas, M. Montfort and J. Casabó, *Transition Met Chem.* 1984, **9**, 707.
4. J. Casabó, T. Flor, F. Teixidor and J. Ribas, *Inorg. Chem.* 1986, **25**, 3166.
5. J. E. House, Jr, *Thermochim. Acta* 1980, **40**, 225.
6. M. E. LeMay and M. W. Babich, *Thermochim. Acta* 1981, **48**, 147.
7. B. E. Douglas (Ed), *Inorg. Synth.* 1978, **18**, 83.
8. M. Linhard and H. Flygare, *Z. Anorg. Chem.* 1950, **262**, 340.
9. W. C. Fernelius (Ed), *Inorg. Synth.* 1946, **2**, 225.
10. T. Flor and J. Casabó, *Synth. React. Inorg. Met–Org. Chem.* 1986, **15**, 795.
11. *Métodos complexométricos de valoración con Titriplex*, 3rd Edn, p. 32. Merck, Darmstadt.
12. M. Ivata and Y. Sayto, *Acta Cryst.* 1973, **B29**, 822.
13. R. L. Carlin, R. Burriel, J. Pons and J. Casabó, *Inorg. Chem.* 1983, **22**, 2832.
14. H. Duggan and R. G. Jungst, *J. Am. Chem. Soc.* 1974, **11**, 3443.
15. (a) D. A. Dows, A. Haim and W. W. Wilmarth, *J. Inorg. Nucl. Chem.* 1961, **21**, 33; (b) R. Castelló, C. Piriz and A. Haim, *Inorg. Chem.* 1972, **10**, 1492; (c) J. Casabó, J. Ribas, J. M. Coronas, M. Montfort and M. 1. Alvarez, *J. Inorg. Nucl. Chem.* 1981, **43**, 3113.
16. R. A. Castelló, C. Piriz and A. Haim, *Inorg. Chem.* 1971, **10**, 203.
17. P. B. Chock, R. B. K. Dewar, J. Holpen and L. Y. Wong, *J. Am. Chem. Soc.* 1969, **912**, 82.
18. J. Casabó and J. Ribas, *J. Inorg. Nucl. Chem.* 1977, **39**, 143.
19. A. Uehara, S. Tanabe and R. Tsuchiya, *Inorg. Chem.* 1983, **22**, 2864.
20. J. E. House, Jr and B. J. Smith, *J. Inorg. Nucl. Chem.* 1977, **39**, 777.

Polyhedron Vol. 6, No. 7, pp. 1571–1576, 1987
Printed in Great Britain

0277–5387/87 $3.00+.00

LIGHT-INDUCED LIGAND-SUBSTITUTION REACTIONS—II. REACTION BETWEEN THE $[CoBr(NH_3)_5]^{2+}$ ION AND ETHYLENEDIAMINETETRAACETATE BY IRRADIATION WITH VISIBLE LIGHT OF AQUEOUS ACID SOLUTION CONTAINING THE TRIS(2,2′-BIPYRIDINE)RUTHENIUM(II) ION

MASARU KIMURA,† TOSHIKO NAKAMURA, HIROKO NAKAMURA and SUZUKO NISHIDA

Department of Chemistry, Faculty of Science, Nara Women's University, Nara 630, Japan

(*Received* 5 *January* 1987; *accepted* 28 *January* 1987)

Abstract—The ligand-substitution reaction of the bromopentaamminecobalt(III) ion, $[CoBr(NH_3)_5]^{2+}$, with ethylenediaminetetraacetate (EDTA) (which denotes all the forms of EDTA, i.e. $edta^{4-}$, $Hedta^{3-}$, H_2edta^{2-} etc.) was induced by irradiation with visible light of aqueous solutions containing the tris(2,2′-bipyridine)ruthenium(II) ion, $[Ru(bpy)_3]^{2+}$. The $[Co(edta)]^-$ ion was efficiently produced in acid solutions at pH 2–3, where $[Ru(bpy)_3]^{2+}$ acts as an inductor and a photocatalyst. The ligand-substitution reaction constitutes a chain reaction composed of a $[Ru(bpy)_3]^{2+}$ and $[Ru(bpy)_3]^{3+}$ cycle, where the substitution reaction is initiated by the quenching reaction of the photoexcited complex $[Ru(bpy)_3]^{2+*}$ with $[CoBr(NH_3)_5]^{2+}$. The formation rate of $[Co(edta)]^-$ by the ligand-substitution reaction between EDTA and $[CoBr(NH_3)_5]^{2+}$ decreased with increasing pH (pH > 3) as well as with decreasing pH (pH < 2), and was at a maximum at pH 2–3. Under conditions of pH 2–3, the photo-induced ligand-substitution reaction between EDTA and $[CoBr(NH_3)_5]^{2+}$ was quantitative, i.e. the $[[Co(edta)]^-]_{formed}/[[CoBr(NH_3)_5]^{2+}]_{decomposed}$ ratio = 1. Reaction mechanisms are discussed.

In a previous work,[1] we studied the photo-induced ligand-substitution reaction between ethylenediaminetetraacetate (EDTA) and $[CoCl(NH_3)_5]^{2+}$. Our interest has arisen from comparing $[CoBr(NH_3)_5]^{2+}$ with $[CoCl(NH_3)_5]^{2+}$ in the same photo-induced reaction composed of a $[Ru(bpy)_3]^{2+}$ and $[Ru(bpy)_3]^{3+}$ cycle. In the initial stage of the present work, we found that the production of $[Ru(bpy)_3]^{3+}$ {or the disappearance of $[Ru(bpy)_3]^{2+}$} due to the quenching reaction between $[Ru(bpy)_3]^{2+*}$ and $[CoBr(NH_3)_5]^{2+}$ was remarkably different from that in the case of $[CoCl(NH_3)_5]^{2+}$ in the previous work[1] (refer to Fig. 1).

When a solution containing $[Ru(bpy)_3]^{2+}$ and $[CoBr(NH_3)_5]^{2+}$ {or $[CoCl(NH_3)_5]^{2+}$} was irradiated with visible light, the $[Ru(bpy)_3]^{2+}$ ion was oxidized to the $[Ru(bpy)_3]^{3+}$ ion by the bimolecular quenching reaction of $[Ru(bpy)_3]^{2+*}$ with $[CoBr(NH_3)_5]^{2+}$ {or $[CoCl(NH_3)_5]^{2+}$}. The $[Ru(bpy)_3]^{3+}$ ion once formed could react with the solvent water or other reducing species such as the Br^- ion in solution, being reduced to the $[Ru(bpy)_3]^{2+}$ ion. Consequently, the difference in the disappearance of $[Ru(bpy)_3]^{2+}$ { or the production of $[Ru(bpy)_3]^{3+}$} due to the quenching reaction of $[Ru(bpy)_3]^{2+*}$ with $[CoBr(NH_3)_5]^{2+}$ and $[CoCl(NH_3)_5]^{2+}$ is attributable to the Br^- and Cl^- ions, the latter ion not being oxidized by $[Ru(bpy)_3]^{3+}$ but the Br^- ion being oxidized by $[Ru(bpy)_3]^{3+}$: the Br^- or Cl^- ion is liberated by the quenching reaction of $[Ru(bpy)_3]^{2+*}$ with $[CoBr(NH_3)_5]^{2+}$ or $[CoCl(NH_3)_5]^{2+}$. Despite the remarkably different behavior in the quenching reactions of $[CoBr(NH_3)_5]^{2+}$ and $[CoCl(NH_3)_5]^{2+}$, the photo-induced ligand-substitution reaction of both complexes with EDTA was found to proceed similarly.

† Author to whom correspondence should be addressed.

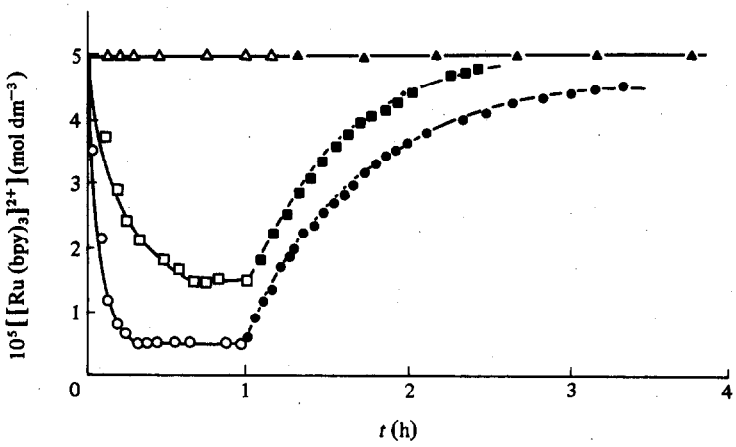

Fig. 1. Variation in the $[Ru(bpy)_3]^{2+}$ ion concentration by the oxidative quenching reactions of $[Ru(bpy)_3]^{2+*}$ with $[CoBr(NH_3)_5]^{2+}$ and $[CoCl(NH_3)_5]^{2+}$. Conditions: 5×10^{-5} mol dm^{-3} $[Ru(bpy)_3]Cl_2$ and 5×10^{-3} mol dm^{-3} $[CoBr(NH_3)_5]Br_2$ for plots △ and ▲, 1×10^{-3} mol dm^{-3} $[CoBr(NH_3)_5](ClO_4)_2$ for plots □ and ■, and 5×10^{-3} mol dm^{-3} $[CoCl(NH_3)_5]Cl_2$ for plots ○ and ●; 0.05 mol dm^{-3} acetic acid and sodium acetate (pH 4.75), nitrogen saturated, 25°C. Plots △, □ and ○ indicate the results with continuous irradiation of visible light by four 100-W tungsten lamps, and plots ▲, ■ and ● indicate the results obtained when the photo-reacted solution stood in the dark after irradiation for 1 h.

EXPERIMENTAL

Chemicals

$[Ru(bpy)_3]Cl_2\cdot6H_2O$[2] and $[CoBr(NH_3)_5](ClO_4)_2$[3] were prepared as described in the literature[2,3] and recrystallized twice. Disodium dihydrogen ethylenediaminetetraacetate ($Na_2[H_2edta]$) and other chemicals used were of guaranteed-reagent grade. Deionized water was further distilled with and without addition of permanganate in a glass still.

Procedure

The procedure is essentially the same as described in the previous paper.[1] The pH of the reaction solution was adjusted with perchloric acid and sodium acetate.

RESULTS AND DISCUSSION

As seen in Fig. 1, when the solution containing $[Ru(bpy)_3]^{2+}$ and $[CoBr(NH_3)_5]^{2+}$ or $[CoCl(NH_3)_5]^{2+}$ in the absence of EDTA was irradiated with visible light the $[Ru(bpy)_3]^{2+}$ ion was oxidized to the $[Ru(bpy)_3]^{3+}$ ion by a bimolecular quenching reaction with the photoexcited species $[Ru(bpy)_3]^{2+*}$, and the $[Ru(bpy)_3]^{3+}$ ion could be reduced rapidly to the $[Ru(bpy)_3]^{2+}$ ion by the Br^- ion (see plot Δ in Fig. 1), and thus the variation curve for the $[Ru(bpy)_3]^{2+}$ ion concentration using $[CoBr(NH_3)_5]^{2+}$ as a quencher was very different from that using the $[CoCl(NH_3)_5]^{2+}$ ion. On the other hand, when a reaction mixture of the same constituents as in Fig. 1 contained some EDTA, the $[Ru(bpy)_3]^{2+}$ ion concentration did not change at all with $[CoBr(NH_3)_5]Br_2$, $[CoBr(NH_3)_5](ClO_4)_2$ and $[CoCl(NH_3)_5]Cl_2$ during irradiation by light, and instead the $[Co(edta)]^-$ complex was produced in proportion to the irradiation time (t), at least for the initial stage of the reaction (see Figs 2 and 3).

This fact indicates that the $[Ru(bpy)_3]^{3+}$ ion once formed is rapidly reduced to the $[Ru(bpy)_3]^{2+}$ ion by the Co(II)EDTA† ion produced by the reaction between EDTA and Co^{2+}_{aq} {or $[CoBr(NH_3)_5]^+$} [see eqn (4)]. The latter species could be formed first by the quenching reaction of the $[Ru(bpy)_3]^{2+*}$ ion with $[CoBr(NH_3)_5]^{2+}$, and dissociates rapidly to Co^{2+}_{aq}, Br^- and NH_3 (or NH_4^+) [see eqn (3)]. It was found that the formation rate of $[Co(edta)]^-$ was indifferent to the Br^- ion over the initial concentration range 0–0.02 mol dm^{-3} in the reaction mixture: the formation rate $d[[Co(edta)]^-]/dt$ was 2.56×10^{-7}, 2.66×10^{-7} and 2.60×10^{-7} mol

† The formula Co(II)EDTA used in the present paper represents a mixture of $[Co(edta)]^{2-}$ and $[Co(Hedta)]^-$; the equilibrium constant $K=[[Co(Hedta)]^-]/\{[[Co(edta)]^{2-}][H^+]\}$ for the reaction $[Co(edta)]^{2-}+H^+\rightleftharpoons[Co(Hedta)]^-$ is $10^{3.1}$ dm^3 mol^{-1} at an ionic strength of 0.10 mol dm^{-3} and 20°C.[4] Thus, the species $[Co(Hedta)]^-$ should be dominant in acid solutions of pH 2–3.

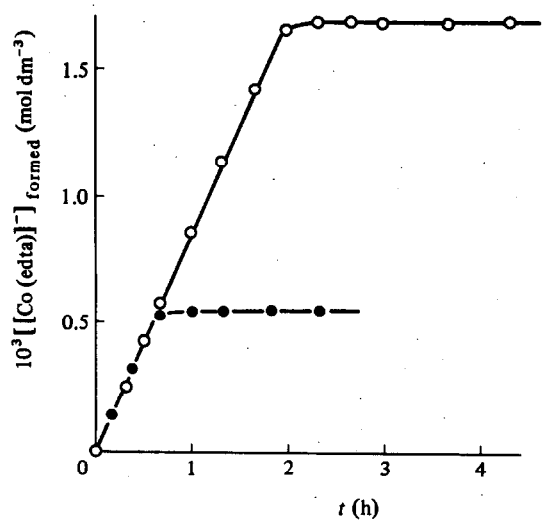

Fig. 2. Examples of $[[Co(edta)]^-]_{formed}$ vs t. Conditions: pH 2.2 (0.02 mol dm^{-3} $HClO_4$), ionic strength 0.21 mol dm^{-3}; initial concentrations are 1×10^{-2} mol dm^{-3} $[CoBr(NH_3)_5](ClO_4)_2$, and 1.7×10^{-3} mol dm^{-3} and 5.4×10^{-4} mol dm^{-3} $Na_2[H_2edta]$ for plots ○ and ●, respectively; and 5×10^{-5} mol dm^{-3} $[Ru(bpy)_3]Cl_2$. The other conditions are the same as those in Fig. 1 with irradiation by four lamps (see footnote ‡ on p. 1575).

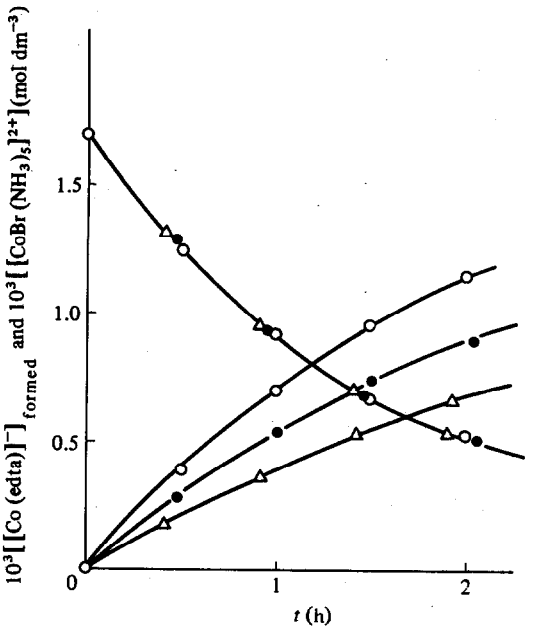

Fig. 3. Variations in the $[[Co(edta)]^-]_{formed}$ and $[[CoBr(NH_3)_5]^{2+}]$ concentrations at pH 4.75. Conditions: 5×10^{-5} mol dm^{-3} $[Ru(bpy)_3]Cl_2$, 1.7×10^{-3} mol dm^{-3} $[CoBr(NH_3)_5](ClO_4)_2$, 0.05 mol dm^{-3} acetic acid and sodium acetate (pH 4.75), and 1×10^{-3}, 2×10^{-3} and 4×10^{-3} mol dm^{-3} EDTA for plots ○, ● and △, respectively. Other conditions are the same as in Fig. 2.

dm^{-3} s^{-1} in 0, 0.004 and 0.02 mol dm^{-3} Br^-, respectively.†

Effect of hydrogen ion concentration on the formation rate of $[Co(edta)]^-$

The initial rate of formation of the $[Co(edta)]^-$ ion [V_i in eqn (8)] was determined from plots of $[[Co(edta)]^-]_{formed}$ vs t for various hydrogen ion concentrations. As seen in Fig. 4, the formation rate of $[Co(edta)]^-$ decreased at pH < 2 and pH > 3, and was maximum at pH 2–3.

The decrease in the formation rate of $[Co(edta)]^-$ at pH < 2 would be due to the increase in the protonated species of EDTA, i.e. H_4edta, H_3edta^- etc., and due to the decrease in the equilibrium concentration of $[Co(edta)]^{2-}$ in such acid solutions. While the decrease in the formation rate of $[Co(edta)]^-$ at pH > 3 is caused by the occurrence of a reaction between EDTA and $[Ru(bpy)_3]^{3+}$ which competes with the formation reaction of $[Co(edta)]^-$, i.e. the reaction between Co(II)EDTA and $[Ru(bpy)_3]^{3+}$ [eqn (5)]. At pH 2–3, the formation rate of $[Co(edta)]^-$ was independent of the EDTA concentration in the reaction mixture, and the concentration of the $[Co(edta)]^-$ formed was

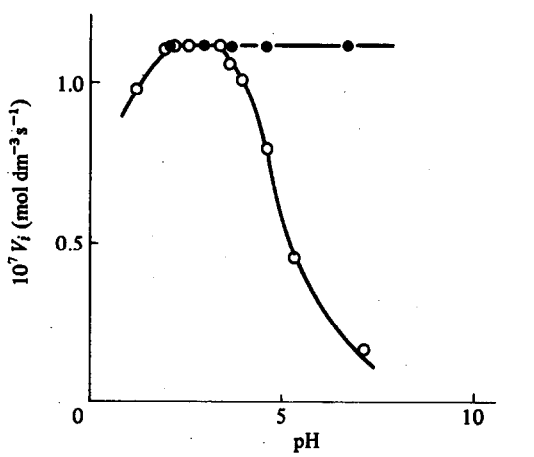

Fig. 4. Effect of pH on the formation rate of $[Co(edta)]^-$. Conditions for plot ○: 5×10^{-5} mol dm^{-3} $[Ru(bpy)_3]Cl_2$, 2×10^{-3} mol dm^{-3} $[CoBr(NH_3)_5](ClO_4)_2$, 2×10^{-3} mol dm^{-3} $Na_2[H_2edta]$, and ionic strength 0.09 mol dm^{-3}. Other conditions are as in Fig. 2. Conditions for plot ●: all the conditions are the same as in plot ○, except for 2×10^{-3} mol dm^{-3} $CoSO_4$, which is equivalent to the EDTA concentration added before starting the reaction.

† The rate constants for the oxidation reactions of water (H_2O), Br^- and Co(II)EDTA by the $[Ru(bpy)_3]^{3+}$ ion are 3.2×10^{-4} s^{-1},[1] 0.44 dm^3 mol^{-1} s^{-1}, and $\geqslant 10^4$ dm^3 mol^{-1} s^{-1}, respectively. Thus, the reaction between Co(II)EDTA and $[Ru(bpy)_3]^{3+}$ could occur predominantly in the presence of Br^- in aqueous solutions.

Table 1. Formation of $[Co(edta)]^-$ and decomposition of $[CoBr(NH_3)_5]^{2+}$ by the photo-induced reaction[a]

t (h)	$10^3[[Co(edta)]^-]_{formed}$ (mol dm^{-3})	$10^3[[CoBr(NH_3)_5]^{2+}]_{decomposed}$ (mol dm^{-3})	$\frac{[[Co(edta)]^-]_{formed}}{[[CoBr(NH_3)_5]^{2+}]_{decomposed}}$
0.5	0.39	0.39	1.00
1.0	0.70	0.70	1.00
1.5	0.97	1.01	0.96
2.0	1.14	1.11	1.03
			Av. 1.00 ± 0.02

[a] Conditions are the same as for plot ○ in Fig. 2, except for 2×10^{-3} mol dm^{-3} $[CoBr(NH_3)_5](ClO_4)_2$.

equal to that of the $[CoBr(NH_3)_5]^{2+}$ decomposed due to the photo-induced ligand-substitution reaction (see Table 1).

Therefore, the stoichiometry and overall reaction at pH 2–3 may be written as follows:

$$[CoBr(NH_3)_5]^{2+} + EDTA \xrightarrow[[Ru(bpy)_3]^{2+}]{h\nu} [Co(edta)]^- + Br^- + 5NH_4^+ \quad \text{(at pH 2–3).} \quad (1)$$

When some $CoSO_4$ concentrations were added to the reaction mixture before starting the reaction, and when all the EDTA species existed as Co(II)EDTA,† the formation rate of $[Co(edta)]^-$ was independent of pH over the range 2–7 and was equal to that at pH 2–3 without addition of $CoSO_4$ (see plot ● in Fig. 4). At pH 4.75, the rate of the decrease in the $[CoBr(NH_3)_5]^{2+}$ ion concentration in the photo-induced reaction system was not dependent on the EDTA concentration, but the formation rate of the $[Co(edta)]^-$ ion decreased with increasing EDTA concentration (see Fig. 3), and the $[[Co(edta)]^-]_{formed}/[[CoBr(NH_3)_5]^{2+}]_{decomposed}$ ratio was 0.7, 0.6 and 0.5 at 0.001, 0.002 and 0.004 mol dm^{-3} EDTA, respectively, at the start of the reaction. These ratio values were smaller than unity being quite different from the corresponding value of 1.0 at pH 2–3 (see Table 1). Consequently, the photo-induced ligand-substitution reaction between $[CoBr(NH_3)_5]^{2+}$ and EDTA proceeds most efficiently (at an efficiency of 100%) at pH 2–3, and proceeds less efficiently at the other pH values of the reaction solution. The experiments hereafter will be carried out at pH 2.2 in a solution of 0.02 mol dm^{-3} $HClO_4$.

Dependence of reaction rate on the $[CoBr(NH_3)_5]^{2+}$ *ion concentration*

The initial rate of formation of $[Co(edta)]^-$ [V_i in eqn (8)] was determined from plots as in Fig. 2, and the reciprocal V_i was plotted against the reciprocal $[CoBr(NH_3)_5]^{2+}$ concentrations at the start of the reaction. As seen in Fig. 5, the V_i^{-1} vs $[[CoBr(NH_3)_5]^{2+}]_i^{-1}$ plots showed a straight line with an intercept. The intercept was hardly dependent on the temperature as well as on the ionic strength, but the slope decreased with increasing temperature or ionic strength (see Fig. 5 and Table 2).

Effect of the irradiated-light intensity on formation of $[Co(edta)]^-$

No substitution reaction between EDTA and $[CoBr(NH_3)_5]^{2+}$ and no formation of $[Co(edta)]^-$ were found in the dark, and the rate of formation of $[Co(edta)]^-$ was proportional to the number of lamps used for irradiation. The initial rate of formation of $[Co(edta)]^-$ was 1.78×10^{-8}, 6.07×10^{-8}, 9.72×10^{-8}, 1.29×10^{-7} and 1.56×10^{-7} mol dm^{-3} s^{-1} with room light, one, two, three and four lamps, respectively, under the same conditions as those at pH 2.2 in Fig. 4.

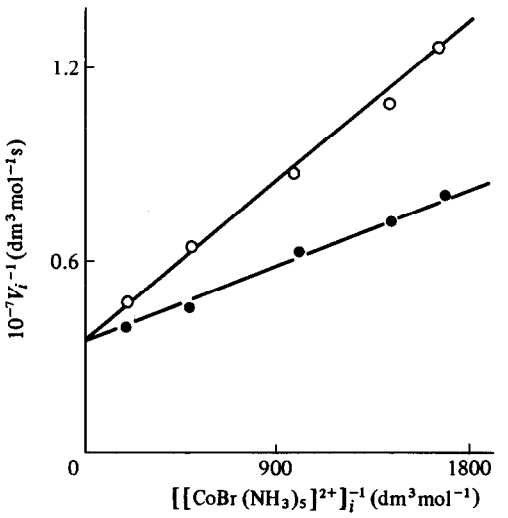

Fig. 5. Plots of V_i^{-1} vs $[[CoBr(NH_3)_5]^{2+}]_i^{-1}$ [eqn (8)]. Conditions: pH 2.2 (0.02 mol dm^{-3} $HClO_4$); other conditions as for plot ○ in Fig. 4. Plots ○ and ● indicate the results obtained at ionic strengths of 0.09 and 0.21 mol dm^{-3}, respectively.

† See footnote † on p. 1572.

Table 2. Values of parameters in eqns (7) and (8)[a]

T (°C)	Ionic strength (mol dm^{-3})	$10^7 I_a\Phi$ (mol dm^{-3} s^{-1})	k_q/k_0 (dm^3 mol^{-1})	$10^{-9}k_q$ (dm^3 mol^{-1} s^{-1})
5	0.09	2.7	550	
15	0.09	2.8	625	
25	0.09	2.7	722	1.09, 0.91[b]
35	0.09	2.8	772	
25	0.21	3.0, 2.4[c]	1102	1.67
		Av. 2.7 ± 0.3		

[a] Conditions as in Fig. 5.
[b] Value obtained by measurement of the luminsecence of $[Ru(bpy)_3]^{2+*}$ which is quenched by the $[CoBr(NH_3)_5]^{2+}$ ion; the Stern–Volmer constant was 601 dm^3 mol^{-1}.
[c] This value has been obtained from the slope in Fig. 2 [see eqn (7″)].

It was also confirmed that the aquation of the $[CoBr(NH_3)_5]^{2+}$ ion during the occurrence of the photo-induced ligand-substitution reaction was negligible under any conditions employed in the present study and that the concentration of the $[Ru(bpy)_3]^{2+}$ ion remained constant during the photo-induced reaction.

Reaction mechanism

The following reaction mechanism could be proposed to account for the results obtained at pH 2–3:

$$[Ru(bpy)_3]^{2+} + h\nu \xrightarrow{I_a} [Ru(bpy)_3]^{2+*}$$

$$[Ru(bpy)_3]^{2+*} \xrightarrow{k_0} \begin{cases} [Ru(bpy)_3]^{2+} + h\nu' \\ [Ru(bpy)_3]^{2+} + \Delta \end{cases} \quad (2)$$

$$[Ru(bpy)_3]^{2+*} + [CoBr(NH_3)_5]^{2+} \xrightarrow{k_q} [Ru(bpy)_3]^{3+} + [CoBr(NH_3)_5]^{+}$$

$$\xrightarrow{H^+} Co^{2+}_{aq} + 5NH_4^+ + Br^-, \quad (3)$$

$$Co^{2+}_{aq}\ \{\text{or } [CoBr(NH_3)_5]^{+}\} + EDTA \rightleftharpoons Co(II)EDTA, \quad (4)\dagger$$

$$Co(II)EDTA + [Ru(bpy)_3]^{3+} \xrightarrow{k_1} [Co(edta)]^- + [Ru(bpy)_3]^{2+}, \quad (5)\dagger$$

$$[Ru(bpy)_3]^{2+*} + [Co(edta)]^- \xrightarrow{k'_q} [Ru(bpy)_3]^{3+} + Co(II)EDTA. \quad (6)$$

The overall reaction is the same as in the stoichiometric eqn (1). Although the quenching rate constant k'_q is as large as k_q [$k_q = (1.1\text{–}1.7) \times 10^9$ dm^3 mol^{-1} s^{-1} (see Table 2) and $k'_q = 2 \times 10^9$ dm^3 mol^{-1} s^{-1}], the reaction of eqn (3) proceeds predominantly when $[[CoBr(NH_3)_5]^{2+}] \gg [[Co(edta)]^-]$. Such conditions $\{[[CoBr(NH_3)_5]^{2+}] \gg [[Co(edta)]^-]\}$ should be satisfied at least for the initial period of the reaction even if the photoreaction started at a relatively low $[CoBr(NH_3)_5]^{2+}$ ion concentration. When the reaction of eqn (6) is neglected, the following rate law can be derived:

$$\frac{d[[Co(edta)]^-]}{dt} = \frac{I_a\Phi k_q[[CoBr(NH_3)_5]^{2+}]}{k_0 + k_q[[CoBr(NH_3)_5]^{2+}]}, \quad (7)\ddagger$$

where I_a indicates the amount of light absorbed, Φ indicates the quantum yield for the excited species $[Ru(bpy)_3]^{2+*}$, and, thus, $I_a\Phi$ corresponds to the formation rate of the excited species. Thus, the initial rate of formation of the $[Co(edta)]^-$ ion (V_i) is written as follows:

$$V_i^{-1} = \frac{1}{I_a\Phi} + \frac{k_0}{I_a\Phi k_q}[[CoBr(NH_3)_5]^{2+}]_i^{-1}. \quad (8)$$

Plots of V_i^{-1} vs $[[CoBr(NH_3)_5]^{2+}]_i^{-1}$ are illustrated in Fig. 5, and the intercept and slope are $1/(I_a\Phi)$ and $k_0/(I_a\Phi k_q)$, respectively. Consequently, the values of $I_a\Phi$ and k_q/k_0 are obtained from the plots, and these

† See footnote † on p. 1572.

‡ When $k_q[[CoBr(NH_3)_5]^{2+}] \gg k_0$, eqn (7) should be written as follows:

$$d[[Co(edta)]^-]/dt = (I_a\Phi) \quad (7')$$

and

$$[[Co(edta)]^-]_{formed} = (I_a\Phi)t, \quad (7'')$$

where the term $I_a\Phi$ is constant (see text and Table 2), and thus the $[[Co(edta)]^-]_{formed}$ should be proportional only to t, irrespective of the $[[CoBr(NH)_3]_5]^{2+}$ ion as well as the EDTA concentration. This is actually the kind of case given in Fig. 2, in which the value of $k_q[[CoBr(NH_3)_5]^{2+}]_i$ is 10-fold larger than the k_0 of 1.5×10^6 s^{-1},[5] and is also much larger than the $k'_q[[Co(edta)]^-]_{formed}$ values during the formation reaction of the $[Co(edta)]^-$ ion.

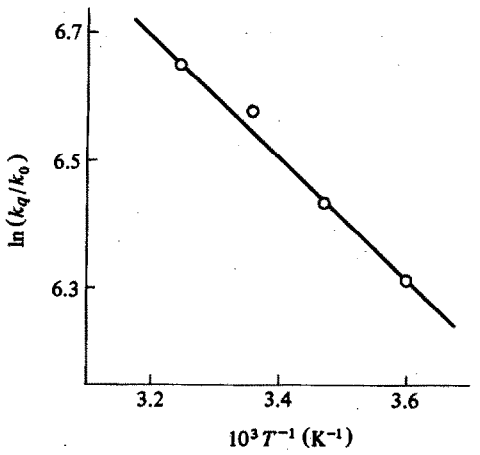

Fig. 6. Arrhenius plots for k_q/k_0. Conditions as in Table 2.

values are given in Table 2. The $I_a\Phi$ values were independent of the temperatures as well as of the ionic strength, while k_q/k_0 values were rather dependent on the temperature as well as on the ionic strength. The plot of $\ln(k_q/k_0)$ vs T^{-1} showed a straight line, giving the activation energy $E_q - E_0 = 8.31$ kJ mol^{-1} (Fig. 6).

We can evaluate the k_q values from k_q/k_0 by using $k_0 = 1.52 \times 10^6$ s^{-1}.[5] The k_q values were obtained under various conditions and are given in Table 2 together with $I_a\Phi$ and k_q/k_0 values. For comparison, the k_q value was determined by measurement of the luminescence of $[Ru(bpy)_3]^{2+*}$ in various $[CoBr(NH_3)_5]^{2+}$ concentrations with determination of the Stern–Volmer constant. The result is given in Table 2 together with values obtained by using eqn (8). They are in good agreement with each other under the given conditions. This also supports the reaction mechanism of eqns (2)–(6), and the rate law of eqns (7) and (8) is practically valid.

At pH > 3, the concentrations $[Co(edta)]^-$ ion which was formed became less than those of the $[CoBr(NH_3)_5]^{2+}$ ion which decomposed to Co^{2+}_{aq}, Br^- and NH_4^+, and the $[[Co(edta)]^-]_{formed}/[[CoBr(NH_3)_5]^{2+}]_{decomposed}$ ratio decreased with increasing EDTA concentration (see Fig. 3). This fact could be attributed to the occurrence of the reaction between EDTA and $[Ru(bpy)_3]^{3+}$. This consideration is reasonable because the reaction rate of $[Ru(bpy)_3]^{3+}$ with EDTA becomes much faster with increasing pH of the solution; e.g. the second-order rate constant for the reaction between $[Ru(bpy)_3]^{3+}$ and EDTA is 8×10^3 and 2×10^6 dm^3 mol^{-1} s^{-1} at pH 4 and pH 7, respectively.[6] The reaction of $[Ru(bpy)_3]^{3+}$ with EDTA competes with that of $[Ru(bpy)_3]^{3+}$ with Co(II)EDTA [eqn (5)], and the reaction rate of the formation of the $[Co(edta)]^-$ ion becomes slower according to the increase in the EDTA concentration at pH > 3 (see Fig. 3).

REFERENCES

1. M. Kimura, M. Yamashita and S. Nishida, *Inorg. Chem.* 1985, **24**, 1527.
2. T. Tachibana, M. Nakahara and M. Shibata (Eds), *Shin Jikken-Kagaku Koza* 8, p. 1475, Japan Chemical Society, Maruzen (1975); R. A. Palmer and T. S. Piper, *Inorg. Chem.* 1966, **5**, 964; I. Fujita and H. Kobayashi, *Ber. Bunsenges. Phys. Chem.* 1972, **76**, 115.
3. T. Tachibana, M. Nakahara and M. Shibata (Eds), *Shin Jikken-Kagaku Koza* 8, p. 1212, Japan Chemical Society, Maruzen (1975).
4. G. Anderegg, *Helv. Chim. Acta* 1964, **47**, 1801.
5. J. N. Demas and A. W. Adamson, *J. Am. Chem. Soc.* 1973, **95**, 5195.
6. D. Miller and G. McLendon, *Inorg. Chem.* 1981, **20**, 950.

Polyhedron Vol. 6, No. 7, pp. 1577–1585, 1987
Printed in Great Britain

0277–5387/87 $3.00+.00

MONOMERIC FIVE-COORDINATE RHENIUM DIAZENIDO AND HYDRAZIDO COMPLEXES WITH AROMATIC THIOLATE LIGANDS: X-RAY STRUCTURES OF $[Re(NNC_6H_4\text{-}4\text{-}Br)_2(SC_6H_3\text{-}2,5\text{-}Me_2)(PPh_3)_2]$ AND $[ReO(NNMePh)(SPh)_3]$, AND OF THE SYNTHETIC PRECURSOR $[Re(NNC_6H_4\text{-}4\text{-}Br)_2Cl(PPh_3)_2]$

TERRENCE NICHOLSON, PAUL LOMBARDI and JON ZUBIETA*

Department of Chemistry, State University of New York at Albany, Albany, NY 12222, U.S.A.

(*Received* 17 *November* 1986; *accepted* 4 *February* 1987)

Abstract—Reaction of $[ReOCl_3(PPh_3)_2]$ with bromophenylhydrazine in methanol yields $[ReCl(N_2C_6H_4Br)_2(PPh_3)_2]$ (**1**). Complex **1** reacts with arylthiolates to give mixtures of $[Re(SAr)(N_2C_6H_4Br)_2(PPh_3)_2]$ (**2**) and $[Re_2(SAr)_7(NNR)_2]^-$. Complexes **1** and **2** display trigonal bipyramidal geometries with the phosphine ligands occupying the axial sites. A significant feature of the structures is the nonequivalence of the rhenium–diazenido moieties, such that for **1** the Re—N(1) and N(1)—N(2) distances are 1.80(2) and 1.24(3) Å, while Re—N(3) and N(3)—N(4) are 1.73(2) and 1.32(3) Å, and for **2** the Re—N distances are 1.73(1) and 1.80(2)° with corresponding N—N distances of 1.32(2) and 1.25(2) Å. Reaction of $(PPh_4)[ReO(SPh)_4]$ (**3**) with unsymmetrically disubstituted hydrazines affords complexes of the type $[ReO(SPh)_3(NMRR')]$ (R = Me, R′ = Ph for **4**). Complexes **3** and **4** display distorted square pyramidal geometries with the oxo groups apical. The significant feature of the structure of **4** is the nonlinear Re—N(1)—N(2) linkage, exhibiting an angle of 145.6(10)°. The angle does not appear to correlate with a significant contribution from a valence form with sp^2 hybridization at the α-nitrogen. *Crystal data*: **1**: monoclinic space group, $P2_1/n$, $a = 12.216(2)$ Å, $b = 19.098(2)$ Å, $c = 20.257(4)$ Å, $\beta = 106.20(1)°$, $V = 4538.3(8)$ Å^3 to give $Z = 4$; structure solution and refinement based on 1905 reflections converged at $R = 0.070$. **2**: monoclinic space group $P2_1/n$, $a = 14.393(2)$ Å, $b = 18.842(3)$ Å, $c = 20.717(4)$Å, $\beta = 110.26(1)°$, $V = 5270.5(8)$ Å^3 to give $Z = 4$ for $D = 1.53$ g cm^{-1}; structure solution and refinement based on 4249 reflections to give $R = 0.070$. **3**: monoclinic space group $P2_1/n$, $a = 12.531(2)$ Å, $b = 24.577(4)$ Å, $c = 16.922(3)$ Å, $\beta = 99.06(1)°$, $V = 5146.2(9)$ Å^3, $D = 1.36$ g cm^{-3} for $Z = 4$, 2912 reflections, $R = 0.050$. **4**: monoclinic space group $p2_1/n$, $a = 16.137(2)$ Å, $b = 9.863(2)$ Å, $c = 16.668(2)$ Å, $\beta = 111.12(1)°$, $V = 2474.7(6)$ Å^3, $D = 1.74$ g cm^{-3} for $Z = 4$, 2940 reflections, $R = 0.066$.

Although there have been extensive recent studies of transition-metal complexes with sulfur ligands,[1] relatively few simple monomeric rhenium thiolato complexes have been reported.[2–4] In particular, examples of rhenium thiolato species incorporating small organic molecules are rare. As part of our studies of the binding of small molecules to metal sulfur sites, we have prepared a number of diazeonido– and hydrazido(2−)–rhenium complexes with aromatic thiolato coligands.

The organodiazenido group $(NNR)^+$ is formally isoelectronic with the nitrosyl ligand NO^+ and chemically related to the diazenide unit, —NNH, a potential intermediate in the reduction of dinitrogen to ammonia. Structural studies have confirmed that the organodiazenido ligand may adopt a variety of geometries: "singly bent",[5] "doubly bent"[6] and bridging.[7]

Unsymmetrically disubstituted organohydrazines may function as hydrazido(2−) ligands, —NNRR′, which arise formally and often in practice, from the protonation of the terminal nitrogen of the organodiazenido ligand. Once again linear[8]

* Author to whom correspondence should be addressed.

and bent[9] M–N–N frameworks have been observed.

In this paper we report the synthesis and structural characterization of the five-coordinate mononuclear rhenium diazenido and hydrazido(2−) complexes $[Re(NNC_6H_4Br\text{-}4)_2(SC_6H_3\text{-}2,5\text{-}Me_2)(PPh_3)_2]$ (**2**) and $[ReO(NNMePh)(SC_6H_5)_3]$ (**4**), respectively. Complex **2** was prepared by the reaction of $[ReCl(NNC_6H_4Br\text{-}4)_2(PPh_3)_2]$ (**1**) with 2,5-dimethylthiophenol. Although the five-coordinate species **1** had been isolated previously,[10] some ambiguity existed with respect to the structural identity, whether mononuclear or chloro-bridged binuclear. This study establishes the mononuclear trigonal bipyramidal structure, analogous to that of $[MoCl(NNMe_2)_2(PPh_3)_2]^+$.[11]

The oxo-hydrazido(2−) species (**4**) was isolated from the reaction of $[ReO(SPh)_4]^-$ (**3**) with the disubstituted hydrazine by replacement of a thiophenolate group. Although the retention of the oxo group was unanticipated, a similar reaction trend has been observed for $[MoO(SPh)_4]^-$ with disubstituted hydrazines.

DISCUSSION

The most frequently employed synthetic routes to aryldiazenido complexes employ oxidative addition of a diazonium salt or insertion into a metal–hydrogen bond to give a diazene complex which is subsequently deprotonated.[12] The silylated diazene Me_3SiN_2Ph has also been shown to provide an efficient method of introducing the aryldiazenido function.[13] Finally, direct reaction of a metal oxo species with an arylhydrazine may proceed by a condensation mechanism, followed by deprotonation, to yield a metal–aryldiazenido complex.[14] Employing the latter methodology, the rhenium(V)–oxo complex $[ReOCl_3(PPh_3)_2]$ reacts with excess *p*-bromophenylhydrazine in methanol to give **1** as a red–orange precipitate in 70–80% yield The complex exhibits a strong IR band at 1520 cm^{-1} assigned to ν(N=N). The X-ray diffraction studies discussed below have established the identity of this species as a mononuclear complex, analogous to the manganese complex $[MnX(N_2Ph)_2(PPh_3)_2]$.[15]

Suspension of **1** in warm benzene or methylene chloride gives a red-maroon material with strong IR bands at 1560 and 1520 cm^{-1}. We suspect the occurrence of a dimerization reaction in aprotic solvents giving a doubly chloro-bridged species (**1a**), implying both linear and bent diazene ligands functioning as three- and one-electron donors.

Complex **1** reacts with excess HCl in methanol to give a red-orange material analyzing for $[ReCl_2(NNHC_6H_4Br\text{-}4)(NNC_6H_4Br\text{-}4)(PPh_3)_2]$ (**1b**). The complex shows strong IR bands at 1625 and 1572 cm^{-1} assigned to ν(N—N) for the hydrazido(2−)- and diazenido-type ligands. Complex **1b** appears to be structurally analogous to the previously reported $[ReBr_2(N_2Ph)(NNHPh)(PPh_3)_2]$ where protonation occurs at the β-nitrogen of the nitrogen ligand.[10]

Addition of an excess of 2,5-dimethylthiophenol to **1** results in a dark red solution from which orange crystals of **2** are observed to form in several hours. The characteristic IR bands at 1545 and 1515 cm^{-1} confirm the presence of the bisorganodiazenido–rhenium unit. In the reaction with unsubstituted phenylthiolate, a second crop of lustrous black crystals separates from the mother liquor after several days. This species has been identified as the formally rhenium(II) complex $[Re_2(SAr)_7(NNC_6H_4Br\text{-}4)_2]^-$, isolated as the triethylammonium salt. The structural and chemical properties of this class of complexes have been discussed previously.[16] Although displacement of the chloro ligand of **1** by thiophenolate occurs readily, under the reaction conditions employed substitution of the phosphine ligands and one organodiazenido group by thiolate ligands occurs only slowly to yield the stable triply thiolato-bridged species $[Re_2(SAr)_7(NNR)_2]^-$.

In contrast to the behavior of **1**, complex **2** reacts with HCl to produce intractable materials, presumably as a result of protonation at the coordinated thiolate sulfur rather than at nitrogen. This preferential protonation at the thiolate site appears to be characteristic of diazenido–thiolate complexes.

Although there are now several examples of molybdenum hydrazido(2−) complexes with thiolate coligands,[17] analogous rhenium complexes have not been reported. In an attempt to isolate rhenium species of this type, $[ReOCl_3(PPh_3)_2]$ was treated with an excess of an unsymmetrically disubstituted organohydrazine, such as $H_2NNMePh$, to yield a crystallizine, light orange material analyzing for $[ReCl(NNMePh)_2(PPh_3)_2]$. Both —$NNR_2$ ligands cannot serve as four-electron donors, since the metal would have a 20-electron count, suggesting that one —NNR_2 group is bent at the α-nitrogen and functions as a two-electron donor.

Reaction of $[ReCl(NNMePh)_2(PPh_3)_2]$ with excess thiophenol in benzene yields **4** in low yield as a diamagnetic bright red crystalline material. The presence of the oxo group is confirmed by a strong IR band at 945 cm^{-1}, while the band at 1545 cm^{-1} is attributed to the hydrazido(2−) ligand. The oxo ligand is apparently introduced from residual oxygen in the reaction solvent, and yields may be considerably improved by carrying out the synthesis in

Table 1. Relevant bond lengths (Å) for structures **1–4**

1		**2**		**3**		**4**	
Re—Cl(1)	2.436(9)			Re—O(1)	1.661(11)	Re—O(1)	1.658(12)
		Re—S(1)	2.376(4)	Re—S(1)	2.326(4)	Re—S(1)	2.339(4)
Re—P(1)	2.449(8)	Re—P(1)	2.457(4)	Re—S(2)	2.350(5)	Re—S(2)	2.354(4)
Re—P(2)	2.457(9)	Re—P(2)	2.454(4)	Re—S(3)	2.323(5)	Re—S(3)	2.331(4)
				Re—S(4)	2.333(4)		
Re—N(1)	1.798(19)	Re—N(1)	1.730(13)			Re—N(1)	1.858(9)
N(1)—N(2)	1.241(29)	N(1)—N(2)	1.324(17)			N(1)—N(2)	1.255(15)
Re—N(3)	1.726(24)	Re—N(3)	1.798(16)				
N(3)—N(4)	1.315(36)	N(3)—N(4)	1.249(23)				

oxygenated solvents. The oxo–hydrazido complex (**4**) may also be prepared by reaction of $[ReO(SPh)_4]^-$ (**3**) with $H_2NNMePh$. Although we anticipated the replacement of the oxo group of **3** by a hydrazido(2−) ligand, **3** reacted with the 1,1-disubstituted hydrazine with retention of the oxo group and replacement of a thiophenolate group by the hydrazido(2−) ligand to give **4**. This is not a simple methathesis reaction as concomitant oxidation of the metal from Re^{V} to Re^{VII} occurs. A hydrazido(1−) species such as $[Re(NHNMePh)O(SPh)_3]^-$ may be an intermediate. The formation of a rhenium–nitrogen multiple bond may provide the driving force for oxidative elimination of the hydrogen on the α-nitrogen.

DESCRIPTION OF THE STRUCTURES

Relevant bond lengths and angles are tabulated in Tables 1 and 2, and ORTEP views of the structures are presented in Figs 1–4.

Table 2. Relevant bond angles (°) for structures **1–4**

1		**2**	
Re—N(1)—N(2)	172.0(27)	Re—N(1)—N(2)	160.9(2)
Re—N(3)—N(4)	164.7(18)	Re—N(3)—N(4)	178.1(2)
N(1)—Re—N(3)	119.4(12)	N(1)—Re—N(3)	120.0(6)
P(1)—Re—P(2)	174.8(2)	P(1)—Re—P(2)	177.5(2)
P(1)—Re—C(1)	89.7(3)	P(1)—Re—S(1)	84.2(1)
P(2)—Re—C(1)	86.5(3)	P(2)—Re—S(1)	97.2(1)
P(1)—Re—N(1)	93.6(8)	P(1)—Re—N(1)	90.0(5)
P(2)—Re—N(1)	91.3(8)	P(2)—Re—N(1)	91.1(5)
P(1)—Re—N(3)	87.4(9)	P(1)—Re—N(3)	90.3(5)
P(2)—Re—N(3)	91.7(9)	P(2)—Re—N(3)	87.2(5)
C(1)—Re—N(1)	118.1(10)	S(1)—Re—N(1)	121.1(5)
C(1)—Re—N(3)	122.5(7)	S(1)—Re—N(3)	118.6(4)
N(1)—N(2)—C(71)	120.0(26)	N(1)—N(2)—C(71)	119.8(13)
N(3)—N(4)—C(81)	116.2(23)	N(3)—N(4)—C(81)	117.6(14)
3		**4**	
		Re—N(1)—N(2)	145.6(10)
O(1)—Re—S(1)	109.3(4)	O(1)—Re—S(1)	109.9(4)
O(1)—Re—S(2)	106.7(4)	O(1)—Re—S(2)	104.8(4)
O(1)—Re—S(3)	109.2(4)	O(1)—Re—S(3)	109.4(4)
O(1)—Re—S(4)	107.0(4)	O(1)—Re—N(1)	108.2(5)
S(1)—Re—S(2)	84.8(2)	S(1)—Re—S(2)	77.4(1)
S(1)—Re—S(3)	141.5(2)	S(1)—Re—S(3)	140.0(2)
S(1)—Re—S(4)	84.8(2)	S(2)—Re—S(3)	85.7(1)
S(2)—Re—S(4)	146.3(2)	S(1)—Re—N(1)	88.8(3)
S(3)—Re—S(4)	83.4(2)	S(2)—Re—N(1)	146.9(4)
		S(3)—Re—N(1)	86.1(4)
		N(1)—N(2)—C(1)	118.8(12)
		N(1)—N(2)—C(7)	122.0(11)

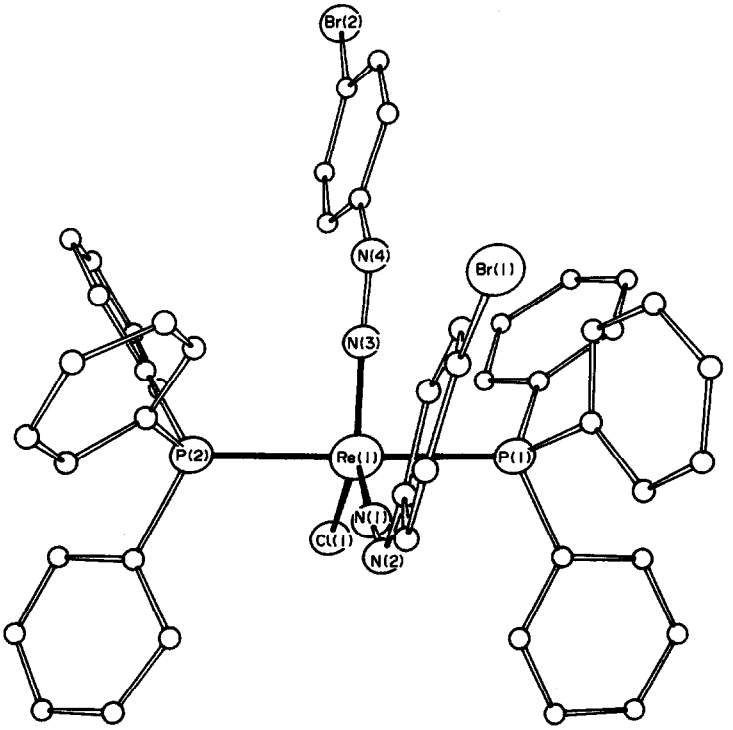

Fig. 1. ORTEP view of the structure of $[ReCl(NNC_6H_4\text{-}Br\text{-}4)_2(PPh_3)_2]$, showing the atom-labelling scheme.

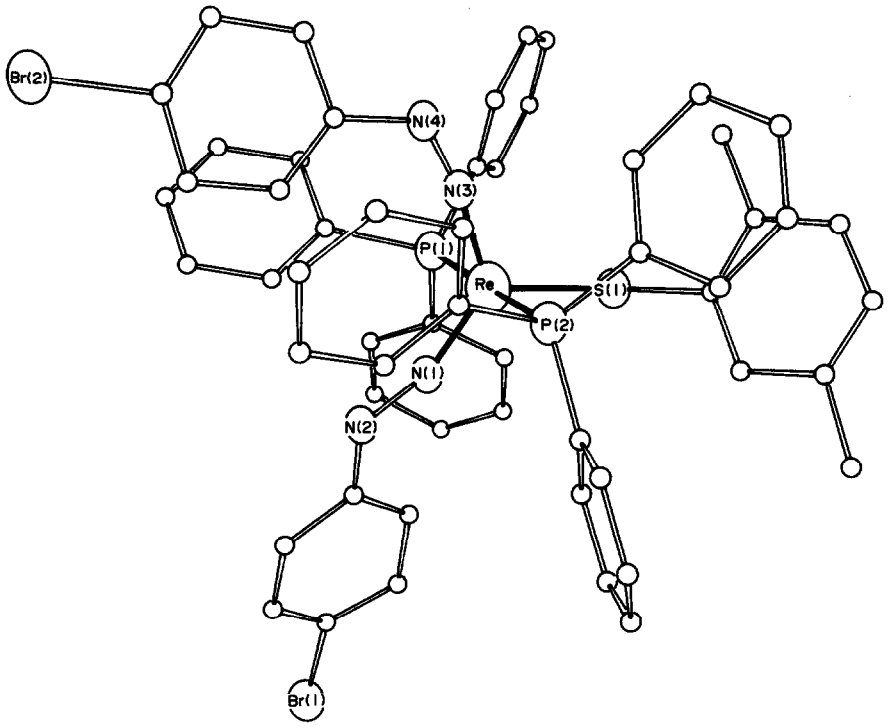

Fig. 2. Perspective views of the structure of $[Re(SC_6H_3\text{-}2,5\text{-}Me_2)(NNC_6H_4\text{-}Br\text{-}4)_2(PPh_3)_2]$.

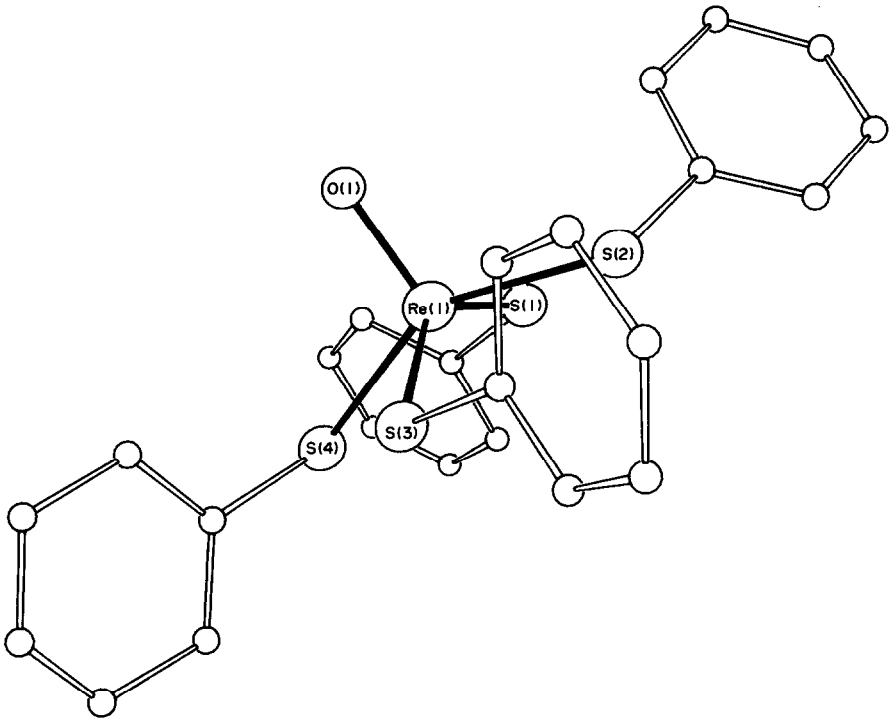

Fig. 3. ORTEP view of the structure of $[ReO(SPh)_4]^-$, crystallized as the $(PPh_4)^+$ salt.

The structure of **1** consists of discrete monomeric units. The geometry about the rhenium is best described as a trigonal bipyramidal, with the phosphine ligands axial and the equatorial plane defined by the chloro group and the α-nitrogen atoms of the diazenido ligands. The rhenium–phosphorus and rhenium–chlorine distances are unexceptional. However, an unusual feature of the structure is the inequivalence of the two rhenium–diazenido units. The Re(1)—N(1) distance of 1.80(1) Å is significantly longer than the Re(1)—N(3) distance [1.73(2) Å]. This unequivalence is reflected in the N(1)—N(2) and N(3)—N(4) distances of 1.24(2) and 1.32(3) Å, respectively, and in the Re—N(1)—N(2) and Re—N(2)—N(3) angles of 172.0(23) and 164.7(18)°. As shown in Table 3, this feature is also observed in the structures of **2** and the molybdenum(VI) cationic species $[MoCl(NNMe_2)_2(PPh_3)_2]^+$ [16] which is structurally analogous to **1** and **2**. Since there are no apparent steric interactions between the —NNR or —NNR_2 ligands and the phosphine groups, this does not appear to be simply a solid-state effect.

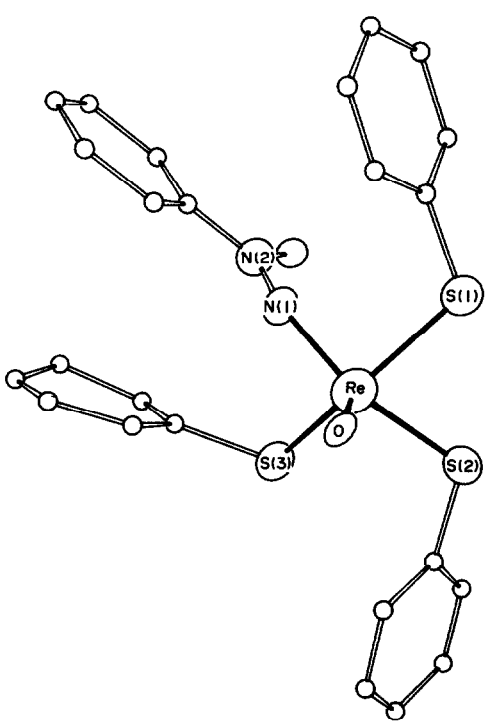

Fig. 4. ORTEP view of the structure of [ReO(NNMePh)$(SPh)_3$], showing the atom labelling.

The gross structural features of **2** are essentially identical to those of **1**, with the exception of the substitution of the thiophenolate ligand for the chloro group in the equatorial plane. The inequivalence of the diazenido ligands is pronounced, suggesting varying contributions of canonical forms **I** and **II** to the overall structure of the diazenido ligands. The Re—N(3) and N(3)—N(4) distances of 1.80(2) and 1.24(2) Å closely approximate the limiting formalism **I**, for which distances of 1.80 and 1.24 Å have been calculated.[18] On the other

Table 3. Comparison of geometric features of five-coordinate rhenium and molybdenum diazenido and hydrazido(2−) complexes

Complex	Coordination geometry[a]	M—N (Å)	N—N (Å)	M—N—N (°)	Reference
$[ReCl(NNC_6H_4Br\text{-}4)_2(PPh_3)_2]$	tbp	1.73(2)	1.32(3)	164.7(18)	This work
		1.80(2)	1.24(2)	172.0(23)	
$[Re(SC_6H_3\text{-}2,5\text{-}Me_2)(NNC_6H_4Br\text{-}4)_2(PPh_3)_2]$	tbp	1.73(1)	1.32(2)	160.9(13)	This work
		1.80(1)	1.25(2)	178.1(13)	
$[MoCl(NNMe_2)_2(PPh_3)_2]^+$	tbp	1.76(1)	1.34(2)	165.2(10)	14
		1.76(1)	1.25(1)	173.9(9)	
$[ReO(NNMePh)(SPh)_3]$	sq. pyr.	1.858(9)	1.26(2)	145.6(10)	This work
$[MoO(NNMe_2)(SPh)_3]^-$	sq. pyr.	1.821(9)	1.29(1)	152.5(10)	11

[a] tbp = trigonal bypiramidal, sq. pyr. = square pyramidal.

hand, the Re—N(1) and N(1)—N(2) distances of 1.73(1) and 1.32(2) Å suggest a significant contribution from **II** and a degree of valence isomerism for the diazenido–rhenium units of these structural types.

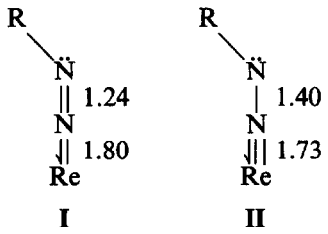

The structure of **3**, crystallized as the tetraphenylphosphonium salt, is identical to that of the tetraphenylarsonium salt, previously reported.[2] The geometry about the rhenium is square pyramidal with an apical oxo group. The Re—O distance of 1.66(1) Å is similar to those observed for the $(Ph_4As)^+$ salt, and for $[ReO(SCH_2CH_2S)_2]^-$[4] and $[ReO(SC_6H_2Me_3)_4]^-$.[19]

The geometry about the rhenium in **4** is best described as distorted square pyramidal with the oxo ligand occupying the apical position. The basal plane is defined by three thiolato sulfur atoms and the α-nitrogen of the hydrazido(2−) ligand. The Re atom lies *ca* 0.7 Å above the mean NS_3 basal plane.

The Re—O distance of 1.66(1) Å is identical to that observed for the parent anion (**3**), and the average Re—S distance of 2.341(6) Å is similar to that of 2.333(6) Å in **3**. The Re—S(3) distance is longer than the average of the Re—S(1) and Re—S(2) distances [2.354(4) vs 2.335(4) Å], presumably reflecting a *trans* influence of the hydrazido(2−) ligands in the pseudo-*trans* position.

The overall square pyramidal geometry adopted by **4** is similar to that observed for $[MoO(NNMe_2)(SPh)_3]^-$.[11] The presence of the oxo group in the apical position is consistent with the tendency of cylindrically symmetrical π-donors to occupy this site in order to maximize overlap with the metal d_{xz}- and d_{yz}-orbitals.[20]

The Re—N(1) and N(1)—N(2) distances of 1.858(9) and 1.26(2) Å, respectively, lie within the range found for metal hydrazido(2−) complexes,[21] and are consistent with extensive delocalization of the π-bonding throughout the Re—N(1)—N(2) unit. Although the —NNMePh ligand lies in the basal plane, the Re—N(1) distance indicates strong π-bonding to the rhenium. The hydrazido group has two orbitals available for π-bonding, the *p*-orbital on N(1) in the N(1)–N(2)–C(1)–C(7) plane and the N–N π-antibonding orbital perpendicular to this plane. The N(1)–N(2)–C(1)–C(7) plane eclipses the Re—O bond vector, ensuring that the N(1) *p*-orbital overlaps with the metal D_{z^2} orbital. The π-antibonding orbital has the correct symmetry to interact with the metal d_{xy}-orbital.

The most unusual feature of the structure is the non-linearity of the Re—N(1)—N(2) angle [145.6(10)°]. Simple electron counting suggests that $—NNR_2$ unit functions as a four-electron donor in the hydrazido(2−) formalism. Although the short N(1)—N(2) distance supports this argument, the Re—N(1)—N(2) angle suggests a contribution from a valence form with sp^2 hybridization at the α-nitrogen. This latter description of the bonding appears unlikely in view of the short Re—N(1) distance and the electronic requirements of the metal. Recent *ab initio* calculations indicate that the energies between different geometric forms of $—NNR_2$ ligand types may often be very small and that the angle at the α-nitrogen is a rather insensitive indicator of hybridization mode.[22] Consequently, extrapolating from the observed structure to an inferred charge distribution may be inappropriate.

Five-coordinate geometries appear to be quite common for rhenium complexes with strongly π-

bonding ligands, such as oxo groups and hydrazido or diazenido units. The limiting geometry, whether trigonal bipyramidal or square-based pyramidal, may be dictated in part by the steric requirements of the coligands. Thus, in the presence of bulky coligands, such as phosphines, the trigonal bipyramidal geometry is adopted with the bulky groups occupying the axial sites. Cylindrically symmetrical π-donors, such as oxo groups, appear to favor the apical position of the square-based pyramid.

Table 4. Summary of crystal data and experimental details for the structures of $[ReCl(NNC_6H_4Br\text{-}4)_2(PPh_3)_2]$ (**1**), $[Re(SC_6H_3\text{-}2,5\text{-}Me_2)(NNC_6H_4Br\text{-}4)_2(PPh_3)_2]$ (**2**), $(PPh_4)[ReO(SPh)_4]$ (**3**) and $[ReO(NNR_2)(SPh)_3]$ (**4**)

	1	**2**	**3**	**4**
	(A) Crystal parameters at 23°C[a]			
a (Å)	12.216(2)	14.393(3)	12.531(2)	16.137(2)
b (Å)	19.098(3)	18.842(3)	24.577(4)	9.863(2)
c (Å)	20.257(4)	20.717(4)	16.922(3)	16.668(2)
α (°)	90.00	90.00	90.00	90.00
β (°)	106.20(1)	110.26(1)	99.06(1)	111.12(1)
γ (°)	90.00	90.00	90.00	90.00
V (Å^3)	4538.3(8)	5270.5(8)	5146.2(9)	2474.7(6)
Space group	$P2_1/n$	$P2_1/n$	$P2_1/n$	$P2_1/n$
Z	4	4	4	4
D_{calc} (g cm^{-3})	1.63	1.53	1.36	1.74
	(B) Measurement of intensity data			
Crystal dimension (mm)	$0.20\times0.20\times0.25$	$0.15\times0.20\times0.22$	$0.18\times0.22\times0.15$	$0.18\times0.18\times0.18$
Instrument	Nicolet R3m			
Radiation	Mo-K_α ($\lambda = 0.71069$ Å)			
Scan mode	Coupled θ(crystal)–2θ(counter)			
Scan rate (° min^{-1})	7–30			
Scan range (°)	$2 > 2\theta \leqslant 45$			
Scan length (°)	From $[2\theta(K_{\alpha1})-1.0]$ to $[2\theta(K_{\alpha2})+1.0]$			
Background measurement	Stationary crystal, stationary counter, at the beginning and end of each 2θ scan, each for the time taken for the scan.			
Standard	3 collected every 197			
Number of reflections collected	4757	8550	5363	4922
Number of independent reflections used in solution	1905	4249	2912	2940
	(C) Reduction of intensity data and summary of structure solution and refinement[b]			
Data corrected for background, attenuators, Lorentz and polarization effects in the usual fashion				
Absorption coefficient (cm^{-1})	67.91	58.41	44.24	92.25
Absorption correction	Based on ψ scands for five reflections with χ near 90 or 270°			
T_{max}/T_{min}	1.09	1.14	1.03	1.11
Structure solution	Patterson synthesis yielded the Re positions, all remaining non-hydrogen atoms were located via standard Fourier technique			
Atomic scattering factors[c]	Neutral atomic scattering factors were used throughout the analysis			
Anomalous dispersion[d]	Applied to all non-hydrogen atoms			
Final discrepancy factor[e]	$R = 0.070$	0.070	0.050	0.066
	$R_w = 0.070$	0.070	0.052	0.066
Goodness of fit (GOF)[f]	1.337	1.369	1.172	1.496

[a] From a least-squares fitting of the setting angle of 25 reflections.

[b] All calculations were performed on a Data General Nova 3 computer with 32K of 16-bit words using local versions of the Nicolet SHELXTL interactive crystallographic software package as described in G. M. Sheldrick, *Nicolet SHELXTL Operations Manual*. Nicolet XRD, Cupertino, CA (1979).

[c] D. T. Cromer and J. B. Mann, *Acta Cryst.* 1968, **A24**, 321.

[d] International Tables for X-ray Crystallography, Vol. 3. Kynoch Press, Birmingham (1962).

[e] $R = \Sigma[|F_o|-|F_c|/\Sigma|F_o|]$, $R_w = (\Sigma w(|F_o|-|F_c|)^2/\Sigma w|F_o|^2]^{1/2}$, $w = 1/\delta^2(F_o)+g^*(F_o)$, $g = 0.0005$.

[f] GOF $= [\Sigma w(|F_o|-|F_c|)^2/(N_O-N_V)]^{1/2}$, where N_O is the number of observations and N_V is the number of variables.

EXPERIMENTAL

Materials and methods

All preparative reactions were performed in reagent grade solvents with no special precautions to eliminate atmospheric oxygen. $[ReOCl_3(PPh_3)]$ was prepared by the literature method.[23] All other reagents were obtained from standard commercial sources and used without further purification.

The following instruments were used in this work: IR, Perkin–Elmer 283B IR spectrophotometer; X-ray crystallography, Nicolet R3m diffractometer.

All compounds were isolated as crystalline solids. Microanalytical data were obtained by MicAnal, Tucson, AZ.

Preparation of compounds

$[ReCl(PPh_3)_2(NNC_6H_4Br\text{-}4)_2]$ (**1**). Oxotrichlorobis-(triphenylphosphine) rhenium (2.0 g), *p*-bromophenyl hydrazine hydrochloride (4.3 g) and triethylamine (15 cm^3) were heated under reflux with stirring in 150 cm^3 methanol for 30 min. The resulting red-brown solution is filtered, and the red precipitate washed with dry methanol, then air-dried giving 70% yield. Found: C, 51.3; H, 3.3; N, 5.0. Calc. for $[ReCl(PPh_3)_2(NNC_6H_4Br)_2]$: C, 51.7; H, 3.4; N, 5.0%.

$[Re(SC_6H_3\text{-}2,5\text{-}Me_2)(PPh_3)_2(NNC_6H_4Br\text{-}4)_2]$ (**2**). Chlorobis(triphenylphosphine) bis(*p*-bromophenyldiazenido) rhenium (0.5 g), 2,5-dimethylthiophenol (0.43 g), and diisopropylethylamine (0.5 cm^3) were warmed gently with stirring in benzene (150 cm^3) overnight. The resulting deep red solution was filtered and the benzene removed by rotary evaporation. The red oil was dissolved in dichloromethane and layered with methanol–diethyl ether. Large red crystals form within 24 h. Found: C, 55.1; H, 3.9; N, 4.5. Calc. for $[Re(SC_6H_3\text{-}2,5\text{-}Me_2)(PPh_3)_2(NNC_6H_4Br\text{-}4)_2]$: C, 55.3; H, 3.9; N, 4.6%.

$(PPh_4)[ReO(SPh)_4]$ (**3**). Was prepared by literature method with substitution of tetraphenyl phosphonium bromide for the arsonium salt.

$[ReO(NNMePh)(SPh)_3]$ (**4**). $(PPh_4)[ReO(SPh_4)]$ (1.0 g) 1,1-methylphenyl hydrazine (0.57 cm^3) and diisopropylethylamine (1.0 cm^3) were refluxed in 100 cm^3 of methanol with stirring. The color gradually changed from purple-black to red, after which the solution is filtered. The methanol was removed by rotary evaporation giving a red oil. This material is redissolved in methanol and layered with diethyl ether, giving bright red-orange crystals. Found: C, 45.9; H, 3.5; N, 4.2. Calc. for $ReO(NNMePh)(SPh)_3$: C, 46.2; H, 3.6; N, 4.3%.

X-ray crystallography

The experimental details of the data collections and structure solutions are summarized in Table 4. A complete description of crystallographic protocols may be found in Ref. 24.

Final atomic positional and thermal parameters, bond lengths and angles and F_o/F_c values have been deposited as supplementary material with the Editor, from whom copies are available on request. Atomic coordinates have also been submitted to the Cambridge Crystallographic Data Centre.

REFERENCES

1. I. G. Dance, *Polyhedron* 1986, **5**, 1037.
2. A. C. McDonnell, T. W. Hambley, M. R. Snow and A. G. Wedd, *Anst. J. Chem.* 1983, **36**, 253.
3. P. J. Blower, J. R. Dilworth, J. P. Hutchinson and J. A. Zubieta, *J. Chem. Soc., Dalton Trans.* 1985, 1533.
4. P. J. Blower, J. R. Dilworth, J. P. Hutchinson, T. Nicholson and J. Zubieta, *J. Chem. Soc., Dalton Trans.* 1986, 1339.
5. D. Sutton, *Chem. Soc. Rev.* 1975, **4**, 443; G. Avitable, P. Ganis and M. Nemiroff, *Acta Cryst.* 1971, **B27**, 725; U. F. Duckworth, P. G. Douglas, R. Mason and B. L. Shaw, *J. Chem. Soc., Chem. Commun.* 1970, 1083; W. E. Carroll and F. J. Lalor, *J. Chem. Soc., Dalton Trans.* 1973, 1754; J. A. Ibers and B. L. Haymore, *Inorg. Chem.* 1975, **14**, 1369; J. V. McArdle, A. J. Schulz, B. J. Corden and R. Eisenberg, *Inorg. Chem.* 1973, **12**, 1676; M. Cowie, B. L. Haymore and J. A. Ibers, *Inorg. Chem.* 1975, **14**, 2617; B. L. Haymore and J. A. Ibers, *Inorg. Chem.* 1975, **14**, 1369.
6. A. P. Gaughan and J. A. Ibers, *Inorg. Chem.* 1975, **14**, 352.
7. E. W. Abel, C. A. Burton, M. R. Churchill and K.-K. G. Lin, *J. Chem. Soc., Chem. Commun.* 1974, 268.
8. P. G. Douglas, A. R. Galbraith and B. L. Shaw, *Transition Met. Chem.* 1975, **1**, 17; R. Mason, K. M. Thomas, J. A. Zubieta, P. G. Douglas, A. R. Galbraith and B. L. Shaw, *J. Am. Chem. Soc.* 1974, **96**, 265; J. Chatt, M. E. Fakley, P. B. Hitchcock, R. L. Richards, N. T. Luong-Thi and D. L. Hughes, *J. Organomet. Chem.* 1979, **172**, C55 (see also Ref. 8 for reformulation); V. W. Day, T. A. George, S. D. A. Iske and S. D. Wagner, *J. Organomet. Chem.* 1976, **112**, C55; F. C. March, R. Mason and K. M. Thomas, *J. Organomet. Chem.* 1975, **96**, C43.
9. F. W. B. Einstein, T. Jones, A. J. L. Hanlan and D. Sutton, *Inorg. Chem.* 1982, **21**, 2585.
10. J. R. Dilworth, S. A. Harrison, D. R. M. Walton and E. Schwede, *Inorg. Chem.* 1985, **24**, 2595.

11. R. J. Burt, J. R. Dilworth, G. J. Leigh and J. A. Zubieta, *J. Chem. Soc., Dalton Trans.* 1982, 2295.
12. D. Sutton, *Chem. Soc. Rev.* 1975, 443.
13. E. W. Abel, C. A. Burton, M. R. Churchill and K. K. Lin, *J. Chem. Soc., Chem. Commun.* 1974, 268; J. R. Dilworth, H. J. de Liefde Meyer and J. H. Teuben, *J. Organomet. Chem.* 1978, **159**, 47.
14. J. Chatt, B. A. L. Crichton, J. R. Dilworth, P. Dahlstrom, R. Gutkoska and J. A. Zubieta, *Transition Met. Chem.* 1979, **4**, 271.
15. B. L. Haymore, *J. Organomet. Chem.* 1977, **137**, C11.
16. T. Nicholson and J. Zubieta, *Inorg. Chim. Acta* 1985, **100**, L35; T.-C. Hsieh, T. Nicholson and J. Zubieta, *Inorg. Chem.* (submitted).
17. B. A: L. Crichton, J. R. Dilworth, P. Dahlstrom and J. Zubieta, *Transition Met. Chem.* 1980, **5**, 316.
18. G. L. Hillhouse, B. L. Haymore, S. A. Bistram and W. A. Hermann, *Inorg. Chem.* 1983, **22**, 314.
19. P. J. Blower, J. R. Dilworth, J. Hutchinson, T. Nicholson and J. Zubieta, *Inorg. Chim. Acta* 1984, **90**, L27.
20. A. R. Rossi and R. Hoffmann, *Inorg. Chem.* 1975, **14**, 365.
21. J. Chatt, B. A. L. Crichton, J. R. Dilworth, P. Gutksoke and J. Zubieta, *Inorg. Chem.* 1982, **21**, 2383.
22. J. R. Dilworth, A. Carcia-Rodriguez, G. J. Leigh and J. N. Murrell, *J. Chem. Soc., Dalton Trans.* 1983, 455.
23. J. Chatt and G. A. Rowe, *J. Chem. Soc. A* 1962, 4019.
24. A. Bruce, J. L. Corbin, P. L. Dahlstrom, J. R. Hyde, M. Minelli, E. I. Stiefel, J. T. Spence and J. Zubieta, *Inorg. Chem.* 1982, **21**, 917.

Polyhedron Vol. 6, No. 7, pp. 1587–1592, 1987
Printed in Great Britain

0277–5387/87 $3.00+.00

CHARACTERIZATION OF MAGNESIUM–ALUMINUM DOUBLE HYDROXIDE PREPARED FROM ALKOXIDES AND ITS PRODUCTS OF THERMOLYSIS

OSAMU YAMAGUCHI,* HIROYUKI TAGUCHI, YUTAKA MIYATA, MASARU YOSHINAKA and KIYOSHI SHIMIZU

Department of Applied Chemistry, Faculty of Engineering, Doshisha University, Kyoto 602, Japan

(*Received* 5 *January* 1987; *accepted* 6 *February* 1987)

Abstract—A magnesium–aluminum double hydroxide was prepared by the simultaneous hydrolysis of magnesium and aluminum alkoxides. Pure double hydroxide is obtained between 0.6 and 0.8 in the $Mg^{2+}/(Mg^{2+}+Al^{3+})$ mole ratio. Infrared spectra were compared with those of $4Mg(OH)_2 \cdot Al(OH)_3$ synthesized by Feitknecht and Gerber, and the naturally occurring mineral $Mg_6Al_2(OH)_{18} \cdot 4H_2O$. The compounds MgO and $MgAl_2O_4$ crystallize slowly above $\approx$ 500°C and $\approx$ 800°C, respectively. Powders for the double hydroxide gave large aggregates of small particles. Definite signs of particle growth and a marked increase in crystallite growth were seen in powders produced above 1100°C. Specific surface areas of powders heated at low temperatures are very high and did not fall below 10 m^2/g until the heating temperature was raised above 1100°C.

A magnesium–aluminum double hydroxide is one of compounds of layer lattice structures that were shown by Feitknecht[1] to form by the combination of divalent and trivalent ions of similar atomic radii. A study dealing with the Mg–Al double hydroxide was first carried out by Feitknecht and Gerber[2] in which precipitations were prepared from magnesium and aluminum chloride solution in the presence of excess sodium hydroxide. The formula of the double hydroxide was given as $4Mg(OH)_2 \cdot Al(OH)_3$. Mortland and Gastuche[3] synthesized the double hydroxide from mixed chloride solution at pH 10 by the use of sodium carbonate. However, no data for the characterization of the double hydroxide, except for the X-ray[2,3] and infrared spectrum[2] analyses, and its heating products have been reported. Aside from the preparation of the double hydroxide, a new magnesium–aluminum hydroxide mineral $Mg_6Al_2(OH)_{18} \cdot 4H_2O$, termed as meixnerite, was recently found in cracks of a serpentine rock near Ybbs-Persenbeug (Lower Austria).[4]

In the present study, a Mg–Al double hydroxide was found to form by the simultaneous hydrolysis of magnesium and aluminum alkoxides. The present paper deals with the characterization of the double hydroxide and its products of thermolysis.

EXPERIMENTAL PROCEDURE

Magnesium methoxide $Mg(OCH_3)_2$ was prepared by the reaction of magnesium foil (> 99.99%) and analytical-grade methanol containing ethyl bromide (MeOH/EtBr = 4:1) at room temperature.[5] Aluminum isopropoxide $Al(OC_3H_7)_3$ was synthesized by heating aluminum metal (> 99.99%) in an excess of analytical-grade 2-propanol with mercury(II) chloride (10^{-4} mol/mol of metal) as a catalyst for 10 h at 82°C.[6] The mixed alkoxides in various compositions shown in Table 1 were refluxed for 10 h and then, except for the mole ratio $Mg^{2+}/(Mg^{2+}+Al^{3+}) = 0.9$, hydrolyzed by adding conductivity water containing ammonium hydroxide ($H_2O/NH_4OH = 2:1$) at room temperature. The temperature was slowly increased to 75°C while the resulting suspensions were stirred. The hydrolysis products were separated from the suspensions by filtration, washed 15 times in hot water, and dried at 80°C under reduced pressure. On the other hand, in the mole

* Author to whom correspondence should be addressed.

Table 1. Chemical compositions and phases identified in starting powders

Starting powder	$(Mg^{2+}/Mg^{2+}+Al^{3+})$ mole ratio	Phase identified
A	0.5	Mg–Al double hydroxide, AlO(OH)
B	0.6	Mg–Al double hydroxide
C	0.7	Mg–Al double hydroxide
D	0.8	Mg–Al double hydroxide
E	0.9	Mg–Al double hydroxide, $Mg(OH)_2$

Table 2. X-ray data for Mg–Al double hydroxides

Starting powder B				Starting powder C			Starting powder D		
d_{obs}/nm	d_{calc}/nm	I/I_0	*hkl*	d_{obs}/nm	d_{calc}/nm	I/I_0	d_{obs}/nm	d_{calc}/nm	I/I_0
0.76	0.76	100	003	0.77	0.77	100	0.79	0.79	100
0.378	0.378	70	006	0.382	0.382	70	0.396	0.396	65
0.258	0.257	50	102	0.258	0.257	50	0.260	0.259	35
0.249	0.249	15	103	0.250	0.250	15	0.252	0.252	10
0.228	0.228	25	105	0.229	0.229	20	0.233	0.232	20
0.1931	0.1931	15	108	0.1943	0.1943	15	0.1978	0.1978	10
0.1523	0.1523	30	110	0.1526	0.1526	30	0.1533	0.1533	30
0.1493	0.1493	25	113	0.1496	0.1496	25	0.1505	0.1505	25
Hexagonal; $a = 0.3046$ nm, $c = 2.268$ nm.				Hexagonal; $a = 0.3051$ nm, $c = 2.293$ nm.			Hexagonal; $a = 0.3066$ nm, $c = 2.373$ nm.		

ratio $Mg^{2+}/(Mg^{2+}+Al^{3+}) = 0.9$ an aqueous solution of sodium hydroxide was added to the mixed alkoxide at room temperature with stirring to adjust the pH to the optimum value of 11.* The resulting suspension was warmed slowly to 75°C with stirring. Subsequent operations were made by using the same technique as described above.

RESULTS AND DISCUSSION

Identification of starting powder

The starting powders were examined by X-ray diffraction (XRD) using Ni-filtered CuKα radiation (Table 1). The starting powder A contained two crystalline phases identified as boehmite AlO(OH) and a Mg–Al double hydroxide. The double hydroxide was obtained as a single phase in B through D. The starting powder E was a mixture of $Mg(OH)_2$ and the double hydroxide. According to Feitknecht and Gerber,[2] the stability of the double hydroxide is due, in part, to Cl^- ions that compensate for the induced positive charges resulting from the substitution of Al^{3+} for Mg^{2+} ions. The formation of the double hydroxide in the present study is probably due to the Br^- ions generated from ethyl bromide used in preparing the magnesium methoxide. Table 2 shows the X-ray data for B through D; the diffraction lines were shifted at higher angles with increasing Mg^{2+} content. They were indexed as a hexagonal unit cell with lattice parameters presented in Table 2. The values of the lattice parameters were generally consistent with those of $4Mg(OH)_2 \cdot Al(OH)_3$ ($a = 0.309$ nm, $c = 2.37$ nm)[2] and $Mg_6Al_2(OH)_{18} \cdot 4H_2O$ ($a = 0.30463$ nm, $c = 2.2932$ nm).[4]

Emission spectroscopic analysis showed that the impurities in starting powder B were 10 Fe, 10 Ca, 50 Pb, 50 K, 100 Si, and 100 ppm Na. All other cation impurities were present in amounts less than 10 ppm.

Experimental results obtained from starting powder B will hereinafter be described.

Thermal analysis

Thermogravimetry (TG) and differential thermal analysis (DTA) were conducted in air at a heating

* Aqueous NaOH solution was used because $Mg(OH)_2$, being one of hydrolysis products, was dissolved by NH_4OH.

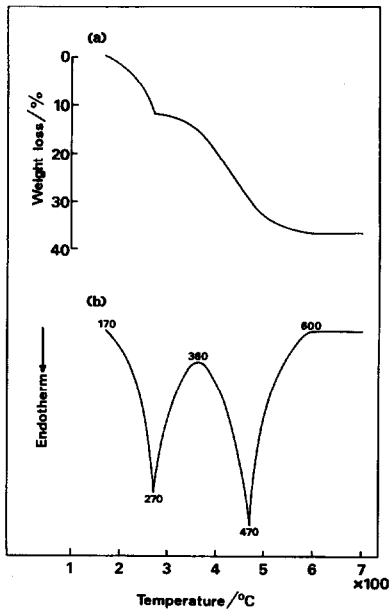

Fig. 1. (a) Thermogravimetry and (b) differential thermal analysis curves for starting powder B.

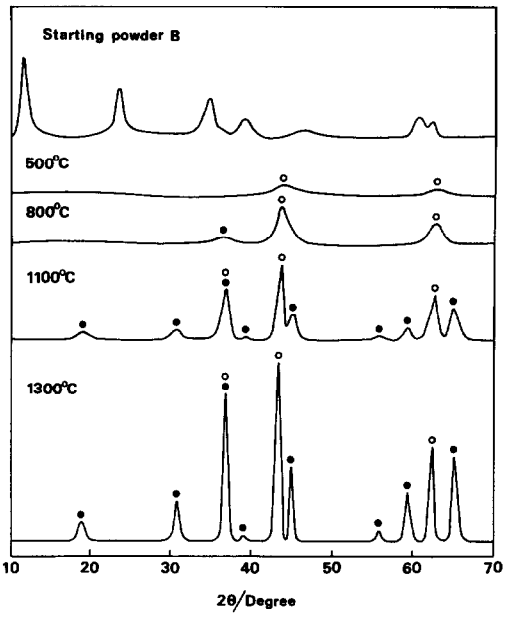

Fig. 2. X-ray diffraction patterns for starting powder B and specimens quenched after heating to various temperatures. Phases: ○, MgO; ●, $MgAl_2O_4$.

rate of 10°C/min; α-alumina was used as the reference for the DTA. Figure 1(a) shows a TG curve of starting powder. The dehydration proceeded in two steps and it was essentially completed at 600°C. The 36.7% weight loss was more than the theoretical value (32.6%) due to the release of adsorbed CO_2, as will be described in the latter section. The DTA curve reveals two endothermic peaks at 170° to 360°C and 360° to 600°C [Fig. 1(b)]; these correspond to two steps of dehydration. Although MgO and spinel $MgAl_2O_4$ crystallized slowly above $\approx$ 500°C in the latter stages of dehydration and $\approx$ 800°C, respectively, no exothermic peaks due to the crystallization were observed throughout the heating process.

Product of thermolysis

The specimens were heated at a rate of 10°C/min and then quenched and examined by XRD. Figure 2 shows the X-ray diffraction patterns for starting powder and products of thermolysis. The lines of the double hydroxide decreased in intensity with increasing temperature above 170°C and disappeared at 600°C. The lines corresponding to MgO and $MgAl_2O_4$ began to appear at $\approx$ 500°C and $\approx$ 800°C, respectively, and their intensities increased slowly up to 1100°C. The specimen heated at 1100°C gave the characteristic pattern of the mixture, although the lines were broadened. Both phases with sharp lines developed rapidly above 1100°C.

Infrared spectra

Infrared spectroscopy was performed on a dispersion in potassium bromide using the pressed-disc technique. The IR spectra of the starting powder is shown in Fig. 3 and compared with those of $4Mg(OH)_2 \cdot Al(OH)_3$[2] and $Mg_6Al_2(OH)_{18} \cdot 4H_2O$;[4] these spectra were very similar in shape. The absorption band resulting from the O–H stretching vibration based on interlayer water was observed at 3450 cm^{-1}. The bands at 3000 and 1625 cm^{-1} are due, respectively, to the O–H stretching and bending vibrations of H_2O and, on the basis of preparation history, represent adsorbed water. The mineral $Mg_6Al_2(OH)_{18} \cdot 4H_2O$ contained 2% CO_2.[4] In addition, Feitknecht and Gerber[2] reported that considerable amounts of CO_2 were adsorbed on the surface of the double hydroxide because aqueous NaOH solution was used in preparation. The absorption bands resulting from CO_3^{2-} stretching vibrations, as well as the data reported, were present at 1410, 1360, 1050, and 865 cm^{-1}; this is probably due to the NH_4OH solution containing CO_2 used in hydrolysis. These bands disappeared in the specimen heated at 600°C. Characteristic bands derived from the structure of the Mg–Al double hydroxide were observed at 780, 680, 555, and 450 cm^{-1}. The spectrum of the specimen after heating at 600°C showed the presence of the bands at 775, 690, 515, and 430 cm^{-1} and their intensities increased with increasing temperature up to 1100°C. The IR spectra for the specimen obtained by heating at 1300°C,

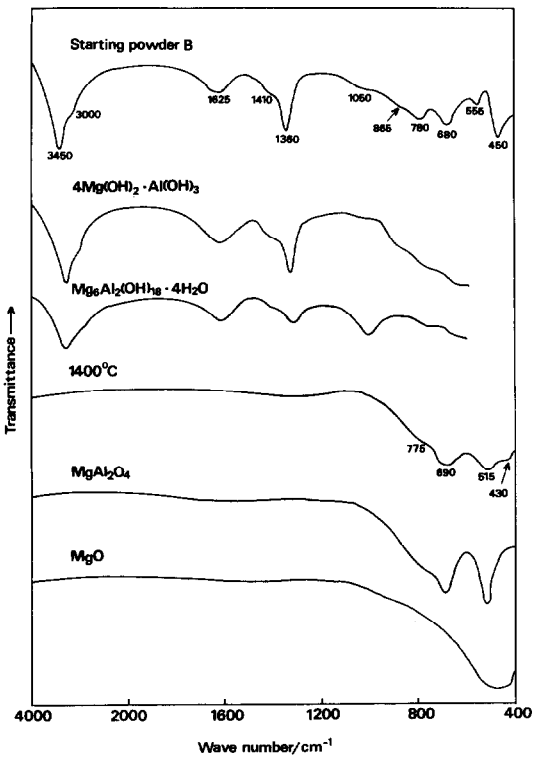

Fig. 3. Infrared absorption spectra for starting powder B, $4Mg(OH)_2 \cdot Al(OH)_3$, $Mg_6Al_2(OH)_{18} \cdot 4H_2O$, specimen quenched after heating B to 1300°C, $MgAl_2O_4$, and MgO.

$MgAl_2O_4$,* and MgO† are also shown in Fig. 3. The data for $MgAl_2O_4$ and MgO were in good agreement with those reported previously.[7-9] The spectrum pattern of the specimen, being the mixture of MgO and $MgAl_2O_4$, is similar to that of pure $MgAl_2O_4$. According to the $MgAl_2O_4$ data,[7,8] the bands in the 500–800 cm^{-1} range are assigned to the Al–O stretching vibration of AlO_6 octahedra. On the other hand, MgO is characterized by only a strong band due to the Mg–O streching vibration between 430 and 550 cm^{-1}.[9] Accordingly, the bands at 775, 690, and 515 cm^{-1} of the specimen can be assigned to Al–O stretching vibrations. The band at 430 cm^{-1} is due to Mg–O stretching vibration.

Powder characterization

Powders for electron microscopic examination were dispersed in amyl acetate by a 5 min ultrasonic treatment. Drops of the dispersion were dried on carbon film. Examination was carried out under a 100 keV beam. Electron micrographs of starting powder and specimens heated to various temperatures are shown in Fig. 4. The starting powder gave large aggregates of small particles. At 600° and 1000°C smaller aggregates (< 1 μm) were formed. Definite signs of particle growth were seen in powders produced above 1100°C.

The variation of crystallite size with increasing temperature was determined from X-ray line broadening.[11] Pure $MgAl_2O_4$ and MgO, described in the former section, were used as the samples of unbroadened line widths. The lines used were the (400) and (311) reflections for $MgAl_2O_4$ and the (200) and (220) reflections for MgO. Figure 5 shows the curves for crystallite growth of MgO and $MgAl_2O_4$ in the products with increasing temperature. A marked increase in crystallite growth of both compounds occurred above 1100°C. These results agree with observations made by the electron microscope.

Specific surface area of the specimens obtained at various temperatures was measured with a BET method using N_2 adsorption after they were dried at 200°C in vacuum. A continuous decrease in surface area with increasing temperature is shown in Fig. 6. Surface areas at low temperatures were very high and did not drop below 10 m^2/g until the heating temperature was raised above 1100°C. As described above, MgO and $MgAl_2O_4$ crystallized slowly from $\approx$ 500°C and $\approx$ 800°C, respectively, to $\approx$ 1100°C. High surface areas at low temperatures must be associated with amorphous phases.

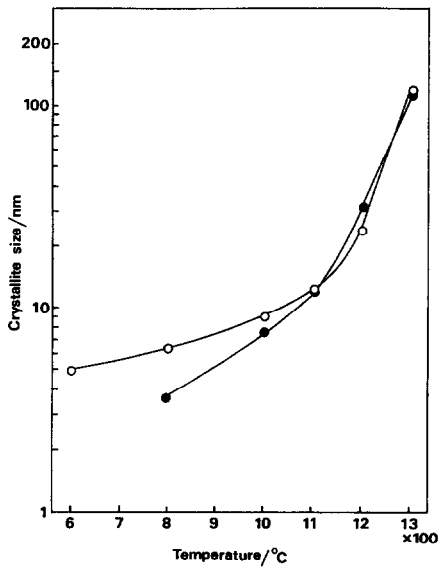

Fig. 5. Crystallite size of MgO and $MgAl_2O_4$ in products obtained from starting powder B with increasing temperature. Phases: ○, MgO; ●, $MgAl_2O_4$. Heating rate is 10°C/min.

*$MgAl_2O_4$ was prepared by solid state reaction between MgO and Al_2O_3 for 10 h at 1500°C.

†MgO was prepared by decomposition of $Mg(OH)_2$ for 3 h at 1200°C.

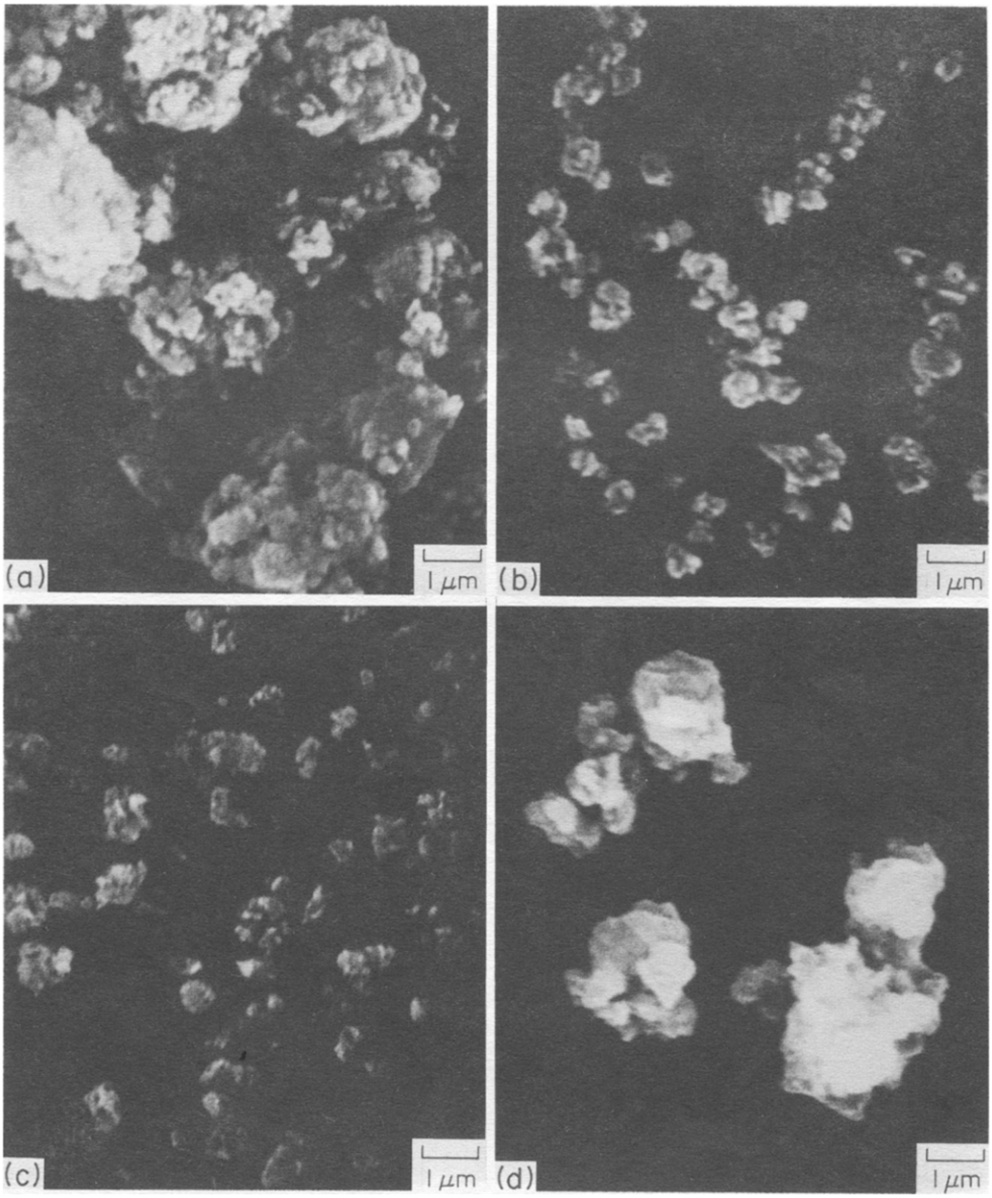

Fig. 4. Electron micrographs for (a) starting powder B, (b) 600°C, (c) 1000°C, and (d) 1300°C. Heating rate is 10°C/min.

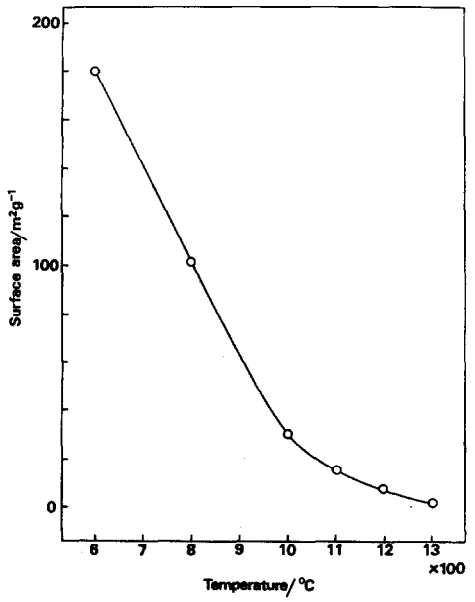

Fig. 6. Surface area of products obtained from starting powder B with increasing temperature. Heating rate is 10°C/min.

Acknowledgement—The authors wish to thank Meijo Kinzoku Co., Ltd. for the emission spectroscopic analyses.

REFERENCES

1. W. Feitknecht, *Helv. Chim. Acta* 1942, **25**, 555.
2. W. Feitknecht and M. Gerber, *Helv. Chim. Acta* 1942, **25**, 131.
3. M. M. Mortland and M. C. Gastuche, *Compt. Rend.* 1962, **255**, 2131.
4. S. Koritnig and P. Suesse, *Tschermarks Min. Petr. Mitt.* 1975, **22**, 79.
5. O. Yamaguchi, H. Matsumoto, S. Morikawa and K. Shimizu, *J. Am. Ceram. Soc.* 1983, **66**, C169.
6. O. Yamaguchi, K. Sugiura, A. Mitsui and K. Shimizu, *J. Am. Ceram. Soc.* 1985, **68**, C44.
7. V. A. Kolesova, *Opt. i Spectroscopia* 1959, **6**, 38.
8. R. A. Schroeder and L. L. Lyons, *J. Inorg. Nucl. Chem.* 1966, **28**, 1155.
9. R. A. Nyquist and R. O. Kagel, *Infrared Spectra of Inorganic Compounds*, p. 207. Academic Press (1971).
10. N. F. M. Henry, H. Lipson and W. A. Wooster, *Interpretation of X-ray Diffraction Photographs*, p. 212. D. Van Nostrand, New York (1951).

Polyhedron Vol. 6, No. 7, pp. 1593–1597, 1987
Printed in Great Britain

0277–5387/87 $3.00+.00
Pergamon Journals Ltd

SYNTHESIS AND CHARACTERIZATION OF NOVEL CHALCOGEN AND PNICTOGEN COORDINATED Bi(III) COMPLEXES—THE FIRST Se,Se′ COORDINATED Bi METALLACYCLE

Th. KLAPÖTKE

Institute of Inorganic and Analytical Chemistry, Technical University of Berlin, Straße des 17. Juni 135, D-1000 Berlin 12, F.R.G.

(*Received* 14 *January* 1987; *accepted* 6 *February* 1987)

Abstract—Inorganic and organometallic Bi(III) complexes with five-membered heterocycles were studied. The preparation, properties, and spectroscopic characterization (^{1}H NMR, IR, MS-fragmentation behaviour) of the new compounds are reported. The first member of Se coordinated Bi metallacycles is presented. Bi organyles with the *o*-aminobenzenethiol ligand system, at present widely investigated, are described as *o*-aminobenzenethiolate and *o*-aminobenzenethioldiate derivatives.

Several Bi(III) heterocycles with O,O′ and S,S′ coordinated five-membered chelate ring systems were prepared by a reaction of $CH_3Bi(OC_2H_5)_2$, obtained from CH_3BiBr_2 and $NaOC_2H_5$, with dioles or dithioles under C_2H_5OH elimination.[1] By means of this reaction the analogous pyrocatechol derivatives were prepared:[1]

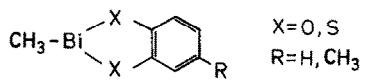

Recently an equivalent synthesis of the corresponding (S,S′ and O,O′ coordinated) eight-membered Bi(III) ring systems was reported,[2] the ψ-tetrahedral sphere of coordination (X-ray structure determination) showing the stereochemical activity of the lone pair of electrons. Triphenylbismuth, reacting with thiosalicylic acid, lost two phenyl groups and the product was a six-membered cyclic O,S coordinated derivative:[3]

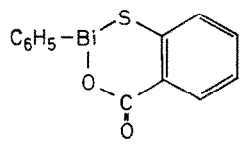

By the methods described above the synthesis of Bi containing five-membered heterocycles was possible. $Bi(C_6H_5)_3$ or $RBi(OC_2H_5)_2$ (Bi: $\delta+$; C, O: $\delta-$), reacting with the free ligand acid R–X–H (X = O, S; R: $\delta-$; H: $\delta+$) gave the desired metallacycles by benzene or ethanol elimination, respectively. Se,Se′ and Te,Te′ coordinated five-membered Bi(III) heterocycles are not yet known. The reason for this may be the difficult preparation of diselenoles or ditelluroles (e.g. hydrolysis of 1,2-$(LiX)_2C_6H_4$, X = Se, Te).

Although some organyl Bi(III)–N compounds have been produced,[4] the synthesis of five-membered metallacycles was restricted to chalcogen coordinated derivatives. In recent publications, however, Bi(III) complexes of *o*-aminothiophenol with Bi–S bondings of tris(2-aminothiobenzenethiolato)bismuth(III) were reported.[5,6] On the other hand *o*-aminothiophenol seems to be an interesting ligand in the synthesis of S,N coordinated five-membered Bi heterocycles as they exist already as members of the subgroups IV and VI.[7,8]

EXPERIMENTAL

Commercially available reagents $BiBr_3$ (Alfa), $Bi(C_6H_5)_3$ (Alfa), 1,2-$Br_2C_6H_4$ (Fluka), and 1,2-$(SH)_2C_6H_4$ (Merck) were used without further purification, *o*-aminothiophenol (Fluka) was distilled under argon and reduced pressure. CH_3BiBr_2,[9,10] $(C_6H_5)_2BiBr$,[11] *cis*-1,2-$(NaS)_2C_2(CN)_2$,[12] and 1,2-$(LiSe)_2C_6H_4$ were prepared as described in the works cited.[13]

All reactions took place in an inert gas atmos-

phere (Ar), using the Schlenk technique. The solvents were purified, dried and argon-saturated.

All melting points are uncorrected. The spectroscopic characterization was carried out with the following equipment:

Elemental analysis: Hewlett–Packard C–H–N analyser 185.

Molar mass determination: Analytische Laboratorien, Elbach.

^{1}H NMR: Bruker WP 80, samples under vacuum.

IR: Perkin–Elmer PE 457 and Perkin–Elmer 580 B, KBr technique.

MS: Varian MAT 311 A, EI, 70 eV; metastable transitions: linked scan, calculated for the following isotopes: ^{32}S, ^{79}Br, ^{80}Se, and ^{209}Bi.

Preparation of (benzene-1,2-dithiolato)bromobismuth(III) [$BiBr(S_2C_6H_4)$] (*complex* **I**)

The equivalent amount (69.32 mmol) of *n*-butyllithium in hexane at 10°C was dropped into the stirred solution of 4.93 g (34.66 mmol) 1,2-$(SH)_2C_6H_4$ in 280 cm^3 benzene. The suspension of 1,2-$(LiS)_2C_6H_4$ was stirred for 2 h and allowed to warm to 25°C and 15.55 g (34.66 mmol) $BiBr_3$ were added and stirred for 4 h. The solvent having been evaporated, the remaining residue was extracted with CH_2Cl_2 and the dark red product recrystallized from acetone.

Yield: 6.40 g (43%). Found: C, 17.0; H, 1.1. Calc. for $C_6H_4BiBrS_2$ [429.11] C, 16.8; H, 0.9%. Fp. decomposition > 200°C. ^{1}H NMR (DMSO-d_6): δ [ppm] (int.). 6.32 (2.00) m, 5.86 (2.09) m. IR: $\tilde{\nu}$ [cm^{-1}]. 3070m (ν-CH,C_6H_4), 1640s, 1435m (ν-CC,C_6H_4), 1265m, 1100w, 1030w, 750vs (γ-CH,C_6H_4). MS (210°C): *m/z* (int.). 428 (20) M^+, 349 (100) M^+-Br, 288 (8) $BiBr^+$, 241 (11) BiS^+, 209 (92) Bi^+, 140 (13) $C_6H_4S_2^+$, 108 (5) $C_6H_4S^+$.

Preparation of (cis-1,2-*dicyano-ethene*-1,2-*dithiolato*)*bromo-bismuth(III)* [$BiBr(S_2C_2(CN)_2)$] (*complex* **II**)

1.20 g (2.69 mmol) $BiBr_3$ were reacted with 0.50 g (2.69 mmol) $(NaS)_2C_2(CN)_2$ in 50 cm^3 THF at 25°C and stirred for 1 h. After filtration the resulting deep red solution was evaporated and the dark red violet residue extracted with CH_2Cl_2. Yield: 0.62 g (54%). Found: C, 11.4; N, 6.1. Calc. for $C_4BiBrN_2S_2$ [429,07] C, 11.2; N, 6.5%. Fp. decomposition under atmospheric conditions. IR: $\tilde{\nu}$ [cm^{-1}]. 2200s (ν-CN,CN). MS (140°C): *m/z* (int.). 428 (43) M^+, 352 (100) $BrBiS_2^+$, 349 (52) M^+-Br, 288 (5) $BiBr^+$, 209 (10) Bi^+.

Preparation of methyl(benzene-1,2-diselenolato) bismuth(III) [$Bi(CH_3)(Se_2C_6H_4)$] (*complex* **III**)

1.08 g (4.34 mmol) of 1,2-$(LiSe)_2C_6H_4$, dissolved in 200 cm^3 of ether, were reacted at −15°C with 1.66 g (4.33 mmol) CH_3BiBr_2 and refluxed for 30 min. The solvent was evaporated, the residue extracted with ether and the precipitated red orange solid collected by filtration, washed with ether and benzene and dried in a vacuum. Yield: 1.23 g (62%). Found: C, 18.1; H, 1.2. Calc. for $C_7H_7BiSe_2$ [458.03] C, 18.4; H, 1.5%. Fp. 142–147°C, decomposition. ^{1}H NMR (acetone-d_6): δ [ppm] (int.). 7.22 (2.00) m, 6.56 (1.98) m, 1.96 (1.52) s, 1.59 (1.59) s. IR: $\tilde{\nu}$ [cm^{-1}]. 3070m (ν-CH,C_6H_4), 2880s (ν-CH,CH_3), 1640s, 1430m (ν-CC,C_6H_4), 1265m, 1100w, 1030w, 750vs (γ-CH,C_6H_4). MS (125°C): *m/z* (int.). 460 (25) M^+, 445 (63) M^+-CH_3, 418 (1) Bi_2^+, 380 (8) M^+-Se, 369 (4) $BiSe_2^+$, 365 (5) M^+-Se-CH_3, 289 (18) $BiSe^+$, 254 (22) $Bi(CH_3)_3^+$, 239 (26) $Bi(CH_3)_2^+$, 224 (19) $BiCH_3^+$, 209 (100) Bi^+, 156 (7) $SeC_6H_4^+$.

Preparation of bis(phenyl)-o-aminothiophenolato-bismuth(III) [$Bi(C_6H_5)_2(SC_6H_4NH_2)$] (*complex* **IV**)

1.19 g (9.47 mmol) *o*-aminothiophenol and 4.17 g (9.47 mmol) triphenylbismuth were dissolved in 50 cm^3 benzene, refluxed for 2 h and stirred for 12 h at 25°C. The yellow solution was concentrated to 20 cm^3 and allowed to stand overnight yielding an orange microcrystalline solid. The product was collected by filtration and washed twice with benzene, methylenechloride, carbondisulfide, and ether. Yield. 3.00 g (65%). Found: C, 44.3; H, 3.1; N, 2.6. Calc. for $C_{18}H_{16}BiNS$ [487.38] C, 44.4; H, 3.3; N, 2.9%. Fp. 105–110°C. Molecular weight by vapor pressure osmometry (solvent N,N-DMF): 469 g/mol. Calc. for M: 487 g/mol. IR: $\tilde{\nu}$ [cm^{-1}]. 3435m (ν-NH,NH_2), 3350m (ν-NH,NH_2), 3060m (ν-CH,C_6H_4), 1598vs (δ-NH,NH_2), 1570m (δ-NH,NH_2), 1480m, 1450m, 1435s (ν-CC,C_6H_4), 1170w, 1060w, 1030w, 1010m, 765m, 745vs (γ-CH,C_6H_4), 735sh, 705s (ν-CS,CS). MS (170°C): *m/z* (int.). 487 (7) M^+, 410 (8) M^+-C_6H_5, 409 (6) M^+-C_6H_6, 363 (5) $Bi(C_6H_5)_2^+$, 333 (5) M^+-$2C_6H_5$, 332 (30) M^+-C_6H_6-C_6H_5, 286 (25) $BiC_6H_5^+$, 248 (30) $(SC_6H_4NH_2)_2^+$, 209 (100) Bi^+, 201 (46) $C_6H_4NH_2SC_6H_5^+$, 154 (8) $(C_6H_5)_2^+$, 125 (68) $H_2NC_6H_4SH^+$, 124 (92) $H_2NC_6H_4S^+$, 108 (2) $SC_6H_4^+$.

Preparation of methyl-o-aminothiophenoldiato-bismuth(III) [$BiCH_3(SC_6H_4NH)]_n$ (*complex* **V**)

The dilithium-*o*-aminothiophenoldiate was prepared in 50 cm^3 benzene by the reaction of 0.61 g

(4.87 mmol) *o*-aminothiophenol with 9.75 mmol *n*-butyllithium in hexane. 1.87 g (4.87 mmol) CH_3BiBr_2 were added and stirred for 8 h at 25°C. The yellow solution was evaporated and the remaining residue extracted with ether. The extract was concentrated to 20 cm^3 and allowed to stand for 12 h. The slightly soluble yellow product thus prepared was collected by filtration and washed three times with ether. Yield: 1.05 g (62%). Found: C, 24.5; H, 2.5; N, 3.8. Calc. for C_7H_8BiNS [347.19] C, 24.2; H, 2.3; N, 4.0%. Fp. 165°C. Molecular weight by vapor pressure osmometry (solvent N,N-DMF): 835 g/mol. Calc. for M_n: $n = 2$, 694; $n = 3$, 1041 g/mol. IR: $\tilde{\nu}$ [cm^{-1}]. 3580m (ν-NH,NH_2), 3420m (ν-NH,NH_2), 3080w (ν-CH,C_6H_4), 2880m (ν-CH,CH_3), 1600m (δ-NH,NH_2), 1480 m, 1450m (ν-CC,C_6H_4), 760sh, 758s (γ-CH,C_6H_4). MS (150°C): *m/z* (int.). 457 (3) $CH_3Bi(SC_6H_4NH_2)(SC_6H_5)^+$, 363 (37) $(CH_3)_2Bi(SC_6H_4NH_2)^+$, 349 (23) $CH_3Bi(H)(SC_6H_4NH_2)^+$, 348 (96) $CH_3Bi(SC_6H_4NH_2)^+$, 347 (8) M^+, 333 (92) $Bi(SC_6H_4NH_2)^+$, 332 (55) M^+-CH_3, 248 (48) $(SC_6H_4NH_2)_2^+$, 239 (18) CH_3BiNH^+, 224 (24) CH_3Bi^+, 209 (96) Bi^+, 125 (98) $HSC_6H_4NH_2^+$, 124 (100) $SC_6H_4NH_2^+$.

RESULTS AND DISCUSSION

Bi(III) *dithiolato derivatives*

The reaction of $BiBr_3$ with equimolar amounts of the appropriate alkali metal dithiolate ligand salts yielded for the first time by a new reaction route some five-membered Bi(III) metallacycles (complex **I** and **II**), which were only inorganically coordinated to the Bi central atom.

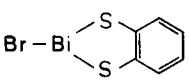

I

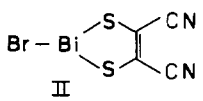

II

Generally **I** and **II** are just moderately soluble, but they are very soluble in DMF and DMSO, **II** in THF too. The ^1H NMR and IR spectra show all the expected signals in the normal ranges. The mass spectra of both complexes have as peak with the highest *m/z* value an intense signal according to the molecular ion; and under MS conditions they are more stable than the corresponding organometallic Bi(III) derivatives.[1]

The first Bi(III) *diselenolato heterocycle*

The synthesis of Se coordinated five-membered Bi(III) metallacycles, analogous to O and S derivatives, had not been achieved on the conventional reaction route because of the difficult preparation of *cis*-1,2-diselenoles. In the present work the first Se,Se′ coordinated five-membered heterocyclic bismuth organyl (complex **III**) is reported as the product of treating CH_3BiBr_2 with an equimolar amount of the easier available dilithium ligand salt of benzene-1,2-diselenol (Fig. 1). The identity of complex **III** was proved by elemental analysis, ^1H NMR, IR, and mass spectra. The IR spectrum shows the typical absorptions of the symmetrical *o*-disubstituted benzene ring system and those of the methyl group. The aromatic range of the ^1H NMR spectrum shows two multiplets, equal in intensity, according to the AA′BB′ system of the C_6H_4 protons. In addition to the solvent quintet of CD_3COCD_2H in the methyl area two sharp singlets with a signal splitting $\Delta\nu$ of 29.6 Hz appear, similar but not equal in intensity (1.00 : 1.05) (Fig. 2). The integration relative to the C_6H_4 protons resulted in approximately a half methyl group for each singlet. This may be explained by the stereochemical activity of the lone pair of electrons and a ψ-tetrahedral geometry of **III** at the Bi central atom. Because of the anisotropy effect of the aromatic ring system (Fig. 1) two conformers with an *endo* or *exo* standing CH_3 group to the five-folded heterocyclic ring system in envelope conformation may exist with a different chemical shift of the methyl protons. In the temperature dependent ^1H NMR spectrum between +60°C and −60°C no significant effect was observable; the coalescence temperature may be higher than +60°C and by this the activation free energy of the ring inversion of the five-membered heterocycle $\Delta G^{\neq}$ can be expected to be higher than 70 kJ/mol.

The mass spectrum of **III** shows an intense peak of the molecular ion with the highest *m/z* value and the signal of the Bi^+ ion as the base peak, as is usual in the case of many Bi organyles. The transitions $(M^+) \rightarrow (M^+\text{-}CH_3)$, $(M^+\text{-Se}) \rightarrow (M^+\text{-Se-}CH_3)$, $(M^+\text{-Se}) \rightarrow (Bi^+)$, and $(CH_3Bi^+) \rightarrow (Bi^+)$ could be clarified by pursuing the metastable transitions using the linked scan technique.

o-*Aminothiophenol derivatives*

Although $Bi(C_6H_5)_3$ reacts with mercaptans with formation of Bi–S bonds and benzene elimination,

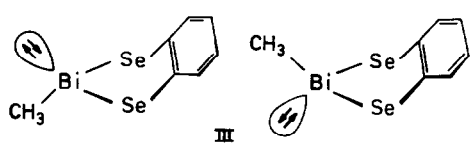

III

Fig. 1. Conformations of **III** with an exo (left) and an endo (right) standing methyl group.

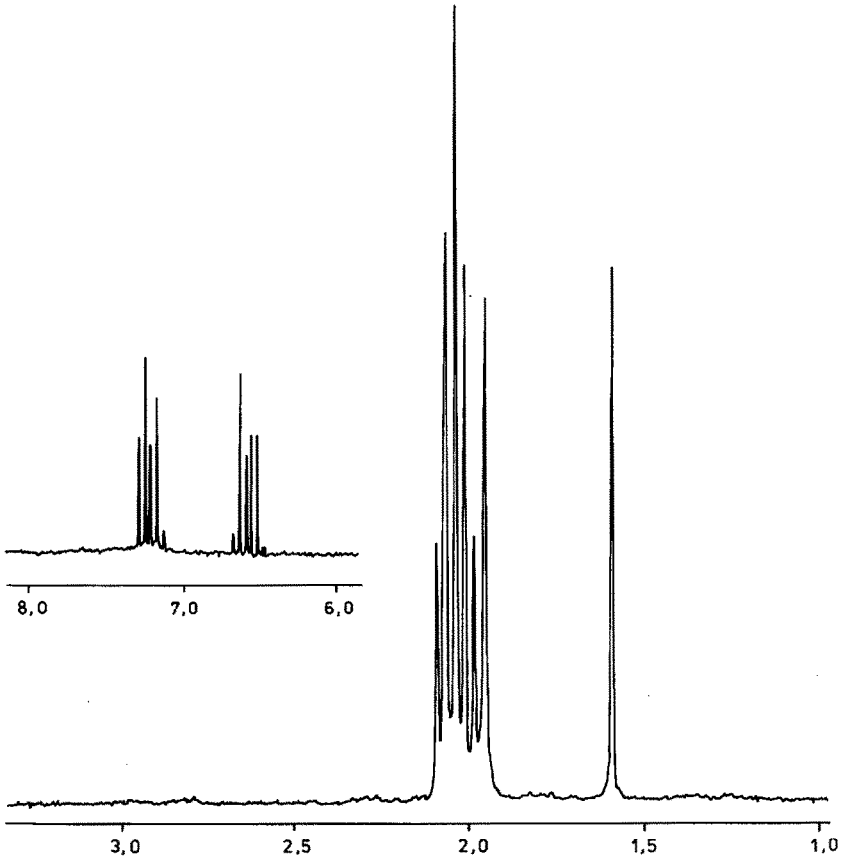

Fig. 2. ^{1}H NMR spectrum of **III**, methyl and aromatic range, −24°C, δ in ppm, solvent: acetone-d_6 (99%D).

the acidity of an aromatic substituted amino group is too low for Bi–N bond formation. Treating $Bi(C_6H_5)_3$ with equimolar amounts of *o*-aminothiophenol yielded the monosubstituted complex **IV** only, and not the desired S,N coordinated derivative **IVa**. By refluxing of $Bi(C_6H_5)_3$ with 1,2-$(NH_2)_2C_6H_4$ in benzene no reaction was observed.

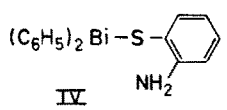

IV

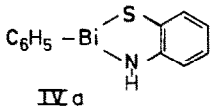

IVa

The identity of the new complex **IV** was proved by elemental analysis, IR, ^{1}H NMR, and mass spectra, its monomeric structure in DMF solution having been determined by vapor pressure osmometry. The compound **IV** was identical with the product we isolated from the reaction of $(C_6H_5)_2BiBr$ with 1,2-$(LiS)(NH_2)C_6H_4$. The transition from **IV** to **IVa** ($m/z = 409$) by benzene elimination and a further fragmentation of a phenyl group from **IVa** to **IVa**-Ph ($m/z = 332$), proved by metastable transition, was observed under the conditions in the mass spectrometer (Fig. 3). On the other hand the non-cyclic M^+(IV)-Ph ($m/z = 410$) was identified and significantly classified because of the isotope purity of Bi (see $m/z = 209$, Bi^+; Fig. 3). With this result the synthesis of an S,N coordinated cyclic Bi derivative seemed to be possible and CH_3BiBr_2 was reacted with the dilithium *o*-aminothiophenoldiate. According to the analytical and spectroscopic data the isolated product **V** corresponds to a complex of the composition $CH_3Bi(SC_6H_4NH)$. The complex **V**, in most organic solvents barely soluble or insoluble, is moderately soluble in DMF ($\approx$ 20 mg/mL). Nevertheless it has no five-membered heterocyclic structure but is an oligomeric polynuclear compound as shown by vapor pressure osmometry and mass spectrometry. Like **IV** the derivative **V** also shows the signal of an ion ($m/z = 347$) which could be the desired monomeric five-membered metallacycle. As is usual for Bi organyles the mass spectra show many decomposition products as well as very intense signals of the Bi^+ ion.

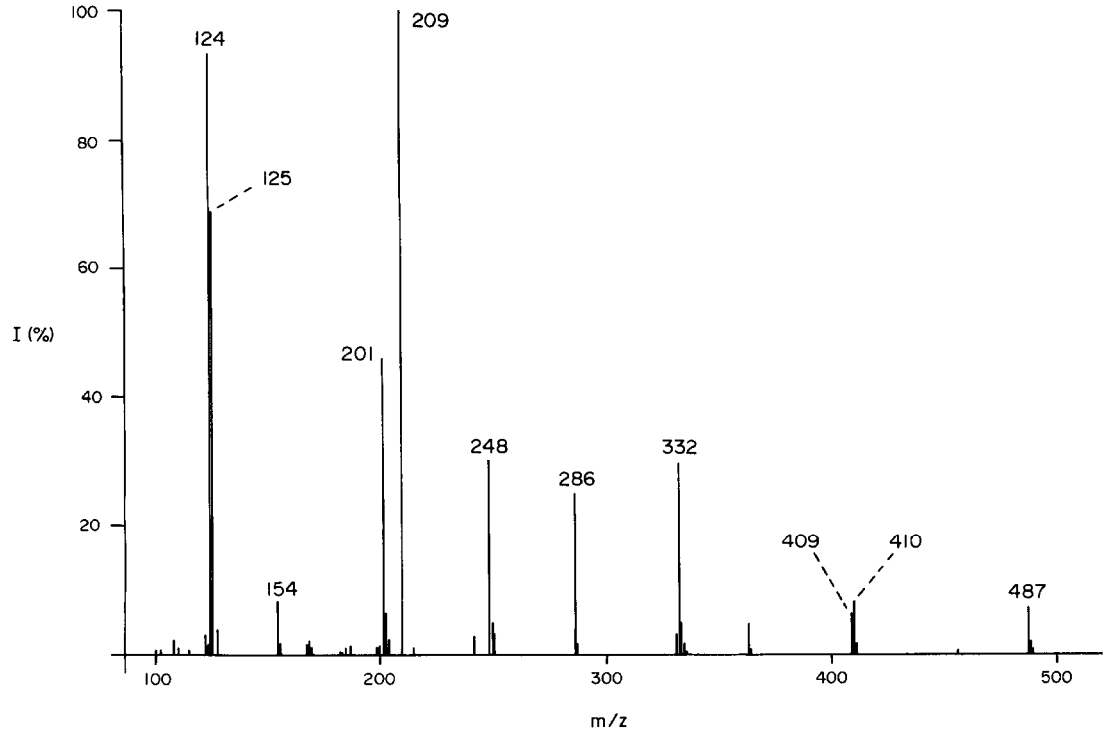

Fig. 3. Mass spectrum of **IV**, EI, 70 eV, 170°C, int. $\geqslant$ 0.2%, $m/z \geqslant 100$.

CONCLUSIONS

In the present work the preparation and spectroscopic characterization of some novel non-organometallic five-membered Bi(III) dithia heterocycles and the first diselena Bi(III) metallacycle are reported. The structure of the selenium derivative is discussed on the basis both of its metastable transition behaviour in the mass spectrum and an unexpected effect in the ^{1}H NMR spectrum; using temperature dependent measurement no dynamic effect could be observed. The synthesis of five-membered Bi(III) heterocycles by the substitution of a chalcogen atom with the isolobal NH group was not successful, although these compounds could be observed in the mass spectra. But instead of these a new interesting *o*-aminothiophenolato complex was obtained by two different reaction routes. Pnictogen coordinated five-membered Bi(III) metallacycles are still unknown under "normal" conditions, but a reference to their existence could be given and their synthesis should be carried out in the future.

Acknowledgements—Our thanks are due to A. Stöckel for mass spectra, M. Dettlaff for NMR spectra and D. Bernhard for elemental analysis.

REFERENCES

1. M. Wieber and U. Baudis, *Z. Anorg. Allg. Chem.* 1976, **423**, 40.
2. M. Dräger and B. M. Schmidt, *J. Organomet. Chem.* 1985, **290**, 133.
3. H. Gilman and H. L. Yale, *J. Am. Chem. Soc.* 1951, **73**, 2880.
4. O. Scherer, P. Hornig and M. Schmidt, *J. Organomet. Chem.* 1966, **6**, 259.
5. G. Alonzo, *Inorg. Chim. Acta* 1983, **73**, 141.
6. E. Casassas and T. Visa, *Polyhedron* 1986, **5**, 1513.
7. H. Köpf and Th. Klapötke, *Chem. Ber.* 1986, **119**, 1986.
8. E. Gore, M. L. H. Green, M. G. Harris, W. E. Lindsell and H. Shaw, *J. Chem. Soc. A* 1969, 1982.
9. A. Marquardt, *Ber. Dtsch. Chem. Ges.* 1887, **20**, 1516.
10. F. Challenger and C. F. Allpress, *J. Chem. Soc.* 1921, **119**, 913.
11. A. Gillmeister, *Ber. Dtsch. Chem. Ges.* 1897, **30**, 2843.
12. G. Bähr and G. Schleitzer, *Chem. Ber.* 1957, **90**, 438.
13. K. Lerstrup, M. Lee, F. M. Wiygul, Th. J. Kistenmacher and D. O. Cowan, *J. Chem. Soc., Chem. Commun.* 1983, 294.

Polyhedron Vol. 6, No. 7, pp. 1599–1601, 1987
Printed in Great Britain

0277–5387/87 $3.00+.00

SYNTHESIS AND MOLECULAR STRUCTURE OF CHLOROTRIS(TRIMETHYLSILYLMETHYL)TRIMETHYLSILYL-METHYLIDYNE RHENIUM(VII)

PAUL D. SAVAGE and GEOFFREY WILKINSON*

Chemistry Department, Imperial College, London SW7 2AY, U.K.

and

MAJID MOTEVALLI and MICHAEL B. HURSTHOUSE*

Chemistry Department, Queen Mary College, Mile End Road, London E1 4NS, U.K.

(*Received* 19 *January* 1987; *accepted* 6 *February* 1987)

Abstract—The complex $Re(CSiMe_3)(CH_2SiMe_3)_3Cl$ has been isolated as yellow crystals in low yield from the reaction of $ReCl_4(THF)_2$ with Me_3SiCH_2MgCl and characterised by X-ray crystallography. The molecule has a trigonal bipyramidal geometry with the alkylidyne and chlorine ligands axial.

The first monomeric alkylidyne complexes, *trans*-$X(CO)_4M{\equiv}CR$ (M = Mo and W), were prepared by treating an alkylidene complex with BX_3.[1] Higher oxidation state species of the type $M(CCMe_3)(CH_2CMe_3)_3$ have been prepared by treating $MoCl_5$ or WCl_6 with five or six equivalents of neopentyllithium.[2]

We now report the synthesis of the first monomeric rhenium(VII) trimethylsilylmethylidyne complex. The alkylation of $ReCl_4(THF)_2$ in tetrahydrofuran leads to the dinitrogen complex,[3] $[Re(CH_2SiMe_3)_4]_2N_2$, as well as low yields of bis(μ-trimethylsilylmethylidyne) tetrakis (trimethylsilylmethyl) dirhenium.[4] A third minor product from this reaction, a hexane soluble yellow air-sensitive crystalline solid $ReCl(CSiMe_3)(CH_2SiMe_3)_3$ has now been isolated.

The molecular structure as determined by X-ray crystallography is shown in Fig. 1, and confirms the structure predicted by Schrock *et al.*,[5] for the analogous neopentyl neopentylidyne complex $ReCl(CCMe_3)(CH_2CMe_3)_3$. Selected bond lengths and angles are given in Table 1. The metal has a trigonal bipyramidal configuration, with the trimethylsilylmethylidyne and chlorine ligands axial. The Re–C bonds to the equatorial trimethylsilylmethyl ligands are bent away slightly from the multiply bonded alkylidyne, as is usually found, and the Re–C–Si angles in the alkyls are somewhat greater than tetrahedral due to steric repulsions involving the $SiMe_3$ groups. Otherwise, geometry parameters are as expected.

The spectroscopic data are in agreement with the structure as determined. There are singlets in the ^1H NMR spectrum at δ 0.22 and 0.15 p.p.m. (relative intensity 27:9) indicating the trimethylsilylmethyl and trimethylsilylmethylidyne methyl protons respectively; a singlet at δ 3.22 (relative intensity 6) can be assigned to the methylene hydrogens, whose

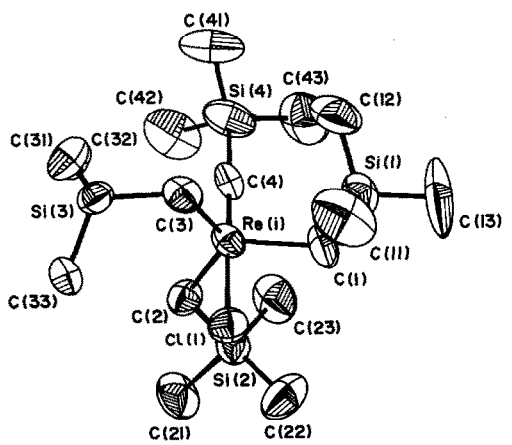

Fig. 1. The structure of $ReCl(CSiMe_3)(CH_2SiMe_3)_3$.

* Authors to whom correspondence should be addressed.

Table 1. Selected bond lengths and angles for $Re(CSiMe_3)(CH_2SiMe_3)_3Cl$

	(a) Bond lengths (Å)		
Cl(1)—Re(1)	2.523(6)	C(1)—Re(1)	2.084(13)
C(2)—Re(1)	2.059(12)	C(3)—Re(1)	2.052(12)
C(4)—Re(1)	1.726(11)	C(1)—Si(1)	1.850(13)
C(11)—Si(1)	1.831(18)	C(12)—Si(1)	1.826(20)
C(13)—Si(1)	1.751(19)	C(2)—Si(2)	1.868(12)
C(21)—Si(2)	1.845(15)	C(22)—Si(2)	1.859(16)
C(23)—Si(2)	1.860(16)	C(3)—Si(3)	1.927(14)
C(31)—Si(3)	1.842(14)	C(32)—Si(3)	1.852(14)
C(33)—Si(3)	1.845(15)	C(4)—Si(4)	1.893(12)
C(41)—Si(4)	1.819(16)	C(42)—Si(4)	1.843(18)
C(43)—Si(4)	1.805(18)		
	(b) Bond angles (deg.)		
C(1)—Re(1)—Cl(1)	87.9(4)	C(2)—Re(1)—Cl(1)	86.1(4)
C(2)—Re(1)—C(1)	118.2(5)	C(3)—Re(1)—Cl(1)	85.4(4)
C(3)—Re(1)—C(1)	119.5(5)	C(3)—Re(1)—C(2)	121.2(5)
C(4)—Re(1)—Cl(1)	179.5(3)	C(4)—Re(1)—C(1)	92.0(6)
C(4)—Re(1)—C(2)	94.4(5)	C(4)—Re(1)—C(3)	94.3(5)
C(11)—Si(1)—C(1)	111.2(7)	C(12)—Si(1)—C(1)	113.0(8)
C(12)—Si(1)—C(11)	105.2(10)	C(13)—Si(1)—C(1)	106.0(8)
C(13)—Si(1)—C(11)	110.6(12)	C(13)—Si(1)—C(12)	110.9(11)
C(21)—Si(2)—C(2)	105.8(6)	C(22)—Si(2)—C(2)	113.0(6)
C(22)—Si(2)—C(21)	107.6(8)	C(23)—Si(2)—C(2)	110.5(6)
C(23)—Si(2)—C(21)	109.3(7)	C(23)—Si(2)—C(22)	110.5(8)
C(31)—Si(3)—C(3)	105.8(7)	C(32)—Si(3)—C(3)	110.4(6)
C(32)—Si(3)—C(31)	110.6(6)	C(33)—Si(3)—C(3)	112.8(6)
C(33)—Si(3)—C(31)	107.6(7)	C(33)—Si(3)—C(32)	109.6(7)
C(41)—Si(4)—C(4)	109.7(7)	C(42)—Si(4)—C(4)	108.8(7)
C(42)—Si(4)—C(41)	111.2(10)	C(43)—Si(4)—C(4)	105.1(8)
C(43)—Si(4)—C(41)	111.3(9)	C(43)—Si(4)—C(42)	110.5(8)
Si(1)—C(1)—Re(1)	118.7(7)	Si(2)—C(2)—Re(1)	119.5(7)
Si(3)—C(3)—Re(1)	116.2(6)	Si(4)—C(4)—Re(1)	178.8(6)

low field value is characteristic of rhenium trimethylsilylmethyl compounds.[6] The mass spectrum shows the molecular ion m/e 568 (13%) with the correct rhenium isotope pattern, although the base mass is m/e 553 (M^+–Me). Sequential loss of the CH_2SiMe_3 groups are not well defined, due to the facile loss of CH_3 groups.

EXPERIMENTAL

Microanalysis by Pascher, Remagen. Spectrometers. I.R., Perkin–Elmer 683 (spectra in nujol mulls); NMR, Jeol FX-90Q (in C_6D_6, p.p.m. relative to $SiMe_4$); mass, Kratos MS 902 at 70 eV. Solvents were refluxed over sodium-benzophenone under nitrogen and distilled before use. All operations were carried out under vacuum or purified nitrogen.

Synthesis of $Re(CSiMe_3)(CH_2SiMe_3)_3Cl$

To a stirred suspension of $ReCl_4(THF)_2$[7] (0.51 g, 1.08 mmol) in THF (50 cm^3) at −78°C was added trimethylsilylmethylmagnesium chloride (6.0 cm^3 of a 0.73 mol dm^{-3} solution in diethylether, 4.3 mmol) under nitrogen. The solution was warmed slowly and held at room temperature for 1 h. The resulting purple solution was evaporated and the residue extracted into hexane (3×30 cm^3), concentrated to about 50 cm^3 and cooled −20°C overnight. Yield: 0.06 g, 10%; m.p. 120–122°C. Found: C, 33.3; H, 7.4; Cl, 6.1. Calc. for $ReC_{16}H_{42}Si_4Cl$: C, 33.8; H, 7.4; Cl, 6.2%. I.R. (cm^{-1}): 1410m, 1336s, 1248vs, 1179s, 1060w, 1020w, 971sh, 935sh, 906s, 845vs, 780sh, 755m, 701sh, 679m and 622m. NMR ^1H: 3.22 (6H, S, $C\underline{H}_2$–$SiMe_3$), 0.22 (27H, s, $CH_2Si\underline{Me}_3$) and 0.15 (9H, s, $Re{\equiv}C$–$Si\underline{Me}_3$). Mass spectrum: m/e, 568 (13%), $Re(\equiv CSiMe_3)$

$(CH_2SiMe_3)_3Cl^+$; 553 (100%), $Re(\equiv CSiMe_3)(CH_2SiMe_3)_3Cl{-}Me^+$; 73 (87%), $SiMe_3^+$.

X-ray crystallography. The crystal used for X-ray study was sealed under argon in a thin walled glass capillary. All X-ray measurements were made using a Nonius CAD4 diffractometer operating in the $\omega/2\theta$ scan mode and graphite monochromated Mo–Kα radiation ($\lambda = 0.71069$ Å). The structure was solved via routine application of the heavy atom method and developed and refined using Fourier and full-matrix least squares methods. Non-hydrogen atoms were refined anisotropically; hydrogens were located experimentally and included with group U_{iso} values, but with geometrical constraints applied to retain idealised geometries at the relevant carbon atoms. Crystal data and details of the data collection and refinement are as follows.

Crystal data

$C_{16}H_{42}ClSi_4Re$, $M = 568.505$, monoclinic, $P2_1/a$, $a = 17.991(2)$, $b = 12.616(2)$, $c = 12.296(2)$ Å, $\beta = 91.66(2)°$, $V = 2790.00$ Å^3, $Z = 4$, $D_c = 1.35$ g cm^{-3}, μ(Mo–K) = 46.78 cm^{-1}, $F(000) = 1144$.

Data collection

Crystal size $0.55 \times 0.45 \times 0.30$ mm, scan width $\omega = 0.8 + 0.35 \tan\theta$, scan times 1.35–6.77 deg min^{-1}, $1.5 \leqslant \theta \leqslant 25$. 4924 unique data, 2207 observed [$I > 2\sigma(I)$].

Structure refinement

No. of parameters = 202. Weights = $[\sigma^2(F) + 0.0002(F_o)^2]^{-1}$, $R = 0.0392$, $R_w = 0.0349$.*

Acknowledgement—We thank the SERC for provision of X-ray facilities.

REFERENCES

1. E. O. Fischer, G. Kreis, C. G. Kreiter, J. Müller, G. Hüttner and H. Lorentz, *Angew. Chem. Int. Ed. Engl.* 1973, **12**, 564.
2. D. N. Clark and R. R. Schrock, *J. Am. Chem. Soc.* 1978, **100**, 6774; R. R. Schrock, D. N. Clark, J. Sancho, J. H. Wengrovius, S. M. Rocklage and S. F. Pedersen, *Organometallics* 1982, **1**, 1645.
3. A. F. Masters, K. Mertis, J. F. Gibson and G. Wilkinson, *Nouv. J. Chim.* 1977, **1**, 389.
4. M. Bochmann, G. Wilkinson, A. M. R. Galas, M. B. Hursthouse and K. M. A. Malik, *J. Chem. Soc., Dalton Trans.* 1980, 1797.
5. D. S. Edwards, L. V. Biondi, J. W. Ziller, M. R. Churchill and R. R. Schrock, *Organometallics* 1983, **2**, 1505.
6. P. Stavropoulos, P. G. Edwards, G. Wilkinson, M. Motevalli, K. M. A. Malik and M. B. Hursthouse, *J. Chem. Soc., Dalton Trans.* 1985, 2167.
7. E. A. Allen, N. P. Johnson, D. T. Rosevear and W. Wilkinson, *J. Chem. Soc.* (A), 1969, 788.

*Final atomic positional and thermal parameters, bond lengths and angles and F_o/F_c values have been deposited as supplementary material with the Editor, from whom copies are available on request. Atomic coordinates have also been submitted to the Cambridge Crystallographic Data Centre.

Polyhedron Vol. 6, No. 7, pp. 1603–1610, 1987
Printed in Great Britain

0277–5387/87 $3.00+.00

THE DINUCLEAR UNIT μ-AQUA-BIS(μ-CARBOXYLATO)DIMETAL. X-RAY STRUCTURE AND MAGNETISM OF COBALT AND NICKEL(II) COMPOUNDS CONTAINING BRIDGING CARBOXYLATO GROUPS AND A BRIDGING WATER MOLECULE

URHO TURPEINEN and REIJO HÄMÄLÄINEN

Department of Chemistry, University of Helsinki, SF-00100 Helsinki 10, Finland

and

JAN REEDIJK*

Department of Chemistry, Leiden University, P.O. Box 9502, 2300 RA Leiden, The Netherlands

(*Received* 14 *October* 1986; *accepted after revision* 18 *February* 1987)

Abstract—The syntheses, characterization, X-ray structure and magnetism of a number of dinuclear compounds, with general formula $M_2(\mu\text{-}OH_2)(\mu\text{-}O_2CR)_2(O_2CR)_2(tmen)_2$ are described. In this formula M = Co(II), Ni(II), R = CH_3, CH_2Cl, $CHCl_2$, and CCl_3, and tmen stands for *N,N,N′,N′*-tetramethyl-1,2-diaminoethane.

The X-ray structures of two examples, M = Co and R = CCl_3(I) and M = Co, Ni and R = CH_2Cl(II) are described in detail. Compound I crystallizes in space group $P2_1/c$, with $a = 23.610(7)$, $b = 10.439(2)$ and $c = 17.920(4)$ Å, $\beta = 110.43(4)°$ and $Z = 4$. Using 5196 measured reflections collected on a diffractometer with graphite monochromatized Mo-Kα radiation, the structure was refined to $R = 0.089$. The dimeric units $Co_2(OH_2)(O_2CCl_3)_2$ [Co . . . Co = 3.696(3) Å, angle Co–O–Co = 116.1(6)°] resemble very much those of earlier reported structures with M = Ni, Co and other bridging carboxylato anions. Apart from the two bridging carboxylato anions, two monodentate $CCl_3CO_2^-$ anions are present, in addition to the normal bidentate tmen ligands, completing the octahedral geometry for each metal ion. The dimeric structure, with the bridging water ligand, appears to be highly stabilized by intramolecular hydrogen bonding with one of the oxygens of the monodentate $CCl_3CO_2^-$ ligands (O . . . O contacts of 2.56–2.60 Å). This stabilization by hydrogen bonding appears to be very similar to the proposed hydrogen bonding in hemerythrine, in which the coordinated dioxygen seems to be hydrogen bonded with the bridging –OH group.

Compound II has essentially the same basic structure; it crystallizes also in the space group $P2_1/c$, with $a = 16.034(7)$, $b = 13.114(7)$, $c = 15.344(7)$, $\beta = 91.20(4)$ and $Z = 4$. From 4701 measured reflections the structure was refined to $R = 0.043$. The dimeric units exhibit a Co-Ni distance of 3.596(1) Å, with a Ni-O-Co angle of 116.5°. The slightly smaller distances around Ni(II) made distinction from Co(II) possible.

The metal ions in these Co and Ni compounds are antiferromagnetically coupled, just as the Fe ions in hemerythrine. This antiferromagnetic interaction has been studied by low-temperature magnetic susceptibility measurements. The magnitude of the coupling appears to vary as a function of the metal, the M . . . M distance and the M–O–M angle.

* Author to whom correspondence should be addressed.

Bridging carboxylato groups are quite common in coordination compounds, and a variety of coordination geometries and bridging modes have been described during the last three decades. The classical example, $Cu_2(OAc)_4(H_2O)_2$, a centrosymmetric structure with four bridging acetates, first described[1] in 1953, has initiated research on this type of compound and derivatives. Reviews about this topic, describing compounds with variations in the apical ligands, and with different carboxylates as the bridges are available.[2] Other classical examples of such compounds are[3,4] $Zn_4O(OAc)_6$ and $Fe_3O(OAc)_6(pyridine)_3$.

In nature, the oxygen transport protein hemerythrine has been known for some time to contain the bridging unit Fe(Glu)(Asp)(OH_x)Fe, in which the value of $x = 0$ or 1, depending upon the conditions. It is now generally accepted that in the deoxy form, the two iron ions are bridged by an OH group, whereas upon oxygenation (at one iron), the OH bridge changes into an oxo bridge,[5-7] in which the hydrogen is transferred to the coordinated peroxo ligand, thereby changing to a hydrogenperoxido, OOH^-.

Very recently, Lippard and Wieghardt independently reported synthetic coordination compounds, mimicking the active site of hemerythrin, at least for the dinuclear $Fe_2O(O_2CR)_2$ unit.[8-10] Apart from the iron(III) compounds, also the Mn(III) dimers,[11] and (very recently[12]) also the Fe(II) dimer could be isolated. This latter compound oxidizes easily and is difficult to study in detail.

It appears that the role of the hydrogen bond between the bridging OH (or O) and the coordinated dioxygen ligand (hydrogenperoxido) is very important for the stability of dinuclear unit and in particular for the binding of the dioxygen. It therefore seems useful to study the details of such dimeric units with a bridging oxygen (O, OH or H_2O) by spectroscopy and magnetism.

Unfortunately with iron, the access to a great variety of compounds seems rather small, due to oxidation and dissociation problems, although Lippard[13] has reported exchange of carboxylates by phosphates. With Co^{2+} and Ni^{2+} much more stable systems having the $M_2(OH_2)(O_2CR)_2$ bridging unit have been known for about a decade,[14-17] with $R = CH_3$, CF_3, CH_2Cl, $CHCl_2$ and CCl_3. In these compounds the bridging H_2O molecule is strongly hydrogen bonded to a non-bridging carboxylato group, see Fig. 1.

This hydrogen bonding is very similar to the pattern proposed in hemerythrin,[6,7] and in fact occurs to each of the metals. It seemed of great interest to study the details of the dimeric structure and to correlate magnetic exchange coupling with M–M, O...O and other contacts and also to study the reactivity of these compounds. The first results deal with the magnetic exchange of some Co^{2+} and Ni^{2+} dimers with *N,N,N',N'*-tetramethyl-1,2-diaminoethane(tmen) as the terminal ligand and with a variety of carboxylates, as well as with the X-ray structure of one example.

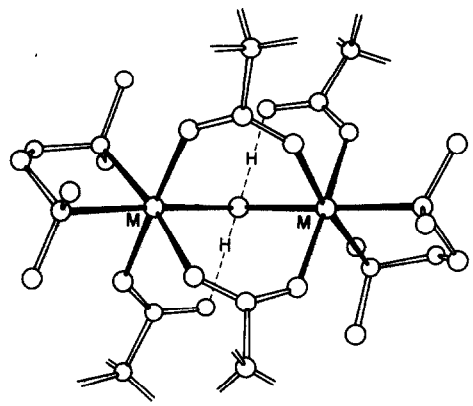

Fig. 1. Schematic structure of $M_2(OH_2)(O_2CR)_4(tmen)_2$ compounds.

EXPERIMENTAL

Starting materials and syntheses

The metal acetates and tmen were used as commercially available, without further purification. The other metal salts were prepared from the metal carbonates and the corresponding acid. Powdered microcrystalline compounds were easily obtained upon slow evaporation of aqueous ethanol solutions of the metal salts and tmen in stoichiometric ratio. The mixed-metal complex was prepared by adding 0.01 mol of green $Ni_2(C_2H_2ClO_2)_4(C_6H_{16}N_2)H_2O$ and 0.01 mol of red–brown $Co_2(C_2H_2ClO_2)_4(C_6H_{16}N_2)_2H_2O$ to 100 cm^3 ethanol. The reaction mixture was refluxed at −78°C for 5 h. After cooling of the solution to room temperature, crystallization was allowed to continue for two weeks. When the most of the solvent was evaporated large light red–brown crystals were collected by filtration. Microscopic examination suggested that crystals were homogeneous.

Characterization and analyses

The compounds were characterized by their infrared spectra and by analysis of their nickel content. The Co(II) and Ni(II) compounds were found to be isomorphous for each counter ion. Determination of nickel and cobalt contents in the mixed-

metal species revealed that the composition was $CoNi(C_2H_2ClO_2)_4(C_6H_{16}N_2)_2H_2O$. Ligand-field spectra were recorded in the diffuse reflectance mode on a Perkin–Elmer 330 instrument. Infrared spectra were taken as Nujol mulls and as KBr discs on a Perkin–Elmer 180 instrument.

Magnetic susceptibility

Powder magnetic susceptibilities were obtained in the 2–80 K region, using a PAR vibrating sample magnetometer, as described by Engelfriet[18] and calibrated with $CoHg(SCN)_4$. ESR spectra were recorded on a Varian E3 instrument at X-band frequencies.

X-ray data collection and refinement

A crystal of $Co_2(Cl_3C_2O_2)_4(C_6H_{16}N_2)_2H_2O$, **I**, used for data collection had dimensions of $0.2 \times 0.3 \times 0.4\ mm^3$. Crystal data and relevant information about the data collection and refinement have been summarized in Table 1. The data were corrected for Lorentz and polarization effects. A mixed-metal crystal of $CoNi(ClH_2C_2O_2)_4(C_6H_6N_2)_2H_2O$, **II**, used for data collection had dimensions $0.28 \times 0.35 \times 0.30\ mm^3$. Crystal data and relevant information about the data collection and refinement have been summarized in Table 2. The absorption effect was checked by empirical ϕ-scan methods, but was so insignificant that correction was excluded. The structure of **I** was solved by direct and Fourier methods using the XRAY 76 program system[19] on a UNIVAC 1100 computer. The chlorine atoms of two trichloroacetate groups appeared to be disordered and two positions were given each of these atoms. The quality of data did not allow the determination of the hydrogen atom positions. Least squares refinement with anisotropic temperature factors of Co and Cl atoms and isotropic temperature factors of the other atoms yielded final $R = 0.087$ and $R_w = 0.115$, with $w = 1/(40 + |F_o| + 0.01|F_o|^2)$. The structure determination of **II** was simplified by the observation that it is isomorphous with corresponding nickel(II) compound. The atomic parameters were taken directly from the refinement of the nickel(II) compound, and refinement with anisotropic temperature factors for non-H atoms and isotropic temperature factor for the H atoms of the water molecule gave $R = 0.042$ and $R_w = 0.038$, with $w = 1/\sigma^2(F)$. The other H atoms with $U = 0.08$ were included at idealized positions (C–H = 1.0 Å) and held fixed. During the refinement the metal ion with the shortest M–O and M–N distances was assigned as nickel. Scattering factors, including anomalous dispersion, were taken from the litera-

Table 1. Crystal and diffraction data of $Co_2(Cl_3C_2O_2)_4(C_6H_{16}N_2)_2H_2O$

M_r	1017.8
Space group	$P2_1/c$
a, Å	23.610(7)
b, Å	10.439(2)
c, Å	17.920(4)
β, deg	110.43(4)
V, Å^3	4139
Z	4 (dimers)
D_{measd}, Mg m^{-3}	1.63
D_{calcd}, Mg m^{-3}	1.63
$F(000)$	2048
2θ, range, deg	4–45
Measd reflens	5196
Significant reflens [$I > 2\sigma(I)$]	2189
μ, cm^{-1}	16.5
Final R value ($\Sigma \|\|F_o\| - \|F_c\|\|/\|F_o\|$)	0.089
Final R_w value ($[\Sigma w(\|F_o\| - \|F_c\|)^2/\Sigma w\|F_o\|^2]^{1/2}$)	0.115
Diffractometer	Syntex $P2_1$
Monochromator	Graphite
Radiation	MoKα
Scanning type	ω-scan
Scan speed °/min	2.5–30

Table 2. Crystal and diffraction data of CoNi $(C_2H_2ClO_2)_4(C_6H_{16}N_2)_2H_2O$

M_r	742.1
Space group	$P2_1/c$
a, Å	16.034(7)
b, Å	13.114(7)
c, Å	15.344(7)
β, deg	91.20(4)
V, Å^3	3226
Z	4 (dimers)
D_{measd}, Mg m^{-3}	1.52
D_{calcd}, Mg m^{-3}	1.53
$F(000)$	1540
2θ, range, deg	5–46
Measd reflens	4701
Significant reflens [$I > 2\sigma(I)$]	2986
μ, cm^{-1}	15.0
Final R value ($\Sigma \|\|F_o\| - \|F_c\|\|/\|F_o\|$)	0.043
Final R_w value ($[\Sigma w(\|F_o\| - \|F_c\|)^2/\Sigma w\|F_o\|^2]^{1/2}$)	0.038
Diffractometer	Nicolet P3
Monochromator	Graphite
Radiation	MoKα
Scanning type	ω-scan
Scan speed °/min	2.5–30

ture.[20] Atomic coordinates, listings of F_o and F_c values and anisotropic thermal parameters have been deposited as supplementary material with the Editor, from whom copies are available on request. Atomic coordinates have also been deposited with the Cambridge Crystallographic Data Centre.

RESULTS AND DISCUSSION

Description of the structure of $Co_2(OH_2)(O_2CCl_3)_4(tmen)_2$

A projection of the molecular structure is depicted in Fig. 2. A pseudo-twofold rotation axis goes through O9 and the Co–Co vector. Relevant bond distances and angles are listed in Table 3. Hydrogen-bonded intramolecular contacts are indicated by dashed lines in Fig. 2. Although the hydrogen atoms could not be located in this structure determination, the close resemblance with other, earlier reported structures,[14–17] and with the other structure described below, leads to the conclusion that a coordinated water molecule is present. The O...O contacts of 2.56–2.60 Å indicate very strong hydrogen bonding. This hydrogen bonding is confirmed by the infrared spectra (see below). The Co...Co distance of 3.696 Å is the longest contact so far observed in compounds of this type. The Co–N and Co–O distances are about the same as those found in related compounds.[14–17]

Description of the structure of $CoNi(OH_2)(O_2CCH_2Cl)_4(tmen)_2$

A projection of the molecular unit of **II** is given in Fig. 3. The structure is very similar to the structure of **I** and earlier reported ones,[14–17] as is also seen from the geometric information given in Table 4. In this structure the hydrogen atoms of the water molecule could be located. The O...O contacts of 2.54 and 2.55 Å are again indicative for a very short hydrogen bond contact, also evident from the IR spectra. The Co–O, Co-N, Ni–O and Ni–N distances are in the range normally observed.[14–17]

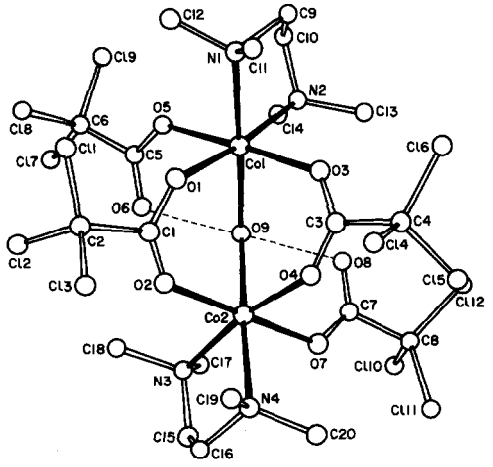

Fig. 2. Drawing of the structure and labeling of atoms of $Co_2(OH_2)(CCl_3CO_2)_4(tmen)_2$. Distances and angles are given in Table 3.

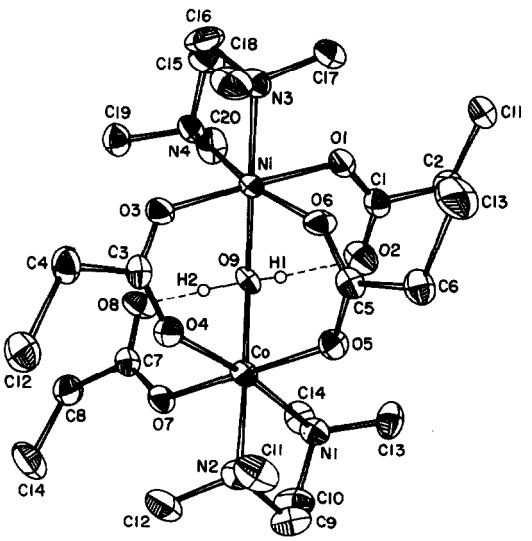

Fig. 3. ORTEP drawing and labeling of the structure of $CoNi(OH_2)(CCl_2HCO_2)_4(tmen)_2$. Geometric information is given in Table 4.

Comparison of structures

Comparing the present structures with the $Fe_2^{II}(OH)$ and the $Fe_2^{III}O$ dimers reported earlier,[8–10,12] shows that the metal–metal interactions are much shorter in the iron compounds, i.e. 3.32 Å for Fe(II) and about 3.15 Å for Fe(III). This seems to be related to the shorter Fe–O distances in Fe_2OH and Fe_2O units, compared to bridging OH_2. This also seems to influence the magnitude of the magnetic exchange (*vide infra*). Table 5 compares structural information available up to now for a variety of $M_2(OH_x)(O_2CR)_2$ dimers.

Spectroscopic measurements

The infrared spectra of all compounds show bands typical for coordinated tmen, monodentate carboxylates and bidentate bridging carboxylates.[21] In addition, however, a band for coordinated water is observed. It appears that this band, the asymmetric O–H stretch, is lowered significantly compared to normal water ligands. Depending upon the particular carboxylato ligand and metal ion, two broad bands, often accompanied by a shoulder,

Table 3. Selected interatomic distances (Å) and angles (°) with estimated standard deviations of $Co_2(H_2O)(CCl_3COO)_4(tmen)_2$(I)

Co(1)—O(1)	2.09(1)	O(1)—Co(1)—O(3)	90.8(4)
Co(1)—O(3)	2.07(1)	O(1)—Co(1)—O(5)	88.2(5)
Co(1)—O(5)	2.06(1)	O(1)—Co(1)—O(9)	91.3(5)
Co(1)—O(9)	2.18(1)	O(1)—Co(1)—N(1)	88.5(6)
Co(1)—N(1)	2.18(2)	O(3)—Co(1)—O(9)	89.8(5)
Co(1)—N(2)	2.20(2)	O(3)—Co(1)—N(1)	91.8(6)
Co(2)—O(2)	2.06(1)	O(3)—Co(1)—N(2)	91.4(5)
Co(2)—O(4)	2.08(1)	O(5)—Co(1)—O(9)	88.0(5)
Co(2)—O(7)	2.10(2)	O(5)—Co(1)—N(1)	90.4(6)
Co(2)—O(9)	2.18(1)	O(5)—Co(1)—N(2)	89.9(5)
Co(2)—N(3)	2.21(2)	O(9)—Co(1)—N(2)	96.1(6)
Co(2)—N(4)	2.19(2)	N(1)—Co(1)—N(2)	84.1(7)
N(1)—C(9)	1.59(3)	O(2)—Co(2)—O(4)	92.9(5)
N(1)—C(11)	1.52(3)	O(2)—Co(2)—O(9)	90.0(5)
N(1)—C(12)	1.49(3)	O(2)—Co(2)—N(3)	91.6(7)
N(2)—C(10)	1.47(3)	O(2)—Co(2)—N(4)	92.2(6)
N(2)—C(13)	1.51(3)	O(4)—Co(2)—O(7)	87.7(6)
N(2)—C(14)	1.48(4)	O(4)—Co(2)—O(9)	89.5(4)
C(9)—C(10)	1.41(5)	O(4)—Co(2)—N(4)	89.2(6)
N(3)—C(15)	1.48(2)	O(7)—Co(2)—O(9)	87.4(5)
N(3)—C(17)	1.48(3)	O(7)—Co(2)—N(3)	88.2(7)
N(3)—C(18)	1.48(4)	O(7)—Co(2)—N(4)	90.4(6)
N(4)—C(16)	1.49(4)	O(9)—Co(2)—N(3)	97.8(5)
N(4)—C(19)	1.51(4)	N(3)—Co(2)—N(4)	83.2(7)
N(4)—C(20)	1.48(3)	Co(1)—O(9)—Co(2)	116.1(6)
C(15)—C(16)	1.42(5)	C(9)—N(1)—C(11)	109(2)
C(1)—O(1)	1.24(2)	C(9)—N(1)—C(12)	110(2)
C(1)—O(2)	1.22(2)	C(11)—N(1)—C(12)	106(2)
C(1)—C(2)	1.61(3)	N(1)—C(9)—C(10)	108(2)
C(2)—Cl(1)	1.68(2)	C(10)—N(2)—C(13)	111(2)
C(2)—Cl(2)	1.73(2)	C(10)—N(2)—C(14)	108(2)
C(2)—Cl(3)	1.77(2)	C(13)—N(2)—C(14)	110(2)
C(3)—O(3)	1.21(2)	N(2)—C(10)—C(9)	115(2)
C(3)—O(4)	1.22(2)	C(15)—N(3)—C(17)	109(2)
C(3)—C(4)	1.58(3)	C(15)—N(3)—C(18)	113(2)
C(4)—Cl(4)	1.73(3)	C(17)—N(3)—C(18)	105(2)
C(4)—Cl(5)	1.74(3)	N(3)—C(15)—C(16)	116(3)
C(4)—Cl(6)	1.72(2)	C(16)—N(4)—C(19)	110(2)
C(5)—O(5)	1.24(2)	C(16)—N(4)—C(20)	114(2)
C(5)—O(6)	1.25(3)	C(19)—N(4)—C(20)	106(2)
C(5)—C(6)	1.51(2)	N(4)—C(16)—C(15)	118(2)
C(6)—Cl(7)	1.71(2)	O(1)—C(1)—O(2)	130(2)
C(6)—Cl(8)	1.77(2)	O(1)—C(1)—C(2)	112(2)
C(6)—Cl(9)	1.77(2)	O(2)—C(1)—C(2)	118(1)
C(7)—O(7)	1.19(2)	O(3)—C(3)—O(4)	131(2)
C(7)—O(8)	1.21(2)	O(3)—C(3)—C(4)	115(2)
C(7)—C(8)	1.59(3)	O(4)—C(3)—C(4)	114(1)
C(8)—Cl(10)	1.71(3)	O(5)—C(5)—O(6)	128(2)
C(8)—Cl(11)	1.76(2)	O(5)—C(5)—C(6)	115(2)
C(8)—Cl(12)	1.82(3)	O(6)—C(5)—C(6)	117(2)
O(6)...O(9)	2.56(2)	O(7)—C(7)—O(8)	130(2)
O(8)...O(9)	2.60(2)	O(7)—C(7)—C(8)	117(2)
Co(1)...Co(2)	3.696(3)	O(8)—C(7)—C(8)	113(2)

Table 4. Interatomic distances (Å) and angles (°) of **II**

Ni—O(1)	2.127(4)	Cl(1)—C(2)	1.743(7)	N(1)—C(10)	1.474(8)
Ni—O(3)	2.039(4)	C(1)—C(2)	1.516(9)	N(1)—C(13)	1.469(7)
Ni—O(6)	2.037(4)	C(1)—O(1)	1.236(7)	N(1)—C(14)	1.489(7)
Ni—O(9)	2.106(4)	C(1)—O(2)	1.239(7)	N(2)—C(9)	1.459(8)
Ni—N(3)	2.171(5)	Cl(2)—C(4)	1.745(6)	N(2)—C(11)	1.485(8)
Ni—N(4)	2.201(5)	C(3)—C(4)	1.522(8)	N(2)—C(12)	1.471(8)
Co—O(7)	2.117(4)	C(3)—O(3)	1.260(7)	C(9)—C(10)	1.477(8)
Co—O(5)	2.052(4)	C(3)—O(4)	1.232(7)	N(3)—C(16)	1.480(8)
Co—O(4)	2.054(4)	Cl(3)—C(6)	1.757(6)	N(3)—C(17)	1.476(8)
Co—O(9)	2.123(4)	C(5)—C(6)	1.522(7)	N(3)—C(18)	1.495(8)
Co—N(2)	2.175(5)	C(5)—O(5)	1.263(7)	N(4)—C(15)	1.456(9)
Co—N(1)	2.216(5)	C(5)—O(6)	1.223(7)	N(4)—C(19)	1.468(8)
Co—Ni	3.596(1)	Cl(4)—C(8)	1.737(6)	N(4)—C(20)	1.497(7)
O(2)...O(9)	2.551(5)	C(7)—C(8)	1.502(8)	C(15)—C(16)	1.464(11)
O(8)...O(9)	2.543(5)	C(7)—O(7)	1.256(7)	O(9)—H(1)	0.81(5)
		C(7)—O(8)	1.230(7)	O(9)—H(2)	1.11(5)
O(1)—Ni—O(6)	87.2(1)	O(4)—Co—N(2)	88.6(2)	O(5)—C(5)—O(6)	111.4(5)
O(1)—Ni—O(9)	87.8(1)	O(9)—Co—N(1)	97.6(2)	Cl(4)—C(8)—C(7)	116.4(5)
O(1)—Ni—N(3)	91.9(2)	N(1)—Co—N(2)	83.0(2)	C(8)—C(7)—O(7)	118.4(5)
O(1)—Ni—N(4)	89.0(2)	Ni—O(1)—C(1)	127.4(4)	C(8)—C(7)—O(8)	115.2(5)
O(3)—Ni—O(6)	93.2(1)	Ni—O(3)—C(3)	130.5(4)	O(7)—C(7)—O(8)	126.4(5)
O(3)—Ni—O(9)	90.1(1)	Ni—O(6)—C(5)	136.6(3)	C(10)—N(1)—C(13)	111.8(5)
O(3)—Ni—N(3)	90.3(2)	Co—O(7)—C(7)	128.9(3)	C(10)—N(1)—C(14)	108.1(4)
O(3)—Ni—N(4)	91.0(2)	Co—O(5)—C(5)	130.7(4)	C(13)—N(1)—C(14)	107.7(4)
O(6)—Ni—O(9)	93.2(1)	Co—O(4)—C(3)	136.5(3)	C(9)—N(2)—C(11)	108.8(5)
O(6)—Ni—N(3)	86.6(2)	Co—O(9)—Ni	116.5(1)	C(9)—N(2)—C(12)	111.2(5)
O(9)—Ni—N(4)	96.4(2)	Cl(1)—C(2)—C(1)	115.4(5)	C(11)—N(2)—C(12)	106.7(4)
N(3)—Ni—N(4)	83.7(2)	C(2)—C(1)—O(1)	121.3(5)	N(1)—C(10)—C(9)	112.3(5)
O(7)—Co—O(4)	87.6(1)	C(2)—C(1)—O(2)	110.9(5)	N(2)—C(9)—C(10)	112.5(5)
O(7)—Co—O(9)	87.0(1)	O(1)—C(1)—O(2)	127.8(5)	C(16)—N(3)—C(17)	111.6(5)
O(7)—Co—N(2)	91.3(2)	Cl(2)—C(4)—C(3)	116.0(4)	C(16)—N(3)—C(18)	109.4(5)
O(7)—Co—N(1)	88.8(2)	C(4)—C(3)—O(3)	112.5(5)	C(17)—N(3)—C(18)	107.9(4)
O(5)—Co—O(4)	93.5(1)	C(4)—C(3)—O(4)	118.6(5)	C(15)—N(4)—C(19)	110.6(5)
O(5)—Co—O(9)	91.2(1)	O(3)—C(3)—O(4)	128.9(5)	C(15)—N(4)—C(20)	109.7(5)
O(5)—Co—N(2)	90.5(2)	Cl(3)—C(6)—C(5)	114.6(4)	C(19)—N(4)—C(20)	106.8(4)
O(5)—Co—N(1)	90.3(2)	C(6)—C(5)—O(5)	111.4(5)	N(3)—C(16)—C(15)	112.4(5)
O(4)—Co—O(9)	90.7(1)	C(6)—C(5)—O(6)	120.1(5)	N(4)—C(15)—C(16)	113.1(6)

are observed in the region 2000–2400 cm^{-1}. This enormous lowering compared to free water is ascribed to the very strong hydrogen-bond formation with the monodentate coordinating carboxylato group, resulting in O...O contacts of about 2.5–2.7 Å. The fact that more than one such O...O contact occurs (see Tables 3 and 4 and refs 14–17), nicely agrees with the observation of 2 or 3 IR bands.

Application of the now classical formula of Bellamy and Owen,[22] an O...O contact of 2.60 Å would predict a decrease in the O–H stretch of about 1100 cm^{-1}, just as observed. The other parts of the IR spectrum just show ligand and anion bands. The M–O stretching frequencies, observed in the far-IR are too much overlapping to allow assignments without isotopic labelling, and therefore are not discussed in this paper. The assignment as M–L bands, however, can be easily deduced from the fact that the isomorphous Co and Ni compounds have comparable bands, but with many Ni compounds having the bands some 5–15 cm^{-1} at higher wave numbers.

The ligand field spectra of all compounds are typical[23,24] for (distorted) octahedral geometry. The band maxima nicely agree with a MN_2O_4 chromophore, and are not discussed in detail. Band maxima for the Ni compounds occur at 9100, 15450 and 25900 cm^{-1}, and those for the Co compounds at 8300 and 19500 cm^{-1}. The Co–Ni mixed-metal compound has a spectrum which is the sum of both spectra.

Table 5. Structural comparison for some compounds with the $M_2O(O_2CR)_2$ unit

Compound	M–M (Å)	M–O–M (°)	M–OH_x (Å)	Ref. No.
(a) Ni(tmen) compounds				
Bridge: acetato	3.563	117.2	2.088	26
chloroacetato	3.567	117.4	2.088	14
dichloroacetato	3.657	118.1	2.133	15
trifluoroacetato	3.676	117.2	2.155	16
(b) Co(tmen)				
Bridge: acetato	3.597	115.1	2.132	17
chloroacetato	3.621	113.5	2.165	17
dichloroacetato	3.675	116.4	2.162	25
trichloroacetato	3.696	116.1	2.18	this work
(c) Ni/Co(tmen)				
Chloroacetato	3.596	116.5	2.114	this work
(d) Iron–nane species				
Bridge: acetato/OH	3.32	113	1.990	12
same with acetato/O	?	119.7	1.800	12
(e) Iron–Bpz_3 species				
Bridge: acetato/O	3.146	123.6	1.784	9

Magnetic properties

The most interesting properties of the compounds are, apart from the fascinating H-bridge system that co-stabilizes the dimeric units, the magnetic properties. Therefore magnetic susceptibilities of a number of Co and Ni compounds have been studied, down to 2 K. The results are summarized in Table 6, together with some geometrical data. A representative curve of the susceptibility in the 2–80 K region with a clear maximum is redrawn in Fig. 4. As is seen from the results, the Co compounds generally have maxima at higher temperature than the Ni compounds, indicative for a stronger exchange coupling and originating from the fact that Co(II) has a spin of 3/2. The trend however, appears to be that when the exchange is weak in the case of the cobalt compound, also the nickel compound has a weak exchange. In some cases the Ni compounds are so weakly interacting,

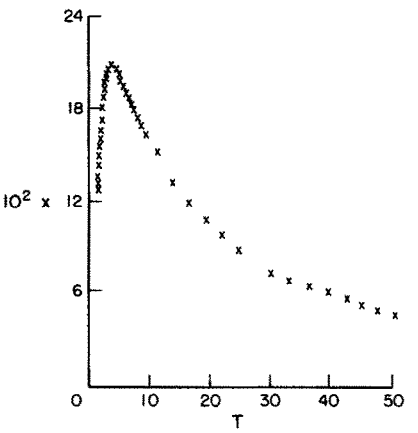

Fig. 4. Plot of the magnetic susceptibility of $Co_2(OH_2)(CCl_3CO_2)_4(tmen)_2$ as a function of temperature.

that no maximum in the susceptibility is observed above 2 K. Apparently the fine details of the exchange interaction are determined by the details

Table 6. Magnetic susceptibility results of some selected Co(II) and Ni(II) compounds with the $M_2(O_2CR)$ unit

Compound	χ_{max} (K)	θ (20–80 K)	μ (80 K) βM	M–O–M (°)
$Co_2(H_2O)(O_2CCl_3)_4(tmen)_2$	4.3	≈ 16	4.8	116.1
$Co_2(H_2O)(O_2CCH_2Cl)_4(tmen)_2$	4.8	≈ 14	4.8	113.5
$Co_2(H_2O)(O_2CCH_3)_4(tmen)_2$	3.0	8.5	4.7	115.1
$Ni_2(H_2O)(O_2CCH_3)_4(tmen)_2$	< 2	1.0	3.0	117.2
$Ni_2(H_2O)(O_2CCH_2Cl)_4(tmen)_2$	3.0	6.0	3.3	117.4
$Ni_2(H_2O)(O_2CHCl_2)_4(tmen)_2$	4.0	5.0	3.1	118.1
$NiCo(H_2O)(O_2CCH_2Cl)_4(tmen)_2$	< 2	6.0	4.0	116.5

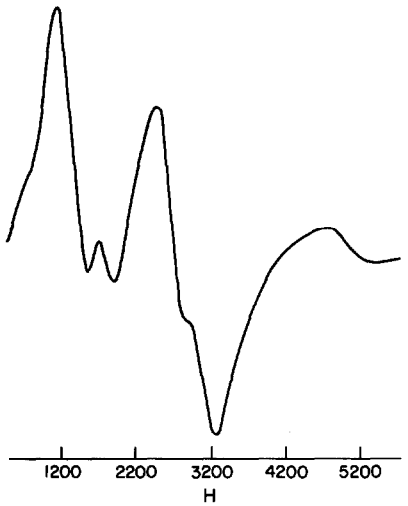

Fig. 5. ESR spectrum at 13 k for the compound $CoNi(OH_2)(CH_2ClCO_2)_4(tmen)_2$.

of the bridging geometry. Therefore, some geometric parameters, as far as available, have been included in Table 6.

In attempts to isolate compounds with two different metal ions, we have prepared several products that contain a 1 : 1 mixture of Co and Ni in the starting solution. Because of the slight asymmetry in the dimeric units, one could expect a possible preference of one site for Co and of the other site for Ni, and in fact the structure described above seems to illustrate this. Magnetic susceptibilities of the compound (see Table 6) indicate that clearly not a physical mixture of the Co_2 and the Ni_2 dimers is present, because in that case a maximum between 3.0 and 4.8 K would be expected. In fact there is no maximum at all above 2 K. Also the ESR-spectrum of the compound, recorded at 13 K and redrawn in Fig. 5, clearly shows that a new species is formed. Further work is planned to do on single-crystal magnetic measurements.

Acknowledgements—The authors are indebted to Mr F. B. Hulsbergen for the spectral measurements, and to Mr R. Prins and Mr W. Vreugdenhill for performing the magnetic susceptibilities.

REFERENCES

1. J. N. van Niekerk and F. R. L. Schoening, *Acta Cryst.* 1953, **6**, 101.
2. M. Melnik, *Coord. Chem. Rev.* 1982, **52**, 259.
3. H. Koyama and Y. Saito, *Bull. Chem. Soc. Japan*, 1954, **52**, 259.
4. J. Catterick and P. Thornton, *Adv. Inorg. Chem. Radiochem.* 1977, **20**, 291.
5. A. K. Shiemke, T. M. Loehr and J. Sanders-Loehr, *J. Am. Chem. Soc.* 1984, **106**, 4951.
6. R. C. Reem and E. I. Solomon, *J. Am. Chem. Soc.* 1984, **106**, 26.
7. R. E. Stenkamp, L. C. Sieker, L. H. Jensen, J. D. McCallum and J. Sanders-Loehr, *Proc. Natl. Acad. Sci. (USA)* 1985, **82**, 713.
8. K. Wieghardt, K. Pohl and W. Gebert, *Angew. Chem. Int. Edn.* 1983, **22**, 727.
9. W. H. Armstrong, A. Spool, G. C. Papaefthymiou, R. B. Frankel and S. J. Lippard, *J. Am. Chem. Soc.* 1984, **106**, 3653.
10. W. H. Armstrong and S. J. Lippard, *J. Am. Chem. Soc.* 1984, **106**, 4632.
11. K. Wieghardt and P. G. Chaudhuri, *J. Chem. Soc. Chem. Commun.* 1985, 69.
12. P. Chaudhuri, K. Wieghardt, B. Nuber and J. Weiss, *Angew. Chem. Int. Edn.* 1985, **24**, 778.
13. W. H. Armstrong and S. J. Lippard, *J. Am. Chem. Soc.* 1985, **107**, 3730.
14. U. Turpeinen, *Finn. Chem. Lett.* 1976, 173; 1977, 36; 1977, 123.
15. M. Ahlgrén, U. Turpeinen and R. Hämäläinen, *Acta Chem. Scand.* 1978, **A32**, 189.
16. M. Ahlgrén and U. Turpeinen, *Acta Cryst.* 1982, **B38**, 276.
17. U. Turpeinen, M. Ahlgrén and R. Hämäläinen, *Acta Cryst.* 1982, **B38**, 1580.
18. D. W. Engelfriet, Ph.D. thesis, Leiden (1980).
19. J. M. Stewart, Ed., *The X-Ray System, Version of 1976*, Technical Report TR-446, Computer Science Center, University of Maryland, College Park (1976).
20. *International Tables for X-ray Crystallography*, Vol. 4. Kynoch Press, Birmingham, U.K. (1974).
21. N. W. Alcock, V. M. Tracy and T. C. Waddington, *J. Chem. Soc. A* 1976, 2243.
22. L. J. Bellamy and A. J. Owen, *Spectrochim. Acta Part A* 1969, **25**, 329.
23. J. Reedijk, P. W. N. M. van Leeuwen and W. L. Groeneveld, *Rec. Trav. Chim.* Pays Bas 1968, **87**, 129.
24. J. Reedijk, W. L. Driessen and W. L. Groeneveld, *Rec. Trav. Chim.* Pays Bas 1969, **88**, 1095.
25. M. Ahlgrén, R. Hämäläinen and U. Turpeinen, *Finn. Chem. Lett.* 1983, 125.
26. U. Turpeinen, M. Ahlgrén and R. Hämäläinen, *Finn. Chem. Lett.* 1977, 146.

Polyhedron Vol. 6, No. 7, pp. 1611–1617, 1987
Printed in Great Britain

0277–5387/87 $3.00+.00
Pergamon Journals Ltd

SYNTHESES AND SPECTROSCOPIC STUDIES ON TETRAAZA MACROCYCLIC COMPLEXES OF PRASEODYMIUM(III)

U. K. PANDEY, O. P. PANDEY, S. K. SENGUPTA* and S. C. TRIPATHI

Department of Chemistry, University of Gorakhpur, Gorakhpur 273009, India

(*Received* 21 *October* 1986; *accepted after revision* 23 *February* 1987)

Abstract—Praseodymium(III) macrocyclic complexes of types $[Pr(L)(H_2O)_2]Cl_3$, $[Pr(mac_1)]Cl_3$ and $[Pr(mac_2)(H_2O)_2]Cl_3$ (L = ligands derived by the condensation of diacetyl or benzil with semicarbazide or thiosemicarbazide; mac_1 = macrocyclic ligands derived by the condensation of diacetyl or benzil with carbohydrazide; mac_2 = macrocyclic ligands derived by the condensation of diacetyl or benzil with semicarbazide, thiosemicarbazide or thiocarbohydrazide) have been prepared and characterized by conductance, magnetic moment, spectral data, thermal and elemental analyses.

The coordination chemistry of polyaza macrocyclic ligands towards lanthanides has been little studied.[1–9] Recently, a number of papers have appeared on crown ether and cryptand complexes of lanthanide ions since they can be used for lanthanide separations, for stabilizing lower oxidation states and for studying high coordinated complexes of lanthanides(III).[10–12] In recent years, the bioinorganic chemistry of the lanthanides has been a research subject. In view of the similarity between the ionic radius of calcium and the trivalent rare earths and the remarkable multitude of spectroscopic and magnetic properties of lanthanides, they are considered to be useful for probing metal ion binding sites of macromolecules of biological interest including amino acids, carbohydrates, nucleotides, sugar-phosphates, porphyrins, phospholipids and membranes.[13,14]

In this paper we report the synthesis and characterization of praseodymium(III) macrocyclic complexes derived from the condensation of diacetyl or benzil with semicarbazide, thiosemicarbazide, carbohydrazide or thiocarbohydrazide.

EXPERIMENTAL

Praseodymium(III) chloride was procured from British Drug House Ltd. Praseodymium was estimated gravimetrically as its oxide, sulphur as $BaSO_4$ and nitrogen by Kjeldahl's method. Estimation of carbon and hydrogen was done by CDRI Lucknow. The details of physical measurements are the same as those described earlier.[15]

(i) *Preparation of ligands* L_1, R_4O_2 [14] *tetraene* $N_4[N_4]$

A solution of diacetyl or benzil (0.04 mol) in ethanol (25 cm^3) was added to a refluxing solution of carbohydrazide (prepared by the method of Möhr *et al.*,[16] 0.04 mol) in aqueous ethanol (30 cm^3) followed by addition of 1 cm^3 concentrated hydrochloric acid. The reaction mixture was refluxed for 4–6 h. After refluxing, the solution was kept overnight. Yellow mass was separated out which was filtered and dried. The product was recrystallized in ethanol.

(ii) *Preparation of ligands* L_2, R_4S_2 [14] *tetraene* $N_4[N_4]$

Ligands of this type were prepared by condensation of diacetyl or benzil with thiocarbohydrazide. The procedure is exactly the same as discussed for L_1. Thiocarbohydrazide was prepared by the method of Bürns.[17]

(iii) *Preparation of ligands* L_3 *and* L_4

Ligands of type L_3 were prepared by condensation of diacetyl or benzil with semicarbazide (molar ratio 1 : 2) and of type L_4 were prepared by

* Author to whom correspondence should be addressed.

condensation of diacetyl or benzil with thiosemicarbazide (molar ratio 1:2) using the same procedure as discussed for L_1

The analytical data of ligands L_1, L_2, L_3 and L_4 are given in Table 1.

(iv) *Preparation of complexes with* L_1 *and* L_2

Praseodymium(III) chloride (0.02 mol) in water (20 cm^3) was added to the refluxing solution of the appropriate ligand (0.02 mol) in ethanol (30 cm^3). The reaction mixture was refluxed for 8–10 h, when the colour of the solution turned yellowish brown. The solvent was removed *in vacuo* and brown or yellowish brown coloured product was obtained. The product was thoroughly washed with dichloromethane to remove the impurities of ligands and dried *in vacuo*. Yield ~ 50–58%.

(v) *Preparation of complexes with* L_3 *and* L_4

Praseodymium(III) chloride (0.02 mol) dissolved in water was added to the appropriate ligand (0.02 mol) dissolved in a mixture of benzene and ethanol (1:1, 30 cm^3). For the preparation of complexes with L_4, small amount of alkali solution (30%, 5 cm^3) was also added. The above solution was refluxed for 10–14 h. The solvent was removed *in vacuo* and the light brown coloured product was obtained. The complex was isolated by crystallizing the product from tetrahydrofuran. Yield ~ 60–62%.

Table 1. Analytical data of ligands

Reactants taken (molar ratio)	Product, yield (%) and colour	Analysis found (calc.) %		
		C	H	N
Diacetyl + carbohydrazide (1:1)	$L_1^{(1)}$ 80 light brown	42.7 (42.8)	5.7 (5.8)	39.5 (40.0)
Benzil + carbohydrazide (1:1)	$L_1^{(2)}$ 88 yellow	69.4 (69.5)	4.6 (4.7)	21.5 (21.6)
Diacetyl + thiocarbohydrazide (1:1)	$L_2^{(1)}$ 66 yellowish brown	38.4 (38.5)	5.1 (5.2)	35.8 (35.9)
Benzil + thiocarbohydrazide (1:1)	$L_2^{(2)}$ 82 yellow	64.3 (64.3)	4.2 (4.3)	19.9 (20.0)
Diacetyl + semicarbazide (1:2)	$L_3^{(1)}$ 76 light yellow	36.0 (36.3)	6.0 (6.2)	42.0 (42.2)
Benzil + semicarbazide (1:2)	$L_3^{(2)}$ 80 yellow	59.3 (59.4)	5.0 (5.2)	25.9 (26.1)
Diacetyl + thiosemicarbazide (1:2)	$L_4^{(1)}$ 68 yellow	31.0 (31.2)	5.2 (5.3)	36.2 (36.3)
Benzil + thiosemicarbazide (1:2)	$L_4^{(2)}$ 72 yellow	53.9 (54.0)	4.5 (4.7)	23.6 (24.0)

where
$L_1^{(1)}$ = 6,7,13,14 Me_4 3,10 O_2 [14] 5,7,12,14 tetraene 1,5,8,12 N_4 [2,4,9,11 N_4].
$L_1^{(2)}$ = 6,7,13,14 Ph_4 3,10 O_2 [14] 5,7,12,14 tetraene 1,5,8,12 N_4 [2,4,9,11 N_4].
$L_2^{(1)}$ = 6,7,13,14 Me_4 3,10 S_2 [14] 5,7,12,14 tetraene 1,5,8,12 N_4 [2,4,9,11 N_4].
$L_2^{(2)}$ = 6,7,13,14 Ph_4 3,10 S_2 [14] 5,7,12,14 tetraene 1,5,8,12 N_4 [2,4,9,11 N_4].
$L_3^{(1)}$ = diacetyl bis(semicarbazone).
$L_3^{(2)}$ = benzil bis(semicarbazone).
$L_4^{(1)}$ = diacetyl bis(thiosemicarbazone).
$L_4^{(2)}$ = benzil bis(thiosemicarbazone).

(vi) *Preparation of complexes with* L_5 *and* L_6

Diacetyl or benzil (0.01 mol) in ethanol (15 cm^3) was added to the complex of praseodymium with L_3 and L_4 dissolved in a mixture of benzene and ethanol (1 : 1, 30 cm^3). Glacial acetic acid (5 cm^3) was added to the above mixture and a clear solution (pH ~ 3) was obtained which was refluxed for 7–8 h, when dark brown coloured precipitate was obtained. The precipitate was filtered, thoroughly washed with benzene and ethanol and dried *in vacuo*. Yield ~ 48–56%.

RESULTS AND DISCUSSION

The condensation reactions of diacetyl or benzil with carbohydrazide, thiocarbohydrazide in ethanol in the presence of small amount of concentrated hydrochloric acid give rise to cyclic products (Table 1):

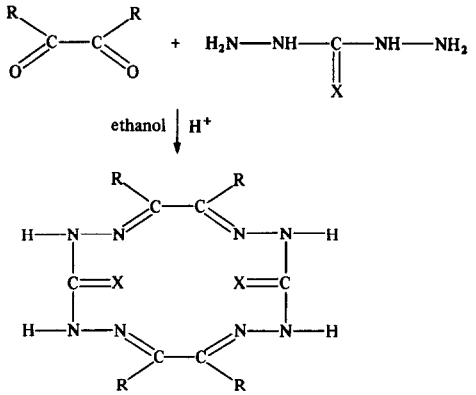

6,7,13,14 R_4 3,10 X_2 [14] 5,7,12,14 tetraene 1,5,8,12 N_4 [2,4,9,11 N_4]

R	X	
CH_3	O	$L_1^{(1)}$
C_6H_5	O	$L_1^{(2)}$
CH_3	S	$L_2^{(1)}$
C_6H_5	S	$L_2^{(2)}$

These ligands react with praseodymium(III) chloride in ethanol and the following two types of products have been isolated:

$$PrCl_3 + L_1 \xrightarrow{\text{ethanol}} [Pr(L_1)]Cl_3$$

$$PrCl_3 + L_2 \xrightarrow{\text{ethanol}} [Pr(L_2)(H_2O)_2]Cl_3$$

The elemental analyses of these complexes reveal 1 : 1 metal to ligand stoichiometry (Table 2). The purity of these complexes was checked by TLC. The complexes are found to be soluble in ethanol, dimethylformamide, dimethylsulphoxide and sparingly soluble in chloroform. The electrical conductance in dimethylformamide indicates 1 : 3 electrolytic nature. The presence of coordinated water molecules in the second type of complex was inferred from thermogravimetric analysis which indicated the loss of two water molecules at 140–180°C.

However, diacetyl or benzil reacted with semicarbazide or thiosemicarbazide in 1 : 2 molar ratio, respectively, and formed open chain ligands (Table 1).

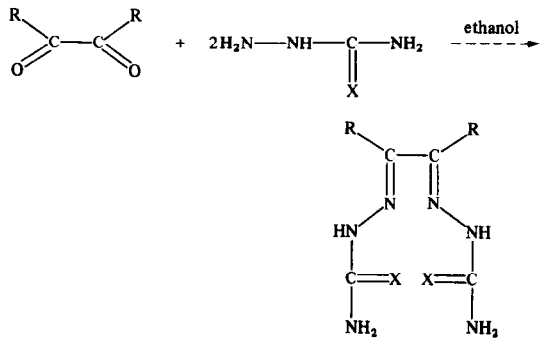

R	X	
CH_3	O	diacetyl bis(semicarbazone); $L_3^{(1)}$
C_6H_5	O	benzil bis(semicarbazone); $L_3^{(2)}$
CH_3	S	diacetyl bis(thiosemicarbazone); $L_4^{(1)}$
C_6H_5	S	benzil bis(thiosemicarbazone); $L_4^{(2)}$

These ligands reacted with praseodymium(III) chloride in 1 : 1 molar ratio and formed open chain complexes.

$$PrCl_3 + L_3 \longrightarrow [Pr(L_3)(H_2O)_2]Cl_3$$

$$PrCl_3 + L_4 \longrightarrow [Pr(L_4)(H_2O)_2]Cl_3$$

It appears that in the above complexes the two terminal amino groups remain uncoordinated and can take part in condensation reactions with α-diketones and, therefore, the reactions of the above complexes with diacetyl or benzil were carried out resulting in the formation of complexes with macrocyclic ligands (L_5 and L_6).

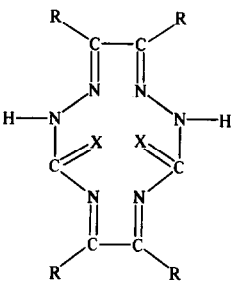

5,6,11,12 R_4 3,8 X_2 [12] 4,6,10,12 tetraene 1,4,7,10 N_4 [2,9 N_2]

R	X	
CH_3	O	$L_5^{(1)}$
C_6H_5	O	$L_5^{(2)}$
CH_3	S	$L_6^{(1)}$
C_6H_5	S	$L_6^{(2)}$

Table 2. Reactions of $PrCl_3$ with ring-open and macrocyclic ligands

Reactants taken (molar ratio)	Refluxing time (h)	Product, yield (%) and colour	Analysis found (calc.) %					
			C	H	N	S	Pr	Cl
$PrCl_3+L_1^{(1)}$ (1:1)	8	$[Pr(L_1^{(1)})]Cl_3$ 52 brown	22.7 (22.8)	3.0 (3.1)	21.2 (21.2)	—	26.7 (26.7)	20.1 (20.2)
$PrCl_3+L_1^{(2)}$ (1:1)	9	$[Pr(L_1^{(2)})]Cl_3$ 56 yellowish brown	46.9 (47.1)	3.1 (3.2)	14.5 (14.6)	—	17.4 (17.4)	13.8 (13.9)
$PrCl_3+L_2^{(1)}$ (1:1)	9	$[Pr(L_2^{(1)})(H_2O)_2]Cl_3$ 55 brown	20.1 (20.2)	3.3 (3.4)	18.8 (18.8)	10.6 (10.8)	23.6 (23.7)	17.8 (17.9)
$PrCl_3+L_2^{(2)}$ (1:1)	10	$[Pr(L_2^{(2)})(H_2O)_2]Cl_3$ 58 brown	42.6 (42.7)	3.3 (3.3)	13.3 (13.3)	7.6 (7.6)	16.7 (16.7)	12.4 (12.6)
$PrCl_3+L_3^{(1)}$ (1:1)	10	$[Pr(L_3^{(1)})(H_2O)_2]Cl_3$ 60 brown	14.7 (14.9)	3.3 (3.3)	17.4 (17.4)	—	29.1 (29.2)	22.1 (22.0)
$PrCl_3+L_3^{(2)}$ (1:1)	9	$[Pr(L_3^{(2)})(H_2O)_2]Cl_3$ 61 brown	31.3 (31.6)	3.3 (3.3)	13.8 (13.8)	—	23.2 (23.2)	17.5 (17.5)
$PrCl_3+L_4^{(1)}$ (1:1)	14	$[Pr(L_4^{(1)})(H_2O)_2]Cl_3$ 60 brown	14.0 (14.0)	3.1 (3.1)	16.2 (16.3)	12.4 (12.4)	27.3 (27.3)	20.6 (20.6)
$PrCl_3+L_4^{(2)}$ (1:1)	14	$[Pr(L_4^{(2)})(H_2O)_2]Cl_3$ 60 brown	30.0 (30.0)	3.1 (3.2)	13.2 (13.1)	10.0 (10.0)	22.1 (22.0)	16.6 (16.6)
$[Pr(L_3^{(1)})(H_2O)_2]Cl_3$+DA (1:1)	7	$[Pr(L_5^{(1)})(H_2O)_2]Cl_3$ 46 dark brown	22.5 (22.5)	3.3 (3.4)	15.7 (15.8)	—	26.4 (26.4)	19.9 (19.9)
$[Pr(L_3^{(2)})(H_2O)_2]Cl_3$+BZ (1:1)	7	$[Pr(L_5^{(2)})(H_2O)_2]Cl_3$ 51 brown	46.0 (46.1)	3.3 (3.4)	10.7 (10.8)	—	18.0 (18.0)	13.6 (13.6)
$[Pr(L_4^{(1)})(H_2O)_2]Cl_3$+DA (1:1)	8	$[Pr(L_6^{(1)})(H_2O)_2]Cl_3$ 56 dark brown	21.2 (21.2)	3.1 (3.2)	14.8 (14.9)	11.3 (11.3)	24.9 (24.9)	18.8 (18.8)
$[Pr(L_4^{(2)})(H_2O)_2]Cl_3$+BZ (1:1)	8	$[Pr(L_6^{(2)})(H_2O)_2]Cl_3$ 57 dark brown	44.2 (44.3)	3.2 (3.2)	10.3 (10.3)	17.8 (17.8)	17.3 (17.3)	12.9 (13.1)

where $L_1^{(1)}$, $L_1^{(2)}$, $L_2^{(1)}$, $L_2^{(2)}$, $L_3^{(1)}$, $L_3^{(2)}$, $L_4^{(1)}$ and $L_4^{(2)}$ are as given in Table 1.
$L_5^{(1)}$ = 5,6,11,12 Me_4 3,8 O_2 [12] 4,6,10,12 tetraene 1,4,7,10 N_4 [2,9 N_2].
$L_5^{(2)}$ = 5,6,11,12 Ph_4 3,8 O_2 [12] 4,6,10,12 tetraene 1,4,7,10 N_4 [2,9 N_2].
$L_6^{(1)}$ = 5,6,11,12 Me_4 3,8 S_2 [12] 4,6,10,12 tetraene 1,4,7,10 N_4 [2,9 N_2].
$L_6^{(2)}$ = 5,6,11,12 Ph_4 3,8 S_2 [12] 4,6,10,12 tetraene 1,4,7,10 N_4 [2,9 N_2].
DA = diacetyl.
BZ = benzil.

The metal to ligand stoichiometry of these macrocyclic products have been established on the basis of elemental analyses (Table 2). The presence of coordinated water molecules was inferred by thermogravimetric study (weight loss at 160–185°C corresponds to two water molecules). These complexes have high melting points and are soluble in dimethylformamide and dimethylsulphoxide. The complexes behave as 1:3 electrolytes in dimethylformamide. Since these cyclic products derived from semicarbazide and thiosemicarbazide could not be isolated in the absence of metal ion,

praseodymium(III) appears to act as a kinetic "template".

Magnetic moments and electronic spectra

As expected the magnetic moments of these complexes (3.50–3.62 BM) show little deviation from the Van Vleck values[18] and those of hydrated sulphate.[19]

The electronic absorption bands of Pr(III) appear due to the transitions from the ground levels $^3H_4$ to the excited J levels of the 4f configuration.[20] Praseodymium(III) complexes show bands around 1700, 20800, 22000 and 23000 cm^{-1} corresponding to the transitions from $^3H_4$ to $^4D_2$, $^2P_0$, $^3P_1$ and $^3P_2$ energy levels, respectively. It has been observed that on complexation the electronic spectral bands shift to lower energy side (nephelauxatic effect). The slight shift in the bands have been attributed by Jorgensen to the effects of crystal fields upon the interelectronic repulsions between the 4f electrons, i.e. to lowering of the interelectron repulsion parameter in the complexes.[21] Further, a marked enhancement in the intensity of the bands, upon complexation, is also observed. Values of nephelauxatic ratio (β) which is defined as ν_c/ν_f where ν_c and ν_f are energies (in cm^{-1}) of the transitions in complex and free ion, respectively, for the present derivatives lie in the range 0.9800–0.9900. From the mean β values, the covalency parameter (δ) (0.8800–1.354) and bonding parameter ($b^{1/2}$) (0.0630–0.0800) were determined using standard procedures.[22] The values of β, which are less than unity, and positive values of δ and $b^{1/2}$ support partial covalent nature of bonding between metal and ligand.

Infrared spectra

(a) *Complexes with ligands* L_1 *and* L_2. The infrared spectra of macrocyclic ligands (L_1) derived by the condensation of carbohydrazide with diacetyl or benzil show bands at ca 1675, 1500, 1260 and 660 cm^{-1} which may be assigned[15,23,24] to amide I (νC=O), amide II (νC—N+δN—H), amide III (δN—H) and amide IV (ϕC=O) vibrations, respectively. In praseodymium(III) complexes all these bands except amide I show upward shift (~ 60–40 cm^{-1}), whereas amide I shows downward shift (~ 30 cm^{-1}). These changes in amide group vibrations indicate[15] that the amide oxygens (ketonic) take part in coordination to metal atom. This has been further confirmed by the appearance of a band at ca 510–470 cm^{-1} in the complexes, assigned to ν(Pr—O). The infrared spectra of macrocyclic ligands (L_2) derived by the condensation of thiocarbohydrazide with diacetyl or benzil show bands at ca 1560, 1210, 1080 and 765 cm^{-1}, which are assigned[25,26] to thioamide I, II, III and IV vibrations, respectively. The ligands containing the HN—C=S group can undergo thione-$\rightleftharpoons$thiol tautomerism. However, the appearance of four thioamide bands in the spectra of ligands indicates[25] the existence of ligands in the thione form. The thioamide IV band has been found to have maximum νC=S contribution. However, in praseodymium(III) complexes all these bands persist at the same position indicating the non-coordination of thiocarbonyl group to the metal atom.

In addition both the ligands of type L_1 and L_2 show a weak band at ca 1640 cm^{-1} which can be assigned to the ν(C=N) vibration of azomethine linkage. The appearance of a weak ν(C=N) band is in accordance with the observations of several other workers.[27,28] In praseodymium(III) complexes the band appears at ca 1620–1610 cm^{-1} suggesting[15] the coordination of azomethine nitrogens to the metal atom. The ν(Pr—N) vibration band appears at ca 420–380 cm^{-1}, in the complexes.

The infrared spectra of praseodymium(III) complexes with ligands L_2 show broad bands at ca 3480–3420 cm^{-1} which are assigned to ν(O—H) vibrations of the coordinated water molecule.

A number of other bands also arise due to phenyl groups and methyl groups but definite assignments of these bands are not possible due to the complexity of the spectra.

(b) *Complexes with ligands* L_3 *and* L_4. The ligands of type L_3 show bands mainly due to the amide groups, amino group and azomethine groups. The infrared spectra of ligands show bands at ca 1650, 1500, 1250 and 650 cm^{-1} which may be assigned[15] to amide I, amide II, amide III and amide IV vibrations, respectively, as with ligands L_1. In the praseodymium(III) complexes amide I band shows downward shift (~ 40–20 cm^{-1}). These changes indicate[15] that amide oxygen (ketonic) takes part in coordination to the praseodymium atom. The (Pr—O) vibration band appears at ca 500–480 cm^{-1}. The ligands also show a weak band at ca 1630–1625 cm^{-1} assignable[27,28] to ν(C=N) of the azomethine linkage. In the complexes this band shifts to lower frequency (ca 30–20 cm^{-1}) suggesting that the nitrogen atoms of azomethines are coordinated to praseodymium atom. This is further supported by the appearance of weak band at ca 400–380 cm^{-1} assignable to ν(Pr—N). The ligands of type L_3 also show a broad band at 3280 cm^{-1} along with two shoulders at 3300 and 3260 cm^{-1}, which may be due to ν_{sym}(N—H) and ν_{asym}(N—H) vibrations.[29] In the complexes all these bands per-

sist indicating the non-coordination of the terminal amino group to the metal.

The ligands of type L_4 show bands mainly due to thioamide groups, amino groups and the azomethine groups. The four thioamide bands appear at ca 1570–1550, 1210, 1080–1070 and 760 cm^{-1}. The thioamide IV band having maximum contribution of $\nu_{C=S}$, undergo shifts to lower frequency ($\sim$ 35–20 cm^{-1}) in the complexes, indicating[25–30] the coordination of sulphur atom to the praseodymium(III). The new band appearing in the complexes at ca 360–325 cm^{-1} may be assigned to ν(Pr—S). A weak band in the spectra of L_4 appears at ca 1630 cm^{-1} assignable[15,25] to ν(C=N). In the complexes this band also shifts to lower frequency ($\sim$ 25 cm^{-1}) indicating the coordination of azomethine nitrogens to the praseodymium atom. The amino group vibrations appear at 3280, 3250 (shoulder) and 3220 cm^{-1} (shoulder). In the praseodymium complexes these bands appear exactly at the same position indicating the non-coordination of the terminal amino groups to the metal atom. All the complexes with L_3 and L_4 ligands show broad bands at ca 3440 cm^{-1} in the infrared spectra suggesting the presence of coordinated water molecules.

(c) *Complexes with ligands* L_5 *and* L_6. The praseodymium(III) complexes with ligands L_3 and L_4 contain terminal amino groups (as evident from above spectral discussion), which may participate in nucleophilic condensation reactions with α-diketones. Therefore the reactions of complexes of L_3 and L_4 with diacetyl or benzil have been carried out in the presence of glacial acetic acid, which causes the ring closure and formation of cyclic product with macrocyclic ligands L_5 and L_6. The infrared spectra of cyclic product show the same pattern of bands for the amide group (L_5) and thioamide group (L_6) and the azomethine group. This indicates that in the macrocyclic complexes with L_5, the ligand is bonded to the metal atom through two azomethine nitrogen atoms and two ketonic oxygen atoms. Similarly in the complexes with ligands L_6 the ligands are coordinated to the metal through two thioamide sulphur atoms and two azomethinenitrogen atoms. However, in both types of complexes, the (νNH_2) band disappears. Only one band is observed in the νN—H region at 3200 cm^{-1} which may be due to a secondary amino group, establishing the condensation of primary amino groups with the carbonyl groups of α-diketones. This is further supported by the appearance of a weak band at ca 1650–1635 cm^{-1}, due to the formation of azomethine linkages.[27] The complexes with ligands L_5 and L_6 also contain coordinated water molecules, as is evident by the presence of a broad band at ca 3480 cm^{-1} in the infrared spectra.

Proton magnetic resonance spectra

The ^1H NMR spectra (90 MHz) of the complexes with ligands L_1, L_2, L_5 and L_6, obtained in deuterated chloroform or in DMSO-d_6 solution with TMS as internal standard show the methyl protons at ca δ 2.2–2.8 ppm and phenyl protons at ca δ 6.8–7.2 ppm. These signals appear downfield compared to the corresponding signals of the ligands indicating coordination of the ligands to the praseodymium ion.

Acknowledgement—One of the authors (U.K.P.) is thankful to the Council of Scientific and Industrial Research, New Delhi for the award of a Fellowship.

REFERENCES

1. C. J. Pedersen, *J. Am. Chem. Soc.* 1967, **89**, 7017.
2. S. Gurrieri, A. Seminara, G. Siracusa and A. Cassal, *Thermochim. Acta* 1975, **11**, 433.
3. W. Radecka-Paryzek, *Inorg. Chim. Acta* 1979, **34**, 5.
4. W. Radecka-Paryzek, *Inorg. Chim. Acta* 1979, **35**, L349.
5. W. Radecka-Paryzek, *Inorg. Chim. Acta* 1980, **45**, L147.
6. W. Radecka-Paryzek, *Inorg. Chim. Acta* 1981, **52**, 216.
7. O. S. Timofeev, N. G. Lukyenenko, T. I. Kirichenko, V. S. Kalishevich, A. V. Bogasskii, A. I. Gren, D. V. Zagorevskii and S. Yu, *Inorg. chim. Acta* 1983, **77**, L245.
8. K. K. Abid, D. E. Feuton, *Inorg. Chim. Acta* 1984, **82**, 223.
9. W. Radecka-Paryzek, *Inorg. Chim. Acta* 1981, **54**, L251.
10. R. B. King and P. R. Heckley, *J. Am. Chem. Soc.* 1974, **96**, 3118.
11. R. J. Jassaux, J. F. Desreux, C. Delchambre and G. Duyckaerts, *Inorg. Chem.* 1980, **19**, 1893 and references therein.
12. M. Ciampolini, C. Mealli and N. Nardi, *J. Chem. Soc., Dalton Trans.* 1980, 376 and references therein.
13. G. L. Eichhorn, *Inorganic Biochemistry*. Elsevier, London (1973).
14. J. Reuben, *Handbook on the Physics and Chemistry of Rare Earths*, Vol. 4, p. 515 (1979).
15. S. K. Sengupta, S. K. Sahni and R. N. Kapoor, *J. Coord. Chem.* 1982, **12**, 113.
16. E. B. Möhr, J. J. Brezinski and L. F. Audrieth, *Inorg. Synth.* **IV**, 32 (1953).
17. G. R. Bürns, *Inorg. Chem.* 1968, **7**, 277.
18. J. H. Van Vleck and A. Frank, *Phys. Rev.* 1929, **34**, 494.
19. D. M. Yost, H. Russel and C. S. Garner, *The Rare*

Earth Elements and Their Compounds. Wiley, New York (1957).
20. G. H. Dieke, *Spectra and Energy Levels of Rare Earths in Crystals*. Interscience, New York (1968).
21. C. K. Jorgensen, *Acta. Chem. Scand.* 1957, **11**, 1981.
22. S. P. Sinha, *J. Inorg. Nucl. Chem.* 1971, **33**, 2205.
23. J. Bould and B. J. Bridon, *Inorg. Chim. Acta* 1976, **19**, 159.
24. M. Nonoyama, S. Tomita and K. Yamasaki, *Inorg. Chim. Acta* 1975, **12**, 33.
25. S. K. Sengupta and S. Kumar, *Synth. React. Inorg. Met.-Org. Chem.* 1983, **13**, 929.
26. S. K. Sahni and V. B. Rana, *Indian J. Chem.* 1977, **15A**, 890.
27. S. K. Sahni, *Transition Met. Chem.* 1979, **4**, 73.
28. S. Kher, S. K. Sahni, V. Kumari and R. N. Kapoor, *Inorg. Chim. Acta* 1979, **37**, 121.
29. K. Nakamoto, *Infrared Spectra of Inorganic and Coordination Compounds*. Wiley Interscience, New York (1970).
30. S. K. Sengupta, S. K. Sahni and R. N. Kapoor, *Synth. React. Inorg. Met.-Org. Chem.* 1980, **10**, 269.

Polyhedron Vol. 6, No. 7, pp. 1619–1620, 1987
Printed in Great Britain

0277-5387/87 $3.00+.00

COMMUNICATION

PROTOLYTIC STABILITY OF PALLADOCYCLES

A. D. RYABOV and A. K. YATSIMIRSKY

Department of Chemistry, Moscow State University, Moscow 119899, U.S.S.R.

and

H.-P. ABICHT*

Department of Chemistry, Martin-Luther-University, DDR-4050 Halle (Saale), G.D.R.

(*Received* 9 *February* 1987; *accepted* 18 *February* 1987)

Abstract—Protonolysis of ortho-palladated asymmetric metallacycles [Pd(o-$C_6H_4CH_2Z_A$)(o-$C_6H_4CH_2Z_B$)] (**3**: $Z_A = NMe_2$, $Z_B = PPh_2$; **4**: $Z_A = NMe_2$, $Z_B = AsPh_2$; **5**: $Z_A = AsPh_2$, $Z_B = PPh_2$) by acetic acid leads to the departure of $PhCH_2NMe_2$ (in the case of **3** and **4**) and $PhCH_2AsPh_2$ (for **5**) and formation of corresponding dimeric acetato bridged complexes **6** and **7**, respectively. The relative stability of the palladocycles is determined by the nature of the donor atom and decreases in the order: P > As > N.

Mechanism of electrophilic cleavage of transition-metal–carbon bonds are still under intensive investigation.[1] Cyclometallated complexes of the type **1**, possessing a rather stable palladium–carbon bond, appear to be useful objects for such studies. We have previously studied the mechanism of protonolysis of complex **1**.[2] The reaction involves the formation of intermediate **2** indicating an important role of a donor group in the course of the palladocycle cleavage. To continue our study of the role of the donor centre, we investigated the protonolysis of complexes **3–5** which contain N-, P- and As-donor palladocycles, by acetic acid with a goal to compare a relative stability of those towards protonolysis.

RESULTS AND DISCUSSION

Addition of D_3CCOOD to a suspension of complexes **3–5** in $CDCl_3$ at room temperature leads to complete dissolution of the starting compounds. The reaction occurs instantaneously in the case of **3**, but it takes 5 and 120 min in the case of **4** and **5**, respectively. The reactivity decreases in the order: **3** > **4** > **5**. The ^{1}H-NMR analysis of the products formed as well as their isolation as solids in the case of **4** and **5** indicates that mixed ligand palladocycles **3–5** lose one cyclopalladated ligand affording acetato bridged dimers **6**, **7** and **6**, respectively. The leaving ligand is $PhCH_2NMe_2$ in the case of **3** and **4**, but $PhCH_2AsPh_2$ in the case of **5**. The relative lability of palladocycles is thus strongly dependent on the nature of donor atom decreases in the order: N > As > P. Note that this sequence does not correspond to that expected on the basis of relative basicity of the elements (N > P > As). A remarkable stability of phosphorus palladocycles is probably due to favourable combination of σ-donor and π-acceptor properties of this donor centre.

It should be pointed out that utilization of rather weak acetic acid allows to perform a selective cleavage of complexes **3–5**, whereas much stronger HCl cleaves both palladocycles.[3] It is also interesting to note that the pathway of decomposition of **3** could be predicted on the basis of recent results on the exchange of cyclopalladated ligands.[4] In the reaction between chloro-bridged *N,N*-dimethylbenzylamine derivative [μ-ClPd(o-$C_6H_4CH_2NMe_2$)]$_2$ and $PhCH_2PPh_2$ in the presence of acetic acid we

* Author to whom correspondence should be addressed.

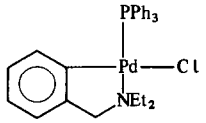

1

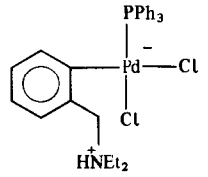

2

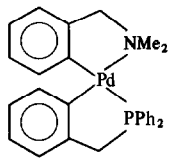

3

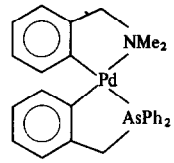

4

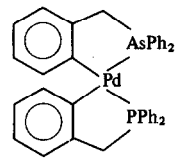

5

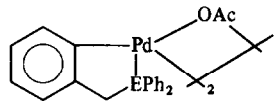

6 E = P
7 E = As

observed the Pd(II) transfer to give $[\mu\text{-ClPd}(o\text{-}C_6H_4CH_2PPh_2)]_2$. Both experiments show the thermodynamic preference of Pd(II) for the P-ligand.

In conclusion, a resistance of palladocycles towards protonolysis is determined by the nature of donor atom increasing in the order: N < As < P.

EXPERIMENTAL

Mixed ligand palladocycles **3–5** were prepared as previously described.[3] ^{1}H-NMR spectra were run on Tesla BS 467 and Bruker CXP 100 instruments. Chemical shifts are given in ppm with respect to TMS.

Protonolysis of complexes **3–5** *in acetic acid (exemplified by* **3**)

{[*o*-(Dimethylaminomethyl)phenyl - C^1, - N] - [*o*-(diphenylphosphinomethyl)phenyl - C^1, - P]} - palladium(II) (**3**) (30 mg) was suspended in 0.5 cm^3 $CDCl_3$. Addition of 0.25 cm^3 D_3CCOOD resulted in rapid dissolution. Hexamethyldisiloxane (0.06 cm^3) was added to the reaction mixture and its ^{1}H-NMR spectrum recorded. The latter contained signals of NCH_2 and NCH_3 protons of free $PhCH_2NMe_2$ at δ = 4.18 and 2.70, respectively, as well as a broad doublet from cyclopalladated $PhCH_2PPh_2$ at δ = 3.06 (J = 13 Hz). On addition of pyridine-d_5, which converts dimeric complexes into monomers of the type **1**, a signal from PCH_2 protons is seen as a sharp doublet at δ = 4.02. These spectral data are in agreement with those reported in the literature for ortho-palladated $PhCH_2PPh_2$ derivatives.[4,5] Similar spectral analyses were performed in the case of **4** and **5**. Compounds **6** and **7** were isolated as solids as described elsewhere.[4] RFA analyses confirmed the absence of As and the presence of P in the complex obtained from **5**. ^{1}H-NMR data of **7**, $\delta(CDCl_3$; py-$d_5)$: 6.77–7.9 m (Ar), 3.79 s ($AsCH_2$), 1.85 s ($OOCCH_3$).

REFERENCES

1. M. D. Johnson, In *The Chemistry of the Metal–Carbon Bond*, Vol. 2, *The Nature and Cleavage of Carbon–Metal-Bonds* (Edited by F. R. Hartley and S. Patai), p. 513. Wiley, Chichester (1985).
2. A. D. Ryabov, *J. Organomet. Chem.* 1984, **268**, 91.
3. H.-P. Abicht and K. Issleib, *J. Organomet. Chem.* 1985, **289**, 201.
4. A. D. Ryabov, A. V. Usatov, V. A. Kalinin and L. I. Zakharkin, *Izv. AN SSSR, Ser. Khim.* 1986, 2790.
5. K. Hiraki, Y. Fuchita and T. Uchiyama, *Inorg. Chim. Acta* 1983, **69**, 187.

Polyhedron Vol. 6, No. 7, pp. 1621–1623, 1987
Printed in Great Britain

0277–5387/87 $3.00+.00
Pergamon Journals Ltd

COMMUNICATION

ANGULAR OVERLAP PARAMETERS FOR RUTHENIUM(II) COMPLEXES

PATRICK E. HOGGARD* and PIERRE P. CLANET

Department of Chemistry, North Dakota State University, Fargo, ND 58105, U.S.A.

(*Received* 29 *May* 1986; *accepted* 6 *March* 1987)

Abstract—Approximate Angular Overlap Model e_π parameters have been obtained for a number of ligands L by comparison of the $t_{2g}(Ru) \rightarrow \pi^*(bpy)$ transition energies in $[Ru(bpy)_2L_2]$ complexes. The filled t_{2g} subshell of Ru(II) limits the effects of otherwise strongly π-donating ligands.

The Angular Overlap Model (AOM) is an additive ligand field theory that factors the ligand potential into σ and π contributions.[1,2] One of the difficulties in applying the AOM is that it is hard to obtain usable experimental values of the parameters e_σ and e_π for particular ligands. Once in hand, however, these parameters should be relatively constant from one complex to another with the same metal ion, although large changes in the electron donating and withdrawing properties of the other ligands can alter this.[3] The e_σ and e_π values may also be transferable, with a multiplicative factor,[4,5] to other metal ions with the same *d* electron configuration. AOM parameter values may, however, be quite different for metal ions with different configurations.

The most common method of determining AOM parameter values is by resolving the splittings of spin-allowed *d–d* bands in MA_5B or MA_4B_2 complexes. There are considerable experimental difficulties here, as often these splittings can only be measured using polarized absorption spectroscopy on single crystals,[6] or by performing a Gaussian curve resolution on bands that may have little or no asymmetry to the eye.[7]

We present here results from a simpler experimental technique to evaluate e_π for a series of ligands through comparison of the metal-to-ligand charge transfer (MLCT) bands in *cis*-$[Ru(bpy)_2L_2]$ complexes (bpy = 2,2′-bipyridine). The lowest-energy MLCT band can be represented as a transition from the highest Ru t_{2g}-remnant orbital, which is degenerate, or nearly so, to the lowest bipyridine π^* orbital. We assume the energy of this π^* orbital to be constant over the entire series of complexes examined, while the energy of the ruthenium orbital can be expressed, assuming all ligands coordinate linearly (which is not true, but is a useful approximation) as

$$E(t_{2g}) = 2e_{\pi bpy} + 2e_{\pi L}.$$

The orbital transition energy is then

$$\Delta E = E(\pi^*) - E(t_{2g}) = E(\pi^*) - 2e_{\pi bpy} - 2e_{\pi L}$$
$$= C - 2e_{\pi L}. \quad (1)$$

We will also assume that other components of the transition energy, including interelectronic repulsion and spin-orbit coupling, can be included in the constant C. If, as is usual in AOM problems, we take a saturated amine as a reference ligand with $e_{\pi L} = 0$, C can be calculated and $e_{\pi L}$ determined for the remaining ligands in the series.

The position of the first absorption band of $[Ru(bpy)_2X_2]$ for each ligand used is listed in Table 1. From the 531 nm value for $[Ru(bpy)_2(en)]$, the constant C in eqn (1) is 18,830 cm^{-1}. The e_π values for each ligand, as calculated from eqn (1), are also listed. Still assuming linear coordination, e_σ may be estimated from $\Delta = 3e_\sigma - 4e_\pi$, if Δ (= 10Dq) is

* Author to whom correspondence should be addressed.

Table 1. Values for angular overlap parameters derived from absorption spectra of $[Ru(bpy)_2L_2]$ complexes

L[a]	λ_1 nm[b]	e_π cm^{-1}[c]	Δ cm^{-1}	e_σ cm^{-1}
F^-	565±10	570	(17,600)[d]	6600
HCO_3^-	560±6	490		
$\frac{1}{2}(acac^-)$	560	490		
Cl^-	559	470	(16,800)[e]	6200
$CH_3CO_2^-$	555±10	410		
$\frac{1}{2}(C_2O_4^{2-})$	553±3	370	(20,900)[f]	7500
BrO_3^-	553	370		
Br^-	551	340	(15,500)[e]	5600
I^-	549.5	320		
$\frac{1}{2}(CO_3^{2-})$	540±5	160		
en	531±7	[0]	28,800[g]	9600
N_3^-	530	−20	(16,800)[h]	5600
SO_3^{2-}	525	−110		
IO_3^-	525	−110		
HCO_2^-	520	−200		
NCS^-	513	−330	(26,900)[i]	8500
$NCSe^-$	505	−490		
CN^-	498	−620	34,800[j]	10800
NO_2^-	473	−1160	(24,700)[d]	6700
bpy	454	−1600		

[a] Abbreviations: bpy = 2,2′-bipyridine, en = 1,2-diaminoethane, Hacac = 2,4-pentanedione.
[b] ±2 nm except as noted.
[c] Values in parentheses from Rh(III) spectra; $\Delta_{Ru} = 0.788\Delta_{Rh}$.
[d] Ref. 8.
[e] Ref. 9.
[f] Ref. 10.
[g] Ref. 11.
[h] Ref. 12.
[i] Ref. 13, from $[Rh(NH_3)_5NCS]^{2+}$.
[j] Ref. 14.

known for that ligand. Only a few octahedral Ru(II) complexes are known for which Δ can be determined from the absorption spectrum. Table 1 lists these, but also estimates values for others taken from the corresponding Rh(III) complexes, using 0.788 as the ratio of Δ_{Ru}/Δ_{Rh}, which is the ratio in the hexaamine complexes.[8,11]

It is instructive to compare the e_π values from this series of complexes to those for Cr(III), a d^3 ion. Table 2 lists values for some representative ligands. These should not be regarded as fixed, but as changing with the molecular environment. The relative values, however, should remain approximately as shown.[15] Examination of Table 2 leads to the conclusion that π-donation is less important with Ru(II) than π-withdrawal. This is not unexpected for low-spin d^6 complexes. The value of e_π depends on a balance between donation by ligand π orbitals

Table 2. Spectrochemical e_π values for Cr(III) and Ru(II) complexes, in cm^{-1}

L	Ru(II)	Cr(III)	Ref[a]
F^-	570	1690	7
Cl^-	470	870	7
Br^-	340	630	7
NCS^-	−330	380	16
CN^-	−620	−290	17

[a] For Cr(III) data.

and withdrawal into ligand π^* orbitals, when accessible. The contrast is quite evident for N-bonding thiocyanate. In Cr(III) complexes the donor effects dominate, while in the bis(bipyridine)ruthenium(II) complexes donor effects are subdued and e_π is negative. Similar behavior is exhibited by many of the ligands from Table 1 with π bonds. Formate is perhaps the most unexpected case, showing net π-withdrawing characteristics, even though acetate is a relatively strong π-donor.

The list of $[Ru(bpy)_2X_2]$ complexes known is extensive. Thus many more ligands may be evaluated and their π-bonding characteristics compared with those studied here. In such comparisons, however, it should be remembered that $[Ru(bpy)_2X_2]$ absorption spectra can be quite sensitive to the solvent.

EXPERIMENTAL

Dimethylformamide was used as the solvent because of the relatively high solubilities of salts generally, and $[Ru(bpy)_3]^{2+}$ salts in particular. If a salt was found that could be dissolved in DMF to yield a 2 M concentration of the desired anion, then $[Ru(bpy)_3]Cl_2$ was added to that solution to a concentration of 0.02 M, and 3 cm^3 photolyzed with a 500-W Hg lamp until a substantial color change had taken place, usually about one hour. The photolysate was then chromatographed on Sephadex LH-20, eluting with DMF. The first band, purple, or sometimes reddish-brown, in color, was in all cases ascribed to the desired *cis*-$[Ru(bpy)_2X_2]$ complex. There were generally two trailing bands, which were *cis*-$[Ru(bpy)_2(DMF)X]^+$ (usually red) and the $[Ru(bpy)_3]^{2+}$ starting material (yellow).[18,19] When a 2 M concentration of anion could not be achieved, the $[Ru(bpy)_3]X_2$ salt was made by preparing a Dowex 1-X8 anion exchange column in the X^- form, passing an aqueous solution of $[Ru(bpy)_3]Cl_2$ through it, and evaporating the eluant. All the

$[Ru(bpy)_3]X_2$ salts prepared in this way were sufficiently soluble in DMF to carry through with the photolysis as above, but with no additional salt present. To prepare $[Ru(bpy)_2(en)]^{2+}$, the perchlorate salt was used and a hundredfold excess of ethylenediamine added. Absorption spectra of the $[Ru(bpy)_2X_2]$ species were recorded on a Cary 14 spectrophotometer.

REFERENCES

1. C. E. Schäffer and C. K. Jørgensen, *Mol. Phys.* 1965, **9**, 401.
2. C. E. Schäffer, *Structure and Bonding* 1968, **5**, 68.
3. R. J. Deeth and M. Gerloch, *Inorg. Chem.* 1985, **24**, 1754.
4. C. K. Jørgensen, *Modern Aspects of Ligand Field Theory*, Chap. 13. North Holland, Amsterdam (1971).
5. C. I. Lepadatu, *Z. Phys. Chem.* (*Frankfurt*) 1968, **57**, 28.
6. M. A. Hitchman, *Inorg. Chem.* 1972, **11**, 2387.
7. J. Glerup, O. Mønsted and C. E. Schäffer, *Inorg. Chem.* 1976, **15**, 1399.
8. H.-H. Schmidtke, *Z. Phys. Chem.* (*Frankfurt*) 1964, **40**, 96.
9. I. P. Alimarin, V. I. Shlenskaya and O. A. Efremenko, *Zh. Neorg. Khim.* (Engl. Transl.) 1970, **15**, 530.
10. R. W. Olliff and A. L. Odell, *J. Chem. Soc.* 1964, 2417.
11. T. Matsubara, S. Efrima, H. I. Mettu and P. C. Ford, *J. Chem. Soc. Faraday Trans. II* 1979, **75**, 390.
12. H.-H. Schmidtke and D. Garthoff, *J. Am. Chem. Soc.* 1967, **89**, 1317.
13. H.-H. Schmidtke, *Ber. Bunsenges. Phys. Chem.* 1967, **71**, 1138.
14. F. Zuloaga and G. Jauregui, *Rev. Latinoamer. Quim.* 1971, **2**, 97.
15. T. J. Barton and R. C. Slade, *J. Chem. Soc. Dalton Trans.* 1975, 650.
16. W. W. Fee and J. N. M. Harrowfield, *Aust. J. Chem.* 1969, **23**, 1049.
17. L. G. Vanquickenborne and A. Ceulemans, *J. Am. Chem. Soc.* 1977, **99**, 2208.
18. P. E. Hoggard and G. B. Porter, *J. Am. Chem. Soc.* 1978, **100**, 1457.
19. W. M. Wallace and P. E. Hoggard, *Inorg. Chem.* 1980, **19**, 2141.

Polyhedron Vol. 6, No. 7, pp. 1625–1628, 1987
Printed in Great Britain

0277–5387/87 $3.00+.00

COMMUNICATION

SYNTHESIS AND MOLECULAR STRUCTURE OF THE FIRST INORGANIC QUADRUPLY-BRIDGED Ir(II) DIMER (Ir–Ir)

F. ALBERT COTTON* and RINALDO POLI

Department of Chemistry and Laboratory for Molecular Structure and Bonding, Texas A&M University, College Station, TX 77843, U.S.A.

(*Received* 17 *February* 1987; *accepted* 9 *March* 1987)

Abstract—Interaction of (COD)Ir(μ-form)$_2$Ir(OCOCF$_3$)$_2$(H$_2$O) (COD = 1,5-cyclooctadiene; form = *N*,*N*′-di-*p*-tolylformamidinate ion) with two equivalents of Hform in toluene affords Ir$_2$(form)$_4$, the first inorganic Ir(II) dimer to be crystallographically characterized. The reaction involves a formal electron redistribution from a dative Ir(I) → Ir(III) to a covalent Ir(II)–Ir(II) bond. The compound crystallizes in the cubic space group Pn$\bar{3}$n with a = 21.300(9) Å. The metal–metal separation, 2.524(3) Å, is the shortest ever reported for a bonding interaction between iridium atoms.

Rh(II) dinuclear compounds containing four monoanionic bridging ligands and a single metal–metal bond of $\sigma^2\pi^4\delta^2\delta^{*2}\pi^{*4}$ electronic configuration are well known.[1] The first one, Rh$_2$(O$_2$CH)$_4$(H$_2$O)$_2$, was reported in 1960,[2a] although not initially recognized as such.[2b] Other dirhodium(II,II) tetracarboxylato compounds have been obtained, mainly by interaction of hydrated RhCl$_3$ with alkali metal carboxylates in alcoholic media.[3] Known compounds with other bridging ligands include Rh$_2$(xhp)$_4$ (xhp = 6-X-substituted hydroxypyridinato ion, X = CH$_3$,[4,5] Cl[5]), Rh$_2$(OC(R)NR′)$_4$ (R = CF$_3$, R′ = H;[6] R = Me, R′ = Ph;[7] R = Ph, R′ = H[8]), Rh$_2$(3,5-Me$_2$pz)$_4$ (pz = pyrazolate ion),[9] Rh$_2$(PhNpy)$_4$,[10] Rh$_2$(N$_2$PhCPh)$_4$[11] and Rh$_2$(form)$_4$ (form = *N*,*N*′-di-*p*-tolylformamidinate ion),[12] some of which contain axially coordinated neutral ligands. A number of Rh_2^{4+} complexes with mixed bridging ligands also exist.[13] On the other hand, Ir(II) complexes having a similar structure have never been reported, in spite of the existence of a large number of structurally different Ir(II) dinuclear complexes, these being generally of the type represented in I[14] or II.[15]

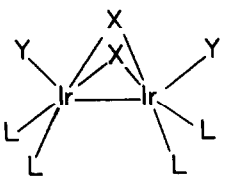

I

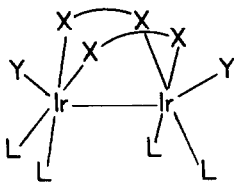

II

Only five diiridium(II,II) compounds that have the two metals in a square planar configuration with the two square planes parallel to each other (with or without additional axial ligands) seem to have been reported in the literature. These are $[Ir_2(TMB)_4I_2]^{2+}$ (TMB = 2,5-dimethyl-2,5-diisocyanohexane)[16] of structure III, Ir$_2$(Tcbiim)$_2$(CO)$_2$(MeCN)$_2$(P(OEt)$_3$)$_2$ (Tcbiim = dianion of tetracyanobiimidazole)[17a] of structure IV, [IrClX(CO)(dppm)]$_2$ [dppm = bis(diphenylphosphino)methane, X = Cl, CH$_3$O$_2$CC=CHCO$_2$CH$_3$][17b] of structure V, and Ir$_2$(OEP)$_2$ (OEP = dianion of octaethylporphirine)[18] of structure VI. The first four have been structurally characterized and exhibit Ir–Ir distances of 2.803[16] and 2.826(2),[17a] 2.786(1) and 3.016(1) (average) Å.[17b] Unfortunately Ir$_2$(OEP)$_2$, which is to be regarded as the only known truly inorganic Ir(II) dimer (this

* Author to whom correspondence should be addressed.

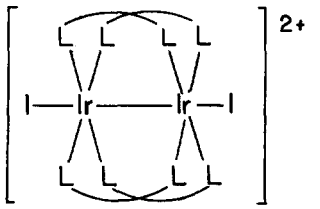

(L-L = $CH_3CH(NC)CH_2CH_2CH(NC)CH_3$)

III

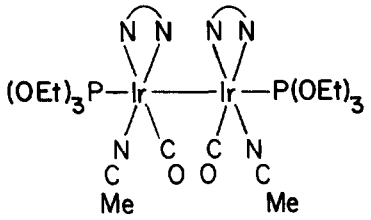

(N-N = TCBIIM)

IV

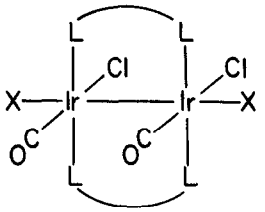

(L-L = DPPM ; X = Cl, $CH_3O_2CC{=}CHCO_2CH_3$)

V

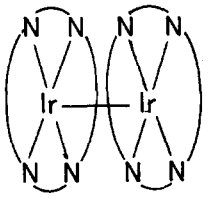

VI

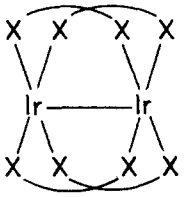

VII

meaning that the coordination sphere around the metal is filled with non-carbon atoms), has not been structurally characterized.

We wish to report here for the first time the synthesis and X-ray crystal structure of an inorganic iridium(II) dimer having a structure of the type VII, i.e. of the same type as the Rh_2^{4+} compounds mentioned above. The mixed-valence Ir(I)–Ir(III) compound, $(COD)Ir(\mu\text{-form})_2Ir(OCOCF_3)_2(H_2O)$ (COD = 1,5-cyclo-octadiene),[19] reacts smoothly in warm toluene with two equivalents of Hform to produce an emerald-green solution from which dark-green crystals of $Ir_2(form)_4$ were obtained in small yields by evaporation to dryness and recrystallization from MeCN.

Such a reaction involves a proton transfer from the weaker acid, Hform, to the stronger one, CF_3COOH. The formation of two new formamidinato bridges between the two iridium centers is presumably the driving force of the reaction. A formal electron redistribution also takes place, from the compound with a dative Ir(I) → Ir(III) bond to

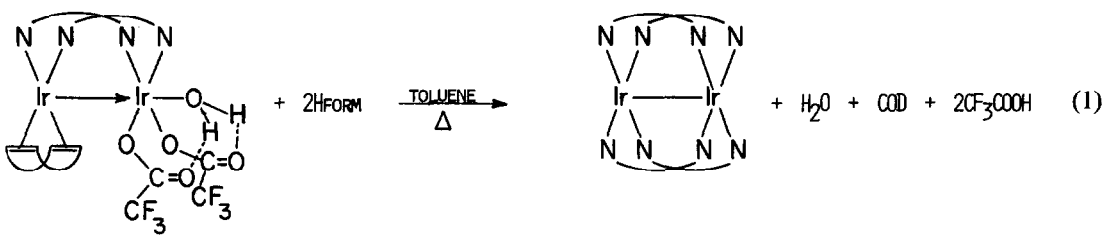

(1)

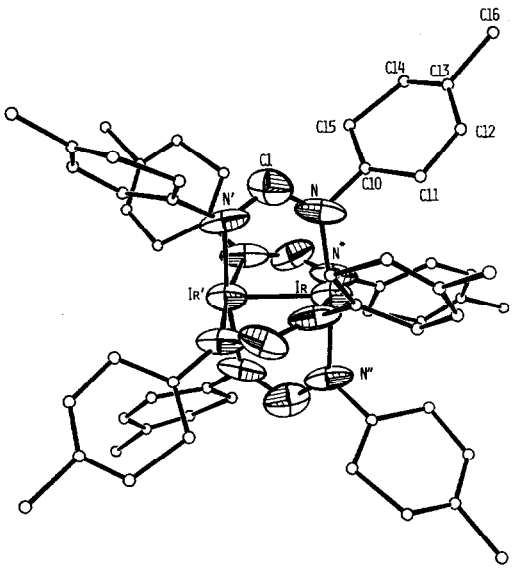

Fig. 1. An ORTEP view of the $Ir_2(form)_4$ molecule. The *p*-tolyl carbon atoms are drawn with arbitrary radii for clarity. Distances: Ir–Ir′, 2.524(3); Ir–N, 2.04(2); N–Cl, 1.34(2); N–ClO, 1.45(4) Å. Angles: Ir′–Ir-N, 85.4(6); N–Ir–N″, 170.9(9), N–Ir–N*, 89.6(7); Ir–N–Cl. 124(1); Ir–N–ClO, 123(2); Cl–N–ClO, 113(2); N–Cl–N′, 116(2)°.

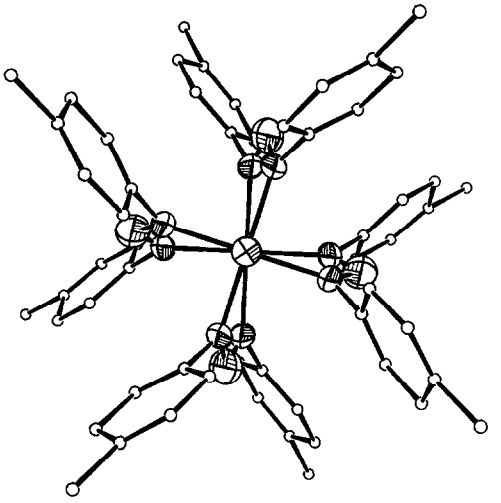

Fig. 2. View of the $Ir_2(form)_4$ molecule along the Ir–Ir′ direction.

the covalently bonded Ir(II)–Ir(II) product. Both CF_3COOH and COD that are obtained along with the iridium product were identified by their ^{1}H-NMR peaks at 13.0 (broad) and 5.55 δ, respectively.

Quite surprisingly, attempts to obtain the same product directly by oxidising $[Ir(form)(COD)]_2$ with Ag(form) failed. No reaction took place under thermal or photochemical conditions or a combination thereof.

The structure of the $Ir_2(form)_4$ molecule is shown in Fig. 1.* The molecule has D_4 imposed symmetry, the fourfold axis passing through the two iridium atoms and the twofold axes passing through and between pairs of trans-methylidyne groups. The compound is isostructural with $Rh_2(form)_4$.[12] Each iridium atom is bonded to four nitrogen atoms in a square planar arrangement. The iridium atom is displaced by 0.16(2) Å from the N_4 plane in the outward direction. The two square planes are twisted away from the eclipsed configuration by 15.6(5)° (see Fig. 2). The metal–metal distance is 2.524(3) Å and is the shortest Ir–Ir bond length ever reported. It is even shorter than the separation in $[Ir(CO)(PPh_3)(\eta\text{-}PPh_2)]_2$, 2.554 Å, for which a bond order of two has been proposed[20] and it is, expectedly, longer than the Rh–Rh separation (2.4336(4) Å) in the analogous compound $Rh_2(form)_4$.[12] The nearest neighbour separation in metallic iridium is 2.714 Å.[21]

Electrochemical, spectroscopic and theoretical studies on $Ir_2(form)_4$ are in progress. The assignment of an electron rich single bond of $\sigma^2\pi^4\delta^2\delta^{*2}\pi^{*4}$ configuration to the metal–metal interaction, however, is strongly suggested by previous work done on similar rhodium compounds.[22]

Acknowledgements—We thank the National Science Foundation for support, and Prof. Piraino for sending us a copy of his manuscript[12] prior to publication.

REFERENCES

1. F. A. Cotton and R. A. Walton, *Multiple Bonds Between Metal Atoms*. Wiley, New York (1982).
2. (a) I. I. Chernyaev, E. V. Shenderetskaya and A. A. Koryagina, *Zh. Neorg. Khim.* 1960, **5**, 1163; (b) I. I. Chernyaev, E. V. Shenderetskaya, L. A. Nazahova and A. S. Antsyshkina, *Abstr. 7th Int. Conf. Coord. Chem.* Stockholm (1962).
3. (a) I. I. Chernyaev, E. V. Shenderetskaya, A. G. Maiorova and A. A. Koryagina, *Zh. Neorg. Khim.* 1965, **10**, 537; (b) *idem*, *Zh. Neorg. Khim.* 1966, **11**, 2575; (c) S. A. Johnson, H. R. Hunt and H. M. Neumann, *Inorg. Chem.* 1963, **2**, 960; (d) T. A. Stephenson, S. M. Morehouse, A. R. Powell, J. P. Heffer and G. Wilkinson, *J. Chem. Soc.* 1965, 3632; (e) G. Winkhaus and P. Ziegler, *Z. Anorg. Allg. Chem.* 1967, **350**, 51; (f) P. Legzdins, R. W. Mitchell, G. L. Rempel, J. D. Ruddick and G. Wilkinson, *J.*

* Crystal data: cubic, space group $Pn\bar{3}n$, $a = 21.300(9)$ Å, $V = 966.4(12)$ Å^3, $Z = 6$, $d_{calc} = 1.317$ g cm^{-3}, $R = 0.0595$ ($R_w = 0.0770$) for 402 reflections having $F_o^2 > 3\sigma(F_o^2)$.

Chem. Soc. (*A*) 1970, 3322; (g) G. A. Rempel, P. Legzdins, H. Smith and G. Wilkinson, *Inorg. Synth.* 1972, **13**, 90.
4. M. Berry, C. D. Garner, I. H. Hillier, A. A. MacDowell and W. Clegg, *J. Chem. Soc., Chem. Comm.* 1980, 494.
5. F. A. Cotton and T. R. Felthouse, *Inorg. Chem.* 1981, **20**, 584.
6. A. M. Dennis, R. A. Howard, D. Lancon, K. M. Kadish and J. L. Bear, *J. Chem. Soc., Chem. Comm.* 1982, 339.
7. J. Duncan, T. Malinski, T. P. Zhu, Z. S. Hu, K. M. Kadish and J. L. Bear, *J. Am. Chem. Soc.* 1982, **104**, 5507.
8. A. R. Chakravarty, F. A. Cotton, D. A. Tocher and J. H. Tocher, *Inorg. Chim. Acta* 1985, **101**, 185.
9. A. R. Barron, G. Wilkinson, M. Motevalli and M. B. Hursthouse, *Polyhedron* 1985, **4**, 1131.
10. D. A. Tocher and J. H. Tocher, *Inorg. Chim. Acta* 1985, **104**, L15.
11. J. C. Le, M. Y. Chavan, L. K. Chau, J. L. Bear and K. M. Kadish, *J. Am. Chem. Soc.* 1985, **107**, 7195.
12. P. Piraino, G. Bruno, S. Lo Schiavo, F. Laschi and P. Zanello, *Inorg. Chem.* in press.
13. (a) J. L. Bear, T. P. Zhu, T. Malinski, A. M. Dennis and K. M. Kadish, *Inorg. Chem.* 1984, **23**, 674; (b) K. M. Kadish, D. Lancon and J. L. Bear. *Inorg. Chem.* 1982, **21**, 2987; (c) M. Y. Chavan, T. P. Zhu, X. Q. Lin, M. Q. Ahsan, J. L. Bear and K. M. Kadish, *Inorg. Chem.* 1984, **23**, 4538; (d) T. P. Zhu, M. Q. Ahsan, T. Malinski, K. M. Kadish and J. L. Bear, *Inorg. Chem.* 1984, **23**, 2; (e) M. Y. Chavan, M. Q. Ahsan, R. S. Lifsey, J. L. Bear and K. M. Kadish, *Inorg. Chem.* 1986, **25**, 3218; (f) P. Piraino, G. Bruno, G. Tresoldi, S. Lo Schiavo and P. Zanello, *Inorg. Chem.* 1987, **26**, 91.
14. (a) A. Thorez, A. Maisonnat and P. Poilblanc, *J. Chem. Soc., Chem. Comm.* 1977, 518; (b) J. J. Bonnet, A. Thorez, A. Maisonnat, J. Galy and R. Poilblanc, *J. Am. Chem. Soc.* 1979, **101**, 5940; (c) B.-K. Teo and P. A. Snyder-Robinson, *J. Chem. Soc., Chem. Comm.* 1979, 255; (d) J. J. Bonnet, P. Kalck and R. Poilblanc, *Angew. Chem., Int. Ed. Engl.* 1980, **19**, 551; (e) B.-K. Teo and P. A. Snyder-Robinson, *Inorg. Chem.* 1981, **20**, 4235; (f) P. Kalck and J. J. Bonnet, *Organometallics* 1982, **1**, 1211; (g) F. A. Cotton, P. Lahuerta, M. Sanau and W. Schwotzer, *J. Am. Chem. Soc.* 1985, **107**, 8284.
15. (a) J. Powell, A. Kuksis, S. C. Nyburg and W. W. Ng, *Inorg. Chim. Acta* 1982, **64**, L211; (b) K. A. Beveridge, G. W. Bushnell, K. R. Dixon, D. T. Eadie, S. R. Stobart, J. L. Atwood and M. J. Zaworotko, *J. Am. Chem. Soc.* 1982, **104**, 920; (c) A. W. Coleman, D. T. Eadie, S. R. Stobart, M. J. Zaworotko and J. L. Atwood, *J. Am. Chem. Soc.* 1982, **104**, 922; (d) G. W. Bushnell, D. O. K. Fjeldsted, S. R. Stobart and M. J. Zaworotko, *J. Chem. Soc., Chem. Comm.* 1983, 580; (e) J. L. Atwood, K. A. Beveridge, G. W. Bushnell, K. R. Dixon, D. T. Eadie, S. R. Stobart and M. J. Zaworotko, *Inorg. Chem.* 1984, **23**, 4050; (f) J. V. Caspar and H. B. Gray, *J. Am. Chem. Soc.* 1984, **106**, 3029; (g) D. G. Harrison and S. R. Stobart, *J. Chem. Soc., Chem. Comm.* 1986, 285.
16. V. M. Miskowski, T. P. Smith, T. M. Loehr and H. B. Gray, *J. Am. Chem. Soc.* 1985, **107**, 7925.
17. (a) P. G. Rasmussen, J. E. Anderson, O. H. Bailey and M. Tamres, *J. Am. Chem. Soc.* 1985, **107**, 279; (b) B. R. Sutherland and M. Cowie, *Organometallics* 1985, **4**, 1801.
18. K. J. Del Rossi and B. B. Wayland, 192*nd ACS National Meeting*, Anaheim, 7–12 September 1986, Comm. INOR 344.
19. F. A. Cotton and R. Poli, *Inorg. Chem.* 1987, **26**, 590.
20. R. Mason, I. Sotofte, S. D. Robinson and M. F. Uttley, *J. Organometal. Chem.* 1972, **46**, C61.
21. L. Pauling, *The Nature of the Chemical Bond*, 3rd ed., p. 410. Cornell University Press, Ithaca, NY (1960).
22. (a) J. G. Norman, Jr. and H. J. Kolari, *J. Am. Chem. Soc.* 1978, **100**, 791; (b) J. G. Norman, Jr., G. E. Renzoni and D. A. Case, *J. Am. Chem. Soc.* 1979, **101**, 5256; (c) B. E. Bursten and F. A. Cotton, *Inorg. Chem.* 1981, **20**, 3042.

Polyhedron Vol. 6, No. 7, pp. 1629–1633, 1987
Printed in Great Britain

0277-5387/87 $3.00+.00
Pergamon Journals Ltd

NEWSLETTER 1987: IUPAC COMMISSION ON NOMENCLATURE OF INORGANIC CHEMISTRY

The objective of this Newsletter is to inform all interested parties about the ongoing activities of the Commission on Nomenclature of Inorganic Chemistry (CNIC), and to draw attention to nomenclature documents that it has published recently. Readers are invited to write to the CNIC chairman about problems involving the nomenclature of inorganic chemistry: Professor Daryle H. Busch, Department of Chemistry, The Ohio State University, 120 West 18th Avenue, Columbus, OH 43210, U.S.A., or to any of its members.*

The first CNIC Newsletter appeared in the following journals: *Transition Metal Chemistry* 1986, **11**, 35; *Polyhedron* 1986, **5**, 925; and *Chemistry International* 1986, **8**, 10.

The favourable response of the chemical community has led the Commission to continue biannual publication of Newsletters.

RECENTLY PUBLISHED DOCUMENTS

The most recent IUPAC–CNIC manual on the nomenclature of inorganic chemistry[1] was published in 1970 and the Commission has published a number of documents about topics that have evolved since that time. Documents appearing in print in 1982 or later deal with isotopically labeled and isotopically substituted compounds,[2] inorganic and coordination polymers[3] (joint with the Nomenclature Commission of the Macromolecular Division of IUPAC), and nitrogen hydrides.[4] Short summaries of these recommendations have been given in Newsletter 1985. A document on heteropolyanions[5] is in press and its synopsis is given below.

NOMENCLATURE OF POLYANIONS

The chemistry of polyanions is a rapidly growing field due particularly to the novelty and significance of some of these compounds. Some species are very large (up to 48 tungsten atoms) and extremely complicated in structure. Many examples of substituted species have been found to exist as isomers. Today the basic compounds are commonly identified among specialists by trivial names and the old rules for naming polyanions (1970 Red Book) are not adequate to treat many of the new species. New rules have been developed. The basic idea is to assign a number to each central atom, the environment of which is then described by letters associated with that number. The document describes various types of polyanions having what is called the Lindqvist structure, the Anderson structure, the Keggin structure, the Dawson structure, and some others derived from them. It is hoped that the examples given in the document will provide a procedure that can be applied to the naming of any new compound of this kind. Since these compounds are very complicated it is not surprising that their names are correspondingly intricate. Shortened names may always be used, for example to describe the composition alone; however, such names invariably will give less information about the details of the actual structure.

ONGOING ACTIVITIES

Because of the development of many new fields and the discovery of many new types of compounds since the publication of the 1970 Red Book, the Commission decided to undertake a complete revision of the rules for the nomenclature of inorganic chemistry. CNIC expects the new basic manual to be published in 1987; the project is described in detail below (1987 Red Book, Part I).

In addition to that basic manual, the Commission intends to publish a Part II that will be made up of chapters dealing with more advanced and detailed recommendations covering more specialized fields, such as those mentioned above[2–5] and organometallic compounds, clusters, inorganic rings, chains and ligand abbreviations (all in preparation).

All interested persons are encouraged to communicate their ideas or suggestions about these topics or to suggest other appropriate subjects to the Commission. Please feel free to share your feelings on topics that are or should be considered by CNIC.

OTHER DOCUMENTS OF RELEVANCE TO INORGANIC CHEMISTRY

The Commission also wants to call attention to nomenclature documents prepared under the supervision of other IUPAC commissions. Of particular note at this time are documents on zeolites,[6] graphite intercalation compounds,[7] use of numerical terms[8] and the application of the λ-convection to treat variable valence in organic nomenclature.[9]

PERIODIC TABLE

The Commission has recommended that the columns of the long form of the Periodic Table be labeled consecutively from left to right with the arabic numerals 1–

* Present titular members of the Commission are: D. H. Busch (chairman), E. Fluck (vice-chairman), P. Fodor-Csanyi, R. Laitinen, J. F. Nixon, J. Reedijk, E. Samuel (secretary) and T. E. Sloan.

18. The environment and nature of this recommendation are reviewed here.

CNIC attempts to be respectful of, and sensitive to, common usage of such basic conventions as those involving the Periodic Table. In the homelands of Mendeleev and J. Lothar Meyer, the classic eight-column short form of the table is understandably still widely used. However, most of the countries in Europe, both East and West, use an 18-column table exclusively, as do Japan and the United States. CNIC expects that, in some countries, use will always be made of the eight-column table. Those users should respect the recommendations of the 1970 Red Book. It remains true, however, the common practice throughout most of the world overwhelmingly supports the 18-column format. Therefore, recommendation of that format cannot be an issue. The labeling of the columns is the only issue.

In 1970 CNIC and IUPAC endorsed a system for column labeling that followed an early precedent for the use of the capital letters A and B to distinguish between the left- and right-side families of elements. While this practice is in common use in Great Britain and much of Europe, it has found acceptance only slowly, if at all, elsewhere. Japan has just accepted this practice while the United States has adhered rigidly to the converse use of the A and B labels. Thus, an unacceptable conflict in column labeling exists.

Exhaustive discussions have been held by CNIC on various formats and labeling schemes for the Periodic Table and representatives of CNIC have promoted public discussions on the subject through national professional organizations. At the meeting of CNIC in 1982, it was concluded that the use of the 18-column table should be encouraged and that that table would be used in the new Red Book, Part I. Further, a majority of the members of CNIC favored the labeling of the columns consecutively, from left to right, with the arabic numbers 1–18. The latter suggestion was offered as a solution to the conflicting use, on opposite sides of the Atlantic Ocean, of the column labels A and B. These conclusions were confirmed by Votes at CNIC meetings in 1983, 1984 and 1985. Now, in 1986, CNIC has reconfirmed these conclusions at its meeting in Heidelberg. While it is neither the purpose nor the intent of CNIC to arbitrarily set the format of the Periodic Table to be used in all parts of the world, it is a reasonable mission for CNIC to offer broadly useful solutions when direct conflicts in usage occur.

At the Heidelberg meeting an attempt was made to evaluate the correspondence on the Periodic Table that was available to CNIC. Least change was most often favored, with no change being most popular of all. Many would like to retain the equivalent of an A–B system. However, this was not found to be acceptable either because of problems with translation or because of the conviction that disguising the problem fails to solve it.

Critics claim that the new labeling system interfers with teaching. Those from users of the eight-column table could not be answered since CNIC expects use of that format to continue in some places. However, it is not appropriate to give credit to CNIC for the evolved dominance of the 18-column form throughout most of the world.

Otherwise, the main concern rests on perceived losses in correlations between column labels and such quantities as positive oxidation numbers and numbers of valence electrons for main-group elements. As has been pointed out by a number of correspondents, no problem of this kind actually exists. One need only show the student that for the "teen columns" the *second* digit of the column number corresponds to the number of valence electrons and to the maximum positive oxidation number. One should also recognize that the CNIC-recommended numbering scheme also displays relationships involving the numbers of electrons for the transition elements. Further, the proposed scheme eliminates the irrational (for the long form) lumping together of three families of elements under a single number (old VIII, new 8–10). In summary, one can teach all that was taught before, plus significantly more, using the proposed labels.

Several correspondents have referred to the use of the roman numerals of the familiar 18-column table in the common parlance of solid-state science; e.g. III/V semiconductors. The behaviors of these materials derive from their electronic (and crystal) structures and not from the labels on the columns of the Periodic Table. It is almost universally agreed that one should not try to reproduce electronic structure precisely in the column headings. Again, the second digit of the column heading relates to the electronic structure for *p*-block elements and the notation III/V remains perfectly rational.

A number of correspondents complained of poor or ineffective communication with regard to the proposed relabeling scheme. CNIC is deeply concerned with this matter. It has been decided that, over whatever length of time is required by appropriate and effective process, ultimate recommendations on the format and labeling of the Periodic Table must be responsive to the user constituency. That constituency ranges from school children to senior scientists and covers such disciplines, in addition to chemistry, as biology, metallurgy, ceramics, solid-state physics, and materials science. Each subgroup of this large population should have the opportunity to seek and present its local consensus. The principal goal of CNIC–IUPAC would be to offer the minimum guidance necessary to eliminate conflicting usages.

CONTENTS OF THE RED BOOK, PART I

In Newsletter 1985 we have only listed the chapter titles. Subsequently, the Commission has approved the contents of the several chapters and the documents are now subject to international public review, as required by IUPAC regulations. Accordingly, synopses of the several chapters have either already appeared or will appear in the coming year, in several journals, about the world. Copies of the chapters can be obtained from the corresponding regional distribution centers. Summaries of the 11 chapters are presented here so that interested readers can consider their contents and see the relationships between the chapters.

Chapter I-1, *general aims*

The opening chapter begins with a brief history of the nomenclature of inorganic chemistry from its birth to the present day. The general aims and functions of nomenclature are then described and the terms "trivial", "semi-systematic" and "systematic" are explained. It is then shown how and why it became necessary to establish rules. This is followed by an explanation of the methodology of name construction.

Various systems of inorganic nomenclature are presented, with examples. The discussion covers binary, additive and replacement nomenclature, and also systems used in organic chemistry and pertinent systems, such as substitutive, subtractive and index nomenclature.

The final section contains information about international collaboration on nomenclature matters, on the formation of working groups on nomenclature, and on the role which IUPAC has assumed in this endeavor. This information is not generally known to the chemical community. A survey of the accomplishments of IUPAC commissions since 1921 is presented, together with bibliographical reference to all of the inorganic nomenclature documents published by this Commission.

Chapter I-2, *grammar*

The purpose of this chapter is to guide the users of nomenclature in building the name or formula of an inorganic compound, and to help them verify that the derived name or formula fully obeys the accepted principles. Chemical nomenclature is a very special language with its own vocabulary, syntax and grammar. This chapter contains a general survey of the "grammatical" rules governing the correct use of the various devices used in the construction of a name or a formula. Sections 1–14 deal with idiomatic symbols (brackets, dots, commas, hyphens, dashes etc.), greek letters and numerals and provide many examples. The various priorities are then discussed in Section 15. The last part, Section 16, deals with suffixes commonly used in inorganic nomenclature. This chapter is an innovation in the presentation of the nomenclature of inorganic chemistry.

Chapter I-3, *elements, atoms, and groups of atoms*

This chapter defines the basic material for inorganic nomenclature, the atomic symbols and names. It also contains definitions of fundamental concepts such as element, atomic charge, and nuclide. The basic methods for indicating ionic charge, atomic number, and mass number are described, as well as a system for naming allotropes of the elements which should be of general if not universal utility.

The final section deals with the indication of groups in the Periodic Table. For the 18-column periodic table, it is recommended that the old A–B system for sub-groups be abandoned because of its inconsistent application in different parts of the world, and that a system with group numbers 1–18 (the last being the inert gases) be adopted generally. Some approved names for particular groups of elements, such as halogens and transition elements, are listed.

Chapter I-4, *formulae*

This chapter is intended to serve as a guide to the users of the nomenclature of inorganic chemistry in writing formulae correctly according to the rules recommended by IUPAC. The chapter contains the definitions of types of formulae, and shows how to indicate proportions, oxidation states, and ionic charges of constituents, and how to use structural modifiers.

The sequence of citation in formulae is based on the alphabetical order of the symbols of the electropositive and electronegative constituents, respectively. A guide to writing the formulae of isotopically modified compounds is included with cross-reference to the detailed IUPAC recommendations. Numerous examples are given to illustrate the rules. Finally, a table summarizes the method for assignment of the formulae of compounds.

The rules of formulae construction are in full agreement with the previously published rules of *Nomenclature of Inorganic chemistry* (1970) (1970 Red Book), but Chap. I-4 gathers together all of the basic information on formulae which was discussed in different chapters of the old Red Book. In addition, some rules, such as that concerning alphabetical ordering, are extended and others explicitly expressed so that it is not necessary to infer them from the examples. This latter method of presentation was used in the 1970 Red Book and has been widely criticized. The number and types of examples have now been increased.

Chapter I-5, *names based on stoichiometry*

This chapter serves as a guide in writing stoichiometric names correctly, including the derivation of names, their assembly into the correct sequence and the indication of proportions. Rules for the names of monoatomic, polyatomic and heteropolyatomic electropositive and electronegative constituents, as well as of addition compounds, are included.

The order of citation in names is based on the alphabetical order of the names of the electropositive and electronegative constituents, respectively. The proportions of the constituents can be indicated either by multiplicative prefixes (numerical prefixes and multiplicative numerals) or by indications of the oxidation numbers or the charges on the ions.

There are no changes in substance between this chapter and the 1970 Red Book; however, the discussion is more extensive and many points are explained more precisely. The chapter contains numerous examples.

Chapter I-6, *solids*

Chapter I-6 of the new Red Book, Part I, deals with the names of solid phases, chemical composition, point defect notation, phase nomenclature, non-stoichiometric phases, polymorphism, amorphous systems and glasses. The chapter is essentially a new one, differing in principle

and detail from corresponding material in 1970 Red Book.

The point defect notation is based on the Kroger–Vink system. It allows the indication of site occupation by using the element symbols as subscripts. Vacant positions are indicated with V and interstitials with the subscript i. Charges are expressed by superscripts; both real and effective charges can be indicated.

Phase nomenclature is derived from the Pearson notation. In the section on non-stoichiometric phases, descriptions are given of modulated structures, crystallographic shear structures, chemical twinning, infinitely adaptive structures and intercalates.

For the distinction between polymorphs, indication of the crystal system in combination with the name or formula is recommended. Some abbreviations are used to designate amorphous systems and glasses.

Chapter I-7, *neutral molecular compounds*

This chapter describes the essential characteristics of the nomenclature of realtively simple neutral compounds, providing guidance for name-construction: (a) for molecules regarded as substitution derivatives of parent hydrides, and (b) for coordination entities.

The principles of substituitive nomenclature are explained and the nomenclature of a chosen set of parent hydrides is described. These principles are extended to cover the nomenclature of oligonuclear hydrides, to various categories of chains of atoms, including branched, and to simple cyclic systems. The case of varying bonding numbers for the central atom, including unsaturation, is treated.

The principles of coordination nomenclature are described and extended from mononuclear coordination entities to dinuclear compounds, and to simple oligonuclear entities. Illustrative examples are provided throughout.

Chapter I-8, *names for ions, radicals and salts*

Cations, anions, radicals and salts are defined, and the two kinds of radicals are distinguished: those consisting of an atom (or groups of atoms) having one or more unpaired electrons and those consisting of a group of atoms for which the name is used as a prefix in substitutive nomenclature. Charged radicals are treated.

The sections on cations and anions deal with species obtained from organic and inorganic molecules after loss or addition of electrons, or hydrogen ions, or of hydride ions. Coordination nomenclature is used when a central atom of metal character is present, whereas substitutive nomenclature is used in other cases. Certain special names are retained (e.g. nitrosyl for NO^+ and kalide for K^-).

Formulae and names of salts are easily constructed by combination of the names of cations and anions. In double salts the cation and anion names are ordered alphabetically unless other requirements mandate an alternative arrangement. Thus, to emphasize structural similarities $AlLaO_3$ is often represented as $LaAlO_3$ (*perovskite*-type).

Chapter I-9, *inorganic oxoacids*

This chapter provides a treatment of the nomenclature of oxoacids which is intended to be comprehensive and useful. The long history of the subject and the importance and widespread use of oxoacid nomenclatures in teaching and industry warrant this extensive coverage. The approach followed involves systematization, whenever possible, based on the principles of coordination nomenclature.

The introductory sections deal with historical considerations. A definition of an oxoacid is given. Then the principles of hydrogen nomenclature and their extension to all oxoacids and their functional derivatives (halogenides, anhydrides, esters and amides) are given, with many examples. This represents a considerable expansion of the 1970 Red Book, but this systematic use was recommended, at that time, only for acids containing ligands other than oxygen and sulfur.

Acid nomenclature is then presented; it has the feature that the number of acidic hydrogens is not explicitly stated. Polynuclear acids are dealt with next. Except for special cases, this nomenclature is based exclusively on that of coordination compounds.

Chapter I-10, *coordination compounds*

The nomenclature of coordination compounds constitutes a major system of addition nomenclature that is based on structural relationships associated with the compounds of the metallic elements. Basic concepts and definitions are presented, and the discussion proceeds on to formulas and names for the simplest coordination compounds. The nomenclature of mononuclear coordination compounds with monodentate ligands is extensively developed with listings of names and abbreviations for many common ligands. Stereochemical descriptors are then presented that designate the geometric arrangements of ligands. Formulas and names for chelate mononuclear complexes follow with special attention being given to the kappa convention for identifying the ligating atoms of ambidentate and polyfunctional ligands, and to stereochemical descriptors for chelated compounds. Chirality symbols are introduced for various polyhedra structures and the skew-line helical reference is presented along with an alternative technique based on the Cahn, Ingold, Prelog priority sequence of ligands. A limited treatment is provided for the nomenclature of more intricate species including polynuclear complexes and clusters, with emphasis given to central atom numbering and bonding notation. A summary of the nomenclature for single-strand coordination polymers is given, and the final section is a brief introduction to the nomenclature of organometallic complexes.

Chapter I-11, *boron hydrides and related compounds*

Just as their structures provided novelty and a challenge to chemistry, the nomenclature of the boron

hydrides must treat distinctive relationships. The bases of boron-hydride nomenclature are discussed, and the polyhedral clusters of boron are presented and classified and the class names are given. Stoichiometric names are presented and the general aspects of structural names are discussed. Numbering schemes, steric descriptors and structural isomers are discussed. The "debor" method is given. The treatment of replacement and substitution in boron clusters is considered, including hydrogen substitution, skeletal subrogation and such species as carbaboranes and metalloboranes.

CORRESPONDENCE, SMALL MATTERS THAT MATTER ETC.

CNIC is a unit of an international public service organization, IUPAC, and we are volunteer chemists from around the world. Since nomenclature is our responsibility, we invite your inquiries and suggestions. We can serve you best if we know your needs and opinions. At worst, we should know someone who can name your cluster—or your ligand! Of course, some people already bring us their questions.

CNIC was formed to eliminate the Tower of Chemical Babel and almost every chemist has both appreciated and despised the tedium of the systematic and proper chemical nomenclature that CNIC is obliged to generate. In this second era of the computer evolution, names, formulae and the like are constrained by the inevitable superliteral reaction of the computer. With sympathy, but because precision and uniformity are increasingly important, we will point out a few conventions that deserve to be observed.

In Newsletter 1985 attention was directed to the use of aqua and the elision of vowels. Other items are: previously, bridging ligands were set out with hyphens as follows: tetrakis-(μ-acetato-)bis(pyridine)dicopper for $Cu_2(OAc)_4(py)_2$. Now, following the ongoing practices of certain journals, we have adopted the simpler convention: tetrakis(μ-acetato)bis(pyridine)dicopper.

REFERENCES

1. International Union of Pure and Applied Chemistry, *Nomenclature of Inorganic Chemistry* (1970), 2nd Edn, Butterworths, London (1971).
2. Nomenclature of isotopically modified compounds, *Pure Appl. Chem.* **54**, 1887 (1981).
3. Nomenclature for regular single-strand and quasi-single-strand inorganic and coordination polymers, *Pure Appl. Chem.* **57**, 149 (1985).
4. The nomenclature of hydrides of nitrogen and derived cations, anions, and ligands, *Pure Appl. Chem.* **54**, 2545 (1982).
5. Nomenclature of heteropolyanions, *Pure Appl. Chem.* (in press).
6. Chemical nomenclature and formulation of compositions of synthetic and natural zeolites, *Pure Appl. Chem.* **51**, 1091 (1979).
7. International cooperation on characterization and terminology of carbon and graphite, *Pure Appl. Chem.* **51**, 1561 (1979).
8. Concerning numerical terms used in organic chemistry, *Pure Appl. Chem.* **55**, 1463 (1983).
9. Treatment of variable valence organic nomenclature, *Pure Appl. Chem.* **56**, 769 (1984).

Polyhedron Vol. 6, No. 8, pp. 1635–1637, 1987
Printed in Great Britain

0277–5387/87 $3.00+.00

DIOXOMOLYBDENUM(VI) COMPLEX WITH *N,N'*-ETHYLENEBIS(SALICYLIDENEIMINE)

LOUIE S. GONZALES and K. S. NAGARAJA*

Department of Chemistry, De La Salle University, Manila, Philippines

(*Received* 19 *November* 1985; *accepted after revision* 7 *May* 1986)

Abstract—The interaction of *N,N'*-ethylenebis(salicylideneimine), H_2salen, with ammonium molybdate yielded the molybdenum(VI) complex MoO_2(salen) with the *cis*-dioxo structure as inferred from IR spectral studies. The ^{1}H NMR chemical shifts of azomethine protons in the free ligand and the complex are 8.14 and 8.39 δ, respectively, suggesting the bonding of the azomethine nitrogen to MoO_2 group. The thermal decomposition behaviour of the complex is discussed.

Several complexes of salen with iron(III)[1], cobalt(II)[2], lanthanoids(III)[3] and uranyl[4] have been reported. Salen may act as a univalent-bidentate or a bivalent-tetradentate ligand. Schiff's base complexes of molybdenum have been reported by Yamanouchi and Yamada[5,6], Dilworth *et al.*[7] and Goh and Lim[8]. We now describe the ^{1}H NMR spectra, thermal decomposition and X-ray powder diffraction data on the oxomolybdenum(VI) complex with salen.

EXPERIMENTAL

Ammonium paramolybdate, salicylaldehyde, ethylenediamine and the solvents used were of laboratory grade. The ligand, H_2salen, was prepared by the condensation of salicylaldehyde with ethylenediamine by following the reported procedure.

Preparation of cis-*dioxo* N,N'-*ethyl-enebis(salicylideneiminato) molybdenum*(VI), MoO_2(*salen*)

Ammonium paramolybdate (0.50 g) was dissolved in water (15 cm^3). H_2salen (2.0 g) in ethanol (50 cm^3) was added and the solution was refluxed for 1 h. The yellow product formed was filtered when the solution was hot. The compound was recrystallized thrice from ethanol to obtain the pure complex.

Yield: 50%. The C, H, N and Mo analyses of the complex was found to be 48.8, 3.6, 7.1, 24.1% which corresponds to the calculated values 48.7, 3.6, 7.1 and 24.3%, respectively for MoO_2(salen). The "d_{hkl}" values for H_2salen and the complex are 2.76(w), 2.92(w) 3.00(m), 3.24(m), 3.86(m), 4.40(w), 4.62(m), 4.87(s), 5.02(m), 5.60(w), 5.91(vs), 6.91(vs), 7.31(s), 11.86(s) and 3.18(s); 4.84(w), 5.13(w), 5.88(s), 6.88(s), 7.21(w), 8.73(m), 10.21(s), 11.73(s), 15.36(w), respectively.

Elemental analyses of the complex were carried out using a Hewlett–Packard CHN analyzer. The IR, far-IR, UV-visible and ^{1}H NMR spectra were recorded on Shimadzu IR-435, Polytech IR 12, Pye–Unicam SP8-100 and Hitachi-R24B 60MHz spectrometers. Thermal analyses was carried out in air on a Shimadzu DTA-30 thermal analyzer using a platinum crucible with a heating rate of 10°C min^{-1}. X-ray powder photographs were taken on a Philipps X-ray diffractometer using CoK_α radiation.

RESULTS AND DISCUSSION

The complex is yellow and has poor solubility in methanol and ethanol. UV-visible spectra of the complex in CH_2Cl_2 has λ_{max} at 410 nm (ε 2870 l mol^{-1} cm^{-1}) which is attributed to a O(p_π)→Mo (d_π) charge-transfer transition. The IR absorption at 1630 cm^{-1} is attributed[7] to ν(C=N), which is characteristic of the azomethine group. The bands at 925 and 900 cm^{-1} due to ν(Mo=O) are characteristic of the *cis*-dioxo structure. The peaks observed at 500 and 305 cm^{-1} are assigned to ν(Mo—O) and ν(Mo—N), respectively.

The ^{1}H NMR is useful in determining the molecular structure of the compound. The spectra of

*Author to whom correspondence should be addressed.

Table 1. ^{1}H NMR spectral data (δ) in ppm with reference to TMS

Compound	—CH_2—	—CH=N—	Aromatic
H_2salen	3.72, 3.29 J = 0.5 Hz	8.15, 8.19 J = 0.3 Hz	6.72, 6.75, 6.85, 6.88, 7.05, 7.16
H_2salen D_2O exchange	3.82	8.21	6.62, 6.70, 6.79, 6.88, 6.91, 7.09, 7.20
MoO_2(salen)	4.01	8.39	6.78, 6.90, 6.91, 7.06, 7.22, 7.32, 7.35, 7.48, 7.50

the ligand and the complex are recorded in $CDCl_3$. The values along with the assignments are given in Table 1. The azomethine (CH=N) and methylene (—CH_2—) protons in the H_2salen appear as a doublet at 8.19, 8.15 and 3.79, 3.72 δ, respectively. The hydrogen bonding to the azomethine N atom splits the signals of CH=N and CH_2 protons. The spectrum of H_2salen treated with D_2O exhibited resonances for CH=N and CH_2 at 8.21 and 3.82 δ as a singlet respectively. The phenolic hydrogen is involved in exchange with D_2O and no hydrogen bonding persists with the azomethine N and so no splitting is observed. The increase in δ values in deuterated H_2salen may be due to the *anti* form of the imine predominating. When hydrogen bonding exists H_2salen may be in the *syn* form.

In the spectra of the complex, MoO_2(salen), the CH=N and CH_2 signals are observed as a singlet at 8.39 and 4.01 δ, respectively, which suggests that the azomethine N is involved in coordination to molybdenum. The spectrum of the complex has more complex multiplet signals for the aromatic protons when compared to free ligand. The inference is that the aromatic protons are experiencing different chemical environments, which is possible for a *cis*-dioxo structure. Thus a *trans*-dioxo symmetrical structure **I** for the complex is ruled out. In structure **II**, the CH=N and CH_2 protons are not identical and the splitting due to coupling is expected. Thus the present ^{1}H NMR spectral studies suggest that the more appropriate structure is **III**.

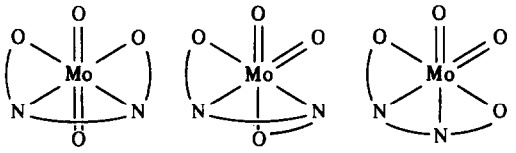

I **II** **III**

Table 2. TG and DTA data

Compound	TG Thermal reaction	TG Weight loss (%) found (calc.)	DTA Temperature range (°C)	DTA Peak	DTA Reaction
H_2salen	—	—	110	Endothermic	Glass transition
	—	—	130	Endothermic	Melting
	Formation of cyclopentadienone	70.1 (70.0)	320–350	Exothermic	Decomposition
		93.0 (—)	450–560	Exothermic	Combustion
MoO_2(salen)	Loss of C_2H_4+2HCN	20.4 (20.8)	235–300	Exothermic	Decomposition
	Formation of Mo metal	75.9 (76.0)	480–550	Exothermic	Decomposition

The thermal decomposition of H_2salen and the complex are given in Table 2. The complex undergoes decomposition at a much lower temperature than the ligand. The hydrogen bonded structure with a pseudo-six-membered ring along with two double bonds may be thermodynamically more stable than a pseudo-heterocyclic ring with molybdenum atom. Further the geometry of the ligand restricts the formation of stronger bonds between molybdenum and donor atoms when compared to a O, N donor ligand such as 8-quinolinol. The end residue is gray and is recognized to be molybdenum metal as evidenced by the percentage weight loss, which was further confirmed by X-ray diffraction studies. The "d_{hkl}" values for the residue are 2.21(s), 1.59(m), 1.27(m), 1.09(w), 0.98(w), which corresponds to molybdenum metal.

The present studies suggests that H_2salen acts as a bivalent tetradentate ligand completing the six coordination around *cis*-dioxomolybdenum as in **III.**

Acknowledgements—The authors thank Ms Elinor L. Bedia and Ms Virginia S. Calix of MSRI, NSTA and PAEC, Quezon City, Philippines for the thermal analysis and X-ray diffraction measurements. Further thanks are due to Science Foundation, RC No. 24 RP(SF) SY 1984–85, for the financial support.

REFERENCES

1. A. van den Bergen, K. S. Murray, M. J. O'Connor, N. Rehak and B. O. West, *Aust. J. Chem.* 1968, **21,** 1505.
2. L. V. Orlova, A. D. Garnovskii, O. A. Osipov and I. J. Kukushkina, *Zhur. Obshchei. Khim.* 1968, **38,** 1850.
3. J. I. Bullock and H. A. Tajmir-Riahi, *J. Chem. Soc., Dalton Trans.* 1978, 36.
4. S. Yamada and A. Takeuchi, *Bull. Chem. Soc., Japan* 1969, **42,** 2549.
5. K. Yamanouchi and S. Yamada, *Inorg. Chim. Acta* 1974, **9,** 83.
6. K. Yamanouchi and S. Yamada, *Inorg. Chim. Acta* 1974, **9,** 161.
7. J. R. Dilworth, C. A. McAuliffe and B. J. Sayle, *J. Chem. Soc. Dalton Trans.* 1977, 849.
8. Wai-kah Goh and Meng-Chay Lim, *Aust. J. Chem.* 1984, **37,** 2235.
9. H. Diehl and C. C. Hach, *Inorg. Synth.* 1950, **3,** 197.
10. M. R. Udupa and K. S. Nagaraja, *Thermochim. Acta* 1982, **58,** 117.

Polyhedron Vol. 6, No. 8, pp. 1639–1645, 1987
Printed in Great Britain

0277–5387/87 $3.00+.00

INFRARED AND MÖSSBAUER INVESTIGATIONS ON DIMETHYLTIN(IV) COMPLEXES WITH POTENTIALLY TRIDENTATE DIANIONIC LIGANDS

L. PELLERITO,* G. DIA, A. GIANGUZZA and M. A. GIRASOLO

Istituto di Chimica Generale, Via Archirafi 26, 90123 Palermo, Italy

and

E. RIZZARELLI and R. PURRELLO

Dipartimento di Scienze Chimiche, Viale A.Doria 6, 95125 Catania, Italy

(*Received* 1 *August* 1986; *accepted after revision* 9 *February* 1987)

Abstract—Dimethyltin(IV) complexes with formulae $Me_2Sn(IMDA)\cdot H_2O$, $Me_2Sn(ODA)\cdot H_2O$ and $[Me_2Sn(OH)]_2(TDA)$ [$IMDA^{2-}$ = iminodiacetate^{2-} (NOO); ODA^{2-} = oxydiacetate^{2-} (OOO); and TDA^{2-} = thiodiacetate^{2-} (SOO donor atoms)] have been obtained and their solid state coordination investigated. Infrared and Mössbauer spectroscopic evidence would suggest tridentate behaviour of the ligands in polymeric *trans*-dimethyl structures for $Me_2Sn(IMDA)\cdot H_2O$ and $Me_2Sn(ODA)\cdot H_2O$ with bridging carboxylate groups; polymeric tetrahedral environments around the two tin(IV) atoms could be inferred with TDA acting as bidentate dianionic ligand through ester type carboxylate groups in $[Me_2Sn(OH)]_2(TDA)$, without involvement of the sulfur atom in coordination.

Organotin(IV) derivatives show biological activity which has been the subject, in recent years, of particular attention by several authors.[1–3] Structure activity correlation has been the aim of a research project for which complexes with biomolecules have been synthesized and, in some case, involved in *in vitro* or *in vivo* investigations.[4–7]

In particular, at concentrations of diorganotin(IV) complexes ranging between 0.5 and 5 nmols/mg of protein, Bu_2SnL (L = ribose and adenosine) inhibited the ATP-ase activity in rat liver mitochondria. Mössbauer measurements carried out at 10 K on rat liver mitochondria pellets, preliminary incubated with the diorganotin(IV) complexes, suggested interaction of the diorganotin(IV) moieties with the thiol groups of the membrane proteins.[6]

Inhibition of development of Ciona intestinalis, Ascidiella aspersa and Ascidia malaca eggs has been shown by R_2SnL complexes (R = Me, Bu, Oct; L = sorbitol, D(+)glucose, D(−)ribose, levulose, D(+)galactose, L(+)galactose and D(+)glyceraldehyde) at concentration of 1×10^{-4} M.[7]

The interaction of diorganotin(IV) and other biofunctional ligands such as adenosine and 5′-triphosphate has been studied in aqueous solution.[8] From the comparison of the stability constants obtained and those of complexes with oxygen and nitrogen donor atom ligands, the coordination of the nucleotide to dimethyltin(IV) through the phosphate oxygen atoms has been suggested.[8]

In order to clarify the above mentioned hypothesis it seemed opportune to investigate the nature of the interaction between the diorganotin(IV) moieties and ligands bearing O, N, S donor atoms, in the solid and in solution phase.

In this paper we report the results obtained in the solid state by infrared and Mössbauer spectroscopy.

EXPERIMENTAL

The complexes $Me_2Sn(IMDA)\cdot H_2O$ and $Me_2Sn(ODA)\cdot H_2O$ were obtained as white

* Author to whom correspondence should be addressed.

solids by mixing methanolic solutions of Me_2SnCl_2 (gift from Schering AG, Bergkamen) (2 mmols of Me_2SnCl_2 in 50 cm^3 of CH_3OH) with solutions of the disodium salts of the iminodiacetic and oxydiacetic acids, respectively (2 mmols of Na_2IMDA or Na_2ODA in 50 cm^3 of 1:1 $H_2O:CH_3OH$ solution).

Attempts to obtain, under the same experimental conditions, the complex $Me_2Sn(TDA)$ were unsuccessful and led to the precipitation of white microcrystalline compounds which analyzed as $[Me_2Sn(OH)]_2(TDA)$. The same complex was obtained in 1:1 $H_2O:CH_3OH$ solution using a ratio $[(CH_3)_2SnCl_2]/[Na_2TDA] = 2$.

The solids were recovered by filtration, recrystallized and analyzed for C, H and Sn contents.

C and H analyses were performed at the Laboratorio di Chimica Organica (Milano). Tin content was determined as SnO_2 in our laboratory as described in the literature.[9]

Analytical data are reported in Table 1.

The thermal decomposition of the complexes was carried out under N_2 atmosphere in a Mettler mod.TA 3000 System.

The samples, contained in small pyrex dishes, were heated from 25 to 600°C.

Infrared spectra were recorded as Nujol and hexachlorobutadiene mulls in the region 4000–200 cm^{-1} using a Perkin Elmer mod. 983 G infrared spectrometer and CsI windows.

^{119}Sn Mössbauer spectra were measured, with a constant acceleration and a triangular waveform, using a Laben mod.8001 multichannel analyzer, a Mössbauer closed refrigerator system mod.21 SC Cryodine Cryocooler CTI-Cryogenics (U.S.A.) and a digital temperature controller mod.DRC-80C Lake Shore Cryotronics (U.S.A.).

Suitable computer programs were used to fit the experimental line to Lorentzian line shapes, in the calculation of ΔE according to the point charge model formalism and in the estimation of the lattice dynamics parameters.

RESULTS AND DISCUSSION

Thermal decomposition

The TG/DT analysis showed a two step process for all of the complexes. The first stage occurred at 125.7, 112.3 and 269°C for $Me_2Sn(IMDA)\cdot H_2O$, $Me_2Sn(ODA)\cdot H_2O$ and $[Me_2Sn(OH)]_2(TDA)$ respectively, which could be ascribed to the loss of one water molecule (exp. 6.36, 6.79 and 4.04, theor. 6.05, 6.03 and 3.79%).

At 275.0, 319.0 and 306.3°C the complexes completely decomposed leaving residues which were analyzed as SnO for $Me_2Sn(IMDA)\cdot H_2O$ (exp. 43.81, theor. 45.22%) and Sn for both $Me_2Sn(ODA)\cdot H_2O$ and $[Me_2Sn(OH)]_2(TDA)$ (exp. 39.88 and 39.66, theor. 39.71 and 39.49%, respectively).

Infrared spectra

The interpretation of the coordination modes of the ligands towards the dimethyltin(IV) Lewis acid can be simplified by taking into account the crystal structure of the free acids and of some of their copper(II) mixed complexes.[10–16]

The iminodiacetic acid, H_2IMDA, possesses a three dimensional network of 10- and 14-membered rings of hydrogen bonded halves of the molecule, with three independent hydrogen bonds, two of the type N–H----O and one of the type O–H----O,[10] while both oxydiacetic, H_2ODA, and thiodiacetic acids, H_2TDA, are formed by infinite chains of hydrogen bonding in pairs of carboxylic groups around the symmetry centre.[11,12]

The more relevant IR bands in the free ligands (Table 2), reflected the above situations, which are

Table 1. Analytical data, found(calc) and experimental Mössbauer parameters

Compound	C%	H%	Sn%	δ^a	$\Delta E_{exp}{}^b$	$\Gamma_{av}{}^c$
$Me_2Sn(IMDA)\cdot H_2O$	23.6 (24.3)	4.2 (4.4)	40.0 (39.8)	1.348	4.05	1.02
$Me_2Sn(ODA)\cdot H_2O$	25.6 (24.1)	3.7 (4.0)	39.4 (39.7)	1.403	3.95	0.98
$[Me_2Sn(OH)]_2(TDA)$	21.3 (20.0)	3.4 (3.7)	50.0 (49.4)	0.934	2.07	1.06

[a] Isomer shift ($\delta \pm 0.002$ mm s^{-1}), with respect to the centroid of a room temperature $CaSnO_3$ spectrum.

[b] Nuclear quadrupole splitting ($\Delta E \pm 0.01$ mm s^{-1}): average values in the temperature range examined.

[c] Full width at half height of the reasonant peaks, average.

Table 2. More relevant IR absorption bands for $Me_2Sn(IV)$ complexes (in the 4000–200 cm^{-1} region)[a]

H_2IMDA[b]	$Me_2Sn(IMDA)\cdot H_2O$	H_2ODA[b]	$Me_2Sn(ODA)\cdot H_2O$	H_2TDA[b]	$[Me_2Sn(OH)]_2(TDA)$	Tentative assignment
					3419 m	ν(OH)
3099 m	3106 m					ν(NH)
3000–2600 s,bd		3000–2600 s,bd		3000–2600 s,bd		ν(OH)+ν(CH)
	2910 s		2929 s		2919 s	ν(CH)
					2900	
			1745			ν_{asym}(COO)
1709 s,bd		1726 s		1693 s		ν(C═O) of unionised H-bonded COOH group
	1642 s		1638 m		1639 s	ν_{asym}(COO)
1582 s	1598 s		1461 s			ν_{asym}(COO)
	1495 m					ν_{sym}(COO)
	1410 s		1413 m		1413 s	ν_{sym}(COO)
1242 m		1246 s		1230 s		ν(C═O)+δ OH of unionised H bonded COOH group
				788 s	788 s	ν_{asym}(CSC)
				658 s	658 s	ν_{sym}(CSC)
	610 s					ν(SnN)
	553 m		551 m		563 m	$\nu_{asym}(SnC_2)$
	520 w		520 w		529 m	$\nu_{sym}(SnC_2)$
	490 w		441 w		510 w	ν(SnO)

[a] Measured in Nujol and hexachlorobutadiene mulls; s = strong; m = medium; w = weak; bd = broad.

[b] H_2IMDA = iminodiacetic acid, $NH(CH_2COOH)_2$; H_2ODA = oxydiacetic acid, $O(CH_2COOH)_2$; H_2TDA = thiodiacetic acid, $S(CH_2COOH)_2$.

varied on coordination to the $Me_2Sn(IV)$ moiety.

In $Me_2Sn(IMDA)\cdot H_2O$ the band present at 3106 m cm^{-1}, slightly shifted with respect to the corresponding band in the free acid (3099 m cm^{-1}), could be attributed to coordinated NH, which did not vary appreciably its electronic surroundings on coordination by substituting one HN—H with HN→Sn bond.

More significant were the shifts which occurred in the 3000–2600 cm^{-1} and 1750–1200 cm^{-1} regions. In fact in the 3000–2600 cm^{-1} region, in the free ligand there were several strong broad bands due to contributions of both OH of hydrogen bonded carboxylic groups and CH stretching. Upon coordination a strong absorption occurred at 2929 s cm^{-1} due to CH stretching.

Only two pairs of bands at 1642 s, 1410 s cm^{-1} ($\Delta\nu = 283$ cm^{-1}) and at 1598 m cm^{-1}, 1495 s cm^{-1} ($\Delta\nu = 103$ cm^{-1}) were present in the complexes, attributable respectively to $\nu_{asym}(COO)$ and $\nu_{sym}(COO)$ of an unidentate carboxylate, the first couple, and to a bridging carboxylate, the second pair.[17] In comparison with the bands at 1709 s,bd, 1454 m and 1242 m cm^{-1} attributable to $\nu(C{=}O)$, CH_2 scissoring+OH bending and to $\delta(OH)$ of unionized carboxylic acid in a polymeric structure[18] and with the bands present at 1582 s and 1394 s,bd cm^{-1} ($\Delta\nu = 188$ cm^{-1}), characteristic of ionised carboxylate.[17]

Absorptions occurring at 610 s, 553 w and 520 w cm^{-1} might be tentatively assigned to $\nu(SnN)$,[19] $\nu_{asym}(SnC_2)$ and $\nu_{sym}(SnC_2)$,[20] with the last two bands a consequence of a distorted CSnC skeleton, while the band at 490 w cm^{-1} could be assigned to a $\nu(SnO)$.[19,20]

Differences in the free and coordinated oxydiacetic acid spectra, were in the region 3000–2600 cm^{-1}, where, according to the hydrogen bonded polymeric structure of H_2ODA,[11] OH and CH stretching absorption occurred.[19] Further variations occurred in the 1750–1200 cm^{-1} range where the two strong bands at 1726 and 1246 s cm^{-1} attributable to $\nu(C{=}O)$ and $\delta(OH)$ of unionised hydrogen bonded COOH group were substituted with bands at 1745 s and 1413 m cm^{-1} ($\Delta\nu = 332$ cm^{-1}, characteristic of unidentate ester type carboxylate) and at 1638 m and 1461 s cm^{-1} ($\Delta\nu = 177$ cm^{-1}, value for bridging carboxylate[17]); between 600 and 200 cm^{-1} bands were present due to $\nu_{asym}(SnC_2)$ at 551 s cm^{-1}, to $\nu_{sym}(SnC_2)$ at 520 m cm^{-1} and to (SnO) at 441 s cm^{-1}.[20,21]

In $[Me_2Sn(OH)]_2(TDA)$ the new band at 3419 m,bd cm^{-1} could be due to OH groups of $Me_2Sn(IV)$ moieties.[22–24]

Analogously to the first two complexes described, in the region 3000–2600 cm^{-1} the strong broad bands of the carboxylic hydrogen bonded OH and of CH are substituted by a couple of bands at 2919 s and 2900 s cm^{-1} ($\nu_{asym}(CH)$ and $\nu_{sym}(CH)$).

The $\Delta\nu$ value (= 226 cm^{-1}) between the pair of bands which occurred at 1639 s [$\nu_{asym}(COO)$] and 1413 s [$\nu_{sym}(COO)$] cm^{-1} would suggest the occurrence of an unidentate ester type carboxylate in the complex[17] [in addition the 1693 s and 1230 s cm^{-1} absorptions in the free ligand could be assigned to $\nu(C{=}O)$ and $\delta(OH)$ respectively[18]]. Coordination of the ethereal sulfur atom could be excluded on the basis of invariance of the 788 s and 658 s cm^{-1} bands, present both in the free and the coordinated ligand, which could be assigned to $\nu_{asym}(CSC)$ and $\nu_{sym}(CSC)$ vibrations.[25] Asymmetric and symmetric CSnC stretchings could be attributed to the bands at 563 m and 529 s cm^{-1} while at 510 vs cm^{-1} a $\nu(SnO)$ could be evidenced.[20,21]

Mössbauer data

The isomer shift, (δ), (Table 1), fell within the range of the values for most diorganotin(IV) compounds,[26] but the lower value for $[Me_2Sn(OH)]_2$ (TDA) would reflect a higher percentage *s*-character of the SnC bonds.[27]

All of the complexes gave a two line quadrupole split spectra, which in the case of the $[Me_2Sn(OH)]_2$(TDA) showed the equivalence of the two tin atoms.

The experimental Nuclear Quadrupole Splittings, (ΔE), (Table 1) for $Me_2Sn(IMDA)\cdot H_2O$ and $Me_2Sn(ODA)\cdot H_2O$ were characteristic of *trans*-R_2Sn octahedral complexes;[26] in principle the experimental ΔE for $[Me_2Sn(OH)]_2$(TDA) did not allow us a choice between octahedral *cis*-Me_2Sn and tetrahedral configurations, which are both $\Delta E_{exp} \approx 2$ mm s^{-1}.

The rationalization of experimental ΔE, according to the point charge model formalism,[26,28–30] was applied to the idealized structures of Fig. 1, octahedral polymeric *trans*-Me_2Sn for $Me_2Sn(IMDA)\cdot H_2O$ (Fig. 1a) and $Me_2Sn(ODA)\cdot H_2O$ (Fig. 1b).

In these configurations, in agreement with the IR data, 6-coordination would be reached by bonding three oxygen atoms, one from the unidentate carboxylate and two from bridging carboxylates and a sixth donor atom, the imino nitrogen atom for $IMDA^{2-}$ complex and the ethereal oxygen atom in ODA^{2-} derivative.

The calculations were carried out by using the partial quadrupole splittings (p.q.s., mm s^{-1}) as extracted or calculated from literature reports.[26,29,31,32]

Octahedral *cis*-Me_2 and tetrahedral were then

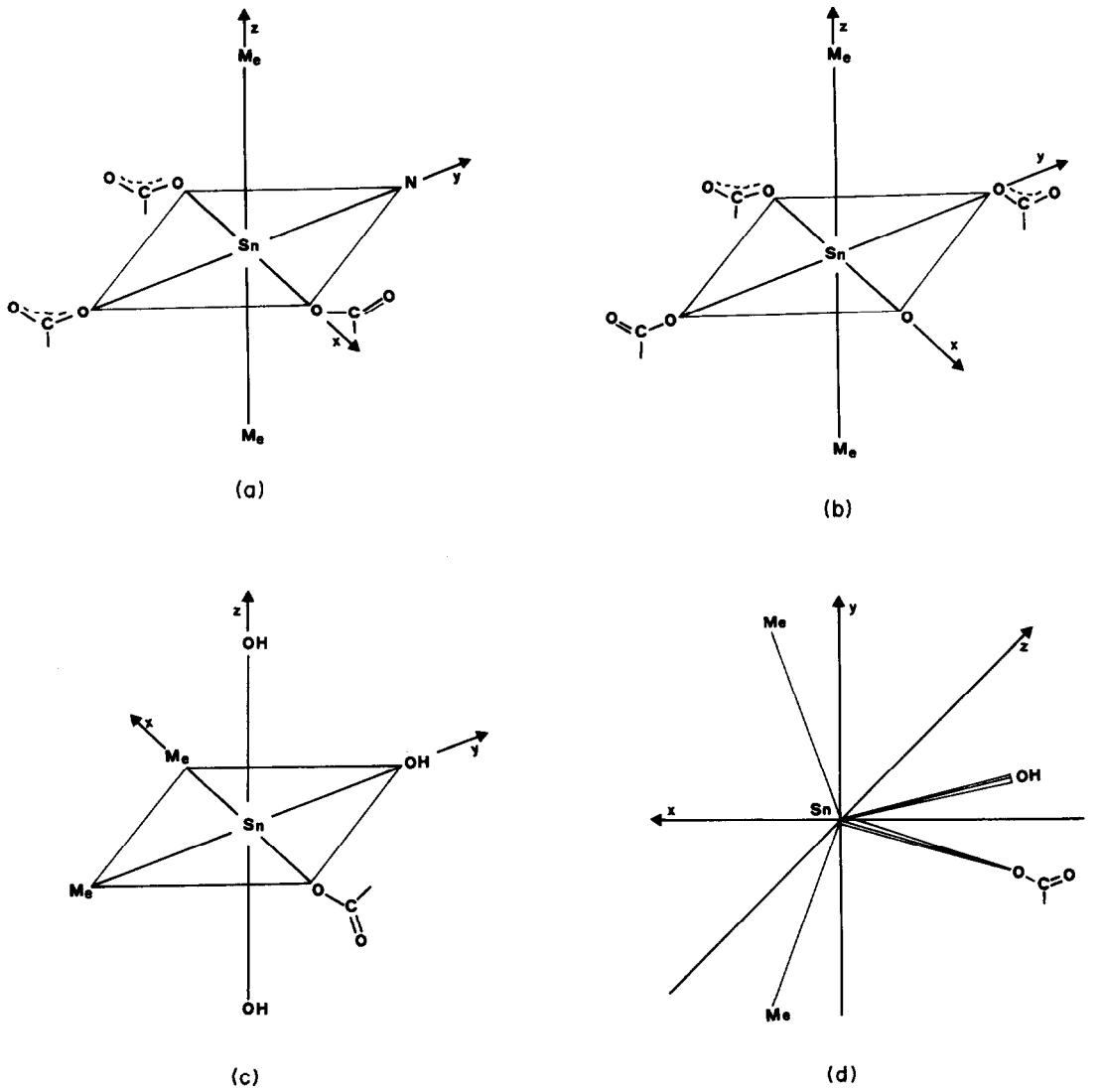

Fig. 1. The idealized structures assumed for point charge calculations of nuclear quadrupole splittings, E, and asymmetry parameter. X, Y, Z are the directions of the principal components of the electric field gradient ($|Vzz| \geq |Vyy| \geq |Vxx|$).

proposed in order to calculate ΔE for $[Me_2Sn(OH)]_2(TDA)$ (Fig. 1c,d).

The six-coordination, in the *cis*-Me_2 octahedral configuration could be obtained by polymerization through three coordinated OH groups.

Table 3 shows that ΔE_{exp} and ΔE_{calc} differed less than the tolerance limit ± 0.4 mm s^{-1} which could justify the proposed structures,[23] so that it clearly appeared that for TDA^{2-} complex both the structures of Fig. 1 (c,d) were equally probable also if there are few cases in which $Me_2Sn(IV)$ derivatives assume a *cis*-Me_2 configuration.[33,34]

Variable temperature Mössbauer studies have been carried out in order to get information on the polymeric or monomeric nature of the investigated complexes.

The more relevant lattice dynamics parameters are summarized in Table 4 together with data referring to the polymer $[-Sn(n\text{-}C_4H_9)_2\text{-}OCH(CCl_3)O-]$[36] and to the monomer Me_4Sn[37] for comparison purpose. The treatment of the data and the relative calculation of the functions were performed as described in detail in the literature[38,39] in the temperature range in which the natural logarithm of the areas under resonant peaks, $\ln A_T$, was a linear function of the temperature. The values of the slopes $d \ln A_T/dT$ obtained (Table 4) were consistent with the existence of polydimensional networks characterized by extensive crosslinking of molecular chains.[39]

These results would be confirmed by the other calculated lattice dynamics parameters (Table 4);

Table 3. Point charge parameters

Compound	ΔE_{exp}	Structure	ΔE_{calc}[a]	η_{calc}[b]
$Me_2Sn(IMDA)\cdot H_2O$	4.05	A	+3.85	0.08
$Me_2Sn(ODA)\cdot H_2O$	3.95	B	+3.71	0.03
$[Me_2Sn(OH)]_2(TDA)$	2.07	C	−2.40	0.81
		D	−1.84	0.00

[a] Point charge values of the nuclear quadrupole splitting and [b] of the asymmetry parameter (Vxx–Vyy)/Vzz. P.q.s., mm s^{-1}, values used are:

$\{(Alk)-(Hal)\}^{oct} = -1.03$; $\{(COO)-(Hal)\}^{oct}_{unid} = -0.11$.

$\{(COO)-(Hal)\}^{oct}_{bridg} = -0.075$; $\{(N)-(Hal)\}^{oct} = -0.01$;

$\{(O)-(Hal)\}^{oct} = -0.144$

$\{(Alk)-(Hal)\}^{tet} = -1.37$; $\{(OH)-(Hal)\}^{tet} = -0.55$

$\{(COO)-(Hal)\}^{tet}_{unid} = -0.15$; $\{(OH)-(Hal)^{oct}_{bridg} = -0.20\}$

Table 4. Lattice dynamics parameters[a]

	Compounds[b]				
	I	II	III	IV	V
Sample thickness (mg $^{119}Sn/cm^2$)	2.161	1.135	1.816	Ref. 31	Ref. 32
Temperature range	30.4–151.4	30.2–142.4	19.6–91.1	77.3–149.5	Ref. 32
No. of point	11	10	7	13	Ref. 32
$d \ln A_T/dT$ ($deg^{-1} \times 10^2$)	−1.011	−1.219	−1.543	−1.367	−2.758
Correlation coefficient	0.996	0.994	0.995	0.994	Ref. 32
f_a^{rel} at 77.3°	0.444	0.431	0.290	0.348	0.065
$\langle X^2 \rangle$(T) ($A \times 10^{-2}$)	0.51–1.62	0.54–1.45	0.53–1.43	0.72–1.40	Ref. 32
θ_D (K)	71.4	83.5	57.4	62.7	65.7
$\bar{\nu}_D$ (cm^{-1})	59.0	58.0	39.8	43.6	45.7
$M\theta_D^2$ (u.m.a. × $deg^2 \times 10^{-6}$)	1.49	1.96	1.38	1.56	0.77

[a] A_T is the total Lorentzian area under resonant peaks; f_a^{rel} the relative recoil free fraction; $\langle X^2 \rangle$ the mean square displacement; θ_D the Debye Mössbauer temperature; $\bar{\nu}_D$ the cutoff frequency and $M\theta_D^2$ the parameter of intermolecular force constant.

[b] I: $Me_2Sn(IMDA)\cdot H_2O$; II: $Me_2Sn(ODA)\cdot H_2O$; III: $[Me_2SnOH]_2(TDA)$; IV: $[\text{-}Sn(n\text{-}C_4H_3)_2\text{-}OCH(CCl_3)O\text{-}]_n$(31); V: Me_4Sn(32).

in particular by the mean square displacements $\langle X^2 \rangle$(T) and by the relative recoil free fraction, f_a^{rel}(T), for all the complexes (Table 4) were fully consistent with that reported for two and three dimensional polymers.[37,40]

Also if the results obtained studying the above systems in solution are not definitive,[41] it is possible to affirm that care must be made in hypothesizing the active species in biological systems and in suggesting structure-activity correlations.

Acknowledgement—The financial support by Ministero della Pubblica Istruzione (Roma) is gratefully acknowledged.

REFERENCES

1. W. N. Aldridge, B. W. Street and J. Noltes, *Chem. Biol. Interactions* 1981, **3**, 223; and refs therein.
2. R. Barbieri, L. Pellerito, G. Ruisi, M. T. Lo Giudice, F. Huber and G. Atassi, *Inorg. Chim. Acta* 1976, **17**, L9.

3. G. Ruisi, A. Silvestri, M. T. Lo Giudice, R. Barbieri, G. Atassi, F. Huber, K. Gratz and L. Lamartina, *J. Inorg. Biochem.* 1985, **25**, 229; and refs therein.
4. J. D. Donaldson, S. M. Grimes, L. Pellerito, M. A. Girasolo, P. J. Smith, A. Cambria and M. Fama, *Polyhedron* 1987, **6**, 383–386.
5. G. Ruisi, M. T. Lo Giudice and L. Pellerito, *Inorg. Chim. Acta* 1984, **93**, 161; and refs therein.
6. M. Fama, L. Pellerito, E. Bertoli, M. A. Girasolo and G. Spampinato, personal communication.
7. C. Mansueto, L. Pellerito and M. A. Girasolo, *Acta Embryol. Morphol. Exper.*, n.s., **XXXII**, n.6, 1985.
8. G. Arena, R. Purrello, E. Rizzarelli, A. Gianguzza and L. Pellerito, *Proc. III Symp. Chimica dei Composti dei Metalli di Non-Transizione*, 37, Parma 27–28 October (1983).
9. W. P. Newman, *Die Organische Chemie des Zinns*. Verlag, Stuttgart (1976).
10. C.-E. Boman, H. Herbertsson and A. Oskarsson, *Acta Cryst.* 1974, **B30**, 378; and refs therein.
11. H. Herbertsson and C. H. Boman, *Acta Chem. Scand.* 1973, **27**, 2234.
12. S. Paul, *Acta Cryst.* 1967, **23**, 491.
13. G. Nardin, L. Randaccio, R. P. Bonomo and E. Rizzarelli, *J. Chem. Soc., Dalton Trans.* 1980, 369.
14. R. P. Bonomo, E. Rizzarelli, N. Bresciani-Pahor and G. Nardin, *Inorg. Chim. Acta* 1981, **54**, L17.
15. R. P. Bonomo, E. Rizzarelli, N. Bresciani-Pahor and G. Nardin, *J. Chem. Soc., Dalton Trans.* 1982, 681.
16. N. Bresciani-Pahor, G. Nardin, R. P. Bonomo and E. Rizzarelli, *J. Chem. Soc., Dalton Trans.* 1983, 1797.
17. G. B. Deacon and R. J. Phillips, *Coord. Chem. Rev.* 1980, **33**, 227; and refs therein.
18. A. A. Ennan, L. Gavrilova, A. N. Chebotarev and N. V. Andreeva, *Russ. J. Inorg. Chem.* 1981, **20**, 26.
19. A. Marchand, M. Riviere Baudet, R. Gassend and M. H. Soulard, *J. Organometal. Chem.* 1976, **118**, 27; and refs therein.
20. F. K. Butcher, W. Gerrard, E. F. Money, R. G. Rees and H. A. Willis, *Spectrochim. Acta* 1964, **20**, 51.
21. J. Mendelshon, A. Marchand and J. Valad, *J. Organometal. Chem.* 1966, **6**, 25.
22. V. Imhof and R. S. Drago, *Inorg. Chem.* 1965, **4**, 426.
23. P. W. N. M. Van Leewen, *Recl. Trav. Chim. Pays-Bas* 1967, **86**, 247.
24. I. Nakagawa and T. Shimanouchi, *Spectrochim. Acta* 1964, **20**, 429.
25. R. A. Nyquist and R. O. Kegel, Organic materials, in *Infrared and Raman Spectroscopy, Part B* (Edited by E. D. Brame, Jr. and J. G. Graselli) Marcel Dekker, New York, Chapter 6 (1977).
26. G. M. Bancroft and R. H. Platt, *Adv. Inorg. Chem. Radiochem.* 1972, **15**, 59.
27. R. V. Parish, *Prog. Inorg. Chem.* 1972, **15**, 101.
28. M. G. Clark, A. G. Maddock and R. H. Platt, *J. Chem. Soc., Dalton Trans.* 1972, 281.
29. G. M. Bancroft, V. G. Kumar Das, T. K. Sham and M. G. Clark, *J. Chem. Soc., Dalton Trans.* 1976, 643.
30. N. N. Greenwood and T. C. Gibb, *Mossbauer Spectroscopy*, Chapman & Hall, London (1971).
31. R. Barbieri, A. Silvestri, F. Huber and C-D. Hager, *Can. J. Spectroscopy* 1981, **26**, 194; and refs therein.
32. I. Korecz, A. A. Saghier, K. Burger, A. Tzschach and K. Jurkschat, *Inorg. Chim. Acta* 1982, **58**, 243.
33. G. C. Stocco, L. Pellerito, M. A. Girasolo and A. G. Osborne, *Inorg. Chim. Acta* 1983, **83**, 79.
34. R. C. Poller and J. R. N. Ruddick, *J. Chem. Soc. (A)* 1969, 2273.
35. K. M. Ali, D. Cunningham, J. D. Donaldson, M. J. Frazer and B. J. Senior, *J. Chem. Soc. (A)* 1969, 2836.
36. R. Barbieri, L. Pellerito, A. Silvestri and G. Ruisi, *J. Organometal. Chem.* 1981, **210**, 43.
37. H. Sano and Y. Mekata, *Chem. Lett.* 1975, 155.
38. R. Barbieri, A. Silvestri, L. Pellerito, A. Gennaro, M. Petrera and N. Burriesci, *J. Chem. Soc. Dalton* 1980, 1983; and refs therein.
39. V. I. Gol'danskii and F. F. Makarov, *Fundamentals of gamma resonance*, in *Chemical Application of Mossbauer Spectroscopy* (Edited by V. I. Gol'danskii and R. Herber), Academic Press, New York, Chapter 1 (1969).
40. R. Barbieri, A. Silvestri, F. Huber and C.-D. Hager, *Inorg. Chim. Acta* 1981, **55**, 113; and refs therein.
41. E. Rizzarelli, R. Purrello, G. Dia, A. Gianguzza and L. Pellerito, preliminary results.

Polyhedron Vol. 6, No. 8, pp. 1647–1652, 1987
Printed in Great Britain

0277–5387/87 $3.00+.00

ELECTROCHEMISTRY OF RHENIUM(V) COMPLEXES WITH N-(2-HYDROXYPHENYL)SALICYLIDENEIMINATE AS SCHIFF BASE LIGAND

RENATO SEEBER*

Dipartimento di Chimica, Università di Sassari, Via Vienna, 2, 07100 Sassari, Italy

GIAN ANTONIO MAZZOCCHIN

Dipartimento di Spettroscopia ed Elettrochimica, Università di Venezia, Dorsoduro 2137, 30123 Venezia, Italy

and

FIORENZO REFOSCO,* ULDERICO MAZZI and FRANCESCO TISATO

Istituto di Chimica e Tecnologia dei Radioelementi del C.N.R., Area della Ricerca, C.so Stati Uniti 4, 35100 Padova, Italy

(*Received* 3 *October* 1986; *accepted* 9 *February* 1987)

Abstract—The anodic and cathodic behaviour of the rhenium(V) complexes nBu$_4$N[ReOCl$_3$(HOPhSal)], nBu$_4$N[ReOCl$_2$(OPhSal)], [ReOCl(OPhSal)(MeOH)] and [ReOCl(OPhSal)(PMe$_2$Ph)] in acetonitrile was studied using platinum and mercury electrodes. Cyclic voltammetry and controlled potential coulometry were the main electroanalytical techniques employed. The nature of the electrolysis products as well as the mechanisms of the electrode oxidation and reduction processes were investigated. In particular a complex of rhenium(VI) containing the group ReO^{4+} and complexes of rhenium(IV) with ReO^{2+} core were electrochemically synthesized. They were characterized by elemental analysis, IR spectroscopy, magnetic susceptibility and conductivity measurements.

A wide variety of oxidation states can be assumed by rhenium in different coordination compounds, depending on the nature of the ligands. Our first series of electrochemical studies has dealt with complexes with the metal in low oxidation states,[1–3] the ligands being typically carbon monoxide, chloride ions and different phosphines. The attention which has been recently devoted to rhenium complexes with Schiff base ligands, together with the interesting properties exhibited by the ReO^{3+} core,[4–7] has suggested the opportunity of studying the electrochemical properties of these compounds, in order to define their oxidation and reduction potentials, to identify species with the rhenium centre in +4 or +6 oxidation states, and possibly to define the nature of the electrode mechanisms.

It is worth noting that studies on the rhenium complexes, in addition to the importance they have for themselves, have often allowed us interesting comparisons with the analogous complexes of technetium.[1–3,8–10] This last aspect is of particular importance taking into account the significance that ^{99m}Tc has assumed in the field of nuclear medicine.

We have reported elsewhere on the electrochemical behaviour of rhenium complexes with the ReO^{3+} core, with bidentate–bidentate and bidentate-tridentate Schiff base ligands.[11] The complexes studied in the present paper contain a single Schiff base ligand, co-ordinated to the metal centre through two or three sites. Their formulas are reported here below.

*Authors to whom correspondence should be addressed.

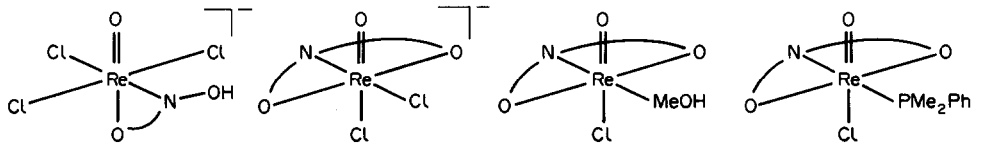

$[ReOCl_3(HOPhSal)]^-$ $[ReOCl_2(OPhSal)]^-$ $ReOCl(OPhSal)(MeOH)$ $ReOCl(OPhSal)(PMe_2Ph)$

EXPERIMENTAL

Acetonitrile (MeCN) (Fluka–Burdick & Jackson, distilled in glass) has been used without further purification; it was stored in nitrogen atmosphere over 0.3 nm molecular sieves (Union Carbide). Tetraethylammonium tetrafluoroborate (Alpha Ventron) was used in most voltammetric and coulometric experiments. It was dried for 48 h at 50°C in a vacuum oven before use.

Recovery and isolation of the electrolysis products involved some problems, mostly with respect to the separation of the supporting electrolyte. Saturated solutions of tetraethylammonium tetraphenylborate were used during exhaustive electrolyses performed with the aim of recovering the reduction products. This salt was prepared by addition of a methanol solution of sodium tetraphenylborate to a methanol solution of tetraethylammonium chloride. The white precipitate was washed repeatedly with water and then recrystallized from hot acetonitrile. The white crystals so obtained were dried for 48 h at 50°C in a vacuum oven before use.

The synthesis of the complexes studied has been described elsewhere.[6]

The solutions studied were deoxygenated by bubbling 99.99% pure nitrogen through.

A PAR 170 Electrochemistry System was used in the voltammetric tests, and the resulting voltammograms were recorded either with a Linseis LY 1800 pen recorder or with a Hewlett–Packard 1223A storage oscilloscope. An electrochemical cell with proper geometry was employed. The working microelectrode was either a platinum disc or a gold sphere freshly covered with mercury; the working electrode was surrounded by a platinum spiral counter electrode, and the reference electrode (saturated calomel electrode—S.C.E.) compartment was connected through a salt bridge ending in a Luggin capillary.

At the end of these tests bis-cyclopentadienyl iron(II) was added to the solution, in order to refer the evaluated $E^r_{1/2}$, taken as experimental approximation of the standard potential, to the corresponding electrochemical parameter of this iron(III)/iron(II) redox couple; in this way the measured quantity results are unaffected by variable liquid junction potentials at the aqueous–organic solvent interface.[12]

An AMEL Model 552 potentiostat with an associated AMEL Model 558 integrator were used in the controlled potential electrolyses, which were carried out in an H-shaped cell with anodic and cathodic compartments separated by a sintered glass disc. The working electrode was a platinum gauze, the auxiliary electrode was a mercury pool and the reference electrode still was a S.C.E.

In order to isolate the electrolysis products different procedures were followed for anodic oxidation and cathodic reduction. The oxidation products resulted scarcely soluble and could be precipitated from the electrolysis solutions, while the reduction products were soluble, so that in this case the solvent was removed under reduced pressure. The resulting solids were washed with CH_2Cl_2 to separate the supporting electrolyte. The solutions recovered by filtration were dried and the dark oils obtained were crystallized by washing with Et_2O. The solids were recrystallized from CH_2Cl_2/Et_2O. The resulting products were characterized by elemental analysis, IR spectroscopy, magnetic susceptibility and conductivity measurements.

IR spectra were recorded on a Perkin–Elmer Model 580B spectrometer. Magnetic moment measurements were performed with an Oxford Instrument at room temperature. Conductivity measurements were carried out at 25 ± 0.1°C using a Metrohm conductometer, Model E 518.

RESULTS AND DISCUSSION

nBu$_4$N[ReOCl$_3$(HOPhSal)]

Figure 1 reports anodic and cathodic behaviour of an acetonitrile solution of nBu$_4$N[ReOCl$_3$(HOPhSal)], containing 0.1 M tetraethylammonium tetrafluoroborate as supporting electrolyte, at a platinum electrode.

As regards the anodic behaviour, coulometric tests at peak A in Fig. 1(a) revealed that 2 mol of electrons are involved in the overall electrode process. The results of cyclic voltammetric tests at potential scan rates from 0.05 to 50 V s^{-1} were in agreement with an e.c.e. mechanism (one electron charge transfer–irreversible chemical reac-

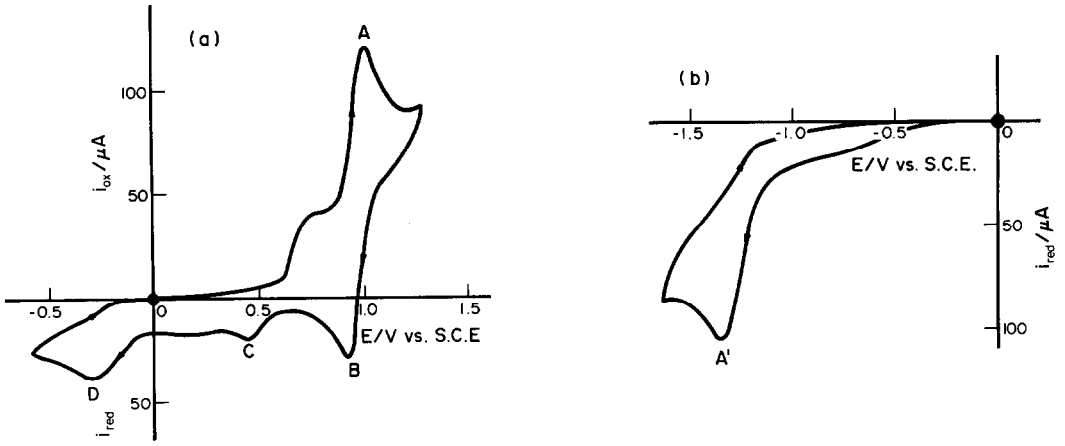

Fig. 1. Cyclic voltammetric curves recorded with a platinum working electrode on a 4.8×10^{-3} M nBu$_4$N [ReOCl$_3$(HOPhSal)], 0.1 M tetraethylammonium tetrafluoroborate, MeCN solution. Potential scan rate 0.2 V s^{-1}. ●, Starting potential; (a) anodic direct scan; (b) cathodic direct scan.

tion–one electron charge transfer). The chemical reaction is too slow to be investigated with voltammetric techniques, since the cathodic–anodic voltammetric response appeared like that of an uncomplicated one electron reversible charge transfer at potential scan rates greater than 0.2 V s^{-1}.

On the basis of the voltammetric responses it was possible to calculate, for the couple [ReOCl$_3$(HOPhSal)]/[ReOCl$_3$(HOPhSal)]$^-$ an $E^r_{1/2}$ value of 0.56 vs $E^r_{1/2}$ of the couple ferricinium ion–ferrocene.

The solutions resulting from exhaustive oxidation showed a voltammetric picture as that reported in Fig. 2. Two most significant peaks can be noted on a cathodic scan starting at the electrolysis potential. Reducing the oxidized solution in correspondence to peak C the complex [ReOCl$_2$(OPhSal)]$^-$ is apparently formed (see below) through a consumption of 1 mol of electrons per mol of starting compound; peak D could be attributed to the reduction of free hydrogen ions.

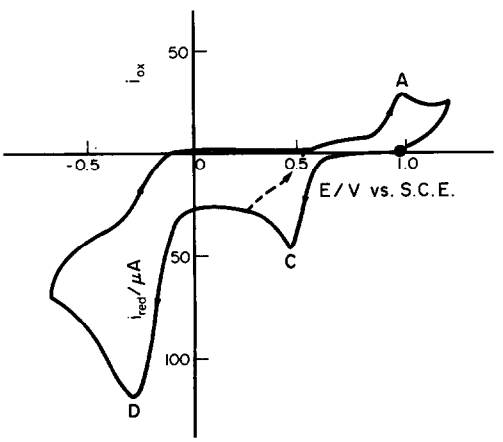

Fig. 2. Cyclic voltammetric curve recorded on the same solution of Fig. 1, after exhaustive electrolysis at +1.0 V vs S.C.E. ●, Starting potential for cathodic direct scan.

The recovery of the oxidation product has allowed us to identify the compound as [ReOCl$_2$(OPhSal)]. The elemental analysis data are as follows (Found: C, 32.5; H, 1.9; N, 3.0; Cl, 14.8. Calc. for $C_{13}H_9NO_3Cl_2Re$: C, 32.2; H, 1.9; N, 2.9; Cl, 14.6%). IR spectra show that a ν(Re=O) absorption is still present at 955 cm^{-1}, close to that noted for the starting complex [ν(Re=O) = 968 cm^{-1}]. The ν(Re—Cl) absorptions are now at 324 and 283 cm^{-1}, while for the starting complex they fall at 315 and 285 cm^{-1}. Magnetic susceptibility measurements on solid samples lead to μ_{eff} = 1.50 B.M., in agreement with a d^1 configuration in a distorted octahedral environment. The compound exhibits a non-conducting behaviour, confirming its non-ionic character. It is soluble in CH_2Cl_2, $CHCl_3$, DMF and acetone, insoluble in Et_2O, CH_3CN, alcohols and hydrocarbons.

The following stoichiometry of the overall oxidation process could account for the results found:

$$[Re(V)OCl_3(HOPhSal)]^- - 2e^- \rightarrow [Re(VI)OCl_2(OPhSal)] + H^+ + \tfrac{1}{2}Cl_2.$$

However, some results can be explained with some difficulty: in addition to the fact that chloride ions can hardly be oxidized at the working potential, as it will be reported below, 2 mol of electrons per mol of starting compound are also spent in the electrode oxidation of [ReOCl$_2$(OPhSal)]$^-$ and the same Re(VI) neutral complex is recovered from these solutions; in the following it will be also shown that the species [Re(VI)OCl$_2$(OPhSal)] is

reduced at potentials much more anodic than those of peak C in Fig. 2. It seems hence more convincing that unidentified products resulting from oxidation of $[ReOCl_3(HOPhSal)]^-$ and of $[ReOCl_2(OPhSal)]^-$ lead to the same, stable rhenium complex, [Re(VI)OCl_2(OPhSal)], as a consequence of reactions occurring during the recovery procedures.

As Fig. 1(b) reports, nBu$_4$N[$ReOCl_3$(HOPhSal)] undergoes electrode reduction [peak A′ of Fig. 1(b)]. No directly associated anodic peak can be recorded, at a potential scan rate as high as 50 V s^{-1}. In controlled potential coulometries 2 mol of electrons per mol of starting complex were spent, and since the voltammetric response is consistent with an e.c. mechanism (one electron reversible charge transfer followed by a fast irreversible chemical reaction), one must suppose the occurrence of a rather complicated overall reduction process, where a further slow chemical reaction must preceed the second, one electron reduction. Any attempt to recover stable rhenium complexes from the electrolysis solution failed, preventing the suggestion of any reliable reduction mechanism.

In order to set the potential range in which the species studied is stable, we report that the cathodic peak potential value at a scan rate of 0.2 V s^{-1} resulted equal to -1.63 V vs $E^r_{1/2}$ of the ferricinium ion-ferrocene couple. Completely similar results were obtained with platinum as well as with mercury working electrodes, indicating an outer sphere charge transfer is operative.[13]

nBu$_4$N[$ReOCl_2$(OPhSal)]

The electrochemical studies of this compound led to results comparable with those obtained with the complex reported previously. The voltammograms recorded on solutions of this compound resulted qualitatively similar to those reported in Fig. 1(a) and (b).

Also in this case the anodic oxidation implies the consumption of 2 mol of electrons per mol of starting compound and consists in two subsequent one electron charge transfers with an interposed irreversible chemical reaction. After exhaustive electrolysis a voltammogram similar to that reported in Fig. 2 could be recorded, the only significant difference being the absence of the peak we had attributed to the reduction of free hydrogen ions. Reducing the oxidized solution in correspondence to peak C of Fig. 2 the starting compound was obtained through the consumption of 1 mol of electrons per mol of starting complex.

As previously mentioned, the product recovered from the oxidized solution could be identified as [Re(VI)OCl_2(OPhSal)], suggesting the solid product separated should be different from that present in the electrolysed solution. In fact its formulation does not account for the consumption of 2 mol of electrons in the oxidation process; moreover, this compound must be reduced in correspondence to the cathodic peak directly associated to the anodic one [see, qualitatively, peak B in Fig. 1(a)], rather than in correspondence to peak C of Fig. 2. The potential difference between the location of these peaks amounts to about 0.45 V.

At high enough potential scan rate we could estimate an $E^r_{1/2}$ value equal to $+0.57$ V vs $E^r_{1/2}$ of the redox couple ferricinium ion–ferrocene, for the redox couple $[ReOCl_2(OPhSal)]/[ReOCl_2(OPhSal)]^-$.

As regards the cathodic reduction, the peak potential value at a potential sweep rate of 0.2 V s^{-1} resulted equal to -1.65 V vs the same reference redox couple.

It is noteworthy that very similar potential values are obtained for oxidation as well as for reduction of both these first compounds studied.

[ReOCl(OPhSal)(MeOH)]

Anodic oxidation of this compound takes place via two subsequent one electron charge transfers with an irreversible interposed chemical reaction; this can be affirmed on the basis of the cyclic voltammetric responses recorded at different potential scan rates and of the results of coulometric tests (2 mol of electrons are spent per mol of electrolysed compound). Although the species primarily formed at the electrode is involved in a chemical reaction faster than that of the complexes studied previously, at fast enough potential scan rate (higher than 10 V s^{-1}) it is possible to prevent the occurrence of the chemical reaction and hence to calculate an $E^r_{1/2}$ value of $+0.66$ V vs ferricinium ion–ferrocene for the couple $[ReOCl(OPhSal)(MeOH)]^+/[ReOCl(OPhSal)(MeOH)]$.

Voltammetric responses recorded on the electrolysed solution only showed ill defined peaks. Anyhow, the recovered oxidation product once more resulted to be [Re(VI)OCl_2(OPhSal)], and the formulation of a reasonable electrode mechanism is not easy.

The starting complex undergoes two subsequent reductions ($E_p = -1.22$ V and -1.61 V vs ferricinium ion–ferrocene couple, at a potential scan rate of 0.2 V s^{-1}). Both peaks do not exhibit any directly associated anodic peak, even at the highest explored scan rates. Coulometric tests at potentials of the less cathodic peak led to the consumption of 1 mol of electrons per mol of starting compound,

and the more cathodic peak is undetectable on the exhaustively reduced solution. This behaviour is consistent with several different electrode mechanisms. However, the analysis of the shape of the responses, together with the fact that after electrolysis at the first peak the second one has disappeared, suggest that chemical reactions must follow the first electrode charge transfer.

The reduction product was recovered and identified as Et_4N [Re(IV)OCl(OPhSal)]. Hence, it can be suggested that the chemical reactions involve the fast release of the MeOH ligand with a subsequent rearrangement to a five-coordinate geometry.

The elemental analysis data are as follows (Found: C, 44.5; H, 5.2; N, 4.6; Cl, 6.3. Calc. for $C_{12}H_{29}N_2O_3ClRe$: C, 43.5; H, 5.0; N, 4.8; Cl, 6.1%).

IR spectra of the recovered reduction product show a significant lowering in the wavenumber of the ν(Re=O) absorption, up to 912 cm^{-1} (976 cm^{-1} in the starting compound). This weakening of the Re=O bond could be explained by the increased negative charge of the rhenium atom. ν(Re—Cl) was observed at 320 cm^{-1}.

Magnetic susceptibility measurements on solid samples lead to $\mu_{eff} = 1.40$ B.M., in agreement with d^3 configuration in a square pyramidal environment.[14]

$\Lambda_{eq} = 1.41\ \Omega^{-1}\ cm^2\ mol^{-1}$ in acetonitrile is in agreement with a 1 : 1 electrolyte.

The product was soluble in CH_2Cl_2, $CHCl_3$, DMF and MeCN; insoluble in Et_2O, hydrocarbons, alcohols and acetone.

[ReOCl(OPhSal)(PMe_2Ph)]

On the basis of the results of cyclic voltammetric tests at different potential scan rates and of coulometric experiments (2 mol of electrons per mol of starting complex) it can be concluded that the oxidation of this compound also takes place through an electrode mechanism in which an irreversible chemical reaction is interposed between two subsequent one electron charge transfers. At high enough potential scan rate the cyclic voltammogram allowed the evaluation of the $E^r_{1/2}$ value of the couple [ReOCl(OPhSal)(PMe_2Ph)]$^+$/[ReOCl(OPhSal)(PMe_2Ph)], which resulted equal to +0.77 V vs $E^r_{1/2}$ of the ferricinium ion–ferrocene couple. Unfortunately, any attempt to recover stable electrolysis products failed.

The electrode reduction of [ReOCl(OPhSal)(PMe_2Ph)] occurs through a single cathodic peak involving, as proved by coulometric tests, a one electron charge transfer. At high enough scan rate the response appeared as that of an uncomplicated reversible charge transfer, allowing us to estimate, for the couple [ReOCl(OPhSal)(PMe_2Ph)]/[ReOCl(OPhSal)(PMe_2Ph)]$^-$, an $E^r_{1/2}$ value of −1.24 V vs ferricinium ion–ferrocene couple.

For the reduction of this complex, as well as for

Table 1. Potentials referred to $E^r_{1/2}$ of the couple ferrocinium–ion/ferrocene

Redox system	$E^r_{1/2}$
[ReOCl(OPhSal)(PMe_2Ph)]$^+$/[ReOCl(OPhSal)(PMe_2Ph)]	+0.77 V
[ReOCl(PhSal)$_2$]$^+$/[ReOCl(PhSal)$_2$]	+0.76 V[a]
[ReOCl(MeSal)$_2$]$^+$/[ReOCl(MeSal)$_2$]	+0.67 V[a]
[ReOCl(OPhSal)(MeOH)]$^+$/[ReOCl(OPhSal)(MeOH)]	+0.66 V
[ReO(OPhSal)(PhSal)]$^+$/[ReO(OPhSal)(PhSal)]	+0.57 V[a]
[ReOCl$_2$(OPhSal)]/[ReOCl$_2$(OPhSal)]$^-$	+0.57 V
[ReOCl(HOPhSal)]/[ReOCl(HOPhSal)]$^-$	+0.56 V
[ReO(OPhSal)(MeSal)]$^+$/[ReO(OPhSal)(MeSal)]	+0.53 V[a]
[ReOCl$_2$(OPhSal)]$^-$/[ReOCl$_2$(OPhSal)]$^{2-}$	−1.65 V*
[ReOCl$_3$(HOPhSal)]$^-$/[ReOCl$_3$(HOPhSal)]$^{2-}$	−1.63 V*
[ReOCl(OPhSal)(MeOH)]/[ReOCl(OPhSal)(MeOH)]$^-$	−1.62 V*
[ReOCl(MeSal)$_2$]/[ReOCl(MeSal)$_2$]$^-$	−1.54 V[a]
[ReOCl(PhSal)$_2$]/[ReOCl(PhSal)$_2$]$^-$	−1.43 V[a]
[ReO(OPhSal)(MeSal)]/[ReO(OPhSal)(MeSal)]$^-$	−1.37 V[a]
[ReO(OPhSal)(PhSal)]/[ReO(OPhSal)(PhSal)]$^-$	−1.33 V[a]
[ReOCl(OPhSal)(PMe_2Ph)]/[ReOCl(OPhSal)(PMe_2Ph)]$^-$	−1.24 V

* Peak potential value measured at a scan rate of 0.2 V s^{-1}; values without thermodynamic significance.

[a] From ref. 11.

all those previously examined, completely similar results were obtained using either platinum or mercury working electrodes.

The recovery of the electrolysis product led to the isolation and identification of the species [ReO(OPhSal)(PMe_2Ph)]. Elemental analysis data are as follows (Found: C, 46.9; H, 3.7; N, 2.2. Calc. for $C_{12}H_{20}NPO_3Re$: C, 45.7; H, 3.6; N, 2.5%). The IR spectrum showed a ν(Re=O) at 913 cm^{-1} (70 cm^{-1} lower than in the starting compound).

Magnetic susceptibility measurements on solid samples gave $\mu = 1.60$ BM, in agreement with a d^3 configuration in a square pyramidal environment. The complex has a non-conducting character confirming a non-ionic compound.

The compound is soluble in CH_2Cl_2, $CHCl_3$, DMF and MeCN; slightly soluble in MeOH, EtOH and acetone; insoluble in Et_2O and hydrocarbons.

It is hence evident that the chemical reaction following the uptake of one electron by the starting compound must consist of the release of the chloride ion. In the likely hypothesis that this reaction is of first order in respect to the rhenium complex concentration, the cyclic voltammetric responses[15] allowed us to estimate a half-life time of about 16 ms for the electrogenerated species [Re(IV) OCl(OPhSal)(PMe_2Ph)]$^-$.

The results of this study confirm our previous finding,[11] i.e. Schiff base type ligands exhibit the interesting property of allowing the Re=O moiety to be retained also with the metal in +4 and +6 oxidation states. In fact, through electrochemical methods it has been possible to prepare and characterize a number of these complexes.

By analysing the $E^r_{1/2}$ values computed in this and in our previous paper,[11] which have been collected in Table 1, we can see that by varying the ligands used the $E^r_{1/2}$ of the oxidation processes lay in quite a narrow range. As to the reduction potentials, the range of the values with thermodynamic significance is also rather narrow. In particular, the product containing phosphine ligand shows the highest $E^r_{1/2}$, and this fact is consistent with the capability of phosphine to delocalize the increased negative charge of the reduced species.

Acknowledgements—The authors thank Mr F. De Zuane for magnetic measurements and Mrs A. Moresco for technical assistance.

REFERENCES

1. R. Seeber, G. A. Mazzocchin, E. Roncari and U. Mazzi, *Transition Met. Chem.* 1981, **6**, 123.
2. E. Roncari, U. Mazzi, R. Seeber and P. Zanello, *J. Electroanal. Chem.* 1982, **132**, 221.
3. R. Seeber, G. A. Mazzocchin, U. Mazzi, E. Roncari and F. Refosco, *Transition Met. Chem.* 1984, **9**, 315.
4. U. Mazzi, E. Roncari, R. Rossi, V. Bertolasi, O. Traverso and L. Magon, *Transition Met. Chem.* 1980, **5**, 289.
5. A. Marchi, A. Duatti, R. Rossi, L. Magon, U. Mazzi and A. Pasquetto, *Inorg. Chim. Acta* 1984, **81**, 15.
6. U. Mazzi, F. Refosco, G. Bandoli and M. Nicolini, *Transition Met. Chem.* 1985, **10**, 121.
7. U. Mazzi, F. Refosco, F. Tisato, G. Bandoli and M. Nicolini, *J. Chem. Soc., Dalton Trans.* 1986, 1623.
8. G. A. Mazzocchin, R. Seeber, U. Mazzi and E. Roncari, *Inorg. Chim. Acta* 1978, **29**, 1.
9. G. A. Mazzocchin, R. Seeber, U. Mazzi and E. Roncari, *Inorg. Chim. Acta* 1978, **29**, 5.
10. U. Mazzi, E. Roncari, R. Seeber and G. A. Mazzocchin, *Inorg. Chim. Acta* 1980, **41**, 95.
11. R. Seeber, G. A. Mazzocchin, U. Mazzi, F. Refosco and F. Tisato, *Polyhedron* 1986, **5**, 1975.
12. G. Gritzner and J. Kuta, *Pure Appl. Chem.* 1984, **56**, 461.
13. V. I. Kravtsov, *J. Electroanal. Chem.* 1976, **69**, 125.
14. R. Hoffman, M. M. L. Chen, M. Elian, A. R. Rossi and D. M. P. Mingos, *Inorg. Chem.* 1974, **13**, 2666.
15. R. S. Nicholson and I. Shain, *Anal. Chem.* 1964, **36**, 706.

Polyhedron Vol. 6, No. 8, pp. 1653–1656, 1987
Printed in Great Britain

0277–5387/87 $3.00+.00
Pergamon Journals Ltd

SYNTHESIS AND CHARACTERIZATION OF SOME NEW NICKEL(II), ZINC(II) AND CADMIUM(II) COMPLEXES OF QUADRIDENTATE SNNS LIGANDS

M. AKBAR ALI,* S. M. GHAUSUL HOSSAIN, S. M. M. H. MAJUMDER and M. NAZIM UDDIN

Department of Chemistry, University of Chittagong, Chittagong, Bangladesh

and

M. T. H. TARAFDER

Department of Chemistry, University of Rajshahi, Bangladesh

(*Received* 7 *October* 1986; *accepted* 9 *February* 1987)

Abstract—Two new quadridentate Schiff base ligands formed from 2,5-hexanedione and S-alkyldithiocarbazic acids and their nickel(II), zinc(II) and cadmium(II) complexes having the general formula [M(SNNS)] ($SNNS^{2-}$ is the dinegatively charged ligands) have been synthesized and characterized by elemental analysis and magnetic and spectroscopic methods. The Ni(SNNS) complexes are diamagnetic and square-planar. The Zn(SNNS) complexes are assigned with polymeric structures with mercapto sulphur-bridging. The Cd(SNNS) complexes presumably have polymeric structures.

During the past 20 years metal complexes of sulphur–nitrogen chelating agents have been studied quite extensively.[1] However, the majority of ligands studied have either the bidentate NS or tridentate NNS donor sequence. Comparatively little work has been directed to the synthesis and characterization of metal complexes of quadridentate sulphur–nitrogen ligands. The quadridentate SNNS ligand, 3-ethoxy-2-oxobutyraldehyde *bis*-(thiosemicarbazone) and its copper(II) and zinc(II) chelates have been shown to possess antineoplastic activities and their interactions with biological systems have been widely investigated.[2–7] In view of their importance as potential antineoplastic agents and as part of our general study of sulphur–nitrogen ligands, we report herein the synthesis and characterization of some new nickel(II), zinc(II) and cadmium(II) chelates of two quadridentate SNNS ligands formed from 2,5-hexanedione and S-alkyldithiocarbazic acids.

* Author to whom correspondence should be addressed.

EXPERIMENTAL

Physical measurements

Conductivity measurements were carried out using a Philips conductivity bridge model PW 9501 equipped with a Philips PW 9515/10 conductivity cell. The IR spectra were recorded in the range 200–4000 cm^{-1} on a Pye Unicam Model SP3-300 IR spectrophotometer using KBr discs. Electronic spectra in Nujol mulls were measured with the help of a Shimadzu UV-120-02 spectrophotometer, PMR spectra in DMSO-d_6 were recorded on a Varian XL-200 Spectrometer using TMS as an internal standard. C, H, N and M analyses were performed as before.[8]

Preparation of the ligands and complexes

S-Methyldithiocarbazate[9] and S-benzyldithiocarbazate[10] were prepared according to literature methods.

Syntheses of the Schiff bases, H_2L_1 *and* H_2L_2. Both the ligands were synthesized by the same

general method: the appropriate S-alkyldithiocarbazate (0.03 mol) was dissolved in abs. ethylalcohol (60 cm^3) and the solution mixed with a solution of 2,5-hexanedione (0.015 mol) in the same solvent (10 cm^3). The mixture was refluxed for a period of ca. 1 h and then left standing to cool. The product which separated out was filtered off and recrystallized from abs. ethylalcohol. H_2L_1: M.p. 135°C. Found: C, 55.7; H, 5.8; N, 11.7. $C_{22}H_{26}N_4S_4$ requires: C, 55.7; H, 5.5; N, 11.8%. H_2L_2: M.p. 150°C. Found: C, 37.5; H, 5.8; N, 17.5. $C_{10}H_{18}N_4S_4$ requires: C, 37.2; H, 5.6; N, 17.4%.

Preparation of the complexes

All the complexes were prepared by the same general method described below: a solution of the metal(II) acetate (2 mmol) in methanol (30 cm^3) was filtered into a boiling solution of the Schiff base (2 mmol) in abs. ethanol (50 cm^3). The mixture was heated on a water-bath for ca. 10–15 min and then left to stand overnight. The product which formed was then filtered off, washed thoroughly with ethanol and dried in a vacuum desiccator over P_4O_{10}.

RESULTS AND DISCUSSION

The reaction of 2 mol of S-alkyldithiocarbazic acid with 1 mol of 2,5-hexanedione results in the formation of stable crystalline Schiff bases represented by the structural formula I (R = —CH_3, —$CH_2C_6H_5$).

These compounds have a proton adjacent to the thione group and consequently, they are capable of existing either as the thioketo form (IA) or as the

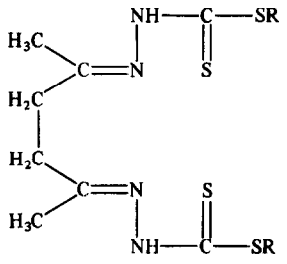

(IA)

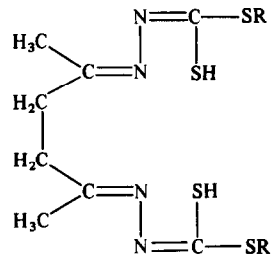

(IB)

enethiol form (IB) or as a mixture of both the thioketo and thioenol forms. The IR spectra of the Schiff bases do not display the ν(S–H) band at ca. 2570 cm^{-1} but show ν(N–H) at 3140–3150 cm^{-1} indicating that in the solid state they remain as the thioketo form IA. The ^1H NMR spectra in $CDCl_3$ also do not display any peak attributable to the S–H proton. It is, therefore, assumed that the Schiff bases remain predominantly in the thioketo forms in $CDCl_3$ solution. However, enethiolization of these ligands seems to be markedly enhanced in the presence of metal ions with the concomitant formation of metal chelates containing the deprotonated ligands. The complexes isolated together with their colours, elemental analyses and molar conductivities are shown in Table 1. The molar conductance data are consistent with the non-electrolytic nature of the complexes. The ligands, therefore, must be acting as dinegatively charged species.

Comparison of the IR spectra (Table 1) of the Schiff bases with those of their metal complexes show that the ν(N–H) of the free ligands are absent in the spectra of the complexes supporting our contention that the ligands are coordinated in deprotonated forms.

The most relevant bands in the IR spectra of the

Table 1. Analytical data, colour, and conductivity of the metal complexes

Compound	Found (calc.) C	H	N	M	Colour	Λ_M (ohm^{-1} cm^2 mol^{-1}) ca. 10^{-3} M at 25°C
$NiL_1 \cdot 0.5H_2O$	48.9 (48.9)	4.8 (4.7)	10.6 (10.4)	11.1 (10.9)	Brown	1.6
$NiL_2 \cdot H_2O$	30.4 (30.2)	4.3 (4.6)	15.1 (14.1)	15.0 (14.8)	Brown	0
$ZnL_1 \cdot 0.5H_2O$	48.5 (48.3)	4.5 (4.4)	10.2 (10.2)	12.6 (11.9)	Yellowish-white	Insoluble
$ZnL_2 \cdot C_2H_5OH$	33.4 (33.4)	5.2 (5.1)	13.0 (13.0)	16.0 (15.1)	Yellow	Insoluble
$CdL_1 \cdot H_2O$	43.9 (43.8)	4.0 (4.3)	9.2 (9.3)	18.9 (18.6)	Yellow	3.4
$CdL_2 \cdot H_2O$	26.4 (26.6)	4.1 (4.0)	12.2 (12.4)	25.8 (24.9)	Yellow	2.8

Table 2. Selected IR absorption bands of the ligands and metal complexes

Compound	IR data					Others	Electronic spectra
	ν(NH)	ν(C=N)	ν(C=S)	ν(N—N)	ν(M—S)	ν(O—H) of solvent	λ_{max} (nm)
H_2L_1	3150 s	1628 s	1050 s	828 m	—	—	
H_2L_2	3140 s	1625 s	1050 s	822 s	—	—	
$NiL_1 \cdot 0.5H_2O$	—	1600 m	970	845 m	370 w	3400 br	265 sh, 307, 355, 445, ca. 535 sh
$NiL_2 \cdot H_2O$	—	1590 s	990 s	818 m	320 s	3450 br	286, 364, 432 sh, 484, 535
$ZnL_1 \cdot 0.5H_2O$	—	1570 m,br	960 s	840 m	320 w	3420 m,br	255 sh, 270, 325 sh
$ZnL_2 \cdot C_2H_5OH$	—	1600 m	950 s	810 m	340 w	3420 m,br 3250 m,br	267, 293 sh, ca. 330 sh
$CdL_1 \cdot H_2O$	—	1590 m	1000 br	845 m	—	3430 br,m	270, 304, 349, 448
$CdL_2 \cdot H_2O$	—	1590 m	1000 s,br	840 m	330 w	3400 s,br	277, 284, 349, ca. 418 sh

complexes and the free ligands are listed in Table 2. The strong band at 1618 cm^{-1} in the IR spectra of the ligands is attributed to ν(C=N) stretching vibration.[11] Upon complexation this band is shifted to lower frequencies by about 20 cm^{-1}, suggesting that the ligands are coordinated to the metal ion via the azomethine nitrogen donor atom. A strong band at 1050 cm^{-1} in the free ligands is tentatively assigned to the ν(C=S) of the thioketo form.[12] This band is substantially lowered in the IR spectra of the metal complexes suggesting that coordination to metal ions occurs through the sulphur atom. This is corroborated by the presence of a weak band in the far IR region (ca. 330 cm^{-1}) attributable to metal-sulphur stretching frequency.[13] All the foregoing evidences support that both the Schiff bases behave as quadridentate SNSN ligands. IR spectra of all the complexes show bands characteristic of lattice waters[14] suggesting that the solvent molecules are not coordinated.

The nickel(II) complexes were obtained as brown solids and their ready solubilities in non-polar solvents suggest that presumably they do not have polymeric structures. The diamagnetism of these complexes (Table 1) implies that they have four-coordinate square–planar configurations. Further evidence in support of a square–planar configuration comes from their electronic spectra (Table 2) which show bands at ca. 307, 355, 445 and 535 nm of which the one at 535 nm may be assigned to the *d–d* transition of square–planar nickel(II) having the NiN_2S_2 chromophore.[15] The ^1H NMR spectral data of the free ligands and their complexes are shown in Table 3. The signal at 2.60 ppm relative to TMS is assigned to the S–CH_3 protons and those at the 1.93 to the C–CH_3 protons.[16] The very small shift of the S–CH_3 proton resonances in the spectra of the complexes is consistent with our assumption that the thioether sulphur is not involved in coordination. Similarly there is also very little change in the position of the peaks due to the S–CH_2– proton resonances in the spectra of the complexes compared to those of the ligands. However, the C–CH_3 protons resonate downfield compared to those in the free ligands indicating deshielding as a result of coordination via the C=N nitrogen atom. The above magnetic, electronic and NMR spectroscopic data support a four-coordinate

Table 3. ^1H NMR spectral data of ligands and complexes (δ ppm) relative to TMS

Compound	—SCH_3	C—CH_3	—CH_2—	—SCH_2—	—C_6H_5—
H_2L_1	—	1.83	2.52	4.36	7.12
H_2L_2	2.60	1.93	2.70	—	—
$NiL_1 \cdot 0.5H_2O$	—	2.35	3.00	4.20	7.20
$NiL_2 \cdot H_2O$	2.46	2.26	2.77	—	—
$CdL_1 \cdot H_2O$	—	2.35	3.15	4.40	7.50
$CdL_2 \cdot H_2O$	2.48	2.35	2.70	—	—

square–planar structure for the nickel(II) complexes with the ligands acting as quadridentate chelating agents bonding the metal ion via the two azomethine nitrogen atoms and the thiolo sulphur atoms as shown in Structure II.

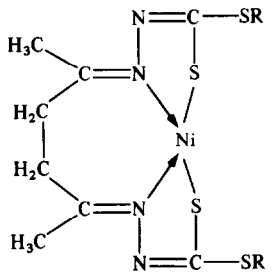

(II)

Such a square–planar structure has, in fact, been confirmed by an X-ray crystal structure determination for the analogous nickel(II) complex of hexene-2,5-dione Schiff base of thiosemicarbazide.[17]

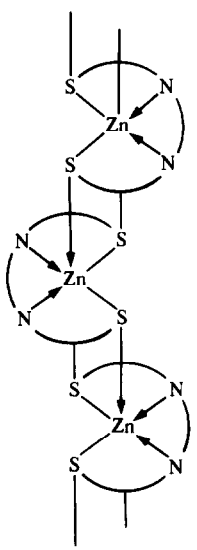

(III)

The zinc(II) complexes Zn(SNNS) were obtained as yellow powders. In contrast with the nickel(II) complexes these compounds were found to be virtually insoluble in all common polar and non-polar solvents suggesting that they probably have polymeric structures. A sulphur-bridged polymeric structure as shown in Structure III will be consistent with the insoluble nature of these complexes.

The cadmium(II) complexes Cd(SNNS) are slightly more soluble than the zinc(II) chelates, but the solubility is not sufficient for molecular weight measurements in solution. These compounds also presumably have polymeric structures like the zinc(II) complexes.

Acknowledgements—We gratefully acknowledge Prof R. W. Hay of Chemistry Department, University of Stirling, Scotland, U.K. for the microanalytical data and the Department of Chemistry, University of Chittagong, Bangladesh for financial assistance.

REFERENCES

1. M. Akbar Ali and S. E. Livingstone, *Coord. Chem. Revs.* 1974, **13**, 101 and references cited therein.
2. D. A. Winkelmann, Y. Bermke and D. H. Petering, *Bioinorg. Chem.* 1974, **3**, 261.
3. D. H. Petering, *Biochem. Pharmacol.* 1974, **23**, 567.
4. C. H. Chan Stier, D. T. Minkel and D. H. Petering, *Bioinorg. Chem.* 1976, **6**, 203.
5. D. T. Minkel, C. H. Chan Stier and D. H. Petering, *Mol. Pharmacol.* 1976, **12**, 1036.
6. D. T. Minkel, A. L. Saryan and D. H. Petering, *Cancer Res.* 1978, **38**, 124.
7. D. T. Minkel and D. H. Petering, *Cancer Res.* 1978, **38**, 117.
8. M. Akbar Ali, Moniruddin, M. Nazimuddin and M. T. H. Tarafder, *Indian J. Chem.* 1986, **25A**, 238.
9. M. Das and S. E. Livingstone, *Inorg. Chim. Acta* 1976, **19**, 5.
10. M. Akbar Ali and M. T. H. Tarafder, *J. Inorg. Nucl. Chem.* 1977, **39**, 1785.
11. G. C. Percy and D. A. Thornton, *J. Inorg. Nucl. Chem. Letters* 1971, **7**, 599; R. A. Kolinski and B. Korybut-Daszkiewicz, *Inorg. Chim. Acta* 1975, **14**, 237.
12. M. T. H. Tarafder and M. Akbar Ali, *Can. J. Chem.* 1978, **56**, 2000.
13. D. M. Adams, *Metal–Ligand and Related Vibrations.* Arnold, London (1967).
14. K. Nakamoto, *Infrared Spectra of Inorganic and Coordination Compounds.* Wiley, New York (1965).
15. M. Akbar Ali and R. N. Bose, *Polyhedron* 1984, **3**, 517.
16. M. F. Iskander, L. El-Sayed, M. Tawfik and M. Arafa, *Inorg. Chim. Acta* 1985, **104**, 125.
17. J. A. McCleverty, *J. Chem. Soc., Chem. Commun.* 1970, 124.

Polyhedron Vol. 6, No. 8, pp. 1657–1667, 1987
Printed in Great Britain

0277–5387/87 $3.00+.00

bis-t-BUTYLIMIDO COMPLEXES OF TUNGSTEN(VI)

ALASTAIR J. NIELSON

Department of Chemistry, University of Auckland, Private Bag, Auckland, New Zealand

(*Received* 13 *November* 1986; *accepted* 9 *February* 1987)

Abstract—WCl_6 reacts with $Me_3SiNHCMe_3$ or Me_3CNH_2 to give $[W(NCMe_3)(\mu\text{-}NCMe_3)Cl_2(NH_2CMe_3)]_2$ which contains *trans* orientated chloro ligands. The reaction does not occur with Me_3SiNHR or RNH_2 (R = Me_2CH-, $MeCH_2$-). An interligand proton transfer between *cis*-orientated *t*-butylamido NH groups gives rise to the imido and amine ligands. $[W(NCMe_3)(\mu\text{-}NCMe_3)Cl_2(NH_2CMe_3)]_2$ reacts with 4-picoline to give $[W(NCMe_3)(\mu\text{-}NCMe_3)Cl_2(4\text{-pic})]_2$ and $[W(NCMe_3)_2Cl_2(4\text{-pic})_2]$ while the bidentate ligands bipy and tmed give $[W(NCMe_3)_2Cl_2(bipy)]$ and $[W(NCMe_3)_2Cl_2(tmed)]$. All the complexes retain the *trans*-chloro orientation. With strong sigma donors, L (L = PMe_3, $PMePh_2$, Me_3CNC), $[W(NCMe_3)(\mu\text{-}NCMe_3)Cl_2(NH_2CMe_3)]_2$ reacts to give the complexes $[W(NCMe_3)(\mu\text{-}NCMe_3)Cl_2(L)]_2$ which contain *cis*-chloro ligands. With *t*-butylamine $[W(NCMe_3)_2(NHCMe_3)_2]$ is formed but less sterically demanding amines (Me_2CHNH_2, $MeCH_2NH_2$) do not react similarly. Reaction of $[W(NCMe_3)(\mu\text{-}NCMe_3)Cl_2(NH_2CMe_3)]_2$ with EtOH and Me_3CNH_2 forms $[W(NCMe_3)_2(OEt)_2]_x$. $WOCl_4$ reacts with $Me_3SiNHCMe_3$ or Me_3CNH_2 to give a complex proposed as $[WO(NCMe_3)Cl_2(NH_2CMe_3)]_x$ which reacts further with bipy to form $[W(NCMe_3)_2Cl_2(bipy)]$ and various uncharacterized oxo complexes by an oxo-imido exchange. The complexes were characterized by analytical data, IR, ^1H and ^{13}C NMR spectroscopy. The position of the *t*-butyl group quaternary carbon in the ^{13}C NMR spectra differentiates between imido, amido and amine ligands.

bis-Organoimido complexes of the group (VI) transition metals[1] are less well-known than the isoelectronic *cis* oxo complexes[2] as general preparative routes have not been established. Recent studies have shown that when the mono-organoimido complexes $[W(NR)Cl_4]_2$ (R = Ph, MePh, Me_2CH, $MeCH_2$, Me) react with the silylamines Me_3SiNHR' (R' = Ph, Me_3C, Me_2CH, $MeCH_2$) the *bis*-organoimido complexes $[W(NR)(NR')Cl_2(NH_2R')]_2$ result[3] which then react with ligands such as 2,2′-bipyridyl or PMe_3 to give the monomeric complexes $[W(NR)(NR')Cl_2(bipy)]$ and $[W(NR)(NR')Cl_2(PMe_3)_2]$.[4] *bis-t*-Butylimido complexes are not available by these methods as the reaction of $WOCl_4$ with RNCO to give the initial mono-organoimido complex, does not occur with *t*-butylisocyanate.[5] Several *bis-t*-butylimido complexes of tungsten are however known, including $[W(NCMe_3)(\mu\text{-}NCMe_3)Me_2]_2$,[6] $[W(NCMe_3)_2(OCMe_3)_2]$[7] and $[W(NCMe_3)_2(PFP)(NH_2CMe_3)]$ (PFP = perfluoropinacol)[8] which are derived from $[W(NCMe_3)_2(NHCMe_3)_2]$,[7] but a general route has so far not been reported.

Previous work in our laboratories has shown[9] that for the pentachlorides of niobium and tantalum, substitution of two chlorides by alkylamido ligands, NHR, results in formation of an alkylimido ligand and coordinated primary amine (eqn 1) by an interligand proton-transfer process which is independent of steric size. A third alkylamido ligand was able to be substituted (eqns 2 and 3) but the complex could not be induced to eliminate HCl and form a second imido function.

$$MCl_5 + 2Me_3SiNHR \rightarrow M(NR)Cl_3(NH_2R) + 2Me_3SiCl \quad (1)$$

$$M(NR)Cl_3(NH_2R) + 2RNH_2 \rightarrow M(NR)(NHR)Cl_2(NH_2R) + RNH_3Cl \quad (2)$$

$$MCl_5 + 6RNH_2 \rightarrow M(NR)(NHR)Cl_2(NH_2R) + 3RNH_3Cl. \quad (3)$$

It was thus of interest to establish whether *bis*-organoimido complexes and, in particular, *bis-t*-butylimido complexes, could be generated from WCl_6 and the silylamines Me_3SiNHR or primary amines RNH_2 (R = alkyl group).

RESULTS AND DISCUSSION

When two equivalents of $Me_3SiNHCMe_3$ were reacted with WCl_6 in benzene, a yellow–brown solution formed which gave rise to a yellow, non-crystalline product analysing as the *bis-t*-butylamido complex $[W(NHCMe_3)_2Cl_4]\cdot\frac{1}{6}C_6H_6$ (1). The ^{13}C NMR spectrum showed a quaternary carbon resonance characteristic of a *t*-butylamido ligand (63.0 ppm) but in addition there were quaternary resonances at 70 and 55 ppm which are characteristic of *t*-butylimido and *t*-butylamine ligands.[9] These features thus suggest the product to be a mixture containing (1) and the imido complex $[W(NCMe_3)Cl_4(NH_2CMe_3)]$ (2). A similar reaction between $Me_3SiNHCHMe_2$ and WCl_6 gave a purple precipitate analysing as $[W(NHCHMe_2)_2Cl_4]$ or alternatively $[W(NCHMe_2)Cl_4(NH_2CHMe_2)]$ (3), but insolubility precluded further characterization by ^{13}C NMR spectroscopy.

Reaction of four equivalents of $Me_3SiNHCMe_3$ with WCl_6, or, reaction of two equivalents of the silylamine with the mixture containing $[W(NHCMe_3)_2Cl_4]$ (1) and $[W(NCMe_3)Cl_4(NH_2CMe_3)]$ (2) gave a yellow complex which analysed as $[W(NCMe_3)_2Cl_2(NH_2CMe_3)]_x$. The ^{13}C NMR spectrum showed *t*-butylimido and *t*-butylamine quaternary carbon resonances at 69.1 and 53.5 ppm respectively and the methyl carbons at 31.3 ppm. In addition the spectrum showed a minor component (ca. 20%, resonances at 68.2, 53.2 and 30.2 ppm) indicating a second species in solution and this was also suggested by the ^1H NMR spectrum, there being three methyl proton resonances of varying intensity and two broad NH_2 proton resonances. The IR spectrum exhibited a single strong absorption at 310 cm^{-1} indicative of *trans* chloro ligands. On the basis of these data, the dimeric structure, $[W(NCMe_3)(\mu\text{-}NCMe_3)Cl_2(NH_2CMe_3)]_2$ (4), is proposed for which some form of dissociation or isomerization in solution occurs to give rise to the NMR spectral features. Repeated crystallizations of the complex have so far given samples with similar spectra. The structure expected is similar to that found by X-ray crystallography for $[W(NCMe_3)(\mu\text{-}NPh)Cl_2(NH_2CMe_3)]_2$.[10] In this complex, however, the chloro ligands are orientated *cis* with characteristic tungsten–chlorine vibrations observed in the IR spectrum at 320 and 290 cm^{-1}.[11]

The results obtained suggest that reactions (1)–(4) occur.

$$WCl_6 + 2Me_3SiNHCMe_3 \rightarrow W(NHCMe_3)_2Cl_4 + 2Me_3SiCl \quad (1)$$

$$W(NHCMe_3)_2Cl_4 \rightarrow W(NCMe_3)Cl_4(NH_2CMe_3) \quad (2)$$

$$W(NCMe_3)Cl_4(NH_2CMe_3) + 2Me_3SiNHCMe_3 \rightarrow W(NCMe_3)(NHCMe_3)_2Cl_2(NH_2CMe_3) + 2Me_3SiCl \quad (3)$$

$$W(NCMe_3)(NHCMe_3)_2Cl_2(NH_2CMe_3) \rightarrow W(NCMe_3)_2Cl_2(NH_2CMe_3) + Me_2CNH_2. \quad (4)$$

A *cis* arrangement of the *bis-t*-butylamido ligands is preferred which can then lead to formation of *t*-butylimido and amine ligands by interligand proton transfer similar to that observed previously for mono-organoimido complexes of niobium and tantalum.[9] The unique feature of the present reaction is that the process is repeated if four chloro ligands are still available, thereby generating a second imido function. A reaction intermediate such as $[W(NHCMe_3)_4Cl_2]$ is unlikely as the strong *trans* influence of the amido ligand would prevent *trans* orientated *t*-butylamido ligands being formed.[12,13] However, a *tris*-amido intermediate, $[W(NHCMe_3)_3Cl_3]$ containing mutually *cis* amido ligands cannot be ruled out.

The silylamine reaction leads to *trans* orientated chloro ligands in (4) and this compares with reactions of the mono-organoimido complexes $[W(NR)Cl_4]_2$ and the silylamines Me_3SiNHR' which give rise to *cis* dichlorides in the resulting $[W(NR)(NR')Cl_2(NH_2R')]$ complexes,[3] the difference apparently arising from steric properties of the *t*-butyl group. Thus, while any steric strain can be relieved in a *cis* amido complex irrespective of R-group size (complex a), after proton transfer a facial arrangement of imido and amine ligands (complex b) is sterically congested if all three ligands contain *t*-butyl groups so that a meridional configuration (c) is then preferred.

The *bis-t*-butylimido complex (4) may also be prepared by reaction of seven equivalents of *t*-butylamine with WCl_6 in benzene. Four equivalents of *t*-butylamine hydrochloride are produced but the yield of complex is lower using this method, the reaction producing a significant amount of petroleum ether soluble, non-crystalline material for which the ^{13}C NMR spectrum shows various *t*-butylimido, amido and amine quaternary carbon

resonances. Other primary amines (Me_2CHNH_2, $EtNH_2$, etc.) do not give clean reactions with WCl_6, producing dark-brown solutions from which characterizable products have not yet been obtained.

With *t*-butylamine, the *t*-butylimido ligands are likely to arise via reactions (5)–(7).

$$WCl_6 + 2Me_3CNH_2 \rightarrow W(NHCMe_3)Cl_5 + Me_3CNH_3Cl \quad (5)$$

$$W(NHCMe_3)Cl_5 + 2Me_3CNH_2 \rightarrow W(NHCMe_3)_2Cl_4 + Me_3CNH_3Cl \quad (6)$$

$$W(NHCMe_3)_2Cl_4 \rightarrow W(NCMe_3)Cl_4(NH_2CMe_3). \quad (7)$$

Proton transfer between amido ligands is not the only process possible, however, as base promoted deprotonation (eqn 8) could also give rise to an imido ligand.

$$W(NHCMe_3)Cl_5 + Me_3CNH_2 \rightarrow W(NCMe_3)Cl_4 + Me_3CNH_3Cl. \quad (8)$$

$[W(NCMe_3)(\mu\text{-}NCMe_3)Cl_2(NH_2CMe_3)]_2$ (4) is a useful source for the preparation of a variety of complexes containing the *bis-t*-butylimido function (scheme 1). When the complex was stirred with two equivalents of 4-picoline, the *t*-butylamine ligand was replaced giving $[W(NCMe_3)(\mu\text{-}NCMe_3)Cl_2(4\text{-pic})]_2$ (5). Refluxing (4) with four equivalents of 4-picoline gave $[W(NCMe_3)_2Cl_2(4\text{-pic})_2]$ (6) while similar reactions with two equivalents of 2,2′-bipyridyl (bipy) or *N,N,N′,N′*-tetramethylethylenediamine (tmed) gave the complexes $[W(NCMe_3)_2Cl_2(bipy)]$ (7) and $[W(NCMe_3)_2Cl_2(tmed)]$ (8). The ^{13}C NMR spectra (Table 2), show a single *t*-butyl group quaternary carbon for each complex, in the vicinity of 71 ppm with associated ^{183}W satellites ($^2J_{W-C}$ ranging from 14.4 to 15.4 Hz) while the ^1H NMR spectra show the correct ratio of *t*-butyl methyl protons to those of the neutral donor ligand. In the IR spectra the complexes exhibit a single strong absorption near 310 cm^{-1} indicating *trans* orientated chloro ligands[10] as in the parent dimer, which necessitate the nitrogen atoms of the amine ligands to lie *trans* to the imido groups.

To maintain an 18-electron count in each of these complexes the *t*-butylimido ligands must donate a total of six electrons. A low temperature X-ray crystal structure determination of $[Mo(NPh)_2(S_2CNEt_2)_2]$[14] has shown some differentiation in W–N bond lengths [1.789(4) and 1.754(4) Å]. However, the four and two electron formalism has not otherwise been observed, structure determinations of $[W(NPh)_2Cl_2(bipy)]$[5] and $[W(NCMe_3)(NPh)Cl_2(bipy)]$[15] for example showing no difference in the W–N bond lengths. A similar situation is thus expected for the *bis-t*-butylimido complexes whereby each imido ligand would have a bond order of approximately 2.5.

When $[W(NCMe_3)(\mu\text{-}NCMe_3)Cl_2(NH_2CMe_3)_2]$ (4) is reacted with trimethylphosphine or diphenylmethyl phosphine, products analysing as $[W(NCMe_3)_2Cl_2(PMe_3)]_x$ and $[W(NCMe_3)_2Cl_2(PMePh_2)]_x$ are formed. The complexes show two bands in the IR spectra near 320 and 280 cm^{-1} characteristic of *cis* dichlorides. The absorptions are analogous to those observed in the IR spectrum of $[W(NCMe_3)(\mu\text{-}NPh)Cl_2(NH_2CMe_3)]_2$ for which the *cis*-arrangement has been confirmed by X-ray crystallography.[11] The ^1H NMR spectra confirm two *t*-butyl groups to one phosphine ligand, the phosphine methyl groups appearing as a doublet. In the ^{13}C NMR spectra, two resonances of similar intensity are observed for both the *t*-butyl group methyl and quaternary carbons. Spectra run at higher field show identical coupling constants indicating the splitting arises from long range coupling to phosphorus[16] rather than different chemical environments for the two *t*-butyl groups (see Fig. 1). The quaternaries show coupling to ^{183}W (Fig. 1), the coupling constants of 13.7 and 12.8 Hz for PMe_3 and $PMePh_2$ complexes, respectively, being slightly smaller than the previous amine complexes. On the basis of the spectral features the complexes are proposed as the dimers $[W(NCMe_3)(\mu\text{-}NCMe_3)Cl_2(PMe_3)]_2$ (9) and $[W(NCMe_3)(\mu\text{-}NCMe_3)Cl_2(PMePh_2)]_2$ (10) [see structure (d)].

As to why the phosphine complexes should adopt a dimeric *cis* chloro structure is not clear. It is apparent however, that a strong σ-donor such as a phosphine cannot be tolerated *trans* to an imido function which exerts a strong *trans* influence, and this feature appears to be general for tungsten organoimido complexes. For example, while complexes such as $[W(NPh)Cl_4 \cdot L]$ (L = amine, nitrile, t.h.f., etc.) can be formed which contain the neutral ligand *trans* to the imido function, phosphines produce gummy materials which reduce to $[W(NPh)Cl_3P_2]$ complexes.[5] For these examples, as with the tungsten IV complexes $[W(NPh)Cl_2P_3]$, X-ray crystal structure determinations[5,17] show a chloro ligand lying *trans* to the imido function. In the trimeric oxo-bridged complex $[W(NPh)(\mu\text{-}O)Me_2(PMe_3)]_3$[18] the phosphine lies *trans* to the bridging oxo group while for the *bis*-phosphine complex, $[W(NCMe_3)(NPh)Cl_2(PMe_3)_2]$, ^1H, ^{13}C and ^{31}P NMR evidence indicates *trans* phosphines which then positions the chloro ligands *trans* to the imido functions.[4] For the present complex $[W(NCMe_3)(\mu\text{-}NCMe_3)Cl_2(NH_2CMe_3)]_2$ (4), reaction with diphenylphosphino ethane (dppe) should

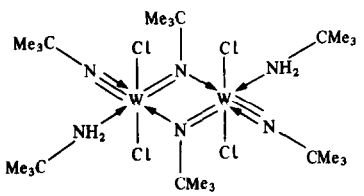

(4)

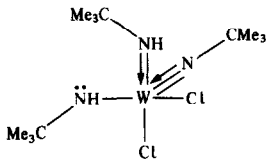

(a)

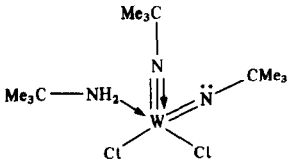

(b)

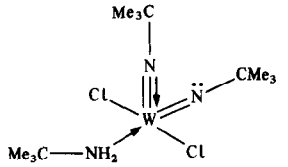

(c)

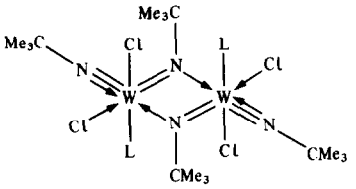

(d)

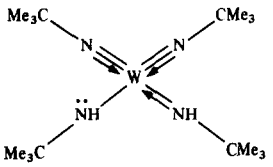

(e)

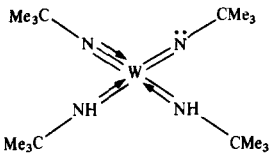

(f)

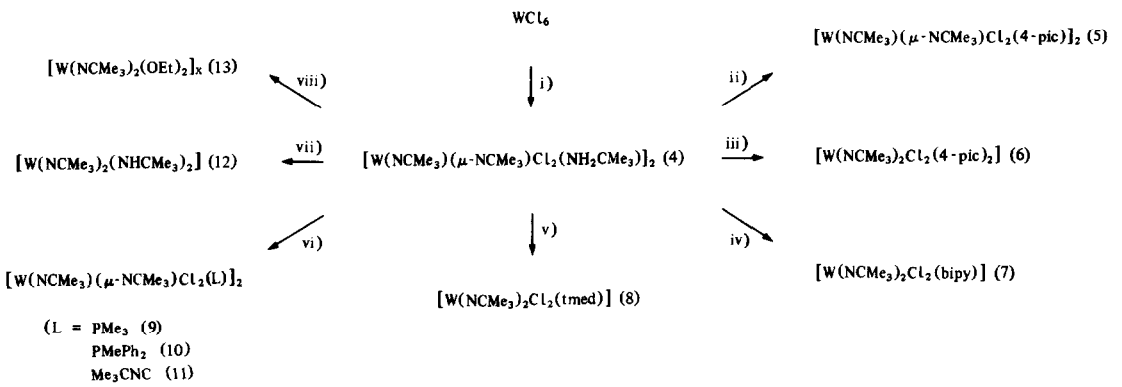

Scheme 1. (i) 4 equivs $Me_3SiNHCMe_3$ or 7 equivs Me_3CNH_2, (ii) 2 equivs 4-picoline, (iii) 4 equivs 4-picoline, (iv) 2 equivs 2,2′-bipyridyl, (v) 2 equivs *N,N,N′,N′*-tetramethylethylenediamine, (vi) 2 equivs L, (vii) 4 equivs Me_3CNH_2, (viii) 2 equivs each of EtOH and Me_3CNH_2.

Table 1. Physical data

Complex	Colour	M.p. (°C)	Analytical data[c] C	H	N	Infrared data[d] W–Cl
$[W(NHCMe_3)_2Cl_4]\cdot\frac{1}{6}C_6H_6$ (1)[a,b]	yellow	> 110 (dec)	22.3 (22.4)	4.5 (4.4)	5.7 (5.8)	320
$[W(NCHMe_2)Cl_4(NH_2CHMe_2)]$ (3)	purple	> 140 (dec)	14.7 (16.3)	4.1 (3.6)	5.3 (6.3)	295
$[W(NCMe_3)(\mu\text{-}NCMe_3)Cl_2(NH_2CMe_3)]_2$ (4)	yellow	162–164	30.2 (30.9)	6.3 (5.8)	9.1 (8.9)	310 (*trans*)
$[W(NCMe_3)(\mu\text{-}NCMe_3)Cl_2(4\text{-pic})]\cdot\frac{1}{4}C_6H_6$ (5)[a]	pale yellow	150–152	36.5 (36.6)	5.3 (5.3)	8.1 (8.3)	322 (*trans*)
$[W(NCMe_3)_2Cl_2(bipy)]$ (7)	pale yellow	> 210 (dec)	38.8 (39.1)	4.8 (4.7)	10.2 (10.1)	305 (*trans*)
$[W(NCMe_3)_2Cl_2(tmed)]$ (8)	pale green	132–134	32.4 (32.8)	6.8 (6.7)	10.7 (10.9)	310 (*trans*)
$[W(NCMe_3)_2(\mu\text{-}NCMe_3)Cl_2(PMe_3)]_2$ (9)	colourless	239–241	28.2 (27.9)	5.8 (5.8)	5.7 (5.9)	318,280 (*cis*)
$[W(NCMe_3)(\mu\text{-}NCMe_3)Cl_2(PMePh_2)]_2$ (10)	pale green	208	41.9 (42.2)	5.6 (5.2)	4.6 (4.7)	318,285 (*cis*)
$[W(NCMe_3)(\mu\text{-}NCMe_3)Cl_2(CNCMe_3)]_2$ (11)	yellow	137	32.4 (32.5)	5.9 (5.7)	8.7 (8.8)	340,300 (*cis*)
$[W(NCMe_3)_2(NHCMe_3)_2]$ (12)	colourless	75–77	39.8 (40.8)	8.3 (8.1)	11.7 (11.9)	—

[a] Solvent molecules supported by ^1H NMR spectrum.
[b] Alternative formulation $[W(NCMe_3)Cl_4(NH_2CMe_3)]$ (2).
[c] Calculated figures in parentheses.
[d] Spectra obtained as nujol mulls between caesium iodide plates.

Table 2. NMR spectra

Complex	^{1}H NMR[a,b,c]	^{13}C NMR[a,c]
$[W(NHCMe_3)_2Cl_4]\cdot\frac{1}{6}C_6H_6$[d] (1)	1.45, 1.52, 1.60 and 1.62 (4s,CMe_3); 7.0 (b,NH)	28.4, 30.0, 31.8, 32.4 (Me_3); 55.2 (NH_2C); 63.0 (NHC); 70.7, 72.9, 74.7 (NC); 128.3 (benzene)
$[W(NCMe_3)(\mu\text{-}NCMe_3)Cl_2(NH_2CMe_3)]_2$ (4)	1.33, 1.40 and 1.45 (3s,27H,3CMe_3); 3.8 and 4.65 (b,4H,2NH_2)	30.2[e] and 31.3 (Me_3); 53.2[e] and 53.5 (NH_2C); 68.2[e] and 69.1 (NC)
$[W(NCMe_3)_2Cl_2(4\text{-pic})_2]$ (6)	1.36 (s,18H,2CMe_3); 2.35 (s,6H,2CH_3); 6.92 (m,4H, β-CH,pic); 8.68 (m,4H,α-CH,pic)	21.4 (Me,pic); 31.2 (Me_3); 67.5 (NC), ^{183}W satellites at 66.5 and 68.5, $^2J_{WC}$ = 14.8 Hz; 124.9 (β-CH,pic); 148.8 (*ipso*-C,pic); 151.1 (α-CH,pic)
$[W(NCMe_3)_2Cl_2(bipy)]$ (7)	1.58 (s,18H,2CMe_3); 7.08–7.64 (m,2H,γ-CH,bipy); 7.64–8.00 (m,4H,β-CH,bipy); 9.75 (d,2H,α-CH, bipy)	32.0 (Me_3); 67.8 (NC), ^{183}W satellites at 66.8 and 68.8, $^2J_{WC}$ = 14.4 Hz; 122.0 and 125.9 (β-CH,bipy); 139.4 (α-CH,bipy); 150.6 (*ipso*-C,bipy); 152.5 (α-CH,bipy)
$[W(NCMe_3)_2Cl_2(tmed)]$ (8)	1.38 (s,18H,2CMe_3); 2.60 (s,4H,2CH_2); 2.68 (s,12H,4Me)	31.4 (Me_3); 51.0 (Me); 57.5 (CH_2); 67.3 (NC), ^{183}W satellites at 66.3 and 68.3, $^2J_{WC}$ = 15.4 Hz
$[W(NCMe_3)(\mu\text{-}NCMe_3)Cl_2(PMe_3)]_2$ (9)	1.38 (s,18H,2CMe_3); 1.64 and 1.86 (d,$^2J_{PH}$ = 11 Hz, 9H,PMe_3)	15.4 and 17.8 (d,$^1J_{PC}$ = 35.4 Hz,PMe_3); 31.8 and 31.9 (Me_3); 69.5 and 69.6 (NC), ^{183}W satellites at 68.7 and 70.5, 68.7 and 70.4, $^2J_{WC}$ = 13.7 Hz
$[W(NCMe_3)(\mu\text{-}NCMe_3)Cl_2(PMePh_2)]_2$ (10)	1.30 (s,18H,2CMe_3); 1.08 and 1.34 (d,$^2J_{PH}$ = 9.6 Hz, 3H,PMe); 7.20–8.00 (m,10H,2Ph)	15.7 and 18.0 (d,$^1J_{PC}$ = 34.2 Hz,PMe); 31.4 and 31.5 (Me_3); 70.2 and 70.3 (NC), ^{183}W satellites at 69.3 and 71.0, 69.4 and 71.1, $^2J_{WC}$ = 12.8 Hz; 128.2, 128.9, 129.6, 131.3, 131.3, 132.9 and 133.6 (PPh_2)
$[W(NCMe_3)(\mu\text{-}NCMe_3)Cl_2(CNCMe_3)]_2$ (11)	1.38 (s,18H,2CMe_3); 1.55 (s,9H,CMe_3)	29.4 (Me_3,isocyanide); 31.8 (Me_3,*t*-butylimido); 59.9 (NC isocyanide); 70.0 (NC), ^{183}W satellites at 69.1 and 70.8, $^2J_{WC}$ = 12.9 Hz; (N≡C, not observed)
$[W(NCMe_3)_2(NHCMe_3)_2]$ (12)	1.19 and 1.33 (2s,36H,4CMe_3); 5.10 (bs,2H,2NH)	33.5 (Me_3); 53.0 (NHC); 65.6 (NC), ^{183}W satellites at 64.7 and 66.6. $^2J_{WC}$ = 14.4 Hz
$[W(NCMe_3)_2(OEt)_2]_x$ (13)	1.10–1.78 (m,18H,2CMe_3,2Me); 4.40–5.22 (q,4H,2CH_2)	19.0 (Me); 32.9, 32.4 (Me_3); 66.3 (NC); 72.2 (OCH_2)

[a] Spectra obtained in $CDCl_3$.
[b] b = broad, d = doublet, m = multiplet, s = singlet.
[c] Assignments for bipy and γ-pic made by comparison with free ligand.
[d] Also contains $[W(NCMe_3)Cl_4(NH_2CMe_3)]\cdot\frac{1}{6}C_6H_6$ (2).
[e] Minor component.

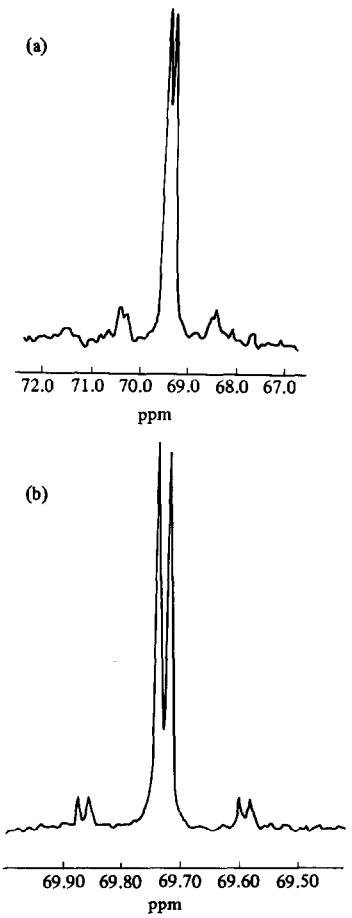

Fig. 1. The *t*-butylimido quaternary carbon resonance in the $^{13}C[^1H]$ NMR spectrum of $[W(NCMe_3)(\mu\text{-}NCMe_3)Cl_2(PMe_3)]_2$ showing coupling to ^{31}P and ^{183}W. (a) 15.04 MHz. (b) 100.61 MHz.

give rise to $[W(NCMe_3)_2Cl_2(dppe)]$ in which at least one phosphorus must lie *trans* to an imido function but the reaction fails to produce an isolatable product.

In a further investigation of the effect of a strong σ-donor, $[W(NCMe_3)(\mu\text{-}NCMe_3)Cl_2(NH_2CMe_3)]_2$ (4) was reacted with four equivalents of *t*-butylisocyanide which gave the complex $[W(NCMe_3)_2Cl_2(CNCMe_3)]_2$ (11). The ^{13}C NMR spectrum showed the methyl group and quaternary carbons of the *t*-butylimido ligands each as single resonances while the IR spectrum again indicated *cis* chlorides. A structure similar to (d) (L = Me_3CNC) is thus preferred for this complex.

$[W(NCMe_3)(\mu\text{-}NCMe_3)Cl_2(NH_2CMe_3)]_2$ (4) does not react further with $Me_3SiNHCMe_3$ but with eight equivalents of *t*-butylamine in petroleum ether, it rapidly dissolves forming four equivalents of Me_3CNH_3Cl and the colourless *bis*-imido-*bis*-amido complex $[W(NCMe_3)_2(NHCMe_3)_2]$ (12).* The ^1H NMR spectrum shows two equal intensity singlets for the *t*-butyl methyl protons while the amido NH protons occur as a broad peak near 5 ppm.[7] In the ^{13}C NMR spectrum the methyl group carbons appear as two distinct singlets and the *t*-butylimido and amido quaternaries appear at 65.6 and 53.0 ppm which are at significantly higher field than usually found for these ligands.

In particular the amido quaternary resonance is found in the region of the *t*-butylamine quaternary of $[W(NCMe_3)(\mu\text{-}NCMe_3)_2Cl_2(NH_2CMe_3)]_2$ (4). These features are apparently a consequence of the unusual geometry that must exist in the molecule. To obtain an 18-electron count, π-bonding is necessary from three nitrogen atoms. As imido and amido ligands possess strong *trans* influencing properties, a mutually *trans* configuration of ligands will not be preferred so that a tetrahedral structure is likely, for which canonicals such as (e) and (f) are needed to maximize the electron count. The coordination geometry involved is apparently stable only for bulky *t*-butyl groups as reactions of $[W(NCMe_3)(\mu\text{-}NCMe_3)Cl_2(NH_2CMe_3)]_2$ (4) or WCl_6 with Me_2CHNH_2 or $EtNH_2$ produce intractable gums.

Attempts to force further proton transfer within the molecule to give a *tris*-*t*-butylimido complex have so far been unsuccessful. $[W(NCMe_3)_2(NHCMe_3)_2]$ (12) remains unchanged after prolonged refluxing in benzene and ligands such as PMe_3 or 4-picoline have no effect. Addition of excess *t*-butylamine gives a dark-brown solution consisting of starting complex and some intractable material.

The chloro ligands of $[W(NCMe_3)(\mu\text{-}NCMe_3)Cl_2(NH_2CMe_3)]_2$ (4) may also be replaced by alkoxides. Reaction of the complex with four equivalents of EtOH in the presence of four equivalents of *t*-butylamine[19] produces Me_3CNH_3Cl and a colorless oil which was identified as $[W(NCMe_3)_2(OEt)_2]_x$ (13) on the basis of the correct methylene to methyl group ratio in the ^1H NMR spectrum while the ^{13}C NMR spectrum contained resonances characteristic of the *t*-butylimido group and ethoxide ligands.[20] In a similar reaction, Me_3COH and $[W(NCMe_3)_2(NHCMe_2)_2]$ have been reported[7] to give $[W(NCMe_3)_2(OCMe_3)_2]$ as a colourless oil.

It was also of interest to prepare complexes containing both oxo and *t*-butylimido ligands in view of the identification of these groups by X-ray crystallography in the trimeric complex $[W(NPh)(\mu\text{-}O)Me_2(PMe_3)]_3$.[18] When benzene solutions of

* This complex was first prepared by Nugent and Haymore by a reaction of WCl_6 with 12 equivalents of *t*-butylamine in petroleum ether.[7] A preliminary X-ray crystal structure determination showed a monomeric molecule but no further structural details have yet been reported.

$WOCl_4$ were reacted with two equivalents of $Me_3SiNHCMe_3$ or four equivalents of Me_3CNH_2, yellow non-crystalline products were obtained which have so far not been fully characterized. The ^{13}C NMR spectra show the presence of both *t*-butylimido and amine quaternary carbons while the IR spectra show vibrations in the vicinity of 800 cm^{-1} which are characteristic of W–O–W bonds.[21] The combined data suggest the presence of $[WO(NCMe_3)Cl_2(NH_2CMe_3)]_x$ but reaction of the material with bipy under reflux produced $[W(NCMe_3)_2Cl_2(bipy)]$ (7) and various as yet unidentified oxo complexes. Thus, if the $WO(NCMe_3)$ moiety is formed in the initial reaction, oxo-imido exchange must occur under the synthetic conditions to give the observed products.

EXPERIMENTAL

All preparations and manipulations were carried out under dry oxygen-free nitrogen using standard bench-top air-sensitive techniques.[22] *N*(trimethylsilyl)-*t*-butylamine was prepared by treating chlorotrimethylsilane with two equivalents of *t*-butylamine and distilling the product.[23] *t*-Butylamine, 4-picoline and *N,N,N′,N′*-tetramethylethylenediamine were dried over and distilled from calcium hydride. Absolute ethanol was distilled from magnesium ethoxide. Trimethylphosphine was prepared by a literature method[24] and tungsten hexachloride was sublimed prior to use. Petroleum ether (B.p. range 40–60°), toluene and benzene were distilled from sodium wire. Infrared spectra were recorded on a Perkin–Elmer 597 spectrometer as Nujol mulls between CsI plates, ^1H NMR spectra on a Varian T60 model spectrometer and ^{13}C NMR spectra on Jeol FX60 and Bruker AM400 spectrometers. Analytical data were obtained by Prof. A. D. Campbell and Associates, University of Otago, New Zealand. Melting points were determined in sealed tubes under N_2 on an electrothermal melting point apparatus and are uncorrected.

bis-t-*Butylamidotetrachlorotungsten(VI)* (**1**) *and* t - *butylamine* - t - *butylimidotetrachlorotungsten(VI)* (**2**)

N(trimethylsilyl)-*t*-butylamine (1.4 cm^3, 7.2 mmol) in benzene (40 cm^3) was added to tungsten hexachloride (1.4 g, 3.5 mmol) dissolved in benzene (70 cm^3) and the mixture was stirred for 24 h. The yellow solution was filtered and the solvent removed to give a flaky yellow material which was washed with petroleum ether and ground up until a yellow powder was formed. Yield: 1.5 g (88%).

IR (Nujol) bands at 3350m, 3100s, 1585m, 1455s, 1398m, 1360s, 1290m, 1250s, 1210s, 1160m, 1050w, 1022w, 960m, 840s, 815s, 795s, 750s, 720s, 675s, 565m, 440m, 320s cm^{-1}.

Tetrachloro - iso - *propylamine* - iso - *propylimidotungsten(VI)* (**3**)

N(trimethylsilyl)-*iso*-propylamine (2.2 cm^3, 12.3 mmol) in benzene (30 cm^3) was added to tungsten hexachloride (1.2 g, 3.0 mmol) dissolved in benzene (100 cm^3) and the mixture was stirred for 14 h. The solution was filtered and the purple product washed with petroleum ether (50 cm^3) and dried *in vacuo*. Yield: 0.6 g (46%).

IR (Nujol) bands at 3350s, 3140s, 1562s, 1458s, 1390m, 1345m, 1320w, 1200s, 1155m, 1120w, 970s, 935m, 920w, 890w, 840w, 790w, 770w, 722m, 600w, 450w, 390m, 320m, 295s cm^{-1}.

bis - t - *Butylaminebis* - t - *butylimidobis*(μ - t - *butylimido*)*tetrachloroditungsten(VI)* (**4**)

(a) *N*(trimethylsilyl)-*t*-butylamine (8.9 cm^3, 46.0 mmol) in benzene (100 cm^3) was added to tungsten hexachloride (4.5 g, 11.4 mmol) dissolved in benzene (140 cm^3) and the mixture was stirred for 20–24 h. The pale green solution was filtered and the solvent volume reduced (ca. 10 cm^3) until a large mass of crystalline material formed. The product was filtered, washed with chilled benzene (5–10 cm^3 portions) until the filtrate was no longer coloured light green, and dried *in vacuo*. The filtrates and mother liquor were combined and the solvent volume again reduced. On standing for several hours, further product crystallized which was washed with chilled benzene (5 cm^3 portions) as before. Overall yield 3.74 g (71%). The complex is sufficiently pure for further use but analytically pure material is obtained by recrystallization from benzene.

IR (Nujol) bands at 3275w, 3155m, 3080m, 2690w, 2580w, 2490w, 2050w, 1600w, 1458m, 1505w, 1390m, 1350s, 1270s, 1250s, 1200s, 1175s, 1127m, 1022w, 924w, 890m, 840w, 802m, 748m, 720m, 692w, 602m, 580w, 555w, 478w, 450w, 420w, 375w, 350w, 310s, 280w cm^{-1}.

(b) *t*-Butylamine (4.8 cm^3, 45.7 mmol) in benzene (50 cm^3) was added to tungsten hexachloride (2.6 g, 6.56 mmol) in benzene (100 cm^3) and the mixture was stirred for 2 h. The light yellow solution was filtered from the precipitate of *t*-butylamine hydrochloride (approx. 3.2 g) and the solvent volume reduced to ca. 5–10 cm^3 whereupon the complex crystallized as yellow prisms. The product was filtered, washed with petroleum ether (10 cm^3) and dried *in vacuo*. Yield: 1.4 g (47%). [Found: C, 30.2;

H, 6.3; N, 9.1. $C_{24}H_{54}Cl_4N_6W_2$ requires C, 30.8; H, 5.8; N, 9.0.] The complex had identical m.p., IR, ^1H and $^{13}C[^1H]$ NMR spectrum to that prepared under (a).

bis - t - *Butylimidobis*(μ - t - *butylimido*)*tetrachlorobis*(4 - *picoline*)*ditungsten(VI)* (**5**)

4-Picoline (0.4 g, 4.2 mmol) in benzene (25 cm^3) was added to *bis-t*-butylaminebis-*t*-butylimidobis (μ-*t*-butylimido)tetrachloroditungsten(VI) (0.9 g, 0.96 mmol) in benzene (50 cm^3) and the mixture was stirred for 2 h. The solution was filtered, the volume reduced and on standing for several weeks a single large crystal of the complex formed.

IR (Nujol) bands at 1600m, 1508m, 1498m, 1398m, 1360s, 1300m, 1270m, 1220s, 1210s, 1138w, 1064m, 1035m, 945m, 880m, 818s, 720s, 585m, 552w, 518w, 498w, 450m, 350w, 322m, 299w, 280w cm^{-1}.

bis - t - *Butylimidodichlorobis*(4 - *picoline*)*tungsten(VI)* (**6**)

4-Picoline (0.5 g, 5.4 mmol) in benzene (30 cm^3) was added to *bis-t*-butylaminebis-*t*-butylimidobis (μ-*t*-butylimido)tetrachloroditungsten(VI) (1.0 g, 1.1 mmol) in benzene (50 cm^3) and the mixture was refluxed for 2 h. The solution was filtered and the solvent removed to give a yellow–green solid which was washed with petroleum ether (40 cm^3) and dried *in vacuo*. Crude yield 1.1 g (89%). The complex was dissolved in toluene (30 cm^3), the solution filtered and the volume reduced to ca. 5 cm^3. On standing at −20° the complex formed as yellow crystals. The product was always surface contaminated with small amounts of a colourless solid and was thus characterized by NMR spectroscopy (Table 2). M.p. (pure crystal) 148°C.

IR (Nujol) bands at 1600m, 1495m, 1395m, 1350s, 1290s, 1250s, 1205s, 1080s, 1015s, 950m, 850m, 800s, 722m, 660m, 590w, 492m, 480m, 445m, 383m, 242m, 200w cm^{-1}.

(2,2-*bipyridyl*)bis-t-*Butylimidodichlorotungsten(VI)* (**7**)

(a) 2,2′-bipyridyl (0.2 g, 1.3 mmol) in benzene (40 cm^3) was added to *bis-t*-butylaminebis-*t*-butylimidobis(μ-*t*-butylimido)tetrachloroditungsten(VI) (0.6 g, 0.64 mmol) in benzene (60 cm^3) and the mixture was refluxed for 30 min. The solution was filtered and the solvent removed to give a light-yellow solid which was extracted with benzene (40 cm^3). The solution was filtered and the volume reduced until the product began to crystallize. The solution was heated until all the solid dissolved and on standing large yellow prisms of the complex formed. Yield: 0.58 g (82%).

IR (Nujol) bands at 1595s, 1560w, 1490w, 1350s, 1308m, 1272s, 1235s, 1210s, 1170w, 1155w, 1135w, 1104w, 1055w, 1042w, 1020m, 970w, 902w, 890w, 800w, 764s, 730s, 650m, 626m, 590m, 564w, 470w, 412w, 355w, 305s cm^{-1}.

(b) *t*-Butylamine (2.15 cm^3, 20.5 mmol) in benzene (30 cm^3) was added to tungstenoxytetrachloride (1.75 g, 5.1 mmol) suspended in benzene (80 cm^3) and mixture was stirred for 3 h. The solution was filtered and the solvent removed to give a yellow solid.

IR (Nujol) bands at 3150m, 3050m, 2700m, 2580m, 2490w, 1604w, 1560w, 1508w, 1396m, 1340s, 1260s, 1210s, 1140w, 1024w, 905w, 835bs, 790bs, 720bs, 675s, 590m, 520m, 450w, 378w, 348w, 295bm cm^{-1}.

^1H NMR $\delta(CDCl_3)$ 1.22–1.65 (several s, CMe_3). ^{13}C NMR $\delta(CDCl_3)$ 30.2, 31.3, 32.2, 33.2 (Me_3); 52.0, 54.0 (NH_2C); broad resonance centred at 60.7 (NHC); broad resonance centred at 70.1 (NC).

The yellow solid (0.9 g) was dissolved in benzene (30 cm^3) and 2,2′-bipyridyl (0.35 g) in benzene (70 cm^3) added. The mixture was refluxed for 2 h, the solution filtered and the solvent removed to give a light-yellow crystalline solid which was washed with warm petroleum ether (50 cm^3) to remove excess 2,2′-bipyridyl. Recrystallization from benzene gave the complex as yellow crystals. [Found: C, 39.2; H, 4.7; N, 10.2. $C_{18}H_{26}Cl_2N_4W$ requires C, 39.1; H, 4.7; N, 10.1.] The complex had identical m.p., IR and NMR spectra to the sample prepared under (a).

(c) *N*(trimethylsilyl)-*t*-butylamine (1.4 cm^3, 7.2 mmol) in benzene (30 cm^3) was added to a suspension of tungsten oxytetrachloride (1.2 g, 3.5 mmol) in benzene (80 cm^3) and the mixture was stirred for 3 h. The solution was filtered and the solvent removed to give a yellow solid. The IR spectrum was similar to the product prepared under (b). ^1H NMR $\delta(CDCl_3)$ 1.20–1.60 (several s, CMe_3); 2.80 and 4.22 (b, NH). ^{13}C NMR $\delta(CDCl_3)$ 30.2, 30.9, 31.3 (Me_3); 52.7, 53.4, 54.6 (NH_2C); 68.1, 69.1, 70.5, 71.5 (NC).

The product (1.3 g) was dissolved in benzene (50 cm^3), 2,2′-bipyridyl (0.5 g) in benzene (30 cm^3) added and the mixture refluxed for 3 h. The solution was filtered, the solvent removed *in vacuo* and the resulting light-yellow solid washed with warm petroleum ether (50 cm^3) to remove excess 2,2′-bipyridyl. The solid was dissolved in hot toluene (20 cm^3), the solution filtered while hot and the volume reduced. On standing for several hours yellow crystals of the complex were formed which were filtered, washed with petroleum ether and dried *in vacuo*.

The product had identical m.p., IR and NMR spectra to the sample prepared under (a).

bis - t - *Butylimidodichloro*(N,N,N′,N′ - *tetramethylethylenediamine*)*tungsten*(*VI*) **(8)**

N,N,N′,N′-tetramethylethylenediamine (0.3 g, 2.6 mmol) in benzene (40 cm^3) was added to *bis-t*-butylaminebis - *t* - butylimidobis(μ - *t* - butylimido) tetrachloroditungsten(VI) (0.9 g, 1.0 mmol) in benzene (60 cm^3) and mixture was refluxed for 2 h. The solution was filtered and the solvent removed to give a colourless crystalline solid. Crude yield 0.7 g (92%). The product was extracted with petroleum ether (40 cm^3), the solution filtered and volume reduced to ca. 5 cm^3. On standing at $-20°$ the complex formed as colourless crystals.

IR (Nujol) bands at 2700w, 2590w, 2500w, 2075w, 1610w, 1510m, 1400m, 1350m, 1300m, 1284m, 1260m, 1244s, 1216s, 1118w, 1095w, 1065w, 1040w, 1032w, 1019m, 958s, 880s, 800s, 775m, 725s, 680m, 590w, 505w, 480w, 452s, 422w, 350s, 310s cm^{-1}.

bis - t - *Butylimidobis*(μ - t - *butylimido*)*tetrachlorobis*(*trimethylphosphine*)*ditungsten*(*VI*) **(9)**

Trimethylphosphine (0.4 cm^3, 3.6 mmol) was added to *bis-t*-butylaminebis-*t*-butylimidobis(μ-*t*-butylimido)tetrachloroditungsten(VI) (0.8 g, 0.86 mmol) in benzene (50 cm^3) and the mixture was stirred for 3 h. The solution was filtered, the solvent removed and the colourless crystalline solid washed with several portions of petroleum ether (10 cm^3) and dried *in vacuo*. Yield: 0.8 g (98%).

IR (Nujol) bands at 3010w, 2700w, 2590w, 2495w, 2060w, 1504w, 1410m, 1395w, 1350s, 1300w, 1280m, 1270s, 1230s, 1204s, 1132w, 964s, 850w, 802w, 745m, 720w, 580w, 464w, 450w, 344w, 318m, 280m, 260w cm^{-1}

bis - t - *Butylimidobis*(μ - t - *butylimido*)*tetrachlorobis*(*diphenylmethylphosphine*)*ditungsten*(*VI*) **(10)**

Diphenylmethyl phosphine (0.4 cm^3, 2.2 mmol) in benzene (50 cm^3) was added to *bis-t*-butylaminebis - *t* - butylimidobis(μ - *t* - butylimido)tetrachloroditungsten(VI) (0.9 g, 0.96 mmol) in benzene (50 cm^3) and the mixture was stirred for 3 h. The solution was filtered and the solvent removed to give the product as a colourless oil which solidified on washing with petroleum ether and drying *in vacuo*. Crude yield 1.1 g (96%). The complex was dissolved in toluene, the solution filtered and the volume reduced to ca. 5 cm^3. On standing at $-20°$ large pale green crystals of the complex were formed.

IR (Nujol) bands at 1600w, 1580w, 1508w, 1400w, 1360s, 1300w, 1268m, 1230m, 1208m, 1135w, 1100m, 1065w, 1022w, 995w, 960w, 880m, 840w, 800w, 740s, 720m, 695s, 594w, 505m, 480w, 450w, 318m, 285m cm^{-1}.

bis - t - *Butylimidobis*(μ - t - *butylimido*)bis - t - *butyl*-iso-*cyanidetetrachloroditungsten*(*VI*) **(11)**

t-Butylisocyanide (0.5 cm^3, 4.4 mmol) in benzene (30 cm^3) was added to *bis-t*-butylaminebis-*t*-butylimidobis(μ-*t*-butylimido)tetrachloroditungsten(VI) (0.8 g, 0.8 mmol) and the mixture was refluxed for 1 h. The solution was filtered, the solvent removed and the crystalline residue washed with petroleum ether (50 cm^3). Crude yield 0.7 g (91%). The solid was dissolved in toluene (30 cm^3), the volume reduced to ca. 5 cm^3 and on standing at $-20°$ yellow crystals of the complex were formed which were filtered, washed with petroleum ether (20 cm^3) and dried *in vacuo*.

IR (Nujol) bands at 2248s, 1464s, 1408w, 1364s, 1282s, 1242s, 1220s, 1200s, 1160m, 1142m, 1052w, 1034w, 980w, 945w, 890w, 852m, 812m, 740m, 728s, 604s, 560w, 538w, 478w, 460w, 400w, 385w, 340s, 300s, 272w cm^{-1}.

bis - t - *Butylamidobis* - t - *butylimidotungsten*(*VI*)[7] **(12)**

t-Butylamine (1.3 cm^3, 12.4 mmol) in petroleum ether (40 cm^3) was slowly added to *bis-t*-butylaminobis - *t* - butylimidobis(μ - *t* - butylimido)tetrachloroditungsten(VI) (1.4 g, 1.5 mmol) suspended in petroleum ether (60 cm^3) and the mixture was stirred for 3 h. The solution was filtered and the solvent removed to give the complex as a colourless solid tinged green with a small amount of impurity. Crude yield 1.2 g (85%). The complex was dissolved in petroleum ether (25 cm^3) and the volume reduced to ca. 10 cm^3. On standing at $-76°$ the complex crystallized as prisms which were washed with petroleum ether (10 cm^3) cooled to $-76°$ and dried *in vacuo*.

IR (Nujol) bands at 3150m, 3050m, 2700m, 2640m, 2500m, 1600w, 1562w, 1525w, 1392m, 1345s, 1255m, 1205m, 1020m, 930w, 835s, 805s, 725s, 595m, 450m, 275w, 250m cm^{-1}.

bis-t-*Butylimidobisethoxytungsten*(*VI*) **(13)**

Ethanol (0.15 cm^3, 2.6 mmol) and *t*-butylamine (0.26 cm^3, 2.6 mmol) in petroleum ether (40 cm^3) were added slowly to *bis-t*-butylaminebis-*t*-butyl-

imidobis(μ-*t*-butylimido)tetrachloroditungsten(VI) (0.6 g, 1.3 mmol) suspended in petroleum ether (80 cm^3) and the mixture was stirred for 4 h. The colourless solution was filtered and the solvent removed to give the product as an oil which failed to crystallize. Yield: 0.42 g (80%).

IR (smear) bands at 1435s, 1345s, 1265s, 1208m, 1140m, 1095s, 1050s, 1025s, 950m, 905s, 878s, 840m, 804m, 720m, 550s, 510s, 445w, 372w cm^{-1}.

Acknowledgement—The assistance of Dr J. M. Coddington in running the high field NMR spectra is gratefully acknowledged.

REFERENCES

1. W. A. Nugent and B. L. Haymore, *Coord. Chem. Rev.* 1980, **31**, 123.
2. W. P. Griffith, *Coord. Chem. Rev.* 1970, **5**, 459.
3. B. R. Ashcroft, A. J. Nielson, D. C. Bradley, R. J. Errington, M. B. Hursthouse and R. L. Short, *J. Chem. Soc., Dalton Trans.* in press.
4. D. C. Bradley, R. J. Errington, M. B. Hursthouse, R. L. Short, B. R. Achcroft, G. R. Clark, A. J. Nielson and C. E. F. Rickard, *J. Chem. Soc., Dalton Trans.* in press.
5. D. C. Bradley, M. B. Hursthouse, K. M. A. Malik, A. J. Nielson and R. L. Short, *J. Chem. Soc., Dalton Trans.* 1983, 2651.
6. D. L. Thorn, W. A. Nugent and B. L. Harlow, *J. Am. Chem. Soc.* 1981, **103**, 357.
7. W. A. Nugent and R. L. Harlow, *Inorg. Chem.* 1980, **19**, 777.
8. D. M.-T. Chan, W. C. Fultz, W. A. Nugent, D. C. Roe and T. H. Tulip, *J. Am. Chem. Soc.* 1985, **107**, 251.
9. T. C. Jones, A. J. Nielson and C. E. F. Rickard, *J. Chem. Soc., Chem. Commun.* 1984, 205; P. A. Bates, A. J. Nielson and J. M. Waters, *Polyhedron* 1985, **4**, 1391.
10. D. C. Bradley, R. J. Errington, M. B. Hursthouse, A. J. Nielson and R. L. Short, *Polyhedron* 1983, **2**, 843.
11. K. Nakamoto, *Infrared and Raman Spectra of Inorganic and Co-ordination Compounds*, 3rd edn, p. 317. John Wiley, New York (1978).
12. M. H. Chisholm, J. C. Huffman and L. S. Tan, *Inorg. Chem.* 1981, **20**, 1859.
13. T. G. Appleton, H. C. Clark and L. E. Manzer, *Coord. Chem. Rev.* 1973, **10**, 335.
14. B. L. Haymore, E. A. Maatta and R. A. D. Wentworth, *J. Am. Chem. Soc.* 1979, **101**, 2063.
15. G. R. Clark, A. J. Nielson and C. E. F. Rickard, unpublished results.
16. L. M. Jackman and S. Sternhell, *Applications of Nuclear Magnetic Resonance Spectroscopy in Organic Chemistry*, 2nd edn, p. 314. Pergamon Press, Oxford (1969).
17. A. J. Nielson and J. M. Waters, *Aust. J. Chem.* 1983, **36**, 243.
18. D. C. Bradley, M. B. Hursthouse, K. M. A. Malik and A. J. Nielson, *J. Chem. Soc., Chem. Commun.* 1981, 104.
19. A. J. Nielson, J. M. Waters and D. C. Bradley, *Polyhedron* 1985, **2**, 285.
20. P. A. Bates, A. J. Nielson and J. M. Waters, *Polyhedron*, 1987, **6**, 163.
21. C. G. Barraclough and J. Stals, *Aust. J. Chem.* 1966, **19**, 741.
22. A. J. Nielson, *Chem. In N.Z.* 1985, **49**, 11.
23. R. M. Pike, *J. Org. Chem.* 1961, **26**, 232 and refs therein.
24. W. Wolfsberger and H. Schmidbaur, *Synth. React. Inorg. Metal-Org. Chem.* 1974, **4**, 149.

Polyhedron Vol. 6, No. 8, pp. 1669–1672, 1987
Printed in Great Britain

0277–5387/87 $3.00+.00

ESR STUDIES ON THE SOLUTIONS OF Cu(II) COMPLEXES WITH TRICOORDINATE SCHIFF BASES DERIVED FROM AMINOACIDS

JULIA JEZIERSKA

Institute of Chemistry, Wrocław University, Wrocław, Poland

(*Received* 26 *September* 1986; *accepted after revision* 23 *February* 1987)

Abstract—Cu(II) complexes with salicylaldimines derived from the following aminoacids: glycine, α-alanine, β-alanine, serine, tyrosine, tryptophane, arginine, ornithine, histidine have been studied by the ESR method. On the basis of room temperature and frozen solution ESR spectra the formation of two types of the adducts have been established. The influence of additional functional groups of aminoacids on adduct formation has been found.

As follows from the literature presented by Wagner and Walker,[1] metal complexes of tridentate Schiff base ligands composed of salicylaldehyde and aminoacids (sal-aminoac), the model systems to investigate the enzymatic reaction of pyridoxal phosphate, have been extensively studied during the last few years.

X-ray analysis of the solids of Cu(sal-aminoac) complexes revealed that the compounds tend to coordinate via phenolic oxygen, one carboxylic oxygen and the imino nitrogen with a water molecule completing the near square planar coordination of Cu(II) ion.[2,3] The same equatorial position of a solvent molecule was postulated for Cu(II) salicylaldimines derived from glycine, α-alanine, phenylglycine, ε-acetyl-lysine and histidine on the basis of ESR of frozen solutions as well as room temperature spectroscopic and titration data.[1,4]

Our own studies of polymeric Cu(II) complexes with tricoordinate Schiff bases[5] indicated that the fourth coordination position taken in the solids by a bridging oxygen atom is replaced in the solutions by the solvent molecule L coordinating via an oxygen or nitrogen atom at a non-equatorial position. Only under specific conditions, when a small amount of a ligand L_1 able to coordinate via nitrogen is added to the solutions of the complexes in oxygen coordinating solvent L, the ligand L_1 binds at equatorial chelate plane. Hence, it is interesting to find out whether or not the tricoordinate character of sal-aminoac ligand would determine the formation of the adducts of Cu(sal-aminoac) in the solutions of a symmetry similar to that stated for the polymeric Cu(II) tridentate Schiff base complexes. Furthermore, the ESR studies presented here show the influence of the aminoacid residues of histidine, ornithine, tyrosine and tryptophane, their additional donor ability or bulky effects on the formation of the adducts of Cu(sal-aminoac).

EXPERIMENTAL

Cu(II) complexes with ligands derived from salicylaldehyde and aminoacids were synthesized according to a general method used by Wagner and Walker.[1] The following aminoacids were used for syntheses: glycine, L-α-alanine, β-alanine, L-serine, L-tyrosine, L-tryptophane, L-arginine, L-ornithine, L-histidine. The elemental analysis for copper, carbon, nitrogen and hydrogen confirms the formation of Cu(II) complexes with tricoordinate Schiff bases formulae: Cu(sal-glycine)·$1\frac{1}{2}H_2O$, Cu(sal-α-alanine)·$2H_2O$, Cu(sal-β-alanine)·H_2O, Cu(sal-serine)·$2H_2O$, Cu(sal-tyrosine)·H_2O, Cu(sal-ornithine)·$1\frac{1}{2}H_2O$, Cu(sal-arginine)·$2H_2O$, Cu(sal-histidine)·$1\frac{1}{2}H_2O$.

The solvents were purified according to the methods described previously.[6] The ESR spectra of liquid solutions of Cu(sal-histidine) appear to be resolved due to copper hyperfine splitting for the concentration of water in dioxan not smaller than 50%. The concentration of pyridine L_1 added as the admixture to oxygen coordinating solvents L is about 0.01 M. The ESR spectra were recorded on

JEOL JES ME X-band spectrometer using a nuclear magnetometer MJ 110R and microwave frequency meter JES-SH-30X.

RESULTS AND DISCUSSION

The complexes presented in Table 1, derived from the following aminoacids: glycine, α-alanine, β-alanine, serine, tyrosine exhibit similar behaviour in the solutions. The same, three-line pattern of syperhyperfine splitting due to one ^{14}N atom bound to copper (of the magnitude between 12–14 G) is observed in the room temperature ESR spectra when the complexes are dissolved in both oxygen or nitrogen coordinating solvents (Fig. 1). This implies, that only the imine nitrogen atom is involved in the superhyperfine interaction with the unpaired electron of the Cu(II) in the xy plane. Consequently, it becomes evident, that in the Cu(sal-aminoac)L adduct (type I), the solvent molecule L occupying the fourth coordinating position is not coplanar with the chelate ring composed of carboxylate oxygen, imine nitrogen and phenolic oxygen.

When a small amount (about 0.01 M) of pyridine is added to all five complexes in oxygen coordinating solvents L, the characteristic change of ESR parameters (decrease of g_{iso} about 0.01 and increase of $|A_{iso}|$ about 6 G) is observed (Table 1, Fig. 1).

According to our studies on tricoordinate Schiff base complexes[5] the new set of ESR parameters

Table 1. ESR parameters for Cu(sal-aminoac) complexes in pure solvents (L) and after addition of pyridine (L_1) to the solution

Aminoacid	Solvent (L)	g_{iso}	A_{iso}	$g_{\parallel}$	$A_{\parallel}$	Pyridine (L_1) added[a] g_{iso}	A_{iso}	$g_{\parallel}$	$A_{\parallel}$
Glycine	3:2 diox–H_2O	2.132	76	2.266	186	2.122	80	2.250	184
	NMF	2.133	76	2.270	182	2.120	81	2.249	186
	DMSO	2.132	68	2.269	185	2.127	80	2.255	181
	pyridine	2.126	70	2.253	180				
α-Alanine	3:2 diox–H_2O	2.129	76	2.267	193	2.118	81	2.253	182
	NMF	2.128	74	2.272	184	2.120	79	2.249	189
	pyridine	2.126	71	2.252	183				
β-Alanine	3:2 diox–H_2O	2.132	72	2.277	186	2.128	77	2.264	178
	NMF	2.131	70	2.285	180	2.126	75	2.266	180
	pyridine	2.130	66	2.262	179				
Serine	3:2 diox–H_2O	2.127	75	2.264	189	2.120	80	2.242	186
	NMF	2.129	73	2.272	184	2.119	82	2.249	187
	pyridine	2.126	70	2.248	187				
Tyrosine	3:2 diox–H_2O	2.128	76	2.265	190	2.119	81	2.254	178
	NMF	2.125	73	2.270	183	2.120	80	2.252	181
	pyridine	2.128	71	2.253	178				
Histidine[b]	2:3 diox–H_2O	2.128	64	2.263	182	2.127	71	2.251	181
	pyridine	2.126	69	2.249	180				
Arginine	3:2 diox–H_2O	2.128	74	2.26	180	2.124	80	2.249	183
	NMF	2.122	76	2.269	188	2.120	79	2.255	185
	pyridine	2.125	66	2.258	175				
Ornithine	3:2 diox–H_2O	2.120	72	2.26	190	2.119	77	2.25	180
	NMF	2.114	66	2.269	184	2.118	73	2.249	186
	pyridine	2.125	64	2.25	180				
Tryptophane	3:2 diox–H_2O	2.113	69	2.260	188	2.110	72	2.251	188
	NMF	2.116	70	2.254	183	2.113	72	2.251	189
	pyridine	2.132	74	2.256	179				

Parameters A are given in 10^{-4} cm^{-1} units. A_{iso} and g_{iso} were measured at 295 K. $A_{\parallel}$ and $g_{\parallel}$ were measured at 150 K.

[a] [pyridine] = 0.01 M.

[b] No hyperfine splitting in NMF solution. diox = dioxane, NMF = N-methylformamide.

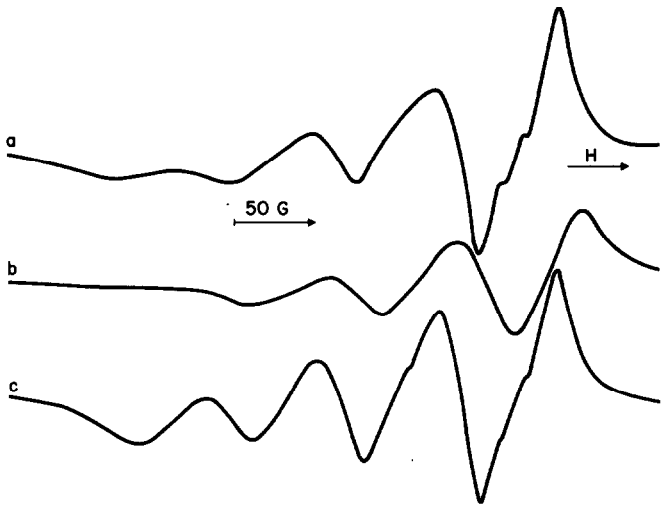

Fig. 1. ESR spectra of Cu(sal-glycine) at 295 K. (a) in 3:2 dioxane–H_2O (L), (b) after addition of L_1 = pyridine (0.01 M) to the 3:2 dioxane–H_2O (L) solution, (c) in pyridine (L).

obtained in this case is characteristic for pentacoordinate adducts. Hence, ESR results indicate the formation of the type II adducts with general formula [Cu(sal-aminoac)(L_1)L]; L_1 = pyridine coordinates probably at the fourth coordination position in the equatorial plane, whereas the oxygen coordinating solvent L transfers into the axial position. It is noteworthy, that type II adducts are formed even in the case of the complexes derived from serine and tyrosine. Thus, -OH and -C_6H_5-4-OH groups do not prevent the transition from type I to type II adducts.

Inspection of Table 1 reveals the considerable decrease of $|A_{iso}|$ and $|A_{\parallel}|$ and the increase of $g_{\parallel}$ for Cu(sal-β-alanine)L in comparison with Cu(sal-α-alanine)L. This trend is compatible with an increasing degree of tetrahedral distortion[7] and may be due to a greater deviation of the solvent molecule L from the chelate ring plane in Cu(sal-β-alanine)L. It is interesting to note other differences between α-alanine and β-alanine derivatives: e.g. contrary to the complex derived from α-alanine no transamination reaction was found in the complex derived from β-alanine which was attributed to the dissimilarities in the bond distances.[8]

The second series of complexes studied consists of Cu(II) salicylaldimines derived from aminoacids with additional functional groups: histidine, ornithine, arginine and tryptophane. The ESR properties (the superhyperfine splitting due to the ligand ^{14}N nucleus and ESR parameters) of the complexes dissolved in the O- or N-coordinating solvents are comparable with these stated for the former series of the compounds (Table 1, Fig. 2). Thus, the adducts of type I are formed for all the complexes.

The result confirms earlier studies[1] on the coordination mode of histidine in Cu(sal-histidine) indicating that the imidazole group is involved in axial interaction while the other three donor atoms are placed in the plane. Attempts to achieve the typical transition: adduct I → adduct II for these complexes results in the smaller effects in comparison with complexes of the former series and the observed changes of ESR parameters are diminished (see Table 1). One possible explanation is that the imidazole nitrogen of histidine and amine

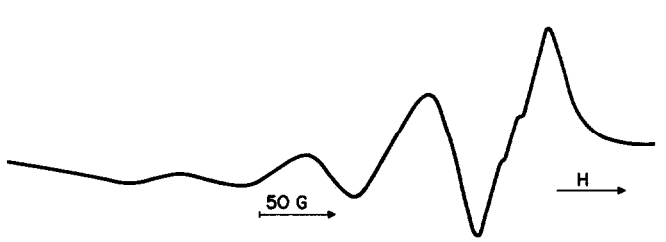

Fig. 2. ESR spectrum of Cu(sal-histidine) in pyridine (L) at 295 K.

nitrogen of ornithine or arginine coordinating at axial position block the lability of the coordination sphere of Cu(II) and hence the transition to type II adduct becomes less probable. In the case of Cu(sal-tryptophane) the indole nitrogen is not able to act as a donor and the observed effect is connected rather with steric hindrance of the bulky residue of the aminoacid.

Acknowledgement—This work was financially supported by the Polish Academy of Sciences.

REFERENCES

1. M. R. Wagner and F. A. Walker, *J. Am. Chem. Soc.* 1983, **22**, 3021.
2. T. Ueki, T. Ashida, Y. Sasada and M. Kakudo, *Acta Cryst.* 1967, **22**, 870.
3. T. Ueki, Y. Sasada and M. Kakudo, *Acta Cryst.* 1969, **B25**, 328.
4. L. A. Zyzyck, F. Frummer and J. F. Villa, *J. Inorg. Nucl. Chem.* 1975, **37**, 1653.
5. J. Jezierska, A. Jezierski, B. Jezowska-Trzebiatowska and A. Ozarowski, *Inorg. Chim. Acta* 1983, **68**, 7.
6. D. D. Perrin, W. L. F. Armarego and D. R. Perrin, *Purification of Laboratory Chemicals*, 2nd edn. Pergamon Press, Oxford (1982).
7. H. Yokoi and A. W. Addison, *Inorg. Chem.* 1977, **16**, 1341.
8. T. Ueki, T. Ashida, Y. Sasada and M. Kaguto, *Acta Cryst.* 1968, **B24**, 1361.

Polyhedron Vol. 6, No. 8, pp. 1673–1676, 1987
Printed in Great Britain

0277–5387/87 $3.00+.00

SYNTHESIS AND CHARACTERIZATION OF CHROMIUM AND TUNGSTEN TETRACARBONYL BOUND TO THE BRIDGING LIGAND 2,3-BIS(2-PYRIDYL)PYRAZINE (DPP)

R. R. RUMINSKI* and I. WALLACE

Department of Chemistry, University of Colorado at Colorado Springs, Colorado Springs, CO 80933-7150, U.S.A.

(*Received* 21 *January* 1987; *accepted* 27 *February* 1987)

Abstract—The synthesis, electronic absorption, infrared and ^{13}C NMR spectra, and electrochemistry of $[Cr(CO)_4]$dpp and $[W(CO)_4]$dpp (dpp = 2,3-bis(2-pyridyl)pyrazine) are reported. Electronic absorption spectra in different solvents show solvatochromic behavior and indicate the metal to ligand charge transfer (MLCT) excited state is lower in energy than the ligand field (LF) excited state. Electrochemical results show the $[Cr(CO)_4]$dpp complex undergoes semi-reversible one electron oxidation, while $[W(CO)_4]$dpp undergoes irreversible one electron oxidation. ^{13}C NMR spectra of both complexes show all carbons in the metal-bound dpp ring shift downfield. The amount of downfield shift for the series $[M(CO)_4]$dpp (M = Cr, Mo, W) is interpreted as indicating better M $d\pi \rightarrow$ dpp $p\pi^*$ back-bonding occurs for Mo and W than for Cr.

Our group has been interested in the preparation and characterization of transition metal complexes bound to nitrogen aromatic ligands, which are highly absorbing in the visible region of the spectrum and possess the ability to coordinate to remote metal centers and form polymetallic complexes.[1,2] Within these criteria, there have been several recent reports of $[M(CO)_4]L$ [M = Cr(0), Mo(0), W(0) and L = 2,2′-bipyrimidine (bpym), 2,5-bis(2-pyridyl)pyrazine (dppz), 3,6-bis(2-pyridyl) 1,2,4,5 tetrazine (dptz) and azo-2,2′-bipyridine (abpy)] type complexes.[3–6] Additionally, these metal complexes also serve as models in understanding the solvatochromic behavior of group 6 metal complexes.[6]

The dpp ligand serves as an effective bidentate ligand in either mono or bimetallic systems,[1,2,7] and the results of previous studies indicate that dpp is more effective at electronically communicating two bound metal centers than most monodentate bridges.[7–9] We report the syntheses and characterization of the highly absorbing $[Cr(CO)_4]$dpp and $[W(CO_4)]$dpp complexes. Electronic spectral, electrochemical and ^{13}C NMR comparisons within the $[M(CO)_4]$dpp (M = Cr, Mo, W) series and with other bridging ligands are presented.

* Author to whom correspondence should be addressed.

EXPERIMENTAL

Materials

$Cr(CO)_6$, $W(CO)_6$, 2,3-bis(2-pyridyl)pyrazine (dpp) and deuterated solvent used for ^{13}C NMR were obtained from Aldrich Chemicals. Other solvents were obtained from Fisher, and used without redistillation. Elemental analyses were performed by Atlantic Microlab, Atlanta, GA.

Instrumentation

Electronic absorption spectra were recorded on a Beckman Model 5240 Spectrophotometer with matching quartz cells.

Cyclic voltammograms were recorded on a Bio Analytic Systems CV-1B Cyclic Voltammograph with Hewlett Packard 7044A XY recorder. All potentials are reported vs. Ag/AgCl, and are uncorrected for junction potentials.

Proton-decoupled ^{13}C NMR were obtained on a Bruker Model WM-250 Fourier Transform NMR operating at 62.9 MHz. Samples were run in a 10.0 mm probe with 30% deuterated dichloromethane as an internal lock and reference (δ = 53.8 ppm).

Infrared spectra were recorded as solid KBr

samples on a Nicolet Model 20DX FTIR with a 1 cm^{-1} resolution.

Syntheses

[$W(CO)_4$]dpp. A mixture of 0.39 g (1.66 mmol) dpp and 0.63 g (1.79 mmol) $W(CO)_6$ in 30 cm^3 toluene was heated at reflux for 30 h under Ar in the dark. After cooling to room temperature, petroleum ether was added and the product refrigerated overnight. The crude red product was collected by filtration on a sintered glass filter funnel, washed with petroleum ether and air dried. The product was then dissolved on the funnel with CH_2Cl_2, and suction filtered. The liquid was loaded on a 25 × 2 cm diameter alumina column that had been washed with CH_2Cl_2. Red [$W(CO)_4$]dpp eluted slowly with CH_2Cl_2. The liquid was collected and rotary evaporated to dryness. The solid was then re-dissolved in CH_2Cl_2, and eluted again through a freshly prepared alumina column. The product was collected and dried as described above, and stored under vacuum in the dark. Yield 0.67 g (1.27 mmol; 76%). Found: C, 40.8; H, 1.9; N, 10.5. Calc. for $C_{18}H_{10}N_4O_4W$: C, 40.8; H, 1.9; N, 10.6%.

[$Cr(CO)_4$]dpp. A mixture of 0.20 g (0.76 mmol) dpp and 0.18 g (0.81 mmol) $Cr(CO)_6$ in 25 cm^3 of toluene was heated at reflux for 9 h under Ar in the dark. The product was precipitated, collected, purified and dried as described above. Yield 0.08 g (0.20 mmol, 27%). Found: C, 53.7; H, 2.6; N, 14.0. Calc. for $C_{22}H_{10}N_4O_4Cr$: C, 54.3; H, 2.5; N, 14.1%.

RESULTS AND DISCUSSION

The [$M(CO)_4$]dpp [M = Cr(0), W(0)] complexes are soluble in a variety of organic solvents, and the electronic spectral data are reported in Table 1. The electronic spectra of both complexes are characterized by highly absorbing ($\varepsilon > 1000\ M^{-1}\ cm^{-1}$) solvent dependent transitions in the visible region of the spectrum with less intense, higher energy solvent independent transitions. The lower energy absorption is similar in position, intensity and solvent dependent behavior with previously reported α-diimine [$M(CO)_4$] metal to ligand charge transfer (MLCT) transitions,[1,3–6,10,11] and by analogy, we assign the lowest energy absorptions of [$Cr(CO)_4$]dpp and [$W(CO)_4$]dpp as being MLCT transitions. The higher energy solvent independent absorptions of [$Cr(CO)_4$]dpp and [$W(CO)_4$]dpp complexes are similar in position and behavior with previously reported [$M(CO)_4$]bpym and [$M(CO)_4$]bpy ligand field absorptions,[5,6,10] and we therefore assign the higher energy absorptions as being $^1A_1, {}^1E_1 \leftarrow {}^1A_1$ ligand field transitions. The large molar absorptivity of the ligand field transition has previously been attributed as being due to some MLCT character in the transition. We assign the highest energy transition at 300 nm to a dpp $\pi^* \rightarrow \pi$ intraligand transition. Based on the comparison of the MLCT energies of the [$M(CO)_4$]dpp vs. [$M(CO)_4$]bpym and [$M(CO)_4$]bpy complexes in a common solvent (dichloromethane), the dpp π^* LUMO appears to be approximately equivalent with the bpym π^* LUMO and lower than the bpy π^* LUMO.

The electrochemistry of [$Cr(CO)_4$]dpp and [$W(CO)_4$]dpp in dichloromethane/0.10 M tetrabutylammonium perchlorate is markedly different (Table 2). The [$Cr(CO)_4$]dpp complex exhibits a quasi-reversible ($E_{anodic} - E_{cathodic} = 160$ mV) cyclic voltammogram for a one electron oxidation, while [$W(CO)_4$]dpp exhibits a cyclic voltammogram with no return cathodic wave after one electron oxidation. The electrochemistry of [$W(CO)_4$]dpp is similar to the previously reported electrochemical irreversibility for [$Mo(CO)_4$]dpp,[1] which also exhibited no return cathodic wave following one electron oxidation. The trend of increasing oxidation potentials ([$Cr(CO)_4$]dpp < [$W(CO)_4$]dpp < [$Mo(CO)_4$]dpp) follows the order of the relative electronegativities of the metals.[12] The electrochemistry of the series of [$M(CO)_4$]dpp (M = Cr, Mo, W) parallels the series of [$M(CO)_4$]L (M = Cr, Mo, W, L = 3,3′-bipyrazine) complexes,[3] with only the [$Cr(CO)_4$]L complex showing a return cathodic wave. No comparative data are available for the [$M(CO)_4$]bpym series.

The infrared spectra of the [$Cr(CO)_4$]dpp and [$W(CO)_4$]dpp complexes were recorded as a solid in KBr and reported in Table 2. The spectra in the carbonyl region (2100–1800 cm^{-1}) reflect the four CO stretching frequencies expected for *cis* disubstituted tetracarbonyl complexes.[11,13]

^{13}C NMR spectra for dpp, [$Cr(CO)_4$]dpp and [$W(CO)_4$]dpp were recorded in deuterated dichloromethane (Table 3). The assignments of dpp ligand signals are based on those for bpy[5,6] and bpym ligands.[5,6,15] Assignment of C(6), C(5), C(6′),(6″) and C(4′),(4″) signals for [$M(CO)_4$]dpp complexes is direct, based on the dpp ligand. The comparative amount of downfield shift of C(6′) (Cr > Mo > W) from the free dpp ligand is opposed to the expected values based on inductive M–N–C through bond interaction, since Cr is the least electronegative metal.[12] The smaller amount of downfield shift in the Mo and W dpp complexes may result from more efficient M $d\pi \rightarrow$ dpp $p\pi^*$ backbonding from the larger Mo and W $d\pi$ orbitals.[14] Assignments for the group of four signals

Table 1. Electronic absorption data for some $[M(CO)_4]L$ complexes

Complex	Solvent	λ_{max} (nm)	ε ($M^{-1}\,cm^{-1} \times 10^{-3}$)	Assignment
$[Cr(CO)_4]$dpp[a]	$CHCl_3$	570	5.0	MLCT
		385 (sh)	3.8	$^1A_1, {}^1E_1 \leftarrow {}^1A_1$
	CH_2Cl_2	555	4.9	MLCT
		380 (sh)	3.8	$^1A_1, {}^1E_1 \leftarrow {}^1A_1$
		310	18	intraligand
	CH_3CN	525	4.0	MLCT
		385 (sh)	3.1	$^1A_1, {}^1E_1 \leftarrow {}^1A_1$
		305	16	intraligand
$[W(CO)_4]$dpp[a]	$CHCl_3$	550	7.4	MLCT
		380 (sh)	4.4	$^1A_1, {}^1E_1 \leftarrow {}^1A_1$
		325 (sh)	17	
		300	20	intraligand
	CH_2Cl_2	530	7.6	MLCT
		375 (sh)	4.5	$^1A_1, {}^1E_1 \leftarrow {}^1A_1$
		300	21	intraligand
	CH_3CN	495	6.4	MLCT
		380 (sh)	3.8	$^1A_1, {}^1E_1 \leftarrow {}^1A_1$
		300	20	intraligand
$[Mo(CO)_4]$dpp[b]	$CHCl_3$	540	6.3	MLCT
		380 (sh)	4.2	$^1A_1, {}^1E_1 \leftarrow {}^1A_1$
	CH_2Cl_2	510	6.3	MLCT
		380 (sh)	4.3	$^1A_1, {}^1E_1 \leftarrow {}^1A_1$
		300	20	intraligand
	CH_3CN	480	5.3	MLCT
		380 (sh)	3.9	$^1A_1, {}^1E_1 \leftarrow {}^1A_1$
		300	21	intraligand
$[Cr(CO)_4]$bpym[c]	CH_2Cl_2	547	2.7	MLCT
		402	6.7	$^1A_1, {}^1E_1 \leftarrow {}^1A_1$
$[W(CO)_4]_2$bpym[c]	CH_2Cl_2	525	4.2	MLCT
		378	7.5	$^1A_1, {}^1E_1 \leftarrow {}^1A_1$
$[Mo(CO)_4]$bpym[d]	CH_2Cl_2	508		
		379		

[a] This work, (sh) shoulder.
[b] Reference 1.
[c] Reference 6.
[d] Reference 5.

Table 2. Infrared and electrochemical[a] data for some $[M(CO)_4]L$ complexes

Complex	Infrared frequencies,[b] cm^{-1} νCO	$E_{1/2}$	Ref.
$[Cr(CO)_4]$dpp	2008, 1906, 1889, 1825	+0.56	[c]
$[Mo(CO)_4]$dpp	2016, 1914, 1882, 1819	+0.90	[c]
$[W(CO)_4]$dpp	2003, 1902, 1872, 1824	+0.82	[c]
$[Cr(CO)_4]$bpy	2010, 1908, 1888, 1833		11
$[Mo(CO)_4]$bpy	2014, 1911, 1882, 1830		11
$[W(CO)_4]$bpy	2008, 1900, 1880, 1829		11
$[Mo(CO)_4]$bpym	2014, 1912, 1869, 1833		5

[a] Oxidation potentials were measured by cyclic voltammetry in CH_2Cl_2, 0.1 M TBAP, at 100 mV/s vs. Ag/AgCl electrode. Potential of the oxidation waves are reported for $[Mo(CO)_4]$dpp and $[W(CO)_4]$dpp.
[b] Infrared samples recorded as solids in KBr.
[c] This work.

Table 3. ^{13}C NMR spectra of dpp and $[M(CO)_4]$dpp (M = Cr(O), Mo(O) and W(O)) complexes

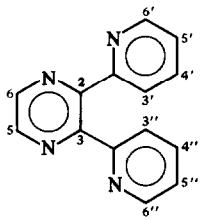

Complex	dpp	$\delta(^{13}C)$, ppm[a] $[Cr(CO)_4]$dpp	$[Mo(CO)_4]$dpp	$[W(CO)_4]$dpp
C(3′)	124.33	126.44	127.17	127.48
C(3″)		124.95	[b]	125.25
C(4′)	136.71	137.91	138.02	138.11
C(4″)		135.53	136.05	135.92
C(5′)	123.30	124.95	[b]	125.96
C(5″)		124.64	124.23	124.44
C(6′)	142.96	145.48	144.59	144.24
C(6″)		142.52	142.68	143.53
C(5)	148.85	149.82	149.82	149.87
C(6)		152.97	152.96	152.55

[a] Chemical shift in CH_2Cl_2 reported vs. TMS.
[b] Signals at 125.30 ppm and 125.13 ppm not specifically assigned, Ref. 1.

between 120–130 ppm for the C(5′),(5″) and C(3′),(3″) of the $[M(CO)_4]$dpp complexes are less certain. If the continued larger downfield shift of the bond ring carbons (C′) vs. non-bound ring carbon (C″) remains consistent, then the two most downfield signals in the group of four are due to C(3′) and C(5′), while the two upfield signals in the same group must be due to C(3″) and C(5″). The previously reported downfield shift of all bridging ligand ring carbons in $M(CO)_4$ complexes,[5,6] has been interpreted as resulting from competitive $Md\pi \rightarrow COp\pi^*$ vs. $Md\pi \rightarrow$ bridging ligand $p\pi^*$ backbonding.

We have recently prepared the $[Cr(CO)_4]_2$dpp and $[W(CO)_4]_2$dpp complexes and are currently working on the preparation and study of the hetero bimetallic complexes.

Acknowledgement—The authors gratefully acknowledge the financial support of this work through a Cottrell Research grant from Research Corporation.

REFERENCES

1. R. R. Ruminski and J. J. Johnson, *Inorg. Chem.* 1987, **26**, 210.
2. K. J. Brewer, R. W. Murphy, Jr., S. R. Spurlin and J. D. Petersen, *Inorg. Chem.* 1986, **25**, 883; J. D. Petersen, W. R. Murphy, Jr., R. Sahai, K. J. Brewer and R. R. Ruminski, *Coord. Chem. Rev.* 1985, **64**, 261.
3. S. Ernst and W. Kaim, *Inorg. Chim. Acta.* 1986, **114**, 123.
4. W. Kaim and S. Kohlman, *Inorg. Chem.* 1986, **25**, 3306.
5. C. Overton and J. A. Connor, *Polyhedron* 1982, **1**, 53.
6. K. J. Moore and J. D. Petersen, *Polyhedron* 1983, **2**, 279.
7. C. H. Braunstein, A. D. Baker, T. C. Strekas and H. D. Gafney, *Inorg. Chem.* 1984, **23**, 857.
8. J. E. Sutton and H. Taube, *Inorg. Chem.* 1981, **20**, 3125.
9. M. J. Powers and T. J. Meyer, *J. Am. Chem. Soc.* 1980, **102**, 1289.
10. M. S. Wrighton and D. L. Morse, *J. Organomet. Chem.* 1975, **97**, 405.
11. M. H. B. Stiddard, *J. Chem. Soc.* 1962, 4712.
12. J. A. Dean, *Lange's Handbook of Chemistry*, 13th edn, Table 3.5. McGraw-Hill, New York (1985).
13. C. L. Lukehart, *Fundamental Transition Metal Organometallic Chemistry*, Brooks Cole, Monterey, CA (1985).
14. J. A. Dean, *Lange's Handbook of Chemistry*, 13th edn, Table 3.10. McGraw-Hill, New York (1985).
15. R. R. Ruminski and J. D. Petersen, *Inorg. Chim. Acta.* 1982, **65**, L177.

Polyhedron Vol. 6, No. 8, pp. 1677–1680, 1987
Printed in Great Britain

0277-5387/87 $3.00+.00

DIAMAGNETIC ANISOTROPY OF M≡M BONDED MOLECULES FOR M = Mo OR W: HOW MUCH π IS THERE AND HOW DO WE SLICE IT?

TIMOTHY P. BLATCHFORD, MALCOLM H. CHISHOLM† and JOHN C. HUFFMAN

Department of Chemistry and Molecular Structure Center, Indiana University, Bloomington, Indiana 47405, U.S.A.

(*Received* 16 *February* 1987; *accepted* 27 *February* 1987)

Abstract—The diamagnetic anisotropies of M≡M bonds for M_2X_6 molecules (M = Mo, W; X = NMe_2, $\frac{1}{2}MeNCH_2CH_2NMe$, OR, $\frac{1}{2}OCMe_2CMe_2O$) calculated by McGlinchey for X=NMe_2 (*Inorg. Chem.* 1980, **19**, 1392) are inadequate to explain the observed chemical shifts of protons located over the M≡M bond in compounds having essentially eclipsed $X_3M{\equiv}MX_3$ skeletons, namely $M_2(MeNCH_2CH_2NMe)_3$ and $M_2(OCMe_2CMe_2O)_3$ molecules. Several causes for errors in the original McGlinchey calculational approach for $\chi_{M\equiv M}$ are noted, the most important of which is the total neglect of the diamagnetic anisotropy of the M–L π bond. This is important for amides and alkoxides. A qualitative correction for this M–L π bonding is introduced and values for $\chi_{M\equiv M}$ recalculated.

Although in 1972 San Filippo[1] indicated that compounds containing metal–metal multiple bonds should have a magnetic anisotropy associated with them which ought to be manifested in their NMR spectra, it was not until recently that efforts to quantify this effect have occurred. Initially qualitative use of this concept was utilized in the interpretation of the NMR spectra of the $M_2(NR_2)_6$ molecules.[2] However, McGlinchey[3] was the first to propose actual values for both the metal–metal triple bond, using the $M_2(NR_2)_6$ molecules as a model, and quadruple bond. Cotton[4] has re-evaluated the magnetic anisotropy of Mo–Mo quadruple bonds based on newer structural and NMR data.

Calculations of values for magnetic anisotropy require three things: (1) quantitative X-ray structural data, (2) measured chemical shift difference from solution NMR spectra and (3) the general equation derived by McConnell,[5] eqn (1).

$$\Delta\sigma_d = \chi\frac{(1-3\cos^2\theta)}{3R^3} \qquad (1)$$

R = distance from M–M bond center to signal nucleus,
θ = angle between R and the M–M bond axis,
σ_d = chemical shift difference,
χ = anisotropy due to M–M bond ($\chi = \chi_\parallel - \chi_\perp$).

Our interest in this area arises from the observed discrepancy (*vide infra*) between values of $\chi_{M\equiv M}$ calculated for $M_2(NR_2)_6$ and $M_2(MeNCH_2CH_2NMe)_3$ molecules (M = Mo, W), respectively. Herein we wish to address this discrepancy in $\chi_{M\equiv M}$ and perhaps provide some insight into the necessary considerations that should enter into obtaining useful values of χ for metal–metal multiple bonded molecules.

RESULTS AND DISCUSSION

$M_2(NR_2)_6$ *and* $M_2(MeNCH_2CH_2NMe)_3$; M = Mo *or* W

McGlinchey's calculated diamagnetic anisotropies for metal–metal triple bonds of molybdenum and tungsten, as determined from the $M_2(NMe_2)_6$ molecules, have given values of $\chi_{M\equiv M}$ of -156×10^{-36} M^3/molecule and -142×10^{-36} M^3/molecule for tungsten and molybdenum, respectively.[3]‡ Analogous calculations on the

† Author to whom correspondence should be addressed.

‡ The more recent literature utilizes SI units, M^3/molecule. To convert from older literature units of cm^3/mole one must multiply by $4\pi\times10^{-6}/N = 2.086\times10^{-29}$, N = Avogadro's Number.

Table 1. Calculated values of R, θ and G[a] for $M_2(MeNCH_2CH_2NMe)_3$; M = Mo, W[b]

	R, Å		θ, °		G ($\times 10^{30}$)		G_{avg} ($\times 10^{30}$)	
	Mo	W	Mo	W	Mo	W	Mo	W
H_1	3.777	3.826	22.27	22.74	−0.009707	−0.009236	−0.004732	−0.004513
H_2, H_3	4.309	4.337	44.26	44.49	−0.002245	−0.002152		
H_4	3.444	3.391	83.68	83.95	−0.007863	−0.008264	−0.005694	−0.005933
H_5	4.132	4.115	73.08	73.32	−0.003524	−0.003601		

[a] Where G is the geometrical factor; $G = (1-3\cos^2\theta)/3R^3$.
[b] H_1, H_2, H_3—distal; H_4, H_5—proximal.

$M_2(MeNCH_2CH_2NMe)_3$ molecules [see eqn (2), Tables 1 and 2] provide values of $\chi_{W\equiv W} = -63\times10^{-36}$ M^3/molecule and $\chi_{Mo\equiv Mo} = -92\times10^{-36}$ M^3/molecule. These results immediately pose two questions which need to be addressed. (1) Why are these values different from those obtained for the $M_2(NMe_2)_6$ compounds? (2) Why is $\chi_{M\equiv M}$ for tungsten now smaller than $\chi_{M\equiv M}$ for molybdenum? We shall address the initial question first. The answer to question 2 will become self-evident.

$$\sigma_{distal} - \sigma_{proximal} = \chi(G_{distal} - G_{proximal}) \qquad (2)$$

If one were to stop and consider: (a) the geometric differences between the two types of molecules, and (b) some convincing arguments made in the past concerning the stabilities and properties of these types of molecules, several points worthy of note lead us to a possible answer to the first question. (1) The $M_2(NMe_2)_6$ and $M_2(MeNCH_2CH_2NMe)_3$ compounds exhibit staggered and (virtually) eclipsed geometries, respectively. (2) Ligand-to-metal π-bonding is a mainstay of these molecules, and together with steric bulk, the reason for their existence as dinuclear rather than polynuclear species. This M ← L π-bonding is manifested in (i) short metal–nitrogen distances, substantially shorter than metal-nitrogen single bond distances,[7,8] (ii) the planarity of the MNC_2 moieties,[8] (iii) the alignment of the MNC_2 units along the M–M axes in the solid state to preclude competition for use of atomic orbitals used in M–M π-bonding,[8] and (iv) barriers to rotation about the M–N bonds.[9] Oxygen-to-metal π-bonding is similarly important in $M_2(OR)_6$ compounds.

Since M ← L π-bonding is unequivocally established for these compounds, it must be reasonable to consider a magnetic anisotropy attributable to the M≡N bond, $\chi_{M\equiv N}$. Therefore, if two M≡N bonds are eclipsed with respect to one another, e.g. as in $M_2(MeNCH_2CH_2NMe)_3$, then the proximal (protons) groups should be subjected to twice the effect due to any magnetic anisotropy associated with the M–N multiple bond, causing the difference in values of $\chi_{M\equiv M}$ obtained for $M_2(NMe_2)_6$ and $M_2(MeNCH_2CH_2NMe)_3$. This suggests original

Table 2. ^1H NMR chemical shifts of $M_2(MeNCH_2CH_2NMe)_3$,[a] $M_2(OC(CH_3)_2C(CH_3)_2O)_3$,[b] M = Mo and W, and the respective free ligands

	Proximal	Distal	Free ligand
$Mo_2(MeNCH_2CH_2NMe)_3$	δ 3.80	δ 2.87	
$W_2(MeNCH_2CH_2NMe)_3$	δ 3.52	δ 2.86	
$CH_3N(H)CH_2CH_2N(H)CH_3$			δ 2.47 —Me; δ 2.73 —CH_2
$Mo_2(OC(CH_3)_2C(CH_3)_2O)_3$	δ 1.49		
$W_2(OC(CH_3)_2C(CH_3)_2O)_3$	δ 1.36		
$HOC(CH_3)_2C(CH_3)_2OH$			δ 1.20 —CH_3
$Mo_2(NMe_2)_6$	δ 4.13	δ 2.41	
$W_2(NMe_2)_6$	δ 4.24	δ 2.36	

[a] Ref. 6a, 6b.
[b] Ref. 10.

estimates of $\chi_{M\equiv M}$ inherently contain some component, $\chi_{M=N}$, and that the effect of magnetic anisotropy on chemical shift separations of proximal and distal groups is the sum or difference of $\chi_{M\equiv M}$ (real) and $\chi_{M=N}$, with the contribution of $\chi_{M=N}$ to the proximal chemical shifts dependent upon the positions of the metal–nitrogen bonds relative to one another on opposing metal atoms.

Let us suppose that for eclipsed M—N bonds that two $\chi_{M=N}$ interactions are the same as one $\chi_{M=N}$ for the distal groups, as they are sufficiently removed from the second M—N bond, and are therefore not abnormally shifted, *c.f.* chemical shifts of distal methyl groups in both the $M_2(NMe_2)_6$ and $M_2(MeNCH_2CH_2NMe)_3$ molecules (Table 2). This means only the proximal protons are affected by two $\chi_{M=N}$ interactions when in an eclipsed conformation. Thus, the discrepancies between values for $\chi_{M\equiv M}$ for both molybdenum and tungsten are a result of an extra $\chi_{M=N}$ contribution. Also, the effect of $\chi_{M=N}$ must be antagonistic to the true $\chi_{M\equiv M}$ since the values found for the eclipsed conformers are much smaller than those determined for their staggered counterparts.

Now, assuming the metal–metal triple bonds for both staggered and eclipsed conformations have the same magnetic anisotropy, assigning $\chi_{M\equiv M}$ and $\chi'_{M\equiv M}$ to the values of magnetic anisotropy derived from $M_2(NMe_2)_6$ and $M_2(MeNCH_2NMe)_3$, respectively, we obtain an expression for $\chi_{M=N}$, eqn (3).

$$\chi_{M\equiv M} - \chi'_{M\equiv M} = \chi_{M=N}. \quad (3)$$

Equation (3) generates $\chi_{M=N}$ of -90×10^{-36} M^3/molecule for W and -50×10^{-36} M^3/molecule for Mo. Using these numbers of $\chi_{M=N}$, McGlinchey's $\chi_{M\equiv M}$, and recalling that $\chi_{M=N}$ is antagonistic to $\chi_{M\equiv M}$ (real), we can generate the real $\chi_{M\equiv M}$, $\chi^*_{M\equiv M}$, where any magnetic anisotropy due to M–N multiple bonding has been eliminated, eqn (4).

$$\chi_{M\equiv M} + \chi_{M=N} = \chi^*_{M\equiv M}. \quad (4)$$

The values obtained from this exercise are given in Table 3. These results: (i) account for M–L π-bonding to at least a first approximation, and (ii) maintain the relative ordering of $\chi_{W\equiv W}$ and $\chi_{Mo\equiv Mo}$.

The answer to question 2 now becomes obvious. Due to the better W–N overlap (bond) relative to that found for Mo–N, the effect of $\chi_{W=N}$ is greater than that of $\chi_{Mo=N}$ to the extent that when doubled and subtracted from $\chi^*_{W\equiv W}$ the relative order of $\chi_{M\equiv M}$ for Mo and W, as calculated from $M_2(MeNCH_2CH_2NMe)_3$ is reversed.

Table 3. Diamagnetic anisotropy of M≡M for M = Mo, W, taking into effect M–L π-bonding [see eqns (3) and (4) in text]

Bond	$\chi\times10^{-36}$ (M^3/molecule)
Mo≡Mo	−192[a]
W≡W	−246[a]
Mo≡Mo	ca. −410[b]

[a] Calculated from ^{1}H NMR data.
[b] Estimated.

Generating useful values of χ

Cotton's recent re-evaluation[4] of $\chi_{Mo\equiv Mo}$ gives results closer to those which might be expected (see Tables 3 and 4). Even though these values are more in line with those anticipated by extrapolation of $\chi_{Mo\equiv Mo}$, they may still be errant. Firstly, one generated value of $\chi_{Mo\equiv Mo}$ is less than $\chi_{Mo\equiv Mo}$, which is unlikely. More reliable estimates may be obtained by taking M ← L π-bonding into account during future calculations. Secondly, the reliability of comparing free ligand chemical shifts to those found in metal–metal multiple bonded systems may be suspect. Efforts to generate $\chi_{M\equiv M}$ using reported chemical shifts of the free ligands and those determined for the proximal protons of the appropriate molecule (see Tables 1, 2 and 5) gave an extremely low value of $\chi_{W\equiv W}$ for $W_2(OC(Me)_2C(Me)_2O)_3$,[10] -44×10^{-36} M^3/molecule. For the $M_2(MeNCH_2CH_2NMe)_3$ molecules values of $\chi_{M\equiv M}$ obtained using this method are -187×10^{-36} M^3/molecule for Mo and -133×10^{-36} M^3/molecule for W. Once again $\chi_{Mo\equiv Mo}$ and $\chi_{W\equiv W}$ are in reverse order, although $\chi_{Mo\equiv Mo}$ is close to our proposed $\chi^*_{Mo\equiv Mo}$. Due to the large difference in results for tungsten, however, we feel the proximity of $\chi_{Mo\equiv Mo}$ to $\chi^*_{Mo\equiv Mo}$, calculated using free ligand chemical shifts, to be fortuitous.

CONCLUDING REMARKS

(1) The use of chemical shift differences between the free and coordinated ligand to calculate $\chi_{M\equiv M}$ gives inadequate results for M = Mo or W. This suggests that this method may not be particularly reliable when applied to other metal–metal multiple bound systems.

(2) Metal–ligand π-bonding should be taken into account when attempting to evaluate $\chi_{M\equiv M}$ in M_2X_6 compounds. Methods for determining the contribution of $\chi_{M=X}$ need to be developed, especially for those molecules that do not easily

Table 4. Diamagnetic anisotropies of M–M multiple bonds and other bonds ignoring M–L π-bonding factors

Compound	$\chi \times 10^{-36}$ (M^3/molecule)	Ref.
$W_2(NMe_2)_6$	-156^a	3
$Mo_2(NMe_2)_6$	-142^a	3
$W_2(MeNCH_2CH_2NMe)_3$	-63^a	this work
$Mo_2(MeNCH_2CH_2NMe)_3$	-92^a	this work
Mo≡Mo	ca. −800	3
$Mo_2(O_2CCH_3)_4$	-239^a	4
$Mo_2(O_2CCH(OH)C_6H_5)_4$	-176^a	4
—C≡C—	−340	[b]

[a] Calculated from ^{1}H NMR data.
[b] Quoted or estimated.

lend themselves to separation of χ_{M-M} (real) and $\chi_{M=X}$.

$\chi_{M\equiv M}$ values determined for metal–metal multiple bonded molecules must be taken *cum grano salis* due to difficulties in accounting for: (i) the magnetic anisotropy of metal–ligand π-bonds, (ii) different conformations for otherwise similar molecules, (iii) methods of determining chemical shift differences (free ligand, proximal–distal), and finally that the assumptions inherent in McConnell's derived equation hold true for these inorganic multiple bonded compounds.

Inherent in our arguments is the assumption that $\chi_{M\equiv M}$ is the same for staggered and eclipsed conformations of M_2X_6 molecules. Arguments have previously been presented to support the view that the $\sigma^2\pi^4$ triple bond is invariant to conformation based on: (i) M≡M distances, (ii) M≡M rotational barriers, (iii) U.V.–visible spectroscopy, (iv) photoelectronspectroscopy and (v) theoretical calculations.[6b]

Table 5. Calculated values of R, θ and G^a for $W_2(OC(CH_3)_2C(CH_3)_2O)_3$[b]

	R, Å	θ, °	G ($\times 10^{30}$)	G_{avg} ($\times 10^{30}$)
H_1	3.218	93.86		
H_2	4.032	74.77	0.005527	
H_3	4.469	90.51		
				0.003643
H_4, H_5	4.727	63.94	0.001759	
H_6	4.970	76.76		

[a] Where G is the geometric factor:
$$G = (1-3\cos^2\theta)/3R^3.$$
[b] Values based on one of the three pinacolate ligands.

Acknowledgement—We thank the National Science Foundation for support.

REFERENCES

1. J. San Filippo, *Inorg. Chem.* 1972, **11**, 3140.
2. (a) M. H. Chisholm, F. A. Cotton, B. A. Frenz, W. W. Reichert, L. W. Shive and B. R. Stults, *J. Am. Chem. Soc.* 1976, **98**, 4469; (b) M. H. Chisholm, F. A. Cotton, M. W. Extine and B. R. Stults, *J. Am. Chem. Soc.* 1976, **98**, 4477.
3. M. J. McGlinchey, *Inorg. Chem.* 1980, **19**, 1392.
4. P. A. Agaskar and F. A. Cotton, *Polyhedron* 1986, **5**, 899.
5. H. M. McConnell, *J. Chem. Phys.* 1957, **27**, 226.
6. (a) T. P. Blatchford, M. H. Chisholm, K. Folting and J. C. Huffman, *Inorg. Chem.* 1980, **19**, 3175; (b) T. P. Blatchford, M. H. Chisholm, K. Folting and J. C. Huffman, *Inorg. Chem.* submitted.
7. For a general review of transition metal dialkylamides, see D. C. Bradley and M. H. Chisholm, *Acc. Chem. Res.* 1976, **9**, 273.
8. (a) M. H. Chisholm, F. A. Cotton, B. A. Frenz, W. W. Reichert, L. W. Shive and B. R. Stults, *J. Am. Chem. Soc.* 1976, **98**, 4469; (b) M. H. Chisholm, F. A. Cotton, M. Extine and B. R. Stults, *J. Am. Chem. Soc.* 1976, **98**, 4477; (c) B. E. Bursten, F. A. Cotton, J. C. Green, E. A. Seddon and G. G. Stanley, *J. Am. Chem. Soc.* 1980, **102**, 4579.
9. (a) M. J. Chetcuti, M. H. Chisholm, K. Folting, D. Haitko, J. C. Huffman and J. Janos, *J. Am. Chem. Soc.* 1983, **105**, 1163; (b) M. H. Chisholm, J. C. Huffman and I. P. Rothwell, *Organomet.* 1982, **1**, 251; (c) M. H. Chisholm, *Chem. Soc. Farad. Symp.* 1980, **14**, 194.
10. (a) for $W_2(OC(Me)_2C(Me)_2O)_3$: C. A. Smith, Ph.D. Thesis, 1985, Indiana University, Bloomington, Indiana; (b) Molecular Structure Report No. 85040; (c) for ^{1}H NMR for $Mo_2(OC(Me)_2C(Me)_2O)_3$; T. P. Blatchford, Ph.D. Thesis, 1986, Indiana University, Bloomington, Indiana.

Polyhedron Vol. 6, No. 8, pp. 1681–1685, 1987
Printed in Great Britain

0277–5387/87 $3.00+.00

A MECHANISTIC INVESTIGATION ON THE FORMATION OF MOLYBDOPHOSPHATE COMPLEXES IN AQUEOUS SOLUTION BY THE USE OF LASER RAMAN SPECTROSCOPY

KATSUO MURATA* and SHIGERO IKEDA

Department of Chemistry, Faculty of Science, Osaka University, Toyonaka, Osaka, Japan 560

(*Received* 28 *October* 1986; *accepted after revision* 6 *March* 1987)

Abstract—Two distinct reaction rates were found in the formation of 12-molybdophosphate complex. These differences in the formation processes were understood by the use of laser Raman spectroscopy. The reaction of isopolymolybdate $(MoO_4)^{2-}(MoO_3)_{11}$ with phosphate PO_4^{3-} proceeds slowly *via* formation of 11- molybdophosphate then to produce 12-molybdophosphate taken for 8 min. This reaction mechanism is considered to undergo first the replacement between MoO_4^{2-} and PO_4^{3-} then the transformation reaction from 11-molybdophosphate into 12-molybdophosphate. On the other hand, the acidification of the mixed solution of molybdate and phosphate rapidly produces 80% of 12-molybdophosphate within 30 s.

A reliable method for the analysis of elements such as P, Si, As, and Ge is based on the formation of polynuclear heteropolymolybdate complexes.[1–5] The mechanism of the formation of these complexes is complex.[6,7] Our previous Raman spectroscopic studies revealed the formation behavior of some species of isopolymolybdate[8] and heteropolymolybdate.[9] Our preliminary experiments showed the difference in the formation rate of 12-molybdophosphate by changing the addition order of phosphate, molybdate, and acid. Crouch *et al.* have studied the kinetics of the formation of heteropolymolybdate blue by spectrophotometric measurements.[10] According to their results, the rate of the formation of phosphomolybdate blue product is independent of the acidity but the spectrophotometric investigation does not clarify much about the configurational information of the chemical species in aqueous solution. The blue product was exclusively followed by measuring the absorbance at 650 nm, which gives no structural information. They lately published the spectrophotometric work in the strong acid[11] and using stopped-flow studies.[12]

We have followed the formation of the molybdophosphate complex by the use of laser Raman spectroscopy. This method has brought much information about the appearance and disappearance of several species.[13,14] It could also shed light on the formation mechanisms of molybdophosphate complexes.

EXPERIMENTAL

Reagents and apparatus

A phosphate solution was prepared of potassium dihydrogen phosphate KH_2PO_4 which was dried at 110°C. A molybdate solution was prepared of sodium molybdate $Na_2MoO_4 \cdot 2H_2O$ of analytical reagent grade and standardized by gravimetric analysis.[15] Hydrochloric acid was used to acidify solutions.

Polynuclear molybdophosphate complexes were produced by means of the mixed solutions of phosphate and molybdate. The following two mixing procedures were examined:

(1) the acidified phosphate solution was mixed with the acidified molybdate solution,

* Author to whom correspondence should be addressed.
Present address: Naruto University of Teacher Education, Naruto, Tokushima, Japan 772.

(2) the mixed solution of phosphate and molybdate was acidified with hydrochloric acid.

A conventional quartz cell was used as a reaction chamber which was kept at 25±1°C. A cell stirrer mixed the phosphate solution (2.0×10^{-2} M, pH 1) of 1 cm^3 with the molybdate solution (2.4×10^{-1} M, pH 1) of 1 cm^3.

Raman spectra were measured with JASCO R800, using 514.5 nm (Ar^+ laser) as the excitation source. The instrument was modified for the data treatment and collection equipped with the Sharp MZ-2000 personal computer. Sodium nitrate was used as an internal standard.

RESULTS AND DISCUSSION

There are two procedures to produce the yellow 12-molybdophosphate complex $[PMo_{12}O_{40}]^{3-}$; (1) acidification of the mixed solution of phosphate and molybdate, (2) mixing with the acidified molybdate solution and the acidified phosphate solution. Although both procedures form the species of 12-molybdophosphate, the rates of formation are quite different. As shown in Fig. 1, the latter procedure exhibits the slower rate in the formation of 12-molybdophosphate, which has a typical Raman band at 996 cm^{-1}.[9] The 12-molybdophosphate complex first appears in 1 min 23 s after the acidified molybdate solution of pH 1 is mixed with the acidified phosphate solution of pH 1. Some other species of polynuclear complex appear and disappear during the progress of the reaction before the 12-molybdophosphate is produced. Figure 1 reveals characteristic features that two peaks at 980 cm^{-1} and at 955 cm^{-1} decrease and correspondingly a new peak at 975 cm^{-1} appears in the initial reaction of the acidified molybdate and phosphate. The previous works[8,9] indicated that the species having the peak at 980 cm^{-1} is $Mo_6O_{19}^{2-}$, the species at 955 cm^{-1} is $(MoO_4)^{2-}(MoO_3)_{11}$, and the species at 975 cm^{-1} is $(PO_4)^{3-}(MoO_3)_{11}$. An important fact is that the first heteropolymolybdate complex formed is not the 12-molybdophosphate but 11-molybdophosphate complex of $(PO_4)^{3-}(MoO_3)_{11}$ when the acidified molybdate is mixed with the acidified phosphate solution. The species of $(PO_4)^{3-}(MoO_3)_{11}$ is produced from the species of $Mo_6O_{19}^{2-}$ and $(MoO_4)^{2-}(MoO_3)_{11}$. The species of 11-molybdophosphate subsequently transforms into 12-molybdophosphate complex: increasing the intensity at 996 cm^{-1} while decreasing the intensity at 975 cm^{-1} observed in the Raman spectra shown in Fig. 1. As shown in Fig. 2, the appearance and disappearance of three species of 11-isopolymolybdate, 11-molybdophosphate, and 12-molybdophosphate were also followed at the constant wavenumber of 955, 975 and 996 cm^{-1}, respectively. Figure 2 clearly indicates that the first heteropolymolybdate formed is not 12-molybdophosphate but 11-molybdophosphate complex. The 12-molybdophosphate complex forms gradually after an induction period of 1 min where 11-molybdophosphate complex is predominantly

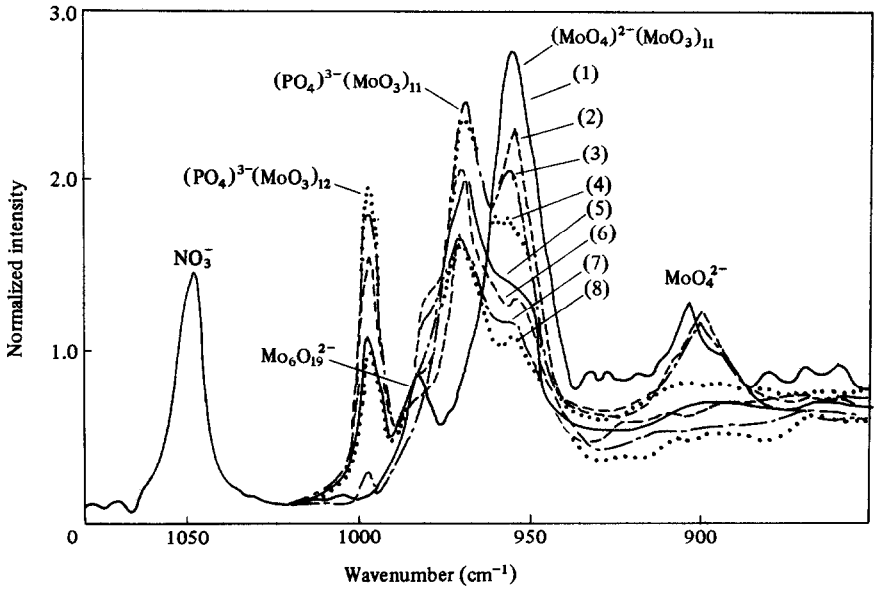

Fig. 1. The reaction of the acidified molybdate with the acidified phosphate solution on Raman spectra ([P] = 1.0×10^{-2} M, [Mo] = 1.2×10^{-1} M, pH 1). The reaction time: (1) 0 s, (2) 31 s, (3) 1 min 23 s, (4) 2 min 14 s, (5) 3 min 5 s, (6) 4 min 47 s, (7) 5 min 38 s, (8) 6 min 29 s.

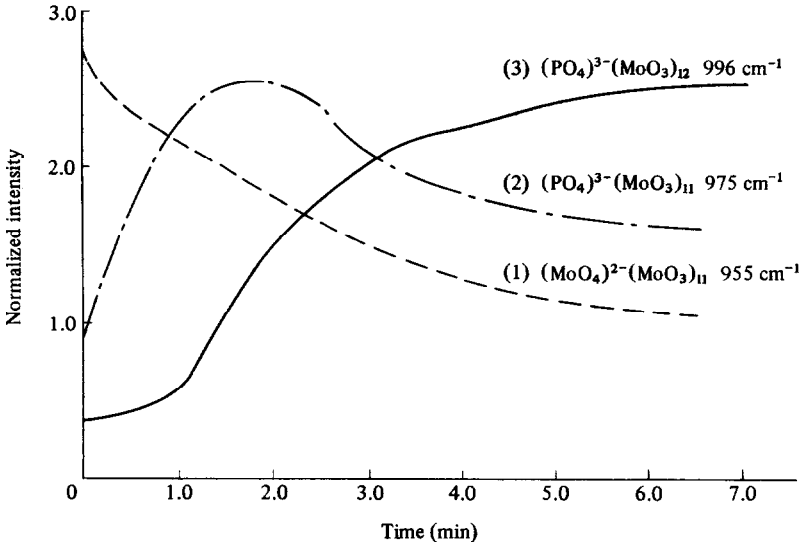

Fig. 2. Formation and decomposition curves of three species observed at each wavenumber. (1) $(MoO_4)^{2-}(MoO_3)_{11}$ at 955 cm^{-1}, (2) $(PO_4)^{3-}(MoO_3)_{11}$ at 975 cm^{-1}, (3) $[PMoO_{40}]^{3-}$ at 996 cm^{-1}.

produced. The formation of the 12-molybdophosphate was completed in 10 min.

On the other hand, the formation rate of the 12-molybdophosphate is extremely fast when the mixed solution of molybdate and phosphate ([P] = 1.0×10^{-2} M, [Mo] = 1.2×10^{-1} M) is acidified to pH 1 as shown in Fig. 3. Within only 31 s, the formation product of 12-molybdophosphate complex proceeds up to 80% of the total amount. After that, the incremental rate is slowed to 20 min 30 s. This contrast in behavior in the formation of the 12-molybdophosphate complex suggests to us the formation mechanism of the heteropoly complex. The acidified molybdate solution of pH 1 contains the predominant species of $(MoO_4)^{2-}(MoO_3)_{11}$ and the minor species of $Mo_6O_{19}^{2-}$.[8] In order to form 11-molybdophosphate from the species PO_4^{3-} and $(MoO_4)^{2-}(MoO_3)_{11}$, the unit of MoO_4^{2-} in the species of $(MoO_4)^{2-}(MoO_3)_{11}$ should be replaced by the unit of PO_4^{3-}. Then this 11-molybdophosphate of $(PO_4)^{3-}(MoO_3)_{11}$ formed should be transformed into 12-molybdophosphate of $[PMo_{12}O_{40}]^{3-}$ like

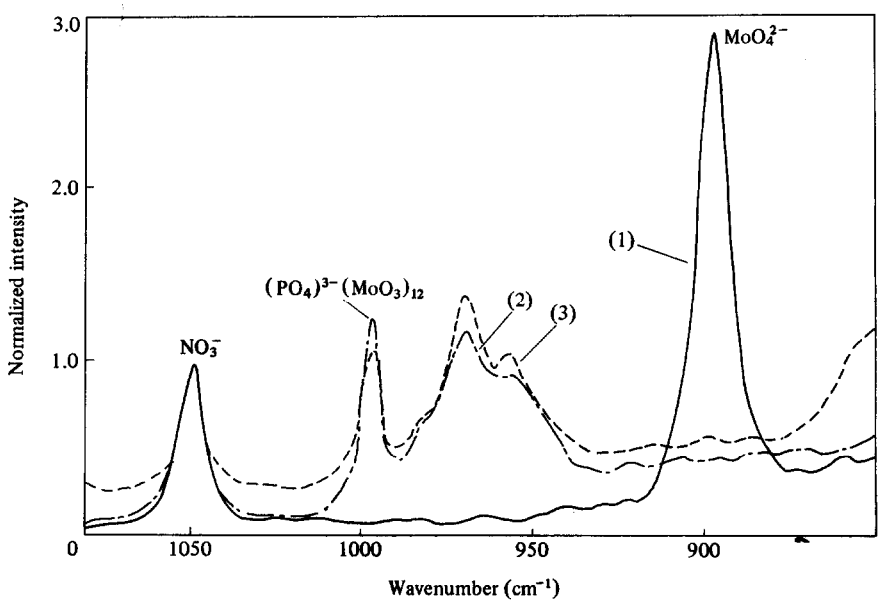

Fig. 3. The acidification of the mixed solution of molybdate and phosphate ([P] = 1.0×10^{-2} M, [Mo] = 1.2×10^{-1} M, pH 1). The reaction time: (1) 0 s, (2) 31 s, (3) 20 min 30 s.

eqns (1) and (2). This formation step takes a considerable time since it proceeds *via* the formation of the 11-molybdophosphate. The observation that the MoO_4^{2-} species appeared around 900 cm^{-1} also supports this mechanism. The MoO_4^{2-} group in the isopolymolybdate species of $(MoO_4)^{2-}(MoO_3)_{11}$ has a Raman peak at 903 cm^{-1} as shown in Fig. 1. In the reaction of isopolymolybdate with phosphate PO_4^{3-}, the free MoO_4^{2-} group is released, giving a band at 897 cm^{-1} in the Raman spectra. The free MoO_4^{2-} disappears again because it is used up to produce the 12-molybdophosphate like in eqn (2). Figure 1 shows no Raman peak of free ion MoO_4^{2-} around 900 cm^{-1} where 12-molybdophosphate is predominantly produced.

$$(MoO_4)^{2-}(MoO_3)_{11}+PO_4^{3-} \rightleftarrows (PO_4)^{3-}(MoO_3)_{11}+MoO_4^{2-} \quad (1)$$

$$(PO_4)^{3-}(MoO_3)_{11}+MoO_4^{2-}+2H^+ \rightleftarrows [PMo_{12}O_{40}]^{3-}+H_2O. \quad (2)$$

In the case of acidifying the mixed solution of molybdate and phosphate, the 12-molybdophosphate is directly formed by the process that the core phosphate shares some molybdate cluster of $Mo_7O_{24}^{6-}$, $Mo_8O_{26}^{4-}$, and $Mo_6O_{19}^{2-}$.[16,17] The formation rate of 12-molybdophosphate is extremely rapid. It is too fast to observe the initial formation behavior since the maximum scan rate of JASCO R800 is 31 s over 200 cm^{-1}. However the following features are obvious. The MoO_4^{2-} species which appeared at 897 cm^{-1} is completely consumed to construct 12-molybdophosphate by acidification as shown in Fig. 3. Around 80% yield of 12-molybdophosphate is attained within 31 s.

These findings suggest the formation mechanisms of isopoly- and heteropolymolybdate. As described in previous work,[9] the optimum acidity of 12-molybdophosphate is around pH 1. When the hetero group anion like PO_4^{3-} is not present in the acidic molybdate solution, isopolymolybdate grows to the large species[8] of $(MoO_4)^{2-}(MoO_3)_{11}$ as given in eqn (3).

$$12MoO_4^{2-}+22H^+ \rightleftarrows (MoO_4)^{2-}(MoO_3)_{11}+11H_2O. \quad (3)$$

Once this large isopolymolybdate species forms in aqueous solution, the formation rate of 12-molybdophosphate $[PMo_{12}O_{40}]^{3-}$ becomes slower because two processes should be gone through: at first the substitution of the MoO_4^{2-} group in $(MoO_4)^{2-}(MoO_3)_{11}$ by PO_4^{3-} group and then the transformation of the formed $(PO_4)^{3-}(MoO_3)_{11}$ into 12-molybdophosphate of $(PO_4)^{3-}(MoO_3)_{12}$ as given in eqns (1) and (2). However the 12-molybdophosphate forms rapidly when the molybdate solution initially contains phosphate PO_4^{3-} as shown in Fig. 3. In this case it is unnecessary to substitute MoO_4^{2-} by PO_4^{3-}. The PO_4^{3-} group directly constructs the 12-molybdophosphate of Keggin structure[18] by the surrounding molybdate clusters: $Mo_7O_{24}^{6-}$, $Mo_8O_{26}^{4-}$, and $Mo_6O_{19}^{2-}$ which are produced by acidification of the molybdate solution.[8,16,19] Despite the relative complexity of these polymolybdate ions, the steps leading to their formation are complete within a few milliseconds.[20,21] In the case of acidification of the mixed solution of phosphate and molybdate, a basic question is whether the heteropoly complex is formed from an initial reaction of phosphate with the monomer MoO_4^{2-} and subsequent polymerization as given in eqn (4) or from an initial polymerization of molybdate followed by a condensation reaction with PO_4^{3-} as given in eqns (5), (6) and (7).

$$12MoO_4^{2-}+PO_4^{3-}+24H^+ \rightleftarrows [PMo_{12}O_{40}]^{3-}+12H_2O \quad (4)$$

$$\begin{cases} 7MoO_4^{2-}+8H^+ \rightleftarrows Mo_7O_{24}^{6-}+4H_2O \\ 7PO_4^{3-}+12Mo_7O_{24}^{6-}+72H^+ \end{cases} \rightleftarrows 7[PMo_{12}O_{40}]^{3-}+36H_2O \quad (5)$$

$$\begin{cases} 8MoO_4^{2-}+12H^+ \rightleftarrows Mo_8O_{26}^{4-}+6H_2O \\ 2PO_4^{3-}+3Mo_8O_{26}^{4-}+12H^+ \end{cases} \rightleftarrows 2[PMo_{12}O_{40}]^{3-}+6H_2O \quad (6)$$

$$\begin{cases} 6MoO_4^{2-}+10H^+ \rightleftarrows Mo_6O_{19}^{2-}+5H_2O \\ PO_4^{3-}+2Mo_6O_{19}^{2-}+4H^+ \end{cases} \rightleftarrows [PMo_{12}O_{40}]^{3-}+2H_2O. \quad (7)$$

There is no evidence in the Raman spectra that the PO_4^{3-} group initially reacts with the monomer MoO_4^{2-} as given in eqn (4). But the interaction between the PO_4^{3-} and isopolymolybdate has been observed.[9,22,23] Moreover the existence of the species $Mo_7O_{24}^{6-}$, $Mo_8O_{26}^{4-}$, and $Mo_6O_{19}^{2-}$ has been investigated and established by several authors.[8,24–26] The latter cases of eqns (5), (6) and (7) seem likely because each isopolymolybdate forms easily and rapidly as above mentioned.

Acknowledgements—Dr. Katsuo Murata wishes to express his thanks to Prof. Donald E. Irish and members of University of Waterloo, Canada for their contributions and hospitality during his stay when this manuscript was finalized. The authors express their thanks to Dr. Iwao Watanabe for electronic modification of the Raman spectroscopic instrument.

REFERENCES

1. E. B. Sandell, *Colorimetric Determination of Trace of Metals*, 3rd. edn, p. 282. Interscience Publishers, New York (1959).
2. I. M. Kolthoff and P. J. Elving, *Treatise on Analytical Chemistry, Part II, Vol. 5, Phosphorus* (Edited by W. Rieman III and J. Benken Kamp), (1961).
3. I. M. Kolthoff and E. B. Sandell, *Textbook of Quantitative Inorganic Analysis*, 3rd. edn, pp. 382, 684. Macmillan, New York (1964).
4. G. Ecket, *Z. Anal. Chem.* 1958, **161**, 421.
5. E. Ebner, *Z. Anal. Chem.* 1964, **206**, 106.
6. M. T. Pope, *Heteropoly and Isopoly Oxometalates*. Springer, New York (1983).
7. T. J. R. Weakley, *Struc. Bonding* 1974, **18**, 131.
8. K. Murata and S. Ikeda, *Spectrochim. Acta* 1983, **39**, 787.
9. K. Murata and S. Ikeda, *Polyhedron* 1983, **2**, 1005.
10. S. R. Crouch and H. V. Malmstadt, *Anal. Chem.* 1967, **39**, 1084.
11. C. C. Kircher and S. R. Crouch, *Anal. Chem.* 1982, **54**, 879.
12. C. C. Kircher and S. R. Crouch, *Anal. Chem.* 1983, **55**, 242.
13. D. E. Irish and H. Chen, *Appl. Spectrosc.* 1971, **25**, 1.
14. D. E. Irish, *Raman Spectroscopy (Theory and Practice)*, p. 224, Plenum Press (1967).
15. M. Borrel and R. Paris, *Analytica Chim. Acta* 1950, **4**, 267.
16. G. A. Tsigdinos, *Heteropoly Compounds of Molybdenum and Tungsten*. Climax Molybdenum Co. Bull. Cdb-12a (1969).
17. K. Tytko and O. Glemster, *Adv. Inorg. Chem. Radiochem.* 1976, **19**, 239.
18. J. F. Keggin, *Proc. R. Soc.* 1934, **144**, 75.
19. G. A. Tsigdinos and C. J. Hallada, *Isopoly Compounds of Molybdenum, Tungsten, and Vanadium*. Climax Molybdenum Co. Bull. Cdb-14 (1969).
20. G. Schwarzenbach and J. Meier, *J. Inorg. Nucl. Chem.* 1958, **8**, 302.
21. D. S. Honig and K. Kustin, *Inorg. Chem.* 1972, **11**, 65.
22. P. Cannon, *J. Inorg. Nucl. Chem.* 1960, **13**, 261.
23. K. Murata and T. Kiba, *J. Inorg. Nucl. Chem.* 1970, **32**, 1667.
24. K. Tytko and B. Schönfeld, *Z. Naturforsch.* 1975, **30b**, 471.
25. G. Johansson, L. Pettersson and N. Ingri, *Acta Chemica Scandinavia* 1979, **A33**, 305.
26. T. Ozeki, H. Kihara and S. Hikime, *Anal. Chem.* 1987, **59**, 945.

Polyhedron Vol. 6, No. 8, pp. 1687–1693, 1987
Printed in Great Britain

0277–5387/87 $3.00+.00

METAL AND ORGANOMETAL COMPLEXES OF OXY- AND THIO-PHOSPHORUS ACIDS—I. O,O-ALKYLENE AND DIALKYL DITHIOPHOSPHATES OF TITANIUM(IV)

J. S. YADAV, R. K. MEHROTRA and G. SRIVASTAVA*

The Chemical Laboratories, University of Rajasthan, Jaipur-302 004, India

(*Received* 19 *September* 1986; *accepted after revision* 17 *March* 1987)

Abstract—O,O-Alkylene and dialkyl dithiophosphates of titanium(IV), $Cl_{4-n}Ti(dtp)_n$ [$n = 2$, 3 and 4; dtp = $S(S)\overline{POCMe_2CMe_2O}$ or $S(S)P(OEt)_2$; $n = 4$ and dtp = $S(S)\overline{POCHMeCHMeO}$, $S(S)\overline{POCH_2CMe_2CH_2O}$ and $S(S)P(OPr^i)_2$] have been synthesized by the reactions of titanium tetrachloride with ammonium or sodium salts of O,O-alkylene and dialkyl dithiophosphoric acids in appropriate stoichiometric ratios in refluxing benzene. All these complexes are hydrolysable, dark red semi-solids or viscous liquids and are soluble in common organic solvents when freshly prepared. Ionic tetrachlorodithiophosphatotitanate(IV) complexes, $[M]^+[TiCl_4(S_2\overline{POCMe_2CMe_2O})]^-$ (M = ammonium or pyridinium) have been obtained as insoluble yellow solids by mixing the reactants in equimolar ratios. All of these compounds have been characterized by elemental analyses, IR and NMR (^1H, ^{13}C and ^{31}P) spectral studies. A few codisproportionation reactions of these dithiophosphato complexes have also been studied by ^{31}P NMR spectroscopy.

The coordination chemistry of titanium(IV) with oxygen donor ligands is confined mainly to 6-coordinate octahedral complexes. Thus, the reaction of titanium tetrachloride with excess acetylacetone stops after the formation of octahedral dichlorotitanium bis(acetylacetonate), $TiCl_2(acac)_2$ as the final product.[1] Similarly 1 : 1 complexes of the type $TiCl_4 \cdot OPCl_3$[2] and $TiCl_4 \cdot CH_3COOEt$[3] dimerise through chlorine bridges to give octahedral structures.

Although titanium is a class A metal, it lies closer to the border-line of class A/class B character and forms a variety of stable complexes with sulphur donor ligands. Among these, titanium(IV) complexes of 1,1′-dithio ligands, particularly *N*,*N*-dialkyldithiocarbamic acids, have generated much interest in recent years.[4] In contrast to β-diketones, the dithiocarbamate ligands have been found to stabilise higher coordination states of titanium, probably due to their low charge and small bite. Thus derivatives of the type $Cl_2Ti(S_2CNR_2)_2$,[5] $ClTi(S_2CNR_2)_3$[6] and $Ti(S_2CNR_2)_4$[7] have been shown to contain 6-, 7- and 8-coordinated titanium atoms, respectively.

O,O-Dialkyl (and alkylene) dithiophosphoric acids behave as versatile dithio ligands[8] and form a variety of complexes with transition[9] as well as non-transition[10] elements. Surprisingly, except for some preliminary investigations[11] on reactions of titanium tetrachloride with ammonium diethyl and diisopropyl dithiophosphates, no systematic work on dithiophosphato complexes of group IV transition metals has been carried out as yet. The present communication deals with the synthesis and characterization of some acyclic and cyclic tetrakis dithiophosphates and mixed chloride dithiophosphates of titanium(IV).

EXPERIMENTAL

Owing to the extremely hydrolysable nature of the derivatives of titanium(IV), rigorous precautions were taken to exclude moisture during experimental manipulations. Solvents (benzene, chloroform, pyridine and DMF) and alcohols (ethanol and isopropanol) were dried before use by standard methods. Titanium tetrachloride (E.

* Author to whom correspondence should be addressed.

Merck) was distilled (b.p. 136.4°C) before use. O,O-Dialkyl[12] and alkylene[13] dithiophosphoric acids and their ammonium/sodium salts were prepared by methods reported in the literature. Sulphur was estimated gravimetrically as barium sulphate. Titanium was estimated as titanium oxide by the cupferon method. Phosphorus was estimated as ammonium magnesium phosphate hexahydrate and chlorine by Volhard's method.

IR spectra were recorded as neat liquids or nujol mulls using a Perkin–Elmer 577 spectrometer in the range 4000–200 cm^{-1} with CsI cell windows. ^1H NMR spectra were recorded in chloroform using a Perkin–Elmer R12B spectrometer using TMS as an external standard. ^{31}P and ^{13}C NMR spectra were recorded in chloroform/benzene using a Jeol FX 90 Q spectrometer with H_3PO_4 and TMS as external standards, respectively.

Synthetic methods

(1) *Reaction of titanium tetrachloride with ammonium O,O-tetramethylethylene dithiophosphate in 1 : 1 molar ratio.* On mixing a suspension of ammonium O,O-tetramethylethylene dithiophosphate (1.35 g, 5.89 mmol) in benzene (~ 30 cm^3) with titanium tetrachloride (1.10 g, 5.79 mmol) in the same solvent (~ 20 cm^3), the solution turned red immediately and an orange solid was precipitated out. The reaction mixture was refluxed for ~ 3 h and the product separated by filtration, washed several times with benzene and dried under reduced pressure to yield an orange powdery solid (2.44 g, 92%), m.p. 206°C. Found: Ti, 11.5; S, 15.3; P, 7.3; Cl, 29.3. Calc. for $C_6H_{16}Cl_4NO_2PS_2Ti$: Ti, 11.4; S, 15.3; P, 7.4; Cl, 29.5%.

(2) *Reaction of titanium tetrachloride with O,O-tetramethylethylene dithiophosphoric acid in presence of pyridine in 1 : 1 molar ratio.* Titanium tetrachloride (0.98 g, 5.16 mmol) in benzene (~ 20 cm^3) was added to O,O-tetramethylethylene dithiophosphoric acid (1.11 g, 5.23 mmol) in ~ 30 cm^3 benzene resulting into a red solution. An orange precipitate was formed on adding pyridine (0.41 g, 5.18 mmol) in ~ 20 cm^3 benzene drop by drop with constant stirring to the above. The contents were stirred for ~ 3 h at room temperature to ensure the completion of the reaction. The precipitate (2.15 gm, 86%) was filtered, washed with benzene and dried under reduced pressure yielding an orange powdery solid, m.p. 196°C. Found: Ti, 10.0; S, 13.3. Calc. for $C_{11}H_{18}Cl_4NO_2PS_2Ti$: Ti, 10.0; S, 13.3%.

(3) *Reactions of titanium tetrachloride with ammonium/sodium O,O-alkylene and dialkyl dithiophosphates in 1 : ⩾ 2 molar ratios.* Titanium tetrachloride in benzene was added to a suspension of ammonium/sodium alkylene or dialkyl dithiophosphate in benzene in different molar ratios (1 : 2, 1 : 3 and 1 : 4). The reaction mixture was refluxed for ~ 3 h and the precipitated ammonium/sodium chloride was removed by filtration, followed by removal of solvent under reduced pressure. The product was finally washed with *n*-hexane and dried.

The relevant data for the above reactions have been summarised in Table 1.

RESULTS AND DISCUSSION

Titanium tetrachloride reacts readily with ammonium O,O-tetramethylethylene dithiophosphate in equimolar ratio in benzene at ambient temperature with precipitation of a 1 : 1 complex, ammonium dithiophosphatotetrachlorotitanate, **I**. A similar pyridinium complex, **II** was also obtained on adding pyridine to an equimolar mixture of titanium tetrachloride and tetramethylethylene dithiophosphoric acid in benzene.

$$TiCl_4 + NH_4S_2\overline{POCMe_2CMe_2O} \rightarrow [NH_4]^+[Cl_4TiS_2\overline{POCMe_2CMe_2O}]^-$$

I

$$TiCl_4 + HS_2\overline{POCMe_2CMe_2O} + C_5H_5N \rightarrow [C_5H_5NH]^+[Cl_4TiS_2\overline{POCMe_2CMe_2O}]^-.$$

II

Both the above complexes are orange solids, insoluble in common organic solvents but soluble in dimethylformamide (DMF). The attachment of the dithiophosphate moiety to titanium is readily indicated by the presence of absorption at 350 and 390 cm^{-1} in the IR spectra of these compounds which could be assigned to ν Ti–S and ν Ti–Cl, respectively. It may be pointed out that anionic titanate complexes containing hexacoordinated titanium, e.g. $[TiX_6]^{2-}$, X = F, Cl and Br and $[TiCl_5(H_2O)]^-$, are well known.[14] The titanate complexes described here may also contain a similar hexacoordinated titanium due to the well known bidentate behaviour of the dithiophosphate moiety.

Interestingly, the ^{31}P NMR chemical shifts of these complexes (**I** and **II**) in DMF are 123.6 and 123.8 ppm respectively which are similar to the values obtained for O,O-tetramethylethylene dithiophosphate anion in the ionic salts (e.g. ammonium tetramethylethylene dithiophosphate shows a shift of 123.8 ppm in DMF). Thus, the ^{31}P NMR data indicate that in DMF solution, the titanate com-

Table 1. Synthesis of titanium(IV) O,O-alkylene and dialkyldithiophosphates

Sl. No.	Reactants (g)		Molar ratio	Product physical state	Compound number	Yield %	Analyses % found (calc.)			
	$TiCl_4$	Amm./Sod. Dithiophosphate					Ti	S	P	Cl
1.	1.43	$NH_4S_2\overline{POCMe_2CMe_2O}$ 3.45	1:2	$Cl_2Ti(S_2\overline{POCMe_2CMe_2O})_2$ Orange sticky solid	III	56	9.0 (8.8)	23.8 (23.7)	11.3 (11.5)	13.0 (13.1)
2.	0.94	3.43	1:3	$ClTi(S_2\overline{POCMe_2CMe_2O})_3$ Orange sticky semisolid	IV	96	6.7 (6.7)	26.7 (26.8)	12.9 (13.0)	4.7 (4.9)
3.	0.60	2.93	1:4	$Ti(S_2\overline{POCMe_2CMe_2O})_4$ Dark red viscous liquid	V	97	5.4 (5.4)	28.8 (28.7)	13.8 (14.0)	—
4.	0.59	$NH_4S_2\overline{POCHMeCHMeO}$ 2.55	1:4	$Ti(S_2\overline{POCHMeCHMeO})_4$ Red sticky solid	VI	97	6.2 (6.1)	32.9 (32.8)	—	—
5.	1.02	$NH_4S_2\overline{POCH_2CMe_2CH_2O}$ 4.63	1:4	$Ti(S_2\overline{POCH_2CMe_2CH_2O})_4$ Red sticky solid	VII	98	5.8 (5.7)	30.7 (30.6)	14.7 (14.8)	—
6.	0.57	$NaS_2P(OEt)_2$ 1.26	1:2	$Cl_2Ti[S_2P(OEt)_2]_2$ Orange semisolid	VIII	93	9.8 (9.8)	26.3 (26.2)	12.5 (12.7)	14.3 (14.5)
7.	0.52	1.73	1:3	$ClTi[S_2P(OEt)_2]_3$ Orange sticky solid	IX	98	7.6 (7.5)	30.2 (30.1)	14.5 (14.6)	5.5 (5.6)
8.	1.13	5.00	1:4	$Ti[S_2P(OEt)_2]_4$ Red viscous liquid	X	93	6.1 (6.1)	32.5 (32.5)	15.5 (15.7)	—
9.	0.24	$NaS_2P(OPr^i)_2$ 1.49	1:4	$Ti[S_2P(OPr^i)_2]_4$ Red viscous liquid	XI	94	5.4 (5.3)	28.5 (28.4)	—	—

plexes undergo solvolysis to generate dithiophosphate anions:

$$[Cl_4TiS_2\overline{POCMe_2CMe_2O}]^- + 2DMF \rightarrow Cl_4Ti \cdot 2DMF + [S_2\overline{POCMe_2CMe_2O}]^-$$

The above solvolysis is further indicated by the conductivity data of complexes **I** and **II**. The molar conductance values (73.0 and 71.2 $ohm^{-1}\ cm^{-1}\ mol^{-1}$, respectively) for 0.01 M DMF solutions of these are almost identical to the values observed for ammonium and pyridinium dithiophosphates (70.3 and 71.7 $ohm^{-1}\ cm^{-1}\ mol^{-1}$, respectively) under similar conditions and these values are consistent with their 1 : 1 electrolytic nature.[15,16] Formation of a stable nonionic 1 : 2 complex between $TiCl_4$ and DMF has already been reported[17] in the literature.

Reactions of ammonium O,O-tetramethylethylene dithiophosphate with titanium tetrachloride in higher than equimolar ratios in refluxing benzene result in replacement of the chlorines by dithiophosphate moieties and by adjusting the molar ratios of the reactants, the bis-, tris- and tetrakis-(dithiophosphates) of titanium can be prepared.

$$TiCl_4 + n NH_4S_2\overline{POCMe_2CMe_2O} \rightarrow Cl_{4-n}Ti[S_2\overline{POCMe_2CMe_2O}]_n + n NH_4Cl$$

III, $n = 2$
IV, $n = 3$
V, $n = 4$.

The products are obtained by filtering off ammonium chloride, removing the solvent and washing the residue with *n*-hexane. These replacement reactions are rather slow. The bis-derivative is obtained in poor yield and for the tetrakis-derivative, a slight excess of the ammonium dithiophosphate and longer refluxing period is required. It seems that ammonium tetrachlorodithiophosphatotitanate (formed initially) and ammonium dithiophosphate are both insoluble in benzene and would react quite sluggishly resulting in a low yield of titanium dichloride bis(dithiophosphate).

The above route was employed for the synthesis of additional examples of titanium tetrakis-(cyclic dithiophosphates):

$$TiCl_4 + 4NH_4dtp \rightarrow Ti(dtp)_4 + 4NH_4Cl$$

VI, dtp = $S_2\overline{POCHMeCHMeO}$
VII, dtp = $S_2\overline{POCH_2CMe_2CH_2O}$

For the sake of comparison, a few selected examples of acyclic dithiophosphate derivatives of titanium have also been prepared by the reaction of titanium tetrachloride with sodium dialkyldithiophosphates in refluxing benzene:

$$TiCl_4 + n Nadtp \rightarrow Cl_{4-n}Ti(dtp)_n + n NaCl$$

VIII, $n = 2$, dtp = $S_2P(OEt)_2$
IX, $n = 3$, dtp = $S_2P(OEt)_2$
X, $n = 4$, dtp = $S_2P(OEt)_2$
XI, $n = 4$, dtp = $S_2P(OPr^i)_2$.

The above reactions appear to be faster than the corresponding reactions of ammonium cyclic dithiophosphates and require less refluxing time.

All of the above dithiophosphate derivatives (**III**–**XI**) are yellowish-red semisolids or highly viscous liquids which are miscible with benzene and chloroform but immiscible with *n*-hexane and can be purified by washing with the latter solvent. These compounds are very susceptible to hydrolysis. The intense colour of the complexes is indicative of the high polarizing capacity of the small titanium atom. For comparison, it may be mentioned that similar complexes of zirconium are white solids.

The purity of these compounds was easily checked by their proton decoupled ^{31}P NMR spectra which show only a single peak. The mixed acyclic derivative **VIII**, however, appears to be prone to disproportionation. The freshly prepared compound in benzene (after filtering off the precipitated sodium chloride) shows a single ^{31}P NMR peak at 84.4 ppm. However, on removing the solvent and redissolving it in benzene after a few days, the compound shows peaks at 88.0, 87.4, 85.7 and 84.2 ppm, thus indicating the presence of all the four disproportionation products $Cl_nTi[S_2P(OEt)_2]_{4-n}$, $n = 0$, 1, 2 and 3. The corresponding cyclic derivative **III**, on the other hand, does not show any tendency to disproportionate under similar conditions.

The highly viscous and hydrolysable nature of titanium dithiophosphates precluded any attempt to determine their molecular weights. The dithiophosphate moieties were changed with the unfulfilled hope to get a crystalline sample for X-ray diffraction data. Titanium(IV) dithiophosphates also show ageing effect, on keeping for longer periods in stoppered flasks at room temperature, their colour is darkened and the solubility in benzene is reduced. The ageing effect is more pronounced in the open chain derivatives which are converted into intractable solids in about a month.

The derivatives **III**–**XI** have been subjected to IR and multinuclear NMR (^1H, ^{13}C and ^{31}P) spectral studies and data are summarised in Table 2.

Table 2. ^{1}H, ^{31}P and ^{13}C NMR spectral data for titanium(IV) O,O-alkylene and dialkyl dithiophosphates

Compound number	^{1}H chemical shift[a] in δ ppm (in chloroform)	^{31}P chemical shift in δ ppm (in benzene)	^{13}C chemical shift[b] in δ ppm
III	1.50, s	94.4	90.63, s (O<u>C</u>—) 23.64, d, (<u>C</u>H$_3$) J = 6.10 Hz
IV	1.40, s	93.7	90.50, s, (O<u>C</u>—) 23.86, d (CH$_3$) J = 6.10 Hz
V	1.45, s	92.4	90.53, s, (O<u>C</u>—) 23.67, d (<u>C</u>H$_3$) J = 4.88 Hz
VI	—	96.4, 95.0	
VII	1.05, S, 24H(-CH$_3$) 3.95, d (J = 15 Hz), 16H (-CH$_2$O)	76.5	
VIII	1.25, t (J = 7 Hz), 12H(–CH$_3$) 3.80–4.50, dq (J = 10 and 6 Hz), 8H(-CH$_2$O)	84.4	
IX	1.20, t (J = 7 Hz), 18H (-CH$_3$) 3.70–4.40, dq (J = 10 and 6 Hz), 12H (-CH$_2$O)	87.3	
X	1.25, t (J = 7 Hz), 24H (-CH$_3$) 3.80–4.50, dq (J = 11 and 6.5 Hz), 16H (-CH$_2$O)	85.6	
XI	1.25, d (J = 6 Hz), 48H (-CH$_3$) 4.40–5.00, m, 8H (-CHO)	82.3	

[a] s = singlet, d = doublet, t = triplet, dq = double quartet and m = multiplet.
[b] III and IV in chloroform, V in benzene.

Infra-red spectral studies

Due to their immiscibility with nujol, suitable mulls for IR spectral study could be made with difficulty. The assignment of relevant peaks have been made on the basis of published literature[9,10,18] on other metal dithiophosphates and on titanium-sulphur bonded compounds.[5,19] A comparison of the spectra of parent ligands (O,O-alkylene and dialkyl dithiophosphoric acids) and the corresponding titanium derivatives reveal the following observations:

(i) The bands due to ν (P)–O–C and ν P–O–(C) present in the region 1150–980 cm^{-1} and 835–770 cm^{-1}, respectively in the parent acids do not show any change in the titanium complexes. In the cyclic derivatives the strong intensity band present at $\sim$ 950 cm^{-1} and attributed to ring vibrations (probably coupled with C–C-stretching vibrations[20,21]) similarly remains unchanged on complexation.

(ii) The band due to ν P=S present at 670–630 cm^{-1} in the acyclic[9] and at 690–670 cm^{-1} in the cyclic[13] derivatives shows a small but notable shift ($\Delta\nu$ = 20–10 cm^{-1}) to lower frequencies in the titanium complexes indicating the involvement of the thiophosphoryl sulphur in bonding to the metal atom.

(iii) All of the titanium complexes have a new band of weak intensity in the region 360–340 cm^{-1} which may be assigned to ν Ti–S vibrations.[5,19] In the complexes **VIII–X**, a regular lowering of this band (**VIII**, 335 cm^{-1}, **IX**, 325 cm^{-1}, **X**, 320 cm^{-1}) may be associated with an increase in the coordination number of titanium atom.

(iv) In the spectra of all the mixed chloride dithiophosphate derivatives, a low intensity band is present in the ν Ti–Cl region of 400–380 cm^{-1}. The position of this band in the monochloride derivative is lower than in the dichloride derivative (e.g. **IX**, 380 cm^{-1}, **VIII**, 400 cm^{-1}) and this may again be attributed to the higher coordination number of titanium in the former.[22]

NMR spectral studies

The ^{1}H and ^{13}C NMR spectra of titanium complexes are remarkably similar to those of the ligand dithiophosphoric acids, probably due to the large distance between the metal atom and these nuclei.

The spectra, however, indicate the presence of single species in each case.

In the ^1H NMR spectra, the signal due to S–H proton is as expected absent. The tetramethylethylene dithiophosphate derivatives show only a singlet, thus indicating negligible ^4J P–H coupling. All other derivatives, however, have hydrogens attached to the α-carbon atoms of the alkoxy or glycoxy groups and these show coupling with phosphorus (^3J P–H being in the range 10–15 Hz).

The ^{13}C NMR spectra of only the tetramethylethylene derivatives (**III** and **IV** in chloroform and **V** in benzene) were measured. In these, the tertiary carbons appears as singlet at ~ 90.5 ppm and the methyl carbons give a doublet around 23.7 ppm, thus showing that whereas there is no observable two-bond C–P coupling, the corresponding three-bond coupling is present in the range of 4–6 Hz. It may be mentioned that in the parent acid (tetramethylethylene dithiophosphoric acid in CCl_4), the coupling of both the types of carbons with phosphorus is observed ($^2J = 2.44$; $^3J = 4.88$ Hz). Interestingly, the ^3J C–P value remains the same in tetrakis-derivative **V**, but increases to 6.66 Hz in the mixed chloride dithiophosphate derivatives (**III** and **IV**).

^{31}P NMR studies of titanium dithiophosphates (Table 2) lead to the following observations:

(i) The chemical shifts of O,O-alkylene and dialkyl dithiophosphoric acids increase in the following order:

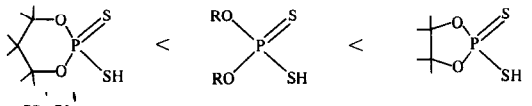

Phosphorus in 6-membered 1,3,2-dioxaphosphorinanes is more shielded where as the same in 5-membered 1,3,2-dioxaphospholanes is less shielded than phosphorus in the corresponding acyclic compounds. Such observations have been made before also with different phosphorinanes and phospholanes.[23]

(ii) The ^{31}P shifts for titanium dithiophosphate complexes are surprisingly almost in the same range as those for the parent acids.

(iii) In tetramethylethylene dithiophosphate complexes (**III–V**), the chemical shift increases, although only slightly, with increasing number of chlorine at the metal. In open chain comlexes also, the same pattern is obtained with the exception of the dichloro derivative.

(iv) All compounds give a single peak when freshly prepared except **IX** (which appears to be contaminated with the tetrakis derivative) and **VI** which may be present as a mixture of diasterioisomers.

(v) Titanium tetrakis (tetramethylethylene dithiophoshate) (**V**) shows ^{31}P signal at 92.4 ppm in benzene. However, in pyridine, it shows two peaks, one of lower intensity at 123.9 ppm and another of higher intensity at 71.3 ppm.

Phosphorus chemical shifts of various metal dithiohosphate complexes have been reported in recent years and an attempt has also been made by Glidewell[24] to correlate the shifts in metal diisopropyl dithiophosphates with the bonding behaviour (monodentate, bidentate or ionic) of the ligand. It was suggested that phosphorus deshielding increases in the order monodentate attachment < bidentate attachment < $[(Pr^iO)_2PS_2]^-$ anion.

Phosphorus chemical shifts in general depend on many factors (e.g. bond angle, steric effect, size of the ring and electronegativity of attached groups)[23,25] and our attempts to correlate the same in metal alkylene dithiophosphates on the lines of Glidewell have not been successful. For example, trimethyltin tetramethylethylene dithiophosphate and dimethyltin bis(tetramethylethylene dithiophosphate) have been shown to contain 4- and 6-coordinated tin respectively on the basis of ^{119}Sn NMR shifts and also by $^1J^{13}C^{-119}Sn$ values.[26] However, the ^{31}P chemical shifts of these two compounds are almost the same (104.5 and 102.1 ppm, respectively).[26]

We, therefore, believe that in titanium dialkyl dithiophosphates also, the ^{31}P chemical shifts are helpful in identification and determination of the purity of compounds, but one should be very cautious in correlating these with the structural features of the compounds. However, the observations that ^{31}P signal of the derivative **V** in pyridine splits into two peaks (one upfield at 71.3 and other down field at 123.9 ppm) can be correlated with the formation of an ionic species of the type **XII** in which there are three monodentate and one ionic dithiophosphate moieties. It is thus an indirect proof of the bidentate

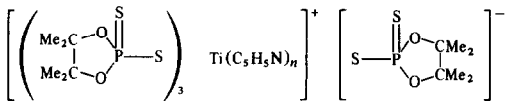

XII

behaviour of all the ligand moieties towards titanium in non polar solvents or in neat compounds. It may be pointed out that a change from bidentate to monodentate behaviour of dithiophosphate moieties in transition metal complexes in the presence of a stronger coordinating ligand has been recorded before. Thus, tetra coordinate $Ni[S_2P(OMe)_2]_2$ forms a 5-coordinate 1 : 1 complex with the bidentate ligand 2,9-dimethyl-1,10-phenanthroline, the crystal structure of which shows one

of the dtp ligands being monodentate.[27] Similarly, palladium and platinum complexes, $M[S_2P(OEt)_2]_2$ react with tertiary phosphines by stepwise cleavage of metal–sulphur bonds to form 4-coordinate 1 : 1 and 1 : 2 adducts having unidentate-bidentate and bidentate-ionic dtp ligands, respectively.[28]

The known titanium-sulphur bonded compounds are very limited in number and in all these cases, titanium shows an enhanced tendency to increase its coordination number. Titanium tetrathiolates are oligomeric in nature (with suggested coordination number eight);[29] the dithiocarbamates, on the other hand, are monomeric with the ligand always acting as bidentate. In case of titanium dithiophosphates also, the IR and ^{31}P NMR spectroscopic data, as discussed earlier, point towards bidentate attachment of the ligand moieties.

Further, due to the similarity between dithiocarbamate and dithiophosphate moieties, the titanium dithiophosphate complexes are expected to be structurally similar to the corresponding dithiocarbamate complexes. On the basis of this comparison the dichloride bis-(dithiophosphate) complexes should be six coordinated octahedral, the monochloride tris-(dithiophosphates) should be 7-coordinated pentagonal bipyramidal and the tetrakis-(dithiophosphates) should be 8-coordinated dodecahedral. The octahedral dichloro bis-(chelate) complexes of titanium (e.g. $Ti(acac)_2Cl_2$,[30] $Ti(dtc)_2Cl_2$[6a] etc.) have invariably *cis* geometry and the same may be expected for the $Ti(dtp)_2Cl_2$ complexes also.

As described earlier, the NMR (^{31}P, ^{13}C and ^1H) data for all the dithiophosphate derivatives of titanium show the presence of only one type of ligand moiety in the molecule at ambient temperature and, thus, indicate the stereochemical non-rigidity of the complexes. Unfortunately variable temperature NMR studies could not be carried out due to lack of facilities. However, it may be worthwhile to mention here that the corresponding dithiocarbamate complexes $Ti(S_2CNR_2)_nCl_{4-n}$ are also stereochemically non-rigid and their variable temperature NMR spectra show that R groups remain equivalent over the temperature range +40 to −90°C.[6a]

Acknowledgement-One of the authors (J.S.Y.) is grateful to the C.S.I.R., New Delhi for providing financial assistance.

REFERENCES

1. R. C. Mehrotra, R. Bohra and D. P. Gaur, *Metal β-diketonates and Allied Derivatives.* Academic Press, London (1978).
2. C. I. Bränden and I. Lindqvist, *Acta. Chem. Scand.* 1960, **14**, 726.
3. L. Brun, *Acta. Cryst.* 1966, **20**, 739.
4. D. Coucouvanis, *Prog. Inorg. Chem.* 1970, **11**, 233; 1979, **26**, 301.
5. E. C. Alyea, B. S. Ramaswamy, A. N. Bhat and R. C. Fay, *Inorg. Nucl. Chem. Lett.* 1973, **9**, 399.
6. (a) A. N. Bhat, R. C. Fay, D. F. Lewis, A. F. Lindmark and S. H. Strauss, *Inorg. chem.* 1974, **13**, 886; (b) D. F. Lewis and R. C. Fay, *J. Am. Chem. Soc.* 1974, **96**, 3843.
7. M. Colapietro, A. Vaciago, D. C. Bradley, M. B. Hursthouse and I. F. Rendel, *J. Chem. Soc., Chem. commun.* 1970, 743; *ibid, J. Chem. Soc. Dalton Trans.* 1972, 1052.
8. I. Haiduc, *Rev. Inorg. Chem.* 1981, **3**, 353.
9. J. R. Wasson, G. M. Wolterman and H. J. Stocklosa, *Topics in Current Chem.* 1973, **35**, 65.
10. R. C. Mehrotra, G. Srivastava and B. P. S. Chauhan, *Coord. Chem. Rev.* 1984, **55**, 207.
11. B. P. S. Chauhan, Ph.D. Thesis, Rajasthan University, India (1980).
12. B. P. Singh, G. Srivastava and R. C. Mehrotra, *J. Organomet. Chem.* 1979, **171**, 35.
13. H. P. S. Chauhan, C. P. Bhasin, G. Srivastava and R. C. Mehrotra, *Phosphorus and Sulphur* 1983, **15**, 99.
14. R. J. H. Clark, *The Chemistry of Titanium and Vanadium.* Elsevier, New York (1968).
15. D. J. Phillips and S. Y. Tyree, *J. Am. Chem. Soc.* 1961, **83**, 1806.
16. R. Ahmad, G. Srivastava and R. C. Mehrotra, *Indian J. Chem.* 1985, **24A**, 557.
17. P. Ehrlich and W. Siebert, *Z. Anorg. Allgem. Chem.* 1960, **303**, 96.
18. D. E. C. Corbridge, *Topics in Phosphorus Chem.* 1969, **6**, 235.
19. S. Kumar and N. K. Kaushik, *Synth. React. Inorg. Met.-Org. Chem.* 1982, **12**, 159.
20. J. Casdeon, W. N. Baxter and W. DeAcetis, *J. Org. Chem.* 1959, **24**, 247.
21. R. A. Y. Jones and A. R. Katritzky, *J. Chem. Soc.* 1960, 4376.
22. D. M. Adams, J. Chatt, J. M. Davidson and J. Gerratt, *J. Chem. Soc.* 1963, 2189.
23. L. D. Quin, *The Heterocyclic Chemistry of Phosphorus.* Wiley Interscience (1981).
24. C. Glidewell, *Inorg. Chim. Acta* 1977, **25**, 159.
25. D. W. Meek and T. J. Mazanec, *Acc. Chem. Res.* 1981, **14**, 266.
26. R. J. Rao, G. Srivastava and R. C. Mehrotra, *J. Organomet. Chem.* 1983, **258**, 155; R. J. Rao, G. Srivastava, R. C. Mehrotra, B. S. Saraswat and J. Mason, *Polyhedron* 1984, **3**, 485; R. J. Rao, Ph.D. Thesis, Rajasthan University, India (1984).
27. P. S. Shitty and Q. Fernando, *J. Am. Chem. Soc.* 1970, **92**, 3964.
28. J. M. C. Alison and T. A. Stephenson, *J. Chem. Soc. Dalton Trans.* 1973, 254.
29. D. C. Bradley and P. A. Hammersley, *J. Chem. Soc.* 1967, 1894.
30. R. C. Fay and R. N. Lowry, *Inorg. Chem.* 1967, **6**, 1512.

Polyhedron Vol. 6, No. 8, pp. 1695–1698, 1987
Printed in Great Britain

0277–5387/87 $3.00+.00

THE MOLECULAR STRUCTURE OF BIS[BIS(TRIPHENYLPHOSPHINE)SILVER] HEXACHLOROOSMIUM(IV)

P. D. ROBINSON

Department of Geology

and

C. C. HINCKLEY,* M. MATUSZ and P. A. KIBALA

Department of Chemistry and Biochemistry, Southern Illinois University, Carbondale, IL 62901, U.S.A.

(*Received* 17 *November* 1986; *accepted after revision* 17 *March* 1987)

Abstract—The molecular structure of a new osmium–silver complex is reported. The compound crystallizes in space group $P\bar{1}$ with $a = 14.486(3)$ Å, $b = 14.711(3)$ Å, $c = 10.233(2)$ Å, $\alpha = 95.55(2)°$, $\beta = 98.75(2)°$, $\gamma = 126.88(1)°$, $V = 1675(2)$ Å^3, and $Z = 1$. Full-matrix least-squares refinement with 3548 independent reflections led to final residual indices of $R = 0.041$ and $R_w = 0.047$. The compound, $OsCl_6Ag_2[P(C_6H_5)_3]_4$, is prepared by precipitation from an acetonitrile solution containing $(n\text{-}Bu_4N)_2OsCl_6$, triphenylphosphine and silver nitrate. The synthesis of $(n\text{-}Bu_4N)_2OsCl_6$ makes use of anhydrous conditions. The molecule is made up of two $Ag(PPh_3)_2$ units which are symmetrically bound to a central $OsCl_6$ group.

The title compound was prepared as part of a study investigating methods of chlorine substitution in $OsCl_6^{2-}$. Osmium–chlorine bonds in the ion are relatively inert, and chlorine substitution represents a synthetic challenge. Legzdins and Nurse[1] made use of silver salts to affect substitutions of iodide in some molybdenum complexes. They obtained silver adducts as isolable intermediates. In the experiment leading to the title compound, a solution of $OsCl_6^{2-}$ with triphenylphosphine was treated with silver nitrate. The result was the formation of excellent dark red crystals in essentially quantitative yield. No reaction of this kind had been reported, and a new silver complex was suspected. An osmium–silver complex was prepared by Clark, and co-workers,[2] who structurally characterized their material and found that it contained an Os–Ag bond. The objective of the work reported in this paper was to structurally characterize the new compound and identify the nature of the silver binding.

* Author to whom correspondence should be addressed.

EXPERIMENTAL

Syntheses

Preparation of $(n\text{-}Bu_4N)_2OsCl_6$. The compound was prepared in a 100 cm^3 round bottom flask equipped with a mantle for warming, a magnetic stirrer, and a reflux condensor. The flask was charged with one ampoule of osmium tetroxide (0.8694 g, 3.42 mmoles) and 10 cm^3 of freshly distilled benzoyl chloride, C_6H_5COCl. In addition to serving as the initial solvent in the preparation, benzoyl chloride insures that solution conditions remain anhydrous throughout the reduction of OsO_4. The reaction mixture was stirred and warmed (50°C) until the OsO_4 dissolved. At this point, 25 cm^3 of 100% ethyl alcohol saturated with gaseous HCl was added through the top of the reflux condensor. The reaction mixture was refluxed for 0.5 h. During the reflux, the color of the reaction mixture changed from pale yellow to deep red and then to orange-yellow. The reaction mixture was allowed to cool, and then evaporated on a rotary evaporator until the solution volume was about 10 cm^3. A

solution of tetra-*n*-butyl ammonium bromide, (*n*-Bu_4N)Br (3.8 g, 11.8 mmoles), in 10 cm^3 of 100% ethyl alcohol was added to the cold (RT) reaction mixture, followed by 100 cm^3 of diethyl ether. The flask was capped and stored overnight in a freezer (−22°C). The precipitate was filtered, washed with diethyl ether and vacuum dried. The yield was 2.107 g (83%) of orange-yellow solid. Found: C, 43.2; H, 8.3; N, 3.1; Cl, 23.9. Calc.: C, 43.3; H, 8.1; N, 3.2; Cl, 24.0%.

Preparation of $OsCl_6Ag_2[P(C_6H_5)_3]_4$. In a typical preparation, 0.2 g (0.2 mmoles) of $(n\text{-}Bu_4N)_2OsCl_6$ was dissolved in 20 cm^3 of acetonitrile together with an excess of triphenylphosphine (0.3 g, 1 mmoles). An excess of silver nitrate (0.1 g, 0.6 mmoles) dissolved in 20 cm^3 of acetonitrile was then added to the solution. The color of the solution became red and small, red crystals precipitated leaving a colorless solution. The solid was filtered, washed first with acetonitrile until tests of the filtrate with Cl^- revealed no remaining Ag^+, and then it was washed with ethyl ether and dried (yield 0.3 g, > 90%). In order to obtain crystals of the size and quality needed for crystal structure analysis, the compound was again prepared (as described above), this time from very dilute solutions (one-fifth the quantities of materials in twice the solvent). An IR spectrum of the compound in the range 400–4000 cm^{-1} exhibited only peaks attributable to triphenylphosphine bound in the complex. Found: C, 52.0; H, 3.6; Cl, 12.9. Calc.: C, 51.8; H, 3.6; Cl, 12.8%.

Crystal data

$OsCl_6Ag_2[P(C_6H_5)_3]_4$; $M = 1667.82$, space group = $P\bar{1}$, $Z = 1$, $a = 14.486(3)$ Å, $b = 14.711(3)$ Å, $c = 10.233(2)$ Å, $\alpha = 95.55(2)°$, $\beta = 98.75(2)°$, $\gamma = 126.88(1)°$, $V = 1675(2)$ $Å^3$, $D_c = 1.65$ g cm^{-3}, $\mu(MoK\alpha)(cm^{-1}) = 29.44$, $F(000) = 824$.

Data collection

Data were collected from a dark red, columnar crystal with dimensions $0.07 \times 0.06 \times 0.12$ mm using a Rigaku AFC-5S diffractometer and graphite monochromatized MoKα radiation ($\lambda = 0.71069$ Å). A total of 25 reflections, in the 2θ range of 9–24° were used for orientation, lattice parameter determination/refinement, and Laue group differentiation. The intensities of 5891 unique reflections were measured (2θ range: 2.5–50°, temperature: 23°C) using θ–2θ scans and a maximum of 3 scan repetitions/reflection in order to obtain $\sigma F/F < 0.10$; 3548 reflections were considered observed with $I > 3\sigma(I)$. Three standard reflections varied −0.20, −0.04 and −1.14% during data collection. All data were corrected for background, Lorentz, polarization, and absorption (numerical method, transmission range: 0.840–0.866).

Structure solution and refinement

Direct methods were used to locate the Os, Ag, Cl, P, and approximately one-half the C atomic sites; the remaining carbons were located by difference Fourier syntheses.

Full matrix least-squares refinement of the non-H atoms proceeded to convergence uneventfully, with all atoms anisotropic. The ring-hydrogens were then placed in geometrically correct positions (C–H = 0.95 Å) and fixed, while all other variables were again refined. The hydrogen generation/refinement procedure was repeated until no significant parameter shifts occured (maximum shift/esd, final cycle: 0.0007). Convergence, with 385 variables, occurred at $R = 0.041$ and $R_w = 0.047$ where $R = \Sigma ||F_o| - |F_c||/\Sigma |F_o|$, $R_w = [\Sigma w(|F_o| - |F_c|)^2/\Sigma w|F_o|^2]^{1/2}$ and $w = 1/\sigma^2(|F_o|)$. The final difference synthesis showed $(\Delta\rho)_{max} = 0.57$ e/$Å^3$ and $(\Delta\rho)_{min} = -0.55$ e/$Å^3$. All calculations were performed with Molecular Structure Corporation's TEXSAN structure analysis package.[3]

The atomic positional and thermal vibration parameters, plus complete distance, angle, and structure factor tables have been deposited with the Editor as supplementary material.

DISCUSSION

The structure of the osmium-silver complex can be described most simply as having a central $OsCl_6$ moiety to which two $Ag(PPh_3)_2$ groups are symmetrically attached (Fig. 1). The osmium atom is located on a center of symmetry within a distorted octahedral array of chloride ions. Each of the silver ions are four-coordinate in distorted tetrahedra formed by two chlorides bridging to the osmium atom and two triphenylphosphine ligands. Selected bond distances and angles are reported in Table 1.

While this compound is unique for osmium, there are several complexes of silver reported in which the silver binding is similar.[4–10] That is, the silver ions are four-coordinate, bridged through two or more atoms to other metal ions, and have two phosphine ligands in their coordination spheres. Of these, the dimer, $\{[(C_6H_5)_3P]_2AgCl\}_2$, may be most directly compared to the osmium-silver complex.[10] In the dimer, the silver ions are bridged by two chloride ions in which the Ag–Cl bond distances are 2.741(2) and 2.596(2) Å. This bond distance asymmetry is typical of halogen bridged silver ions. Bond angles for the dimer are 122.91(7)° for the P–Ag–P angle

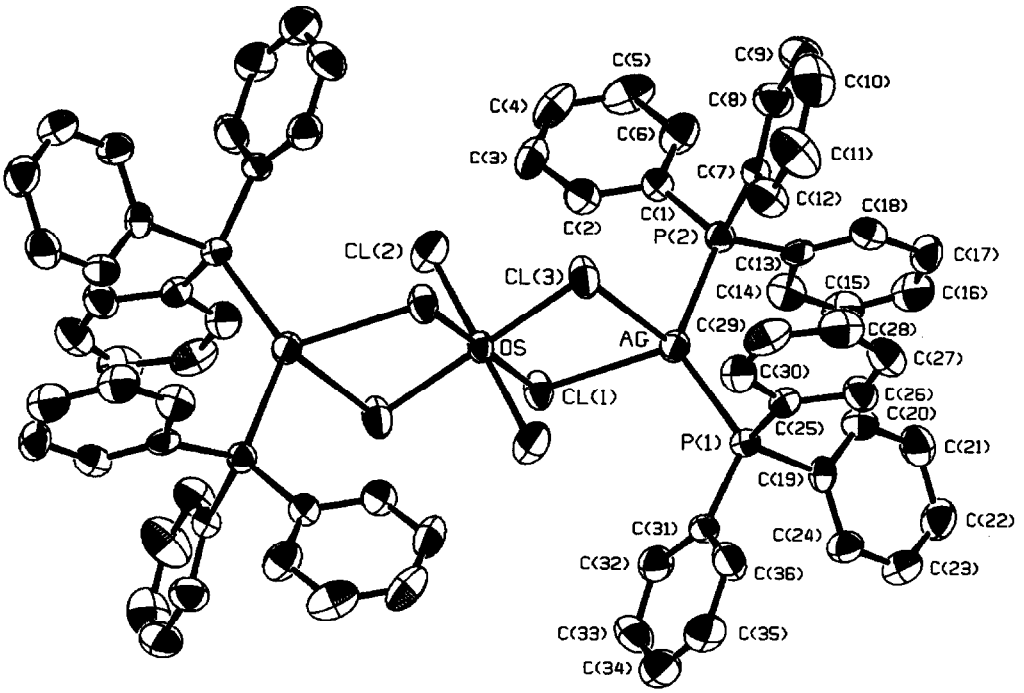

Fig. 1. General view of $OsCl_6Ag_2[P(C_6H_5)_3]_4$ showing labelling scheme. Atoms are represented by their thermal ellipsoids at the 50% probability level. Hydrogen atoms have been omitted for clarity.

and 88.03(6) ° for the Cl–Ag–Cl angle in the bridge.

Silver–chlorine distances in the osmium–silver complex are longer than those in the silver dimer, 2.678(2) and 2.807(3) Å, and the Cl–Ag–Cl bond angle is only 74.05(7)°, a more than 10° reduction from the angle observed in the silver dimer. Silver phosphine distances in the osmium–silver complex are only slightly shorter than those for the dimer, but the P–Ag–P bond angle is significantly larger at 128.49(9)°.

Table 1. Selected bond distances and angles for $OsCl_6Ag_2[P(C_6H_5)_3]_4$

	Bond distances (Å)		
Os—Cl(2)	2.315(3)	P(1)—C(25)	1.82(1)
Os—Cl(3)	2.334(2)	P(1)—C(31)	1.829(9)
Os—Cl(1)	2.356(2)	P(1)—C(19)	1.84(1)
Ag—P(1)	2.452(3)	P(2)—C(1)	1.81(1)
Ag—P(2)	2.455(3)	P(2)—C(13)	1.83(1)
Ag—Cl(1)	2.678(2)	P(2)—C(7)	1.84(1)
Ag—Cl(3)	2.807(3)		
	Bond angles (°)		
Cl(2)—Os—Cl(3)	90.3(1)	C(25)—P(1)—C(19)	105.9(4)
Cl(2)—Os—Cl(1)	90.6(1)	C(25)—P(1)—Ag	107.1(3)
Cl(3)—Os—Cl(1)	89.57(8)	C(31)—P(1)—C(19)	102.7(4)
P(1)—Ag—P(2)	128.49(9)	C(31)—P(1)—Ag	122.8(3)
P(1)—Ag—Cl(1)	111.05(9)	C(19)—P(1)—Ag	112.4(3)
P(1)—Ag—Cl(3)	109.5(1)	C(1)—P(2)—C(13)	103.5(4)
P(2)—Ag—Cl(1)	118.16(9)	C(1)—P(2)—C(7)	105.8(4)
P(2)—Ag—Cl(3)	97.89(9)	C(1)—P(2)—Ag	118.6(3)
Cl(1)—Ag—Cl(3)	74.05(7)	C(13)—P(2)—C(7)	103.6(4)
Os—Cl(1)—Ag	98.26(8)	C(13)—P(2)—Ag	114.5(3)
Os—Cl(3)—Ag	95.28(8)	C(7)—P(2)—Ag	109.5(3)
C(25)—P(1)—C(31)	104.5(4)		

Osmium–chlorine distances in uncomplexed $OsCl_6^{2-}$ average 2.337 Å.[11] When bound to silver in the osmium–silver complex, the Os–Cl distances are 2.356(2) and 2.334(2) Å for the bridging chlorines, and 2.315(3) Å for the chlorine bound only to osmium. Metal–chlorine distances in the bridging structure suggest that each silver ion is relatively strongly bound to one of the bridging chlorines and weakly associated with the other. Cl–Os–Cl angles are essentially 90°, so the asymmetry in the central octahedron is primarily a result of Os–Cl bond distance variation.

REFERENCES

1. P. Legzdins and C. R. Nurse, *Inorg. Chem.* 1982, **21**, 3110.
2. G. R. Clark, C. M. Cochrane, W. R. Roper and L. J. Wright, *J. Organometallic Chem.* 1980, **199**, C35.
3. Molecular Structure Corporation 1985, *TEXSAN Structure Analysis Package*. MSC, 3304 Longmire Drive, College Station, TX 77840.
4. D. M. Ho and R. Bass, *Inorg. Chem.* 1983, **22**, 4073.
5. L. Golic, N. Bulc and W. Dietzsch, *Polyhedron* 1983, **2**, 1201.
6. J. Howatson and B. Morosin, *Cryst. Struct. Commun.* 1973, **2**, 51.
7. J. H. Meiners, J. C. Clardy and J. G. Verkade, *Inorg. Chem.* 1975, **14**, 632.
8. N. W. Alcock, P. Moore, P. A. Lampe and K. F. Mok, *J. Chem. Soc. Dalton* 1982, 207.
9. A. Cassell, *Acta Cryst. B* 1975, **31**, 1194.
10. A. Cassell, *Acta Cryst. B* 1979, **35**, 174.
11. E. E. Kim, K. Eriks and R. Magnuson, *Inorg. Chem.* 1984, **23**, 393.

Polyhedron Vol. 6, No. 8, pp. 1699–1701, 1987
Printed in Great Britain

0277–5387/87 $3.00+.00

METAL COMPLEXES OF HYBRID OXYGEN–ARSENIC LIGANDS—VI. STABILIZATION OF MANGANESE(II)–ARSINE COMPLEXES USING LIGANDS FROM *o*-$R_2AsC_6H_4CO_2Na$

SWARN S. PARMAR,* HARKEERAT K. BHARAJ and MANOHAR L. SAIGHAL

Chemistry Department, Guru Nanak Dev University, Amritsar-143005, India

(*Received* 20 *January* 1987; *accepted after revision* 1 *April* 1987)

Abstract—A reaction of $MnCl_2 \cdot 4H_2O$ with *o*-$R_2AsC_6H_4CO_2$ Na in 1:2 molar ratio in 95% EtOH yields four manganese(II)–monotertiaryarsine complexes [Mn(*o*-$Me_2AsC_6H_4CO_2$)Cl]·$0.5H_2O$, [Mn(*o*-$R_2AsC_6H_4CO_2)_2(H_2O)_2] \cdot nH_2O$ ($n = 0$ and R = Ph or *p*-tolyl; $n = 1$ and R = Et). The stabilization of these four complexes is significant in view of the only two already known.

Manganese(II) has little tendency to form complexes with arsines since these are extremely susceptible to oxidation even by the traces of moisture in the presence of this metal ion.[1] Manganese(II) halides are known to react with $AsPh_3$ to yield manganese(II)–arsine oxide complexes $Mn(OAsPh_3)_2X_2$.[2] Manganese(II)–arsine complexes [Mn(L–L′)$_2X_2$] (X = Cl or Br; L–L′ = $AsMe_2$(*o*-$C_6H_4EMe_2$) with E = As or Sb) have been obtained only in the absence of oxygen and moisture.[3] However, a nitrogen–arsenic hybrid ligand has been reported to stabilize two manganese(II)–monotertiary arsine complexes [Mn($AsMe_2$(*o*-$C_6H_4NH_2$))X_2] (X = Br or ClO_4) even in the presence of both; water being removed azeotropically.[4] We now report the characterization of the products from reactions of $MnCl_2 \cdot 4H_2O$ with (1) (Fig. 1) in 95% EtOH to know if the oxygen–arsenic ligands derived from (1) also stabilize the manganese(II)–arsine complexes in the presence of both oxygen and water.

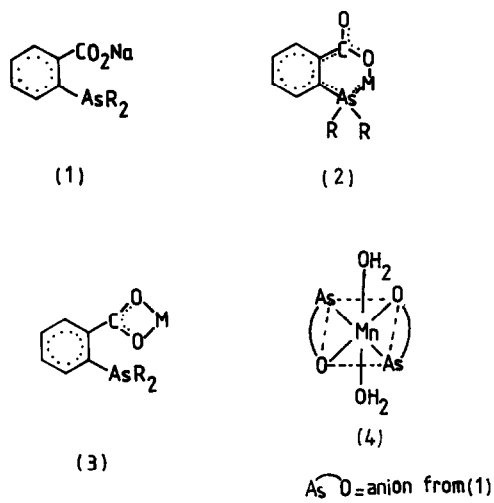

Fig. 1.

EXPERIMENTAL

Mn(*o*-$Me_2AsC_6H_4CO_2$)Cl·$0.5H_2O$, [Mn(*o*-$R_2AsC_6H_4CO_2)_2(H_2O)_2] \cdot nH_2O$ ($n = 0$ *and* R = Ph *or p*-tolyl; $n = 1$ *and* R = Et)

A white solid first formed on the addition of [(1), 6 mmol] in 95% EtOH (20–25 cm^3) to a 95% ethanolic solution (10 cm^3) of $MnCl_2 \cdot 4H_2O$ (0.6 g, 3 mmol) dissolved on shaking. However, these contents on refluxing (30 min for R = Me or Et and 1 h for R = Ph or *p*-tolyl) gave a white† compound which was filtered washed with 95% EtOH (to remove NaCl), EtOH and Et_2O and finally dried in vacuo. Yield: 60%.

Physical methods

Details of spectral and other measurements, preparation of (1) and estimation of arsenic(III) have been published elsewhere.[5,6]

* Author to whom correspondence should be addressed.

† The colour changes to dirty-white or light-pink on drying.

Table 1. Analytical and IR (cm^{-1}) data of manganese(II) complexes

Complex (colour, m.p. ° C)	Found (calc.) (%) C	H	As^{III}	Mn	ν(OH) (δ(HOH))	$\nu_{as}(CO_2)$ ($\nu_s(CO_2)$)
$[Mn(o\text{-}Me_2AsC_6H_4CO_2)Cl]\cdot 0.5H_2O$	34.0	3.7	23.7	16.9	3420m	1590
(dirty white, 198)	(33.3)	(3.4)	(23.1)	(17.0)	(1615sh)	(1388)
$[Mn(o\text{-}Et_2AsC_6H_4CO_2)_2(H_2O)_2]H_2O$	41.3	5.0	—[a]	9.3	3500m	1587
(light pink, 300)	(42.3)	(5.6)		(8.8)	3410br (1610sh)	(1385)
$[Mn(o\text{-}Ph_2AsC_6H_4CO_2)_2(H_2O)_2]$	58.4	4.8	19.6	6.8	3410brm	1590
(light pink, 144)	(57.4)	(4.1)	(19.1)	(7.0)		(1375)
$[Mn(o\text{-}(p\text{-tolyl})_2AsC_6H_4CO_2)_2(H_2O)_2]$	59.9	4.5	17.6	6.6	3410brm	1595
(dirty white, 175)	(59.6)	(4.7)	(17.8)	(6.5)	(1620sh)	(1395)

[a] As^{III} could not be estimated because of its spontaneous oxidation to As^{V} as evidenced by the presence of As=O band in the IR spectrum of the resulting compound.

RESULTS AND DISCUSSION

The analytical (C, H, N, As) TGA and IR data of the reaction products suggests that $MnCl_2\cdot 4H_2O$ reacts with (1) in 1 : 2 molar ratio in 95% EtOH to yield four manganese(II)–arsine complexes $[Mn(o\text{-}Me_2AsC_6H_4CO_2)Cl]\cdot 0.5H_2O$ and $[Mn(o\text{-}R_2AsC_6H_4CO_2)_2(H_2O)_2]\cdot nH_2O$ ($n = 0$ for R = Ph or *p*-tolyl; $n = 1$ for R = Et). The presence of water in these complexes has been indicated by the appearance of broad ν(OH) and shoulder δ(OH) bands.[7,8] The $\rho(H_2O)$ band expected[9] at 800–900 cm^{-1} seems to be obscured by the ligand δ(OCO) band.[10]

Application of the reported criterion for the assignment of the bonding mode of these ligands to the $\nu_{as}(CO_2)$ and $\nu_s(CO_2)$ values (Table 1) of these four complexes suggests the coordination of carboxylate oxygen and arsenic(III) as given in structure (2)[11] and rules out the structure (3).[6,12]

The observed room temperature μ_{eff} values of 5.37–5.98 B.M of these complexes suggest the presence of high-spin manganese(II); the subnormal μ_{eff} value of 5.40 B.M for the chloro complex being attributed to Mn–Cl–Mn bridging indicated by the appearance of a ν(Mn–Cl) band[13] at 280 cm^{-1}. However, the subnormal μ_{eff} value of 5.37 B.M for the complex with R = Et is not understood while the values for the complexes with R = Ph (5.98 B.M) and *p*-tolyl (5.82 B.M) are normal as expected. An octahedral stereochemistry is also favoured by the appearance of doubly forbidden very weak bands in their electronic absorption spectra. Only the complexes with R = Ph and *p*-tolyl give an X-band EPR signal at room temperature as a broad single line with $g \approx 2$ which indicates their nearly-axial symmetry having small distortions from octahedral stereochemistry.[13] Only the complex with R = *p*-tolyl is soluble in $PhNO_2$ and behaves as a nonelectrolyte. These observations favour structure (4) for all the complexes except the chloro complex for which the octahedral stereochemistry may only be achieved if the chloride ion acts as triply bridging and the ligand is tridentate.

The net result of the present work is the stabilization of four new stable manganese(II)–monotertiary arsine complexes which is significant in view of the only two already known.[4] Further McAuliffe's emphasis[1-3,14] on the use of strictly deoxygenated and anhydrous reaction medium does hold good for the soft ligands but the results of the present investigation and those of Chiswell *et al.*[4] clearly suggest that the presence of water and oxygen in a reaction of a manganese(II) salt with an As–O/As–N hybrid ligand does not inhibit the formation of a manganese(II)–arsine complex.

REFERENCES

1. S. Casey, W. Levason and C. A. McAuliffe, *J. Chem. Soc. Dalton Trans.* 1974, 886.
2. W. Levason and C. A. McAuliffe, *J. Inorg. Nucl. Chem.* 1975, **37**, 340.
3. M. H. Jones, W. Levason, C. A. McAuliffe and M. J. Parrott, *J. Chem. Soc. Dalton Trans.* 1976, 1642.
4. B. Chiswell, R. Plowman and K. Verral, *Inorg. Chim. Acta* 1971, **5**, 579.
5. S. S. Parmar and H. Kaur, *Trans. Metal Chem.* 1982, **7**, 79.
6. S. S. Parmar, H. K. Bharaj and M. L. Sehgal, *Polyhedron* 1985, **4**, 959.
7. D. M. Adams, *Metal Ligand and Related Vibrations*. Edward Arnold, London (1967).
8. K. Nakamoto, *Infrared Spectra of Inorganic and*

Coordination Compounds, 2nd edn. Wiley, New York (1970)
9. J. Fujita, K. Nakamoto and M. Kobayashi, *J. Am. Chem. Soc.* 1956, **78**, 3963.
10. M. D. Taylor, C. P. Carter and C. I. Wynter, *J. Inorg. Nucl. Chem.* 1968, **30**, 1503.
11. S. S. Parmar and H. Kaur, *Polyhedron* 1982, **1**, 667.
12. S. S. Parmar and H. K. Bathla, *Indian J. Chem.* 1985, **24A**, 1035.
13. A. Hosseiny, C. A. McAuliffe, K. Minten, M. J. Parrott, R. Pritchard and J. Tames, *Inorg. Chim. Acta* 1980, **39**, 227.
14. C. A. McAuliffe, *J. Organomet. Chem.* 1982, **228**, 255.

Polyhedron Vol. 6, No. 8, pp. 1703–1705, 1987
Printed in Great Britain

0277–5387/87 $3.00+.00
Pergamon Journals Ltd

COMMUNICATION

THE SYNTHESIS AND SPECTRAL PROPERTIES OF THE NOVEL MONODENTATE(S) COORDINATED THIOSEMICARBAZIDE AND THIOSEMICARBAZONE COMPLEXES $[Fe(CO)_2L(\eta^5\text{-}C_5H_5)][PF_6]$ ($L = H_2NNHCSNH_2$, cy-$C_5H_{10}CNNHCSNH_2$ OR $R'R''CNNHCSNH_2$, $R' = R'' = Me$; $R' = H$, $R'' = Ph$; $R' = H$, $R'' = p\text{-}NO_2Ph$, $R' = Me$, $R'' = p\text{-}MePh$)

MICHEL J. M. CAMPBELL,* ELIZABETH MORRISON and VERNON ROGERS

The School of Chemistry, Thames Polytechnic, Wellington Street, London, SE18 6PF, U.K.

and

PAUL K. BAKER*

Department of Chemistry, University College of North Wales, Bangor, Gwynedd LL57 2UW, U.K.

(*Received* 23 *February* 1987; *accepted* 1 *April* 1987)

Abstract—The acetone complex $[Fe(CO)_2(Me_2CO)(\eta^5\text{-}C_5H_5)][PF_6]$ reacts with L ($L = H_2NNHCSNH_2$, cy-$C_5H_{10}CNNHCSNH_2$, or $R'R''CNNHCSNH_2$ where $R' = R'' = Me$; $R' = H$, $R'' = Ph$; $R' = H$, $R'' = p\text{-}NO_2Ph$; $R' = p\text{-}MePh$) in refluxing trichloromethane to give the new complexes $[Fe(CO)_2L(\eta^5\text{-}C_5H_5)][PF_6]$. The complexes are clearly coordinated through the sulphur atom since the thiosemicarbazide complex reacts with benzaldehyde to afford the corresponding thiosemicarbazone compound.

Thiosemicarbazones have been shown to be active against protozoa,[1] influenza,[2] smallpox[3] and certain kinds of tumour,[4] and their activity has often been thought to be due to their ability to chelate trace metals. For example, Liebermeister[5] showed that copper ions enhance the anti-tubercular activity of p-acetamidobenzaldehydethiosemicarbazone.

Many "classical" complexes containing thiosemicarbazide and thiosemicarbazones as coordinated ligands with bidentate coordination through the sulphur and hydrazinic nitrogen atoms have been reported.[6,7] However, there are very few papers describing complexes with monodentate(S) coordination. The only examples of thiosemicarbazide or thiosemicarbazones acting as monodentate ligands reported so far are those of Ag(I),[8] Hg(II)[9,10] and Co(II).[11] Also, very few organo-transition-metal complexes containing attached thiosemicarbazide or thiosemicarbazones have been reported.[12–15] In this communication we wish to describe the synthesis of the new monodentate(S) bonded complexes $[Fe(CO)_2L(\eta^5\text{-}C_5H_5)][PF_6]$ ($L = H_2NNHCSNH_2$, cy-$C_5H_{10}CNNHCSNH_2$, or $R'R''CNNHCSNH_2$, $R' = R'' = Me$; $R' = H$, $R'' = Ph$; $R' = H$, $R'' = p\text{-}NO_2Ph$; $R' = Me$, $R'' = p\text{-}MePh$) and preliminary studies of their reactivity.

Equimolar quantities of $[Fe(CO)_2(Me_2CO)(\eta^5\text{-}C_5H_5)][PF_6]$[16] and L ($L = H_2NNHCSNH_2$, cy-$C_5H_{10}CNNHCSNH_2$ or $R'R''CNNHCSNH_2$, $R' = R'' = Me$; $R' = H$, $R'' = Ph$; $R' = H$,

*Authors to whom correspondence should be addressed.

Table 1. (C, H and N)[a] and IR[b] data of $[Fe(CO)_2L(\eta^5\text{-}C_5H_5)][PF_6]$

	L	Yield (%)	C	H	N	ν(CO) cm^{-1}
(1)	$H_2NNHCSNH_2$	59	22.7 (23.6)	2.4 (2.5)	10.6 (10.2)	2047s 2011s 1997s
(2)	cy-$C_5H_{10}CNNHCSNH_2$	72	33.9 (34.1)	3.6 (3.7)	8.1 (8.5)	2049s 1998s
(3)	$Me_2CNNHCSNH_2$	61	30.1 (29.2)	3.2 (3.1)	9.0 (9.3)	2058s 2051s 2002s
(4)	$C_6H_5CHNNHCSNH_2$	65	35.2 (35.9)	2.8 (2.8)	7.9 (8.4)	2061s 2024s
(5)	p-$NO_2C_6H_4CHNNHCSNH_2$	58	33.0 (33.0)	2.4 (2.4)	10.3 (9.9)	2060s 2016s
(6)	p-$MeC_6H_4CMeNNHCSNH_2$	41	38.8 (38.7)	3.4 (3.5)	7.9 (7.9)	2057s 2009s

[a] Calculated values in parentheses.
[b] Spectra recorded as KBr discs, s, strong.

R″ = p-NO_2Ph; R′ = Me, R″ = p-MePh) react in refluxing $CHCl_3$ to give good yields of the new complexes $[Fe(CO)_2L(\eta^5\text{-}C_5H_5)][PF_6]$ via displacement of acetone. The complexes have been fully characterized by elemental analysis (C, H and N), IR spectroscopy (Table 1) and ^1H NMR spectroscopy.* All of the complexes are stable in the solid state in air and decompose very slowly in solution when exposed to air. The compounds are insoluble in hydrocarbon solvents, sparingly soluble in dichloromethane and trichloromethane and very soluble in dimethyl sulphoxide.

It is revealing that the thiosemicarbazide complex $[Fe(CO)_2(H_2NNHCSNH_2)(\eta^5\text{-}C_5H_5)][PF_6]$ (**1**) reacts smoothly with benzaldehyde to give the benzaldehydethiosemicarbazone complex which can also be prepared by reacting $[Fe(CO)_2(Me_2CO)(\eta^5\text{-}C_5H_5)][PF_6]$ with benzaldehyde thiosemicarbazone in refluxing chloroform. This indicates that the ligands must be bound through the sulphur atom since as expected the complexes $[MoX(CO)_2(H_2NNHCSNH_2)(\eta^3\text{-}C_3H_4R)]$(R = H or 2-Me, X = Cl or Br)[14] with bidentate (SN) coordination do not appear to react with ketones to afford thiosemicarbazone complexes.

The infrared spectrum of the acetone complex $[Fe(CO)_2(OCMe_2)(\eta^5\text{-}C_5H_5)][BF_4]$ shows two metal-carbonyl bands at 2070 and 2028 cm^{-1} which are slightly higher than for the new complexes with a sulphur atom coordinated to the metal which is to be expected. The X-ray crystal structure of free thiosemicarbazide shows the molecule to be in a *trans*-configuration[17] and it is likely that the iron complexes (**2**), (**4**) and (**6**) have the thiosemicarbazone ligand in this configuration [Fig. 1(a)] whereas complexes (**1**), (**3**) and (**5**) show either two cyclopentadienyl or 3 carbonyl bands which are probably due to the *trans*- and *cis*-isomers [Fig. 1(a) and (b)]. Further studies are in progress.

* ^1H NMR data.

1. $[Fe(CO)_2(H_2NNHCSNH_2)(\eta^5\text{-}C_5H_5)][PF_6]$; δ (d_6-DMSO); 5.49 (5H, d (J = 0.4 Hz), C_5H_5), 8.30 (2H, S, $\underline{NH}_2NH$), 9.80 (2H, s, NH_2CS) and 11.21 (1H, s, $NH_2\underline{NH}$).

2. $[Fe(CO)_2(cy\text{-}C_5H_{10}CNNHCSNH_2)(\eta^5\text{-}C_5H_5)][PF_6]$; δ (d_6-DMSO); 1.60–2.55 (10H, m, cy-C_5H_{10}), 5.48 (5H, s, C_5H_5), 8.46 (2H, s, br, NH_2CS) and 11.61 (1H, s, NH).

3. $[Fe(CO)_2(Me_2CNNHCSNH_2)(\eta^5\text{-}C_5H_5)][PF_6]$; δ (d_6-DMSO); 2.08 (6H, s, Me), 5.49 (5H, s, C_5H_5), 8.60 {2H, d (J = 1.8 Hz), NH_2CS} and 11.32 (1H, s, NH).

4. $[Fe(CO)_2(PhCHNNHCSNH_2)(\eta^5\text{-}C_5H_5)][PF_6]$; δ (d_6-DMSO); 5.60 (5H, s, C_5H_5), 7.53–7.92 (5H, m, C_6H_5), 8.28 (1H, s, Ph$\underline{CH}$N), 8.97 (2H, d (J = 6.3 Hz), NH_2CS) and 12.51 (1H, s, NH).

5. $[Fe(CO)_2(p\text{-}NO_2PhCHNNHCSNH_2)(\eta^5\text{-}C_5H_5)][PF_6]$; δ (d_6-DMSO); 5.63 (5H, d (J = 1.7 Hz), C_5H_5), 8.21–8.65 (6H, m, C_6H_4 and NH_2CS) and 12.86 (1H, s, NH).

6. $[Fe(CO)_2\{(p\text{-MePh-, Me-})CNNHCSNH_2\}(\eta^5\text{-}C_5H_5)][PF_6]$; δ (d_6-DMSO); 2.04 (3H, s, p-Me), 2.66 (3H, s, Me-), 5.78 (5H, s, C_5H_5), 7.37–7.71 (6H, m, C_6H_4 and NH_2CS) and 10.27 (1H, s, NH).

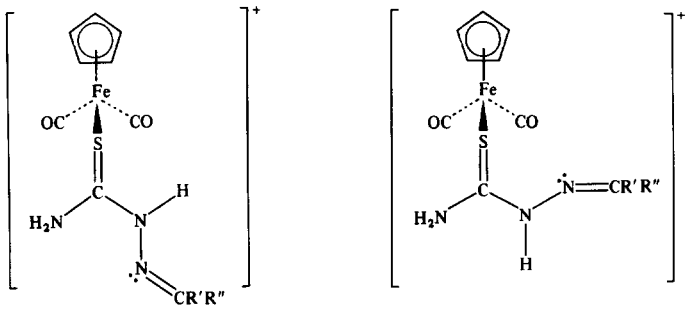

Fig. 1. Proposed structures for the complexes $[Fe(CO)_2L(\eta^5\text{-}C_5H_5)][PF_6]$.

REFERENCES

1. U. S. Pat. 3 266 382 (1968) to K. Butler.
2. N. N. Orlova, V. A. Aksenova, D. A. Selidovkin, N. S. Bogdanova and G. N. Pershin, *Russ. Pharmacol. Toxicol.* 1968, 348.
3. D. J. Baur, L. St. Vincent, C. H. Kemp and A. W. Downe, *Lancet* 1963, **2**, 494.
4. H. G. Petering, H. H. Buiskirk and G. E. Underwood, *Cancer Res.* 1964, **64**, 367.
5. K. Leibermeister, *Z. naturforsch B.* 1950, **5**, 79.
6. M. J. M. Campbell, *Coord. Chem. Rev.* 1975, **15**, 279.
7. S. Padhye and G. B. Kauffman, *Coord. Chem. Rev.* 1985, **63**, 127.
8. (a) M. Nardelli, G. Fava Gasparri and I. Chierici, *Ric. Sci.* 1965, **35**, 11-A, 480. (b) M. Nardelli, G. Fava Gasparri, G. Gioraldi Battistini and A. Musatti, *J. Chem. Soc., Chem. Commun.* 1965, 187. (c) G. Fava Gasparri, A. Mangia, A. Musatti and M. Nardelli, *Acta Cryst. B* 1968, **24**, 367. (d) L. Calzolari Capacchi, G. Fava Gasparri, M. Ferrari and M. Nardelli, *J. Chem. Soc., Chem. Commun.* 1968, 910. (e) L. Calzolari Capacchi, G. Fava Gasparri, M. Ferrari and M. Nardelli, *Ric. Sci.* 1968, **38**, 974.
9. (a) C. Chieh, *Can. J. Chem.* 1977, **55**, 1583. (b) C. Chieh, L. P. C. Lee and C. Chin, *Can. J. Chem.* 1978, **56**, 2526.
10. D. R. Goddard, B. D. Lodam, S. O. Ajayi and M. J. M. Campbell, *J. Chem. Soc. A* 1969, 506.
11. (a) C. Bellitto, A. A. G. Tomlinson, C. Furlani and G. de Munno, *Inorg. Chim. Acta* 1978, **27**, 269. (b) G. Dessey and V. Fares, *J. Chem. Soc. D* 1978, **11**, 1549.
12. P. K. Baker, M. J. M. Campbell and M. V. White, *Inorg. Chim. Acta* 1985, **98**, L27.
13. V. Srivastava, S. Sengupta and S. C. Tripathi, *Synth. React. Inorg. Met.-Org. Chem.* 1985, **15**, 163.
14. M. J. M. Campbell, E. Morrison, V. Rogers and P. K. Baker, *Synth. React. Inorg. Met.-Org. Chem.* 1986, **16**(a), 1237.
15. M. J. M. Campbell, E. Morrison, V. Rogers and P. K. Baker, *Trans. Met. Chem.* 1986, **11**, 381.
16. W. E. Williams and F. J. Lalor, *J. Chem. Soc., Dalton Trans.* 1973, 1329.
17. (a) P. Domiano, G. Fava Gasparri, M. Nardelli and P. Sgarbotto, *Acta Cryst. B* 1969, **25**, 343. (b) G. D. Andreeti, P. Domiano, G. Fava Gasparri, M. Nardelli and P. Sgarbotto, *Acta Cryst. B* 1970, **26**, 1005.

Polyhedron Vol. 6, No. 8, pp. 1707–1708, 1987
Printed in Great Britain

0277–5387/87 $3.00+.00

COMMUNICATION

SYNTHESIS AND CHARACTERIZATION OF A Tc(V) GLYCOLATO COMPLEX

G. HUBER, G. ANDEREGG* and K. MAY

Laboratorium für Anorganische Chemie, ETH Zürich, CH-8092 Zürich, Switzerland

(*Received* 20 *March* 1987; *accepted* 6 *April* 1987)

Abstract—The preparation of the Tc(V) glycolato complex $(C_4H_9)_4N[^{99}TcO(OCH_2CH_2O)_2]$ is described. On the basis of IR, ^{1}H-NMR and ^{13}C-NMR spectra, a structure for the complex is postulated.

As the Tc(IV) alcoholato complexes can be obtained from $TcBr_6^{2-}$ by ligand substitution,[1] an attempt was made to synthesize an oxo-Tc(V) glycolato complex, starting with $Bu_4N[TcOCl_4]$. The substitution of chloride by the chelating glycolate ($OCH_2CH_2O^{2-}$) was carried out in non-aqueous organic solvents because $TcOCl_4^-$ is prone to hydrolysis.

$$TcOCl_4^- + 2HOCH_2CH_2OH + 4Bu_4NOH \xrightarrow{\text{i-propanol}} [TcO(OCH_2CH_2O)_2]^- + 4Bu_4NCl + 4H_2O.$$

It seems that the oxo-Tc(V) unit prefers oxygen as a donor atom as does Tc(IV).

EXPERIMENTAL

$Bu_4N[TcOCl_4]$ was recrystallized from dichloromethane/hexane. Bu_4NOH in dry isopropanol was commercially available.

Synthesis of $Bu_4N[TcO(OCH_2CH_2O)_2]$ **(I)**

15 cm^3 of a solution of 0.1 M Bu_4NOH (1.5 mmol) in isopropanol were added to 160 mg $Bu_4N[TcOCl_4]$ (0.32 mmol) and 0.2 cm^3 ethyleneglycol (3.5 mmol) in an argon atmosphere, and the mixture treated in an ultrasonic vibrator. The colour of the solution changed to deep-violet within 2 min. After all of the $Bu_4N[TcOCl_4]$ had dissolved, the solvent was removed first by a stream of dry argon and then *in vacuo*. The excess ethyleneglycol was removed by distillation under high vacuum. The dark-violet residue was dissolved in 5 cm^3 of dry acetone and mixed with 10 cm^3 dry diethylether. The clear solution was left to stand overnight at −20°C, and virtually all of the chloride precipitated as white Bu_4NCl crystals. The filtered solution was reduced to a total volume of 1 cm^3 by purging with dry argon. Dried ether was added, yielding an opaque violet solution, which was then left to stand for 3 days at −20°C. 105 mg of violet crystals were obtained, which were washed twice with hexane and dried *in vacuo*. Even after recrystallization from deoxygenated chloroform/ether the NMR spectrum showed one ethyleneglycol-unit per three molecules of Tc-complex.

Elemental analysis. Found: C, 49.8; H, 9.4; Tc, 19.8. Calc. for $Bu_4N[TcO(OCH_2CH_2O)_2] \cdot \frac{1}{3}(HOCH_2CH_2OH)$: C, 49.8; H, 9.3; Tc, 19.9%.

The complex is very soluble in water, alcohols, acetone, acetonitrile, dimethylformamide, dimethylsulfoxide, tetrahydrofuran, chloroform, methylenechloride, benzene; slightly soluble in toluene; insoluble in ether and hexane. It decomposes in aqueous solution at pH < 10. The complex is sensitive to oxygen and slowly decomposes particularly in solution into pertechnetate. In paper chromatography the R_f-value of the title complex is 0.5 (CH_3CN/H_2O = 5:2 v/v). The dry crystals can be stored under argon at least for several months.

Spectroscopic properties of the complex. The IR band at 964 cm^{-1} can be assigned to a Tc=O

* Author to whom correspondence should be addressed.

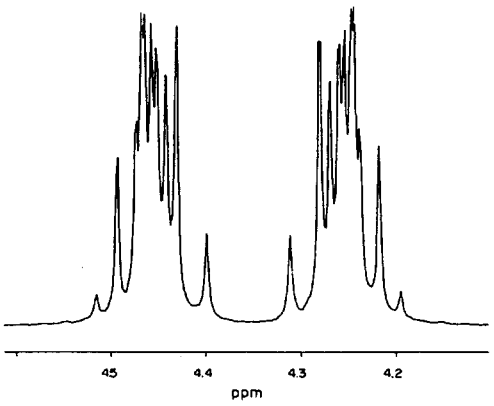

Fig. 1. H-NMR spectrum of coordinated glycolates in $Bu_4N[TcO(OCH_2CH_2O)_2]$.

stretching frequency. This is similar to other five-coordinate oxo-Tc(V) complexes.[2] Moreover, the IR spectrum shows bands characteristic of Bu_4N^+ and ethyleneglycol.

UV–VIS spectrum in dry CH_3OH:

$\lambda_{max} = 249\,nm, \varepsilon = 3000 : sh = 350\,nm, \varepsilon = 50$

$\lambda_{max} = 524\,nm, \varepsilon = 90.$

250 MHz-H-NMR *spectroscopy in* $CDCl_3$. This shows a multiplet centred at $\delta = 4.36$ ppm due to coordinated glycolate. The symmetric structure of the 20 signals points to an aa'bb'-spin-system, while the CH_2-group of ethyleneglycol resonates at $\delta = 3.62$ ppm. The other signals are identical to those of salts containing Bu_4N^+.

63 MHz-^{13}C-NMR *spectroscopy in* $CDCl_3$. The signal of coordinated glycolate is a singlet at 77.5 ppm. The small signal of ethyleneglycol is at 64.4 ppm. The other four signals of Bu_4N^+ are, as expected, at 58.8/24.3/19.9/13.9 ppm.

DISCUSSION

It has long been known that most metal centres with significant A-character form complexes with alcoholates.[3,4,5] Such complexes can also be synthesized with Tc(V), which suggests that Tc(V) also has A-character. The +V oxidation state of Tc can be deduced from chemical measurements and elemental analysis. Known Tc(V) complexes, e.g. the tetraza-dioxo-Tc(V) complex[6] $TcO_2(2,3,2\text{-tet})^+$ using the title compound as starting material, can be obtained in good yields (2,3,2-tet = $NH_2(CH_2)_2NH(CH_2)_3NH(CH_2)_2NH_2$):

$$TcO(OCH_2CH_2O)_2^- \xrightarrow[\text{in MeOH/H}_2O]{\text{2,3,2-tet}} TcO_2(2,3,2\text{-tet})^+.$$

As already mentioned, the glycolato complex is soluble in water and stable at pH > 10 in deoxygenated water. Below pH = 8 the solution darkens quickly (due to formation of TcO_2), and needles of Bu_4NTcO_4 precipitate. Hydrolysis can be prevented by adding a strong ligand. This provides a useful method of synthesizing new Tc(V) complexes directly from aqueous solutions.

A fivefold coordination of Tc(V) in the glycolato complex can be derived from IR- as well as from NMR-spectra. The H-NMR-signals of coordinated glycolates show a pattern typical of an aa'bb'-spin-system, which is consistent either with a square-pyramidal or a trigonal-bipyramidal structure (Fig. 1).

The ^{13}C-NMR spectrum shows only one signal for the coordinated glycolates favoring the square-pyramidal configuration. Analogous results have been obtained elsewhere ($TcO(SCH_2CH_2O)_2^-$,[8] $TcO(SCH_2CH_2S)_2^-$[9]). Since the chemical shift of the glycolate signals is similar to that of related cyclic glycolate esters (4–4.5 ppm), a diamagnetic behaviour of the compound may be tentatively assumed as in some paramagnetic complexes shifts of approximately 20 ppm are observed.[10]

Acknowledgements—The authors thank the Eidgenössischen Institut für Reaktorforschung (EIR), Würenlingen, for financial support (G.H.) of these investigations and especially Dr. P. Bläuenstein (EIR) for technical help.

REFERENCES

1. R. Alberto, G. Anderegg and K. May, *Polyhedron* 1986, **5**, 2107.
2. M. E. Kastner, P. H. Fackler, M. J. Clarke and E. Deutsch, *Inorg. Chem.* 1984, **23**, 4683.
3. E. Bischoff and H. Adkins, *J. Am. Chem. Soc.* 1924, **46**, 256.
4. D. C. Bradley, W. Wardlaw and A. Whitley, *J. Chem. Soc.* 1955, 726.
5. D. C. Bradley, W. Wardlaw and R. K. Multani, *J. Chem. Soc.* 1958, 126.
6. K. Zollinger, Thesis ETH, Zürich, 1984, Nr. 7664, 67.
7. P. Bläuenstein, G. Pfeiffer, P. A. Schubiger, G. Anderegg, K. Zollinger, K. May, Z. Proso, E. Ianovici and P. Lerch, *Int. J. Appl. Radiat. Isot.* 1985, **36**, 315.
8. A. Davison, A. G. Jones and B. V. de Pamphilis, *Inorg. Chem.* 1981, **20**, 1617.
9. J. E. Smith, E. F. Byrne, F. A. Cotton and J. C. Sekutowski, *J. Am. Chem. Soc.* 1978, **100**, 5571.
10. K. Zollinger, private communication.

Polyhedron Vol. 6, No. 8, pp. 1709–1710, 1987
Printed in Great Britain

0277-5387/87 $3.00+.00

COMMUNICATION

THE PREPARATION AND CHARACTERIZATION OF BIS(1,2-BIS(DIPHENYLPHOSPHINO)ETHANE)TRIMETHYLPHOSPHINERUTHENIUM(0)

ADELA ANILLO and RICARDO OBESO ROSETE

Departamento de Quimica Inorganica, Facultad de Quimica, Universidad de Oviedo, 33071-Oviedo, Spain

and

DAVID J. COLE-HAMILTON*

Department of Chemistry, University of St Andrews, St Andrews, Fife KY16 9ST, Scotland, U.K.

(*Received* 24 *March* 1987; *accepted* 6 *April* 1987)

Abstract—Reaction of {Ru(styrene)(dppe)$_2$}, (dppe = 1,2-bis(diphenyl-phosphino)ethane), with trimethylphosphine affords [Ru(dppe)$_2$(PMe$_3$)], which has been characterized spectroscopically, and which is in equilibrium with [RuH(C$_6$H$_4$P(Ph)CH$_2$CH$_2$PPh$_2$)(dppe)] and free PMe$_3$in solution at room temperature.

The preparation of highly electron rich metal centres is a goal of considerable importance since such centres may be useful in the activation of saturated hydrocarbons. To this end, attempts have been made to stabilize ruthenium in oxidation state zero with ligands which are poor π-acceptors, such as tertiary phosphines. This has not proved straight forward, since, although [Ru(P(OMe)$_3$)$_5$] can be isolated,[1] attempts to synthesize the analogous [Ru(PMe$_3$)$_5$] have been unsuccessful and have led[2] to [RuH(CH$_2$PMe$_2$)(PMe$_3$)$_3$], presumably because PMe$_3$ is an insufficiently good π-acceptor to stabilize the ruthenium(0) centre.

Indeed, only two examples of complexes in which ruthenium(0) is coordinated only to phosphine ligands have been reported. Chatt postulated[3] [Ru(dmpe)$_2$(PEt$_3$)], dmpe = 1,2-bis(dimethylphosphino)ethane, from the reaction of [RuH(naphthyl)(dmpe)$_2$] with PEt$_3$, whilst the analogously prepared [Ru(dmpe)$_2$(PMe$_3$)] has recently been structurally characterized.[4]

We have reported[5] upon the chemistry of [Ru(dppe)$_2$styrene], dppe = 1,2-bis(diphenylphosphino)ethane, available from the reaction of [Ru(PPh$_3$)$_2$(styrene)$_2$] with dppe, including the replacement of styrene by CO or P(OMe)$_3$ (L) to give [Ru(dppe)$_2$L]. We now report that an analogous reaction using PMe$_3$ gives [Ru(dppe)$_2$(PMe$_3$)], another example of an all phosphine stabilized ruthenium(0) centre.

Addition of excess PMe$_3$ to [Ru(dppe)$_2$styrene] in tetrahydrofuran (thf) results in an orange solution from which orange-red crystals analysing for [Ru(dppe)$_2$(PMe$_3$)] can be isolated in high yield. Although these crystals are well formed, they do not diffract X-rays so that their characterization relies on spectroscopic investigations. There is no IR or ^{1}H NMR evidence for the presence of a hydride ligand, and combined IR and ^{31}P NMR studies confirm that the dppe ligand has not undergone an internal metallation reaction. Thus, there are no IR absorptions[6] at 1550 or 1410 cm^{-1} and the ^{31}P NMR spectrum consists of a doublet from the four equivalent phosphorus atoms and a quintet from the PMe$_3$ phosphorus atom. There is evidence

* Author to whom correspondence should be addressed.

that PMe_3 dissociates in solution since resonances for free PMe_3 and for [RuH($C_6H_4P(Ph)CH_2CH_2PPh_2$)(dppe)] (III in ref. 5) are observed in the ^{31}P NMR spectrum. These correspond to *ca.* 35% dissociation and do not vary with time, suggesting that equilibrium 1 is established but that exchange of free and bound PMe_3 is slow on the NMR time-scale. The existence of equilibrium 1 is confirmed since addition of excess PMe_3 removes the peaks from [RuH($C_6H_4P(Ph)CH_2CH_2PPh_2$)(dppe)] and only peaks from [Ru(dppe)$_2$(PMe_3)] and PMe_3 are observed in the ^{31}P NMR spectrum.

$$[Ru(dppe)_2(PMe_3)] \rightleftharpoons [RuH(C_6H_4P(Ph)CH_2CH_2PPh_2)(dppe)] + PMe_3. \quad (1)$$

Doublets from both free and bound PMe_3 are also observed in the ^1H NMR spectrum. Observation of this equilibrium lends support in the suggestion,[4] made as a result of kinetic measurements, that exchange of PMe_3 in the related [Ru(dmpe)$_2$(PMe_3)] with $P(CD_3)_3$ or with [$CNCH_2CMe_3$] involves preliminary phosphine dissociation. Metallated species,[3,4] although undetected, may also be present in the dmpe system.

The simple nature of the ^{31}P NMR spectrum suggests that [Ru(dppe)$_2$(PMe_3)] adopts a square pyramidal configuration with apical PMe_3, as has been observed for [Ru(dmpe)$_2$(PMe_3)][4] and [Ru(dppe)$_2$($P(OMe)_3$)][5] rather than the more usual trigonal bipyramidal structure adopted by [Ru(dppe)$_2$(CO)][4] and related molecules.

EXPERIMENTAL

Microanalyses were by the University of Oviedo and NMR spectra were obtained on Perkin–Elmer R12 (60 MHz, ^1H) or Brüker Associates WM250 (^{31}P) spectrometers, the latter operating in the Fourier Transform mode with noise proton decoupling. The melting point was measured on an electrothermal melting point apparatus in a sealed capillary under argon and is uncorrected.

Bis - (1,2 - bis(diphenylphosphino)ethane)(trimethylphosphine)ruthenium(0)

Thf (5 cm^3) was added to a mixture of [Ru(dppe)$_2$(styrene)][5] (0.3 g) and PMe_3 (0.3 cm^3) under argon. The dark-orange solution was stirred for 30 min at room temperature. Petroleum (10 cm^3, 40–60°C bpt) was added before the solution was filtered and cooled to −20°C for 3 days. The solution was filtered again and allowed to stand at −20°C for 3 weeks. The dark-orange crystals, which are indefinitely stable at room temperature under argon and are stable for a few minutes in air, were collected, washed with petroleum and dried *in vacuo*. Yield *ca.* 60%. M.p. 94–96°C.

Found: C, 67.7; H, 6.5%. $C_{55}H_{57}P_5Ru$ requires: C, 67.8; H, 5.9%. IR (λ max/cm^{-1}) 3040 m, 3010 w, 1580 m, 1565 w, 1475 s, 1425 vs, 1302 w, 1290 vw, 1265 w, 1175 sh, 1170 w, 1152 vw, 1115 vw, 1092m, 1080 s, 1065 vs, 1022 m, 995 vw, 965 vw, 940 s, 932 s, 925 sh, 910 m, 875 m, 848 w, 840 w, 802 s, 745 sh, 740 vs, 735 sh, 695 vs, 680 sh, 660 m, 650 sh, 635 m, 625 m, 612 w.

^{31}P NMR (δ to low frequency of external 85% H_3PO_4) 73.5 d, −30.80 qu, J_{PP} = 17.0 Hz, −62.0 s (free PMe_3), 73.9 ddd; 71.9 ddd; 46.6 ddd; 8.5 ddd ([RuH($C_6H_4P(Ph)CH_2CH_2PPh_2$)(dppe)], J as for isomer III in Ref. 5).

^1H NMR (δ, ppm in C_6D_6) 8.8–6.7 (bm, 40, Ph); 1.9 (bm, 8, CH_2); 1.2 (d, J_{PH} = 6.0 Hz, 6, PMe_3 bound); 0.9 (d, J_{PH} = 2.4 Hz, 3, PMe_3, free).

Acknowledgement—We thank CAICYT (Spain) for support (A.A. and R.O.R.).

REFERENCES

1. A. D. English, S. D. Ittel, C. A. Tolman, P. Meakin and J. P. Jesson, *J. Am. Chem. Soc.* 1977, **99**, 117.
2. H. Werner and R. Werner, *J. Organometal. Chem.* 1981, **209**, C60.
3. J. Chatt and J. Davidson, *J. Chem. Soc.* 1965, 843.
4. W. D. Jones and E. Libertini, *Inorg. Chem.* 1986, **25**, 1794.
5. R. Obeso Rosete, D. J. Cole-Hamilton and G. Wilkinson, *J. Chem. Soc. Dalton Trans.* 1984, 2067.
6. D. J. Cole-Hamilton and G. Wilkinson, *J. Chem. Soc. Dalton Trans.* 1977, 797.
7. F. A. Cotton, B. A. Frenz and D. L. Hunter, *J. Chem. Soc. Chem. Commun.* 1974, 755.

Polyhedron Vol. 6, No. 8, pp. 1711–1713, 1987
Printed in Great Britain

0277–5387/87 $3.00+.00

COMMUNICATION

THE STRUCTURE OF THE MIXED-VALENCE, CHLORO-BRIDGED DIMERIC COMPLEX CATION $[Ru_2(NH_3)_6Cl_3]^{2+}$

MARTIN N. HUGHES,*† DESMOND O'REARDON† and ROBERT K. POOLE‡

Departments of †Chemistry and ‡Microbiology, King's College, Campden Hill Road, London W8 7AH, U.K.

and

MICHAEL B. HURSTHOUSE* and MARK THORNTON-PETT

Department of Chemistry, Queen Mary College, Mile End Road, London E1 4NS, U.K.

(*Received* 3 *April* 1987; *accepted* 27 *April* 1987)

Abstract—The cation in the ruthenium blue $[Ru_2(NH_3)_6Cl_3](BPh_4)_2$ is a trichloro-bridged bioctahedral dimer, with a Ru—Ru distance of 2.753 Å.

The intense blue solutions formed either by adding hydrochloric acid to solutions of ruthenium(II) complexes containing *N*-donor ligands or by reducing solutions of ruthenium(III) in hydrochloric acid have been the subject of much controversy. It is now generally accepted that these "ruthenium blues" are mixed-valence dimeric species,[1] although to date no definitive structural work has been carried out due to the difficulties in preparing suitable crystals.

We have studied the biological and chemical properties of the blue Ru(II,III) compound formed by reaction between $[Ru(NH_3)_6]Cl_2$ and hydrochloric acid. Compounds of this type have remarkable biological activity, for example as potent inhibitors of accumulation of calcium by everted membrane vesicles of *Escherichia coli*,[2] and in the elicitation of filamentation in *E. coli*.[3] This activity is not found for the oxidised Ru(III,III) dimer. It should be noted that the mixed-valence dimer is mutagenic.

The mixed-valence dimer has been formulated[4] as a di-chloro-bridged complex, $[Ru_2(NH_3)_6Cl_4(H_2O)]Cl$, partly on the basis of conductivity data, which was judged appropriate for a 1 : 1 electrolyte. However, other evidence is indicative of a doubly charged complex with three bridging chloride groups, $[Ru_2(NH_3)_6Cl_3]Cl_2 \cdot H_2O$. This evidence includes ion-exchange studies, which indicate a doubly-charged complex,[5] and vibrational spectroscopy.[6] Furthermore, it is possible to isolate salts of the type $[Ru_2(NH_3)_6Cl_3]I_2 \cdot H_2O$ and $[Ru_2(NH_3)_6Cl_3]ZnX_4$, where X = Cl, Br.[6] We have prepared the tetraphenylborate salts $[Ru_2(NH_3)_6Cl_3](BPh_4)_2$, which have identical electronic spectra and magnetic properties to the chloride, and now report full details of the crystal structure.[3]

EXPERIMENTAL

Preparation of hexaammine-μ-trichlorodiruthenium(II,III) tetraphenylborate

The complex chloride was prepared by the method of Bottomley and Tong[4] and recrystallized from methanol. It was precipitated as the tetraphenylborate from an aqueous deoxygenated solution by addition of a concentrated solution of sodium tetraphenylborate. The product was separated by centrifugation and recrystallized twice from methanol to give dark blue, rod-like crystals of maximum length about 1 mm. The formulation $[Ru_2(NH_3)_6Cl_3](BPh_4)_2$ was confirmed by analysis for Ru, Cl, C, H, N. Attempts to prepare crystal-

* Authors to whom correspondence should be addressed.

line products with other anionic species were all unsuccessful.

X-ray crystallography

The crystal used for the X-ray work was a rod of maximum dimension 0.6 mm. It was sealed in a thin-walled capillary under argon. All measurements were made using a CAD4 diffractometer operating in the $W/2\theta$ scan mode and graphite-monochromatized Mo–K_α radiation ($\lambda = 0.71069$ Å), following previously detailed procedures.[7] In spite of the size of the crystal used, the scattering was rather weak, and the specimen showed considerable mosaic spread.

The structure was solved by use of the heavy atom method and refined by full-matrix least squares. All non-hydrogen atoms were refined with anisotropic displacement factor coefficients; hydrogen atoms were included in idealised positions and assigned group isotropic coefficients. Experimental data were as follows:

Crystal data. $[Ru_2Cl_3N_6H_{18}]^{2+}[C_{24}H_{20}B]_2^-$, Mr = 1048.56, monoclinic, $P2_1/a$, $a = 18.257(4)$, $b = 18.151(3)$, $c = 18.319(6)$ Å, $\beta = 115.80(2)°$, $U = 5465.6$ Å^3, $Z = 4$, $Dc = 1.27$ g cm^{-3}, μ(Mo–K_α) = 6.56 cm^{-1}.

Data collection. Scan width $\omega = 0.8 + 0.35 \tan\theta$, scan time 1.35–6.77° min^{-1}, $1.5 \leqslant \theta \leqslant 25.0°$. 9012 data recorded, 8437 unique, 4387 observed [$I > 1.5\sigma(I)$]. Data corrected for absorption empirically.

Structural refinement. 470 parameters, weights $= 1/[\sigma^2(Fo) + 0.00045(Fo)^2]$, $R = 0.066$, $R_w = 0.078$. Final atomic parameters, full lists of bond lengths and angles and lists of *Fo/Fc* values have been deposited as supplementary material with the Editor, from whom copies are available on

Table 1. Bond lengths and angles in the cation

Bond lengths (Å)			
N(11)—Ru(1)	2.120(15)	N(12)—Ru(1)	2.114(12)
N(13)—Ru(1)	2.110(13)	Ru(2)—Ru(1)	2.753(4)
Cl(1)—Ru(1)	2.411(6)	Cl(2)—Ru(1)	2.395(5)
Cl(3)—Ru(1)	2.374(7)	N(21)—Ru(2)	2.120(18)
N(22)—Ru(2)	2.096(12)	N(23)—Ru(2)	2.107(13)
Cl(1)—Ru(2)	2.417(5)	Cl(2)—Ru(2)	2.393(6)
Cl(3)—Ru(2)	2.380(7)		
Bond angles (°)			
N(12)—Ru(1)—N(11)	90.1(6)	N(13)—Ru(1)—N(11)	89.8(6)
N(13)—Ru(1)—N(12)	92.5(5)	Ru(2)—Ru(1)—N(11)	128.1(5)
Ru(2)—Ru(1)—N(12)	122.6(4)	Ru(2)—Ru(1)—N(13)	123.4(4)
Cl(1)—Ru(1)—N(11)	90.0(4)	Cl(1)—Ru(1)—N(12)	89.7(4)
Cl(1)—Ru(1)—N(13)	177.8(3)	Cl(1)—Ru(1)—Ru(2)	55.3(2)
Cl(2)—Ru(1)—N(11)	91.7(4)	Cl(2)—Ru(1)—N(12)	177.5(3)
Cl(2)—Ru(1)—N(13)	89.3(4)	Cl(2)—Ru(1)—Ru(2)	54.9(2)
Cl(2)—Ru(1)—Cl(1)	88.6(2)	Cl(3)—Ru(1)—N(11)	177.1(4)
Cl(3)—Ru(1)—N(12)	87.6(5)	Cl(3)—Ru(1)—N(13)	88.7(5)
Cl(3)—Ru(1)—Ru(2)	54.7(2)	Cl(3)—Ru(1)—Cl(1)	91.7(2)
Cl(3)—Ru(1)—Cl(2)	90.6(2)	N(21)—Ru(2)—Ru(1)	126.6(5)
N(22)—Ru(2)—Ru(1)	124.1(3)	N(22)—Ru(2)—N(21)	90.6(6)
N(23)—Ru(2)—Ru(1)	123.2(5)	N(23)—Ru(2)—N(21)	91.3(6)
N(23)—Ru(2)—N(22)	90.9(5)	Cl(1)—Ru(2)—Ru(1)	55.1(2)
Cl(1)—Ru(2)—N(21)	90.1(5)	Cl(1)—Ru(2)—N(22)	90.1(4)
Cl(1)—Ru(2)—N(23)	178.3(4)	Cl(2)—Ru(2)—Ru(1)	54.9(2)
Cl(2)—Ru(2)—N(21)	89.5(5)	Cl(2)—Ru(2)—N(22)	178.6(3)
Cl(2)—Ru(2)—N(23)	90.4(5)	Cl(2)—Ru(2)—Cl(1)	88.5(2)
Cl(3)—Ru(2)—Ru(1)	54.5(2)	Cl(3)—Ru(2)—N(21)	178.5(4)
Cl(3)—Ru(2)—N(22)	89.4(4)	Cl(3)—Ru(2)—N(23)	87.2(5)
Cl(3)—Ru(2)—Cl(1)	91.4(2)	Cl(3)—Ru(2)—Cl(2)	90.5(2)
Ru(2)—Cl(1)—Ru(1)	69.5(2)	Ru(2)—Cl(2)—Ru(1)	70.2(2)
Ru(2)—Cl(3)—Ru(1)	70.8(3)		

request. Atomic coordinates have also been deposited with the Cambridge Crystallographic Data Centre.

RESULTS AND DISCUSSION

The cation has a confacial bioctahedral structure, as shown in Fig. 1. Bond lengths and angles are given in Table 1. The octahedra are very similar in geometry. The presence of the triple chloride bridge is confirmed, while the short Ru—Ru distance of 2.753 Å is consistent with metal–metal interaction. The mean Ru—Cl—Ru bridging angle is 70.2°, close to the value of 70.5° expected for two regular octahedra sharing one face.[8]

The electronic absorption spectra and electronic configuration of the trichloro-bridged species have recently been discussed[9] in terms of a delocalized mixed valence electronic ground state in which both ruthenium atoms are equivalent and the unpaired electron is occupying a σ^* molecular orbital. The structure as found, and especially the Ru—Ru distance, which probably indicates a bond order slightly less than one,[10] is consistent with this picture.

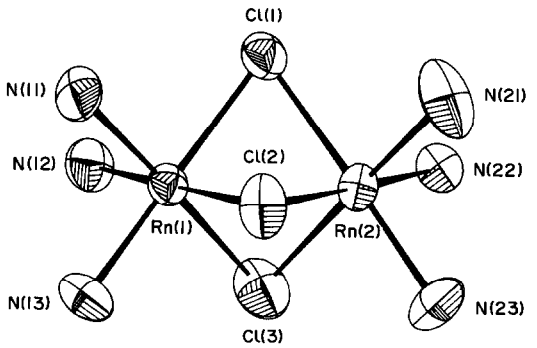

Fig. 1.

Acknowledgements—We thank the S.E.R.C. for support of the X-ray facilities and for a studentship to D.O'R, and Messrs. Johnson Matthey for the loan of ruthenium compounds.

REFERENCES

1. E. E. Mercer and P. E. Dumas, *Inorg. Chem.* 1971, **10**, 2755.
2. J. F. Gibson, R. K. Poole, M. N. Hughes and J. F. Rees, *J. Gen. Microbiol.* 1982, **128**, 2211.
3. J. F. Gibson, R. K. Poole, M. N. Hughes and J. F. Rees, *Arch. Microbiol.* 1984, **139**, 265.
4. F. Bottomley and S. B. Tong, *Can. J. Chem.* 1971, **49**, 3739.
5. E. E. Mercer and L. W. Gray, *J. Am. Chem. Soc.* 1972, **94**, 6426.
6. J. R. Durig, Y. Omura and E. E. Mercer, *J. Mol. Struct.* 1975, **29**, 53.
7. R. A. Jones, M. B. Hursthouse, K. M. A. Malik and G. Wilkinson, *J. Am. Chem. Soc.* 1979, **101**, 4128.
8. F. A. Cotton and D. A. Ucko, *Inorg. Chim. Acta* 1972, **6**, 161.
9. N. S. Hush, J. K. Beattie and V. M. Ellis, *Inorg. Chem.* 1984, **23**, 3339.
10. F. A. Cotton and R. A. Walton, *Multiple Bonds between Metal Atoms*. Wiley, New York (1982).

Polyhedron Vol. 6, No. 8, pp. 1715–1716, 1987
Pergamon Journals Ltd. Printed in Great Britain

BOOK REVIEWS

Structural Methods in Inorganic Chemistry. E. A. V. Ebsworth, David W. H. Rankin and Stephen Cradock, Blackwell Scientific, Oxford, 1987, ISBN 0-632-01592-6 (price unknown)

This is the most enjoyable chemistry book I have read for years. We all have systematic textbooks in inorganic chemistry and I am glad this is not another of those. We all have books as well on the physical methods we specialise in, but not many people are able to take on writing a book which covers the application of nearly all the spectroscopic, diffraction and other techniques we need to solve structural problems. This is what these three authors from Edinburgh have done, and their success shows that the intellectual tradition of the Athens of the North lives on.

Each chapter describes a single, or two similar, techniques. Short theoretical and practical introductions precede penetrating accounts of applications. There is emphasis on the strengths and weaknesses of each method and all the chapters end with a set of testing problems and plenty of references to books, reviews and papers.

When you turn to the end of the book to see if you've got the problems solved you will be surprised to find only half the problems have been given answers. This is because the authors are trying to stimulate us to do some open-ended thinking and discussion. They rightly maintain that a researcher's work is never done and that an interesting piece of chemistry always throws up fresh ideas for more experiments.

After you have recovered from that shock you get another when you find there are no answers at all to the problems in chapter 10. This last chapter is worth the money alone. It consists of 18 case studies, intriguing problems which have fascinated chemists for years. There is the XeF_6 story, the N_2O_3 story, the problem of eclipsed or staggered ferrocene, agostic hydrogens, where the electrons go in reduced or excited dipyridyl complexes, and more. Most of these illustrate the principles that we need to use a combination of techniques to solve structural problems in inorganic chemistry, and that for worthwhile chemistry there are no easy answers.

I particularly enjoyed the crystallography and NMR chapters. The former is the best account I have yet seen for people who may not do it themselves but want to know what it is about, and you will not need to know what a reciprocal lattice is. You can also read how alleged $[ClF_6]^+[CuF_4]^-$ might really be $[Cu(H_2O)_4]^{2+}[SiF_6]^{2-}$.

In the NMR chapter there is a clear critical survey of modern developments, including multiple resonance, multi-pulse methods, applications to the solid state and use of liquid crystals, as well as all those delights like INEPT and INADEQUATE which make the layman think he is. If you want to know what these and other acronyms like MIKES and RIKES stand for there's a good glossary in the first chapter. This is an excellent innovation which all books should have in the space often wasted with accounts of nomenclature rules.

Another good chapter contains a sensible combination of "ordinary" electronic spectra with photoelectron spectra, but the balance favours the second of these unduly. There is still plenty of good work being done on ligand field transitions in electronic spectra. A more extended treatment of these would have allowed a case study in the last chapter on how electronic and ESR spectra can be combined to reveal structure in copper(II) compounds. I was also sorry not to see a chapter about magnetochemistry, which is so closely linked to structure. If this had been covered we could have had a case study on haemocyanin or some other biological system. Some of the necessary space could be generated by omitting the well written but unnecessary sections on quantitative analysis by IR or UV spectra.

Mentioning haemocyanin brings me to my other adverse criticism, that the authors take a slightly restricted view of inorganic chemistry. Nearly all the main text and all the case studies describe work on discrete molecules or ions, but the subject of inorganic chemistry is much wider than this and students in particular would benefit from reading about how ideas developed by the study of molecules can be applied, with adjustment, to proteins, say, or intercalation compounds or electronic materials.

The greatest use of this book ought to be to train Ph.D. students. There is plenty of material here for postgraduate courses and exercises. If your students do get hold of this book, make them read it all, not just use it as a reference book for odd topics or even a few chapters. The writing is fluent and conversational, and even funny, as when $[PtMe_3OH]$ "was reported to explode on combustion, and explosion can lead to inaccurate results", or when the WAHUHA technique in NMR is described as "not an easy experiment to perform successfully, and it is even harder to understand".

I detected no serious errors in any section in which I thought myself knowledgeable and strongly recommend this book to all readers of this journal.

PETER THORNTON

Department of Chemistry
Queen Mary College
Mile End Road
London E1 4NS, U.K.

Gmelin Handbook of Inorganic Chemistry. Gmelin Institute for Inorganic Chemistry of the Max-Planck-Society for the Advancement of Science, 8th edn. Cu-Organocopper Compounds, Part 3. Springer, Berlin, 1986, xii+249 pp. ISBN 3-540-93537-1, DM 1152.

Parts 1 and 2 covered organocopper compounds with alkyl, alkenyl and aryl ligands. The present volume completes the coverage of mononuclear organocopper compounds with ligands bonded through one carbon atom, and contains all derivatives with alkynyl, carbonyl and isocyanide groups.

The copper acetylides, which are extensively used in organic synthesis, occupy the greater part of the volume (187 pages). The literature on the acetylides is first indexed, and their general preparations, structures, properties and reactions are reviewed. The remainder of the chapter (some 50 pages) is then taken up with a tabulation, with extensive footnotes and references, of the compounds RC≡CCu. Their reactions, particularly their conversions to the products RC≡CR′ and RC≡C—C≡CR are listed, and the more complex reactions are described in more detail in subsequent sections.

Acetylides containing copper(I) and a second metal are then dealt with in a similar way, and the volume concludes with sections on copper carbonyls (27 pp.) and isocyanide compounds (24 pp.).

The literature is covered through 1985. The presentation of the material, now wholly in English, is exemplary, as it is in all of these volumes. Organometallic chemists, and organic chemists who need to use organocopper intermediates, are indebted to the authors Helmut Bauer, Jürgen Faust, Rolf Froböse, and Johannes Füssel, and to the Max-Planck Institute and Springer-Verlag, for completing this valuable series.

Department of Chemistry **A. G. DAVIES**
University College London
20 *Gordon Street*
London WC1H 0AJ, U.K.

An Introduction to Organometallic Chemistry. A. W. Parkins and R. C. Poller, Macmillan, Basingstoke, 1986, xii+252 pp. ISBN 0-333-3642-5, ISBN 0-333-36433-3 Pbk, £25.00 (hard back), £9.95 (paper back).

Conventional organic chemistry is concerned with the organic chemistry of some half-dozen electronegative elements. It constitutes a major fraction of any degree course in chemistry and is served by many excellent text books of 1000 pages or more.

Organometallic chemistry on the other hand covers the organic chemistry of some 90 elements (some of them admittedly not very common), and it is necessarily more diverse and varied (and some would say more interesting) then organononmetallic chemistry. Yet organometallic chemistry provides a relatively small fraction of any first degree course, and its text books have to be correspondingly smaller.

Few authors have yet undertaken the difficult task of the drastic compression that is required for a general text book in this field, and the appearance of a new one is very welcome.

Parkins and Poller have chosen an approach which integrates main group and transition metal compounds. They do not discuss particular metals or particular ligands separately at any length, but build up a picture of the preparations, structures and reactions involved in organometallic chemistry as a whole.

The first third of the book deals with the preparation of organometallic compounds and with their structures and the bonding principles which are involved. The approach here is one which most teachers of the subject would approve.

The remaining two-thirds of the book cover the reactions of organometallic compounds, with chapters devoted to carbanion chemistry, carbene chemistry, coordination chemistry, reactions of the bonded organic ligands, stoichiometric applications and catalytic applications. Leading references are given throughout.

Most of the topics which you expect to find are mentioned, if only very briefly. You can quibble about the short shrift with which some of your favourite topics are treated, but on the whole the authors have made a very good job of presenting the salient features of organometallic chemistry. The balanced approach will appeal to teachers of the subject, and renders the book suitable as recommended reading for many university courses in organometallic chemistry.

Department of Chemistry **A. G. DAVIES**
University College London
20 *Gordon Street*
London WC1H 0AJ, U.K.

Gmelin Handbook of Inorganic Chemistry. Gmelin Institute for Inorganic Chemistry of the Max-Planck-Society for the Advancement of Science, 8th edn. Cu-Organocopper Compounds, Part 3. Springer, Berlin, 1986, xii+249 pp. ISBN 3-540-93537-1, DM 1152.

Parts 1 and 2 covered organocopper compounds with alkyl, alkenyl and aryl ligands. The present volume completes the coverage of mononuclear organocopper compounds with ligands bonded through one carbon atom, and contains all derivatives with alkynyl, carbonyl and isocyanide groups.

The copper acetylides, which are extensively used in organic synthesis, occupy the greater part of the volume (187 pages). The literature on the acetylides is first indexed, and their general preparations, structures, properties and reactions are reviewed. The remainder of the chapter (some 50 pages) is then taken up with a tabulation, with extensive footnotes and references, of the compounds RC≡CCu. Their reactions, particularly their conversions to the products RC≡CR′ and RC≡C—C≡CR are listed, and the more complex reactions are described in more detail in subsequent sections.

Acetylides containing copper(I) and a second metal are then dealt with in a similar way, and the volume concludes with sections on copper carbonyls (27 pp.) and isocyanide compounds (24 pp.).

The literature is covered through 1985. The presentation of the material, now wholly in English, is exemplary, as it is in all of these volumes. Organometallic chemists, and organic chemists who need to use organocopper intermediates, are indebted to the authors Helmut Bauer, Jürgen Faust, Rolf Froböse, and Johannes Füssel, and to the Max-Planck Institute and Springer-Verlag, for completing this valuable series.

Department of Chemistry **A. G. DAVIES**
University College London
20 *Gordon Street*
London WC1H 0AJ, U.K.

An Introduction to Organometallic Chemistry. A. W. Parkins and R. C. Poller, Macmillan, Basingstoke, 1986, xii+252 pp. ISBN 0-333-3642-5, ISBN 0-333-36433-3 Pbk, £25.00 (hard back), £9.95 (paper back).

Conventional organic chemistry is concerned with the organic chemistry of some half-dozen electronegative elements. It constitutes a major fraction of any degree course in chemistry and is served by many excellent text books of 1000 pages or more.

Organometallic chemistry on the other hand covers the organic chemistry of some 90 elements (some of them admittedly not very common), and it is necessarily more diverse and varied (and some would say more interesting) then organononmetallic chemistry. Yet organometallic chemistry provides a relatively small fraction of any first degree course, and its text books have to be correspondingly smaller.

Few authors have yet undertaken the difficult task of the drastic compression that is required for a general text book in this field, and the appearance of a new one is very welcome.

Parkins and Poller have chosen an approach which integrates main group and transition metal compounds. They do not discuss particular metals or particular ligands separately at any length, but build up a picture of the preparations, structures and reactions involved in organometallic chemistry as a whole.

The first third of the book deals with the preparation of organometallic compounds and with their structures and the bonding principles which are involved. The approach here is one which most teachers of the subject would approve.

The remaining two-thirds of the book cover the reactions of organometallic compounds, with chapters devoted to carbanion chemistry, carbene chemistry, coordination chemistry, reactions of the bonded organic ligands, stoichiometric applications and catalytic applications. Leading references are given throughout.

Most of the topics which you expect to find are mentioned, if only very briefly. You can quibble about the short shrift with which some of your favourite topics are treated, but on the whole the authors have made a very good job of presenting the salient features of organometallic chemistry. The balanced approach will appeal to teachers of the subject, and renders the book suitable as recommended reading for many university courses in organometallic chemistry.

Department of Chemistry **A. G. DAVIES**
University College London
20 *Gordon Street*
London WC1H 0AJ, U.K.

Polyhedron Vol. 6, No. 9, pp. 1717–1719, 1987
Printed in Great Britain

0277–5387/87 $3.00+.00

THE POTENTIOMETRIC DETERMINATION OF STABILITY CONSTANTS OF SULFITE AND COBALT(II) IN IONIC STRENGTH 2.0 M ($NaClO_4$). USE OF THE MATRIX METHOD

ÉDER TADEU GOMES CAVALHEIRO, ANA MARIA DE GUZZI PLEPIS and GILBERTO ORIVALDO CHIERICE*

Instituto de Física e Química de São Carlos, Departamento de Química e Física Molecular, USP—Cx.P. 369—13.560, São Carlos, SP, Brazil

and

EDUARDO F. A. NEVES

Instituto de Química, USP, São Paulo, SP, Brazil

(*Received* 3 *February* 1987; *accepted* 18 *February* 1987)

Abstract—Determination of the stability constants for the system Co(II)/SO_3^{2-}, was made potentiometrically using SO_3^{2-}/HSO_3^- as buffers. Computation and matrix methods lead to the following overall stepwise constants: $\beta_1 = 4.3 \times 10^2$ M^{-1}, $\beta_2 = 2.2 \times 10^4$ M^{-2} and $\beta_3 = 3.0 \times 10^6$ M^{-3}. The partial constants (M^{-i}) obtained were: $K_1 = 4.3 \times 10^2$, $K_2 = 51$ and $K_3 = 1.4 \times 10^2$. The HSO_3^- competition was eliminated by using the extrapolation procedure.

Although a few studies have been reported on the complexation of amines of Co(III) and sulfite in aqueous solutions,[1,2] the literature is very lacking in data reporting the complexation reaction between cobalt(II) and sulfite. In the present work a potentiometric study[3,4] of the system SO_3^{2-}/HSO_3^-/Co(II), in ionic strength 2.0 M maintained with $NaClO_4$ and temperature of 25°C, is reported.

EXPERIMENTAL

Reagents and solutions

The reagents used in this work were of analytical grade (Merck). $NaClO_4$ was recrystallized and stock solutions 4.0 M were made and standardized gravimetrically by drying at 110°C to constant weight. Sulfite and bisulfite were prepared with boiled and de-aerated water, by passing through N_2 and standardized gravimetrically.[5] Cobalt(II) perchlorate was synthesized by reaction of the pure metal with $HClO_4$, the excess of the acid being evaporated in a sand bath. The pH of the resulting solution was measured from 0.100 M solution in Co(II), at the ionic strength 2.0 M ($NaClO_4$).

Apparatus and procedure

A glass electrode (Metrohm E-6.0203.00), saturated with NaCl and a titroprocessor (Metrohm E-636), with an adequate program for following the pH variations of the system were used in all measurements.

The experiments were taken at 25.0 ± 0.1°C. The conditional pH was measured in relation to solutions of [H^+] concentration of 1.0×10^{-2} M and 1.0×10^{-4} M, with the ionic strength adjusted to 2.0 M with $NaClO_4$, and used in the electrode calibration.

The experimental procedure was based on the titration of 20.00 cm^3 of a mixture of [HSO_3^-]/[SO_3^{2-}] in different relations, whose pH_1, free of metal, was measured with a metallic solution. After each injection of the metallic solution, with conditional hydrogen ion concentration well known, a new pH_2 of equilibria was measured.

The mass balance and volume corrections lead to curves of $\bar{n}$ (the average ligand number) vs [SO_3^{2-}]

* Author to whom correspondence should be addressed.

(concentration of free sulfite). Influence of the bisulfite ions was detected in the measurements and curves of $\bar{n}$ vs $[SO_3^{2-}]$ were taken in various HSO_3^-. Extrapolation of these curves allowed the values of $\bar{n}$ free of $[HSO_3^-]$ to be obtained using a programmable calculator HP-97.

All the measurements were made under N_2 atmosphere maintained in order to prevent the ligand oxidation.

RESULTS AND DISCUSSION

Method utilized

The competitive method,[6] is used based on the variation of the conditional pH (referred to the hydrogen ion concentration instead of its activity) of a sulfite/bisulfite buffer, by the presence of Co(II).

The mass balance applied to the system, based on the pH changes, leads to the final concentration of free sulfite and the average ligand number ($\bar{n}$), as previously discussed.[3]

The conditional pK_a calculated for the weak acid in each solution, instead of the average value, eliminates several sources of errors such as drift in junction potential, reference electrode potential, etc.

The conditional pK_a values obtained, varied in relation to the various buffers, which could be explained by the formation of the $S_2O_5^{2-}$ ion, studied by Golding,[7] according to the equilibria:

$$2HSO_3^- \rightleftharpoons S_2O_5^{2-} + H_2O. \quad (1)$$

Table 1 shows the buffer relations used and the pK_a value obtained. The existence of polynuclear species were not evidenced by the independence of the $\bar{n}$ in relation to the metal concentration.

Four buffer relations were measured each one giving one curve $\bar{n}$ vs $[SO_3^{2-}]$, with the total concentration of sulfite being maintained constant and varying the total concentration of bisulfite. At many points of this curve were taken values of $\bar{n}$ and $C_{HSO_3^-}$, these being values extrapolated to $C_{HSO_3^-}$ equal to zero. Figure 1 shows the set of curves while Fig. 2 presents the final formation curve obtained.

Table 1. Relationship between $C_{SO_3^{2-}}/C_{HSO_3^-}$ used, and their respective pK_a values

Sample	Relationship $C_{SO_3^{2-}}/C_{HSO_3^-}$		pK_a
100:1	10/0.10	20/0.20	6.37
40:1	10/0.25	20/0.50	6.44
20:1	10/0.25	20/1.0	6.48
10:1	10/1	20/2.0	6.52

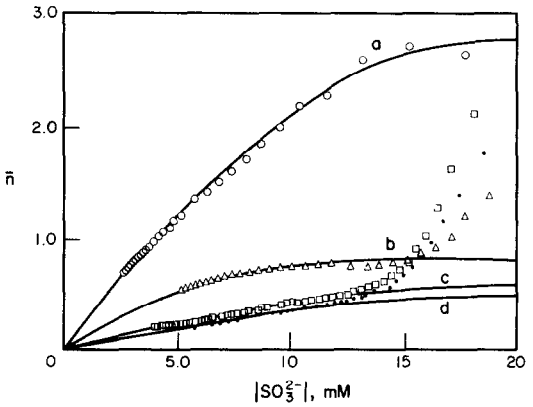

Fig. 1. Formation curves for the solutions measured. The relationship between $C_{SO_3^{2-}}/C_{HSO_3^-}$ were: a = 100:1, b = 40:1, c = 20:1, d = 10:1.

The extrapolation of $\log \bar{n}$ vs $C_{HSO_3^-}$ leads to straight lines, facilitating the extrapolation. After this extrapolations the $\bar{n}$ values obtained (Fig. 2), free of the influence of $C_{HSO_3^-}$, were treated giving the Leden functions,[8] which were treated according to DeFord and Hume[9] giving three complex species.

The overall stepwise constants formation

The curve $\bar{n}$ vs SO_3^{2-}, was integrated,[10] in order to obtain the Leden function, $F_0(x)$, which permits by graphic extrapolation calculation of the value of the overall constants n of equilibria:

$$F_0(x) = 1 + \beta_1[L] + \beta_2[L]^2 + \cdots + \beta_n[L]^n. \quad (2)$$

The graphic treatment leads us to three species, according to the general reaction:

$$Co^{2+} + nSO_3^{2-} \rightleftharpoons Co(SO)_3)_n^{(2-2n)+} \quad (3)$$

with

$$\beta_n = \frac{[Co(SO_3)_n^{(2-2n)+}]}{[Co^{2+}] \cdot [SO_3^{2-}]^n}. \quad (4)$$

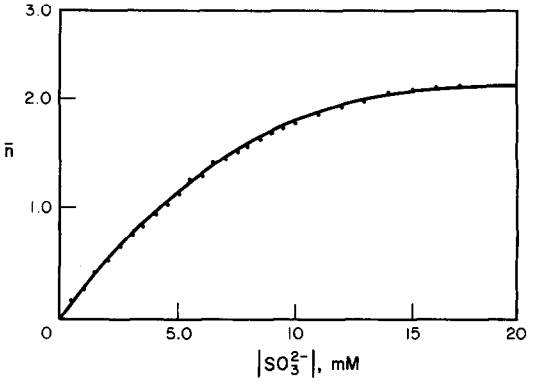

Fig. 2. Definitive formation curve obtained by extrapolation of $\log \bar{n}$ vs $C_{HSO_3^-}$. These data were integrated in order to give the $F_0(x)$ function.

In spite of being an incontestable reference for the calculation of the constants, we must take into account the possibility of subjective errors caused by the extrapolations. Because of this, many methods have been developed for the refinement of data obtained graphically; in this study the matrix method has been chosen, proposed initially by Milcken and Neves.[11] This method is based on a "normalization factor", fi, given by:

$$fi = F_0(x)_{max}/F_0(x) \quad (5)$$

which is introduced in the function $F_0(x)$, by:

$$F_0(x)_{max} = F_0(x)_i fi = fi + fi\beta_1[L] + fi\beta_2[L]^2 + \cdots + fi\beta_n[L]^n. \quad (6)$$

The resolution of the system by matrix method is given by the following constants:

$$\beta_1 = \frac{[CoSO_3]}{[Co^{2+}]\cdot[SO_3^{2-}]} = 4.3\times10^2\,M^{-1}$$

$$\beta_2 = \frac{[Co(SO_3)_2^{2-}]}{[Co^{2+}]\cdot[SO_3^{2-}]^2} = 2.2\times10^4\,M^{-2}$$

$$\beta_3 = \frac{[Co(SO_3)_3^{4-}]}{[Co^{2+}]\cdot[SO_3^{2-}]^3} = 3.0\times10^6\,M^{-3}$$

$$K_1 = \frac{[CoSO_3]}{[Co^{2+}]\cdot[SO_3^{2-}]} = 4.3\times10^2\,M^{-1}$$

$$K_2 = \frac{[Co(SO_3)_2]}{[Co(SO_3)]\cdot[SO_3^{2-}]} = 51\,M^{-1}$$

$$K_3 = \frac{[Co(SO_3)_3]}{[Co(SO_3)_2]\cdot[SO_3^{2-}]} = 1.4\times10^2\,M^{-1}.$$

This set of constants gives an $F_0(x)$ calculated by eqn (1), which differ in $\pm0.91\%$ from the integrated value. This gives a good support for the calculation procedure.

It is important to note that in higher concentrations of the ligand precipitation occurs. In order to help this work, a preliminary study of the K_{ps} of system was conducted.[12] The value obtained was $K_{ps} = 7.3\times10^{-3}$ M^2, in the presence of bisulfite.

Considering the partial constants (K_n), we can see that K_2 is the smaller one, probably because it represents the formation of a charged species from a neutral one. The formation of this neutral species gives to K_1 the biggest numerical value of the set.

Figure 3 shows the distribution curves for the system.

Considering that the coordination number for the cobalt(II) ion is generally 6 and that SO_3^{2-} is doubly charged, it is possible to suppose that the ligand acts like a bidentate ligand in this case, because of the formation of three species.

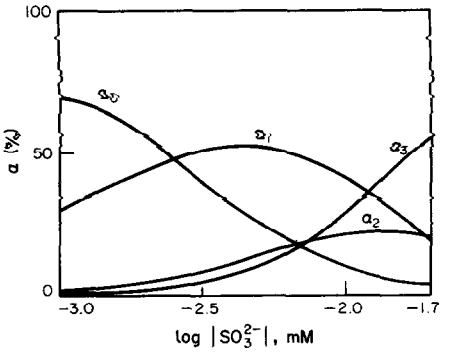

Fig. 3. Distribution curves for the various species of the system Co(II)/SO_3^{2-}.

The possibility must also be considered of the second species to be square planar, because there are known Co(II)(d^7)[13] complexes, having this behavior.

The HSO_3^- anion can influence this system in two ways, the first one like the proper HSO_3^-, or in the form of $S_2O_5^{2-}$ ion, as has been discussed, it coexists with the sulfites in aqueous solution and has variable concentration with the pH and the concentration of HSO_3^- in the media.

REFERENCES

1. L. G. Silén and H. E. Martell, *Stability Constants of Metal Ion Complexes*. The Chemical Society, London (1964).
2. *ibid.* Supplement 1. The Chemical Society, London (1971).
3. E. F. A. Neves, R. Tokoro and M. E. Suarez, *J. Chem. Res.* 1979, **374**, 4401M.
4. G. O. Chierice and E. F. A. Neves, *Polyhedron* 1983, **2**, 31.
5. A. I. Vogel, *Química Analítica Cuantitativa*, Ediutorial Kapeluz S.A. (1974).
6. J. Bjerrum, *Metal Amine Formation in Aqueous Solutions*. P. Haase, Copenhagen (1941).
7. R. M. Golding, *J. Chem. Soc.* 1960, 3711.
8. I. Leden, *Z. Phys. Chem.* 1941, **A188**, 160.
9. D. D. DeFord and D. N. Hume, *J. Am. Chem. Soc.* 1951, **73**, 5321.
10. S. Fronaeus, Thesis, Lund (1943).
11. E. F. A. Neves, M. E. V. Suarez and R. Tokoro, Anais II—Simpósio Brasileiro de Eletroquímica e Eletroanalítica, p. 29. Inst. Química, USP, São Paulo (1980).
12. E. T. G. Cavalheiro and G. O. Chierice, Anais 6º Encontro Regional de Química, São Carlos (1985).
13. J. E. Huheey, *Inorganic Chemistry*. Harper & Row, London (1975).

Polyhedron Vol. 6, No. 9, pp. 1721–1725, 1987
Printed in Great Britain

0277–5387/87 $3.00+.00

CHROMIUM(VI) OXIDATION OF THALLIUM(I)

G. S. GOKAVI and J. R. RAJU*

Department of Chemistry, Karnatak University, Dharwad-580 003, India

(*Received* 13 *November* 1986; *accepted after revision* 6 *March* 1987)

Abstract—The chromium(VI) oxidation of thallium(I) in 3 M hydrochloric acid at ionic strength 4 M and 25°C is studied spectrophotometrically and is found to follow a second-order rate law. The reaction is understood to occur between the species $ClCrO_3^-$ and TlCl and the possible mechanisms are discussed.

The reported standard potentials of the couples, Cr(VI)/Cr(III) and Tl(III)/Tl(I) of 1.33 and 1.25 V in acid solutions[1] do not preclude the possibility of the chromium(VI) oxidation of thallium(I) from occurring yet the reaction does not take place even in concentrated solutions of perchloric and sulphuric acids. In dilute hydrochloric acid solutions, the two potentials are nearly the same but diverge as the acid concentration is increased. The values in 5 M hydrochloric acid at 25°C are 1.17 and 0.606 V for the Cr(VI)/Cr(III) and the Tl(III)/Tl(I) couples respectively and the chromium(VI) oxidation of thallium(I) in such a solution occurs with great facility.[2] Indeed, solutions of 6 M hydrochloric acid have been used in the titrimetric analysis of thallium(I) by chromium(VI).[2,3] The reaction is of considerable interest because of its non-complementary nature and the possibility of a variety of mechanisms involving reactive intermediates such as Cr(V), Cr(IV) and Tl(II) all of which have been encountered in chemical reactions.[4] Moreover, the crucial role of hydrochloric acid, without which the reaction does not occur, needs to be understood.

EXPERIMENTAL

Chemicals

Reagent grade chemicals were used. Doubly distilled water was used for solutions. The Cr(VI) solution was obtained by dissolution of potassium dichromate (BDH,AR) in distilled water and appropriate dilution. The Cr(VI) concentration was ascertained by measuring the absorbance of the Cr(VI) solution at 360 nm in a Bausch and Lomb Spectronic 2000 instrument. The application of Beer's law was tested in the case of the 3 M hydrochloric acid solutions containing 2×10^{-4} to 6×10^{-4} M Cr(VI) using 1 cm cells with $\varepsilon = 1153$. Higher concentrations of Cr(VI) than 6×10^{-4} M were not required in any of the kinetic runs as the solubility of TlCl in 3 M hydrochloric acid was slight (1.6×10^{-3} M). The Tl(I) solution was obtained by dissolving TlCl (BDH) in distilled water and standardization with potassium bromate.[5] Most of this work employed hydrochloric acid, Acid Chem AR, although, at the later stages, Glaxo AR sample was also used. As different samples of hydrochloric acid tended to lead to discrepencies in results, one batch was usually collected and used for related studies to enable comparison of results. Acetic acid was purified by refluxing with chromium(VI) oxide for 5–6 h and distilling.[6] A further distillation gave the product to be used.

Kinetic runs

The ionic strength was maintained at 4 M in most runs with lithium perchlorate. Runs were usually carried out in 3 M hydrochloric acid solutions. In a typical run, the concentrations of Cr(VI) and Tl(I) were 3×10^{-4} and 5×10^{-4} M respectively in 3 M hydrochloric acid at an ionic strength of 4 M. The kinetics were followed by mixing the equilibrated reactant solutions. The resulting reaction mixture was transferred to a 1 cm cell and the absorbance at 360 nm was followed with a Bausch and Lomb Spectronic 2000 Spectrophotometer. The temperature was maintained at 25 ± 0.05°C. Kinetic

* Author to whom correspondence should be addressed.

runs could be reproduced to ±3% or better and runs were usually followed to about four half-lives.

RESULTS

Oxidation of hydrochloric acid by Cr(VI)

The oxidant, Cr(VI), exists mainly in the form of acid chromate ion, $HCrO_4^-$, in dilute acid solutions and, in concentrated hydrochloric acid, the predominant form of the oxidant is the chlorochromate ion,[7] $ClCrO_3^-$. Hence it may be expected that this is the species responsible for oxidation of Tl(I) in concentrated hydrochloric acid solutions. In addition to the main Cr(VI)–Tl(I) redox reaction, there is also a marginal oxidation of hydrochloric acid in the medium. At 25°C, with Cr(VI) and hydrochloric acid concentrations of 3×10^{-4} M and 3 M respectively, the extent of the latter oxidation is very small, only about 0.3% and less than 1% of oxidant being consumed in 30 and 60 min respectively. Under similar conditions, with the Tl(I) concentration at 5×10^{-4} M, 95% of the oxidant is consumed in 30 min. Hence no correction for the Cr(VI) oxidation of hydrochloric acid has been made at this temperature. The reduction of Cr(VI) by hydrochloric acid is accelerated at higher temperatures (0.5% in 15 min) as shown by the data at 32.5°C. However, the rate of the Cr(VI)–Tl(I) redox reaction is also enhanced with temperature, 95% of the reaction taking place in about 15 min at 32.5°C.

Air oxidation

Air oxidation does not occur to any significant extent under the conditions of the present study at 25°C and time durations of the Cr(VI)–Tl(I) reaction as found from runs in the presence and absence of air. At a higher hydrochloric acid concentration of 6 M and 29°C, marginal air oxidation has been reported as occurring in one study[2] while no such air oxidation interfered under similar conditions in another study.[3]

Stoichiometry

Several reaction mixtures were prepared in 3 M hydrochloric acid at ionic strength of 4 M and analysed after keeping for 2 h at 25°C. Cr(VI) was found by measuring the absorption at 360 nm. Tl(I) was determined by titrating 40 ml of the reaction mixture with 2×10^{-3} M potassium bromate and Cr(III) does not interfere. Tl(III) was found as difference of total oxidant titrated by iodometry with 2×10^{-3} M thiosulfate and Cr(VI) found by spectrophotometry. The results are shown in Table 1 and indicate a 2:3 stoichiometry for the Cr(VI) oxidation of $Tl(I) : 2Cr(VI) + 3Tl(I) = 2Cr(III) + 3Tl(III)$.

Effect of added products

The effect of added products, Cr(III) and Tl(III), was studied at an ionic strength of 4 M and hydrochloric acid concentration of 3 M and at constant Cr(VI) and Tl(I) concentrations. The products did not have any significant effect on the reaction.

Rate law

The order of the reaction with respect to Cr(VI) and Tl(I) was found by log (rate) vs log (conc.) plots in the case of the 3 M hydrochloric acid solutions at ionic strength 4 M. The order in Cr(VI) in the concentration range of 2×10^{-4} to 6×10^{-4} M at a constant Tl(I) concentration of 5×10^{-4} M was 0.9; whereas, in the concentration range of 1×10^{-4} to 6×10^{-4} M of Tl(I) at a constant Cr(VI) concentration of 3×10^{-4} M, the order in Tl(I) was 0.64. The fractional orders in Tl(I) and Cr(VI) were taken to be due to the main active species being TlCl and CrO_3Cl^- with the formation equilibrium constants of 3.9 (this work) and 14[7] respectively at 25°C. The formation constant, K_2, of TlCl at 25°C was determined at an ionic strength of 4 M from solubilities in presence of varying concentrations of hydrochloric acid. In view of the slowness of the Cr(VI)–Tl(I) reaction in solutions containing

Table 1. Stoichiometry of chromium(VI)–thallium(I) reaction [HCl] = 3.0; I = 4.0 M; temp. 25°C

$[Tl(I)] \times 10^4$ taken	$[Cr(VI)] \times 10^4$ taken	$[Tl(I)] \times 10^4$ remaining	$[Cr(VI)] \times 10^4$ remaining	$[Tl(III)] \times 10^4$ found
3.0	1.0	1.5	—	1.5
4.0	2.0	1.0	—	3.0
5.0	3.0	0.50	—	4.48
3.0	3.0	Zero	1.0	3.00
5.0	3.0	0.50	—	4.44

hydrochloric acid less than 3 M, the effect of H^+ and Cl^- concentrations on the reaction were studied at an ionic strength of 5 M in solutions containing H^+/Cl^- (4 M) and varying the concentration of the other ion from 1.0 to 4.0 M (data of Table 2); the order in H^+ and Cl^- thus found was 0.97 in either case. The rate law is given by (1) where K_1 and K_2 are the formation equilibrium constants of CrO_3Cl^- and TlCl respectively. Rates of reaction at around 30 different sets of concentrations of Tl(I) and Cr(VI) were found to bear an approximately linear relationship with the product of the two reactant concentrations as shown in Fig. 1(a). Second order plots according to (2) with a and b representing Tl(I) and Cr(VI) concentrations respectively were found to be linear in most cases to about 90% reaction [Fig. 1(b)], k_s giving the second order rate constant.

$$-\frac{d[Cr(VI)]}{dt} = k_o \frac{K_1K_2[H^+][Cl^-]^2}{(1+K_1[H^+][Cl^-])(1+K_2[Cl^-])} \times [Tl(I)][Cr(VI)] \quad (1)$$

$$k_s = \frac{2.303}{t(a-3b/2)} \log \frac{b(a-3x/2)}{a(b-x)} \quad (2)$$

Effect of solvent polarity

The effect of dielectric constant (D) on the reaction was studied by changing the solvent polarity by use of different quantities of acetic acid in the solvent keeping the ionic strength constant at 3 M. The plot of $\log k_s$ vs $1/D$ was linear with positive slope. The dielectric constants used were computed from the values of pure liquids as in earlier work.[8]

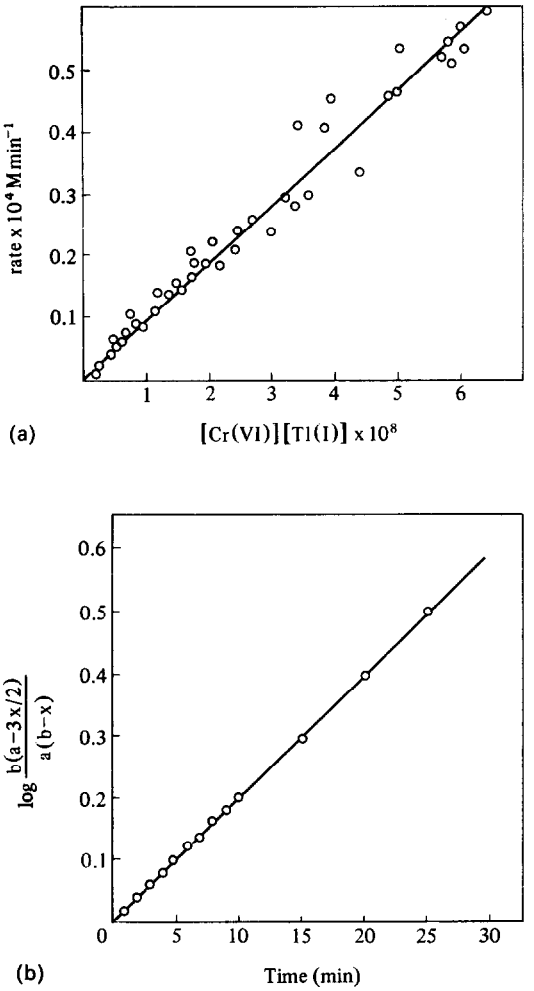

Fig. 1. (a) Graph of rate of Cr(VI)–Tl(I) reaction vs product of reactant concentrations. I = 4.0 M; [HCl] = 3.0; T = 25°C. (b) Second order plot of Cr(VI)–Tl(I) reaction at 25°C. I = 4.0 M; [Cr(VI)] = 3.0×10^{-4}; [Tl(I)] = 5.0×10^{-4}; [HCl] = 3.0.

DISCUSSION

The stoichiometry of the Cr(VI)–Tl(I) redox reaction is found to be 2:3. The marginal reduction of Cr(VI) by the hydrochloric acid present in high concentrations in the reaction medium occurs only to the extent of about 0.3% in 30 min at 25° and that too in the absence of Tl(I). During this time, 95% of the main reaction, i.e. of Cr(VI) oxidation of Tl(I), is complete. There was also no need of excluding air from the reaction under the present conditions although an earlier study found that, at a concentration of 6 M hydrochloric acid, an inert atmosphere was needed[2] while another study[3] under similar conditions did not find it necessary to exclude air from the reaction.

Table 2. Effect of chloride and hydrogen ions on second order rate constant. I = 5.0 M; [Cr(VI)] = 3.0×10^{-4}; [Tl(I)] = 5.0×10^{-4}; temp. 25°C

(a) $[H^+] = 4.0$		(b) $[Cl^+] = 4.0$	
$[Cl^-]$	k_s M^{-1} s^{-1}	$[H^+]$	k_s M^{-1} s^{-1}
1.0	6.6	1.0	7.0
2.0	17	2.0	9.4
3.0	25	3.0	22
4.0	44	4.0	44

The rate law (1) and other results may be accommodated by Scheme I or Scheme II. In both schemes, Cr(VI) and Tl(I) are converted into the species $ClCrO_3^-$ and TlCl respectively in prior equilibria. In Scheme I, these species are involved in a first reversible step giving the reactive intermediates Cr(V) and Tl(II) and the latter species are involved

in further steps. A steady state treatment of Cr(V) and Tl(II) results in the rate law (3). With constant factors on the right hand side identifiable with k_s as 15.6 $M^{-1} s^{-1}$ [Fig. 1(a)] and using an approximate value of k_1 as 19.9 $M^{-1} s^{-1}$, a value of 6.5 is obtained for the ratio k_3k_4/k_2.

$$-\frac{d[Cr(VI)]}{dt} = \left(\frac{k_3k_4}{k_2}\right)\left\{\left(1+\frac{4k_1k_2}{k_3k_4}\right)^{1/2}-1\right\} \times \left\{\frac{K_1K_2[H^+][Cl^-]^2}{(1+K_1[H^+][Cl^-])(1+K_2[Cl^-])}\right\} \times [Tl(I)][Cr(VI)]. \quad (3)$$

Scheme II is essentially the same as Scheme I except that the prior equilibria are succeeded by the rate determining and irreversible step of formation of Cr(V) and Tl(II) followed by other steps as in Scheme I. While this mechanism is in agreement with the results, more often than not in non-complementary reactions involving Cr(VI) or Tl(III), the formation of Cr(V) or Tl(II) involves a reversible step. However, in view of the fact that both Cr(V) and Tl(II) are reactive and are likely to be present in very low concentrations, it is difficult to distinguish between Schemes I and II.

The Cr(VI)–Tl(I) reaction is facile only in the presence of large concentrations of hydrochloric acid and, as mentioned already, the reduction potentials of the couples Cr(VI)/Cr(III) and Tl(III)/Tl(I) become more and more favourable as the hydrochloric acid concentration increases.[2] From the difference in reduction potentials, the equilibrium constant for the reaction in dilute acids and in 6 M hydrochloric acid at 25°C may be calculated to be around 10^5 and 10^{28} respectively showing the facility of the reaction in the latter solution as compared to the dilute sulphuric/perchloric acid medium. In Cr(VI) solutions containing hydrochloric acid concentrations greater than 1 M, the Cr(VI) which is present mainly in the form of the acid chromate ion, $HCrO_4^-$, in dilute acid solutions, is almost entirely transformed into chlorochromate,[9] $ClCrO_3^-$. Hence, it is the latter species that is responsible for the oxidation of Tl(I) in concentrated hydrochloric acid solutions. The Tl(I) in chloride solutions forms chloride species, $(TlCl_n)^{1-n}$, with $n = 1$ and $n = 2$ and higher chloride species may also be expected in concentrated chloride solutions.[10] The major species is TlCl with an equilibrium constant of formation of 3.9 in 3 M hydrochloric acid at an ionic strength of 4 M at 25°C. Thus, the active species is likely to be TlCl which is also supported by the fact that the second order rate constant, k_s, of the Cr(VI)–Tl(I) reaction in such media increases with the decrease of the dielectric constant of the solvent medium. Unfortunately, as the solubility of Tl(I) in hydrochloric acid is severely limited and since analysis of Tl(I) at such low concentrations is difficult, this cannot be further studied under pseudo first order conditions. If the reactants are in the form of $ClCrO_3^-$ and TlCl, they may be expected to form in prior equilibria.

In Scheme I, no Cr(IV) is involved but Cr(V) is. Induction experiments with iodide could not be performed in the present case as one of the products, Tl(III), also oxidises iodide along with Cr(VI) and any Cr(V) that forms. Furthermore, the Cr(V)–Tl(I) reaction, being a complementary one, is expected to be fast and Cr(V), as well as Tl(II), is likely to be present in very low concentrations.

It was observed in the case of the γ-radiation induced reduction of Cr(VI) by Tl(I) in 0.4 M air saturated sulphuric acid, that the OH radicals produced oxidised Tl(I) to Tl(II) and the latter produced Cr(V) by reduction of Cr(VI).[11] The Cr(VI), Cr(V) and any Cr(IV) did not oxidise Tl(I) to Tl(II) nor did Tl(II) oxidise Cr(III). The products, Cr(III) and Tl(III), also did not have any effect on the reaction. In the present case also, the products Cr(III) and Tl(III) do not affect the reaction but Cr(VI) and Cr(V) attack Tl(I) and Tl(II) in Scheme I unlike the γ-ray induced reduction of Cr(VI) in dilute sulphuric acid solution. In the latter solution, the oxidant is mainly present as the acid chromate, $HCrO_4^-$, while in the hydrochloric acid solution, the species, $ClCrO_3^-$, is involved. Moreover, high chloride concentrations favour Tl(I) oxidations[12] and, as in the present case, hydrogen and chloride ions have been found to together facilitate the reduction of Cr(VI) by Tl(I) (Table 2). Chloride ions accelerate the reaction to a greater extent at constant hydrogen ion concentration (Table 2).

$$HCrO_4^- + H^+ + Cl^- \rightleftharpoons ClCrO_3^- + H_2O \quad (K_1)$$
$$Tl^+ + Cl^- \rightleftharpoons TlCl \quad (K_2)$$
$$ClCrO_3^- + TlCl \rightleftharpoons CrO_3^- + TlCl_2 \quad (k_1, k_2)$$
$$ClCrO_3^- + TlCl_2 \rightarrow CrO_3^- + TlCl_2^+ + Cl^- \quad (k_3)$$
$$2(CrO_3^- + TlCl + 6H^+ \rightarrow Cr^{3+} + TlCl^{2+} + 3H_2O) \quad (k_4)$$

Scheme I.

REFERENCES

1. M. C. Day and J. Selbin, *Theoretical Inorganic Chemistry*, p. 229. Reinhold, New York (1962).
2. S. R. Sagi, G. S. Prakasa Raju and K. V. Ramana, *Talanta* 1975, **22**, 93.
3. I. Buzás and L. Erdey, *Talanta* 1963, **10**, 467.

4. J. H. Espenson, in *Homogeneous Inorganic Reactions, Techniques of Chemistry* (Edited by E. S. Lewis), Vol. VI, pp. 584–586. Wiley-Interscience, New York (1974).
5. E. Zintl and G. Rienacker, *Z. Anorg. Allg. Chem.* 1926, **153**, 276.
6. J. A. Riddick and E. E. Toops, Jr., *Organic Solvents, Techniques of Organic Chemistry*, Vol. VII, 2nd edn. p. 390. Interscience, New York (1955).
7. G. P. Haight, Jr., D. C. Richardson and N. W. Coburn, *Inorg. Chem.* 1964, **3**, 1777.
8. P. S. Radhakrishnamurthy and S. C. Pati, *Ind. J. Chem.* 1969, **7**, 687.
9 K. B. Wiberg, in *Oxidation in Organic Chemistry* (Edited by K. B. Wiberg), Part A, p. 72. Academic Press, New York (1965).
10. Kuo-Hao Hu and A. B. Scott, *J. Am. Chem. Soc.* 1955, **77**, 1380.
11. T. J. Sworski, *J. Phys. Chem.* 1959, **63**, 823.
12. I. M. Kolthoff and R. Belcher, *Volumetric Analysis*, Vol. III, pp. 102, 461, 519 and 641. Interscience, New York (1957).

Polyhedron Vol. 6, No. 9, pp. 1727–1735, 1987
Printed in Great Britain

0277–5387/87 $3.00+.00

SYNTHESIS AND CHARACTERIZATION OF NOVEL PLATINUM GROUP METAL COMPLEXES OF BIS[2-(DIPHENYLPHOSPHINO)ETHYL]AMINE

M. M. TAQUI KHAN* and E. RAMA RAO

Discipline of Co-ordination Chemistry and Homogeneous Catalysis, Central Salt & Marine Chemicals Research Institute, Bhavnagar 364002, India

(*Received* 9 *December* 1986; *accepted* 6 *March* 1987)

Abstract—A mixed donor tridentate ligand bis [2-(diphenylphosphino)ethyl]amine (DPEA) was synthesized in its hydrochloride form by a modified procedure and characterized by ^{1}H, ^{13}C and ^{31}P NMR spectral data. Reaction of $RhCl(CO)(PPh_3)_2$ with DPEA · HCl and $NaBPh_4$ in methanol gave the cationic Rh(I) complex $[Rh(DPEA)PPh_3]BPh_4$ but the reaction of $IrCl(CO)(PPh_3)_2$ with DPEA · HCl in boiling benzene gave a unique complex, [Ir(H)(Cl)(CO)(DPEA)]Cl, in which five different donor atoms are coordinated to the single Ir(III) ion. A neutral, Rh(III) complex of the composition $[RhCl_3(DPEA)]$ was prepared by the reaction of $RhCl_3 \cdot xH_2O$ with DPEA · HCl in methanol. Reaction of $PdCl_2(COD)$ with DPEA · HCl in benzene or methanol gave the cationic complex [PdCl(DPEA)]Cl the above reaction conducted in benzene-acetone-methanol mixture gave the 1:2 complex $[Pd(DPEA)_2]Cl_2$. A novel trinuclear Pt(II) complex of the composition $[Pt_3Cl_3(DPEA)_3]Cl_3$ was prepared by the reaction of K_2PtCl_4 and DPEA · HCl in water-acetone mixture. Reaction of K_2PtCl_4, DPEA · HCl and NH_4PF_6 in water ethanol mixture gave the binuclear, cationic complex, $[Pt_2(DPEA)_3](PF_6)_4$. All the complexes were characterized by elemental analysis, conductivity, ^{1}H and ^{31}P NMR spectral data.

Recently we have been interested in the synthesis and chemistry of transition metal complexes of polydentate ligands containing mixed donor atoms like N, P, As.[1–5] Though considerable research interest has been concentrated on mononuclear complexes of polydentate mixed donor ligands, only recently active interest has been evinced in the use of these polydentate ligands in the synthesis of bi- and polynuclear metal complexes,[6–8] mostly due to their catalytic importance.[9–11]

In this paper we report the synthesis of mononuclear platinum group metal complexes of bis[2-(diphenylphosphino)ethyl]amine (DPEA) which has been synthesized by a modified procedure. Binuclear and trinuclear Pt(II) metal complexes of DPEA in which the two metal ions are held apart at a sufficient distance and incapable of forming metal–metal bonds, have also been synthesized. All the complexes and the ligand DPEA are characterized on the basis of their analytical and spectral data.

RESULTS AND DISCUSSION

The ligand DPEA · HCl is soluble in most of the organic solvents and was characterized by analytical and spectral measurements. The ^{1}H NMR spectrum of the ligand DPEA · HCl, exhibits a complex asymetric phenyl proton resonance at 7.3 δ. The resonance of the protons of the CH_2CH_2 bridge are also observed as multiplets centered at 2.9 δ ($-CH_2$ protons attached to diphenylphosphino group) and 2.5 δ ($-CH_2$ protons attached to amine center). The spectrum also exhibits the NH resonance at 1.9 δ, in concurrence with earlier reported values.[12,13] The $^{31}P\{^{1}H\}$ NMR spectrum of the ligand in $CHCl_3$ gave an intense singlet at -20.3 δ. The $^{13}C\{^{1}H\}$ NMR spectrum of DPEA · HCl in $CDCl_3$ gave two well defined doublets centred at 44.4 δ and 24.0 δ in the aliphatic region. The more downfield doublet is assigned to the methylene car-

* Author to whom correspondence should be addressed.

bon of the CH_2CH_2 bridge attached to phosphorus, with larger $^1J(C-P) = 26.4$ Hz and the other high field doublet with $^2J(C-P) = 17.6$ Hz, can be assigned to the methylene carbon attached to nitrogen. The aromatic carbons of the diphenylphosphino moieties gave doublets centred at 136.3, 132.7 and 128.8 δ with J(C–P) values of 13.2, 19.1 and 5.8 Hz assigned to C-2(6), C-1, C-3(5), respectively, whereas C-4 carbon gave a singlet at 129.7 δ.

Platinum group metal complexes

The ligand DPEA · HCl was utilized for the synthesis of various platinum group metal complexes.

The reaction of DPEA · HCl with $RhCl(CO)(PPh_3)_2$ in 1 : 1 molar ratio gave the cationic complex, $[Rh(DPEA)(PPh_3)]BPh_4$ **1** best isolated as its BPh_4^- salt. Complex **1** gave a conductance value indicative of a 1 : 1 electrolyte[14] (Table 1). The $^{31}P\{^1H\}$ NMR spectrum of complex **1** (Fig. 1, Table 2) exhibits an A_2MX pattern of spectrum with a pair of triplets and doublets. The doublets are centred at 41.5 and 38.2 δ with $J(Rh-P_a) = 134.3$ Hz and are assigned to the two equivalent *trans* phosphorus atoms (P_a) of the ligand (structure I). The triplets are centred at 32.0 and 29.3 δ with $J(Rh-P_b) = 117.2$ Hz, $J(P_a-P_b) = 24.4$ Hz, and assigned to triphenyl phosphine (P_b), which is coordinated to rhodium *trans* to the nitrogen of

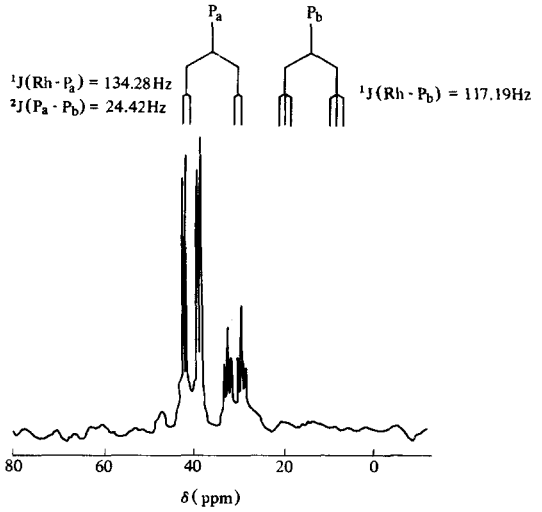

Fig. 1. $^{31}P\{^1H\}$ NMR spectrum of [Rh(DPEA)(PPh$_3$)]BPh$_4$.

DPEA. There is a considerable downfield shift of ^{31}P resonance of the phosphorus atoms of the ligand DPEA upon chelation to form a five-membered ring[15] and also the $^1J(Rh-P_a)$ coupling is larger than that of $^1J(Rh-P_b)$, due to the strong bond of the chelated phosphorus atoms rather than the monodentate phosphorus atom. Complex **1** can be assigned a square-planar structure as shown in Structure I.

Table 1. Analytical and other physical data of metal complexes

Complex[a]	Colour	Melting/ decomposition point (°C)	Elemental analysis[b] %C	%H	%N	%Cl	Conductivity[c] λ_∞ Ω^{-1} cm^2 mol^{-1}
$[Rh(DPEA)(PPh_3)]BPh_4$ **1**	Pale yellow	178	74.7 (74.4)	5.7 (5.7)	1.2 (1.2)	—	32[d]
$[Rh(DPEA)Cl_3]$ **2**	Pale yellow	248	51.6 (50.8)	4.5 (4.5)	2.1 (2.1)	—	32[e]
[Ir(Cl)(H)(CO)(DPEA)]Cl **3**	White	245–247	49.9 (48.9)	4.3 (4.3)	2.0 (1.9)	10.1 (10.1)	65[e]
[Pd(DPEA)Cl]Cl **4**	Yellowish-green	243–245	54.3 (54.1)	4.7 (4.7)	2.2 (2.1)	11.4 (11.4)	106
$[Pd(DPEA)_2]Cl_2$ **5**	Yellow	> 200	63.4 (63.2)	5.7 (5.7)	2.6 (2.5)	—	130[e]
$[Pt_2(DPEA)_2(\mu^3\text{-DPEA})(PtCl_3)]Cl_3$ **6**	White	212–216	47.5 (47.0)	4.1 (4.1)	1.9 (1.9)	—	181
$[Pt_2(DPEA)_2(\mu\text{-DPEA})](PF_6)_4$ **7**	White	228	43.1 (42.8)	3.7 (3.6)	1.7 (1.7)	—	212

[a] DPEA = bis[2-(diphenylphosphino)ethyl]amine.
[b] Found values are in parentheses.
[c] Conductivity measurements were done in methanol at room temperature and values reported for infinite dilution.
[d] Dichloromethane.
[e] DMF.

Table 2. The $^{31}P\{^{1}H\}$ NMR spectral data[a] of the metal complexes

Complex[b]	Solvent	Chemical shifts[c] (δ/ppm) Pa	Pb	Pc	Coupling constant (Hz) J(M–P) J(M–P_a)	J(M–P_b)	J(P–P) J(P_a–P_b)
[Rh(DPEA)(PPh_3)](BPh_4) **1**	$CHCl_3$	41.5(d) 38.2(d)	32.0(t) 29.3(t)	—	134.3	117.2	24.4
[Rh(DPEA)Cl_3] **2**	CH_2Cl_2						
(A) *Mer*		28.4(d)	—	—	84.2	—	—
(B) *Fac*		44.5(d)	—	—	122.1	—	—
[Ir(Cl)(H)(CO)(DPEA)]Cl **3**	$CHCl_3$	27.7(s)	—	—	—	—	—
[Pd(DPEA)Cl]Cl **4**	$CHCl_3$	37.2(s)	—	—	—	—	—
[Pd(DPEA)$_2$]Cl_2 **5**	$CHCl_3$	45.4(d)	15.5(t)	−22.4(s)	—	—	~ 24
[Pt_2(DPEA)$_2$(μ^3-DPEA)($PtCl_3$)]Cl_3 **6**	$CHCl_3$	42.0(d)	−5.3(t)	—	2578	3123	19.5
[Pt_2(DPEA)$_2$(μ-DPEA)](PF_6)$_4$ **7**	CH_2Cl_2	42.0(d)	−7.0(t)	—	2537	3147	19.5

[a] Positive Chemical Shifts Downfield from 85% H_3PO_4.
[b] DPEA = bis(2-(diphenylphosphino)ethyl)amine.
[c] s = singlet, d = doublet, t = triplet.

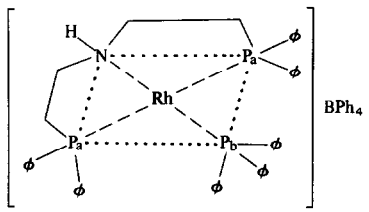

I

Interaction of hydrated rhodium trichloride with DPEA · HCl in 1 : 1 mole ratio gives a neutral, octahedral complex of the composition [$RhCl_3$(DPEA)] **2** which can exist in two isomeric forms: *facial* and *meridional*. The far-infrared spectrum exhibits a broad band at 335 cm^{-1} and also two more bands at 350 and 386 cm^{-1} indicative of ν(Rh–Cl) and cannot be unambiguously assigned to either isomer. However, $^{31}P\{^{1}H\}$ NMR spectrum (Table 2) corroborates the presence of both *facial* and *meridional* isomers. The spectrum displays two doublets centred at 44.5 δ (J(Rh–P) = 122.2 Hz) and 28.4 δ (J(Rh–P) = 84.2 Hz) that can be assigned to the *fac* and *mer* isomers (Structure II, IIa), respectively. The above spectral assignment was based on the following considerations in the *fac* isomer (**II**) the two phosphorus atoms *trans* to a more electronegative and a weak ligand would exhibit a more downfield resonance with a large J(Rh–P) in comparison to the *mer* isomer, in accordance with the earlier observed data.[16,17]

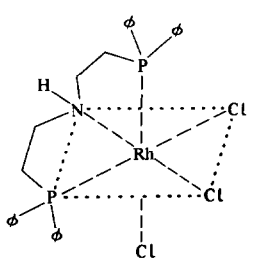

II

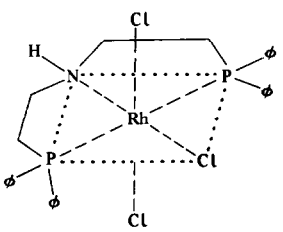

IIa

Interaction of DPEA · HCl with $IrCl(CO)(PPh_3)_2$ in boiling benzene, however gave a unique and interesting complex of the composition [Ir(H)(Cl)(CO)(DPEA)]Cl **3** wherein the metal ion is coordinated to five different donor atoms. Analytical and conductivity data (Table 1) support the above formulation for complex **3**. Complex **3** is obtained by an oxidative-addition of the HCl, derived from the ligand DPEA · HCl, to the Ir(I) complex $IrCl(CO)(PPh_3)_2$ followed by the coordination of Ir(III) to DPEA. The infrared spectrum of complex **3** (Fig. 2) displays an intense peak at 2020 cm^{-1} indicative of the coordinated carbonyl absorption band. This band is red shifted about 50 cm^{-1} compared to that of the starting material (Vaska's complex) and is in support[18] of the oxidation of Ir(I) to Ir(III). The IR spectrum of the complex also exhibits an intense metal-hydride stretching frequency at 2095 cm^{-1} (Fig. 2). The far-infrared spectrum of **3** shows a ν(Ir–Cl) band at 333 cm^{-1}.

The ^{1}H and ^{31}P NMR are of great help in corroborating the above formulation for complex **3**. The ^{1}H NMR spectrum (Fig. 3) exhibits the proton resonance centred at 7.5 δ and two types of the methylene protons at 3.4 and 3.3 δ as broad intense peaks. The proton of the secondary amine gave the resonance at 10.1 δ (Fig. 3) indicating the coor-

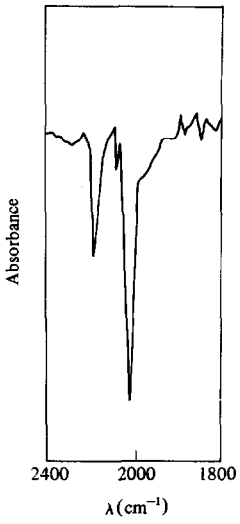

Fig. 2. IR spectrum of [Ir(H)(Cl)(CO)(DPEA)]Cl.

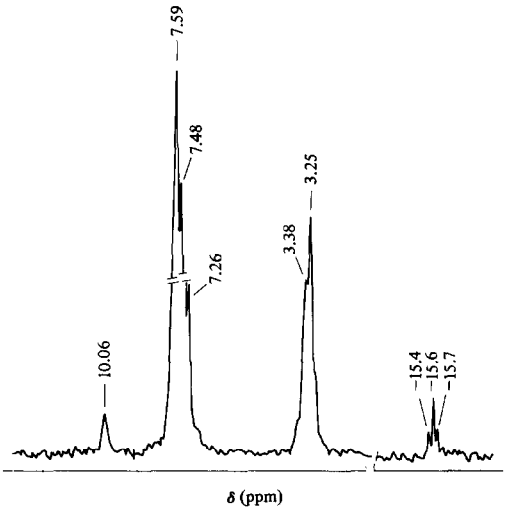

Fig. 3. ^{1}H NMR spectrum of [Ir(H)(Cl)(CO)(DPEA)]Cl.

dination of nitrogen of the secondary amine to the metal ion.[19] The ^{1}H NMR spectrum in the high field region displays a well defined triplet (Fig. 3) centred at -15.6 δ indicating the presence of hydride species in the coordination sphere of the metal ion. The triplet is due to coupling of the hydride with two equivalent *trans* disposed phosphorus atoms of the ligand DPEA (Structure III).

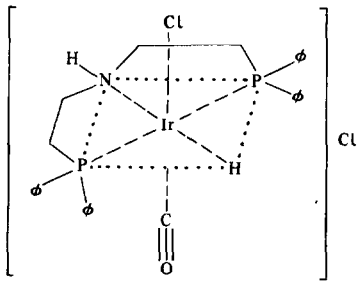

III

The J(P–H) of 12.8 Hz is also in agreement with the *cis* disposition of the hydride to the two phosphorus atoms of the ligand.[20]

The ^{31}P{^{1}H} NMR spectrum exhibits an intense singlet at 27.7 δ in support of structure III for complex **3**.

The reaction of $PdCl_2$(COD) with DPEA·HCl in refluxing methanol or benzene, resulted in the formation of the square planar complex [PdCl(DPEA)]Cl **4**, by the complete displacement of 1,5-COD. The conductance value is consistent with a 1:1 electrolyte[14] (Table 1). The far-infrared spectrum of the complex displays a ν(Pd–Cl) absorption band at 337 cm^{-1}. The ^{31}P{^{1}H} NMR spectrum of complex **4** exhibits a singlet at 37.2 δ indicating the magnetic equivalence of the two *trans* disposed phosphorus atoms of the ligand DPEA, as shown in Structure IV.

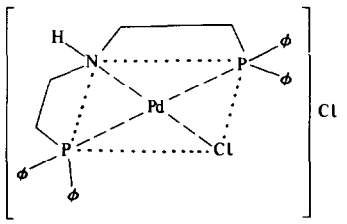

IV

When the reaction of $PdCl_2$ with DPEA·HCl was conducted in a methanol/acetone/benzene mixture a five-coordinated 1:2 complex of the composition $[Pd(DPEA)_2]Cl_2$ **5** resulted. The formulation of complex **5** is corroborated by the elemental analysis, conductance values (Table 1) and the ^{31}P{^{1}H} NMR. The ^{31}P{^{1}H} NMR spectrum of complex **5** displays an interesting spectrum (Fig. 4). The spectrum has a downfield doublet centred at 45.4 δ, a triplet centred at 15.5 δ and a higher field singlet at -22.4 δ. The spectrum suggests that one of the two coordinated DPEA ligands which is potentially terdentate is coordinated to the metal ion through only one of two phosphorus atoms and the other phosphorus donor end (P_c) is free as

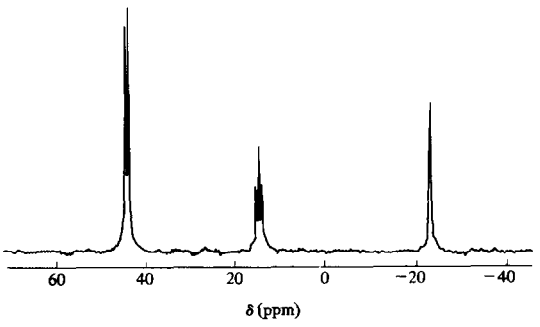

Fig. 4. ^{31}P{^{1}H} NMR spectrum of $[Pd(DPEA)_2]Cl_2$.

evidenced by the high field singlet. Thus the ligand DPEA acts as a bidentate ligand in the complex (Structure V). The doublet is assigned to the two

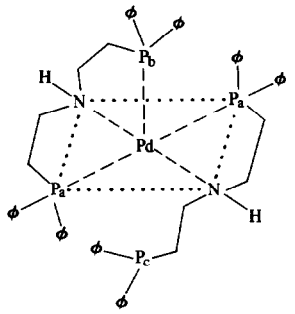

V

equivalent phosphorus donor atoms (P_a) and the triplet to the phosphorus (P_b). The $J(P_a–P_b)$ value of ~ 24 Hz also confirms the *cis* coordination of the phosphorus atoms P_a and P_b as shown in Structure V. The complex is shown with a five coordinated square pyramidal Pd(II) ion. Such a five coordination of Pd(II) was also suggested in other complexes.[21] Five coordination is more common in Pd(II) complexes as compared to those of Pt(II) complexes.

The reaction of $PdCl_2$ with DPEA · HCl in methanol however gave a mixture of complexes **4** and **5** as evidenced by the $^{31}P\{^1H\}$ NMR spectrum in $CHCl_3$ with complex **4** being the predominant species.

The reaction of K_2PtCl_4 with DPEA · HCl in 1 : 1 molar ratio in water–acetone medium gave a trinuclear ligand bridged complex of the composition $[Pt_2DPEA)(\mu^3\text{-}DPEA)(PtCl_3)]Cl_3$ **6**. The above reaction when conducted in water–methanol medium in the presence of NH_4PF_6 resulted in the formation of a binuclear, ligand bridged complex of the composition, $[Pt_2(DPEA)_2(\mu\text{-}DPEA)](PF_6)_4$ **7**. The elemental analysis and conductance data obtained is in confirmation of the above formulations for the complexes **6** and **7**. The far-infrared spectrum of complex **6** displays a broad band at 325 cm^{-1} due to ν(Pt–Cl).

The infrared spectrum of **7** exhibits a strong absorption at 840 cm^{-1} characteristic of ν(P–F) stretching frequency.[22]

The $^{31}P\{^1H\}$ NMR spectrum of complex **6** supports its formulation as a trinuclear ligand bridged species. The $^{31}P\{^1H\}$ NMR spectrum of **6** (Fig. 5) exhibits a doublet centred at 42.0 δ and a triplet centred at -5.3 δ with ^{195}Pt satellites in 2 : 1 ratio, respectively. This also indicates the presence of two different types of phosphorus atoms in accordance with the geometry shown in Structure VI. The doublet is assigned to the two equivalent *trans* disposed phosphorus atoms (P_a) of the ligand DPEA and the triplet to the phosphorus atom (P_b) which is *trans* to a nitrogen donor and *cis* to the two equivalent P_a nuclei. The platinum–phosphorus coupling constants $J(Pt–P_a)$ and $J(Pt–P_b)$ calculated from the platinum satellites are found to be 2578 Hz and 3123 Hz, respectively, in accordance with the earlier observed values.[17,19,23] The $J(Pt–P_b)$ value is larger as compared to that of $J(Pt–P_a)$ due to the fact that the phosphorus atom (P_b) *trans* to a σ-donor nitrogen group is bound strongly to the metal ion with a greater *s* character of the Pt–P

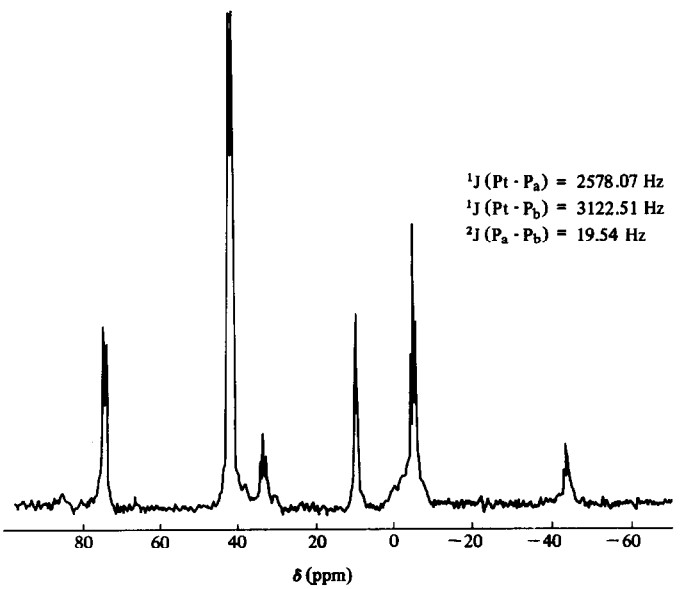

Fig. 5. $^{31}P\{^1H\}$ NMR spectrum of $[Pt_2(DPEA)(\mu^3\text{-}DPEA)(PtCl_3)]Cl_3$.

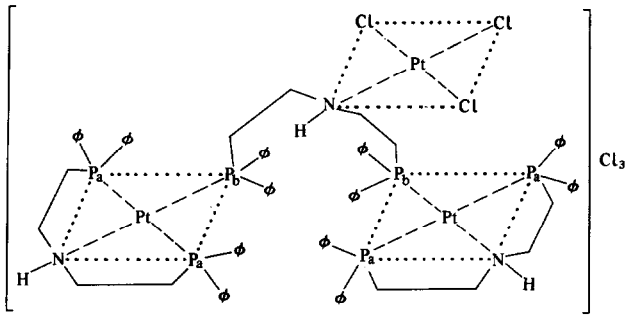

VI

bond as compared to the mutually *trans* phosphorus atom (P_a).[17,23]

The $^{31}P\{^1H\}$ NMR spectrum of complex **7** (Fig. 5) shows a doublet centred at 42.0 δ and a triplet centred at -7.0 δ with ^{195}Pt satellites. The doublet is assigned to *trans* disposed phosphorus aroms (P_a) and the triplet is assigned to the phosphorus atom (P_b) which is *trans* disposed to a σ-donor nitrogen group and *cis* to two P_a atoms as shown in Structure VII. The $^1J(Pt–P_a)$ = 2537 Hz, $^1J(Pt–P_b)$ = 3147 Hz and $^2J(P_a–P_b)$ = 19.5 Hz, values are in accordance with earlier observed data.[17,19,23] The $^{31}P\{^1H\}$ spectrum of complex **7** also displays seven sharp lines (J = 713 Hz) in the high-field region centred at -143.3 δ due to the PF_6^- ion.[24,25] The geometry of complex **7** is shown in Structure VII.

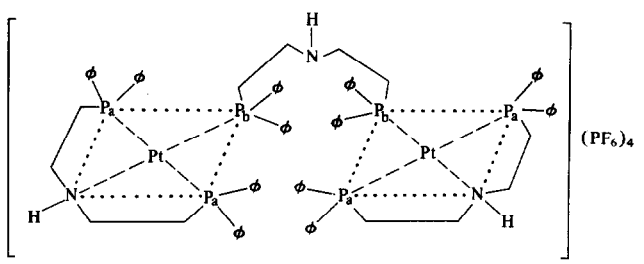

VII

The far-infrared spectra of complexes **1–7** gave bands around 520 cm^{-1} due to ν(M–P).

The electronic spectral data of all the complexes **1–7** agree with the proposed geometries of the complexes. All the square-planar complexes in this work have nd^8 whereas octahedral complexes have nd^6 valence orbital electronic configurations, respectively. Complex **1** gave bands at 340 nm (4160) and 335 nm (3200) assignable to *d–d* transitions and the bands at 272 nm (25120) and 268 nm (25440) are attributed to π–π^* transitions. Similarly, complex **4** displays a band at 353 nm (31840) assigned to *d–d* transition with LMCT character and bands at 288 nm (35360) and 262 nm (24000) are due to LMCT transitions between the metal ion and the ligand. The polynuclear Pt(II) complexes **6** and **7** gave bands at 274 nm (12900) with LMCT character and 360 nm (3360), respectively, assigned to *d–d* transitions. The bands observed at 256 nm (17000), 226 nm (25000) and 266 nm (25600), 250 nm (24000) for **6** and **7**, respectively, are assigned to charge-transfer transitions between metal ion and the ligand. The results obtained are in agreement with the earlier reported work with nd^8 metal ions.[26,27]

The octahedral Rh(III) complex **2** gave bands at 425 nm (11207), 353 nm (64000), 330 nm (11360) and 257 nm (29046) whereas Ir(III) complex **3** gave bands at 355 nm (2160), 290 nm (11360), 272 nm (15040) and 265 nm (16640). The bands around 425 and 350 nm are assigned to the transitions from $^1A_{1g}$ ground state to the $^1T_{1g}$ excited state. Whereas the other high energy bands are assigned to charge-transfer transitions between metal ion and the ligand.

EXPERIMENTAL

The hydrated trichlorides of rhodium and iridium, $PdCl_2$ and K_2PtCl_4 were purchased from Alfa Inorganics (USA) and Johnson Matthey (England). Triphenyl phosphine was purchased from Strem Chemicals Inc. (U.S.A.). $NaBPh_4$ and NH_4PF_6 were obtained from SISCO (India). 1,5-cyclooctadiene obtained from Fluka was used as such. The complexes $RhCl(CO)(PPh_3)_2$,[28]

$IrCl(CO)(PPh_3)_2$,[28] were prepared by published procedures. Diethanolamine, thionyl chloride were of Analar grade and were used without further purification. Bis(2-chloroethyl)amine hydrochloride was prepared by published procedure.[29] All the preparations were carried out in a dry nitrogen atmosphere.

Microanalysis, melting points, infrared spectra, conductivity measurements were done as reported.[30] Proton NMR spectra were recorded on a Jeol FX100 spectrometer operating at 100 MHz using TMS as an internal standard. The carbon-13 NMR spectrum of the ligand was also recorded on the same instrument operating at 24.9 MHz in $CDCl_3$ using TMS as an internal standard. The proton noise decoupled phosphorus-31 NMR spectra of the ligand and complexes were taken in the indicated solvents (Table 2) using the same instrument operating at 40.3 MHz in the FT mode with a deuterium lock. 85% H_3PO_4 was used as an external reference. The electronic spectra of complexes were measured on a Shimadzu UV 240 spectrophotometer.

Synthesis of the ligand

The terdentate mixed donor (N and P) ligand bis[2-(diphenylphosphino)ethyl]amine hydrochloride (DPEA · HCl) was synthesized by modified published procedures,[31,32] as shown in scheme.

$$HN(CH_2CH_2OH)_2 + 2SOCl_2 \xrightarrow{CHCl_3} Cl^-H_2N^+(CH_2CH_2Cl)_2 + 2SO_2 + 2HCl$$

a

$$\mathbf{a} + 10\%NaOH \longrightarrow HN(CH_2CH_2Cl)_2 + 2NaCl + 2H_2O$$

b

$$PPh_3 + 2K \xrightarrow{1,4,dioxan} KPPh_2 + KPh$$

$$\mathbf{b} + 2KPPh_2 \xrightarrow[THF]{1,4,dioxan} HN(CH_2CH_2PPh_2)_2 + 2KCl$$

c

$$\mathbf{c} + 2NHCl \xrightarrow{n\text{-hexane}} Cl^-H_2N^+(CH_2CH_2PPh_2)_2$$

Bis(2-chloroethyl)amine hydrochloride **a** was prepared by the published procedure[28] and its free amine **b** was liberated by the treatment of a stoichiometric amount of 10% NaOH. The free amine was liberated as an insoluble oil and was dried over sodium sulfate prior to its use. Free amine **b** (6.42 g, 0.045 mol) was dissolved in 40 cm^3 of THF and added dropwise with stirring to an orange-red solution of $KPPh_2$, which was obtained previously through the reaction of metallic potassium (7.04 g, 0.18 mol) with PPh_3 (25.66 g, 0.09 mol) in dioxane. Prior to the addition of the organic halide **b**, KPh was destroyed carefully by the addition of NH_4Cl to the reaction mixture containing both KPh and $KPPh_2$. This *in situ* method of reaction is found to be more convenient to us. After the addition of **b** the reaction mixture was refluxed for an hour and poured into a beaker containing ice-cold water before which the unreacted potassium was destroyed by methanol. The ligand DPEA was separated as an insoluble oil **c**, which on treatment with 2N HCl, in *n*-hexane with vigorous stirring gave a solid white crystalline ligand **d** in its hydrochloride form. The ligand DPEA · HCl was purified by recrystallizing from hot acetonitrile. Yield: 90%. M.p. 175°C; mol wt. 477.5 (calculated), 470 (experimental, osmometric in chloroform). Found: C, 70.1; H, 6.3; N, 2.9. Calc. for $C_{28}H_{30}NClP_2$: C, 70.4; H, 6.3; N, 2.9%.

Preparation of metal complexes

(1) *Triphenylphosphinebis*[2 - (*diphenylphosphino*)*ethyl*]*aminerhodium*(I)*tetraphenylborate*, [Rh(DPEA)(PPh_3)]BPh_4. To a refluxing methanolic solution of DPEA · HCl (0.11 g, 0.22 mmol) was added $RhCl(CO)(PPh_3)_2$ (0.15 g, 0.22 mmol) and further refluxed for 3 h to get a dark yellowish orange solution. An excess of $NaBPh_4$ was then added to the above solution, which on concentration gave a crystalline yellow compound. The compound was filtered, washed with benzene, methanol and recrystallized from dichloromethane-*n*-hexane mixture. Yield: 0.2 g (82%).

(2) *Trichlorobis*[2 - (*diphenylphosphino*)*ethyl*]-*aminerhodium*(III), $RhCl_3$(DPEA). $RhCl_3 \cdot 3H_2O$ (0.11 g, 0.42 mmol) in methanol was reacted with the ligand DPEA · HCl (0.2 g, 0.42 mmol) to give a yellow solution. After refluxing the solution for 6–7 h, the solution was concentrated to a small volume by a vacuum rotary evaporator and diethyl-ether added to get a yellow precipitate. The complex was filtered, washed with benzene, diethyl ether and recrystallized from dichloromethane-*n*-hexane mixture. Yield: 0.17 g (63%).

(3) *Chlorohydridocarbonylbis* [2 - (*diphenylphosphino*)*ethyl*]*amineiridium*(III) *chloride*, [Ir(Cl)(H)(CO)(DPEA)]Cl. The ligand DPEA · HCl (0.1 g, 0.21 mmol) and $IrCl(CO)(PPh_3)_2$ (0.11 g, 0.21 mmol) in benzene were refluxed for 6 h, to get a pale yellow crystalline complex. The complex was filtered, washed with benzene and dried *in vacuo*. Yield: 0.11 g (73%).

(4) *Chlorobis*[2-(*diphenylphosphino*)*ethyl*]*aminepalladium* (II) *chloride*, [PdCl(DPEA)]Cl. To the refluxing benzene solution of DPEA·HCl (0.2 g, 0.42 mmol) was added $PdCl_2$(COD) (0.12 g, 0.42 mmol), when a clear solution was obtained. The refluxing was continued till a yellowish green crystalline compound separated. The complex was filtered, washed with benzene and recrystallized from dichloromethane-*n*-hexane mixture. Yield: 0.21 g (72%).

The above reaction when conducted in refluxing methanol also gave the same product.

(5) *Bis* (*bis* [2 - (*diphenylphosphino*) *ethyl*] *aminepalladium* (II) *chloride*, $[Pd(DPEA)_2]Cl_2$. The reaction of $PdCl_2$ (0.10 g, 0.56 mmol) with DPEA·HCl (0.27 g, 0.56 mmol) was conducted in a mixture of 25 cm^3 of benzene, 5 cm^3 of acetone and 5 cm^3 of methanol. The above reaction mixture was refluxed for 2 h, and the solution concentrated to a small volume by a vacuum rotary evaporator. The addition of diethyl ether gave a yellow complex which was filtered, washed with diethyl ether and recrystallized from dichloromethane-*n*-hexane mixture. Yield: 0.48 g (80%).

(6) *Bis*(*bis*[2 - (*diphenylphosphino*)*ethyl*] *amine* - μ^3 - *bis*[2 - (*diphenylphosphino*)*ethyl*]*aminediplatinum* (II)*trichloroplatinum*(II)*trichloride*, [(DPEA) $\overline{Pt(Ph_2PCH_2CH_2}$ $\overline{N(H)CH_2CH_2PPh_2}](PtCl_3)$ Pt (DPEA)] Cl_3. To a 1:1 water acetone mixture of K_2PtCl_4 (0.13 g, 0.42 mmol) was added DPEA·HCl (0.2 g, 0.42 mmol) in hot acetone. On addition of the ligand the solution is decolourized and the reaction mixture was refluxed for 6 h. After removing the acetone by rotary vacuum evaporator, the compound was extracted by dichloromethane. The extracted solution was dried over Na_2SO_4, concentrated to a small volume and the complex precipitated by the addition of *n*-hexane. The complex was filtered, washed with benzene and *n*-hexane and recrystallized from dichloromethane-*n*-hexane mixture. Yield 0.23 (76%).

(7) *Bis*(*bis*[2-(*diphenylphosphino*)*ethyl*]*amine*-μ-*bis*[2-(*diphenylphosphino*)*ethyl*]*aminediplatinum*(II) *hexafluorophosphate*, $[Pt_2(DPEA)_2(\mu\text{-DPEA})](PF_6)_4$. To an aqueous solution of K_2PtCl_4 (0.13 g, 0.42 mmol) was added an ethanolic solution of the ligand DPEA·HCl (0.2 g, 0.42 mmol) to get a colourless solution. The reaction mixture was stirred for about 2 h at room temperature and then refluxed for 5 h. To the refluxing solution NH_4PF_6 (0.1 g, 0.62 mmol) was added and the refluxing continued for a further period of 2 h. Ethanol was completely removed by a vacuum rotary evaporator and an addition quantity of 10 cm^3 of water was added to the solution. On keeping the solution overnight crystalline flakes were obtained. The complex was filtered, washed with water, benzene and recrystallized from dichloromethane-*n*-hexane mixture. Yield: 0.29 g (78%).

REFERENCES

1. M. M. Taqui Khan, H. C. Bajaj, M. R. H. Siddiqui, B. T. Khan, M. Satyanarayana Reddy and K. Veera Reddy, *J. Chem. Soc. Dalton Trans.* 1985, 2603.
2. M. M. Taqui Khan and V. Vijay Sen Reddy, *Inorg. Chem.* 1986, **25**, 208.
3. M. M. Taqui Khan and B. Swamy, *Inorg. Chem.* 1986, **25**, 178.
4. M. M. Taqui Khan, V. Vijay Sen Reddy and H. C. Bajaj, *Polyhedron* 1987 (in press).
5. M. M. Taqui Khan, A. Purshotham Reddy, V. Vijay Sen Reddy and E. Rama Rao, *Inorg. Chem.* 1986 (communicated).
6. T. G. Schenck, J. M. Downes, C. R. C. Milne, P. B. Mackenzie, H. Boucher, J. Whelan and B. Bosnich, *Inorg. Chem.* 1985, **24**, 2334.
7. J. P. Farr, *Inorg. Chem.* 1983, **22**, 1229.
8. F. E. Wood, M. M. Olmstead and A. L. Balch, *J. Am. Chem. Soc.* 1983, **105**, 6332.
9. M. M. Taqui Khan, B. T. Khan, Safia Begum and S. M. Ali, *J. Mol. Cat.* 1986, **34**, 283 and references therein.
10. T. Suarez and B. Fontal, *J. Mol. Cat.* 1985, **32**, 191.
11. T. G. Schenck, C. R. C. Milne, J. F. Sawyer and B. Bosnich, *Inorg. Chem.* 1985, **24**, 2338.
12. J. R. Dyer, *Applications of Absorption Spectroscopy of Organic Compounds.* Prentice-Hall, New Jersey (1969).
13. A. Purshotham Reddy, Ph.D. Thesis, Osmania University, India (1986).
14. W. J. Geary, *Coord. Chem. Rev.* 1971, **7**, 81.
15. P. E. Garrou, *Chem. Rev.* 1981, **81**, 229.
16. D. F. Steele and T. A. Stephenson *J. Chem. Soc.*(*A*) 1972, 2161.
17. J. F. Nixon and A. Pidcock, *Ann. Rev. N.M.R. Spectroscopy* 1969, **2**, 345.
18. J. P. Farr and A. L. Balch, *Inorg. Chem.* 1983, **22**, 1229.
19. D. Hedden and D. M. Roundhill, *Inorg. Chem.* 1985, **24**, 4152.
20. L. E. Johnson and R. Eisenberg, *J. Am. Chem. Soc.* 1985, **107**, 3148.
21. F. A. Cotton and G. Wilkinson, *Advanced Inorganic Chemistry*, 4th edn. John Wiley, New York (1980).
22. K. Nakamoto, *Infrared and Raman Spectra of Inorganic and Coordination Compounds*, 3rd edn. John Wiley, New York (1978).
23. G. K. Anderson and Ravi Kumar, *Inorg. Chem.* 1984, **23**, 4064.
24. J. F. Nixon and R. Schmutzler, *Spectrochim. Acta* 1964, **20**, 1835.
25. R. B. King and J. C. Cloyd, *Inorg. Chem.* 1975, **14**, 1550.
26. W. E. Hill, D. M. A. Minahan and C. A. McAuliffe, *Inorg. Chem.* 1983, **22**, 3382.

27. G. L. Geoffory, M. S. Wrighton, G. S. Hammond and H. B. Gray, *J. Am. Chem. Soc.* 1974, **96**, 3105.
28. *Inorganic Synthesis*, (Edited by W. L. Jolly), Vol. XI, pp. 100–101 (1968).
29. J. P. Mason and D. J. Gosch, *J. Am. Chem. Soc.* 1938, **60**, 2816.
30. M. M. Taqui Khan and K. Veera Reddy, *J. Coord Chem.* 1982, **12**, 71.
31. L. Sacconi and R. Morassi, *J. Chem. Soc.* (*A*) 1968, 299.
32. M. E. Wilson, R. G. Nuzzo and G. M. Whitesides, *J. Am. Chem. Soc.* 1978, **100**, 2269.

Polyhedron Vol. 6, No. 9, pp. 1737–1740, 1987
Printed in Great Britain

0277–5387/87 $3.00+.00

HALOGENATION OF 4,5-DICARBA-ARACHNO-NONABORANE(13),4,5-$C_2B_7H_{13}$

TOMÁŠ JELINEK, BOHUMIL ŠTIBR,* FRANTIŠEK MAREŠ, JAROMIR PLEŠEK and STANISLAV HEŘMÁNEK

Institute of Inorganic Chemistry, Czechoslovak Academy of Sciences, 250 68 Řež near Prague, Czechoslovakia

(*Received* 10 *February* 1987; *accepted* 6 *March* 1987)

Abstract—The AlX_3-catalyzed (X = Cl, Br, and I) halogenation of *arachno*-4,5-$C_2B_7H_{13}$ with anhydrous hydrogen halides produces a series of 6-substituted derivatives, 6-X-4,5-$C_2B_7H_{12}$. The same compounds along with 6,8-I_2-4,5-$C_2B_7H_{11}$ are obtained in non-catalyzed reactions with elemental halogens. The electrophile-induced nucleophilic substitution concept (EINS) of the substitution with hydrogen halides is suggested. The constitution of all compounds isolated was unambiguously determined via ^1H, ^{13}C, ^{11}B, and two-dimensional (2-D) ^{11}B-^{11}B NMR spectra.

The *arachno*-4,5-$C_2B_7H_{13}$ carborane (**1**) (Fig. 1) was first reported by Rietz and Schaeffer[1] in 1973; however, it has been only recently that a high-yield synthesis of this compound has been developed in our laboratory.[2,3] Nevertheless, carborane (**1**) has been for almost 15 years taken as "*nido*-4,5-$C_2B_7H_{11}$" or, alternatively, as "*nido*-2,6-$C_2B_7H_{11}$" according to the latest trend in nomenclature.[4] Just recently, its structure has been unambiguously reinterpreted in our laboratory[5] on the basis of multinuclear NMR measurements. This paper reports on halogenation reactions of (**1**) with hydrogen halides and elemental halogens.

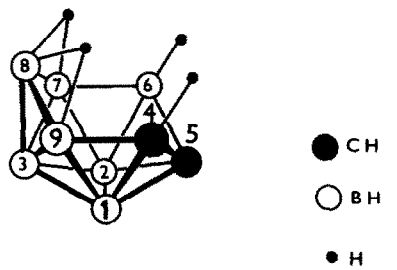

Fig. 1. Simplified structure and numbering system of *arachno*-4,5-$C_2B_7H_{13}$ (**1**).

EXPERIMENTAL

^1H (200 MHz), ^{13}C (50.31 MHz), and ^{11}B (64.18 MHz) pulse Fourier transform NMR spectra were recorded in deuteriochloroform on a Varian XL-200 spectrometer, and data manipulation utilized standard Varian software. Chemical shifts are given in δ [ppm, referenced to TMS (^1H and ^{13}C) and $BF_3 \cdot OEt_2$ (^{11}B); positive shifts downfield]. Two-dimensional (2-D) ^{11}B-^{11}B NMR spectra were produced on all samples via procedures described elsewhere.[6] Unit resolution mass spectra in the NI mode (chemical ionization of negative ions) were obtained on a GC/MS MAT 44S spectrometer. TLC was performed on Silufol sheets (silica gel on aluminium foil; detection by iodine vapours followed by $AgNO_3$ spray) in 1 : 2 benzene–hexane.

Chemicals and syntheses

Carborane (**1**) was prepared by the previously reported method.[3] Hydrogen bromide was prepared in the reaction of bromine with refluxing tetraline and hydrogen iodide by adding dropwise concentrated hydroiodic acid to excess P_4O_{10}; both products were condensed at −78°C and then generated by slow evaporation. Benzene and hexane were distilled with sodium metal prior to use and other commercially available chemicals were reagent grade and were used as purchased. Except where otherwise indicated, all syntheses and standard isolation procedures were conducted in an inert atmosphere or *in vacuo*.

* Author to whom correspondence should be addressed.

Table 1. Signal assignments in the ^1H and ^{13}C NMR spectra of halogenated derivatives of *arachno*-4,5-$C_2B_7H_{13}$

Substituent	^1H NMR (δ)[a]				^{13}C NMR (δ)[b]	
	C(5)H	exo-C(4)H	endo-C(4)H	μH	C(5)	C(4)
6-Cl (**2a**)	2.83	1.86	1.72	−1.28	—	—
6-Br (**2b**)	2.94	1.85	1.68	−1.26	29.34(184)	8.94(165)
6-I (**2c**)	3.02	1.81	1.44	−1.24	—	—
6,8-I_2 (**2d**)	3.29	1.98	1.65	−1.27	29.01(163)	9.32(161)

[a] Singlets of relative intensities 1 : 1 : 1 : 2.
[b] Doublets and triplets of equal intensities, J(CH) in parentheses(in Hz).

Arachno-6-Cl-4,5-$C_2B_7H_{12}$ (**2a**). (a) Dry HCl was slowly introduced for 2 h at ambient temperature to a stirred solution of (**1**) (1.1 g; 0.01 mol) in benzene (60 cm^3) in the presence of $AlCl_3$ (0.13 g; 1 mmol). After the hydrogen evolution had ceased (*ca.* 3 h), the mixture was filtered, the filtrate was reduced in volume to *ca.* 20 cm^3, and hexane (40 cm^3) was carefully added onto the surface of the solution. The two-layer mixture was left standing overnight to separate white crystals which were isolated by filtration, washed with cold hexane and vacuum-dried to give 1.4 g (95%) of IIb; mass spectrum, high mass m/z 149, corresponding to $[^{12}C_2{}^{11}B_7{}^1H_{11}{}^{37}Cl]^-$ (P-1, C_2B_7Cl pattern). For NMR spectra see Tables 1–4.

(b) Gaseous chlorine was slowly passed through a solution of (**1**) (1.1 g; 0.01 mol) in hexane (60 cm^3) under stirring at −30°C until carborane (1) had disappeared from the solution (checked by TLC, R_F 0.4). The separated white crystals were isolated by filtration, washed with cold hexane and vacuum-dried to afford 0.7 g (47%) of (**2a**).

Arachno-6-Br-4,5-$C_2B_7H_{12}$ (**2b**). (a) Dry HBr was slowly passed through a stirred mixture of $AlBr_3$ (0.27 g; 1 mmol) and a solution of (**1**) (1.1 g; 0.01 mol) in benzene (60 cm^3) at ambient temperature until carborane (**1**) had disappeared from the mixture (*ca.* 3 h). Analogous work-up as in the preceding experiment (a) led to the isolation of 1.6 g (83%) of (**2b**); high mass m/z 193, corresponding to $[^{12}C_2{}^{11}B_7{}^1H_{11}{}^{81}Br]^-$ (P-1, C_2B_7Br pattern). For NMR data see Tables 1–4.

When the $AlBr_3$ catalyst was replaced by $AlCl_3$ (1 : 1 molar ratio of the latter and carborane (**1**)) and the reaction was conducted exactly in the way described above, 1.4 g of *ca.* 4 : 1 mixture of (**2a**) and (**2b**) was obtained, as assessed by ^{11}B NMR by comparing the signal intensities of the B(6) resonances of both compounds at δ_B −16.47 and −22.87, respectively.

(b) A solution of (**1**) (1.1 g; 0.01 mol) in benzene (30 cm^3) was treated with a solution of bromine (0.6 cm^3; 0.02 mol) in benzene (20 cm^3) under stirring at 5°C. After the colour of bromine disappeared, the solution was reduced in volume to *ca.* 20 cm^3 and filtered. Further work-up as in the preceding experiment with Cl_2 (b) produced 0.7 g (36%) of (**2b**).

Arachno-6-I-4,5-$C_2B_7H_{12}$ (**2c**). (a) Dry HI was slowly introduced into a stirred mixture of AlI_3 (0.41 g; 1 mmol) and a solution of (**1**) (1.1 g; 0.01 mol) in benzene (60 cm^3) at ambient temperature until the hydrogen evolution had ceased (*ca.* 3 h). Further work-up as in the preceding experiment (a)

Table 2. Signal assignments in the ^{11}B NMR spectra[a] of halogenated derivatives of *arachno*-4,5-$c_2B_7H_{13}$

Substituent	B(7)[b]	B(9)	B(2)	B(1)	B(8)	B(6)[c]	B(3)
6-Cl (**2a**)	12.47/156	2.75/161[b]	−2.91/165	−3.41/168	−5.92/178[b]	−16.47/147	−56.21/162
6-Br (**2b**)	11.54/163	3.40/164/22	−2.93/182	−3.25/157	−5.79/176[b]	−22.87/151	−56.04/157
6-I (**2c**)	10.95/145	4.22/162/31	−2.96/166[d]	−2.96/166[d]	−5.24/177[b]	−36.61/151	−55.47/159
6,8-I_2 (**2d**)	12.99/156	5.72/147[b]	−5.30/171	−3.40/156	−18.09/0/48[e]	−36.12/147	−51.78/162

[a] δ_B/J(BH)/J(B-μH), assignments based on 2-D spectra, all signals in proton coupled spectra are doublets.
[b] Signals are broadened, but J(B-μH) is not measurable.
[c] Doublets of the monosubstituted BH_2 group.
[d] Overlapping doublets.
[e] Singlet.

Table 3. Cross-peaks indicated in the 2-D ^{11}B–^{11}B NMR spectra of halogenated derivatives of *arachno*-4,5-$C_2B_7H_{13}$

Substituent	Cross peaks[a]
6-Cl (**2a**)	B(7)[B(2)^s,B(3)^m,B(6)^w,B(8)^w] B(9)[B(1)^m,B(3)^m,B(8)^m] B(2)[B(1)^s,B(3)^s,B(6)^w,B(7)^s] B(1)[B(2)^s,B(3)^m,B(9)^m] B(8)[B(3)^s,B(7)^w,B(9)^m] B(6)[B(2)^w,B(7)^w] B(3)[B(1)^m,B(2)^s,B(7)^m,B(8)^s,B(9)^m]
6-Br (**2b**)	B(7)[B(2)^s,B(3)^m,B(6)^w,B(8)^w] B(9)[B(1)^0,B(3)^m,B(8)^m] B(2)[B(1)^b,B(3)^s,B(6)^w,B(7)^s] B(1)[B(2)^b,B(3)^s,B(9)^0] B(8)[B(3)^s,B(7)^w,B(9)^m] B(6)[B(2)^w,B(7)^w] B(3)[B(1)^s,B(2)^s,B(7)^m,B(8)^s,B(9)^0]
6-I (**2c**)	B(7)[B(2)^s,B(3)^m,B(6)^m,B(8)^m] B(9)[B(1)^m,B(3)^s,B(8)^s] B(2)[B(1)^b,B(3)^s,B(6)^m,B(7)^s] B(1)[B(2)^b,B(3)^s,B(9)^m] B(8)[B(3)^s,B(7)^0,B(9)^s] B(6)[B(2)^m,B(7)^m] B(3)[B(1)^s,B(2)^s,B(7)^m,B(8)^s,B(9)^s]
6,8-I_2 (**2d**)	B(7)[B(2)^s,B(3)^m,B(6)^m,B(8)^w] B(9)[B(1)^w,B(3)^m,B(8)^m] B(2)[B(1)^s,B(3)^0,B(6)^m,B(7)^s] B(1)[B(2)^s,B(3)^s,B(9)^w] B(8)[B(3)^s,B(7)^m,B(9)^m] B(6)[B(2)^m,B(7)^m] B(3)[B(1)^s,B(2)^0,B(7)^m,B(8)^s,B(9)^m]

[a] Atoms giving cross peaks with the observed atom (on diagonal) are listed in brackets with right superscipts indicating relative intensities of the off-diagonal interactions (s-strong, m-medium, w-weak, 0-zero interaction). Observed atoms (off brackets) are listed upfield.

[b] The cross peaks cannot be unambiguously defined due to a high degree of overlap.

resulted in the isolation of 1.1 g (80%) of (**2c**); mass spectrum, high mass m/z 239, corresponding to $[^{12}C_2{}^{11}B_7{}^1H_{11}{}^{127}I]^-$ (P-1, C_2B_7I pattern). For NMR data see Tables 1–4.

(b) A solution of (**1**) (1.1 g; 0.01 mol) in benzene (30 cm^3) was refluxed with iodine (2.5 g; 0.02 mol) for 48 h. The mixture was then shortly evacuated, shaken with solid Na_2SO_3 to remove excess iodine, filtered and reduced in volume to *ca.* 20 cm^3. Analogous work-up as in the experiment with Cl_2 (b) led to the isolation of 1.1 g (60%) of (**2c**).

Arachno-6,8-I_2-4,5-$C_2B_7H_{11}$ (**2d**). Carborane (**1**) (0.6 g; 5 mmol) was added to solid iodine (1.3 g; 0.01 mol). After the initial exothermic reaction had ceased, the reaction was finished by heating at 90°C for 1 h. The decolourized melt was dissolved in benzene (20 cm^3), the solution was filtered and the filtrate was reduced in volume to *ca.* 10 cm^3. Hexane (30 cm^3) was added onto the surface and the two-layer mixture was left standing overnight to separate pale yellow crystals which were washed with cold hexane and vacuum-dried to give 1.1 g (60%) of (**2d**); mass spectrum, high mass m/z 238, corresponding to $[^{12}C_2{}^{11}B_7{}^1H_{10}{}^{127}I]^-$ (P-1-HI, C_2B_7I pattern). For NMR data see Tables 1–4.

RESULTS AND DISCUSSION

The AlX_3-catalyzed reactions (X = Cl, Br, and I) of (**1**) with anhydrous hydrogen halides in benzene at ambient temperature give rise to a series of monohalogenated compounds of the general formula 6-X-4,5-$C_2B_7H_{13}$ [(**2a**), X = Cl; (**2b**), X = Br, and (**2c**), X = I, for numbering see Fig. 1] with the evolution of one mole of hydrogen. It is to be noted that these reactions do not proceed without catalysis at any measurable rate. In contrast, there is evidence for direct involvement of AlX_3 in the halogenation process. When the reaction of (**1**) with hydrogen

Table 4. ^{11}B NMR shift changes ($\Delta\delta_B$)[a] for halogenated derivatives of *arachno*-4,5-$C_2B_7H_{13}$

Substituent	B(1)	B(2)	B(3)	B(6)	B(7)	B(8)	B(9)	$\Delta\bar{\delta}_B$[b] (k_2)[c]
6-Cl (**2a**)	1.14	1.64	0.47	13.74	2.87	0.58	−1.12	0.93(1.77)
6-Br (**2b**)	1.30	1.62	0.64	7.34	1.94	0.71	−0.47	0.96(0.75)
6-I (**2c**)	1.59	1.59	1.21	−6.40	1.35	1.26	0.35	1.23(0.20)
6,8-I_2 (**2d**)	1.15	−0.75	4.90	−5.93	3.39	−11.59	1.85	2.10(4.65)

[a] δ_B(substituted) − δ_B(parent compound[5]).

[b] Mean shift for unsubstituted atoms defined as $\Delta\bar{\delta} = 1/n \sum_{i=1}^{i=n} \Delta\delta_i$ (*n*-number of unsubstituted atoms).

[c] Variance of the shift from the mean value defined as $k_2 = 1/n-1 \sum_{i=1}^{i=n} (\Delta\delta_i - \Delta\bar{\delta})^2$.

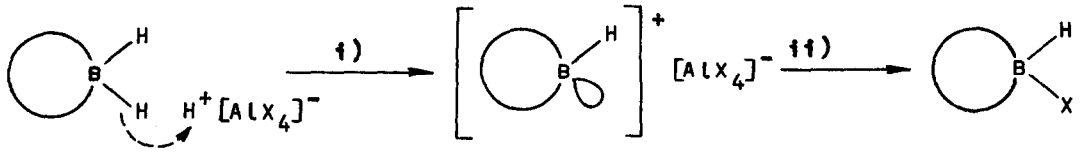

Scheme 1. Electrophile-induced nucleophilic substitution of the cage BH_2 group of (1) by hydrogen halides; (i) H^+ attack, $-H_2$: (ii) X^- attack, $-AlX_3$.

bromide is carried out in the presence of an equimolar amount of $AlCl_3$, *ca.* 4:1 mixture of 6-Cl and 6-Br derivatives of (**1**) is obtained, as assessed from ^{11}B NMR. The observed parallel substitution on the cage $B(6)H_2$ group by Cl and Br is consistent with a proton attack by $H^+[AlX_4]^-$ at the B(6) exo-hydrogen to remove the H^- anion and evolve dihydrogen. The vacant exohedral molecular orbital thus formed is subsequently filled with X^- (from AlX_4^-) to recover AlX_3 and form exohedral B(6)H-X bond as in Scheme 1.

In view of this approach, the substitution process outlined above can be regarded as an electrophile-induced nucleophilic substitution reaction (EINS). This EINS concept, characteristic by hydride removal on the attack by the electrophilic particle with a subsequent attack by the nucleophilic particle, can be applied more generally to other "electrophilic" reactions of boron hydrides. The difference between these reactions and electrophilic Friedel–Crafts substitutions on organic aromatic substrates[7] obviously consists both in the hydridic character of the BH bond and in the electron deficient nature of the boron atom under attack.

The same series of compounds (**2a–c**) is also obtained in noncatalyzed reactions of (**1**) with elemental halogens (Cl_2, $-30°C$; Br_2, 5°C, and I_2, reflux) in hexane or benzene. Spontaneous solid-phase reaction of (**1**) with iodine, finished by heating at 90°C, results in the formation of 6,8-I_2-4,5-$C_2B_7H_{11}$ (**2d**). The observed relative ease of the noncatalyzed halogenation seems to consist of a strong hydridic character of the cage $B(6)H_2$ group.

NMR spectra of compounds (**2a–d**) (Tables 1 and 2) exhibit general features of those published for parent 4,5-$C_2B_7H_{13}$.[5] ^1H NMR spectra show 1:1:1:2 patterns of singlets due to three CH resonances [C(5)H, $C(4)H_{exo}$, and $C(4)H_{endo}$] and two coincidentally overlapping bridge proton signals. ^{13}C NMR spectra of (**2b**) and (**2d**), exhibiting one doublet and one triplet of equal intensities, clearly evidence the presence of one CH and one CH_2 groups. The relevant ^{11}B NMR data of (**2a–d**) unambiguously indicate the presence of seven non-equivalent boron environments with three borons coupled to hydrogen bridges. The most interesting feature is the presence of the doublet of the monohalogenated $B(6)H_2$ group.

Additional insight was given by 2-D ^{11}B–^{11}B measurements on (**2a–d**). In the scheme presented in Table 3, all adjacent borons give rise to observed cross peaks expected in 2-D spectra for the geometry depicted in Fig. 1 except for those between the B(1)-B(9), B(7)-B(8) and B(2)-B(3) nuclei which are not observable in a few cases.

Table 4 reflects the influence of the B(6) halogen substitution on the ^{11}B NMR shifts in terms of $\Delta\delta$, $\Delta\tilde{\delta}$, and k_2 values. The trends seen in this table for substituted borons are similar to those observed with other substituted borane systems, e.g. $B_{10}H_{14}$,[8] 2,4-$C_2B_5H_7$,[9] and 6,9-$C_2B_8H_{14}$.[10] Taking unsubstituted boron atoms of (**2a–d**) into account, a regular trend of increase in $\Delta\tilde{\delta}$ and a decrease in k_2 values is seen on going through the 6-Cl, 6-Br, and 6-I series; similar trends were observed with all monohalogenated derivatives of $B_{10}H_{14}$,[8] but not with 1-haloderivatives of 6,9-$C_2B_8H_{14}$.[10] To draw more general conclusions, more derivatives substituted on other cage atoms should be isolated and characterized.

Acknowledgements—The authors wish to thank Drs I. Koruna and M. Ryska of the Research Institute for Pharmacy and Biochemistry, Prague, for mass spectral measurements.

REFERENCES

1. R. R. Rietz and R. Schaeffer, *J. Am. Chem. Soc.* 1973, **95**, 6254.
2. J. Plešek, B. Štibr and S. Heřmánek, *Chem. Ind. (London)* 1980, 626.
3. B. Štibr, J. Plešek and S. Heřmánek, *Inorg. Synth.* 1983, **22**, 237.
4. J. B. Casey, W. J. Evans and W. H. Powell, *Inorg. Chem.* 1983, **22**, 2236.
5. S. Heřmánek, T. Jelinek, J. Plešek, B. Štibr and J. Fusek, *J. Chem. Soc. Chem. Commun.* in press.
6. S. Heřmánek, J. Fusek, B. Štibr, J. Plešek and T. Jelinek, *Polyhedron* 1986, **5**, 1303.
7. E. S. Gould, *Mechanism and Structure in Organic Chemistry*. Rinehart and Winston, New York (1959).
8. R. F. Sprecher, B. E. Aufderheide, G. W. Luther III and J. C. Carter, *J. Am. Chem. Soc.* 1974, **96**, 4404.
9. N. G. Bradford, T. Onak, T. Banuleos, F. Gomes and E. W. DiStefano, *Inorg. Chem.* 1985, **24**, 4091.
10. B. Štibr, Z. Janoušek, J. Plešek, T. Jelinek and S. Heřmánek, *Collec. Czech. Chem. Commun.*, in press.

Polyhedron Vol. 6, No. 9, pp. 1741–1745, 1987
Printed in Great Britain

0277–5387/87 $3.00+.00

DIRECT SYNTHESIS FROM $MoCl_3(THF)_3$ OF A COMPLEX CONTAINING THE $[Mo_3S_4]^{4+}$ CORE

F. ALBERT COTTON* and ROSA LLUSAR

Department of Chemistry and Laboratory for Molecular Structure and Bonding, Texas A&M University, College Station, TX 77843, U.S.A.

(*Received* 12 *January* 1987; *accepted* 9 *March* 1987)

Abstract—By reaction of $MoCl_3(THF)_3$ with NaSH in tetrahydrofuran, followed by addition of $Me_2PCH_2CH_2PMe_2$(dmpe), then chromatography on silica-gel, and finally addition of NH_4PF_6, the compound $[Mo_3S_4Cl_3(dmpe)_3]PF_6 \cdot CH_3OH$ was prepared in moderate yield. X-ray crystallography showed the presence of a chiral cation based on a Mo_3S_4 core with chelating dmpe units arranged like the blades of a ship's screw. The three Cl atoms fill the remaining octahedral sites on each metal atom. The compound crystallizes in space group R3c with (hexagonal) cell dimensions of $a = 15.310(7)$ Å, $c = 30.640(3)$ Å and $Z = 6$. The $[Mo_3S_4Cl_3(dmpe)_3]^+$ ion and the PF_6^- ion each have crystallographic C_3 symmetry. The principal distances and theirs esds are: Mo–Mo, 2.766(4) Å; Mo–(μ_3-S), 2.360(9) Å; Mo–(μ_2-S), 2.290(7) Å, 2.336(7) Å; Mo–P, 2.534(8) Å, 2.605(8) Å; Mo–Cl, 2.473(7) Å; P–F, 1.56(2) Å, 1.64(3) Å. The correct enantiomer was obtained by refining both to convergence, which give $R = 0.059$ and $R = 0.064$.

The synthetic chemistry leading to compounds containing the $Mo_3S_4^{4+}$ core has recently been developing very rapidly. The following types of synthetic entry to this field have been reported:

(1) Those in which the Müller complex,[1] $[Mo_3(\mu_3\text{-}S)(\mu_2\text{-}S_2)_3(S_2)_3]^{2-}$ (1) is treated with desulfurizing reagents. Examples are:

$$1 + 12CN^- \rightarrow [Mo_3S_4(CN)_9]^{5-} + 3SCN^- + 3S_2^{2-} \quad (1)^2$$

$$1 + 3[SCH_2CH_2S]^{2-} \rightarrow Mo_3S_4(SCH_2CH_2S)_3]^{2-} + \text{polysulfur species.} \quad (2)^3$$

(2) Desulfurization of 1 without the use of any exogenous S-atom acceptor:[4]

$$1 + 3H_3NTA \rightarrow [Mo_3S_4(NTA)(HNTA)_2]^{2-} + S_n^{2-} \text{ species}$$

$$1 + 3H_2C_2O_4 \rightarrow [Mo_3S_4(C_2O_4)(HC_2O_4)_2(H_2O)_3] + S_n^{2-} \text{ species.}$$

(3) Degradation of an $[Mo_4S_4]^{n+}$ unit, which proceeds in 60% yield[5] under appropriate conditions:

$$[Mo_4S_4(NCS)_{12}]^{6-} + 3[9]aneN_3 \rightarrow [Mo_3S_4([9]aneN_3)_3]^{4+}.$$

(4) Coalescence of $[Mo_2(\mu\text{-}S)_2O_2(cys)_2]^{2-}$ dimers to give an Mo_4S_4 intermediate that degrades *in situ* to $Mo_3S_4^{4+}$.[6]

We now report a new, convenient, non-aqueous method for making $[Mo_3S_4]^{4+}$ derivatives. Because the method is non-aqueous it allows access to types of compounds not heretofore obtained. We describe and illustrate the method by providing full preparative and crystallographic details for the compound $[Mo_3S_4Cl_3(dmpe)_3]PF_6 \cdot CH_3OH$.

EXPERIMENTAL

Materials

NaSH[7] and $MoCl_3(THF)_3$[8] were prepared as described elsewhere. 1,2-bis(dimethylphosphino) ethane (dmpe) was obtained from Strem Chemicals and used as received.

* Author to whom correspondence should be addressed.

Synthesis of $[Mo_3S_4Cl_3(dmpe)_3]PF_6 \cdot CH_3OH$

NaSH (40 mg, 0.072 mmol) was added to a solution of $MoCl_3(THF)_3$ (300 mg, 0.072 mmol) in 15 cm^3 of THF under argon. This mixture was cooled to −78°C and the dmpe (120 μL, ca. 0.72 mmol) was introduced. Addition of 3 cm^3 of MeOH (to dissolve the NaSH) followed by slow warming to room temperature produced a mixture consisting of a dark precipitate and a green solution.

This green solution was filtered under argon and it seemed to be air stable, at least for several days. It was taken to dryness in vacuum, the residue redissolved in CH_2Cl_2 and the solute adsorbed on a silica-gel column. After washing the column with acetone, the green band that remained on the top was eluted with methanol. The UV–visible spectrum of this green solution showed a band at 625 nm. Addition of NH_4PF_6 to the above solution followed by slow evaporation in air afforded green crystals suitable for X-ray diffraction studies. Yield: ca. 40%. These crystals were characterized as $[Mo_3S_4Cl_3(dmpe)_3]PF_6 \cdot CH_3OH$.

X-ray diffraction studies

A green crystal of dimensions $0.1 \times 0.15 \times 0.15$ mm was mounted on the top of a glass fiber with epoxy cement. Data were collected on a CAD-4 four-circle diffractometer using monochromated Mo Kα radiation. Preliminary cell parameters were determined from 25 reflections and confirmed by axial photographs. Data pertaining to the crystallographic procedures are given in Table 1. During data collection three intensity standards were collected every hour. No decay was observed during the 47.5 h of exposure to X-rays.

Corrections for polarization and Lorentz factors were applied to the measured intensities. An absorption correction was based on the variation in the intensities of reflections at Eulerian angle χ

Table 1. Crystal data for $[Mo_3S_4Cl_3(dmpe)_3]PF_6 \cdot CH_3OH$

Formula	$Mo_3S_4Cl_3P_7F_6OC_{19}H_{52}$
Formula weight	1149.87
Space group	R3c
Systematic absences	$(hkil) = -h+k+l = 3n$; $(h\bar{h}0l): h+l = 3n, l = 2n$; $(000l)\ l = 6n$
a, Å	15.310(7)
c, Å	30.640(3)
V, $Å^3$	6216
Z	6
d_{calc}, g/cm^3	1.84
Crystal size, mm	$0.1 \times 0.15 \times 0.15$
$\mu(MoK_\alpha)$, cm^{-1}	15.749
Data collection instrument	CAD-4
Radiation (monochromated in incident beam)	MoK_α ($\lambda_{\bar{a}} = 0.71073$ Å)
Orientation reflections, number, range (2θ)	25, 6-25
Temperature, °C	15°C
Scan method	ω-2θ
Data col. range, 2θ, deg	4-45
No. unique data, total	1391
with $F_o^2 > 3\sigma(F_o^2)$	872
Number of parameters refined	114
Trans. factors, max., min.	1.27, 0.84
R^a	0.059
R_w^b	0.064
Quality-of-fit indicator[c]	1.19
Largest shift/esd, final cycle	0.01
Largest peak, $e/Å^3$	1.12

[a] $R = \Sigma ||F_o| - |F_c|| / \Sigma |F_o|$.

[b] $R_w = [\Sigma w(|F_o| - |F_c|)^2 / \Sigma w|F_o|^2]^{1/2}$; $w = 1/\sigma^2(|F_o|)$.

[c] Quality-of-fit = $[\Sigma x(|F_o| - |F_c|)^2 / (N_{obs} - N_{parameters})]^{1/2}$.

close to 90° during azimuthal scans (ψ-scans). Five sets of reflections were averaged to produce an absorption profile for the crystal with maximum, minimum and average experimental transmission factors of 1.27, 0.84 and 0.99, respectively.

The crystal belongs to the Laue class $\bar{3}m$. Systematic absences limited the possible space groups to R3c and R$\bar{3}$c. The unit cell volume suggested $Z = 6$, which would require the trinuclear unit to be located on a special position such that a three-fold axis of crystallographic symmetry would be in accord with the molecular symmetry. The trinuclear unit could be accommodated in an ordered model only in the non-centrosymmetric space group R3c because in R$\bar{3}$c the location of the molecule around the three fold axis requires the presence of an inversion center. Since the amount of data was limited by the small size of the crystal, Friedel pairs (which are independent observations in a noncentrosymmetric space group) were collected to improve the data to parameter ratio.

The position of the unique Mo atom was obtained from direct methods, MULTAN, and the remainder of the molecule was located and refined by alternating difference Fourier maps and least squares cycles, employing the Enraf-Nonius Structure Determination Package. All the atoms in the cluster and the anion, except three of the carbon atoms in the phosphine were refined anisotropically. C(2), C(5) and C(6) had to be refined isotropically. After location and refinement of the cluster and the anion, two peaks, one in a special position (3-fold axis) and one in a general position, remained in the difference Fourier map. The distance between them was suggestive of a methanol molecule and they were refined with isotropic thermal parameters as C and O atoms. The C–O distance calculated after the last cycle of refinement was slightly short (1.22 ± 0.12 Å), but acceptable under the circumstances.

RESULTS AND DISCUSSION

The preparative procedure described here differs from all others previously used in that it provides access to the $Mo_3S_4^{4+}$ moiety by a non-aqueous route, thus making it possible to prepare derivatives that are, or contain ligands which are not amenable to handling in aqueous media. At some stage the Mo(III) present in the starting material is oxidized to Mo(IV) but this, as well as other aspects of the procedure, remains to be elucidated.

The identity and structure of the green product were conclusively established by X-ray crystallography. The trinuclear cation is shown in Fig. 1. It has a crystallographically imposed three-fold axis of symmetry. The bond distances and angles within it are listed in Tables 2 and 3.

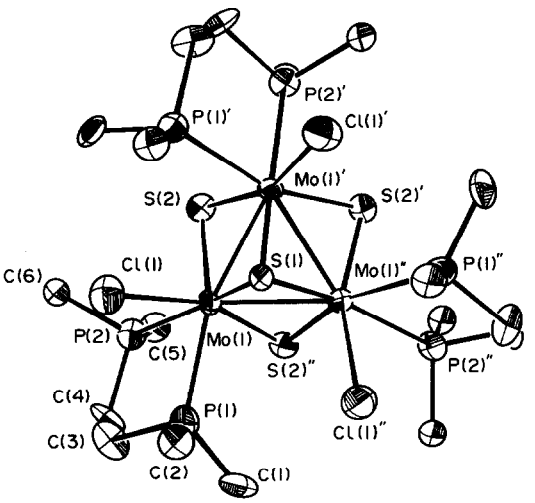

Fig. 1. The $[Mo_3S_4Cl_3(dmpe)_3]^+$ ion viewed approximately along the three-fold axis. The labeling scheme employs primes and double primes to identify symmetry equivalent atoms.

There are some small but real deviations from C_{3v} symmetry in the Mo_3S_4 core, attributable to the arrangement of the two P and one Cl atom in the external sites on each Mo atom. The Mo–Mo and Mo–(μ_3-S) distances are, of course all equal, but there are two kinds of Mo–(μ_2-S) distances and some attendant slight differences in the two sorts of Mo–Mo–(μ_2-S) angles. The Mo–(μ_2-S) distance that is roughly *trans* to an Mo–P bond is significantly longer, by 0.046(10) Å, than the one that is roughly *trans* to an Mo–Cl bond. The two types

Table 2. Table of bond distances in Å and their estimated standard deviations for the $[Mo_3S_4Cl_3(dmpe)_3]^+$ ion

Atom 1	Atom 2	Distance
Mo(1)	Mo(1)'	2.766(4)
Mo(1)	Cl(1)	2.473(7)
Mo(1)	S(1)	2.360(9)
Mo(1)	S(2)	2.336(7)
Mo(1)	S(2)"	2.290(7)
Mo(1)	P(1)	2.605(8)
Mo(1)	P(2)	2.534(8)
P(1)	C(1)	1.89(3)
P(1)	C(2)	1.88(3)
P(1)	C(3)	1.79(3)
P(2)	C(4)	1.88(3)
P(2)	C(5)	1.81(3)
P(2)	C(6)	1.88(3)
C(3)	C(4)	1.58(3)

Numbers in parentheses are estimated standard deviations in the least significant digits.

Table 3. Table of bond angles in degrees and their estimated standard deviations for the $[Mo_3S_4Cl_3(dmpe)_3]^+$ ion

Atom 1	Atom 2	Atom 3	Angle
Mo(1)″	Mo(1)′	Mo(1)	60.00(0)
Mo(1)″	Mo(1)	Cl(1)	136.7(2)
Mo(1)″	Mo(1)	S(1)	54.1(2)
Mo(1)″	Mo(1)	S(2)	98.4(2)
Mo(1)″	Mo(1)	S(2)″	54.0(2)
Mo(1)″	Mo(1)	P(1)	99.1(2)
Mo(1)″	Mo(1)	P(2)	140.9(2)
Mo(1)′	Mo(1)	Cl(1)	101.3(2)
Mo(1)′	Mo(1)	S(1)	54.1(2)
Mo(1)′	Mo(1)	S(2)	52.5(2)
Mo(1)′	Mo(1)	S(2)″	99.5(2)
Mo(1)′	Mo(1)	P(1)	146.6(2)
Mo(1)′	Mo(1)	P(2)	134.7(2)
Cl(1)	Mo(1)	S(1)	82.9(2)
Cl(1)	Mo(1)	S(2)	97.9(3)
Cl(1)	Mo(1)	S(2)″	158.8(3)
Cl(1)	Mo(1)	P(1)	75.4(3)
Cl(1)	Mo(1)	P(2)	81.0(2)
S(1)	Mo(1)	S(2)	105.1(2)
S(1)	Mo(1)	S(2)″	106.6(3)
S(1)	Mo(1)	P(1)	92.7(3)
S(1)	Mo(1)	P(2)	163.1(3)
S(2)	Mo(1)	S(2)″	97.8(4)
S(2)	Mo(1)	P(1)	160.2(3)
S(2)	Mo(1)	P(2)	82.2(3)
S(2)″	Mo(1)	P(1)	85.0(3)
S(2)″	Mo(1)	P(2)	87.0(2)
P(1)	Mo(1)	P(2)	78.3(3)
Mo(1)	S(1)	Mo(1)″	71.8(3)
Mo(1)	S(2)	Mo(1)′	73.4(2)

Numbers in parentheses are estimated standard deviations in the least significant digits.

Table 4. Comparison of the $[Mo_3S_4]^{4+}$ core dimensions, Å, in various compounds

	Outer ligands					
Type of bond	$Cl_3(dmpe)_3$	9CN	$(HNTA)_2(NTA)$	$(SCH_2CH_2S)_3$	$(C_2O_4)_3(H_2O)_3$	$([9]aneN_3)_3$
Mo–Mo	2.766(4)	2.765(7)	2.769(1)	2.78	2.738(5)	2.773(1)
Mo–(μ_3-S)	2.360(9)	2.363(4)	2.344(5)	2.35	2.33(1)	2.36(1)
Mo–(μ_2-S)	2.290(7) 2.336(7)	2.312(5)	2.298(3)	2.30	2.28(1)	2.278(9)
Ref.	This work	9	4	3	10	5

of Mo–P distance also differ, by 0.071(11) Å, with the one *trans* to the capping sulfur atom being shorter. We may also note that in this electron-poor type of cluster the Mo–Cl distance is appreciably shorter than the Mo–P distances, a quite common situation in early transition metal phosphine complexes.

Finally, in Table 4, we compare the dimensions of the Mo_3S_4 unit in the present compound with those previously reported for other compounds. It is clear that despite differences in the sets of external ligands, the three principal types of distances that characterize this unit are substantially the same in all cases.

In further exploratory work spectroscopic measurements (UV–visible) have shown that this compound can also be prepared by reaction of $MoCl_3$ and NaSH with dmpe in MeOH at −78°C followed by a workup of the solution similar to the one described previously.

Similar reactions have been observed with other halides (MoI_3) or other phosphines (dmpm). The compounds obtained in those cases appear to be less stable. Reactions with monodentate phosphines seem to follow quite different pathways. Efforts to establish the nature of these products are in progress.

Acknowledgement—We thank the Robert A. Welch Foundation, Grant No. A-494, for support.

REFERENCES

1. A. Müller, S. Pohl, M. Dartmann, J. P. Cohen, J. M. Bennett and R. M. Kirchner, *Z. Naturforsch. Teil B* 1979, **34**, 434.
2. A. Müller and U. Reinsch, *Angew. Chem. Int. Ed. Engl.* 1980, **19**, 72.
3. T. R. Halbert, K. McGauley, W.-H. Pau, R. S. Czernuszewicz and E. I. Stiefel, *J. Am. Chem. Soc.* 1984, **106**, 1849.
4. F. A. Cotton, R. Llusar, D. O. Marler, W. Schwotzer and Z. Dori, *Inorg. Chim. Acta* 1985, **102**, L25. H_3NTA = nitrilotriacetic acid; $H_2C_2O_4$ = oxalic acid.
5. F. A. Cotton, Z. Dori, R. Llusar and W. Schwotzer, *Inorg. Chem.* 1986, **25**, 3654. [9]aneN_3 = 1,4,7-triazacyclononane.
6. P. Kathirgamanathan, M. Martinez and A. G. Sykes, *J. Chem. Soc. Chem. Commun.* 1985, 1437.
7. R. E. Eibeck, *Inorg. Synth.* 1963, **7**, 128.
8. J. R. Dilworth and J. A. Zubieta, *J. Chem. Soc. Dalton Trans.* 1983, 397.
9. N. C. Howlader, G. P. Haight, Jr., T. W. Hambley, G. W. Lawrance, K. M. Rahmoeller and M. R. Snow, *Aust. J. Chem.* 1983, **36**, 377.
10. F. A. Cotton, Z. Dori, R. Llusar and W. Schwotzer, *J. Am. Chem. Soc.* 1985, **107**, 6734.

Polyhedron Vol. 6, No. 9, pp. 1747–1755, 1987
Printed in Great Britain

0277–5387/87 $3.00+.00

PREPARATION AND CHARACTERIZATION OF HEXACYCLOHEXOXIDO- AND TRISPINACOLATO-DITUNGSTEN (M≡M). A COMPARISON OF STAGGERED AND ECLIPSED ETHANE-LIKE $O_3W{\equiv}WO_3$ UNITS

MALCOLM H. CHISHOLM,* KIRSTEN FOLTING, MARK HAMPDEN-SMITH and CRYSTAL A. SMITH

Department of Chemistry and Molecular Structure Center, Indiana University, Bloomington, Indiana 47405, U.S.A.

(*Received* 9 *March* 1987; *accepted* 17 *March* 1987)

Abstract—The reactions between $W_2(OBu^t)_6$ and each of pinacol (3 equiv) and cyclohexanol (> 6 equiv) yield the title compounds $W_2(OCMe_2CMe_2O)_3$, **I**, and $W_2(OCy)_6$, **II** (Cy = cyclohexyl) as yellow needles, which are sparingly soluble in hydrocarbon solvents. In the solid-state both compounds form infinite chains. Compound **I** has three pinacolate ligands which span the W≡W bond: W–W = 2.2738(8) Å, W–O = 1.90 Å (av) and W–W–O = 99° (av). The three bridging ligands lead to a near eclipsed W_2O_6 skeleton having O–W–W–O torsion angles = 10° (av). The infinite chain is caused by weak intermolecular oxygen-to-tungsten bonding, W...O = 2.9 Å. The $W_2(OCy)_6$ molecule has crystallographically imposed C_{2h} symmetry and the central W_2O_6 moiety is staggered (virtual D_{3d}) with W–W = 2.340(1) Å, W–O = 1.87 Å (av) and W–W–O = 107° (av). The infinite chain in the solid-state results from the stacking of the cyclohexyl ligands. The intermolecular contacts are essentially identical to the intramolecular ones. In solution $W_2(OCMe_2CMe_2O)_3$ undergoes rapid enantiomerization such that a time-averaged eclipsed W_2O_6 moiety is seen on the NMR time-scale. The cyclohexyl rings in $W_2(OCy)_6$ are not inverting (chair ⇌ boat ⇌ chair) on the NMR time-scale.

Albright and Hoffmann's[1] provocative claim that M_2X_6(M≡M) dimers[2,3] "should prefer the eclipsed conformation" stimulated several theoretical appraisals of these molecules (M = Mo and W, and X = a uninegative ligand).[4–7] While the other calculations generally supported the view that there should be no electronic preference for either geometry, it is easy to see why the original suggestion was made. If the M_2X_6 dimers are constructed from two MX_3 fragments then the M–M bonding will reflect the geometry of the MX_3 fragments. If MX_3 fragments derived from an octahedron[8] are brought together, the eclipsed geometry will be preferred. However, if two trigonal planar ML_3 fragments are used to form the M_2X_6 unit then no electronic preference is predicted. Calculations employing EHMO and other methods naturally prefer to employ ligands such as H, Cl or CH_3 for which there are no known M_2X_6 (M≡M) compounds.[2,3] These compounds are not likely to be isolable either, so it was a challenge for the synthetic chemist to address the points raised by the theoreticians.

We recently described in full our comparative studies of staggered and eclipsed M_2N_6 moieties in $M_2(NMe_2)_6$ and $M_2(MeNCH_2CH_2NMe)_3$ compounds.[9] We describe here our preparation and characterization of two new compounds $W_2(OCMe_2CMe_2O)_3$ and $W_2(OCy)_6$. These provide the appropriate comparison of staggered and eclipsed $O_3W{\equiv}WO_3$ units and provide the first examples of structurally characterized unligated $W_2(OR)_6$ compounds.[10]

RESULTS AND DISCUSSION

Syntheses

Both new compounds were prepared by the addition of the alcohol to a hydrocarbon solution of $W_2(OBu^t)_6$. This obviates problems associated

* Author to whom correspondence should be addressed.

with oxidative addition reactions and the formation of dimethylamine adducts.[11]

In reactions involving cyclohexanol, the $W_2(OCy)_6$ compound, **II**, is precipitated as a pale yellow microcrystalline powder. It is only sparingly soluble in toluene and benzene and even less soluble in aliphatic hydrocarbons. It is more soluble in THF and was recrystallized from warm THF/toluene solvent mixtures. **II** does not undergo the reversible dimerization that we have recently observed for $W_2(O\text{-}i\text{-}Pr)_6$ under identical conditions.[10]

In reactions involving pinacol an initial dark-purple crystalline compound is formed which is formulated as a pinacol adduct $W_2(OCMe_2CMe_2O)_3$(pinacol). Even when only 3 equivalents of pinacol are used this is formed leaving some unreacted $W_2(OBu^t)_6$. The ^1H NMR spectrum reveals six inequivalent pinacolate Me resonances of equal intensity and a downfield signal *ca.* δ 10 ppm indicative of the hydroxyl group, together with a singlet of three times the intensity of the other methyl signals. Regrettably it is not possible to formulate a unique structure based on these data. However, the initially formed pinacol adduct slowly loses pinacol in THF or hydrocarbon solutions containing pyridine to give $W_2(OCMe_2CMe_2O)_3$, **I**, as fine yellow needles. [It seems that the donor molecules assist in the disruption of the hydrogen-bonded pinacolate adduct.] The crystals obtained for the X-ray study were obtained by recrystallization from warm THF. **I** is only sparingly soluble in aromatic hydrocarbon solvents and essentially insoluble in alkanes.

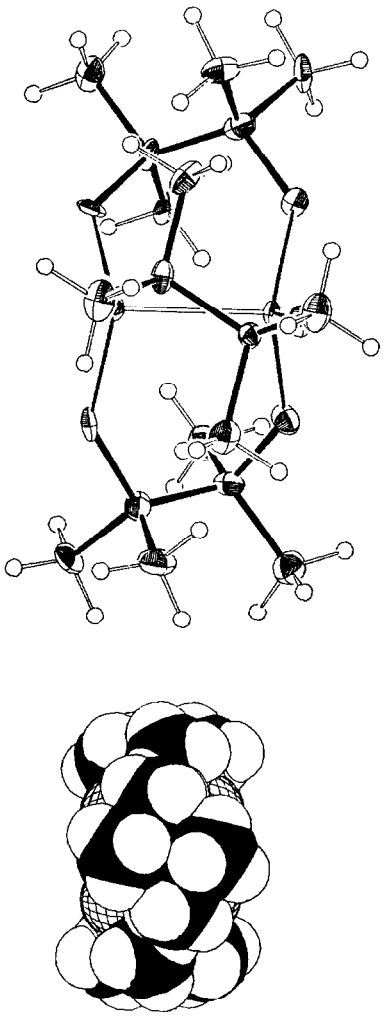

Fig. 1. An ORTEP view of the $W_2(OCMe_2CMe_2O)_3$ molecule looking down one of the virtual C_2 axes. A space filling drawing of the same view is shown below.

Solid-state and molecular structures

$W_2(OCMe_2CMe_2O)_3$. Crystallizes from THF as a 1 : 1 solvent complex, though the THF molecule is not coordinated to any tungsten atom. An ORTEP view of the $W_2(OCMe_2CMe_2O)_3$ molecule is shown in Fig. 1 and a view looking down the W–W bond with the atom number scheme is given in Fig. 2. The molecule has virtual D_3 symmetry as a result of the tris-bridging pinacolate ligands which form $M_2O_2C_2$ six membered rings in the skew-boat conformation. The average syn-O–W–W–O torsion angle is 10°. Selected bond distances and angles are given in Table 1.

$W_2(OCy)_6$. Has a crystallographically imposed mirror plane containing the M–M bond and a C_2 axis perpendicular to this, i.e. C_{2h} molecular symmetry. An ORTEP plot giving the atom number scheme is shown in Fig. 3 and a view looking down the M–M bond is given in Fig. 4. Pertinent bond distances and bond angles are given in Table 2. The most striking feature of this structure is the orientation of the cyclohexyl ligands which are all essentially perpendicular to the M–M axis.

The infinite chains. Compounds containing multiple bonds between metal atoms provide interesting building blocks for molecular design of new solid-state materials and metalloorganic liquid crystal phases. (1) The architectural signature of the M–M quadruple bond, for example, in $M_2(O_2CR)_4$ compounds is the four bladed paddle wheel while that of the $(M{\equiv}M)^{6+}$ moiety (M = Mo or W) is the staggered or ethane-like $X_3M{\equiv}MX_3$ moiety. (2) The subunits tend to stack due to weak intermolecular interactions involving either the metal atoms or the ligands. In the two compounds reported here we see an example of each phenomenon.

The pinacolate compound **I** consists of infinite chains of $W_2(OCMe_2CMe_2O)_3$ units which are

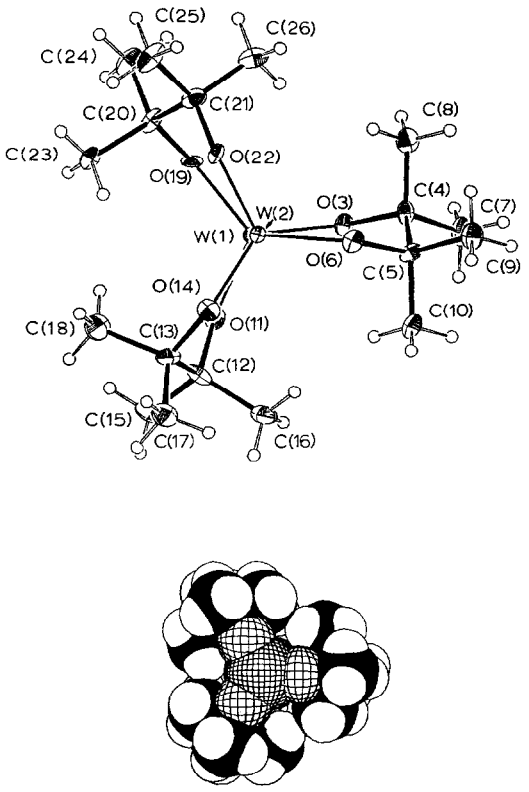

Fig. 2. A view of the $W_2(OCMe_2CMe_2O)_3$ molecule, with the atom number scheme used in the tables, looking down the W–W bond emphasizing the near eclipsed O_3WWO_3 moiety. A space filling drawing of the same view is shown below.

propagated along the *a* axis. The intermolecular O...to...W distances are *ca.* 2.9 Å. See Fig. 5. In the cyclohexoxide, the stacking is caused entirely by the hydrocarbon interactions. See Fig. 6. Again the infinite chains grow along the *a* axis but now the O...to...W distances along the chain are *ca.* 4.5 Å. Note also the intermolecular and intramolecular cyclohexyl ring distances are essentially identical.

We mention here these interesting fundamental stacking properties of M–M multiple bonded compounds because they have drawn little attention this far but are clearly of potential interest with respect to the molecular design of linear polymers. Note also the cavities within the chain may readily accommodate guest molecules as is seen for THF in the solid-state structure of $W_2(OCMe_2CMe_2O)_3 \cdot THF$.

Comparisons of molecular parameters for M_2X_6 *moieties.* The orientation of the cyclohexyl ligands in **II** and the pinacolate ligands in **I** are such that the $W_2(OC)_6$ skeletons of the two molecules differ only significantly with respect to the staggered and eclipsed W_2O_6 moieties. The W–O–C angles in I span a range 133° to 139° while in **II** the W–O–C angles are 141 and 145°. In both molecules the W–O–C units are aligned along the M–M axis in the proximal manner.

Table 1. Selected bond distances (Å) and bond angles (°) for the $W_2(O_2CMe_2CMe_2O)_3$ molecule

A	B	Distance
W(1)	W(2)	2.2738(8)
W(1)	O(3)	1.895(7)
W(1)	O(11)	1.890(7)
W(1)	O(19)	1.931(7)
W(2)	O(6)	1.915(7)
W(2)	O(14)	1.885(8)
W(2)	O(22)	1.901(7)
O(3)	C(4)	1.473(12)
O(6)	C(5)	1.453(12)
O(11)	C(12)	1.447(13)
O(14)	C(13)	1.445(14)
O(19)	C(20)	1.454(12)
O(22)	C(21)	1.440(13)
O(30)	C(29)	1.468(23)
O(30)	C(31)	1.422(24)

A	B	C	Angle
W(2)	W(1)	O(3)	99.53(21)
W(2)	W(1)	O(11)	98.72(21)
W(2)	W(1)	O(19)	100.03(22)
O(3)	W(1)	O(11)	117.6(3)
O(3)	W(1)	O(19)	117.8(3)
O(11)	W(1)	O(19)	116.7(3)
W(1)	W(2)	O(6)	99.88(2)
W(1)	W(2)	O(14)	99.19(22)
W(1)	W(2)	O(22)	99.98(21)
O(6)	W(2)	O(14)	116.4(3)
O(6)	W(2)	O(14)	117.0(3)
O(14)	W(2)	O(22)	118.3(3)
W(1)	O(3)	C(4)	136.0(6)
W(2)	O(6)	C(5)	136.4(6)
W(1)	O(11)	C(12)	139.0(6)
W(2)	O(14)	C(13)	139.1(7)
W(1)	O(19)	C(20)	133.3(6)
W(2)	O(22)	C(21)	135.0(6)

The oxygen lone-pairs which may be termed[12] σ and π are thus orientated in the same way in **I** and **II**. The π-lone pairs will principally interact with the metal d_{xy} and $d_{x^2-y^2}$ orbitals and the σ lone-pairs will be largely non-bonding.

In the pinacolate two oxygen σ-lone pairs, one at each tungsten atom, are in fact weakly bonded to neighbouring W_2 units, W(1)...O(19) = 2.83(1) Å and W(2)...O(6) = 2.91(1) Å. This is the range of M–to–O distances that we have previously termed semi-bridging. It is worth noting that the oxygen atoms involved in this "intermolecular" interaction

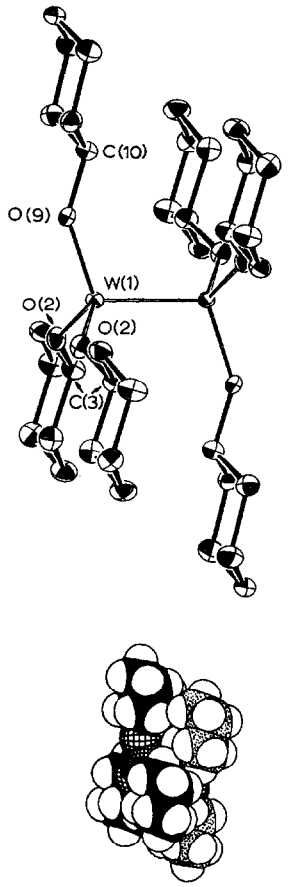

Fig. 3. An ORTEP view of the $W_2(OCy)_6$ molecule giving the atom number scheme used in the tables. A space filling drawing of the same view is shown below.

Table 2. Selected bond distances (Å) and angles (°) for the $W_2(OCy)_6$ molecule

A	B	Distance
W(1)	W(1)′	2.340(1)
W(1)	O(2)	1.880(4)
W(1)	O(9)	1.856(6)
O(2)	C(3)	1.432(7)
O(9)	C(10)	1.437(10)
C	C	1.52(1) (av) cyclohexyl

A	B	C	Angle
W(1)′	W(1)	O(2)	107.22(13)
W(1)′	W(1)	O(9)	107.62(18)
O(2)	W(1)	O(9)	111.39(15)
O(2)	W(1)	O(2)′	111.74(27)
W(1)	O(2)	C(3)	141.0(4)
W(1)	O(9)	C(10)	144.9(5)

form somewhat longer intramolecular W–O distances, W(1)–O(6) = 1.915(7) Å and W(2)–O(19) = 1.971(7) Å. There is little doubt that this weak intermolecular W . . . O bonding is responsible for the formation of the infinite chain structure and for the low solubility in hydrocarbon solvents.

In Table 3 we compare W–W, W-X and proximal W–X–C angles for the compounds $W_2(NMe_2)_6$, $W_2(MeNCH_2CH_2NMe)_3$, **I** and **II**. Three points are worthy of note. (1) The M–M distances are shorter in the eclipsed $X_3M{\equiv}MX_3$ compounds. (2) The M–M distances decrease as the M–M–X angles decrease for X = O and N. (3) The M–X–C proximal angles of the bridged molecules are smaller than those in the staggered molecules.

Regrettably it is impossible to separate the steric from the electronic factors in this series and the effective constraints imposed by the bridging chelates. For example, for alkoxides, the bulkier the alkyl group the greater the steric repulsion across the M–M bond. This will lead to larger M–M–O and M–O–C angles both of which will tend to lead to a lengthening of the M–M bond as a competition for M–M and M–O π-bonding sets in. For M–M–O angles equal 90° and M–O–C angles of *ca.* 120° with the M–O–C planes aligned along the M–M axis, the oxygen *p*-to-metal-*d* π-donation will not be mixed with M–M π-bonding. The two e sets, (d_{xz}, d_{yz}) and (d_{xy}, $d_{x^2-y^2}$), will be involved in M–M π and M–O π-bonding, respectively. As the M–M–O angle increases the e sets mix and O–to–M π-bonding competes with M–M π-bonding. The same is

Table 3. Comparison of selected structural parameters for eclipsed and staggered $X_3M{\equiv}MX_3$ containing molecules

Compound	M–M (Å)	M–M–X°	M–X–C°	Ref.
$W_2(NMe_2)_6$	2.294(1)	103.8(3)	132.6(6)	[a]
$W_2(MeNCH_2CH_2NMe)_3$	2.265(1)	101.6(5)	130.1(14)	9
$W_2(OCy)_6$	2.340(1)	107.4(2)	143(2)	this work
$W_2(OCMe_2CMe_2O)_3$	2.274(1)	99.8(4)	136(3)	this work

[a] M. H. Chisholm, F. A. Cotton, M. W. Extine and B. R. Stults, *J. Am. Chem. Soc.* 1976, **98**, 4477.

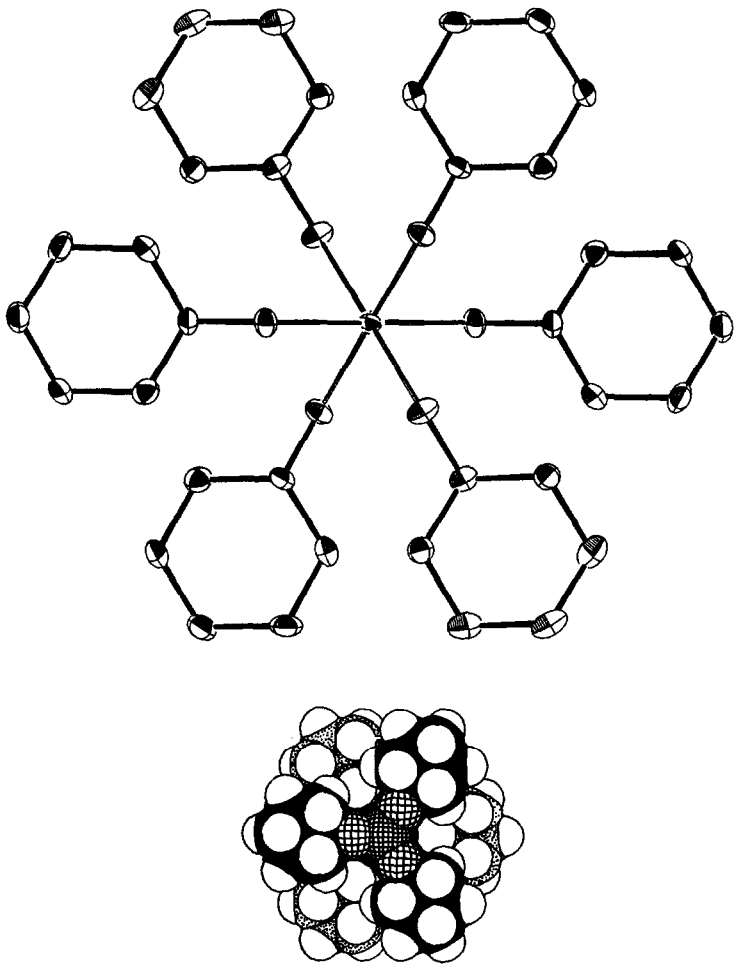

Fig. 4. An ORTEP view of the $W_2(OCy)_6$ molecule looking down the W–W bond emphasizing the staggered O_3WWO_3 moiety. A space filling drawing of the same view is shown below.

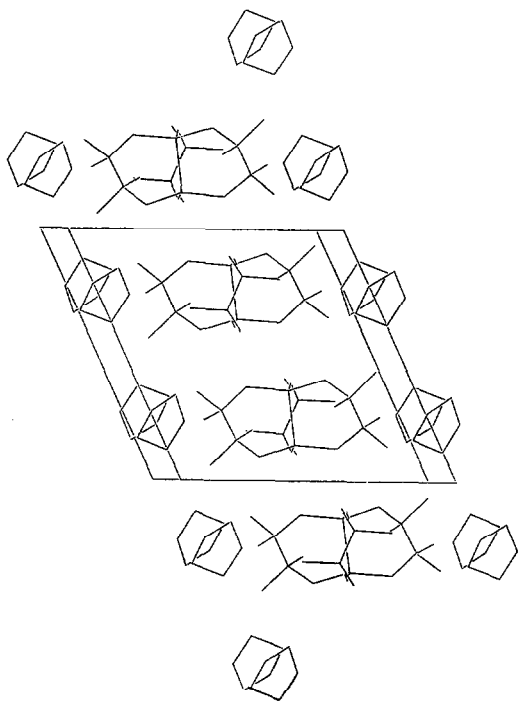

Fig. 5. A view of the unit cell of $W_2(OCMe_2CMe_2O)_3 \cdot THF$ looking down the *b* axis showing the stacking of the W_2 units along the *a* axis and the positions of the THF molecules.

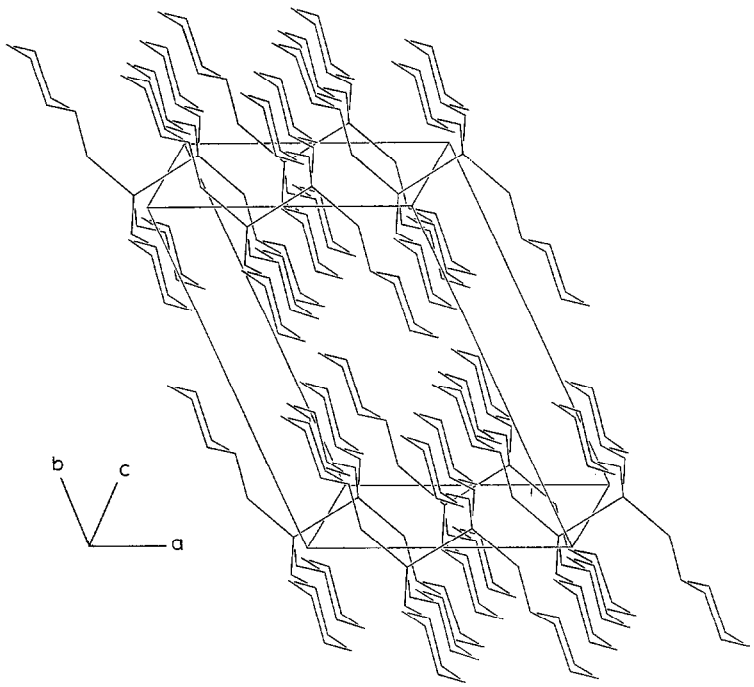

Fig. 6. A view of the unit cell of $W_2(OCy)_6$ showing chains of the W_2 units propagated along the *a* axis.

true as the M–O–C angle goes from 120° to 180°, even though the M–M–O angle remains 90°. A specific bridging chelate will have a geometrically preferred M–M–O and M–O–C angle which, whether eclipsed or staggered, will influence the M–M distance. In the present case the pinacolate ligand favors the factors which favor short M≡M distances.

NMR studies

The ^{1}H NMR spectrum of **I** shows only one methyl signal at room temperature at 360 MHz. This implies that the enantiomerization must be rapid on the NMR time-scale; i.e. the time averaged syn-O–W–W–O torsion angles are zero. A similar result was found for $M_2(MeNCH_2CH_2NMe)_3$ compounds.[9]

$W_2(OCy)_6$ shows a single downfield multiplet at *ca.* δ 5.4 assignable to its methyne proton. This is similar to that of the isopropoxy methyne resonances in $M_2(O\text{-}i\text{-}Pr)_6$ compounds (M = Mo, W) and presumably reflects the proximity of the methyne hydrogen to the M≡M bond as indeed is seen in the molecular structures in the solid-state. The remaining cyclohexyl proton resonances appear in the region 2.5 to 1.2 ppm as partially overlapping multiplets. It is, however, apparent that ring inversion is slow on the NMR time-scale at 360 MHz, and 25°C. This is not surprising since ring inversion in cyclohexanol is also virtually frozen-out under these conditions (360 MHz, 25°C).

Concluding remarks

The present work shows that little shortening of the W≡W bond occurs in going from a staggered to an eclipsed $O_3W{\equiv}WO_3$ moiety, the difference being 0.07 Å in compounds **I** and **II**. The origin in the lengthening could be ascribed to either electronic or steric factors (or a combination of both) but is unlikely to be associated with the W_2O_6 conformation. The reactivity of **I** is currently under investigation. It is noticeably different from other $W_2(OR)_6$ compounds in having a hydrocarbon girth around the W≡W bond and uniquely exposed tungsten atoms along the metal–metal axis.

EXPERIMENTAL

Dry and oxygen-free solvents were used in all experiments. All manipulations were carried out under inert atmospheres using standard Schlenk techniques. $W_2(OBu^t)_6$ was prepared by the addition of Bu^tOH to $W_2(NMe_2)_6$ according to literature procedures.[13]

^{1}H NMR spectra were recorded on a Nicolet NT-360 spectrometer at 360 MHz using toluene-d_8 or benzene-d_6 as solvents. The cyclohexyl resonances of **II** were assigned by a combination of homonuclear decoupling and 2D ^{1}H NMR experiments.

Single frequency decoupling of the multiplet at 2.39 ppm collapsed the resonance of H_α to a triplet with vicinal $J_{H-H} = 9$ Hz. The resonance at 2.39 ppm was therefore assigned to the two H^e_β proton (where the superscript represents axial (a) or equatorial (e), and the subscript the position on the ring). Decoupling the multiplet at 1.65 ppm collapsed H_α to a triplet $^3J_{H-H} = 4$ Hz. The resonance at 1.65 ppm was therefore assigned to H^a_β. The remaining resonances could be assigned from a 2D ^{1}H NMR chemical shift correlated contour plot assuming $J^{ae}_{gem} \simeq J^{aa}_{vic} > J^{ee}_{vic} > J^{ae}_{vic}$. 2D Matrix: 128×512, 8 scans, total acquisition time 27 min. Elemental analyses were obtained by Bernhard Analytical Laboratories, West Germany. Cyclohexanol was dried over, and distilled from finely divided magnesium.

$W_2(OCMe_2CMe_2O)_3$. $W_2(OBu^t)_6$ (500 mg, 0.62 mmol) was dissolved in hexane (20 cm^3) and 0.45 M pinacol in toluene (5.6 cm^3, 2.5 mmol) was added. The resulting red solution was cooled immediately to 0°C. After 24 h, the solution had become deep purple. On reducing the volume, deep purple-black crystals were obtained. The compound which is formulated as $W_2(OCMe_2CMe_2O)_3(HOCMe_2CMe_2OH)$ is formed nearly quantitively in this reaction. ^{1}H NMR data at 22°, toluene-d_8: δ(Me) 0.86(3H, s), 1.22(3H, s), 1.26(3H, s), 1.61(3H, s), 1.75(3H, s), 1.94(3H, s), 1.36(9H, s), δ(OH) 10.2(1H, no coupling to ^{183}W). $W_2(OCMe_2CMe_2O)_3(HOCMe_2CMe_2OH)$ (180 mg, 0.22 mmol) was dissolved in THF (10 cm^3). After stirring at ambient temperature for *ca.* 18 h, the solution had become pale yellow. The solvent was removed *in vacuo* and the resultant pale yellow solid was washed with toluene (5 cm^3) to remove any residual traces of pinacol. $W_2(OCMe_2CMe_2O)_3$ was recrystallized from THF solution in *ca.* 80% yield.

^{1}H NMR data, 22°C in $CDCl_3$: δ(Me) = 1.46(s); in toluene-d_8: δ(Me) = 1.43(s).

Found: C, 30.1; H, 5.0. Calc. for $W_2O_6C_{18}H_{36}$: C, 30.2; H, 5.1%.

$W_2(OCy)_6$. To W_2(O-t-Bu)$_6$ (700 mg, 0.87 mmol), dissolved in 20 cm^3 of hexane, 2 cm^3 (20.7 mmol) of dry cyclohexanol was added dropwise. The solution darkened as the alcohol was added and after about 5 min a yellow precipitate had formed. The mixture was stirred for 1 h at 25°C, filtered, the yellow solid washed with 2×6 cm^3 portions of hexane and 575 mg (0.60 mmol) of $W_2(OCy)_6$ (**II**) was recovered in 70.0% yield. Crystallization of **II** from toluene resulted in formation of long, pale yellow needles unsuitable for X-ray diffraction, however, larger crystals were grown from an 80% toluene/20% THF mixture at 40°C.

^{1}H NMR data, 22°C in toluene-d_8: $\delta(H\alpha) = 5.38$ ppm, (t of t) $^3H_{H_\alpha-H^a_\beta} = 9$ Hz, $^3J_{H_\alpha-H^e_\beta} = 4$ Hz; $\delta H^e_\beta = 2.39$ (m); $\delta H^e_\gamma = 1.86$ (m); $\delta H^a_\beta = 1.65$ (m); $\delta H^e_\delta = 1.50$ (m); $\delta H^a_\gamma = 1.40$ (m); $\delta H^a_\delta = 1.22$ (m). ^{13}C NMR data, 22°C, toluene-d_8: $\delta(C\alpha) = 87.7$ ppm; $\delta(C\beta) = 37.2$ ppm; $\delta(C\gamma) = 24.6$ ppm; $\delta(C\delta)$ = not obs. UV–visible spectrum, 22°C in THF: $\lambda = 347$ nm ($\varepsilon = 2317$ mol^{-1} cm^{-1}), $\lambda = 420$ nm. (sh.)

Crystallographic studies

General operating procedures and listings of programs have been described previously.[14] A summary of crystal data is given in Table 4.

$W_2(OCMe_2CMe_2O)_3 \cdot$THF. A suitable sample was cleaved from a larger crystal using standard inert atmosphere handling techniques and transferred to the goniostat where it was cooled to −158°C for characterization and data collection. A systematic search of a limited hemisphere of reciprocal space revealed a set of diffraction maxima which could be indexed as monoclinic, space group $P2_1/c$. Subsequent solution and refinement confirmed the choice.

The structure was solved by a combination of direct methods (MULTAN78) and Fourier techniques, and refined by full-matrix least squares. Although hydrogen atoms were visible in a difference Fourier phased on the non-hydrogen atoms, no attempt was made to refine them. They were included as fixed idealized contributors in the final cycles. No attempt was made to include hydrogen atoms for the THF solvent molecule in the structure.

A final difference Fourier was featureless, the largest peak being 1.21 e/Å^3, located at one of the metal sites.

$W_2(OCy)_6$. A suitable crystal was located and transferred to the goniostat using standard inert atmosphere handling techniques employed by the Indiana University Molecular Structure Center and cooled to −158°C for characterization and data collection.

A systematic search of a limited hemisphere of reciprocal space located a set of diffraction maxima with symmetry and systematic absences corresponding to a C centered monoclinic space group. Initial solution was in the noncentrosymmetric space group C2, but examination of the structure revealed additional symmetry and the space group C2/m was selected. Subsequent refinement of the structure confirmed this choice.

Data were collected in the usual manner using a continuous θ-2θ scan with fixed backgrounds. Data were reduced to a unique set of intensities and

Table 4. Summary of crystal data

	I	II
Empirical formula	$W_2C_{18}H_{36}O_6 \cdot C_4H_8O$	$W_2O_6C_{36}H_{66}$
Color of crystal	yellow	orange-yellow
Crystal dimensions (mm)	$0.16 \times 0.22 \times 0.20$	$0.13 \times 0.13 \times 0.15$
Space group	$P2_1/c$	C2/m
Cell dimensions		
Temperature (°C)	−158	−158
a (Å)	11.383(2)	8.128(3)
b (Å)	21.840(6)	22.314(12)
c (Å)	11.499(2)	22.602(5)
beta (deg)	114.14(1)	114.27(2)
2 (molecules/cell)	4	2
Volume (Å^3)	2608.68	1918.39
Calculated density (gm/cm^3)	2.007	1.666
Wavelength (Å)	0.71069	0.71069
Molecular weight	788.29	962.61
Linear absorption coefficient (cm^{-1})	90.384	61.591
Detector to sample distance (cm)	22.5	22.5
Sample to source distance (cm)	23.5	23.5
Average omega scan width at half height	0.25	0.25
Scan speed (deg/min)	4.0	4.0
Scan width (deg + dispersion)	2.0	2.0
Individual background (s)	6	8
Aperture size (mm)	3.0×4.0	3.0×4.0
Two-theta range (deg)	6–45	6–55
Total number of reflections	3830	4959
Number of unique intensities	3413	2277
Number with $F > 3.00\sigma(f)$	2841	1993
$R(F)$	0.0409	0.0336
$R_w(F)$	0.0476	0.0326
Goodness of fit for the last cycle	1.859	0.715
Maximum delta/sigma for last cycle	0.05	0.05

I = $W_2(OCMe_2CMe_2O)_3 \cdot$ THF. II = $W_2(OCy)_6$.

associated sigmas in the usual manner. The structure was solved by a combination of direct methods (MULTAN78) and Fourier techniques. The positions of all hydrogen atoms were clearly visible in a difference Fourier phased on the non-hydrogen atoms, and the coordinates and isotropic thermal parameters for hydrogens were varied in the final cycles of refinement.

The molecule lies at a crystallographic 2/m symmetry site, with the 2-fold axis perpendicular to and bisecting the metal-metal bond.

A final difference Fourier was essentially featureless, with the largest peak being 0.85 e/Å^3, lying near the W site.

Acknowledgements—We thank the National Science Foundation, the Wrubel Computing Center and the Indiana University Foundation for support of this work.

Crystallographic Data. Complete listings of bond distances and bond angles have been deposited with the Editor at Queen Mary College and atomic positional parameters are available from the Director, Cambridge Crystallographic Data Center.

REFERENCES

1. T. A. Albright and R. Hoffmann, *J. Am. Chem. Soc.* 1978, **100**, 7736.
2. M. H. Chisholm and F. A. Cotton, *Acc. Chem. Res.* 1978, **11**, 356.
3. M. H. Chisholm, *Angew. Chem. Int. Edit. Engl.* 1986, **25**, 21.
4. B. E. Bursten, F. A. Cotton, J. C. Green, E. A. Seddon and G. G. Stanley, *J. Am. Chem. Soc.* 1980, **102**, 4579.
5. M. B. Hall and R. A. Kok, *Inorg. Chem.* 1983, **22**, 728; *idem, J. Am. Chem. Soc.* 1980, **102**, 204.
6. K. D. Dobbs, M. M. Frankel and W. J. Hehre, *Inorg. Chem.* 1984, **23**, 24.

7. T. Zeigler, *J. Am. Chem. Soc.* 1983, **105**, 7543.
8. M. Elian and R. Hoffmann, *Inorg. Chem.* 1975, **14**, 1058; M. Elian, M. M. L. Chieu, D. M. P. Mingos and R. Hoffmann, *Inorg. Chem.* 1976, **15**, 1148; T. A. Albright, P. Hoffmann and R. Hoffmann, *J. Am. Chem. Soc.* 1977, **99**, 7546.
9. T. P. Blatchford, M. H. Chisholm and J. C. Huffman, *Inorg. Chem.*, in press. A preliminary publication has appeared: T. P. Blatchford, M. H. Chisholm, K. Folting and J. C. Huffman, *Inorg. Chem.* 1980, **19**, 3175.
10. Since the initiation of this work we have characterized a crystal containing a 1:1 mixture of $W_4(O\text{-}i\text{-}Pr)_{12}$ and $W_2(O\text{-}i\text{-}Pr)_6$: M. H. Chisholm, D. L. Clark, K. Folting and J. C. Huffmann, *Angew. Chem. Int. Edit. Engl.* 1986, **25**, 1014.
11. M. H. Chisholm, J. C. Huffman and C. A. Smith, *J. Am. Chem. Soc.* 1986, **108**, 222.
12. M. H. Chisholm and D. L. Clark, *Comments on Inorg. Chem.* 1987, **6**, 23.
13. M. Akiyama, M. H. Chisholm, F. A. Cotton, M. W. Extine, D. A. Haitko, D. Little and P. E. Fanwick, *Inorg. Chem.* 1979, **18**, 2266.
14. M. H. Chisholm, K. Folting, J. C. Huffman and C. C. Kirkpatrick, *Inorg. Chem.* 1984, **23**, 1021.

Polyhedron Vol. 6, No. 9, pp. 1757–1763, 1987
Printed in Great Britain

0277–5387/87 $3.00+.00

SYNTHESIS AND THERMAL BEHAVIOUR OF A SERIES OF PENTACYANOLIGANDFERRATE(II) COMPLEXES*

ELSA E. SILEO, MÓNICA G. GARCÍA POSSE, PEDRO J. MORANDO† and MIGUEL A. BLESA†

Departamento de Química Inorgánica, Analítica y Química Física, Facultad de Ciencias Exactas y Naturales, Universidad de Buenos Aires; Ciudad Universitaria, Pabellón II, 1428 Buenos Aires, República Argentina; and Departamento Química de Reactores, Comisión Nacional de Energía Atómica

HUMBERTO A. HERRERA

Laboratorio de Fisicoquímica, Facultad de Agronomía y Agroindustria, Universidad Nacional de Santiago del Estero, Av. Bellgrano 1912, (4200) Santiago Del Estero, Argentina

CARLOS O. DELLA VEDOVA

Programa QUINOR, Facultad de Ciencias Exactas, Universidad Nacional de La Plata, Calle 47 y 115; (1900) La Plata, Argentina

and

A. ESTEBAN

Departamento Combustibles Nucleares, Comisión Nacional de Energía Atómica, Centro Atomico Constituyentes; Av. Constituyentes y General Paz, (1650) Buenos Aires, Argentina

(*Received* 27 *August* 1986; *accepted after revision* 17 *March* 1987)

Abstract—$[M_mFe(CN)_5L \cdot xH_2O]$ (M = Mn, Fe, Co, Ni, Cu; L = pyridine or pyrazine derivative) have been synthesized, and their UV–vis and IR spectral characteristics are reported. Thermolysis of the solids leads to water release, ligand release and/or decomposition, redox interaction between Fe^{3+} (or Cu^{2+}) with CN^- or L, and redox interaction between M^{2+} (or Cu^+) and CN^-, yielding elemental metal and metal carbides.

Mixed metal cyanides have been studied extensively from the point of view of the intervalence bands appearing in their visible or near infrared spectra.[1–6] Structural characterizations have been also carried out, showing that in $M_m[M(CN)_6]_n \cdot xH_2O$ two types of M′ ions may be found, i.e. hydrated interstitial cations,[7–12] and cations coordinated to nitrile nitrogen. The thermal behaviour of simple and complex cyanides has also been the subject of much work. The decomposition has been shown to involve cyanogen release, usually with nitrogen evolution, and formation of metal carbides.[13–18] The characteristics of the resulting solids however have not been studied, partly because of their "intractable nature".[13]

In the present paper we report the preparation, characterization and thermal behaviour of several complexes of the type $[M_mFe(II)(CN)_5L \cdot xH_2O]$, where M is a divalent or trivalent transition metal cation and L is an aromatic amine derived from pyridine or pyrazine. The main questions addressed in this paper are: (1) the nature of the water molecules of hydration and their corresponding thermal dehydration behaviour; (2) spectroscopic evidence on the interaction between anions and cations, including the possibility of Fe–CN–M and/or Fe–L–M bridges; (3) the unambiguous characterization of a $Fe(CN)_5$ derivative as the

* Presented in part at 8th International Conference on Thermal Analysis, Bratislava, Czechoslovakia, 1985 that was published in summary form in *Therm. Act.* 1985, **92**, 835.

† Authors to whom correspondence should be addressed.

original decomposition product. In the case of ferrocyanides, $Fe(CN)_5^{3-}$ may be formed at relatively low temperatures (ca. 200°C, for Prussian Blues);[13] (4) the influence of the nature of M on the thermal behaviour of these compounds; (5) the composition and morphology of the solids formed at high temperature (ca. 900°C).

EXPERIMENTAL

Preparation of the complexes

$Na_n[Fe(CN)_5L]\cdot xH_2O$ complexes for L = nicotinamide (nide), isonicotinamide (isonide), pyrazinamide (pzide), nicotinate (nic) and isonicotinate (isonic) were prepared from $Na_3[Fe(CN)_5NH_3]\cdot 3H_2O$ by literature methods.[19,20] The complexes $M_m[Fe(CN)_5L]\cdot xH_2O$ [M = Mn(II), Fe(II), Fe(III), Co(II), Ni(II) and Cu(II)] were precipitated by adding a threefold excess of aqueous metal sulphate or nitrate solution to an aqueous solution of $Na_m[Fe(CN)_5L]\cdot xH_2O$]. After stirring for 15 min the solid thus obtained was collected, washed with distilled water, ethanol and diethylether and then dried over $CaCl_2$ in a desiccator for several days. In some instances, oily products were formed; in these cases, precipitation was achieved by adding NaI and working with cooled materials and solvents.

Elemental analysis

C, H and N microanalyses were performed by UMYMFOR, UBA using standard techniques. The results, although only of semiquantitative value because of carbide formation (see below), confirmed the presence of $Fe(CN)_5L^{n-}$ moieties. Metal contents were determined in a Varian Techtron A-A5R atomic absorption spectrometer. About 30–40 mg of each complex were treated in concentrated sulphuric and/or nitric/or hydrochloric acid and diluted with distilled water. The ratio Fe : L was in all cases (except for M = Fe) unity, and the ratio Fe : M was in agreement with a simple precipitation process [i.e. the ratio was two for anionic L^- and M(II), etc.].

Thermogravimetric analysis

Thermograms were obtained in a Mettler Recording Thermoanalyser 1 with samples of about 15 mg in N_2 atmosphere in the temperature range 25–900°C.

Spectral characterization

IR measurements were made using a Perkin–Elmer 580 B spectrophotometer in KBr disks. Reflectance and transmittance UV-visible spectra were recorded for solid samples or 10^{-4} M solutions using a Shimadzu 110 A spectrophotometer.

RESULTS AND DISCUSSION

Characterization of the starting solids

Amorphous materials were obtained in all cases showing no X-ray diffraction peaks. The $[Fe(CN)_5L]^{n-}$ moiety remained intact as apparent from chemical analysis and spectral data. For all cations other than Fe(III) and Cu(II) the electronic spectra in the visible range is dominated by the metal to ligand charge transfer (MLCT) band typical of the anion. These bands are located in the range 374–401 nm for nide, 415–460 nm for isonide, 479–543 nm for pzide, 338–385 nm for nic and 391–440 nm for isonic. The nature of the counter cation does not alter the energy sequence of the MLCT bands as the ligand L is charged; the wavelength increases in the order nic < nide < isonic < isonide < pzide. This is a well known effect of the electron-accepting properties of the heterocycles.[21,22] For Fe(III) and Cu(II), an intervalence band is also observed, in the ranges 650–670 and 480–540 nm respectively. Co(II) complexes also exhibit a second maximum in addition to the MLCT at ca. 600–620 nm characterized by a rather low absorptivity ($\varepsilon = 116\ M^{-1}\ cm^{-1}$) that is assigned to a *d–d* transition of Co(II) in a quasi-tetrahedral environment.[23,24]

In the IR spectra, cyanide stretching values for M(II) salts are very similar to those for hexacyanoferrate(II) complexes.[25] In several cases the absorption profiles exhibit faint shoulders or humps in the range 2130–2170 cm^{-1}, but the lack of resolution prevents any further elaboration (symmetry splitting, or distinct cis- and trans-CN). The frequency increases from ca. 2045–2050 cm^{-1} (sodium salts) following the sequence Mn < Fe < Co < Ni < Cu, the highest values for divalent M being in the range 2093–2100 cm^{-1}. This trend follows the Irwing–Williams series and reflects the formation increasingly stronger of Fe(II)–CN–M(II) bridges.[26–28] For Fe(III) complexes cyanide stretching frequencies are in the same range (2065–2075) cm^{-1}, as found earlier by Fluck[27] for L = H_2O, NH_3 and CO. Hydration water does not influence appreciably the value of ν_{CN}; upon dehydration at ca. 100°C, the observed frequency remains unchanged.

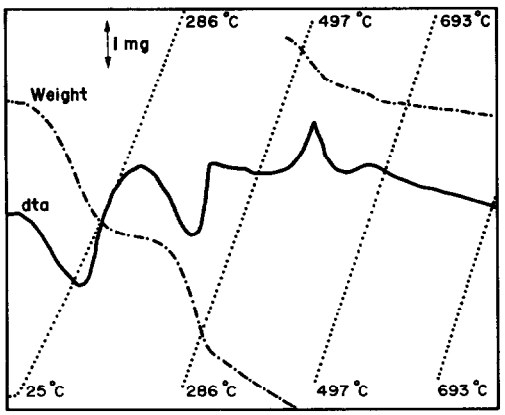

Fig. 1. TGA (-·-·-) and DTA (——) curves for $Ni_3[Fe(CN)_5(isonida]_2 \cdot 13.5H_2O$.

The possibility of chelation of M by carboxylate or amide groups is ruled out by the values of the symmetric and antisymmetric CO_2 stretching, the C=O stretching and NH_2 deformation, that are similar to those of the sodium salt. Similar results have been reported for sodium and copper nicotinate and isonicotinate, and for copper isonicotinamide and nicotinamide complexes.[29,30]

Thermal behaviour

A typical thermogram, obtained in N_2 atmosphere is shown in Fig. 1. Thermograms for other compounds are similar in general, except as noted below. Dehydration, ligand L release and cyanogen plus dinitrogen evolution occur at stages reasonably well delimited. A summary of the observed peaks is given in Tables 1 and 2.

Table 2. Ligand release or decomposition temperature data (°C)[a]

Compound	nide	isonide	pzide	nic	isonic
Na	277	252	320	401	436
Mn	309	331	400	428	415
Fe(II)	290	305	300	400	390
Co	358	362	392	391	390
Ni	291	316	388	397	370
Cu	210 325	235 315	[b]	180 335	230 320
Fe(III)	295	275	[b]	270 360	250 340

[a] Those values within the rectangular field correspond to reasonably neat ligand evolution without decomposition; other values indicate release of gases arising from decomposition of ligand that can be resolved from peaks corresponding to cyanide decomposition.

[b] Not measured.

Dehydration

The differentiation between physisorbed and constituent water molecules is difficult to establish. Different hydration numbers are obtained by thermal analysis, depending on the previous drying procedure of the sample. Samples dried in a desiccator over $CaCl_2$ for 24 h or more yield solids that usually show H_2O : M ratios between 3 and 5. Samples previously dried for 24 h or more in vacuum at 40°C

Table 1. DTG/DTA water release peak maxima (°C) and H_2O : M ratio (in parentheses)

	Ligand				
M	nide	isonide	pzide	nic	isonic
Mn	120 (1.8)	120 (1.9)	116 (2.3)	106 (2.7)	133 (1.6)
Fe(II)	110 (1.3)	107 (1.7) 105* (2.1)	110 (2.0)	100 (1.9)	120 (1.6)
Co	107 (2.2)	94 (1.3) 95* (3.1)	116 (2.7)	83 (2.5)	98 (1.1)
Ni	94 (2.0)	107 (2.7) 127* (4.5)	94 (2.0)	103 (3.5)	115 (1.8)
Cu	90* (3.5)	105* (3.7)	—	80* 105* (3.5)	120* (3.8)
Fe(III)	100* (5.0)	100* (5.0)	—	100* (4.1)	100* (4.1)

Solids previously dried in vacuum at 40°C for 24 h, except those noted by *, corresponding to samples dried over $CaCl_2$ in vacuum at room temperature. Selected cases showing the result of applying both procedures on the same sample are included.

lose water upon heating that corresond typically to H_2O : M ratios between one and three (see Table 1). The difference is probably related to the initial formation of solids containing partially hydrated cations, and the existence of cation hydration and crystallization water molecules. Thermograms run at 5°C min^{-1} do not resolve both types of water molecules, although humps are usually apparent in the DTA and DTG peaks. The usual release temperature for all the water molecules, in samples dried by either procedure, is 90–120°C. Experiments under static air atmosphere give indication of sequential (although not completely resolved) water loss.

Ligand release

IR spectra of samples heated up to 150°C demonstrate that the complex anion suffers no change during dehydration. Ligand L release takes place in the temperature range 280–400°C, except for Cu(II); it is a simple process in the case of neutral L species in salts of all cations other than Fe(III) and Cu(II). In favourable cases weight loss and peak profiles are in good agreement with the stoichiometry (1), but usually separation from following peaks is not complete.

$$M_3[Fe(CN)_5L]_2(s) \rightarrow M_3[Fe(CN)_5]_2(s) + 2L(g). \quad (1)$$

Operation of process (1) is demonstrated also by IR characterization of the condensed evolved gaseous products: neutral L ligands remain undercomposed during release. The behaviour is similar to that of sodium salts[31] although ligand release from Fe(III) complexes is characterized by a rather broad peak that may reflect a more complex process (or the overlap with ensuing cyanide release).

Table 2 shows a summary of the temperatures of the DTA–DTG peaks, under the constant condition of our measurements; both neutral and anionic ligands are included. For neutral L, the temperature generally increases in the sequence: nide < isonide < pzide. This indicates that the thermolysis is governed by the breaking of the Fe(II)–L bond in the anion, as the bond strength increases in the same order.[22,31] The reverse order nide > isonide found in the sodium salts,[31] in disagreement with the general trends, was related earlier to an exothermic peak that produced local heating in the isonide complex. Our present observations reinforce the idea that the order of release of isonide and nide in the sodium salts is anomalous. In all the thermograms of isonide complexes an exothermic peak is observed, but in the present cases this unexplained feature takes place only after ligand L release (see Fig. 1 for a typical example).

M–L interactions are secondary in determining thermal stability. There is however also an ordering for the decomposition temperatures of the various M salts of a given $Fe(CN)_5L^{n-}$ anion, that is generally valid for the studied neutral ligands; the decomposition temperature increases in the order: Na < Fe < Ni < Mn < Co.

As can be seen from Table 2, anionic L ligands are decomposed and released at higher temperatures: carbon dioxide is one of the evolved products, as shown by the formation of $BaCO_3$ upon bubbling in $Ba(OH)_2$ solution; the other decomposition products of the organic ligand were not characterized. This process overlaps with cyanogen release (see below).

For Cu(II), neutral L are released at substantially lower temperatures, in a complex process that shows typical "ripples" in the DTA curve prior to the main weight loss. This suggests a redox process, with possible generation of Cu(I). In iron(III) complexes neutral ligands loss may also overlap with redox processes (see above), but this is not clearly demonstrated by the thermograms. In fact, for Cu(II) and Fe(III) solids the thermal behaviour in this temperature range is governed by the redox chemistry of the metal centre, and there are no substantial differences between neutral and anionic L ligands. Depending on the nature of L and M electron transfer may take place either solely from cyanide or both from cyanide and L. Thus, either $(CN)_2$ or mixtures $(CN)_2 + CO_2 +$ other decomposition products are expected in the evolved gas. The presence of $(CN)_2$ and CO_2 was detected through the formation of AgCN upon bubbling in $AgNO_3$ solution, and the formation of $BaCO_3$ upon bubbling in $Ba(OH)_2$ solutions. For Cu(II) the decomposition takes place at lower temperatures and involves essentially cyanogen release, e.g.

$$Cu_3[Fe(CN)_5L]_2 \rightarrow Cu_3Fe_2(CN)_7L_2 + (3/2)(CN)_2(g). \quad (2)$$

The milder oxidizing power of Fe(III) is reflected in higher decomposition temperatures. In this range, ligand L decomposition overlaps with CO_2 release. Oxidation of carboxylates by Cu(II) and Fe(III) are known to proceed with a rather low activation energy and in the temperature range 220–400°C.[33]

The nature of the decomposition products of L in our Fe(III) and Cu(II) complexes is not known; ligand loss takes place over a wide temperature range, with some indications of more than one step and this is probably related to fragmentation of the

ligand. For example, for L = isonicotinate, M = Fe(III), weight loss analysis and chemical characterization of the evolved gas suggest that CO_2 is the main (if not only) released product at ca. 250°C. Also, carbonization is suggested by the chemical analysis of the solid residues obtained upon calcination at 900°C: the carbon percentage is too high to be compatible with complete release of the ligand. The same situation is found for L = nide and M = Fe(III).

The nature of the solid phases formed upon ligand release was investigated in more detail in experiments carried out with controlled heating up to previously selected temperatures and subsequent isothermal decomposition until nearly constant weight was achieved. The behaviour of the solids in these experiments was sensitive to the nature of M but was very similar for different L complexes of a given M. In the case of M = Cu, as explained above ν_{CN} decreased alongside with L bands; ν_{CN} shifts at first to lower wavenumbers (i.e. from 2070 to 2040 cm^{-1} for L = nide) and its intensity decreases relative to the intensity of ligand L bands in agreement with (2). The shift to lower wavenumbers may be attributed to the replacement of Cu(II) by Cu(I) in the solid. At longer heating times, ν_{CN} shifts to higher wavenumbers (for instance, to 2100 cm^{-1} in the noted L = nide case); this effect may be related to an increasing Cu(I)–NC interaction[26] (for polymeric CuCN, featuring Cu–CN–Cu bridges, ν_{CN} = 2172 cm^{-1} has been reported[26]).

For M = Ni, after nearly complete removal of L, in the ν_{CN} region two bands were apparent, the more intense one being centred at 2168 cm^{-1}, and the weaker one at 2036 cm^{-1}; cobalt complexes behave similarly. For M = Mn, the most intense band in the ligand-free residue is located at 2036 cm^{-1} and a much weaker band is seen at 2150–2180 cm^{-1}. The high frequency band is attributable to bridged Fe–CN–M groups[32] but may also be explained through other processes involving the rupture of the $Fe(CN)_5$ moiety (note that 2176 cm^{-1} is the ν_{CN} frequency in $Ni(CN)_2$[26]). Thus, there is no conclusive evidence regarding the nature of the thermolysis product in Ni complexes. On the other hand, the low frequency value of 2036 cm^{-1} can be reasonably attributed to $Fe(CN)_5$ moieties where Fe interacts most weakly with a sixth ligand; no evidence of ligand scrambling is apparent, and thus the solid is best formulated as $Mn_3[Fe(CN)_5]_2$.

Cyanide release

Cyanide ions start to break down at temperatures that in some cases overlap with ligand L release temperatures. These temperatures, for Cu(II) are as low as 200°C. In the usual case, cyanide decomposes in a wide temperature range starting around 400°C or higher. In agreement with previous work,[13–16] weight loss is indicative of metal carbide and elemental carbon formation in varying degrees. X-

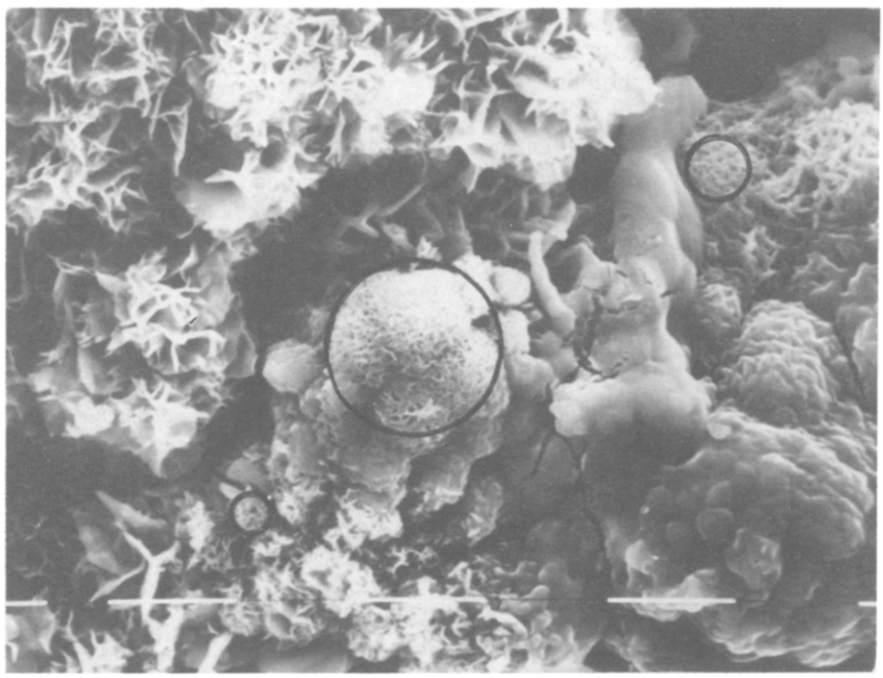

Fig. 2. SEM picture (1700×) of the pyrolysis (700°C) product of $Co_3[Fe(CN)_5nide]_2 \cdot 9H_2O$. Circles indicate Co-rich regions according to EDAX; other regions are Fe-rich.

ray diffraction of the solid residues indicates the presence of mixtures of both metals and cementite. For neutral L the overall stoichiometry arises from the overlap of (3) and (4):

$$M_3Fe_2(CN)_{10} \rightarrow 3M + 2Fe + 2xC + xN_2 + (5-x)(CN)_2 \quad (3)$$

$$M_3Fe_2(CN)_{10} \rightarrow 3M + (2/3)Fe_3C + (2x-2/3)C + xN_2 + (5-x)(CN)_2. \quad (4)$$

Eventually metal M carbides may also form. Cyanogen is detected in the evolved gas by reaction with $AgNO_3$. Carbide formation in general and cementite formation in particular is well documented in the literature.[16,18,33]

The prevalence of (3) or (4) may reflect the influence of M on the stability of the carbide. In the case of Fe(III) solids, X-ray diffraction and iron analysis of the residues indicates that cementite Fe_3C is the main reaction product. On the other hand, in Cu solids, the residue is made up essentially of pure copper and iron in the expected ratio, with little carbon in it; again, weight losses are compatible with X-ray diffraction and chemical analysis. In the case of other M(II) cations, intermediate situations are found, corresponding to the formation of both carbides and elemental metals. Weight loss data in all cases indicates substantial carbon contents in the residual solid.

In some cases (M = Co) the nature of the solid residue was characterized by SEM and EDAX, see Fig. 2. It is apparent that both metals are segregated in the process, and complex morphologies arise. Thus, the thermolysis of mixed metal cyanides, although potentially suited to produce high area intermetallics, in fact yield the individual metals in an intimate mixture. Segregation is possible because the absolute temperature of the process is as high as 0.5–0.6 times the melting point of the metals.

The following competing events may therefore be visualized: (a) cyanide oxidation by Fe(II) and M(II) (or Cu(I)) to yield Fe(0) + M(0) + cyanogen; (b) cyanide decomposition to yield cementite, M(0) and N_2. Depending on the nature of M, either (a) or (b) may be favoured. In general, only M = Fe favours strongly carbide formation. The initial solid product of pathway (a) should be an intermetallic FeM_m that then evolves to yield Fe + mM.

Acknowledgements—To A. M. Olmedo for the scanning electron micrographs; to Prof. E. Gros for the elemental analyses; to Prof. O. Troccoli for the use of the atomic absorption spectrophotometer. To CONICET and CIC for partial support. PJM, MAB and CODV are members of CONICET.

REFERENCES

1. M. A. Robin, *Inorg. Chem.* 1962, **1**, 337.
2. A. C. Sharpe, *The Chemistry of Cyano Complexes of the Transition Metals*. Academic Press, New York (1976).
3. P. Day, *Comments Inorg. Chem.* 1981, **1**, 55.
4. R. Glauser, U. Hanser, F. Herren, A. Ludi, E. Schmidt, H. Siegenthaler and F. Wenk, *J. Am. Chem. Soc.* 1973, **95**, 8457.
5. A. Ludi and H. U. Güdel, *Struct. Bonding* (Berlin) 1973, **14**, 1.
6. H. E. Toma and L. A. A. Oliveira, *Inorg. Chim. Acta* 1979, **33**, L143.
7. A. Ben Altabef, S. A. Brandan and N. E. Katz, *Polyhedron* 1985, **4**, 227.
8. D. F. Shriver, S. A. Shriver and S. E. Anderson, *Inorg. Chem.* 1965, **4**, 725.
9. D. F. Shriver and D. Basset Brown, *Inorg. Chem.* 1969, **8**, 42.
10. D. Basset Brown and D. F. Shriver, *Inorg. Chem.* 1969, **8**, 37.
11. G. S. B. Megni, S. A. Brandán, A. Ben Altabef and N. E. Katz, *Monatsch Chem.*, in press.
12. P. G. Rasmussen and E. A. Meyers, *Polyhedron* 1984, **3**, 183.
13. M. M. Chamberlain and A. F. Greene, Jr, *J. Inorg. Nucl. Chem.* 1963, **25**, 1471, and references therein.
14. G. B. Seifer, *Zh. Neorg. Khim.* 1960, **5**, 68.
15. G. B. Seifer, *Zh. Neorg. Khim.* 1962, **7**, 482.
16. J. I. Kunrath, C. S. Müller and E. Frank, *J. Therm. Anal.* 1978, **14**, 253.
17. E. Frank, J. I. Kunrath and C. S. Müller, *An. Quim.* 1981, **77**, 307.
18. L. A. Gentil, J. A. Olabe, E. J. Baran and P. J. Aymonino, *J. Therm. Anal.* 1975, **7**, 279.
19. P. J. Morando, Ph.D. Thesis, Universidad Nacional de La Plata, Argentina (1981).
20. P. J. Morando, V. I. E. Bruyère, M. A. Blesa and J. A. Olabe, *Trans. Met. Chem.* 1983, **8**, 99.
21. H. E. Toma and J. M. Malin, *Inorg. Chem.* 1973, **12**, 1039.
22. P. J. Morando and M. A. Blesa, *J. Chem. Soc. Dalton Trans.* 1982, 2147.
23. B. N. Figgis, *Introduction to Ligand Fields*, Chapter 9, p. 239. Interscience Publishers, New York (1967).
24. A. B. S. Lever, *Inorganic Electronic Spectroscopy*, 2nd edn. Elsevier, Amsterdam (1984).
25. M. G. Emschwiller, *Compt. Rend.* 1954, **238**, 1414.
26. A. Dows, A Haim and W. K. Wilmarth, *J. Inorg. Nucl. Chem.* 1961, **21**, 33.
27. E. Fluck, H. Inoue, M. Nagao and S. Yanagisawa, *J. Inorg. Nucl. Chem.* 1979, **41**, 287.
28. S. N. Ghosh, *J. Inorg. Nucl. Chem.* 1974, **36**, 2465.
29. M. Paris, H. Thomas and J. C. Merrin, *Mem. Soc. Chim. France* 1961, **5**, 707.
30. K. Nagano, H. Kinoshita and A. Hirakawa, *Chem. Pharm. Bull.* 1964, **12**, 1198.

31. P. J. Morando, V. I. E. Bruyère, M. A. Blesa and A. Esteban, *Therm. Act.* 1983, **62**, 249.
32. K. Nakamoto, *Infrared Spectra of Inorganic and Coordination Compounds*. J. Willys, New York (1963).
33. W. E. Brown, D. Dollimore and A. K. Galwey, *Comprehensive Chemical Kinetics*, Vol. 22, Chapter 4, p. 228 (Edited by Ch. Bamford and C. F. H. Tipper). Elsevier, Amsterdam (1982).

Polyhedron Vol. 6, No. 9, pp. 1765–1774, 1987
Printed in Great Britain

0277–5387/87 $3.00+.00

STERICALLY CONGESTED *TRIS* PHENOXIDE COMPLEXES OF TANTALUM(V). THE X-RAY CRYSTAL STRUCTURES OF [$TaCl_2$(2,6-DI-t-BUTYLPHENOXIDE)$_3$] AND [$Ta_2Cl(\mu\text{-}Cl)_2$(2,6-DI-ISOPROPYLPHENOXIDE)$_5(\mu\text{-}O)$]

GEORGE R. CLARK, ALASTAIR J. NIELSON* and CLIFTON E. F. RICKARD

Department of Chemistry, University of Auckland, Private Bag, Auckland, New Zealand

(*Received* 8 *December* 1986; *accepted* 25 *March* 1987)

Abstract—$TaCl_5$ reacts with two equivalents of lithium 2,6-di-t-butylphenoxide in benzene to give [$TaCl_3$(2,6-di-t-butylphenoxide)$_2$] (**1**) in 70% yield and with three equivalents of the lithium phenoxide in diethyl ether to give [$TaCl_2$(2,6-di-t-butylphenoxide)$_3$] (**2**) which can also be prepared by reaction of (**1**) with one equivalent of the lithium phenoxide. Three equivalents of lithium 2,6-di-isopropylphenoxide react with $TaCl_5$ to give [$TaCl_2$(diethyl-ether)(2,6-di-isopropylphenoxide)$_3$] (**4**) which, on attempted recrystallization in the presence of air, gave [$Ta_2Cl(\mu\text{-}Cl)_2$(2,6-di-isopropylphenoxide)$_5(\mu\text{-}O)$] (**5**). Complexes (**1**), (**2**), and (**4**) were characterized by elemental analysis, IR, and ^1H and ^{13}C NMR spectra. Coordination of the phenoxide ligand in (**2**) is accompanied by downfield shifts of the phenyl ring *ipso*, *ortho* and *para* carbon resonances of 9.6, 3.6 and 3.1 ppm respectively, compared with the free ligand. For complex (**4**) the relative shifts are 5.9, 6.1 and 2.9 ppm. The structures of (**2**) and (**5**) have been determined by single-crystal X-ray diffraction methods. Crystals of (**2**) are monoclinic, space group $P2_1/c$ with $a = 18.902(6)$ Å, $b = 10.815(8)$ Å, $c = 20.259(4)$ Å and $\beta = 92.62(2)°$; crystals of (**5**) are monoclinic, space group $P2_1/c$ with $a = 11.174(1)$ Å, $b = 20.402(4)$ Å, $c = 27.143(3)$ Å and $\beta = 94.58(1)°$. Both structures were solved by Patterson and Fourier methods and refined to R values of 0.063 for the 1690 observed data for (**2**) and 0.062 for the 3693 observed data for (**5**). Complex (**2**) is monomeric with a square pyramidal coordination geometry about Ta. Observed distances are: $Ta\text{–}O_{axial}$ 1.83(2) Å; $Ta\text{–}O_{basal}$ each 1.90(2) Å; $Ta\text{–}Cl_{basal}$ each 1.37(1) Å. Complex (**5**) is binuclear with a distorted octahedral geometry about each tantalum atom. The structure consists essentially of $TaCl_2$(2,6-di-isopropylphenoxide)$_3$ and $TaCl_2$(O)(2,6-di-isopropylphenoxide)$_2$ units bridged through the oxygen and Cl atoms. Observed distances are $Ta\text{–}O_{bridge}$ 1.69(1) and 2.10(1) Å; $Ta\text{–}Cl_{bridge}$ 2.498(7), 2.396(8), 2.634(7) and 2.781(7) Å; $Ta\text{–}Cl_{terminal}$ 2.309(8) Å. The $Ta\text{–}O_{phenoxide}$ distances range from 1.77(2) to 2.19(2) Å. In both (**2**) and (**5**) the phenyl rings are orientated such as to minimise interactions between the 2- and 6-substituents. In both molecules electron counts are maximized using π-electron density from the terminal ligands.

There are now many examples of early transition metal complexes which contain the phenoxide ligand (-OPh).[1,2] Recent interest has centred on complexes containing alkyl substituents at the 2,6 positions of the phenoxide phenyl ring, as unusual coordination geometries and coordinatively unsaturated molecules can result.[3–10] In general, the structures of complexes containing bulky ligands cannot be rationalised on steric grounds alone, as there is always a subtle interplay of both steric and electronic factors.[11,12] However, where a series of related complexes can be prepared in which the steric size of a particular ligand is able to be varied structural changes may be related more specifically to steric effects.

For tantalum(V), a variety of phenoxide complexes have been synthesised. The pentaphenoxide

* Author to whom correspondence should be addressed.

$[Ta(OPh)_5]$, and the mixed chloro-phenoxides $[TaCl_{5-x}(OPh)_x]$ have been prepared from $TaCl_5$ and phenol.[13,14] Reactions between a series of lithium 2,6-disubstituted phenoxides and $TaCl_5$ have given the *penta* phenoxide complex using lithium 2,6-dimethylphenoxide, the *tris* phenoxide complex using lithium 2-t-butyl-6-methylphenoxide and *bis*-phenoxide complexes using lithium 2,6-di-isopropylphenoxide and lithium 2,6-di-t-butylphenoxides.[15] Of the complexes prepared, only $[TaCl_3(2,6\text{-di-t-butylphenoxide})_2]$ has been characterised by X-ray crystallography.[15]

As part of our studies of the chemistry of group V transition metals we have prepared complexes containing three sterically demanding phenoxide ligands. We report here the preparation and characterisation of *tris* 2,6-di-isopropylphenoxide and *tris* 2,6-di-t-butylphenoxide complexes of tantalum(V) and the X-ray crystal structures of $[TaCl_2(2,6\text{-di-t-butylphenoxide})_3]$ and $[Ta_2Cl(\mu\text{-Cl})_2(2,6\text{-di-isopropylphenoxide})_5(\mu\text{-O})]$.

RESULTS AND DISCUSSION

2,6-*Di-t-butylphenoxide complexes*

It has previously been reported that tantalum pentachloride reacts with an excess of lithium 2,6-di-t-butylphenoxide in benzene to give the *bis* phenoxy complex $[TaCl_3(2,6\text{-di-t-butylphenoxide})_2]$ (**1**) in 30–40% yield.[15] We have found however that the complex can be obtained in an improved yield of up to 71% if two equivalents of the lithium phenoxide are employed.

The ^{13}C NMR spectrum of (**1**) shows that on coordination of the phenoxide the *ipso* carbon signal shifts downfield by 9.9 ppm compared with the free ligand, the *ortho* and *para* carbon resonances each shift by 5.5 ppm, while the *meta* carbon resonance shifts by 1.1 ppm.

Deshielding of these carbons indicates electron withdrawal from the aromatic ring.[16] The methyl carbons of the t-butyl group show a single resonance, shifted 2 ppm downfield from the free ligand, while the quaternary carbon resonance position is unchanged.

When tantalum pentachloride was reacted with slightly more than three equivalents of lithium 2,6-di-t-butylphenoxide in diethyl ether for up to 24 h, an orange coloured solution formed from which the *bis* phenoxy complex (**1**) could again be obtained. However, when the reaction was carried out for longer periods, the solution colour paled to yellow. After a total reaction period of 3 days, isolation of the product gave a gummy material containing the *tris* phenoxy complex $[TaCl_2(2,6\text{-di-t-butylphenoxide})_3]$ (**2**). This complex could also be obtained by reacting the *bis* phenoxy complex (**1**) with slightly more than one equivalent of the lithium phenoxide reagent.

The gummy *tris* phenoxide product obtained from these reactions failed to solidify and we have been unable to crystallise the product directly from hydrocarbon solvents in which it is very soluble. However it is only slightly soluble in acetonitrile, addition of which causes the complex to precipitate out analytically pure, in a yield of approximately 40%. Further complex can be obtained from the washings, bringing the total yield to *ca.* 50%. The success of this procedure results from the complex being suitably non-polar whereas the lithium phenoxide reagent, the phenol and the *bis* phenoxy complex (**1**) are all sufficiently polar to dissolve in acetonitrile.

Pure $[TaCl_2(2,6\text{-di-t-butylphenoxide})_3]$ (**2**) decomposes slowly in air but more rapidly in solution. It is soluble in hydrocarbon solvents and is best crystallised from benzene solution from which large yellow crystals are obtained. In the infrared spectrum the OH absorption of the free ligand is absent, and in the 1300–1000 cm^{-1} region where ν(C–O)Ta is characteristically observed[17] there are two strong absorptions at 1160 and 1088 cm^{-1}. In addition, the spectrum contains absorbances at 880, 875, 690, 463 and 320 cm^{-1} which are not present in the free ligand. The bands at 463 and 320 cm^{-1} are assigned to Ta–O and Ta–Cl vibrations respectively on the basis of tentative assignments made for similar bands in the *bis*-phenoxy complex (**1**).[15]

The ^1H NMR spectrum of (**2**) (Table 1) shows only one resonance for the methyl protons of the t-butyl group, no phenol OH proton resonance and an aromatic multiplet similar to that found for the free ligand. In the ^{13}C NMR spectrum only one set of resonances for the three phenoxide ligands is observed. The *ipso* carbon resonance is shifted downfield 9.6 ppm compared with the free ligand while the *ortho*, *para* and *meta* carbon resonances show downfield shifts of 3.6, 3.1 and 1.3 ppm respectively. The *ortho* and *para* carbon shifts are smaller than those observed for the *bis* phenoxide complex (**1**) which suggests slightly less electron withdrawal from the aromatic rings when three phenoxide ligands are present. This feature may be related to the overall π-bonding properties of the ligands (see later).

Crystal structure of $[TaCl_2(2,6\text{-di-t-butylphenoxide})_3]$ (**2**)

A crystal structure determination of $[TaCl_2(2,6\text{-di-t-butylphenoxide})_3]$ (**2**) was carried out to com-

Table 1. NMR spectra[a]

Complex	^{1}H NMR[b]		^{13}C NMR[b,c]				
	substituent	aromatics	substituent	*ipso*	*ortho*	*meta*	*para*
2,6-di-t-butylphenol	1.45(s,18H,6Me) 5.19(s,1H,OH)	6.64–7.0(m,1H,H_{para}) 7.05–7.35(m,2H,H_{meta})	30.3(Me_3) 34.3(C)	153.8	135.8	124.8	119.6
[$TaCl_3$(2,6-di-t-butylphenoxide)$_2$] (**1**)	1.34(s,36H,12Me)	6.66–7.0(m,2H,H_{para}) 7.00–7.35(m,4H,H_{meta})	32.9(Me_3) 35.8(C)	163.6 (+9.9)	141.3 (+5.5)	125.9 (+1.1)	125.1 (+5.5)
[$TaCl_2$(2,6-di-t-butylphenoxide)$_3$] (**2**)	1.36(s,54H,18Me)	6.63–7.0(m,3H,H_{para}) 7.02–7.40(m,6H,H_{meta})	33.1(Me_3) 36.3(C)	163.4 (+9.6)	139.4 (+3.6)	126.1 (+1.3)	122.7 (+3.1)
2,6-di-isopropylphenol	1.23(d,12H,4Me) 3.15(sep,2H,2CH) 4.90(b,1H,OH)	6.82–7.31(m,3H,$H_{meta,para}$)	22.7(Me_2) 27.0(CH)	149.8	133.6	123.3	120.5
[$TaCl_2$(diethylether)(2,6-di-isopropylphenoxide)$_3$] (**4**)[d]	1.10(d,36H,12H) 3.78(bsep,6H,6CH)	6.70–7.20(m,9H,$H_{meta,para}$)	25.4(Me_2) 25.9(CH)	155.7 (+5.9)	139.7 (+6.1)	123.4 (+0.1)	123.4 (+2.9)

[a] Spectra obtained in dry $CDCl_3$, values in ppm downfield from internal TMS.
[b] Assignments in parentheses, b = broad, d = doublet, m = multiplet, s = singlet, sep = septet.
[c] Figures in parentheses show downfield shift (+ve values) compared with free ligand.
[d] Diethyl ether resonances: ^{1}H NMR, 1.24 (triplet, 6H, 2Me), 3.45–4.20 (obscured quartet, 4H, $2CH_2$); ^{13}C NMR, 12.7 (CH_3), 66.6 (CH_2).

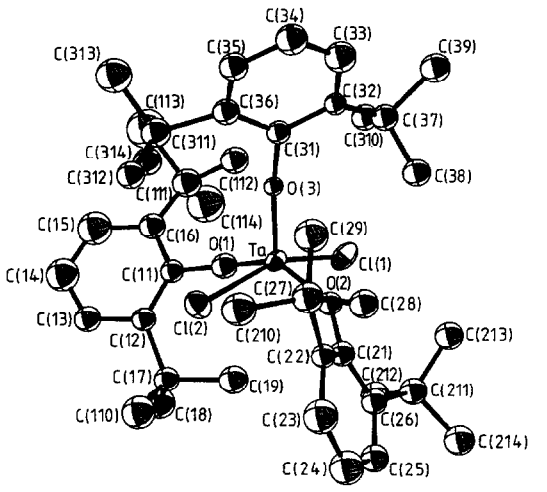

Fig. 1. Molecular geometry and atomic numbering for [$TaCl_2$(2,6-di-t-butylphenoxide)$_3$] (**2**).

pare its geometry with those of the *bis* phenoxy complexes [$TaCl_3$(2,6-di-t-butylphenoxide)$_2$] (**1**)[15] and [$Ta(Me)_3$(2,6-di-t-butylphenoxide)$_2$] (**3**).[18] The molecular structure of (**2**) is shown in Fig. 1 and bond lengths and angles are contained in Table 2. The molecule adopts a square pyramidal geometry about the tantalum atom with one 2,6-di-t-butylphenoxide ligand occupying the axial position and the other two occupying opposite sites of the square pyramid base. The two chloro ligands fill the remaining basal positions. The geometry is thus similar to that observed for the *bis* phenoxy complex (**1**) but it differs from the trigonal bipyramidal geometry of [$Ta(Me)_3$(2,6-di-t-butylphenoxide)$_2$] (**3**).[18]

The axial Ta–O bond length (1.83(2) Å) is considerably shorter than the two basal Ta–O bond lengths (each 1.90(2) Å), as was found in the *bis* phenoxy complex (**2**) (Table 3 compares data for complexes (**1**) and (**2**).) The axial Ta–O–C bond angle 162(2)° is larger than the two basal Ta–O–C bond angles (153(2)° and 148(2)°). All these angles are significantly smaller than those observed for the *bis* phenoxy complex (**1**). The two Ta–Cl bond lengths are slightly longer than the equivalent bond lengths in [$TaCl_3$(2,6-di-t-butylphenoxide)$_2$] (**1**) but lie within the range found for other tantalum(V) complexes.

Several features relating to π-bonding arise from the molecular dimensions observed. The Ta–O and Ta–Cl bond distances are all shorter than expected for single bonds and this is apparently a consequence of the low formal electron count for the molecule. If the chloro and phenoxide ligands are regarded formally as one-electron donors for purposes of the 18-electron rule then the molecule has an electron count of 10. Adoption of the square-pyramidal geometry increases the ability for ligand to metal π-bonding,[18] thus increasing the formal electron count. In general, -OR ligands are better π-donors than are chloro ligands.[19] In complex (**2**), where three phenoxides are capable of donating π-electron density to the metal, the Ta–Cl bonds are slightly longer than those in the *bis* phenoxy complex (**1**) (see Table 3). An 18-electron count can theoretically be attained if three phenoxides and just one of the chloro ligands act as 3-electron donors, with the remaining chloride acting as a 1-electron donor. However, the structure shows that all of the Ta–O and Ta–Cl bonds are relatively short, indicating that all are involved in π-bonding to the metal. The Ta–O(3) bond (1.83(2) Å) is sufficiently short to suggest that the axial phenoxide acts as a full 3-electron donor with the basal ligands sharing the remaining contribution

Table 2. Selected bond lengths and angles for [$TaCl_2$(2,6-di-t-butylphenoxide)$_3$] (**2**)

	(a) Bond lengths (Å)		
Ta—Cl(1)	2.37(1)	Ta—O(3)	1.83(2)
Ta—Cl(2)	2.37(1)	O(1)—C(11)	1.38(4)
Ta—O(1)	1.90(2)	O(2)—C(21)	1.42(4)
Ta—O(2)	1.90(2)	O(3)—C(31)	1.47(4)
	(b) Bond angles (°)		
Cl(1)—Ta—Cl(2)	156.4(4)	O(1)—Ta—O(2)	145.3(8)
Cl(1)—Ta—O(1)	84.9(7)	O(1)—Ta—O(3)	106.2(8)
Cl(1)—Ta—O(2)	89.7(6)	O(2)—Ta—O(3)	108.4(8)
Cl(1)—Ta—O(3)	102.9(6)	Ta—O(1)—C(11)	153(2)
Cl(2)—Ta—O(1)	86.0(7)	Ta—O(2)—C(21)	148(2)
Cl(2)—Ta—O(2)	85.6(6)	Ta—O(3)—C(31)	162(2)
Cl(2)—Ta—O(3)	100.5(7)		

Table 3. Comparison of selected structural data for $[TaCl_3(2,6\text{-di-t-butylphenoxide})_2]$ (**1**)[a] and $[TaCl_2(2,6\text{-di-t-butylphenoxide})_3]$ (**2**)[b]

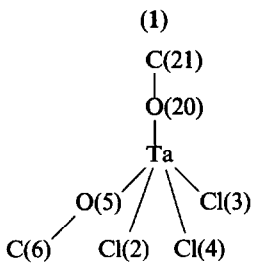

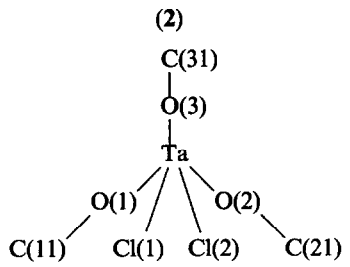

(a) Bond distances (Å)

Ta—Cl(2)	2.339(2)	Ta—Cl(1)	2.37(1)	
Ta—Cl(3)	2.358(2)	—		
Ta—Cl(4)	2.335(2)	Ta—Cl(2)	2.37(1)	
Ta—O(20)	1.836(4)	Ta—O(3)	1.83(2)	
Ta—O(5)	1.872(5)	Ta—O(1)	1.90(2)	
—		Ta—O(2)	1.90(2)	

(b) Bond angles (°)[c]

Cl(2)—Ta—Cl(4)	143.8(1)	Cl(1)—Ta—Cl(2)	156.4(4)	[+12.6]
Cl(3)—Ta—O(5)	155.8(1)	O(2)—Ta—O(1)	145.3(8)	[−10.5]
O(5)—Ta—O(20)	104.2(2)	O(1)—Ta—O(3)	106.2(8)	[+2.0]
Cl(3)—Ta—O(20)	100.0(1)	O(2)—Ta—O(3)	108.4(8)	[+8.4]
Cl(2)—Ta—O(20)	105.8(1)	Cl(1)—Ta—O(3)	102.9(6)	[−2.9]
Cl(4)—Ta—O(20)	110.1(1)	Cl(2)—Ta—O(3)	100.5(7)	[−9.6]
Cl(2)—Ta—O(5)	87.5(1)	Cl(1)—Ta—O(1)	84.9(7)	[−2.6]
Cl(2)—Ta—Cl(3)	84.0(1)	Cl(1)—Ta—O(2)	89.7(6)	[+5.7]
Cl(3)—Ta—Cl(4)	85.1(1)	Cl(2)—Ta—O(2)	85.6(6)	[+0.5]
Cl(4)—Ta—O(5)	88.6(1)	Cl(2)—Ta—O(1)	86.0(7)	[−2.6]

[a] Data taken from Reference 15.

[b] Data from present work.

[c] Values in square parentheses show change in bond angles (**2**) compared with those of (**1**). Positive values indicate angle opens, negative values angle closes relative to $[TaCl_3(2,6\text{-di-t-butylphenoxide})_2]$ (**1**).

to the π-bonding through a series of PhO⇄Ta and Cl⇄Ta canonicals. The basal Ta–O–C bond angles are smaller in complex (**2**) compared with (**1**) but the bond lengths are not sufficiently different to confirm less π-donation from the phenoxide oxygens in (**2**).

While the overall geometries of the *bis* and *tris* phenoxy complexes are similar, it is of interest to examine the effect of adding the third bulky phenoxide ligand. Bond angles for the two complexes are compared in Table 3. The O(1)–Ta–O(3) bond angle in (**2**) is similar to the equivalent bond angle in (**1**). In both molecules the t-butyl groups of the axial phenoxide are positioned over the basal chlorine ligands while the plane of the two phenyl rings is approximately perpendicular (for (**2**) the angle made by the two planes is 115(1)°). Addition of the third phenoxide ligand opens up the Cl–Ta–Cl bond angle by 12.6° and decreases the equivalent Cl(2)–Ta–O(3) bond angle by 9.6° while the O(2)–Ta–O(3) bond angle (equivalent to the Cl(3)–Ta–O(20) bond angle in (**1**)) opens up by 8.4° resulting in a decrease of the equivalent O(1)–Ta–O(2) bond angle by 10.5°. Changes in the other bond angles are comparatively small.

The phenyl rings in complex (**2**) are positioned to minimise steric interactions between t-butyl substituents. The aromatic ring of the third phenoxide lies somewhat below the basal plane at an angle of 57° to the plane made by the axial phenoxide phenyl ring. As observed in the *bis* phenoxy complex the t-butyl group attached to C(12) in (**2**) occupies the "open" site *trans* to the axial Ta–O bond. We have been unable to refine the positions of the hydrogens on the methyl groups but a non-bonded metal–proton interaction similar to that found in (**1**)[15]

is likely to be present. However the ^1H NMR spectrum indicates that in solution all protons are equivalent.

2,6-*Di-isopropylphenoxide complexes*

Tantalum pentachloride reacts with three equivalents of lithium 2,6-di-isopropylphenoxide in diethyl ether to give a yellow-orange coloured solution which pales considerably when the reaction period is extended to 20–36 h. The product isolated persisted as a yellow gum and we have so far been unable to obtain reliable analytical data. However, on the basis of the chlorine analysis and spectroscopic data, the product was characterised as $[TaCl_2(diethylether)(2,6\text{-}di\text{-}isopropylphenoxide)_3]$ (**4**). The complex is very soluble in hydrocarbons and in polar solvents such as MeCN or $MeNO_2$, but resisted crystallisation from these media.

The infrared spectrum does not contain OH absorptions and there are bands at 1262 and 1200 cm^{-1} characteristic of ν(C–O)M.[1] In the far infrared the Ta–Cl stretch occurs at 295 cm^{-1}. In the ^1H NMR spectrum the methyl protons of the isopropyl group appear as a slightly broadened doublet, the methine proton as a broadened septet shifted 0.6 ppm downfield compared with the free ligand and the spectrum does not contain an OH proton resonance. In addition, the spectrum contains a quartet and a triplet which integrate as one diethyl ether molecule for every three phenoxide ligands. In the ^{13}C NMR spectrum there is only one set of phenoxide resonances. The *ipso* carbon resonance shows a downfield shift of 5.9 ppm compared with the free ligand, while the *ortho*, *para* and *meta* carbon resonances show downfield shifts of 6.1, 2.9 and 0.1 ppm respectively. The methyl and methine carbons of the isopropyl groups show small downfield shifts of 1.7 and 1.1 ppm.

During attempts to crystallise $[TaCl_2(diethylether)(2,6\text{-}di\text{-}isopropylphenoxide)_3]$ (**4**) from petroleum ether, air was inadvertently admitted into the crystallisation flask. After several weeks a small quantity of yellow crystals was obtained, which are identified as $[Ta_2Cl(\mu\text{-}Cl)_2(2,6\text{-}di\text{-}isopropylphenoxide)_5(\mu\text{-}O)]$ (**5**) by X-ray crystallography.

Crystal structure of $[Ta_2Cl(\mu\text{-}Cl)_2(2,6\text{-}di\text{-}isopropylphenoxide)_5(\mu\text{-}O)]$ (**5**)

The crystal structure determination shows the complex to be binuclear (Figs 2 and 3) in which the two tantalum atoms are in distorted octahedral geometries and are bridged by oxo and two chloro ligands. The oxo ligand lies *trans* to a chloro ligand

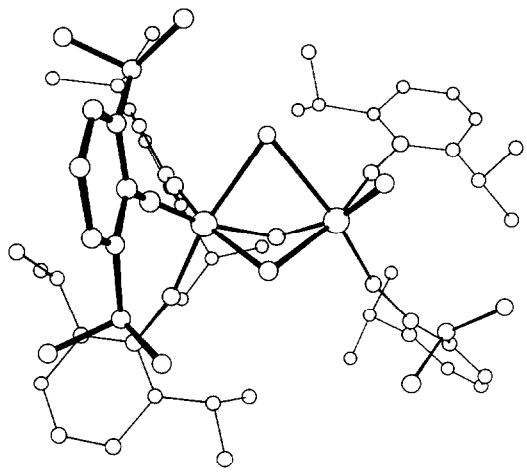

Fig. 2. Molecular geometry for $[Ta_2Cl(\mu\text{-}Cl)_2(2,6\text{-}di\text{-}isopropylphenoxide)_5(\mu\text{-}O)]$ (**5**).

on one tantalum atom and *trans* to a 2,6-di-isopropylphenoxide ligand on the other. Both bridging chlorides lie *trans* to phenoxide ligands. Bond distances and angles for the molecule are contained in Table 4.

The short Ta(1)–O(1) bond distance (1.69(1) Å) and long Ta(2)–O(1) bond distance (2.10(1) Å) indicate an asymmetric bridge in which oxygen forms a double bond to Ta(1) and a 2-electron sigma bond to Ta(2). The two Ta–Cl–Ta bridges are also asymmetric, the Ta–Cl bond lengths indicating that both Cl(1) and Cl(3) form essentially single bonds to Ta(1). The Ta(1)–Cl(3) bond length at 2.781(7) Å is extremely long and probably represents the limit of lone pair donation from chlorine to a tantalum(V) centre. By comparison, in $[TaCl_2(\mu\text{-}Cl)(NPh)(SMe_2)]_2$ the Ta–Cl bond length *trans* to the phenylimido ligand (which exerts a strong *trans*

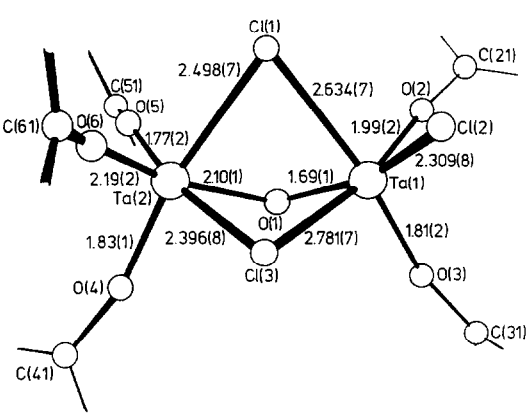

Fig. 3. Inner coordination geometry for $[Ta_2Cl(\mu\text{-}Cl)_2(2,6\text{-}di\text{-}isopropylphenoxide)_5(\mu\text{-}O)]$ (**5**).

Table 4. Selected bond lengths and angles for $[Ta_2Cl(\mu\text{-}Cl)_2(2,6\text{-di-isopropylphenoxide})_5(\mu\text{-}O)]$ (**5**)

	(a) Bond lengths (Å)		
Ta(1)—Cl(1)	2.634(7)	Ta(2)—Cl(1)	2.498(7)
Ta(1)—Cl(2)	2.309(8)	Ta(2)—Cl(3)	2.396(8)
Ta(1)—Cl(3)	2.781(7)	Ta(2)—O(1)	2.10(1)
Ta(1)—O(1)	1.69(1)	Ta(2)—O(4)	1.83(1)
Ta(1)—O(2)	1.99(2)	Ta(2)—O(5)	1.77(2)
Ta(1)—O(3)	1.81(2)	Ta(2)—O(6)	2.19(2)
O(2)—C(21)	1.50(3)	O(4)—C(41)	1.29(2)
O(3)—C(31)	1.41(2)	O(5)—C(51)	1.32(3)
		O(6)—C(61)	1.58(6)
	(b) Bond angles (°)		
Cl(1)—Ta(1)—O(1)	83.3(5)	Cl(1)—Ta(2)—O(1)	79.5(5)
Cl(1)—Ta(1)—Cl(3)	73.1(2)	Cl(1)—Ta(2)—Cl(3)	82.5(2)
Cl(1)—Ta(1)—Cl(2)	73.2(3)	Cl(1)—Ta(2)—O(5)	86.5(5)
Cl(1)—Ta(1)—O(2)	95.4(5)	Cl(1)—Ta(2)—O(6)	85.6(4)
Cl(1)—Ta(1)—O(3)	170.1(5)	Cl(1)—Ta(2)—O(4)	168.7(5)
Cl(2)—Ta(1)—Cl(3)	74.4(2)	Cl(3)—Ta(2)—O(6)	78.7(5)
Cl(2)—Ta(1)—O(1)	150.0(5)	O(1)—Ta(2)—O(6)	158.5(6)
Cl(2)—Ta(1)—O(2)	103.0(5)	O(5)—Ta(2)—O(6)	110.0(6)
Cl(2)—Ta(1)—O(3)	107.3(5)	O(4)—Ta(2)—O(5)	101.8(7)
Cl(3)—Ta(1)—O(1)	81.1(5)	Cl(3)—Ta(2)—O(1)	84.1(5)
Cl(3)—Ta(1)—O(2)	168.6(5)	Cl(3)—Ta(2)—O(5)	165.5(5)
Cl(3)—Ta(1)—O(3)	97.4(5)	Cl(3)—Ta(2)—O(4)	88.0(5)
O(1)—Ta(1)—O(2)	97.5(7)	O(1)—Ta(2)—O(5)	84.6(6)
O(1)—Ta(1)—O(3)	92.7(7)	O(1)—Ta(2)—O(4)	93.5(6)
O(2)—Ta(1)—O(3)	94.0(6)	O(4)—Ta(2)—O(6)	98.6(6)
Ta(1)—Cl(1)—Ta(2)	71.5(2)	Ta(1)—Cl(3)—Ta(2)	70.4(3)
Ta(1)—O(1)—Ta(2)	104.4(7)	Ta(2)—O(5)—C(51)	158.7(13)
Ta(1)—O(2)—C(21)	174.5(14)	Ta(2)—O(6)—C(61)	161.5(12)
Ta(1)—O(3)—C(31)	162.8(12)	Ta(2)—O(4)—C(41)	161.9(13)

influence) is shorter at 2.751(3) Å.[20] The two Ta–Cl–Ta bond angles in the phenoxide dimer are 70.4(2) and 71.5(2)° which are considerably smaller than those observed in $[TaCl_2(\mu\text{-}Cl)(NPh)(SMe_2)]_2$ (103.6°).[20] The Cl–Ta–O(1) bond angles are similar on both sides of the dimer, while the Cl(1)–Ta(1)–Cl(3) bond angle is 11° smaller than the Cl(1)–Ta(2)–Cl(3) bond angle.

For the 2,6-di-isopropylphenoxide ligands, the Ta-O bond lengths range from 1.77(2) to 2.19(2) Å, a wider range than that found in the *tris* 2,6-di-t-butylphenoxide complex (**2**) (1.83(2) to 1.90(2) Å). The ligands about each tantalum atom are considerably distorted from ideal octahedral geometry (see Table 4) as a result of the two halves of the molecule being chemically distinct. For example, the O(2)–Ta(1)–O(3) angle is 94.0(6)° whereas the three O–Ta(2)–O bond angles average 103.5°; Cl(1)–Ta–Cl(3) is 73.1(2)° whereas Cl(1)–Ta(2)–Cl(3) is 82.5(2)°.

The Ta–O–C bond angles range from 161(1)° to 174(2)° and on average are larger than the Ta–O–C bond angles observed for the *tris* 2,6-di-t-butylphenoxide ligands in complex (**2**). At Ta(1) the angles are such as to push the phenyl rings away from the bridge structure. At Ta(2) the Ta–O–C angles are such that the equatorial phenoxides bend away from each other while the axial phenoxide ligand bends into the space between them. In this way the isopropyl substituents at the 2,6-positions of the phenyl rings are able to minimise steric repulsions.

All the phenyl rings orientate on either side of the molecule so as to minimise interactions between the isopropyl groups (see Fig. 3). The isopropyl groups themselves are rotated so that all the methyl groups project away from the metal centres. A corollary is the methine hydrogens in each case project towards the metal centres. However none of these hydrogens make particularly close approaches to Ta, Cl or O atoms.

The structural features thus show that the molecule is able to maintain a +5 oxidation state for

each tantalum atom as it consists essentially of $TaCl(phenoxide)_2(O)$ and $TaCl_2(phenoxide)_3$ fragments which form a binuclear structure using lone pairs from the oxo and chloro ligands. As such, the Ta(1) fragment is formally a 14-electron species and the Ta(2) fragment is a 12-electron species, but the ligands about each metal centre contribute additional electron density through π-bonds. The Ta(1)–Cl(2) bond length of 2.310(7) Å is significantly shorter than the two Ta(2)–Cl bonds in which the chloro ligands can only act as one-electron donors to Ta(2). Thus Ta(1) uses π-electron density from Cl(2) (as well as that from the two phenoxide ligands) to increase its electron count. It is interesting to note that the terminal chlorine can π-bond to the metal when lying *trans* to the 2-electron donor bridging oxo group. In high-valent monomeric complexes containing the terminal oxo ligand or the isoelectronic organoimido ligand, both of which act as 4-electron donors to the central atom, only lone pair donation from a ligand in the *trans* position has been observed.[20–23] However, in lower-valent complexes, chlorides are found *trans* to such ligands but in these cases the M–Cl bonds are considerably lengthened.[24,25]

A formal electron count for Ta(2) gives 12 electrons but this also is increased by π-electron density from the phenoxide ligands. The Ta(2)–O(6) bond distance (2.19(2) Å) is however significantly longer than the Ta(2)–O(4) and Ta(2)–O(5) distances (1.83(1) and 1.77(2) Å) so that the π-electron contribution comes mainly from O(4) and O(5).

The effect of phenoxide π-bonding on the *trans* ligand is also apparent in the molecule. About each tantalum centre the phenoxides are placed *trans* to ligands co-ordinating by σ-electron density only. The phenoxides orientate *cis* to one another which allows the metal atoms maximum use of oxygen π-electron density. *trans*-Orientated phenoxides would result in a competitive π-bonding situation leading to less effective use of the electron density available. This feature is similarly found in dialkylamido complex of tantalum(V). Crystal structure determinations of $[Ta(NMe_2)_3Cl_3(NHMe_2)]$, $[\{Ta(NMe_2)Cl_2(NHMe_2)\}O]$ and $[Ta(NMe_2)_3Cl_2]_2$ show the dimethylamido ligands are orientated *cis*.[26]

CONCLUSION

The studies show that when three of the chloro ligands in $TaCl_5$ are replaced by 2,6-di-alkylphenoxide ligands, octahedral geometry is possible when the alkyl substituents are isopropyl groups. However, when three or even two of the chloro ligands are replaced by 2,6-di-t-butylphenoxide ligands the steric size of the t-butyl substituents is sufficient to force a square-pyramidal geometry on the molecule. The results thus suggest that electronic effects are less important, the change in geometry apparently arising from steric factors alone.

EXPERIMENTAL

Lithium phenoxides were prepared by adding one equivalent of *n*-butyllithium to the phenol in petroleum ether and stirring for 2 h. Tantalum pentachloride was sublimed prior to use. Acetonitrile was dried over and distilled from calcium hydride. Petroleum ether (bpt range 40–60°), benzene and diethyl ether were distilled over sodium. All distillations were carried out under N_2 treated to remove oxygen and water, as were manipulations, using bench-top air sensitive techniques.[27] Infrared spectra were recorded on a Perkin–Elmer 597 spectrometer, ^1H NMR on a Varian T60 Model spectrometer and ^{13}C NMR spectra on a Jeol FX60 spectrometer. Analytical data were obtained by Prof. A. D. Campbell and Associates, University of Otago, New Zealand. Melting points were determined in sealed tubes under N_2 on an Electrothermal melting point apparatus and are uncorrected.

Trichlorobis(2,6 - *di* - *t* - *butylphenoxo*)*tantalum*(*V*) (1)

Lithium 2,6-di-t-butylphenoxide (3.2 g, 15.1 mmol) in benzene (50 cm^3) was added to a suspension of tantalum pentachloride (2.6 g, 7.3 mmol) in benzene (80 cm^3) and the mixture was stirred for 20 h. The orange solution was separated from the precipitate by centrifuging and the solvent removed to give an orange-red gum which was washed several times with petroleum ether. On drying *in vacuo* the complex was obtained as an orange powder. Yield: 3.6 g (71%). (Found: C, 48.6; H, 5.7%. $C_{28}H_{42}Cl_3O_2Ta$ requires C, 48.2; H, 6.1%.)

IR(Nujol) bands at 1570w, 1370s, 1358s, 1252s, 1192s, 1175s, 1150s, 1104s, 1080s, 1020w, 915s, 895s, 864m, 819m, 790s, 780m, 732s, 688m, 670w, 630w, 568w, 538w, 519w, 460w, 440w, 354s, 345s and 300m cm^{-1}.

Dichlorotris(2,6 - *di* - *t* - *butylphenoxo*)*tantalum*(*V*) (2)

(a) A suspension of lithium 2,6-di-t-butylphenoxide (4.2 g, 19.8 mmol) in diethyl ether (100 cm^3) was added slowly to a suspension of tantalum pentachloride (2 g, 5.6 mmol) in diethyl ether (200

cm^3) and the reaction mixture was stirred for 3 days. The yellow solution was filtered and the solvent removed giving a yellow crystalline solid which was contaminated with an orange gummy substance. The product was extracted several times with petroleum ether (200 cm^3 in all) until the residue was no longer coloured yellow, the extracts were combined and the solvent removed. The resulting yellow orange gum was washed with acetonitrile (3 cm^3) leaving the complex as a yellow solid which was dissolved in petroleum ether (150 cm^3). The complex was obtained as yellow micro-crystals on reducing the solution volume and standing at −20°C. Yield: 2.3 g (48%). [M.p. 120–122°C] (Found: C, 57.8; H, 7.3; Cl, 7.8%. $C_{42}H_{63}Cl_2O_3Ta$ requires C, 58.1; H, 7.3; Cl, 8.2%.)

IR(Nujol) bands at 1570w, 1465m, 1420m, 1380s, 1358s, 1310w, 1258m, 1225m, 1194m, 1160s, 1088s, 1020w, 880s, 875s, 820m, 804w, 785m, 740s, 720w, 690m, 635w, 565w, 522w, 464w, 442w, 418w, 378w, and 320m cm^{-1}.

(b) A suspension of lithium 2,6-di-t-butylphenoxide (1 g, 1.43 mmol) in diethyl ether (50 cm^3) was added to trichloro*bis*(2,6-di-t-butylphenoxy) tantalum(V) (0.35 g, 1.64 mmol) in diethyl ether (100 cm^3) and the mixture was stirred for 2 days. The yellow solution was filtered, the solvent removed, and the residue extracted with petroleum ether (120 cm^3). The solution was filtered, the solvent removed, and the residue washed with acetonitrile (5 cm^3) leaving the complex as a yellow solid. Yield: 0.54 g (43%). The complex had identical m.p., IR, ^{13}C NMR spectra to the sample prepared under (a). Recrystallisation from benzene gave the complex as large yellow crystals.

Dichlorodiethylethertris(2,6 - *di* - *isopropylphenoxo*) *tantalum*(*V*) (**4**)

Lithium 2,6-di-isopropylphenoxide (4.0 g, 21.6 mmol) in diethyl ether (100 cm^3) was added to tantalum pentachloride (2.5 g, 7.0 mmol) suspended in diethyl ether (150 cm^3) and the mixture was stirred for 36 h. The solution was filtered and the solvent removed to give a gum which failed to solidify. The product was dissolved in petroleum ether, the solution filtered, and the solvent removed to give the complex as a gummy material which failed to completely solidify even when held under vacuum for extended periods. Yield: 5.2 g (87%). (Found: Cl, 8.0%. $C_{40}H_{61}Cl_2O_4Ta$ requires: Cl, 8.3%.) The complex was further characterised by spectral properties.

IR (Nujol) bands at 1600w, 1490s, 1335s, 1262s, 1200s, 1152m, 1110m, 1065w, 1050m, 1020w, 930s, 902m, 985w, 830m, 800s, 755s, 720s, 660w, 610w, 550w, 510w, 440w, 320m and 295m cm^{-1}.

Chloro(*μ* - *dichloro*)*penta*(2,6 - *di* - *isopropylphenoxo*) (*μ* - *oxo*)*ditantalum*(*V*) (**6**)

Air was admitted to a solution of dichlorodiethylethertris(2,6 - di - isopropylphenoxy)tantalum(V) in petroleum ether. The flask was stoppered and allowed to stand at −20°C whereupon a small quantity of yellow crystals was formed. The complex was filtered, washed with petroleum ether, chilled to ice temperature and dried *in vacuo*. Characterisation was made by X-ray crystallography.

Crystallographic studies

Single crystals of $[TaCl_2(2,6\text{-di-t-butylphenoxide})_3]$ (**2**) and $[Ta_2Cl(\mu\text{-}Cl)_2)(2,6\text{-di-isopropylphenoxide})_5(\mu\text{-}O)]$ (**5**) were grown from benzene and toluene solutions respectively and sealed under nitrogen in glass capillaries. They were mounted on an Enraf-Nonius CAD-4 diffractometer.

Crystal data: *Complex* (**2**). $C_{42}H_{63}Cl_2O_3Ta$, $M = 866.8$, monoclinic, $a = 18.902(6)$ Å, $b = 10.815(8)$ Å, $c = 20.259(4)$ Å, $\beta = 92.62(2)°$, $U = 4137.1$; space group $P2_1/c$, $Z = 4$, $D_c = 1.392$ g cm^{-1}, $F(000) = 1784$, $\mu(\text{Mo-}K_\alpha) = 29.6$ cm^{-1}.

Crystal data: *Complex* (**5**). $C_{60}H_{85}Cl_5O_6Ta_2$, $M = 1440.2$, monoclinic, $a = 11.174(1)$ Å, $b = 20.402(3)$ Å, $c = 27.143(3)$ Å, $\beta = 94.57(1)°$, $U = 6168.2$; space group $P2_1/c$, $Z = 4$, $D_c = 1.551$ g cm^{-1}, $F(000) = 2896$, $\mu(\text{Mo-}K_\alpha) = 40.0$ cm^{-1}.

Data collection. Accurate unit cell parameters were determined by least-squares fits to the setting angles of 25 reflections measured using Mo-K_α ($\lambda = 0.71069$ Å) radiation. Data collection was by $2\theta/\omega$ scans with a background/peak count-time ratio of 1/2. For complex (**2**) reflections were counted for 60 s or until $\sigma(I)/I$ was 0.02, a total of 6258 reflections being measured to θ_{max} of 22°. The intensity of three reflections monitored throughout the collection showed an isotropic decline with time. For complex (**5**) decomposition in the X-ray beam was more severe and the maximum count time was reduced to 40 s. Even so, it was necessary to use four crystals to measure 2567 reflections to θ_{max} of 19°.

The data were corrected for Lorentz, polarisation, crystal decay and absorption.[28] Each crystal for (**5**) was treated separately and the data placed on a common scale by comparison of common reflections. Subsequently separate scale factors were refined for each crystal.

Structural solutions and refinements. Both structures were solved by Patterson and Fourier methods and refined by the full-matrix least-squares technique. Computing was carried out using the SDP suite of programs on a PDP-11 computer and SHELX-76 in an IBM 4341 computer. The function minimised was $\Sigma w(|F_o|-|F_c|)^2$. Atomic scattering factors and dispersion corrections were for neutral atoms. After initial isotropic refinement, anisotropic thermal parameters were refined for the heavier atoms. Final residuals R and R_w were 0.063 and 0.061 for the 1690 observed data of complex (**2**) and 0.062 and 0.068 for the 3693 observed data of complex (**5**).

Final atomic coordinates for both complexes, tables of thermal parameters, and listings of observed and calculated structure factors have been deposited with the Editor as supplementary material.*

REFERENCES

1. D. C. Bradley, R. C. Mehrotra and D. P. Gaur, *Metal Alkoxides*. Academic Press, London (1978).
2. K. C. Malhotra and R. L. Martin, *J. Organomet. Chem.* 1982, **239**, 159.
3. L. Chamberlain, J. Keddington and I. P. Rothwell, *Organometallics* 1982, **1**, 1098.
4. R. A. Jones, J. G. Hefner and T. C. Wright, *Polyhedron* 1984, **3**, 1121.
5. L. R. Chamberlain and I. P. Rothwell, *J. Am. Chem. Soc.* 1983, **105**, 1665.
6. S. L. Latesky, J. Keddington, A. K. McMullen, I. P. Rothwell and J. C. Huffman, *Inorg. Chem.* 1985, **24**, 995.
7. A. Shah, A. Singh and R. C. Mehrotra, *Polyhedron* 1986, **5**, 1285.
8. A. W. Duff, R. A. Kamarudin, M. F. Lappert and R. J. Norton, *J. Chem. Soc., Dalton Trans.* 1986, 489 and refs therein.
9. M. R. Churchill, J. W. Ziller, J. H. Freudenberger and R. R. Schrock, *Organometallics* 1984, **3**, 1554; K. C. Wallace, J. C. Dewan and R. R. Schrock, *Organometallics* 1986, **5**, 2162.
10. L. R. Chamberlain, I. P. Rothwell and J. C. Huffman, *J. Am. Chem. Soc.* 1986, **108**, 1502.
11. M. H. Chisholm, L-S. Tan and J. C. Huffman, *J. Am. Chem. Soc.* 1982, **104**, 4879.
12. C. Heath and M. B. Hursthouse, *J. Chem. Soc., Chem. Commun.* 1971, 143.
13. V. H. Funk and W. Z. Baumann, *Anorg. Allg. Chem.* 1937, **231**, 264.
14. K. C. Malhotra, U. K. Bannerjee and S. C. Chaudhry, *J. Indian Chem. Soc.* 1980, **57**, 868.
15. L. R. Chamberlain, I. P. Rothwell and J. C. Huffman, *Inorg. Chem.* 1984, **23**, 2575.
16. G. C. Levy, R. L. Lichter and G. L. Nelson, *Carbon-13 Nuclear Magnetic Resonance Spectroscopy*, 2nd edn, p. 102. Wiley, New York (1980).
17. C. G. Barraclough, D. C. Bradley, J. Lewis and I. M. Thomas, *J. Chem. Soc.* 1961, 2601; C. T. Lynch, K. S. Mazdiyasni, J. S. Smith and W. J. Crawford, *Anal. Chem.* 1964, **36**, 2332.
18. L. Chamberlain, J. Keddington, J. C. Huffman and I. P. Rothwell, *Organometallics* 1982, **1**, 1538.
19. M. H. Chisholm, *Polyhedron* 1983, **2**, 681.
20. J. M. Canich, F. A. Cotton, S. A. Duraj and W. J. Roth, *Polyhedron* 1986, **5**, 895.
21. J. C. Taylor and A. B. Waugh, *J. Chem. Soc., Dalton Trans.* 1980, 2006.
22. H. Hess and H. Hartung, *Z. Anorg. Chem.* 1966, **344**, 157.
23. M. B. Drew and I. B. Tomkins, *J. Chem. Soc. A* 1969, 2412.
24. D. C. Bradley, M. B. Hursthouse, K. M. A. Malik, A. J. Neilson and R. L. Short, *J. Chem. Soc., Dalton Trans.* 1983, 2651.
25. A. J. Nielson and J. M. Waters, *Aust. J. Chem.* 1983, **36**, 243.
26. M. H. Chisholm, J. C. Huffman and L. S. Tan, *Inorg. Chem.* 1981, **20**, 1859.
27. A. J. Nielson, *Chem. in New Zealand* 1985, **49**, 11.
28. A. C. T. North, D. C. Phillips and F. S. Mathews, *Acta Cryst.* 1968, **A24**, 351.

* Atom coordinates for these structures have also been deposited with the Cambridge Crystallographic Data Centre for inclusion in their Data Base. Copies are available on request from the Editor at Queen Mary College.

Polyhedron Vol. 6, No. 9, pp. 1775–1779, 1987
Printed in Great Britain

0277–5387/87 $3.00+.00

TRIS-PENTASULFIDORHODATES(III). X-RAY STRUCTURE OF $(NH_4)_3[Rh(S_5)_3](H_2O)_2$

PETER CARTWRIGHT and R. D. GILLARD*

Department of Chemistry, University College, P.O. Box 78, Cardiff CF1 1XL, Wales, U.K.

REIJO SILLANPAA

Department of Chemistry, University of Turku

and

JUSSI VALKONEN

Department of Chemistry, University of Jyvaskyla, 40100 Jyvaskyla, Finland

(*Received* 5 *January* 1987; *accepted* 25 *March* 1987)

Abstract—The crystal structure of the racemic dihydrated ammonium salt of the *tris*-pentasulfidorhodate(III) anion is compared with those of salts of the *tris*-pentasulfidoplatinate(IV) ion.

Notwithstanding growing interest in transition metal polysulfides,[1] the homoleptic polysulfides of rhodium have hardly been examined, despite an early report[2] by Hofmann of the iridium system $(NH_4)_3[IrS_{15}]$. Two reports by Krause remain the only studies of such homoleptic systems,[3,4] although Malatesta and Turner characterized[5] the mixed complex of rhodium(III) formed from "dimethylglyoxime" H_2DMG and yellow ammonium sulfide as $H[Rh(HDMG)_2S_6]_n$. We have repeated Krause's preparation of $(Nh_4)_3RhS_{15}$ and obtain only the dihydrate $(NH_4)_3RhS_{15}\cdot 2H_2O$. We have also been able to prepare unsolvated $[N(C_2H_5)_3H]_3RhS_{15}$ by using CH_3CN–THF solutions. We report here these preparations, and the crystal structure of $(NH_4)_3Rh(S_5)_3\cdot 2H_2O$.

EXPERIMENTAL

Ammonium *tris*-pentasulfidorhodate(III) dihydrate, $(NH_4)_3Rh(S_5)_3\cdot 2H_2O$, was prepared by bubbling H_2S through 50 cm^3 of concentrated ("880") ammonia solution, which contained sulfur (20 g) until all dissolved. $Na_3RhCl_6\cdot 12H_2O$ (2.35 g) in water (10 cm^3) was added, causing a darkening of the solution. The system was well stirred and then filtered through celite. The dark brown red prismatic crystals formed from the filtrate during a few days at room temperature. Yield (1.5 g) was about 57%. Found: H, 2.2; N, 5.9; H_2O, 5.5. Calc. for $(NH_4)_3RhS_{15}\cdot 2H_2O$: H, 2.4; N, 6.2; H_2O, 5.3%. (Thermogravimetric analysis gave 15.0% residue at 1000°C, calculated for metal 15.3%.) However, sulfur analyses for this compound gave consistently low values *ca.* 64% versus the calculated value 71%. The analyses were done by oxidizing S to SO_4^{2-} by OH^-/H_2O_2, a method which had given good results[6] in ammonium and other salts of $[PtS_x]^{2-}$ anions.

The crystals of this compound are very soluble in water, DMF and DMSO, but sparingly soluble in methanol, ethanol, acetonitrile, THF and NH_3 solution, and insoluble in hydrocarbons. The compound was unstable in water and DMF. After dissolving it in water, a yellow precipitate rapidly appeared. In fresh DMF solution, the salt had λ_{max} at 320 nm ($\varepsilon = 14670$ 1 mol^{-1} cm^{-1}, this molar extinction coefficient calculated from the mass of $(NH_4)_3[RhS_{15}]2H_2O$ used) and 24 h later λ_{max} was still at 320 nm, but the apparent value of ε was 9660 1 mol^{-1} cm^{-1}.

* Author to whom correspondence should be addressed.

As the above properties might suggest some kind of polymer structure for $(NH_4)_3RhS_{15}\cdot 2H_2O$, a single crystal X-ray study was undertaken, as a precursor to our work on optical resolution.

Preparation of tri-ethylammonium tris(pentasulfido)rhodate(III), $[NEt_3H]_3RhS_{15}$

The preparation of the above salt was undertaken making two important solvent changes. The polysulfide (S_5^{2-}) solution was prepared by weighing 2.55 g sulfur into a 3 necked flask, adding 6 cm^3 NEt_3, 35 ml dry MeCN, 35 cm^3 dry THF (dried by reflux over Na benzophenone). H_2S was bubbled slowly through until all sulfur dissolved. (Prior degassing of solutions was performed.)

The Rh(III) complex used was prepared by stirring 660 mg $RhCl_3\cdot 3H_2O$ in 50 cm^3 ethanol for 45 min, filtering off any undissolved material and evaporating the filtrate to dryness, taking up the residue in the minimum amount of ethanol (20 cm^3). Three 5 cm^3 portions were taken and (1) 6.7 cm^3, (2) 11.2 cm^3, (3) 22.4 cm^3 S_5^{2-} solution (i.e. a 3-fold, 5-fold, 10-fold excess respectively of polysulfide solution) was added.

From (1) a very dark crystalline material formed after 15 min which was filtered off and washed with ether. After 2 h (2) had some small red needle-like crystals, and the flask was left in the refrigerator overnight. Unfortunately, the red crystals had become a dark crystalline material after 18 hours, (400 mg) which was filtered off and washed with toluene and ether. Flask (3) after 3 days yielded 100 mg of very nice acicular red crystals which were collected by filtration and washed with toluene and then ether.

Another similar S_5^{2-} solution and Rh(III) solution in 18 cm^3 ethanol were prepared. To two batches of 9 cm^3 of the Rh(III) solution were added (1) 22.6 cm^3 S_5^{2-} (5-fold excess), (2) 45.2 cm^3 S_5^{2-} (10-fold excess). After 90 min 470 mg of red microcrystals were filtered from (1), washed with toluene and ether. After 48 h nice acicular red crystals (150 mg) were collected from flask (2), and washed first with toluene, then with ether.

The materials are very soluble in DMF, DMSO, quite soluble in MeCN, CH_3NO_2, slightly soluble in MeOH, $CHCl_3$, H_2O and insoluble in EtOH, acetone, THF. The red crystals seem to be light sensitive decomposing to a blackish substance over a few weeks in "lab. light".

The TG of the products are similar, as are the infrared spectra and indicate no solvent of crystallization.

Crystal data

Dark brown red prismatic crystals of $(NH_4)_3Rh(S_5)_3\cdot 2H_2O$ ($M_r = 673.95$) are monoclinic, space group $C_{2/c}$, $a = 2597.8(6)$, $b = 1182.7(3)$, $c = 1591.6(2)$ pm, $\beta = 109.69(2)$; $Z = 8$, $D_c = 1.94$ g cm^{-3}. Single crystal, X-ray diffraction data were collected on an Enraf-Nonius CAD4 diffractometer using Mo–K_α radiation. The data were corrected for Lorentz and polarization effects. The structure was solved by direct methods and refined by least-squares techniques to an R value of 0.047 ($R_w = 0.056$) for 1228 independent reflections having $I > 3\sigma(I)$.* Hydrogen atoms were not included in refinements and two oxygen atoms were refined with lower population parameters giving the calculated number of water molecules as 1.25 though thermogravimetric analyses of bulk samples had clearly indicated that the salt is a dihydrate.

DISCUSSION

The structure is made of water molecules, ammonium and *tris*-pentasulfidorhodate(III) $[Rh(S_5)_3]^{3-}$ ions. The crystal is held together by ionic interaction and by hydrogen bonds from N–H and O–H hydrogens to S and O atoms. Water molecules are in the large holes between the ions. This water of crystallization is easily lost from the crystals.

The anion is illustrated in Fig. 1. Each rhodium atom is surrounded by six sulfur atoms and these form a distorted octahedron around rhodium. Rh–S bond distances are from 234.7(4) to 240.5(5) pm, the mean being 237.4. In rhodium(III)-thiolate and -thioether structures Rh–S bond lengths are[7,8] in the range from 231.4 to 236.9 pm. The present S–S bond distances are from 202.1(9) to 207.9(8) pm. All RhS_5 rings have a chair conformation.

There is a three-fold axis through the rhodium ion, relating the three chelate rings, so that the complex ion has the symmetry C_3. There is, of course, another possible conformer, with C_1 symmetry. Both conformers were indeed detected, in the case of $[Pt(S_5)_3]^{2-}$, by the temperature variation[9] of the ^{195}Pt magnetic resonance spectrum. The C_1-isomer, judging on a statistical basis alone, would be the more probable. Nevertheless, in the present

*Final atomic coordinates, tables of thermal parameters and observed and calculated structure factors have been deposited with the Editor as supplementary data; atomic coordinates have also been deposited with the Cambridge Crystallographic Data Centre.

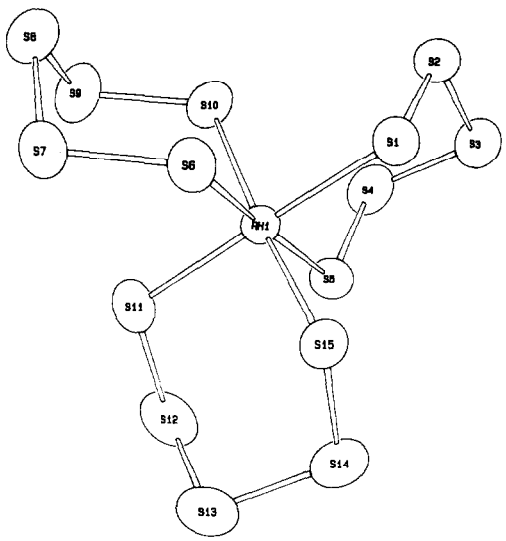

Fig. 1. Ortep drawing of $Rh(S_5)_3^{3-}$ anion showing the labelling scheme.

case for the $[Rh(S_5)_3]^{3-}$ ion and in the 3 known structures[10-12] of solid salts of the $[Pt(S_5)_3]^{2-}$ anion, the more symmetrical C_3 conformer is found. It may well be that efficient packing is easier to achieve with the more compact C_3-isomer.

There is, by virtue of the relative sizes of the sulfide atoms and of the rhodium(III) ion, one unusual feature in the *tris*-chelated anions, which is that the angles within the chelate rings (we use the general symbol α) are all greater than 90°. As shown in Table 3, the angles S_1RhS_5, S_6RhS_{10} and $S_{11}RhS_{15}$ are 92.7(2), 92.4(2) and 93.1(2) respectively. For the recently discovered[12] and analyzed dimorph of the platinum(IV) analogue, $(NH_4)_2[Pt(S_5)_3]2H_2O$, also crystallizing in the $C_{2/c}$ space group, the three intra-chelate ring angles α are S_1PtS_5, S_6PtS_{10}, $S_{11}PtS_{15}$ 90.9(2), 92.6(2), and 92.8(2) respectively.

Most of the examples of homoleptic compounds whose structures are known in detail have angles α within their chelate rings less than 90°. Currently, the nature of the electronic transition giving rise to the observed Cotton effects for *tris*-chelated octahedral ions is uncertain. Several theories[13] utilize the "trigonal splitting parameters" (or an equivalent quantity) which describes the effect on octahedral (O_h) levels (for example, $^1T_{1g}$ of spin-paired cobalt(III) in $[Co(NH_3)_6]^{3+}$) of imposing a trigonal field, as in $[Co(en)_3]^{3+}$, where en = 1,2-diaminoethane. Where the intra-chelate angles α at the metal ion are $< 90°$, the trigonal splitting for example, between A and E components of $^1T_{1g}$ in Co(III) is of one sign, and where these angles α are $> 90°$, it is of the opposite sign. That is, the circular dichroism of 2 *tris*-chelated molecules of the same absolute stereochemistry—say D or $S(C_3)$—will appear enantiomeric if the intra-chelate angle α is $< 90°$ in one case and $> 90°$ in the other.

The test cannot yet be made for the present molecule $[Rh(S_5)_3]^{3-}$ (with $\alpha > 90°$) as against say $(-)[Rh(en)_3]^{3+}$ or $[Rh(C_2O_4)_3]^{3-}$ (with $\alpha < 90°$) because we have not yet succeeded in resolving the racemic-*tris*-pentasulfidorhodate(III) into its enantiomers (although attempts continue). For the platinum(IV) analogue, where we do have the enantiomers,[6] the lowest energy absorptions are not *d–d* in character.

As a final point, whereas most racemic solid *tris*-chelated species crystallize in space groups such that neighbouring three-bladed propellers are of opposite hands (stacking —DLDLDL—), the present case $(NH_4)_3[Rh(S_5)_3]2H_2O$, with its $C_{2/c}$ space

Table 1. Microanalysis of samples of $[(C_2H_5)_3NH]_3[Rh(S_5)_3]$

	Calculated				Found			
	C	H	N	% TG[a] residue	C	H	N	% TG[a] residue
Prep (1) 3 × excess				14.3% to Rh_2O_3	24.7	5.7	3.5	13.5
5 × excess	24.3	5.4	4.7	11.6% to	24.0	4.9	3.6	13.8
10 × excess				*metal*	22.1	4.1	3.8	14.5
Prep (2) 5 × excess				14.3% to				
	24.3	5.4	4.7	Rh_2O_3	24.9	5.8	3.4	15.0
10 × excess				11.6% to *metal*	23.5	5.7	3.7	

[a] Thermogravimetric analyses were carried out in a dynamic nitrogen atmosphere, heating rate 20°C min^{-1}, up to 900°C.

Table 2. Bond distances (Å) for $(NH_4)_3Rh(S_5)_3 \cdot 2H_2O$

Atom 1	Atom 2	Distance	Atom 1	Atom 2	Distance	Atom 1	Atom 2	Distance
Rh1	S1	2.405(5)	S12	S13	2.037(11)	N1	S1	3.39(2)
Rh1	S5	2.361(6)	S13	S14	2.079(8)	N1	S5	3.34(2)
Rh1	S6	2.385(6)	S14	S15	2.021(9)	N1	S6	3.401(15)
Rh1	S10	2.373(6)	Rh1	S2	3.724(6)	N1	S15	3.46(2)
Rh1	S11	2.347(4)	Rh1	S4	3.640(7)	N2	S4	3.50(2)
Rh1	S15	2.375(6)	Rh1	S7	3.689(7)	N2	S5	3.47(2)
S1	S2	2.038(9)	Rh1	S9	3.637(6)	N2	S10	3.38(2)
S2	S3	2.067(10)	Rh1	S12	3.615(6)	N2	S10	3.46(2)
S3	S4	2.055(7)	Rh1	S14	3.704(7)	N2	O2	3.00(4)
S4	S5	2.024(8)	O1	S12	3.32(2)	N3	S11	3.26(2)
S6	S7	2.034(7)	O1	S12	3.32(2)	N3	S13	3.48(2)
S7	S8	2.056(9)	O1	N3	3.04(2)	N3	S15	3.33(2)
S8	S9	2.046(11)	O1	N3	3.04(2)	N3	O1	3.04(2)
S9	S10	2.036(8)	O1	O2	3.00(4)	N3	O1	3.04(2)
S11	S12	2.025(9)	O1	O2	3.00(4)			

Numbers in parentheses are estimated standard deviations in the least significant digits.

Table 3. Bond angles (°) for $(NH_4)_3Rh(S_5)_3 \cdot 2H_2O$

Atom 1	Atom 2	Atom 3	Angle	Atom 1	Atom 2	Atom 3	Angle	Atom 1	Atom 2	Atom 3	Angle
S1	Rh1	S5	92.7(2)	S6	Rh1	S11	92.9(2)	Rh1	S6	S7	112.9(3)
S1	Rh1	S6	83.0(2)	S6	Rh1	S15	82.5(2)	S6	S7	S8	104.5(3)
S1	Rh1	S10	91.5(2)	S10	Rh1	S11	92.4(2)	S7	S8	S9	103.0(4)
S1	Rh1	S11	174.5(2)	S10	Rh1	S15	172.7(2)	S8	S9	S10	107.6(4)
S1	Rh1	S15	82.7(2)	S11	Rh1	S15	93.1(2)	Rh1	S10	S9	110.9(3)
S5	Rh1	S6	173.8(2)	Rh1	S1	S2	113.6(3)	Rh1	S11	S12	111.3(3)
S5	Rh1	S10	92.2(2)	S1	S2	S3	105.6(4)	S11	S12	S13	107.5(4)
S5	Rh1	S11	91.1(2)	S2	S3	S4	102.4(3)	S12	S13	S14	101.3(4)
S5	Rh1	S15	92.5(2)	S3	S4	S5	105.4(4)	S13	S14	S15	105.5(4)
S6	Rh1	S10	92.4(2)	Rh1	S5	S4	112.0(3)	Rh1	S15	S14	114.6(4)

Numbers is parentheses are estimated standard deviations in the least significant digits.

group is exactly similar to the second dimorph[12] of $(NH_4)_2[Pt(S_5)_3]2H_2O$ (space group $C_{2/c}$) where the 8 molecules of the unit cell are made up of 4 in one half cell of one hand of propeller (say D) and the other 4 in the other reflection related half cell of the other hand (L), so that the stacking is —DDLLD-DLLDDLL—. These are the only known cases of such stacking.

The structural parameters of the present anion have nearly the same values as found in the $Pt(S_5)_3^{2-}$ anion.[10] For example, the average Rh–S distance is 237.4 pm as the average Pt–S distance is 239.0 pm. The average S–S bond distance in the rhodium compound is 204.1 pm and in the platinum compound 204.9 pm.

In general, the $Pt(S_5)_3^{2-}$ anion seems to be more stable (or at least easier to handle) than the $Rh(S_5)_3^{3-}$ anion. In the light of the similar structural results, the differences are due to kinetics. Anionic Rh(III) complexes are often labile, but anionic Pt(IV) complexes are inert. The redox couples Rh(I)/Rh(III) and Pt(II)/Pt(IV) may play an important role in the stabilities of the above anions: we hope to evaluate this possibility through optical activity studies.

Acknowledgements—We thank the University of Turku for leave for ERJS, during the tenure of which at University College Cardiff, this project started. We also thank the Science and Engineering Research Council for financial support (P.S.C.).

REFERENCES

1. M. Draganjac and T. B. Rauchfuss, *Angew. Chem. Int. Ed. Engl.* 1985, **24**, 742.
2. K. A. Hofmann and F. Hochtlen, *Chem. Ber.* 1904, **37**, 245.
3. R. A. Krause, *Inorg. Nucl. Chem. Lett.* 1971, **7**, 973.
4. R. A. Krause, A. Wickenden Kozlowski and J. L. Cronin, *Inorg. Synth.* 1982, **31**, 12.
5. L. Malatesta and F. Turner, *Gazz. Chim. Ital.* 1942, **72**, 489.
6. R. D. Gillard, F. L. Wimmer and J. P. G. Richards, *J. Chem. Soc. Dalton Trans.* 1985, 253.
7. R. Beckett and B. F. Hoskins, *Inorg. Nucl. Chem. Lett.* 1972, **8**, 683.
8. R. Ricter, J. Kaiser, J. Sieler and L. Kutschabsky, *Acta Cryst. B.* 1975, **31**, 1642.
9. F. G. Riddell, R. D. Gillard and F. L. Wimmer, *J. Chem. Soc. Chem. Commun.* 1982, 332.
10. P. E. Jones and L. Katz, *Acta. Cryst. B.* 1969, **25**, 745; modified by *idem*, *ibid*, 1972, **28**, 3438. First polymorph of $(NH_4)_2[Pt(S_5)_3]2H_2O$.
11. $K_2[Pt(S_5)_3]$. Isostructural with ammonium salt of ref. 10: M. Spangenberg and W. Bronger, *Z. Naturforsch. B.* 1978, **33**, 482.
12. E. H. M. Evans, R. D. Gillard, J. P. G. Richards and F. L. Wimmer, *Nouveau Journal de Chimie*, 1986, **10**, 783. Second polymorph ($C_{2/c}$) of $(NH_4)_2[Pt(S_5)_3]2H_2O$.
13. R. D. Gillard, in H. A. O. Hill and P. Day, *Advanced Methods in Physical Inorganic Chemistry*, J. Wiley (1967), and references therein.

Polyhedron Vol. 6, No. 9, pp. 1781–1784, 1987
Printed in Great Britain

0277–5387/87 $3.00+.00

REACTIVITY OF [M(CO)$_3$(NN)(THIOUREAS)] (M = Mo, W; NN = 2,2′BIPYRIDINE, 1,10-PHENANTHROLINE) COMPLEXES TOWARDS SYSTEMS WITH MERCURY–HALIDES BONDS. TRIMETALLIC COMPOUNDS WITH X–M–Hg–M′–X (M′ = Mo, W; X = Cl, Br, I) BONDINGS

P. CORREA, M. E. VARGAS* and J. GRANIFO*

Departamento de Ciencias Químicas, Facultad de Ingeniería, Universidad de La Frontera, Casilla 54-D, Temuco, Chile

(*Received* 5 *January* 1987; *accepted* 6 *April* 1987)

Abstract—New heterotrimetallic complexes were isolated by reaction of M(CO)$_3$(NN)L (M = Mo, W; NN = bipy, phen; L = thioureas) either with HgX_2 (X = Cl, Br, I) giving complexes of the formula [M(CO)$_3$(NN)(X)]$_2$Hg or with M′(CO)$_3$(NN′)(Cl)(HgCl) (M′ = Mo, W; NN′ = bipy, phen) producing compounds of the type (Cl)(NN)(CO)$_3$M–Hg–M′(CO)$_3$(NN′)(Cl). These new photosensitive substances were characterized through IR spectroscopy and conductivity measurements. Structures involving X–M–Hg–M′–X bonding are proposed and the reactions are discussed in terms of an insertion of the fragment M(CO)$_3$(NN) into the Hg–X bonds.

Mixed derivatives of the formula *fac*-M(CO)$_3$(NN)L (M = Mo, W; NN = 2,2′-bipyridine (bipy), 1,10-phenantroline (phen) L being a wide range of unidentate Lewis bases are well known,[1–6] but their reaction with mercuric halides, $HgCl_2$, has been reported when L is triphenylphosphine or derivative,[7,8] pyridine[9] and thiourea,[10] giving tricarbonyl complexes containing either M–Hg or M–Hg–M bonds.

The formation of the metal–mercury compounds above has been considered to be a Lewis acid-base reaction, the metal complex being the nucleophilic centre, yielding HgCl or $HgCl_2$ complexes. The reaction would occur without elimination of the ligands in the complexes M(CO)$_3$(NN)PPh_3,[7] due to the soft character of the phosphorus atom in PPh_3 and the chelate nature of the bipy or phen,[11] but when L is a p-substituted triphenylphosphine it would be displaced,[8] the same would pass with the thiourea[10] while the pyridine complexes would show both types of behavior.[9]

The aim of this work is to clarify the way of the reaction of *fac*-M(CO)$_3$(NN)L complexes with mercuric halides, HgX_2 (X = Cl, Br, I). In this regard we chose L to be several N-substituted thioureas. The results of this investigation show that the active species towards the Hg–X bonds are the M(CO)$_3$(NN) fragments.

RESULTS AND DISCUSSION

The only known complex of the type M(CO)$_3$(NN)L (M = Mo, W; NN = bipy, phen) in which L is thiourea is the Mo(CO)$_3$(NN)(thiourea)[6,10] procedure prepared by Houk and Dobson.[6] In this work the above synthesis route was modified, using less drastic conditions, introducing the thioureas through a substitution reaction in the complex M(CO)$_3$(NN)(CH_3CN),[6] by refluxing in methanol.

The reaction of the complexes M(CO)$_3$(NN)(thioureas) with mercury halides, HgX_2 (X = Cl, Br, I), in the molar ratio 1/1 or more in acetone gave, in all cases, complexes of the formula [M(CO)$_3$(NN)]$_2$$HgX_2$. Nevertheless, in some cases the quoted reaction products were obtained contaminated with the mercury thiourea compounds, HgX_2(thiourea)$_2$.

The new compounds are air stable, orange or red colored microcrystalline solids, but they undergo rapid decomposition on exposure to sunlight or on heating, as manifested by mercury deposition. They are insoluble in non-polar organic solvents and very

* Authors to whom correspondence should be addressed.

slightly soluble in methanol or acetone. In DMFA no conductivity was detected, but an increase with the time was observed probably due to the displacement of the halide by the solvent.[12]

When the reaction was carried out in the presence of a large excess of the mercury halide, the seven-coordinate metal complexes $M(CO)_3(NN)(X)(HgX)$ were precipitated. These have been prepared by other authors[13,14] through the reaction of HgX_2 with the tetracarbonyls $M(CO)_4(NN)$. The crystal structure of one of them, $Mo(CO)_3(bipy)(Cl)(HgCl)$, shows the presence of the Mo-HgCl and Mo–Cl bonds.[15]

The IR spectra of the compounds $[M(CO)_3(NN)]_2HgX_2$ reveals the absence of the thioureas but the presence of the bipy and phen. The position of these latter bands show no significant differences compared to those of the parent complex $M(CO)_3(NN)$(thioureas).

The CO stretching region (Table 1, compounds 1–12) shows two strong absorptions; that of lower frequency is broad and in some cases split into two. Furthermore, no significant displacements of their positions occur by changing the halide. On the other hand, in the $[M(CO)_3(NN)(X)(HgX)]$ complexes these bands are shifted to higher frequencies.[13,14] A similar behaviour was observed in comparing the complexes $[(\eta\text{-}C_5H_5)M(CO)_3]_2Hg$ and $(\eta\text{-}C_5H_5)M(CO)_3(HgX)$, which are connected by an exchange process with HgX_2.[16]

Accordingly, these antecedents permit us to suggest the existence of a new tricarbonyl complex system related by the reaction:

$$[M(CO)_3(NN)]_2HgX_2 + HgX_2 = 2M(CO)_3(NN)(X)(HgX). \quad (1)$$

There are two possible structures for the halides $[M(CO)_3(NN)]_2HgX_2$: $[M(CO)_3(NN)]_2HgX_2$ or $[M(CO)_3(NN)(X)]_2Hg$. In both situations M–Hg–M bonding would be present and the mercury atom would have a coordination number of four in the first case and of two in the second one. Nevertheless, in related compounds co-ordination numbers higher than two for the mercury atom were not observed.[16] Hence, the second possibility seems to be more plausible. Moreover, in this way the seven-coordinate metal atom would reach the inert gas configuration.

With the above discussion, the structure for the complexes $[M(CO)_3(NN)(X)]_2Hg$ implies the existence of the X–M–Hg–M–X system. Hence, it seems reasonable to interpret the mechanism of formation of these compounds as the insertion of the fragment

Table 1. Analytical and infrared spectra for the complexes $[(X)(NN)(CO)_3M\text{–}Hg\text{–}M'(CO)_3(NN')(X)]$

	Compound					Analysis (%)[a]			
	X	NN	M	M′	NN′	C	H	N	ν(CO)[b]
1[c]	Cl	bipy	Mo	Mo	bipy	33.4(33.1)	1.9(1.7)	6.1(5.9)	1938, 1833
2	Br					30.1(30.2)	1.5(1.6)	5.5(5.4)	1940, 1832
3	I					28.1(27.7)	1.6(1.4)	4.9(5.0)	1939, 1830
4	Cl	phen	Mo	Mo	phen	35.9(36.3)	1.8(1.6)	5.7(5.6)	1933, 1837
5	Br					33.2(33.3)	1.7(1.5)	5.3(5.2)	1940, 1823
6	I					30.9(30.7)	1.6(1.4)	4.9(4.8)	1930, 1818
7	Cl	bipy	W	W	bipy	27.6(27.9)	1.5(1.4)	5.1(5.0)	1936, 1824
8	Br					25.9(25.8)	1.3(1.3)	4.7(4.6)	1935, 1820
9	I					24.1(24.0)	1.2(1.2)	4.2(4.3)	1937, 1822
10	Cl	phen	W	W	phen	30.7(30.9)	1.5(1.4)	4.9(4.8)	1939, 1826
11	Br					28.7(28.7)	1.4(1.3)	4.5(4.5)	1934, 1823
12	I					26.6(26.7)	1.1(1.2)	4.2(4.1)	1940, 1825
13	Cl	bipy	W	W	phen	29.3(29.4)	1.3(1.4)	4.8(4.9)	1932, 1825
14	Cl	bipy	W	Mo	phen	32.2(31.9)	1.6(1.5)	5.4(5.3)	1934, 1822
15	Cl	bipy	W	Mo	bipy	30.3(30.3)	1.5(1.6)	5.5(5.4)	1937, 1826
16	Cl	phen	W	Mo	bipy	31.7(31.9)	1.6(1.5)	5.2(5.3)	1929, 1817
17	Cl	phen	W	Mo	phen	33.4(33.4)	1.4(1.5)	5.3(5.2)	1936, 1816
18	Cl	phen	Mo	Mo	bipy	34.9(34.7)	1.8(1.7)	5.8(5.8)	1935, 1820

[a] Required values are given in parentheses.
[b] Nujol mulls, in cm^{-1}, all bands are strong.
[c] Compound prepared before; see ref. 8.

$M(CO)_3(NN)$ between the atoms of the Hg-X bond:

$$M(CO)_3(NN)L + X-Hg-X = M(CO)_3(NN)(X)(Hg-X) + L \quad (2)$$

$$M(CO)_3(NN)L + M(CO)_3(NN)(X)(Hg-X) = [M(CO)_3(NN)(X)]_2Hg + L. \quad (3)$$

The concept of the insertion behavior of the groups $M(CO)_3(NN)$ enabled us to isolate a series of new asymmetric trimetallic M–Hg–M′ complexes just based in the eqn (3) (M′ = Mo, W; NN′ = bipy, phen):

$$M(CO)_3(NN)L + M'(CO)_3(NN')(Cl)(Hg-Cl) = (Cl)(NN)(CO)_3M-Hg-M'-(CO)_3(NN')(Cl) + L. \quad (4)$$

The IR spectra of these asymmetric trimetallic complexes (Table 1, compounds 13–18) do not show any noticeable difference with those of the symmetric ones, except in the fact of the simultaneous appearance of the bands of the bipy and phen ligands.

In addition, the insertion fragment $M(CO)_3NN$ was made to react with the complex $Fe(CO)_4(HgCl)_2$,[17] yielding $[M(CO)_3(NN)(Cl)]_2Hg$ and the polymeric $[HgFe(CO)_4]_n$. This result may be explained by the insertion between the Hg–Cl bonds, giving an unstable complex in which Hg(I) disproportionates.

The behavior of the system under study showed that the thioureas are good leaving ligands, but they can cause contamination of the reaction products. This prompted us to find a clean source of $M(CO)_3(NN)$ fragments, and so the $M(CO)_3(NN)(CH_3CN)$ complexes achieved successfully all the requirements.

EXPERIMENTAL

All the reactions were carried out under nitrogen and with de-aerated solvents. The compounds $M(CO)_3(NN)(CH_3CN)$ (M = Mo, W; NN = bipy, phen)[6] and $M(CO)_3(NN)(X)(HgX)$[13,14] were prepared by similar methods to those described in the literature. Mercury salts and substituted thioureas (e.g. thiourea, *N*-methylthiourea, *N*,*N*-dimethylthiourea, *N*-phenylthiourea, *N*,*N*-dimethyl *N*′-phenylthiourea, tetramethylthiourea) were of commercial origin and used without further purification. The $M(CO)_3(NN)$(thioureas) compounds were characterized by their elemental analysis and their IR spectra. The shapes and positions of these latter bands are in agreement with literature data for sulphur bonded ligands.[6] The IR spectra were obtained using a Perkin–Elmer 577 spectrophotometer. The conductivity was measured at room temperature in DMFA with a direct lecture L. Pusl instrument.

Synthesis of $[M(CO)_3(NN)(X)]_2Hg$ (X = Cl, Br, I)

These compounds were synthesised by reaction of the complexes $M(CO)_3(NN)L$ (L = thioureas or acetonitrile) and HgX_2 in acetone. All these substances were either orange or red colored microcrystalline solids. The following synthesis is described as a typical one.

$[Mo(CO)_3(bipy)(Cl)]_2Hg$: A solution of $Mo(CO)_3$(bipy)(tetramethylthiourea) (0.241 g; 0.51 mmol) and $HgCl_2$ (0.70 g; 0.25 mmol) in 10 cm^3 acetone was vigorously stirred in the dark for 30 min. The solution became yellowish and an orange precipitate was formed. It was then filtered and washed 3–4 times with 5 cm^3 portions of acetone. 0.14 g of an orange colored microcrystalline solid were obtained. The results of the elemental analysis are presented in Table 1.

Synthesis of $[(Cl)(NN)(CO)_3M-Hg-M'(CO)_3(NN')(Cl)]$ (M′ = Mo, W; NN′ = bipy, phen)

The general procedure was the addition of half of the stoichiometric quantity of solid $M'(CO)_3(NN')(Cl)(HgCl)$ to a solution of $M(CO)_3(NN)(CH_3CN)$ in acetonitrile. All these reaction products were orange-red colored microcrystalline solids. The following reaction is given as an example.

$[(Cl)(bipy)(CO)_3Mo-Hg-W(CO)_3(bipy)(Cl)]$: $W(CO)_3$(bipy)(Cl)(HgCl) (0.14 g; 0.2 mmol) was added to a freshly prepared solution of $Mo(CO)_3$(bipy)(CH_3CN) (0.15 g; 0.4 mmol) in acetonitrile and was vigorously stirred for 2 h. The orange-red precipitate was filtered and washed 3–4 times with 5 cm^3 portions of acetonitrile and finally with acetone. 0.15 g of the microcrystalline compound was obtained. The elemental analysis of these compounds are given in Table 1.

Acknowledgements—Financial support given by the Dirección de Investigación de la Universidad de La Frontera (Project N°1032126–862-3) and the Comisión Nacional de Investigación Científica y Tecnológica (Project N°5007/85) to carry out this work is gratefully acknowledged. A gift of some metal hexacarbonyls from Merck Química Chile is also gratefully acknowledged.

REFERENCES

1. W. Hieber and F. Mühlbauer, *Z. anorg. Chem.* 1935, **221**, 337.
2. W. Hieber and E. Romborg, *Z. anorg. Chem.* 1935, **221**, 349.
3. M. H. B. Stiddard, *J. Chem. Soc.* 1963, 756.
4. H. Behrens and N. Harder, *Chem. Ber.* 1964, **97**, 433.
5. L. W. Houk and G. R. Dobson, *J. Chem. Soc.* 1966, 317.
6. L. W. Houk and G. R. Dobson, *Inorg. Chem.* 1966, **5**, 2119.
7. M. P. Pardo and M. Cano, *J. Organomet. Chem.* 1983, **247**, 293.
8. M. Panizo and M. Cano, *J. Organomet. Chem.* 1984, **266**, 247.
9. M. P. Pardo and M. Cano, *J. Organomet. Chem.* 1984, **270**, 311.
10. A. López, M. Panizo and M. Cano, *J. Organomet. Chem.* 1986, **311**, 145.
11. M. A. Lobo, M. F. Perpiñan, M. P. Pardo and M. Cano, *J. Organomet. Chem.* 1983, **254**, 325.
12. R. Kummer and W. A. G. Graham, *Inorg. Chem.* 1968, **7**, 310.
13. K. E. Edgar, B. F. G. Johnson, J. Lewis and S. B. Wild, *J. Chem. Soc.* (*A*) 1968, 2851.
14. R. T. Jernigan and G. R. Dobson, *Inorg. Chem.* 1972, **11**, 81.
15. P. D. Brotherton, J. M. Epstein, A. H. White and S. B. Wild, *Aust. J. Chem.* 1974, **27**, 2667.
16. M. J. Mays and J. D. Robb, *J. Chem. Soc.* (*A*) 1968, 329.
17. J. Lewis and S. B. Wild, *J. Chem. Soc.* (*A*) 1966, 69.

Polyhedron Vol. 6, No. 9, pp. 1785–1789, 1987
Printed in Great Britain

0277–5387/87 $3.00+.00

1,3-INTRAMOLECULAR METAL SHIFTS IN SOME PENTACARBONYL-CHROMIUM AND -TUNGSTEN DERIVATIVES OF BIS-, TRIS- AND TETRAKIS(METHYLTHIO)METHANE AND BIS(METHYLSELENO)METHANE. A DYNAMIC NUCLEAR MAGNETIC RESONANCE INVESTIGATION

EDWARD W. ABEL,* THOMAS E. MACKENZIE, KEITH G. ORRELL and VLADIMIR ŠIK

Department of Chemistry, University of Exeter, Exeter, EX4 4QD, U.K.

(*Received* 24 *March* 1987; *accepted* 6 *April* 1987)

Abstract—The mononuclear complexes $[M(CO)_5(CH_3E)_nCH_{4-n}]$ ($n = 2$, M = Cr and W, E = S and Se; $n = 3$, M = Cr and W, E = S; $n = 4$, M = Cr, E = S) have been synthesized and characterized. In addition to the facile atomic inversions of the metal co-ordinated sulphur and selenium atoms, there are intramolecular 1,3-metallotropic shifts among all the available co-ordination sites on each ligand. From dynamic NMR studies activation energies have been determined for these metal commutations.

The metal complexes of organosulphur and selenium ligands have been shown to possess a striking array of fluxional phenomena.[1] Cyclic sulphide ligand complexes of pentacarbonyl-chromium, -molybdenum and -tungsten have been observed to undergo 1,3-metallotropic shifts,[2–5] as also have the complexes of the acyclic 2-selena-4-thiapentane.[6] We have now sought to extend the complexity of these motions by presenting to metal pentacarbonyl moieties the opportunity to commute over either two, three or four isosteric sulphur atoms in the ligands bis(methylthio)methane, $(CH_3S)_2CH_2$, tris-(methylthio)methane, $(CH_3S)_3CH$, and tetrakis (methylthio)methane, $(CH_3S)_4C$, and between two selenium atoms in bis(methylseleno)methane $(CH_3Se)_2CH_2$. We report herein the synthesis and characterization of pentacarbonylmetal derivatives of these ligands. These complexes all display 1,3-metal chalcogen shifts, and we have determined accurate energy barriers for all of these processes utilizing well developed spectral line-shape analysis techniques.[7]

* Author to whom correspondence should be addressed.

EXPERIMENTAL

Materials and preparations

Metal hexacarbonyls were used directly as obtained commercially. $(CH_3S)_2CH_2$,[8] $(CH_3S)_3CH$,[9] $(CH_3S)_4C$,[9] $(CH_3Se)_2CH_2$,[10] $[(C_2H_5)_3O]^+BF_4^-$[11] and $[WBr(CO)_5]^-N(C_2H_5)_4^+$[12] were prepared as previously reported. All reactions and purification procedures were carried out under nitrogen.

Pentacarbonylbis(methylthio)methanetungsten(O) $[(CO)_5WS(CH_3)CH_2SCH_3]$. Tetraethylammonium bromopentacarbonyltungstate (1.32 g, 2.91 mmol) and bis(methylthio)methane (0.36 g, 3.3 mmol) were dissolved in dichloromethane (5 cm^3). A solution of triethyloxonium tetrafluoroborate, $(C_2H_5)_3OBF_4$ (0.57 g, 3.00 mmol) in dichloromethane (2 cm^3) was added with stirring causing an immediate clearing of the cloudy solution, and a change of colour to light orange. Solvent was removed under reduced pressure to leave a yellow residue which was extracted with hexane (2×30 cm^3). The combined hexane extracts were filtered through a medium glass frit, reduced in volume (low pressure) at 20°C, and then left at −20°C for

Table 1. Characterization of the complexes $[M(CO)_5L]$, M = Cr or W and L = $(CH_3S)_2CH_2$, $(CH_3Se)_2CH_2$, $(CH_3S)_3CH$ and $(CH_3S)_4C$

Complex	Colour	Yield	M.p. (°C)	Elemental analysis (%) C Calc.	C Obt.	H Calc.	H Obt.	I.R. data ν(CO) cm^{-1} (Hexane solution)
$[W(CO)_5(CH_3S)_2CH_2]$	orange	67	56	22.2	22.1	1.9	1.7	
$[Cr(CO)_5(CH_3S)_2CH_2]$	yellow	71	42	32.0	31.8	2.7	2.6	2080 w, 1948 m, 1944 sh
$[W(CO)_5(CH_3S)_3CH]$	orange	43	44	22.6	22.0	2.1	1.9	
$[Cr(CO)_5(CH_3S)_3CH]$	yellow	31	oil	31.2	32.0	2.9	3.2	2065 w, 1944 m, 1935 w
$[Cr(CO)_5(CH_3S)_4C]$	yellow	28	dec.	30.4	29.9	3.1	3.2	2075 w, 1953 m, 1935 w
$[W(CO)_5(CH_3Se)_2CH_2]$	yellow	54	73	16.6	16.4	1.4	1.5	
$[Cr(CO)_5(CH_3Se)_2CH_2]$	yellow	58	46	21.7	22.2	1.8	1.9	2063 w, 1945 m, 1935 w

three days to produce yellow crystals of $[(CO)_5WS(CH_3)CH_2SCH_3]$ (0.84 g, 1.9 mmol) (67% yield).

Pentacarbonyltungsten and pentacarbonylchromium complexes of $(CH_3S)_2CH_2$, $(CH_3Se)_2CH_2$, $(CH_3S)_3CH$ and $(CH_3S)_4C$ were all prepared in analogous ways and are characterized in Table 1.

NMR spectra. All of the compounds studied were sensitive to decomposition by air in solution, hence solutions were made up in standard 5 mm bore tubes with Taperlock joints (Wilmad Glass Co. Inc.). Reference material and solvent were distilled under vacuum onto the sample, and tube and contents were subsequently flushed with nitrogen. Variable temperature ^1H NMR spectra were recorded using a JEOL PS/PFT–100 spectrometer operating at 100 MHz. Sample temperatures were controlled by a standard JES-VT-3 accessory and measured with a digital thermometer (Comark Ltd). Temperatures recorded are accurate to at least $\pm 1°C$ over the reported range. NMR bandshape analyses were carried out as described[13] previously.

RESULTS

^1H NMR studies

$[M(CO)_5(CH_3E)_2CH_2]$ *complexes,* M = Cr *and* W, E = S *and* Se. The NMR spectra of all four of these complexes (Table 2) consist of three separate signals with integrated peak intensities of 2 : 3 : 3. This would be the anticipated spectrum for such compounds with a methylene group along with one metal co-ordinated methylthio/seleno group and one pendant methylthio/seleno group as in Fig. 1. As illustrated, however, the two protons of the methylene group should be anisochronous due to the chiral nature of the co-ordinated sulphur/selenium atom. In view of the extensive data already reported on inversion barriers in sulphur/selenium co-ordinated metal pentacarbonyls it is reasonable to assume that rapid inversion about the co-ordinated pyramidal sulphur/selenium atom is causing equilibration of the protons in the prochiral methylene group. On cooling the solutions

Table 2. Room temperature ^1H NMR chemical shifts[a] for $M(CO)_5L$ complexes, M = Cr or W and L = $(CH_3S)_2CH_2$, $(CH_3Se)_2CH_2$, $(CH_3S)_3CH$ and $(CH_3S)_4C$

Complex	$\delta(CH_2)$	$\delta(CH)$	$\delta(SCH_3)$	$\delta(M \leftarrow SCH_3)$	$\delta(SeCH_3)$	$\delta(M \leftarrow SeCH_3)$
$[W(CO)_5(CH_3S)_2CH_2]$	3.83		2.27	2.72		
$[Cr(CO)_5(CH_3S)_2CH_2]$	3.62		2.22	2.39		
$[W(CO)_5(CH_3S)_3CH]$		4.45	2.22	2.70		
$[Cr(CO)_5(CH_3S)_3CH]$		4.45	2.28	2.48		
$[Cr(CO)_5(CH_3S)_4C]$			2.29	2.61		
$[W(CO)_5(CH_3Se)_2CH_2]$	3.84				2.18	2.59
$[Cr(CO)_5(CH_3Se)_2CH_2]$	3.66				2.15	2.34

[a] Relative to $(CH_3)_4Si$.

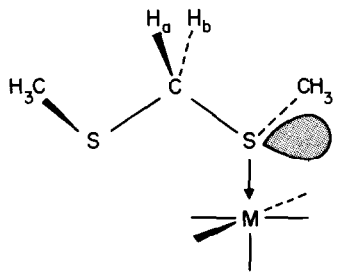

Fig. 1. $[M(CO)_5(CH_3S)_2CH_2]$, illustrating the pendant CH_3S group and the prochiral methylene group of the ground state.

Table 3. Free energy of activation for 1,3-metallotropic shifts in the complexes $[M(CO)_5L]$

Complex	$\Delta G^{\ddagger}(298)$/kJmol^{-1}
$[W(CO)_5(CH_3S)_2CH]$	84.3±0.8
$[W(CO)_5(CH_3Se)_2CH_2]$	85.8±0.5
$[Cr(CO)_5(CH_3S)_3CH]$	72.9±0.5
$[W(CO)_5(CH_3S)_3CH]$	78.6±2.5
$[Cr(CO)_5(CH_3S)_4C]$	67.0±3.7

of the complexes $[M(CO)_5(CH_3Se)_2CH_2]$, M = Cr and W to −60°C the room temperature methylene singlet resolves to the expected AB quartet with the slowing/cessation of inversion about the co-ordinated selenium atom. We were, however, unable to bring about the geminal proton chemical shift distinction at reduced temperature for the complexes $[M(CO)_5(CH_3S)_2CH_2]$. This may be attributable to either (or both) of the following reasons: (i) accidental chemical shift degeneracy, or (ii) still rapid equilibration of proton environments by sulphur atom inversion. Despite our best efforts, we have been unable to resolve these protons, but we still believe co-ordinated chalcogen atom inversion to be one of the fluxional characteristics of each of these complexes.

On recording NMR spectra at above room temperature, lineshape changes become evident at about 70°C whence the two methylthio/seleno signals in each complex are observed to broaden and proceed towards coalescence at *ca* 120°C. The absence of inter-broadening of complexed ligand and free ligand signals, or any concentration effects on the bandshape indicate that an intramolecular process is responsible for the observed methyl equilibrations. This we interpret as a shuttling of the metal between two chalcogen atoms as depicted in Fig. 2. The exchange broadened SMe/SeMe bandshapes due to this 1,3-shift process may be simulated as a simple 2-site exchange problem with no scalar coupling.

Due to the high temperatures required for observation of the phenomenon, some complexes underwent partial decomposition, and consequently the recorded spectra were not always ideal for computer simulation. Only cases where the spectral fittings produced reliable values of $\Delta G^{\ddagger}$ for the 1,3-commutation process are reported in Table 3.

The graph diagram in Fig. 3 illustrates interchange pathways by atomic inversion and by 1,3-shift for the four co-ordination topomers of the complexes $[M(CO)_5(CH_3E)_2CH_2]$.

$[M(CO)_5(CH_3S)_3CH]$ *complexes*, M = Cr *and* W. The NMR spectra of these two complexes (Table 2) consist of three separate signals with integrated peak intensities 1 : 3 : 6 corresponding to methine, ligand co-ordinated methylthio and two unco-ordinated methylthio groups respectively. It can be assumed, at room temperature, that metal co-ordinated sulphur atom inversion is rapid, thus rendering the potentially anisochronous unco-ordinated methylthio groups equivalent. Between 60 and 110°C the signals of the co-ordinated and unco-ordinated methylthio groups coalesce with an absence of any exchange with the signal of the free ligand present in solution. This observation is the result of intramolecular commutation of the metal pentacarbonyl moiety among all three methylthio

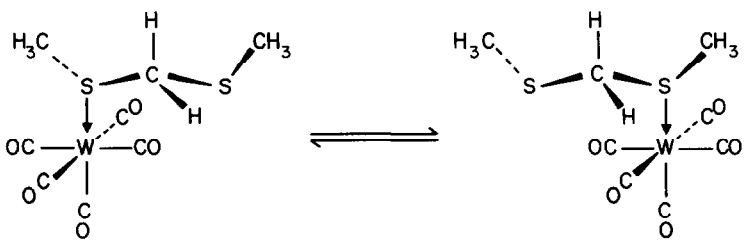

Fig. 2. 1,3-Metal commutation illustrated for the complex $[W(CO)_5(CH_3S)_2CH_2]$.

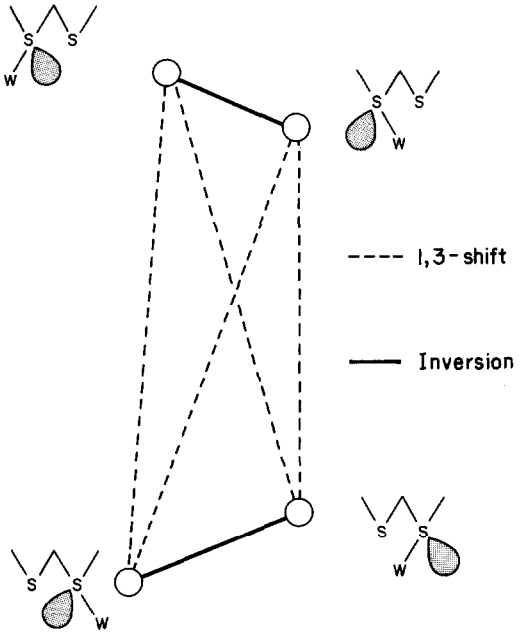

Fig. 3. Graph diagram illustrating the four topomers of $[W(CO)_5(CH_3S)_2CH_2]$ and their exchange pathways.

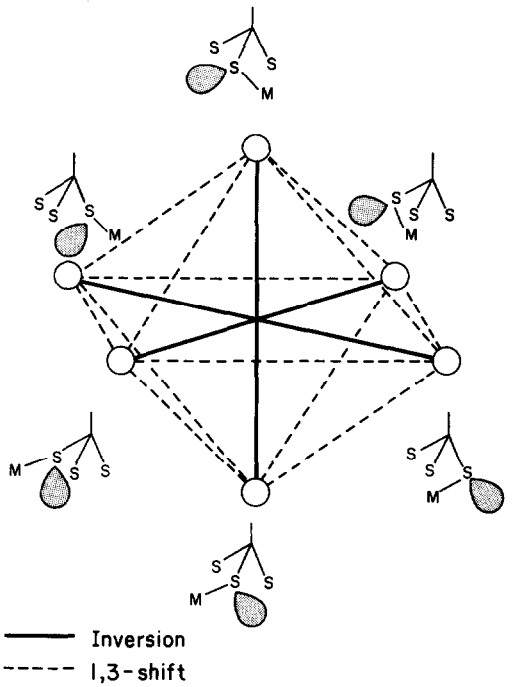

Fig. 4. Graph diagram illustrating the six topomers of $[M(CO)_5(CH_3S)_3CH]$ and their exchange pathways.

groups of the ligand. This results in a total of six possible topomers, and Fig. 4 illustrates how each topomer may access four others by the 1,3-metallotropic shift and the other by sulphur atom inversion. Simulation of the spectra was straightforward as the rapid sulphur inversion rendered the spin problem for the exchanging methylthio groups as $A \rightleftharpoons B_2$, and the energy barriers so obtained are recorded in Table 3.

$[Cr(CO)_5(CH_3S)_4C]$. Pure samples of $[W(CO)_5(CH_3S)_4C]$ could not be obtained, but we were able to prepare, characterize and investigate the chromium analogue fully. The NMR spectrum shows a 1 : 3 signal ratio in its methylthio region, resulting from one only of the four methylthio groups being co-ordinated to the chromium pentacarbonyl moiety. The temperature collapse of the methylthio signals indicates the onset of the intramolecular 1,3-metallotropic shift which moves the chromium pentacarbonyl group over the surface of the ligand. The eight sites of attachment yield the eight topomers of this species. The graph diagram of Fig. 5 illustrates their interconversion pathways either by sulphur atom inversion or by 1,3-metal commutation.

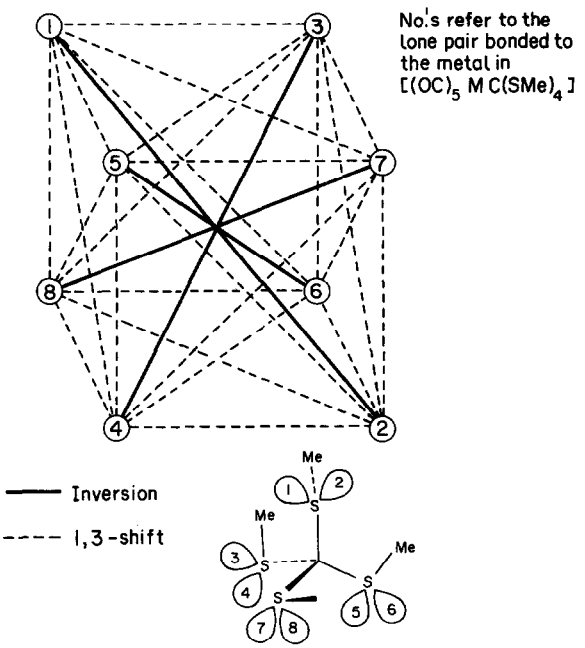

Fig. 5. Graph diagram illustrating the eight topomers of $[M(CO)_5(CH_3S)_4C]$. Numbers at the cube corners identify the topomer corresponding to the metal pentacarbonyl moiety co-ordinated at the corresponding numbered position on the ligand illustration. It is not possible in such a graph digram to give identical processes the same geometrical values. Thus all edges and face-diagonals represent 1,3-commutations and the remaining trans-cube diagonals represent interchange of topomers by ligand atom inversion.

DISCUSSION

1,3-Metallotropic shifts have been extensively reported[2-5] for cyclic ligands, and the cor-

responding process in the acyclic 2-selena-4-thiapentane has been studied.[6] Now, the complexes reported herein have either two, three or four completely identical ligand sulphur/selenium atoms for co-ordination to a metal pentacarbonyl moiety in an acyclic ligand.

In all cases we observe temperature variable ^1H NMR spectra which we associate with 1,3 metal commutation between all available co-ordination sites on the molecule. In all species we find the rates to be independent of concentration. This fact coupled with an absence of any exchange between the signals of complexed ligand and free ligand, suggest a completely intramolecular process. In the transition state we envisage the $M(CO)_5$ moiety as being equally bonded to the two methylthio/seleno groups between which it commutes. In such an intermediate, the metal may be thought of as pseudo seven co-ordinate and as such be stereochemically non-rigid, with a resultant possibility for scrambling of the carbonyl groups. A recent report[14] on the 1,2-metallotropic shifts of metal pentacarbonyls on organic disulphides, however, indicates that in these commutations the $M(CO)_5$ group remains rigid, with non-exchanging axial and equatorial carbonyl groups. The stereochemistry of the $M(CO)_5$ moiety in a wide range of 1,3-commutations in both cyclic and acyclic ligands is now under investigation, and will be reported later.

In Table 3 the considerable decrease in free energy of activation for the 1,3-metal commutation is notable as the number of methylthio groups on the ligand increases. In each case the transition state involves simultaneous co-ordination of two methylthio groups to the metal, and changes in other groups on the central carbon atom appear unlikely to effect the steric requirements of the transition state. In the ground state, however, the steric congestion increases significantly as the number of methylthio groups on the ligand increases from two to three to four. This would therefore suggest that the decreasing activation energy for the 1,3 shifts with increasing methylthio groups is due to steadily increasing ground state energies in $[M(CO)_5(MeS)_2CH_2]$, $[M(CO)_5(MeS)_3CH]$ and $[M(CO)_5(MeS)_4C]$ rather than changes in the transition state energy.

Acknowledgements—We wish to thank the Science and Engineering Research Council for support of this work, and Dr. P. K. Mittal for help in a synthesis.

REFERENCES

1. E. W. Abel, S. K. Bhargava and K. G. Orrell, *Prog. Inorg. Chem.* 1984, **32**, 1.
2. W. A. Schenk and M. Schmidt, *Z. Anorg. Allg. Chem.* 1975, **416**, 311.
3. E. W. Abel, M. Booth, K. G. Orrell and G. M. Pring, *J. Chem. Soc., Dalton Trans.* 1981, 1944.
4. E. W. Abel, G. D. King, K. G. Orrell, G. M. Pring and V. Šik, *Polyhedron* 1983, **2**, 1117.
5. E. W. Abel, G. D. King, K. G. Orrell and V. Šik, *Polyhedron* 1983, **2**, 1363.
6. E. W. Abel, S. K. Bhargava, T. E. MacKenzie, P. K. Mittal, K. G. Orrell and V. Šik, *J. Chem. Soc., Chem. Comm.* 1982, 1983; *J. Chem. Soc., Dalton Trans.* 1987, in press.
7. G. Binsch and H. Kessler, *Angew. Chem., Int. Ed.* 1980, **19**, 411.
8. F. Feher and K. Vogelbruch, *Chem. Ber.* 1958, **91**, 996.
9. W. Seebach, K.-H. Greiss, A. K. Beck, B. Graf and H. Daum, *Chem. Ber.* 1972, **105**, 3280.
10. D. V. Ende, W. Dumont and A. Krief, *Angew. Chem. Int. Edn.* 1975, **14**, 700.
11. H. Meerwein, *Organic Syntheses* 1966, **46**, 113.
12. E. W. Abel, I. S. Butler and J. G. Reid, *J. Chem. Soc.* 1963, 2068.
13. E. W. Abel, A. R. Khan, K. Kite, K. G. Orrell and V. Šik, *J. Chem. Soc., Dalton Trans.* 1980, 2208.
14. E. W. Abel, I. Moss, K. G. Orrell, V. Šik and D. Stephenson, *J. Chem. Soc. Chem. Comm.* 1986, 1724.

Polyhedron Vol. 6, No. 9, pp. 1791–1796, 1987
Printed in Great Britain

0277–5387/87 $3.00+.00
Pergamon Journals Ltd

FORMATION OF SPINEL FROM METAL ORGANIC COMPOUNDS

OSAMU YAMAGUCHI,* HIROYUKI TAGUCHI and KIYOSHI SHIMIZU

Department of Applied Chemistry, Faculty of Engineering, Doshisha University, Kyoto 602, Japan

(*Received* 24 *March* 1987; *accepted* 6 *April* 1987)

Abstract—A magnesium–aluminum product, which can be used to form spinel, is prepared by the simultaneous hydrolysis of magnesium acetylacetonate and aluminum isopropoxide. Infrared spectrum and X-ray diffraction analyses show that the product is a magnesium substituted γ-alumina-like amorphous material. Spinel is formed slowly at $\approx$ 700–1250°C at a heating rate of 10°C min^{-1}. A marked increase in crystallite size occurs between 1100 and 1200°C. Spinel powders consist of aggregates of plate-like particles. The kinetics of crystallization of spinel have been studied by X-ray measurements. The initial stage at each temperature proceeds rapidly in a short time. The final stage can be described in terms of the contracting square equation $1-(1-f)^{1/2} = kt$, the activation energy being 164 kJ mol^{-1}.

Magnesium aluminate spinel $MgAl_2O_4$ is usually prepared by solid state reaction between MgO and Al_2O_3. Preparation conditions require heating for 100 h at 1302°C even when submicron reactants are used.[1] In contrast, chemical methods[2–7] permit the preparation of spinel at lower temperatures. Bratton[2,3] showed that the coprecipitate prepared from aqueous solutions of $MgCl_2 \cdot 6H_2O$ and $AlCl_3 \cdot 6H_2O$ by ammonium hydroxide was an intimate mixture of $2Mg(OH)_2 \cdot Al(OH)_3$ and gibbsite $Al(OH)_3$. Sugiura and Kamigaito[7] reported that the hydrolysis products of magnesium aluminum double alkoxide $MgAl_2(OC_3H_8)_8$ depended on the atmosphere; thus, under inert gas, an AlO(OH) boehmite-like compound was formed, but in air, a variety of compounds were formed because of the influence of carbon dioxide. However, no kinetic study of the formation of spinel has been carried out using the specimens prepared by chemical methods.

In the present study, the simultaneous hydrolysis product of magnesium acetylacetonate and aluminum isopropoxide was amorphous. The present paper deals with the formation of spinel from metal organic compounds.

EXPERIMENTAL

Magnesium acetylacetonate $Mg(C_5H_7O_2)_2$ (> 99% pure) as-received was dissolved in 2-propanol. Aluminum isopropoxide $Al(OC_3H_7)_3$ was synthesized by heating 99.9% aluminum metal in an excess of analytical-grade 2-propanol with mercury (II) chloride (10^{-4} mol/mol of metal) as a catalyst for 10 h at 82°C.[8] The mixed solution prepared in the mole ratio $Mg^{2+}:2Al^{3+}$ was refluxed for 10 h and then hydrolyzed at room temperature in air by adding drops of ammonia water (28%) with stirring. After the termination of dropping, the resulting suspension was further stirred for 30 min at room temperature. The hydrolysis product was separated from the suspension by filtration, washed 10 times in conductivity water, and dried at 80°C under reduced pressure. The powder obtained is termed "starting powder".

Thermal analyses (TG, DTA) were conducted in air at a heating rate of 10°C min^{-1}; α-alumina was used as the reference for the DTA. The starting powder and specimens heated at a rate of 10°C min^{-1} and then quenched were examined by X-ray diffraction using Ni-filtered CuKα radiation. The kinetics of crystallization of spinel were followed by X-ray measurements. The starting powder was preheated as will be described. The specimens were

* Author to whom correspondence should be addressed.

placed in an electric furnace equipped with a temperature regulator, heated for the desired time, and then quenched rapidly to room temperature. The fraction of crystallization was determined from the intensity ratio of the spinel line (311) to the spinel $+CaF_2$ line (220) as an internal standard, using a calibration curve prepared with known compositions. Powders for electron microscopic observation were dispersed in amyl acetate by an ultrasonic treatment for 5 min. The dispersed drops were dried on carbon film, and observed under a 35 keV beam. Infrared spectroscopy was performed on a dispersion in potassium bromide using the pressed-disk technique.

RESULTS AND DISCUSSION

Characterization of starting powder

X-Ray diffraction analysis showed that the starting powder was amorphous. The average particle size, determined by electron microscopy, was ≈ 60 nm (Fig. 1). Figure 2(A) shows the IR spectrum of starting powder. The absorption bands at 3450 and 1630 cm^{-1} are due, respectively, to the O–H stretching and bending vibrations of H_2O[9] and, on the preparation history, represent adsorbed water and water of hydration. The bands resulting from CO_3^{2-} stretching vibrations were present at 1545, 1415 and 1055 cm^{-1};[10] this is probably due to CO_2 absorbed in the aqueous ammonia. Two main spectral bands for ammonia (gas, solid) are located in the vicinity of 3380 and 1640 cm^{-1}.[11,12] They may be overlapped with the bands due to water described above. No bands due to NH_4^+ were observed. According to the Deo *et al.*[13] data for 2-propanol adsorbed on γ-alumina, six bands are located at 2960, 2930, 2870, 1465, 1170 and 650 cm^{-1}. Therefore, the bands at 2925, 2850, 1465 and 1160 cm^{-1} must be assigned, as shown in Fig. 2(A), by reference to their data. The spectrum pattern below 1000 cm^{-1} is similar to that of γ-alumina* (spinel-type structure) shown in Fig. 2(B). On the basis of the γ-alumina[14] data, a broad band at 530 to 845 cm^{-1} in starting powder is assigned to the Al–O stretching vibration. From the results of X-ray diffraction, no species other than spinel were observed throughout the heating process. Thus, it

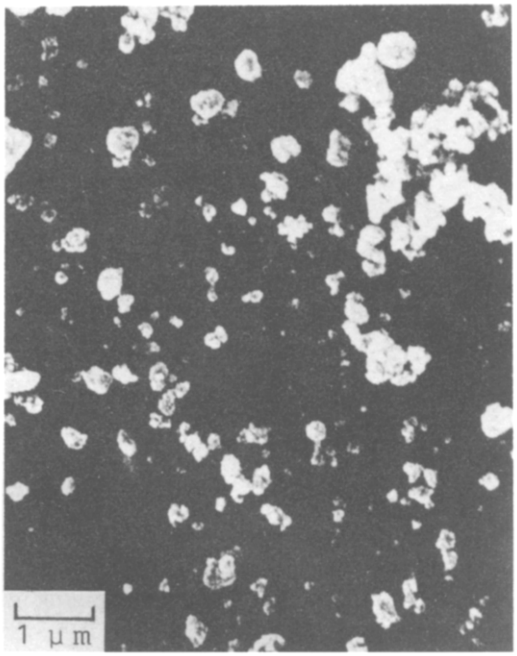

Fig. 1. Scanning electron micrograph for starting powder.

can be considered that the starting powder is Mg^{2+}-substituted γ-alumina-like amorphous containing water, ammonia, 2-propanol, and carbon dioxide.

Thermal analysis

Thermogravimetric examination of starting powder showed that the weight decrease was essentially completed at 540°C [Fig. 3(A)]. This can be attributed to the release of ammonia, water and organic residues from the parent alcohol. In addition, the weight decrease of 2.5% was recognized at 540–900°C; IR spectrum data suggested the release of water and carbon dioxide. A DTA curve is shown in Fig. 3(B). Except for an endothermic peak due to the release of ammonia and water, and an exothermic peak to the combustion of organic residues, no peak due to the crystallization of spinel was clearly detected in the DTA, although it was observed above $\approx$ 700°C as will be described.

Formation of spinel

Figure 4 shows the X-ray diffraction patterns of specimens with increasing temperature. The starting powder did not change up to 650°C. The (311) and (400) lines for spinel began to appear after heating at 700°C. Other lines were recognized when heated at 800°C. The intensity of the lines increased gradually with increasing temperature. Well-crystallized spinel was obtained by heating at 1250°C.

* Boehmite gel, prepared by the hydrolysis at room temperature of aluminum isopropoxide using conductivity water, was heated to 900°C at a heating rate of 10°C/min.

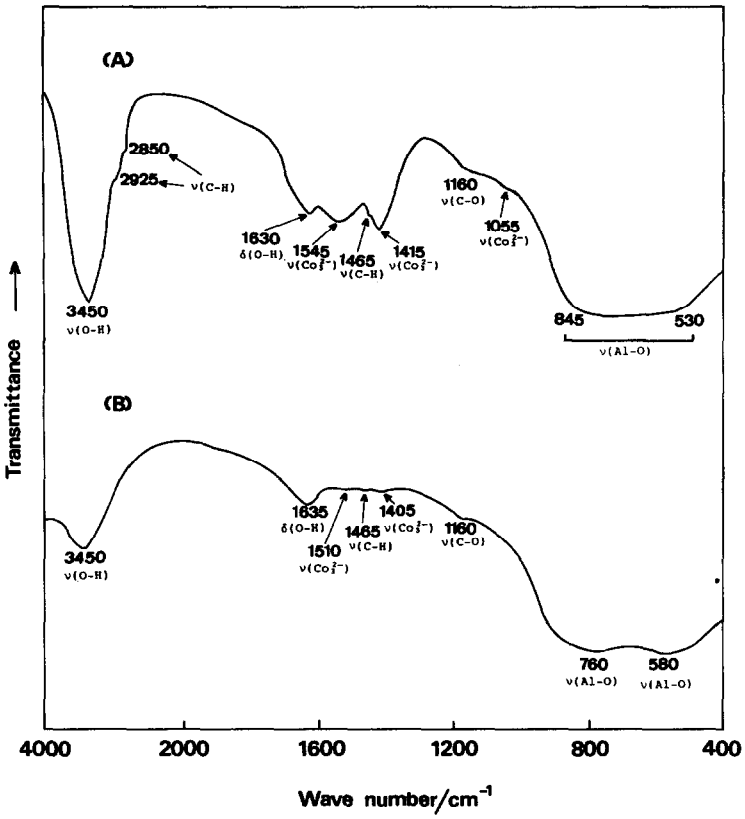

Fig. 2. Infrared spectra for (A) starting powder and (B) γ-Al_2O_3.

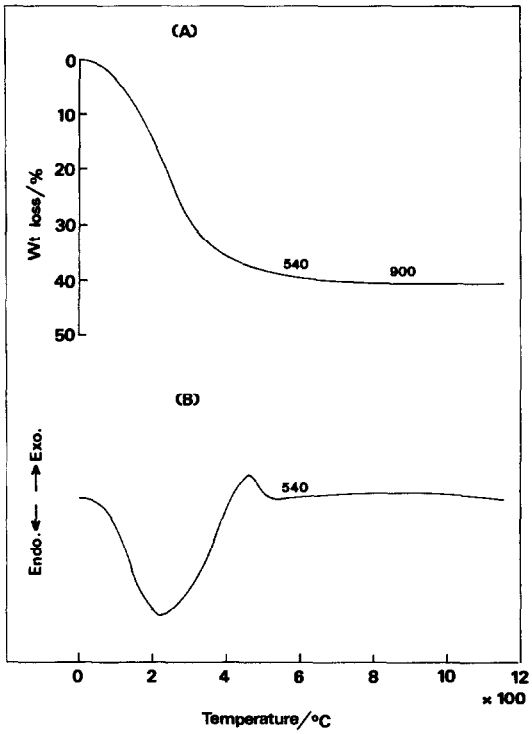

Fig. 3. (A) TG and (B) DTA curves for starting powder.

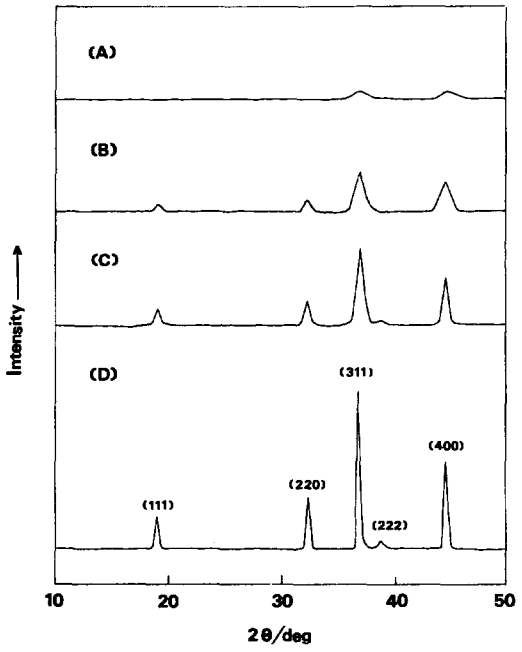

Fig. 4. X-ray diffraction patterns for specimens heated at (A) 700, (B) 1000, (C) 1100 and (D) 1250°C.

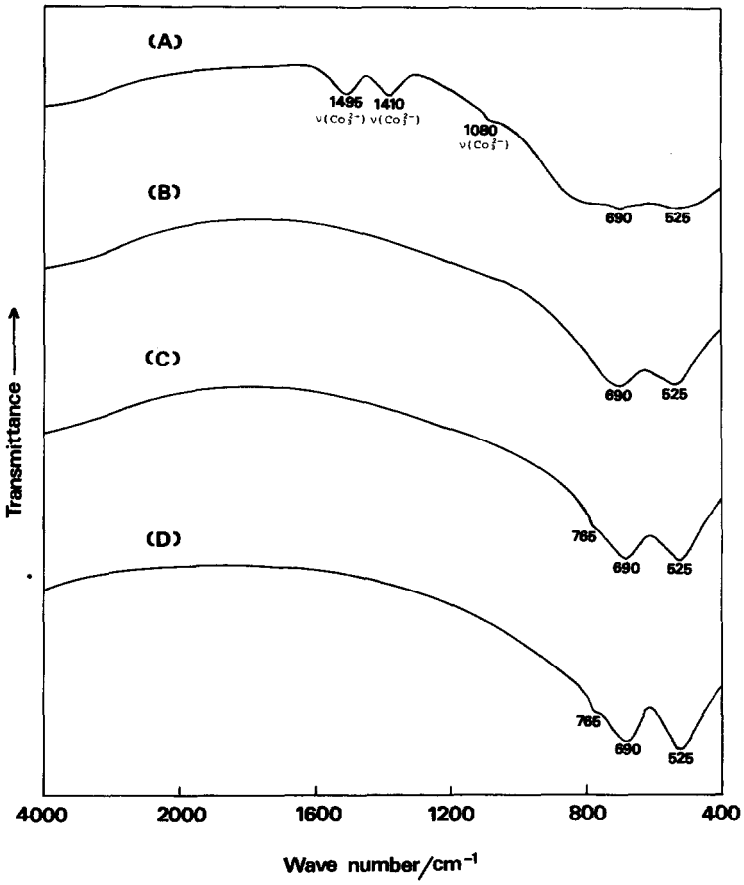

Fig. 5. Infrared spectral patterns for specimens heated at (A) 700, (B) 1000, (C) 1100 and (D) 1250°C.

The infrared spectral patterns of specimens heated to various temperatures are shown in Fig. 5. In accordance with the results of X-ray diffraction, IR spectrum data indicated that the characteristic bands of spinel at 690 and 525 cm^{-1} come to appear at 700°C;[15] however, the specimen contained carbon dioxide. The intensity of both bands increased with further increase in the heating temperature. The characteristic pattern of spinel with a shoulder at 765 cm^{-1} was observed above 1100°C.

From the above mentioned results, the crystallization of spinel was found to proceed slowly at $\approx$ 700–1250°C. The variation of crystallite size with increasing temperature was determined from X-ray line-broadening measurements.[16] The formula $D = K\lambda/\beta\cos\theta$ was used, where D is the mean crystallite dimension, K the crystalline-shape constant, λ the X-ray wavelength, β the corrected line breadth, and θ the Bragg angle. A spinel standard, which was prepared by solid state reaction between MgO and Al_2O_3 for 12 h at 1500°C, was used to obtain unbroadened line widths of the (311) and (400) reflections. A mean crystallite size was calculated by using an averaged broadening $\bar{\beta}_{12}$ defined as $\sqrt{\beta_1\beta_2}$ where $\beta_1 = B-b$ and $\beta_2^2 = B^2-b^2$; B is the width of a broadened line and b is the width of a standard line. Figure 6 shows the curve for crystallite growth of the spinel powders. A marked increase in crystallite size occurred between 1100 and 1200°C. Spinel powders consisting of aggregates of plate-like particles are shown in Fig. 7; the morphology is in agreement with that of particles reported.[3,7] The lattice constant of spinel obtained by heating for 3 h at 1250°C was estimated as a = 0.8084 nm, comparing with the value of a standard (a = 0.8083 nm)[2] prepared by solid state reaction between MgO and Al_2O_3.

Kinetics of crystallization of spinel

The fraction of crystallization of spinel was determined as a function of time at different temperatures. The starting powder had been heated previously up to 540°C at a rate of 10°C min^{-1}. A well-crystallized specimen was obtained by heating the starting powder for 3 h at 1250°C. As shown in

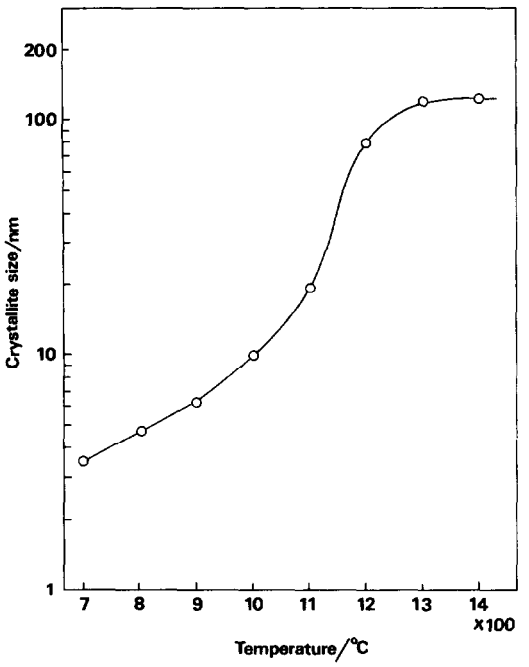

Fig. 6. Crystallite size of spinel with increasing temperature.

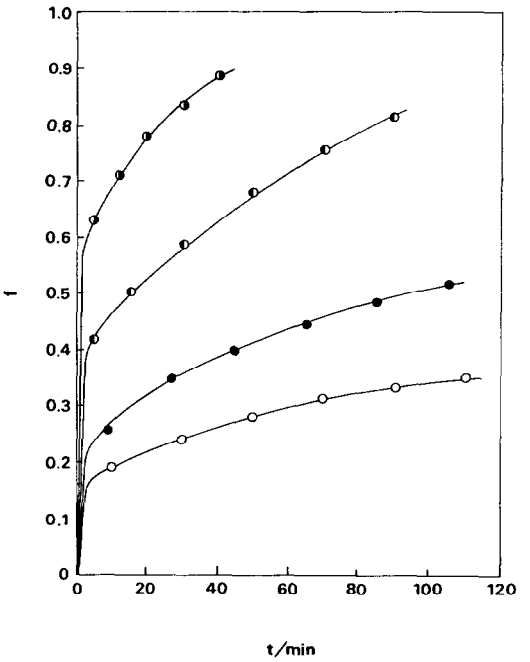

Fig. 8. Isotherms for crystallization of spinel at (○) 960, (●) 1020, (◐) 1100 and (◑) 1160°C.

Fig. 8, the initial stage of crystallization at each temperature proceeded rapidly in a short time; this may represent the process of nucleation. The data in the final stage can be described in terms of the contracting square equation (1)[17] (Fig. 9):

$$1-(1-f)^{1/2} = kt \qquad (1)$$

where f, t and k are the fractional crystallization, time, and rate constant, respectively. Equation (1), which has been employed to explain the kinetics of thermal decomposition of solids, is equivalent to one of the limiting forms of the Mampel equation.[18] In the present case, it indicates that crystallization is controlled by the rate of advance of interfacial

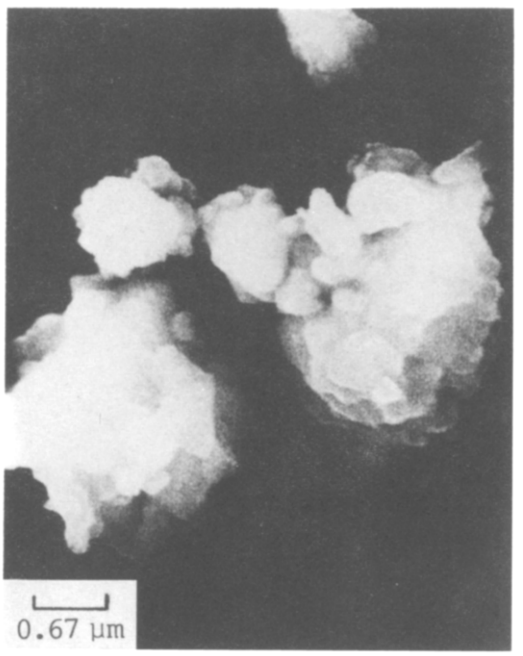

Fig. 7. Scanning electron micrograph for spinel powder.

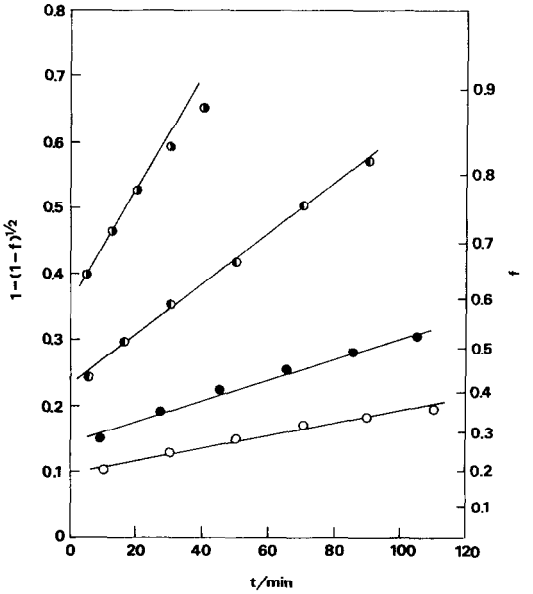

Fig. 9. Plots of $1-(1-f)^{1/2}$ vs time t of the data shown in Fig. 8. f is the fraction of spinel crystallized in time t. See Fig. 8 for key.

growth. An Arrhenius plot of the rate constants gave an activation energy of 164 kJ mol^{-1}.

REFERENCES

1. J. Beretka and T. Brown, *J. Am. Ceram. Soc.* 1983, **66**, 383.
2. R. J. Bratton, *Am. Ceram. Soc. Bull.* 1969, **48**, 759.
3. R. J. Bratton, *Am. Ceram. Soc. Bull.* 1969, **48**, 1069.
4. M. Dimitrov and I. Bakalova, *God. Vissh. Khimikotekhnol. Inst., Sofia* 1971, **16**, 171.
5. D. R. Messier and G. E. Gazza, *Am. Ceram. Soc. Bull.* 1972, **51**, 692.
6. P. W. D. Mitchell, *J. Am. Ceram. Soc.* 1972, **55**, 484.
7. M. Sugiura and O. Kamigaito, *Yogyo Kyokai Shi* 1984, **92**, 605.
8. O. Yamaguchi, K. Sugiura, A. Mitsui and K. Shimizu, *J. Am. Ceram. Soc.* 1985, **68**, C44.
9. M. L. Hair, *Infrared Spectroscopy in Surface Chemistry*, p. 198. Marcel Dekker, New York (1967).
10. M. P. Rosynek and D. T. Magnuson, *J. Catal.* 1977, **46**, 402.
11. R. D. Waldron and D. F. Hornig, *J. Am. Chem. Soc.* 1953, **76**, 6079.
12. M. M. Mortland, J. J. Fripiat, J. Chaussidon and J. Uytterhoeven, *J. Phys. Chem.* 1963, **67**, 248.
13. A. V. Deo, T. T. Chuang and I. G. D. Lana, *J. Phys. Chem.* 1971, **75**, 234.
14. G. A. Dorsey, Jr., *Anal. Chem.* 1968, **40**, 971.
15. P. Tarte, *Spectrochim. Acta* 1967, **23A**, 2127.
16. N. F. M. Henry, H. Lipson and W. A. Wooster, *Interpretation of X-Ray Diffraction Photograph*, p. 212. Van Nostland, New York (1951).
17. J. S. Sharp, G. W. Brindley and B. N. N. Achar, *J. Am. Ceram. Soc.* 1966, **49**, 379.
18. K. L. Mampel, *Z. Phys. Chem. Abt. A* 1940, **43**, 235.

Polyhedron Vol. 6, No. 9, pp. 1797–1802, 1987
Printed in Great Britain

0277-5387/87 $3.00+.00

THE DIMERIZATION OF DIPHENYL(CYCLOPENTADIENYL)PHOSPHINE LIGANDS BY DIELS–ALDER ADDITION

GREGORY G. GARVIN, TIMOTHY J. SLOAN and RICHARD J. PUDDEPHATT*

Department of Chemistry, University of Western Ontario, London, Canada N6A 5B7

(*Received* 5 *March* 1987; *accepted* 10 *April* 1987)

Abstract—Reaction of diphenyl(cyclopentadienyl)phosphine, **1**, with $[PdCl_2(PhCN)_2]$, $[PtCl_2(SMe_2)_2]$ or $[M(CO)_4(norbornadiene)]$, where M = Mo or W, gave the complexes $[PdCl_2\{(Ph_2P)_2C_{10}H_{10}\}]$, $[PtCl_2\{(Ph_2P)_2C_{10}H_{10}\}]$ or $[M(CO)_4\{(Ph_2P)_2C_{10}H_{10}\}]$ respectively, in which the ligand underwent dimerization by Diels–Alder addition. The reaction occurs in a very selective way and this is rationalized in terms of a template effect, in which two ligands **1** in mutually *cis* positions undergo the Diels–Alder reaction. In contrast, the complex $[Fe(CO)_4(Ph_2PC_5H_5)]$ is stable to Diels–Alder addition. The structures of the complexes were deduced by ^1H, ^{13}C and ^{31}P NMR spectroscopy. The major product contains a six-membered chelate ring while a minor product, formed in the palladium and platinum systems only, contains a five-membered chelate ring.

Cyclopentadienyldiphenylphosphine, **1**, has been shown to exist as a mixture of isomers **1a** (85%) and **1b** (15%), with none of the third possible isomer **1c**. Exchange between **1a** and **1b** was shown to be slow on the NMR time scale at room temperature.[1]

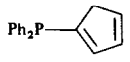

1a

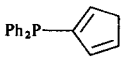

1b

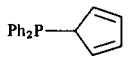

1c

The phosphine **1** did not undergo dimerization by Diels–Alder addition of cyclopentadienyl groups but, on oxidation to the phosphine oxide or sulfide or the methylphosphonium ion, dimerization did occur to give the Diels–Alder adduct identified as **2a** or **2b** (A = Ph_2PO, Ph_2PS or Ph_2PMe^+).[1] Both **2a** and **2b** would be formed from the major isomeric form of the oxidized phosphine **1a**.

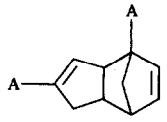

2a

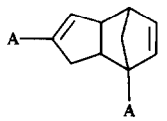

2b

The ligand **1**, in its deprotonated form $[Ph_2PC_5H_4]^-$, has proved to be very useful for bridging between two different metal atoms. The preferred synthetic method has been to coordinate the C_5H_4 unit first to give an η^5-$C_5H_4PPh_2$ complex and then to coordinate a second metal through the phosphine group.[2] In ferrocene, the phosphino groups can be added later and $[Fe(\eta^5\text{-}C_5H_4PPh_2)_2]$ and its derivatives have been used to great effect as bidentate diphosphine ligands.[3] An alternative approach would be to coordinate the phosphine of **1** first, followed by deprotonation and coordination to a second metal via the cyclopentadienyl group. This article shows that this approach is likely to be limited to a single bridging ligand, since rapid Diels–Alder addition occurs when two of the ligands **1** are coordinated in mutually *cis* positions. The nature of this reaction is of considerable interest and gives two new bidentate diphosphine ligands $(Ph_2P)_2C_{10}H_{10}$.

RESULTS

Reaction of two equivalents of cyclopentadienyldiphenylphosphine, **1**, with $[PdCl_2(PhCN)_2]$ or $[PtCl_2(SMe_2)_2]$ gave the corresponding complexes $[PdCl_2\{(Ph_2P)_2C_{10}H_{10}\}]$, **3**, and $[PtCl_2\{(Ph_2P)_2C_{10}H_{10}\}]$, **4**, respectively. Simi-

* Author to whom correspondence should be addressed.

larly, reaction of $[M(CO)_4(NBD)]$, NBD = norbornadiene, with two equivalents of **1** gave $[Mo(CO)_4\{(Ph_2P)_2C_{10}H_{10}\}]$, **5**, or $[W(CO_4)\{(Ph_2P)_2C_{10}H_{10}\}]$, **6**, respectively. It was immediately apparent that the ligands had undergone Diels–Alder addition. Thus a complex $M(Ph_2PC_5H_5)_2$, with the ligand in either isomeric form **1a** or **1b**, should give a ^1H NMR spectrum with integration of olefinic : aliphatic protons = 3 : 2, whereas either **5** or **6** gave this integration = 3 : 7 as previously found for the Diels–Alder adduct **2**.[1] The situation was more complex for **3** and **4** as discussed below, but it was still clear that Diels–Alder addition had occurred. The structures were studied by ^1H, ^{13}C and ^{31}P NMR spectroscopy and the data are given in Tables 1–3.

If a template effect is assumed in the Diels–Alder coupling then, because of the constraints imposed by the dicyclopentadiene bridge, only five- or six-membered chelate rings are possible, and the coupling must be different from that observed in forming **2**.[1] The size of a diphosphine chelate ring can be determined from the ^{31}P chemical shifts and from the magnitudes of the coupling $^2J(PMP)$, using established empirical correlations.

The ^{31}P NMR spectra of the complexes **5** and **6** showed them to be single isomers, each giving an "AX" spectrum containing two doublet resonances. The chemical shifts were characteristic of a six-membered ring (Table 3). In addition, the magnitudes of $^2J(PP)$ of $\geqslant 20$ Hz are characteristic of a six-membered chelate ring (Table 3) but much too large for a five-membered ring.[4]

The nature of the dicyclopentadiene bridge was studied by ^{13}C and ^1H NMR spectroscopy (Tables 1 and 2), by comparison with the known spectra of endo- and exo-dicyclopentadiene, **7a** and **7b**.[5] The spectra are complex and assignments for the molybdenum complex **5** were confirmed by recording the 2D ^{13}C–^1H chemical shift correlated spectrum and the 2D ^1H–^1H correlated spectrum. The ^1H–^1H correlation identified H^2 and H^3 as a coupled pair and hence H^8 was identified as the remaining olefinic hydrogen. The corresponding carbon atoms were identified from the ^{13}C–^1H correlation and the signal for C^9 identified as the only remaining olefinic carbon. The aliphatic carbon and hydrogen signals could be assigned similarly and hence the overall connectivity determined. The NMR data thus determine the skeleton as **I** or **II**, formed by endo- or exo-addition respectively. The positions of the phosphorus atoms are confirmed by the magnitudes of the couplings $^1J(PC^1)$ and $^1J(PC^9)$. Consideration of molecular models indicates that both **I** and **II** are possible structures, with neither having significant ring strain. The spectra of the tungsten

Table 1. ^1H NMR data for the complexes

Complex	δ(H)/ppm									J/Hz				
	H^2	H^3	H^4	H^5	$H^{5'}$	H^6	H^7	$H^{7'}$	H^8	H^9	H^{10}	$J_{2,3}$	$J_{6,7}$	$J_{5,5'}$	$J_{7,7'}$	$J_{8,9}$
$[PdCl_2(LL)]$	6.72	6.38	2.95	1.60	1.95	2.95	2.42	1.86	5.48	—	3.16	6	8	9	19	—
$[PtCl_2(LL)]$	6.80	6.32	2.92	1.72	1.95	2.92	2.35	1.88	5.37	—	3.08	6	8	8	20	—
$[Mo(CO)_4(LL)]$	6.72	6.21	3.00	0.77	2.04	2.78	2.30	1.83	5.23	—	3.00	6	10	9	19	—
$[W(CO)_4(LL)]$	6.73	6.22	3.04	0.79	2.04	2.82	2.33	1.86	5.26	—	3.04	6	10	8.5	19	—
$[PdCl_2(LL')]$	6.34	6.24	2.91	1.30	1.92	3.02	2.37	1.72	5.14	5.52	—	6	8	8	19	6
$[PtCl_2(LL')]$	6.28	6.28	2.95	1.15	1.80	3.11	2.18	1.75	5.11	5.47	—	[a]	8	8	18	6
endo-Dicp	5.92	5.92	2.75	1.25	1.53	2.60	2.13	1.63	5.44	5.44	3.17	5.8	9.6	8.0	17	5.6
exo-Dicp	6.08	6.08	2.55	1.51	1.30	2.24	2.42	1.86	5.54	5.75	2.74	5.8	10.8	8.0	17.5	5.6

[a] Not resolved.

Table 2. ^{13}C NMR data for the complexes

Complex	δC/ppm (J[PC]/Hz)									
	C^1	C^2	C^3	C^4	C^5	C^6	C^7	C^8	C^9	C^{10}
$[PdCl_2(LL)]$	53.0	135.7	147.0	46.5	51.7	44.5	36.3	134.6	126.5	59.1
	(36)	(11.5)	(9)	(6.5)	(6.5)	(5,7)	(11.5)	(11.5)	(55,14)	(15,6)
$[Mo(CO)_4(LL)]$	55.8	135.7	145.0	45.1	51.2	43.4	35.5	134.2	137.0	60.1
	(23)	(11)	(6)	(7)	(6)	(5,7)	(9)	(9)	(35,4)	(18,11)
$[W(CO)_4(LL)]$	56.3	135.6	145.0	45.2	51.4	43.4	35.6	134.2	136.7	60.1
	(28)	(11)	(5)	(8)	(5.5)	(5,8)	(9)	(9)	(31)	(17,10)
endo-Dicp	45.3	131.9	132.2	46.3	50.3	41.3	34.7	132.1	135.6	54.8
exo-Dicp	45.5	137.2	137.0	48.0	41.3	41.8	36.5	132.9	132.0	51.4

and molybdenum complexes are almost identical and clearly indicate the same structure for both compounds; this chelate ligand is labelled LL in the tables and has structure **I** as shown below.

The situation was more complex for the palladium and platinum complexes **3** and **4**. The ^{31}P NMR spectra showed the presence of two isomers in each case, each giving an "AX" spectrum. The ^{31}P chemical shifts of each (with chelate ligands labelled LL′ and LL) showed that both five-membered (LL′) and six-membered (LL) chelate rings were formed,[4] with the ratio of LL:LL′ being approximately 70:30 in each case. For the palladium complex **3**, the major isomer $[PdCl_2(LL)]$ could be separated by fractional crystallization but the minor isomer was not isolated pure. However, multiple partial separations using thin layer chromatography followed by recrystallization gave a sample containing ~ 75% $[PdCl_2(LL')]$/25% $[PdCl_2(LL)]$ and the ^1H NMR spectrum of $[PdCl_2(LL')]$ (Table 1) was obtained from this impure sample. Separation was also difficult for the platinum complexes, but in one case a small amount of $[PtCl_2(LL')]$ was isolated in pure form. The spectrum of $[PtCl_2(LL)]$ was obtained on a sample containing ~ 15% $[PtCl_2(LL')]$, as determined by ^{31}P NMR. The coupling constants $^1J(PtP)$ for these compounds are also characteristic of chelate ring size[4] and confirm the conclusion based on the ^{31}P chemical shifts.

The ^1H and ^{13}C NMR spectra of the major palladium complex, containing the six-membered chelate ring $[PdCl_2(LL)]$ (Tables 1 and 2), were assigned using 2D NMR as described for the molybdenum

Table 3. ^{31}P NMR data for the complexes

Complex[a]	δ(P)	$^1J(MP)$	$^2J(PP)$	Complex[a]	δ(P)	$^1J(MP)$	$^2J(PH)$
$[PdCl_2(dppe)]$	68.3	—	—	$[PdCl_2(dppp)]$	12.9	—	—
$[PdCl_2(LL')]$	85.3	—	2	$[PdCl_2(LL)]$	30.6	—	2
	59.4	—	2		13.5	—	2
$[PtCl_2(dppe)]$	45.3	3618	—	$[PtCl_2(dppp)]$	−5.6	3420	—
$[PtCl_2(LL')]$	58.1	3644	11	$[PtCl_2(LL)]$	10.9	3555	18
	34.5	3558	11		−4.8	3496	18
$[Mo(CO)_4(dppe)]$	54.7	—	5	$[Mo(CO)_4(dppp)]$	21.0	—	28
				$[Mo(CO)_4(LL)]$	35.7	—	25
					21.8	—	25
$[W(CO)_4(dppe)]$	40.1	231	4	$[W(CO)_4(dppp)]$	0.0	222	22
				$[W(CO)_4(LL)]$	17.9	230	20
					4.4	229	20

[a] dppe = $Ph_2PCH_2CH_2PPh_2$, dppp = $Ph_2PCH_2CH_2CH_2PPh_2$. Values for dppe and dppp taken from ref. 4.

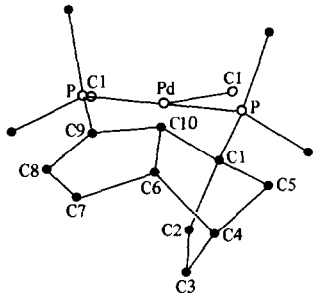

Fig. 1. Ball and stick diagram of the structure of $[PdCl_2\{(Ph_2P)_2C_{10}H_{10}\}]$, **3-I**. Atoms are shown as spheres of arbitrary size; carbon atoms are closed spheres; only ipso carbon atoms of phenyl rings are shown. Typical distances (Å): C2–C3, 1.32(1); C8–C9, 1.35(1); other C–C distances of $C_{10}H_{10}$ unit, 1.49(1)–1.56(1); P–C, 1.793(6)–1.816(7); P–Pd, 2.260(2), 2.263(2); Pd–Cl, 2.341(3), 2.349(2).

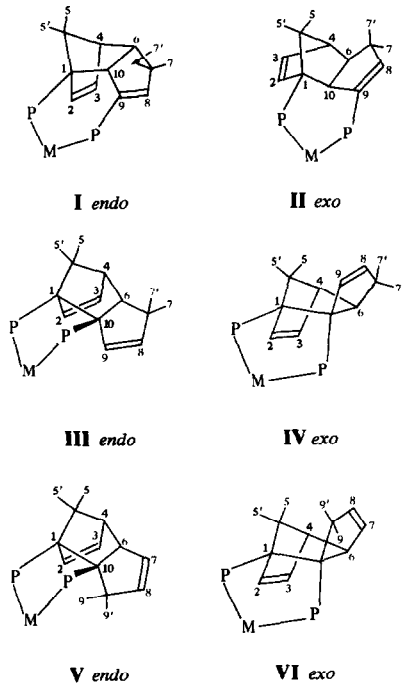

I *endo* **II** *exo*

III *endo* **IV** *exo*

V *endo* **VI** *exo*

complex. The close similarity in spectra strongly suggest the same structure **I** or **II** for the diphosphine ligand LL in all cases, and the endo structure **I** was established by X-ray crystallography for the palladium complex (Fig. 1).[6]

Satisfactory ^{13}C NMR spectra of the minor complexes $[PdCl_2(LL')]$ and $[PtCl_2(LL')]$ shown by ^{31}P NMR to contain a five-membered chelate ring, could not be obtained and the structure of the dicyclopentadiene bridge is deduced only from the ^1H NMR spectra. In these complexes four olefinic protons were identified, consistent with the structures **III**–**VI**. The exo structures **IV** and **VI** are more strained than the endo structures **III** and **V** and are therefore considered unlikely. In the ^1H NMR spectra of both $[PdCl_2(LL')]$ and $[PtCl_2(LL')]$, the signal for H^7 appears as a broad doublet of doublets with $^2J(H^7H^{7'}) = 18$–19 Hz and a second coupling of 8 Hz, as expected for isomer **III** due to the vicinal coupling $^3J(H^6H^7)$ (Table 1) but not for structure **V**. The signal due to H^6 is partially obscured but also appears as a doublet with J(HH) ~ 8 Hz. It is therefore tentatively concluded that the structure is **III** for the ligand LL′.

Reaction of $PPh_2(C_5H_5)$ with $[Fe(CO)_5]$ gave $[Fe(CO)_4\{PPh_2(C_5H_5)\}]$, which did not readily dimerize by intermolecular Diels–Alder addition. The complex existed as a single isomer (^{31}P NMR evidence) with the ligand present in form **1a** or **1b** (^1H NMR evidence) and the cyclopentadienyl group could be deprotonated reversibly.

DISCUSSION

There are a number of interesting features of the above reactions. The increased rate of Diels–Alder addition on complexation of the ligand **1** could be due simply to an electronic effect, just as oxidation of the phosphorus atom of **1** to the oxide, sulfide or methylphosphonium derivative leads to increased reactivity to dimerization.[1] However, the complex $[Fe(CO)_4\{PPh_2(C_5H_5)\}]$ does not readily dimerize, whereas all of the complexes containing two phosphine ligands underwent rapid dimerization of the cyclopentadienyl substituents. This indicates clearly that a template effect is primarily responsible for the increased reaction rate of the Diels–Alder addition. Such an effect is expected since the entropy term is usually a major component of the activation energy for Diels–Alder additions, which have a highly ordered transition state.[7]

The selectivity of the observed Diels–Alder reactions is impressive. The free phosphine ligand exists as a mixture of 85% **1a** and 15% **1b**, and the probabilities of pairs of phosphines **1a**·**1a**, **1a**·**1b** and **1b**·**1b** are therefore 72%, 26% and 2% respectively.[1] The complexes formed contained the coupled ligands, LL, in structure **I** which is formed by coupling of **1a**·**1b** pairs as either the major or only product (eqn 1). The diene is **1a** and the dienophile is **1b**. The minor products with ligands LL′ are thought to have structure **III** which is also formed by coupling of **1a**·**1b** pairs (eqn 2). These observations can only be understood if hydrogen migration, which is necessary to interconvert **1a** ⇌ **1b** (in either free or complexed form), is faster than the Diels–Alder addition reaction. Otherwise the major products should be formed by coupling of **1a**·**1a** pairs.

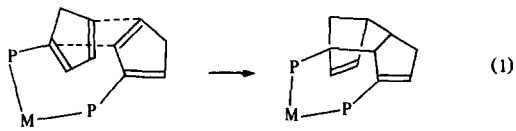

(1)

I

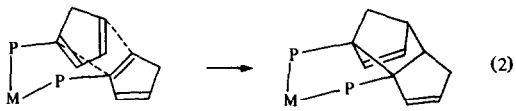

(2)

III

Why are the isomeric forms **I** and **III** formed? We note that both are formed by *endo*-addition, which is the favored mode of Diels–Alder addition of cyclopentadiene itself.[7] There is still some debate in the organic literature about the reasons for *endo* rather than *exo* addition.[7] In the present case, it is clear that the template effect is primarily responsible for the selectivity of the addition. Molecular models clearly show that the diene in the Diels–Alder addition must be in form **1a**, as is observed experimentally. In form **1b** the diphenylphosphino group would be at C^2 in the product and chelation would not be possible. Now, the six-membered chelate ring can only be formed if the dienophile is in form **1b** (eqn 1) rather than **1a**. Form **1c** would be allowed, but this appears to be of too high energy to be formed. The formation of **I** thus follows naturally from the template effect.

The five-membered ring could be formed with the dienophile in either form **1a** or **1b**, but it seems that the product is formed selectively from the form **1b**. Since the ligand structure **III** is tentative in this case, no further comment is justified. The preference for formation of the six-membered ring **I**, rather than the five-membered ring **III**, is probably due to a slightly less strained transition state. In the absence of such effects, the five-membered ring **III** would be expected to be thermodynamically more stable than **I**.

EXPERIMENTAL

^1H NMR spectra were recorded using Varian XL100 or XL200 spectrometers. Chemical shifts are given with respect to Me_4Si (^1H, ^{13}C) or 85% H_3PO_4 (^{31}P).

The ligand $PPh_2(C_5H_5)$ was prepared by the literature method.[1]

$[PtCl_2(Ph_2PC_{10}H_{10}PPh_2]$, 4

A solution of $[PtCl_2(SMe_2)_2]$ (0.83 g) in CH_2Cl_2 (25 cm^3) was added dropwise to a solution of $PPh_2(C_5H_5)$ (1.08 g) in tetrahydrofuran (40 cm^3). The mixture was allowed to stir for 2 h, the solvents were evaporated under vacuum and the residue was crystallized from CH_2Cl_2/MeOH to give colorless crystals of the product (1.26 g) m.p. 220°C (decomp.). Found: C, 53.1; H, 4.0; Cl, 9.1. Calc. for $C_{34}H_{30}Cl_2P_2Pt$: C, 53.3; H, 3.9; Cl, 9.3%. The pure isomer **4–III** was obtained by repeated recrystallization.

$[PdCl_2(Ph_2PC_{10}H_{10}PPh_2)]$, 3

This was prepared similarly from $[PdCl_2(PhCN)_2]$ (1.00 g) and $PPh_2(C_5H_5)$ (1.30 g) and purified by crystallization from $CHCl_3$/MeOH. M.p. 210°C (decomp.). Found: C, 59.8; H, 4.3; Cl, 10.7. Calc. for $C_{34}H_{30}Cl_2P_2Pd$: C, 60.3; H, 4.4; Cl, 10.5%.

The pure isomer **3-I** was obtained by repeated recrystallization from CH_2Cl_2/MeOH. Found: C, 55.2; H, 4.0. Calc. for $C_{34}H_{30}Cl_2P_2Pd \cdot CH_2Cl_2$: C, 55.4; H, 4.2%.

$[Mo(CO)_4(Ph_2PC_{10}H_{10}PPh_2)]$, 5

A solution of $[Mo(CO)_4(NBD)]$, NBD = norbornadiene (0.72 g) in CH_2Cl_2 (10 cm^3) was added to a solution of $PPh_2(C_5H_5)$ (1.68 g) in $CHCl_2$ (10 cm^3). The mixture was stirred for 2 h, the solvent was evaporated and the product was purified by recrystallization from $CHCl_3$/pentane at 0°C. Yield 0.96 g. Found: C, 64.2; H, 4.2; P, 8.4. Calc. for $C_{38}H_{30}O_4P_2Mo$: C, 64.4; H, 4.2; P, 8.8%.

$[W(CO)_4(Ph_2PC_{10}H_{10}PPh_2)]$, 6

A solution of $[W(CO)_4(NBD)]$ (0.20 g) and $PPh_2(C_5H_5)$ (0.33 g) in CH_2Cl_2(10 cm^3) was stirred at room temperature for 20 h. The solvent was evaporated and the product was purified by recrystallization from $CHCl_3$/pentane (0.35 g). Found: C, 57.3; H, 3.6; P, 7.2. Calc. for $C_{38}H_{30}O_4P_2W$: C, 57.3; H, 3.8; P, 7.8%.

$[Fe(CO)_4(Ph_2PC_5H_5)]$

$Fe(CO)_5$ (3.92 g) was added to a refluxing solution of $PPh_2(C_5H_5)$ (2.50 g) in toluene (50 cm^3) containing $CoBr_2 \cdot 3H_2O$ (0.08 g) as catalyst. After 1 h the volume was reduced and the product was purified by chromatography on 5 g/20 g/20 g $CoBr_2 \cdot 6H_2O$/alumina/silica column with benzene eluent. Recrystallization from CH_2Cl_2/hexane gave the product as a red solid. Yield 91%. ^1H NMR: δ = 6.90, 6.75, 6.60 (*m*, 3H, =CH); 3.20 (m, CH_2). ^{31}P NMR: δ = 55.8 (s, ^{31}P). IR: 2040, 1980, 1940

[ν(CO)]. Found: C, 60.3; H, 3.7. Calc. for $C_{21}H_{15}FeO_4P$: C, 60.3; H, 3.6%.

Reaction of the above complex with TlOEt in toluene gave a precipitate of [$Fe(CO)_4(Ph_2PC_5H_4Tl)$] as a brown powder. The complex was too insoluble for characterization by NMR, but addition of CF_3CO_2H to a suspension of the complex in C_6D_6 gave [$Fe(CO)_4(Ph_2PC_5H_5)$], characterized by its NMR spectrum.

Acknowledgements—We thank NSERC (Canada) for financial support.

REFERENCES

1. F. Mathey and J.-P. Lampin, *Tetrahedron* 1975, **31**, 2685.
2. See for example: (a) F. Mathey and J.-P. Lampin, *J. Organomet. Chem.* 1977, **128**, 297; (b) M. D. Rausch, B. H. Edwards, R. D. Rogers and J. L. Atwood, *J. Am. Chem. Soc.* 1983, **105**, 3881; (c) A. W. Rudie, D. W. Lichtenberg, M. L. Katcher and A. Davison, *Inorg. Chem.* 1978, **17**, 2859; (d) J. C. Leblanc, C. Moise, A. Maisonnet, R. Poilblanc, C. Charrier and F. Mathey, *J. Organomet. Chem.* 1982, **231**, C43; (e) C. P. Casey, R. M. Bullock, W. C. Fultz and A. L. Rheingold, *Organometallics* 1982, **1**, 1591; (f) J. J. Bishop and A. Davison, *Inorg. Chem.* 1971, **10**, 826 and 832; (g) C. P. Casey, R. M. Bullock and F. Nief, *J. Am. Chem. Soc.* 1983, **105**, 7574; (h) C. P. Casey and R. M. Bullock, *Organometallics* 1984, **3**, 1100.
3. For recent references, see: I. R. Butler and W. R. Cullen, *Organometallics* 1986, **5**, 2537; A. Davison and J. J. Bishop, *Inorg. Chem.* 1971, **10**, 826.
4. (a) P. E. Garrou, *Chem Rev.* 1981, **81**, 229; (b) S. O. Grim, R. C. Barth, J. D. Mitchell and J. DelGaudio, *Inorg. Chem.* 1977, **16**, 1776; (c) S. O. Grim, R. Barth, W. Briggs, C. A. Tolman and J. P. Jesson, *Inorg. Chem.* 1974, **13**, 1095; (d) A. R. Sanger, *J. Chem. Soc. Dalton Trans.* 1977, 1971; (e) T. G. Appleton, M. A. Bennett and I. B. Tomkins, *J. Chem. Soc. Dalton Trans.* 1976, 439; (f) A. J. Carty, D. K. Johnson and S. E. Jacobson, *J. Am. Chem. Soc.* 1979, **101**, 5612.
5. (a) K. C. Ramey and D. C. Lini, *J. Mag. Res.* 1970, **3**, 94; (b) R. G. Foster and M. C. McIvor, *J. Chem. Soc. B* 1969, 188; (c) K. Nakagawa, S. Iwase, Y. Ishii, S. Hamanaka and M. Ogawa, *Bull. Chem. Soc. Jap.* 1977, **50**, 2391.
6. T. J. Sloan, M.Sc. thesis, University of Western Ontario, 1984. One of the phenyl rings of the complex is severely disordered. The details of the crystallography will be published separately.
7. (a) T. L. Gilchrist and R. C. Storr, *Organic Reactions and Orbital Symmetry*, 2nd edn, chap. 5. Cambridge University Press, Cambridge (1979); (b) J. G. Martin and R. K. Hill, *Chem. Rev.* 1961, **61**, 537; (c) R. R. Schmidt, *Angew. Chem. Int. Ed. Engl.* 1973, **12**, 212; (d) W. Oppolzer, *Angew. Chem. Int. Ed Engl.* 1977, **16**, 10; (e) R. B. Woodward and R. Hoffmann, *Angew. Chem. Int. Ed. Engl.* 1969, **8**, 781; (f) W. C. Herndon and L. H. Hall, *Tetrahedron Lett.* 1967, 3095; (g) J. Sauer, *Angew. Chem. Int. Ed. Engl.* 1967, **6**, 16.

Polyhedron Vol. 6, No. 9, pp. 1803–1805, 1987
Printed in Great Britain

0277–5387/87 $3.00+.00

COMMUNICATION

A PARTIALLY CLOSED-MODE PLATINUM DIMER BASED ON A BINUCLEATING HEXAPHOSPHINE LIGAND SYSTEM: CRYSTAL STRUCTURE OF $[Pt_2Cl_2(eHTP)^{2+}][PF_6^-]_2$ (eHTP = $(Et_2PCH_2CH_2)_2PCH_2P(CH_2CH_2PEt_2)_2$

SUZANNE E. SAUM and GEORGE G. STANLEY*

Department of Chemistry, Louisiana State University, Baton Rouge, LA 70803-1804, U.S.A.

(*Received* 9 *December* 1986; *accepted after revision* 29 *April* 1987)

Abstract—The reaction of two equivalents of K_2PtCl_4 with the hexaphosphine ligand system $(Et_2PCH_2CH_2)_2PCH_2P(CH_2CH_2PEt_2)_2$, eHTP, quantitatively yields the diamagnetic dimer species, $Pt_2Cl_2(eHTP)^{2+}$, **3**. The single-crystal X-ray structure of the PF_6^- salt of **3** reveals a distorted square-planar environment about the metal atoms with the eHTP ligand adopting a symmetrical *bis*chelating/bridging, partially closed-mode coordination geometry with a Pt—Pt distance of 4.6707(9) Å.

Our studies of the coordination chemistry of the powerful binucleating hexatertiaryphosphine ligand, $(Et_2PCH_2CH_2)_2PCH_2P(CH_2CH_2PEt_2)_2$, eHTP, have revealed that the ligand's ability to both bridge and *bis*-chelate two metal centers has so far produced only open-mode complexes of the general type **1b**[1] or **1c**,[2] while the closed-mode conformer **1a** has not yet been crystallographically characterized. Van der Waal energy calculations on the nickel complex $Ni_2Cl_2(eHTP)^{2+}$, **2**, have revealed that the closed-mode configuration should be inaccessible for an eHTP arrangement in which two terminal phosphine groups are *trans* to one another, i.e. for square-planar coordination geometries.[2] In light of these results, we would like to report the synthesis and structural characterization of the platinum(II) complex, $[Pt_2Cl_2(eHTP)^{2+}][PF_6^-]_2$, **3**, in which the eHTP ligand has adopted a square-planar coordination and a partially closed-mode conformation.

The reaction of two equivalents of K_2PtCl_4 with eHTP[1] in ethanol under inert atmosphere conditions, followed by addition of $NaPF_6$, produces the air-stable, colorless, diamagnetic binuclear complex $[Pt_2Cl_2(eHTP)^{2+}][PF_6^-]_2$, **3**, in very high yields. A single-crystal X-ray structure (Fig. 1, selected bond distances and angles are listed in Table 1) on **3** shows that the eHTP ligand adopts a tridentate, distorted square-planar geometry about each

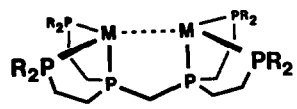

1a

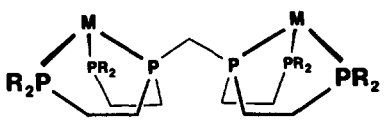

1b

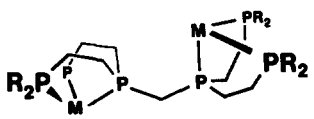

1c

* Author to whom correspondence should be addressed.

of the two platinum centers.† The distortion from square-planar coordination about each platinum atom is considerable, as indicated by the *trans* P—Pt—P angle of 163.6(2)°. This distortion is undoubtably related to the strain induced by the placement of two fused 5-member chelate rings in a transoidal geometry. The presence of ethylene bridges in eHTP favors *confacial* rather than *meridional* type coordination for each tridentate half of the ligand.[3] Although other mononuclear Pt(II) halide complexes with two-carbon bridged tridentate phosphine ligands have been reported, this represents the first structurally characterized complex.[4–7]

What is immediately evident from the structure is that the eHTP ligand adopts a rather different rotomeric conformation about the central P—CH_2—P linkage from anything we have previously seen. The related nickel complex, $[Ni_2Cl_2(eHTP)^{2+}][BF_4^-]_2$, for example, has a structure that corresponds to **1c**, while the chloride salt has a structure midway between **1b** and **1c**.[2] The platinum structure, however, is approaching that of a closed-mode configuration, **1a**, with a Pt—Pt distance of 4.6707(9) Å. The rotational orientation of the eHTP ligand can be clearly seen in Fig. 1 which also shows an orthogonal view of the molecule looking down the P1···P4 vector. The Pt1—P1···P4—Pt2 torsional (dihedral) angle is 62°, where 0°, represents the closed-mode form **1a**.

A remarkable feature of the structure of **3** is that the central P—CH_2—P angle has a value of

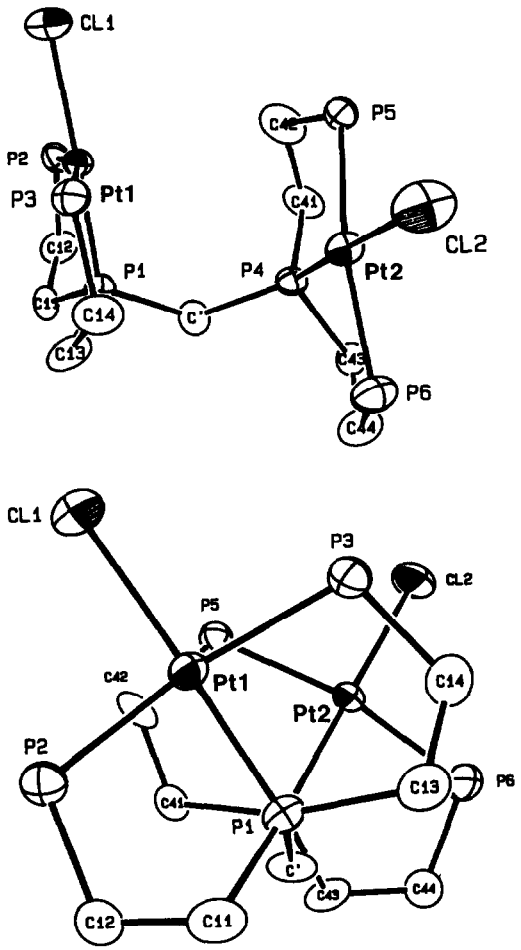

Fig. 1. ORTEP plots of $Pt_2Cl_2(eHTP)^{2+}$ showing views parallel and perpendicular to the central P1···P4 vector. Ethyl groups on the external phosphorus atoms have been omitted for clarity. Probability ellipsoids are shown at a 33% level.

129.7(9)°. This can be contrasted to typical P—CH_2—P angles seen in other *bis*(phosphino)methane bridged structures which are in the range of 109–118°.[8] This angle is also 8° greater than that seen in the analogous isoelectronic nickel complex, **2**,[2] and even surpasses the P—CH_2—P angle of 127.7(3)° seen in $Co_2(CO)_4(eHTP)^{2+}$.[1] Indeed, this is one of the largest angles observed about a methylene bridge, on par with that observed for *bis*(9-triptycyl)methane which has a C—CH_2—C angle of 129.3°.[9] The M—M bond distances in eHTP complexes are, of course, related to the rotational orientation of the ligand with the cobalt complex having the maximum M—M separation of 6.697(1) Å, while the nickel systems show M—M bond distances of 5.9333(8) Å and 5.7505(6) Å. **3**, with its partially closed-mode structure, has the shortest M—M distance observed in an eHTP

†X-ray analysis: Compound **3** crystallizes in the orthorhombic space group $P2_12_12_1$ with $a = 13.418(3)$ Å; $b = 17.795(6)$ Å; $c = 18.906(4)$ Å; $V = 4514(4)$ Å^3; $Z = 4$. 5930 Friedel pair reflections were collected at 25°C on a Nicolet P3 diffractometer using Mo Kα radiation and the ω scan data collection technique with a maximum 2θ angle of 45°. The structure was solved using the MULTAN direct methods programs and refined using 2529 reflections with $F_o^2 > 3\sigma(F_o^2)$ to give discrepancy indices of $R = 0.035$ and $R_w = 0.047$ for 352 variables representing 37 anisotropic non-hydrogen atoms (the flourine atoms on the PF_6^- groups were refined isotropically). An empirical absorption correction using Friedel pair reflections and program DIFABS was performed.

Supplementary Materials Available. Tables of fractional coordinates and thermal parameters have been deposited with the Cambridge Crystallographic Data Centre. Tables of data collection and structure solving details, full listings of bond distances and angles, and observed and calculated structure factor tables have been deposited with the Editor at Indiana University and are also available from the author.

Table 1. Selected bond distances and angles for $Pt_2Cl_2(eHTP)^{2+} \cdot 2PF_6^-$[a]

	Bond distances (Å)		
Pt(1)—Pt(2)	4.6707(9)	Pt(2)—P(5)	2.320(5)
Pt(1)—P(1)	2.197(4)	Pt(2)—P(6)	2.317(5)
Pt(1)—P(2)	2.302(5)	Pt(2)—Cl(2)	2.348(5)
Pt(1)—P(3)	2.325(5)	P(1)—C′	1.82(2)
Pt(1)—Cl(1)	2.352(5)	P(4)—C′	1.83(2)
Pt(2)—P(4)	2.200(4)		
	Bond angles (°)		
P(1)—Pt(1)—Cl(1)	177.5(2)	P(4)—Pt(2)—Cl(2)	176.8(3)
P(1)—Pt(1)—P(2)	85.3(2)	P(4)—Pt(2)—P(5)	86.7(2)
P(1)—Pt(1)—P(3)	86.9(2)	P(4)—Pt(2)—P(6)	85.0(2)
P(2)—Pt(1)—P(3)	163.7(2)	P(5)—Pt(2)—P(6)	163.5(2)
		P(1)—C′—P(4)	129.7(9)

[a] Numbers in parentheses represent esd's. A complete set of bond distances and angles is given in supplementary material.

complex so far with a Pt—Pt distance of 4.6707(9) Å.

An important question one must ask is why **3** adopts such a large P—CH_2—P angle allowing access to the partially closed-mode eHTP orientation. One possible answer is that crystal packing forces are responsible, just as they cause rotational differences in the nickel structures.[2] Although it is rather difficult to predict the effects or magnitudes of crystal packing forces, it would appear unlikely that they represent the sole factor in determining the extremely large P—CH_2—P angle and unusual (for a square-planar complex) eHTP conformation observed. It is very difficult at this point to determine whether it is the flexibility of the P—CH_2—P bond angle that allows access to the partially closed-mode conformation or whether there is some driving force favoring this conformation that is forcing the methylene bridge angle open to its remarkable value. As with most physical explanations it is most probably a subtle mixture of several features. We feel that some of the important factors that work together to influence the molecular conformation are: considerable low-energy flexibility of the P—CH_2—P linkage; increased *intra*molecular steric contacts due to chelate ring puckering differences caused by the larger terminal Pt—P bond distances (approx. 0.1 Å greater than the nickel or cobalt systems); and the possible presence of a *weak* Pt—Pt bonding interaction which could help overcome the steric and electrostatic factors favoring the open-mode conformations. We plan to further explore these points through van der Waal energy calculations and solution NMR experiments to study the conformational preferences of **3**.

Acknowledgements—This work was supported by a grant from the National Science Foundation and the Petroleum Research Fund of the American Chemical Society. We would also like to acknowledge a young faculty research support grant from Monsanto Co.

REFERENCES

1. F. R. Askham, G. G. Stanley and E. C. Marques, *J. Am. Chem. Soc.* 1985, **107**, 7423.
2. S. A. Laneman and G. G. Stanley, *Inorg. Chem.* 1987, **26**, 1177.
3. T. E. Nappier, D. W. Meek, R. M. Kirchner and J. A. Ibers, *J. Am. Chem. Soc.* 1973, **95**, 4195.
4. R. B. King, P. N. Kapoor and R. N. Kapoor, *Inorg. Chem.* 1971, **10**, 1841.
5. R. B. King and J. C. Cloyd Jr., *Inorg. Chem.* 1975, **14**, 1550.
6. R. B. King, J. A. Zinich and J. C. Cloyd Jr., *Inorg Chem.* 1975, **14**, 1554.
7. R. B. King, J. C. Cloyd Jr. and R. H. Reimann, *Inorg. Chem.* 1976, **15**, 449.
8. *c.f.* (a) L. Manojlovic-Muir, K. W. Muir, A. A. Frew, S. S. Ling, M. A. Thompson and R. J. Puddephatt, *Organometallics* 1984, **3**, 1637; (b) C. P. Kubiak and R. Eisenberg, *Inorg. Chem.* 1980, **19**, 2726; (c) C. P. Kubiak, C. Woodcock and R. Eisenberg, *ibid* 1980, **19**, 2733; (d) M. Cowie and S. K. Dwight, *ibid* 1980, **19**, 2500; (e) M. Cowie and S. K. Dwight, *ibid* 1979, **18**, 2700.
9. C. A. Johnson, M. Guenzi, R. B. Nachbar Jr., J. F. Blount, O. Wennerstrom and K. Mislow, *J. Am. Chem. Soc.* 1982, **104**, 5163.

Polyhedron Vol. 6, No. 10, pp. 1807–1812, 1987
Printed in Great Britain

0277–5387/87 $3.00+.00
Pergamon Journals Ltd

SYNTHESIS AND ELECTRICAL PROPERTIES OF VANADYL(V)CHLORIDE COMPLEXES OF *N*-2(4,5,6-MONOSUBSTITUTED PYRIDYL)-*N'*-ARYL SUBSTITUTED THIOUREAS

K. L. MADHOK

School of Studies in Chemistry, Jiwaji University, Gwalior-474011 (M.P.), India

(*Received* 10 *September* 1986; *accepted* 6 *March* 1987)

Abstract—$VOCl_3$ formed six-coordinated complexes with *N*-aryl-*N'*-2(4,5,6-monosubstituted pyridyl)thioureas of the general formula $[VOCl_3(RNHC{=}SNHR')]$, where R = pyridyl, 5-nitropyridyl, 4-methylpyridyl, 6-methylpyridyl groups and R' = $-C_6H_5$, *o*-$C_6H_5(CH_3)$ and *p*-$C_6H_4(CH_3)$. The complexes have been characterized by means of elemental analysis, molar conductance, magnetic susceptibility, IR, UV–VIS, and ^1H NMR spectral data. The thermally stimulated depolarization effect was studied in samples polarized under different conditions. The results indicate two distinct transitions in the temperature range 92–100°C and 120–125°C for the ligands, whereas the $VOCl_3$-complexes show no breaks. The polarization–depolarization phenomena were correlated with the physicochemical changes occurring in the matrix. Depolarization kinetic data such as activation energy (E_a) and relaxation time (τ) of the electrets are reported.

Vanadium halides and oxyhalides are reported to form a number of complexes with mono, bi and polydentate ligands, but very little is known about the vanadyl(V)chloride complexes. Metal complexes of the substituted thioureas having heterocyclic group as one of the substituents have been studied by many workers.[1–3] Electrical properties of several metal Cu(II), Co(II), Ni(II) and Pt(II)-phthalocynin complexes have been reported.[4–5] Earlier communications[6–14] have described the metal chelates of C=S, C=O and C=NH donor ligands. However, less work is available on the synthesis and physiochemical properties of $VOCl_3$ complexes with *N*-aryl-*N'*-2(4,5,6-monosubstituted pyridyl)thioureas. A literature survey reveals that a number of phase transitions have been reported in ferroelectric materials like substituted thioureas.[15–19] Thus it was of interest to see what the electrical behaviour of such a ferroelectric substance will be, when incorporated in a complex matrix. The present study on $VOCl_3$-complexes with the title ligands was undertaken with the view to study the electrical changes.

EXPERIMENTAL

All the solvents and reagents used were guaranteed reagents. 2-aminopyridine, 2-amino-4-methyl, 2-amino-6-methyl and 2-amino-5-nitro pyridines were of Aldrich chemicals. The mustard oils like phenyl, orthotolyl, paratolyl-isothiocyanates were prepared by reported methods.[20] Vanadyl(V) chloride was prepared by refluxing equimolar quantities of V_2O_5 and $SOCl_2$ for 6–8 h and the product was distilled and the $VOCl_3$ fraction obtained at 125–127°C. The ligand *N*-aryl-*N'*-2(4,5,6-monosubstituted pyridyl)thioureas were prepared by the method reported earlier.[13]

GENERAL METHOD OF THE PREPARATION OF $VOCl_3$-COMPLEXES

All the operations in the preparation of metal complexes were carried out in a dry box. To a requisite amount of ligand (0.02 M) in $CHCl_3/CCl_4$ mixture was added 0.03 M CCl_4 solution of $VOCl_3$ drop by drop with constant stirring and was ice-cooled maintaining in each case a slight excess of the ligand. The mixture was shaken and allowed to stand for 8 h to attain equilibrium. The intensely coloured complexes were separated out, filtered washed with CCl_4 and $CHCl_3$. The complexes were analysed for V, S and Cl after fusion with alkali.

Magnetic measurements were carried out on a Gouy balance using a field strength of 5×10^3 Gauss

and mercury tetrathiocyanato cobaltate (II) as standard. Molar conductances were determined in *N,N*-dimethylformamide with conductivity meter type LBR of Wissenschaftlich technisch Werkenstatten, Germany using a dip-type cell. The IR spectra of the ligands and their metal-complexes were determined using KBr pellets on an infrared spectrophotometer of the type Beckman-20. Absorption spectra of $VOCl_3$ complexes were measured by standard methods using Perki–Elmer UV–VIS spectrophotometer model 139. Transition energy (E_T) was calculated by the relation

$$E_T = \frac{2.859 \times 10^5}{\lambda_{max}(\text{in Å})}$$

and the oscillatory strength "f" was calculated from the equation

$$f = 4.32 \times 10^{-9} \int E_{dv}.$$

Utilizing

$$E_{max}\Delta\bar{v} = \int E_{dv}$$

where $\Delta\bar{v}$ is the wave number of the half band width.

All the electrical measurements were made on pellets pressed at a load of 9 tons at room temperature. The pellets were sandwiched between two aluminium electrodes. The capacitance was measured with a standard LCR bridge (Systronics 921) at 1 and 10 kHz as a function of temperature. The area A of the pellet was measured geometrically and graphically and the thickness d of the pellet was measured by a micrometer screw reading up to 0.001 cm. The dielectric constant ε was calculated from the equation

$$\varepsilon = C_0 d/(\varepsilon_0 A)$$

where $\varepsilon_0 = 8.85 \times 10^{-14}$ F cm^{-1}.

The sample was polarized at conditions $T_p = 90°C$, $E_p = 2.50 \times 10^3$ V cm^{-1}, $t_p = 2$ h. The heating rate was maintained at 6°C min^{-1}.

TSD spectra was recorded in the temperature range of 20 to 200°C. Activation energy, E_a was calculated by the initial rise method of Garlick and Gibson,[21] from the slope of the straight line curve of log current (i) vs $1/T$ for the first lower half of the TSD peak.

$$\log i(T) = \text{constant} - \frac{E_a}{T}$$

where E_a = activation energy, T = absolute temperature and K = Boltzmann's constant.

Relaxation time of polarization created by ionic motion or by dipoles orientation is given by the Arrhenius equation

$$\tau(T) = \tau_o \exp(-E_a/KT)$$

where $\tau(T)$ is the temperature dependent relaxation time of the dipoles in a dielectric, τ_o is the time constant and can be written as

$$\tau_o = \frac{kT_{max}}{\beta E_a \exp(E_a/k\bar{T}_{max})}$$

where β = heating rate and T_{max} = peak temperature.

RESULTS AND DISCUSSIONS

All the $VOCl_3$ complexes are dark yellow–green coloured and soluble in chloroform, DMF, THF and nitrobenzene. All of them decompose above 225°C. The analytical results (Table 1) correspond to the general empirical formula $VOCl_3 \cdot L$ where L is a bidentate ligand molecule. Since there is no loss of chlorine (wt%) in the complexes, reduction of V(V) to V(IV) may not be taking place. The electrolytic conductance measurements of these complexes (29–60 Ohm^{-1} cm^2 mole^{-1} in freshly distilled DMF solution indicate non-electrolytic nature of these complexes. The molar conductance of uni-univalent electrolytes are 80–90 mhos.[22] It seems that partial replacement of chloride by solvent may be taken place as follows

$$[VOCl_3(L)] + S \rightleftharpoons [VOCl_2(L)S]^+ + Cl^-$$

where S is solvent. The magnetic susceptibility of the complexes were found in the range -0.043 to -0.71×10^{-6} G. The negative values of susceptibility indicate the diamagnetic nature of $VOCl_3$ complexes.

The electronic spectral bands of the complexes are listed in Table 2. All these bands are due to M ← S charge-transfer absorption. Moor and Larsen[23] have earlier observed that S → M charge-transfer in xanthate complexes appears at 6000 cm^{-1} below that of the corresponding dithiocarbamate complexes, and have suggested that xanthates are much greater reducing agents than dithiocarbamates. From the spectral data in our case, it is observed that the present ligands are not reducing agents.

The IR spectra of substituted thioureas and their $VOCl_3$ complexes are quite complicated, and therefore the effect of substitution could not be studied with a degree of certainty. The bands appearing at 3000–3400 cm^{-1} have been assigned to ν_s(NH) and ν_{as}(NH), the latter being the higher frequency band. A medium broad band appearing at 3000–

Table 1. Analytical data of $VOCl_3$ complexes

Compound	Colour	M.p. (°C)	Analysis of the complexes % found V	S	Cl	% calculated V	S	Cl
$VOCl_3$	Reddish	—	29.9	—	61.7	29.4	—	61.4
$VOCl_3$(PyPTU)	Green	225	12.4	7.9	26.4	12.6	7.9	26.4
$VOCl_3$(4MePyPTU)	Green	145	12.2	7.7	25.5	12.2	7.7	25.5
$VOCl_3$(6MePyPTU)	Green	120	12.2	7.5	25.5	12.2	7.7	25.5
$VOCl_3$(5NPyPTU)	Yellow	162d	11.4	7.1	23.7	11.4	7.1	23.8
$VOCl_3$(5NPy·*o*TTU)	Yellow	178	11.0	6.9	23.0	11.0	6.9	23.0
$VOCl_3$(5NPy·*p*TTU)	Yellow	186d	11.0	6.8	22.9	11.0	6.9	23.0
$VOCl_3$(6MePy·*o*TTU)	Green	182	11.6	7.2	24.6	11.8	7.4	24.7
$VOCl_3$(6MePy·*p*TTU)	Green	180	11.8	7.4	24.6	11.8	7.4	23.7
$VOCl_3$(Py·*o*TTU)	Green	215	12.0	7.7	25.5	12.2	7.7	25.5
$VOCl_3$(Py·*p*TTU)	Green	192d	12.1	7.6	25.0	12.2	7.7	25.5

d = decomposed.

3100 cm^{-1} has been assigned to 2-aminopyridine vibrations. Bands appearing at 1600 and 1640 cm^{-1} are assignable to ν(C=C+C=N) modes of aryl groups. In the case of metal complexes there is a little change in this band. The bands appearing at 1132–1010 cm^{-1} due to ν(NCS+C=S) modes in the case of ligands are either reduced in intensity or shifted to the higher frequency side in most of the complexes. The ν(C=S) mode occurring at 750–775 cm^{-1} in ligands is also shifted to the lower frequency side (20–25 cm^{-1}) in $VOCl_3$ complexes. The behaviour of the bands assigned to ν(C=C+V=N) is of considerable importance in deciding whether or not the heterocyclic nitrogen is

Table 2. Magnetic susceptibility, molar conductance and UV–VIS spectral data of $VOCl_3$-complexes

Complex	Magnetic susceptibility ($\times 10^{-6}$)	Molar conductance, Λ_M cm^2 mole Ω^{-1}	UV-spectral data in ethanol λ_{max}	E_{max} (l $mole^{-1}$/ cm^{-1})	E_T (K cal/ mole)	"*f*"
$VOCl_3$(PyPTU)	−0.302	29.8	275	24690	104.00	0.095
			311	20950	91.91	0.085
$VOCl_3$(4MePyPTU)	−0.430	40.2	278	16290	102.80	0.039
			309	13920	92.51	0.032
$VOCl_3$(6MePyPTU)	−0.420	50.50	281	25570	101.70	0.088
			315	22870	90.76	0.067
$VOCl_3$(5NPyPTU)	−0.717	52.20	276	18860	103.60	0.030
			309	14110	92.51	0.142
$VOCl_3$(5NPy·*o*TTU)	−0.420	56.20	276	28230	103.60	0.142
			311	24100	91.91	0.136
$VOCl_3$(5NPy·*p*TTU)	−0.380	58.20	282	31090	101.40	0.127
			314	26740	91.05	0.092
$VOCl_3$(6MePy·*o*TTU)	−0.458	45.80	265	39320	107.90	0.722
			318	34400	90.76	0.301
$VOCl_3$(6MePy·*p*TTU)	−0.318	60.00	290	18740	105.90	0.170
			308	18350	92.81	0.096
$VOCl_3$(Py·*o*TTU)	−0.436	35.70	259	30950	110.40	0.334
			308	28790	92.81	0.161
$VOCl_3$(Py·*p*TTU)	−0.471	38.80	264	30540	108.50	0.511
			305	26130	93.74	0.170

involved in the coordination with the metal ion. This band has been reported to be shifted to higher frequency in the case of coordinated pyridyl nitrogen.[1] In the present vanadyl(V)chloride complexes the band is increased by 10–30 cm^{-1}, which indicates that the ring nitrogen is also involved in the bond formation.

The frequency of the band assignable to V=O stretching mode in $VOCl_3$ is in agreement with the reported values.[23] (V=O stretch at 1035 cm^{-1} and νV–Cl at 408 cm^{-1}), which in the present case have been shifted to lower frequencies 950 cm^{-1} (V=O) and 315–400 cm^{-1} (V–Cl).

The ^{1}H NMR spectra of PyPTU, Py·*o*TTU, Py·*p*TTU and 4MePyPTU indicate four distinct resonances: (i) a sharp singlet (δ 7.4–7.8 ppm) due to $-C_6H_5$ ring protons, (ii) a broad multiplet (δ 3.2–3.4 ppm) due to *o,p*-$CH_3C_5H_4$ ring protons, (iii) a sharp signal (δ 2.3–2.4 ppm) due to the protons of CH_3 groups and (iv) a doublet at (δ 4.35–4.42 ppm) due to NH protons of S=C—NH group. Finally a singlet at δ 8.4–8.6 ppm is possibly due to protons of the pyridyl ring. On account of poor solubility, the NMR spectra of $VOCl_3$ complexes with the above ligands were taken in deuterated DMSO. The spectra of V(V) complexes show the signal due to —CNH group without any shift. The positions of the C_6H_5 and *o,p*-$CH_3C_5H_4$ ring protons remain unperturbed ruling out the possibility of coordination of —NH group of NHC_6H_5. The lone pair of electrons on the nitrogen of the pyridyl ring causes a paramagnetic shielding of the 2- and 6-protons.[24] Formation of the dative bonds using this electron pair greatly reduces the paramagnetic shielding giving a significant upfield shift for the adjacent protons. In other words we can say that there is a decrease in the electron density of the pyridine ring upon complex formation. This decrease causes a reduction of the paramagnetic anisotropic effect. This will result in the almost uniform upfield shift for all the ring protons. In the $VO(V)Cl_3$ complexes of PyPTU, Py·*o*TTU, Py·*p*TTU and 4MePyPTU, an upfield shift of heterocyclic ring protons by 3.0 to 4.8 ppm is observed confirming the coordination through pyridyl nitrogen.

All these observations show that ligands are coordinated to the vanadium metal though thio-keto sulphur and pyridyl ring nitrogen atoms.

$VOCl_3$ has been reported to have a distorted tetrahedral structure[25] which possibly has the d^2sp hybridization. It seems possible that the distorted tetrahedral symmetry of $VOCl_3$ has been changed to six coordinated irregular octahedral configuration with d^2sp^3 hybridization. On the basis of the information, the complexes of $VOCl_3$ with the title ligands may be represented by Structure I.

ELECTRICAL PROPERTIES

Eley[26,27] first observed the semiconducting properties of organic ligands and proposed that conductivity arose through thermal or optical excitation of electrons from the highest filled to the lowest empty orbital. The mechanism of conductivity is associated with the mobile electrons of the ligand rings. Earlier Day *et al.*[28] reported the resistivity of Fe-*p*H-thalocyanin as 4×10^9 Ω cm by a single crystal method. The present data on $VOCl_3$

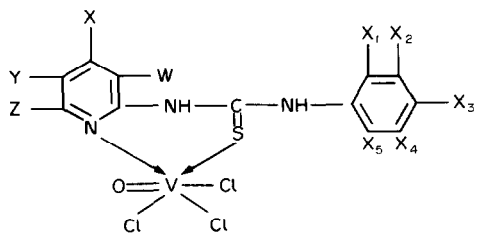

Structure I.

For L

PyPTU;	$X_1,X_2,X_3,X_4,X_5 = H$; W,X,Y,Z = H
4MePyPTU;	$X_1-X_5 = H$; W = H; X = CH_3; Y = H; Z = H
6MePyPTU;	$X_1-X_5 = H$; Z = CH_3; W = H, X = H; Y = H
5NPyPTU;	Y = $-NO_2$; W,X,Z = H; $X_1-X_5 = H$
5NPY·*o*TTU;	Y = $-NO_2$; W,X,Z = H; $X_1 = CH_3$, $X_2-X_5 = H$
5NPy·*p*TTU;	Y = $-NO_2$; W,X,Z = H; $X_3 = CH_3$, $X_1-X_4,X_5 = H$
6MePy·*o*TTU;	Z = CH_3, W,X,Y = H; $X_1 = CH_3$, $X_2-X_5 = H$
6MePy·*p*TTU;	Z = CH_3, W,X,Y = H; $X_3 = CH_3$, $X_1,X_2,X_4,X_5 = H$
Py·*p*TTU;	W,X,Y,Z = H, $X_3 = CH_3$, $X_1,X_2,X_4,X_5 = H$
Py·*o*TTU;	W,X,Y,Z = H, $X_1 = CH_3$, X_2-X_5 = H.

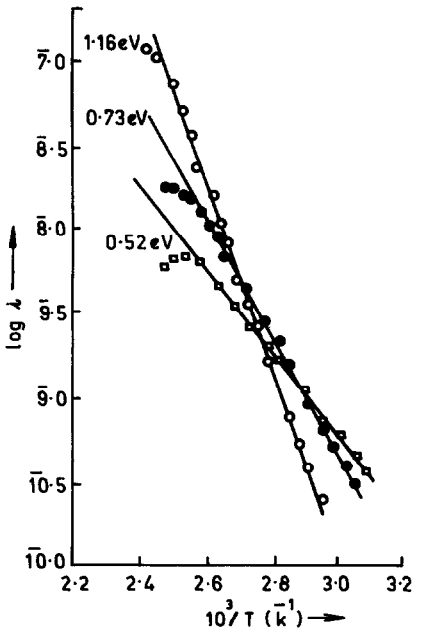

Fig. 1. Current (i) vs $1/T$ for determination of activation energy (E_a) at T_{max}: ○, 138°C; ●, 130°C, □. 122°C; for o-TP$_y$TU.

complexes is plotted as log × current as a function of temperature in Fig. 1. At room temperature ρ is of the order of 4.7×10^{11} Ω cm and decreases with increasing temperature (3.1×10^{11} Ω cm at 98°C). The log i vs $1/T$ plot is linear showing breaks at 92–100°C and 120–125°C for ligands. Activation energies, E_a have been calculated from the semi-logarithmic plots of current (i) in the initial rise of the depolarization peak vs $1/T$. The corresponding values of relaxation times were also calculated using Arrhenius equation from E_a values obtained in the initial rise method and are listed in Table 3.

As T_p increases, the t.s.d. peak shifts to higher temperatures. It is well known that, in homogeneous systems, polarization and depolarization phenomena are associated with dipoles and space charge effect, while the Maxwell–Wagner effect (interfacial polarization) becomes operative in a heterogeneous system. For example, in the presence of an air gap, heterogeneity is created giving rise to t.s.d. peaks. In the present study t.s.d. peaks were obtained from samples coated with aluminium as well as sandwiching them between aluminium electrodes. In both the cases similar types of t.s.d. peaks are obtained indicating the presence of no air gap in the samples, avoiding the possibility of interfacial polarization due to an air gap. Since the charging voltages are low (10^3 V cm^{-1}), the homocharges by injection may not be present. Hence only polarization by dipole orientation and space charge effect are considered. Thus though the data taken together cannot conclusively establish the mechanism of depolarization, the trends are indicative of space-charge polarization. Beside physical effects, Stupp and Carr have shown that chemical changes can be associated with the t.s.d. peaks. In the present case heating will lead to further condensations, which would effect the t.s.d. peaks. Both the ligands and their $VOCl_3$ complexes show high dielectric constants. The dielectric constant of the ligands and complex are plotted as a function of temperature (Fig. 2). A broad shoulder is observed in the region 90–150°C in the PyPTU. On heating the dielectric constant of the complexes increases rapidly above 150°C, thus exhibiting the pyroelectric effect.

Thus, the electrical measurements along with the variations in IR spectral data, indicate the presence of two distinct transition temperature ranges 92–100°C and 120–125°C. It is proposed that up to 92–100°C trapped water as well is present in the matrix. This is reflected in a decrease in resistivity.[30] On continuous heating chain mobility is increased. Thus it is proposed that the t.s.d. peaks at 92–100°C

Table 3. Activation energies (E_a) and depolarization kinetic data obtained for o-TP$_y$TU and $VOCl_3 \cdot o$-TP$_y$TU

Compound	E_a (eV)	T_{max} (°C)	$\tau_{T_{max}}$ (S)	$\tau_{T_{max}}$ (day)
o-TPyTU	0.52	122	4.05×10^2	0.00468
	0.73	130	2.93×10^2	0.00339
	1.16	138	1.91×10^2	0.00221
$VOCl_3 \cdot o$-TP$_y$TU	0.39	122	5.20×10^2	0.00680
	0.89	138	2.315×10^2	0.00303

E_a is activation energy.
T_{max} is temperature of the t.s.d. peak.
$\tau_{T_{max}}$ is the relaxation time at T_{max}.

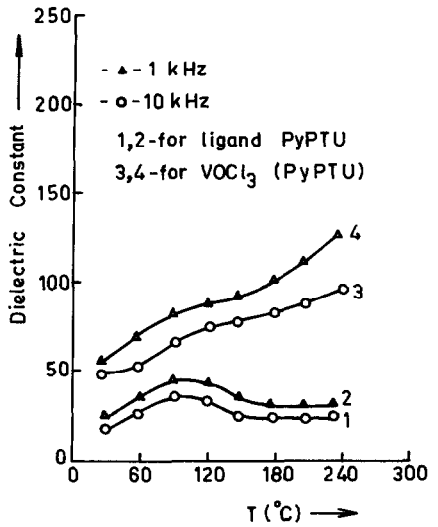

Fig. 2. Plot of Dielectric Constant versus temperature at 1 and 10 kHz.

are due to a physical effect associated with trapped water and the one at 120–125°C is attributed to both physical and chemical transitions.

Acknowledgement—The author is thankful to the Director, D.R.D.E., Gwalior for taking NMR-spectra.

REFERENCES

1. D. Banerjee and I. P. Singh, *Ind. J. Chem.* 1968, **6**, 34.
2. C. Dijkgraff, *Spectrochim. Acta* 1965, **21**, 1419.
3. G. W. A. Fowles, *Prog. Inorg. Chem.* 1964, 61.
4. P. E. Fielding and F. Gutmann, *J. Chem. Phys.* 1957, **26**, 411.
5. W. Filmayer and I. Wolf, *J. Electrochem. Soc.* 1958, **105**, 2280.
6. K. L. Madhok and K. P. Srivastava, *Ind. J. Chem.* 1980, **A19**, 808.
7. K. L. Madhok, *Proc. Ind. Acad. Sci. (Chem. Sci.)* 1982, **91**, 165.
8. K. L. Madhok, *Inorg. Chim. Acta* 1982, **61**, 103.
9. K. P. Srivastava and K. L. Madhok, *Ind. J. Chem.* 1978, **16A**, 359.
10. K. P. Srivastava and K. L. Madhok, *J. Inorg. Nucl. Chem.* 1978, **40**, 1821.
11. K. P. Srivastava and K. L. Madhok, *J. Chem. Engng Data (ACS)* 1978, **23**, 256.
12. K. P. Srivastava, G. P. Srivastava, S. K. Arya and K. L. Madhok, *J. Chem. Engng Data (ACS)* 1980, **25**, 173.
13. K. P. Srivastava, I. K. Jain and K. L. Madhok, *Proc. Ind. Acad. Sci. (Chem. Sci.)* 1981, **90**, 309.
14. K. L. Madhok, *Polyhedron* 1984, **3**, 39.
15. K. L. Madhok, *Prod. Ind. Acad. Sci. (Chem. Sci.)* 1983, **92**, 605.
16. G. J. Goldsmith and J. C. White, *J. Chem. Phys.* 1959, **31**, 1175.
17. N. E. Hill, W. E. Vanghan, A. H. Price and M. Davies, *Dielectric Properties and Molecular Behaviour*. Von Nostrand Reinhold, London (1969).
18. A. F. Devonshire, *Adv. Phys.* 1954, **3**, 85.
19. D. R. McKenzie, *J. Phys.* 1985, **C8**, 1607.
20. A. I. Vogel, *Practical Organic Chemistry*. Longman, Green, London (1964).
21. G. F. J. Garlick and A. F. Gibson, *Proc. Phys. Soc.* 1948, **60**, 574.
22. A. R. Nicholson and G. J. Sutton, *Austral. J. Chem.* 1969, **22**, 1543.
23. McCormick B. Jack, *Inorg. Chem.* 1968, **7**, 1965.
24. E. F. Mooney and M. A. Qaseem, *J. Inorg. Nucl. Chem.* 1968, **30**, 1439.
25. C. Dijkgraaf, *Spectrochim. Acta* 1965, **21**, 1419.
26. D. D. Eley, *Nature* 1948, **162**, 819.
27. D. D. Eley, G. D. Perfitt, M. J. Perry and D. H. Taysum, *Trans Faraday Soc.* 1953, **49**, 79.
28. P. Day, G. Scregg and R. J. P. Williams, *Nature* 1963, **197**, 589.
29. S. I. Stupp and S. H. Carr, *J. Polym. Sci. Polym. Physa. Edn* 1977, **15**, 485.
30. H. S. Nalwa and P. Vasudavan, *Eur. Polym. J.* 1981, **17**, 145.

Polyhedron Vol. 6, No. 10, pp. 1813–1821, 1987
Printed in Great Britain

0277–5387/87 $3.00+.00

^{51}V AND ^{17}O NMR STUDIES OF THE MIXED METAL POLYANIONS IN AQUEOUS V–Mo SOLUTIONS

R. I. MAKSIMOVSKAYA* and N. N. CHUMACHENKO

Institute of Catalysis, Novosibirsk 630090, U.S.S.R.

(*Received* 1 *December* 1986; *accepted* 25 *March* 1987)

Abstract—$NaVO_3$–Na_2MoO_4 solutions acidified with HCl were studied at the atomic V/Mo ratios equal to 3 : 1, 1 : 1, 1 : 3, 1 : 6 and vanadium concentration [V] = 0.1, 0.04, 0.004 and 0.0004 M in the range pH 7–2. Their ^{51}V NMR spectra (measured at $H_o = 7$ T) were compared with those of V–W solutions containing mixed metal complexes of known composition. The $VMo_5O_{19}^{3-}$ (^{51}V NMR chemical shift relative to $VOCl_3$, δ, −502 ppm), $V_2Mo_4O_{19}^{4-}$ (δ −494), $HV_2Mo_4O_{19}^{3-}$ (δ −507), $V_9MoO_{28}^{5-}$ (δ −422, −492, −501, −512, −521.5) and $HV_9MoO_{28}^{4-}$ polyanions (p.a.) have been found to be dominant mixed species in Na–V–Mo solutions. Along with them the $V_xMo_{13-x}O_{40}^{-x-3}$ p.a. ($x \sim 2$–3) of the Keggin type (δ −496, −498, −516, −522) are supposed to be formed at pH < 4 in concentrated solutions ([V] > 0.01 M). The $V_2Mo_6O_{26}^{6-}$ p.a., isolated at pH ~ 5 as the sodium salt (solid state δ −482), seem to be present in concentrated Na–V–Mo solutions only as minor species. On dissolving the salt the $V_2Mo_6O_{26}^{6-}$ p.a. mainly disproportionates into the complexes mentioned. From solutions containing mainly the $V_9MoO_{28}^{5-}$ p.a. the sodium salt of $V_{10}O_{28}^{6-}$ is crystallized. The $V_9WO_{28}^{5-}$ p.a. are detected in V–W solutions at V/W > 1. ^{17}O and ^{95}Mo NMR spectra of some mixed complexes are described. The distribution diagrams for V–Mo and V-W solutions at [V] = 0.004 M and V/Mo(W) = 1 : 3, derived from their ^{51}V NMR spectra, are given.

In acid aqueous V–Mo solutions several mixed metal complexes are formed, the exact number and composition of which have not been established yet.[1] From potentiometric and spectrophotometric studies of dilute solutions[2–4] complexes with the atomic V/Mo ratios equal to 1 : 1, 1 : 2, 1 : 5 and 9 : 1 were supposed to form, but they were not isolated. Only one mixed complex of the composition $Na_6[V_2Mo_6O_{26}]\cdot 16H_2O$ was isolated from weak acid Na–V–Mo solutions at different V/Mo ratios.[5] Its discrete polyanions have the same structure as α-$Mo_8O_{26}^{4-}$.[6] The $VMo_5O_{19}^{3-}$, is isostructural with the hexaniobate, and was isolated only from nonaqueous solutions as the tetrabutylammonium(TBA) salt.[7]

From weak acid K–V–Mo solutions the $K_7[Mo_8V_5O_{40}]\cdot 8H_2O$ and $K_8[Mo_4V_8O_{36}]\cdot 12H_2O$ crystals, containing discrete polyanions, were also obtained and their structures were determined.[6]

The preparation of a red-orange compound with V/Mo = 1 : 6 at high acidity (pH < 3) was described in [8]. That complex was extracted from solutions with ether. From chemical analysis the composition of the complex was supposed to be $H_6V_2Mo_{12}O_{44}$ but it was not supported by any structural data.

We hoped to obtain some new data on the composition of the V–Mo complexes in solutions by means of ^{51}V NMR, which was shown to be a very informative method in studying V–W and some other solutions containing vanadium.[9–12] It allows one to observe directly different complexes of V(V), which are simultaneously present in a solution, and to find their concentration. On the basis of chemical similarity of Mo and W(VI) it is reasonable to expect an analogy in the compositions of some of their complexes with V(V) and in the way they manifest themselves in the NMR spectra as well. The high concentration sensitivity of ^{51}V NMR allows measurements to be made in a wide concentration range including dilute solutions, which were studied earlier by potentio and spec-

* Author to whom correspondence should be addressed.

trophotometric techniques. In this paper the ^{51}V and ^{17}O NMR data on the V–Mo solutions are reported and assignments of several resonances are given, mostly for the first time. A comparison is made with the V-W system containing several mixed metal polyanions of known composition.

EXPERIMENTAL

^{51}V NMR spectra of V–M (M = Mo, W) solutions were studied at the atomic V/M ratios equal to 3 : 1, 1 : 1, 1 : 3, 1 : 6 and vanadium concentrations, [V], equal to 0.1, 0.04, 0.004 and 0.0004 M in the case of Mo–V and to 0.004 M in the case of W–V solutions. The 0.1 and 0.04 M solutions were prepared from $NaVO_3 \cdot 2H_2O$ and $Na_2MO_4 \cdot 2H_2O$ of reagent grade and acidified with dilute HCl. The degree of acidification P = [HCl]/[V+M] was changed in the range 0.1 to 1.8–2.5. The 0.004 and 0.0004 M solutions were prepared by diluting the 0.04 series. After storing the solutions at 20° for several days their pH values and NMR spectra were measured. $Na_6[V_2Mo_6O_{26}] \cdot 16H_2O$ was prepared as described in Fig. 5.

The pH values were measured on a pH-meter "pH-262" with the silver chloride electrode. NMR spectra were measured on a BRUKER CXP-300 spectrometer using a high power probe head and cylindrical 8 mm o.d. (1.5 ml solution volume) horizontal sample tubes without sample spinning. The ^{17}O spectra were obtained at 40.7 MHz with a spectral width of 50 kHz and a pulse duration of 10 μs. The number of transients was about 50,000, the pulse delay was 0.02 s. All spectra were obtained at natural abundance of ^{17}O. For obtaining the $Na_6[V_2Mo_6O_{26}]$ solution, water enriched with ^{17}O ($\sim$ 1%) was used as well. Because of the baseline roll the ^{17}O peak intensities were measured from peak areas and not from integrals and were checked by recording under various conditions (delay, spectral and pulse width). An average uncertainty in measuring ^{17}O peak intensities was about 20%. The chemical shifts (δ) are given in ppm relative to solvent H_2O.

^{51}V spectra were obtained at 78.88 MHz with a spectral width of 25 kHz, a pulse duration of 7 μs and a pulse delay of 0.1 s. For dilute solutions the number of transients was about 2000. The concentrations of different vanadium forms were found from peak intensities which were measured from integrals and peak areas. The overlapped peaks were resolved graphically. An average uncertainty was about 15%. The chemical shifts are given relative to $VOCl_3$ as an external standard.

^{95}Mo spectra were obtained at 19.56 MHz. The spectrum width was 20 kHz, the pulse width was 10 μs and the pulse delay was 0.3 s. The number of transients was 1000–5000. The 1 M Na_2MoO_4 solution was used as an external standard. For all nuclei the downfield shifts are taken as positive.

^{51}V NMR spectra of solid samples were measured using the magic angle spinning (MAS) technique.

RESULTS

The ^{51}V NMR spectra of the isopolyvanadates are rather well known.[9–11] The 0.004 M solution of $NaVO_3$ (pH $\sim$ 7.1) contains vanadium in the meta- (mainly with $\delta = -573$ ppm) and diprotonated ortho- and pyrovanadate forms (-556 and -568). On mixing with Na_2MoO_4 new complexes are not formed. The titration curve of one of the V–Mo solutions is shown in Fig. 1. On acidifying up to P = 0.1–0.3 a yellow colour appears and a modified spectrum of dacavanadate, containing five peaks instead of the usual three (noted as I, Table 1, Figs 2 and 3), arises. At P = 0.1–0.4 (depending upon the V/Mo ratio) a peak at -494 appears, which is displaced upfield with the increase in acidity (Fig. 4). In more acid solutions (P = 0.6–1.0) a peak at -502 is observed and another modified spectrum of the decavanadate type (II, Table 1, Fig. 3) appears. There is also a weak peak at -533 in the spectra of the 1 : 3 and 1 : 6 solutions at pH 5.5–4. This peak is more intense in the 1 : 6 series. At pH < 3 the VO_2^+ oxycations are formed in the solutions.

At [V] = 0.0004 M the -494 and -502 peaks and weak spectrum I are again observed. The total amount of vanadium in the V–Mo complexes decreases relative to free vanadium, which is present at that concentration only as $H_2VO_4^-$, transforming into VO_2^+ at pH < 4.

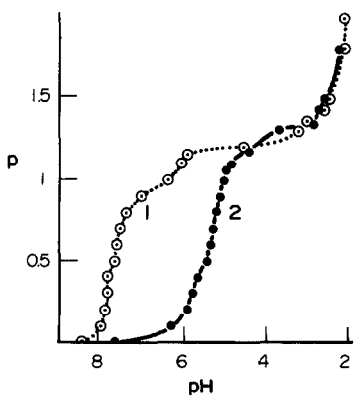

Fig. 1. The curves of titration of the $NaVO_3$–Na_2MO_4 solutions with HCl solution; V/M = 1 : 3, [V] = 0.004 M, M = W(1) and Mo(2).

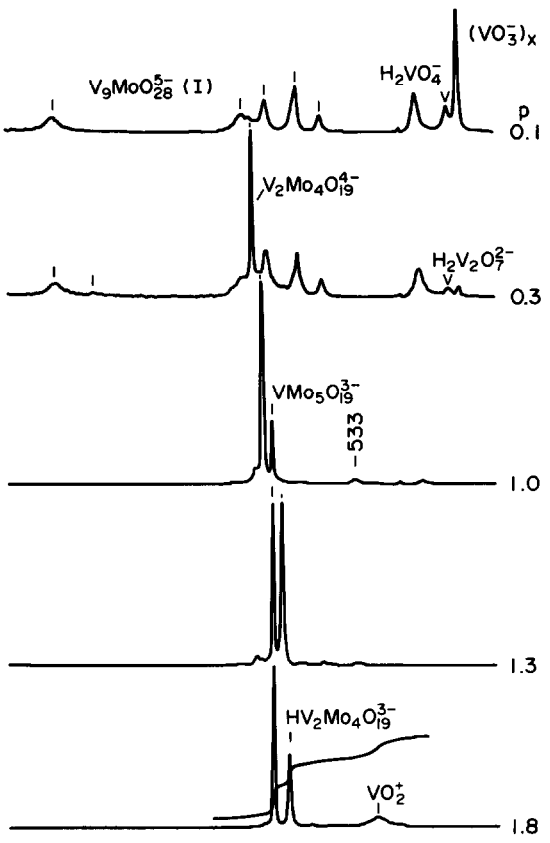

Fig. 2. ^{51}V NMR spectra of the $NaVO_3$–Na_2MoO_4 solutions (V/Mo = 1:3, [V] = 0.004 M) at different acidifications.

Thus, only four different mixed metal complexes are formed in dilute V–Mo solutions.

The same signals are observed in the spectra at [V] = 0.04 and 0.1 M and at pH > 4, but the relative intensities of spectra I and II increase and there appears one more modified decavanadate spectrum, (III Table 1, Fig. 3). The relative intensity of the −533 peak also increases and in some spectra a new peak is observed at −536 ppm.

On storing the orange 1:3 and 1:6 solutions (pH ~ 5.5) at 20° colourless or slightly yellow prismatic crystals were gradually formed, which were shown to be $Na_6[V_2Mo_6O_{26}]\cdot nH_2O$.

At pH < 4 the composition of the concentrated solutions is markedly different from that of the dilute solutions. Besides the above mentioned signals there is a new group of relatively broad peaks at −522, −516, −498 and −496 ppm. At pH < 3 the VO_2^+ peak (δ −541) and broad peaks at −600 and −628 ppm also appear. The same spectra are observed for solutions prepared as described in ref. 8. On heating, the solutions become darker red-orange, the intensity of the −522 signal increases and the signal is split into several components due to their narrowing. On storing the solutions at 20° the precipitates of hydrated oxides are formed in several days, with the intensity of the −541, −600 and −628 peaks decreasing considerably.

In the case of V–W solutions ([V] = 0.004 M) a yellow colour appears on mixing $NaVO_3$ and Na_2WO_4 without additional acidification, with pH value increasing as compared with that of the initial solutions. In the ^{51}V NMR spectra of these solutions a weak peak of $V_2W_4O_{19}^{4-}$ (noted as V_2W_4) is visible at −507 ppm[10,12] (Fig. 5). On acidifying the solutions the peak intensity increases. At V/W > 1 the modified decavanadate spectrum of type (I) is also observed. In more acid solutions the $VW_5O_{19}^{3-}$ species (VW_5) are formed (δ −522) and the V_2W_4 peak is shifted upfield (Fig. 4). At pH < 3 the VO_2^+ oxycations are produced.

DISCUSSION

The V–W polyanions are known to have either $M_6O_{19}^{n-}$ or Keggin structures.[1] As it can be seen (Fig. 5), only two of them, VW_5 and V_2W_4, are produced at [V] = 0.004 M. The $V_3W_3O_{19}^{5-}$ (V_3W_3) and $V_xW_{13-x}O_{40}^{x-3}$ ($x = 3$ and 4) polycomplexes are formed in more concentrated solutions.[10,12]

From the data available on the V–Mo complexes[1-4] and by the anology with the V–W system one can expect first of all the $V_xMo_{6-x}O_{19}^{2-x}$ polyanions to be present in the V–Mo dilute solutions. The peculiarities of the ^{51}V NMR spectra of the corresponding V–W species were discussed elsewhere.[12] They contain single relative narrow signals, which are shifted downfield and broadened in the order $VW_5 \rightarrow V_2W_4 \rightarrow V_3W_3$. As the vanadium content in the polyanions increases the pH range of their stability shifts to a less acid region, the V_3W_3 species existing in solutions only at pH > 7. The more highly charged V_3W_3 and V_2W_4 species are protonated at pH < 8.7 and < 4, respectively, which can be concluded from the upfield shift of their signals.

From careful analysis of all data obtained we can conclude that the VMo_5 and V_2Mo_4 species are formed in V–Mo solutions and that their signals are those at −502 and −494 ppm. Actually the −502 peak is the only one in the ^{51}V spectrum at [V] = 0.0002, [Mo] = 0.01 M and at pH 3, when according to the data[3] there is only the 1:5 mixed complex in the solution. The assignment of the −494 peak to the V_2MO_4 species is also confirmed by the ^{17}O NMR spectrum, and will be discussed below.

The shift of the V_2Mo_4 peak with acidity (Fig. 4) indicates the presence of the increasing amount of the HV_2Mo_4 species and the fast exchange between

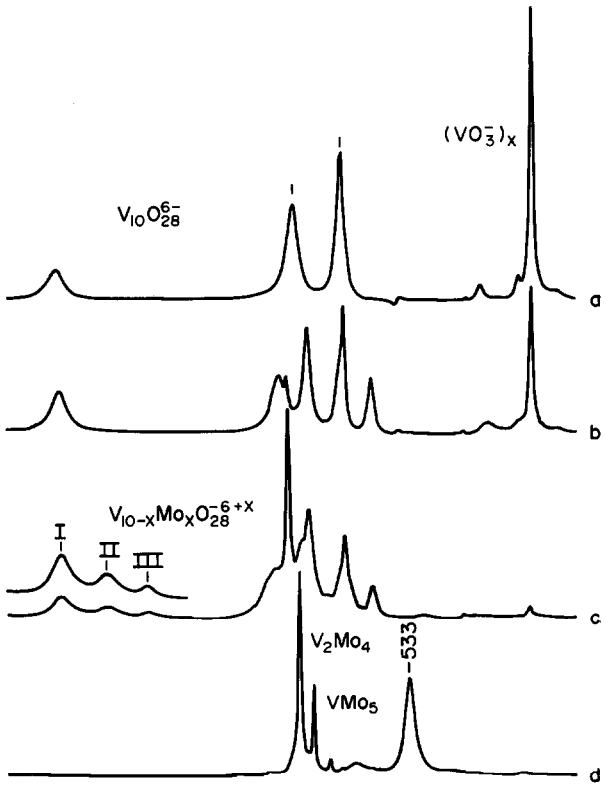

Fig. 3. ^{51}V NMR spectra of solutions: $V_{10}O_{28}^{6-}$ and $(VO_3^-)_x$, [V] = 0.05 M, pH 6.45 (a); $NaVO_3$–Na_2MoO_4, 1 : 1, [V] = 0.04 M, pH 6.25 (b); [V] = 0.1 M, pH 5.8 (c); [V] = 0.04 M, pH 4.9 (d).

Table 1. ^{51}V and ^{95}Mo NMR chemical shifts of polyanions

Polyanion	^{51}V NMR δ ±0.5 ppm	^{95}Mo NMR δ ±2 ppm
$V_{10}O_{28}^{6-}$, pH 5.4	−420(2), −495(4), −511(4)	
$V_9MoO_{28}^{5-}$ (I)	−422(2), −492(2), −512(2), −501(2), −521.5(1)	+115, 300 Hz
$V_{10-x}Mo_xO_{28}^{6+x}$ (II)	−435(2), −486(2), −500, −497, −513(2)	
(III)	−449, −489, −506, −498, −514	
$V_9WO_{28}^{5-}$ (I)	−424(2), −492(2), −511(2), −503(2), −522(1)	
$VMo_5O_{19}^{3-}$	−502, 25 Hz	
$V_2Mo_4O_{19}^{4-}$	−494, 50 Hz	+130, 200 Hz
$V_2Mo_4O_{19}H^{3-}$	−507	+126
$Mo_7O_{24}^{6-}$, pH 6		+210(1), +33(6)
pH 4.1		+200(1), +28(6) 550 Hz, 300 Hz
$Na_6[V_2Mo_6O_{26}]\cdot 16H_2O$	−482±3, 5.5 kHz 0.9 kHz (MAS)	
$V_xMo_{13-x}O_{40}^{n-}$,[a] $x \sim 2$–3	−496, −498, −516, −522	
$VMo_6O_{24}^{7-}$[a]	−506, −533	

( ) is the relative intensity.
[a] Is the supposed composition.

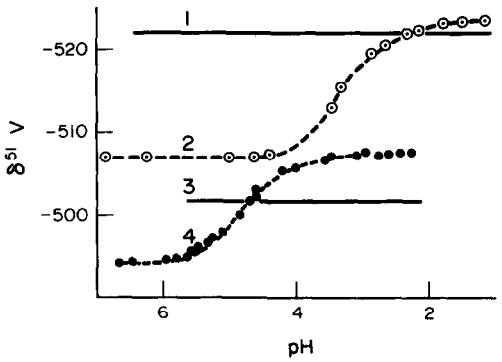

Fig. 4. The plot of the ^{51}V NMR δ value against pH for $VW_5O_{19}^{3-}$, $V_2W_4O_{19}^{4-}$ (1,2) and $VMo_5O_{19}^{3-}$, $V_2Mo_4O_{19}^{4-}$ (3,4).

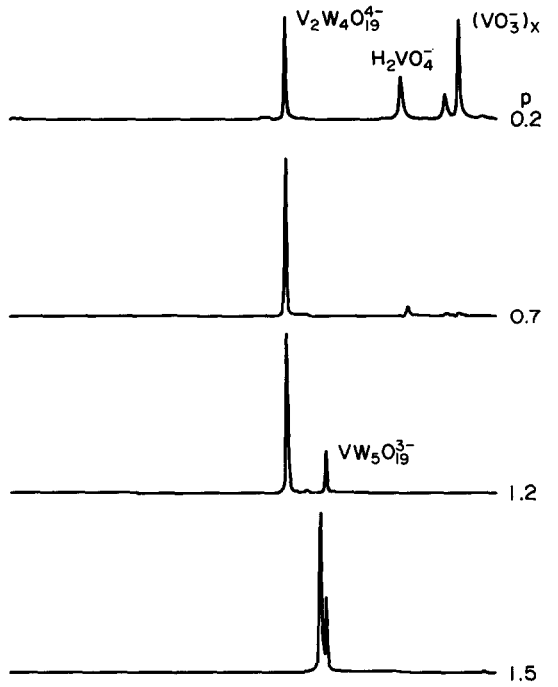

Fig. 5. ^{51}V NMR spectra of the $NaVO_3$–Na_2WO_4 solutions (V/W = 1:3, [V] = 0.004 M) at different acidifications.

the two forms. The observable δ value depends on their proportion, which allows us to evaluate the amount of each form. At pH < 4.5 the V_2Mo_4 signal is shifted upfield relative to the VMo_5 signal. The horizontal part of curve 4 (Fig. 4) corresponds to the complete $V_2Mo_4 \rightarrow HV_2Mo_4$ conversion. The V_2W_4 anions are protonated in more acid solutions (curve 2, Fig. 4) and the VW_5 and V_2W_4 signals are interchanged at pH < 2, where the HV_2W_4 polyanions are not stable and can only be observed at V/W > 1 immediately after acidification of the solution.

Unlike the V–W system in the V–Mo system a mixed complex, based on the decavanadate structure, predominates in the 1:3 and 1:6 series at low acidity and in the 1:1 and 3:1 series in the whole pH range studied. The $V_{10}O_{28}^{6-}$ species contains V atoms of the three types (Fig. 6).[14] There are three peaks with the intensity ratio 2:4:4 in their ^{51}V NMR solution spectrum. The weaker signal at −420 ppm arises from the two V_{III} atoms. The assignment of the two other signals has been recently made with the use of ^{17}O $\{^{51}V\}$ decoupling experiments.[16] In the modified decavanadate spectrum (I) these two signals are split into four in the intensity ratio 2:2:2:1 showing that one of either V_I or V_{II} atoms is replaced by the Mo atom, i.e. that the $V_9MoO_{28}^{5-}$ species is formed.

Further support for this composition comes from the ^{17}O NMR spectra (Fig. 6, Table 2). In case of $V_9MoO_{28}^{5-}$ the number of the terminal O=V peaks increases as compared with $V_{10}O_{28}^{6-}$ and a new peak arises from an O=Mo oxygen atom. The peak of the two sixfold bridging O_A atoms is split into two peaks, one of them being shifted upfield. Two peaks of equal intensities appear instead of the peak of four threefold bridging O_B atoms. A new peak arises from oxygen in the V–O–Mo bridge, its intensity corresponding approximately to two atoms. The peak of four quasi-terminal O_E atoms is split into two peaks of equal intensities. The δ values and the number of the V–O–V peaks also change. A spectrum like that seems to correspond better to the substitution of one of the V_I than the V_{II} atoms.

It is very imortant that there is a possibility of comparing the spectra of the isostructural $V_9MoO_{28}^{5-}$ and $V_9WO_{28}^{5-}$ complexes as the O atoms of the same type bound to the Mo and W atoms should have different chemical shifts. In the ^{17}O NMR spectrum of $V_9WO_{28}^{5-}$ the A, B and C peaks are displaced slightly further upfield than in the $V_9MoO_{28}^{5-}$ spectrum, the other peaks having very similar splittings and δ values (Table 2). This shows that exactly the O_B atoms as well as the O_C and O_A atoms have a direct contact with the alien atom, which is only possible for the V_I position.

Two other mixed complexes (II and III, Table 1), based on the decavanadate structure, which were only observed in V–Mo solutions, may be supposed to be either the two other positional isomers of $V_9MoO_{28}^{5-}$ or $V_{10-x}Mo_xO_{28}^{6+x}$ complexes with $x > 1$. Due to overlapping ^{51}V NMR spectra of several complexes we were unable to determine the exact number and the intensity ratio of the peaks in each spectrum and to distinguish between these alternative possibilities.

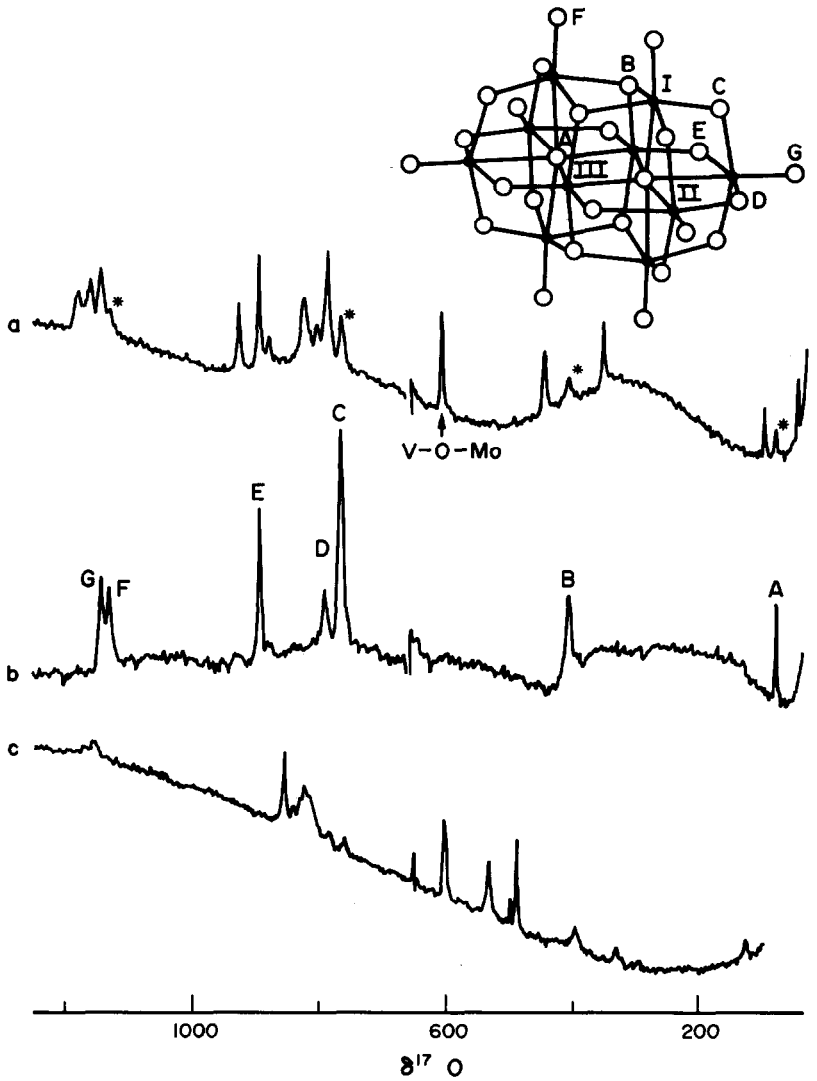

Fig. 6. ^{17}O NMR spectra of solutions of $V_9MoO_{28}^{5-}$ (* are the decavanadate peaks) (a) and $V_{10}O_{28}^{6-}$ (at natural ^{17}O content) (b) and of the $Na_6[V_2Mo_6O_{26}]$ solution (in enriched water) (c); idealized bond structure of $V_{10}O_{28}^{6-}$.

It is to be noted that on mixing the $Na_6V_{10}O_{28}$ and $Na_6Mo_7O_{24}$ solutions (V/Mo ~ 9:1) the $V_9MoO_{28}^{5-}$ polyanions were formed during several days. That shows that the V_1 position is more preferable for the exchange with cations from a solution.

The ^{51}V NMR spectrum of $V_9Mo(W)O_{28}^{5-}$ is usually overlapped with that of $V_{10}O_{28}^{6-}$, but the admixture of the latter is not large and can be evaluated from the intensities of the −512 and −521.5 signals (at pH 5.5). The V–Mo solution contains about 85% of vanadium as $V_9MoO_{28}^{5-}$ at V/Mo = 9:1.5 and [V] = 1 M. However, we have failed in isolating $V_9MoO_{28}^{5-}$ from such a solution. The less soluble sodium salt of $V_{10}O_{28}^{6-}$ is crystallized instead and equilibrium in the solution is gradually shifted to V_2Mo_4.

The ^{51}V NMR peaks of $V_{10}O_{28}^{6-}$ begin to be displaced upfield at pH < 5.5 and those of $V_9MoO_{28}^{5-}$ at pH < 4 due to protonation and the mutual position of their spectra is changed with acidity.

The $Na_6[V_2Mo_6O_{26}]\cdot nH_2O$ salt is crystallized from solutions at V/Mo < 1 and pH 5.5. The crystals give an isotropic ^{51}V NMR signal 5.5 kHz in width at δ −482 ppm. Rotating the sample at a magic angle narrows the signal up to 0.9 kHz. Such a signal shows a rather high symmetry of the nearest oxygen environment of the V atoms and corresponds to the VO_4 tetrahedra with nearly equal V–O bonds,[15] which is consistent with the

Table 2. ^{17}O NMR chemical shifts of some mixed metal polyoxoanions[a]

Polyanion	OV	OMo	VOV	VOM	MoOMo	OM_3	OM_4	OM_6	Ref.
$Mo_6O_{19}^{2-}$		933(6)			560(12)			−32(1)	7
$VMo_5O_{19}^{3-}$	1200(1)	885(5)		665(4)	541(4) 531(4)			−22(1)	7
$V_2Mo_4O_{19}^{4-}$	1165(2)	862(4)	(1)	604(6)	498(1) 489(4)			(1)	
α-$Mo_8O_{26}^{4-}$		866(12) 775(2)			495(6)	396(6)			7
$Mo_7O_{24}^{6-}$ 300 K		819(8)			757(2) 397(2)	340(2)	122(2)		
	G,F	E	D C			B	A[a]		
$V_{10}O_{28}^{6-}$ pH 5.4	1150(4) 1140(4)	895(4)	790(2) 765(8)			397(4)		63(2)	
$V_9MoOO_{28}^{5-}$	1190(3) 1169(2) 1153(2)	880(1) 895(2) 929(2)	801(1) 786(4) 822(3)	604(2)		436(2) 342(2)		80(1) 27(1)	
$V_9WO_{28}^{5-}$	1195(3) 1174(2) 1160(2)	904(2) 933(2)	807(1) 788(4) 825(3)	495(2)		439(2) 298(2)		82(1) 14(1)	

( ) is the relative intensity.
[a] Corresponds to Fig. 6.

structural data.[6] The downfield shift of this signal relative to that of the orthovanadate VO_4^{3-} anion (δ −535) may result from the decrease in the electron density transferred from oxygen to vanadium in the O–V bonds due to their lengthening.

On dissolving the slightly yellow crystals of $Na_6V_2Mo_6O_{26}$ give a bright orange solution with pH 5.5. The ^{51}V NMR spectrum of this solution is closely similar to that of the mother liquor having V/Mo = 1 : 3. There is a strong signal at −494, the −533 signal, modified decavanadate spectrum (II) and a weak peak at −485 ppm in this spectrum. ^{17}O and ^{95}Mo NMR show MoO_4^{2-} and $Mo_7O_{24}^{6-}$ to be present in the solution as well. The question arises, which of the ^{51}V peaks may be ascribed to $V_2Mo_6O_{26}^{6-}$. The chemical shift of −485 is almost equal to the δ value of the complex in solid state, but the −485 peak is too weak. We may then suppose the −494 signal, which is dominant in the spectrum, to arise from $V_2Mo_6O_{26}^{6-}$ when in solution, although the signal with the same δ value has been concluded from the ^{51}V NMR data to arise from V_2Mo_4. In order to elucidate this point it is necessary to examine the ^{17}O NMR spectrum of this solution.

The $V_2Mo_6O_{26}^{6-}$ species is known to be isotypic with α-$Mo_8O_{26}^{4-}$,[6] the ^{17}O NMR spectrum of which is also described.[7] We could expect the $V_2Mo_6O_{26}^{6-}$ spectrum to be of the similar type with some modification caused by introducing two V atoms into the structure. However, in the ^{17}O NMR spectrum of the $Na_6[V_2Mo_6O_{26}]$ solution (Fig. 6c) we did not find a set of peaks that could be attributed to $V_2Mo_6O_{26}^{6-}$. On the contrary, all the peaks observed besides those of MoO_4^{2-} and $Mo_7O_{24}^{6-}$ can be assigned to a V–Mo complex of a hexaniobate type. All these peaks are displaced upfield relative to the VMo_5 peaks.[7] Although we were unable to evaluate all the peak intensities with high accuracy, we could conclude the spectrum to arise from $V_2Mo_4O_{19}^{4-}$. On the whole this spectrum is like that of $V_2W_4O_{19}^{4-}$,[12] especially the narrow resonances of the Mo–O–Mo bridges, which are split in the intensity ratio 1 : 4 exactly as the corresponding resonances of the W–O–W bridges. We were unable to detect only the weakest two peaks arising from a sixfold bridging O atom and from one atom in the V–O–V bridge probably due to their overlap with other more intense signals (H_2O, $Mo_7O_{24}^{6-}$).

Thus, the ^{51}V and ^{17}O NMR spectra together show that on dissolving in water $V_2Mo_6O_{26}^{6-}$ mainly disproportionates into V_2Mo_4, $Mo_7O_{24}^{6-}$ and some other complexes. Only the weak peak at −485 seems to arise from $V_2Mo_6O_{26}^{6-}$ in solution.

We tried to obtain the TBA salt of $V_2Mo_6O_{26}^{6-}$ in order to dissolve it then in nonaqueous solvent

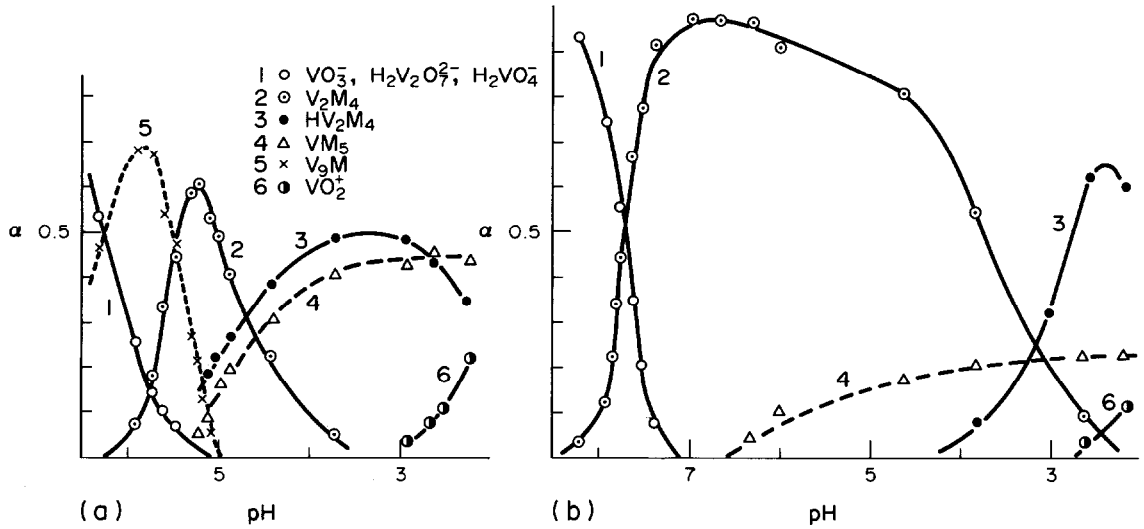

Fig. 7. Distribution diagrams of V(V) for the $NaVO_3$–Na_2MO_4 solutions (1:3, [V] = 0.004 M), M = Mo (a) and W (b).

therefore preventing hydrolysis. On dissolving $Na_6[V_2Mo_6O_{26}]$ in the aqueous solution of TBA · Br a yellow precipitate was gradually formed. However, the ^{17}O NMR spectrum of the CH_3CN solution of this precipitate shows that the TBA salt of VMo_5 has really been obtained.

We have not identified a mixed complex observed at δ_V −533. From relative intensity variations of this peak for the different V–Mo series we may only conclude the V/Mo ratio in it to be < 1/5. The pH interval of the formation of this complex coincides with that of $Mo_7O_{24}^{6-}$. If $NaVO_3$ and $Na_6Mo_7O_{24}$ are mixed in the ratio V/Mo = 1/20, nearly all vanadium is observed by this peak. Probably the complex in question is obtained by replacing a Mo atom with a V atom in the $Mo_7O_{24}^{6-}$ species. However, further studies of the true composition of this complex are needed.

At high concentration and acidity (pH < 4) VW_5 and V_2W_4 are known to convert to the darker coloured complexes having the Keggin structure.[1,10] The similarity of the V–Mo and V–W systems in forming the V_xM_{6-x} species allows us to suppose the V–Mo red-orange complexes (δ_V −496 to −522 ppm), which are formed under similar conditions, to be of the Keggin type too. The pH range of their formation and the ability to form etherate complexes are typical for polyanions having the Keggin structure. Besides, their ^{51}V NMR spectra consisting of several rather broad peaks showing a number of different positions of the V atoms and the larger dimensions than in the case of the V_xM_{6-x} species, these spectra are similar to those of the 1:12 PMoV, PWV and WV complexes. But the corresponding $V_xMo_{13-x}O_{40}^{n-}$ species ($x \sim 2$ and 3) seem to be less stable. They can exist in equilibrium with VMo_5, HV_2Mo_4 and cationic V and Mo forms. At the given pH value equilibrium strongly depends on concentration and temperature. However, further studies of these complexes are necessary.

^{95}Mo was used mainly for studying rather concentrated solutions ([Mo] > 0.1 M). The MoO_4^{2-} and $Mo_7O_{24}^{6-}$ anions as well as mixed V_2Mo_4 and V_9Mo species were detected in the solutions studied (Table 1).

Thus, most of the mixed polyanions observed by ^{51}V NMR in dilute Na–V–Mo solutions ([V] < 0.01) have been identified in this work. That makes it possible to compose the distribution diagrams for dilute V–Mo as well as V-W solutions, which show the ratio between vanadium in a V or V–M complex to total vanadium as evaluated from the ^{51}V NMR peak intensities. The diagrams for [V] = 0.004 M and V/M = 1:3 are shown in Fig. 7. MoO_4^{2-} and $Mo_7O_{24}^{6-}$ are not included as their content has not been examined in the 0.004 M solutions due to the low concentration sensitivity of the ^{95}Mo and ^{17}O NMR.

It can be seen that the mixed species prevailing in Na–V–Mo solutions are not crystallized and some minor species are crystallized instead probably due to the lower solubility of their Na salts. This can partly explain the contradiction of the data available on the composition of the V–Mo complexes, which were obtained from studies of solutions and crystal phases. Besides, we have also found that the

cations (Na, K, NH_4) influence the composition of the concentrated V–Mo solutions. As a result some other complexes can be isolated from K(NH_4)–V–Mo solutions.

REFERENCES

1. M. T. Pope, *Heteropoly and Isopoly Oxometalates*. Springer, Berlin (1983).
2. F. Chauveau, *Bull. Soc. Chim. Fr.* 1960, 834.
3. G. W. Wallace and M. G. Mellon, *Analyt. Chim. Acta* 1960, **23**, 35.
4. F. Chauveau and P. Souchay, *Bull. Soc. Chim. Fr.* 1963, 561.
5. A. A. Amirbekova and A. K. Ilyasova, *Izv. Akad. Nauk Kaz. SSR, Ser. Khim.* 1969, 81.
6. A. Björnberg, *Acta Cryst.* 1979, **B35**, 1989, 1995; 1980, **B36**, 1530.
7. M. Filowitz, R. K. C. Ho, W. G. Klemperer and W. Shum, *Inorg. Chem.* 1979, **18**, 93.
8. N. A. Polotebnova and E. F. Tkatch, *Zh. Neorg. Khim.* 1969, **14**, 1040.
9. L. P. Kazansky and V. I. Spytsin, *Dokl. Akad. Nauk SSSR* 1975, **223**, 381.
10. S. E. O'Donnel and M. T. Pope, *J. Chem. Soc. Dalton Trans.* 1976, 2290.
11. O. Heath and O. W. Howarth, *J. Chem. Soc. Dalton Trans.* 1981, 1105.
12. R. I. Maksimovskaya, A. K. Ilyasova, D. U. Begalieva, D. F. Takezhanova and A. K. Akhmetova, *Izv. Akad. Nauk SSSR, Ser. Khim.* 1984, 2169.
13. L. P. Kazansky, *Koord. Khim.* 1977, **3**, 327.
14. H. T. Evans, *Perspec. Struct. Chem.* 1971, **4**, 1.
15. V. M. Mastikhin, O. B. Lapina, V. V. Krasilnikov and A. A. Ivakin, *React. Kinet. Catal. Lett.* 1984, **24**, 119.
16. C. J. Besecker, W. G. Klemperer, D. J. Maltbie and D. A. Wright, *Inorg. Chem.* 1985, **24**, 1027.

Polyhedron Vol. 6, No. 10, pp. 1823–1831, 1987
Printed in Great Britain

0277–5387/87 $3.00+.00

A NEW MODE OF FORMATION OF THE PHOSPHORUS–PHOSPHORUS BOND: SYNTHESIS AND CRYSTAL STRUCTURE DETERMINATION OF 1,5-DICHLORO-2,4-DIMETHYL-2,4-DIAZA-1,5-DIPHOSPHA-1,5-DIPHENYLPENTAN-3-ONE AND OF 1,4-DIMETHYL-2,3-DIPHENYL-1,4,3,2-DIAZADIPHOSPHOLIDIN-5-ONE-2-OXIDE AND ITS OXIDATION WITH TETRACHLOROORTHOBENZOQUINONE

GERHARD BETTERMANN and REINHARD SCHMUTZLER*

Institut für Anorganische und Analytische Chemie der Technischen Universität, Hagenring 30, D-3300 Braunschweig, F.R.G.

SIEGFRIED POHL

Fachbereich Chemie der Universität, Carl von Ossietzky-Straße, 2900 Oldenburg, F.R.G.

and

ULF THEWALT

Sektion Röntgen- und Elektronenbeugung der Universität, Oberer Eselsberg, D-7900 Ulm, F.R.G.

(*Received* 31 *October* 1986; *accepted* 20 *March* 1987)

Abstract—Reaction of phenyldichlorophosphine, **2b**, with *N,N'*-dimethyl-*N,N'*-bis(trimethylsilyl)urea, **1**, leads to a symmetrical diphosphorylation product, **3b**. A mechanism for the formation of **3b**, on the basis of ^{31}P NMR-data, is proposed. **3b** reacts with oxalic acid bis(trimethylsilyl)ester, **5**, with intramolecular P–P-coupling and formation of the λ^3P–λ^4P-mixed-valence diphosphorus compound, 1,4-dimethyl-2,3-diphenyl-1,4,3,2-diazadiphospholidin-5-one-2-oxide, **6**, which has been oxidized by means of tetrachloroorthobenzoquinone (TOB), **7**, to the λ^4P–λ^5P-compound, **8**. The structures of **3b**, **6** and **8** have been elucidated by ^{1}H- and ^{31}P-NMR-spectroscopy; single crystal X-ray diffraction studies of **3b** and of **6** have been conducted. The identity of both compounds has been confirmed. In the acyclic diphosphorus compound, **3b**, a remarkably short non-bonding P–P distance of 280.6 pm has been found while the P–P bond length in the cyclic compound **6** is of the usual order of magnitude (221.1 and 221.8 pm, respectively).

Recently, the reaction of *N,N'*-dimethyl-bis(trimethylsilyl)-urea, **1**, with methyldichlorophosphine, **2a**, has been shown to yield a symmetrical diphosphorylation product, **3a**, which has been found to undergo various further transformations.[1,2] We have now prepared the related compound, **3b**, as a crystalline solid from **1** and phenyldichlorophosphine, **2b**:

* Author to whom correspondence should be addressed.

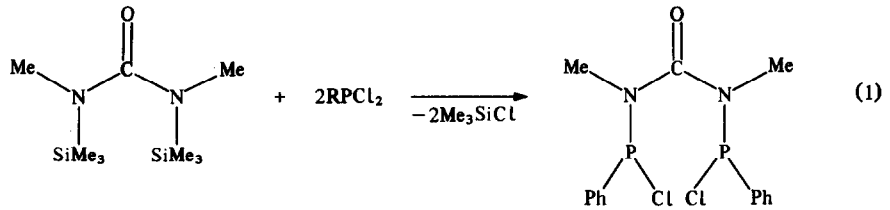

(1)

1 **2a** R = Me **3a** R = Me
2b R = Ph **3b** R = Ph

The reaction of **1** with **2b**, in a molar ratio 1 : 1, has already been described by Roesky and his co-workers, with formation of different products.[3] In a subsequent publication a possible pathway has been suggested,[4] and it would seem reasonable to assume the reactions to proceed via a common intermediate. In a ^{31}P NMR investigation of the reaction of **2b** with $(Me_3Si)(Me)NC(:O)N(Me)(SiMe_3)$, **1**, only the signals for $PhPCl_2$, **2b** (δ_P +160) and for the product, Ph(Cl)P(Me)NC(:O)N(Me)P(Cl)Ph, **3b**, (δ_P +120) were observed at room temperature. No evidence for an intermediate product was found. In an experiment, conducted in an NMR tube at −45°C between $PhPCl_2$, **2b** and **1** in a molar ratio 2 : 1 evidence for a two-step reaction was obtained, however. Upon warming the sample in the NMR tube two strong signals, one at δ_P 160 ($PhPCl_2$), and one for an intermediate product (δ_P 124.8), and a weak signal for **3b** (δ_P 120) were noted. In the following spectrum, recorded within about 1 min of the first one, a reversal of the signal intensities was already noted. Finally, in a spectrum recorded at room temperature 5 min later only the product **3b** (δ_P +120) was observed.

On the basis of the above evidence the following pathway is suggested for the reaction:

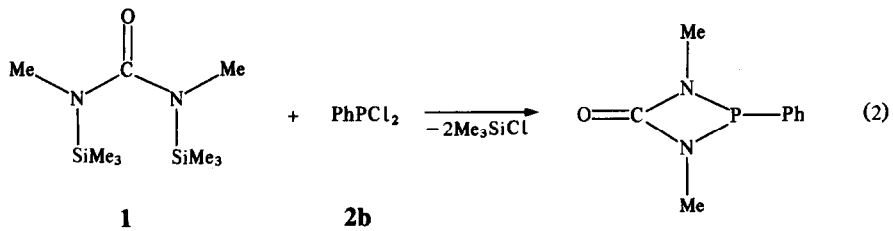

(2)

1 **2b**

In a second step, insertion of $PhPCl_2$ into the P–N bond is suggested to occur:

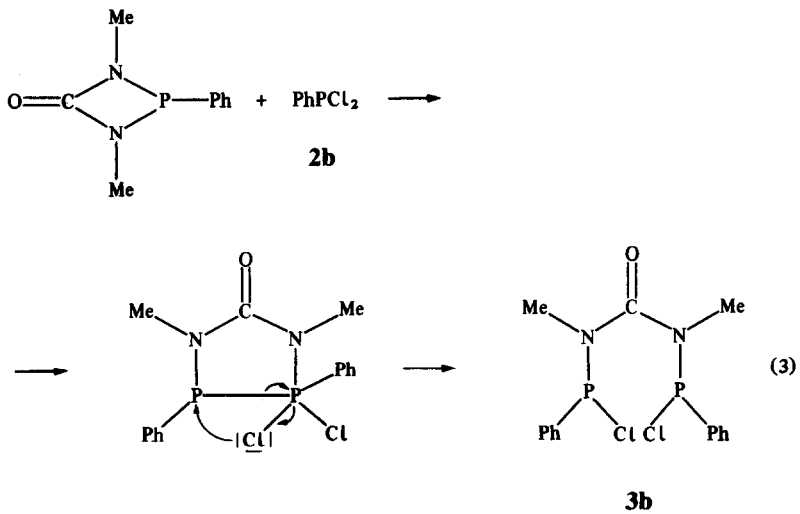

(3)

3b

The reaction is accompanied, presumably, by simultaneous migration of chlorine and cleavage of the P–P bond, with formation of **3b**.

As both compounds, **3a** and **3b**, show a triplet in the ^{1}H NMR spectrum for the N–Me-protons, indicating coupling between the phosphorus atoms,[5] a single crystal X-ray structure determination of **3b** was carried out, in order to support the evidence for this interaction.

The most remarkable finding originating from the structure determination of **3b** is the unusually low P–P-distance of 280.6 pm in the solid state which may, perhaps, be represented in terms of contributions by the mesomeric structures depicted below:

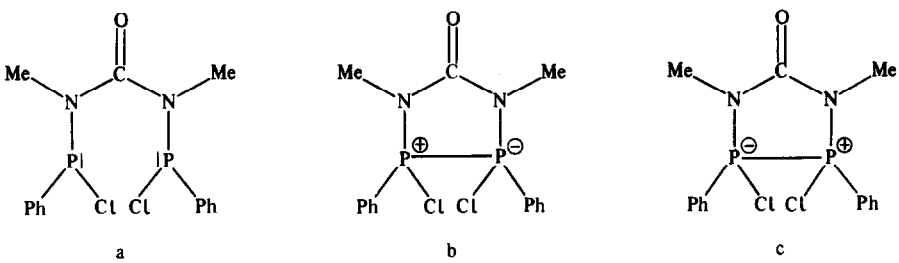

3b

In b and c the urea grouping may function as a kind of "electron sink" which serves to compensate or alleviate the consequences of a shift of electron density. It cannot be ascertained to which extent the remarkable proximity of the two phosphorus atoms in **3b** persists in the solution state.

It may well be of some relevance to the ease of P–P bond formation when the transformation of **3b** into **6** is effected [eqn (4)].

Since bonds involving the negatively charged hypervalent phosphorus atom are probably weakened to the same extent to which those to the positively charged phosphorus are strengthened, the P–Cl, P–N and P–C bonds, as a consequence of these effects, would appear to be normal single bonds. The coordination of both phosphorus atoms is rather similar. While it cannot be described in terms of a regular polyhedron it may, perhaps be referred to as strongly distorted ψ-trigonal bipyramidal. The five-membered ring invoked in structures b and c is non-planar (see also Fig. 2). The phosphorus atoms are situated *ca* 60 pm above and below the plane, respectively, in which the atoms, N1, N2 and C1 are situated (see Fig. 1).

An attempt was undertaken at the intramolecular coupling of the two phosphorus atoms in **3b**, with formation of the cyclic diphosphorus compound, **4b**, the P,P′-dimethyl analogue of which, **4a**, is known.[2]

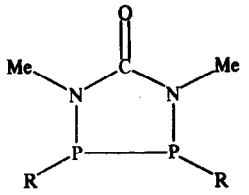

4a R = Me
4b R = Ph

As a new reagent which, it was hoped, would bring about this intramolecular dehalogenating condensation, oxalic acid bis(trimethylsilyl)ester,[6] **5**, was employed. A smooth reaction, involving P–P coupling, was indeed observed but, instead of **4b**,

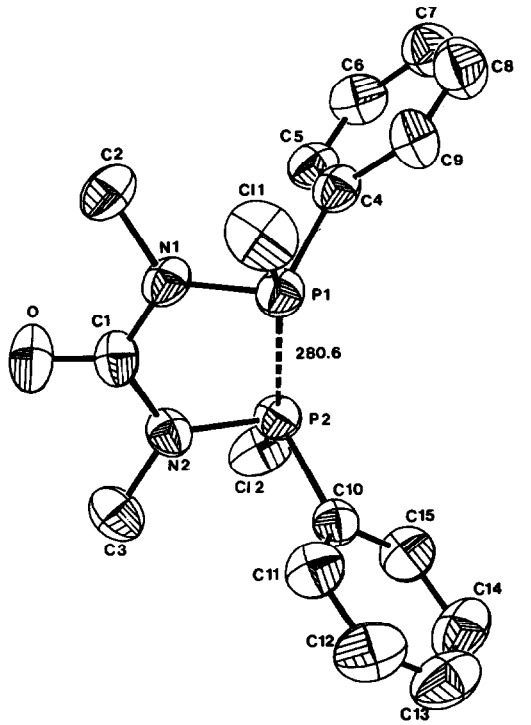

Fig. 1. Molecule of **3b** showing the atom number; r(P–P) in pm; vibrational ellipsoids with 50% probability (excluding hydrogen atoms).

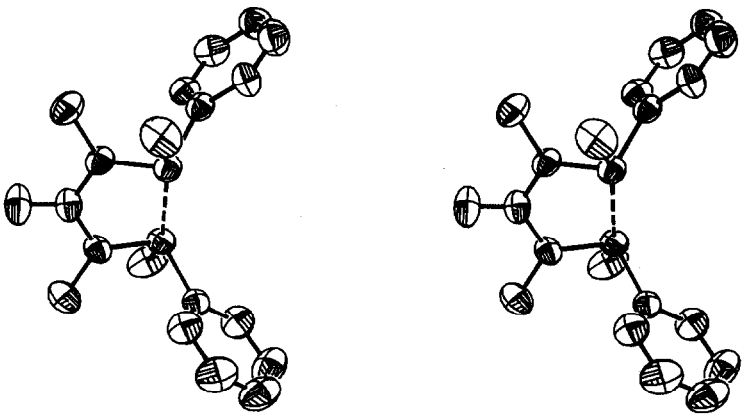

Fig. 2. Stereoview of a molecule of **3b**.

the mixed valence diphosphorus compound, **6**, was formed, in accord with eqn (4).

It may be envisaged that, in subsequent steps, from one molecule each of **3b** and **5** an initial cyclic product is formed which undergoes loss of CO and CO_2, as indicated, to give the λ^3P–λ^4P diphosphorus compound, **6** [eqn (4)]. The NMR spectra of **6** (Table 1) suggest the existence of the compound in two stereoisomeric forms, **6a** and **6b**, which are believed to differ with regard to the positions, relative to each other, of the phenyl groups at the phosphorus–phosphorus bond. According to the X-ray

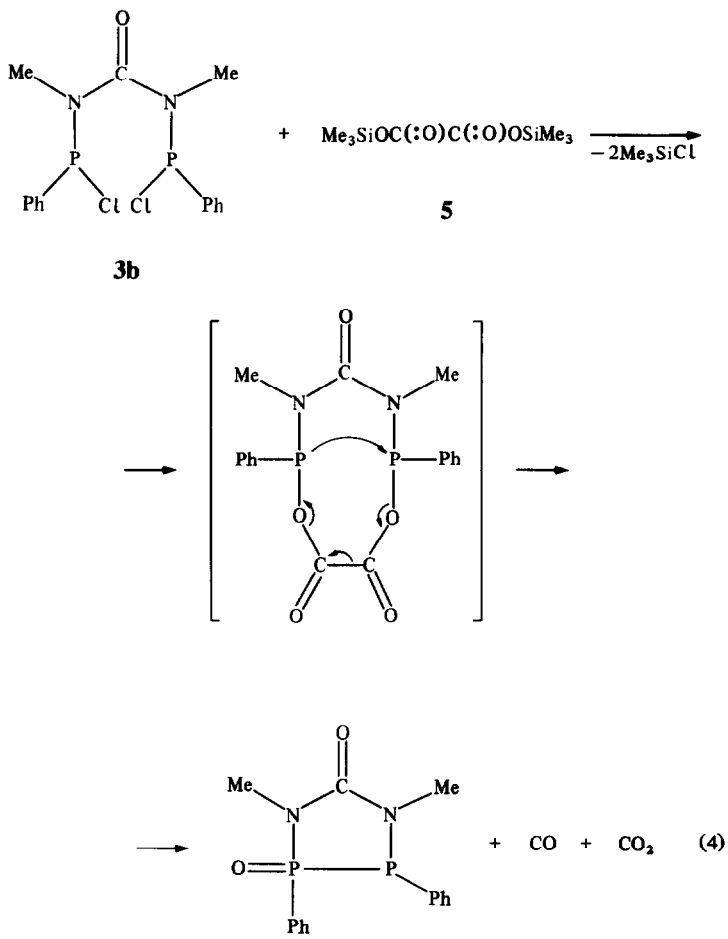

6

Table 1. ^{1}H and ^{31}P NMR spectra of **6**[a] (in $CDCl_3$)

		Isomer **6a**		Isomer **6b**
^{31}P:	δ (λ^3P)	33.1(d)		29.7 (d)
	δ (λ^4P)	14.6 (d)		11.2 (d)
	^{1}J(PP)	169 Hz[b]		182 Hz[b]
^{1}H	δ λ^4P-NC$\underline{H}_3$	3.77	^{3}J(HP) 9.5 Hz (d)	3.74
	δ λ^3P-NC$\underline{H}_3$	2.90	^{3}J(HP) 7.5 Hz (d)	2.90
	Ph	7.0	center of multiplet	7.0

[a] Shift values to high field of the reference have been given a negative sign.

[b] Roesky and his co-workers[7] have not reported ^{1}J(PP) for their compound, and a comparison is thus impossible.

Table 2. Bond lengths (pm) and bond angles in compound **3b**

P(1)—Cl(1)	210.0(2)	Cl(1)—P(1)—N(1)	100.7(1)
P(1)—N(1)	170.2(3)	Cl(1)—P(1)—C(4)	98.6(1)
P(1)—C(4)	182.1(4)	N(1)—P(1)—C(4)	101.4(2)
P(2)—Cl(2)	209.6(1)	Cl(2)—P(2)—N(2)	101.5(1)
P(2)—N(2)	170.6(3)	Cl(2)—P(2)—C(10)	99.5(1)
P(2)—C(10)	182.3(4)	N(2)—P(2)—C(10)	101.9(2)
O—C(1)	120.9(5)	P(1)—N(1)—C(1)	122.1(2)
N(1)—C(1)	138.3(4)	P(1)—N(1)—C(2)	121.6(2)
N(1)—C(2)	148.2(5)	C(1)—N(1)—C(2)	114.8(3)
N(2)—C(1)	138.1(4)	P(2)—N(2)—C(1)	121.2(2)
N(2)—C(3)	146.5(4)	P(2)—N(2)—C(3)	121.4(3)
C(4)—C(5)	138.8(6)	C(1)—N(2)—C(3)	115.5(3)
C(4)—C(9)	138.7(5)	O—C(1)—N(1)	121.7(3)
C(5)—C(6)	137.4(6)	O—C(1)—N(2)	121.4(3)
C(6)—C(7)	137.2(6)	N(1)—C(1)—N(2)	117.0(3)
C(7)—C(8)	138.6(7)	P(1)—C(4)—C(5)	121.0(3)
C(8)—C(9)	137.2(6)	P(1)—C(4)—C(9)	120.0(3)
C(10)—C(11)	138.6(6)	C(5)—C(4)—C(9)	118.7(4)
C(10)—C(15)	137.6(6)	C(4)—C(5)—C(6)	120.3(3)
C(11)—C(12)	137.7(6)	C(5)—C(6)—C(7)	121.2(4)
C(12)—C(13)	137.4(7)	C(6)—C(7)—C(8)	118.4(4)
C(13)—C(14)	136.7(8)	C(7)—C(8)—C(9)	121.1(4)
C(14)—C(15)	138.3(6)	C(4)—C(9)—C(8)	120.3(4)
P(1)—P(2)	280.6(2)	P(2)—C(10)—C(11)	121.1(3)
		P(2)—C(10)—C(15)	119.9(3)
		C(11)—C(10)—C(15)	118.5(4)
		C(10)—C(11)—C(12)	120.8(4)
		C(11)—C(12)—C(13)	120.1(5)
		C(12)—C(13)—C(14)	119.6(4)
		C(13)—C(14)—C(15)	120.5(4)
		C(10)—C(15)—C(14)	120.5(4)
		P(2)···P(1)—Cl(1)	157.7(1)
		P(1)···P(2)—Cl(2)	156.0(1)
		P(2)···P(1)—N(1)	77.7(1)
		P(1)···P(2)—N(2)	78.7(1)
		P(2)···P(1)—C(4)	103.5(1)
		P(1)···P(2)—C(10)	104.0(1)

Table 3. Bond lengths (pm) and bond angles in compound **6**

Atoms	Molecule A	Molecule B	Atoms	Molecule A	Molecule B
P(1)—P(2)	221.1(2)	221.8(2)	P(2)—P(1)—N(1)	89.2(2)	89.3(2)
P(1)—N(1)	172.3(4)	173.2(4)	P(2)—P(1)—C(4)	101.1(2)	100.4(2)
P(1)—C(4)	182.3(5)	183.9(5)	N(1)—P(1)—C(4)	103.4(2)	104.0(2)
P(2)—N(2)	167.8(4)	167.4(4)	P(1)—P(2)—N(2)	93.7(2)	93.7(2)
P(2)—O(2)	148.2(4)	147.7(4)	P(1)—P(2)—O(2)	113.3(2)	114.9(2)
P(2)—C(10)	179.1(5)	179.5(5)	P(1)—P(2)—C(10)	113.7(2)	113.4(2)
N(2)—C(1)	139.5(8)	138.6(8)	N(2)—P(2)—O(2)	116.4(2)	115.0(2)
N(2)—C(3)	148.9(6)	149.0(6)	N(2)—P(2)—C(10)	105.5(2)	105.0(2)
C(1)—N(1)	136.4(7)	135.9(6)	O(2)—P(2)—C(10)	112.8(2)	113.1(2)
C(1)—O(1)	123.7(6)	123.4(6)	P(2)—N(2)—C(1)	118.1(3)	119.8(3)
N(1)—C(2)	148.2(9)	149.1(8)	P(2)—N(2)—C(3)	121.4(4)	120.4(4)
C(4)—C(5)	139.2(7)	139.4(7)	C(1)—N(2)—C(3)	118.3(4)	119.0(4)
C(5)—C(6)	139.3(8)	139.9(8)	N(2)—C(1)—N(1)	114.5(4)	114.5(4)
C(6)—C(7)	137.7(8)	137.7(8)	N(2)—C(1)—O(1)	121.5(5)	122.1(5)
C(7)—C(8)	138.0(9)	138.4(9)	N(1)—C(1)—O(1)	123.9(6)	123.3(5)
C(8)—C(9)	138.8(9)	139.0(8)	C(1)—N(1)—P(1)	121.9(4)	122.1(4)
C(9)—C(4)	139.2(7)	136.1(7)	C(1)—N(1)—C(2)	118.7(4)	117.9(4)
C(10)—C(11)	138.7(8)	138.0(8)	P(1)—N(1)—C(2)	119.4(3)	119.2(3)
C(11)—C(12)	137.4(8)	139.2(8)			
C(12)—C(13)	138.3(9)	136.5(9)			
C(13)—C(14)	138.4(10)	139.2(10)			
C(14)—C(15)	136.8(7)	138.3(8)			
C(15)—C(10)	140.6(7)	140.5(7)			

crystal structure determination of **6**, however, only one species is present in the solid state (*vide infra*).

The mass spectrum of **6** reveals its thermal stability, in that the base peak of the spectrum corresponds to the molecular ion. Based on the observation of two metastable ions, the loss of one methyl group (m* 288.71; 318 → 303; Δm = 15) and of methyl isocyanate (m* 214.22; 318 → 261; Δm = 57) is indicated.

The NMR spectra of **6** both for ^{1}H and ^{31}P (Table 1) are different for each isomer. Isomer **6a** is present in excess over **6b** which is thought to be a consequence of less steric hindrance (*trans* arrangement of phenyl groups), compared to **6b** (*cis*).

The preparation of **6** by a thermolytic reaction, apparently in a lower state of purity (reported m.p. 118°; our m.p. 150°) has been reported.[7] An attempted X-ray crystal structure determination of **6** confirmed its identity, but a structure refinement has been reported as being impossible, due to the unsatisfactory quality of the crystals.[7] We have, therefore, undertaken a new single crystal X-ray determination of **6**.

The present X-ray investigation confirms the preliminary results of Sheldrick *et al.*[7] There are two crystallographically independent molecules of **6** per asymmetric unit. As Fig. 3 shows, the two molecules (labeled A and B) have the same configuration (with the phenyl groups *cis* relative to the heterocyclic ring, as opposed to **3b** where the phenyl groups are trans). Furthermore A and B have an almost identical conformation.* The molecular packing is illustrated in Fig. 4. The heterocyclic rings are slightly puckered. The deviations (in pm) of atoms from the respective least squares planes defined by the ring atoms are for A: P(1a) 2; P(2a) −5; N(2a) 8; C(1a) −6; N(1a) 1; for B: P(1b) 3; P(2b) −4; N(2b) 6; C(1b) −3; N(1b) −2. The phosphorus–phosphorus bond lengths in **6** of 221.1(2) (A) and 221.8(2) pm (B) fall in the range typical of phosphorus–phosphorus single bonds (c.f. e.g.[8]).

Since there are only very few examples of P–P compounds involving the λ^4P–λ^5P-structural unit,[8] and as only one example of a product of direct oxidation of TOB to a λ^4P–λ^5P compound is known,[8c] we were interested in the oxidation of **6** by TOB. In many cases investigated previously, the P–P bond was broken upon oxidation.[9]

The reaction proceeded as shown below, eqn (5); the P–P bond remained intact; P–P coupling,

* Bond distances and angles are listed in Table 3.

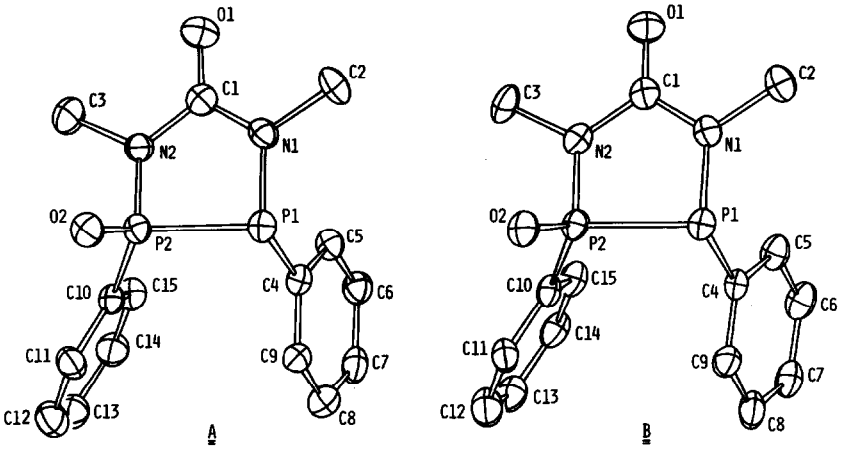

Fig. 3. ORTEP drawings of the two crystallographically independent molecules of **6**.

$^1J_{P-P}$ = 350 Hz was observed. In the ^{1}H NMR spectrum two isomers were observed, too, the $NC\underline{H}_3$ resonance line for one isomer being shifted by only 0.01 ppm, relative to the other.

tallized from either dichloromethane or benzene. Yield of **3b**, 6.6 g (76%); m.p. 155–156°. Found: C, 47.4; H, 4.3; Cl, 18.2. $C_{15}H_{16}Cl_2OP_2$ (373.17) requires: C, 48.3; H, 4.5; Cl, 19.0%. NMR spectra

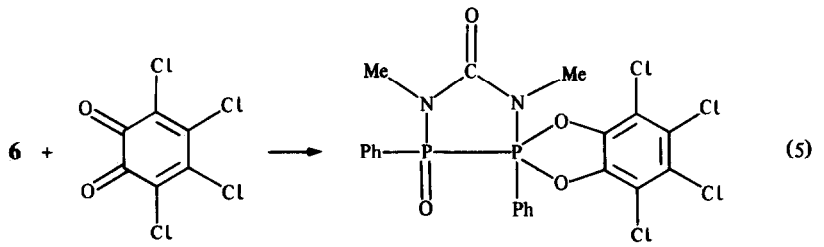

7 **8**

EXPERIMENTAL

The usual precautions with regard to exclusion of air and moisture were observed in the course of the experiments. ^{1}H and ^{31}P NMR spectra: JEOL JNM-60 HL with TMS (ext.) and 85% H_3PO_4 (ext.) standards. IR spectra: Beckman IR 4260. Mass spectra AEI MS 9.

Preparation of 1,5-*dichloro*-2,4-*dimethyl*-2,4-*diaza*-1,5-*diphospha*-1,5-*diphenylpentan*-3-*one*, **3b**

N,N'-Bis(trimethylsilyl)-*N,N'*-dimethyl-urea, **1** (5.3 g; 0.023 mol) was added dropwise with stirring to a solution of $PhPCl_2$, **2b** (23 g; 0.13 mol) in 20 cm^3 of dichloromethane. After stirring had been continued for 20 h volatile products were removed *in vacuo*, and the remaining solid was collected by filtration. It was washed with ether and recrys-

(in $CDCl_3$):

^{1}H: $NC\underline{H}_3$: δ+2.90, 'triplet' (separation of components 2.1 Hz)
$C_6\underline{H}_5$ δ+7.5 (center of multiplet)
^{31}P δ+120.

Mass spectrum (rel. intensities of the characteristic fragments, based on m/e 143 = 100%, in parentheses); m/e 337 (1): M^+–Cl; 302 (6): M^+–2Cl; 230 (12): M^+–PhPCl; 178 (82): $PhPCl_2^+$; 143 (100): $PhPCl^+$; 124 (43): $PhPO^+$; 60 (48): $MePN^+$. IR (Nujol mull): ν(C=O)(vs) at 1675 cm^{-1}.

Reaction of **3b** *with oxalic acid bis(trimethylsilyl)ester*, **5**: *preparation of* 1,4-*dimethyl*-2,3-*diphenyl*-1,4,2,3-*diazadiphospholidin*-5-*one*-2-*oxide*, **6**

The solid reactants, **3b** (6.2 g; 0.017 mol) and **5** (3.9 g; 0.017 mol) were thoroughly mixed. The

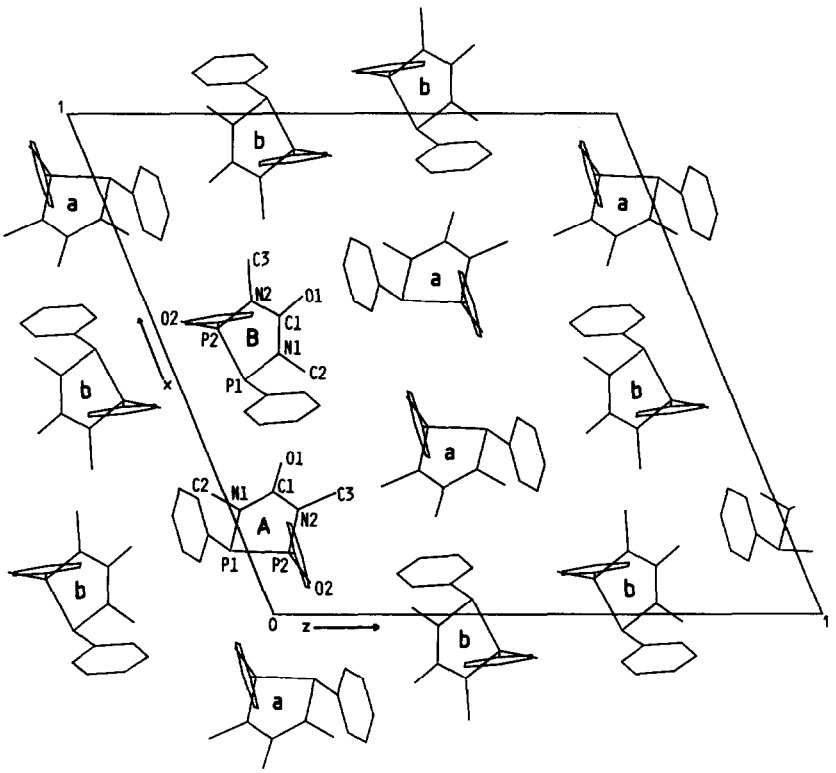

Fig. 4. Projection of the crystal structure of **6** along the *y* axis.

reaction with formation of gas commenced upon dropwise addition of 30 cm^3 dichloromethane over 0.5 h while the mixture was stirred. After an 0.5 h period of reflux, solvent and other volatile products were removed *in vacuo*. The solid product thus remaining was obtained as white crystals of m.p. 150° upon recrystallization from dichloromethane/ether. Yield 4.2 g (80%). Found: C, 56.4; H, 5.1; P, 19.8. $C_{15}H_{16}N_2O_2P_2$ (318.27) requires: C, 56.6; H, 5.1; P, 19.5%.

For NMR data of **6**, see Table 1. Mass spectrum (rel. intensities of the characteristic fragments, based on m/e 318 = 100%, in parentheses): m/e 318 (100): M^+; 303 (1): M^+–Me; 261 (69): M^+–MeNCO; 201 (67): Ph_2PO^+; 60 (65): $MeNP^+$. IR (solution in CH_2Cl_2) ν(C=O)(vs) 1685 cm^{-1}.

Reaction of **6** *with tetrachloroortho-benzoquinone*, **7**: *preparation of spiro-(4,5,6,7)-tetrachloro-(1,3,2)benzodioxaphosphole - 2,3' - 1',4' - dimethyl-2',3' - diphenyl - 1',4',2',3' - diazadiphospholidin - 5'-one-2'-oxide*, **8**

To a solution of **6** (2.6 g; 0.008 mol) in 10 cm^3 of dichloromethane was added dropwise a solution of **7** (2 g; 0.008 mol) in 10 cm^3 of dichloromethane. The intensely red solution of **7** lost its colour almost instantaneously. After addition of about half of the amount of **7** a colourless precipitate began to form. After the addition of **7** had been completed the mixture was stirred for 24 h and the volatile components were removed *in vacuo*. The solid residue was recrystallized from dichloromethane/ether. Yield of **8** 4.2 g (91%); m.p. 164° (dec.). Found: C, 44.0; H, 2.8; P, 10.5. $C_{21}H_{16}Cl_4N_2O_4P_2$ (564.13) requires: C, 44.2; H, 2.9; P, 11.0%.

NMR spectra (in CD_2Cl_2):

^{1}H: $NC\underline{H}_3$ (P=O)	δ+3.12 (d)	^{3}J(HP) 12 Hz
$NC\underline{H}_3$ ($PO_2C_6Cl_4$)	δ+3.19 (d)	^{3}J(HP) 8 Hz.

Two isomers are observed from the NCH_3 resonances, the second (about 40%) shifted from isomer one by $\Delta\delta$ = 0.01 ppm downfield (isomer one *vide supra*)

PhP	δ+7.5	(center of multiplet)		
^{31}P	δ+19.36	(d)	λ^4P	^{1}J(PP) 350 Hz
	δ−34.42	(d)	λ^5P	^{1}J(PP) 350 Hz.

Mass spectrum (rel. intensities of the characteristic fragments, based on m/e 371 = 100%, in parentheses): m/e 371 (100): $(O_2C_6Cl_4P(:O)Ph$; 355 (83): $O_2C_6Cl_4PPh$; 277 (87): $O_2C_6Cl_4$; 153 (76): PhP(:O)NMe; 124 (60): PhP(:O); 107 (66): PhP;

77 (73) : Ph ; 60 (66) MeNP. IR (Solution in CH_2Cl_2) ν(C═O)(vs) 1694 cm^{-1}. Crystals of **3b** and **6**, suitable for a single crystal X-ray crystal structure determination, were obtained by slowly evaporating the solvent, dichloromethane, over P_4O_{10}.

Crystal structure determination of **3b**

Colourless prisms of **3b** were employed for the X-ray determination conducted on a Syntex $P2_1$ diffractometer, (Mo-K_α radiation; graphite monochromator; λ (K$\bar{\alpha}$) 71.069 pm); the crystal dimensions were $0.3 \times 0.3 \times 0.4$ mm, triclinic; space group $P\bar{1}$. Cell parameters: $a = 808.2(3)$; $b = 948.9(3)$; $c = 1201.2(4)$ pm; $\alpha = 80.12(3)$; $\beta = 90.58(3)$; $\gamma = 75.67(3)$. Cell volume 877.96×10^6 pm^3 ($Z = 2$). Intensity data were collected to a θ_{max} of 24°, yielding a total of 2760 independent reflexions of which 2108 ($I > 2\sigma(I)$) were used in the subsequent calculations, using direct methods (programme SHELXTL; computer CM S 140). Final values for R and R_w, 0.048 and 0.054, respectively (hydrogens in fixed positions, remaining atoms refined with anisotropic temperature factors); weighting scheme: $w = (\sigma^2(F_o) + 0.01F_o^2)^{-1}$.

Crystal structure determination of **6**

Crystals of **6** were colourless and transparent, and of isometric habitus. A crystal of 0.24 mm average diameter was used for the X-ray measurements on a Philips PW 1100 diffractometer (graphite monochromator; (Mo-K$\bar{\alpha}$) = 71.069 pm). Cell parameters: $a = 1948.0(6)$, $b = 875.9(3)$, $c = 1973.9(4)$ pm; $\beta = 112.32(3)°$.

The space group (from systematic absences) is $P2_1/n$. $D_{calc} = 1.357$ g/cm^3 for $Z = 8$. Intensity data were collected to a θ_{max} of 22°, yielding a total of 3828 independent data. The 3143 reflexions with $F_o > 2.5\sigma(F_o)$ were used in the subsequent calculations. The structure was solved by Patterson techniques. All hydrogen atoms could be located in difference Fourier maps. The final values for R and R_w were 0.063 and 0.069, respectively (hydrogens in fixed positions, remaining atoms refined with anisotropic temperature factors). The weighting scheme was given by $w = 1.18(\sigma^2(F_o) + 0.003F_o^2)^{-1}$.* The calculations were carried out using the SHELX system.[10]

Acknowledgements—Thanks are due to Bayer A.G. and to Hoechst A.G. for generous gifts of chemicals. The support of Fonds der Chemischen Industrie is gratefully acknowledged.

REFERENCES

1. N. Weferling and R. Schmutzler, *Am. Chem. Soc. Symp. Series*, No. 171, Phosphorus Chemistry (L. D. Quin and J. G. Verkade, Ed), 1981, 425.
2. N. Weferling, R. Schmutzler and W. S. Sheldrick, *Liebigs Ann. Chem.* 1982, 167.
3. H. W. Roesky, K. Ambrosius, M. Banek and W. S. Sheldrick, *Chem. Ber.* 1980, **113**, 1847.
4. H. W. Roesky, H. Zamankhan, W. S. Sheldrick, A. H. Cowley and S. K. Mehrota, *Inorg. Chem.* 1981, **20**, 2910.
5. R. K. Harris, *Can. J. Chem.* 1964, **42**, 2275.
6. G. Schott and G. Henneberg, *Z. anorg. allg. Chem.* 1963, **323**, 228.
7. W. S. Sheldrick, S. Pohl, H. Zamankhan, M. Banek, D. Amirzadeh-Asl and H. W. Roesky, *Chem. Ber.* 1981, **114**, 2132.
8. (a) D. Schomburg, N. Weferling and R. Schmutzler, *J. Chem. Soc. Chem. Comm.* 1981, 609; (b) H. W. Roesky and H. Djarrah, *Inorg. Chem.* 1982, **21**, 844; (c) H. W. Roesky and D. Amirzadeh-Asl, *Z. Naturforsch.* 1983, **38b**, 460; (d) G. Bettermann, H. Buhl, R. Schmutzler, D. Schomburg and U. Wermuth, *Phosphorus and Sulfur* 1983, **18**, 77.
9. Ph.D. Thesis, N. Weferling, Braunschweig (1981).
10. G. M. Sheldrick, SHELX-76, Program for Crystal Structure Determination.

* Final atomic positional and thermal parameters, bond lengths and angles and F_o/F_c values have been deposited as supplementary material with the Editor, from whom copies are available on request. Atomic coordinates have also been submitted to the Cambridge Crystallographic Data Centre.

Polyhedron Vol. 6, No. 10, pp. 1833–1837, 1987
Printed in Great Britain

0277–5387/87 $3.00+.00

COORDINATION CHEMISTRY OF ALKALI AND ALKALINE EARTH CATIONS—SYNTHESIS AND X-RAY STRUCTURAL ANALYSIS OF SODIUM(PICRATE)-(1,10-PHENANTHROLINE)$_2$

JAN A. KANTERS and PIETER F. W. STOUTEN

Laboratorium voor Kristal-en Structuurchemie, Rijksuniversiteit Utrecht, Transitorium 3, Padualaan 8, 3584 CH Utrecht, The Netherlands

and

VIKSITA VIJAYWARGIA and NARINDER S. POONIA*

IRCS, Research Oasis, 68 Vishnupuri, Indore 452001, India

(*Received* 20 *May* 1986; *accepted after revision* 23 *April* 1987)

Abstract—The complex Na(Pic)(PHEN)$_2$ (Pic = picrate, Phen = 1,10-phenanthroline) is unique in being a cluster with two independent Na ions in the asymmetric unit. Na(1) is seven-coordinated involving two N atoms of two Phen molecules (Na—N, 2.492–2.622 Å), phenoxide O (Na—O$^-$, 2.381 Å) and an *o*-nitro-oxygen (Na—ONO, 2.584 Å) of Pic(1) and also to the phenoxide O (Na—O$^-$, 2.656 Å) of Pic(2). Na(2) is six-coordinated through four N atoms of the two other Phen molecules (Na—N, 2.510–2.570 Å), phenoxide O (Na—O$^-$, 2.317 Å) and *o*-nitro-oxygen (Na—ONO, 2.592 Å) of Pic(2). Thus Pic(2) serves as a linkage residue between two clusters. The Phen molecules are planar and nearly perpendicular to each other in either cluster.

With the aim of understanding the vital bioinorganic functions of Na, K, Mg and Ca,[1] we have been interested in unravelling the fundamental coordination chemistry of alkali (M^+) and alkaline earth (M^{2+}) cations (general abbr. M^{z+}). In order to understand the individual Lewis acid behaviour of each M^{z+}, a wide range of chemical and crystallographic investigations[2] have been undertaken on the systems of the type $M^{z+}(X)_z^-$(ligand)$_x$ and $M^{z+}(L)_z^-$(ligand)$_x$ where X and L are inorganic and organic charge neutralizers, respectively. The ligand may be a macrocycle such as benzo-15-crown-5,[3] a protic acyclic multidentate such as tetraethyleneglycol (Teg)[4] or triethanolamine (Tea),[5] or an aprotic conventional bidentate such as 2,2-bipyridine (Bipy)[6] or 1,10-phenanthroline (Phen).[7–9] The macrocycles have the advantage of the macrocyclic effect,[10] the protic Teg and Tea type of ligands enjoy the advantage of being double action[2] in that they coordinate the M^{z+} while also stabilizing (bridging) the counteranion. Bipy and Phen carry fairly anionic N-sites[11] and bind efficiently the hard M^{z+} in the capacity of being "anionic ligands".

During our extensive chemical[7–9] work on the ML_z-Phen systems under the solvating effect of the diverse protic and aprotic media, we realized that Na^+ and Ca^{2+}, for Pic (picrate) as L, display outstanding ability to yield solid Phen-complexes. Their complexes insolubilize easily irrespective of the solvating medium, in particular from water. To know about the chemical principles related to this conspicuous feature we have undertaken X-ray structural analysis of selected ML_z-Phen complexes with the hope that it would add to the understanding of the chemical differentiation of Na and Ca from their biologically important analogues K and Mg. In this paper we report on the structural results of Na(Pic)(Phen)$_2$.

* Author to whom correspondence should be addressed.

EXPERIMENTAL

Synthesis of $Na(Pic)(Phen)_2$

A 1 : 2 reaction mixture of Na(Pic) (0.002 mmol) and Phen-monohydrate was dissolved by warming in 5 cm^3 ethanol and set aside in a closed beaker at room temperature to allow a slow crystallization of the title complex. Bright yellow crystals (m.p. 280°C), recovered by filtration, were subjected to structural analysis.

X-ray structural analysis

From a yellow, transparent rod shaped crystal of dimensions $0.4 \times 0.2 \times 0.1$ mm, mounted on an Enraf–Nonius CAD-4 Diffractometer, 5057 reflections were measured for one half of the reflection sphere with Zr-filtered MoKα radiation up to $2\theta = 44°$ using ω-2θ scan technique. Lattice constants were determined by least squares refinement of the setting angles of 24 reflexions.

Crystal data

$Na^+(C_6H_2N_3O_7)^-(C_{12}H_8N_2)_2$, $M_r = 611.55$, triclinic with $a = 12.535(11)$, $b = 13.364(8)$, $c = 17.664(6)$ Å, $\alpha = 93.20(4)$, $\beta = 94.36(5)$, $\nu = 110.97(6)°$, $V = 2744$ Å^3, space group $P\bar{1}$ with $Z = 4$, $d_c = 1.436$ g cm^{-3}, (MoKα) = 0.71069 Å, μ(MoKα) = 1.1 cm^{-1}, $F(000) = 1256$, $T = 298$ K. Final R for 4614 observed reflections was 0.043.

The structure was determined by direct methods. MULTAN 80[12] yielded Fourier maps that could not be interpreted; however, SHELX 84[13] gave all but two non-hydrogen atoms. Subsequent Fourier methods revealed the remaining two atoms.

Isotropic refinement of the 90 non-hydrogen atoms was carried out with the SHELX 76[14] program on the Cyber 855 computer of the University of Utrecht and converged at $R = 0.14$. Subsequent refinement was performed on an in-house DG-Eclipse s/230 mini-computer, using a locally modified SHELX 76[14] implementation. Anisotropic non-hydrogen refinement converged at $R = 0.07$. All 36 H-atoms were placed at idealized aromatic C(sp^2)-H positions with a C—H distance of 1.08 Å and were kept fixed during refinement. The H-atoms were assigned an overall isotropic temperature parameter, which refined to a final value of 0.13. Scattering factors were taken from the *International Tables for X-ray Crystallography*.[15] The molecular geometry was calculated and the illustrations were prepared with the EUCLID-package.[16]

RESULTS AND DISCUSSION

The atom numbering of the phenanthroline and picrate molecules are shown in Fig. 1. There are two types of Na^+ ion, the coordination of which are shown in Figs 2 and 3. The numbering of atoms in Figs 2–4 is derived from the number of the corresponding moiety, i.e. O(201) denotes O(1) of picrate (2). Coordination geometry around Na(1) and Na(2) is detailed in Table 1. Other bond distances, angles, torsion angles and positional and thermal parameters have been deposited in the supplementary material.

There are only a few M^{z+}-Phen complexes the structural analysis of which have been reported. The $Sr(ClO_4)_2(Phen)_4 \cdot 4H_2O$ and $Ba(ClO_4)_2(Phen)_4 \cdot 4H_2O$ systems[17] are isomorphous wherein the cation is within the environment of only two bidentate Phen molecules and the four water molecules. More details for the Ba-system are available in our recent publication.[18] Bonding modes of Ba in $Ba(Pic)_2(Phen)_2$ acetone[19] and $Ba(Dnp)_2(Phen)_3$[20] (Dnp = 2,4-dinitrophenolate) have also been examined. In the $M(Onp)(Phen)_2$ (M = K or Rb; Onp = *o*-nitro-phenolate) complexes[21] the cation is within the environment of the two bidentate Phen molecules, the chelating Onp, and the unused nitro-oxygen belong to the Onp of the adjoining molecule in the lattice. The analogous $Na(Onp)(Phen)_2$ is not dimerized in this way but exists in discrete molecules[21] containing a 6-coor-

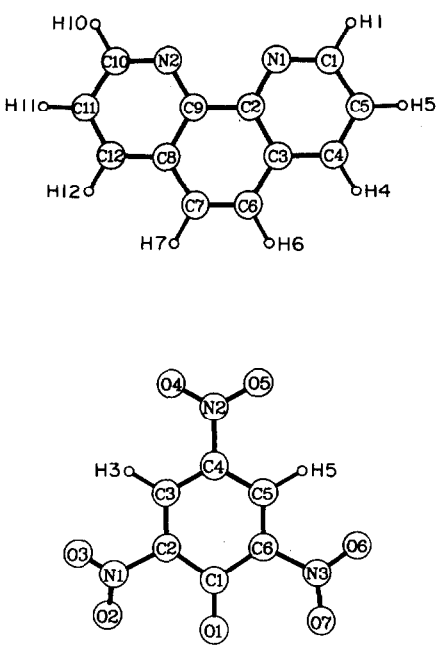

Fig. 1. Atom numbering of phenanthroline and picrate residues.

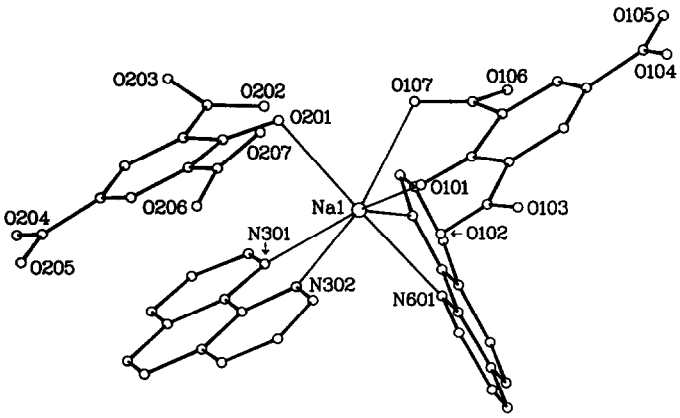

Fig. 2. Coordination of Na(1). [The residue number precedes the atom number, e.g. O(201) is atom O(1) of picrate(2), and N(301) is atom N(1) of phen(3) etc.]

dinated cation (Na—N, 2.444–2.557 Å; Na—O^-, 2.281 Å; and Na—ONO, 2.421 Å).

The present complex represents a unique example of being a cluster (Fig. 4) wherein there are two crystallographically different Na ions for each asymmetric unit. One cation, Na(1), is seven coordinated through the two bidentate Phen molecules (Na—N, 2.492–2.622 Å), the Pic(1) phenoxide (Na—O^-, 2.381 Å), an ortho-nitro-oxygen of the same Pic (Na—O, 2.584 Å) and also the Pic(2) phenoxide through a rather long contact (Na—O^-, 2.656 Å). The other cation, Na(2), is six coordinated through the two bidentate Phen molecules (Na—N, 2.510–2.570 Å), the Pic(2) phenoxide (Na—O^-, 2.317 Å) and an ortho-oxygen of this Pic (Na—O, 2.592 Å).

The two Phen molecules in each cluster are planar (ave. σ plane, 0.025 Å), nearly perpendicular to each other (88.2 and 84.0°) with the uniqueness that one C—N bond of each is consistently short (ave. 1.323 Å) while the other is distinctly longer (ave. 1.354 Å). As seen in Table 1, the two Na—N bond lengths for each Phen with a given cation, Na(1) or Na(2), are different, especially for the Phen molecule roughly in plane with Pic (and approaching the cation from the direction opposite to it); in fact it forms the shortest and the longest Na—N bonds and the effect is more pronounced for Na(1) which is in contact with two anionic oxygens. Similar differences are traceable for the $Na(Onp)(Phen)_2$ complex although, both Phen molecules in this compound are equally inclined to the Onp moiety.[21] Recently, the compound $NaMoO(CN)_3(Phen)_3 \cdot MeOH \cdot H_2O$ has been examined crystallographically[22] and has been found to contain Na within the cationic moiety of the complex $[Na(Phen)_2 \cdot MeOH,H_2O]^+[MoO(NC)_3(Phen)]^-$ wherein it is six-coordinated through two bidentate Phen

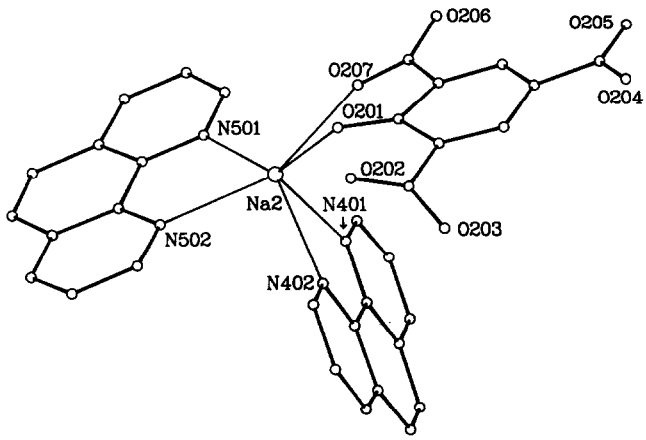

Fig. 3. Coordination of Na(2).

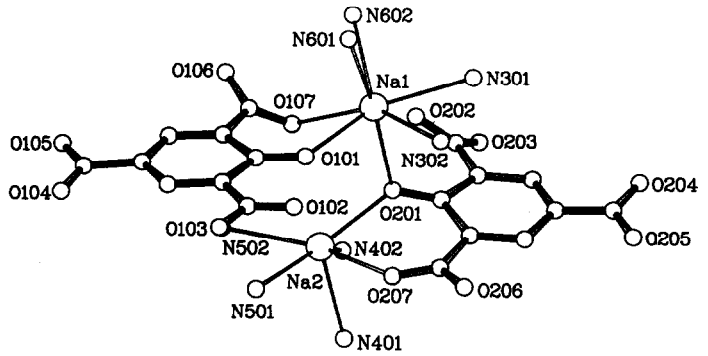

Fig. 4. The asymmetric unit consisting of two interlinked Na clusters.

molecules (Na—N, 2.500–2.521 Å), the water molecule (Na—OH_2, 2.380 Å), and methanol (Na—O, 2.413 Å). Na^+ is not under formal pairing with any charge neutralizer but the intriguing deformation of one Phen molecule still takes place which yields the shortest (2.500 Å) and the longest (2.521 Å) distance. The phenomenon is, therefore, an inherent feature of the Phen molecule.

The aromatic rings of Pic(1) and Pic(2) are also planar (σ plane, 0.055 and 0.020 Å) but nitro groups of both are rotated to different degrees (0.0, 4.5 and 33.3°, and 35.9, 6.5 and 16.4°, respectively). It

Table 1. Selected bond lengths and angles

	(a) Bond lengths (Å)		
Na(1)—O(201)	2.381(3)	Na(2)—O(101)	2.317(3)
Na(1)—N(302)	2.492(3)	Na(2)—N(501)	2.510(3)
Na(1)—N(601)	2.546(3)	Na(2)—N(502)	2.527(3)
Na(1)—N(602)	2.569(4)	Na(2)—N(401)	2.542(3)
Na(1)—O(207)	2.584(3)	Na(2)—N(402)	2.565(4)
Na(1)—N(301)	2.622(3)	Na(2)—O(107)	2.592(4)
Na(1)—O(101)	2.656(3)		
	(b) Angles (°)		
O(201)—Na(1)—N(302)	90.3(1)	O(101)—Na(2)—N(501)	137.4(1)
O(201)—Na(1)—N(601)	82.7(1)	O(101)—Na(2)—N(502)	132.6(1)
O(201)—Na(1)—N(602)	119.3(1)	O(101)—Na(2)—N(401)	113.0(1)
O(201)—Na(1)—O(207)	66.4(1)	O(101)—Na(2)—N(402)	84.1(1)
O(201)—Na(1)—N(301)	154.8(1)	O(101)—Na(2)—O(107)	66.2(0)
O(201)—Na(1)—O(101)	87.4(0)	N(501)—Na(2)—N(502)	65.5(1)
N(302)—Na(1)—N(601)	87.3(1)	N(501)—Na(2)—N(401)	89.7(1)
N(302)—Na(1)—N(602)	133.4(1)	N(501)—Na(2)—N(402)	138.3(1)
N(302)—Na(1)—O(207)	148.9(1)	N(501)—Na(2)—O(107)	84.7(1)
N(302)—Na(1)—N(301)	64.7(1)	N(502)—Na(2)—N(401)	106.1(1)
N(302)—Na(1)—O(101)	88.6(0)	N(502)—Na(2)—N(402)	90.0(1)
N(601)—Na(1)—N(602)	64.3(1)	N(502)—Na(2)—O(107)	149.4(1)
N(601)—Na(1)—O(207)	108.6(1)	N(401)—Na(2)—N(402)	64.2(1)
N(601)—Na(1)—N(301)	98.6(0)	N(401)—Na(2)—O(107)	79.4(1)
N(601)—Na(1)—O(101)	169.3(1)	N(402)—Na(2)—O(107)	118.5(1)
N(602)—Na(1)—O(207)	77.5(1)		
N(602)—Na(1)—N(301)	83.0(1)		
N(602)—Na(1)—O(101)	124.8(0)		
O(207)—Na(1)—N(301)	134.8(1)		
O(207)—Na(1)—O(101)	70.8(0)		
N(301)—Na(1)—O(101)	88.5(0)		

indicates a different conformation for the two Pic moieties. Rotation of nitro groups of the nitrophenolates is a common feature of Onp[21,23,24] and Dnp[20] and in particular Pic.[25,26] Yet other chemically significant features of Pic in the present complex are the shortening of the C—O^- bond, elongation of the two C—C bonds next to C—O compared to the rest and decrease of the C—C—C angle at the C—O^-. This effect is practically the same as noted for Onp in K(Onp)·H_2O,[23] Rb(Onp)(Phen)$_2$[21] and K(Onp. isonitrosoacetophenone)[24] and to a decreased extent for Pic in K(Pic)[25] and Ba(Pic)$_2$(benzo-15-crown-5)·H_2O.[26] The origin of these deformities is the electron donating nature of the phenoxide and electron withdrawing nature of the nitro group, and the consequent hybridization change of the connected carbons.[27,28]

The Na—O^- and Na—ONO distances in the present complex are distinctly longer (Na—O^-, 2.381, 2.317 and 2.656 Å (bridging); Na—ONO, 2.584 and 2.592 Å) compared to the analogous distances in Na(Onp)(Phen)$_2$ (Na—O^-, 2.281; Na—ONO, 2.421 Å) suggesting a diminished anionic state of oxygens in Pic and an enhanced ionicity in the present complex. This feature, apparently relates itself to its inert (insoluble) characteristics in water medium; the Ca(Pic)$_2$(Teg)·H_2O,[29] which is highly inert in protic media and is rather quantitatively insoluble in isoproponal, is found through structural analysis to be practically charge separated. A vital clarification at this juncture is in order in that chemical inertness (insolubility) of ionic compounds in protic media, including water, increases with the ionicity of the compound.[2] The cross linkage of Na(1) with phenoxide of Pic(2) may add to the chemical inertness of the complex; Ba(Onp)$_2$, which we have found through X-ray analysis[30] to be an intricately Ba—O cross-linked, displays typical chemical inertness.

REFERENCES

1. R. J. P. Williams, *Q. Rev. Chem. Soc.* 1970, **24**, 331; *Membranes and Ion Transport*, Vol. 1 (Edited by E. E. Bittar). Wiley-Interscience, New York (1970).
2. N. S. Poonia and A. V. Bajaj, *Chem. Rev.* 1979, **79**, 389.
3. N. S. Poonia, P. Bagdi and K. S. Sidhu, *J. Inclusion Phenomena* 1986, **4**, 43.
4. N. S. Poonia, S. K. Sarad, A. Jayakumar and G. C. Kumar, *J. Inorg. Nucl. Chem.* 1979, **41**, 1759; N. S. Poonia, G. C. Kumar, A. Jayakumar, P. Bagdi and A. V. Bajaj, *J. Inorg. Nucl. Chem.* 1981, **43**, 2159.
5. J. A. Kanters, W. J. J. Smeets, K. Venkatasubramanian and N. S. Poonia, *Acta Cryst.* 1984, **C40**, 1701; J. A. Kanters, A. De Koster, A. Schouten, K. Venkatasubramanian and N. S. Poonia, *Acta Cryst.* 1985, **C41**, 1585.
6. J. Sharma and N. S. Poonia, work in progress.
7. N. S. Poonia and M. R. Truter, *J. Chem. Soc., Dalton Trans.* 1972, 1791.
8. N. S. Poonia, *Inorg. Chim. Acta* 1977, **23**, 5.
9. N. S. Poonia, *J. Indian Chem. Soc.* 1979, **56**, 22.
10. D. K. Cabbiness and D. W. Margerum, *J. Am. Chem. Soc.* 1969, **91**, 6540; F. P. Hinz and D. W. Margerum, *J. Am. Chem. Soc.* 1974, **96**, 4993.
11. C. Longuet-Higgins and C. A. Coulson, *J. Chem. Soc.* 1949, 971.
12. *MULTAN 80, A System of Computer Programs for Automatic Solution of Crystal Structures from X-ray Diffraction Data* (Edited by P. Main). University of York, U.K. and Louvain, Belgium (1980).
13. *SHELX 84, Program for Crystal Structure Solution* (Edited by G. M. Sheldrick). University of Gottingen, F.R.G. (1984).
14. *SHELX 76, Program for Crystal Structure Determination* (Edited by G. M. Sheldrick). University of Cambridge, U.K. (1976).
15. *International Tables for X-ray Crystallography*. Kynoch Press, Birmingham, U.K. (1974).
16. A. L. Spek, *The EUCLID Package in Computational Crystallography* (Edited by D. Sayre), p. 528. Clarendon Press, Oxford (1982).
17. G. Smith, E. J. Reilly, C. H. L. Kennard and A. H. White, *J. Chem. Soc., Dalton Trans* 1977, 1184.
18. R. L. Stanfield, S. R. Ernst, M. L. Hackert, V. Vijaywargiya, K. Venkatasubramanian and N. S. Poonia, *Acta Cryst.* 1984, **C40**, 1681.
19. R. Postma, J. A. Kanters, A. J. M. Duisenberg, K. Venkatasubramanian and N. S. Poonia, *Acta Cryst.* 1983, **C39**, 1221.
20. J. A. Kanters, R. Postma, A. J. M. Duisenberg, K. Venkatasubramanian and N. S. Poonia, *Acta Cryst.* 1983, **C39**, 1519.
21. D. L. Hughes, *J. Chem. Soc., Dalton Trans.* 1973, 2347.
22. S. S. Basson, J. G. Leipoldt and I. M. Patgieter, *Inorg. Chim. Acta.* 1984, **90**, 57.
23. J. P. G. Richards, *Z. Krist.* 1961, **116**, 468.
24. M. A. Bush and M. R. Truter, *J. Chem. Soc.* (*A*) 1971, 745.
25. K. Maartmann-Moe, *Acta Cryst.* 1969, **B25**, 1452.
26. K. Venkatasubramanian, N. S. Poonia, K. Clinger, S. R. Ernst and M. L. Hackert, *J. Inclusion Phenomena* 1984, **2**, 319.
27. H. A. Bent, *J. Inorg. Nucl. Chem.* 1961, **19**, 43.
28. O. L. Carter, A. T. McPhail and G. A. Sim, *J. Chem. Soc.* (*A*) 1966, 822.
29. T. P. Singh, R. Reinhardt and N. S. Poonia, *Inorg. Nucl. Chem. Lett.* 1980, **16**, 293.
30. J. A. Kanters, W. J. J. Smeets, A. J. M. Duisenberg, K. Venkatasubramanian and N. S. Poonia, *Acta Cryst.* 1984, **C40**, 1699.

Polyhedron Vol. 6, No. 10, pp. 1839–1842, 1987
Printed in Great Britain

0277–5387/87 $3.00+.00

X-RAY CRYSTAL STRUCTURE OF $W(OAlBr_3)(CH_2t\text{-}Bu)_3Br$, A MODEL FOR CATALYST–COCATALYST INTERACTION

J. FISCHER, J. KRESS, J. A. OSBORN,* L. RICARD and M. WESOLEK

Laboratoire de Chimie des Métaux de Transition et de Catalyse (UA au CNRS 424), Université Louis Pasteur, Institut Le Bel, 4 rue Blaise Pascal, 67000 Strasbourg, France

(*Received* 9 *January* 1987; *accepted* 23 *April* 1987)

Abstract—The crystal structure of the acid-base adduct obtained from $WO(CH_2t\text{-}Bu)_3Br$ and $AlBr_3$ is described. The interaction between the Lewis acid and the oxo ligand of the tungsten compound is discussed on the basis of bond distances and bond angles in the Br—W—O—Al linkage. The role of the W—O—Al linkage in homogeneous catalysis and of such interactions modelling the catalyst-support interactions in heterogeneous catalysis are briefly considered.

In recent years the organometallic chemistry of transition metals in formally high oxidation states has been greatly developed. The wide expansion of this field has emphasized the need for the use of π-donor ligands such as alkoxo, amido, oxo, imido or nitrido groups, which were shown to stabilize the generally electron deficient high oxidation state compounds. The oxo ligand has elicited interest for at least two further reasons: it has been suggested that it can serve as a "spectator" group in certain catalytic reactions[1] or as a reactive entity in both chemical and biochemical[2] oxidation processes. In this report, we describe an additional possible role for the oxo group, that of a bridge between catalyst and cocatalyst in certain catalytic reactions.

Previously[3] we have reported that tungsten(VI)–oxo-alkyl complexes of the type $WO(CH_2t\text{-}Bu)_3X$ (X = halide, alkoxide, ...) become catalytically active for the metathesis of olefins after addition of suitable Lewis acids such as boron, aluminum, gallium or tin halides. Acid-base interaction between the Lewis acid and the oxo function, both in the initial trialkyl precursors and in the propagating tungsten carbene derivatives, was suggested to be at the origin of this catalytic activity. We now report the X-ray structure of one of the initiating addition products, i.e. that formed from $WO(CH_2t\text{-}Bu)_3Br$ and $AlBr_3$.

* Author to whom correspondence should be addressed.

EXPERIMENTAL

Suitable single crystals of the title compound **1** were obtained from a saturated toluene solution at low temperature under argon in the absence of light. A systematic search in reciprocal space using a Philips PW1100/16 automatic diffractometer showed that crystals of **1** belong to the orthorhombic system. The unit-cell dimensions and their standard deviations were obtained and refined at room temperature with CuKα radiation (λ = 1.5405 Å) by using 25 carefully selected reflections and the standard Philips software. Crystal data: $C_{15}H_{33}OAlBr_4W$, M = 759.9, a = 18.643(6) Å, b = 15.996(5) Å, c = 17.092(6) Å, V = 5097 Å^3, Z = 8, d_{calc} = 1.98 g cm^{-3}, μ = 162.94 cm^{-1}, F_{000} = 2864, space group Pbca.

A crystal of 0.14 × 0.18 × 0.22 mm was sealed in a Lindemann glass capillary and mounted on a rotation free goniometer head. All quantitative data were obtained from a Philips PW1100/16 four circle automatic diffractometer, controlled by a P 852 computer, using graphite monochromated radiation and standard software. The vertical and horizontal apertures in front of the scintillation counter were adjusted so as to minimize the background counts without loss of net peak intensity at 2σ level. The total scan width in $\theta/2\theta$ flying step-scan used was $\Delta\theta = 1.0+0.143tg(\theta)$ deg. a step width of 0.05 deg. and a scan speed of 0.024 deg s^{-1}. 3785 hkl reflections were recorded ($4° < \theta < 57°$). The

resulting data-set was transferred to a PDP 11/60 computer, and for all subsequent computations, the Enraf-Nonius SDP/PDP package was used,[4] with the exception of a local data-reduction program. Three standard reflections measured every hour during entire data-collection period has a mean loss of 16% in intensity which was corrected using a time-dependent linear interpolation function.

The raw step-scan data were converted to intensities using the Lehmann–Larson method[5] and then corrected for Lorentz, polarisation and absorption factors, the latter computed by the numerical integration method of Busing and Levy[6] (transmission factors between 0.08 and 0.31). A unique data set of 1333 reflections having $I > 3\sigma(I)$ was used for determining and refining the structure.

The structure was solved using the heavy atom method. After refinement of heavy atoms, a difference-Fourier map revealed maxima of residual electronic density close to the positions expected for hydrogen atoms; they were introduced in structure factor calculations by their computed coordinates (C—H = 0.95 Å) and isotropic temperature factors of the form B(H) = 1 + *Beqv*(*C*) Å^2 but not refined. Full least-squares refinement minimizing $\Sigma\omega(|Fo|-|Fc|)^2$ converged to $R(F) = 0.060$ and $R_w(F) = 0.073$, $w = (\sigma^2_{\text{counts}}+(pI)^2)^{-1}$. The unit weight observation was 1.38 for $p = 0.08$. A final difference map revealed no significant maxima. The scattering factors coefficients and anomalous dispersion coefficients come respectively from Refs 7 and 8.

Tables of atomic positional parameters [Table 2 (1 page), Tables 3_1 (1 p.), and 3_2 (1 p.)] and thermal parameters [Table 4 (1 p.)] and lists of *Fo*/*Fc* values (*10, Table 5 (6 pp.)), have been deposited as supplementary data with the Editor, from whom copies are available on request. Atomic coordinates have also been deposited with the Cambridge Crystallographic Data Centre.

RESULTS

The crystal consists of discrete molecular units separated by normal Van der Waals distances. There are no unusual intermolecular contacts. An ORTEP view of the molecular unit is displayed in Fig. 1 along with the atom labelling scheme. Selected bond distances and bond angles are given in Table 1.

The molecule consists of a central tungsten(VI) atom which has a slightly distorted trigonal bipyramidal coordination geometry. The equatorial positions are occupied by the three neopentyl groups,

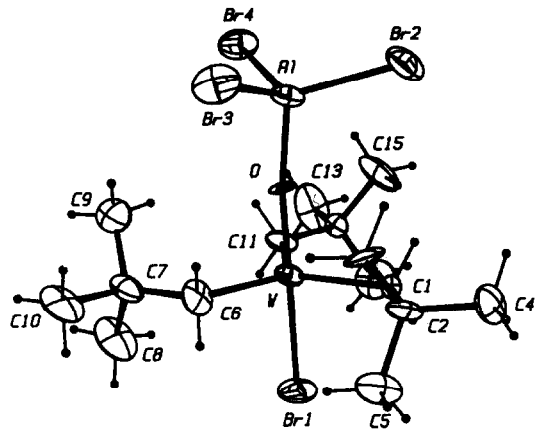

Fig. 1. ORTEP view of complex 1 (50% probability thermal ellipsoids).

and the axial positions by the oxo and bromo ligands. The oxo oxygen is linked to the aluminum of the $AlBr_3$ moiety resulting in a distorted tetrahedral arrangement about Al.

The three neopentyl groups adopt a helical arrangement about the tungsten centre, the β carbon atoms C(2), C(7) and C(12) being located almost within the plane defined by the α carbons C(1), C(6), C(11). The tungsten atom lies out of this plane by only 0.01 Å, being displaced towards the Br(1) axial ligand. The three W—C bonds, as well as the three C—W—C and W—C—C angles are not significantly different from each other with normal mean values of 2.11 Å, 120° and 121° respectively (Table 1) similar to those observed in $[WO(CH_2t\text{-}Bu)_3]_2(\mu\text{-}O)$.[9]

The oxo bridge between tungsten and aluminum is characterized by an almost linear alignment of the three atoms (W—O—Al = 172°). The short Al—O distance (1.79 Å)[10,11] is indicative of a strong coordination bond. The tungsten–oxygen bond distance (1.77 Å), although *ca* 0.1 Å longer than in other W(VI) oxo compounds,[9,12–15] is consistent with the presence of a double bond. The W—Br(1) bond distance, on the other hand, is particularly short (2.428 Å),[16–18] despite the location of the bromine in position *trans* to the oxo ligand. Both axial O and Br(1) are slightly tipped with respect to normal of the plane defined by the equatorial atoms C(1), C(6), C(11) (3.1 and 2.7° respectively), with a Br(1)–W–O angle of 177°.

The $AlBr_3$ moiety is linked to the oxygen so that the three bromine atoms are staggered with respect to the three neopentyl ligands in a gear-type arrangement. The three Al—Br bond distances as well as the O—Al—Br bond angles are very similar and show no unexpected feature.

Table 1. Selected bond lengths (Å), bond angles (deg.) and averages with their estimated standard deviations

W—Br1	2.428(3)		W—O—Al	172(1)	
W—O	1.77(1)		W—C1—C2	120(2)	
W—C1	2.11(2)		W—C6—C7	120(2)	121
W—C6	2.08(3)	2.11(1)	W—C11—C12	123(2)	
W—C11	2.14(2)		Br1—W—O	177.4(5)	
Al—O	1.79(1)		C1—W—C6	120(1)	
Al—Br2	2.241(9)		C1—W—C11	119(1)	120
Al—Br3	2.243(9)	2.248(5)	C6—W—C11	120(1)	
Al—Br4	2.260(10)		Br1—W—C1	87.6(6)	
C1—C2	1.56(3)		Br1—W—C6	91.3(7)	
C6—C7	1.53(4)	1.52(2)	Br1—W—C11	91.9(6)	
C11—C12	1.47(3)		O—W—C1	92.0(7)	
C2—C3	1.53(3)		O—W—C6	86.7(9)	
C2—C4	1.53(3)		O—W—C11	90.5(7)	
C2—C5	1.47(3)		O—Al—Br2	109.6(6)	
C7—C8	1.48(3)		O—Al—Br3	104.2(6)	
C7—C9	1.50(4)	1.51(1)	O—Al—Br_4	103.7(6)	
C7—C10	1.57(4)				
C12—C13	1.52(3)				
C12—C14	1.46(4)				
C12—C15	1.50(3)				

DISCUSSION

The overall geometry observed for the complex is clearly consistent with the minimization of steric interactions within the molecule.

As predicted from spectroscopic[3] and theoretical[19] studies, the Lewis acid $AlBr_3$ is shown to interact with the oxo function of $WO(CH_2t\text{-}Bu)_3Br$ (**2**) which thereby acts as a Lewis base. The W—O—Al bond angle near to 180° is not surprising according to both steric and electronic[19] considerations. The Al—O bond length, but also the two other bond lengths of the quasi linear Br(1)—W—O—Al linkage, allow us an insight into the nature of the acid-base interaction and its effects on the electronic structure in the molecule.

The most surprising result would seem to be the very short W—Br(1) bond length (2.428 Å) when compared to tungsten–bromine distances observed in other W(VI) complexes such as $W[C(CH_2)_3CH_2](OCH_2t\text{-}Bu)_2Br_2$ (2.566 Å)[18] and even the highly electron deficient $WOBr_4$ (2.444 Å).[17] This indicates the presence of a substantial Br to W π-donating interaction, compensating undoubtedly for the loss of O to W π-donation when the Lewis acid binds to the oxo group.

The strong donor–acceptor nature of the oxygen–aluminum bond results in the very short Al—O bond distance (1.79 Å) compared to those observed in the relatively strong THF adducts Al(Ph)C=C(Ph)Al(Ph)C=C(Ph)·2THF (1.907 Å)[10] and $AlCl_3$·2THF (1.99 Å).[11] These differences can only partly be accounted for by the change in oxygen hybridisation[20] (*sp* and sp^3 respectively), and we propose result from π-donation of oxygen lone pairs in vacant *d* orbitals on Al. The essentially double bond character of the tungsten–oxygen bond is indicated by a distance of 1.77 Å which although similar to that observed in the unsymmetrically oxo-bridged $WOBr_4$ (1.78 Å),[17] is *ca* 0.1 Å longer than for the terminal oxo atoms in $[WO(CH_2t\text{-}Bu)_3]_2(\mu\text{-}O)$ (1.71 Å),[9] $WOBr_4$ (gaseous phase) (1.70 Å),[12] $WO(CHt\text{-}Bu)(PEt_3)Cl_2$ (1.66 Å),[13] $WO(CHt\text{-}Bu)(PMe_3)_2Cl_2$ (1.69 Å)[14] and $WOCp(CH_2SiMe_3)_3$ (1.66 Å).[15] In these latter compounds significant O to W π-donation and bond orders superior to two are present. We note further that coordination of the oxo grouping to aluminum also causes ^1H NMR resonance of $WO(CH_2t\text{-}Bu)_3Br$ (**2**) to be shifted *ca* 1 ppm downfield after coordination to $AlBr_3$.[3]

As discussed earlier,[3] the adduct $W(OAlBr_3)(CH_2t\text{-}Bu)_3Br$ when dissolved in chlorobenzene under ambient light is a moderately effective catalyst for the metathesis of olefins,[21] whereas compound $WO(CH_2t\text{-}Bu)_3Br$ by itself is inactive. The interest of the present structural characterisation of the W–O–Al interaction between the transition metal "catalyst" and the Lewis acid "cocatalyst" is thus evident. More generally, this interaction can

also be considered as a model for catalysts supported on alumina or silica surfaces. Similar Al-O-M,[22] Si–O–M[23] or Ti–O–M[24] interactions have thus been shown to occur in such supported metal catalysts for the hydrogenation or the polymerisation of olefins. They might also be involved in olefin metathesis reactions catalysed by molybdenum or tungsten alkyls supported on SiO_2 or Al_2O_3.[25]

REFERENCES

1. A. K. Rappe and W. A. Goddard III, *J. Am. Chem. Soc.* 1982, **104**, 448.
2. R. A. Sheldon and J. K. Kochi, *Metal-Catalysed Oxidations of Organic Compounds*. Academic Press, New York (1981).
3. J. Kress, M. Wesolek, J. P. Le Ny and J. A. Osborn, *J. Chem. Soc., Chem. Commun.* 1981, 1039.
4. B. A. Frenz, in *Computing in Crystallography* (Edited by H. Schenk, R. Olthof-Hazekamp, H. von Koningsveld and G. C. Bassi). Delft University Press, Delft, The Netherlands (1978).
5. M. S. Lehmann and F. K. Larsen, *Acta Cryst.* 1974, **A30**, 580.
6. W. R. Busing and H. A. Levy, *Acta Cryst.* 1957, **10**, 180.
7. D. T. Cromer and J. T. Waber, *International Tables for X-Ray Crystallography*, Vol. 4, Tables 2–2b. Kynoch Press, Birmingham, U.K. (1974).
8. D. T. Cromer, *International Tables for X-Ray Crystallography*, Vol. 4, Table 2.3.1. Kynoch Press, Birmingham, U.K. (1974).
9. I. Feinstein-Jaffe, D. Gibson, S. J. Lippard, R. R. Schrock and A. Spool, *J. Am. Chem. Soc.* 1984, **106**, 6305.
10. H. Hoberg, V. Gotor, A. Milchereit, C. Krüger and J. C. Sekutowski, *Angew. Chem.* 1977, **89**, 563.
11. A. H. Cowley, M. C. Cushner, R. E. Davis and P. E. Riley, *Inorg. Chem.* 1981, **20**, 1179.
12. N. Ya Shishkin, I. M. Zharskii and G. I. Novikov, *J. Mol. Struct.* 1981, **73**, 249.
13. M. R. Churchill, J. R. Missert and M. J. Youngs, *Inorg. Chem.* 1981, **20**, 3388.
14. M. R. Churchill and A. L. Rheingold, *Inorg. Chem.* 1982, **21**, 1357.
15. P. Legzdins, S. J. Rettig and L. Sanchez, *Organometallics* 1985, **4**, 1470.
16. F. A. Cotton, L. R. Falvello and J. H. Meadows, *Inorg. Chem.* 1985, **24**, 514.
17. U. Müller, *Acta Cryst.* 1984, **C40**, 915.
18. A. Aguero, J. Fischer, J. Kress, J. A. Osborn and M. T. Youinou, in prep.
19. S. Nakamura and A. Dedieu, *Nouv. J. Chimie* 1982, **6**, 23.
20. C. A. Coulson, Valence, Oxford University Press, New York and London (1961).
21. For a recent review see K. J. Ivin, *Olefin Metathesis*. Academic Press, London (1983).
22. F. B. M. Duivenvoorden, D. C. Koningsberger, Y. S. Uh and B. C. Gates, *J. Am. Chem. Soc.* 1986, **108**, 6254 and refs therein.
23. Y. I. Yermakov, *Catal. Rev., Sci. Engng* 1976, **13**, 77 and refs therein.
24. P. B. Smith, S. L. Bernasek, J. Schwartz and G. S. McNulty, *J. Am. Chem. Soc.* 1986, **108**, 5654.
25. J. Smith, W. Mowat, D. A. Whan and E. A. V. Ebsworth, *J. Chem. Soc., Dalton Trans* 1974, **16**, 1742.

Polyhedron Vol. 6, No. 10, pp. 1843–1847, 1987
Printed in Great Britain

0277–5387/87 $3.00+.00

COBALT(II) AND NICKEL(II) HALIDE COORDINATION COMPOUNDS WITH 1,6-BIS(BENZIMIDAZOL-2-YL)-2,5-DITHIAHEXANE AND 1,7-BIS(BENZIMIDAZOL-2-YL)-2,6-DITHIAHEPTANE. THE CRYSTAL AND MOLECULAR STRUCTURE OF DIBROMO(1,6-BIS(BENZIMIDAZOL-2-YL)-2,5-DITHIAHEXANE)NICKEL(II)

JAN M. M. SMITS, RON JANSSEN and PAUL T. BEURSKENS

Crystallography Laboratory, University of Nijmegen, Toernooiveld, 6525 ED Nijmegen, The Netherlands

and

JACOBUS VAN RIJN and JAN REEDIJK*

Department of Chemistry, Gorlaeus Laboratories, Leiden University, P.O. Box 9502, 2300 RA Leiden, The Netherlands

(*Received* 5 *January* 1987; *accepted* 23 *April* 1987)

Abstract—The synthesis and characterization by spectroscopic techniques of compounds with general formulae MX_2(bbdh) and MX_2(bbdhp) is described. In these formulae M = Co(II), Ni(II); X = Cl, Br bbdh = 1,6-bis(benzimidazol-2-yl)-2,5-dithiahexane and bbdhp = 1,7-bis(benzimidazol-2-yl)-2,6-dithiaheptane. The compounds have been characterized by chemical analysis, infrared spectra, ligand field spectra, X-ray powder diagrams and in one case by a single crystal structure analysis. The metal ions are octahedrally (all Ni compounds and the Co compound of bbdh) or tetrahedrally (Co compounds of bbdhp) coordinated by the ligands and the anions. The detailed structure of $NiBr_2$(bbdh) was determined by X-ray methods at 290 K. Crystals of $C_{18}H_{18}Br_2N_4NiS_2$, M_r = 572.995, crystallized in the orthorhombic space group Pnc2, with a = 8.502(3), b = 13.748(2), c = 8.794(3) Å, V = 1027.96(57) Å^3, Z = 2, D_x = 1.851 Mg/m^3, were studied with CuKα radiation (using monochromator, λ = 1.54178 Å), μ(CuKα) = 7.931 mm^{-1}, F(000) = 568. The final conventional R-factor = 0.064, (R_w = 0.083) for 1600 "observed" reflections and 122 variables. The structure was solved using Patterson and DIRDIF techniques and refined by SHELX. The coordination around Ni(II) is octahedral with a *cis*-geometry of the two bromide anions (Ni—Br = 2.543(2) Å), a *trans*-arrangement of the benzimidazole ligands (Ni—N = 2.132(8) Å) and a *cis*-geometry of the thioether groups (Ni—S = 2.441(3) Å). The packing in the crystal results in hydrogen bond interactions between the N–H groups of the imidazoles and bromine atoms of nearby units. The structures of the nickel compounds and the isomorphous Co(II) bbdh compound are believed to be essentially the same, as deduced from spectroscopic analysis. The Co(II) compounds of bbdhp, however, appear to be tetrahedrally coordinated, as deduced from ligand field spectra. It seems that in this case the thioether groups are not coordinated to the Co(II) ion.

Chelating ligands containing imidazole-type ligands have been the subject of many investigations during the last decade.[1–4] A major aim to study such compounds originates from the fact that a very large number of metalloproteins contain at least one imidazole group from a histidine side chain as a ligand for the metal in the protein. Knowledge of this type of coordination, especially when more than one imidazole ligand is present, will lead to a better understanding of the structure and reactivity

* Author to whom correspondence should be addressed.

of metalloproteins that contain histidine ligands. Most of the work with this type of ligand has dealt with Cu(I) and Cu(II) compounds, since all copper proteins that play a role in redox reactions, have at least two histidine ligands.

However, this type of ligand is also of interest for other metal ions, such as cobalt(II), zinc(II) and nickel(II), because these metal ions are easily studied by spectroscopic methods such as ligand–field spectra. Moreover, Cu(II) is known to have very flexible coordination requirements, whereas the other metal ions, and especially nickel(II), have stronger preferences for more regular structures, such as octahedral and tetrahedral.

Therefore we have decided to study the coordination chemistry of two ligands, i.e. 1,6-bis (benzimidazol-2-yl)-2,5-dithiahexane (abbreviated bbdh), and bis(benzimidazol-2-yl)-2,6-dithiaheptane (abbreviated bbdhp), with known[2,3] coordination properties towards Cu(II) and having different steric constraints. The results described in this paper deal with Co, Ni and Zn metal ions, with Cl and Br as counterions. To prove the coordination geometry, the crystal structure has been determined in the case of $NiBr_2$(bbdh).

EXPERIMENTAL

Starting materials

The ligands bbdh and bbdhp were synthesized as described in earlier work.[2,3] Metal salts were used as the commercially available hydrates. Reagent grade solvents were used.

Synthesis

The solid coordination compounds were obtained by mixing 1 : 1 solutions of the metal salt and the ligand in ethanol. The desired compounds were obtained upon standing while slowly cooling. In a few cases addition of a small amount of diethyl ether facilitated the precipitation. The products were isolated as finely divided crystalline powders and isolated by filtration. In the case of $NiBr_2$(bbdh) crystals were grown by slow evaporation of the ethanol solution.

Characterization

The compounds were characterized by elemental analysis, infrared spectra, ligand–field spectra, X-ray powder diagrams and NMR spectra, using standard techniques and equipment, previously described.[2,3] Analysis showed the compounds to be MX_2(L).

X-RAY DATA COLLECTION AND STRUCTURE DETERMINATION OF $NiBr_2$(bbdh)

An irregularly shaped crystal of approximately $0.30 \times 0.26 \times 0.19$ mm, mounted in a capillary tube, was used during the measurements. Throughout the experiment CuKα radiation was used with a graphite crystal monochromator on a Nonius CAD4 single crystal diffractometer ($\lambda = 1.54178$ Å). The unit cell dimensions, $a = 8.502(3)$, $b = 13.748(2)$, $c = 8.794(3)$ Å, $V = 1027.96(57)$ Å^3, were determined from the angular settings of 25 reflections with $10° < \theta < 44°$. The space group was determined to be Pnc2 from the systematic absences: $0kl$, $k+l = 2n+1$, $h0l$, $l = 2n+1$, $0k0$, $k = 2n+1$ and $00l$, $l = 2n+1$ and from the structure determination. The intensity data of 7817 reflections (the full sphere up to $\theta = 70°$), were measured, using the ω–2θ scan technique, with a scan angle of 1.80° and a variable scan rate with a maximum scan time of 15 s per reflection. The intensity of the primary beam was checked throughout the data collection by monitoring three reference reflections every 30 min. The final drift correction factors were between 1.00 and 1.15. A decline in the intensities of approximately 11% occurred over the course of the data collection. A smooth curve based on the reference reflections was used to correct for this drift. On all reflections profile analysis was performed,[5,6] the crystal shape and the capillary tube used, prevented a description of the crystal for an analytical absorption correction, but an empirical absorption correction was applied, using psi-scans,[7] μ(CuKα) = 7.931 mm^{-1} (correction factors were in the range 0.88 to 1.00). Symmetry equivalent reflections were averaged, $R_{int} = \Sigma(I - \langle I \rangle)/\Sigma I = 0.053$, resulting in 1960 unique reflections of which 1600 were observed with $I > 3\sigma(I)$. Lorentz and polarization corrections were applied and the data were reduced to $|Fo|$ values.

The nickel and bromine atoms were found using Patterson techniques. All non-hydrogen atoms were found with DIRDIF[8] (direct methods applied to difference structure factors). The structure was refined by full-matrix least-squares on $|F|$ values, using SHELX.[9] The origin was fixed in the c direction by keeping the z-parameter of bromine fixed during the refinement. Scattering factors were taken from International Tables (1974).[10] Hydrogen atoms were included in fixed idealized positions 1.08 Å from the carbon c.q. nitrogen atom to which they were bonded. Isotropic refinement converged to $R = 0.079$. At this stage an additional empirical absorption correction was applied,[11] resulting in a

further decrease of R to 0.077 (correction factors were in the range 0.719–1.632).

After completion of the isotropic refinement the Bijvoet coefficient was calculated,[12] resulting in a value of −0.97(3), based on 118 Friedel pairs. The structure was therefore inverted before continuing the refinement. During the final stages of the refinement the positional parameters of all atoms and the anisotropic thermal parameters of the non-hydrogen atoms were refined. The hydrogen atoms had fixed isotropic temperature factors of 0.07 Å.^{2} The final conventional agreement factors were $R = 0.064$ and $R_w = 0.083$ for the 1600 "observed" reflections and 122 variables. The function minimized was $\Sigma w(Fo-Fc)^2$ with $w = 1/(\sigma^2(Fo) + 0.00400Fo^2)$ with $\sigma(Fo)$ from counting statistics. The maximum shift over error ratio in the last full matrix least-squares cycle was less than 0.05. The final difference Fourier map showed a number of peaks around Br up to 3 e/Å^3, around Ni up to 2 e/Å^3 and around S up to 1 e/Å^3 in the remaining space no peaks higher than 0.5 e/Å^3 were found. The quality of the intensity data would not allow a better parameterization because an accurate absorption correction was impossible.

Plots were made with PLUTO.[3] Final atomic coordinates and thermal parameters for the non-hydrogen atoms, hydrogen atom parameters and anisotropic thermal parameters are given as supplementary material, together with a table of observed and calculated structure factors. Atomic coordinates have also been deposited with the Cambridge Crystallographic Data Centre.

RESULTS AND DISCUSSION

General aspects and spectroscopy

All compounds have been listed in Table 1, with some relevant spectroscopic data. From the similarities in the infrared spectra and the X-ray powder diffraction diagrams, it is easily seen that all four bbdh compounds must have similar structures. The ligand field maxima for the cobalt and the nickel compounds with bbdh agree with octahedrally based coordination geometry.[14,15]

The ligand field maxima listed in Table 1 for these compounds agree nicely with an $MN_2S_2X_2$ (X = Cl, Br) geometry. Apparently the splittings in the bands due to the low symmetry are not large enough to be resolved. This is not uncommon in *cis*-distorted octahedral compounds.[16] In case of the ligand bbdhp the spectral data of the Ni(II) compounds agree with octahedrally based coordination, whereas the data of the cobalt compounds indicate clearly a tetrahedrally based coordination geometry.

To determine the precise coordination geometry of the ligand, when coordinated to the metal, it was decided to perform a single-crystal X-ray analysis. The compound $NiBr_2$(bbdh) appeared to yield crystals suitable for X-ray diffraction, and the results of the structure determination are described below.

Crystal structure of $NiBr_2$(bbdh)

The most important geometrical data have been given in Table 2, whereas a stereoview of the molecule is depicted in Fig. 1. The molecular unit with the numbering system used is given in Fig. 2.

Detailed inspection of Table 2 and the Figs, shows that no unusual geometrical features are present. The observed Ni—Br, Ni—S and Ni—N distances all fall in the range normally observed for octahedral Ni(II).[17] The *cis*-orientation of the bromide ligands is like one would expect from geometrical consideration of the bbdh ligand. A *trans*-orientation would require a tetradentate square planar geometry for the Ni(bbdh) unit, which would

Table 1. Cobalt and nickel coordination compounds with bbdh and bbdhp, together with some spectroscopic data

Formula	X-ray type	IR type	Ligand-field maxima in cm^{-1} 10^3				
$CoBr_2$(bbdh)	I	A	7.9	9.9sh	16.0w	18.0sh	19.0
$CoCl_2$(bbdh)	I	A	8.0	9.6sh	16.7w	18.0	19.0
$NiCl_2$(bbdh)	I	A	9.4		15.8	26.0	
$NiBr_2$(bbdh)	I	A	9.3		15.0	24.4	
$CoCl_2$(bbdhp)	II	B	6.0	7.4	9.0	16.2	17.5sh
$CoBr_2$(bbdhp)	II	B	6.0	7.0	8.5	15.9	17.2sh
$NiCl_2$(bbdhp)	III	C	9.5		16.0	25.7	
$NiBr_2$(bbdhp)	III	C	9.3		15.2	24.8sh	

Table 2. Bond lengths in Å (with esd's) and bond angles in ° (with esd's) for $NiBr_2$(bbdh)

Ni(1)—Br(1)	2.543(2)	C(3)—C(3)	1.328(39)	C(4)—C(9)	1.413(14)
Ni(1)—S(2)	2.441(3)	N(1)—C(2)	1.374(12)	C(5)—C(6)	1.384(16)
Ni(1)—N(3)	2.132(8)	N(1)—C(9)	1.378(14)	C(6)—C(7)	1.383(17)
C(1)—S(2)	1.825(12)	C(2)—N(3)	1.320(11)	C(7)—C(8)	1.375(17)
C(1)—C(2)	1.450(17)	N(3)—C(4)	1.385(12)	C(8)—C(9)	1.367(15)
S(2)—C(3)	1.819(17)	C(4)—C(5)	1.376(16)		

Br(1)—Ni(1)—S(2)	90.3(1)	Ni(1)—N(3)—C(4)	136.5(6)
Br(1)—Ni(1)—N(3)	91.2(2)	C(2)—N(3)—C(4)	107.7(8)
S(2)—Ni(1)—N(3)	81.7(2)	N(3)—Ni(1)—N(3)	164.0(4)
Br(1)—Ni(1)—Br(1)	91.0(1)	N(3)—C(4)—C(5)	131.3(9)
S(2)—C(1)—C(2)	109.4(8)	N(3)—C(4)—C(9)	108.4(9)
Ni(1)—S(2)—C(1)	96.9(4)	C(5)—C(4)—C(9)	120.3(9)
Ni(1)—S(2)—C(3)	98.9(5)	C(4)—C(5)—C(6)	116.7(9)
C(1)—S(2)—C(3)	110.0(9)	C(5)—C(6)—C(7)	122.5(10)
S(2)—Ni(1)—S(2)	88.3(2)	C(6)—C(7)—C(8)	121.1(11)
C(2)—N(1)—C(9)	108.6(8)	C(7)—C(8)—C(9)	116.8(11)
C(1)—C(2)—N(1)	122.4(9)	N(1)—C(9)—C(4)	105.1(8)
C(1)—C(2)—N(3)	127.4(9)	N(1)—C(9)—C(8)	132.5(10)
N(1)—C(2)—N(3)	110.1(9)	C(4)—C(9)—C(8)	122.4(11)
Ni(1)—N(3)—C(2)	115.7(6)		

result in serious steric hindrance of the benzimidazole groups.

The benzimidazole ligands are planar within experimental error, and the intraligand distances and angles are also normal for benzimidazole ligands.[2,3] The packing of the molecules in the solid state is determined by van der Waals interactions and N(1)–H(1)...Br(1′) hydrogen bonds (N(1)...Br(1′) = 3.35(1) Å, H(1)...Br(1′) = 2.35(5) Å for Br(1′) at x, $0.5-y$, $-0.5+z$).

CONCLUSIONS

The compounds described in the present paper indicate clearly that the bis(benzimidazole) thioether ligands bbdh and bbdhp are good tetradentate chelating ligands for Co(II) and Ni(II). A comparison with the previously studied copper coordination compounds with these ligands is appropriate. In case of Cu(II) the bbdh ligand yields a five-coordinated $[Cu(bbdh)Cl]^+$ species, although a six-coordinate species $Cu(bbdh)Cl_2$ could be detected spectroscopically.[2] With the ligand bbdhp, rapid reduction occurs to the Cu(I) state, yielding a coordination entity consisting of $[Cu(bbdhp)]^+$ with very long—and hardly coordinating—Cu–S distances.[3] When we look at our Cobalt(II) compounds, the ligand bbdh yields octahedral species $Co(bbdh)X_2$, whereas bbdhp yields tetrahedrally coordinated $Co(bbdhp)X_2$. In this

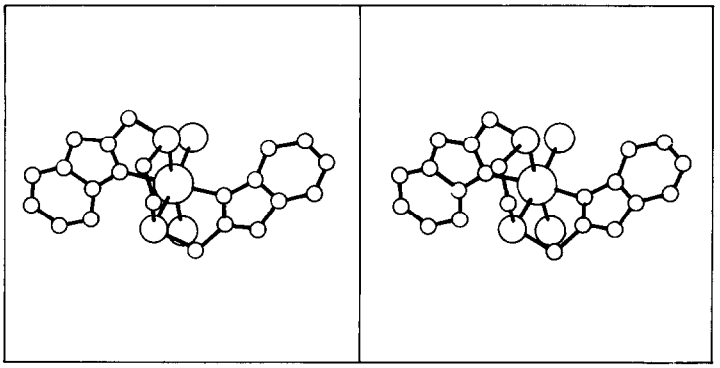

Fig. 1. Stereoview of $NiBr_2$(bbdh) showing the molecular configuration. (ANTNI stereoview in minimum overlap).

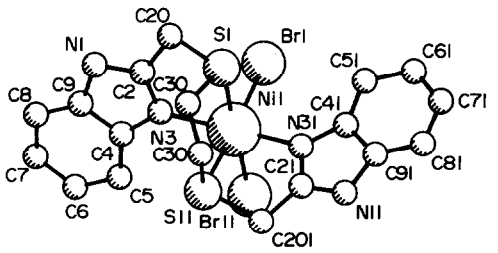

Fig. 2. Crystallographic numbering scheme of $NiBr_2$(bbdh). Hydrogen atoms omitted for clarity. (ANTNI minimum overlap with atomic numbering).

case one could ask whether the thioethers are coordinated to the halides. Study of the details of the ligand-field spectra immediately shows that the chromophore is an N_2X_2 chromophore,[16,18] so that the thioether groups of bbdhp do not coordinate to Co(II). A study of molecular models immediately makes clear that in a tetrahedral geometry the Co...S contacts can indeed be very large so that one cannot speak of coordination anymore.

Finally, when considering the nickel compounds, the spectral data indicate an octahedrally based coordination for all species. Knowing the preference of Ni(II) for octahedral coordination, it can be understood that the extra CH_2-group of bbdhp is unable to distort the octahedral coordination significantly, contrary to the case of Co(II), where a relatively large preference for tetrahedral geometry is imposed by the cation.

In other words, the ligand bbdhp is a ligand that imposes all kinds of geometries, depending upon the nature of the metal ion actually present.

Acknowledgement—The authors are indebted to Mr. F. B. Hulsbergen (Leiden) for synthetic and spectroscopic assistance.

REFERENCES

1. K. D. Karlin and J. Zubieta, *Biological and Inorganic Copper Chemistry*. Adenine Press (1986), and refs cited therein.
2. P. J. M. W. L. Birker, J. Helder, G. Henkel, B. Krebs and J. Reedijk, *Inorg. Chem.* 1982, **21**, 357.
3. M. J. Schilstra, P. J. M. W. L. Birker, G. C. Verschoor and J. Reedijk, *Inorg. Chem.* 1982, **21**, 2637.
4. K. Takahashi, Y. Nishida and S. Kida, *Polyhedron* 1984, **3**, 113.
5. M. S. Lehman and F. K. Larsen, *Acta Cryst.* 1974, **A30**, 580.
6. D. F. Grant and E. J. Gabe, *J. Appl. Cryst.* 1978, **11**, 114.
7. A. C. T. North, D. C. Philips and F. S. Mathews, *Acta Cryst.* 1968, **A24**, 351.
8. P. T. Beurskens, W. P. Bosman, H. M. Doesburg, Th. E. M. Van den Hark, P. A. J. Prick, J. H. Noordik, G. Beurskens, R. O. Gould and V. Parthasarathi, *Conformation in Biology* (Edited by R. Srinivasan and R. H. Sarma), pp. 389–406. Adenine Press, New York (1982).
9. G. M. Sheldrick, *SHELX. A Program for Crystal Structure Determination*. University Chemical Laboratory, Cambridge, U.K. (1976).
10. *International Tables for X-ray Crystallography*, Vol. IV. Kynoch Press, Birmingham (1974).
11. N. Walker and D. Stuart, *Acta Cryst.* 1983, **A39**, 158.
12. G. Beurskens, J. H. Noordik and P. T. Beurskens, *Cryst. Struct. Comm.* 1980, **9**, 23.
13. W. D. S. Motherwell, *PLUTO. A Program for Plotting Molecular and Crystal Structures*. University Chemical Laboratory, Cambridge, U.K. (1976).
14. J. Reedijk, P. W. N. M. Van Leeuwen and W. L. Groeneveld, *Rec. Trav. Chim.* 1968, **87**, 129.
15. J. Reedijk, W. L. Driessen and W. L. Groeneveld, *Rec. Trav. Chim.* 1969, **88**, 1095.
16. A. B. P Lever, *Inorganic Electronic Spectroscopy*. Elsevier, Amsterdam (1984).
17. *Cambridge Crystallographic Datafile* (1986).
18. J. Reedijk, *Rec. Trav. Chim.* 1971, **90**, 234.

Polyhedron Vol. 6, No. 10, pp. 1849–1858, 1987
Printed in Great Britain

0277–5387/87 $3.00+.00

THE MOLECULAR STRUCTURES OF PENTABORANE(9) AND PENTABORANE(11) IN THE GAS PHASE AS DETERMINED BY ELECTRON DIFFRACTION

ROBERT GREATREX and NORMAN N. GREENWOOD*

School of Chemistry, University of Leeds, Leeds LS2 9JT, U.K.

and

DAVID W. H. RANKIN and HEATHER E. ROBERTSON

Department of Chemistry, University of Edinburgh, West Mains Road, Edinburgh EH9 3JJ, U.K.

(*Received* 25 *March* 1987; *accepted* 23 *April* 1987)

Abstract—The structure of gaseous *arachno*-B_5H_{11} has been redetermined by electron diffraction and shown to be similar to that found in the solid state at low temperature (93 K) except that the inner basal interatomic distance B(3)—B(4) appears to be somewhat shorter in the gas phase. The data are consistent with the presence of asymmetric B(2)—H(2,3)—B(3) and B(5)—H(4,5)—B(4) bridges with the two halves of each bridge differing in length by *ca.* 12 pm. The unique *endo*/face-capping H atom attached to the apical B(1) atom has not been located with high precision, but the best fit to the data is obtained for an asymmetric structure with the distances B(2)...$H(1)_{endo}$ and B(5)...$H(1)_{endo}$ differing by 31 pm. For comparison, the structure of *nido*-B_5H_9 has also been redetermined by electron diffraction. The interatomic distances are in excellent agreement with those previously obtained from microwave data. The directly-bonded B–H(bridge) distances reveal an unusually large amplitude of vibration of the bridging H atoms but it was not possible to establish whether this was a real effect or whether the structure has a lower symmetry than that expected.

There is an unresolved problem in the structure of *arachno*-B_5H_{11}. The boron framework has long been established as that of an open-sided tetragonal pyramid (structure **I**) but there is some uncertainty about the precise location of the unique *endo*/face-capping H atom attached to the apical B(1) atom. Early X-ray diffraction work[1] suggested that the H atom was asymmetrically disposed above the open triangular face (structure **II**), but subsequent refinement of the data favoured C_s symmetry (structure **III**) rather than C_1 (structure **II**).[2]

Later, a more precise low-temperature study clearly established that the molecule has C_1 point symmetry in the crystalline state.[3] The most recent theoretical study, involving complete optimization at the 3-21G level, whilst favouring C_1 symmetry, points to a very low barrier (7 kJ mol^{-1}) for the C_1–C_s–C_1 fluxional process.[4] It is therefore not surprising that the proton and boron NMR spectra on

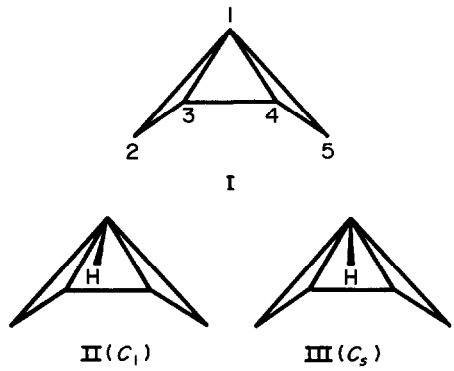

Structures I–III.

* Author to whom correspondence should be addressed.

the neat liquid revealed no evidence for the asymmetry.[5] The question therefore remains as to whether the asymmetry observed in the X-ray diffraction study is the result of crystal-packing forces, or whether it arises from some more deep-seated electronic-bonding effect. There has been no accurate determination of the structure of the gaseous molecule, the interpretation of early electron diffraction data being either palpably incorrect[6] or yielding no direct information about the hydrogen atom positions.[7]

In order to define as accurately as possible the positions of the atoms, including the so-called "anomalous" *endo*/face-capping hydrogen atom, we have now re-investigated the structure of the gaseous *arachno*-B_5H_{11} molecule by electron diffraction. Because it was readily available in the laboratory, we have also taken the opportunity of redetermining the molecular parameters of *nido*-B_5H_9 by the same technique for comparison with the results obtained by previous electron diffraction[8] and X-ray diffraction[3,9] studies and in particular with the more recent microwave data.[10]

EXPERIMENTAL

Preparation and purification of materials

The boranes were handled in a conventional high-vacuum system equipped with greaseless O-ring taps and spherical joints [J. Young (Scientific Glassware) Ltd]. *Nido*-B_5H_9 was supplied by Dr R. E. Williams (Chemical Systems, Inc. California). *Arachno*-B_5H_{11} was prepared from B_4H_{10} by the general method of Shore and coworkers.[11] Specifically, deprotonation was achieved using KH in dimethyl ether, and BCl_3 was used as the hydride-abstracting agent. The B_4H_{10} intermediate was prepared by the action of BF_3 on $[NMe_4][B_3H_8]$.[11] The B_5H_{11} was purified by repeated fractionation on a low-temperature fractional distillation column,[12] the effluent from which was sampled continuously by mass spectrometry. Traces of B_5H_9 are difficult to remove from B_5H_{11} and are also difficult to detect by mass spectrometry because of the similarity of the spectra of the two compounds. The sample of B_5H_{11} used in the electron diffraction study was shown by ^{11}B NMR to contain $< 0.5\%$ B_5H_9 as the only detectable impurity; its vapour pressure at 0°C was 52.5 mmHg, in excellent agreement with the published value.[13]

Electron diffraction

Electron diffraction scattering intensities were recorded on Kodak electron image plates, using the Edinburgh apparatus,[14] with nozzle-to-plate distances of 128 and 285 mm, and an accelerating voltage of *ca.* 44 kV. The nozzle was maintained at room temperature, 285 K, during the experiments and the samples were kept at room temperature (B_5H_9) or 250 K (B_5H_{11}). We have noticed that plates for boranes and related compounds have often shown dark patches, suggesting that there is some reaction between sample and emulsion, and this problem was particularly severe with B_5H_{11}. To minimize these effects, the plates were pumped for 24 h before being removed from the diffraction apparatus, and they were then washed thoroughly with water before development.

Data were obtained in digital form using a computer-controlled Joyce-Loebl MDM6 microdensitometer at the S.E.R.C. Laboratory, Daresbury, using the scanning program described previously.[15] Electron wavelengths were determined from the scattering patterns of gaseous benzene, recorded on the same occasions as the sample data. Calculations were carried out using standard data-reduction[16] and least-squares refinement programs. Weighting points used in setting up the off-diagonal weight matrices are given in Table 1, with other pertinent data. In all calculations the complex scattering factors of Schäfer *et al.*[17] were used.

RESULTS AND DISCUSSION

Refinement of the structure of B_5H_9

For almost all refinements it was assumed that B_5H_9 had C_{4v} symmetry, with one terminal hydro-

Table 1. Weighting functions, correlation parameters and scale factors

Compound	Camera height (mm)	Wavelength (pm)	Δs	s_{min}	sw_1	sw_2 (nm^{-1})	s_{max}	Correlation parameter	Scale factor
B_5H_9	285.7	5.690	2	20	40	124	144	0.486	0.651(11)
	128.3	5.689	4	60	80	300	340	−0.037	0.580(14)
B_5H_{11}	285.4	5.717	2	20	40	124	144	0.463	0.540(10)
	128.3	5.688	4	60	80	300	352	0.471	0.594(13)

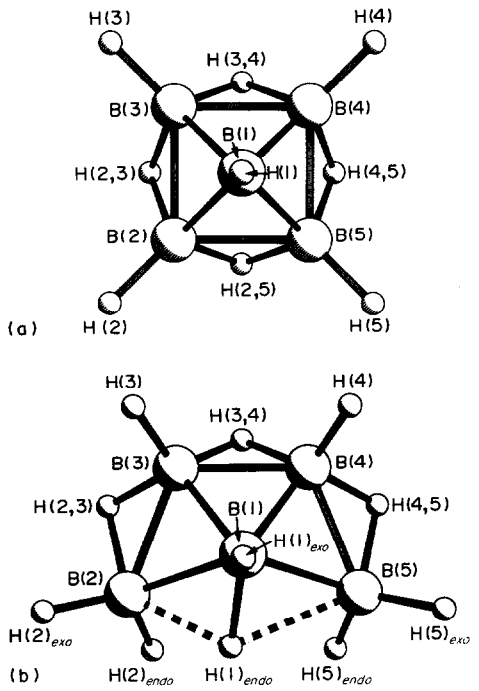

Fig. 1. Structures of (a) B_5H_9 and (b) B_5H_{11}, showing the atom numbering scheme used in this work.

gen atom associated with each boron atom, and with four bridging hydrogen atoms, each one bonding equally to two boron atoms. The atom numbering scheme used in this work is shown in Fig. 1(a). The structure was then defined by the two different B—B interatomic distances (base–base and base–apex), the mean B—H distance, the difference between bridging and mean terminal B—H distances, the difference between the lengths of the basal and apical terminal B—H bonds, and two angles defining the positions of the terminal and bridging hydrogens associated with the base of the pyramid. These angles were chosen to be B(1)B(2)H(2), and the angle between the base plane and the plane BH(bridge)B, which is labelled "H(2,3)dip" in Table 2.

Table 2. Molecular parameters for B_5H_9 (distances in pm, angles in degrees)

p_1	r(B—B) (base–base)	181.1(4)
p_2	r(B—B) (base–apex)	169.4(4)
p_3	r(B—H) (mean)	127.1(8)
p_4	Δr(B—H) (bridge–terminal)	16.7(18)
p_5	$\angle$B(1)B(2)H(2)	125.4(73)
p_6	H(2,3)dip	68.8(29)
p_7	Δr(B—H) (terminal, base–apex)	0.5(fixed)

All geometrical and vibrational parameters relating to the B_5 pyramid refined easily, as did the mean B–H distance and the difference between terminal and bridging B—H bond lengths, and the amplitudes of vibration for both terminal and bridging bonds. The small difference in lengths of the two types of terminal bonds could not be refined, and was fixed at the value found by microwave spectroscopy.[10c]

The two remaining parameters, defining the positions of hydrogen atoms, were much more difficult to determine, because there are five different non-bonding B...H distances between 240 and 280 pm, and the non-bonding B...B distance also falls in this region. In the end it was possible to refine three vibrational parameters for the B...H atom pairs, as well as the two angles, but strong correlations between these parameters [Table 3(a)] make their estimated standard deviations relatively large. The refined parameters are listed in Table 2, and interatomic distances and vibrational amplitudes are given in Table 4. In both these tables the quoted errors are estimated standard deviations obtained in the least-squares analysis, increased to allow for systematic errors.

In this refinement the amplitudes of vibration for the atom pairs B(2)...H(5) and B(2)...H(1) were assumed to be equal, and that for B(1)...H(2) was fixed at a value close to that obtained for the other two, as all of these relate to a boron atom and a terminal hydrogen on an adjacent boron atom. However, the values obtained for these atom pairs are *smaller* than that for the directly-bonded B—H(bridge) pairs. This unusually large value suggests that either the bridging hydrogen atoms are involved in a large-amplitude vibration in which they move tangentially to the C_4 axis (an a_2 mode) or they are displaced from the positions equidistant from the neighbouring boron atoms, so that the molecular symmetry is reduced to C_4. Tests using a model with C_4 symmetry showed that substantial displacements of these atoms could be accommodated with little effect on the quality of the fit. For this purpose an additional parameter was introduced, representing the difference between the lengths of the two parts of the B—H—B bridges. The possibility of simultaneous displacement of the other basal hydrogen atoms was not investigated. With the difference between the lengths of the two parts of the bridge set to 20 pm, the R factor (R_G) rose only from 0.0874 to 0.0875, and the amplitude of vibration for the two bridge distances reduced from 13.9 to 11.5 pm. The results are therefore inconclusive on this point.

The results quoted in Tables 2–4 are for the C_{4v} model. Atomic coordinates are given in Table 5(a),

Table 3. Least-squares correlation matrices showing all elements ⩾ 50%

(a) B_5H_9

Geometrical parameter	Vibrational amplitudes						Scale factor	
p_7	u_1	u_2	u_3	u_5	u_9	u_{11}	k_1	
		55						p_1
	57							p_2
				77				p_3
			−78	−74	55			p_4
87					−67	−59		p_6
					−64			p_7
		87						u_1
				54				u_3
						68		u_6
	60	63					53	k_2

(b) B_5H_{11}

Geometrical parameters				Vibrational amplitudes				Scale factors		
p_2	p_4	p_5	p_6	u_1	u_5	u_7	u_{14}	k_1	k_2	
74	94	−65			60					p_1
	71				51					p_2
56		75		−69						p_3
					56					p_4
					−53					p_5
						8				p_6
			−57			−61				p_7
							76			p_{10}
							61	−71	−57	p_{11}
				52					8	k_1
				57						k_2

Table 4. Interatomic distances (r_a/pm) and amplitudes of vibration (u/pm) for B_5H_9

		Distance	Amplitude
r_1	B(2)—B(3)	181.1(4)	5.8(4)
r_2	B(1)—B(2)	169.4(4)	5.4(4)
r_3	B(2)—H(2)	121.0(12)	8.9(8)
r_4	B(1)—H(1)	120.5(12)	
r_5	B(2)—H(2,3)	137.4(11)	13.9(13)
r_6	B(2)...B(4)	256.1(6)	7.0(8)
r_7	B(2)...H(5)	278.5(21)	11.9(12)
r_8	B(2)..H(1)	264.5(14)	
r_9	B(2)...H(3,4)	255.3(38)	15.9(37)
r_{10}	B(1)...H(2)	259.1(85)	11.3(fixed)
r_{11}	B(1)...H(2,3)	243.5(18)	10.3(25)
r_{12}	B(2)...H(4)	374.8(30)	12.4(19)

Note: H...H distances were also included in the refinement but are not listed here.

so that angles of interest may be calculated. The observed and final weighted difference molecular scattering intensities are shown in Fig. 2, and the radial distribution curve in Fig. 3.

Refinement of the structure of B_5H_{11}

The numbering of atoms is shown in Fig. 1(b).

The boron framework. This structure was defined by five parameters—the mean nearest neighbour B—B interatomic distance, the difference of the average interatomic distance between neighbouring basal boron atoms from the average of those between base and apex, the difference between distances B(1)—B(2) and B(1)—B(3), the difference between B(3)—B(4) and B(2)—B(3), and the angle at the apex of the open face, ∠B(2)B(1)B(5). In all refinements the mean B—B distance was close to

Table 5. Atomic coordinates (pm)

Atom	x	y	z
(a) B_5H_9			
B(1)	0.0	0.0	110.9
B(2)	128.1	0.0	0.0
H(1)	0.0	0.0	231.5
H(2)	245.7	0.0	28.6
H(2,3)	90.4	−90.4	−96.3
Coordinates of the remaining atoms are given by applying C_4 operations about the z axis to B(2), H(2) and H(2,3).			
(b) B_5H_{11}			
B(1)	0.0	52.6	95.6
B(2)	−154.5	0.0	0.0
B(3)	−88.0	168.5	0.0
B(4)	88.0	168.5	0.0
B(5)	154.5	0.0	0.0
$H(1)_{exo}$	0.0	49.8	214.8
$H(1)_{endo}$	−17.2	−68.2	43.5
$H(2)_{exo}$	−261.8	−20.4	47.9
$H(2)_{endo}$	−125.9	−80.3	−83.3
H(3)	−139.6	244.4	76.1
H(4)	139.6	244.4	76.1
$H(5)_{exo}$	261.8	−20.4	47.9
$H(5)_{endo}$	125.9	−80.3	−83.3
H(2,3)	−184.2	118.6	−66.9
H(3,4)	0.0	210.2	−91.3
H(4,5)	184.2	118.6	−66.9

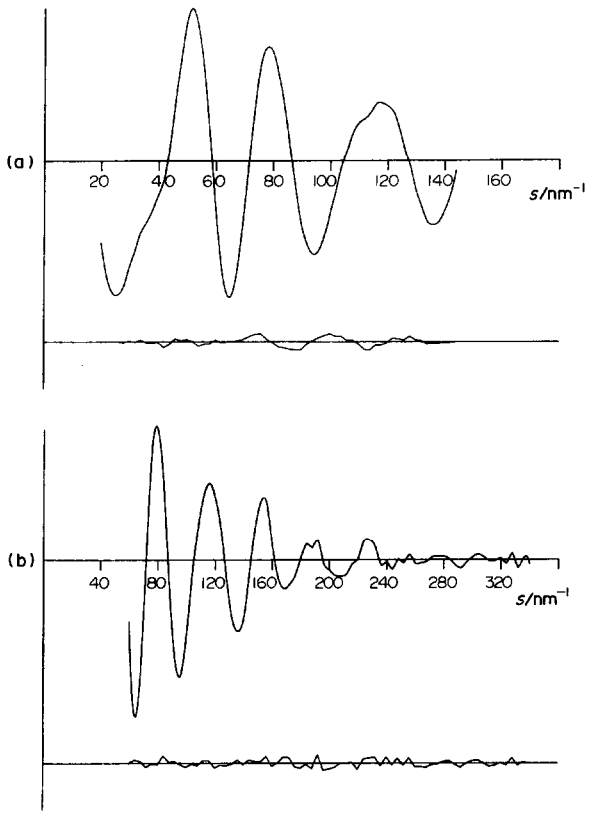

Fig. 2. Observed and final weighted difference molecular scattering intensities for B_5H_9 at nozzle-to-plate distances of (a) 285 and (b) 128 mm.

179 pm, and the angle B(2)B(1)B(5) was around 109°. The interatomic distances B(1)—B(2) were always substantially longer than for B(1)—B(3) so the apical boron atom is displaced away from the open edge of the base. The interatomic distances around the base were consistently shorter than those to the apex, but the difference varied, depending on the refinement conditions. In all the best refinements the difference was around −4 or −5 pm. Similarly, the basal distance B(3)—B(4) was always less than B(2)—B(3), but here the difference varied from −2 to −9 pm, being close to −5 pm in the best refinements.

Hydrogen atoms [*not including the face-capping hydrogen*, $H(1)_{endo}$]. It was assumed that all terminal B—H distances were equal. The B(3)H(3,4)B(4) bridge was assumed to be symmetrical, with bonds equal in length to the mean of all the bridge bond lengths. The other bridges, B(2)H(2,3)B(3) and B(5)H(4,5)B(4) were asymmetric, with the bonds B(2)—H(2,3) and B(5)—H(4,5) longer than the mean, and the other bonds shorter than the mean by an equal amount. The positions of hydrogen atoms were then defined by the following angle parameters:

$H(1)_{exo}$ "tilt"-angle between B(1)—$H(1)_{exo}$ bond and z axis (defined as perpendicular to plane of basal boron atoms). A positive tilt is towards the open face of the cluster.

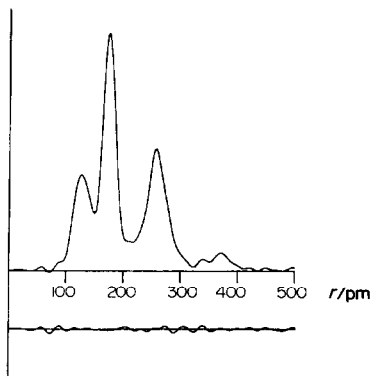

Fig. 3. Observed and final difference radial distribution curves, $P(r)/r$, for B_5H_9. Before Fourier inversion the data were multiplied by $s\exp[-0.00002s^2/(Z_B-f_B)(Z_H-f_H)]$.

$H(2)_{exo}$"dip"-angle of B(2)—$H(2)_{exo}$ bond below base plane.
$H(2)_{exo}$"wag"-angle between projection of B(2)—$H(2)_{exo}$ bond in base plane and x axis [defined as parallel to B(2)...B(5)].
$H(2)_{endo}$"dip" and "wag"—defined as for $H(2)_{exo}$.
H(3)"dip"-angle defined as for $H(2)_{exo}$. The projection of the bond B(3)—H(3) was assumed to bisect the angle B(2)B(3)B(4).
H(2,3)"dip"-angle of B(2)H(2,3)B(3) below base plane.
H(3,4)"dip"—defined as for H(2,3).

The two B—H interatomic distances both refined consistently, and their values did not change significantly during the whole series of refinements. All the other angles were refined at some time, but only four of the eight could be included in the final refinement. Quoted errors are therefore probably under-estimates. The difference between the lengths of the bridging B—H bonds and the mean was not refined, but was fixed at various values between 0 and 6 pm. The best fit to the data was found with it set at 6 pm, which corresponds to the value reported for the solid phase structure.[2(a),3]

The face-capping hydrogen $H(1)_{endo}$. Tests on the position of the anomalous hydrogen atom $H(1)_{endo}$ bound to B(1) were carried out with all positional parameters for terminal hydrogens $H(1)_{exo}$, $H(2/5)_{exo}$, $H(2/5)_{endo}$ and H(3/4) fixed, except for the mean B—H(terminal) bond length. The position of $H(1)_{endo}$ was defined by three parameters, B(1)—$H(1)_{endo}$, the angle between this bond and the z axis, which is perpendicular to the plane of the basal boron atoms, and a wag angle, which represented displacement of this bond from the mirror plane. With B(1)—$H(1)_{endo}$ fixed at 126 pm and the wag set at 5°, the remaining angle [called $H(1)_{endo}$ tilt] was refined to 116.7(26)° indicating that the hydrogen atom did indeed lie over the open face of the boron cluster. The distances B(2)...$H(1)_{endo}$ and B(5)...$H(1)_{endo}$ were 161 and 179 pm. Refinements with the wag angle fixed at various values between 0 and 20° showed a minimum R factor at about 8°, and this angle was then allowed to refine to 8.7(31)°. The tilt angle decreased systematically as the wag increased, and when both angles were refined the tilt went to 111.3(44)°. With this structure the distances B(2)...$H(1)_{endo}$ and B(5)...$H(1)_{endo}$ were 159 and 190 pm. Finally, the B(1)—$H(1)_{endo}$ distance was also allowed to refine, to 132(10) pm, and under these conditions the tilt and wag angles were 113.0(67) and 8.1(36)° respectively, and the B(2)...$H(1)_{endo}$ and B(5)...$H(1)_{endo}$ distances were 159(4) and 190(10) pm.

The parameters, interatomic distances and amplitudes of vibration obtained in the final refinement, for which R_G was 0.063, are given in Tables 6 and 7, and the least-squares correlation matrix is listed in Table 3(b). This last table shows substantial correlations between refining parameters, and it must be realized that correlations with fixed parameters

Table 6. Molecular parameters for B_5H_{11} (distances in pm, angles in degrees)

p_1	r(B—B) (mean)	179.4(4)
p_2	Δr(B—B), [(base–base) minus (base–apex)]	−4.0(7)
p_3	Δr(B—B), [B(1)—B(2) minus B(1)—B(3)]	15.0(8)
p_4	Δr(B—B), [B(3)—B(4) minus B(2)—B(3)]	−5.3(13)
p_5	∠ B(2)B(1)B(5)	109.5(7)
p_6	r(B—H) terminal	119.2(4)
p_7	r(B—H) bridge (mean)	133.4(7)
p_8	Δr(B—H) bridge[a]	6.0(fixed)
p_9	$H(1)_{exo}$ tilt[a]	−1.3(fixed[b])
p_{10}	H(3,4) dip[a]	65.5(60)
p_{11}	H(3) dip[a]	−39.7(33)
p_{12}	$H(2)_{exo}$ dip[a]	−23.7(fixed[b])
p_{13}	$H(2)_{exo}$ wag[a]	169.2(fixed[b])
p_{14}	$H(2)_{endo}$ dip[a]	44.3(fixed[b])
p_{15}	$H(2)_{endo}$ wag[a]	70.4(26)
p_{16}	H(2,3) dip[a]	43.2(30)
p_{17}	r[B(1)—$H(1)_{endo}$]	132.7(fixed[b])
p_{18}	$H(1)_{endo}$ tilt[a]	113.1(fixed[b])
p_{19}	$H(1)_{endo}$ wag[a]	8.1(fixed[b])

[a] For definition of parameters, see text.
[b] Not included in final refinement, but refined earlier: see text.

Table 7. Interatomic distances (r_a/pm) and amplitudes of vibration (u/pm) for B_5H_{11}[a]

		Distance	Amplitude
r_1	B(1)—B(2)	189.2(6)	6.3(7)
r_2	B(1)—B(3)	174.2(8)	5.9
r_3	B(2)—B(3)	181.2(7)	6.1 (tied to u_1)
r_4	B(3)—B(4)	176.0(12)	5.9
r_5	B(2)...B(5)	309.1(10)	7.2(8)
r_6	B(2)...B(4)	295.3(6)	
r_7	B(1)—H(1)$_{exo}$	119.2(4)	6.8(8)
r_8	B(2)—H(2,3)	139.4(7)	
r_9	B(3)—H(2,3)	127.4(7)	7.3 (tied to u_7)
r_{10}	B(3)—H(3,4)	133.4(7)	
r_{11}	B(1)—H(1)$_{endo}$	132.7[b]	8.5
r_{12}	B(2)—H(1)$_{endo}$	159.4(9)	10.0
r_{13}	B(5)—H(1)$_{endo}$	189.9(9)	10.0
r_{14}	B(1)...H(3)	238.1(35)	
r_{15}	B(1)...H(2)$_{exo}$	275.9(7)	
r_{16}	B(1)...H(2)$_{endo}$	256.0(19)	
r_{17}	B(1)...H(2,3)	254.4(13)	
r_{18}	B(1)...H(3,4)	244.5(20)	
r_{19}	B(2)...H(3)	256.5(16)	
r_{20}	B(2)...H(1)$_{exo}$	269.3(8)	
r_{21}	B(2)...H(3,4)	276.4(41)	10.5(10)
r_{22}	B(3)...H(1)$_{exo}$	260.8(8)	
r_{23}	B(3)...H(2)$_{exo}$	261.2(9)	
r_{24}	B(3)...H(2)$_{endo}$	265.2(16)	
r_{25}	B(3)...H(4)	251.7(16)	
r_{26}	B(3)...H(4,5)	284.7(16)	
r_{27}	B(3)...H(1)$_{endo}$	250.9(13)	
r_{28}	B(4)...H(1)$_{endo}$	262.7(12)	
r_{29}	B(2)...H(4)	390.0(24)	
r_{30}	B(2)...H(4,5)	365.1(21)	
r_{31}	B(2)...H(5)$_{exo}$	419.6(11)	15.0(fixed)
r_{32}	B(2)...H(5)$_{endo}$	303.4(29)	
r_{33}	B(3)...H(5)$_{exo}$	400.4(8)	
r_{34}	B(3)...H(5)$_{endo}$	338.6(25)	

[a] 31 H...H distances were also included in the refinements, but are not listed here.

[b] Fixed in final refinement: see text.

would increase these values further. Atomic coordinates listed in Table 5(b) enable bond angles to be calculated. Molecular scattering intensities are shown in Fig. 4 and the radial distribution curve in Fig. 5.

GENERAL CONCLUSIONS

The main results of the present structural determinations of gaseous pentaborane(9) and pentaborane(11), based on electron-diffraction data, are compared in Tables 8 and 9 with those derived from various other methods. The interatomic distances for B_5H_9 are seen to correspond well with the earlier electron diffraction results, but are now defined with considerably improved precision and agree to within 1% with the microwave data. The unusually large value observed for the amplitude of vibration of the directly-bonded B—H(bridge) pairs is worthy of comment, but unfortunately we are unable to say whether this is a real effect or whether the structure is of lower symmetry than expected. The rotational spectrum[10c] indicated that the molecule must have some low-frequency mode, but the rotation constants themselves are insensitive to a distortion of a_2 symmetry.

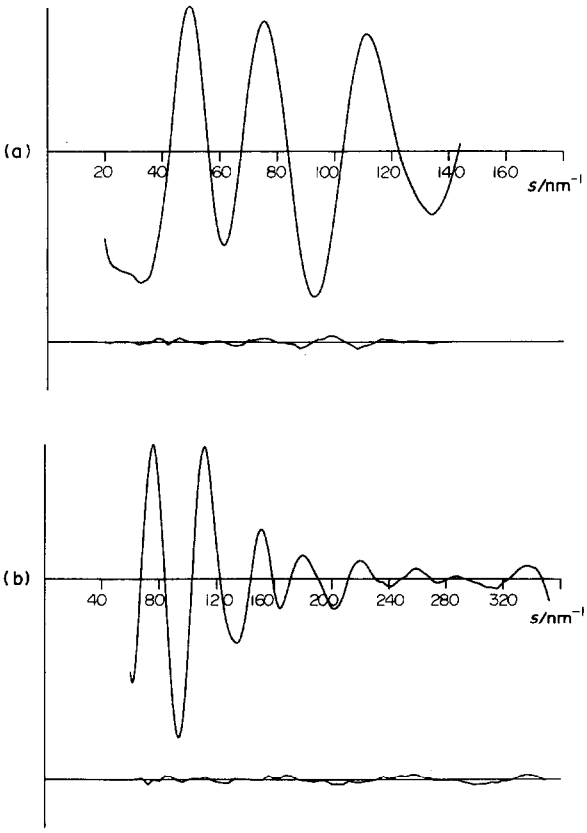

Fig. 4. Observed and final weighted difference molecular scattering intensity curves for B_5H_{11} at nozzle-to-plate distances of (a) 286 and (b) 128 mm.

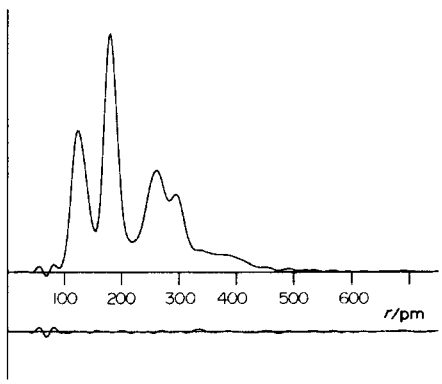

Fig. 5. Observed and final difference radial distribution curves, $P(r)/r$, for B_5H_{11}. Before Fourier transformation the data were multiplied by $s\exp[-0.00002s^2/(Z_B-f_B)(Z_H-f_H)]$.

In the case of B_5H_{11} the structure of the boron framework is marked by the length of the interatomic distances to the boron atoms at the open edge. For all reasonable positions of hydrogen atoms the parameters relating to the cluster vary little, and its structure is well determined. The interatomic distances are close to those reported for the compound in the crystalline phase,[2a,3] except that B(3)—B(4) is apparently shorter in the gas phase. Admittedly the interatomic distances B(2)—B(3) and B(4)—B(5) have been held equal in the present

Table 8. A comparison of the molecular parameters of pentaborane(9) as determined by various methods[a]

Parameter	Electron diffraction[b]	X-ray[c]	Microwave[d]	Electron diffraction[e]
(a) Distances/pm				
B(1)—B(2)	170.0(17)	165.3(10)	169.0(2)	169.4(4)
B(2)—B(3)	180.5(14)	175.1(6)	180.3(2)	181.1(4)
B(1)—H(1)	123.4(66)[f]	114(8)	118.1(2)	120.5(12)[g]
B(2)—H(2)	123.4(66)[f]	107(3)	118.6(2)	121.0(12)[g]
B(2)—H(2,3)	135.9(77)	127(2)	135.2(4)	137.4(11)
(b) Angles/°				
B(1)—B(2)—H(2)	120(20)	130.05(215)	128.72	125.4(73)
B(2)—B(1)—B(3)		63.97(37)		
B(2)—H(2,3)—B(3)		87.28(102)		
B(3)—B(2)—H(2,3)		46.38(102)		
B(2)—B(1)—H(1)		131.49(34)		
B(1)—B(2)—B(3)		58.01(19)		
B(3)—B(2)—H(2)		106.61(28)		
H(2,3) dip				68.8(29)

[a] Estimated standard deviations are given in parentheses where values are available. [b]Ref. 8. [c]Ref. 3. [d]Ref. 10(c). [e]This work. [f]The B(1)—H(1) and B(2)—H(2) distances were assumed to be equal. [g]See text. The small difference in length of the two types of terminal bonds was fixed at the value found by microwave spectroscopy.

Table 9. A comparison of interatomic distances in pentaborane(11) as determined by various methods[a]

Interatomic distance	X-ray[b]	Theoretical[c] C_1	Theoretical[c] C_1[d]	Electron diffraction
B(1)—B(2)	187.4(3)	191.45	187.35	189.2(6)[e]
B(1)—B(5)	187.4(3)	193.26	187.47	
B(1)—B(3)	172.3(3)	175.69	172.26	174.2(8)[e]
B(1)—B(4)	171.6(3)	175.74	171.53	
B(2)—B(3)	179.6(3)	184.63	179.62	181.2(7)[e]
B(4)—B(5)	175.1(3)	175.34	175.12	
B(3)—B(4)	179.1(3)	184.55	179.10	176.0(12)
B(2)...B(5)	—	310.93	304.87	309.1(10)
B(2)...B(4)	—	—	—	295.3(6)
B(1)—H(1)$_{exo}$	107(1)	117.99	118.00	119.2(4)
B(1)—H(1)$_{endo}$	106(2)	122.76	122.59	132.7[f]
B(2)—H(2)$_{exo}$	106(2)	118.16	118.17	
B(2)—H(2)$_{endo}$	111(2)	118.69	118.70	
B(3)—H(3)	106(2)	117.59	117.58	119.2(4)[e]
B(4)—H(4)	110(2)	117.53	117.52	
B(5)—H(5)$_{exo}$	111(2)	118.38	118.38	
B(5)—H(5)$_{endo}$	112(2)	118.31	118.40	
B(2)—H(2,3)	134(2)	146.76	143.03	139.4(7)[e]
B(5)—H(4,5)	130(2)	139.70	143.31	
B(3)—H(2,3)	119(2)	124.00	124.15	127.4(7)[e]
B(4)—H(4,5)	119(2)	125.17	125.21	
B(3)—H(3,4)	125(2)	134.44	133.23	133.4(7)[g]
B(4)—H(3,4)	128(1)	132.14	130.84	
B(2)...H(1)$_{endo}$	155(2)	157.73	155.36	159.4(9)
B(5)...H(1)$_{endo}$	183(2)	—	—	189.9(9)

[a] Distances in pm. Estimated standard deviations are given in parentheses where values are available. [b] Ref. 3. [c] Ref. 4. Complete optimization at 3-21G level assuming C_1 symmetry. [d] Boron framework fixed to experimental dimensions in Ref. 3. [e] This work; the interatomic distances were constrained to be equal as indicated. [f] Refined to 132(10) pm, but fixed in final refinement, see text. [g] B(3)—H(3,4)—B(4) bridge assumed to be symmetrical.

study, but it is unlikely that this alone is responsible for the observed effect on B(3)—B(4).

The asymmetrical nature of the B(2)—H(2,3)—B(3) and B(5)—H(4,5)—B(4) bridges in gaseous B_5H_{11} has been confirmed. In the present study the best fit to the data was found when the difference between the two halves of the bridge was set at the value reported for the solid phase structure,[2a,3] i.e. 12 pm, leading to values of 139.4(7) and 127.4(7) pm. The average B—H bridge distance is of course substantially longer than is found by X-ray diffraction, as we are looking at nuclear positions and not at centres of electron density. Unsymmetrical B—H—B bridges are a common feature of many polyhedral boranes, including for example B_3H_7CO,[18] B_4H_{10},[19] B_6H_{10},[3] $B_6H_{10}(PPh_3)_2$,[20] and $B_{10}H_{14}$.[21]

As regards the position of the face-capping hydrogen atom H(1)$_{endo}$, the results are to some extent inconclusive. There is no doubt that the best fit to the data has been obtained with an asymmetric structure, but the improvements observed on relaxing the symmetry requirement were not so great that the symmetric structure can be entirely ruled out. The evidence that H(1)$_{endo}$ lies over the open face B(2)B(1)B(5) is fairly strong—the angle of tilt has at no time had an uncertainty of more than 9°. The effect of fixing the parameters relating to other hydrogen atoms and many amplitudes of vibration on the quoted errors cannot be determined but must be substantial. All we can say therefore is that the hydrogen atom may well be asymmetrically located above the B(2)B(1)B(5) face, the best fit being obtained when the distances B(2)...H(1)$_{endo}$ and

B(5)...H(1)$_{endo}$ are 159(4) and 190(10) respectively, the difference of 31 pm being 2.2 times the sum of the estimated errors.

Acknowledgement—We thank the SERC for financial support.

REFERENCES

1. (a) L. R. Lavine and W. N. Lipscomb, *J. Chem. Phys.* 1953, **21**, 2087; (b) *ibid.* 1954, **22**, 614; (c) W. N. Lipscomb, *ibid.* 1954, **22**, 985.
2. (a) E. B. Moore, R. E. Dickerson and W. N. Lipscomb, *J. Chem. Phys.* 1957, **27**, 209; (b) G. S. Pawley, *Acta Cryst.* 1966, **20**, 631.
3. J. C. Huffman, Ph.D. Thesis, Indiana University, 1974.
4. M. L. McKee and W. N. Lipscomb, *Inorg. Chem.* 1981, **20**, 4442.
5. (a) R. Schaeffer, J. N. Schoolery and R. Jones, *J. Am. Chem. Soc.* 1957, **79**, 4606; (b) R. E. Williams, S. G. Gibbins and I. Shapiro, *J. Chem. Phys.* 1959, **30**, 320; (c) R. E. Williams, F. J. Gerhart and E. Piers, *Inorg. Chem.* 1965, **4**, 1239; (d) T. Onak and J. B. Leach, *J. Am. Chem. Soc.* 1970, **92**, 3513; (e) R. R. Rietz, R. Schaeffer and L. G. Sneddon, *ibid.* p. 3514; (f) J. B. Leach, T. Onak, J. Spielman, R. R. Rietz, R. Schaeffer and L. G. Sneddon, *Inorg. Chem.* 1970, **9**, 2170; (g) A. O. Clouse, D. C. Moody, R. R. Rietz, T. Roseberry and R. Schaeffer, *J. Am. Chem. Soc.* 1973, **95**, 2496.
6. S. H. Bauer, *J. Am. Chem. Soc.* 1938, **60**, 805.
7. M. E. Jones, K. Hedberg and V. Schomaker, private communication referred to by W. N. Lipscomb, *J. Chem. Phys.* 1954, **22**, 985, ref. 29.
8. K. Hedberg, M. E. Jones and V. Schomaker, *J. Am. Chem. Soc.* 1951, **73**, 3538; *Proc. Natl. Acad. Sci. U.S.* 1952, **38**, 679.
9. W. J. Dulmage and W. N. Lipscomb, *J. Am. Chem. Soc.* 1951, **73**, 3539; *Acta Cryst.* 1952, **5**, 260.
10. H. J. Hrostowski, R. J. Myers and G. C. Pimentel, *J. Chem. Phys.* 1952, **20**, 518; (b) H. J. Hrostowski and R. J. Myers, *ibid.* 1954, **22**, 262; (c) D. Schwoch, A. B. Burg and R. A. Beaudet, *Inorg. Chem.* 1977, **16**, 3219.
11. M. A. Toft, J. B. Leach, F. L. Himpsl and S. G. Shore, *Inorg. Chem.* 1982, **21**, 1952.
12. D. F. Shriver, *The Manipulation of Air-sensitive Compounds*, p. 90. McGraw-Hill, New York (1969).
13. A. B. Burg and H. I. Schlesinger, *J. Am. Chem. Soc.* 1933, **55**, 4009.
14. C. M. Huntley, G. S. Laurenson and D. W. H. Rankin, *J. Chem. Soc.* 1980, 954.
15. S. Cradock, J. Koprowski and D. W. H. Rankin, *J. Mol. Struct.* 1981, 77, 113.
16. A. S. F. Boyd, G. S. Laurenson and D. W. H. Rankin, *J. Mol. Struct.* 1981, **71**, 217.
17. L. Schäfer, A. C. Yates and R. A. Bonham, *J. Chem. Phys.* 1971, **55**, 3055.
18. J. D. Glore, J. W. Rathke and R. Schaeffer, *Inorg. Chem.* 1973, **12**, 2175.
19. C. J. Dain, A. J. Downs, G. S. Laurenson and D. W. H. Rankin, *J. Chem. Soc. Dalton Trans.* 1981, 472.
20. M. M. Mangion, J. R. Long, W. R. Clayton and S. G. Shore, *Cryst. Struct. Commun.* 1975, **4**, 501.
21. (a) A. Tippe and W. C. Hamilton, *Inorg. Chem.* 1969, **8**, 464; (b) V. S. Mastryukov, O. V. Dorofeeva and L. V. Vilkov, *J. Struct. Chem.* 1975, **16**, 110.

Polyhedron Vol. 6, No. 10, pp. 1859–1861, 1987
Printed in Great Britain

0277–5387/87 $3.00+.00
Pergamon Journals Ltd

SYNTHESIS AND CRYSTAL STRUCTURE OF CARBONYLCHLOROBIS(TRIPHENYLPHOSPHINE)DITHIOFORMATORUTHENIUM(II)TETRAHYDROFURAN $[C_{42}H_{39}ClO_2P_2S_2Ru]$*

SARADA GOPINATHAN, I. R. UNNI and C. GOPINATHAN†

Inorganic Chemistry Division, National Chemical Laboratory, Pune 411 008, India

and

VEDAVATI G. PURANIK, S. S. TAVALE and T. N. GURU ROW

Physical Chemistry Division, National Chemical Laboratory, Pune 411 008, India

(*Received* 7 *May* 1986; *accepted after revision* 27 *April* 1987)

Abstract—The title complex $[RuCl(CO)(PPh_3)_2(S_2CH)](thf)$ has been prepared by the insertion of carbon disulphide into the Ru—H bond of $[RuHClCO(PPh_3)_2(4\text{-Vp})]$ followed by crystallization from a mixture of benzene and thf (4-Vp = 4-vinyl pyridine). Its structure has been determined by single crystal X-ray diffraction methods. The crystals are triclinic, space group $P\bar{1}$, $z = 2$, $a = 10.042(1)$, $b = 11.216(1)$, $c = 17.772(2)$ Å, $\alpha = 99.80(1)$, $\beta = 93.26(1)$ and $\gamma = 90.86(1)°$. The structure, which has been refined to $R = 0.078$ for 4949 reflections, is a distorted octahedron.

Phosphine substitution in the complex $RuHCl(CO)(PPh_3)_3$ (I) has been reported to be carried out using phosphites, phosphonites and phosphinites.[1] Recently we reported the synthesis of monosubstitution products of the complex (I) using nitrogen heterocyclics.[2] The 4-vinylpyridine ruthenium(II) complex $RuHCl(CO)(PPh_3)_2(4\text{-Vp})$ (II) reacts with a variety of bidentate chelating ligands containing potential hydroxyl groups in the presence of a base to give chelated ruthenium complexes having O—O coordination with the elimination of chlorine and 4-vinyl pyridine.[3] Activated olefins can readily be inserted into the Ru—H bond in the complex (II) to yield insertion products.[4] We have extended this reaction by the synthesis of a dithioformate complex of Ru(II) using carbon disulphide.

EXPERIMENTAL

Reactions were carried out in a dry, oxygen-free nitrogen atmosphere, using dried, freshly distilled and degassed solvents.

(a) *Carbonylchlorohydridobis (triphenylphosphine) (4-vinylpyridine)ruthenium(II)*

Freshly distilled 4-vinyl pyridine (0.84 g; 8 mmol) was added to a suspension of $RuHCl(CO)(PPh_3)_3$ (0.95 g; 1 mmol) in thf (50 cm^3) in a Schlenk tube. The solution was stirred at 25° for 20 h to yield a white solid. This was filtered through a sintered disc, washed with thf and dried at 60° at 1 mm pressure, m.p. 199°C. Yield 0.62 g (78%). Found: C, 66.3; H, 4.9; P, 8.0. Calc. for $C_{44}H_{38}ClNOP_2Ru$: C, 66.4; H, 4.8; P, 7.8.

(b) *Carbonylchlorobis (triphenylphosphine) dithioformatoruthenium(II)*

To a suspension of $RuHCl(CO)(PPh_3)_2(4\text{-Vp})$ (0.20 g; 0.25 mmol) in benzene (25 cm^3) was added carbon disulphide (5 cm^3). The contents turned brown in 2 h and were kept at room temperature for 24 h. The yellow crystals separated were filtered and dried at 60°C at 1 mm pressure for 2 h. M.p. 223°C. Found: C, 59.5; H, 4.1; P, 8.0. Calc. for $C_{38}H_{31}ClOP_2S_2Ru$: C, 59.5; H, 4.1; P, 8.1. A portion of the product was crystallized from a benzene–

* NCL Communication No. 4028.

† Author to whom correspondence should be addressed.

thf mixture (90 : 10, vol./vol.) to get crystals for X-ray studies.

(c) *X-ray studies*

A crystal of dimension $0.7 \times 0.35 \times 0.17$ mm was used for data collection. Formula weight 838.37, triclinic, $P\bar{1}$; $a = 10.042(1)$, $b = 11.216(1)$, $c = 17.772(2)$ Å, $\alpha = 99.80(1)$, $\beta = 93.26(1)$, $\gamma = 90.96(1)°$ and $V = 1968.6$ Å^3; $z = 2$, density (by flotation) 1.412 g/cm^3 (calc. 1.414 g/cm^3), μ(Mo–K$_\alpha$) = 6.76 cm^{-1}, $F(000) = 860$.

Intensity data were collected on an Enraf Nonius CAD 4F-11M diffractometer using the $\omega/2\theta$ scan technique with Mo–K$_\alpha$ ($\lambda = 0.7107$ Å, graphite monochromated) radiation. Cell dimensions were taken from 20 reflections ($32 \leqslant 2\theta \leqslant 39°$). A total of 6438 reflections ($\theta < 23.5°$) were collected with three standard reflections measured every 1000 s. The variations in these standard reflections were within 3%. A total of 4949 reflections with $|F_o| \leqslant 3\sigma|F_o|$ were used in the final refinement of structural parameters. The structure was solved using a modified[5] MULTAN 78[6] package. The crystallographic numbering of the atoms is shown in Fig. 1.

Full-matrix least squares refinement[7] of scale, positional, anisotropic thermal parameters for Ru, S, P and Cl atoms, and isotropic thermal parameters for the rest of the non-hydrogen atoms (hydrogen atoms were geometrically fixed and were not refined) gave an R value of 0.078. A final difference Fourier map was featureless. Atomic scattering factors used were from the International Tables for X-ray Crystallography.[8] Lists of observed and calculated structure factors, final positional and equivalent temperature factors for all non-hydrogen atoms, atomic coordinates for hydrogen atoms and anisotropic thermal parameters have been deposited with the Editor. Atomic coordinates have also been submitted to the Cambridge Crystallographic Data Centre.

RESULTS AND DISCUSSION

The complex [RuHCl(CO)(PPh$_3$)$_2$(4-Vp)] reacts with carbon disulphide in benzene at an ambient temperature to yield the insertion product as an air-stable yellow crystalline solid with the elimination of 4-vinyl pyridine. Upon crystallization from benzene–thf mixture, one molecule of tetrahydrofuran is retained in the crystal as seen by X-ray diffraction studies but it can be removed by heating the crystals at 60°C at 1 mm pressure. The thf-free sample was used for spectral studies. This yellow product shows IR absorption bands in the carbonyl region at 1945 cm^{-1} characteristic of a terminal carbonyl group. The bands at 1235 and 930 cm^{-1} are attributable to δ(HCS) and ν_{as}(CS$_2$) respectively, which suggest the presence of a chelated dithio ligand.[9,10]

^{1}H NMR spectrum comprises of a triplet at δ 11.88, ^{4}J(PH) ~ 8 Hz due to the coupling of dithioformate proton (S$_2$CH) with *trans* phosphorus nuclei.

Crystal structure of [C$_{42}$H$_{39}$ClO$_2$P$_2$S$_2$Ru]

A perspective view of the molecule is given in Fig. 2. Table 1 gives interatomic bond distances and bond angles along with e.s.d.'s in parentheses. The molecule has a distorted octahedral coordination around the ruthenium atom. The two sulphur atoms are *cis* with respect to each other which enables chelation with the metal atom, thereby closing a four membered ring. The two triphenylphosphine groups are also *cis* to each other while the carbonyl group is *trans* to the chlorine atom. The bite angle of the dithioformate group is 70.5° and is nearly equal to that in bis(dithioformato)-bis(triphenylphosphine)ruthenium(II) (71°).[11] There is a delocalization in the HCS$_2$ ligand [C(1)—S(1) = C(1)—S(2) = 1.67(1) Å]. Similar delocalization is found in the rhenium complex[12] Re(CO)$_2$(HCS$_2$)$_2$(PPh$_3$)$_2$, in Pd(S$_2$CPh)$_2$ and its nickel analogue.[13]

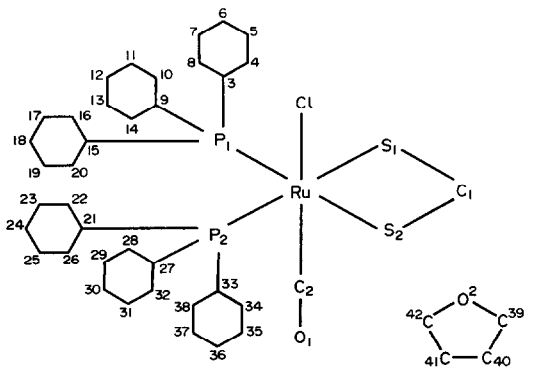

Fig. 1.

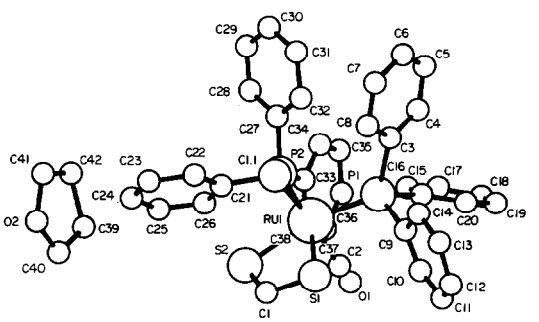

Fig. 2.

Table 1. Some selected bond distances (Å) and bond angles (°) with e.s.d.'s in parentheses

Bond lengths (Å)	
Ru—Cl	2.421(3)
Ru—S(1)	2.447(2)
Ru—S(2)	2.427(2)
Ru—P(1)	2.396(2)
Ru—P(2)	2.398(2)
Ru—C(2)	2.064(17)
S(1)—C(1)	1.670(14)
S(2)—C(1)	1.667(14)
C(2)—O(1)	0.755(21)
Bond angles (°)	
Cl—Ru—S(1)	85.2(1)
Cl—Ru—S(2)	87.8(1)
Cl—Ru—P(1)	94.5(1)
Cl—Ru—P(2)	89.9(1)
Cl—Ru—C(2)	172.2(5)
S(1)—Ru—S(2)	70.5(1)
S(1)—Ru—P(1)	93.1(1)
S(1)—Ru—P(2)	160.6(1)
S(1)—Ru—C(2)	87.2(5)
S(2)—Ru—P(1)	163.3(1)
S(2)—Ru—P(2)	90.6(1)
S(2)—Ru—C(2)	87.9(5)
P(1)—Ru—P(2)	105.9(1)
P(1)—Ru—C(2)	87.8(5)
P(2)—Ru—C(2)	96.7(5)
Ru—S(1)—C(1)	86.9(5)
Ru—S(2)—C(1)	87.6(5)
S(1)—C(1)—S(2)	115.0(10)

The distances of all coordinating atoms are normal. However, the C(2)—O(1) is too short (0.76 Å). A strikingly similar value is seen in the structure of *trans*-carbonylbis(triphenylphosphine)rhodium(I) chloride.[14] The difference Fourier map does not indicate any disorder in this region and also the temperature factor associated with this oxygen atom is normal. The crystal structure has a molecule of tetrahydrofuran (thf) of crystallization and there are no significant interactions of this moiety with the structure. The thermal vibrations associated with the thf molecule are large; however the bond lengths and the bond angles are about normal. The crystal structure is stabilized by van der Waal's interactions.

REFERENCES

1. C. L. Creswel, S. D. Robinson and A. Sahajpal, *Polyhedron* 1983, **2**, 517.
2. J. W. Gilje, R. Schmutzler, W. S. Sheldrick and V. Wrey, *Polyhedron* 1983, **2**, 603.
3. S. Gopinathan, I. R. Unni, S. S. Deshpande and C. Gopinathan, *Ind. J. Chem.* 1986, **25A**, 1015.
4. S. Gopinathan, I. R. Unni and C. Gopinathan, *Polyhedron*, 1986, **5**, 1921.
5. S. S. Tavale and T. N. Ruru Row, *Proc. Ind. Acad. Sci. (Chem. Sci.)* 1986, **97**, 209.
6. P. Main, S. E. Hull, L. Lessinger, G. Germain, J. P. Declereg and M. M. Woolfson, MULTAN 78. A system of computer programs for automatic solution of crystal structures from X-ray diffraction data, Universities of York, U.K. and Louvain, Belgium (1978).
7. P. K. Gantzel, R. A. Sparks and K. N. Trueblood, LALS A program for the full-matrix least squares refinement of positional and thermal parameters and scale factors, University of California, Los Angeles (1961).
8. *International Tables for X-ray Crystallography*, Vol. IV. Kynoch Press, Birmingham (1974).
9. I. S. Butler and A. E. Fenster, *J. Organomet. Chem.* 1974, **66**, 161.
10. F. W. Einstein, E. Enwall, N. Filtcroft and J. M. Leach, *J. Inorg. Nucl. Chem.* 1972, **34**, 885.
11. R. O. Harris, L. S. Sadavoy, S. C. Nyburg and F. H. Pickard, *J. Chem. Soc., Dalton Trans.* 1973, 2646.
12. V. G. Albano, P. L. Bellon and G. Ciani, *J. Organomet. Chem.* 1971, **31**, 75.
13. C. Furlani and M. L. Luciani, *Inorg. Chem.* 1968, **7**, 1586.
14. A. Del Pra, G. Zanotti and P. Segala, *Cryst. Struct. Commun.* 1979, **8**, 959.

Polyhedron Vol. 6, No. 10, pp. 1863–1867, 1987
Printed in Great Britain

0277–5387/87 $3.00+.00

STUDY OF CATION EFFECTS ON INORGANIC CYCLOPHOSPHATES HYDROLYSIS IN AQUEOUS SOLUTIONS

GENICHIRO KURA

Department of Chemistry, Fukuoka University of Education, Akama, Munakata, Fukuoka 811-41, Japan

(*Received* 26 *January* 1987; *accepted* 27 *April* 1987)

Abstract—The ionic strength dependence of cyclophosphates hydrolysis rates was investigated at constant acid concentration. The rates decreased with the increase in the ionic strength, and hence the degree of association of cyclophosphate anions with hydrogen ions strongly affects the hydrolysis rates. In alkaline solutions, the hydrolysis rates for each phosphate decrease in the order: LiOH > NaOH > KOH > $N(CH_3)_4OH$. When copper(II) ion of concentration 5×10^{-3} M was added, the hydrolysis rates of the phosphates were accelarated. The "metaphosphate abstraction" was briefly discussed.

Of the inorganic condensed phosphates, the cyclic phosphates containing P—O—P bonds are very interesting and useful electrolytes, having multivalent anionic charge on their comparatively compact molecules, (e.g. $P_3O_9^{3-}$, $P_4O_{12}^{4-}$, $P_6O_{18}^{6-}$ and $P_8O_{24}^{8-}$).[1] We have extensively studied various chemical properties of these phosphates.[2–14] The present study was undertaken to understand the cation effects on the hydrolysis of the cyclophosphates in acidic, neutral and alkaline conditions. These cyclophosphates are very stable in neutral aqueous solution even if they are boiled for up to one hour provided a large amount of cation is not present. However, it has been elucidated by our previous study that in acidic solutions the hydrolysis rates of cyclophosphates increase rapidly.[11,13] The cyclophosphate ions are not so strong as a Brønsted base, however, the interactions between the phosphate ions and hydrogen ions were observed at higher H^+ concentrations.[5] This is considered to be the main reason to accelerate the hydrolysis reaction. In this study, the ionic strength dependence of the hydrolysis rate at a constant hydrogen ion concentration was determined and it is verified that the bond formation between the phosphate ions and H^+ is the major factor to catalyze the hydrolysis rates. As a supporting electrolyte to keep the ionic strength at a constant, tetramethylammonium chloride was used.

In alkaline solutions, the hydrolysis rates are affected not only by the hydroxide concentration but by the presence of other cations. Great discrepancies in the rates were observed when NaOH or $N(CH_3)_4OH$ was used as an alkali.[14] In $N(CH_3)_4OH$ solution, the hydrolysis rates of cyclophosphates decrease with the increase in the polymerization degree. The reverse tendency was found for the hydrolysis of linear phosphates.[15] In the present study, LiOH and KOH were used as the alkali to investigate the effect of Li^+ and K^+ on the cyclophosphate hydrolysis. By comparing the results in $N(CH_3)_4OH$ and NaOH with those in LiOH and KOH, the hydrolysis rates in the LiOH solution were shown to be fastest for each cyclophosphate. This explains the strongest interactions of Li^+ ion with cyclophosphate anions and the interactions might facilitate the nucleophilic attack of the OH^- ion on the P atom.

Cyclophosphate anions have such high negative charges on their compact molecules that they form complexes (or ion-pairs) with various cations and the stability constants of some complexes have been determined.[3–5,7,12] The effect of copper(II) ion on the cyclophosphate hydrolysis at pH 5 was investigated. At this pH, the hydrolysis of copper(II) and cyclophosphate ions are negligible. The hydrolysis rates were accelerated by the addition of copper(II) ion. This might be due to the complex formation of the copper(II) ion with the cyclophosphate ions.

The hydrolysis rates of the cyclophosphate ions

thus have been affected not only by the H^+, OH^- ions but by the ionic strength and cations present.

In this paper, cyclophosphates and linear phosphates are abbreviated as P_{nm} and P_n, respectively, where n is the degree of the polymerization.

EXPERIMENTAL

Materials

Sodium salts of cyclo-tri-, cyclo-tetra-, cyclohexa- and cyclo-octaphosphates were prepared by the methods described previously.[2] As the copper(II) salt, the perchlorate was used. The other chemicals used were reagent grade and commercially available.

Analysis

Hydrolysis products were analyzed by anion-exchange chromatography. The chromatographic system consisted of a Hitachi 655 A-11 pump, a Hitachi 655-0300 reaction pump and a Hitachi 228A spectrophotometer as a detector. As an anion-exchanger, TSK gel SAX, particle sice 10 μm, was used and the column dimension was 250×4 mm I.D. The flow system is similar to that schematically represented in our previous paper[11] and the elution condition is also the same as that used previously.[11]

Details of the hydrolysis procedure have been described in a previous paper.[11]

RESULTS AND DISCUSSION

The analysis of the hydrolysis products was achieved by liquid chromatography using an anion-exchange column. As an example, the chromatograms of the hydrolysis samples were shown in Fig. 1(a) and (b). In the chromatograms, the first peaks were characterized as a mixture of linear polymers as the hydrolysis products of cyclo-octaphosphate.[11] The concentration of the parent species can be calculated from the area of its chromatogram.

Hydrolysis reactions of cyclophosphates have been known as first-order for the phosphates under various experimental conditions.[8-11] If the total concentration of the phosphates to be degraded is designated as c, the rate can be presented as

$$-\frac{dc}{dt} = k_{obs}c. \quad (1)$$

The apparent rate constant, k_{obs} was determined in each case. The hydrolysis rates of cyclophosphates are most strongly affected by the hydrogen ions and depend on its concentration.[13] The effect might be

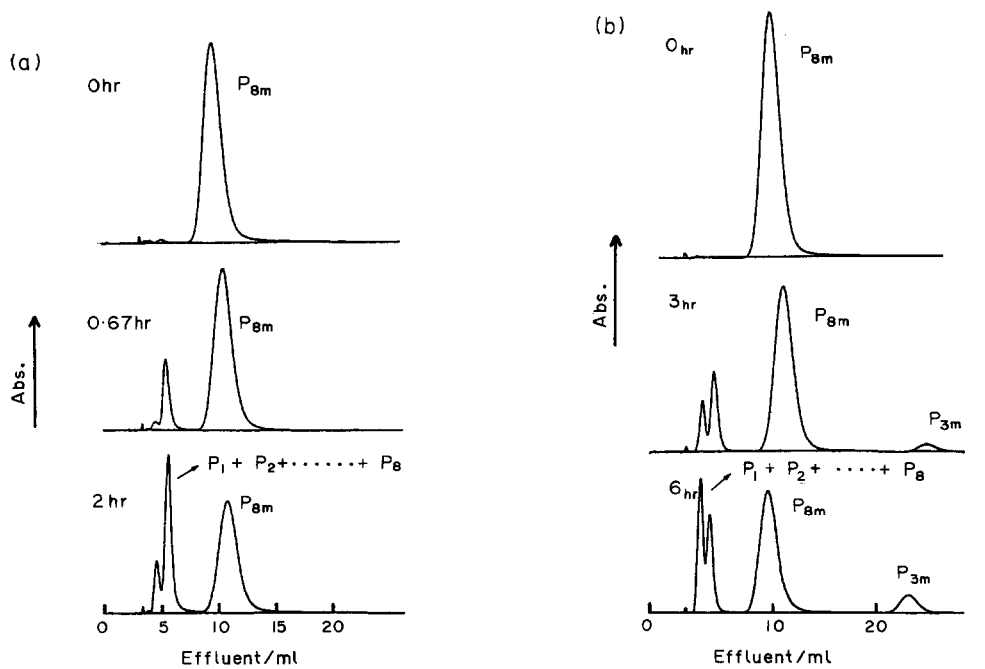

Fig. 1. Chromatograms of the hydrolysis samples of $P_8O_{24}^{8-}$ in (a) 0.75 M LiOH at 50°C and (b) 0.005 M HCl at 40°C.

due to the bonding of the hydrogen ions with PO^- on the PO_4 tetrahedra. In this study, the ionic strength dependence of the hydrolysis rates of the phosphates at a constant acid concentration was investigated to verify the above assumption. The variation of the rate constants, k_{obs}, at a hydrogen concentration of 0.05 M at 40°C, in the ionic strength range 0.05–1 were determined. The ionic strength was controlled by adding tetramethylammonium chloride as an inert electrolyte. The results obtained are shown in Table 1 and Fig. 2. The significant decrease in the k_{obs} was observed with increase in the ionic strength. For each cyclophosphate, the k_{obs} is reduced to one-half or a quarter of the initial value by changing the ionic strength from 0.05 to 1. The results correspond to the decrease in the degree of bonding of H^+ with $P_nO_{3n}^{n-}$, with the increase in the ionic strength.

As summarized above, in the acidic solution, hydrogen ions play an important role to catalyze the hydrolysis rates. In the alkaline solutions, it has been elucidated that the hydrolysis rates depend not only on the concentration of OH^- which attacks the P atoms but on the kinds and concentration of the cations present.[14] In this study, the hydrolysis rates using KOH and LiOH as an alkali were further determined. In the tetramethylammonium hydroxide solution, the hydrolysis reaction is first-order for OH^- since the rate determining step is the nucleophilic attack of OH^- on the P atom.[14] Accordingly, the rate equation can be written as

$$-\frac{dc}{dt} = k[OH^-]c \qquad (2)$$

where if

$$k[OH^-] = k_{obs} \qquad (3)$$

we can obtain the same equation as eqn (1). The $\log k_{obs}$ obtained for the hydrolysis of the cyclophosphates in 0.5 M LiOH and KOH at 50°C are shown in Fig. 3 and Table 2 with data for 0.5 M NaOH and $N(CH_3)_4OH$. This result suggests that Li^+ interacts most strongly with the cyclophosphate anions and the intensity of the interaction decreases from Na^+ to K^+. This decrease is in accord with the increase in the crystal radii of the cation. In the tetramethylammonium hydroxide solution, the cyclophosphate with the larger ring is rather stable, however, in other alkaline solutions, the hydrolysis rate of cyclo-octaphosphate begins to increase again. This tendency was observed in the case of the hydrolysis in the acidic solution.[13] The higher-membered cyclo-octaphosphate has a much larger ring structure with higher flexibility, and conse-

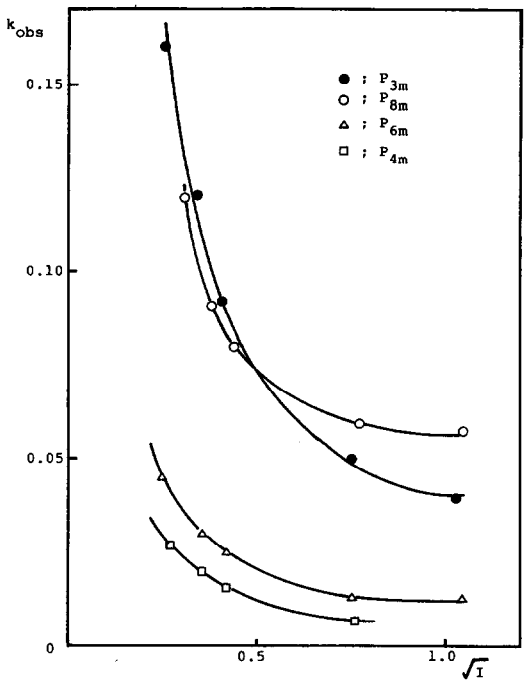

Fig. 2. Ionic strength dependence of the hydrolysis rate constants of cyclophosphates in 0.05 M HCl at 40°C.

Table 1. Ionic strength dependence of the rate constants of cyclophosphates in 0.05 M HCl at 40°C

$\sqrt{I}$	k_{obs} (h^{-1})
P_{3m}	
0.255	0.16
0.339	0.12
0.406	0.092
0.752	0.050
1.03	0.040
P_{4m}	
0.274	0.026
0.354	0.020
0.418	0.016
0.758	0.0070
P_{6m}	
0.276	0.045
0.355	0.030
0.420	0.025
0.759	0.014
1.04	0.013
P_{8m}	
0.308	0.12
0.381	0.091
0.442	0.080
0.771	0.060
1.05	0.058

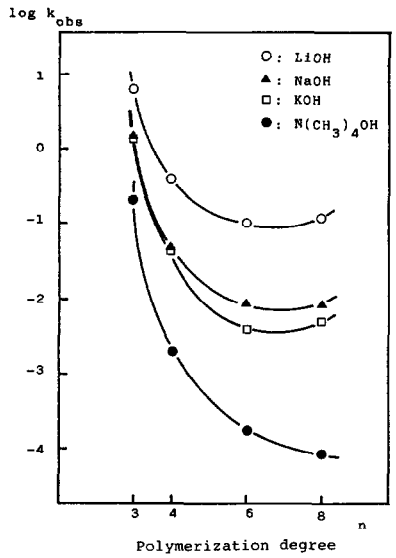

Fig. 3. The hydrolysis rate constants of cyclophosphates in various alkaline solutions at 50°C.

quently the interaction of the anions with H^+, Li^+, Na^+ or K^+ ions increases.[5,12]

When the effect of multi-valent cations on the cyclophosphates hydrolysis is investigated, the concentration of the cations is limited within the lower value to prevent the formation of a precipitate. Thus, the hydrolysis rates at the same concentration of mono- and multi-valent cations for each cyclophosphate could not be compared with each other. In this study, copper(II) ion of concentration 5×10^{-3} M was added to each cyclophosphate solution and the rates were determined. The concentration of each cyclophosphate was 2.5×10^{-3} M for cyclo-tri and cyclo-tetraphosphate, and 1.25×10^{-3} M for cyclo-hexa- and cyclo-octaphosphate. The pH of the mixed solution to be hydrolyzed was adjusted to 5.0 to prevent the formation of OH^- complexes of the copper(II) ion. At this pH, the hydrolysis rates of the four above cyclophosphates were negligibly slow[13] and the effects of hydrogen ions on the hydrolysis rates can be ignored. The rate acceleration observed is due to the copper(II) ion effect. The hydrolysis reaction under this condition were first-order for the phosphates and half-lives at 50°C for cyclo-tri-, cyclo-tetra-, cyclo-hexa- and cyclo-octaphosphates were 5.8, 68, 70 and 72 hr, respectively. The hydrolysis reaction of the phosphates is accelerated by the copper(II) ion. At higher copper(II) ion concentrations, the enhanced promotion of the hydrolysis rates might be expected.

From the chromatograms shown in Fig. 1, the following speculation is deduced. At a similar stage during the hydrolysis of cyclo-octaphosphate in acidic or alkaline solutions, cyclo-triphosphate as a side product could not be observed after the alkaline hydrolysis. On the other hand, in the case of acidic hydrolysis, an appreciable amount of cyclo-triphosphate was observed. The neutralization of the charges on the linear phosphates produced by the cyclo-octaphosphate hydrolysis with hydrogen ions might permit coiling of the linear polymers and cyclo-triphosphate is also formed by the mechanism called "metaphosphate abstraction".[15] While, at much higher pH, the coiled structure becomes difficult due to the repulsion between charges of PO^- ion on the linear phosphate chain. At even higher concentrations of LiOH, Li^+ did not catalyze the "metaphosphate abstraction". This suggests that Li^+ form looser bonds with the linear phosphate anions than the H^+ ions do. For the hydrolysis reactions studied in all the alkaline solutions "metaphosphate abstraction" was not observed.

Table 2. The rate constants of cyclophosphates in 0.5 M alkaline solutions at 50°C

	log (k_{obs}/h^{-1})			
	LiOH	NaOH	KOH	$N(CH_3)_4OH$
P_{3m}	0.76	0.15	0.11	−0.70
P_{4m}	−0.44	−1.31	−1.37	−2.70
P_{6m}	−1.02	−2.10	−1.42	−3.78
P_{8m}	−0.95	−2.05	−1.33	−4.06

Acknowledgements—The author wishes to thank Miss Miyuki Suzuki and Miss Junko Tsutsumi for their help with the experiments.

REFERENCES

1. J. R. Van Wazer, *Phosphorus and its Compounds.* Interscience, New York (1958).
2. G. Kura and S. Ohashi, *J. Chromatogr.* 1971, **56**, 111.
3. G. Kura and S. Ohashi, *J. Inorg. Nucl. Chem.* 1972, **34**, 3899.
4. G. Kura, S. Ohashi and S. Kura, *J. Inorg. Nucl. Chem.* 1974, **36**, 1605.
5. G. Kura and S. Ohashi, *J. Inorg. Nucl. Chem.* 1976, **38**, 1151.
6. S. Ohashi, G. Kura, Y. Shimada and M. Hara, *J. Inorg. Nucl. Chem.* 1977, **39**, 1513.
7. M. Koganemaru, H. Waki, S. Ohashi and G. Kura, *J. Inorg. Nucl. Chem.* 1979, **41**, 1457.
8. G. Kura, *J. Chromatogr.* 1981, **211**, 87.

9. G. Kura, T. Nakashima and F. Oshima, *J. Chromatogr.* 1981, **219**, 385.
10. G. Kura, *J. Chromatogr.* 1982, **246**, 73.
11. G. Kura, *Bull. Chem. Soc. Jpn* 1983, **56**, 3769.
12. G. Kura, *Polyhedron* 1986, **5**, 2097.
13. G. Kura, *Polyhedron* 1987, **6**, 531.
14. G. Kura, *Bull. Chem. Soc. Jpn* 1987, **60**, in press.
15. R. K. Osterheld, in *Topics in Phosphorus Chemistry* (Edited by M. Grayson and E. J. Griffith), Vol. 7, p. 103. Interscience, New York (1972).

Polyhedron Vol. 6, No. 10, pp. 1869–1874, 1987
Printed in Great Britain

0277–5387/87 $3.00+.00

INTERACTION OF METAL IONS WITH HUMIC-LIKE MODELS—X. SYNTHESIS, SPECTRAL PROPERTIES AND THERMAL DECOMPOSITION OF COPPER(II) METHOXY- AND DIMETHOXY-BENZOATES

LILIANA STRINNA ERRE and GIOVANNI MICERA*

Dipartimento di Chimica, Universitá di Sassari, Via Vienna 2, 07100 Sassari, Italy

and

FRANCO CARIATI

Dipartimento di Chimica Inorganica e Metallorganica and Centro C.N.R., Universitá di Milano, Via G. Venezian 21, 20133 Milan, Italy

(*Received* 27 *January* 1987; *accepted* 27 *April* 1987)

Abstract—Cu(II) complexes of 2-methoxybenzoic acid (MBH), 2,*x*-dimethoxybenzoic acids (2,*x*-DMBH; $x = 3$, 4, 5 and 6) and 3,*y*-dimethoxybenzoic acids (3,*y*-DMBH; $y = 4$ and 5) have been prepared and characterized by spectroscopic methods. They involve tetracarboxylate bridged dimeric arrangements of the copper(II) acetate monohydrate-type. The thermal decomposition of such complexes has been studied by thermogravimetric measurements and spectroscopic as well as mass spectrometric analysis of the evolved products and the intermediate residues. A mechanism which involves the shift of a CH_3 group from a ligand molecule to the carboxylic group of a second ligand, to give the methyl ester of the parent methoxy- or dimethoxy-benzoic acid, has been substantiated. Simultaneously, monomeric copper(II) complexes involving a 1 : 1 metal to ligand ratio and metal coordination by a carboxylate and a phenolate group are formed in the residues.

In the course of a study on the metal complexes formed by simple humic-like molecules, namely dihydroxy- and dimethoxy-substituted benzoic acids, we have recently reported the structure of the complexes of 2,6-dimethoxybenzoic acid with some divalent metal ions.[1–9] Dimeric arrangements of the copper(II) acetate monohydrate-type were observed for the Cu(II) compounds,[4] while polymeric aqua-bridged structures were found in the case of Mn, Co, Ni and Zn.[9]

For the latter compounds the thermal decomposition was also investigated and a mechanism leading to the formation of complexes of 2-hydroxy-*o*-anisic acid, in the 1 : 1 metal to ligand molar ratio, plus methyl 2,6-dimethoxybenzoate was substantiated.[3]

We report here the synthesis and the spectroscopic characterization of the Cu(II) complexes formed by 2-methoxybenzoic, 2,*x*- and 3,*y*-dimethoxybenzoic acids ($x = 3$, 4 or 5; $y = 4$ or 5), together with a thermal study on these complexes and on the previously described Cu(II)–dimethoxybenzoates.

EXPERIMENTAL

Materials

The acids, purchased from Fluka, were twice recrystallized from water or aqueous ethanol and dried *in vacuo*. Copper(II) acetate monohydrate (Carlo Erba) was the metal source.

Preparation of complexes

The preparation methods were similar for all the complexes. Typically, a solution or a suspension of

* Author to whom correspondence should be addressed.

Table 1. Analytical data[a]

Complex	C%	H%	H_2O%[b]
$[Cu_2(MB)_4(H_2O)_2]$	50.6 (50.1)	4.4 (4.2)	4.5 (4.7)
$[Cu_2(2,3\text{-DMB})_4(H_2O)_2]$	49.2 (48.7)	4.7 (4.5)	4.0 (4.1)
$[Cu_2(2,4\text{-DMB})_4(H_2O)_2]$	49.0 (48.7)	4.6 (4.5)	4.0 (4.1)
$[Cu_2(2,5\text{-DMB})_4(H_2O)_2]\cdot H_2O$	48.0 (47.7)	4.8 (4.7)	6.0 (6.0)
$[Cu_2(3,4\text{-DMB})_4(H_2O)_2]\cdot 4H_2O$	45.4 (45.0)	4.7 (5.0)	11.0 (11.3)
$[Cu_2(3,5\text{-DMB})_4(H_2O)_2]\cdot 2H_2O$	47.6 (46.8)	4.7 (4.8)	7.0 (7.8)

[a] Calculated values in parentheses.
[b] Thermogravimetric determination.

3.2 mmol of acid in 50 cm^3 of warm water was stirred while slowly adding 50 cm^3 of an aqueous solution containing 1.6 mmol of copper(II) acetate. Microcrystalline precipitates formed rapidly or after a few hours. They were filtered, washed with warm water and air-dried. Analytical data are listed in Table 1. The $[Cu_2(2,6\text{-DMB})_2(O_2CCH_3)_2(H_2O)_2]$ and $[Cu_2(2,6\text{-DMB})_4(H_2O)_2]$ complexes, were those described previously.[4]

Instruments

Thermogravimetric data were obtained by using a Perkin–Elmer TGS-2 apparatus in nitrogen or air atmosphere. A scanning rate of 5°C min^{-1} was employed. Chemical analyses for C and H were performed on a Perkin–Elmer 240 B elemental analyser. IR spectra were recorded on a Perkin–Elmer 683 B spectrophotometer. Electronic diffuse reflectance spectra were obtained on a Beckman Acta M IV spectrophotometer using $BaSO_4$ as the reference sample. ^1H NMR spectra were recorded on a Varian XL-200 spectrometer. ESR spectra were obtained on a Varian E 9 spectrometer at the X-band frequency. Mass spectra data were obtained on a VG Analytical 7070 EQ instrument. Acetic acid was identified by GLC analysis (Perkin–Elmer F 30 gas chromatograph; 2.3 m × 2.5 mm column packed with SP 2100 10% on Chromosorb WAW at 300°C).

Dissociation constants of ligands

The dissociation constants of the acids (except 3,5-DMBH which has a too low solubility in water) were determined by potentiometric titration in aqueous solution with 0.1 M $NaClO_4$ as the supporting electrolyte. The following pK_a values were obtained: 3.97 (MBH), 3.47 (2,3-DMBH), 4.24 (2,4-DMBH), 3.85 (2,5-DMBH), 3.40 (2,6-DMBH) and 4.26 (3,4-DMBH).

RESULTS

Spectral data

All the complexes exhibit spectral properties (Fig. 1 and Table 2) consistent with dimeric structures of the copper(II) acetate monohydrate-type, just as in the case of the structurally known 2,6-DMB derivative $[Cu_2(2,6\text{-DMB})_4(H_2O)_2]$.[4] Thus, their description needs no further comment. As is usual for such a type of complex, the slight differences between the observed solid-state spectral parameters may be attributed to minor differences in the copper(II) coordination geometry, e.g. the metal–water distances.

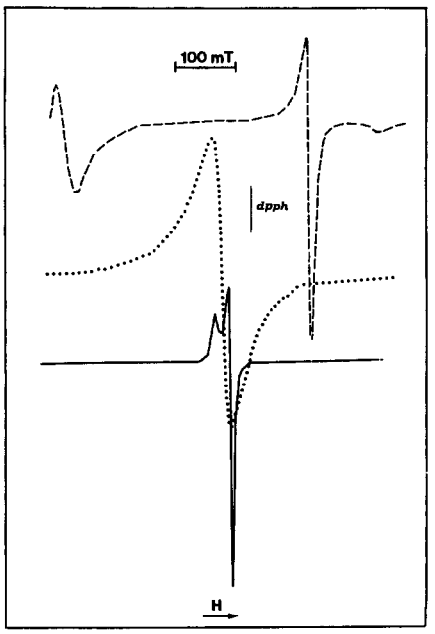

Fig. 1. X-band ESR spectra recorded at room-temperature on $[Cu_2(2,4\text{-DMB})_4(H_2O)_2]$ (– – –), $[Cu_2(2,4\text{-DMB})_4]$ (· · ·) and its intermediate residue after evolution of methyl 2,4-dimethoxybenzoate (——).

Table 2. Spectral data for complexes and their residues

Complex	Hydrated dimer				Residue after evolution of ester		
	Abs. max. (10^3 cm^{-1})	$g_\parallel$	$g_\perp$	D (cm^{-1})	$g_\parallel$	$A_\parallel$ (10^{-4} cm^{-1})	$g_\perp$
$[Cu_2(MB)_4(H_2O)_2]$	14.1	2.35	2.07	0.34	2.26		2.06
$[Cu_2(2,3\text{-DMB})_4(H_2O)_2]$	13.9	2.35	2.07	0.35	2.33	158	2.08
$[Cu_2(2,4\text{-DMB})_4(H_2O)_2]$	14.1	2.34	2.07	0.34	2.26		2.06
$[Cu_2(2,5\text{-DMB})_4(H_2O)_2]\cdot H_2O$	13.8	2.35	2.07	0.34	2.26		2.06
$[Cu_2(2,6\text{-DMB})_4(H_2O)_2]$	13.5	2.36	2.08	0.35	2.28	166	2.07
$[Cu_2(2,6\text{-DMB})_2(O_2CCH_3)_2(H_2O)_2]$	14.8	2.36	2.06	0.34	2.28	166	2.07
$[Cu_2(3,4\text{-DMB})_4(H_2O)_2]\cdot 4H_2O$	13.7	2.34	2.08	0.34	2.29	167	2.07
$[Cu_2(3,5\text{-DMB})_4(H_2O)_2]\cdot 2H_2O$	14.1	2.35	2.06	0.34	2.29	167	2.07

Also the IR absorptions are typical for tetracarboxylate-bridged copper(II) complexes, the carboxylate bands falling within the expected ranges (ν_{as}: 1580–1620 cm^{-1}; ν_s: 1385–1420 cm^{-1}; $\Delta\nu$: 190–230 cm^{-1}).

Thermal data

The thermogravimetric curves of the complexes (Figs 2 and 3) show distinct steps due to the release of water and decomposition of the anhydrous compounds. The onset of the decomposition step appears to be dependent on the ring substitutions of the ligands. Namely, 2-methoxy-substituted ligands yield complexes which are substantially less stable than the other ones, thus suggesting that a methoxyl group in an *ortho*-position to the carboxylate function activates the thermal decomposition process. At first glance, however, no immediate information concerning the decomposition mechanism may be drawn from the thermogravimetric curves, which,

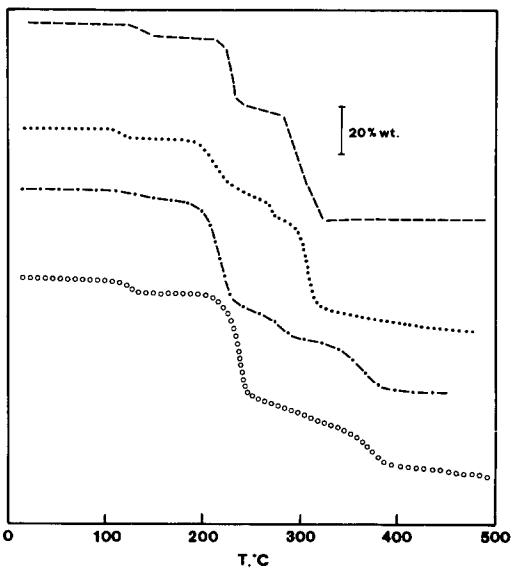

Fig. 2. Thermogravimetric curves (nitrogen atmosphere): $[Cu_2(MB)_4(H_2O)_2]$ (– – –), $[Cu_2(2,3\text{-DMB})_4(H_2O)_2]$ (· · ·), $[Cu_2(2,4\text{-DMB})_4(H_2O)_2]$ (· – ·) and $[Cu_2(2,5\text{-DMB})_4(H_2O)_2]\cdot H_2O$ (o o o).

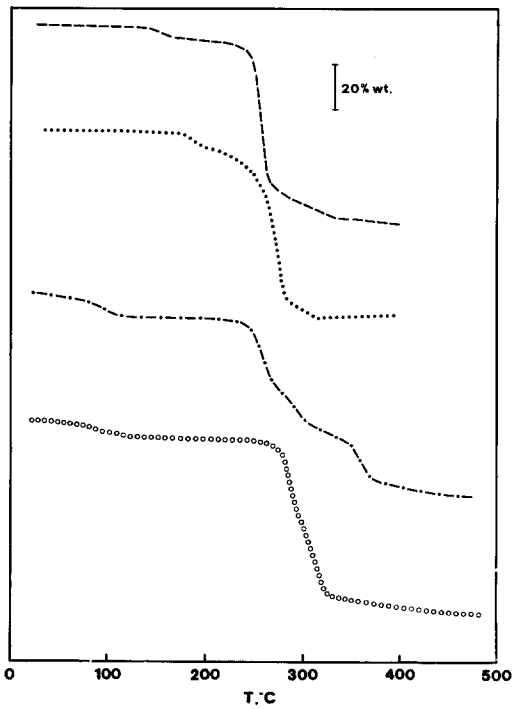

Fig. 3. Thermogravimetric curves (nitrogen atmosphere): $[Cu_2(2,6\text{-DMB})_4(H_2O)_2]$ (– – –), $[Cu_2(2,6\text{-DMB})_2(O_2CCH_3)_2(H_2O)_2]$ (· · ·), $[Cu_2(3,4\text{-DMB})_4(H_2O)_2]\cdot 4H_2O$ (· – ·) and $[Cu_2(3,5\text{-DMB})_4(H_2O)_2]\cdot 2H_2O$ (o o o).

Table 3. Evolved products and analytical data

Complex	Evolved product	^{1}H NMR ($CDCl_3$), δ (ppm)	Mass spectrum, *m/e* (relative intensity)
$[Cu_2(MB)_4(H_2O)_2]$	Methyl 2-methoxybenzoate	7.80 (d,1H), 7.48 (t,1H), 7.02–6.97 (m,2H), 3.91 (s,3H), 3.90 (s,3H)	77 (100), 135 (95), 166 (M^+,68), 133 (64), 92 (59), 105 (35), 120 (27), 133 (17), 134 (14), 153 (13)
$[Cu_2(2,3\text{-}DMB)_4(H_2O)_2]$	Methyl 2,3-dimethoxybenzoate	7.32–7.04 (m,3H), 3.89 (s,6H), 3.86 (s,3H)	165 (100), 196 (M^+,97), 163 (86), 107 (32), 122 (28), 77 (28), 149 (25), 135 (22), 92 (12), 153 (11)
$[Cu_2(2,4\text{-}DMB)_4(H_2O)_2]$	Methyl 2,4-dimethoxybenzoate	7.85 (d,1H), 6.50–6.46 (m,2H), 3.88 (s,3H), 3.84 (s,6H)	165 (100), 196 (M^+,41), 163 (17), 122 (13), 166 (13), 135 (12), 150 (10), 107 (10), 77 (9), 79 (8)
$[Cu_2(2,5\text{-}DMB)_4(H_2O)_2]\cdot H_2O$	Methyl 2,5-dimethoxybenzoate	7.33–6.88 (m,3H), 3.88 (s,3H), 3.84 (s,3H), 3.77 (s,3H)	150 (100), 196 (M^+,87), 165 (59), 107 (41), 182 (35), 181 (34), 163 (28), 151 (26), 79 (23), 135 (22)
$[Cu_2(3,4\text{-}DMB)_4(H_2O)_2]\cdot 4H_2O$	Methyl 3,4-dimethoxybenzoate	7.73–6.86 (m,3H), 3.93 (s,6H), 3.89 (s,3H)	165 (100), 196 (M^+,97), 79 (24), 182 (23), 77 (19), 120 (12), 121 (11), 124 (11), 137 (11), 107 (8)
$[Cu_2(3,5\text{-}DMB)_4(H_2O)_2]\cdot 2H_2O$	Methyl 3,5-dimethoxybenzoate	7.18 (d,2H), 6.64 (t,1H), 3.90 (s,3H), 3.82 (s,6H)	182 (100), 71 (50), 135 (46), 109 (35), 122 (32), 183 (31), 111 (25), 152 (21), 77 (20), 196 (M^+,19)
$[Cu_2(2,6\text{-}DMB)_4(H_2O)_2]$	Methyl 2,6-dimethoxybenzoate	7.28 (t,1H), 6.55 (d,2H), 3.90 (s,3H), 3.81 (s,6H)	165 (100), 196 (M^+,51), 107 (42), 150 (35), 77 (22), 135 (17), 122 (16), 166 (16), 164 (13), 92 (11)
$[Cu_2(2,6\text{-}DMB)_2(O_2CCH_3)_2(H_2O)_2]$	Methyl 2,6-dimethoxybenzoate	7.28 (t,1H), 6.55 (d,2H), 3.90 (s,3H), 3.81 (s,6H)	165 (100), 196 (M^+,51), 107 (42), 150 (35), 77 (22), 135 (17), 122 (16), 166 (16), 164 (13), 92 (11)

in most cases, apparently involve overlapping weight-losses.

Evolved products

To obviate the above lack of information, 0.5–1.0 g samples of the complexes were decomposed under static air in a round-bottomed flask kept at constant temperature (*ca.* 200°C) and fitted with a reflux condenser. Volatile products evolved during decomposition were collected along the condenser and analyzed by IR, ^{1}H NMR and mass spectrometry. In all cases (Table 3) these products were identified as the methyl esters of the ligands. For $[Cu_2(2,6\text{-DMB})_2(O_2CCH_3)_2(H_2O)_2]$, methyl 2,6-dimethoxybenzoate and acetic acid (the latter analysed also by GLC) were the evolved products.

By examination of the thermogravimetric curves it may be observed that in some cases (2,4- and 2,5-DMB complexes) the weight-loss subsequent to dehydration corresponds well to the release of a molecule of ester. In other cases, e.g. for $[Cu_2(MB)_4(H_2O)_2]$, the change of the operative conditions (Fig. 4) allowed an almost theoretical weight-loss for a molecule of ester. This may suggest that the first decomposition step of all the complexes involves the formation of a molecule of ester, but TG weight-losses of rather complex shape can result because (i) the ester, with increasing temperature, may decompose instead of being evolved as such, or (ii) its release can overlap with subsequent decomposition steps.

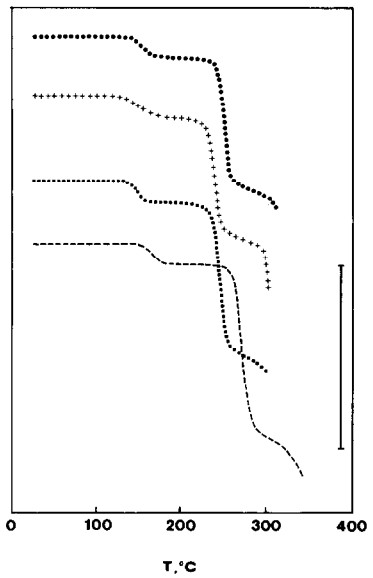

Fig. 4. Thermogravimetric curves of $[Cu_2(MB)_4(H_2O)_2]$: (● ● ●) nitrogen atmosphere, 5°C min^{-1}; (+ + +) static air, 5°C min^{-1}; (■ ■ ■) static air plus nitrogen purge, 5°C min^{-1}; (– – –) static air plus nitrogen purge, 10°C min^{-1}. The vertical bar represents the loss-weight corresponding to a molecule of methyl 2-methoxybenzoate (43.3 wt.%).

Residues

After evolution of volatile products, the residues were washed with $CHCl_3$ and dissolved in dilute aqueous HCl to separate the copper from ligands. By concentrating the solutions, the ligands were isolated and analysed by IR, ^{1}H NMR and mass spectrometry. In some cases, they were identified as pure compounds differing from the parent acid by having a phenolic function in the place of a methoxyl group (2-hydroxy-4 (or 5)-methoxybenzoic acid from 2,4- and 2,5-DMB complexes, respectively). In other cases, the precipitates were a mixture, easily distinguishable, containing the phenolic derivative and the undecomposed parent acid. In particular, the residue of $[Cu_2(MB)_4(H_2O)_2]$ gave salicylic acid, while those of $[Cu_2(2,6\text{-DMB})_4(H_2O)_2]$ and $[Cu_2(2,6\text{-DMB})_2(O_2CCH_3)_2(H_2O)_2]$ gave 2-hydroxy-6-methoxy-benzoic acid. Finally, it was impossible to isolate the intermediate residues of 2,3-, 3,4- and 3,5-DMB complexes, due to their thermal instability, in agreement with the thermogravimetric results.

Spectral study of residues

The decomposition of the complexes was also followed by spectroscopic (reflectance absorption and ESR) methods. After evolution of esters, the residues exhibited ESR signals attributable to magnetically dilute species (Table 2 and Fig. 1). On the other hand, a band around 450 nm, which could be assigned as a phenolate oxygen to Cu(II) transition,[10] was observed in the reflectance spectra.

DISCUSSION

The result of this study are in full agreement with those found previously for the $[M(2,6\text{-DMB})_2(H_2O)_3]\cdot H_2O$ complexes (M = Mn, Co, Ni and Zn). They support the view that the thermal decomposition of complexes formed by methoxy-substituted benzoic acids proceeds through a general pathway. This involves the intermolecular shift of an ethereal methyl group from a ligand molecule to the carboxylate moiety of a second ligand. As a consequence, the former ligand is demethylated and forms a phenolate bond with the metal ion, while the latter is transformed into the corresponding methyl ester.

Support for the proposed mechanisms is given by all the experimental data:

(i) all the released esters and most of phenolic ligands, which are the primary decomposition products, have been isolated and fully characterized;

(ii) ESR and electronic spectra of all the intermediate residues after evolution of ester indicate the presence of magnetically dilute Cu(II) complexes, where the metal ion is bound to a carboxylate and a phenolate group.

The temperature over which such a process occurs is clearly dependent on the position of the substituents within the aromatic ring of the ligands. Particularly, it appears that the decomposition of complexes formed by *ortho*-substituted ligands occurs at temperatures which are substantially lower than those for the 3,4- and 3,5-DMB analogues. Therefore the formation of intermediates with a 1 : 1 metal to ligand ratio, involving chelation by phenolate and carboxylate groups in *ortho*-positions, is a factor favouring the first decomposition step.

With increasing temperature, the 1 : 1 intermediates decompose but, if this process is too near to the first decomposition step, low yields are expected when attempting to isolate the 1 : 1 intermediates. Accordingly, the maximum yield of phenolic ligands is obtained for 2,4- and 2,5-DMB complexes whose thermogravimetric curves are consistent with almost theoretical weight-losses for a decomposition occurring in two steps distinct enough to allow the isolation of 1 : 1 intermediates.

Turning to the first decomposition stage, the detection of acetic acid as a volatile product evolved by $[Cu_2(2,6\text{-DMB})_2(O_2CCH_3)_2(H_2O)_2]$ in static air is clear evidence that the acetate is, at least in part, hydrolysed by water vapour, analogously to the findings, e.g. for nitrate.[11] Acetic acid is also evolved by heating copper(II) acetate under the same conditions (static air), also the mechanisms under nitrogen flow could be different. Therefore, the thermal behaviour of the complex $[Cu_2(2,6\text{-DMB})_2(O_2CCH_3)_2(H_2O)_2]$ may be reasonably interpreted as that of a mixture of copper(II) acetate and copper(II) 2,6-dimethoxybenzoate.

Finally, a further comment is needed on the absence of complexes involving mixed bridges (acetate and methoxy- or dimethoxy-benzoate) for all ligands except 2,6-DMB, in spite of the similar synthetic procedures used. 2,6-DMBH differs from the other ligands by having the most acidic carboxylic group and two methoxyl substituents in *ortho* positions to the carboxylic function. The pK_a value is, however, comparable to that of 2,3-DMBH. Thus, the most likely reason for the isolation of the "mixed" complex is the steric hindrance produced by the bulky *o*-methoxy substituents, which, in the presence of acetate, disfavours the formation of a binary 2,6-DMB complex.

Acknowledgement—The authors wish to thank Mr S. Cossu for GLC analyses.

REFERENCES

1. F. Cariati, L. Erre, G. Micera, A. Panzanelli, G. Ciani and A. Sironi, *Inorg. Chim. Acta* 1983, **80**, 57.
2. F. Cariati, L. Erre, G. Micera, A. Panzanelli and P. Piu, *Thermochim. Acta* 1983, **66**, 1.
3. G. Micera, P. Piu, L. Strinna Erre, F. Cariati and A. Pusino, *Thermochim. Acta* 1984, **77**, 67.
4. L. Strinna Erre, G. Micera, P. Piu, F. Cariati and G. Ciani, *Inorg. Chem.* 1985, **24**, 2297.
5. G. Micera, L. Strinna Erre, F. Cariati, D. A. Clemente, A. Marzotto and M. Biagini Cingi, *Inorg. Chim. Acta* 1985, **109**, 135.
6. G. Micera, L. Strinna Erre, F. Cariati, D. A. Clemente, A. Marzotto and G. Valle, *Inorg. Chim. Acta* 1985, **109**, 173.
7. G. Micera, L. Strinna Erre, P. Piu, F. Cariati, G. Ciani and A. Sironi, *Inorg. Chim. Acta* 1985, **107**, 223.
8. G. Micera, L. Strinna Erre, F. Cariati, G. Ciani and A. Sironi, *Inorg. Chim. Acta* 1985, **108**, L1.
9. L. Strinna Erre, G. Micera, F. Cariati, G. Ciani, A. Sironi, H. Kozłowski and J. Baranowski, *J. Chem. Soc., Dalton Trans.*, in press.
10. E. I. Solomon, K. W. Penfield and D. E. Wilcox, *Struct. Bonding (Berlin)* 1983, **53**, 1.
11. D. Dollimore, G. A. Gamlen and T. J. Taylor, *Thermochim. Acta* 1985, **86**, 119.

Polyhedron Vol. 6, No. 10, pp. 1875–1878, 1987
Printed in Great Britain

0277–5387/87 $3.00+.00

TRIFLUOROMETHANESULFONATO COMPLEXES OF (1,4,8,11-TETRAAZACYCLOTETRADECANE)COBALT(III) AND RUTHENIUM(III) WITH *TRANS* GEOMETRY

PAUL V. BERNHARDT and GEOFFREY A. LAWRANCE*

Department of Chemistry, The University of Newcastle, New South Wales 2308, Australia

(*Received* 28 *January* 1987; *accepted* 27 *April* 1987)

Abstract—Reaction of *trans*-[M(cyclam)Cl_2]Cl (M = Co, Ru; cyclam = 1,4,8,11-tetraazacyclotetradecane) with anhydrous CF_3SO_3H at elevated temperatures formed initially *trans*-[M(cyclam)Cl(OSO_2CF_3)](CF_3SO_3), with *trans*-[M(cyclam)(OSO_2CF_3)$_2$](CF_3SO_3) formed after extended reaction time. The complexes were characterized by spectroscopy, and rate constants for the rapid aquation of the bound $CF_3SO_3^-$ determined. In the case of the cobalt(III) complexes, derivatives were prepared by substitution of the $CF_3SO_3^-$ ligand by the neutral ligands acetonitrile and dimethylformamide.

The coordination chemistry of the weakly nucleophilic trifluoromethanesulfonate (triflate) anion has been well documented in recent years, since it has proved to be an excellent leaving group from a range of inert metal ions.[1,2] The lability of bound triflate is comparable to that of the perchlorate ligand; however, complexes of the former are inherently safer to handle as the triflate anion is non-oxidizing. The use of triflato complexes as precursors in inorganic chemistry has been demonstrated by the development of facile and high yielding routes to a range of previously inaccessible complexes.[2] For inert metal complexes, introduction of the triflato ligand to the coordination sphere is usually and conveniently achieved by reaction of the chloro complex with anhydrous acid (CF_3SO_3H). The elimination of hydrogen chloride drives the reaction, and yields of the triflato complexes are essentially quantitative.

Although there are a range of examples of *mono*, *bis* and even *tris* triflato complexes of octahedral metal amines, there are very few examples of stable complexes in which the triflato ligand is *trans* to any ligand other than an ammine or amine.[1,2] For cobalt(III), the only known complex is the ion *trans*-[Co(en)$_2$Cl(OSO_2CF_3)]$^+$ reported during the course of this work, and prepared by reaction of *trans*-[Co(en)$_2$Cl$_2$]$^+$ with CF_3SO_3H at −5°C for several hours.[3] Replacement of the second chloro ligand was not possible without isomerization to the *cis* isomer during reaction. Previously, reaction at elevated temperature showed *cis*-[Co(en)$_2$(OSO_2CF_3)$_2$]$^+$ to be the sole product of reaction from either *cis*- or *trans*-[Co(en)$_2$Cl$_2$]$^+$,[4] consistent with *cis* isomers being more stable in polar solvents than *trans* isomers. For *bis*(1,2-ethanediamine) complexes, it is only with the more stereoretentive Rh(III) and Ir(III) that *trans*-[M(en)$_2$Cl(OSO_2CF_3)]$^+$ complexes can be prepared at elevated temperatures.[5]

Greater structural rigidity of metal complexes can be imposed by replacing *bis*(1,2-ethanediamine) ligands by a cyclic tetraamine such as 1,4,8,11-tetraazacyclotetradecane (cyclam). There exist cyclam complexes of most transition metals, especially those in higher oxidation states stabilized by the strong ligand field of the macrocycle.[6,7] Geometric isomers of cyclam complexes exist with the preferred configuration (*cis* or *trans*) dependent on the ionic radius of the metal and the absolute configuration of the asymmetric nitrogen donor atoms. The cyclam complexes of cobalt(III) show a preference for the *trans* geometry compared with *bis*(1,2-diaminoethane) analogues, although *cis* isomers are known with both unidentate and particularly chelating ligands in the other two coordination sites.[8] This preference suggests that *trans*-dichloro(cyclam)cobalt(III) may provide a route to the first stable *trans*-chloro(triflato) and *trans*-

* Author to whom correspondence should be addressed.

bis(triflato) complexes of cobalt(III). Further, although both *cis*- and *trans*-$[Ru(cyclam)Cl_2]^+$ complexes are known, the *trans* isomer is thought to be more stable,[9] and it may also yield *trans*-triflato complexes. Reaction of both of these *trans*-dichloro ions with CF_3SO_3H has been probed in this work.

EXPERIMENTAL

trans-$[Co(cyclam)Cl(OSO_2CF_3)](CF_3SO_3)$

To *trans*-$[Co(cyclam)Cl_2]Cl$[8] (3 g) in a three-necked round bottomed flask (100 cm^3) fitted with a gas bubbler was carefully added anhydrous CF_3SO_3H (8 cm^3). A stream of nitrogen was bubbled through the solution as it was warmed in an oil bath at 100°C for 90 min. The flask was then allowed to cool with the gas supply maintained. Dropwise addition of diethyl ether (70 cm^3) to the rapidly stirring solution precipitated a green solid, which was collected on a fine porosity sintered glass frit. The green powder was washed several times with diethyl ether (30 cm^3), and dried *in vacuo* (4.7 g, 96%). The product is stable indefinitely if stored in a desiccator. Found: C, 22.7; H, 3.8; N, 7.8. $C_{12}H_{24}ClCoF_6N_4O_6S_2 \cdot \frac{1}{2}CF_3SO_3H$ requires: C, 22.5; H, 3.7; N, 8.35%. Vis. spectrum (CF_3SO_3H): 630 nm (ε 22 dm^3 mol^{-1} cm^{-1}), 410 (ε 35).

trans-$[Co(cyclam)(OSO_2CF_3)_2](CF_3SO_3)$

Anhydrous CF_3SO_3H (8 cm^3) was added cautiously to *trans*-$[Co(cyclam)Cl_2]Cl$ (2 g) in a three-necked flask fitted with a gas bubbler. A gentle stream of nitrogen was passed through the solution, which was heated in an oil bath at 100°C for 50 h. The green product was precipitated with diethyl ether (70 cm^3) and isolated as above (3.5 g, 90%). Found: C, 20.1; H, 3.4; N, 6.6. $C_{13}H_{24}CoF_9N_4O_9S_3 \cdot CF_3SO_3H$ requires: C, 19.7; H, 3.0; N, 6.5%. Vis. spectrum (CF_3SO_3H): 635 nm (ε 83 dm^3 mol^{-1} cm^{-1}), 410 (ε 151).

trans-$[Co(cyclam)(NCCH_3)Cl](CF_3SO_3)_2$

A solution of *trans*-$[Co(cyclam)Cl(OSO_2CF_3)](CF_3SO_3)$ (0.5 g) in dry acetonitrile (20 cm^3) was stirred at room temperature for 2 h, then added to rapidly stirring diethyl ether (100 cm^3). The resulting oil was separated from the supernatant by decantation, the oil was dissolved in ethanol (20 cm^3) and the product precipitated as a red powder by addition of diethyl ether (100 cm^3) with stirring. The product was collected, washed with ether, and dried *in vacuo* (0.27 g, 50%). Found: C, 25.9; H, 4.1; N, 10.3. $C_{14}H_{27}ClCoF_6N_5O_6S_2 \cdot H_2O$ requires: C, 25.8; H, 4.15; N, 10.7%. ^1H NMR (D_2O): δ 2.57 ($C\underline{H}_3CN$; 2.06, free CH_3CN), 2.0–3.0 ($-C\underline{H}_2-$, multiplets). Vis. spectrum (water): 535 nm (ε 33 dm^3 mol^{-1} cm^{-1}), 420 nm (ε 48). IR spectrum (KBr disc): 2340, 2380 cm^{-1} (nitrile stretch).

trans-$[Co(cyclam)(OCH \cdot N(CH_3)_2)Cl](CF_3SO_3)_2$

A solution of *trans*-$[Co(cyclam)Cl(OSO_2CF_3)](CF_3SO_3)$ (0.5 g) in dry dimethylformamide (20 cm^3) was stirred at room temperature for 2 h, then isolated as described for the nitrile analogue. The green product (0.34 g, 60%) was dried *in vacuo*. Found: C, 25.5; H, 4.6; N, 9.5. $C_{15}H_{31}ClCoF_6N_5O_7S_2 \cdot 2H_2O$ requires; C, 25.65; H, 5.0; N, 9.9%. ^1H NMR (D_2O): δ 7.95 ($-C\underline{H}O$), 3.02, 2.87 ($-C\underline{H}_3$), 2.0–3.0 ($-C\underline{H}_2-$, multiplets). Vis. spectrum (water): 580 nm (ε 21 dm^3 mol^{-1} cm^{-1}), 410 (ε 35). IR spectrum (KBr): 1670 cm^{-1} (amide).

trans-$[Co(cyclam)(NCCH_3)_2](CF_3SO_3)_3$

A solution of *trans*-$[Co(cyclam)(OSO_2CF_3)_2](CF_3SO_3) \cdot CF_3SO_3H$ (0.5 g) was dissolved in dry acetonitrile (20 cm^3) and stirred for 4 h at room temperature. The product was isolated by addition of diethyl ether (100 cm^3), as an oil. After decanting the ether solution, the oil was dissolved in ethanol (10 cm^3) and added with vigorous stirring to diethyl ether (100 cm^3). The orange powder precipitated was collected, washed with ether, and dried *in vacuo* (0.31 g, 60%). Found: C, 23.6; H, 3.9; N, 8.8. $C_{17}H_{30}CoF_9N_6O_9S_3 \cdot C_2H_5OH \cdot HOSO_2CF_3$ requires: C, 23.2; H, 3.8; N, 8.55%. The product may be recrystallized as a perchlorate, but was (apart from detected ethanol) pure by NMR measurement. ^1H NMR (D_2O): δ 2.57 ($C\underline{H}_3CN$), 2.0–3.0 ($-C\underline{H}_2-$, multiplets). Vis. spectrum (water): 495 nm (ε 86 dm^3 mol^{-1} cm^{-1}), 405 (ε 125). IR spectrum (KBr): 2320 cm^{-1} (nitrile stretch).

trans-$[Co(cyclam)(OCH \cdot N(CH_3)_2)_2](CF_3SO_3)_3$

A solution of *trans*-$[Co(cyclam)(OSO_2CF_3)_2](CF_3SO_3)$ (0.5 g) was dissolved in dimethylformamide (20 cm^3) and stirred at room temperature for 4 h. The green product was isolated as described for the acetonitrile analogue, and dried *in vacuo* (0.39 g, 65%). Found: C, 26.9; H, 4.5; N, 9.8. $C_{19}H_{38}CoF_9N_6O_{11}S_3$ requires: C, 26.75; H, 4.5; N, 9.85%. ^1H NMR (D_2O): δ 7.95 ($-C\underline{H}O$), 3.01, 2.85 ($C\underline{H}_3-$), 2.0–3.0 ($-C\underline{H}_2-$, multiplets). Vis.

spectrum (water): 535 nm (ε 53 $dm^3\ mol^{-1}\ cm^{-1}$), 410 (ε 87). IR spectrum (KBr): 1670 cm^{-1} (amide).

trans-[Ru(cyclam)Cl(OSO_2CF_3)](CF_3SO_3)

To *trans*-[Ru(cyclam)Cl_2]Cl[9] (2.0 g) in a three-necked round bottomed flask fitted with a gas bubbler was added anhydrous CF_3SO_3H (6 cm^3). A stream of nitrogen was passed through the solution, which was heated in an oil bath at 100°C for 2 h. After the mixture had been allowed to cool, the nitrogen flow was disconnected and precipitation of the product was achieved by careful addition of diethyl ether (50 cm^3) with vigorous stirring. The brown solid was collected, washed several times with diethyl ether, and dried in a vacuum desiccator (2.95 g, 95%). The product was stable if stored in a desiccator in the dark. Found: C, 21.1; H, 3.5; N, 7.9. $C_{12}H_{24}ClF_6N_4O_6S_2Ru$ requires: C, 21.6; H, 3.6; N, 8.4%. Vis. spectrum (CF_3SO_3H): 370 nm (ε 1520 $dm^3\ mol^{-1}\ cm^{-1}$).

trans-[Ru(cyclam)(OSO_2CF_3)$_2$](CF_3SO_3)

A solution of *trans*-[Ru(cyclam)Cl_2]Cl (2.0 g) in CF_3SO_3H (6 cm^3) was reacted at 100°C for 24 h under nitrogen. It was isolated as described above for the other ruthenium complex (3.3 g, 90%). Found: C, 19.9; H, 3.5; N, 7.1. $C_{13}H_{24}F_9N_4O_9S_3Ru \cdot 2H_2O$ requires: C, 20.0; H, 3.6; N, 7.1%. To permit accurate analysis of this moisture-sensitive compound, it was hydrated and analyzed as the aqua complex; all other triflato compounds were analyzed as isolated.

Physical methods

Electronic spectra were recorded using a Hitachi 220A spectrophotometer, while infrared spectra were recorded with the complexes dispersed in KBr discs on a Nicolet MX-1 fourier-transform infrared spectrometer. Proton magnetic resonance spectra of complexes dissolved in D_2O were recorded using a Jeol FX-90Q spectrometer. Rates of hydrolysis of triflato complexes were determined from absorbance–time responses determined spectrophotometrically, using standard computational methods.

RESULTS AND DISCUSSION

The facile and high yielding synthesis of triflato complexes from chloro precursors developed earlier[1–5] has been applied successfully to the synthesis of *trans*-chloro(triflato) and *trans-bis*(triflato) complexes of (cyclam)cobalt(III) and ruthenium(III). The *trans-bis*(triflato) complexes are the first reported for any complex, *cis* stereochemistry being common.[1] Spectroscopic evidence detailed later defines the *trans* geometry. Since synthesis and isolation is performed in strongly acidic conditions, preservation of the geometry is expected since many isomerization reactions of polyamine complexes involve deprotonation of secondary amine groups, which cannot occur under the experimental conditions employed. Although the lability of triflate forbids recrystallization, the compounds as isolated were of acceptable purity, and derivatives of microanalytical and spectroscopic purity were prepared directly from the triflato precursors. The lability of the triflato ligand was demonstrated by the ready substitution by acetonitrile (AN), *N*,*N*-dimethylformamide (DMF) and even acetone at room temperature.

It was apparent from the electronic spectra of both triflatocobalt(III) precursors and their derivatives that *trans* geometry was maintained. A striking feature of the spectra was the large splitting of the octahedral $^1T_1$ state under the tetragonal field to give a ^1E and a $^1A_2$ state with the former of lower energy. Transitions (from a $^1A_1$ ground state) to these states occurred in the visible region; the ultraviolet region was dominated by intense bands due to charge transfer or intra-ligand transitions which masked the other *d–d* transition to the $^1T_2$ state. The two bands in the visible region (see Experimental) converged with increasing strength of the *trans* ligand. Spectra of triflato complexes were recorded in anhydrous CF_3SO_3H, since variation in the spectra in dry acetone indicates that even that weak ligand may displace triflate, as previously observed.[4] Observed spectra are consistent with the earlier location of $CF_3SO_3^-$ near Cl^- in the spectrochemical series,[5] since maxima for *trans*-dichloro (625, 420 nm), *trans*-chloro(triflato) (630, 410 nm) and *trans-bis*(triflato) (635, 410 nm) are similar. Substitution of $CF_3SO_3^-$ by DMF or AN causes significant shifts of the low energy maxima to higher energy, as expected.

The low frequency infrared spectra of the triflato complexes displayed evidence for coordinated as well as ionic triflate. The spectrum of ionic triflate has been studied in detail[1,10] and by comparison with the spectrum of the cobalt triflate complexes assignments to coordinated triflate were possible. One obvious difference was the appearance of a peak at 655 cm^{-1}, adjacent to the resonance of ionic triflate at 640 cm^{-1}. This higher energy peak, which was more intense in the *bis*(triflato) complex, disappeared on substitution of the triflato ligands by both DMF and AN. Earlier, it has been noted that the band at 1280 cm^{-1} for ionic triflate is shifted

approximately 100 cm^{-1} higher in energy on coordination.[4]

The IR absorption frequencies associated with the cyclam ligand are essentially invariant for all complexes of cobalt(III), consistent with retention of geometry. For derivatives, characteristic vibrations of carbonyl or nitrile groups were observed also. For the ruthenium(III) complexes, the region from 800 to 1000 cm^{-1} is useful for identifying *cis* and *trans* cyclam complexes.[11] The bands in this region, assigned to methylene group rocking, differ significantly, with a doublet near 890 cm^{-1} and a singlet at 805 cm^{-1} being indicative of *trans* geometry. The *cis* dichloro isomer shows a more complicated series of bands which are mutually exclusive with those in the *trans* complex. The spectra of the triflato complexes showed bands common with those of the *trans* dichloro complex, consistent with retention of geometry throughout.

The lability of the triflato ligand was quantified by measurement of rates of aquation for complexes. The chloro(triflato)cobalt(III) complex hydrolyzes rapidly under acidic conditions ($k_{obs} = 0.048$ s^{-1}, 25°C, 0.1 mol dm^{-3} H^+) to the *trans*-aqua chloro complex; further reactions are slow, and were not pursued. This rate constant is similar to that reported for the simple $[Co(NH_3)_5(OSO_2CF_3)]^{2+}$ ion (0.024 s^{-1}, 25°C). The chloro(triflato)ruthenium(III) also aquates rapidly ($k_{obs} = 0.060$ s^{-1}, 25°C, 0.1 mol dm^{-3} H^+), again with a rate constant similar to that reported for $[Ru(NH_3)_5(OSO_2CF_3)]^{2+}$ (0.093 s^{-1}, 25°C). The *bis*(triflato) cobalt(III) complex displayed two successive relatively fast aquation processes ($k_1 = 0.038$ s^{-1}, $k_2 = 0.0017$ s^{-1}, 25°C, 0.1 mol dm^{-3} H^+) assigned to successive hydrolyses of triflato ligands. Notably, the aquation rate constant for $[Co(cyclam)Cl(OSO_2CF_3)]^+$ is very close to that for $[Co(cyclam)(OSO_2CF_3)_2]^+$ (0.048 s^{-1} vs 0.019 s^{-1}, dividing the latter by two for statistical correction), indicating that the *trans* labilizing influence of $CF_3SO_3^-$ is not a lot less than that of Cl^-. Further, aquation of the *trans*-aqua(triflato) intermediate is approximately twenty times slower than aquation of the *trans*-chloro(triflato) complex, which may be related to the greater *trans* labilizing effect of chloro compared with aqua ligand. The lability of coordinated triflate observed in these complexes is consistent with general observations.[1]

The lability of coordinated triflate permitted ready substitution by coordinating solvents, with the O-donor DMF and the N-donor AN introduced into the coordination sphere of the cobalt(III) systems to illustrate the process. Products isolated in high yield were microanalytically pure, and exhibited characteristic electronic and infrared spectra. Further, proton NMR spectra in D_2O defined coordination clearly. For all derivatives a series of multiplets associated with the cyclam ligand were seen in the region 2.0–3.0 p.p.m., comparable with known *trans*-cyclam complexes. Coordinated AN was apparent from the appearance of a singlet from the methyl of AN in both chloro(acetonitrile) and *bis*(acetonitrile) complexes at 2.57 p.p.m., shifted substantially from the resonance for free AN in the same solvent at 2.06 p.p.m. Both *mono* and *bis* DMF complexes exhibited signals at 3.02 and 2.87 p.p.m., from the two non-equivalent methyl groups on the DMF ligand, as well as a singlet at 7.95 p.p.m. from the amide proton, again shifted as a result of coordination.

Syntheses of labile *trans*-$[M(cyclam)(OSO_2CF_3)_2]^+$ complexes (M = Co, Ru) from dichloro precursors have been developed, and facile syntheses of derivatives demonstrated for cobalt(III) complexes. The cobalt(III) complexes are the first geometrically stable cobalt triflato complexes with *trans* geometry, and their synthesis may provide a route to previously inaccessible complexes, including polymetallic chains with bridging ligands replacing the labile triflates.

REFERENCES

1. G. A. Lawrance, *Chem. Rev.* 1986, **86**, 17.
2. N. E. Dixon, G. A. Lawrance, P. A. Lay, A. M. Sargeson and H. Taube, *Inorg. Synth.* 1985, **24**, Chap. 5.
3. P. Comba, N. J. Curtis, W. G. Jackson and A. M. Sargeson, *Aust. J. Chem.* 1986, **39**, 1297.
4. N. E. Dixon, W. G. Jackson, M. A. Lancaster, G. A. Lawrance and A. M. Sargeson, *Inorg. Chem.* 1981, **20**, 1470.
5. N. E. Dixon, G. A. Lawrance, P. A. Lay and A. M. Sargeson, *Inorg. Chem.* 1984, **23**, 2940.
6. G. A. Melson, ed., *Coordination Compounds of Macrocyclic Complexes*. Plenum, New York (1982).
7. L. F. Lindoy and D. H. Busch, *Prep. Inorg. React.* 1971, **6**, 1.
8. B. Bosnich, C. K. Poon and M. L. Tobe, *Inorg. Chem.* 1965, **4**, 1102; 1109; C. K. Poon and M. L. Tobe, *J. Chem. Soc. A* 1968, 1549.
9. C. K. Poon and L. M. Che, *J. Chem. Soc., Dalton Trans.* 1980, 756.
10. H. Burger, K. Burczyk and A. Blaschette, *Monatsh. Chem.* 1970, **101**, 102.
11. S. S. Isied, *Inorg. Chem.* 1980, **19**, 911.

Polyhedron Vol. 6, No. 10, pp. 1879–1884, 1987
Printed in Great Britain

0277–5387/87 $3.00+.00

CATIONIC CARBONYL COMPLEXES OF MANGANESE(I) WITH DIPHENYLPHOSPHINE

G. A. CARRIEDO, V. RIERA,* M. L. RODRÍGUEZ and J. J. SAINZ-VELICIA

Departamento de Química Organometálica, Universidad de Oviedo, 33071 Oviedo, Spain

(*Received* 12 *March* 1987; *accepted* 27 *April* 1987)

Abstract—The cationic complexes $[Mn(CO)_{6-n}(PHPh_2)_n]ClO_4$, for $n = 1$ to 4 and $[Mn(CO)_{4-n}(L\frown L)(PHPh_2)_n]A$ ($L\frown L$ = dppm or dppe, $n = 1$, $A = ClO_4$; $L\frown L$ = bipy or phen, $n = 1$ or 2, $A = ClO_4$ or PF_6) have been prepared from $PHPh_2$ and $Mn(OClO_3)(CO)_5$ or *fac*-$MnX(CO)_3(L\frown L)$ respectively (X = Br or $OClO_3$). The *fac*-tricarbonyls *fac*-$[Mn(CO)_3(PHPh_2)_3]ClO_4$ and *fac*-$[Mn(CO)_3(L\frown L)(PHPh_2)]ClO_4$ for $L\frown L$ = dppm or dppe, isomerize upon heating to the corresponding *mer*-tricarbonyls, and the dicarbonyl *cis*-$[Mn(CO)_2(PHPh_2)_4]ClO_4$ gives the *trans* isomer under UV irradiation.

It is known that the reaction of the neutral perchlorate complex $Mn(OClO_3)(CO)_5$ with monodentate ligands (L) gives $[Mn(CO)_5L]ClO_4$ or *fac*-$[Mn(CO)_3L_3]ClO_4$, and that, in the case of the phosphites $[P(OR)_3]$, the more substituted products $[Mn(CO)_2L_4]ClO_4$ can be obtained.[1] The tetracarbonyls $[Mn(CO)_4L_2]ClO_4$ were not made from $Mn(OClO_3)(CO)_5$, but the BF_4 salts can be prepared by other routes.[2] We have found that the reaction of the secondary phosphine $PHPh_2$ with $Mn(OClO_3)(CO)_5$ leads to the cationic carbonyl complexes $[Mn(CO)_{6-n}(PHPh_2)_n]ClO_4$ for $n = 1$ to 4 by varying the reaction conditions. Herein we describe the preparation of those complexes and of the related species $[Mn(CO)_{4-n}(L\frown L)(PHPh_2)_n]A$, where for $L\frown L$ = dppm† or dppe, $n = 1$ and for $L\frown L$ = bipy or phen $n = 1$ or 2 and $A = ClO_4$ or PF_6.

EXPERIMENTAL

All reactions were carried out under dry, oxygen-free argon. The NMR spectra were recorded with a JEOL FX 90Q instrument and the IR with a Perkin–Elmer 298 spectrometer. The compounds $Mn(OClO_3)(CO)_5$,[1] *fac*-$[Mn(OClO_3)(CO)_3(L\frown L)]$ ($L\frown L$ = dppm or dppe,[9] $L\frown L$ = bipy or phen[10] were prepared by published methods.

$[Mn(CO)_5(PHPh_2)]ClO_4$ (I)

A mixture of the complex $Mn(OClO_3)(CO)_5$ (0.32 g, 1 mmol) and the phosphine $PHPh_2$ (0.19 cm^3, 1 mmol) in dichloromethane (40 cm^3), was stirred for 17 h at room temperature and evaporated almost to dryness. The residue was washed repeatedly with diethyl ether and crystallized from CH_2Cl_2: Et_2O as a pale yellow microcrystalline solid (0.45 g, 86%). The compound was stored cooled and under dry argon

cis-$[Mn(CO)_4(PHPh_2)_2]ClO_4$ (II)

A mixture of $Mn(OClO_3)(CO)_5$ (0.22 g, 0.75 mmol) and $PHPh_2$ (0.39 cm^3, 2.24 mmol) in ethanol (8 cm^3) was refluxed for 75 min and cooled to room temperature. The white crystalline precipitate was separated from the mother liquor and recrystallized from CH_2Cl_2: Et_2O (0.32 g, 67.5%). From the mother liquor a mixture of **II** and **III** was obtained by concentrating and precipitating with ether.

fac-$[Mn(CO)_3(PHPh_2)_3]ClO_4$ (III)

A solution of $Mn(OClO_3)(CO)_5$ (0.4 g, 1.36 mmol) in acetone (15 cm^3) was refluxed for 90 min and allowed to cool to room temperature. To the resulting solution of *fac*-$[Mn(CO)_3(Me_2CO)_3]ClO_4$, the phosphine $PHPh_2$ (0.85 cm^3, 4.9 mmol) was added and the mixture was stirred for 2 h at room temperature. Part of the product precipitated as a

* Author to whom correspondence should be addressed.

† Throughout this paper dppm = $Ph_2PCH_2PPh_2$, dppe = $Ph_2PCH_2CH_2PPh_2$, bipy = 2,2′-bipyridine and phen = 1,10-orthophenanthroline.

white solid. Excess of diethyl ether was added and the precipitate was separated and washed with ether. Recrystallization from CH_2Cl_2: Et_2O gave white microcrystalline **III** (0.78 g, 72%).

Isomerization of **III**

The salt **III** (0.1 g, 0.125 mmol) was heated in refluxing *n*-butanol (10 cm^3) for 1 h and the resulting solution was allowed to cool to room temperature. Addition of a small amount of diethylether gave a first precipitate that was mainly the *mer* isomer (**V**), and from the mother liquor the remaining *fac*-tracarbonyl mixed with some **V** was precipitated with hexane.

cis-$[Mn(CO)_2(PHPh_2)_4]ClO_4$ (**IV**)

To a solution of **III** (0.10 g, 0.13 mmol) and $PHPh_2$ (0.1 cm^3, 0.57 mmol) in acetone (12 cm^3), freshly sublimed $ONMe_3$ (0.01 g, 0.13 mmol) was added and the mixture was stirred at room temperature for 5 h. The volatiles were removed *in vacuo* and the residue was washed with diethylether. The resulting solid was recrystallized from CH_2Cl_2: Et_2O as pale yellow microcrystals (0.06 g, 49%).

trans-$[Mn(CO)_2(PHPh_2)_4]ClO_4$ (**VI**)

A mixture of **III** (0.16 g, 0.2 mmol) and $PHPh_2$ (0.8 cm^3, 4.6 mmol) in CH_2Cl_2 (10 cm^3) was irradiated at $-15°C$ until the IR of the solution no longer showed the $\nu(CO)$ absorptions of the starting material. The solution was concentrated to *ca.* 3 cm^3 and diethylether was added to give a pale yellow microcrystalline precipitate (0.1 g, 52%) that was recrystallized from CH_2Cl_2: Et_2O.

fac-$[Mn(CO)_3(\widehat{L\ L})(PHPh_2)]ClO_4$ (**VII**)

A solution of *fac*-$Mn(OClO_3)(CO)_3(dppe)$ (0.74 g, 1.16 mmol) and $PHPh_2$ (0.36 cm^3, 2.1 mmol) in CH_2Cl_2 (40 cm^3) was stirred for 7 h. The solvent was removed *in vacuo* and the residue was washed with ether. Recrystallization from CH_2Cl_2: Et_2O gave pale yellow microcrystalline **VIIb** (0.88 g, 92.5%).

The other *fac*-tricarbonyls **VII** were similarly prepared from the corresponding *fac*-$[Mn(OClO_3)(CO)_3(\widehat{L\ L})]$ with the following reaction times and yields: $\widehat{L\ L}$ = dppm, 48 h, 61%; $\widehat{L\ L}$ = bipy, 17 h, 60% (made in acetone); $\widehat{L\ L}$ = phen, 16 h, 64% (made in acetone).

fac-$[Mn(CO)_3(bipy)(PHPh_2)]PF_6$ (**VIIe**)

A mixture of *fac*-$[MnBr(CO)_3(bipy)]$ (0.3 g, 0.8 mmol), $PHPh_2$ (0.24 cm^3, 1.38 mmol) and $TlPF_6$ (0.4 g, 1.14 mmol) in CH_2Cl_2 (15 cm^3) was stirred for 5 h at room temperature and filtered through celite. Evaporation of the solvent *in vacuo* gave an oil that was washed several times with hexane. Recrystallization from CH_2Cl_2: Et_2O gave yellow–brown microcrystalline **VIIe** (0.49 g, 98%).

Isomerization of fac-$[Mn(CO)_3(\widehat{L\ L})(PHPh_2)]ClO_4$ ($\widehat{L\ L}$ = dppm *or* dppe)

The compound *fac*-$[Mn(CO)_3(dppm)(PHPh_2)]ClO_4$ (0.5 g, 0.62 mmol) was heated in refluxing *n*-butanol (25 cm^3) for 4.5 h and the mixture was cooled to room temperature. After concentrating (*in vacuo*) to half the volume, hexane was added and the yellow precipitate was washed with hexane to give 0.42 g of *mer*-$[Mn(CO)_3(dppm)(PHPh_2)]ClO_4$ mixed with some *cis*-$[Mn(CO)_2(dppm)_2]ClO_4$.

Similarly, the dppe compound gave a mixture of the corresponding *mer*-tricarbonyl and *trans*-$[Mn(CO)_2(dppe)_2]ClO_4$.

cis-trans-$[Mn(CO)_2(bipy)(PHPh_2)_2]PF_6$ (**VIII**)

A mixture of **VIIe** (0.10 g, 0.16 mmol) and $PHPh_2$ (0.05 cm^3, 0.29 mmol) in toluene (10 cm^3) was refluxed for 1 h and allowed to cool to room temperature. On standing an orange precipitate was formed that was recrystallized from CH_2Cl_2: Et_2O (0.10 g, 78%).

RESULTS AND DISCUSSION

Stirring a 1:1 molar mixture of $Mn(OClO_3)(CO)_5$ and $PHPh_2$ in CH_2Cl_2 at room temperature (i in Scheme 1) gave the cationic pentacarbonyl $[Mn(CO)_5(PHPh_2)]ClO_4$ (**I**), characterized by the data in Tables 1 and 2. This compound could be purified by precipitation with Et_2O from CH_2Cl_2 solutions under argon, but when a solution in CH_2Cl_2: EtOH (free or $PHPh_2$) was concentrated by heating at reduced pressure, it was almost quantitatively transformed into the previously known dimer $[Mn_2(CO)_8(\mu\text{-}PPh_2)_2]$[3] with concomitant formation of CO and $HClO_4$, as evidenced by the strong acidity of the mother liquor. This decomposition also occurred by heating the pure cationic pentacarbonyl **I** in ethanol and also in CH_2Cl_2 solutions in the presence of H_2O* or

* The IR spectrum of **I** in CH_2Cl_2 solution was better obtained using CaF_2 windows. On some occasions when NaCl windows were used, particularly in the presence of water vapour, the formation of the dimer was observed, probably favoured by the heat of the IR source.

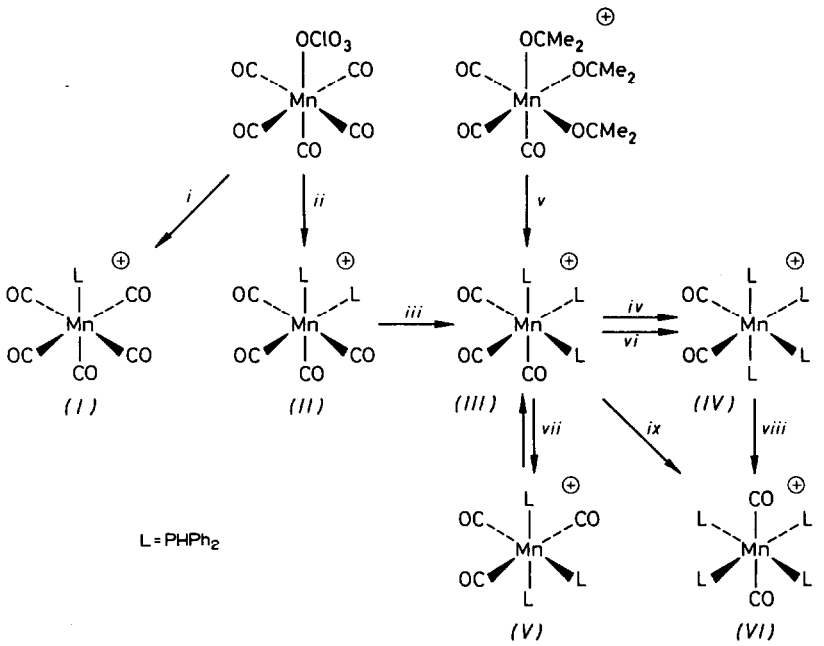

Scheme 1. Key to reagents and conditions. (i) $PHPh_2$ (1 : 1) in CH_2Cl_2 at room temperature, (ii), (iii) and (iv) $PHPh_2$ (excess) in refluxing ethanol, (v) $PHPh_2$ (3 : 1) in Me_2CO at room temperature, (vi) $PHPh_2$ (excess) and $ONMe_3$ in CH_2Cl_2 at room temperature, (vii) refluxing *n*-butanol, (viii) and (ix) in CH_2Cl_2 at $-15°C$ with U.V. irradiation.

Na_2CO_3, although in the latter case the dimer was formed along with another red unidentified product. These transformations are clearly favoured by the stability of the diphenylphosphido bridged species, and by the enhanced acidity of the $PHPh_2$ ligand coordinated to the $Mn(CO)_5^+$ fragment. On the other hand, **I** reacted very quickly with Bu^n_4NBr in refluxing CH_2Cl_2 to give the known tetracarbonyl *cis*-$[MnBr(CO)_4(PHPh_2)]$,[3] indicating that one CO is labilized in the cationic pentacarbonyl.

The reaction of the perchlorate complex $Mn(OClO_3)(CO)_5$ with a two- or three-fold excess of $PHPh_2$ in refluxing ethanol (ii in the scheme) gave the tetracarbonyl *cis*-$[Mn(CO)_4(PHPh_2)_2]ClO_4$ (**II**) as a crystalline precipitate. The ^1H NMR of this compound in $CDCl_3$ solution showed a pattern consistent with an AA′XX′ system similar to that described for the analogous neutral molybdenum complex $Mo(CO)_4(PHPh_2)_2$.[4] In Table 2 only the centre of the multiplet and the separation (in Hz) between the two more intense signals (the external ones) are given. The preparation of the tetracarbonyl **II** by reaction of $PHPh_2$ with $Mn(OClO)_3(CO)_5$ is similar to the result obtained with the ligand tetramethylthiourea (TMTU),[5] but contrasts with the observation that the reaction of the perchlorate complex with other monodentate ligands gives the tricabonyls *fac*-$[Mn(CO)_3L_3]ClO_4$, probably passing through the tetracarbonyls, although the latter are not detected by monitoring the reaction by IR.[1] In the reaction (ii in scheme) the *fac*-tricarbonyl *fac*-$[Mn(CO)_3(PHPh_2)_3]ClO_4$ (**III**) was also observed, but its formation from **II** (iii in Scheme) was slow in refluxing ethanol and on prolonged heating it was obtained together with some remaining **II** and the *cis*-dicarbonyl *cis*-$[Mn(CO)_2(PHPh_2)_4]ClO_4$ (**IV**). The latter compound could be prepared from the tricarbonyl **III** and excess of $PHPh_2$ in refluxing ethanol (iv in scheme) but only in poor yield because it had to be carefully crystallized out from the mixture before the reaction is completed otherwise some decomposition to an unidentified dicarbonyl begins.

The cationic tricarbonyl **III** could be conveniently obtained pure in good yield from $PHPh_2$ and *fac*-$[Mn(CO)_3(Me_2CO)_3]ClO_4$[1] in acetone (reaction v in the scheme). The dicarbonyl **IV** was easily prepared, also in good yield, by reacting **III** with $PHPh_2$ in CH_2Cl_2 in the presence of $ONMe_3$, (vi in scheme) a method often employed to promote CO substitution,[6] that in some cases has led to unexpected isomers.[7] Heating the *fac*-tricarbonyl **III** in refluxing *n*-butanol (viii in scheme) resulted in the formation of *mer*-$[Mn(CO)_3(PHPh_2)_3]ClO_4$ (**V**), as evidenced by the changes in the $\nu(CO)$ IR spectrum

Table 1. Melting point, conductivity, analytical and IR data for the compounds

Compound	M.p.[a] (°C)	Λ (Ω^{-1} cm^2 mol^{-1})[b]	Analysis [found (calc)%] C	H	N	IR (cm^{-1})[c] ν(CO)[d]
$[Mn(CO)_5(PHPh_2)]ClO_4$ (I)	80	120	42.8 (42.5)	2.46 (2.31)		2150m, 2102m, 2062s
cis-$[Mn(CO)_4(PHPh_2)_2]ClO_4$ (II)	186	136	52.7 (52.7)	3.46 (3.47)		2102m, 2037s, 2022s, 1999sh
fac-$[Mn(CO)_3(PHPh_2)_3]ClO_4$ (III)[e]	183	144	58.6 (58.8)	4.19 (4.14)		2038s, 1965s.br
cis-$[Mn(CO)_2(PHPh_2)_4]ClO_4$ (IV)	171	123	62.8 (62.9)	4.61 (4.61)		1964s, 1909s
trans-$[Mn(CO)_2(PHPh_2)_4]ClO_4$ (VI)	149	133	62.6 (62.9)	4.47 (4.61)		1916s[f]
fac-$[Mn(CO)_3(dppm)(PHPh_2)]ClO_4$ (VIIa)[g]	120	106	60.0 (59.4)	4.05 (4.11)		2030s, 1955s.br
fac-$[Mn(CO)_3(dppe)(PHPh_2)]ClO_4$ (VIIb)[h]	110	120	59.0 (59.8)	4.30 (4.29)		2033s, 1958s.br
fac-$[Mn(CO)_3(phen)(PHPh_2)]ClO_4$ (VIIc)	177[i]	132	53.0 (53.6)	3.09 (3.17)	4.49 (4.63)	2045s, 1970s, 1935s
fac-$[Mn(CO)_3(bipy)(PHPh_2)]ClO_4$ (VIId)	136[i]	140	50.7 (51.7)	3.19 (3.30)	4.67 (4.82)	2045s, 1972s, 1938s
fac-$[Mn(CO)_3(bipy)(PHPh_2)]PF_6$ (VIIe)	156[i]	125	47.3 (47.9)	3.28 (3.03)	4.15 (4.47)	2045s, 1972s, 1938s
cis-trans-$[Mn(CO)_2(bipy)(PHPh_2)_2]PF_6$ (VIII)	224	131	55.0 (55.1)	3.78 (3.82)	3.47 (3.57)	1952s, 1884s

[a] With decomposition.
[b] In 5×10^{-4} M acetone solution.
[c] In CH_2Cl_2 solution.
[d] The ν(PH) band could not be clearly observed. Ambiguities came because of the near coincidence with the CO_2 absorptions in this region.
[e] For the *mer* isomer ν(CO): 2040w, 1972s.br.
[f] ν(PH) at 2330 cm^{-1}.
[g] For the *mer* isomer ν(CO): 2050w, 1965s.br.
[h] For the *mer* isomer ν(CO): 2040w, 1960s.br.
[i] Before melting the colour changed from yellow to red.

[from two equally strong bands to one weaker than the other (Table 1)]. This process is similar to that observed in the case of many other cationic tricarbonyls with phosphorus ligands;[1] however, the isomerization could not be completed after prolonged heating and a mixture of the two isomers **III** and **V** was obtained. This suggests that at high temperatures, the equilibrium vii shown in the Scheme is established. The $^{31}P(^1H)$NMR spectrum of **III** featured a very broad signal even at −90°C centred at *ca.* 33 ppm with $\Delta\nu_{1/2} = 750$ Hz. (920 Hz at −60°C) while the spectrum of the mixture having more of the *mer*-isomer taken at −60°C, showed also a doublet centred at 43.6 ppm and a triplet centred at 26.1 ppm with intensity ratio 2:1 and with $^2J(P,P) = 39$ Hz. In the non-decoupled ^{31}P NMR spectrum the doublet centred at 43.7 ppm was split into two broad multiplets separated by *ca.* 360 Hz and the triplet was split into two broad multiplets separated by *ca.* 390 Hz. The ^1H NMR spectrum of **III** showed a complex multiplet centred at 6.43 ppm with a separation of 396 Hz between the two extreme and more intense peaks. In the ^1H NMR spectrum of the isomer mixture, two complex multiplets assignable to the *mer*-tricarbonyl were observed, one was centred at 6.35 ppm with a separation between the more intense peaks of 369 Hz but only half of the other multiplet (at 3.46 ppm) could be observed, the other half probably being hidden by the strong signal of the PPh_2 groups. All these features are consistent with the structures proposed for **III** and **V**.

The *cis*-dicarbonyl **IV** could be converted into the isomer *trans*-$[Mn(CO)_2(PHPh_2)_4]ClO_4$ (**VI**) by

Table 2. NMR data for the compounds

Compound	^{1}H NMR[a]	^{31}P{^{1}H} NMR[b]
I	7.53(413)	11(v.br.)[c]
II	7.41(417)	23
III	6.50(398)	33(v.br.)[d]
IV	6.80(370),[e] 5.89(350)[e]	53.4(2P, t, ^{1}J(PP) = 36, $PHPh_2$), 34.7(2P, t, ^{1}J(PP) = 36, $PHPh_2$)[f]
V	6.35(369), 5.63[g](390)	43.6(2P, d, ^{1}J(PP) = 39, $PHPh_2$), 26.1(1P, t, ^{1}J(PP) = 39, $PHPh_2$)
VI	6.46(382)	43.6
VIIb	[h]	66.6(2P, d, ^{1}J(PP) = 39, dppe), 33.1(1P, t, ^{1}J(PP) = 40, $PHPh_2$)
VIIe	[h]	39.9
VIII	6.23(351)[i]	54.4

[a] In $CDCl_3$ unless otherwise stated. Measured at room temp. in ppm with ref. to TMS. Only the centre of the multiplet corresponding to the $PHPh_2$ proton is quoted; in parentheses is given the separation between the two more intense peaks that corresponds closely to the ^{1}J(PH) coupling constant (in Hz).

[b] In CH_2Cl_2 solution measured at −60°C with reference to downfield of external 85% H_3PO_4 (in ppm). Coupling constants in Hz.

[c] $\Delta\nu_{1/2}$ *ca.* 1000 Hz.

[d] $\Delta\nu_{1/2}$ = 920 Hz.

[e] Pseudotriplet with peak separation of *ca.* 8 Hz.

[f] The spectrum is in fact a AA'BB' system, that has been measured directly from the spectrum as a first-order approximation.

[g] Estimated.

[h] Not observed because of the Ph protons.

[i] In d_6-acetone.

irradiating a CH_2Cl_2 solution with UV light at −15°C (viii in scheme), a reaction that resembles the UV promoted isomerization of the cationic dicarbonyl *cis*-$[Mn(CO)_2(dppm)_2]ClO_4$.[8] The spectroscopic data obtained for both isomeric dicarbonyls (Tables 1 and 2) were in accord with the structures proposed. The salt **VI** could be conveniently prepared directly from **III** and $PHPh_2$ under UV irradiation (ix in scheme).

Replacement of the coordinated $OClO_3$ ligand by $PHPh_2$ from the neutral complexes *fac*-$[Mn(OClO_3)(CO)_3(L\frown L)]$, gave the cationic carbonyls *fac*-$[Mn(CO)_3(L\frown L)(PHPh_2)]ClO_4$ [$L\frown L$ = dppm (**VIIa**), dppe (**VIIb**), phen (**VIIc**) or bipy (**VIId**)]. The analogous salt *fac*-$[Mn(CO)_3(bipy)(PHPh_2)]PF_6$ (**VIIe**) could be prepared directly from *fac*-$[MnBr(CO)_3(bipy)]$ and $PHPh_2$ in the presence of $TlPF_6$. Heating the *fac*-tricarbonyls containing the diphosphines resulted in the isomerization to the *mer*-tricarbonyls [ν(CO) IR: 2050 w, 1965 s.br (dppm) and 2040 w, 1960 s.br (dppe)]. This behaviour is similar to that observed for other cationic tricarbonyls with diphosphines,[9] however the *mer*-tricarbonyls with $PHPh_2$ were accompanied by the dicarbonyls *cis*-$[Mn(CO)_2(dppm)_2]ClO_4$ (in the case of the dppm complex) and *trans*-$[Mn(CO)_2(dppe)_2]ClO_4$ (in the dppe compound) and were not obtained pure.

By contrast, heating the *fac*-tricarbonyls with bipy or phen, resulted in decomposition giving the red dicarbonyls *cis-trans*-$[Mn(CO)_2(N\frown N)(PHPh_2)_2]ClO_4$ ($N\frown N$ = bipy or phen). This was confirmed by reacting the PF_6 salt **VIIe** with $PHPh_2$ in refluxing toluene that gave the complex *cis-trans*-$[Mn(CO)_2(bipy)(PHPh_2)_2]PF_6$ (**VIII**), characterized by the data in Tables 1 and 2 and that is analogous to other cationic *cis-trans* dicarbonyls with bipyridine or phenenthroline and two monodentate phosphorus ligands already known.[10]

Acknowledgement—We thank the Spanish C.A.I.C.Y.T. for financial support.

REFERENCES

1. R. Usón, V. Riera, J. Gimeno, M. Laguna and P. Gamasa, *J. Chem. Soc., Dalton Trans* 1979, 996.
2. P. J. Harris, S. A. R. Knox and F. G. A. Stone, *J. Chem. Soc., Dalton Trans* 1978, 1009.
3. P. M. Treichel, W. K. Dean and W. M. Douglas, *J. Organomet. Chem.* 1972, **42**, 145; R. G. Hayter, *J. Am. Chem. Soc.* 1964, **86**, 823.
4. J. G. Smith and D. T. Tompson, *J. Chem. Soc. A* 1967, 1694.
5. C. Carriedo, M. Sanchez, G. A. Carriedo, V. Riera,

X. Solans and M. L. Valin, *J. Organomet. Chem.* (in press).
6. J. A. S. Howell and P. M. Burkinshaw, *Chem. Rev.* 1983, **83**, 557.
7. F. J. García Alonso, V. Riera, F. Villafañe and N. Vivanco, *J. Organomet. Chem.* 1984, **276**, 39.
8. G. A. Carriedo, J. B. Parra-Soto, V. Riera, M. L. Valin, D. Moreiras and X. Solans, *J. Organomet. Chem.* (in press).
9. G. A. Carriedo and V. Riera, *J. Organomet. Chem.* 1981, **205**, 371.
10. R. Usón, V. Riera, J. Gimeno and M. Laguna, *Trans Met. Chem.* 1977, **2**, 123.

Polyhedron Vol. 6, No. 10, pp. 1885–1899, 1987
Printed in Great Britain

0277–5387/87 $3.00+.00

ADDUCTS OF COORDINATION COMPOUNDS—XIII.* NITRATES, HYDROGEN AND SILVER DINITRATES, AND POLYSILVER NITRATES OF *TRANS*-DIHALOTETRAKISPYRIDINERHODIUM(III) AND IRIDIUM(III) IONS

R. D. GILLARD† and S. H. MITCHELL‡

Department of Chemistry, University College, P.O. Box 78, Cardiff CF1 1XL, U.K.

(*Received* 14 *July* 1986; *accepted after revision* 5 *May* 1987)

Abstract—The synthesis and characterization, chiefly as salts of the anions $[X(ONO_2)_2]^-$ ($X = H^+$ or Ag^+) (by analysis, X-ray powder photography, vibrational spectra and thermogravimetry) of adducts of the nitrates *trans*-$[M(L)_4X_2](NO_3)$ (M = Rh or Ir; L = pyridine, perdeuteriopyridine or 4-methylpyridine; X = Cl or Br) with hydrogen nitrate and silver nitrate are described.

Salts (usually nitrates) with incorporated "extra" nitric acid or silver nitrate have been known for over a century. $CsNO_3 \cdot HNO_3$, described by Schultz[2] in 1862, was the first example of a hydrogen dinitrate salt,§ although unrecognized as such at the time.

Double salts containing silver nitrate have also been known for a long time. Silver halide–silver nitrate combinations, $nAgX \cdot AgNO_3$ (X = Cl or Br, n = 1; X = I, n = 1–4) are among the earliest described.[3] The double salts $CNO_3 \cdot AgNO_3$ ($C = K^+$ or NH_4^+) were first made[4] in 1877, but their structures have been determined[5] only recently.

In 1935, Poulenc reported[6] the synthesis of salts of the complex cation *trans*-$[Rhpy_4Br_2]^+$ containing "extra" nitric acid, silver nitrate and silver bromide; he formulated them as $[Rhpy_4Br_2]NO_3 \cdot HNO_3$, $[Rhpy_4Br_2Ag](NO_3)_2$ and $[Rhpy_4Br_2Ag]Br_2$. The nitric acid adduct and some analogues have received much attention. The existence of the hydrogen dinitrate anion was first recognized by Gillard and Ugo[7] in this compound. Our IR spectra indicated that the structure involved pairs of nitrate ions linked through oxygen atoms by symmetrical hydrogen bonds thus giving the hydrogen dinitrate anion.

trans-$[Rhpy_4Cl_2]^+$ has proved useful for isolating unusual species as stable adducts; besides its salts with $[H(ONO_2)_2]^-$, $(X_3)^-$ [X = Cl, Br or I], or Br_2Cl^- as gegen-ions, double salts with $(H_5O_2)^+$ have been described.[8] In contrast to the fairly well understood adducts of Brønsted acids, there are no published studies on the two argentous adducts of Poulenc since his original report, though Miss Davies confirmed[9] their existence.

The compounds known (from diffraction work) to contain hydrogen dinitrate anions are listed in Table 1. Two distinct conformations are known for the anion (**1** and **2**). The initial confusion

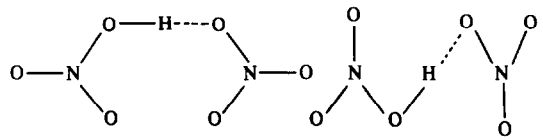

(1) **(2)**

for $CsH(ONO_2)_2$ and *trans*-$[Rhpy_4Cl_2]H(NO_3)_2$, where the two nitrate groups were said to form a distorted tetrahedron[14,15] around the proton, arose because, although the individual hydrogen dinitrate

* For part XII see ref. 1.

† Author to whom correspondence should be addressed.

‡ Present address: Department of Chemistry, University of Otago, Dunedin, New Zealand.

§ We name these compounds of $[H(\underline{O}NO_2)_2]^-$ as hydrogen dinitrates [on the pattern of "hydrogen difluoride" for $(HF_2)^-$]. By analogy, we call the ion $[Ag(\underline{O}NO_2)_2]^-$ silver dinitrate, though dinitratoargentate(I) would be more fully descriptive.

Table 1. Structures of hydrogen dinitrate salts

	Conformation	X-ray/neutron	Ref.
$CsH(NO_3)_2$	**1**	n	10
trans-$[Rhpy_4Cl_2]H(NO_3)_2$	**1**	n	11
trans-$[Rupy_4Cl_2]H(NO_3)_2$	**1**	X	12
$Ph_4AsH(NO_3)_2$	**2**	X	13

anions in those salts have the structure **1**, they occur disordered throughout the lattice.[10,11]

Oligonitric acid adducts have also been isolated and studied by infrared and Raman spectroscopy,[16–18] and one crystal structure has been determined,[19] that of $NH_4NO_3 \cdot 2HNO_3$.

Hydrogen dinitrate and oligonitric acid adducts are not confined to the solid or solution phases. A large number of such anions have been proposed[20–23] as components of the troposphere and stratosphere. Families of nitrate- and/or sulphate-containing species form the bulk of the ions "identified" (by mass spectrometry): $NO_3^-(HNO_3)_n$; $HSO_4^-(HNO_3)_n$; $HSO_4^-(H_2SO_4)_n$ ions (n = 1 and 2) are dominant[22] below about 27 km. The enthalpy, ΔH^0, of the dissociation, in the vapour phase,

$$NO_3^- \cdot HNO_3 \rightarrow NO_3^- + HNO_3 \qquad (1)$$

is given[23a] by Kebarle as > 26.4 kcal mol^{-1} (i.e. > 110.4 kJ mol^{-1}), an estimate relying on a value for

$$NO_3^- \cdot H_2O + HNO_3 \rightleftharpoons NO_3^- \cdot HNO_3 + H_2O \qquad (2)$$

in the vapour phase, of $\Delta G_{300} \geqslant -7.3$ kcal mol^{-1} (i.e. 30.5 kJ mol^{-1}).

EXPERIMENTAL

Source complex cations were prepared first as chloride salts of chloro-complexes using published methods,[24] with minor variations. Bromo-analogues were then prepared[24] from these:

$$trans\text{-}[RhL_4Cl_2]^+ \xrightarrow[\Delta,NaBr]{EtOH/H_2O} trans\text{-}[RhL_4Br_2]^+. \qquad (3)$$

Subsequently, all halide salts were converted into nitrate salts by metathesis. The following complexes were prepared: *trans*-$[Rhpy_4Cl_2]NO_3 \cdot 5H_2O$, *trans*-$[Rh(py\text{-}d5)_4Cl_2]NO_3 \cdot 5H_2O$, *trans*-$[Irpy_4Cl_2]NO_3 \cdot 5H_2O$, *trans*-$[Rh(4\text{-}pic)_4Cl_2]NO_3 \cdot 2H_2O$, *trans*-$[Ir(4\text{-}pic)_4Cl_2]NO_3 \cdot 2H_2O$, *trans*-$[Rh(4\text{-}pic)_4Br_2]NO_3 \cdot 2H_2O$. (4-pic = 4-methylpyridine).

Nitric acid adducts were prepared by heating the parent complex in concentrated nitric acid. Crystals, usually flakes, were produced on cooling: these were filtered off, washed with 8 M HNO_3, and air dried.

The silver nitrate salts were made by dissolving the parent nitrate salt in ethanol, and adding silver nitrate dissolved in a drop or two of water. Most solutions were then cooled to 0°C, and kept at that temperature for crystallization. The concentrations and ratios of reactants used are shown in Table 2. Usually from 0.5–2 cm^3 of solution were prepared for each experiment. The conditions were chosen with the following requirements in mind: (i) that the parent nitrate does not precipitate on addition of silver nitrate through the "common ion" effect, (ii) silver nitrate itself does not form and (iii) product formation occurs sufficiently rapidly that the

Table 2. Preparative details for silver nitrate adducts

Product	$M \times 10^{-3}$	Ag : Rh (Rh = 1)	Yield (%)	Formation
trans-$[Rhpy_4Cl_2]Ag(NO_3)_2$	9.9	2.5		rapid
trans-$[Rh(py\text{-}d5)_4Cl_2]Ag(NO_3)_2$	24	2.9	32.5	rapid
trans-$[Irpy_4Cl_2]Ag(NO_3)_2$	43	1.7	60.5	rapid
trans-$[Rh(4\text{-}pic)_4Cl_2]Ag(NO_3)_2$	26	3.1	—	overnight
trans-$[Rh(4\text{-}pic)_4Cl_2]NO_3 \cdot 3AgNO_3$	18	11.2	64.0	few hours
trans-$[Rh(4\text{-}pic)_4Br_2]Ag(NO_3)_2$	20	2.9	74.4	few hours
trans-$[Rh(4\text{-}pic)_4Br_2]NO_3 \cdot 4AgNO_3$	44	8.8	28.1	rapid[a]
trans-$[Ir(4\text{-}pic)_4Cl_2]NO_3 \cdot 3AgNO_3$	20	15.2	60.0	few hours

[a] Then more slowly forms the $3AgNO_3$ salt.

Table 3. Chemical and thermogravimetric analyses of parents and silver nitrate adducts

		C	H	N	M	H_2O
trans-$[Rhpy_4Cl_2]NO_3 \cdot 5H_2O$	found	37.5	4.6	10.9	16.1	13.9
	expected	37.4	4.7	10.9	16.0	14.0
trans-$[Rhpy_4Cl_2]Ag(NO_3]_2$	found	32.4	2.7	11.4	29.2	
	expected	33.3	2.8	11.6	29.2	
trans-$[Irpy_4Cl_2]Ag(NO_3)_2$	found	29.6	2.8	10.6	36.5	
	expected	29.6	2.5	10.4	37.0	
trans-$[Rh(4\text{-pic})_4Cl_2]NO_3 \cdot 1.7H_2O$	found	45.1	4.9	11.0	16.0	5.0
	expected	45.1	5.0	11.0	16.1	4.8
trans-$[Rh(4\text{-pic})_4Cl_2]Ag(NO_3)_2$	found				27.1	
	expected				27.1	
trans-$[R(4\text{-pic})_4Cl_2]NO_3 \cdot 3AgNO_3$	found	27.5	3.6	10.5	36.5	
	found	26.9	3.2	9.4	34.0	
	expected	25.8	2.5	10.0	38.1	
trans-$[Ir(4\text{-pic})_4Cl_2]NO_3 \cdot 2H_2O$	found	39.7	4.4	9.2	25.1	5.0
	expected	39.3	4.4	9.5	26.2	4.9
trans-$[Ir(4\text{-pic})_4Cl_2]NO_3 \cdot 3AgNO_3$	found	24.8	2.4	9.6	41.2	
	expected	23.9	2.3	9.3	42.7	
trans-$[Rh(4\text{-pic})_4Br_2]NO_3 \cdot 2H_2O$	found				14.1	4.5
	expected				14.0	4.9
trans-$[Rh(4\text{-pic})_4Br_2]Ag(NO_3)_2$	found	33.2	3.4	9.3	22.1	
	expected	33.2	3.3	9.7	24.3	
trans-$[Rh(4\text{-pic})_4Br_2]NO_3 \cdot 4AgNO_3$	found	19.6	2.5	8.5	37.6	
	expected	20.9	2.0	9.2	38.8	

silver ion does not abstract the halide from the complex. The same requirements, especially (iii), have so far prevented growth of single crystals large enough for X-ray work, though powder pictures for $[Mpy_4Cl_2][Ag(NO_3)_2]$ are good.

The pyridine complexes readily crystallize from solution as their silver dinitrate salts. For the 4-picoline complexes the usual procedure for formation of silver nitrate salts gave several products, depending on the concentration and ratio of factors.

Thermogravimetric and chemical analysis

Chemical analyses for carbon, hydrogen and nitrogen are consistent with compounds containing pyridine (or picoline) and nitrate. With metal analyses from the thermogravimetric runs, they enable the compositions to be calculated (Table 3).

The residue found from thermogravimetric runs could not always be relied on as an analytical result. There are several sources of error; (i) the residue was not entirely metallic: silver and rhodium oxides sometimes formed that could not be decomposed on prolonged heating at 900°C and (ii) sublimation of silver halide sometimes occurred before a metallic phase was reached. When these effects were gross they were readily observed, and the analysis rejected. There were only two instances of extensive sublimation, involving AgCl and AgBr. However, sublimation of trace amounts might have gone unnoticed, leading to under-estimation of silver content. The loss of silver from the residue is not unexpected because silver halides and nitrates melt at low temperatures[25] (Cl^-, 455; Br^-, 432; NO_3^-, 212°C). Silver analysis by atomic absorption gave unsatisfactory results. For all compounds, the silver contents found were much too low (when compared with the content deduced from the thermogram and CHN analysis) probably due to the formation in solution of AgX (X = Cl or Br).

Tables 3 and 4 give analytical details.

X-ray powder diffraction

X-ray powder diffraction patterns were recorded using a Guinier camera and CuK_α radiation (unfiltered). Exposure was from 2 to 5 h; α-Al_2O_3 was included as a reference. The data have been deposited as supplementary material.*

* The tabulated data on X-ray powder diffraction are available from the Editor on request.

Table 4. Thermogravimetric analysis for *trans*-$[ML_4X_2]H(NO_3)_2 \cdot nHNO_3$

M	L	X	"free" HNO_3 (%)	HNO_3 (n)	HNO_3 (%o)	HNO_3 (%c)	T[a] °C	Metal residue (%o)	Metal residue (%c)
Rh	py	Cl	29.1	4.0	~ 7.0	7.3	180	12.0	11.8
Ir	py	Cl	3.0	0.3	9.0	8.7	180	26.6	26.5
Rh	4-pic	Cl	13.4	1.6	~ 7.8	8.1	146	13.3	13.3
Ir	4-pic	Cl	9.2	1.2	7.7	7.5	160	22.6	22.9
Rh	4-pic	Br	0	0	~ 8.6	8.3	133	13.6	13.5
Rh	4-pic	Br	10.0	1.3	~ 7.6	7.5	146	12.0	12.2

[a] Decomposition temperature of $[H(NO_3)_2]^-$.

Infrared spectra

Mulls were prepared using Nujol, fluorolube, hexachlorobutadiene, acetone or carbon tetrachloride on caesium iodide plates. Attempts to prepare potassium bromide discs usually resulted in decomposition of the compounds, shown as a reversion to a pattern containing bands of free nitrate ion. Compounds containing an excess of nitric acid were dried by heating on a thermobalance to constant weight. An excess of nitric acid results in rapid decomposition and deterioration of the spectrum, extra bands appear and iodine forms. Similarly, with acetone mulls, there is fairly rapid decomposition, nitrate is liberated and extra unidentified bands appear.

Infrared spectra are illustrated in Figs 1–3, and tables of data have been deposited as supplementary data.* The figures are composites of spectra recorded in Nujol, acetone and CCl_4. No bands due to the mulling agent are present, except where indicated. Nujol-free spectra (estimated from acetone mulls) are shown in Figs 1 and 3.

RESULTS

IR spectra of the parent nitrate and halide salts were used as a basis for identifying bands of the nitric acid and silver nitrate adducts. The changes in the spectrum of pyridine on its coordination to metal ions are well documented, and most bands may be readily assigned.[26] Differences between compounds are chiefly confined to changes in the splitting pattern of the B_2 modes (ν23–ν27), which are particularly sensitive to the crystal environment. There are of course also differences in the region (below about 400 cm^{-1}) where the M—X/L bands occur (Table 5).

Nitrate hydrates

All the parent hydrated nitrate salts readily lose water to a drying atmosphere, either as the normal laboratory atmosphere or in a stream of nitrogen as used in the thermobalance. Consequently, samples were kept in a humidity chamber ($Na_2SO_4 \cdot 10H_2O$, RH 93% at 20°C) for at least 12 h prior to analysis. Also, when available, large crystals were used in preference to powders or small crystals. On heating, water loss is complete by 80°C, and if heating is stopped water will be reabsorbed, giving back the original hydrate. The pyridine complexes were all found to be pentahydrates, and the 4-picoline complexes dihydrates.

The main weight loss from the anhydrous material begins with a rapid loss of pyridine or 4-picoline from 226–280°C. This loss corresponds to between 2 and 3 mol of base per mol of metal. In general, loss of pyridine and 4-picoline occurs at a similar temperature for a given metal. Iridium complexes are more stable to heat than their rhodium analogues. The rate of subsequent losses (halide and remaining organic material) begins slowly, gradually increasing until a metal residue remains.

Table 5. Metal–halide and N-heterocycle infrared bands[a] in *trans*-$[ML_4X_2]NO_3 \cdot nH_2O$

Rh—Cl/py	Rh—Cl/py-d5	Ir—Cl/py
365s	355m	337m
311w	305w	261m
249m	242m	
Rh—Cl/4-pic	**Ir—Cl/4-pic**	**Rh—Br/4-pic**
396w	335w	none
349w	296m	above
282m		~ 240 cm^{-1}
266w		

[a] Raman band frequencies for some related compounds (e.g. *trans*-$[Rhpy_4Cl_2][H(\underline{O}NO_2)_2]$) are in Ref. 12.

* The tables of IR data are available from the Editor on request.

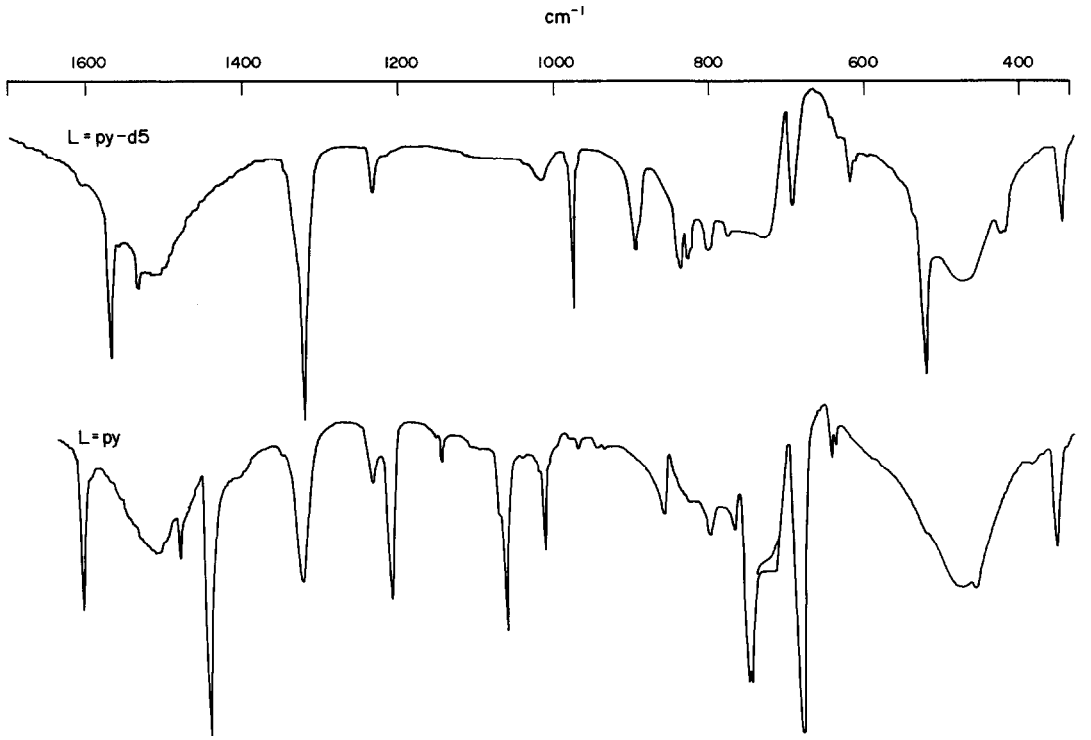

Fig. 1. Infrared spectra of *trans*-$[RhL_4Cl_2][H(ONO_2)_2]$; upper spectrum, $L = C_5D_5N$: lower spectrum, $L = C_5H_5N$. In this, and in both spectra of Fig. 3, in the region of 720 cm^{-1}, the lower curve of lesser absorption represents the Nujol-free spectrum.

Two phases of pyridine complex were identified by X-ray powder diffraction. *trans*-$[Rhpy_4Cl_2]NO_3 \cdot 5H_2O$ and *trans*-$[Irpy_4Cl_2]NO_3 \cdot 5H_2O$ crystallize as different phases, while both these phases were found for *trans*-$[Rh(py\text{-}d5)_4Cl_2]NO_3 \cdot 5H_2O$. The governing factors were not studied. However, in related work, we found that the chlorides *trans*-$[Mpy_4Cl_2]Cl \cdot 6H_2O$ (M = Ir or Rh) each crystallized from water in two forms. The crystal structure of the "low temperature form" for iridium is known.[27]

Nitric acid adducts

When prepared in concentrated nitric acid, most salts incorporated nitric acid in excess over that required for $H(NO_3)_2^-$. Apparently dry samples showed an initial loss of weight on heating from

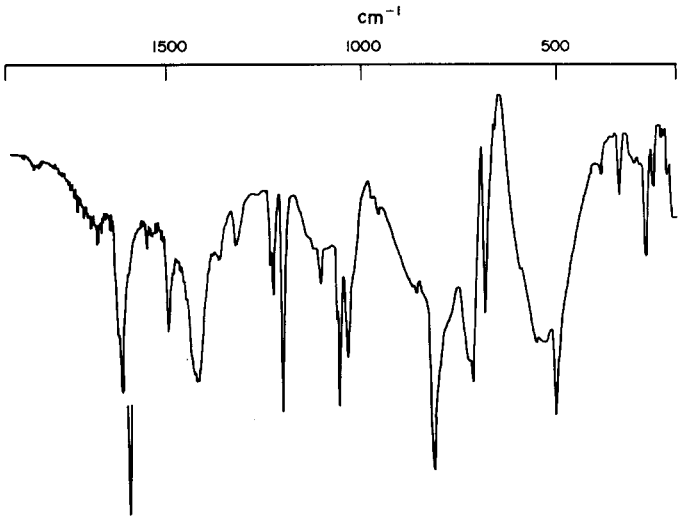

Fig. 2. Infrared spectrum (1900–200 cm^{-1}) of *trans*-$[Rh(4\text{-methylpyridine})_4Cl_2][H(ONO_2)_2]$.

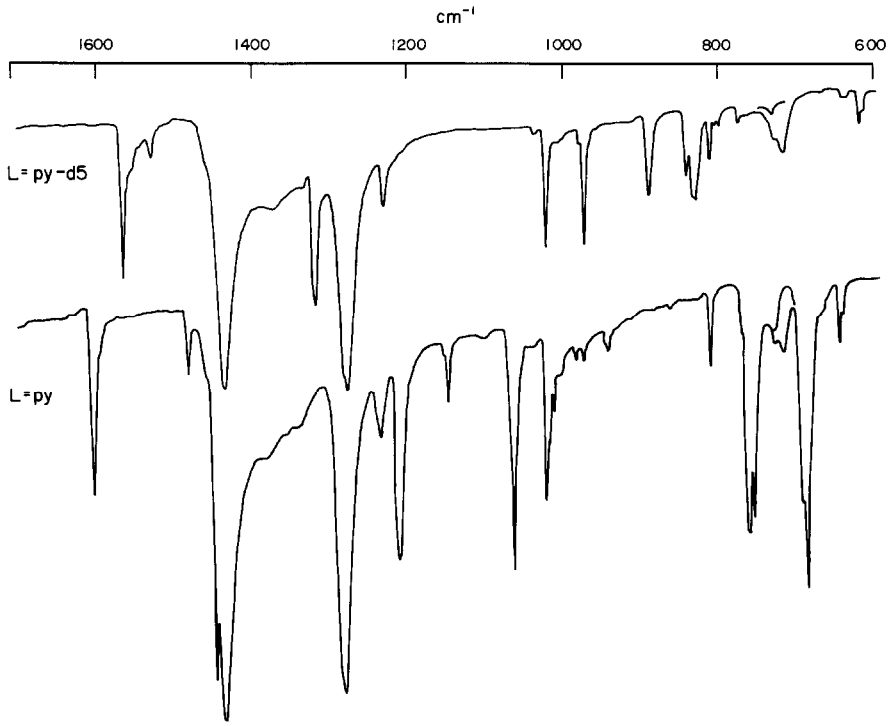

Fig. 3. Infrared spectrum (1700–600 cm^{-1}) of *trans*-$[RhL_4Cl_2][Ag(ONO_2)_2]$: upper spectrum, L = C_5D_5N; lower spectrum, L = C_5H_5N. (See note in caption of Fig. 1.)

room temperature. A stable stage is reached, the $H(NO_3)_2^-$ salt, which loses no more nitric acid until about 145°C. This loss may merge with decomposition of the complex unit, 250°C for Rhpy and 240°C for Rh(4-pic) (heating rate 5°C/min).

Diffraction lines of *trans*-$[Rhpy_4Cl_2]H(NO_3)_2$ are assigned to 2.913 Å (reflection 063). Assignments were made by comparison with line positions calculated from the known[11] orthorhombic cell of *trans*-$[Rhpy_4Cl_2]H(NO_3)_2$. There was good agreement between the observed and calculated patterns. The iridium analogue gives an almost indistinguishable pattern, indicative of a similar structure, and the pattern was similarly assigned (available from the Editor).

The three compounds *trans*-$[M(4\text{-pic})_4Cl_2]H(NO_3)_2$ (M = Rh, Ir) and *trans*-$[Rh(4\text{-pic})_4Br_2]H(NO_3)_2$ give almost identical powder diffraction patterns (available from the Editor), but since no crystallographic details are yet known, lines cannot be assigned. With non-dried samples, a few new lines are observed, which are probably due to the presence of oligonitric acid adducts.

Silver nitrate adducts

Pyridine complexes: as already noted, the complex cations *trans*-$[Mpy_4X_2]^+$ readily form silver dinitrate salts. In contrast to the picoline cases, no compounds with silver nitrate contents higher than one per complex unit were found.

The X-ray powder diffraction patterns of the hydrogen and silver dinitrate salts of *trans*-$[Mpy_4Cl_2]^+$ (M = Rh or Ir) are sufficiently similar in terms of line position and intensity that their structures may be considered isomorphous. Thus lines in the pattern of the silver dinitrate salts were assigned by analogy with the known line assignments of the hydrogen dinitrate salt. Using these lines, the unit cell dimensions were calculated by solving simultaneous equations for all possible combinations of these lines. This gave for *trans*-$[Mpy_4Cl_2]Ag(NO_3)_2$;

Rh $a = 7.71(5)$, $b = 21.55(12)$, $c = 14.97(24)$ Å

Ir $a = 7.72(3)$, $b = 21.57(23)$, $c = 15.05(10)$ Å

from which a powder pattern was calculated (Rh only) and the remaining lines assigned.

Thermograms of the silver nitrate adducts follow a pattern of decomposition similar to those of the anhydrous nitrates. The initial loss of pyridine occurs at a slightly lower temperature (190 vs 240°C). Decomposition of the silver nitrate merges with decomposition of the complex. A stage is

reached where the residue comprises of rhodium or iridium and silver metals: limited oxidation of the silver may occur soon after and on prolonged heating this returns to silver metal.

Silver dinitrate infrared bands were located in the same manner as hydrogen dinitrate bands. The spectrum is shown in Fig. 3 and a table of these bands has been deposited with the Editor.

Picoline complexes: There was considerable difficulty with the analysis of these compounds, because—in part—of their intractable nature, and (for some) rapid decomposition. The formulae given may not completely describe each compound: they are used chiefly to indicate separate compounds, and their probable composition. A compound is recognized by its X-ray powder diffraction pattern (tables deposited with Editor). No assignment of the diffraction lines was made because there are no data available for single crystals of these compounds.

Thermograms begin with an unexpected low temperature loss. The temperature of this loss is much lower than that of coordinated 4-picoline as found in the nitrate salts, and although ethanol or water is implicated in some compounds, this loss is probably premature loss of 4-picoline.

The formulations were arrived at by using %mol ratios in the following way. The only source of carbon is from 4-picoline and that provides the rhodium content, %Rh, all of which is found in the residue. The percentage of silver is derived from the difference total %M (residue) minus %Rh. The nitrogen content arises from 4-picoline and nitrate: the amount due to 4-picoline has been fixed by the carbon analysis and thus the difference, the nitrate content, may be apportioned first to that part neutralizing the single positive charge of the complex, and the remainder to silver. As a final check on the validity of the above scheme the figures for silver and nitrate(silver) should be the same.

The infrared bands arising from "nitrate" for all the complexes examined are collected in Table 6.

Table 6. Infrared "nitrate" bands of *trans*-[Rh(4-pic)$_4$X$_2$]NO$_3$·A

X =	Cl	Cl	Br	Cl
A =	$AgNO_3$	$AgNO_3$. solvate	$AgNO_3$. solvate	$3AgNO_3$
		3415w[a]	3430w[a]	
			1422w	
	[b]		1398s	1400s
		1362s	1370sh	1367s
	1285wsh	1285wsh		1314s
	1272m	1272m	1300s	1290s
	1022m	1024w		

[a] From solvent.
[b] The region 1400–1300 cm^{-1} was not studied.

Preparations based on trans-[Rh(4-pic)$_4$Cl$_2$]NO$_3$

At low mol ratio (1 complex : 3 $AgNO_3$) yellow crystals slowly form. These are the silver dinitrate salt. Raising the mol ratio to 1 : 11 gave fine golden yellow crystals of *trans*-[Rh(4-pic)$_4$Cl$_2$]NO$_3$·3AgNO$_3$.

trans-[Rh(4-pic)$_4$Cl$_2$]Ag(NO$_3$)$_2$. This preparation was done thrice. Crystals (a) were grown overnight at room temperature. A thermogram of the product begins with a steady (0.15%/C° heating rate 10°/min) weight loss from 133°C, that becomes very rapid at 215°C and culminates in a steady decomposition leaving metal residue (27.1%), the figure expected for *trans*-[Rh(4-pic)$_4$Cl$_2$]Ag(NO$_3$)$_2$. Its X-ray powder pattern and IR spectrum (which showed no bands of solvent) have been deposited with the Editor.

When crystals (b) from a second preparation (mol ratio 1 : 3.1, [Rh] = 2.62×10^{-2} M, grown at 0°C) were removed from solution they immediately went opaque. Their thermogram is the same as that of (a) above 145°C, but there is an early loss below 145°C: it begins at 55°C, and there are two distinct loss steps, of 2.9 and 3.5%. Crushing (b) released ethanol (smell) which may account for the loss of weight at low temperature. The IR spectrum has a weak band at 3375 cm^{-1} which might indicate ethanol or water. If ethanol is indeed present, then the thermogram indicates about 1 mol per formula unit. A diffraction pattern (of a sample which had been aged and crushed) shows a mixture of compounds; the pattern of (a), that of silver chloride, and lines not identified with any other salt. The strongest new lines occur at 10.28, 7.00, 4.91 and 4.13 Å.

Crystals (c) from the third preparation (mol ratio 1 : 4.5, [Rh] = 3.93×10^{-2} M) were like (b) in going opaque, but if quickly returned to the mother liquor, transparency returned. The diffraction pattern is extremely similar to that recorded from (a), and the infrared spectrum has a band at 3415 cm^{-1}, indicating that the compound contains a solvent.

The nitrate bands from this compound are recorded in Table 6. Unfortunately, decomposition occurs on the plates (CsI) and the bands at 1400–1300 cm^{-1} increase in intensity at the expense of the pair at 1300–1260 cm^{-1}.

trans-[Rh(4-pic)$_4$Cl$_2$]NO$_3$·3AgNO$_3$. This com-

pound was also prepared three times, and gave thermograms substantially identical in form. There is a minor loss (1.5–2.0%) as a distinct step, beginning at 90°C and accompanied by the formation of a brown tar and AgCl. The major loss begins at 175°C with no distinct stages, and a metal residue is produced (% obs: 32.1, 34.0 and 36.5). There was a considerable amount of sublimed AgCl in the furnace from the first of these. A table of IR spectra has been deposited with the Editor.

Preparations based on trans-$[Ir(4\text{-pic})_4Cl_2]NO_3$. The mol ratio 1 : 15.2 gave a product of *trans*-$[Ir(4\text{-pic})_4Cl_2]NO_3 \cdot 3AgNO_3$; the thermogram is similar to that of the analogous rhodium complex, with the initial minor loss beginning at 150°C. Infrared spectra and X-ray powder patterns are identical with those of the rhodium analogue.

Preparations based on trans-$[Rh(4\text{-pic})_4Br_2]NO_3$. The silver dinitrate salt was produced at low mol ratio (1 : 3) of factors. At high mol ratio (1 : 9) the product that forms first is a $4AgNO_3$ salt as orange–brown flakes; the $3AgNO_3$ salt crystallizes later.

trans-$[Rh(4\text{-pic})_4Br_2]Ag(NO_3)_2$. This formed during several hours as orange crystals, which behave like their chloro-analogue in that when removed from solution they go opaque. There is a weak band at 3430 cm^{-1} in the IR spectrum.

The thermogram begins with a low temperature (33°C) loss of variable duration, magnitude (5.8–11%), and form. It may be due in part to loss of ethanol but during this loss AgBr (X-ray powder picture) is formed. The subsequent losses follow the pattern already established for *trans*-$[Rh(4\text{-pic})_4Cl_2][Ag(NO_3)_2]$.

trans-$[Rh(4\text{-pic})_4Br_2]NO_3 \cdot 3AgNO_3$. This compound has the same X-ray powder diffraction pattern as that found for its rhodium and iridium chloro-analogues. While recording a thermogram, silver bromide sublimed into the furnace.

trans-$[Rh(4\text{-pic})_4Br_2]NO_3 \cdot 4AgNO_3$. This has a thermogravimetric pattern similar to that of the corresponding silver dinitrate salt, except that a much higher residue is finally obtained. The first slow loss begins at 38°C. There is a weak band at 3390 cm^{-1} which may indicate solvent (ethanol) in the lattice.

In each instance (except *trans*-$[Rh(4\text{-pic})_4X_2][Ag(NO_3)_2]$) where ethanol is thought to be present in the structure, its calculated content is small (less than 2%) and cannot itself account for all the low temperature loss seen in the thermograms. Its loss may however initiate decomposition. The easy decomposition of *trans*-$[Rh(4\text{-pic})_4X_2][Ag(NO_3)_2]$ (X = Cl or Br) shows that this first loss is related to changes in the coordination sphere.

DISCUSSION

Hydrogen dinitrate

The crystal structures of $CsH(NO_3)_2$ and of *trans*-$[Rhpy_4Cl_2]H(NO_3)_2$ contain hydrogen dinitrate anions with C_2 symmetry on C_2 sites: this corresponds to Speakman's class A hydrogen bonding.[28] In both structures, two hydrogen dinitrate anions occur disordered throughout the lattice.[10,11]

The anions have similar geometry. The O—H—O bonds are, as far as can be determined, symmetrical, the O...O distances are the same, and thus the strengths of the O—H bonds must be similar. The only major difference is in the dihedral angle between the places of the nitrate groups. With $CsH(NO_3)_2$ this angle is 75.4(4)°, and in *trans*-$[Rhpy_4Cl_2]H(NO_3)_2$ 96(3) and 91(4)°.

The O—H—O bonds between the nitrate groups are considerably bent: 167.5(14)° (Rh) and 172.6(7)° (Cs). This bending does not destroy the point group symmetry but may contribute to determining the band positions in the IR spectrum.

The X-ray study of *trans*-$[Rupy_4Cl_2][H(NO_3)_2]$ gives[12] the O...O distance for the hydrogen bond as 2.88 Å, much larger than expected for a strong hydrogen bond, or as indicated by the position given for the O—H stretch. Our present recalculation of this distance from the coordinates given indeed leads to the reported result. In the isomorphous rhodium complex, this distance is[10] 2.461(18) and 2.480(18) Å.

However, a large O...O distance was also found for the other hydrogen dinitrates before allowance is made for disorder of hydrogen dinitrate in their lattices.

The "C_{2h}" form of hydrogen dinitrate (**2**) found[13] in $Ph_4AsH(NO_3)_2$ may be considered as one extreme of the C_2 structure with a nitrate–nitrate dihedral angle of 180°. This gives it higher symmetry than C_2, and changes symmetry-related properties. However it occupies a site in the lattice with site symmetry ($\bar{1}$), which lowers its point group from C_{2h} (E, C_2, i, σ) to C_i (E, i): even so, the nitrate groups are coplanar.[13]

Infrared spectra. The symmetry of the hydrogen dinitrate anion is so different from that of nitrate that designations of molecular motion are not readily transferred. Treating it as a perturbed nitrate allows only the qualitative estimation of a few band positions and gives no indication where the many new modes will occur. In summary, the isolated hydrogen dinitrate anion has 21 vibrational degrees of freedom, which occur as the following species for the geometries of symmetry C_2, C_{2h} and C_i:

C_2: 11A, 10B—all IR and Raman active

C_{2h}: $7A_g$, $2B_g$—Raman active; $4A_u$, $8B_u$—IR active

C_i: $9A_g$—Raman active; $12A_u$—IR active.

Normal coordinate calculations have been done[29] for the geometries of hydrogen dinitrate found in $CsH(NO_3)_2$ and $Ph_4AsH(NO_3)_2$, assuming C_{2h} symmetry in the latter. The same set of derived force constants was used to calculate frequencies, but torsion modes, of which there are five, were not included in the analysis. Comparison between observed and calculated (fitted) spectra show good agreement for the Cs salt, but less so for Ph_4As as the gegen ion because just over half the bands were not located. One important result of the calculation is the indication of considerable mixing of hydrogen bond modes with nitrate modes.

Other authors have assigned bands using as a model a perturbed nitrate group with D_{3h}, C_{2v} or C_s symmetry.[7,12,30,31] Although the spectra appear simple, this simplified approach to assignment leaves problematic the location of modes involving the hydrogen bonds. In broad terms, the descriptions of some bands agree with those found from the normal coordinate analyses.

Nitrate and hydrogen dinitrate bands were located in our present work by comparison between spectra of the chloride, nitrate (hydrate and dehydrated), and hydrogen dinitrate salts of the pyridine, perdeuteropyridine, and 4-picoline complexes. Spectra are shown in Figs 1 and 2 and the data have been deposited with the Editor. In particular, the bands identified as arising from hydrogen dinitrate or from its influence are given in Tables 7 and 8.

The nitric acid adducts examined here divide into two groups according to their IR spectra; these are typified by *trans*-$[Mpy_4Cl_2]H(NO_3)_2$ and *trans*-$[M(4\text{-pic})_4X_2]H(NO_3)_2$.

trans-$[Mpy_4Cl_2]H(NO_3)_2$ (M = Rh *or* Ir; py = py *or* py-d5)

The spectrum of hydrogen dinitrate in *trans*-$[Rhpy_4Cl_2]H(NO_3)_2$ is[30] the same as in the dichlorocobalt(III) analogue (which is isomorphous[30] with

Table 7. Hydrogen dinitrate IR bands of *trans*-$[RhL_4Cl_2]H(NO_3)_2$

Description (follows Ref. 29)	Calc.[29]	py	py-d5
$\nu^a_{N=O}$, $\delta^a_{NO_2}$	1542	1510sbr	1509sbr
$\nu^{a'}_{N=O}$, $\delta^{a'}_{NO_2}$	1531		
δ'_{OHO}, δ_{NOH}	1419		
$\nu^{s'}_{N=O}$, $\delta^{s'}_{NO_2}$, ν'_{N-O}	1330	1326s	1330sh
$\nu^s_{N=O}$, $\delta^s_{NO_2}$, ν_{N-O}	1331		
δ^2_{OHO}, δ'_{NOH}, $\nu^{s'}_{N=O}$ ν'_{N-O}	1037		
			1018w
$\nu^s_{N=O}$, ν_{N-O}	1008		
$\nu^{s'}_{N=O}$, δ'_{NOH}	986		
window +		865m	
−			
window +			841m(+py-d^5)
−			836w
+			831m(+py-d^5)
γ_{NO_3}	801	805w	806w(+py-d^5)
γ'_{NO_3}	800		
window +		775w	
−		770w	
$\nu^a_{N=O}$, $\delta^a_{NO_2}$	743	728sbr	730sbr
$\nu^{a'}_{N=O}$, $\delta^{a'}_{NO_2}$	733		
$\nu^s_{N=O}$, $\delta^s_{NO_2}$, $\nu_{N=O}$	687	690(+py)	696m
$\nu^{s'}_{N=O}$, $\delta^{a'}_{NO_2}$, ν'_{N-O}	685		
ν'_{OHO}	619		
		600wsh	
		483sbr	481sbr
ν_{OHO}	213		

Table 8. Hydrogen dinitrate IR bands[a] of *trans*-[Rh(4-pic)$_4$Cl$_2$]H(NO$_3$)$_2$

δ'_{OHO} δ'_{NOH}	1683mbr
	1428m[b]
$\nu^{s}_{N=O}$ $\delta^{s}_{NO_2}$ ν_{N-O}	1326w[b]
	1115wbr
ν_{NO_3}	810sbr
$\nu^{a}_{N=O}$ $\delta^{a}_{NO_2}$	730m
$\nu^{s}_{N=O}$ $\delta^{s}_{NO_2}$ ν_{N-O}	691m
	615wsh
	535sbr
	315wbr[b]

[a] Tentative assignments, based[29] on C_{2h} symmetry.
[b] Of dubious validity as hydrogen dinitrate bands.

the *bromo*-complex *trans*[Rhpy$_4$Br$_2$][H(ONO$_2$)$_2$]) but simpler than in CsH(NO$_3$)$_2$: it is however complicated by ligand modes. The pattern calculated for CsH(NO$_3$)$_2$ may serve as a model for assigning the modes of *trans*-[Rhpy$_4$Cl$_2$]H(NO$_3$)$_2$, although the differences in structure must modify the pattern especially in respect of torsion modes. Hydrogen dinitrate bands from *trans*-[RhL$_4$Cl$_2$]H(NO$_3$)$_2$ (L = py, py-d5) are given in Table 7.

The spectrum (*Fig. 1*). 1800–900 cm^{-1}: In this region there are three bands. Modes ν_1 and ν_2, and ν_3 and ν_4 (see Table 7 for descriptions, following Ref. (29) are well separated ($\Delta \sim 180$ cm^{-1}), but neither shows the further splitting found for CsH(NO$_3$)$_2$, the extent of which was said[30] to be dependent on the nitrate–nitrate torsion angle. The third band (1018 cm^{-1}) might be ν_6, ν_7 or both; whichever is the case, it is of symmetric components $\nu_{N=O}$ and ν_{N-O}. This region contains a group of bands reported[7,12,31] as belonging to the hydrogen dinitrate anion (1000–945 cm^{-1}). They are here identified as pyridine bands, since they also crop up in the spectra of *trans*-[Mpy$_4$Cl$_2$]Cl and[26] *mer*-[Mpy$_3$Cl$_3$] (M = Rh or Ir).

900–600 cm^{-1}: This region is difficult to interpret because Evans windows and ligand bands are superimposed on anion band(s). There are hydrogen dinitrate bands at 806, 728 and 696 cm^{-1}. The broad structure between $\sim$ 850 and 710 cm^{-1} may contain several broad bands (e.g. ν_9 and ν_{10}) or be the high frequency wing of a very asymmetric band peaking at 730 cm^{-1}.

The ν_{OHO} band has been placed here but calculations indicate a lower frequency. Discussion of its location follows.

600–300 cm^{-1}: There are two bands in this region. One at $\sim$ 482 cm^{-1} is strong and roughly symmetrical while the other is a weak shoulder at higher energy ($\sim$ 600 cm^{-1}).

trans-[M(4-pic)$_4$X$_2$]H(NO$_3$)$_2$ (M = Rh, X = Cl *or* Br; M = Ir, X = Cl)

The spectra from the three compounds in this second isomorphous group are essentially identical, except for the expected differences in the M—X/M—L stretching region, which are the same as found in the parent nitrate salts. Thus comments and descriptions are made only on the spectrum of *trans*-[Rh(4-pic)$_4$Cl$_2$]H(NO$_3$)$_2$ (Fig. 2). They apply, *mutatis mutandis*, to the others.

This spectrum is not complicated by Evans windows, but unfortunately a number of 4-picoline and hydrogen dinitrate bands coincide: probable values for the latter are given in Table 8 (with caveats).

The spectrum (*Fig. 2*). 1800–1000 cm^{-1}: There are two broad bands in this region, and another two that are possibly hydrogen dinitrate bands. The moderately strong picoline band at $\sim$ 1430 cm^{-1}, of irregular shape in the chloride and nitrate salts, is broader and more regular in the hydrogen dinitrate salt. This may indicate the presence of an underlying hydrogen dinitrate band. The 1334 cm^{-1} picoline band (identified from Cl$^-$ salt) changes slightly, becoming broader and in some mulls appearing as a doublet: its structure may be due either to genuine splitting or to superposition of a weak hydrogen dinitrate mode on a picoline band.

1000–200 cm^{-1}: This region is in many respects similar to that of the pyridine analogue, but without the complicating Evans windows. There are six bands. The only band of dubious nature is at $\sim$ 315 cm^{-1} (weak and broad). It is not present in chloride or nitrate salts or the dibromo-rhodium hydrogen dinitrate analogue.

Acetone mulls of the complex deteriorate rapidly (minutes). Only the limited range 900–400 cm^{-1} was examined. The bands at $\sim$ 810 and 535 cm^{-1} rapidly disappear to reveal weak bands at 860 and 618 cm^{-1}, while the medium bands at 730 and 691 cm^{-1} are weakened.

The hydrogen bond

If a hydrogen bond is considered to be the interaction of a base and a proton donor as in —O—H...O then as the hydrogen bond strength increases the O—H bond is weakened, and becomes longer. Thus the O—H stretching mode shifts to lower wavenumber, becomes asymmetric and broadens considerably.[28,32] Eventually, with the proton midway between the oxygen atoms, there is no distinction between O—H and H...O stretching modes.

Recently there has been detailed discussion[33–35] of infrared band shaping mechanisms, applied to

hydrogen stretching modes in particular. Although, strictly speaking this is restricted to non-crystalline phases, we adopt it here. The main band-shaping mechanism is anharmonic coupling with external modes, responsible[35] for the asymmetry and large band width. The broadened band can have a smooth profile or have many sub-bands. The sub-bands arise from Fermi coupling with low frequency fundamentals or combination bands, shown as regions of enhanced transmission, with "ABC" type structures[36] or Evans windows.[37] Recent theory suggests that rather than continuing to broaden as the hydrogen bond gets stronger (i.e. very strong) the band becomes narrower and symmetrical.[35]

Evans windows are regions of enhanced transmission observed on broad bands. Evans showed[38] that they may be accounted for by Fermi coupling of a vibration capable of adopting many energy states with a sharply peaked transition of similar energy. The result of the interaction is to produce the broad-band regions of enhanced and decreased transmission connected by a sharp change of intensity, or, if the band maxima coincide—a symmetrical window. The effect is seen at 856–865 and 775–770 cm^{-1} in the spectrum of the pyridine complex and at about 836 cm^{-1} in the deuteropyridine complex.

In the particular cases of *trans*-$[Rhpy_4Cl_2][H(NO_3)_2]$, $Cs[H(NO_3)_2]$ and $[Ph_4As][H(NO_3)_2]$, the hydrogen bonds are very short ($O\ldots O < 2.5$ Å) and must be considered as being very strong. In each of these compounds, one nitrate half of the anion is related to the other by lattice symmetry. This would indicate possible class A hydrogen bonding in Speakman's classification.

Strictly, such class A hydrogen bonding would require[28] that the proton lie on a centre or along a two-fold proper or improper rotation axis. This would seem likely in the present compounds and would give equivalent O—H bonds. However, this may represent only the average situation, because it is not possible[39] even by neutron diffraction to distinguish between a proton occupying a single minimum potential well, or a symmetric double minimum well where the minima are less than 0.1 Å apart.

There is a third possibility, unlikely in the present case because the nitrate groups are symmetry related, that the proton occupies an asymmetric double minimum potential well, which is disordered throughout the lattice giving apparently a symmetric double minimum well.

The $\nu_{O—H}$ mode in *trans*-$[Rhpy_4Cl_2][H(NO_3)_2]$ might be expected at similar energy to that in $CsH(NO_3)_2$ (observed[30] at ~ 600 cm^{-1}) in view of the similarity of structure. The differences, in particular the nitrate–nitrate torsion angle and O—H—O bend, are unlikely of themselves to determine to any great extent the position of the $\nu_{O—H}$ mode.

The accepted position for the O—H stretching mode of *trans*-$[Rhpy_4Cl_2][H(NO_3)_2]$ and analogous compounds is[12] the broad feature between 850–700 cm^{-1}, peaking at 785–750 cm^{-1}. Its position may be estimated from the figure of Novak,[32] in which the O—H stretching frequencies for a number of compounds are plotted against $r_{O—H}$. Given $r_{O—H} = 1.23$ Å, a frequency of 690 cm^{-1} is indicated for $\nu_{O—H}$. This is lower than the accepted position. Calculation of its position in $CsH(NO_3)_2$ and $Ph_4AsH(NO_3)_2$ indicates still lower stretching frequencies, 619 and 621 cm^{-1} respectively, while inelastic neutron scattering experiments on $CsH(NO_3)_2$ point[40] to an even lower frequency (450(30) cm^{-1}). This latter technique is particularly sensitive to proton motion and so should give a reasonable indication of the stretching frequency.

Thus one of the two bands found below 700 cm^{-1} might not be a torsion mode but instead the O—H stretching mode, while the broad feature above 700 cm^{-1} is—at least in part—the nitrate bending mode γNO_3 which is expected in this region.

There is a good deal of similarity between the IR spectra of *trans*-$[Rhpy_4Cl_2]H(NO_3)_2$ and $CsH(NO_3)_2$. It may be a little unreasonable to expect exact correspondence between bands of the two series in view of the differences in structure of the anion and lattice. The crystal environment must be important in determining the exact geometry of the anion.

The analogous 4-picoline hydrogen dinitrate salts are new. Their IR spectra indicate that they have a different structure for the hydrogen dinitrate moiety from that in *trans*-$[Rhpy_4Cl_2]H(NO_3)_2$. However the pattern does have features similar to those of $Ph_4AsH(NO_3)_2$, $CsH(NO_3)_2$ and *trans*-$[Rhpy_4Cl_2]H(NO_3)_2$.

All these nitric acid adducts give similar spectra over the region 1000–400 cm^{-1}, indicating some similarity of structure. Since this region contains the O—H stretching mode, *trans*-$[Rh(4\text{-pic})_4X_2]H(NO_3)_2$ must be like the others in having a short and probably symmetrical hydrogen bond.

Between 1800 and 1000 cm^{-1}, its pattern is most closely similar to that of $Ph_4AsH(NO_3)_2$. The modes $\nu^a_{(N=O)}$ and $\nu^s_{(N=O)}$ should aid assignment of its stereochemistry. If $\nu^a_{(NO)}$ is at ~ 1430 cm^{-1} and $\nu^s_{(NO)}$ is absent, then the hydrogen dinitrate species contains a centre of symmetry. The band at 1683 cm^{-1} has an analogue in $[Ph_4As][H(NO_3)_2]$; this was first assigned[31] as ν^a_{NO} at 1670 cm^{-1}, later as[30]

$\nu^{s}_{NO_2}$ at 1705 cm^{-1} and finally re-assigned[29] as bending modes δ_{OHO} and ε_{NOH}, these last calculated to be at least 1688 cm^{-1}. However, the vibrational assignments are still insecure because over half the 27 fundamental modes of the anion in $[Ph_4As][H(ONO_2)_2]$ have not been observed.

Silver nitrate adducts

There are quite a few reports of double compounds or adducts containing silver nitrate. Table 9 lists some of them.

The silver halide–silver nitrate double salts all have structures[41-45] in which silver is coordinated irregularly by halide, and mono and bidentate nitrate ions. Some nitrate is also present as a counter ion. These compounds include some "inverse complexes".

$HgI_2 \cdot 2AgNO_3 \cdot H_2O$ has a polymeric structure, the silver ions alternating with mercury in a chain linked by iodide ions; nitrate acts only as a counter ion. The structures of $[Ag(bipy)_2](NO_3)_2 \cdot AgNO_3 \cdot HNO_3$ and $Ag[Ni(acac)_3] \cdot AgNO_3$ are not known, but the latter compound probably has a structure similar to that of $Ag[Ni(acac)_3] \cdot 2AgNO_3 \cdot H_2O$. There, the silver ions are bonded to the "active methylene" carbons and oxygen atoms of the acetylacetonate (2,4-pentanedionate) ligands. Of the three unique silver ions, one binds intermolecularly, while the others bind intramolecularly and are also coordinated to nitrate. The coordination geometry is approximately tetrahedral about each silver.

$CAg(NO_3)_2$ ($C = K^+$, NH_4^+ or Rb^+) are the only compounds of those in Table 9 where the sole ligand available is nitrate. Its structure is composed of $_{\infty}^{1}[Ag_2(NO_3)_4]^{2-}$ chains. Bridging monodentate nitrate and silver ions form a spiral parallel to *b*, and bridging bidentate nitrates link together every other silver. We made $KAg(NO_3)_2$ to examine nitrate bands in its IR spectrum. The data on its preparation, X-ray powder pattern and IR spectrum have been deposited.

Table 9. Adducts of silver nitrate

$AgCl \cdot AgNO_3$	Ag_2ClNO_3	41, 42
$AgBr \cdot AgNO_3$	Ag_2BrNO_3	43
$AgI \cdot AgNO_3$	Ag_2INO_3	44
$AgI \cdot 2AgNO_3$	$Ag_3I(NO_3)_2$	45
$CNO_3 \cdot AgNO_3$	$CAg(NO_3)_2$ ($C = K^+$, NH_4^+ or Rb^+)	5
$HgI_2 \cdot 2AgNO_3 \cdot H_2O$	$HgAgI_2(NO_3)_2 \cdot H_2O$	46
$[Ag(bipy)_2](NO_3)_2 \cdot AgNO_3 \cdot HNO_3$		47
$Ag[Ni(acac)_3] \cdot 2AgNO_3 \cdot H_2O$		48, 49
$Ag[Ni(acac)_3] \cdot AgNO_3$		49

The only other compound that might have a structure with discrete silver-containing anions analogous to silver dinitrate (itself, of course, like other $[AgX_2]^-$, where $X^- = Cl^-$ or Br^-) is[50] $[Ag(NH_3)_2][Ag(NO_2)_2]$. However, that structure contains linear diamminosilver ions, and an $Ag—NO_2$ framework in which one silver ion is coordinated by four nitrite ions to give a distorted tetrahedron.

Given that the monomeric anion silver dinitrate does exist in the solid state, then it follows that it must also exist at some concentration in solution. Its known salts are "insoluble" and so its concentration need not be large.

There have been many studies on the species present in solutions or melts containing silver nitrate. Chief and most useful among these are the Raman spectroscopic studies. In aqueous solution a number of species have been established.[51-53] They have been resolved from each other by fitting curves to the observed bands arising from nitrate. The species proposed and their relationship are described by eqn 4:

$$Ag^{+}_{(aq)} + NO^{-}_{3(aq)} = (Ag \cdot H_2O \cdot NO_3)^{0}_{(aq)} = (Ag \cdot NO_3)^{0}_{(aq)} = (Ag \cdot nNO_3)^{(n-1)-}_{(aq)} \quad (4)$$

No bands due to vibration of Ag—O were identified in the Raman spectrum, and at high concentration (> 6 M), the last species has been described[53] as a "second inner-sphere complex".

Silver dinitrate has not been thought to be a participant species in concentrated solutions of silver nitrate, but might actually be one of the inner sphere complexes described. Its symmetry might well be such that there is only one Raman active Ag—O stretching mode, and this at a frequency as yet unidentified.

The situation is much the same in melts of $AgNO_3$ or $AgNO_3$–alkali metal nitrates. There is[54] preferential association of silver and nitrate ions, more along the lines of a salt-like structure in which Ag^+ ions occupy holes in a lattice of nitrate ions, rather than specific coordination of silver by nitrate.

There have been no studies on the species present in solutions of silver nitrate in ethanol or ethanol–water mixtures. But it must be that as the concentration of silver and nitrate ions increase, they associate to a greater extent. Because ethanol's dielectric constant is lower than that of water, an ethanol–water mixture would be expected to favour a higher concentration of associated species including silver dinitrate.

The isomorphism of the silver and hydrogen dini-

trate salts of *trans*-$[Rhpy_4Cl_2]^+$ indicates that they may have similar structures in respect of the anion, namely monomeric C_2 (**1**). One factor controlling the size of the unit cell is the volume occupied by the anion. Replacing a proton (with OHO *ca* 2.5 Å) by silver (OAgO *ca* 4.8 Å) might—by increasing the size of the anion—be expected to produce a significantly larger unit cell. However, the hydrogen dinitrate anions do occupy a larger volume, through disorder, than they would in an ordered arrangement, and if the silver dinitrate anions are ordered then the difference in cell dimensions might not be so large.

Assuming a linear sequence O—X—O in the dinitrate ions, then for X = H the O...O distance is known[11] at 2.5 Å, and given a Ag—O(nitrate) distance[5] of 2.4 Å (the smallest of several) then the O...O distance is 4.8 Å, nearly twice that of hydrogen dinitrate. The O...O line lies parallel to the *ac* plane and so expansion would not affect the *b* axis. For *trans*-$[Rhpy_4Cl_2]X(NO_3)_2$ (X = H and Ag) expansion is 0.18 Å in *a* and 0.25 Å in *c*, as against X = H, but there is contraction by 0.17 Å in *b* from X = H to X = Ag.

The isomorphous series found are indicated in Table 10.

Most of these relationships are not too unexpected, particularly when the only difference is at the metal centre. What is surprising is that the 4-picoline silver dinitrate complexes do not form an isomorphous group. Perhaps they are (like so many coordination compounds) polymorphic, and it happens that different phases have been produced; the nitrate infrared bands do indicate that the structures of the anions may differ.

Table 10. Isomorphous relationships

trans-$[Rh(py\text{-}d5)_4Cl_2]NO_3 \cdot 5H_2O$[a]
trans-$[Irpy_4Cl_2]NO_3 \cdot 5H_2O$
trans-$[Rhpy_4Cl_2]NO_3 \cdot 5H_2O$
trans-$[Rh(py\text{-}d5)_4Cl_2]NO_3 \cdot 5H_2O$[b]
trans-$[Rhpy_4Cl_2]H(NO_3)_2$
trans-$[Irpy_4Cl_2]H(NO_3)_2$
trans-$[Rhpy_4Cl_2]Ag(NO_3)_2$
trans-$[Irpy_4Cl_2]Ag(NO_3)_2$
trans-$[Rh(4\text{-}pic)_4Cl_2]NO_3 \cdot 2H_2O$
trans-$[Ir(4\text{-}pic)_4Cl_2]NO_3 \cdot 2H_2O$
trans-$[Rh(4\text{-}pic)_4Br_2]NO_3 \cdot 2H_2O$
trans-$[Rh(4\text{-}pic)_4Cl_2]H(NO_3)_2$
trans-$[Ir(4\text{-}pic)_4Cl_2]H(NO_3)_2$
trans-$[Rh(4\text{-}pic)_4Br_2]H(NO_3)_2$
trans-$[Rh(4\text{-}pic)_4Cl_2]NO_3 \cdot 3AgNO_3$
trans-$[Ir(4\text{-}pic)_4Cl_2]NO_3 \cdot 3AgNO_3$
trans-$[Rh(4\text{-}pic)_4Br_2]NO_3 \cdot 3AgNO_3$

[a] This compound exists in two phases.
[b] The second phase.

The infrared spectrum of silver dinitrate (see Fig. 3) in *trans*-$[Rhpy_4Cl_2]Ag(NO_3)_2$ is, not unexpectedly, quite different from that of free nitrate, being more akin to hydrogen dinitrate but with fewer bands.

A nitrate group with D_{3h} symmetry has four vibrational modes, three of which are IR active. Coordinating a single nitrate group lowers its symmetry from D_{3h} to C_{2v} or C_s species. This means that there are (at least potentially) six active bands and additionally an X—ONO_2 mode.[55-57] The coordination modes of nitrato-groups have been reviewed by Addison and his colleagues[56] and Rosenthal.[57] However, no features of the spectra were found to be sufficiently reliable to distinguish consistently between them. With two nitrate groups coordinated to the same centre, the situation is exacerbated because the variety of species and number of vibrations is greater. However, some indication of the structure and geometry of $Ag(NO_3)_2^-$ can be obtained from its spectrum.

First, the nitrate bands derived from $\nu_3(E')$ are narrow with half-widths of 30 cm^{-1} at 1439 cm^{-1} and 20 cm^{-1} ar 1279 cm^{-1}. In contrast, broad bands are found in the spectra of $AgNO_3$ and $KAg(NO_3)_2$, the half-widths being 65 cm^{-1} at 1386 cm^{-1}, and 395 cm^{-1} over the three $\nu_{N=O}$ bands, respectively. Each nitrate in these structures[5,58,59] binds together two or three silver atoms into chains. The lengths of the Ag—O bonds are between 2.37 and 2.70 Å. The narrow bands we find for the present anion indicate that it does not have a chain structure but is probably monomeric. The broad bands of hydrogen dinitrate are either hydrogen bond modes or out of plane deformation modes of nitrate; its nitrate stretching modes are comparatively narrow.

Secondly, the ν_3 mode of free nitrate is split [see Table 11] into two components, at 1438 and 1281 cm^{-1}. Thus the symmetry of the nitrate in the silver dinitrates is lower than D_{3h} namely C_s or C_{2v}.

Thirdly the band at 1281 cm^{-1} is further split. If this results from nitrate–nitrate coupling across silver, then the molecule cannot contain a centre (otherwise coupling would give rise to two bands, one IR active and the other Raman active only).

There are no bands found above 230 cm^{-1} that can be associated with Ag—O stretching modes.

All this, and isomorphism with *trans*-$[Rhpy_4Cl_2]H(NO_3)_2$ tend to confirm that the silver dinitrate anion has the same structure as hydrogen dinitrate.

The case of the 4-picoline complexes is more

Table 11. Infrared bands due to silver dinitrate in *trans*-$[RhL_4Cl_2]Ag(NO_3)_2$

L =	py	py-d5
$\nu_{N=O}$	1438s	1439s
$\nu_{N=O}$	1281s[a]	1279s[a]
ν_{N-O}	1024m	1027m
ν_{NO_3}	816w	817w
δ_{NO_2}	733w	733w

[a] Doublet.

difficult to resolve. The table of IR bands has been deposited with the Editor. Unfortunately bands from 4-picoline occur where some of the nitrate bands would be expected. Further it is not known to what extent loss of solvent changed the spectrum of those compounds.

In each compound except *trans*-$[Rh(4\text{-pic})_4Cl_2]NO_3 \cdot 4AgNO_3$, for which no spectrum was recorded, the ν_3 mode of nitrate is split into ν_s and ν_{as} components by 70–81 cm^{-1}, and its band width is increased over that of *trans*-$[Rhpy_4Cl_2]Ag(NO_3)_2$. The two monosilver nitrate salts each have one component of the split ν_3 band further split, but these splittings are on different components. These salts may require solvent (in the lattice, on a ligand, or even coordinated to the silver) to maintain their structure.

The splitting pattern of all these 4-picoline complexes is similar in form to that of *trans*-$[Rhpy_4Cl_2]Ag(NO_3)_2$, and so similar constraints must apply to the symmetry of the nitrate. The structures, however, of the $[Ag(ONO_2)_2]^-$ moieties must all be quite different from that in the pyridine complex because the primary splitting of ν_3 is by comparison quite small, while the secondary splitting (coupling between the two nitrate units linked to silver) is quite large.

Coordination of silver to halide (to give a silver halide molecule as ligand) as Poulenc envisaged[6] is unlikely for these compounds because the Rh—X/L band system remains unchanged from that of the nitrate salt. However, there are a number of facts which should encourage the search for intact silver halide molecules as ligands.

(i) Halide (X) bridges are increasingly common; (where say M = W^{III})

$$(M—X—M)^{(n-1)+}.$$

The structures of solid silver halides contain the elements

$$(Ag—X—Ag)^+$$

so that the "average" situation

$$(M—X—Ag)^{n+}$$

is to be expected, as in mixed halides of silver and transition metals.

The "inverse" or "metallo-" complexes $(Ag_2Br)^+$ and the like (responsible for the solubility of silver halides in excess of aqueous silver salt solutions) may, of course, be regarded as a silver halide ligand coordinated to a silver ion

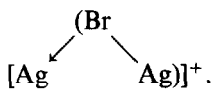

(ii) Many complexed pseudo-halides form bridges to other metal ions as in

$$\{[Fe(CN)_6]Hg(CN)_2\}^{3-}$$

and

$$[(H_3N)_5Co(NCS)Ag]^{3+}.$$

(iii) Silver ions often promote the solvolysis of halide coordinated to kinetically inert metal ions, e.g. Co(III)—Cl, presumably via $[Co—Cl—Ag]^{3+}$ intermediates, some of which may have reasonable lifetimes.

(iv) Werner isolated compounds like *trans*-$[Co(en)_2Cl_2]Cl \cdot AgCl$ which he believed to contain silver chloride ligands. However, we reformulated Poulenc's very similar 1 : 1 adduct of silver bromide, "*trans*-$[Rhpy_4Br(BrAg)]Br_2$" as *trans*-$[Rhpy_4Br_2][AgBr_2]$.

Finally, we extend the present comparison between two-coordinated silver ion and two-coordinated proton to other systems. There are many linear species $[MX_2]^+$ for M = H^+ or Ag^+ and X = an uncharged Brønsted base, like water, pyridine, or pyridine-N-oxide. Similarly, for $[MY_2]^-$, for both H^+ and Ag^+ as M, there are isolable derivatives for Y = halide or NO_3^- as in the present work. For Y = $(RCO_2)^-$ [where, with R = CH_3, we have a 24-electron system, isoelectronic with $(ONO_2)^-$], the species $\{(RCOO)_2H\}^-$ are very well-known. The corresponding dicarboxylato-argentates(I) seem not to have been isolated, though they certainly exist. In aqueous media, silver ion remains in solution at pH > 7 when acetate is present, "through formation of $[Ag(OOC \cdot CH_3)_2]^-$".[60]

In view of Emsley's work on the remarkably stable mixed species $[RCOO \cdot H \cdot F]^-$, where R = H or CH_3, we could expect mixed species like $[Ag(\underline{O}NO_2)(OOC \cdot R)]^-$ and $[AgF(\underline{O}NO_2)]^-$ to have reasonable stability.

REFERENCES

1. Nabila S. Al Zamil, E. H. M. Evans, R. D. Gillard, D. W. James, T. E. Jenkins, R. J. Lancashire and P. A. Williams, *Polyhedron* 1982, **1**, 525.
2. C. Schultz, *Z. Chem.* 1862, **5**, 531.
3. J. W. Mellor, *A Comprehensive Treatise*, Vol. 3, p. 466. Longmans, London (1921).
4. W. J. Russell and N. S. Maskelyne, *Proc. Roy. Soc.* 1877, **26**, 357.
5. E. Zobetz, *Mh. Chem.* 1980, **111**, 1253.
6. P. Poulenc, *Annals Chim.* 1935, ser. 11, **4**, 567.
7. R. D. Gillard and R. Ugo, *J. Chem. Soc. A* 1966, 549.
8. A. W. Addison and R. D. Gillard, *J. Chem. Soc., Dalton Trans.* 1973, 2009.
9. R. A. Davies and R. D. Gillard, unpublished work (1969–70).
10. J. Roziere, M.-T. Roziere-Bories and J. M. Williams, *Inorg. Chem.* 1976, **15**, 2490.
11. J. Roziere, M. S. Lehmann and J. Potier, *Acta Cryst.* 1979, **B35**, 1099.
12. N. S. Al-Zamil, E. H. M. Evans, R. D. Gillard, D. W. James, T. E. Jenkins, R. J. Lancashire and P. A. Williams, *Polyhedron* 1982, **1**, 525.
13. B. D. Faithful and S. C. Wallwork, *J. Chem. Soc., Chem. Commun.* 1967, 1211.
14. G. C. Dobinson, R. Mason and D. R. Russell, *J. Chem. Soc., Chem. Commun.* 1967, 62.
15. J. M. Williams, N. Dowling, R. Gunde, D. Hadzi and B. Orel, *J. Am. Chem. Soc.* 1976, **98**, 1581.
16. L. Diop and J. Potier, *J. Mol. Struct.* 1977, **36**, 191.
17. M. Pham Thi, M. H. Herzog-Cance, A. Potier and J. Potier, *J. Raman Spec.* 1981, **11**, 96.
18. L. Diop, *Spectrochim. Acta* 1982, **38A**, 509.
19. J. R. C. Duke and F. J. Llewellyn, *Acta Cryst.* 1950, **3**, 305.
20. E. Arijs, D. Nevejans, P. Frederick and J. Ingels, *Geophys. Res. Lett.* 1981, **8**, 121.
21. D. Smith, N. G. Adams and E. Alge, *Planet. Space Sci.* 1981 **29**, 449.
22. F. Arnold, A. A. Viggiano and H. Schlager, *Nature* 1982, **297**, 371.
23. H. Heitmann and F. Arnold, *Nature* 1983, **306**, 747.

23a. P. Kebarle, *Ann. Rev. Phys. Chem.* 1977, **28**, 445.

24. A. W. Addison, K. Dawson, R. D. Gillard, B. T. Heaton and H. Shaw, *J. Chem. Soc., Dalton Trans.* 1972, 589.
25. *CRC Handbook of Chemistry and Physics*, 59th edn, (Edited by R. C. Weast) (1979).
26. S. H. Mitchell, The complex *mer*-trichlorotris ligand metal(III) and its solvates. M.Sc. Thesis, University of Wales: University College, Cardiff (1981).
27. R. D. Gillard, S. H. Mitchell, P. A. Williams and R. S. Vagg, *J. Coord. Chem.* 1984, **13**, 325.
28. J. C. Speakman, *Structure and Bonding*, 1972, **12**, 141.
29. B. Barlic, D. Hadzi and B. Orel, *Spectrochim. Acta* 1981, **37A**, 1047.
30. S. Detoni, L. Diop, R. Gunde, D. Hadzi, B. Orel, A. Potier and J. Potier, *Spectrochim. Acta* 1979, **35A**, 443.
31. B. D. Faithful, R. D. Gillard, D. G. Tuck and R. Ugo, *J. Chem. Soc. (A)* 1966, 1185.
32. A. Novak, *Structure and Bonding*, 1974, **18**, 177.
33. S. Bratos, *J. Chem. Phys.* 1975, **63**, 3499.
34. E. G. Weidemann and A. Hayd, *J. Chem. Phys.* 1977, **67**, 3713.
35. S. Bratos and H. Ratajczak, *J. Chem. Phys.* 1982, **76**, 77.
36. M. F. Claydon and N. Sheppard, *J. Chem. Soc., Chem. Commun.* 1969, 1431.
37. J. C. Evans and N. Wright, *Spectrochim. Acta* 1960, **16**, 352.
38. J. C. Evans, *Spectrochim. Acta* 1960, **16**, 994.
39. W. C. Hamilton and J. A. Ibers, *Hydrogen Bonding in Solids*. A. Benjamin, Hamburg (1968).
40. J. Roziere and C. V. Berney, *J. Am. Chem. Soc.* 1976, **98**, 1582.
41. G. Zhou and B. Wu, Hua Hsueh Hsueh Pao, 1981, **39**, 319. *Chem. Abstr.* 1981, **95**: 179134.
42. K. Persson, *Acta Cryst.* 1979, **B35**, 1432.
43. K. Persson and B. Holmberg, *Acta Cryst.* 1977, **B33**, 3768.
44. K. Persson, *Acta Cryst.* 1979, **B35**, 302.
45. R. Birnstock and D. Britton, *Z. Krist.* 1970, **132**, 87.
46. K. Persson and B. Holmberg, *Acta Cryst.* 1982, **B38**, 904.
47. G. T. Morgan and F. H. Burstall, *J. Chem. Soc.* 1930, 2594.
48. W. H. Watson and C.-T. Lin, *Inorg. Chem.* 1966, **5**, 1074.
49. R. J. Kline, C. S. Grinsburg and C. H. Oestreich, *Spectrochim. Acta* 1966, **22**, 1923.
50. H. M. Maurer and A. Weiss, *Z. Krist.* 1977, **146**, 227.
51. D. E. Irish, *Ionic Interactions* (Edited by S. Petrucci). Academic Press, New York (1971).
52. T.-C. G. Chang and D. E. Irish, *J. Solution Chem.* 1974, **3**, 175.
53. R. L. Frost and D. W. James, *J. Chem. Soc., Faraday Trans.* 1982, **78**, 3263.
54. B. Holmberg and G. Johansson, *Acta Chem. Scand.* 1983, **A37**, 367.
55. B. O. Field and C. J. Hardy, *Quart. Rev.* 1964, **18**, 361.
56. C. C. Addison, N. Logan, S. C. Wallwork and C. D. Garner, *Quart. Rev.* 1971, **25**, 289.
57. M. R. Rosenthal, *J. Chem. Ed.* 1973, **50**, 331.
58. P. Meyer, A. Rimsky and R. Chevalier, *Acta Cryst.* 1978, **B34**, 1457.
59. P. F. Lindley and P. Woodward, *J. Chem. Soc. A* 1966, 123.
60. A. F. Clifford, *Inorganic Chemistry of Qualitative Analysis*, p. 302. Prentice-Hall, London (1961).

Polyhedron Vol. 6, No. 10, pp. 1901–1907, 1987
Printed in Great Britain

0277–5387/87 $3.00+.00

TRANSITION METAL COMPLEXES WITH THE THIOSEMICARBAZIDE-BASED LIGANDS—I. NICKEL(II) COMPLEXES WITH THE QUADRIDENTATE LIGANDS BASED ON S-METHYLISOTHIOSEMICARBAZIDE; X-RAY CRYSTAL STRUCTURE OF (ACETYL-ACETONE N(1)-SALICYLIDENE-S-METHYLIZOTHIOSEMICARBAZONATO)NICKEL(II)

VUKADIN M. LEOVAC,* VLADIMIR DIVJAKOVIĆ and VALERIJA I. ČEŠLJEVIĆ

Faculty of Sciences, University of Novi Sad, I. Djuričića 4, 21000 Novi Sad, Yugoslavia

and

PETER ENGEL

Laboratory for Chemical and Mineralogical Crystallography, University of Bern, 3012 Bern, Switzerland

(*Received* 17 *December* 1986; *accepted after revision* 5 *May* 1987)

Abstract—The reaction of a warm ethanolic solution of [Ni(SALSMeTSC-H)Py]Cl·0.5Py (SALSMeTSC = salicylaldehyde S-methylisothiosemicarbazone) with salicylaldehyde and acetylacetone (HACAC), yielded the corresponding square-planar complexes [Ni(SAL_2SMeTSC-2H)] (**A**) and [Ni(SALACACSMeTSC-2H)] (**B**) (SAL_2SMeTSC, and SALACACSMeTSC = quadridentate 2O2N ligand: N(1),N(3)-*bis*(salicylidene)-S-methyl-isothiosemicarbazide, and acetylacetone N(1)-salicylidene-S-methylisothiosemicarbazone, respectively). An X-ray analysis of complex **B** showed that in the reaction of the starting complex with HACAC a rearrangement of the salicylaldehyde moiety takes place (while the C—N(3) bond of the azomethine group is ruptured) and its binding to the N(1) nitrogen. At the same time, HACAC is simultaneously bonded to the liberated N(3)-nitrogen of the hydrazine fragment. Crystal data for the complex B ($NiC_{14}H_{15}N_3O_2S$) are: $M_r = 348.0$, orthorhombic, space group $Pna2_1$, $a = 7.484(3)$, $b = 21.995(8)$, $c = 8.866(3)$ Å; $V = 1459.44$ Å^3, $Z = 4$, $F(000) = 720$, $Dc = 1.58$ g cm^{-1}, $Do = 1.56$ g cm^{-1}, $\mu(MoK\alpha) = 14.45$ cm^{-1}. The structure was solved by the heavy-atom method and refined anisotropically to an R value of 0.078 for 1174 non-zero reflections. The complex molecules are planar, the Ni—Ni distance of nearest molecules being about 3.76 Å. The compounds have been characterized by elemental analysis as well as by IR and electronic spectra.

It has been shown[1,2] that in the presence of some ions, such as VO(II), Ni(II), Cu(II) and Fe(III) a template condensation reaction takes place between salicylaldehyde thiosemicarbazone and its S-alkyl derivatives, yielding the complexes of these metal ions with the quadridentate (2O2N) ligand, N(1),N(3)-*bis*(salicylidene)-S-alkylisothiosemicarbazide, HO-C_6H_4-CHN(3)N(2)C(-SR)-N(1)CH-C_6H_4-OH, SAL_2SRTSC. To our knowledge, there has been no report on the preparation of metal complexes with the ligands which would contain some other carbonyl compound instead of one salicylaldehyde moiety. Therefore, the objective

* Author to whom correspondence should be addressed.

of this work was to investigate the conditions for the synthesis and to determine the structure of the [Ni(SALACACSMeTSC-2H)] complexes, where SALACACSMeTSC is acetylacetone N(1)-salicylidene-S-methylisothiosemicarbazone. Also, we propose here a novel procedure for the synthesis of the earlier described Ni(II) complex with N(1),N(3)-*bis*(salicylidene)-S-methylisothiosemicarbazide, [Ni(SAL_2SMeTSC-2H)].[1]

EXPERIMENTAL

Chemicals and methods

The starting complex [Ni(SALSMeTSC-H)Py] Cl·0.5Py was prepared according to the procedure described earlier.[3] Salicylaldehyde and acetylacetone (HACAC) were puriss grade ("Fluka").

Nickel was determined as *bis*(dimethylglyoximato)-nickel(II), while C, H and N were determined by standard micro-methods.

Magnetic measurements were performed by Gouy balance, and melting points were determined by Kofler apparatus with no correction. IR (KBr pellet) and solution electronic spectra ($C \sim 4 \times 10^{-5}$ mol/dm^3 in EtOH and Py) were obtained on a Perkin–Elmer 457 and on a Unicam SP 800 spectrophotometer, respectively.

Structure solution of complex **B**

Crystal data: $M_r = 348.0$, formula $NiC_{14}H_{15}N_3O_2S$, orthorhombic, Laue symmetry mmm, $a = 7.484(3)$, $b = 21.995(8)$, $c = 8.866(3)$ Å; $V = 1459.44$ Å^3, $Z = 4$, $F(000) = 720$ $Dc = 1.58$ g cm^{-1}, $Do = 1.56$ g cm^{-1}, $\mu(MoK\bar{\alpha}) = 14.45$ cm^{-1}. Systematic extinctions: $0kl$ for $k+1 = 2n+1$, $h0l$ for $h = 2n+1$, ($h00$ for $h = 2n+1$, $0k0$ for $k = 2n+1$ and $00l$ for $l = 2n+1$) define the possible space-groups Pnam (No. 62) or $Pna2_1$ (No. 33). Since $Z = 4$ and the molecule does not have the required symmetry ($\bar{1}$ or m) for Pnam, $Pna2_1$ was chosen and shown to be correct by the subsequent successful structure analysis. The density was measured by flotation in benzene/methyl iodide. Preliminary data on lattice parameters, crystal symmetry and space group were determined from rotation and Weissenberg diffraction patterns. Accurate cell dimensions and X-ray intensity data were measured on a PHILIPS PW 1100 computer-controlled four-circle diffractometer using graphite monochromatized MoK$\bar{\alpha}$ radiation ($\lambda = 0.71069$ Å) and the ω–2θ scan technique. Unit cell parameters were refined from measurements on 14 carefully centred reflections. Intensities were collected in the range $0 < 2\theta < 50°$, h: 0–9, k: 0–26, l: 0–10. A total of 1195 independent reflections were measured of which 1174 with $I > 3\sigma(I)$ were considered as observed and were used in the structure analysis. All intensities were corrected for Lorentz and polarization factors but no absorption correction was applied.

The intensity statistics confirmed the non-centrosymmetric space group (theoretical values are given in parentheses): $\langle E \rangle = 0.885$ (0.886); $\langle E^2 \rangle = 1.000$ (1.000); $\langle |E^2 - 1| \rangle = 0.748$ (0.736). The structure was solved by the heavy-atom method; the positions of the Ni atoms are found from a three dimensional Patterson function. The positions of the non-hydrogen atoms were determined by subsequent Fourier maps. The structure was refined with full-matrix least-squares calculations using anisotropic temperature factors. The final agreement index was $R = 0.078$. A correction for extinction was not applied. Atomic scattering factors including the corrections for anomalous dispersion were taken from the International Tables for X-ray Crystallography.[4] Final atomic coordinates, thermal parameters and a list of Fo/Fc values were deposited as supplementary material; copies are available on request. Bond distances and bond angles are given in Table 1.

Preparation of complexes

[Ni(SAL_2SMeTSC-2H)] (**A**): 0.50 g of [Ni(SALSMeTSC-H)Py] Cl·0.5Py[3] was dissolved by heating in 5 cm^3 of EtOH to which was then added 1.0 cm^3 of salicylaldehyde. The red solution was heated mildly with stirring for about 10 min and left at room temperature for about 12 h. The obtained needle-like crystals of cherry-red colour were filtered off and washed with the EtOH–Et_2O (1 : 1) mixture, and finally with Et_2O. Yield: 0.30 g. Found: Ni, 15.6; C, 52.1; H, 3.3; N, 11.2. Calc. for [Ni(SAL_2SMeTSC-2H)]: Ni, 15.9; C, 51.9; H, 3.5; N, 11.3%.

[Ni(SALACACSMeTSC-2H)] (**B**): This complex was prepared in an analogous way, i.e. by the reaction of 1.0 g of the starting complex, dissolved in 10.0 cm^3 of EtOH and by adding 3.0 cm^3 of HACAC. The red solution was heated for about 30 min with reflux. After keeping the solution for several days at room temperature, the dark-red crystals were filtered off and washed carefully with the EtOH–Et_2O (1 : 1) mixture and with Et_2O. Yield: 0.25 g. Found: Ni, 16.7; C, 48.6; H, 4.2; N, 12.4. Calc. for [Ni(SALACACSMeTSC-2H)]: Ni, 16.9; C, 48.3; H, 4.3; N, 12.1%.

Table 1. Bond distances (Å) and bond angles (°)

Ni—O(1)	1.852(7)	C(9)—O(1)—Ni	125.8(6)
Ni—O(2)	1.836(7)	C(11)—O(2)—Ni	127.1(8)
Ni—N(1)	1.824(9)	C(1)—N(1)—Ni	112.4(7)
Ni—N(3)	1.818(8)	C(3)—N(1)—Ni	128.1(8)
S—C(1)	1.723(11)	C(3)—N(1)—C(1)	119.6(9)
S—C(2)	1.804(14)	C(1)—N(2)—N(3)	110.4(8)
O(1)—C(9)	1.314(10)	N(2)—N(3)—Ni	117.4(6)
O(2)—C(11)	1.265(11)	N(2)—N(3)—C(13)	114.3(8)
N(1)—C(3)	1.307(13)	C(13)—N(3)—Ni	128.3(7)
N(1)—C(1)	1.411(12)	N(1)—C(1)—S	122.4(7)
N(2)—C(1)	1.324(13)	N(2)—C(1)—S	121.4(8)
N(2)—N(3)	1.374(13)	N(1)—C(1)—N(2)	116.2(9)
N(3)—C(13)	1.343(12)	N(1)—C(3)—C(4)	123.5(9)
C(3)—C(4)	1.421(16)	C(3)—C(4)—C(5)	117.3(11)
C(4)—C(5)	1.434(10)	C(3)—C(4)—C(9)	122.0(7)
C(5)—C(6)	1.380(19)	C(5)—C(4)—C(9)	120.7(11)
C(6)—C(7)	1.357(21)	C(4)—C(5)—C(6)	118.8(14)
C(7)—C(8)	1.418(14)	C(5)—C(6)—C(7)	121.4(10)
C(8)—C(9)	1.423(13)	C(6)—C(7)—C(8)	121.4(12)
C(9)—C(4)	1.401(15)	C(7)—C(8)—C(9)	118.9(11)
C(10)—C(11)	1.490(14)	C(8)—C(9)—C(4)	118.7(8)
C(11)—C(12)	1.399(16)	C(8)—C(9)—O(1)	116.0(9)
C(12)—C(13)	1.397(15)	C(4)—C(9)—O(1)	125.3(8)
C(13)—C(14)	1.513(15)	C(10)—C(11)—O(2)	116.4(10)
		C(10)—C(11)—C(12)	119.8(9)
O(1)—Ni—O(2)	85.9(3)	C(12)—C(11)—O(2)	123.8(10)
O(1)—Ni—N(1)	95.2(3)	C(11)—C(12)—C(13)	125.9(8)
O(2)—Ni—N(3)	95.3(3)	C(12)—C(13)—N(3)	119.5(9)
N(1)—Ni—N(3)	83.5(4)	C(12)—C(13)—C(14)	122.0(9)
C(1)—S—C(2)	102.5(5)	C(14)—C(13)—N(3)	118.5(10)

RESULTS AND DISCUSSION

Synthesis and general characteristics of complexes

It is well known from the literature,[5-7] that thiosemicarbazide, $H_2N(3)—N(2)HC(=S)—N(1)H_2$, is condensed with monocarbonyl compounds solely via the hydrazine nitrogen N(3), while the amide nitrogen N(1) does not enter such reaction. However, it has been shown recently[1] that this nitrogen atom can, under special reaction conditions, take part in similar reactions. Thus, the method of template condensation of salicylaldehyde thiosemicarbazone and salicylaldehyde itself, in a basic medium and in the presence of VO(II), Ni(II) and Cu(II) yielded the complexes of general formula $M'[M(SAL_2TSC\text{-}3H)]\cdot nH_2O$ (M' = Na, K; M = VO(II), Ni(II), Cu(II) and SAL_2TSC = quadridentate ligand $HO—C_6H_4—CHNNC(—SH)NCH—C_6H_4—OH$).[1] The compounds obtained can react with CH_3I giving the corresponding complexes of the non-electrolyte type $[M(SAL_2SMeTSC\text{-}2H)]$.[1] It has been established that the above condensation reaction in the case of Ni(II) can proceed only in an alkaline medium (KOH or NaOH). However, in the present work we have shown that $[Ni(SAL_2SMeTSC\text{-}2H)]$ can be prepared in another way, with no OH^- ions present in the solution.

The reaction of hot ethanolic solution of $[Ni(SALSMeTSC\text{-}H)Py]Cl\cdot 0.5Py$[3] (SALSMeTSC = salicylaldehyde S-methylisothiosemicarbazone) and salicylaldehyde appeared to be the route for obtaining the desired complex. Such a course of the reaction can be explained by the coordination of salicylaldehyde S-methylisothiosemicarbazone from $[Ni(SALSMeTSC\text{-}H)Py]Cl\cdot 0.5Py$ which is also established, apart from the oxygen of the deprotonated OH group and the hydrazine nitrogen, via the nitrogen atom of the amide group.[3] The configuration formed is favourable for the occurrence of the template condensation reaction which is in addition catalysed by the coordination effect of the NH_2 group.

With the aim to employ the same condensation reaction for preparation of the complexes with an

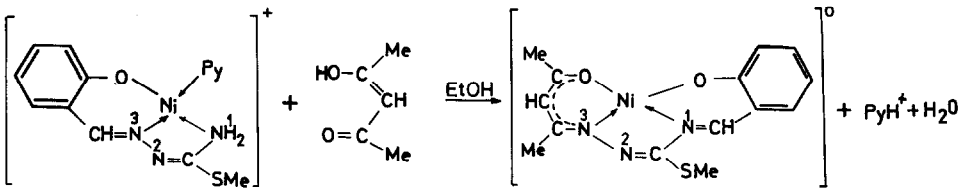

Scheme 1.

asymmetric quadridentate ligand containing some other carbonyl compound, we have tried out (under same conditions) the reaction of acetylacetone with the above Ni(II) complex. It appeared, as concluded from an X-ray analysis of the resulting compound, that HACAC has not entered the condensation reaction with the non-condensed amide group. Instead, an unexpected rearrangement of the salicylaldehyde moiety took place, accompanied by its binding to the azomethine nitrogen, and preceded by the rupture of the C—N bond. At the same time HACAC was bound to the newly liberated nitrogen atom of the hydrazine fragment N(3). The general reaction can be represented by Scheme 1.

Such a course of the reaction can be explained by the difference in reactivity of the corresponding hydrazine and amide group of thiosemicarbazide (TSC) and S-methylisothiosemicarbazide (SMeTSC), respectively, as well as by different condensation capabilities of aldehydes and ketones. Namely, it is well known that the condensation reactions with NH_2 groups proceed more readily with aldehydes than with ketones, and the hydrazine group of both TSC and SMeTSC is more reactive than the amide NH_2 group.*

With regard to the nature of the compound obtained and the ligand, respectively, it can be concluded that the rupture of the bond salicylidene–hydrazine moiety [followed by the bonding of the latter to the amide nitrogen N(1)] is energetically preferable to the formation of an ACAC—N(1) bond.

Both complexes are well soluble in common organic solvents, (DMF, $CHCl_3$, C_6H_6, MeOH, EtOH, Me_2CO), less soluble in Et_2O and insoluble in water.

Their molar conductivities are close to zero, which is in agreement with their coordination formulae.

As it could be expected, complex **A** exhibits greater thermal stability (m.p. = 297°C), compared to complex **B** (m.p. = 208°C).

Finally, the complexes are diamagnetic, both crystalline and in solution, which also confirms their square-planar structure.

Descriptions of the structure of complex **B**

The shape of the molecule, atomic numbering scheme and the packing of the molecules are indi-

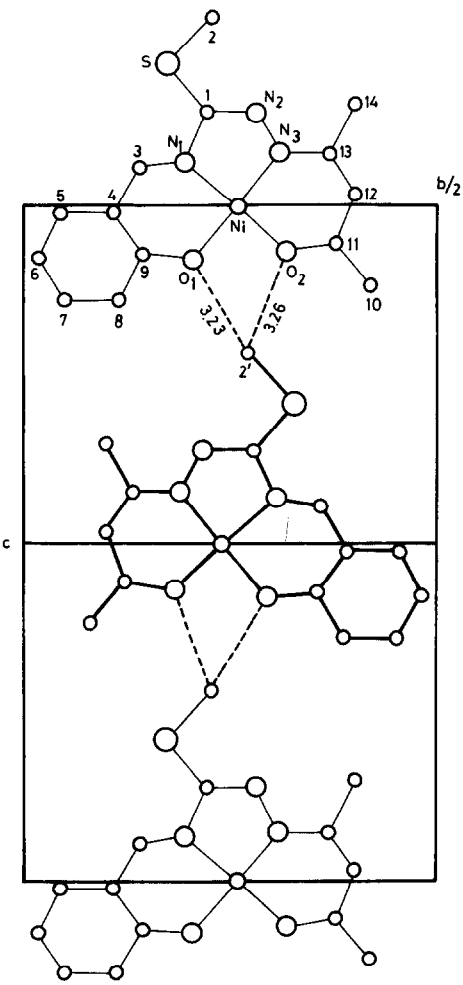

Fig. 1. Arrangement of molecules in two asymmetric units viewed along the *a* axis. The thin lines represent molecules with $a \approx 0$, and the thick lines those with $a \approx 0.5$. Van der Waals contacts are in Å.

* Apparently, the latter difference disappears under special reaction conditions (alkaline medium, presence of a suitable transition metal ion) when, due to the template effect, the condensation of TSC with salicylaldehyde takes place via the two terminal nitrogen atoms.[1]

cated in Fig. 1. The neutral complex molecules are almost planar, in which the ligand is the quadridentate (2O2N) doubly deprotonated acetylacetone N(1)-salicylidene-S-methylisothiosemicarbazone. The ligand coordination around the nickel atom is square-planar with a deviation from the best-plane not exceeding 0.01 Å (compare Table 2). The distances Ni—N(1) and Ni—N(3) of 1.824 and 1.818 Å respectively, agree well with those found in similar compounds having square-planar coordination around the Ni atom. The distance Ni—O(1) (1.852 Å) and Ni—O(2) (1.836 Å) are in good agreement with the corresponding values observed in the structure of ammine(salicylaldehyde 4-phenylthiosemicarbazonato)nickel(II).[8] In the present structure the salicylidene fragment of the ligand is bonded via the amide nitrogen N(1) to the S-methylisothiosemicarbazide moiety instead, as it would be expected, via the hydrazine nitrogen N(3). Such a configuration of salicylidene and S-methylisothiosemicarbazide was found in some transition metal complexes with the similar ligands[9–11] in which two salicylidene fragments were coupled to both N(1) and N(3). The bond distances and bond angles found in the salicylidene and S-methylisothiosemicarbazide fragments of the title compound are in good agreement with the corresponding values from the above references. The bond distances C(1)—N(1) (1.411 Å) and C(1)—N(2) (1.324 Å) indicate a partial delocalization of the electronic density within the carbazide fragment of the ligand. In this case the delocalization is realized in an opposite way with respect to the similar π-electronic delocalization (in the same moiety) of some transition metal complexes with different derivatives of S-methylisothiosemicarbazones in which the ligands appear in an imido form.[12] In the deprotonated acetylacetone fragment, an asymmetric delocalization of electronic charge takes place. As a result, the C—C bond lengths are 1.399 and 1.397 Å, while the C—N and C—O bond distances are 1.343 and 1.265 Å, respectively. The observed C—CH_3 bond lengths are 1.513 and 1.490 Å. These values correspond to those observed in the *bis*(acetylacetone)Ni(II) dihydrate.[13]

The quadridentate ligand chelating the nickel atom forms two (acetylacetoneimine and salicylidene) six-membered, and one (S-methylisothiosemicarbazide) five-membered ring. The ligand molecule as a whole lies approximately in one plane with the largest deviation from the best-plane of 0.06 Å (compare Table 2) for the carbon atom of the thiomethyl group. The S—C(2) bonding is in the *trans*-position with respect to the C(1)—N(1) bond.

The ligand molecules are mutually linked by van der Waals contacts in the layers perpendicular to the *b* axis (Fig. 1). Van der Waals contacts are realized via methyl carbon and both oxygens |C(2′)H_3...O(1) = 3.23 Å, C(2)H_3...O(2) = 3.27 Å|.

These intermolecular contacts are slightly shorter compared to the sum of van der Waals radii of the methyl group (2.0 Å) and oxygen (1.4 Å).[14] The shortest Ni—Ni distance of neighbouring complexes is 3.76 Å.

Table 2. The best-planes in the complex molecule

Plane 1. $0.93387^aX+0.00293^aY-0.35759^aZ = 0.60581$

Atom	Distance (Å) from the best-plane
O(1)	−0.00216
O(2)	0.00217
N(1)	0.00223
N(3)	−0.00225
Ni[a]	−0.00632

Plane 2. $0.93779^aX+0.00920^aY-0.34707^aZ = 0.65401$

Atom	Distance (Å) from the best-plane	Atom	Distance (Å) from the best-plane
S	0.32631	C(5)	0.01995
O(1)	0.00327	C(6)	0.03022
O(2)	0.01438	C(7)	0.01686
N(1)	−0.03039	C(8)	−0.01396
N(2)	−0.04507	C(9)	−0.01382
N(3)	−0.02182	C(10)	0.00936
C(1)	−0.01712	C(11)	0.01724
C(2)	0.05734	C(12)	0.04817
C(3)	−0.03965	C(13)	−0.00825
C(4)	−0.02682	C(14)	−0.02598

[a] Atoms not forming the plane.

IR spectra

The character of the IR spectra is in concordance with the established structure of the ligands and complexes. Their prominent feature is the absence of the ν(OH) and ν(NH) vibrations in the region 3600–3050 cm^{-1}. On the other hand, in the region 1615–1510 cm^{-1} there are five strong bonds which, apart from ν(C=C) vibrations of the benzene ring, can be ascribed to the valence vibrations ν(C=O), ν(C=N) and ν(C=N).[15] The three strong and clearly split bands appearing at 1440–1370 cm^{-1} are characteristic of $\delta(CH_3)$ of the acetylacetone moiety,[15] as well as of δ(Cγ—H).[16] The only significant band appears in the spectrum of complex

Table 3. Electronic spectral data (cm^{-1})

Complex	*d–d* bands	Other bands		
[Ni(SAL$_2$SMeTSC-2H)]	19,880[a]	25,300[a]	30,770[a]	39,200[a]
	(2300)	(5580)	(5650)	(15,350)
	19,840[b]	24,750[b]	33,300[a]	41,670[a]
	(7070)	(7070)	(6980)	(18,800)
[Ni(SALACACSMeTSC-2H)]	21,280[a]	24,750[a]	27,900[a]	42,550[a]
	(6670)	(8700)	(10,430)	(35,360)
	20,660[b]	24,270[b]	34,480[a]	43,860[a]
	(6950)	(7540)	(15,650)	(36,810)

[a] In EtOH.
[b] In Py. Molar extinction coefficient (ε, $dm^3\ mol^{-1}\ cm^{-1}$) in parentheses.

A at about 1450 cm^{-1}, which makes the principal difference in the appearance of the spectra of the two compounds. This is in agreement with the absence of the acetylacetone moiety in complex **A**, since this band is obviously due to the skeleton vibrations of the benzene ring. The band in the spectrum of complex **B** is overlapped with $\delta_{as}(CH_3)$ and $\delta(C\gamma—H)$ vibrations.[16] The strong band at about 1160 cm^{-1} in both the spectra is due to $\nu(C_{Ar—O})$ of the coordinated phenolic hydroxyl. Finally, the bands of medium intensity at 750 cm^{-1} can be unambigously ascribed to the 1,2-substituted benzene ring, i.e. to the out-of-plane vibrations of four neighbouring hydrogen atoms.[17]

Electronic spectra

The position and intensity of *d–d* bands ($\sim$ 20.000 cm^{-1} for **A**, and $\sim$ 21.000 cm^{-1} for **B**) in the electronic absorption spectra of the complexes (Table 3) recorded in EtOH and Py, suggest that the square-planar structure is also preserved in the solution.[18] The practically identical position of the bands obtained in both solvents, as well as the absence of lower energy bands ($<$ 15.000 cm^{-1})[19,20] indicate the lack of Ni—Py interactions, i.e. the coordination number of Ni(II) has not been changed even in a solvent of strong donor character, such as pyridine. The explanation should be based on a very strong ligand field of both ligands so that the alteration of electronic structure of Ni(II) ion, i.e. of its spin state, would require a larger amount of energy than it would obtain on account of an axial coordination with solvent molecules.

A further support to the square-planar structure of the complexes in the solution is their dark-red colour, as well as their established diamagnetic properties.

Acknowledgement—The authors acknowledge partial financial support from the Scientific Fund of SAP Vojvodina.

REFERENCES

1. N. V. Gerbeleu, *Reaktsii na Matritsakh*. Shtiintsa, Kishinev (1980).
2. M. A. Yampol'skaya, S. G. Shova, N. V. Gerbeleu, Yu. A. Simonov, V. K. Bel'skii and A. A. Dvorkin, *Zh. Neorg. Khim.* 1983, **28**, 1744.
3. V. M. Leovac, D. M. Petrović, D. Ž. Obadović and N. V. Gerbeleu, *Z. anorg. allg. Chem.* 1984, **512**, 211.
4. *International Tables for X-Ray Crystallography*. Kinoch Press, Birmingham (1969).
5. C. Neuberg and W. Neimann, *Ber.* 1902, **35**, 2049.
6. M. Freund and W. Schander, *Ber.* 1902, **35**, 2602.
7. Yu. P. Kitaev and B. I. Buzykin, *Gidrazony*. Nauka, Moskow (1974).
8. M. Sariano-Garcia, R. A. Toscano, J. Valdes-Martinez and J. M. Fernandez-G, *Acta Cryst.* C 1985, **41**, 498.
9. M. A. Yampol'skaya, S. G. Shova, N. V. Gerbeleu, V. K. Bel'skii and Yu. A. Simonov, *Zh. Neorg. Khim.* 1982, **27**, 2551.
10. Yu. A. Simonov, N. V. Gerbeleu, M. D. Revenko, S. G. Shova, V. E. Zavodnik and V. G. Rusu, *Kristallographiya* 1985, **30**, 1090.
11. Yu. A. Simonov, M. A. Yampol'skaya, S. G. Shova, V. K. Bel'skii and N. V. Gerbeleu, *Dokl. Akad. Nauk SSSR* 1985, **282**, 895.
12. V. Divjaković, B. Ribar, V. M. Leovac and N. V. Gerbeleu, *Z. Kristallogr.* 1981, **154**, 83.
13. R. W. G. Wyckoff, *Crystal Structures*. Wiley-Interscience, New York (1966).
14. L. Pauling, *Die Natur der Chemischen Bindungen*. Verlag Chemie, Weinheim (1973).
15. K. Nakamoto, *Infrared and Raman Spectra of Inorganic and Coordination Compounds* (3rd edn). Wiley-Interscience, New York (1978).
16. V. P. Nekhoroshkov, G. L. Kamalov, I. I. Želtvai, A.

K. Ososkov and E. D. Berestetskaya, *Koord. Khim.* 1984, **10**, 459.
17. K. Nakanishi, *Infrared Absorption Spectroscopy*. Holden–Day, San Francisco (1962).
18. A. B. P. Lever, *Inorganic Electronic Spectroscopy*. Elsevier, Amsterdam (1968).
19. L. Cacconi, P. Nannelli, N. Nardi and U. Campigli, *Inorg. Chem.* 1965, **4**, 943.
20. C. A. Root and D. H. Busch, *Inorg. Chem.* 1968, **7**, 789.

Polyhedron Vol. 6, No. 10, pp. 1909–1912, 1987
Printed in Great Britain

0277–5387/87 $3.00+.00

FORMATION OF CYANIDE COMPLEXES OF COBALT(II) AND MANGANESE(II)

EFRAIM AVŞAR* and BETÜL BAŞARAN

Department of Chemistry, Technical University of Istanbul, Maslak, 80 626 Istanbul, Turkey

(*Received* 3 *March* 1987; *accepted* 5 *May* 1987)

Abstract—The formation of complexes of the cyanide ion with Co(II) and Mn(II) has been studied potentiometrically in an aqueous sodium perchlorate medium of unit ionic strength at 298 K. Studies of the equilibria in the cobalt(II)–cyanide system show that at least one strong mononuclear complex exists, while in the manganese(II)–cyanide system two mononuclear complexes can be formed in the concentration range studied.

Despite the large number of studies carried out so far[1–7] to indicate the number and nature of complexes formed when cyanide is added to an aqueous solution of cobalt(II) salts, our knowledge is by no means complete. A common opinion is that a strong fifth mononuclear complex exists in cobalt(II) cyanide solutions; but no value for the formation constant seems to have been evaluated. Besides, to the best of our knowledge no equilibrium studies dealing with the formation of cyanide complexes of manganese(II) have ever been reported.

The aim of the present work was to determine the step-wise complex formation equilibria in the cyanide systems of Co(II) and Mn(II).

Potentiometry has been the main technique used for studying the complex formation in aqueous solution.[8] Potentiometric measurements may be applied to a central ion-ligand system if a suitable electrode is available. Here, the most suitable method for ligand determination seems to be pH and/or direct [L], i.e. free ligand, measurements in a buffer of the ligand ion and the corresponding acid by using both glass and cyanide-specific electrodes. From such measurements the free ligand concentration [L] and the average ligand number $\bar{n}$ can be found.[9] All measurements in this study have been carried out at 298.15 K in an aqueous medium of ionic strength $I = 1.0$ M with sodium perchlorate as an inert electrolyte.

* Author to whom correspondence should be addressed.

EXPERIMENTAL

Chemicals

Co(II) perchlorate solution was prepared from $Co(ClO_4)_2 \cdot 6H_2O$ (Fluka, purum). Mn(II) perchlorate was made by dissolving Mn(II) carbonate (Fluka, purum) in perchloric acid (Merck, p.a.) and recrystallizing several times. Co(II) and Mn(II) were analysed as before.[9] The free acid concentrations in the stock solutions have been determined potentiometrically. The perchloric acid (Merck, p.a.) solutions were standardized against borax. Sodium perchlorate was prepared and analysed as described before.[10] Sodium cyanide (Merck, p.a.) solutions were prepared daily. The NaCN solutions were standardized with a standard $AgNO_3$ solution. Oxygen-free nitrogen was used for deaeration. The Ag, AgCl electrodes were prepared as described previously.[11]

Apparatus and procedure

A Metrohm E580 ion-activity-meter and/or a Metrohm E500 digital pH meter equipped with a Metrohm EA-306-CN ion-specific electrode and a Radiometer type G202 C glass electrode have been used for the potentiometric measurements. The slopes of both the electrodes have been checked repeatedly and found to be 59.2 ± 0.2 mV. The reproducibility in the measurements was usually within ± 1 mV for the Co(II)–CN^- system, but

much better, ±0.4 mV, for the Mn(II)–CN^- system. All solutions in the cobalt(II)–cyanide system were de-oxygenated by purging with purified nitrogen for about 15 min before titrations. A magnetic stirrer was used for mixing. The e.m.f.s of the following cell were measured.

$$-RE//C_M\ M\ Me(ClO_4)_2, C_L\ M\ NaCN,$$
$$C_H\ M\ HClO_4, NaClO_4$$
$$\text{to } I = 1\ M/\text{glass of cyanide electrode} +$$

where

$$RE// = Ag, AgCl/0.025\ M\ NaCl,$$
$$0.975\ M\ NaClO_4/1.00\ M\ NaClO_4/.$$

Here, Me denotes Co or Mn. Both the cyanide and glass electrodes were used in the Co(II)–CN^- system, while in the Mn(II)–CN^- system, measurements were performed with a glass electrode. The measurements were arranged as titrations where the solutions in the right-hand half-cell were obtained by adding a known volume v (cm^3) of a ligand solution to V_0 (cm^3) of metal perchlorate solution. Special attention has been paid to obtain reliable measurements. The precipitate of $Co(CN)_2$ is slightly soluble; therefore the measurements were performed at very low cobalt ion concentrations, *ca* 10^{-4} M, in order to avoid the precipitation. The e.m.f.s have been read within as short a time as possible after each addition. All solutions used in the cobalt(II)–cyanide system have been carefully de-oxygenated and kept under an inert atmosphere during the measurements.

Calculations

The step-wise formation constants have been evaluated both graphically and numerically. The graphical method has been described elsewhere.[9,11] The numerical calculations have been carried out by using different programs designed by Sandell.[12] In order to calculate the formation constants from these measurements, it is necessary to know the acidity constant of HCN under the same conditions. This has therefore been determined in separate measurements and found to be $K_a = (1.12 \pm 0.01)\ 10^{-9}$ M.

RESULTS AND DISCUSSION

Co(II)–*cyanide system*

Potentiometric titrations were carried out on five different C_M, i.e. 0.245, 0.490, 0.633, 0.980 and 1.960 mM at constant acid concentrations of 0.0468, 0.0537, 0.217, 0.0277 and 0.0554 mM, respectively. A free ligand ion concentration up to ~ 1 mM could be reached in the measurement. Thus, the possible formation of a hexacyanide could have been studied.

Both the graphical and numerical evaluations of constants clearly indicate the formation of more than one complex, and the mononuclear pentacyanide complex strongly dominates the complex formation. Furthermore, these calculations show that both $\beta_1 = 0$ and $\beta_6 = 0$. The graphical calculations indicate the existence of ML_3, ML_4 and ML_5 mononuclear complexes. Another one, namely ML_2, might be present but no significant value could be obtained. In the numerical calculations, on the other hand, the fifth complex is well established. However, it is not possible to decide with certainty the sufficiency of the complex ML_5 alone to describe the experimental material. However, in all models to be tested ML_5 has to be included. Nevertheless calculations showed that the introduction of the the third, or fourth, complex gives a much better fit to experimental data. For a model containing ML_4 and ML_5 $\beta_4 = (1.2 \pm 1.8)\ 10^{18}\ M^{-4}$ and $\beta_5 = (1.0 \pm 0.8)10^{23}\ M^{-5}$ are found. Another calculation by considering ML_3 and ML_5 gave a better fit with the results of $\beta_3 = (5 \pm 4)10^{13}\ M^{-3}$ and $\beta_5 = (1.0 \pm 0.6)10^{23}\ M^{-5}$. Thus, introducing the third, or fourth, complex gives a better fit but increases the uncertainties in the estimates. On the other hand, including the three mononuclear complexes, such as $ML_3+ML_4+ML_5$, $ML_2+ML_3+ML_5$ etc. or taking account of all the possible combinations of the probable six complexes always results in very large errors. Moreover, some runs with polynuclear complexes and/or hydrolytic species such as $ML_5(OH)$, have been performed but no estimates could ever be obtained. Such combinations should thus be discarded. This means that the experimental data can adequately be described by just two parameters.

Table 1.

Method	β_1	β_2	β_3	β_4	β_5	β_6
Graphical	0	$\sim < 5 \times 10^8$	$< 2 \times 10^{14}$	$< 6 \times 10^{19}$	$(5 \pm 2)10^{23}$	0
Numerical	0	0	$(5 \pm 4)10^{13}$	0	$(1.0 \pm 0.6)10^{23}$	0

The results of these calculations are shown in Table 1. Obviously, only the value of β_5 is well established. The errors given in the numerical calculations correspond to confidence limits at the 99.9% level of significance.

Since the best fit to the potentiometric data is obtained with the model including only ML_3 and ML_5, this has been accepted to be the best representation of this system. The distribution of the complexes ML_3 and ML_5 as a function of [L], calculated from the formation constants, is shown in Fig. 1(a).

Table 2. Over-all formation constants of the Co(II)– and Mn(II)–cyanide systems at 298.15 K and $I = 1.0$ M: errors given correspond to confidence limits at the 99.9% level of significance

System	j	β_j (M^{-j})
Co(II)–cyanide	3	$(5\pm4)10^{13}$
	5	$(1.0\pm0.6)10^{23}$
Mn(II)–cyanide	1	75 ± 11
	2	$(2.3\pm0.5)10^{3}$

Mn(II) *cyanide system*

Titrations were performed with four different values of C_M, namely 10, 20, 30 and 40 mM. Higher metal ion concentrations were used without any precipitations, which permit the study of the system in a wider range of concentration. The acid concentrations, constant during the titrations, were 10 mM for $C_M = 10$ mM, 20 and 40 mM for $C_M = 20$ mM, 15 mM for $C_M = 30$ mM, 20 and 40 mM for $C_M = 40$ mM. A free ligand ion concentration up to $\simeq 80$ mM could have been reached in these measurements. Higher free ligand concentrations were not allowed due to a blue precipitate of the hexacyanide complex.[13] No systematic deviations could be observed when both C_M and C_H were varied, which shows that neither polynuclear nor acid complexes seem to exist.

The mononuclear complexes are formed in the concentration range studied. The consecutive formation constants were evaluated both graphically[8] and numerically by a high-speed computer using the data program UNINUX.[12] Both methods gave the same estimates: $\beta_1 = 75\pm11$ M^{-1}, $\beta_2 = (2.3\pm0.5)\,10^3$ M^{-2}. The distribution curves of the complexes are shown in Fig. 1(b), and the results of this work are collected in Table 2.

The cyanide system of Co(II) shows an unusual course of complex formation, in which a strong pentacoordinate is dominating. Potentiometric data indicates further the formation of complexes in small quantities before the main pentacyanide. The experimental difficulties do not allow the studies of other complex equilibria in a wider range of concentrations. However, the formation of the third complex can be detected with a formation constant of the order of 10^{13} M^{-3}. In this respect, the Co(II)–CN^- system is reminiscent of another cyanide system, i.e. Ni(II)–CN^-. Also in this system a very strong complex of tetracyanide with $\beta_4 = 1.16\times10^{31}$ M^{-4} was found, while the formation of other complexes could have been discarded.[14]

Comparing with Co(II) complexes, Mn(II)-cyanides have markedly lower stabilities. This, of course, is expected as all Mn(II) complexes show the same trend. In the range of cyanide concentration studied

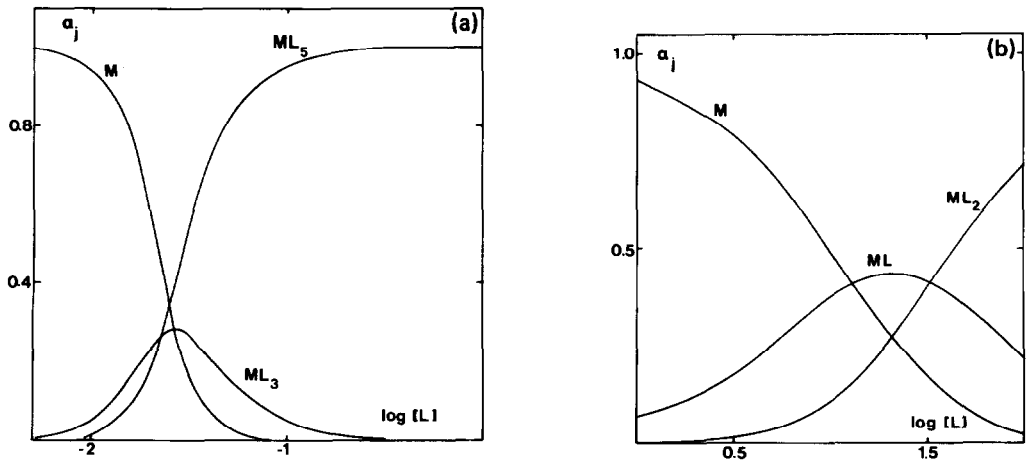

Fig. 1. Distribution of (a) cobalt(II) and (b) manganese(II) between the different ML_j complexes with varying cyanide ion concentrations ([L] in mM).

only the formation of the first two complexes takes place in appreciable amounts. Addition of further cyanide causes a blue precipitate of the hexacoordinate complex,[13] which changes colour on storing. The cyanide ligand can be bonded to a metal ion essentially by covalent bonds. Most metal cyanide complexes have metal-carbon rather than metal-nitrogen bonds. As a very soft ligand the cyanide forms strong complexes with the most transition-elements.

Acknowledgement—We are grateful to Dr Arvid Sandell from the University of Lund, Lund, Sweden, for invaluable help with computer calculations and for fruitful discussions.

REFERENCES

1. J. M. Pratt and R. J. P. Williams, *J. Chem. Soc.* (*A*) 1967, 1291.
2. R. G. S. Banks and J. M. Pratt, *ibid.* 1968, 854.
3. R. M. Izatt, G. D. Watt, C. H. Bartholomew and J. J. Christensen, *Inorg. Chem.* 1968, **7**, 2236.
4. A. Haim and W. K. Wilmarth, *J. Am. Chem. Soc.* 1961, **83**, 509.
5. B. M. Chadwick and A. G. Sharpe, *Adv. Inorg. Chem. Radiochem.* 1966, **8**, 83.
6. A. W. Adamson, *J. Am. Chem. Soc.* 1951, **73**, 5710.
7. R. Lykvist, Undersökningar av Några Reaktioner an Pentacyanokoboltat(II). Dissertation, University of Lund, Lund, Sweden (1984).
8. S. Fronaeus, In H. B. Jonassen and A. Weisberger, *Techniques of Inorganic Chemistry*, Vol. 1, Ch. 1. Interscience, New York (1963).
9. E. Avşar, *J. Inorg. Nucl. Chem.* 1980, **42**, 881.
10. S. Ahrland and E. Avşar, *Acta Chem. Scand.* 1975, **A29**, 881.
11. E. Avşar and F. B. Erim, *Polyhedron* 1986, **5**, 1335.
12. A. Sandell, personal communication.
13. W. P. Griffith, *Coord. Chem. Rev.* 1975, **17**, 177.
14. H. Persson, *Acta Chem. Scand.* 1974, **A28**, 885.

Polyhedron Vol. 6, No. 10, pp. 1913–1917, 1987
Printed in Great Britain

0277–5387/87 $3.00+.00

SYNERGISTIC COMPLEXES OF URANYL ION WITH 1-PHENYL-3-METHYL-4-ACETYL-PYRAZOLONE-5 AND SOME OXO-DONORS

M. S. NAGAR, P. B. RUIKAR and M. S. SUBRAMANIAN*

Radiochemistry Division, Bhabha Atomic Research Centre, Trombay, Bombay-400085, India

(*Received* 17 *February* 1987; *accepted* 11 *May* 1987)

Abstract—Complexes of uranyl ion with 1-phenyl-3-methyl-4-acetyl-pyrazolone-5(PMAP) and various oxo-donors such as aliphatic sulphoxides [R_2SO, where R = *i*-C_5H_{11}(DISO), *n*-C_6H_{13}(DHSO), *n*-C_7H_{15}(DSSO), *n*-C_8H_{17}(DOSO), *n*-C_9H_{19}(DNSO), *n*-$C_{10}H_{21}$(DDSO), *n*-$C_{11}H_{23}$(DUDSO) and *n*-C_4H_9(DBUSO)] tributylphosphate (TBP) and tri-*n*-octyl phosphine oxide (TOPO) have been synthesised and characterized. Analytical data establish that they have the stoichiometry $UO_2(PMAP)_2X$ where X is the oxo-donor. The IR spectra of the sulphoxide complexes in the S—O stretching region indicate that the ligands R_2SO are O-bonded. The methyl protons of the pyrazole ring and acetyl group in the PMAP ligand are equivalent giving rise to a single sharp peak in the PMR spectra, whereas in the synergistic complexes with the oxo-donors, two deshielded peaks of equal intensity are observed which indicate the non-equivalence of the methyl groups. The peak which is more deshielded has been ascribed to the methyl of the acetyl group. The higher deshielding of these methyl protons arises due to the transfer of electron density to the metal atom on complexation.

4-aroyl pyrazolones, such as 1-phenyl-3-methyl-4-benzoyl-pyrazolone-5(PMBP) are being increasingly used as extractants for several metal ions[1–10] in view of their relatively lower cost[11] and their ability to extract metal ions from relatively acidic solutions.[2,6,12] This has resulted in the investigation of extraction of several metal ions by various workers. However, relatively little is known about the stabilities and structure of metal chelates of pyrazolones.

We have been investigating the synthesis, infrared and NMR spectra of solid synergistic complexes of uranyl ion with pyrazolones and oxo-donors such as sulphoxides and phosphorus oxides.[13] Rao and Arora[14] have reported the synthesis and infrared spectra of uranyl-PMBP adducts with tributyl phosphate(TBP) and tri-*n*-octyl phosphine oxide (TOPO). Recently, Okafor[15] has isolated the lanthanide chelates of PMAP and investigated their spectroscopic properties. The present paper reports on the synthesis, characterization, infrared and PMR spectra of synergistic complexes of uranyl ion with PMAP and the oxo-donor aliphatic sulphoxides and tributyl phosphate and tri-*n*-octyl phosphine oxide.

* Author to whom correspondence should be addressed.

EXPERIMENTAL

Reagents

All chemicals used were of B.D.H./A.R. grade. PMAP was synthesised by a modified Jensens' method[16] described by Okafor and recrystallized from hexane to obtain yellow crystals of the enol form m.p. = 67°C, C = 66.6%, H = 5.6%, N = 12.9%; required for $C_{12}H_{12}O_2N_2$, m.p. = 67°C, C = 66.8%, H = 5.6%, N = 13.0%. All the sulphoxides were prepared by a general method reported earlier for the synthesis of long chain aliphatic sulphoxides.[17] TOPO was obtained from Koch Light Co. and used as such. TBP was purified and distilled by the usual procedure.

Preparation of the complexes

The complexes were prepared by solvent extraction of 50 cm^3 of uranyl nitrate solution (1 mM) at a pH 2 with 50 cm^3 of benzene solution containing 2 mM of PMAP and 1 mM of the neutral oxo-donor. The benzene layer was dried with anhydrous sodium sulphate, evaporated to dryness in a rotary evaporator and the product recrystallized twice from *n*-hexane.

Characterization of the complexes

Table 1 summarises the analytical data of the complexes. Melting points were determined using an automatic melting point apparatus, Mettler FP-61. Carbon and hydrogen were determined by microanalysis using the empty tube combustion method described by Belcher and Spooner.[18] Sulphur was by combustion in an oxygen filled flask and conductometric titration of the sulphate in neutral solution with standard barium acetate solution in alcohol–water medium. Uranium was determined by back-extracting from benzene, a weighed amount of the complex with 5 N sulphuric acid, passing through a Jones' reductor to convert to U(IV) and titrating with standard cerium(IV) solution using ferroin as indicator. It was also obtained from the weight of the oxide residue (U_3O_8) after C—H combustion. Infrared spectra were measured in Nujol mulls between CsI discs in the range of 4000–200 cm^{-1} using a Perkin–Elmer 577 infrared grating spectrophotometer. Proton magnetic resonance spectra were measured in $CDCl_3$ with a Varian EM-360, 60 MHz NMR spectrophotometer using 0.1 M solutions and TMS as internal standard.

RESULTS AND DISCUSSION

A few typical bands in the infrared spectra of these complexes have been assigned empirically

Table 1. Analytical data of $UO_2(PMAP)_2X$ complexes

X	Colour	% yield	M.p. (°C)	%C	%H	%N	%S	%U
H_2O	yellow	61	Dec.	40.2	3.4	7.6		32.8(G), 32.9(V)
				40.0	3.3	7.8		33.0
TBP	orange	71	163.2	44.6	5.2	6.0		24.7(G), 24.6(V)
				44.6	5.3	5.8		24.6
TOPO	yellow	89	125.4	53.4	6.9	4.9		21.5(G), 21.9(V)
				52.9	6.7	5.2		21.9
DISO	orange	78	238.1	46.2	5.0	6.2	3.8	26.6(G), 26.8(V)
				45.7	4.9	6.3	3.6	26.7
DHSO	yellow	65	152.0	46.5	5.3	6.0	3.6	26.0(G), 26.0(V)
				46.9	5.2	6.1	3.5	26.0
DSSO	yellow	63	164.2	48.1	5.5	5.9	3.3	25.2(G), 25.1(V)
				48.1	5.5	5.9	3.4	25.1
DOSO	yellow	82	156.2	49.1	5.7	6.0	3.4	24.4(G), 25.4(V)
				49.3	5.7	5.8	3.3	24.4
DNSO	yellow	58	133.1	50.1	5.9	5.7	3.4	23.8(G), 23.7(V)
				50.2	6.0	5.6	3.2	23.8
DDSO	yellow	66	130.0	51.1	6.3	5.5	3.3	23.1(G), 22.7(V)
				51.2	6.2	5.4	3.1	23.1
DUDSO	yellow	67	126.3	51.3	6.0	5.5	3.0	22.2(G), 22.5(V)
				52.1	6.4	5.3	3.0	22.5
DBUSO	yellow	71	196.0	46.6	5.0	6.3	3.8	26.0(G), 25.4(V)
				44.4	4.6	6.5	3.7	27.7

Second line entry under each heading indicates calculated values. In TBP and TOPO complexes, the final product of decomposition has been assumed to be $(UO_2)_2P_2O_7$. DISO = i-$(C_5H_{11})_2SO$; DHSO = $(n$-$C_6H_{13})_2SO$; DSSO = $(n$-$C_7H_{15})_2SO$; DOSO = $(n$-$C_8H_{17})_2SO$; DNSO = $(n$-$C_9H_{19})_2SO$; DDSO = $(n$-$C_{10}H_{21})_2SO$; DUDSO = $(n$-$C_{11}H_{23})_2SO$; DBUSO = $(n$-$C_4H_9)_2SO$.

Table 2. Characteristic infrared bands of $UO_2(PMAP)_2X$ complexes

X	S=O; P=O	O—U—O	M—O(Pyr)	M—O(donor)	νCH	Py.ring str.	CH in plane def.
H_2O		927			750	1525	1075
TOPO	1083	915	495	400	753	1530	1082
TBP	1210	920	490	395	752	1535	1080
DUDSO	965	910	485	395	756	1530	1080
DNSO	965	905	490	395	760	1530	1078
DSSO	970	910	485	392	755	1530	1080
DOSO	967	910	490	400	760	1530	1081
DHSO	967	905	490	396	755	1530	1083
DISO	968	916	490	395	760	1530	1082
DBUSO	960	908	490	400	755	1528	1083

Table 3. Pmr spectral data of chelate protons of $UO_2(PMAP)_2X$ complexes in $CDCl_3$ at 60 MHz (δ ppm)

	Phenyl protons								Pyrazolone methyl protons			
	ortho				m.p.							
X	B	I	M	J	B	I	M	J	B	I	M	J
TBP	8.33	4	multiplet		7.43	6	multiplet		2.51 2.77	6	1	—
TOPO	8.40	4	multiplet		7.45	6	multiplet		2.53 2.82	6	1	—
DBUSO	8.48	4	multiplet		7.42	6	multiplet		2.56 2.75	6	1	—
DISO	8.45	4	multiplet		7.46	6	multiplet		2.60 2.90	6	1	—
DSSO	8.40	4	multiplet		7.40	6	multiplet		2.60 2.90	6	1	—
DOSO	8.40	4	multiplet		7.40	6	multiplet		2.60 2.88	6	1	—
DDSO	8.42	4	multiplet		7.40	6	multiplet		2.58 2.88	6	1	—
DHSO	8.45	4	multiplet		7.45	6	multiplet		2.60 2.88	6	1	—
DNSO	8.45	4	multiplet		7.47	6	multiplet		2.60 2.85	6	1	—
DUDSO	8.40	4	multiplet		7.50	6	multiplet		2.58 2.85	6	1	—
MPP[a]	7.86	2	multiplet		7.32	3	multiplet		2.15 3.40	3 2	1 1	0 (CH_2)
PMAP[a]	7.85	2	multiplet		7.42	3	multiplet		2.44 11.30	6 1	1 1	 (OH)

[a] Denote free ligands.

B = Band position; I = Intensity; M = Multiplicity; J = Coupling constant.

(Table 2). These indicate a small shift of the carbonyl vibration indicating chelation. The S=O stretching frequency in the sulphoxide adducts has been observed as a strong band in the region of 960–970 cm^{-1}. Since these are reduced with respect to the free sulphoxides, it has been concluded that the bonding is through the oxygen atom of the sulphoxide. A band at 1083 cm^{-1} and another at 1210 cm^{-1} have been ascribed to the P=O stretching frequencies in the TOPO and TBP complexes respectively. In all these complexes, the O—U—O asymmetric stretch has been observed as a strong band at 910–920 cm^{-1}. This is lower than the frequency observed at about 950 cm^{-1} in ionic uranyl compounds indicating the presence of the uranyl group in the complexes. In all these complexes a band at 485–490 cm^{-1} which is absent in the free PMAP ligand is observed and this has been attributed to the U—O (pyrazolone) stretching frequency. This compares with the assignment made by Okafor for the M—O stretching frequency of lanthanide chelates of PMAP.[15] Another band at 390–400 cm^{-1} which is absent in the free ligand has been ascribed to the M—O(oxo-donor) stretching frequency. No correlation of this frequency with the base strength of the oxo-donor has been observed. Strong bands at 755 and at 1080 cm^{-1} have been assigned to the νCH and CH in-plane deformation modes respectively as observed by Okafor for lanthanide chelates of PMAP.

In the PMR spectra, two sets of signals of the phenyl protons are observed due to the ortho protons and *m,p* protons in the synergistic complexes of PMAP and oxo-donors (Table 3). The chemical shift of the *ortho* protons occurring at 8.45 ppm shows significant deshielding as compared to the PMAP ligand (7.85 ppm) whereas no shift is observed in the case of the *m,p* protons. This can be attributed to the bonding site being nearer to the *ortho* protons of the phenyl ring. The methyl protons of the pyrazole ring and those of the acetyl group give only a single signal at 2.44 ppm in the PMAP ligand. However, in the synergistic complexes, they are deshielded with respect to the ligand and occur as two sharp separate signals at 2.60 and 2.85 ppm. The latter is ascribed to the methyl protons of the acetyl group as it is more deshielded with respect to the methyl protons of the pyrazole ring due to the transfer of electron density to the metal on coordination. The single peak corresponding to the enolic proton occurring at 11.3 ppm in PMAP disappears in the synergistic complexes on the formation of the chelate. The alpha methylene protons of the sulphoxide groups (Table 4) in these complexes show the expected multiplet (8 lines) at 3.15 ppm corresponding to the ABX_2

Table 4. PMR spectral data of oxodonor protons of $UO_2(PMAP)_2X$ complexes in $CDCl_3$ at 60 MHz (δ ppm)

	Oxodonor protons											
	Alpha CH_2				Other CH_2				Methyl protons			
X	B	I	M	J	B	I	M	J	B	I	M	J
TBP	4.24	6	4	6	1.4	12	multiplet		0.83	9	3	7
TOPO			multiplet		2.23	36	1	—	0.88	9	3	7
DBUSO	3.15		multiplet		—	8	multiplet		0.80	6	3	7
DISO	3.12		multiplet		1.70	6	multiplet		0.87	12	3	6
DSSO	3.10		multiplet		1.20	6	multiplet		0.83	6	3	5
					1.90	4	3	(B—CH_2)				
DOSO	3.15		multiplet		1.20	20	1	—	0.82	6	3	5
					1.90	4	3	6—(B—CH_2)				
DDSO	3.15		multiplet		1.23	28	1	—	0.85	6	3	5
					1.90	4	multiplet(B—CH_2)					
DHSO	3.15		multiplet		1.20	12	multiplet		0.80	6	3	5
					1.88	4	3	5—(B—CH_2)				
DNSO	3.18		multiplet		1.20	24	1	—	0.85	6	3	6
					1.90	4	multiplet(B—CH_2)					
DUDSO	3.15		multiplet		1.22	32	1	—	0.85	6	3	6
					1.90	4	multiplet(B—CH_2)					

B = Band position; I = Intensity; M = Multiplicity; J = Coupling constant.

pattern as observed in complexes with TTA as the chelating ligand.[19,20] In the $UO_2(PMAP)_2 \cdot TBP$ complex however, these protons are observed as a quartet occurring at 4.24 ppm due to coupling with the adjacent P-31 nuclei. The methyl protons of the oxo-donor are found to occur at much higher fields of 0.85 ppm compared to those of the methyl protons of pyrazolone due to the inductive effect of the adjacent methylene groups. In addition, these peaks appear as triplets with a J value of 5–7 Hz due to coupling by the adjacent methylene protons whereas the pyrazolone methyls occur only as single sharp peaks in these complexes.

CONCLUSIONS

Solid synergistic complexes of uranyl ion with PMAP and oxo-donors have the stoichiometry, $UO_2(PMAP)_2 \cdot X$ where X is the oxo-donor. These are similar to the PMBP systems in which the oxo-donor binds giving a possible coordination number of seven for uranium.

Acknowledgement—The authors wish to express their sincere thanks to Dr P. R. Natarajan, Head of the Radiochemistry Division for his keen interest in the work.

REFERENCES

1. B. Y. Myasoedov, N. E. Kochetkova and M. K. Chmutova, *Zh. Anal. Khim.* 1972, **27**, 678; 1973, **28**, 1723.
2. G. N. Rao and J. S. Thakur, *J. Sci. Ind. Res.* 1975, **34**, 110.
3. J. Hala and J. Primoda, *Collect. Czech. Chem. Commun.* 1978, **43**, 2890.
4. O. Navaratil, *Collect. Czech. Chem. Commun.* 1980, **45**, 1221.
5. M. Y. Mirza and F. I. Nwabue, *Radiochim. Acta* 1980, **27**, 47.
6. S. Umetani, M. Matsui, J. Toei and T. Shigematsu, *Anal. Chim. Acta* 1980, **113**, 315.
7. M. S. Bhatti and I. H. Quershi, *J. Radioanal. Chem.* 1980, **56**, 65.
8. M. Y. Mirza and F. Y. Nwabue, *Talanta* 1981, **28**, 49.
9. Y. Akama, T. Nakai and F. Kawamura, *Analyst* 1981, **106**, 250.
10. S. A. Pai and M. S. Subramanian, *J. Radioanal. Nucl. Chem.* 1985, **89**, 423.
11. Yu. A. Zolotov, *Extraction of Chelate Compounds*, p. 227. Ann Arbor–Humphrey Scientific Publishers (1970).
12. A. Roy and K. Nag, *J. Inorg. Nucl. Chem.* 1978, **40**, 331.
13. M. S. Subramanian, A: K. Sabnis and M. S. Nagar, *Synth. React. Inorg. Met. Org. Chem.* 1983, **13**, 1067.
14. G. N. Rao and H. C. Arora, *J. Inorg. Nucl. Chem.* 1977, **39**, 2057.
15. E. C. Okafor, *Polyhedron* 1983, **2**, 309.
16. B. S. Jensen, *Acta Chem. Scand.* 1959, **13**, 1890.
17. M. Guy Laurence and H. Normant, *C.R. Acad. Sc. Paris* 1969, **269**, 352.
18. R. Belcher and C. E. Spooner, *J. Chem. Soc.* 1943, 13.
19. M. S. Subramanian, S. A. Pai and V. K. Manchanda, *Aust. J. Chem.* 1973, **26**, 85.
20. M. M. Dinghra and M. S. Subramanian, *Chem. Phys. Letts.* 1975, **30**, 83.

Polyhedron Vol. 6, No. 10, pp. 1919–1921, 1987
Printed in Great Britain

0277–5387/87 $3.00+.00

COMMUNICATION

EFFECT OF COUNTERCATIONS IN CATALYTIC PHOTOOXIDATION OF ISOPROPYL ALCOHOL BY DECATUNGSTATE ISOPOLYANION

KENJI NOMIYA,* SEIICHIRO MATSUBARA, KIYOTSUGU YAMASHITA and MAKOTO MIWA

Department of Industrial Chemistry, Faculty of Engineering, Seikei University, Musashino, Tokyo 180, Japan

(*Received* 6 *April* 1987; *accepted* 5 *May* 1987)

Abstract—By utilizing homogeneous decatungstate solution, we have found a novel catalyst system for photooxidation of isopropyl alcohol under excess of O_2. The decatungstate with countercation ratio of K : TBA (tetrabutylammonium) = 3 : 1 shows an activity about double that of the homogeneous K or TBA salt of decatungstate. A new redox cycle considering the ion-pair between decatungstate and countercations is proposed.

Under excess of O_2, a catalytic photooxidation of isopropyl alcohol to acetone, initiated by irradiation (> 300 nm) of the charge-transfer bands of decatungstate isopolyanion $[W_{10}O_{32}]^{4-}$ proceeds in conjunction with a redox cycle of the polyanion between oxidized (pale yellow) and $2e^-$-reduced (blue) forms.[1–3] The reoxidation of $2e^-$-reduced species is attained by reaction with O_2. Recently we have found spectrophotometrically for homogeneous solution containing K or TBA salt that the relative velocity of redox cycle is markedly influenced by the countercations, i.e. a photoreduction of polyanion proceeds faster for the K salt than for the TBA salt, but a reoxidation of the reduced polyanion by reaction with O_2 proceeds slower for the K salt than for the TBA salt.[2] In spite of such a difference, however, the conversion of isopropyl alcohol to acetone and the catalytic turnover are almost unchanged for the two salts. In order to seek a more active catalyst using decatungstate, we have studied the photooxidation of isopropyl alcohol by mixed-countercation species of decatungstate, $K_n(TBA)_{4-n}[W_{10}O_{32}]$, under excess of O_2.

* Author to whom correspondence should be addressed. Present address: the laboratory of Prof. R. G. Finke, Department of Chemistry, University of Oregon, Eugene, Oregon 97403, U.S.A.

EXPERIMENTAL

All chemicals used were of analytical grade. $K_4[W_{10}O_{32}]\cdot 4H_2O$ and $(TBA)_4[W_{10}O_{32}]$ were prepared as previously described.[1,2] Solvent was used as a 1 : 1 mixture of CH_3CN and water (pH 2.5, H_2SO_4). A sample solution (50 cm^3) was prepared using two decatungstate salts at a constant concentration of $[W_{10}O_{32}]^{4-}$ (2×10^{-3} mol dm^{-3}) containing various molar ratios of K : TBA (4 : 0, 3.5 : 0.5, 3 : 1, 2.5 : 1.5, 2 : 2, 1 : 3, 0 : 4), into which isopropyl alcohol (0.4 mol dm^{-3}) as a substrate and benzene (0.24 mol dm^{-3}) as an internal reference for gas chromatography had been added. Apparatus for the photoreaction, comprising of a 75-W mercury lamp (SHL 100-UV, Toshiba Corporation) for an external irradiation and 75 cm^3 Pyrex reaction-flask, was described elsewhere. Actinometry was performed by irradiation with 2-hexanone and the light intensity was 1.0×10^{-4} einstein h^{-1}. Decrease of substrate and production of acetone during irradiation (> 300 nm) under excess of O_2 were monitored by TCD gas chromatography (Shimadzu GC-8A) on a PEG 20M glass-column (3 m) and the data were treated by Chromatopak (Shimadzu C-R3A). The formation of reduced decatungstate under N_2 and the reoxidation of it by reaction with O_2 were monitored by a spectrophotometer (Hitachi-340).

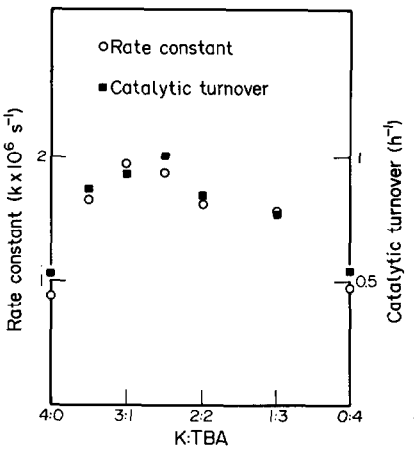

Fig. 1. Relation of the countercation-ratio of decatungstate to the rate constant of decreasing isopropyl alcohol determined by the assumed first-order kinetics and to the catalytic turnover per hour for production of acetone. Conditions: [decatungstate] = 2×10^{-3} mol dm^{-3} and [isopropyl alcohol] = 0.4 mol dm^{-3} in 50 cm^3 solution containing benzene as an internal reference for gas chromatography. Solvent: 1:1 mixed media of Ch_3CN and water (pH 2.5, H_2SO_4).

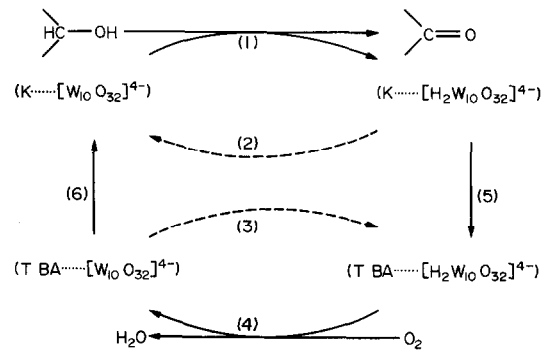

Fig. 2. Proposed redox cycle of decatungstate for catalytic photooxidation of isopropyl alcohol.

RESULTS AND DISCUSSION

Since the stoichiometry between consumed isopropyl alcohol and produced acetone is retained, side-reactions do not need to be considered. For each countercation ratio of decatungstate, the rate constant for decreasing isopropyl alcohol deter-

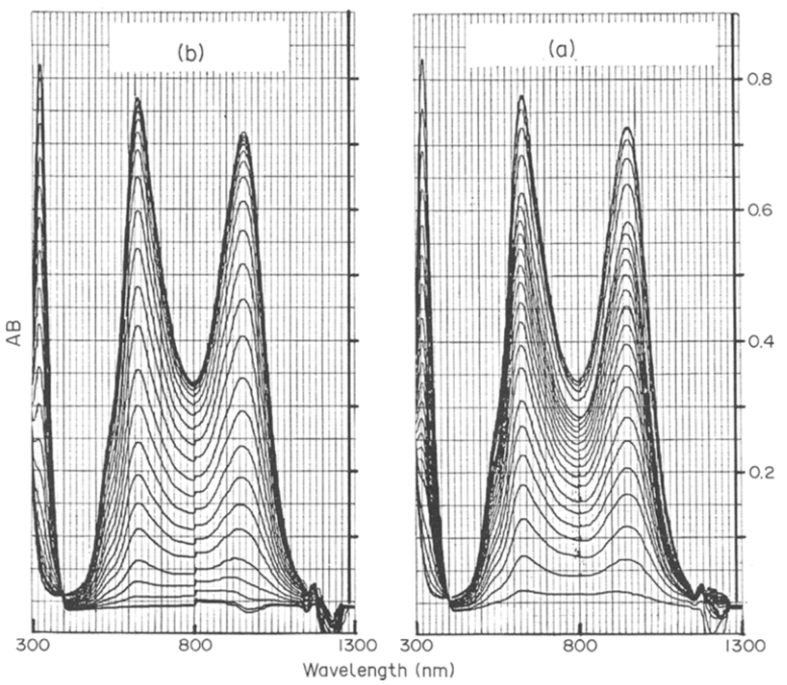

Fig. 3. Absorption spectral changes of photoreduced decatungstate under N_2 (a) and of reoxidation process of reduced decatungstate by reaction with O_2 (b). Irradiation is performed for the decatungstate with the cation-ratio K : TBA = 3 : 1 ([decatungstate] = 6.25×10^{-5} mol dm^{-3}), isopropyl alcohol (5×10^{-3} mol dm^{-3}) and benzene (1.6×10^{-3} mol dm^{-3}) in the 1 : 1 mixed media of CH_3CN and water (pH 2.5, H_2SO_4). The spectra in (a) are recorded for 18 min each after 1-min irradiation and then for each after 5-min irradiation. The spectra of reoxidation (b) are recorded after exposure to air of the solution of saturated photoreduced species obtained in the experiment of (a).

mined by the assumed first-order kinetics and the catalytic turnover, or the molar ratio of decatungstate to produced acetone, per hour are depicted in Fig. 1. Significant effects by countercations are seen in the cases, other than when the K:TBA ratio is 4:0 and 0:4. Such mixed-cation systems show a higher activity about 1.5–2 times than that of the decatungstate with homogeneous countercation composition. A maximal activity is especially observed when the countercation ratio is 3 : 1–2.5 : 1.5. These facts could not be explained by the redox cycle of only a polyanion-moiety, but by the cycle of an ion-pair, or an outer-sphere complex between decatungstate and countercations.

In Fig. 2, we propose a new redox cycle involving ion-pairs with countercations. The paths (1) and (3) show the photoreduction of decatungstate and the paths (2) and (4) the reoxidation of reduced decatungstate by reaction with O_2. $(K\ldots[W_{10}O_{32}]^{4-})$ and $(TBA\ldots[W_{10}O_{32}]^{4-})$ represent the ion-pair of oxidized decatungstate, and $(K\ldots[H_2W_{10}O_{32}]^{4-})$ and $(TBA\ldots[H_2W_{10}O_{32}]^{4-})$ the ion-pair of $2e^-$-reduced decatungstate. For the homogeneous K salt, the redox cycle consists of paths (1) and (2), and for the homogeneous TBA salt, it consists of paths (3) and (4). It has been spectrophotometrically evident that the paths (1) and (4) proceed faster than those of (2) and (3).[2] For the mixed-countercation system, the paths (1)–(5)–(4)–(6) form a new redox cycle, where the paths (5) and (6) are assumed as a process comprising of a rearrangement of countercations.

Figure 3 shows the absorption spectral changes of photoreduction of decatungstate with a K : TBA ratio of 3 : 1 during irradiation under N_2 and of the reoxidation of saturated $2e^-$-reduced decatungstate by exposure to air. These spectra show that both of these processes are well balanced. They markedly contrast to recently reported spectra for homogeneous K or TBA salt, where both processes are unbalanced.[2] The proposed redox cycle is consistent with these spectral changes.

REFERENCES

1. K. Nomiya, Y. Sugie, T. Miyazaki and M. Miwa, *Polyhedron* 1986, **5**, 1267.
2. K. Nomiya, T. Miyazaki, K. Maeda and M. Miwa, *Inorg. Chim. Acta* 1987, **127**, 65.
3. K. Nomiya, K. Maeda, T. Miyazaki and M. Miwa, *J. Chem. Soc., Dalton Trans.* 1987, **4**, 961.

Polyhedron Vol. 6, No. 10, pp. 1923–1924, 1987
Printed in Great Britain

0277–5387/87 $3.00+.00

COMMUNICATION

SYNTHESIS AND RING INVERSION OF THE FIRST HAFNOCENE DITELLUROLENE CHELATE: $[(\eta^5\text{-}C_5H_5)_2Hf(1,2\text{-}Te_2C_6H_4)]$

TH. KLAPÖTKE,* H. KÖPF and P. GOWIK

Institut für Anorganische und Analytische Chemie, Technische Universität Berlin, D-1000 Berlin 12, F.R.G.

(*Received* 23 *April* 1987; *accepted* 11 *May* 1987)

Abstract—$[(cp)_2Hf(1,2\text{-}Te_2C_6H_4)]$ (**1**) (cp = η^5-C_5H_5) was obtained from $[(cp)_2HfCl_2]$ and equivalent amounts of $1,2\text{-}(LiTe)_2C_6H_4$ as the first hafnocene ditellurolene metallacycle and the last missing member of the widely investigated subgroup IV metallocene dichalcogenolene chelate complexes of the type $[(cp)_2M(1,2\text{-}X_2C_6H_4)]$ (M = Ti, Zr, Hf; X = S, Se, Te). Hafnocene benzene-1,2-ditellurolate (**1**) was shown by temperature-dependent ^1H NMR spectroscopy to exist in toluene solution in an envelope conformation, the five-membered $HfTe_2C_2$ chelate ring undergoing rapid inversion at room temperature.

Metallocene heterocycles of subgroup IV with S,S-[1–6] and Se,Se-coordinated[7–8] benzene-1,2-dichalcogenolato chelate ligands have been synthesized. Recently there were reports about the preparation of the analogous tellurium derivatives of the titanocene[9] and zirconocene[10] systems using different reaction routes and that no metallacycle could be obtained analogous to the synthesis of the Zr complex when the metal was Hf.[10] We now report on the synthesis and spectroscopic characterization of hafnocene benzene-1,2-ditellurolate (**1**), the first example of a Te containing hafnocene metallacycle and the last missing member of the metallocene ditellurolene chelates of subgroup IV.

The reaction in an argon atmosphere and exclusion of air and moisture of hafnocene dichloride $[(cp)_2HfCl_2]$[11] (5.14 mmol) with $1,2\text{-}(LiTe)_2C_6H_4$[12] (5.19 mmol) in 200 cm^3 tetrahydrofurane (thf)/ether (1:1) at −78°C afforded the desired hafnocene ditellurolene metallacycle (**1**) as a deep red solid, sensitive towards air and moisture (Scheme 1). The product was recrystallized from dry toluene and gave **1** in 37% yield with satisfactory elemental analysis and spectroscopic results in agreement with the expected theoretical values: IR (KBr) $\tilde{\nu}$: ν (CH, cp) 3105, ω (CC, cp) 1435, δ (CH, cp) 1010, γ (CH, cp) 800, γ (CH, 1,2-C_6H_4) 720 cm^{-1}; ^1H NMR (toluene-d_8): 8.30–6.75 (m, 4H, 1,2-C_6H_4), and 5.74 (s, 10H, cp) ppm; MS (EI, 70 eV, 180°C) *m/z*: 640 (46%) M^+, 564 (20) $M^+-C_6H_4$, 512 (25) M^+-Te, 436 (19) $M^+-C_6H_4-Te$, 384 (60) M^+-2 Te, 308 (100) $M^+-Te_2C_6H_4$, 243 (11) $M^+-Te_2C_6H_4-cp$, 178

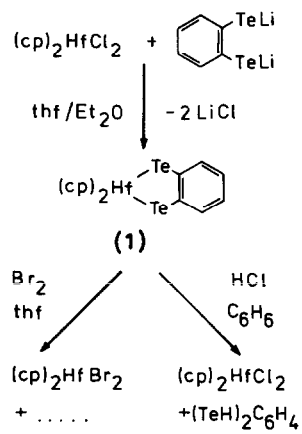

Scheme 1. Preparation and reaction behavior of **1**, cp = η^5-C_5H_5.

* Author to whom correspondence should be addressed.

Table 1. ^{1}H NMR data[a] and activation parameters of $[(cp)_2M(1,2\text{-}X_2C_6H_4)]$

M	X	δ (cp) (ppm)	T_c (°C)	$\Delta\nu$ (Hz)	$\Delta G_c^{\ddagger}$ (kJ mol^{-1})	Ref.
Ti	Te	5.76	−38	10.0	51	9
Zr	Te	5.96[b]	−30	20.9	51	10
Hf	Te	5.74	−50	9.4	48	present work
Hf	Se	5.46	−75	—	—	8
Hf	S	5.46	−64	20.0	45	6

[a] Solvent: $CD_3C_6D_5$; [b] cp = η^5-^{t}BuC$_5$H$_4$.

(28) Hf^+; (values given relate to ^{178}Hf and ^{128}Te); Fp: 225°C, decomposition. **1** reacts with halides such as bromine, dissolved in thf, or hydrogen halides as with hydrogen chloride saturated benzene yielding the corresponding hafnocene dihalides (Scheme 1).

In the dynamic ^{1}H NMR spectrum the singlet due to the ten equivalent cp protons at room temperature was subject to a coalescence phenomenon at a lower temperature and was split into two sharp singlets of equal intensity at temperatures below −50°C (Fig. 1). From this result an envelope conformation of the five-membered chelate ring, folded along the Te---Te axis and undergoing rapid inversion at room temperature, can be derived (Fig. 2). The activation parameters of the chelate ring inversion of **1** and the analogous titanocene and zirconocene derivatives as well as those of the S or Se coordinated hafnocene complexes are given in Table 1. With regard to an estimation of the error of these $\Delta G_c^{\ddagger}$ values (±13%) surprisingly there is no significant connection between this activation parameter and the central atom or the coordinating chalcogen atom.

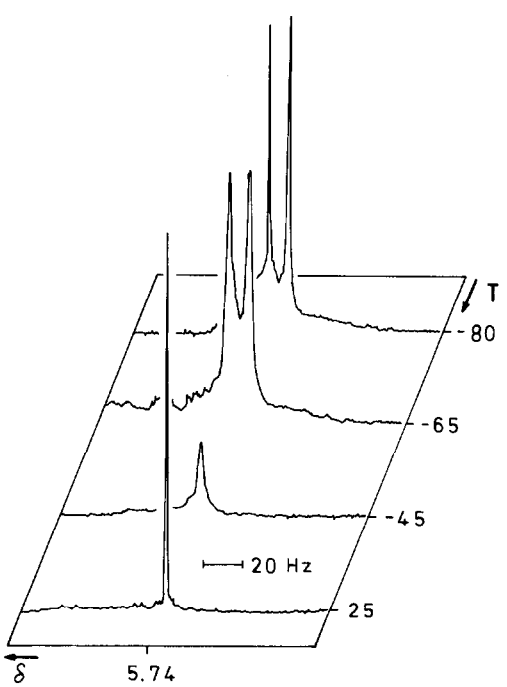

Fig. 1. Temperature-dependent ^{1}H NMR spectrum (cp region) of **1** in $CD_3C_6D_5$, δ in ppm, T in °C.

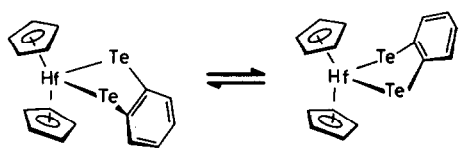

Fig. 2. Chelate ring inversion of **1**.

Acknowledgements—We are grateful to the Fonds der Chemischen Industrie for financial support, A. Stöckel for mass spectra, and M. Dettlaff for NMR spectra.

REFERENCES

1. H. Köpf, *Z. Naturforsch.* 1968, **23b**, 1531.
2. H. Köpf and M. Schmidt, *J. Organomet. Chem.* 1965, **4**, 426.
3. M. A. Chaudhari and F. G. A. Stone, *J. Chem. Soc. A* 1966, 838.
4. R. B. King and C. A. Eggers, *Inorg. Chem.* 1968, **7**, 340.
5. H. Köpf, *J. Organomet. Chem.* 1968, **14**, 353.
6. H. Köpf and Th. Klapötke, *Z. Naturforsch.* 1985, **40b**, 1338.
7. B. Gautheron, G. Tainturier, S. Pouly, F. Théobald, H. Vivier and A. Laarif, *Organometallics* 1984, **3**, 1495.
8. H. Köpf and Th. Klapötke, *J. Organomet. Chem.* 1986, **310**, 303.
9. H. Köpf and Th. Klapötke, *J. Chem. Soc., Chem. Commun.* 1986, 1192.
10. P. Meunier, B. Gautheron and A. Mazouz, *J. Organomet. Chem.* 1987, **320**, C39.
11. E. Samuel, *Bull. Soc. Chim. France* 1966, 3548.
12. K. Lerstrup, M. Lee, F. M. Wiygul, T. J. Kistenmacher and D. O. Cowan, *J. Chem. Soc., Chem. Commun.* 1983, 294.

Polyhedron Vol. 6, No. 10, pp. 1925–1927, 1987
Printed in Great Britain

0277–5387/87 $3.00+.00

COMMUNICATION

ISOLATION OF THE COMPLEXES $(n\text{-}Bu_4N)_2[(Re_2Cl_7)_2\{\mu\text{-}(L—L)\}]$, WHERE L—L = $Ph_2PC{\equiv}CPPh_2$ OR *TRANS*-$Ph_2PCH{=}CHPPh_2$. THE FIRST EXAMPLES OF QUADRUPLY BONDED DIRHENIUM(III) ANIONS OF THE TYPE $[Re_2Cl_7L]^-$

MOHAMMED BAKIR and RICHARD A. WALTON†

Department of Chemistry, Purdue University, West Lafayette, IN 47907, U.S.A.

(*Received* 23 *March* 1987; *accepted* 27 *May* 1987)

Abstract—The reactions of $(n\text{-}Bu_4N)_2Re_2Cl_8$ with the bidentate bridging phosphine ligands (L—L) = $Ph_2PC{\equiv}CPPh_2$ or *trans*-$Ph_2PCH{=}CHPPh_2$ in methanol–conc. HCl give the salts $(n\text{-}Bu_4N)_2[(Re_2Cl_7)_2\{\mu\text{-}(L—L)\}]$, the first examples of quadruply bonded dirhenium(III) anions of the type $[Re_2Cl_7L]^-$. Their spectroscopic properties and reactivity have been examined.

The octahalodirhenate(III) anions $[Re_2X_8]^{2-}$ (X = Cl or Br) react with monodentate phosphine ligands (PR_3) to form the neutral quadruply-bonded species $Re_2X_6(PR_3)_2$, and from thence to the lower valent complexes $Re_2X_5(PR_3)_3$ (Re—Re bond order 3.5) or $Re_2X_4(PR_3)_4$ (Re—Re bond order 3) depending upon the reducing propensity of the phosphine ligand.[1] In no instance has a salt of the intermediate monoanionic mono-substituted type $[Re_2X_7(PR_3)]^-$ been isolated. We report for the first time the isolation of such species as present in the salts $(n\text{-}Bu_4N)_2[(Re_2Cl_7)_2\{\mu\text{-}(L—L)\}]$ (**1**), in which L—L is the bidentate bridging phosphine $Ph_2PC{\equiv}CPPh_2$(dpa) or *trans*-$Ph_2PCH{=}CHPPh_2$ (*t*-dppee).

$(n\text{-}Bu_4N)_2[Cl_4ReReCl_3\{\mu\text{-}(L—L)\}Cl_3ReReCl_4]$

L—L = $Ph_2PC{\equiv}CPPh_2$ (**1a**)

L—L = *trans*-$Ph_2PCH{=}CHPPh_2$ (**1b**)

A representative recipe is as follows.‡ A mixture of $(n\text{-}Bu_4N)_2Re_2Cl_8$[2] (0.20 g, 0.175 mmol), dpa (0.09 g, 0.228 mmol) and 10 cm^3 of methanol, to which 10 drops of conc. HCl had been added, was stirred at room temperature for one day. The resulting insoluble purple precipitate was filtered off, washed with methanol, hexanes, diethyl ether and dried *in vacuo*; yield 0.17 g (91%). Found: C, 34.1; H, 4.6; Cl, 22.9. Calc. for $C_{58}H_{92}Cl_{14}N_2P_2Re_4$: i.e. $(n\text{-}Bu_4N)_2[(Re_2Cl_7)_2\{\mu\text{-}(Ph_2PC{\equiv}CPPh_2)\}]$: C, 32.9; H, 4.4; Cl, 23.4. The slightly high C and H microanalyses reflect the difficulty of purifying such an insolublc complex.§

A similar procedure gave $(n\text{-}Bu_4N)_2[(Re_2Cl_7)_2\{\mu\text{-}(trans\text{-}Ph_2PCH{=}CHPPh_2)\}]$ as a green solid in a yield of 86%.

Although both complexes display very limited solubility properties we were, nonetheless, able to adequately characterize them although neither could be obtained in single crystal form. We favor a structure such as that depicted below in which the individual dirhenium units retain the eclipsed

† Author to whom correspondence should be addressed.

‡ Bis(diphenylphosphino(acetylene (dpa) and *trans*-1,2-bis(diphenylphosphino)ethylene (*t*-dppee) were purchased from Strem Chemicals and used as received. Solvents used in the preparation of complexes were of commercial grade and were thoroughly deoxygenated prior to use. All reactions were performed in a nitrogen atmosphere using standard vacuum line techniques.

§ When the reaction which gave this complex was carried out in methanol in the absence of conc. HCl, a brown solid precipitated. Although this product has not yet been fully characterized, it is not $Re_2Cl_6(dpa)_2$.

rotational geometry of the parent $[Re_2Cl_8]^{2-}$,[1] (see Structure 1).

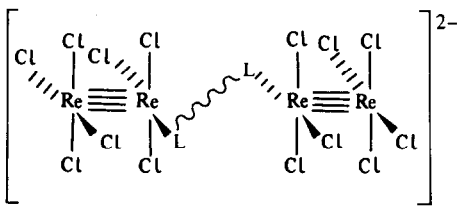

The electronic absorption spectrum of **1a**, recorded as a Nujol mull, has a band at ~ 740 nm, assigned to the $\delta \rightarrow \delta^*$ transition,[1] weak absorptions at ~ 540 and 480 nm, and more intense features at 390 and 325 nm. In CH_2Cl_2 solution, the spectrum is very similar to this, with absorptions (relative intensities in parentheses) at 730(9), ~ 540(2), ~ 470(2), 380sh(13) and 315(34) nm. The Nujol mull spectrum of (**1b**) shows the $\delta \rightarrow \delta^*$ transition at 735 nm, a weak band at ~ 570 nm, a shoulder at ~ 410 nm and an intense absorption at 290 nm. Although (**1a**) and (**1b**) decompose in CH_3CN (*vide infra*), the ^1H NMR spectrum of a freshly prepared solution of (**1a**) in CD_3CN shows proton resonances due to the dpa ligand and *n*-Bu_4N^+ cation in the expected intensity ratio of 1 : 2.

Further evidence for the identity of these salts as derivatives of the quadruply bonded Re_2^{6+} core was obtained from reactions with monodentate phosphines. (**1a**) reacts with PEt_3 in ethanol to form $Re_2Cl_4(PEt_3)_4$ in 55% yield, while $PMePh_2$ and $PEtPh_2$ under these same conditions form $Re_2Cl_5(PMePh_2)_3$ and $Re_2Cl_5(PEtPh_2)_3$, respectively, in yields of ~ 80%. These yields are similar to those in which $Re_2Cl_5(PMePh_2)_3$ and $Re_2Cl_5(PEtPh_2)_3$ are formed (90% and 75%, respectively) from $(n\text{-}Bu_4N)_2Re_2Cl_8$.[3] (**1b**) shows this same reactivity behavior; it forms $Re_2Cl_4(PEt_3)_4$ in 68% yield and $Re_2Cl_5(PMePh_2)_3$ in 85% yield. These products, which are the ones expected from such a quadruply bonded Re_2^{6+} starting material,[3] were identified on the basis of their spectroscopic and electrochemical properties.[3,4]

Of special note is the reaction of (**1a**) with PPh_3 in hot ethanol. An excess of PPh_3 affords an almost quantitative yield of green insoluble $Re_2Cl_6(PPh_3)_2$ (94%), whereas 2 equivs of PPh_3 gives $Re_2Cl_6(PPh_3)_2$ (49%) and from the filtrate a mixture of dpa and $(n\text{-}Bu_4N)_2Re_2Cl_8$.† These observations imply that the following reactions are occurring:

(1) $[Re_2Cl_7(\mu\text{-dpa})Re_2Cl_7]^{2-} + 2PPh_3 \rightarrow Re_2Cl_6(PPh_3)_2 + (n\text{-}Bu_4N)_2Re_2Cl_8 + dpa$

(2) $(n\text{-}Bu_4N)_2Re_2Cl_8 + 2PPh_3 \rightarrow Re_2Cl_6(PPh_3)_2 + 2n\text{-}Bu_4NCl.$

In this same context we have observed that (**1a**) reacts slowly with CH_3CN to give $(n\text{-}Bu_4N)_2Re_2Cl_8$ (36% yield of isolated product) together with an as yet unidentified blue Re_2^{6+} complex (λ_{max} at 656 nm for its $\delta \rightarrow \delta^*$ transition). When the latter reaction is carried out at room temperature in the presence of an excess of *n*-Bu_4NCl for 2 h, the blue salt $(n\text{-}Bu_4N)_2Re_2Cl_8$ can be precipitated in quantitative yield upon the addition of an excess of diethylether. The yield of pure recrystallized product (from methanol/conc. HCl) was ~ 80%. These reactions not only confirm the structural identity of (**1a**) but, furthermore, demonstrate the lability of the μ-dpa ligand.

The cyclic voltammogram (CV) of (**1a**) in 0.1 M *n*-Bu_4NPF_6 (TBAH)-CH_2Cl_2 shows a pair of closely spaced couples at $E_{1/2} \simeq -0.31$ V and -0.43 V vs Ag/AgCl (Fig. 1) which signify that the reductions of the two dpa-coupled Re_2^{6+} cores occur at different potentials.[5] A similar phenomenon is seen in the CV of (**1b**) with $E_{1/2}$ values of $\simeq -0.40$ V and -0.52 V vs Ag/AgCl. These potentials are, as expected, intermediate between those for the one-electron reductions of $Re_2Cl_6(PR_3)_2$[1,4] and $[Re_2Cl_8]^{2-}$.[1,6,7] When acetonitrile is added to a solution of (**1a**) in 0.1 M TBAH-CH_2Cl_2, the CV changes with time and shows the formation of $[Re_2Cl_8]^{2-}$ ($E_{1/2} \simeq +1.5$ V and $E_{1/2} \simeq -0.93$ V vs Ag/AgCl)[6,7] together with a couple at $\simeq -0.7$ V which must be associated with another Re_2^{6+} species.

Studies on the chemistry of these systems

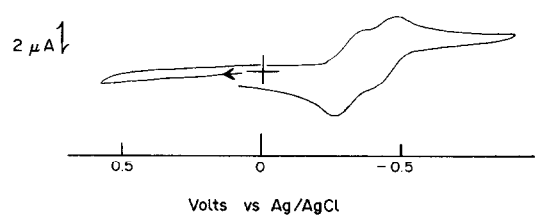

Fig. 1. Cyclic voltammogram (recorded at $v = 200$ mV s^{-1} using a Pt-bead electrode) for a 0.1 M *n*-Bu_4NPF_6-CH_2Cl_2 solution of $(n\text{-}Bu_4N)_2[(Re_2Cl_7)_2(\mu\text{-dpa})]$. For each of the closely spaced couples at $E_{1/2} = -0.31$ V and -0.43 V, the peak separations ΔE_p ($= E_{p,a} - E_{p,c}$) are $\simeq 100$ mV. Under our experimental conditions the ferrocenium/ferrocene reference standard had $E_{1/2} = +0.47$ V.

† The dissociation of dpa in this reaction under non-acidic conditions is in marked contrast to the reaction of $(n\text{-}Bu_4N)_2Re_2Cl_8$ with dpa in methanol to give (**1a**) which requires the presence of HCl.

are continuing. We note that the reaction of *trans*-dppee with $(n\text{-}Bu_4N)_2Re_2Cl_8$ in methanol–conc. HCl to give (**1b**) is different from that with chelating *cis*-dppee. In the latter case, cleavage of the Re≡Re bond predominates to give *trans*-$[ReCl_2(dppee)_2]Cl$.[8]

Acknowledgement—We thank the National Science Foundation for support of this work (Grant No. CHE85-06702 to R.A.W.).

REFERENCES

1. F. A. Cotton and R. A. Walton, *Multiple Bonds between Metal Atoms*. Wiley, New York (1982) and refs cited therein.
2. T. J. Barder and R. A. Walton, *Inorg. Chem.* 1982, **21**, 2510.
3. J. R. Ebner and R. A. Walton, *Inorg. Chem.* 1975, **14**, 1987.
4. P. Brant, D. J. Salmon and R. A. Walton, *J. Am. Chem. Soc.* 1978, **100**, 4424.
5. For experimental details of the electrochemical set-up, see B. J. Brisdon, K. A. Conner and R. A. Walton, *Organometallics* 1983, **2**, 1159.
6. C. J. Cameron, S. M. Tetrick and R. A. Walton, *Organometallics* 1984, **3**, 240.
7. D. G. Nocera, A. W. Maverick, J. R. Winkler, C. Che and H. B. Gray, *Am. Chem. Soc. Symp. Ser.* 1983, **211**, 21.
8. M. Bakir, P. E. Fanwick and R. A. Walton, *Polyhedron* 1987, **6**, 907.

Polyhedron Vol. 6, No. 10, pp. 1929–1931, 1987
Printed in Great Britain

0277–5387/87 $3.00+.00

COMMUNICATION

LOSS OF WATER AND HYDROGEN CYANIDE FROM AQUOPENTAMMINECOBALT(III) HEXACYANOFERRATE(III)

J. E. HOUSE, Jr.* and FADZILAH MOHD TAHIR

Department of Chemistry, Illinois State University, Normal, IL 61761, U.S.A.

(*Received* 4 *March* 1987; *accepted* 27 *May* 1987)

Abstract—Previous studies on the non-isothermal decomposition of $[Co(NH_3)_5H_2O][Fe(CN)_6]$ showed that H_2O and three molecules of HCN are lost simultaneously but the results of the isothermal studies reported here show that these processes can be partially separated. It was found that the first reaction involves the loss of H_2O and two molecules of HCN and the second reaction results in the loss of an additional molecule of HCN. Kinetic studies have been performed and kinetic parameters are reported here and possible mechanisms are discussed.

Since our initial proposal of a defect-diffusion mechanism for solid state reactions,[1] numerous dehydration reactions have shown the utility of this description for such reactions.[2] Many of the reactions similar to that first reported by Haim *et al.*[3]

$$[Co(NH_3)_5H_2O][Co(CN)_6](s) \rightarrow [(NH_3)_5Co\text{-}NC\text{-}Fe(CN)_5](s)+H_2O(g) \quad (1)$$

have been studied by Ribas and co-workers.[2] These reactions include the dehydration of double complex salts containing two different metals. Our TGA study of the process shown in eqn (1) showed that it follows first order kinetics and has an activation energy of 232 ± 40 kJ mol^{-1}[4] while Simmons and Wendlandt reported 239 kJ mol^{-1}. However, an isothermal study on the reaction showed it to be a first order process with an activation energy of 144 kJ mol^{-1}.[5] Other complexes of this type which have been studied include $[Co(NH_3)_5H_2O][Cr(NCS)_6]$, $[Co(NH_3)_5H_2O][Cr(CN)_6]$, and $[Co(NH_3)_5H_2O][Fe(CN)_6]$.[4,7] Ribas and co-workers have also studied a series of complexes of the type $[M(NH_3)_5H_2O][Co(CN)_6]$ where M is Co(III), Rh(III) or Ir(III).[8] These can be dehydrated without further decomposition. In the case of $[Co(NH_3)_5H_2O][Fe(CN)_6]$ the study using TGA showed that H_2O and three molecules of HCN per molecule of complex were lost in a single reaction. Analysis of the data showed that the reaction is second order with an activation energy of 224 ± 8 kJ mol^{-1}.[4] Since the behavior of $[Co(NH_3)_5H_2O][Fe(CN)_6]$ is so different from that of other hexacyanometallates, we have studied this decomposition using isothermal techniques in an effort to separate the dehydration reaction from the loss of HCN and to determine the kinetic parameters for the processes. This report presents the results of that work.

EXPERIMENTAL

The $[Co(NH_3)_5H_2O][Fe(CN)_6]$ was prepared by mixing equal numbers of mols of $[Co(NH_3)_5H_2O]Br_3$ amd $K_3[Fe(CN)_6]$ in equal volumes of water.[4] After the precipitate of $[Co(NH_3)_5H_2O][Fe(CN)_6]$ formed, it was removed by filtration, washed with water, absolute ethanol and ether. The product was allowed to dry in air for two days.

Kinetic studies were performed using a Perkin–Elmer Thermogravimetric System model TGS-2. Samples were contained in platinum pans and were heated at constant temperature in a dry nitrogen atmosphere with a flow rate of 20 cc min^{-1}. Carrying out the first reaction at low temperature (100–

* Author to whom correspondence should be addressed.

120°C) resulted in the loss eventually of H_2O and two molecules of HCN per molecule of complex. When higher temperatures were used (180–195°C), an additional molecule of HCN was lost. The fraction of the reaction complete, α, was obtained by measuring the mass loss with time. Each reaction was studied at several temperatures. The data were analyzed by fitting the data to 14 kinetic models for solid state reactions.[9]

RESULTS AND DISCUSSION

The results of mass loss studies on $[Co(NH_3)_5H_2O][Fe(CN)_6]$ heated isothermally show that a partial separation of the loss of H_2O and HCN can be effected. While TGA studies showed that three molecules of HCN per molecule of complex were lost during dehydration,[4] prolonged heating at temperatures of 100–120°C results in a mass loss corresponding to the reaction:

$$[Co(NH_3)_5H_2O][Fe(CN)_6](s) \rightarrow [(NH_3)_3Co(NH_2)_2NCFe(CN)_3](s) + H_2O(g) + 2HCN(g). \quad (2)$$

The solid product appears to have one CN and two NH_2 bridges. This reaction is different from that indicated earlier by non-isothermal techniques where H_2O and three molecules of HCN were lost.[4] Heating the complex which had already lost H_2O and two HCN molecules at 185–195°C resulted in the loss of one molecule of HCN per molecule of complex:

$$[(NH_3)_3Co(NH_2)_2NCFe(CN)_3](s) \rightarrow [(NH_3)_2Co(NH_2)_3NCFe(CN)_2](s) + HCN(g). \quad (3)$$

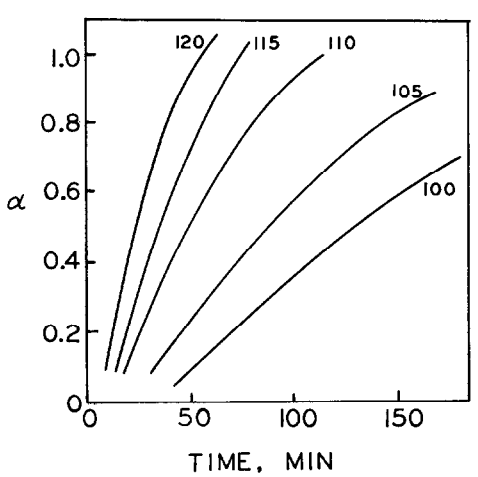

Fig. 1. Extent of reaction vs time for loss of H_2O and two molecules of HCN [eqn (2)].

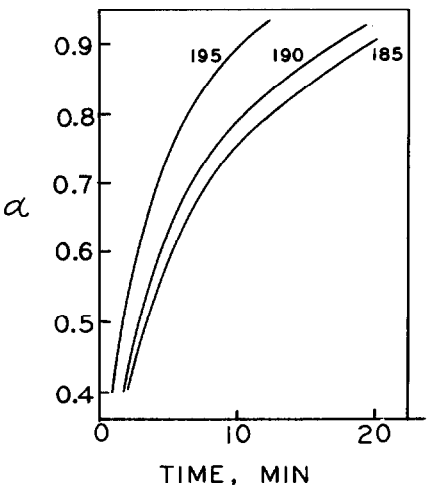

Fig. 2. Extent of reaction vs time for loss of the third molecule of HCN [eqn (3)].

Consequently, it is possible to perform kinetic studies on both of the reactions that are shown in eqns (2) and (3). Figures 1 and 2 show the plots of α, the fraction of reaction complete vs time for the reactions shown in eqns (2) and (3), respectively. These curves are characteristic of solid state reactions of this type.

The usual analysis of the kinetics of solid state reactions involves representing some function of α as a function of time. Theoretical models result in fourteen commonly used functions.[9] Fitting the α, t data for the first reaction to these models results in the best fit being the function $f(\alpha) = 1-(1-\alpha)^{1/2}$. This function corresponds to a two dimensional diffusion controlled process. As far as the physical process is concerned, the diffusion controlled mechanisms frequently result when gaseous products are lost. Although the rate law provides some indication of this aspect of the mechanism, it does not give insight as to how the H_2O and HCN are lost from the coordination spheres.

Analysis of the α and time data shown in Fig. 1 using the rate law $f(\alpha) = 1-(1-\alpha)^{1/2}$ yields the rate constants shown in Table 1. Applying the Arrhenius

Table 1. Rate constants for the reaction shown in eqn (2)

Temperature (°C)	k (min^{-1})	Uncertainty in k	Corr. coeff.
100	3.128×10^{-3}	3.364×10^{-5}	09993
105	4.623×10^{-3}	5.102×10^{-5}	0.9992
110	8.362×10^{-3}	5.812×10^{-5}	0.9998
115	13.911×10^{-3}	4.065×10^{-4}	0.9983
120	18.346×10^{-3}	2.068×10^{-4}	0.9998

equation to these rate constants leads to an activation energy of 113 ± 7 kJ mol^{-1} and a pre-exponential factor of 2.19×10^{13} min^{-1}. This value for the activation energy is much smaller than the 224 ± 8 kJ mol^{-1} found from non-isothermal measurements when H_2O and three molecules of HCN are lost.[4]

The second reaction, the loss of the third HCN, gave the best fit to the data when $f(\alpha) = -\ln(1-\alpha)$, which corresponds to the unimolecular growth controlled mechanism. It would be expected that this process would be unimolecular since the last molecule of HCN lost is probably the result of an intramolecular process in $[(NH_3)_3Co(NH_2)_2NCFe(CN)_3]$. Apparently, in this case, diffusion of the HCN from the solid product is not the rate-controlling process. The structure of the product, $[(NH_3)_2Co(NH_2)_3NCFe(CN)_2]$, would be of interest since it may contain Fe^{3+} with a coordination number of four.

Analysis of the α and time data shown in Fig. 2 for the loss of the third molecule of HCN yields the data shown in Table 2. These rate constants yield an activation energy of 96.8 kJ mol^{-1}. This reaction takes place readily at the temperatures used but could not be studied successfully at lower temperatures. Because of this, only a narrow range of temperatures could be employed and relatively few data points were obtainable, especially at the higher temperatures. As a result, the error limits are large for this activation energy, being about ± 40 kJ mol^{-1}. The pre-exponential factor for the reaction is 7.28×10^9 min^{-1}. It is interesting to note that the sum of the activation energies for the two reactions studied here, about 210 kJ mol^{-1}, is within experimental error of the 224 ± 8 kJ mol^{-1} found for the loss of the H_2O and three HCN molecules studied as a single process using TGA.[4]

Table 2. Rate constants for reaction shown in eqn (3)

Temperature (°C)	k (min^{-1})	Uncertainty in k	Corr. coeff.
185	0.1046	2.148×10^{-3}	0.9983
190	0.1177	2.424×10^{-3}	0.9985
195	0.1802	7.415×10^{-3}	0.9975

This work has shown that by using isothermogravimetry it is possible to study the loss of H_2O and two molecules of HCN from $[Co(NH_3)_5H_2O][Fe(CN)_6]$ in one step and the loss of the third HCN in another. The first step follows a rate law for a two dimensional diffusion controlled process, perhaps because three molecules of gaseous products are produced. The second process does not follow such a rate law and that may be a reflection of the fact that only one HCN is lost and the rate is not diffusion limited.

REFERENCES

1. J. E. House, Jr., *Thermochim. Acta* 1980, **38**, 59.
2. M. Corbella and J. Ribas, *Inorg. Chem.* 1986, **25**, 4390 and refs therein.
3. R. A. deCastello, C. P. Mac-Coll, N. B. Egan and A. Haim, *Inorg. Chem.* 1969, **8**, 699.
4. C. A. Jepsen and J. E. House, Jr., *J. Inorg. Nucl. Chem.* 1981, **43**, 953.
5. E. L. Simmons and W. W. Wendlandt, *J. Inorg. Nucl. Chem.* 1971, **33**, 3588.
6. J. E. House, Jr. and B. J. Smith, *J. Inorg. Nucl. Chem.* 1977, **39**, 777.
7. J. E. House, Jr. and C. A. Jepsen, *Thermochim. Acta* 1980, **37**, 49.
8. J. Ribas, A. Escuer and M. Monfort, *Thermochim. Acta* 1984, **76**, 201.
9. J. Sestak and G. Berggren, *Thermochim. Acta* 1971, **3**, 1.

Polyhedron Vol. 6, No. 10, pp. 1933–1934, 1987
Pergamon Journals Ltd. Printed in Great Britain

ANNOUNCEMENTS

FIFTH INTERNATIONAL SYMPOSIUM ON THE EFFECT OF TIN UPON MALIGNANT CELL GROWTH

18–20 JULY 1989
BRUSSELS, BELGIUM

ORGANIZATION

Chairman Marcel Gielen (Free University of Brussels V.U.B.) is being assisted by a Local Organizing Committee and an International Scientific Committee. The Symposium will be supported by the Free Universities of Brussels, industrial sponsors, government sources, the Federation of the European Chemical Societies and the Belgian Chemical Societies.

DATE AND LOCATION

The Fifth International Symposium on the Effect of Tin upon Malignant Cell Growth will be held in Brussels, Belgium from Tuesday to Thursday, 18–20 July 1989. The scientific sessions of the symposium will take place on the campus of the Free University of Brussels V.U.B.

SCOPE

The technical sessions of the symposium will be concerned with the synthesis and characterization, *in vitro* and *in vivo* activity, fate in living organisms, mechanisms of action, physiological effects, toxicity, experimental and clinical therapeutics, and pharmacology of tin-based anti-tumour drugs.

ACCOMMODATION

Inexpensive housing will be available in single rooms of the Free University of Brussels dormitories.

SOCIAL PROGRAMMES

A welcoming reception will be held on Tuesday evening. A banquet and special events are planned for the symposium participants and their guests.

YOUNG SCIENTISTS

Participation of young scientists will be especially encouraged through reduced registration fees for graduate students and post-doctoral research associates, and by Conference Fellowships. Details will be included in the second circular.

PRE-REGISTRATION

Individuals interested in receiving the second circular describing the symposium, to be mailed in July 1988, are asked to complete and return the preliminary registration form **before 1 May 1988.** The second circular will contain a list of the major speakers, final registration forms, instructions for preparing and submitting abstracts, housing information, special events and social activities.

All correspondence should be addressed to: **5th TUC, Prof. Dr Marcel Gielen, Free University of Brussels V.U.B., AOSC Unit, 8G512, Pleinlaan 2, B-1050 Brussels, Belgium.** Phone: (2) 6413279.

SIXTH INTERNATIONAL CONFERENCE ON THE ORGANOMETALLIC AND COORDINATION CHEMISTRY OF GERMANIUM, TIN AND LEAD

23–28 JULY 1989
BRUSSELS, BELGIUM

ORGANIZATION

Chairman Marcel Gielen (Free University of Brussels V.U.B.) is being assisted by a Local Organizing Committee and an International Scientific Committee. The Symposium will be supported by the Free Universities of Brussels, industrial sponsors, government sources, the Federation of the European Chemical Societies (124th event of FECS) and both Belgian Chemical Societies.

DATE AND LOCATION

The 6th ICCC GeSnPb will be held in Brussels, Belgium from Sunday to Friday, 23-28 July 1989. The scientific sessions of the symposium will take place on the campus of the Free University of Brussels V.U.B.

SCOPE

The technical sessions will be concerned with theoretical, structural, mechanistic and synthetic aspects of the chemistry of these elements, together with applications in areas including agriculture, biology/medicine, catalysis, electronics, environmental, polymer and solid-state chemistry, and organic synthesis.

ACCOMMODATION

Inexpensive housing will be available in single rooms of the Free University of Brussels dormitories.

SOCIAL PROGRAMMES

A welcoming reception will be held on Sunday evening. A banquet and special events are planned for the symposium participants and their guests.

YOUNG SCIENTISTS

Participation of young scientists will be especially encouraged through reduced registration fees for graduate students and post-doctoral research associates, and by Conference Fellowships. Details will be included in the second circular.

PRE-REGISTRATION

Individuals interested in receiving the second circular describing the symposium, to be mailed in July 1988, are asked to complete and return the preliminary registration form **before 1 May 1988.** The second circular will contain a list of the major speakers, final registration forms, instructions for preparing and submitting abstracts, housing information, special events and social activities.

All correspondence should be addressed to: **Prof. Dr Marcel Gielen, Free University of Brussels V.U.B., AOSC Unit, 8G512, Pleinlaan 2, B-1050 Brussels, Belgium.** Phone: (2) 6413279.

Polyhedron Vol. 6, No. 11, pp. 1935–1958, 1987
Printed in Great Britain

0277–5387/87 $3.00+.00
Pergamon Journals Ltd

POLYHEDRON REPORT NUMBER 22

FROM METALLABORANES TO TRANSITION METAL BORIDES: THE CHEMISTRY OF METAL-RICH METALLABORANE CLUSTERS

CATHERINE E. HOUSECROFT

University Chemical Laboratory, Lensfield Road, Cambridge CB2 1EW, U.K.

CONTENTS

INTRODUCTION

This report is aimed at highlighting the syntheses, structures, bonding and chemistry of metallaboranes which exhibit a metal to boron ratio of greater than or equal to one; that is, metallaboranes possessing equal numbers of metal and boron atoms, or else, possessing more metal nuclei than boron nuclei in their framework. Several classes of compounds are excluded from the review. These exclusions are monometallic borohydride complexes of type $L_xM[BH_4]_y$,[1] complexes in which the source of boron is an organo-borane or -borate ligand, and metallocyclic complexes. Excellent reviews covering the area of metallaboranes with emphasis on the boron-rich cluster compounds have recently been presented by Kennedy.[2] Comprehensive surveys have also been compiled by Shore *et al.*[1] and Grimes.[1] A review of boron containing metallocycles has been provided by Herberich.[3]

In the last few years, metallaborane chemistry has developed rapidly. In particular, the prolific results from Greenwood *et al.*[2] illustrate the extent to which metallaborane cluster chemistry has expanded, and a diversity of fascinating structural types has now been characterized. Perturbation

of a borane cage by a metal fragment is thus well documented. On the other hand, cluster chemistry exhibits a plethora of transition metal aggregates with a very rich associated chemistry, a fair proportion of which involves organic ligands of one type or another. In most of these transition metal-hydrocarbon clusters, the metal nuclei outnumber the organic carbon centres in a given cluster core. Despite the adjacent position of boron to carbon in the periodic table, there are only limited examples of metal hydrocarbon complexes which have metallaborane analogues.[4] As is now quite commonly exemplified, transition metal–carbon interactions extend to metal carbide (i.e. bare carbon) clusters.[5,6] Carbon is not the only naked hetero-atom encapsulated within a transition metal framework; for example, metal nitride,[7] oxide,[8] and phosphide[9] clusters have been characterized. And yet, the trail from a boron-rich metallaborane to a metal-rich metallaborane or a discrete metal boride cluster is only now beginning to be laid.

BOROHYDRIDE (BH_4^-) COMPLEXES

There are several unusual borohydride complexes which deserve a mention because each exhibits a BH_4^- ligand coordinated to multi-metal centres. On the basis of infra-red data, it is proposed that $[(Ph_3P)_4Cu_2BH_4]^+$ [Fig. 1(a)] contains a borohydride ligand bridging through two hydrogens to

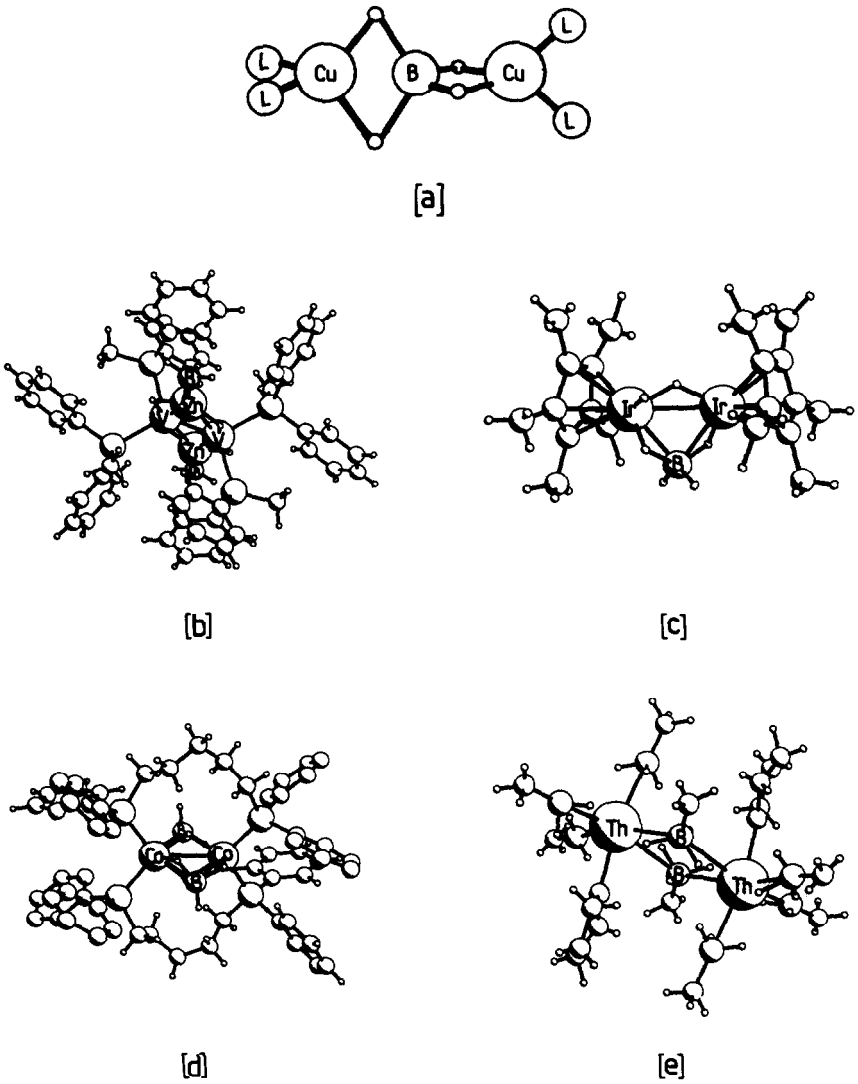

Fig. 1. (a) Proposed structure of $[L_4Cu_2BH_4]^+$;[10] (b) Molecular structure of $V_2Zn_2H_4(BH_4)_2(PPh_2Me)_4$;[11] (c) Molecular structure of $[(C_5Me_5)Ir]_2H_3(BH_4)$;[12] (d) Molecular structure of $Co_2(BH_4)_2(Ph_2P[CH_2]_5PPh_2)_2$;[13] (e) Molecular structure of $\{Th(BH_3CH_3)_4\}_2 \cdot THF$.[14]

each of two copper centres.[10] Although clearly not a "cluster" compound, this complex is of interest because it exemplifies a borohydride ligand in which there are no terminal hydrogen atoms. This is an unusual feature for ligated BH_4^-. A hydrogen-rich borohydride derivative, $V_2Zn_2H_4(BH_4)_2(PPh_2Me)_4$, [Fig. 1(b)] has been made in 50% yield from the reaction of $\{V_2(\mu\text{-}Cl)_3(THF)_6\}_2Zn_2Cl_6$ with PPh_2Me and BH_4^-.[11] The structure is described in terms of two $Zn(BH_4)^+$ units interacting with a divanadium polyhydride anion rather than as containing BH_4^- ligands interacting with a cationic metal centre. Another polyhydride complex containing a borohydride ligand is $\{(C_5Me_5)Ir\}_2H_3(BH_4)$,[12] [Fig. 1(c)]. The complex has the unusual feature that the borohydride ligand bridges between two metal atoms thereby making the complex "metal-rich" as regards the metal to boron atom ratio. In addition, whereas it is usual for bridging and terminal hydrogen atoms in coordinated BH_4^- ligands to undergo exchange on the NMR timescale, those in $\{(C_5Me_5)Ir\}_2H_3(BH_4)$ do not. Nor do the iridium associated metal hydrides exchange with the Ir—H—B bridge hydrogen atoms. Bridging of two metal centres by BH_4^- has also been observed in $Co_2(BH_4)_2(Ph_2P\{CH_2\}_5PPh_2)_2$[13] [Fig. 1(d)], and the related methyltrihydroborate complexes $\{Th(BH_3CH_3)_4\}_2 \cdot L$ (L = OEt_2; THF),[14] [Fig. 1(e)]. It is interesting to ponder whether or not these complexes can be usefully classified as clusters rather than as simple coordination complexes. For example, in $Co_2(BH_4)_2(Ph_2P[CH_2]_5PPh_2)_2$, counting each CoL_2 unit as a one electron cluster fragment and breaking down each borohydride ligand into a cluster BH unit plus three *endo*-hydrogen atoms provides six electron pairs for cluster bonding. On the basis of PSEPT,[15] the Co_2B_2 core is predicted to be a *nido*-cluster, either a tetrahedron or an open butterfly (internal dihedral angle of 140° for an ideal homonuclear cage). However, the observed Co_2B_2 core has an internal dihedral angle of 170° if one defines the Co—Co vector to lie along the butterfly hinge; i.e. the four atoms are virtually coplanar. In addition, the Co—Co distance of 2.869 Å is too long to be considered a bonding interaction. Presumably, the deviation from an obvious cluster bonding picture may be a steric consequence of the bidentate phosphine ligands. Nonetheless, the compound $Co_2(BH_4)_2(Ph_2P[CH_2]_5PPh_2)_2$ does seem to present us with an appropriate bridge from borohydride ligand complexes to clusters.

CLUSTERS WITH METAL:BORON RATIO 1:1

The air and light sensitive diiron–diboron cluster $Fe_2(CO)_6B_2H_6$ has been prepared from the reaction of $Fe(CO)_5$ and B_5H_9 in yields of less than 10%.[16] This ferraborane is also a by-product in the reaction of $Fe(CO)_5$, $BH_3 \cdot THF$ and $LiBEt_3H$ in hexane, (0°C for 3 h), followed by acidification,[17] and in the reaction of $[Fe(CO)_4COCH_3]PPN$ with $BH_3 \cdot THF$ (1 : 3 equivalents) in hexane at 60°C followed by acidification.[18] Formulation is deduced from mass spectroscopic data and a proposed structure is given on the basis of infra-red and multinuclear NMR spectra. Initially, 100 MHz room temperature NMR results were interpreted as being consistent with a diborane-like fragment interacting with a diiron hexacarbonyl unit [Fig. 2(a)].[16] The structure recently proposed for $Fe_2(CO)_6B_2H_6$ [Fig. 2(b)] is postulated from Mössbauer spectroscopic data and the results of a 300 MHz variable temperature ^1H NMR study.[17] The resonances at δ −10.3 and 0.2, originally[16] assigned to four equivalent Fe—H—B protons and two terminal B—H protons respectively, are now observed to be the coalesced signals of three Fe—H—B protons (two at δ −15.6 and one at δ −12.9) and one terminal B—H proton (δ 2.3), and of one terminal B—H hydrogen (δ 2.3), and one bridge B—H—B proton (δ −2.4) respectively.[17] The electronic structure of $Fe_2(CO)_6B_2H_6$ has been probed by UV–photoelectron spectroscopy and by extended Hückel and Fenske–Hall quantum chemical techniques. [The geometrical structure assumed for the calculations is that shown in Fig. 2(a).] The results permit a comparison between the bonding in $Fe_2(CO)_6B_2H_6$ and $Fe_2(CO)_6S_2$,[19] and suggest a greater $Fe_2(CO)_6^{\delta+}B_2H_6^{\delta-}$ charge separation than $Fe_2(CO)_6^{\delta+}S_2^{\delta-}$ separation (1.16 vs 0.07 electrons by the Fenske-Hall method). The results also imply that the B—B bond should exhibit significant Lewis basicity. Indeed, in the more recently postulated structure [Fig. 2(b)], the B—B bond is "protonated". Deprotonation of $Fe_2(CO)_6B_2H_6$ by methanol/PPNCl or methanol/Ph_4AsCl leads to the removal of an Fe—H—B rather than a B—H—B bridging proton. Two isomeric anions are proposed [Fig. 2(c)].[17]

Cobaltaboranes provide examples of *closo*-metal-rich metallaboranes containing equal numbers of metal and boron atoms. The air-stable solids 1,2,3-$\{(C_5H_5)Co\}_3B_3H_5$[20–22] and $[(C_5H_5)Co]_4$

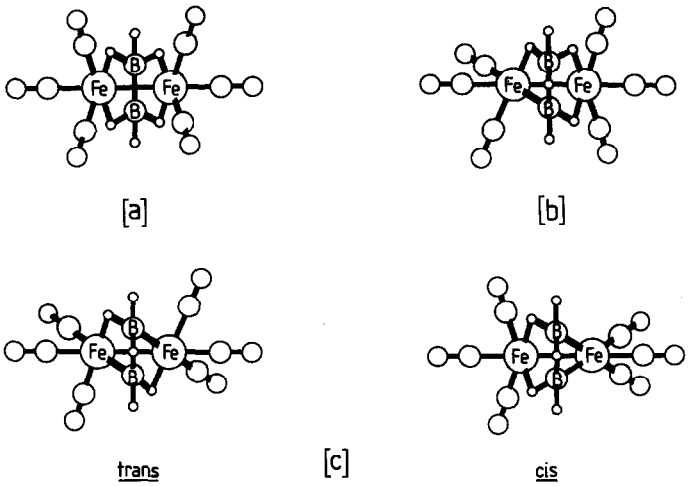

Fig. 2. Proposed structures of $Fe_2(CO)_6B_2H_6$ (a) Ref. 16; (b) on the basis of low temperature 300 MHz ^1H NMR;[17] (c) proposed structures of *trans*- and *cis*-isomers of $[Fe_2(CO)_6B_2H_5]^-$.[17]

B_4H_4[21-23] are minor products of the reaction of $[B_5H_8]^-$ with cobalt(II) chloride and $[C_5H_5]^-$. Interestingly, however, the pentamethylcyclopentadienyl analogues of these clusters have not been detected in an analogous reaction using $[C_5Me_5]^-$ in place of $C_5H_5^-$.[21] The structure[20] of 1,2,3-$\{(C_5H_5)Co\}_3B_3H_5$ [Fig. 3(a)] consists of staggered B_3 and Co_3 triangles which make up an octahedron. Each boron atom is therefore adjacent to two cobalt and two boron atoms. The same

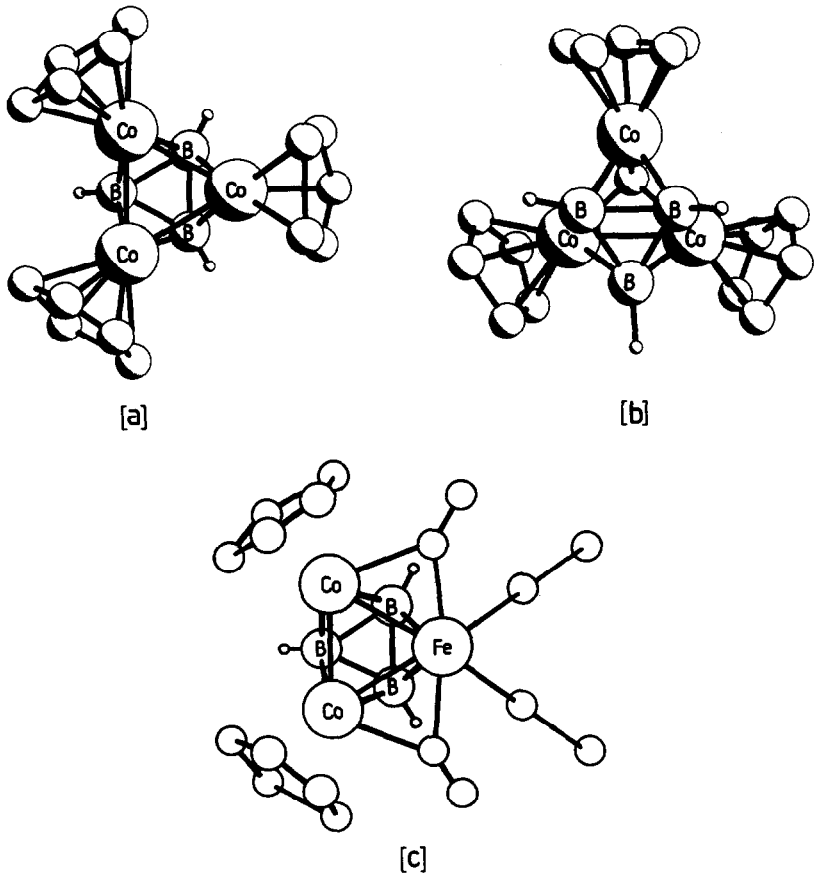

Fig. 3. Molecular structures of the cobaltaboranes (a) 1,2,3-$[(C_5H_5)Co]_3B_3H_5$;[20] (b) 1,2,3-$[(C_5H_5)Co]_3B_3H_3(\mu_3\text{-}CO)$;[24] (c) 1,2,3-$[(C_5H_5)Co]_2Fe(CO)_4B_3H_3$ (proposed).[26]

cluster core is present in 1,2,3-$\{(C_5H_5)Co\}_3B_3H_3(\mu_3\text{-}CO)$[24,25] [Fig. 3(b)], which is prepared in 2.7% yield by reacting cobalt vapour and cyclopentadiene with B_5H_9. The source of the cluster-bound CO is unproven but may originate either from metal oxide impurities in the cobalt powder used in the reaction, or from THF used to extract the products. When the preparation is carried out in the presence of carbon monoxide, the yield of 1,2,3-$\{(C_5H_5)Co\}_3B_3H_3(\mu_3\text{-}CO)$ rises to 6.4%.[24] In 1,2,3-$\{(C_5H_5)Co\}_3B_3H_5$, it is deduced from ^1H and ^{11}B NMR spectroscopy and electron difference maps that the two non-terminal protons occupy disordered bridging sites along the three Co—Co edges.[20] The two electrons provided by the two *endo*-hydrogens in 1,2,3-$\{(C_5H_5)Co\}_3B_3H_5$ are donated by the μ_3-carbonyl ligand in $\{(C_5H_5)Co\}_3B_3H_3(\mu_3\text{-}CO)$. Just as the *endo*-hydrogen atoms are associated with the metal atoms, so too is the carbonyl ligand. There is, however, no suggestion that the two clusters interconvert in the presence of H_2 or CO respectively. This type of interconversion is exemplified for another pair of metal-rich metallaboranes, $[Fe_3(CO)_9BH_4]^-$ and $[Fe_3(CO)_{10}BH_2]^-$, described below.

1,2,3-$\{(C_5H_5)Co\}_2Fe(CO)_4B_3H_3$ is prepared by the photochemically initiated reaction of 2-$(C_5H_5)CoB_4H_8$ with $Fe(CO)_5$.[26] The structure [Fig. 3(c)] of this mixed metal cluster is deduced from spectroscopic data and assumed to be related to that of 1,2,3-$[(C_5H_5)Co]_3B_3H_5$. Two bridging carbonyl ligands are invoked to provide the molecular twofold symmetry required by the NMR spectra.

$\{(C_5H_5)Co\}_4B_4H_4$ and $\{(C_5H_5)Ni\}_4B_4H_4$ are the highest nuclearity (i.e. total metal plus boron nuclei) metal-rich metallaboranes yet reported. The cobaltaborane is among the products of the reaction of $Na[B_5H_8]$ with excess $CoCl_2$ and $Na[C_5H_5]$ carried out in THF below 20°C.[27] It is a green, air-stable solid. The brown, air-stable $\{(C_5H_5)Ni\}_4B_4H_4$ is a product of the reaction of $Na[B_5H_8]$ with nickelocene in cold THF in the presence of one equivalent of sodium amalgam.[28]

$\{(C_5H_5)Co\}_4B_4H_4$[23] and $\{(C_5H_5)Ni\}_4B_4H_4$[29] both exhibit closed cages, although they are not isostructural. From Fig. 4, it is apparent that the cobalt atoms in $[(C_5H_5)Co]_4B_4H_4$ occupy sites of high connectivity, whereas the nickel atoms in $[(C_5H_5)Ni]_4B_4H_4$ occupy sites of low connectivity on the dodecahedral skeleton. The $(C_5H_5)Co$ and BH fragments in $\{(C_5H_5)Co\}_4B_4H_4$ can contribute a total of eight electron pairs to cluster bonding (i.e. one pair short of the number required by PSEPT for a *closo* dodecahedral cluster structure). On the other hand, the cluster fragments of

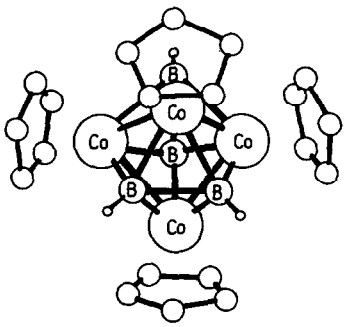

[a]

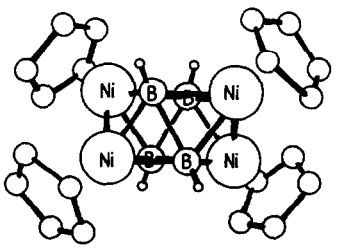

[b]

Fig. 4. Molecular structures of (a) $[(C_5H_5)Co]_4B_4H_4$[23] and (b) $[(C_5H_5)Ni]_4B_4H_4$.[29]

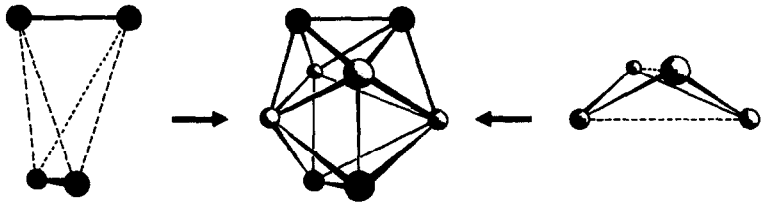

Fig. 5. Schematic representation of the combination of elongated and flattened tetrahedra to generate a D_{2d} dodecahedron.

$\{(C_5H_5)Ni\}_4B_4H_4$ provide ten electron pairs, (i.e. one pair in excess of the PSEPT requirement). An extended Hückel analysis of the dodecahedral cluster in terms of its formation from the interpenetration (Fig. 5) of two tetrahedra, one flattened and one elongated, has been used to rationalize this structural difference.[30] Since the energies of the metal fragment orbitals are always lower than the energies of the BH fragment MO's, the metal–boron cluster bonding orbitals will exhibit more metal than boron character. Thus, the metal will tend to be predominant in the cluster bonding. If the metal fragments occupy the vertices designated by the flattened tetrahedron, then the electron requirement will reflect those of that tetrahedron; i.e. eight cluster bonding pairs are available in $\{(C_5H_5)Co\}_4B_4H_4$ and so the cobalt atoms define the flattened tetrahedron. In $\{(C_5H_5)Ni\}_4B_4H_4$, the electron pair availability fits the needs of the elongated tetrahedron. Alternatively, Wade[31] had demonstrated that the degeneracy of the highest occupied molecular orbitals of the parent dodecahedral cluster $B_8H_8^{2-}$ (which is *closo* with nine cluster bonding electron pairs) allows flexibility in the number of bonding electrons required. Single occupancy of the degenerate set leads to the "normal" *closo* cluster. In $\{(C_5H_5)Co\}_4B_4H_4$, the degenerate MO set is left unoccupied and becomes, therefore, the LUMO of the complex. In $\{(C_5H_5)Ni\}_4B_4H_4$, both these MO's are fully occupied. Wade[31] has explained this in terms of the charge distribution over the cluster surface; the nickel fragment is a three electron donor and will occupy the site of low connectivity which corresponds to the site of highest electron density in the parent $B_8H_8^{2-}$.

A cluster which categorises as "pseudo metal-rich" is 4,6-$\{(C_5H_5)Co\}_2$-3,5-$S_2B_2H_2$.[32] The "pseudo" description is used here only because the sulphur atoms might be seen as isoelectronic main group replacements for BH_3 units in the hypothetical parent metallaborane $\{(C_5H_5)Co\}_2B_4H_8$. 4,6-$\{(C_5H_5)Co\}_2$-3,5-$S_2B_2H_2$ has an interesting *nido*-structure based on a pentagonal bipyramid (Fig. 6). Six-vertex eight electron pair carboranes and metallaboranes tend to adopt pentagonal pyramidal structures. The structure of 4,6-$\{(C_5H_5)Co\}_2$-3,5-$S_2B_2H_2$ illustrates a vacancy at a low rather than a high connectivity site on the parent polyhedron (inset in Fig. 6). This is attributed to a maximising of the Co···Co and S···S separations.

CLUSTERS WITH METAL:BORON RATIO 3:2

The presence of two boron atoms together in a cluster brings to mind derivatives of B_2H_6. A cluster involving B_2H_6 interacting with a diiron fragment has been described above. B_2H_6 interacting

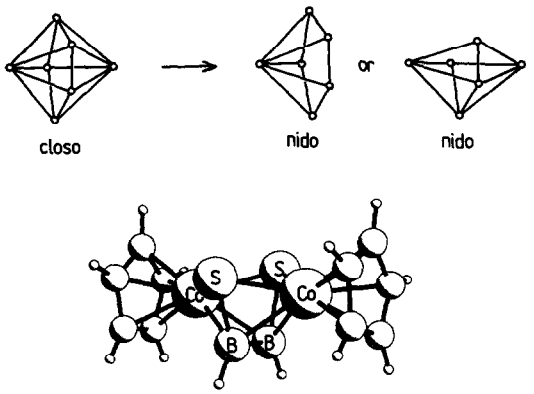

Fig. 6. Molecular structure of 4,6-$[(C_5H_5)Co]_2$-3,5-$S_2B_2H_2$.[32]

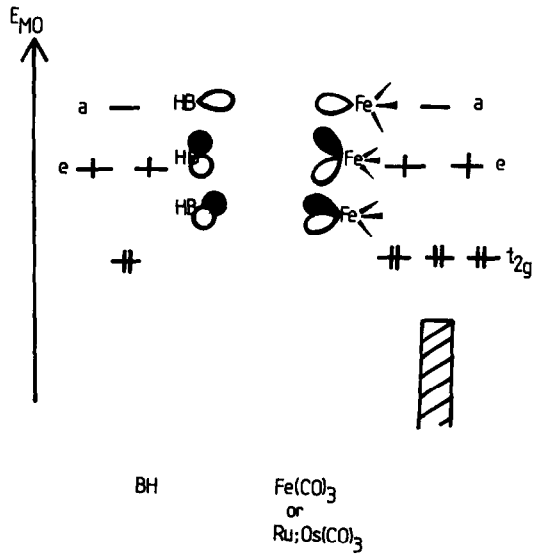

Fig. 7. Comparison of the frontier molecular orbitals of BH and $M(CO)_3$ (M = Fe, Ru, Os) cluster fragments. Energy scales are arbitrary.

with a trinuclear metal framework has been reported for $Ru_3(CO)_9B_2H_6$.[33] The reaction of $Ru_3(CO)_{12}$ with sodium borohydride in refluxing THF leads to a mixture of metal cluster products, two of which are boron-containing. On the basis of spectroscopic data, these are formulated as $Ru_3(CO)_9B_2H_6$ and $Ru_4(CO)_{12}BH_3$. The latter cluster is discussed along with its iron analogue in detail below. No NMR data were recorded for $Ru_3(CO)_9B_2H_6$ and hence, no structural assignment was made.[33] At this stage, it is useful to apply the isolobal analogy; BH and C_{3v} $M(CO)_3$ (M = Fe, Ru, Os) fragments each provide two cluster bonding electrons and exhibit frontier orbitals of the same symmetry. This is schematically represented in Fig. 7. Thus, the bonding requirements of a BH fragment in a cluster may be mimicked by an $M(CO)_3$ fragment. By comparing $Ru_3(CO)_9B_2H_6$ with the related metallaboranes $Fe(CO)_3B_4H_8$[34] and $Fe_2(CO)_6B_3H_7$[18,35] and by considering its parentage as arising from B_5H_9,[36] several isomeric structures can be postulated based on a *nido*-square pyramidal geometry (Fig. 8). It is interesting that no iron analogue of $Ru_3(CO)_9B_2H_6$ has

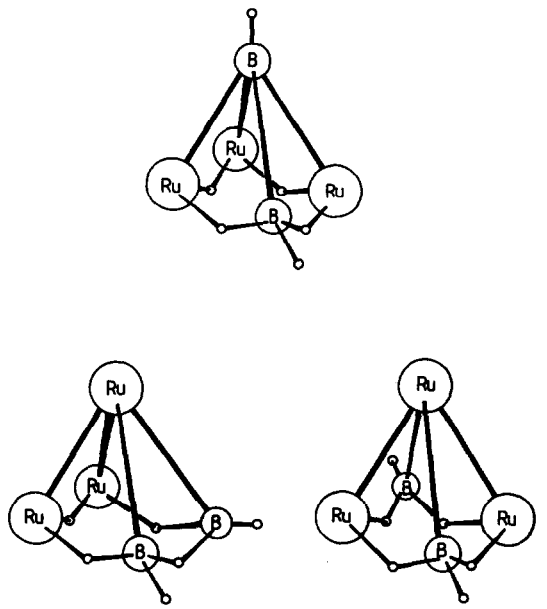

Fig. 8. Possible isomers for $Ru_3(CO)_9B_2H_6$ based on a square pyramid.

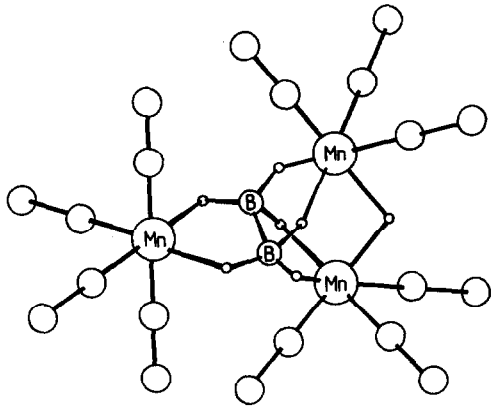

Fig. 9. Structure of $HMn_3(CO)_{10}B_2H_6$.[37]

been characterized to date and that $Fe_3(CO)_9B_2H_6$ remains an elusive member of the $\{Fe(CO)_3\}_x\{BH\}_{5-x}H_4$ series of metallaboranes.

$HMn_3(CO)_{10}B_2H_6$ has been structurally characterized and exhibits an ethane-like diborane fragment bridging between three manganese carbonyl units (Fig. 9).[37] Hydrogen atoms were not refined in the crystal structure but infrared data indicate an absence of terminal BH bonds and the presence of Mn—H—B bridges. Six Mn—H—B bridging protons are suggested on the grounds of equivalent Mn—B bond distances (mean value 2.30(2) Å) and from electron-counting arguments.[37] The presence of the bridging hydrogen atoms also allows each of the metal atoms to maintain an octahedral environment. A broad ^1H NMR resonance at δ −19 is attributed to the Mn—H—Mn bridging hydrogen atom in $HMn_3(CO)_{10}B_2H_6$, but no signals due to the boron associated protons are reported.

CLUSTERS WITH METAL:BORON RATIO 2:1

Upon entering this category of metallaborane cluster, we are truly considering clusters which are "metal-rich". Exemplars of this class are scarce. Recently, the cluster $\{(C_5H_5)Co\}_4B_2H_4$ (Fig. 10) has been structurally characterized.[38] The compound is prepared in 16% yield by the reaction of $(Ph_3P)Co(C_5H_5)(Et_2C_2)$ with $BH_3\cdot THF$ in toluene at 60°C. It is a member of the class of cobaltaboranes $\{(C_5H_5)Co\}_x\{BH\}_{6-x}H_2$,[20,22,27,39,40] but is the first member of the series in which metal atoms outnumber boron atoms in the skeleton. The compound is also noteworthy because of its relationship to the tetrametal acetylene complex, $Co_4(CO)_{10}C_2H_2$.[41] The Co_4X_2 (X = B or C) core is common to both $\{(C_5H_5)Co\}_4B_2H_4$ and $Co_4(CO)_{10}C_2H_2$ with the two main group atoms being adjacent to one another within the octahedral skeleton. The preparation of $\{(C_5H_5)Co\}_4B_2H_4$ illustrates a novel use of $BH_3\cdot THF$.[38,42] The borane acts as a dual reagent, removing phosphine and acetylene ligands from the metal precursor, and then condensing with $\{Co(C_5H_5)\}$ fragments

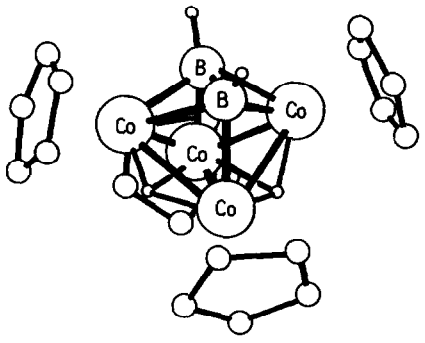

Fig. 10. Molecular structure of $\{(C_5H_5)Co\}_4B_2H_4$.[38]

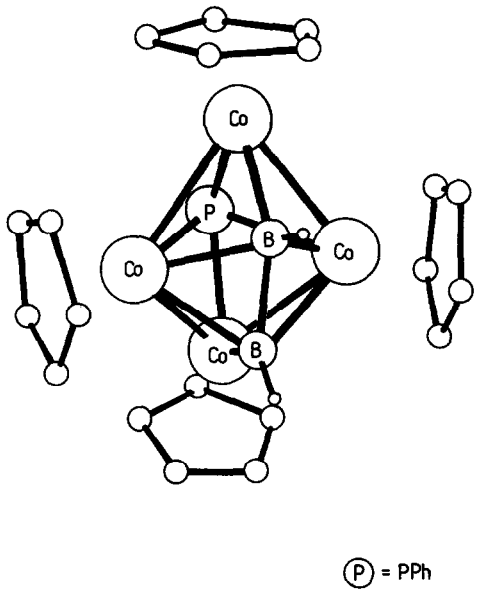

Fig. 11. Molecular structure of 2-Ph-1,3,6,7,2-$\{(C_5H_5)Co\}_4PB_2H_2$.[42]

to form the product cluster. The products formed are sensitive to reaction conditions.[42] Related to $\{(C_5H_5)Co\}_4B_2H_4$ is 2-Ph-1,3,6,7,2-$\{(C_5H_5)Co\}_4PB_2H_2$[42] (Fig. 11). Again, this metallaborane has a close metal-hydrocarbon analogue, *viz.* $Ru_4(CO)_{11}C_2Ph_2PPh$.[43] $\{(C_5H_5)Co\}_4B_2H_4$ and 2-Ph-1,3,6,7,2-$\{(C_5H_5)Co\}_4PB_2H_2$ are seemingly related by the insertion of a PPh unit into a Co—Co bond of, and elimination of two hydrogen atoms from, the former cluster. However, attempts to form 2-Ph-1,3,6,7,2-$\{(C_5H_5)Co\}_4PB_2H_2$ by reacting $\{(C_5H_5)Co\}_4B_2H_4$ with PPh_3 and eliminating two moles of benzene have failed.[42]

Although a metallacarborane rather than a metallaborane, $\{(C_5H_5)(CO)_2W\}_2(CMe)(BHEt)$[44] is worthy of inclusion here, not only because it is metal-rich, but also because its synthesis involves an interesting reduction of the $CH_3C{\equiv}W$ fragment in $(C_5H_5)(CO)_2W{\equiv}CMe$ by $BH_3 \cdot THF$ and subsequent transfer of the ethyl group so-formed onto the boron atom. The structure of $\{(C_5H_5)(CO)_2W\}_2(CMe)(BHEt)$ is shown in Fig. 12. The W—H—B bridging hydrogen atom is an unusual feature.

CLUSTERS WITH METAL:BORON RATIO 3:1

Clusters with metal atoms outnumbering boron atoms 3:1 represent a group which has been the subject of detailed bonding analyses and reactivity studies. However, until recently, only one such reported metal–boron cluster had been reported. This was the tricobalt derivative $Co_3(CO)_9BNEt_3$ (Fig. 13) which is a product of the reaction of $[Co(CO)_4]^-$ with BBr_3 in the presence of a

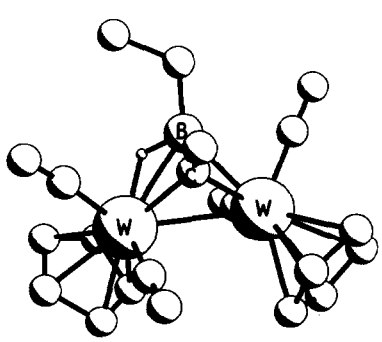

Fig. 12. Molecular structure of $\{(C_5H_5)(CO)_2W\}_2(CMe)(BHEt)$.[44]

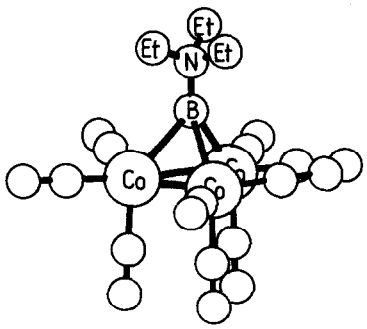

Fig. 13. Proposed structure of $Co_3(CO)_9BNEt_3$.[45]

stoichiometric amount of triethylamine:

$$3[Co(CO)_4]^- + BBr_3 + NEt_3 \xrightarrow{C_6H_6} Et_3NBCo_3(CO)_9 + 3Br^- + 3CO.$$

The nature of the cluster was determined by cryoscopic weight measurements.[45] No structural confirmation of this type of trimetalmonoboron cluster geometry was available until Shore *et al.* characterized $(\mu\text{-H})_3Os_3(CO)_9BCO$[46] [Fig. 14(a)]. The preparation of $(\mu\text{-H})_3Os_3(CO)_9BCO$ is interesting because it formally involves the insertion of boron into an Os—CO bond, but the success of the reaction depends on the presence of catalytic amounts of $BH_3 \cdot NEt_3$. The proposed mechanism is represented in Fig. 15.[46] $(\mu\text{-H})_3Os_3(CO)_9BCO$ is air-stable and is obtained in 85% yield. However, when $BH_3 \cdot THF$ replaces $BH_3 \cdot NEt_3$, a fascinating boroxine derivative, $[(\mu\text{-H})_3Os_3(CO)_9CO]_3B_3O_3$, containing pendant cluster units surrounding a central boroxine ring, is produced along with $(\mu\text{-H})_3Os_3(CO)_9BCO$.[46,47] Transformations at the boron-attached carbonyl in $(\mu\text{-H})_3Os_3(CO)_9BCO$ have been explored[46,48-50] and are summarized in Fig. 16. The unique carbonyl ligand is subject to nucleophilic substitution by PMe_3 to yield exclusively $(\mu\text{-H})_3Os_3(CO)_9BPMe_3$. There is no indication that phosphine substitution at the metal centres competes with substitution at the boron atom.[46,48] An indirect route is used to produce $(\mu\text{-H})_3Os_3(CO)_8(PPh_3)BCO$ from $(\mu\text{-H})_3Os_3(CO)_9BCO$.[48] Reaction of $(\mu\text{-H})_3Os_3(CO)_8(PPh_3)BCO$ with PMe_3 produces a mixture of $(\mu\text{-H})_3Os_3(CO)_9BPMe_3$

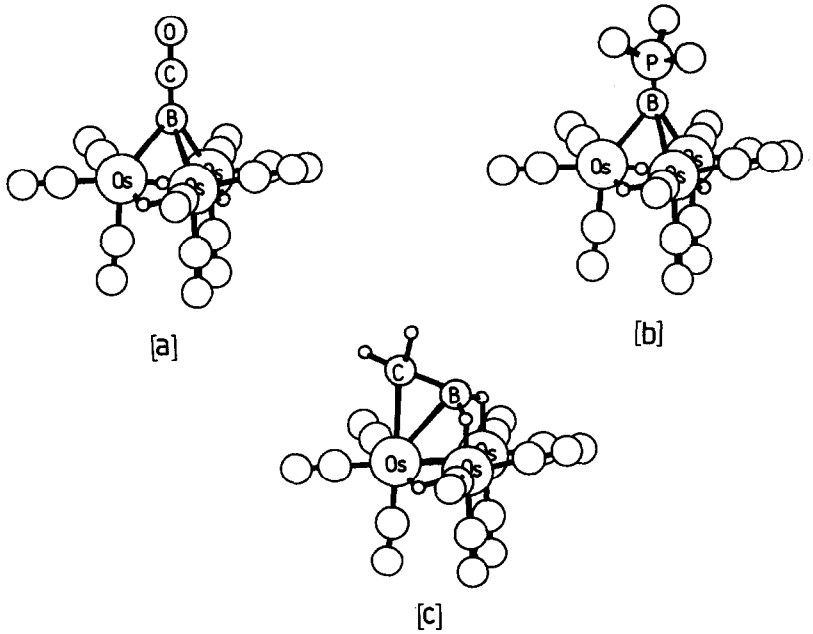

Fig. 14. Molecular structures of (a) $(\mu\text{-H})_3Os_3(CO)_9BCO$;[46] (b) $(\mu\text{-H})_3Os_3(CO)_9BPMe_3$;[48] (c) $(\mu\text{-H})_3Os_3(CO)_9B{=}CH_2$.[49]

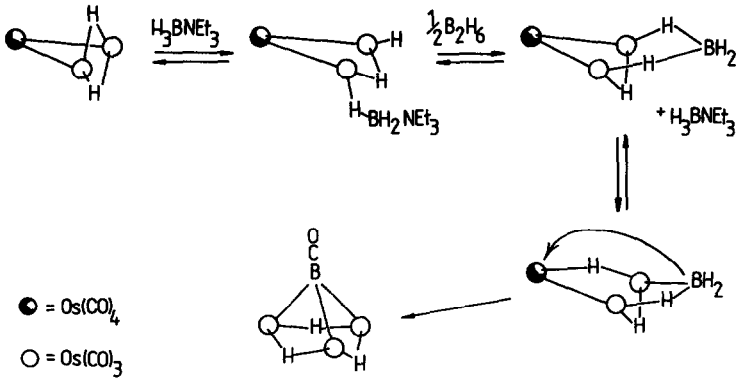

Fig. 15. Proposed mechanism for the formation of $(\mu\text{-H})_3Os_3(CO)_9BCO$.[46]

and $(\mu\text{-H})_3Os_3(CO)_8(PPh_3)BPMe_3$. Kinetic studies on this system suggest that the incoming nucleophile initially attacks the boron atom, resulting in tetrahedral cage opening at an Os—B bond to give a "butterfly" intermediate which subsequently closes, extruding either a CO or a PPh_3 ligand.[48]

UV–photoelectron spectroscopic and Fenske–Hall quantum chemical studies of the clusters $(\mu\text{-H})_3Os_3(CO)_9BCO$ and $(\mu\text{-H})_3Os_3(CO)_9BPMe_3$ have recently been made.[51] The results indicate that the boron is acting as a "pseudo-metal atom". In a comparison between $(\mu\text{-H})_3Os_3(CO)_9BCO$ and $(\mu\text{-H})_2Os_3(CO)_9CCO$, it is shown that the energies of the BCO molecular orbitals are better matched to those of the trimetal fragment than are those of the CCO fragment. This results in their being greater interaction between the metal framework and the BCO unit than between the metal triangle and the CCO fragment. An important observation is that the MO calculations provide evidence for a synergic interaction between the boron and its carbonyl ligand. Again, this suggests a metal-like boron atom.

Reaction of $(\mu\text{-H})_3Os_3(CO)_9BCO$ with $BH_3 \cdot THF$ (Fig. 16) yields an unprecedented triosmium borylidene carbonyl cluster, $(\mu\text{-H})_3Os_3(CO)_9B{=}CH_2$,[49] which can be likened to a trimetal vinylidene system, $(\mu\text{-H})_2Os_3(CO)_9C{=}CH_2$.[52] A comparison of the bonding of the $B{=}CH_2$ and $C{=}CH_2$ fragments to a trimetal framework has been made.[49] It is worth pointing out one salient feature of the structure of $(\mu\text{-H})_3Os(CO)_9B{=}CH_2$ as compared to other characterized $(\mu\text{-H})_3Os_3(CO)_9BX$ clusters: $(\mu\text{-H})_3Os_3(CO)_9B{=}CH_2$ alone exhibits both Os—H—Os and B—H—Os bridges whereas $(\mu\text{-H})_3Os_3(CO)_9BCO$ and $(\mu\text{-H})_3Os_3(CO)_9BPMe_3$ exhibit solely Os—H—Os bridging hydrogen atoms. Presumably, reorientation of the B—X ligand from a vertical (as in X = CO or PMe_3) position to a tilted position (as in X = CH_2) results in a rehybridization of orbitals at the boron

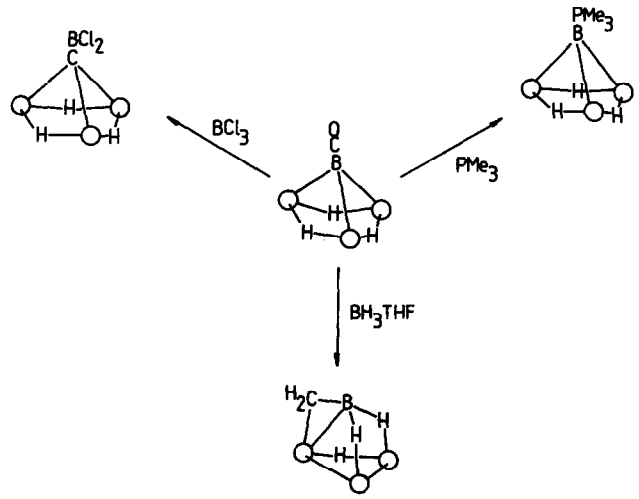

Fig. 16. Reactions of the cluster bound BCO unit in $(\mu\text{-H})_3Os_3(CO)_9BCO$.[46,48–50]

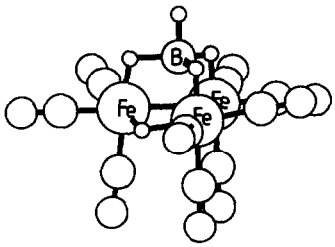

Fig. 17. Molecular structure of $Fe_3(CO)_9BH_5$.[53,54]

atom and a redistribution of electron density on the cluster surface in the hypothetical $[Os_3(CO)_9BX]^{3-}$ anion. The protons will tend to migrate to the regions of highest electron density.

The triiron–borane clusters $(\mu\text{-H})Fe_3(CO)_9BH_4$ and $(\mu\text{-H})Fe_3(CO)_{10}BH_2$, and their conjugate bases $[(\mu\text{-H})Fe_3(CO)_9BH_3]^-$ and $[(\mu\text{-H})Fe_3(CO)_{10}BH]^-$, have been studied in detail. $(\mu\text{-H})Fe_3(CO)_9BH_4$ is prepared by the reaction of two equivalents of $BH_3\cdot THF$ with $[Fe(CO)_4COCH_3]Na$ in THF at 65°C. After acidification, $(\mu\text{-H})Fe_3(CO)_9BH_4$ is produced in 5% yield. The ferraborane has been structurally characterized (Fig. 17).[53,54] The mode of bonding of the borane fragment is particularly interesting. It may be envisaged as the first example of a $\mu_3\text{-}BH_4$ ligand binding to three metal centres via three M—H—B bridges. On the other hand, the 300 MHz variable temperature ^1H NMR spectrum[54] illustrates that three of the borane ligand's four hydrogen atoms are intimately associated with the Fe_3B cluster core while one hydrogen remains terminally attached to the boron atom. This suggests that the $[BH_4]^-$ fragment has lost its ligand identity. There are two separate fluxional processes involving the cluster *endo*-hydrogen atoms in $(\mu\text{-H})Fe_3(CO)_9BH_4$. At −100°C, the protons are static. Warming to −50°C renders the three Fe—H—B protons equivalent, while further warming to 80°C allows exchange of all four *endo*-hydrogen atoms.

Deprotonation of $(\mu\text{-H})Fe_3(CO)_9BH_4$ is readily accomplished with weak bases.[54] Infra-red, multinuclear NMR and Mössbauer spectra indicate that an Fe—H—B bridging proton is removed in preference to either the Fe—H—Fe or terminal protons [Fig. 18(a)]. The terminal BH would not be the expected site of deprotonation since this would leave an exposed boron lone pair, radially

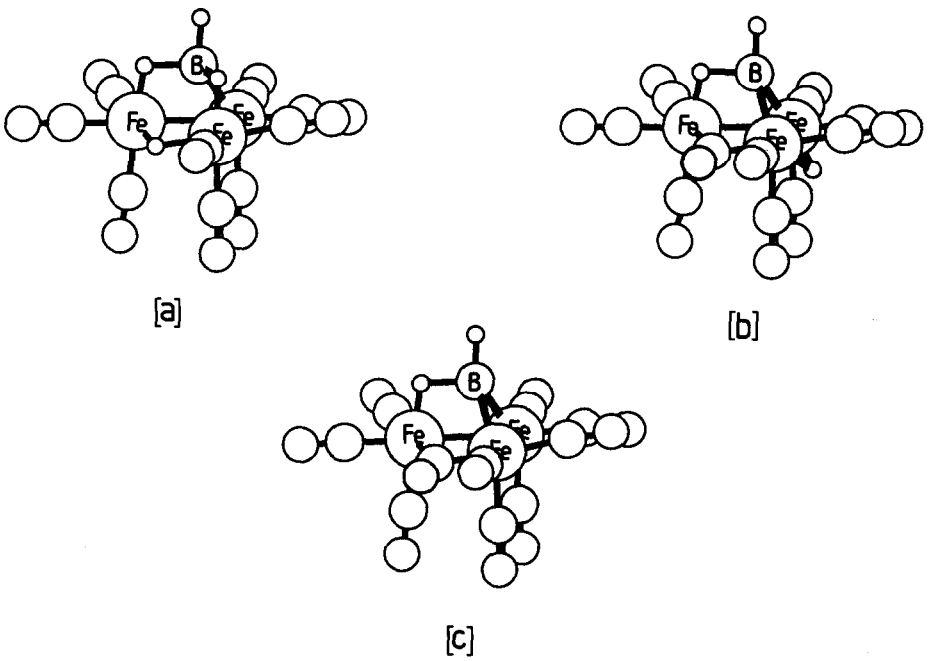

Fig. 18. Proposed structures of (a) $[Fe_3(CO)_9BH_4]^-$; (b) $Fe_3(CO)_{10}BH_3$; (c) $[Fe_3(CO)_{10}BH_2]^-$.[54,57]

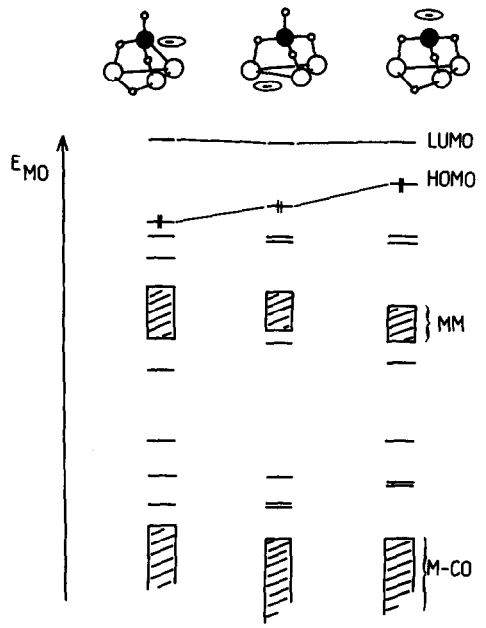

Fig. 19. Comparison of the molecular orbital energies of some isomers of $[Fe_3(CO)_9BH_4]^-$.[55]

disposed and pointing out from the cluster. The relative stabilities of several possible isomers of $[(\mu\text{-}H)Fe_3(CO)_9BH_3]^-$ can be probed by comparing the HOMO–LUMO energy separation obtained from Fenske–Hall calculations.[55] However, it should be noted that the calculations are known to artificially favour M—H—B over M—H—M bridging sites.[56] Figure 19 compares the energies of the MO's of some isomers and we note that the calculations appear to predict a structure in line with experimental observations.

If the conditions of synthesis for $(\mu\text{-}H)Fe_3(CO)_9BH_4$ are modified by adding two equivalents of $Fe(CO)_5$, the favoured product is $(\mu\text{-}H)Fe_3(CO)_{10}BH_2$ [Fig. 18(b)].[57] $(\mu\text{-}H)Fe_3(CO)_{10}BH_2$ is related to $(\mu\text{-}H)Fe_3(CO)_9BH_4$ via the formal replacement of two hydrogen atoms, (each a one electron donor), by a bridging carbonyl ligand, (a two electron donor). Spectroscopic evidence shows that, on going from $(\mu\text{-}H)Fe_3(CO)_9BH_4$ to $(\mu\text{-}H)Fe_3(CO)_{10}BH_2$, two hydrogens "migrate" from Fe—H—B edges on to the trimetal framework and are placed by an edge bridging carbonyl ligand. This migration is a formalism only. The transformation is reported not to take place experimentally; $(\mu\text{-}H)Fe_3(CO)_{10}BH_2$ does not react with H_2 to give $(\mu\text{-}H)Fe_3(CO)_9BH_4$, nor does $(\mu\text{-}H)Fe_3(CO)_9BH_4$ react with CO to give $(\mu\text{-}H)Fe_3(CO)_{10}BH_2$.[57]

In contrast to $(\mu\text{-}H)Fe_3(CO)_9BH_4$, $(\mu\text{-}H)Fe_3(CO)_{10}BH_2$ deprotonates via loss of the Fe—H—Fe proton [Fig. 18(c)].[57] Interestingly, although neutral $(\mu\text{-}H)Fe_3(CO)_9BH_4$ is reported not to react with CO to eliminate hydrogen gas, $[(\mu\text{-}H)Fe_3(CO)_{10}BH]^-$ can be formed in 80% yield by the passage of CO through a solution of $[(\mu\text{-}H)Fe_3(CO)_9BH_4]^-$ at 45°C.[58]

The reactivity of $PPN[(\mu\text{-}H)Fe_3(CO)_9BH_3]$ towards Lewis bases[58] is illustrative of two features. Firstly, it indicates the factors which control whether the incoming nucleophile attacks the boron centre or a metal atom. Secondly, it emphasises the competition between ligand substitution and cluster fragmentation, a problem which Pöe has described as the "Achilles' heel" of cluster substitution.[59] For the Lewis bases H_2O and NEt_3, the expected affinity for boron over a metal centre is observed. However, for $PhMe_2P$, there are three competing reaction pathways as illustrated in Fig. 20. Interestingly, the phosphine substituted product observed in path A is a result of hydrogen, and not CO, elimination. When $PPN[(\mu\text{-}H)Fe_3(CO)_{10}BH]$ reacts with one equivalent of $PhMe_2P$, substitution of a carbonyl ligand is observed as the only reaction. The kinetics of the reaction of $PPN[(\mu\text{-}H)Fe_3(CO)_9BH_3]$ with $PhMe_2P$ show that the reaction is first order with respect to both cluster and Lewis base.[58]

The special significance which the *endo*-hydrogen atoms impart to $[(\mu\text{-}H)Fe_3(CO)_9BH_3]^-$ is noted not only in the reaction of this ferraborane anion with phosphine, but also in its reactivity towards

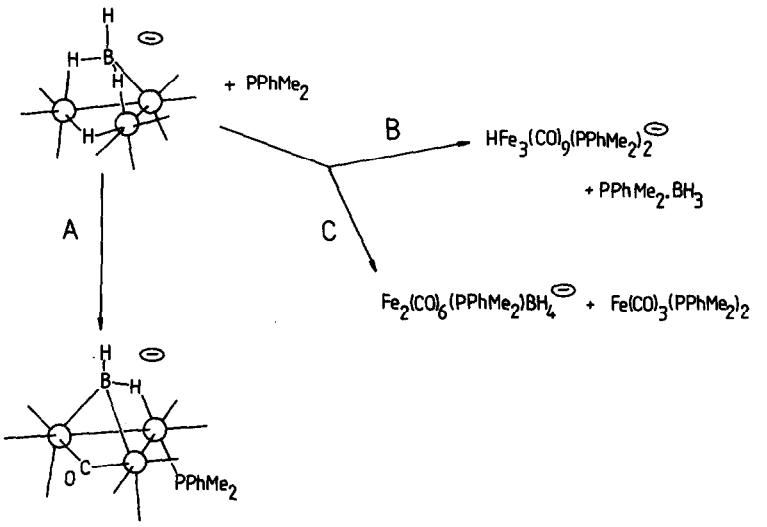

Fig. 20. Competitive pathways for the reaction of $PhMe_2P$ with $[Fe_3(CO)_9BH_4]^-$; pathway **A** is favoured at low concentrations of $PhMe_2P$, while pathways **B** and **C** compete at high $[PhMe_2P]$.[58]

$Fe_2(CO)_9$. The expansion of the triiron cluster to a tetrairon cluster $[(\mu\text{-H})Fe_4(CO)_{12}BH]^-$ is achieved by reacting $PPN[(\mu\text{-H})Fe_3(CO)_9BH_3]$ with two equivalents of $Fe_2(CO)_9$ at room temperature.[56,60] The mild conditions, heterogeneous nature of the reaction mixture, and fact that the cluster reaction takes place quantitatively, are remarkable. The stoichiometry of the reaction has been fully established:

$$[(\mu\text{-H})Fe_3(CO)_9BH_3]^- + 2Fe_2(CO)_9 \rightarrow [(\mu\text{-H})Fe_4(CO)_{12}BH]^- + H_2 + 3Fe(CO)_5.$$

The cluster building sequence is schematically illustrated in Fig. 21. This cluster construction closely parallels a geometrical description and molecular orbital fragment analysis of $(\mu\text{-H})Fe_4(CO)_{12}CH$[61] which is isoelectronic with $[(\mu\text{-H})Fe_4(CO)_{12}BH]^-$. The metallaborane $[(\mu\text{-H})Fe_4(CO)_{12}BH]^-$ will be discussed in the section, metal : boron ratio of 4 : 1.

Alkylated derivatives of $(\mu\text{-H})Fe_3(CO)_9BH_4$ are major products of the reaction of $Fe(CO)_5$, $BH_3 \cdot THF$ and $Li[BEt_3H]$ in hexane.[54] The methylated derivative of $(\mu\text{-H})Fe_3(CO)_{10}BH_2$, $(\mu\text{-H})Fe_3(CO)_{10}BH(CH_3)$, (Fig. 22) is also formed, but in low yield. Significantly higher yields of the alkylated species $(\mu\text{-H})Fe_3(CO)_9BH_3R$ are obtained if one equivalent of $Fe_2(CO)_9$ is initially present in the reaction mixture.[62] Orange, air-sensitive $(\mu\text{-H})Fe_3(CO)_9BH_3R$ ($R = CH_3$, C_2H_5) is a crystalline solid at room temperature. It is interesting that this particular synthetic route does not produce the all hydrogenated ferraborane, $(\mu\text{-H})Fe_3(CO)_9BH_4$. Separation of the methyl and ethyl derivatives (Fig. 23) has not been achieved.[62] Both derivatives display similar spectroscopic characteristics; the ^{11}B NMR resonances are at δ 22.1 (R = Me) and δ 25.4 (R = Et), while the ^1H NMR resonances are indistinguishable for the two derivatives.[55] The effect of substituting an alkyl group for a terminal hydrogen atom on the boron is to lower the energy barrier to *endo*-hydrogen mobility. Whereas for R = H, the limiting low temperature 300 MHz ^1H NMR spectrum shows that all *endo*-hydrogen motion is frozen out, for R = Me or Et, the three Fe—H—B protons remain equivalent

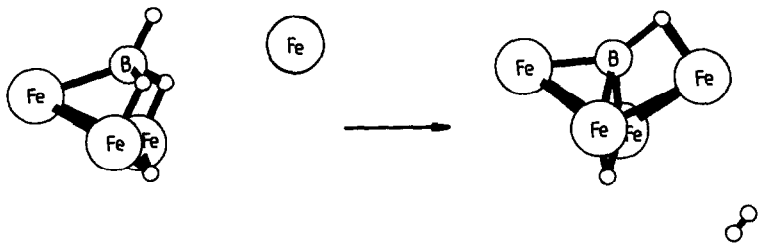

Fig. 21. A schematic representation of the expansion of $[Fe_3(CO)_9BH_4]^-$ to $[HFe_4(CO)_{12}BH]^-$ via the elimination of H_2.[56,60]

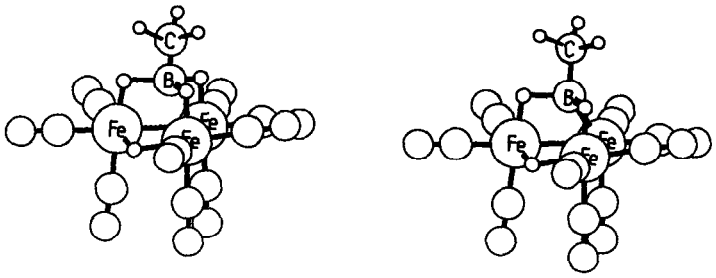

Fig. 22. Proposed structures of $Fe_3(CO)_{10}BH_2(CH_3)$ and $[Fe_3(CO)_{10}BH(CH_3)]^-$.[58]

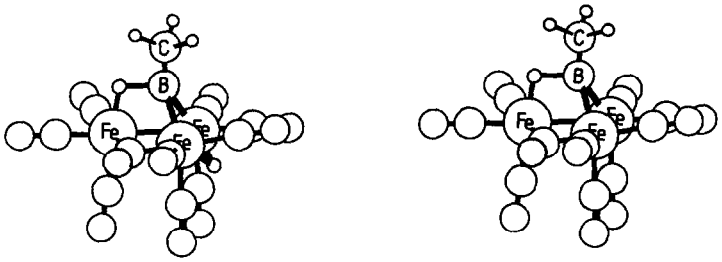

Fig. 23. Proposed structures for $Fe_3(CO)_9BH_4(CH_3)$ and $[Fe_3(CO)_9BH_3(CH_3)]^-$. The ethyl derivatives have the same structures with C_2H_5 replacing CH_3.[54]

at $-80°C$ despite there being two geometrical positions (Fig. 24). This equivalence could be due either to exchange of the Fe—H—B protons themselves, or to scrambling of the Fe—H—Fe proton around the triiron base of the cluster. As with $(\mu\text{-H})Fe_3(CO)_9BH_4$, deprotonation of $(\mu\text{-H})Fe_3(CO)_9BH_3R$ takes place readily at an Fe—H—B site.[54]

$(\mu\text{-H})Fe_3(CO)_{10}BH(CH_3)$ displays similar NMR spectral properties to the hydrogenated parent cluster $(\mu\text{-H})Fe_3(CO)_{10}BH_2$.[58] It deprotonates readily, as does the parent, by loss of an Fe—H—Fe bridging proton (Fig. 22).

CLUSTERS WITH METAL:BORON RATIO 4:1

The formation of $PPN[(\mu\text{-H})Fe_4(CO)_{12}BH]$ via a designed cluster expansion reaction was described above. Historically, the conjugate acid, $(\mu\text{-H})Fe_4(CO)_{12}BH_2$, was the first fully char-

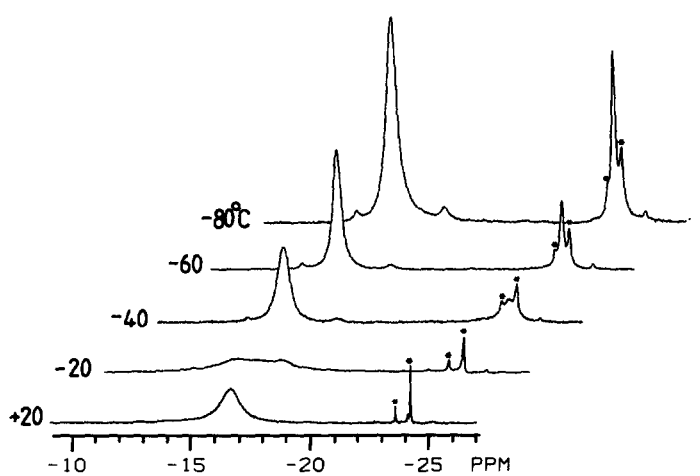

Fig. 24. 300 MHz variable temperature ^1H NMR in CD_2Cl_2 for $Fe_3(CO)_9BH_4R$ (R = Me, Et).[55] Signals labelled * are due to $H_3Fe_3(CO)_9CR$.

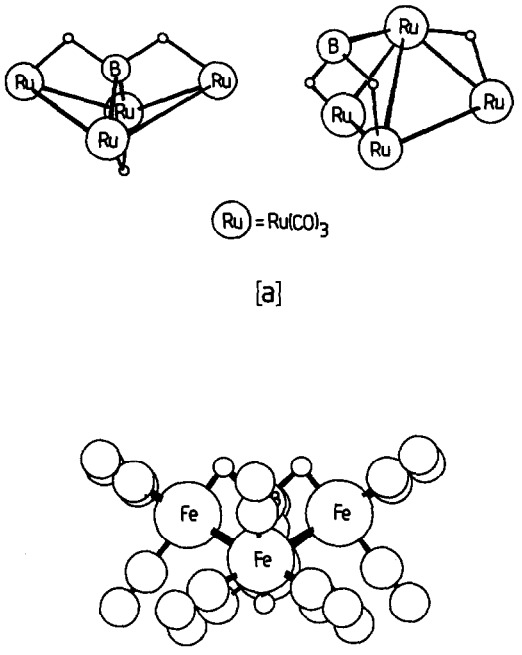

Fig. 25. (a) Proposed structures of $HRu_4(CO)_{12}BH_2$[33] and (b) molecular structure of $HFe_4(CO)_{12}BH_2$.[63,64]

acterized four-metal monoboron cluster.[63,64] A few years earlier, the ruthenium analogue, (μ-H)$Ru_4(CO)_{12}BH_2$ was reported[33] to accompany $Ru_3(CO)_9B_2H_6$ as a minor product in the reaction of $Ru_3(CO)_{12}$ with Na[BH_4]. Two structures [Fig. 25(a)] were proposed for (μ-H)$Ru_4(CO)_{12}BH_2$ on the basis of mass spectroscopic and ^{1}H NMR data. No ^{11}B NMR data were reported. One of the proposed structures for (μ-H)$Ru_4(CO)_{12}BH_2$ was confirmed by X-ray analysis for the ferraborane analogue [Fig. 25(b)].[63,64] In (μ-H)$Fe_4(CO)_{12}BH_2$, the boron atom interacts with a butterfly of four iron atoms (internal dihedral angle 114°), and lies only 0.3 Å above a line joining the two wing-tip metal atoms. All hydrogen atoms are *endo* with respect to the cluster. These structural observations tend to suggest that the boron atom should be described as being *interstitial* with respect to the metal atoms. Note that the BH_2 group is isoelectronic with CH, N and O^+, all of which have been characterized in interstitial environments within butterfly arrays of metal atoms.[7,8,65] The interstitial nature of the boron atom in (μ-H)$Fe_4(CO)_{12}BH_2$ is further indicated by the results of Fenske–Hall MO calculations.[64]

Mono-deprotonation of (μ-H)$Fe_4(CO)_{12}BH_2$ by loss of an Fe—H—B proton takes place readily in the presence of a weak base to form the conjugate base, [(μ-H)$Fe_4(CO)_{12}BH]^-$.[56] Several hours' exposure to triethylamine[55] deprotonates PPN[(μ-H)$Fe_4(CO)_{12}BH$] to the dianion.[66] With *n*-butyl lithium, stepwise deprotonation of (μ-H)$Fe_4(CO)_{12}BH_2$ to the trianion is achieved (Fig. 26).[66] This occurs via alternate loss of Fe—H—B and Fe—H—Fe protons. The replacement of an Fe—H—B interaction by a direct Fe—B interaction as one moves along the series (μ-H)$Fe_4(CO)_{12}BH_2$ to [(μ-H)$Fe_4(CO)_{12}BH]^-$ to $[Fe_4(CO)_{12}BH]^{2-}$ to $[Fe_4(CO)_{12}B]^{3-}$ has a significant effect both on the chemical shift (see Appendix I) and the line width of the ^{11}B NMR resonance.[66] $[Fe_4(CO)_{12}B]^{3-}$ is isoelectronic with $[Fe_4(CO)_{12}C]^{2-}$[67] and is the first example of a transition metal cluster exhibiting an exposed boron atom; i.e. it is a discrete metal boride cluster.

The *endo*-hydrogen atoms of the monoanion, [(μ-H)$Fe_4(CO)_{12}BH]^-$, are fluxional at room temperature on the 300 MHz NMR timescale. A comparison[56] between the fluxional processes that operate in [(μ-H)$Fe_4(CO)_{12}BH]^-$ and the isoelectronic and isostructural cluster (μ-H)$Fe_4(CO)_{12}CH$[68] indicates that exchange of the Fe—H—Fe and Fe—H—X (X = B or C) is more facile for the ferraborane than for the iron hydrocarbyl complex. At low temperatures, the ^{13}C NMR spectrum of (μ-H)$Fe_4(CO)_{12}CH$[65] exhibits equivalence of the two wing-tip $Fe(CO)_3$ units. This can

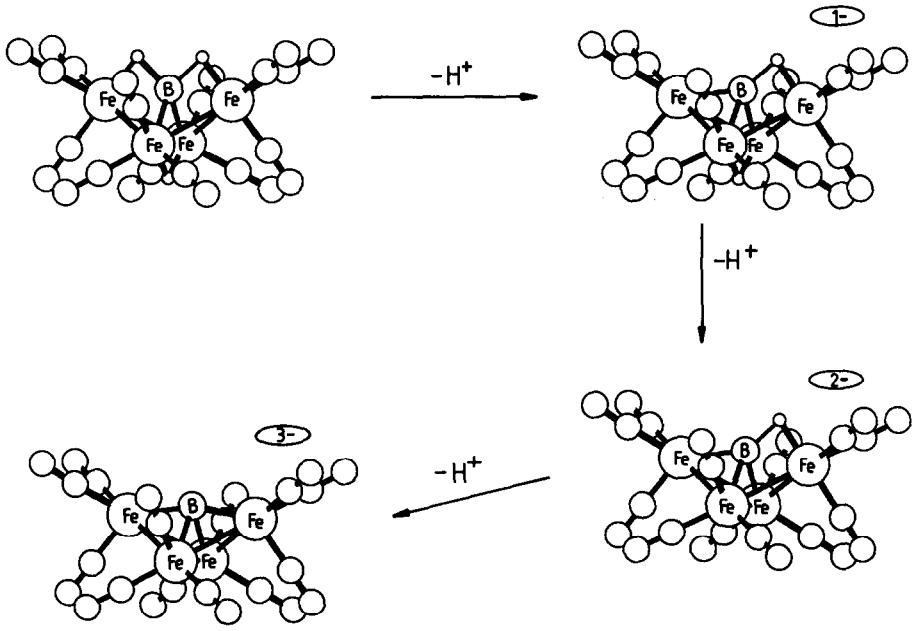

Fig. 26. Stepwise deprotonation of $HFe_4(CO)_{12}BH_2$ leading to $[Fe_4(CO)_{12}B]^{3-}$.[66]

be explained by a process such as a "flip" of the Fe—H—C bridge proton between the two equivalent wing-tip iron-carbon sites. An analogous process in $[(\mu\text{-H})Fe_4(CO)_{12}BH]^-$ has a higher activation energy and is not observed in this case. It is concluded that in $[(\mu\text{-H})Fe_4(CO)_{12}BH]^-$, the Fe—H—B proton is more strongly bound to the iron atom than to the carbon atom, whereas in $(\mu\text{-H})Fe_4(CO)_{12}CH$, the Fe—H—C proton is more closely associated with the carbon than with the iron atom.[56]

The reactivity of $[(\mu\text{-H})Fe_4(CO)_{12}BH]^-$ towards Lewis bases has been studied.[56,69] With one equivalent of $PhMe_2P$, $[(\mu\text{-H})Fe_4(CO)_{12}BH]^-$ reacts smoothly via an associative mechanism to give the monosubstituted derivative $[(\mu\text{-H})Fe_4(CO)_{11}(PhMe_2P)BH]^-$. A further equivalent of phosphine leads to $[Fe_4(CO)_{10}(PhMe_2P)_2BH_2]^-$ (again via an associative mechanism), but its formation is accompanied by significant cluster fragmentation. In both the mono- and di-phosphine substituted derivatives, multinuclear NMR data evidence that substitution occurs at an equatorial site on a wing-tip iron atom. The relative stability of this versus other sites is illustrated using extended Hückel MO calculations.[56] It is noteworthy, firstly, that in going from $[(\mu\text{-H})Fe_4(CO)_{12}BH]^-$ to $[(\mu\text{-H})Fe_4(CO)_{11}(PhMe_2P)BH]^-$, the activation barrier to *endo*-hydrogen exchange is raised; secondly, in going from $[(\mu\text{-H})Fe_4(CO)_{11}(PhMe_2P)BH]^-$ to $[Fe_4(CO)_{10}(PhMe_2P)_2BH_2]^-$, the stable locations for the *endo*-hydrogens change from being one Fe—H—B and one Fe—H—Fe to both protons occupying Fe—H—B bridge sites (Fig. 27). The *endo*-hydrogen atoms play an important role in

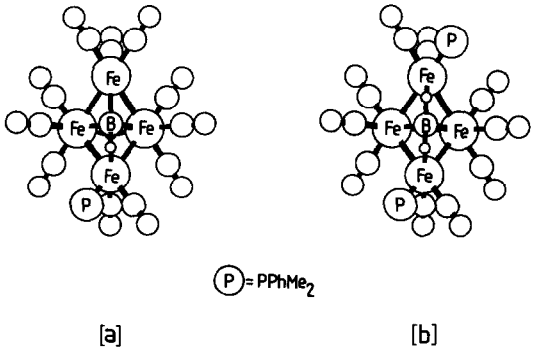

Fig. 27. Proposed structures for (a) $[HFe_4(CO)_{11}(PhMe_2P)BH]^-$ and (b) $[Fe_4(CO)_{10}(PhMe_2P)_2BH_2]^-$.[56,59]

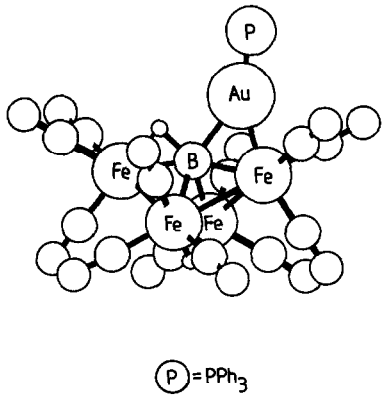

Fig. 28. Proposed structure of $HFe_4(CO)_{12}(AuPPh_3)BH$.[72]

"absorbing" changes in electronic charge which occur at the wing-tip iron atoms as a result of phosphine substitution.[56]

CLUSTERS WITH METAL:BORON RATIO 5:1

The isolobal relationship between H^+ and $AuPR_3^+$[70,71] has been exploited in order to increase the metal to boron ratio in $(\mu\text{-H})Fe_4(CO)_{12}BH_2$ from 4:1 to 5:1; $PPN[(\mu\text{-H})Fe_4(CO)_{12}BH]$ reacts with one equivalent of $AuPPh_3Cl$ at room temperature in CH_2Cl_2 to give $(\mu\text{-H})Fe_4(CO)_{12}(AuPPh_3)BH$.[72] The structure shown in Fig. 28 is proposed on the basis of spectroscopic data. Little change occurs in the ^{11}B NMR chemical shift upon going from $[(\mu\text{-H})Fe_4(CO)_{12}BH]^-$ to $(\mu\text{-H})Fe_4(CO)_{12}(AuPPH_3)BH$; it has previously been noted that, unlike association with protons, association of the boron atom with $AuPR_3$ fragments causes minimal perturbation to the ^{11}B NMR shift.[73] This fact, in conjunction with the observation of ^1H NMR shifts at δ −7.4 (Fe—H—B) and

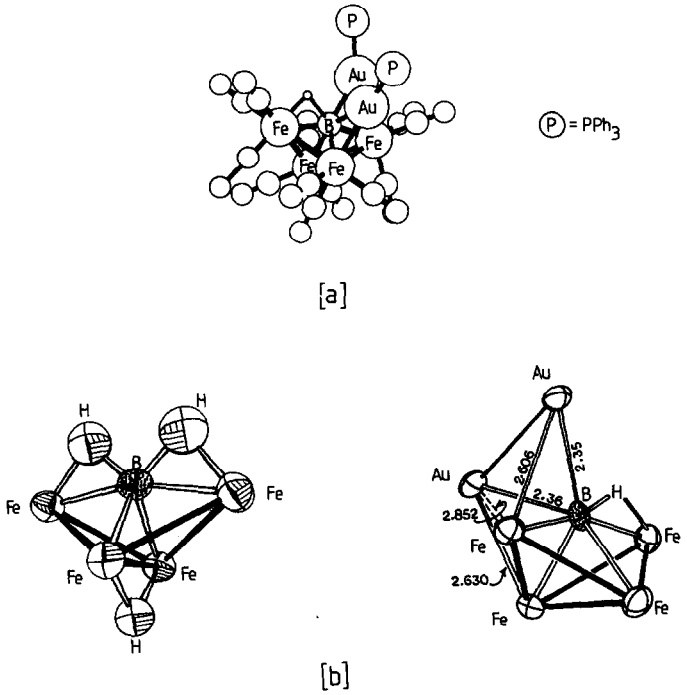

Fig. 29. (a) Molecular structure of $Fe_4(CO)_{12}(AuPPh_3)_2BH$[73,74] and (b) comparison of the Fe_4BH_3 core structure of $HFe_4(CO)_{12}BH_2$ with the Fe_4Au_2BH core of $Fe_4(CO)_{12}(AuPPh_3)_2BH$.

−24.9 (Fe—H—Fe), indicates that $(\mu\text{-H})Fe_4(CO)_{12}(AuPPH_3)BH$ retains the cluster core structure of $(\mu\text{-H})Fe_4(CO)_{12}BH_2$ with a $AuPPh_3$ unit replacing one Fe—H—B bridging proton.

CLUSTERS WITH METAL:BORON RATIO 6:1

Until 1986, the only discrete cluster reported to contain six metal atoms and one boron atom was $Co_6(CO)_{16}B$.[45] This cluster is produced either by the reaction of $Co_2(CO)_8$ with BBr_3 at 60°C, or by treatment of $Co_2(CO)_8$ with 8–10 atmospheres of B_2H_6. Characterization was by elemental analysis and infrared spectroscopy only.

The reaction of $[(\mu\text{-H})Fe_4(CO)_{12}BH]^-$ with excess $AuPPh_3Cl$ in CH_2Cl_2 leads to the high yield formation of $Fe_4(CO)_{12}(AuPPh_3)_2BH$.[73,74] In view of the isolobal analogy between H^+ and $AuPPh_3^+$, one might have expected the cluster structure of $Fe_4(CO)_{12}(AuPPh_3)_2BH$ to mimic that of $Fe_4(CO)_{12}BH_3$. However, the crystallographically characterized isomer of this compound possesses an unprecedented M_6X cluster core [Fig. 29(a)] with one $AuPPh_3$ fragment bridging an Fe(hinge)—B edge and one bridging an Fe(wing)—B edge of the parental Fe_4B cluster core.[73,74] A comparison between the core structures of $Fe_4(CO)_{12}(AuPPh_3)_2BH$ and $Fe_4(CO)_{12}BH_3$ is made in Fig. 29(b). A comparative molecular orbital analysis of the bonding in the two compounds has been made.[74] Certainly, the spatial requirements of the *endo*-hydrogen atom in $Fe_4(CO)_{12}(AuPPh_3)_2BH$ must be responsible for the observed distortion from the symmetrical octahedral M_6 skeleton which encapsulates a carbon atom (isoelectronic with BH) in the related compounds $[Fe_6(CO)_{16}C]^{2-}$[75] and $Fe_4(CO)_{12}(AuPEt_3)_2C$.[76] The two phosphorus environments in $Fe_4(CO)_{12}(AuPPh_3)_2BH$ were not originally observed in the 36 MHz ^{31}P NMR spectrum.[73] However, recent 162 MHz ^{31}P NMR variable temperature studies illustrate that the two phosphorus environments can be frozen out.[72]

It is pertinent to illustrate at this point how molecular orbital calculations can use the known heavy atom structure of a neutral cluster to aid in the location of hydrogen atoms which are not refined in a structure determination. For example, in the crystallographic determination of $Fe_4(CO)_{12}(AuPPh_3)_2BH$, refinement allows the cluster geometry to be known with certainty.[73,74] We can consider the hypothetical anion $[Fe_4(CO)_{12}(AuPPh_3)_2B]^-$ to have the refined core structure of the neutral $Fe_4(CO)_{12}(AuPPh_3)_2BH$. Thus the HOMO of this anion should exhibit a region of high electron density (Lewis basicity) at the site of protonation. Figure 30 illustrates this feature.[55] ($CuPH_3$ fragments are used to model $AuPPh_3$ units in the calculations.[74]) It is, however, crucial to remember that this procedure in *no way* predicts the structure of the real anion, $[Fe_4(CO)_{12}(AuPPh_3)_2B]^-$, but rather uses the known heavy atom structure of the neutral cluster to predict the location of the *endo*-hydrogen in the neutral complex.

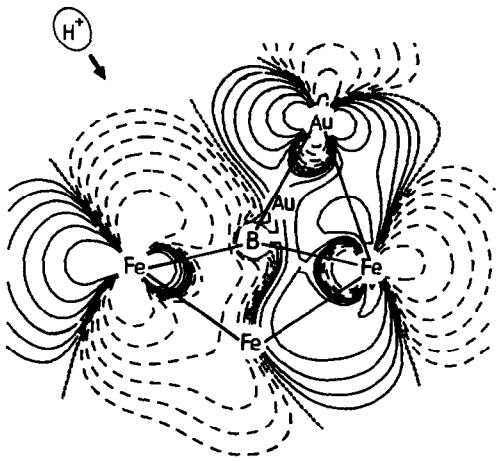

Fig. 30. Amplitude contour plot of the HOMO of $[Fe_4(CO)_{12}(CuPH_3)_2B]^-$ used to model $[Fe_4(CO)_{12}(AuPPh_3)_2B]^-$; the anion has a hypothetical structure derived from the crystallographically refined positions of the non-hydrogen atoms in $Fe_4(CO)_{12}(AuPPh_3)_2BH$. The plot is in the plane containing wing-tip iron atoms, boron atom and Fe(wing)—B bridging gold(I) fragment and shows only core atoms. The other core atoms are projected onto the plane of the plot. The largest contour is 0.05 electron au^{-3}, and each succeeding contour differs from the last by a factor of 2.

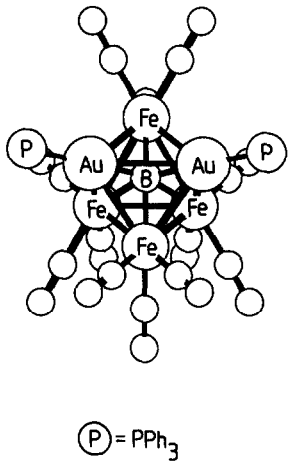

Fig. 31. Proposed structure of $[Fe_4(CO)_{12}(AuPPh_3)_2B]^-$.[72]

Deprotonation of $Fe_4(CO)_{12}(AuPPh_3)_2BH$ with triethylamine leads to a single anionic product.[72] The extreme downfield ^{11}B NMR shift (δ 192) indicates that the boron atom is interacting directly with all four iron atoms. This, in conjunction with a single, temperature invariant ^{31}P NMR resonance suggests that, once rid of the steric requirements of the proton, $[Fe_4(CO)_{12}(AuPPh_3)_2B]^-$ becomes isostructural with its isoelectronic analogue $Fe_4(CO)_{12}(AuPPh_3)_2C$, rather than retaining the distorted octahedral structure found in $Fe_4(CO)_{12}(AuPPh_3)_2BH$. Thus, a boridic environment is proposed for $[FE_4(CO)_{12}(AuPPh_3)_2B]^-$ (Fig. 31).

CONCLUSIONS

The aim of this article has been to illustrate recent developments in the field of metal-rich metallaboranes and this particular survey is timely in view of the burgeoning number of publications in this area. The transition from metallaboranes to discrete metal boride clusters is being made and there should now follow a wealth of new and exciting chemistry. It is many years since Lipscomb pointed out the analogies between borane clusters and bulk metal boride systems.[77] The links between the two extremes are now beginning to be understood.

ABBREVIATIONS

PPN	*bis*(triphenylphosphine)nitrogen(1+) cation
THF	tetrahydrofuran
HOMO	highest occupied molecular orbital
LUMO	lowest unoccupied molecular orbital
PSEPT	polyhedral skeletal electron pair theory
Me	CH_3
Et	C_2H_5
Ph	C_6H_5

Acknowledgements—The Cambridge Crystallographic Data Centre is gratefully acknowledged for providing data for some of the structural figures. I thank Dr E.C. Constable, Miss K. S. Harpp and Mr M. S. Shongwe for helpful suggestions made during the preparation of this manuscript. I should also like to thank Prof. T. P. Fehlner for communicating results prior to publication.

REFERENCES

1. S. Boocock, K. B. Gilbert and S. G. Shore, *Comprehensive Organometallic Chemistry* (Edited by E. W. Abel, F. G. A. Stone and G. Wilkinson), Vol. 6, p. 879. Pergamon Press, Oxford (1982); R. N. Grimes *ibid.* Vol. 1, p. 459.
2. J. D. Kennedy, *Prog. Inorg. Chem.* 1984, **32**, 519; J. D. Kennedy, *Prog. Inorg. Chem.* 1986, **34**, 211.

3. G. E. Herberich, *Comprehensive Organometallic Chemistry* (Edited by E. W. Abel, F. G. A. Stone and G. Wilkinson). Vol. 1, p. 381. Pergamon Press, Oxford (1982).
4. T. P. Fehlner and C. E. Housecroft, *Adv. Organomet. Chem.* 1982, **21**, 57.
5. J. S. Bradley, *Adv. Organomet. Chem.* 1983, **22**, 1.
6. E. L. Muetterties, *Prog. Inorg. Chem.* 1981, **28**, 203.
7. See for example: D. E. Fjare and W. L. Gladfelter, *Inorg. Chem.* 1981, **20**, 3532; M. L. Blohm and W. L. Gladfelter, *Organometallics* 1985, **4**, 45.
8. C. K. Schauer and D. F. Shriver, 193rd Am. Chem. Soc. Nat. Meeting, INORG 256, Denver, U.S.A. (Apr. 1987).
9. S. B. Colbran, C. M. Hay, B. F. G. Johnson, F. J. Lahoz, J. Lewis and P. R. Raithby, *J. Chem. Soc., Chem. Commun.* 1986, 1766 and references therein.
10. F. Cariati and L. Naldini, *J. Inorg. Nucl. Chem.* 1966, **28**, 2243.
11. R. L. Bansemer, J. C. Huffman and K. G. Caulton, *J. Am. Chem. Soc.* 1983, **105**, 6163.
12. T. M. Gilbert, F. J. Hollander and R. G. Bergman, *J. Am. Chem. Soc.* 1985, **107**, 3508.
13. D. G. Holah, A. N. Hughes, S. Maciaszek and V. R. Magnuson, *J. Chem. Soc., Chem. Commun.* 1983, 1308.
14. R. Shinomoto, J. G. Brennan, N. M. Edelstein and A. Zalkin, *Inorg. Chem.* 1985, **24**, 2896.
15. D. M. P. Mingos, *Nature* 1972, **236**, 99; R. W. Rudolph, *Acc. Chem. Res.* 1976, **9**, 446; K. Wade, *Adv. Inorg. Chem. Radiochem.* 1976, **18**, 1; R. E. Williams, *Adv. Inorg. Chem. Radiochem.* 1976, **18**, 67.
16. E. L. Andersen and T. P. Fehlner, *J. Am. Chem. Soc.* 1978, **100**, 4606.
17. E. L. Andersen, F.-E. Hong, C. E. Housecroft, G. B. Jacobsen, M. L. Buhl, G. J. Long and T. P. Fehlner, submitted for publication.
18. C. E. Housecroft, *Inorg. Chem.* 1986, **25**, 3108.
19. E. L. Andersen, R. L. DeKock and T. P. Fehlner, *Inorg. Chem.* 1981, **20**, 3291.
20. J. R. Pipal and R. N. Grimes, *Inorg. Chem.* 1977, **16**, 3255.
21. T. L. Venable and R. N. Grimes, *Inorg. Chem.* 1982, **21**, 887.
22. V. R. Miller, R. Weiss and R. N. Grimes, *J. Am. Chem. Soc.* 1977, **99**, 5646.
23. J. R. Pipal and R. N. Grimes, *Inorg. Chem.* 1979, **18**, 257.
24. G. J. Zimmerman, L. W. Hall and L. G. Sneddon, *Inorg. Chem.* 1980, **19**, 3642.
25. J. M. Gromek and J. Donohue, *Cryst. Struct. Commun.* 1981, **10**, 849.
26. R. Weiss, J. B. Bowser and R. N. Grimes, *Inorg. Chem.* 1978, **17**, 1522.
27. V. R. Miller and R. N. Grimes, *J. Am. Chem. Soc.* 1976, **98**, 1600.
28. J. R. Bowser and R. N. Grimes, *J. Am. Chem. Soc.* 1978, **100**, 4623.
29. J. R. Bowser, A. Bonny, J. R. Pipal and R. N. Grimes, *J. Am. Chem. Soc.* 1979, **101**, 6229.
30. D. N. Cox, D. M. P. Mingos and R. Hoffmann, *J. Chem. Soc., Dalton Trans.* 1981, 1788.
31. M. E. O'Neill and K. Wade, *Inorg. Chem.* 1982, **21**, 464.
32. R. P. Micciche, P. J. Carroll and L. G. Sneddon, *Organometallics* 1985, **4**, 1619.
33. B. F. G. Johnson, C. R. Eady and J. Lewis, *J. Chem. Soc., Dalton Trans.* 1977, 477.
34. N. N. Greenwood, C. G. Savory, R. N. Grimes, L. G. Sneddon, A. Davison and S. S. Wreford, *J. Chem. Soc., Chem. Commun.* 1974, 718.
35. E. L. Andersen, K. J. Haller and T. P. Fehlner, *J. Am. Chem. Soc.* 1979, **101**, 4390; K. J. Haller, E. L. Andersen and T. P. Fehlner, *Inorg. Chem.* 1981, **20**, 309.
36. T. P. Fehlner, *Boron Chemistry* (Edited by R. W. Parry and G. Kodama), p. 95. Pergamon Press, Oxford (1980).
37. H. D. Kaesz, W. Fellmann, G. R. Wilkes and L. F. Dahl, *J. Am. Chem. Soc.* 1965, **87**, 2753.
38. T. P. Fehlner, J. Feilong and A. L. Rheingold, *J. Am. Chem. Soc.* 1987, **108**, 1860.
39. V. R. Miller and R. N. Grimes, *J. Am. Chem. Soc.* 1973, **95**, 5078.
40. J. R. Pipal and R. N. Grimes, *Inorg. Chem.* 1979, **18**, 252.
41. L. F. Dahl and D. L. Smith, *J. Am. Chem. Soc.* 1962, **84**, 2450.
42. T. P. Fehlner, J. Feilong and A. L. Rheingold, 193rd Am. Chem. Soc. Nat. Meeting, INORG 215, Denver, U.S.A. (Apr. 1987).
43. J. Lunniss, S. A. MacLaughlin, N. J. Taylor, A. J. Carty and E. Sappa, *Organometallics* 1985, **4**, 2066.
44. G. A. Carriedo, G. P. Elliott, J. A. K. Howard, D. B. Lewis and F. G. A. Stone, *J. Chem. Soc., Chem. Commun.* 1984, 1585.
45. G. Schmid, V. Batzel, G. Elzrodt and R. Pfeil, *J. Organomet. Chem.* 1975, **86**, 257.
46. S. G. Shore, D.-Y. Jan, L.-Y. Hsu and W.-L. Hsu, *J. Am. Chem. Soc.* 1983, **105**, 5923.
47. S. G. Shore, D.-Y. Jan, W.-L. Hsu, L.-Y. Hsu, S. Kennedy, J. C. Huffman, T.-C. Lin Wang and A. Marshall, *J. Chem. Soc., Chem. Commun.* 1984, 392.
48. D.-Y. Jan, L.-Y. Hsu and S. G. Shore, 188th Am. Chem. Soc. Nat. Meeting, INORG 180, Philadelphia, U.S.A. (Aug. 1984).
49. D.-Y. Jan and S. G. Shore, *Organometallics* 1987, **6**, 428.

50. D.-Y. Jan, L.-Y. Hsu, D. Workman and S. G. Shore, 191st Am. Chem. Soc. Nat. Meeting, INORG 417, New York, U.S.A. (Apr. 1986).
51. R. D. Barreto, T. P. Fehlner, L.-Y. Hsu, D.-Y. Jan and S. G. Shore, *Inorg. Chem.* 1986, **25**, 3572.
52. A. J. Deeming and M. Underhill, *J. Chem. Soc., Dalton Trans.* 1974, 1415.
53. J. C. Vites, C. Eigenbrot and T. P. Fehlner, *J. Am. Chem. Soc.* 1984, **106**, 4633.
54. J. C. Vites, C. E. Housecroft, C. Eigenbrot, M. L. Buhl, G. J. Long and T. P. Fehlner, *J. Am. Chem. Soc.* 1986, **108**, 3304.
55. C. E. Housecroft, unpublished results.
56. C. E. Housecroft, T. P. Fehlner, M. L. Buhl and G. J. Long, *J. Am. Chem. Soc.* 1987, **109**, 3323.
57. J. C. Vites, C. E. Housecroft, G. B. Jacobsen and T. P. Fehlner, *Organometallics* 1984, **3**, 1591.
58. C. E. Housecroft and T. P. Fehlner, *J. Am. Chem. Soc.* 1986, **108**, 4867.
59. N. Brodie, A. Poe and V. J. Sekhar, *J. Chem. Soc., Chem. Commun.* 1985, 1090.
60. C. E. Housecroft and T. P. Fehlner, *Organometallics* 1986, **5**, 379.
61. C. E. Housecroft and T. P. Fehlner, *Organometallics* 1984, **3**, 764.
62. K. S. Harpp, C. E. Housecroft and M. S. Shongwe, unpublished results.
63. K. S. Wong, W. R. Scheidt and T. P. Fehlner, *J. Am. Chem. Soc.* 1982, **104**, 1111.
64. T. P. Fehlner, C. E. Housecroft, W. R. Scheidt and K. S. Wong, *Organometallics* 1983, **2**, 825.
65. M. A. Beno, J. M. Williams, M. Tachikawa and E. L. Muetterties, *J. Am. Chem. Soc.* 1981, **103**, 1485.
66. T. P. Fehlner and N. P. Rath, *J. Am. Chem. Soc.* 1987, **109**.
67. J. H. Davis, M. A. Beno, J. M. Williams, J. Zimmie, M. Tachikawa and E. L. Muetterties, *Proc. Natl. Acad. Sci. U.S.A.* 1981, **78**, 668.
68. M. Tachikawa and E. L. Muetterties, *J. Am. Chem. Soc.* 1980, **102**, 4541.
69. C. E. Housecroft and T. P. Fehlner, *Organometallics* 1986, **5**, 1279.
70. D. G. Evans and D. M. P. Mingos, *J. Organomet. Chem.* 1982, **232**, 171.
71. J. W. Lauher and K. Wald, *J. Am. Chem. Soc.* 1981, **103**, 7648.
72. K. S. Harpp and C. E. Housecroft, manuscript in preparation.
73. C. E. Housecroft and A. L. Rheingold, *J. Am. Chem. Soc.* 1986, **108**, 6420.
74. C. E. Housecroft and A. L. Rheingold, *Organometallics* 1987, **6**, 1332.
75. M. R. Churchill and J. Wormald, *J. Chem. Soc., Dalton Trans.* 1974, 2410.
76. B. F. G. Johnson, D. A. Kaner, J. Lewis, P. R. Raithby and M. J. Rosales, *J. Organomet. Chem.* 1982, **231**, C59.
77. W. N. Lipscomb, *J. Less-Common Metals* 1981, **82**, 1.

APPENDIX I: ^{11}B NMR CHEMICAL SHIFTS FOR METAL-RICH METALLABORANES

Compound	Fig.	^{11}B shift[a] (ppm) (*Observed frequency MHz*)	Solvent	Ref.
$V_2Zn_2H_4(BH_4)_2(PPh_2Me)_4$	1(b)	−30.6	C_6D_6	11
$\{(C_5Me_5)Ir\}_2H_3(BH_4)$	1(c)	5.5[b]	$C_6D_5CD_3$	12
$Fe_2(CO)_6B_2H_6$	2(a,b)	−24.2 (*96.3*)	CD_2Cl_2	17
$[Fe_2(CO)_6B_2H_5]^-$	2(c)	−17.4 (*96.3*)	CD_2Cl_2	17
1,2,3-$\{(C_5H_5)Co\}_3B_3H_5$	3(a)	62.7 (*32.1*)	$CDCl_3$	22
1,2,3-$\{(C_5H_5)Co\}_3B_3H_3(\mu_3\text{-}CO)$	3(b)	89.9 (*115.5*)	CH_2Cl_2	24
1,2,3-$\{(C_5H_5)Co\}_2Fe(CO)_4B_3H_3$	3(c)	87.5(1B) 73.0(2B) (*32.1*)	$CDCl_3$	25
$\{(C_5H_5)Co\}_4B_4H_4$	4(a)	121.4 (*32.1*)	$CDCl_3$	22, 27
$\{(C_5H_5)Ni\}_4B_4H_4$	4(b)	56.2 (*32.1*)	$CDCl_3$	29
4,6-$\{(C_5H_5)Co\}_2$-3,5-$S_2B_2H_2$	6	17.6 (*32.1*)	C_6D_6	32

Appendix I—*continued*

Compound	Fig.	^{11}B shift[a] (ppm) (*Observed frequency MHz*)	Solvent	Ref.
$\{(C_5H_5)Co\}_4B_2H_4$	10	104 (*96.2*)	$(CD_3)_2CO$	38
2-Ph-1,3,6,7,2-$\{(C_5H_5)Co\}_4PB_2H_2$	11	103.8 (*96.2*)	—	42
$\{(C_5H_5)(CO)_2W\}_2(CMe)(BHEt)$	12	−30.0 —	C_6D_6	44
$(\mu\text{-}H)_3Os_3(CO)_9BCO$	14(a)	19.4 —	CD_2Cl_2	46
$(\mu\text{-}H)_3Os_3(CO)_9BPMe_3$	14(b)	60.9 —	$CDCl_3$	48
$(\mu\text{-}H)_3Os_3(CO)_9B{=}CH_2$	14(c)	53.5 —	$C_6D_5CH_3$	49
$Fe_3(CO)_9BH_5$	17	1.8 (*96.2*)	C_6D_6	53, 54
$[Fe_3(CO)_9BH_4]^-$	18	6.2 (*96.2*)	$(CD_3)_2CO$	54
$Fe_3(CO)_{10}BH_3$	18	56.0 (*96.2*)	C_6D_6	57
$[Fe_3(CO)_{10}BH_2]^-$	18	57.4 (*96.2*)	$(CD_3)_2CO$	57
$Fe_3(CO)_9BH_4(CH_3)$	23	22.1 (*96.2*)	CD_2Cl_2	54
$Fe_3(CO)_9BH_4(C_2H_5)$	23	25.4 (*96.2*)	CD_2Cl_2	55
$[Fe_3(CO)_9BH_3(CH_3)]^-$	23	29.3 (*96.2*)	$(CD_3)_2CO$	54
$[Fe_3(CO)_9BH_3(C_2H_5)]^-$	23	26.5 (*96.2*)	$(CD_3)_2CO$	55
$Fe_3(CO)_{10}BH_2(CH_3)$	22	76.4 (*96.2*)	$(CD_3)_2CO$	58
$[Fe_3(CO)_{10}BH(CH_3)]^-$	22	74.5 (*96.2*)	$(CD_3)_2CO$	58
$[Fe_3(CO)_9(PhMe_2P)BH(CH_3)]^-$	—	72.7 (*96.2*)	$(CD_3)_2CO$	58
$HFe_4(CO)_{12}BH_2$	25(b)	116.0[c] (*96.2*)	C_6D_6	56
$[HFe_4(CO)_{12}BH]^-$	26	150.0 (*96.2*)	$(CD_3)_2CO$	56, 60
$[Fe_4(CO)_{12}BH]^{2-}$	26	153.0 (*96.2*)	C_4H_8O	66
$[HFe_4(CO)_{11}(PhMe_2P)BH]^-$	27(a)	141.7 (*96.2*)	$(CD_3)_2CO$	56, 69
$[Fe_4(CO)_{10}(PhMe_2P)_2BH_2]^-$	27(b)	117.9 (*96.2*)	$(CD_3)_2CO$	56, 69
$HFe_4(CO)_{12}(AuPPh_3)BH$	28	137.5 (*128.7*)	CD_2Cl_2	72
$Fe_4(CO)_{12}(AuPPh_3)_2BH$	29	141.3 (*28.7*)	$(CD_3)_2CO$	73, 74
$[Fe_4(CO)_{12}(AuPPh_3)_2B]^-$	31	192.2 (*128.4*)	$(CD_3)_2CO$	72

[a] δ ^{11}B with respect to $BF_3 \cdot OEt_2$. Positive shifts are downfield.
[b] Referenced with respect to $[BF_4]^-$ in methanol.
[c] This resonance was originally recorded at 32.1 MHz at δ 106.[63]

APPENDIX II: ^{1}H NMR CHEMICAL SHIFTS FOR M—H—B BRIDGING PROTONS IN METAL-RICH METALLABORANES

Compound	Fig.	^{1}H NMR shift[a] for M—H—B proton (ppm) (*Observed frequency MHz*)	Solvent	Ref.
$\{(C_5Me_5)Ir\}_2H_3(BH_4)$	1(c)	−14.18	C_6D_6	12
$Fe_2(CO)_6B_2H_6$	2(b)	−12.4(1H) −15.9(2H) (*300*)	CD_2Cl_2	17
$[Fe_2(CO)_6B_2H_5]^-$	2(c)	−14.2 (*300*)	CD_2Cl_2	17
$\{(C_5H_5)(CO)_2W\}_2(CMe)(BHEt)$	12	−10.23	—	44
$(\mu\text{-H})_3Os_3(CO)_9B{=}CH_2$	14(c)	−12.26 −13.45 —	$C_6D_5CD_3$	49
$Fe_3(CO)_9BH_5$	17	−12.8(1H) −15.8(2H) (*300*)	$C_6D_5CD_3$	54
$[Fe_3(CO)_9BH_4]^-$	18	−13.1 (*300*)	$(CD_3)_2CO$	54, 57
$Fe_3(CO)_{10}BH_3$	18	−13.7 (*300*)	$C_6D_5CD_3$	57
$[Fe_3(CO)_{10}BH_2]^-$	18	−11.1 (*300*)	$(CD_3)_2CO$	57
$Fe_3(CO)_9BH_4(CH_3)$	23	−14.6 (*300*)	CD_2Cl_2	54
$Fe_3(CO)_9BH_4(C_2H_5)$	23	−14.6 (*300*)	CD_2Cl_2	55
$[Fe_3(CO)_9BH_3(CH_3)]^-$	23	−12.9 (*300*)	$(CD_3)_2CO$	54
$[Fe_3(CO)_9BH_3(C_2H_5)]^-$	23	−12.9 (*300*)	$(CD_3)_2CO$	55
$Fe_3(CO)_{10}BH_2(CH_3)$	22	−13.2 (*300*)	CD_2Cl_2	58
$[Fe_3(CO)_{10}BH(CH_3)]^-$	22	−10.3 (*300*)	$(CD_3)_2CO$	58
$[Fe_3(CO)_9(PhMe_2P)BH(CH_3)]^-$	—	−10.3	$(CD_3)_2CO$	58
$HRu_4(CO)_{12}BH_2$	25(a)	−8.5 (*100*)	—	33
$HFe_4(CO)_{12}BH_2$	25(b)	−11.9 (*100*)	CD_2Cl_2	63
$[HFe_4(CO)_{11}(PhMe_2P)BH]^-$	27(a)	−8.4 (*300*)	$(CD_3)_2CO$	56, 69
$[Fe_4(CO)_{10}(PhMe_2P)_2BH_2]^-$	27(b)	−11.6 (*300*)	$(CD_3)_2CO$	56, 69
$HFe_4(CO)_{12}(AuPPh_3)BH$	28	−7.4 (*400.0*)	CD_2Cl_2	72
$Fe_4(CO)_{12}(AuPPh_3)_2BH$	29	−9.1 (*89.6*)	$(CD_3)_2CO$	73, 74

[a] δ ^{1}H with respect to TMS. Positive shifts are downfield.

Polyhedron Vol. 6, No. 11, pp. 1959–1970, 1987
Printed in Great Britain

0277–5387/87 $3.00+.00

ESR STUDY ON THE REACTIONS OF IRON CARBONYLS WITH NITRO AND NITROSOPARAFFINES. A MECHANISM OF THE REDUCTIVE CARBONYLATION OF NITRO COMPOUNDS

Yu. A. BELOUSOV* and T. A. KOLOSOVA

A. N. Nesmeyanov Institute of Organoelement Compounds, USSR Academy of Sciences, 28 Vavilov Str., 117813 Moscow, U.S.S.R.

(*Received* 26 *March* 1987; *accepted* 27 *April* 1987)

Abstract—The interaction of $Fe_n(CO)_m$ (n and m equal 1 and 5, 2 and 9, 3 and 12, respectively) with 2-methyl-2-nitrosopropane and sodium salts of nitromethane and nitrocyclohexane was studied. The initial stages of the process, following the activating complex-formation, involves redox disproportionation to give rise to the radical Fe(I) carbonyl complexes and radical anions $Fe_2(CO)_8^-$ (**I**) $Fe_3(CO)_{11}^-$ (**II**), $Fe_4(CO)_{13}^-$ (**III**) and $Fe_3(CO)_{12}^-$ (**IV**). Also, radical anions **I–IV** are formed in the interaction of salts of carbonyl ferrate anions $Na_2Fe(CO)_4 \cdot 1.5$ diox and $PPN_2[Fe_n(CO)_{m-1}]$ (where PPN = $(PPh_3)_2N^+$), with nitro- and nitroso-tert-butane.

Radical anions **I–III** act as catalytically active species in the coordination sphere of which the nitro compounds undergo a successive deoxygenation to nitrene radical complexes with their subsequent carbonylation to isocyanates. A scheme of the reductive carbonylation is proposed.

Reactions of iron carbonyls with nucleophilic agents and bases have been under study for more than 60 years. Owing mainly to the studies of Hieber and coworkers[1,2] it is known that these reactions represent redox disproportionation whose thermodynamics are controlled by formation of Fe(II) salts with the carbonyl ferrate anion Fe(-II) as the counterion. The bi- and trinuclear iron carbonyl complexes were often isolated as intermediates.[3] These complexes contain a variety of fixed products resulting from the conversions of the parent substrates. The complexes were considered to be intermediate catalytic species[4,5] in the carbonylation of nitro[5] and a variety of other nitrogenated compounds[6–8] catalysed with metal, particularly iron carbonyls.

However, only little attention has been paid in these studies to the redox disproportionation of the carbonyls, and its catalytic role has not been disclosed.

On the other hand, electrochemical, ESR and ion cyclotron resonance studies gave evidence of the paramagnetic radical ions of iron carbonyls having a formal charge on metal (-I), such as $Fe_2(CO)_8^-$ (**I**), $Fe_3(CO)_{11}^-$ (**II**), $Fe_4(CO)_{13}^-$ (**III**) and $Fe_3(CO)_{12}^-$ (**IV**). They are generated either by means of the traditional reducing agents or electrochemically.[9–13]

However, these studies do not trace relations between radical anions **I–IV** and redox disproportionation of the iron carbonyls either.

One of the present authors has shown for the first time that such radical anions of iron carbonyls result from the one-electron transfer at the first stage of redox disproportionation of the iron carbonyls under the effect of the nitrogenous nucleophiles, anions of azoles,[14] and that these radical anions are catalytically active species where the reduction of the nitro compounds takes place.[15] The purpose of the present study is to discuss this problem.

EXPERIMENTAL

ESR spectra were taken with an ERS-221 (ZWG DDR) instrument in an X-range with a 100 kHz

* Author to whom correspondence should be addressed.

modulation. The reactions were conducted directly in an ampoule placed in the ESR spectrometer cavity with the equimolar reagents ratio of *ca.* 10^{-1} M of THF and toluene. When using 2-methyl-2-nitrosopropane as the spin trap, its concentration was *ca.* 10^{-3} M. The samples were conditioned in a vacuum of 10^{-4} torr by freeze–pump–thaw cycles by the use of THF and toluene dehydrated over benzophenone ketyl, or nitromethane dehydrated over 4 Å molecular sieves. All the studies using 2-methyl-2-nitrosopropane were made in the dark.

Syntheses of the parent compounds

All the syntheses were carried out in an argon atmosphere. Potassium and sodium nitrites were those commercially available, without preliminary purification. The iron pentacarbonyl was purified by sublimation. The iron pentacarbonyl $^{57}Fe(CO)_5$[16] as well as $Na_2Fe(CO)_4 \cdot 1.5diox$,[17] $PPN_2[Fe_2(CO)_8]$,[18,19] $PPN_2[Fe_3(CO)_{11}]$,[20] $PPN_2[Fe_4(CO)_{13}]$,[21] $PPN[Fe(CO)_3NO]$,[22] $PPN(NO_2)$,[23] t-C_4H_9NO,[24] $FcPF_6$ where Fc is ferricenium,[25] $Fe_2(CO)_6(N\text{-}t\text{-}Bu)_2$, $Fe_3(CO)_9(N\text{-}t\text{-}Bu)_2$, $Fe_2(CO)_6[(t\text{-}BuN)_2CO]$[26] and t-BuNCO[27] were synthesized by the known methods. The sodium salts of the nitro compounds were obtained from the corresponding nitro compounds and sodium hydride in THF.

RESULTS AND DISCUSSION

1. *Reactions of the iron carbonyls* $Fe(CO)_5$ *and* $Fe_3(CO)_{12}$ *with the sodium salts of nitromethane and nitrocyclohexane*

Iron pentacarbonyl is known to interact with aliphatic nitro compounds under the effect of ultraviolet irradiation, radiolysis or high temperatures. If in reactions with iron carbonyls the sodium salts of nitro compounds are used (thereby increasing the basicity of the reagents) the reactions in THF at room temperature for the most inert iron carbonyl, *viz.* pentacarbonyl, will terminate in no more than a few minutes. When the reaction takes place directly in the ESR spectrometer cavity at −80°C, one can observe a successive formation of radical anions **I–IV** whose g-factors are in good agreement with those reported by Krusic *et al.*[10] Note that these four radicals are always formed in the reactions, irrespective of which iron carbonyl is used initially. The only difference is the order in which they are formed as well as the rate of their accumulation and consumption at the different reaction stages.

Starting with $Fe_3(CO)_{12}$, the order in which the radical anions appear is as follows: **IV, II, I, III.**

In addition to these species, reactions of iron pentacarbonyl gave a series of radicals with the corresponding signals: a broadened singlet ($g = 2.0461$) from **V** which was formed at the initial reaction stages; a broad signal ($g = 2.0327$) from **VI**; a 1 : 2 : 3 : 2 : 1 quintet ($g = 2.0217$ and $a_N = 1.6$ G) from **VII** and broadened singlet ($g = 2.0182$) from **VIII**. A 1 : 3 : 6 : 7 : 6 : 3 : 1 heptet ($g = 1.9914$ and $a_N = 4.7$ G) from **IX** is also detectable (see Table 1), probably $Fe(CO)(NO)_3^{\cdot}$.[28]

We believe that the earlier proposed scheme[14] of redox disproportionation of iron carbonyls under the effect of anionic nucleophiles is applicable to nitro compound salts, as well. For the reaction with iron pentacarbonyl the following scheme can be written down:

$$Fe(CO)_5 + (R_2CNO_2)^- \rightleftharpoons [Fe(CO)_{5-n} \cdot (R_2CNO_2)]^-$$

$$[Fe(CO)_{5-n} \cdot (R_2CNO_2)]^- + Fe(CO)_5 \xrightarrow[-CO]{} [Fe(CO)_4 \cdot (R_2CNO_2)]^{\cdot} + Fe(CO)_5^- \quad (1)$$

$$R = H, -R-R- = -(CH_2)_5-.$$

The ambiguity of the n value (0 or 1) is caused by the order in which one or another process, i.e. CO group elimination or electron transfer, takes place. A detailed discussion of the interaction of iron carbonyls with Lewis bases will be given elsewhere.[29]

The resulting $Fe(CO)_5^-$ is unstable.[30] It interacts with the iron pentacarbonyl to yield radical anions **I–IV**, i.e. Fe(-I) compounds. Thereby the reductive part of the iron carbonyl redox disproportionation is realized.

Among the Fe(I) species $Fe(CO)_3(NO)^{\cdot}$ **(VI)** can be regarded as a reliably identified radical. At −60°C the corresponding signal exhibits a structure typical of a 1 : 1 : 1 unresolved triplet with a Lorenzian line shape to give, as reported elsewhere,[31] $a_N = 2.1$ G. The labelled ^{57}Fe yields a doublet on the iron, $a_{^{57}Fe} = 7.9$ G.

Radical **VI** was also obtained by us via an alternative synthesis, by the reaction:

$$PPN[Fe(CO)_3(NO)] + Fc^+PF_6^- \rightarrow Fe(CO)_3(NO)^{\cdot} + Fc. \quad (2)$$

It is detected at −80°C at the initial reaction stages. The extended reaction time gives rise to the other radicals with a multiplet structure of the signals in this region, whose superposition impedes spectrum interpretation.

Using 2-methyl-2-nitrosopropane as the spin trap

Table 1. ESR data on the reactions of iron carbonyls with nitro and nitrozoparaffines[a,b]

Radical number	Radical structure[c]	g-factor[d]	Hyperfine splitting constants (Gauss)[e] a_N	$a_{(x)}$	Reaction number
I	$Fe_2(CO)_8^-$	2.0385			1, 3, 7, 8, 12, 13
II	$Fe_3(CO)_{11}^-$	2.0498			1, 3, 5, 7, 8, 11–13
III	$Fe_4(CO)_{13}^-$	2.0135			1, 3, 7, 8, 12
IV	$Fe_3(CO)_{12}^-$	2.0013			1, 3, 5, 7, 8, 12
V	$[Fe(CO)_4(H_2CNO_2)]^-$?	2.0461			1, 4
VI	$Fe(CO)_3NO^-$	2.0327[f]	2.1[f] (t)	7.9(^{57}Fe) (d)	1–5
VII		2.0217	1.6 (g)		1, 3
VIII		2.0182		1.8(^{57}Fe) (1:3:3:1)	1, 3
IX	$Fe(CO)(NO)_3^-$?	1.9914	4.7 (h)		1
X	$(CO)_3(NO)FeN(\dot{O})$-t-Bu	2.0040[g]	16.9[g] (t) 0.65[g] (t)	1.7(^{57}Fe)[g] (d)	5, 6h
XI	$[Fe(CO)_4(NO_2)]^-$?	2.0376	13.2		3
XII	$Fe(CO)_2(NO)_2^+$	2.0286	2.8 (q)		3
XIII	tBu_2NO^-	2.0060	15.4 (t)		5, 6d
XIV	$tBuNO^-$	2.0060	10.7 (t)		6b, 6g
		2.0059[h]	12.3[h] (t)		8
		2.0061[i]	12.1[i] (t)	1.5 (Na)[i] (1:1:1:1)	8
XV	t-BuNOH	2.0060	13.1 (t)	10.7 (H) (d)	6
XVI	$[Fe(CO)_{5-n}(t\text{-BuNO})_2]^+$?	2.0222	2.8 (q)		6b
XVII	$t\text{-BuNO}_2^-$	2.0060	25.4 (t)		8
XVIII		2.0063	15.8 (t)		8
XIX		2.0054	16.7 (t)		8
XX	$Fe_3(CO)_9(N\text{-}t\text{-Bu})^-$	2.0267	1.8 (t)		8, 11
XXI	$Fe_3(CO)_{10}(N\text{-}t\text{-Bu})^-$	2.0251	2.1 (t)		8, 11
XXII		2.0365			8, 11
XXIII		2.0037	15.5 (t)		8
XXIV		2.0054			8
XXV		2.0036	16.7 (t)		8
XXVI		2.0062	15.7 (t), 2.3 (t)		8
XXVII		2.0059	14.0 (t), 2.0 (t)		8
XXVIII	$Fe_3(CO)_9(N\text{-}t\text{-Bu})_2^-$	2.0135	1.8 (q)		11, 13
XXIX		2.0054	14.8 (t), 2.3 (t)		9
XXX	$Fe_2(CO)_6(\text{-N-}t\text{-Bu})_2^-$	2.0335	2.9 (q)		13
XXXI	$Fe_2(CO)_6[OC(N\text{-}t\text{-Bu})_2]^-$	2.0084	8.2 (q)		

[a] Some weak or overlapping hardly detectable signals are ommitted.

[b] THF; −80°C.

[c] The question mark means that the identification is not ultimate.

[d] *f*-Factor was calculated relatively to the standard sample of Cr^{3+}/MgO with $g = 1.9796 \pm 0.0001$.

[e] The multiplicity and intensities of multiplets are placed in brackets: triplet (t) (1:1:1), quintet (q) (1:2:3:2:1), heptet (h) (1:3:6:7:6:3:1) splitting on ^{14}N, doublet (d) splitting on ^{1}H and ^{57}Fe.

[f] −60°C.

[g] +20°C.

[h] 0°C.

[i] −60°C.

makes it possible to detect the spin adduct of this radical, $(CO)_3(NO)Fe—N(O^{\cdot})—t\text{-Bu}$ (X), $g = 2.0040$. The signal has a triplet-of-triplets structure ($a_{N_1} = 16.9$ G, $a_{N_2} = 0.65$ G) (see Fig. 1). When using $^{57}Fe(CO)_5$, one can observe a doubling on a single Fe atom, $a^{57}_{Fe} = 1.7$ G. The final structure of this radical was confirmed by an alternative synthesis in the reaction of PPN[$Fe(CO)_3NO$] with $Fc^+PF_6^-$ in the presence of *t*-BuNO. It should be noted that the literature reports on the spin adducts isoelectronic to radical X, e.g. $ClFe(CO)_4—N(O^{\cdot})—t\text{-Bu}$, $g = 2.0049$, $a_N = 16.0$ G in $CHCl_3$.[32]

The absence of an organic substituent at the nitrogen atom in the resultant radical $Fe(CO)_3NO^{\cdot}$ has made it possible to assume that the formation of the Fe(I) complexes involves a cleavage of the C—N bond in the nitro compound salt.

The cleavage of this bond in nitro compounds is observed in reactions with sodium alcoholates, leading to the formation of a nitrite ion.[33] In reactions with iron carbonyls such a cleavage is likely due to the fact that during the disproportionation an inorganic coordination sphere is formed first around Fe^+ and then Fe^{2+}. Therefore we decided to carry out ESR studies of the reactions of the iron pentacarbonyl with the nitrites such as $Kat^+NO_2^-$, where $Kat^+ = Na^+$, K^+ and PPN^+. Concerning a set of radical products, this reaction turned out to be close to that with the nitro paraffine salts. The formation and consumption of radicals **I–IV** as well as **VI–VIII** is the same for the two reactions (see Table 1).

However, these reactions differ at the initial stages. In reactions with nitrites, radical **V** is absent but instead a strong 1 : 1 : 1 triplet ($g = 2.0376$ and $a_N = 13.2$ G) from **XI** is observed.

Moreover, there appears the radical $Fe(CO)_2(NO)_2^+$ ($g = 2.0286$, $a_N = 2.8$ G) (a 1 : 2 : 3 : 2 : 1 quintet), also obtained via an alternative synthesis by the reaction $Fe(CO)_2(NO)_2 + Fc^+PF_6^- \rightarrow Fe(CO)_2(NO)_2^+ + Fc$.

The reaction of the carbonyls with the nitrite ion as the nucleophile will occur as follows:

$$Fe(CO)_5 + NO_2^- \rightarrow [Fe(CO)_{5-n} \cdot NO_2]^-$$

$$[Fe(CO)_{5-n} \cdot NO_2]^- + Fe(CO)_5 \xrightarrow[-CO]{} [Fe(CO)_4 \cdot NO_2]^{\cdot} + Fe(CO)_5^- \quad (3)$$

$$\xrightarrow[FeCO_5]{} Fe_2(CO)_8^-, Fe_3(CO)_{11}^-, Fe_3(CO)_{12}^-$$

$$n = 0 \text{ or } 1.$$

* Dark reactions.

Fig. 1. ESR-signal from $(CO)_3(NO)FeN(O^{\cdot})—t\text{-Bu}$ (X) in THF at +20°C.

Thus we assume that the structure of radical **V** appearing at the initial stages is $[Fe(CO)_4(R_2CNO_2)]^{\cdot}$ in Scheme 1, and that of radical **XI**–$[Fe(CO)_4 \cdot NO_2]^{\cdot}$ in Scheme 3. Then the appearance of $Fe(CO)_3NO^{\cdot}$ in reactions with the nitroparaffin salts can be explained as follows:

$$[Fe(CO)_4 \cdot (R_2CNO_2)]^{\cdot} \rightarrow [Fe(CO)_4 \cdot NO_2]^{\cdot} \rightarrow Fe(CO)_3NO^{\cdot}. \quad (4)$$

After losing the CO groups and oxidation, the radical $Fe(CO)_3NO^{\cdot}$ in Scheme (4) converts to the Fe(II) complexes. This process is responsible for the thermodynamics of the iron carbonyl redox disproportionation.

Thus the interaction of the nitroparaffin salts with the iron carbonyls represents a redox process accompanied by the appearance of radical anions **I–IV** and Fe(+I) complexes. The formation of the latters coordination sphere involves the cleavage of the C—N bond in the nitro compounds.

2. *Reactions of the iron carbonyls* $Fe(CO)_5$ *and* $Fe_3(CO)_{12}$ *with 2-methyl-2-nitrosopropane**

Nitroso compound complexes are considered to be intermediates during the reductive carbonylation of nitro compounds.[5,34] However, usually the reduction proceeds to immediately reach the lower states of nitrogeneous derivative oxidation.

Therefore it was advisable to study the reactions of the iron carbonyls with nitroso compounds. Used as such a compound was 2-methyl-2-nitrosopropane which also acts as the spin trap.

The reaction of $Fe_3(CO)_{12}$ with 2-methyl-2-nitrosopropane in THF yielded initially the radicals **IV** and **II** as well as two nitroxyl radicals, *viz.* $(t\text{-Bu})_2NO^{\cdot}$ (**XIII**), giving a triplet ($g = 2.0060$, $a_N = 15.4$ G at 20°C[35]) and the spin adduct **X** which has already been detected by us in reactions with the nitroparaffin salts.

Thus, as in the case of the nitroparaffin salts, the interaction of $Fe_3(CO)_{12}$ with *t*-BuNO can be described by the redox disproportionation scheme:

$$Fe_3(CO)_{12} + t\text{-BuNO} \rightleftharpoons [Fe_3(CO)_{12-n} \cdot (t\text{-BuNO})]$$

$$[Fe_3(CO)_{12-n} \cdot (t\text{-BuNO})] + Fe_3(CO)_{12} \xrightarrow[-CO]{} [Fe_3(CO)_{11} \cdot t\text{-BuNO}]^{+} + Fe_3(CO)_{12}^{-}$$

$$[Fe_3(CO)_{11} \cdot t\text{-BuNO}]^{+} \rightarrow Fe(CO)_3(NO)^{\cdot} + t\text{-Bu}^{\cdot}$$

$$Fe_3(CO)_{12}^{-} \xrightarrow{-CO} Fe_3(CO)_{11}^{-}$$

$$Fe(CO)_3(NO)^{\cdot} \xrightarrow{t\text{-BuNO}} (CO)_3(NO)Fe{-}N(O^{\cdot}){-}t\text{-Bu}$$

$$t\text{-Bu}^{\cdot} \xrightarrow{t\text{-BuNO}} t\text{-Bu}_2NO^{\cdot} \qquad (5)$$

As in the case of the nitroparaffin salts, the cleavage of the C—N bond during the formation of the Fe(I) coordination sphere is typical of the nitroso compounds, as well. The reaction of 2-methyl-2-nitrosopropane with iron pentacarbonyl in THF or toluene differs greatly from the previous one. At 20°C the reaction has a fairly long induction period, *ca.* 20 min. At the end of this period the spectra begin to show the rapidly growing signals from $Fe(CO)_3NO^{\cdot}$ and $t\text{-BuNO}^{-}$ ($g = 2.0060$, $a_N = 10.7$ G) (**XIV**).[35] Then the signals from the radicals $t\text{-Bu}_2NO^{\cdot}$ and $(CO)_3(NO)FeN(O^{\cdot})\text{—}t\text{-Bu}$ appear. Low intensity signals from $t\text{-BuNOH}^{\cdot}$ ($g = 2.0060$, $a_N = 13.1$ G, $a_H = 10.7$ G) (**XV**) can also be detected (see Table 1). In this case an appreciable amount of radical anions, primarily **IV**, appear at the terminal reaction stages or, if the reaction starting at 20°C is allowed to occur overnight at −196°C.

Such a difference in the behaviour of iron pentacarbonyl as compared to that of dodecacarbonyl can be explained by considering the fact that the one-electron reduction of the nitroso compound to the radical anion ($E_{1/2\,red} = -1.36$ V in acetonitrile[36]) is more facile than that of pentacarbonyl ($E_{1/2\,red} = -1.64$ to -1.77 V in THF). For iron dodecacarbonyl $E_{1/2\,red} = -0.32$ V in THF so that in Scheme 5 the carbonyl itself undergoes reduction.

Thus the redox disproportionation in the reaction of iron pentacarbonyl with 2-methyl-2-nitrosopropane can be described as follows: in Scheme 6b $Fe(CO)_5$ should be replaced by *t*-BuNO so that

$$Fe(CO)_5 + (t\text{-BuNO})_2 \rightarrow [Fe(CO)_{5-n} \cdot (t\text{-BuNO})_2] \qquad (6a)$$

$$[Fe(CO)_{5-n} \cdot (t\text{-BuNO})_2] + t\text{-BuNO} \rightarrow [Fe(CO)_{5-n} \cdot t\text{-BuNO}]^{+} + t\text{-BuNO}^{-} \qquad (6b)$$

Then the second limiting stage occurs in which the charges become separated. It is this fact which is responsible for the prolonged induction period.

In principle, the reaction can be catalysed by impurity-type nucleophiles, e.g. water, or by the effect of light. In this case the induction period is much shorter. In the absence of these factors the dimer $(t\text{-BuNO})_2$ is likely to act as the nucleophile. Radical cation **XVI** appearing at stage 6b has $g = 2.0222$ and $a_N = 2.8$ G (1:2:3:2:1).

These are not the only differences. Then the decomposition of $t\text{-BuNO}^{-}$ occurs to yield $t\text{-Bu}_2NO^{\cdot}$:[35]

$$t\text{-BuNO}^{-} \rightarrow t\text{-Bu}^{\cdot} + NO^{-} \qquad (6c)$$

$$t\text{-Bu}^{\cdot} + t\text{-BuNO} \rightarrow t\text{-Bu}_2NO^{\cdot}. \qquad (6d)$$

The resulting nitrosyl anion NO^{-} triggers the already known scheme of the $Fe(CO)_5$ redox disproportionation under the effect of the anionic nucleophile. The scheme is distinguished by the fact that as long as the trap is not exhausted, the formation of the radical anion $Fe(CO)_5^{-}$ and, hence, the remaining radical anions **I**–**IV**, remains inhibited:

$$Fe(CO)_5 + NO^{-} \xrightarrow[-CO]{} Fe(CO)_3(NO)^{-} \qquad (6e)$$

$$Fe(CO)_3(NO)^{-} + Fe(CO)_5 \xrightarrow[-CO]{} Fe(CO)_3(NO)^{\cdot} + Fe(CO)_5^{-} \qquad (6f)$$

$$Fe(CO)_5^{-} + t\text{-BuNO} \rightarrow Fe(CO)_5 + t\text{-BuNO}^{-} \qquad (6g)$$

$$Fe(CO)_3(NO)^{\cdot} + t\text{-BuNO} \rightarrow (CO)_3(NO)Fe{-}\underset{\displaystyle O^{\cdot}}{\overset{\displaystyle |}{N}}{-}t\text{-Bu}. \quad (6h)$$

It should be noted that after the induction period (Scheme 6b) the process goes in a chain mode which is effected through the decomposition and formation of tBuNO^{-} (Schemes 6g and 6c, respectively).

If $Fe(CO)_5$ is taken in an excess amount relative to t-BuNO, then after the reduction of the whole of the nitroso compound one can observe the consumption of the appearing **XIII**. This is likely due to the reduction of this species to the hydroxylamine anion ($E_{1/2\,red} = -1.63$ V in acetonitrile[37]).

Thus this scheme can be regarded as an alternative mechanism of the redox disproportionation of the iron carbonyls, by which the organic substrate is reduced and the whole of the Fe(0) from $Fe(CO)_5$ passes to Fe(I).

Such a mechanism is likely to take place if the telomerization is initiated by iron pentacarbonyl in the presence of, e.g. CCl_4 ($E_{1/2\,red} = -0.71$ to -0.78 V[38]), assuming that CCl_4, in this process, is similar to t-BuNO. So stage 6c for CCl_4 is presented in the form:

$$[CCl_3 \ldots Cl]^{-} \rightarrow CCl_3^{\cdot} + Cl^{-}. \quad (6c')$$

In this case one can clearly understand the role of cocatalysts such as nucleophilic agents (amines, dimethyl formamide, etc.[39]) which afford the redox disproportionation of iron pentacarbonyl at the initial stages of the process.

Thus the initial stage in the mechanism of the reductive carbonylation of the nitro and nitroso compounds is represented by the process of the redox disproportionation of the iron carbonyls under the effect of nucleophilic agents. As this takes place, depending on the ratio of the reduction potentials for a given iron carbonyl and an organic substrate, the redox process occurs either with the formation of the Fe(I) and Fe(−I) carbonyl complexes or Fe(I) complexes alone and reduction of the organic substrate. Therefore the thermodynamics of such reactions is controlled, in the long run, by the redox process.

3. *Reactions of carbonyl ferrate anions with nitro- and nitroso-tert-butane*

The interaction of iron carbonyls[26] and carbonyl ferrate anions[40,41] with nitro compounds is known to give rise to the nitro group reduction products such as amines, isocyanates and ureas.

On the other hand, it follows[42] that the iron carbonyl radical anions **IV** and **II** resulting from the one-electron reduction exhibit a very labile coordination sphere and can participate in the ETC and NCE processes in which their CO groups are partially substituted by such stable ligands as phosphines. However, these studies have not revealed such an important property of the iron carbonyl radical anions as their deoxygenating catalytic activity. One of us has shown that the iron carbonyl radical anions **I**–**IV** appearing at the stage of iron carbonyl redox disproportionation reduce the nitro- and nitroso compounds.[15] This section is devoted to a more detailed study of the catalytic function of the iron carbonyl radical anions in the reductive carbonylation of the nitro and nitroso compounds as well as their deoxygenating function.

For this purpose we have studied the processes in which the iron carbonyl radical anions are generated by an independent method, *i.e.* oxidation of the corresponding carbonyl ferrate anions with a ferricenium cation[10] to be then reacted with the nitro- and nitroso compounds such as tertiary nitroso- and nitrobutane:

$$Fe_n(CO)_{m-1}^{2-} \xrightarrow{Fe^{+}PF_6^{-}} Fe_n(CO)_{m-1}^{-} \xrightarrow{BuNO_x} \quad (7)$$

$$n = 1, m = 5; n = 2, m = 9; n = 3, m = 12; n = 4, m = 14, x = 1, 2.$$

However, oxidation with ferricenium (Scheme 7) gives rise to a fast uncontrollable formation of the iron carbonyls $Fe(CO)_5$ and $Fe_3(CO)_{12}$, whose interaction with the nitrogeneous compounds yields side processes. Another inconvenience is the fact that the strong signals appearing at the initial stages of the processes from the initially formed iron carbonyl radical anions **I**, **II**, **IV** prevents the weak signals of the other species being clearly identified.

A different method in which the nitro- or nitroso compounds themselves were used as the oxidants for the carbonyl ferrate anions turned out to be preferred. However, it should be noted that for the tertiary nitrobutane this method is applicable to the reaction with the mono- and binuclear carbonyl ferrate anions ($x = 2$, $n \leqslant 2$) whereas for 2-methyl-2-nitrosopropane, probably to that with the trinuclear carbonyl ferrate anion ($x = 1$, $n \leqslant 3$).

Such behaviour of the carbonyl ferrate anions in reactions with the nitro- and nitroso compounds can be readily understood based on the redox potentials of the carbonyl ferrate anions, iron carbonyl radical anions and organonitrogen radical anions (E_M^{2-}, E_M^{-} and E_L^{-}, respectively, in Fig. 2).

If the E_M^{2-} value of the carbonyl ferrate anions is more negative than that of the t-BuNO$_2^{-}$ ($E_{L^{-}} = -1.62$ to -1.77 V),[36] the process will take place

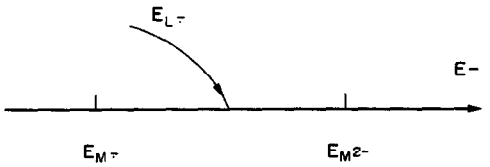

Fig. 2. The comparative scale of redox potentials of carbonyl ferrate radicals (M^-), organic ligands (L^-) and carbonyl ferrate anions (M^{2-}).

as follows:

$$Fe_n(CO)_{m-1}^{2-} + t\text{-}BuNO_x \rightarrow Fe_n(CO)_{m-1}^{-} + t\text{-}BuNO_x^{-}. \quad (8)$$

This gives rise to the radical anions of the corresponding carbonyl ferrate anions. This holds for $Fe(CO)_4^{2-}$ whose E_M^{2-} value, as reported by different authors,[11,12] lies in the range between -1.64 and -1.77 V. If the process takes place directly in the ESR cavity, the first stage will give the signals of the corresponding iron carbonyl radical anions and in some cases those of the nitroso and nitro compounds.

t-$BuNO^-$ (**XIV**) and *t*-$BuNO_2^-$ (**XVII**) (Table 1) are formed in reactions of the corresponding compounds with $Na_2Fe(CO)_4 \cdot 1.5$ diox. Note that in the case of *t*-$BuNO^-$ at the initial stages of the process one can observe the temperature-dependent ion-pair equilibrium *t*-$BuNO^-$ ... solv. ... $Na^+ \rightleftharpoons$ *t*-$BuNO^-$ ... Na^+. At -60°C there appears a triplet of quadruples (a_N = 12.1, a_{Na} = 1.5 G), and at 0°C, a triplet (a_N = 12.3 G).

Due to the fact that the rate of formation of the radical anions by Scheme 8 depends on the relationship between the parent carbonyl ferrate anion and nitrogen containing compound, the further stages of the process of the reduction of R-NO_x (x = 1, 2) may be different, therefore first we shall concentrate on the discussion of the particular cases.

(1) The reaction of $Na_2Fe(CO)_4 \cdot 1.5$ diox with *t*-BuNO proceeds vigorously. The first stages of the process, between -80 and -60°C, give rise to the iron caronyl radical anions **I**, **IV**, **II** and *t*-$BuNO^-$. Then the nitroxyl radical (g = 2.0063, a_N = 15.8–15.7 G (**XVIII**)) and (g = 2.0054, a_N = 16.7 G (**XIX**) are formed. In the middle of the process one can observe the accumulation of the radicals with a triplet splitting on the nitrogen atom (g = 2.0267, a_N = 1.8 G (**XX**) and g = 2.0251, a_N = 2.3 G (**XXI**) (Fig. 3)), the former slowly passing to the latter. One of the products of their further conversions is likely to be a radical (g = 2.0365) generating a broad singlet (ΔH = 4.6 G at -80°C) (**XXII**).

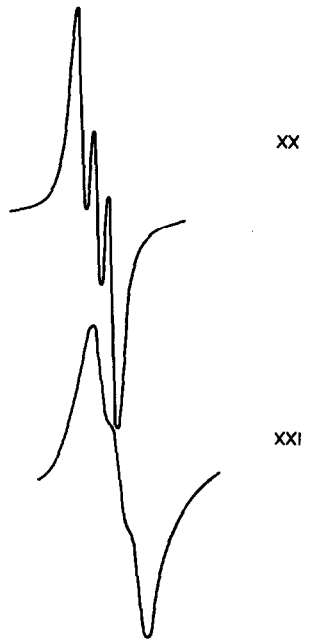

Fig. 3. ESR-spectra of radicals **XX** and **XXI** in THF at -80°C.

If *t*-BuNO is present in an excessive amount, then the terminal stages of the process will show in the ESR spectra at room temperature the presence of signals from *t*-$Bu_2NO^{\cdot}$ and **X** alone, resulting from the reaction of *t*-BuNO with $Fe(CO)_5$ (Schemes 6a–h), appearing during oxidation of the carbonyl ferrate anions.

(2) The reaction of $Na_2Fe(CO)_4 \cdot 1.5$ diox with *t*-$BuNO_2$ is also rather vigorous. At the first instant at -80°C one can observe the formation of the iron carbonyl radical anions **I**, **II**, **IV** and a strongly broadened triplet (g = 2.0060, a_N = 25.4 G), from **XVII**, probably as a result of the ion pair interaction of *t*-$BuNO_2^-$ with Na^+. The spectrum also shows the presence of a broad triplet (**XXIII**) (g = 2.0037, a_N = 15.5 G) and a broad signal (g = 2.0054) from **XXIV**. At the later stages of the process the spectrum begins showing two more nitroxyl radicals (g = 2.0036, a_N = 16.7 G) (**XXV**) and (g = 2.0053, a_N = 16.7 G (**XIX**)) as well as the three earlier mentioned signals from **XX**–**XXII**.

(3) The reactions of $(PPN)_2[Fe_2(CO)_8]$ with *t*-BuNO and *t*-$BuNO_2$ occur much more slowly than the first two processes. In the first case signals from the iron carbonyl radical anions **I**, **II**, **IV**, a weak signal from **XX**, a triplet of triplets in the nitroxyl region (g = 2.0062, a_{N_1} = 15.7 G, a_{N_2} = 2.3 G (**XXVI**)), and a doublet of triplets from **XV** are detected in the spectra. The reaction with tertiary nitrobutane gives signals from the iron carbonyl

radical anions **I, II, IV** as well as very weak signals from t-$Bu_2NO^{\cdot}$.

(4) The reaction of $(PPN)_2[Fe_3(CO)_{11}]$ is only possible with t-BuNO. Initially there appears the iron carbonyl radical anions **II, I, IV** and radical **XX**, a triplet of triplets ($g = 2.0059$, $a_{N_1} = 14.0$ G, $a_{N_2} = 2.0$ G (**XXVII**)). Then one can observe the appearance of t-$Bu_2NO^{\cdot}$ and t-$BuNOH^{\cdot}$.

(5) The reaction of $(PPN)_2[Fe_4(CO)_{13}]$ with t-BuNO when kept for a long time at room temperature gives a signal from radical **XXVII** and a weak signal from **IV**.

In other words, the reduction of the nitro- and nitroso-tertbutane in these reactions involves the formation of the radical products which can be divided into three groups:

First, the known nitroxyl radicals[35] ($g = 2.0059$–2.0063), typical of the reduction of 2-methyl-2-nitrosopropane.

Second, the hitherto unknown unstable radicals, whose g-factors (2.0036–2.0054) and hyperfine splitting constants (15.5–17.7) also lie in the nitroxyl region. Due to the fact that these radicals do not appear at the first stages of the reaction of the iron carbonyl radical anions **I–IV** with t-BuNO, then, they represent, in all likelihood, the spin adducts not of these anions themselves but rather their conversion products.

Third, the hitherto unknown nitrogen-containing radicals ($g = 2.025$–2.036).

To establish the structure of the radicals belonging to the second and third groups, we have conducted an additional series of reactions, i.e. the reduction of the diamagnetic complexes $Fe_3(CO)_9(N\text{-}t\text{-}Bu)_2$, $Fe_2(CO)_6(N\text{-}t\text{-}Bu)_2$, $Fe_2(CO)_6[(N\text{-}t\text{-}Bu)_2CO]$ on a sodium mirror in the presence of the spin trap, t-BuNO, at -80°C, in THF. These complexes are products of the reaction of $Fe_2(CO)_9$ with t-$BuNO_2$.[26]

(a) Initially the reduction of $Fe_3(CO)_9(N\text{-}t\text{-}Bu)_2$ gives rise to a quintet ($g = 2.0135$, $a_N = 1.8$ G (**XXVIII**)) which then rapidly disappears. This is followed by the formation of radical anions **II, IV, I** and a strong triplet from **XX** which then, upon temperature increase to -40°C, converts to **XXI**.

In the presence of the spin trap the signal from **XXVIII** passes to a triplet of triplets ($g = 2.0054$, $a_{N_1} = 14.8$ G, $a_{N_2} = 2.3$ G (**XXIX**)). Also, the spectrum shows the presence of signals from **XIX**.

(b) The reduction of $Fe_2(CO)_6(N\text{-}t\text{-}Bu)_2$ results in the appearance of signals from **I, II, IV**. Initially there is also a quintet ($g = 2.0335$, $a_N = 2.9$ G (**XXX**)), part of which lies on the shoulder of the strong signal from **I**.

The reduction in the presence of t-BuNO yields spin adduct **XXV**.

(c) At the first stages of the reduction of $Fe_2(CO)_6[(N\text{-}t\text{-}Bu)_2CO]$ at -80°C it is possible to detect a broad quintet-type signal ($g = 2.0084$, $a_N = 8.2$ G (**XXXI**)). At the later stages there will appear two broadened singlets ($g = 2.0287$ ($\Delta H = 2.8$ G) (**XXXII**) and $g = 2.0417$ ($\Delta H = 4.6$ G) (**XXXIII**)).

Thus the initial stages of the reduction give rise to the radical anions of the corresponding complexes $Fe_3(CO)_9(N\text{-}t\text{-}Bu)_2^{-}$ (**XXVIII**), $Fe_2(CO)_6(N\text{-}t\text{-}Bu)_2^{-}$ (**XXX**) and $Fe_2(CO)_6[(N\text{-}t\text{-}Bu)_2CO]^{-}$ (**XXXI**) having an extra electron.

Further conversion of the system goes either through elimination of the ligands or rearrangement of the iron cluster skeleton. In the presence of the spin trap it may happen that the unpaired electron is localized on the organic ligand which, upon interaction with the trap, forms a spin adduct. In this case a closed electron shell is formed on the metallo fragment. This fact may be attributed to the appearance of the second group of radicals ($g = 2.0037$–2.0054). Thus, for example:

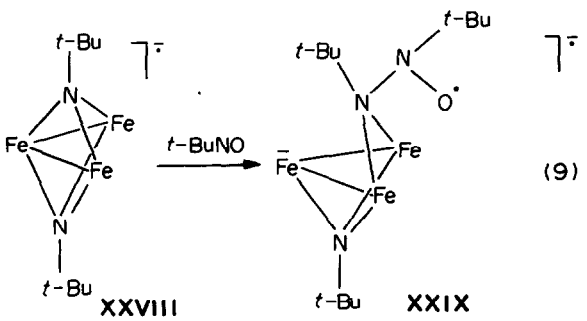

XXVIII **XXIX** (9)

CO-ligands are ommitted in the Schemes 9, 11.

Here one can observe a hyperfine splitting at two nitrogen atoms. The formation of the spin adduct is also possible by means of the addition of the spin trap to the CO group with no secondary splitting in this case.

The intensive triplet from **XX** as a result of the reduction of $Fe_3(CO)_9(N\text{-}t\text{-}Bu)_2$ is attributed by us to the formation of a comparatively stable iron carbonyl trinuclear radical anion containing a single nitrene fragment. It is likely that it appears as a result of the structural rearrangement of the trinuclear cluster with elimination of the nitrene fragment.

Based on the published data concerning the transformation of the diamagnetic complexes

$$Fe_3(CO)_8L(NPh)_2 \xrightarrow{CO} Fe_3(CO)_{10}(NPh) \qquad (10)$$

where L = C(Ph)OEt,[43] as well as on the fact that in our case the reduction of $Fe_3(CO)_9(N\text{-}t\text{-}Bu)_2$ on the sodium mirror involves a rapid exchange of the CO ligands to give the iron carbonyl radical anions

IV, II, I, it can be assumed that the formation of XX and its conversion to XXI take place as follows:

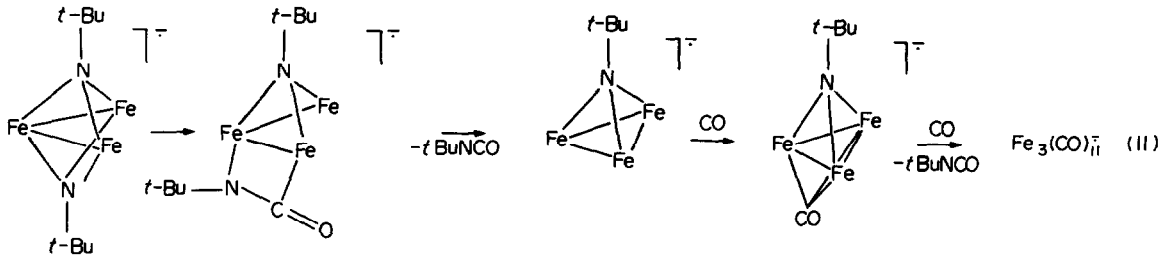

XXVIII XX XXI II

Such a rearrangement of the coordination sphere in the form of a butterfly-trigonal bipyramid is assumed to take place in the trinuclear iron carbonyl complexes with phosphene ligands.[43] It is likely that radical XXI is formed from XX as a result of a variation in metallo fragment nuclearity.

An attempt to pass through this scheme in the reverse direction, i.e. using $Fe_3(CO)_{11}^{-}$ and *t*-BuNO to detect compounds XX and XXI is of little success because the appropriate signals lie on the shoulder of the intensive signal from I appearing from II due to their mutual conversions. However, the signals from XX and XXI become detectable if the ampoule containing the iron carbonyl $Fe_n(CO)_m$, where $n = 1$, $m = 5$; $n = 2$, $m = 9$; $n = 3$, $m = 12$, and tert-butyl-isocyanate BuNCO is irradiated with a filament lamp at −80°C. In this case it is possible to control the intensity growth of signal from I.

Thus the appearance of radicals XX and XXI in the reactions of carbonyl ferrate anions with tertiary nitro- and nitrosobutane as well as in those of the iron carbonyls with tert-butyl isocyanate indicate that isocyanate is formed as a result of carbonylation of the nitrene radical complexes. These in turn are obtained during the reduction of the nitro and nitroso compounds in the coordination sphere of the iron carbonyl radical anions.

4. *The catalytic role of the iron carbonyl radical anions* I–IV. *Scheme of the reductive carbonylation*

Schemes for the reduction of nitro and nitroso compounds with iron carbonyls or carbonylferrate anions have been put forward by some authors.[6,40,41] In this case the reduction process initially goes owing to the CO groups of a certain intermediate carbonyl complex, these groups being oxidized to CO_2. The role of such a complex is assigned, for example, to the adduct of the type

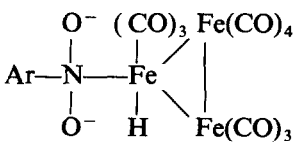

However, these schemes can be constructed assuming the appearance of either a coordinatively unsaturated iron carbonyl species which is short of two electrons to complete its electronic configuration, ($Fe(CO)_4$), or those with an O—Fe bond. But the existence of such intermediates in solution is most unlikely.

In our hypotheses we used the following facts.

First, the conditions of the nitro compound reduction coincide with those when the radical anions I–IV are formed either due to the redox disproportionation of the iron carbonyls or oxidation of the carbonyl ferrate anions.

Second, the resultant iron carbonyl radical anions I–III have an open electronic shell containing 33, 47 and 59 cluster valence electrons, respectively. Radical anion IV contains 49 electrons but it can readily and reversibly convert to II in the CO elimination. This ensures the lability of the coordination sphere, and the resultant activity of the ligand exchange process.[42]

Third, the reduction of the nitro and nitroso compounds involves the formation of similar intermediate radical species XX and XXI as is the case in the reaction of the iron carbonyls with *t*-BuNCO as well as in the reduction of the diamagnetic nitrene complex $Fe_3(CO)_9(N\text{-}t\text{-}Bu)_2$.

The totality of these facts makes it possible to put forward the following scheme:

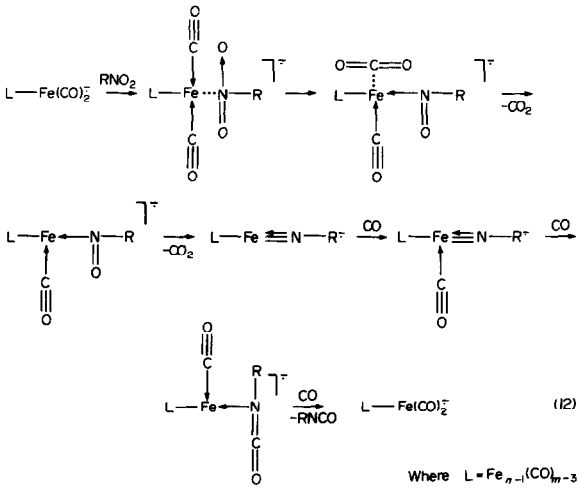

The scheme illustrates the case when the coordination sphere of the iron carbonyl cluster contains a nitro compound molecule. The initial stages of the process consist of a successive reduction of the nitro compound coordinated to the iron carbonyl radical anion, through the nitroso compound to the nitrene complexes. The reduction is realized through the coordinated CO groups which are abstracted in the form of CO_2. Then, if the process goes in the catalytic mode, the intermediate complexes undergo carbonylation to yield isocyanates and the parent iron carbonyl radical anions.

The addition of the second nitro compound molecule in the process of reduction is responsible for the appearance of a variety of intermediate radical species similar to **XVIII, XIX, XXIII–XXVII** as well as formation of diazo compounds as the final products.

If the reaction is carried out at the stoichiometric quantities of the reagents, the reduction of the nitrogen-containing ligand can terminate after the nitrene structures have been formed, which, by loosing an unpaired electron, convert to the well known diamagnetic complexes $Fe_2(CO)_6(N\text{-}t\text{-}Bu)_2$, $Fe_2(CO)_6[(t\text{-}BuN)_2CO]$ and $Fe_3(CO)_9(N\text{-}t\text{-}Bu)_2$. This leads to the withdrawal of the nitrene species out of the catalytic cycle.

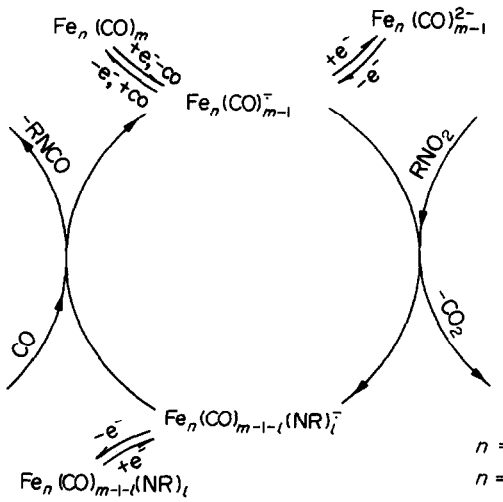

(13)

$n = 2,\ m = 9,\ l = 2$
$n = 3,\ m = 12,\ l = 1, 2$

It should be pointed out that the electron-deficient negatively charged species **I–III** are catalytically active. However the electron-deficiency can be lost during the catalytic process on the successive addition of the CO ligands as, for example, is the case with the transition

$$Fe_3(CO)_{11} \xrightarrow{CO} Fe_3(CO)_{12}.$$

Nevertheless, the electron-excessive system can be rearranged into an electron-deficient one. This is possible, first, when the excess electron goes towards the ligand. As this takes place, a new bond, e.g. CO—NR, RN—NR, between the coordinated ligands can be formed or such ligands, e.g. RNH, can be reduced. Usually the reaction medium should contain proton donors.

Second, the rearrangement can be effected at the expense of the cluster skeleton, by cleaving the Fe—Fe or Fe—N bonds. The ability of the iron carbonyl radical anions to be rearranged in such a way is also responsible for their catalytic activity.

Schemes 12 and 13 explain the conversions occurring in an aprotic medium, therefore the final products contain isocyanates and diazo compounds. More complicated processes take place in a proton medium where, along with $Fe_n(CO)^-_{m-1}$, their protonated analogues $HFe_n(CO)_{m-1}$ are formed,[44] which are expected to participate in the reduction processes to yield amines, formamide and various urea derivatives.

CONCLUSIONS

The interaction of the iron carbonyls with the nitro and nitroso compounds therefore depends on the following factors.

The initial stages of the process consist of the activating complex formation of the iron carbonyls and Lewis bases, then occurs the redox stage and, as a result of a one-electron transfer, there appears the radical Fe(I) complexes and the iron carbonyl radical anions **I–III** which are just these species that control the catalytic properties of the iron carbonyl–base system.

The iron carbonyl radical anions **I–III** that are capable of a fast exchange in the coordination sphere can deoxygenate the nitro and nitroso com-

pounds to nitrene complexes and then undergo carbonylation to give isocyanates.

We believe that the disclosed deoxygenation and carbonylation ability is of the same nature. This permits, using the same principles, to study a variety of processes involving iron carbonyls, such as carbonylation of various nitrogen-containing compounds (amines, azines, diazo compounds),[6,7] and olefins,[45] telomerization,[39] Fischer–Tropsch process,[46] formation of bi- and trinuclear chalcogene and nitrogen-containing compounds of carbonyl complexes.[3,47] Based on the new conceptions it is possible to provide a fresh approach to the catalytic effect of the iron carbonyls in WGSR and understand the conflicting information.[48,49] We believe that here, as in the case of the nitro compounds, water deoxygenation to H_2 occurs in a catalytic cycle, similar to that presented in Scheme 13 where RNO_2 should be replaced by H_2O. Note that along with the radical anions **I–III** their protonated analogues can also participate in this process.

Acknowledgements—The authors wish to thank Profs V. N. Babin and S. P. Solodovnikov for the useful discussions.

REFERENCES

1. W. Hieber and N. Kahlen, *Chem. Ber.* 1958, **96**, 2223.
2. W. Hieber and A. Lipp, *Chem. Ber.* 1959, **92**, 2075.
3. A. N. Nesmeyanov, M. I. Rybinskaya and L. V. Rybin, *Usp. Khim.* 1979, **3**, 393.
4. M. Dekker and G. R. Knox, *J. Chem. Soc. Chem. Commun.* 1967, 1243.
5. (a) V. I. Manov-Yuvensky and B. K. Nefedov, *Usp. Khim.* 1981, **5**, 889; (b) V. I. Manov-Yuvensky and B. K. Nefedov, *Khim. Promyshl.* 1983, **5**, 287.
6. H. Alper and J. T. Edward, *Can. J. Chem.* 1970, **48**, 1543.
7. A. Rosenthal and I. Wender, *Organic Syntheses via Metal Carbonyls*, Vol. 1. Interscience, New York (1968).
8. B. D. Dombek and R. J. Angelici, *J. Catal.* 1977, **48**, 433.
9. P. Miholova, J. Klima and A. A. Vlček, *Inorg. Chim. Acta* 1978, **27**, L67.
10. P. J. Krusic, J. San Filippo, Jr., B. Hutchinson, R. L. Hance and L. M. Daniels, *J. Am. Chem. Soc.* 1981, **103**, 2129.
11. N. E. Murr and A. Chaloyard, *Inorg. Chem.* 1982, **21**, 2206.
12. A. M. Bond, P. A. Dawson, B. M. Peake, B. H. Robinson and G. Simpson, *Inorg. Chem.* 1977, **9**, 2199.
13. J. Wronka and D. P. Ridge, *J. Am. Chem. Soc.* 1984, **106**, 67.
14. V. N. Babin, Yu. A. Belousov, V. V. Gumenyuk, R. M. Salimov, R. B. Matetikova and N. S. Kochetkova, *J. Organomet. Chem.* 1983, **241**, 41.
15. Yu. A. Belousov and E. I. Mysov, *IV Int. symp. on homogeneous catalysis*, Vol. 4, p. 30. Leningrad, 1984.
16. B. Bernard, L. Daniels, R. Hance and B. Hutchinson, *Synth. React. Inorg. Met.-Org. Chem.* 1980, **10**, 1.
17. R. G. Finke and J. N. Sorrebl, *Org. Synth.* 1979, **59**, 102.
18. K. Farmery, M. Kilner, R. Greatrex and N. N. Greenwood, *J. Chem. Soc. A* 1969, **16**, 2339.
19. H. B. Chin, M. B. Smith, R. D. Wilson and R. R. Rau, *J. Am. Chem. Soc.* 1974, **96**, 5285.
20. H. A. Hodali and D. E. Shriver, *Inorg. Synth.* 1980, **20**, 212.
21. K. Whitmire, J. Ross, C. B. Cooper and D. F. Shriver, *Inorg. Synth.* 1983, **21**, 66.
22. N. G. Conelly and C. J. Gardner, *J. Chem. Soc., Dalton Trans.* 1976, 1525.
23. A. Martinsen and J. Songstad, *Acta Chim. Scand.* 1977, **A31**, 645.
24. J. C. Storwell, *J. Org. Chem.* 1971, **36**, 3055.
25. I. R. Lyatifov, S. P. Solodovnikov, V. N. Babin and R. B. Materikova, *Z. Naturforsch.* 1979, **34b**, 863.
26. H. Alper, *Inorg. Chem.* 1972, **11**, 976.
27. A. Bühler and H. F. Fietz-David, *Helv. Chim. Acta* 1943, **26**, 2123.
28. C. Couture, J. R. Morton, K. F. Preston and S. J. Strach, *J. Magn. Reson.* 1980, **41**, 88.
29. Yu. A. Belousov, T. A. Kolosova and V. N. Babin, *Polyhedron* to be published.
30. B. M. Peake, M. R. Symons and J. L. Wyatt, *J. Chem. Soc., Dalton Trans.* 1983, 1171.
31. *Atlas of the Electron Spin Resonance Spectra*, Akad. Nauk SSSR, Moscow (1962).
32. R. G. Gasanov and R. Kh. Freidlina, *Dokl. Akad. Nauk SSSR* 1977, **235**, 1309.
33. A. K. Hoffmann, W. G. Hodgson, D. L. Maricle and W. H. Jura, *J. Am. Chem. Soc.* 1964, **86**, 631.
34. E. Köerner von Gustorf, M. C. Henry and R. E. Sacher, *Z. Naturforsch.* 1966, **B21**, 1152.
35. I. I. Bilkis and S. M. Shein, *Tetrahedron* 1975, **31**, 969.
36. H. Sayo, Y. Tsukitani and M. Masui, *Tetrahedron* 1968, **24**, 1717.
37. A. K. Hoffmann and A. T. Henderson, *J. Am. Chem. Soc.* 1961, **83**, 467.
38. M. Stackelberg and W. Stracke, *Z. Elektrochem.* 1949, **53**, 118.
39. E. C. Chukovskaya, R. G. Gasanov, I. I. Kandror and R. Kh. Friedlina, *Zh. vses. khim. Obshch.* 1978, **2**, 161.
40. J. M. Landesberg, L. Katz and C. Olsen, *J. Org. Chem.* 1972, **7**, 930.
41. H. Abbayes and H. Alper, *J. Am. Chem. Soc.* 1977, **99**, 98.
42. M. Arewgoda, B. H. Robinson and J. Simpson, *J. Am. Chem. Soc.* 1983, **105**, 1893.
43. G. D. Williams, G. L. Geoffrey and R. R. Whittle, *J. Am. Chem. Soc.* 1985, **107**, 729.
44. P. J. Krusic, D. Jones and C. Roe, *Organometallics* 1986, **5**, 456.

45. Ya. T. Eydus, E. Z. Gildenberg, V. A. Shvets, A. L. Lapidus and V. B. Kazansky, *Kinet. Katal.* 1975, **16**, 1077.
46. A. L. Lapidus, M. M. Savelyev, L. M. Muranova, S. D. Sominsky, L. T. Kondratyev, I. T. Borisovich and V. E. Vasserberg, *Izv. Akad. Nauk SSSR, Ser. Khim.* 1985, **1**, 24.
47. W. Heiber and J. Gruber, *Z. anorg. Allg. Chem.* 1957, **296**, 91.
48. R. J. Trautman, D. C. Cross and P. C. Ford, *J. Am. Chem. Soc.* 1985, **107**, 2355.
49. K. R. Lane, R. E. Lee, L. Sallans and R. S. Squires, *J. Am. Chem. Soc.* 1984, **106**, 5767.

Polyhedron Vol. 6, No. 11, pp. 1971–1974, 1987
Printed in Great Britain

0277–5387/87 $3.00+.00

THE INTERACTION OF 1-OXY-2,6-DI[(*N*,*N*-BISCARBOXYMETHYL)AMINOMETHYL]4-CHLOROBENZENE WITH LANTHANIDES

B. ZARLI,* A. CASSOL, U. RUSSO, P. L. ZANONATO and M. VIDALI

Dipartimento di Chimica Inorganica, Metallorganica e Analitica, Università di Padova, Via Loredan 4,35135 Padova, Italy

(*Received* 16 *February* 1987; *accepted* 11 *May* 1987)

Abstract—This paper reports on some complexes of lanthanum(III) and europium(III) with the title ligand (H_5L) which possesses two similar coordination sites: mononuclear and homo- and hetero-dinuclear species are described. The isolated compounds have the formulas $[M(H_2L)\cdot 3H_2O]$, $[M_2LNO_3\cdot 4H_2O]$, (M = La, Eu); $[MM'LOH\cdot nH_2O]$ (M = Fe, M′ = La, $n = 2$; M = Eu, M′ = La, $n = 4$). In addition $[Li_2LaL\cdot 3H_2O]$ and $[CuLaL\cdot 3H_2O]$ have also been obtained. Relevant IR and visible spectral data and magnetic moment values are given and discussed.

Research on polynuclear complexes has increased in recent years, stimulated by the large interest developed in areas such as metallo-enzymes, heterogeneous catalysis and physicochemical properties. A large series of heterobinuclear complexes containing compartmental ligands and *d*- or *f*-block metal ions have been reported by reaction of the pure mononuclear chelates with the required metal salt.[1] To our knowledge, few papers concerning polynuclear chelates of these ligands with lanthanides(III) ions have been reported.[2]

This work reports the synthesis and characterization of mononuclear and binuclear complexes of lanthanide(III) ions with a new binucleating ligand with two similar coordination sites. Homobinuclear complexes of this ligand with transition metals of the *d*-series have already been reported.[3]

EXPERIMENTAL

The ligand 1-oxy-2,6-di[(*N*,*N*-biscarboxymethyl) aminomethyl]-4-chlorobenzene(H_5L) was prepared according to the literature method.[4]

Preparation of the mononuclear complexes

The ligand (1 mmol) was suspended in methanol (40 cm^3) and then LiOH (3 mmol) was added. The lanthanide(III) nitrate (1 mmol), dissolved in methanol (80 cm^3), was added dropwise with stirring to the clear solution. The resulting mixture precipitated the product either immediately or after heating the solution on a steam bath. In each case the solution was refluxed for 4 h, filtered, and the precipitate washed several times with methanol and diethyl ether and then dried *in vacuo* over P_4O_{10}.

Preparation of the homobinuclear complexes

Homobinuclear complexes were prepared by two general methods:

(a) The ligand (1 mmol) and LiOH (5 mmol) dissolved in methanol (80 cm^3) was added dropwise to the lanthanide(III) nitrate (2 mmol) dissolved in the same solvent (40 cm^3). The resulting mixture was heated for 4 h and a precipitate was obtained. It was filtered, washed several times with methanol and dried *in vacuo* over P_4O_{10}.

(b) The mononuclear chelate (1 mmol) was suspended in methanol and lithium hydroxide (2 mmol) was added. After a clear solution was obtained, the appropriate metal salt (1 mmol) dissolved in methanol was added. The resulting mixture was heated under stirring for 4 h. A precipitate was formed, filtered and washed with methanol and diethyl ether, and then dried *in vacuo* over P_4O_{10}.

* Author to whom correspondence should be addressed.

Table 1. Elemental analyses and magnetic moments of prepared compounds

Compound	C% Calc.	C% Found	H% Calc.	H% Found	N% Calc.	N% Found	μ_{eff} (BM)[a]
$La(H_2L)\cdot 3H_2O$	31.5	31.5	3.6	3.4	4.6	4.7	diam.
$La_2LNO_3\cdot 4H_2O$	23.3	23.7	2.7	2.7	5.1	5.5	diam.
$Eu(H_2L)\cdot 3H_2O$	30.9	30.7	3.5	3.4	4.5	4.6	3.58
$Eu_2LNO_3\cdot 4H_2O$	22.6	22.7	2.6	2.5	4.9	4.8	3.20
$Li_2LaL\cdot 3H_2O$	30.9	30.8	3.2	3.4	4.6	4.5	diam.
$FeLaLOH\cdot 2H_2O$	29.0	29.1	2.9	3.0	4.6	4.5	5.87
$CuLaL\cdot 3H_2O$	28.7	28.4	3.0	3.1	4.2	4.3	1.67
$EuLaLOH\cdot 4H_2O$	24.2	24.3	2.9	2.8	3.5	3.7	2.90
$EuLi_2L\cdot 3H_2O$	30.3	29.8	3.2	3.2	4.4	4.3	3.26

[a] Magnetic moments are given per atom.

Preparation of the heterobinuclear complexes

The heterobinuclear complexes were prepared according to method (b) above.

Chemical and physical measurements

Elemental analyses were performed in the microanalytical laboratory of the Department of Inorganic Chemistry. Infrared spectra were obtained by a Perkin–Elmer model 580 spectrophotometer on samples suspended in a KBr matrix or mulled with mineral oil. Electronic spectra were carried out on a Cary 17 spectrophotometer in aqueous solution. Magnetic susceptibilities were measured by the Faraday method by using an Oxford instrument; the apparatus was calibrated with $Nien_3(ClO_4)_2$.

RESULTS AND DISCUSSION

The interactions of metal salts with 1-oxy-2,6-di[(*N*,*N*-biscarboxymethyl)aminomethyl]-4-chlorobenzene (H_5L) in methanol are illustrated in Scheme 1. The mononuclear Eu(III) and La(III) complexes were prepared by stoichiometric reaction of the ligand with the lanthanide(III) nitrate. Their formulation as $[H_2LLn(H_2O)_3]$ is supported by analytical and spectroscopic data. The IR spectra shows a broad band at 3400 cm^{-1} corresponding to the ν(OH) of the water bound to the cation. The strong band at about 1590 cm^{-1} in both the compounds is assigned to the coordinated carboxylate groups, while the uncoordinated ones were found at 1730 cm^{-1}. The weak band observed at 1285 cm^{-1} in the free ligand, which shifts to about

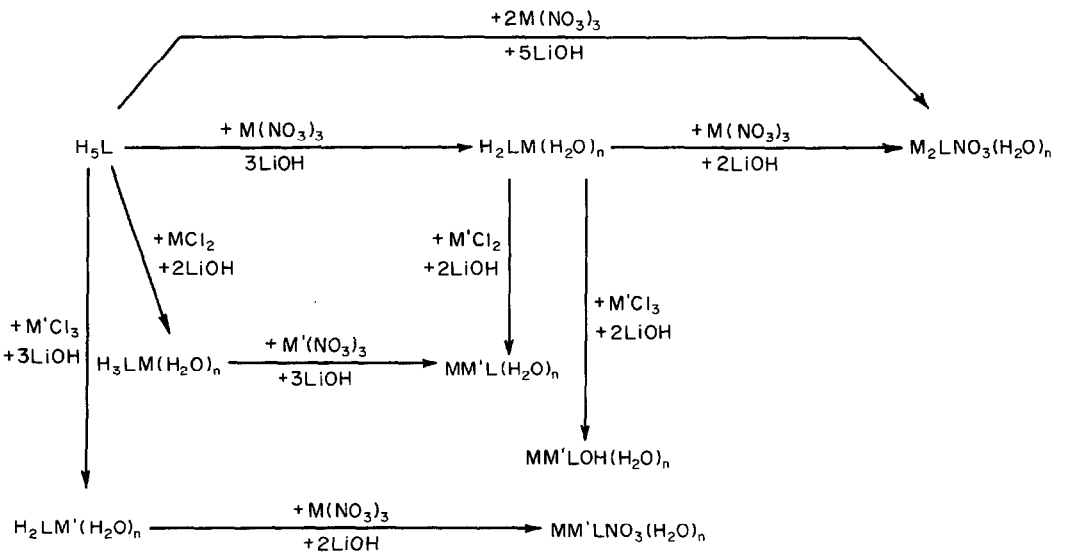

Scheme 1. Reaction pathways of the metal salts with the ligand in methanol.

1295 cm^{-1} in the chelates, is assigned to the phenolic (CO) group. This small shift may be ascribed to the delocalization of electronic density from the oxygen atom to the lanthanide(III) ion resulting in a slight ionic character of the Ln—O bond and consequently in a slight increase in the ν (CO) frequency.

Homo- and hetero-binuclear complexes have been obtained. The former can be prepared by reacting either the ligand with metal nitrate in a molar ratio of 1:2 or the mononuclear chelate with a stoichiometric amount of the metal salt. The latter complexes were synthesized by successive steps; the preparation of the mononuclear complex and then its reaction with the second metal salt.

The homobinuclear compounds present different infrared spectra than those of the corresponding mononuclear chelates. The absorption peak due to the coordinated carboxylic groups is found at 1590 cm^{-1} for $[Eu_2LNO_3(H_2O)_4]$ and 1600 cm^{-1} for $[La_2LNO_3(H_2O)_4]$. The band due to uncoordinated carboxylic groups is absent. The phenolic C—O stretching vibration, which occurs at 1295 cm^{-1} in the mononuclear chelates, lies at the same frequency in the binuclear chelates (about 1300 cm^{-1}). The strong absorptions found at 1490–1470 and 1300–1280 cm^{-1} in the nitrato complexes indicate that the nitrate group acts as a bidentate ligand towards the metal atoms (Fig. 1), a result which is in agreement with the conductivity values in methanol ranging from 10 to 30 mhos at concentrations 10^{-3} M.

The heterobinuclear complexes, prepared from the mononuclear compound (Scheme 1), show a broad band at 3400 cm^{-1}, which corresponds to the ν(OH) of the coordinated water. The strong band observed at about 1600 cm^{-1} is assigned to the characteristic asym. mode of the coordinated carboxylic groups. The phenolic C—O vibration is

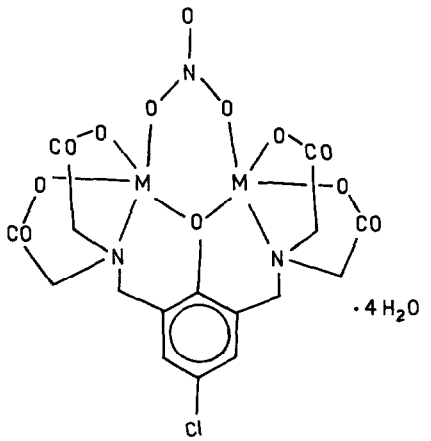

Fig. 1. Proposed coordination geometry of the binuclear complexes.

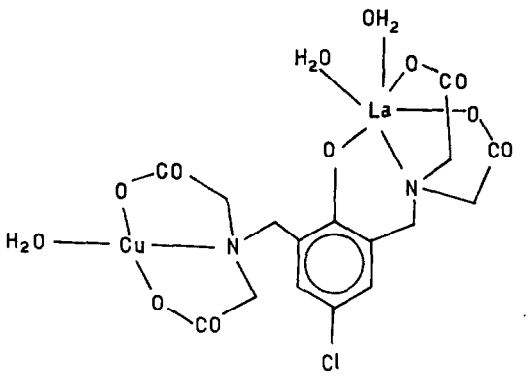

Fig. 2. Proposed coordination geometry of the $CuLaL \cdot 3H_2O$ complex.

found at 1290–1295 cm^{-1}, that is the same frequency of the mononuclear lanthanide complexes.

The purple Fe/La complex dissolved in aqueous solution gives an electronic spectrum (λ_{max} = 515 nm) similar to that observed for the iron(III) complex with N-(*o*-hydroxybenzyl)-N-(carboxymethyl) glycine[5] and the mononuclear iron complexes with analogous ligand.[6] Its magnetic moment (5.87 BM) is that expected for isolated high spin iron(III) complexes with an octahedral geometry. The electronic spectrum of the Cu/La complex, in aqueous solution (λ_{max} = 740 nm) and its low magnetic moment at room temperature (1.67 BM) suggest a pseudo-tetrahedral coordination geometry around the copper atom[7] (Fig. 2). The value of the magnetic moment is similar to that of an isolated copper(II) ion and hence magnetic exchange between two copper atoms in different molecules can probably be ruled out. To confirm this, we are carrying out variable temperature measurements of its susceptibility. The Eu/La complex shows a magnetic moment close to that of the mononuclear Eu(III) complex indicating that the environment of the Eu ion is not affected by the presence of the second ion.

As conclusion, it is in our opinion that the binuclear complexes are monomeric species similar to the di-iron complex with an analogous ligand, whose molecular structure has been resolved by X-ray analysis,[6] even if the possibility of oligomerisation could not definitively be excluded.

Acknowledgements—We wish to acknowledge Mr L. Turiaco and F. De Zuane (ICTR-CNR) for technical assistance and M.P.I. (Italy) for financial support.

REFERENCES

1. D. E. Fenton, S. E. Gayda, U. Casellato, P. A. Vigato and M. Vidali, *Inorg. Chim. Acta* 1978, **27**, 9.

2. G. Condorelli, I. Fragalà, S. Giuffrida and A. Cassol, *Z. Anorg. Allg. Chemie* 1975, **412**, 251; D. E. Fenton, U. Casellato, P. A. Vigato and M. Vidali, *Inorg. Chim. Acta* 1983, **94**, 6; A. Chisari, A. Musumeci, M. Vidali and A. Seminara, *Inorg. Chim. Acta* 1984, **81**, L19.
3. U. Russo, M. Vidali, R. Purrello, G. Maccarrone and B. Zarli, *Inorg. Chim. Acta* 1986, **120**, L11.
4. G. Schwarzenbach, G. Anderegg and R. Sallmann, *Helv. Chim. Acta* 1952, **35**, 1785.
5. W. R. Harris, R. J. Motekaitis and A. E. Martell, *Inorg. Chem.* 1975, **14**, 974.
6. B. P. Murch, P. D. Boyle and L. Que, Jr., *J. Am. Chem. Soc.* 1985, **107**, 6728.
7. A. B. P. Lever, *Inorganic Electronic Spectroscopy*, p. 359. Elsevier, London (1968).

Polyhedron Vol. 6, No. 11, pp. 1975–1980, 1987
Printed in Great Britain

0277–5387/87 $3.00+.00

AQUEOUS REDOX CHEMISTRY OF DINUCLEAR CLUSTERS. A MECHANISTIC STUDY OF PROTON OXIDATIVE ADDITION TO THE $Mo_2Cl_8^{4-}$ ION AND THE HOMOGENEOUS REDUCTION OF $Mo_2(\mu\text{-}X)(\mu\text{-}Cl)_2Cl_6^{3-}$, X = H, Cl BY AQUEOUS CHROMIUM(II)

CONSTANTINOS MERTIS,* MYRSINI KRAVARITOU, ADNAN SHEHADEH and DIMITRIS KATAKIS

University of Athens, Inorganic Chemistry Laboratory, Navarinou 13A, 10680 Athens, Greece

(*Received* 23 *February* 1987; *accepted* 11 *May* 1987)

Abstract—The kinetics of the oxidative addition of hydrochloric acid (6–12 M) to the quadruply bonded $Mo_2Cl_8^{4-}$ ion, **1**, to produce the triply bonded hydride $Mo_2(\mu\text{-}H)(\mu\text{-}Cl)_2(Cl)_6^{3-}$, **2**, are first order in the concentration of the acid, and first order in the Mo_2^{4+} reactant. The rate is strongly affected by axial coordination. At lower acid concentrations (< 6 M) the reaction is complicated by hydrolysis. The hydride **2** and the analogous nonachlorodimolybdate $Mo_2(\mu\text{-}Cl)_3Cl_6^{3-}$, **3**, undergo a two-electron reduction by chromous chloride in HCl (6M) to give **1**; the Mo_2^{6+}/Mo_2^{4+} couple catalyzes the anaerobic oxidation of Cr(II) to Cr(III).

The Redox chemistry of dinuclear clusters is of interest[1] and can be accomplished chemically or electrochemically. Molybdenum compounds are receiving special attention in this context because of the involvement of the metal in many chemical and biochemical reactions.[2] One-electron proton addition to the quadruply bonded (configuration $\sigma^2\pi^4\delta^2$) octachlorodimolybdate anion $Mo_2Cl_8^{4-}$, **1**, is a well established reaction[3] yielding the formally triply bonded [configuration $(a')^2(e')^4$] bioctahedral hydride, $Mo_2(\mu\text{-}H)(\mu\text{-}Cl)_2Cl_6^{3-}$, **2**.

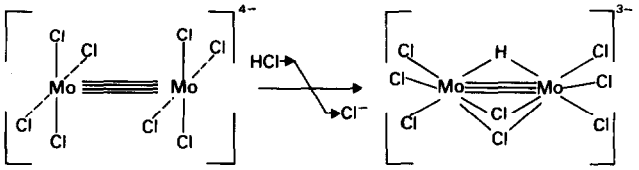

(1)

The molybdenum hydride **2** was first isolated[4] by treating $Mo_2(acet)_4$ with 12 M HCl at 60°C. It has also been obtained photochemically[5] and electrochemically[6] from 6 M HCl solutions of **1**. Aqueous acidic solutions of **2** and also of the isostructural[7] nonachlorodimolybdate $Mo_2(\mu\text{-}Cl)_3Cl_6^{3-}$, **3**, undergo heterogeneously[8] (amalgamized zinc) a two-electron reduction to give **1**. By contrast, electrochemical reduction[4,6] of **2** and **3** in 6 M HCl produce, respectively, **3** and **2**, instead of **1**. There are several mechanistic studies of proton addition on mononuclear metallic centres,[9] but none on metal–metal multiple bonds which we know of. In this paper we describe the kinetics and discuss the mechanism of reaction (1) and also report the homogeneous reduction of **2** and **3** by chromous chloride in HCl solutions to give **1**.

EXPERIMENTAL

The potassium salts of $Mo_2Cl_8^{4-}$, $Mo_2HCl_8^{3-}$ and the ammonium salt of $Mo_2Cl_9^{3-}$ were prepared by

* Author to whom correspondence should be addressed.

the literature methods.[4,10,11] Experiments were performed under oxygen-free nitrogen or argon. Solvents were thoroughly degassed by freeze pumping. All reagents were of analytical grade and purified before use. Chromous chloride was supplied by Ventron and all other compounds by Fluka. Samples for kinetic measurements were prepared on a thermostated Schlenk tube and the resulting clear solution was quickly transferred via a stainless tube and under positive argon pressure to a (previously purged by argon) 1 cm spectrophotometric cell. Microanalyses were performed in this laboratory and at the Research Centre, Demokritos. Electronic spectra were recorded with a Hitachi and a Carry 17.

Reaction of tripotassium 1,1-*trichloro*-2,2,2-*trichloro*-μ-*hydrido*-*bis*-μ-*chloro*-*dimolybdenum*(III) *with* $CrCl_2$

Into a solution (10 cm^3 HCl 6 M) of $K_3Mo_2HCl_8$ (0.105 g, 0.17 mmol) and KCl (0.012 g, 0.17 mmol) is added slowly a solution (10 cm^3 HCl 6 M) of $CrCl_2$ (0.085 g, 0.68 mmol) at room temperature with stirring. The colour of the solution darkens to deep green–brown and gas evolution (H_2) is observed. The mixture was left to react for *ca.* 2 h, the solvent was removed *in vacuo* at room temperature, and the residues were extracted with tetrahydrofuran (20 cm^3). The deep green solution was removed by filtering and the red residue was washed with small portions of tetrahydrofuran until they remained colourless, dried *in vacuo*, and identified by analysis and spectroscopy to be $K_4Mo_2Cl_8$. Yield, 97% based on $Mo_2HCl_8^{3-}$.

Reaction of tris-n-*tetrabutylammonium*-1,1,1-*trichloro*-2,2,2-*trichloro*-*tris*-μ-*chloro*-*dimolybdenum* (III) *with* $CrCl_2$

Into a solution (20 cm^3 HCl 6 M) of a mixture of $[(n\text{-}C_4H_9)_4N]_3Mo_2Cl_9$ (0.363 g, 0.34 mmol) and $(n\text{-}C_4H_9)_4NCl$ (0.363 g, 0.34 mmol) is added a solution (20 cm^3 HCl 6 M) of $CrCl_2$ (0.17 g, 1.36 mmol) at room temperature with stirring. The mixture was left to react for *ca.* $2\frac{1}{2}$ h and treated as described above. The red product was identified as $[(n\text{-}C_4H_9)_4N]_4Mo_2Cl_8$. Yield, 95% based on $[(n\text{-}C_4H_9)_4N]_3Mo_2Cl_9$.

RESULTS AND DISCUSSION

In aqueous solutions $K_4Mo_2Cl_8$ is unstable; it hydrolyzes within a few minutes and the initial red colour becomes brown–yellow. Hydrolysis is slower in hydrochloric acid solutions, the extent of the equilibrium

$$Mo_2Cl_8^{4-} \underset{+Cl^-}{\overset{-Cl^-}{\rightleftharpoons}} Mo_2Cl_{8-x}(H_2O)_x^{4-x} \qquad (2)$$

depending on the acid concentration. The development of the spectra in 6 M and 0.5 M HCl is given in Figs 1 and 2, respectively.

The reaction taking place in 6 M HCl, where hydrolysis is limited is given by eqn (1). The structures of **1** and **2** are assumed to be the same as those determined in the solid.[12,13] The presence of isosbestic points in Fig. 1 indicates that at 6 M HCl $Mo_2HCl_8^{3-}$ is the only appreciably absorbing product. In contrast, at 0.5 M HCl there is no isosbestic point, presumably because of hydrolysis. Never-

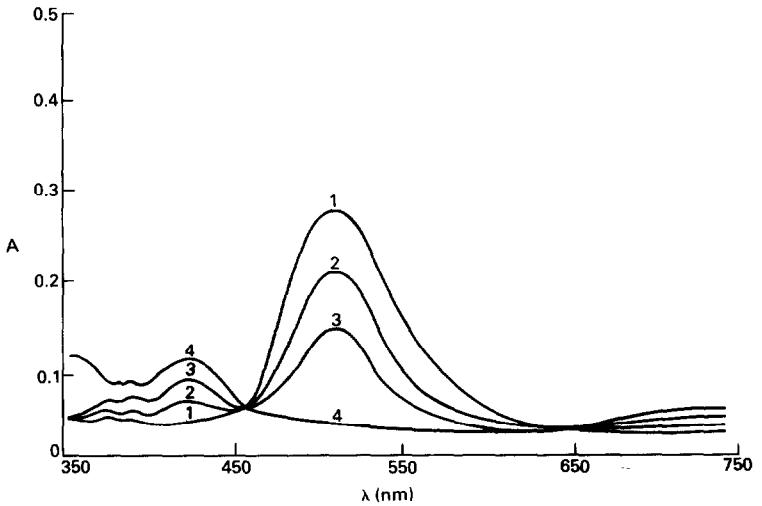

Fig. 1. Spectral changes of a $K_4Mo_2Cl_8$ (3×10^{-4} M) solution in 6 M HCl at 25°C, recorded after 1, 2 and 48 h.

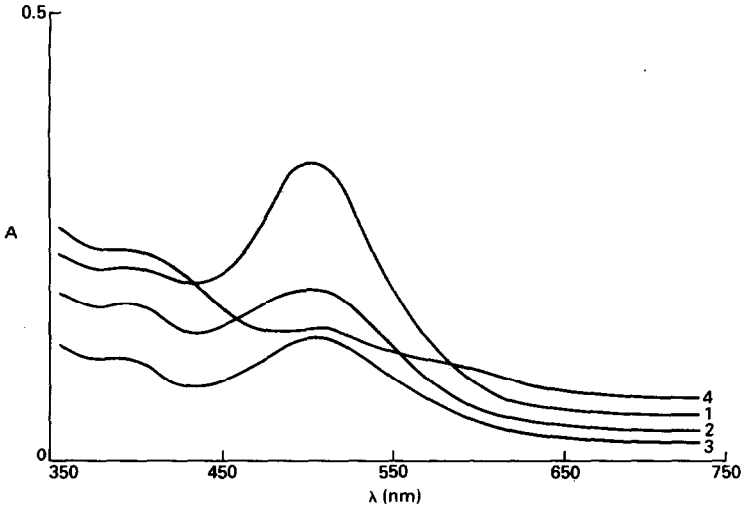

Fig. 2. Spectral changes of a $K_4Mo_2Cl_8$ (6.5×10^{-2} M) solution in 0.5 M HCl at 25°C recorded after 1, 2 and 72 h.

theless here too there is no shift in the peak at 520 nm but the peak of the products (at *ca.* 420 nm in 6 M HCl) is shifted. Accordingly the reaction was followed by monitoring the absorption at 520 nm. The complexity at low acid and the relative simplicity at high acid is also reflected in the kinetics (Fig. 3). At low acid concentrations there is an initial decrease in absorbance, again attributed to hydrolysis. In the acid concentration range between 3–6 M, this initial stage is clearly shown, but it is not too extensive and it does not seem to much influence the subsequent (first order) part, which is attributed to oxidative addition similar to that shown in eqn (1) but with participation of hydrolyzed species. In this acid range the slope of the linear part increases with increasing acid concentration. At lower acid (0.5–3 M) hydrolysis and/or condensation have rates comparable to oxidative addition, the results are not reproducible, and the final absorption at *ca.* 420 nm is relatively small (Fig. 2). In the acid range between 6–12 M, the plots do not have non-linear initial parts (Fig. 4) and the first order kinetics are attributed to reaction (1). In this range the quadruple bond absorption at 520 nm disappears, being replaced by the triple bond absorption at 420 nm. The dependence

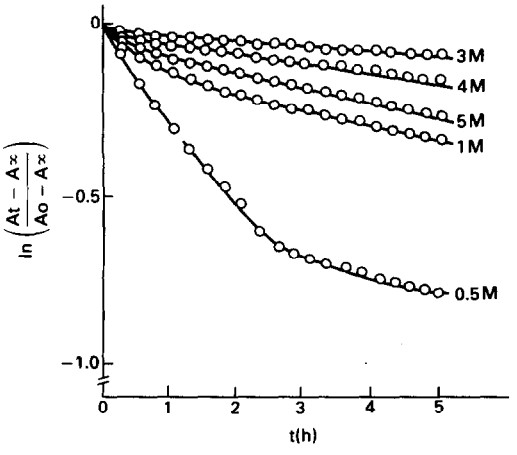

Fig. 3. First order plots in HCl 0.5–5 M at 25°C.

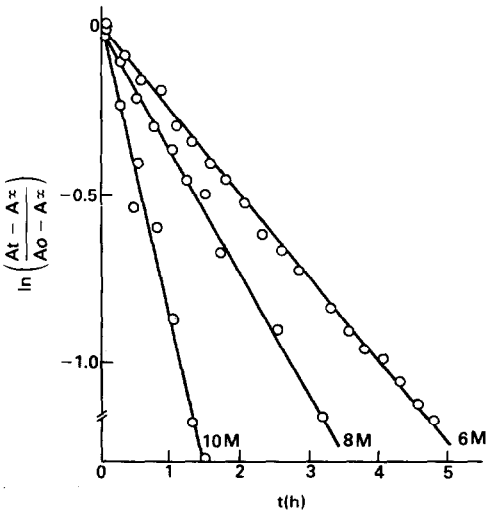

Fig. 4. Typical first order plots (6, 8 and 10 M HCl), at 25°C.

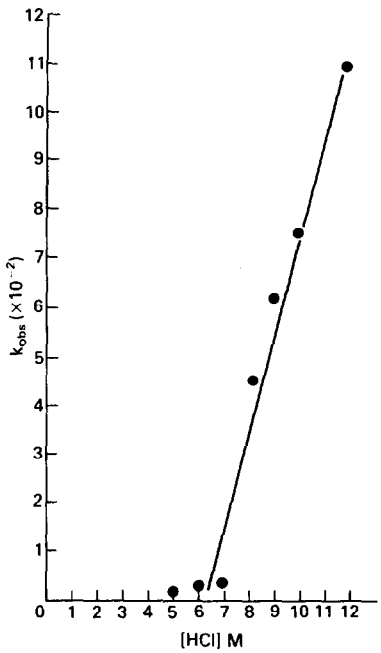

Fig. 5. Dependence of the observed pseudo-first order rate constant on the concentration of HCl.

of the first order rate constant on acid for [HCl] $\geqslant$ 3 M is shown in Fig. 5. Above 6 M the plot is linear, below this concentration it is not, and the rates are relatively slow, because of the postulated participation of hydrolyzed species. Within experimental error the addition of 2 M KCl to a solution of **1** in 2 M HCl had no measurable effect. Addition of KCl or NaCl at higher acid concentrations is limited by solubility. However, hydrogen ion concentration can be changed considerably by addition of p-toluenesulfonic acid (PTSH). The spectrophotometric results are shown in Fig. 6. The rate constant for the disappearance of **1** at 25°C, in 6 M HCl, 6 M PTSH is 2.5×10^{-4} s^{-1} whereas at 6 M HCl it is only 3.3×10^{-5} s^{-1}. The results indicate that the rate determining step in the formation of the hydride **2** is the addition of the proton to the quadruple bond. The activation probably originates in the reorganization involved, including some rotation around the molecular axis and a lengthening of the metal–metal bond. However, the destabilization caused by the approach of the positive charge and the removal of bonding electron density eventually leads to the breaking of the δ-bond which is replaced by three bridges, albeit not without considerable weakening as indicated by the dramatic increase in bond length,[12,13] from 2.139 Å to 2.780 Å. At lower acid where some of the chloride ligands have been replaced by water molecules complete destruction of the multiple bond prevails.[14] The rate constant in 6 M HCl and 6 M PTSH is considerably smaller compared to the value (Fig. 6) 1.9×10^{-3} s^{-1} at 12 M HCl. The difference could partly be attributed to medium effects but a more plausible explanation is that it is caused by the axial coordination of the negatively charged chloride ligands, which causes a weakening of the metal–metal bond, and a simultaneous increase of the proton nucleophilicity of **1**. The increase in bond length caused by axial coordination is well known.[15] With the non-complexing PTS^- some of the chloride ligands are replaced by water molecules, which are decreasing the nucleophilicity. An analogous effect is

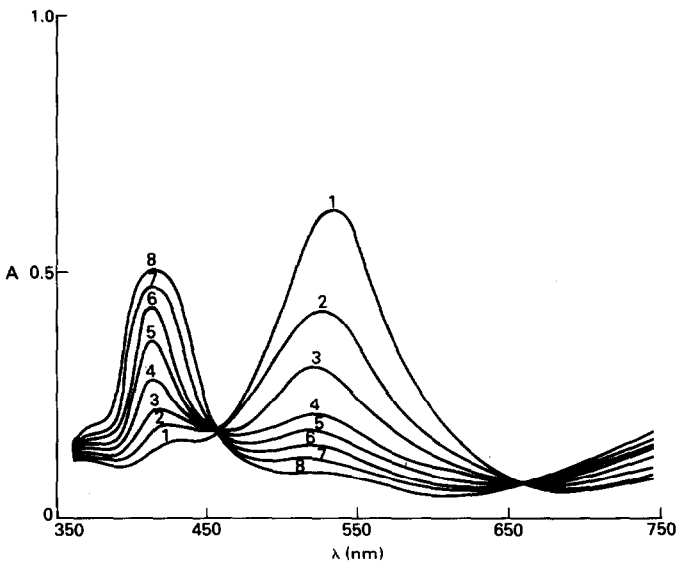

Fig. 6. Spectral changes of a $K_4Mo_2Cl_8$ (10^{-4} M) solution in a mixture of HCl (6 M) and PTSH (6 M) recorded at 10 min intervals.

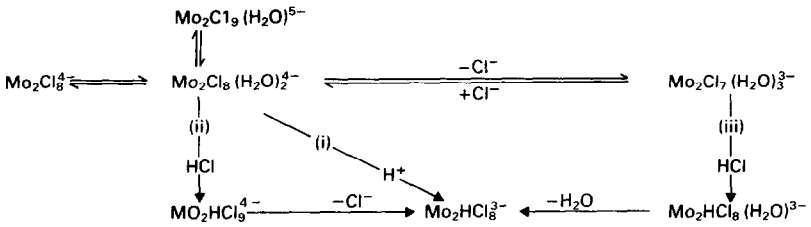

Scheme 1. Proposed pathways of the formation of $Mo_2HCl_9^{3-}$ from $Mo_2Cl_8^{4-}$ by proton oxidative addition.

expected at lower acid concentrations. The *bis*-end coordinated aqua adduct $Mo_2Cl_8(H_2O)_2^{4-}$ can be isolated[12] in 6 M HCl but not from 12 M HCl,[9] whereas the anion $Mo_2Cl_9(H_2O)^{5-}$, where one water molecule is replaced by chloride, has been structurally characterized as the pyridinium salt.[15b] The implication is that apart from hydrolysis the following equilibrium occurs,

$$Mo_2Cl_8(H_2O)_2^{4-} \underset{-Cl^-}{\overset{+Cl^-}{\rightleftharpoons}} Mo_2Cl_9(H_2O)^{5-}. \quad (3)$$

Thus, the mechanism can be summarized as in Scheme 1.

The formation of the hydride **2** can be simply viewed as the protonation of the quadruple bond of **1** and subsequent fast rearrangement [path(i)] or as step-wise addition of HCl across the metal–metal bond producing $Mo_2HCl_9^{4-}$, followed by loss of chloride ion and chloride bridge formation [path (ii)]. At lower acid concentration HCl is added to the metathetical derivative[16] $Mo_2Cl_7(H_2O)^{3-}$ [path (iii)]. The last route has been proposed for the corresponding bromide.[17] At this stage it is not possible to distinguish between paths (i) and (ii).

The mechanistic scheme just described is further supported by observations made with the anion $W_2Cl_8^{4-}$, which is transformed[18] into the corresponding hydride, $W_2HCl_8^{3-}$, much easier (at $-10°C$). The difference in the reactivity[19] can be attributed to the higher energy of the HOMO of W_2^{4+}, compared to Mo_2^{4+}, which implies that bonding electrons are more accessible and the disruption of the weaker δ-bond easier. A similar effect has also been demonstrated by comparing the reaction[20] of benzoic acid with $Mo_2X_4(PR_3)_4$, which yields $Mo_2X_2(PR_3)_2(OOCPh)_2$, with the reaction[21] of this compound with $W_2Cl_2(PBu^n_3)_4$, which gives $W_2Cl_2(PBu^n_3)_2(OOCPh)_2(\mu\text{-H})(\mu\text{-Cl})$ resulting from facile oxidative addition of the generated HCl to the initially formed $W_2Cl_2(PBu^n_3)_2(OOCPh)_2$.

The hydride **2** is stable in 6 M HCl (peak at 420 nm, $\varepsilon = 1082$) whereas Cr(II) is oxidized to Cr(III):

$$Cr^{2+} + H^+ \rightarrow Cr^{3+} + \tfrac{1}{2}H_2. \quad (4)$$

Reactions (1) and (4) depend on the acid concentration and under the above conditions reaction (1) is completed in *ca.* 48 h and (4) in *ca.* 3 h.

When thoroughly deoxydenated freshly prepared

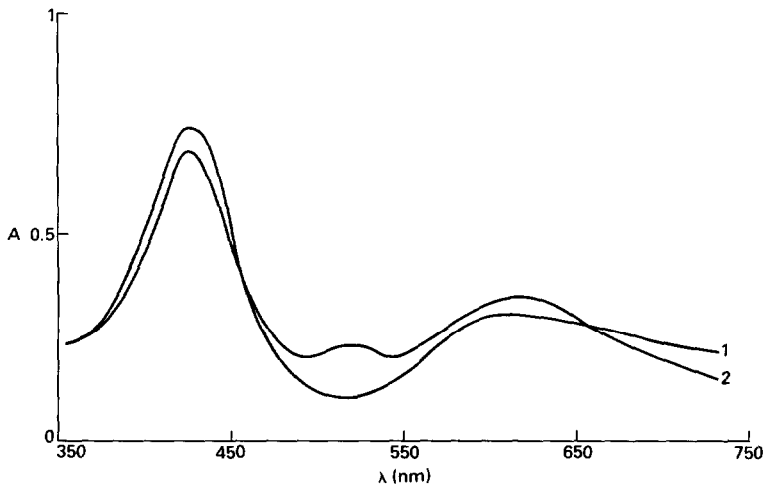

Fig. 7. Spectra of a mixture of $K_3Mo_2HCl_8$, 8.5×10^{-5} M and $CrCl_2$, 3.4×10^{-4} M in 6 M HCl at 25°C; (a) after 15 min from the start of the reaction, (b) after 1 h.

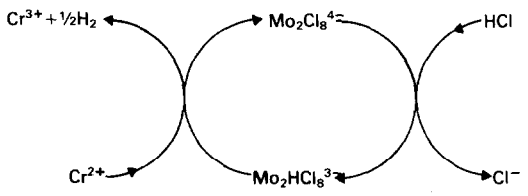

Scheme 2.

HCl 6 M solutions of an excess of chromous chloride and a mixture of $K_3Mo_2HCl_8/KCl$ are mixed at room temperature the colour changes from light yellow–green to dark green–brown and gas evolution (H_2) is observed. The reaction can be followed spectrophotometrically, Fig. 7. The absorbance at 420 nm due to the hydride **2** diminishes whereas a new peak attributed to **1** appears and chromium(II) is oxidized to chromium(III). The reaction taking place is

$$Mo_2HCl_8^{3-} + 2Cr^{2+} + H^+ \rightarrow Mo_2Cl_8^{4-} + 2Cr^{3+} + H_2 \quad (5)$$

but the measured stoichiometry is little more than two Cr^{2+} ions for each $Mo_2HCl_8^{3-}$, because of the parallel reaction (4). There is also a peak at 615 nm attributed to a mixture of $[Cr(H_2O)_5Cl]^{2+}$ and $[Cr(H_2O)_4Cl_2]^+$ which absorbs[22] at 605 and 635 nm, respectively. A similar mixture is obtained in reaction (4). At the end of reaction (5) the solvent is removed *in vacuo*, the residues are extracted with tetrahydrofuran leaving behind a red solid identified as **1**; the green filtrate contains Cr(III) in the form of the dichloro-complex (peaks at 445 and 640 nm). In HCl the product **1** is converted back to **2**, hence the dimolybdenum couple participates in the cycle shown (Scheme 2). With $[(n\text{-}C_4H_9)_4N]_3Mo_2Cl_9$ the reaction is similar yielding **1** and Cr(III).

The Mo_2^{6+} core effectively oxidizes Cr(II) to Cr(III) thus comparing to the behaviour of the olefinic and acetylenic compounds,[23,24] except that here the bond order increases rather than decreases, from three to four.

The system is of interest and it it desirable to pay more attention to its mechanistic aspects in order to establish:

(i) The mechanism of reaction (1).

(ii) Whether the electron transfer in reaction (5) occurs via a chloride bridged activated complex (inner sphere) or by direct metal–metal interaction (Mo—Cr).

(iii) How the bridges over the molybdenum ions open and the implications to homogeneous catalysis.

Acknowledgements—We thank the Greek Ministry of Science and Technology for Support.

REFERENCES

1. F. A. Cotton and R. A. Walton, (a) *Multiple Bonds Between Metal Atoms*. Wiley, New York (1982); (b) *Structure and Bonding* 1985, **62**, 2, and refs therein; (c) M. H. Chisholm, *Polyhedron* 1986, **5**, 25, and refs therein.
2. (a) J. Chatt, J. R. Dilworth and R. L. Richards, *Chem. Rev.* 1977, **78**, 589; (b) R. A. Henderson, G. J. Leigh and C. J. Pikett, *Adv. Inorg. Chem. Radiochem.* 1983, **27**, 198.
3. F. A. Cotton, *Acc. Chem. Res.* 1978, **11**, 225.
4. M. J. Bennet, J. V. Brencic and F. A. Cotton, *Inorg. Chem.* 1969, **8**, 1060.
5. W. C. Trogler, D. K. Erwin, G. L. Geoffroy and H. B. Gray, *J. Am. Chem. Soc.* 1978, **100**, 1160.
6. J. San Filippo, Jr. and M. A. Schaefer King, *Inorg. Chem.* 1976, **15**, 1228.
7. See ref. 1(a), p. 235.
8. A. Bino and D. Gibson, *J. Am. Chem. Soc.* 1980, **102**, 4277.
9. J. P. Collman and L. S. Hegedus, *Principles and Applications of Organotransition Metal Chemistry*. University Science, Milk Valley, California (1980).
10. J. V. Brencic and F. A. Cotton, *Inorg. Chem.* 1970, **9**, 351.
11. W. H. Delphin and R. A. D. Wentworth, *Inorg. Chem.* 1974, **13**, 2037.
12. J. V. Brencic and F. A. Cotton, *Inorg. Chem.* 1969, **8**, 7.
13. A. Bino and F. A. Cotton, *Angew. Chem. Int. Ed.* 1979, **18**, 332.
14. (a) A. R. Bowen and H. Taube, *J. Am. Chem. Soc.* 1971, **93**, 3285; *Inorg. Chem.* 1974, **13**, 2245; (b) M. Ardon and A. Pernick, *Inorg. Chem.* 1974, **13**, 2275.
15. (a) F. A. Cotton and G. Wilkinson, *Advanced Inorganic Chemistry* (4th edn), pp. 1102–1105. Wiley (1980) and refs therein; (b) J. V. Brencic and F. A. Cotton, *Inorg. Chem.* 1970, **9**, 346.
16. A. Bino, F. A. Cotton and W. Kaim, *Inorg. Chem.* 1979, **18**, 3030.
17. F. A. Cotton and B. J. Kalbacher, *Inorg. Chem.* 1969, **8**, 7.
18. A. P. Sattelberger, K. W. McLaughlin and J. C. Huffman, *J. Am. Chem. Soc.* 1981, **103**, 2880.
19. F. A. Cotton, J. L. Hubbard, D. L. Lichtenberger and I. Shim, *J. Am. Chem. Soc.* 1982, **104**, 679.
20. J. San Filippo, Jr., *Inorg. Chem.* 1976, **15**, 2215.
21. F. A. Cotton and G. N. Mott, *J. Am. Chem. Soc.* 1982, **104**, 5978.
22. P. J. Elving and B. Zemel, *J. Am. Chem. Soc.* 1957, **97**, 1281.
23. (a) C. E. Castro and R. D. Stephens, *J. Am. Chem. Soc.* 1964, **86**, 4358; (b) R. S. Bottei and W. A. Joern, *J. Am. Chem. Soc.* 1968, **90**, 297.
24. D. Katakis, J. Konstantatos and E. Vrachnou-Astra, *J. Organomet. Chem.* 1985, **279**, 131.

Polyhedron Vol. 6, No. 11, pp. 1981–1986, 1987
Printed in Great Britain

0277-5387/87 $3.00+.00

SOME ELECTROPHILIC SUBSTITUTION REACTIONS OF *CLOSO*-[1-$CB_{11}H_{12}$]$^-$ AND ONE-BORON INSERTION INTO *NIDO*-7-L-7-$CB_{10}H_{12}$ (L = H^- OR Me_3N) COMPOUNDS. ISOLATION OF ALL THREE B-SUBSTITUTED *CLOSO*-Me_3N-1-$CB_{11}H_{11}$ DERIVATIVES

TOMÁŠ JELÍNEK, JAROMÍR PLEŠEK, FRANTIŠEK MAREŠ, STANISLAV HEŘMÁNEK and BOHUMIL ŠTÍBR*

Institute of Inorganic Chemistry, Czechoslovak Academy of Sciences, 250 68 Řež near Prague, Czechoslovakia

(*Received* 3 *March* 1987; *accepted* 27 *May* 1987)

Abstract—Electrophilic deuteration of *closo*-[1-$CB_{11}H_{12}$]$^-$ in the DCl/D_2O system confirmed the expected order of reactivity on individual skeletal atoms, decreasing in the series B(12) > B(7–11) > B(2–6) > C(1). In contrast, electrophilic B-substitution of *closo*-[1-$CB_{11}H_{12}$]$^-$ with H_2NOSO_3H is consistent with the preference of the B(7)-substitution to suggest a different mechanism for almost exclusive formation of 7-H_3N-*closo*-1-$CB_{11}H_{11}$. 7-Me_3N-*closo*-1-$CB_{11}H_{11}$ was isolated along with the remaining 2- and 12-Me_3N-1-$CB_{11}H_{11}$ isomers as side products of the thermal decomposition of [$BH_2(NMe_3)_2$]$^+$[*nido*-7-$CB_{10}H_{13}$]$^-$ at 270°C, which is inconsistent with a specific insertion of the $BNMe_3$ fragment into the open face of *nido*-[7-$CB_{10}H_{13}$]$^-$. Nevertheless, clean ^{10}B-insertion was observed in the reactions of $Et_3N^{10}BH_3$ with both *nido*-[7-$CB_{10}H_{13}$]$^-$ and 7-Me_3N-*nido*-7-$CB_{10}H_{12}$ to give respectively *closo*-[1-$CB_{11}H_{12}$]$^-$ and [1-Me_2N-1-$CB_{11}H_{11}$]$^-$ labelled by ^{10}B exclusively at the B(2) site. Cage rearrangement was observed, however, in the reaction of 7-Me_3N-8-$PhCH_2$-*nido*-7-$CB_{10}H_{11}$ with Et_3NBH_3 under similar conditions to produce only the 1-Me_3N-7-$PhCH_2$-1-$CB_{11}H_{10}$ *closo*-isomer.

Recently, we have reported[1] electrophilic substitution reactions of the *closo*-[1-$CB_{11}H_{12}$]$^-$ anion (Fig. 1) with halogens, leading to multiple substitution of the B(7–12) atoms with chlorine and bromine, and to the substitution at the B(7,12) sites with iodine. Acid-catalyzed reaction of [1-$CB_{11}H_{12}$]$^-$ with dimethyl sulphoxide[1] proceeded exclusively on the B(12) atom to produce *closo*-12-Me_2S-1-$CB_{11}H_{11}$ as the main product. With respect to relative rates of halogenation in the series of isoelectronic 12-vertex *closo*-compounds, the decrease in reactivity in the order [$B_{12}H_{12}$]$^{2-}$ > [$CB_{11}H_{12}$]$^-$ > $C_2B_{10}H_{12}$ can be clearly estimated. The skeletal carbon, bearing a partial net positive charge, reduces the reactivity towards electrophilic reagents. Previous work has shown that, apart from the disproportionation of *nido*-[7-$CB_{10}H_{13}$]$^-$ at higher temperatures,[2] the *closo*-[1-$CB_{11}H_{12}$]$^-$ anion and its C-amine derivatives can be prepared by more convenient one-boron insertion into the framework of *nido*-7-L-7-$CB_{10}H_{12}$ compounds[1–3] (L = H^-, H_3N and Me_3N). This paper reports some new aspects of this insertion reaction along with some supplementary results on electrophilic substitution reactions of *closo*-[1-$CB_{11}H_{12}$]$^-$.

EXPERIMENTAL

Physical measurements

The ^{11}B (64.18 MHz) and two-dimensional (2-D) ^{11}B–^{11}B NMR spectra were recorded on a Varian XL-200 spectrometer in hexadeuterioacetone, chemical shifts are given in δ (ppm, referenced to $BF_3 \cdot OEt_2$, positive shifts downfield). 2-D ^{11}B–^{11}B

* Author to whom correspondence should be addressed.

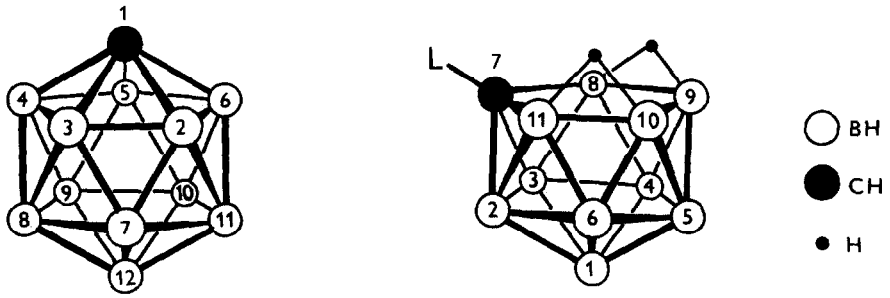

Fig. 1. Simplified structure and numbering system of *closo*-$[1\text{-}CB_{11}H_{12}]^-$ anion and *nido*-7-L-7-$CB_{10}H_{12}$ compounds.

NMR spectra were produced on selected samples via procedures described elsewhere.[4] The following short notation of the off-diagonal interactions (cross peaks) found in 2-D spectra is used: boron atoms found to interact with the observed boron atom (on diagonal) are given in brackets with right superscripts (s—strong, m—medium, w—weak, 0—zero interaction) indicating relative intensities of the cross peaks observed. ^1H (60 MHz) NMR spectra were obtained on Tesla BS-467 equipment in hexadeuterioacetone, chemical shifts are given in δ (ppm, referenced to TMS). Mass spectra were collected at 70 eV using a GC/MS HP-5989 device. TLC was performed on Silufol (silica gel on aluminium foil; detection by I_2 vapour followed by $AgNO_3$ spray) in 1:3 acetonitrile–chloroform. Melting points were determined in sealed capillaries under nitrogen and are uncorrected.

Chemicals

Diethyl ether and tetrahydrofuran were distilled with $NaAlH_2(OC_2H_4OCH_3)_2$ prior to use and other solvents were purified by standard distillation procedures. A concentrated solution of DCl in D_2O was prepared by the absorption of dry DCl, generated in the reaction of benzoyl chloride with D_2O (Merck, 99.9%) at 120–140°C, in D_2O. Compounds 7-L-7-$CB_{10}H_{12}$ (L = H_3N or Me_3N),[5–7] $[1\text{-}CB_{11}H_{12}]^-$,[3] 6-$PhCH_2B_{10}H_{13}$,[8] $[BH_2(NMe_3)_2]^+I^-$,[9] and $Et_3N^{10}BH_3$[10] were prepared by literature methods. Other commercially available chemicals were reagent grade and were used as purchased.

Syntheses

Except where otherwise indicated, all syntheses were conducted under an inert atmosphere. Operations connected with solvent evaporations were performed *in vacuo* on a standard rotatory evaporator.

Deuteration of closo-$[1\text{-}CB_{11}H_{12}]^-Na^+$. A NMR tube was charged with a 1 M D_2O-solution of $[1\text{-}CB_{11}H_{12}]^-Na^+$ (*ca.* 3 cm^3) prepared as in the following experiment. The solution was acidified by three drops of concentrated DCl/D_2O and the ^{11}B NMR spectrum was monitored in 15 min, 1 h, 2 h, and 24 h intervals. The H–D exchange rate on individual B-atoms was estimated by monitoring the collapse of the two low-field doublets into singlets (Fig. 2). The final product of the exchange

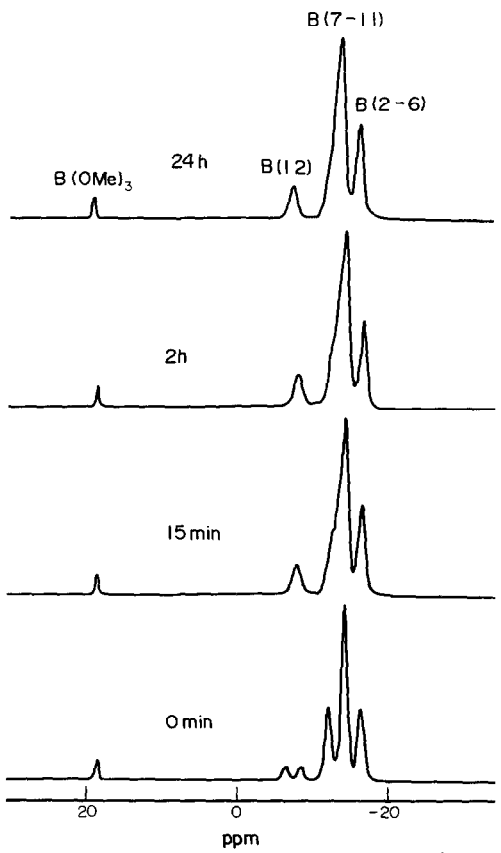

Fig. 2. Proton-coupled ^{11}B NMR spectra of the *closo*-$[1\text{-}CB_{11}H_{12}]^-Na^+/DCl/D_2O$ system in different time intervals.

was [7,8,9,10,11,12-D_6-1-$CB_{11}H_6$]$^-$Na$^+$; connectivities from the 2-D ^{11}B–^{11}B NMR spectrum: B(12) [B(7–11)^s], B(7–11) [B(2–6)^s, B(12)^m], B(2–6) [B(7–11)^s].

7-H_3N-1-$CB_{11}H_{11}$. The [1-$CB_{11}H_{12}$]$^-$$NMe_3H^+$ salt (2.2 g; 0.01 mol) was treated with aqueous 1 M NaOH (10 cm^3) at 50°C, the solution was filtered and the trimethylamine evolved was removed *in vacuo*. The residual solution was extracted with ether (30 cm^3) and the organic layer was separated and evaporated. The semi-solid residue (hydrated [1-$CB_{11}H_{12}$]$^-$Na$^+$) obtained after removing the solvents, was dissolved in water (50 cm^3), acidified with acetic acid to pH 6 and treated with H_2NSO_3H (7.0 g; 0.06 mol). The mixture was heated at 80°C for 10 h, cooled to an ambient temperature and the unreacted [1-$CB_{11}H_{12}$]$^-$ was precipitated with 3 M aqueous $Et_3N \cdot HCl$. The white precipitate was isolated by filtration, washed with water and vacuum-dried to recover 1.5 g (59%) of [1-$CB_{11}H_{12}$]$^-$$NEt_3H^+$, as assessed by ^{11}B NMR. The clear filtrate was extracted with ether (2 × 20 cm^3) and the ether layer was evaporated, leaving a white solid which was recrystallized from benzene (20 cm^3) and vacuum-dried to give 0.25 g (39%) of 7-H_3N-1-$CB_{11}H_{11}$; m.p. > 280°C; R_F 0.25; *m/z* 161; ^{1}H NMR: δ 6.54 [s, 3H, H_3N], 2.51 [s, 1H, H(1)]; ^{11}B NMR: δ_B −5.28 [s, 1B, B(7)], −6.90 [d, 1B, J(BH) 156, B(12)], −13.60 [d, 2+2B, 136, B(8,11)/B(9,10)], −16.79 [d, 2+2B, 164, B(2,3)/B(4,6)], −19.41 [d, 1B, 160, B(5)]. As assessed by ^{11}B NMR, the product was slightly contaminated by the 12-H_3N-isomer (singlet at δ_B −0.60).

closo-7-Me_3N-1-$CB_{11}H_{11}$. A sample of 7-H_3N-1-$CB_{11}H_{11}$ (0.2 g; 1.25 mmol) was dissolved in 5% sodium hydroxide (10 cm^3) and the resultant solution was treated with dimethyl sulphate (0.8 cm^3; 8.4 mmol). The mixture was stirred at room temperature for 1 h to deposit white material and treated with concentrated ammonia (5 cm^3) for 0.5 h. The product was isolated by filtration, washed with water, vacuum-dried and dissolved in 1:1 dichloromethane/benzene. The solution was slowly reduced in volume to *ca.* 10 cm^3 to precipitate white crystals which were filtered, washed with benzene (*ca.* 5 cm^3) and vacuum-dried to afford 0.2 g (75%) of 7-Me_3N-1-$CB_{11}H_{11}$; m.p. 268–270°C; R_F (benzene) 0.20; *m/z* 203; ^{1}H NMR: δ 3.08 [s, 9H, Me_3N], 2.59 [s, 1H, H(1)]; ^{11}B NMR: δ_B 2.57 [s, 1B, B(7)], −7.39 [d, 1B, 138, B(12)], −13.89 [d, 2+2B, 166, B(8,11/9,10)], −16.98 [d, 2+2B, 152, B(2,3/4,6)], −18.65 [d, 1B, 151, B(5)], the unresolved signals assigned to B(8,11/9,10) and B(2,3/4,6) were partially resolved in the "window area" of the 2-D spectrum. Connectivities from 2-D ^{11}B–^{11}B NMR: B(7) [B(12)^m, B(8,11)^s, B(2,3)^s], B(12) [B(7)^m, B(8,11/9,10)^s], B(8,11/9,10) [B(12)^s, B(7)^s, B(2,3/4,6)^s, B(5)^s], B(2,3/4,6) [B(7)^s, B(8,11/9,10)^s, B(5)^s], B(5) [B(2,3/4,6)^s, B(9,10)^s].

Thermal decomposition of nido-[7-$CB_{10}H_{13}$]$^-$[$BH_2(NMe_3)_2$]$^+$. The title salt (2.65 g; 0.01 mol), prepared by the precipitation of 0.2 M aqueous *nido*-[7-$CB_{10}H_{13}$]$^-$Na$^+$ (50 cm^3) with [$BH_2(NMe_3)_2$]$^+$I$^-$ (2.6 g; 0.01 mol), was heated *in vacuo* at 270°C for 3 h in a reaction flask equipped with a glass sublimation tube. The white sublimate and residual solids were digested with dichloromethane (2 × 20 cm^3) and the resultant mixture was filtered. Silica gel (5 g) was added to the filtrate and the solids obtained after removing the solvent were placed onto a column (2.5 × 30 cm) packed with silica gel. Benzene developed three main fractions of R_F 0.42, 0.25 and 0.20 (checked by TLC in benzene) which were evaporated, washed with hexane and vacuum-dried. The first fraction (0.36 g; 18%) was identified as *closo*-12-Me_3N-1-$CB_{11}H_{11}$; m.p. 163–164°C; *m/z* 203; ^{1}H NMR: δ 2.92 [s, 9H, Me_3N], 4.49 [s, 1H, H(1)]; ^{11}B NMR: δ_B 7.73 [s, 1B, B(12)], −12.43 [d, 5B, 148, B(7–11)], −17.23 [d, 5B, 160, B(2–6)]; connectivities from 2-D ^{11}B–^{11}B NMR: B(12) [B(7–11)^s], B(7–11) [B(2,6)^s, B(12)^s], B(2–6) [B(7–11)^s]. The product from the second fraction, (0.1 g; 5%) was identified as *closo*-2-Me_3N-1-$CB_{11}H_{11}$; m.p. 206–207°C; *m/z* 203; ^{1}H NMR: δ 3.22 [s, 9H, Me_3N], 4.71 [s, 1H, H(1)]; ^{11}B NMR: δ_B 19.02 [s, 1B, B(2)], −3.15 [d, 1B, 147, B(12)], −11.15 [d, 2B, 157, B(7,11)], −14.72 [d, 5B, 157, B(3–6,9)], −19.59 [d, 2B, 154, B(8,10)]; connectivities from 2-D ^{11}B–^{11}B NMR: B(2) [B(3–6,9)^m, B(7,11)^s], B(12) [B(7,11)^w, B(8,10)^s, B(3,6/4,5/9)^w], B(7,11) [B(8,10)^s, B(12)^w, B(2)^s, B(3,6/4,5/9)^m], B(3,6/4,5/9) [B(7,11)^m, B(8,10)^s, B(12)^w], B(8,10) [B(3,6/4,5/9)^s, B(7,11)^s, B(12)^s]. The third fraction was identified from ^{11}B NMR as 7-Me_3N-1-$CB_{11}H_{11}$, which was characterized in the preceding experiment. The dichloromethane insoluble portion was treated with boiling 5% potassium hydroxide (30 cm^3) and filtered. The filtrate was precipitated with 1 M tetramethylammonium chloride, the white solid was isolated by filtration and recrystallized from aqueous acetone to recover 1.3 g (59%) of *closo*-[1-$CB_{11}H_{12}$]$^-$$NMe_4^+$, as assessed from ^{11}B NMR.[3]

^{10}B-*insertion into nido*-[7-$CB_{10}H_{13}$]$^-$. A mixture of [7-$CB_{10}H_{13}$]$^-$Cs$^+$ (2.7 g; 0.01 mol) and $Et_3N^{10}BH_3$ (6.8 g; 0.06 mol) was heated at 200°C for 6 h and the triethylamine evolved was removed by distillation. After being cooled to room temperature, the mixture was treated with a mixture of ethanol (50 cm^3) and concentrated hydrochloric acid (30 cm^3). After the initial exothermic reaction

had ceased, the mixture was heated at 80°C for an additional 4 h, diluted with water (100 cm^3), filtered with activated charcoal and extracted with ether (2 × 30 cm^3). The ether layer was evaporated with water (15 cm^3) and the remaining aqueous solution was precipitated with 1 M NMe_4Cl (10 cm^3). The precipitate was isolated by filtration, washed with water and recrystallized from aqueous acetone to give 1.2 g (55%) of *closo*-[2-^{10}B-1-$CB_{10}H_{12}$]$^-$ NMe_4^+ (for ^{10}B and ^{11}B NMR spectra see Fig. 3).

^{10}B *Insertion into nido*-7-Me_3N-7-$CB_{10}H_{12}$. A mixture of 7-Me_3N-7-$CB_{10}H_{12}$ (1.9 g; 0.01 mol) and $Et_3N^{10}BH_3$ (2.8 g; 0.02 mol) was heated at 200°C for 4 h to evolve hydrogen and triethylamine. After being cooled to room temperature, the mixture was decomposed with a mixture of ethanol (50 cm^3) and concentrated hydrochloric acid (30 cm^3) as in the preceding experiment. The solids were decanted and treated with 10% NaOH (30 cm^3) and the alkaline solution was filtered. The filtrate was stirred with dimethyl sulphate (7.6 g; 0.06 mol) for 1 h and the excess dimethyl sulphate was removed by adding concentrated ammonia (10 cm^3) under stirring for 0.5 h. The white product was isolated by filtration and recrystallized from acetone to obtain 0.8 g (42%) of *closo*-1-Me_3N-2-^{10}B-1-$CB_{10}H_{11}$; ^{11}B NMR: δ_B −7.40 [d, 1B, 141, B(12)], −13.65 [d, 5B, 140, B(7–11)], −15.07 [d, 4B, B(3–6)].

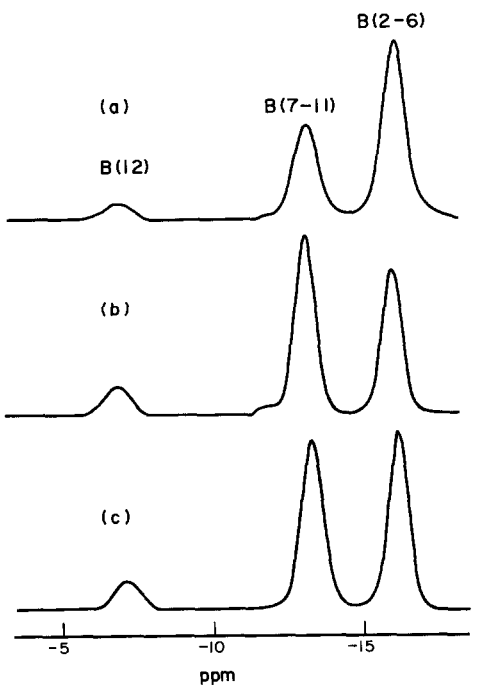

Fig. 3. (a) $^{10}B\{^1H\}$ NMR spectrum of the *closo*-[2-^{10}B-1-$CB_{10}H_{12}$]$^-$ anion; (b) $^{11}B\{^1H\}$ NMR spectrum of *closo*-[2-^{10}B-1-$CB_{10}H_{12}$]$^-$; (c) $^{11}B\{^1H\}$ NMR spectrum of the *closo*-[1-$CB_{11}H_{12}$]$^-$ anion with natural isotopic abundance.

nido-8-$PhCH_2$-7-Me_3N-7-$CB_{10}H_{11}$. A solution of *nido*-6-$PhCH_2B_{10}H_{13}$ (3.2 g; 0.015 mol) in hexane (30 cm^3) was added to a solution of sodium cyanide (2.2 g; 0.045 mol) in water (30 cm^3) and the mixture was stirred for 2 h. The aqueous layer was separated, cooled to 0°C and acidified with dilute (1 : 5) hydrochloric acid (30 cm^3). The deposited white solid was washed with water and vacuum-dried to afford 3.0 g (83%) of 8-$PhCH_2$-7-H_3N-7-$CB_{10}H_{11}$; R_F 0.5; m.p. > 280°C; ^{1}H NMR: δ 7.12 [m, 5H, Ph], 5.43 [s, 3H, H_3N], 2.45 [m, 2H, CH_2], −3.25 [br.s, 2H, μH]; ^{11}B NMR: δ_B −1.18 [d+s, 1+1B, B(5/8)], −8.48 [d, 1B, 147, B(3)], −10.68 [d, 1+1B, 132, B(2/11)], −21.46 [d, 1B, 168, B(9)], −23.02 [d, 1B, 169, B(10)], −26.04 [d, 1B, 149, B(1)], −31.01 [d, 1B, 147, B(4)], −33.86 [d, 1B, 148, B(6)]. The product was dissolved in 5% potassium hydroxide (40 cm^3) and dimethyl sulphate (8.5 cm^3; 0.09 mol) was added dropwise under stirring for 1 h. The precipitate was isolated by filtration, washed with water (100 cm^3) and vacuum-dried to obtain 3.2 g (75% based on 6-$PhCH_2B_{10}H_{13}$ consumed) of 8-$PhCH_2$-7-Me_3N-7-$CB_{10}H_{11}$; R_F 0.71; m.p. 266–268°C; *m/z* 283; ^{1}H NMR: δ 7.15 [m, 5H, Ph], 3.38 [s, 9H, Me_3N], 2.50 [q, 2H, CH_2], −3.35 [br.s, 2H, μH]; ^{11}B NMR: δ_B 0.62 [d, 1B, 140, B(5)], −3.18 [s, 1B, B(8)], −8.20 [d, 1B, 163, B(3)], −11.16 [d, 1B, 165, B(2)], −13.75 [d, 1B, 153, B(11)], −19.76 [d, 1B, 146, B(9)], −24.12 [d, 1B, 138, B(10)], −26.52 [d, 1B, 144, B(1)], −30.90 [d, 1B, 149, B(4)], −33.83 [d, 1B, 152, B(6)]; connectivities from 2-D ^{11}B–^{11}B NMR: B(5) [B(9)^m, B(10)^s, B(1)^s, B(4)^m, B(6)^s], B(8) [B(3)^o, B(4)^s, B(9)^m], B(3) [B(8)^o, B(2)^s, B(1)^m, B(4)^m], B(2) [B(3)^s, B(11)^m, B(1)^s, B(6)^o], B(11) [B(2)^m, B(6)^s, B(10)^s], B(9) [B(5)^m, B(10)^s, B(4)^m], B(10) [B(5)^s, B(9)^s, B(6)^s, B(11)^s], B(1) [B(5)^s, B(3)^m, B(2)^m, B(4)^m, B(6)^s], B(4) [B(5)^m, B(8)^s, B(3)^m, B(9)^m, B(1)^s], B(6) [B(5)^s, B(2)^o, B(11)^s, B(1)^s].

closo-[1-Me_2N-7-$PhCH_2$-1-$CB_{11}H_{10}$]$^-$$NMe_4^+$. A mixture of *nido*-7-$Me_3N$-8-$PhCH_2$-7-$CB_{10}H_{11}$ (3.0 g; 0.011 mol) and Et_3NBH_3 (5 cm^3; 0.04 mol) was heated at 220°C for 5 h under distillation until the trimethylamine evolved. After being cooled to room temperature, the mixture was treated with a mixture of methanol (10 cm^3) and dilute (1 : 5) hydrochloric acid (30 cm^3) and refluxed for 3 h. The resulting mixture was alkalised with solid sodium hydroxide under cooling, filtered, and the filtrate was extracted with two portions of ether (30 cm^3). The ether was removed from the organic layer by evaporation and the residual aqueous solution was precipitated with 1 M NMe_4Cl (20 cm^3). The white precipitate was filtered, washed with water (20 cm^3) and recrystallized from methanol to give 2.9 g (78%) of *closo*-[1-Me_2N-7-$PhCH_2$-1-

$CB_{11}H_{10}]^-NMe_4^+$; R_F 0.40; ^{1}H NMR: δ 7.03 [m, 5H, Ph], 3.43 [s, 12H, NMe_4^+], 3.06 [s, 6H, NMe_2], 2.25 [m, 2H, CH_2]; ^{11}B NMR: δ_B −4.78 [s, 1B, B(7)], −10.56 [d, 1B, 131, B(12)], −14.16 [d, 2+2B, 148, B(2,3/8,11)], −15.29 [d, 2+2B, B(4,6/9,10)], −17.94 [d, 1B, 164, B(5)]; connectivities from 2-D ^{11}B–^{11}B NMR: B(7) [B(12)^m, B(2,3/8, 11)^s], B(12) [B(7)^m, B(2,3/8,11)^s, B(4,6/9,10)^s], B(2,3/8,11) [B(7)^s, B(12)^s, B(4,6/9,10)^s], B(4,6/9,10) [B(12)^s, B(2,3/8,11)^s, B(5)^m], B(5) [B(4,6/9,10)^m]. The product (1.2 g; 2.85 mmol) was shaken with ether (10 cm^3) and dilute (1:3) hydrochloric acid (20 cm^3) until the solid had disappeared. The ether was removed from the organic layer by evaporation and the solid was dissolved in 5% potassium hydroxide (30 cm^3). The mixture was methylated with dimethyl sulphate (0.7 cm^3: 7.4 mmol) under stirring for 1 h and the excess dimethyl sulphate was removed by treatment with concentrated ammonia (5 cm^3) for 15 min. The white precipitate was isolated by filtration, vacuum-dried and recrystallized from benzene to afford 0.8 g (96%) of *closo*-1-Me_3 N-7-$PhCH_2$-1-$CB_{11}H_{10}$; R_F 0.65; m.p. 165–167°C; *m/z* 293; ^{1}H NMR: δ 7.05 [M, 5H, Ph], 3.37 [s, 9H, Me_3N], 2.19 [m, 2H, CH_2]; ^{11}B NMR: δ_B −2.82 [s, 1B, B(7)], −6.33 [d, 1B, 141, B(12)], −12.86 [d, 2+2B, 150, B(4,6/9,10)], −14.15 [d, 2B, 149, B(8,11)], −15.47 [d, 2B, 167, B(2,3)], −18.56 [d, 1B, 154, B(5)].

RESULTS AND DISCUSSION

Previously reported results[1] suggested the following order of reactivity towards electrophilic substitution on individual cage atoms of the *closo*-[1-$CB_{11}H_{12}]^-$ anion (Fig. 1): B(12) > B(7–11) > B(2–6) > C(1). The observed course of the acid-catalyzed deuteration of the latter anion in the DCl/D_2O system, monitored by the ^{11}B NMR spectrum (Fig. 2), is in agreement with this presumption. The H–D exchange occurs primarily at the B(12) position with subsequent exchange at the B(7–11) equatorial belt to give the B(7–12) hexadeuterated compound as a final product. The reaction is in agreement with the results of the electrophilic deuteration of *closo*-1,2-$C_2B_{10}H_{12}$ occurring on boron atoms nonadjacent to carbon.[11]

A different result was obtained, however, in an attempt to introduce amine functionality directly onto the *closo*-[1-$CB_{11}H_{12}]^-$ cluster in its reaction with excess hydroxylamine-*O*-sulphonic acid in weakly acidic solution. The reaction affords *closo*-7-H_3N-1-$CB_{11}H_{11}$ contaminated with a small amount of the 12-H_3N-1-$CB_{11}H_{11}$ isomer. On the other hand, the observed, even though a little surprising enhanced reactivity at B(7), which is indicative of a different substitution mechanism, is comparable to the reported[12,13] less favoured equatorial substitution of the *closo*-$[B_{10}H_{10}]^{-2}$ anion by the H_3N group under similar conditions. The compound 7-H_3N-1-$CB_{11}H_{11}$ can be smoothly methylated in alkaline medium to give its N-trimethyl derivative, *closo*-7-Me_3N-1-$CB_{11}H_{11}$.

All of the three possible B-substituted Me_3N-derivatives of the general formula *closo*-Me_3N-1-$CB_{11}H_{11}$ were isolated as side products of the thermal decomposition of the $[BH_2(NMe_3)_2]^+[7\text{-}CB_{10}H_{13}]^-$ salt at 270°C to produce the parent *closo*-$[1\text{-}CB_{11}H_{12}]^-$ as the main product. The relative ratio of the 2-, 7- and 12-Me_3N-1-$CB_{11}H_{11}$ derivatives isolated is *ca.* 3:1:10, respectively. The described reaction represents another interesting way of boron insertion into open borane clusters, however, the found type of insertion is inconsistent with the expected regioselective entry of the B-NMe_3 fragment into the open pentagonal face of the *nido*-$[7\text{-}CB_{10}H_{13}]^-$ anion (Fig. 1); this process should produce exclusively *closo*-2-Me_3N-1-$CB_{11}H_{11}$. Since 1-Me_3N-1-$CB_{11}H_{11}$ and 7-Me_3N-1-$CB_{11}H_{11}$ do not undergo thermal rearrangement at 320°C for 10 h, the thermal migration of the exohedral substituent seemingly does not account for the observed course of the reaction.

Nevertheless, this result prompted us to examine boron insertion reactions in more detail. In comparison with the preceding reaction, the results of ^{10}B-insertion reactions of $Et_3N^{10}BH_3$ with both *nido*-$[7\text{-}CB_{10}H_{13}]^-$ and *nido*-7-Me_3N-7-$CB_{10}H_{12}$[14,15] at 200°C are in good agreement with the respective formation of $[1\text{-}CB_{11}H_{12}]^-$ and 1-Me_3N-1-$CB_{11}H_{11}$ (on methylation of the $[1\text{-}Me_2N\text{-}1\text{-}CB_{11}H_{11}]^-$ intermediate), both labelled by ^{10}B exclusively at the B(2) site, as documented via ^{10}B and ^{11}B NMR spectra (Fig. 3). The spectra indicate clearly the desired ^{10}B-enrichment on the B(2–6) equatorial belt, which is in agreement with a clean ^{10}B insertion into the open pentagonal face of the eleven-vertex nido-system.

The Et_3NBH_3 insertion approach has also been employed in a similar reaction conducted on *nido*-7-Me_3N-8-$PhCH_2$-1-$CB_{10}H_{11}$. Unlike the preceding case, only the *closo*-1-Me_3N-7-$PhCH_2$-1-$CB_{11}H_{10}$ derivative has been obtained instead of the 2-$PhCH_2$-isomer expected on applying the insertion scheme outlined above. The result is compatible with a regioselective cage rearrangement which manifests the steric effect of the two bulky Me_3N and $PhCN_2$-exohedral substituents at vicinal positions.

The constitution of all isolated compounds of both *nido*-7-L-7-$CB_{10}H_{12}$ and *closo*-$[1\text{-}CB_{11}H_{12}]^-$ series was established unambiguously from ^{1}H and

^{11}B NMR spectra. From the known cage geometries, the 2-D ^{11}B–^{11}B NMR spectra were interpreted and the resonances in the 1-D spectra assigned to specific boron nuclei. In the relevant connectivity schemes (see Experimental), most adjacent borons gave rise to the cross peaks observed in the 2-D spectra, even though the results are complicated due to the overlap of closely spaced resonances in a few cases.

Acknowledgement—The authors wish to thank Dr Z. Weidenhoffer for the mass spectral measurements.

REFERENCES

1. T. Jelínek, J. Plešek, S. Heřmánek and B. Štibr, *Collect. Czech. Chem. Commun.* 1986, **51**, 819.
2. W. H. Knoth, *Inorg. Chem.* 1971, **10**, 598.
3. J. Plešek, T. Jelínek, E. Drdáková, S. Heřmánek and B. Štibr, *Collect. Czech. Chem. Commun.* 1984, **49**, 1559.
4. S. Heřmánek, J. Fusek, B. Štibr, J. Plešek and T. Jelínek, *Polyhedron* 1986, **5**, 1303.
5. W. H. Knoth and E. L. Muetterties, *J. Inorg. Nucl. Chem.* 1961, **20**, 66.
6. W. H. Knoth, J. L. Little, J. R. Lawrence, F. R. Scholer and L. J. Todd, *Inorg. Synth.* 1968, **11**, 33.
7. T. Jelínek, J. Plešek, S. Heřmámek and B. Štibr, *Collect. Czech. Chem. Commun.* 1986, **50**, 1376.
8. R. J. Palchak, J. H. Norman and R. E. Williams, *J. Am. Chem. Soc.* 1961, **83**, 3380.
9. J. Plešek, T. Jelínek, S. Heřmánek and B. Štibr (unpublished results).
10. J. Plešek, B. Štibr, E. Drdáková and T. Jelínek, *Czech. Pat.* 1986, 242,064.
11. B. Štibr, S. Heřmánek, Z. Janoušek, J. Dolanský, Z. Plzák and J. Plešek, *Polyhedron* 1982, **1**, 822.
12. W. R. Hertler and M. S. Raasch, *J. Am. Chem. Soc.* 1964, **86**, 3661.
13. W. H. Knoth, J. C. Sauer, D. C. England, W. R. Hertler and E. L. Meutterties, *J. Am. Chem. Soc.* 1964, **86**, 3973.
14. D. E. Hyatt, R. F. Scholer, L. J. Todd and J. L. Warner, *Inorg. Chem.* 1967, **6**, 2229.
15. W. H. Knoth, *J. Am. Chem. Soc.* 1967, **89**, 1274.

Polyhedron Vol. 6, No. 11, pp. 1987–1991, 1987
Printed in Great Britain

0277–5387/87 $3.00+.00

SYNTHESIS AND MOLECULAR AND CRYSTAL STRUCTURE OF THE OCTANUCLEAR PALLADIUM CLUSTER $Pd_8(\mu_3\text{-}CO)_2(\mu_2\text{-}CO)_6(PMe_3)_7$

MANFRED BOCHMANN* and IAN HAWKINS

School of Chemical Sciences, University of East Anglia, Norwich NR4 7TJ, U.K.

and

MICHAEL B. HURSTHOUSE* and RICHARD L. SHORT

Department of Chemistry, Queen Mary College, London E1 4NS, U.K.

(*Received* 27 *April* 1987; *accepted* 27 *May* 1987)

Abstract—Treatment of *bis*(dibenzylideneacetone)palladium with trimethylphosphine under a carbon monoxide atmosphere gives the title complex in good yield. X-ray crystallography has shown the structure of the complex to consist of an octahedron of palladium atoms which is bicapped by two further palladium atoms in an asymmetric fashion. Seven of the eight palladium centres carry terminal trimethylphosphine ligands. Two face-bridging and six edge-bridging CO molecules complete the ligand shell.

Clusters of zerovalent palladium carrying carbonyl and phosphine ligands, $Pd_n(CO)_x(PR_3)_y$, are known for nuclearities n ranging from 3–23.[1] Although all are synthesised under very similar and mild conditions, the process of cluster formation appears to be highly sensitive to the palladium source and the reaction medium. For example, the carbonylation of $Pd(NO_2)_2(PPh_2Me)_2$ in dichloromethane gives $Pd_4(CO)_5(PPh_2Me)_4$,[2] and $Pd(\eta^1,\eta^3\text{-}C_8H_{12})(PMe_3)$ generates $Pd_7(CO)_7(PMe_3)_7$,[3] while $Pd(OAc)_2$ in H_2O/Ac_2O or dioxane results in the synthesis of $Pd_{12}(CO)_{17-x}(PR_3)_{5+x}$ ($x = 0, 2$)[4] and of $Pd_{10}(CO)_{12}(PBu^n_3)_6$,[5] respectively. We report here the high-yield preparation and the crystal and molecular structure of a new member of this family, $Pd_8(CO)_8(PMe_3)_7$ (**1**).

EXPERIMENTAL

Preparation of $Pd_8(CO)_8(PMe_3)_7$

To a solution of 1.75 g (3.04 mmol) *bis*(dibenzylideneacetone)palladium[11] in 40 cm^3 dry dichloromethane under nitrogen was added 0.31 cm^3 (3.0 mmol) trimethylphosphine at room temperature. CO was bubbled through this solution for 1 min and the colour of the mixture changed from yellow–brown to maroon. Stirring was continued for 1 h under 1 bar CO. After removal of volatiles the residue was washed with 4×10 cm^3 diethylether, leaving a dark-red powder which was recrystallized from dichloromethane–diethylether to give 400 mg of **1** (0.24 mmol, 65%). Shiny deep red-to-black plates suitable for X-ray diffraction were obtained by the slow evaporation of a dichloromethane solution of **1** through a rubber septum.

X-ray crystallography

The crystal used for X-ray work was mounted under nitrogen in a thin-walled glass capillary. The orientation matrix and associated cell dimensions and intensity data were obtained at 291 K following previously described procedures,[12] using an Enraf–Nonius CAD4 diffractometer operating in the ω–2θ scan mode and graphite monochromatised Mo-K_α radiation [λ(Mo-K_α) = 0.71069 Å]. The structure was solved by direct methods (SHELXS86),[13] developed via difference synthesis and refined via

* Authors to whom correspondence should be addressed.

full matrix least squares, with scattering factor data taken from reference 14. During the refinement process it became clear that some of the PMe_3 groups were orientationally disordered and it was possible to refine the carbon atoms in the isotropic mode only. Pd and P atoms were treated anisotropically. Crystallographic data were as follows: $Pd_8(CO)_8(PMe_3)_7$, $M_r = 1607.83$, orthorhombic, $a = 11.106(4)$, $b = 11.248(2)$, $c = 42.302(4)$ Å, $V = 5284.1$ Å^3, space group $P2_12_12_1$, $Z = 4$, $d_c = 2.02$ g cm^{-3}, $\mu = 26.5$ cm^{-1}. 5258 intensities measured, 5221 unique and 4080 observed [$F_o > 3\sigma(F_o)$]. The final R, R_w values were 0.055 and 0.064 respectively, with weights $\omega = 1/[\sigma^2(F_o) + 0.0003F_o^2]$. Final atomic parameters, full lists of bond lengths and angles and F_o/F_c values have been deposited as supplementary material with the Editor, from whom copies are available on request. Atomic coordinates have also been deposited with the Cambridge Crystallographic Data Centre.

RESULTS AND DISCUSSION

Treatment of a solution of *bis*(dibenzylideneacetone)palladium in dichloromethane with one equivalent of trimethylphosphine under a CO atmosphere at room temperature gives black–purple crystals of the title complex (**1**) in 60–70% yield. The infrared spectrum of solid **1** (Nujol mull) indicates the presence of bridging and the absence of terminal CO ligands (ν_{CO} 1763 (m), 1775 (m), 1803 (sh), 1810 (s), 1843 (m), 1878 (s) cm^{-1}); a simpler spectrum is observed in dichloromethane solution (ν_{CO} 1817 (s), 1877 (m) cm^{-1}). The presence of PMe_3 ligands is indicated by bands at 1281 (m) and 955 (vs) cm^{-1}.

The structure of (**1**) was elucidated by X-ray diffraction. Six of the eight palladium atoms are arranged to form a regular octahedron. The two remaining Pd atoms cap two opposite triangular faces of the octahedron and interact with the same octahedral vertex Pd atom [Pd(1)] which, as a consequence, is the only metal centre of the cluster not to carry a terminal PMe_3 ligand. Two of the eight carbonyl ligands bridge the two octahedral faces adjacent to those capped by palladium; the others are edge-bridging. The structure and atomic numbering scheme are given in Fig. 1; selected bond lengths and angles are collected in Tables 1 and 2.

The octahedral core of the cluster is subject to only minor distortions due to a shortening of CO bridged edges (on average 2.78 vs 2.85 Å). The shortest Pd—Pd distances are found between the singular octahedral atom Pd(1) and the two capping atoms Pd(7) and Pd(8). The capping is highly asymmetric; one Pd—Pd interaction between each cap and the core is significantly weaker than the other

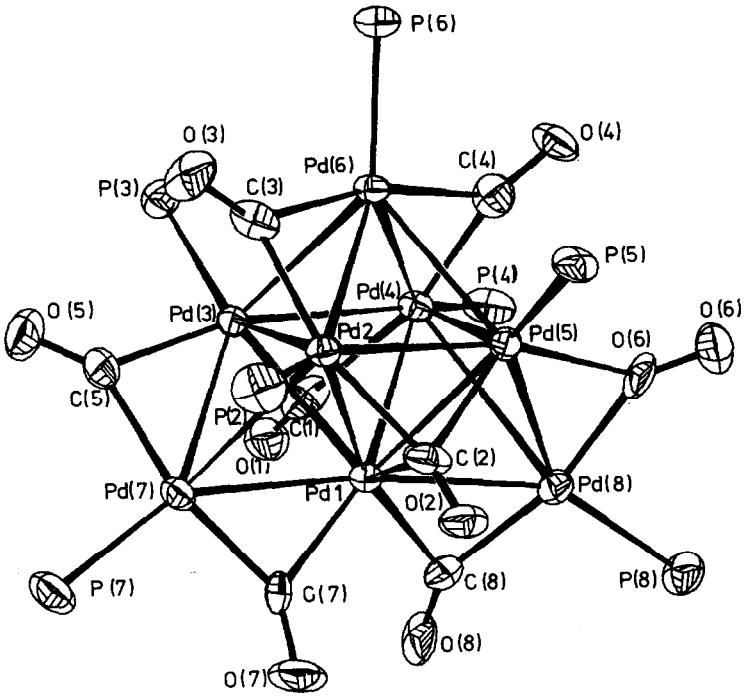

Fig. 1. The molecule structure of **1**, showing the atomic numbering scheme. Ellipsoids correspond to 50% probability.

Table 1. Selected bond lengths of **1** (Å)

Pd(1)—Pd(2)	2.859(5)	Pd(1)—C(1)	2.420(25)
Pd(1)—Pd(3)	2.824(5)	Pd(3)—C(1)	2.198(25)
Pd(1)—Pd(7)	2.703(5)	Pd(4)—C(1)	2.036(24)
Pd(2)—Pd(3)	2.872(5)	Pd(2)—C(3)	2.061(24)
Pd(2)—Pd(5)	2.754(5)	Pd(6)—C(3)	2.043(23)
Pd(2)—Pd(6)	2.780(5)	Pd(3)—C(5)	2.050(25)
Pd(2)—Pd(7)	3.138(5)	Pd(7)—C(5)	2.060(25)
Pd(3)—Pd(6)	2.838(5)	Pd(1)—C(7)	2.092(23)
Pd(3)—Pd(7)	2.730(5)	Pd(7)—C(7)	1.927(24)
Pd(2)—P(2)	2.309(10)	Pd(3)—C(3)	2.634(25)
Pd(3)—P(3)	2.321(8)	Pd(5)—C(4)	2.670(23)
Pd(6)—P(6)	2.307(9)	C(1)—O(1)	1.188(27)
Pd(7)—P(7)	2.289(10)	C(3)—O(3)	1.191(28)

two, with an average Pd—Pd bond length of 3.18 Å between the capping atoms and two mutually opposite octahedral vertices.

This asymmetry of bonding of the capping palladium units is reflected in the Pd—C distances of the triply bridging CO ligands. Three sets of significantly different Pd—C bond lengths are observed, from the shortest (2.04 Å) between C(1,2) and the Pd atoms least involved in bonding to a capping metal [Pd(2,4)], to the longest towards Pd(1) (> 2.3 Å). Two of the six edge-bridging CO ligands, C(3) and C(4), also show a strong tendency towards a face-bridging position and are inclined towards Pd(3) and Pd(5), i.e. the Pd(2)—C(3)—Pd(6) plane deviates by 47.9° from the Pd(2)—Pd(4)—Pd(6) plane (48.1° for the Pd(4)—C(4)—Pd(6) plane), while angles of 0° would have been expected for truly edge-bridging

Table 2. Selected bond angles of **1** (deg.)

Pd(3)—Pd(1)—Pd(2)	60.7(2)	P(6)—Pd(6)—Pd(2)	135.6(2)
Pd(4)—Pd(1)—Pd(3)	58.5(2)	P(6)—Pd(6)—Pd(3)	135.0(2)
Pd(5)—Pd(1)—Pd(2)	57.7(2)		
Pd(5)—Pd(1)—Pd(3)	89.9(2)	Pd(1)—C(1)—Pd(3)	75.2(8)
Pd(5)—Pd(2)—Pd(1)	61.0(2)	Pd(4)—C(1)—Pd(1)	79.2(8)
Pd(6)—Pd(2)—Pd(1)	90.8(2)	Pd(4)—C(1)—Pd(3)	81.8(9)
Pd(6)—Pd(2)—Pd(5)	61.6(2)		
Pd(7)—Pd(1)—Pd(2)	68.6(2)	Pd(2)—C(3)—Pd(6)	85.3(9)
Pd(7)—Pd(1)—Pd(3)	59.1(2)	Pd(3)—C(5)—Pd(7)	83.2(9)
Pd(7)—Pd(1)—Pd(4)	117.1(2)	Pd(1)—C(7)—Pd(7)	84.4(10)
Pd(7)—Pd(1)—Pd(5)	126.2(2)	C(5)—Pd(7)—C(7)	158.9(9)
Pd(7)—Pd(1)—Pd(8)	171.9(1)	C(3)—Pd(6)—C(4)	165.1(8)
Pd(7)—Pd(2)—Pd(3)	53.8(2)	C(1)—Pd(1)—C(2)	147.0(8)
Pd(7)—Pd(2)—Pd(6)	114.0(2)	C(1)—Pd(1)—C(7)	113.7(10)
Pd(7)—Pd(2)—Pd(1)	53.3(2)		
Pd(7)—Pd(3)—Pd(1)	58.2(2)		
Pd(7)—Pd(3)—Pd(2)	68.1(2)		
Pd(7)—Pd(3)—Pd(4)	119.1(2)		
Pd(7)—Pd(3)—Pd(6)	126.2(2)		
P(2)—Pd(2)—Pd(1)	129.5(3)		
P(2)—Pd(2)—Pd(6)	139.4(2)		
P(2)—Pd(2)—Pd(7)	91.4(3)		
P(3)—Pd(3)—Pd(1)	152.7(2)		
P(3)—Pd(3)—Pd(2)	140.5(2)		
P(3)—Pd(3)—Pd(6)	91.3(3)		
P(3)—Pd(3)—Pd(7)	137.1(2)		

ligands. However, the Pd(3)—C(3) and Pd(5)—C(4) distances of 2.63 and 2.67 Å are too long to be interpreted as bonding interactions.

For steric reasons, the trimethylphosphine ligands coordinated to Pd(3) and Pd(5) are bent out of the octahedral "equatorial" plane towards Pd(6) by 37.7 and 37.2°, respectively, while P(2) and P(4) are slightly inclined towards Pd(1) below this plane by 3.7 and 8.4°, respectively.

The cluster possesses 110 cluster valence electrons (CVE) and its geometry is in agreement with this electron count.[6,7] Examples for octanuclear 110 CVE clusters are very limited; the dianion $[Os_8(CO)_{22}]^{2-}$ (**2**),[8] the mixed-metal cluster $Os_6Pt_2(CO)_{17}(C_8H_{12})_2$ (**3**)[9] and the carbide cluster $[Re_8C(CO)_{24}]^{2-}$[10] have been structurally characterized. A comparison of the structure of **1** with that of the isoelectronic Os cluster $[Os_8(CO)_{22}]^{2-}$ (**2**)[8] reveals significant differences in the distribution of metal–metal bond lengths (Fig. 2). While both in **1** and **2** the shortest interactions are those between the basal octahedron vertex and the two capping atoms, in **2** each of these caps forms a nearly regular tetrahedron with its three neighbours in the octahedral core and the longest Os—Os distances are found not between capping and core atoms but for the non-CO bridged vertices between the apical and two equatorial Os atoms of the octahedral core. Asymmetric capping as observed in **1** is a feature typical of d^{10} metal centres and is found to varying degrees in the mixed-metal Os_6Pt_2 cluster **3**[9a] (Fig. 2) as well as in $Pd_7(CO)_7(PMe_3)_7^3$ and $Pd_{10}(CO)_{12}(PBu^n_3)_6^5$* (Fig. 3). It has been argued[3,6]

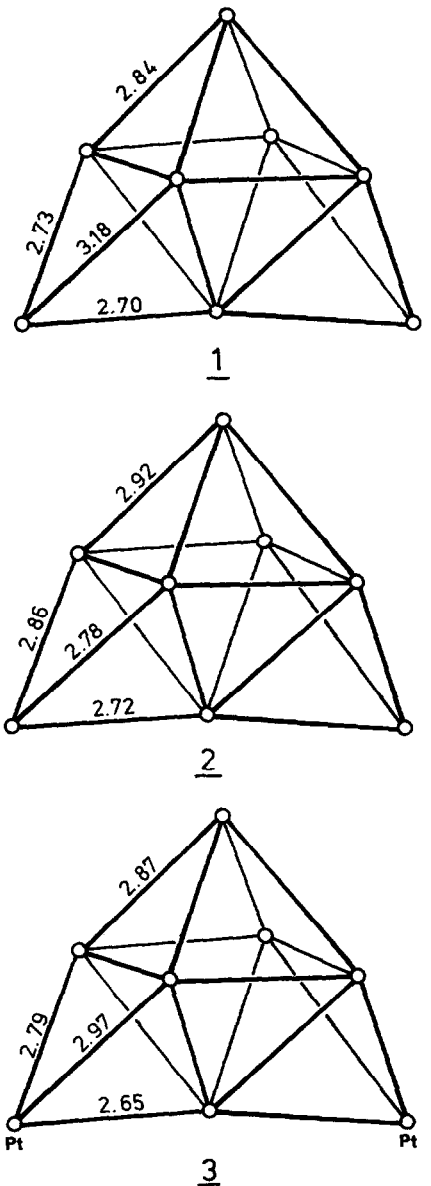

Fig. 2. Comparison of the structures of the octanuclear 110 CVE clusters $Pd_8(CO)_8(PMe_3)_7$ (**1**), $[Os_8(CO)_{22}]^{2-}$ (**2**) and $Os_6Pt_2(CO)_{17}(C_8H_{12})_2$ (**3**) (bond lengths in Å).

* By contrast, asymmetric-face capping Pd units are absent from $Pd_{23}(CO)_{22}(PEt_3)_{10}$, which consists of a four-fold edge bridged Pd_{19} octahedron in a cubic close packed arrangement.[1] The Pd_8 geometry of (**1**) may be regarded as part of a Pd_{19} structure.

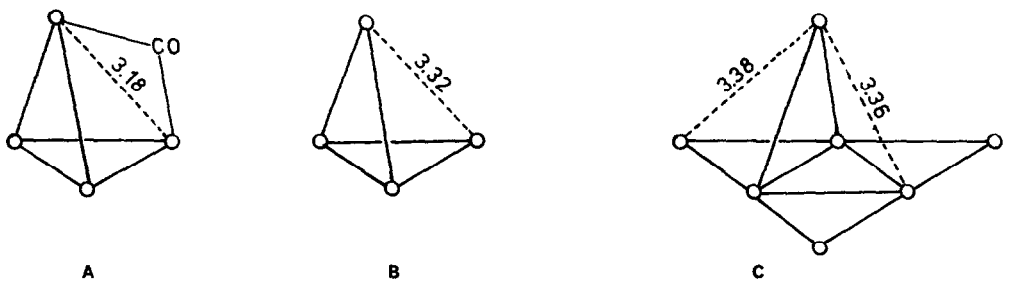

Fig. 3. Partial structures of $Pd_7(CO)_7(PMe_3)_7$[3] (**A**), $Pd_{10}(CO)_{12}(PBu^n_3)_6$[5] (**B**), and $Pd_{23}(CO)_{22}(PEt_3)_{10}$[1] (**C**), illustrating two types of asymmetric face capping (**A**,**B**) and the only example of symmetrical edge bridging (**C**) palladium.

that the reason for metal–metal bond lengthening as observed in **1** lies in the energetic separation between the metal *p* orbitals from the *s* and *d* levels which increases as one moves across the transition series towards heavier elements. A high energy (relative to *d* levels) would make the *p* orbitals less available for bonding, resulting in a deficiency of metal–metal bonding MO's in the cluster and an occupation of low-lying antibonding MO's and consequently a distortion of the cluster geometry.

Acknowledgements—We thank the University of East Anglia for support (to I.H.) and the SERC for the provision of X-ray facilities.

REFERENCES

1. E. G. Mednikov, N. K. Eremenko, Y. L. Slovokhotov and Y. T. Struchkov, *J. Organomet. Chem.* 1986, **301**, C35.
2. J. Dubrawski, J. C. Kriege-Simondsen and R. D. Feltham, *J. Am. Chem. Soc.* 1980, **102**, 2089.
3. R. Goddard, P. W. Jolly, C. Krüger, K. P. Schick and G. Wilke, *Organometallics* 1982, **1**, 1709.
4. E. G. Mednikov, N. K. Eremenko and S. P. Gubin, *J. Organomet. Chem.* 1980, **202**, C102.
5. E. G. Mednikov, N. K. Eremenko, V. A. Mikhailov, S. P. Gubin, Y. L. Slovokhotov and Y. T. Struchkov, *J. Chem. Soc., Chem. Comm.* 1981, 989.
6. J. W. Lauher, *J. Am. Chem. Soc.* 1978, **100**, 5305.
7. D. M. P. Mingos, *Acc. Chem. Res.* 1984, **17**, 311; B. K. Teo, *Inorg. Chem.* 1984, **23**, 1251.
8. P. F. Jackson, B. F. G. Johnson, J. Lewis and P. R. Raithby, *J. Chem. Soc., Chem. Comm.* 1980, 60.
9. (a) C. Couture, D. H. Farrar and R. J. Goudsmit, *Inorg. Chim. Acta* 1984, **89**, L29; (b) C. Couture and D. H. Farrar, *J. Chem. Soc., Dalton Trans.* 1986, 1395.
10. G. Ciani, G. D'Alfonso, M. Freni, P. Romiti and A. Sironi, *J. Chem. Soc., Chem. Comm.* 1982, 705.
11. Y. Takahashi, T. Ito, S. Sakai and Y. Ishii, *J. Chem. Soc., Chem. Comm.* 1970, 1065. (Dibenzylideneacetone = 1,5-diphenyl-1,4-pentadien-3-one.)
12. M. B. Hursthouse, R. A. Jones, K. M. A. Malik and G. Wilkinson, *J. Am. Chem. Soc.* 1979, **101**, 4128.
13. G. M. Sheldrick, SHELXS 86, University of Göttingen, F.R.G. (1986).
14. *International Tables for X-ray Crystallography*, Vol. 4. Kynoch Press, Birmingham (1974).

Polyhedron Vol. 6, No. 11, pp. 1993–1997, 1987
Printed in Great Britain

0277–5387/87 $3.00+.00

SPECTROPHOTOMETRIC STUDY OF THE COMPLEXATION EQUILIBRIA OF COBALT(II) WITH 4-(5′-METHYL-3′-ISOXAZOLYLAZO)-RESORCINOL AND DETERMINATION OF COBALT(II)

Z. SOSA, J. P. PÉREZ TRUJILLO, J. J. ARIAS and F. GARCÍA MONTELONGO*

Department of Analytical Chemistry, University of La Laguna, 38204-La Laguna, Spain

(*Received* 24 *April* 1987; *accepted* 27 *May* 1987)

Abstract—The reaction of cobalt(II) with 4-(5′-methyl-3′-isoxazolylazo)-resorcinol (MIAR) in 4% v/v ethanol–water medium at $I = 0.1$ M ($NaClO_4$) was investigated spectrophotometrically. Graphical and numerical calculation methods were used to establish the equilibria in solution and to evaluate the stability constant of the complexes formed ($\log\beta_{101} = 7.48 \pm 0.06$, $\log\beta_{111} = 12.77$ max 12.99, $\log\beta_{102} = 16.41 \pm 0.07$). The optimum conditions for the spectrophotometric determination of Co(II) with MIAR were established and the method applied to its determination in some low alloy steels and hydrofining catalysts.

Heteroazo-phenols and -naphthols have been widely used as chromogenic reagents and metallochromic indicators for many metal ions,[1,2] but in general little attention has been paid to study their complexation equilibria in solution.

In a previous paper[3] the acid–base behaviour, Table 1, of 4-(5′-methyl-3′-isoxazolylazo)-resorcinol (MIAR) as well as its complexation equilibria with cadmium(II) were studied.

The present paper deals with the spectrophotometric study of the complexation equilibria of MIAR and Co(II), the species in solution and their stability constants established by graphical and numerical calculation methods, and a method is developed for the spectrophotometric determination of cobalt, which is applicable to its determination in some low alloy steels and hydrofining catalysts.

EXPERIMENTAL

4-(5′-methyl-3′-isoxazolylazo)-resorcinol (MIAR) 10^{-3} M solution in absolute ethanol. Standard 10^{-1} M $Co(ClO_4)_2$ solution prepared from cobalt nitrate by perchloric acid treatment and standardized complexometrically.[4] A hexamine/$HClO_4$ buffer solution (pH = 7.5) was used as indicated. The ionic strength, I, of the solution was kept constant at 0.1 m ($NaClO_4$).

Analytical reagent grade chemicals and de-ionized water were used throughout with no further purification.

The pH measurements were carried out with a Radiometer PHM64 digital pH-meter with a glass–calomel combination electrode. Absorption measurements were made on a Hitachi Perkin–Elmer 200 recording spectrophotometer provided with 1 cm matched quartz cells. Measurements were performed at 25 ± 0.1°C. Calculations were carried out on a Digital VAS/VMX 11/780 (V.4) computer.

Table 1. Optical characteristics of MIAR species (4% v/v ethanol–water, $I = 0.1$ M $NaClO_4$)

Species	λ_{max} (nm)	ε (l mol^{-1} cm^{-1})	pKa
H_2R	365	18,351	pKa_3 5.51
HR^-	385	26,171	pKa_4 10.52
R^{2-}	463	29,244	

* Author to whom correspondence should be addressed.

Spectrophotometric determination of cobalt

To the sample, 8.75–30.00 μg of cobalt(II) in a 25 cm^3 measuring flask, 5 ml of 10^{-3} M MIAR, 5 cm^3 of hexamine/$HClO_4$ buffer solution (pH = 7.5), 1 cm^3 of 2.5 M $NaClO_4$ was added and made up to volume with de-ionized water. After 5 min the absorbance was measured at 465 nm against a reagent blank.

Spectrophotometric determination of cobalt in low alloy steels and hydrofining catalysts

1 g amounts of the steel or catalyst were weighed accurately and treated with 30 cm^3 of HCl (1 : 1) and 5 cm^3 of concentrated HNO_3 in the case of the steel, and with 30 cm^3 of HCl (1 : 1) in the case of the catalyst, heated in a water-bath until dissolved and then taken almost to dryness. The residue was redissolved and made up to 100 cm^3 in a calibrated flask with 6 M HCl. Suitable aliquots were analysed as described above, iron being previously removed with di-*iso*-propyl ether.

RESULTS AND DISCUSSION

Solutions containing 4-(5′-methyl-3′-isoxazolylazo)-resorcinol, MIAR and Co(II) show an orange colouration over a wide pH range. The absorption spectra as a pH function of the MIAR–Co solutions where $C_{Co}/C_R = 20/1$, Fig. 1, show at the greatest acid pHs an absorption maximum that corresponds to the free reagent and at pH ⩾ 5 an absorption maximum is defined at 465 nm, indicative of the complex species formed.

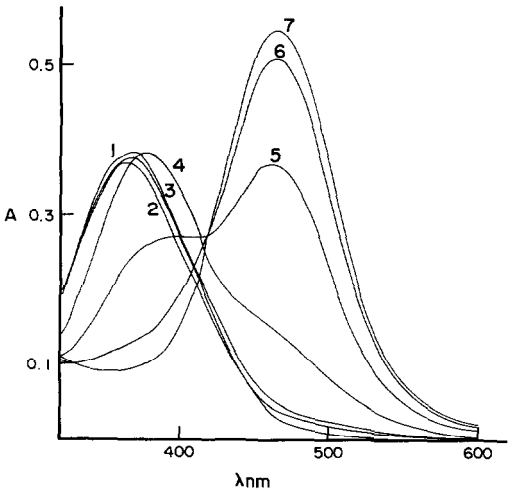

Fig. 1. Absorption spectra of the system Co(II)–MIAR. $C_R = 2.10^{-5}$ M; $C_{Co} = 4.10^{-4}$ M; $I = 0.1$ M ($NaClO_4$); 4% (v/v) ethanol–water; pH = (1) 2.86, (2) 3.96, (3) 4.76, (4) 5.27, (5) 6.25, (6) 6.80, (7) 7.30.

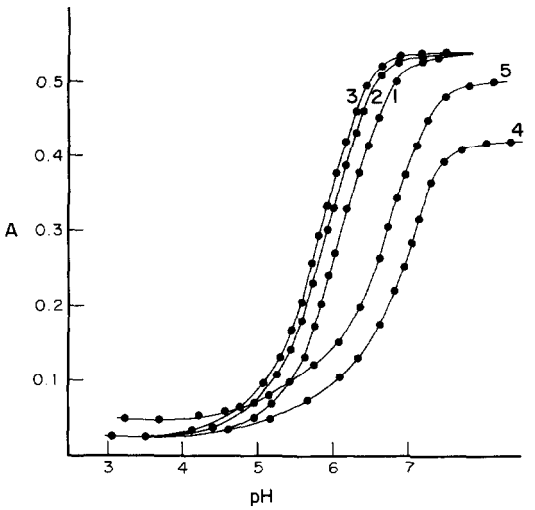

Fig. 2. Absorption–pH curves for the system Co–MIAR. $C_R = 2.10^{-5}$ M, $I = 0.1$ M ($NaClO_4$); 4% (v/v) ethanol–water; 465 nm; C_R/C_{Co} = (1) 1/20, (2) 1/40, (3) 1/60, (4) 1/1, (5) 5/1.

The absorbance–pH curves, at 465 nm, for solutions with different C_{Co}/C_R ratios, Fig 2, show that the complexation begins at pH ≃ 5 and stabilizes at pH ⩾ 6.5.

The stoichiometry, determined at pH = 7.5 and 465 nm by the continuous variations and the molar ratio methods, indicated the formation of a 1 : 2, Co : R species, Fig. 3.

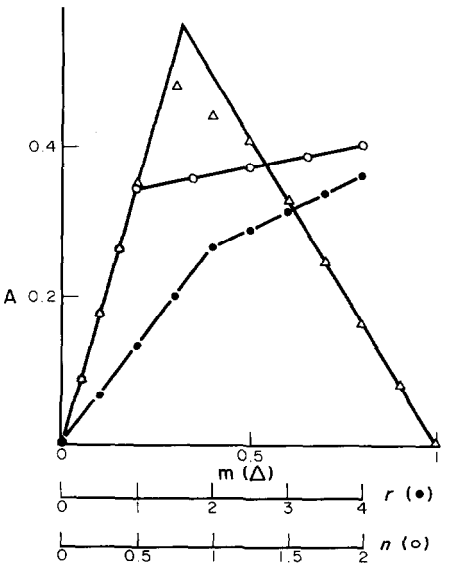

Fig. 3. Stoichiometry of the Co(II)–MIAR system. $I = 0.1$ M ($NaClO_4$); pH = 7.5; 4% (v/v) ethanol–water; 465 nm; (1) $m = C_{Co}/C_R + C_{Co}$; $C_t = 4.10^{-5}$ M, (2) $n = C_{Co}/C_R$; C_R = const. = 2.10^{-5} M, (3) $r = C_R/C_{Co}$; C_{Co} = const. = 10^{-5} M.

Comparison of the absorption spectra in the presence of oxidants or reducers confirmed the presence of cobalt(II) in the complex.

In order to calculate the formation constant of the complex a method of graphical analysis of the A–pH curves derived from that of Sommer *et al.*[5] was used. In accordance with the range of pHs in which complexation took place and the pK_a values of the reagent, it could be admitted that the H_2R and HR^- species of the reagent were those that took part in the complexation reactions, written as follows

$$Co^{2+} + mH_2R \overset{K_{1am}}{\rightleftharpoons} CoH_aR_m + nH^+ \qquad (a = 2m-n) \quad (A)$$

$$Co^{2+} + mHR^- \overset{K_{1bm}}{\rightleftharpoons} CoH_bR_m + pH^+ \qquad (b = m-p) \quad (B)$$

to which the following set of equations can be applied:

$$\log \frac{(AZ - C_R\bar{\varepsilon}_R)(\varepsilon Z - m\bar{\varepsilon}_R)^m}{(C_M\varepsilon Z - C_M m\bar{\varepsilon}_R - AZ + C_R\bar{\varepsilon}_R)(C_R\varepsilon - mA)^m} = \log K + n\,\mathrm{pH} \quad (1)$$

$$\frac{C_R}{A} = \frac{m}{\varepsilon} + \frac{1}{\varepsilon K^{1/m}} \times \left[\frac{(AZ - C_R\bar{\varepsilon}_R)(\varepsilon Z - m\bar{\varepsilon}_R)^m |H^+|^n}{A^m(C_M\varepsilon Z - C_M m\bar{\varepsilon}_R - AZ + C_R\bar{\varepsilon}_R)}\right]^{1/m} \quad (2)$$

where

$$Z = |H^+|/Ka_3 + 1 + Ka_4/|H^+|;$$

$$\bar{\varepsilon}_R = \varepsilon_2 \frac{|H^+|}{Ka_3} + \varepsilon_1 + \varepsilon_0 \frac{Ka_4}{|H^+|}$$

ε_2, ε_1, ε_0 and ε are the molar absorptivities of species H_2R, HR^- and R^{2-} of the reagent and the complex, respectively.

Upon applying the logarithmic equation for $m = 2$, straight lines with a slope of value four were obtained for pH > 6 for the first equilibrium and a value of two for the second equilibrium, indicating that the species formed was CoR_2, while the points of pH > 6 were not in alignment. The fact that not all the points were alligned within a straight line indicated the possible existence of more than one complex species in solution.

Once the values of m, n, and p became known, eqn (2) was applied for pH > 6. The results obtained for equilibrium B are presented in Table 2, where it is observed that the values of K_{102} and ε_{102} for the species CoR_2 are slightly different for solutions with metal excess than in equimolar and excess reagent solutions.

The numerical calculation method was next applied, using the LETAGROP–SPEFO programme.[6] In this treatment, we initially divided the experimental data into two parts: one corresponding to the solutions in excess of metal ion and the other to the equimolar and excess reagent solutions the most suitable model was defined and then applied to the whole of the experimental data.

The data presented in Table 3 indicate that for the ratios in excess of metal ion and in accordance with the values of U and $\sigma(A)$ the fit to a model of a single species is not correct, even with the species CoR_2. The best fit was achieved for a model formed by the species CoHR, CoR and CoR_2, although the constant of the species CoHR was not well defined. The results obtained for the equimolar and excess reagent ratios also indicate that the best fit is obtained with the three-species model deduced in the previous calculations.

Table 2. Values of log K and ε for the system Co-MIAR calculated by graphical methods

Equation	C_R/C_M	Straight line[a]	ε_{102}	$\log K_{102}$
(1)	1/60	$Y = -3.49 + 1.96\,X$		−3.49
	1/40	$Y = -3.74 + 1.99\,X$		−3.74
	1/20	$Y = -3.46 + 1.90\,X$		−3.64
	1/1	$Y = -4.04 + 1.95\,X$		−4.04
	5/1	$Y = -4.73 + 2.02\,X$		−4.73
(2)	1/60	$Y = 3.66\times10^{-5} + 1.40\times10^{-3}\,X$	54,644	−3.78
	1/40	$Y = 3.67\times10^{-5} + 1.52\times10^{-3}\,X$	54,455	−3.84
	1/20	$Y = 3.77\times10^{-5} + 1.78\times10^{-3}\,X$	53,051	−3.92
	1/1	$Y = 4.04\times10^{-5} + 3.69\times10^{-3}\,X$	49,504	−4.52
	5/1	$Y = 4.14\times10^{-5} + 3.89\times10^{-3}\,X$	48,320	−4.55

[a] Correlation coefficients better than 0.997.

Table 3. Values of U, $\alpha(A)$, $\log \beta_{pqr}$ and ε_{pqr} for the different models tested by the LETAGROP-SPEFO method

Species	U	$\sigma(A)$	$\log \beta_{pqr}$	ε_{pqr}
(a) solutions in metal ion excess				
CoH_2R_2	0.393	0.071	—	—
$CoHR_2$	0.188×10^{-1}	0.015	—	—
CoR_2	0.484×10^{-1}	0.025	—	—
CoH_xR_2 CoR_2	0.650×10^{-2}	0.009	—	—
CoR_2 CoOHR	0.661×10^{-2}	0.009	—	—
CoR CoR_2	0.636×10^{-2}	0.009	—	—
CoHR CoR	0.720×10^{-2}	0.009	—	—
CoHR			12.77 max 12.99	44,241 ± 1130
CoR	0.266×10^{-2}	0.006	7.39 ± 0.23	28,812 ± 497
CoR_2			16.73 ± 0.13	54,640 ± 568
(b) equimolar and reagent excess solutions				
CoR_2	0.875×10^{-2}	0.011	—	—
CoR CoR_2	0.320×10^{-2}	0.008	—	—
CoHR			12.77 max 12.99	44,241 ± 1130
CoR	0.246×10^{-2}	0.007	7.39 ± 0.23	28,812 ± 497
CoR_2			16.43 ± 0.08	50,171 ± 268
CoHR CoR CoR_2 CoR_3	0.583×10^{-2}	0.009	—	—
CoHR CoR CoR_2 CoH_xR_2	0.604×10^{-2}	0.010	—	—
(c) all data together				
CoHR			12.77 max 12.99	44,241 ± 1130
CoR	0.252×10^{-2}	0.007	7.48 ± 0.06	30,811 ± 191
CoR_2			16.41 ± 0.07	50,704 ± 313

The values obtained for the formation constants and molar absorptivities of the different complex species that form the most suitable model are given in Table 3.

In accordance with the values obtained for the whole of the experimental data and using the HALTAFALL programme,[7] the distribution diagrams of species for the proposed model at different metal–ligand ratios, were established as clearly seen in Fig. 4 the slight concentration of the CoHR species justifies the fact that its stability constant is not well defined by mathematical calculation.

The results obtained evidence the limitations presented by applying the graphical method to the study of complexation equilibria in which mixtures of complexes in solution co-exist.

Spectrophotometric determination of cobalt with MIAR

The complex CoR_2, the predominant species in excess of reagent, at pH = 7.5 and 465 nm conforms to Beer's law between 0.12 and 1.65 ppm, according to the equation:

$$A = 9.3 \times 10^{-4} + 0.659|Co^{2+}(ppm)| \quad c.c = 0.999$$

Table 4. Spectrophotometric determination of cobalt with MIAR in the presence of foreign ions, $|Co^{2+}|$ taken = 0.235 ppm, pH = 7.5, λ = 465 nm

|interferent|/|$[Co^{2+}]$|	interference
100/1[a]	F^-, Ca^{2+}, Cl^-, Br^-, Ag^+, I^-, Mg^{2+}, Al^{3+}
50/1	SCN^-, $S_2O_3^{2-}$
25/1	Tl^+, $C_2O_4^{2-}$, WO_4^{2-}, MoO_4^{2-}
1/1	Mn^{2+}, Au^{3+}, tartrate, citrate
	Cu^{2+}, Ni^{2+}, Pd^{2+}, UO_2^{2+}, Cd^{2+}, Zn^{2+}
1/1	EDTA, DCTA, NTA
	(high interference)

[a] Maximum amount tested.

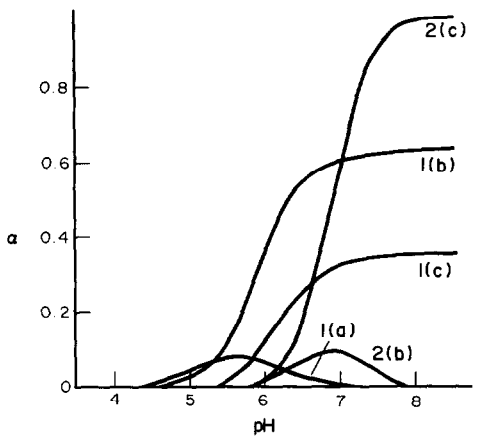

Fig. 4. Distribution diagram of species for Co–MIAR system calculated by HALTAFALL programme, (a) CoHR, (b) CoR, (c) CoR_2; C_{Co}/C_R = (1) 60/1, (2) 1/5.

with 3.89×10^4 as molar absorptivity and 0.23–1.18 ppm as optimum concentration range in accordance with the Ringbom graph with 1.8% as photometric error.

From the statistical study carried out with ten samples each containing 0.235 ppm of cobalt, 0.233 ppm was obtained as the mean value, with a standard deviation of 3.24×10^{-3} and a relative error of 1% (P = 0.05).

The results obtained upon studying the interferences originated by different cations and anions in the determination of cobalt are presented in Table 4.

The method developed was applied to the determination of cobalt in a low alloy steel, Artillería J-5 (4.935% Co), containing Ni and Cu in amounts smaller than those of Co, after previous removal of iron with di-*iso*-propyl ether, and to a hydrofining catalyst, Hydrobon HS-9 (3.23% Co), with recoveries of 4.92% and 3.22%, respectively, as mean values of three determinations.

REFERENCES

1. H. R. Hovind, *Analyst* 1975, **110**, 1196.
2. S. Shibata, *Chelates in Analytical Chemistry*, Vol. 2. Dekker, New York (1972).
3. Z. Sosa, J. P. Pérez Trujillo, J. J. Arias and F. García Montelongo, *Quim. Anal.* (in press).
4. G. Schwarzenbach and H. Flaschka, *Complexometric Titrations*. Methuen, London (1969).
5. L. Sommer and S. P. Mushran, *Coll. Czech. Chem. Commun.* 1969, **34**, 3695.
6. L. G. Sillén and B. Warnqvist, *Arkiv. Kemi.* 1969, **31**, 377.
7. N. Ingri, W. Kakolowicz, L. G. Sillén and B. Warnqvist, *Talanta* 1967, **14**, 1261.

Polyhedron Vol. 6, No. 11, pp. 1999–2002, 1987
Printed in Great Britain

0277–5387/87 $3.00+.00

AMIDE RHODIUM AND IRIDIUM COMPLEXES DERIVED FROM *Z*-*N*-PHENYL,*β*-(AMINO)-4-METHYL-STYRYLDIPHENYLPHOSPHA-1 λ^5-AZENE

MARIA J. FERNANDEZ, JESUS J. DEL VAL and LUIS A. ORO*

Departamento de Química Inorgánica, Instituto de Ciencia de Materiales de Aragón, Universidad de Zaragoza-C.S.I.C., 50009-Zaragoza, Spain

and

FRANCISCO PALACIOS and JOSE BARLUENGA

Departamento de Química Organometálica, Facultad de Química, Universidad de Oviedo, 33071 Oviedo, Spain

(*Received* 28 *April* 1987; *accepted* 27 *May* 1987)

Abstract—Mononuclear amide rhodium and iridium complexes of the formulae M(LH)(COD) and M(LH)(CO)(PPh_3) (M = Rh, Ir; COD = 1,5-cyclooctadiene; LH = deprotonated *Z*-*N*-phenyl, *β*-(amino)-4-methylstyryldiphenylphospha-1 λ^5-azene) are described. The related amine ionic compounds $[M(COD)(LH_2)]ClO_4$, $[Rh(CO)_2(LH_2)]ClO_4$, $[Rh(CO)(PPh_3)(LH_2)]ClO_4$, $[M(COD)(LH_2)][M(Cl)_2(COD)]$ and $[Rh(CO)_2(LH_2)][Rh(Cl)_2(CO)_2]$ have also been obtained.

There has been an increasing interest in the chemistry of amide complexes of rhodium[1–9] and iridium.[4–11] In this context, we have recently reported the preparation of new dinuclear rhodium[3,7] and iridium[7] amide complexes containing the deprotonated diaminenaphthalene group, in which the ligand is bound to the two metals in a bridging and chelating manner, as well as dinuclear rhodium(I) complexes with phenyl(2-pyridyl)amido ligands.[9] Following our studies, we report here the synthesis of new chelated rhodium and iridium complexes derived from primary *Z*-*β*-enaminophospha-λ^5-azene (Fig. 1). This ligand can be easily deprotonated with bases to give amide compounds. Furthermore, the ligand contains a phospha-λ^5-azene group which in coordination chemistry has not received extensive attention.[11]

EXPERIMENTAL

Reactions were carried out under a nitrogen atmosphere using standard Schlenk techniques. $[Ir(\mu\text{-OMe})(COD)]_2$,[12] $[Rh(\mu\text{-OMe})(COD)]_2$,[12] $[Ir(\mu\text{-Cl})(COD)]_2$[13] and $[Rh(\mu\text{-Cl})(COD)]_2$[14] and LH_2[15] were prepared as previously reported. IR spectra were recorded on a Perkin–Elmer 783 spectrophotometer. Elemental analyses were carried out with a Perkin–Elmer 240B microanalyzer. Conductivities were measured at 20°C with *ca.* 4×10^{-4} M acetone solutions using a Philips PW 9509 conductimeter. Molecular weights were measured in *ca.* 10^{-3} M chloroform solutions with a Perkin–Elmer 115 osmometer.

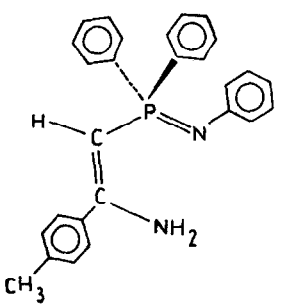

Fig. 1.

* Author to whom correspondence should be addressed.

Preparation of M(LH)(COD) *complexes*

The M(LH)(COD) (M = Rh, Ir) compounds were prepared by reaction of $[M(\mu\text{-OMe})(COD)]_2$ with LH_2 in dichloromethane. In a typical procedure, $[Rh(\mu\text{-OMe})(COD)]_2$ (50 mg, 0.1 mmol) was added to a solution of LH_2 (84 mg, 0.2 mmol) in dichloromethane. The mixture was allowed to react for 30 min, after which the solution was evaporated to dryness to leave a yellow solid. Yield 83 mg (67%).

Preparation of $M(LH)(CO)(PPh_3)$ *complexes*

The $M(LH)(CO)(PPh_3)$ (M = Rh, Ir) complexes were prepared by similar methods. In a typical procedure, carbon monoxide was bubbled through a solution of Rh(LH)(COD) (255 mg, 0.4 mmol) in dichloromethane for 30 min, after which PPh_3 (108 mg, 0.4 mmol) was added. The solution was stirred for 30 min, then concentrated and addition of hexane gave a yellow precipitate, which was filtered off, washed with hexane and air-dried. Yield 262 mg (82%).

Preparation of $[M(COD)(LH_2)]ClO_4$ *complexes*

The $[M(COD)(LH_2)]ClO_4$ complexes were prepared by similar methods. As a typical example, a mixture of $[Rh(\mu\text{-Cl})(COD)]_2$ (40 mg, 0.08 mmol) and $AgClO_4$ (33 mg, 0.16 mmol) in acetone was stirred for 30 min. The AgCl was filtered off and LH_2 (66 mg, 0.16 mmol) was added to the filtrate. After concentration of the solution, the addition of diethyl ether gave a yellow precipitate, which was filtered off, washed with diethyl ether and air-dried. Yield 23 mg (20%).

Preparation of $[Rh(CO)_2(LH_2)]ClO_4$

Carbon monoxide was bubbled through a solution of $[Rh(COD)(LH_2)]ClO_4$ (100 mg, 0.14 mmol) in dichloromethane for 30 min. The yellow solution was concentrated and diethyl ether was added to yield a yellow solid, which was filtered off, washed with diethyl ether and air-dried. Yield 64 mg (69%).

Preparation of $[Rh(CO)(PPh_3)(LH_2)]ClO_4$

PPh_3 (85 mg, 0.32 mmol) was added to a solution of $[Rh(CO)_2(LH_2)]ClO_4$ (213 mg, 0.32 mmol) in dichloromethane. The solution was stirred for 30 min, then concentrated and addition of diethyl ether gave a yellow precipitate which was filtered off, washed with diethyl ether and air-dried. Yield 247 mg (86%).

Preparation of $[M(COD)(LH_2)][M(Cl)_2(COD)]$ *complexes*

The $[M(COD)(LH_2)][M(Cl)_2(COD)]$ complexes were prepared by similar methods. In a typical procedure, $[Rh(\mu\text{-Cl})(COD)]_2$ (60 mg, 0.12 mmol) was added to a solution of LH_2 (50 mg, 0.12 mmol) in dichloromethane and the solution was left to react for 15 min. The solution was concentrated and addition of hexane gave a yellow precipitate which was filtered off, washed with hexane and air-dried. Yield 62 mg (58%).

Preparation of $[Rh(CO)_2(LH_2)][Rh(Cl)_2(CO)_2]$

$[Rh(\mu\text{-Cl})(CO)_2]_2$ (40 mg, 0.1 mmol) was added to a solution of LH_2 (42 mg, 0.1 mmol) in dichloromethane. The solution was left to react for 30 min, after which the solution was concentrated and addition of hexane gave a yellow precipitate which was filtered off, washed with hexane and air-dried. Yield 57 mg (70%).

RESULTS AND DISCUSSION

Reaction of *Z-N*-phenyl, *β*-amino-4-methylstyryldiphenylphospha-1 λ^5-azene (LH_2) with $[M(\mu\text{-OMe})(COD)]_2$ (M = Rh, Ir) leads to the formation of the chelated amide complexes M(LH)(COD), according to the following equation:

$$[M(\mu\text{-OMe})(COD)]_2 + 2LH_2 \rightarrow 2M(LH)(COD) + 2MeOH.$$

As we have previously reported,[7] the methoxy dimers are good starting materials for the preparation of amide complexes via deprotonation of an amine ligand.

Treatment of M(LH)(COD) with carbon monoxide gives the $M(LH)(CO)_2$ complexes as can be deduced by the presence of two metal carbonyl bands of approximately equal intensity in the IR spectra, typical of *cis*-dicarbonylated complexes [$\nu(C{\equiv}O)$: 1990, 2060 cm^{-1} (M = Rh); 1965, 2040 cm^{-1} (M = Ir)]. The $M(LH)(CO)_2$ complexes have not been isolated due to their solubility in aprotic solvents. Reaction of $M(LH)(CO)_2$ with PPh_3 leads to the displacement of one CO ligand and subsequent formation of $M(LH)(CO)(PPh_3)$.

IR spectra (Table 1) show the presence of ν(N—H) bands from the deprotonated ligand and ν(P=N) bands in the region 1102–1110 cm^{-1} corresponding to the phospha-λ^5-azene group, whose frequency drops to around 200 cm^{-1} confirming the coordination of the P=N group as a two electron

Table 1. Analytical and physical data for the neutral compounds

Compound	Analyses [Found(Calc.)] N (%)	C	H	M.W.[a] [Found (Calc.)]	Selected IR bands (cm^{-1})
Rh(LH)(COD)	4.2	68.7	6.5	623	3330,[b] 1105[c]
	(4.5)	(68.0)	(5.8)	(618)	
Ir(LH)(COD)	3.9	58.8	5.3	706	3320,[b] 1102[c]
	(3.9)	(58.4)	(5.1)	(707)	
Rh(LH)(CO)(PPh_3)	3.2	68.1	4.8	785	3358,[b] 1110[c]
	(3.5)	(69.0)	(4.9)	(800)	1955[d]
Ir(LH)(CO)(PPh_3)	2.7	60.6	4.5	914	3368,[b] 1110[c]
	(3.1)	(62.0)	(4.4)	(889)	1942[d]

[a] *Ca.* 2×10^{-3} M chloroform solutions. [b] ν(NH). [c] ν(P=N)(Nujol mulls). [d] ν(C≡O) (CH_2Cl_2 solutions).

nitrogen donor.[16,17-18] Furthermore, molecular weight measurements on the complexes in chloroform solution by vapour pressure osmometry confirm the mononuclear formulation.

The $[M(COD)(LH_2)]ClO_4$ (M = Rh, Ir) complexes are obtained by reaction of LH_2 with $[M(COD)(acetone)_x]ClO_4$, prepared *in situ* by reacting $[M(\mu\text{-Cl})(COD)]_2$ with $AgClO_4$ in acetone. $[Rh(COD)(LH_2)]ClO_4$ reacts with carbon monoxide to give $[Rh(CO)_2(LH_2)]ClO_4$, which on treatment with PPh_3 leads to the formation of $[Rh(CO)(PPh_3)(LH_2)]ClO_4$. The coordinated amine group ($-NH_2$) in $[Rh(CO)_2(LH_2)]ClO_4$ can be easily deprotonated by treatment with a methanol solution of potassium hydroxide leading to the amide complex $Rh(LH)(CO)_2$; this reaction can be reversed by addition of perchloric acid, according to the following equation:

$$[Rh(CO)_2(LH_2)]ClO_4 \underset{HClO_4}{\overset{KOH/MeOH}{\rightleftharpoons}} Rh(LH)(CO)_2.$$

Reaction of $[M(\mu\text{-Cl})(COD)]_2$ (M = Rh, Ir) with LH_2 in dichloromethane results in the formation of the ionic pair $[M(COD)(LH_2)][M(Cl)_2(COD)]$. Similarly reaction of $[Rh(\mu\text{-Cl})(CO)_2]_2$ with LH_2 in dichloromethane gives $[Rh(CO)_2(LH_2)][Rh(Cl)_2(CO)_2]$. The latter complex can also be obtained by treatment of $[Rh(COD)(LH_2)][Rh(Cl)_2(COD)]$ with carbon monoxide. It shows four metal carbonyl bands in the IR spectrum corresponding to $[Rh(CO)_2(LH_2)]^+$ (ν(C≡O) = 2020, 2085 cm^{-1}) and $[Rh(Cl)_2(CO)_2]^-$ (ν(C≡O) = 1990, 2070

Table 2. Analytical and physical data for the ionic compounds

Compound	Analyses[Found(Calc.)] N (%)	C	H	Λ_M[a] ($ohm^{-1}\,cm^2\,mol^{-1}$)	Selected IR bands (cm^{-1})
$[Rh(COD)(LH_2)]ClO_4$	4.1	57.7	5.1	135	3228[b]
	(4.0)	(58.4)	(5.1)		
$[Ir(COD)(LH_2)]ClO_4$	3.4	52.2	4.4	122	3215[b]
	(3.5)	(52.0)	(4.6)		
$[Rh(CO)_2(LH_2)]ClO_4$	3.9	51.6	3.8	133	3200–3300,[b]
	(4.2)	(52.2)	(3.7)		2025,[c] 2085[c]
$[Rh(CO)(PPh_3)(LH_2)]ClO_4$	2.8	61.2	4.4	113	3200–3300,[b]
	(3.1)	(61.3)	(4.4)		1995[c]
$[Rh(COD)(LH_2)][Rh(Cl)_2(COD)]$	3.1	57.9	5.7	54	3100–3200[b]
	(3.1)	(57.3)	(5.4)		
$[Ir(COD)(LH_2)][Ir(Cl)_2(COD)]$	2.5	47.3	4.6	62	3100–3200[b]
	(2.6)	(47.8)	(4.5)		
$[Rh(CO)_2(LH_2)][Rh(Cl)_2(CO)_2]$	3.6	47.0	3.4	97	3150–3250,[b]
	(3.5)	(47.1)	(3.2)		1990,[c] 2020,[c]
					2070,[c] 2085[c]

[a] *Ca.* 2×10^{-3} M acetone solutions. [b] ν(N—H)(Nujol mulls). [c] ν(C≡O)(CH_2Cl_2 solutions).

cm^{-1}).[19–21] These reactions are analogous to that found with chelating bidentate nitrogen donor ligands,[19–21] and support the tendency of this ligand to act as a chelate due to the stability conferred by the formation of a six membered ring with a π electronic delocalization. Analytical and physical data for the ionic complexes are given in Table 2.

REFERENCES

1. B. Centikaya, M. F. Lappert and S. Torroni, *J. Chem. Soc., Dalton Trans.* 1979, 843.
2. G. J. Organ, M. K. Cooper, K. Henrick and M. McPartlin, *J. Chem. Soc., Dalton Trans.* 1984, 2377.
3. L. A. Oro, M. J. Fernández, J. Modrego, C. Foces-Foces and F. H. Cano, *Angew. Chem. Int. Ed.* 1984, **23**, 913.
4. C. W. G. Ansell, M. K. Cooper, K. P. Dancey, P. A. Duckworth, K. Henrick, M. McPartlin, G. Organ and P. A. Tasker, *J. Chem. Soc., Chem. Comm.* 1985, 437.
5. A. Nutton and P. M. Maitlis, *J. Chem. Soc., Dalton Trans.* 1981, 2339.
6. M. D. Fryzuk and P. A. MacNeil, *Organometallics* 1983, **2**, 355; M. D. Fryzuk, P. A. MacNeil and S. J. Retting, *Organometallics* 1986, **5**, 2469.
7. L. A. Oro, M. J. Fernández, J. Modrego and J. M. López, *J. Organomet. Chem.* 1985, **287**, 409.
8. D. Hedden and D. M. Roundhill, *Inorg. Chem.* 1986, **25**, 9.
9. F. J. Lahoz, F. Viguri, M. A. Ciriano, L. A. Oro, C. Foces-Foces and F. H. Cano, *Inorg. Chim. Acta* 119, **128**, 1987.
10. M. D. Fryzuk and P. A. MacNeil, *Organometallics* 1983, **2**, 682.
11. S. Pack, D. Hedden and D. M. Roundhill, *Organometallics* 1986, **5**, 2151.
12. R. Usón, L. A. Oro and J. A. Cabeza, *Inorg. Synth.* 1985, **23**, 126.
13. J. L. Herde, J. C. Lambert and C. V. Senoff, *Inorg. Synth.* 1974, **15**, 18.
14. J. Powell and B. L. Shaw, *J. Chem. Soc.* (*A*) 1968, 211.
15. J. Barluenga, F. López and F. Palacios, *J. Chem. Res.* 1985 (s), 211, (M) 2541.
16. E. W. Abel and S. A. Mucklejohn, *Inorg. Chim. Acta* 1979, **37**, 107.
17. J. S. Miller, M. O. Visscher and K. G. Caulton, *Inorg. Chem.* 1974, **13**, 1632.
18. H. Alper, *J. Organomet. Chem.* 1977, **127**, 385.
19. B. Crociani, V. Belluco and P. Sandrini, *J. Organomet. Chem.* 1979, **177**, 385.
20. F. Pruchnik and K. Wajda, *J. Organomet. Chem.* 1979, **164**, 71.
21. M. A. Garralda and L. Ibarlucea, *J. Organomet. Chem.* 1986, **311**, 225.

Polyhedron Vol. 6, No. 11, pp. 2003–2007, 1987
Printed in Great Britain

0277–5387/87 $3.00+.00

THE ^{1}H NMR SPECTRA OF 8-QUINOLINOLATO COMPLEXES OF Mn(III)

PHILIPPA ADDY, DENNIS F. EVANS* and QUERO DE SOUZA

Inorganic Chemistry Laboratories, Imperial College of Science and Technology, London SW7 2AY, U.K.

(*Received* 28 *April* 1987; *accepted* 27 *May* 1987)

Abstract—^{1}H NMR spectra are reported for *tris*(8-quinolinolato)manganese(III), *tris*(2-methyl-8-quinolinolato)manganese(III) and mixtures of *tris*(acetylacetonato)manganese(III) and *tris*(8-quinolinolato)manganese(III). In the latter case, mixed complexes are formed in equilibrium, with only one of the three possible isomers of acetylacetonato *bis*(8-quinolinolato)manganese(III) being present in detectable amounts. The spectra were assigned making extensive use of selective deuteriation.

There has been considerable interest recently in complexes of Mn(III), partly because a number of enzymes contain manganese in this oxidation state.[1] One technique for studying Mn(III) complexes is ^{1}H NMR spectroscopy. Although a number of low-spin porphyrin complexes have recently been characterized,[2,3] and the low-spin $Mn(CN)_6^{3-}$ anion has been known for some considerable time, the great majority of Mn(III) complexes are high-spin.[4] Species of this type which have been studied by ^{1}H NMR spectroscopy include those with β-diketones,[5,6] tropolones,[7] porphyrins,[8–10] and some sulphur-bonding ligands.[11] In general, the ^{1}H NMR resonances have moderate bandwidths.

The present work is concerned with the ^{1}H NMR spectra of complexes derived from 8-quinolinol (8-hydroxyquinoline), i.e. *tris*(8-quinolinolato)manganese(III), $Mn(hq)_3$, *tris*(2-methyl-8-quinolinolato)manganese(III) and 8-quinolinolatoacetylacetonato mixed species. The rather complex spectra were assigned with the extensive use of selective deuteriation.

EXPERIMENTAL

Trisacetylacetonato manganese(III) ($Mn(acac)_3$). This was prepared by the method of Bhattacharjee and Chaudhuri.[12]

$Mn(hq)_3$[13]—To a solution of $Mn(acac)_3$ (0.89 g, 0.0025 mol) in ethanol (30 cm^3) was added 8-quinolinol (1.45 g, 0.01 mol) dissolved in ethanol (20 cm^3). After 1 h at *ca.* 4°C, the crystals were filtered off, washed with ethanol and dried *in vacuo*. The coordinated ethanol[14] was finally removed by heating at 170–180°C for 1 h. Yield 0.92 g (75%). The deuteriated complexes were prepared similarly, using a molar ratio 8-quinolinol-d_n: $Mn(acac)_3$ of 3.5 : 1.

Tris(2-*methyl*-8-*quinolinolato*)*manganese*(III). This was prepared as described by Burns *et al.*[14] or from $Mn(acac)_3$ and excess 2-methyl-8-quinolinol in ethanol.

Selective ring deuteriation of 8-*quinolinol*

Except where otherwise stated, materials were sealed in glass tubes of appropriate wall-thickness in an Ar atmosphere, and the selectivity of deuteriation was $\geqslant$ 90%.

8-*quinolinol*-$d_{5,7}$. 8-quinolinol (1 g, 6.9×10^{-3} mol), D_2O (5 cm^3) and *either* triethylamine (0.5 cm^3, 3.5×10^{-3} mol) *or* NaOD (0.14 g, 3.5×10^{-3} mol) were heated at 100°C for 24 h. The solution was saturated with CO_2, the solid filtered off, washed with H_2O, and dried *in vacuo* over $CaCl_2$. Yield 0.72 g (70%).

To distinguish between the five and seven positions, 8-quinolinol (0.5 g), 38% DCl (2.4 cm^3) and D_2O (2.4 cm^3) were heated in a screw-top vial at *ca.* 95°C for 48 h. The ^{1}H NMR spectrum of the solution after dilution with an equal volume of D_2O showed that the ratio $[H_7]/[H_5]$ was *ca.* 2.3, with the other ring protons being unaffected. The solution

* Author to whom correspondence should be addressed.

was made slightly alkaline with $NaOH_{aq}$ and the product isolated as above. Yield 0.36 g (70%).

8-*quinolinol*-$d_{2,5,7}$. 8-quinolinol (0.6 g) and D_2O (5 cm^3) were heated at 218°C for 24 h. After cooling, the solid was filtered off and dried as above. Yield 0.43 g (70%).

8-*quinolinol*-$d_{2,3,4,5,6,7}$. 8-quinolinol HCl (0.7 g, obtained by adding HCl gas in diethyl ether to a solution of 8-quinolinol in diethyl ether) and D_2O (12 cm^3) were heated at 255°C for 4–6 days. After cooling, $NaHCO_3$ (0.4 g) dissolved in a little water was added to precipitate the product. Yield 0.36 g (62%).

The largest amount of residual protium was at the six position.

To characterize H_6 further, Na (0.17 g, 7.4×10^{-3} mol) was added in portions to D_2O (5 cm^3) with cooling and in an Ar atmosphere, followed by 1.0 g (6.9×10^{-3} mol) of 8-quinolinol. The mixture was heated in a rocking stainless steel bomb under Ar for *ca.* 1 h at *ca.* 200°C. The contents were diluted with a little H_2O, filtered to remove some debris caused by attack on the stainless steel, and the filtrate adjusted with HCl_{aq} to pH 7. Yield 0.62 g (60%). The ^1H NMR spectrum showed that all ring protons were largely deuteriated, with the exception of H_6.

To distinguish between H_3 and H_4, a solution similar to that used to prepare 8-quinolinol-$d_{2,3,4,5,6,7}$ was heated at 250–255°C for 24 h only. The ^1H NMR spectrum (DCl solution) of the deuteriated product so obtained showed that the ratio $[H_4]/[H_3]$ was *ca.* 3.5.

8-*quinolinol*-$d_{2,3,4,6}$. 8-quinolinol-$d_{2,3,4,5,6,7}$ (0.4 g), H_2O (10 cm^3) and NaOH (0.11 g) were heated at 100°C for 24 h and the product isolated as for 8-quinolinol-$d_{5,7}$.

$2CD_3$-8-*quinolinol*-$d_{5,7}$. The preparation was similar to that for 8-quinolinol-$d_{5,7}$, using NaOD and $2CH_3$-8-quinolinol. In addition to H_5 and H_7, the CH_3 group was almost completely deuteriated. Yield 85%.

Mn(acac-d_1)$_3$. Acetylacetone (1.1 g) dissolved in D_2O (10 cm^3) was left overnight. Finely powdered AnalaR $KMnO_4$ (0.25 g) was added with vigorous stirring. After 10 min the crystals were filtered off, washed with water and dried *in vacuo*. Yield 0.4 g. ^1H NMR and mass spectroscopy showed that the isotopic purity was *ca.* 85%.

Mn(acac-d_6)$_3$. Acetylacetone-d_8[15] (1.2 g) dissolved in H_2O (10 cm^3) was left overnight, and the procedure for Mn(acac-d_1)$_3$ was then followed. The isotopic purity was *ca.* 93%.

The ^1H NMR spectra of the manganese complexes were measured at 250 MHz on a Bruker WM-250 FT spectrometer, and the deuteriated 8-quinolinols similarly or at 90 MHz on a Perkin–Elmer R32 spectrometer.

RESULTS AND DISCUSSION

The ^1H NMR spectrum of Mn(hq)$_3$ is shown in Fig. 1, and indicates that the complex exists as the meridional isomer, since in the facial isomer all three rings are equivalent. The *mer* configuration is also found in the solid state for Mn(hq)$_3$[16] and Cr(hq)$_3$[17] from X-ray studies, and for Al(hq)$_3$,[18,19] Ga(hq)$_3$,[19] Co(hq)$_3$[18] and Rh(hq)$_3$[18] from ^1H NMR spectroscopy. The spectrum was assigned by studying deuteriated samples of Mn(hq)$_3$, prepared from 8-quinolinol which had been selectively deuteriated in all six ring positions. The ^1H NMR spectrum[20] of 8-quinolinol in $CDCl_3$ solution (220 MHz) shows some overlap of the ring resonances. However, by

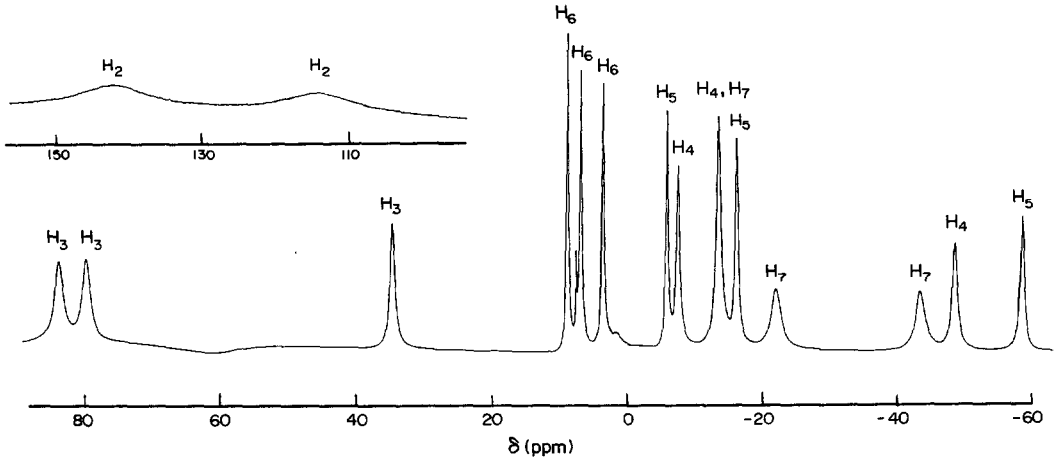

Fig. 1. The ^1H NMR spectrum of Mn(hq)$_3$ in $CDCl_3$ at 301 K.

using, where necessary, solutions in D_2O containing NaOD or DCl, complete resolution could be obtained even at 90 MHz. Standard techniques for the deuteriation of aromatic compounds were used,[21,22] i.e. heating 8-quinolinol with D_2O under neutral, acid or alkaline conditions (see Experimental Section). Since the ^{1}H NMR spectrum of a deuteriated 8-quinolinol was compared with that of the complex prepared from it, highly selective deuteriation was not required. In the present work, the minimum value for $[H_x]/[H_y]$, where x and y are two positions to be distinguished, was greater than 2, although smaller ratios would have been adequate.

Table 1 presents the observed chemical shifts. The only omission is one resonance from H_2, which could not be located. It can be seen that the chemical shifts for the three rings vary greatly, with two resonances for each proton lying close together, and the third considerably up-field. This could be explained by a large pseudo-contact contribution. However, for other Mn(III) complexes the general conclusion is that pseudo-contact shifts are comparatively small[5,9] and it seems more likely that the observed variations are largely due to differing σ- and π-delocalization of the metal d electrons onto the ligands.[23]

The linewidths of the proton resonances vary greatly (Fig. 1). Two coupling mechanisms can contribute to the linewidths, dipolar broadening (proportional to r^{-6}, where r is the distance between the manganese nucleus and the proton) and scalar broadening. Calculations using a molecular model suggest that the linewidths are largely, though not entirely, governed by the dipolar mechanism. This is also found for other Mn(III) complexes,[9] and can enable probable assignments to be made in the absence of selective deuteriation experiments.

The ^{1}H NMR spectrum of *tris*(2-methylquinolinolato)manganese(III) could be largely assigned [in conjunction with that for $Mn(hq)_3$] from the line positions and widths. An ambiguity concerning H_4 and H_5 was resolved by measuring the spectrum of the complex obtained from $2CD_3$-8-quinolinol-$d_{5,7}$ which also enabled two partly overlapped CH_3 resonances to be located unambiguously. The results are given in Table 1.

Mixed 8-quinolinolato-acetylacetonato manganese(III) *complexes*

Figure 2 shows the ^{1}H NMR spectrum of a solution prepared from $Mn(hq)_3$ and $Mn(acac)_3$. From the complexity of the spectrum it is clear that ligand

Table 1. Proton chemical shifts (δ) of 8-quinolinolato complexes of manganese(III) in $CDCl_3$ at 301°

Compound	Resonance	δ (ppm)			Paramagnetic shifts[a] (ppm)		
$Mn(hq)_3$	H_2	142,	114,	—	133.4,	105.4,	—
	H_3	83.4,	79.2,	34.4	76.6,	67.6,	26.8
	H_4	−8.1,	−14.1,	−48.6	−16.4,	−22.4,	−56.9
	H_5	−6.4,	−16.8,	−58.6	−13.4,	−23.8,	−65.6
	H_6	8.4,	6.4,	3.1	0.9,	−1.1,	−4.4
	H_7	−14.1,	−22.5,	−43.7	−21.3,	−29.7,	−50.9
tris(2-CH_3-8-quinolinolato) manganese(III)	CH_3	56.8,	17,	9			
	H_3	82.1,	75.0,	17.7			
	H_4	−1.1,	−3.9,	−33.5			
	H_5	−6.3,	−21.0,	−58.8			
	H_6	5.9,	5.1,	1.6			
	H_7	−9.4,	−26.4,	−43.5			
$Mn(acac)_2hq$	H_3		(65.6)				
	H_5		−28.9				
	H_7		−26.3				
	CH_3	42.9,	29.9,	24.1, 9.7			
$Mn(acac)(hq)_2$ (Isomer *A* or *B*)	H_3		(57.2)				
	H_4		(−27.6)				
	H_5		−41.3				
	H_6		(3.8)				
	H_7		−35.1				
	CH_3		19.2				

[a] Relative to $In(hq)_3$.[19]

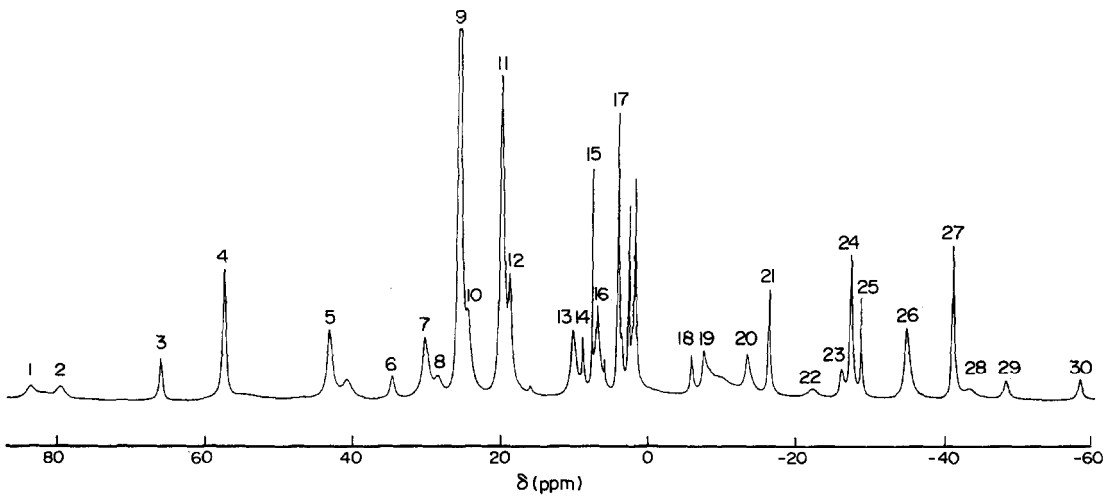

Fig. 2. The ^1H NMR spectrum of a mixture of 0.05 M $Mn(acac)_3$ and 0.05 M $Mn(hq)_3$ in $CDCl_3$ at 301 K. Assignments (1) $Mn(hq)_3$, H_3; (2) $Mn(hq)_3$, H_3; (3) $Mn(acac)_2(hq)$, (H_3); (4) $Mn(acac)(hq)_2$, (H_3); (5) $Mn(acac)_2hq$, CH_3; (6) $Mn(hq)_3$, H_3; (7) $Mn(acac)_2hq$, CH_3; (8) mixed, acac CH; (9) $Mn(acac)_3$, CH_3; (10) $Mn(acac)_2hq$, CH_3; (11) $Mn(acac)(hq)_2$, CH_3; (12) $Mn(acac)_3$, CH; (13) $Mn(acac)_2hq$, CH_3; (14) $Mn(hq)_3$, H_6; (15) $CHCl_3$; (16) $Mn(hq)_3$, H_6; (17) $Mn(acac)(hq)_2$, (H_6); (18) $Mn(hq)_3$, H_5; (19) $Mn(hq)_3$, H_4; (20) $Mn(hq)_3$, H_4, H_7; (21) $Mn(hq)_3$, H_5; (22) $Mn(hq)_3$, H_7; (23) $Mn(acac)_2hq$, H_7; (24) $Mn(acac)(hq)_2$, (H_4); (25) $Mn(acac)_2(hq)$, H_5; (26) $Mn(acac)(hq)_2$, H_7; (27) $Mn(acac)(hq)_2$, H_5; (28) $Mn(hq)_3$, H_7; (29) $Mn(hq)_3$, H_4; (30) $Mn(hq)_3$, H_5. Sharp peaks in the region δ 0–10 arise from diamagnetic impurities.

exchange has occurred to give mixed complexes in equilibrium with $Mn(hq)_3$ and $Mn(acac)_3$ (δ CH_3 25.2 ppm, δ CH 18.2 ppm). A solid analysing as $Mn(acac)(hq)_2$ has been reported by Yamaguchi and Sawyer.[24] The possible isomers for $Mn(acac)_2hq$ and $Mn(acac)(hq)_2$ are shown in Table 2 together with the number of resonances expected for each isomer. To assign the spectrum shown in Fig. 2, the ^1H NMR spectra of $Mn(acac)_3$, $Mn(acac\text{-}d_1)_3$ (deuteriated in the CH groups), $Mn(acac\text{-}d_6)_3$ (deuteriated in the CH_3 groups), $Mn(hq\text{-}d_6)_3$ and $Mn(hq\text{-}d_{2,3,4,6})_3$ were studied in various combinations. By a comparison of the three spectra obtained from $Mn(hq\text{-}d_6)_6$ mixed with $Mn(acac)_3$, $Mn(acac\text{-}d_1)_3$ and $Mn(acac\text{-}d_6)_3$, all the CH_3 resonances in the mixed complexes could be characterized. It was only possible to locate one acac CH resonance of a mixed complex (at $\delta = 28.4$ ppm), with the other presumably being overlapped. The spectrum of a mixture of $Mn(acac\text{-}d_6)_3$ and $Mn(hq\text{-}d_{2,3,4,6})_3$ enabled the H_5 and H_7 resonances in the mixed complexes to be picked out and confirmed that only one of the three possible isomers of $Mn(acac)(hq)_2$ was present in any detectable amount, i.e. either isomer *A* or *B*. The H_5 and H_7 resonances were distinguished by their relative linewidths (see above).

Resonances from the two mixed isomers $Mn(acac)_2hq$ and $Mn(acac)(hq)_2$ could be distinguished on intensity grounds. For a solution initially equi-

Table 2. Possible isomers of $Mn(acac)_2hq$ and $Mn(acac)(hq)_2$ and expected ^1H NMR spectra

		Expected resonances	Relative intensity
$Mn(acac)_2hq$			
		4 CH_3	3
		2 CH(acac)	1
		6 hq	1
$Mn(acac)(hq)_2$			
A	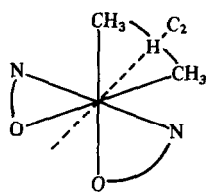	1 CH_3 1 CH 6 hq	6 1 2
B	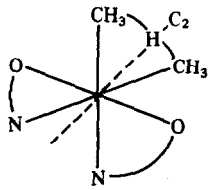	1 CH_3 1 CH 6 hq	6 1 2
C	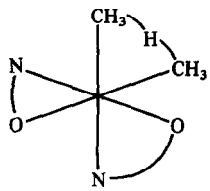	2 CH_3 1 CH 12 hq	3 1 1

molar in $Mn(acac)_3$ and $Mn(hq)_3$, we have $[Mn(acac)_2hq] = [Mn(acac)(hq)_2]$. As confirmation, some spectra were recorded with different initial ratios of $Mn(acac)_3$ and $Mn(hq)_3$ or deuteriated analogues.

A number of other hq resonances in the mixed complexes could be tentatively assigned on the basis of their line positions and widths. The final assignments are given in Fig. 2 and Table 1. Quantitative intensity measurements showed that in the equilibrium $Mn(acac)_3 + Mn(hq)_3 \rightleftharpoons Mn(acac)_2hq + Mn(acac)(hq)_2$, the mixed complexes were favoured. In a solution initially 0.05 M in both $Mn(acac)_3$ and $Mn(hq)_3$, the ratio of the concentrations of the mixed isomers to those of $Mn(acac)_3$ and $Mn(hq)_3$ was *ca.* 1.6.

Acknowledgements—We thank the S.E.R.C. for a postgraduate studentship (to Q. de S.) and Ms S. Johnson for measurements of ^{1}H NMR spectra.

REFERENCES

1. J. L. Seela, K. Folting, R. Wang, J. C. Huffman, G. Christou, H. Change and D. N. Hendrickson, *Inorg. Chem.* 1985, **24**, 4454.
2. J. T. Landrum, K. Hatona, W. Scheidt and C. A. Reed, *J. Am. Chem. Soc.* 1980, **102**, 6729.
3. A. P. Hanson and H. M. Goff, *Inorg. Chem.* 1984, **23**, 4519.
4. L. J. Boucher, *Coord. Chem. Rev.* 1972, **7**, 289.
5. D. R. Eaton, *J. Am. Chem. Soc.* 1965, **87**, 3097.
6. J. G. Gordon, M. J. O'Connor and R. H. Holm, *Inorg. Chim. Acta* 1971, **5**, 381; G. W. Everett and A. Johnson, *J. Am. Chem. Soc.* 1972, **94**, 6397.
7. S. S. Eaton, G. R. Eaton, R. H. Holm and E. L. Muetterties, *J. Am. Chem. Soc.* 1973, **95**, 1116.
8. T. R. Janson, L. J. Boucher and J. J. Katz, *Inorg. Chem.* 1973, **12**, 940.
9. G. N. La Mar and F. A. Walker, *J. Am. Chem. Soc.* 1973, **95**, 6950; *ibid*, 1975, **97**, 5103.
10. C. G. Hill and M. W. Williamson, *Inorg. Chem.* 1985, **24**, 2836; *ibid*, 3024.
11. G. Henkel, K. Greuwe and B. Krebs, *Angew. Chem. Int. Ed. Engl.* 1985, **24**, 117; R. M. Golding, *Aust. J. Chem.* 1974, **27**, 2081.
12. M. N. Bhattacharjee and M. K. Chaudhuri, *J. Chem. Soc., Dalton Trans.* 1982, 669.
13. M. M. Ray, J. N. Adhya, D. Biswas and S. N. Poddar, *Aust. J. Chem.* 1966, **19**, 1737.
14. A. R. Burns, T. J. Cardwell and R. W. Cattrall, *Aust. J. Chem.* 1971, **24**, 661.
15. W. Egan, G. Gunnarson, T. E. Bull and S. Forsen, *J. Am. Chem. Soc.* 1977, **99**, 4568.
16. R. Herns, T. J. Cardwell and M. F. Mackay, *Aust. J. Chem.* 1975, **28**, 443.
17. K. Folting, M. H. Cox, J. W. Moore and L. L. Merrit, *J. Chem. Soc., Chem. Commun.* 1968, 1170.
18. B. C. Baker and D. T. Sawyer, *Anal. Chem.* 1968, **40**, 1945.
19. P. Addy, D. F. Evans and R. S. Sheppard, *Inorg. Chim. Acta* 1987, **127**, L19.
20. A. Corsini, W. J. Louch and M. Thompson, *Talanta* 1974, **21**, 252.
21. A. F. Thomas, *Deuterium Labelling in Organic Chemistry*. Meredith, New York (1971).
22. N. H. Werstiuk and G. Timmens, *Can. J. Chem.* 1981, **59**, 1022.
23. G. N. La Mar, W. De W. Horrocks and R. H. Holm, *NMR of Paramagnetic Molecules*. Academic Press, New York (1973).
24. K. Yamaguchi and D. T. Sawyer, *Inorg. Chem.* 1985, **24**, 971.

Polyhedron Vol. 6, No. 11, pp. 2009–2018, 1987
Printed in Great Britain

0277–5387/87 $3.00+.00

SYNTHESIS AND CHARACTERIZATION OF TRANSITION METAL COMPLEXES OF A NEW BIDENTATE LIGAND {2-(DIPHENYLPHOSPHINO)ETHYL}BENZYLAMINE

M. M. TAQUI KHAN*

Discipline of Coordination Chemistry and Homogeneous Catalysis, Central Salt and Marine Chemicals Research Institute, Bhavnagar 364 002, India

and

A. PURSHOTHAM REDDY

Department of Chemistry, Osmania University, Hyderabad 500 007, India

(*Received* 5 *May* 1987; *accepted* 2 *June* 1987)

Abstract—A new bidentate ligand {2-(diphenylphosphino)ethyl}benzylamine (DPEBA) was synthesized and characterized based on the IR, mass and ^{1}H, ^{13}C and ^{31}P NMR spectra. Various complexes of platinum group metal ions and Ni(II) and Co(II) ions with the ligand were synthesized. Reaction of $RuCl_2(PPh_3)_3$ or $RuCl_2(Me_2SO)_4$ with the ligand DPEBA, resulted in formation of a penta-coordinate, Ru(II) species of the composition $[RuCl(DPEBA)_2]Cl$. Carbonylation of $[RuCl(DPEBA)_2]Cl$ gave an octahedral carbonyl complex of the type $[RuCl(CO)(DPEBA)_2]Cl$. The reaction of $RuCl_3 \cdot 3H_2O$ or $RuCl_3(AsPh_3)_2MeOH$ with a twofold excess of the ligand gave an octahedral Ru(III) cationic species $[Ru(DPEBA)_2Cl_2]Cl$. Carbonylation of the Ru(III) complex gave rise to a carbonyl complex $[RuCl(CO)(DPEBA)_2]Cl_2$. The ligand DPEBA reacts with cobalt(II) chloride in methanol to give the 1 : 1 complex $[Co(DPEBA)Cl_2]$. A series of Rh(I) complexes $[Rh(DPEBA)_2Cl]$, $[RhCl(CO)(DPEBA)]$ and $[Rh(DPEBA)_2]Cl$ were synthesized by the reaction of DPEBA with $RhCl(PPh_3)_3$, $RhCl(CO)(PPh_3)_2$ and $[Rh(COD)Cl]_2$, respectively. Reaction of $[Ir(COD)Cl]_2$ and $IrCl(CO)(PPh_3)_2$ with the ligand DPEBA, gave the square-planar complexes $[Ir(DPBA)_2]Cl$ and $[Ir(DPEBA)(CO)Cl]$, respectively. Octahedral cationic complexes of the type $[M(DPEBA)_2Cl_2]Cl$ (M = Rh(III), Ir(III)) were synthesized by the reaction of the ligand DPEBA and rhodium and iridium trichlorides. Reaction of $NiCl_2 \cdot 6H_2O$ with DPEBA in 1 : 2 molar equivalents, in boiling butanol gave an octahedral neutral complex $[Ni(DPEBA)_2Cl_2]$ which readily rearranges to the square-planar complex $[Ni(DPEBA)_2]Cl_2$ in methanol. Reaction of Pd(II) and Pt(II) chlorides with DPEBA gave square-planar, cationic complexes of the type $[M(DPEBA)_2Cl]Cl$ (M = Pd, Pt). All the complexes were characterized on the basis of their analytical and spectral data.

Recently we have synthesized transition metal complexes of bi- and poly-dentate ligands[1–4] containing mixed donor atoms like N, P, As and O, because of their increasing importance in the area of catalysis.[5–7] Bidentate ligands with one weak and one strong donor site have been a subject matter of many reports.[8] These ligands can act both as chelating ligands as well as bridging ligands with metal ions and readily provide a coordination site for the incoming substrates by the displacement of the weak donor atom. This factor, the susceptibility of the weak donor site to displacement by the incoming substrate along with the stability of the catalyst precursor in the absence of the substrate by chelate effect, has a tremendous utility in the field of homogeneous catalysis.[9–11]

In this paper we report the synthesis of one such

* Author to whom correspondence should be addressed.

ligand {2-(diphenylphosphino)ethyl}benzylamine (DPEBA) which contains a set of mixed donor atoms N and P. This ligand has been synthesized and characterized by ^{1}H, $^{13}C\{^{1}H\}$ and $^{31}P\{^{1}H\}$ NMR spectra and mass spectra. The ligand DPEBA was used in the synthesis of Ni(II), Co(II) and platinum group metal complexes which were characterized by analytical and spectral data.

RESULTS AND DISCUSSION

The mixed donor bidentate ligand DPEBA is soluble in almost all organic solvents. The infrared spectrum of the ligand exhibits a characteristic ν(N—H) at 3300 cm^{-1} and a band of the quaternary ammonium salt was observed at 2800 cm^{-1} in addition to the other ligand absorptions.

The ^{1}H NMR spectrum of DPEBA, exhibits resonances from the phenyl protons around δ 7.5. The resonance of the protons of the CH_2CH_2 bridge are observed as multiplets centred at δ 2.8 (CH_2 protons attached to amine centre) and δ 4.2 (-CH_2 protons attached to diphenylphosphino group), due to the interaction of the neighbouring methylene protons and also by the ^{31}P nuclear spin. Two singlets at δ 3.5 and δ 1.7 were assigned to the CH_2 protons of the benzyl group and the N—H proton, respectively. The $^{31}P\{^{1}H\}$ NMR spectrum of the ligand exhibits a singlet at δ −19.3 in $CHCl_3$. The $^{13}C\{^{1}H\}$ NMR spectrum of DPEBA exhibits two well defined doublets at δ 48.3 and δ 22.5. The more downfield doublet is assigned to the methylene carbon of the CH_2CH_2 bridge attached to phosphorus, with larger $^{1}J(C—P) = 30.5$ Hz and the other doublet with $^{2}J(C—P) = 17.1$ Hz, can be assigned to the methylene carbon attached to nitrogen. A singlet at δ 56.7 is assigned to the methylene carbon CH_2 of the benzyl group. Two well defined multiplets in the range δ 129.4–131.4 are assigned to the aromatic carbons of the diphenylphosphino moiety and the phenyl of the benzyl group. The mass spectral fragmentation of the ligand DPEBA is presented in the experimental section and shows general features similar to those reported earlier on some polytertiary phosphines, arsines and phosphinoarsines[12,13] and confirms the above formulation of the ligand.

Metal complexes of the ligand DPEBA

Ru(II) *and* (III) *complexes of DPEBA*. The reaction of $RuCl_2(PPh_3)_3$ or $RuCl_2(Me_2SO)_4$ with the ligand DPEBA in 1 : 2 molar ratio gave rise to the five-coordinate, cationic Ru(II) species [RuCl(DPEBA)$_2$]Cl (**1**). Complex **1** exhibits conductivity consistent with a 1 : 1 electrolyte[14] (Table 1). A band at 310 cm^{-1} in the far-infrared spectrum is assigned to ν(Ru—Cl). Complex **1** can exist in square-pyramidal or trigonal-bipyramidal geometries. The $^{31}P\{^{1}H\}$ NMR spectrum of **1** is however consistent with a square-pyramid geometry (structure **I**). The

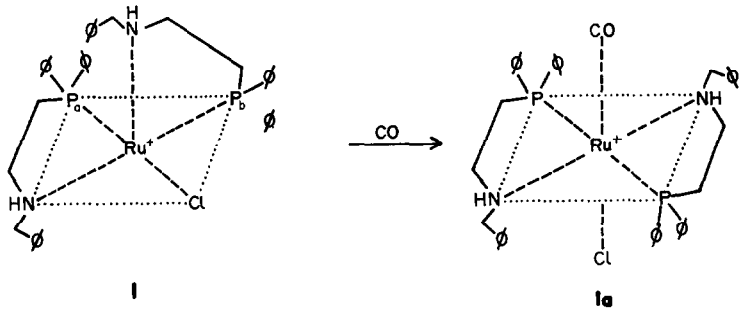

I **Ia**

^{31}P NMR spectrum exhibits two doublets at δ 45.9 and 42.9 (Table 2) indicating the presence of two magnetically non-equivalent phosphorus atoms. Based on this spectrum all the other isomers with equivalent phosphorus atoms can be ruled out as they would give rise to a singlet. The other trigonal-bipyramidal isomer where one of the phosphorus atoms lies in the equatorial plane and the other in an axial plane can also be excluded on the basis of the chemical shift values. In this isomer one expects a large chemical shift difference between the two ^{31}P resonances.[2] Based on the chemical shift values a square-pyramidal geometry in which one of the phosphorus atom is *trans* to Cl (doublet at δ 45.9) and the other *trans* to N (doublet at δ 42.9) can be proposed for the complex (Structure **I**). The $J(P_a–P_b)$ value of 39 Hz is also typical for the coupling constant of non-equivalent phosphorus nuclei *cis* to one another in ruthenium(II)-tertiary phosphine complexes.[15,16]

Carbonylation of complex **1** yielded an octahedral carbonyl species [Ru(DPEBA)Cl(CO)]Cl **1a**. Complex **1a** is a 1 : 1 electrolyte (Table 1) and exhibits an intense CO infrared absorption band at 1940 cm^{-1}. The $^{13}C\{^{1}H\}$ NMR spectrum displays a sin-

Table 1. Analytical and other physical data for metal complexes

Complex		Colour	M.p.[a] (°C)	Conductivity[b] λ_∞, Ω^{-1} cm^2 mol^{-1}	Elemental analysis[c] %C	%H	%N
[Ru(DPEBA)$_2$Cl]Cl	(1)	Red	229	80	62.2 (61.7)	5.4 (5.4)	3.4 (3.3)
[RuCl(CO)(DPEBA)$_2$]Cl	(1a)	Green	> 200	76	60.1 (60.2)	5.3 (5.2)	3.3 (3.3)
[Ru(DPEBA)$_2$Cl$_2$]Cl	(2)	Red	255	89	59.4 (60.4)	5.2 (5.2)	3.3 (3.1)
[RuCl(CO)(DPEBA)$_2$]Cl$_2$	(2a)	Brown	> 200	135	57.7 (57.6)	5.0 (5.0)	3.2 (3.1)
[Co(DPEBA)Cl$_2$]	(3)	Bluish-green	300	6(A)	65.6 (64.8)	5.7 (5.6)	3.6 (3.5)
[Rh(DPEBA)$_2$Cl]	(4)	Yellow	268	21	64.8 (63.9)	5.6 (5.5)	3.6 (3.6)
[Rh(DPEBA)$_2$]Cl	(5)	Yellow	269	60	55.8 (55.3)	5.4 (5.3)	2.7 (2.7)
[Ir(DPEBA)$_2$]Cl	(6)	Pale yellow	263	80	58.2 (58.1)	5.0 (5.0)	3.2 (3.2)
[Rh(DPEBA)(CO)Cl]	(7)	Yellow	275	25	54.3 (53.8)	4.5 (4.4)	2.8 (2.8)
[Ir(DPEBA)(CO)Cl]	(8)	Yellow	279	25	45.9 (45.5)	3.8 (3.6)	2.4 (2.3)
[Rh(DPEBA)$_2$Cl$_2$]Cl	(9)	Yellow	235	68	59.4 (60.5)	5.2 (5.3)	3.3 (3.0)
[Ir(DPEBA)$_2$Cl$_2$]Cl	(10)	Yellow	293	85	53.1 (52.9)	4.6 (4.6)	2.9 (2.8)
[Ni(DPEBA)$_2$Cl$_2$]	(11)	Blue	265–269	4(A) 178(M)	65.5 (65.3)	5.7 (5.6)	3.6 (3.6)
[Pd(DPEBA)$_2$Cl]Cl	(12)	Yellow	293	70	61.7 (61.5)	5.3 (5.2)	3.4 (3.4)
[Pt(DPEBA)$_2$Cl]Cl	(13)	Pale yellow	285	79	55.6 (56.2)	4.9 (4.9)	3.1 (3.0)

[a] Decomposition temperatures.
[b] Measured in DMF solution except where mentioned, A = acetone, M = methanol.
[c] Found values are given in parentheses.

glet at δ 196.2 indicative of a coordinated carbonyl group. The $^{31}P\{^1H\}$ NMR spectrum of **1a** exhibits a singlet at δ 20.3 which is typical of the presence of *trans* phosphorus atoms (Structure **Ia**).

Interaction of $RuCl_3(AsPh_3)_2MeOH$ or $RuCl_3 \cdot 3H_2O$ with the ligand DPEBA in 1 : 2 molar equivalents resulted in the formation of the cationic Ru(III) complex $[Ru(DPEBA)_2Cl_2]$ (**2**). Complex **2** is a 1 : 1 electrolyte (Table 1) and exhibits a magnetic moment of 1.98 μ_B corresponding to one unpaired electron as expected for a low-spin, Ru(III) species. The *trans* coordination of the chloride is indicated by the presence of a single (Ru—Cl) band at 326 cm^{-1}. The $^{31}P\{^1H\}$ NMR spectrum of **2** exhibits a rather broad singlet at δ 37.2 due to the paramagnetic nature of the complex. Based on the ^{31}P chemical shift value an octahedral geometry in which the phosphorus atoms of the ligand DPEBA lie *cis* to each other is proposed (Structure **II**).

Carbonylation of **2** in MeOH–CH_2Cl_2 solvent gave the carbonyl complex $[RuCl(CO)(DPEBA)_2]Cl_2$ (**2a**) by the displacement of one of the chlorines present in **2**. Complex **2a** is a 1 : 2 electrolyte (Table 1) and its infrared spectrum gave the ν(CO) band at 1940 cm^{-1}. The $^{13}C\{^1H\}$ NMR spectrum of **2a** exhibits the resonance of CO at δ 208.0. The $^{31}P\{^1H\}$ NMR spectrum of **2a** exhibits a more upfield broad singlet at δ 20.2 indicating a *trans* geometry for the two coordinated phosphorus atoms of the ligands (Structure **IIa**) unlike that of **2** where the phosphorus atoms are *trans* to a N donor group. The magnetic susceptibility of com-

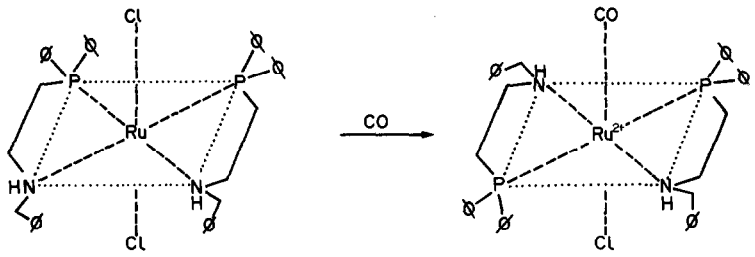

II IIa

plex **2a** gave a value of 1.95 μ_B corresponding to a low spin t_{2g}^5 Ru(III) complex. The oxidation state of ruthenium (+3) in the complex is also supported by the further downfield shift of the CO resonance at δ 208.0 indicative of a weaker Ru(III)—CO bond.

Co, Rh and Ir complexes of DPEBA. The reaction of $CoCl_2 \cdot 6H_2O$ and DPEBA in refluxing methanol, gave the greenish-blue, neutral, high-spin complex $[CoCl_2(DPEBA)]$ (**3**). The complex is a non-electrolyte (Table 1), with chlorides coordinated to the metal ion as evidenced by the presence of ν(Co—Cl) at 366 and 322 cm^{-1}. The electronic spectrum of **3** in dichloromethane is consistent with a tetrahedral geometry. The band at 707 nm in the visible region is assigned to the $^4A_2(F) \rightarrow {}^4T_1(P)(\nu_3)$ transition,[17] which is split into a number of components indicating a considerable deviation from the T_d symmetry. The magnetic moment, 4.41 μ_B also corroborates a tetrahedral, high spin, cobalt(II) species, with paramagnetism nearer to the spin-only value.[18,19] No $^{31}P\{^1H\}$ signal for complex **3** was obtained. Based on the above spectral data a tetrahedral geometry is proposed for complex **3**.

The reaction of the ligand DPEBA with $RhCl(PPh_3)_3$, $[RhCl(COD)]_2$ and $[IrCl(COD)]_2$

Table 2. $^{31}P\{^1H\}$ NMR spectral data for metal complexes

Complex[a]		Solvent	Chemical shift[b] (δ)	Coupling constants (Hz) J(M–P)	J(P–P)
$Ph_2PCH_2CH_2N(H)CH_2Ph \cdot HCl$		$CHCl_3$	−19.3(s)	—	—
$[Ru(DPEBA)_2Cl]Cl$	(**1**)	Methanol	45.8(d)	—	—
			42.9(d)		
$[RuCl(CO)(DPEBA)_2]Cl$	(**1a**)	$CHCl_3$	20.3(s)	—	—
$[Ru(DPEBA)_2Cl_2]Cl$	(**2**)	$CHCl_3$	37.2(bs)	—	—
$[RuCl(CO)(DPEBA)_2]Cl_2$	(**2a**)	$CHCl_3$	20.2(bs)	—	—
$[Rh(DPEBA)_2Cl]$	(**4**)	Methanol	36.1(d)	115	25
			33.2(d)		
			22.3(2)	115	
			19.6(d)		
$[Rh(DPEBA)_2]Cl$	(**5**)	Methanol	52.7(d)	154.00	—
$[Ir(DPEBA)_2]Cl$	(**6**)	$CHCl_3$	−22.0(s)	—	—
$[Rh(DPEBA)(CO)Cl]$	(**7**)	Methanol	22.7(d)	126.95	—
$[Ir(DPEBA)COCl]$	(**8**)	$CHCl_3$	−7.2(s)	—	—
$[Rh(DPEBA)_2Cl_2]Cl$	(**9**)	$CHCl_3$	8.7(d)	86.89	—
$[Ir(DPEBA)_2Cl_2]Cl$	(**10**)	$CHCl_3$	−22.9(s)	—	—
$[Ni(DPEBA)_2Cl_2]$	(**11**)	Acetone	62.3(s)[c]	—	—
$[Pd(DPEBA)_2Cl]Cl$	(**12**)	$CHCl_3$	47.3(d)	—	40
			13.0(d)		
$[Pt(DPEBA)_2Cl]Cl$	(**13**)	$CHCl_3$	34.0(d)	3768.9	18
			−0.99(d)	3259.3	

[a] DPEBA = $Ph_2PCH_2CH_2N(H)CH_2Ph \cdot HCl$.

[b] Chemical shift values (δ) in ppm relative to 85% H_3PO_4, with positive values downfield from reference, s = singlet; d = doublet, bs = broad singlet.

[c] See the text.

resulted in the formation of $[Rh(DPEBA)_2Cl]$ **4**, $[Rh(DPEBA)_2]Cl$ **5** and $[Ir(DPEBA)_2]Cl$ **6**, respectively. Complex **4** is a non-electrolyte, whereas **5** and **6** are 1 : 1 electrolytes (Table 1). A band at 330 cm^{-1} in the IR spectrum of **5** is assigned to ν(Rh—Cl).

The $^{31}P\{^1H\}$ NMR spectrum of **4** displays an AMX type of spectrum with a pair of doublets of doublets (Table 2) indicating the presence of two non-equivalent phosphorus atoms and also suggests that one of the ligands DPEBA, which is potentially bidentate, is coordinated to the metal ion through its phosphorus donor atom only and the other donor atom N being free as shown in Structure **III**.

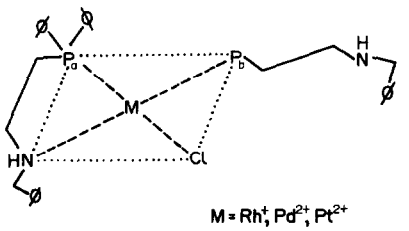

III

Based on the chemical shift, the doublet of doublets at δ 34.7 can be attributed to the phosphorus atom (P_a) *trans* to Cl and the other doublet of doublets at δ 21.0 is assigned to the phosphorus atom (P_b) of the unidentate DPEBA. The larger downfield chemical shift δ 20 of P_a in comparison to P_b is due to the involvement of P_a in a five-membered ring and also the *trans* disposition to Cl.[20] The $^1J(Rh—P_a)$ and $^1J(Rh—P_b)$ coupling constant values of about 115 Hz and the $^2J(P_a—P_b)$ of 25 Hz are in agreement with the earlier reported work[21] and confirm the square-planar geometry as shown in (**III**).

The $^{31}P\{^1H\}$ NMR spectra of complexes **5** and **6**, however, display doublets at δ 52.7 (with $^1J(Rh—P) = 154$ Hz) for complex **5** and a singlet at δ −22.04 for complex **6** (Table 2). The ^{31}P NMR spectral data of **5** and **6** support the coordination of all the donor atoms to the metal ions with *cis* phosphorus as shown in **IV**.

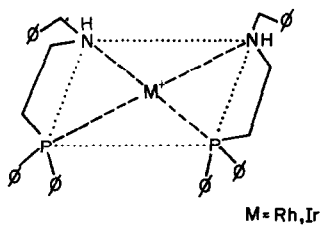

IV

Complex [RhCl(CO)(DPEBA)] **7** and [IrCl(CO)(DPEBA)] **8** were synthesized by the interaction of one equivalent of the ligand DPEBA with the complexes $MCl(CO)(PPh_3)_2$ (M = Rh, Ir). Complexes **7** and **8** exhibit intense infrared absorptions at 1970 and 2020 cm^{-1} respectively, indicative of the coordinated CO. The ν(Rh—Cl) and ν(Ir—Cl) are observed at 348 and 325 cm^{-1} in complexes **7** and **8**, respectively.

The $^{31}P\{^1H\}$ NMR spectra (Table 2) displays a doublet at δ 27.7 for complex **7** with $^1J(Rh—P) = 126$ Hz and a singlet at δ −7.2 for complex **8**, respectively. A square-planar geometry with phosphorus either *trans* to Cl or CO can therefore be proposed. However the chemical shift values suggest that the phosphorus is *trans* to a CO group[15] (Structure **V**).

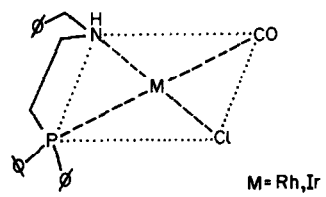

V

The Rh(III) and Ir(III) complexes $[MCl_2(DPEBA)_2]Cl$ (M = Rh **9**, Ir **10**) show conductance values indicative of 1 : 1 electrolytes. The ν(Rh—Cl) and ν(Ir—Cl), in **9** and **10** are observed at 310 and 340 cm^{-1}, respectively. The $^{31}P\{^1H\}$ NMR spectra of **9** and **10** exhibits a doublet at δ 8.7 with $^1J(Rh—P) = 86$ Hz and a singlet at δ −22.9, respectively. An octahedral geometry with a *cis* disposition of phosphorus atoms and *trans* chlorides is proposed for **9** and **10**.

The $^{31}P\{^1H\}$ NMR data (Table 2) of complexes **4**, **5**, **7** and **9** reveal the fact that the $^1J(Rh—P)$ of Rh(I) complexes are larger than the $^1J(Rh—P)$ coupling values of Rh(III) complexes as was observed earlier.[22] The $^1J(Rh—P)$ in Rh(I) complexes are of the order 115–154 Hz whereas it is around 86 Hz in the Rh(III) complex. The ^{31}P NMR chemical shifts of coordination complexes are generally observed downfield as compared to that of the free ligand due to the strong σ-donor bond from phosphorus to metal with a small d_π–d_π back donation. However in the case of iridium complexes **6**, **8** and **10** the chemical shift (δ) values are observed at higher field values particularly for the complexes **6** and **10** where the chemical shifts are observed at δ −22.0 and −22.9 respectively.

The $^{31}P\{^1H\}$ chemical shifts of the third transition series of elements are usually close to the free ligand value or at values more upfield to that of the free ligand.[23] The upfield shift in the δ values can be accounted in terms of a weak metal phosphorus σ-bond and a strong metal to ligand d_π–d_π back bonding interaction.[24,25]

Ni(II), Pd(II) *and* Pt(II) *complexes of DPEBA.* The reaction of $NiCl_2 \cdot 6H_2O$ with the ligand DPEBA in boiling butanol gave a deep blue, neutral, octahedral 1 : 2 complex $[Ni(DPEBA)_2Cl_2]$ (**11**). The presence of a ν(Ni—Cl) band at 321 cm^{-1} is due to the *trans* chlorides.

The electronic spectrum of **11** in acetone displays three bands at 635, 560 and 325 nm, which are assigned to $^3A_{2g} \rightarrow {}^3T_{2g}$, $^3A_{2g} \rightarrow {}^3T_{1g}(F)$ and $^3A_{2g} \rightarrow {}^3T_{1g}(P)$ transitions, respectively, characteristic of an octahedral, Ni(II) species. When complex **11** is dissolved in methanol the deep-blue colour of the complex rapidly changes to a bright red colour and the electronic spectrum of this solution exhibits a single absorption band at 414 nm, which can be attributed to a square-planar Ni(II) species **11a** derived from a change of the octahedral Ni(II) geometry to a diamagnetic square-planar geometry. The change from **11** to **11a** can be brought about by slow addition of methanol to the acetone solution **11** and observe the decrease in the intensities of the peaks in the UV-Vis spectrum at 635, 560 and 325 nm and simultaneously the increase in the intensity of 414 nm. This change is further corroborated by studying the conductivity (Table 1) and $^{31}P\{^1H\}$ NMR of **11** and **11a**. The complex **11** is neutral, whereas **11a** is a 1 : 2 electrolyte. The $^{31}P\{^1H\}$ NMR spectrum of **11** in acetone at room temperature does not give a well resolved spectrum but at −30°C it gives a singlet at δ 62.3. This large chemical shift may be due to the disposition of the two phosporus atoms *trans* to Cl (Structure **VI**). The $^{31}P\{^1H\}$ NMR spectrum of **11a** in methanol displays a sharp singlet but at a much higher field of δ 29.18 when compared to that for **11**, suggesting the equivalence of the phosphorus atoms in either a *cis* or a *trans* configuration as shown in **VIa**. The square-planar complex **11a** is not converted back to **11** on the addition of acetone.

Interaction of K_2MCl_2 (M = Pd, Pt) with the ligand DPEBA in a 1 : 2 molar equivalents in water–acetone mixture give rise to cationic complexes of the type $[MCl(DPEBA)_2]Cl$ (M = Pd **12**; Pt **13**). The 1 : 1 electrolytic nature of these complexes and the presence of ν(M—Cl)[26] at 325 and 310 cm^{-1} in **12** and **13** support the configuration of the complexes **12** and **13** as shown above. The $^{31}P\{^1H\}$ NMR of both complexes **12** and **13** confirm the unidentate nature of one of the DPEBA ligands coordinated to the metal ion. The ^{31}P NMR spectrum of **12** exhibits two doublets at δ 47.3 and 13.0 indicating the presence of two non-equivalent phosphorus atoms. The doublet at δ 47.3 can be assigned to phosphorus atom (P_a) (Structure **III**) *trans* to Cl and associated in a five-membered ring.[27] The doublet at δ 13.0 can be assigned to the phosphorus atom (P_b) of the ligand DPEBA acting in a monodentate fashion with the nitrogen end free. The $J(P_a–P_b)$ value of 39.2 Hz is also typical of *cis*-phosphorus atoms and the square-planar geometry is assigned as shown in **III**.

The $^{31}P\{^1H\}$ NMR spectrum (Fig. 1) of complex **13** displays two doublets at δ 34.0 and −0.99 with ^{195}Pt satellites confirming the unidentate nature of

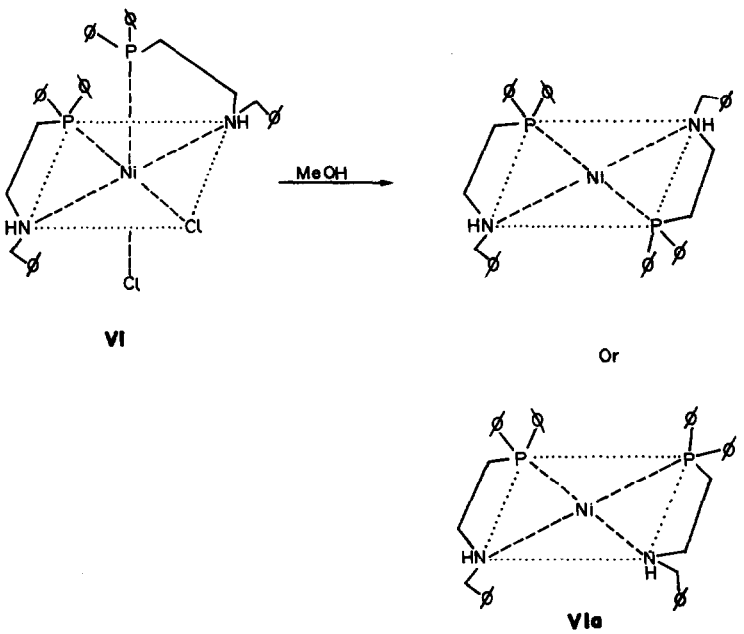

VI **VIa**

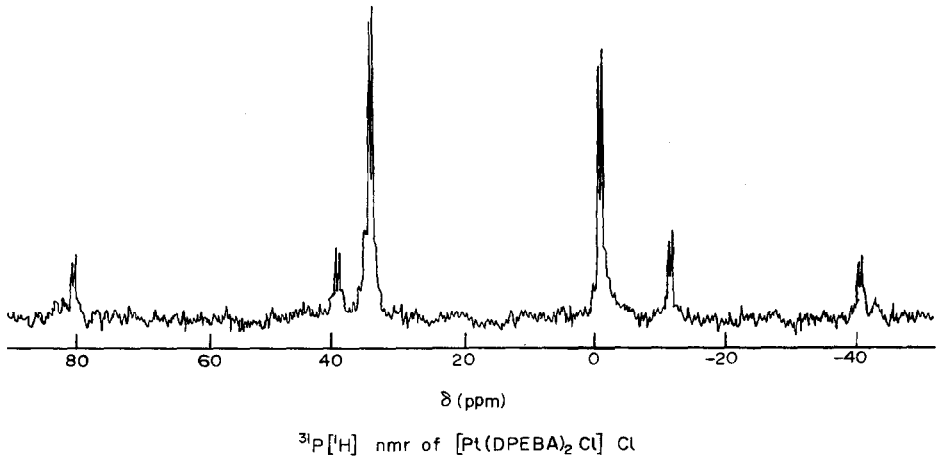

Fig. 1. $^{31}P\{^{1}H\}$ NMR spectrum of $[PtCl(DPEBA)_2]Cl$.

one of the two ligands DPEBA. The former doublet at δ 34.0 can be assigned to P_a of the ligand DPEBA involved in a five-membered ring(III) and the latter δ −0.99 to the P_b of the unidentate ligand. The $^{1}J(Pt—P_a)$ value of 3768 Hz and $^{1}J(Pt—P_b)$ of 3259 Hz are typical of a phosphine *trans* to chloride and *trans* to an amine, respectively.[28,29] The $^{2}J(P_a–P_b)$ of 18 Hz is also typical of mutually *cis* phosphines[29] as shown in (**III**).

The ^{31}P NMR chemical shifts (δ) (Table 2) of all the complexes reveal that there is a good correlation between the size of the metal ion and chemical shifts. In the group Co, Rh, Ir and Ni, Pd, Pt the coordination chemical shifts are largest for the first member of the triad and decreases in the order Co > Rh > Ir and similarly Ni > Pd > Pt as the size increases and electronegativity decreases. It was also observed that the chemical shift values decrease in the order Ru(III) > Rh(III) > Ir(III).

EXPERIMENTAL

The Ru(III), Ir(III) and Rh(III) trichloride trihydrates, K_2PdCl_4 and K_2PtCl_4 were obtained from Johnson Matthey (U.K.) or Alfa Inorganics (U.S.A.). The ligand triphenyl-phosphine was purchased from Strem Chemicals Inc. (U.S.A.). The complexes $RuCl_2(PPh_3)_3$,[30] $RuCl_2(Me_2SO)_4$,[31] $RuCl_3(AsPh_3)_2MeOH$,[27] $RhCl(PPh_3)_3$,[32] $RhCl(CO)(PPh_3)_2$,[33] $IrCl(CO)(PPh_3)_2$[33,34] and $[M(COD)Cl]_2$ (M = Rh, Ir[35]) were synthesized by published procedures. Ethanolamine, benzyl chloride and thionyl chloride were of Analar reagent grade and were used without further purification. All solvents used in this work were of reagent grade and were purified and dried before use. All the preparations were carried out under an atmosphere of nitrogen. Microanalysis, melting points, infrared spectra, conductivity and magnetic susceptibility measurements were done as reported.[36] Proton NMR spectra of the ligand DPEBA was recorded on a Bruker 270 MHz spectrometer in $CDCl_3$. The Carbon-13 NMR spectra of the ligand was recorded on a Jeol FX100 spectrometer operating at 24.99 MHz in $CDCl_3$ using TMS as an external reference. Phosphorus-31 NMR spectra of the ligand and complexes were taken in the indicated solvents (Table 2) with a Jeol FX100 spectrometer operating at 40.3 MHz in the Fourier transform mode with proton noise decoupling and a deuterium lock. The samples were placed in a 10 mm NMR tube and a capillary with deuterium oxide was placed in for the lock. Phosphoric acid (85%) was used as an external standard. The electronic spectra of complexes were measured on a Shimadzu UV240 spectrophotometer. Molecular weight and mass spectral measurements of the ligands were done as reported earlier.[2]

Microanalytical data, conductivity, melting point and magnetic susceptibility data of the ligand and complexes were presented in Table 1. The $^{31}P\{^{1}H\}$ NMR spectral data are presented in Table 2.

Synthesis of the ligand DPEBA. The new bidentate ligand {2-(diphenylphosphino)ethyl}benzylamine (DPEBA) was synthesized employing the reaction as shown in Scheme 1.

$$PhCH_2Cl + H_2NCH_2CH_2OH \xrightarrow[\text{ethanol}]{K_2CO_3} PhCH_2N(H)CH_2CH_2OH$$

a

$$\mathbf{a} \xrightarrow[\text{(ii) 10\% NaOH}]{\text{(i) } SOCl_2} PhCh_2N(H)CH_2CH_2Cl$$

b

$$\mathbf{b} + KPPh_2 \cdot 2diox \xrightarrow{1,4\text{-dioxane}} PhCH_2N(H)CH_2CH_2PPh_2$$

c

$$\mathbf{c} + HCl \xrightarrow{methanol} PhCH_2N(H)CH_2CH_2PPh_2 \cdot HCl$$

(Ph = C_6H_5, diox = dioxane)

The compound $PhCH_2N(H)CH_2CH_2OH$, **a** was prepared by the reaction of benzyl chloride (51.8 g, 0.41 mol) with ethanolamine (25.0 g, 0.41 mol) and potassium carbonate (29.5 g, 0.20 mol) in 100 cm^3 of absolute alcohol. The halide **b** was obtained[37] by the reaction of **a** with thionyl chloride in a 1 : 1 ratio in the form of a quaternary ammonium salt which on treatment with 10% NaOH gave the free amine **b** as an insoluble oil. A dioxane solution of the above oil (dried over Na_2SO_4 prior to its use) was added dropwise with stirring to an orange–red suspension of $KPPh_2$[38] in dioxane, in a stoichiometric amount under cold conditions (15–20°C). The reaction mixture was then allowed to reflux for 1 h. During the course of reaction a sharp decolouration of the orange–red colour occurred. The reaction contents were then poured into ice-water to get a crude oil **c** which was then separated and stirred with 2N HCl in 20 ml of methanol to get a white crystalline precipitate **d**. The ligand **d** was recrystallized from methanol–petroleum ether mixture with a yield of about 65%; m.p. 98–100°C; mol.wt. 355.5(calculated), 350(experimental, osmometric in chloroform). Found: C, 70.6; H, 6.4; N, 3.8. Calc. for $C_{21}H_{23}PNCl$: C, 70.9; H, 6.5; N, 3.9%.

Mass spectral fragmentation of DPEBA

$PhCH_2N(H)CH_2CH_2PPh_2^+$ (10),

$PhCH_2—N^+—CH_2CH_2PPh_2$ (42),

$PhCH{=}N^+(H)CH_2CH_2Ph$ (30),

$C_7H_7^+$ (100), P^+Ph_2 (18),

$\overline{C_6H_4P^+C_6H_4}$ (10), PhP^+ (8).

(Ph=C_6H_5).

Preparation of complexes

(1) *Chloro (bis (2 - (diphenylphosphino) ethyl) benzylamine) ruthenium* (II) *chloride*, $[RuCl(DPEBA)_2]Cl$. The complex $RuCl_2(PPh_3)_3$ (0.15 g, 0.16 mmol) and the ligand DPEBA (0.17 g, 0.47 mmol) were refluxed for 12 h in acetone. During the course of the reaction the original brown colour of the solution changed to red. The solution was then reduced to a small volume and diethyl ether added to get a pinkish-red complex which was filtered, washed with benzene and recrystallized from a dichloromethane–diethyl ether mixture. Yield: 71%. Alternatively, the same complex was obtained by the reaction of DPEBA and $RuCl_2(Me_2SO)_4$ in benzene. When carbon monoxide was passed through a MeOH—CH_2Cl_2 solution of $[RuCl(DPEBA)_2]Cl$ the colour of the solution immediately changed to green to give a carbonyl complex of the composition $[RuCl(CO)(DPEBA)_2]Cl$.

(2) *Dichloro(bis(2-(diphenylphosphino)ethyl)benzylamine) ruthenium* (III) *chloride*, $[Ru(DPEBA)_2Cl_2]Cl$. The ligand DPEBA (0.841 g, 1.14 mmol) dissolved in 10 cm^3 of methanol was added to a refluxing methanolic solution of $RuCl_3 \cdot 3H_2O$ (0.2 g, 0.38 mmol). After refluxing the solution for an additional 6 h, the reddish complex was filtered, washed with methanol, diethyl ether and dried *in vacuo*. Yield: 63%. Alternatively, the same complex was obtained by the reaction of DPEBA with $RuCl_3(AsPh_3)_2MeOH$ in benzene. When CO was bubbled through a MeOH—CH_2Cl_2 solution of $[RuCl_2(DPEBA)_2]Cl$, a brown carbonyl complex of the composition $[RuCl(CO)(DPEBA)_2]Cl_2$ resulted.

(3) *Dichloro* (2 - (*diphenylphosphino*) *ethyl*) *benzylamine*) *cobalt* (II), $[Co(DPEBA)Cl_2]$. A solution of the ligand DPEBA (0.45 g, 1.26 mmol) dissolved in methanol was added to a refluxing methanolic solution of $CoCl_2 \cdot 6H_2O$. The colour of the solution changed to greenish-blue immediately. After refluxing the solution for 6 h it was concentrated to a small volume by a vacuum rotary evaporator and the complex precipitated by the addition of diethyl ether. The greenish-blue complex was filtered, washed with CCl_4, diethyl ether and dried *in vacuo*. The complex was recrystallized from a dichloromethane–diethyl ether mixture. Yield: 70%.

(4) *Chloro (bis (2 - (diphenylphosphino) ethyl) benzylamine) rhodium* (I), $[Rh(DPEBA(_2Cl]$. The complex $RhCl(PPh_3)_3$ (0.15 g, 0.16 mmol) and the ligand DPEBA (0.15 g, 0.324 mmol) in 30 cm^3 of benzene were refluxed for 12 h. The solution was concentrated to a small volume and diethyl ether added to get a yellow precipitate which was filtered, washed with CCl_4, diethyl ether and recrystallized from a methanol–diethyl ether mixture. Yield: 78%.

(5) (*Bis* (2 - (*diphenylphosphino*) *ethyl*) *benzylamine*) *rhodium* (I) *chloride*, $[Rh(DPEBA)_2]Cl$. The complex $[Rh(COD)Cl]_2$ (0.15 g, 0.30 mmol) and the ligand DPEBA (0.43 g, 1.21 mmol) were refluxed for 7 h in acetone. The solution was then concentrated to a small volume and by the addition of diethyl ether the precipitated complex was

filtered, washed with diethyl ether and recrystallized from a dichloromethane–*n*-hexane mixture. Yield: 55%.

(6) *(Bis (2 - (diphenylphosphino) ethyl) benzylamine) iridium* (I) *chloride*, $[Ir(DPEBA)_2]Cl$. The ligand DPEBA (0.27 g, 0.75 mmol) was added to a refluxing benzene solution of $[Ir(COD)Cl]_2$ (0.13 g, 0.19 mmol). After refluxing the solution for 6 h, the yellow crystalline complex separated was filtered and washed with benzene. Yield: 78%.

(7) *Chlorocarbonyl(2-(diphenylphosphino)ethyl) benzylamine)rhodium*(I), [RhCl(CO)(DPEBA)]. The ligand DPEBA (0.15 g, 0.42 mmol) dissolved in 10 cm^3 of benzene was added to a refluxing benzene solution of $RhCl(CO))(PPh_3)_2$ (0.29 g, 0.42 mmol). After refluxing the solution for 6 h, the solution was cooled and a yellow crystalline complex was obtained. The complex was filtered, washed with benzene, diethyl ether and dried *in vacuo*. Yield: 84%.

(8) *Chlorocarbonyl(2-(diphenylphosphino)ethyl) benzylamine) iridium* (I), [IrCl(CO)(DPEBA)]. To a suspension of $IrCl(Co)(PPh_3)_2$ (0.24 g, 0.31 mmol), the ligand DPEBA (0.11 g, 0.31 mmol) was added and refluxed for 6 h. The solution was concentrated to a small volume by a rotary vacuum evaporator. The addition of diethyl ether gave a yellow complex which was filtered, washed with CCl_4 and recrystallized from a methanol–diethyl ether mixture. Yield: 65%.

(9) *Dichloro (bis (2 - (diphenylphosphino) ethyl) benzylamine)rhodium*(III)*chloride*, $[RhCl_2(DPEBA)_2]$ Cl. To a refluxing methanolic solution of $RhCl_3 \cdot 3H_2O$ (0.17 g, 0.63 mmol), the ligand DPEBA (0.67 g, 1.80 mmol) was added and the solution further refluxed for 10 h. The solution was then evaporated to a small volume on a rotary vacuum evaporator and diethyl ether added to get a yellow crystalline complex. The compound was filtered, washed with diethyl ether and recrystallized from a dichloromethane–*n*-hexane mixture. Yield: 72%.

(10) *Dichloro(bis(2-(diphenylphosphino)ethyl)benzylamine)iridium*(III)*chloride*, $[IrCl_2(DPEBA)_2]$ Cl. A mixture of 0.1 g (0.28 mmol) of $IrCl_3 \cdot 3H_2O$ and the ligand DPEBA (0.31 g, 0.85 mmol) in ethanol was refluxed for 6 h. During the course of the reaction the colour of the solution changed to pale-yellow. The solution was concentrated to a small volume by a vacuum rotary evaporator and the complex precipitated by the addition of diethyl ether. The pale-yellow complex was filtered, washed with water, CCl_4 and recrystallized from a dichloromethane–*n*-hexane mixture. Yield: 55%.

(11) *Dichloro (bis (2 - (diphenylphosphino) ethyl) benzylamine) nickel* (II), $[NiCl_2(DPEBA)_2]$. A mixture of hydrated nickel(II) chloride (0.20 g, 0.84 mmol) and the ligand DPEBA (0.59 g, 1.6 mmol) were refluxed in 30 cm^3 of degassed butanol for 4 h. A deep-blue crystalline complex was obtained, which was filtered, washed with hot butanol and diethyl ether and dried *in vacuo*. Yield: 85%.

(12) *Chloro(bis(2-(diphenylphosphino)ethyl)benzylamine)palladium*(II)*chloride*, [PdCl(DPEBA)]Cl.

(13) *Chloro(bis(2-(diphenylphosphino)ethyl)benzylamine)platinum*(II)*chloride*, [PtCl(DPEBA)]Cl. For the preparation of **12** and **13** aqueous solutions of K_2PdCl_4 (0.1 g, 0.31 mmol) and K_2PtCl_4 (0.2 g, 0.48 mmol) were added separately to a refluxing acetone solution of the ligand DPEBA (0.61 g, 0.61 mmol and 0.34 g, 0.96 mmol). The solutions after refluxing for 3 h were evaporated to dryness by a rotary vacuum evaporator to get pale-yellow complexes of the composition [PdCl(DPEBA)]Cl **12** and [PtCl(DPEBA)]Cl **13**. The complexes were filtered, washed with diethyl ether and recrystallized from a dichloromethane–diethyl ether mixture. Yield: 75% **12**; 60% **13**.

REFERENCES

1. M. M. Taqui Khan, V. Vijay Sen Reddy and H. C. Bajaj, *Polyhedron* 1987, **6**, 921.
2. M. M. Taqui Khan and V. Vijay Sen Reddy, *Inorg. Chem.* 1986, **25**, 208.
3. M. M. Taqui Khan and B. Swamy, *Inorg. Chem.* 1987, **26**, 178.
4. M. M. Taqui Khan, K. Nazeeruddin and H. C. Bajaj, *J. Chem. Soc., Dalton Trans.* 1986 (Communicated).
5. M. M. Taqui Khan, B. T. Khan and Begum Safia, *J. Mol. Cat.* 1986, **9**, 34 and references therein.
6. T. Suarez and B. Fontal, *J. Mol. Cat.* 1985, **32**, 191.
7. D. M. Roundhill, R. A. Bechtold and S. G. N. Roundhill, *Inorg. Chem.* 1980, **19**, 284 and references therein.
8. M. Haib, H. Trujillo, C. A. Alexander and B. N. Storhoff, *Inorg. Chem.* 1985, **24**, 2344 and references therein.
9. J. A. Davies and F. R. Hartley, *Chem. Rev.* 1981, **81**, 79.
10. R. R. Schrock J. A. Osborn, *J. Am. Chem. Soc.* 1976, **98**, 2134.
11. A. Sen and T. W. Lai, *Organometallics* 1982, **1**, 415.
12. R. Colton and Q. N. Porter, *Aust. J. Chem.* 1968, **21**, 2215.
13. R. B. King and P. N. Kapoor, *J. Am. Chem. Soc.* 1971, **93**, 4158.
14. W. J. Geary, *Coord. Chem. Rev.* 1971, **7**, 81.
15. J. B. Letts, T. J. Mazanec and D. W. Meek, *J. Am. Chem. Soc.* 1982, **104**, 3898.
16. J. C. Briggs, C. A. McAuliffe and G. Dyer, *J. Chem. Soc., Dalton Trans.* 1984, 423.

17. L. Sacconi and R. Morassi, *J. Chem. Soc. A* 1968, 2997.
18. J. A. Bertrand and D. L. Plymale, *Inorg. Chem.* 1966, **5**, 879.
19. B. N. Figgis and R. Nyholm, *J. Chem. Soc.* 1959, 338.
20. P. E. Garrou, *Chem. Rev.* 1981, 229.
21. K. D. Tau, D. W. Meek, T. Sorrel and J. A. Ibers, *Inorg. Chem.* 1978, **17**, 3454.
22. A. Pidcock and J. F. Nixon, *Ann. Rev. NMR Spectra* 1969, **2**, 345.
23. A. Pidcock, R. E. Richards and L. M. Venanzi, *J. Chem. Soc. A.* 1966, 1707.
24. T. Kruch and W. Lang, *Z. Anorg. Chem.* 1968, **118**, 356.
25. J. G. Smith and D. T. Thompson, *J. Chem. Soc. A* 1967, 1694.
26. F. R. Hartley, *The Chemistry of Platinum and Palladium*. Applied Science, Barking (1973).
27. Ruiz-Ramirez, L. Stephenson and T. A. Switkes, *J. Chem. Soc., Dalton Trans.* 1973, 1770.
28. G. K. Anderson, H. C. Clark and J. A. Davies, *Inorg. Chem.* 1983, **22**, 434.
29. G. K. Anderson and Ravi Kumar, *Inorg. Chem.* 1984, **24**, 4064.
30. T. A. Stephenson and G. J. Wilkinson, *Inorg. Nucl. Chem.* 1966, **28**, 945.
31. I. P. Evans, A. Spencer and G. Wilkinson, *J. Chem. Soc., Dalton Trans.* 1973, 204.
32. J. A. Osborn, F. A. Jardine, J. F. Young and G. Wilkinson, *J. Chem. Soc. A.* 1966, 1711.
33. W. L. Jolly, Ed., *Inorg. Synth.* Vol. XI, p. 101.
34. L. Vaska and J. W. Di Luzio, *J. Am. Chem. Soc.* 1961, **83**, 1262.
35. J. Herde, J. Lambert and C. V. Senott, *Inorg. Synth.* 1974, **15**, 18.
36. M. M. Taqui Khan and K. Veera Reddy, *J. Coord. Chem.* 1982, **12**, 71.
37. J. P. Mason and D. J. Gosc, *J. Am. Chem. Soc.* 1938, **60**, 2816.
38. K. Isslieb and A. Tzschach, *Chem. Ber.* 1959, **92**, 1118.

Polyhedron Vol. 6, No. 11, pp. 2019–2026, 1987
Printed in Great Britain

0277–5387/87 $3.00+.00

THE CHEMISTRY OF STERICALLY CROWDED ARYLOXIDE LIGANDS—VII. SYNTHESIS, STRUCTURE AND SPECTROSCOPIC PROPERTIES OF SOME GROUP 4 AND GROUP 5 METAL DERIVATIVES OF 2,6-DIPHENYLPHENOXIDE

ROBERT W. CHESNUT, LOREN D. DURFEE, PHILLIP E. FANWICK and IAN P. ROTHWELL*

Department of Chemistry, Purdue University, West Lafayette, IN 47907, U.S.A.

and

KIRSTEN FOLTING and JOHN C. HUFFMAN

Molecular Structure Center, Indiana University, Bloomington, IN 47405, U.S.A.

(*Received* 16 *March* 1987; *accepted* 24 *June* 1987)

Abstract—A series of early transition metal organometallic derivatives containing the ancillary ligand 2,6-diphenylphenoxide (OAr–2,6Ph_2) have been synthesized. Compounds of stoichiometry Ti(OAr–2,6Ph_2)$_2$(R)$_2$ (R = CH_3, CH_2SiMe_3, CH_2Ph and Ph) and Ti(OAr–2,6Ph)$_3$(R) (R = CH_3, CH_2SiMe_3) are obtained by treating the corresponding homoleptic alkyl, TiR_4, with the required amount of phenol, HOAr–2,6Ph_2. For the Group 5 metals Nb and Ta, the methyl derivatives M(OAr–2,6Ph_2)$_2$(CH_3)$_3$ and M(OAr–2,6Ph_2)$_3$(CH_3)$_2$ are obtained via methylation of the corresponding chloro-aryloxides. Besides routine spectroscopic characterization the diphenyl Ti(OAr–2,6Ph_2)$_2$(Ph)$_2$ and mono-alkyl Ti(OAr–2,6Ph_2)$_3$(CH_2SiMe_3) have been structurally characterized by X-ray diffraction techniques. Both molecules contain a pseudo-tetrahedral environment about the titanium atom with short 1.794(3)–1.806(2) Å, Ti—O distances and large, 153–179°, Ti—O—Ar angles. The Ti—C distances appear normal for these types of compounds.

The last few years have seen a considerable research effort into the study of the inorganic and organometallic chemistry associated with 2,6-dialkylphenoxide, (OAr) and 2,6-dialkylthiophenoxide, (SAr) ligation. In the case of the phenoxide ligands a diverse range of chemistry has been supported.[1–4] The related thiophenoxide ligands have also been extensively used with a wider range of transition metals to generate systems of possible relevance to biological thiolate environments.[5–8] Following our work on the sterically very demanding 2,6-di-*tert*-butylphenoxide ligand which has been shown to sometimes undergo the mild activation of the aliphatic carbon-hydrogen bonds of the *tert*-butyl groups,[9,10] we have begun an investigation of the ligand 2,6-diphenylphenoxide on similar metal systems.[11] This ligand has the possibility of forming related six-membered metallacycle rings, albeit this time via activation of an aromatic CH bond. Recent work by our group on molybdenum has confirmed this postulate.[12] We wish to report here our synthesis of a number of Group

* Author to whom correspondence should be addressed. Camille and Henry Dreyfus Teacher–Scholar, 1985–1990; Fellow of the Alfred P. Sloan Foundation, 1986–1990.

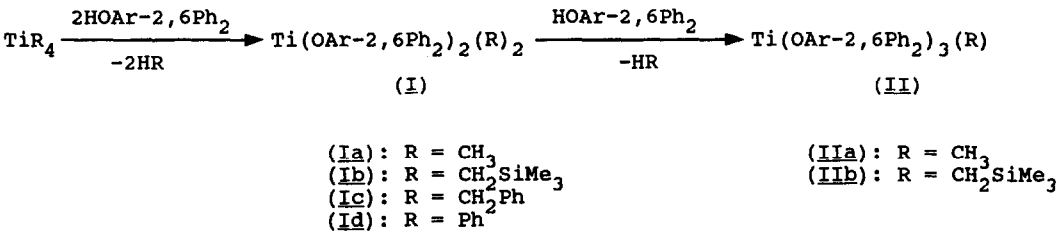

Scheme 1.

4 and Group 5 metal organometallic derivatives of this ligand as well as their structural and spectroscopic properties. While this work was in progress we became aware that some related studies were being carried out by Dilworth and coworkers[13,14] to complement the interesting work they had previously completed on the related 2,6-diphenylthiophenoxide group.[5]

RESULTS AND DISCUSSION

Synthesis of compounds

Two general synthetic strategies for the synthesis of organometallic derivatives containing 2,6-diphenylphenoxide ligation were employed. The first involved the treatment of homoleptic alkyls of titanium and zirconium[15] with the parent phenolic reagent in hydrocarbon solvents. This resulted in the sequential protonolysis of alkyl groups to directly generate mixed alkyl, phenoxides of this ligand. For zirconium the treatment of $Zr(CH_2SiMe_3)_4$ with HOAr–2,6Ph_2 led to the rapid replacement of all alkyl groups and formation of sparingly soluble $Zr(OAr–2,6Ph_2)_4$ in essentially quantitative yields. However, with titanium alkyls the substitution reaction was more controlled and allowed the synthesis in moderate yields of a number of compounds of general formulae $Ti(OAr–2,6Ph_2)_2(R)_2$ (**I**) and $Ti(OAr–2,6Ph_2)_3(R)$ (**II**) (Scheme 1). The tetra-alkyl substrate TiR_4 was either isolated ($R = CH_2SiMe_3$) or else generated *in situ* ($R = CH_3$, CH_2Ph, Ph) before being reacted with HOAr–2,6Ph_2. The phenoxide derivatives (**I**) and (**II**) were thermally much more robust than the corresponding homoleptic alkyls, undergoing little noticeable decomposition either in the solid state or hydrocarbon solution at 20–30°C over periods of weeks. These deep red or yellow crystalline materials proved only slightly soluble in hexane but much more soluble in aromatic hydrocarbon solvents.

For the Group 5 metals niobium and tantalum a synthetic route via the mixed chloro, phenoxide intermediates was investigated (Scheme 2). Treatment of the pentahalides MCl_5 (M = Nb, Ta) with HOAr–2,6Ph_2 (2 equivalents) in benzene led to the corresponding trichlorides $M(OAr–2,6Ph_2)_2Cl_3$ in good yields. It was then found possible to further substitute one more chloride ligand by using LiOAr–2,6Ph_2, again in hydrocarbon solvents, to yield the dihalide derivatives. Treatment of these halide substrates with the alkylating agent $LiCH_3$ resulted in the formation of the corresponding methyl compounds, $M(OAr–2,6Ph_2)_2(CH_3)_3$ (**III**) and $M(OAr–2,6Ph_2)_3(CH_3)_2$ (**IV**) as yellow (M = Nb) or colorless (M = Ta) crystalline solids (Scheme 2). Treatment of the dimethyl species (**IV**) with excess $LiCH_3$ resulted initially in the formation of (**III**) with loss of LiOAr–2,6Ph_2, but on extended

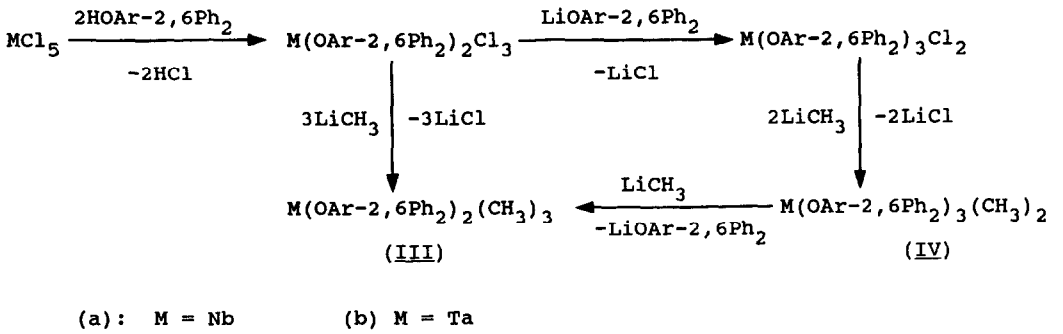

Scheme 2.

exposure decomposition, presumably via formation of $M(CH_3)_5$, took place. This reactivity pattern is similar to that found for other 2,6-di-alkylphenoxide complexes of these metals.[1]

Spectroscopic properties

Some selected NMR data are collected in Table 1. As is to be expected the ^1H and ^{13}C NMR spectra of the 2,6-diphenylphenoxide ligand itself are not very informative, all resonances being grouped in the δ 6–7.5 ppm and δ 110–160 ppm regions. However, the ligand does have some influence on the NMR resonances of other groups contained in the metal coordination sphere. This is a consequence of the phenyl substituents of the aryloxide ligand which, due to their associated diamagnetic anisotropy, tend to shield some of the proton and carbon nuclei of adjacent groups. This effect was also noticed in dimolybdenum amido and tantalum alkylidyne derivatives of this ligand.[11] Table 1 contains some selected ^1H and ^{13}C NMR data for the organometallic compounds obtained in this study. Hence, considering the methyl derivatives one finds that the M-CH_3 protons resonate at values of δ 0.53 (**Ia**), −0.41 (**IIa**), 0.09 (**IIIa**), −0.26 (**IIIb**), 0.18 (**IVa**) and −0.21 ppm (**IVb**) compared to values of δ 1–2 ppm typically found for methyl derivatives of these metals containing other 2,6-dialkylphenoxide ligands. Similar upfield shifts of the resonances of other protons in the alkyl ligands are also evident (Table 1).

Solid state structures of $Ti(OAr\text{–}2,6Ph_2)_2(Ph)_2$ (**Id**) *and* $Ti(OAr\text{–}2,6Ph_2)_3(CH_2SiMe_3)$ (**IIb**)

In order to more fully characterize the coordination properties of the 2,6-diphenylphenoxide ligand in these systems, X-ray diffraction analyses of the diphenyl compound (**Id**) and mono-trimethylsilylmethyl derivative (**IIb**) were carried out. Although a complete data set was also collected on the trimethyl $Ta(OAr\text{–}2,6Ph_2)_2(CH_3)_3$, the structure proved impossible in our hands to solve.[16] Attempts to solve the structure of the niobium analogue by Dilworth and co-workers were also unsuccessful.[13] Figures 1 and 2 contain the ORTEP views of (**Id**) and (**IIb**) respectively while Tables 2 and 3 contain some selected bond distances and angles. The diphenyl compound (**Id**) was found to contain one molecule of benzene per unit cell. It can be seen that both compounds (**Id** and **IIb**) contain a pseudo-tetrahedral arrangement of oxygen and carbon atoms about the titanium metal center. The five Ti—O distances lie in the narrow range of 1.794(3)–1.806(2) Å and can be compared with distances of 1.780(3) and 1.781(3) Å in $Ti(OAr\text{–}2,6Pr^i_2)_4$[17] and 1.782(8), 1.802(7) and 1.810(9) in $Ti(OAr\text{–}2,6Bu^t_2)_3I$.[18] In the less crowded diphenyl (**Id**) the Ti—O—Ar angles are 153.0(3) and 162.2(3)° while in the much more sterically congested $Ti(OAr\text{–}2,6Ph_2)_3(CH_2SiMe_3)$ (**IIb**) this angle opens up to values of 164.6(2), 170.7(2) and 179.1(2)°. These latter values are on average significantly larger than found in the stoichiometrically related iodide compound $Ti(OAr\text{–}2,6Bu^t_2)_3I$; 155.2(4), 158.2(4) and 159.1(4)°.[18]

The short Ti—O distances found in these compounds are consistent with the presence of considerable oxygen-*p* to metal-*d* π-bonding. The almost linear Ti—O—Ar angles also can be attributed to this effect and are characteristic of the coordination of 2,6-dialkylphenoxide ligands to early transition metal centers[19] and allow some relief of the steric congestion at the metal caused by the bulky substituents. Similar structural

Table 1. Selected spectroscopic data

Compound	^1H NMR (δ)[a]	^{13}C NMR (δ)[a]
$Ti(OAr\text{–}2,6Ph_2)_2(CH_3)_2$ (**Ia**)	0.53 (s, Ti–CH_3)	66.1 (Ti–CH_3), ^1J = 125 Hz
$Ti(OAr\text{–}2,6Ph_2)_2(CH_2SiMe_3)_2$ (**Ib**)	0.85 (s, Ti–CH_2); −0.05 ($SiMe_3$)	90.0 (Ti–CH_2), ^1J = 112 Hz; 6.6 ($SiMe_3$)
$Ti(OAr\text{–}2,6Ph_2)_2(CH_2Ph)_2$ (**Ic**)	1.87 (s, Ti–CH_2)	99.2 (Ti–CH_2), ^1J = 131 Hz
$Ti(OAr\text{–}2,6Ph_2)_2(Ph_2)$ (**Id**)	—	202.9 (Ti–C_6H_5)
$Ti(OAr\text{–}2,6Ph_2)_3(CH_3)$ (**IIa**)	−0.41 (s, Ti–CH_3)	66.7 (Ti–CH_3), ^1J = 129 Hz
$Ti(OAr\text{–}2,6Ph_2)_3(CH_2SiMe_3)$ (**IIb**)	0.27 (s, Ti–CH_2); −0.77 ($SiMe_3$)	101.0 (Ti–CH_2) 5.6 ($SiMe_3$)
$Nb(OAr\text{–}2,6Ph_2)_2(CH_3)_3$ (**IIIa**)	0.09 (s, Nb–CH_3)	52.0 (Nb–CH_3)
$Ta(OAr\text{–}2,6Ph_2)_2(CH_3)_3$ (**IIIb**)	−0.26 (s, Ta–CH_3)	58.7 (Ta–CH_3)
$Nb(OAr\text{–}2,6Ph_2)_3(CH_3)_2$ (**IVa**)	0.18 (s, Nb–CH_3)	62.0 (Nb–CH_3)
$Ta(OAr\text{–}2,6Ph_2)_3(CH_3)_2$ (**IVb**)	−0.21 (s, Ta–CH_3)	64.8 (Ta–CH_3)

[a] In C_6D_6 at 30°C.

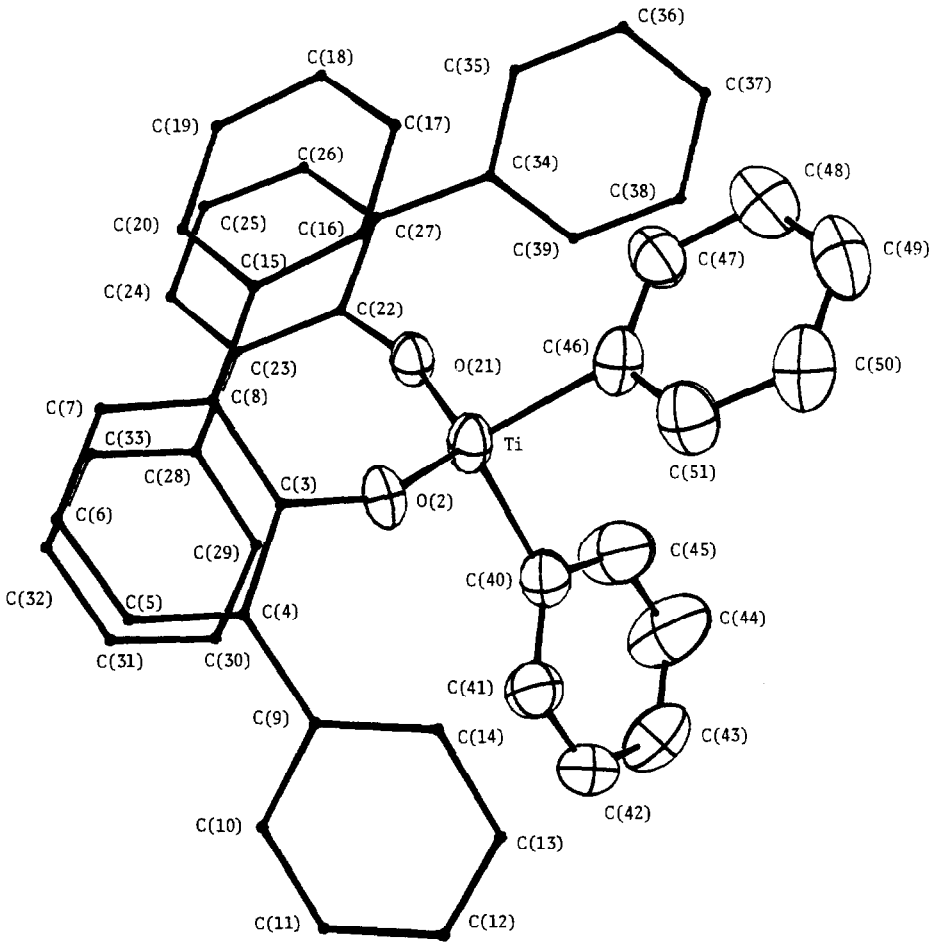

Fig. 1. ORTEP view of $Ti(OAr\text{–}2,6Ph_2)_2(Ph)_2$ (**Id**) emphasizing the central coordination sphere and Ti—Ph groups.

features were reported by Dilworth for $Ti(OAr\text{–}2,6Ph_2)_2Cl_2$.[13] The Ti—C(phenyl) distances of 2.070(5) and 2.106(5) Å in $Ti(OAr\text{–}2,6Ph_2)_2(C_6H_5)_2$ (**Id**) are slightly shorter than the distance of 2.272(14) Å reported for the metallocene derivative $Cp_2Ti(C_6H_5)_2$.[20] The Ti—C distance of 2.051(4) Å in (**IIb**) is also slightly shorter than found in the mono-cyclometallated complex $Ti(OC_6H_3Bu^t CMe_2CH_2)(OAr\text{–}2,6Bu^t_2)(CH_2SiMe_3)(py)$, 2.131(6) Å.[9] However, we do not believe these shorter distances in these derivatives of 2,6-diphenylphenoxide are significant.

EXPERIMENTAL

All reactions were carried out under an atmosphere of dry, oxygen-free nitrogen using standard Schlenk and glove box techniques. Solvents were distilled under nitrogen from sodium benzophenone and stored under nitrogen. The halides $TiCl_4$, $NbCl_5$ and $TaCl_5$ were obtained commercially (Alfa) as was 2,6-diphenylphenol ($HOAr\text{–}2,6Ph_2$, Aldrich). ^1H and ^{13}C NMR spectra were recorded on a Varian Associates XL-200 spectrometer. Microanalyses were obtained in-house at Purdue University.

Preparations

Due to similarities of the procedures used full details of the synthesis of only representative compounds will be given. Considerable difficulty in obtaining good microanalyses of derivatives of 2,6-diphenylphenoxide was experienced. Typically carbon percentages were suppressed probably due to the formation of metal carbides. However, full microanalytical data that were obtained on all new compounds are reported.

$Ti(OAr\text{–}2,6Ph_2)_2(CH_3)_2$ (**Ia**). To a solution of $IMgCH_3$ (0.11 mol) in diethylether (250 cm^3) cooled to −78°C was slowly added $TiCl_4$ (0.026 mol) in hexane (15 cm^3). The resulting yellow mixture con-

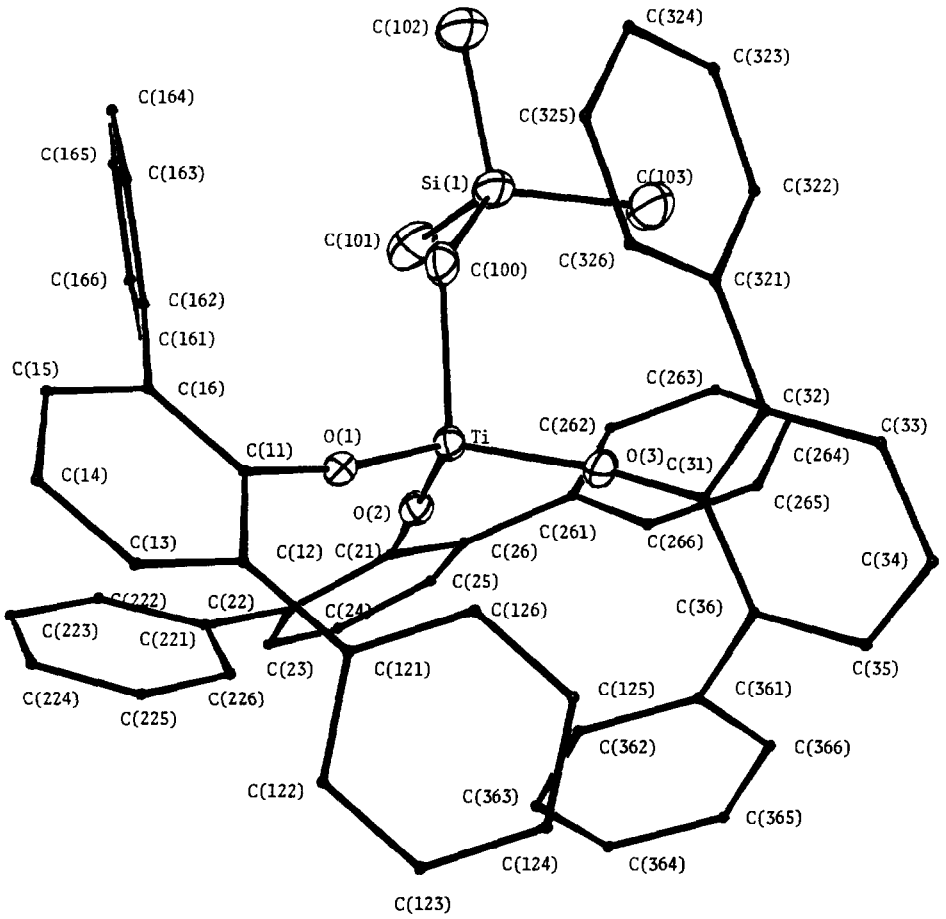

Fig. 2. ORTEP view of $Ti(OAr\text{–}2,6Ph_2)_3(CH_2SiMe_3)$ (**IIb**) emphasizing the central coordination sphere and alkyl group.

taining $Ti(CH_3)_4$ was stirred for 1 h at −78°C before $HOAr\text{–}2,6Ph_2$ (13.9 g, 2 equiv per Ti) was added slowly as a toluene (50 cm^3) solution. The color of the mixture darkened to orange and methane was evolved. After being allowed to warm slowly to room temperature, all solvent was removed *in vacuo* to yield a dark solid residue. Extraction of the residue with a 50/50 hexane/benzene mixture and evaporation gave the crude product as an off-yellow crystalline powder. Recrystallization with hexane and cooling to −15°C gave the pure product as lemon–yellow crystals. Yield = 6.28 g (42%). Found: C, 79.7; H, 5.5. Calc. for $TiC_{38}H_{32}O_2$: C, 80.3; H, 5.7%.

$Ti(OAr\text{–}2,6Ph_2)_2(CH_2SiMe_3)_2$ (**Ib**). To a yellow solution of $Ti(CH_2SiMe_3)_4$ (1.0 g) in benzene (20

Table 2. Selected bond distances and angles for $Ti(OAr\text{-}2,6Ph_2)_2(C_6H_5)_2 \cdot C_6H_6$ (**Id**)

Ti(1)—O(2)	1.794(3)	Ti(1)—C(40)	2.106(5)
Ti(1)—O(21)	1.797(3)	Ti(1)—C(46)	2.070(5)
O(2)—Ti—O(21)	122.99(14)	Ti—O(2)—C(3)	153.0(3)
O(2)—Ti—C(40)	108.97(18)	Ti—O(21)—C(22)	162.2(3)
O(2)—Ti—C(46)	107.14(18)	Ti—C(40)—C(41)	120.7(5)
O(21)—Ti—C(40)	106.09(18)	Ti—C(40)—C(45)	126.3(4)
O(21)—Ti—C(46)	109.24(18)	Ti—C(46)—C(47)	122.7(4)
C(40)—Ti—C(46)	100.01(20)	Ti—C(46)—C(51)	118.9(4)

Table 3. Selected bond distances and angles for $Ti(OAr\text{-}2,6Ph_2)_3(CH_2SiMe_3)$ (**IIb**)

Ti—O(1)	1.797(2)	Ti—O(3)	1.802(2)
Ti—O(2)	1.806(2)	Ti—C(100)	2.051(4)
O(1)—Ti—O(2)	115.42(8)	O(3)—Ti—C(100)	104.7(2)
O(1)—Ti—O(3)	111.27(9)	Ti—O(1)—C(11)	170.7(2)
O(1)—Ti—C(100)	102.5(2)	Ti—O(2)—C(21)	179.1(2)
O(2)—Ti—O(3)	114.39(9)	Ti—O(3)—C(31)	164.6(2)
O(2)—Ti—C(100)	107.2(2)	Ti—C(100)—Si(1)	126.4(2)

cm^3) was added solid $HOAr\text{–}2,6Ph_2$ (1.24 g, 2 equiv) with vigorous stirring. The resulting mixture was stirred overnight before the solvent was removed *in vacuo* to yield the crude product as a yellow powder. The compound can be readily recrystallized from saturated hexane solution on cooling as large yellow blocks. Yield = 1.08 g (60%). Found: C, 73.2; H, 7.0. Calc. for $TiC_{44}H_{48}O_2Si_2$: C, 70.8; H, 6.7%.

$Ti(OAr\text{–}2,6Ph_2)_2(CH_2Ph)_2$ (**Ic**). An essentially identical procedure used for (**Ia**) except using $ClMgCH_2Ph$ (0.16 mol) and $TiCl_4$ (0.04 mol) yielded the di-benzyl (**Ic**) as deep-red crystals from hexane. Yield = 24.6 g (84%). Found: C, 80.9; H, 5.7. Calc. for $TiC_{50}H_{40}O_2$: C, 83.3; H, 5.5%.

$Ti(OAr\text{–}2,6Ph_2)_2(Ph)_2 \cdot C_6H_6$ (**Id**). Addition of $HOAr\text{–}2,6Ph_2$ (14.8 g, 2 equiv) to a preformed solution of $TiPh_4$ (PhMgBr, 0.12 mol; $TiCl_4$, 0.03 mol) using the procedures outlined for (**Ia**) above yielded a dark brown mixture. The crude product was purified by recrystallization from hexane/benzene mixture as large yellow blocks. Yield = 3.5 g (17%). Found: C, 82.2; H, 5.5. Calc. for $TiC_{48}H_{36}O_2 \cdot C_6H_6$: C, 84.1; H, 5.5%.

$Ti(OAr\text{–}2,6Ph_2)_3(CH_3)$ (**IIa**). A yellow solution of $Ti(OAr\text{–}2,6Ph_2)_2(CH_3)_2$ (**Ia**) (0.5 g) and $HOAr\text{–}2,6Ph_2$ (0.22 g) in toluene (10 cm^3) was stirred at 25°C. Methane evolution occurred, but no color change was evident. After 30 min the solution was cooled slowly to yield the product as yellow crystals. Yield = 0.50 g (73%). More product could be obtained on cooling the mother liquor. Found: C, 81.4; H, 5.2. Calc. for $TiC_{55}H_{42}O_3$: C, 82.7; H, 5.3%.

$Ti(OAr\text{–}2,6Ph_2)_3(CH_2SiMe_3)$ (**IIb**). A mixture of $Ti(CH_2SiMe_3)_4$ (1.0 g) and $HOAr\text{–}2,6Ph_2$ (1.86 g, 3 equiv) in toluene (30 cm^3) was refluxed for 4 h. The solvent was removed to give the crude product as a yellow powder which was recrystallized from a toluene/hexane mixture. Yield = 0.6 g (27%). Found: C, 79.6; H, 6.0. Calc. for $TiC_{58}H_{50}SiO_3$: C, 80.8; H, 5.8%.

$Nb(OAr\text{–}2,6Ph)_2(Cl_3)$. A solution of $HOAr\text{–}2,6Ph_2$ (18.16 g) in benzene was added slowly to a solution of $NbCl_5$ (9.96 g) also in benzene. The resulting mixture was stirred for 3 h before the solvent, along with generated HCl, was removed *in vacuo* to leave the crude product as an orange solid. Recrystallization from a saturated toluene solution gave the pure product. Yield = 24.0 g (94.4%). Found: C, 62.5; H, 4.3; Cl, 14.2. Calc. for Nb, $C_{36}H_{26}O_2Cl_3$: C, 62.7; H, 3.8; Cl, 15.4%.

$Ta(OAr\text{–}2,6Ph_2)_2Cl_3$. This was obtained as a yellow solid using an identical procedure using $TaCl_5$ instead of $NbCl_5$. Found: C, 56.9; H, 3.9; Cl, 12.2. Calc. for Ta, $C_{36}H_{26}O_2Cl_3$: C, 55.6; H, 3.4; Cl, 13.7%.

$Nb(OAr\text{–}2,6Ph_2)_3Cl_2$. Addition of $LiOAr\text{–}2,6Ph_2$ (0.37 g) to a solution of $Nb(OAr\text{–}2,6Ph_2)_2Cl_3$ (1.0 g) in benzene gave a yellow–orange suspension. After being stirred overnight the mixture was filtered and the filtrate stripped to yield the crude product as a yellow–orange solid. (Recrystallization from saturated hexane solutions gave the pure product.) Yield = 1.25 g (96.2%). Found: C, 72.3; H, 4.6; Cl, 7.1. Calc. for $NbC_{54}H_{39}O_3Cl_2$: C, 72.1; H, 4.4; Cl, 7.9%.

$Ta(OAr\text{–}2,6Ph_2)_3Cl_2$. An identical procedure using $Ta(OAr\text{–}2,6Ph_2)_2Cl_3$ gave the product as a pale yellow solid. Found: C, 64.2; H, 4.4; Cl, 8.7. Calc. for $TaC_{54}H_{39}O_3Cl_2$: C, 65.6; H, 4.0; Cl, 7.2%.

$Nb(OAr\text{–}2,6Ph_2)_2(CH_3)_3$ (**IIa**). Slow addition of $LiCH_3$ (190 mg, 3 equiv) to a solution of $Nb(OAr\text{–}2,6Ph_2)_2Cl_3$ (2.0 g) in benzene causes a lightening of the solution from orange to pale yellow. Filtration and removal of the solvent *in vacuo* gave the product as a yellow powder. Recrystallization from hexane yielded the pure products as well formed yellow crystals. Yield = 1.1 g (68.1%). Found: C, 70.7; H, 5.4. Calc. for $NbC_{39}H_{35}O_2$; C, 74.5; H, 5.6%.

$Ta(OAr\text{–}2,6Ph_2)_2(CH_3)_3$ (**IIIb**). An identical procedure using $Ta(OAr\text{–}2,6Ph_2)_2Cl_3$ yielded (**IIb**) as well formed, white blocks from hexane. Found: C, 65.0; H, 5.1. Calc. for $TaC_{39}H_{35}O_2$: C, 65.3; H, 4.9%.

$Nb(OAr\text{–}2,6Ph_2)_3(CH_3)_2$ (**IVa**). Obtained from

$Nb(OAr\text{–}2,6Ph_2)_3Cl_2$ and $LiCH_3$ (2 equiv) in benzene. Recrystallized from hexane on cooling. Found: C, 78.3; H, 5.4. Calc. for $NbC_{56}H_{45}O_3$: C, 78.3; H, 5.3%.

$Ta(OAr\text{–}2,6Ph_2)_3(CH_3)_2$ (**IVb**). Obtained by reacting $Ta(OAr\text{–}2,6Ph_2)_3Cl_2$ with $LiCH_3$ (2 equiv) in benzene. An identical procedure to that used for (**IIa**) yielded the product as a white crystalline solid. Found: C, 70.3; H, 4.7. Calc. for $TaC_{56}H_{45}O_3$: C, 71.0; H, 4.8%.

Crystallographic studies

Crystal data are summarized in Table 4. One of the structures was determined at the Indiana University Molecular Structure Center while the second was determined in-house at Purdue.

$Ti(OAr\text{–}2,6Ph_2)_2(Ph)_2 \cdot C_6H_6$ (**Id**). General operating procedures and a listing of programs have been published previously.[21] A suitable small crystal was selected and transferred to the goniostat for characterization and data collection. Attempts at cooling the crystal to our usual operating temperature of −150°C resulted in fracturing of the crystal, possibly due to a phase transition. At about −94°C the crystal was stable, and this temperature was used for characterization and data collection. A systematic search of a limited hemisphere of reciprocal space yielded a set of reflections which exhibited monoclinic symmetry and extinctions corresponding to the space group $P2_1/c$.

The structure was solved by direct methods, all non-hydrogen atoms were readily located after some initial difficulty resulting from the placement of the Ti atom almost on a twofold screw axis. After initial refinement the hydrogen atoms were located

Table 4. Crystal structure determination data

	(Id)	(IIb)
Formula	$TiC_{48}H_{36}O_2 \cdot C_6H_6$	$TiC_{61}H_{57}SiO_3$
fw	770.82	914.12
Space group	$P2_1/c$	$P\bar{1}$
a, Å	10.959(2)	11.923(2)
b, Å	36.309(1)	11.887(3)
c, Å	10.859(2)	19.446(5)
$\alpha°$	—	90.19(2)
$\beta°$	110.29(1)	92.69(2)
$\gamma°$	—	115.96(2)
Z	4	2
V, Å^3	4053.16	2474.0
Density (calc.) g cm^{-3}	1.263	1.227
Crystal size	0.30 × 0.30 × 0.40	0.65 × 0.36 × 0.24
Crystal color	orange	yellow
Radiation	MoKα (λ = 0.71069 Å)	MoKα (λ = 0.71069 Å)
Linear abs coeff., cm^{-1}	2.48	2.37
Temp. deg. C	−94	−167
Detector aperture	3.0 mm wide × 4.0 mm high	(1.5 + tan θ) mm wide 4.0 mm high
Takeoff angle, deg.	2.0	4.90
Scan speed, deg. min^{-1}	5.0	variable
Scan width, deg.	1.2 + dispersion	0.8 + 0.35 tan θ
bkgd counts, s	6	50% of scan time
2θ range, deg.	6–45	4–45
Unique data	5321	6442
Unique data with $Fo > 3.00\,\sigma$	3754	5151
$R(F)$	0.0647	0.052
$Rw(F)$	0.0651	0.076
Goodness of fit	1.171	1.515
Largest Δ/σ	0.05	0.11

and refined. The full matrix least-squares refinement was completed using anisotropic thermal parameters on all non-hydrogen atoms and isotropic thermal parameters on the hydrogen atoms. The final difference map was essentially featureless, the largest peak was 0.6 e/Å. The asymmetric unit contained one molecule of benzene solvent. The atoms in the solvent are numbered C(52) through to C(57).

$Ti(OAr\text{–}2,6Ph_2)_3(CH_2SiMe_3)$ (**IIb**). A suitable crystal was located and mounted in a 0.5 mm capillary surrounded by epoxy resin. Data collection and refinement were carried out using the standard procedures of the Purdue Crystallographic facility.[11]

Hydrogens were located such that the hydrogen–carbon bond was 0.95 Å and the angles were correct. For methyl groups, one hydrogen was located in the Fourier map, its position was idealized, and the remaining hydrogen positions were calculated based on it. Hydrogen temperature factors and positions were not refined.

Acknowledgements—We thank the National Science Foundation (Grant CHE-8612063) to I.P.R. for support of this research. We also thank the National Science Foundation Chemical Instrumentation Program (Grant CHE-8204994) for support of the X-ray diffraction facility at Purdue. I.P.R. also gratefully acknowledges the Camille and Henry Dreyfus Foundation for the award of a Teacher–Scholar Grant and the Alfred P. Sloan Foundation for a fellowship. L.D.D. gratefully acknowledges Amoco for the award of a fellowship.

REFERENCES

1. L. R. Chamberlain, L. D. Durfee, P. E. Fanwick, L. Kobriger, S. L. Latesky, A. K. McMullen, I. P. Rothwell, K. Folting, J. C. Huffman, W. E. Streib and R. Wang, *J. Am. Chem. Soc.* 1987, **109**, 390; T. W. Coffindaffer, I. P. Rothwell, K. Folting and J. C. Huffman, *J. Chem. Soc., Dalton Trans.* 1987, 155; L. R. Chamberlain and I. P. Rothwell, *J. Chem. Soc., Dalton Trans.* 1987, 163; S. L. Latesky, A. K. McMullen, I. P. Rothwell and John C. Huffman, *Organometallics* 1985, **4**, 902; L. R. Chamberlain, I. P. Rothwell and J. C. Huffman, *Inorg. Chem.* 1984, **23**, 2575.
2. C. J. Schaverien, J. C. Dewan and R. R. Schrock, *J. Am. Chem. Soc.* 1986, **108**, 2771; I. A. Latham, L. R. Sita and R. R. Schrock, *Organometallics* 1986, **5**, 1508; K. C. Wallace, J. C. Dewan and R. R. Schrock, *Organometallics* 1986, **5**, 2161; M. R. Churchill, J. W. Ziller, J. H. Freudenberger and R. R. Schrock, *Organometallics* 1984, **3**, 1554.
3. A. W. Duff, R. A. Kamarudin, M. F. Lappert and R. J. Norton, *J. Chem. Soc., Dalton Trans.* 1986, 489 and refs therein.
4. B. D. Murray, H. Hope and P. P. Power, *J. Am. Chem. Soc.* 1985, **107**, 169 and refs therein.
5. P. T. Bishop, P. J. Blower, J. R. Dilworth and J. A. Zubieta, *Polyhedron* 1986, **5**, 363; P. T. Bishop, J. R. Dilworth and J. A. Zubieta, *J. Chem. Soc., Chem. Comm.* 1985, 257; P. T. Bishop, J. R. Dilworth, T. Nicholson and J. A. Zubieta, *J. Chem. Soc., Chem. Comm.* 1986, 1123; P. J. Blower, P. T. Bishop, J. R. Dilworth, T. C. Hsieh, J. Hutchinson, T. Nicholson and J. Zubieta, *Inorg. Chim. Acta* 1985, **101**, 63; P. J. Blower, J. R. Dilworth, J. Hutchinson, T. Nicholson and J. A. Zubieta, *J. Chem. Soc., Dalton Trans.* 1985, 2639; R. J. Burt, J. R. Dilworth, G. J. Leigh and J. A. Zubieta, *J. Chem. Soc., Dalton Trans.* 1982, 2295.
6. M. H. Chisholm, J. Corning and J. C. Huffman, *J. Am. Chem. Soc.* 1983, **105**, 5924; P. J. Blower, J. R. Dilworth and J. Zubieta, *Inorg. Chem.* 1985, **24**, 2866.
7. E. Roland, E. C. Walborsky, J. C. Dewan and R. R. Schrock, *J. Am. Chem. Soc.* 1985, **107**, 5795; M. L. Listemann, J. C. Dewan and R. R. Schrock, *J. Am. Chem. Soc.* 1985, **107**, 7207.
8. R. Fikor, S. A. Koch and M. M. Millar, *Inorg. Chem.* 1985, **24**, 3311; S. L. Soong, V. Chebolv, S. A. Koch, T. O'Sullivan and M. M. Miller, *Inorg. Chem.* 1986, **25**, 4067.
9. I. P. Rothwell, *Polyhedron* 1985, **4**, 177.
10. S. L. Latesky, A. K. McMullen, I. P. Rothwell and J. C. Huffman, *J. Am. Chem. Soc.* 1985, **107**, 5981; L. R. Chamberlain, I. P. Rothwell and J. C. Huffman, *J. Am. Chem. Soc.* 1986, **108**, 1502; L. Chamberlain and I. P. Rothwell, *J. Am. Chem. Soc.* 1983, **105**, 1665.
11. A. E. Ogilvy, P. E. Fanwick and I. P. Rothwell, *Organometallics* 1987, **6**, 73; T. W. Coffindaffer, W. M. Westler and I. P. Rothwell, *Inorg. Chem.* 1985, **24**, 4565.
12. J. L. Kerschner and I. P. Rothwell, *J. Am. Chem. Soc.*, in press.
13. J. R. Dilworth, J. Hanich, M. Krestel, J. Beuk and J. Strahle, *J. Organomet. Chem.* 1986, **351**, C9. We thank the authors for a preprint of this work prior to publication.
14. J. R. Dilworth, personal communication.
15. *Comprehensive Organometallic Chemistry* (Edited by G. Wilkinson, F. G. A. Stone and E. Abel). Pergamon Press, Oxford (1982).
16. P. E. Fanwick, personal communication.
17. L. D. Durfee, I. P. Rothwell and J. C. Huffman, *Inorg. Chem.* 1985, **24**, 4569.
18. S. L. Latesky, A. K. McMullen, J. Keddington, I. P. Rothwell and J. C. Huffman, *Inorg. Chem.* 1985, **24**, 995.
19. T. W. Coffindaffer, I. P. Rothwell, K. Folting, J. C. Huffman and W. E. Streib, *J. Chem. Soc., Chem. Comm.* 1985, 1519; T. W. Coffindaffer, I. P. Rothwell and J. C. Huffman, *Inorg. Chem.* 1983, **22**, 2906.
20. V. Kocman, J. C. Rucklidge, R. J. O'Brian and W. Santo, *J. Chem. Soc., Chem. Comm.* 1971, 1340.
21. M. H. Chisholm, K. Folting, J. C. Huffman and C. C. Kirkpatrick, *Inorg. Chem.* 1984, **23**, 1021.

Polyhedron Vol. 6, No. 11, pp. 2027–2029, 1987
Printed in Great Britain

0277–5387/87 $3.00+.00

COMMUNICATION

ELECTRON DELOCALIZATION IN RHODIUM (1+) *BIS* DIISOCYANOBIPHENYL CHLORIDE POLYMERS WITH DIRECT RHODIUM–RHODIUM INTERACTIONS

S. A. LAWRENCE,* K. A. K. LOTT, P. A. SERMON and E. L. SHORT

Department of Chemistry, Brunel University, Uxbridge, Middlesex UB8 3PH, U.K.

and

I. FEINSTEIN-JAFFE

Department of Materials Science, The Weizmann Institute of Science, Rehovot, Israel 76000

(*Received* 9 *April* 1987; *accepted* 2 *June* 1987)

Abstract—It is shown in the present work that hexagonal and tetragonal forms of Rh(I) *bis*-4,4′-diisocyanobiphenyl chloride polymers containing stacks of rhodium ions in the integral +1 state show *d*-electron delocalization in one dimension along Rh^+—Rh^+ chains at and below ambient temperature at atmospheric pressure.

Although most organometallic solids are insulators,[1] their structural and electronic properties can be modified by overlap of metal orbitals[2] or π-ligand orbitals[3] to allow formation of conduction bands. In the present study on rhodium diisocyanide polymers, both types of overlap may contribute towards the overall electronic conductivity.

Hexagonal and tetragonal rhodium(I) *bis* 4,4′-diisocyanobiphenyl chloride polymers ($[Rh(CN\text{-}C_6H_4\text{-}C_6H_4\text{-}NC)_2]^+Cl)_n$, have been prepared from the reaction of 4,4′-diisocyanobiphenyl[4] with tetracarbonyl di-μ-chloro dirhodium.[5,6,7] These and similar polymers have shown catalytic hydrogenation properties[8,9] as well as electrical[10] and photoconductivities.[11]

Powder X-ray diffractometry on these materials has revealed ordered structures of "graphite-like" two-dimensional laminae with interlayer separations of 3.54 and 3.40 Å for the hexagonal[6] and tetragonal[10] modifications respectively. Interlayer spacing of this order (3–4 Å) are found in many planar molecule charge-transfer salts.[3] For the materials reported here, the interplanar spacings most probably arise from overlap of electron density between adjacent ligand sheets and rhodium(I) ions. Both structural modifications of the rhodium polymer satisfy all of the preconditions necessary for one-dimensional metals,[12] and the interplanar spacing is at about the maximum critical distance (i.e. 3.44 Å+a contribution for polarizability) required for delocalization of electrons within Rh—Rh bonded systems[13] provided that vertical alignment of Rh^+ ions is present.

A band found in the electronic spectra of both structural forms of the material at ~ 700 nm has been attributed to an $a_{1g}(d_z^2) \rightarrow a_{2u}(p_z, \pi^*)$ transition (which shifted from 520 nm because of overlap of adjacent metal–metal d_z^2 orbitals[14]), providing the first evidence for Rh—Rh interactions therein.[5,6] However, to date, the existence of one-dimensional molecular metals in these compounds has not been proved conclusively. The applicability of Raman spectroscopy to the study of weak metal–metal interactions has been well detailed[15] and a weak Raman-active band has been detected at 130 cm^{-1} for the rhodium polymers discussed here. This band

* Author to whom correspondence should be addressed.

is attributed to a symmetric Rh—Rh stretching vibration and is reported here for the first time as further evidence for direct metal–metal interactions in these polymeric solids. The weak intensity of this band together with its low vibration frequency in the Raman spectrum (a band at 170 cm^{-1} had previously been detected for νRh—Rh in rhodium(II) acetate[16]) indicate that only a weak metal–metal interaction is present here.

We find that both hexagonal and tetragonal polymers exhibit weak paramagnetism; this is surprising, as a fully spin-paired d^8 ground state electronic configuration would have been predicted for Rh^+ in D_{4h} symmetry. This unpaired spin electron density probably arises from either paramagnetic rhodium impurities or from donation of electron density from the antibonding σ-lone pair on the C atom from ArNC to the metal. A shift of 24 cm^{-1} has been observed for the νC≡N stretching mode in the infrared spectra of the ligand after complexation and this confirms that net electron donation occurs from the ligand to the metal (and not the reverse) for these particular polymeric solids.

The unpaired electron spin density on the rhodium centres proved to be amenable to detection by electron paramagnetic resonance spectroscopy; three EPR spectra of the hexagonal and tetragonal polymers are shown in Fig. 1. Both polymeric solids exhibit EPR spectra with two peaks. The peak at $g \approx 2.00$ is attributed to unpaired electron density on the rhodium ions and the peak at the larger g value is thought to be due to delocalized electron density in the material's solid state conduction bands. Similar conduction electron EPR spectra to those shown in Fig. 1 have been reported for colloidal metal particle sols[17] and for the molybdenum hexafluoride intercalated graphite samples[18] and the peak assignments given are consistent with those suggested here. Samples of tetratolyl isocyano rhodium(I) perchlorate, prepared by the action of tolyl isocyanide on rhodium trichloride in the presence of sodium perchlorate,[19] gave no detectable EPR signal. For this reason it is thought unlikely that the EPR spectra recorded for the two polymers here result from spin-orbital coupling within paramagnetic rhodium centres in an anisotropic field.

Temperature-dependent EPR studies in the range 78 to 420 K show that the total integrated peak area decreases with temperature and that the conduction band is the most susceptible peak of the two to changes in temperature. At room temperature, calibration of the EPR spectra gave total spin densities of 4.55×10^{-4} for each Rh site in the hexagonal polymer and 1.36×10^{-4} for each Rh site in the tetragonal polymer. The values obtained for the conduction–electron spin densities at room temperature for the same species were 1.8×10^{20} spins per mol for the hexagonal polymer and 4.9×10^{18} spins per mol for the tetragonal polymer.

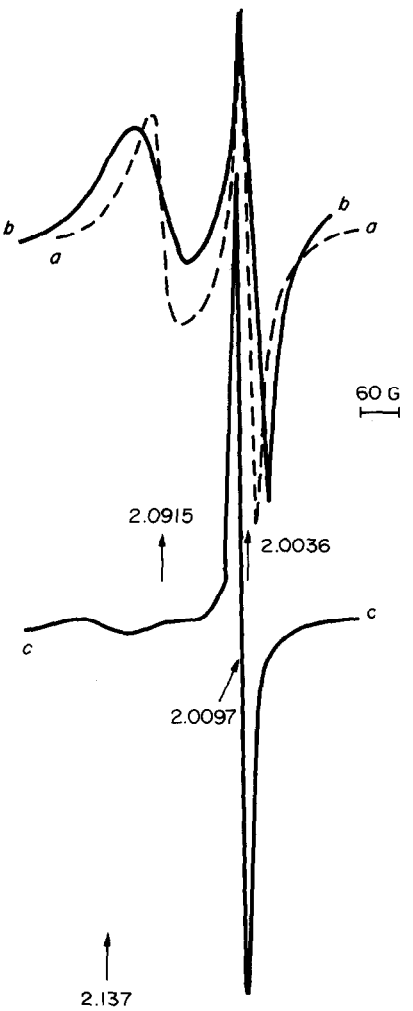

Fig. 1. EPR spectra of Rh(I) *bis*-diisocyanobiphenyl chloride polymers obtained on a Varian EPS3 instrument in air: (a) in the hexagonal configuration at 78 K shows two peaks (g = 2.0915, 45 G and g = 2.0036, 40 G), (b) in the hexagonal configuration at 333 K also shows two peaks (g = 2.0915, 85 G and g = 2.0036, 60 G), and (c) in the tetragonal configuration at 333 K, which shows two peaks (g = 2.137 72 G and g = 2.0097, 5 G).

The "dark" electrical conductivities of polycrystalline samples of the two different polymers were determined in a low-pressure conductivity cell[20] and show $\sigma_{hex} > \sigma_{tet}$ (2×10^{-6} ohm^{-1} cm^{-1} and 1×10^{-7} ohm^{-1} cm^{-1} respectively). This is in agreement with the results obtained from EPR spectroscopy. The intrinsic electrical conductivities of both of these polymers had been interpreted previously in terms of a summation of intralayer and interlayer contributions.[10] However, infra-red spectral data indicate that electron transfer may occur one way only, from the ligands to the metal and

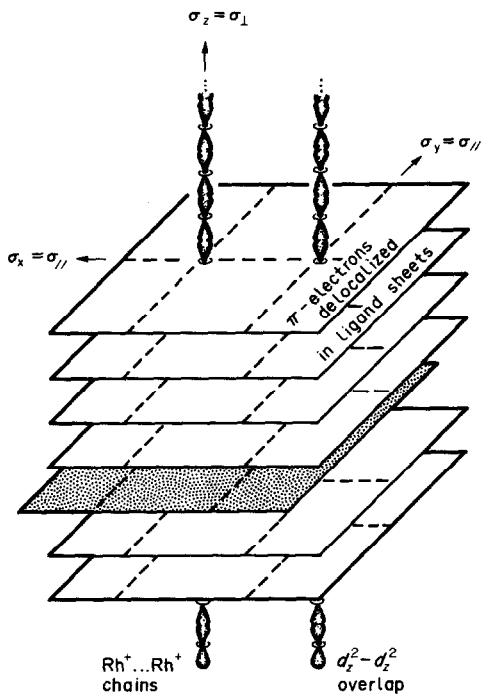

Fig. 2. Electronic conductivity of Rh(I) *bis*-diisocyanobiphenyl chloride polymers. $\sigma_\parallel$ denotes conductivity within (or parallel to) diisocyanobiphenyl sheets. $\sigma_\perp$ denotes conductivity perpendicular to these sheets which predominantly involves d_z^2–d_z^2 overlap of Rh^+ centres (in essentially integral +1 oxidation states) forming Rh^+—Rh^+—Rh^+ chains which are broken only by translational defects resulting in a mismatch of Rh^+—Rh^+ ions in adjacent laminae (mismatched sheet breaking Rh^+—Rh^+—Rh^+ chain is shaded). – – – denotes the diisocyanobiphenyl ligands between Rh^+ centres in the laminae involving π-bond delocalization).

EPR shows no peak splitting due to coupling of unpaired electron density on the rhodium centres with nitrogen atoms in the ligands. In the light of the results reported here, it may be concluded that the intralayer contribution $\sigma_\parallel$ (see Fig. 2) to the total electrical conductivity must be very small when compared with the interlayer contribution $\sigma_\perp$ (see Fig. 2).

Total numbers of unpaired electrons per rhodium site suggest that the overall oxidation state of the rhodium ions present in these materials is $(1 \pm x)$, where x is a factor which takes into account the electron donating power of the ligands as well as the effects of interlayer electronic delocalization within the solid state.

As mentioned earlier, the Rh—Rh distance in these polymers is very close to the critical limiting distance for delocalization of *d*-electrons. Thus for either of the two systems considered here only a relatively small stacking fault (i.e. translational dislocation) would be required to disrupt the one-dimensional metallic character (see Fig. 2). The electronic charge is able to move freely along the *straight* Rh^+—Rh^+—Rh^+ segments but requires an activation energy input to hop over from one chain to the next. The kinetics involved in electron transfer of this kind are critical in defining the level of electronic conduction in this a similar class of material[21] and are dependent upon relaxation rates along the metal atom and chain lengths. Further research is being carried out in this area to define and modify the magnetic and electronic properties in this and related one-dimensional systems.

Acknowledgement—The authors thank Johnson Matthey Ltd., for the loan of rhodium trichloride. I.F.-J. acknowledges the financial support of N.C.R.D. (Israel) for parts of this research programme.

REFERENCES

1. A. E. Underhill and D. N. Watkins, *Chem. Soc. Rev.* 1980, **9**, 429.
2. I. D. Parker, R. H. Friend, P. I. Clemenson and A. E. Underhill, *Nature* 1986, **324**, 547.
3. M. R. Bryce, *Nature* 1986, **324**, 510.
4. A. Efraty, I. Feinstein, L. Wackerle and A. Goldman, *J. Org. Chem.* 1980, **45**, 4059.
5. A. Efraty, I. Feinstein, F. Frolow and L. Wackerle, *J. Am. Chem. Soc.* 1980, **102**, 6341.
6. A. Efraty, I. Feinstein and F. Frolow, *Inorg. Chem.* 1982, **21**, 485.
7. I. Feinstein-Jaffe, F. Frolow, L. Wackerle, A. Goldman and A. Efraty, *Inorg. Chem.*, in press.
8. I. Feinstein-Jaffe and A. Efraty, *J. Mol. Catal.* 1987, **40**, 1.
9. A. Efraty and I. Feinstein, *Inorg. Chem.* 1982, **21**, 3115.
10. I. Feinstein-Jaffe and A. Efraty, *Macromol.* 1986, **19**, 2076.
11. I. Feinstein-Jaffe and H. Flaischer, *Mol. Cryst. Liq. Cryst.* 1987, **145**, 159.
12. A. E. Underhill, *Phil. Trans. R. Soc. Lond. A.* 1985, **314**, 125.
13. J. B. Goodenough, *Magnetism and the Chemical Bond*, 2nd edn, p. 296. Interscience, New York (1986).
14. J. C. Gordon, R. Williams, C. H. Hsu, E. Cuellar, S. Samson, K. Mann, H. B. Gray, V. Hadek and R. R. Somoano, *R. Ann N.Y. Acad. Sci.* 1978, **313**, 580.
15. T. G. Spiro, *Prog. Inorg. Chem.* 1970, **11**, 1.
16. J. S. Filippo and H. J. Snaidoch, *Inorg. Chem.* 1973, **12**, 2326.
17. K. Kimura and S. Bandow, *Surf. Sci.* 1985, **156**, 883.
18. D. Vaknin, D. Davidov, H. Selig and Y. Yeshurun, *J. Chem. Phys.* 1983, **83**, 3859.
19. L. Malatesta and L. Vallarino, *J. Chem. Soc.* 1956, 1867.
20. S. A. Lawrence, K. Mavadia, P. A. Sermon and S. Stevenson, *Proc. R. Soc. Lond. A* 1987, **411**, 95.
21. J. Friedal, *Phil. Trans. R. Soc. Lond. A* 1985, **314**, 189.

Polyhedron Vol. 6, No. 11, pp. 2031–2033, 1987
Printed in Great Britain

0277–5387/87 $3.00+.00

COMMUNICATION

SYNTHESIS AND X-RAY CRYSTAL STRUCTURE OF $[\{(C_5H_4Me)Fe(CO)_2\}_2BiCl]_3$: A COMPOUND CONTAINING A PLANAR SIX-MEMBERED Bi_3Cl_3 RING

WILLIAM CLEGG, NEVILLE A. COMPTON, R. JOHN ERRINGTON* and NICHOLAS C. NORMAN*

Department of Inorganic Chemistry, The University of Newcastle upon Tyne, Newcastle upon Tyne NE1 7RU, U.K.

(*Received* 16 *March* 1987; *accepted June* 1987)

Abstract—The reaction between $BiCl_3$ and two equivalents of $Na[(C_5H_4Me)Fe(CO)_2]$ affords the title complex, $[\{(C_5H_4Me)Fe(CO)_2\}_2BiCl]_3$, containing a planar six-membered Bi_3Cl_3 ring in which each bismuth is bonded to two chlorine atoms and two $(C_5H_4Me)Fe(CO)_2$ fragments.

Organotransition metal complexes containing transition metal–bismuth bonds are uncommon. Examples of known complexes include $[Bi\{Co(CO)_4\}_3]$,[1] $[Bi\{Ir(CO)_3\}_3]$,[2] $[W_3Bi_2(CO)_{15}]$,[3] $[W_2(CO)_8(\mu\text{-}\eta^2\text{-}Bi_2)(\mu\text{-}Bi(Me)W(CO)_5)]$[4] and recently a range of iron carbonyl–bismuth clusters has been reported by Whitmire *et al.*[5] As part of a study of such systems, we have investigated the reaction of the cyclopentadienylirondicarbonyl anion with bismuth trichloride, since there appear to be no literature reports of transition metal–bismuth complexes containing the cyclopentadienyl ligand.

Treatment of a THF solution of $BiCl_3$ with two equivalents of $[(C_5H_5)Fe(CO)_2]^-$ in THF at room temperature produces a deep emerald green solution from which, after filtration and recrystallization from THF/hexane, dark green crystals of **1a** can be isolated in moderate yield. Analogous reactions involving the alkylated cyclopentadienyl ligands, C_5H_4Me and C_5Me_5, afford the derivatives **1b** and **1c** respectively. ^1H and ^{13}C NMR† analysis of **1a–c** indicated a single cyclopentadienyl environment while infra-red spectroscopy revealed only terminal carbonyl absorptions.† However, since these data gave little indication as to the nature of **1a–c**, a single crystal X-ray diffraction study of **1b** was undertaken, the result of which is shown in Fig. 1 and Table 1.‡ The molecule consists of a planar six-membered Bi_3Cl_3 ring in which each bismuth atom is bonded to two chlorine atoms (mean Bi–Cl = 2.907 Å) and two $(C_5H_4Me)Fe(CO)_2$ fragments (mean Bi–Fe = 2.680 Å) as represented in the diagram. Each bismuth atom resides in a tetrahedral environment but this is considerably distorted, as evidenced by the large Cl–Bi–Cl angles (153.2

* Authors to whom correspondence should be addressed.

† Spectroscopic Data for complexes **1a–c**. **1a**: NMR; ^1H (d^8 THF), 5.01 (s, 5H, C_5H_5). $^{13}C\{^1H\}$ (d^8 THF), 86.1 (s, C_5H_5), 203.5 (s, CO). IR; $\nu_{C\equiv O}$ (THF) 2046(w), 2008(s), 1976(s), 1952(s). **1b**: NMR; ^1H (d^8 THF), 2.0 (bs, 3H, C_5H_4Me), 4.9 (bs, 4H, C_5H_4Me). $^{13}C\{^1H\}$ (d^8 THF), 13.2 (s, C_5H_4Me), 85.3 and 86.5 (s, C_5H_4Me, ring C-H), 103.4 (s, C_5H_4Me, ring C-Me), 204.0 (s, CO). IR; $\nu_{C\equiv O}$ (THF), 2041(w), 2006(s), 1973(s), 1948(s). **1c**: NMR; ^1H (d^8 THF), 1.86 (s, 15H, C_5Me_5). $^{13}C\{^1H\}$ (d^8 THF), 9.9 (s, C_5Me_5), 97.0 (s, C_5Me_5), 203.2 and 206.2 (s, CO). IR; $\nu_{C\equiv}$ (Nujol mull) 2020(m), 1980(s), 1950(m). Satisfactory microanalytical data were obtained for **1a** and **1b**.

‡ Crystal Data for **1b**: $C_{48}H_{42}Bi_3Cl_3Fe_6O_{12}$, $M_r = 1879.2$, monoclinic, $a = 21.440(7)$, $b = 12.480(4)$, $c = 20.315(6)$ Å, $\beta = 95.00(4)°$, $V = 5415$ Å^3, $Z = 4$, $D_c = 2.305$ g cm^{-3}, $F(000) = 3528$, $\mu(MoK\alpha) = 11.45$ mm^{-1}, $\lambda = 0.71073$ Å, space group $C2/c$; $R = 0.054$, $wR = 0.058$ for 3142 unique reflections with $F > 4\sigma(F)$, measured on a Siemens AED2 diffractometer at room temperature and corrected for absorption. The least-squares weighting scheme was $w^{-1} = \sigma^2(F) + 0.0004F^2$, with anisotropic thermal parameters and no hydrogen atoms (327 parameters).

Table 1. Selected bond lengths (Å) and angles (°) for $[\{(C_5H_4Me)Fe(CO)_2\}_2BiCl]_3$, **1b**

Bi(1)—Cl(1)	2.914(4)	Bi(1)—Fe(1)	2.668(2)
Bi(2)—Cl(1)	2.852(4)	Bi(2)—Fe(2)	2.705(2)
Bi(2)—Cl(2)	2.955(4)	Bi(2)—Fe(3)	2.668(2)
Cl(1)—Bi(1)—Fe(1)	94.1(1)	Cl(1)—Bi(1)—Cl(1*a*)	153.2(2)
Fe(1)—Bi(1)—Cl(1*a*)	101.6(1)	Fe(1)—Bi(1)—Fe(1*a*)	107.6(1)
Cl(1)—Bi(2)—Cl(2)	154.9(1)	Cl(1)—Bi(2)—Fe(2)	94.1(1)
Cl(2)—Bi(2)—Fe(2)	103.2(1)	Cl(1)—Bi(2)—Fe(3)	99.2(1)
Cl(2)—Bi(2)—Fe(3)	91.8(1)	Fe(2)—Bi(2)—Fe(3)	110.3(1)
Bi(1)—Cl(1)—Bi(2)	86.0(1)	Bi(2)—Cl(2)—Bi(2*a*)	84.4(1)

Symmetry operator for atoms labelled *a*: $1-x, y, 1/2-z$.

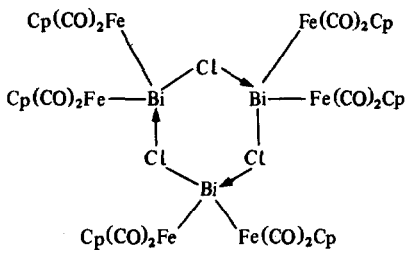

1a – Cp = C_5H_5
b – Cp = C_5H_4Me
c – Cp = C_5Me_5

and 154.9°), which in turn leads to a small angle at each chlorine (86.0 and 84.4°). These distortions are probably a result of a stereochemically active lone pair on each bismuth, which presumably lies in the Fe_2Bi plane and bisects the Cl–Bi–Cl angle. An alternative explanation invoking Bi—Bi interactions, which might result in similar distortions, is considered unlikely due to the large internuclear separation (mean Bi···Bi = 3.944 Å). Typical Bi—Bi distances in complexes containing mutually bonded dibismuth fragments range from 2.796 to 3.092 Å[3,4,5d] while in the cluster $[Bi_4Fe_4(CO)_{13}]^{2-}$,[5b] containing a tetrahedron of bismuth atoms, the Bi—Bi separations range from 3.140 to 3.473 Å, these being associated with some degree of Bi–Bi interaction. The Bi—Bi distance in bismuth metal is 3.10 Å.[6] The $(C_5H_4Me)Fe(CO)_2$ fragments are arranged such that the cyclopendienyl ligands are chemically equivalent, consistent with the observed solution NMR properties of **1a–c**. The carbonyls, however, fall into two sets; six pointing in towards the centre of the Bi_3Cl_3 ring and six pointing out. The observation of only one carbonyl resonance in the ^{13}C NMR spectrum of **1a** and **1b** implies an exchange process in solution at room temperature (presumably rotation about the Fe—Bi bonds). In **1c**, however, two CO signals are observed, consistent with a static structure in solution, possibly due to hindered rotation resulting from the increased size of the C_5Me_5 ligands.

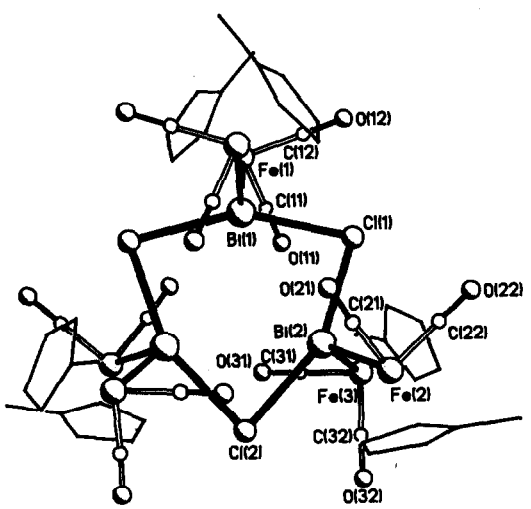

Fig. 1. A diagram of the molecular structure of **1b** showing the atom numbering scheme adopted, except for the C_5H_4Me ligands. A crystallographic two-fold axis passes through Bi(1) and Cl(2).

The structure of **1b** is formally derived from a cyclotrimerization of $\{(C_5H_4Me)Fe(CO)_2\}_2BiCl$ fragments resulting from a Lewis acid–base interaction between bismuth and a second chlorine. The Lewis acidity of tricoordinate bismuth is well known and a similar interaction occurs in the related chloro-bismuthinidene complex, **2**.[7] Fur-

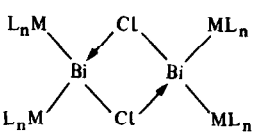

2 $ML_n = (C_5H_5)Mn(CO)_2$

there studies in related systems and on the reactivity of **1** are in progress.

Acknowledgements—We thank the SERC, the Research Corp. Trust and Nuffield Foundation for financial support.

Note added in proof—After submission of this manuscript a publication appeared reported the synthesis and structural characterisation of **1a**. J. M. Wallis, G. Müller and H. Schmidbaur, *J. Organomet. Chem.* 1987, **327**, 159.

REFERENCES

1. G. Etzrodt, R. Boese and G. Schmid, *Chem. Ber.* 1979, **112**, 2574.
2. W. Kruppa, D. Bläser, R. Boese and G. Schmid, *Z. Naturforsch* 1982, **B37**, 209.
3. G. Huttner, U. Weber and L. Zsolnai, *Z. Naturforsch* 1982, **B37**, 707.
4. A. M. Arif, A. H. Cowley, N. C. Norman and M. Pakulski, *Inorg. Chem.* 1986, **25**, 4836.
5. (a) K. H. Whitmire, C. B. Lagrone, M. R. Churchill, J. C. Fettinger and L. V. Biondi, *Inorg. Chem.* 1984, **23**, 4227; (b) K. H. Whitmire, T. A. Albright, S.-K. Kang, M. R. Churchill and J. C. Fettinger, *Inorg. Chem.* 1986, **25**, 2799; (c) K. H. Whitmire, C. B. Lagrone and A. L. Rheingold, *Inorg. Chem.* 1986, **25**, 2472; (d) K. H. Whitmire, K. S. Raghuveer, M. R. Churchill, J. C. Fettinger and R. F. See, *J. Am. Chem. Soc.* 1986, **108**, 2778.
6. A. F. Wells, *Structural Inorganic Chemistry*, 4th edn. Clarendon Press, Oxford (1975).
7. J. von Seyerl and G. Huttner, *J. Organomet. Chem.* 1980, **195**, 207.

Polyhedron Vol. 6, No. 11, p. 2035, 1987
Pergamon Journals Ltd. Printed in Great Britain

BOOK REVIEW

Preparative Polar Organometallic Chemistry Vol. 1. By Lambert Brandsma and Hermann D. Verkruijsse. Springer, Berlin, 1987. ISBN 3-540-19616-4, 240pp., DM 78.

This book is the first in a new organometallic series and is devoted to polar organometallics derived from *sp*2 compounds. The first chapter discusses the use of strong bases such as alkali metal amides, metal dialkyl amides and alkyllithiums. Aspects such as reagent stability, solvent purification, additives such as HMPA, safety precautions and practical tips are all covered. In chapter two the general reactivities of polar organometallics are discussed, with detailed reference to alkylation, acylation, halogenation, etc. These two first chapters form an excellent introduction to synthesis using strong bases and organometallics, and are illustrated with plenty of examples and full experimental procedures in the style of "Organic Syntheses".

The remainder of the book then describes the preparation and reactions of *sp*2 organometallics derived from four main groups: olefins and allenes, hetero-substituted unsaturated systems, hetero-aromatics and aromatics. In each section a general introduction is followed by full experimental procedures for preparation of a variety of products. Three useful indexes allow rapid location of a particular metallation reaction, or type of functionalization and over 240 references are included.

The book serves both as an excellent reference collection of organometallic preparations and as an informative lab. manual useful for researchers in all areas of synthetic chemistry.

Department of Chemistry **NIGEL S. SIMPKINS**
Queen Mary College
Mile End Road
*London E*1 *4NS, U.K.*

Polyhedron Vol. 6, No. 12, pp. 2037–2052, 1987
Printed in Great Britain

0277–5387/87 $3.00+.00

^{17}O AND ^{14}N NMR STUDIES OF THE Co(II), Cu(II) AND Mn(II) COMPLEXES OF L-PROLINE IN AQUEOUS SOLUTION

EFSTATHIOS D. GOTSIS* and DANIEL FIAT†

Department of Physiology and Biophysics, University of Illinois College of Medicine at Chicago, P.O. Box 6998, Chicago, IL 60680, U.S.A.

(*Received* 27 *May* 1986; *accepted after revision* 17 *March* 1987)

Abstract—The ^{17}O and ^{14}N paramagnetic transverse relaxation time and chemical shift of proline as well as of water, in aqueous solutions of Co(II), Cu(II) and Mn(II) were measured as a function of pH, temperature, and metal ion concentration. The relaxation results were fitted to a theoretical equation linking the Swift–Connick equation to the stability constants of the major complexes in equilibrium. Stability constants for the major complexes of the three ions in this work were determined, along with thermodynamic parameters for some of the complexes. Two complexes of Co(II) were detected directly by ^{17}O NMR at basic pH, and were assigned to $CoPro_2$ and $CoPro_3^-$. The hyperfine coupling constant for these two complexes, A/h, was determined directly from the isotropic shift and was found to be -0.63 and -0.31 MHz, respectively. $CoPro_2$ could be detected in the pH range 6–12, for Co(II) concentrations greater than 0.04 M, and its chemical shift was around 700 ppm downfield from free proline, at 300 K. $CoPro_3^-$ was detected only at pH 11, in the temperature range 275–284 K, with a chemical shift of 390 ppm downfield from free proline.

Transition metal ion complexes of amino acids and their equilibria in aqueous solution have been the subject of a number of investigations.[1–5] Among the various methods, ^1H and ^{13}C NMR have been used extensively, with varying success. Both the ^1H and the ^{13}C nuclei, though, are not involved directly in the binding to the paramagnetic ions, and consequently there is an inevitable attenuation of the paramagnetic effects arising from the greater distances to the paramagnetic center. On the other hand, both ^{17}O and ^{14}N nuclei are binding sites, and as such they should manifest the effects of the paramagnetic ions in a more pronounced way. The above considerations, together with an overwhelming lack of ^{17}O and ^{14}N NMR studies of transition metal ion complexes with amino acids, led us to the undertaking of this work.

The inherent difficulties associated with ^{17}O NMR, due to the low natural abundance of the ^{17}O nucleus (0.037%), low sensitivity and broad spectral lines resulting from an effective quadrupolar relaxation mechanism, are difficult to overcome without isotopic enrichment.[6] The above difficulties, coupled with the requirement of a high-power transmitter and probe (not standard equipment in most laboratories) and rather expensive isotopic enrichment, had kept ^{17}O NMR from realizing its full potential.

Of the three metal ions in this work, the Co(II)–Proline complexes have been investigated the least. The only stability constants that could be found in the literature[7–9] were for $CoPro^+$ and $CoPro_2$, thus comparison with literature cannot be made for the remaining complexes.

EXPERIMENTAL

For the ^{17}O NMR measurements, proline enriched to 30% ^{17}O at the carboxyl site by methods described previously,[10–11] was used after being passed through a chelex column twice, for further

* Present address: Department of Chemistry, University of Illinois at Chicago, P.O. Box 4348, Chicago, IL 60680, U.S.A.

† Author to whom correspondence should be addressed.

purification. For ^{14}N NMR, commercially available L-proline was used as bought from the manufacturer.

The NMR measurements were obtained using two spectrometers: a Bruker CXP-180 high-power spectrometer, operating in the Pulsed Fourier Transform mode at frequencies of 24.4 and 13.0 MHz for ^{17}O and ^{14}N NMR, respectively, and a home-made NSF-250 high-power spectrometer at the Regional NMR Center of the University of Illinois in Champaign-Urbana, operating in the Pulsed Fourier Transform mode at frequencies of 33.926 and 18.075 MHz for ^{17}O and ^{14}N NMR, respectively. Whenever appropriate, many measurements were performed on both spectrometers, to determine possible field effects, as well as to ascertain reproducibility of results.

Normally, 2,000–10,000 scans were sufficient for a well-resolved spectrum, and typical spectroscopic parameters were a spectral width of 50 kHz, pulse width for a 90° pulse of 10 μs, pulse delay of 10 μs, recycle delay of 70 ms and 4k spectral points for signal averaging.

Experimental errors in both ^{17}O and ^{14}N NMR shifts are within ± 0.5 ppm for narrow lines (20–400 Hz), and no more than ± 2.0 ppm for broader lines. The accuracy of the measured linewidths is within $\pm 5\%$.

A Bruker temperature control unit, with the thermocouple external to the sample, was used to monitor the temperature of the samples to within ± 0.5 K, with the CXP-180 spectrometer, whereas a Varian Associates temperature control unit operating along the same principles was employed with the NSF-250 spectrometer. In both cases, a minimum time of 15 min was allowed for the temperature to equilibrate each time is was changed.

The pH of the solutions was adjusted by the addition of NaOH or HCl and measured on a Corning model 125 pH meter, equipped with a combined electrode. The pH of the solution was measured before and after spectral acquisition, and, if different, the average value was recorded, provided that the variation was small.

Stock solutions of $CoCl_2$, $CuCl_2$ and $MnCl_2$ were prepared from salts of the ions that were dried at 105°C, for 36 h. The concentration of proline was determined by weighing an amount of dried in vacuum powder of proline, and whose purity was checked with an amino acid analyzer. The amino acid analyzer was used at least twice for each sample. The accuracy of the calculated concentration of proline is estimated to be within $\pm 10\%$, to allow for humidity that was inevitably absorbed by the hydrophilic proline, as well as other measuring errors.

THEORETICAL

A. *Chemical exchange*

The Bloch equations were modified by McConnell[12] to take into account the effects of chemical exchange between different magnetic environments. The McConnell equations were subsequently applied to the limiting conditions of a predominant diamagnetic site (the bulk water), in chemical exchange with one or more paramagnetic sites at considerably lesser concentrations (aqueous complexes of paramagnetic ions), by Swift and Connick.[13] In addition to the predominance of the diamagnetic site, chemical exchange among the paramagnetic sites was considered negligible to a first approximation, thus simplifying the solution of the modified Bloch equations. As a result, analytical expressions for the paramagnetic relaxation rate, $1/T_{2p}$, and chemical shift, $\Delta\omega_a$, of the diamagnetic site in the presence of the paramagnetic ions can be derived. For the benefit of the reader, a discussion of the Swift and Connick equations will follow, for they are an integral part of the theoretical treatment of our data.

The paramagnetic relaxation rate, $1/T_{2p}$, and the paramagnetic chemical shift, $\Delta\omega_a$, were found by Swift and Connick to be:

$$1/T_{2p} = \sum_{j=b}^{n} \frac{1}{\tau_a} \frac{T_{2j}^{-2} + (\tau_j T_{2j})^{-1} + \Delta\omega_j^2}{(\tau_j^{-1} + T_{2j}^{-1})^2 + \Delta\omega_j^2} \qquad (1)$$

and

$$\Delta\omega_a = -\sum_{j=b}^{n} \frac{1}{\tau_a \tau_j} \frac{\Delta\omega_j}{(\tau_j^{-1} + T_{2j}^{-1})^2 + \Delta\omega_j^2} \qquad (2)$$

where τ_a is the lifetime of the nucleus in the predominant diamagnetic site, τ_j is the lifetime of the nucleus in each of the paramagnetic sites, T_{2j} is the transverse relaxation time of the nucleus in the paramagnetic site and $\Delta\omega_j$ is the frequency difference, in rads/s, between the bulk and each of the paramagnetic sites.

In the special case of only one paramagnetic site exchanging with the diamagnetic site, eqs (1) and (2) can be reduced to simpler ones:

$$1/T_{2p} = \frac{1}{\tau_a} \frac{T_{2m}^{-2} + (\tau_m T_{2m})^{-1} + \Delta\omega_m^2}{(\tau_m^{-1} + T_{2m}^{-1})^2 + \Delta\omega_m^2} \qquad (3)$$

and

$$\Delta\omega_a = -\frac{1}{\tau_a \tau_m} \frac{\Delta\omega_m}{(\tau_m^{-1} + T_{2m}^{-1})^2 + \Delta\omega_m^2} \qquad (4)$$

where the subscript m refers to the paramagnetic site.

Some distinctions about the mechanism of transfer of the paramagnetic effects to the bulk can now

be made, depending on the relative size of T_{2m} and $\Delta\omega_m$. Thus, if $T_{2m}^{-2} \gg \Delta\omega_m^2$, it is referred to as the "T_{2m}" mechanism, whereas in the opposite case it is referred to as the "$\Delta\omega_m$" mechanism. In each case we further distinguish between slow and fast exchange, depending on the magnitude of the exchange rate, $1/\tau_m$. The following limiting equations describe all possible cases.

(1) The "$\Delta\omega_m$" mechanism:

$\Delta\omega_m^2 \gg T_{2m}^{-2}$, and eqs (3) and (4) become:

$$1/T_{2p} = (1/\tau_a)[\Delta\omega_m^2/(\tau_m^{-2}+\Delta\omega_m^2)] \tag{5}$$

and

$$\Delta\omega_a = -(1/\tau_a\tau_m)\Delta\omega_m/(\tau_m^{-2}+\Delta\omega_m^2). \tag{6}$$

We can now distinguish two cases, depending on the rate of chemical exchange, $1/\tau_m$. Thus, for $\Delta\omega_m^2 \gg \tau_m^{-2}$,

$$1/T_{2p} = 1/\tau_a = p_m/\tau_m \tag{5a}$$

and

$$\Delta\omega_a = (\tau_a\tau_m\Delta\omega_m)^{-1} \tag{6a}$$

where p_m is the ratio of the number of nuclei in the paramagnetic site divided by that of the bulk.

For $\tau_m^{-2} \gg \Delta\omega_m^2 \gg (T_{2m}\tau_m)^{-1}$,

$$1/T_{2p} = p_m\tau_m\Delta\omega_m^2 \tag{5b}$$

and

$$\Delta\omega_a = -p_m\Delta\omega_m. \tag{6b}$$

(2) The "T_{2m}" mechanism:

$T_{2m}^{-2} \gg \Delta\omega_m^2$, which results in:

$$1/T_{2p} = p_m/(\tau_m+T_{2m}) \tag{7}$$

and

$$\Delta\omega_a = -p_m\Delta\omega_m T_{2m}^2/(\tau_m+T_{2m})^2. \tag{8}$$

Again, we distinguish two cases, depending on the rate of chemical exchange, $1/\tau_m$, with respect to $1/T_{2m}$. For $T_{2m}^{-2} \gg \tau_m^{-2}$,

$$1/T_{2p} = 1/\tau_a = p_m/\tau_m \tag{7a}$$

and

$$\Delta\omega_a = -p_m\Delta\omega_m(T_{2m}/\tau_m)^2. \tag{8a}$$

For $\tau_m^{-2} \gg T_{2m}^{-2}$,

$$1/T_{2p} = p_m/T_{2m} \tag{7b}$$

and

$$\Delta\omega_a = -p_m\Delta\omega_m. \tag{8b}$$

Granot and Fiat[14] have distinguished one more case in the "$\Delta\omega_m$" mechanism. If $(\tau_m T_{2m})^{-1} \gg T_{2m}^{-2}$, $\Delta\omega_m^2$ then,

$$1/T_{2p} = p_m/T_{2m}. \tag{5c}$$

In this last case, the exchange is very rapid, so that the term $(\tau_m T_{2m})^{-1}$ becomes important and it can no longer be ignored in eq. (5).

The temperature dependence of τ_m is given by the Eyring equation,[15] indicative of first-order exchange processes:

$$\tau_m = (h/kT)\exp(\Delta H\dagger/RT-\Delta S\dagger/R) \tag{9}$$

where $\Delta H\dagger$ and $\Delta S\dagger$ are the enthalpy and entropy of activation for the first-order reaction of exchange between the diamagnetic and paramagnetic sites.

The frequency difference between the paramagnetic and diamagnetic sites is given by:

$$\Delta\omega_p = \Delta\omega_a+\Delta\omega_m. \tag{10}$$

The temperature dependence of $\Delta\omega_p$ and its relationship to the hyperfine coupling constant, A/h, is given by the equation of Bloembergen:[16]

$$(\Delta\omega_p/\omega) = -S(S+1)A(\gamma_e/\gamma_n)/3kT \tag{11}$$

where S is the spin of the paramagnetic ion, γ_e and γ_n are the magnetogyric ratios of the free electron and the nucleus under consideration, respectively, and the other constants have their usual meaning. At the point of intersection of the two limiting cases of $\ln T_{2p}$ vs $1/T$, $\Delta\omega_m\tau_m = 1$. Thus, having determined τ_m from the slow exchange region of $\ln T_{2p}$ vs $1/T$, eq. (5a), one can determine $\Delta\omega_m$, and consequently A/h from eq. (11). Such parameters were determined for aqueous complexes of several transition metal ions,[17-20] with considerable accuracy.

B. *Paramagnetic relaxation*

The relaxation of the ^{17}O and ^{14}N nuclei in a paramagnetic complex could occur by dipolar and hyperfine interactions with the unpaired electrons of the paramagnetic ion[17,21-23] in addition to their quadrupolar relaxation, and the transverse relaxation rate, $1/T_{2m}$, is given by:

$$1/T_{2m} = (1/T_{2m})_{DP}+(1/T_{2m})_{HF} \tag{12}$$

where DP stands for dipolar and HF for hyperfine:

$$(1/T_{2m})_{DP} = (1/15)[S(S+1)g^2\beta^2\gamma_n^2/r^6] \times (B+C+D+D+E+F) \tag{13}$$

and

$$(1/T_{2m})_{HF} = (1/3)S(S+1)(2\pi A/h)^2(G+H). \tag{14}$$

The terms A, B, C, D, E, F, G and H are given

by:

$$B = 4\tau_1$$

$$C = \tau_2/[1+(\omega_n-\omega_e)^2\tau_2^2]$$

$$D = 3\tau_1/(1+\omega_n^2\tau_1^2)$$

$$E = 6\tau_2/(1+\omega_e^2\tau_2^2)$$

$$F = 6\tau_2/[1+(\omega_n+\omega_e)^2\tau_2^2]$$

$$G = \tau_1$$

$$H = \tau_2/[1+(\omega_n-\omega_e)^2\tau_2^2]$$

where τ_1 and τ_2 are correlation times characterizing the interactions, r is the distance between the nucleus and the unpaired electrons and ω_n and ω_e are the nuclear and electronic precessional frequencies, respectively. The rest of the terms have their usual meaning.

Equations (13) and (14) can be further simplified, considering the relative size of ω_n, ω_e and the correlation times, τ_1 and τ_2. Thus, since $\omega_e \gg \omega_n$ and $\omega_n^2\tau^2 \ll 1$, eqs (13) and (14) become:

$$(1/T_{2m})_{DP} = (1/15)[S(S+1)g^2\beta^2\gamma_n^2/r^6] \times [7\tau_1+13\tau_2/(1+\omega_e^2\tau_2^2)] \quad (15)$$

and

$$(1/T_{2m})_{HF} = (1/3)(2\pi A/h)^2S(S+1) \times [\tau_1+\tau_2/(1+\omega_e^2\tau_2^2)]. \quad (16)$$

Similar equations[17,23] exist for T_{1m}:

$$1/T_{1m} = (1/T_{1m})_{DP}+(1/T_{1m})_{HF} \quad (17)$$

where,

$$(1/T_{1m})_{DP} = [(2/15)S(S+1)g^2\beta^2\gamma_n^2/r^6] \times [3\tau_1+7\tau_2/(1+\omega_e^2\tau_2^2)] \quad (18)$$

and

$$(1/T_{1m})_{HF} = (2/3)S(S+1)(2\pi A/h)^2[\tau_2/(1+\omega_e^2\tau_2^2)]. \quad (19)$$

C. *Quadrupolar relaxation*

The ^{17}O quadrupolar relaxation ($I = 5/2$) in the extreme motional narrowing limit is given by the following equation:[23]

$$(1/T_2)_q = (3/125)(1+\eta^2/3)(e^2qQ/\hbar)^2\tau_c \quad (20)$$

where η is the asymmetry parameter, $e^2qQ/\hbar$ is the quadrupolar coupling constant and τ_c is the rotational correlation time.

D. *Complex equilibria*

For aqueous solutions of amino acids or peptides, containing small quantities of paramagnetic ions, such that [L] ≫ [M], where L and M refer to the ligand amino acid or peptide and metal ion, respectively, the complex equilibria in solution can be described by the general equation:[24]

$$pM^{2+}+qH^+ + rL^{y-} \overset{\beta_{pqr}}{\rightleftharpoons} M_pH_qL_r^{(2p+q-yr)}. \quad (21)$$

β_{pqr} is the overall stability constant for each metal ion complex:

$$\beta_{pqr} = [M_pH_qL_r]/([M]^p[H]^q[L]^r). \quad (22)$$

Since the concentration of the metal ions in this work is much smaller than that of the ligands, the probability for polymeric species is negligible and only monomeric species are considered with $p = 1$. L-Proline can exist in three forms: the ionic form, L^-, with $q = 0$, the zwitterionic form, $HL^{\pm}$, with $q = 1$, and the cationic form, H_2L^+, with $q = 2$. Considering that there are two possible binding sites per amino acid, and assuming hexa-coordinated complexes of the metal ions in this work, there can be up to three amino acids per metal ion. Thus $r = 1$, 2 or 3.

From the mass balance equation for $[M]_{total}$ and $[L]_{total}$ we get:

$$[M] = [M]_{total}\Big/\left(1+\sum_q\sum_r\beta_{1qr}[H]^q[L]^r\right) \quad (23)$$

and

$$[L] = [L]_{total}\Big/\left(1+\sum_q\beta_{0q1}[H]^q\right). \quad (24)$$

Thus, by calculating $[L^-]$ as a function of pH (easily accomplished with the aid of the Henderson–Hasselbalch equation), one can calculate the free metal ion concentration, provided that the stability constants are known and consequently the concentration of each of the complexes in solution. The validity of the above approximation has been tested by Beattie *et al.*[5] with an iterative solution of the complete mass balance equations using the method of Ingri and Sillén.[25] We can now combine the complex equilibria equations with the Swift–Connick equation and get:

$$1/T_{2p} = \sum_q\sum_r p_{1qr}f(\tau, T_2, \Delta\omega)_{1qr} \quad (25)$$

where τ_{1qr}, $(T_2)_{1qr}$ and $\Delta\omega_{1qr}$ refer to the lifetime, transverse relaxation time and frequency difference, in rads/s, from the free ligand, for each of the complexes. p_{1qr} is the ratio of the number of exchanging nuclei in each of the complexes divided by the number of nuclei in the free ligand. Since the free ligand concentration is much larger than the concentration of any of the complexes, the total concentration of

the ligand in solution is being taken as the concentration of the free ligand, to a first approximation. Thus,

$$p_{1qr} \approx r[MH_qL_r]/[L]_{total}. \quad (26)$$

Since $[MH_qL_r] = \beta_{1qr}[M][H][L]$, we can now substitute in (25) and get:

$$1/T_{2p} = \sum_q \sum_r r[M][H]^q[L]^r \beta_{1qr} f(\tau, T_2, \Delta\omega)_{1qr}/[L]_{total}. \quad (27)$$

Substituting eq. (23) into (26) for [M], we get:

$$1/T_{2p} = \frac{([M]/[L])_{total} \sum_q \sum_r r\beta_{1qr}[H]^q[L]^r f(\tau, T_2, \Delta\omega)_{1qr}}{\left(1+\sum_q \sum_r \beta_{1qr}[H]^q[L]^r\right)}. \quad (28)$$

Equation (28) thus links the paramagnetic relaxation rate, $1/T_{2p}$, of the free ligand, to the stability constants of all possible complexes and their perspective NMR parameters. Thus, it is possible to determine the stability constants of the complexes through a multi-parameter fit of the experimental relaxation data to eq. (28). In this work, the variation of the stability constants and NMR parameters was done semi-manually, starting with published values of stability constants (whenever possible), and having the computer determine $1/T_{2p}$ for any given combination of parameters. The best fits were then determined graphically, and the correlation coefficients were found to be in the range 0.97–0.99.

E. *The solvent signal*

In addition to the relaxation results for the free proline, there is a second set of data that indirectly gives information about the degree of formation of the various complexes, namely the paramagnetic relaxation rate of H_2O:

$$1/T_{2p} = p_m f(\tau_m, T_{2m}, \Delta\omega_m) \quad (29)$$

where p_m is the ratio of the bound water molecules divided by the number of molecules in the bulk water:

$$p_m = n_{eff}[M]_{total}/(55.5 - n_{eff}[M]_{total}). \quad (30)$$

Since $[M] \ll 55.5$, p_m is approximated by:

$$p_m \approx n_{eff}[M]_{total}/55.5. \quad (31)$$

In a pure aqueous solution of the metal ions in this work, n_{eff} is 6, assuming a hexa-coordinated structure.[17-20] In the presence of the amino acid, though, some of the water molecules in the metal ion complexes get replaced by the amino acid, reducing, thus, the effective number of coordinated water molecules. Consequently, the paramagnetic relaxation rate of water is reduced in a predictable way, since it depends linearly on n_{eff} and also on $f(\tau_m, T_{2m}, \Delta\omega_m)$. Thus in general n_{eff} can be calculated from the ratio of the paramagnetic relaxation of water in the presence and absence of proline, respectively:

$$n_{eff} = [6(1/T_{2p})^*/(1/T_{2p})] \times [f(\tau_m, T_{2m}, \Delta\omega_m)/f^*(\tau_m, T_{2m}, \Delta\omega_m)] \quad (32)$$

where the asterisk denotes the presence of proline in the solution, and all parameters subscripted by m are weighted average quantities over the various complexes in which water can be bound.

Equation (32) can be useful only when $f(\tau_m, T_{2m}, \Delta\omega_m)/f^*(\tau_m, T_{2m}, \Delta\omega_m)$ is known, or assumptions can be made about its magnitude. Assuming that $f(\tau_m, T_{2m}, \Delta\omega_m)/f^*(\tau_m, T_{2m}, \Delta\omega_m) = 1$, however, simplifies eq. (32) to:

$$n_{eff} = 6(1/T_{2p})^*/(1/T_{2p}) \quad (32a)$$

which is the equation that we have used in plotting the experimental results. The validity of this approximation will be discussed in a subsequent section.

Another way of calculating n_{eff} is by taking the weighted average of the number of water molecules in each complex, i.e.

$$n_{eff} = (1/[M]_{total})\{6[M(H_2O)_6]^{2+} + 5[MHL^{2+} \cdot 5H_2O] + \cdots + 1[MHL_3 \cdot H_2O]\}$$

which can be written in compact form as:

$$n_{eff} = (1/[M]_{total}) \sum_q \sum_r (6+q-2r)[MH_qL_r]. \quad (33)$$

Assuming that the concentrations of the complexes are known (i.e. the stability constants are known) one can calculate the effective coordination number of water molecules per metal ion, n_{eff}, in two ways: from eqs (32a) and (33). A good agreement between the results of the two equations will assure that the assumption made to get eq. (32a) is valid, and/or the stability constants are correct. Alternatively, divergence of the results of eqs (32a) and (33) means that the assumption that $[f(\tau_m, T_{2m}, \Delta\omega_m)/f^*(\tau_m, T_{2m}, \Delta\omega_m)] = 1$ is not valid and/or the stability constants used in eq. (33) are not correct. A further discussion of these points will follow in the next section.

RESULTS AND DISCUSSION

A. *The* Co(II)-*proline system*

(1) ^{17}O *NMR*. The pH dependence of the paramagnetic transverse relaxation rate of proline, $1/T_{2p}$, at 300 K, for a solution containing 0.13 M proline and 7.7 mM $CoCl_2$ (Solution A) is depicted in Fig. 1. The experimental results were least-squares fitted to eq. (28), and the stability constants and NMR parameters for each complex are given in Tables 1 and 2. Unlike other amino acids, for which several stability constants have been reported, the only stability constants for Co(II)–proline complexes that could be found in the literature were K_1 and β_2, for $CoPro^+$ and $CoPro_2$, respectively,[7–9] which are included in Table 1 for comparison. The following equations define the stability constants for all complexes assumed to exist in non-negligible concentrations:

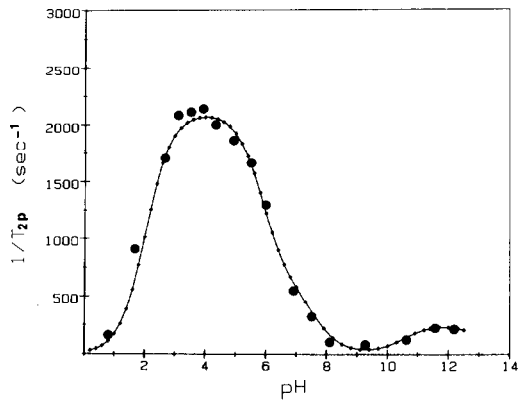

Fig. 1. Dependence of the ^{17}O paramagnetic transverse relaxation rate of proline upon the measured pH of a solution containing 0.126 M L-Proline and 7.7 mM $CoCl_2$ (Solution A). The experimental points were recorded at 24.4 MHz, 300 K and the dotted line is the least-squares fit of the experimental points to eq. (28), with the constants of Tables 1 and 2.

Table 1. Log stability constants of the major Co(II)–proline complexes in aqueous solution

Complex	Constant	This work	Ref.	
$CoHPro^{2+}$	k'_1	1.01 ± 0.1		
$Co(HPro)_2^{2+}$	k''_2	1.62 ± 0.25		
$CoHPro_2^+$	k'_2	1.41 ± 0.2		
$CoHPro_3$	k'_3	0.11 ± 0.15		
$CoPro^+$	K_1	5.05 ± 0.1	5.05[a]	4.89[b]
$CoPro_2$	β_2	9.30 ± 0.3	9.27[a]	9.30[c]
$CoPro_3^-$	β_3	10.75 ± 0.2		

[a] Ref. 9.
[b] Ref. 7.
[c] Ref. 8.

$$Co^{2+} + HPro^+ \overset{k'_1}{\rightleftharpoons} CoHPro^{2+} \quad \text{(I)}$$

$$Co^{2+} + 2HPro^+ \overset{k''_2}{\rightleftharpoons} Co(HPro)_2^{2+} \quad \text{(II)}$$

$$CoPro^+ + HPro^+ \overset{k'_2}{\rightleftharpoons} CoHPro_2^+ \quad \text{(III)}$$

$$CoPro_2 + HPro^+ \overset{k'_3}{\rightleftharpoons} CoHPro_3 \quad \text{(IV)}$$

$$CoPro_2 + Pro^- \overset{K_3}{\rightleftharpoons} CoPro_3^- \quad \text{(V)}$$

$$Co^{2+} + Pro^- \overset{K_1}{\rightleftharpoons} CoPro^+ \quad \text{(VI)}$$

$$Co^{2+} + 2PRo^- \overset{\beta_2}{\rightleftharpoons} CoPro_2 \quad \text{(VII)}$$

$$Co^{2+} + 3PRo^- \overset{\beta_3}{\rightleftharpoons} CoPro_3^-. \quad \text{(VIII)}$$

Table 2. Thermodynamic and NMR parameters of the Co(II)–proline complexes in aqueous solution[a]

Complex	$f(\tau_m, \Delta\omega_m)$ (s^{-1})	τ_m (s)	A/h (MHz)	$\Delta H\dagger$ (Kcal/mol)	$\Delta S\dagger$ (e.u.)
$CoHPro^{2+}$	4.80×10^4	1.6×10^{-6}	-1.2 ± 0.2	9.3	-8.6
$Co(HPro)_2^{2+}$	5.20×10^4				
$CoHPro_2^+$	1.15×10^4				
$CoHPro_3$	3.10×10^2				
$CoPro^+$	3.14[b]				
$CoPro_2$	39.0[b]		-0.63 ± 0.02		
$CoPro_3^-$	1.38×10^3	6.75×10^{-4}	-0.31 ± 0.05	7.1	-10.1
		9.5×10^{-5}[c]		7.1[c]	-8.8[c]

[a] All parameters are calculated at 300 K.
[b] Ref. 9.
[c] From ^{14}N NMR measurements.

First-order dissociation of $CoPro^+$ and $CoPro_2$ cannot be a major source of broadening, because of the long lifetimes of complexes of this type (in the order of 10^{-1} to 10^{-2} s),[9,26] thus their contribution to the relaxation rate of proline was neglected, to a first approximation. (A rough calculation shows that the contribution of these two complexes to $1/T_{2p}$ is less than 0.5 Hz, certainly negligible.) Incidentally, the small deviation of the experimental points from the theoretical line in the pH range 3–5 is due to copper impurities that are found in the titrating base. As will be seen in the Cu(II)–proline results, very large broadening is observed in the pH range 3–4 for comparatively small copper concentrations.

Taking the existence of $Co(HPro)_2^{2+}$ into account was dictated by the value of n_{eff} in the acidic pH range, Fig. 2. Without $Co(HPro)_2^{2+}$, an unreasonably large stability constant for $CoHPro^{2+}$ would have to be assumed to justify a value of about 5 for n_{eff} at pH 4–5. Similar considerations were also made in the case of glycine and alanine[27] for Co^{2+} but not for Cu^{2+} and Mn^{2+}, for which the best fits were obtained without considering the complex $M(HL)_2^{2+}$ as a major species. The solid circles in Fig. 2 were determined from eq. (32a). The deviation from the dotted line [eq. (33)] shows clearly that $f(\tau_m, T_{2m}, \Delta\omega_m)/f^*(\tau_m, T_{2m}, \Delta\omega_m) = 1$ is not a good assumption for $n_{eff} < 5$. In fact, $f(\tau_m, T_{2m}, \Delta\omega_m)/f^*(\tau_m, T_{2m}, \Delta\omega_m)$ was found to vary nonlinearly from 1 at very acidic pH to about 5 at pH 8, (Solution C, data not included).

Figure 3 shows the distribution of all Co^{2+}-containing species in Solution A, as a function of pH, constructed with the stability constants of Table 1. The existence of $CoHPro_3$ was postulated on the fact that the zwitterionic form of proline is predominant in the pH range 3–10, thus eq. (IV) should be considered. The best fit for $1/T_{2p}$ could be obtained with $\log k'_3 = 0.11$, but there is an uncertainty of ± 0.15 associated with the above value, due to the small paramagnetic broadening in the pH range where $CoHPro_3$ reaches its maximum concentration. The distribution of $CoHPro_3$ follows that of $CoPro_2$, except in the high pH range where the concentration of the zwitterion of proline diminishes and reaction (IV) is negligible.

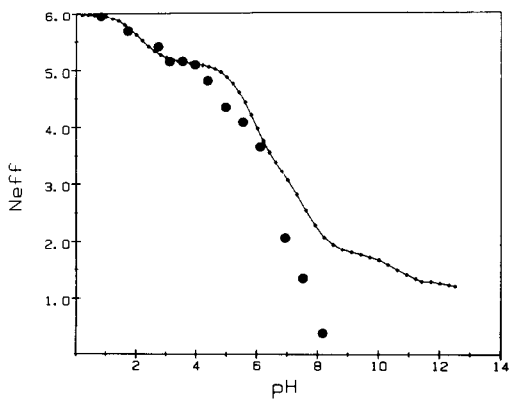

Fig. 2. Dependence of the effective coordination number of water upon pH, for Solution A. The solid circles represent the experimental data calculated from eq. (32a), while the dotted line is the theoretical prediction of eq. (33).

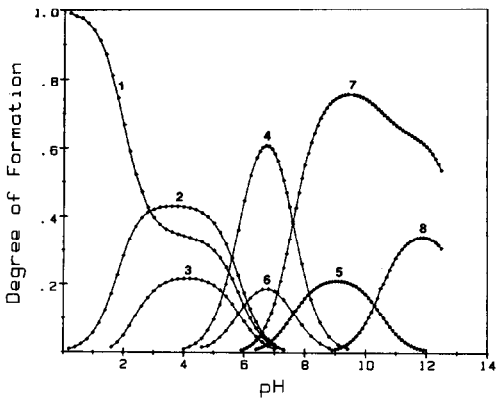

Fig. 3. Dependence of the relative concentration of all Co^{2+}-containing species upon pH, for Solution A. All curves were constructed with the stability constants of Table 1. 1 is the free Co^{2+}, 2, 3, 4, and 5 are the protonated complexes $CoHPro^{2+}$, $Co(HPro)_2^{2+}$, $CoHPro_2^+$ and $CoHPro_3$, respectively, whereas 6, 7 and 8 are the bidentate complexes $CoPro^+$, $CoPro_2$ and $CoPro_3^-$, respectively.

Second-order processes were neglected, but the shorter lifetimes calculated from the ^{14}N NMR data for $CoPro_3^-$ at basic pH indicate that second-order exchange does play a role when the concentration of the free ligand is larger than 0.5 M. The low concentration of proline in Solution A, though, justifies neglecting of second-order effects, included in:

$$1/\tau_m = k_1 + k_2[Pro^-] \tag{34}$$

with k_2 defined by:

$$CoPro_r + (Pro^-)^* \overset{k_2}{\rightleftharpoons} CoPro^*_{(r-1)}Pro + Pro^-. \tag{35}$$

The reaction of the type shown in eq. (35) has been considered in several ^1H NMR studies of amino acids and metal ions.[5,28,29]

The relatively small paramagnetic broadening in the basic pH range, where $CoPro_3^-$ is the predominant species, indicates the formation of strong coordination bonds between proline and Co^{2+}, with a slow rate of chemical exchange on the NMR time scale. From the temperature dependence of T_{2p}, the enthalpy and entropy of activation for the first-

order process (V) were calculated along with the lifetime of $CoPro_3^-$ and its hyperfine coupling constant, A/h, are presented in Table 2.

Figure 4 contains several ^{17}O spectra of Solution B at various pH values. In addition to free proline, a second signal can be seen at around 700 ppm from free proline. Considering the stoichiometry of the solution in the pH range 7–12 this signal was assigned to $CoPro_2$. The concentration of $CoPro_2$ determined from the relative areas of the signals (compared to the signal of water that was considered as constant to a first approximation) reaches a maximum at pH 9.5, and then decreases slightly above that pH. The concentration of free proline, on the other hand, decreases dramatically above pH 9, reflecting the formation of $CoPro_3^-$. Note that the total concentrations of proline and Co^{2+} in Solution B are 0.28 and 0.055 M, respectively, thus at basic pH where $CoPro_2$ and $CoPro_3^-$ are the predominant complexes, more than half of the proline is bound to Co^{2+}. Of course, the Swift and Connick equations are not expected to hold true in this case, because the condition of a predominant diamagnetic case is not met. The high concentration of Co^{2+}, though, was necessary in order to make detection of $CoPro_2$ possible.

The minimum linewidth of $CoPro_2$ (1,700 Hz) occurs in the pH range 6–8 and it is taken to be the natural linewidth of $CoPro_2$ (no contributions from chemical exchange to it). This assumption is substantiated by $T_1 = 0.19$ ms that was determined for $CoPro_2$ at pH 9, which corresponds to about 1,700 Hz. Above pH 8, the linewidth of $CoPro_2$ increases non-linearly with pH (from 1900 Hz at pH 9 to 3700 Hz at pH 11.7). The long lifetime of $CoPro_2$ (2.5×10^{-2} s)[9] rules out the importance of first-order exchange. Second-order exchange broadening of $CoPro_2$ must then be considered and that is given by:

$$1/T_{2p} = k_2[Pro^-] \tag{36}$$

whereas the second-order broadening of free proline is given by:

$$1/T_{2p} = k_2[CoPro_2][Pro^-]/[Pro]_{total}. \tag{37}$$

Comparing eqs (36) and (37) it is obvious that the second-order broadening of $CoPro_2$ is greater than that of free proline by a factor of $[Pro]_{total}/$

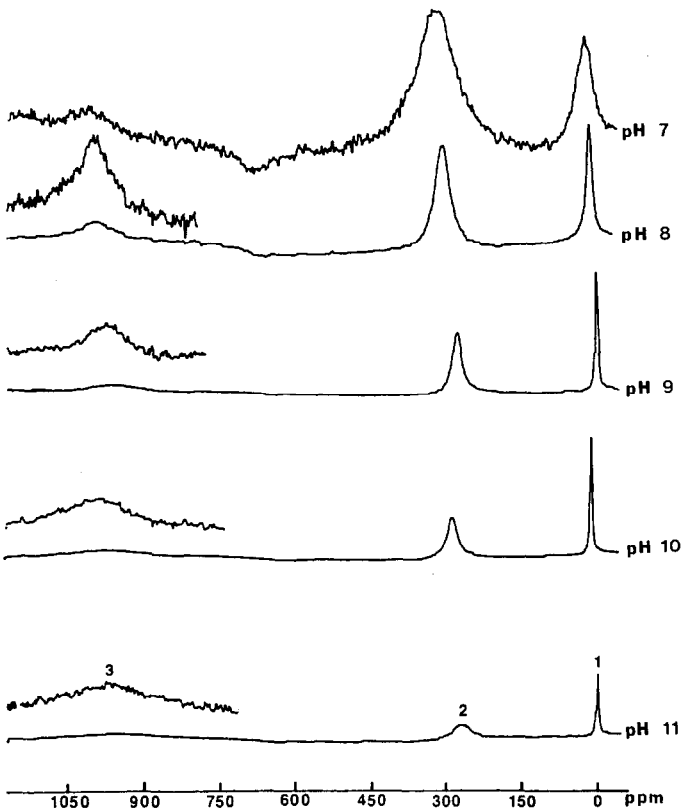

Fig. 4. ^{17}O NMR spectra of a solution containing 0.28 M proline and 55 mM $CoCl_2$ (Solution B), At several pH values. The spectra were recorded at 24.4 MHz, 300 K, with a spectral width of 50 KHz, pulse width of 10 μs, delay time of 10 μs, recycle delay of 70 ms and with 4k spectral points for signal acquisition.

[$CoPro_2$]. For Solution A at pH 11.7, this factor is about 40, thus if second-order exchange broadens the free proline signal by 20 Hz, $CoPro_2$ would be broadened by 800 Hz, certainly non-negligible.

The question that must be answered is whether the signal that was assigned to $CoPro_2$ is the weighted average of all ^{17}O nuclei in $CoPro_2$ or is it due only to the non-coordinated carbonyl oxygens in that complex. The "narrow" linewidth of 1,700 Hz suggests that the quadrupolar interaction be the principal mechanism of relaxation. In fact, if one uses eq. (33) with $\eta = 0.45$,[30] $e^2qQ/h = 10.2$ MHz determined from the ^{17}O quadrupolar splittings of [^{17}O]urea dissolved in a lyotropic liquid crystal (M. I. Burgar and D. Fiat, unpublished data), and $\tau_c = 7.6 \times 10^{-11}$ s calculated from the Moniz–Gutowski–BPP equation[31,32] (taking $d = 1$ g/cm^3) the quadrupolar relaxation rate is expected to be 7860 s^{-1}, larger than the observed value of 5340 s^{-1}. This estimate shows that the quadrupolar relaxation alone can account for the observed relaxation rate of $CoPro_2$. It also shows that the correlation time calculated from the Moniz–Gutowski–BPP equation is longer than what one calculates from the quadrupolar relaxation rate, a finding that has been reported quite often.[31,33,34]

The contribution of the dipolar and hyperfine mechanisms to the relaxation rate of $CoPro_2$ can be determined from eqs (15) and (16), respectively, provided that the hyperfine coupling constant, correlation times and the distance between the ^{17}O nucleus and Co^{2+} are known. The hyperfine coupling constant was determined from the observed paramagnetic shift of $CoPro_2$ and was found to be -6.3×10^5 Hz. The correlation time for the aqueous and methanol complexes of Co^{2+} was taken to be the electronic relaxation time, which at 298 K was found to be 7×10^{-13} s.[18,19] Using this value for the electronic relaxation time in the case of $CoPro_2$ is not necessarily a good assumption (in view of the negative charge of the carboxylate group of each proline molecule) but it should serve as a guide since no better estimate could be found. The distance between the metal ion and the non-coordinated carbonyl oxygen was taken to be 4 Å, in line with similar values measured for complexes of proline with Mn^{2+} and Cu^{2+} (3.99 and 4.04 Å, respectively).[4,35] With these values, eqs (15) and (16) give 4 and 27 s^{-1}, respectively, for the dipolar and hyperfine contributions to the relaxation rate of $CoPro_2$.

The predominance of the quadrupolar mechanism and the small hyperfine coupling constant of $CoPro_2$ support the hypothesis that the signal arises from the non-coordinated carbonyl oxygens in $CoPro_2$ (one from each proline molecule). The paramagnetic shift of $CoPro_2$ was taken to be the difference of the observed chemical shift of $CoPro_2$ from that of the carbonyl oxygen of methyl ester (970 and 350 ppm, respectively), rather than from the signal of free proline, which is the weighted average signal of a double bonded and a single bonded carboxylic oxygen exchanging rapidly with respect to the NMR time scale. Thus the methyl ester carbonyl oxygen seems to be a better-suited reference in the present case.

Figure 5 shows the pH dependence of the paramagnetic chemical shift, $\Delta\omega_a$, of proline in Solution A. The decline from pH 3 to 4 is probably due to experimental error (at this pH the broadest lines are observed, with an uncertainty of ± 2.0 ppm). A plateau is more likely to reflect the concentration profile of $CoHPro^{2+}$ and $Co(HPro)_2^{2+}$ in this pH range, and the additional shift from pH 4–7 is apparently due to the formation of $CoHPro_2^+$ in this pH range. Thus, the paramagnetic chemical shift also reflects the distribution of the complexes as a function of pH.

Figures 6 and 7 show the temperature dependence of T_{2p} of free proline in Solution C, at pH 3 and 6, respectively. In this pH range, where the monodentate complexes $CoHPro^{2+}$ and $Co(HPro)_2^{2+}$ predominate, both the slow and the fast exchange regions are accessible in the temperature range of 274–370 K. Incidentally, room temperature falls in the intermediate exchange region, where maximum broadening occurs, and neither the slow nor the fast exchange approximation is valid for $1/T_{2p}$. At the point of intersection of the slow and fast exchange curves in Figs 6 and 7, $\Delta\omega_m\tau_m = 1$, and eq. (5) reduces to:

$$1/T_{2p} = (1/2)p_m/\tau_m. \tag{38}$$

The above simplification serves as a useful con-

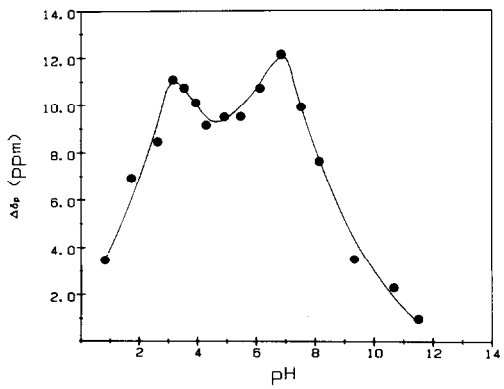

Fig. 5. Dependence of the ^{17}O paramagnetic chemical shift of proline upon pH, for Solution A, 300 K and a spectrometer frequency of 24.4 MHz.

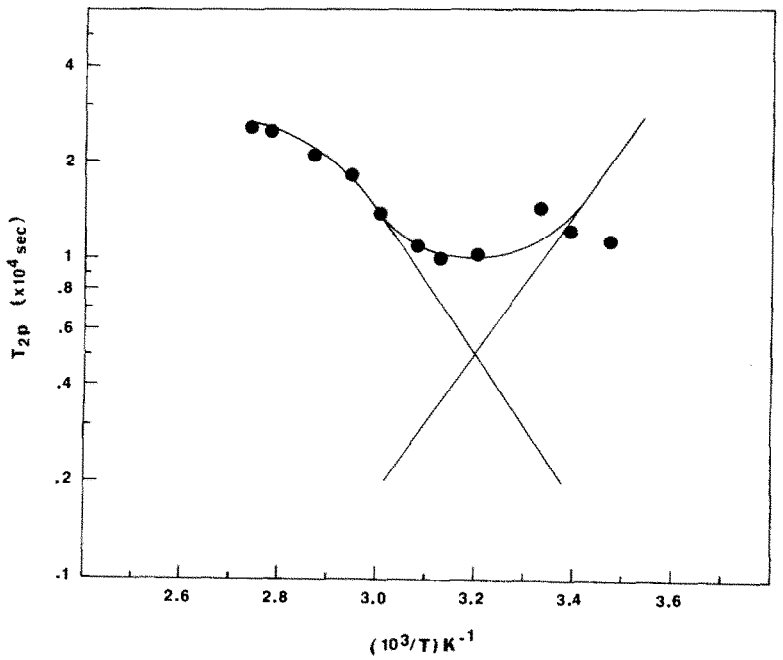

Fig. 6. Dependence of the ^{17}O paramagnetic transverse relaxation time of proline upon inverse temperature at pH 3, for a solution containing 0.3 M proline and 22 mM $CoCl_2$ (Solution C). The data were recorded at 33.926 MHz.

straint on the data analysis: the slow and fast exchange approximation lines intersect at a point at exactly half the experimental value at that temperature.

If an average p_m is assumed, i.e. including $CoHPro^{2+}$, $Co(HPro)_2^{2+}$ and $CoHPro_2^+$, an average value of A/h for these three complexes can be calculated. Unfortunately, although the relative distribution of these complexes can be determined at a given temperature by a least-squares fitting of eq. (28) to the experimental paramagnetic relaxation data, the temperature dependence of the stability constants and the rate of chemical exchange are not known, thus the relative contribution of each complex to the overall relaxation rate, $1/T_{2p}$, as a function of temperature, cannot be assessed. As a result, only an average value (or at best some estimates) for all thermodynamic parameters, as

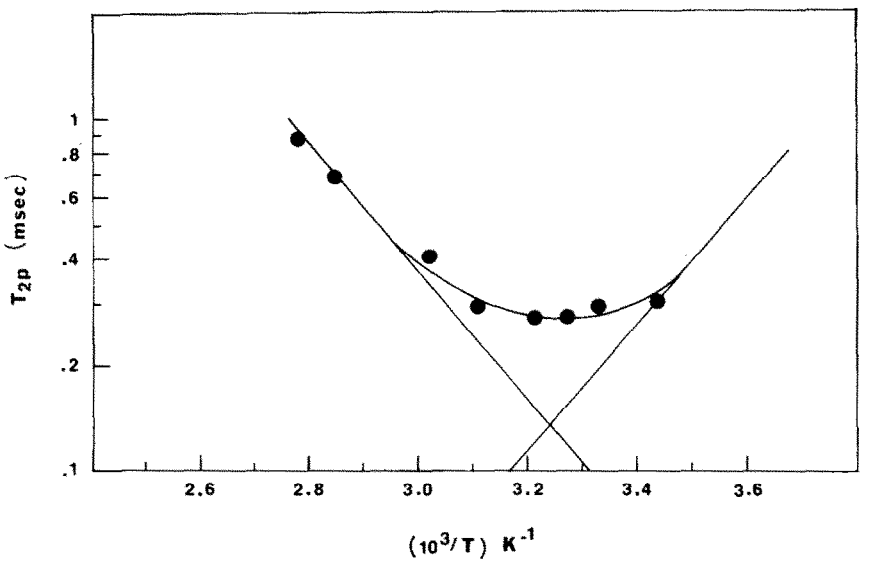

Fig. 7. Dependence of the ^{17}O paramagnetic transverse relaxation time of proline upon inverse temperature, in Solution C, at pH 6 and at a spectrometer frequency of 33.926 MHz.

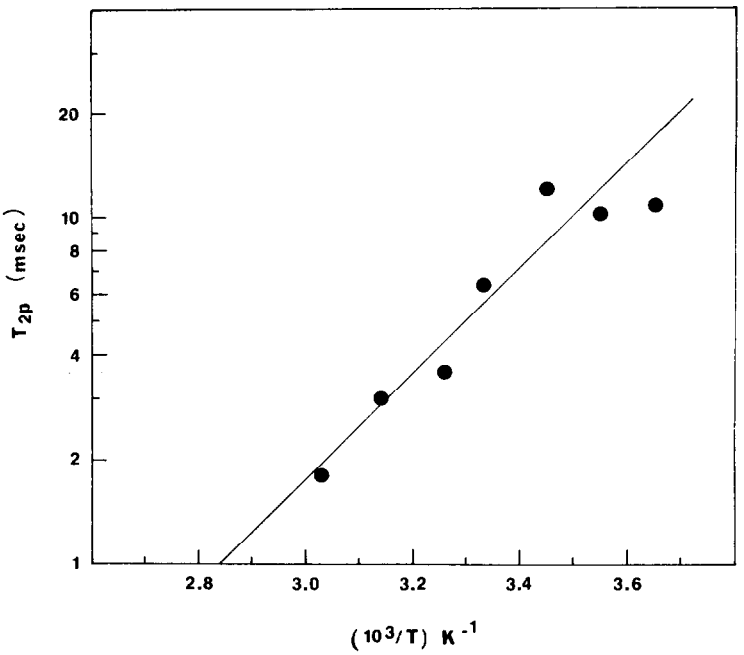

Fig. 8. Dependence of the ^{17}O paramagnetic transverse relaxation time of proline upon inverse temperature, at pH 11, for a solution containing 0.26 M proline and 0.01 M $CoCl_2$ (Solution D). Spectrometer frequency is 33.926 MHz.

well as for the hyperfine coupling constant, A/h, can be determined.

Figure 8 shows the temperature dependence of T_{2p} of proline for Solution D, at pH 11. Only the slow exchange region is accessible in the temperature range 275–330 K. The deviation from linearity at the lower temperatures is probably due to a non-linear increase in the viscosity of the solution. From the slow exchange region, the lifetime of $CoPro_3^-$, the enthalpy and entropy of activation of the first-order exchange of this complex are determined and shown in Table 2.

(2) ^{14}N *NMR results.* Figure 9 shows the pH dependence of the ^{14}N transverse paramagnetic relaxation rate, $1/T_{2p}$, of proline for Solution E and F, containing Co^{2+} and Cu^{2+}, respectively. The complete lack of broadening below pH 8 is consistent with the ^{17}O results, indicating that the first-order exchange in reaction (V) and second-order exchange [eq. (35)] are responsible for the observed broadening in the basic pH region. Thus, ^{14}N NMR can be used as a complementary method to ^{17}O NMR, but alone it lacks the wealth of information provided by ^{17}O NMR. The broadening of the proline signal above pH 9 follows the formation of $CoPro_3^-$. Thus, the temperature dependence of T_{2p} at high pH, can provide the thermodynamic parameters associated with reaction (V), to a first approximation, i.e. neglecting second-order effects. Table 2 summarizes the results obtained from both ^{17}O and ^{14}N NMR experiments.

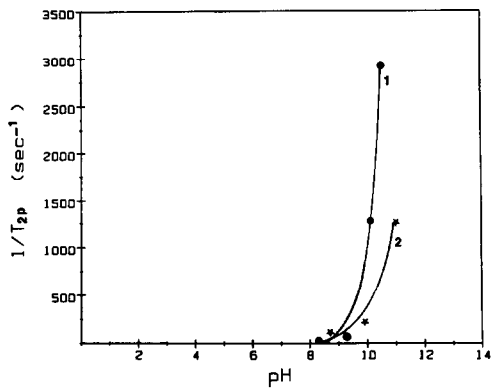

Fig. 9. Dependence of the ^{14}N paramagnetic transverse relaxation rate of proline upon pH, for Solution E (1.5 M proline and 0.02 M $CoCl_2$) and Solution F (1.0 M proline and 1.0 mM $CuCl_2$), at 300 K. The spectrometer frequency was 18.075 MHz.

B. *The* Cu(II)-*proline system*

(1) ^{17}O *NMR results.* Figure 10 shows the pH dependence of the ^{17}O paramagnetic transverse relaxation rate, $1/T_{2p}$, of proline for Solution G, at 300 K. The dotted line was constructed through eq. (28), with the stability constants of Table 3 and the NMR parameters of Table 4.

Figure 11 shows the distribution of all Cu(II)-containing species in Solution G, as a function of

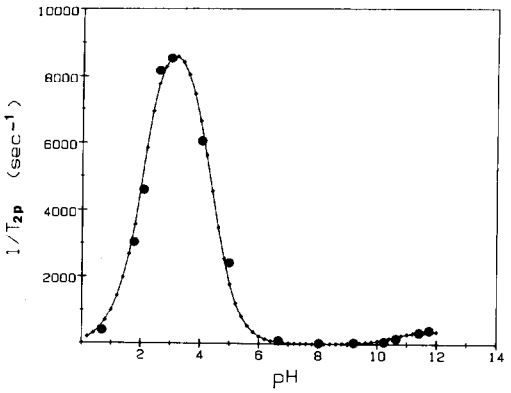

Fig. 10. Dependence of the ^{17}O paramagnetic transverse relaxation rate of proline upon the measured pH of a solution containing 0.25 M proline and 0.3 mM $CuCl_2$ (Solution G). The experimental points were recorded at 24.4 MHz, and 300 K, and the dotted line is the least-squares fit of the experimental points to eq. (28), with the constants of Tables 3 and 4.

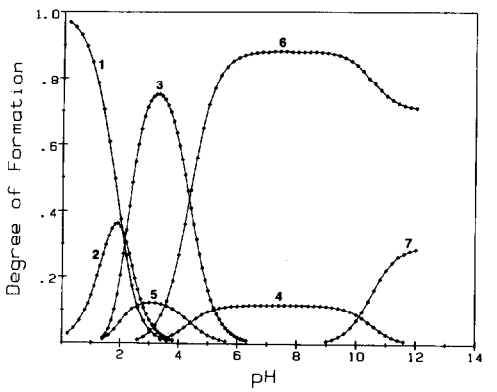

Fig. 11. Dependence of the relative concentration of all Cu^{2+}-containing species upon pH, for Solution F. All curves were constructed with the stability constants of Table 3. 1 is the free Cu^{2+}, 2, 3 and 4 are the protonated complexes $CuHPro^{2+}$, $CuHPro_2^+$ and $CuHPro_3$, respectively, and 5, 6 and 7 are the bidentate complexes $CuPro^+$, $CuPro_2$ and $CuPro_3^-$, respectively.

Table 3. Log of stability constants of the major Cu(II)–proline complexes in aqueous solution[a]

Complex	Constant	This work	Ref. 2	Ref. 36	Ref. 37
$CuHPro^{2+}$	k'_1	0.85	0.98 ± 0.27		
$CuHPro_2^+$	k'_2	1.39	1.10 ± 0.19		
$CuHPro_3$	k'_3	−0.05			
$CuPro^+$	K_1	8.70	8.69	8.76	8.72
$CuPro_2$	β_2	16.34	16.03	16.31	16.35
$CuPro_3^-$	β_3	16.54			

[a] The stability constants of this work were determined at 300 K, while those of Ref. 2 were recorded at 310 K. The remaining constants are reported at 298 K.

Table 4. Thermodynamic and NMR parameters of the Cu(II)–proline complexes in aqueous solution[a]

Complex	$f(\tau_m, T_{2m})$ (s^{-1})	τ_m (s)	$\Delta H\dagger$ (Kcal/mol)	$\Delta S\dagger$ (e.u.)
$CuHPro^{2+}$	2.68×10^6			
$CuHPro_2^+$	2.17×10^6			
$CuHPro_3$	2.5×10^4			
$CuPro^+$	3.0[b]			
$CuPro_2$	5.9[b]			
$CuPro_3^-$	1.68×10^5	1.2×10^{-6}[c]	5.8[c]	−14.0[c]

[a] All parameters are calculated at 300 K.
[b] Taken from Ref. 9.
[c] From ^{14}N NMR.

pH, constructed with the stability constants of Table 3. For comparison, the stability constants reported by other investigators are also given in Table 3. The overall good agreement confirms the validity of the method used in this work.

The n_{eff} data of water could not be used in this case, due to the small paramagnetic broadening of the water signal, for the concentration of $CuCl_2$ used in this work. Considering the experimental uncertainty of ± 5 Hz associated with narrow lines, and the total paramagnetic broadening of 20 Hz, the uncertainty in n_{eff} was $\pm 0.25 \times 6$ or ± 1.5, totally unacceptable.

The values of $f(\tau_m, T_{2m}, \Delta\omega_m)$ associated with each Cu(II)–Proline complex are one to three orders of magnitude larger than those of the corresponding Co(II)–Proline complexes. The relevant mechanism of transfer of the paramagnetic effects of Cu(II) to the bulk is the "T_{2m}" mechanism, given by eq. (7). Thus, either the rate of chemical exchange in cases of slow exchange, or the transverse relaxation rate of the complexes in cases of fast exchange, are one to three orders of magnitude larger than those of the corresponding Co(II)–proline complexes. This is also the case with the aqueous complexes of the aforementioned metal ions.[13] The Jahn–Teller interactions that characterize the coordination of Cu^{2+} cause the formation of elongated octahedral complexes, with unequal equatorial and axial coordination, whereas the complexes of Co(II) are distinguished by regular octahedral symmetry, with all six coordination sites equivalent. Thus, the long electronic relaxation times of Cu^{2+}, coupled with possible interconversion of the axial and equatorial coordination sites, may be the principal reasons for the apparent short NMR relaxation times and/or lifetimes of its complexes.

The relaxation results in the basic pH region are completely different from those in the Cu(II)–Glycine and Cu(II)–Alanine systems, in which cases the broadening in the basic pH was larger than that in the acidic pH.[27] This result must be due to the cyclic structure of proline and the fact that it is a more basic amino acid (pK_a of proline is an order of magnitude larger than that of glycine and alanine). Consequently, $CuPro_3^-$ is more tightly bound than $CuGly_3^-$ or $CuAla_3^-$, and as a result it has a longer lifetime. The overall result is less broadening of the free proline signal in the basic pH.

The stability constant that was determined for $CuHPro_3$ suffers from the same uncertainty as that of $CoHPro_3$, for the reasons discussed previously, but its overall effect on the stability constants of the other species in the pH range that it exists was minimal. Thus, omitting $CuHPro_3$ from the fitting would require slightly different stability constants for $CuHPro_2$, $CuPro_2$ and $CuPro_3^-$ to obtain a good fit, but the resulting best fit had a smaller correlation coefficient than the best fit obtained including $CuHPro_3$. Thus $CuHPro_3$ was included in the fitting.

(2) ^{14}N *NMR results.* The pH dependence of the ^{14}N paramagnetic transverse relaxation rate of proline, $1/T_{2p}$, for Solution F, is depicted in Fig. 9. As in the case of the Co(II)–Proline system, there is no broadening in the acidic and neutral pH, but only in the basic pH, following the formation of $CuPro_3^-$. Thus, no information could be provided in the acidic and neutral pH, limiting, therefore, ^{14}N NMR as a self-sufficient method in ion binding studies with amino acids.

Figure 12 depicts the temperature dependence of the ^{14}N paramagnetic transverse relaxation time of proline at pH 11, for Solution H. The thermodynamic parameters derived from the temperature dependence of τ_m of $CuPro_3^-$ are given in Table 4. Slow exchange characterizes the Cu(II)–Proline system for the entire temperature range of 275–360 K. At the lower end of the temperature range, the non-linear increase in the viscosity of the solution causes additional broadening, and that explains the deviation from linearity.

C. *The* Mn(II)*-proline system*

(1) ^{17}O *NMR results.* Figure 13 shows the pH dependence of the ^{17}O paramagnetic transverse relaxation rate of proline, for Solution I. The dotted line is the least-squares best fit of the experimental results to eq. (28). The stability constants and NMR parameters are shown in Table 5. The small deviation from the theoretical line around pH 3 is caused by the inevitable contamination of the solution with copper impurities, that despite all precautions persist in the titrating base. As it was seen in the previous section, copper causes the largest broadening around pH 3. While one can reduce the amount of impurities in the solution by extreme caution, some trace of the copper impurity will always persist for all practical applications.

The most striking difference from the Co(II)–proline and Cu(II)–proline systems lies in the fact that one species predominates in the pH range 0–8, namely $MnHPro^{2+}$. The spherical symmetry in the electronic charge density of Mn^{2+}, resulting in small stability constants of its complexes, is the reason that $MnHPro^{2+}$ is the predominant species in the pH range 0–8.

The distribution of the Mn(II)–proline complexes as a function of pH, for the same Solution H, is given in Fig. 14. The same types of complexes that

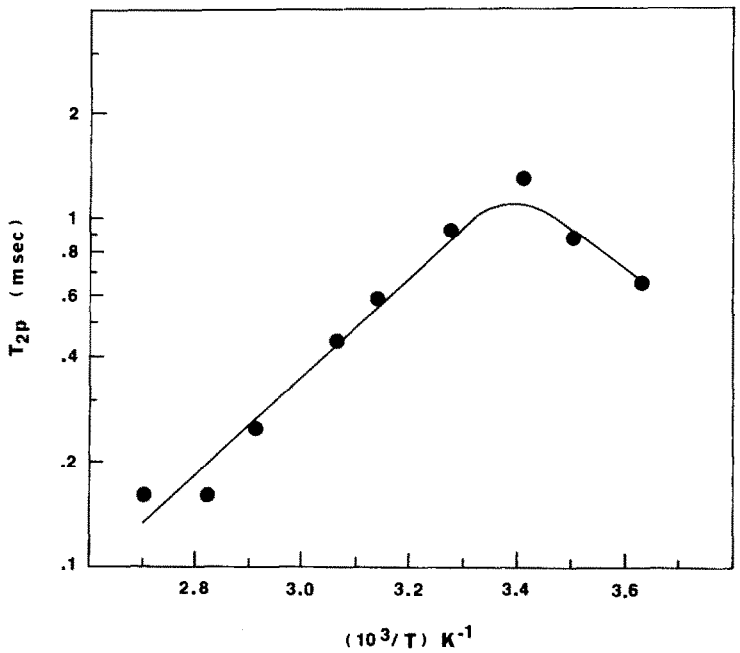

Fig. 12. Dependence of the ^{14}N paramagnetic transverse relaxation time of proline upon inverse temperature, for a solution containing 1.5 M proline and 2.0 mM $CuCl_2$ (Solution H), at pH 11. The spectrometer frequency was 18.075 MHz.

were discussed in previous sections also exist in the Mn(II)–proline system, except that their maximum concentration is shifted to much higher pH. The stability constants reported by Childs and Perrin[2] were used almost unchanged, as can be seen from Table 5, and this confirms the validity of the overall method used in this work.

Figure 15 shows the pH dependence of n_{eff} of water for Solution I. Since there are only two Mn(II)-containing species in the pH range 0–8, namely $Mn(H_2O)_6^{2+}$ and $MnHPro^{2+}$ ($5H_2O$), and assuming $f(\tau_m, T_{2m}, \Delta\omega_m)/f^*(\tau_m, T_{2m}, \Delta\omega_m) \approx 1$, then the stability constant of $MnHPro^{2+}$ can be calculated easily from n_{eff}, since the concentrations of both free Mn^{2+} and $MnHPro^{2+}$ are deduced from n_{eff}:

$$[MnHPro^{2+}]/[Mn(H_2O)_6] = (6-n_{eff})/(n_{eff}-5) \quad (39)$$

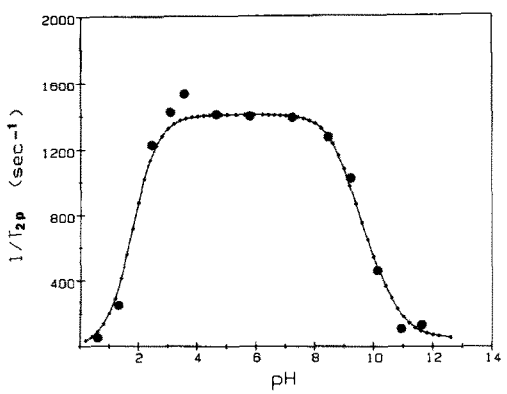

Fig. 13. Dependence of the ^{17}O paramagnetic transverse relaxation rate of proline upon the measured pH of a solution containing 0.08 M proline and 0.34 mM $MnCl_2$ (Solution I), at 300 K. The experimental points were recorded at 24.4 MHz and the dotted line is the least-squares fit of the experimental points to eq. (28), with the constants of Tables 5 and 6.

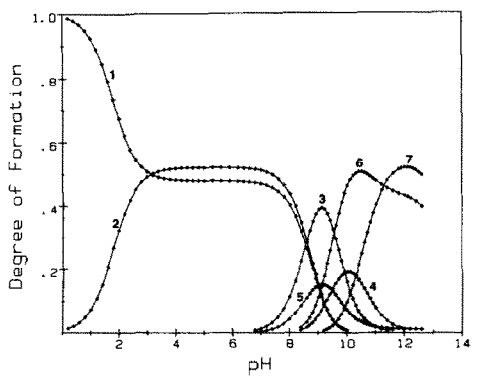

Fig. 14. Dependence of the relative concentration of all Mn^{2+} containing species upon pH, for Solution I, at 300 K. All curves were constructed with the stability constants of Table 5. 1 is the free Mn^{2+}, 2, 3, and 4 are the protonated complexes $MnHPro^{2+}$, $MnHPro_2^+$ and $MnHPro_3$, respectively, whereas 5, 6 and 7 are the bidentate complexes $MnPro^+$, $MnPro_2$ and $MnPro_3^-$, respectively.

Table 5. Log stability constants of the major Mn(II)–proline complexes and NMR parameters in aqueous solution[a]

Complex	$f(\tau_m, T_{2m})$ (s^{-1})	Constant	This work	Ref. 2	
$MnHPro^{2+}$	6.03×10^5	k'_1	1.15	1.50 ± 0.12	
$MnHPro_2^+$	1.82×10^5	k'_2	1.53	1.74 ± 0.21	
$MnHPro_3$	1.10×10^3	k'_3	0.17 ± 0.13		
$MnPro^+$		K_1	2.84	2.84	3.34[b]
$MnPro_2$		β_2	5.53	5.53	5.5[c]
$MnPro_3^-$	1.78×10^4	β_3	6.74	6.74	

[a] The parameters calculated in this work are reported at 300 K, whereas those of Ref. 2 are reported at 310 K.
[b] Taken from Ref. 38.
[c] Taken from Ref. 7.

and

$$k'_1 = [HPro^+]^{-1}(6-n_{eff})/(n_{eff}-5). \quad (40)$$

Needless to say that one need not see the signal of proline to derive the stability constant for $MnHPro^{2+}$, for only the signal of water in the absence and presence of proline at constant Mn^{2+} concentration is required. Thus, non-enriched proline is sufficient for such a task. The excellent agreement between the theoretical and experimental values of n_{eff} in Fig. 15 justifies the assumption that when only one water molecule is replaced by an amino acid in an aqueous complex of a metal ion, $f(\tau_m, T_{2m}, \Delta\omega_m)$ for the remaining water molecules is not changed drastically with respect to that in $M(H_2O)_6^{2+}$.

The temperature dependence of the paramagnetic transverse relaxation time of proline at pH 11, where $MnPro_3^-$ predominates, showed that conditions of fast exchange prevail in the temperature range 275–330 K. In this range, $1/T_{2p} = p_m/T_{2m}$, thus the transverse relaxation time of $MnPro_3^-$ can be calculated. At 33°C, T_{2m} was found to be 6.18 μs, from which a correlation time of 1.4×10^{-10} s was calculated, taking a value of 1.97×10^{-8} cm derived by Henry *et al.*[4] from ^{13}C NMR data. Henry *et al.* also report a value of 1.28×10^{-10} s for the rotational correlation time of $MnPro_3^-$, at the same temperature, which is in good agreement with our value. At 60°C, though, they report a value of 4.6×10^{-11} s, while at the same temperature we calculated a value of 8.4×10^{-11} s for the rotational correlation time of $MnPro_3^-$, almost two times longer. No clear explanation exists other than possible experimental error, either theirs or ours.

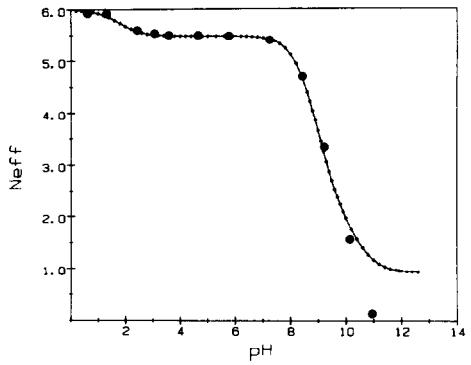

Fig. 15. Dependence of the effective coordination number of water upon pH, for Solution H. The experimental points were calculated from the ratio of the paramagnetic transverse relaxation rate of water in the presence and absence of proline, respectively, and the dotted line is the prediction of eq. (33).

CONCLUSIONS

This work showed that the combination of ^{17}O and ^{14}N NMR can be a powerful probe in ion binding studies of amino acids and information not afforded easily by any other method can be extracted from such studies. Thus, stability constants, hyperfine coupling constants and the corresponding thermodynamic parameters characterizing the dynamical behavior of the metal ion complexes can be determined from the ^{17}O and ^{14}N NMR studies.

With regard to the complexes of proline, in particular, the stability constants of $CoHPro^{2+}$, $Co(HPro)_2^{2+}$, $CoHPro_2^+$ $CoHPro_3$ and $CoPro_3^-$ were determined for the first time, in this work. Furthermore, the direct observation of $CoPro_2$ and $CoPro_3^-$ allowed the accurate determination of the hyperfine coupling constant, A/h, of these complexes, as well as the characterization of the

mechanism of interaction between the unpaired electrons of Co^{2+} and the ^{17}O nucleus.

Acknowledgements—This work was supported by NIH Grant GM24813. We would like to thank Drs A. Steinschneider and D. Dhawan for labeling and purifying proline for the ^{17}O NMR studies. We would also like to thank Dr Eric Oldfield, Dennis Warrenfeltz and Dr David Wright at the Regional NMR Center at the University of Illinois at Champaign-Urbana and the RRC facilities of the University of Illinois at Chigaco for their assistance. We would also like to thank Dr Robert E. Connick at the University of California, Berkeley, for some helpful discussions.

REFERENCES

1. E. Tiezzi, *J. Chem. Soc., Perkin II* 1975, 769.
2. C. W. Childs and D. D. Perrin, *J. Chem. Soc. (A)* 1969, 1039.
3. B. Henry, M. Rappeneau, J.-J. Boubel and J. J. Delpuech, *Adv. Mol. Relax. Inter. Process.* 1980, **16**, 29.
4. B. Henry, M. Rappeneau and J.-J. Delpuech, *Polyhedron* 1982, **1**, 113.
5. J. K. Beattie, D. J. Fensom and H. C. Freeman, *J. Am. Chem. Soc.* 1976, **98**, 500.
6. B. Valentine, T. St. Amour, R. Walter and D. Fiat, *Org. Mag. Res.* 1980, **13**, 232.
7. K. K. Girdhar, K. K. Vaidya and P. S. Relam, *J. Ind. Chem. Soc.* 1970, **47**, 715.
8. A. Albert, *Biochem. J.* 1950, **47**, 531.
9. K. Kustin and S. T. Liu, *J. Chem. Soc., Dalton Trans.* 1973, 278.
10. A. Steinschneider, M. I. Burgar, A. Buku and D. Fiat, *Int. J. Pept. Protein Res.* 1981, **18**, 324.
11. A. Steinschneider, T. St. Amour, B. Valentine, M. I. Burgar and D. Fiat, *J. Appl. Rad. Isotopes* 1981, **32**, 120.
12. H. M. McConnell, *J. Chem. Phys.* 1958, **28**, 430.
13. T. J. Swift and R. E. Connick, *J. Chem. Phys.* 1962, **37**, 307.
14. J. Granot and D. Fiat, *J. Mag. Res.* 1974, **15**, 540.
15. H. Eyring, *Chem. Rev.* 1935, **17**, 65.
16. N. Bloembergen, *J. Chem. Phys.* 1957, **27**, 595.
17. R. E. Connick and D. Fiat, *J. Chem. Phys.* 1966, **44**, 4103.
18. A. M. Chmelnick and D. Fiat, *J. Chem. Phys.* 1967, **47**, 3986.
19. D. Fiat, Z. Luz and B. L. Silver, *J. Chem. Phys.* 1968, **49**, 1376.
20. A. M. Chmelnick and D. Fiat, *J. Am. Chem. Soc.* 1971, **93**, 2875.
21. I. Solomon and N. Bloembergen, *J. Chem. Phys.* 1956, **25**, 261.
22. N. Bloembergen and L. O. Morgan, *J. Chem. Phys.* 1961, **34**, 842.
23. A. Abragam, *The Principles of Nuclear Magnetism.* Oxford University Press (Clarendon), London and New York (1961).
24. R. Osterberg and B. Sjoberg, *J. Biol. Chem.* 1968, **243**, 3038.
25. N. Ingri and L. G. Sillén, *Acta Chem. Scand.* 1962, **16**, 173.
26. G. G. Hammes and J. I. Steinfeld, *J. Am. Chem. Soc.* 1962, **84**, 4639.
27. E. D. Gotsis, ^{17}O and ^{14}N NMR studies of the Co(II), Cu(II) and Mn(II) complexes with amino acids and peptides in solution, Ph.D Thesis, University of Illinois at Chicago (1985).
28. I. Nagypal, E. Farkas, F. Debreczeni and A. Gergely, *J. Phys. Chem.* 1978, **82**, 1548.
29. I. Nagypal, F. Debreczeni and R. E. Connick, *Inorg. Chim. Acta* 1981, **48**, 225.
30. C. P. Cheng and T. L. Brown, *J. Am. Chem. Soc.* 1979, **101**, 2327.
31. W. B. Moniz and H. S. Gutowski, *J. Chem. Phys.* 1963, **38**, 1155.
32. N. Bloembergen, E. M. Purcell and R. V. Pound, *Phys. Rev.* 1948, **73**, 679.
33. D. Rogers and M. T. Rogers, *J. Mag. Res.* 1972, **7**, 30.
34. B. Valentine, A. Steinschneider, D. Dhawan, M. I. Burgar, T. St. Amour and D. Fiat, *Int. J. Pept. Protein Res.* 1984, **25**, 56.
35. N. Shamala, *Cryst. Struct. Comm.* 1973, **8**, 5.
36. M. M. Petit-Ramel and M. R. Paris, *Bull. Soc. Chim. France* 1968, 2791.
37. I. Khalil and M. M. Petit-Ramel, *Bull. Soc. Chim. France* 1973, 1908.
38. H. M. Kroll, *J. Am. Chem. Soc.* 1952, **74**, 2034.

Polyhedron Vol. 6, No. 12, pp. 2053–2065, 1987
Printed in Great Britain

0277-5387/87 $3.00+.00

^{17}O AND ^{14}N NMR STUDIES OF THE Co(II), Cu(II) AND Mn(II) COMPLEXES OF GLYCINE IN AQUEOUS SOLUTION

EFSTATHIOS D. GOTSIS* and DANIEL FIAT†

University of Illinois College of Medicine at Chicago, Department of Physiology and Biophysics, P.O. Box 6998, Chicago, IL 60680, U.S.A.

(*Received* 27 *May* 1987; *accepted* 29 *June* 1987)

Abstract—The ^{17}O and ^{14}N paramagnetic relaxation rates and chemical shifts of glycine as well as of water, in aqueous solutions of Co(II), Cu(II), and Mn(II) were measured as a function of pH, temperature and metal ion concentration; the relaxation results were fitted to a theoretical equation linking the Swift–Connick equation to the stability constants of all major complexes in equilibrium. As a result, the stability constants of all major complexes were determined, and from the temperature-dependent measurements the thermodynamic parameters for some of these complexes were also calculated. In addition to the bidentate complexes ML^+, ML_2 and ML_3^-, monodentate complexes of the type MHL^{2+} and $M(HL)_2^{2+}$, mixed complexes of the type MHL_2^+ and MHL_3 were also considered. In the case of the Cu(II)–glycine system at pH > 12 two additional species were considered, namely $ML_2(OH)^-$ and $ML_2(OH)_2^{2-}$, suggested by the drastic reduction of the paramagnetic broadening in that pH range.

Glycine is the smallest and structurally simplest of all amino acids and its complexes with transition metal ions in aqueous solution have been the subject of a number of investigations.[1–5] Use of ^{17}O NMR however has been conspicuously absent, especially if one considers that the carboxylic oxygen is a potential binding site and should therefore be a sensitive probe to assess the paramagnetic effects. Similarly, the amino nitrogen is also a potential binding site, thus a combination of ^{17}O and ^{14}N NMR should be a good probe to use for ion binding studies. The above considerations, led us to the undertaking of this work.

Of the three metal ions in this work, Cu(II) has certainly attracted most of the attention, not only in NMR but in ESR studies as well.[6,7] Mn(II) complexes of glycine have also received attention, but Co(II) complexes of glycine have not been studied as thoroughly. For example, no information could be found in the literature for $CoHG^{2+}$, $Co(HG)_2^{2+}$, $CoHG_2^+$, and $CoHG_3$. The stability constants for these species were determined in this work.

EXPERIMENTAL

For the ^{17}O NMR measurements, glycine enriched to 30% ^{17}O at each carboxyl site by methods described previously,[8,9] was used after being passed through a chelex column twice, for further purification. For ^{14}N NMR, commercially available glycine was used as bought from the manufacturer.

The NMR measurements were obtained on a Bruker CXP-180 high-power spectrometer, at 24.4 and 13.0 MHz for ^{17}O and ^{14}N NMR, respectively, and a home-made NSF-250 spectrometer at the Regional NMR Center of the University of Illinois in Champaign-Urbana, at 33.926 and 18.075 MHz respectively. Whenever appropriate many measurements were performed on both spectrometers, to determine possible field effects, as well as to ascertain reproducibility of results. Most measurements were repeated at least twice.

Typical spectroscopic parameters were a spectral width of 20 kHz, pulse width for a 90° pulse of 10 μs, pulse delay of 25 μs, recycle delay of 110 msec and 4k spectral points for signal acquisition.

Experimental errors in both ^{17}O and ^{14}N NMR shifts are within ± 0.5 ppm for narrow lines (20–300 Hz), and no more than ± 2.0 ppm for broader

* Present address: Department of Chemistry, University of Illinois at Chicago, P.O. Box 4348, Chicago, IL 60680, U.S.A.

† Author to whom correspondence should be addressed.

lines. The accuracy of the measured linewidths is within ±5%.

The pH of the solutions was adjusted by the addition of NaOH or HCl and measured on a Corning Model 125 pH meter, equipped with a combined electrode. The pH of the solution was measured before and after spectral acquisition, and, if different, the average value was recorded, provided that the variation was small.

The purity of the enriched glycine was checked with an amino acid analyzer. The amino acid analyzer was used at least twice for each sample. The accuracy of the calculated concentration of glycine is within ±10%, to allow for all measuring errors.

The ^{17}O chemical shifts are reported (unless otherwise stated) with respect to external water, at the same temperature. The dependence of the chemical shift of water upon inverse temperature was found to be linear in a wide temperature range, thus the chemical shift at any temperature could be extrapolated from the linear plot. ^{14}N chemical shifts were measured with respect to external NH_4NO_3.

THEORETICAL

(A) *Chemical exchange*

The effect of chemical exchange between a predominant diamagnetic site (the bulk) and a much less concentrated paramagnetic site (the coordination sphere of the metal ions) on the relaxation rate and chemical shift of the bulk has been determined by Swift and Connick,[10] along the lines of the McConnell[11] equations. A detailed description of the Swift–Connick equations and their connection to the stability constants of all complexes in solution was given in a previous paper,[12] thus only a brief summary of the equations used in this work will follow here.

The paramagnetic relaxation rate, $1/T_{2p}$, and the paramagnetic chemical shift, $\Delta\omega_a$, were found by Swift and Connick to be:

$$1/T_{2p} = \sum_{j=b}^{n} \frac{1}{\tau_a} \frac{T_{2j}^{-2} + (\tau_j T_{2j})^{-1} + \Delta\omega_j^2}{(\tau_j^{-1} + T_{2j}^{-1})^2 + \Delta\omega_j^2} \quad (1)$$

and

$$\Delta\omega_a = -\sum_{j=b}^{n} \frac{1}{\tau_a \tau_j} \frac{\Delta\omega_j}{(\tau_j^{-1} + T_{2j}^{-1})^2 + \Delta\omega_j^2} \quad (2)$$

where τ_a is the lifetime of the nucleus in the predominant diamagnetic site, referred to as the bulk henceforth, τ_j is the lifetime of the nucleus in each of the paramagnetic sites, T_{2j} is the transverse relaxation time of the nucleus in the paramagnetic site, and $\Delta\omega_j$ is the frequency different, in rads/s, between the bulk and each of the paramagnetic sites.

The temperature dependence of τ_j is given by the Eyring equation:[13]

$$\tau_j = (h/kT)\exp(\Delta H\dagger/RT - \Delta S\dagger/R) \quad (3)$$

where $\Delta H\dagger$ and $\Delta S\dagger$ are the enthalpy and entropy of activation for the first-order reaction of exchange between the diamagnetic and paramagnetic sites.

The temperature dependence of $\Delta\omega$ and its relationship to the hyperfine coupling constant, A/h, is given by the equation of Bloembergen:[14]

$$(\Delta\omega/\omega) = -S(S+1)A(\gamma_e/\gamma_n)/3kT \quad (4)$$

where S is the spin of the paramagnetic ion, γ_e and γ_n are the magnetogyric ratios of the free electron and the nucleus under consideration, respectively, and the other constants have their usual meaning.

(B) *Complex equilibria*

For aqueous solutions of amino acids or peptides, containing small quantities of paramagnetic ions, such that $[L] \gg [M]$ (ligand and metal ion concentrations, respectively), the complex equilibria in solution can be described by the general equation:[15]

$$pM^{2+} + qH^{+} + rL^{y-} \underset{}{\overset{\beta_{pqr}}{\rightleftharpoons}} M_pH_qL_r^{(2p+q-yr)} \quad (5)$$

where β_{pqr} is the overall stability constant for each metal ion complex:

$$\beta_{pqr} = [M_pH_qL_r]/([M]^p[H]^q[L]^r). \quad (6)$$

From the mass balance equation for $[M]_{total}$ and $[L]_{total}$ we get:

$$[M] = [M]_{total} \Big/ \left(1 + \sum_q \sum_r \beta_{1qr}[H]^q[L]^r\right) \quad (7)$$

and

$$[L] = [L]_{total} \Big/ \left(1 + \sum_q \beta_{0q1}[H]^q\right). \quad (8)$$

The validity of the above approximation was tested by Beattie *et al.*[1] by an iterative solution of the complete mass balance equations using the method of Ingri and Sillen.[16] Combining the complex equilibria equations with the Swift–Connick equation we get:

$$1/T_{2p} = \frac{([M]/[L])_{total} \sum_q \sum_r r\beta_{1qr}[H]^q[L]^r f(\tau, T_2, \Delta\omega)_{1qr}}{\left(1 + \sum_q \sum_r \beta_{1qr}[H]^q[L]^r\right)}. \quad (9)$$

Equation (9) links the paramagnetic relaxation rate, $1/T_{2p}$, of the free ligand, to the stability constants of all possible complexes and their NMR parameters. Thus, it is possible to determine the stability constants of the complexes through a multi-parameter fit of the experimental relaxation data to eqn (9). The correlation coefficients of the final fitted lines were found to be in the range of 0.97–0.99.

(C) *The solvent signal*

In addition to the data of glycine, a second set of data indirectly gives information about the degree of formation of the various complexes, namely the paramagnetic relaxation rate of H_2O:

$$1/T_{2p} = p_m \frac{1}{\tau_m} \frac{T_{2j}^{-2} + (\tau_j T_{2j})^{-1} + \Delta\omega_j^2}{(\tau_j^{-1} + T_{2j}^{-1})^2 + \Delta\omega_j^2} = p_m f(\tau_m, T_{2m}, \Delta\omega_m) \quad (10)$$

where p_m is the ratio of the bound water molecules divided by the number of molecules in the bulk water:

$$p_m = n_{\text{eff}}[M]_{\text{total}}/(55.5 - n_{\text{eff}}[M]_{\text{total}}). \quad (11)$$

Since $[M] \ll 55.5$, p_m is approximated by:

$$p_m \approx n_{\text{eff}}[M]_{\text{total}}/55.5. \quad (12)$$

In a pure aqueous solution of the metal ions in this work, n_{eff} is 6, assuming a hexa-coordinated structure.[11,17–19] In the presence of the amino acid, though, some of the water molecules in the metal ion complexes get replaced by the amino acid, reducing, thus, the number of sites coordinated to water. n_{eff} can be calculated from the ratio of $1/T_{2p}$ of water in the presence and absence of the amino acid, respectively:

$$n_{\text{eff}} = [6(1/T_{2p})^*/(1/T_{2p})]/[f(\tau_m, T_{2m}, \Delta\omega_m)/f^*(\tau_m, T_{2m}, \Delta\omega_m)] \quad (13)$$

where the asterisk denotes the presence of the amino acid in the solution. The above equation is useful if $f(\tau_m, T_{2m}, \Delta\omega_m)/f^*(\tau_m, T_{2m}, \Delta\omega_m)$ is known or assumptions about its magnitude can be made. Assuming it to be 1, eqn (13) reduces to:

$$n_{\text{eff}} = 6(1/T_{2p})^*/(1/T_{2p}). \quad (13a)$$

Another way of calculating n_{eff} is by taking the weighted average of the number of water molecules in each complex, i.e.

$$n_{\text{eff}} = (1/[M]_{\text{total}}) \sum_q \sum_r (6+q-2r)[MH_qL_r]. \quad (14)$$

Equation (14) is of course the correct equation to use, provided that the stability constants of the complexes are known, but equation (13a) has some limited usefulness under conditions which will be discussed in a subsequent section.

(D) *Second-order exchange*

In addition to first-order exchange, the linewidth of free glycine may be broadened by second-order chemical exchange with some of the complexes. Such a process can be described by the following equation:

$$ML_r + {}^*L^- \overset{k_r}{\rightleftharpoons} ML^*_{(r-1)}L + L^-. \quad (15)$$

The lifetime of the ligand in ML_r can be determined from:

$$\tau_m = (k_1 + k_r[L^-])^{-1} \quad (16)$$

where k_1 is the first-order rate constant and k_r is the second-order rate constant involving the species ML_r.

It is obvious that second-order exchange leads to concentration-dependent lifetimes, thus one can reach fast exchange not only by raising the temperature, as is done with first-order exchange, but also by increasing the pH. The effects of second-order exchange broadening are described by the following equation:

$$(1/T_{2p})^{**} = k_2[ML_r][L^-]/[L]_{\text{total}} \quad (17)$$

where the double asterisk indicates second-order exchange broadening. Equation (17) must be added to eqn (9) whenever second-order exchange processes are considered.

RESULTS AND DISCUSSION

(A) *The* Co(II)*–glycine system*

(1) ^{17}O *NMR.* The pH dependence of the paramagnetic transverse relaxation rate, $1/T_{2p}$, of glycine at 300 H, for Solution A, is depicted in Fig. 1. The dotted line is the least-squares best fit of eqn (9) to the experimental results, with the stability constants of Table 1, and the NMR parameters of Table 2. The following equations define the stability constants of the major complexes of glycine considered in this work, using the notation of Childs and Perrin,[2] except in (II), (IX) and (X):

$$M^{2+} + HG^+ \overset{k_1'}{\rightleftharpoons} MHG^{2+} \quad (I)$$

$$M^{2+} + 2HG^+ \overset{k_2''}{\rightleftharpoons} M(HG)_2^{2+} \quad (II)$$

$$MG^+ + HG^+ \overset{k_2'}{\rightleftharpoons} MHG_2^+ \quad (III)$$

Table 1. Log of stability constants of the major Co(II)–glycine complexes in aqueous solution

Complex	Constant	This work	Ref. 23	Ref. 29	Ref. 30
$CoHG^{2+}$	k'_1	0.76			
$Co(HG)_2^{2+}$	k''_2	1.02			
$CoHG_2^+$	k'_2	1.04			
$CoHG_3$	k'_3	−0.45			
CoG^+	K_1	4.96	4.51	5.23	5.5
CoG_2	β_2	9.18	8.16	9.25	9.0
CoG_3^-	β_3	10.43	10.43		11.3

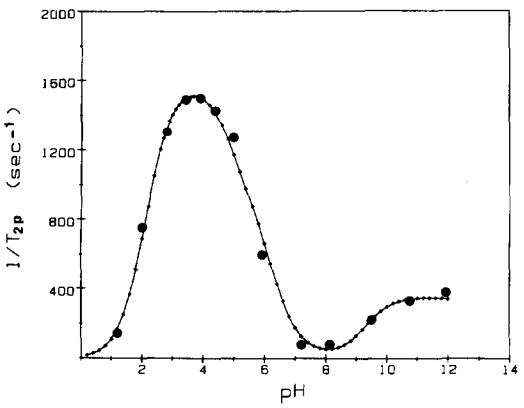

Fig. 1. Dependence of the ^{17}O paramagnetic transverse relaxation rate of glycine upon the measured pH of a solution containing 0.31 M glycine and 5.0 mM $CoCl_2$ (Solution A). The experimental points were recorded at 24.4 MHz, 300 K, and the dotted line is the least-squares best fit of the experimental points to eqn (9), with the constants of Tables 1 and 2.

$$MG_2 + HG^+ \overset{k'_3}{\rightleftharpoons} MHG_3 \quad \text{(IV)}$$

$$MG_2 + G^- \overset{K_3}{\rightleftharpoons} MG_3^- \quad \text{(V)}$$

$$M^{2+} + G^- \overset{K_1}{\rightleftharpoons} MG^+ \quad \text{(VI)}$$

$$M^{2+} + 2G^- \overset{\beta_2}{\rightleftharpoons} MG_2 \quad \text{(VII)}$$

$$M^{2+} + 3G^- \overset{\beta_3}{\rightleftharpoons} MG_3^- \quad \text{(VIII)}$$

$$MG_2 + OH^- \overset{K_{OH}}{\rightleftharpoons} MG_2(OH)^- \quad \text{(IX)}$$

$$MG_2 + 2OH^- \overset{K_{2OH}}{\rightleftharpoons} MG_2(OH)_2^{2-} \quad \text{(X)}$$

where M stands for Co^{2+}, Cu^{2+} or Mn^{2+}. Equations (IX) and (X) were used only in the Cu(II)–glycine system.

The low n_{eff} for water in the acidic pH, Fig. 2, suggested that the existence of $Co(HG)_2^{2+}$ be taken

Table 2. Thermodynamic and NMR parameters of the Co(II)–glycine complexes in aqueous solution[a]

Complex	$f(\tau_m, \Delta\omega_m)$ (s^{-1})	τ_m (s)	A/h (MHz)	$\Delta H\dagger$ (Kcal/mole)	$\Delta S\dagger$ (e.u.)
$CoHG^{2+}$	8.95×10^4	5.0×10^{-6}	-1.2 ± 0.2	7.3	−9.6
$Co(HG)_2^{2+}$	1.02×10^5				
$CoHG_2^+$	3.37×10^4	1.0×10^{-5}	-0.7 ± 0.2	7.5	−9.1
$CoHG_3$	3.83×10^2	2.6×10^{-3}			
CoG^+	10.0[b]				
CoG_2	39.0[b]		-0.72 ± 0.1		
CoG_3^-	7.1×10^3	1.4×10^{-4}		7.8[c]	−13.2[c]
		9.5×10^{-5}[c]			

[a] All parameters are calculated at 300 K.
[b] Ref. 23.
[c] From ^{14}N NMR measurements.

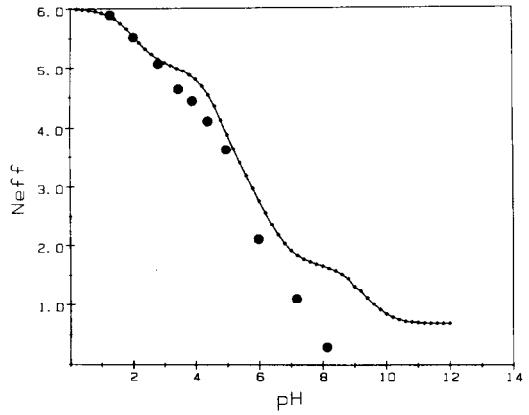

Fig. 2. Dependence of the effective coordination number of water upon pH, for Solution A. The solid circles represent the experimental data calculated from eqn (13a), while the dotted line is the theoretical prediction of eqn (14).

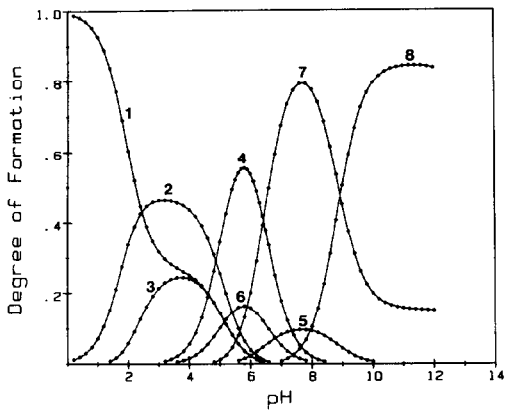

Fig. 3. Dependence of the relative concentration of all Co^{2+}-containing species upon pH, for Solution A. All curves were constructured with the stability constants of Table 1. (1) Is the free Co^{2+}; (2), (3), (4) and (5) are the protonated complexes $CoHG^{2+}$, $Co(HG)_2^{2+}$, $CoHG_2^+$ and $CoHG_3$, respectively; whereas (6), (7) and (8) are the bidentate complexes CoG^+, CoG_2 and CoG_3^-, respectively.

into account, otherwise an unreasonably large stability constant for $CoHG^{2+}$ would have to be assumed in order to fit the acidic pH data, but then the relaxation results at neutral pH were overestimated. Similar conclusions were drawn from the Co(II)–proline, and to a lesser degree the Co(II)–alanine systems.[20]

The agreement between theoretical and experimental values of n_{eff} requires that $f(\tau_m, T_{2m}, \Delta\omega_m)/f^*(\tau_m, T_{2m}, \Delta\omega_m)$ of water as a function of pH remain unchanged, and of course the correct stability constants of the complexes. The first condition can be met approximately in the pH range 0–4, in which $f(\tau_m, T_{2m}, \Delta\omega_m)/f^*(\tau_m, T_{2m}, \Delta\omega_m)$ was found to be 1 ± 0.15, whereas values as high as 5 were found at pH 8 for a solution containing proline[21] and Co^{2+}. The second condition is expected to be met throughout the pH range, within the accuracy of the present method.

Figure 3 shows the distribution of all Co^{2+}-containing species as a function of pH, constructed with the stability constants of Table 1. The existence of $CoHG_3$ was postulated on the fact that the zwitterionic form of glycine is predominant in the pH range 3–8, thus reaction (IV) should be taken into account. The best fit for $1/T_{2p}$ was obtained with $k'_3 = 0.3$, but there is an uncertainty of ± 0.25 associated with the above value, due to the small paramagnetic broadening in the pH range 7–9 where this species reaches its maximum concentration.

The distribution of $CoHG_3$ follows that of CoG_2, as can be seen in Fig. 3, except in the high pH range where the concentration of the zwitterionic form of glycine diminishes and reaction (IV) is negligible.

The relatively small paramagnetic broadening in the basic pH range, where CoG_3^- is the predominant species, is indicative of the slow rate of chemical exchange. Hammes and Steinfeld[4] report a value of $3.8 \times 10^3\ s^{-1}$ for the rate constant of CoG_3^-, whereas we found $7.1 \times 10^3\ s^{-1}$ with ^{17}O NMR and an even higher value with ^{14}N NMR. Pearson and Lanier[5] report a first-order rate constant of $5.7 \times 10^3\ s^{-1}$, and a second-order constant of $4.8 \times 10^3\ M^{-1}\ s^{-1}$ from ^1H NMR studies. With these constants at pH 11, a total rate constant ($1/\tau_m = k_1 + k_2[L^-]$) of $7.14 \times 10^3\ s^{-1}$ for $[L] = 0.3$ M that was used for our ^{17}O NMR measurements, and $10.5 \times 10^3\ s^{-1}$ for $[L] = 1.0$ M that was used for the ^{14}N NMR measurements. Certainly, both the ^{17}O and ^{14}N NMR results are in excellent agreement with the results of Pearson and Lanier. Thus, since the concentrations used in the ^{17}O NMR experiments are not particularly large, in the range of 0.1–0.3 M, the assertion that second-order mechanisms do not contribute appreciably to the observed broadening is basically valid. With the second-order constant of Pearson and Lanier, the second-order contribution to the observed broadening would range from 8 to 20%, for concentrations of glycine ranging from 0.1 to 0.3 M, at pH 11. The lifetimes for CoG_3^- reported in Table 2 are then the combined effects of both first- and second-order exchange processes, especially those derived from the ^{14}N measurements.

Figure 4 shows the pH dependence of the paramagnetic chemical shift of glycine for Solution A, at 300 K. The first peak in the pH range 3–4 reflects

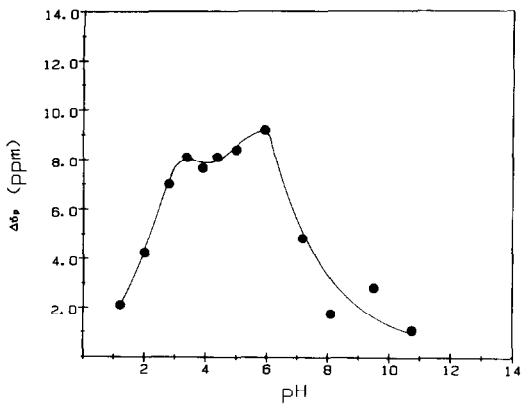

Fig. 4. Dependence of the ^{17}O paramagnetic chemical shift of glycine upon pH, for Solution A, 300 K and a spectrometer frequency of 24.4 MHz.

the maximum concentration of $CoHG^{2+}$ and $Co(HG)_2^{2+}$, whereas the additional shifts in the pH range 4–6 are due to $CoHG_2^+$, as can be seen from Fig. 3. The small paramagnetic shifts at basic pH are due to the slow exchange with CoG_3^-. Thus, the paramagnetic chemical shift does reflect the distribution of the complexes as a function of pH, in harmony with the relaxation results.

Figure 5 shows the temperature dependence of T_{2p} of free glycine at pH 3, for Solution B. At this pH, the monodentate complex $CoHG^{2+}$ predominates, and $Co(HG)_2^{2+}$ makes a small contribution (less than 15% of the total broadening of the free glycine at 300 K is due to $Co(HG)_2^{2+}$). As can be seen in Fig. 5, both the slow as well as the fast exchange regions are accessible in the temperature range of 274–335 K. Incidentally, room temperature falls in the intermediate exchange rate, where maximum broadening occurs, and neither the slow nor the fast exchange approximation is valid for $1/T_{2p}$. At the point of intersection of the slow and fast exchange approximation lines in Figs 5 and 6, $\Delta\omega_m\tau_m = 1$, and eqn (5) reduces to:[22]

$$1/T_{2p} = (1/2)p_m/\tau_m. \tag{18}$$

The above constraint was used to draw the slow and fast exchange approximation lines, for the point of intersection must be half the experimental value at that same temperature.

The hyperfine coupling constant of $CoHG^{2+}$, calculated from the intersection of the slow and fast exchange limits in Fig. 5 is approximately the same as that obtained for $CoHPro^{2+}$ and $CoHAla^{2+}$ ($+1.2\pm0.2$ MHz).[12,20] The enthalpy and entropy

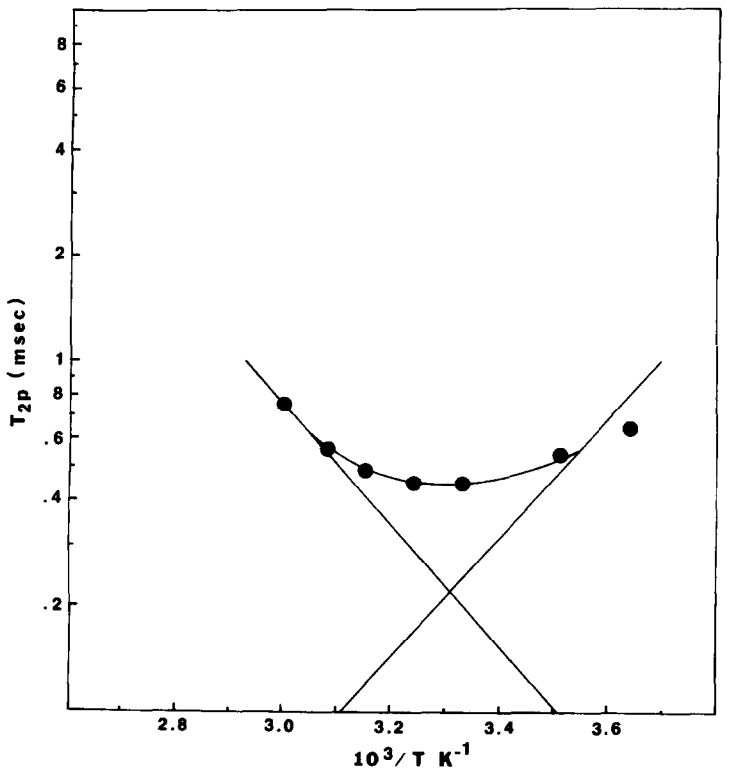

Fig. 5. Dependence of the ^{17}O paramagnetic transverse relaxation time of glycine upon inverse temperature at pH 3, for a solution containing 0.115 M glycine and 5.0 mM $CoCl_2$ (Solution B). The data were recorded at 24.4 MHz.

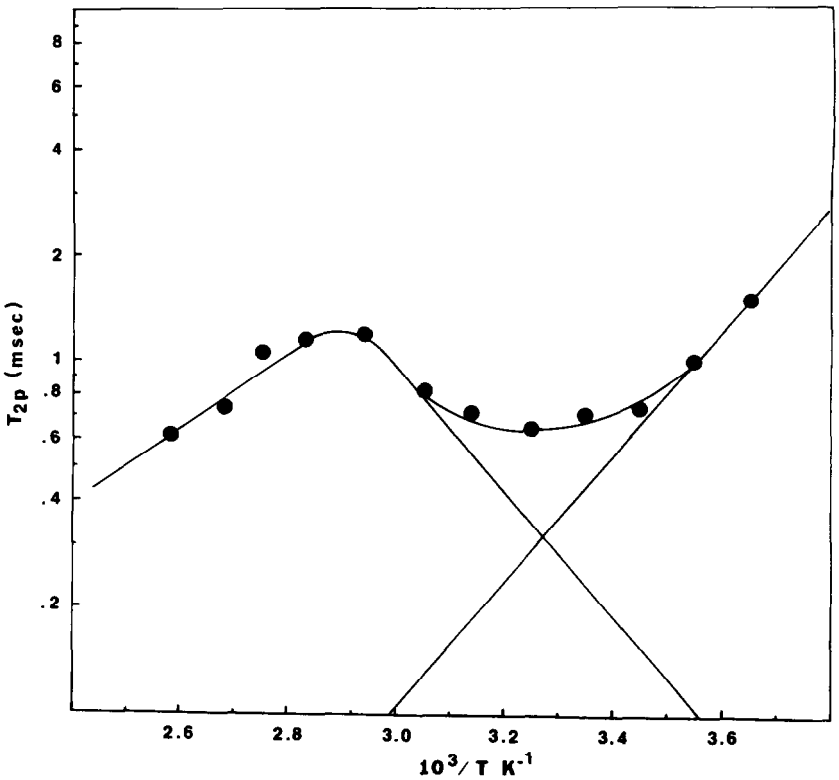

Fig. 6. Dependence of the ^{17}O paramagnetic transverse relaxation time of glycine upon inverse temperature, in a solution containing 0.19 glycine and 10.0 mM $CoCl_2$ (Solution C), at pH 6.1 and a spectrometer frequency of 33.926 MHz.

of activation for the first-order dissociation of $CoHG^{2+}$ were also calculated from the slow exchange region of Fig. 5 and are also included in Table 2. The values, though, were calculated from the total paramagnetic relaxation time (to which $Co(HG)_2^{2+}$ makes a contribution), thus $\pm 25\%$ uncertainty is to be expected with those values.

Figure 6 depicts the dependence of T_{2p} of glycine upon inverse temperature, for Solution C, at pH 6. At this pH, $CoHG_2^+$ is the predominant complex and it causes the observed broadening. This complex is similar to CoG_2 with respect to the number of negatively charged carboxylic oxygens per Co^{2+}, but one glycine molecule is bound only through the oxygen site. The hyperfine coupling constant, A/h, for $CoHG_2^+$ is in the order of 0.7 MHz, a value similar to that of CoG_2 that could be determined directly from the chemical shift of that complex, and its lifetime was found to be about 10^{-5} s. The high-temperature bend from linearity in Fig. 6 may be due to an increased contribution from CoG^+ and CoG_2, which was neglected at low temperatures because of their long lifetimes at those temperatures.[23]

Although much effort was made to detect directly CoG_2, as it was done easily for the corresponding complex in the Co(II)–proline system,[12] we were successful only once, at pH 10. The signal was detected at the same frequency that $CoPro_2$ was detected, but it was much broader (around 6,000 Hz, as opposed to about 2,000 Hz recorded for $CoPro_2$), making detection difficult. The lack of reproducibility of results, then, makes the single observation suspect, and the possibility of an artifact cannot be excluded entirely, although the usual tests for determining whether a signal is "real" or not were performed and proven to be positive.

(2) ^{14}N *NMR results.* The pH dependence of the ^{14}N transverse paramagnetic relaxation rate, $1/T_{2p}$, of glycine for Solution D is depicted in Fig. 7. Broadening occurs only above pH 7, indicating that the first- and second-order exchange processes with CoG_3^- are responsible for the observed broadening. Thus, ^{14}N NMR can be used as a complementary method to ^{17}O NMR, for the information that it offers is limited in the basic pH only, where the amino nitrogen binds directly to the metal ion. From the temperature dependence of T_{2p} at pH 11 (Fig. 8), the thermodynamic parameters describing CoG_3^- were determined. Those results are shown in Table 2. Note the shorter lifetime for CoG_3^- calculated from ^{14}N NMR, compared to that deter-

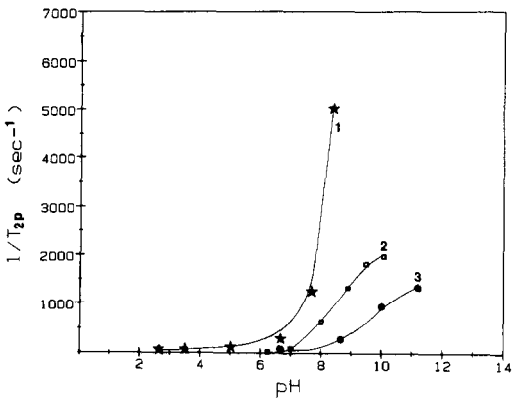

Fig. 7. Dependence of the ^{14}N paramagnetic transverse relaxation rate of glycine upon pH, for Solutions D (1.0 M glycine and 0.01 M $CoCl_2$), E (1.0 M glycine and 1.0 mM $CuCl_2$), and F (1.0 M glycine and 1.0 mM $MnCl_2$), at 300 K. The spectrometer frequency was 18.075 MHz.

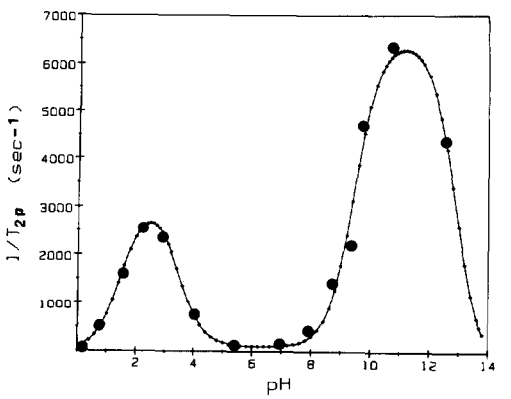

Fig. 9. Dependence of the ^{17}O paramagnetic transverse relaxation rate of glycine upon the measured pH of a solution containing 0.29 M glycine and 0.2 mM $CuCl_2$ (Solution G). The experimental points were recorded at 24.4 MHz, 300 K, and the dotted line is the least-squares best fit of the experimental points to eqn (9), with the constants of Tables 3 and 4.

mined from ^{17}O NMR, as a result of a greater contribution from second-order exchange to the total rate constant, arising from the higher concentration of glycine used in the ^{14}N NMR measurements.

(B) *The* Cu(II)*–glycine system*

(1) ^{17}O *NMR results.* Figure 9 shows the pH dependence, at room temperature, of the ^{17}O paramagnetic transverse relaxation rate, $1/T_{2p}$, of gly-

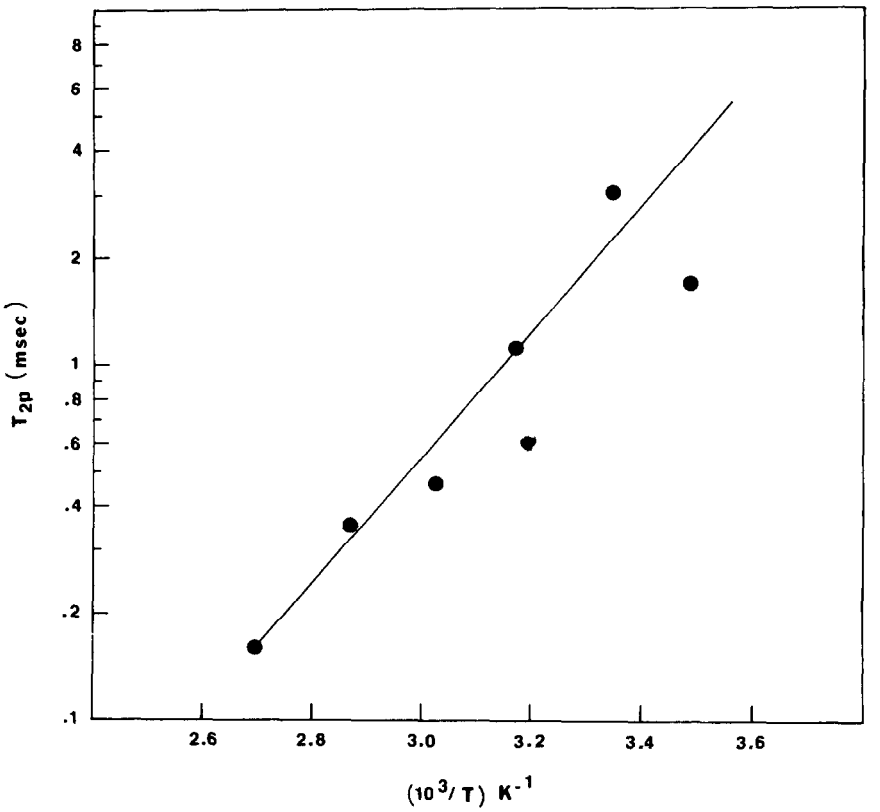

Fig. 8. Dependence of the ^{14}N paramagnetic transverse relaxation time of glycine in Solution D upon inverse temperature, at pH 11. The spectrometer frequency was 18.075 MHz.

Table 3. Log of stability constants of the major Cu(II)–glycine complexes in aqueous solution

Complex	Constant	This work	Ref. 1	Ref. 2
$CuHG^{2+}$	k'_1	1.22	0.92	1.53 ± 0.2
$CuHG_2^+$	k'_2	0.94	0.58	1.34 ± 0.2
$CuHG_3$	k'_3	−0.56		
CuG^+	K_1	8.02	8.3	8.056
CuG_2	β_2	15.2	15.2	14.784
CuG_3^-	β_3	15.43	15.43	
$CuG_2(OH)^-$	K_{OH}	1.46		
$CuG_2(OH)_2^{2-}$	K_{2OH}	1.56		

cine for Solution G. The dotted line is a least-squares best fit of eqn (9) to the experimental relaxation results, with the stability constants of Table 3 and the NMR parameters of Table 4. $Cu(HG)_2^{2+}$ was not considered as a major species, and there was no compelling evidence to the contrary. The paramagnetic relaxation rate of water could not be used in the case of Cu^{2+} because it was too small for the concentrations used in this work. Typically, the maximum broadening of the water signal in the presence of Cu^{2+} was about 20 Hz. Given the ±5 Hz uncertainty in the linewidth of water, the uncertainty in n_{eff} was $\pm(5/20) \times 6 = \pm 1.5$, totally unacceptable.

The Cu(II)–glycine system has been the subject of several authors, with particular emphasis on ^1H NMR, ESR as well as potentiometric studies.[1,2,6,7,24,25] In this work we have extended our studies to the entire pH range 0–14, for the decrease of the broadening above pH 11.5 indicated the formation of complexes involving OH^-. The best fit was obtained by considering two additional complexes in the basic pH, namely $CuG_2(OH)^-$ and $CuG_2(OH)_2^{2-}$, with the stability constants defined in eqns (IX) and (X), respectively.

Table 3 contains some values from the literature, for comparison, particularly those from Beattie *et al.*[1] and Childs and Perrin.[2] There are several interesting comparisons that can be made to the studies of Beattie *et al.* First, the minimum broadening that they observed in their ^1H paramagnetic relaxation rate was around pH 4, and the broadening above pH 4 was assigned to second-order processes with CuG_2, and first-order processes with CuG_3^-. Our ^{17}O paramagnetic relaxation data show a minimum broadening in the pH range 6–8, in which CuG_2 is the predominant species. The ^{17}O paramagnetic relaxation in the acidic pH follows closely the concentration profiles of $CuHG^{2+}$ and $CuHG^+$ and their first-order dissociation. The results at basic pH were fitted by considering the first-order dissociation of CuG_3^- and second-order exchange broadening with CuG_2. A second-order rate constant of $1.5 \times 10^7\ M^{-1}\ s^{-1}$ (taken from Beattie *et al.*[1]) was used, whereas a value of $2.27 \times 10^6\ s^{-1}$ was used for $f(\tau_m, T_{2m})$ of CuG_3^-. Note that the stability constants for CuG_2 and CuG_3^- are identical to those determined by Beattie *et al.* (Table 2).

Pearson and Lanier[5] have reported a second-order rate constant of $8.2 \times 10^6\ M^{-1}\ s^{-1}$ for CuG_2,

Table 4. Thermodynamic and NMR parameters of the Cu(II)–glycine complexes in aqueous solution[a]

Complex	$f(\tau_m, T_{2m})$ (s^{-1})	τ_m (s)	$\Delta H\dagger$ (Kcal/mole)	$\Delta S\dagger$ (e.u.)
$CuHG^{2+}$	3.40×10^6			
$CuHG_2^+$	1.85×10^6			
$CuHG_3$	2.71×10^5	1.1×10^{-6}	7.5	−12.3
CuG^+	23[b]			
CuG_2	120[b]			
CuG_3^-	2.27×10^6			

[a] All parameters are calculated at 300 K.
[b] Taken from Ref. 26.

whereas Nagypal *et al.*[25] determined a value of 7.7×10^7 M^{-1} s^{-1}. Using the value of Nagypal *et al.* and assuming that the broadening at pH 11 is due entirely to the second-order exchange with CuG_2, a broadening of 14,870 s^{-1} is predicted, while the experimental value is 6,270 s^{-1}. Clearly, the second-order rate constant of Nagypal *et al.* is overestimated by a factor of more than two. The value reported by Beattie *et al.* seems to be in better agreement without ^{17}O NMR results.

In the pH range 6–8, though, neither first- nor second-order exchange with CuG_2 could justify the relaxation results. If the existence of $CuHG_3$ were not taken into account, the observed broadening would have to be assigned to CuG_2, and an unreasonably short lifetime for this complex would be calculated from the relaxation results (in the order of 10^{-5} s). This value is two to three orders of magnitude shorter than values reported for complexes of this type,[26] thus first-order exchange with CuG_2 has to be excluded as a major source of broadening. On the other hand, if second-order exchange with CuG_2 was considered as the major source of broadening, then a value of 20 s^{-1} is calculated at pH 7.3 with $k_2 = 1.5 \times 10^7$ M^{-1} s^{-1} (Beattie *et al.*[1]), whereas the experimental value is about 160 s^{-1}. Thus if one calculates the second-order rate constant from the relaxation results at neutral pH ignoring the existence of $CuHG_3$, a value of 1.2×10^8 M^{-1} s^{-1} is calculated, which is in total disagreement with the relaxation results at basic pH. Clearly, CuG_2 alone cannot justify the relaxation results at neutral pH, thus the existence of $CuHG_3$ seems to be fairly well-established. Incidentally, the existence of $CuHG_3$ was suggested by Beattie *et al.*,[1] in view of their ^1H relaxation results at neutral pH, and some spectrophotometric evidence.

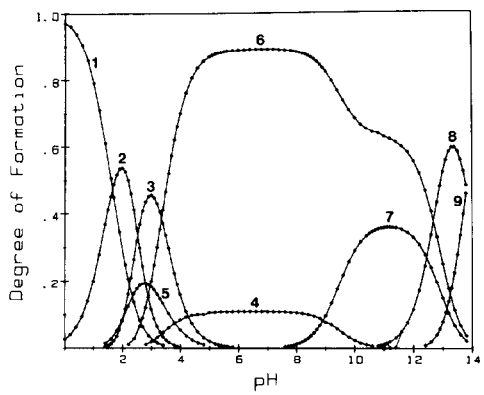

Fig. 10. Dependence of the relative concentration of all Cu^{2+}-containing species upon pH, for Solution G. All curves were constructed with the stability constants of Table 3. (1) Is the free Cu^{2+}; (2), (3) and (4) are the protonated complexes $CuHG^{2+}$, $CuHG_2^+$ and $CuHG_3$, respectively; (5), (6) and (7) are the bidentate complexes CuG^+, CuG_2 and CuG_3^-, respectively; (8) and (9) refer to the complexes $CuG_2(OH)^-$ and $CuG_2(OH)_2^{2-}$, respectively.

The dependence of T_{2p} of glycine upon inverse temperature, in Solution H at pH 7.3, is depicted in Fig. 11. The deviation from linearity at the lower end of the temperature range is probably due to non-linear viscosity effects. Since the major source of broadening at this pH was shown to be $CuHG_3$, and enthalpy and entropy of activation for the first-order dissociation of this complex were found to be 7.5 Kcal/mole and -12.3 e.u., respectively, and its lifetime at 300 K was found to be *ca.* 10^{-6} s.

The second maximum around pH 11, Fig. 9, reflects the concentration profile of CuG_3^-, Fig. 10. The decrease of the concentration of CuG_3^- above pH 11 is due to the formation of $CuG_2(OH)^-$, initially, and $CuG_2(OH)_2^{2-}$ at even higher pH. The stability constant for CuG_3^- used was $K_3 = 1.7$, as determined by Beattie *et al.* James and Williams[27] have reported $K_3 = 2.95$, but most authors have failed to determine K_3, including Childs and Perrin,[2] with whom we are in fairly good agreement for most of the stability constants.

A pH dependence of $1/T_{2p}$ at 323 K (not shown) produced reduced broadening in the pH range 0–7 (with respect to the results at 300 K), whereas above pH 7, the broadening was more pronounced. These results indicate that conditions of fast exchange prevail in the acidic pH range where the monodentate complexes predominate, whereas in the basic pH where the first-order dissociation of CuG_3^- and the second-order exchange with CuG_2 are responsible for the observed broadening, conditions of slow exchange prevail. (Both first- and second-order rate constants increase with increasing temperature).

(2) ^{14}N *NMR results.* The pH dependence of the ^{14}N paramagnetic transverse relaxation rate of glycine, for Solution E, are depicted in Fig. 7. The small broadening in the pH range 5–7 is indicative of second-order exchange with CuG_2, for the first-order dissociation of $CuHG_3$ cannot be a major source of broadening to the ^{14}N nucleus. The steep increase above pH 7 is the combined result of the first-order dissociation of CuG_3^- and the increasing contribution of the second-order exchange with CuG_2. Very broad lines at high pH prevented us from extending the measurements to higher pH. Thus, the ^{14}N relaxation results provide an additional source of information about the complexes, but the lack of information in the acidic pH limits ^{14}N NMR as a self-sufficient method in the entire pH range.

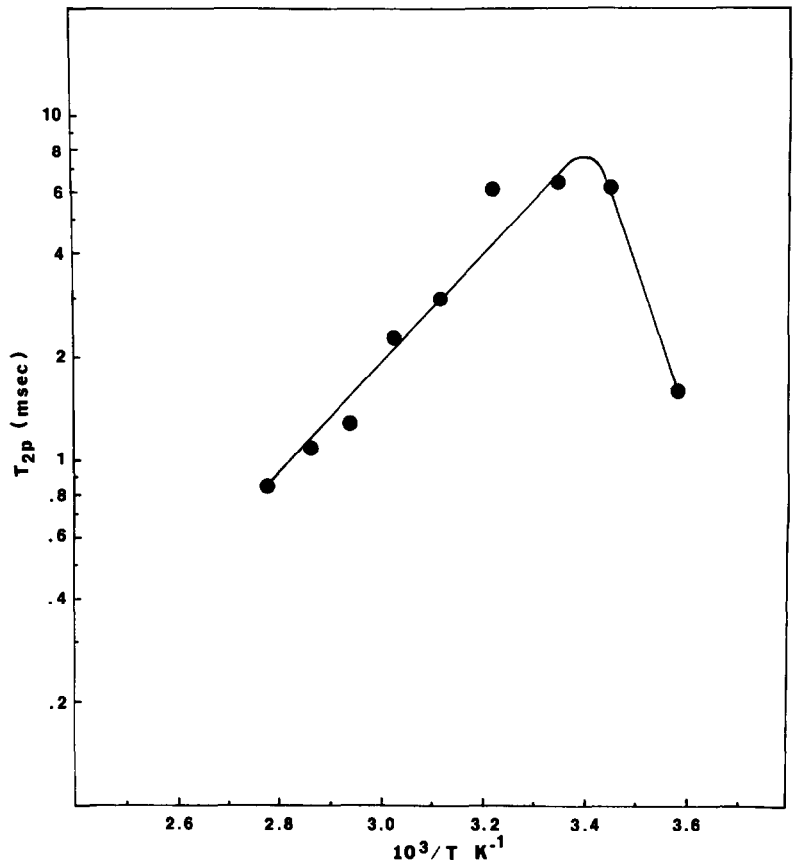

Fig. 11. Dependence of the ^{17}O paramagnetic relaxation time of glycine upon inverse temperature, in a solution containing 0.19 M glycine and 1.0 mM $CuCl_2$ (Solution H), at pH 7.3. The spectrometer frequency was 33.926 MHz.

(C) *The* Mn(II)–*glycine system*

(1) ^{17}O *NMR results.* Figure 12 shows the pH dependence of the ^{17}O paramagnetic transverse relaxation rate of glycine, for Solution I, at 300 K. The dotted line is the least-squares best fit of eqn (9) to the experimental results and the resulting stability constants and NMR parameters are shown in Table 5.

The most striking difference from the Co(II)–glycine and Cu(II)–glycine systems lies in the fact that one species predominates in the pH range 0–7, namely $MnHG^{2+}$. This is due to the small stability constants of the bidentate complexes, which is characteristic of Mn^{2+}.

The distribution of the Mn(II)–glycine complexes as a function of pH, for the same Solution I, is given in Fig. 13. The same types of complexes that were

Table 5. Log of stability constants of the major Mn(II)–glycine complexes and NMR parameters in aqueous solution[a]

Complex	$f(\tau_m, T_{2m})$ (s^{-1})	Constant	This work	Ref. 2
$MnHG^{2+}$	1.43×10^6	k'_1	0.80	0.64 ± 0.49
$MnHG_2^+$	6.85×10^5	k'_2	0.92	0.80 ± 0.42
$MnHG_3$	1.14×10^6	k'_3	0.08	
MnG^+		K_1	2.71	2.71
MnG_2		β_2	4.76	4.755
MnG_3^-	4.50×10^5	β_3	5.57	5.52

[a] All parameters of this work are reported at 300 K, whereas those of Ref. 2 are reported at 310 K.

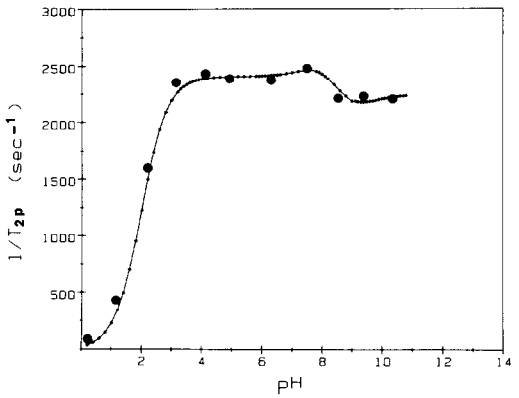

Fig. 12. Dependence of the ^{17}O paramagnetic transverse relaxation rate of glycine upon the measured pH of a solution containing 0.20 M glycine and 0.6 mM $MnCl_2$ (Solution I), at 300 K. The experimental points were recorded at 24.4 MHz and the dotted line is the least-squares fit of the experimental points to eqn (9), with the constants of Table 5.

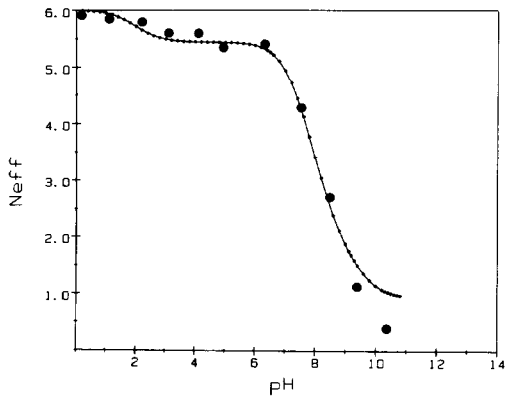

Fig. 14. Dependence of the effective coordination number of water upon pH, for Solution I. The experimental points were calculated from the ratio of the paramagnetic transverse relaxation rate of water in the presence and absence of glycine, respectively, and the dotted line is the theoretical prediction of eqn (14).

discussed in previous sections also exist in the Mn(II)–glycine system, only at much higher pH. The stability constants for the bidentate species in the basic pH were found to be almost identical to those reported by Childs and Perrin,[2] as can be seen from Table 5, and this once more confirms the validity of the overall method used in this work. A fairly good agreement also exists with regard to the values reported by those authors about $MnHG^{2+}$ and $MnHG_2^+$.

Figure 14 shows the pH dependence of n_{eff} of water for Solution I. Since there are only two Mn^{2+}-containing species in the pH range 0–7, namely $Mn(H_2O)_6^{2+}$ and $MnHG^{2+} \cdot 5H_2O$, and assumming that $f(\tau_m, T_{2m})/f^*(\tau_m, T_{2m})$ is approximately 1, then the stability constant of $MnHG^{2+}$ can be calculated easily from n_{eff}, since the concentrations of both free Mn^{2+} and $MnHG^{2+}$ are deduced from n_{eff}:[22]

$$[MnHG^{2+}]/[Mn(H_2O)_6^{2+}] = (6-n_{eff})/(n_{eff}-5) \quad (19)$$

and

$$k'_1 = [HG^+]^{-1}(6-n_{eff})/(n_{eff}-5). \quad (20)$$

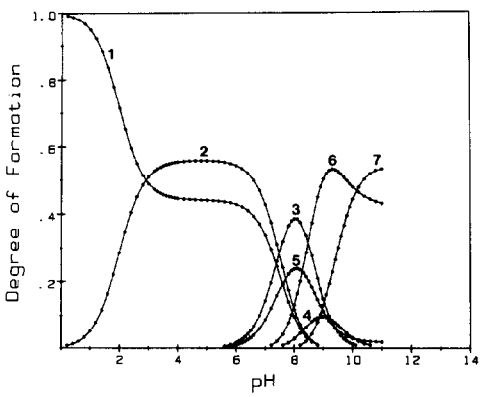

Fig. 13. Dependence of the relative concentration of all Mn^{2+} containing species upon pH, for Solution I, at 300 K. All curves were constructed with the stability constants of Table 5. (1) Is the free Mn^{2+}, (2), (3) and (4) are the protonated complexes $MnHG^{2+}$, $MnHG_2^+$ and $MnHG_3$, respectively, whereas (5), (6) and (7) are the bidentate complexes MnG^+, MnG_2 and MnG_3^-, respectively.

The dependence of T_{2p} of glycine upon inverse temperature, at pH 6.6, where $MnHG^{2+}$ is the predominant complex, showed that conditions of slow exchange prevail at 300 K. The enthalpy and entropy of activation for the first-order exchange of glycine were found to be 5 Kcal/mole and -17 e.u., respectively, and the lifetime of $MnHG^{2+}$ at 300 K was found to be 4×10^{-6} s. At higher temperatures (*ca.* 330 K), conditions of intermediate exchange prevail, at which point $1/T_{2p} = (1/2)p_m/T_{2m}$. T_{2m} can be then calculated from the experimental value of T_{2p}. Taking a value of 10^{-8} s for the electronic relaxation time of Mn^{2+} (a value of 2.18×10^{-8} s was assumed by Henry *et al.*[28] for $MnPro_3^-$) we can get an estimate of the hyperfine coupling constant, A/h, assuming the Fermi contact mechanism to be predominant. With the above assumptions, a value of -0.5 MHz was found for A/h.

Precipitation above pH 11, where MnG_3^- predominates, precluded us from conducting temperature dependent studies at that pH, to derive the thermodynamic parameters for that complex. Even when a lower concentration of Mn^{2+} was used in an attempt to prevent precipitation, it still occurred

at elevated temperatures, after only one hour, thus the results were discarded. Considering the scarcity of enriched materials no further experimentation was attempted.

CONCLUSIONS

The stability constants of all major complexes of glycine in aqueous solutions of Co^{2+}, Cu^{2+}, and Mn^{2+} were determined in this work by utilizing the paramagnetic relaxation rate of glycine as a function of pH. The thermodynamic parameters of some complexes were also determined. The existence of the species MHG_3 was taken into account, and estimates of its stability constant are given. Similarly, the stability constants of $CuG_2(OH)^-$ and $CuG_2(OH)_2^{2-}$ were determined for the first time in this work, along with stability constants for the monodentate complexes of Co^{2+}. Overall, the ^{17}O paramagnetic relaxation of amino acids has been shown to be a fairly reliable method for determining stability constants and certainly the method of choice for determining the dynamical involvement of oxygen in complexes of paramagnetic ions.

Acknowledgements—The authors would like to thank Drs A. Steinschneider and D. Dhawan for labeling and purifying the ^{17}O enriched glycine used in this work. Our long cooperation with the Regional NMR Center at Champaign-Urbana and Dr Eric Oldfield in particular is greatly appreciated. Special thanks to Dr David Wright and Dennis Warrenfeltz, also at Champaign-Urbana. We would also like to thank the RRC Facilities at the University of Illinois at Chicago.

REFERENCES

1. J. K. Beattie, D. J. Fensom and H. C. Freeman, *J. Am. Chem. Soc.* 1976, **98**, 500.
2. C. W. Childs and D. D. Perrin, *J. Chem. Soc. (A)* 1969, 1039.
3. E. Tiezzi, *J. Chem. Soc. Perkin II*, 1975, 769.
4. G. G. Hammes and J. I. Steinfeld, *J. Am. Chem. Soc.* 1962, **84**, 4639.
5. R. G. Pearson and R. D. Lanier, *J. Am. Chem. Soc.* 1964, **86**, 765.
6. M. Fujimoto and J. Janecka, *J. Chem. Phys.* 1971, **55**, 1152.
7. A. M. Dezor, *Acta Physica Polonica* 1979, **A56**, 385.
8. A. Steinschneider, M. I. Burgar, A. Buku and D. Fiat, *Int. J. Pept. Protein Res.* 1981, **18**, 324.
9. A. Steinschneider, T. St. Amour, B. Valentine, M. I. Burgar and D. Fiat, *J. Appl. Rad. isotopes* 1981, **32**, 120.
10. T. J. Swift and R. E. Connick, *J. Chem. Phys.* 1962, **37**, 307.
11. H. M. McConnell, *J. Chem. Phys.* 1958, **28**, 430.
12. E. D. Gotsis and D. Fiat, *Polyhedron* 1987, **6**, 2037.
13. H. Eyring, *Chem. Rev.* 1935, **37**, 65.
14. N. Bloembergen, *J. Chem. Phys.* 1957, **27**, 595.
15. R. Osterberg and B. Sjoberg, *J. Biol. Chem.* 1968, **243**, 3038.
16. N. Ingri and L. G. Sillen, *Acta Chem. Scand.* 1962, **16**, 173.
17. A. M. Chmelnick and D. Fiat, *J. Chem. Phys.* 1967, **47**, 3986.
18. D. Fiat, F. Luz and B. L. Silver, *J. Chem. Phys.* 1968, **49**, 1376.
19. A. M. Chmelnick and D. Fiat, *J. Am. Chem. Soc.* 1971, **93**, 2875.
20. E. D. Gotsis, ^{17}O and ^{14}N NMR studies of complexes of paramagnetic ions with amino acids and peptides in solution. Ph.D Thesis, University of Illinois at Chicago (1985).
21. E. D. Gotsis and D. Fiat, *Magn. Reson. Chem.* 1987, **25**, 407.
22. E. D. Gotsis and D. Fiat, *J. Chem. Phys.* 1986, **85**, 3701.
23. D. Hopgood and D. L. Leussing, *J. Am. Chem. Soc.* 1969, **91**, 3740.
24. I. Nagypal, E. Farkas, F. Debreczeni and A. Gergely, *J. Phys. Chem.* 1978, **82**, 1548.
25. I. Nagypal, F. Debreczeni and R. E. Connick, *Inorg. Chim. Acta* 1981, **48**, 225.
26. J. W. Brubaker, Jr., J. E. Pearlmutter, J. E. Stuehr and T. V. Vu, *Inorg. Chem.* 1974, **13**, 559.
27. B. R. James and R. J. P. Williams, *J. Chem. Soc.* 1961, 2007.
28. B. Henry, M. Rappeneau and J.-J. Delpeuch, *Polyhedron* 1982, **1**, 113.
29. C. B. Monk, *Trans. Farday Soc.* 1951, **47**, 285.
30. V. Jokl, *J. Chromatog.* 1964, **14**, 71.

Polyhedron Vol. 6, No. 12, pp. 2067–2071, 1987
Printed in Great Britain

0277–5387/87 $3.00+.00

SYNTHESIS OF THE DIMETAL COMPOUNDS [FeW{μ-$PPh_2 \cdot CH \cdot CH_2 \cdot C(C_6H_4Me\text{-}4)$}$(CO)_5(\eta^5\text{-}C_5Me_5)$] AND [FeMo{$\mu$-$PPh_2 \cdot CH \cdot CH_2 \cdot C(C_6H_4Me\text{-}4)$}$(CO)_5(\eta^5\text{-}C_5H_5)$]; MOLECULAR STRUCTURE OF THE IRON–TUNGSTEN COMPOUND

JOACHIM HEIN, JOHN C. JEFFERY, FRANK MARKEN and F. GORDON A. STONE*

Department of Inorganic Chemistry, The University of Bristol, Bristol BS8 1TS, U.K.

(*Received* 9 *July* 1987; *accepted* 13 *July* 1987)

Abstract—Reactions between diphenyl(vinyl)phosphine and the compounds [FeW(μ-$CC_6H_4Me\text{-}4$)$(CO)_5(\eta^5\text{-}C_5Me_5)$] and [FeMo($\mu$-$CC_6H_4Me\text{-}4$)$(CO)_6(\eta^5\text{-}C_5H_5)$] result in a coupling of the vinyl and *p*-tolylmethylidyne groups at the dimetal centres to produce the $PPh_2 \cdot CH \cdot CH_2 \cdot C(C_6H_4Me\text{-}4)$ fragment, which bridges the metal–metal bonds. This was confirmed by an X-ray diffraction study on [FeW{μ-$PPh_2 \cdot CH \cdot CH_2 \cdot C(C_6H_4Me\text{-}4)$}$(CO)_5(\eta^5\text{-}C_5Me_5)$].

The availability of the compounds [FeW(μ-$CC_6H_4Me\text{-}4$)$(CO)_5(\eta^5\text{-}C_5Me_5)$] (**1**)[2] and [FeMo($\mu$-$CC_6H_4Me\text{-}4$)$(CO)_6(\eta^5\text{-}C_5H_5)$] (**2**)[2] has allowed extensive studies to be made on the reactivity of an alkylidyne ligand when bridging two dissimilar metal centres. For example, both species react under mild conditions with oxygen, sulphur, alkynes or diazomethane. Coupling of these reagents with the alkylidyne groups occurs and new C—O, C—S and C—C bonds are formed.[1–4] The molybdenum complex (**2**),[5] and its tungsten analogue [FeW(μ-$CC_6H_4Me\text{-}4$)$(CO)_6(\eta^5\text{-}C_5H_5)$],[6] also readily react with tertiary phosphines with displacement of a CO group at the iron centre. These studies have led us to investigate reactions of (**1**) and (**2**) with $P(CH:CH_2)Ph_2$ and the results are reported herein. It was anticipated that the phosphine would initially coordinate at the iron atom, with the vinyl group subsequently playing a non-spectator role, the nature of which could not be readily predicted.

RESULTS AND DISCUSSION

Treatment of the iron–tungsten compound (**1**) with $P(CH:CH_2)Ph_2$ in CH_2Cl_2 at ambient temperatures afforded a yellow–orange crystalline complex [FeW{μ-$PPh_2 \cdot CH \cdot CH_2 \cdot C(C_6H_4Me\text{-}4)$}$(CO)_5(\eta^5\text{-}C_5Me_5)$] (**3**). A similar reaction occurred in thf (tetrahydrofuran) between $P(CH:CH_2)Ph_2$ and the iron–molybdenum compound (**2**), yielding a product (**4**) which on the basis of spectroscopic data was evidently structurally similar to (**3**). However, from the ^1H and $^{13}C\text{-}\{^1H\}$ NMR results it was not possible to establish the structures of these compounds, and hence an X-ray diffraction study was carried out on (**3**) for which suitable single crystals were available.

Important structural parameters obtained from the X-ray diffraction study are listed in Table 1 and the structure is shown in Fig. 1. It will be seen that the Fe—W bond is spanned by a $PPh_2 \cdot CH \cdot CH_2 \cdot C(C_6H_4Me\text{-}4)$ fragment in such a manner that the phosphorus atom ligates the iron atom. The μ-$C(C_6H_4Me\text{-}4)$ group is σ bonded to both metal centres and the CH group is σ bonded to the tungsten atom. The latter, as expected, carries the η^5-C_5Me_5 ligand and two carbonyl groups, and the iron atom is coordinated by three essentially orthogonal CO groups.

It is interesting to compare the interatomic distances in (**3**) with those found in some other recently reported iron-tungsten compounds. The Fe—W separation is 2.828(1) Å and is thus long compared with those in [FeW{μ-$C(C_6H_4Me\text{-}4)C(O)O$}$(CO)_5(\eta^5\text{-}C_5Me_5)$] [2.605(1) Å],[1] [FeW($\mu$-$CC_6H_4Me\text{-}4$)$(CO)_5${$HB(pz)_3$}] [{$HB(pz)_3$ = hydrotris(pyrazol-1-yl)borate}, 2.612(2)Å],[6] [NEt_4][FeW(μ-$CC_6H_3Me_2\text{-}2,6$)$(CO)_5(\eta^5\text{-}C_2B_9H_9Me_2)$] [2.600(1) Å],[7]

*Author to whom correspondence should be addressed.

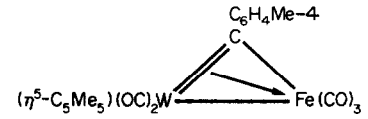

(1)

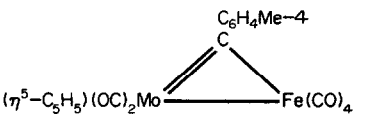

(2)

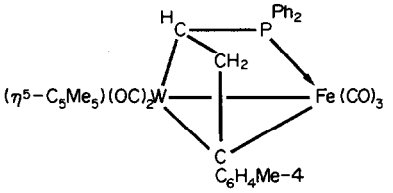

(3)

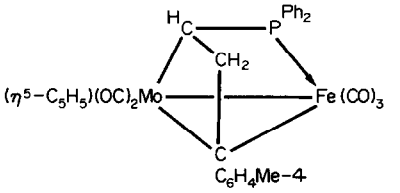

(4)

[FeW{μ - C(C_6H_4Me - 4)C(O)C(Me)C(Me)}$(CO)_5$ (η^5-C_5Me_5)] [2.722(1) Å][4] and [FeW{μ-C(C_6H_4Me-4) C(Me)C(Me)}$(CO)_5$(η-C_5H_5)] [2.720(1) Å].[8]

The μ-C(10)—Fe [2.141(4) Å] and μ-C(10)—W [2.188(4) Å] distances may be compared with the respective μ-C(C_6H_4Me-4)—Fe and μ-C(C_6H_4Me-4)—W separations in [FeW{μ-C(C_6H_4Me-4)C(O)C(Me)C(Me)}$(CO)_5$(η^5-C_5Me_5)] [2.103(6), and 2.193(5) Å],[4] and [FeW{μ-C(C_6H_4Me-4)C(Me)C(Me)}$(CO)_5$(η^5-C_5H_5)] [2.047(6) and 2.194(6) Å].[8] The Fe—P bond [2.248(1) Å] in (**3**) is of very similar length to that [2.184(9) Å] in the dimetal compound [FeW(μ-PPh_2)$(CO)_5$ {$HB(pz)_3$}].[9]

Having established the molecular structure of (**3**) by X-ray diffraction it became possible to interpret the NMR data for this species, and for (**4**) also. Since the latter displayed similar resonances it was evidently isostructural. The ^{13}C-{^1H} NMR spectrum of (**3**) measured at room temperature in CD_2Cl_2–CH_2Cl_2 showed doublet signals for the two CO groups bonded to tungsten [δ 230.1 and 225.3 ppm, with J(PC) 12 and 14 Hz, respectively], and three broad resonances for the $Fe(CO)_3$ fragment (δ 216.5, 213.2 and 212.8 ppm). The latter observation suggested site-exchange of the three CO groups at the iron centre. At −60°C, however, in a ^{13}C spectrum measured in CD_2Cl_2–CH_2Cl_2 the tricarbonyliron group gave rise to three sharp doublet signals at δ 216.5, 213.2 and 212.5 ppm with J(PC) 23, 41 and 30 Hz, respectively. For compound (**4**), the ^{13}C-{^1H} NMR spectrum at ambient temperatures showed five distinct resonances for the CO ligands, each a doublet, at δ 236.5, 235.0 (Mo—CO), 214.7, 212.4 and 210.8 ppm, with J(PC) 10, 15, 24, 44 and 29 Hz, respectively.

The ^{13}C-{^1H} NMR spectra of (**3**) and (**4**) show several peaks in the range *ca* δ 120–155 ppm due to the Ph and C_6H_4 moieties. However, doublet signals in each spectrum characteristic for the μ-CC_6H_4Me-4 group are seen at δ 131.6 ppm with J(PC) 7 Hz. The resonance for the C(H)M (M = W or Mo) group occurs as a doublet in the spectra of both compounds at *ca* δ −8.2 ppm, with J(PC) 7 Hz. The assignment is confirmed by the appearance of ^{183}W satellite peaks [J(WC) 24 Hz] on this resonance in the spectrum of (**3**). In a fully-coupled ^{13}C spectrum of (**4**), measured in $CDCl_3$, the signal for the C(H)Mo group (δ −8.1 ppm) occurs as a doublet

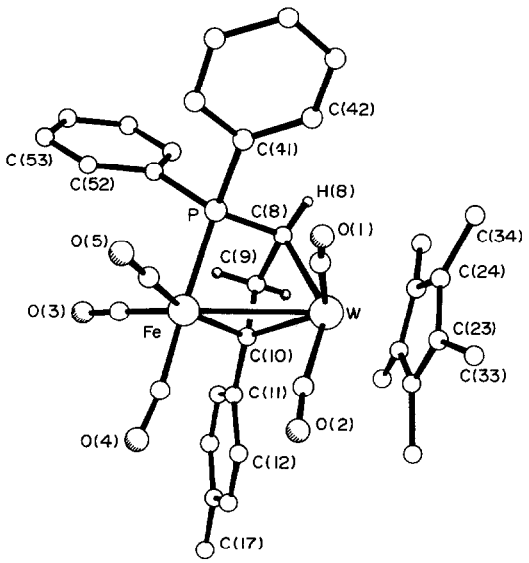

Fig. 1. The molecular structure of the complex [FeW{μ-PPh_2·CH·CH_2·C(C_6H_4Me-4)}$(CO)_5$(η^5-C_5Me_5)].

Table 1. Selected internuclear distances (Å) and angles (°) for [FeW{μ-PPh$_2$·CH·CH$_2$·C(C$_6$H$_4$Me-4)}(CO)$_5$(η-C$_5$Me$_5$)] (**3**) with estimated standard deviations in parentheses

W—Fe	2.828(1)	W—C(1)	1.998(5)	W—C(2)	2.000(4)	W—C(8)	2.315(4)
W—C(10)	2.188(4)	Fe—P	2.248(1)	Fe—C(3)	1.781(5)	Fe—C(4)	1.801(4)
Fe—C(5)	1.786(5)	Fe—C(10)	2.141(4)	P—C(8)	1.755(4)	P—C(41)	1.838(4)
P—C(51)	1.838(4)	C(1)—O(1)	1.148(7)	C(2)—O(2)	1.142(6)	C(3)—O(3)	1.130(6)
C(4)—O(4)	1.134(6)	C(5)—O(5)	1.131(7)	C(8)—C(9)	1.521(5)	C(9)—C(10)	1.519(5)
C(10)—C(11)	1.482(5)	range W—(η-C$_5$Me$_5$)	2.295(4)–2.404(4)				
C(1)—W—C(2)	78.8(2)	Fe—W—C(8)	70.8(1)	Fe—W—C(10)	48.5(1)	C(8)—W—C(10)	62.3(1)
W—Fe—P	74.3(1)	C(3)—Fe—C(4)	91.6(2)	C(3)—Fe—C(5)	109.4(2)	C(4)—Fe—C(5)	88.8(2)
W—Fe—C(10)	49.9(1)	P—Fe—C(10)	84.1(1)	Fe—P—C(8)	96.6(1)	Fe—P—C(41)	125.9(2)
C(8)—P—C(41)	108.5(2)	Fe—P—C(51)	114.0(1)	C(8)—P—C(51)	112.1(2)	C(41)—P—C(51)	100.0(2)
W—C(1)—O(1)	171.0(4)	W—C(2)—O(2)	170.7(4)	Fe—C(3)—O(3)	178.0(4)	Fe—C(4)—O(4)	171.2(4)
Fe—C(5)—O(5)	177.4(5)	W—C(8)—P	98.2(2)	W—C(8)—C(9)	91.0(2)	P—C(8)—C(9)	105.0(2)
C(8)—C(9)—C(10)	100.1(3)	W—C(10)—Fe	81.6(1)	W—C(10)—C(9)	96.1(2)	Fe—C(10)—C(9)	109.6(2)
W—C(10)—C(11)	129.1(3)	Fe—C(10)—C(11)	118.7(2)	C(9)—C(10)—C(11)	115.9(4)		

of doublet of doublets [J(PC) 7, J(HC) 150 and 7]. Evidently ^{1}H–^{13}C coupling occurs between C(H)Mo and only one proton of the adjacent CH_2 moiety. The resonance for the latter was not observed in the ^{13}C-{^{1}H} spectrum of (**4**) when measured in CD_2Cl_2–CH_2Cl_2, being masked by the solvent peaks, but is seen in the ^{13}C spectrum (in $CDCl_3$) at δ 54.6 ppm as a triplet [J(HC) 129 Hz] of doublets [J(PC) 14 Hz].

The ^{1}H NMR spectra of (**3**) and (**4**) show the expected three signals for the CH·CH$_2$ fragment. For (**3**), these occur at δ 0.78 [d of d, CH, J(PH) 14, J(HH) 4], 3.05 [d of d of d, CH$_2$, J(PH) 50, J(HH) 15, 4] and 4.50 [d of d, CH$_2$, J(PH)17, J(HH) 15 Hz], while for (**4**) the resonances are at δ 1.76 [d of d, CH, J(PH) 12, J(HH) 4], 3.57 [d of d of d, CH$_2$, J(PH) 50, J(HH) 15, 4] and 4.13 [d of d, CH$_2$, J(HH) 15, 4 Hz].

The μ-PPh$_2$·CH·CH$_2$·C(C$_5$H$_4$Me-4) group present in compounds (**3**) and (**4**) can be visualized as having been formed in a step-wise manner at the dimetal centre. Based on previous observations,[5] it is probable that initially the phosphine coordinates at the iron centres of (**1**) and (**2**), a process which would require release of CO from the latter species. Subsequent addition of the vinyl group to the C═M (Mo or W) bond would produce the M·CH(PPh$_2$)·CH$_2$·C(C$_6$H$_4$Me-4) ring system found in the products. Reaction of the vinyl group present in P(CH:CH$_2$)Ph$_2$ with the μ-alkylidyne groups of (**1**) and (**2**) provides a further demonstration of the reactivity of these heteronuclear dimetal species.

EXPERIMENTAL

All experiments were carried out under nitrogen, using Schlenk tube techniques. Solvents were rigorously dried before use. NMR spectra were recorded with JNM FX 90Q, FX 200 or GX 400 instruments and IR spectra were recorded with Nicolet MX 10 or MX 5 spectrophotometers. For NMR data all chemical shifts are in ppm and coupling constants are in Hz. Phosphorus-31 chemical shifts are positive to high frequency of 85% H_3PO_4 (external). The compounds [FeW(μ-CC$_6$H$_4$Me-4)(CO)$_5$(η^5-C$_5$Me$_5$)] and [FeMo(μ-CC$_6$H$_4$Me-4)(CO)$_6$(η^5-C$_5$H$_5$)] were prepared by methods previously described.[1,2] Light petroleum refers to that fraction of b.p. 40–60°C.

Synthesis of the complexes

(i) Compound (**1**) (0.16 g, 0.26 mmol) in CH_2Cl_2 (20 cm^3) was treated with P(CH:CH$_2$)Ph$_2$ (0.055 g,

0.052 cm^3, 0.26 mmol) and the mixture was stirred at ambient temperatures for *ca* 4 h. The volume was reduced *in vacuo* to *ca* 5 cm^3 and the mixture was chromatographed at 10°C on a Florisil column (3 × 15 cm, 100–200 mesh). Elution with light petroleum–CH_2Cl_2 (3:2) afforded a yellow eluate. Removal of solvent *in vacuo*, followed by crystallization of the residue from CH_2Cl_2–light petroleum (1:5) at −78°C gave yellow–orange *needles* of $[FeW\{\mu\text{-}PPh_2\cdot CH\cdot CH_2\cdot C(C_6H_4Me\text{-}4)\}(CO)_5(\eta^5\text{-}C_5Me_5)]$ (**3**) (0.18 g, 83%) [Found: C, 51.4; H, 4.5%. $C_{37}H_{35}FeO_5PW$ requires C, 53.5; H, 4.3%]. ν_{max} (CO) at 2024s, 1956s, 1948s and 1877w cm^{-1} (in CH_2Cl_2). NMR: ^1H (in CD_2Cl_2), δ 0.78 [d of d, 1 H, CH·P, *J*(PH) 14, *J*(HH) 4], 1.81 (s, 15 h, C_5Me_5), 2.24 (s, 3 H, Me-4), 3.05 [d of d of d, 1 H, CH_2, *J*(PH) 50, *J*(HH) 15 and 4], 4.50 [d of d, 1 H, CH_2, *J*(PH) 17, *J*(HH) 15], 6.97 (m, 4 H, C_6H_4), and 7.29–7.71 (m, 10 H, Ph); $^{13}C\text{-}\{^1H\}$ (in CD_2Cl_2–CH_2Cl_2), δ 230.1 [d, WCO; *J*(PC) 12], 225.3 [d, WCO, *J*(PC) 14], 216.5, 213.2, 212.8 [3 × br s, $Fe(CO)_3$], 154.2–121.8 (C_6H_4, Ph), 131.6 [d, CC_6H_4 Me-4, *J*(PC) 7], 100.5 (C_5Me_5), 21.6 [d, CH_2, *J*(PC) 14], 21.1 (Me-4), 9.5 (C_5Me_5) and −8.2 [d, P·CH, *J*(PC) 7, *J*(WC) 24]; ^{13}C (at −60°C), δ 230.5 [d, WCO, *J*(PC) 12], 224.9 [d, WCO, *J*(PC) 14], 216.5 [d, FeCO, *J*(PC) 23], 213.2 [d, Fe(CO), *J*(PC) 41], 212.5 [d, FeCO, *J*(PC) 30], 131.6 [d, CC_6H_4Me-4, *J*(PC) 7] and −8.2 [d of d, CH·P, *J*(PC) 7, *J*(HC) 159]. In the ^{13}C NMR at −60°C the CH_2 resonance at 51.6 is obscured by a strong solvent peak. $^{31}P\text{-}\{^1H\}$ (in CD_2Cl_2), δ 41.4.

(ii) Compound (**2**) (0.20 g, 0.41 mmol) in thf (50 cm^3) was treated with $P(CH:CH_2)Ph_2$ (0.095 g, 0.45 mmol) at room temperature and the mixture was stirred for 3 h. Solvent was removed *in vacuo* and the brown residue was dissolved in CH_2Cl_2 (2 cm^3) and light petroleum (8 cm^3), and the solution chromatographed on an alumina column (3 × 30 cm, Brockman Activity II). Elution with CH_2Cl_2–light petroleum (1:4) afforded a yellow eluate. Removal of solvent *in vacuo* gave yellow *microcrystals* of $[FeMo\{\mu\text{-}PPh_2\cdot CH\cdot CH_2\cdot C(C_6H_4Me\text{-}4)\}(CO)_5(\eta^5\text{-}C_5H_5)]$ (**4**) (0.22 g, 77%) [Found: C, 57.0; H, 4.2%. $C_{32}H_{25}FeMoO_5P$ requires C, 57.2; H, 3.8%]. ν_{max} (CO) at 2029s, 1996w, 1964vs, 1945w and 1898w(br) cm^{-1} (in CH_2Cl_2). NMR: ^1H (in CD_2Cl_2), δ 1.76 [d of d, 1 H, CH·P, *J*(PH) 12, *J*(HH) 4], 2.27 (s, 3 H, Me-4), 3.57 [d of d of d, 1 H, CH_2, *J*(PH) 50, *J*(HH) 15 and 4], 4.13 [d of d, 1 H, CH_2, *J*(PH) 14, *J*(HH) 15], 5.02 (s, 5 H, C_5H_5), 7.03 [m, 4 H, C_6H_4], and 7.20–7.70 (m, 10 H, Ph); $^{13}C\text{-}\{^1H\}$ (in CD_2Cl_2–CH_2Cl_2), δ 236.5 [d, MoCO, *J*(PC) 10], 235.0 [d, MoCO, *J*(PC) 15], 214.7 [d, FeCO, *J*(PC) 24], 212.4 [d, FeCO, *J*(PC) 44], 210.8 [d, FeCO, *J*(PC) 29], 157.1 [$C^1(C_6H_4)$], 141.0–124.0 (C_6H_4 and Ph), 131.6 [d, CC_6H_4Me-4, *J*(PC) 7], 92.1 (C_5H_5), 21.1 (Me-4) and −8.2 [d, CH·P, *J*(PC) 7]; ^{13}C ($CDCl_3$), δ 54.6 [t of d, CH_2, *J*(HC) 129, *J*(PC) 14] and −8.11 [d of d of d, CH·P, *J*(PC) 7, *J*(HC) 150, 7]; $^{31}P\text{-}\{^1H\}$, δ 43.2 ppm.

X-ray crystallographic data

Red crystals of (**3**) were grown from CH_2Cl_2–light petroleum. Diffraction data were collected on a Nicolet P3 diffractometer at 298 K using a crystal of dimensions *ca* 0.50 × 0.40 × 0.35 mm. Of the 6511 intensities measured (Wyckoff ω-scans, $2\theta \leqslant 50°$), 5389 had $F \geqslant 5\sigma(F)$ and only these were used in the solution and refinement of the structure. Intensity data were corrected for Lorentz, polarization, and X-ray absorption effects. The latter by a procedure based upon azimuthal scan data.[10]

Crystal data for (**3**). $C_{37}H_{35}FeO_5PW$, $M = 830.4$, triclinic, $a = 8.583(3)$, $b = 10.529(4)$, $c = 19.989(8)$ Å, $\alpha = 88.43(3)$, $\beta = 84.58(3)$, $\gamma = 67.66(3)°$, $U = 1663(1)$ $Å^3$, $Z = 2$, $D_c = 1.66$ g cm^{-3}, $F(000) = 824$, space group $P\bar{1}$, $\mu(Mo\text{-}K_\alpha) = 40.5$ cm^{-1}, Mo-K_α X-radiation ($\bar{\lambda} = 0.71069$ Å, graphite monochromator).

The structure was solved, and all non-hydrogen atoms were located, by conventional heavy-atom and difference Fourier methods. Hydrogen atoms were included in calculated positions with fixed isotropic thermal parameters (aryl, CH_2 and CH), or common refined isotropic thermal parameters (methyl). All remaining atoms were given anisotropic thermal parameters. Refinement by blocked-cascade least-squares converged at $R = 0.024$ ($R_w = 0.026$) with a weighting scheme of the form $w^{-1} = [\sigma^2(F) + 0.0005|F|^2]$.* The final electron-density difference synthesis showed no peaks >0.7 e $Å^{-3}$. Scattering factors were from ref. 11. All calculations were carried out on a Data General "Eclipse" computer with the SHELXTL system of programs.[10]

Acknowledgement—We thank the Deutscher Akademischer Austauschdienst for a Scholarship to J.H.

*Atomic positional and thermal parameters, bond lengths and angles, and structure factor values have been deposited as supplementary material with the Editor. Atomic Coordinates have also been submitted to the Cambridge Crystallographic Data Centre.

REFERENCES

1. E. Delgado, J. Hein, J. C. Jeffery, A. L. Ratermann, F. G. A. Stone and L. J. Farrugia, *J. Chem. Soc., Dalton Trans.* 1987, 1191.

2. M. E. Garcia, J. C. Jeffery, P. Sherwood and F. G. A. Stone, *J. Chem. Soc., Dalton Trans.* 1987, 1209.
3. P. G. Byrne, M. E. Garcia, J. C. Jeffery, P. Sherwood and F. G. A. Stone, *J. Chem. Soc., Dalton Trans* 1987, 1215; *J. Chem. Soc., Chem. Commun.* 1987, 53.
4. J. Hein, J. C. Jeffery, P. Sherwood and F. G. A. Stone, *J. Chem. Soc., Dalton Trans.* 1987, 2211.
5. P. G. Byrne, M. E. Garcia, N. H. Tran-Huy, J. C. Jeffery and F. G. A. Stone, *J. Chem. Soc., Dalton Trans.* 1987, 1243.
6. M. Green, J. A. K. Howard, A. P. James, A. N. de M. Jelfs, C. M. Nunn and F. G. A. Stone, *J. Chem. Soc., Dalton Trans.* 1986, 1697.
7. F.-E. Baumann, J. A. K. Howard, R, J. Musgrove, P. Sherwood and F. G. A. Stone, *J. Chem. Soc., Dalton Trans.* in press.
8. J. C. Jeffery, K. A. Mead, H. Razay, F. G. A. Stone, M. J. Went and P. Woodward, *J. Chem. Soc., Dalton Trans.* 1984, 1383.
9. S. V. Hoskins, A. P. James, J. C. Jeffery and F. G. A. Stone, *J. Chem. Soc., Dalton Trans.* 1986, 1709.
10. G. M. Sheldrick, SHELXTL programs for use with the Nicolet X-ray system, University of Cambridge (1976); updated Göttingen (1981).
11. *International Tables for X-ray Crystallography*, Vol. 4. Kynoch Press, Birmingham (1974).

Polyhedron Vol. 6, No. 12, pp. 2073–2075, 1987
Printed in Great Britain

0277–5387/87 $3.00+.00

SYNTHESIS AND CRYSTAL STRUCTURE OF $[Re_2Cl_2(CO)_6(SeCH_2CMe_2CH_2Se)]$

EDWARD W. ABEL,* PRAMOD K. MITTAL and KEITH G. ORRELL

Department of Chemistry, University of Exeter, Exeter, U.K.

and

HELEN DAWES and MICHAEL B. HURSTHOUSE*

Department of Chemistry, Queen Mary College, Mile End Road, London E1 4NS, U.K.

(*Received* 15 *June* 1987; *accepted* 10 *July* 1987)

Abstract—The dinuclear complex $[Re_2Cl_2(CO)_6SeCH_2CMe_2CH_2Se]$ has been prepared and characterized in the solid state by X-ray crystallography. Proton NMR spectroscopy has shown the structure to be stereochemically rigid in solution.

Syntheses and structures of complexes of general formula $[Re_2X_2(CO)_6L]$, (X = Cl, Br, I, L = R_2S_2, R_2Se_2) where the open chain ligands bridge two rhenium atoms are now well characterized.[1–3] In the case of the complexes of dialkyl disulphides and diselenides, the chalcogen atoms have been reported to undergo pyramidal inversions.[3] The aims of the present work are to examine whether analogous complexes can be formed with cyclic dichalcogen ligands and to study any stereochemical non-rigidity in solution.

EXPERIMENTAL

The cyclic diselenide $SeCH_2CMe_2CH_2Se$[4] and the dirhenium complex $[Re_2Cl_2(CO)_6(THF)_2]$[5] were prepared by literature methods. The diselenide in excess (0.205 mmol) in chloroform (5 cm^3) was added to a stirred solution of $[Re_2Cl_2(CO)_6(THF)_2]$ (0.155 mmol) in chloroform. After stirring under nitrogen (4 h) the solvent was removed under vacuum from the pale brown solution. Dissolution of the residue in dichloromethane (10 cm^3) and filtration gave a yellow solution to which was added heptane (4 cm^3). Slow cooling to −20°C yielded yellow/brown crystals of $[Re_2Cl_2(CO)_6(SeCH_2CMe_2CH_2Se)]$ (0.088 mmol 57%) (Found: C, 15.9; H, 1.3. Calc: C, 15.7; H, 1.2%). (ν_{CO} 2060, 2038, 1958, 1937 and 1905 cm^{-1}). The mass spectrum gave a complex pattern for $[M]^+$ which corresponded exactly to the computer simulated isotope pattern, with maximum intensity $[M]^+$ at 840.

X-ray crystallography. X-ray diffraction measurements were made on a small crystal, of dimensions approx. $0.16 \times 0.12 \times 0.06$ mm^3, sealed inside a thin-walled glass capillary. Orientation matrix and cell dimensions were determined accurately and intensity data recorded at room temperature with graphite monochromatised Mo-K_α radiation ($\lambda = 0.71069$ Å) using a CAD4 diffractometer and previously detailed procedures.[6]

Crystal data

$C_{11}H_{10}Cl_2O_6Re_2Se_2$, $M = 839.427$, space group $P2_1/n$, $a = 9.9996(16)$ Å, $b = 18.0336(31)$ Å, $c = 10.8639(12)$ Å, $\beta = 111.673(10)°$, $U = 1820.568$ $Å^3$, $Z = 4$, $D_c = 3.06$ g cm^{-3}, μ(Mo-K_α) = 169.3 cm^{-1}. Of the 2461 data measured in the range $1.5 \leqslant \theta \leqslant 22.0°$, 2232 were unique and 1716 observed [$I > 2.5\sigma(I)$]. The structure was solved via interpretation of a Patterson Function followed by standard heavy atom phasing procedures. The intensity data were corrected for absorption (ABSC in SHELX76).[7] Non-hydrogen atoms were refined anisotropically; hydrogens were inserted in idealized positions and assigned group U_{iso} values. The final R, R_w values were 0.0396 and 0.0340 for 230 parameters, with a weighting scheme $w = 1/[\sigma^2(F) + 0.0007F_o^2]$.

* Authors to whom correspondence should be addressed.

Tables of atomic coordinates and displacement factor coefficients, and lists of F_o/F_c values have been deposited as supplementary data with the Editor, from whom copies can be obtained on request. Atomic coordinates have also been deposited with the Cambridge Crystallographic Data Centre.

DISCUSSION

There are many parallels between the structural moieties $PtXMe_3$ and $ReX(CO)_3$. The metal centres are isoelectronic, and with similar ligands isostructural products usually result. We have reported the acyclic diselenide $[(PtXMe_3)_2(RSeSeR)]$[8] and Calderazzo and his co-workers[1,2] have reported the corresponding $[\{ReX(CO)_3\}_2(RSeSeR)]$ complexes. The structures of both types of complex show there to be invariably a *trans* relationship between the two ligand organic groups, and there is a synchronous or correlated pyramidal atomic inversion process about the coordinated selenium atoms.[3,9] Notably the activation parameters for these processes are considerably higher for the rhenium comlexes.[3]

Table 1. Bond lengths (Å) and angles (deg)

Bond lengths			
Se(1)—Re(1)	2.601(5)	Cl(1)—Re(1)	2.503(8)
Cl(2)—Re(1)	2.509(7)	C(11)—Re(1)	1.820(22)
C(12)—Re(1)	1.878(22)	C(13)—Re(1)	1.879(22)
Se(2)—Re(2)	2.611(5)	Cl(1)—Re(2)	2.498(7)
Cl(2)—Re(2)	2.509(7)	C(21)—Re(2)	1.875(24)
C(22)—Re(2)	1.913(24)	C(23)—Re(2)	1.883(25)
Se(2)—Se(1)	2.395(5)	C(1)—Se(1)	1.999(21)
C(5)—Se(2)	1.982(22)	O(11)—C(11)	1.182(21)
O(12)—C(12)	1.169(20)	O(13)—C(13)	1.196(22)
O(21)—C(21)	1.204(23)	O(22)—C(22)	1.159(22)
O(23)—C(23)	1.204(23)	C(2)—C(1)	1.504(28)
C(3)—C(2)	1.556(25)	C(4)—C(2)	1.503(25)
C(5)—C(2)	1.555(29)		
Bond angles			
Cl(1)—Re(1)—Se(1)	87.4(2)	Cl(2)—Re(1)—Se(1)	86.2(2)
Cl(2)—Re(1)—Cl(1)	80.6(2)	C(11)—Re(1)—Se(1)	90.3(7)
C(11)—Re(1)—Cl(1)	176.6(6)	C(11)—Re(1)—Cl(2)	96.7(7)
C(12)—Re(1)—Se(1)	90.7(7)	C(12)—Re(1)—Cl(1)	93.8(6)
C(12)—Re(1)—Cl(2)	173.7(5)	C(13)—Re(1)—Se(1)	177.7(5)
C(13)—Re(1)—Cl(1)	93.8(7)	C(13)—Re(1)—Cl(2)	92.1(7)
C(12)—Re(1)—C(11)	88.8(9)	C(13)—Re(1)—C(11)	88.4(9)
C(13)—Re(1)—C(12)	91.1(9)	Cl(1)—Re(2)—Se(2)	87.5(2)
Cl(2)—Re(2)—Se(2)	86.6(2)	Cl(2)—Re(2)—Cl(1)	80.7(2)
C(21)—Re(2)—Se(2)	91.0(6)	C(21)—Re(2)—Cl(1)	178.5(5)
C(21)—Re(2)—Cl(2)	98.8(7)	C(22)—Re(2)—Se(2)	92.2(6)
C(22)—Re(2)—Cl(1)	92.4(6)	C(22)—Re(2)—Cl(2)	173.1(5)
C(23)—Re(2)—Se(2)	176.0(5)	C(23)—Re(2)—Cl(1)	93.1(6)
C(23)—Re(2)—Cl(2)	89.6(6)	C(22)—Re(2)—C(21)	88.0(9)
C(23)—Re(2)—C(21)	88.3(8)	C(23)—Re(2)—C(22)	91.7(8)
Se(2)—Se(1)—Re(1)	105.5(2)	C(1)—Se(1)—Re(1)	103.3(7)
C(1)—Se(1)—Se(2)	91.2(7)	Se(1)—Se(2)—Re(2)	104.6(2)
C(5)—Se(2)—Re(2)	103.6(7)	C(5)—Se(2)—Se(1)	91.9(7)
Re(2)—Cl(1)—Re(1)	97.1(2)	Re(2)—Cl(2)—Re(1)	96.6(2)
O(11)—C(11)—Re(1)	177.0(17)	O(12)—C(12)—Re(1)	178.1(16)
O(13)—C(13)—Re(1)	178.2(18)	O(21)—C(21)—Re(2)	176.2(16)
O(22)—C(22)—Re(2)	175.7(16)	O(23)—C(23)—Re(2)	175.5(16)
C(2)—C(1)—Se(1)	110.6(14)	C(3)—C(2)—C(1)	106.9(17)
C(4)—C(2)—C(1)	112.3(17)	C(4)—C(2)—C(3)	109.0(19)
C(5)—C(2)—C(1)	109.7(18)	C(5)—C(2)—C(3)	106.9(16)
C(5)—C(2)—C(4)	111.7(17)	C(2)—C(5)—Se(2)	110.3(14)

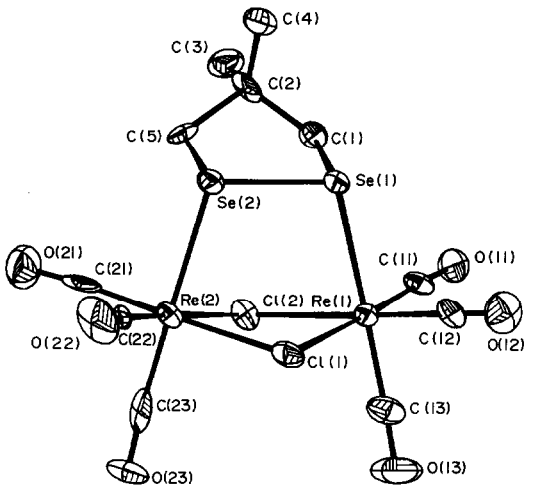

Fig. 1.

The formation of a diselenide complex of Pt(IV) with a *cis* relationship between the two carbon atoms attached to the seleniums of the ligand was achieved with the cyclic diselenide $SeCH_2CMe_2CH_2Se$, and this was found to undergo a synchronous inversion of the selenium atom pairs with an energy about 20 kJ mol^{-1} higher than the usual single site inversion energies.[10]

The displacement of THF from $[Re_2Cl_2(CO)_6(THF)_2]$ by 4,4-dimethyl-1,2-diselenacyclopentane gave a good yield of $[Re_2Cl_2(CO)_6(SeCH_2CMe_2CH_2Se)]$.

This structure is the first example of a bis $ReX(CO)_3$ moiety bridged by a cyclic dichalcogen ligand. The X-ray crystal structure is shown in Fig. 1, and important bond lengths and angles are given in Table 1.

We have been unable to detect, to date, any selenium pyramidal inversion for this species in solution. This is not unexpected as any such process will necessarily involve both Se atoms inverting synchronously. From previous experience with dinuclear Pt(IV) complexes[10] this is a relatively high energy process, and not surprisingly in the present complex is apparently too slow to produce any exchange broadening of the ligand methylene and methyl signals in the high temperature range accessible for our NMR studies.

REFERENCES

1. I. Bernal, J. L. Atwood, F. Calderazzo and D. Vitali, *Gazz. Chim. Ital.* 1976, **106**, 971; *Israel J. Chem.* 1976–1977, **15**, 153.
2. J. Korp, I. Bernal, J. L. Atwood, F. Calderazzo and D. Vitali, *J. Chem. Soc., Dalton* 1979, 1492.
3. E. W. Abel, S. K. Bhargava, M. M. Bhatti, M. A. Mazid, K. G. Orrell, V. Šik, M. B. Hursthouse and K. M. A. Malik, *J. Organomet. Chem.* 1983, **250**, 373.
4. G. Bergson and A. Biezais, *Arkiv. Für Kemi.* 1964, **22**, 475.
5. D. Vitali and F. Calderazzo, *Gazz. Chim. Ital.* 1972, **102**, 587.
6. M. B. Hursthouse, R. A. Jones, K. M. A. Malik and G. Wilkinson, *J. Am. Chem. Soc.* 1979, **101**, 4128.
7. G. M. Sheldrick, University of Cambridge, U.K. (1976).
8. E. W. Abel, A. R. Khan, K. Kite, M. B. Hursthouse, K. M. A. Malik and M. A. Mazid, *J. Organomet. Chem.* 1982, **235**, 121.
9. E. W. Abel, A. R. Khan, K. Kite, K. G. Orrell and V. Šik, *J. Chem. Soc., Dalton* 1980, 2208, 2220.
10. E. W. Abel, P. K. Mittal, K. G. Orrell and V. Šik, *J. Chem. Soc., Dalton* 1986, 961.

Polyhedron Vol. 6, No. 12, pp. 2077–2079, 1987
Printed in Great Britain

0277–5387/87 $3.00+.00

SYNTHESIS AND CHARACTERIZATION OF A NEW COORDINATION COMPOUND OF GOLD(III) WITH TRIPHENYLARSINE OXIDE(TPAsO)

GONG YUQIU* and XIA SHIHUA

Department of Chemistry, Hangzhou University, Hangzhou, China

(*Received* 6 *May* 1987; *accepted* 19 *June* 1987)

Abstract—A new solid coordination compound of the type 1 : 1 of TPAsO to gold(III) was prepared firstly by means of the extraction method, but only the coordination compound of the type 2 : 1 was obtained by the method of direct synthesis. It was found in polar solvents that the 1 : 1 type coordination compound could transform to that of the 2 : 1 type slowly. By the data of thermoanalyses, a mechanism was suggested for thermal decomposition of the above two coordination compounds.

Potts[1] synthesized a solid coordination compound of the type 2 : 1 of TPAsO to gold(III) more than ten years ago, but he failed to prepare the 1 : 1 type. When researching the extraction behavior of gold(III) with TPAsO, we obtained the new compound of the 1 : 1 type successfully, and the comparison with that of the 2 : 1 type was made. It was discovered that the composition of the solid coordination compound of the 1 : 1 type was the same as that of the extracted species of gold(III) with TPAsO.

EXPERIMENTAL

UV spectra were obtained using a UV-210A type doublebeam UV and visible spectrophotometer. IR spectra were recorded on a Perkin–Elmer 683 spectrophotometer. ^{1}H NMR spectra were recorded on a JEOL FX-90Q spectrometer at 90 Hz. Elemental analyses of carbon and hydrogen were measured with a Perkin–Elmer EA-240C type analyser and gold analyses were carried out by gravimetric methods. The TG/DTA data were recorded on a DT-30 simultaneous thermal analyser, the rate of heating was 10°C per min. Molar conductance were measured with a DDS-11A type conductance meter.

TPAsO was prepared as reported by Shriner,[2] after recrystallizing using 1,2-dichloroethane and petroleum ether, drying in vacuum, the product obtained was white crystals, m.p. = 189°C. Tetrachloroaurate (A.R.) was purchased from the second factory of chemicals in Peking. Other reagents used were of chemical or analytical grade.

Preparation of coordination compounds

Direct synthetic method. 2.43 mmol $HAuCl_4 \cdot 4H_2O$ (dissolved in 10 cm^3 1.0 M HCl) was added to 2.43 mmol, 4.86 mmol and 7.29 mmol TPAsO solutions (dissolved in 10 cm^3 ethanol for each), respectively and yellow products precipitated immediately. After filtering, washing several times with ethanol, pale yellow crystal were obtained for each (Compd **I**).

Extraction method. 2.43 mmol $HAuCl_4 \cdot 4H_2O$ (dissolved in 10 cm^3 1.0 M HCl) were added to 2.43 mmol TPAsO (in 10 cm^3 1,2-dichloroethane). On shaking for a few minutes, the organic phase was separated and solid product was obtained after evaporating the solvent. The solid product was recrystallized by 1,2-dichloroethane and petroleum ether, a deep yellow crystal was obtained after drying in air (Compd **II**).

RESULTS AND DISCUSSION

The elemental analyses and some physical properties of the coordination compounds, which were prepared by the direct synthetic method and the extraction method, are shown in Table 1. From Table 1, it can be seen that the composition of the

* Author to whom correspondence should be addressed.

Table 1. Analytical and physical data

Solid compds	Synthetic method TPAsO:Au	Method	Colour	M.p. (°C)	Elemental analyses C%	H%	Au%
	1:1	Direct syn.	Pale yellow	174–5	43.5 (43.9)[a]	3.2 (3.2)	
$[H(TPAsO)_2]AuCl_4$ (I)	2:1	*ibid.*	*ibid.*	*ibid.*	44.0 (43.9)	3.1 (3.2)	20.0
	3:1	*ibid.*	*ibid.*	*ibid.*	44.1 (43.9)	3.2 (3.2)	(19.6)
$[H(TPAsO)]AuCl_4$ (II)	1:1	Extrn	Deep yellow	149.5–50	32.9 (32.6)	2.4 (2.4)	29.5 (29.7)

[a] Figures in parentheses are calculated ones.

coordination compound obtained by the extraction method was the same as that of the extracted species of gold(III) and TPAsO.[3] However, the attempt to synthesize the 1:1 type solid coordination compound by the direct synthetic method did not succeed. The experiments showed that only the 2:1 type product was obtained when any ratios of TPAsO to gold(III) were used, this might be why Potts could not synthesize the 1:1 type coordination compound.

IR spectra showed the stretching frequency of free As=O bond was at 881 cm^{-1}, but after coordination, this absorption peak shifted to 770 cm^{-1} (Compd **I**) and 745 cm^{-1} (Compd **II**), respectively, and in coordination compound (**I**), the vibrating peaks of hydrogen bonds appeared at 1030 cm^{-1} and 1280 cm^{-1}; but in compound (**II**), a characteristic peak appeared at 2940 cm^{-1}, this might be ascribed to the absorption peak of the hydroxy group (O—H) formed by the bonding of As=O and H^+. Apparently, that is why the stretching frequency of As=O in compound (**I**) was lower than that in compound (**II**) due to the O—H covalent bond formed in coordination compound (**II**).

When dissolving coordination compounds in $CDCl_3$ and TMS as internal references, we discovered the hydrogen proton resonance peak in compound (**II**) was at 6.12 ppm, but the relative resonance peak of compound (**I**) was at 7.40 ppm, this indicated the electron density of the hydrogen proton in compound (**II**) was higher than that of compound (**I**). Apparently, this was because of the formation of an O—H covalent bond between As=O bond and H^+ in compound (**II**). However, only a hydrogen bond was formed between H^+ and two TPAsO molecules, so the proton resonance peak shifted to lower field in compound (**II**). This result was consistent with the conclusion obtained from IR spectra.

The 10^{-4} M solutions of compounds were made using dichloromethane and ethanol as solvents and UV absorption spectra of them were recorded (results shown in Table 2). The absorption curves of the two coordination compounds were almost the same as that of tetrachloroaurate in water, suggesting the $AuCl_4^-$ anionic complex existed in them.[4]

Table 2. UV spectra of coordination compounds λ_{max} (nm), ε (cm^{-1} mol^{-1} l)

Compds	Solvents CH_2Cl_2	C_2H_5OH	H_2O
	$\varepsilon \times 10^{-3}$		
(I)	3.05(324)[a]	4.62(322)	
(II)	4.08(323)	2.75(321)	
$HAuCl_4$			5.60(313)

[a] Figures in parentheses were maximum absorption peaks.

The solid coordination compounds dissolved in many polar organic solvents, e.g. ethanol, trichloromethane, dichloromethane and 1,2-dichloroethane etc. but did not dissolve in non-polar solvents such as benzene and toluene. The molar conductance values of the two compounds in ethanol and dichloromethane are presented in Table 3.

Table 3. The molar conductance of coordination compounds, Λ_M (Ω^{-1} cm^2 M^{-1}), 25°C

Compds.	Solvents C_2H_5OH	CH_2Cl_2
(I)	34.0	50
(II)	39.5	40
KNO_3	37.0	[a]

[a] KNO_3 can not dissolve in CH_2Cl_2.

Table 4. TG/DTA analyses of coordination compounds

Compds	Percentage of loss of weight: First loss of weight	Second loss of weight	Total loss of weight
(I)	72.40	6.47	78.87
	(73.50)[a]	(6.45)	(79.93)
(II)	61.30	9.15	70.45
	(60.66)	(9.59)	(70.25)

[a] Figures in parentheses are calculated ones.

From Table 3, it can be seen that the two compounds are 1 : 1 electrolytes.

It must be noted that when the above solutions of compound (II) were left for several days, it was discovered that the molar conductance of it apparently increased. If the solvents were evaporated and the product was recrystallized by ethanol and petroleum ether, a pale yellow crystal was obtained. Elemental analyses of it showed the product was coordination compound (I). It appears that compound (II) could transform gradually in polar organic solvents as follows:

$$2[H(TPAsO)][AuCl_4] \xrightarrow[\text{dichloromethane}]{\text{in ethanol or}} [H(TPAsO)_2][AuCl_4] + HAuCl_4.$$

Thermogravimetric and differential thermal analyses showed coordination compounds had endothermic peaks at 175°C (Compd I) and 152°C (Compd II), respectively, but no loss of weight occurred in the thermogravimetric curves. It was believed that the positions of endothermic peaks were relative to their melting points. The TG/DTA curves of them were almost the same, the first loss of weight was finished between 200–300°C. At 400°C the second loss of weight started and ended at *ca.* 500°C, from then no loss of weight occurred. The final products of thermal decomposition were a yellow powder of gold. By the above experiments, it was suggested that procedures of thermal decompositions of the two compounds could be written as follows:

$$[H(TPAsO)n]AuCl_4 \xrightarrow[(1)]{200\text{–}300^\circ C} Au(CO)Cl \xrightarrow[(2)]{400\text{–}500^\circ C} Au$$

where $n = 1$ or 2.

By the above procedures of thermal decompositions of coordination compounds, theoretical percentage loss of weight for each stage coincided very well with the values measured by experiments (shown in Table 4).

From the results of the above experiments, the structures of the two compounds may be suggested as follows:

Compd I

$$[TPAsO \ldots H^+ \ldots OAsPT]AuCl_4^-.$$

Compd II

$$[TPAsO^+—H]AuCl_4^-.$$

Acknowledgements—The project was supported by the National Natural Science Foundation of China.

REFERENCES

1. R. A. Potts, *Inorg. Chem.* 1970, **9**, 1284.
2. R. L. Shriner, *Org. Syn.* 1963, **4**, 910.
3. Gong Yuqiu and Xia Shihua, XXV, ICCC. Nanking, China (1987).
4. Gong Yuqiu, Xia Shihua and Yang Jian, *Science Bull.* 1986, **31**, 1112.

Polyhedron Vol. 6, No. 12, pp. 2081–2084, 1987
Printed in Great Britain

0277–5387/87 $3.00+.00

NEW SEVEN-COORDINATE THIOUREA AND *N,N,N′,N′*-TETRAMETHYLTHIOUREA COMPLEXES OF MOLYBDENUM(II) AND TUNGSTEN(II)

PAUL K. BAKER* and STUART G. FRASER

Department of Chemistry, University College of North Wales, Bangor, Gwynedd LL57 2UW, U.K.

(*Received* 8 *May* 1987; *accepted* 19 *June* 1987)

Abstract—The compounds $[MI_2(CO)_3(NCMe)_2]$ (M = Mo or W) react with one equivalent of thiourea (tu) in MeOH or *N,N,N′,N′*-tetramethylthiourea (tmtu) in CH_2Cl_2 at room temperature to initially afford the monoacetonitrile compounds $[MI_2(CO)_3(NCMe)L]$ (L = tu or tmtu) which rapidly transform to the isolated iodide bridged dimers, $[M(\mu\text{-}I)I(CO)_3L]_2$ with loss of acetonitrile. Reaction of $[WI_2(CO)_3(NCMe)_2]$ with two equivalents of tu or tmtu gave the expected mononuclear seven-coordinate compounds $[WI_2(CO)_3L_2]$. However, reaction of $[MoI_2(CO)_3(NCMe)_2]$ with two equivalents of tu or tmtu rapidly affords the iodide-bridged dimers $[Mo(\mu\text{-}I)I(CO)_2L_2]_2$ with loss of carbon monoxide from $[MoI_2(CO)_3L_2]$. The low temperature (−70°C) ^{13}C NMR spectrum of $[Mo(\mu\text{-}I)I(CO)_2\{SC(NMe_2)_2\}_2]_2$ suggests the complex is based on two capped octahedra with a carbonyl ligand capping each octahedral face.

Although there are a wide variety of examples of complexes of molybdenum(II) and tungsten(II) containing anionic sulphur ligands such as dithiocarbamates and xanthates: in particular the compounds $[M(CO)_n(S_2CNR_2)_2]$ (M = Mo or W; $n = 2$ or 3; R = Me, Et and ^{i}Pr)[1] hitherto very few seven-coordinate halocarbonyl complexes containing neutral sulphur donor ligands have been reported. Wilkinson and Mannerskantz[2] reported the reaction of the zerovalent complexes $[M(CO)_4(dth)]$ (M = Mo or W; dth = 2,5-dithiahexane) with X_2 (X = Br or I) under controlled conditions to give the seven-coordinate complexes $[MX_2(CO)_3(dth)]$. Also Tsang, Meek and Wojcicki[3] reported the preparation of some seven-coordinate complexes with neutral sulphur donor ligands attached to molybdenum(II) and tungsten(II) such as diphenyl(*o*-methylthiophenyl)phosphine and phenylbis(*o*-methylthiophenyl)phosphine.

Although the zerovalent six-coordinate complexes $[Mo(CO)_3\{SC(NH_2)_2\}_3]$,[4] $[Mo(CO)_3(bipy)\{SC(NH_2)_2\}]$[5] and very recently $[Cr(CO)_5\{SC(NR_2)_2\}]$ (R = H, Me, p-tol or ^{t}Bu)[6] have been previously reported, hitherto there are no examples of seven-coordinate complexes of molybdenum(II) or tungsten(II) containing thiourea as an attached ligand. In this paper we describe the preparation and properties of some new mononuclear and dinuclear seven-coordinate complexes of molybdenum(II) and tungsten(II) containing $SC(NH_2)_2$ or $SC(NMe_2)_2$ as attached ligands.

EXPERIMENTAL

The synthesis and purification of the complexes described were carried out under an atmosphere of dry nitrogen. The compounds $[MI_2(CO)_3(NCMe)_2]$ (M = Mo or W) were prepared by the published method,[7] and $[M(CO)_6]$, acetonitrile, I_2, $SC(NH_2)_2$ and $SC(NMe_2)_2$ were purchased from commercial sources.

The low temperature (−70°C) ^{13}C NMR spectrum of (7) was recorded on a Bruker WH-400 MHz NMR spectrometer at the University of Warwick (the spectrum was calibrated against tetramethylsilane). Infrared spectra were recorded on a Perkin–Elmer 197 infrared spectrophotometer. Elemental analyses for carbon, hydrogen and nitro-

* Author to whom correspondence should be addressed.

gen were carried out by Mr E. Lewis of the Department of Chemistry, UCNW, on a Carlo Erba Elemental Analyser MOD 1106 (using helium carrier gas). Molecular weight determinations were carried out using Rast's method[8] using camphor as the solvent. Magnetic susceptibilities were determined using a Johnson–Mathey magnetic susceptibility balance.

(3) $[Mo(\mu\text{-}I)I(CO)_3\{SC(NMe_2)_2\}]_2$

To $[MoI_2(CO)_3(NCMe)_2]$ (0.195 g, 0.378 mmol) dissolved in CH_2Cl_2 (15 cm^3) with continuous stirring under a stream of dry nitrogen was added $SC(NMe_2)_2$ (0.05 g, 0.378 mmol). After stirring the solution for two minutes, filtration and removal of the solvent *in vacuo* gave brown crystals of $[Mo(\mu\text{-}I)I(CO)_3\{SC(NMe_2)_2\}]_2$ (yield = 0.17 g, 80%), which were recrystallized from CH_2Cl_2. Molecular weight for $C_{16}H_{24}N_4I_4Mo_2O_6S_2$: Calc. 1132; found 1062.

Similar reactions of $[MI_2(CO)_3(NCMe)_2]$ with $L = SC(NH_2)_2$ in CH_3OH and $SC(NMe_2)_2$ in CH_2Cl_2 gave the new compounds $[M(\mu\text{-}I)I(CO)_3L]_2$ (1), (2) and (4). Molecular weight for (4): $C_{16}H_{24}N_4I_4W_2O_6S_2$: Calc. 1308; found 1172.

(6) $[WI_2(CO)_3\{SC(NH_2)_2\}_2]$

To $[WI_2(CO)_3(NCMe)_2]$ (0.23 g, 0.381 mmol) dissolved in MeOH (15 cm^3) with continuous stirring under a stream of dry nitrogen was added $SC(NH_2)_2$ (0.058 g, 0.762 mmol). After stirring the solution for 4 min, filtration and removal of the solvent *in vacuo* gave green crystals of $[WI_2(CO)_3\{SC(NH_2)_2\}_2]$ yield = 0.16 g, 62%), which were recrystallized from MeOH.

In a similar reaction, $[WI_2(CO)_3(NCMe)_2]$ with $SC(NMe_2)_2$ in CH_2Cl_2 gave the new compound $[WI_2(CO)_3\{SC(NMe_2)_2\}_2]$ (8).

(7) $[Mo(\mu\text{-}I)I(CO)_2\{SC(NMe_2)_2\}_2]_2$

To $[MoI_2(CO)_3(NCMe)_2]$ (0.195 g, 0.378 mmol) dissolved in CH_2Cl_2 (15 cm^3) with continuous stirring under a stream of dry nitrogen was added $SC(NMe_2)_2$ (0.1 g, 0.756 mmol). After stirring the solution for 6 min, filtration and removal of the solvent *in vacuo* gave brown crystals of $[Mo(\mu\text{-}I)I(CO)_2\{SC(NMe_2)_2\}_2]_2$ (yield = 0.18 g, 71%), which were recrystallized from CH_2Cl_2. Molecular weight for $C_{24}H_{48}N_8I_4Mo_2O_4S_4$: Calc. 1340, found 1154.

In a similar reaction, $[MoI_2(CO)_3(NCMe)_2]$ with $SC(NH_2)_2$ in MeOH gave the new compound $[Mo(\mu\text{-}I)I(CO)_2\{SC(NH_2)_2\}_2]_2$ (5).

RESULTS AND DISCUSSION

The addition of one equivalent of $SC(NH_2)_2$(tu) or $SC(NMe_2)_2$(tmtu) to $[MI_2(CO)_3(NCMe)_2]$ (M = Mo or W) at room temperature after rapid filtration and removal of the solvent *in vacuo* gave good yields of the iodide-bridged compounds $[M(\mu\text{-}I)I(CO)_3L]_2$ (L = tu or tmtu). Reaction of two equivalents of tu or tmtu with $[WI_2(CO)_3(NCMe)_2]$ afforded good yields of the mononuclear seven-coordinate compounds $[WI_2(CO)_3L_2]$. Whereas reaction of $[MoI_2(CO)_3(NCMe)_2]$ with two equivalents of tu or tmtu after rapid filtration and removal of solvent *in vacuo* gave good yields of the iodide-bridged dimers $[Mo(\mu\text{-}I)I(CO)_2L_2]_2$ with loss of carbon monoxide. All the complexes (1)–(8) are very air-sensitive in solution and rapidly decompose in the solid state in air. The compounds are also thermally unstable (particularly the iodide-bridged dimers), although they can be stored for several hours in the solid state under nitrogen at 0°C. The thiourea complexes are much less soluble than their tetramethylthiourea counterparts. The complexes are not very soluble in chlorinated solvents such as $CHCl_3$ or CH_2Cl_2 but are much more soluble in MeOH. All the complexes have been characterized by elemental analysis (C, H and N) (Table 1), IR spectroscopy (Table 2) and for the tetramethylthiourea complexes molecular weight studies using Rast's method[8] indicated that the complexes (3), (4) and (7) were dimeric (see Experimental). The magnetic susceptibilities of compounds (1)–(8) were determined and the results showed all the complexes to be diamagnetic.

Reaction of the complexes $[MI_2(CO)_3(NCMe)_2]$ (M = Mo or W)[7] with one equivalent of L (L = tu or tmtu) must initially afford the monoacetonitrile complexes $[MI_2(CO)_3(NCMe)L]$ via displacement of acetonitrile probably by a dissociative mechanism since seven-coordinate complexes are highly crowded. This type of complex $[MI_2(CO)_3(NCMe)L]$ has been isolated from the reaction of $[MI_2(CO)_3(NCMe)_2]$ with one equivalent of L (L = PPh_3, $AsPh_3$ or $SbPh_3$)[9] which are good π-acceptor ligands and hence stabilize these seven-coordinate monomers by lowering the electron density on the metal and hence increasing the strength of the M—N bond. Whereas tu and tmtu are better σ-donors and poorer π-acceptors than PPh_3, $AsPh_3$ or $SbPh_3$ and hence the electron density at the metal is greater which weakens the M—N bond. Acetonitrile is mainly a σ-donor ligand and rapid loss of acetonitrile occurs via attack of the iodide lone pair to give the iodide bridged complexes $[M(\mu\text{-}I)I(CO)_3L]_2$.

Reaction of $[WI_2(CO)_3(NCMe)_2]$ with two equi-

Table 1. Physical and analytical data[a] for the complexes

Complex		Colour	Yield (%)	Analysis (%) C	H	N
(1)	$[Mo(\mu\text{-}I)I(CO)_3\{SC(NH_2)_2\}]_2$	Black	68	7.5(9.4)	1.1(0.8)	5.3(5.5)
(2)	$[W(\mu\text{-}I)I(CO)_3\{SC(NH_2)_2\}]_2$	Green	77	8.1(8.0)	1.0(0.7)	5.0(4.7)
(3)	$[Mo(\mu\text{-}I)I(CO)_3\{SC(NMe_2)_2\}]_2$	Brown	80	16.9(17.0)	2.3(2.1)	5.3(5.0)
(4)	$[W(\mu\text{-}I)I(CO)_3\{SC(NMe_2)_2\}]_2$	Green	66	15.4(14.7)	1.9(1.9)	4.0(4.3)
(5)	$[Mo(\mu\text{-}I)I(CO)_2\{SC(NH_2)_2\}_2]_2$	Black	86	8.9(8.6)	1.8(1.5)	10.0(10.0)
(6)	$[WI_2(CO)_3\{SC(NH_2)_2\}_2]$	Green	62	8.8(8.9)	1.4(1.2)	8.4(8.3)
(7)	$[Mo(\mu\text{-}I)I(CO)_2\{SC(NMe_2)_2\}_2]_2$	Brown	71	21.3(21.5)	3.7(3.6)	8.3(8.4)
(8)	$[WI_2(CO)_3\{SC(NMe_2)_2\}_2]$	Brown	77	19.8(19.9)	3.3(3.1)	7.3(7.1)

[a] Calculated values in parentheses.

valents of tu or tmtu gives the expected mononuclear compounds $[WI_2(CO)_3L_2]$ with facile displacement of two acetonitrile ligands. The molybdenum complex $[MoI_2(CO)_3(NCMe)_2]$ reacts with two equivalents of L and initially gives $[MoI_2(CO)_3L_2]$ which rapidly dimerizes with loss of carbon monoxide to give the iodide-bridged dimers $[Mo(\mu\text{-}I)I(CO)_2L_2]_2$. This tendency for molybdenum complexes of the type $[MoX_2(CO)_3L_2]$ (L = phosphorus donor ligands) to dimerize with loss of carbon monoxide more readily than their tungsten analogues has been previously observed.[10] Molecular weight and magnetic susceptibility measurements on (7) confirm the dimeric nature of this complex (see Experimental).

Most of the previously reported X-ray crystal structures of d^4-seven-coordinate complexes have capped octahedral geometry.[11] It is very likely that the $[WI_2(CO)_3L_2]$ complexes will have a similar geometry since their infrared carbonyl pattern closely resembles the seven-coordinate complexes which have been shown to have capped octahedral geometry from X-ray crystallography.[11] Colton and Kevecordes[12] have shown how low temperature (−70°C) ^{13}C NMR spectroscopy can be used to find out if there is a carbonyl ligand in the capping position in capped octahedral compounds. Unfortunately the low temperature (−70°C) ^{13}C NMR spectra of $[WI_2(CO)_3L_2]$ did not reveal any carbonyl resonances due to instability and low solubility in CD_3OD at low temperature. However, the low temperature (−70°C) ^{13}C NMR spectrum of $[Mo(\mu\text{-}I)I(CO)_2\{SC(NMe_2)_2\}_2]_2$ (recorded in CD_3OD) shows carbonyl resonances at δ = 207.7(s) and 239.6(s) ppm. The low field resonance at δ = 239.6 ppm is highly likely to be due to a carbonyl ligand in the unique capping position. Hence the structure of (7) probably has the two molybdenum atoms in capped octahedral environments with a carbonyl ligand capping a $[MoI_3(CO)\{SC(NMe_2)_2\}_2]$ octahedron. It is interesting to note that Cotton and co-workers[13] recently reported the X-ray crystal structure of $[W(\mu\text{-}Br)Br(CO)_4]_2$ which shows the two tungsten atoms to be in capped octahedral environments with a carbonyl ligand capping a $[WBr_3(CO)_3]$ octahedron, i.e. similar to our suggested structure of (7). We have tried without success to grow crystals of (1)-(8) for X-ray crystallography.

The complexes $[MX_2(CO)_3L_2]$ (M = Mo or W;

Table 2. IR data[a] for the complexes

Complex	ν(CO)/cm^{-1}	ν(CS)/cm^{-1}
(1)	2065(m), 2010(s) and 1935(s)	1650(s)
(2)	2070(m), 2010(s), 1932(s) and 1880(m)	1630(s)
(3)	2075(s), 2025(s) and 1944(m)	1575(s)
(4)	2070(s), 2010(s), 1934(s) and 1878(m)	1578(s)
(5)	2030(s), 1929(s) and 1869(s)	1630(s)
(6)	2015(m), 1921(s) and 1870(s)	1640(s)
(7)	2065(s), 2015(s) and 1939(s)	1570(s)
(8)	2060(s), 2000(s) and 1920(s)	1570(s)

[a] Spectra recorded in $CHCl_3$. (m), medium; (s), strong.

X = Cl or Br; L = PPh_3 or $AsPh_3$) have recently been found to be catalysts for the ring-opening polymerization of norbornene and norbornadiene,[14] and in view of this work we are currently investigating the catalytic activity of the $[WI_2(CO)_3L_2]$ compounds.

Acknowledgement—We wish to thank Dr O. W. Howarth for measuring the low temperature (−70°C) ^{13}C NMR spectrum of the complex $[Mo(\mu\text{-}I)I(CO)_2\{SC(NMe_2)_2\}_2]_2$ and we thank the S.E.R.C. for support.

REFERENCES

1. (a) R. Colton, G. R. Scollary and I. B. Tomkins, *Aust. J. Chem.* 1968, **21**, 15; (b) G. J.-J. Chen, R. O. Yelton and J. W. McDonald, *Inorg. Chim. Acta* 1977, **22**, 249; (c) J. A. Broomhead and C. G. Young, *Aust. J. Chem.* 1982, **35**, 277; (d) J. R. Morrow, J. L. Templeton, J. A. Bandy, C. Banister and C. J. Prout, *Inorg. Chem.* 1986, **25**, 1923.
2. H. C. E. Mannerskantz and G. Wilkinson, *J. Chem. Soc.* 1962, 4454.
3. W. S. Tsang, D. W. Meek and A. Wojcicki, *Inorg. Chem.* 1968, **7**, 1263.
4. F. A. Cotton and F. Zingales, *Inorg. Chem.* 1962, **1**, 145.
5. L. W. Houk and G. R. Dobson, *Inorg. Chem.* 1966, **5**, 2119.
6. J. A. Costamagna and J. Granifo, *Inorg. Synth.* 1986, **23**, 1.
7. P. K. Baker, S. G. Fraser and E. M. Keys, *J. Organomet. Chem.* 1986, **309**, 319.
8. F. G. Mann and B. C. Saunders, *Practical Organic Chemistry*, pp. 342–344. Longman's Green.
9. P. K. Baker and S. G. Fraser, *Polyhedron* 1986, **5**, 1381.
10. J. R. Moss and B. L. Shaw, *J. Chem. Soc.* (*A*) 1970, 595.
11. (a) A. Mawby and G. E. Pringle, *J. Inorg. Nucl. Chem.* 1972, **34**, 517; (b) M. G. B. Drew, *J. Chem. Soc., Dalton Trans.* 1972, 626; (c) M. G. B. Drew, *J. Chem. Soc., Dalton Trans.* 1975, 1984; (d) G. Schmid, R. Boese and E. Welz, *Chem. Ber.* 1975, **108**, 260; (e) R. Boese and U. Müller, *Acta Cryst.* 1976, **B32**, 582; (f) M. G. B. Drew and J. D. Wilkins, *J. Chem. Soc., Dalton Trans.* 1977, 557.
12. R. Colton and J. Kevekordes, *Aust. J. Chem.* 1982, **35**, 895.
13. F. A. Cotton, L. R. Falvello and J. H. Meadows, *Inorg. Chem.* 1985, **24**, 514.
14. (a) L. Bencze and A. Kraut-Vass, *J. Mol. Catal.* 1985, **28**, 369; (b) L. Bencze, A. Kraut-Vass and L. Prókai, *J. Chem. Soc., Chem. Commun.* 1985, 911.

Polyhedron Vol. 6, No. 12, pp. 2085–2090, 1987
Printed in Great Britain

0277–5387/87 $3.00+.00

ELECTRON PARAMAGNETIC RESONANCE STUDY OF THE REACTIONS OF TETRATHIOMOLYBDATE WITH ROUSSIN SALTS AND ESTERS, AND WITH SOME RELATED IRON NITROSYLS

ANTHONY R. BUTLER, CHRISTOPHER GLIDEWELL,* IAN L. JOHNSON and JOHN C. WALTON

Department of Chemistry, University of St Andrews, St Andrews, Fife KY16 9ST, U.K.

(*Received* 23 *February* 1987; *accepted* 24 *June* 1987)

Abstract—The tetrathiomolybdate ion $[MoS_4]^{2-}$ reacts in DMF solution with Roussin esters $Fe_2(SR)_2(NO)_4$ (R = Me, Et, *n*-Pr, *i*-Pr, *n*-Bu, *t*-Bu, *n*-C_5H_{11}) to yield the paramagnetic iron nitrosyls $[Fe(NO)_2(SR)_2]^-$ (**1**), $[Fe(NO)_2(S_2MoS_2)]^-$ (**2**) and $[Fe(NO)(S_2MoS_2)_2]^{2-}$ (**3**). The new complexes (**2**) and (**3**) have been characterized by EPR spectroscopy and the assignment to them of constitutions based respectively upon tetrahedral and square pyramidal iron is supported by EHMO calculations. $Fe_2(SPh)_2(NO)_4$ with $[MoS_4]^{2-}$ yields only $[Fe(NO)_2(SPh)_2]^-$, and preformed (**3**) reacts with PhS^- to give firstly EPR-silent species, and then $[Fe(NO)_2(SPh)_2]^-$. The mononitrosyl (**3**) can also be formed by reaction of $[MoS_4]^{2-}$ with $[Fe_4S_3(NO)_7]^-$, $Fe_4S_4(NO)_4$, or $Fe_2I_2(NO)_4$.

We have recently shown[1] that the diamagnetic Roussin esters $Fe_2(SR)_2(NO)_4$ (R = Me, Et, *i*-Pr, *t*-Bu, $PhCH_2$) are readily converted, by means of RS^- to the paramagnetic mononuclear complexes $[Fe(NO)_2(SR)_2]^-$: the formal oxidation state of iron remains as Fe(−I). The characterization[1] of $[Fe(NO)_2(SR)_2]^-$ by EPR spectroscopy has allowed definitive identification of a family of iron–nitrosyl complexes widely[2] observed in animal tissues following administration of certain chemical carcinogens. The primary products of similar reactions of RS^- with the tetra-nuclear nitrosyl cluster $[Fe_4S_3(NO)_7]^-$, in which all the nitrosyl ligands are present[3] as NO^+ and in which the basal $Fe(NO)_2$ groups formally contain Fe(−I) and the apical Fe(NO) group contains Fe(I),[4] are[1] $[Fe(NO)_2(SR)_2]^-$ (from the basal irons) and $[Fe(NO)(SR)_3]^-$ (from the apical iron). Again the initial reaction with RS^- proceeds without change of oxidation state at iron.

However in the presence of the non-chelating RS^- ligands $[Fe(NO)]^{2+}$ groups are[1] fairly rapidly converted to $[Fe(NO)_2]^+$, while in the presence of chelating ligands such as $[Me_2NCS_2]^-$ the reverse transformation of $[Fe(NO)_2]^+$ fragments into $[Fe(NO)]^{2+}$ readily occurs: thus $[Me_2NCS_2]^-$ reacts[1] with both $Fe_2(SMe)_2(NO)_4$ and $[Fe_4S_3(NO)_7]^-$ to yield the well-known paramagnetic complex $Fe(NO)(S_2CNMe_2)_2$, and in this case no paramagnetic dinitrosyl intermediate could be detected. The interconversion of $[Fe(NO)_2]^+$ and $[Fe(NO)]^{2+}$ fragments in mono-nuclear iron–sulphur nitrosyl complexes appears[1] to be common and dependent primarily on the nature of the sulphur ligands present.

In the present paper we present the results of an EPR study of the reactions of the chelating ligand tetrathiomolybdate $[MoS_4]^{2-}$ with a range of Roussin esters $Fe_2(SR)_2(NO)_4$, with the tetra-nuclear species $[Fe_4S_3(NO)_7]^-$ and $Fe_4S_4(NO)_4$, and with $Fe_2I_2(NO)_4$.

RESULTS

Reactions of $Fe_2(SR)_2(NO)_4$, R = *alkyl*

The reactions of $Fe_2(SR)_2(NO)_4$ for R = Me, Et, *n*-Pr, *i*-Pr, *n*-Bu, *t*-Bu and *n*-C_5H_{11} with tetrathiomolybdate all follow a common pattern.

Addition of $[MoS_4]^{2-}$ to $Fe_2(SR)_2(NO)_4$, for R = alkyl as above, in DMF solution such that the overall molar ratio Mo : Fe was 1 : 1 yielded in every

* Author to whom correspondence should be addressed.

case an EPR spectrum showing the presence of three paramagnetic iron–nitrosyl complexes, (**1**)–(**3**): complexes (**1**) and (**2**) were dinitrosyl species and (**3**) was a monitrosyl.

The EPR parameters for (**1**) permitted its identification in each case as a member of the known[1] series $[Fe(NO)_2(SR)_2]^-$. The dinitrosyl complex (**2**) was characterized by $g = 2.027$ and $A(^{14}N) = 2.0$ G, while the mononitrosyl (**3**) was characterized by $g = 2.024$ and $A(^{14}N) = 15.0$ G. When the molar ratio Mo : Fe was increased from 1 : 1 to 5 : 1, the spectra of complexes (**1**) and (**2**) disappeared while the spectrum of (**3**) was enhanced.

The EPR parameters, g and $A(^{14}N)$, for (**2**) were independent of the identity of R in the initial ester $Fe_2(SR)_2(NO)_4$ and hence (**2**) contains no RS group: on the other hand these parameters are very similar to those observed[1] for $[Fe(NO)_2(SR)_2]^-$ and suggest that (**2**) also contains a tetrahedral $S_2Fe(NO)_2$ fragment. We therefore assign the constitution $[Fe(NO)_2(S_2MoS_2)]^-$ to complex (**2**):

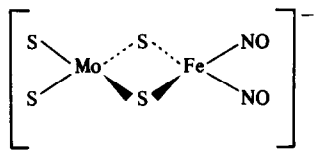

(**2**)

This assignment is supported by molecular orbital calculations, discussed below.

The formation of complexes (**1**) and (**2**) is therefore entirely straightforward, eqs (1) and (2):

$$Fe_2(SR)_2(NO)_4 + 2[MoS_4]^{2-} \rightarrow 2RS^- + 2[Fe(NO)_2(S_2MoS_2)]^- \quad (1)$$
(**1**)

$$Fe_2(SR)_2(NO)_4 + 2RS^- \rightarrow [Fe(NO)_2(SR)_2]^- \quad (2)$$
(**2**)

Nucleophilic displacement of RS^- from $Fe_2(SR)_2(NO)_4$ by $[MoS_4]^{2-}$ yields the complex (**2**), while the known[1] reaction of $Fe_2(SR)_2(NO)_4$ with excess RS^- yields (**1**).

In the presence of a large excess of the chelating ligand $[MoS_4]^{2-}$ both (**1**) and (**2**) are converted to (**3**). The EPR parameters of (**3**) are again independent of the identity of R in the initial $Fe_2(SR)_2(NO)_4$ and closely resemble those of $Fe(NO)(S_2CNMe_2)_2$: in particular both (**3**) and $Fe(NO)(S_2CNMe_2)_2$ have large $A(^{14}N)$ values, 15.0 and 13.6 G respectively in DMF solution. Molecular orbital calculations (discussed below) suggest that these large $A(^{14}N)$ values are characteristic of square pyramidal $Fe(NO)S_4$ species, having a C_{2v} (approximate C_{4v}) symmetry. Hence we assign to complex (**3**) the constitution $[Fe(NO)(S_2MoS_2)_2]^{2-}$: the analogous square pyramidal thiotungstate complexes $[Fe(NO)(S_2WS_2)_2]^{2-}$ and $[Co(NO)(S_2WS_2)_2]^{2-}$ have recently been described.[5]

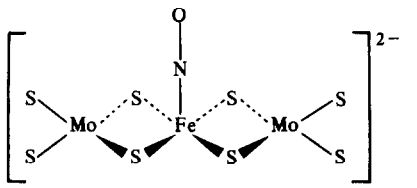

(**3**)

The formation of (**3**) from (**1**) and (**2**) is entirely analogous to the formation of $Fe(NO)(S_2CNMe_2)_2$ from $Fe_2(SR)_2(NO)_4$ or $[Fe_4S_3(NO)_7]^-$: $[Fe(NO)_2]^+$ fragments are converted into $[Fe(NO)]^{2+}$. The main difference between $[MoS_4]^{2-}$ and $[Me_2NCS_2]^-$ in this content is that no dinitrosyl species analogous to (**2**) were detected[1] in reactions involving $[Me_2NCS_2]^-$.

The relative abundances of complexes (**2**) and (**3**) were temperature dependent; when the Mo : Fe ratio was 1 : 1 and in the temperature range 220–300 K, the relative abundance of (**3**) rose steadily. However at 280 K, complex (**3**) although initially more abundant than (**2**), had a shorter life-time: when the EPR spectrum of such a mixture was monitored continuously at 280 K, the spectrum of (**3**) disappeared within *ca.* 30 min, while that of (**2**) disappeared only after *ca.* 2 h. When species (**2**) and (**3**) had both disappeared, presumably as a result of irreversible conversion to EPR-silent species, there remained only the weak EPR spectra of two mononitrosyl complexes (**4**), having $g = 2.042$, $A(^{14}N) = 3.3$ G, and (**5**) having $g = 2.041$, $A(^{14}N) = 3.4$ G. Of these (**5**) is the more robust and was the sole paramagnetic species detectable in mixtures of $Fe_2(SR)_2(NO)_4$ and $[MoS_4]^{2-}$ after 3 h at 280 K.

The relative abundance of the dinitrosyl complexes of (**1**) and (**2**) was somewhat dependent upon the identity of R, when the Mo : Fe ratio was 1 : 1. For R = *i*-Pr, the dominant dinitrosyl was (**2**) while for R = *t*-Bu the dominant dinitrosyl was (**1**): for other alkyl groups (**1**) and (**2**) were present in rather similar abundance, although accurate measurement of the molar ratio was not possible because of spectral overlaps.

Reactions of $Fe_2(SR)_2(NO)_4$, R = *aryl*

When $[MoS_4]^{2-}$ was added to a DMF solution of $Fe_2(SPh)_2(NO)_4$, to give a molar ratio Mo : Fe of 1 : 1, the weak spectrum of the solvo-complex[1] was rapidly replaced by the spectrum of a dinitrosyl complex, together with a trace only of complex (**3**).

The dinitrosyl had $g = 2.027$, $A(^{14}N) = 2.5$ G and was identical with an authentic sample of $[Fe(NO)_2(SPh)_2]^-$, prepared in the usual way[1] from $Fe_2(SPh)_2(NO)_4$ and PhS^-. The assignment was checked using the reactions of $Fe_2(SPh_2)(^{15}NO)_4$ with PhS^- and $[MoS_4]^{2-}$, both separately and together. The spectrum was independent of temperature in the range 220–320 K. Increase of the ratio Mo : Fe first to 5 : 1 and then to 10 : 1 caused no increase in the abundance of (**3**) but weak features due to complexes (**4**) and (**5**) appeared. The behaviour of $Fe_2(SC_6H_4CH_3\text{-}p)_2(NO)_4$ with $[MoS_4]^{2-}$ was identical: the major product was $[Fe(NO)_2(SC_6H_4CH_3\text{-}p)_2]^-$, $g = 2.027$, $A(^{14}N) = 2.5$ G, with only a trace of complex (**3**). No (**2**) was detected in either reaction.

The very low abundances of complexes (**2**) and (**3**) in the reactions of $Fe_2(S\text{-aryl})(NO)_4$ with $[MoS_4]^{2-}$ may possibly be the result of their reaction with ArS^- to form EPR-silent products. This idea was tested as follows: a solution was prepared, from $Fe_2(SBu^t)_2(NO)_4$ and $[MoS_4]^{2-}$, containing $[Fe(NO)_2(SBu^t)_2]^-$ and $[Fe(NO)(S_2MoS_2)_2]^{2-}$ in roughly equal abundance, and this solution was then titrated in the EPR spectrometer against a DMF solution of PhS^-. Initial aliquots of PhS^- caused the disappearance firstly of $[Fe(NO)_2(SBu^t)_2]^-$ and then of $[Fe(NO)(S_2MoS_2)_2]^{2-}$, followed upon further addition of PhS^-, by the appearance of $[Fe(NO)_2(SPh)_2]^-$. The two complexes initially present apparently reacted with PhS^- to yield EPR silent species, while further addition of PhS^- yielded the EPR active complex $[Fe(NO)_2(SPh)_2]^-$.

Whereas when R = alkyl, $[MoS_4]^{2-}$ competes effectively with RS^- for Fe coordination sites, when R = aryl, RS^- is the more effective ligand. Hence when R = alkyl, complexes (**2**) and (**3**) are generally dominant, but when R = aryl, complex (**1**) is dominant.

Reactions of $[Fe_4S_3(NO)_7]^-$

Addition of $[MoS_4]^{2-}$ to a DMF solution of $Na[Fe_4S_3(NO)_7]H_2O$ to give a 1 : 1 Mo : Fe ratio, yielded a very complex spectrum containing $[Fe(NO)(S_2MoS_2)_2]^{2-}$ and the known[1,6] complexes $[Fe(NO)_2(SH)_2]^-$ and $[Fe(NO)(SH)_3]^-$: $[Fe(NO)(SH)_3]^-$ has[6] $g = 2.020$ and $A(^{14}N) = 5.0$ G. The relative abundances of these three complexes were temperature dependent, varying widely as the temperature was raised from 220 to 320 K, but the changes were fully reversible when the temperature was lowered again to 220 K. At 220 K $[Fe(NO)_2(SH)_2]^-$ was most abundant and $[Fe(NO)(SH)_3]^-$ least: at 240 K, all three species were of similar abundance, but from 260 to 320 K, $[Fe(NO)(SH)_3]^-$ was the most abundant and $[Fe(NO)_2(SH)_2]^-$ the least. At 300 K and above $[Fe(NO)_2(SH)_2]^-$ was scarcely detectable, although it reverted to high abundance when the temperature was lowered to 220 K. Thus the net effect of increasing temperature appears to be to shift the equilibrium of eq. (3) to the right:

$$[Fe(NO)_2(SH)_2]^- \rightleftharpoons [Fe(NO)(SH)_3]^- \quad (3)$$

so providing another example of the very ready interconversion of $[Fe(NO)_2]^+$ and $[Fe(NO)]^{2+}$ fragments. It should be emphasized that with the Mo : Fe molar ratio at 1 : 1, the temperature variation of the EPR spectrum of the $[Fe_4S_3(NO)_7]^-/[MoS_4]^{2-}$ system was entirely reversible.

However when the Mo : Fe ratio was increased to 5 : 1 the effects observed on change of temperature are non-reversible. At 220 K, the EPR spectrum showed the same three species $[Fe(NO)(S_2MoS_2)_2]^{2-}$ (**3**), $[Fe(NO)_2(SH)_2]^-$ and $[Fe(NO)(SH)_3]^-$ as before, together with very weak indications of species (**4**) and (**5**). The spectral variation upon raising the temperature was such that at 320 K only (**3**), (**4**) and (**5**) were detectable. On reducing the temperature to 320 K only (**3**) was detectable and throughout a further temperature cycle 220 → 260 → 220 K, (**3**) was the sole complex detectable by EPR spectroscopy. Thus, as with $Fe_2(SR)_2(NO)_4$ as starting iron complex, so with $[Fe_4S_3(NO)_7]^-$, when high Mo : Fe ratios were employed the equilibria in solution shift so that $[Fe(NO)(S_2MoS_2)_2]^{2-}$ is the dominant paramagnetic species present. As usual,[1] $[Fe(NO)_2(SH)_2]^-$ is formed by attack of HS^- (from hydrolysis of $[MoS_4]^{2-}$) at the basal iron atoms in $[Fe_4S_3(NO)_7]^-$ and $[Fe(NO)(SH)_3]^-$ by attack at the apical iron: in both cases substitution occurs without change of the oxidation state at iron.

Reactions of $Fe_4S_4(NO)_4$

In contrast to the reactions of $Fe_2(SR)_2(NO)_4$ or $[Fe_4S_3(NO)_7]^-$ with $[MoS_4]^{2-}$, the reaction of $Fe_4S_4(NO)_4$ with $[MoS_4]^{2-}$ yielded EPR spectra which were essentially independent of the Mo : Fe ratio between 1 : 1 and 5 : 1.

Immediately after addition of $[MoS_4]^{2-}$ to a DMF solution of $Fe_4S_4(NO)_4$, a complex EPR spectrum appeared. Three species were present: (**3**), $[Fe(NO)_2(SH)_2]^-$ and a new mononitrosyl complex (**6**) characterized by $g = 2.023$, $A(^{14}N) = 13.5$ G, characteristic of a complex having a SOMO σ orbital along the Fe—N—O vector (see Discussion section, below). At 220 K the relative abundances were: $[Fe(NO)_2(SH)_2]^-$ > (**3**) ≃ (**6**): as the tem-

perature was raised the relative abundance of $[Fe(No)_2(SH)_2]^-$ diminished the fastest so that at 280 K the relative abundances were (3) > (6) > $[Fe(NO)_2(SH)_2]^-$, and at 300 K only (3) was detectable, accompanied by traces of (4) and (5). When the temperature was then cycled, thus: 300 → 230 → 300 → 230 K, complex (6) was the only species detectable. After heating to 350 K however and recooling to 220 K, only $[Fe(NO)_2(SH)_2]^{2-}$ remained, all other complexes presumably having undergone irreversible thermal decomposition above 300 K.

Reaction of $Fe_2I_2(NO)_4$

Finally, we have studied the reaction of $[MoS_4]^{2-}$ with $Fe_2I_2(NO)_4$, which, as we have shown[7] previously, reacts readily with sulphur-donor ligands via the intermediacy of mono-nuclear paramagnetic complexes.

A solution of $Fe_2I_2(NO)_4$ in DMF gives[7] a strong EPR spectrum showing the presence of $[Fe(NO)_2]^+$, $Fe(NO)_2I$ and $[Fe(NO)_2I_2]^-$, the first two of which are presumably solvated by DMF to give four-coordination. Upon addition of $[MoS_4]^{2-}$ such that the molar ratio of Mo : Fe was 1 : 1, the original EPR spectrum was immediately replaced, at 220 K, by a spectrum showing primarily (3), but with (2) and $[Fe(NO)_2(SH)_2]^-$ in lesser abundance. As the temperature was raised to 280 K, the relative abundance of (3) increased, although at 300 K the whole spectrum was very weak. On cooling from 300 to 220 K, only $[Fe(NO)_2(SH)_2]^-$ remained. As in the solution derived from $Fe_4S_4(NO)_4$, $[Fe(NO)_2(SH)_2]^-$ is the complex most robust at 300 K.

The EPR parameters of new complexes are collected in Table 1 and the reaction products are summarized in Table 2.

Table 1. EPR parameters of new complexes

Complex	g	$A(^{14}N)$ G^{-1}
$[Fe(NO)_2(S_2MoS_2)]^-$ (2)	2.027	2.0
$[Fe(NO)(S_2MoS_2)_2]^{2-}$ (3)	2.024	15.0
$[Fe(NO)_2(SPh)_2]^-$	2.027	2.5
$[Fe(NO)_2(SC_6H_4CH_3\text{-}p)_2]^-$	2.027	2.5
(4)	2.042	3.3
(5)	2.041	3.4
$[Fe(NO)(SH)_4]^{2-}$ (6)	2.023	13.5
$[Fe(NO)(SH)_3]^-$	2.020	5.0

DISCUSSION

The di-nuclear complex (2), $[Fe(NO)_2(S_2MoS_2)]^-$, is similar in stoichiometry to, but differs in redox level from, the diamagnetic di-anion $[Fe(NO)_2(S_2MoS_2)]^{2-}$ isolated[8] from the reaction $[Fe(S_2MoS_2)_2]^{2-}$ with NO gas, and characterized[8] by X-ray crystallography.

The tri-nuclear complex (3) $[Fe(NO)(S_2MoS_2)_2]^{2-}$, represents a further example of a trimetallic system containing "linear"[9] MoS_2Fe units. Complexes of this previously reported include the Mo—Fe—Fe type,[10] as in $[(S_2MoS_2)FeS_2Fe(SAr)_3]^{3-}$ and the Fe—Mo—Fe type,[11] as in $[Cl_2FeS_2MoS_2FeCl_2]^{2-}$: the present complex (3) contains a Mo—Fe—Mo system, $[(S_2MoS_2)Fe(NO)(S_2MoS_2)]^{2-}$, analogous to the W—Fe—W system[5] $[Fe(NO)(S_2WS_2)_2]^{2-}$.

The large difference in $A(^{14}N)$ values between (3) and $Fe(NO)(S_2CNMe_2)_2$ on the one hand ($A \sim 13$–15 G), and (2) and $[Fe(NO)_2(SR)_2]^-$ on the other ($A \sim 2$–4 G)[1] can be traced to the different forms of the SOMO in these complexes, as determined using EHMO calculations. In each of $Fe(NO)(S_2CNMe_2)_2$ and $[Fe(NO)(S_2MoS_2)_2]^{2-}$, containing square pyramidal $Fe(NO)S_4$ groups, the SOMO is of σ type and it lies along the linear Fe—NO bond, Fig. 1. In contrast, in $[Fe(NO)_2(SR)_2]^-$, of C_{2v} symmetry, the SOMO is

Table 2. Formation of paramagnetic iron nitrosyls from $[MoS_4]^{2-}$ and di- or tetra-iron nitrosyls[a]

	(1)	(2)	(3)	$[Fe(NO)_2(SH)_2]^-$	$[Fe(NO)(SH)_3]$	$[Fe(NO)(SH)_4]^-$
$Fe_2(S\text{-alkyl})_2(NO)_4$	+	+	+	−	−	−
$Fe_2(SPh)_2(NO)_4$	+	−	[b]	−	−	−
$Na[Fe_4S_3(NO)_7]\cdot H_2O$	−	−	+	+	+	−
$Fe_4S_4(NO)_4$	−	−	+	+	−	+[c]
$Fe_2I_2(NO)_4$	−	+	+	+	−	−

[a] All systems except $Fe_2I_2(NO)_4$ yielded also species (4) and (5) (see text).
[b] Trace only.
[c] Tentative assignment only.

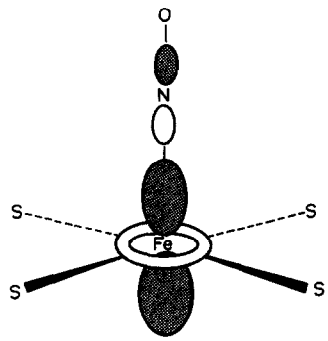

Fig. 1. The SOMO in the square pyramidal complexes $[Fe(NO)(SH)_4]^{2-}$, $Fe(NO)(S_2CNMe_2)_2$ and $[Fe(NO)(S_2MoS_2)_2]^{2-}$.

of b_2 symmetry and is of approximately π type with respect to the Fe—N bonds, Fig. 2. The poorer overlap in the SOMO of $[Fe(NO)_2(SR)_2]^-$ prevents spin density from reaching the nitrogens and this is the origin of the much reduced A value.

This simple connection between the $A(^{14}N)$ value and the form of the SOMO allows a more detailed consideration of the assignment of two families of paramagnetic mono-nitrosyl iron complexs observed in earlier work.[1,6] Reaction of *i*-PrSH with $Fe_2I_2(NO)_4$ in THF/Et_3N yields,[6] in addition to $[Fe(NO)_2(SPr^i)_2]^-$, a paramagnetic mono-nitrosyl characterized by $g = 2.040$ and $A(^{14}N) = 13.5$ G, but showing no hyperfine coupling to hydrogen in SR groups: similar species were obtained[1] from the reactions of $Fe_4S_4(NO)_4$ with SH^- or with *t*-BuS^-. The 13.5 G species were tentatively assigned[1,6] a constitution of type $[Fe(NO)(SR)_3]^{x-}$ where $x > 1$. From the foregoing discussion it is clear that these species, of whatever composition, must have a SOMO which is of a σ type along with Fe—N direction.

The second family of mono-nitrosyl complexes observed,[1] of type $[Fe(NO)(SR)_3]^-$, were obtained along with $[Fe(NO)_2(SR)_2]^-$ by reaction of RS^- with $[Fe_4S_3(NO)_7]^-$. If this reaction occurs without any change of oxidation state at iron, then $[Fe(NO)_2(SR)_2]^-$ arises from the basal $[Fe(NO)_2]^+$ groups in $[Fe_4S_3(NO)_7]^-$ and $[Fe(NO)(SR)_3]^-$ from the apical $[Fe(NO)]^{2+}$ group. The magnitude of $A(^{14}N)$ in the complexes $[Fe(NO)(SR)_3]^-$, ranging[1] between 3.9 and 5.0 G, strongly indicates a constitution having a SOMO which is of π type with respect to the Fe—N vector (in iron di-nitrosyl complexes having a π-type SOMO, the observed range of $A(^{14}N)$ is 2.0–6.0 G).

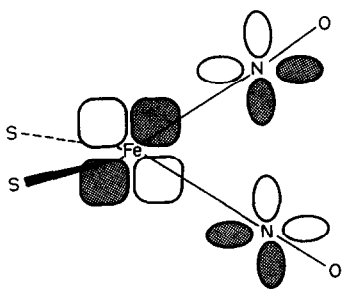

Fig. 2. The SOMO in complexes of types $[Fe(NO)_2(SR)_2]^-$ and $[Fe(NO)_2(S_2MoS_2)]^-$.

EHMO calculations on mononitrosyl complexes of the following constitutions: tetrahedral $[Fe(NO)(SR)_3]^-$, tetrahedral $[Fe(NO)(SR)_3]^{3-}$ and square-pyramidal $[Fe(NO)(SR)_4]^{2-}$ show that while in $[Fe(NO)(SR)_3]^-$ the SOMO is of π type in the Fe—N bond, it is of σ type in the other two complexes. The calculations thus support the assignment[1] of the constitution $[Fe(NO)(SR)_3]^-$ to the low $A(^{14}N)$ mononitrosyls, but cannot distinguish between $[Fe(NO)(SR)_3]^{3-}$ (as suggested earlier[1]) and $[Fe(NO)(SR)_4]^{2-}$ for the $g = 2.040$ complexes. The slow conversion,[1] in the presence of excess RS^-, of $[Fe(NO)(SR)_3]^-$ to the $g = 2.040$ species is perhaps more consistent with a redox reaction, yielding $[Fe(NO)(SR)_3]^{3-}$ and RSSR, than with a simple ligand addition to yield $[Fe(NO)(SR)_4]^{2-}$. If the $g = 2.040$ complexes having $A(^{14}N)$ of 13.5 are on this basis assigned the constitution $[Fe(NO)(SR)_3]^{3-}$, then complex (**6**), formed along with (**3**) and $[Fe(NO)_2(SH)_2]^-$ in the reaction of $[MoS_4]^{2-}$ with $Fe_4S_4(NO)_4$ and having $g = 2.023$ and $A(^{14}N) = 13.5$ G, may be tentatively assigned as square-pyramidal $[Fe(NO)(SH)_4]^{2-}$.

Complexes (**4**) and (**5**) which are formed in low abundance in almost all the systems described in this work, are each on the basis of the foregoing discussion a mononitrosyl species having a SOMO which is of π type with respect to the Fe—N bond, but having a g value rather higher than all other complexes listed in Table 1: these complexes remain at present unidentified, but the possibility that they are ologomeric cannot be excluded. Certainly neither can be assigned as NO, for which $A(^{14}N)$ is 10.6 G.[12]

CONCLUDING REMARKS

We have found ready routes to the formation of the paramagnetic iron nitrosyls (**2**) and (**3**), containing $Fe(\mu\text{-}S)_2Mo$ fragments: these may prove to be useful synthetic intermediates for the construction of diamagnetic oligonuclear mixed iron–molybdenum nitrosyls, analogous to $[Fe_4S_3(NO)_7]^-$ or $Fe_4S_4(NO)_4$.

EXPERIMENTAL

Literature methods were used for the preparation of $Fe_2(SR)_2(NO)_4$[13] and $(NH_4)_2[MoS_4]$:[14] ^{15}N labelled compounds [except for $Fe_2(S\text{-}CH_2Ph)_2(^{15}NO)_4$] were similarly prepared[13] using 99% $Na[^{15}NO_2]$ (MSD Isotopes). DMF of AnalaR quality was dried over barium oxide, distilled under reduction pressure and stored under dry nitrogen.

EPR spectra were measured, in 1 mm quartz capillaries, using a Bruker ER200D spectrometer: di-*t*-butyl nitroxide was used as the standard for the measurement of line positions and diphenyl picryl hydrazyl as the standard in the measurement of intensities. Spectral assignments were confirmed where necessary by the use of ^{15}N labelling: spectral parameters for new species are in Table 1.

Molecular orbital calculations employed the EHMO method.[15,16] Atomic parameters, for a basis set including *d* orbitals for S, Fe, and Mo, and *s* and *p* orbitals only for N and O, were as published.[17] Molecular geometries were based upon those observed[8,18-20] for $[Fe(NO)_2(S_2MoS_2)]^{2-}$, $[Fe(S_2MoS_2)_2]^{3-}$, $Fe(NO)(S_2CNMe_2)_2$ and $[Fe(NO)_2(SPh)_2]^-$.

Bis(μ-toluene-α-thiolato)bis[di(^{15}N*)nitrosyliron]*, $Fe_2(SCH_2Ph)_2(^{15}NO)_4$

$Fe_2(SCH_2Ph)_2(CO)_6$ (0.68 g, 1.3 mmol) was dissolved in DMF (30 cm^3) and $Na[^{15}NO_2]$ (0.50 g, 7.1 mmol) was added. The mixture was stirred at ambient temperature, under nitrogen, and the reaction was monitored by infrared spectroscopy. After 3 h toluene (500 cm^3) was added and the mixture was then filtered through Hyflo-supercel. The filtrate was evaporated to dryness and the residue was dissolved in CH_2Cl_2 (40 cm^3). This solution was washed with nitrogen-flushed distilled water (10×300 cm^3). The organic fraction was dried over Na_2SO_4, filtered and reduced to small volume: addition of an equal volume of ice-cold methanol precipitated the product (yield 40%). The compound was identified by ^1H NMR and by infrared spectroscopy: $\nu(^{15}NO)$ 1745, 1718 cm^{-1}.

Acknowledgement—We thank the Ministry of Agriculture, Fisheries and Food for financial support.

REFERENCES

1. A. R. Butler, C. Glidewell, A. R. Hyde and J. C. Walton, *Polyhedron* 1985, **4**, 797.
2. (a) J. C. Woolum and B. Commoner, *Biochim. Biophys. Acta* 1970, **201**, 631; (b) R. W. Chiang, J. C. Woolum and B. Commoner, *Biochim. Biophys. Acta* 1972, **257**, 452; (c) C. Nagata, Y. Ioki, M. Kodama, Y. Tagashira and M. Nakadate, *Ann. N.Y. Acad. Sci.* 1973, **222**, 1031; (d) A. F. Vanin and V. Ya. Varich, *Studia Biophys.* 1981, **86**, 177; (c) V. Ya. Varich and A. F. Vanin, *Biophysica* 1983, **28**, 1125.
3. A. R. Butler, C. Glidewell, A. R. Hyde and J. McGinnis, *Inorg. Chem.* 1985, **24**, 2931.
4. S.-S. Sung, C. Glidewell, A. R. Butler and R. Hoffmann, *Inorg. Chem.* 1985, **24**, 3856.
5. A. Müller, *Polyhedron* 1986, **5**, 319.
6. A. R. Hyde, Ph.D. Thesis, University of St Andrews, 1984.
7. A. R. Butler, C. Glidewell, A. R. Hyde and J. C. Walton, *Polyhedron* 1985, **4**, 303.
8. D. Coucouvanis, E. D. Simhon, P. Stremple and N. C. Baenziger, *Inorg. Chim. Acta* 1981, **53**, L135.
9. K. S. Bose, P. E. Lamberty, J. E. Kovacs, E. Sinn and B. A. Averill, *Polyhedron* 1986, **5**, 393.
10. B. K. Teo, M. R. Antonio, R. H. Tieckelmann, H. C. Silvis and B. A. Averill, *J. Am. Chem. Soc.* 1982, **104**, 6126.
11. D. Coucouvanis, N. C. Baenziger, E. D. Simhon, P. Stremple, D. Swenson, A. Simopoulos, A. Kostikas, V. Petrouleas and V. Papaefthymiou, *J. Am. Chem. Soc.* 1980, **102**, 1732.
12. R. Beringer and J. G. Castle, *Phys. Rev.* 1950, **78**, 581.
13. A. R. Butler, C. Glidewell, A. R. Hyde, J. McGinnis and J. E. Seymour, *Polyhedron* 1983, **2**, 1045.
14. S. H. Laurie, D. E. Pratt and J. H. L. Yong, *Inorg. Chim. Acta* 1984, **93**, L57.
15. R. Hoffmann, *J. Chem. Phys.* 1963, **39**, 1397.
16. J. Howell, A. Rossi, D. Wallace, K. Haraki and R. Hoffmann, QCPE No. 344.
17. (a) P. Kubaček, R. Hoffmann and Z. Havlas, *Organometallics* 1982, **1**, 180; (b) T. A. Albright, R. Hoffmann, J. C. Thibeault and D. L. Thorn, *J. Am. Chem. Soc.* 1979, **101**, 3801; (c) T. Hughbanks and R. Hoffmann, *J. Am. Chem. Soc.* 1983, **105**, 3528; (d) K. I. Goldberg, D. M. Hoffmann and R. Hoffmann, *Inorg. Chem.* 1982, **21**, 3863; (e) S. D. Wijeyesekera and R. Hoffmann, *Inorg. Chem.* 1983, **22**, 3287.
18. D. Coucouvanis, E. D. Simhon and N. C. Baenziger, *J. Am. Chem. Soc.* 1980, **102**, 6644.
19. G. R. Davies, J. A. J. Jarvis, B. T. Kilbourn, R. H. B. Mais and P. G. Owston, *J. Chem. Soc.* (*A*) 1970, 1275.
20. H. Strasdeit, B. Krebs and G. Henkel, *Z. Naturforsch.* 1986, **41B**, 1357.

Polyhedron Vol. 6, No. 12, pp. 2091–2094, 1987
Printed in Great Britain

0277–5387/87 $3.00+.00

ISOTOPIC EXCHANGE REACTIONS BETWEEN IRON–SULPHUR–NITROSYL CLUSTERS AND NITRITE

ANTHONY R. BUTLER, CHRISTOPHER GLIDEWELL* and IAN L. JOHNSON

Chemistry Department, University of St Andrews, St Andrews, Fife KY16 9ST, U.K.

(*Received* 26 *May* 1987; *accepted* 24 *June* 1987)

Abstract—The anion $[Fe_4S_3(NO)_7]^-$ undergoes slow exchange with labelled nitrite $[^{15}NO_2]^-$ to yield a product $[Fe_4S_3(^{14}NO)(^{15}NO)_6]^-$ in which complete isotopic exchange has occurred at the basal $Fe(NO)_2$ groups, but with no exchange at the apical Fe(NO) group. The neutral $Fe_4S_4(NO)_4$ reacts rapidly with $[^{15}NO_2]^-$ to give fully exchanged $[Fe_4S_3(^{15}NO)_7]^-$, and it is proposed that the conversion proceeds by fragmentation, followed by complete isotopic exchange and rapid reassembly. The binuclear anion $[Fe_2S_2(NO)_4]^{2-}$ also yields, with $[^{15}NO_2]^{2-}$ in CD_2Cl_2 solution, the fully exchanged $[Fe_4S_3(^{15}NO)_7]^-$, and a mechanism involving successive fragmentation, exchange and reassembly steps is proposed; however in aqueous solution, a clean exchange reaction occurs to give $[Fe_2S_2(^{15}NO)_4]^{2-}$. Neutral binuclear esters $Fe_2(SR)_2(NO)_4$ (R = Me, Et, or Ph) with $[^{14}NO_2]^-$ yield the mononuclear paramagnetic $[Fe(^{14}NO)_2(^{14}NO_2)_2]^-$, and with $[^{15}NO_2]^-$, the analogous $[Fe(^{15}NO)_2(^{15}NO_2)_2]^-$.

We have recently observed,[1] using ^{13}C and ^{15}N NMR spectroscopy, that the nitrosyl ligand in the nitroprusside anion $[Fe(CN)_5^{14}NO]^{2-}$ undergoes rapid and complete isotopic exchange with excess of labelled nitrite, $[^{15}NO_2]^-$. Similar rapid and complete isotopic exchange was observed[2,3] by EPR spectroscopy both for the neutral iron nitrosyl $Fe(NO)(S_2CNMe_2)_2$ and for the two series of anionic complexes $[Fe(NO)_2(SR)_2]^-$ and $[Fe(NO)(SR)_3]^-$, for R = H, Me, Et, *i*-Pr, *t*-Bu, and $PhCH_2$, where the facile replacement of the ligand ^{14}NO by ^{15}NO was of great value in making the assignment of the EPR spectra in the $[Fe(NO)_2(SR)_2]^-$ and $[Fe(NO)(SR)_3]^-$ series.[2,3] In addition, infrared spectroscopy has been used[4] to monitor the isotopic exchange reactions of *cis*- and *trans*-$Fe(NO)(NO_2)(S_2CNEt_2)_2$ with both ^{15}NO and $[^{15}NO_2]^-$. If general, such isotopic exchange reactions would, by removing the need for *de novo* synthesis of isotopically labelled complexes, greatly facilitate the NMR and EPR spectroscopy of metal nitrosyl systems.

We now report the results of a ^{15}N NMR study of the nitrosyl exchange reactions between nitrite and Roussin salts and esters, and some related metal cluster nitrosyls.

RESULTS AND DISCUSSION

$[Fe_4S_3(NO)_7]^-$ *and* $[Fe_4Se_3(NO)_7]^-$

The ^{15}N NMR spectrum of the isotopically labelled Roussin anion $[Fe_4S_3(^{15}NO)_7]^-$ in CD_2Cl_2 solution consists[1] of a singlet at $\delta = +7.7$, due to the apical nitrosyl ligand and an AX spectrum having δ_A +76.1, δ_X +36.0 and $J = 4.3$ Hz, due to the basal $Fe(NO)_2$ groups in which the axial and equatorial nitrosyl ligands are different and distinguishable:[5] we have never observed any exchange processes involving the nitrosyl groups in $[Fe_4S_3(^{15}NO)_7]^-$, either within the basal $Fe(NO)_2$ groups or between basal and apical nitrosyl ligands. When either $Na[Fe_4S_3(^{14}NO)_7]$ was mixed with $Na[^{15}NO_2]$ in D_2O solution or $(PNP)[Fe_4S_3(^{14}NO)_7]$ $[(PNP)^+ \equiv (Ph_3PNPPh_3)^+]$ was mixed with $(PNP)[^{15}NO_2]$ in acetone-d_6 solution such that the overall ratio $^{14}N:{}^{15}N$ was 1:5, no exchange was apparent within 4 h of mixing the solutions. After 3 days in aqueous solution, or 20 days in acetone solution, exchange of the basal nitrosyl ligands was complete, as judged by the

* Author to whom correspondence should be addressed.

sharp AX spectrum due to basal $Fe(^{15}NO)_2$ groups: residual $Fe(^{14}NO)(^{15}NO)$ groups would provide singlets rather than doublets at δ 76 and 36. However, despite the complete exchange of the basal ligands, no exchange at all was detectable for the apical nitrosyl ligand. These observations show that the apical Fe(NO) group, containing formally[6] d^7 Fe(I), undergoes exchange much more slowly than the basal $Fe(NO)_2$ groups which contain formally d^9 Fe(−I): attempts to monitor the exchange reaction of the apical ligands over longer periods of time than 20 days were not conclusive, as the $[Fe_4S_3(NO)_7]^-$ anion begins to decompose after long periods in solution, even under a dinitrogen atmosphere. These observations also confirm very elegantly the lack of exchange between basal and apical nitrosyl ligands.

For the selenium analogue $Na[Fe_4Se_3(NO)_7]$ of Roussin's black salt, we employed sodium salts in aqueous solutions, as these conditions had given the fastest exchange with $[Fe_4S_3(^{14}NO)_7]^-$: when saturated aqueous solutions of $Na[Fe_4Se_3(^{14}NO)_7]$ and $Na[^{15}NO_2]$ were mixed, no exchange at all was detectable after 1 h: the ^{15}N spectrum was monitored at intervals, but it was clear that the rate of decomposition of $Na[Fe_4Se_3(NO)_7]$ comfortably exceeded the rate of any exchange, and at no time did this mixed solution exhibit the characteristic[1] ^{15}N spectrum of the selenium anion $[Fe_4Se_3(^{15}NO)_7]^-$.

$Fe_4S_4(NO)_4$

The cubane-like cluster $Fe_4S_4(^{15}NO)_4$ exhibits[1] a single sharp resonance in its ^{15}N NMR spectrum, at δ 12.8 in CD_2Cl_2 solution. When a solution of $Fe_4S_4(^{14}NO)_4$ in CD_2Cl_2 was mixed with a $(PNP)[^{15}NO_2]$ solution, the ^{15}N NMR spectrum recorded immediately after mixing shows no labelled $Fe_4S_4(NO)_4$ at all, but rather the three chemical shifts characteristic of $[Fe_4S_3(^{15}NO)_7]^-$. When the overall ratio of $^{14}N:{}^{15}N$ was 1:1 the spectrum of the partially labelled $[Fe_4S_3(NO)_7]^-$ comprised three singlets, but when the $^{14}N:{}^{15}N$ ratio was 1:10 the full spectrum of $[Fe_4S_3(^{15}NO)_7]^-$ was observed. As in our previous observations[1,2] on isotopic exchange using $[^{15}NO_2]^-$, the exchange is an equilibrium which is forced effectively to the ^{15}N side by addition of sufficient $[^{15}NO_2]^-$.

The behaviour of $Fe_4S_4(NO)_4$ with nitrite is thus markedly different from that of $[Fe_4S_3(^{14}NO)_7]^-$. First there is a stoichiometric change from $Fe_4S_4(NO)_4$ to $[Fe_4S_3(NO)_7]^-$; secondly, the product has incorporated ^{15}NO ligands at all the sites, rather than at just the basal sites, as for preformed $[Fe_4S_3(^{14}NO)_7]^-$; finally, the overall exchange process is very much faster than in preformed $[Fe_4S_3(NO)_7]^-$. The stoichiometric change is equivalent to that effected by reduction[5,7] of $Fe_4S_4(NO)_4$, and we envisage the transformation of $Fe_4S_4(NO)_4$ to $[Fe_4S_3(NO)_7]^-$ as proceeding via electron transfer[7] leading to cluster fragmentation followed by rapid spontaneous self assembly. If the initial cluster undergoes fragmentation into mono-iron complexes, as occurs with other nucleophiles,[2,6] then the known[2] rapid nitrosyl mobility in $[Fe(NO)]^{2+}$ and $[Fe(NO)_2]^+$ fragments is sufficient to explain our observations on the reaction between $Fe_4S_4(NO)_4$ and $(PNP)[^{15}NO_2]$. It is necessary for the exchange of ^{14}NO ligands with $[^{15}NO_2]^-$ to occur before rather than after the self-assembly process to give $[Fe_4S_3(NO)_7]^-$ in order to rationalize both the rate of the exchange process and the completeness of substitution in the final product $[Fe_4S_3(^{15}NO)_7]^-$.

$[Fe_2S_2(NO)_4]^{2-}$

The red Roussin anion $[Fe_2S_2(NO)_4]^{2-}$ has been characterized[8] by X-ray methods as its $(Me_4N)^+$ salt, in which it has approximately D_{2h} symmetry. The nucleophilic reactivity of the sodium salt in THF solution has also been investigated.[9] In previous work, we observed[1] that analytically pure samples of $(PNP)_2[Fe_2S_2(^{15}NO)_4]$ were rapidly and cleanly converted, in CD_2Cl_2 solution, to $[Fe_4S_3(^{15}NO)_7]^-$ as the only species detectable by ^{15}N NMR spectroscopy. We have now observed that analytically pure $(Et_4N)_2[Fe_2S_2(^{14}NO)_4]$ cleanly undergoes conversion, with $(PNP)[^{15}NO_2]$ in CD_2Cl_2 to $[Fe_4S_3(^{15}NO)_7]^-$, again as the sole product detectable by ^{15}N NMR. Because of the complete isotopic substitution in $[Fe_4S_3(NO)_7]^-$, including the apical nitrosyl ligand, the mechanism for conversion of $[Fe_2S_2(NO)_4]^{2-}$ to $[Fe_4S_3(NO)_7]^-$ probably again involves fragmentation followed by isotopic exchange and finally by spontaneous self-assembly to give the product $[Fe_4S_3(NO)_7]^-$.

However, despite the facile conversion of $[Fe_2S_2(NO)_4]^{2-}$ to $[Fe_4S_3(NO)_7]^-$ in CD_2Cl_2, we have found that reaction of a 2% aqueous solution of $Na_2[Fe_2S_2(^{14}NO)_4]$ with $Na^{15}NO_2$, such that $^{14}N:{}^{15}N$ is 1:10 gives a single sharp resonance, in addition to excess $^{15}NO_2^-$, at δ +37.8, identical with that observed for preformed $Na_2[Fe_2S_2(^{15}NO)_4]$. There was no sign of the characteristic spectrum of $[Fe_4S_3(NO)_7]^-$ nor, in contrast to the behaviour of neutral di-iron complexes $Fe_2(SR)_2(NO)_4$ (see below), was there any evidence for the formation of appreciable concentrations of paramagnetic intermediates.

$Fe_2(SR)_2(NO)_4$

When either of the neutral Roussin esters $Fe_2(SEt)_2(NO)_4$ and $Fe_2(SPh)_2(NO)_4$ was mixed with (PNP)[$^{15}NO_2$] in CD_2Cl_2 solution, the resulting ^{15}N NMR spectrum exhibited only very broad unresolved absorptions, suggestive of the presence of persistent paramagnetic species. This was confirmed by EPR spectroscopy. Reaction of $Fe_2(SR)_2(^{14}NO)_4$ (R = Me, Et or Ph) with (PNP)[$^{14}NO_2$] in CH_2Cl_2 solution gave a strong EPR spectrum, characterized by $g = 2.036$, $A(^{14}N) = 6.5$ G (2N), 2.2 G (2N); the spectral assignment was confirmed by use of $Fe_2(SCH_3)_2(^{15}NO)_4$ and (PNP)[$^{15}NO_2$]. The simplest system which contains two equivalent nitrogen ligands of one type, and two others of a second type is $[Fe(NO)_2(NO_2)_2]^-$, formed as in eq. (1):

$$Fe_2(SR)_2(NO)_4 + 4NO_2^- \rightarrow 2RS^- + 2[Fe(NO)_2(NO_2)_2]^- \quad (1)$$

This is an example of a more general reaction of Roussin esters with nucleophilic anions, eq. (2):

$$Fe_2(SR)_2(NO)_4 + 4X^- \rightarrow 2RS^- + 2[Fe(NO)_2X_2]^- \quad (2)$$

This has been observed both for X = R'S,[2] and for a wide range of other nucleophiles.[10]

At low temperatures (220 K in DMF or 190 K in acetone) the EPR spectrum of $[Fe(NO)_2(NO_2)_2]^-$ showed two A values, as noted above. However upon raising the temperature by 20–30 K, the g value remained unchanged but the spectrum showed a symmetric pattern of nine lines with mean A value of 4.3 G. This indicated that all the nitrogen nuclei had become equivalent, with an A value which is the average of the two A values (6.5 G and 2.2 G) observed at low temperature, and was thus consistent with a rapid scrambling of the NO and NO_2 ligands, as indicated schematically in eq. (3).

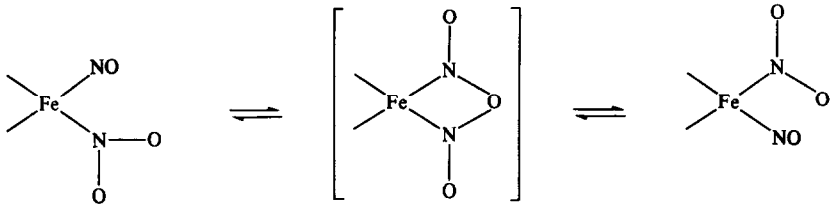

(3)

Such an exchange process can account for the formation of $[Fe(^{15}NO)_2(^{15}NO_2)_2]^-$ from $Fe_2(SR)_2(^{14}NO)_4$ and $[^{15}NO_2]^-$.

Mononuclear iron-nitrosyls

We have noted previously[2] the rapid exchange between $Fe(^{14}NO)(S_2CNMe_2)_2$ and $[^{15}NO_2]^-$, observed by EPR spectroscopy. We have now observed using ^{15}N NMR spectroscopy, rapid exchange between $[^{15}NO_2]^-$ and $Fe(^{14}NO)(^{14}NO_2)(S_2CNMe_2)_2$. Reaction of (PNP)[$^{15}NO_2$] with *cis*-$Fe(^{14}NO)(^{14}NO_2)(S_2CNMe_2)_2$ in CD_2Cl_2 solution with an overall ratio $^{14}NO_x$: $^{15}NO_x$ of 1 : 5 gave two sharp singlets in the ^{15}N spectrum at δ +84.7 and −27.1: we assign these respectively to $^{15}NO_2$ and ^{15}NO ligands in *cis*-$Fe(^{15}NO)(^{15}NO_2)(S_2CNMe_2)_2$. Even after one day at normal temperature, when full equilibration of ^{15}N between the NO and NO_2 ligands should be complete (the half-life for exchange between these ligand at 295 K in $CHCl_3$ solution is less than 1 h[4]), no $^2J(^{15}NFe^{15}N)$ coupling between the ^{15}NO and $^{15}NO_2$ ligands could be resolved. Under the conditions of our experiments, *trans*-$Fe(^{14}NO)(^{14}NO_2)(S_2CNMe_2)_2$ was converted to the *cis*-isomer too rapidly for its exchange reaction with $[^{15}NO_2]^-$ to be studied.

The mononuclear salt (PNP)[$Fe(CO)_3(^{15}NO)$], for which δ is +15.2 in 2% solution in CD_2Cl_2 underwent complete exchange within 3 h with a tenfold molar excess of (PNP)[$^{14}NO_2$]. Whereas the exchange is fast[1] for $[Fe(CN)_5NO]^{2-}$, the corresponding ruthenium analogue $[Ru(CN)_5NO]^{2-}$ showed no rapid exchange.

EXPERIMENTAL

Literature methods were employed for the preparation of (PNP)[$^{15}NO_2$][11] [$(PNP)^+ \equiv (Ph_3PNPPh_3)^+$], (PNP)[$Fe(CO)_3NO$],[11] $Na_2[Fe_2S_2(NO)_4]$, $Na[Fe_4S_3(NO)_7]$,[12] (PNP)[$Fe_4S_3(NO_7)$],[13] $Na[Fe_4Se_3(NO)_7]$,[13] $Fe_4S_4(NO)_4$,[1,7] $Fe_2(SR)_2(NO)_4$[1,13] and $Fe(NO)(NO_2)(S_2CNMe_2)_2$.[4,14] Isotropically labelled materials where required were prepared by appropriate modifications[1] of these procedures, using Na[$^{15}NO_2$] (99% enriched, MSD Isotopes) as a source of ^{15}N. $(Et_4N)_2[Fe_2S_2(NO)_4]$, prepared[8] by reaction of $(Et_4N)OH$ with $Na[Fe_4S_3(NO)_7]$ had C, 34.1; H, 7.2; N, 14.9%: $(Et_4N)_2[Fe_2S_2(NO)_4]$, $C_{16}H_{40}Fe_2N_6O_4S_2$ requires C, 34.5; H, 7.2; N, 15.1%; $(Et_4N)[Fe_4S_3(NO)_7]$, $C_8H_{20}Fe_4N_8O_7S_3$ requires C, 14.6; H, 3.1; N, 17.0%.

All ^{15}N NMR spectra were recorded at 36.51 MHz and 25°C relative to external $CH_3{}^{15}NO_2$ using the Bruker WH-360 spectrometer of the SERC

regional NMR service at the University of Edinburgh: spectral parameters were as described previously.[1] All spectra were recorded using 1% or 2% *w/w* solutions in the appropriate solvent (D_2O, $(CD_3)_2CO$, or CD_2Cl_2).

EPR spectra were recorded in 1 mm quartz capillaries using a Bruker ER200D spectrometer, with di-*t*-butyl nitroxide as the standard for the measurement of line positions.

Acknowledgement—We thank the Ministry of Agriculture, Fisheries and Food for financial support, and Dr D. Reed for help in obtaining the ^{15}N NMR spectra.

REFERENCES

1. A. R. Butler, C. Glidewell, A. R. Hyde and J. McGinnis, *Inorg. Chem.* 1985, **24**, 2931.
2. A. R. Butler, C. Glidewell, A. R. Hyde and J. C. Walton, *Polyhedron* 1985, **4**, 797.
3. A. R. Hyde, Ph.D. Thesis, St Andrews (1984).
4. O. A. Ileperuma and R. D. Feltham, *J. Am. Chem. Soc.* 1976, **98**, 6039.
5. C.T.-W. Chu and L. F. Dahl, *Inorg. Chem.* 1977, **16**, 3245.
6. S.-S. Sung, C. Glidewell, A. R. Butler and R. Hoffmann, *Inorg. Chem.* 1985, **24**, 3856.
7. C.T.-W. Chu, F. Y.-K. Lo and L. F. Dahl, *J. Am. Chem. Soc.* 1982, **104**, 3409.
8. Lin Xian-ti, Zheng An, Lin Shan-huo, Huang Jinling and Lu Jia-xi, *J. Struct. Chem.* (*Wuhan*) 1982, **1**, 8.
9. D. Seyferth, M. K. Gallagher and M. Cowie, *Organometallics* 1986, **5**, 539.
10. A. R. Butler, C. Glidewell and I. L. Johnson, to be published.
11. R. E. Stevens and W. L. Gladfelter, *Inorg. Chem.* 1983, **22**, 2034.
12. G. Brauer, *Handbuch der Präparativen Anorganischen Chemie* 2nd Edn, Vol. II. F. Enke, Stuttgart (1960).
13. A. R. Butler, C. Glidewell, A. R. Hyde, J. McGinnis and J. E. Seymour, *Polyhedron* 1983, **2**, 1045.
14. H. Büttner and R. D. Feltham, *Inorg. Chem.* 1972, **11**, 971.

Polyhedron Vol. 6, No. 12, pp. 2095–2098, 1987
Printed in Great Britain

0277–5387/87 $3.00+.00

STUDIES ON THE CHELATION OF ALUMINIUM FOR BIOLOGICAL APPLICATION—IV. AMP, ADP AND ATP

GRAHAM E. JACKSON* and KUKU V. VOYI

Department of Inorganic Chemistry, Rondebosch 7700, South Africa

(*Received* 28 *April* 1987; *accepted* 10 *July* 1987)

Abstract—Aluminium complexes of AMP, ADP and ATP have been studied at 25°C and an ionic strength of 0.15 mol dm^{-3}, using glass electrode potentiometry. A novel formation function has been used as an aid to the interpretation of the data. For the Al^{3+}/ADP system the major species formed, under the experimental conditions, was ML, while for the Al^{3+}/ATP system the MLH species predominated.

Aluminium is one of the most abundant elements in the earth's crust and its uptake by plants is determined by the pH of the soil, being high in acidic and low in alkaline soil.[1] Aluminium in its pure metallic state is highly reactive but quickly becomes coated with a passive oxide layer. In aluminium cooking utensils this amphoteric layer is solubilized by various foodstuffs.[2] Aluminium compounds are also additives in many common household products. Despite a high dietary intake of aluminium it is of limited toxicity.[3] The reasons for this are two fold (i) the insolubility of its metal hydroxides and (ii) its very high affinity for membrane phosphates.

Notwithstanding the relatively low toxicity of aluminium, this metal-ion has been implicated in "dialysis dementia",[4] phosphate depletion syndrome,[5] Alzheimers disease,[6,7] decreased serum adenosine triphosphate levels[8] and increased prothrombrin times.[9] More recently aluminium(III) has been found to inhibit cholinergic enzyme acetylcholinesterase[10] and influence the activity of a range of phosphatase enzymes.[11,12,13]

In the light of the biomedical interest in aluminium(III) and in particular its interaction with biological phosphates, we have studied, using glass electrode potentiometry, the Al^{3+}, AMP, ADP and ATP systems.

EXPERIMENTAL

Solutions were prepared using distilled deionized and degassed water. All titrations were carried out under an atmosphere of nitrogen which had been successively washed in 15 g of 1,2,3-trihydroxybenzene in 100 cm^3 of 30% KOH, 50% KOH and 150 mmol dm^{-3} NaCl. The ionic strength was maintained at a chloride concentration of 150 mmol dm^{-3} using NaCl. Aluminium stock solutions were prepared from $AlCl_3 \cdot 6H_2O$ and standardized by complexometric titration using EDTA[14] and by a Gran plot[15] for hydrogen ion concentration. NaOH solutions (100 mmol dm^{-3}) were prepared weekly from standard ampoules, under nitrogen and standardized using potassium hydrogen phthalate.

AMP, ADP and ATP (Sigma Chemical Co.) were used without purification. In order to avoid hydrolysis prior to potentiometric measurements, samples of the nucleotides were weighed out as the solid and added to the reaction vessel just prior to performing the titration. The titrations were performed in a double walled vessel, thermostated at 25°C. Potentiometric measurements were made on a Radiometer PHM84 research pH meter equipped with a Metrohm glass electrode and a Ag/AgCl reference electrode with a renewable liquid junction of 150 mmol dm^{-3} NaCl. Because of the relatively slow kinetics of aluminium(III) complexation reactions, data were only collected once an emf drift of

*Author to whom correspondence should be addressed.

<0.1 mV min^{-1} was established. The data were analysed using the computer program ESTA.[16]

RESULTS AND DISCUSSION

Adenosine-5′-monophosphate

AMP shows two protonation constants, both of which are assigned to the phosphate group. The experimental values compare well with the literature considering the different conditions under which they were obtained. Attempts to measure formation constants for the Al^{3+}–AMP system failed. Under the conditions used in this study no metal complexes were detected before the onset of precipitation. This was so even at a ligand to metal ratio of 7 : 1.

Adenosine-5′-diphosphate

ADP has three protonation sites, of which only two could be titrated above pH 2.0. Agreement with the literature is fair as far as pK_{a2} is concerned (3.81 and 3.93[17]) but poor with respect to pK_{a1}. The concentration of the ligand was kept low to avoid any ring stacking which might occur.[18] The objective function is low, with good statistical agreement between the calculated and experimental results.

Figure 1(a) shows the formation curves for the Al^{3+}/ADP system at different ligand to metal ratios. These are somewhat unusual and require some comment. The horizontal region of the curve from pA 4–7 is an indication of the presence of a ML species. Clearly this is present even at the start of the titration. Below pA = 4, the formation curves begin to fan out, indicating the formation of hydroxy species.

Inspection of the deprotonation curves [Fig. 1(b)] shows that from pH 2.5–5.0, the average number of protons on the complex is zero. Above pH = 5.0 hydroxy species are formed with a final stoichiometry at pH 7 of MLOH. Both these conclusions are consistent with the observations made

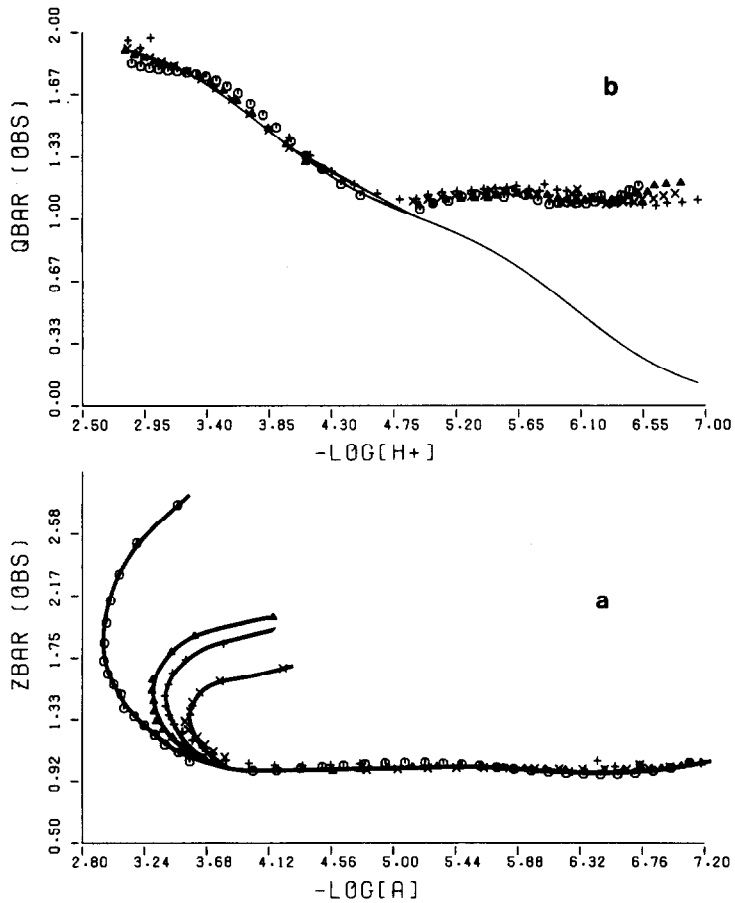

Fig. 1. (a) Experimental formation curves of $\bar{Z}$ vs $-\log$ (free ligand) for the aluminium(III) ADP system at 25°C and 0.15 mol dm^{-3} (Na)[Cl]. The full line represents the theoretical curve obtained using the formation constants given in Table 1. (b) Experimental deprotonation curves of $\bar{Q}$ vs pH. The full line represents the $\bar{n}$ function. ADP : AL^{3+} ratios: 0.0071 : 0.0024, 0.0078 : 0.0038, 0.0081 : 0.0042, 0.0081 : 0.005.

from the formation function. The final set of constants refined from these data are presented in Table 1. In this case, while the standard deviation in the beta values and also the objective function are very good, the statistical R factor is relatively high. The agreement between the theoretical and experimental formation function show this model to be a reasonable description of the data.

Adenosine-5′-triphosphate

This ligand has four protonation sites. Only two have been titrated in this study. The constants obtained after ESTA[16] refinement of the data are presented in Table 1, together with relevant literature values. Once again the agreement is not good. The most likely reason for this discrepancy is the different ionic medium used in the two studies. However, because the theoretical and experimental curves are superimposable and also because the statistical analysis of the data is so good, we have confidence in our results. The pK_a's of the third and fourth protonation sites are below the range (i.e. pH 2.0) of the glass electrode and so could not be determined.

The aluminium formation curves are presented in Fig. 2(a). These are not easily interpreted, but suggest the formation of MLH at pA = 7, followed by deprotonation to ML at pA = 3. The deprotonation function [Fig. 2(b)] is more easily interpreted. At the start of the titration (pH 2.0) $\bar{Q} = 1$ and $\bar{n} = 2$, which implies a stoichiometry of MLH. As the pH is raised deprotonation occurs until at pH 5.0, $\bar{Q} = \bar{n} = 1$ and ML is the major species in solution. Notwithstanding the fact that the presence of only two main species is indicated by the formation function, numerous other species were tested for, using the BETA task of ESTA.[16] No significant improvement in the model was achieved by the inclusion of any of these species and so the simplest model was chosen. The final results obtained are given in Table 1.

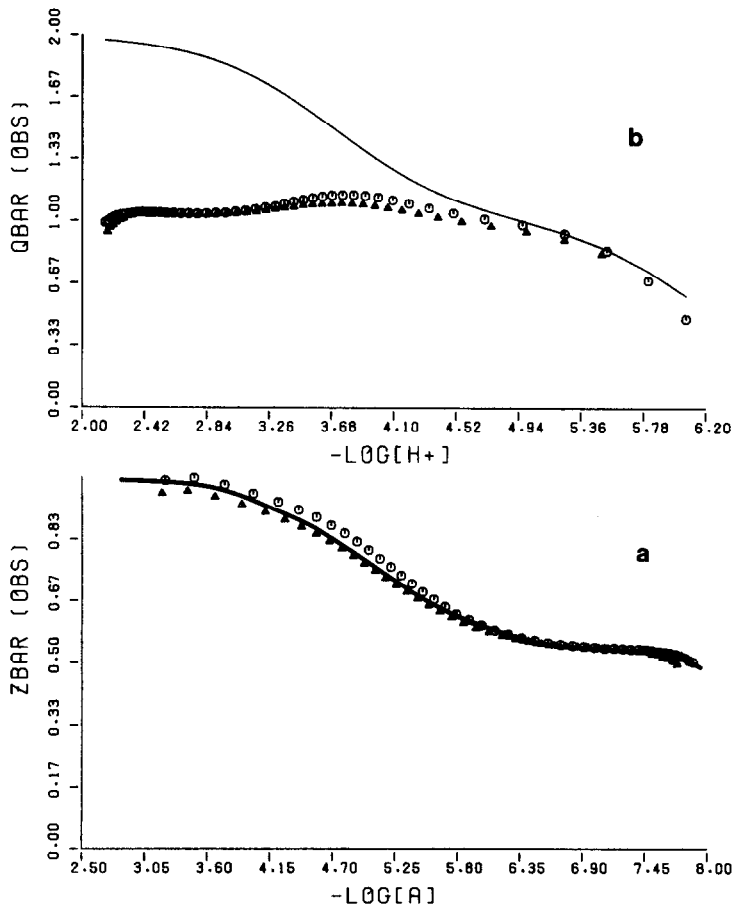

Fig. 2. (a) Experimental formation curves of $\bar{Z}$ vs $-\log$(free ligand) for the aluminium(III) ATP system at 25°C and 0.15 mol dm^{-3} (Na)[Cl]. The full line represents the theoretical curve obtained using the formation constants given in Table 1. (b) Experimental deprotonation curves of $\bar{Q}$ vs pH. The full line represents the $\bar{n}$ function. For clarity only selected points have been plotted.

Table 1. Log β for the species $A_pB_qH_r$ at 25°C and $I = 0.150$ M NaCl. A = ligand, B = Al^{3+}, H = H^+, R = crystallographic R factor and U = ESTA objective function

p	q	r	log β	Lit.[17]	R	U	pH	range
AMP								
1	0	1	6.04(2)	6.21	0.002	2.5	2.0	7.8
1	0	2	9.77(3)	10.02				
ADP								
1	0	1	6.08(6)	6.40	0.007	30.0	2.0	6.8
1	0	2	9.89(7)	10.36				
1	1	0	10.03(2)		0.012	18.9	2.5	7.0
1	1	−1	4.18(4)					
ATP								
1	0	1	6.24(4)	6.53	0.009	10.9	2.0	6.0
1	0	2	9.94(6)	10.59				
1	1	1	12.47(3)					

Standard deviations in log β are given in parentheses.

Of the three ligands examined in this study, AMP was found to form very weak complexes with aluminium(III). Similar results have been found for other metal ions,[17] where the AMP complexes are considerably less stable than the corresponding ADP and ATP complexes. In this case the AMP complex is so weak that hydrolysis of the aluminium occurs before complexation.

The structure of the Al^{3+}/ATP complex has been studied by NMR[19] and the metal found to coordinate to the β and γ phosphates. The effect of Mg^{2+} on the ^{31}P nmr spectrum of ATP is not as simple but coordination to α and β phosphates is postulated.[20] These observations are consistent with our observation that the Al^{3+}/ADP complex is more stable than the corresponding ATP complex, while the Mg^{2+}/ATP complex is more stable (log $K = 4.22$) than the Mg^{2+}/ADP complex−(log $k = 3.17$).[21] In conclusion the Al^{3+}, ADP and ATP complexes are fairly stable and hence it is very possible that aluminium exerts its pathological potential via coordination to one of these high energy phosphates.

Acknowledgements—We gratefully acknowledge the award of an AECI Fellowship to K.V.V. and research grants from the University of Cape Town and the CSIR.

REFERENCES

1. C. R. Lee, *Agron. J.* 1971, **63**, 363.
2. G. A. Trapp and J. B. Cannon, *N. Engl. J. Med.* 1981, **304**, 172.
3. J. Sorenson, *Environ. Health Perspectives* 1971, **8**, 3.
4. J. J. Ferera, *J. Am. Med. Technol.* 1980, **42**, 342.
5. I. S. Parkinson, M. K. Ward, T. G. Feest, R. W. P. Fawcett and D. N. S. Kerr, *Lancet* 1979, 406.
6. U. de Boni, A. Otvos, J. Scott and D. Crapper, *Acta Neuropathol.* 1976, **35**, 285.
7. D. B. Perl and A. R. Brody, *Science* 1980, **208**, 297.
8. M. Lotz, E. Zisman and F. C. Bartter, *N. Engl. J. Med.* 1968, **228**, 409.
9. D. Waldron-Edwards, P. Chan and S. C. Skoryna, *Can. Med. Assoc. J.* 1978, **105**, 1297.
10. J. K. Marquis and A. J. Lerrick, *Biochem. Pharmacol.* 1982, **31**, 1437.
11. J. Bigay, P. Deterre, C. Pfister and M. Chabre, *FEBS Lett.* 1985, **191**, 181.
12. A. J. Lange and W. J. Arion, *J. Biol. Chem.* 1986, **261**, 101.
13. P. F. Blackmore, S. B. Bocckino, L. E. Waynick and J. H. Exton, *J. Biol. Chem.* 1985, **260**, 14477.
14. A. I. Vogel, *A Text-Book of Quantitative Inorganic Analysis*. Longman, London (1961).
15. G. Gran, *Analyst* 1952, **77**, 661.
16. K. Murray and P. M. May, ESTA. Equilibrium simulation for titration analysis. UWIST, Cardiff (1984).
17. A. E. Martell and R. E. Smith, *Critical Stability Constants*. Plenum Press, New York (1974).
18. S. S. Danyluk and F. E. Hvuska, *Biochemistry* 1968, **7**, 1038.
19. J. L. Bock and D. E. Ash, *J. Inorg. Biochem.* 1980, **13**, 105.
20. F. Ramirez and J. F. Marecek, *Biochim. Biophys. Acta* 1980, **21**, 589.
21. M. M. Taqui Khan and A. E. Martell, *J. Am. Chem. Soc.* 1967, **87**, 5585.

Polyhedron Vol. 6, No. 12, pp. 2099–2102, 1987
Printed in Great Britain

0277–5387/87 $3.00+.00

LIQUID–LIQUID EXTRACTION OF TRIVALENT ACTINIDES AND LANTHANIDES WITH 1-PHENYL-3-METHYL-4-TRIFLUOROACETYL PYRAZOLONE-5

J. N. MATHUR and P. K. KHOPKAR*

Radiochemistry Division, Bhabha Atomic Research Centre, Trombay, Bombay 400085, India

(*Received* 5 *March* 1987; *accepted* 24 *June* 1987)

Abstract—Extraction of the trivalent actinides Am, Cm and Cf and lanthanides Eu, Tb, Tm and Lu has been studied with 1-phenyl-3-methyl-4-trifluoroacetyl pyrazolone-5(HPMTFP) in chloroform and benzene. The formation of a self-adduct species $M(PMTFP)_3 \cdot HPMTFP$ has been observed with Am, Cm and Eu but only the chelate species $M(PMTFP)_3$ with Cf, Tb, Tm and Lu. The reasons for the formation of a self-adduct species with lighter actinides and lanthanides and not with the heavier ones of the pyrazolones have been discussed.

The extraction of trivalent actinides and lanthanides with β-diketones alone as well as their mixtures with neutral donors has been a subject of great interest.[1–3] A new class of extractants namely 1-phenyl-3-methyl-4-acyl (or aroyl) pyrazolone-5 has found varied applications in the extraction and separation of trivalent metal ions from acidic solutions due to the lower pK_a values of the pyrazolones as compared to those of other β-diketones.[4–9] Freiser *et al.*[6] studied the extraction of lanthanides by pyrazolones having decanoyl or substituted benzoyl (in the 4-position) groups. In a recent study[7] they have used halogen substituted 4-acyl-pyrazolones for the uptake of the lanthanides. Among the halogen substituted pyrazolones, 1-phenyl-3-methyl-4-trifluoroacetyl pyrazolone-5 (HPMTFP) is of particular interest since it has a reasonably low pK_a value (2.73) and extracts the trivalent metal ions from acidic solutions in a much better way as compared to 1-phenyl-3-methyl-4-benzoyl pyrazolone-5 (HPMBP) (pK_a 4.01). In earlier studies we have examined the extraction behaviour of trivalent actinides and lanthanides with HPMBP and 1-phenyl-3-methyl-4-(3 : 5-dinitrobenzoyl) pyrazolone-5 (HDMPP).[8–10] The present study deals with the extraction of trivalent Am, Cm, Cf, Eu, Tb, Tm and Lu with HPMTFP in chloroform and benzene.

EXPERIMENTAL

The tracer solutions of ^{241}Am, ^{244}Cm, Cf (mainly ^{252}Cf), $^{152,154}Eu$, ^{160}Tb, ^{170}Tm and ^{177}Lu were prepared and assayed as described earlier.[11,12] HPMTFP in the keto from (m.p. 144°C) was prepared in this laboratory by the procedure described by Jensen.[13] Chloroform, benzene and the other chemicals used were of A.R. grade. The experimental details of HPMTFP and pH variations were as given in Ref. 9 with an exception that the solutions had to be shaken vigorously (0.5 h) on a wrist shaker and then slow rotation (2 h) as against 1 h slow rotation for the attainment of equilibrium.

RESULTS AND DISCUSSION

In earlier solvent extraction studies with HPMBP and HDMPP[5,8–10] it was observed that equilibrium is attained in 1 h by slow rotation in a thermostated bath, but in the present study with HPMTFP it was not attained even after 2 h. However, equilibrium was attained when the tubes were vigorously shaken for 0.5 h on a wrist shaker and then by slow rotation for 2 h. Freiser *et al.*[7] while using HPMTFP for the extraction of trivalent lanthanides found it necessary to use vigorous shaking for 1 h in order to attain

* Author to whom correspondence should be addressed.

Table 1. Absorption spectra of HPMTFP as a function of time in chloroform and benzene

Time elapsed	Chloroform Main peak (nm)	Chloroform O.D.	Benzene Main peak (nm)	Benzene O.D.
0.00 h	~ 406	No peak detected	~ 406	No peak detected
4.00 h	406	0.211	406	0.208
23.00 h	411	0.346	413	0.329
28.00 h	412	0.383	414	0.383
4 days	412	0.409	413	0.398
5 days	411	0.411	413	0.364
7 days	411	0.411	413	0.351

equilibrium, whereas with 8-hydroxyquinoline only 0.5 h was sufficient for the same.[14] It is probable that in the HPMTFP systems (similar to the thenoyltrifluoroacetone (HTTA) systems[15]) the keto–enol equilibrium is attained rather slowly. A vigorous and longer shaking probably helps to attain the equilibrium in a comparatively shorter time. The results of absorption spectral studies of HPMTFP dissolved in chloroform and benzene (0.02 M) using a Beckman DU-7 spectrophotometer are given in Table 1. Absence of any peak at 406 nm in the beginning and its subsequent appearance and gradual increase in intensity may be taken as an indication of the slow attainment of the keto–enol equilibrium and is probably one of the reasons for the longer and more vigorous shaking required to reach an equilibrium in this system.

Figure 1 gives the plots of log D (distribution coefficient) vs log[HPMTFP] in chloroform and benzene for different actinides and lanthanides at pH 2.70. In this range of HPMTFP concentration (0.01–0.02 M) straight lines with a slope of 4 are obtained for Am, Cm and Eu and only of 3 for Cf, Tb, Tm and Lu. The lower slope of 3 observed in such plots for heavier actinides and lanthanides (smaller ionic radii) could possibly have arisen due to the increased hydrolysis of these metal ions as was observed earlier in *N*-benzoyl-*N*-phenyl hydroxylamine-trivalent metal ion systems at pH 4.5.[16] The HPMTFP variation experiments carried out with Lu(III) (smallest ionic radius) in the same concentration range of HPMTFP but at a lower pH of 2.03 (HCl) giving a straight line with a slope of 3 only (Fig. 1 lower Lu curve) completely ruled out the possibility of hydrolysis at pH 2.70. Figure 2 shows the plots of log D vs pH at a fixed HPMTFP concentration (0.02 M) in both the diluents. The straight lines with a slope of 3 suggest an inverse third power dependence on the $[H^+]$ for all the

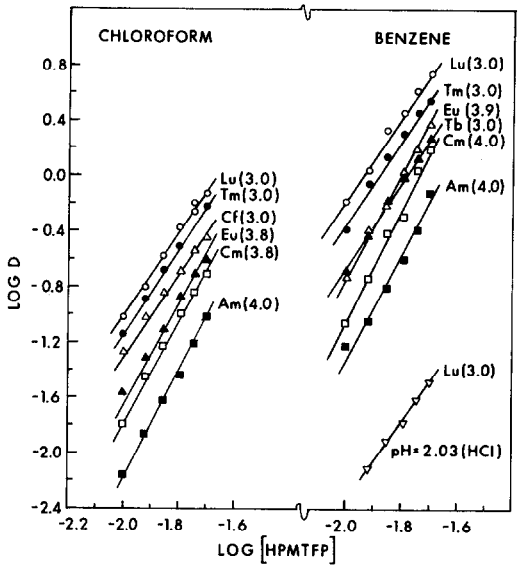

Fig. 1. Variation of log D of trivalent actinides and lanthanides as a function of HPMTFP concentration. Aqueous phase: pH 2.70 (0.01 M chloroacetate buffer containing 0.1 M $NaClO_4$) in all systems except the lower curve for Lu having pH 2.03 (HCl). Org. phase: 0.01–0.02 M, HPMTFP in chloroform or benzene.

metal ions. The extraction equilibria may, therefore, be represented either by the adduct formation mechanism:

$$M^{3+}_{aq} + 4HPMTFP_{org} \rightleftharpoons M(PMTFP)_3 \cdot HPMTFP_{org} + 3H^+_{aq} \quad (1)$$

where M = Am, Cm or Eu, or by a simple chelate

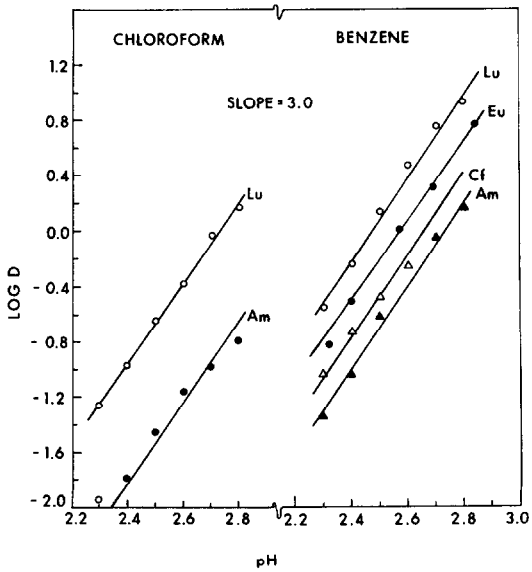

Fig. 2. Variation of log D trivalent actinides and lanthanides as a function of pH.

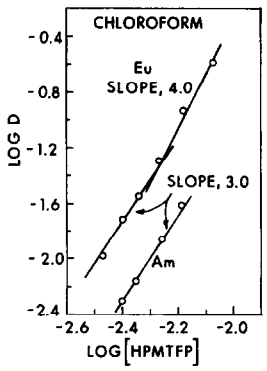

Fig. 3. Variation of log D of trivalent Am and Eu as a function of HPMTFP concentration. Aqueous phase: pH 3.0 chloroacetate buffer. Org. phase: 0.0034–0.0085 M HPMTFP in chloroform.

formation mechanism:

$$M^{3+}_{aq} + 3HPMTFP_{org} \rightleftharpoons M(PMTFP)_{3org} + 3H^{+}_{aq} \quad (2)$$

where M = Cf, Tm or Lu.

In the cases of Am(III) and Eu(III) where the formation of a self-adduct species has been observed, it was decided to carry out the extraction studies at lower HPMTFP concentrations. Figure 3 shows the plots of log D vs log[HPMTFP] for Am(III) and Eu(III) at such HPMTFP concentrations (0.0034–0.0085 M). The straight lines with a slope of 3 suggest the formation of the chelate species $M(PMTFP)_3$ at lower HPMTFP concentrations. Freiser *et al.*[7] have also obtained a slope of 3 in similar plots for Eu(III) extraction by HPMTFP in chloroform at similar low concentrations. As seen from the above experiments it is clear that simple chelates are formed at lower reagent concentrations while the self-adducts $M(PMTFP)^3 \cdot HPMTFP$ are obtained at higher concentrations.

Formation of "self-adduct" species in different metal chelate extraction systems has been established by many workers.[14,17–22] In the chloroform solutions of HPMBP, HDMPP and HPMTFP, it has been observed that (a) with HPMBP, Am, Bk, Cf and Eu are extracted as self-adducts and Cm as a chelate,[9,10] (b) with HDMPP, all these metal ions are extracted as the chelate species[9] and (c) with HPMTFP, Am, Cm and Eu are extracted as self-adducts and Cf, Tm and Lu as chelate species. From the above observations it may be concluded that the formation of a self-adduct species depends mainly on the basicity of the neutral pyrazolone molecule. As seen from the pK_a values (Table 2), the basicity of HDMPP is minimum and it does not form a self-adduct at all. The next in the basicity order being HPMTFP, it forms self-adducts with lighter trivalent actinides and lanthanides whereas with HPMBP (highest basicity) the self-adducts are formed with elements up to Cf (Cm being an exception due to the "tetrad effect").

The formation of a self-adduct species with Am, Cm and Eu and only the chelate species with the rest of metal ions studied in the HPMTFP-chloroform (or benzene) systems could be explained as due to the formation of stronger complexes of the metal ions of higher Z (smaller ionic radii) with $PMTFP^-$ anions in the aqueous phase. This leaves a smaller residual charge (δ^+) on their metal chelate species which is insufficient to attract a less basic HPMTFP molecule. Under similar conditions HPMBP forms a self-adduct species because of its higher basicity.

Table 3 gives the equilibrium constant (K) values of the two phase reactions of the trivalent actinides and lanthanides with HPMTFP in chloroform and benzene. In case of Am, Cm and Eu (all forming a self-adduct) the log K values follow the order Am < Cm < Eu and in the case of other metal ions, where a chelate species is formed the order is Am < Eu < Cf < Tm < Lu. These orders are just

Table 2. Two phase equilibrium constant (K) values for Am(III) and Eu(III) with β-diketones in chloroform

	Reaction	log K Am	log K Eu	pK_a of β-diketone	Ref.
Self-adduct	$M^{3+}_{aq} + 4HPMTFP_{org} \rightleftharpoons M(PMTFP)_3 \cdot HPMTFP_{org} + 3H^{+}_{aq}$	−2.30	−1.80	2.73	Present work
	$M^{3+}_{aq} + 4HPMBP_{org} \rightleftharpoons M(PMBP)_3 \cdot HPMBP_{org} + 3H^{+}_{aq}$	−3.67	−3.37	4.01	10
	$M^{3+}_{aq} + 3HDMPP_{org} \rightleftharpoons M(DMPP)_{3org} + 3H^{+}_{aq}$	−2.81	−2.01	2.00	10
Chelate	$M^{3+}_{aq} + 3HPMTFP_{org} \rightleftharpoons M(PMTFP)_{3org} + 3H^{+}_{aq}$	−4.10	−3.54	2.73	Present work
	$M^{3+}_{aq} + 3HBTFA_{org} \rightleftharpoons M(BTFA)_{3org} + 3H^{+}_{aq}$	−9.65	−8.55	6.15	10
	$M^{3+}_{aq} + 3HTTA_{org} \rightleftharpoons M(TTA)_{3org} + 3H^{+}_{aq}$	−8.72	−8.25	6.25	10

Table 3. Two phase equilibrium constant (K) values for trivalent actinides and lanthanides—HPMTFP in chloroform and benzene

Reaction	log K Chloroform	Benzene
$Am^{3+}_{aq} + 4HA_{org} \rightleftharpoons AmA_3 \cdot HA_{org} + 3H^+_{aq}$	−2.30	−1.44
$Cm^{3+}_{aq} + 4HA_{org} \rightleftharpoons CmA_3 \cdot HA_{org} + 3H^+_{aq}$	−1.94	−1.14
$Cf^{3+}_{aq} + 3HA_{org} \rightleftharpoons CfA_{3org} + 3H^+_{aq}$	−3.42	−2.76
$Eu^{3+}_{aq} + 4HA_{org} \rightleftharpoons EuA_3 \cdot HA_{org} + 3H^+_{aq}$	−1.80	−0.90
$Tb^{3+}_{aq} + 3HA_{org} \rightleftharpoons TbA_{3org} + 3H^+_{aq}$	—	−2.77
$Tm^{3+}_{aq} + 3HA_{org} \rightleftharpoons TmA_{3org} + 3H^+_{aq}$	−3.25	−2.45
$Lu^{3+}_{aq} + 3HA_{org} \rightleftharpoons LuA_{3org} + 3H^+_{aq}$	−3.10	−2.28
$Am^{3+}_{aq} + 3HA_{org} \rightleftharpoons AmA_{3org} + 3H^+_{aq}$	−4.10	—
$Eu^{3+}_{aq} + 3HA_{org} \rightleftharpoons EuA_{3org} + 3H^+_{aq}$	−3.54	—
$AmA_{3org} + HA_{org} \rightleftharpoons AmA_3 \cdot HA_{org}$	+1.80	—
$EuA_{3org} + HA_{org} \rightleftharpoons EuA_3 \cdot HA_{org}$	+1.74	—

the reverse of the order of ionic radii of these metal ions. In the case of Am and Eu where the experimental data for both the chelate and self-adduct formation was available, the equilibrium constant for the organic phase reaction

$$M(PMTFP)_{3org} + HPMTFP_{org} \rightleftharpoons M(PMTFP)_3 \cdot HPMTFP_{org} \quad (3)$$

has also been calculated. The log K values for Am (1.80) and Eu (1.74) are as expected much lower than the organic phase synergistic constants involving neutral donors.[1,9,10]

Table 2 gives the two-phase equilibrium constant (K) values of Am(III) and Eu(III) with different β-diketones in chloroform along with the pK_a values of the β-diketones. It is evident that the log K values for both these metal ions follow an increasing order (separately for the chelate and self-adduct species) with decrease in pK_a value of the β-diketones. It may be inferred that in the extraction of the trivalent Am and Eu with the above β-diketones, the higher stability of the complexes of β-diketones (in the aqueous phase) does not play an important role (higher pK_a gives higher metal chelate stability) while other factors like ionization and partition coefficient of β-diketones and partition coefficient of the metal chelates are probably of special significance.

Acknowledgement—The authors thank Dr P. R. Natarajan, Head, Radiochemistry Division, B.A.R.C., for his interest in this work.

REFERENCES

1. J. N. Mathur, *Solv. Extr. Ion Exch.* 1983, **1**, 349.
2. G. Duyckaerts and J. F. Desreux, *Int. Solv. Extr. Conf.*, p. 73. Toronto, CIM, Montreal (1977).
3. T. V. Healy, *Solvent Extraction Research*, p. 257. Wiley, New York (1969).
4. B. F. Myasoedov, M. K. Chmutova and I. A. Lebedov, *Proc. Int. Solv. Extr. Conf.* 1971; *J. Soc. Chem. Ind.* 1971, **1**, 815.
5. J. N. Mathur and P. K. Khopkar, *Solv. Extr. Ion Exch.* 1983, **1**, 597.
6. Y. Sasaki and H. Freiser, *Inorg. Chem.* 1983, **22**, 2289.
7. H. Chun-Hui and H. Freiser, *Solv. Extr. Ion Exch.* 1986, **4**, 41.
8. J. N. Mathur and P. K. Khopkar, *Sep. Sci. Technol.* 1982, **17**, 985.
9. J. N. Mathur and P. K. Khopkar, *Polyhedron* 1984, **3**, 1125.
10. J. N. Mathur and P. K. Khopkar, *Radiochem. Radioanal. Lett.* 1983, **57**, 259.
11. P. K. Khopkar and J. N. Mathur, *J. Radioanal. Chem.* 1980, **60**, 131.
12. P. K. Khopkar and J. N. Mathur, *J. Inorg. Nucl. Chem.* 1977, **39**, 2063.
13. B. S. Jensen, *Acta. Chem. Scand.* 1959, **13**, 1668.
14. T. Hori, M. Kawashima and H. Freiser, *Sep. Sci. Technol.* 1980, **15**, 861.
15. E. L. King and W. H. Reas, *J. Am. Chem. Soc.* 1951, **73**, 1806.
16. J. N. Mathur and P. K. Khopkar, *Radiochim. Acta.* 1986, **39**, 77.
17. D. Dyrssen, *Sven. Kem. Tidskr.* 1955, **67**, 311.
18. L. Newman and P. Klotz, *Inorg. Chem.* 1966, **5**, 461.
19. O. Navratil, *Proc. Int. Solv. Extr. Conf. Liège*, 1980, **3**, 2585. Association des Ingénieurs Sortis de l'Université de Liège (1980).
20. S. Peterson, *J. Inorg. Nucl. Chem.* 1960, **14**, 126.
21. E. L. King, *USAEC Report TID-5290*, paper 34, p. 269 (1958).
22. G. A. Pribylova, M. K. Chmutova and B. F. Myasoedov, *Radiokhimiya* 1981, **23**, 521.

Polyhedron Vol. 6, No. 12, pp. 2103–2110, 1987
Printed in Great Britain

0277–5387/87 $3.00+.00

X-RAY AND ELECTROCHEMICAL INVESTIGATION OF A SERIES OF COBALT COMPLEXES WITH TETRA- AND QUINQUEDENTATE SCHIFF BASE LIGANDS AND THEIR CATALYTIC PROPERTIES IN THE OXIDATION OF 2,6-DITERTBUTYLPHENOL BY MOLECULAR OXYGEN

I. SASAKI,* D. PUJOL and A. GAUDEMER

Laboratoire de Chimie de Coordination Bioorganique, UA 255, ICMO 91405, Orsay Cédex, France

and

A. CHIARONI and C. RICHE

Laboratoire de Cristallochimie ICSN, CNRS 91190, Gif-sur-Yvette, France

(*Received* 19 *March* 1987; *accepted* 24 *June* 1987)

Abstract—Complexes of cobalt(II) with Schiff-bases obtained by condensation of 5-formyl pyrimidine bases with di- or tri-amines have been synthesized and characterized by visible spectroscopy and magnetic susceptibilities. Their catalytic efficiency in the oxidation of 2,6-ditertbutylphenol by molecular oxygen was studied. The molecular structure of a cobalt(III) complex was reported.

Cobalt(II) complexes have been the subject of numerous studies because of their similarities to natural dioxygen carriers[1,2] and also of their ability to catalyze the insertion of oxygen into organic substrates.[3,4] Among them, cobalt phtalocyanines[5] and porphyrins,[6] Co SalN-Medpt,[7] Co acacen[8] and cobaloxime derivatives[9] all form dioxygen adducts and have been found to be efficient catalysts in the oxidation of hindered phenols.

On the other hand, some antibiotics owe their biological activity to their complexing properties towards metal cations such as Fe^{2+} for bleomycin[10] and Cu^{2+} for streptonigrin.[11] Though the detailed mechanisms of their action are not known, it appears well-established that the chelated metal is able to bind molecular oxygen, leading by reduction to an activated species which efficiently induces strand-scissions of DNA.

We describe here the synthesis and characterization of cobalt(II) complexes of a series of Schiff-base ligands derived from the pyrimidine bases, uracil and dimethyl barbituric acid. We present the results of an electrochemical study of these complexes in order to establish a relationship between their structure, their redox potential and their catalytic efficiency in the oxidation of 2,6-ditertbutyl phenol by molecular oxygen. We also report the crystal and molecular structure of a cobalt(III) complex determined by single-crystal X-ray diffraction.

EXPERIMENTAL

Synthesis

The synthesis of the Schiff bases derived from 5-formyl uracil and 5-formyl dimethyl-1,3 barbituric acid was previously described.[12,13] Co Salen, Co Salpen and Co SalN–Medpt were prepared according to known procedures.[14] All complexes were prepared under argon.

Co Urapen

1 mmol of 5-formyluracil was partially dissolved

* Author to whom correspondence should be addressed.

in 20 cm^3 of degassed 95% ethanol. To this suspension was added 0.5 mmol of 1,3 diaminopropane and 0.5 mmol of cobalt acetate dissolved in 10 cm^3 of methanol. The mixture turned violet then pale pink. Heating was maintained for 4 h and the pink precipitate filtered off and dried under argon.

Co Uradpt

2 mmol of Uradpt were partially dissolved in 40 cm^3 of refluxing 95% ethanol. 1 mmol of cobalt acetate in 15 cm^3 of methanol was added to this suspension. After refluxing for 4 h then cooling, the grey–green precipitate was filtered off and dried under argon.

Cobalt complexes with ligands derived from dimethyl barbituric acid

To 0.5 mmol of ligand in 25 cm^3 of methanol was added 1 mmol of NaOH (pellets). After stirring at room temperature for 1 h, 1.1 equivalents of $Co(OAc)_2$ dissolved in 10 cm^3 of methanol were added to the suspension of the ligand and the mixture heated to reflux for 3 h. After cooling, the complex was recovered as a precipitate which was filtered off, washed with degassed methanol and dried under argon.

Co(III) DiMeBardpt OAc

The same procedure described for the preparation of the Co(II) complexes is followed using 30 cm^3 of methanol instead of 5 cm^3. Ater leaving the solution in contact with air, at room temperature for a few days, brown crystals appeared.

In the case of Co DiMeBardpt, only 5 cm^3 of methanol was used due to the greater solubility of this complex.

Electrochemistry

Spectroscopic grade DMSO (Merck) was dried on 0.3 nm molecular sieves. The supporting electrolytes (Fluka), tetraethylammonium perchlorate (TEAP) and tetrabutylammonium hexafluorophosphate (TBH), were dried in a vacuum oven and used without purification. Argon bubbling was used to remove oxygen from tested solutions.

Cyclic voltammetry was performed using an EG and G Princeton applied research model 362 scanning potentiostat.

In all electrochemical experiments, an aqueous saturated calomel electrode (S.C.E.) was used as reference electrode; the reported potential values are accurate to ± 0.02 V. The temperature was controlled at 20 ± 0.5°C.

The concentration of the different complexes was 0.6 mM in DMSO.

X-ray crystal structure of Co DiMeBardpt OAc

Crystals suitable for X-ray diffraction were obtained by evaporation of an ethanolic solution. A small crystal sealed in a Lindemann capillary with a drop of mother liquor was used for data collection and determination of the unit cell parameters.

Crystal data: $(C_{22}H_{30}O_8N_7)Co$, 0.5EtOH. M.W. = 579.46 + 46.07, monoclinic system, space group $P2/n$, $Z = 4$; $a = 14.831(5)$, $b = 9.955(3)$, $c = 20.292(6)$ Å, $\beta = 107.46(3)°$; $V = 2857.92(9)$ $Å^3$, $d_c = 1.40$, $\mu(\text{CuK}\alpha) = 49.92$ cm^{-1}, $F(000) = 1260$.

Data were collected on a Philips PW1100 diffractometer using graphite monochromatized CuKα radiation ($\lambda\text{CuK}\alpha = 1.5418$ Å) and the θ–2θ scan technique. Three standard reflections monitored every 2 h showed loss in intensity and a correction was made for crystal decomposition. A total of 7591 reflections were collected of which 2361 independent ones with $I > 3\sigma(I)$ were considered as observed and used for the structure calculations. The cobalt atom was located from the Patterson function, then Fourier syntheses gave all the other atoms of the molecule. The structure was refined by least-squares method, minimizing the function $\Sigma w(Fo - |Fc|)^2$. An empirical correction for absorption was made[15] reducing the isotropic R factor from 0.134 to 0.107. At the end of the anisotropic refinement, difference Fourier maps showed some hydrogen atoms and the presence of an ethanol solvent molecule. The ethanol atoms displayed high thermal motion, and so the molecule was refined as a rigid group with arbitrary occupation factors of 0.5 and a group isotropic thermal factor.

Hydrogen atoms were introduced at theoretical positions (dC—H = 1.08 Å) with an isotropic temperature factor equivalent to that of the bonded atom.

Final R values were 0.086 ($R = \Sigma(Fo - Fc)/\Sigma Fo$) and 0.0942 [$Rw = \Sigma w^{1/2}|Fo - |Fc||/\Sigma w^{1/2} Fo$ with a weighting scheme $w^{-1} = \sigma^2(Fo) + 0.0186(Fo)^2$], max $\Delta P = 0.76$, min $\Delta P = -0.90$ e $Å^{-3}$ on the final difference Fourier map.

All calculations were performed on a Mini-6 Bull computer using SHELX76[16] with coefficients for analytical approximation to the scattering factor and anomalous corrections from International Tables. Final coordinates, thermal parameters and a list of observed and calculated structure factors

have been deposited as supplementary material with the Crystallographic Data Centre in Cambridge.

Magnetic measurements

Magnetic susceptibility measurements at ambient temperature were performed on polycrystalline samples weighing about 5 mg, with a Faraday-type magnetometer. $HgCo(NCS)_4$ was used as calibrant. The molar susceptibilities were corrected for ligand diamagnetism, using Pascal's constants.

General procedure for the oxidation of 2,6-ditert-butylphenol

To 0.15 mmol of the starting phenol in 5 cm^3 of acetonitrile was added the catalyst (0.015 mmol) in 0.5 cm^3 of DMSO. The solution was stirred in a two-necked flask connected to a gas-burette containing oxygen (pressure 1 atm). At the end of the reaction, the different products were extracted by hexane. The hexane phase was evaporated to dryness and the percentage of the various products evaluated by NMR spectroscopy.

^1H NMR spectra were recorded on a Perkin–Elmer R-32 spectrometer using $CDCl_3$ solutions or DMSO d_6 solutions and $SiMe_4$ as internal reference.

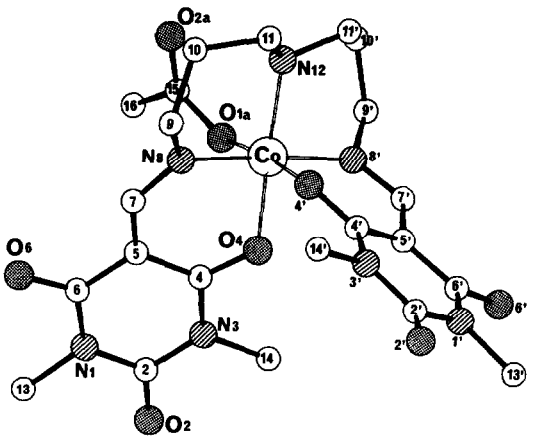

Fig. 1. Structure of Co DiMeBardpt OAc.

RESULTS AND DISCUSSION

(1) *Synthesis*

The cobalt complexes of the Schiff-bases derived from uracil were obtained simply by refluxing a suspension of the ligand in the presence of an equal amount of cobalt acetate. However in the cases of the ligands derived from 1,3-dimethyl barbituric acid, two equivalents of base must be added to accomplish complexation with cobalt(II). Barbituric acid is in fact a much stronger acid (pKa = 4.7) than uracil which is a base. The ligands with their abbreviated notation are shown in the Structures.

(2) *X-ray analysis*

The X-ray analysis establishes that an acetate group was linked to the cobalt atom as shown in Fig. 1. The cobalt atom, surrounded by three nitrogen and three oxygen atoms in two perpendicular planes assumes an octahedral geometry: it lies exactly in the plane of the four atoms: O4, N8, N12 and N8′ of the Schiff base ligand, the atoms O4′ and O1a being respectively 1.876(5) and 1.887(6) Å distance from the central cobalt atom (Table 1). Therefore, the two dimethyl barbituric acid moieties are in a *cis* geometry, the dihedral angle between the pyrimidine rings being 94.3° (Table 2). An intramolecular hydrogen bond bridges the second oxygen atom of the acetate group to the nitrogen atom N12 (O2a—N12 = 2.81 Å, O2a—H12 = 1.79 Å, angle O2a—H12—N12 = 154.5°), making the molecule more rigid.

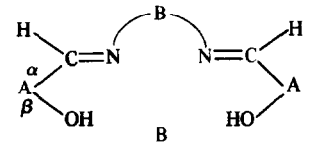

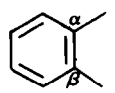

Sal

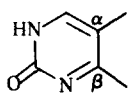

Ura

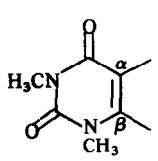

DiMeBar

$(CH_2)_2$
en

$CH-CH_2$
CH_3
Meen

$(CH_2)_3$
Pen

$(CH_2)_3NH(CH_2)_3$
dpt

$(CH_2)_3\ N\ (CH_2)_3$
CH_3
N–Medpt

Table 1. Interatomic distances (Å) of Co DiMeBardpt OAc

Co—O4	1.924(5)	C11—N12	1.486(11)
Co—N8	1.945(6)	N12—C11′	1.486(12)
Co—N12	1.961(7)	N1′—C2′	1.379(11)
Co—O4′	1.874(5)	N1′—C6′	1.401(11)
Co—N8′	1.920(7)	N1′—C13′	1.490(12)
Co—O1A	1.898(6)	C2′—O2′	1.211(10)
N1—C2	1.361(13)	C2′—N3′	1.362(11)
N1—C6	1.398(12)	N3′—C4′	1.396(10)
N1—C13	1.484(14)	N3′—C14′	1.487(11)
C2—O2	1.232(11)	C4′—O4′	1.259(10)
C2—N3	1.382(12)	C4′—C5′	1.413(11)
N3—C4	1.391(10)	C5′—C6′	1.404(12)
N3—C14	1.468(12)	C5′—C7′	1.411(11)
C4—O4	1.271(10)	C6′—O6′	1.249(10)
C4—C5	1.401(12)	C7′—N8′	1.298(10)
C5—C6	1.412(13)	N8′—C9′	1.473(10)
C5—C7	1.409(11)	C9′—C10′	1.486(14)
C6—O6	1.253(12)	C10′—C11′	1.501(14)
C7—N8	1.287(10)	O1A—C15	1.304(13)
N8—C9	1.495(10)	O2A—C15	1.231(15)
C9—C10	1.496(13)	C15—C16	1.472(19)
C10—C11	1.524(15)	OH—CH2	1.377(47)
		CH2—CH3	1.462(41)

In the packing of the molecules only Van der Waals contacts are noted. The ethanol molecule is placed in a hole of the crystal and does not establish any hydrogen bond with the complex molecules.

The structure of this complex can be compared to that of the complex formed from the corresponding Schiff-base derived from salicylaldehyde.[17] No significant difference in the geometry around the metal centre appears between the two molecules. As noticed by the authors, the same geometry of the Schiff-base ligand is observed in the peroxy-quinolato cobalt(III) complex[18] and in the binuclear μ-peroxo cobalt(III) complex[19] whereas it is *trans* in the dioxygen complex.[20]

(3) *Characterization of the cobalt complexes*

In addition to the results of elemental chemical analyses, the complexes have been characterized by IR, Visible and U.V. spectral studies and magnetic susceptibility measurements.

(a) IR spectroscopy of all the complexes are similar: they show very strong IR-active bands near 1650–1600 cm^{-1} which are assigned to the conjugated C=N, C=O and C=C stretching vibrations of the amide and imine chelated bonds. Compared to the free ligands these bands are shifted to lower energy in the complexes. Additional bands are also observed at 1695 and 1550 cm^{-1} for DiMeBar type and Ura type complexes respectively.

(b) Due to the low solubility of the various complexes which are not soluble in most organic solvents, we have measured their spectra in DMSO solution (Table 3). The spectra of the Co Salen and Co SalN–Medpt were also measured in chloroformic and DMSO solutions for the sake of comparison. Whatever the solvent, the values of λ max do not vary much and show that Co Salen is square-planar and Co SalN–Medpt is a trigonal bipyramid.[21]

All the complexes with Schiff-bases derived from uracil, Co DiMeBarpen and Co DiMeBardpt exhibit the same type of spectra: a shoulder at $\approx$ 1000 nm and a maximum at 550 nm.

These values are consistent with an octahedral geometry[21] with one or two molecules of DMSO when the ligands are respectively penta- or tetradentate. Co DiMeBaren and Co DiMeBarMeen are probably square-planar as indicated by the absence of absorption at 500 nm. After complexation a bathochromic shift of 20–30 nm was observed in the UV spectra.

(c) Magnetic susceptibility measurements (Table 4) reveal that Co DiMeBaren which probably has a square planar geometry is the only low-spin complex. As indicated by the microanalysis, this complex crystallizes with a molecule of solvent (MeOH) which can be either in the lattice or directly bound to the metal, in which case the axial ligand field would not be increased sufficiently to give a high-spin complex. The other five complexes are high-spin. In the case of Co DiMeBarMeen the presence of two water molecules creates an axial ligand field which is relatively strong compared to the equatorial ligand field and leads to a high-spin complex. As expected the tetrahedral Co Urapen and Co DiMeBarpen and the five coordinate Co Uradpt and Co DiMeBardpt exhibit magnetic moments in the range of 4.2–4.6 BM.

(4) *Electrochemistry*

(a) Cyclic voltammetry. The voltammogram of Co DiMeBaren shows the typical behavior of tetracoordinated cobalt complexes: in the range +0.5 to −1.8 V (vs SCE), a reversible process is seen, including an anodic current peak at +0.15 V and a cathodic one at +0.25 V. Increasing the scan rate does not modify these values. A second anodic current peak is observed at −1.3 V which is associated to a cathodic current peak at −1.2 V, which probably corresponds to the reduction of Co(II) to Co(I).

The voltammograms of pentacoordinate com-

Table 2. Valence angles (°) of Co DiMeBardpt OAc

O4—Co—N8	90.2(2)	N1′—C2′—O2′	121.1(8)
O4—Co—N12	175.5(3)	N1′—C2′—N3′	116.8(7)
O4—Co—O4′	89.5(2)	O2′—C2′—N3′	122.0(8)
O4—Co—N8′	85.3(3)	C2′—N3′—C4′	123.7(7)
O4—Co—O1A	84.5(2)	C2′—N3′—C14′	118.0(6)
N8—Co—N12	93.4(3)	C4′—N3′—C14′	118.3(6)
N8—Co—O4′	87.4(2)	N3′—C4′—O4′	116.5(7)
N8—Co—N8′	176.2(3)	N3′—C4′—C5′	117.8(7)
N8—Co—O1A	90.6(3)	O4′—C4′—C5′	125.6(7)
N12—Co—O4′	91.9(3)	Co—O4′—C4′	123.3(5)
N12—Co—N8′	90.4(3)	C4′—C5′—C6′	120.5(7)
N12—Co—O1A	94.2(3)	C4′—C5′—C7′	119.6(7)
O4′—Co—N8′	91.6(3)	C6′—C5′—C7′	119.3(7)
O4′—Co—O1A	173.7(2)	N1′—C6′—C5′	117.0(7)
N8′—Co—O1A	89.9(3)	N1′—C6′—O6′	117.7(7)
C2—N1—C6	124.2(8)	C5′—C6′—O6′	125.2(7)
C2—N1—C13	115.7(8)	C5′—C7′—N8′	125.8(7)
C6—N1—C13	120.1(8)	Co—N8′—C7′	122.5(5)
N1—C2—O2	121.3(9)	Co—N8′—C9′	119.0(5)
N1—C2—N3	116.9(8)	C7′—N8′—C9′	118.2(7)
O2—C2—N3	121.8(8)	N8′—C9′—C10′	110.0(7)
C2—N3—C4	122.4(7)	C9—C10′—C11′	116.2(9)
C2—N3—C14	116.7(7)	N12—C11′—C10′	111.4(8)
C4—N3—C14	120.8(7)	Co—O1A—C15	130.0(7)
N3—C4—O4	114.6(7)	O1A—C15—O2A	123.6(11)
N3—C4—C5	119.5(7)	O1A—C15—C16	114.5(10)
O4—C4—C5	125.8(8)	O2A—C15—C16	121.9(11)
Co—O4—C4	122.7(5)		
C4—C5—C6	119.1(8)		
C4—C5—C7	120.3(7)		
C6—C5—C7	119.1(8)		
N1—C6—C5	117.7(8)		
N1—C6—O6	119.4(9)		
C5—C6—O6	122.9(9)		
C5—C7—N8	126.2(8)		
Co—N8—C7	122.5(5)		
Co—N8—C9	121.2(5)		
C7—N8—C9	115.3(7)		
N8—C9—C10	113.1(7)		
C9—C10—C11	116.9(8)		
C10—C11—N12	110.6(8)		
Co—N12—C11	116.6(6)		
Co—N12—C11′	115.0(6)		
C11—N12—C11′	110.7(7)		
C2′—N1′—C6′	124.0(7)		
C2′—N1′—C13′	116.7(7)		
C6′—N1′—C13′	119.0(7)		

plexes are less simple: we have chosen Co DiMeBardpt as an example. The first redox process [Co(III)/Co(II)] is fast and reversible. Reduction of Co(II) to Co(I) is not observed under the experimental condition used (Pt, DMSO, TEAP). With a graphite electrode which enables the exploration of a larger range of potentials, it is possible to see an anodic current peak at ≈ -1.8 V which probably corresponds to the reduction of Co(II) to Co(I). This process is also reversible but the Co(I) complexes are probably reacting with the solvent leading to an electroactive species which is oxidized at ≈ -1.8 V.

(b) Linear voltammetry. We have compared the values of $E_{\frac{1}{2}}$ of the reference complexes (e.g. Co Salen and Co SalN–Medpt) with those of the Co(II)

Table 3. Visible and near IR spectra of cobalt(II) complexes (nm)

Complex	Solid (KBr)	$CHCl_3$	DMSO
Co Salen		1200	1240
Co SalN–Medpt		1580(12) 680(26)	1660(10) 680(26)
Co Urapen	580(sh) 510 485		1040(sh) 550(sh) 525(sh) 475(sh)
Co Uradpt			1000(sh) 540(sh) 520(43) 490(sh) 455(sh)
Co DiMeBaren			1040(370)
Co DiMeBarMeen			1000(17)
Co DiMeBarpen			1020(10) 550(sh) 522(30)
Co DiMeBardpt			1000(8) 550(sh) 522(30) 482(sh) 435(sh)

complexes derived from pyrimidine bases (Table 5).

If we first examine the values measured for the complexes with Schiff-bases derived from salicylaldehyde, we can see that the oxidation potential Co(II)/Co(III) is more negative for Co SalN–Medpt than for Co Salen,[22] indicating that Co(II) is more difficult to oxidize in the latter complex. This is probably due to the fact that Co Salen is tetracoordinate in DMSO whereas Co SalN–Medpt is pentacoordinate as shown by visible spectroscopy. This observation agrees well with the results of Basolo,[23] who suggested that the oxidation potential of cobalt(II) is strongly dependent on the electron density at the metal centre. Co Salpen is the least easily oxidized complex probably because of its nearly tetrahedral geometry.

Table 4. Magnetic data of cobalt(II) complexes

	μBM
Co Urapen	4.63
Co Uradpt	4.36
Co DiMeBaren	2.72
Co DiMeBarMeen	4.58
Co DiMeBarpen	4.64
Co DiMeBardpt	4.49

As for the two complexes derived from uracil, the values of the oxidation [Co(II)/Co(III)] and of the reduction [Co(II)/Co(I)] potentials are higher than for Co Salen or Co SalN–Medpt. On the other hand, for a given type of ligand, the reduction of the Co(II) complexes is more difficult than the reduction of the corresponding Cu(II) complexes as noticed previously by Deutsch.[24] The differences observed in the values of $E_{\frac{1}{2}}$ between the two series of complexes, are a consequence of the decreased electron-donating character of the uracil ring compared to the phenoxyl group, therefore making the metal cation more easily reduced and less easily oxidized.

Concerning the complexes derived from dimethyl barbituric acid, the presence of an extra hydroxyl group and two methyl groups on the pyrimidine ring has no great influence on the values of $E_{\frac{1}{2}}$ [Co(II)/Co(III)] compared to those of Co Urapen or Co Uradpt. Except for DiMeBarpen, the values of $E_{\frac{1}{2}}$ [Co(II)/Co(III)] are nearly the same for the three other complexes whether the ligand is tetra- or pentadentate.

Well above in the scale in each series are Co DiMeBarpen and Co Urapen with value of $E_{\frac{1}{2}}$ of $+0.51$ V and > 0.5 V respectively. This is in agreement with the more positive potential for [Co(III)/Co(II)] reduction of Co Salpen compared

Table 5.

Compound	$E_{\frac{1}{2}}$ (V)[a]		% of quinone after 2 h[b]
Co Salen	−0.1;	−1.33	100
Co Salpen	+0.12;	−1.58	0
Co SalN–Medpt	−0.26;	−2.28(Hg)	70
Co Urapen	>0.5 V	−1.6(Hg)	0
Co Uradpt	+0.09;	−1.6(Hg)	0
Co DiMeBaren	+0.15;	−1.3	30
Co DiMeBarMeen	+0.17;	−1.29	100
Co DiMeBarpen	+0.54;	−1.6	0
Co DiMeBardpt	+0.14;	−1.9(C)	95

[a] Half-wave potentials of Co(II) complexes.
[b] Oxidation of 2,6-ditertbutylphenol by mol. O_2 catalyzed by Co(II) compounds. See text for experimental conditions.

to Co Salen, probably reflecting slightly different geometries. We confirm also that the presence of a methyl group on the ethylene bridge has no influence on the stability of Co(II), as already shown by Averill.[25]

(5) *Electron paramagnetic resonance*

In order to test the ability of these complexes to bind dioxygen, we have measured the ESR spectrum of two complexes: Co Uradpt and Co DiMeBardpt which show similar values of $E_{\frac{1}{2}}$ [Co(II)/Co(III)].

Co Uradpt being soluble only in DMSO, was dissolved in this solvent in the presence of oxygen; whatever the temperature, no signal corresponding to the complex Co—O_2 could be detected. However under the same conditions Co DiMeBardpt shows a change of colour from green (solid) to maroon (solution) and exhibits a weak signal corresponding to the oxygen adduct, that is with eight lines because of the coupling of the cobalt nucleus and the electron from Co—O_2^-. The coupling constant is 15 G, which was already observed for other Co Saldpt complexes.[26,27] When acetonitrile was used instead of DMSO, a much stronger signal was observed. The heights of the lines varied with temperature and reached a maximum at room temperature. Addition of a trace of DMSO to the acetonitrile solution caused a strong decrease of the signal. This demonstrated that DMSO competes with oxygen as a ligand.

Thus, two complexes with very similar values of $E_{\frac{1}{2}}$[Co(II)/Co(III)] behave quite differently towards dioxygen. We will propose a possible explanation in the conclusion. We have also tested their catalytic activity in the oxidation of 2,6-ditertbutyl phenol by molecular oxygen.

(6) *Catalytic oxidation of 2,6-ditertbutyl phenol*

2,6-ditertbutyl phenol is readily oxidized by molecular oxygen in the presence of various cobalt(II) complexes giving only two products: parabenzoquinone (PBQ) and diphenoquinone (DPQ) as shown in the Scheme. We have compared the efficiency of the different cobalt complexes mentioned in this study with that of Co Salen and Co SalN–Medpt under the same standard conditions: 1 atm pressure of oxygen, room temperature, solvent: H_3CC N/DMSO, 10/1 in order to increase the solubility of the complexes, ratio: catalyst/phenol = 0.1.

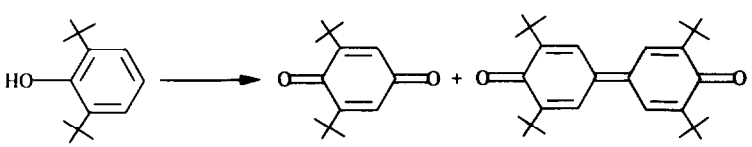

PBQ DPQ

All complexes are not efficient catalysts (Table 5), but when they are, they exhibit the same high selectivity, the only reaction product being the benzoquinone PBQ. As expected, Co DiMeBardpt which binds O_2 shows an efficiency which is similar to that of good catalysts in this reaction such as Co SalN–Medpt whereas Co Uradpt which does not bind O_2 does not catalyze the reaction.

We noticed also that when the reaction is carried out in pure acetonitrile, the yield in oxidation product become quantitative with Co SalN–Medpt but drops to 70% with Co Salen instead of 100% in the mixture DMSO/CH_3CN (1/10). We interpret these apparently surprising results by assuming that in the case of Co SalN–Medpt, DMSO can act as a sixth ligand, thus preventing the binding of O_2. By contrast, with Co Salen it would act as a fifth ligand thus increasing the ability of the cobalt atom to bind O_2. Although the values of $E_{\frac{1}{2}}$ for Co DiMeBaren and Co DiMeBarMeen are similar, the yields in quinone are very different. This might be due to a lower solubility of Co DiMeBaren under the conditions we have used. The complexes derived from 1,3-propylene diamine (as Co Salpen for instance) are totally inefficient probably due to the high value of their Co(III)/Co(II) potential.

We conclude that complexes which have similar Co(II)/Co(III) redox potential values can exhibit very different catalytic efficiency. The latter is certainly a function of the redox potential but also depends on other factors such as the steric hindrance at the metal centre.[31] One should also bear in mind that these $E_{\frac{1}{2}}$ values concern a complex which is only the precursor of the active catalyst namely the oxygen adduct and that many other cobalt complexes are involved as intermediates in the catalytic oxidation.[28–30] Therefore, it seems very hazardous to establish a direct relationship between $E_{\frac{1}{2}}$ values and the catalytic efficiency of cobalt(II) complexes.

Acknowledgements—We wish to thank Dr J. Huet for the ESR spectra.

REFERENCES

1. R. D. Jones, D. A. Summerville and F. Basolo, *Chem. Rev.* 1978, **79**, 139.
2. E. C. Niederhoffer, J. H. Timmons and A. E. Martell, *ibid.* 1984, **84**, 137.
3. A. Nishinaga, *Chem. Lett.* 1975, 273.
4. A. Zombeck, D. E. Hamilton and R. S. Drago, *J. Am. Chem. Soc.* 1982, **104**, 6782; *ibid.* 1987, **109**, 374.
5. V. M. Kothart and I. J. Tazurma, *J. Catal.* 1976, **41**, 180.
6. M. N. Dufour, A. L. Crumbliss, G. Johnston and A. Gaudemer, *J. Mol. Catal.* 1980, **7**, 277.
7. T. Matsuura, K. Watanabe and A. Nishinaga, *J. Chem. Soc. C.* 1970, 163.
8. A. McKillop and S. Ray, *Synthesis* 1977, 847.
9. L. I. Simandi, *Inorg. Chem. Acta* 1980, **44**, 2107.
10. T. Suzuki, J. Kuwahara and Y. Sugiura, *Biochem.* 1985, **24**, 4719.
11. R. Cone, S. K. Hasan, J. W. Lown and A. R. Morgan, *Can. J. Biochem.* 1976, **54**, 219.
12. I. Sasaki, M. N. Dufour, A. Gaudemer, A. Chiaroni, C. Riche, D. Parquer-Decrouez and P. Boucly, *Nouv. J. Chim.* 1984, **4**, 237.
13. I. Sasaki, A. Gaudemer, A. Chiaroni and C. Riche, *Inorg. Chim. Acta* 1986, **112**, 119.
14. B. H. Bailes and M. Calvin, *J. Am. Chem. Soc.* 1947, **69**, 1886.
15. N. Walker and D. Stuart, *Acta Cryst.* 1983, **A39**, 158.
16. G. M. Sheldrix, SHELX76, Program for crystal structure determination. University of Cambridge, U.K. (1976).
17. N. Matsumoto, M. Imaizumi and A. Ohyoshi, *Polyhedron* 1983, **2**, 137.
18. A. Nishinaga, H. Tomita, K. Nishizawa, T. Matsuura, S. Ooi and K. Hirotsu, *J. Chem. Soc., Dalton Trans.* 1981, 1504.
19. L. A. Lindblom, W. P. Schaeffer and R. E. Marsh, *Acta Cryst.* 1971, **B27**, 1461.
20. R. Cini and P. Orioli, *J. Chem. Soc., Dalton Trans.* 1983, 2563.
21. L. Banci, A. Bencini, C. Benelli, D. Gatteschi and C. Zancaini, *Structure and Bonding* 1982, **52**, 37.
22. O. Reyes-Salas, Thèse, Paris VI (1982).
23. M. J. Carter, D. P. Rillema and F. Basolo, *J. Am. Chem. Soc.* 1974, **96**, 392.
24. D. F. Rohrbach, W. R. Heineman and E. Deutsch, *Inorg. Chem.* 1979, **18**, 2536.
25. D. F. Averill and R. F. Broman, *ibid.* 1978, **17**, 3389.
26. M. D. Braydich, J. J. Fortman and S. C. Cummings, *ibid.* 1983, **22**, 484.
27. R. H. Niswander and L. T. Taylor, *J. Magn. Res.* 1977, **26**, 491.
28. A. Nishinaga, A. Tomita, K. Nishizawa and J. Matsuura, *J. Chem. Soc., Dalton Trans.* 1981, 1504.
29. B. B. Corden, R. S. Drago and R. P. Perito, *J. Am. Chem. Soc.* 1985, **107**, 2903.
30. M. Frostin-Rio, D. Pujol, C. Bied-Charreton, M. Perree-Fauvet and A. Gaudemer, *J. Chem. Soc., Perkin Trans.* 1984, **I**, 1971.
31. C. Busetto, F. Cariati, A. Fusi, M. Gullotti, A. Pasini, R. Ugo and V. Valenti, *ibid.* 1973, 754.

Polyhedron Vol. 6, No. 12, pp. 2111–2118, 1987
Printed in Great Britain

0277-5387/87 $3.00+.00
Pergamon Journals Ltd

MOLYBDENUM–MOLYBDENUM QUADRUPLE BONDS: AN ASYMMETRICALLY SUBSTITUTED DIMER CONTAINING A SINGLE ACETATE BRIDGE. CRYSTAL AND MOLECULAR STRUCTURE OF $[Mo_2Cl_3(\mu\text{-}OAc)(PMe_3)_3]\cdot PhMe$

PAUL A. BATES, ALASTAIR J. NIELSON* and JOYCE M. WATERS†

Department of Chemistry, University of Auckland, Private Bag, Auckland, New Zealand

(*Received* 30 *March* 1987; *accepted* 24 *June* 1987)

Abstract—$[Mo_2(OAc)_4]$ reacts with three or more equivalents of lithium chloride and PMe_3 in thf to give $[Mo_2Cl_3(\mu\text{-}OAc)(PMe_3)_3]0.75thf$ (**1**). The IR spectrum of the complex shows Mo—O and Mo—Cl stretches at 350 and 300 cm^{-1} respectively and the ^1H and ^{13}C NMR spectra suggest several species are present in solution. $[Mo_2Cl_3(\mu\text{-}OAc)(PMe_3)_3]$ converts slowly in thf to $[Mo_2Cl_4(PMe_3)_4]$ and $[Mo_2(OAc)_4]$. The structure of $[Mo_2Cl_3(\mu\text{-}OAc)(PMe_3)_3]0.5C_6H_5Me$ (**2**) has been determined by single-crystal X-ray diffraction methods. Crystals of the toluene solvate are tetragonal with $a = 20.726(2)$, $c = 11.776(2)$ Å, space group = $I4cm$. The structure was solved by Patterson and Fourier methods and refined to R of 0.035 for the 539 observed data. The molecule contains two metal centres each of which shows 5-fold coordination. The two molybdenum atoms are linked by an acetate bridge and a short Mo—Mo bond of 2.121(3) Å. Remaining coordination sites are occupied on Mo(1) by two Cl and one PMe_3 and on Mo(2) by one Cl and two PMe_3 groups.

Preparations of dinuclear molybdenum(II) complexes containing chloro and phosphine ligands have traditionally used $[Mo_2(OAc)_4]$ as the source material for the molybdenum–molybdenum quadruple bond.[1] Reaction with ammonium chloride to give $(NH_4)_5Mo_2Cl_9\cdot H_2O$ followed by treatment with the phosphine has been the usual route.[2] McCarley *et al.* have reported that $[Mo_2Cl_4(PEt_3)_4]$ could be synthesized by reacting $[Mo_2(OAc)_4]$ with excess Me_3SiCl in the presence of PEt_3.[3] More recently Green *et al.* found that $[Mo_2Cl_2(OAc)_2(P)_2]$ complexes could be prepared by the reaction of $[Mo_2(OAc)_4]$ with two equivalents of Me_3SiCl in the presence of a variety of phosphine ligands.[4] This latter reaction showed that complexes containing both acetate and chloro ligands could be prepared for molybdenum as had been found with rhenium.[5]

The stepwise deacetylation of $[Mo_2(OAc)_4]$ to produce $[Mo_2Cl_4(P)_4]$ complexes can be envisaged to proceed through the following intermediates

$$[Mo_2(OAc)_4] \rightarrow [Mo_2Cl(OAc)_3P] \rightarrow [Mo_2Cl_2(OAc)_2P_2] \rightarrow [Mo_2Cl_3(OAc)P_3] \rightarrow [Mo_2Cl_4P_4].$$

In this sequence only the *mono-* and *tri*-chloro complexes remain to be discovered. We report here results of work in which attempts were made to prepare and characterize these two complexes using PMe_3 as the phosphine ligand. In particular the X-ray structural characterization of a $[Mo_2Cl_3(OAc)P_3]$ complex is presented.

RESULTS AND DISCUSSION

During reactions carried out between Me_3CPLi_2 and $[Mo_2(OAc)_4]$ in the presence of PMe_3 using thf as solvent, we have observed the formation of small quantities of a red–purple complex for which analytical and spectral data indicated a molybdenum compound containing chloro and PMe_3 ligands. Since it was suspected that the chloro ligands resulted from a reaction between $[Mo_2(OAc)_4]$ and lithium chloride present in our solutions of

* Author to whom correspondence should be addressed.

† Present address: Department of Chemistry and Biochemistry, Massey University, Palmerston North, New Zealand.

Me_3CPLi_2, the interaction of these two reagents was studied further.

When $[Mo_2(OAc)_4]$ was reacted with three or more equivalents of LiCl in thf in the presence of PMe_3, the mixture rapidly became purple and lithium acetate was precipitated. The red–purple complex extracted from this reaction mixture had similar spectral properties to the complex formed when the dilithium phosphide reagent was present. Recrystallization of the product from thf gave a complex which analyzed as $[Mo_2Cl_3(OAc)(PMe_3)_3]$ 0.75 thf (**1**). The IR spectrum showed a broad C=O absorption band at 1450 cm^{-1} and there were bands due to PMe_3 and thf at 960 and 855 cm^{-1} respectively. In the far-IR, bands at 350 and 300 cm^{-1} were identified as Mo—O and Mo—Cl stretches respectively.[6] In the ^1H NMR spectrum there were several PMe_3 methyl resonances in the vicinity of 1.8 ppm; a singlet was observed for the acetate methyl carbon and the methylene protons of the thf appeared as multiplets in the vicinity of 1.8 and 3.7 ppm. In the $^{13}C[^1H]$ NMR spectrum there were several resonances present for the PMe_3 methyl carbons and singlets for the acetate methyl carbon as well as the α- and β-carbons of the thf solvate. In addition there were three resonances of different intensity for the acetate group quarternary carbon. The $^{13}C[^1H]$ NMR spectrum thus indicated the presence of several species present in solution.

When the red–purple complex is allowed to stand for long periods in thf (i.e. several weeks) the solution changes colour from purple to blue and molybdenum tetra-acetate precipitates. From the blue–purple solution $[Mo_2Cl_4(PMe_3)_4]$[7,8] and the red–purple complex (**1**) were isolated.

The solvated complex (**1**) was best prepared from $[Mo_2(OAc)_4]$ in thf by the addition of three equivalents of both LiCl and PMe_3. It was also formed when Me_3SiCl was used in place of LiCl. Reactions of $[Mo_2(OAc)_4]$ with one or two equivalents of LiCl and PMe_3 in thf invariably lead to mixtures containing various uncharacterized molybdenum complexes. When $[Mo_2(OAc)_4]$ was reacted with two equivalents of Me_3SiCl and PMe_3 in thf, a pink product was formed which we believe to be $[Mo_2(OAc)_2Cl_2(PMe_3)_2]$ but attempts to obtain pure product by crystallization led only to the red–purple complex.

Crystal structure studies

The crystal structure of the red–purple complex recrystallized from toluene was determined and found to be the toluene solvate, $[Mo_2Cl_3(\mu\text{-}OAc)(PMe_3)_3]0.5C_6H_5Me$ (**2**). The molecular structure is shown in Fig. 1. It consists of an asymmetric

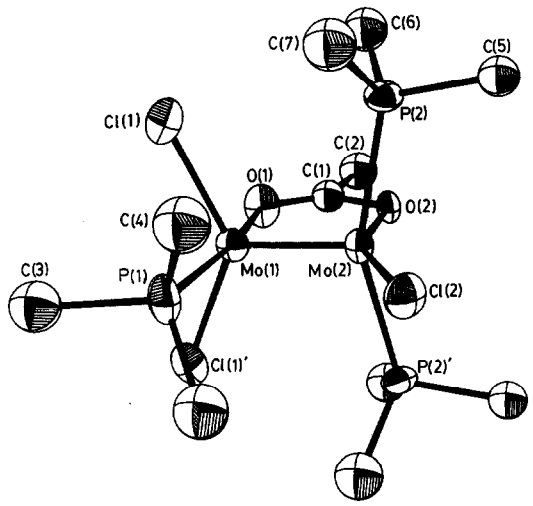

Fig. 1. Molecular structure of $[Mo_2Cl_3(\mu\text{-}OAc)(PMe_3)_3]0.5PhMe$. Ellipsoids are drawn at the 40% probability level. Hydrogen atoms have been omitted.

dinuclear species in which a single acetate ligand bridges two molybdenum atoms which in turn are joined by a short metal–metal bond of 2.121(2) Å. The remaining coordination sites are occupied on Mo(1) by two Cl and one phosphine and on Mo(2) by one Cl and two phosphine ligands. As a result the donor atoms *trans* to the acetate oxygens are not the same for the two metal centres. Bond distances and angles are given in Table 1. These latter indicate the deviations from ideal 5-fold coordination which occur. At Mo(1) the angles Cl(1)–Mo(1)–Cl(1)′ and P(1)–Mo(1)–O(1) of 134.2(2) and 170.6(6)° respectively, more closely resemble a trigonal bipyramidal geometry whereas P(2)–Mo(2)–P(2)′ (156.2(2)°) and Cl(2)–Mo(2)–O(2) (149.8(5)°) are more indicative of the square pyramidal arrangement.

A comparison of distances and angles observed for (**2**) and other related complexes is given in Tables 2 and 3. The Mo(1)—Mo(2) separation of 2.121(2) Å lies within the range of values (2.086(2)–2.153(6) Å) found for complexes containing a Mo—Mo quadruple bond. These compounds may be further subdivided into complexes either with, or without, an acetate bridge. In complexes in which two or more acetate bridges are present the Mo—Mo separation is a little shorter (2.093(1)–2.113(1) Å) than that observed where no acetate bridges occur (2.130(1)–2.153(6) Å). In (**2**) the Mo—Mo distance of 2.121(3) seems to lie between the two ranges. The Mo(1)—Cl(1) and Mo(2)—Cl(2) distances of 2.420(7) and 2.431(8) Å respectively do not differ significantly from one another despite the differences in their *trans* neigh-

Table 1. Selected bond lengths and bond angles for $[Mo_2Cl_3(\mu\text{-}OAc)(PMe_3)_3]\cdot 0.5\ PhMe$(2)

	Bond lengths (Å)		
Mo(1)—Mo(2)	2.121(2)	P(1)—C(3)	1.86(3)
Mo(1)—Cl(1)	2.420(7)	P(1)—C(4)	1.82(2)
Mo(1)—P(1)	2.517(9)	P(2)—C(5)	1.82(2)
Mo(1)—O(1)	2.14(2)	P(2)—C(6)	1.81(2)
Mo(2)—Cl(2)	2.431(8)	P(2)—C(7)	1.80(2)
Mo(2)—P(2)	2.550(6)	C(1)—O(1)	1.19(4)
Mo(2)—O(2)	2.06(2)	C(1)—O(2)	1.36(4)
		C(1)—C(2)	1.59(3)
	Bond angles (°)		
Mo(2)—Mo(1)—Cl(1)	112.9(2)	Mo(1)—P(1)—C(3)	111.4(10)
Mo(2)—Mo(1)—P(1)	99.9(3)	Mo(1)—P(1)—C(4)	116.5(7)
Mo(2)—Mo(1)—O(1)	89.6(6)	C(3)—P(1)—C(4)	100.1(11)
Cl(1)—Mo(1)—Cl(1)′	134.2(2)	Mo(2)—P(2)—C(5)	110.0(7)
Cl(1)—Mo(1)—P(1)	85.8(2)	Mo(2)—P(2)—C(6)	115.1(6)
Cl(1)—Mo(1)—O(1)	90.6(3)	Mo(2)—P(2)—C(7)	120.1(7)
P(1)—Mo(1)—O(1)	170.6(6)	C(5)—P(2)—C(6)	102.9(11)
Mo(1)—Mo(2)—Cl(2)	115.7(3)	C(5)—P(2)—C(7)	102.8(11)
Mo(1)—Mo(2)—P(2)	101.6(1)	C(6)—P(2)—C(7)	103.9(10)
Mo(1)—Mo(2)—O(2)	94.5(5)	Mo(1)—O(1)—C(1)	118(2)
Cl(2)—Mo(2)—P(2)	87.7(2)	Mo(2)—C(2)—O(2)	113(1)
Cl(2)—Mo(2)—O(2)	149.8(5)	O(1)—C(1)—O(2)	125(2)
P(2)—Mo(2)—P(2)′	156.2(2)	O(1)—C(1)—C(2)	124(3)
P(2)—Mo(2)—O(2)	86.1(2)	O(2)—C(1)—C(2)	111(3)

(atoms Cl(1)′ and P(2)′ refer to equivalent sites $\frac{1}{2}+y, \frac{1}{2}+x, z$)

Table 2. M—M separations in Mo—Mo dimers

Complex	Mo—Mo distance (Å)	Ref.
(a) Complexes with no bridging ligands		
$[K_4Mo_2Cl_8]\cdot 2H_2O$	2.139(4)	9
$[(enH_2)_2Mo_2Cl_8]\cdot 2H_2O$	2.134(1)	10
$[(NH_4)_5Mo_2Cl_9]\cdot H_2O$	2.150(5)	11
$[Mo_2Cl_4(pic)_4]\cdot CHCl_3$	2.153(6)	12
$[Mo_2Cl_4)(PMe_3)_4]$	2.130(1)	8
$[Mo_2Cl_4(PPh_3)_2(CH_3OH)_2]$	2.143(1)	13
$[Mo_2Cl_4(SEt_2)_4]$	2.144(1)	14
	Range 2.130(1)–2.153(6)	
(b) Complexes with acetate bridges		
$[Mo_2(OAc)_4]$	2.0934(8)	15
$[Mo_2Cl_2(OAc)_2(PBu_3)_2]$	2.099(1)	4
$[Mo_2Cl_2OAc)_2(PEt_3)_2]$—red	2.113(1)	16
$[Mo_2Cl_2(OAc)_2(PEt_3)_2]$—orange	2.0984(4)	16
$[Mo_2(O_2CCPh)_4]$	2.096(1)	17
$[Mo_2(O_2CCMe_3)_4]$	2.088(1)	17
$[Mo_2(OAc)_2Cl_4]^{2-}$	2.086(2)	6
	Range 2.086(1)–2.113(1)	

bours. They lie within the range observed (2.410(4)–2.437(3) Å) for other similar dinuclear complexes as shown in Table 3. Some differences are noted in the Mo—P bond lengths with Mo(1)—P(1) (2.517(9) Å), which is *trans* to an acetate oxygen, being a little shorter than Mo(2)—P(2) (2.550(6) Å) where the *trans* group is another phosphine ligand. This finding is in accord with the proposal of

Table 3. Structural data on some dinuclear molybdenum complexes

Complex	Mo—Cl (Å)	Trans group (*X*)	Cl—Mo—X (deg)	Mo—P (Å)	Trans group (*Y*)	P—Mo—Y (deg)	Ref.
$[Mo_2(OAc)Cl_3(PMe_3)_3]$	2.420(7)	Cl	134.2	2.550(6)	P	156.2	[a]
	2.431(8)	O	149.8(5)	2.517(9)	O	170.6(6)	
$[Mo_2Cl_4(PMe_3)_4]$	2.415(1)	Cl	135.27(4)	2.546(1)	P	155.55(4)	8
	2.413(1)	Cl	135.85(4)	2.544(1)	P	155.18(4)	
$[Mo_2(OAc)_2Cl_2(PBu_3)_2]$	2.427(2)	P	139.8(1)	2.501(3)	Cl	139.8( )	4
$[Mo_2(O_2CCMe_3)_2Cl_2(PEt_3)_2]$ (red isomer)	2.415(4)	O	152.6(3)	2.529(4)	O	163.9(3)	16
	2.410(4)	O	151.5(3)	2.558(4)	O	165.0(3)	
$[Mo_2CCMe_3)_2Cl_2(PEt_3)_2]$ (orange isomer)	2.428(5)	P	142.2(2)	2.513(4)	Cl	142.2(2)	14
$[Mo_2Cl_4(SEt_2)_4]$	2.398(7)	Cl	142.42(9)				
	2.415(7)	Cl	142.42(9)				
	2.413(7)	Cl	143.10(8)				
	2.417(6)	Cl	143.10(8)				
$[Mo_2(OAc)_2Cl_4]^{2-}$	2.437(3)	Cl	141.8(1)				
	2.430(4)	Cl	141.8(1)				

Complex	Mo—O (Å)	Trans group	O—Mo—X	C—O[b]	Ref.
$[Mo_2(OAc)Cl_3(PMe_3)_3]$	2.14(2)	P	170.3(6)	1.19(4)	[a]
	2.06(2)	Cl	149.8(6)	1.36(4)	
$[Mo_2(OAc)_2Cl_2(PBu_3)_2]$	2.109(5)	O	176.2(2)	1.28(1)	4
	2.100(6)	O	176.2(2)	1.27(1)	
$[Mo_2(O_2CCMe_3)_2Cl_2PEt_3)_2]$ (red isomer)	2.051(8)	Cl	152.6(3)	1.29(2)	16
	2.136(8)	P	165.0(3)	1.24(2)	
	2.063(9)	Cl	151.5(3)	1.29(2)	
	2.106(9)	P	163.9(3)	1.20(2)	
$[Mo_2(O_2CCMe_3)_2Cl_2(PEt_3)_2]$ (orange isomer)	2.105(5)	O	176.4	1.267(6)	16
	2.105(5)	O	176.4	1.264(6)	
$[Mo_2(OAc)_4]$	2.110(4)	O	176.3(2)	1.279(8)	15
	2.107(5)	O	176.3(2)	1.272(8)	
	2.137(4)[c]	O	176.5(2)	1.284(7)	
	2.121(4)	O	176.5(2)	1.273(7)	
$[Mo_2(O_2CCMe_3)_4]$	2.111(6)	O	176.0(2)	1.28(1)	17
	2.110(6)	O	175.7(2)	1.276(9)	
	2.126(5)[c]	O	175.9(2)	1.29(1)	
	2.100(6)	O	175.5(2)	1.26(1)	
	2.098(5)	O	176.0(2)	1.265(9)	
	2.135(5)[c]	O	175.7(2)	1.270(9)	
	2.109(6)	O	175.9(2)	1.28(1)	
	2.103(6)	O	175.5(2)	1.29(1)	
$[Mo_2(O_2CCPh)_4]$	2.092(3)	O	176.3(1)	1.280(4)	17
	2.131(3)	P	176.3(1)	1.281(5)	
	2.104(3)	O	176.6(1)	1.268(5)	
	2.099(3)	O	176.6(1)	1.272(5)	

[a] This work.

[b] The 2 C—O distances within the same acetate group follow one another.

[c] The oxygen is involved in an intermolecular bonding interaction.

Arenivar *et al.*[16] that the *trans* effect of a phosphine is greater than that attributed to acetate. However the variation in Mo—P distances in the red isomer of $[Mo_2(O_2CCMe_3)_2Cl_2(PEt_3)_2]$[16] cannot be explained in this way. In (**2**), the Mo(1)—O(1) bond length of 2.14(2) Å is longer than Mo(2)—O(2) (2.06(2) Å) and at least part of the difference can be attributed to the differing *trans* effect exerted by phosphine and Cl. The distances C(1)—O(1) (1.19(4) Å), C(1)—O(2) (1.36(4) Å) appear to differ significantly from one another at the 3σ level suggesting an asymmetry in the bridging acetate. Such an effect has not been observed in the di- and tetra-acetate bridged species listed in Table 3.

Inspection of the bond angles given in Table 3 shows that for each of the three groups Cl—Mo—X, P—Mo—X and O—Mo—X the angles fall into three ranges of decreasing value as X varies from O through P to Cl. If steric effects were solely responsible for this then it is surprising that the P—Mo—Cl angles of 139.8 and 142.2° are observed in the complexes $[Mo_2(OAc)_2Cl_2(PBu_3)_2]$ and $[Mo_2(O_2CCMe_3)_2Cl_2(PEt_3)_2]$ respectively where the smaller angle is associated with the bulkier phosphine group.

The crystal structure determination highlights several features. The complex is the first structurally characterized molybdenum complex containing a single acetate bridge. To retain the Mo^{2+} formalism for each molybdenum atom, O(1) must act as a 2-electron σ-donor to Mo(1). In other chloro-carboxylate complexes, a distinction between bonding modes is not always apparent by inspection or more importantly from structural data. For example in $[Mo_2(OAc)_4]$ the bond lengths observed do not distinguish between the two bonding modes.[15] In the red isomer of $[Mo_2Cl_2(OAc)_2(PBu_3)_3]$ the two longer Mo—O bonds lie *trans* to the phosphorous atoms[16] which suggest that the anion may bind *trans* to the chloride. However, this is not a certainty since a difference in bond length is to be expected due to the trans effect. For $[Re_2Cl_4(\mu\text{-}Cl)(\mu\text{-}O)(\mu\text{-}O_2CEt)(PPh_3)_2]$ (Re^{4+} dimer containing a Re≡Re double bond) in which the oxygen atoms of the single acetate bridge lie *trans* to chloro ligands, the Re—O distances are equivalent at 2.097(11) and 2.092(12) Å.[18] In the present complex (**2**), the Mo(1)—O(1) distance (2.14(2) Å) differs from the Mo(2)—O(2) distance (2.06(2) Å) by just over 3σ which may reflect a significant difference in the two modes of bonding. Further, this is accompanied by a difference in the C—O bond length (1.19(4) and 1.36(4) Å for C(1)—O(1) and C(1)—O(2) respectively) which, although small, is at least consistent with O(2) being involved in π-bonding.

Another feature of the structure is the asymmetry in the molecule. One end contains a *trans* Cl—Mo—Cl structure and the other a *trans* P—Mo—Cl structure. Two of the phosphine ligands are eclipsed which has not been observed in the other chloro-phosphine complexes structurally characterized. As a result of this geometry the P(1)—Mo—O(1) bond angle is widened to 170.6(6)° which compares with 163.9(2) and 165.0(3)° in the orange isomer of $[Mo_2Cl_2(OAc_2)(PEt_3)_2]$ in which phosphine and chloro ligands are *trans* to one another.[16] As a consequence of the acetate bridging mode the Mo(1)—P(1) bond represents a phosphine ligand lying *trans* to a 2-electron oxygen sigma donor. The Mo(1)—P(1) bond length (2.517(9) Å) is similar to that found for the equivalent position in the red isomer of $[Mo_2Cl_2(OAc)_2(PEt_3)_2]$ (2.529(4) Å)[9] but is much shorter than for the *trans* oriented phosphines in $[Mo_2Cl_4(PMe_3)_4]$ (Mo—P bond distances 2.546(1) and 2.544(1) Å).[8]

Analysis of the species formed when the acetate ligands of $[Mo_2(OAc)_4]$ are replaced in a stepwise manner by chloro and phosphine ligands, taking into account the origin of the O=C—O^- function, suggests that the complex characterized is not an intermediate in the transformation of $[Mo_2(OAc)_4]_2$ to $[Mo_2Cl_4(PMe_3)_4]$, but results from an isomerization of one of the stepwise transformed intermediates. The coordination geometry observed about Mo(1) could give rise to the *trans* orientation of ligands in (**a**) and (**b**) [see Fig. (2)] whereas the geometry about Mo(2) could result in the *cis* structures (**c**) and (**d**). The characterized complex itself is likely to give rise to the *trans–cis* structure (**e**). The complex could result from (**f**), being an isomerized product of (**g**), which itself is the stepwise replaced product from the *tris*-acetate (**h**), or from an isomerization of a $[Mo_2Cl_3(\mu\text{-}OAc)(PMe_3)_3]$ product produced by the stepwise replacement of an acetate in a $[Mo_2Cl_2(OAc)_2(PMe_3)_2]$ molecule. The ^{13}C NMR spectrum of the complex indicates that more than one species is present and this suggests that the solution chemistry is more complicated than the solid state structure would suggest.

EXPERIMENTAL

Lithium chloride was dried by heating to 100°C under vacuum for 24 h. Trimethyl phosphine was prepared by a literature method.[19] $[Mo_2(OAc)_4]$ was prepared by refluxing $[Mo(CO)_6]$ in a mixture of acetic acid and acetic anhydride.[20] Tetrahydrofuran (thf) was distilled from sodium hydroanaphthylide. All preparations and manipulations were carried out under dry, oxygen-free nitrogen using standard bench-top air-sensitive techniques.[21]

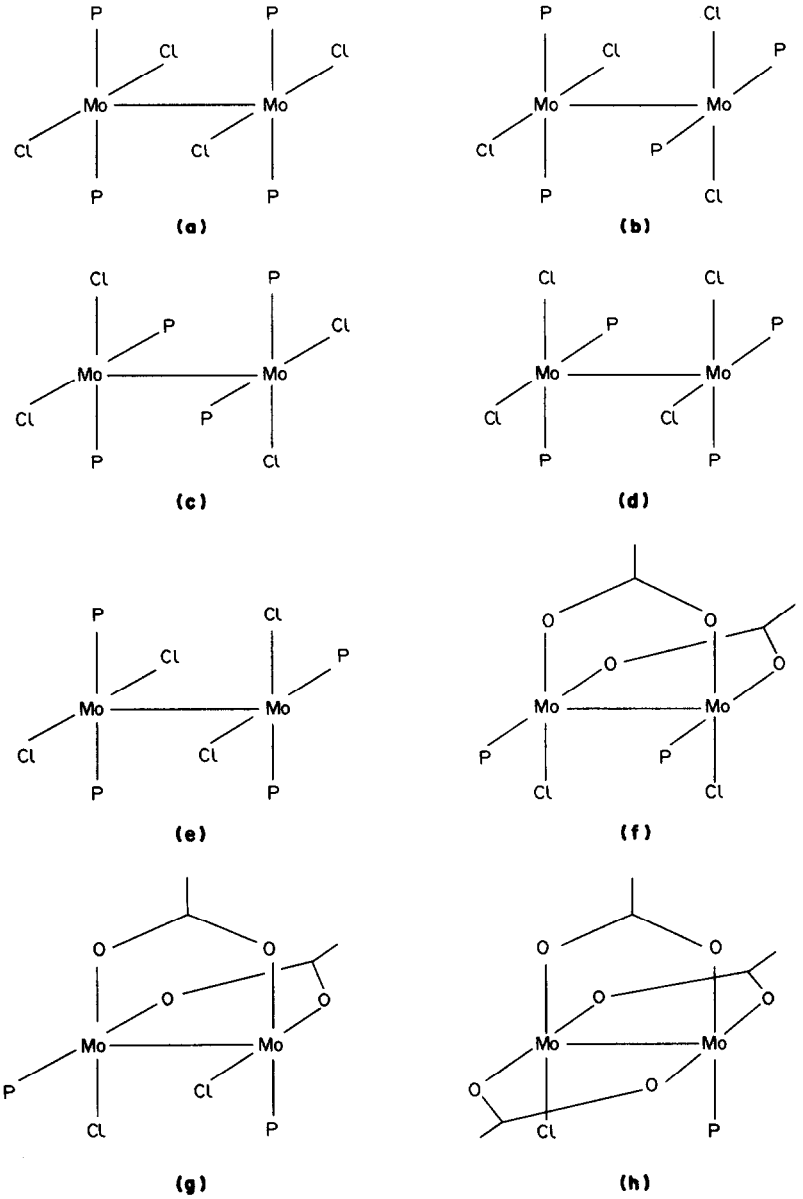

Fig. 2.

IR spectra were recorded on a Perkin–Elmer 597 spectrometer as Nujol mulls between CsI plates. ^{1}H and ^{13}C NMR spectra on a JEOL FX60 spectrometer. Analytical data were obtained by Prof. A. D. Campbell and his associates, University of Otago, New Zealand.

μ - Acetato - trichlorotris (trimethylphosphine) dimolybdenum (II)

Trimethyl phosphine (0.8 cm^3, 7.3 mmol) was added to a suspension of dimolybdenum tetraacetate (1.0 g, 2.3 mmol) in tetrahydrofuran (50 cm^3) and the mixture was stirred rapidly while a suspension of lithium chloride in tetrahydrofuran (30 cm^3) was added. The mixture was stirred for a further 20 h and the solution filtered from the precipitate which was then extracted with tetrahydrofuran (10 cm^3 portions) until the washings were no longer coloured purple. The extracts were combined, filtered and the solvent removed *in vacuo* to give the complex as purple–red crystals. Yield 1.3 g (96%). An analytically pure sample was obtained by dissolving the bulk sample in thf, filtering the solution and reducing the volume until crystallization commenced. On standing, the complex formed as red–purple needles which were filtered, washed with cooled thf (5 cm^3)

and dried *in vacuo*. (Found: C, 26.4; H, 5.6%. $C_{14}H_{36}Cl_3Mo_2O_{2.75}P_3$ (i.e. $[Mo_2Cl_3(\mu\text{-OAc})(PMe_3)_3]$ 0.75 thf requires C, 26.3; H, 5.7%.)

IR (Nujol) bands at 1450s, 1304m, 1285m, 1070m, 1055w, 1030w, 960s, 855m, 740m, 675m, 600w, 350m and 300m cm^{-1}. ^1H NMR ($CDCl_3$) 1.38–1.70 (m, 27H, $3PMe_3$); 1.70–2.0 (m, β Hs, thf); 2.75 (s, 3H, Me); 3.55–3.82 (m, α-Hs, thf). ^{13}C NMR, 10.7, 11.6, 12.2, 13.1, 14.0 (PMe_3); 23.5 (Me); 25.6 (β-Cs, thf); 67.9 (α-Cs, thf); 184.8, 185.7, 186.3 ($-CO_2$).

The complex was dissolved in tolune (30 cm^3) and the volume reduced to *ca.* 5 cm^3. On standing at $-20°$ red–purple crystals of the complex were formed which were filtered and washed with chilled toluene (2 cm^3). The product was crushed to a powder and dried for 3 h under vacuum. (Found: C, 27.1; H, 5.6; P, 14.5%. $C_{14.5}H_{34}Cl_3Mo_2O_2P_3$ (i.e. $[Mo_2Cl_2(\mu\text{-OAc})(PMe_3)_3]$0.5PhMe) requires C, 27.6; H, 5.4; P, 14.7%.)

A sample of the complex (0.5 g) was dissolved in thf (15 cm^3) and the solution allowed to stand at room temperature for several weeks giving a blue solution and a yellow precipitate of $[Mo_2(OAc)_4]$. On crystallization, the filtrate gave rise to the thf solvate of $[Mo_2Cl_3(\mu\text{-OAc})(PMe_3)_3]$ and $[Mo_2Cl_4(PMe_3)_4]$. The complexes were separated manually and identified by spectral comparison with authentic samples.

Crystallographic studies

Crystal data. Compound recrystallized from toluene at $-20°C$, $[Mo_2(\mu\text{-}O_2CMe)Cl_3(PMe_3)_3]$0.5 C_7H_8: $C_{11}H_{30}O_2P_3Cl_3Mo_2$0.5$C_7H_8$, $M = 631.63$, tetragonal, $a = 20.726(2)$, $c = 11.776(2)$ Å, $U = 5059$ Å^3, space group $I4cm$, $Z = 8$, $Dc = 1.66$ g cm^{-1}, $F(000) = 2536$, μ(Mo-$K\alpha$) = 14.8 cm^{-1}.

Data collection. CAD4 diffractometer, Mo-$K\alpha$ radiation (0.71069 Å), graphite monochromator $\omega/2\theta$ scan mode. Crystal ($0.30 \times 0.12 \times 0.11$ mm) sealed under N_2 in a capillary tube, 808 unique data measured ($\theta_{max} = 22°$). The intensities of three standard reflections, monitored during the data collection showed a variation of less than 3.5%; corrections were made for absorption,[22] minimum and maximum correction factors being 0.917 and 1.000 respectively.

Structure solution and refinement. The structure was solved by Patterson and Fourier methods and refined by a full-matrix least-squares technique.[23] The final refinement cycle converged to values of 0.034 and 0.035 for R and Rw respectively for the 121 variables and 539 data for which $F^2 > 3\sigma(F^2)$; the weight, w, is defined as $0.9337/[\sigma^2(F) + 0.001194F^2]$. The compound crystallized as the toluene solvate and disordered sites for the atoms of the solvent molecule were located about the four-fold axis. The six carbon atoms of the aromatic ring were treated as a rigid group (C—C 1.395 Å) for inclusion in the calculations with an occupancy factor of 0.25 but because of the nature of the disorder no attempt was made to include the methyl substituent. Anisoptropic thermal motion was assumed for all atoms other than hydrogen with the exception of C(1), C(2), C(3) and the solvent atoms. All hydrogen temperature factors were fixed at $U = 0.1$ e Å^{-2}. The atomic scattering factors were taken from the tabulations of Cromer and Mann,[24] anomalous dispersion corrections were by Cromer and Liberman.[25] Final atomic coordinates, tables of thermal parameters, hydrogen atom coordinates and lists of Fo/Fc have been deposited with the editor as supplementary material.*

Acknowledgement—We thank the N.Z. University Grants Committee for funding for equipment.

REFERENCES

1. F. A. Cotton and R. A. Walton, *Multiple bonds between Metal Atoms*. John Wiley, New York (1982).
2. J. San Filippo, Jr., *Inorg. Chem.* 1972, **11**, 3140.
3. R. E. McCarley, T. R. Ryan and C. C. Torardi, *ACS Symp. Ser.* 1981, **155**, 41.
4. M. L. H. Green, G. Parkin, J. Bashkin, J. Fail and K. Prout, *J. Chem. Soc., Dalton Trans.* 1982, 2519.
5. F. A. Cotton, C. Oldham and W. R. Robinson, *Inorg. Chem.* 1966, **5**, 1798; F. A. Cotton, C. Oldham and R. A. Walton, *Inorg. Chem.* 1967, **6**, 214; F. A. Cotton, R. Eiss and B. M. Foxman, *Inorg. Chem.* 1969, **8**, 950.
6. W. Clegg, C. D. Garner, S. Parkes and I. B. Walton, *Inorg. Chem.* 1979, **18**, 2250.
7. R. A. Anderson, R. A. Jones and G. Wilkinson, *J. Chem. Soc., Dalton Trans.* 1978, 446.
8. F. A. Cotton, M. W. Extine, T. R. Felthouse, B. W. S. Holthammer and D. G. Lay, *J. Am. Chem. Soc.* 1981, **103**, 4040.
9. J. V. Brencic and F. A. Cotton, *Inorg. Chem.* 1969, **8**, 7.
10. J. V. Brencic and F. A. Cotton, *Inorg. Chem.* 1969, **8**, 2698.
11. J. V. Brencic and F. A. Cotton, *Inorg. Chem.* 1970, **9**, 346.

*Atomic coordinates for the non-hydrogen atoms have also been deposited with the Cambridge Crystallographic Data Centre for inclusion in their Data Base. Copies are available on request from the Editor at Queen Mary College.

12. J. V. Brencic, L. Golic, I. Leban and P. Segedin, *Monatsh Chem.* 1979, **110**, 1221.
13. F. A. Cotton and B. M. Foxman, *Inorg. Chem.* 1968, **7**, 1784.
14. F. A. Cotton and P. E. Fanwick, *Acta Cryst.* 1980, **B36**, 457.
15. F. A. Cotton, Z. C. Mester and T. R. Webb, *Acta Cryst.* 1974, **B30**, 2768.
16. J. D. Arenivar, V. V. Mainz, H. Ruben, R. A. Anderson and A. Zalkin, *Inorg. Chem.* 1982, **21**, 2649.
17. F. A. Cotton, M. Extine and L. D. Gage, *Inorg. Chem.* 1978, **17**, 172.
18. R. N. McGinnis, T. R. Ryan and R. E. McCarley, *J. Am. Chem. Soc.* 1978, **100**, 7900.
19. W. Wofsberger and H. Schmidbauer, *Synth. React. Inorg. Met.-Org. Chem.* 1974, **4**, 149.
20. T. A. Stephenson, E. Bannister and G. Wilkinson, *J. Chem. Soc.* 1964, 2538.
21. A. J. Nielsen, *Chem. N.Z.* 1985, **49**, 11.
22. A. C. T. North, D. C. Phillips and F. S. Mathews, *Acta Cryst.* 1968, **A24**, 351.
23. G. Sheldrick, *SHELX*-76, *Program for Crystallographic Structure Determination*, University of Cambridge, U.K. (1976).
24. D. T. Cromer and J. B. Mann, *Acta Cryst.* 1968, **A24**, 321.
25. D. T. Cromer and D. Liberman, *J. Chem. Phys.* 1970, **53**, 1891.

Polyhedron Vol. 6, No. 12, pp. 2119–2128, 1987
Printed in Great Britain

0277–5387/87 $3.00+.00

STUDIES ON SPIROBORATE COMPLEXES—II.* STRUCTURAL ELUCIDATION OF BISCATECHOL SPIROBORATE AND ITS ANALOGS BY NMR AND MS SPECTROSCOPY

YOSHIHISA OKAMOTO† and YUKA TAKEI

Division of Chemistry, College of Liberal Arts and Sciences, Kitasato University, 1-15-1, Kitasato, Sagamihara-shi, Kanagawa-ken 228, Japan

and

KANAME TAKAGI

Central Research Laboratories, Zeria Pharmaceutical Co. Ltd. 2512-1, Oshikiri, Konan-mura, Saitama-ken 360-01, Japan

(*Received* 21 *May* 1987; *accepted* 24 *June* 1987)

Abstract—Nine spiroborate complexes (**7–15**) were analyzed by NMR and MS spectroscopy and the characteristic spectra and fragmentation patterns are reported. On the basis of these results, the structure of Meulenhoff's free acid is re-investigated.

There have been considerable studies on reactions between boric acid and diols in connection with the changes of conductivity, acidity and rotatorypolarization.[2] Hermans pointed out that the changes of these physical properties are due to the formation of a spiroborate complex (**1**) which is produced from those reactions in a solution.[3] The first isolation of the spiroborate complex was performed by Böeseken and co-workers[4] who synthesized potassium biscatechol spiroborate (**2**) from the reaction of catechol with potassium borate in water, although they failed to get satisfactory elemental analyses. Later, Meulenhoff confirmed the structure as the spirane type by measurement of the rotatory polarization of some substituted biscatechol spiroborates.[5] Moreover, the free acid (**3**), which is called Meulenhoff's free acid, was reported to be obtained by sublimation of anilinium biscatechol spiroborate (**5**) *in vacuo*.[5] However, the structure of this free acid is still ambiguous and furthermore, NMR and MS spectral analyses of both biscatechol spiroborate and its analogs are little known. In this paper, we describe the structural elucidation of Meulenhoff's free acid on the basis of its spectral data, which are compared with those of its related compounds.

EXPERIMENTAL

All 2-amino-4-methylpyridinium spiroborate complexes (**7–15**) were obtained by our previously reported method.[1] ^{1}H-NMR and ^{13}C-NMR were obtained using Varian T-60 (60 MHz) or EM-90 (90 MHz) and XL-400 (400 MHz) spectrometers, respectively. ^{1}H-NMR spectra of all spiroborates **7–15** were measured in a solution of dimethylsulfoxide-d_6 using tetramethylsilane as an internal standard and all chemical shifts were attributed in a previous paper.[1] Similarly, spiroborates **2** and **5** were also submitted to ^{1}H-NMR and ^{13}C-NMR measurements. MS spectral data were obtained on a JEOL JMS DX-300 (equipped with JMA 3100; ionization voltage, 70 eV) and a JEOL JMS D-100 (ionization voltage, 20 eV) spectrometers.

RESULTS AND DISCUSSION

In a previous study, we reported a new synthesis of 2-amino-4-methylpyridinium biscatechol spi-

* For Part I, see ref. 1.

† Author to whom correspondence should be addressed.

roborate (7) and its analogs (**8–15**) by the reaction of 2-amino-4-methylpyridine borane (**6**) with catechol and its related diols in the presence of orthoester.[1] To confirm the spirane structure, we converted Böeseken's complex **2** into anilinium complex **5** and 2-amino-4-methylpyridinium complex **7** by exchange of potassium cation with the corresponding protonated amines, respectively. When these two spiroborates (**5**) and (**7**) were sublimed *in vacuo* by Meulenhoff's method, the pure starting spiroborates were recovered, respectively, but not the free acid (**3**). Therefore, we used a subliming apparatus as shown in Fig. 1 which is equipped with a dish where concentrated sulphuric acid is poured to remove aniline from gaseous **5**. The sublimation was repeated twice at 140°C below 2 mmHg, and colourless powder was obtained. Hereafter, we used it as Meulenhoff's free acid (MFA). In 1961, Dale and co-workers proposed structure (**4**) instead of structure (**3**) for MFA by speculation about the result that an open structure of a crystalline bis(2,2,5,5-tetramethylhexane-3,4-diol)borate has been confirmed by the presence of an OH absorption band in the infrared (IR) spectrum.[6,7] These facts prompted us to re-examine the structure of MFA by NMR and MS analyses.

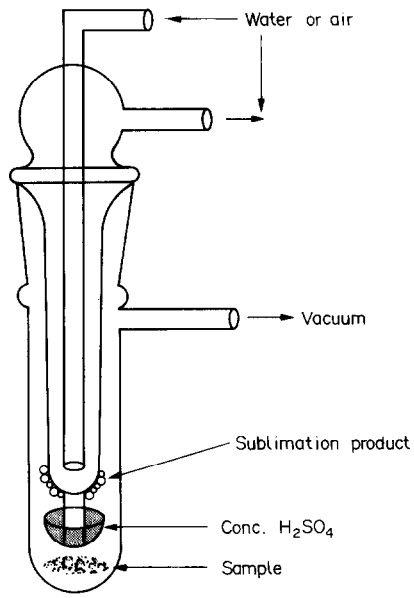

Fig. 1. Subliming apparatus.

NMR spectra

A few NMR studies have been reported on certain spiroborates,[8,9] but not on biscatechol spiroborate and its analogs. Previously, we measured ^{1}H-NMR of spiroborates **7–15**,[1] and have studied their spectral data as well as those of **2** and **5** and two characteristic phenomena were found. Firstly the signal patterns of anion moieties of the spiroborates **7–15** changed when deuterium oxide was added to the solution and secondly the signal of spirans **2** was unchanged by addition of deuterium oxide. As Fig. 2(a) shows, when the counter cation of the biscatechol spiroborate is potassium ion, the singlet signal at 6.47 ppm due to the atomic protons was unchanged by addition of deuterium oxide, whereas when the counter cation is a protonated amine such as anilinium or 2-amino-4-methylpyridinium, the singlet signal at 6.47 ppm of the anion moiety was partially changed to a multiplet by addition of deuterium oxide. Figures 2(b) and (c) show two other examples. The ratio of the signal at 2.15 ppm to the signal at 2.12 ppm due to methyl protons (6H) of spirans **8** was changed by addition of deuterium oxide. Similarly, the signal at 4.43 ppm due to methylene protons (4H) of spi-

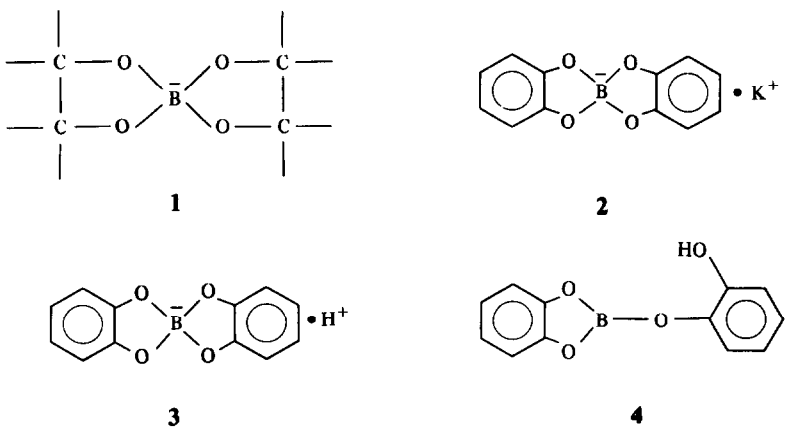

1 **2** **3** **4**

Scheme 1.

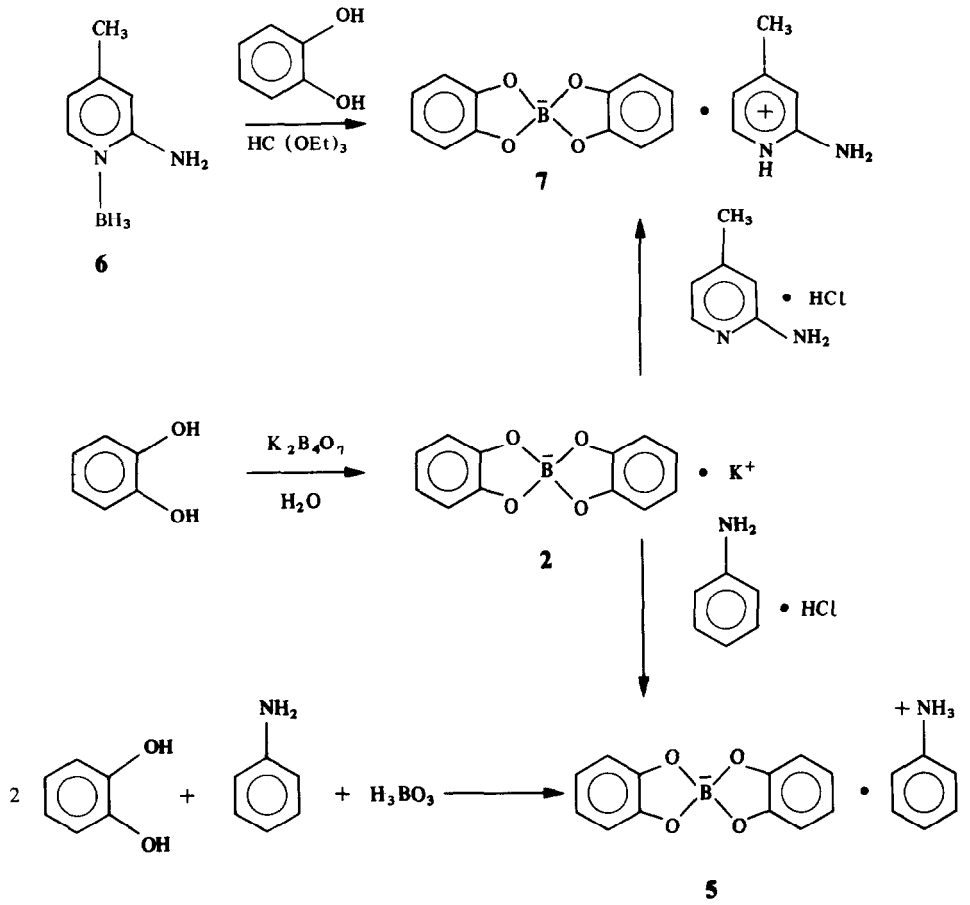

Scheme 2.

rans **11** was clearly changed to a doublet (4.40 and 4.45 ppm) by addition of deuterium oxide. Namely, the proton of anilinium or of the 2-amino-4-methylpyridinium ion would assist hydrolysis of the anion moiety of the spiroborate complex.

Since some spiroborates have already been hydrated in their crystals and also a little amount of water is contained in the NMR solvent, hydrolysis of the spiroborates would occur to a small extent even without adding deuterium oxide. In fact, Fig. 3 shows a small signal of AA′BB′ pattern near the singlet signal at 6.47 ppm at least below 50°C, although deuterium oxide was not added to the solution. The signal of the AA′BB′ pattern coalesced with the singlet signal when the solution was heated above 70°C and after cooling the spectrum again showed the same pattern as that at 32°C. Therefore, the AA′BB′ pattern at 32°C resulted from hydrolysis of the spiroborate where water was contained in the NMR solvent. The equilibrium equation would be expressed as eq. (1).

The ^{13}C-NMR spectrum of spiroborate **2** was

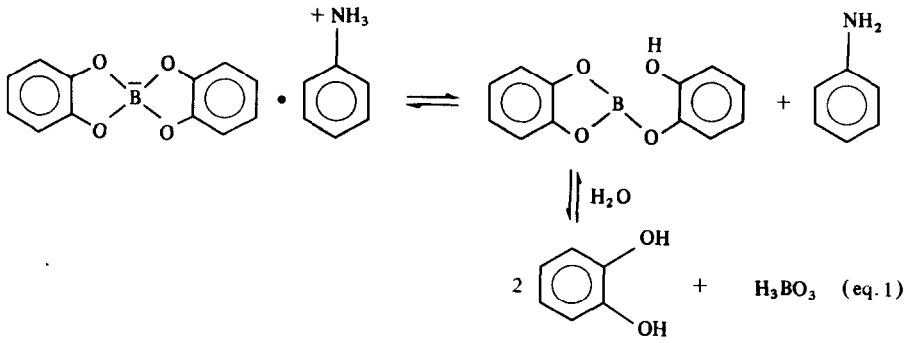

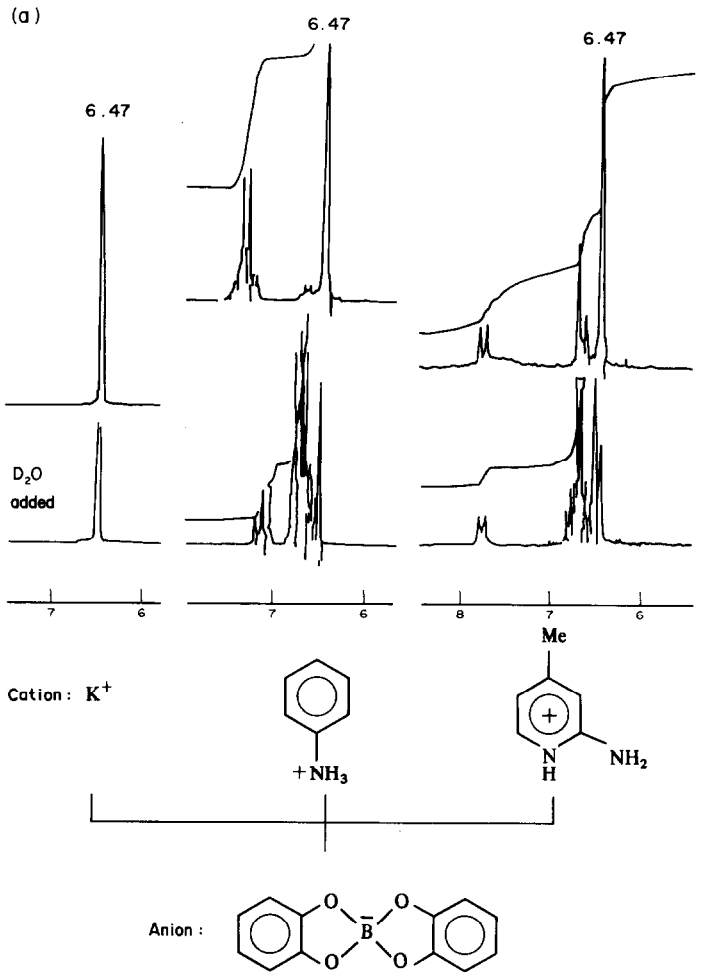

Fig. 2. (a) ^{1}H-NMR spectra of spiroborates 2, 5 and 7 (90 MHz) (deuterium oxide was added in the spectra below). (b) ^{1}H-NMR spectra of spiroborate 8 (90 MHz). (c) ^{1}H-NMR spectra of spiroborate 11 (60 MHz).

compared with that of catechol and Table 1 shows the difference of the chemical shifts between catechol and **2**. Those chemical shifts of **2** were attributed to DEPT and ^{13}C-^{1}H COSY. Clearly, electrons of the oxygen atom of **2** flow into the boron atom because the C-1 signal of **2** shifted to the lower field in the range of 6.28 ppm comparing it with catechol. Magnetic anisotropy of the boron atom was especially observed at C-2.

Table 1. ^{13}C-NMR spectral data (ppm)

Compound	C-1	C-2	C-3
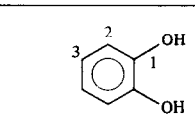	145.37	115.80	119.41
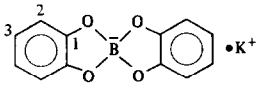 •K$^+$	151.65	107.72	117.43
Difference	−6.28	+8.08	+1.98

MS spectra

Tables 2 and 3 show the results of MS analysis of spiroborates **7**–**15**. In compound **7**, for example, when R is defined as a 2-(1,3,2-benzodioxaborolyl) group, typical fragment ions such as RO––OR (*m*/*Z* 346), R—O—R (*m*/*Z* 254), RO––OH (*m*/*Z* 228) and R—OH (*m*/*Z* 136) were observed including the molecular ion peaks of the catechol (*m*/*Z* 110) and 2-amino-4-methylpyridine (*m*/*Z* 108). This fragmentation pattern was in common with other spiroborates **8**, **12** and **13**. On the other hand, as Table 3 shows, *o*-substituted spiroborates **9**, **10** and **11**, and spiroborates with a carboxyl group as the

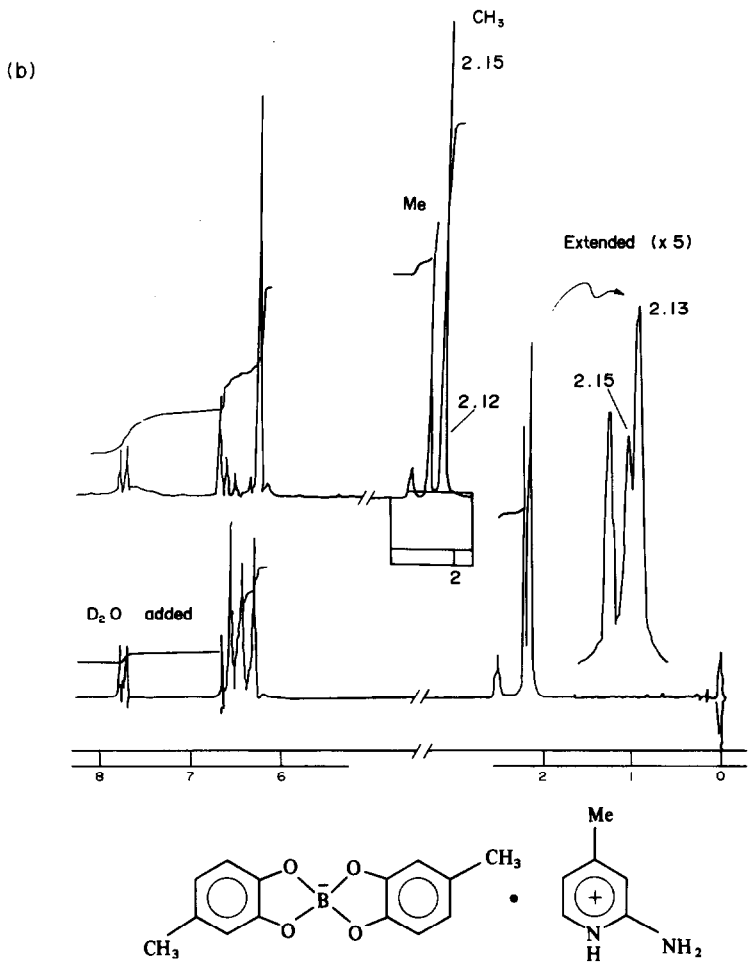

Fig. 2—*continued*

ligand (**14** and **15**) did not afford the characteristic fragmentation pattern of this kind. Especially, **15** did not give any fragment ion of boron contained moiety even by the In Beam method. MS spectrum of **2** was not obtained and this result corresponded with the fact that **2** is hard to combust.[5]

Although relative intensities of these typical fragment ions were dependent on their sample temperature for measurement, the fragment ion of bisdiol trigonal borate (RO––OH) showed the strongest intensity among the boron contained fragment ions in Table 2. It is worth noting that any kind of amine in the protonated counter cation does not affect the MS fragmentation of the spiroborate anion (compare **7** in Table 2 with **5** in Table 4). Therefore, both the characteristic fragmentation pattern and the strongest fragment ion shown in Table 2 could become the clue to clarify whether the structure of a certain borate is spirane or simple trigonal.

Structural elucidation of MFA

On the basis of the above results, we attempted to elucidate the structure of MFA. Table 4 shows the fragment ions of MFA in comparison with those of **5**. Since one of the typical fragment ions, RO––OR (*m*/*Z* 346), was not observed and the relative intensity of the fragment ion R—OH (*m*/*Z* 136) was very strong instead of RO––OH (*m*/*Z* 228), MFA could not be **3**. Interestingly, the molecular ion peak of aniline was observed. Meanwhile, Fig. 4 shows ^{1}H-NMR spectra of MFA where signals of deuterium exchangable protons (7.85 ppm) and aromatic protons of both aniline (7.23–7.60 ppm) and catechol (6.40–6.83 ppm) were observed in addition to an aromatic singlet signal at 6.47 ppm (the left spectra). When treated with deuterium oxide, the spectral patterns were changed to those of aniline (5H, 6.97–7.43 ppm) and catechol (8H, 6.50–6.87 ppm), and the signal at 6.47 ppm disappeared

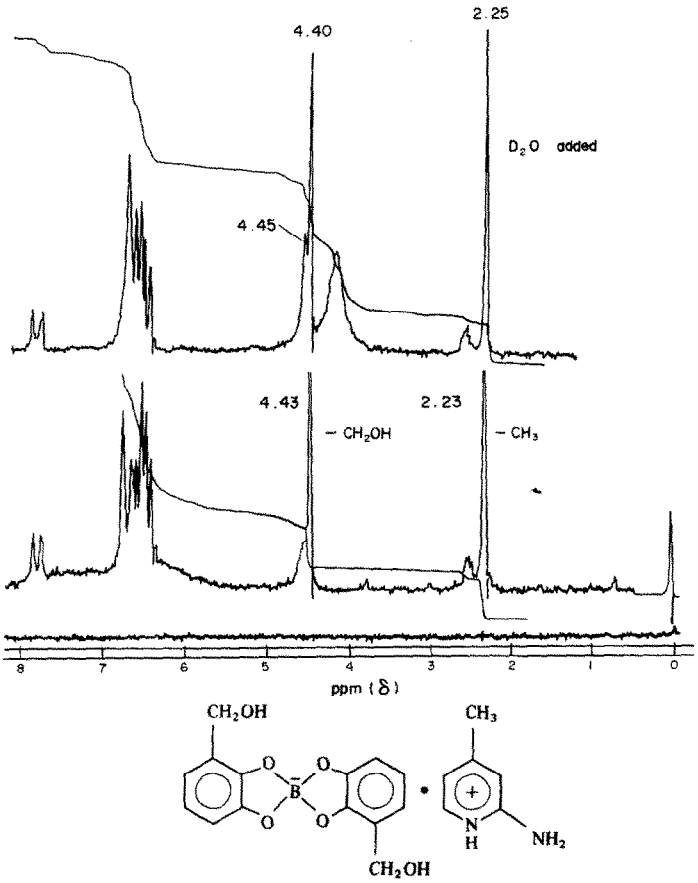

Fig. 2—*continued*

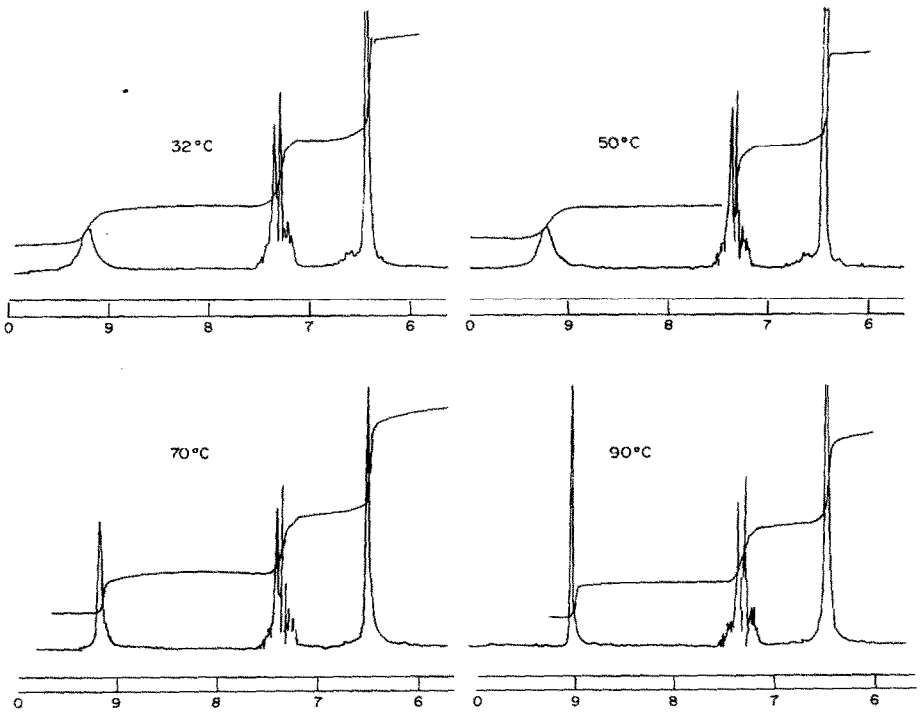

Fig. 3. ^{1}H-NMR spectra of spiroborate 5 at various temperatures (90 MHz).

Table 2. MS spectral data on spiroborates (2-amino-4-methylpyridinium salts)

Spiroborate	R	X	Fragment ion (m/Z; relative intensity %) RO–∿∿–OR	R—O—R	RO–∿∿–OH	R—OH
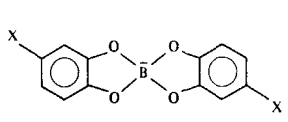	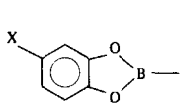	H	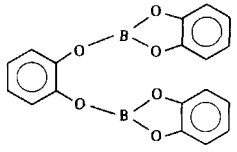	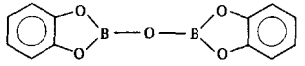	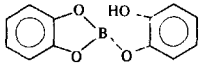	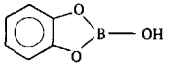
7 : X = H 8 : X = CH_3			346(33%)	254(24%)	228(100%)	136(44%)
		CH_3	388(51%)	282(13%)	256(100%)	150(15%)
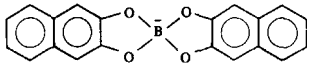 12	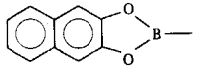		496(66%)	354(28%)	328(100%)	186(39%)
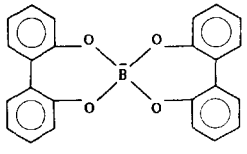 13	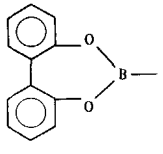		574(100%)	406(19%)	380(100%)	212(83%)

Table 3. MS spectral data on spiriborates (2-amino-4-methylpyridinium salts)

Spiroborate	R	X	Fragment ion (m/Z; relative intensity %) RO—⋀—OR	R—O—R	RO—⋀—OH	R—OH	Others
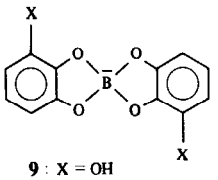 **9** : X = OH **10** : X = CHO **11** : X = CH_2OH	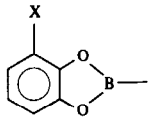	OH	—	—	260(100%)	152(88%)	536(24%) 535(22%) 402(92%) 401(61%)
		CHO	—	—	284(36%)*	164(100%)	374(9%)[a] 328(9%)[a]
		CH_2OH	—	—	—	166	—
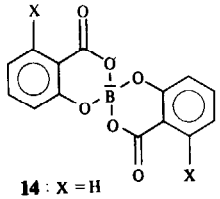 **14** : X = H **15** : X = OH	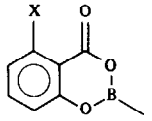	H	—	310(76%)	—	164(100%)	520(21%) 400(40%) 355(30%)
		OH	—	—	—	—	—

[a] In beam method.

Table 4. MS spectral data on spiroborate 5 and MFA (Relative intensity %)

Compound	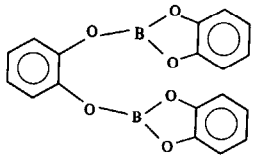 (346)	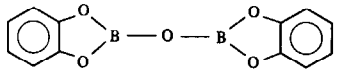 (254)	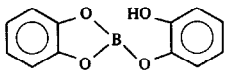 (228)	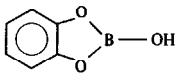 (136)	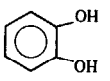 (110)	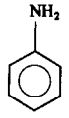 (93)
5	33%	24%	100%	44%	61%	96%
MFA	—	4%	3%	100%	98%	73%

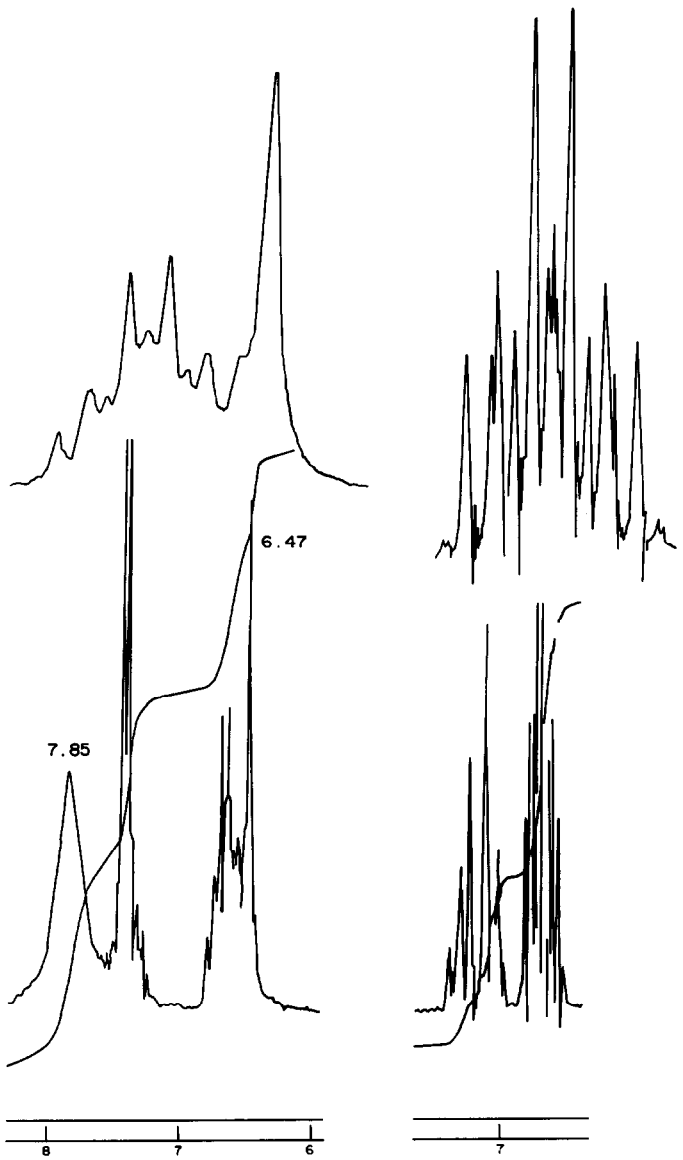

Fig. 4. ^{1}H-NMR spectra of MFA (90 MHz). (The right shows the spectra after addition of D_2O. The upper shows the extended spectra (× 5) in the region of 6–7 ppm).

entirely (the right spectra). These data clearly indicate that aniline cannot be removed from **5** by the sublimation method even over concentrated sulphuric acid. We believe that MFA might be a mixture of catechol, aniline and an unknown compound which would readily be hydrolyzed so that the signal at 6.47 ppm disappeared upon addition of deuterium oxide. Since *o*-phenylene borate like compound **4** is known to be hydrolyzed readily,[10] the unknown compound might be the aniline adduct of compound **4**.

In conclusion, spiroborates of certain kinds derived from catechol and its analogous diols showed characteristic spectra, and especially the proton of the counter cation in the spiroborate complex plays an important role in the ^{1}H-NMR and MS spectroscopic measurements.

REFERENCES

1. Y. Okamoto, T. Kinoshita, Y. Takei and Y. Matsumoto, *Polyhedron* 1986, **5**, 2051.
2. J. Böeseken, *Adv. Carbohydrate Chem.* 1949, **4**, 189 and literatures cited therein.
3. P. H. Hermans, *Z. Anorg. Allgem. Chem.* 1925, **142**, 83.

4. J. Böeseken, A. Obreen and A. van Haeften, *Rec. Trav. Chem.* 1918, **37**, 184.
5. J. Meulenhoff, *Z. Anorg. Allgem. Chem.* 1925, **142**, 373.
6. A. J. Hubert, B. Hargitay and J. Dale, *J. Chem. Soc.* 1961, 931.
7. J. Dale, *J. Chem. Soc.* 1961, 910.
8. M. Mazurek and A. S. Perlin, *Can. J. Chem.* 1963, **41**, 2403.
9. H. R. Morales, H. Tlahuext, F. Santiesteban and R. Contreras, *Spectrochim. Acta* 1984, **40A**, 855.
10. R. C. Mehrotra and G. Srivastava, *J. Chem. Soc.* 1961, 4045.

Polyhedron Vol. 6, No. 12, pp. 2129–2135, 1987
Printed in Great Britain

0277-5387/87 $3.00+.00

A "VERTEX ELECTRON PAIR" SCHEME (VEPS) FOR DESCRIBING THE SKELETAL ELECTRON DISTRIBUTION IN BORANE-TYPE CLUSTERS

RONALD J. GILLESPIE

Chemistry Department, McMaster University, Hamilton, Ontario L85 4M1, Canada

WILLIAM W. PORTERFIELD

Chemistry Department, Hampden-Sydney College, Hampden-Sydney, Virginia 23943, U.S.A.

and

KENNETH WADE*

Chemistry Department, Durham University, South Road, Durham DH1 3LE, U.K.

(*Received* 21 *May* 1987; *accepted* 24 *June* 1987)

Abstract—A predominantly localized electron pair scheme is outlined for describing the electron distribution and bonding in *closo* borane anions $B_nH_n^{2-}$ and related electron deficient deltahedral clusters, in which a skeletal electron pair is assigned to each vertex, one pair being regarded as delocalized just inside the roughly spherical surface on which the skeletal atoms lie. The scheme gives a clearer picture of the electron distribution than is conveyed by resonating 2- and 3-centre bonds in the polyhedron edges and faces, and allows the bond orders of the polyhedron edge links to be calculated readily. The consequence of formal removal of BH^{2+} units from closo species $B_nH_n^{2-}$ to generate *nido* species $B_{n-1}H_{n-1}^{4-}$ and *arachno* species $B_{n-2}H_{n-2}^{6-}$ is explored, and seen to allow rationalization of two features of such deltahedral-fragment clusters: (i) why a high-connectivity vertex is left vacant and (ii) why the frontier orbitals of such species concentrate electronic charge around their open faces. Moreover, in the case of D_{4h} $B_4H_4^{6-}$ (cf. $C_4H_4^{2-}$) and D_{5h} $B_5H_5^{6-}$ (cf. $C_5H_5^-$), the approach leads directly to the familiar picture for aromatic ring systems in which the highest filled, doubly degenerate π-bonding molecular orbital concentrates electronic charge in rings above and below the polygon on which the skeletal nuclei lie. It also leads to the expectation that *arachno* clusters with non-adjacent vacant vertices will be more stable than those with adjacent vacant vertices.

In previous papers[1,2] in which we have separately discussed the bonding in cluster compounds, we have advocated the use of localized valence shell electron pair schemes for treating the bonding in certain highly symmetrical polyhedral clusters in which the numbers of edges or faces coincide with the numbers of bond pairs available. For example, a regular octahedral arrangement of six bond pairs over the edges of the tetrahedral P_4 molecule allows its bonding to be described in terms of six 2-centre 2-electron (2c2e) bonds, while a tetrahedral arrangement of the four skeletal bond pairs over the faces of the tetrahedral boron halide B_4Cl_4 satisfactorily accounts for its bonding in terms of four 3-centre 2-electron (3c2e) bonds. Similar treatments are possible for the metal–metal bonding in the octahedral clusters $Mo_6Cl_8^{4+}$ (twelve 2c2e edge bonds) and $Nb_6Cl_{12}^{2+}$ (eight 3c2e face bonds). The advantages of these treatments are that they give a clear picture of the symmetrical distribution of the

* Author to whom correspondence should be addressed.

electronic charge in such clusters, and give a useful indication of the strength of the bonding (edges associated with a pair of electrons clearly correspond to bonds of order 1.00; those shared between faces containing 3c2e bonds, effectively acquiring one-third of a bond pair from each such bond, have a bond order of 0.66′).

Closo borane anions $B_nH_n^{2-}$ and related clusters contain too few electrons to allow comparably simple treatments of their bonding. They contain $(n+1)$ skeletal bond pairs with which to hold together their n BH units, which are located at the n vertices of deltahedra with $2(n-2)$ faces and $3(n-2)$ edges (Fig. 1).[2-6] If each skeletal atom was to participate in three skeletal bonds (a condition that must be met if each skeletal atom is to use all four of its valence shell orbitals) then the $(n+1)$ skeletal bond pairs would have to be allocated to three 2c2e edge bonds and $(n-2)$ 3c2e face bonds.[4,7,8] However, none of the polyhedra in Fig. 1 has the appropriate symmetry to allow such a combination of 2c2e and 3c2e bonds to be allocated in a unique manner to match the skeletal symmetry. In each case, a relatively large number of resonance canonical forms has to be considered (e.g. 24 in the case of $B_6H_6^{2-}$, 10 in the case of $B_7H_7^{2-}$) any one of which gives a distorted picture of the actual electron distribution.[9,10] The average number of electrons associated with each type of polyhedron edge is difficult to deduce from such bond schemes, which are therefore rarely used for *closo* clusters, even though 2c2e BH and BB bonds and 3c2e BHB and BBB bonds have been found to be extremely helpful for describing the bonding in *nido* and *arachno* boranes B_nH_{n+4} and B_nH_{n+6} ever since Lipscomb developed his elegant topological treatment of borane bonding a quarter century ago.[7,11]

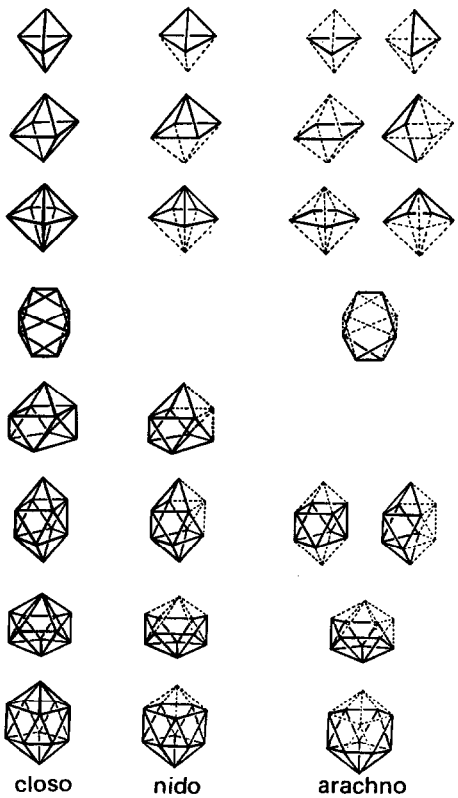

Fig. 1. The deltahedral skeletal structures of *closo* borane anions $B_nH_n^{2-}$ and isoelectronic carboranes $C_2B_{n-2}H_n$, and polyhedral fragment structures of *nido* species $B_{n-1}H_{n+3}$ and *arachno* species $B_{n-2}H_{n+4}$.

Because of the complexity of 2- and 3-centre bond schemes for *closo* borane anions $B_nH_n^{2-}$ and related clusters, it is usual to treat their skeletal bonding in terms of molecular orbital schemes that delocalize the electrons over the whole molecular skeleton.[6,12,13] Such schemes help one understand the numbers of electrons needed, but (like the 2c2e and 3c2e bond schemes) convey little feeling for the electron distribution or the numbers of electrons associated with individual polyhedron edges. It is to overcome this problem that we put forward in this paper a predominantly *localized* electron pair scheme for *closo* clusters that associates a skeletal bond pair with each polyhedron *vertex* as outlined below. This scheme, which we refer to as a "Vertex Electron Pair Scheme" (VEPS), not only conveys a feeling for the electron distribution in deltahedral (*closo*) clusters, but also allows the electron distribution in polyhedral fragment (*nido* and *arachno*) clusters to be deduced easily, reproducing quite well the electron distribution deduced from MO calculations on such clusters. Moreover, it underlines the relationship between *closo* clusters like $B_6H_6^{2-}$ or $B_7H_7^{2-}$ and *arachno* aromatic ring systems like $C_4H_4^{2-}$ or $C_5H_5^-$ respectively.

THE VERTEX ELECTRON PAIR SCHEME (VEPS)

Our approach exploits the fundamental feature of *closo* borane anions $B_nH_n^{2-}$, that each of the n BH units contributes two electrons for skeletal bonding. Since in the cluster it shares these with similar BH units, it is reasonable to suppose that the overall distribution of skeletal electron density over the surface of the polyhedron still leaves each boron atom's share as effectively two electrons centred on the boron nucleus and so on the polyhedron vertex. (Actually, for clusters with more than one type of vertex, the atoms at vertices of low connectivity end up with a slightly greater share—a small fraction of an electron charge—of the skeletal electrons than those at vertices of high connec-

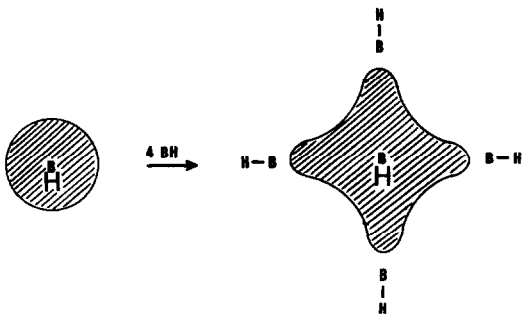

Fig. 2. Polarization of a BH unit's skeletal electron pair by four neighbouring skeletal boron atoms.

tivity.[2,4,9,13,14]) Compared to an isolated BH unit, with its available skeletal electron pair cylindrically symmetrically disposed about the B—H axis, the skeletal pair associated with a BH unit in a cluster will become polarized under the attractive influence of the neighbouring boron nuclei (Fig. 2).

In addition to retaining effective control over two skeletal electrons, each BH unit in a fully symmetrical *closo* cluster anion $B_nH_n^{2-}$ will also acquire a supplementary electronic charge of $-2/n$, that being its share of the extra, $(n+1)$th skeletal electron pair.

This is illustrated schematically in Fig. 3 for

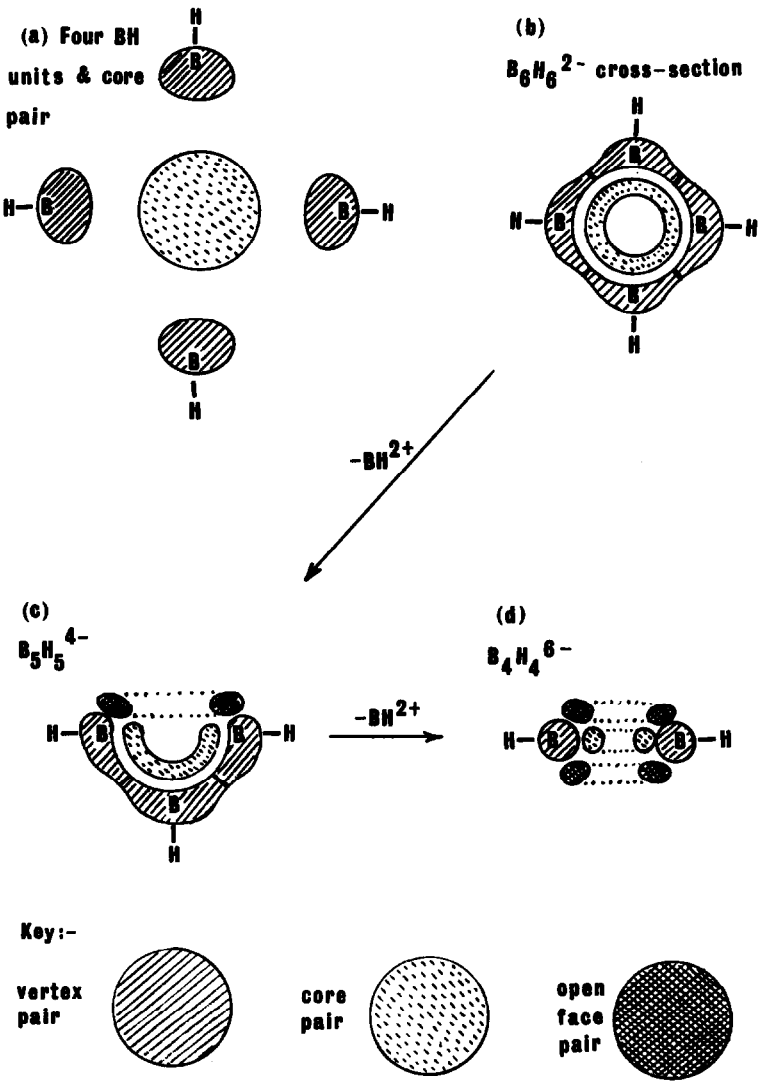

Fig. 3. Distribution of the skeletal electron pairs in O_h $B_6H_6^{2-}$ (illustrated as a cross-section in a B_4 plane) and in the *nido* C_{4v} $B_5H_5^{4-}$ and *arachno* D_{4h} $B_4H_4^{6-}$ derivable therefrom by successive removal of two BH^{2+} units. (a) Four BH units and core-centred pair in exploded form. (b) Cross-section of O_h $B_6H_6^{2-}$ in a B_4 plane. (c) Cross-section of C_{4v} $B_5H_5^{4-}$ in a B_3 plane. (d) Cross-section of D_{4h} $B_4H_4^{6-}$ in a B_2 plane.

$B_6H_6^{2-}$. Figure 3(a) shows a cross-section of this octahedral cluster in exploded form, with four BH units, each contributing a pair of electrons for skeletal bonding, surrounding the extra, $(n+1)$th pair of electrons. When these BH units are brought together [Fig. 3(b)] to the interatomic distances appropriate for $B_6H_6^{2-}$, there are two major consequences for the skeletal electron pairs. Those associated with the BH units acquire the C_{4v} distortion already referred to (Fig. 2), as they are attracted towards adjacent nuclei, while the $(n+1)$th electron pair, which initially may be considered to lie at the cluster centre, spreads out to form an octahedrally distorted spherical shell of electronic charge just inside the sphere on which the boron nuclei lie.

Such a distribution of the skeletal electron pairs, responding to the attractions of the boron nuclei, conveys (in essentially localized electron pair terms) the electron distribution implicit in molecular orbital treatments of *closo* clusters.[7,12-15] Invariably, there is a unique, strongly bonding MO of A symmetry (S^{σ}-type in A. J. Stone's nomenclature[16-18]) resulting from a fully in-phase combination of inward-pointing *sp* hybrid orbitals. This molecular orbital concentrates electronic charge in a roughly spherical shell just inside the sphere on which the boron atoms lie. It is this orbital which is represented by the unique, $(n+1)$th (delocalized) electron pair in our treatment, centred on the middle of the cluster but concentrated near to the boron nuclei. The remaining n bonding MO's all arise primarily from interactions of tangentially oriented p AO's that concentrate electron density on the roughly spherical surface of the polyhedron (illustrated for $B_6H_6^{2-}$ in Fig. 4).[15]

POLYHEDRON EDGE BOND ORDERS

The approach we have outlined can be used to calculate the fractional bond orders of the B—B polyhedron edge bonds of *closo* borane anions $B_nH_n^{2-}$ and related clusters very simply. If each BH unit is allocated $(2+2/n)$ electrons as its share of the $(n+1)$ skeletal electron pairs and it shares these equally between the k 2-centre links it forms to neighbouring boron atoms (where k is the skeletal connectivity—the number of polyhedron edges radiating from the vertex in question), then a polyhedron edge linking two boron atoms of skeletal connectivities k_1 and k_2 can be allocated $(2+2/n)(1/k_1+1/k_2)$, i.e. $2(n+1)(k_1+k_2)/nk_1k_2$ electrons and so has a bond order, $\bar{n}$, of $(n+1)(k_1+k_2)/nk_1k_2$. For octahedral $B_6H_6^{2-}$, for which $n=6$, $k_1=k_2=4$, all edges have formal bond order $7/12=0.58$. For pentagonal bipyramidal $B_7H_7^{2-}$, for which $n=7$, $k_1=4$, $k_2=5$, the axial–equatorial edges have formal bond order of 18/35, i.e. 0.51, while the equatorial edges have a bond order of 4/7, i.e. 0.57. These and other bond orders, $\bar{n}_{VEPS}$, calculated similarly for the various types of edge in *closo* borane anions $B_nH_n^{2-}$ ($n=5$–12) are listed in Table 1, together with the edge lengths L. For comparison, Table 1 also lists some relevant data taken from Refs 10 and 19. These include bond indices I calculated by the Molecular Orbital Bond Index (MOBI) method,[20] and bond orders estimated by two other methods, (i) $\bar{n}_L$, edge bond orders calculated directly from their known lengths L and (ii) $\bar{n}_{2c3c}$, bond orders deduced from the distributions of 2- and 3-centre bonds compatible with their topologies. In comparing them, one should note that the calculated bond indices I integrate to values that *exceed* the numbers of skeletal electron pairs, whereas $\Sigma\bar{n}_{VEPS}$ and $\Sigma\bar{n}_{2c3c}$ equal the numbers of skeletal bond pairs, $(n+1)$. The values of $\bar{n}_{VEPS}$ in Table 1 provide an encouragingly reliable guide to the way the edge bonds vary in strength (and so in length) in these *closo* clusters, though necessarily failing to discriminate between bonds of identical connectivity type that occupy non-equivalent sites (as in the cases of $B_8H_8^{2-}$, $B_9H_9^{2-}$, $B_{10}H_{10}^{2-}$ and $B_{11}H_{11}^{2-}$). However, the values of $\bar{n}_{VEPS}$ underestimate the *extent* to which bonds vary in strength with connectivity, for the reason

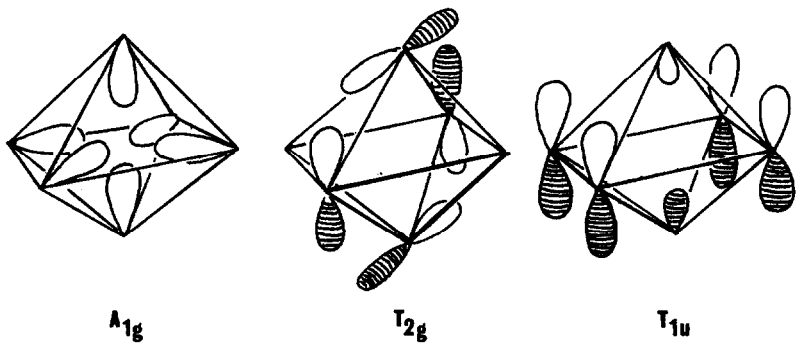

Fig. 4. Skeletal molecular orbitals of $B_6H_6^{2-}$.

Table 1. Interatomic distances L (Å), bond indices I and bond orders $\bar{n}$ for *closo* borane anions $B_nH_n^{2-}$

Species	L	k_1, k_2	I	$\bar{n}_L$	$\bar{n}_{VEPS}$	$\bar{n}_{2c3c}$
$B_5H_5^{2-}$	1.64[a]	3, 4	0.93	0.68	0.70	0.83
	1.83[a]	4, 4	0.42	0.36	0.60	0.33
$B_6H_6^{2-}$	1.686	4, 4	0.68	0.58	0.58	0.58
$B_7H_7^{2-}$	1.63[a]	4, 4	0.85	0.71	0.57	0.58
	1.79[a]	4, 5	0.53	0.41	0.51	0.43
$B_8H_8^{2-}$	1.559	4, 4	0.93	0.91	0.56	0.83
	1.717	4, 5	0.70	0.52	0.50	0.83
	1.756	4, 5	0.53	0.46	0.50	0.33
	1.926	5, 5	0.46	0.27	0.45	0.33
$B_9H_9^{2-}$	1.708	4, 5	0.66	0.54	0.50	0.58
	1.837	5, 5	0.46	0.36	0.44	0.33
	1.906	5, 5	0.45	0.29	0.44	0.33
$B_{10}H_{10}^{2-}$	1.678	4, 5	0.67	0.60	0.50	0.58
	1.796	5, 5	0.51	0.40	0.44	0.42
	1.810	5, 5	0.50	0.39	0.44	0.38
$B_{11}H_{11}^{2-}$	1.655	4, 5	0.77	0.64	0.49	0.75
	1.745	4, 6	0.58	0.48	0.45	0.50
	1.771	4, 5	0.51	0.44	0.49	0.75
	1.788	5, 5	0.53	0.42	0.44	0.38
	2.012	5, 6	0.38	0.22	0.40	0.33
$B_{12}H_{12}^{2-}$	1.775	5, 5	0.54	0.43	0.43	0.43

[a] Calculated values[19]: these and other values of L, I, $\bar{n}_L$ and $\bar{n}_{2c3c}$ are taken from Refs 10 and 19. Bond orders $\bar{n}_L$ were calculated from bond lengths L[19]; bond orders $\bar{n}_{2c3c}$ were calculated from 2c- and 3c-electron pair bond schemes.[10]

noted above—that the atoms of lower connectivity attract a slightly greater share of the skeletal electronic charge.

NIDO AND *ARACHNO* SPECIES

It is possible to extend our approach to *nido* or *arachno* clusters with shapes that are clearly fragments of the same series of polyhedra as the *closo* boranes. *Nido* boranes B_nH_{n+4} are formally protonated derivatives of hypothetical anions $B_nH_n^{4-}$ whose polyhedral fragment structures (Fig. 1) resemble those of *closo* species $B_{n+1}H_{n+1}^{2-}$, but with one vertex (normally that of highest skeletal connectivity) left vacant. The *nido* anion $B_nH_n^{4-}$ can thus be generated in principle by removal of a BH^{2+} unit from a highly-connected vertex of a parent *closo* species $B_{n+1}H_{n+1}^{2-}$. Figure 3(c) illustrates the consequence of this for the skeletal electrons. The electrons originally associated with the vertex from which BH^{2+} is removed, losing their electrostatic attraction to that vertex, spread out towards the neighbouring nuclei. The core-centred delocalized skeletal pair also moves away from the vacant vertex. The effect of these shifts in the electron distribution is to build up electron density around the open face, with only a marginal increase in electron density elsewhere. Again, this is consistent with the picture conveyed by MO calculations: typically, the HOMO of *nido* clusters concentrates electronic charge around the open face,[2,7,12,16–18,21–26] making this region most suitable for protonation in generating neutral species B_nH_{n+4}. The high connectivity of the vertex vacated is also intelligible in that the ring of electronic charge generated will be stabilized increasingly with the number of nuclei around the open face.

Similar arguments apply to *arachno* clusters B_nH_{n+6} whose skeletal anions $B_nH_n^{6-}$ have shapes formally derivable from *closo* parents $B_{n+2}H_{n+2}^{2-}$ by removal of two BH^{2+} units. Figure 2(d) illustrates this for the removal of a second BH^{2+} unit from a vertex opposite the first vacated. Again, the electron pair originally assigned to the vertex vacated spreads out to form a ring of charge adjacent to the neighbouring nuclei and the core-centred, delocalized skeletal pair likewise relaxes towards those nuclei.

The *arachno* $B_4H_4^{6-}$ species depicted schematically as the end product of these successive removals of two BH^{2+} units from $B_6H_6^{2-}$ is a square planar species, analogous to the cyclobutadiene dianion, $C_4H_4^{2-}$. The rings of electronic charge generated, above and below the plane of the four boron atoms, correspond directly to the electron distribution arising from the doubly degenerate HOMO of a species like $C_4H_4^{2-}$. Similar removal of the axial BH^{2+} units from a pentagonal bipyramidal *closo* parent $B_7H_7^{2-}$ would generate an *arachno* pentagonal species $B_5H_5^{6-}$ (cf. the isoelectronic cyclopentadienide anion $C_5H_5^-$). Again, the electron distribution in rings above and below the $B_5H_5^{6-}$ plane reproduces exactly that appropriate for the doubly degenerate HOMO of an aromatic ring system like $C_5H_5^-$.

The cyclic *arachno* species $B_4H_4^{6-}$ and $B_5H_5^{6-}$ just considered, derived from parent *closo* species $B_6H_6^{2-}$ and $B_7H_7^{2-}$ respectively by removal of two BH^{2+} units from opposite vertices, would clearly be more stable entities than hypothetical alternatives in which the BH^{2+} units were removed from adjacent vertices, since the stabilization of the electron pairs associated with the open face would involve fewer boron nuclei and so be less in the latter case. Indeed, the approach outlined here leads to the prediction that, for *arachno* species in general, the most stable isomer will be that in which *non*-adjacent, high connectivity vertices will be left vacant. Among known

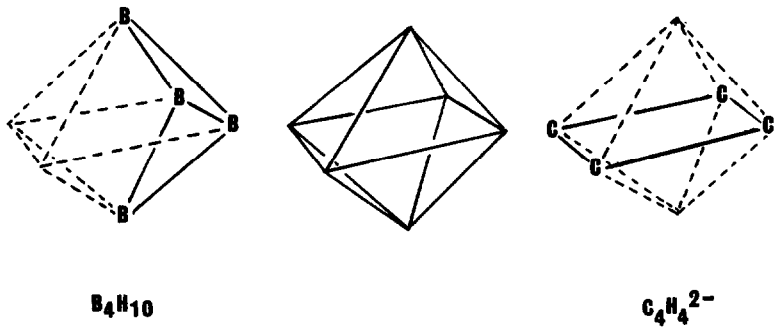

Fig. 5. Alternative skeletal shapes possible for *arachno* species based on an octahedron.

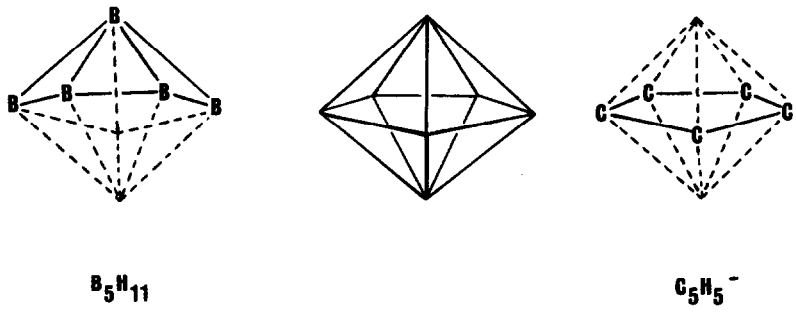

Fig. 6. Alternative skeletal shapes possible for *arachno* species based on a pentagonal bipyramid.

arachno boranes, B_nH_{n+6}, however, the preferred isomer is one that leaves adjacent vertices vacant. Tetraborane(10) B_4H_{10}, for example, has a butterfly-shaped arrangement of its four skeletal boron atoms (Fig. 5) (contrast the square planar shape expected for $C_4H_4^{2-}$) while pentaborane(11), B_5H_{11}, has the nonplanar tent-like shape shown in Fig. 6 (contrast planar $C_5H_5^-$). We shall show elsewhere[26] that EHMO calculations support the qualitative conclusions drawn here, that the more stable skeleton is that with non-adjacent vacant vertices, but that the extra six hydrogen nuclei that *arachno* boranes need to convert their $B_nH_n^{6-}$ frameworks into neutral molecules B_nH_{n+6} are better accommodated if that framework has adjacent *vacant* vertices.

Acknowledgement—The approach outlined here evolved during the tenure of visiting professorial appointments by WWP at Durham and by KW at McMaster. Financial support from the Mednick (WWP) and Hooker (KW) Foundations is gratefully acknowledged.

REFERENCES

1. R. J. Gillespie, *Chem. Soc. Rev.* 1979, **8**, 315.
2. K. Wade, *Advan. Inorg. Chem. Radiochem.* 1976, **18**, 1.
3. K. Wade, *J. Chem. Soc. Chem. Commun.* 1971, 791.
4. K. Wade, *Electron Deficient Compounds*. Nelson, London (1971).
5. K. Wade, *Inorg. Nucl. Chem. Letts* 1972, **8**, 823.
6. D. M. P. Mingos, *Chem. Soc. Rev.* 1986, 31.
7. W. N. Lipscomb, *Boron Hydrides*. Benjamin, New York (1963).
8. W. N. Lipscomb, *Inorg. Chem.* 1979, **18**, 2328.
9. M. E. O'Neill and K. Wade, *Inorg. Chem.* 1982, **21**, 461.
10. M. E. O'Neill and K. Wade, *Polyhedron* 1984, **3**, 199.
11. W. N. Lipscomb, *Advan. Inorg. Chem. Radiochem.* 1959, **1**, 117.
12. W: N. Lipscomb, *Boron Hydride Chemistry* (Edited by E. L. Muetterties) Chap. 2, pp. 29–78. Academic Press, New York (1975).
13. R. L. Middaugh, *Boron Hydride Chemistry* (Edited by E. L. Muetterties) Chap. 8, pp. 273–300. Academic Press, New York (1975).
14. M. F. Hawthorne, D. C. Young, T. D. Andrews, D. V. Howe, R. L. Pilling, A. D. Pitts, M. Reintjes, L. F. Warren, Jr. and P. A. Wegner, *J. Am. Chem. Soc.* 1968, **90**, 879.
15. H. C. Longuet-Higgins, *Quart. Rev. Chem. Soc. (London)* 1957, **11**, 121.
16. A. J. Stone, *Inorg. Chem.* 1981, **20**, 563.
17. A. J. Stone and M. J. Alderton, *Inorg. Chem.* 1982, **21**, 2297.
18. A. J. Stone, *Polyhedron* 1984, **3**, 1299.

19. C. E. Housecroft, R. Snaith, K. Moss, R. E. Mulvey, M. E. O'Neill and K. Wade, *Polyhedron* 1985, **4**, 1875.
20. D. R. Armstrong, P. G. Perkins and J. J. P. Stewart, *J. Chem. Soc., Dalton Trans.* 1973, **838**, 2273.
21. E. B. Moore, L. L. Lohr, Jr. and W. N. Lipscomb, *J. Chem. Phys.* 1961, **35**, 1329.
22. G. B. Dunks and M. F. Hawthorne, *Boron Hydride Chemistry* (Edited by E. L. Meutterties) Chap. 11, pp. 383–430. Academic Press, New York (1975).
23. M. F. Hawthorne and T. D. Andrews, *Chem. Commun.* 1965, 443.
24. R. N. Grimes, *Metal Interactions with Boron Clusters*. Plenum, New York (1982).
25. R. N. Grimes, *Comprehensive Organometallic Chemistry* (Edited by G. Wilkinson, F. G. A. Stone and E. W. Abel) Vol. 4, p. 459. Pergamon, Oxford (1982).
26. M. E. Jones, W. W. Porterfield and K. Wade, unpublished work.

Polyhedron Vol. 6, No. 12, pp. 2137–2143, 1987
Printed in Great Britain

0277–5387/87 $3.00+.00

CHEMICAL BEHAVIOUR OF *o,o'*-DIAMINOAZOBENZENE. SPECTROPHOTOMETRIC DETERMINATION OF Pd(II)

L. VICH, J. M. ESTELA* and V. CERDÁ

Department of Chemistry, University of the Illes Balears, 07071 Palma de Mallorca, Spain

and

E. CASASSAS and S. HERNÁNDEZ

Department of Analytical Chemistry, University of Barcelona, Spain

(*Received* 3 *June* 1987; *accepted* 24 *June* 1987)

Abstract—A study of several physicochemical and analytical properties of *o,o'*-diaminoazobenzene (DAB) is reported and its chemical behaviour discussed from the point of view of Pearson's theory. DAB has been applied to the determination of palladium by means of a new extractocolorimetric method.

The azocompounds, mainly those derived from benzene and naphthalene, are widely used as analytical reagents.[1–5] Their importance both theoretical and practical, is based on their complexing reactions. The great influence of the donor atoms that are present as substituents in the *ortho* position to the azo group is well known. Among these substituents are the phenolic, carboxyl, amino groups or a heteroatom of the ring, such as nitrogen or sulphur, in the *ortho* position. The azo group also acts as a donor when chelate compounds are formed.

Redox reactions take place in the case of several ions. Thus, with Cr^{2+}, V^{2+} and Ti^{3+} a reduction to the colourless *leuco*form is produced; whereas with dichromate, permanganate, VO_2^+, Fe^{3+} and Tl^{3+} there is an oxidation to *o*- or *p*-quinones under analogous conditions.

Some azo dyes yield, in basic media, adsorption or coprecipitation of coloured chelates on metallic hydroxides whose mechanisms are not well known. These reactions, that can be initially interpreted through adsorption phenomena, in diluted solutions give stoichiometric compounds or coloidal solutions.

One of the main difficulties in the determination of the complexation constants and also in the acid–base dissociation study, is the possibility of aggregation, (usually dimerization), which can easily be produced for concentrations of about 10^{-3} M.[6]

Great efforts were made in order to establish the laws of chemical behaviour of chelates, mainly by Irving and Williams and more recently by Pearson with the theory of hard and soft acids and bases.

A bibliographic review shows that azo compounds with substituents decreasing the basic strength of the ligand have been scarcely studied. Therefore we chose *o,o'*-diaminoazobenzene as an analytical reagent in order to determine its behaviour with metallic ions.

Following Pearson's theory, a decrease of stability is expected for alkaline, alkaline-earth and lanthanide elements, whereas more stable comlexes with divalent transition and platinum family elements will probably be formed.

EXPERIMENTAL

Reagents

o,o'-Diaminoazobenzene was synthesized using the following procedure.† 10.8 g of *o*-phenylendiamine and 4.3 g of methyltrioctylammonium chloride were placed in a round-bottomed flask; 100 cm^3 of benzene and 100 cm^3 aqueous solution

* Author to whom correspondence should be addressed.

† We acknowledge Prof. Mendoza of the Department of Organic Chemistry of the University Autonoma of Madrid for providing the product to initiate this research.

of 50% NaOH added, the mixture was refluxed for 96 h at 60°C. The black precipitate formed was purified by column chromatography using a mixture of benzene and chloroform. A red compound was isolated with a yield of 47%. M.p. 133°C.

Purity of DAB was controlled by thin layer chromatography using several solvents (*Rf* in silicagel 60 F_{254} Merck 0.2 mm : 0.18 chloroform, 0.18 benzene, 0.22 chloroform–benzene 1 : 1, 0.68 chloroform–methanol 9 : 1, 0.75 methanol–water 8 : 2, 0.77 ether, 0.83 methanol, 0.89 ethylacetate). Only one spot was observed. All other chemicals were of analytical grade.

Apparatus

Beckman ACTA CIII spectrophotometer with 1 cm quartz cells. Digital 112 Corning potentiometer with Corning 476051 glass and AgCl/Ag reference electrodes.

Extracto-colorimetric procedure for Pd(II) determination

Place a sample volume in a 100 cm^3 separatory funnel (0.5–5 ppm concentration range) and add 1 cm^3 of DAB 2.8 10^{-3} M in ethanol, 10 cm^3 of Prideaux buffer[7] and deionized water to a final volume of 20 cm^3. Extraction with 10 cm^3 of isoamyl alcohol is performed by shaking for 5 min. Let it settle for 5 min and filter the organic phase through a filter paper. Absorbance is measured at 585 nm using isoamyl alcohol as reference.

Palladium in 5% palladized active carbon determination procedure

Treat 0.1490 g of the sample first with aqua regia, then with HNO_3–H_2SO_4 mixture. Evaporate to dryness and dissolve with diluted HCl. Adjust to pH 2, transfer to a 250 cm^3 flask and dilute with deionized water to the mark. Continue as stated in the extracto-colorimetric proposed method.

RESULTS AND DISCUSSION

Physicochemical properties

Solubilities of DAB in several solvents were determined using the Wittemberg method.[8] This compound is scarcely soluble in water (0.066%), more in alcohols (0.94% isoamylic, 2.50% ethanol and 3.76% methanol) and soluble in MIBK (13.9%). The spectral behaviour of the compound obtained agreed with that expected for DAB (IR: 3460 cm^{-1} NH_2 asym., 3340 NH_2 sym., 3060–3025 C—H ar., 1600 NH_2 bend, 1480–1460 Ø, 1330–1315 N—Ø, 1260–1225 C—H rock, 1140 NH_2 rock, 860 NH_2 twist, 755–745 4H adj. wag.; ^{1}H NMR in $CDCl_3$: 4.20–4.80 ppm NH_2broad, 6.66–6.87 *m* 4H (H_3H_5), 7.17 *d d d* J = 7.5, 7.4 and 1.6 Hz(H_4), 7.68 *d d* 2H J = 8.2, 1.5 Hz (H_6)). UV-visible spectra of DAB were run for several pH values (Fig. 1) in a 50% methanol–water mixture. There is only one maximum in the visible zone: λ_{max} = 440 nm in neutral (ε = 8100) and 0.1 M NaOH media (ε = 7000) and stable for at least 60 min in neutral medium, 24 h, 0.1 M HCl and unstable in 0.1 M NaOH.

Acid-base equilibria

Dissociation constants of DAB were potentiometrically determined. Electrode calibration was performed by the Gran method, titrating HCl with NaOH[9–11] in water at 25.0±0.1°C and I = 0.1 M KCl. Resulting values were refined by means of the MINIPOT program,[12] which allowed us to obtain several parameters necessary for further calculations (pK_w = 13.783±0.001, log j_H = 0.00, log j_{OH} = 0.90, E^0 = 362.95±0.05 mV, g = 59.157, U = 1.60 mV^2, s = 0.22 mV.

DAB was then dissolved in HCl, which also was used to calibrate (*in situ*) the electrodes, and then titrated with NaOH in analogous conditions. Only one constant could be observed. The data resulting from the potentiometric titration were refined by means of the MINIPOT program, which only accepted one protonation constant, log β = 3.24±0.02, E^0 = 362.2±0.1 mV, U = 3.41 mV^2 and s = 0.3 mV.

Reactionability

The analytical behaviour of DAB in 1% ethanol was studied using 59 inorganic ions (1 g l^{-1}) at different pH values: HCl, AcOH, NH_3, NaOH (2N) and neutral media. Positive tests were repeated in the presence of masking agents: fluoride, cyanide, tartrate and EDTA; and extractants: ether, chloroform, toluene, isoamyl alcohol and MIBK both without and with trioctylmethylammonium chloride 5 g l^{-1} which in some cases, enabled extractable ion-pair formation. Results are summarized in Tables 1 and 2, showing that DAB reacts with 16 of the 59 ions. Therefore selectivity is quite good in acid media, sensitivities proved to be high, with p*D*s values ranging between 4–6, the follow-

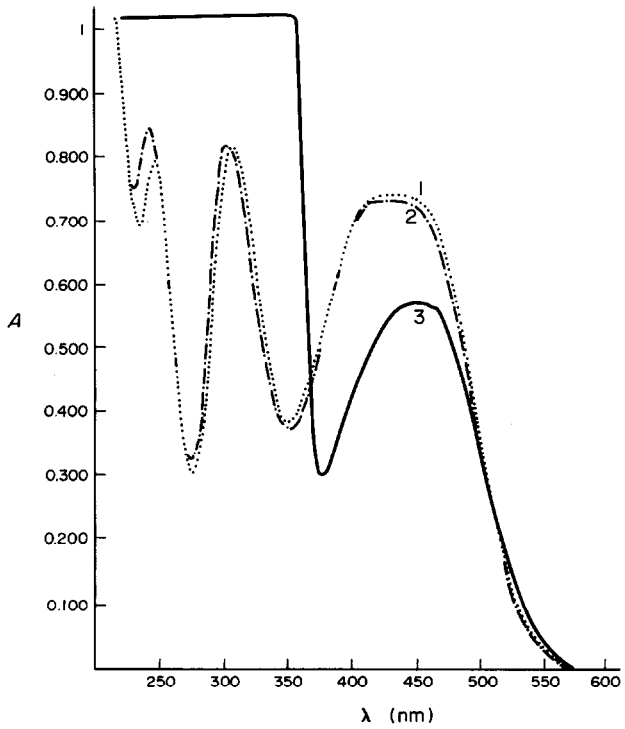

Fig. 1. pH influence on the spectra of DAB (50% MeOH/H_2O): (1) neutral, [DAB] = 9×10^{-5} M; (2) NaOH 0.1 M, [DAB] = 1.04×10^{-4} M; (3) HCl 0.1 M, [DAB] = 2.16×10^{-4} M.

Table 1. Reactionability of *o,o'*-diaminoazobenzene with inorganic ions in different media

Ion	Medium	Reaction	*pD*	Masking agents
Cu(II)	AcOH	c.yellow	4.8	CN^-,EDTA
	Water	c.violet	6.0	CN^-
	NH_3	c.violet	6.0	CN^-,F^-
		pp.violet	3.3	CN^-,F^-
	NaOH	c.violet	5.8	CN^-,F^-
Au(III)	HCl	c.brown	6.0	CN^-
	AcOH	c.brown	5.4	CN^-
	Water	c.brown	5.7	CN^-
	NH_3	c.brown	5.7	CN^-
	NaOH	c.brown	5.7	CN^-
Co(II)	HCl	c.gray	3.9	CN^-,EDTA
	AcOH	c.brown	4.5	CN^-,EDTA
	Water	c.blue	6.0	CN^-,EDTA
	NH_3	c.green	6.0	CN^-
	NaOH	c.blue	6.0	CN^-
V(V)	HCl	c.yellow	5.3	
	AcOH	c.brown	5.3	
Fe(III)	AcOH	c.brown	5.0	
	Water	c.brown	6.0	CN^-,F^-

Table 1 (*continued*)

Ion	Medium	Reaction	*pD*	Masking agents
Pd(II)	HCl	pp.violet	4.6	
	AcOH	c.violet	5.7	
		pp.violet	5.3	
	Water	c.violet	6.0	
		pp.violet	5.3	
	NH_3	c.red	6.3	
		pp.violet	4.6	
	NaOH	c.violet	6.0	
		pp.violet	4.6	
Ni(II)	Water	c.brown	5.0	CN^-
	NH_3	c.violet	6.0	CN^-
		pp.violet	4.3	CN^-
	NaOH	c.blue	6.3	CN^-
		pp.blue	4.0	CN^-
Hg(II)	AcOH	c.red	3.6	CN^-
	Water	c.red	5.0	CN^-
	NH_3	c.brown	5.0	CN^-
		pp.brown	4.0	CN^-
	NaOH	c.blue	5.7	CN^-
		pp.blue	4.0	CN^-
Hg(I)	Water	c.red	5.0	CN^-,EDTA
	NH_3	c.brown–red	5.7	CN^-,EDTA
	NaOH	c.brown–red	6.0	CN^-
Mg(II)	NH_3	pp.red	5.0	F^-,T
Ag(I)	NaOH	c.brown	4.6	CN^-
		pp.brown	3.6	CN^-
BrO_3^-	HCl	c.red	5.0	
		pp.orange	3.3	
IO_4^-	AcOH	c.brown	5.0	
CrO_4^{2-}	HCl	c.yellow–brown	4.6	
	AcOH	c.brown–red	5.3	
NO_2^-	HCl	c.red	5.7	
	AcOH	c.red	5.3	
MnO_4^-	NaOH	c.green	4.6	
		pp.green	4.0	

pp: precipitate, c: colour, T = tartrate.

ing giving the greatest: Cu(II), Au(III), Co(II), Fe(III), Pd(II), Ni(II) and Hg(II).

As was initially expected, a shift of the ligand properties to a softer basic behaviour, reacting especially with soft acids, takes place on substituting OH groups by $-NH_2$ in the azocompounds. The use of extractants and/or maskings increases both selectivity and sensibility, effects which have been exploited in further experiments.

Qualitative applications

From the reactionability table, two qualitative tests can be proposed:

(1) *Procedure for* Pd(II) *identification.* Place 0.5 cm^3 of the sample in a test tube (previously neutralized if it is basic), add 0.5 cm^3 of HCl(2N), 0.5 cm^3 of DAB (1% in ethanol) and shake. A violet precipitate shows the presence of Pd(II) ($pD = 4.6$). This sensitivity can be increased to $pD = 6.0$ by means of extraction with isoamyl alcohol. This test is specific.

(2) *Procedure for* Mg(II) *identification.* Place 0.5 cm^3 of neutral sample in a test tube, add 0.5 cm^3 of DAB (1% in ethanol), 0.5 cm^3 of NH_3(2N) and shake. An orange precipitate is produced in presence of Mg(II) ($pD = 5$). In presence of CN^- only Pd(II) interferes.

Table 2. Positive extraction test

Ion	Medium	Extractant	Colour of the organic phase
Cu(II)	AcOH	Chl,Is.A.,MIBK	Yellow
	Water	Et+Ad,Chl+Ad,Tol+Ad, Is.A.,MIBK	Red
	NH_3	Chl,Is.A.,MIBK	Violet
	NaOH	Et,Chl,Is.A.,MIBK	Violet
Au(III)	HCl	Et,Chl,Tol,Is.A.,MIBK	Brown
	AcOH	Et,Chl,Tol,Is.A.,MIBK	Brown
	Water	Et,Chl,Tol,Is.A.,MIBK	Brown
	NH_3	Et,Chl,Tol,Is.A.,MIBK	Brown
	NaOH	Et,Chl,Tol,Is.A.,MIBK	Brown
Co(II)	HCl	Chl,Is.A.,MIBK	Brown
	AcOH	Et,Chl,Tol,Is.A.,MIBK	Brown
	Water	Et,Chl,Tol,Is.A.,MIBK	Blue
	NH_3	Et,Chl,Tol,Is.A.,MIBK	Green
	NaOH	Et,Chl,Tol,Is.A.,MIBK	Blue
V(V)	AcOH	Et,Chl,Tol+Ad,Is.A.,MIBK	Brown
Pd(II)	HCl	Et,Chl,Tol,Is.A.,MIBK	Violet
	AcOH	Et,Chl,Tol,Is.A.,MIBK	Violet
	Water	Et,Chl,Tol,Is.A.,MIBK	Violet
	NH_3	Et,Chl,Tol,Is.A.,MIBK	Red
	NaOH	Et,Chl,Tol,Is.A.,MIBK	Violet
Ni(II)	Water	Et,Chl,Tol,Is.A.,MIBK	Brown
	NH_3	Et,Chl,Tol,Is.A.,MIBK	Violet
	NaOH	Et,Chl,Tol,Is.A.,MIBK	Blue
Hg(II)	AcOH	Is.A.	Red
	Water	Is.A.	Red
	NH_3	Et,Chl,Tol,Is.A.,MIBK	Brown
	NaOH	Et,Chl,Tol,Is.A.,MIBK	Blue
Hg(I)	Water	MIBK,Is.A.	Red
	NaOH	Et,Chl,Is.A.,Tol,MIBK	Red
Ag(I)	NaOH	Et,Chl,Tol,Is.A.,MIBK	Brown
IO_4^-	AcOH	Et,Chl,Tol,Is.A.,MIBK	Brown
CrO_4^{2-}	HCl	Chl+Ad,Et+Ad,Is.A.+Ad, MIBK+Ad	Brown
	AcOH	Tol+Ad	Red
NO_2^-	AcOH	Et,Chl,Tol,Is.A.,MIBK	Red
MnO_4^-	NaOH	Et,Chl,Tol,Is.A.,MIBK	Green

Chl = chloroform, Et = ether, Tol = toluene, Is.A. = isomylalcohol, MIBK = methylisobutylketone, Ad = adogen.

Quantitative applications

Extracto-colorimetric determination of Pd(II). Both selectivity of the qualitative test and the increase of the sensibility of the extraction procedure, encouraged us to develop a new method for Pd(II) determination. Influence of pH has been studied by using the Prideaux buffer.[7] For different pH values the corresponding spectra of DAB and its Pd(II) complexes can be observed in Fig. 2. Since maxima differences were observed at pH 2 for an analytical wavelength of 585 nm, these values were selected for further experiments. The absorbance of the complex is constant if the molar ratio of DAB to Pd is greater than 2:1. A 1.4×10^{-4} M concentration of DAB was selected. Best results were obtained for an addition order of Pd(II)–DAB–buffer. Although 5 min shaking time was chosen it

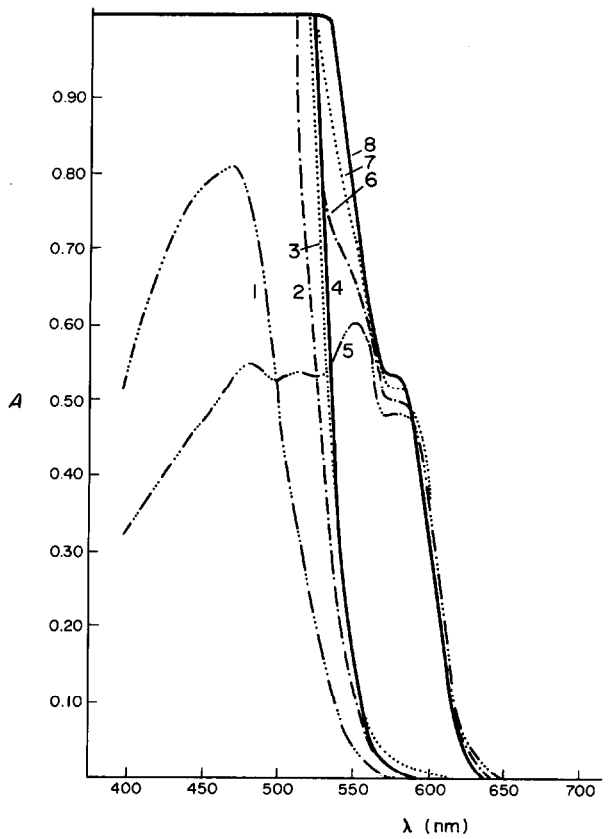

Fig. 2. pH influence on the spectra of DAB and its Pd(II) complex extracted with isoamilic alcohol. [DAB] = 27.8×10^{-5} M; [Pd(II)] = 2.8×10^{-5} M. Curves 1, 2, 3 and 4: DAB reagent at pH 2.1, 3.2, 4.0 and 5.1. Curves 5, 6, 7 and 8: DAB-Pd(II) complex at pH 2.1, 3.2, 4.0 and 5.1.

had no influence on the absorbance values. The absorbance of the extracted complex is constant for at least 90 min.

Stoichiometry of the complex was determined by Job's method, giving 1 : 1 with a molar absorptivity of 16625 l mol^{-1} cm^{-1}. The Lambert–Beer's law is obeyed in the 0.5–5 ppm Pd(II) concentration range, the Ringbom minimum error zone being between 1–5 ppm, where the relative error is 3.3%. Statistical values ($n = 11$, 95% confidence level) were determined with a 3 ppm Pd(II) content; standard deviation 5.83×10^{-3}, average standard deviation 0.0017, C.V. $= \sigma \times 100/x_m = 0.18\%$, $E = \pm t \times \sigma \times 100/x_m = \pm 0.18\%$.

Table 3. Tolerance of different ions in Pd(II) (3 ppm) determination for a 5% photometric error

Ion	Tolerance (ppm)
Au(III)	12
Fe(III)	12
V(V)	25
Hg(II)	100
Cu(II)	12
Co(II)	50
BrO_3^-	100
CrO_4^-	12
NO_2^-	0.75
Tartrate	100
EDTA	100
F^-	100
CN^-	1

In Table 3 the effect of different ions on Pd(II) determination can be observed. Concentrations producing a 5% photometric error are also indicated, 100 ppm was the maximum quantity tested. EDTA, tartrate and fluoride can be used as masking agents.

Palladium in a 5% palladized active carbon was determined by the proposed extracto-colorimetric procedure, using both the standard addition and the calibration curve methods. Results were of 4%, which agree with those of A. A. spectrophotometry.

Acknowledgements—Financial support of CAICYT (GR85-0049) is gratefully acknowledged.

REFERENCES

1. L. Sommer and M. Hnilickova, *Folia Prirodovedecka*. Faculty University, J.E. Purkyne Brne, 1964, 133.
2. E. Casassas and L. Eek, *Anal. de Quim.* 1965, **61**, 557.
3. E. Casassas, L. Eek and J. Rosal, *Inform. Quim. Anal.* 1965, **19**, 135.
4. E. Casassas, L. Eek and N. Salvatella, *Inform. Quim. Anal.* 1967, **21**, 48.
5. L. Eek and E. Casassas, *Inform. Quim. Anal.* 1970, **24**, 1.
6. E. Coates, B. Tigg, R. Murton and D. H. Smith, *J. Soc. Dyers and Col.* 1963, **79**, 465.
7. C. Mongay and V. Cerdá, *Talanta* 1977, **24**, 747.
8. W. Wittemberger, *Chemische Laboratorium Technik*. Springer, Wien (1950).
9. G. Gran, *Analyst* 1952, **77**, 661.
10. G. Gran, A. Johansson and S. Johansson, *Analyst*. 1981, **106**, 1109.
11. J. Cantallops, J. M. Estela and V. Cerdá, *Anal. Chim. Acta* 1985, **169**, 397.
12. F. Gaizer and A. Puskás, *Talanta* 1981, **28**, 565.

Polyhedron Vol. 6, No. 12, pp. 2145–2149, 1987
Printed in Great Britain

0277–5387/87 $3.00+.00

SPECTROPHOTOMETRIC STUDY OF COMPLEXATION EQUILIBRIA BETWEEN $HCrO_4^-$ AND Cl^- IONS

N. MIRALLES,* A. SASTRE and M. AGUILAR

Departament de Química, Escola Tècnica Superior d'Enginyers Industrials de Barcelona, Diagonal 647, 08028 Barcelona, Spain

(*Received* 8 *June* 1987; *accepted* 24 *June* 1987)

Abstract—The complex equilibria between $HCrO_4^-$ and Cl^- ions has been studied spectrophotometrically at a constant ionic strength of 3.0 mol dm^{-3} and the data have been analyzed both graphically and numerically by means of the program LETAGROP-SPEFO (L. G. Sillen and B. Warnquist, *Arkiv. kemi.* 1968, **31**, 377). The experimental results can be explained on the basis of the following reaction:

$$HCrO_4^- + H^+ + Cl^- = CrO_3Cl^- + H_2O \qquad (\log\beta_{11} = 1.37 \pm 0.08).$$

Molar absorptivities of $HCrO_4^-$ and CrO_3Cl^- were also reported.

Preliminary studies on the extraction of chromium(VI) with long chain amines[2] have shown that the distribution of the metal between the aqueous and the organic phase depends principally on the nature of the ionic medium used in the aqueous phase.

When hydrochrloric acid is used the extraction of chromium(VI) is much higher than with other mineral acids,[3–5] probably due to the extraction of the CrO_3Cl^- species. On the other hand, it has been demonstrated that the extraction is higher when the concentration of hydrochloric acid is increased.

The studies by Haight *et al.*,[6] Halloway[7] and Tong and Johnson[8] indicate that the addition of hydrochloric acid, sulphuric acid and phosphoric acid changes the $HCrO_4^-$ absorption spectrum over the range 260–400 nm. It has been assumed that these changes are due to the formation of the species CrO_3Cl^-, $CrSO_7^{2-}$, $H_2CrPO_7^-$ respectively. Dikshitulu *et al.*[9] obtained similar results from kinetic studies of the reduction of chromium(VI) by tellurium(IV). Formation constants of these species were also determined under several experimental conditions.

The present work is a detailed study of formation equilibria of CrO_3Cl^-. This study has been carried out spectrophotometrically at the wavelengths 320, 330 and 340 nm and 25°C. An ionic strength of 3.0 mol dm^{-3} has been utilized which allows a wide variation in chloride concentration.

EXPERIMENTAL

It is known that acid solutions of chromium(VI) in concentration lower than 4×10^{-4} mol dm^{-3} follow the Beer–Lambert law between 320 and 350 nm.[6]

It has been tested experimentally that Beer's law is obeyed in solutions of the following composition: B mol dm^{-3} Cr(VI), 10^{-2} mol dm^{-3} H^+, 3.0 mol dm^{-3} (Na^+, ClO_4^-), where the concentration B of chromium(VI) was kept in the range $1.5\ 10^{-4} \leqslant B \leqslant 7.5\times10^{-4}$ mol dm^{-3}. Values of molar absorptivities ε_{10} for $HCrO_4^-$ were determined from the slope of the straight line obtained by plotting absorbance against chromium(VI) concentration for different wavelengths and these are given in Table 1.

For determining the variation of absorbance as a function of chloride ion concentration, solutions of the following composition were prepared: B mol dm^{-3} Cr(VI), 10^{-2} mol dm^{-3} H^+, C mol dm^{-3} Cl^-, $(3.0-C)$ mol dm^{-3} ClO_4^-, 3.0 mol dm^{-3} Na^+. For each series, the concentration B of chromium(VI) was kept constant and the concentration C was varied between 0 and 3.0 mol dm^{-3}. Values of B were in the range between 2.6×10^{-4} mol dm^{-3}

* Author to whom correspondence should be addressed.

Table 1. Molar absorptivities ε_{10} of $HCrO_4^-$ for different wave lengths

$\lambda = 320$ nm	$\varepsilon_{10} = 817$
$\lambda = 330$ nm	$\varepsilon_{10} = 1156$
$\lambda = 340$ nm	$\varepsilon_{10} = 1466$

and 3.1×10^{-4} mol dm^{-3} for all series. This range allows the neglect of the $Cr_2O_7^{2-}$ and CrO_4^{2-} concentrations.[8]

Reagents and solutions

Sodium perchlorate, Merck p.a., used as ionic medium, was prepared as described previously.[10]

Potassium dichromate, primary standard grade "Baker Analyzed", was dried at 110°C before use. Chromium(VI) solutions were prepared by weighing the appropriate amount of potasium dichromate.

Sodium chloride, Probus, was recrystallized twice in distilled water and the stock solution analyzed using silver nitrate.[11]

Perchloric acid, Merck, p.a. A stock solution of approximate 0.1 mol dm^{-3} was standardized with HgO and NaI.[12]

Equipment

The spectrophotometric measurements were obtained using a visible–UV Perkin–Elmer 554 spectrophotometer, using Hellma K 282/2X 10 × 10 mm cells.

RESULTS AND DISCUSSION

The experimental data have been analyzed both graphically and numerically using the program LETAGROP-SPEFO,[1] in order to determine the formation constant of CrO_3Cl^- as well as the molar absorptivities at different wavelengths.

Graphical treatment

In the experimental conditions employed the following reaction can be assumed:

$$HCrO_4^- + H^+ + Cl^- = CrO_3Cl^- + H_2O \quad (1)$$

with β_{11} being the constant of reaction (1) defined by:

$$\beta_{11} = \frac{[CrO_3Cl^-]}{[H^+][Cl^-][HCrO_4^-]}. \quad (2)$$

Since the hydrogen ion and chloride concentrations were always much higher than chromium(VI) concentrations, it was assumed that the concentration of these species were equal to their stoichiometric concentrations. On the other hand, the chromium concentrations employed were in a region of negligible dimeric species. In such conditions, the absorbance A of the solutions can be written as:

$$A = \varepsilon_{10}[HCrO_4^-] + \varepsilon_{11}[CrO_3Cl^-] \quad (3)$$

where ε_{10} and ε_{11} are the molar absorptivities of $[HCrO_4^-]$ and $[CrO_3Cl^-]$ respectively.

Taking into account eq. (2), the mass balance for chromium(VI) can be written:

$$B = [HCrO_4^-] + [CrO_3Cl^-] = [HCrO_4^-](1 + \beta_{11}[H^+][Cl^-]). \quad (4)$$

By substituting (4) in eq. (3) we obtain:

$$A = \frac{B}{1 + \beta_{11}[H^+][Cl^-]}(\varepsilon_{10} + \varepsilon_{11}\beta_{11}[H^+][Cl^-]). \quad (5)$$

Rearranging eq. (5) it follows:

$$\log\frac{B\varepsilon_{10} - A}{B} \log(\varepsilon_{10} - \varepsilon_{11}) = \log\frac{\beta_{11}[H^+][Cl^-]}{1 + \beta_{11}[H^+][Cl^-]}. \quad (6)$$

Two new variables Y and u can be defined as:

$$Y = \frac{B\varepsilon_{10} - A}{B}\frac{1}{(\varepsilon_{10} - \varepsilon_{11})} \quad (7)$$

$$u = \beta_{11}[H^+][Cl^-]. \quad (8)$$

Substituting eqs (7) and (8) in (6) we get:

$$\log Y = \log\frac{u}{1+u}. \quad (9)$$

By comparison of the experimental data plotted as $\log(B\varepsilon_{10} - A)/B$ vs $\log[Cl^-]$ with the theoretical function $\log Y$ vs $\log u$, the values of β_{11} and ε_{11} can be obtained by reading off the differences:

$$\log\frac{B\varepsilon_{10} - A}{B} - \log Y = \log(\varepsilon_{10} - \varepsilon_{11}) \quad (10)$$

$$\log u - \log[Cl^-] + pH = \log\beta_{11} \quad (11)$$

in the position of the best adjust.

The experimental results as well as the theoretical function $\log Y$ vs $\log u$ in the position of the best adjust are plotted in Figs 1–3 for different wavelengths. Values of β_{11} and ε_{11} are given in Table 2.

Numerical treatment

A refinement of the values of β_{11} and ε_{11} was performed using a version of the general minimizing

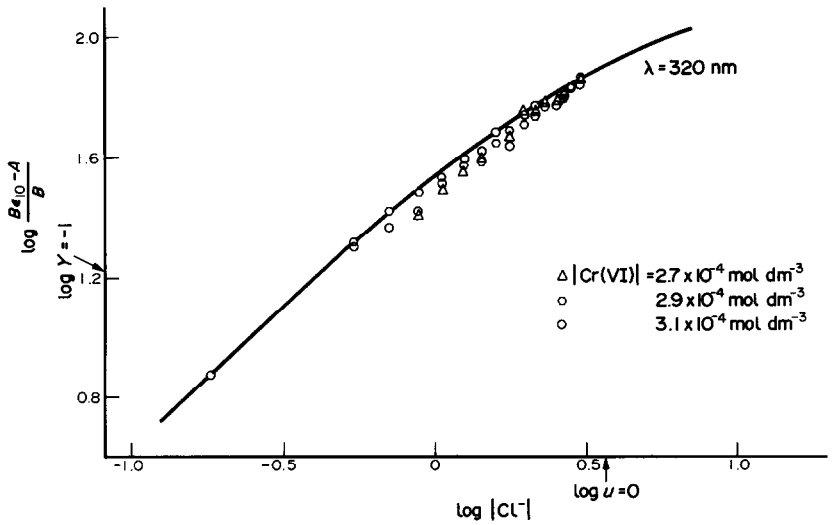

Fig. 1. $-\log(B\varepsilon_{10}-A)/B$ plotted vs $\log[Cl^-]$ at $\lambda = 320$ nm for different chromium(VI) concentration. The full drawn line gives $\log Y$ as a function of $\log u$ in the position of the best adjust.

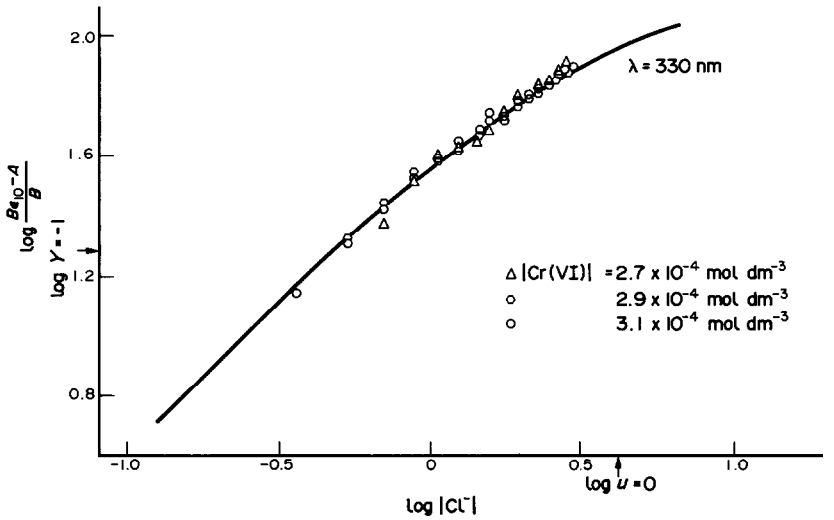

Fig. 2. $-\log(B\varepsilon_{10}-A)/B$ plotted vs $\log[Cl^-]$ at $\lambda = 330$ nm for different chromium(VI) concentration. The full drawn line gives $\log Y$ as a function of $\log u$ in the position of the best adjust.

Table 2. Values of β_{11} and the molar absorptivities ε_{10} and ε_{11} found graphically and numerically

	$\log\beta_{11}$	ε_{10}	ε_{11}	Method
$\lambda = 320$	1.43	—	651	graphic
$\lambda = 330$	1.38	—	965	graphic
$\lambda = 340$	1.40	—	1288	graphic
$\lambda = 320$		820 ± 1	634 ± 3	Letagrop
$\lambda = 330$		1158 ± 1	949 ± 3	Letagrop
$\lambda = 340$		1467 ± 1	1264 ± 3	Letagrop

$\log\beta_{11} = 1.37\pm0.08$.

program LETAGROP,[13] especially adapted to the treatment of spectrophotometric data LETAGROP-SPEFO.[1]

As input, experimental data of absorbance at different wavelength, concentrations of chromium(VI) and values of β_{11}, ε_{10} and ε_{11} calculated graphically, were given. The program searches for the best set of constants that would minimize the error square sum defined by

$$U = \sum(A_{calc}-A_{exp})^2 \qquad (12)$$

where A_{exp} is the value of absorbance measured

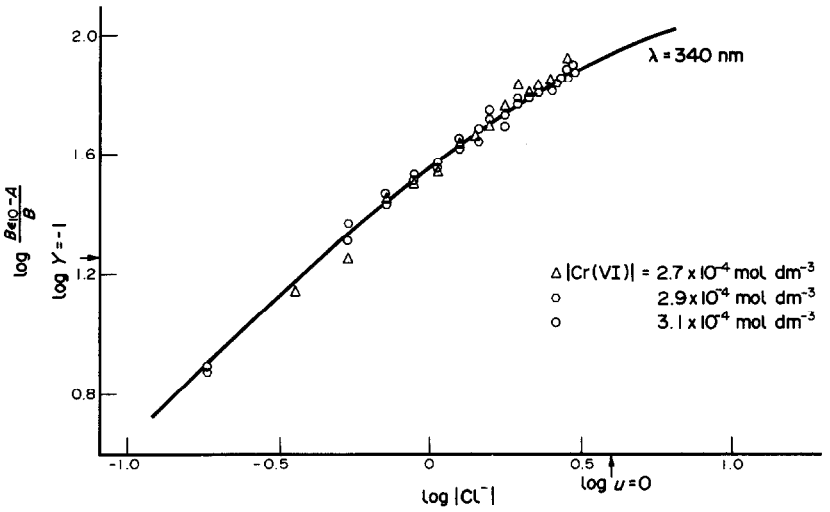

Fig. 3. $-\log(B\varepsilon_{10}-A)/B$ plotted vs $\log[Cl^-]$ at $\lambda = 340$ nm for different chromium(VI) concentration. The full drawn line gives $\log Y$ as a function of $\log u$ in the position of the best adjust.

experimentally and A_{calc} is the calculated A obtained assuming a set of complexes and their formation constants. The program also calculates the standard deviation $\sigma(A)$ defined by:

$$\sigma(A) = \left[\frac{\sum (A_{calc}-A_{exp})^2}{N_p}\right]^{1/2} \qquad (13)$$

where N_p are the number of experimental points.

The fit of the data is illustrated in Fig. 5, where $A_{calc}-A_{exp}$ has been plotted against $[Cl^-]$.

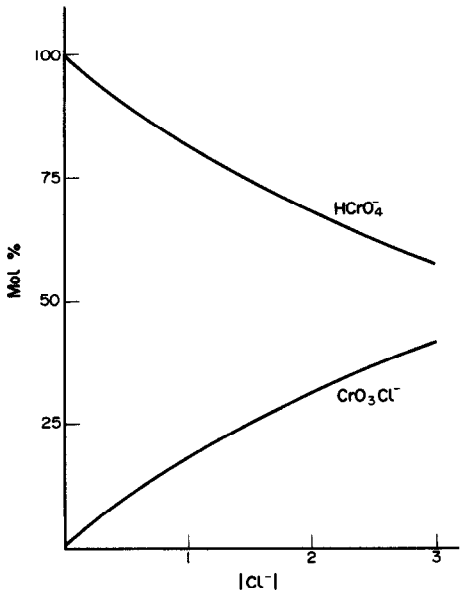

Fig. 4. The mol percent of the different chromium(VI) species as a function of the chloride concentration.

In Table 2 the value of $\log\beta_{11}$, ε_{10} and ε_{11} are given for different methods. It is seen from this table, that normalized curves and least-square methods give, practically the same constants.

The calculations give a value of $\log\beta_{11} = 1.37$. This value could be corrected to 1.0 mol dm^{-3} ionic strength to be compared with the values found in the literature. The activity coefficients γ could be calculated using the extended Debye–Hückel equation[15]

$$\log\gamma = \frac{-z^2 0.511\sqrt{I}}{1+1.5\sqrt{I}} + 0.102z^2 I \qquad (14)$$

where I is the ionic strength and z is the charge of the ion.

From these calculations, it was found that $\log\beta_{11} = 1.04$. As seen the value of the formation constant obtained seems to agree with those found in the literature (Table 3).

Table 3. Values of formation constants of CrO_3Cl^-, β_{11} found in the literature

T (°C)	I	$\log\beta_{11}$	Ref.
25	1.0	1.23	6
25	1.0	1.05	8
20	1.0	0.93	14
15	1.0	1.03	8
35	1.0	1.09	8
31	1.0	1.30	9
25	3.0	1.37±0.08	This work

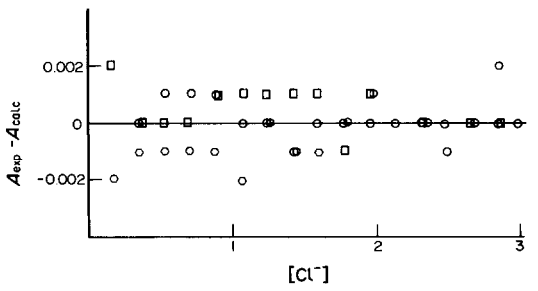

Fig. 5. $A_{exp} - A_{calc}$ plotted as a function of $[Cl^-]$ for different chromium(VI) concentrations at $\lambda = 330$ nm.

From the results of this work, the mol percent of the different chromium(VI) species was calculated and plotted as a function of chloride ion concentration at pH = 2 (Fig. 4). This plot shows that the $HCrO_4^-$ species is predominant in the range of concentration studied.

REFERENCES

1. L. G. Sillen and B. Warnquist, *Arkiv. kemi.* 1968, **31**, 377.
2. A. Sastre, N. Miralles and M. Aguilar, *An. Quim.* 1984, **80**, 546.
3. M. Niitsu and T. Sekine, *J. Inorg. Nucl. Chem.* 1976, **38**, 1057.
4. S. A. Kats, W. M. McNabb and J. F. Mezel, *Anal. Chim. Acta* 1962, **27**, 405.
5. D. G. Tuck and R. M. Walters, *J. Chem. Soc.* 1963, 1111.
6. G. P. Haight, D. C. Richardson and N. H. Corbun, *Inorg. Chem.* 1964, **3**, 1777.
7. F. Halloway, *J. Am. Chem. Soc.* 1952, **75**, 225.
8. J. I. Tong and R. L. Johnson, *Inorg. Chem.* 1966, **5**, 1902.
9. L. S. A. Dikshitulu and D. Satyanarayana, *J. Inorg. Nucl. Chem.* 1976, **38**, 1843.
10. *Some Laboratory Methods in Current Use at the Department of Inorganic Chemistry*, The Royal Institute of Technology, Mimeograph (1959).
11. A. I. Vogel, *Quimica Analitica Cuantitativa* (Edited by Kapelusz), p. 553 (1960).
12. *Ibid.* p. 331.
13. N. Ingri and L. G. Sillen, *Arkiv. Kemi.* 1964, **23**, 97.
14. O. Lukkari, *Suom. Kemi.* 1962, **35**, 91.
15. H. S. Harned and B. B. Owen, *The Physical Chemistry of Electrolytic Solutions*, 3rd edn. Reihold, New York (1958).

Polyhedron Vol. 6, No. 12, pp. 2151–2153, 1987
Printed in Great Britain

0277–5387/87 $3.00+.00

REACTION ENTROPY FOR THE ELECTROREDUCTION OF BIS(BIPHENYL)CHROMIUM(I) IN DIFFERENT SOLVENTS

JAN S. JAWORSKI

Department of Chemistry, University of Warsaw, 1 Pasteur Street, 02-093 Warszawa, Poland

(*Received* 27 *April* 1987; *accepted* 29 *June* 1987)

Abstract—The reaction entropy, ΔS_r°, for the electroreduction of bis(biphenyl)chromium(I) has been measured in eight solvents using a non-isothermal cell arrangement. A correlation between the solvent acceptor number and the ΔS_r° values has been observed. The measured reaction entropies are higher than those for ferrocene/ferricenium ion and bis(benzene)chromium(0)/bis(benzene)chromium(I) couples.

The electrochemical reaction entropy, ΔS_r°, i.e. the entropy difference between the reduced and oxidized forms of a redox couple can be obtained from the temperature dependence of the electrode potential using a non-isothermal cell.[1] The ΔS_r° values are suitable for detailed examination of ionic solvation as well as electron-transfer processes and thus, they were reported for numerous transition-metal redox couples and many earlier results were discussed by Hupp and Weaver.[2] Among sandwich complexes the reaction entropy in a variety of solvents was measured only for the two couples: ferrocene/ferricenium ion, Fc/Fc^+,[3] and its derivative.[4] Recently, some entropy data for other metallocenes and bis(benzene)chromium(0)/bis(benzene)chromium(I) couple were also reported.[5] In the same solvent the obtained values were similar, in full agreement with the empirical prediction[2] for redox couples with identical charge numbers and similar radii.

It is interesting to investigate electrochemical reaction entropies for bis(biphenyl)chromium(0)/bis(biphenyl)chromium(I), BCr/BCr^+, for the sake of a possibility to examine the influence of reactant size as well as for a comparison with reaction entropies for Fc/Fc^+, because these two couples have been recently recommended as reference redox systems for the reporting electrode potentials in nonaqueous solvents.[6]

EXPERIMENTAL

Dimethylformamide (DMF), dimethylsulphoxide (DMSO), dimethylacetamide (DMA), propylene carbonate (PC), acetonitrile (ACN) and N-methylformamide (NMF) were purified and dried as described previously.[7–9] Methanol (POCh) (MeOH) and formamide (IE, Windsor) (FA) were purified in a conventional manner.[10] A small amount of NaOH was added to FA to avoid an acidic decomposition of BCr^+ cation. The concentration of bis(biphenyl)chromium tetraphenylborate was 0.5 mM and 0.1 M tetraethylammonium perchlorate (TEAP) was used as the supporting electrolyte.

The reaction entropy was obtained from the temperature dependence of the reversible polarographic half-wave potential using a non-isothermal cell; details have been described previously.[7–9] The reference electrode consisted of a silver wire in a solution containing 0.09 M TEAP and 0.01 M $AgNO_3$ (or $AgClO_4$ in the case of PC) in the solvent of interest,[8] with the exception of measurements in NMF and FA where a silver electrode in ACN was used.

RESULTS AND DISCUSSION

Linear coefficients of temperature variations in the half-wave potentials for the reduction of BCr^+,

$dE_{1/2}/dT$, measured in different solvents and errors determined on the basis of the "Student's" distribution with a confidence level of 0.95 are given in Table 1. The reaction entropies calculated for the one-electron reversible reduction from:

$$\Delta S_r^\circ = F dE_{1/2}/dT \qquad (1)$$

where F denotes Faraday's constant, are positive (Table 1). Similarly, the positive ΔS_r° values were observed[2] for the reduction of other cationic couples due to a greater extent of solvent polarization in the vicinity of an oxidized form with a higher ionic charge.

The inspection of the ΔS_r° values collected in Table 1 indicates that the reaction entropy becomes smaller in protic solvents with molecules associated via hydrogen bonding. The analogous behaviour observed for the Fc/Fc^+ couple[3] and its derivative (*n*-ferrocenemethylene-*p*-toluidine[4]) was rationalized in terms of a significant donor–acceptor interaction between the solvent hydrogens and the cyclopentadienyl rings of the Fc molecule, which has a greater electron density than those of the Fc^+ ion.[3,4] Alternatively, the negative contribution to entropy change arising from the disordering of the original solvent structure by the charged Fc^+ ion was considered.[2,4] The solvent acceptor number, *AN*,[11] was proposed as a measure of both the above effects.[3,4]

Plots of the ΔS_r° values against the solvent acceptor number for BCr/BCr^+ as well as Fc/Fc^+ [3,4] and $(C_6H_6)_2Cr^{0/+}$ [5] couples are shown in Fig. 1. A weighted regression line for BCr/BCr^+ system holds with the correlation coefficient 0.984 and χ^2-test 2.3, which indicates that the deviations from the line are explained completely by experimental errors in the

Table 1. Temperature coefficients of $E_{1/2}$ and the reaction entropies for the reduction of bis(biphenyl)chromium(I) in a variety of solvents

Solvent	AN[a]	$dE_{1/2}/dT$ ($mV\,K^{-1}$)	n^b	r^c	ΔS_r° (J mol^{-1} K^{-1})
DMA	13.6	1.2±0.2	5	0.992	116
DMF	16.0	1.0±0.4	5	0.934	96
PC	18.3	0.8±0.1	5	0.992	85
ACN	18.9	0.9±0.2	5	0.981	87
DMSO	19.3	1.0±0.1	5	0.997	96
NMF	32.1	0.5±0.3	4	0.995	48
FA	39.8	0.3±0.1	5	0.983	29
MeOH	41.3	0.3±0.1	6	0.985	29

[a] Solvent acceptor number from Ref. 11.
[b] Number of data sets (different temperatures).
[c] Correlation coefficient of $E_{1/2}$ on T.

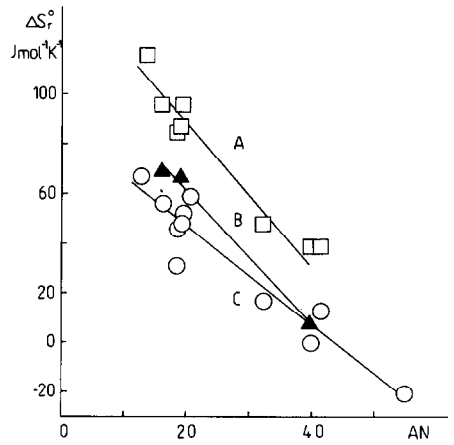

Fig. 1. Plots of the reaction entropy for the electroreduction of BCr^+ (A), $(C_6H_6)_2Cr^+$ (B) and Fc^+ (C) against the solvent acceptor number. Entropic data for B and C were taken from Refs 3–5.

ΔS_r° values. A similar solvent effect on the reaction entropy for the BCr/BCr^+ and Fc/Fc^+ couples (Fig. 1) is not surprising if one takes into account that differences between the redox potentials for these systems were found[6] to be almost constant in 22 solvents.

On the other hand, in each solvent the highest reaction entropy was found for the largest reactant, BCr/BCr^+. The above result does not agree with the empirical equation proposed by Hupp and Weaver[2] in which the reaction entropy is proportional to the reciprocal of the reactant radius. Differences in the method of the ΔS_r° measurements used in this paper and by Weaver and coworkers are not responsible for that finding. For the oxidation of ferrocene at a dropping mercury electrode in ACN a reaction entropy equal to 47 ± 5 J K^{-1} mol^{-1} has been obtained, in full agreement with Weaver's value of 48 J K^{-1} mol^{-1} determined by cyclic voltammetry and using a different cell and electrodes.[3]

Two alternative explanations for the presented result can be suggested: a difference in short range donor–acceptor interactions with solvent molecules due to a distinct charge distribution on aromatic rings of the considered couples and greater increase in the metal-ring distances during the electroreduction process for the BCr^+/BCr couple. The first possibility corresponds to the observation found[7,12] for systems of organic heteraromatic molecules and their radical-ions, that ΔS_r° values are related to a spin density at a heteroatom in a radical-ion. However, the same number of hyperfine components in ESR spectra of BCr^+ and $(C_6H_6)_2Cr^+$ cations suggests[13] for the former a delocalization of an unpaired electron only on one benzene ring in each biphenyl system. Then, a similar effect of a spin

distribution can be expected for both the considered cations.

Concerning the second possibility it should be added, that a significant contribution to ΔS_r° values proportional to a relative change in the metal–ligand bond distances between the reduced and oxidized species has been recently found[14] for a number of transition-metal redox couples, including aquo ligands and complexes of cobalt. However, we are not in a position to discuss that possibility in detail because for sandwich complexes the metal-ring distances in both oxidation states are not known with sufficient accuracy.

Acknowledgements—The author is grateful to Dr W. Linert, Vienna, for a sample of bis(biphenyl)chromium tetraphenylborate. This work was supported as a part of CPBP 01.15 programme.

REFERENCES

1. E. L. Yee, K. L. Guyer, P. D. Tyma and M. J. Weaver, *J. Am. Chem. Soc.* 1979, **101**, 1131.
2. J. T. Hupp and M. J. Weaver, *Inorg. Chem.* 1984, **23**, 3639.
3. S. Sahami and M. J. Weaver, *J. Sol. Chem.* 1981, **10**, 199.
4. J. T. Hupp and M. J. Weaver, *J. Electrochem. Soc.* 1984, **131**, 619.
5. T. Gennett, D. F. Milner and M. J. Weaver, *J. Phys. Chem.* 1985, **89**, 2787.
6. G. Gritzner and J. Kuta, *Pure Appl. Chem.* 1984, **56**, 461.
7. J. S. Jaworski, *Monatsh. Chem.* 1986, **117**, 151.
8. J. S. Jaworski, *Electrochim. Acta* 1986, **31**, 85.
9. J. S. Jaworski, *J. Electroanal. Chem.* 1987, **219**, 209.
10. C. K. Mann, In *Electroanalytical Chemistry* (Edited by A. J. Bard) Vol. 3, Chap. 2. Marcel Dekker, New York (1969).
11. V. Gutmann, *The Donor–Acceptor Approach to Molecular Interactions*. Plenum Press, New York (1978).
12. J. S. Jaworski, *Z. Phys. Chem.* (*NF*), in press.
13. G. Wilkinson and F. A. Cotton, In *Progress in Inorganic Chemistry* (Edited by F. A. Cotton), Vol. 1, p. 77. Interscience, New York (1959).
14. J. S. Jaworski, in preparation.

Polyhedron Vol. 6, No. 12, pp. 2155–2160, 1987
Printed in Great Britain

0277–5387/87 $3.00+.00

EXTRACTION OF Fe(III) BY *n*-DODECANOIC ACID DISSOLVED IN TOLUENE

M. P. ELIZALDE,* J. M. CASTRESANA and A. I. ELORRIAGA

Departamento de Química Analítica, Facultad de Ciencias, Universidad del País Vasco, Apartado 644, 48080 Bilbao, Spain

(*Received* 28 *April* 1987; *accepted* 29 *June* 1987)

Abstract—The extraction of Fe(III) from a nitrate medium of ionic strength 1.0 mol dm^{-3} by *n*-dodecanoic acid (HA) dissolved in toluene has been studied by distribution measurements. Experimental data, treated by different graphical and numerical methods, have been explained assuming the extraction of the species $(FeA_3)_3$ into the organic phase as well as the formation of a Fe(III)–HA complex in the aqueous phase.

The solvent extraction of metal ions by carboxylic acids has aroused a great interest from both theoretical and practical points of view. Being one of the cheapest available kind of extractant reagents, the studies were first focussed on the possibilities of hydrometallurgical applications. Later on, detailed series of studies concerning the distribution equilibria of metal ions were carried out, giving rise to several reviews on the subject reported by Fletcher and Flett,[1] Flett and Jaycock,[2] Ashbrook,[3] Miller,[4] Rice,[5] Brzóska and Rózycki[6] and Yamada and Tanaka.[7] Most of the work basically agrees on the presence of monomer–polymer equilibria between metallic carboxylates, although the complexity of the systems has resulted in serious discrepancies in the composition of the extracted species.

The reported enhancements of the extraction of metals by carboxylic-containing synergic mixtures[8–10] has revealed the importance of having self-consistent data on individual systems in order to explain satisfactorily the results obtained with the mixtures.

With regard to iron(III) extraction, the influence of the diluent and the type of carboxylic acid over the composition of the extracts seems to be open to question since trimers,[11,12] dimers of several compositions[13–15] and monomers[16,17] have been proposed as main organic complexes in different conditions.

In the present work, the study of the extraction of Fe(III) from a nitrate medium by *n*-dodecanoic acid dissolved in toluene has been carried out in order to determine the stoichiometries of the complexes extracted as well as their stoichiometric extraction constants.

EXPERIMENTAL

Reagents

$Fe(NO_3)_3 \cdot 9H_2O$, Merck, p.a., was twice crystallized from distilled deionized water. *n*-Dodecanoic acid, Merck, r.s., was purified by successive recrystallization in ethanol and acetone.[18] Sodium nitrate and toluene, Merck, p.a., were used as supplied. All other chemicals were analytical-reagent grade.

Experimental procedure

Equal volumes (10 cm^3) of both organic and aqueous phases were mechanically shaken in special stoppered test tubes for 4 h. The initial acidity of the aqueous phase was gradually adjusted during the extraction process, always keeping the pH value below 3.3 in order to avoid the evolution of iron(III) hydroxide. Previous experiments showed that, under the conditions used, equilibrium was reached in about 2 h and no changes in the distribution coefficient were noticed up to 12 h after mixing. The concentration of *n*-dodecanoic acid in toluene was varied from 0.100–0.400 mol dm^{-3}. The aqueous phases contained Fe(III) in the concentration range 0.2–1.0 mmol dm^{-3} in $NaNO_3$ (1.0 mol dm^{-3}).

* Author to whom correspondence should be addressed.

After phase separation by centrifugation, the H^+ concentration was measured potentiometrically, using a combined glass electrode. The iron content in both phases was determined by atomic absorption spectroscopy. The iron concentration in the organic solutions was determined by stripping the metal into 1.0 mol dm^{-3} HNO_3. Any data which did not fulfil the mass balance for iron within 5% were rejected.

When necessary, the sodium content in both phases was determined by atomic absorption spectroscopy.

RESULTS

The extraction of iron(III) by *n*-dodecanoic acid (HA) can be described by the following general equilibrium:

$$j\mathrm{Fe}^{3+} + \tfrac{1}{2}(m+n)j(\mathrm{HA})_{2,\mathrm{org}} \rightleftharpoons (\mathrm{FeA}_m(\mathrm{HA})_n)_{j,\mathrm{org}} + mj\mathrm{H}^+ \quad (1)$$

where the known predominance of the carboxylic acid as a dimer in toluene has been considered.[19]

Taking into account that the total concentration of Fe(III) in the organic phase is given by:

$$C_{\mathrm{Fe,org}} = \sum_m \sum_n \sum_j j|(\mathrm{FeA}_m(\mathrm{HA})_n)_j|_{\mathrm{org}} \quad (2)$$

and k_{mnj} being the stoichiometric equilibrium constant for reaction (1), the distribution coefficient of the metal ion can be expressed as:

$$D = C_{\mathrm{Fe,org}}/C_{\mathrm{Fe,aq}} = \sum_m \sum_n \sum_j jk_{mnj}\alpha_{\mathrm{Fe}}^{-1} \times |\mathrm{Fe}^{3+}|^{j-1}|(\mathrm{HA})_2|^{1/2(m+n)j}|\mathrm{H}^+|^{mj} \quad (3)$$

where α_{Fe} is the side reaction coefficient of Fe(III) due to the formation of hydroxo[20] and nitrate[21] complexes in the aqueous phase and can be calculated from the equation:

$$\alpha_{\mathrm{Fe}} = 1 + \beta_1|\mathrm{NO}_3^-| + \beta_{11}|\mathrm{OH}^-| + \beta_{12}|\mathrm{OH}^-|^2 + \beta_{14}|\mathrm{OH}^-|^4 + \beta_{22}|\mathrm{Fe}^{3+}||\mathrm{OH}^-|^2 + \beta_{34}|\mathrm{Fe}^{3+}|^2|\mathrm{OH}^-|^4. \quad (4)$$

In Fig. 1 the experimentally determined $\log D$ values are plotted as a function of equilibrium pH at constant total metal concentration. On the other hand, Fig. 2 shows $\log D$ vs pH data at constant *n*-dodecanoic acid concentration and several C_{Fe} levels.

Both the high slope values, larger than the charge of the metal ion, obtained in the low D range for all the sets of data in Fig. 1 and the shifts to lower pH values of the experimental curves in Fig. 2 when increasing the iron content point to the polimerization of the extracted iron complexes.

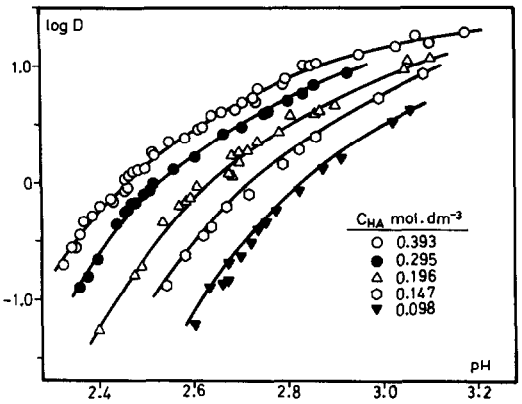

Fig. 1. Extraction of Fe(III) at various *n*-dodecanoic acid concentrations and $C_{\mathrm{Fe}} = 5.0 \times 10^{-4}$ mol dm^{-3}. Continuous lines have been drawn using the equilibrium constants proposed in Table 2.

Each type of data was first considered separately but the whole of the experimental information was subsequently treated both graphically and numerically.

GRAPHICAL TREATMENT

Data at constant iron concentration

An estimation of the polymerization degree of the extracted species can be achieved from the data collected at constant metal iron concentration. Assuming the formation of one single compound in the organic phase, eq. (2) takes the form:

$$\log C_{\mathrm{Fe,org}} = \log jk_{mnj} + \tfrac{1}{2}(m+n)j \times \log|(\mathrm{HA})_2|_{\mathrm{org}} + j(\log|\mathrm{Fe}^{3+}| + m\mathrm{pH}). \quad (5)$$

The function $\log C_{\mathrm{Fe,org}} = f(\log|\mathrm{Fe}^{3+}| + m\mathrm{pH})$ at constant extractant concentration was evaluated

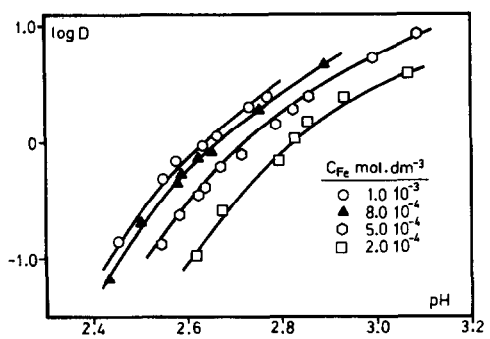

Fig. 2. The effect of total Fe(III) concentration on the extraction with *n*-dodecanoic acid at $C_{\mathrm{HA}} = 0.174 \times$ mol dm^{-3}. Continuous lines have been drawn using the equilibrium constants proposed in Table 2.

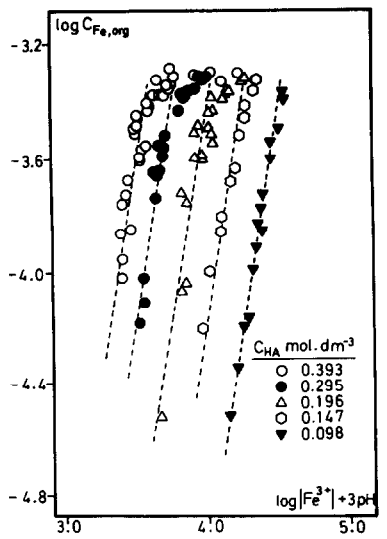

Fig. 3. Plot of the function $\log C_{Fe,org} = f(\log|Fe^{3+}| + 3pH)$ for the experimental data collected at constant total Fe(III) concentrations.

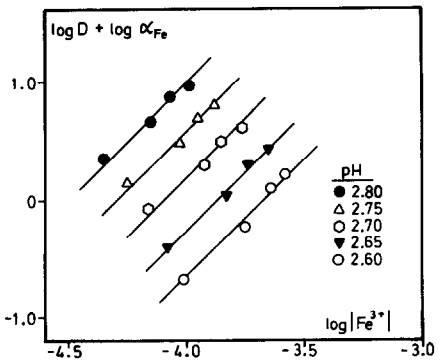

Fig. 4. Plot of the function $\log D + \log \alpha_{Fe} = f(\log|Fe^{3+}|)$ for the experimental data collected at different total Fe(III) concentrations.

for selected integer m values until straight lines were found. $|Fe^{3+}|$ values were calculated from the measured $C_{Fe,aq}$ according to eq. (5) by means of the program SOLGASWATER.[22]

Although in the higher D range deviations from linearity were observed for all the m values tried, linear plots were only found for $m = 3$, and a value of $j = 3$ was deduced from the slopes obtained (Fig. 3). Since straight lines of slope 4.5 were obtained in the plots $\log C_{Fe,org} = f(\log|(HA)_2|_{org})$ at several constant $(\log|Fe^{3+}| + 3pH)$ values, it can be deduced that $n = 0$ and consequently that a trimer of stoichiometry $(FeA_3)_3$ is extracted in the organic phase. From the intercepts of the former plots an extraction constant value of $\log k_{303} = -11.6$ was obtained.

Data at different iron concentration

In order to confirm the validity of the former extraction model, a graphical analysis of the experimental data at constant C_{HR} and different iron concentration (Fig. 2) was performed. Assuming the extraction of a single species, eq. (2) can be reduced to:

$$\log D + \log \alpha_{Fe} = \log k' + (j-1)\log|Fe^{3+}| \quad (6)$$

where, at constant pH values, k' is a conditional extraction constant defined by:

$$\log k' = \log jk_{mnj} + \tfrac{1}{2}(m+n) \times \log|(HA)_2|_{org} + mj\,pH. \quad (7)$$

Figure 4 shows the plots of the function $\log D + \log \alpha_{Fe} = f(\log|Fe^{3+}|)$ at several constant pH values. The straight lines of slope 2.0 ($j = 3$) obtained, further confirm the degree of polymerization of the extracted complex. An extraction constant value of $\log k_{303} = -11.5$, in good agreement with the one deduced from data at constant metal concentration was obtained by plotting the intercepts in Fig. 4 as a function of pH.

Treatment of all the data

The extraction of the species $(FeA_3)_3$ does not explain the whole set of data since deviations from the expected behaviour are found mainly at the highest studied range of extractant concentration. All the graphical analysis performed assuming the extraction of more metallic species, including OH-containing complexes, did not improve the fit to the data. A similar procedure using the highest formation constant values quoted in the literature for the iron(III)-hydroxo complexes confirmed that deviations cannot be attributed only to the presence of these species in the aqueous phase. Moreover, additional experiments showed that coextraction of sodium from the ionic medium, with the resulting decrease of *n*-dodecanoic acid concentration, was negligible in the pH range of the study. Accordingly, a graphical treatment of all the experimental data taking into account the possibility of the formation of iron carboxylate species in the aqueous phase was carried out. The biphasic equilibria for this reaction can be described as:

$$zFe^{3+} + \tfrac{1}{2}(x+y)z(HA)_{2org} \rightleftharpoons [FeA_x(HA)_y]_z + xzH^+. \quad (8)$$

Considering the mass balance equations for iron(III) in both phases:

$$C_{Fe,org} = 3[(FeA_3)_3]_{org} \quad (9)$$

$$C_{Fe,aq} = |Fe^{3+}|\alpha_{Fe} + z[(FeA_x(HA)_y)_z] \quad (10)$$

and the free iron concentration:

$$|Fe^{3+}| = [k_{303}^{-1}[(FeA_3)_3]_{org} \times |H^+|^9[(HA)_2]_{org}^{9/2}]^{1/3} \quad (11)$$

the following expression can be derived by combination of eqs (9), (10) and (11):

$$\frac{(3k_{303})^{1/3}C_{Fe,aq}|(HA)_2|_{org}^{3/2}}{C_{Fe,org}^{1/3}|H^+|^3\alpha_{Fe}} = 1 + zk_{xyz} \times (3k_{303})^{(1-z)/3}|(HA)_2|_{org}^{(1/2)[3+z(x+y-3)]} \times |H^+|^{z(3-x)-3}C_{Fe,org}^{(z-1)/3}\alpha_{Fe}^{-1} \quad (12)$$

where k_{xyz} is the stoichiometric constant for reaction (8).

Experimental functions $[\log C_{Fe,aq} + 3pH - (1/3)\log C_{Fe,org} - \log \alpha_{Fe}] = f[(z(3-x)-3)\log|H^+| + (z-1)/3 \log C_{Fe,org} - \log \alpha_{Fe}]$, at constant extractant concentration and different x and z values, were compared with the theoretical $\log Y = \log(1+X) = f(\log X)$, where Y and X are two normalized variables:

$$Y = (3k_{303})^{1/3}C_{Fe,aq} \times |(HA)_2|_{org}^{3/2}C_{Fe,org}^{-1/3}|H^+|^{-3}\alpha_{Fe}^{-1} \quad (13)$$

and X being the second term in eq. (12).

The best fit was found for $x = 3$ and $z = 2$ (Fig. 5), although it is noteworthy that the goodness of the fit is slightly sensible to changes on the degree of polymerization, z.

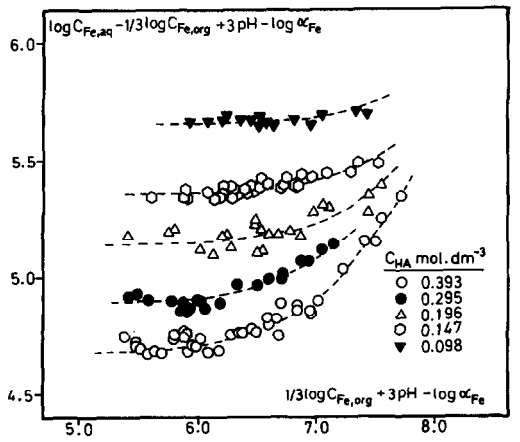

Fig. 5. Positions of best fit between the experimental function $\log C_{Fe,aq} - (1/3)\log C_{Fe,org} + 3pH - \log \alpha_{Fe} = f((1/3)\log C_{Fe,org} + 3pH - \log \alpha_{Fe})$ and the theoretical $\log Y = f(\log X)$.

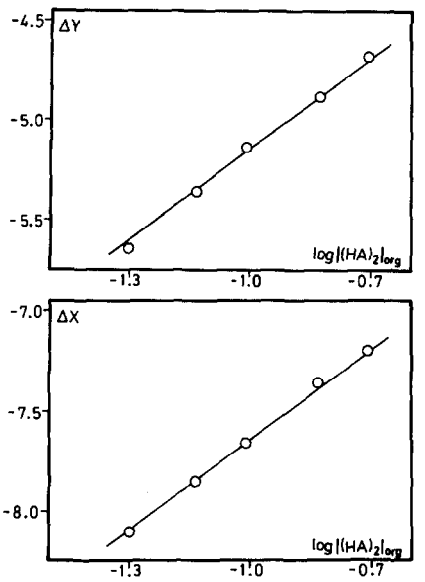

Fig. 6. Plots of the differences ΔY and ΔX as a function of free *n*-dodecanoic acid concentration.

Differences on both axes in the position of best fit between the experimental and the theoretical functions depend on $|(HA)_2|$, according to:

$$\Delta Y = \log Y - [\log C_{Fe,aq} - (1/3)\log C_{Fe,org} + 3pH - \log \alpha_{Fe}] = (1/3)\log 3k_{303} + (3/2)\log|(HA)_2|_{org} \quad (14)$$

$$\Delta X = \log X - [3pH + (1/3)\log C_{Fe,org} - \log \alpha_{Fe}] = 2\log k_{3y2} - (1/3)\log 3k_{303} + \tfrac{1}{2}(2y+3)\log|(HA)_2|_{org}. \quad (15)$$

Plots of these differences as a function of $|(HA)_2|$ are shown in Fig. 6. Since the points fall on a straight line of slope 1.5, it can be deduced that $y = 0$ and therefore the stoichiometry $(FeA_3)_2$ for the aqueous species can be deduced. Values of the constants obtained from the intercepts are given in Table 1.

NUMERICAL TREATMENT

Computer calculations were carried out in order to search for the chemical model which best explains the experimental data as well as to refine the extraction constant values graphically derived. The LETAGROP-DISTR program[23] was used in the calculations, the error square sum being:

$$U = \sum(\log D_{calc} - \log D_{exp})^2 \quad (16)$$

the function chosen for the minimization.

For each model tried, the program finds the set

Table 1. Values of the stoichiometric equilibrium constants obtained by graphical and numerical treatments of all the extraction data

Species	Method	$\log k_{mnj} \pm 3\sigma(\log k)$	$\log k_{xyz} \pm 3\sigma(\log k)$
$(FeA_3)_{3,org}$	Curve fitting	−11.4	
	Letagrop	−11.31 ± 0.04	
$(FeA_3)_{2,aq}$	Curve fitting		−10.1
	Letagrop		−10.01 ± 0.09

of equilibrium constants which gives the minimum value of U (U_{min}) as well as the standard deviation $\sigma(\log D)$, the best model being the one with the lowest values of both U_{min} and $\sigma(\log D)$. The results of the calculations are summarized in Table 2, confirming that the model graphically derived provides the best fit to the data. Table 1 compares the values of the constants obtained by the program and those derived by graphical analysis.

The fit to the data can be observed in Figs 1 and 2, where the continuous lines have been drawn using the equilibrium constants calculated by the program.

CONCLUSIONS

The presence in the organic phase of the unsolvated trimer quantitatively explains the extraction of Fe(III) from 1.0 mol dm^{-3} $NaNO_3$ by *n*-dodecanoic acid dissolved in toluene. Both graphical and numerical treatments of extraction data carried out at different metal ion and extractant concentrations confirm the absence of any other species in the organic phase. This result is in agreement with that obtained by Kholk'in *et al.*[12] and Tanaka *et al.*[11] for the extraction of Fe(III) by *n*-octanoic and *n*-decanoic acids, respectively, and seems to confirm the view of Yamada and Tanaka[7] that monomeric and dimeric iron(III) long chain carboxylates are not realistic in non-polar solvents. The extraction constant value obtained is higher than the one reported by Kholk'in *et al.* for the extraction by *n*-octanoic acid in benzene ($\log k_{303} = -14.63$) and the difference could be qualitatively explained by the higher distribution constant of *n*-dodecanoic in our system.

Deviations of the extraction data in the highest pH range studied can be only quantitatively

Table 2. Values of U_{min} and $\sigma(\log D)$ for some of the different models of species tried

Species $(FeA_m(HA)_n)_j$ $(m,n)j$	U_{min}	$\sigma(\log D)$	Rejected species
$(3,0)3_{org}$	2.1332	0.1327	
$(3,0)1_{org}$	3.9912	0.1816	
$(3,0)2_{org}$	1.7791	0.1213	
$(3,0)4_{org}$	3.1565	0.1615	
$(3,0)3_{org}$; $(3,0)2_{org}$	1.7780	0.1217	
$(3,0)3_{org}$; $(3,0)1_{org}$	1.9474	0.1274	
$(3,1)3_{org}$	5.7306	0.2176	
$(3,0)3_{org}$; $(3,0)1_{aq}$	0.3228	0.0519	
$(3,0)2_{org}$; $(3,0)1_{aq}$	0.8135	0.0823	
$(3,0)3_{org}$; $(3,0)2_{aq}$	0.3183	0.0515	
$(3,0)2_{org}$; $(3,0)2_{aq}$	0.8329	0.0833	
$(3,0)3_{org}$; $(3,0)3_{aq}$	0.3210	0.0517	
$(3,0)3_{org}$; $(3,0)4_{aq}$	0.3263	0.0522	
$(3,0)3_{org}$; $(3,1)2_{aq}$	0.4255	0.0595	
$(3,0)3_{org}$; $(3,0)1_{org}$; $(3,0)1_{aq}$	0.3228	0.0519	$(3,0)1_{org}$
$(3,0)3_{org}$; $(3,0)2_{org}$; $(3,0)1_{aq}$	0.3230	0.0521	$(3,0)2_{org}$
$(3,0)3_{org}$; $(3,0)1_{aq}$; $(3,0)2_{aq}$	0.3189	0.0517	
$(3,0)3_{org}$; $(3,0)1_{org}$; $(3,0)2_{aq}$	0.3183	0.0517	$(3,0)1_{org}$

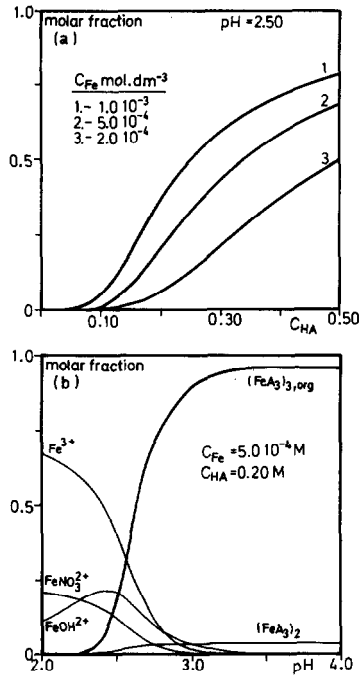

Fig. 7. Distribution diagrams in the system Fe(III)–$NaNO_3$/HA–toluene. (a) Molar fraction of the trimer, $(FeA_3)_3$, in the organic phase as a function of C_{HA} at constant pH and different total metal concentration. (b) Molar fraction of the main species in both phases as a function of pH at constant metal and *n*-dodecanoic acid concentration.

explained by the formation of iron carboxylate complexes of general composition $(FeA_3)_n$. Although the best fit is obtained for $n = 2$, the aggregation degree should be considered only as an average and species with a different n value cannot be disregarded.

Finally, the distribution diagrams in Fig. 7 show the influence of iron concentration on the extraction and the variation of the molar fraction of the main iron-containing species in both phases as a function of pH at constant metal and extractant concentrations. It can be easily appreciated that the aqueous iron carboxylate predominates in the aqueous phase in the range of high extraction, keeping the extraction percentage practically unchanged in a wide pH range.

REFERENCES

1. A. W. Fletcher and D. S. Flett, *Solvent Extraction Chemistry of Metals*, p. 359. Macmillan, New York (1966).
2. D. S. Flett and M. J. Jaycock, *Ion Exchange and Solvent Extraction*, Vol. 3, p. 1. Marcel Dekker, New York (1973).
3. A. W. Ashbrook, *Miner. Sci. Eng.* 1973, **3**, 169.
4. F. Miller, *Talanta* 1974, **21**, 685.
5. N. M. Rice, *Hydrometal.* 1978, **3**, 111.
6. Z. Brzózka and C. Rózycki, *Chem. Anal. (Warsaw)* 1980, **25**, 3.
7. H. Yamada and M. Tanaka, *Adv. Inorg. Chem. Radiochem.* 1985, **29**, 143.
8. M. Cox and D. S. Flett, *Proc. ISEC'71*, p. 204. Le Hague (1971).
9. V. I. Lakshmanan and G. J. Lawson, *Proc. ISEC'74*, p. 1169. Lyon (1974).
10. M. P. Elizalde, J. M. Castresana, M. Aguilar and M. Cox, *Solv. Ext. Ion Exch.* 1986, **4**, 1095.
11. M. Tanaka, N. Nakasuka and S. Goto, *Solvent Extraction Chemistry*, p. 154. North-Holland, Amsterdam (1967).
12. A. I. Kholk'in, L. M. Gindin, K. S. Luboshnikova, P. Mühl and K. Gloe, *J. Radioanal. Chem.* 1976, **30**, 383.
13. A. Bold and S. Fisel, *An. Stünt. Univ. Iasi. Sect. 1C* 1971, **17**, 19.
14. A. J. Van der Zeeuw, *Hydrometal.* 1979, **4**, 21.
15. A. Bartecki and W. Apostoluk, *Hydrometal.* 1980, **5**, 367.
16. R. W. Cattrall and M. J. Walsh, *J. Inorg. Nucl. Chem.* 1974, **36**, 1643.
17. H. Einaga, *Proc. ISEC'74*, p. 1691. Lyon (1974).
18. D. D. Perrin, W. L. F. Armarego and D. R. Perrin, *Purification of Laboratory Chemicals*. Pergamon Press, Oxford (1980).
19. G. K. Schweitzer and D. K. Morris, *Anal. Chim. Acta* 1969, **45**, 65.
20. C. F. Baes Jr. and R. E. Mesmer, *The Hydrolysis of Cations*. Wiley Interscience, New York (1976).
21. R. M. Smith and A. E. Martell, *Critical Stability Constants*. Plenum Press, New York (1977).
22. G. Erikson, *Anal. Chim. Acta* 1979, **112**, 375.
23. D. H. Liem, *Acta Chem. Scand.* 1971, **25**, 1521.

Polyhedron Vol. 6, No. 12, pp. 2161–2164, 1987
Printed in Great Britain

0277–5387/87 $3.00+.00

ALKOXY DERIVATIVES OF TRITHIAZYLTRICHLORIDE

RAY JONES, IVAN P. PARKIN, DAVID J. WILLIAMS and J. DEREK WOOLLINS*

Department of Chemistry, Imperial College of Science and Technology, South Kensington, London SW7 2AY, U.K.

(*Received* 5 *May* 1987; *accepted* 29 *June* 1987)

Abstract—Reaction of trithiazyltrichloride, $(NSCl)_3$, with NaOR in ROH (R = Me, Et, ^{i}Pr, ^{n}Pr, ^{n}Bu, ^{t}Bu, pentyl, amyl, cyclohexyl, benzyl) gives $(NSOR)_3$. The compounds have been characterized by IR and mass spectroscopy and in the case of R = methyl, (**2a**) and benzyl, (**2e**) by X-ray crystallography. In the structures of both (**2a**) and (**2e**) the S_3N_3 ring adopts a flattened chair cyclohexane conformation with the substituents being axial.

Trithiazyltrichloride, $(NSCl)_3$, (**1**), has been known for many years.[1] It is readily prepared[2] and unlike many other sulphur–nitrogen species, not especially hazardous. However, unlike the related phosphorus–nitrogen ring system, $(PNCl_2)_3$, substitution reactions of (**1**) are not common; with ring cleavage readily occurring. There has recently been a brief report[3] on the use of sodium alkoxides (NaOR; R = Me, ^{i}Pr) in the preparation of $(NSOR)_3$, (**2**), from (**1**). Neither the generality of the reaction nor the structure and properties of (**2**) were described. Here we report on our studies into the preparation of (**2**) for a wide variety of R groups. Vibrational and mass spectroscopy have been used to characterize the compounds. In the cases of R = methyl and benzyl the X-ray crystal structures are reported.

EXPERIMENTAL

General. All reactions were performed under an inert atmosphere of nitrogen or argon using dried solvents. Alcohols were dried over 3 Å molecular sieves and petroleum ether was dried over sodium. Trithiazyltrichloride was prepared by the literature method.[2] IR spectra were recorded as thin films or nujol mulls using a PE497. UV/vis spectra were measured on a Pye SP8-400.

Preparation of $(NSOR)_3$ R = Me, Et, *n*-Pr, *i*-Pr. Sodium (0.6 g, 0.026 mol) was added to the appropriate alcohol (20 cm^3), after dissolution of the metal petroleum ether (5 cm^3) was added and the reaction cooled to 0°C. A slurry of $S_3N_3Cl_3$ (3.0 g, 0.012 mol) in alcohol (20 cm^3) was added over 10 min. The reaction was stirred and allowed to warm to room temperature (2 h) during which time it turned red. The solvent was evaporated under reduced pressure and the oily solid remaining was extracted with *n*-hexane (3 × 20 cm^3). Removal of the *n*-hexane *in vacuo* gave the final products. Analytical and spectroscopic data are in Tables 1 and 2. For R = Me the volume of *n*-hexane was reduced to *ca* 20 cm^3 and the solution cooled to −20°C, Yield 1.4 g, 50%. Crystals of (**2a**) suitable for X-ray crystallography were obtained by slow evaporation of an *n*-hexane solution at 4°C.

R = *n*-Bu, *t*-Bu, *n-pentyl*, *amyl*, *cyclohexyl*. Sodium (0.2 g, 8.7 mmol) was dissolved in the

Table 1. Microanalytical data and yields

R	M.p./°C	Yield	C	H	N
2a Me	32	51	15.4 (15.6)	3.6 (3.8)	17.7 (18.2)
2b Et	liq.	36	27.4 (26.2)	5.8 (5.5)	14.3 (15.3)
2c *n*-Pr	liq.	32	34.5 (34.3)	6.9 (6.7)	12.9 (13.3)
2d *i*-Pr	liq.	34	34.3 (34.3)	6.8 (6.7)	13.3 (13.3)
2e benzyl	74	23	54.6 (54.8)	4.6 (4.6)	9.05 (9.1)
2f amyl	liq.	22	45.4 (45.1)	8.4 (8.3)	10.0 (10.5)

* Author to whom correspondence should be addressed.

Table 2. IR and NMR data

R	ν(CO)	ν(SN)				ν(SO)	δ(ring)	^{1}H NMR δ/ppm
Me								
IR	1043s	994s	910	730s	701s	640s	510mw	3.80(s)
Raman	—	998w	954w	730w	709s	637s	512m	
Et	1040s	980s	890s	730s	700s	670s	530m	1.36(t,4) 4.07(q,3)
n-Pr	1020s	928s	900s	730s	710s	680s	535m	1.00(t,3) 1.76(m,2) 3.96(t,3)
i-Pr	1020s	—	905s	740s	—	680s	540m	1.31(d,6) 4.49(septet,1)
n-Pent	1030s	955s	890s	740s	696s	650s	540m	0.91(t,3) 1.36(m,4) 1.74(m,2) 3,83(t,2)
amyl	1020s	925s	842(?)	738s	—	680s	540m	—
bz								
IR	1005s	930s	900s	723s	675s	630s	523m	4.70, 4.92 7.25(m,5)
Raman	1004s	948w	—	720m	—	632s	525m	

appropriate alcohol (20 cm^3) and pet. ether (20 cm^3) added. With the solution at 35°C solid $S_3N_3Cl_3$ (1.0 g, 4.0 mmol) was added. Stirring and heating was maintained for 3 h after which time the reaction was worked up as above.

R = *Benzyl.* Sodium (0.23 g, 10 mmol) was dissolved in benzyl alcohol at 0°C. To this solution was added solid $S_3N_3Cl_3$ (0.8 g, 3.2 mmol). After 2 h the alcohol was removed *in vacuo* and the residue extracted with pet. ether (2 × 20 cm^3). The ether solution was reduced to *ca* 20 cm^3 and cooled to −20°C to give the product as crystals suitable for X-ray studies.

Crystal Data. (**2a**), $C_3H_9N_3O_3S_3$, $M = 231.3$, rhombohedral, $a = 12.147(6)$, $c = 11.368(6)$ Å, $U = 1453(1)$ Å^3, space group $R\bar{3}$, $Z = 6$, $D_c = 1.59$ g cm^{-3}, colourless air stable irregular polyhedron, crystal dimensions 0.15 × 0.15 × 0.2 mm. μ(Cu-K$_\alpha$) = 67.8 cm^{-1}, $\lambda = 1.54178$ Å, $F_{(000)} = 720$.

(**2e**), $C_{21}H_{21}N_3O_3S_3$, $M = 459.6$, monoclinic, $a = 9.373(2)$, $b = 13.581(3)$, $c = 17.507(5)$ Å, $\beta = 90.08(2)$, $U = 2229(1)$ Å^3, space group $P2_1/n$, $Z = 4$, $D_c = 1.37$ g cm^{-3}, colourless, air stable irregular polyhedron, crystal dimensions 0.16 × 0.18 × 0.15 mm, μ(Cu-K_α) = 32.2 cm^{-1}, $\lambda = 1.54178$ Å, $F_{(000)} = 960$.

Data collections and processing

Nicolet R3m diffractometer, ω-scan method [$2\theta \leqslant 116$ (**2a**) and 100° (**2e**)], graphite monochromated Cu-K_α radiation. 437 and 2198 independent reflections of which 269 and 1692 respectively considered observed [$|F_o| > 3\sigma(|F_o|)$] for (**2a**) and (**2e**), corrected for Lorentz and polarization factors; empirical absorption correction based on 360 azimuthal scans for both data sets.

Structure analysis and refinement

Both structures were solved by direct methods and non-hydrogen atoms refined anisotropically in each case. The methyl group in (**2a**) was treated as a rigid body. The hydrogen atoms in (**2e**) were idealized (C—H = 0.96 Å), assigned isotropic thermal parameters [$U(H) = 1.2U_{eq}(C)$] and allowed to ride on their parent carbons. Refinement was by block-cascade full-matrix least-squares to give for (**2a**) $R = 0.107$, $R_w = 0.122$ ($w^{-1} = \sigma^2(F) + 0.00278F^2$) and for (**2e**) $R = 0.050$, $R_w = 0.053$ ($w^{-1} = \sigma^2(F) + 0.00072F^2$) ($R = \Sigma|(F_o - F_c)|/\Sigma|F_o|$). The maximum residual electron densities in the final ΔF maps were 0.74 and 0.22 e Å^{-3} for (**2a**) and (**2e**) respectively. The mean and maximum shifts/error in the final refinement cycles were for (**2a**) 0.016 and 0.107 and for (**2e**) 0.005 and 0.017. Computations were carried out on an Eclipse S140 computer using the SHELXTL system.[4]*

RESULTS AND DISCUSSION

The *cyclo*-trialkoxytrithiazenes, $(NSOR)_3$, (**2**), are readily prepared by reaction of trithiazyltrichloride with the appropriate sodium alkoxide in alcohol [eq. (1)]. Yields varied between 51 and 10%, with lower yields being obtained in reactions involving bulky alcohols

$$(NSCl)_3 + 3NaOR \rightarrow (NSOR)_3 + 3NaCl. \quad (1)$$

Microanalytical data for those compounds obtained pure is given in Table 1; when using less volatile alcohols it was not possible to free the pro-

* Final positional parameters and F_o/F_c values have been deposited as supplementary data with the Editor, from whom copies are available on request. Atomic coordinates have also been deposited with the Cambridge Crystallographic Data Centre.

duct of the parent alcohol even after sustained pumping under high vacuum. Since we found that (**2**) are somewhat thermally unstable they could not be distilled. The reaction does not proceed in solvents other than the parent alcohol. Asymmetrically substituted compounds are also readily prepared. For example, reaction of NaOEt/NaO*i*-Pr (in ethanol/isopropanol) with (**1**) gives all possible products, $S_3N_3(OEt)_n(OiPr)_{3-n}$ (in the statistically expected proportions); observed by ^1H NMR and mass spectrometry.

IR and NMR data for selected compounds are given in Table 2. In (**2**) the ^1H resonances are shifted downfield relative to the parent alcohol. For the observed (*vide infra*) C_{3v} symmetry four ν(SN) vibrations together with ν(SO) and ν(CO) vibrations are expected. Seven characteristic bands are observed. The band at *ca* 1025 cm^{-1} is assigned as ν(CO) because of its sensitivity to the R group. The ν(SO) and ν(SN) vibrations fall between 1000–630 cm^{-1}; although individual assignments are difficult it seems likely that ν(SO) is the lowest frequency band of this group (at around 640 cm^{-1}). The moderate intensity band at *ca* 520 cm^{-1} is probably a ring deformation. The mass spectra consist of weak peaks due to M^+ with the principle fragments being $S_3N_3(OR)_2^+$ and $(S_2N_2OR)^+$. The UV spectra of (**2**) exhibit one absorption centred at 208 nm of moderate intensity ($\varepsilon \approx 1800$ mol^{-1} dm^3 cm^{-1}).

The X-ray crystal structure of (**2e**) (Fig. 1) is analogous to that of (**1**) having a flattened chair-like six-membered ring which is substituted axially. The whole structure has approximate non-crystallographic C_3 symmetry. The bond lengths and angles (Table 3) are not significantly different within the ring suggesting a delocalized system. The SN bond lengths (range 1.588(4)–1.611(4) Å) are shorter than the single bonds in *cyclo*-$S_4(NCH_2Ph)_2$, (**3**), [1.713(4)–1.720(3)][5] and are within statistical significance the same as those in

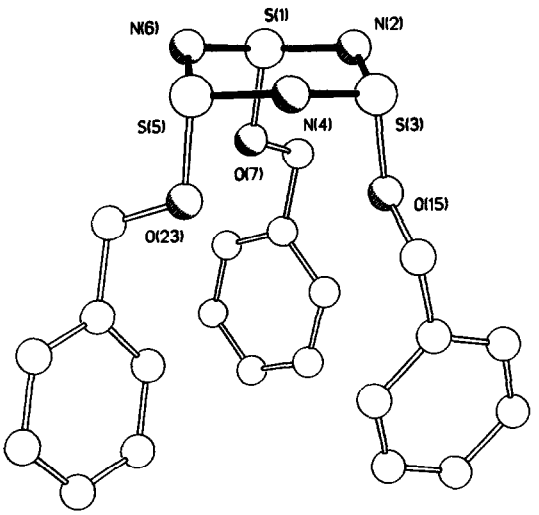

Fig. 1. The X-ray crystal structure of $(NSOBz)_3$, (**2e**).

$(NSCl)_3$.[6] The SNS and NSN angles [range 121.2(3)–122.5(2) and 112.2(2)–113.3(2)°] in (**2e**) indicate trigonal and distorted tetrahedral environments for nitrogen and sulphur respectively. The structure of (**2a**) though of limited accuracy (the determination being carried out close to the melting point) displays the same axial substitution pattern and flattened chair cyclohexane conformation. The errors in the structural parameters preclude any meaningful comparisons. The chair form appears to be general for S(IV) rings[1,6] although β-$(SNOCl)_3$ adopts a distorted boat conformation with the chlorines axial and the oxygens equatorial.[7]

It is interesting to compare the relative planarity of (**2e**) and (**3**) since this may provide an indication of the extent of π-delocalization in (**2**). In (**2e**) the S(1)—S(3)—N(4)—N(6) plane is inclined to the S(1)—N(2)—S(3) and N(4)—S(5)—N(6) planes by 32 and 27° respectively with N(2) and S(5) lying 0.38 and 0.42 Å above and below this plane. In (**3**)

Table 3. Selected bond distance (Å) and angles (°) in $(NSOBz)_3$, (**2e**)

S(1)—N(2)	1.593(4)	S(1)—N(6)	1.614(4)
S(3)—N(2)	1.603(4)	S(3)—N(4)	1.611(4)
S(5)—N(4)	1.604(4)	S(5)—N(6)	1.588(4)
S(1)—O(7)	1.636(3)	S(3)—O(15)	1.646(3)
S(5)—O(23)	1.634(3)	O(7)—C(8)	1.441(6)
O(15)—C(16)	1.432(7)	O(23)—C(24)	1.461(6)
N(2)—S(1)—N(6)	112.1(2)	N(2)—S(3)—N(4)	112.4(2)
N(4)—S(5)—N(6)	113.3(2)	S(1)—N(2)—S(3)	122.5(2)
S(1)—N(6)—S(5)	121.2(3)	S(3)—N(4)—S(5)	121.2(3)
N(2)—S(1)—O(7)	107.0(2)	N(2)—S(3)—O(15)	99.0(2)
N(4)—S(5)—O(23)	99.4(2)	S(1)—O(7)—C(8)	113.9(3)
S(3)—O(15)—C(16)	112.8(3)	S(5)—O(23)—C(24)	114.6(3)

the S—S—S—S and S—N—S planes are inclined by 63° whereas the comparable angles in (**1**) are 23 and 18° respectively.* The flattening of the ring in (**1**) and (**2e**) relative to (**3**) is presumably a consequence of a π system based on nitrogen *p* and sulphur *d* orbitals. This type of bonding scheme has been developed previously.[8] The noticeably flattening in the structure of (**1**) relative to (**2e**) is due to the increased steric repulsion between the three chlorine substituents *cf.* the oxygen atoms in (**2e**). In (**1**) the Cl···Cl distances are 3.61, 3.61, and 3.78 Å whilst in (**2e**) the O···O distances are 3.06, 3.13 and 3.17 Å.

The compounds reported here are sulphur–nitrogen analogues of $(PNR_2)_3$ and as such may provide useful starting materials in the synthesis of substituted SN polymers. Further work is under way.

*The equivalent values for the alternative S(1)—N(2)—N(4)—S(5) plane are 30 and 29° and for the N(2)—S(3)—S(5)—N(6) plane are 29 and 28°. In all three instances the larger dihedral angle is associated with the out of plane nitrogen atom.

Acknowledgements—We are grateful to the University of London Central Research Fund for support and to J. Bilton for measuring the mass spectra.

REFERENCES

1. *Gmelin Handbook of Inorganic Chemistry*, 8th edn, Sulphur, Sulphur–Nitrogen Compounds Part 2. Springer, Berlin (1985).
2. W. L. Jolly and K. D. Maguire, *Inorg. Synth.* 1967, **9**, 102.
3. M. Meissner, K. H. Kohnickt and H. Schumann, *Chem. Zeitung.* 1982, **106**, 409.
4. G. M. Sheldrick, SHELXTL, An Integrated System for Solving, Refining and Displaying Crystal Structures from Diffraction Data. University of Göttingen, Göttingen, FRG (1978), Revision 4.1 (August 1983).
5. R. Jones, D. J. Williams and J. D. Woollins, *Angew. Chem. Int. Ed.* (*Engl.*) 1985, **24**, 760.
6. G. A. Wiegers and A. Vos, *Acta Cryst.* 1966, **20**, 192.
7. R. Jones, unpublished observation.
8. R. Gleiter, *Angew. Chem. Int. Ed.* (*Engl.*) 1981, **20**, 444.

Polyhedron Vol. 6, No. 12, pp. 2165–2168, 1987
Printed in Great Britain

0277–5387/87 $3.00+.00

PREPARATION AND X-RAY CRYSTAL STRUCTURES OF MIXED LIGAND COMPLEXES CONTAINING THE S_3N^- LIGAND

RAY JONES, THOMAS G. PURCELL, DAVID J. WILLIAMS and J. DEREK WOOLLINS*

Department of Chemistry, Imperial College of Science and Technology, South Kensington, London SW7 2AY, U.K.

(*Received* 29 *May* 1987; *accepted* 10 *July* 1987)

Abstract—Reaction of $Hg(S_7N)_2$ with *cis*-$PtCl_2(PR_3)_2$ (PR_3 = PPh_3, PPh_2Me, $PPhMe_2$, PEt_3) in the presence of $Na[PF_6]$ gives $[Pt(S_3N)(PR_3)_2][PF_6]$ in 32–46% yield. The complexes have been characterized by IR, NMR and microanalyses. The X-ray crystal structures of two examples (PR_3 = PPh_2Me and PEt_3) show that the S_3N^- ligand coordinates in a bidentate fashion via two sulphur atoms.

Metalla–sulphur–nitrogen complexes include terminally bonded fragments and stretch from 5 to 8 membered rings.[1,2] We are investigating the stabilization of reactive sulphur–nitrogen anions using transition metal centres for a number of reasons. New insights into the solution equilibria of SN species might be gained; synthetic reagents can be prepared and structurally interesting materials are available. In this latter regard we have recently reported[3] on the synthesis of mixed ligand platinum stacking compounds, $[Pt(S_2N_2H)(PR_3)_2]X$, (**1**) containing the $S_2N_2H^-$ group. There has previously been substantial work on $M(S_2N_2H)_2$ and $M(S_3N)_2$ complexes[4] and it is clear that the $S_2N_2H^-$ and S_3N^- ligand are isoelectronic (NH = S). We have therefore developed a simple synthesis of $[Pt(S_3N)(PR_3)_2][PF_6]$, (**2**), to enable us to investigate the effect of replacement of an NH group by a sulphur atom on the stacking properties of (**1**).

Previously, complexes containing the S_3N^- ligand have been obtained from reactions involving explosive S_4N_4;[4] directly from salts of S_3N^-[5,6] or by *in situ* formation of the anion using base and S_7NH.[7–10] All of these three routes have problems. S_4N_4 is rather hazardous and should be avoided wherever possible. Salts of S_3N^- are not particularly easy to prepare, are air sensitive, equilibrate in solution to S_4N^- and have not been particularly successful in the preparation of Group VIII complexes. The deprotonation reactions of S_7NH are useful but give complex products. Finally, none of these routes has been used in reactions with metal phosphine complexes. Here, we report on the usefulness of the readily prepared and easily handled reagent $Hg(S_7N)_2$ in the synthesis of $[Pt(S_3N)(PR_3)_2]$, (**2**). The X-ray crystal structures of two examples (PR_3 = PPh_2Me and PEt_3) are reported.

EXPERIMENTAL

General experimental procedures and preparation of platinum starting materials were as described previously.[4,11] $Hg(S_7N)_2$ was prepared by the reported method[12] and stored at −18°C in the dark. All reactions were performed under an inert atmosphere (N_2 or Ar) but the work-ups were carried out in air.

Preparation of S_3N^- *complexes.* In a typical reaction $PtCl_2(PPh_3)_2$ (100 mg, 0.126 mmol), $Hg(S_7N)_2$ (86 mg, 0.126 mmol) and $NaPF_6$ (23 mg, 0.136 mmol) were stirred together in dichloromethane (20 cm^3) at room temperature for 24 h. During this time the initial cream suspension turned into a dark purple solution. The solution was filtered through Celite and its volume reduced to *ca* 3 cm^3 before preparative thin layer chromatography (CH_2Cl_2 eluent). The product (r_f 0.3) was extracted from the silica using CH_2Cl_2/thf. After evaporation of this solution, *in vacuo*, to near dryness the orange/brown product was precipitated

*Author to whom correspondence should be addressed.

Table 1. Yields and microanalytical data

Complex	Yield/%	M.p./°C	C%	H%	N%
$[Pt(S_3N)(PEt_3)_2]PF_6$ (**2a**)	37	137–138	21.0 (21.0)	4.4 (4.4)	2.0 (2.0)
$[Pt(S_3N)(PMe_2Ph)_2]PF_6$ (**2b**)	46	146–147	26.4 (27.0)	3.0 (3.1)	1.9 (1.8)
$[Pt(S_3N)(PMePh_2)_2]PF_6$ (**2c**)	33	141–142	36.7 (35.0)	3.1 (3.2)	1.6 (2.0)
$[Pt(S_3N)(PPh_3)_2]PF_6$ (**2d**)	39	154–156	44.3 (44.2)	3.1 (3.0)	1.4 (1.5)

Table 2. ^{31}P-{^1H} NMR data

PR_3	^{31}P-{^1H} NMR δ_A/ppm	δ_X/ppm	^1J_A/Hz	^1J_X/Hz	^2J/Hz
(2a) PEt_3	7.30	9.17	2373	2842	27
(2b) PMe_2Ph	−19.80	−17.18	2439	2927	24
(2c) $PMePh_2$	−10.08	−6.48	2485	2979	26
(2d) PPh_3	7.08	11.39	2566	3120	22

using *n*-hexane. Yields, and properties of the complexes are reported in Tables 1 and 2. Samples suitable for X-ray crystallography were obtained by diffusion of hexane into dichloromethane solutions.

Crystal data

2(a) $[Pt(S_3N)(P(C_2H_5)_3)_2][PF_6]$, $M = 686.6$, orthorhombic, $a = 12.540(4)$, $b = 13.754(5)$, $c = 27.542(8)$ Å, $U = 4750(3)$ Å^3, space group *Pcab*, $Z = 8$, $D_c = 1.93$ g cm^{-3}, red air stable truncated octahedron, crystal dimensions $0.2 \times 0.1 \times 0.1$ mm, μ(Cu-$K\alpha$) = 160 cm^{-1}, $\lambda = 1.54178$ Å, $F(000) = 2671$.

2(b) $[Pt(S_3N)(PCH_3(C_6H_5)_2)_2][PF_6]\cdot(X_{11})_{0.25}$*, M* = 883.7, monoclinic, $a = 18.759(4)$, $b = 19.168(5)$, $c = 12.498(2)$ Å, $\beta = 124.34(2)$, $U = 3711(1)$ Å^3, space group $C2/c$, $Z = 4$, D_c* = 1.59 g cm^{-3}, red air stable prism, crystal dimensions $0.3 \times 0.2 \times 0.1$ mm, μ(Cu-$K\alpha$)* = 104 cm^{-1}, $\lambda = 1.54178$ Å, $F(000)$* = 1722.

Data collections and processing

Nicolet R3m diffractometer, ω-scan method ($2\theta \leqslant 100°$ for (**a**) and $2\theta \leqslant 116°$ for (**b**)), graphite monochromated Cu-$K\alpha$ radiation. For (**1**) and (**2**): 2003 and 2590 independent measured reflections of which 1915 and 2371 respectively were considered observed ($|F_o| > 3\sigma(|F_o|)$), corrected for Lorentz and polarization factors; numerical absorption corrections (face indexed crystals).

Structure analysis and refinement

Structure (**2a**) was solved by the heavy atom technique and (**2b**) by direct methods. In (**2a**) all the non-hydrogen atoms were located from successive ΔF maps and refined anisotropically. In (**2b**) the structure was initially solved in space-group *Cc*. The thermal ellipsoids for the N(1) and S(2) atoms in the PtS_3N ring indicated the structure to be disordered about the axis passing through the Pt atom and bisecting the P—Pt—P angle. Further inspection of the coordinates of the atoms in the two phosphine ligands showed that they also could be related by this 2-fold axis. The PF_6 anion could also be accommodated on an independent 2-fold axis. Subsequent refinement of the disordered model was carried out in space-group $C2/c$ which though resulting in the expected small increase in R gave significantly improved standard deviations. All non-hydrogen atoms were refined anisotropically with the exception of the 50% occupancy nitrogen atom N(1) and the disordered solvent, for which five carbon atoms were refined isotropically in general positions with occupancies of 25% and one carbon atom was refined isotropically on a crystallographic centre of symmetry with an occupancy of 12.5%.

*Contains a contribution from an unknown disordered solvent fragment refined as $(C_{11})_{0.25}$.

In both structures the PF_6 anions were refined as rigid bodies. The methyl groups were also refined as rigid bodies, all other hydrogen atoms [in (**2a**) and (**2b**)] were idealized (C—H = 0.96 Å), assigned isotropic thermal parameters [$U(H) = 1.2U_{eq}(C)$] and allowed to ride on their parent carbon atoms. Refinement was by block cascade full-matrix least-squares to give for (**2a**) $R = 0.042$, $R_w = 0.034$ ($w^{-1} = \sigma^2(F) + gF^2$, where g converged to a value of less than 0.00001) and for (**2b**) $R = 0.063$, $R_w = 0.067$ ($w^{-1} = \sigma^2(F) + 0.00738F^2$) ($R = \Sigma|F_o - F_c|/\Sigma|F_o|$). The maximum residual electron densities in the final ΔF maps were 0.60 and 1.92 eÅ^{-3} for (**2a**) and (**2b**) respectively. The mean and maximum shifts/error in the final refinement cycles were, for (**2a**), 0.011 and 0.082 and, for (**2b**), 0.002 and 0.026. Computations were carried out on an Eclipse S140 computer using the SHELXTL[13] program system and published[14] scattering factors.

RESULTS AND DISCUSSION

Reaction of $Hg(S_7N)_2$ with $PtCl_2(PR_3)_2$ and $NaPF_6$ at room temperature gives reasonable yields of $[Pt(S_3N)(PR_3)_2][PF_6]$.

$$Hg(S_7N)_2 + PtCl_2(PR_3)_2 + NaPF_6 \rightarrow [Pt(S_3N)(PR_3)_2][PF_6] + HgCl_2$$

The products were characterized by $^{31}P\text{-}\{^1H\}$ NMR and IR spectroscopy and this data together with the microanalytical results are shown in Tables 1 and 2. The driving force for the reaction is the formation of $HgCl_2$ but the mechanism is not obvious. During purification using preparative thin layer chromatography we isolated S_4N_2 as a major side-product. A number of pathways thus seem possible. (1) Decomposition of $Hg(S_7N)_2$ to form S_4N_2 which then reacts with *cis*-$PtCl_2(PR_3)_2$ to give (**2**). (2) Initial formation of a complex containing the S_7N^- ligand which then eliminates sulphur. (3) Formation of S_7N^- which equilibrates to S_4N^-/S_3N^-. We do not favour (3) since the characteristic blue colour of S_4N^- is not observed during the reaction. There has recently been a report on the formation of an S_7N^- complex[10] and this lends some support for (2). Stirring $Hg(S_7N)_2$ overnight (with formation of S_4N_2 as evidenced by TLC) followed by treatment with $PtCl_2(PMe_2Ph)_2$ did not result in formation of (**2**). Direct reaction of sublimed S_4N_2 with $Pt(C_2H_4)(PR_3)_2$ gives $Pt(S_2N_2)(PR_3)_2$. We therefore favour pathway (2).

The $^{31}P\text{-}\{^1H\}$ NMR of (**2**) are AB type with platinum satellites. The magnitudes of $^2J(^{31}P—^{31}P)$ and $^1J(^{31}P—^{195}Pt)$ are appropriate for Pt(II) complexes. Assignment of individual resonances is difficult. Comparison with (**1**) and $Pt(S_2N_2)(PR_3)_2$, (**3**), which are related to (**2**) by replacement of a sulphur atom by an NH group and an N^-, is of interest but not particularly helpful. As was the case with (**1**) and (**3**) there is a linear increase in the magnitude of ^1J on replacing methyl groups by phenyl groups in the phosphines. To be consistent with our previous assignments we tentatively assign δ_A (with the lower ^1J values) to P(1) which is *trans* to S(1). The Pt—P bond lengths are however not crystallographically distinguishable because of disorder problems.

The IR spectra of the complexes are dominated by absorptions due to phosphines. However, in the PEt_3 case two ν(SN) vibrations (1010(sh) 709(m) cm^{-1}), a ν(SS) (529(m) cm^{-1}) and two ν(PtS) (338(w), 320(vw) cm^{-1}) vibrations may be assigned by analogy with $Pt(S_3N)_2$.[4]

The X-ray structures of (**2a**) (Fig. 1) and (**2b**) have been determined. The cations have the expected *cis* square planar geometry. Unfortunately, in each case, disorder about the pseudo two-fold axis (Fig. 2) of the cation precludes any detailed discussion of bond lengths and angles for the sulphur–nitrogen portions of the molecules. The degree of disorder, as evidenced by the thermal elipsoids, is somewhat less in (**2a**) than in (**2b**). Disorder of this type is apparent in a number of other related complexes.[10,15] Comparison with $Cu(S_3N)(PPh_3)_2$ and $PPN[Cu(S_3N)_2]$,[5] neither of which are reported to be disordered, shows an apparent reversal in the lengths of the bonds at nitrogen for (**2a**) relative to the copper complexes [in (**2a**) S(2)—N(1) 1.502(11), N(1)—S(3) 1.632(10) Å; the equivalent distances in

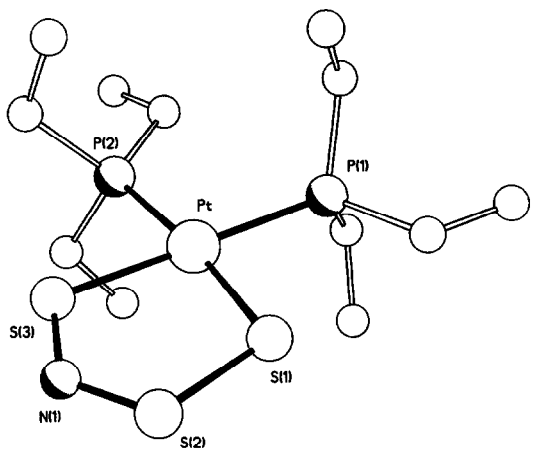

Fig. 1. The X-ray crystal structure of the cation in (**2a**); selected bond lengths and angles S(1)—S(2) 2.034(5), S(2)—N(1) 1.502(11), N(1)—S(3) 1.632(10), Pt—S(1) 2.287(3), Pt—S(3) 2.290(3), Pt—P(1) 2.321(3), Pt—P(2) 2.319(3) Å, S(1)—Pt—S(3) 89.8(1), Pt—S(1)—S(2) 103.6(1), S(1)—S(2)—N(1) 111.7(4), S(2)—N(1)—S(3) 124.8(7), N(1)—S(3)—Pt 110.1(4)°.

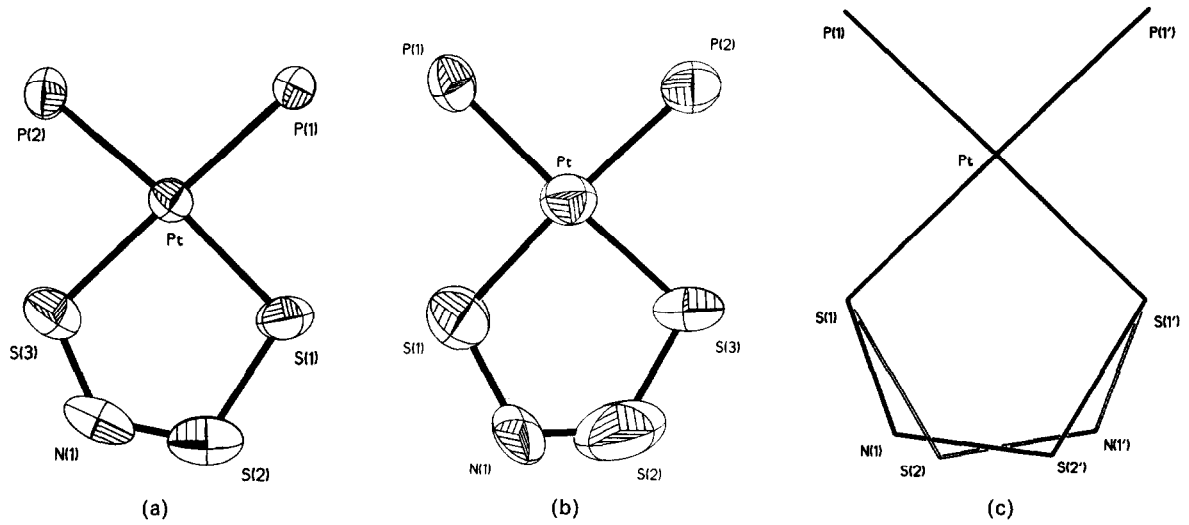

Fig. 2. (a) 50% probability thermal ellipsoid plot of the cation in (**2a**). (b) 50% probability thermal ellipsoid plot of the cation in (**2b**) when refined in space-group *Cc* showing the disorder affecting the metallacycle (carbon atoms omitted for clarity). (c) A line drawing showing the disordered model, refined in space-group *C*2/*c*, for (**2b**) where the two orientations of the ring are related by a crystallographic two-fold axis passing through the Pt atom and bisecting the P—Pt—P angle.

PPN[Cu(S_3N)$_2$] are 1.652(9) and 1.512(11) Å]. This apparent reversal may be an artifact of the disorder present in (**2a, b**), nonetheless, the structures do confirm the gross geometry of the cations to be as expected. The Pt—P and Pt—S bond lengths are as expected for Pt(II) complexes and are not significantly different from those observed in analogous $S_2N_2^{2-}$ and $S_2N_2H^-$ complexes.[11,16] Neither structure shows the type of stacking of cations observed in the isoelectronic $S_2N_2H^-$ complexes, (**1**).

Acknowledgements—We are grateful to Johnson Matthey for loans of precious metal and to the University of London Central Research Fund for an equipment grant.

REFERENCES

1. P. F. Kelly and J. D. Woollins, *Polyhedron* 1986, **5**, 607.
2. T. Chivers and F. Edelmann, *Polyhedron* 1986, **5**, 1661.
3. R. Jones, P. F. Kelly, C. P. Warrens, D. J. Williams and J. D. Woollins, *J. Chem. Soc., Chem. Commun.* 1986, 711.
4. J. D. Woollins, R. Grinter, M. K. Johnson and A. J. Thomson, *J. Chem. Soc., Dalton Trans*, 1980, 1910.
5. J. Bojes, T. Chivers and P. W. Codding, *J. Chem. Soc., Chem. Commun.* 1981, 1171.
6. J. Bojes, T. Chivers, W. G. Laidlaw and M. Trsic, *J. Am. Chem. Soc.* 1982, **104**, 4837.
7. J. D. Woollins, *Polyhedron*, 1984, **3**, 1365.
8. J. Weiss, *Angew. Chem. Int. Ed. Engl.* 1982, **21**, 705.
9. J. Weiss, *Z. anorg. allg. Chem.* 1985, **521**, 44.
10. J. Weiss, *Z. anorg. allg. Chem.* 1986, **542**, 137.
11. P. A. Bates, M. B. Hursthouse, P. F. Kelly and J. D. Woollins, *J. Chem. Soc., Dalton Trans.* 1986, 2367.
12. R. J. Ramsay, H. G. Heal and H. Garcia-Fernandez, *J. Chem. Soc., Dalton Trans.* 1976, 234.
13. G. M. Sheldrick, SHELXTL, An integrated system for solving, refining and displaying crystal structures from diffraction data. University of Gottingen, FRG (1978); Revision 4.1 (1983).
14. *International Tables for X-ray Crystallography*, Vol. IV, pp. 99–149. Kynoch Press, Birmingham, U.K. (1974).
15. U. Thewalt, *Z. Naturforsch.* 1982, **B37**, 276.
16. R. Jones, P. F. Kelly, D. J. Williams and J. D. Woollins, *J. Chem. Soc., Dalton Trans.* accepted.

Polyhedron Vol. 6, No. 12, pp. 2169–2175, 1987
Printed in Great Britain

0277–5387/87 $3.00+.00

SYNTHETIC POSSIBILITIES OF THE 2,4-PENTANEDIONE-1,2-DIAMINOETHANE SYSTEM: AN OVERALL VIEW

J.-P. COSTES

Laboratoire de Chimie de Coordination du CNRS, Unité n° 8241 liée par convention à l'Université Paul Sabatier, 205, route de Narbonne, 31077 Toulouse Cedex, France

(*Received* 25 *April* 1987; *accepted* 10 *July* 1987)

Abstract—Single condensation of acetylacetone (AcacH) with 1,2-diaminoethane (En) yields the terdentate "half-unit" 7-amino-4-methyl-5-aza-3-hepten-2-one (abbreviated as AEH). In the presence of a metal ion, this ligand leads to the macrocycle 5,7,12,14-tetramethyl-1,4,8,11-tetraazacyclo tetradeca-4,6,11,13-tetraene, which can be considered as resulting from the condensation of two molecules of (AcacH) with two molecules of (En). This "half-unit" can also be used to obtain acyclic ligands and complexes made with one (AcacH) molecule and two (En) molecules (1 : 2) or conversely two (AcacH) molecules and one (En) molecule (2 : 1). Using reagents other than (AcacH) and (En), this "half-unit" may yield homo and heterodinuclear complexes, macrocyclic compounds and non-symmetrical tetradentate Schiff bases.

Within the large family of Schiff bases, one of the most frequently named is *N,N'*-ethylene-bis(acetyl acetoneimine) ($BAEH_2$)* [*Cf.* Fig. 1(C)]. It is generally suggested that ($BAEH_2$) is the only product resulting from the reaction of 1,2-diaminoethane with 2,4-pentanedione, whatever the proportion of the two reagents.[1] After deprotonation it may be reacted with divalent metal ions M(II) to yield MBAE complexes.[2–4] It is noteworthy that these complexes may be obtained through different synthetic pathways, such as the reaction of $Ni(En)_2Cl_2$ with (AcacH),[5] that of $Ni(CH_3COO)_2 \cdot 4H_2O$ with an equimolar mixture of (En) and (AcacH), or the reaction of bis(4-amino-3-penten-2-onato)nickel(II) with (En).[6] On the contrary, no reaction occurs on mixing $Ni(Acac)_2 \cdot H_2O$ and (En). This absence of reactivity has been attributed to a $p\pi$-$d\pi$ cyclo conjugation between the metal centre and the 2,4-pentanedionato anion.[7]

It has been reported that $NiCl_2 \cdot 6H_2O$ reacts with a mixture of (En) and (AcacH), in the presence of acetic acid, to yield the compound (**H**).[8] This compound is also obtained by reacting (AcacH) with $Ni(En)_2Cl_2$.[9] In the Au^{3+} chemistry, a similar reaction not only yields the complex (**H**) but also a macrocyclic compound of the (**J**) type.[10] This macrocycle was also synthesized by reaction of (En) with 4-amino-3-penten-2-one[11] or with the thio analog of ($BAEH_2$),[12] subsequent to the activation of the ketone or thioketone functions by Et_3OBF_4. Finally, from a literature survey it appears that the synthetic possibilities of the (En)/(AcacH) system are restricted to the preparation of the (**C**), (**H**) and (**J**) compounds. The diazepine (**F**) resulting from the double condensation of (AcacH) and (En) in strong acidic medium must be added to this list.[13] Furthermore, low yields characterize the reported synthesis of (**H**) and (**J**).

In this paper, our aim is to show that the possibilities of the (En)/(AcacH) system largely exceed these three compounds. This increase is based on the synthesis of the "half-unit" (AEH) [Fig. 1 (**A**)]. We have recently shown that suitable experimental conditions allow for the monocondensation of diaminoethane and 2,4-pentanedione, leading to (AEH), a stable, easily handled compound.[14] A similar approach for 2,4-pentanedione-*ortho*-

*The following abbreviations will be used in this paper: (AcacH) for 2,4-pentanedione, (En) for 1,2-diaminoethane, ($BAEH_2$) for *N,N'*-ethylene-bis(acetylacetoneimine), (AEH) for 7-amino-4-methyl-5-aza-3-hepten-2-one. The less common compounds will be pointed out by letters, as indicated in Fig. 1.

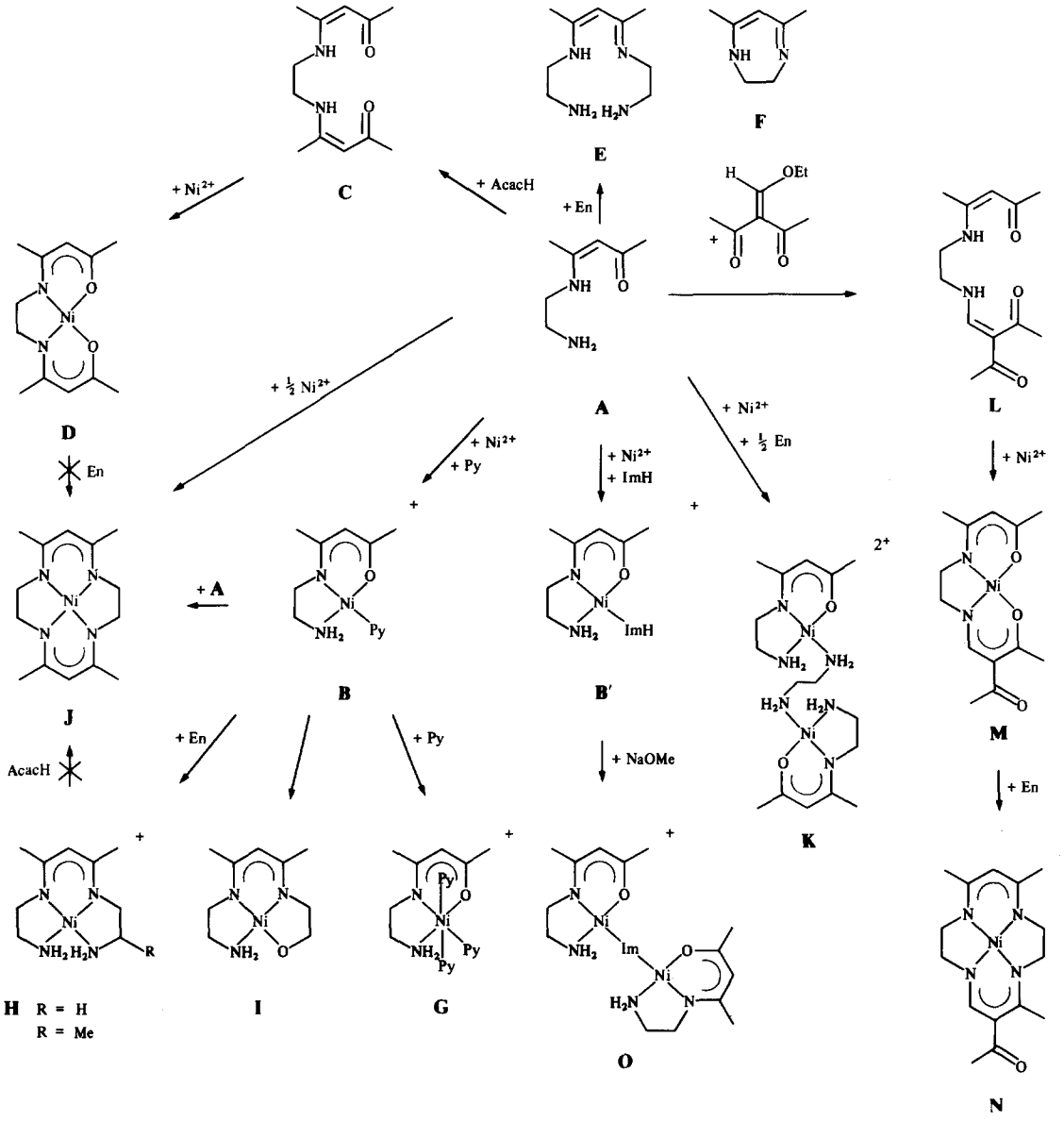

Fig. 1. Synthetic possibilities of the 2-4-pentanedione-1,2-diaminoethane system.

phenylenediamine recently appeared in the literature.[15,16] The authors suggested that the key compound was a monoanil or "half-unit" which, however, was not isolated. The occurrence of such "half-units" was evidenced in the hydrolysis of benzodiazepines[17] also suggested by Nelson[18] in more complicated systems.

RESULTS AND DISCUSSION

Reactivity of the "half-unit" (AEH)

The whole set of reactions made from the free (AEH) or complexed (**B**) ligand appears in Fig. 1.

Chronologically, the first use of (AEH) was to give an easy access to tetradentate non-symmetrical Schiff bases.[19–24] This possibility is illustrated in Fig. 1 by the reaction of (AEH) with 3-(ethoxymethylene)2,4-pentanedione, leading to the ligand (**L**). Its complexed form, (**M**), can subsequently react with (En) to give a functionalized macrocyclic complex, (**N**), in quantitative yield. Such a reaction is governed by the "thermodynamic and kinetic template effect"[24] and also by the inductive effect exerted by the -C(O)Me group. Conversely, complex (**D**), NiBAE, does not react with (En) to give (**J**).

The free (AEH) ligand can lead to ($BAEH_2$) (**C**), the diazepine (**F**) and in low yield, to the ligand (**E**). The most interesting reaction concerns self-

condensation of (AEH) to give the macrocyclic compound (**J**). This reaction necessitates the presence of (AEH), sodium methoxide and Py_2NiCl_2 as a source of nickel ions. The macrocycle is isolated under its complexed form in 30% yield. A mixture of free (AEH) and complex (**B**), where the (AEH) ligand is complexed, also yields the complex (**J**) but with a lower yield. It is interesting to recall here that the reaction of (AEH) with nickel(II) ions in the absence of any base leads to (**D**).

A promising opportunity results from the tridentate nature of (AEH) which cannot saturate the possibilities of coordination at the metal ion. Thus, at least, a second ligand such as pyridine can enter the coordination sphere, as it is the case for complexes (**B**) and (**G**). Interestingly, the second ligand may be (AEH) itself but in this instance, the nature of the resulting products depends on the nature of the metal ions. For cobalt (III), an octahedral complex $[Co(AE)_2]^+$ is obtained while in the case of the nickel(II) ion cyclization occurs, leading to the macrocyclic (**J**) complex. A trinuclear complex, $[(AECu)_3OH]^{2+}$, is isolated in high yield for the copper(II) ion.[25]

In (**B**), substituting pyridine, a monodentate ligand, by bidentate ligands offers new possibilities toward the preparation of dinuclear species such as (**O**) with imidazole[26] or (**K**) with 1,2-diaminoethane. At this stage, the versatility of (En) has to be emphasized. Depending on the experimental conditions, the system $(AEH)/Ni^{2+}/(En)$ can yield either the dinuclear complex (**K**) or the mononuclear species (**H**). In the first case, (En) makes a bridge between two nickel ions, while in the other case one of the two NH_2 groups reacts with the keto function of the (AE) ligand. Substituting 2-aminoethanol for (En) leads to the complex (**I**).

Until now, we have restricted our presentation to the nickel complexes since due to their diamagnetic behaviour they are easily characterized by NMR. Nevertheless, similar reactions work in the case of copper(II): only (**I**) and (**J**) are not obtained. This is not surprising in the case of (**J**) because it has been recently shown in the literature[27] that during the reaction of the free macrocycle with copper salts, the concentration of the macrocyclic complex (**J**) goes through a maximum, then decreases as decomposition takes place in solution. Indirect preparations with other metal ions can be carried out through demetallation of the nickel complexes and complexation by these ions.[28]

Characterization and properties

NMR results (^1H *and* ^{13}C). Free ligands and nickel(II) complexes are easily characterized by NMR (^1H and ^{13}C). The chemical shifts are reported in Tables 1 and 2. The ^1H NMR spectrum of (AEH) presents three singlets (two CH_3 and one CH group), a triplet–quadruplet set (two CH_2 groups) and two large signals attributable to the NH_2 and NH groups, the latter being strongly deshielded ($\delta \sim 11$ ppm). Selective irradiation of this signal changes the quadruplet (CH_2) into a triplet while irradiation of the second CH_2 signal (triplet) changes the quadruplet into a doublet. The appearance of two complex CH_2 signals is quite good evidence for the formation of (AEH) for they clearly show the inequivalence of the two methylene signals resulting from the monocondensation of 2,4-pentanedione with (En). Furthermore, the results of irradiation confirm the tautomeric form (**A**) for the "half-unit", conversely to the first suggestion.[14] The presence of a hydrogen bond —NH···OC— must be responsible for the deshielding of the NH signal. Most probably, the triplet–quadruplet set for the two CH_2 groups is due to the identity of the coupling constants $^3J_{HNCH} = {}^3J_{HCCH} = 6$ Hz.

The ^{13}C NMR spectrum displays seven signals corresponding to the seven types of carbon atoms present in (AEH): attributions were made, based on proton off-resonance decoupling experiments.[29]

The spectra of ligands (**C**), (**F**), (**L**) and that of complex (**D**) are identical to previously published results.[24,30–32]

The ligand (**E**) presents an interesting NMR spectrum. The two singlets related to the CH_3 groups display rather similar shifts (1.98 and 2.00 ppm). These values are consistent with the substitution of the keto function of (AEH) by an imine function. By analogy to (AEH), the triplet at 2.72 ppm, corresponds to the CH_2 group adjacent to the NH_2 functions. A multiplet centred at 3.30 ppm can be considered as resulting from the superposition of a triplet and a quadruplet of the CH_2N and CH_2NH groups, respectively. The other nuclei gave signals at 3 ppm (NH_2, broad signal), 7.75 ppm (NH, triplet) and 7.98 (CH, singlet). Coupling constants $^3J_{HNCH}$ and $^3J_{HNCH}$ are equal to 5 Hz.

NMR data for complex (**B**) have previously been published.[33] Complex (**J**) gives simple spectra: three

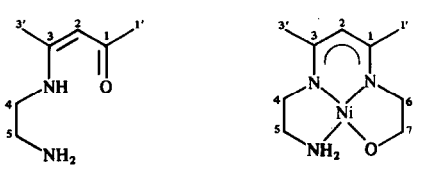

Fig. 2. Numbering of the different atoms used in ^1H and ^{13}C NMR tables.

Table 1. ^{1}H NMR data (numbering as in Fig. 2)

	CH_3			CH_2				CH			
	1′	3′	6′	4	5	6	7	2	NH_2	NH	Solvent
A	1.90	1.94	—	3.27(q)	2.87(t)	—	—	4.94	1.27	10.80	$CDCl_3$
B[a]	1.72	1.95	—	3.17(t)	2.61(m)	—	—	5.06	2.61	—	$CDCl_3$
C	1.93	2.00	—	3.47(d+s)	3.47(d+s)	—	—	4.98	—	11.40	$CDCl_3$
D	1.85	1.85	—	3.08	3.08	—	—	4.86	—	—	$CDCl_3$
E	1.97	2.00	—	3.28(m)	2.82(t)	2.82(t)	3.28(m)	7.97	3.00	7.75	$CDCl_3$
	2.00	1.97									
F	1.88	1.88	—	3.42	3.42	—	—	4.40	—	7.76	$CDCl_3$
H											
R = H	2.05	2.05	—	3.23(t)	2.77(m)	2.77(m)	3.32(t)	4.85	3.47	—	Acetone-d_6
R = CH_3	2.02	2.04	1.39(d)		(2.73–3.48)			4.83	3.60	—	Acetone-d_6
	2.04	2.02									
I	1.89	1.83	—	3.16[c]	2.55[c]	3.62[c]	3.16[c]	4.60	3.62	—	$CDCl_3$
	1.83	1.89									
J	1.90	1.90	—	3.12	3.12	3.12	3.12	4.58	—	—	$CDCl_3$
K[b]	1.85	2.05	—	3.15(m)	2.61(m)	—	—	4.94	2.97	—	Acetone-d_6

[a] Other resonances: 8.71, 7.43, 7.83 (pyridine).
[b] Other resonances: 2.97 (CH_2, diaminoethane), 6.90–7.57 (tetraphenylborate).
[c] Bad resolution.
s: singlet, d: doublet, t: triplet, q: quadruplet, m: multiplet.

singlets for ^{1}H NMR and four singlets for ^{1}H-decoupled ^{13}C spectra. ^{1}H NMR spectra of (**H**) are identical to literature results[9] when R = H, while ^{13}C NMR spectra display three CH_3 signals and two CN signals when R = CH_3. In order to characterize (**K**) by ^{1}H NMR, it is necessary to substitute perchlorate ions by tetraphenylborate ions. Its ^{1}H NMR spectrum is quite similar to that of the (**B**) complex, with a supplementary broad singlet at 2.97 ppm which corresponds to the CH_2+NH_2 groups of the bridge (En).

Infrared results. Complexes (**H**) and (**K**) display four bands between 3320–3080 cm^{-1} due to NH_2 functions whereas two bands are observed in this area for (**B**) complexes (symmetrical and antisymmetrical stretching vibrations). The increase in the number of bands is presumably due to hydrogen bonds between perchlorate ions and NH_2 groups. The two bands at *ca* 1590 and 1520 cm^{-1} may be assigned to the "double bonds" C=O, C=C and C=N. The band at 1590 cm^{-1} which is lacking in the (**J**) spectrum can be confidently attributed to

Table 2. ^{13}C NMR data (numbering as in Fig. 2)

	CH_3			CH_2				CH	CO	CN	
	1′	3′	6′	4	5	6	7	2	1	3	Solvent
A	27.4	17.5	—	45.5	40.8	—	—	94.0	193.1	162.1	$CDCl_3$
B[a]	24.0	21.6	—	54.1	43.9	—	—	100.7	176.0	166.5	$CDCl_3$
C	28.6	18.4	—	43.4	43.4	—	—	95.9	195.3	162.7	$CDCl_3$
D	24.2	20.9	—	52.9	52.9	—	—	99.4	176.8	164.5	$CDCl_3$
H											
R = H	21.1	21.1	—	54.1	43.5	—	—	98.8	159.1	159.1	Acetone-d_6
R = CH_3	20.3	20.3	17.9	54.0	44.1	51.7	60.0	98.6	159.2	159.0	Acetone-d_6
I	20.6	20.7	—	54.4	43.6	66.8	54.4	98.4	158.0	158.9	$CDCl_3$
	20.7	20.6							158.9	158.0	
J	21.5	21.5	—	53.7	53.7	53.7	53.7	97.2	158.7	158.7	$CDCl_3$

[a] Other resonances: 151.0, 125.5, 138.6 (pyridine).

ν(C=O). The broad band at 1090 cm^{-1} and the sharper one at 625 cm^{-1} are attributed to the perchlorate ion (ν_3 and ν_4). The absence of these bands in (**I**) confirms the deprotonation of the OH function of 2-aminoethanol.

A particular case: *the macrocyclic complex* (**J**), 5,7,12,14 - *tetramethyl* - 1,4,8,11 - *tetraaza* - 4,6,11,13 - *cyclotetradecatetraenato* (2-) *Nickel* (II)

The importance of macrocyclic complexes gives a particular interest to (**J**) which is readily prepared from (AEH). Seemingly, (**J**) has been previously prepared by Holm.[11] However, the physical characteristics of the two samples are not fully identical. For instance, our complex appears as a green microcrystalline powder whereas Holm's complex is described as a red–brown powder.

Analytical results agree with the formula $C_{14}H_{22}N_4Ni$ which is also consistent with mass spectra results. The most important peak is centred at 304 a.m.u., with higher isotopic peaks corresponding to the proposed formulation. Secondary peaks are attributable to deprotonated species, particularly those resulting from the loss of two or four protons. This agrees with the data reported by Holm who showed that (**J**) could be converted to a sixteen-electron π complex with a parent peak at 300 a.m.u.[11]

The NMR results (*vide supra*) are in accordance with the proposed structure. Regarding the electrochemical behaviour, (**J**) does not reduce at potentials of *ca* -2.0 V but undergoes apparent one-electron oxidation at -0.094 V (*vs* Ag/AgCl) in our case while the oxidation is reported to occur at $+0.110$ V (*vs* SCE) for the red–brown compound.

The most important difference between these two complexes is the colour but it is quite difficult to link this difference to a spectral modification since diffuse reflectance spectrum of the red–brown one was not reported. In the present case, the large *d-d* band moves from 16,800 cm^{-1} (solid) to 17,700 cm^{-1} (solution in acetone). Such an effect generally arises from a modification of electronic interactions between the next molecules in the solid state[34] and could be the reason for the difference between these two compounds. Another cause could be the conformation of the pentagonal Ni–N–C–C–N-cycles. Known structural studies show that these cycles have a *left* configuration. For (**J**), three stereochemical possibilities: two enantiomers, $\delta\delta$ and $\lambda\lambda$, and one diastereoisomer $\lambda\delta$, can be envisaged. The template effect of the nickel ion, which is essential for the synthesis of (**J**) could favour one of these forms or alter the *left* configuration of the pentagonal cycles. It is noteworthy that a green complex of the (**J**) type prepared from *ortho*-phenylenediamine presents two flat pentagonal cycles. In our case, structural studies of related complexes of the "half-unit"[25,26] point to a *left* configuration for the diamine chain. Furthermore, breaking of the (AEH) ligands may be discarded since this would result in the formation of (**D**) and (**H**) species which, as previously noted, cannot lead to (**J**). Finally, we suggest that the favoured isomer is the $\lambda\lambda$ enantioner.

Surprisingly compound (**J**) which from static susceptibility measurements is diamagnetic, shows an EPR signal in the solid state. Several samples resulting from different preparations present a thin signal (20 G) centred at $g = 2.0027$. The intensity of this signal does not vary even after exposure to air for a long time. This behaviour is similar to that observed for several diamagnetic metallo-phtalocyanins.[35,36] The g value and a peak-to-peak separation of 20 G are suggestive of the occurrence of π-cation radical species.

Conclusion

A view of Fig. 1 shows the prominent part of the "half-unit" (AEH) [(**A**) and (**B**)] to increase the reactive possibilities of the (AcacH)/(En) system. Kinetic and thermodynamic template effects play a major role in this chemistry, as in the synthesis of macrocycles (**N**).

In this article, reactions of the "half-unit" with (AcacH) and (En) deserve a detailed examination. Under its free (**A**) or complexed (**B**) forms, (AEH) reacts with an excess of (AcacH) or (En) to give terdentate compounds with N_2O_2 (**C, D**) or N_4 sites (**E, H**) that do not undergo further reaction to give the (**J**) macrocycle. Furthermore, if (En) is used in stoichiometric ratio and at ambient temperature, we do not observe a condensation reaction but formation of a dinuclear species (**K**). The formation of (**J**) necessitates the use of the preformed (AEH) exclusively, in the presence of nickel ions. These differences of behaviour are justified within the context of the mechanism recently proposed by Melson.[37]

The first step of the process in going from (**B**) to (**H**) could be the formation of a pentacoordinated $(\mathbf{B}.En)^+$ or hexacoordinated $(\mathbf{B}.2En)^+$ adduct in which one or two (En) molecules acting as monodentate ligands would be axially bound to nickel. The second step would involve deprotonation of the coordinated amine by the base, followed by the nucleophilic attack of the deprotonated amine NH^- at the CO group of the ligand to give (**H**). In this instance, the metal plays two important functions:

(i) it is used for orienting the reactant molecules and (ii) it acts as a positively charged centre able to induce suitable polarization of the coordinated amine and keto functions. The choice between a penta- or hexacoordinated intermediate would necessitate a detailed kinetic study, but we can suggest that, considering the preference of the nickel ion for six-coordination, the intermediate is (**B**.2En)$^+$ while in the case of the copper ion, a pentacoordinated intermediate seems more reliable. Such a model explains the autocondensation of (AEH) leading to (**J**). The intermediate species must involve two "half-units" orthogonally arranged around the hexacoordinated nickel. A similar complex has been isolated with cobalt (III).[14] Eventually, the decisive step would be the formation of an unstable penta- or hexacoordinated complex; the impossibility to form such a compound could explain the lack of reaction between (**H**) and (AcacH) or between (**D**) and (En). We found[29] that (**D**) remains diamagnetic in the presence of pyridine, while (**B**) becomes paramagnetic owing to the formation of a hexacoordinated species (**G**).

We can also recall the abnormal properties of the (**J**) macrocycle which need further study and particularly, a structural determination.

EXPERIMENTAL

Microanalyses were preformed by the Service Central de Microanalyses du CNRS, Lyon. Infrared spectra of KBr discs were recorded using a Perkin–Elmer 577 spectrometer, visible spectra using a Cary 14 spectrophotometer. Mass spectra were obtained using a VG Micromass 7070F spectrometer. Proton and ^{13}C NMR spectra were run on a Bruker WH90 using TMS (^1H spectra) and $CDCl_3$ (^{13}C spectra) as internal references. All chemical shifts (^1H and ^{13}C) are given in ppm *vs* TMS using CD_3COCD_3 or $CDCl_3$ as solvent. EPR spectra were obtained on a Bruker 200 TT spectrometer. Polarographic measurements were obtained with a "home-made microcomputer-controlled instrument" according to the following experimental conditions: 10^{-3} M in CH_3CN/Et_4NClO_4 (Fluka) 0.1 M medium; ambient temperature, potential measured *vs* Ag/AgCl (0.1 M KCl) as reference electrode.

Preparations

Some of the compounds and ligands were prepared according to literature processes, *viz.* (AEH),[14] (**B**),[33] (**B′** and **O**),[26] (**C** and **D**),[3,4] (**L, M** and **N**).[24]

(**E**) *ligand.* To an aqueous solution of (AEH) was added another aqueous solution containing one equivalent of (En) and of acetic acid. The mixture was stirred overnight. An aqueous Na_2CO_3 solution then was added and finally chloroform. The organic layer was dried and concentrated. Addition of ether caused a small amount of a precipitate to appear which was then filtered and dried.

(**F**) *ligand.* Addition of NH_4Cl to an alcoholic solution of (AEH) yielded the salt of diazepine (**F, HX**) (70% yield) which was isolated and neutralized to give (**F**).

(**K**) *complexes.* To a solution of (AEH) (7×10^{-3} M) in MeOH (50 cm^3) was added upon stirring the equivalent amount of a MeOH solution of NaOMe. A few minutes later, $NiClO_4 \cdot 6H_2O$ (2.57 g in 20 cm^3 of MeOH), then an (En) solution (3.3×10^{-3} M in 10 cm^3 of MeOH) were added. An orange precipitate appeared readily which was filtered, washed with MeOH and dried (80% yield). Calc. (Found) for $C_{16}H_{34}Cl_2N_6Ni_2O_{10}$: C, 29.2 (29.1); H, 5.2 (5.2); N, 12.8 (12.7); Ni, 17.7 (17.2); Cl, 10.8 (10.7)%.

With $CuClo_4 \cdot 6H_2O$, a similar experimental procedure yielded a blue product (80% yield). Calc. (Found) for $C_{16}H_{34}Cl_2Cu_2N_6O_{10}$: C, 28.7 (28.6); H, 5.1 (5.1); N, 12.6 (12.4); Cu, 19.0 (19.2); Cl, 10.6 (10.5)%.

(**J**) *complex.* To (AEH) (2 g, 1.410^{-2} M) in MeOH (60 cm^3) were added the equivalent amount of NaOMe (1.4×10^{-2} M) and Py_2NiCl_2[38] (2 g, 0.7×10^{-2} M). The mixture was heated for 20 min at 50°C under argon. The solution turned from yellow to red and gave a green precipitate. After cooling and filtration, the precipitate was taken back by boiling toluene and filtered again. After cooling, green microcrystals appeared. They were isolated and dried under reduced pressure (30% yield). This compound could also be obtained using (**B**) and (AEH) according to the procedure of the (**H**) complexes but the yield was lower. Calc. (Found) for $C_{14}H_{22}N_4Ni$: C, 55.3 (54.9); H, 7.2 (7.2); N, 18.4 (18.0); Ni, 19.1 (19.0)%.

(**H**) *and* (**I**) *complexes.* (**B**) (1 g) was suspended in water (30 cm^3). Addition of (En) (0.4 cm^3) and NaOH (0.1 g) caused the solubilization of the nickel complex. The mixture was brought to boiling for 15 min and left to stand overnight. The resulting red crystals were filtered and dried (50% yield). Calc. (Found) for $C_9H_{19}ClN_4NiO_4$: C, 31.7 (31.5); H, 5.6 (5.7); N, 16.4 (16.2)%. Substituting 1,2-diaminopropane for 1,2-diaminoethane yielded a more soluble, red compound (30% yield). Calc. (Found) for $C_{10}H_{21}ClN_4NiO_4$: C, 33.8 (33.5); H, 5.9 (6.0); N, 15.8 (15.6)%.

Use of ethanolamine yielded the red product (**I**). The mass spectrum of this compound gives the par-

ent peak at 241 a.m.u. (100) corresponding to the $C_9H_{17}N_3NiO$ formula while (**H**) complexes do not give such parent peaks in the same experimental conditions. Calc. (Found) for $C_9H_{17}N_3NiO$: C, 44.8 (44.1); H, 7.0 (7.2); N, 17.4 (16.9)%. In the case of [CuAEPy](ClO_4) and (En), a green product appeared (35% yield). Calc. (Found) for $C_9H_{19}ClCN_4O_4$: C, 31.2 (31.2); H, 5.5 (5.6); N, 16.2 (15.9)%.

Acknowledgement—The author is deeply indebted to Dr J.-P. Laurent for invaluable discussions and for his constant interest throughout this work.

REFERENCES

1. W. N. Wallis and S. C. Cummings, *Inorg. Chem.* 1974, **13**, 991.
2. A. Combes and C. Combes, *C. R. Acad. Sc., Paris* 1889, **108**, 1252.
3. G. Morgan and H. Smith, *J. Chem. Soc.* 1925, 2030; 1926, 918.
4. P. J. McCarthy, R. J. Hovey, K. Ueno and A. E. Martell, *J. Am. Chem. Soc.* 1955, **77**, 5820.
5. E. J. Olszewski, L. J. Boucher, R. W. Oehmke, J. C. Bailar Jr. and D. F. Martin, *Inorg. Chem.* 1963, **2**, 661.
6. R. D. Archer, *Inorg. Chem.* 1963, **2**, 292.
7. R. P. Hanzlik, *Inorganic Aspects of Biological and Organic Chemistry*. Academic Press, New York (1976).
8. W. H. Elfring and N. J. Rose, *Inorg. Chem* 1975, **14**, 2759.
9. L. F. Lindoy, W. E. Moody, J. Lewis and T. W. Matheson, *J. Chem. Soc., Dalton Trans.* 1976, 1965.
10. J. H. Kim and G. W. Everett Jr., *Inorg. Chem.* 1979, **18**, 3145.
11. T. J. Truex and R. H. Holm, *J. Am. Chem. Soc.* 1972, **94**, 4529.
12. S. C. Tang, S. Koch, G. N. Weinstein, R. W. Lane and R. H. Holm, *Inorg. Chem.* 1973, **12**, 2589.
13. G. Scharzenbach and K. Lutz, *Helv. Chim. Acta* 1940, **23**, 1139.
14. J.-P. Costes and G. Cros, *C. R. Acad. Sc., Paris, Ser. B* 1982, **294**, 173.
15. A. R. Cutler, C. S. Alleyne and D. Dolphin, *Inorg. Chem.* 1985, **24**, 2276.
16. A. R. Cutler, C. S. Alleyne and D. Dolphin, *Inorg. Chem.* 1985, **24**, 2281.
17. D. Lloyd, R. H. McDougall and D. R. Marshall, *J. Chem. Soc.* 1965, 3785.
18. S. M. Nelson, *Pure Appl. Chem.* 1980, **52**, 2461.
19. J.-P. Costes, G. Cros, M.-H. Darbieu and J.-P. Laurent, *Inorg. Chim. Acta* 1982, **60**, 111.
20. J.-P. Costes, G. Cros, M.-H. Darbieu and J.-P. Laurent, *Trans. Met. Chem.* 1982, **7**, 219.
21. H. Adams, N. A. Bailey, I. S. Baird, D. E. Fenton, J.-P. Costes, G. Cros and J.-P. Laurent, *Inorg. Chim. Acta* 1985, **101**, 7.
22. J.-P. Costes, *Inorg. Chim. Acta* 1987, **130**, 17.
23. R. C. Coombes, J.-P. Costes and D. E. Fenton, *Inorg. Chim. Acta* 1983, **77**, L173.
24. J.-P. Costes, G. Cros and J.-P. Laurent, *Inorg. Chim. Acta* 1985, **97**, 211.
25. J.-P. Costes, F. Dahan and J.-P. Laurent, *Inorg. Chem.* 1986, **25**, 413.
26. J.-P. Costes, J.-F. Serra, F. Dahan and J.-P. Laurent, *Inorg. Chem.* 1986, **25**, 2790.
27. M. Fujiwara, T. Matsushita and T. Shono, *Polyhedron* 1984, **3**, 1357.
28. D. P. Riley and D. H. Busch, *Inorg. Synth.* 1978, **18**, 36.
29. J.-P. Costes, G. Commenges and J.-P. Laurent, *Inorg. Chim. Acta*, in press.
30. G. O. Dudek and R. H. Holm, *J. Am. Chem. Soc.* 1961, **83**, 2099.
31. H. A. Staab and F. Vogtle, *Chem. Ber.* 1965, **98**, 2701.
32. L. F. Lindoy, W. E. Moody and D. Taylor, *Inorg. Chem.* 1977, **16**, 1962.
33. J.-P. Costes, *Trans. Met. Chem.* 1985, **10**, 185.
34. S. M. Peng and V. L. Goedken, *J. Am. Chem. Soc.* 1976, **98**, 8500.
35. E. C. Johnson, T. Niem and D. Dolphin, *Can. J. Chem.* 1978, **56**, 1381.
36. J. B. Raynor, M. Robson and A. S. M. Torrens-Burton, *J. Chem. Soc., Dalton Trans.* 1977, 2360.
37. G. A. Melson and L. A. Funke, *Inorg. Chim. Acta* 1984, **82**, 19.
38. N. S. Gill and R. S. Nyholm, *J. Inorg. Nucl. Chem.* 1961, **18**, 88.

Polyhedron Vol. 6, No. 12, pp. 2177–2180, 1987
Printed in Great Britain

0277–5387/87 $3.00+.00

PREPARATION AND X-RAY CRYSTAL STRUCTURE OF HEXAKIS(1-METHYLIMIDAZOLINE-2(3H)-THIONE)TETRAKIS(NITRATO)DILEAD(II)

STUART BRISTOW* and JAYNE A. HARRISON

Department of Chemistry, University of Exeter, Exeter EX4 4QD, U.K.

and

LOUIS J. FARRUGIA*

Department of Chemistry, University of Glasgow, Glasgow G12 8QQ, U.K.

(*Received* 4 *June* 1987; *accepted* 10 *July* 1987)

Abstract—The title complex, prepared by reacting lead(II) nitrate with a stoichiometric amount of 1-methylimidazoline-2(3H)-thione (mimt) in water, crystallizes in the triclinic space group $P\bar{1}$ with $a = 9.334(2)$, $b = 11.340(4)$, $c = 11.398(3)$ Å, $\alpha = 108.24(2)$, $\beta = 95.69(2)$, $\gamma = 100.27(2)°$ and $Z = 1$. In the solid state, the molecules show an unusual dimeric structure, with the formula $[(mimt)_2(NO_3)_2Pb(\mu\text{-}mimt)_2Pb(NO_3)_2(mimt)_2]$.

Imidazoline-2-thiones are familiar as ligands to a number of metals, including Cr,[1] Co,[2–5] Ni,[6–8] Cu,[9–10] Zn,[4,5,11] Pd,[12] Cd,[4] and Pt[13] complexes which have been well characterized. The coordination behaviour of ligands of this type is of interest as they serve as partial models for the biological imidazoline-2-thione derivative, ergothioneine found in erythrocytes.

Herein, we report the preparation and characterization of a complex of lead(II) with 1-methylimidazoline-2(3H)-thione. An X-ray crystal structure shows that the complex consists of discrete dimeric units with the formula $[Pb_2(C_4H_6N_2S)_6(NO_3)_4]$ per dimer.

EXPERIMENTAL

Preparation of hexakis (1-methylimidazoline-2(3H)-thione)tetrakis(nitrato)dilead(II)

To a hot (70°C) solution of lead(II) nitrate (0.66 g, 2.0 mmol) in water (10 cm^3) was added a hot (70°C) solution of 1-methylimidazoline-2(3H)-thione (Aldrich; 0.69 g, 6.0 mmol) in water (5 cm^3). The resulting green–yellow solution was evaporated to approximately one quarter its original volume, cooled and scratched with a glass rod, whereupon a yellow, microcrystalline solid was deposited. The product was isolated by filtration, washed with a little cold water and dried over anhydrous $CaCl_2$. Yield 0.97 g, 72%. M.p. 148–148.5°C. (Found: C, 21.2; H, 2.7; N, 16.5; Pb, 31.1. $C_{24}H_{36}N_{16}O_{12}Pb_2S_6$ requires C, 21.4; H, 2.7; N, 16.6; Pb, 30.8%.) Crystals suitable for X-ray diffraction studies were grown by slow evaporation of a solution of the complex in water.

Analytical and spectroscopic measurements

Microanalyses were carried out by Butterworth Laboratories Ltd., Teddington, Middlesex, U.K. Melting points were measured using a Gallenkamp MF-370 melting point apparatus and are uncorrected. Infrared spectra were recorded, for samples mulled in liquid paraffin and in hexachlorobutadiene, and held between NaCl plates, in the range 4000–600 cm^{-1} on a Perkin–Elmer PE 297 spectrophotometer. U.V.–visible absorbance measurements were recorded for samples dissolved in water and contained in matched silica cells (path-

* Authors to whom correspondence should be addressed.

length = 1 cm) on a Pye–Unicam SP6-500 spectrophotometer. The ^{1}H NMR spectrum was recorded at 250 MHz on a Bruker AM-250 spectrometer, at 30°C, using a sample dissolved in ^2H_2O, and was referenced to $Na^+(CH_3)_3Si(CH_2)_3SO_3^-$.

Crystal structure determination

Crystal data. $C_{24}H_{36}N_{16}O_{12}Pb_2S_6$, $M = 1347.43$. Triclinic, $a = 9.334(2)$, $b = 11.340(4)$, $c = 11.398(3)$ Å, $\alpha = 108.24(2)$, $\beta = 95.69(2)$, $\gamma = 100.27(2)°$, $V = 1111.9(6)$ Å^3 (by least-squares fit to the setting angles of 25 reflections, $\theta \geqslant 12°$), Mo-K_α radiation ($\lambda = 0.71069$ Å), space group $P\bar{1}$ (No. 2, C_i^1), $Z = 1$, $D_x = 2.01$ g cm^{-3}. Pale cream prisms. Crystal dimensions *ca* $0.6 \times 0.5 \times 0.3$ mm. $F(000) = 648$, μ(Mo-K_α) = 79.6 cm^{-1}.

Data collection and processing. Enraf–Nonius CAD4F diffractometer, $\theta/2\theta$ scan mode. A unique hemisphere of data (h, 0–11, k, −13–13, l, −13–13) totalling 4161 observations, $2 \leqslant \theta \leqslant 25°$ were collected, yielding 3897 independent reflections, of which the 3345 reflections having $I > 3.0\sigma(I)$ were deemed observable and used for structure solution and refinement. The intensities of 3 reflections (016, $\bar{1}\bar{5}5$, and $\bar{3}4\bar{5}$) were monitored during data collection, and a linear decay correction (equivalent to *ca* 10% over 10,000 reflections) was applied to all data. Data were also corrected for Lorentz/polarization effects, and for absorption using the method of Walker and Stuart.[14]

Structure solution and refinement. Patterson and Fourier methods for all non-hydrogen atoms. H atoms included at fixed, calculated positions (methyl C—H 1.084, ring C—H and N—H 1.073 Å). Full-matrix least squares refinement, with all non-hydrogen atoms anisotropic, minimizing $w(|F_o| - |F_c|)^2$ with the weighting scheme $w = 1/\sigma^2(F)$ used and judged satisfactory, gave final discrepancy indices R and R_w of 0.031 and 0.037, respectively. A final difference-Fourier synthesis showed no peaks greater than 1.16 nor less than −1.29 e Å^3, the largest features being in the vicinity of the Pb atom. Scattering factors were taken from ref. 15, with corrections for anomalous dispersion. All calculations were carried out on a Gould–SEL 32/27 minicomputer using the GX suite of programs.[16] Selected bond lengths and interbond angles are given in Table 1.*

RESULTS AND DISCUSSION

The reaction between $Pb(NO_3)_2$ and 1-methylimidazoline-2(3H)-thione (mimt) in water at 70°C gives a yellow product which has been shown by X-ray crystallography to exist in the solid state as discrete dimeric units, $[\{(mimt)_2(NO_3)_2Pb\text{-}(\mu\text{-}mimt)\}_2]$ (Fig. 1) separated by normal van der Waals distances. The two lead atoms in the formula unit are related by a crystallographic centre of symmetry and are bridged by the sulphur atoms of two mimt ligands. The distances between lead and the bridging S atoms are 3.053(2) and 3.195(2) Å; and the Pb—S_b—Pb and S_b—Pb—S_b angles are 82.0(1) and 98.0(1)° respectively, giving a Pb—Pb distance of 4.102(1) Å. Two more mimt ligands are coordinated to the Pb in positions essentially *trans* to the bridging ligands. Thus, S(1)—Pb—S(3) = 165.8(1)° and S(1′)—Pb—S(2) = 170.4(1)°. As expected, the Pb—S bond lengths to the nonbridging mimt ligands are shorter than those to the bridging ligands: Pb—S(2) = 2.850(2) Å and Pb—S(3) = 2.826(2) Å. These distances may be compared with Pb—S distances of *ca* 3.05 Å (bridging) and *ca* 2.96 Å (nonbridging) in a related lead–thiourea complex.[17] The overall geometry of the $\{(mimt)_2Pb(\mu\text{-}mimt)_2Pb(mimt)_2\}$ unit is reminiscent of the core structure found[18] for a nickel ethanethiolate complex, $[Ni_2(SEt)_6]^{2-}$, in that the bridging ligands adopt an *anti* configuration and the thione coordination about lead is distorted square planar. The mimt ligands are unremarkable in geometry compared to that found in 1,3-dimethylimidazoline-2-thione.[19] In particular, the C—S bond lengths in the complex (mean = 1.699(7) Å) are close to that in 1,3-dimethylimidazoline-2-thione (1.696(5) Å), and are indicative of partial C=S character. However, there is clearly some contribution to the electronic structure of the mimt ligand from a canonical resonance form involving a thiolate-type sulphur.[19] In addition, the mimt ligands are all essentially planar, with the greatest deviation from the mean plane defined by the five ring atoms being 0.012(8) Å for C(24).

The coordination sphere of lead is completed by two nitrato groups, one monodentate, the other bidentate, giving an overall coordination number of seven. However, the coordination geometry about lead can be described as distorted octahedral if the bidentate nitrate is considered to occupy a single coordination site. The conventional geometries for seven-coordination[20] are pentagonal bipyramidal, capped octahedral or capped trigonal prismatic:

* Atomic co-ordinates, thermal parameters, full lists of bond lengths and angles, and lists of F_o/F_c values have been deposited as supplementary data with the Editor, from whom copies are available on request. Atomic co-ordinates have also been deposited with the Cambridge Crystallographic Data Centre.

Table 1. Selected bond lengths (Å) and bond angles (°) for $[(mimt)_2(NO_3)_2Pb\text{-}(\mu\text{-}mimt)_2Pb(NO_3)_2(mimt)_2]$

Bonds			
Pb···Pb	4.102(1)	Pb—O(12)	2.811(5)
Pb—S(1)	3.053(2)	Pb—O(21)	2.524(5)
Pb—S(1′)	3.195(2)	Pb—O(22)	2.748(6)
Pb—S(2)	2.850(2)	S(1)—C(12)	1.698(6)
Pb—S(3)	2.826(2)	S(2)—C(22)	1.697(6)
		S(3)—C(32)	1.701(7)
Imidazoline rings (mean values)			
N_1—C(Methyl)	1.459[6]	N_1—C_2	1.339[5]
C_2—N_3	1.336[5]	N_3—C_4	1.379[6]
C_4—C_5	1.325[7]	N_1—C_5	1.385[5]
Angles			
Pb—S(1)—Pb′	82.0(1)	S(1)—Pb—S(1′)	98.0(1)
Pb—S(1)—C(12)	103.8(3)	S(1)—Pb—S(2)	89.1(1)
Pb′—S(1)—C(12)	114.9(3)	S(1)—Pb—O(12)	106.7(2)
Pb—S(2)—C(22)	98.2(3)	S(3)—Pb—S(1′)	86.0(1)
Pb—S(3)—C(32)	101.4(3)	S(1′)—Pb—O(12)	81.7(2)
S(1)—Pb—O(CT)[a]	81.9	S(2)—Pb—S(3)	88.6(1)
S(1′)—Pb—O(CT)[a]	83.9	S(2)—Pb—O(12)	90.2(2)
S(2)—Pb—O(CT)[a]	103.6	S(3)—Pb—O(12)	87.3(2)

[a] O(CT) is centroid of O(21) and O(22).

none of these geometries adequately describes the irregular stereochemistry found in this complex. This may be due to a stereochemically active lone pair of electrons. However, the geometry is irregular, whatever basis is chosen to describe the coordination polyhedron. Thus, we choose to describe the geometry as distorted octahedral, with the bidentate nitrato ligand occupying a single site. If the mean position of the coordinated oxygen atoms of the bidentate nitrato group is O(CT) then S(1)—Pb—O(CT) = 81.9°, S(1′)—Pb—O(CT) = 83.9°, and S(2)—Pb—O(CT) = 103.6°, values which support our description of the geometry. The appearance of a dimeric unit in the solid-

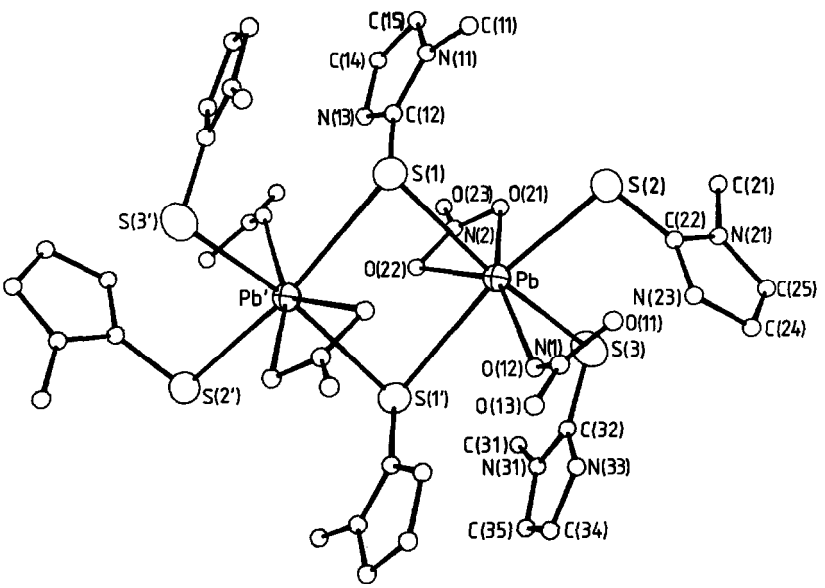

Fig. 1. Molecular structure of $[(mimt)_2(NO_3)_2Pb(\mu\text{-}mimt)_2Pb(NO_3)_2(mimt)_2]$.

state structure was unexpected and is unusual for complexes of this ligand.[1-13] Related complexes of Pb with thiourea (tu) have structures which are almost exclusively one-dimensionally non-molecular.[17] An exception is the triclinic form of $[Pb(tu)_6](ClO_4)_2$,[21] which consists of discrete, distorted octahedral $[Pb(tu)_6]^{2+}$ cations and ClO_4^- anions. Thus, this structure is unusual in being merely dimeric.

Confirmation of the presence of an N—H group in the compound is found in the infrared spectrum, where a fairly weak band is seen at 3150 cm^{-1}, compared with 3120 cm^{-1} in the free ligand. No S—H absorption around 2600 cm^{-1} was detected, confirming the thione tautomer. There are several bands in the region 1000–1500 cm^{-1}, where vibrations of coordinated NO_3^- should occur.[22] However, these are obscured by mimt ligand vibrations in the same region. There is little agreement on the position of C—S stretching vibrations.[23] Several bands in the spectrum might be assigned to this vibration, including one at 740 cm^{-1}.

The title compound dissolves in water to give a yellow solution ($\lambda_{max} = 208$ nm, $\varepsilon = 3.9 \times 10^4$ dm^3 mol^{-1} cm^{-1}; $\lambda_{max} = 255$ nm, $\varepsilon = 4.2 \times 10^4$ dm^3 mol^{-1} cm^{-1} per dimer), which has resonances in its ^1H NMR spectrum at $\delta = 3.58$ ppm (s, CH_3); 6.95 ppm (d, $J = 2.3$ Hz, CH) and 7.03 ppm (d, $J = 2.3$ Hz, CH). This apparent equivalence of the mimt ligands in solution suggests that the dimer does not remain intact in solution, but dissociates—perhaps to form monomeric $[Pb(mimt)_3]^{2+}$ cations.

REFERENCES

1. E. S. Raper, S. Redshaw and J. R. Creighton, *Inorg. Chim. Acta* 1984, **87**, L1.
2. E. M. Holt, S. L. Holt and K. J. Watson, *J. Am. Chem. Soc.* 1970, **92**, 2721.
3. E. S. Raper and I. W. Nowell, *Acta Cryst. B* 1979, **35**, 1600.
4. E. S. Raper and I. W. Nowell, *Inorg. Chim. Acta* 1980, **43**, 165.
5. E. S. Raper and P. H. Crackett, *Inorg. Chim. Acta* 1981, **50**, 159.
6. E. S. Raper, M. E. O'Neill and J. A. Daniels, *Inorg. Chim. Acta* 1980, **41**, 201.
7. M. E. O'Neill, E. S. Raper, I. W. Nowell and J. A. Daniels, *Inorg. Chim. Acta* 1981, **54**, L243.
8. R. E. Oughtred, E. S. Raper and I. W. Nowell, *Inorg. Chim. Acta* 1984, **84**, L5.
9. L. P. Battaglia, A. B. Corradi, M. Nardelli and M. E. V. Tani, *J. Chem. Soc., Dalton Trans.* 1976, 143.
10. E. R. Atkinson, D. J. Gardiner, A. R. W. Jackson and E. S. Raper, *Inorg. Chim. Acta* 1985, **98**, 35.
11. I. W. Nowell, A. G. Cox and E. S. Raper, *Acta Cryst. B* 1979, **35**, 3047.
12. L. M. Butler, J. R. Creighton, R. E. Oughtred, E. S. Raper and I. W. Nowell, *Inorg. Chim. Acta* 1983, **75**, 149.
13. M. E. O'Neill, E. S. Raper, J. A. Daniels and I. W. Nowell, *Inorg. Chim. Acta* 1982, **66**, 79.
14. N. Walker and D. Stuart, *Acta Cryst. A* 1983, **39**, 158.
15. D. T. Cromer, *International Tables for X-ray Crystallography*, Vol. IV. Kynoch Press, Birmingham (1974).
16. P. R. Mallinson and K. W. Muir, *J. Appl. Cryst.* 1985, **18**, 51.
17. F. H. Herbstein and M. Kaftory, *Acta Cryst. B* 1972, **28**, 405.
18. A. D. Watson, C. P. Rao, J. R. Dorfman and R. H. Holm, *Inorg. Chem.* 1985, **24**, 2820.
19. G. B. Ansell, *J. Chem. Soc., Perkin Trans.* 2, 1972, 841.
20. D. L. Kepert, *Prog. Inorg. Chem.* 1979, **25**, 41.
21. I. Goldberg and F. H. Herbstein, *Acta Cryst. B* 1972, **28**, 400.
22. K. Nakamoto, *Infrared and Raman Spectra of Inorganic and Coordination Compounds*, 3rd Edn, pp. 244–247. Wiley, New York (1978).
23. L. J. Bellamy, *The Infrared Spectra of Complex Molecules*, 3rd Edn, p. 401. Chapman & Hall, London (1975).

Polyhedron Vol. 6, No. 12, pp. 2181–2186, 1987
Printed in Great Britain

0277–5387/87 $3.00+.00

COMMUNICATION

OXYGEN ABSTRACTION FROM TETRAHYDROFURAN BY MOLYBDENUM–IODIDE COMPLEXES. X-RAY MOLECULAR STRUCTURE OF $[Mo_2(\mu\text{-}O)(\mu\text{-}I)(\mu\text{-}O_2CCH_3)I_2(THF)_4][MoOI_4(THF)]$ (THF = TETRAHYDROFURAN)

F. ALBERT COTTON* and RINALDO POLI

Department of Chemistry and Laboratory for Molecular Structure and Bonding, Texas A&M University, College Station, TX 77843, U.S.A.

(*Received* 30 *March* 1987; *accepted* 1 *July* 1987)

Abstract—The interaction between $Mo_2(O_2CCH_3)_4$, Me_3SiI and I_2 in THF resulted in oxygen abstraction from the solvent and formation of $[Mo_2(\mu\text{-}O)(\mu\text{-}I)(\mu\text{-}O_2CCH_3)I_2(THF)_4]^+[MoOI_4(THF)]^-$ and $I—(CH_2)_4—I$. The molybdenum complex has been characterized by X-ray diffractometry. *Crystal data*: triclinic, space group $P\bar{1}$, $a = 13.827(3)$ Å; $b = 15.803(7)$ Å; $c = 9.950(3)$ Å; $\alpha = 93.34(4)°$; $\beta = 102.40(2)°$; $\gamma = 90.09(2)°$; $V = 2120(2)$ Å^3; $Z = 2$; $d_{calc} = 2.559$ g cm^{-3}; $R = 0.0476$ ($R_w = 0.0613$) for 370 parameters and 3938 data with $F_0^2 > 3\sigma(F_0^2)$. The metal-metal distance in the cation is 2.527(2) Å and indicates a strong interaction. The magnetic behavior is consistent with the assignment of one unpaired electron to the Mo_2^{7+} core of the cation and one to the d^1 Mo(V) center of the anion. The interaction between $Mo(CO)_6$ and I_2 in THF also results in the formation of 1,4-diiodobutane.

We have recently been investigating the relatively unexplored chemistry of molybdenum–iodide complexes.[1–3] Among other things, we spent some time trying to obtain the tetrahydrofuran adduct of molybdenum(III), $MoI_3(THF)_3$, as this might be expected to be a good starting material for the synthesis of the virtually unknown class of molybdenum(III)–iodide derivatives. We were eventually able to prepare the compound by iodine oxidation of low-valent molybdenum carbonyl derivatives.[3] Among other unsuccessful strategies, we also tried to obtain the above mentioned material by iodine oxidation of quadruply bonded molybdenum(II) iodide dimers, $Mo_2I_4L_4$. This led to the discovery of a quite complex reactivity which involves oxygen abstraction from the solvent and formation of a metal complex with a higher average oxidation state. We report here this chemistry and the X-ray molecular structure of the peculiar molybdenum product.

EXPERIMENTAL

All operations were carried out under an atmosphere of prepurified argon with standard Schlenk-tube techniques. Solvents were dried by conventional methods and distilled under dinitrogen prior to use. Instruments used were as follows: IR, Perkin–Elmer 783; ^{1}H-NMR, Varian XL-200; GC-MS, HP 5995; magnetic susceptibility, Johnson–Matthey JME. $Mo_2(O_2CCH_3)_4$ was prepared as described in the literature,[4] while Me_3SiI was obtained from Aldrich and used as received.

Preparation of $[Mo_2OI_3(O_2CCH_3)(THF)_4][MoOI_4(THF)]$

$Mo_2(O_2CCH_3)_4$ (1.09 g, 2.54 mmol) was suspended in 15 cm^3 of THF and treated with Me_3SiI (1.50 cm^3, 10.5 mmol). Most of the insoluble mo-

* Author to whom correspondence should be addressed.

lybdenum compound, but not all, rapidly dissolved to afford a deep yellow solution. The appearance of the mixture did not change upon brief reflux. Treatment with an additional 0.50 cm^3 of Me_3SiI (3.5 mmol) caused the complete disappearance of the yellow solid. A solution of I_2 (0.43 g, 1.68 mmol) in 15 cm^3 of THF was then added dropwise at room temperature. The solution first turned green and then a dark grey solid started to precipitate. At the end of the addition there was much precipitate, while the supernatant liquid had a dark red color. The product was filtered off, washed with THF and dried *in vacuo*. Yield: 0.91 g [33% with respect to the molybdenum(II) acetate, 100% with respect to I_2 and the stoichiometry of eq. (2), see Discussion]. IR (nujol mull): 2340 w (br), 1265 w, 1440 vs (br), 1380 s, 1345 s, 1055 m, 1025 m, 945 w, 680 s, 620 m, 595 w, 385 s, and 345 s cm^{-1}. $\chi_g = 2.20 \times 100^{-6}$ c g s; $\mu_{eff} = 3.14$ BM [diamagnetic correction (molar) $= -553.1 \times 10^{-6}$ c g s]. A GC-MS analysis of the filtered solution showed the presence of $I—(CH_2)_4—I$ (M^+, $m/e = 310$).

A single crystal for the X-ray analysis was obtained as follows: $Mo_2(O_2CCH_3)_4$ (0.21 g, 0.50 mmol) in THF (5 cm^3) was treated with 0.30 cm^3 of Me_3SiI (2.1 mmol). After brief stirring the mixture was filtered and a solution of I_2 (0.08 g, 0.31 mmol) in 10 cm^3 of *n*-hexane was carefully layered on top of it. A mixture of well-formed black and yellow crystals was produced upon diffusion. A black crystal was used for the subsequent X-ray analysis. A yellow crystal was selected and its cell constants determined from its X-ray diffraction pattern. These correspond to those reported[5] for $Mo_2(O_2CCH_3)_4$. The identity of the black crystals with the grey microcrystalline material obtained in the above described procedure was confirmed by IR analysis.

Reaction between $Mo(CO)_6$ *and* I_2 *in* THF

$Mo(CO)_6$ (4.62 g, 17.5 mmol) was treated with I_2 (6.69 g, 26.4 mmol) in THF (50 cm^3). The mixture was refluxed for 3 days. IR monitoring in the carbonyl stretching region showed the disappearance of the carbonyl starting material (band at 1979 cm^{-1}). The final mixture contained a black insoluble solid, whose nature was not further investigated. After filtration, the solution was reduced in volume by room temperature evaporation at reduced pressure. A dense liquid remained at the end of the treatment. Distillation of this residue under reduced pressure yielded 4.48 g of colorless $I—(CH_2)_4—I$ (b.p. 69–80°C at *ca* 6×10^{-2} mm Hg), identified by IR, ^{1}H-NMR and MS (55% yield with respect to I_2).

X-ray crystallography for $[Mo_2OI_3(O_2CCH_3)(THF)_4][MoOI_4(THF)]$

A single crystal was glued under argon to the inside of a thin-walled capillary and mounted on the diffractometer. The cell constant determination, data collection and reduction were routine. A semi-empirical absorption correction based on the variation of intensity during azimuthal (ψ) scans for nine standard reflections having an Eulerian angle χ close to 90° was applied.[6] The structure was solved with the SHELXS-86[7] direct methods program package and refined by alternating cycles of full-matrix least-squares and difference Fourier maps. An additional absorption correction was applied at the end of isotropic refinement.[8] The agreement factor R was then 0.122. Anisotropic refinement converged at $R = 0.0476$ ($R_w = 0.0613$). The highest peaks in the final difference Fourier map, having a height of > 1 e $Å^{-3}$, were all located at < 1.0 Å distance from the iodine atoms and were attributed to series termination errors and/or deficiencies in the absorption correction. Pertinent crystal data are assembled in Table 1 and selected bond distances and angles are in Table 2.*

RESULTS AND DISCUSSION

We allowed $Mo_2(O_2CCH_3)_4$ to interact with four equivalents of Me_3SiI in THF as solvent, with the hope that this would afford the reactive intermediate $Mo_2I_4(THF)_4$ according to eq. (1).

$$Mo_2(O_2CCH_3)_4 + 4Me_3SiI + 4THF \rightarrow Mo_2I_4(THF)_4 + 4Me_3SiO_2CCH_3. \quad (1)$$

The same strategy has been employed for the preparation of chloride,[9,10] bromide[11] and iodide derivatives[12] of the Mo_2^{4+} core containing phosphine ligands, although higher nuclearity clusters were sometimes obtained.[9] We have evidence that reaction 1 does not proceed to completion when a $Me_3SiI/Mo_2(O_2CCH_3)_4$ ratio of 4:1 is employed. Some molybdenum acetate remains unreacted in these conditions and even the use of an excess of the silyl reagent over the 4:1 ratio results in the formation of a final product where one acetate group is still present. We believe that the incom-

* A full list of bond distances and angles, positional parameters, anisotropic displacement parameters and F_o/F_c data have been deposited with the Editor as supplementary materials. The atomic coordinates have also been deposited with the Cambridge Crystallographic Data Centre.

Table 1. Crystal data for $[Mo_2(\mu\text{-}O)(\mu\text{-}I)(\mu\text{-}O_2CCH_3)I_2(THF)_4][MoOI_4(THF)]$

Formula	$C_{22}H_{43}I_7Mo_3O_9$
Formula weight	1627.73
Space group	$P\bar{1}$
Systematic absences	none
a, Å	13.827(3)
b, Å	15.803(7)
c, Å	9.950(3)
α, deg	93.34(4)
β, deg	102.40(2)
γ, deg	90.09(2)
V, Å^3	2120(2)
Z	2
d_{calc}, g cm^{-3}	2.559
Crystal size, mm	$0.1 \times 0.5 \times 0.9$
$\mu(MoK_\alpha)$, cm^{-1}	59.586
Data collection instrument	CAD-4
Radiation (monochromated in incident beam)	MoK_α ($\lambda_\alpha^- = 0.71073$ Å)
Orientation reflections, number, range (2θ)	25, 15–25
Temperature, °C	20
Scan method	$\omega - 2\theta$
Data col. range, 2θ, deg	4–45
No. unique data, total with $F_0^2 > 3\sigma(F_0^2)$	4986, 3938
Number of parameters refined	370
Trans. factors, max., min.	1.000, 0.377
R^a	0.0476
R_w^b	0.0613
Quality-of-fit indicator^c	1.77
Largest shift/esd, final cycle	0.43
Largest peak, e Å^{-3}	1.33

[a] $R = \Sigma ||F_o| - |F_c|| / \Sigma |F_o|$.
[b] $R_w = [\Sigma w(|F_o| - |F_c|)^2 / \Sigma w|F_o|^2]^{1/2}$; $w = 1/\sigma^2(|F_o|)$.
[c] Quality-of-fit $= [\Sigma w(|F_o| - |F_c|)^2 / (N_{obs} - N_{parameters})]^{1/2}$.

pleteness of reaction 1 is caused by a competitive interaction of Me_3SiI with the solvent (*vide infra*).

Once the interaction between $Mo_2(O_2CCH_3)_4$ and Me_3SiI is completed, a subsequent treatment with I_2 causes the formation of a precipitate, identified as $[Mo_2(\mu\text{-}O)(\mu\text{-}I)(\mu\text{-}O_2CCH_3)I_2(THF)_4]^+[MoOI_4(THF)]^-$ by X-ray analysis. The stoichiometry of the reaction is represented in eq. (2). The formation of 1,4-diiodobutane has been confirmed by GC-MS analysis.

$$3Mo_2(O_2CCH_3)_4 + 10Me_3SiI + 6I_2 + 14THF \rightarrow 2[Mo_2OI_3(O_2CCH_3)(THF)_4][MoOI_4(THF)] + 10Me_3SiO_2CCH_3 + 4I{-}(CH_2)_4{-}I. \quad (2)$$

We suggest that the oxophilicity and the Lewis acidity of the molybdenum center make a molybdenum-assisted iodide cleavage of THF possible, as shown in Scheme 1.

It is well known that ethers can be cleaved by HI and also by HX (X = Br, Cl) in the presence of Lewis acids such as $ZnCl_2$.[13] Me_3SiI has also been found to be effective in the cleavage reaction of ethers.[14] The room temperature interaction between THF and Me_3SiI in $CDCl_3$ as solvent was reported to take place rapidly with formation of $Me_3Si{-}O{-}(CH_2)_4{-}I$ followed by slow conversion to $I{-}(CH_2)_4{-}I$.[14a] We cannot therefore exclude *a priori* that 1,4-diiodobutane is produced only by interaction of Me_3SiI with THF and that the oxygen atom is then in some way transferred from the silicon to the molybdenum centers. We observe, however, that in our system the molybdenum acetate dimer will compete with THF for the silyl reagent according to eq. (1). The observed fast dissolution of the insoluble $Mo_2(O_2CCH_3)_4$ upon treatment with Me_3SiI indicates that reaction between these two compounds does occur. The competitive interaction between Me_3SiI and THF may, however, account for the incompleteness of reaction 1.

That the molybdenum center is capable of assisting the cleavage reaction of THF by iodide is proved by the result of the interaction between $Mo(CO)_6$ and I_2 in THF. The interaction between $Mo(CO)_6$ and I_2 in a 2:3 ratio in refluxing benzene–toluene

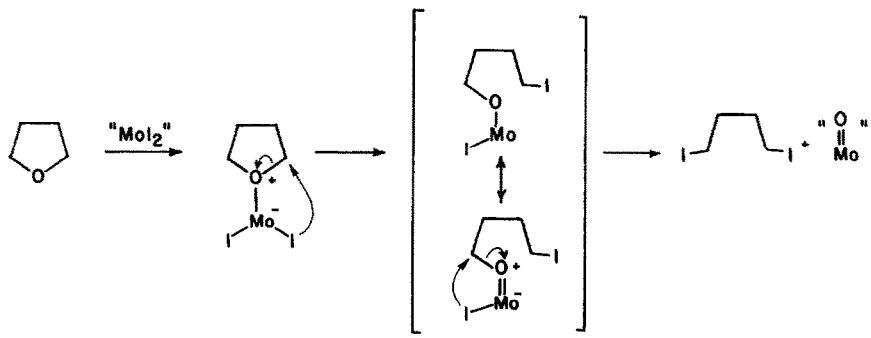

Scheme 1.

Table 2. Selected bond distances (Å) and angles (deg.) for $[Mo_2(\mu\text{-}O)(\mu\text{-}I)(\mu\text{-}O_2CCH_3)I_2(THF)_4][MoOI_4(THF)]$

Atom 1	Atom 2	Distance	Atom 1	Atom 2	Distance	Atom 1	Atom 2	Distance
Mo1	Mo2	2.527(2)	Mo2	I2	2.710(1)	Mo3	I4	2.724(2)
Mo1	I1	2.700(1)	Mo2	I12	2.732(1)	Mo3	I5	2.752(2)
Mo1	I12	2.737(1)	Mo2	O2	2.197(8)	Mo3	I6	2.749(2)
Mo1	O1	2.197(9)	Mo2	O4	2.213(9)	Mo3	O8	1.644(11)
Mo1	O3	2.207(9)	Mo2	O6	2.088(7)	Mo3	O9	2.402(10)
Mo1	O5	2.081(7)	Mo2	O7	1.880(8)			
Mo1	O7	1.859(8)	Mo3	I3	2.761(2)			

Atom 1	Atom 2	Atom 3	Angle	Atom 1	Atom 2	Atom 3	Angle	Atom 1	Atom 2	Atom 3	Angle
Mo2	Mo1	I1	105.54(5)	O5	Mo1	O7	90.6(3)	O4	Mo2	O7	161.2(3)
Mo2	Mo1	I12	62.38(4)	Mo1	Mo2	I2	104.50(4)	O6	Mo2	O7	91.1(3)
Mo2	Mo1	O1	127.1(2)	Mo1	Mo2	I12	62.58(4)	Mo1	I12	Mo2	55.04(3)
Mo2	Mo1	O3	146.9(3)	Mo1	Mo2	O2	126.2(3)	Mo1	O7	Mo2	85.0(3)
Mo2	Mo1	O5	85.9(2)	Mo1	Mo2	O4	147.0(2)	I3	Mo3	I4	92.63(5)
Mo2	Mo1	O7	47.8(3)	Mo1	Mo2	O6	85.9(2)	I3	Mo3	I5	171.60(6)
I1	Mo1	I12	92.40(4)	Mo1	Mo2	O7	47.1(2)	I3	Mo3	I6	87.45(5)
I1	Mo1	O1	91.7(2)	I2	Mo2	I12	94.23(4)	I3	Mo3	O8	94.3(4)
I1	Mo1	O3	89.2(2)	I2	Mo2	O2	91.7(2)	I3	Mo3	O9	84.4(2)
I1	Mo1	O5	167.9(2)	I2	Mo2	O4	89.6(2)	I4	Mo3	I5	89.09(5)
I1	Mo1	O7	100.2(2)	I2	Mo2	O6	169.4(2)	I4	Mo3	I6	165.69(7)
I12	Mo1	O1	167.9(3)	I2	Mo2	O7	97.6(2)	I4	Mo3	O8	95.3(4)
I12	Mo1	O3	88.0(3)	I12	Mo2	O2	167.6(3)	I4	Mo3	O9	83.1(2)
I12	Mo1	O5	89.2(2)	I12	Mo2	O4	87.0(2)	I5	Mo3	I6	88.85(5)
I12	Mo1	O7	110.0(3)	I12	Mo2	O6	88.5(2)	I5	Mo3	O8	93.7(4)
O1	Mo1	O3	80.7(4)	I12	Mo2	O7	109.5(2)	I5	Mo3	O9	87.7(2)
O1	Mo1	O5	84.4(3)	O2	Mo2	O4	82.1(3)	I6	Mo3	O8	98.9(4)
O1	Mo1	O7	80.4(4)	O2	Mo2	O6	83.8(3)	I6	Mo3	O9	82.7(2)
O3	Mo1	O5	78.8(3)	O2	Mo2	O7	80.4(3)	O8	Mo3	O9	177.9(4)
O3	Mo1	O7	159.1(3)	O4	Mo2	O6	80.3(3)				

Numbers in parentheses are estimated standard deviations in the least significant digits.

is a good synthetic method for anhydrous MoI_3.[15] When, however, we carried out the same interaction in boiling THF [hoping to produce the THF adduct, $MoI_3(THF)_3^3$], significant amounts of 1,4-diiodobutane were obtained together with an uncharacterized black solid, presumably an oxo-iodide of molybdenum.

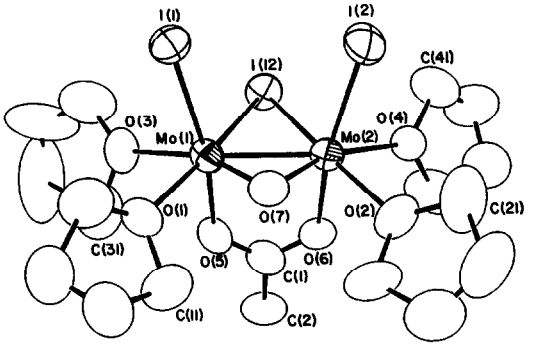

Fig. 1. An ORTEP view of the $[Mo_2OI_3(O_2CCH_3)(THF)_4]^+$ ion.

Molecular structure

A view of the cation is illustrated in Fig. 1, while the anion is shown in Fig. 2. The assignment of the

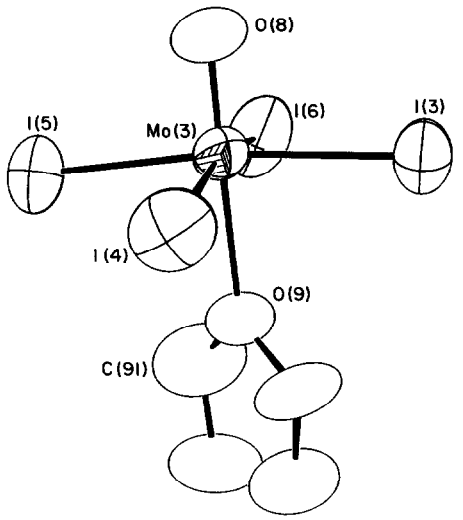

Fig. 2. An ORTEP view of the $[MoOI_4(THF)]^-$ ion.

charge to the two ions is based on the existence in the literature of another salt of the $[MoOI_4L]^-$ anion (L = H_2O).[16] Also, this assignment fits well with the observed magnetic properties of the compound (*vide infra*).

The cation is a dinuclear complex with a distorted edge-sharing bioctahedral arrangement of the ligands. A bridging oxygen atom and a bridging iodine atom are the ligands defining the shared edge. An axially coordinated acetate group also bridges the two metal centers. The coordination spheres are completed by one axial iodide ligand and two equatorial THF groups per molybdenum atom. This cation therefore contains three different bridges between the metal atoms. An identical configuration has been found for the rhenium compound $Re_2OCl_5(O_2CC_2H_5)(PPh_3)_2$,[17] the two metal atoms being bridged there by an oxygen atom, a chlorine atom and a propionato group.

There are several reasons for the deviation of the geometry from the ideal edge-sharing bioctahedral one. The first one is the different bond lengths to the two bridging atoms in the shared edge (average values are given): Mo—(μ-O), 1.87 Å; Mo—(μ-I), 2.734 Å. Another is the close contact between the two axial iodide ligands (I···I: 3.931 Å), which is less than the sum of the van der Waals radii (4.30 Å).[18] These two atoms thus push each other away from the ideal axial positions (the average I—Mo—O angle involving the acetate oxygen atom is 168.6°). The equatorial donor atoms show only slight deviations from the respective least-squares planes. Each molybdenum atom, on the other hand, is displaced away from its own local equatorial plane by 0.140(1) Å towards the axial iodine atom. The two planes form a dihedral angle of 21.2(4)°.

The metal–metal separation of 2.527(2) Å indicates a strong bonding interaction. A Mo_2^{7+} core is present in the cation, with five electrons available for metal–metal bonding. These may be distributed among the orbitals of the dimetal core either in the $\sigma^2\pi^2\delta^1$ or in the $\sigma^2\pi^2\delta^{*1}$ order.[19] In either case a paramagnetism for the ion is expected corresponding to one unpaired electron. A distance of 2.789(1) has been reported for the d^3–d^3 compound $Mo_2Cl_6(dppm)_2$ [dppm = bis(diphenylphosphino) methane], which is believed to have a $\sigma^2\pi^2\delta^{*2}$ configuration. No edge-sharing bioctahedral compound of Mo(IV) with a metal–metal bonding interaction seems to have been reported. The edge-sharing bioctahedral $[Mo_2Cl_{10}]^{2-}$ complex has a metal–metal separation of 3.80 Å, which indicates no bonding interaction.[20] The compound $Mo_2S_2(SCNPr_2)_2(S_2CNPr_2)_2$, however, has been described as containing a double bond between Mo(IV) centers,[21] with a metal–metal distance of 2.705(2) Å. The shorter distance in our compound might then be due to the occupation of the δ orbital by the fifth electron, but it is also possible that the two metals are forced closer to each other by the presence of the small oxo bridge.

The average separation between molybdenum and terminal iodine atoms is a little shorter (2.705 Å) than those involving the bridging iodine atom. These Mo—I bond lengths are shorter than those commonly found for other molybdenum–iodide complexes,[1-3,22] in agreement with the higher oxidation state and the positive charge of the ion. The Mo—(μ-O) distances are slightly shorter than those typical of Mo—(μ-O)—Mo moieties in trinuclear clusters of molybdenum(IV) (the latter being in the 1.91–1.94 Å range)[23] and may indicate some double bond character. The Mo—O distances involving the acetato group (average 2.084 Å) compare with those found in $Mo_2(O_2CCH_3)_4$ (2.10–2.21 Å),[5] while those involving the THF ligands (2.19–2.21 Å) are in the same range found in $MoI_3(THF)_3$.[3]

The anion (see Fig. 2) is a distorted octahedral complex of Mo(V). The structural parameters compare well with those of the very similar anion $[MoOI_4(H_2O)]^-$.[16] The Mo—I distances are longer than those found in the cation (*vide supra*) in spite of the higher oxidation state in the anion. This may be due to the different charge of the two ions. The Mo—O(THF) bond length is also substantially longer in the anion, mainly because of the well-known strong *trans* influence of the oxo group. The molybdenum atom is displaced away from the least-squares plane of the four iodine atoms by 0.265(1) Å, towards the oxo ligand.

A d^1 electronic configuration for the Mo(V) center is present in the anion. The salt $[Mo_2OI_3(O_2CCH_3)(THF)_4][MoOI_4(THF)]$ is therefore expected to have two unpaired electrons, one in the cation and one in the anion. A magnetic susceptibility measurement agrees with this view, as an effective magnetic moment of 3.14 BM is found at room temperature.

Acknowledgements—We are grateful to the National Science Foundation for support of this work and to Prof. D. H. R. Barton for helpful discussion.

REFERENCES

1. F. A. Cotton and R. Poli, *J. Am. Chem. Soc.* 1986, **108**, 5628.
2. F. A. Cotton and R. Poli, *Inorg. Chem.* 1986, **25**, 3624.
3. F. A. Cotton and R. Poli, *Inorg. Chem.* 1987, **26**, 1514.

4. A. B. Brignole and F. A. Cotton, *Inorg. Synth.* 1972, **13**, 81.
5. F. A. Cotton, Z. C. Mester and T. R. Webb, *Acta Cryst.* 1974, **B30**, 2768.
6. A. C. T. North, D. C. Phillips and F. S. Mathews, *Acta Cryst.* 1968, **A24**, 351.
7. G. M. Sheldrick, SHELXS-86, University of Cambridge (1986).
8. N. Walker and D. Stuart, *Acta Cryst.* 1983, **A39**, 158.
9. R. E. McCarley, T. R. Ryan and C. C. Torardi, in *Reactivity of Metal–Metal Bonds* (Edited by M. H. Chisholm) No. 155, pp. 41–60. American Chemical Society; Washington, D.C., U.S.A. (1981).
10. (a) J. D. Arenivar, V. V. Mainz, H. Ruben, R. A. Andersen and A. Zalkin, *Inorg. Chem.* 1982, **21**, 2649; (b) P. A. Agaskar and F. A. Cotton, *Inorg. Chim. Acta* 1984, **83**, 33; (c) P. A. Agaskar, F. A. Cotton, I. F. Fraser and R. D. Peacock, *J. Am. Chem. Soc.* 1984, **106**, 1851; (d) P. A. Agaskar and F. A. Cotton, *Inorg. Chem.* 1984, **23**, 3383.
11. F. L. Campbell, III, F. A. Cotton and G. L. Powell, *Inorg. Chem.* 1984, **23**, 4222.
12. (a) F. A. Cotton, K. R. Dunbar and M. Matusz, *Inorg. Chem.* 1986, **25**, 3641; (b) F. A. Cotton, K. R. Dunbar and R. Poli, *Inorg. Chem.* 1986, **25**, 3700.
13. N. L. Allinger, M. P. Cava, D. C. De Jongh, C. R. Johnson, N. A. Lebel and C. L. Stevens, *Organic Chemistry*, 2nd edn, pp. 439–440. Worth Publishers, New York (1976).
14. (a) M. E. Jung and M. A. Lyster, *J. Org. Chem.* 1977, **42**, 3761; (b) G. A. Olah, S. C. Narang, B. G. B. Gupta and R. Malhotra, *J. Org. Chem.* 1979, **44**, 1247.
15. A. D. Westland and N. Muriithi, *Inorg. Chem.* 1973, **12**, 2356.
16. A. Bino and F. A. Cotton, *Inorg. Chem.* 1979, **18**, 2710.
17. F. A. Cotton and B. M. Foxman, *Inorg. Chem.* 1968, **7**, 1984.
18. L. Pauling, *The Nature of the Chemical Bond*, 3rd edn, p. 260. Cornell University Press, Ithaca (1960).
19. (a) S. Shaik, R. Hoffmann, C. R. Fisel and R. H. Summerville, *J. Am. Chem. Soc.* 1980, **102**, 4555; (b) A. R. Chakravarty, F. A. Cotton, M. P. Diebold, D. B. Lewis and W. J. Roth, *J. Am. Chem. Soc.* 1986, **108**, 971.
20. E. Hen, F. Weller and K. Dehnicke, *Z. Anorg. Allg. Chem.* 1984, **508**, 84.
21. L. Ricard, J. Estienne and R. Weiss, *Inorg. Chem.* 1973, **12**, 2182.
22. F. A. Cotton and R. Poli, *Inorg. Chem.* 1986, **25**, 3703.
23. F. A. Cotton, Z. Dori, R. Llusar and W. Schwotzer, *Inorg. Chem.* 1986, **25**, 3654 and references therein.

Polyhedron Vol. 6, No. 12, pp. 2187–2189, 1987
Printed in Great Britain

0277–5387/87 $3.00+.00

COMMUNICATION

RAPID THERMAL HYDROGEN PRODUCTION FROM 2,3-BUTANEDIOL CATALYZED BY HOMOGENEOUS RHODIUM CATALYSIS

DAVID MORTON and DAVID J. COLE-HAMILTON*

Chemistry Department, University of St. Andrews, St. Andrews, Fife KY16 9ST, U.K.

and

JOHN A. SCHOFIELD and ROBERT J. PRYCE

Sittingbourne Research Centre, Shell Biosciences Division, Sittingbourne, Kent, ME9 8HG, U.K.

(*Received* 25 *April* 1987; *accepted* 11 *May* 1987)

Abstract—Thermal production of hydrogen from butane-2,3-diol is achieved with rates of up to 125 catalyst turnovers per hour using the homogeneous rhodium catalysts, $[Rh(bipy)_2]Cl$, $[RhH(P^iPr_3)_3]$ and $[RhCl(PPh_3)_3]$. (bipy = 2,2′-bipyridyl).

High grade fuel oils can be obtained from the hydrogenation of biomass,[1] but the need for external hydrogen has meant that such processes are not generally commercially viable. The ability to produce hydrogen from biomass, or from products that are readily formed from biomass might allow such hydrogenations to be carried out in a one or two stage system without the need for other sources of hydrogen.

One material that can readily be produced by fermentation reactions is butane-2,3-diol and we now report the rapid thermal dehydrogenation of this compound under mild conditions.

Heating butane-2,3-diol with $[Rh(bipy)_2]Cl$, $[RhCl(PPh_3)_3]$ or $[RhH(P^iPr_3)_3]$ in the presence of base produces hydrogen at initial rates corresponding to 66–125 mol of hydrogen per mol of catalyst per hour (Table 1). These rates, which correspond to up to 1.1 l of hydrogen per l of catalyst solution per hour are considerably higher than is normally observed for alcohol dehydrogenation reactions, although comparable to those obtained from high boiling alcohols using $[Ru(PPh_3)_2(CO)(O_2CCF_3)_2]$[2] or from ethanol using $[Rh(bipy)_2]Cl$.[3] The initial fast rates fall slightly after *ca.* 2 h, but sustained hydrogen production at 40–90 turnovers per hour can be achieved for at least 24 h.

Although for $[Rh(bipy)_2]Cl$, similar rates of hydrogen production can be obtained using ethanol as substrate,[3] hydrogen is only produced in very low yields for thermal reactions of ethanol catalyzed by $[RhH(P^iPr_3)_3]$ or $[RhCl(PPh_3)_3]$. We attribute the much higher yields and rates of hydrogen production from butane-2,3-diol to the absence of the facile decarbonylation of alkanals (the products of dehydrogenation of primary alcohols) by rhodium(I) complexes and the stability of the carbonyl species formed towards CO loss. In the case of $[Rh(bipy)_2(CO)]^+$, CO can be lost by water–gas shift type chemistry[3,4] and for $[RhH(CO)P^iPr_3)_2]$, CO can be lost photochemically, accounting for the activity of $[RhH(P^iPr_3)_3]$ for photochemical decomposition of primary alcohols.[5]

Since butane-2,3-diol is a secondary alcohol, the possible reaction products, acetoin and butane-2,3-

* Author to whom correspondence should be addressed.

Table 1. Rates of hydrogen production (r/mol [mol catalyst]$^{-1}$ h^{-1}) from butane-2,3-diol (at 140°C) and propan-2-ol (at 120°C) catalyzed by rhodium(I) complexes

Substrate (5 cm^3)	Catalyst	[Catalyst] (10^{-4} mol dm^{-3})	[NaOH] (mol dm^{-3})	Time (h)	r
butane-2,3-diol	$RhCl(PPh_3)_3$	3.70	1.0	2	125
butane-2,3-diol	$RhCl(PPh_3)_3$	3.90	1.0	18	89
butane-2,3-diol	$RhCl(PPh_3)_3$	3.90	1.0	23[a]	55
butane-2,3-diol	$RhH(P^iPr_3)_3$	5.86	1.0	3	66
butane-2,3-diol	$RhH(P^iPr_3)_3$	3.46	1.0	17	41
butane-2,3-diol	$RhH(P^iPr_3)_3$	3.46	1.0	23[a]	43
butane-2,3-diol	$[Rh(bipy)_2]Cl$	3.48	1.0	2	117
butane-2,3-diol	$[Rh(bipy)_2]Cl$	2.60	1.0	15	50
butane-2,3-diol	$[Rh(bipy)_2]Cl$	2.60	1.0	20[a]	56
propan-2-ol	$[RhCl(PPh_3)_3]$	5.22	0.25	3	119
propan-2-ol	$[RhH(P^iPr_3)_3]$	5.22	0.25	3	35
propan-2-ol	$[Rh(bipy)_2]Cl$	3.04	0.25	2	115

[a] Reaction was evacuated after 18, 17 or 15 h and continued for a further 5, 6 or 5 h.

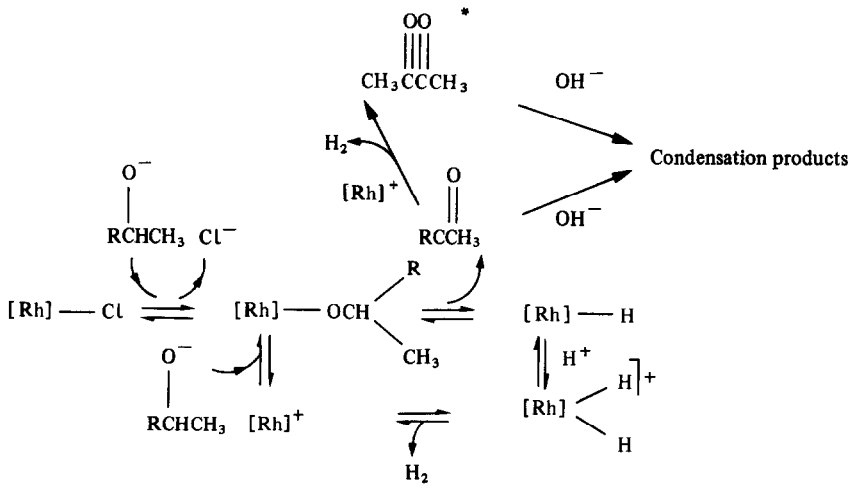

Scheme 1. Proposed mechanism for hydrogenation of secondary alcohols catalyzed by [RhCl$(PPh_3)_3$][Rh] = $[Rh(PPh_3)_2]$, R = Me or MeCH(OH). Similar mechanisms can be proposed for the other catalysts employed in this study. * R = $CH_3CH(OH)^-$.

dione* are not susceptible to decarbonylation hence poisoning of the catalyst does not occur and efficient hydrogen production is observed. Consistent with this explanation is the observation that all of the compounds efficiently dehydrogenate secondary alcohols, e.g. propan-2-ol, although less basic conditions are required for this reaction (Table 1).

In the absence of base, the activity of the catalysts drops markedly presumably because the equilibrium constants for reactions such as (1) are much higher than those for reaction (2).

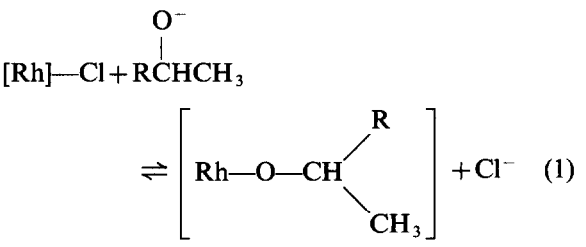

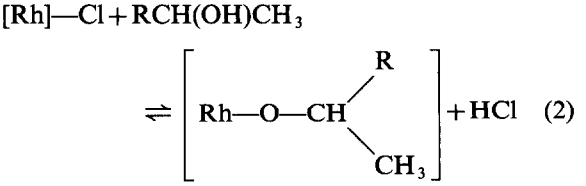

* These are not detected as reaction products by g.l.c. analysis of the liquid phase, but condensation products, which are readily formed under the basic reaction conditions can be observed.

We are currently carrying out detailed experiments aimed at elucidating the mechanisms of these interesting reactions, but preliminary results suggest mechanisms of the type shown in Scheme 1.

REFERENCES

1. E. M. Goodger, *Alternative Fuels; Chemical Energy Resources*. Macmillan, London (1980).
2. A. Dobson and S. D. Robinson, *Inorg. Chem.* 1977, **16**, 137.
3. D. Morton and D. J. Cole-Hamilton, *J. Chem. Soc., Chem. Commun.* 1987, 248.
4. D. Mahajon, C. Creutz and N. Sutin, *Inorg. Chem.* 1985, **24**, 2063.
5. E. Delgado Leita, M. A. Luke, R. F. Jones and D. J. Cole-Hamilton, *Polyhedron* 1982, **1**, 839.

Polyhedron Vol. 6, No. 12, pp. 2191–2192, 1987
Printed in Great Britain

0277-5387/87 $3.00+.00

COMMUNICATION

THE SYNTHESIS OF ORGANO–IMIDO COMPLEXES OF Cr(IV) AND Fe(III)

ROBYN L. ELLIOTT, PETER J. NICHOLS and BRUCE O. WEST*

Department of Chemistry, Monash University, Clayton, Victoria 3168, Australia

(*Received* 1 *July* 1987; *accepted* 10 *July* 1987)

Abstract—The reaction of *p*-tolylazide with (5,10,15,20-tetraphenylporphyrinato) chromium(II) (Cr(TPP)) yields the high spin chromium(IV) organo–imido complex, $CH_3C_6H_4N{=}Cr(TPP)$. *N,N'*-ethylene-bis-(salicylideneiminato)iron(II), (Fe(salen)), however reacts with arylazides to produce iron(III) organo–imido-bridged compounds of general formula, $[Fe(salen)]_2NR$ showing magnetic coupling between the Fe(III) centres.

The synthesis and study of transition metal organo–imido complexes (M=NR) is of considerable current interest.[1] However, relatively few examples are yet known of compounds in which chelating ligands are attached to the metal in addition to the organo–imido group.[2–5] One synthetic route which seems to have potential application to a wide variety of metals involves reaction between arylazides and metal chelate complexes which are readily oxidizable by a two electron process to give the organo–imide with nitrogen as the second product thus,

$$(Lig)M^n + N_3R \rightarrow (Lig)M^{n+2}(NR) + N_2.$$

This type of reaction has been used with particular success in synthesizing $(Lig)_2Mo(VI)(NR)_2$ complexes from Mo(II)[3,4] and Mo(IV)[5] starting materials with Lig = dithiocarbamato or dithiophosphato ligands.

We wish to report the synthesis of the first chromium porphyrin organo–imido complex, *p*-$CH_3C_6H_4N{=}Cr(TPP)$ by reaction of the air sensitive metalloporphyrin, Cr(II)(TPP), with excess *p*-tolylazide in toluene with rigorous exclusion of moisture and air. When solutions of the reagents are mixed at room temperature, a gradual change in colour is observed over 10 min from the brown of Cr(II)(TPP) to the green–brown solution containing the product. Nitrogen is evolved during the reaction. The complex is precipitated as a green–brown solid by addition of hexane.

The molecular ion $[CH_3C_6H_4N \cdot Cr(TPP)]^{+\cdot}$ is observed as a low intensity peak in the mass spectrum of the compound together with $[Cr(TPP)]^{+\cdot}$ and $[CH_3C_6H_4NH]^{+\cdot}$, the latter peak being particularly intense. Elemental microanalyses and mass spectroscopy indicate the presence of one further molecule of toluene in the product. The magnetic moment for the complex in the solid state at 293K is 2.7 BM, consistent with a spin free d^2, Cr(IV) system. This may be compared with the diamagnetism (or at least very low paramagnetism) found for a variety of Cr(IV) oxo porphyrin[6] (O=Cr(IV)(P)) derivatives, including the isoelectronic O=Cr(TPP).

The UV/visible spectrum of the complex in toluene displays a Soret band at 423 nm with a further low intensity band at 537 nm. O=Cr(TPP) has similar bands at 431 and 544 nm.[6] Addition of tetrahydrofuran (THF) or N-methylimidazole (N-MeIm) causes shifts in the position of the Soret band and the appearance of several new bands at higher wavelengths, indicating coordination of these donor molecules to the Cr atom in the organo–imido complex thus†

THF/toluene λ_{max} = 410sh, 433, 555, 594 nm

N–MeIm/toluene λ_{max} = 417sh, 439, 558, 604 nm.

Tetrahydrofuran binds notably more strongly to the organo–imido complex than to O=Cr(TPP)

*Author to whom correspondence should be addressed.

†The determination of accurate extinction coefficients has been found to be very difficult because of the combination of low solubility and sensitivity to moisture of this complex.

since the addition of comparable amounts of THF to a toluene solution of O=Cr(TPP) causes no change in position or intensity of the absorption maxima.

It has not been possible to determine unambiguously a value for the Cr—N(imido) stretching frequency in this complex because of the multitude of ligand vibrations in the 850–1150 cm^{-1} region where the frequency may be expected.[7]

The complex reacts with PPh_3 in toluene yielding the phosphine–imide $CH_3C_6H_4N{=}PPh_3$, this product being identified by its mass spectrum after evaporation of the reaction mixture under vacuum and extraction of the phosphine–imide together with excess PPh_3 by hexane. Cr(II)(TPP), the second product formed, was detected in the reaction mixture by its characteristic Soret absorption band at 421 nm.[6] Oxygen transfer from O=Cr(TPP) to PPh_3 has been shown to occur readily.[8]

We have also observed that the readily oxidised complex, Fe(II)(salen), undergoes smooth reactions at room temperature with a variety of arylazides.

Thus, when Fe(salen) reacted with *p*-tolylazide in dry CH_2Cl_2 under nitrogen the initial red–brown colour of the mixture lightened rapidly and nitrogen was evolved. Addition of hexane precipitated a black, microcrystalline complex whose microanalysis indicated a solvated product of formula $[Fe(salen)]_2NC_6H_4CH_3 \cdot CH_2Cl_2$. The mass spectrum of the product does not display the molecular ion of the complex but peaks due to $[Fe(salen)]^{+\cdot}$ and $[CH_3C_6H_4NH]^{+\cdot}$ were dominant once the very volatile CH_2Cl_2 had been removed. The compound has a magnetic moment $\mu_{eff} = 2.8$ BM per dimer at 293K similar to that found for the μ-oxo derivative[9] ($\mu_{eff} = 2.7$ BM). Solutions of the complex in CH_2Cl_2 rapidly turn orange in colour when exposed to air due to the formation of an Fe(III)(salen) hydrolysis product while *p*-toluidine is also recovered. The complex does not react with triphenylphosphine.

Unsolvated complexes have been isolated from toluene solution using *p*-tolyl, *p*-chloro and phenylazides. Their general properties and magnetism, each similar to those described for the CH_2Cl_2 solvated *p*-tolyl derivative, strongly indicate that they are organo–imido bridged derivatives as in (**a**). The reduced magnetic moments observed for these complexes are no doubt due to extensive spin-coupling through the organo–imido bridge as found for the complexes $[Fe(III)(salen)]_2X$, X = O[9] and S.[10] Detailed magnetic studies on several of the complexes will be reported elsewhere.

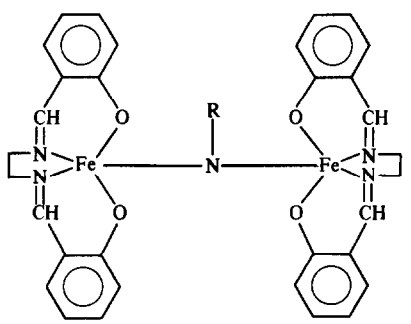

(a)

A number of homobinuclear[1,11] and trinuclear[12,13] bridged organo–imido derivatives have been reported with carbonyl or cyclopentadienyl groups attached to the metal. The present iron complexes appear to be the first examples of organo–imido bridged compounds involving simple chelating ligands.

Acknowledgements—This work was supported by a grant from the Australian Research Grants Scheme (to BOW and PJN) and the award of a Commonwealth Postgraduate Scholarship (to RLE).

REFERENCES

1. W. A. Nugent and B. L. Haymore, *Coord. Chem. Rev.* 1980, **31**, 123.
2. J. W. Buchler and S. Pfeifer, *Z. Naturforsch*, 1985, **40B**, 1362 (V–porphyrin); J. P. Mahy, P. Battioni, D. Mansuy, J. Fisher, R. Weiss, J. Mispelter, I. Morgenstern-Badarau and P. Gans, *J. Am. Chem. Soc.* 1984, **106**, 1699 (Fe–porphyrin); R. Rossi, H. Marchi, A. Duatti, L. Magon, V. Casellato, R. Graziani and G. Polizzotti, *Inorg. Chim. Acta* 1984, **90**, 121 (Re–salicylaldimine); L. S. Tan, G. V. Golden and B. L. Haymore, *Inorg. Chem.* 1983, **22**, 1744 (Nb.Ta–dithiocarbamate).
3. B. L. Haymore, E. A. Maatta and R. A. D. Wentworth, *J. Am. Chem. Soc.* 1979, **101**, 2063.
4. A. W. Edelblut and R. A. D. Wentworth, *Inorg. Chem.* 1980, **19**, 1110.
5. E. A. Maatta and R. A. D. Wentworth, *Inorg. Chem.* 1979, **18**, 2409.
6. D. J. Liston and B. O. West, *Inorg. Chem.* 1985, **24**, 1568.
7. J. H. Osborne and W. C. Trogler, *Inorg. Chem.* 1985, **24**, 3098; J. H. Osborne, A. L. Rheingold and W. C. Trogler, *J. Am. Chem. Soc.* 1985, **107**, 7945.
8. J. T. Groves, W. J. Kruper, R. C. Haushalter and W. M. Butler, *Inorg. Chem.* 1982, **21**, 1363.
9. K. S. Murray, *Coord. Chem. Rev.* 1974, **12**, 1.
10. J. R. Dorfman, J.-J. Girerd, F. D. Simhon, T. D. P. Stack and R. H. Holm, *Inorg. Chem.* 1984, **23**, 4407.
11. M. L. H. Green and K. J. Moynihan, *Polyhedron* 1986, **5**, 921.
12. D. C. Bradley, M. B. Hursthouse, A. N. de M. Jelfs and R. L. Short, *Polyhedron* 1983, **2**, 849.
13. S. Bhaduri, K. S. Gopalkrishnan, G. M. Sheldrick, W. Clegg and D. Stalke, *J. Chem. Soc., Dalton Trans.* 1983, 2339; *Acta Cryst. Series C* 1984, **40**, 927; S. Bhaduri, K. S. Gopalkrishnan, W. Clegg, P. G. Jones, G. M. Sheldrick and D. Stalke, *J. Chem. Soc., Dalton Trans.* 1984, 1765.

AUTHOR INDEX